

Contents of Volume

Number 1	
Acid-catalysed acylation of carbonyl compounds S M Lukyanov, A V Koblik	1
Dibenzo-<i>p</i>-dioxins. Methods of synthesis, chemical properties, and hazard assessment A D Kunzevich, V F Golovkov, V R Rembovskii	27
Heterylferrocenes. Synthesis and use M A Shvekhgeimer	41
The nature and dynamics of nonlinear excitations in conducting polymers. Polyacetylene V I Krinichnyi	81
Number 2	
Nonlinear theory of multicomponent sorption dynamics and chromatography A I Kalinitchev	95
Computer-aided studies of reaction mechanisms A V Zeigarnik, L G Bruk, O N Temkin, V A Likholobov, L I Maier	117
Chemistry of methylenecyclobutane M G Vinogradov, A V Zinenkov	131
Synthesis and properties of sultines, cyclic esters of sulfinic acids O B Bondarenko, L G Saginova, N V Zyk	147
Synthesis of monodisperse functional polymeric microspheres for immunoassay N I Prokopov, I A Gritskova, V R Cherkasov, A E Chalykh	167
Number 3	
Electrochemistry of hydride-forming intermetallic compounds and alloys O A Petrii, S Ya Vasina, I I Korobov	181
Direct high-pressure gas-phase oxidation of natural gas to methanol and other oxygenates V S Arutyunov, V Ya Basevich, V I Vedeneev	197
Coordination chemistry of hydrophosphorane compounds K N Gavrilov, I S Mikhel	225
Cardo polyheteroarylenes. Synthesis, properties, and characteristic features S V Vinogradova, V A Vasnev, Ya S Vygodskii	249
Titanium compounds as catalysts for esterification and transesterification M I Siling, T N Laricheva	279
Number 4	
Design of inorganic compounds with tetrahedral anions B I Lazoryak	287

The tautomerism of heterocyclic thiols. Five-membered heterocycles E D Shtefan, V Yu Vvedenskii	307
The reactivity of metal β-diketonates in the thermal decomposition reaction E I Tsyganova, L M Dyagileva	315
Catalytic asymmetric synthesis of β-hydroxyacids and their esters E I Klabunovskii	329
Gradient interpenetrating polymer networks: formation and properties L M Sergeeva, L A Gorbach	345
Interaction of bleomycin and its oligonucleotide derivatives with nucleic acids D S Sergeev, V F Zarytova	355
Number 5	
Phase equilibria in M–X–X' and M–Al–X ternary systems (M = transition metal; X, X' = B, C, N, Si) and the crystal chemistry of ternary compounds A I Gusev	379
Synthesis and application of sulfenamides I V Koval'	421
Natural aliphatic oxygenated unsaturated acids. Synthesis and biological activity. A G Tolstikov, G A Tolstikov	441
Number 6	
Ternary carbides and nitrides based on transition metals and subgroup IIIB, IVB elements: electronic structure and chemical bonding A L Ivanovskii	461
Stabilisation of metal ions in unusual oxidation states and electron dynamics in oxide glasses A I Aleksandrov, A I Prokof'ev, N N Bubnov	479
Reactivity of hydrocarbons and their individual C–H bonds with peroxy radicals W W Pritzkow, V Ya Suprun	497
Cyclic mechanisms of chain termination in the oxidation of organic compounds E T Denisov	505
The nature and dynamics of nonlinear excitations in conducting polymers. Heteroaromatic polymers V I Krinichnyi	521
Positively charged lipids: structure, methods of synthesis and applications I D Konstantinova, G A Serebrennikova	537
Number 7	
Adamantane derivatives containing heterocyclic substituents in the bridgehead positions. Synthesis and properties M A Shvekhgeimer	555
Aromatic polyimides with flexible and rigid chains Z B Shifrina, A L Rusanov	599
Catalytic properties of metal-phthalocyanines in reactions involving hydrogen E M Sul'man, B V Romanovskii	609

Prospects for the development of methods for the processing of organohalogen waste. Characteristic features of the catalytic hydrogenolysis of halogen-containing compounds L N Zanaveskin, V A Aver'yanov, Yu A Treger	617
Selective oxidation of gaseous hydrocarbons by bacterial cells G A Kovalenko	625
Number 8	
The problem of the quantitative evaluation of the inductive effect: correlation analysis A R Cherkasov, V I Galkin, R A Cherkasov	641
Methods for the measurement of ion mobilities and applications G V Karachevtsev	657
Physicochemical aspects of the adsorption of sulfur dioxide by carbon adsorbents S A Anurov	663
The influence of chemical structure on the relaxation properties of heat-resistant aromatic polymers A A Askadskii	677
Methods for the covalent attachment of nucleic acids and their derivatives to proteins G Ya Sheflyan, E A Kubareva, E S Gromova	709
Bacterial polyesters. Synthesis, properties, and application B E Geller	725
Number 9	
Unusual monosaccharides: components of O-antigenic polysaccharides of microorganisms N K Kochetkov	735
Natural peroxides. Chemistry and biological activity G A Tolstikov, A G Tolstikov, O V Tolstikova	769
Polycondensation reactions catalysed by Ni and Pd complexes as the method for the synthesis of carbo- and hetero-cyclic polyarylenes A L Rusanov, I A Khotina	785
Prospects in the application of alkoxo-technology in heterogeneous catalysis Yu M Rodionov, E M Slyusarenko, V V Lunin	797
The influence of the medium on the mechanical properties of catalysts E D Shchukin, L Ya Margolis, S I Kontorovich, Z M Polukarova	813
Number 10	
Inner valence molecular orbitals and the structure of X-ray photoelectron spectra Yu A Teterin, S G Gagarin	825
Low-temperature functionalisation of alkanes and cycloalkanes by 'classical' and 'non-classical' (superacidic) Friedel–Crafts complexes I S Akhrem, A V Orlinkov, M E Vol'pin	849
The structure and properties of block poly(vinylidene fluoride) and systems based on it V V Kochervinskii	865
Number 11	

Capillary gas-solid chromatography V G Berezkin	915
Fluoroalkoxy-derivatives of trivalent phosphorus: synthesis and reactivity V F Mironov, I V Konovalova, L M Burnaeva, E N Ofitserov	935
Dependence of the extaction ability of orgaic compounds on their structure A M Rozen, B V Krupnov	973
Electrochemical syntheses based on elemental phosphorous and phosphorus acid esters A P Tomilov, I M Osadchenko, A V Khudenko	1001
 Number 12	
Spatial and electronic structure of vinyl and allenyl chalcogenides L M Sinegovskaya, B A Trofimov	1009
Thermodynamics of polyolefines B V Lebedev	1039
Thermodynamics of polylactones B V Lebedev	1063
Michael synthesis of esters of β-amino acids: stereochemical aspects N N Romanova, A G Gravis, Yu G Bundel'	1083

Acid-catalysed acylation of carbonyl compounds

S M Luk'yanov, A V Koblik

Contents

I. Introduction	1
II. Acylals	1
III. Enol acylates	4
IV. α -Haloalkyl acylates	6
V. Acyloxycarbenium ions	7
VI. Direct <i>O</i> -acylation of aldehydes and ketones	13
VII. Acid-catalysed <i>C</i> -acylation of carbonyl compounds	17
VIII. Electrophilic catalysis by acyl cations	18

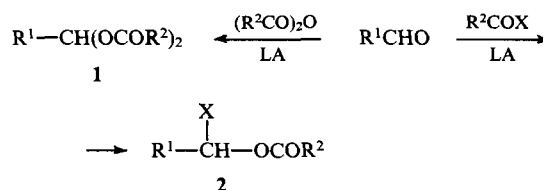
Abstract. Data concerning the *O*- and *C*-acylation of carbonyl compounds under acid catalytic conditions are surveyed. The properties of little-studied products of these reactions, i.e., acylals, α -haloalkyl acylates, and enol acylates are described. The acyloxycarbenium ions formed by the acylation of aldehydes and ketones are characterised. The recently discovered new reactions of carbonyl compounds that lead to various heterocyclic and polyfunctional compounds are discussed. The bibliography includes 275 references.

I. Introduction

The acylation of carbonyl compounds is traditionally considered as a means of lengthening a carbon chain together with the introduction of the carbonyl function. Such reactions include ester condensation and related reactions (i.e., Claisen, Dieckmann, Darzens reactions, etc.).^{1–6} These processes are catalysed by bases, while *O*-acylation which sometimes occurs is usually regarded as an undesirable side reaction. The preparative application of these methods was so successful and fruitful that the analogous acid-catalysed conversions were considered only as theoretically, rather than practically, interesting reactions. Only in some cases, when acid and base catalysis results in different products (e.g., acylation of asymmetric ketones), have syntheses been developed.^{1,2} Perhaps only acylation of ketones by anhydrides in the presence of boron trifluoride is an exception.^{5,6}

The technique of base-catalysed acylation of carbonyl compounds has been improved and modified (e.g., in Taylor–McKillop and Passerini reactions,^{7,8} phase-transfer catalysis,⁹ and the application of acyl anions¹⁰), whereas acid-catalysed reactions have remained much less investigated until now. This is explained by difficulties in the effective stabilisation of cationoid intermediates, as cationoid chemistry has been less well studied than carbanion chemistry.¹¹

Although the importance of the reaction between carbonyl compounds and aprotic acids was noted thirty years ago,¹² few publications concerning this problem are available. On the other hand, two reactions of aldehydes with anhydrides and acid halides in the presence of Lewis acids have been known since the beginning of this century. These reactions lead to the acylals **1** and the α -haloalkyl acylates **2**, respectively.



LA — Lewis acid; X = Cl, Br.

The attitude of synthetic chemists towards acid-catalysed carbonyl reactions can be illustrated by the history of compounds **1** and **2**: the properties of the acylals **1** have been very little investigated until now. The α -haloesters **2** were recalled in the sixties only as subjects of a series of studies under the common title 'A forgotten carbonyl reaction' (see Section IV).

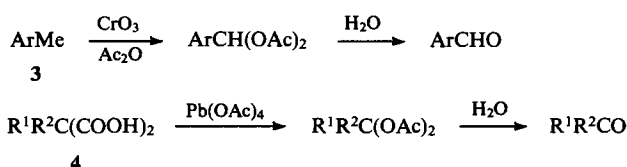
II. Acylals

The esters formed from geminal diols (i.e., acylals, also called aldehyde diacylates) have been known for more than 120 years. Chloral diacetate was described as one of the first acylals.¹³ The synthesis based on the acid-catalysed *O*-acylation of aliphatic and aromatic aldehydes by acetic anhydride in the presence of various catalysts was elaborated later.^{14,15} Scant information about acylals can be found in some monographs.^{5,16–18} For a long time, acylals were regarded only as convenient intermediates for the preparation of aldehydes and ketones from methylarenes **3** by oxidation with a $\text{CrO}_3\text{—Ac}_2\text{O}$ mixture^{5,18,19} as well as by oxidative decarboxylation of malonic acid derivatives **4**.⁵

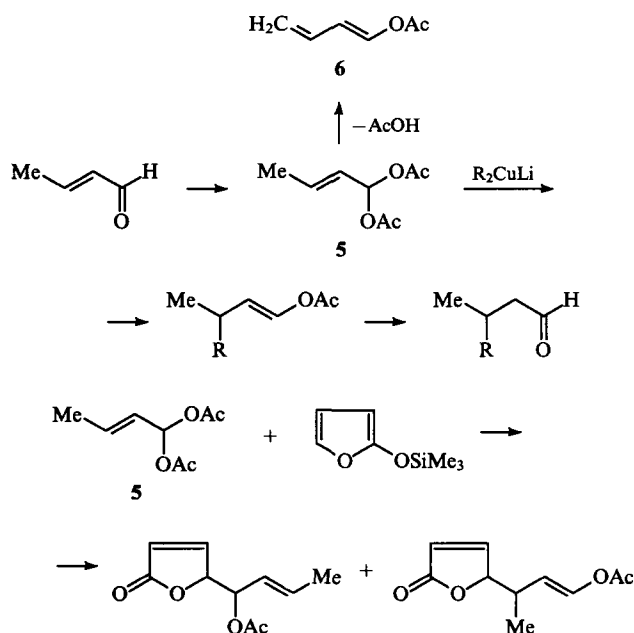
S M Luk'yanov, A V Koblik Institute of Physical and Organic Chemistry, Rostov State University, Prosp. Stachki 194/3, 344104 Rostov-on-Don, Russian Federation. Fax (7-863) 228 56 67. Tel (7-863) 228 08 94

Received 24 April 1995

Uspekhi Khimii 65(1) 3–28 (1996); translated by S S Veselyi

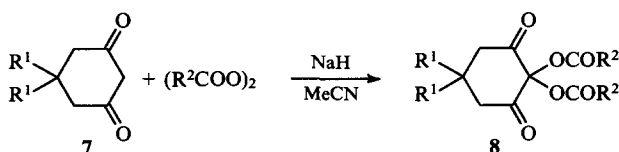


Only recently have acylals attracted special attention as compounds having independent synthetic value. Acylals can serve as convenient precursors of not only aldehydes but also of enol acylates, e.g., in the conversion of crotonaldehyde into 1-acetoxybutadiene **6**²⁰ and other synthetically difficult compounds.^{21,22}



The *gem*-diacetate moiety turned out to be quite stable toward dilute acids, but it is easily removable in weakly alkaline solutions.²¹ This group can therefore serve as a suitable complement of the well-known acetal protection for aldehydes.²³ Examples of acylal protection have been mentioned in the literature, but this topic is outside the scope of the present review, which is devoted to the activation rather than the passivation of the carbonyl function.

In the early eighties, several authors reported the preparation of acylals by the acid-catalysed acylation of aldehydes with acetic anhydride. Diacetates of aliphatic and aromatic aldehydes can be obtained in high yields in the presence of PCl_3 (Ref. 24 and the references cited therein). The use of FeCl_3 instead of PCl_3 allows one to extend the aldehyde series and to reduce the duration of the acylal synthesis; detailed spectroscopic data (IR, ^1H NMR and ^{13}C NMR) and mass spectra for the acylals were also obtained.²¹ The undesirable treatment of reaction mixtures with water can be excluded using the solid superacid 'Nafion-H', which also allows one to simplify the isolation of the acylation products.²⁵ The preparation of acylals in the presence of protic acids (e.g., sulfuric, perchloric, methanesulfonic acids) was reported in several studies.²⁶⁻²⁹ A series of acylals **8** have been obtained by the acyloxylation of cyclohexane-1,3-diones **7** with diacyl peroxides.³⁰

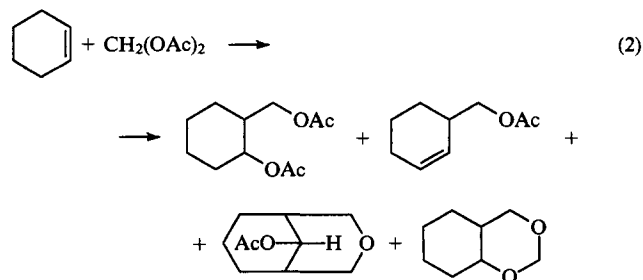
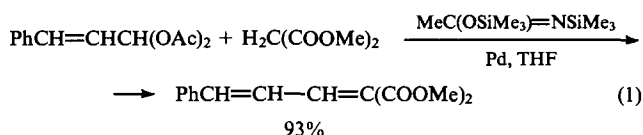


$\text{R}_2^1 = \text{Me}_2, -(\text{CH}_2)_5-$; $\text{R}^2 = \text{Ar}, \text{PhCH}_2\text{O}$.

Compounds **8** are ketone acylals. It has been mentioned in earlier publications that ketones do not yield *gem*-diacetates.¹⁴ Subsequently, it was shown that cyclohexanone and its 4-alkyl derivatives react with an $\text{Ac}_2\text{O}-\text{H}_2\text{SO}_4$ mixture to form the corresponding enol acetates, but hitherto unknown 1,1-diacetates were also isolated in low yields from these reaction mixtures.³¹ However, cyclopentanone affords only an acylal under the same conditions.³² Mazur and coworkers^{33,34} have described the preparation of ketone acylals by the action of trichloroacetic anhydride without a catalyst. However, the reactions of ketones (mainly cyclic ones) with Ac_2O require the presence of an acid.³⁴ It is remarkable that cyclobutanone reacts with Ac_2O and HClO_4 to yield only the 1,1-diacetate.³⁴ Obviously, the strain in small rings prevents the transformation of acylals into enol acylates.

The mechanism of the formation of acylals derived from both aldehydes and ketones was studied using mixed anhydrides²¹ as well as initial ketones labelled with the ^{18}O isotope.^{33,34} It has been shown that acylation, which is a reversible reaction, occurs with the participation of two anhydride molecules. Conditions for the conversion of acylals into carbonyl compounds by hydrolysis³⁵⁻³⁷ and for the transformation of diacylates into enol acylates were also described.^{31,33,38}

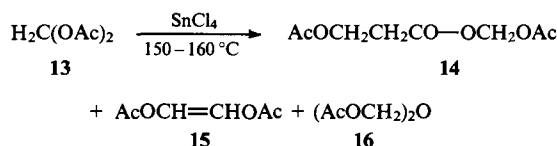
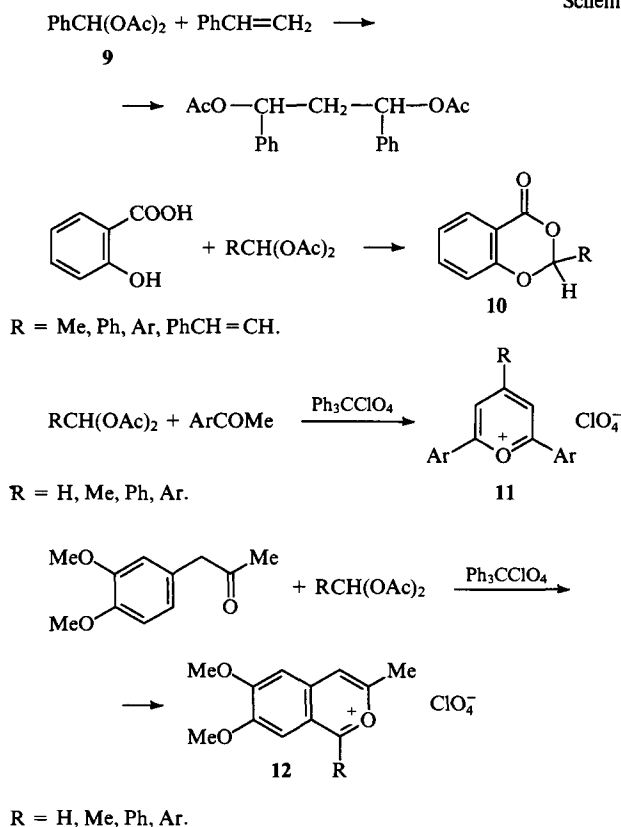
Acylals undergo many reactions typical of aldehydes, such as condensations with CH -acids³⁹ and with alkenes according to the Prins reaction scheme [Eqns (1) and (2)].⁴⁰⁻⁴²



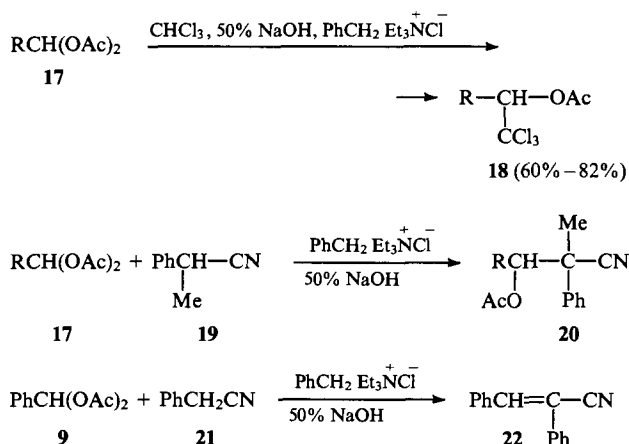
On the other hand, syntheses based on acylals were described in which the aldehydes themselves proved to be ineffective. Thus, in the reaction of benzylidene diacetate **9** with styrene, it is possible to avoid the telomerisation usually occurring in reactions between aldehydes and carboxylic acids (Scheme 1).⁴³ Acid-catalysed reactions of aldehydes with salicylic acid involve the alkylation of the aromatic ring, whereas the use of acylals yielded a series of 2-substituted 4-oxo-1,3-benzodioxanes **10**.⁴⁴ Acylals react with methyl ketones in the presence of triphenylmethyl perchlorate to form the pyrylium salts **11** and the 2-benzopyrylium salts **12**.²⁹

Methylene diacetate **13** undergoes self-condensation in the presence of SnCl_4 to give the ester and ether derivatives **14-16**.⁴⁵ It was found recently^{46,47} that aliphatic and aromatic aldehyde diacetates **17** react with CHCl_3 under phase-transfer catalytic conditions. These reactions proceed with substitution of an acetoxy group by a CCl_3 group with lengthening of the carbon chain by one atom to yield acetates of α -trichloromethyl carbinols **18** (Scheme 2). Apparently, this reaction is general and can also be expanded for other carbanion precursors. For example, analogous conversions were carried out with phenylmethylacetonitrile **19** and phenylacetonitrile **21** (Scheme 2).⁴⁸

Scheme 1

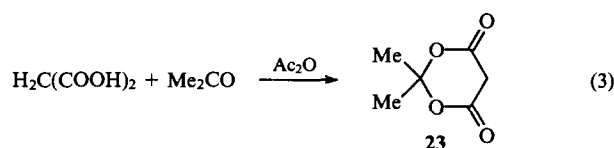


Scheme 2

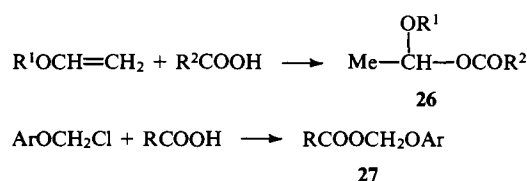


The substitution products obtained (18, 20, and 22) are valuable intermediates for subsequent transformations.

At present, isopropylidene malonate, Meldrum's acid 23, is the best known acylal (see the relevant reviews^{49–51}). This acid, which is an important precursor of many synthons and carbon suboxide and is a valuable starting material for the preparation of aliphatic-aromatic ketones and synthetically difficult 1,3,5-tricarbonyl compounds,^{52,53} has recently attracted keen attention. Meldrum's acid can be prepared by the acid-catalysed acetylation of acetone with acetic anhydride and malonic acid [Eqn (3)]⁵⁴ as well as by the acidolysis of isopropenyl acetate 24.⁵⁵

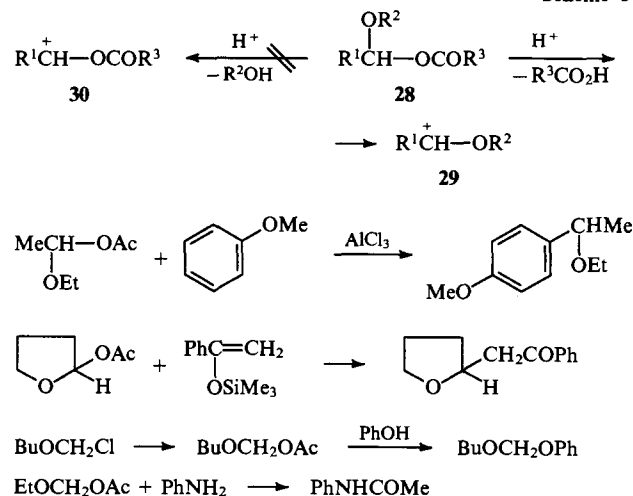


Mixed geminal α -acyloxyalkyl ethers 26 and 27, that can be obtained in reactions of carboxylic acids with vinyl ethers^{56–59} or aryl chloromethyl ethers,⁶⁰ are also called acylals in the chemical literature.

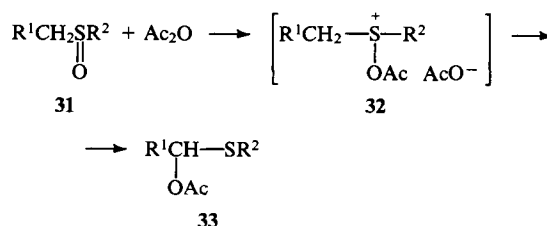


Compounds 26, 27, and 28 are noteworthy because their conversions always proceed with substitution of the acyloxy- rather than alkoxy-group, i.e. the more stable alkoxy-carbocations 29 arise (see Section V). Kinetic investigations confirmed this observation.⁶¹ Some examples of such reactions are shown in Scheme 3.^{62–65}

Scheme 3



It is appropriate to mention in this Section the unusual sulfur-containing hetero-analogues of acylals 33, which are products of the Pummerer reaction.^{7,66} This reaction is, in essence, acylation of the sulfoxides 31, which are sulfur analogues of ketones.

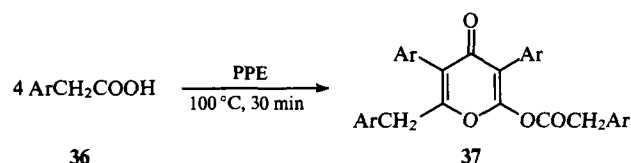
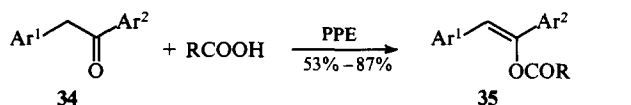


Acylals formed by ketones and an inorganic acid, the geminal diperchlorates $\text{R}^1\text{R}^2\text{C(OCIO}_3)_2$, have also been described.⁶⁷

III. Enol acylates

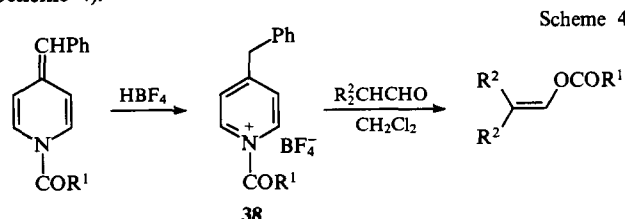
Compared with acylals, vinyl esters, i.e. enol acylates, particularly vinyl acetate, are better known because they are widely used. Syntheses based on enol acylates are of great importance, particularly in steroid chemistry. The extensive literature concerning enol acylates has been surveyed in several reviews.⁶⁸⁻⁷¹ A series of papers have been devoted to modifications of well-known preparative methods, for example, the acetoxymercuration of alkynes,^{72,73} as well as to the formation of enol acylates under unusual conditions (thermal opening of cyclobutene derivatives,⁷⁴ electrochemical acylation of indenones⁷⁵) and the syntheses of unusual enol acylates (benzenesulfonates,⁷⁶ triflates⁷⁷⁻⁷⁹). The syntheses of enol acylates from α -halogenated aldehydes and ketones by the action of acid halides in the presence of zinc are of interest.^{80,81}

As to syntheses of enol acylates by the acid-catalysed acylation of carbonyl compounds, new variants of this approach were also reported side by side with new examples of traditional procedures (e.g. treatment of ketones with Ac_2O in the presence of perchloric⁸² or sulfuric acid⁸³). For example, deoxybenzoins **34** react with carboxylic acids or their anhydrides in polyphosphoric ester (PPE) to give the *O*-acylation products **35**.⁸⁴ It was found that the arylacetic acids **36** can undergo fourfold self-acylation to form the α -acyloxy- γ -pyrones **37** under these conditions.⁸⁵

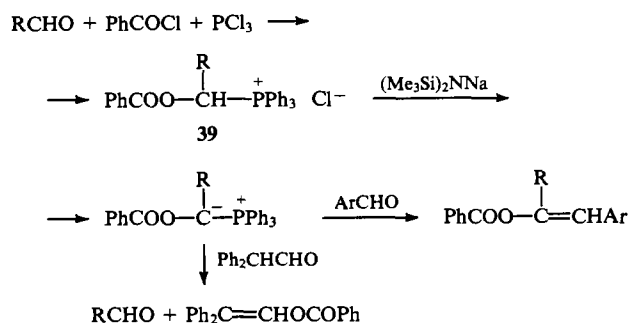


Ar = Ph, 4- $\text{NO}_2\text{C}_6\text{H}_4$.

The use of an $\text{Ac}_2\text{O} + \text{Me}_3\text{SiCl}$ mixture represents a new method for the preparation of enol acylates from ketosteroids.⁸⁶ This mixture acts as an acylating reagent because trimethylsilyl chloride cleaves Ac_2O to give trimethylsilyl acetate and acetyl chloride.⁸⁶ *N*-Acylpyridinium salts **38**⁸⁷ and acyloxyacylphosphonium salts **39**⁸⁸ have also been used as acylating agents (Scheme 4).



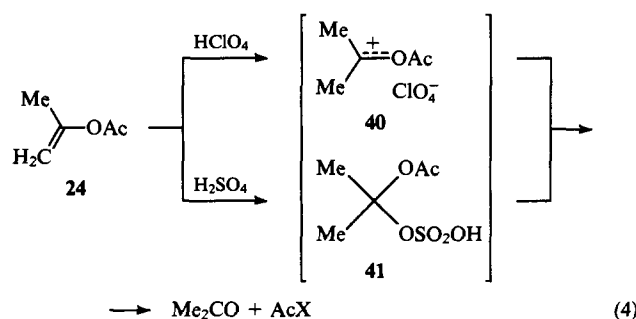
$\text{R}^1 = \text{Pr}^i, \text{Ph}, \text{Ar}; \text{R}^2 = \text{Me}, \text{Ph}$.



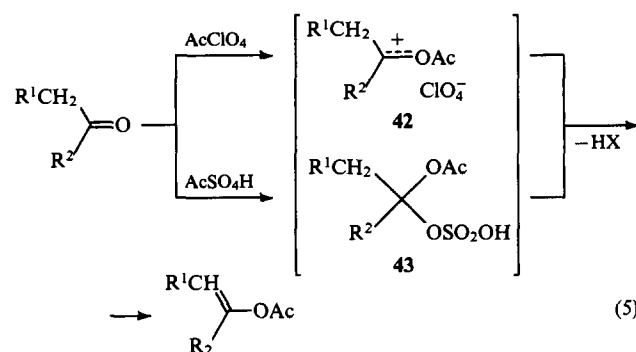
Scheme 4

Investigations of the behaviour of labelled (^{18}O) ketones confirmed that acylals are intermediates in the formation of enol acylates by the acid-catalysed acylation of ketones with acetic anhydride.³⁴ A correlation between the rate of this reaction and the nucleophilicity of the anion of the protic acid was demonstrated. Thus, in the acylation of cyclohexanone by Ac_2O the degree of conversion of the ketone into the corresponding enol acetate reaches 80% after 20 min in the presence of HClO_4 , in contrast to only 10% after 10 h in the presence of H_2SO_4 .³⁴ The reactions of cyclic ketones with isopropenyl acetate **24** in the presence of both perchloric and sulfuric acids were described in the same paper.³⁴ According to ^1H NMR data, these reactions occur considerably faster in the presence of HClO_4 than with H_2SO_4 , because in the former case the intermediates **40** and **42** have a cationoid structure, in contrast to the predominantly covalent nature of the intermediates **41** and **43** in the latter case (Scheme 5).

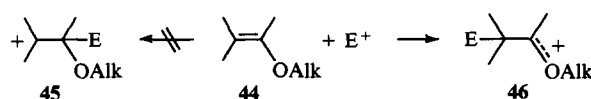
Scheme 5



X = ClO_4 , SO_4H .

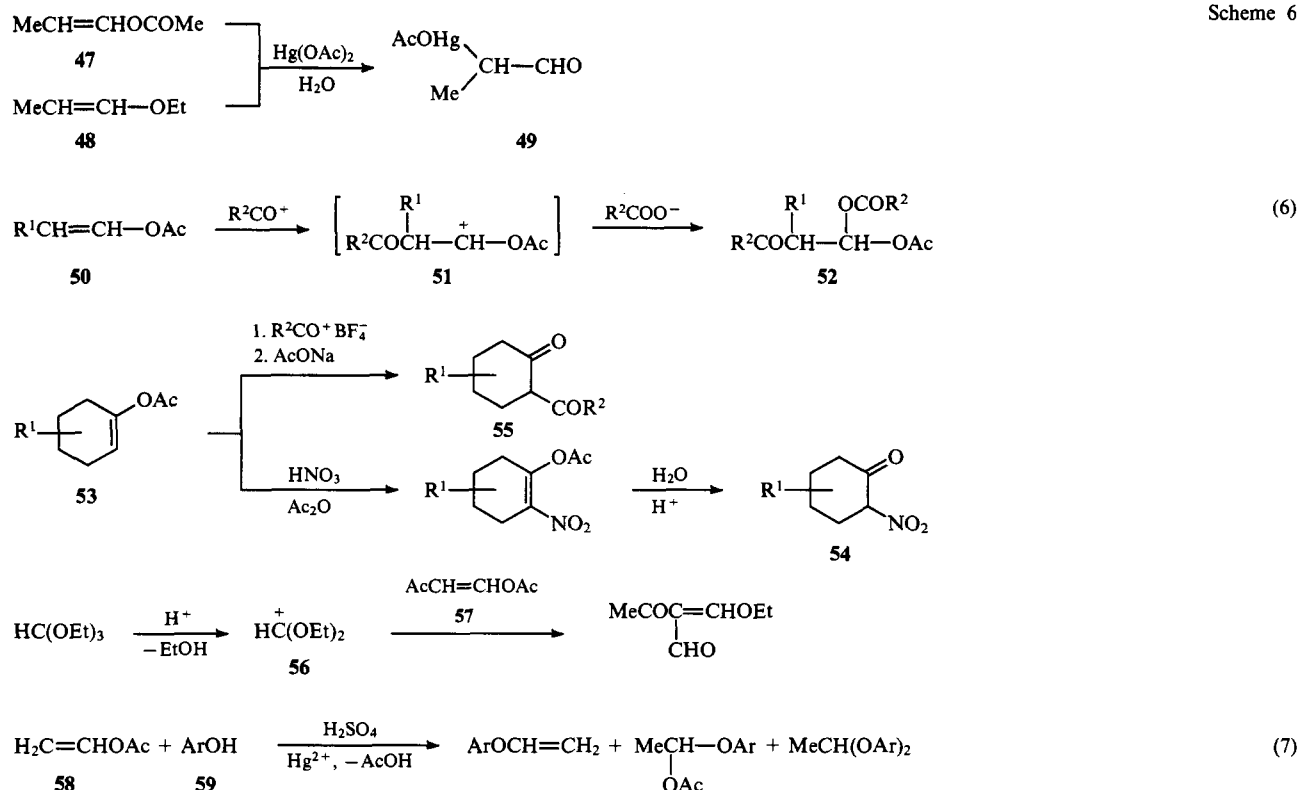


Among enol acylate reactions, the interaction of the latter with cationoid electrophiles (E) is of particular interest. It is generally known that vinyl ethers **44** always combine with an electrophile at the double bond carbon atom most remote from the oxygen atom and are then converted into carbonyl compounds [see Kulish et al.,⁸⁹ Shostakovskii,⁹⁰ and also Barton and Ollis⁷⁰ (p. 351)]. This is due to the formation of the alkoxy-carbenium ions **46**, which are much more stable than the alternative carbocation **45** (even tertiary ones).^{91,93}



This difference in the stability of cations **45** and **46** explains the pinacol rearrangement with group migration from the carbon atom linked to the ether oxygen atom^{94,95} (see Ref. 1, p. 461). It should be noted that the concept of carbocation resonance stabilisation by heteroatoms at the carbenium centre is so common now that any carboxonium ions are regarded as *a priori* stable. If this were really so, there would be no need to continue this review.

Scheme 6



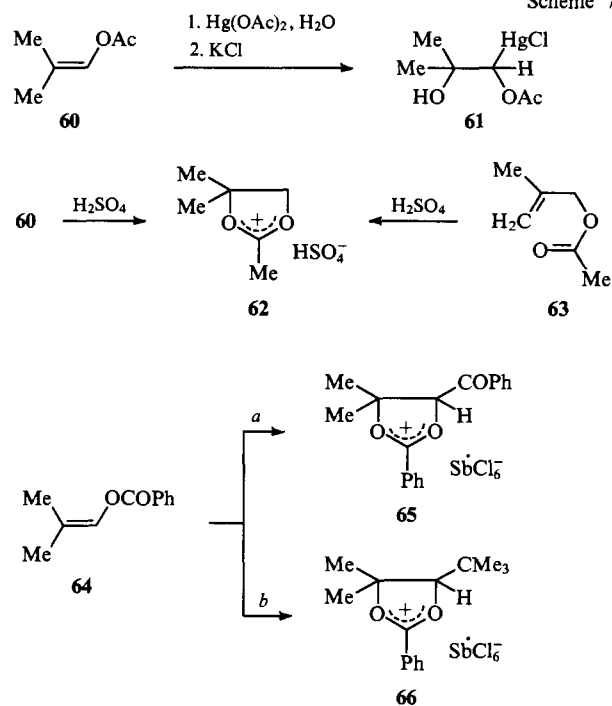
Many of the reactions involving electrophilic addition to vinyl esters reported in the literature are fully consistent with the above ideas. Thus, both the enol acetate of propanal **47** and ethyl propenyl ether **48** react with mercuric acetate to form α -acetoxymercuriopropenal **49** (Scheme 6).^{96,97} Acylation of vinyl acetates **50** leads to the β -ketoaldehyde acylals **52** via the acyloxycarbenium ions **51**.^{98,99} Nitration of 1-acetoxycyclohexenes **53** gives the nitroketones **54**,¹⁰⁰ while its acylation affords the 1,3-diketones **55**.¹⁰¹ The diethoxycarbenium **56** formed from ethyl orthoformate also attacks the enol acetate of 3-oxobutanal **57** at the position as the C=C double bond most distant from the ether oxygen atom.¹⁰²

The addition of phenols **59** to the C(α) atom bearing an acetoxy-group in vinyl acetate **58** occurs due to protonation of the latter at the methylene group.¹⁰³ All of the enol acylates used in the above reactions contained a primary or secondary carbon atom at the position in the double bond most distant from the oxygen atom (which will be, for convenience, henceforth called the β -carbon atom).

However, it was found recently that enol acylates containing a tertiary β -carbon atom react with electrophiles in a fundamentally different way. Thus, the enol acetate of isobutyraldehyde **60** gives under acyloxymercuration conditions⁹⁶ a 1,2-diol derivative **61** rather than an aldehyde.¹⁰⁴ Dissolution of the enol acetate **60** in 98% sulfuric acid yields a 1,3-dioxolanylium salt **62**, the ¹H NMR spectrum of which is fully identical to that of the product of protonation of methylallyl acetate **63**.¹⁰⁵ Benzoylation and alkylation of the enol benzoate **64** in weakly nucleophilic media yield 4-benzoyl-**65** and 4-*tert*-butyl-1,3-dioxolanylium salts **66**, respectively.¹⁰⁴ It should be emphasised that the above 1,3-dioxolanylium salts **62**, **65**, and **66** are derivatives of 1,2-glycols, into which they can be readily converted by hydrolysis¹⁰⁶ (Scheme 7).

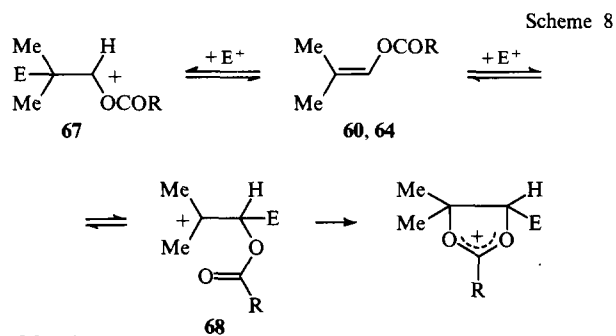
Thus, if an enol acylate is branched at the position in the C=C double bond most distant from the oxygen atom, the addition of an electrophilic species occurs at the α -carbon atom linked to the oxygen atom. Hence, the energies of the alternative cations, i.e. the acyloxycarbenium cations **67** and the tertiary carbenium cation **68**, are almost the same (see Section VI) (Scheme 8).

Scheme 7



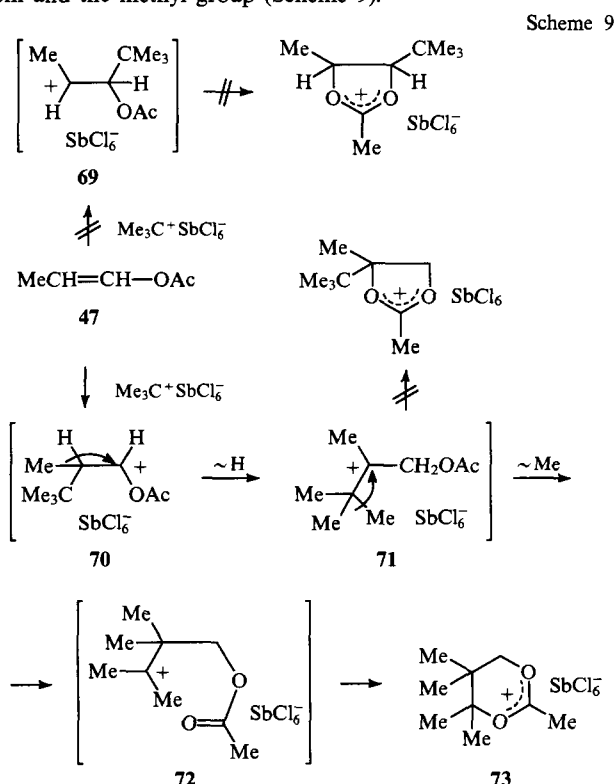
a: $\text{PhCO}^+\text{SbCl}_6^-$, -10°C , CH_3NO_2 ;

b: $\text{Me}_3\text{C}^+\text{SbCl}_6^-$, -60°C , CH_2Cl_2 .



R = Me, Ph.

This conclusion is in good agreement with the results of the alkylation of the enol acetate **47** under the same conditions leading to 1,3-dioxanylium hexachloroantimonate **73**.¹⁰⁴ The reaction mechanism presupposes the formation of the acyloxy-carbenium ion **70**, which is more stable than the secondary carbocation **69**, and two consecutive migrations of a hydrogen atom and the methyl group (Scheme 9).



It should be noted in conclusion that the acid-catalysed acylation of aldehydes and ketones leads to enol acylates, provided that the reaction mixtures contain bases capable of eliminating a proton from the product of the *O*-acylation of the carbonyl compound. This function can be performed by isopropenyl acetate,³⁴ pyridine,⁸⁷ or the acetate anion at elevated temperatures. In the cold, nucleophilic addition of acylate anions takes place and is accompanied by the formation of acylals. If other acylating reagents are used, such as acyl halides, then the halogen atom should play the role of the nucleophile.

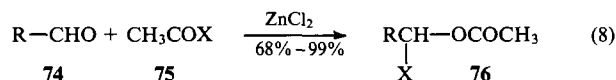
IV. α -Haloalkyl acylates

The acid-catalysed acylation of aldehydes by acid chlorides was discovered in 1901.^{107,108} The α -chloroalkyl carboxylates **2** were obtained from formaldehyde and acetaldehyde in the presence of anhydrous zinc chloride. Later several studies were published in which this reaction was extended to higher aldehydes and acrolein.^{109–112}

The α -haloalkyl acylates **2** have aroused interest only since the middle of this century. This was connected with the possible use of these compounds for the preparation of vinyl monomers,¹¹³ but primarily for application in studies of the nucleophilic substitution mechanism. In the sixties and seventies, Euranto and coworkers published the results of very detailed investigations of the noncatalytic hydrolysis of various α -haloesters under a wide range of conditions (see the relevant communications^{114–120} and the references therein). The methods for the preparation of α -haloalkyl acylates reported up to that time were surveyed in a separate article,¹²¹ in which the merits and drawbacks of ten different approaches were listed. Preference was given to methods involving the chlorination of alkyl carboxylates as well as the halogenation and hydrohalogenation of enol acylates. Five of these procedures, including the acylation of aldehydes, were used for the preparation of samples employed in kinetic investigations.¹²¹ Brief historical surveys concerning the topic discussed were also given in Refs 109 and 113.

However, a preparative application of the reaction of carbonyl compounds with acyl halides was not found until the late sixties, when Neuenschwander and coworkers^{122,123} developed a new method to prepare fulvenes. It was found that only α -chloroalkyl acetates are capable of reacting effectively with cyclopentadiene to form differently substituted fulvenes in up to 70% yields.^{122–125} Neither their precursors, i.e. carbonyl compounds, nor the related simple α -chloroesters react in this way. A detailed investigation of the mechanism of the formation of the key starting materials, i.e. α -haloalkyl acylates (acyloxy-chloromethanes), became the subject of a series of papers. Two papers^{126,127} reported the applicability of the haloacylation of carbonyl compounds to the synthesis of α -haloalkyl acylates.

The equilibrium of the reaction between the aliphatic aldehydes **74** and the acetyl halides **75** is so shifted towards the products **76** that the equilibrium constant cannot be determined by ¹H NMR spectroscopy. The authors believe that the reaction considered was rarely used for preparative purposes because of the poor yields of the target products **76** resulting from imperfect techniques for the isolation of the latter. This problem can be solved by using low temperatures (from -10 to 0°C) and by removing the catalyst (ZnCl_2) before the fractional distillation of the reaction mixtures.

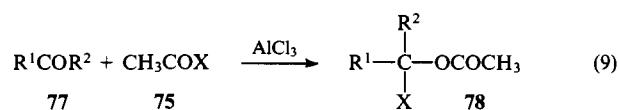


R = H, Me, Et, Pr, Prⁱ, Bu, Buⁱ, Bu^t, CH=CH₂, CH=CHOAc,

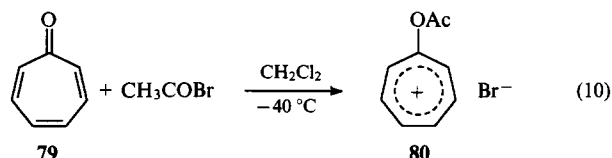
CH=CHCl, C \equiv CH, Ph, Ar, , X = Cl, Br.

The haloacylation of α,β -unsaturated aldehydes occurs readily (68%–94% yields).¹²⁷ In contrast to the situation with aliphatic aldehydes, the equilibrium position of the reaction involving aromatic aldehydes is measurable; substituents having +*M* and +*I* effects shift this equilibrium to the left. Therefore, excess acetyl chloride should be used in reactions involving starting aldehydes such as 4-methoxy- and 4-dimethoxy-amino-benzaldehydes. Other aromatic aldehydes afford the products **76** in 96%–99% yields.

The haloacylation of ketones **77** gives the products **78** in 76%–93% yields, which were observed to depend on the ring size of the alicyclic ketones. In the case of cyclobutanone and cyclohexanone, the equilibrium position is shifted towards the product **78**, whereas for cyclopentanone and cycloheptanone it is nearer to the starting reactants. Aromatic ketones such as acetophenone practically do not form α -haloalkyl esters. Tropone **79**, which gives the acylation product **80** with an ionic structure, occupies a particular position.¹²⁷



$\text{R}^1, \text{R}^2 = \text{Me}, -(\text{CH}_2)_n-, n = 3, 5; \text{X} = \text{Cl}, \text{Br}$

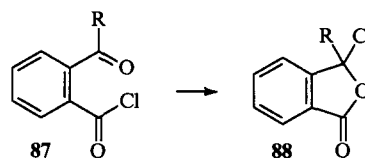


An analysis of the side products formed by the haloacetylation of aldehydes has been carried out¹²⁸ in order to optimise the synthesis conditions. The structure of the aliphatic aldehydes, the reaction time, the concentrations of the catalysts and starting reactants, as well as the polarity of the solvent were varied during this investigation. It was concluded that (a) dilute solutions, (b) nonpolar solvents, (c) higher concentrations of acetyl halides, achieved by the dropwise addition of the aldehyde to the reaction mixture, (d) low temperatures, and (e) higher concentrations of the catalyst dissolved in the acyl halide should be used for the successful suppression of side reactions mentioned above.

The dependence of the equilibrium position on the reaction conditions in the above processes [Eqns (8) and (9)] was considered in detail in Ref. 129. The equilibrium constants were measured as a function of the structure of the carbonyl component, the composition of the acyl halide, solvent polarity, and temperature. The results of exact measurements¹²⁹ fully agree with the practical recommendations specified above.¹²⁸

Finally, the possible mechanisms of the haloacylation of carbonyl compounds, namely, the two 'polar mechanisms' (a, b), the synchronous mechanism (c), and the ketene mechanism (d) have been thoroughly discussed¹³⁰ (Scheme 10). It was shown by ¹H NMR kinetic measurements that aliphatic acyl halides react according to the 'polar mechanism' b via the intermediates **84** and **85**, i.e. without ionisation, while aromatic acyl chlorides follow the mechanism a with the participation of the acyloxycarbocations **82**.¹³⁰ This can be attributed to the lower energy (i.e. higher stability) of the benzoyl cations **81** ($\text{R}^1 = \text{Ar}$) in comparison with that of aliphatic acyl cations.

In relation to the facts considered above, we should also mention the long known intramolecular interaction between the functional groups in the chlorides of γ - and δ -keto- and aldehydo-carboxylic and *o*-acylbenzoic acids **87**.

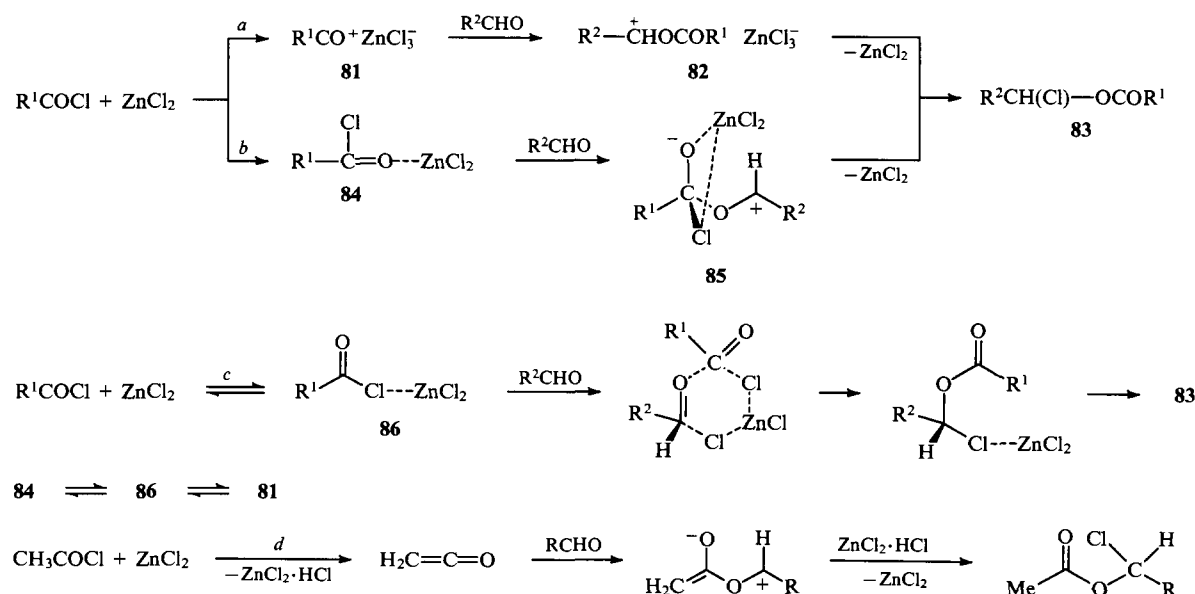


The majority of such compounds are stable only as cyclic α -chloroalkyl acylates **88**, and only a few examples are known where steric hindrance prevents cyclisation.^{131–134} More than a hundred of such structures, both aliphatic and aromatic, were considered in a review¹³⁵ containing an extensive bibliography. The existence of tautomeric equilibrium between the open form **87** and the cyclic form **88** is completely rejected in Refs 133–135.

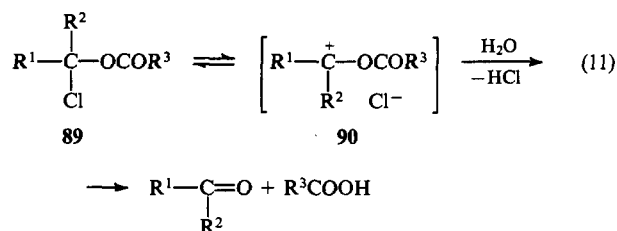
As mentioned above, until now there has been little information about the synthetic application of α -haloalkyl acylates. These compounds can be used as alkylating reagents in reactions with 2-(trimethylsilyloxy)furan,²² pyridine,¹¹³ secondary amines,¹³⁶ silver salts of *N*-nitrosohydroxylamines,¹³⁷ and phenols,¹³⁸ as well as for forming carbon–manganese bonds.¹³⁹ However, the same α -haloesters behave as acylating agents under other conditions.^{136, 138, 140} The chlorine atom in α -chloroalkyl acetates, similarly to that in acylals (see Section II), can be substituted by the trichloromethyl group under phase-transfer catalytic conditions.¹⁴¹ However, the most interesting properties of α -chloroesters were found when the latter were used for the synthesis of oxygen-containing heterocyclic compounds (see Section V).

V. Acyloxycarbenium ions

It was shown by kinetic studies of the hydrolysis of the α -haloesters **83** and **89** that the majority of the latter react according to a *S_N1* mechanism^{114–120} via the acyloxycarbenium ions **82** and **90** as intermediates.

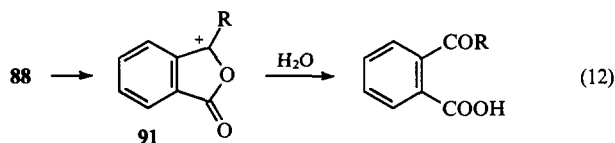


Scheme 10



It was established¹¹⁵ that α -chloroethyl benzoate **89** ($\text{R}^1 = \text{Me}$, $\text{R}^2 = \text{H}$, $\text{R}^3 = \text{Ph}$) hydrolyses via a unimolecular $\text{S}_{\text{N}}1$ mechanism almost 100 times more quickly than chloromethyl benzoate **89** ($\text{R}^1 = \text{R}^2 = \text{H}$, $\text{R}^3 = \text{Ph}$), the solvolysis of which occurs by an $\text{S}_{\text{N}}2$ mechanism. Secondary α -haloalkyl acylates **89** ($\text{R}^1, \text{R}^2 = \text{Alk}$, $\text{R}^3 = \text{Me, Et, CCl}_3$) are hydrolysed a thousand times more quickly than the corresponding primary esters **89** ($\text{R}^1 = \text{Alk}$, $\text{R}^2 = \text{H}$, $\text{R}^3 = \text{Ph}$).¹¹⁶ α -Chlorobenzyl esters **89** ($\text{R}^1 = \text{Ar}$, $\text{R}^2 = \text{H}$, $\text{R}^3 = \text{Ph}$) also undergo substitution of the chlorine atom by a unimolecular mechanism.^{118, 119}

The formation of cyclic acyloxycarbocations **91** is suggested by kinetic data for the hydrolysis of the cyclic α -chloroalkyl acylates **88** mentioned above.^{133, 134, 142}



The hydrolysis of the acylals **1** can also occur by different pathways. Ethylidene diacetate $\text{MeCH}(\text{OAc})_2$ reacts by an $\text{A}_{\text{AC}}2$ mechanism,³⁶ like *p*-nitrobenzylidene diacetate, $4\text{-O}_2\text{NC}_6\text{H}_4\text{-CH}(\text{OAc})_2$.³⁷ However, *p*-methoxybenzylidene diacetate, $4\text{-MeOC}_6\text{H}_4\text{CH}(\text{OAc})_2$, undergoes unimolecular hydrolysis via acyloxycarbocation ions.³⁷ It was shown that primary α -chloroalkyl esters react with oxygen- and nitrogen-containing nucleophiles by a bimolecular mechanism,^{136, 138} whereas the analogous α -chloroalkyl ethers react by an $\text{S}_{\text{N}}1$ mechanism.⁹⁴ It is known that vinyl ethers hydrolyse via the same mechanism 10⁴ times more quickly than vinyl acetate, which was supposed to form a π -complex with the proton.⁸⁹ However, the next homologue, isopropenyl acetate **24**, can be readily transformed into the acyloxycarbocation **40**,^{143, 144} which was detected by ¹H NMR spectroscopy.¹⁴⁵ It was assumed that both the acetolysis of

α -acetoxystyrene, $\text{PhC}(\text{OAc})=\text{CH}_2$,¹⁴⁶ and the formation of phthalides from *o*-aroylbenzoic acids¹⁴⁷ proceed with formation of acyloxycarbocation ions.

These results allow us to conclude that the generation of the acyloxycarbocations **90** requires a considerably higher energy than the formation of the related alkoxy carbocations **46** and depends very strongly on both the precursor structure (acylal, enol acylate, or α -haloalkyl acylate) and on reaction conditions. The high energy of the acyloxycarbocations follows from the unusual mode of electrophilic addition to β -branched enol acylates (see Section III) and from some indirect evidence, such as the possibility of an equilibrium between the acyloxycarbocation ion **92** (in this case, considerably stabilised) and the acylium ion **93** (Scheme 11).¹⁴⁸

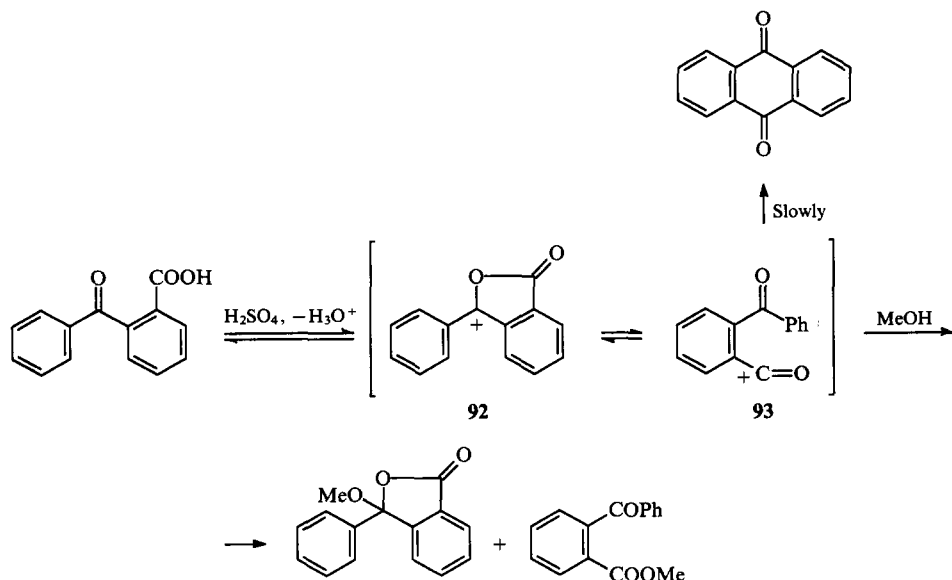
Thus, an acyloxy group linked to a carbocation centre stabilises the latter, but to a much lower extent than a hydroxy- or alkoxy-group. Apparently, the relatively high stability of acylals in weakly acid media²¹ (see Section II) can be explained by difficulties in their ionisation (in comparison with acetals).

Perhaps the fact that acyloxycarbocation ions have never been mentioned in any of the reviews dealing with carboxonium ions⁹¹⁻⁹³ can be explained only by their unpredictable formation conditions and behaviour. At the same time, the information presented above suggests that these species cannot be regarded as just one example of the ion series $\text{R}^1\text{R}^2\text{C}^+-\text{OR}^3$. In addition to the high energy of acyloxycarbocations, their tendency to decompose into a carbonyl compound and a quite stable acylium cation should be taken into account as their characteristic feature.^{129, 149, 150} However, since acyloxycarbocation ions are intermediates not only in the acid-catalysed acylation of carbonyl compounds but also in the reactions of its products, it is quite appropriate to make a compilation of the scattered data on these species.

In addition to the instances presented above [reactions (3)-(6), (10)-(13); Schemes 9 and 10], the acyloxycarbocations **95**, **98**, **100**, and **101** were assumed as intermediates in a number of reactions of carbonyl compounds with acylating agents: the reaction of succinic anhydride with 2-acetoxybut-2-ene **94** for the preparation of the key intermediate **96** in steroid syntheses;¹⁵¹ the conversion of 2,6-diphenyl-4-pyrone **97** into cyanine dyes;¹⁵² the reaction of 3,5-di-*tert*-butyl-1,2-benzoquinone **99** with acetic anhydride (Scheme 12).^{153, 154}

The acyloxycarbocation ions **103**, **104**, and **106** are formed by the acylation of the α, β -unsaturated carbonyl compounds **102** and **105**.^{155, 156}

Scheme 11



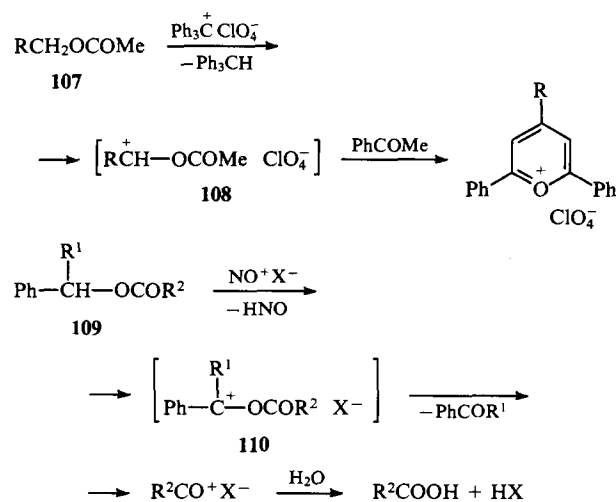
(13)

Scheme 12

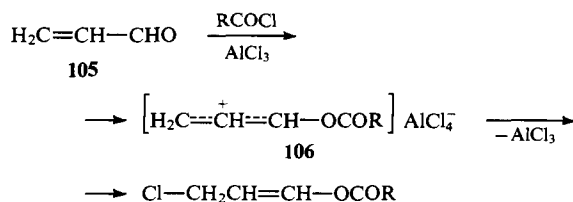
Scheme 12 illustrates the synthesis of 1,2-dimethylcyclopentanone and 1,2,4,6-tetra-*tert*-butyl-3,5-diacetoxycyclohexa-2,5-diene.

Top Reaction: Succinic anhydride reacts with 4-methyl-3-penten-2-one (**94**) in the presence of AlCl_3 and PhNO_2 to form 1,2-dimethylcyclopentanone (**96**). The mechanism involves the formation of a complex intermediate (**95**), which is a 1,2-dimethyl-3-(2-oxocyclopentyl)propan-1-one derivative, followed by rearrangement and elimination to yield **96**.

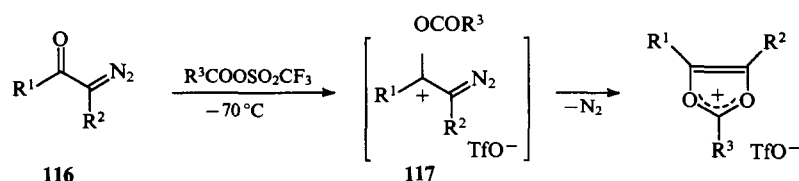
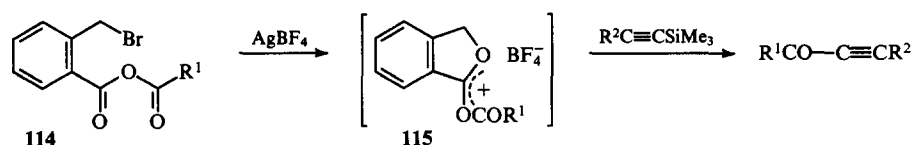
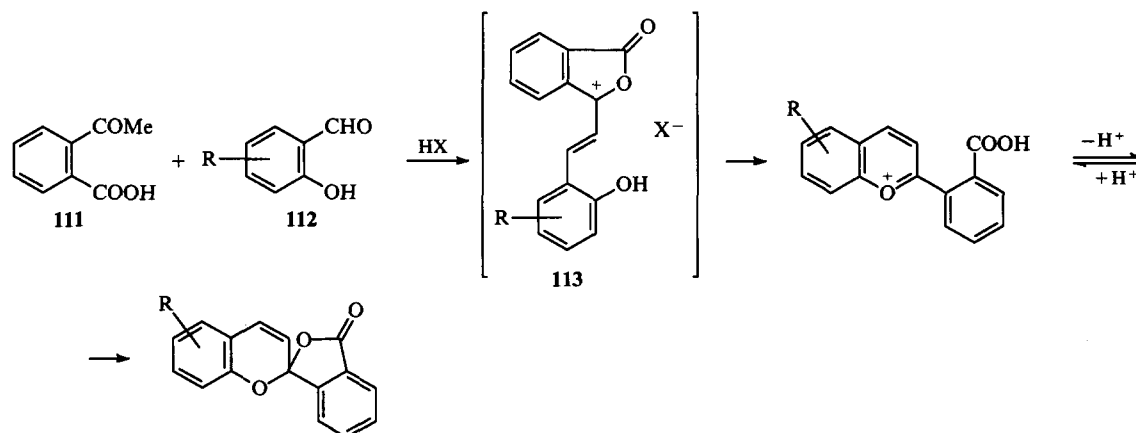
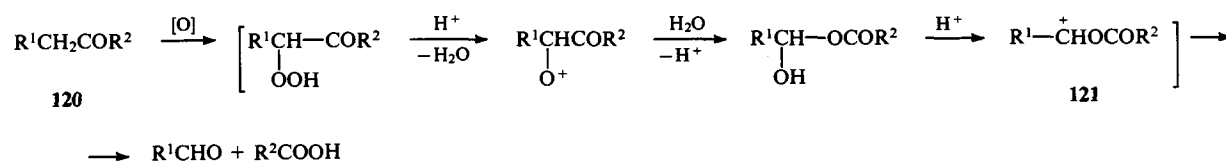
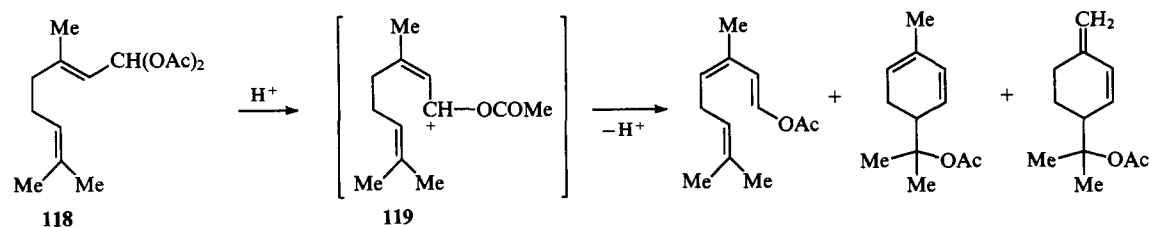
Bottom Reaction: 1,4-dimethyl-2,5-cyclohexadien-1-one (**97**) reacts with Ac_2O to form a resonance-stabilized cationic intermediate (**98**), which is a 1,4-dimethyl-2,5-cyclohexadien-1-yl cation with an OCOMe group and an AcO^- counterion. This intermediate then reacts with AcO^- to form a 1,4-dimethyl-2,5-cyclohexadien-1-yl cation with an OAc group and a ClO_4^- counterion. This cationic intermediate reacts with Ac_2O and HClO_4 to form a 1,4-dimethyl-2,5-cyclohexadien-1-yl cation with two OAc groups and a ClO_4^- counterion (**101**). Finally, **101** reacts with Me_3C^+ and ClO_4^- to yield 1,2,4,6-tetra-*tert*-butyl-3,5-diacetoxycyclohexa-2,5-diene.



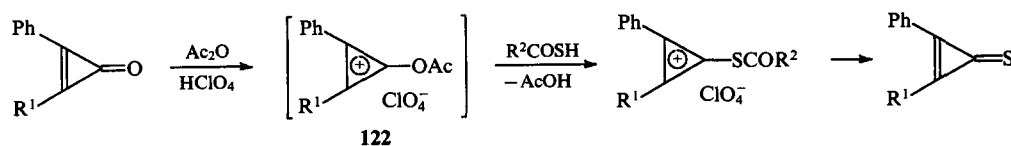
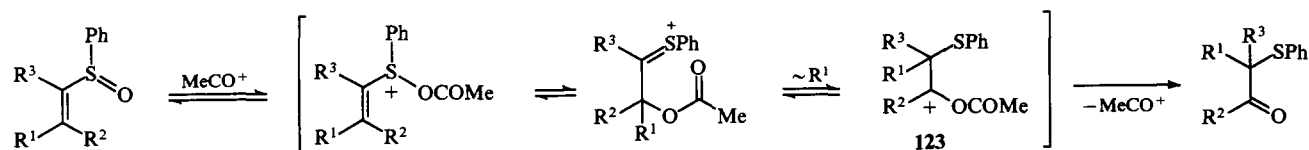
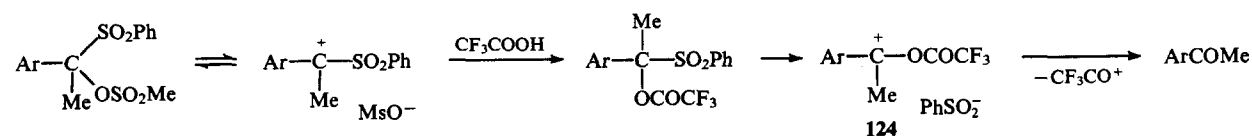
Both the nitration of cyclohexanone enol acetates **53**¹⁰⁰ and the formylation of formylacetone mono-enol acetate **57**¹⁰² considered above (see Section III) also proceed via acyloxy-carbenium ions as intermediates. It was assumed that the latter (compounds **122**–**124**) can serve as intermediates in acid-catalyzed transformations of sulfur-containing compounds (Scheme 14).^{164–166}



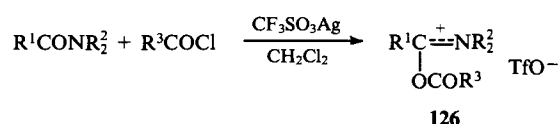
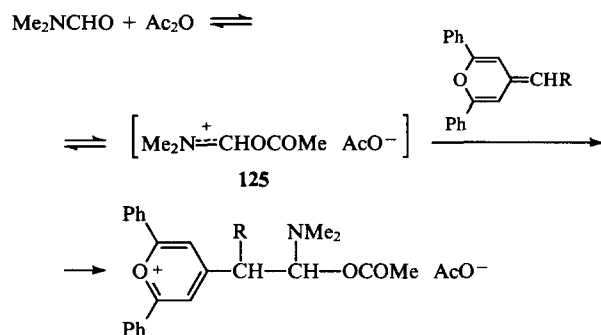
Scheme 13

Tf = SO₂CF₃.

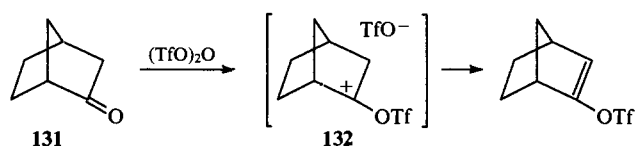
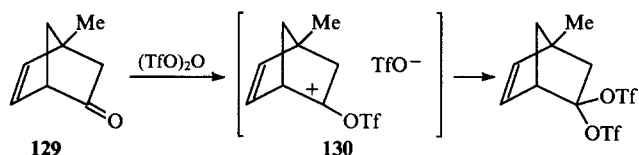
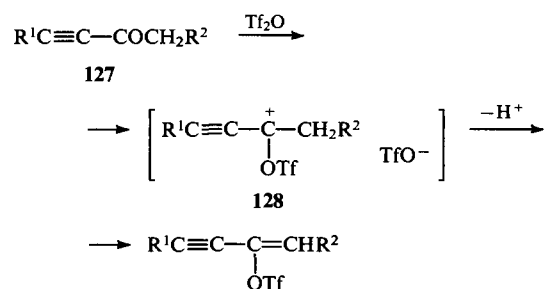
Scheme 14

R¹ = Me, Ph; R² = Me, Ar.R¹ = H, Me.

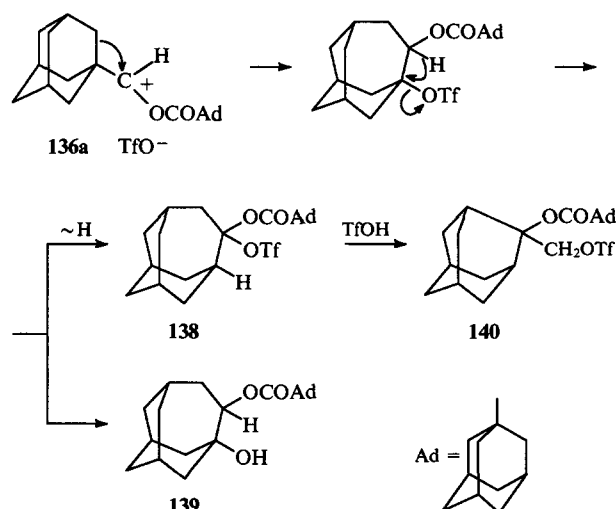
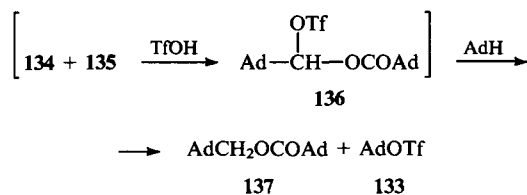
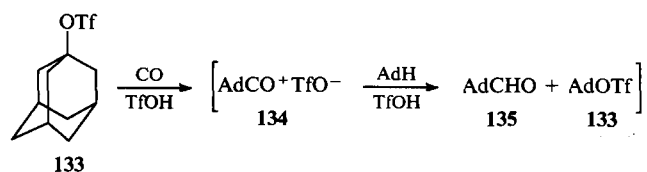
The unusual cationoid species **125** and **126** are formed by the *O*-acylation of amides.^{167, 168}



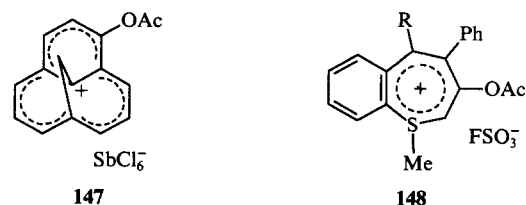
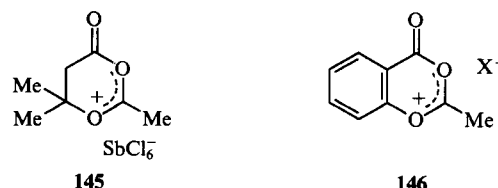
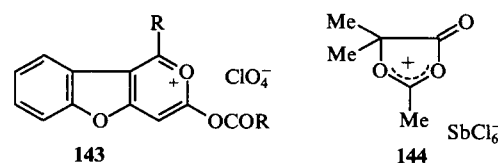
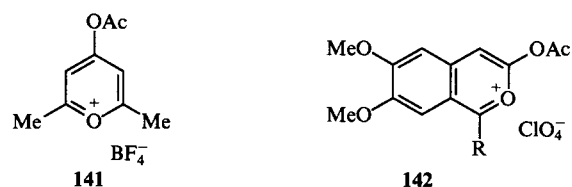
The carbocations **128**, **130**, and **132** are intermediates in reactions of trifluoromethanesulfonic anhydride with the butyrones **127**¹⁶⁹ and the terpene ketones **129** and **131**.^{170, 171}



The reaction of 1-adamantyl triflate **133** with carbon monoxide and adamantane (AdH) in the presence of trifluoromethanesulfonic acid (TfOH) gives the products **137**, **139**, and **140**, the formation of which was explained by the participation of acyloxycarbenium intermediates **136**, **136a**, and **138**.¹⁷² Although one of them (**136**) was represented as a covalent structure,¹⁷² its ability to be a hydride acceptor and to undergo a rearrangement suggests that it is readily transformed into the cation **136a** (the low nucleophilicity of the triflate anion is well known¹⁷³).



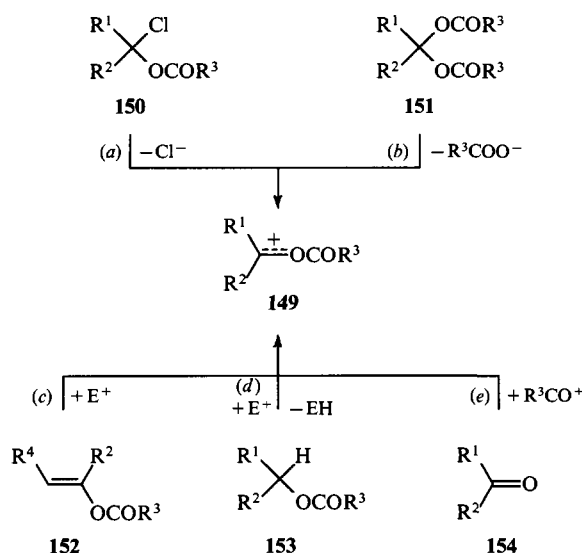
Finally, stable acyloxycarbenium salts have been described: acyloxypyrylium (**141**, **142**, and **143**),^{174–176} 4-oxo-1,3-dioxolan-2-ylum (**144**), and 4-oxo-1,3-dioxolan-2-ylum (**145**),¹⁷⁷ as well as 4-oxo-1,3-dioxolan-2-ylum (**146**)¹⁷⁸ salts. Papers dealing with the synthesis of the carbocyclic and heterocyclic systems **147** and **148** containing an acetoxy group as a substituent have been published.^{179, 180}



To sum up the above information, five general methods for the generation of the acyloxycarbeniums **149** can be distinguished: (a) ionisation of the α -chloroalkyl acylates **150**,¹¹⁹

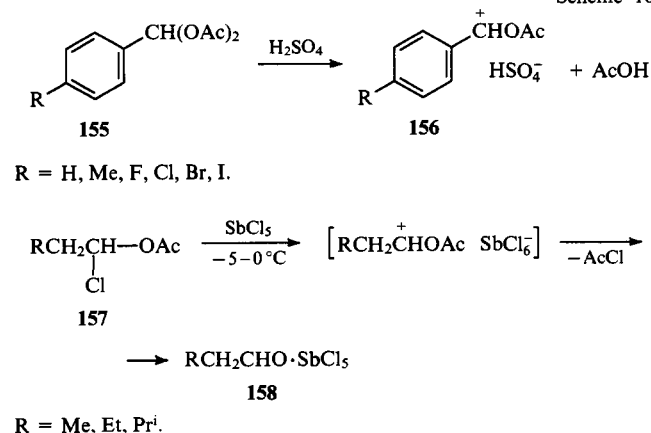
(b) ionisation of the acylals **151**;³⁷ (c) addition of cationoid electrophiles to the enol acylates **152**;¹⁴⁵ (d) oxidative dehydrogenation of the esters **153**;^{149, 157} and (e) direct *O*-acylation of the carbonyl compounds **154**;¹⁵⁶ (Scheme 15).

Scheme 15

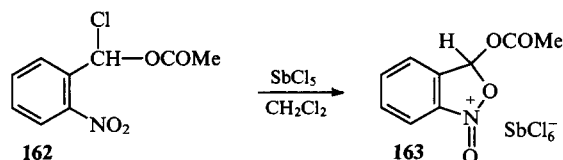
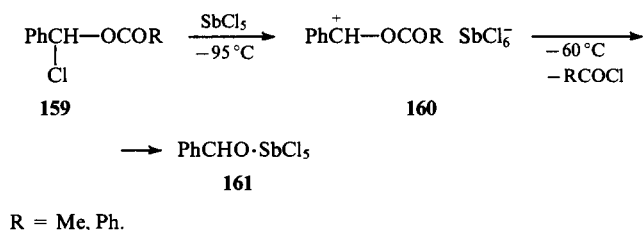


It is known that the stability of highly reactive species such as carbocations can be characterised by the conditions of their existence as salts. Many hydroxy- and alkoxy-carbenium ions are so stable that they can readily be detected in solution by ¹H NMR spectroscopy or even isolated as salts with nonnucleophilic anions.^{91, 92} The conversion of the diacetates of benzaldehyde and its substituted derivatives **155** into arylacyloxycarbenium perchlorates **156**, characterised by ¹H NMR spectra of the acylals **155** in solutions in concentrated H₂SO₄, have been reported.¹⁸¹ The chemical shifts presented¹⁸¹ agree well with those for methoxycarbenium ions formed from dimethyl acetals of the same aldehydes.⁹² However, the author's statement¹⁸¹ concerning the isolation of solid acyloxycarbenium salts is doubtful. As shown in another study,¹⁸² treatment with SbCl₅ of the α-chloroalkyl acetates **157** derived from aliphatic aldehydes leads only to complexes of the latter with SbCl₅ (**158**). Mixing the α-chlorobenzyl acylates **159** with SbCl₅ at temperatures higher than -60 °C also gives the colourless complexes **161**.¹⁸³ Only at -95 °C were bright yellow precipitates of the salts **160** obtained and could be characterised by IR spectra. Heating their suspensions in CH₂Cl₂ to -60 °C results in their decomposition. The product **163** of the reaction between α-chloro-*o*-nitrobenzyl acetate **162** and SbCl₅ turned out to be somewhat more stable.¹⁸³ Its stability (10 to 15 min at 20 °C) can be explained by the participation of the *ortho*-nitro group in cyclisation¹⁸⁴ (Scheme 16).

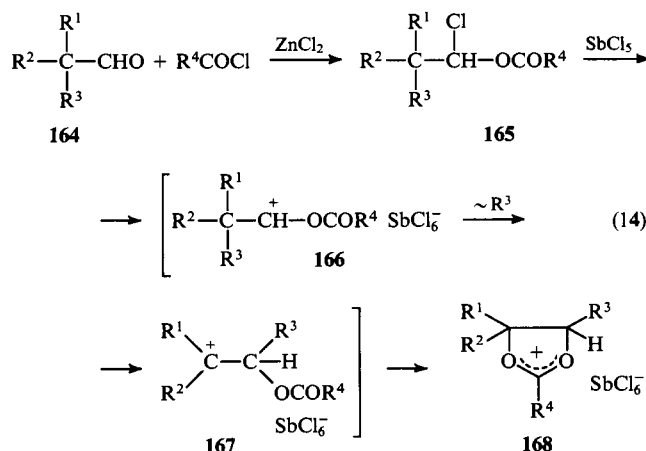
Scheme 16



Scheme 16 continued



As in *Ad_E* reactions of enol acylates (see Section III), the situation changes sharply when the α-chloroalkyl acylates **165**, obtained from the α-branched aldehydes **164**, are treated with SbCl₅. Colourless stable salts were isolated in quantitative yields; according to ¹H NMR and IR spectroscopic data, these turned out to be 1,3-dioxolanylium hexachloroantimonates **168**.^{182, 185, 186}

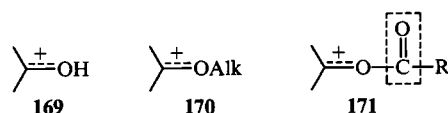


R¹ = Me, Ph;

R² = Me, Et, Ph; R¹ + R² = -(CH₂)₄-, -(CH₂)₅-;

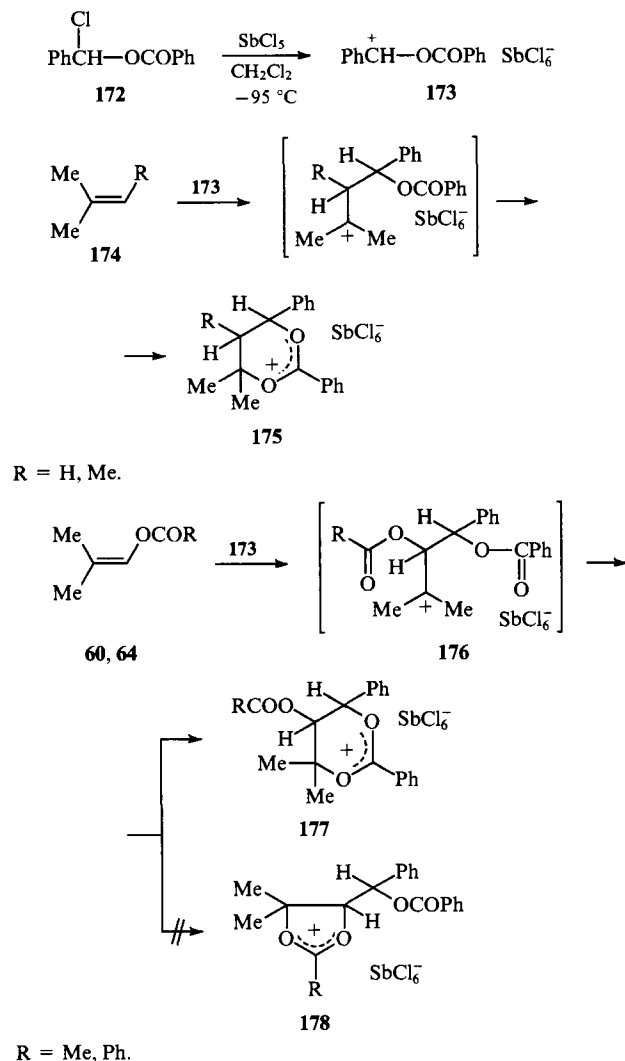
R³ = H, Ph, PhCH₂; R⁴ = Me, Et, Ph.

Thus, the same 1,3-dioxolanylium salts as those derived from branched enol acylates **60** and **64** are formed from the α-chloroesters **165**. However, isomerisation of the acyloxycarbenium ions **166** to the tertiary carbenium ions **167**, already shown above (see Scheme 9), occurs in this reaction. It must be emphasised that rearrangements with 1,2-migration to a carbon atom linked to an oxygen atom (see Section VI) are not typical of carboxonium ions and thus differentiate sharply the acyloxy-carbenium ions **171** from the well-known hydroxy-(**169**) and alkoxy-carbenium (**170**) ions.



Moreover, an important feature of the cations **171** is the combination of electrophilic (the carbenium atom) and nucleophilic (the carbonyl oxygen atom) centres within the same species. This makes them suitable for interaction with unsaturated compounds in polar 1,4-cycloaddition reactions.¹⁸⁷ Thus, benzyloxyphenylcarbenium hexachloroantimonate **173**, obtained beforehand from α-chlorobenzyl benzoate **172**, reacts with the

alkanes **174** to give the 1,3-dioxanylium salts **175**.¹⁸³ The 5-acyloxy-1,3-dioxanylium salts **177** can be derived from the enol acylates **60** and **64** as unsaturated components.¹⁸³



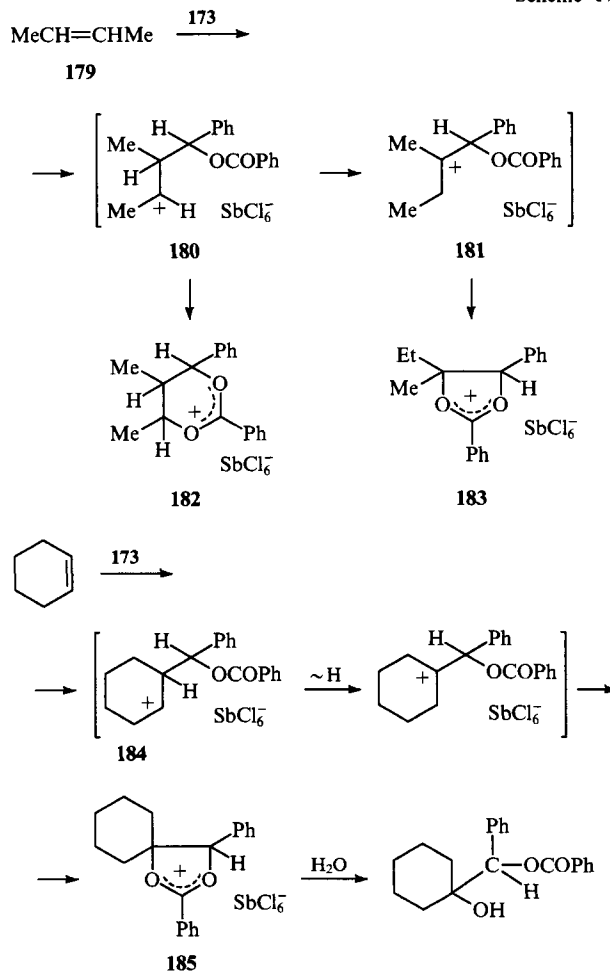
Hydrolysis of 1,3-dioxanylium salts **175** readily yields 1,3-diols with a branched skeleton.¹⁸⁸ Correspondingly, the salts **177** can be precursors of 1,2,3-triol derivatives.

The interaction of the carboxonium salt **173** with 2-butene **179** leads to a separable mixture of the isomers **182** and **183** in a 6:1 molar ratio. It is obvious that cyclisation of the secondary cationoid intermediate **180** is accompanied by partial isomerisation of the latter to the more stable tertiary cation **181**.¹⁸³ However, cyclohexene reacts with the salt **173** to give only the 1,3-dioxolanylium derivative **185**. Apparently, immediate cyclisation in the less flexible structure **184** is difficult (Scheme 17).¹⁸³

A contradiction is evident in the above cycloaddition processes. On the one hand, no five-membered heterocycles **178** arise in the reaction of the enol acylates **60** and **64** with the salt **173** by the pathway described in Section III. Cyclisation through one of the two acyloxy groups in the intermediate **176** results only in the 1,3-dioxanylium salts **177**, which supports the concerted 1,4-addition of the cation **173** to the C=C double bond. On the other hand, the addition to cyclohexene has an obviously stepwise mechanism.

As shown by ¹H NMR spectroscopy,^{188, 189} the concerted and stepwise cycloaddition mechanisms can operate simultaneously, and the structure of the end-products is determined by the configuration of at least two transition states arising from the differing chirality of α-chlorobenzyl benzoate **172**.¹⁸⁸

Scheme 17



VI. Direct O-acylation of aldehydes and ketones

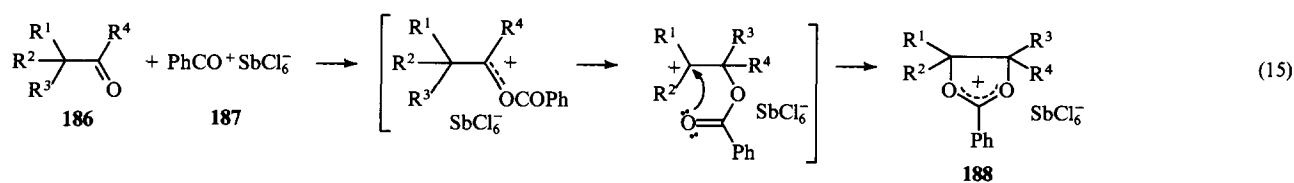
The use of acylals, enol acylates, and α-haloalkyl acylates for preparative syntheses of acyloxycarbocations suffers from several drawbacks. On the one hand, these approaches are in essence 'two steps forward and one step back' because carbonyl compounds acylated under acid catalytic conditions are common starting materials in all these reactions. On the other hand, only aldehydes can be employed successfully, since ketones usually do not form stable acylals and α-haloesters.

Therefore, attempts were made to perform the above syntheses by obtaining the required acyloxycarbocations directly from aldehydes and ketones by path *e* (see Scheme 15). To solve this problem, some requirements had to be fulfilled. First, it was necessary to exclude from the reaction mixtures both any 'external' nucleophiles, such as halide, acylate, and hydroxide anions to avoid the formation of the adducts **1** or **2**, and any bases to prevent the deprotonation of the acyloxycarbocations to give enol acylates or the fragmentation of the former with loss of an acyl cation. Obviously, the presence of protons as competing electrophiles is also undesirable.

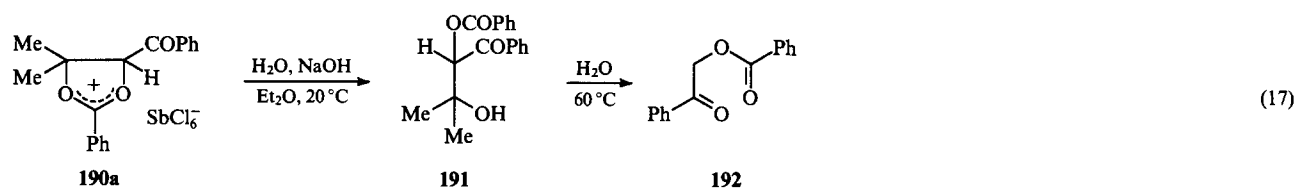
All of these requirements can be satisfied by employing cationoid complexes, namely, acylium salts that have recently found extensive use for the controlled and directed functionalisation of unsaturated compounds under *Ad_E* reaction conditions.^{190–192} The benzoyl and *tert*-butyl hexachloroantimonates (see Schemes 7 and 9) can be used as such cationoid complexes.

The interaction of a series of aldehydes and ketones **186** with benzoyl hexachloroantimonate **187** gave the 1,3-dioxolanylium salts **188** in 32%–86% yields.^{193–195} It was found that nitromethane is the optimum solvent for these processes as it can

Scheme 18


$$R^1, R^2 = \text{Me, Ph, PhCH}_2; \quad R^3 = \text{H, Me, Ph, PhCH}_2; \quad R^4 = \text{H, Me, Et, Pr}^i, \text{Ph.}$$


R = Me, Ph.



effectively stabilise the cationoid intermediates.¹⁹⁴ The acylation of the ketoaldehydes **189** under the same conditions gave the hitherto unknown 4-acyl-1,3-dioxolanylium salts **190**. Hydrolysis of the salt **190a** yielded the polyfunctional compounds **191** and **192**.¹⁹⁶ 1,3-Diketone **193** behaves similarly (Scheme 18).¹⁹⁶

Studies of the structures of the products of these reactions, **190** and **194**, and compositions of the reaction mixtures [Eqns (16) and (18)] showed that these processes involve 1,2-acyl migrations.¹⁹⁶ It should be noted that 1,2-shifts of acyl groups between carbon atoms in cations are very rare and have been studied only in the ketoxirane series.^{197–200} However, the isomerisation of the acyloxycarbobocations already mentioned in Sections V and VI [Eqns (14)–(16) and (18); Scheme 9] is worthy of particular consideration.

Sextet rearrangements so typical of carbenium ions^{94, 201} are not in any way characteristic of the carboxonium cations **169** and **170**, which arise in acid-catalysed reactions of carbonyl compounds. The Danilov aldehyde-ketone isomerisation,²⁰² the acyloin rearrangement,⁹⁴ as well as the dienone-phenol rearrangement¹² are perhaps the only ones known. Therefore, the isomerisation discovered in reactions involving acyloxycarocations at once attracted attention. The isomerisation is, in essence, the transformation of carbonyl compounds into 1,2-diols, i.e. the reverse of the pinacol (diol-ketone) rearrangement; hence it was described as a retopinacol rearrangement. This term is about 90 years old and is most frequently used for the conversion of pinacol into tetramethylethene. However, this conversion is in fact not a retro-reaction relative to the pinacol rearrangement. This fact has been repeatedly noted, and it was even proposed to exclude altogether this inappropriate term.²⁰³

The discovery of a reaction actually corresponding to this concept required reasoned criteria to determine the place of the process among other rearrangements. Structural, functional, and redox features were proposed for this purpose, according to

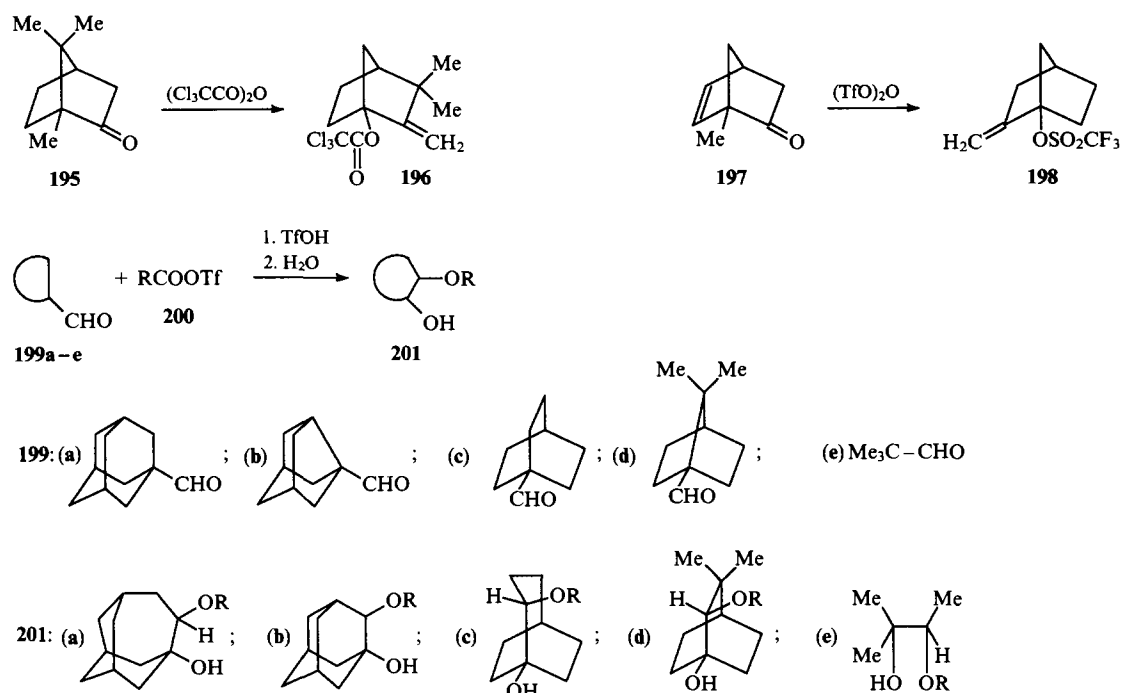
which this conversion of carbonyl compounds is fully the reverse of the pinacol rearrangement.^{194, 195, 204–206}

A few further examples of the retropinacol rearrangement, also proceeding upon acylation of carbonyl compounds, have been described in the literature. The action of trichloroacetic anhydride on camphor **195**³³ and of trifluoromethanesulfonic anhydride on 1-methylnorborn-5-en-2-one **197**¹⁷⁰ leads to the allyl alcohol derivatives **196** and **198**. These reactions are the reverse of the second variant of the pinacol rearrangement, viz. the L'vov-Sheshukov reaction (conversion of allyl alcohols into aldehydes²⁰²). The acylation of the aldehydes **199** by the acyl triflates **200** also occurs through the retropinacol rearrangement to give the 1,2-diols **201**.²⁰⁷ An analogous transformation of the aldehyde **199a** by treatment with benzoyl chloride in the presence of AlCl₃ was recently described.²⁰⁸ Pinacolone **202** undergoes a rearrangement on treatment with SO₃ (Scheme 19).²⁰⁹

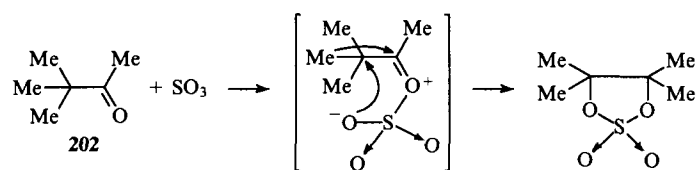
All these reactions are possible owing to the high energy of the acyloxycarbenium intermediates. According to quantum chemical calculations, the energy of the latter is almost equal to that of tertiary carbenium ions [ΔH_f (**166**) = 94.8 kcal mol⁻¹; ΔH_f (**167**) = 97.2 kcal mol⁻¹].²¹⁰

Such a low stability of the acyloxycarbenium ions **171** relative to the carboxonium ions **169** and **170** permits other conversions that are also unusual for carbonyl compounds. Fragmentation of the cationoid intermediate with cleavage of the C–C bond can occur under conditions complicating the rearrangement. Thus, not migration but loss of the benzoyl group in the intermediate **204** takes place upon the benzylation of 1,1-dibenzoylcyclopentane **203**.¹⁹⁶ Under the same conditions, the β -branched ketone **206** gives the acyloxycarbocation **207**, which is incapable of rearrangement (which would result in a less stable secondary carbocation) and therefore undergoes fragmentation. C-Acylation of its products **208–210** gives the pyrylium salt **211**¹⁹⁶ (Scheme 20).

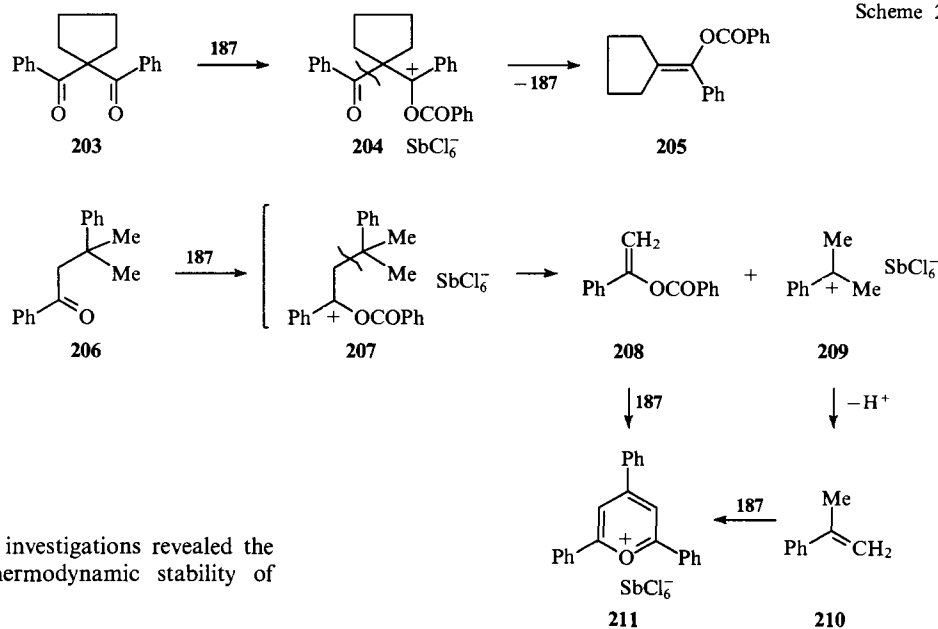
Scheme 19



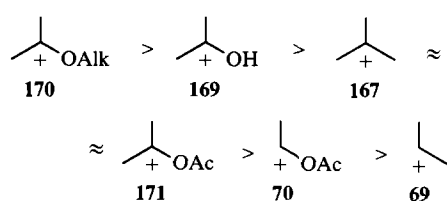
R = H, Ph, 1-adamantyl.



Scheme 20



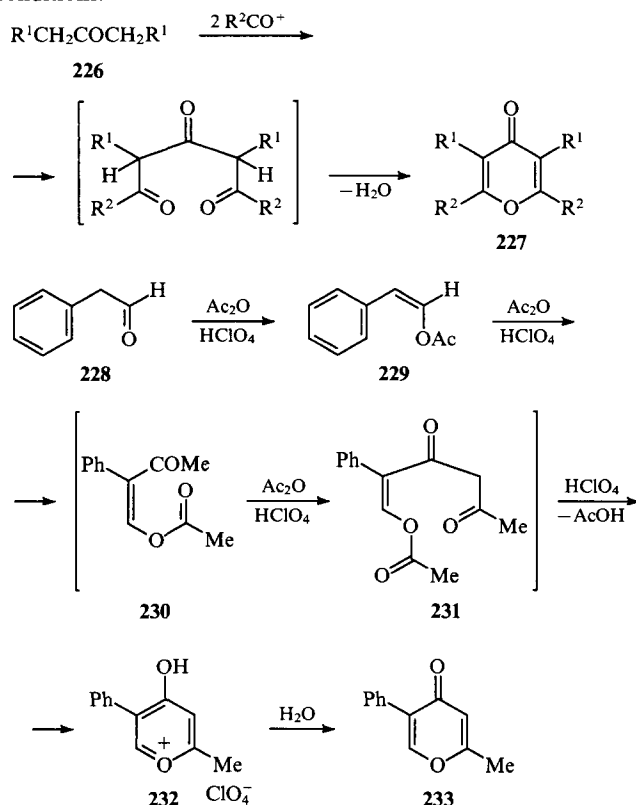
Information from this series of investigations revealed the following series based on the thermodynamic stability of cations.¹⁰⁴



VII. Acid-catalysed C-acylation of carbonyl compounds

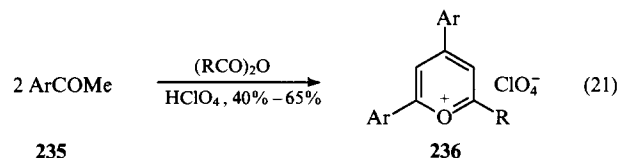
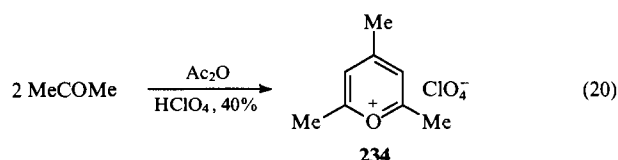
The aforementioned (see Section I) method of synthesis of 1,3-diketones by the acylation of ketones in the presence of boron trifluoride⁶ has never been widely used. This was prevented by various side reactions (acylation of diketones, see Section VI) as well as the successful development of alternative approaches using fixed enolic derivatives of ketones, particularly silyl enol ethers (see, for example, Tirpak and Rathke²¹⁹ and a review²²⁰). On the other hand, these side reactions were the basis of many one-pot syntheses of oxygen-containing heterocyclic compounds. These syntheses involve the repeated acylation of the starting carbonyl compounds and intermediates, and are in essence chains of consecutive conversions of cationoid (or similar) structures, terminated by cyclisations to highly stable heterocyclic cations.

Syntheses of the 4-pyrones **227** by the acylation of acetone and its symmetrical homologues **226** have been reported. In these processes, carboxylic acids or their anhydrides in the presence of polyphosphoric acid²²¹ or acetyl chloride with AlCl_3 ²²² were used as acylating agents. Repeated acylation of phenylethanol **228** gives the unsymmetrical 4-pyrones **233**.²²³ This reaction involves successive lengthening of the carbon chain via the intermediates **230** and **231**, which are represented as uncharged species but can hardly remain uncharged under these reaction conditions.

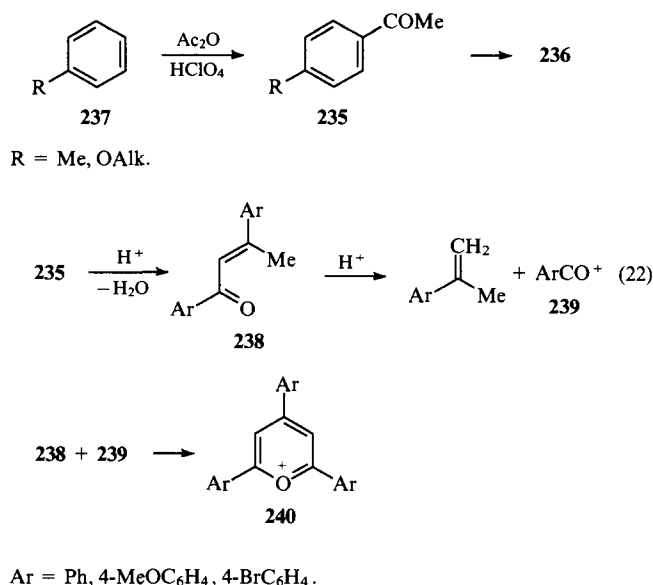


However, pyrylium salts (e.g. **225** and **232**) occupy a dominant position among the heterocyclic compounds discussed. Practically all the information concerning these compounds is concentrated in two comprehensive reviews^{224, 225} and in several papers.^{91, 174, 226} Therefore, the methods of synthesis of pyrylium salts by the acylation of carbonyl compounds will be outlined only briefly in the present review.

It turned out that the mixture of acetic anhydride with 70% perchloric acid was the most suitable acylating agent for the synthesis of pyrylium salts.²²⁶ This mixture converts acetone into 2,4,6-trimethylpyrylium perchlorate **234**;²²⁷ unsymmetrical 6-alkyl-2,4-diarylpyrylium salts **236** were obtained from the aryl methyl ketones **235** under the same conditions.¹⁷⁴

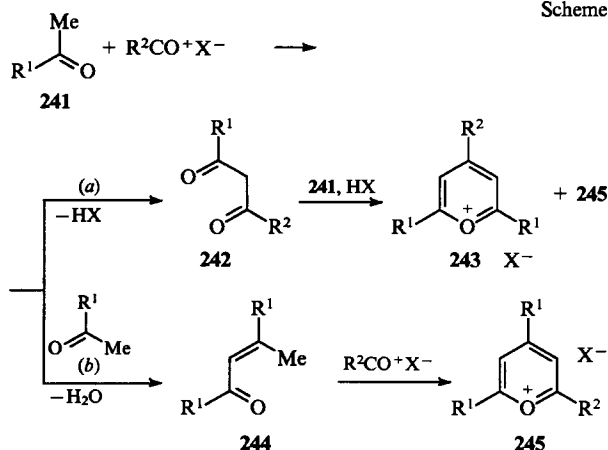


Noteworthy modifications of the latter process are acylation of aromatic compounds **237** having electron-donating substituents and protonation of the aryl methyl ketones **235** with strong inorganic acids.²²⁴ In the former case, the initial Friedel-Crafts ring C-acylation to the ketone **235** is followed by its reaction according to Eqn (21). In the latter case, the interaction involves self-condensation of the ketone **235** to the dypnone **238**, which is partially deacylated by the acid [Eqn (22)].^{224, 228} It should be mentioned that this reaction [Eqn (22)] is of a rather theoretical interest because abundant charring takes place, whereas the yields of the salts **240** do not exceed 12%–15%.



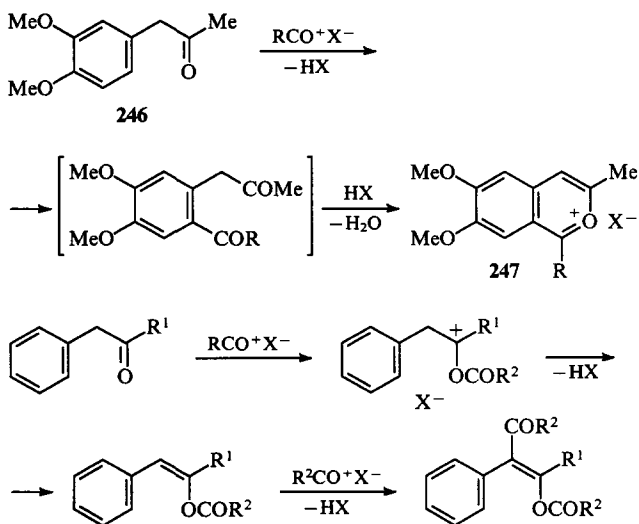
Until recently, there were no commonly accepted opinions concerning the pathway of the methyl ketone acylation [Eqns (20) and (21)]. Arguments have been put forward in the literature both in favour of the initial C-acylation of the starting ketones **241** to give the 1,3-diketones **242**, which subsequently react with a second molecule of the ketone **241** (pathway *a*), and in favour of the preliminary crotonic condensation of the ketones **241** to give the α,β -unsaturated ketones **244**, which then undergo C-acylation (pathway *b*).²²⁴ Recently, investigations showed that condensations of the unsymmetrical 1,3-diketones **242** ($\text{R}^1 \neq \text{R}^2$) with methyl ketones **241** always lead to mixtures of isomeric pyrylium salts **243** and **245**, while acylation of the ketones **241** gives only the asymmetric isomers **236** and **245**.²²⁹ Hence, it was concluded that the latter reaction occurs by pathway *b* (Scheme 22).

Scheme 22

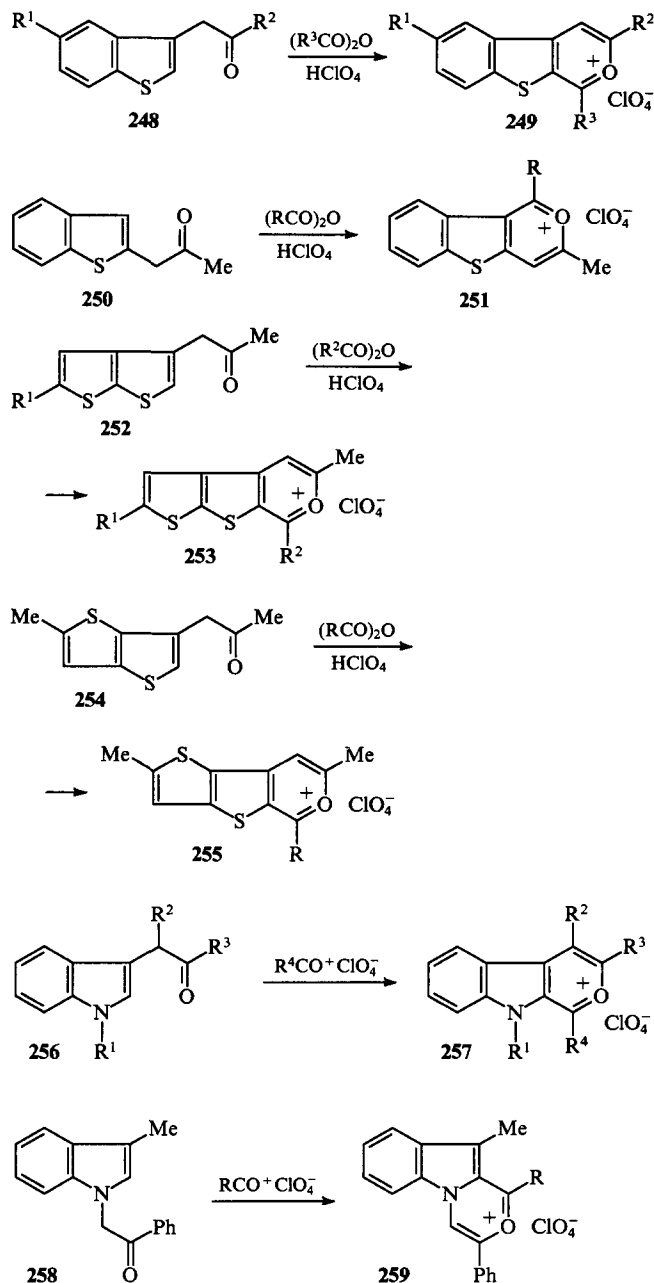


The acylation of the α, β -unsaturated ketones **244** represented by Scheme 22 is one more widely used method for synthesising pyrylium salts,²²⁴ particularly when salts **245** containing definite substituents at positions 2 and 4 are required. The use of dypnone [1,3-diphenyl-2-buten-1-one (Ed.)] and mesityl oxide has been reported most frequently.²²⁴ Evidently, the process occurs by Eqn (19) including isomerisation to a β, γ -unsaturated ketone (or the corresponding enol acylate **244**).²¹⁸

Finally, one more reaction, very important in pyrylium chemistry, cannot be disregarded, namely, the acylation of the benzyl ketones **246** to give the 2-benzopyrylium salts **12** and **247**.²³⁰ These salts can be readily transformed into isoquinolines, including natural alkaloids which are difficult to obtain. The key step of this process is acylation of the aromatic ring which must contain electron-donating substituents (this is possibly the only preparative restriction of this method). In the absence of such substituents, competitive *O*-acylation prevails, which prevents the formation of the target products **247**.



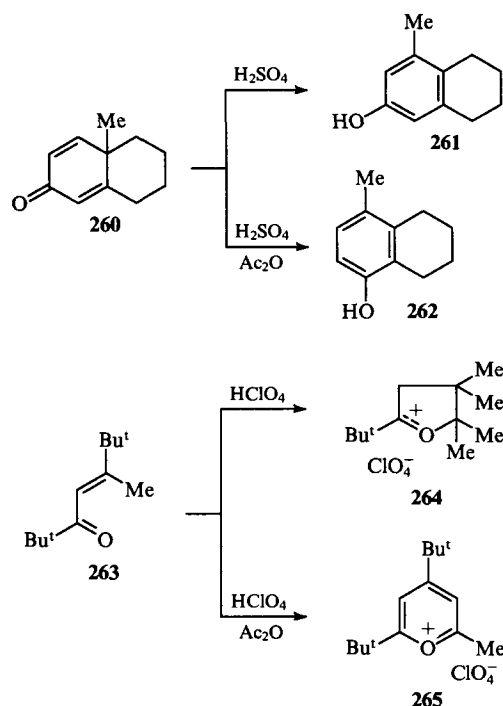
The benzyl ketones **246** can be regarded as fixed β, γ -unsaturated ketones undergoing *C*-acylation at the γ -position.^{231, 232} The reaction considered was discovered in 1966²³³ and was later extended to various heterocyclic ketones (**248**, **250**, **252**, **254**, and **256**). As a result, fused polyheterocyclic derivatives such as the thienopyrylium salts **249**,²³⁴ **251**,²³⁵ **253**, and **255**,²³⁶ as well as the indolopyrylium salts **257**²³⁷ were obtained. These salts can be converted into the corresponding pyridine derivatives, particularly, β -carbolines.²³⁷ The novel indolo-1,4-oxazinium salts **259** were prepared by the acylation of 1-phenacyl-3-methylindole **258**.²³⁸



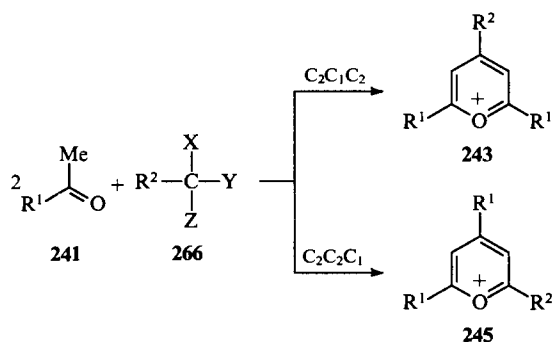
The products **259** are interesting as precursors of indolopyrazines used as psychotropic preparations and antibiotics.²³⁸

VIII. Electrophilic catalysis by acyl cations

While investigating the acid-catalysed reactions of carbonyl compounds, it was observed long ago that the addition of acetic anhydride to an acidic reaction medium can change the direction of such processes. Thus, isomerisation of dienone **260** occurs by the usual mechanism involving the dienone-phenol rearrangement with migration of the methyl group to form the phenol **261**, but the anomalous product **262** was obtained in the presence of Ac_2O .^{239, 240} Protonation of the α, β -unsaturated ketone **263** gives the dihydrofurylium salt **264**,²⁴¹ while the addition of acetic anhydride leads to the pyrylium salt **265**.²⁴²

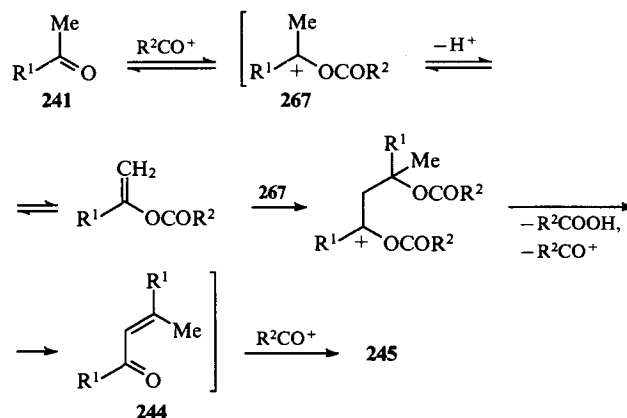


One of the three-component syntheses of pyrylium salts presented above [see Eqns (20) and (21) and Scheme 22, pathway *b*] involves the interaction of the methyl ketone **241** (the C_2 -component) with the precursor of the acyl cation (the C_1 -component). According to the formation pattern of the five-carbon chain of the ring, this synthetic method can be represented as $C_2C_2C_1$.^{224,225} Other precursors of carboxonium ions can be also employed as C_2 -components: aromatic aldehydes **266** ($X = H, Y + Z = O$, hydroxycarbocations), acetals **266** ($X = H, Y = Z = OAlk$, alkoxy carbocations), orthoesters **266** ($X = Y = Z = OAlk$, dialkoxy carbocations).^{224,225} However, these processes give symmetrical pyrylium salts **243** via the $C_2C_1C_2$ pathway.

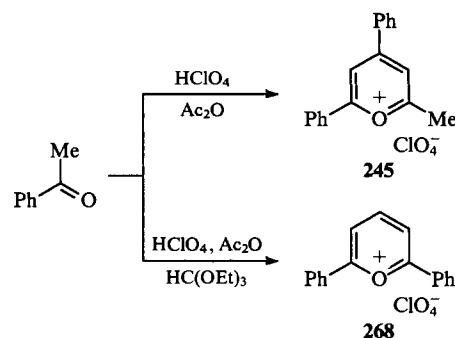


It was found that the reactions of the methyl ketones **241** with analogues of the above C_1 -components, e.g. α -chloroalkyl acylates **266** ($X = H, Y = Cl, Z = OAc$), chloromethyl methyl ether **266** ($R^2 = X = H, Y = Cl, Z = OMe$), as well as alkyl α, α -dichloromethyl ethers **266** ($R^2 = H, X = Y = Cl, Z = OAlk$), preferentially follow the $C_2C_2C_1$ path.^{224,225,243} This fact evidently implies initial fast self-condensation of the methyl ketone **241** to the α, β -unsaturated ketone **244** (Scheme 22). It should be noted that reactions using these α -chloroethers and α -chloroesters were carried out in AcOH. It was found that the formation of unsymmetrical pyrylium salts **245** predominates when acylium ions are present in the reaction mixture or conditions for the generation of these ions in situ are created.²⁴³

Hence acyl cations are the factor that promotes the rapid self-condensation of the methyl ketones **241** in accordance with the assumed scheme.²⁴³

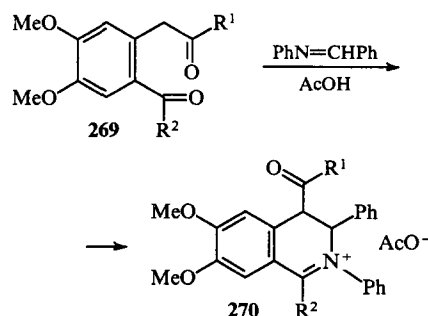


If the *O*-acylation of the keto-component **241** is suppressed, the reaction follows the $C_2C_1C_2$ path. Thus, the addition of ethyl orthoformate (which irreversibly binds the acyl cations to form the corresponding ester and to liberate diethoxycarbenium ions) to the same mixture, 'acetophenone + acetic anhydride + perchloric acid', leads to 2,6-diphenylpyrylium perchlorate (**268**) in high yield.²⁴⁴

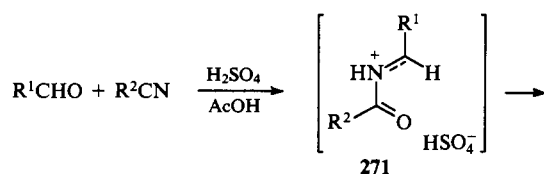


As shown recently, the 1,5-dicarbonyl compounds **269** react with azomethines in AcOH to give the dihydroisoquinolines **270**; this reaction does not occur either in acetonitrile or in *N,N*-dimethylformamide.²⁴⁵

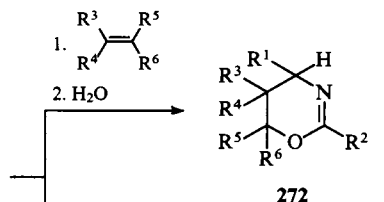
Although acyl cations do in fact participate in the conversions of carbonyl compounds considered, they are included among the end-products only provided that the process involves *C*-acylation. In other words, here we deal with electrophilic catalysis by acylium ions in reactions of carbonyl compounds with weak nucleophiles; such catalysis involves the conversion of an aldehyde or ketone into the highly reactive acyloxycarbenium ions **267** (see Section V).



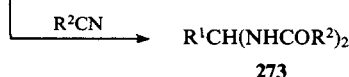
The most typical example of the application of catalysis by acyl cations is the interaction between carbonyl compounds and nitriles. The syntheses of 1,3-oxazine derivatives **272** from aldehydes, nitriles and alkenes are usually carried out with a mixture of sulfuric and acetic acids, although the role of the latter in the reaction has not been clarified.²⁴⁶⁻²⁴⁸



271



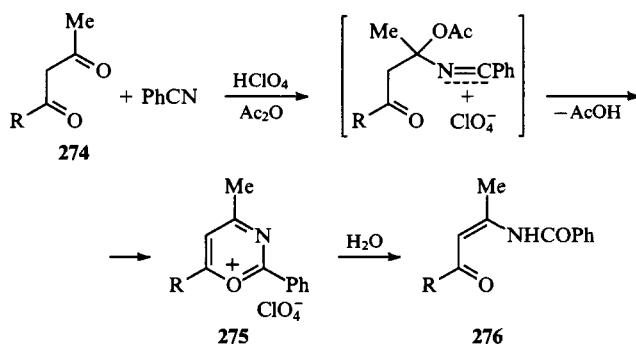
272



273

In the absence of an alkane component, the *N*-acyliminium intermediates **271** combine with another nitrile molecule to give the geminal bis-amides **273**.²⁴⁹

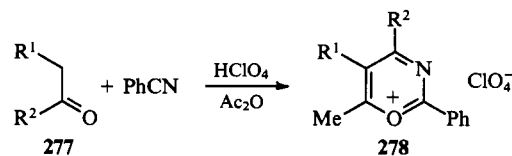
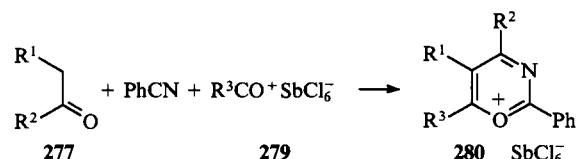
These reactions are well-known in the aldehyde series; however, attempts to extend them to ketones have failed until recently.^{249, 250} This problem was solved using $HClO_4 + Ac_2O$ as the acylating mixture. The 1,3-diketones **274** readily react with benzonitrile in the presence of this mixture to yield the little-known 3-azapyrylium salts **275**, the hydrolysis of which gives the β -acylamino vinyl ketones **276**.²⁵¹



R = Me, Ph.

Under the same conditions, the alkyl aryl ketones **277** give the 3-azapyrylium salts **278**, which are structurally isomeric with compounds **275**.²⁵² These reactions do not occur in the absence of acetic anhydride (when the nitrile is absent, the reaction follows Schemes 21 and 22).

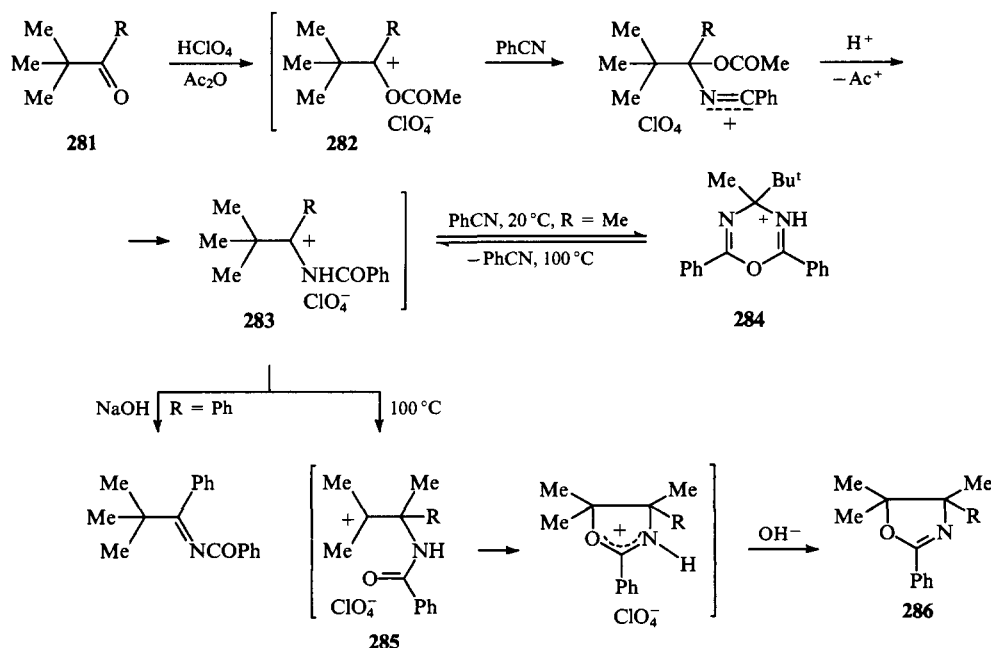
The large series of 3-azapyrylium salts **280** were obtained by treating mixtures of benzonitrile and the ketones **277** with the acylium salts **279**.²⁵³

R¹ = H, Me; R² = Ph, 4-MeC₆H₄.

R¹ = Me, Et, Bu^t, Ph; R² = H, Me; R¹ + R² = -(CH₂)₄-;
R³ = Me, Et.

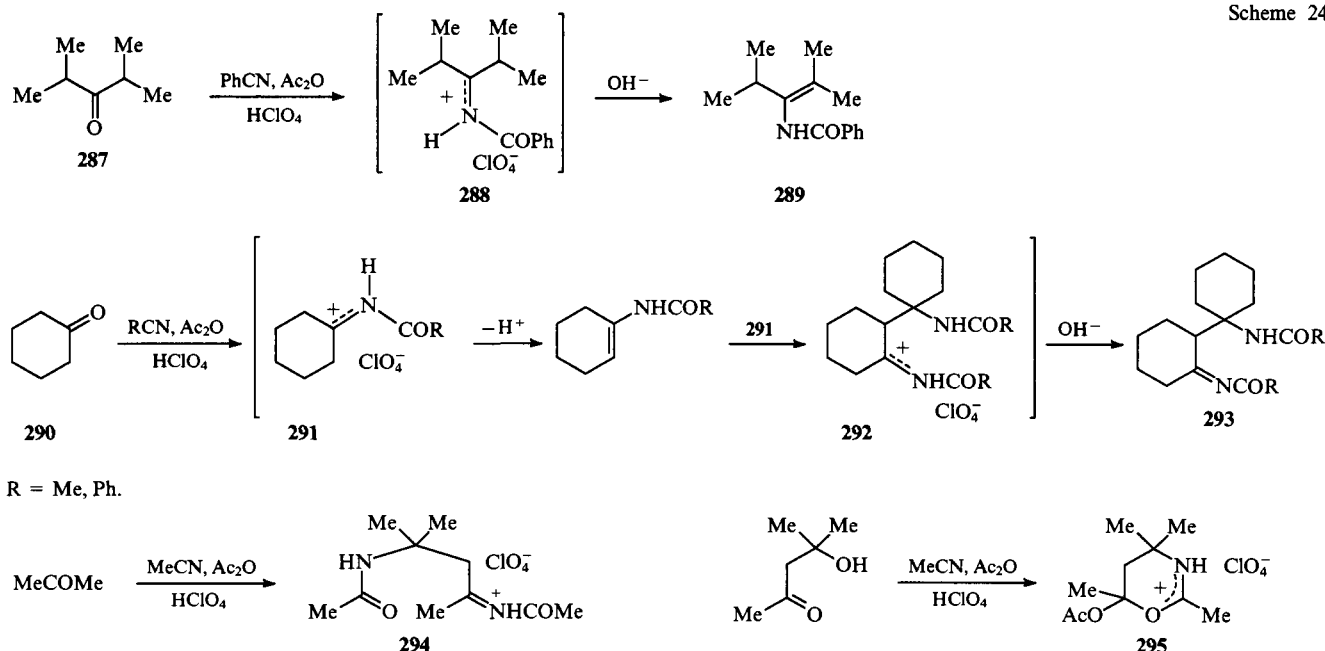
The transformations of a series of aliphatic ketones under the conditions of electrophilic catalysis by acyl cations were described in Ref. 254. Pinacolone **281** (R = Me) combines with benzonitrile in the presence of the $HClO_4 + Ac_2O$ mixture to furnish 1,3,5-oxadiazinium perchlorate **284**, which is decomposed on heating to form the *N*-acyliminium intermediate **283**. The latter, which is a heteroanalogue of **282**, can isomerise to the tertiary carbocation **285**. This process is another variant of the retropinacol rearrangement (see Section VI), which is the reverse of the Tiffeneau and MacKenzie reactions²⁵⁴ (it should be noted that the 2-oxazolines **286** are direct derivatives of 1,2-aminoalcohols). Pivalophenone **281** (R = Ph) behaves similarly. Its transformations also occur in the presence of Ac_2O , but the acyl fragment is not included in the product structure (Scheme 23).

Scheme 23



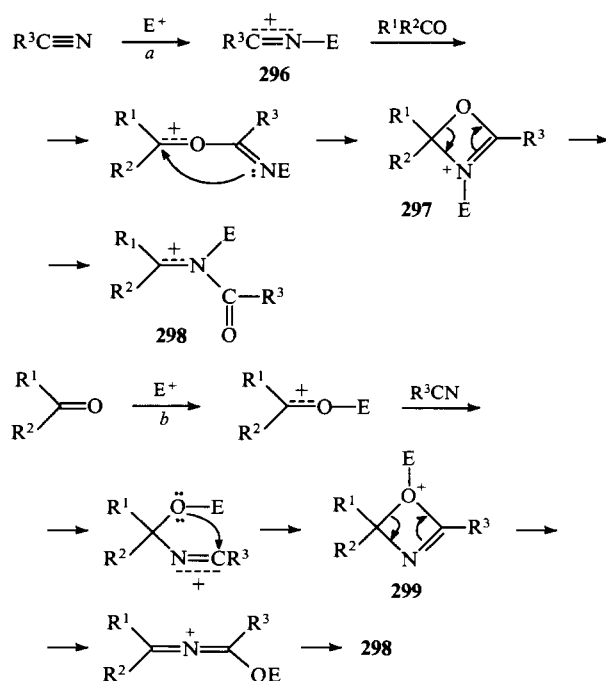
R = Me, Ph.

Scheme 24



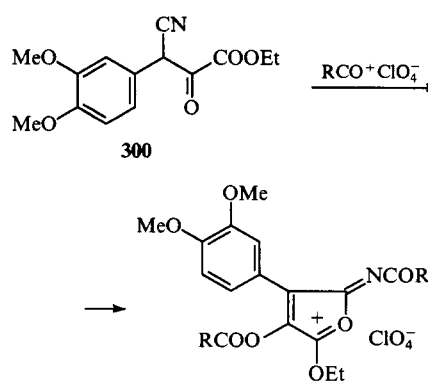
The structure of the products obtained from diisopropyl ketone **287** and cyclohexanone **290** under the same conditions suggest that the *N*-acyliminium ions **288** and **291** are formed as intermediates.²⁵⁴ The hypothesis that the aldol condensation of the ketone may initially occur has been disproved, for example, by obtaining different products (**294** and **295**) from acetone and diacetone alcohol²⁵⁴ (Scheme 24).

As shown by experiment and quantum-chemical calculations, the interaction of carbonyl compounds with nitriles occurs by different pathways depending on whether the process is catalysed by protic acids or acylium ions.^{255–258} In the former case, the nitrile component undergoes electrophilic activation (protonation, pathway *a*, E = H). The nitrilium cation **296** formed attacks a molecule of the carbonyl compound. On the other hand, in the presence of acylium ions, the carbonyl component undergoes electrophilic activation (pathway *b*, E = Ac). Both pathways lead to the *N*-acyliminium ions **298** via the intermediates **297** and **299**.



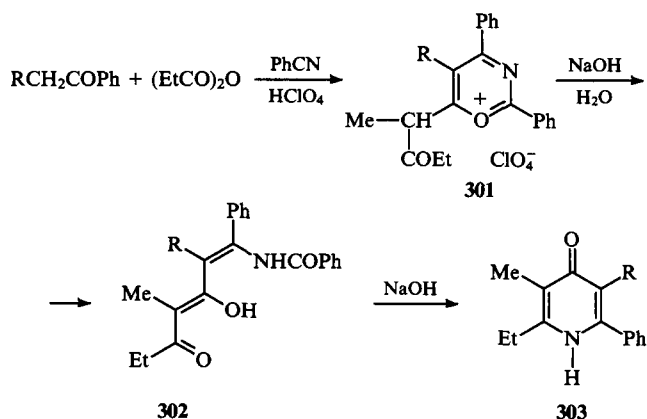
While pathway *b* is analogous to the Ritter reaction (but fundamentally differs from it in a number of features^{255, 257}), the interaction following pathway *a* was unknown until recently. Only recently has it been found that the nitrilium salts **296** (E = Alk) prepared beforehand (they are, incidentally, heteroanalogues of acylium ions) readily react with carbonyl compounds to give the *N*-acyliminium ions **298** (E = Alk).^{259–261} Some aspects of the interaction of aldehydes and ketones with nitriles were thoroughly discussed in a recent review.²⁶²

Remarkable processes take place in the acylation of compounds containing both a keto-group and a nitrile moiety (e.g. compound **300**).^{263–266}

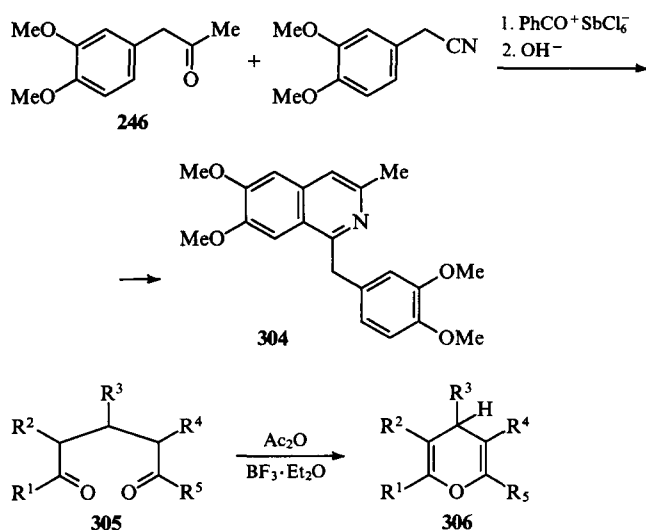


R = Me, Et.

Acylation of propiophenone or butyrophenone with propionic anhydride in benzonitrile leads to the 6-acylmethyl-3-azapyrylium salts **301**, which can be converted into derivatives of the 1,3,5-triketones **302**, which are difficult to synthesise, and into the pyridones **303**.²⁶⁷



Electrophilic catalysis by acylium ions was found to be the most effective means for the transformation of the benzyl ketone **246** into a natural alkaloid of the isoquinoline series **304**,²⁶⁸ as well as for the cyclisation of the polysubstituted 1,5-diketones **305** to the pyrans **306**.²⁶⁹ These reactions did not occur in the presence of other acid catalysts.


$$R^1, R^2 = \text{Ar, cyclo-Alk};$$
$$R^3 = H, Alk, Ar; \quad R^4 = H, R^5 = Ph.$$

* * *

The examples presented above illustrate the wide scope of the synthetic application of acyl cations as catalysts in condensations and cyclisations of carbonyl substrates. Moreover, going beyond the limits of this review, it should be mentioned that the applicability of the above reactions can be considerably extended using derivatives of carbonyl compounds. Some of them, such as acylals, α -haloalkyl acylates, enol acylates and acetals, have been described in this review. Vinyl halides and ethynes also belong to this series. For example, the reactions of acylium salts with *tert*-butylethyne and the chloroalkenes $R^1-CH=C(Cl)R^2$ present one more example of the retropinacol rearrangement.^{270, 271} The same rearrangement, i.e. conversion of ketones into vicinal chloroamides, occurs via highly reactive chlorocarbenium ions in the interaction of geminal dichlorohydrocarbons with nitriles.²⁷² β,γ -Unsaturated chloroketones, allenic 1,5-diketones, and 4-chloropyrylium salts can be obtained by the acylation of vinyl chlorides.^{271, 273} Vinyl chlorides react with nitriles to give pyrimidines in the presence of trifluoromethanesulfonic acid²⁷⁴ or 3-azapyrylium hexachloroantimonates in the presence of acylium salts.²⁵³ Finally, pyrimidines and 3-azapyrylium salts

can be prepared by the interaction of vinyl chlorides with nitrilium salts.²⁷⁵

Thus, the acid-catalysed acylation of carbonyl compounds is not only an alternative to traditional methods using base catalysis but is also a new approach to the activation of aldehydes and ketones in reactions with various carbo- and hetero-nucleophiles. Previously unknown reactions of carbonyl compounds, rearrangements, and fundamentally new methods of synthesis of valuable oxygen- and nitrogen-containing heterocyclic and polyfunctional compounds have already been found in this promising synthetic field.

The authors are grateful to the International Science Foundation for financial support of this work (grant no. RV000).

References

1. D J Cram, G S Hammond, in *Organic Chemistry* (New York: McGraw-Hill, 1964) p. 323
2. R C Fuson, in *Reaction of Organic Compounds* (New York: Wiley, 1962) p. 427
3. H G O Becker, in *Einführung in die Elektronentheorie Organisch-chemischer Reaktionen* (Berlin: VEB Deutscher Verlag der Wissenschaften, 1974) p. 327
4. In *Organikum* (Berlin: VEB Deutscher Verlag der Wissenschaften, 1974) Vol. II, p. 127
5. J March *Advanced Organic Chemistry* (New York: Wiley-Interscience, 1985) Vols 1-4
6. C R Hauser, F W Swamer, J T Adams *Org. React.* **8** 59 (1954)
7. K V Vatsuro, G L Mishchenko, in *Imennye Reaktsii v Organicheskoi Khimii* (Named Reactions in Organic Chemistry) (Moscow: Khimiya, 1976)
8. I G Tishchenko, O N Bubel', Yu L Ptashenkov *Dokl. Akad. Nauk BSSR* **24** 719 (1980)
9. L A Yanovskaya, S S Yufit, in *Organicheskii Sintez v Dvukhfaznykh Sistemakh* (Organic Synthesis in Two-phase Systems) (Moscow: Khimiya, 1982) p. 72
10. D Seyferth, R M Weinstein, W-L Wang, R C Hui *Tetrahedron Lett.* **24** 4907 (1983)
11. A F Bochkov, V A Smit, in *Organicheskii Sintez* (Organic Synthesis) (Moscow: Nauka, 1987) p. 99
12. S Patai (Ed.), in *The Chemistry of the Carbonyl Group* (New York: Wiley-Interscience, 1966) p. 457
13. V Meyer, L Dulk *Liebigs Ann. Chem.* **171** 65 (1874)
14. E Knoevenagel *Liebigs Ann. Chem.* **402** 111 (1914)
15. M Bakunin *Ann. Chim. Appl.* **5** 243 (1916); *Chem. Zentralblatt* **2** (17/18) 523 (1917)
16. Houben-Weyl, in *Methoden der Organischen Chemie* (Stuttgart: Georg Thieme, 1954) Vol. VII/1, p. 442
17. I Houben, in *Methoden der Organischen Chemie* (Translated into Russian; Moscow: Izd. ONTI, 1935) Vol. III/2, p. 473
18. L F Fieser, M Fieser, in *Reagents for Organic Synthesis* (New York: Wiley, 1968) Vol. IV, p. 181
19. J Thile, E Winter *Liebigs Ann. Chem.* **311** 353 (1900)
20. B B Snider, S G Amin *Synth. Commun.* **8** 177 (1978)
21. K S Kochhar, B S Bal, R P Deshpande, S N Rajadhyaksha, H W Pinnick *J. Org. Chem.* **48** 1765 (1983)
22. M Asaoka, N Sugimura, H Takei *Bull. Chem. Soc. Jpn.* **52** 1953 (1979)
23. L A Yanovskaya, S S Yufit, V F Kucherov *Khimiya Atsetalei* (The Chemistry of Acetals) (Moscow: Nauka, 1975)
24. J K Michie, J A Miller *Synthesis* 824 (1981)
25. G A Olah, A K Mehrotra *Synthesis* 962 (1982)
26. F Freeman, E M Karchefski *J. Chem. Eng. Data* **22** 355 (1977)
27. H O House, W C Liang, P D Weeks *J. Org. Chem.* **39** 3102 (1974)
28. J A Marshall, P G M Wuts *J. Org. Chem.* **42** 1794 (1977)
29. G N Dorofeenko, S M Luk'yanov, T I Davidenko *Zh. Org. Khim.* **11** 163 (1975)
30. R Schank, R Blattner, V Schmidt, H Hasenfratz *Chem. Ber.* **114** 1938 (1981)
31. I V Machinskaya *Zh. Obshch. Khim.* **23** 569 (1953)
32. I V Machinskaya, V A Barkhash, V I Molchanov *Zh. Obshch. Khim.* **23** 756 (1953)
33. J Libman, M Sprecher, Y Mazur *Tetrahedron* **25** 1679 (1969)

34. J Libman, Y Mazur *Tetrahedron* **25** 1699 (1969)
35. P Salomaa *Acta Chem. Scand.* **11** 247 (1957)
36. R P Bell, B Lukianenko *J. Chem. Soc.* 1686 (1957)
37. M J Gregory *J. Chem. Soc. B* 1201 (1970)
38. I V Machinskaya *Zh. Obshch. Khim.* **22** 1159 (1952)
39. B M Trost, J Vercauteren *Tetrahedron Lett.* **26** 131 (1985)
40. G Ferrand, J Huet *Bull. Soc. Chim. Fr.* 3122 (1973)
41. G Ferrand, J Huet *Bull. Soc. Chim. Fr.* 356 (1975)
42. G Ferrand, J Huet *Bull. Soc. Chim. Fr.* 1709 (1975)
43. R Merten, G Müller *Angew. Chem.* **74** 866 (1962)
44. D T Mowry *J. Am. Chem. Soc.* **69** 2362 (1947)
45. V S Markevich, O N Petrenko *Zh. Org. Khim.* **18** 2219 (1982)
46. G V Kryshchal', V S Bogdanov, L A Yanovskaya, Yu P Volkov, E I Trusova *Izv. Akad. Nauk SSSR, Ser. Khim.* 2820 (1981)
47. G V Kryshchal', V S Bogdanov, L A Yanovskaya, Yu P Volkov, E I Trusova *Tetrahedron Lett.* **23** 3607 (1982)
48. G V Kryshchal', M Monkosha, M Fedoryn'skii, L A Yanovskaya *Izv. Akad. Nauk SSSR, Ser. Khim.* 663 (1983)
49. H McNab *Chem. Soc. Rev.* **7** 345 (1978)
50. B-C Chen *Heterocycles* **32** 529 (1991)
51. M F Strozhev, I E Lielbriedis, O Ya Neiland *Khim. Geterotsikl. Soedin.* 579 (1991)
52. D G Desai, R B Mane *Indian J. Chem. B, Org. Incl. Med.* **20** 504 (1981)
53. D W Brooks, N Gastro de Lee, R Peevey *Tetrahedron Lett.* **25** 4623 (1984)
54. A N Meldrum *J. Chem. Soc.* **93** 598 (1908)
55. D Davidson, S A Bernhard *J. Am. Chem. Soc.* **70** 3426 (1948)
56. M F Shostakovskii, N A Gershtein, V A Neterman *Izv. Akad. Nauk SSSR, Otd. Khim. Nauk* 2011 (1959)
57. T Fujita, S Watanabe, K Suga, T Isobe, N Miura *Synthesis* 910 (1979)
58. R R Gallucci, R C Going *J. Org. Chem.* **47** 3517 (1982)
59. N A Nedolya, M Ya Khil'ko, B A Trofimov *Zh. Org. Khim.* **23** 1181 (1987)
60. S Tabbache, B Loubinoux *Synthesis* 665 (1982)
61. N H Fife, N C De J. *Am. Chem. Soc.* **96** 6158 (1974)
62. C Hurd, T Iwashige *J. Org. Chem.* **24** 1321 (1959)
63. S Murata, R Noyori *Tetrahedron Lett.* **23** 2601 (1982)
64. N V Kuznetsov, N K Makhnovskii *Ukr. Khim. Zh.* **45** 1016 (1979)
65. A F Grapov, A S Remizov *Zh. Obshch. Khim.* **53** 1541 (1983)
66. N V Fedorov, A V Anisimov, E A Viktorova *Khim. Geterotsikl. Soedin.* 1299 (1989)
67. K Baum *J. Am. Chem. Soc.* **92** 2927 (1970)
68. I V Machinskaya, V A Barkhash, in *Reaktsii i Metody Issledovaniya Organicheskikh Soedinenii* (Reactions and Methods for the Investigation of Organic Compounds) (Ed. B A Kazanskii, I L Knunyants, M M Shemyakin, N N Mel'nikov) (Moscow: Khimiya, 1964) Vol. 12, p. 299
69. V G Neroznik, B G Zadontsev, Yu M Sivergin *Sintez Slozhnykh Vinilovykh Efirov* (Synthesis of Vinyl Esters) (Donetsk, 1982) Article deposited at ONIITEKhim No. 747khp-D82 Cherkassy (1982); *Chem. Abstr.* **100** 52 033r (1984)
70. D Barton, W D Ollis (Eds), in *Comprehensive Organic Chemistry* Vol. 1 (Oxford: Pergamon Press, 1979) Vol. 2, p. 583
71. D Barton, W D Ollis (Eds), in *Comprehensive Organic Chemistry* Vol. 2 (Oxford: Pergamon Press, 1979) Vol. 4, p. 307
72. P F Hudrlik, A M Hudrlik *J. Org. Chem.* **38** 4254 (1973)
73. R D Bach, R A Woodard, T J Anderson, M D Glick *J. Org. Chem.* **47** 3707 (1982)
74. J F Weana, H R Taneja, M Erion *Synth. Commun.* **12** 167 (1982)
75. N Takano, N Takeno, M Morita, Y Otsuji *Bull. Chem. Soc. Jpn.* **58** 2417 (1985)
76. E Hirsch, S Hünig, H-U Reissig *Chem. Ber.* **115** 3687 (1982)
77. M A Garcia, F A Herrera, A R Martinez *An. Quim. Publ. Real. Soc. Esp. Fis. Quim., Ser. C* **76** 87 (1980); *Chem. Abstr.* **94** 83 464u (1981)
78. M A Garcia, F A Herrera, A R Martinez, M G Sanchez *An. Quim. Publ. Real. Soc. Esp. Fis. Quim., Ser. C* **77** 28 (1981); *Chem. Abstr.* **97** 5840m (1982)
79. J E McMurphy, W J Scott *Tetrahedron Lett.* **24** 979 (1983)
80. V V Shchepin, N Yu Russkikh, in *Sinteticheskie Metody na Osnove Elementoorganicheskikh Soedinenii* (Synthetic Methods Based on Organoelement Compounds) (Perm': Izd. Perm'sk. Gos. Univ., 1982) p. 23; *Chem. Abstr.* **99** 194 570y (1983)
81. V V Fotin, V V Shchepin, S V Sinani *Zh. Org. Khim.* **24** 1934 (1988)
82. T Tanaka, S Kurozumi, T Toru, M Kobayashi, S Miura, S Ishimoto *Tetrahedron Lett.* **16** 1535 (1975)
83. A S Wendel, T Reffstrup, P M Boll *Tetrahedron* **35** 2181 (1979)
84. I V Shcherbakova, N N Potemkina, G N Dorofeenko, E V Kuznetsov *Zh. Org. Khim.* **13** 1341 (1977)
85. E V Kuznetsov, I V Shcherbakova, G N Dorofeenko *Khim. Geterotsikl. Soedin.* 705 (1977)
86. P K Chowdhury, R P Sharma, J N Barua *Tetrahedron Lett.* **24** 3383 (1983)
87. E Anders, W Will, T Gassner *Chem. Ber.* **116** 1506 (1983)
88. E Anders, T Gassner *Chem. Ber.* **117** 1034 (1984)
89. A F Kulish, L A Kiprianova, A F Redasheva *Ukr. Khim. Zh.* **33** 934 (1967)
90. M F Shostakovskii *Prostye Vinilovye Efiroy* (Vinyl Ethers) (Moscow: Izd. Akad. Nauk SSSR, 1952)
91. H Perst *Oxonium Ions in Organic Chemistry* (New York: Academic Press, 1971)
92. D L Rakhmankulov, R T Akhmatdinov, E A Kantor *Usp. Khim.* **53** 1523 (1984) [*Russ. Chem. Rev.* **53** 888 (1984)]
93. G A Olah *Angew. Chem.* **85** 183 (1973)
94. C K Ingold *Structure and Mechanism in Organic Chemistry* (Ithaca: Cornell University Press, 1969)
95. O A Reutov, in *Teoreticheskie Osnovy Organicheskoi Khimii* (Theoretical Principles of Organic Chemistry) (Moscow: Izd. Mosk. Gos. Univ., 1964) p. 538
96. D Y Curtin, M J Hurwitz *J. Am. Chem. Soc.* **74** 5381 (1952)
97. W Fukuda, H Sato, H Kakiuchi *Bull. Chem. Soc. Jpn.* **59** 751 (1986)
98. A Wagner, U Rall *Angew. Chem.* **71** 193 (1959)
99. N K Kochetkov, E E Nifant'ev *Usp. Khim.* **30** 31 (1961) [*Russ. Chem. Rev.* **30** 15 (1961)]
100. H Özal, W W Zajac *J. Org. Chem.* **46** 3082 (1981)
101. N Ya Grigor'eva, V A Smit, V F Kucherov *Izv. Akad. Nauk SSSR, Ser. Khim.* 154 (1973)
102. T Benneche, K Undheim *Acta Chem. Scand., Ser. B* **36** 529 (1982)
103. G G Gareev, A M Belousov, Yu M Belousov, N A Cherkashina *Zh. Org. Khim.* **11** 2229 (1975)
104. Yu A Zhdanov, S M Luk'yanov, S V Borodaev *Zh. Org. Khim.* **21** 2067 (1985)
105. C U Pittman, S P McManus *Tetrahedron Lett.* **10** 39 (1969)
106. L V Mezheritskaya, G N Dorofeenko *Khim. Geterotsikl. Soedin.* 869 (1975)
107. M Descude C. R. *Hebd. Seances Acad. Sci.* **132** 1567 (1901)
108. M Descude *Bull. Soc. Chim. Paris* **27** 867 (1902)
109. R Adams, E H Vollweiler *J. Am. Chem. Soc.* **40** 1732 (1918)
110. H E French, R Adams *J. Am. Chem. Soc.* **43** 651 (1921)
111. L H Ulich, R Adams *J. Am. Chem. Soc.* **43** 660 (1921)
112. A Kirmann *Bull. Soc. Chim. Fr.* **5** 256 (1938)
113. A Ya Yakubovich, V V Razumovskii, Z N Vostrukhina, S M Rozenshtein *Zh. Obshch. Khim.* **28** 1930 (1958)
114. E K Euranto *Suom. Kemistil. B* **33** 41 (1960)
115. E K Euranto, T Yrjänä *Suom. Kemistil. B* **38** 214 (1965)
116. E K Euranto *Acta Chem. Scand.* **21** 721 (1967)
117. E K Euranto, N J Cleve *Suom. Kemistil. B* **45** 154 (1972)
118. N J Cleve, E K Euranto *Acta Chem. Scand.* **27** 1841 (1973)
119. E K Euranto, M Lankinen, K Lappalainen *Acta Chem. Scand., Ser. B* **30** 455 (1976)
120. E K Euranto, L T Kanerva *Bull. Soc. Chim. Belg.* **91** 394 (1982)
121. E K Euranto, A Noponen, T Kujanpää *Acta Chem. Scand.* **20** 1273 (1966)
122. H Schaltegger, M Neuenschwander, D Meuche *Helv. Chim. Acta* **48** 955 (1965)
123. R Kyburz, H Schaltegger, M Neuenschwander *Helv. Chim. Acta* **54** 1037 (1971)
124. M Neuenschwander, R Iseli *Helv. Chim. Acta* **60** 1061 (1977)
125. J Furrer, P Bönzli, A Frey, M Neuenschwander, P Engel *Helv. Chim. Acta* **70** 862 (1987)
126. P Bigler, H Mühle, M Neuenschwander *Synthesis* 593 (1978)
127. M Neuenschwander, P Bigler, K Christen, R Iseli, R Kyburz, H Mühle *Helv. Chim. Acta* **61** 2047 (1978)
128. P Bigler, S Schöholz, M Neuenschwander *Helv. Chim. Acta* **61** 2059 (1978)
129. P Bigler, M Neuenschwander *Helv. Chim. Acta* **61** 2165 (1978)
130. P Bigler, M Neuenschwander *Helv. Chim. Acta* **61** 2381 (1978)

131. R E Valter *Usp. Khim.* **42** 1060 (1973) [*Russ. Chem. Rev.* **42** 464 (1973)]
132. R E Valter, A E Batse *Izv. Latv. SSR, Ser. Khim.* **455** (1988)
133. M V Bhatt, S H El Ashry, M Balakrishnan *Proc. Indian Acad. Sci., Sect. A* **88** 421 (1979)
134. M V Bhatt, S H El Ashry, V Somayaji *Proc. Indian Acad. Sci., Chem. Sci.* **89** 7 (1980)
135. M V Bhatt, S H El Ashry, V Somayaji *Indian J. Chem. B, Org. Incl. Med.* **19** 473 (1980)
136. K B Sloan, S A V Koch *J. Org. Chem.* **48** 635 (1983)
137. O A Luk'yanov, T I Zhiguleva *Izv. Akad. Nauk SSSR, Ser. Khim.* **1422** (1982)
138. K B Sloan, S A V Koch *J. Org. Chem.* **48** 3777 (1983)
139. B D Dombek *J. Am. Chem. Soc.* **101** 6466 (1979)
140. G Barcelo, J-P Senet, G Sennyey, J Bensoam, A Loffet *Synthesis* **627** (1986)
141. D Dvorzhak, E Arnol'd, G V Kryshnal', L A Yanovskaya *Izv. Akad. Nauk SSSR, Ser. Khim.* **351** (1983)
142. M V Bhatt, S H El Ashry *Indian J. Chem. B, Org. Incl. Med.* **19** 487 (1980)
143. D S Noyce, R M Pollack *J. Am. Chem. Soc.* **91** 119 (1969)
144. D S Noyce, R M Pollack *J. Am. Chem. Soc.* **91** 7158 (1969)
145. J A Landgrebe *J. Org. Chem.* **30** 2105 (1965)
146. J-P Montheard, M Camps, M Chatzopoulos, M O Ait Yahia, R Guilluy, D Deruaz *J. Chem. Res. (S)* **224** (1983); *Chem. Abstr.* **100** 5483c (1984)
147. H Burton, D A Munday *J. Chem. Soc.* **1727** (1957)
148. M S Newman *J. Am. Chem. Soc.* **64** 2324 (1942)
149. T-L Ho, G A Olah *Synthesis* **418** (1977)
150. K E Teo, E W Warnhoff *J. Am. Chem. Soc.* **95** 2728 (1973)
151. V J Grenda, G W Lindberg, N L Wendler, S H Pines *J. Org. Chem.* **32** 1236 (1967)
152. M Simalty, J Carretto, S Sib *Bull. Soc. Chim. Fr.* **3926** (1970)
153. L Yu Ukhin, N A Dolgoplova, Z S Morkovnik, L G Kuz'mina, Yu T Struchkov *Khim. Geterotsikl. Soedin.* **454** (1983)
154. B R Davis, D M Gash, P D Woodgate, S D Woodgate *J. Chem. Soc., Perkin Trans. 1* **1499** (1982)
155. J Singh, K P Agarwal, G Singh *Tetrahedron Lett.* **22** 3775 (1981)
156. I I Ibragimov, V G Dzhaifarov, V A Tarasov *Dokl. Akad. Nauk SSSR* **275** 892 (1984)
157. S M Luk'yanov, L N Etmetchenko, A V Koblik, O A Rakina, G N Dorofeenko *Zh. Org. Khim.* **13** 287 (1977)
158. R Sato, M Okazaki *J. Chem. Soc. Jpn., Chem. Ind. Chem.* **2146** (1975); *Chem. Abstr.* **84** 59 147r (1976)
159. D A Oparin, T G Melent'eva, L A Pavlova *Khim. Geterotsikl. Soedin.* **1299** (1986)
160. S Fukuoka, H Nanri, T Katsuki, M Yamaguchi *Tetrahedron Lett.* **28** 6205 (1987)
161. W Lorenz, G Mass *J. Org. Chem.* **52** 375 (1987)
162. M B Erman, I M Pribytkova, O O Volkova, N A Novikov, I S Aul'chenko, V B Mochalin *Zh. Org. Khim.* **23** 233 (1987)
163. A L Perkel', S G Voronina, B G Freidin *Usp. Khim.* **63** 793 (1994)
164. H Yoshida, M Nakajima, T Ogata, K Matsumoto *Bull. Chem. Soc. Jpn.* **55** 1973 (1982)
165. O De Lucchi, G Marchioro, G Modena *J. Chem. Soc., Chem. Commun.* **513** (1984)
166. X Creary, M E Mehrsheikh-Mohammadi, M D Eggers *J. Am. Chem. Soc.* **109** 2435 (1987)
167. H Khedija, H Strzelecka, M Simalty *Bull. Soc. Chim. Fr.* **218** (1973)
168. W E Bottomley, G V Boyd *J. Chem. Soc., Chem. Commun.* **790** (1980)
169. M Hanack, J R Hassdenteufel *Chem. Ber.* **115** 764 (1982)
170. M A Garcia, A R Martinez, V E Teso, A M R Gomez *An. Quim. Publ. Real. Soc. Esp. Quim., Ser. C* **77** 196 (1981); *Chem. Abstr.* **97** 91 397b (1982)
171. M A Garcia, G J M Sanches, A A Nunez *An. Quim. Publ. Real. Soc. Esp. Quim., Ser. C* **77** 209 (1981); *Chem. Abstr.* **97** 38 265f (1982)
172. K Takeuchi, T Miyazaki, I Kitagawa, K Okamoto *Tetrahedron Lett.* **26** 661 (1985)
173. P J Stang, M Hanack, L B Subramanian *Synthesis* **85** (1982)
174. G N Dorofeenko, E I Sadekova, E V Kuznetsov *Preparativnaya Khimiya Pirilievyykh Solei* (Preparative Chemistry of Pyrylium Salts) (Rostov-on-Don: Izd. Rostovsk. Gos. Univ., 1972); *Chem. Abstr.* **78** 43 238 (1973)
175. G N Dorofeenko, V G Korobkova *Khim. Geterotsikl. Soedin.* **1601** (1971)
176. G N Dorofeenko, V G Korobkova, V I Volbushko *Khim. Geterotsikl. Soedin.* **553** (1977)
177. H Brinkmann, C Rüchardt *Tetrahedron Lett.* **13** 5221 (1972)
178. R E Valter *Kol'chato-tsepnaya Izomeriya* (Ring-Chain Isomerism) (Riga: Zinatne, 1978)
179. R Neidlein, H Zeiner *Monatsh. Chem.* **113** 1151 (1982)
180. H Hofmann, A Molnar, C Göttfert *Leibigs Ann. Chem.* **425** (1983)
181. T Fairwell, P M Nair *Indian J. Chem.* **9** 660 (1971)
182. S M Luk'yanov, S V Borodaev, S V Borodaeva *Zh. Org. Khim.* **19** 2154 (1983)
183. S M Luk'yanov, S V Borodaev *Zh. Org. Khim.* **22** 510 (1986)
184. Yu S Shabarov, S S Mochalov, V I Daineko *Izv. Sib. Otd. Akad. Nauk, Ser. Khim. Nauk* **7** (3) 43 (1980)
185. S V Borodaev, S M Luk'yanov, G N Dorofeenko *Zh. Org. Khim.* **17** 1106 (1981)
186. G N Dorofeenko, S V Borodaev, S M Luk'yanov *Zh. Org. Khim.* **17** 2233 (1981)
187. R R Schmidt *Angew. Chem.* **85** 235 (1973)
188. S V Borodaev, S M Luk'yanov *Zh. Org. Khim.* **24** 1399 (1988)
189. S V Borodaev, S M Luk'yanov *Zh. Org. Khim.* **19** 1780 (1983)
190. W A Smit *Sov. Sci. Rev. B, Chem.* **7** 155 (1985)
191. Sh O Badanyan, G G Melikyan, G R Mkhitaryan, K A Atanesyan *Arm. Khim. Zh.* **34** 926 (1981)
192. O V Lyubinskaya, V A Smit, A S Shashkov, V A Chertkov, M I Kanishchev, V F Kucherova *Izv. Akad. Nauk SSSR, Ser. Khim.* **397** (1978)
193. S M Luk'yanov, S V Borodaev *Zh. Org. Khim.* **19** 458 (1983)
194. Yu A Zhdanov, S M Luk'yanov, S V Borodaev, S V Borodaeva *Zh. Org. Khim.* **22** 1173 (1986)
195. S V Borodaev, S M Luk'yanov, Yu A Zhdanov *Dokl. Akad. Nauk SSSR* **287** 862 (1986)
196. Yu A Zhdanov, S M Luk'yanov, S V Borodaev, S V Borodaeva *Zh. Org. Khim.* **22** 2376 (1986)
197. R D Bach, M W Tubergen, R C Klix *Tetrahedron Lett.* **27** 3565 (1986)
198. J Kagan, D A Agdeppa, D A Mayers, S P Singh, M J Walters, R D Wintermute *J. Org. Chem.* **41** 2355 (1976)
199. M I Kanishev, A A Schegolev, W A Smit, R Caple, M J Kelner *J. Am. Chem. Soc.* **101** 5660 (1979)
200. C Le Drian, P Vogel *Tetrahedron Lett.* **28** 1523 (1987)
201. D Bethell, V Gold *Carbonium Ions* (London: Academic Press, 1967)
202. S N Danilov, in *Reaktsii i Metody Issledovaniya Organicheskikh Soedinenii* (Reactions and Methods for the Investigation of Organic Compounds) (Moscow: Goskhimizdat, 1956) Vol. 4, p. 159
203. H G O Becker, in *Einführung in die Elektronentheorie Organisch-chemischer Reaktionen* (Berlin: VEB Deutscher Verlag der Wissenschaften, 1964) (Translated into Russian; Moscow: Mir, 1965, p. 485)
204. S M Luk'yanov, in *Khimicheskaya Entsiklopediya* (Encyclopaedia of Chemistry) (Moscow: Izd. Bol'shaya Rossiiskaya Entsiklopediya, 1992) Vol. 3, p. 516
205. S M Luk'yanov *Zh. Org. Khim.* **31** 866 (1995)
206. S V Borodaev, Candidate Thesis in Chemical Sciences, Rostov State University, Rostov-on-Don, 1985
207. K Takeuchi, I Kitagawa, F Akiyama, T Shibata, M Kato, K Okamoto *Synthesis* **612** (1987)
208. A N Santiago, K Takeuchi, Y Ohga, M Nishida, R A Rossi *J. Org. Chem.* **56** 1581 (1991)
209. J C Sheehan, U Zoller *J. Org. Chem.* **39** 3415 (1974)
210. M E Kletsii, S M Luk'yanov, S V Borodaev, R M Minyayev, V I Minkin *Zh. Org. Khim.* **25** 1345 (1989)
211. T T Tidwell *Angew. Chem.* **96** 16 (1984)
212. J-P Begue, M Charpentier-Morize *Acc. Chem. Res.* **13** 207 (1980)
213. M Maleki, A C Hopkinson, E Lee-Ruff *Tetrahedron Lett.* **24** 4911 (1983)
214. K Takeuchi, M Yoshida, Y Ohga, A Tsugeno, T Kitagawa *J. Org. Chem.* **55** 6063 (1990)

215. S V Borodaev, M E Kletskii, S M Luk'yanov, R M Minyaev *Zh. Org. Khim.* **27** 1557 (1991)
216. K Matsui, M Motoi, T Nojiri *Bull. Chem. Soc. Jpn.* **46** 562 (1973)
217. N V Shibaeva, S V Borodaev, S M Luk'yanov, A I Pyshchev *Zh. Org. Khim.* **24** 2630 (1988)
218. G N Dorofeenko, S M Luk'yanov, E P Olekhovich, T I Davidenko *Khim. Geterotsikl. Soedin.* **735** (1973)
219. R E Tirpak, M W Rathke *J. Org. Chem.* **47** 5099 (1982)
220. P Brownbridge *Synthesis* **1**, 85 (1983)
221. A N Sagredos, J D Mikusch *Liebigs Ann. Chem.* **697** 111 (1966)
222. A T Balaban, G D Mateescu, C D Nenitzescu *Rev. Chim. Acad. Repub. Pop. Roum.* **6** 295 (1961)
223. E V Kuznetsov, A I Pyshchev, G N Dorofeenko *Khim. Geterotsikl. Soedin.* **152** (1972)
224. A T Balaban, W Schroth, G Fischer *Adv. Heterocycl. Chem.* **10** 241 (1969)
225. A T Balaban, A Dinculescu, G N Dorofeenko, G W Fischer, A V Koblik, V V Mezheritskii, W Schroth *Adv. Heterocycl. Chem., Suppl.* **2** (1982)
226. G N Dorofeenko, Yu A Zhdanov, V I Dulenko, S V Krivun *Khlornaya Kislota i ee Soedineniya v Organicheskoy Sintez* (Perchloric Acid and its Derivatives in Organic Synthesis) (Rostov-on-Don: Izd. Rostovsk. Gos. Univ., 1965)
227. G N Dorofeenko, S V Krivun *Ukr. Khim. Zh.* **29** 1058 (1963)
228. R C Elderfield, T P King *J. Am. Chem. Soc.* **76** 5437 (1954)
229. S M Luk'yanov, S V Borodaev, S B Polovinko, A G Starikov, V P Metlushenko, A G Abolin *Zh. Org. Khim.* **25** 1008 (1989)
230. E V Kuznetsov, I V Shcherbakova, A T Balaban *Adv. Heterocycl. Chem.* **50** 157 (1990)
231. G N Dorofeenko, V I Dulenko *Dokl. Akad. Nauk SSSR* **157** 361 (1964)
232. Yu A Nikolyukin, S L Bogza, V I Dulenko *Khim. Geterotsikl. Soedin.* **465** (1990)
233. S V Krivun, V I Dulenko, L V Dulenko, G N Dorofeenko *Dokl. Akad. Nauk SSSR* **166** 359 (1966)
234. V I Dulenko, S V Tolkunov, N N Alekseev *Khim. Geterotsikl. Soedin.* **1351** (1981)
235. N N Alekseev, S V Tolkunov *Khim. Geterotsikl. Soedin.* **848** (1980)]
236. V I Dulenko, S V Tolkunov, N N Alekseev *Khim. Geterotsikl. Soedin.* **37** (1983)
237. V I Dulenko, I V Komissarov, A T Dolzhenko, Yu A Nikolyukin, in *β -Karboly. Khimiya i Neurobiologiya* (β -Carbolines. Their Chemistry and Neurobiology) (Kiev: Naukova Dumka, 1992) p. 76
238. A V Kibal'nyi, Yu A Nikolyukin, V I Dulenko *Khim. Geterotsikl. Soedin.* **1041** (1994)
239. R B Woodward, T Singh *J. Am. Chem. Soc.* **72** 494 (1950)
240. A S Dreiding, W J Pummer, A J Tomaszewski *J. Am. Chem. Soc.* **75** 3159 (1953)
241. W Rundel, K Besserer *Tetrahedron Lett.* **9** 333 (1968)
242. M A Kudinova, V V Kurdyukov, A I Tolmachev *Dokl. Akad. Nauk Ukr. SSR, Ser. B* **51** (1985)
243. S M Luk'yanov, S V Borodaev, S B Polovinko, A G Starikov, O V Zubkova *Zh. Org. Khim.* **27** 1588 (1991)
244. A L Pikus, V M Feigel'man, V V Mezheritskii *Zh. Org. Khim.* **25** 2603 (1989)
245. D E Tosunyan, Candidate Thesis in Chemical Sciences, Rostov State University, Rostov-on-Don, 1994
246. C Giordano, L Abis Gazz. *Chim. Ital.* **104** 1181 (1974)
247. S M Weinreb, P M Scola *Chem. Rev.* **89** 1525 (1989)
248. B S Drach, V S Brovarets, O B Smolii *Sintezy Azotsoderzhashchikh Geterotsiklicheskich Soedinenii na Osnove Amidoalkiliryushchikh Agentov* (Syntheses of Nitrogen Containing Heterocyclic Compounds with the use of Amidoalkylating Reagents) (Kiev: Naukova Dumka, 1992)
249. E N Zil'berman, in *Reaktsii Nitrilov* (Reactions of Nitrile) (Moscow: Khimiya, 1971) p. 289
250. A Ya Khorlin, O S Chizhov, N K Kochetkov *Zh. Obshch. Khim.* **29** 3411 (1959)
251. N V Shibaeva, S V Borodaev, A I Pyshchev, S M Luk'yanov *Zh. Org. Khim.* **24** 1561 (1988)
252. N V Shibaeva, S V Borodaev, A I Pyshchev, S M Luk'yanov *Zh. Org. Khim.* **24** 2232 (1988)
253. S V Borodaev, O V Zubkova, N V Shibaeva, A P Knyazev, A I Pyshchev, S M Luk'yanov *Zh. Org. Khim.* **27** 1986 (1991)
254. S V Borodaev, N V Shibaeva, O V Zubkova, A P Knyazev, S M Luk'yanov, A I Pyshchev *Zh. Org. Khim.* **25** 2416 (1989)
255. M E Kletskii, S V Borodaev, S M Luk'yanov, N V Shibaeva, A I Pyshchev, R M Minyaev *Zh. Org. Khim.* **27** 2470 (1991)
256. M E Kletskii, S V Borodaev, N V Shibaeva, A I Pyshchev, O V Zubkova, S M Luk'yanov, R M Minyaev *Zh. Org. Khim.* **27** 2479 (1991)
257. S M Lukyanov, M E Kletskii, S V Borodaev, N V Shibaeva, A I Pyshchev, R M Minyaev *Mendeleev Commun.* **73** (1991)
258. O V Zubkova, Candidate Thesis in Chemical Sciences, Rostov State University, Rostov-on-Don, 1991
259. S M Luk'yanov, S V Borodaev, V I Rusakov, O V Zubkova, A P Knyazev *Zh. Org. Khim.* **28** 2569 (1992)
260. J C Jochims, M O Glocker, J Hofmann, H Fischer *Tetrahedron* **47** 205 (1991)
261. J C Jochims, R Abu-El-Halawa, M O Glocker, L Zsolnai, G Huttner *Synthesis* **763** (1990)
262. S M Luk'yanov, in *The Chemistry of Enamines* (Ed. Z Rappoport) (Chichester: Wiley, 1994) p. 1441
263. S L Bogza, Yu A Nikolyukin, V I Dulenko *Khim. Geterotsikl. Soedin.* **990** (1990)
264. S L Bogza, Candidate Thesis in Chemical Sciences, Institute of Physical Organic and Coal Chemistry, Academy of Sciences, Ukraine, Donetsk, 1992
265. S L Bogza, Yu A Nikolyukin, M Yu Zubritskii, V I Dulenko *Zh. Org. Khim.* **29** 1480 (1993)
266. S L Bogza, Yu A Nikolyukin, M Yu Zubritskii *Zh. Org. Khim.* **29** 1638 (1993)
267. I I Nechayuk, Candidate Thesis in Chemical Sciences, Rostov State University, Rostov-on-Don, 1994
268. V G Brovchenko, N V Shibaeva, A I Pyshchev, E V Kuznetsov *Khim. Geterotsikl. Soedin.* **363** (1992)
269. A F Blinokhvatov, O V Markovtseva, M N Nikolaeva *Khim. Geterotsikl. Soedin.* **320** (1992)
270. S V Borodaev, E V Naumova, S M Luk'yanov *Zh. Org. Khim.* **22** 1789 (1986)
271. S V Borodaev, O V Zubkova, S M Luk'yanov *Zh. Org. Khim.* **24** 1843 (1988)
272. S V Borodaev, O V Zubkova, S M Luk'yanov, A G Gasanov *Zh. Org. Khim.* **24** 2333 (1988)
273. O V Zubkova, S V Borodaev, S M Luk'yanov *Zh. Org. Khim.* **27** 2376 (1991)
274. S V Borodaev, O V Zubkova, S M Luk'yanov *Zh. Org. Khim.* **24** 2330 (1988)
275. S M Luk'yanov, S V Borodaev, O V Zubkova *Zh. Org. Khim.* **28** 2577 (1992)

Dibenzo-*p*-dioxins.

Methods of synthesis, chemical properties, and hazard assessment

A D Kunzevich, V F Golovkov, V R Rembovskii

Contents

I. Introduction	27
II. Nomenclature and structure	27
III. Methods for the formation of the tricyclic system of dibenzo- <i>p</i> -dioxin	28
IV. Reactions of dibenzo- <i>p</i> -dioxins	31
V. Toxic properties of compounds of the dibenzo- <i>p</i> -dioxin class	35
VI. Formation and occurrence in nature	36
VII. Conclusion	36

Abstract. The review surveys and gives a systematic account of the data on the methods of synthesis and chemistry of dibenzo-*p*-dioxins including their halogenated derivatives. The hazard of these compounds to mammals is discussed. The bibliography includes 219 references.

I. Introduction

Never before has the world community been so concerned about the hazard caused by any class of chemicals as in the case of dibenzo-*p*-dioxins. Year after year scientists from all over the world have met at conferences in an attempt to assess the hazard due to these substances generated during the industrialisation of human society.

The first representatives of dibenzo-*p*-dioxins were synthesised late in the 19th century. However, over a long period they remained known only to a narrow circle of researchers, until the terrible consequences of the chemical warfare in Vietnam (1961–1971) and an accident in Seveso (Italy, 1976) demonstrated to the whole world the potential danger inherent in these compounds.

The above and some other events associated with the discharge of halodibenzo-*p*-dioxins into the atmosphere have stimulated research dealing with their properties. The development of national ecological programmes in which dibenzo-*p*-dioxins occupy an important place has begun in many countries.

A large number of papers including reviews have been devoted to dibenzo-*p*-dioxins. This comes as no surprise in view of the hazard associated with some representatives of these compounds. The surprising thing is that no surveys of the chemistry of dibenzo-*p*-dioxins have yet been published. The published papers^{1–5} do not provide exhaustive information. We have, therefore, ventured to fill this gap to some extent.

Since the danger coming from dibenzo-*p*-dioxins is attributed to their halogenated derivatives, these compounds receive

particular attention in the literature. While preparing the present review we also used our practical experience in working with these substances.

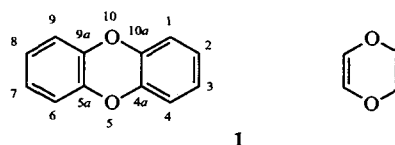
The first mentions of dibenzo-*p*-dioxins date back to 1872, when Merz and Weith⁶ obtained octachlorodibenzo-*p*-dioxin while heating potassium perchlorophenoxide at a high temperature and described its properties. In 1894, Zinke⁷ found that octachlorodibenzo-*p*-dioxin is produced on heating many other chlorinated compounds. The same was observed by Biltz⁸ in 1904 and again by Zinke⁹ in 1908.

The parent compound of this class, dibenzo-*p*-dioxin, was synthesised by Ullman and Stein¹⁰ in 1906. Later, various derivatives of dibenzo-*p*-dioxin were prepared by several workers^{11–19} and up to the 1970s many of them were regarded as promising compounds for practical purposes. Attempts have been made to develop dyes^{20–23} and medicinal preparations^{24–28} based on these compounds. It has been suggested that some halogenated dibenzo-*p*-dioxins be used as fireproofing agents.^{26,29,30} The possibility of developing promising polymeric materials based on some dibenzo-*p*-dioxin derivatives has been studied.^{31,32}

In view of the events mentioned above, since the middle 1970s the primary emphasis has shifted to the investigation of polyhalogenated dibenzo-*p*-dioxins (PHDD) as potential ecotoxins. In 1972–1976, the main approaches to synthesis of these compounds were developed. At present, all the possible polychlorinated dibenzo-*p*-dioxins (PCDD) have been prepared in a pure state; bromine-, fluorine-, and iodine-containing dibenzo-*p*-dioxins as well as compounds incorporating functional groups (NO₂, CN, CH₃, CF₃, etc) have been synthesised.

II. Nomenclature and structure

The molecule of dibenzo-*p*-dioxin **1** is a fused heterocyclic system formed by two benzene rings and an inner six-membered heterocycle incorporating two oxygen atoms. In conformity with the IUPAC rules,³³ the name of dibenzo-*p*-dioxin is based on fusing 1,4-dioxin **2** with two benzene rings. {The names dibenzo-1,4-dioxin and dibenzo[*b,e*]dioxin for **1** and *para*-dioxin for **2** can also be found in the literature}.



A D Kunzevich, V F Golovkov, V R Rembovskii Ecotoximetry Centre,
Russian Academy of Sciences, ul. Kosygina 4, 117977 Moscow,
Russian Federation. Fax (7-095) 938 2156

Received 28 August 1995

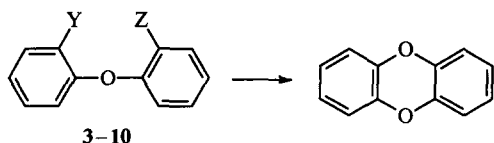
Uspekhi Khimii 65 (1) 29–42 (1996); translated by Z P Bobkova

The molecule of dibenzo-*p*-dioxin is planar. The crystal and molecular structures of compound **1** and some of its derivatives have been discussed in a number of papers.^{34–41} The dipole moment of compound **1** is zero or close to zero, and the dipole moments of some alkyl- and halo-substituted dibenzo-*p*-dioxins have been reported.^{42,43} The IR spectra of dibenzo-*p*-dioxins exhibit characteristic absorption bands in the region of 1330–1280 cm⁻¹,^{1,44,45} which are due to antisymmetric vibrations of the C–O–C group. An exception is provided by octahalo-derivatives, whose absorption in this region is weak.⁴⁵ The ¹H NMR spectrum of dibenzo-*p*-dioxin is an AA'BB' system centred at 6.89 ppm.⁴⁶ The ¹H NMR spectra of almost all the halogenated dibenzo-*p*-dioxins have also been obtained.^{46–53} In concentrated sulfuric acid in the presence of an oxidising agent, dibenzo-*p*-dioxins produce a characteristic green-blue colour (dioxin test), which is attributed to the formation of radical-cations.^{54,55} The EPR spectra and the properties of these radical-cations have been discussed in a number of papers.^{56–60}

III. Methods for the formation of the tricyclic system of dibenzo-*p*-dioxin

1. Self-condensation of diphenyl ethers

Among diphenyl ethers, *o*-phenoxyphenols, the so-called pre-dioxins, are of practical interest for the preparative synthesis of dibenzo-*p*-dioxins. Various dibenzo-*p*-dioxins can be prepared from these compounds, their yields being frequently quantitative.⁶¹



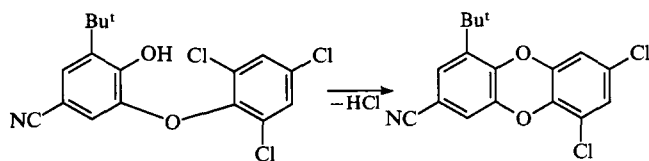
3–10

Z = Y = OH (**3**), OMe (**4**), NH₂ (**5**);

Z = OH, Y = H (**6**), NH₂ (**7**), Br (**8**), Cl (**9**);

Z = OMe, Y = Cl (**10**).

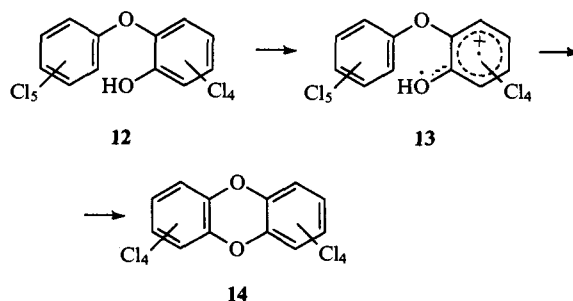
The condensation is often carried out by heating the corresponding ether (**3** and **4**) in hydrobromic acid in the presence of phosphorus.¹⁰ Two functional groups in the ortho-positions are not required for cyclisation to take place. For example, compound **1** can be formed on treatment of 2-hydroxyphenyl phenyl ether **6** with nitrobenzene or selenium.⁶² The diphenyl ethers **8–10** containing a hydroxy- (or methoxy-) group and a halogen atom in the ortho-positions undergo condensation in the presence of hydrogen chloride acceptors. The best results have been achieved by using K₂CO₃ in an appropriate solvent.^{50,61,63} Electron-donating groups facilitate condensation,⁶⁴ as is the case with *tert*-butyl in compound **11**.



11

The tricyclic dibenzo-*p*-dioxin system has also been obtained by the diazotisation of the corresponding amines.^{62,65} For example, compound **1** can be obtained from 2-aminophenyl 2-hydroxy-phenyl ether **7** or di(2,2'-aminophenyl) ether **5**.

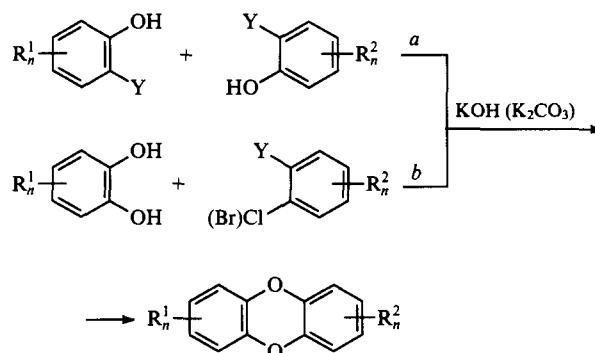
The closure of the ring in *o*-phenoxyphenols can also occur under the action of UV irradiation in the presence of sensitizers.^{66,67} In this case, 3,4,5,6-tetrachloro-2-(pentachlorophenoxy)phenol **12** is converted into octachlorodibenzo-*p*-dioxin **14** (OCDD, **14**). Cyclisation is supposed to occur via the biradical-cation **13**.



Fairly pure specimens, suitable as reference materials, can be obtained from diphenyl ethers. However, this method has not found wide application owing to the low availability of the starting compounds.

2. Condensation of halogenated phenols and other hydroxy-compounds

Generally, condensation of halogenated phenols occurs according to Scheme 1.



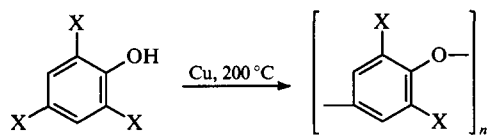
Scheme 1

R¹, R² = Hal, CN, NO₂, Alk;

Y = Hal, NO₂; n = 1–4.

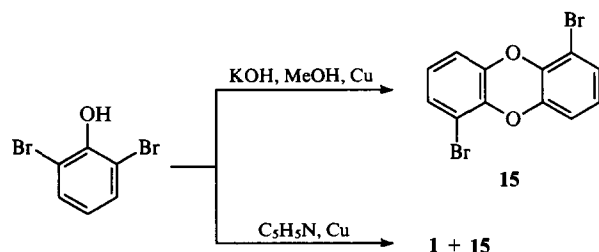
The first representative of halogenated dibenzo-*p*-dioxins, octachlorodibenzo-*p*-dioxin **14**, was synthesised in this way by heating potassium perchlorophenoxide to a high temperature.⁶ Octafluorodibenzo-*p*-dioxin⁶⁸ and some other PCDD have been obtained in a similar way.⁶⁹ Potassium salts are most frequently used for the condensation of halogenated phenols. They are prepared by the following general method. The corresponding phenol is added to a methanol solution of potassium methoxide or potassium hydroxide or to a methanol suspension of potassium carbonate, and the solvent is evaporated. However, potassium phenoxides are normally not isolated in a pure state. Instead, a mixture of phenol and a 5–10-fold excess of the alkaline reagent are refluxed in an appropriate solvent. The use of a calcium salt has also been reported; compound **14** was obtained in 28% yield by heating perchlorophenol in the presence of marble.⁷⁰

Copper and its salts are used as condensation catalysts.^{6,45,68–70,71–73} An example of using a palladium-copper catalyst has been reported.⁷⁴ However, pure copper is preferred. For example, by heating *o*-bromophenol in the presence of the Cu + Cu(OAc)₂ system, compound **1** was obtained in 40% yield.⁷¹ When pure copper was used, the yield increased to 65%.⁷¹ The replacement of *o*-bromophenol by *o*-chloro- or *o*-iodophenol does not result in an increase in the yield. In the latter case, it amounted to 8%.⁷¹ Under similar conditions, *o*-chlorophenol affords compound **1** in 25% yield. When polyhalogenated dibenzo-*p*-dioxins are synthesised using copper without a solvent, the yields usually do not exceed 20%.^{45,70,72,73} The main side reaction that decreases the yields of dibenzo-*p*-dioxins is polyoligomerisation.^{63,72}



Pyrolytic condensation of potassium chlorophenoxides has been used to prepare 22 isomers of tetrachlorodibenzo-*p*-dioxins.⁷⁵ However, purification of the products obtained by this method requires the combination of liquid and gas chromatography, which seriously restricts the applicability of the method.

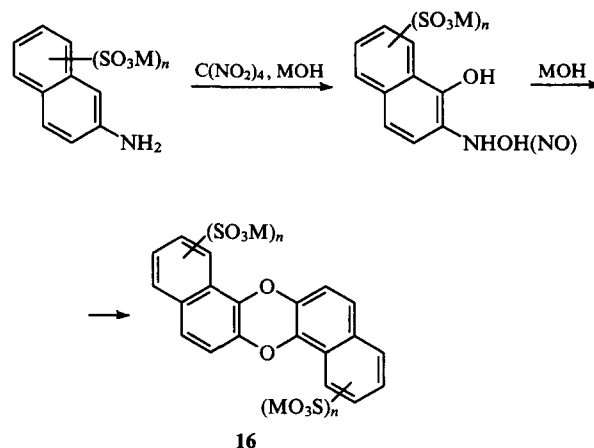
The condensation of phenols containing functional groups is frequently accompanied by partial elimination of these groups,^{76,77} and therefore this method is not used for preparing functionally substituted dibenzo-*p*-dioxins. In some cases, the abstraction of halogen atoms has also been observed.^{45,78,79} In fact, whereas the condensation of potassium 2,6-dibromophenoxide in methanol yields 1,6-dibromodibenzo-*p*-dioxin^{45,78} **15**, the condensation of the same salt in pyridine⁷⁸ gives a mixture of compounds **1** and **15**.



It is not strictly necessary to use salts of phenols. Some workers^{1,6-8,45,70,80,81} have shown that pyrolysis of perhalogenated phenols and a number of oxo-compounds gives the corresponding octahalodibenzo-*p*-dioxins. However, it should be noted that this reaction occurs via a different mechanism.

Among other hydroxy-compounds, naphthols^{76,82} and hydroxyquinolines⁸³⁻⁸⁵ can be involved in the condensation. The properties of the resulting naphthalene and other analogues

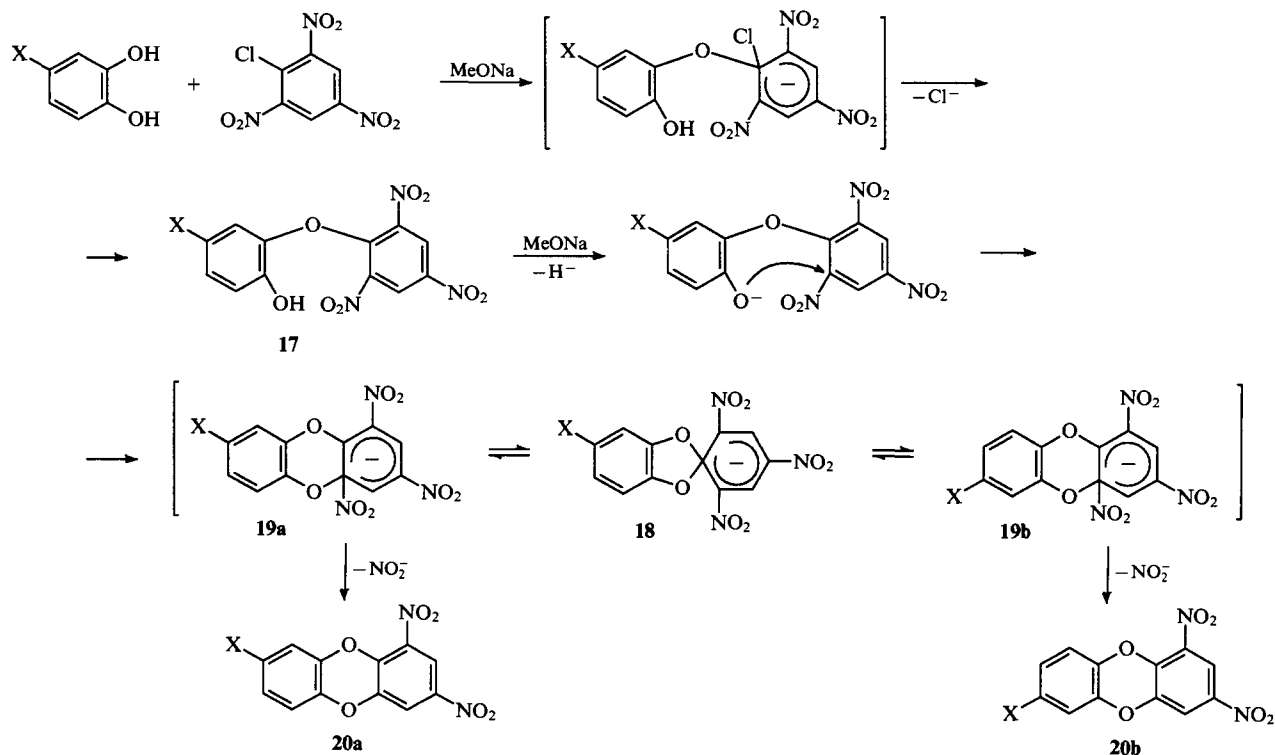
of dibenzo-*p*-dioxins have scarcely been studied. At the same time, these compounds may be formed as minor products in the production of dyes. For example, it has been found⁸⁶ that in the presence of tetranitromethane in an alkaline medium, aminonaphthalenesulfonic acids are converted into the corresponding salts of sulfodinaphtho[5,6-*b,e*]-1,4-dioxin **16**. This reaction was assumed to proceed via the oxidation of the CH and NH₂ groups in the 1- and 2-positions to COH and NHOH (NO) groups followed by the condensation of two molecules.



3. Condensation of catechols with halobenzenes

The method of condensation of catechols with halobenzenes⁴⁶ suggested in 1972 is, perhaps, the most convenient way of preparing various dibenzo-*p*-dioxins including those incorporating functional groups^{47,87-91} (see Scheme 1, pathway *b*). This method is preferred when a high-purity compound is needed. The analytical standards for 22 tetrachlorodibenzo-*p*-dioxins,^{92,93} some pentachloro- and heptachlorodibenzo-*p*-dioxins,^{49,94} and some other compounds,^{79,95-97} including mixed bromine- and chlorine-containing dibenzo-*p*-dioxins,⁹⁶ have been prepared by

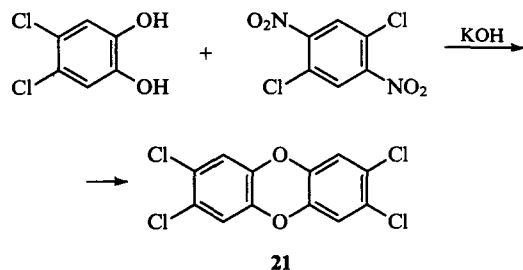
Scheme 2



this procedure. Fluorine-containing dibenzo-*p*-dioxins have also been synthesised and suggested as internal standards for gas-chromatographic and mass-spectrometric analyses of PCDD.⁹⁸⁻¹⁰⁰

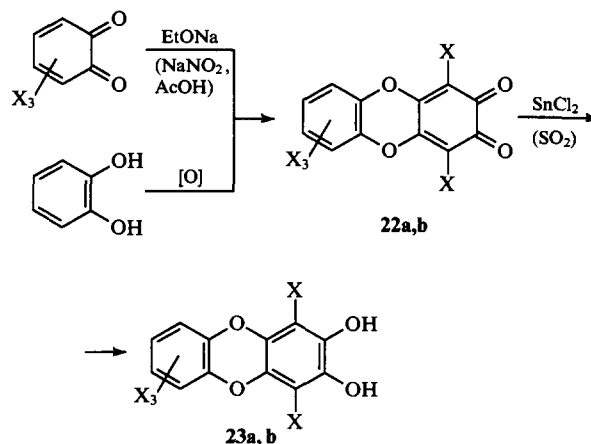
The condensation of catechols is carried out under mild conditions by refluxing a mixture of reactants in a solvent. DMSO, DMF, acetone, or, more rarely, alcohols are used as solvents in this reaction. The yield of reaction products is fairly high and obviously does not depend substantially on the nature of the halogen in the halogenated benzene. In fact, the replacement of dichlorobenzene by dibromobenzene in the condensation with catechol^{65,101} does not result in a substantial increase in the yield of compound 1. Good results have been obtained by Kunzevich et al.,¹⁰² who carried out the condensation of the disodium salt of catechol with various chlorine-containing benzenes in hexamethylphosphoramide. The yields of dibenzo-*p*-dioxins varied from 40% to 66% depending on the chlorine-containing reagent used.

Better results are achieved when the catechol or benzene molecule contains a strong electron-withdrawing group (or several groups). This group generally acts as the leaving group, other functional groups remaining unaffected.⁹¹ For example, the condensation of catechol with picryl chloride (see Scheme 2)¹¹ affords 1,3-dinitrodibenzo-*p*-dioxin (20a, 20b, X = H) in 85% yield.¹¹ Catechol reacts with 2,4-dinitrochlorobenzene¹⁰³ just as easily. It has been found that a nitro group in the lateral position is replaced by a halogen. Therefore, the condensation of 4,5-dichlorocatechol with 2,5-dichloro-1,4-dinitrobenzene gives 2,3,7,8-tetrachlorodibenzo-*p*-dioxin (TCDD, 21) in 90% yield.¹⁰⁴



Halogenated *o*-quinones also undergo condensation. For example, in a study of the properties of tetrabromo(or chloro)-*o*-quinones, it has been found¹⁰⁵⁻¹⁰⁷ that these compounds can condense to give halogenated dibenzo-*p*-dioxin-2,3-quinones 22a. Reduction of the latter gives the corresponding hydroxy-compounds 23.

In the presence of strong dehydrating reagents, for example, P₂O₅, the condensation of catechol to compound 1 has been observed,⁶⁵ while in the presence of oxygen or sodium nitrite, dibenzo-*p*-dioxin-2,3-quinone 22b is produced.^{105,108,109} The reaction occurs via a radical mechanism involving the oxidation of the dimer 24, formed from the radical in the first stage of the process, to the quinone 25, which then undergoes rapid heterolytic ring closure to give compounds 22b (Scheme 3).



X = Cl, Br (a), H (b).

o-,*p*-Quinones^{105-107,110} and cyclic triketones¹¹¹ also undergo cyclisation.

4. The mechanism of the formation of the tricyclic dibenzo-*p*-dioxin system

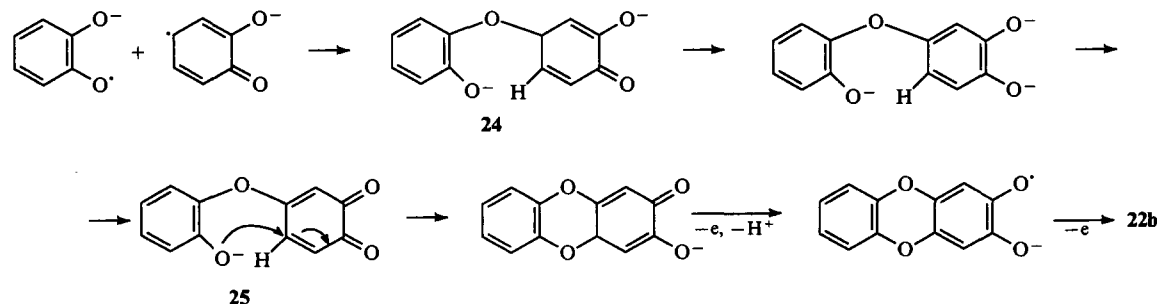
The condensation of halophenols and catechols (or their salts) with halobenzenes is based on aromatic nucleophilic substitution. This substitution must occur by an S_N2Ar mechanism¹¹² (in other sources,¹¹³ this mechanism has also been called S_NAr). We can follow this mechanism in relation to the condensation of catechol with 2,4,5-trinitrochlorobenzene¹⁰³ (see Scheme 2).

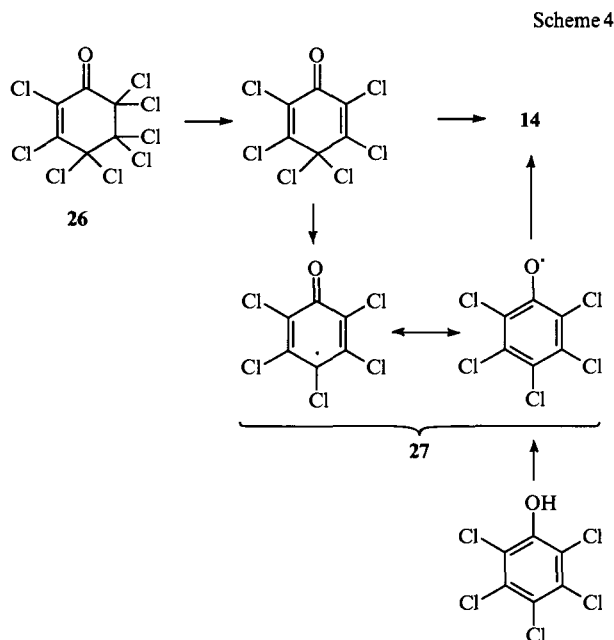
The first stage of this process gives *o*-diphenoxyphenol (predioxin, 17), whose subsequent cyclisation is intramolecular and yields the Meisenheimer spiro-complex 18. The latter complex is formed as an intermediate in the Smiles rearrangement,¹¹⁴ and in the example under consideration¹⁰³ it was isolated in a pure state (X = H) as the sodium salt. The spiro-complex is then converted to complex 19a,b, from which the dioxin ring is formed (compounds 20a and 20b) after the abstraction of the NO₂ group. The presence of two isomers in the reaction mixture has been accounted for^{63,73,115} by the Smiles rearrangement. The fact that some predioxins^{61,63} yield mixtures of isomers of dibenzo-*p*-dioxins is also evidence in support of the rearrangement.^{61,63}

The pyrolysis of phenols and other hydroxy-compounds proceeds unlike the reactions of the salts, via a radical mechanism (Scheme 4). In particular, some researchers^{1,7,8,18,80} have studied the formation of octachloro- and octabromodibenzo-*p*-dioxins in the pyrolysis of perhalophenols or a number of oxo-compounds, for example, octachlorocyclohexenone 26 and found that these reactions involve the formation of the pentachlorophenoxy radical 27.

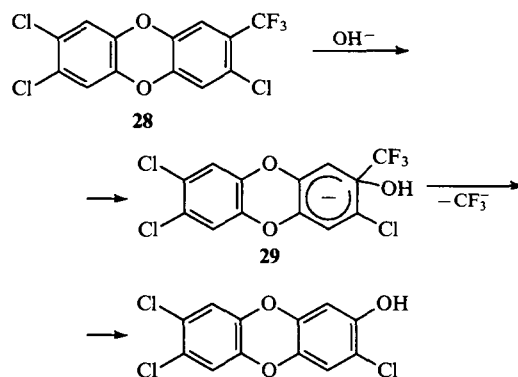
In all probability, the condensation of other phenols occurs by the same mechanism. Octabromo- and 1,2,4,6,7,9-hexabromo-3,8-dichlorodibenzo-*p*-dioxins have been obtained in this way, and it was suggested that the method may find wide application.¹⁸

Scheme 3





with this system occurs via a transition state with a fairly low activation energy. In the case of compound **28**, the stable σ -complex **29** is formed, whose existence is in all probability caused by the presence of the CF_3 group, which has a strong inductive effect. Hydroxylation is the rate-determining step of this process. The radical substitution of chlorine (or CF_3) by the OH group proceeds more slowly than the nucleophilic substitution by a factor of approximately 3.



IV. Reactions of dibenzo-*p*-dioxins

The molecular structure of dibenzo-*p*-dioxin allows one to treat it as a cyclic aromatic diether. Accordingly, dibenzo-*p*-dioxins enter into all the reactions characteristic of aromatic compounds, namely, electrophilic and nucleophilic substitution in the benzene rings, radical reactions, as well as reactions of functional groups. Among the reactions typical of the heterocyclic nucleus, one should note the relatively easy formation of the radical-cation and reactions peculiar to it, and also reactions involving the cleavage of the C–O–C linkage.

There are almost no papers devoted to the general reactivity of dibenzo-*p*-dioxins, including their halo-derivatives. A comparative analysis of the nucleophilic and radical substitution of the functional groups in the aromatic systems of dibenzo-*p*-dioxins by the hydroxy-group has been carried out.¹¹⁶ In relation to 2-trifluoromethyl-3,7,8-trichlorodibenzo-*p*-dioxin **28** and model compounds (4,5-dichlorocatechol and 5-chloro-4-trifluoromethylcatechol), it has been shown that the reaction of the OH^- anion

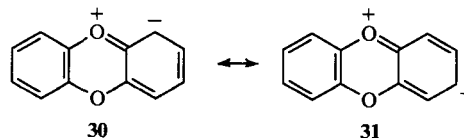
1. Electrophilic substitution reactions

a. Halogenation of dibenzo-*p*-dioxins

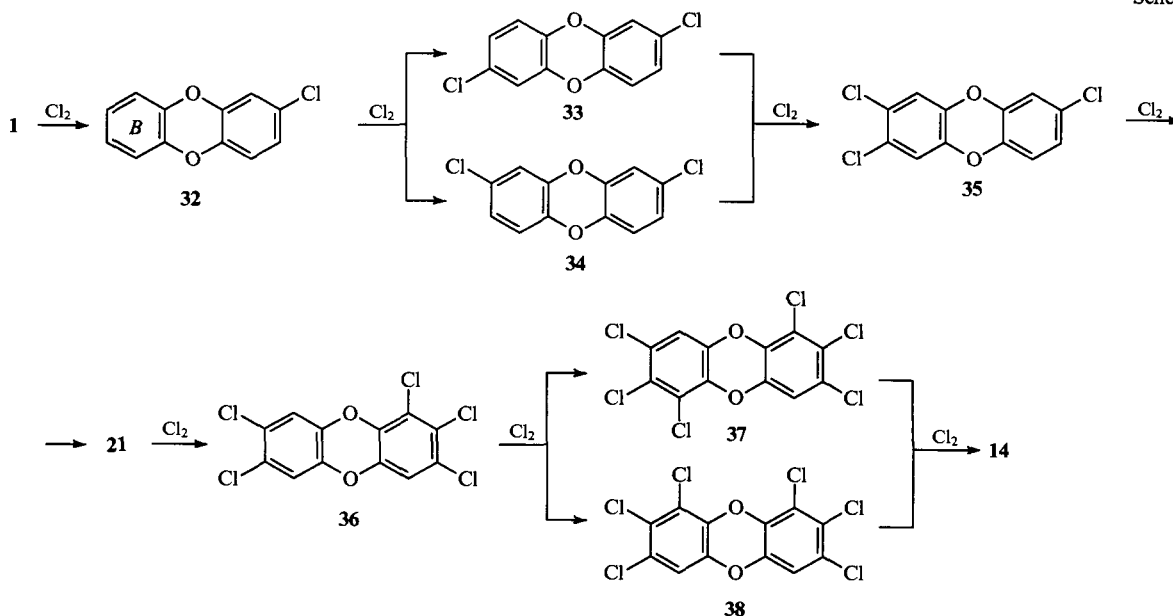
Direct halogenation of dibenzo-*p*-dioxin occurs according to the rules common to aromatic compounds. This process may be used for preparing PCDD.

The presence of the heterocycle influences the order in which the hydrogen atoms in the dibenzo-*p*-dioxin molecule are replaced. This is determined by the overall mesomeric and inductive effects of the oxygen atom on the benzene ring.^{112, 117}

The mesomeric effect is illustrated by the resonance structures **30** and **31**, which determine the occurrence of ortho- or para-substitution with respect to the oxygen atoms in the dioxin ring.



Scheme 5

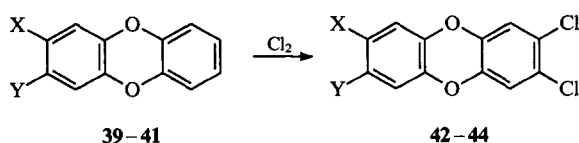


However, the ortho-position is deactivated by the inductive effect of oxygen to a larger extent than the para-position. Therefore, the first stage of the halogenation of dibenzo-*p*-dioxin **1** yields the isomer **32** (Scheme 5). The order in which subsequent substitution occurs is an interesting theoretical problem. Due to the deactivating influence of the first halogen atom, the second substitution should occur in ring *B*. The most theoretically probable substitution positions are 7 and 8 (compounds **33** and **34**). When further halogenation is carried out, the hydrogen atoms in the 3- and 7-(or 8)-positions, which are equivalent in terms of the substitution order, are successively replaced by the halogen. As a result, the highly toxic 2,3,7,8-tetrahalodibenzo-*p*-dioxin **21** is formed. Further substitution involves the 1-position (compound **36**) and then the 6- or 9-position (compounds **37** and **38**). The remaining free positions are equivalent in terms of the substitution order, and exhaustive halogenation yields the weakly toxic octahalodibenzo-*p*-dioxin **14**. According to published data, the toxicities of the remaining halogenated dibenzo-*p*-dioxins are intermediate between those of 2,3,7,8-tetra- and octahalo-substituted compounds.^{2,118}

The chlorination of dibenzo-*p*-dioxin **1** proceeds to a greater extent than the bromination. It has been shown^{46,119} that chlorination yields a mixture of products with various degrees of substitution that are difficult to separate. Therefore, this method was⁴⁶ considered to be unsuitable for the synthesis of individual chlorinated dibenzo-*p*-dioxins. Bromination of dibenzo-*p*-dioxin **1** normally comes to a halt at the stage where 2,3,7,8-tetrabromodibenzo-*p*-dioxin is formed.^{102,120} Under certain conditions, this compound can be obtained in a quantitative yield.¹⁰²

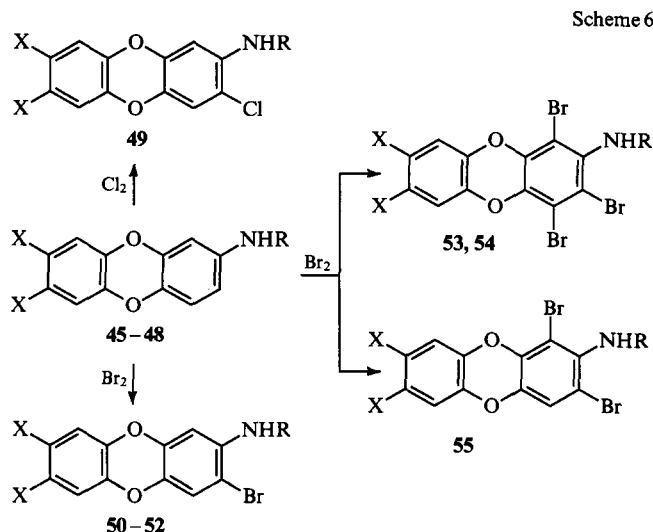
It has been reported that chlorination in the second stage gives mostly the 2,7-isomer, while in the case of bromination, the 2,8-isomer predominates;^{19,102} however, this conclusion is questionable. In fact, the yield of the 2,7-dichloro-isomer obtained by the chlorination of dibenzo-*p*-dioxin **1** was only 3%. This fact made it possible to suggest⁴⁶ that the 2,8-dichloro-isomer is more soluble and this is why it had not been isolated by the authors of the previous paper.¹⁹ In any case, there are no serious reasons for believing that chlorination in this stage differs from bromination.

The foregoing considerations are also valid for the halogenation of dibenzo-*p*-dioxins in which the hydrogen atoms of one ring have been completely replaced by chlorine:⁴⁶ substitution occurs in the 7- and 8-positions of the free ring. The presence of other halogens in the molecule also does not change the order in which substitution occurs. In the chlorination of 2,3-dibromo-**(39)** and 2,3-difluoro-**(40)** derivatives, 2,3-dibromo-7,8-dichloro-**(42)** and 2,3-difluoro-7,8-dichlorodibenzo-*p*-dioxins **(43)** have been isolated.¹¹⁹ The nitro-group deactivates ring *A* to such an extent that 2-nitrodibenzo-*p*-dioxin **(41)** is halogenated in the unsubstituted ring *B*,^{121,122} yielding 7,8-dichloro-2-nitrodibenzo-*p*-dioxin **44**.



X = Y = Br (**39**, **42**), F (**40**, **43**); X = H, Y = NO₂ (**41**, **44**).

Conversely, the amino group activates dibenzo-*p*-dioxin. For example, bromination of amino- or acetamido-derivatives **45-48** occurs fairly readily^{121,123} and substitution involves the ring containing the amino-group (Scheme 6, compounds **50-55**). Unlike bromination, the chlorination of the amino-derivatives **45** and **47** is accompanied by the resinification of the reaction mixture.¹²¹ The corresponding acetyl-derivatives **46** and **48** are susceptible to resinification to a lesser degree. For example, the chlorination of 2-acetamido-7,8-dichlorodibenzo-*p*-dioxin **46** gave 2-acetamido-3,7,8-trichlorodibenzo-*p*-dioxin **49** in good yield.^{121,123}



X = Cl, R = H (**45**), Ac (**46**, **49**, **50**, **53**);

X = Br, R = H (**47**, **51**, **55**), Ac (**48**, **52**, **54**).

The influence of various catalysts on the process of chlorination of dibenzo-*p*-dioxins has been described.¹²² The authors found that among the catalysts studied, namely I₂, FeCl₃ + I₂ and 18-crown-6, the last named is the most active. The chlorination pattern in all these cases is the same. In particular, irrespective of the nature of the catalyst, the chlorination of dibenzo-*p*-dioxin **1** affords a mixture of products in which, in addition to TCDD **21**, 2,3,7-trichloro-**(35)** and 1,2,3,7,8-pentachlorodibenzo-*p*-dioxins **(36)**, have been detected.

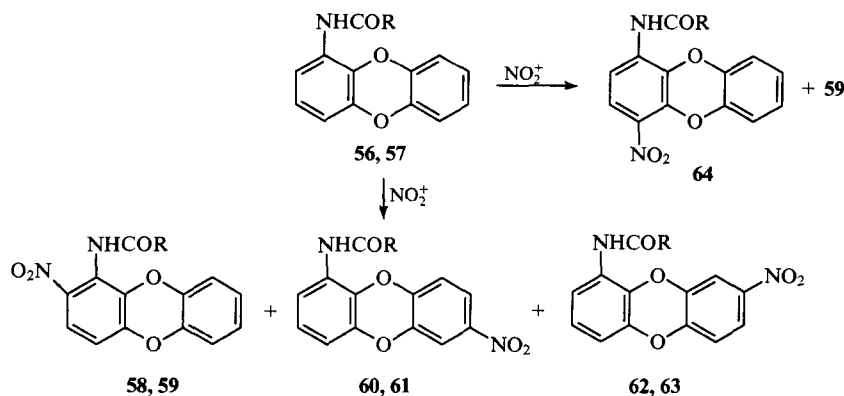
It is likely that the presence of catalysts can result in more extensive bromination. For example, the bromination of dibenzo-*p*-dioxin in the presence of FeCl₃ gave¹¹⁹ a mixture of compounds containing, in addition to 2,3,7,8-tetrabromodioxin, the products of its further bromination. Therefore, while brominating compound **1** by bromine in the presence of a catalyst, one should take into account the possibility of the formation of polybrominated compounds.

b. Nitration of dibenzo-*p*-dioxin and its derivatives

Dibenzo-*p*-dioxin **1** can be nitrated by conventional nitration reagents such as nitric acid or nitric acid in concentrated sulfuric acid.^{16,124-130} Depending on the reaction conditions, a series of successive substitution products are formed, and the order in which substitution occurs follows the rules which govern halogenation. Owing to the strong deactivating effect of nitro-groups, nitration proceeds only until 2,3,7,8-tetranitrodibenzo-*p*-dioxin is formed.¹³⁰

The influence of various substituents and various nitrating agents on the nitration process has been studied.^{124,125,128,131,132} For example, depending on the reaction conditions, the first substitution in the nitration of 1-acetyldibenzo-*p*-dioxins **(56 and 57)** may involve either the ring containing the functional group or the unsubstituted ring as well, as shown in Scheme 7. The ratio between the isomers obtained and their quantity depends on the nature of the substituent and the nitrating agent. When an excess of the latter is used, 2-, 7-, or 8-nitro-derivatives (compounds **58-63**) are formed. However, in some cases, this order of nitration may be violated. For example, when compound **57** is nitrated by the NH₄NO₃ - (CF₃CO)₂O - THF mixture, substitution involves only the ring containing the functional group and mostly the 4-position of this ring (compound **64**).¹²⁹ Some instances where the acetyl group is replaced by the nitro-group during nitration have also been reported.¹²⁵ Dibenzo-*p*-dioxins incorporating methyl or methoxy groups are readily nitrated by nitric acid in either sulfuric or acetic acid.^{124,131,132}

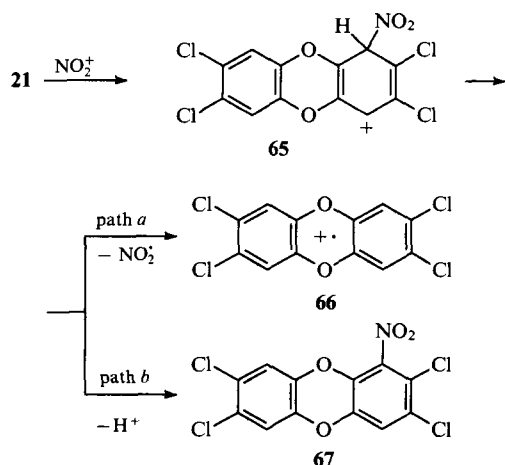
Scheme 7



R = Me (56, 58, 60, 62), CF₃ (57, 59, 61, 63, 64).

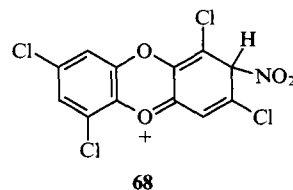
The nitration of halogen-containing dibenzo-*p*-dioxins presents certain difficulties associated with the deactivating effect of the halogens. For example, it has been noted that 1,6-dibromodibenzo-*p*-dioxin **15** does not undergo nitration with nitric acid in concentrated sulfuric acid.¹²⁴ This task can be accomplished by using fuming nitric acid in acetic acid at $T = 70^\circ\text{C}$;¹³¹ this nitrating agent can also be used successfully in other cases, for example, to nitrate mono- and dihalo-substituted dibenzo-*p*-dioxins.^{121, 123, 130, 133} Good results have also been obtained in the nitration by this mixture of polyhalogenated dibenzo-*p*-dioxins containing halogens in one ring, in particular, of 1,2,3,4-tetrachlorodibenzo-*p*-dioxin.^{121, 123, 133} The nitro group goes to the unsubstituted ring. 2,3,7-Trihalo-substituted derivatives are also nitrated under these conditions to give the mono-substitution product.¹³³

Tetrahalo-derivatives are more stable. The most stable are isomers with a lateral arrangement of the halogens. In particular, TCDD **21** does not react with a mixture of nitric and acetic acids¹²⁸ and is destroyed on treatment with fuming nitric acid in sulfuric acid.⁹⁵ This behaviour can be explained, on the one hand, by the low stability of the σ -complex **65** arising in the course of the reaction (which is due to the fact that the positive charge in this complex cannot be delocalised owing to the electron pairs of the oxygen atoms) and, on the other hand, by the decomposition of the σ -complex **65** via pathway *a* to the radical-cation **66** and the NO₂[•] radical.¹³⁴ Under these conditions, oxidation processes leading to the destruction of the dioxin nucleus prevail. In the case where complex **65** decomposes via pathway *b*, nitration affording compound **67** takes place.¹³³



In the nitration of 2,3,7,8-tetrachloro-derivative **21**, satisfactory results have been obtained¹³⁵ by using nitronium tetrafluoroborate in sulfolane at $T = 125^\circ\text{C}$. This reaction yields a

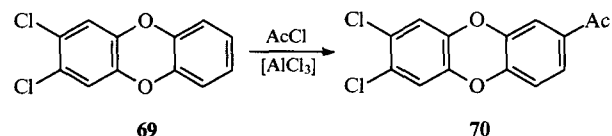
disubstitution product. Compound **21** can also be nitrated by an NH₄NO₃–(CF₃CO)₂O–MeNO₂ mixture. In this case, substitution involves the 1-position and gives compound **67** (yield 1%–2%).¹³⁷ The tetrahalo-derivatives in which the arrangement of halogen atoms is other than lateral form the more stable σ -complexes **68**. Therefore, 1,3,6,8-tetrachloro- and 1,3,7,8-tetrachloro-dibenzo-*p*-dioxins are readily nitrated by the NH₄NO₃–(CF₃CO)₂O–MeNO₂ mixture.^{87, 136}



c. Acylation and alkylation of dibenzo-*p*-dioxin and its derivatives

Dibenzo-*p*-dioxins are fairly smoothly acylated by acyl chlorides in the presence of aluminium chloride (or bromide).^{15, 22, 27, 125, 129, 137–145} The reaction is most frequently carried out in carbon disulfide. The hydrogen atoms in the 2- and 7-positions are substituted preferentially. If these positions are occupied, substitution involves the 3-position. For example, acylation of 2,7-dihalodibenzo-*p*-dioxins by acetyl chloride gives the corresponding 2-acetyl-3,8-dihalodibenzo-*p*-dioxins.¹⁴⁵ If the 1-position is occupied by a substituent, the reaction may involve the 4- and 9-positions.¹⁴²

The third halogen atom deactivates the nucleus to such an extent that, for example, 2,3,7-trichlorodibenzo-*p*-dioxin **35** cannot be acylated by acetyl chloride even in the presence of aluminium chloride.¹³³ Compound **21** also does not undergo acylation. In the case where the halogen atoms are located in one ring, the unsubstituted ring is acylated. For example, by acylating 2,3-dichlorodibenzo-*p*-dioxin **69** by acetyl chloride, one can obtain 2-acetyl-7,8-dichlorodibenzo-*p*-dioxin **70**.¹³³



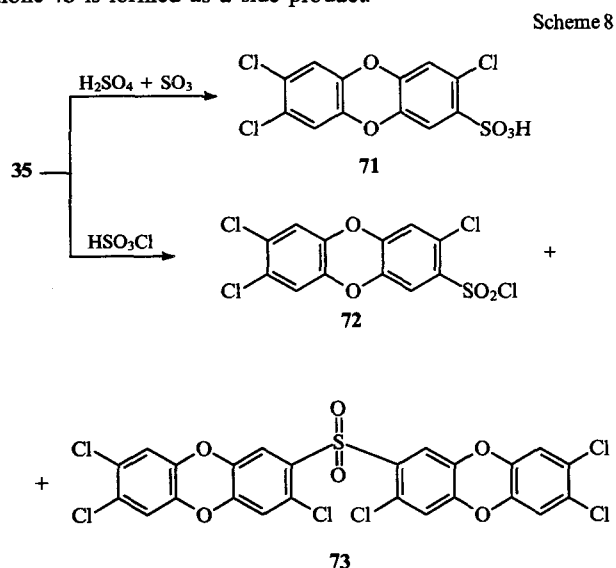
The alkylation of dibenzo-*p*-dioxin **1** has been studied in detail¹⁹ and has some peculiarities. In particular, it was found that in the alkylation of compound **1** by isopropyl chloride, the second substitution in the resulting 2-isopropyl-dibenzo-*p*-dioxin involves the 3-position, in contrast to halogenation, nitration, or acylation. After that, the 7-position is substituted. Exhaustive alkylation is not observed even when an excess of isopropyl chloride is employed. Under these conditions, the authors cited isolated

one of the possible hexaisopropyl derivatives. If there is steric hindrance, for example if the alkylation is carried out with *tert*-butyl chloride, only a disubstitution product is formed, the second substitution involving the 7- or 8-position.

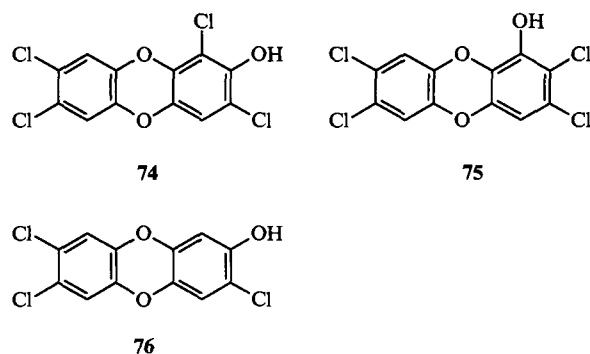
No examples of the alkylation of halogenated dibenzo-*p*-dioxins have been reported. However, from general considerations, it may be suggested that this process would be substantially hampered owing to the deactivating effect of the halogens.

d. Sulfonation (sulfochlorination) of dibenzo-*p*-dioxin and its derivatives

Sulfonation of dibenzo-*p*-dioxin **1** by sulfuric acid or oleum gives the 2,7-disulfonic acid.¹⁴⁶ When chlorosulfonic acid is used, the 2-chlorosulfonyl chloride is formed.³² Halodibenzo-*p*-dioxins are sulfonated under similar conditions.¹³³ For example, when the sulfonation of 2,3,7-trichlorodibenzo-*p*-dioxin **35** is carried out with oleum at room temperature, the hydrogen atom in a lateral position is replaced by the sulfo group and the reaction yields the sulfonic acid **71** (Scheme 8). Sulfochlorination of dioxin **35** gives¹³³ 2-chlorosulfonyl-3,7,8-trichlorodibenzo-*p*-dioxin **72**; the sulfone **73** is formed as a side product.



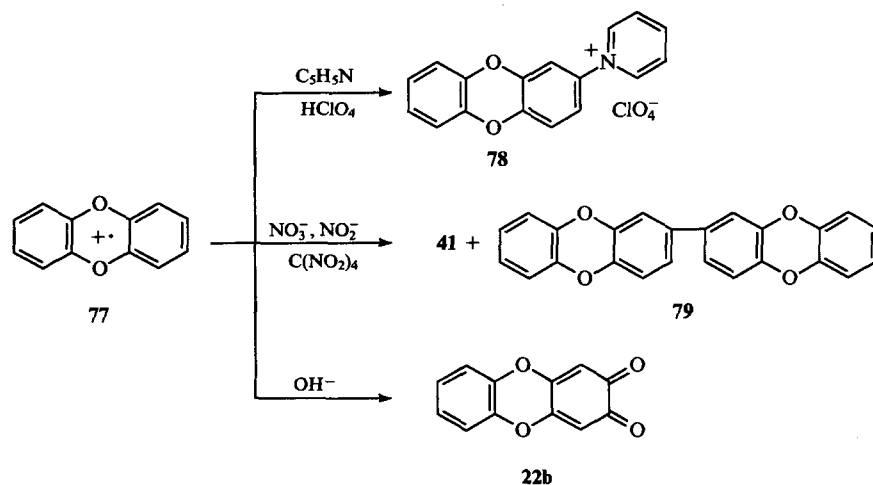
and hydrogen peroxide¹⁴⁸ have been suggested for the practical removal of PCDD from the gas phase. It is believed that, among all the chemical methods recommended for the detoxification of PCDD-containing waste, the alkaline dehydrochlorination technology, applicable to both liquid and solid waste, is the most promising.¹⁴⁹ In addition, nucleophilic species are known to participate directly or indirectly in many processes involving PCDD and occurring in the environment and in the organs of mammals.^{4,150} For example, it has been found that ring hydroxylation is the dominant route in the metabolism of chlorinated dibenzo-*p*-dioxins.^{151,152} It was found that the metabolism of dioxin **21** involves hydroxylation in lateral positions with migration of chlorine to the 1-position and gives 2-hydroxy-1,3,7,8-tetrachlorodibenzo-*p*-dioxin¹⁵¹ **74**. 1-Hydroxy-2,3,7,8-tetrachlorodibenzo-*p*-dioxin **75** and 2-hydroxy-3,7,8-trichlorodibenzo-*p*-dioxin **76** are also metabolites of TCDD. Dibenzo-*p*-dioxins chlorinated to lesser degrees are converted into 2- and 3-hydroxy-derivatives.¹⁵³ The metabolism in dogs and rats may involve the cleavage of the dioxin nucleus to give bis(dichlorohydroxyphenyl) ether¹⁵¹ and 4,5-dichlorocatechol.¹⁵⁴



Dibenzo-*p*-dioxins are capable of forming radical cations when treated with strong oxidising agents in combination with photoirradiation.^{155,156} The radical-cations of functionally substituted dibenzo-*p*-dioxins are generated, for example, on treatment with concentrated sulfuric acid in the presence of potassium nitrate,⁵⁶ nitric acid, potassium perchlorate, manganese dioxide, hydrogen peroxide,⁵⁸ or antimony pentachloride¹⁵⁷ and also during electrochemical oxidation.^{54,158–160} The chemical and physical properties and the EPR spectra of the radical-cation derived from compound **1** and a large number of its substituted derivatives have been studied.^{57,58,157,161–166} It was shown that the dibenzo-*p*-dioxin radical-cation **77** (Scheme 9), stabilised by an anion, possesses a certain stability. For example, stable acetonitrile solutions of the tetrafluoroborate of the radical-cation **77** have been obtained by treating compound **1** with NO^+BF_4^- .¹⁶⁷

2. Reactions involving nucleophiles

Despite the fact that nucleophilic substitution plays a significant role in the chemistry of dibenzo-*p*-dioxins, this problem has not been adequately addressed in the literature. Methods based on the nucleophilic substitution of hydroxy groups for chlorine atoms on treatment with potassium hydroxide^{2,147} or potassium carbonate



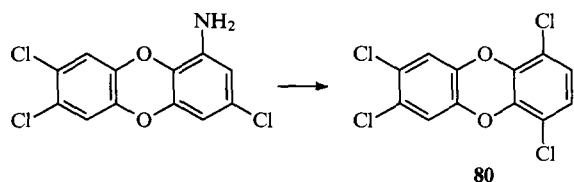
In another study,¹⁵⁸ the perchlorate of the radical-cation **77** was isolated and its reactivity was studied. The radical-cation **77** was found to react with pyridine giving *N*-(2-dibenzo-*p*-dioxinyl)pyridinium perchlorate **78**. The nitrite anion reacts with the radical-cation as a nucleophilic agent to form 2-nitro-dibenzo-*p*-dioxin **41**. The nitro compound **41** was also obtained when the radical-cation **77** was treated with nitrate anions or with tetranitromethane. In addition to the perchlorate of the radical-cation **77** the dimer of dibenzo-*p*-dioxin **79** was isolated,¹⁵⁸ however, its structure was not discussed. Taking into account the melting point of the compound obtained, one may suggest that it is 2,2'-bis(dibenzo-*p*-dioxin), which was described previously.¹²⁷ It has also been found^{54,159} that the perchlorate of the radical-cation **77** in solution reacts with water to give dibenzo-*p*-dioxin-2,3-quinone **22b**.

Apart from the reaction products, the initial dibenzo-*p*-dioxin **1** has been recovered in all cases. Reactions with other nitrogen-containing nucleophiles (CH₃, NH₃, RNH₂) led only to the recovery of compound **1**. It is believed¹⁵⁸ that, for nucleophilic substitution to occur, a stronger nucleophile is required.

3. Reactions of functional groups

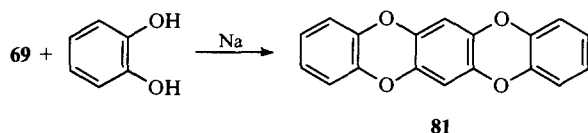
Among the functionally substituted dibenzo-*p*-dioxins, the nitro- and amino-derivatives are of prime interest and have been the most thoroughly studied.^{47,128,136,168–170} These compounds are more frequently encountered than is believed.¹⁶⁸ They present a severe hazard to mammals and are environmental pollutants.¹²³ Aminodibenzo-*p*-dioxins have found application in the development of a radio-immune method for the assay of PCDD.^{171,172}

No data have been published that would make it possible to speak of any influence of the dioxin nucleus on the reactivity of nitro- and amino-derivatives. In some studies, the Sandmeyer reaction has been used to prepare halogenated dibenzo-*p*-dioxins from the corresponding amino-derivatives.^{95,104,136,173} It was noted that in some cases the reaction is complicated by a rearrangement and consequently may give unexpected products, for example, compound **80**.¹⁰⁴



Nitro-derivatives can be reduced, and this reaction is the main method of synthesis of amino-containing dibenzo-*p*-dioxins. Various reducing reagents have been used,^{121,130,136,173–175} however, the highest yield was achieved in the case of tin dichloride.¹²¹ Aminodibenzo-*p*-dioxins are readily acylated,¹²³ enter into the Skraup reaction to form the corresponding quinoline derivatives,^{176,177} and condense with quinones¹⁷⁸ to give phenazines. Hydroxy-derivatives are acylated in a similar way.¹⁷⁹

Halogen-containing dibenzo-*p*-dioxins can condense,^{102,127} affording products with enlarged structures.



V. Toxic properties of compounds of the dibenzo-*p*-dioxin class

1. Toxic properties

It is believed, with good reason, that PCDD are products of human technological activity.^{4,180} The pathways to the formation

of PCDD are known and have been fairly extensively studied, but the formation of functionally substituted dibenzo-*p*-dioxins still remains unexplored. There are data showing that halogenated nitro-derivatives of dibenzo-*p*-dioxins are formed on the fly ash from incinerators via the nitration of the corresponding dibenzo-*p*-dioxins by the nitrogen dioxide present in the exhaust gases.¹⁶⁸ Although the potential hazard of functionally substituted dibenzo-*p*-dioxins is quite considerable,^{87,123} they have scarcely been studied.

The urgent need to study dibenzo-*p*-dioxin class compounds arises primarily from the results of toxicological studies. A large number of publications, including several detailed reviews, have been devoted to this problem.^{2,181–183} Analysis of these and other data makes it possible to make some generalisations concerning the toxicology of compounds of this class.

Among dibenzo-*p*-dioxins and compounds with similar structures—polychlorinated dibenzofurans, biphenyls, and naphthalenes—those substances in whose molecules all the lateral positions are occupied by halogen atoms are the most toxic. It has been found that TCDD **21** exhibits the highest toxicity toward the most sensitive species (guinea pigs), while 2,3,7,8-tetrachloronaphthalene has the lowest toxicity. When the number of halogen atoms in the ring decreases or increases, the toxicity diminishes sharply.^{2,183} Completely halogenated compounds exhibit virtually no toxicity, at least, under the conditions of an acute experiment.

The positions of the halogen atoms in the ring are significant for biological activity. For example, symmetrical derivatives are as a rule more toxic than their nonsymmetrical analogues.

TCDD possesses the highest biological activity among all the classes of compounds under consideration. It comes as no surprise that most of the published data are devoted to the toxicology of this compound.

The high toxicity of TCDD for warm blooded animals is combined with pronounced interspecific differences in sensitivity to it.¹⁸⁴ The coefficient of interspecific differences is as high as four orders of magnitude.^{150,183–186} Another important feature of the biological action of TCDD is the presence of clear-cut individual intraspecific distinctions, which is indicated by the fact that the slopes of 'dose-effect' plots are small, compared with those for other xenobiotics.¹⁸⁷ Interstrain differences in the sensitivity to TCDD are fairly clear-cut (~250 for rats and ~20 for mice).¹⁸³ The presence of paradoxical behaviour in the 'dose-effect' relations should be regarded as significant evidence in support of intraspecific polymorphism in the sensitivity to TCDD and its analogues.¹⁸⁸

Studies of the chronic action of small TCDD doses have demonstrated the presence of pronounced supercumulative effects,^{184,189–191} which is significant for the regulation of the maximum permissible concentrations of this compound in the environment.

The most general symptoms of the TCDD poisoning of various types of warm blooded animals are liver enlargement, thymus atrophy, progressive weight loss, and a clear-cut latent period of up to 10–15 days after contact with the poison. Other clinical manifestations are fairly polymorphic. In fact, in mice, rats, and rabbits, apart from hepatomegaly, pronounced centrolobular necrosis of liver tissue, in some cases turning into hepatargia, has been observed.^{183,189,192} The edematous syndrome, accompanied by intense secretion of transudate in pericardial, pleural, and abdominal cavities, is typical for chickens. In the case of guinea pigs and monkeys (rhesus, macaque), the prevailing symptoms are those indicating deep suppression of the immune system. The data concerning symptoms of the effects of TCDD on humans are less definite, because they have been obtained in relation to accidental contacts with the xenobiotic or by examining the personnel engaged in the production of 2,4,5-trichlorophenol containing TCDD as an impurity.

Nevertheless, it has been reported^{192,193} that the TCDD intoxication in humans is manifested as skin changes (chloracne), weight loss, high susceptibility to fatigue, muscle

asthenia, insomnia, high irritability, decrease in libido, reduction of sensory functions, tendency to hepatomegaly, decrease in the concentration of serum lipids, increase in the prothrombin time, and porphyria. In addition, there are data on more severe pathologies: the people under examination suffered more frequently from soft tissue sarcoma.¹⁹¹ This last fact is the reason why studies dealing with remote consequences of the action of TCDD, and, in particular, with mutagenic, carcinogenic, teratogenic, and embryotoxic effects, are urgently required.

In 1972, a mutagenic effect of solutions of TCDD was observed in bacterial test systems, and a mechanism of this phenomenon, involving the intercalation of TCDD with the DNA helix, was suggested.¹⁹³ Somewhat earlier, Courtney and Moore,¹⁹⁴ who carried out experiments with various strains of mice and rats, discovered embryotoxic and teratogenic effects of TCDD: the cleaving of the hard palate and defects in kidney embryogenesis. Discussions concerning the character of the carcinogenic effect of TCDD still continue.¹⁹⁵ The authors of another study¹⁹⁶ are apt to regard TCDD as a pronounced promoter of carcinogenesis, at least in rodents. In conformity with their data, the tumour-stimulating effect of PCDD is comparable with that of aflatoxin B₁. According to other data,¹⁹⁷ at concentrations that can occur in an organism, TCDD is neither a classical carcinogen nor a mutagen. One may speak only of its promoting effect with respect to some carcinogens, such as nitrosamines.

2. The mechanism of action

To explain the mechanism of the toxic action of TCDD, several hypotheses have been put forward.

1. The toxic effect of TCDD arises through bonding to the highly specific cytosol Ah-receptor. The complex is then translocated to the nucleus and expresses the DNA sections, responsible for the synthesis of pools and the RNA initiating the synthesis of cytochrome P-450 (or 448)-dependent monooxygenases.^{183, 198} This hypothesis adequately explains the extraordinarily high degrees of induction of microsomal monooxygenases.

2. TCDD exhibits a thyroxine-like action, which is indicated by a number of hyperthyroid symptoms, enhancement of the catabolism of lipids and biopolymers, weight loss, additivity of the toxic effects of TCDD and thyroid hormones.^{183, 199}

3. The toxic action of TCDD is due to the relative deficiency of carotinoids.^{183, 200} This hypothesis was based on the sharp decrease in the concentration of carotinoids, in particular vitamin A, in the liver of rats exposed to TCDD. This approach is supported by the syndrome (skin changes, hyperkeratosis, lesion of the sclera and the cornea, etc.) in laboratory animals poisoned by TCDD.

Among other attempts to explain the mechanism of the toxic action of TCDD, the assumption that disturbance of the flavin metabolism, in particular the metabolism of riboflavin, whose structure is similar to that of TCDD, plays the key role in the pathogenesis of TCDD intoxication deserves attention.²⁰¹ The above structural similarity accounts for the fairly successful use of riboflavin preparations in the experimental therapy of TCDD poisoning. It should be noted that none of these hypotheses concerning the pathogenesis of TCDD toxification can explain fully by itself the whole diversity of the clinical pattern of the poisoning and especially the very pronounced inter- and intra-specific differences in the sensitivity to this xenobiotic.

At the same time, there is the noteworthy possibility that all the above approaches can be interpreted in terms of the disturbance of the equilibrium between the pro- and antioxidant systems in an organism. In fact, the hypothesis of the leading role of the Ah-locus accounts for the activation of prooxidant processes. Thyroid hormones also exert an indirect prooxidant effect. Carotinoids as well as tocopherols are obligatory constituents of the antioxidant protection of an organism.

We believe that all the above hypotheses could be accommodated within the framework of a unified theory of the pathogenesis of the intoxication by polychlorinated polyaromatic hydrocarbons, which would be based on the assessment of the

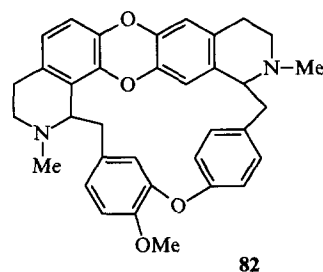
degree of prooxidant action and on the determination of the actual balance between the pro- and antioxidant systems, especially since the intensification of the peroxide oxidation of lipids and the enhancement of the generation of active oxygen forms in an organism under the influence of TCDD (i.e. the existence of prooxidant action) are established facts.²⁰² Such activity is manifested by the characteristic features of the functioning of pro- and antioxidant systems in various species.

VI. Formation and occurrence in nature

The causes of the formation of technogenic PHDD and the pathways by which they arrive in the environment have been studied quite extensively.^{4, 180, 181, 185} However, dibenzo-*p*-dioxins of natural origin have scarcely been studied. At the same time, the presence of a large number of hydroxy-derivatives of benzene in plants makes it possible to infer that the compounds under consideration are not rarities.²⁰³ The oxidation of hydroxy-compounds is most probably the main pathway to the formation of the tricyclic dibenzo-*p*-dioxin system in plants. For example, dibenzo-*p*-dioxin is known to be formed on oxidation of *p*-benzoquinone,¹¹⁰ catechol,^{106, 108} and certain pyrogallol derivatives.^{109, 204} It has been established^{205–208} that such oxidation can occur in plants through the action of certain enzymes. In fact, an enzyme that oxidises catechol to dibenzo-*p*-dioxin-2,3-quinone²⁰⁸ with a high specificity has been isolated from an extract of *Tecoma stans* leaves. In another study,²⁰⁷ this quinone was isolated in a pure state after the oxidation of catechol by polyphenol oxidase, and its structure was confirmed by an alternative synthesis.

In a study of keto-derivatives of inositol,¹¹¹ it was found that the acetylation of these compounds in the presence of an acid catalyst yields completely hydroxylated dibenzo-*p*-dioxin. It was suggested that dibenzo-*p*-dioxin derivatives may be synthesised via this route in nature.

The discovery of the alkaloid trilobine and the determination of its structure served as direct confirmation of the formation of dibenzo-*p*-dioxin in nature. In 1924, Kondo and Nakasato studied an extract from the roots of cocculus (*Cocculus trilobus* DC) and isolated an alkaloid which was called trilobine.²⁰⁹ Eight years later, Kondo and Tomita found that the trilobine structure is based on the heterocyclic system of dibenzo-*p*-dioxin.²¹⁰ In 1942, Tomita and Tani^{211, 212} published the full formula of trilobine **82**.



The alkaloid micranthine, isolated from the plant *Daphnandra micrantha*,²¹³ as well as the alkaloids tiliacresine, tiliacorine, and tiliacoronine, obtained from the plant *Tiliacora racemosa*,^{214–216} have structures similar to that of trilobine.

VII. Conclusion

The data presented in this review indicate that studies devoted to dibenzo-*p*-dioxins are progressing vigorously. The methods of synthesis of compounds of this class are being improved, and insight is being gained into processes occurring in nature and in the organs of animals involving halo-derivatives of dibenzo-*p*-dioxins. However, the knowledge accumulated does not yet make it possible to speak of an ultimate solution of the problem of dioxin-like xenobiotics. Although the latter have mostly been created by human activity, one should keep in mind that the

dibenzo-*p*-dioxin structure has been invented by nature. From this viewpoint, this class of compounds remains poorly investigated. For this reason, humankind has probably been deprived of many useful things, ranging from medicines to various materials. However, in recent years some studies dealing with this problem have been published. These were mostly attempts to develop new medicines.²¹⁷

Comprehensive investigation of halogenated dibenzo-*p*-dioxins has been the dominant factor in the development of the chemistry of dibenzo-*p*-dioxins. One significant property of these compounds that has not yet received the due attention of scientists is noteworthy, namely that, in some cases, it is expedient to treat dibenzo-*p*-dioxin (and its halo-derivatives) as a crown ether (dibenzo-6-crown-2). Some of the properties of PCDD, including their toxic properties may be associated with the ionophoric and complex-forming capacities of these compounds. In any case, the toxicity of octabromodibenzo-18-crown-6 is comparable with that of 2,3,7,8-tetrabromodibenzo-*p*-dioxin.¹⁰² In addition, TCDD exhibits a growth-stimulating activity with respect to herbaceous plants, typical of crown ethers.²¹⁸

The complex-forming capacity of dibenzo-*p*-dioxins forms the basis of a photometric determination of PCDD.²¹⁹

Thus, the data considered in the present review indicate that careful study of the properties of dibenzo-*p*-dioxins may lead to new possibilities in the investigation of the physiological activity of compounds of this sort.

References

1. L Denivelle, R Fort, P Van Hai *Bull. Soc. Chim. Fr.* 1538 (1960)
2. V I Vysochin *Dioksin i Rodstvennye Soedineniya. Analiticheskii Obzor* (Dioxins and Related Compounds. Analytical Review) (Novosibirsk: State Patent Scientific Technical Library, Siberian Branch of the Russian Academy of Sciences, 1989)
3. N Humppi *Chemosphere* 15 2003 (1986)
4. L A Fedorov *Dioksiny kak Ekologicheskaya Opasnost': Retrospektiva i Perspektivy* (Dioxins as an Ecological Danger: Retrospection and Prospects) (Moscow: Nauka, 1993)
5. M Buch-ta, B Dolesal *Chem. Listy* 85 158 (1991)
6. V Merz, W Weith *Ber. Dtsch. Chem. Ges.* 5 458 (1872)
7. T Zincke *Ber. Dtsch. Chem. Ges.* 27 557 (1894)
8. H Biltz *Ber. Dtsch. Chem. Ges.* 37 4003 (1904)
9. T Zincke, W Broeg *Liebigs Ann. Chem.* 363 221 (1908)
10. F Ullman, A Stein *Ber. Dtsch. Chem. Ges.* 39 622 (1906)
11. H W Hillyer *Am. Chem. J.* 23 125 (1900)
12. H W Hillyer *Am. Chem. J.* 26 361 (1901)
13. S Ueo *Bull. Chem. Soc. Jpn.* 16 177 (1941)
14. M Tomita *Chem. Zentr.* 3131 (1933)
15. M Tomita *Chem. Zentr.* 1053 (1935)
16. M Tomita *Chem. Zentr.* 2552 (1936)
17. M Kulka *Can. J. Chem.* 39 1973 (1961)
18. J J Dietrich *Dissertation Abstr.* 79 2810 (1957)
19. H Gilman, J J Dietrich *J. Am. Chem. Soc.* 79 1439 (1957)
20. German P. 223 367; *Chem. Zentr.* 349 (1990)
21. Fr. P. 799 627; *Chem. Abstr.* 30 7867 (1936)
22. German P. 668 875; *Chem. Abstr.* 33 5006 (1939)
23. Swiss P. 238 627; *Chem. Abstr.* 43 4484 (1949)
24. Br. P. 870 298; *Chem. Abstr.* 55 27 756 (1961)
25. M Tomita, W Watande *J. Pharm. Soc. Jpn.* 72 478 (1952)
26. Can. P. 702 144; *Chem. Abstr.* 62 16 261 (1965)
27. G Vasilu, I Basiu *Ann. Univ. Bucharest, Ser. Chem.* 38 15 (1969)
28. Fr. P. 2 053 020; *Chem. Abstr.* 76 140 759 (1972)
29. Belg. P. 616 197; *Chem. Abstr.* 59 2828 (1963)
30. BRD P. 1 930 259; *Chem. Abstr.* 74 64 250 (1971)
31. BRD P. 1 905 651; *Chem. Abstr.* 71 92 080 (1969)
32. Br. P. 1 163 975; *Chem. Abstr.* 71 113 498 (1969)
33. *Nomenklaturnye Pravila I Yu PAK po Khimii T. 2* (IUPAC Nomenclature of Chemistry, Vol. 2) (Moscow: Izd. VINITI, 1979)
34. R G Wood, G Williams *Philos. Mag.* 31 115 (1941)
35. A I Kitaigorodskii, P M Zorkii, V K Bel'skii *Stroenie Organicheskogo Veshchestva* (The Structure of Organic Matter) (Moscow: Nauka, 1982)
36. M Senma, Z Taira, T Taga, K Osaki *Cryst. Struct. Commun.* 2 311 (1973)
37. M A Neuman, P P North, F P Boer *Acta Crystallogr., Sect. B, Struct. Crystallogr.* 28 2313 (1972)
38. F P Boer, M A Neuman, O Aniline *Acta Crystallogr., Sect. B, Struct. Crystallogr.* 28 2878 (1972)
39. F P Boer, F P Van Remoortere, P P North, M A Neuman *Acta Crystallogr., Sect. B, Struct. Crystallogr.* 28 1023 (1972)
40. F P Boer, P P North *Acta Crystallogr., Sect. B, Struct. Crystallogr.* 28 1613 (1972)
41. J S Cantrell, N C Webb, A J Mabis *Acta Crystallogr., Sect. B, Struct. Crystallogr.* 25 150 (1969)
42. G M Bennet, D P Earp, S Glasstone *J. Chem. Soc.* 1179 (1934)
43. K Higasi *Sci. Pap. Inst. Phys. Chem. Res. (Jpn.)* 38 331 (1941)
44. M Narisada *Yakugaku Zasshi* 79 183 (1959)
45. M Tomita, Sh Ueda *Yakugaku Zasshi* 79 186 (1959)
46. A E Pohland, G C Yang *J. Agric. Food Chem.* 20 1093 (1972)
47. K Chae, L K Cho, J D McKinney *J. Agric. Food Chem.* 25 1207 (1977)
48. A S Kende, J J Wade, D Ridge, A Poland *J. Org. Chem.* 39 931 (1974)
49. A P Gray, S P Cepa, I J Solomon, O Aniline *J. Org. Chem.* 41 2435 (1976)
50. N Humppi, K Heinola *J. Chromatogr.* 331 410 (1985)
51. L T Gelbaum, D G Patterson, D L Ashley, D F Groce *Chemosphere* 17 551 (1988)
52. D G Patterson, V V Reddy Jr, E R Barnhart, D L Ashley, C R Lapeza Jr, L R Alexander, L T Gelbaum *Chemosphere* 19 233 (1989)
53. A P Gray, S D Cepa, J S Cantrell *Tetrahedron Lett.* 33 2873 (1975)
54. G Cauquis, M Maurey *C. R. Hebd. Seances Acad. Sci., Ser. C* 266 1021 (1968)
55. W Schrott, R Bopsdorf, J Seidler *Z. Chem.* 10 147 (1970)
56. M Tomita, Sh Ueda, Y Nakai, Y Deguchi, H Takaki *Tetrahedron Lett.* 4 1189 (1963)
57. T N Toser, L D Tuck *J. Chem. Phys.* 38 3035 (1963)
58. M Tomita, Sh Ueda *Chem. Pharm. Bull.* 12 33 (1964)
59. Sh Ueda *Yakugaku Zasshi* 84 212 (1964)
60. R J Wratten, M A Ali *Mol. Phys.* 13 233 (1967)
61. N Humppi *Chemosphere* 15 2003 (1986)
62. M Tomita *J. Pharm. Soc. Jpn.* 56 814 (1936)
63. O Aniline, in *Chlorodioxins—Origins and Fate* (Advances in Chemistry Series) Vol. 120 (Ed. E H Blair) (Washington, DC: American Chemical Society, 1973) p. 126
64. A Rieker *Chem. Ber.* 98 714 (1965)
65. N M Cullinane, H G Davey, J H Padfield *J. Chem. Soc.* 716 (1934)
66. P K Freeman, S Ramauyian *J. Agric. Food Chem.* 31 775 (1983)
67. P K Freeman, S Ramauyian *J. Org. Chem.* 51 3939 (1986)
68. L Denivelle, R Chesneau, H-A Hoa *C. R. Hebd. Seances Acad. Sci., Ser. C* 271 192 (1970)
69. A J Dobbs, J Jappi, A E Wadham *Chemosphere* 12 481 (1983)
70. W Sandermann, H Stockman, R Casten *Chem. Ber.* 90 690 (1957)
71. M Tomita, T Nacano, K Hirai *J. Pharm. Soc. Jpn.* 74 934 (1954)
72. M M Julia, M Baillarge *Bull. Soc. Chem. Fr.* 644 (1953)
73. A P Grey, S P Cepa, J S Cantrell *Tetrahedron Lett.* 33 2873 (1975)
74. US P. 3 679 704; *Chem. Abstr.* 77 114 413 (1972)
75. T J Nestrick, L L Lamparski, R H Stehl *Anal. Chem.* 51 2273 (1979)
76. M Tomita *Chem. Zentr.* 3131 (1933)
77. M Tomita *J. Pharm. Soc. Jpn.* 52 139 (1932)
78. Sh Ueda, A Teraoka *Yakugaku Zasshi* 83 552 (1963)
79. A J Dobbs, J Jappi, A E Wadham *Chemosphere* 12 481 (1983)
80. US P. 2 802 037 (1957)
81. M Kulka *Can. J. Chem.* 39 1973 (1961)
82. M Tomita *J. Pharm. Soc. Jpn.* 52 900 (1932)
83. M Tomita, N Yoshida *J. Pharm. Soc. Jpn.* 72 718 (1952)
84. E Fujita, T Saijoh, N Takao *J. Pharm. Soc. Jpn.* 73 453 (1953)
85. K Nagarajan, A N Goud, V R Ranga, R K Shah, S J Shenoy *Proc. Indian Acad. Sci., Chem. Sci.* 104 549 (1992)
86. A G Manyats, V V Erina, V S Kuz'min, S S Gordeichuk, Yu N Burtsev *Zh. Org. Khim.* 28 1722 (1992)
87. K C Donnelly, H H Jones, S Safe *Chemosphere* 15 1961 (1986)
88. M Romkes, S Safe, J Piskorska-Pliszczynska, T Fujita *Chemosphere* 16 1710 (1987)
89. G Mason, S Safe *Chemosphere* 15 2081 (1986)

90. A Poland, E Glover *J. Biol. Chem.* **251** 4936 (1976)
91. T Savahata, J R Olston, R A Neal *Biochem. Biophys. Res. Commun.* **105** 341 (1982)
92. D G Patterson, L R Alexander, L T Gelbaum, R C O'Connor, V Maggio, L L Needham *Chemosphere* **15** 1601 (1986)
93. E R Barnhart, D G Patterson *Chemosphere* **18** 827 (1989)
94. L T Gelbaum, D G Patterson, D F Groce, in *Chlorinated Dioxins and Dibenzofurans in Perspective* (Eds C Rappe, G Choudhary, L H Keith) (Chelsea, MI: Lewis, 1986) p. 479
95. J E Oliver, W R Lisby *J. Heterocycl. Chem.* **15** 689 (1978)
96. B Ramalingam, T Mazer, D J Wagel, in *Chlorinated Dioxins and Dibenzofurans in Perspective* (Eds C Rappe, G Choudhary, L H Keith) (Chelsea, MI: Lewis, 1986) p. 485
97. K A Francesconi, E L Ghisalberti *Aust. J. Chem.* **38** 1271 (1985)
98. N A Klyuev, V F Golovkov, S A Chernov, E S Brodskii, G M Shuiskii *Khim. Geterotsikl. Soedin.* **7** 902 (1994)
99. K N Ivanov, T D Chernova, A B Rummyantsev, in *Pervaya Konf. po Dioksinovym Ksenobiotikam (Tez. Dokl.)* [The First Conference on Dioxin Xenobiotics (Abstracts of Reports)] (Vol'sk, 1992) p. 8
100. K Chae, P W Albro, J D McKinney *J. Environ. Sci.* **17** 441 (1985)
101. M Tomita *J. Pharm. Soc. Jpn.* **52** 429 (1932)
102. A D Kunzevich, V F Golovkov, S F Chernov, V R Rembovskii, N M Troshkin, S I Baulin *Dokl. Akad. Nauk* **332** 461 (1993)
103. V N Drozd, V N Knyazev, A A Klimov *Zh. Org. Khim.* **10** 826 (1974)
104. J W Apsimon, T L Collier, N D Venayak *Chemosphere* **14** 881 (1985)
105. F R Hewgill, T J Stone, W A Waters *J. Chem. Soc.* **408** (1964)
106. A Critchlow, E Halsam, R D Haworth, P B Tincer, N M Waldron *Tetrahedron* **23** 2829 (1967)
107. J Frejka, B Sefranek, J Zika *Collect. Czech. Chem. Commun.* **9** 238 (1937)
108. C L Jackson, F W Russe *Ber. Dtsch. Chem. Ges.* **38** 419 (1905)
109. C L Jackson, R D M Laurin *Ber. Dtsch. Chem. Ges.* **38** 4103 (1905)
110. J Y Savoie, P Brassard *Can. J. Chem.* **47** 733 (1969)
111. A J Fatiadi *Carbohydr. Res.* **12** 130 (1970)
112. P Saiks *Mekhanizmy Reaktsii v Organicheskoi Khimii* (Mechanisms of Reactions in Organic Chemistry) (Ed. V F Traven) (Moscow: Khimiya, 1991)
113. J March *Advanced Organic Chemistry. Reactions, Mechanisms, and Structure* Vol. 3 (New York: Wiley, 1985)
114. K V Vatsuro, G L Mishchenko *Imennye Reaktsii v Organicheskoi Khimii* (Named Reactions in Organic Chemistry) (Moscow: Khimiya, 1976)
115. A S Kende, M DeCamp *Tetrahedron Lett.* **33** 2877 (1975)
116. A D Kunzevich, V F Golovkov, S Ya Pichkhidze, G M Shuiskii *Dokl. Akad. Nauk* **331** 320 (1993)
117. J March *Advanced Organic Chemistry. Reactions, Mechanisms, and Structure* Vol. 2 (New York: Wiley, 1985)
118. F Cattabeni, A Cavallaro, G Galli (Eds) *Dioxin. Toxicological and Chemical Aspects* Vol. 1 (New York: Spectrum, 1978)
119. W D Munslow, G W Sovocool, J R Donnelly, R K Mitchum *Chemosphere* **16** 1661 (1987)
120. C Teuffl, R Dumler, D Lenoir, O Hutzinger *VDI-Ber.* **634** 257 (1987)
121. A D Kunzevich, V F Golovkov, S A Chernov *Zh. Obshch. Khim.* **63** 1831 (1993)
122. A D Kunzevich, V F Golovkov, S A Chernov *Dokl. Akad. Nauk* **327** 92 (1993)
123. A D Kunzevich, V F Golovkov, V R Rembovskii, S A Chernov *Dokl. Akad. Nauk* **330** 333 (1993)
124. A K Prokof'ev *Usp. Khim.* **59** 1799 (1990) [*Russ. Chem. Rev.* **59** 1051 (1990)]
125. T R Govindachari, S S Sathe, N Viswanathan *Indian J. Chem.* **5** 128 (1967)
126. M Tomita *J. Pharm. Soc. Jpn.* **55** 205 (1935)
127. H Gilman, E A Weipert, J J Dietrich, F N Hayes *J. Org. Chem.* **23** 361 (1958)
128. J E Oliver *J. Heterocycl. Chem.* **21** 1073 (1984)
129. M Tomita *J. Pharm. Soc. Jpn.* **54** 165 (1934)
130. H Gilman, J Dietrich *J. Am. Chem. Soc.* **80** 366 (1958)
131. Sh Ueda, A Teraoka *Yakugaku Zasshi* **83** 552 (1963)
132. M Tomita, Sh Ueda *Yakugaku Zasshi* **80** 953 (1960)
133. A D Kunzevich, V F Golovkov, K N Ivanov, S A Chernov *Zh. Obshch. Khim.* **64** 1722 (1994)
134. V A Koptug Arenonievye Iony. *Stroenie i Reaktsionnaya Sposobnost'* (Arenium Ions. Structure and Reactivity) (Novosibirsk: Nauka, 1983)
135. A S Kende, J J Wade *Environ. Health Perspect.* **5** 49 (1973)
136. J E Oliver, J M Ruth *Chemosphere* **12** 1497 (1983)
137. I Baci, I Tanasescu *Rev. Chim. (Bucharest)* **22** 654 (1971)
138. M Tomita *J. Pharm. Soc. Jpn.* **54** 891 (1934)
139. M Tomita *J. Pharm. Soc. Jpn.* **56** 906 (1936)
140. M Tomita *J. Pharm. Soc. Jpn.* **58** 130 (1938)
141. M Tomita *J. Pharm. Soc. Jpn.* **58** 498 (1938)
142. M Tomita, J Yagi *Yakugaku Zasshi* **78** 581 (1958)
143. G Olah (Ed.) *Friedel-Crafts and Related Reactions* Vol. 3 (New York: Interscience, 1963-1965)
144. G Vasiliu, J Baci *Rev. Chim. (Bucharest)* **22** 6 (1971)
145. G Vasiliu, J Baci *Rev. Chim. (Bucharest)* **23** 523 (1972)
146. M Tomita, Sh Ueda *J. Pharm. Soc. Jpn.* **8** 796 (1960)
147. D J Brunelle, D A Singleton *Chemosphere* **14** 173 (1985)
148. P Tundo, S Facchetti, W Tumiatti *Chemosphere* **14** 403 (1985)
149. P E Rosiers *Chemosphere* **12** 727 (1983)
150. I B Tsyrl'ov *Khlorigovannye Dioksiny: Biologicheskie i Meditsinskie Aspekty. Analiticheskii Obzor* (Chlorinated Dioxins: Biological and Medical Aspects. Analytical Review) (Novosibirsk: State Patent Scientific Technical Library, Siberian Branch of the Russian Academy of Sciences, 1990)
151. H Poiger, H-R Buser, in *Human and Environmental Risk of Chlorinated Dioxins and Related Compounds* (Eds R E Tucker, A L Young, A P Grey) (New York: Plenum, 1984) p. 483
152. H Poiger, H-R Buser, H Weber, U Zweifel *Experientia* **38** 484 (1982)
153. M T Tulp, O Hutzinger *Chemosphere* **9** 761 (1978)
154. H Poiger, H-R Buser, in *Biological Mechanisms of Dioxin Action* Vol. 18 (Eds A E Pohland, R D Kimbrough) (New York: Cold Spring Harbor Laboratory, 1984) p. 39
155. A E Pohland, G C Yang, N Brown *Environ. Health Perspect.* **5** 9 (1973)
156. G C Yang, A E Pohland, in *Chlorodioxins — Origin and Fate (Advances in Chemistry Series)* Vol. 120 (Ed. E H Blair) (Washington, DC: American Chemical Society, 1973) p. 33
157. M Tomita, Sh Ueda *J. Pharm. Soc. Jpn.* **12** 40 (1964)
158. H J Shine, L R Shade *J. Heterocycl. Chem.* **11** 139 (1974)
159. G Cauquis, M Maurey *Bull. Soc. Chim. Fr.* **3588** (1972)
160. C Barry, G Cauquis, M Maurey *Bull. Soc. Chim. Fr.* **2510** (1966)
161. R Bell, A Gara, in *Chlorinated Dioxins and Dibenzofurans in the Total Environment* (Eds L Keith, C Rappe, G Choudhary) (Stoneham: Butterworth, 1985) p. 3
162. T S Zhuravleva *Zh. Strukt. Khim.* **7** 516 (1966)
163. G C Yang, A E Pohland *J. Phys. Chem.* **76** 1504 (1972)
164. S P Sorensen, W H Brining *J. Am. Chem. Soc.* **94** 6352 (1972)
165. R J Wratten, V A Ali *Mol. Phys.* **13** 233 (1967)
166. B Lamotte, G Berther *J. Chim. Phys., Phys. Chim. Biol.* **63** 369 (1966)
167. B K Bandlish, H J Shine *J. Org. Chem.* **42** 561 (1977)
168. G A Eiceman, H O Rghei *Chemosphere* **13** 1025 (1984)
169. K C Donnelly, D H Jones, S Safe *Chemosphere* **15** 1961 (1986)
170. H O Rghei, G A Eiceman *Chemosphere* **14** 252 (1985)
171. T L Collier, J W Apsimon, J P Sherry *Chemosphere* **20** 301 (1990)
172. C A Bradfield, A S Kende, A Poland *Mol. Pharm.* **34** 229 (1988)
173. K Chae, L K Cho, J D McKinney *J. Agric. Food Chem.* **25** 1207 (1977)
174. M Tomita, Sh Ueda *Yakugaku Zasshi* **80** 353 (1960)
175. G S-R Ruf, B Lobert *Bull. Soc. Chim. Fr.* **183** (1974)
176. M Tomita *J. Pharm. Soc. Jpn.* **56** 65 (1936)
177. M Tomita *Chem. Zentr.* **2914** (1936)
178. M Tomita *J. Pharm. Soc. Jpn.* **55** 1060 (1935)
179. M Tomita *J. Pharm. Soc. Jpn.* **56** 490 (1936)
180. L A Fedorov, B F Myasoedov *Usp. Khim.* **59** 1818 (1990) [*Russ. Chem. Rev.* **59** 1063 (1990)]
181. V Marshall *Major Chemical Hazards* (New York: Wiley, 1987)
182. O B Chastnikova, N E Polyakova, D V Mitrofanova, in *Pervaya Konf. po Dioksinovym Ksenobiotikam (Tez. Dokl.)* [The First Conference on Dioxin Xenobiotics (Abstracts of Reports)] (Vol'sk, 1992) p. 50
183. H Greim, K Rosman *VDI-Ber.* **34** 399 (1987)

184. A D Kunzevich, N M Troshkin, S I Baulin, V F Golovkov, Yu K Nedoshivin, V R Rembovskii *Dokl. Akad. Nauk* **340** 268 (1995)
185. A V Fokin, A F Kolomiets *Priroda (Moscow)* **3** 3 (1985)
186. B J Cociba, O Cabey *Chemosphere* **14** 449 (1985)
187. V R Rembovskii, V N Shapovalov, in *Pervaya Konf. po Dioksinovym Ksenobiotikam (Tez. Dokl.)* [The First Conference on Dioxin Xenobiotics (Abstracts of Reports)] (Vol'sk, 1992) p. 7
188. A E Gusakov, in *Pervaya Konf. po Dioksinovym Ksenobiotikam (Tez. Dokl.)* [The First Conference on Dioxin Xenobiotics (Abstracts of Reports)] (Vol'sk, 1992) p. 11
189. E McConnel, in *Biological Mechanisms of Dioxin Action* Vol. 18 (Eds A E Pohland, R D Kimbrough) (New York: Cold Spring Harbor Laboratory, 1984) p. 27
190. N Nelson, P B Hammoud, C T Nisbet, A F Serafirm, W H Drury *Environ. Res.* **5** 249 (1972)
191. S I Baulin, in *Pervaya Konf. po Dioksinovym Ksenobiotikam (Tez. Dokl.)* [The First Conference on Dioxin Xenobiotics (Abstracts of Reports)] (Vol'sk, 1992) p. 47
192. E E McConnel, J A Moore, in *Dioxin. Toxicological and Chemical Aspects* Vol. 1 (Eds F Cattabeni, A Cavallaro, G Galli) (New York: Spectrum, 1978) p. 137
193. S Hussain, V Ehrenberg, L Lofoth, G Glivalet *Ambio* **1** 32 (1972)
194. B D Courtney, J A Moore *Toxicol. Appl. Pharm.* **20** 369 (1971)
195. S Garattini, A Vecchi, M Sironi, A Montovani, in *Chlorinated Dioxins and Related Compounds. Impact on the Environment* (Oxford: Pergamon Press, 1982) p. 275
196. K E Appel, A Y Hilderbrandt, W Lingk, H W Kunz *Chemosphere* **15** 1825 (1986)
197. D Neubert, R Meister *VDI-Ber.* **634** 443 (1987)
198. A E Pohland, E Glover *Mol. Pharm.* **9** 736 (1973)
199. J D McKinney, J Fawres, S Jordan, K Chac, S Oatley, R E Coleman, W Briner *Environ. Health Perspect.* **61** 41 (1985)
200. T Thunberg, U Ahlberg, B Wahlston *Arch. Toxicol.* **55** 16 (1984)
201. B N Filatov, E V Kozhevnikov, in *Pervaya Konf. po Dioksinovym Ksenobiotikam (Tez. Dokl.)* [The First Conference on Dioxin Xenobiotics (Abstracts of Reports)] (Vol'sk, 1992) p. 58
202. S P Krechetov, L M Udintseva, V M Gerashchenko, in *Pervaya Konf. po Dioksinovym Ksenobiotikam (Tez. Dokl.)* [The First Conference on Dioxin Xenobiotics (Abstracts of Reports)] (Vol'sk, 1992) p. 54
203. T W Goodwin, E I Mercer *Introduction to Plant Biochemistry* Vol. 2 (New York: Pergamon Press, 1983)
204. N M Waldron *J. Chem. Soc., C* **15** 1914 (1968)
205. C Kandaswami, P V Subba Rao, P M Nair, C S Vaidyanathan *Can. J. Biochem.* **47** 375 (1969)
206. P M Nair, L C Vining *Arch. Biochem. Biophys.* **106** 422 (1964)
207. W G C Forsyth, V C Quesnel, J B Roberts *Biochem. Biophys. Acta* **37** 322 (1960)
208. C Kandaswami, C S Vaidyanathan *Biochem. J.* **128** 30 (1972)
209. H Kondo *J. Pharm. Soc. Jpn.* **511** 1 (1924)
210. H Kondo, M Tomita *J. Pharm. Soc. Jpn.* **52** 139 (1932)
211. M Tomita, C Tani *J. Pharm. Soc. Jpn.* **62** 468 (1942)
212. M Tomita, C Tani *J. Pharm. Soc. Jpn.* **62** 481 (1942)
213. I R C Bick, A R Todd *J. Chem. Soc.* **6** 1606 (1950)
214. B Anjaneyulu, T R Govindachari, N Viswanathan *Tetrahedron* **27** 439 (1971)
215. B Anjaneyulu, T R Govindachari, S S Sathe, N Viswanathan, K W Gopinath, B R Pai *Tetrahedron* **25** 3091 (1969)
216. A K Ray, G Mikhopadhyay, S S Mitra, R P Guna, Biswapati Mukherjee, Atta-ur-Rahman, Aisha Nelofar *Phytochemistry* **29** 1020 (1990)
217. H H Lee, B D Palmer, M Boyg, B C Baguley, W A Denny *J. Med. Chem.* **35** 252 (1992)
218. A D Kunzevich, V F Golovkov, S A Chernov, S I Baulin, N M Troshkin, V R Rembovskii *Dokl. Akad. Nauk* **341** 693 (1995)
219. A D Kunzevich, E V Kuchinskii, I T Polyakov, V F Golovkov, A A Druzhinin, V N Syutkin *Dokl. Akad. Nauk* **335** 326 (1994)

Heterylferrocenes. Synthesis and use

M-G A Shvekhgeimer

Contents

I. Introduction	41
II. Compounds containing three-membered heterocycles	41
III. Compounds containing four-membered heterocycles	43
IV. Compounds containing five-membered heterocycles	43
V. Compounds containing six-membered heterocycles	62
VI. Compounds containing heterocycles with more than six atoms	74
VII. Biological activities and applications of heterylferrocenes	76

Abstract. Data on the synthesis of ferrocene derivatives containing heterocyclic substituents linked directly to the ferrocene system or separated from it by a chain of carbon atoms are described systematically and surveyed. Data on the biological activities and applications of these compounds are presented. The bibliography includes 229 references.

I. Introduction

In 1951, Kealy and Pauson¹ reported for the first time the synthesis of ferrocene and in the same year the first organic compound containing the ferrocenyl and heterocyclic groups was obtained.² Such compounds immediately attracted the attention of many investigators and in subsequent years ferrocene derivatives were synthesised in which there are various heterocyclic substituents both linked directly to the ferrocene system and separated from it by a chain of carbon atoms. The considerable interest in heterylferrocene was aroused not only by the unusual chemical behaviour of the ferrocene system, which enters into electrophilic and radical substitution reactions, but also by the unusual properties of the heterocyclic residue due to the presence of the ferrocene fragment. In addition, diverse biological activities of these compounds were observed. It is also significant that heterylferrocenes have found extensive practical applications as medicinal preparations, as components of nonsilver photosensitive compositions and materials, as dyes, and also as additives improving the most important characteristics of rocket fuels and explosives.

The first review devoted to the synthesis of ferrocene derivatives with heterocyclic groups appeared in 1971.³ It presented an analysis of studies published up to the middle of 1971. The literature data on the synthesis of compounds containing heterocyclic nuclei condensed with the ferrocene system were surveyed in a later communication.⁴ The present

author's previous review⁵ was fully devoted to the chemistry of heterylferrocenes, but it dealt mainly with studies which had been published up to 1972.

The present review gives a systematic account and surveys data published after 1971. Earlier studies containing interesting and important results which were not reflected in subsequent publications are considered as an exception. The review includes data on the synthesis of compounds containing the ferrocenyl group linked directly to an atom of the heterocycle as well as compounds in which the ferrocenyl and heterocyclic groups are separated by a chain of carbon atoms. Compounds in which the ferrocenyl system is condensed with the heterocyclic nucleus, ferrocenophanes, as well as compounds containing the ferrocenyl and heterocyclic groups separated by heterocycles or chains incorporating heteroatoms are not considered. The review presents data on the biological activities and applications of heterylferrocenes.

Sections II–VI present information about the synthesis of compounds containing heterocyclic nuclei with three, four, five, six, and more atoms. In each of these sections, the derivatives of ferrocene containing nitrogen, oxygen, and sulfur atoms in the heterocyclic nuclei are considered in succession. Next compounds with heterocycles containing simultaneously nitrogen and oxygen, nitrogen and sulfur, or oxygen and sulfur atoms are described. At the end of each section, data are presented on other heterocyclic systems. Each section deals at the beginning with compounds in which the ferrocenyl group is linked directly to an atom of the heterocycle and then with compounds containing the ferrocenyl and heterocyclic groups separated by a chain of carbon atoms. If the compound contains two or more heterocyclic nuclei (condensed or noncondensed), then its location in a particular section is determined by the heterocyclic system closest to the ferrocenyl nucleus.

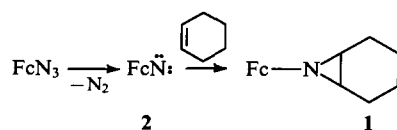
II. Compounds containing three-membered heterocycles

When ferrocenyl azide is irradiated with UV light in cyclohexene, the aziridine derivative **1** is formed in a low yield.⁶ The reaction evidently proceeds via the intermediate generation of the nitrene **2**, which adds to the double bond of cyclohexene. It has been noted that the aziridine **1** is formed both under nitrogen and under oxygen atmospheres. Consequently the nitrene **2** exists in the singlet state.⁶

M-G A Shvekhgeimer Department of Organic Chemistry and the Chemistry of Dyes, Kosygin Moscow State Textile Academy, ul. Malaya Kaluzhskaya 1, 117918 Moscow, Russian Federation. Fax (7-095) 952 14 40. Tel. (7-095) 955 35 96

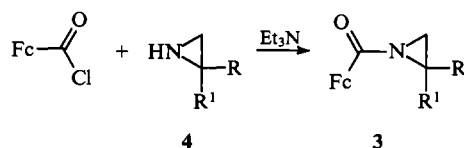
Received 13 June 1995

Uspekhi Khimii 65 (1) 43–83 (1996); translated by A K Grzybowski



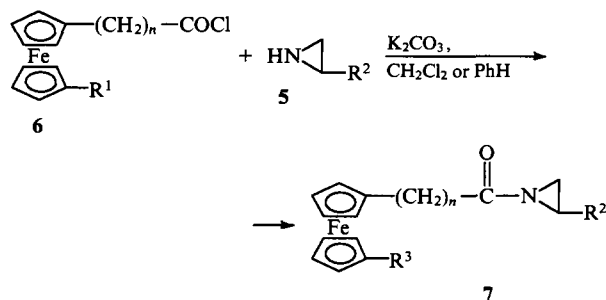
Here and henceforth Fc = ferrocenyl ($\eta^5\text{-C}_5\text{H}_4\text{Fe}(\eta^5\text{-C}_5\text{H}_5)$).

When the aziridine derivatives **4** interact with the chloride of ferrocenecarboxylic acid in the presence of triethylamine, *N*-ferrocenoylaziridines **3** are obtained.⁷



R, R¹ = H, Me.

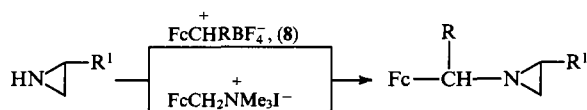
On *N*-acylation of the monosubstituted aziridine derivatives **5** by the chlorides of ferrocenyl-substituted monocarboxylic and dicarboxylic acids **6** in the presence of potassium carbonate at 10–30 °C, compounds **7** are produced in 40%–90% yields.^{8,9}



$n = 0-3$; R¹ = H, COCl; R² = H, Me, Et;

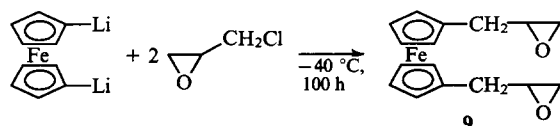
R³ = H, $\text{—C(=O)—N} \begin{array}{c} \diagup \text{R}^2 \diagdown \end{array}$.

The tetrafluoroborates of the α -ferrocenylcarbonium ions **8** and trimethylferrocenylmethylammonium iodide have been used recently for the *N*-alkylation of aziridine derivatives.¹⁰

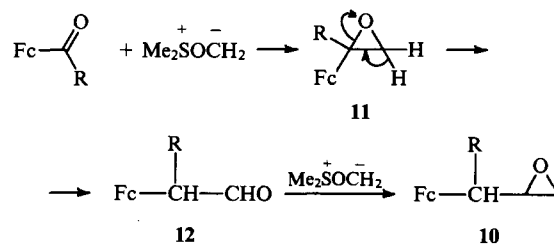


R = H, Me, Ph, Fc; R¹ = H, Me, Et.

Compound **9**, containing two epoxy-groups, has been synthesised in 44% yield by the reaction of 1,1'-dilithioferrocene with epichlorohydrin at –40 °C.¹¹

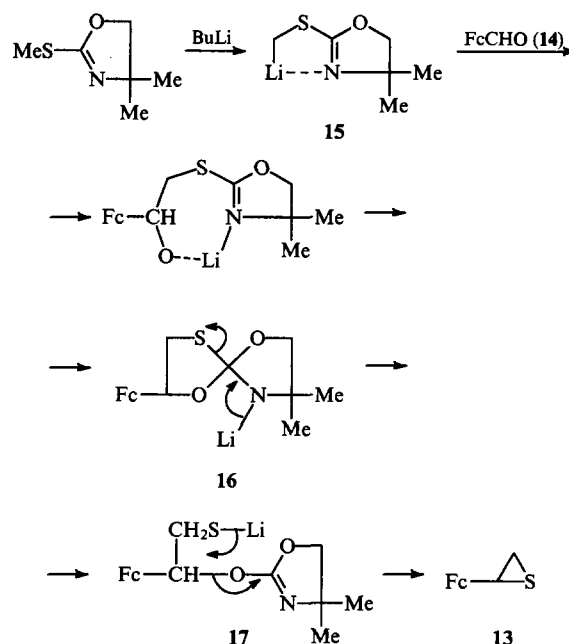


A novel method of synthesis of the epoxy-compounds **10** has been described.¹² The authors believe that, in the reactions of the carbonyl derivatives of ferrocene with dimethyloxosulfonium methylide, the epoxides **11** are formed in the first stage and are converted into the aldehydes **12** under the reaction conditions. The latter react with a further molecule of the methylide and are converted into compound **10**.

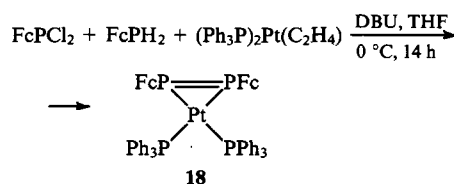


R = H, Me.

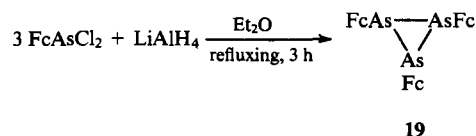
A mechanism involving the lithiation of the methyl group attached to the sulfur atom, the interaction of the aldehyde **14** with the lithio-derivative **15**, the conversion of the reaction product into the spiro-compound **16**, and the rearrangement of the latter to a new oxazoline derivative **17** and its cleavage to the thiirane **13** has been put forward for the synthesis of ferrocenylthiirane **13** from formylferrocene **14** and 2-methylthio-4,4-dimethyloxazoline.^{13,14}



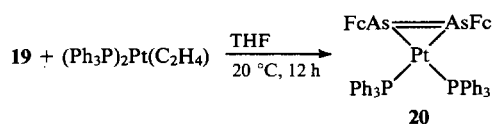
German investigators¹⁵ synthesised unusual heterocyclic compounds containing ferrocenyl groups. Thus the reaction of FcPCL_2 , FcPH_2 , and $(\text{Ph}_3\text{P})_2\text{Pt}(\text{C}_2\text{H}_4)$ in the presence of diazabicycloundecene (DBU) resulted in the formation of (diferrocenyldiphosphene)bis(triphenylphosphine)platinum(0) **18** in a quantitative yield.



Triferrocenyltriarsirane (**19**) has been synthesised in 66% yield by the reduction of FcAsCl_2 with lithium tetrahydroaluminate in boiling ether.¹⁵

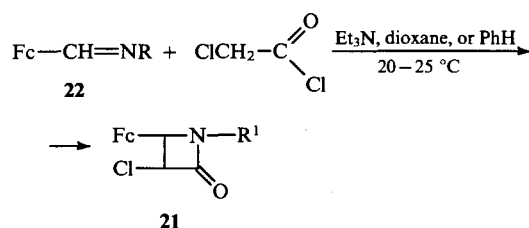


The latter was made to react with $(\text{Ph}_3\text{P})_2\text{Pt}(\text{C}_2\text{H}_4)$ at room temperature, which led to compound **20** in 68% yield.



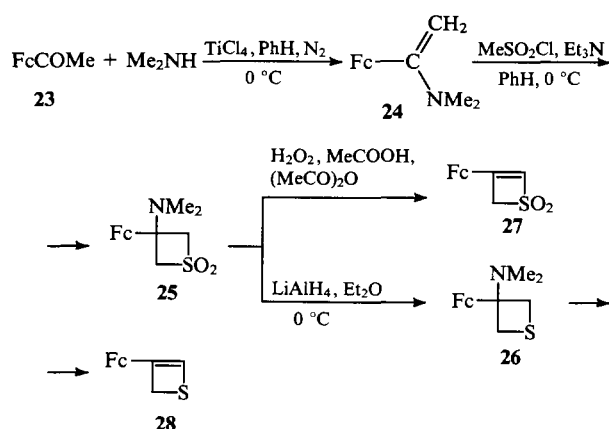
III. Compounds containing four-membered heterocycles

Numerous derivatives of 4-ferrocenylazetidin-2-ones **21** have been synthesised by the addition of chloroketene (synthesised from chloroacetyl chloride) to ferrocenylmethylideneimines **22**.^{16–20} The reactions were carried out in dioxane at 20–25 °C, the reaction time (ranging from several hours to several days) depending on the structure of the initial imine **22**. The reaction products and their yields are listed in Table 1.

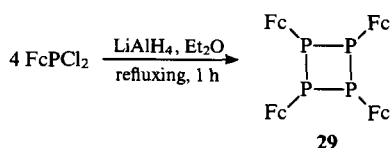


There are no literature data on the derivatives of ferrocene containing four-membered heterocyclic rings with oxygen atoms in the ring.

A series of 3-ferrocenylthiete derivatives have been synthesised from acetylferrocene **23**.²¹ Thus its treatment with dimethylamine in the presence of TiCl_4 leads to α -dimethylaminovinylferrocene **24** (yield 89%), which affords the sulfone **25** (yield 46%) on treatment with methanesulfonyl chloride in the presence of triethylamine. The sulfone may be reduced to the thietane **26** (yield 78%) and also deaminated by treatment with H_2O_2 in an acid medium to 3-ferrocenyl-2*H*-thiete dioxide **27** (yield 34%). Compound **26** was converted in two stages into 3-ferrocenylthiete **28** (yield 36%).²¹

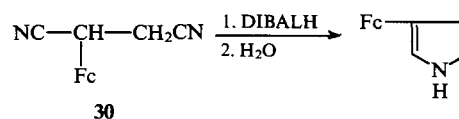


On heating ferrocenyldichlorophosphine with lithium tetrahydroaluminate in ether, tetraferrocenyltetraphosphetane **29** is formed in 11% yield.¹⁵

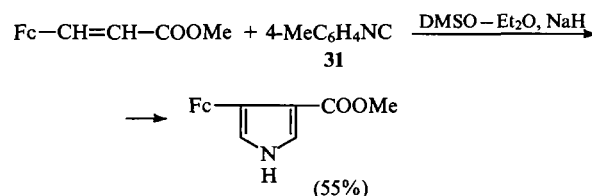


IV. Compounds containing five-membered heterocycles

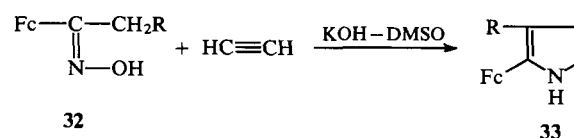
3-Ferrocenylpyrrole is formed in 21% yield on reduction of the dinitrile of 2-ferrocenylsuccinic acid **30** with diisobutylaluminium hydride (DIBALH) and subsequent hydrolysis.²²



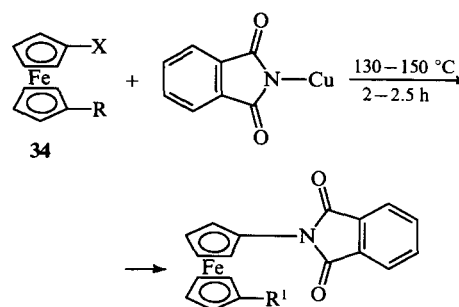
In the presence of sodium hydride, methyl 3-ferrocenylacrylate reacts with the isonitrile **31**, affording 3-ferrocenyl-4-methoxycarbonylpyrrole.²³



The cyclocondensation of the oximes of the acylferrocenes **32** with ethyne on treatment with alkali leads to the pyrrole derivatives **33**.²⁴ It has been noted that, when the reaction is carried out in a microwave oven, the yield of the reaction products increases appreciably.

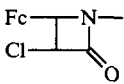
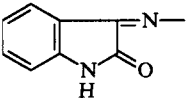
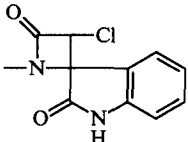
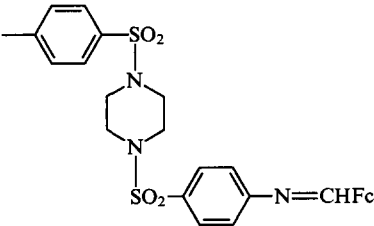
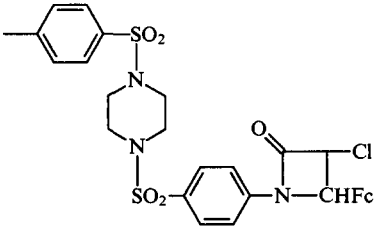
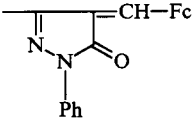
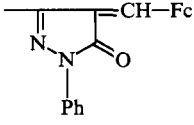
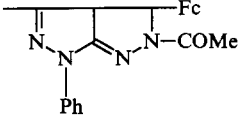
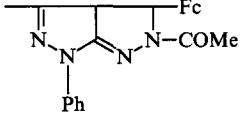
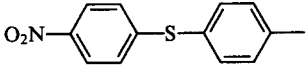
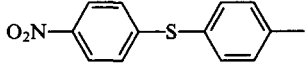
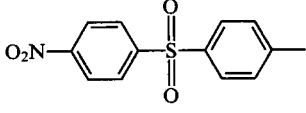
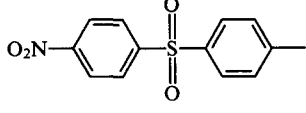
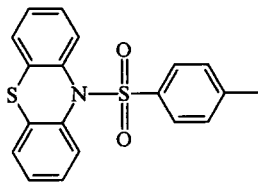
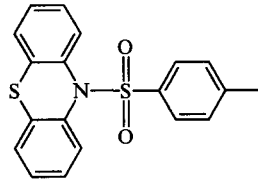
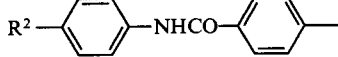
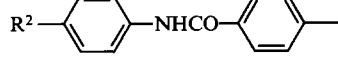


Ferrocene derivatives containing a phthalimide residue have been synthesised by heating the halo-derivatives **34** with copper phthalimide.^{25–27}

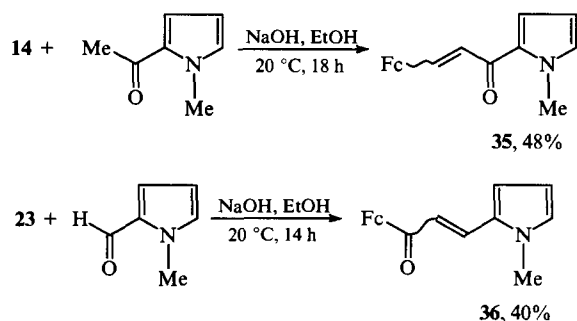


X	R	R ¹	Yield (%)
Br			37
Cl	Ph	Ph	49
Br	Br	H	8.5
Br	Br		47
I	H	H	73
I	I		35

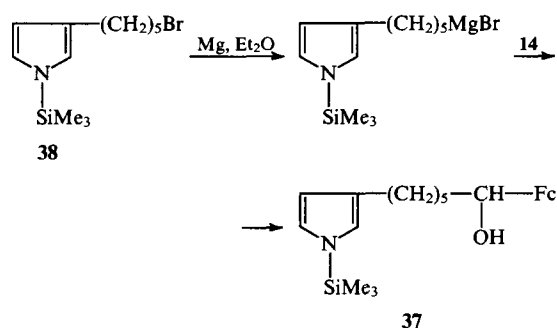
Table 1. The initial imines **22** and the 4-ferrocenylazetidin-2-one derivatives **21**.

R	R ¹	Yield of 21 (%)	Ref.
2-Py	2-Py	12	16
FcCH=N—		10	16
H ₂ NCONH—	H ₂ NCONH—	22	16
H ₂ NCSNH—	H ₂ NCSNH—	18	16
		14	16
		15	16
		50	17
		70	17
		32	18
		100	18
		40	19
		70	20
(R ² = H, Cl)	(R ² = H, Cl)		

In the presence of an alcoholic solution of NaOH, the aldehyde **14** condenses with 2-acetyl-1-methylpyrrole, while the ketone **23** condenses with 2-formyl-1-methylpyrrole to form the corresponding chalcones **35** and **36**.²⁸



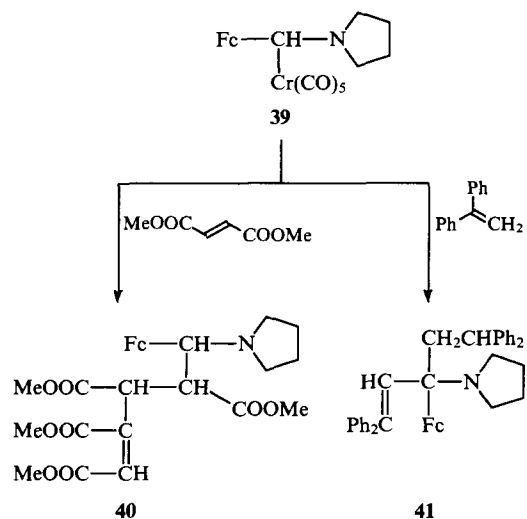
The alcohol **37** has been synthesised from the bromo-derivative **38** and FcCHO **14**.²⁹



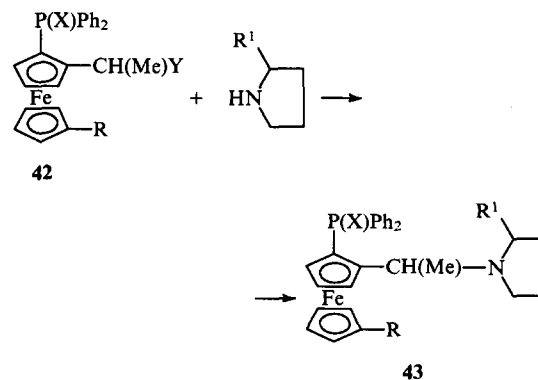
The synthesis of *N*-(2-ferrocenylethyl)pyrrole from 2-hydroxyethylferrocenyl toluene-*p*-sulfonate and potassium pyrrolide has been described.³⁰

Two procedures have been proposed for the synthesis of *N*-ferrocenylmethylpyrrolidine: the interaction of ferrocenylmethyl(trimethyl)ammonium iodide with pyrrolidine in the presence of aqueous sodium hydroxide^{31,32} and condensation of ferrocene with formaldehyde and pyrrolidine (yield 50%).³³

Unusual compounds have been obtained by the reactions of complex **39** with unsaturated compounds.³⁴ The interaction with fumaric acid ester affords the tetraester **40** (solvent – pyridine, refluxing for 2.5 h, yield 44%), while the reaction with 1,1-diphenylethene gives rise to the derivative **41** (inert atmosphere, in the dark, heating up to 136 °C for 3.5 h, yield 7%).

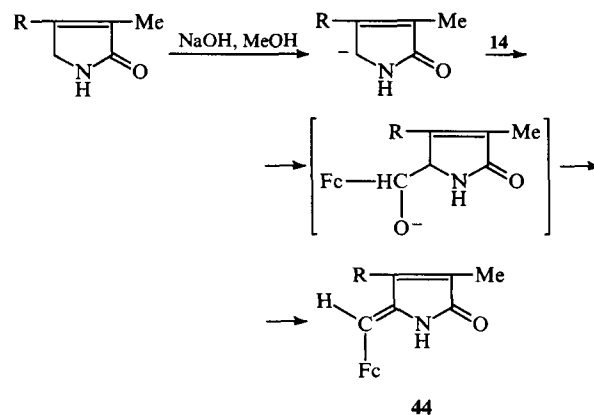


The group Y in compound **42** is substituted on treatment with pyrrolidine or its derivatives (refluxing in methanol for 5–8 h or maintenance in acetonitrile at 20 °C for 12 h); the yields of the products **43** are 55%–88%.^{35,36}



X	Y	R	R ¹
O	NMe ₂	H	H
—	OAc	H	CH ₂ NMe ₂
—	OAc	H	Me
—	OAc	PPh ₂	H
—	OAc	H	H

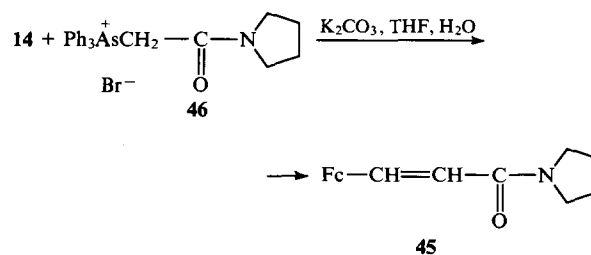
The reaction of 3,4-dimethylpyrrolone-2-one with FcCHO results in the formation of the product **44** of the kinetically controlled addition almost exclusively in the form of the (*Z*)-isomer.³⁷



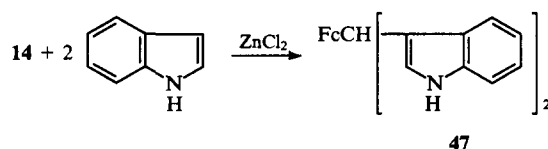
R = H, Me.

If 3-methylpyrrolin-2-one is made to react with the aldehyde **14**, then the product **44** (R=H) is formed as a 1 : 1 mixture of the (*Z*)- and (*E*)-isomers.³⁸

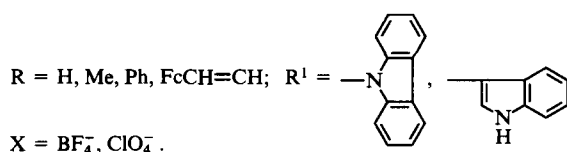
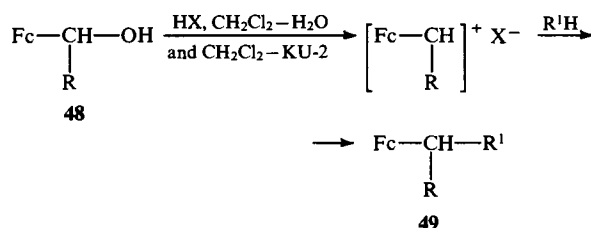
In the synthesis of the amide **45**, the reaction of FcCHO with the arsonium salt **46** was carried out in the presence of potassium carbonate in aqueous tetrahydrofuran (THF).³⁹



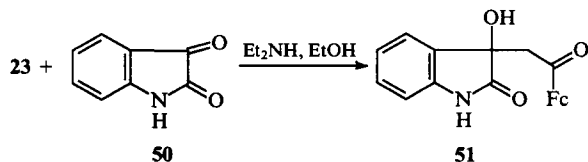
In the presence of ZnCl₂, the aldehyde **14** reacts with two molecules of indole, producing the ferrocene derivative **47**.⁴⁰



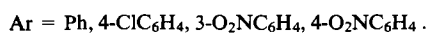
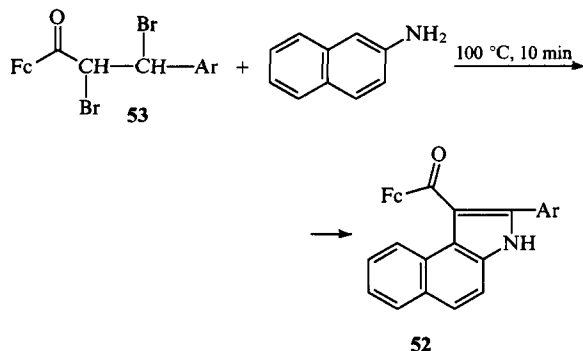
When the ferrocenyl carbinols **48** are treated with strong acids, highly reactive α -carbonium ions are formed. However, when strong acids are employed, the reaction is complicated by oxidation-reduction processes due to the presence of the ferrocene fragment in the substrate. In order to suppress these processes, the reaction is carried out in the CH_2Cl_2 - H_2O two-phase system and the KU-2 cation-exchange resin is employed instead of strong acids.⁴¹⁻⁴⁵ The $[\text{Fc}-\text{CHR}]^+$ cations readily react with nitrogen heterocycles, affording the ferrocene derivatives **49** in 60%–80% yields.



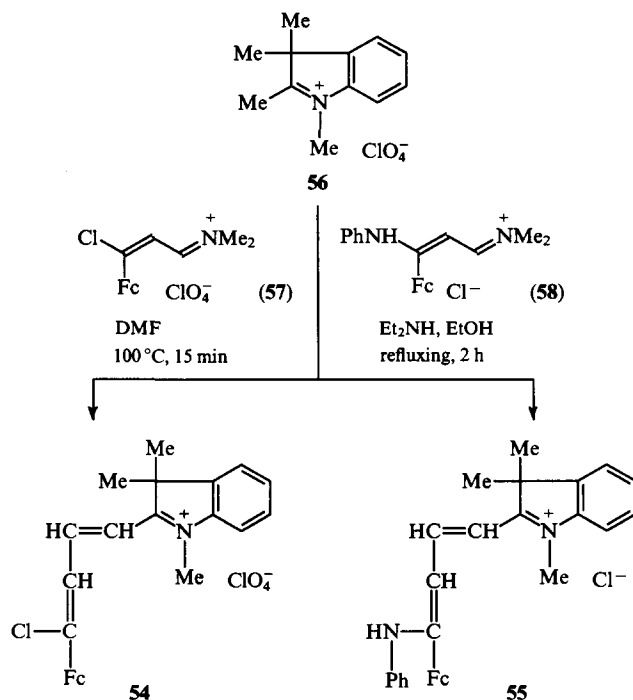
Refluxing of an alcoholic solution of FcCOMe **23** and isatin **50** in the presence of diethylamine for 1 h and subsequent standing at room temperature for several days led to the synthesis of compound **51** in 93% yield.⁴⁶



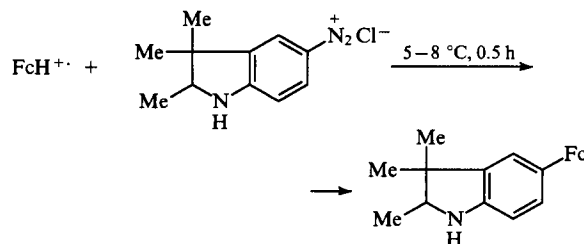
The naphthopyrrole derivatives **52** have been obtained in 80%–85% yields by heating the dibromo-derivative **53** with 2-aminonaphthalene.⁴⁷



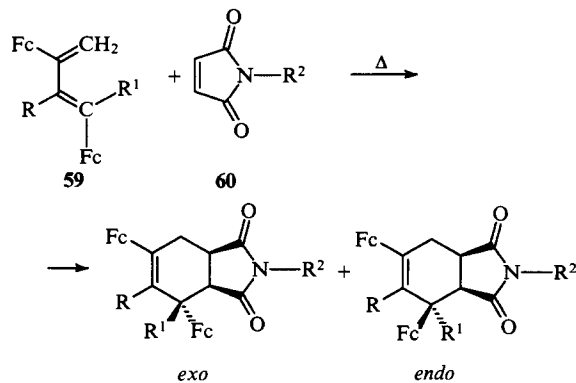
The dyes **54** and **55**, containing the ferrocenyl group, are formed as a result of the condensation of the perchlorate **56** with the immonium salts **57** and **58**.⁴⁸



The ferrocenium cation, arising on interaction of ferrocene with concentrated sulfuric acid, reacts with diazotised 5-amino-2,3,3-trimethylindolenine, which results in the formation of 5-ferrocenyl-2,3,3-trimethylindolenine in 23% yield.⁴⁹

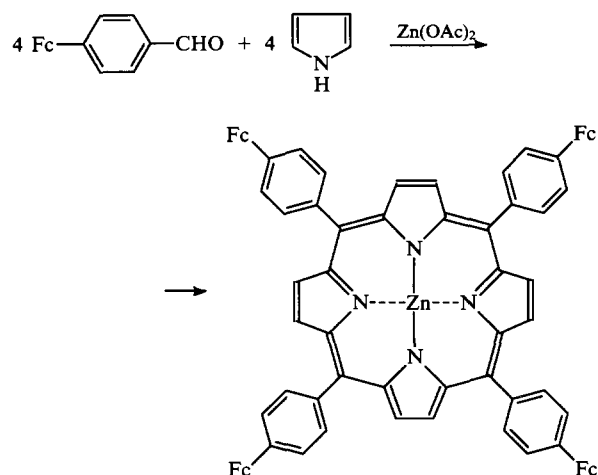


The 1,3-dienes **59**, containing a ferrocenyl substituent, are capable of undergoing the diene synthesis reaction with *N*-substituted maleic acid imides **60**.^{50,51} A mixture of the *endo*- and *exo*-isomers is formed as a rule and the *endo*-isomer has been obtained exclusively only in the case of the diene **59** ($\text{R} = \text{Me, R}^1 = \text{H}$).

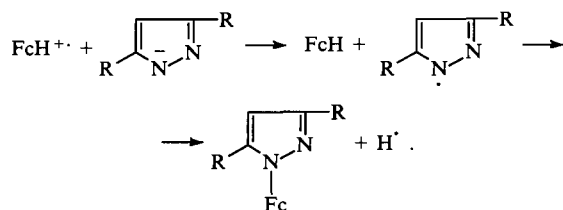


R	R ¹	R ¹
H	H	Ph
H	H	PhCH ₂
Me	H	Ph
H	Me	Ph

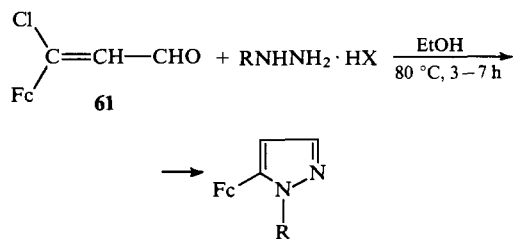
Schmidt et al.⁵² synthesised *meso*-tetrakis(4-ferrocenylphenyl)porphyrin by condensing 4-ferrocenylbenzaldehyde with pyrrole.



The direct conversion of ferrocene into a heteryl derivative has been achieved by treating ferrocenium hexafluorophosphate with the sodium derivatives of pyrazole or 3,5-dimethylpyrazole.⁵³ 1-Ferrocenylpyrazole and 1-ferrocenyl-3,5-dimethylpyrazole were synthesised. The following process mechanism has been put forward:



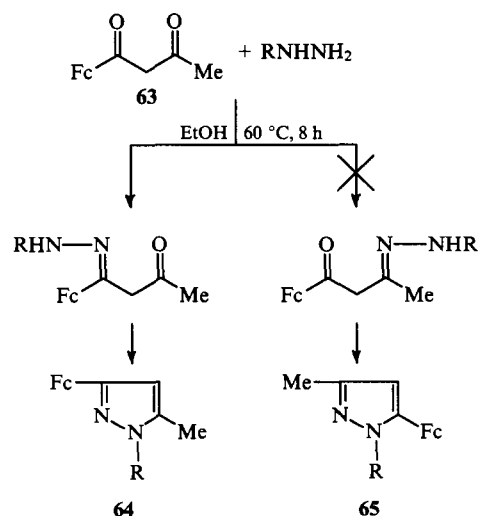
3-Chloro-3-ferrocenylacrylic aldehyde **61** and 3-chloro-3-ferrocenylacrylonitrile **62** are convenient starting compounds for the synthesis of ferrocenylpyrazoles. Thus the condensation of the aldehyde **61** with hydrazine hydrate or phenylhydrazine hydrochloride leads to the formation of 5-ferrocenylpyrazole and 5-ferrocenyl-1-phenylpyrazole respectively.⁵⁴



R	HX	Yield (%)
H	H ₂ O	18
Ph	HCl	41

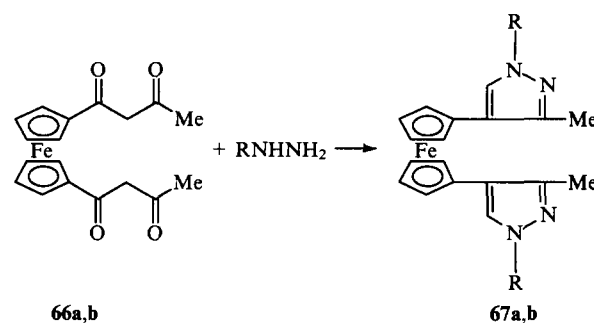
If the nitrile **62** is introduced into the reaction with hydrazine hydrate, then the product is 3-amino-5-ferrocenylpyrazole (yield 68%).

The reactions of acetoacetylferrocene **63** with hydrazine and its derivatives may lead to the formation of the two isomeric pyrazoles **64** and **65**. However, only the isomers **64** have been isolated from the reaction mixture.⁵⁵ The author explained this by the smaller steric hindrance in the cyclisation stage.



R	H	Me	Ph	2,4-(O ₂ N) ₂ C ₆ H ₃	CONH ₂
Yield (%)	81	30	70	21	90

A similar situation is observed in the condensation of the tetraketone **66** with hydrazine and its derivatives. Out of the three possible regioisomers, only the isomer **67** is formed. Together with steric factors, the stability of the corresponding intermediate hydrazones apparently plays a no less important role.⁵⁵

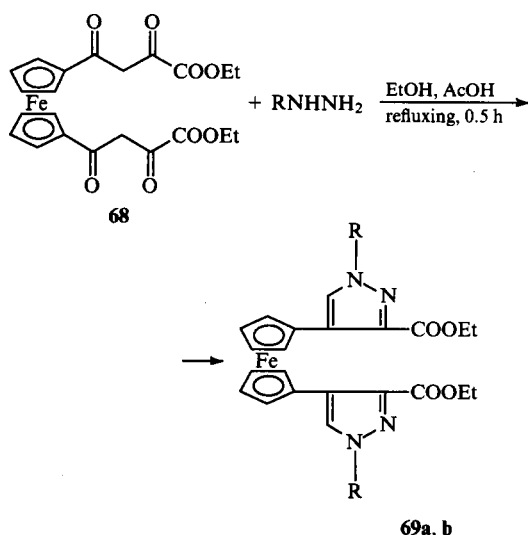


Compound	R	Yield (%)
a	H	60
b	CONH ₂	80

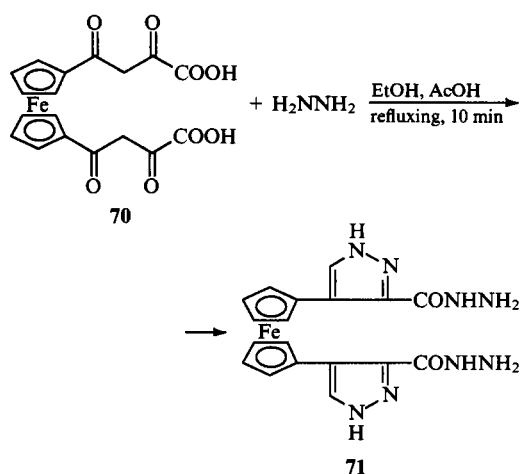
1-Benzoyl-1'-(5-trifluoromethylpyrazol-3-yl)ferrocene has been synthesised by condensing 1-benzoyl-1'-(4,4,4-trifluoro-3-oxobutanoyl)ferrocene with hydrazine.⁵⁶

An unusual method of synthesis of 3-ferrocenylpyrazol has been described.⁵⁷ Acetylferrocene **23** was treated with ethyl formate in the presence of sodium ethoxide in toluene, after which the reaction mixture was treated initially with hydrazine hydrochloride in water and then with hydrazine hydrate in methanol. The yield of 3-ferrocenylpyrazole reached 61%.

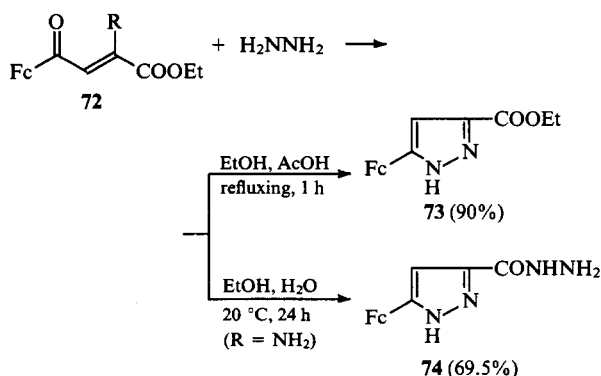
α,γ -Diketoacids of the ferrocene series and their esters have been used successfully as the starting compounds in the synthesis of ferrocenylpyrazoles. Thus condensation of the diester **68** with hydrazine (in the presence of acetic acid) or with phenylhydrazine afforded the corresponding pyrazole-containing diesters **69** (the yields of compound **69a** and **69b** were 56% and 52% respectively).⁵⁸ It was shown in the same study that the dihydrazide **71** is formed in 76.5% yield after brief refluxing of the dicarboxylic acid **70** with an excess of hydrazine.



$R = H$ (a), Ph (b)



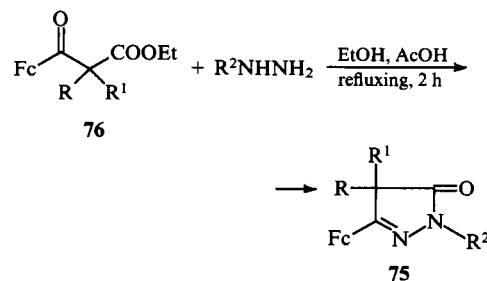
Depending on the reaction conditions, either 3-ethoxycarbonyl-5-ferrocenylpyrazole **73** or the hydrazide of 5-ferrocenylpyrazole-3-carboxylic acid **74** may be obtained from the ethyl esters of α -hydroxy- or α -amino- β -ferrocenoylacrylic acids **72** and hydrazine.⁵⁹



$R = NH_2, OH, NHMe, NHEt, NHPr^i, NHPh, NHC_6H_4Cl-m, NHC_6H_4OMe-o$.

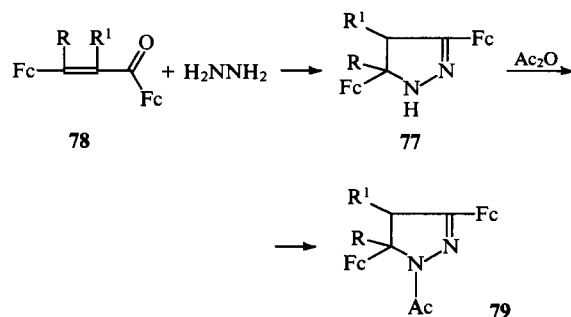
It is of interest that the reaction of β -ferrocenoyl- α -hydroxyacrylic acid with semicarbazide in the presence of sodium acetate and sodium bicarbonate afforded 5-ferrocenylpyrazole-3-carboxylic acid.⁵⁹ Consequently semicarbazide serves as a source of hydrazine under these conditions.

Derivatives of ferrocenylpyrazolones **75** are formed when the esters of the ketoacids **76** interact with hydrazine or phenylhydrazine in the presence of acetic acid.⁶⁰



$R, R^1 = H, Me; R^2 = H, Ph$.

The most general method of synthesis of ferrocenylpyrazolines involves the reaction of the vinyl ketones $FcCR=CR^1-COR^2$ or $FcCO-CH=CHR$ with hydrazine or its derivatives. As a rule, ferrocenylpyrazolines with a hydrogen atom at the N(1) atom are unstable and are therefore converted into the *N*-acetyl derivatives. For example, when the pyrazoline derivatives **77**, obtained from the vinyl ketones **78** and hydrazine, were treated with acetic anhydride, the *N*-acetyl derivatives **79** were isolated in 72%–75% yields.⁶¹

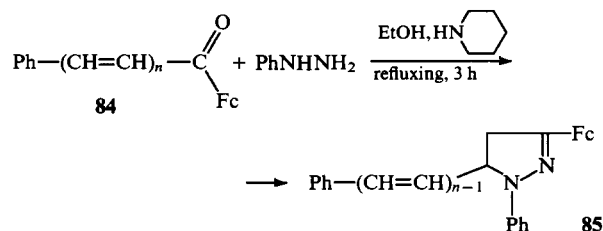


$R, R^1 = H, Me$.

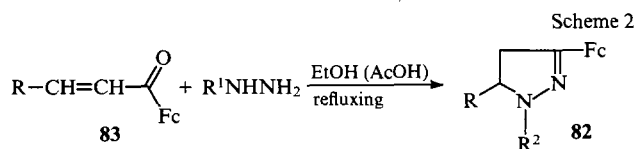
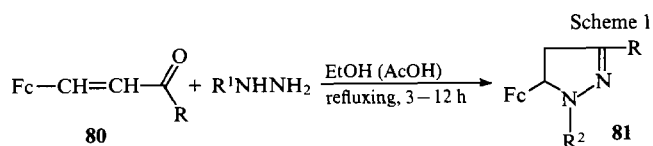
The reactions of the vinylketones **80** with hydrazine and its derivatives have been investigated in a series of studies;^{62–67} the pyrazoline derivatives **81** (Scheme 1) were obtained in 60%–95% yields. When the reaction was carried out in the presence of acetic acid, the reaction products were the *N*-acetyl derivatives. For $R^1 = Ph$, the reaction was carried out in the presence of piperidine.

The pyrazoline derivatives **82** with a different disposition of the substituents have been synthesised by the cyclocondensation of the vinyl ketones **83** with hydrazine and its derivatives;^{47,62,64,65} the yields were 60%–95% (Scheme 2).

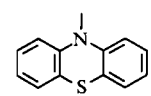
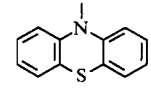
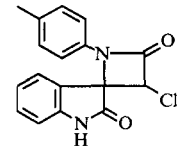
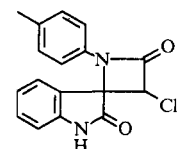
The behaviour of polyene ketones in their reactions with hydrazine and its derivatives has been studied in fair detail. The ketones **84**, containing two or three conjugated double bonds, react regioselectively with phenylhydrazine in the presence of piperidine, affording the pyrazoline derivatives **85** in 86%–91% yields.⁶⁸



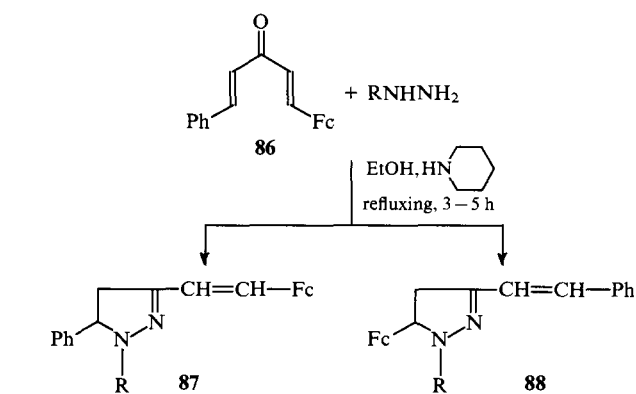
$n = 2, 3$.



R	R ¹	R ²	Ref.
Me	H	Ac	62
Me	Ph	Ph	62
Et	H	Ac	62
Et	Ph	Ph	62
Ph	H	Ac	62
Ph	H	H	65
Ph	Ph	Ph	62, 65
C ₆ H ₄ Et-4	H	Ac	62
C ₆ H ₄ Et-4	Ph	Ph	62
Ph	SO ₂ Ph	SO ₂ Ph	63
C ₆ H ₄ Ph-4	SO ₂ Ph	SO ₂ Ph	63
C ₆ H ₄ Br-4	SO ₂ Ph	SO ₂ Ph	63
C ₆ H ₄ Cl-4	SO ₂ Ph	SO ₂ Ph	63
C ₆ H ₄ OMe-4	SO ₂ Ph	SO ₂ Ph	63
C ₆ H ₄ Me-4	SO ₂ Ph	SO ₂ Ph	63
C ₆ H ₄ Et-4	SO ₂ Ph	SO ₂ Ph	63
Ph	SO ₂ C ₆ H ₄ NHAc-4	SO ₂ C ₆ H ₄ NHAc-4	63
C ₆ H ₄ Ph-4	SO ₂ C ₆ H ₄ NHAc-4	SO ₂ C ₆ H ₄ NHAc-4	63
C ₆ H ₄ Br-4	SO ₂ C ₆ H ₄ NHAc-4	SO ₂ C ₆ H ₄ NHAc-4	63
C ₆ H ₄ Cl-4	SO ₂ C ₆ H ₄ NHAc-4	SO ₂ C ₆ H ₄ NHAc-4	63
C ₆ H ₄ OMe-4	SO ₂ C ₆ H ₄ NHAc-4	SO ₂ C ₆ H ₄ NHAc-4	63
C ₆ H ₄ Me-4	SO ₂ C ₆ H ₄ NHAc-4	SO ₂ C ₆ H ₄ NHAc-4	63
C ₆ H ₄ Et-4	SO ₂ C ₆ H ₄ NHAc-4	SO ₂ C ₆ H ₄ NHAc-4	63
(η ⁵ -C ₅ H ₄)Mn(CO) ₃	H	H	64
Fc	H	H	64, 65
Fc	Ph	Ph	64, 65
(η ⁵ -C ₅ H ₄)Mn(CO) ₃	Ph	H	64
C ₆ H ₄ OMe-4	H	H	65
C ₆ H ₄ OMe-4	Ph	Ph	65
C ₆ H ₄ Br-4	Ph	Ph	65
Ph	Fc	Fc	65

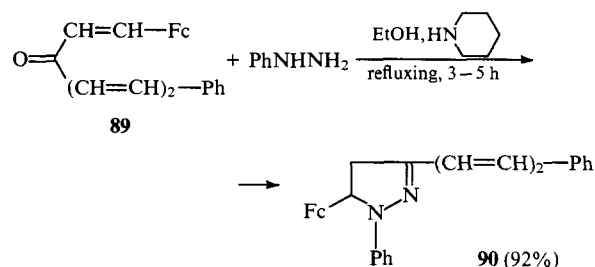
	H	Ac	66
	Ph	Ph	66
	Ph	Ph	67
	H	H	67

The addition of RNHNH₂ (R = H, Ph) to the divinyl ketone derivative **86** leads to a mixture of the isomeric pyrazolines **87** and **88**.⁶⁸ The regioselectivity of the reaction in favour of the formation of compound **88** has been noted and has been explained by the greater electron-donating capacity of the ferrocenyl substituent compared with the phenyl substituent.

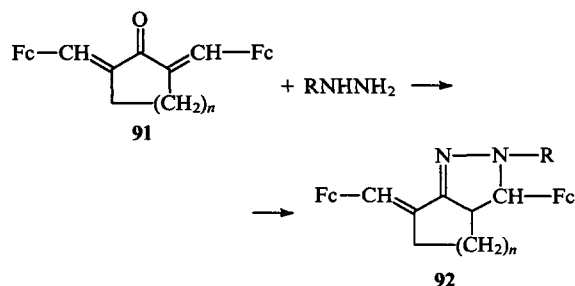


R = H, Ph

In the case of the ketone **89**, the addition of hydrazine takes place regioselectively,⁶⁸ whereupon the pyrazoline **90** is formed. Apart from the electronic factors quoted above, the proximity of the carbonyl group and the Fc fragment apparently plays a role.

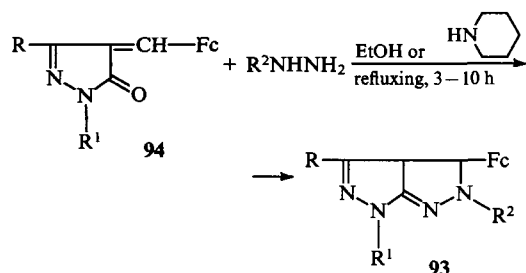


The ferrocenylmethylidene-substituted cyclic ketones **91** are converted into the bicyclic compounds **92** on condensation with hydrazine or its derivatives.



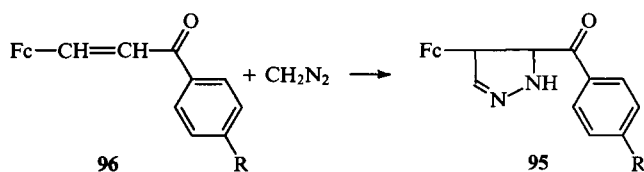
R = H, 2,4-(O₂N)₂C₆H₃; n = 1, 2.

The ferrocene derivatives **93** with two condensed pyrazoline rings have been synthesised by the reaction of the ferrocenylmethylidenepyrazolones **94** with hydrazine or phenylhydrazine (in the presence of piperidine) in alcohol (10 h) or dioxane (3 h), the product yield amounting to 50%–70%.^{17, 69}



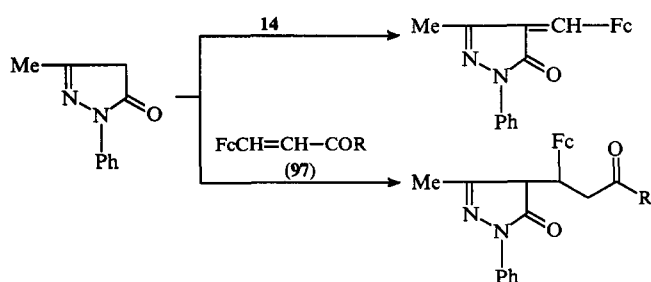
R	R ¹	R ²
Me	Ph	H
Me	2,4-(O ₂ N) ₂ C ₆ H ₃	H
Me	Ph	Ph
Me	2,4-(O ₂ N) ₂ C ₆ H ₃	Ph
FcCH=N–	Ph	Ph

A series of pyrazoline derivatives **95** have been synthesised by the cycloaddition of the vinyl ketones **96** to diazomethane.⁶³



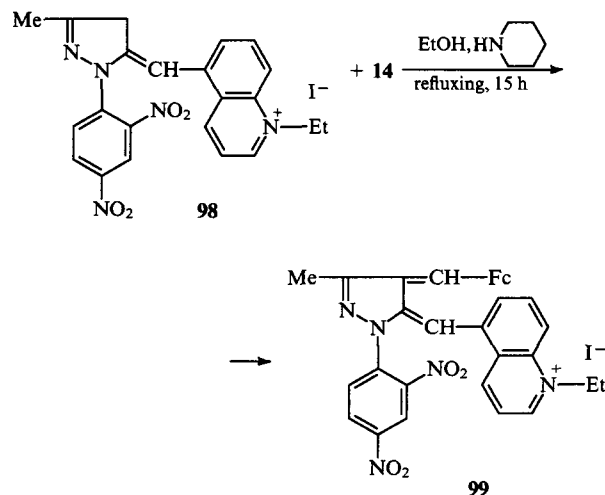
R = H, Cl, Br, Me, Et, OMe, Ph.

Two methods of synthesis of pyrazolone derivatives containing the ferrocenyl group in the side chain have been described: by the condensation of formylferrocene **14** with 3-methyl-1-phenylpyrazol-5-one or by the addition of the latter to the double bond of the vinyl ketones **97**.⁶⁹

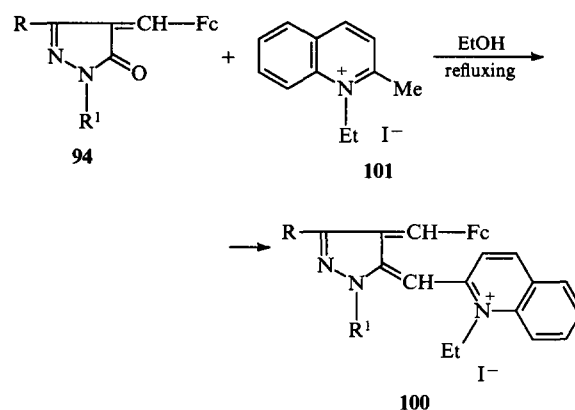


R = 4-MeC₆H₄, 4-ClC₆H₄, 4-BrC₆H₄, 4-MeOC₆H₄, 4-PhC₆H₄.

When the aldehyde **14** is heated with the salt **98** in alcohol in the presence of piperidine, the monomethinecyanine **99** is formed in 50% yield.⁷⁰



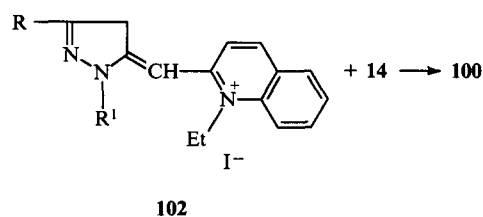
The cyanine dyes **100** have been synthesised by condensing the pyrazolone derivatives **94** with 1-ethyl-2-methylquinolinium iodide **101** in the presence of piperidine.^{17, 69}



R = Me, R¹ = Ph, 2,4-(O₂N)₂C₆H₃; R = FcCH=N–, R¹ = Ph.

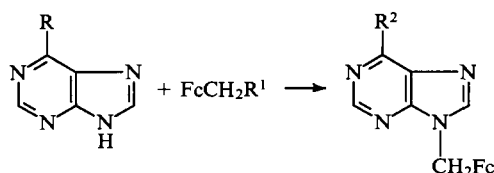
An analogue of the salt **100** (R = Me, R¹ = Ph), with a pyridine instead of a quinoline ring, has been obtained by the same procedure.⁶⁹

Compounds **100** are also formed as a result of the condensation of the salts **102** with FcCHO.⁶⁹



R = Me; R¹ = Ph, 2,4-(O₂N)₂C₆H₃.

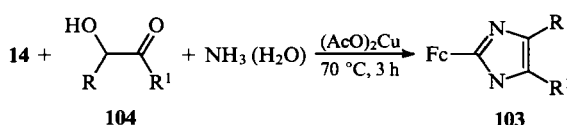
The ferrocenylmethyl group can also be introduced into the purine nucleus in two ways: as a result of the alkylation of 6-X-purines (X = NH₂, Cl) by ferrocenylmethyl-(trimethyl)ammonium iodide or aminomethylferrocene.⁷¹



R	R ¹	R ²	Conditions	Yield (%)
NH ₂	N ⁺ Me ₃ I ⁻	NH ₂	H ₂ O, refluxing, 6 h	47
Cl	NH ₂	NHCH ₂ Fc	MeOCH ₂ CH ₂ OH, refluxing, 3 h	21

N-Ferrocenylimidazole has been synthesised by treating the sodio-derivative of the imidazole with ferrocenium hexafluorophosphate.⁵³

2-Ferrocenylimidazole and its derivatives **103** are formed in 15%–50% yields as a result of the condensation of FcCHO **14** with the α -hydroxycarbonyl compounds **104** and ammonia in the presence of copper acetate.⁷²

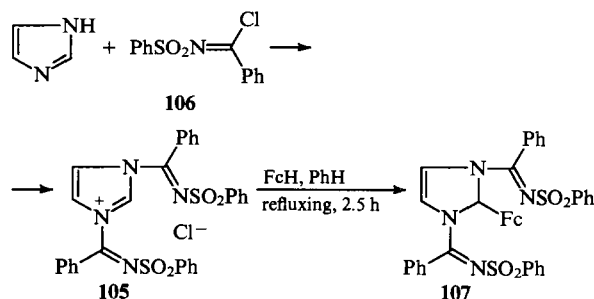


R = H: R¹ = H, Me, Ph;

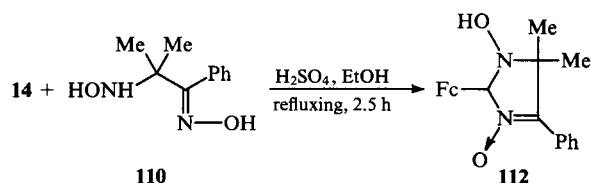
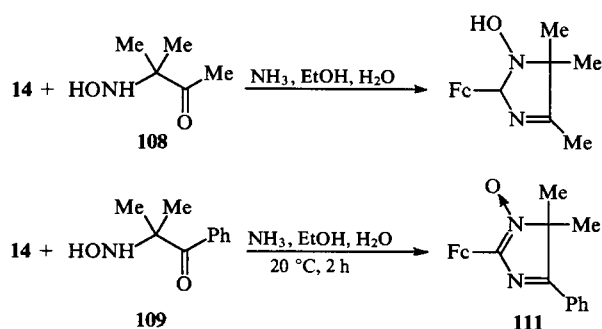
R = Me: R¹ = Me, Ph;

R = R¹ = Ph; R + R¹ = -(CH₂)₄-.

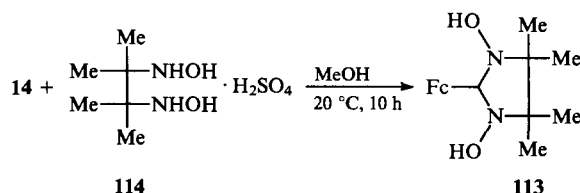
The salt **105**, which is obtained from imidazole and benzenesulfonylbenzimidoyl chloride **106**, is converted into 1,3-bis(benzenesulfonylbenzimidoyl)-2-ferrocenylimidazoline **107** on heating with ferrocene in benzene.⁷³



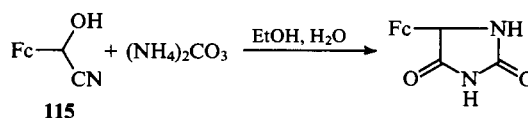
The selectivity of the reaction of FcCHO with the hydroxylamine derivatives **108**–**110** is influenced by the nature of the substituent at the keto-group.⁷⁴ 2-ferrocenyl-1-hydroxy-4,5,5-trimethylimidazoline is formed from the methyl ketone **108** (the reaction was carried out at 0 °C for 0.5 h with subsequent maintenance at 20 °C for 0.5 h; the yield was 30%); the *N*-oxides **111** and **112** were obtained from the phenyl ketone **109** and the oxime **110** (in 25% and 60% yields respectively). It has been suggested that compound **111** is formed as a result of the rapid oxidation in solution of the intermediate hydroxyimidazoline.⁷⁴



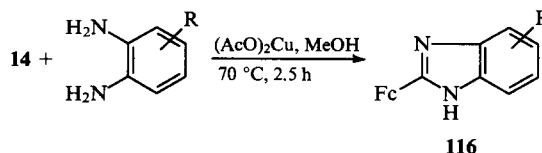
The salt **114** was used as the starting material for the synthesis of 2-ferrocenyl-1,3-dihydroxy-4,4,5,5-tetramethylimidazoline **113**.⁷⁵



5-Ferrocenylhydantoin has been obtained in 85% yield from the cyanohydrin **115** and ammonium carbonate in aqueous alcohol (the reaction was carried out at 50 °C for 2 h with subsequent maintenance at 20 °C for two days).⁷⁶



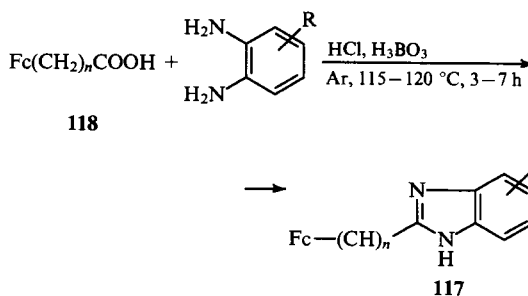
German investigators⁷² synthesised a series of derivatives of 2-ferrocenylbenzimidazole **116** (in 70%–90% yield) by condensing FcCHO **14** with substituted 1,2-diaminobenzenes in the presence of copper acetate.



R = H, 4-Me, 5-Me, 5,6-Me₂, 4-Cl, 5-Cl, 5-Br, 4-NO₂,

5-NO₂, 5-CN, 5-OMe, 5-NH₂, 4,5-(-CH=CH-CH=CH-).

The benzimidazole derivatives **117**, containing the ferrocenyl group linked directly to the heterocycle or separated from it by a chain of 1–5 carbon atoms, are formed in 45%–98% yields on heating ferrocenyl-substituted carboxylic acids **118** with substituted 1,2-diaminobenzenes under an argon atmosphere in the presence of hydrochloric and boric acids.⁷²

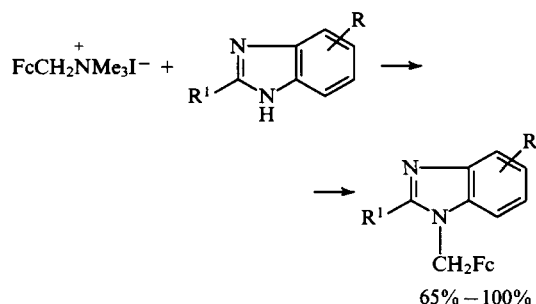


R = H ($n = 1-5$), 4-Me ($n = 0, 1$), 5-Me ($n = 1$), 5,6-Me₂ ($n = 1$), 4-Cl ($n = 1$), 5-Cl ($n = 1$), 5-OMe ($n = 1$), 4,5-(-CH=CH-CH=CH-) ($n = 1$).

Their analogues **117**, methylated at the N(1) atom, have been obtained under similar conditions from the acids **118** ($n = 0, 1$) and 1-amino-2-methylaminobenzene, while the *N*-phenylated

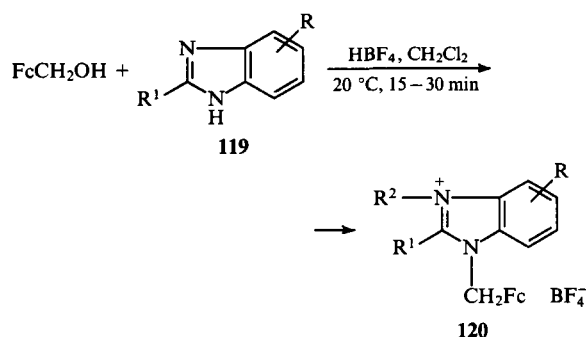
analogue **117** has been obtained from the acid **118** ($n = 1$) and 1-amino-2-phenylaminobenzene.⁷² The yields of compounds **117** were 54%–81%.

When benzimidazoles are treated with ferrocenylmethyl-(trimethyl)ammonium iodide, the N(1) atom is ferrocenylmethylated.^{77, 78}



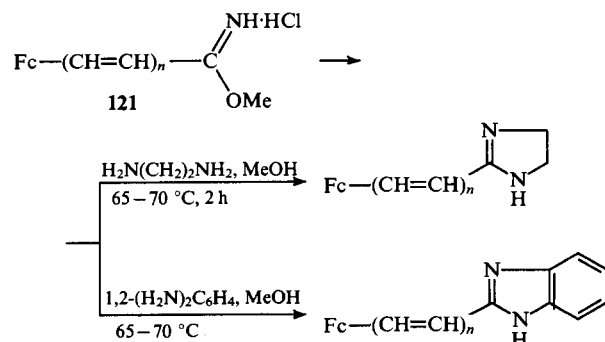
R = H: R¹ = H, Me, Ph;
R = 5-NO₂: R¹ = H, Me.

The FcCH₂ substituent can also be introduced at the nitrogen atoms of the benzimidazole derivatives **119** by the reaction with hydroxymethylferrocene in the presence of tetrafluoroboric acid. Depending on the ratios FcCH₂OH:119:HBF₄, one or both nitrogen atoms of the heterocycle are alkylated. The mono-alkylated products **120** (R² = H) are obtained for the ratios 1:1:2, while the dialkylated products **120** (R² = FcCH₂) are formed for the ratios 2:1:2.⁷⁸



R	R ¹	R ²	Yield (%)
H	Me	H	55
H	Me	FcCH ₂	68
6-NO ₂	H	H	71
6-NO ₂	Me	H	75
6-NO ₂	H	FcCH ₂	65
6-NO ₂	Me	FcCH ₂	62

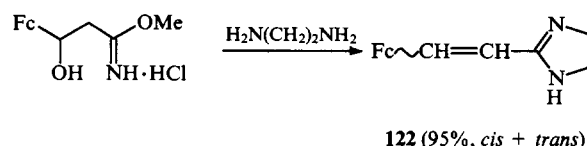
Ferrocene-containing imidazolines and benzimidazoles are formed in high yields (80%–93%) on condensation of the iminoester hydrochlorides **121** with ethylenediamine or 1,2-diaminobenzene.^{79, 80}



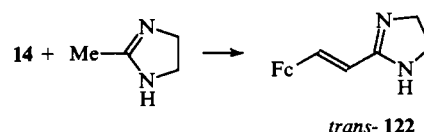
$n = 0, 1$.

The configuration of the ethene fragment in the product is the same as in the initial iminoester **121** ($n = 1$).^{81, 82}

The reaction of ethylenediamine with the hydrochloride of the iminoester of 3-ferrocenyl-3-hydroxypropionic acid results in the formation of 1-ferrocenyl-2-(2-imidazolyl)ethene **122** in the form of a mixture of the *cis*- and *trans*-isomers.⁸²

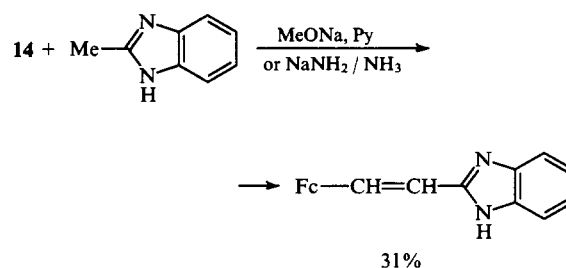


The condensation of the aldehyde **14** with 2-methylimidazoline constitutes a stereoselective method of synthesis of the *trans*-isomer of the imidazoline **122**.^{82–84}

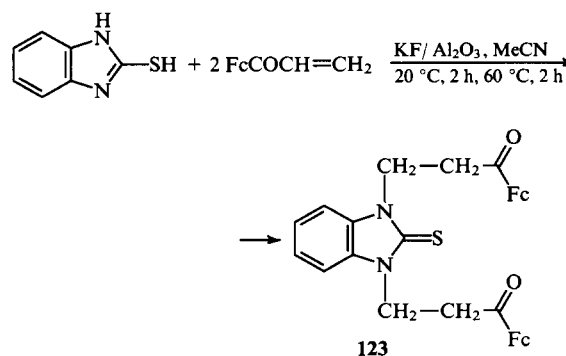


Conditions	Yield of 122 (%)
RONa, ROH (R = Me, Et)	54
KU-2, PhH	32

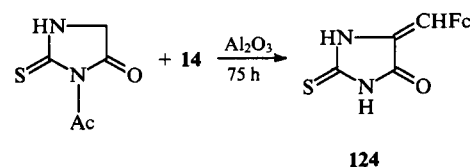
2-(2-Benzimidazolyl)-1-ferrocenylethene has been obtained similarly from 2-methylbenzimidazole.^{83, 84}



2-Mercaptobenzimidazole reacts in the thiono-form with two molecules of ferrocenyl vinyl ketone in the presence of potassium fluoride, affording the adduct **123** in 94% yield.⁸⁵

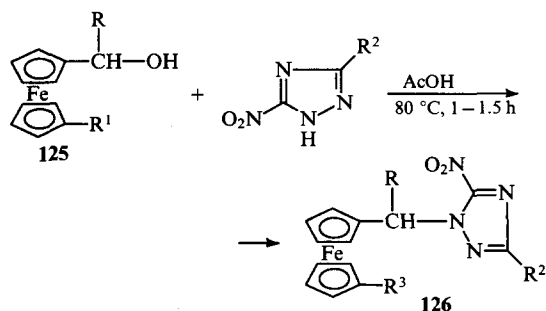


In the reaction of 3-acetyl-2-thiohydantoin with FcCHO on aluminium oxide, deacetylation takes place together with ferrocenylmethylation; the reaction product is compound **124** (yield 75%).⁸⁶



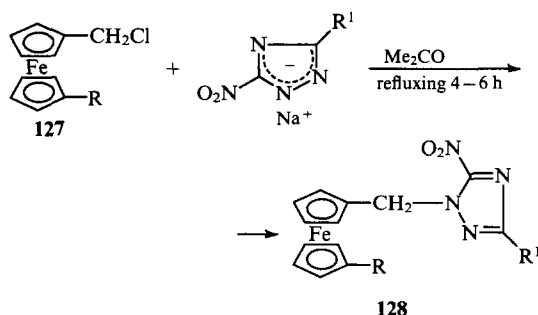
The synthesis of 2-ferrocenyl-5-mercapto-4-phenyl-1,2,4-triazoline by the condensation of phenyl isothiocyanate with the hydrazide of ferrocenecarboxylic acid has been described.⁸⁷

In the presence of acetic acid, the ferrocenylcarbinols **125** react regiospecifically with 5-nitro- and 3,5-dinitro-1,2,4-triazoles, forming the products of alkylation at the N(1) atom.⁸⁸ The ferrocene derivatives **126** with heteryl-containing substituents in both rings can be obtained under these conditions.



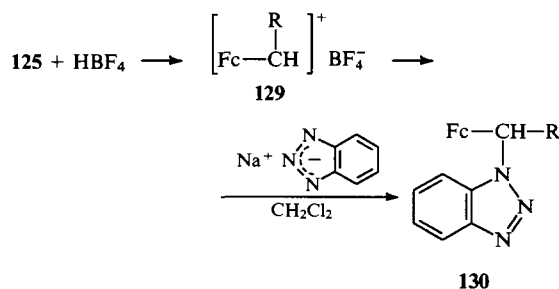
R	R ¹	R ²	R ³	Yield (%)
H	H	H	H	42
Me	H	H	H	57
Ph	H	H	H	18
H	H	NO ₂	H	12
Me	H	NO ₂	H	14
H	CH ₂ OH	H		60
Me	CH(Me)OH	H		53
Me	CH(Me)OH	NO ₂		14

The alkylation of the sodio-derivatives of 5-nitro- and 3,5-dinitro-1,2,4-triazoles by chloromethyl- and 1,1'-di(chloromethyl)-ferrocenes **127** also takes place regiospecifically at the N(1) atom. The yields of the products **128** are 50%–80%.^{89,90}



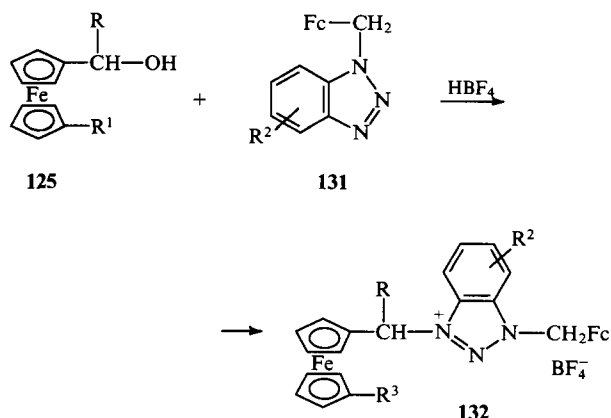
R	R ¹	R ²
H	H	H
H	NO ₂	H
CH ₂ Cl	H	
CH ₂ Cl	NO ₂	

The reaction of the sodio-derivative of benzotriazole with the salts **129**, formed from the ferrocenylcarbinols **125** and HBF₄, leads to *N*-substituted benzotriazoles **130** in 54%–96% yields.⁴³ According to the authors, the reaction proceeds via a stage involving the one-electron oxidation of the benzotriazole anion.

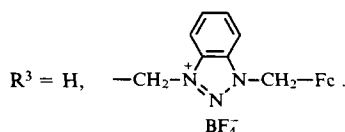


R	H	Me	Ph	FcCH=CH	Fc	
Reaction time/h	0.25	1.25	1.75	20	0.5	0.5

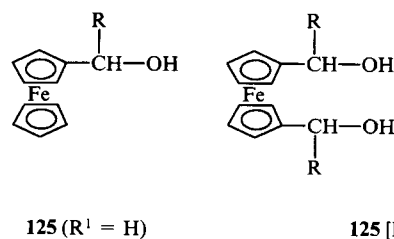
The alkylation of the substituted benzotriazoles **131** by treatment with the ferrocenylcarbinols **125** in 48% aqueous HBF₄ in the course of 3–5 min leads to the salts **132** in 92%–96% yields.⁹¹

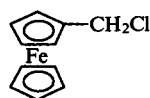


R = H, Me; R¹ = H, CH₂OH; R² = H, Me, Br, NO₂;

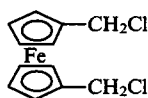


The alkylation of tetrazole and its derivatives **133** by various cationoid ferrocene-containing reagents has been investigated.^{88,92} The reagents employed were the alcohols **125** of the ferrocene series, which readily generate α -ferrocenyl-carbonium ions in an acid medium, as well as α -haloalkyl-ferrocenes **127**. In these reactions, electrophilic functional groups were present in only one as well as in both rings of the ferrocene system.

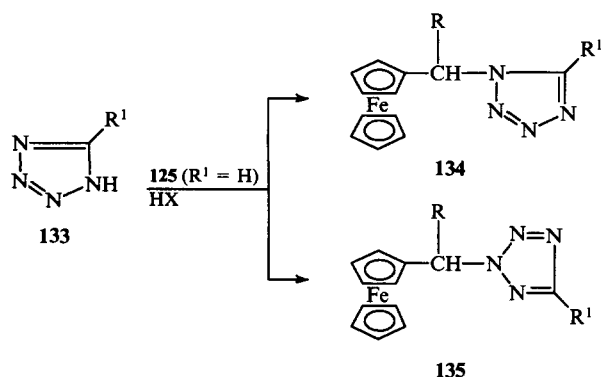




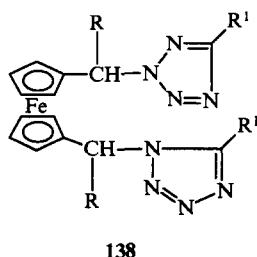
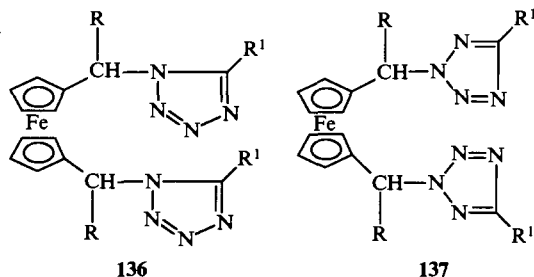
127 (R = H)

127 (R = CH₂Cl)

Treatment of tetrazole (or 5-R¹-tetrazole) **133** or of its sodio-derivative by the above reagent gave the products of alkylation at the N(1) atom (compound **134**) or the N(2) atom of the tetrazole ring (compound **135**).



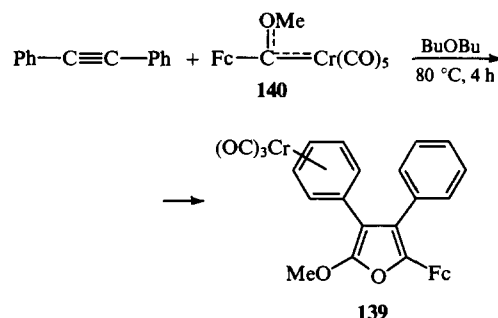
It has been observed that tetrazole and its alkyl derivatives (R¹ = H, Alk) are alkylated nonselectively, which results in the formation of a mixture of regioisomers (compounds **134**, **135**, and **136–138**). The introduction of electron-accepting or aromatic substituents (R¹ = Ar, NO₂) into the tetrazole ring promotes substitution at the N(2) atom. In the case of 5-nitrotetrazole, only the N(2)-alkylated derivatives are obtained (compounds **135** and **137**).



138

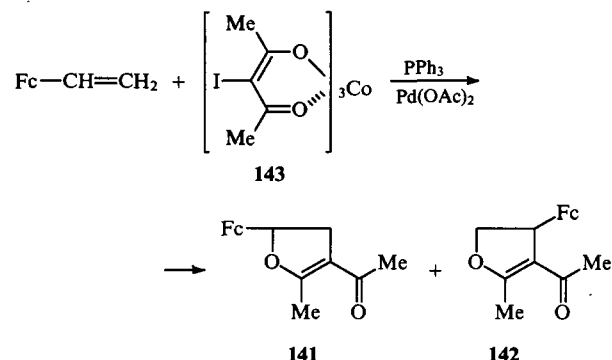
The influence of the acidity of the medium on the selectivity of the alkylation of tetrazole by the alcohols **125** has been investigated.⁹³ It was found that alkylation at the N(1) atom predominates in an acid medium.

The ferrocenylfuran derivative **139** has been obtained in 45% yield by heating a mixture of diphenylethyne with pentacarbonyl[ferrocenyl(methoxy)carbene]chromium(0) **140** in dibutyl ether.⁹⁴



139

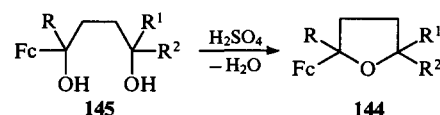
A mixture of the two dihydrofuran derivatives **141** and **142** is formed as a result of the reaction of vinylferrocene with tris(3-iodopentane-2,4-dionato)cobalt **143** in the presence of palladium acetate and triphenylphosphine.⁹⁵



141

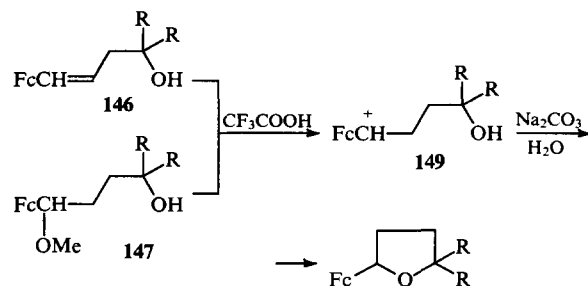
142

2-Ferrocenyltetrahydrofuran and its derivatives **144** have been synthesised in 90%–95% yields by the dehydrocyclisation of the corresponding 1,4-diols **145** on treatment with sulfuric acid or on heating in vacuo.^{96,97}



R	R ¹	R ²
H	H	H
Ph	Me	Me
Ph	Me	Et
Ph	Pr	Pr
Ph	-(CH ₂) _n - (n = 4, 5)	

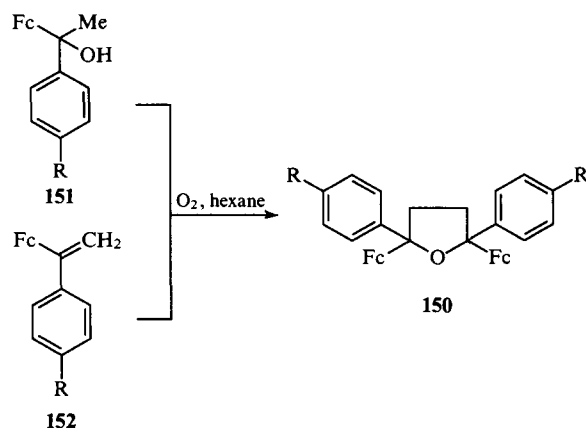
The unsaturated alcohols **146** or the 1,4-diol monoethers **147** are converted into the tetrahydrofuran derivatives **148** by the reaction with trifluoroacetic acid and subsequent treatment with an aqueous solution of sodium carbonate. According to the authors,⁹⁸ the reaction proceeds via a stage involving the formation of the carbonium ions **149**. The yields of compounds **148a, b** were 84% and 88% respectively.



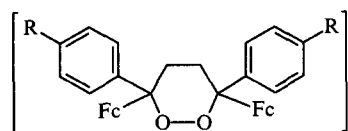
R = H (a), Me (b)

148a,b

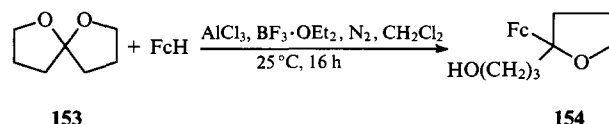
Japanese investigators have described a new method of synthesis of 2,5-diferrocenyltetrahydrofuran derivatives **150**.^{99,100} They treated the alcohols **151** or the alkenes **152** with oxygen in hexane in the presence of silica gel or acid aluminium oxide.



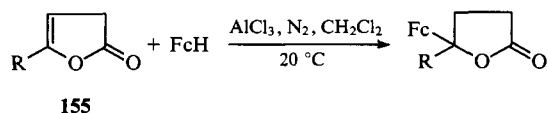
The authors believe that the reaction proceeds via the intermediate formation of a peroxide as a result of the oxidative dimerisation of the initial compounds.



When 1,6-dioxaspiro[4.4]nonane **153** is activated by Lewis acids (AlCl_3 , BF_3), it is capable of alkylating ferrocene with the opening of one of the rings of the spiro-system.^{101,102} After treatment with water, 2-ferrocenyl-2-(3-hydroxypropyl)tetrahydrofuran **154** is formed in 55%–89% yield.



Ferrocene adds to the dihydrofuranone derivative **155** under similar conditions.¹⁰³

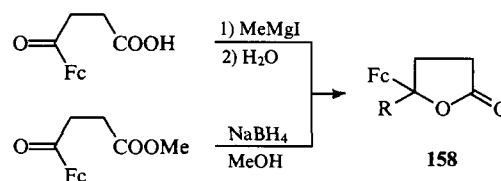
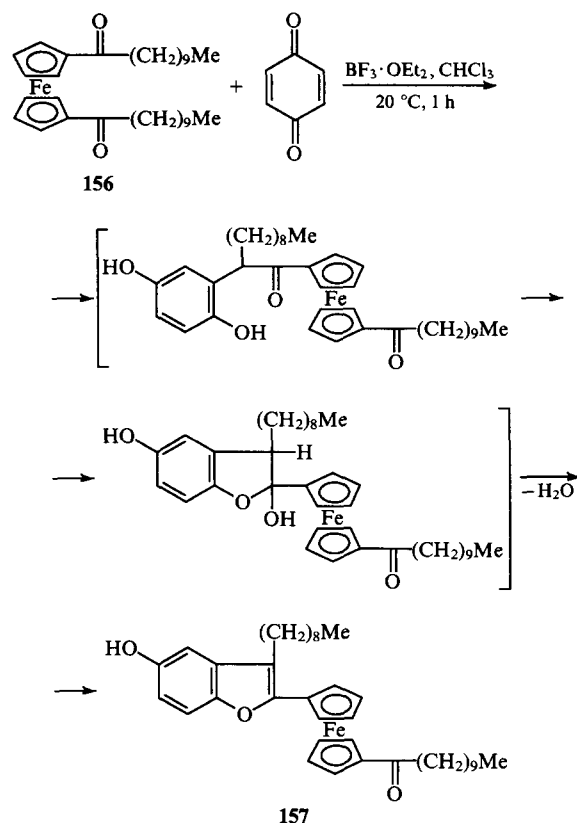


2-Ferrocenylfuran-5-carboxylic acid has been synthesised by the cyclocondensation of 3-chloro-3-ferrocenylacrolein **61** with glycolic acid. It was noted that, when the reaction is carried out in a microwave oven, the yield of the cyclocondensation product increases appreciably.²⁴

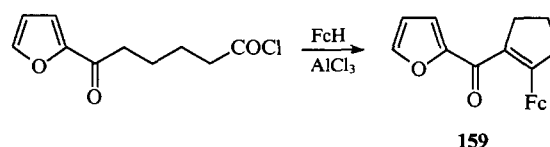
The interaction of the diketone **156** with benzoquinone in the presence of $\text{Et}_2\text{O} \cdot \text{BF}_3$ results in the formation of the benzofuran derivative **157** in 30% yield.¹⁰⁴

The alcohols obtained from 3-ferrocenylpropionic acid or its methyl ester cyclise to the tetrahydrofuranone derivative **158** on treatment with MeMgI or NaBH_4 in situ.^{98,105}

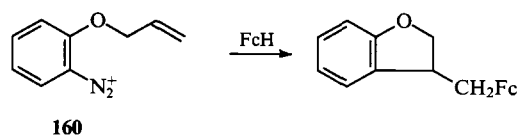
The acylation of ferrocene by the chloride of 5-(2-furoyl)-valeric acid in the presence of aluminium chloride is accompanied by the intramolecular crotonic condensation; the final reaction product is 2-ferrocenyl-1-(2-furoyl)cyclopentene **159**.¹⁰⁶



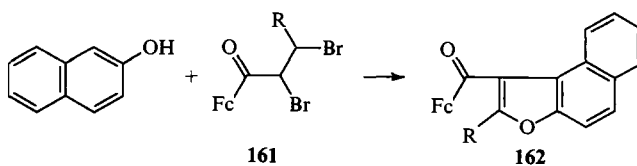
R = H, Me.



Australian investigators¹⁰⁷ described a novel method of synthesis of 3-ferrocenylmethyl-2,3-dihydrobenzofuran by the cyclocondensation of ferrocene with the diazonium cation **160**.

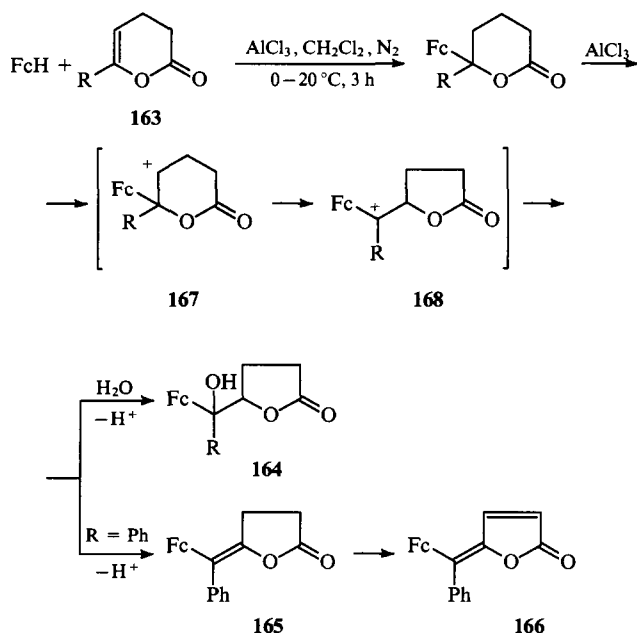


The naphthofuran derivatives **162** have been synthesised in 70%–78% yields by heating a mixture of β -naphthol and the dibromo-derivatives **161** above the melting point.⁴⁷

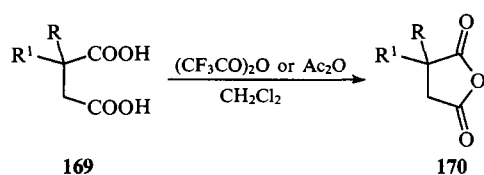


R = Ph, 4- ClC_6H_4 , 3- $\text{O}_2\text{NC}_6\text{H}_4$, 4- $\text{O}_2\text{NC}_6\text{H}_4$.

The reaction of ferrocene with the lactones **163** in the presence of aluminium chloride¹⁰³ leads to compounds **164–166** with five-membered rings, which are formed as a result of the carbonium ion rearrangement **167** → **168**.

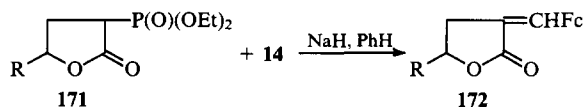


The synthesis of the ferrocenyl-substituted succinic anhydrides **170** from the corresponding acids **169** on treatment with Ac_2O or $(\text{CF}_3\text{CO})_2\text{O}$ has been described.^{108–110}



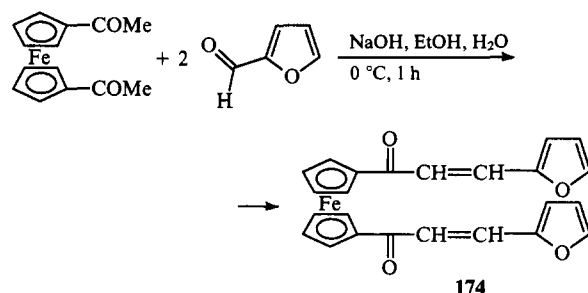
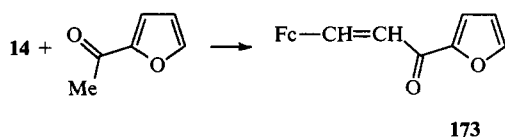
R	R ¹	Yield (%)	Ref.
H	FcCH ₂	80–88	109
	Fc(Me)C=	100	108
	Fc(Ph)C=	90	108
	FcHC=	53	110

The Horner–Emmons interaction of FcCHO **14** with the phosphonates **171** leads to the unsaturated lactones **172**.¹¹¹

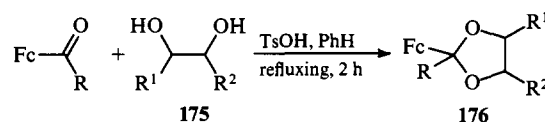


R = H, Me.

The ferrocene-containing chalcones **173** and **174** have been obtained^{112,113} by condensing compound **14** with 2-acetylfuran (on treatment with aqueous alkali at 20 °C for 24 h or on treatment with piperidine in methanol) and also by condensing 1,1'-diacetylferrocene with furfural.

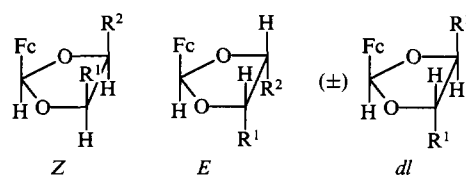


On treatment with the glycols **175** in the presence of toluene-*p*-sulfonic acid, the aldehyde **14** and acetylferrocene **23** afford the corresponding dioxolanes **176** (yield 68%–77%).^{114,115}

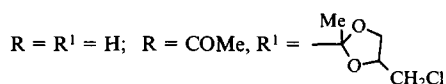
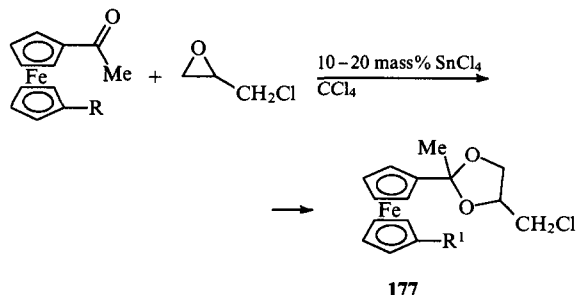


R	R ¹	R ²	Ref.
Me	H	H	114
H	Me	H	115
H	Me	Me	115

It has been established by ¹H NMR spectroscopy¹¹⁵ that the reaction with aldehyde **14** proceeds stereoselectively: for R¹ = Me and R² = H, a 6:5 mixture of (*Z*)- and (*E*)-isomers is formed; the *dl*- and (*E*)-isomers are formed in proportions of 6:1 from the symmetrical diol, where R¹ = R² = Me.



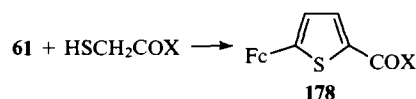
The introduction of the dioxolane fragment into the ferrocene system is also possible on treatment with epichlorohydrin in the presence of tin(IV) chloride.^{114,116} The maximum yields of the products **177** have been obtained for the ratio ferrocene derivative: epichlorohydrin = (1:2)–(1:4).



A method of synthesis of 1,1'-bis(2-thienyl)ferrocene, involving the reaction of 1,1'-dibromoferrocene with an excess of (2-thienyl)magnesium iodide has been patented.¹¹⁷

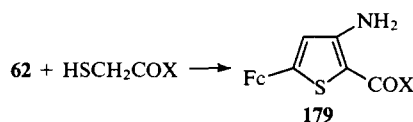
The cyclocondensation of 3-chloro-3-ferrocenylacrolein **61** with thioglycolic acid in the presence of triethylamine [60–80 °C, dimethylformamide (DMF)]^{24,118} leads not only to the expected 2-ferrocenylthiophene-5-carboxylic acid (yield 12%) but also to its decarboxylation product — 2-ferrocenylthiophene (yield 20%).

The condensation of ethyl thioglycolate proceeds without complications¹¹⁸ and the corresponding thiophene derivative **178** (X = OEt) has been isolated in 63% yield. The amide **178** (X = NHPh) has been obtained in 36% yield from the anilide of thioglycolic acid.



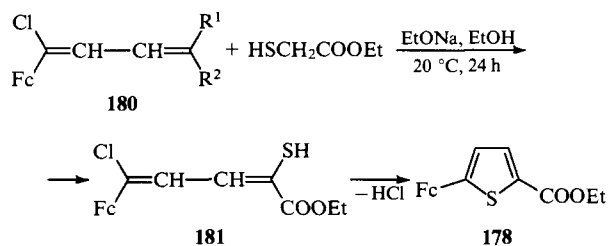
X = OEt, NHPh.

The same communication reports the synthesis of the amino-derivatives **179** (X = OEt, yield 49%; X = NHPh, yield 65%) when the 3-chloro-3-ferrocenylacrylonitrile **62** is condensed with thioglycolic acid derivatives.

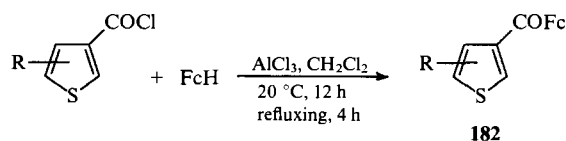


X = OEt, NHPh.

In a basic medium, the diene derivative **180** undergo transcondensation with ethyl thioglycolate. This leads to the product **181**, unstable under the reaction conditions, which cyclises to the thiophene derivative **178** (X = OEt).¹¹⁹

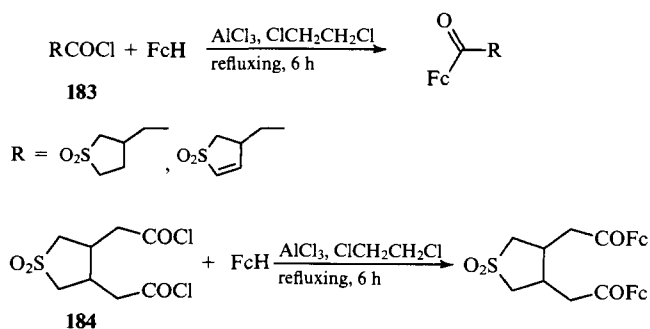


When ferrocene is acylated by the chlorides of thiophene-3-carboxylic acids, the ketones **182** are formed in low yields (14%–20%).¹²⁰

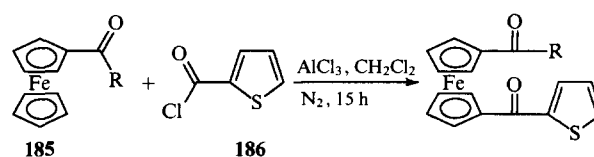


R = 2-COOMe, 4-COOMe.

The acylation of ferrocene by the acid chlorides **183** and **184**, containing a sulfolane or sulfolene fragment, is also ineffective for preparative purposes (the product yields are 14%–20%).¹²¹



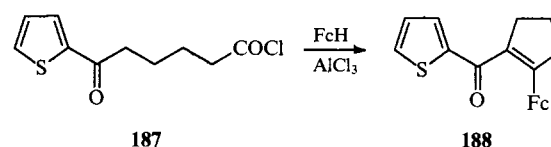
When the acylferrocenes **185** are acylated by the chloride of thiophene-2-carboxylic acid **186**, the attack by the electrophile is directed to the unsubstituted cyclopentadienyl fragment.¹²²



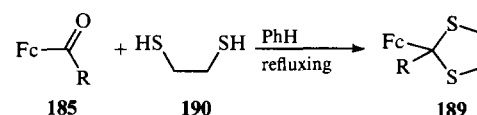
R = Me (80%), Et (83%), Ph (81%), PhCH₂ (85%).

When 1-acetyl-1'-ethylferrocene is used as the substrate, substitution takes place in the ring with the alkyl substituent (the yield of the acylation product is 16%).¹²²

The acylation of ferrocene by the chloride **187** under the conditions of the Friedel-Crafts reaction is accompanied by cyclisation with formation of the ketone **188**.¹⁰⁶

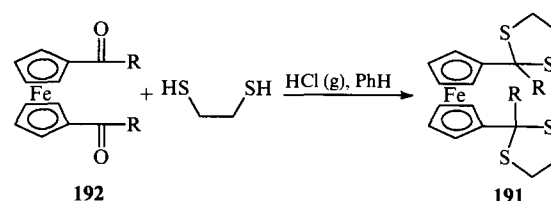


The 1,3-dithiolanes **189** have been synthesised in 51%–81% yields by the thioketalisation of the acylferrocenes **185** on treatment with the 1,2-dithiols **190** in the presence of acid catalysts.¹¹⁵



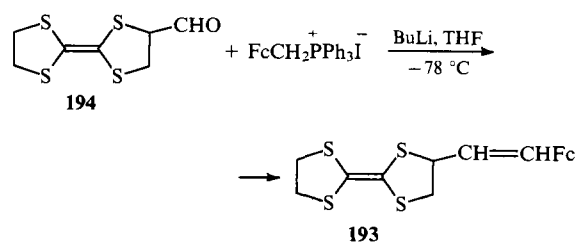
R = H, Me, Ph.

More severe conditions are required for the synthesis of the bistioketals **191** from 1,1'-diacylferrocenes **192**, the product yields being 29%–31%.

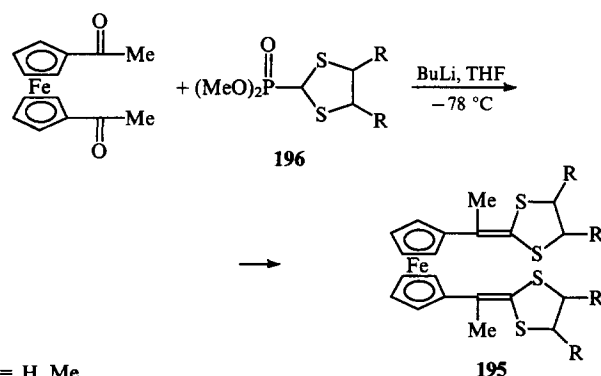


R = Me, Ph.

The vinylferrocene derivative **193** has been synthesised by the Wittig reaction from the aldehyde **194** and ferrocenylmethyl-(triphenyl)phosphonium iodide in 58% yield.¹²³

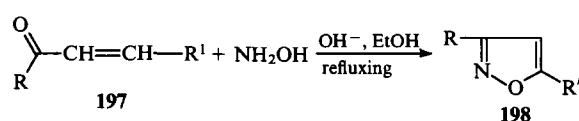


Compounds **195** have been obtained from 1,1'-diacetylferrocene and the reagents **196** by the Horner-Emmons method in 60%–70% yields.¹²³



R = H, Me.

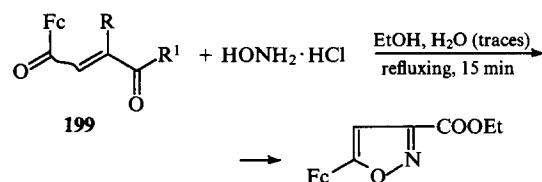
On heating the unsaturated ketones **197** with hydroxylamine in the presence of alkali, the adduct was unexpectedly readily aromatised, the isoxazoles **198** being obtained instead of the isoxazolines.¹²⁴



R = Fc; R¹ = Fc, Ph, , R = *p*-FC₆H₄, R¹ = Fc.

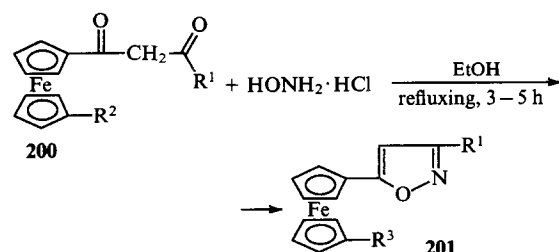
5-Ferrocenylisoxazole has been synthesised in 25% yield by heating the aldehyde **61** with the hydrochloride of hydroxylamine in methanol. On treatment with hydroxylamine in the presence of sodium ethoxide, the nitrile **62** affords a 56% yield of 3-amino-5-ferrocenylisoxazole.⁵⁴

The ethyl ester of 5-ferrocenylisoxazole-3-carboxylic acid is formed in 61%–86% yield in the reaction of 3-ferrocenylacrylic acid derivatives **199** with hydroxylamine hydrochloride.⁵⁹



R = NH₂, R¹ = OEt; R = OH, R¹ = OH.

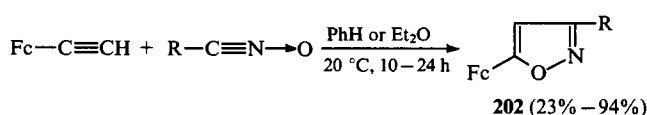
The ferrocene derivatives **201**, containing isoxazole fragments in one or both cyclopentadienyl rings, have been obtained in 47%–81% yield by the cyclocondensation of the diketone-derivatives **200** on refluxing with HONH₂·HCl in alcohol.^{55,58} For R¹ = Me in the initial diketone-derivative **200**, the reaction is carried out in the presence of pyridine.



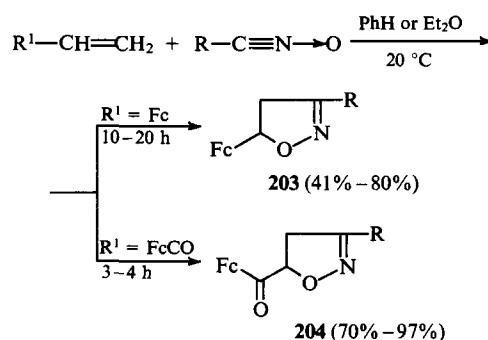
R ¹	R ²	R ³
Me	H	H
Me		
COOEt		

3-(10-Phenothiazinyl)-5-ferrocenylisoxazoline has been synthesised in 40% yield by refluxing a mixture of 10-(3-ferrocenyl-1-oxoprop-2-en-1-yl)phenothiazine with hydroxylamine in ethanol for 6 h.⁶⁶

The 1,3-dipolar addition of the *N*-oxides of carboxylic acid nitriles to unsaturated ferrocene derivatives is a convenient method of synthesis of 5-ferrocenylisoxazole and 5-ferrocenylisoxazoline derivatives. Ferrocenylethyne, vinylferrocene, and ferrocenyl vinyl ketone have been used as the dipolarophiles. Their cycloaddition to the *N*-oxides of aliphatic and aromatic acid nitriles led to the series of derivatives **202**–**204**.¹²⁵

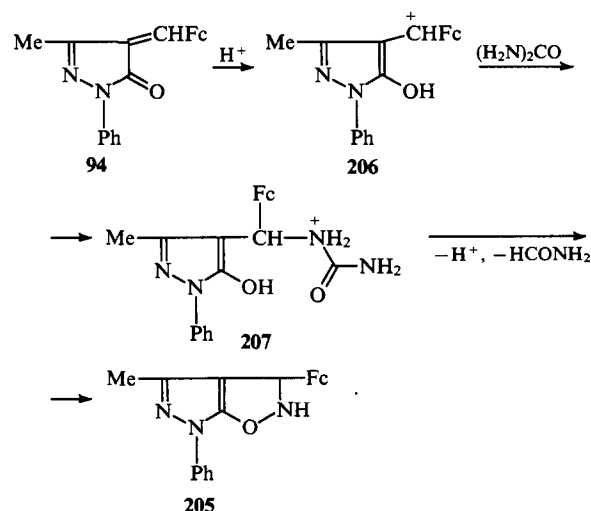


R = Me, Et, COMe, COOEt, Ph, 3-O₂NC₆H₄, 4-O₂NC₆H₄.

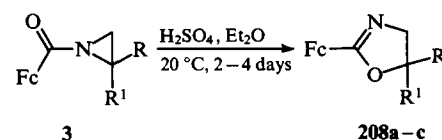


R = Me, Et, COMe, COOEt, Ph, 3-O₂NC₆H₄, 4-O₂NC₆H₄.

Compound **205** with two condensed heterocyclic rings is formed in 60% yield as a result of the interaction of the pyrazolone derivative **94** (R = Me, R¹ = Ph) with urea in boiling acetic acid.⁶⁹ The following reaction mechanism has been proposed:



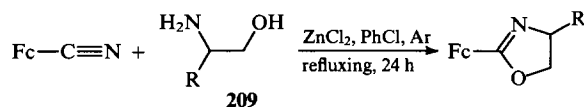
Treatment of 1-ferrocenylaziridines **3** with sulfuric acid in the dark leads to the expansion of the ring and the formation of the oxazoline derivatives **208** (yields 24%–58%).⁷



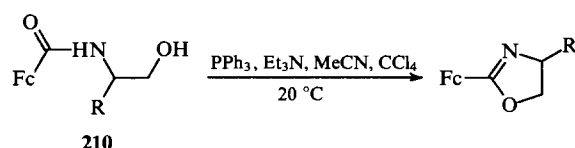
R = R¹ = H (a); R = H, R¹ = Me (b); R = R¹ = Me (c).

A further two methods of synthesis of the oxazolines **208** have been patented: by the reaction of FeCN with 1-aminopropan-2-ol (compound **208b** is obtained) or by the reaction of FeCOCl with 2,2-dimethylaziridine (compound **208c** is obtained).¹²⁶

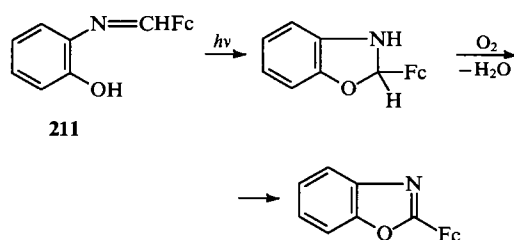
A method has been proposed recently for the synthesis of 4-substituted 2-ferrocenyloxazolines from cyanoferrocene and the aminoalcohols **209** in the presence of zinc chloride (yields 15%–38%).¹²⁷ Best results are achieved when the β -hydroxyamides **210** are cyclised on treatment with triphenylphosphine (yield 77%–92%).¹²⁸



R = Me, Prⁱ, Buⁱ, Bu^t, Ph, PhCH₂.

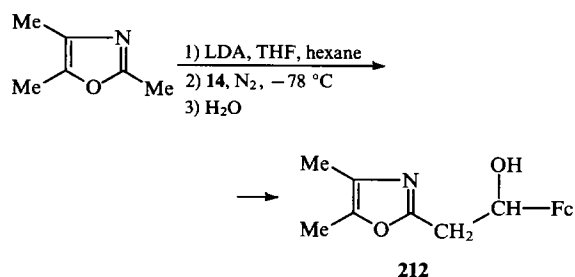

$$R = H, Pr^i.$$

Cyclocondensation of the hydrochloride of the methyl iminoester of ferrocenecarboxylic acid with *o*-aminophenol in boiling methanol leads to 2-ferrocenylbenzoxazole in 84% yield.⁷⁹ The latter has also been obtained in 70% yield by irradiating the imine **211** with light of 348 nm wavelength in boiling toluene for 10 s.¹²⁹ The unstable 2-ferrocenylbenzoxazoline, which is rapidly oxidised, is formed as an intermediate.

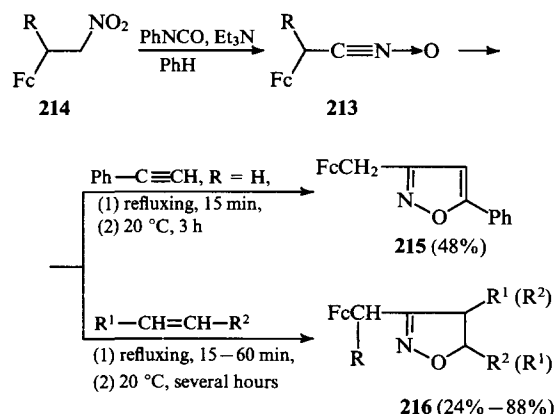


An alternative route to 2-ferrocenylbenzoxazole involves the treatment of the imine **211** with lead tetraacetate in glacial acetic acid.¹²⁹

The lithium derivative, formed on deprotonation of 2,4,5-trimethyloxazole by treatment with lithium diisopropylamide (LDA), reacts with FcCHO **14**, affording (after hydrolytic treatment) the alcohol **212** (yield 57%).¹³⁰

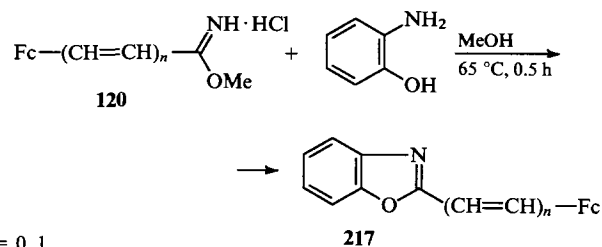


The *N*-oxides of the carboxylic acid nitriles **213**, generated by the dehydration of the primary nitro-compounds **214** by phenyl isocyanate in the presence of triethylamine, were made to undergo the 1,3-dipolar cycloaddition to phenylethyne or alkenes.^{131, 132} This resulted in the synthesis of 3-ferrocenylmethyl-5-phenylisoxazole **215** or of the isoxazoline derivatives **216**.



R	R ¹	R ²
H	H	CN
H	H	Ph
H	H	n-C ₅ H ₁₁
H	H	cyclo-C ₆ H ₁₁
H	H	SiMe ₃
H	H	OAc
H	H	CH ₂ OCO(CF ₂) ₂ CF ₃
H	H	COOCH ₂ (CF ₂) ₅ CF ₃
Me	H	CN
Me	H	OAc
OEt	COOMe	<i>trans</i> -COOMe
Ph	COOMe	<i>trans</i> -COOMe
OMe	COOMe	<i>trans</i> -COOMe

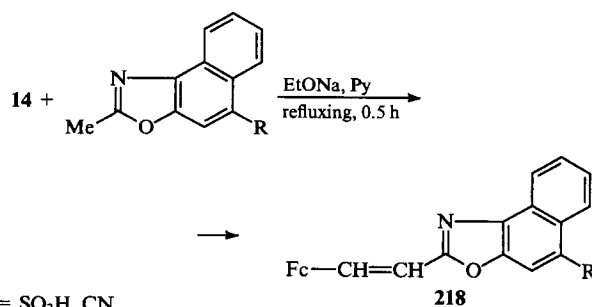
Interaction of the hydrochlorides of the iminoesters **120** with *o*-aminophenol results in the formation of the benzoxazole derivatives **217** in 84%–100% yields.^{82,133}

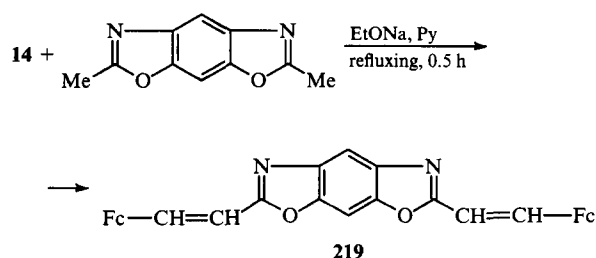

$$n = 0, 1.$$

It has been found that the cyclocondensation does not affect the configuration of the double bond.⁸¹ The individual *cis*- and *trans*-iminoesters **120** ($n = 1$) afforded the corresponding diastereoisomers **217** in 90%–93% yields.

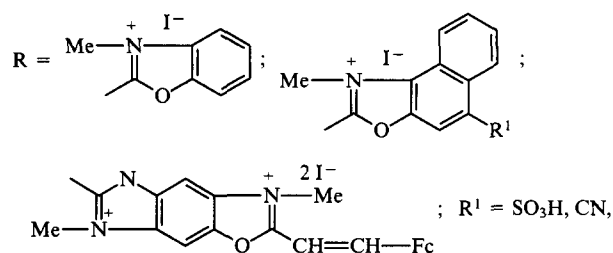
Compound **217** ($n = 1$) has been synthesised by condensing the aldehyde **14** with 2-methylbenzoxazole in the presence of bases (MeONa, NaNH₂).^{83, 84, 133} If the substrate is 2,3-dimethylbenzoxazolium iodide, the condensation product is the corresponding salt of the *N*-methyl derivative **217**.

A condensation of the same type has been used to synthesise the more complex ferrocene-containing benzoxazoles **218** and **219** (yields 75%–80%).⁸⁴


$$R = \text{SO}_3\text{H}, \text{CN}$$

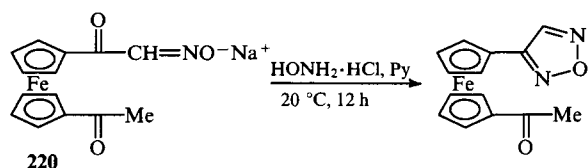


Ferrocene-containing cyanines having the general formula $\text{FcCH}=\text{CHR}$ have been synthesised from the aldehyde **14** and the methiodides of 2-methylbenzoxazole and its derivatives.⁸⁴ The compounds with

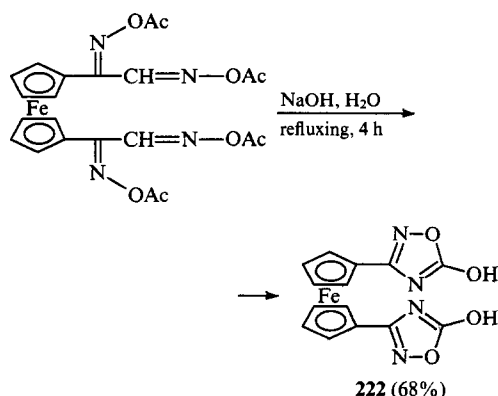
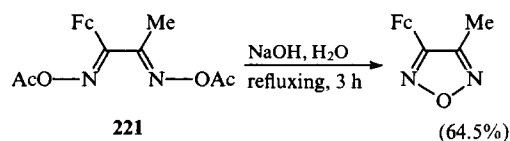


have been described.

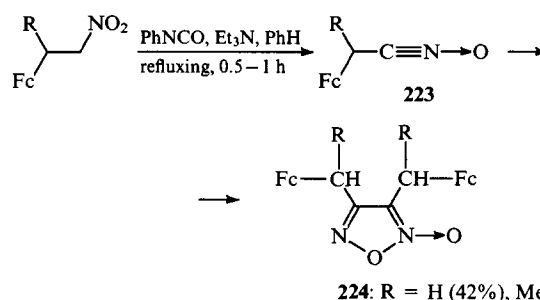
The condensation of the salt **220** with hydroxylamine results in the formation of 1-acetyl-1'-(1,2,5-oxadiazol-4-yl)ferrocene in 73% yield.¹³⁴



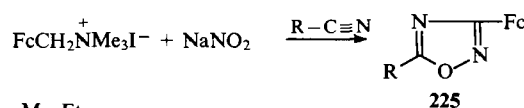
Refluxing of the diacetate of 1-ferrocenyl-2-methylglyoxime **221** in aqueous alkali leads to 5-ferrocenyl-4-methyl-1,2,5-oxadiazole.¹³⁵ On the other hand, when there is a hydrogen atom attached to the carbonyl carbon atom in the glyoxime derivative, the 1,2,4-oxadiazole derivative **222** is formed under the same conditions.



The *N*-oxides of the nitriles **223**, generated from primary nitro-compounds on treatment with phenyl isocyanate in the presence of triethylamine, dimerise in the absence of dipolarophiles and are converted into the furoxanes **224**.^{131, 132}

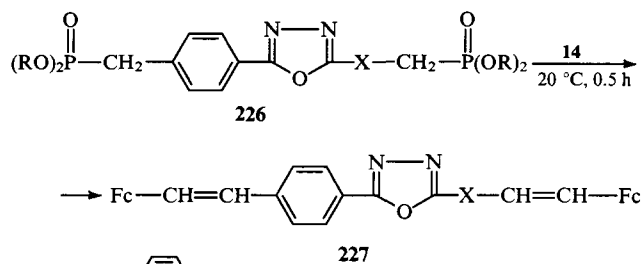


The 1,2,4-oxadiazole derivatives **225** have been obtained¹³⁶ by the reaction of ferrocenylmethyl(trimethyl)ammonium iodide with sodium nitrite in acetonitrile or propionitrile.



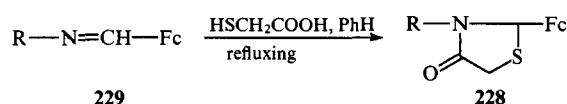
Apparently the *N*-oxide of the nitrile $\text{FcC}\equiv\text{N} \rightarrow \text{O}$ is formed as an intermediate, undergoing subsequently the 1,3-dipolar cycloaddition reaction with the nitrile group.

The phosphonic acid derivatives **226**, containing the 1,3,4-oxadiazole ring, react under very mild conditions with the aldehyde **14** to form compounds **227**.¹³⁷



5-Ferrocenylisothiazole has been synthesised from the aldehyde **61** on treatment with ammonium thiocyanate (refluxing in acetone for 20 min; yield 42%).⁵⁴

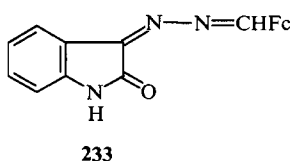
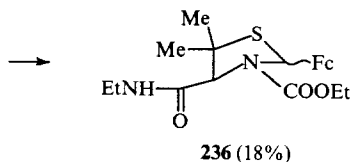
The cyclocondensation of the imines **229** with thioglycolic acid is frequently used to synthesise 2-ferrocenylthiazolin-4-one **228**.^{16, 18-20}



R	Yield (%)	Ref.
	14	16
	54	18
	100	18
	—	20
	—	19

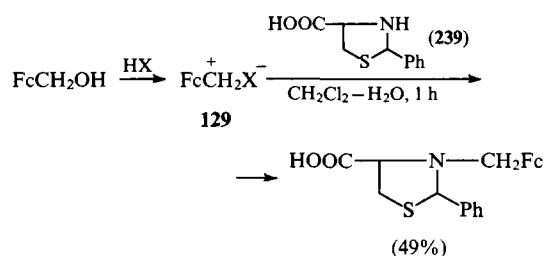
$$\text{RNH}-\text{N}=\text{CH}-\text{Fc} \xrightarrow[\text{refluxing}]{\text{HSCH}_2\text{COOH, PhH}} \text{RNH}-\text{N}(\text{C}_4\text{H}_4\text{S})-\text{Fc}$$

231 230

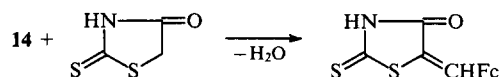
c1ccc2c(c1)sc3ccccc23C(=O)C
$$\text{RCH}=\text{N}-\text{N}=\text{CHFc} \xrightarrow[\text{refluxing}]{2\text{HSCH}_2\text{COOH, PhH}} \text{Product } 234$$

$$\text{FcCHO} + \text{BrCMe}_2\text{CHO} + \text{NH}_3 + \text{CO}_2 + \text{NaSH} + \text{EtNC} \xrightarrow{\text{EtOH}}$$

$$\text{Fc-X-COOH} + \text{2-aminobenzenethiol} \longrightarrow \text{Fc-X-2-((1H-benzotriazol-2-yl)thio)phenyl}$$

238 237

2-Phenylthiazolidine-4-carboxylic acid **239** is alkylated at the N atom of the heterocycle on treatment with ferrocenylmethyl perchlorate or tetrafluoroborate **129**, which are generated from ferrocenylmethanol under phase-transfer conditions.^{41,44}

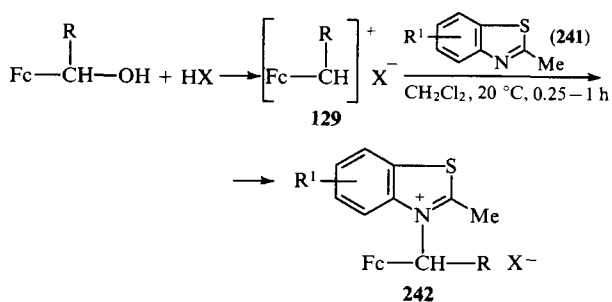


The condensation of the aldehyde **14** with rhodanine yields 5-ferrocenylmethylidene-4-oxo-2-thionothiazolidine.¹⁴²

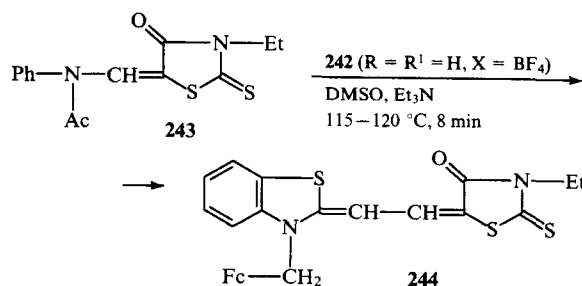

$$\text{Fc}-\overset{\text{R}}{\underset{|}{\text{CH}}}-\text{OH} + \text{benzothiazole} \xrightarrow[20^\circ\text{C, 4 h}]{\text{KU-2, CH}_2\text{Cl}_2} \text{benzothiazole-2-yl}-\overset{\text{R}}{\underset{|}{\text{CH}}}-\text{Fc}$$

240

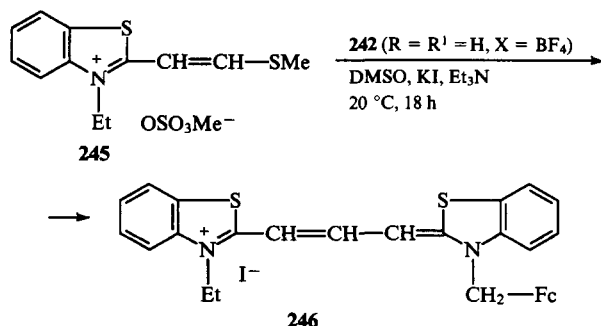
When the α -carbonium ion salts **129** were allowed to react with the 2-methylbenzothiazole derivatives **241**, the nitrogen atom of the heterocycles was alkylated and the corresponding salts **242** were formed in 77%–100% yields.^{143, 144}



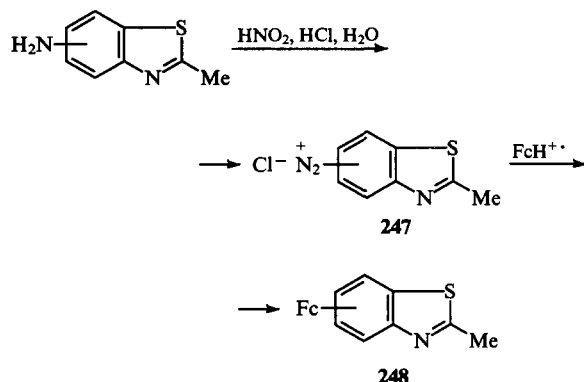
The methyl group at the C(2) atom of the heterocycle in 3-ferrocenylmethyl-2-methylbenzothiazolium tetrafluoroborate **242** (R = R¹ = H, X = BF₄) contains mobile hydrogen atoms and is able to condense with 5-acetylphenylaminomethylene-3-ethylrhodanine **243** to form dimethinemerocyanine **244** (yield 39%).⁴²



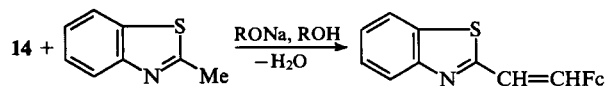
The carbocyanine **246** has been obtained in 64% yield by treating 3-ethyl-2-(2-methylthiovinyl)benzothiazolium methanesulfate **245** with the reagent **242** ($R = R^1 = H$, $X = BF_4$).⁴²



Compounds **248** have been synthesised (yields 7%–9%) by the reaction of the ferrocenium cation, formed when ferrocene is treated with concentrated sulfuric acid, and 5- and 6-diazo-2-methylbenzothiazolium chloride **247**.⁴⁹



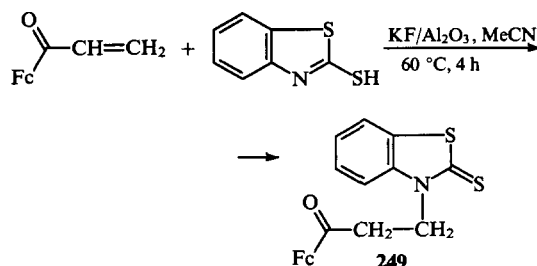
It has been shown^{83,84} that in the presence of bases 2-methylbenzothiazole condenses with $FcCHO$ **14** to form 2-(2-ferrocenylvinyl)benzothiazole.



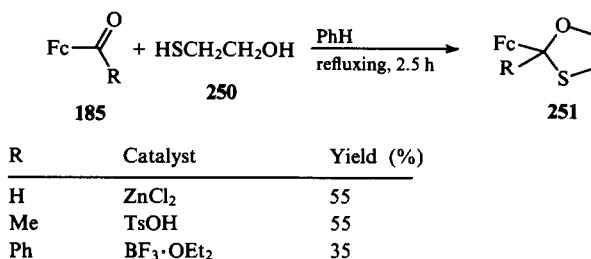
Solvent	Reaction time/h	Yield (%)	Ref.
MeOH	0.5	65	83
EtOH	12	65	84
EtOH, Py	0.5	97	83, 84

2,3-Dimethylbenzothiazolium iodide, in which the mobility of the H atoms of the methyl group at the C(2) atom is greater, reacts more readily with $FcCHO$ ⁸³ and 2-(2-ferrocenylvinyl)-3-methylbenzothiazolium iodide is formed in a virtually quantitative yield in the presence of piperidine.

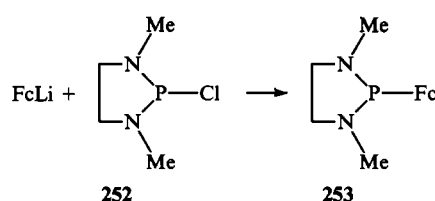
Ferrocenyl vinyl ketone is a Michael acceptor in relation to 2-mercaptobenzothiazole.⁸⁵ When the radiation is carried out on aluminium oxide, a 96% yield of the adduct **249** is attained.



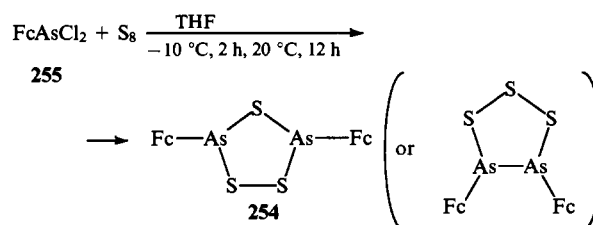
The acylferrocenes **185** react with 2-mercaptoethanol **250** to form the 1,3-oxathiolane derivatives **251**. It has been established¹¹⁵ that, depending on the nature of R, various catalysts are required for the successful synthesis.



On treatment with ferrocenyllithium, the chlorine atom in compound **252** is substituted by the ferrocenyl group, whereupon 1-ferrocenyl-2,5-dimethyl-1,2,5-diazaphospholane **253** is formed.¹⁴⁵

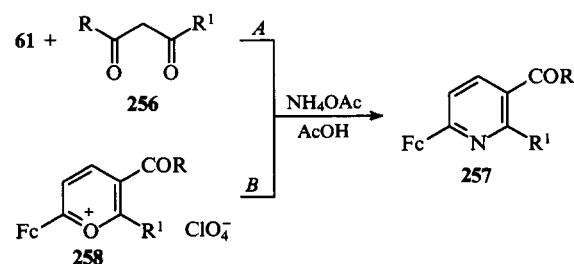


Compound **254** has been obtained in 49% yield as a result of the reaction of dichloro(ferrocenyl)arsine **255** with sulfur in the presence of 2,4,6-tris(*tert*-butyl)phenylphosphine and diazabicycloundecene.¹⁵



V. Compounds containing six-membered heterocycles

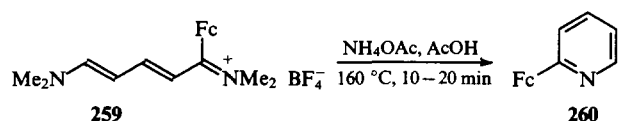
Condensation of the aldehyde **61** with the β -dicarbonyl compound **256** in the presence of ammonium acetate leads to the 3-acyl-6-ferrocenylpyridine derivatives **257**.¹⁴⁶ The same result has been achieved by treating the pyrilium salts **258** with ammonium acetate.¹⁴⁷



R	R ¹	Yield (%)	
		A	B
Ph	Ph	34	25
Me	Me	27	10
Me	EtO	43	
EtO	Me		43
—CH ₂ —CMe ₂ —CH ₂ —		45	21

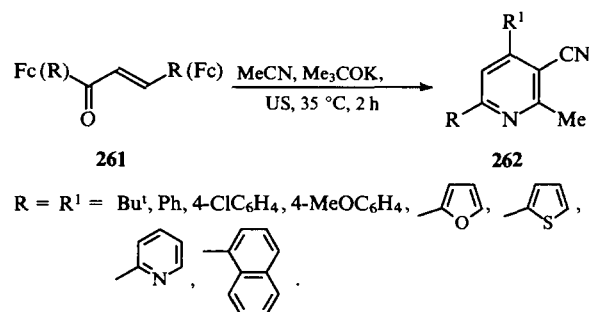
4-Ferrocenyl-2,6-dimethylpyridine is formed in 63% yield on treatment of 4-ferrocenyl-2,6-dimethylpyrylium perchlorate with aqueous ammonia.¹⁴⁸ A similar transformation of 6-ferrocenyl-2,4-diphenylpyrylium perchlorate into 6-ferrocenyl-2,4-diphenylpyridine requires more severe conditions: refluxing with an alcoholic solution of ammonia for 10 min (yield 45%–51%)¹⁴⁹ or heating with an alcoholic solution of ammonia in a sealed tube at 100 °C for 7 h (yield 27%).¹⁵⁰

When the salt **259** was heated with ammonium acetate in aqueous acetic acid, 2-ferrocenylpyridine **260** was obtained in 57% yield.¹⁵¹

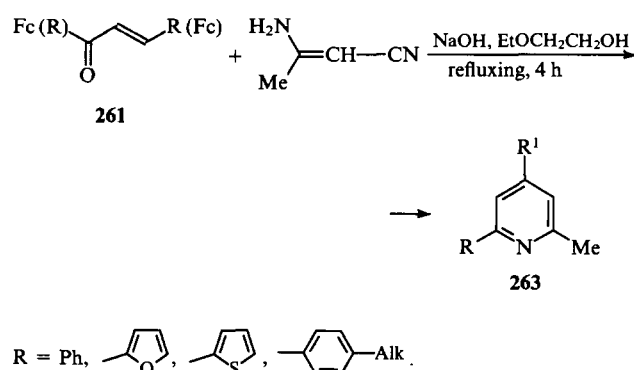


3,5-Dicyano-4-ferrocenyl-2,6-dimethyl-1,4-dihydropyridine, formed as a result of the condensation of FcCHO with diacetonitrile (refluxing for 1 h in acetic acid under a nitrogen atmosphere), is converted into 3,5-dicyano-4-ferrocenyl-2,6-dimethylpyridine on oxidation with chloranil.¹⁵²

The accelerating effect of ultrasound on chemical reactions has been demonstrated by Japanese investigators.¹⁵³ They showed that the sonolysis of unsaturated ferrocenyl-substituted ketones **261** in acetonitrile at 35 °C for 2 h leads to the pyridine derivatives **262** in 60%–85% yields. The authors¹⁵³ believe that diacetonitrile, generated from acetonitrile under the reaction conditions, participates in the formation of the pyridines.

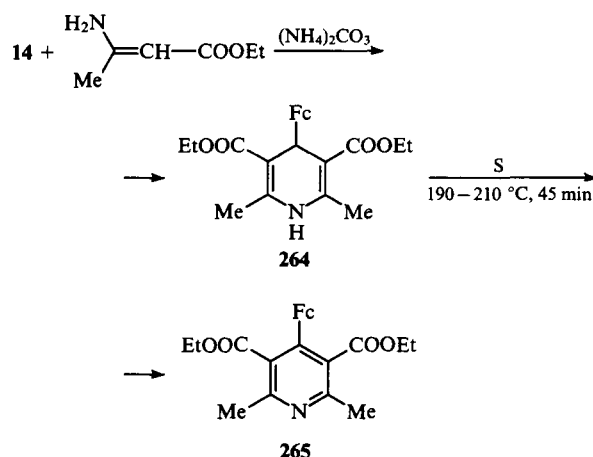


In the presence of bases, the unsaturated ketones **261** react with 3-aminocrotonitrile. If the reaction is carried out in 2-ethoxyethanol,¹⁵⁴ then the products are the substituted pyridines **263**.

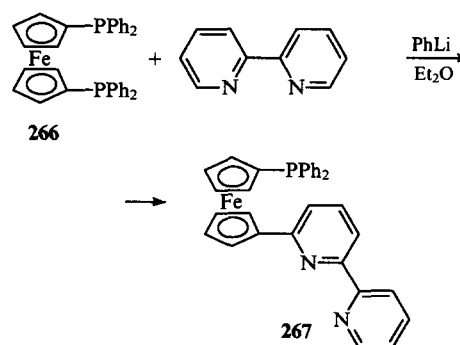


When the condensation is carried out in butanol with subsequent heating of the reaction products with water, substituted nicotinamides are obtained.¹⁵⁴

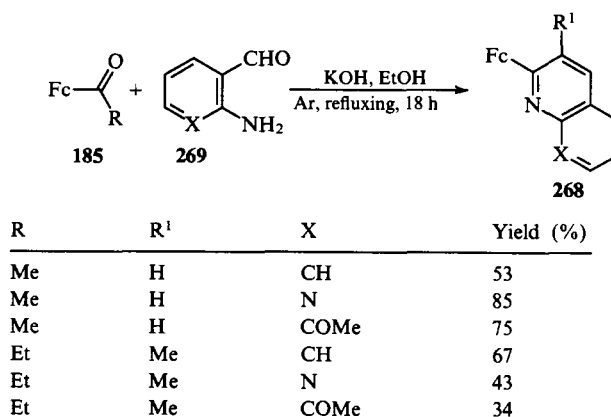
The condensation of the aldehyde **14** with ethyl 3-amino-crotonate in the presence of ammonium carbonate leads to the 1,4-dihydropyridine derivative **264**, which is oxidised by sulfur and is converted into 3,5-bis(ethoxycarbonyl)-4-ferrocenyl-2,6-dimethylpyridine **265**.¹⁵⁵



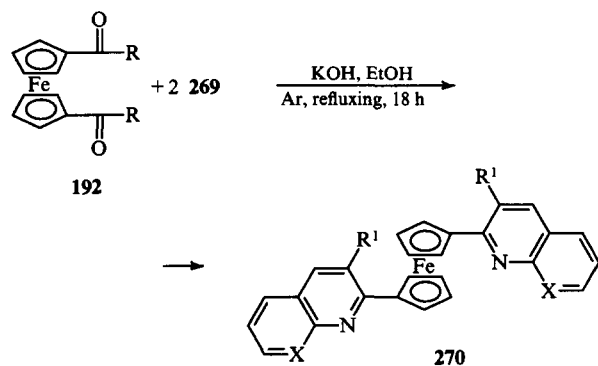
In the diphosphine **266**, one of the PPh_2 groups is substituted by the 2,2'-bipyridyl group on treatment with the lithium derivative formed from 2,2'-bipyridyl and phenyllithium.¹⁵⁶



A series of quinoline and naphthyridine derivatives **268**, containing the ferrocenyl group, have been synthesised by the Friedlaender reaction from acylferrocenes **185** and the aminoaldehydes **269**.¹⁵⁷

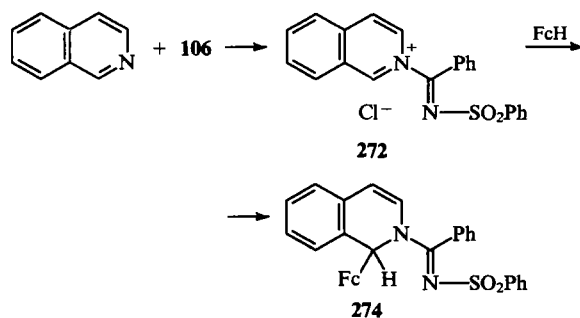
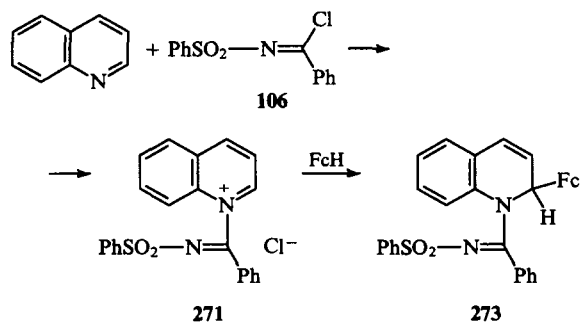


Compounds **270** are obtained under similar conditions from the 1,1'-diacylferrocenes **192** and 2 mol of the aminoaldehydes **269**.



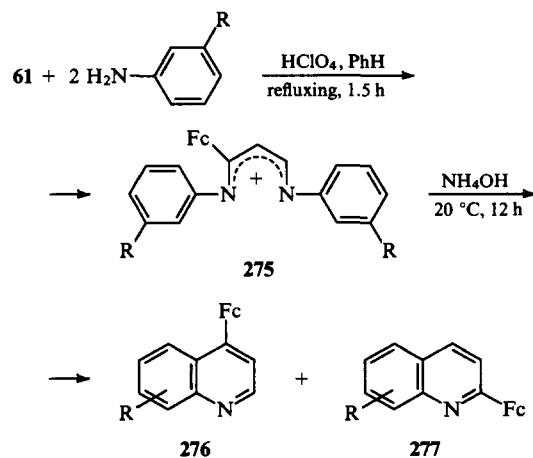
R	R ¹	X	Yield (%)
Me	H	CH	75
Me	H	N	75
Me	H	COMe	62
Et	Me	CH	26
Et	Me	N	40
Et	Me	COMe	24

Benzenesulfonylbenzimidoyl chloride **106** adds to quinoline or isoquinoline with formation of the salts **271** or **272**, which alkylate ferrocene (refluxing in benzene for 2.5 h), affording compounds **273** or **274** in 42% or 51% yields respectively.⁷³

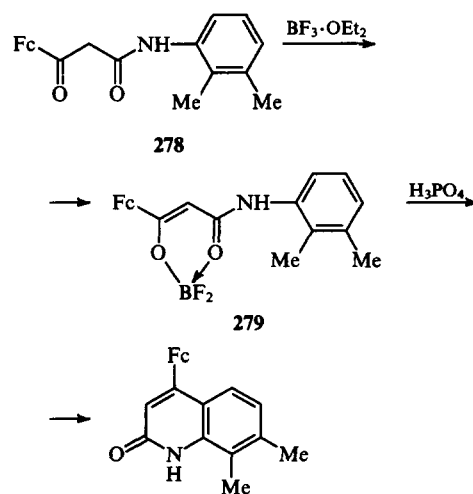


The aldehyde **61** reacts with two molecules of 3-hydroxy- or 3-methoxyaniline with formation of the salts **275**, the subsequent treatment of which with aqueous ammonia leads to cyclisation to the quinoline derivatives **276** and **277**.¹⁴⁶ ¹H NMR data revealed the regioselectivity of the cyclisation in favour of compound **277**. In the case of unsubstituted aniline, the reaction stops at the stage involving the formation of the salt **275** (R = H).

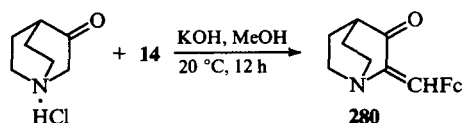
On treatment with boron trifluoride etherate, the amide **278** gives rise to the chelate **279**, which cyclises on heating with orthophosphoric acid and is converted into 4-ferrocenyl-7,8-dimethyl-2-quinolone.¹⁵⁸



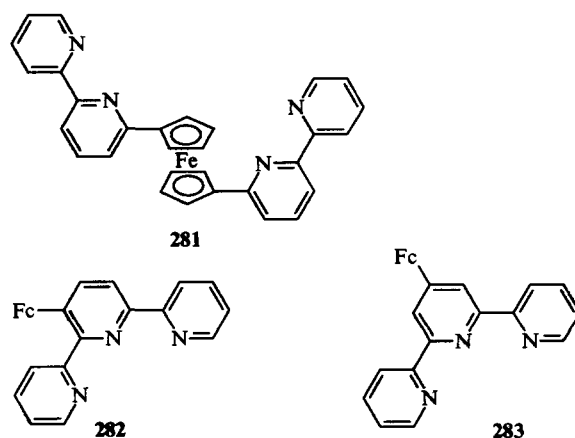
R = OH (15%), OMe (44%).



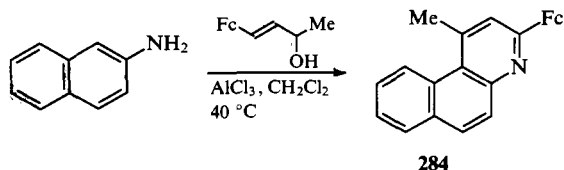
In the presence of alkali, the aldehyde **14** condenses with the hydrochloride of quinuclidin-3-one, which affords 2-ferrocenyl-methylidenequinuclidin-3-one **280**.¹⁵⁹



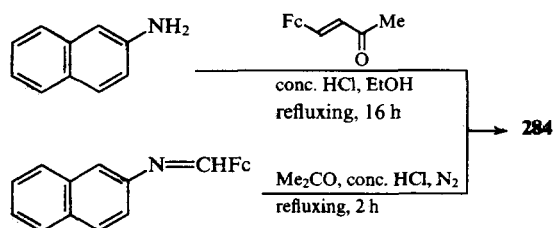
Methods for the synthesis of a series of ferrocene-containing derivatives of bipyridyl (compounds **281**) and terpyridyl (compounds **282** and **283**) have been developed based on the carbonyl derivatives of ferrocene.¹⁶⁰⁻¹⁶²



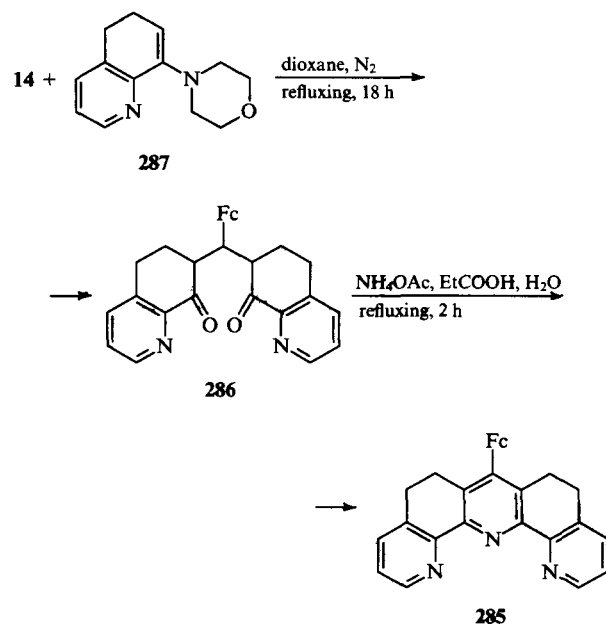
The method of synthesis of 2-ferrocenyl-4-methyl-5,6-benzoquinoline **284**, proposed in a patent,¹⁶³ involves the condensation of 4-ferrocenylbut-3-en-1-ol with β -naphthylamine in the presence of aluminium chloride.



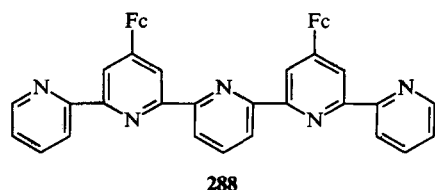
Two other methods of synthesis of compound **284** are based on the acid-catalysed condensation of carbonyl compounds with β -naphthylamine or *N*-ferrocenylmethylidene- β -naphthylamine.¹⁶⁴



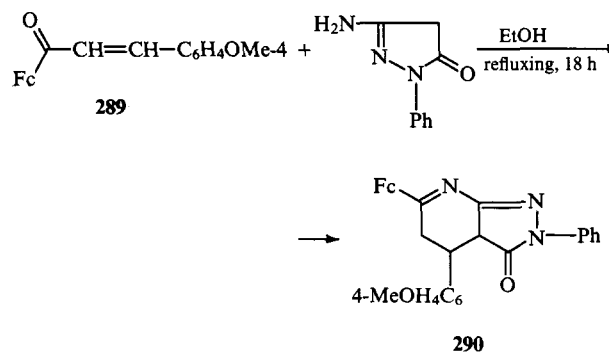
Compound **285**, in which condensed pyridine and cyclohexadienyl rings alternate, has been synthesised in 26% yield by treating with ammonium acetate the product **286** formed when the aldehyde **14** reacts with the enamine **287**.¹⁶⁵



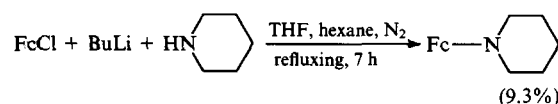
Compound **288**, containing two ferrocenyl groups and five pyridine rings, has been obtained by a two-stage synthesis from the aldehyde **14** and 2,6-diacetylpyridine.¹⁶⁶



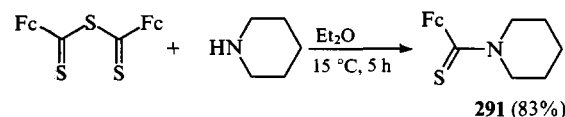
The pyridopyrazole derivative **290** is formed in 70% yield on refluxing the chalcone **289** with 3-amino-1-phenylpyrazol-5-one in ethanol.¹⁶⁷



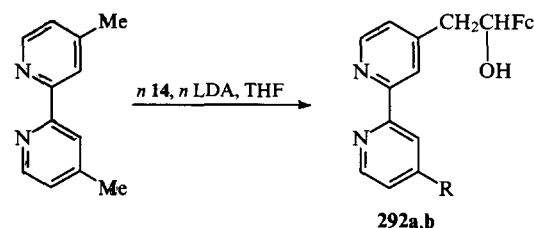
A single example of the synthesis of 1-ferrocenylpiperidine by the reaction of chloroferrocene with piperidine in the presence of butyllithium has been described.¹⁶⁸



Bis(ferrocenylcarbothionyl) sulfide thioacylates piperidine, affording *N*-(ferrocenylcarbothionyl)piperidine **291**.¹⁶⁹



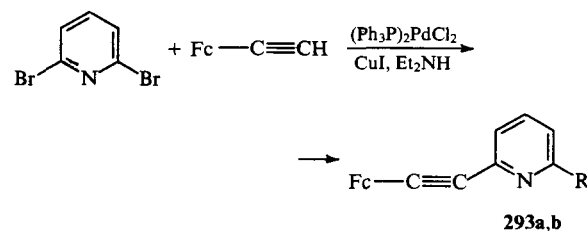
The mono- and di-lithio-derivatives of 4,4'-dimethyl-2,2'-bipyridyl, generated by treatment with LDA, add to the carbonyl group of compound **14**, which leads to the alcohol **292a** or the diol **292b**.¹⁷⁰



292a: $n = 1$, $R = \text{Me}$ (77%);

292b: $n = 2$, $R = \text{CH}_2\text{CH}(\text{OH})\text{Fc}$ (55%).

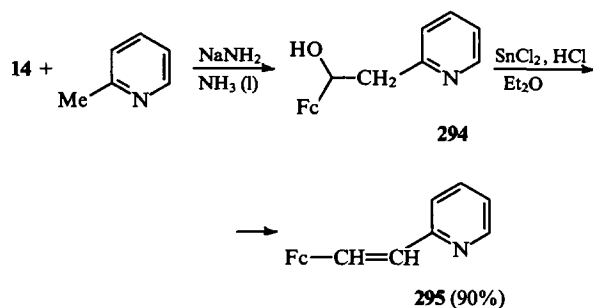
Bis(triphenylphosphine)palladium dichloride catalyses the nucleophilic substitution of the halogen atoms in 2,6-dibromopyridine on treatment with ferrocenylethyne in the presence of bases and copper(I) salts.¹⁷¹ After reaction for 1.5 h, the mono-substitution product **293a** is formed in 78% yield. When the reaction is carried out over a period of 24 h, the disubstitution product **293b** is formed in 90.4% yield.



$R = \text{Br}$ (**a**), $\text{C}\equiv\text{C}-\text{Fc}$ (**b**).

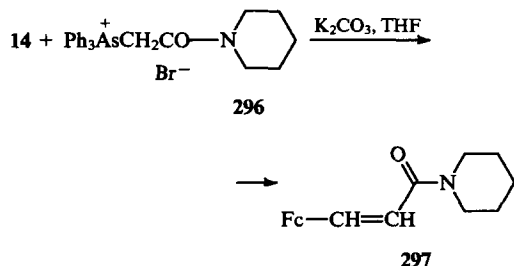
It was shown in the same investigation that both bromine atoms in 3,3'-dibromo-2,2'-bipyridyl are substituted by the FcC≡C group [the yield of 3,3'-bis(2-ferrocenylethynyl)-2,2'-bipyridyl was 89% after 48 h].

The condensation of the aldehyde **14** with 2-methylpyridine on treatment with sodium in liquid ammonia leads to the alcohol **294** in 57% yield.⁸³ It may be dehydrated to 2-(2-ferrocenylvinyl)pyridine **295** by treatment with tin(II) chloride.

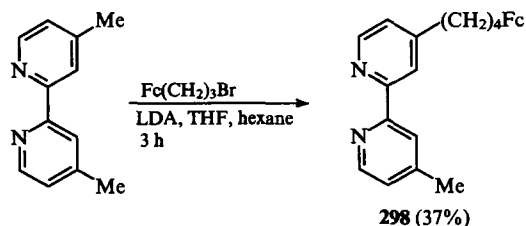


When an excess of sodium amide⁸³ or sodium alkoxide in pyridine⁸⁴ is used, the alkene **295** is formed in 51% yield. 2-(2-Ferrocenylvinyl)quinoline has been obtained similarly (yield 94%).

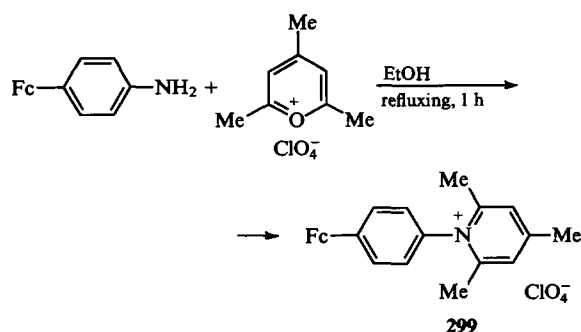
The amide **297** has been synthesised by converting the aldehyde **14** into an alkene by treatment with the arsonium salt **296** in the presence of potassium carbonate in THF containing traces of water.³⁹



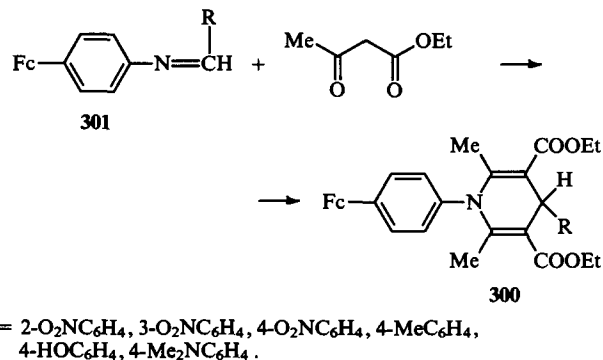
The alkylation of the lithio-derivative of 4,4'-dimethyl-2,2'-bipyridyl with 3-bromopropylferrocene affords compound **298**.¹⁷²



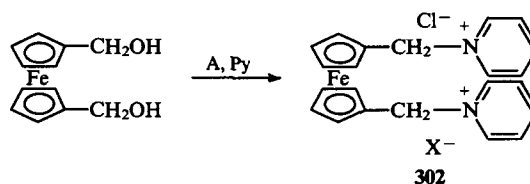
N-(4-Ferrocenylphenyl)-2,4,6-trimethylpyridinium perchlorate **299** has been obtained in 65% yield as a result of the substitution of the oxygen atom in the heterocyclic nucleus of 2,4,6-trimethylpyrylium perchlorate on treatment with *p*-ferrocenylaniline.¹⁵⁵



The 1,4-dihydropyridine derivative **300** is formed on cyclocondensation of the imines **301** with acetoacetic ester.¹⁵⁵

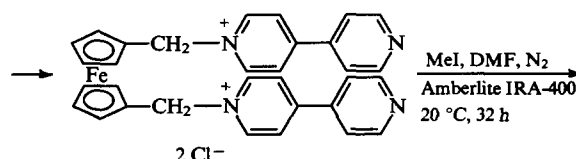
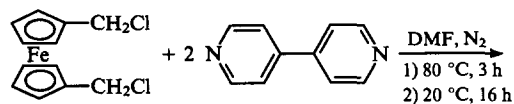
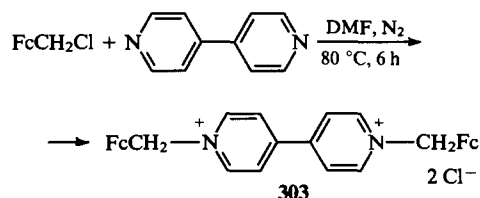


1,1'-Bis(hydroxymethyl)ferrocene is able to alkylate pyridine at the nitrogen atom on activation with toluene-*p*-sulfonyl chloride or thionyl chloride.¹⁷³ The mixed salt **302** (X = OTs) and a dichloro-derivative are formed in the first and second cases respectively.



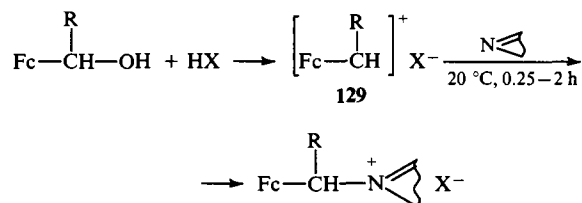
A = 4-MeC₆H₄SO₂Cl, X = OSO₂C₆H₄Me-4;
A = SOCl₂, X = Cl.

The synthesis of compounds with fragments of viologens (*N,N'*-dialkyl-4,4'-bipyridyls) linked covalently to photosensitive groups constitutes a complex task. The study¹⁷⁴ in which a method was described for the preparation of the viologen-metalloenes (ferrocenyl-containing viologens) **303** and **304**, capable of displacing hydrogen from water in the presence of catalysts, is therefore of significant interest.

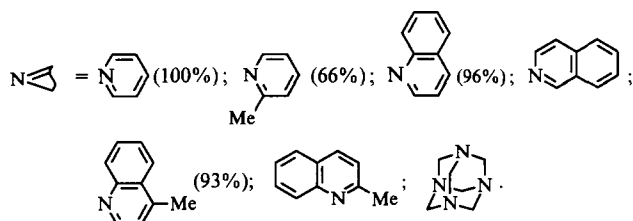


Boev and coworkers^{42,45,143,144} investigated the reactions of hydroxymethylferrocene and 1-ferrocenylethanol with six-membered nitrogen heterocycles in the presence of HBF₄ or HClO₄.

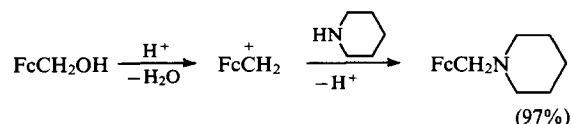
It was found that the reaction proceeds via a stage involving the formation of the salts **129**, which attack the heterocyclic nucleophiles. This is confirmed by the finding that salts of the heterocycles with HX obtained beforehand do not react under the conditions investigated with the alcohols FcCH(R)OH .¹⁴⁴



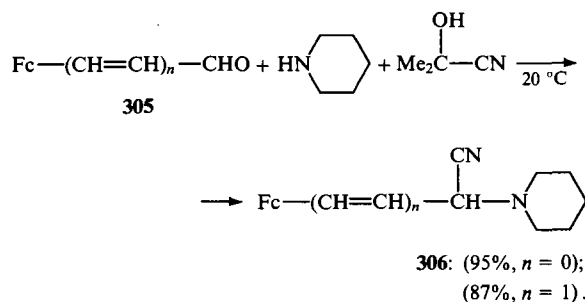
R = H, Me; X = BF_4 , ClO_4 ;



Piperidine is alkylated similarly by hydroxymethylferrocene in the presence of an acid.¹⁷⁵

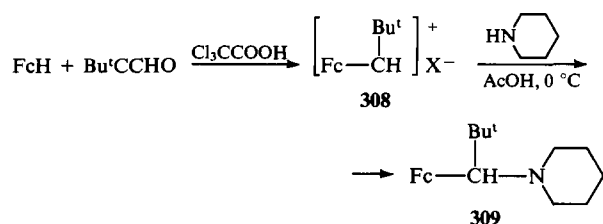


The amins formed from the aldehydes **305** and piperidine undergo transcondensation with acetone cyanohydrin, affording the aminonitriles **306**.¹⁷⁶

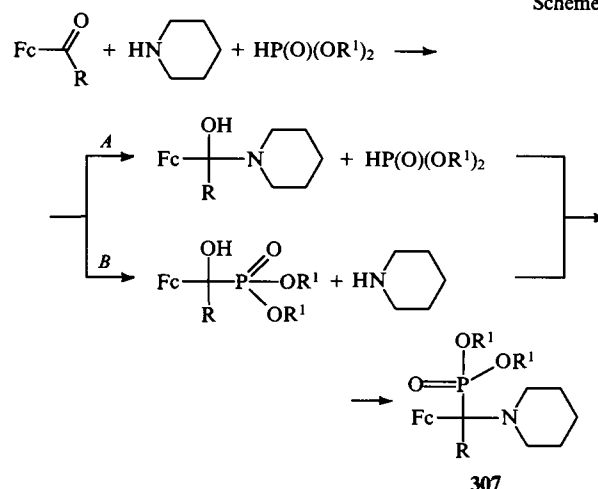


When the aldehyde **14** or the ketone **23** interacts with phosphorous acid esters and piperidine, the α -aminophosphonates **307** are formed.¹⁷⁷ Of the two possible mechanisms (*A* and *B*, Scheme 3), the first is preferable since it has been shown¹⁷⁷ that piperidine does not displace phosphorous acid esters from specially prepared α -ferrocenyl- α -hydroxyalkylphosphonates (150–160 °C, 10–12 h).

In the presence of trichloroacetic acid, electrophilic substitution in the ferrocene nucleus by treatment with



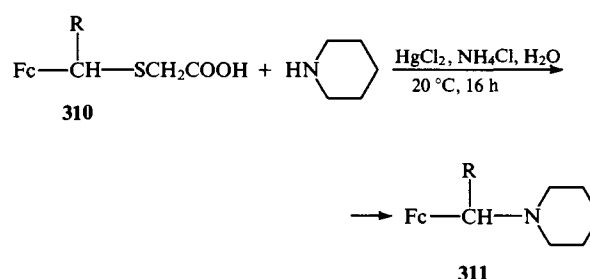
Scheme 3



R	R ¹	Yield (%)
H	Me	55
Me	Me	50
H	Et	76
Me	Et	56
H	Pr	80
Me	Pr	52
Me	Pr ⁱ	43
Me	Bu	45
Me	Bu ⁱ	45

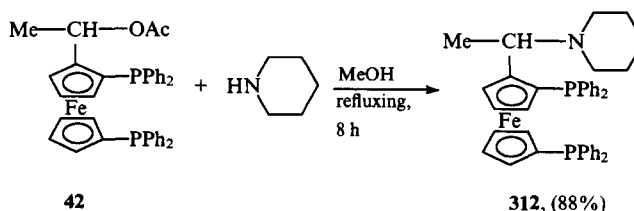
trimethylacetaldehyde and subsequent protonation and dehydration lead to the salt **308**, which is converted into *N*-(1-ferrocenyl-2,2-dimethylpropyl)piperidine **309** in 68% yield on treatment with piperidine.¹⁷⁸

The alkylation of piperidine by α -carbonium ion intermediates (generated from the sulfides **310** on treatment with mercury salts), leading to the amines **311**, takes place similarly.¹⁷⁹

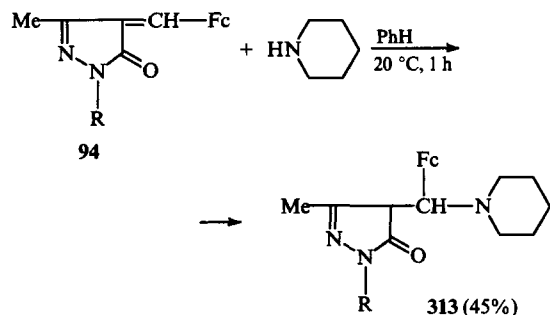


R = H (30%), Me (90%).

On refluxing in methanol, piperidine substitutes the acetoxy-group in compound **42**.³⁵

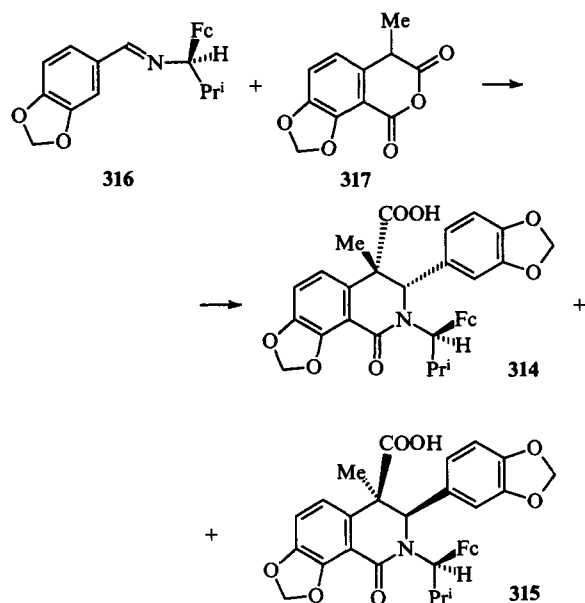


Another method for the introduction of the piperidiny group into ferrocene derivatives involves the Michael addition of piperidine to the pyrazolones **94**, which leads to compound **313**.⁶⁹

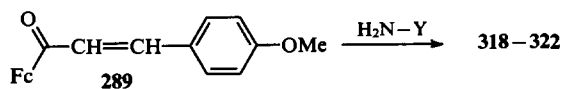


R = Ph, 2,4-(O₂N)₂C₆H₃.

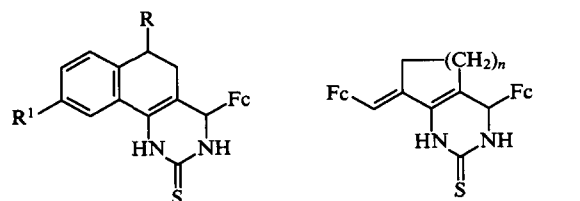
A mixture of the two isomeric tetrahydroisoquinolinone derivatives **314** and **315** has been obtained (in 10% and 81% yields respectively) by refluxing the imine **316** and compound **317** in benzene for 82 h.¹⁸⁰



Indian investigators^{167, 181} made a detailed study of the reaction of 1-ferrocenyl-2-(*p*-methoxyphenyl)ethene with primary heterocyclic amines and guanidine. The structures of the products and the yields of compounds **318**–**322** are presented in Table 2.



The derivatives of dihydropyrimidine-2-thione **323**–**326** have been synthesised by condensing α,β -unsaturated cyclic ferrocene-containing ketones with thiourea in the presence of alkali in ethanol.¹⁸²

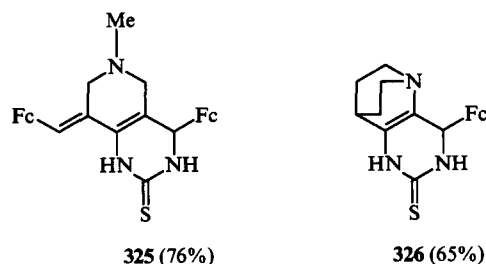


323a: R = R¹ = H (95%);
323b: R = H, R¹ = OMe (95%);
323c: R = OMe, R¹ = H (90%).
324, n = 1 (95%), 2 (75%).

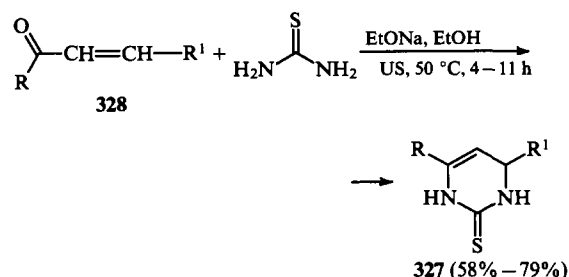
Table 2. The reactions of 1-ferrocenyl-2-(*p*-methoxyphenyl)ethene with nitrogen-containing heterocyclic compounds and guanidine.

H ₂ N–Y	Product	Yield (%)	Ref.
		50	167
		51	181
		65	167
		56	181
		75	167

Note. The reactions were carried out in boiling ethanol for 18–24 h. The group R in the reaction product is 4-MeOC₆H₄.



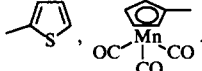
A series of similar compounds (compounds **327**) have been synthesised from the ketones **328** and thiourea with irradiation by ultrasound (US).¹⁸³



R = Fc: R¹ = Ph, 4-MeC₆H₄, 4-MeOC₆H₄, 4-ClC₆H₄,
 3,4-(OCH₂O)C₆H₃;
 R = 4-MeOC₆H₄, R¹ = Fc.

A wider range of the ketones **328** were later involved in this reaction^{184,185} and conditions were found under which the products **327** are obtained in yields from 70% to 95%. Here

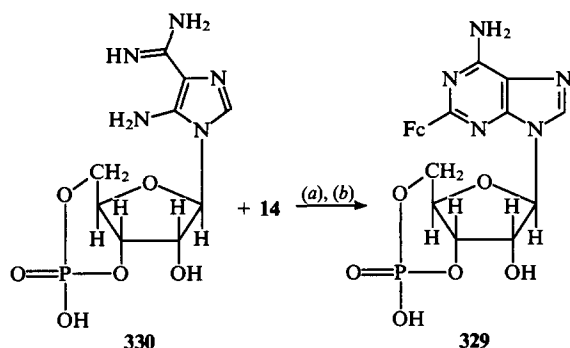
$R = \text{Fc}$, $R^1 = 4\text{-Me}_2\text{NC}_6\text{H}_4$;

$R^1 = \text{Fc}$, $R = \text{Ph}$, $4\text{-FC}_6\text{H}_4$, $4\text{-IC}_6\text{H}_4$, 

The synthesis of 5-ferrocenylmethylidenearbituric acid (yield 94%) by condensing barbituric acid with the aldehyde **14** has been patented.¹⁸⁶

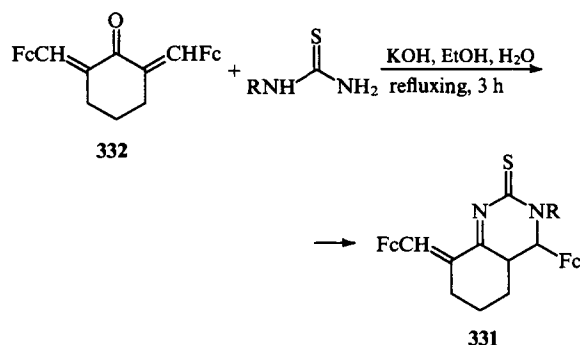
The coupling of ferrocenylethyne with 5-chloromercurio-derivatives of uracil, cytosine, and adenine, as well as the corresponding nucleosides, which leads to compounds having the general formula $\text{FcC}\equiv\text{C}-\text{R}$, where R is a group derived from a heterocyclic base or a nucleoside, has been described.¹⁸⁷

The adenosine derivative **329** has been obtained in 19% yield as a result of the condensation of the aldehyde **14** with compound **330** and subsequent aromatisation under the influence of palladium.^{188,189}



a: NaOH, MeOH, 20 °C, 3 days; b: Pd/C, EtOH, H₂O, 80 °C.

The dihydropyrimidine-2-thione derivatives **331** are formed in 58%–79% yield on interaction of the ketone **332** with thiourea or phenylthiourea.⁶²

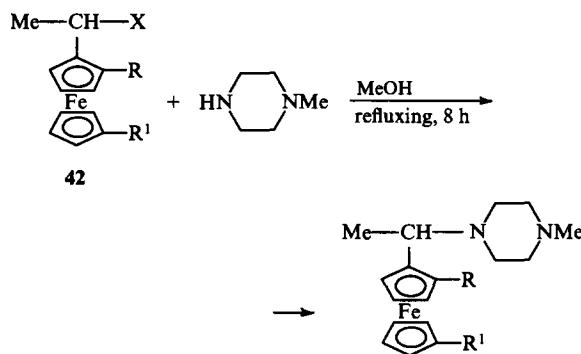


$R = \text{H}$, Ph .

High-molecular-mass compounds containing quinoxaline nuclei have been obtained by the polycondensation of 1,2,4,5-tetraaminobenzene or 3,4,3',4'-tetraaminobiphenyl with 1,1'-bis-(glyoxalyl)ferrocene.

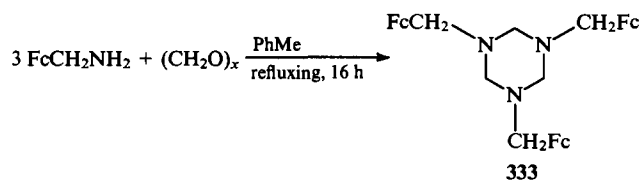
The chloride of ferrocenecarboxylic acid acylates piperazine or 1-(2-aminoethyl)piperazine (at 25 °C for 24 h) with formation of 1,4-bis(ferrocenoyl)piperazine or 1-(2-ferrocenoylaminoethyl)-4-ferrocenoylpiperazine.¹⁹⁰

Ferrocene derivatives containing piperazine fragments have been synthesised by the nucleophilic substitution of the $\text{N}^+\text{Me}_3\text{I}^-$ or OAc groups in compound **42** on treatment with N-methylpiperazine.^{35,36}

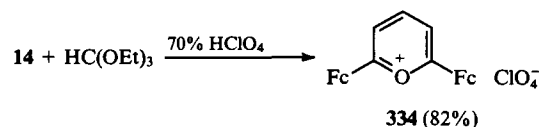


R	R ¹	X	Ref.
P(O)Ph ₂	H	$\text{N}^+\text{Me}_3\text{I}^-$	35
PPh ₂	PPh ₂	OAc	35, 36

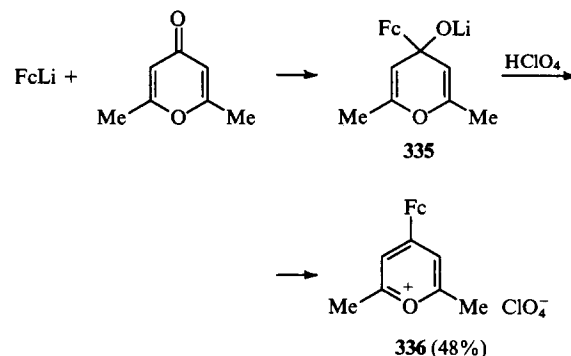
1,3,5-Tris(ferrocenylmethyl)hexahydro-1,3,5-triazine **333** has been obtained in 85% yield by the cyclocondensation of aminomethylferrocene with paraformaldehyde.¹⁹¹



Two methods of synthesis of ferrocenylpyrylium salts have been patented.¹⁴⁸ 2,6-Diferrocenylpyrylium perchlorate **334** has been synthesised by the reaction of the aldehyde **14** with orthoformic ester in the presence of perchloric acid.

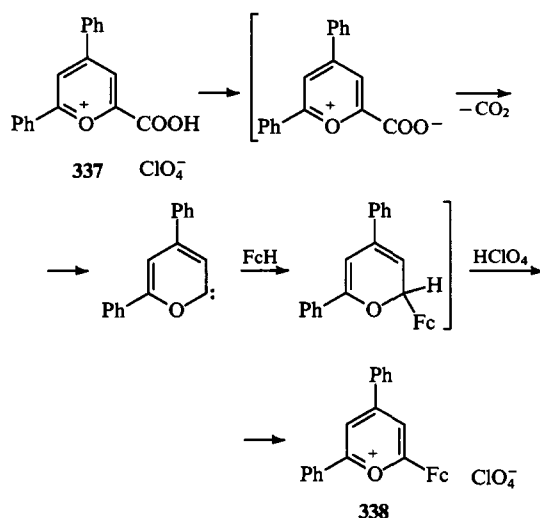


4-Ferrocenyl-2,6-dimethylpyrylium perchlorate has been synthesised by another method—treatment of the lithio-derivative **335**, obtained from 2,6-dimethyl-4-pyrone and ferrocenyllithium, with perchloric acid.

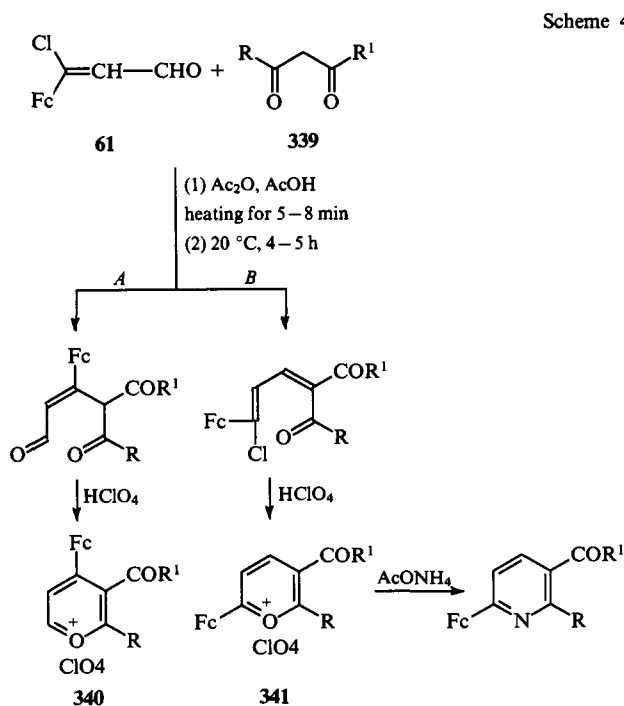


The thermal decarboxylation of the acid salt **337** in boiling acetic acid in the presence of ferrocene leads to the formation of the ferrocenylpyrylium salt **338** (yield 47%).¹⁵⁰ The authors postulate a mechanism involving the insertion of a carbene intermediate in the $\text{Fc}-\text{H}$ bond.

The salt **338** has also been obtained as a result of the interaction of acetylferrocene with the chalcone $\text{PhCH}=\text{CH}-\text{COPh}$ in the presence of perchloric acid.¹⁵⁰

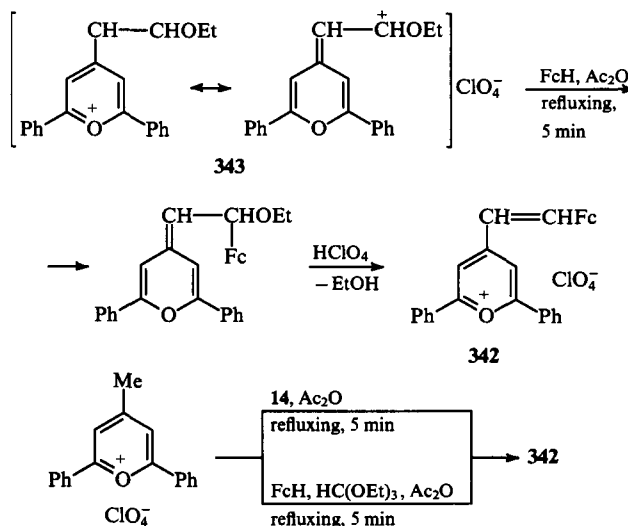


The interaction of the aldehyde **61** with the β -dicarbonyl compounds **339** on treatment with acetic anhydride in acetic acid can lead to various intermediates, which should be converted into the pyrylium salts **340** or **341** on treatment with perchloric acid (Scheme 4). It was found that treatment of the primary reaction product with ammonium acetate affords 3-acyl-6-ferrocenylpyrylium derivatives, which may be formed only from the salts **341**, demonstrating that the reaction proceeds via route *B*.¹⁴⁷



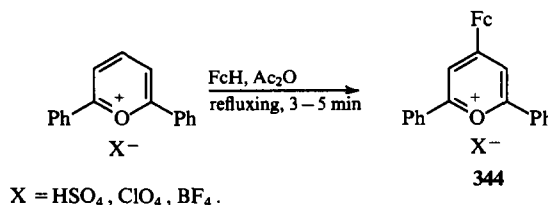
R	R ¹	Yield (%)
Ph	Ph	100
Me	Me	100
Me	OEt	68
-CH ₂ -CMe ₂ -CH ₂ -		72

4-(2-Ferrocenylvinyl)-2,6-diphenylpyrylium **342** has been synthesised by three procedures:¹⁴⁹ by the reaction of the salt **343** with ferrocene (yield 55%), by the condensation of 4-methyl-2,6-diphenylpyrylium perchlorate with the aldehyde **14** (yield 88%), or by the condensation with ferrocene and orthoformic acid ester (yield 46%).

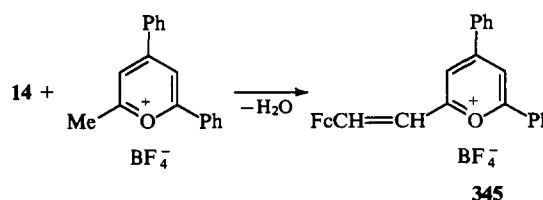


4-(2-Ferrocenylvinyl)-2,6-dimethylpyrylium perchlorate has been obtained by the last method from 2,4,6-trimethylpyrylium perchlorate (in 52% yield).¹⁴⁹

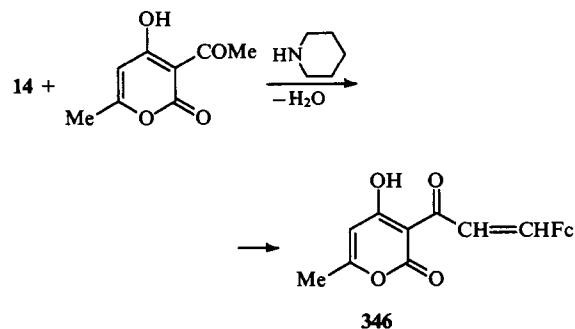
The 4-ferrocenylpyrylium salts **344** are formed in 81%–82% yields on refluxing the corresponding 2,6-diphenylpyrylium salts with ferrocene in acetic anhydride.¹⁴⁹



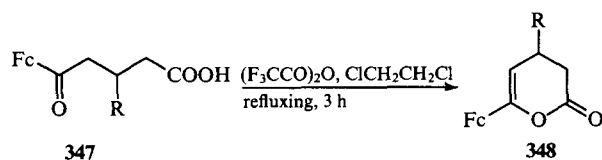
The methyl group in 2-methyl-4,6-diphenylpyrylium tetrafluoroborate exhibits an enhanced reactivity and condenses with the aldehyde **14** to form the derivative **345**.¹⁹²



In the presence of piperidine, the aldehyde **14** reacts with 3-acetyl-4-hydroxy-6-methyl-2-pyrone, affording the vinyl ketone **346**.¹⁹³



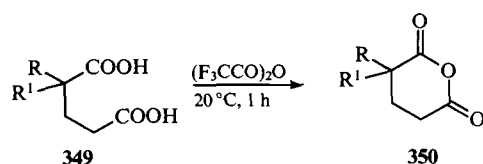
3-Aryl-5-ferrocenyl-5-oxovaleric acids **347** are dehydrated by trifluoroacetic anhydride and are converted into the dihydropyrone derivatives **348** in 92%–98% yields.¹⁹⁴



R = Ph, 4-MeOC₆H₄, 4-O₂NC₆H₄.

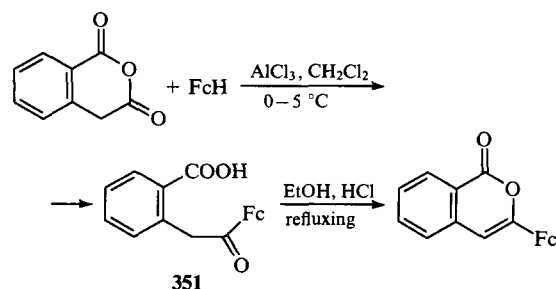
The cyclodehydration of 1-ferrocenylpentane-1,5-diol results in the formation of 2-ferrocenyltetrahydropyran.⁹⁶

The dehydration of the glutaric acid derivatives **349** by treatment with trifluoroacetic anhydride in CH₂Cl₂¹⁰⁹ or dichloroethane¹⁹⁵ with formation of the derivative **350** has been described.

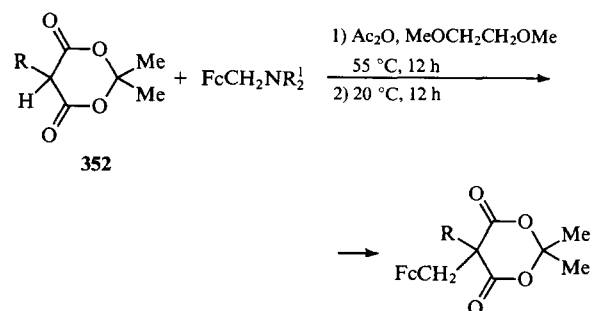


R	R ¹	Yield (%)	Ref.
FcCH ₂	H	70	109
FcCH=		98	196

The ketoacid **351**, obtained as a result of the acylation of ferrocene with homophthalic anhydride, is converted into 3-ferrocenylisocoumarin on refluxing with a solution of HCl in ethanol.¹⁹⁶

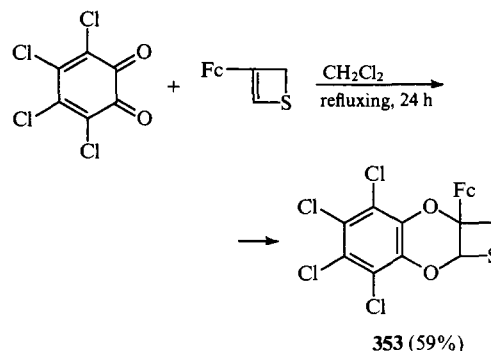


The substitution of a hydrogen atom in compounds **352** by the ferrocenylmethyl group has been achieved by treatment with dialkylaminomethylferrocene derivatives in the presence of acetic anhydride.¹⁹⁷

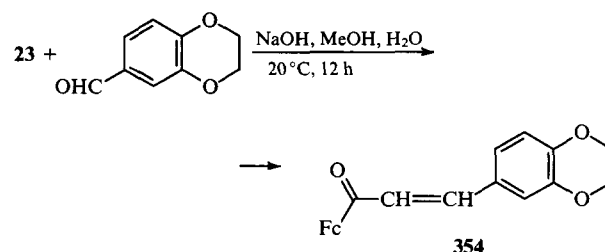


R = Me (70%), Et (66%), Ph (92%); R¹ = Me, Et.

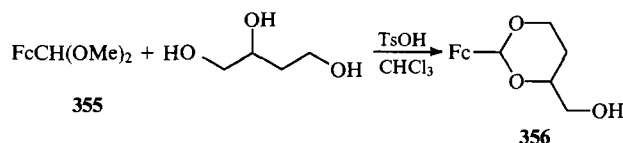
The tricyclic compound **353**, containing a 1,4-dioxane fragment, has been synthesised by heating 3,4,5,6-tetrachloro-*o*-benzoquinone with 3-ferrocenylthiethene.¹⁹⁸



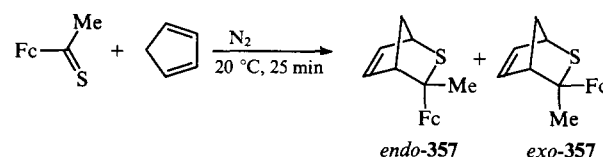
The condensation of the ketone **23** with 6-formyl-1,4-benzodioxane leads to compound **354** in 54% yield.¹¹²



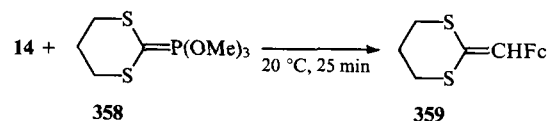
The acid-catalysed transesterification¹⁹⁹ of the acetal **355** leads to the 1,3-dioxane derivative **356**.



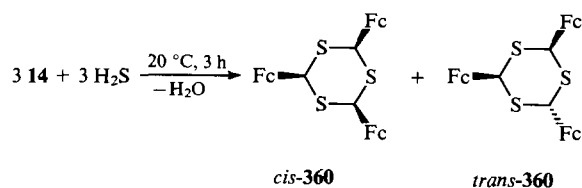
Thioacetylferrocene plays the role of the dienophile in relation to cyclopentadiene.²⁰⁰ The adduct **357** is obtained even at room temperature in the form of a mixture of the *endo*- and *exo*-isomers.



The reaction involving the conversion of the aldehyde **14** into an alkene by the ylide **358** afforded 2-ferrocenylmethylidene-1,3-dithiane **359** in 63% yield.²⁰¹

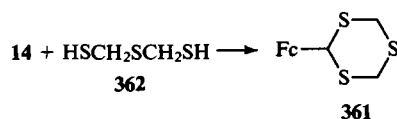


The preparation and certain properties of the isomeric *cis*- and *trans*-1,3,5-trithiacyclohexanes **360**, containing ferrocenyl substituents, have been described.²⁰²

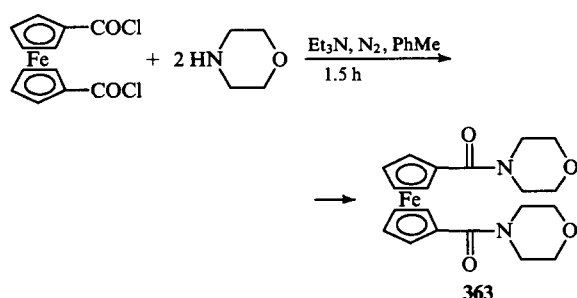


The ratio of the *cis*- and *trans*-isomers depends on the medium in which the reaction is carried out. The ratio is 5:1 in EtOH-HCl and 1:4 in concentrated HCl. When the reaction is carried out in concentrated HCl in the presence of Na₂S₂O₃·5H₂O, mainly the *cis*-trithiane (yield 35%) and traces of the *trans*-isomer are formed.²⁰²

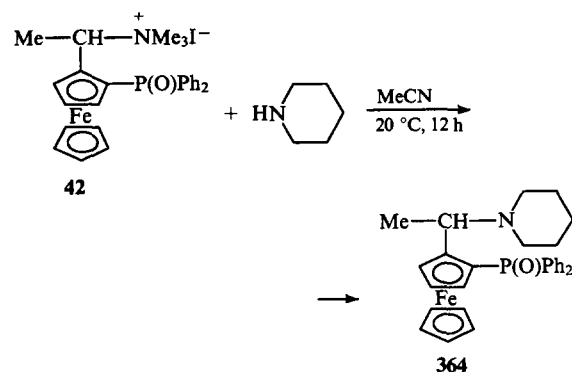
The synthesis of 2-ferrocenyl-1,3,5-trithiane **361** from the aldehyde **14** and bis(mercaptomethyl) sulfide **362** has been reported recently.²⁰³



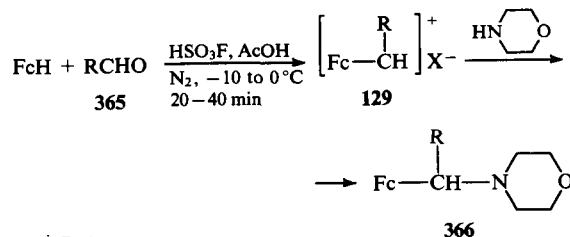
The *N*-acylation of morpholine by the chloride of ferrocene-1,1'-dicarboxylic acid affords the dimorpholide **363** (yield 83%).²⁰⁴



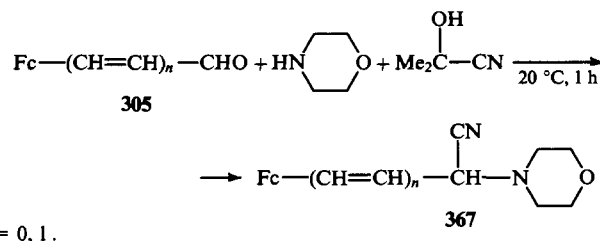
The quaternary ammonium salt **42** alkylates morpholine, whereupon the N⁺Me₃I⁻ group is substituted by the heterocyclic group. The product **364** is formed in 92% yield.³⁵



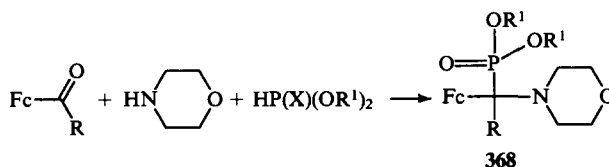
Electrophilic substitution in the ferrocene nucleus on treatment with the aldehydes **365** under superacid conditions leads to the salts **129** (formed as a result of the acid-catalysed dehydration of the intermediate carbinols), which are converted on treatment with morpholine into α-morpholino-derivatives of ferrocene **366**, with yields of 49% to 59%.¹⁷⁸



The aldehydes **305** react with acetone cyanohydrin and morpholine, which affords the aminonitriles **367** (yields 93%–96%).¹⁷⁶

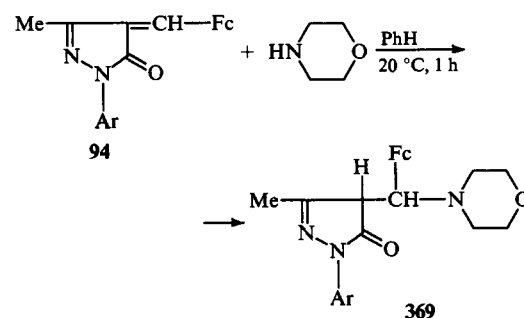


Compounds **368** have been synthesised by condensing carbonyl compounds of the ferrocene series with morpholine and phosphorous or phosphorothious acid esters.^{177, 205}



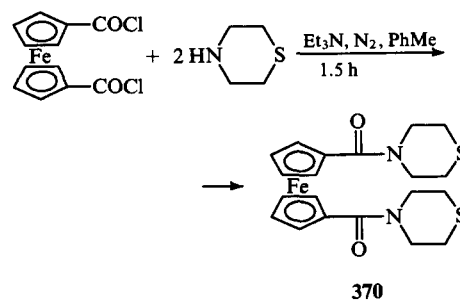
R	R ¹	X	Yield (%)	Ref.
H	Et	S	60	205
H	Me	O	55	177
H	Et	O	81	177
Me	Et	O	33	177

The addition of morpholine to the enones **94** leads to the pyrazolone derivatives **369** in 47%–57% yields.⁶⁹

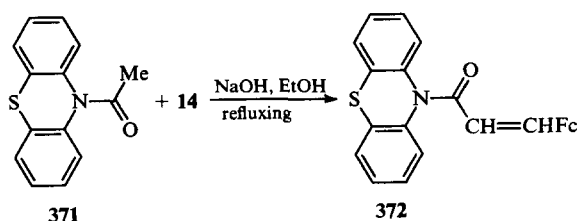


Ar = Ph, 2,4-(O₂N)₂C₆H₃.

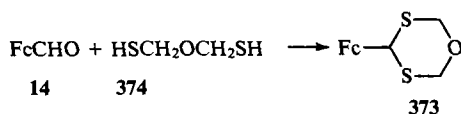
The chloride of ferrocene-1,1'-dicarboxylic acid acylates thiomorpholine with formation of the product **370** (yield 85%).²⁰⁴



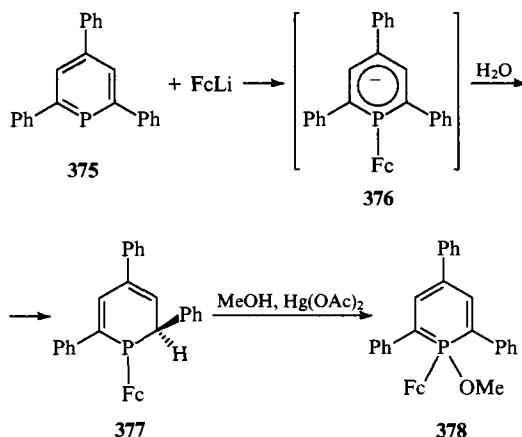
In the presence of alcoholic alkali, 10-acetylphenothiazine **371** condenses with the aldehyde **14**; the reaction product is the unsaturated amide **372**.⁶⁶



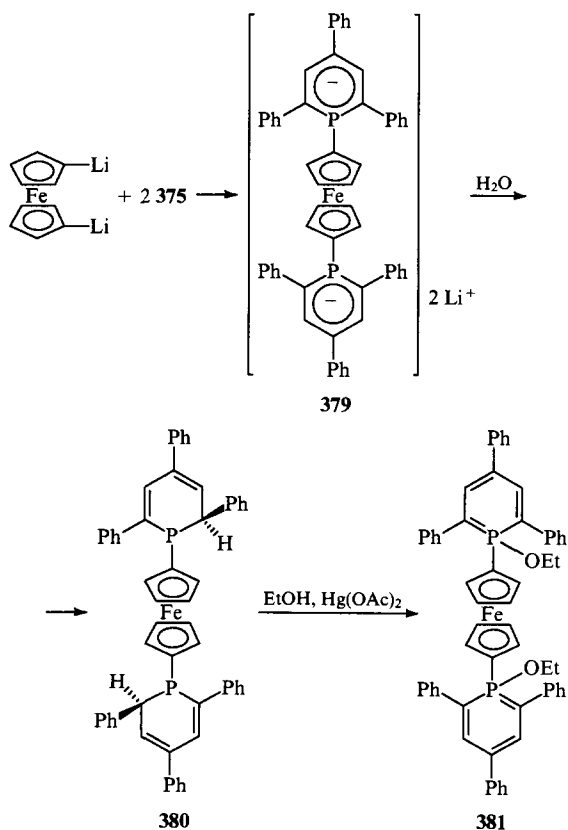
2-Ferrocenyl-1,3-dithia-5-oxacyclohexane **373** has been synthesised from FcCHO and di(mercapto)ether **374**.²⁰³



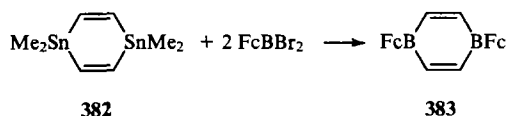
On treatment with ferrocenyllithium, 2,4,6-triphenylphosphinine **375** gives rise to the anion **376**, which, on treatment with water, is converted into 1-ferrocenyl-2,4,6-triphenyl-1,2-dihydrophosphinine **377**. As a result of oxidative alkoxylation, the latter affords 1-ferrocenyl-1-methoxy-2,4,6-triphenylphosphinine **378**.²⁰⁶



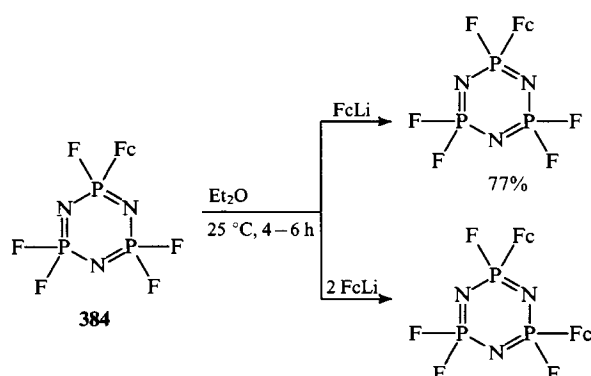
The interaction of the phosphorine **375** with 1,1'-dilithioferrocene takes place similarly.²⁰⁶ The diphosphorylated ferrocene **379** is converted on treatment with water into the dihydrophosphinine **380**, which is converted into compound **381** after treatment with mercury acetate in ethanol.



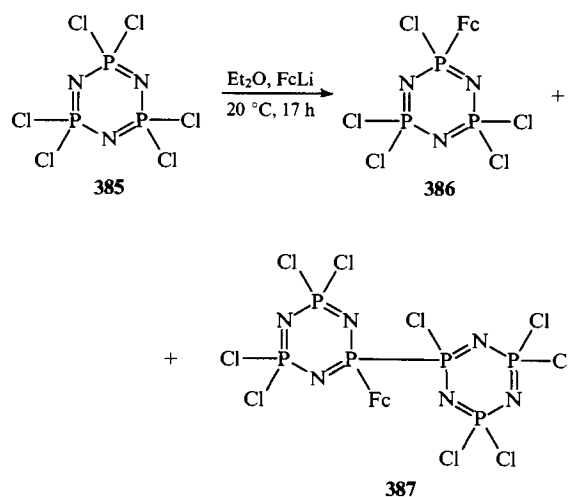
The transmetalation of 1,1,4,4-tetramethyl-1,4-distannacyclohexa-2,5-diene **382** on treatment with dibromo(ferrocenyl)borane leads to 1,4-diferrocenyl-1,4-diboracyclohexa-2,5-diene **383**.²⁰⁷



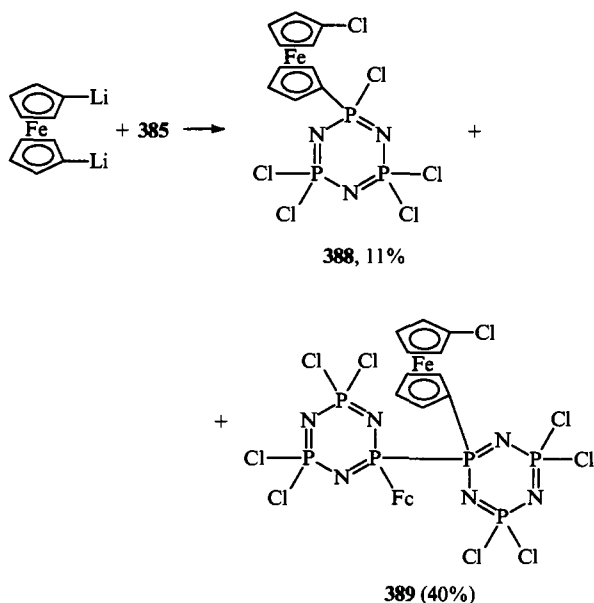
One²⁰⁸ or two²⁰⁹ fluorine atoms in 2,2,4,4,6,6-hexafluorocyclotriphosphazene **384** can be substituted by ferrocenyl groups on treatment with ferrocenyllithium.



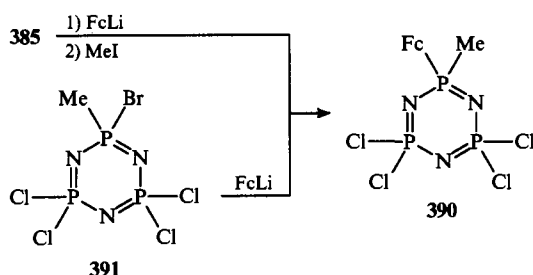
Apart from the monosubstitution product **386** (yield 31%), compound **387** was obtained (yield 20%) in the reaction of ferrocenyllithium with 2,2,4,4,6,6-hexachlorocyclotriphosphazene **385**. Compound **387** is evidently formed as a result of the interaction of the product **386** with the initial cyclophosphazene **385**.²⁰⁹



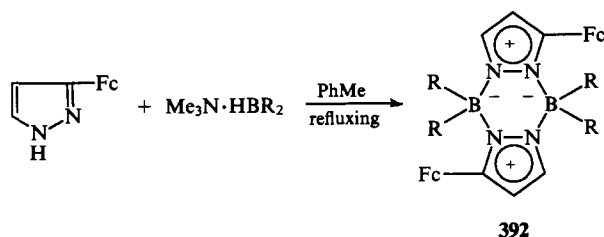
The interaction of the hexachloro-derivative **385** with 1,1'-dilithioferrocene proceeds in a more complex manner: the reaction products **388** and **389** contain a heterocyclic substituent only in one of the ferrocene rings.²⁰⁹



Two methods of synthesis of 2,2,6,6-tetrachloro-4-ferrocenyl-4-methylcyclotriphosphazene **390** were described in the same investigation: by treatment with iodomethane of the product of the reaction of FcLi with the hexachloro-derivative **385** or by the reaction of 4-bromo-2,2,6,6-tetrachloro-4-methylcyclotriphosphazene **391** with FcLi .

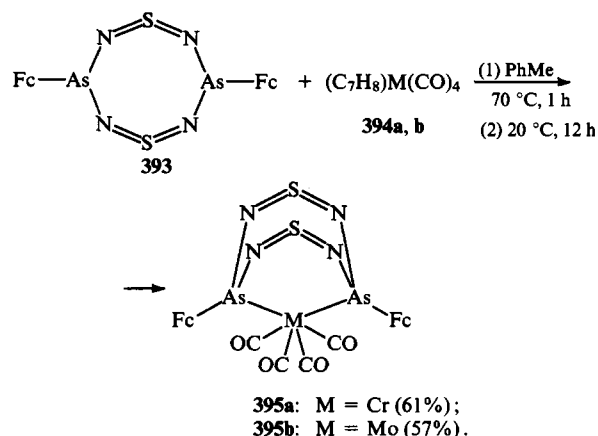


Interesting and unusual heterocyclic compounds—pyrazaboles **392**—have been synthesised by the reaction of 3-ferrocenylpyrazole with trimethylamine–borane or trimethylamine–diethylborane in boiling toluene.⁵⁷



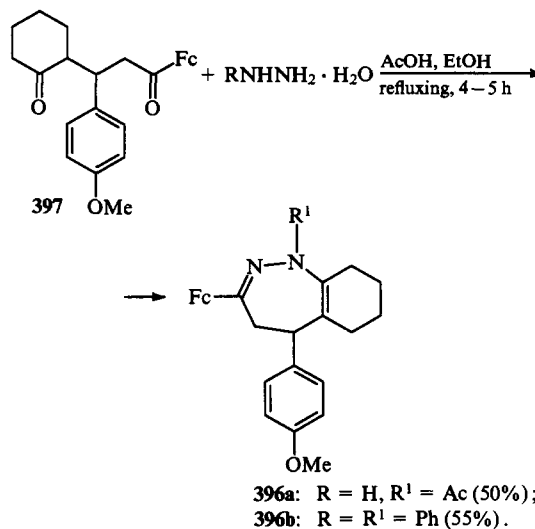
R	Reaction time/h	Yield (%)
H	1	—
Et	8	35

The interaction of diferrocenyldithiatetraazadiarsocine **393** with norbornadienenchromium tetracarbonyl **394a** or norbornadienemolybdenum tetracarbonyl **394b** results in the formation of the complex tetracarbonyl(diferrocenyldithiatetraazadiarsocine)-chromium(0) **395a** and the corresponding molybdenum(0) complex **395b**.¹⁵

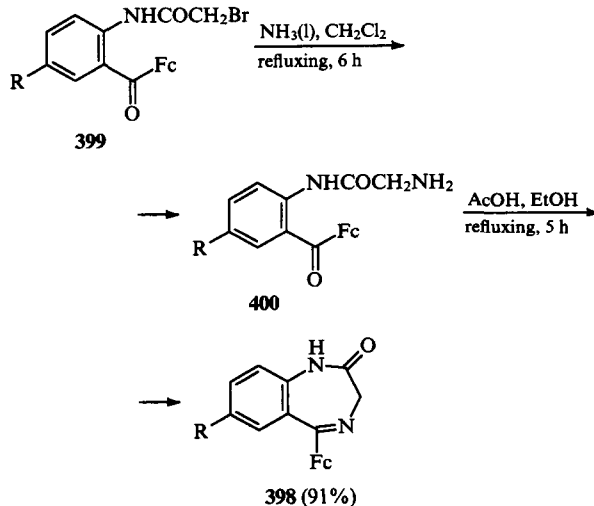


VI. Compounds containing heterocycles with more than six atoms

The synthesis of dihydro-1,2-diazepine derivatives **396a, b** from the diketone **397** on treatment with hydrazine or phenylhydrazine has been described.¹⁸¹

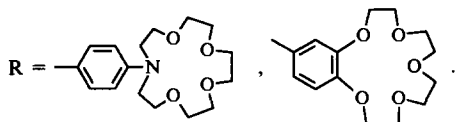
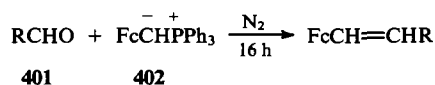


The 1,3-dihydrobenzo-1,4-diazepin-2-one derivatives **398** have been synthesised in two stages: by treating the ketoamides **399** with liquid ammonia and the subsequent cyclisation of the aminoketones **400** formed.²¹⁰

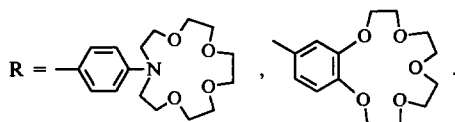
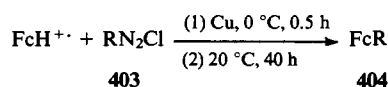


R = H, I.

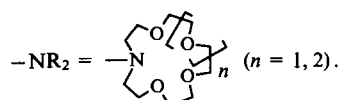
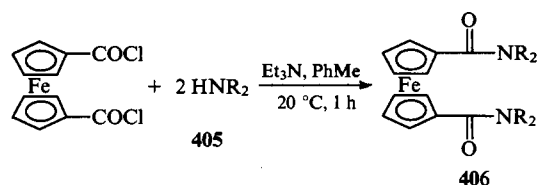
The Wittig insertion of the ferrocenylvinyl fragment into the crown-ether derivatives **401** has been achieved²¹¹ by treatment with the ylide **402** under an inert atmosphere in the absence of light.



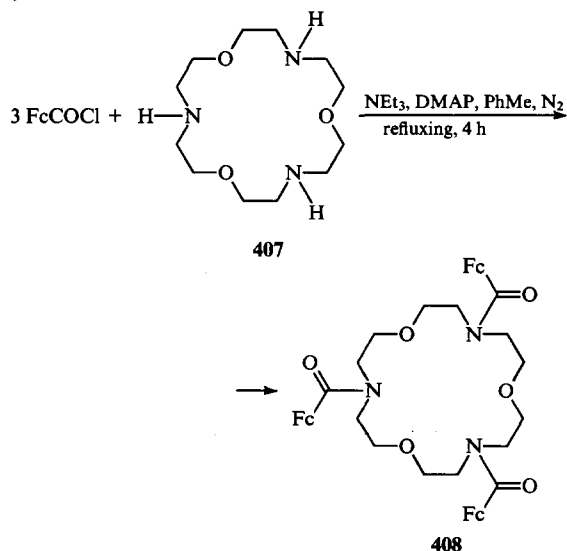
The crown-ethers **404**, containing a ferrocenyl substituent, have been synthesised (yields 25%–30%) by coupling the ferrocenium cation with the diazonium salts **403**.²¹²



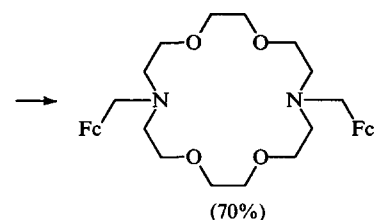
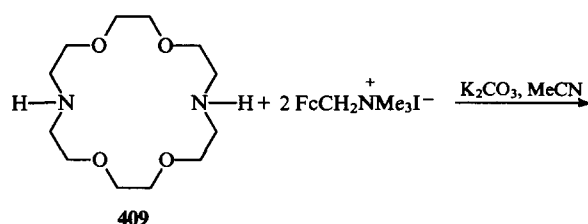
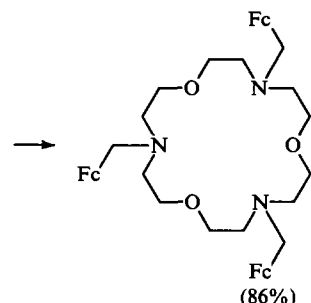
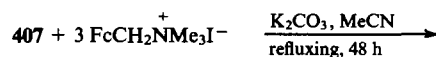
The ferrocene derivatives **406**, containing two crown-ether fragments in the molecule, are formed in 80%–85% yields as a result of the acylation of the aza-crown-ethers **405** by the dichloride of ferrocene-1,1'-dicarboxylic acid in the presence of triethylamine.²¹³



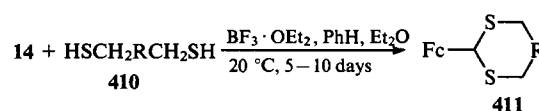
Three ferrocenyl groups have been introduced into the triaza-crown-ether **407** by treatment with the ferrocenecarboxylic acid chloride in the presence of triethylamine and 4-dimethylaminopyridine (DMAP) (the yield of the product **408** was 85%).²¹⁴



The aza-crown-ethers **407** and **409** are smoothly alkylated by ferrocenylmethyl(trimethyl)ammonium iodide, affording the corresponding ferrocenylmethyl-substituted macrocycles.²¹⁴



The ferrocenyl-substituted crown-ethers **411**, containing oxygen and sulfur atoms in the ring, have been obtained from the aldehyde **14** by its conversion into an acetal with the aid of the bismercapto-derivatives **410** in the presence of Lewis acids.^{203, 215, 216}

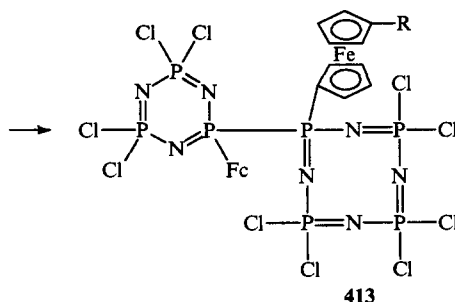
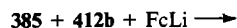
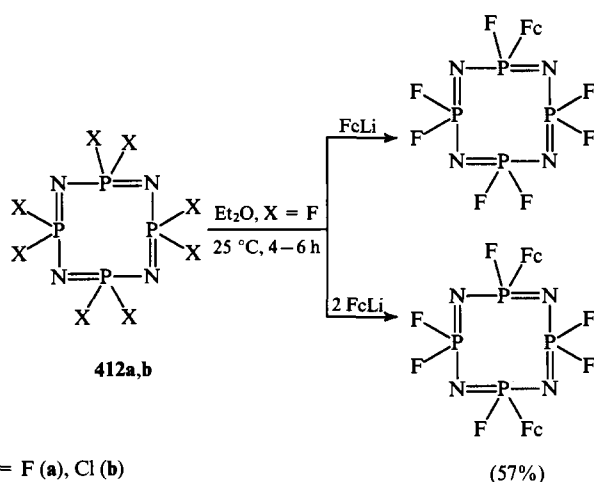


R	Yield (%)
OCH ₂ CH ₂ SCH ₂ CH ₂ O	—
CH ₂ OCH ₂	84
CH ₂ OCH ₂ CH ₂ OCH ₂	72
CH ₂ O(CH ₂ CH ₂ O) ₂ CH ₂	92
CH ₂ O(CH ₂ CH ₂ O) ₃ CH ₂	62
CH ₂ O(CH ₂ CH ₂ O) ₄ CH ₂	64
CH ₂ SCH ₂	31
CH ₂ OCH ₂ CH ₂ SCH ₂ CH ₂ OCH ₂	78
CH(OH)CH(OH)(CH ₂) ₂	—
CH ₂ SCH ₂	—

The reaction of 2,2,4,4,6,6,8,8-octafluorocyclotetraphosphazene **412a** with ferrocenyllithium results in the formation of the products of the substitution of one or two fluorine atoms by the Fc groups (Scheme 5).^{208, 209}

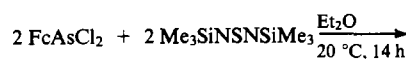
Treatment of a mixture of hexachlorocyclotriphosphazene **385** and octachlorocyclotetraphosphazene **412b** with ferrocenyllithium leads to the formation of compounds **413**, containing cyclotriphosphazene and cyclotetraphosphazene fragments in the molecule.²¹⁷

Scheme 5

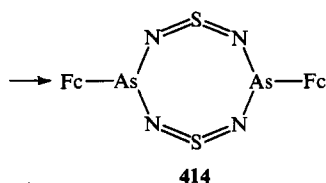


R = H, Cl.

Diferrocenyldithiatetraazadiarsocine **414** has been synthesised in 73% yield from dichloro(ferrocenyl)arsine and compound **415**.¹⁵



415



VII. Biological activities and applications of heterylferrocenes

It has been found that many heterylferrocenes exhibit a biological activity. Thus ferrocenyl-containing derivatives of 6-aminopenicillanic or 7-aminocephalosporanic acids have been recommended as effective antibiotics and inhibitors of β -lactamase.^{218, 219} The tetrafluoroborates and perchlorates of benzothiazolium derivatives inhibits the growth of staphylococci and streptococci as well as the yeast fungi of the genus *Candida*.¹⁴³ Derivatives of ferrocene-containing fragments of the diethyl esters of phosphonic and phosphonotheic acids and morpholine¹⁷⁷ or 1,3,4-triazole²⁰⁵ as well as thiophene and 1,3-thiazolidin-2-one rings¹³⁹ in the molecule exhibit an antimicrobial activity against both Gram-positive and Gram-negative microorganisms.

3-Ferrocenyl-1-(2-furyl)cyclopent-1-ene has been patented as an agent counteracting the anaemia induced by iron deficiency in

the organism.¹⁰⁶ The product of the condensation of 2,4,6-trichloro-1,3,5-triazine with the disodium salt of ferrocene-1,1',-dicarboxylic acid is active against a series of bacteria.²²⁰

The nonsilver photosensitive compositions and materials frequently include charge-transfer complexes (CTC). It has been stated that CTC based on the copolymer of vinylferrocene with *N*-vinylcarbazole and 2,4,7-trinitrofluorenone²²¹ as well as the copolymer based on 4-cyano(or phenyl)-3-ferrocenylisoxazolines and CBr₄ have been synthesised.^{131, 222} The products of the condensation of FcCHO with benzothiazole derivatives or with 1,3-diazolidine-2,4-dione have been recommended as components of nonsilver photosensitive compositions.¹⁹² Compounds containing the FcCH=CH groups and 1,3,4-oxadiazole rings may be used as electrophotographic materials.¹³⁷ Derivatives of 2,3-bis(2-ferrocenylvinyl)quinoxaline are electrophotographic semiconductors and are used in compositions for the preparation of effective and long-lived printing plates, which make it possible to obtain many thousands of impressions.²²³

2-Ferrocenyl-1,4-dimethyl-5,6-benzoquinolinium iodide is a dye for polyamide and polyester fibres.¹⁶⁴ Derivatives of ferrocene-containing quinoline and pyrazoline rings have been recommended as cyanine dye-sensitisers.^{17, 69, 70} Ferrocenyl-containing cyanine dyes with an indole ring fragment in the molecule have been described.⁴⁸

Heterylferrocenes are used as modifying agents which improve the operational characteristics of rocket fuels and explosive compositions. *N*-Ferrocenylmethylpyrrolidine has been used as an additive improving the ballistic and mechanical characteristics of rocket fuels.^{31, 32} 1,4-Bis(*N*-ferrocenyl)piperazine and analogous compounds,¹⁹⁰ 2-ferrocenyltetrahydrofuran,²²⁴ and 2-ferrocenyl-1-isopropenylcarborane²²⁵ may be used to regulate the rate of combustion of rocket fuels based on NH₄ClO₄. 2-Ferrocenyl-2-(hydroxypropyl)tetrahydrofuran has been proposed as a catalyst for the combustion of rocket fuel.¹⁰² 2-Ferrocenyltetrahydrofuran increases the rate of combustion of rocket fuel and its efficiency.²²⁶ 5-Ferrocenylmethylenebarbituric acid is a catalyst of the combustion of explosive compositions based on nitramines.¹⁸⁶

Crown-ethers containing a ferrocenyl group are interesting as regards practical use.^{212, 213, 216}

The polymers obtained by condensing furfural with ferrocene in the presence of AlCl₃ have been proposed as thermostable and radiation-resistant coatings, adhesives, and insulators.²²⁸ 6-(2-Ferrocenylvinyl)-2,4-diphenylpyrylium tetrafluoroborate has been patented as a dye-hardening agent for gelatin in photographic compositions.¹⁹² The polymer formed on heating ferrocenyldihydrobenzofuranone in the presence of ZnCl₂ or AlCl₃ exhibits an effective thermal stability and may be used in many fields: as a coating, as an adhesive, as an insulator, as an ion-exchange resin, as a combustion catalyst, as films resistant to irradiation, and as an inhibitor of the ageing of silicone rubbers and other elastomers.²²⁸

Isoxazoline derivatives containing ferrocenylalkyl groups in the 3-position exhibit pesticidal, herbicidal, acaricidal, and fungicidal activities and are plant growth regulators.¹³¹ It has been reported²²⁹ that the 4,5-diphenyloxazole derivative containing the NHN=CHFc group in the 2-position may be used to combat plant viruses.

References

1. T J Kealy, P L Pauson *Nature (London)* **168** 1039 (1951)
2. J W Huffman, D J Rabb *J. Org. Chem.* **26** 3588 (1951)
3. F D Popp, E B Moynahan *Adv. Heterocycl. Chem.* **13** 1 (1971)
4. H Volz, H Kowarsch *Heterocycles* **7** 1319 (1977)
5. M-G A Shvekhgeimer *Khim. Geterotsikl. Soedin.* 147 (1991)
6. R A Abramovitch, C I Azogu, R G Sutherland *J. Chem. Soc., Chem. Commun.* 134 (1971)
7. G Schmitt, P Klein, W Ebertz *J. Organomet. Chem.* **234** 63 (1982)

8. F Li, G Ning, A He *Huaxue Shiji* **7** 291 (1985); *Chem. Abstr.* **105** 24418 (1986)
9. Zh Bian, F Li *Chem. J. Chin. Univ.* **7** 701 (1986); *Chem Abstr.* **107** 59 206 (1987)
10. Zh Bian, G Li, G Wen, Sh Wu *Huaxue Shiji* **15** 73 (1993); *Chem. Abstr.* **119** 139 471 (1993)
11. S L Sosin, V P Alekseeva, M D Litvinova, V V Korshak, A F Zhigach *Vysokomol. Soedin., Ser. B* **18** 703 (1976)
12. J P Sevenair, D H Lewis, B W Ponder *J. Org. Chem.* **37** 4061 (1972)
13. A J Meyers, M E Ford *Tetrahedron Lett.* **16** 2861 (1975)
14. A J Meyers, M E Ford *J. Org. Chem.* **41** 1735 (1976)
15. C Sprang, F T Edelmann, M Noltemeyer, H W Roesky *Chem. Ber.* **122** 1247 (1989)
16. Kh M Hassan Z. *Naturforsch.* **33** 1508 (1978)
17. Kh M Hassan, M A El-Maghraby, H S El-Kashef *Indian J. Chem. B, Org. Ind. Med.* **16** 326 (1978)
18. M A Abbady, Kh M Hassan, M A El-Maghraby *Indian J. Chem. B, Org. Ind. Med.* **16** 499 (1978)
19. Kh M Hassan, S R El-Ezbawy, A A Abdel-Wahab *J. Indian Chem. Soc.* **56** 290 (1979)
20. Kh M Hassan, M A Abbady *Indian J. Chem. B, Org. Ind. Med.* **18** 44 (1979)
21. Th C Sederger, D C Dittmer *J. Org. Chem.* **52** 695 (1987)
22. T L Rose, A B Kon *Inorg. Chem.* **32** 781 (1993)
23. N H Nemeroff, M E McDonnell, J M Axsten, L J Buckley *Synth. Commun.* **3271** (1992)
24. M Puciova, P Ertl, S Toma *Collect. Czech. Chem. Commun.* **59** 175 (1994)
25. A N Nesmeyanov, N N Sedova, V A Sazonova, L S Borodina *Dokl. Akad. Nauk SSSR* **207** 617 (1972)
26. A N Nesmeyanov, V A Sazonova, N N Sedova, E N Stakheeva *Izv. Akad. Nauk SSSR, Ser. Khim.* **2141** (1979)
27. M Sato, S Ebine *Synthesis* **472** (1981)
28. S Toma, J Federic, E Solcaniova *Collect. Czech. Chem. Commun.* **46** 2531 (1981)
29. T Inagaki, M Hunter, X Q Yang, T A Skotheim, Y Okamoto *J. Chem. Soc., Chem. Commun.* **126** (1988)
30. A Haimerl, A Merz *Angew. Chem.* **98** 179 (1986)
31. US P. 3 925 410; *Chem. Abstr.* **84** 59 752 (1976)
32. US P 3 765 965; *Chem. Abstr.* **80** 61 709 (1974)
33. M Th Wu, G S Shaw, Ch J Jong, J J Liang, C S Hsu *J. Organomet. Chem.* **297** 205 (1985)
34. J A Connor, J P Lloyd *J. Chem. Soc., Perkin Trans. 1* **17** (1973)
35. T Hayashi, T Mise, M Fukushima, M Kagotani, N Nagashima, Y Hamada, A Matsumoto, S Kawakami, M Komishi, K Yamamoto, M Kumada *Bull. Chem. Soc. Jpn.* **53** 1138 (1980)
36. M Kumada, T Hayashi, T Mise, A Katsumora, N Nagashima, M Fukushima *Kenkyu Hokoku-Asahi Garasu Kogyo Gijitsu Shoreikai* **37** 69 (1980); *Chem. Abstr.* **96** 85 708 (1982)
37. H Falk, K Grubmayr, O Hofer *Monatsh. Chem.* **106** 301 (1975)
38. H Falk, K Grubmayr, O Hofer, F Neufinger *Monatsh. Chem.* **106** 991 (1975)
39. J Huang, H Jiang, Yu Huang *J. Organomet. Chem.* **419** 337 (1991)
40. J Meng, D Du, Yo Wang, R Wang, H Wang *Chin. Chem. Lett.* **3** 247 (1992); *Chem. Abstr.* **117** 69 988 (1992)
41. V I Boev, A V Dombrovskii *Zh. Obshch. Khim.* **52** 1693 (1982)
42. V I Boev, M S Lyubich, S M Larina *Zh. Org. Khim.* **21** 2195 (1985)
43. N S Kochetkova, V I Boev, L V Popova, V N Babin *Izv. Akad. Nauk SSSR, Ser. Khim.* **1397** (1985)
44. V I Boev, A V Dombrovskii *Zh. Obshch. Khim.* **54** 1863 (1984)
45. V I Boev, A V Dombrovskii *Zh. Obshch. Khim.* **57** 938 (1987)
46. F D Popp, B F Donigan *J. Pharm. Sci.* **68** 519 (1979)
47. A M El-Khawaga, Kh M Hassan, A A Khalaf Z. *Naturforsch. B, Chem. Sci.* **36** 119 (1981)
48. V I Boev, A V Dombrovskii *Zh. Obshch. Khim.* **54** 1617 (1984)
49. V I Boev, M S Lyubich *Zh. Org. Khim.* **19** 1066 (1983)
50. A N Chekhlov, V N Solov'ev, A N Pushchin, V A Sazonova, E I Klimova, I V Martynov *Izv. Akad. Nauk SSSR, Ser. Khim.* **701** (1986)
51. A N Pushchin, E I Klimova, V A Sazonova *Zh. Obshch. Khim.* **57** 1102 (1987)
52. E S Schmidt, Th S Calderwood, Th C Bruce *Inorg. Chem.* **25** 3718 (1986)
53. V N Babin, Yu A Belousov, V V Gumenyuk, V V Materikova, R B Salimov, N S Kochetkova *J. Organomet. Chem.* **214** C13 (1983)
54. G A Shvekhgeimer, V I Zvolinskii, M Litim, P B Terent'ev *Metallog. Khim.* **5** 376 (1992)
55. B V Polyakov, V P Tverdokhlebov, I V Tselinskii, N M Bakstova, G M Frolova *Zh. Obshch. Khim.* **53** 2046 (1983)
56. Y Zhou, Yu Lui *Lazhou Daxue Xuebao Z. K.* **21** 105 (1985); *Chem. Abstr.* **106** 50 382 (1987)
57. K Niedenzu, J Serwatowski, S Trofimenko *Inorg. Chem.* **30** 524 (1991)
58. M Lacan, R Sarac-Arneri *Croat. Chem. Acta* **43** 215 (1971)
59. M Lacan, V Rasic *Croat. Chem. Acta* **44** 317 (1972)
60. N Oda, T Osaki, Sh Nagai, I Ito *Chem. Pharm. Bull.* **26** 359 (1978)
61. E I Klimova, V N Postnov, V A Sazonova *Dokl. Akad. Nauk SSSR* **263** 358 (1982)
62. A M Osman, Kh M Hassan, M A El-Maghraby *Indian J. Chem. B* **14** 282 (1976)
63. Kh M Hassan, M M Aly, G M El-Nagkar *J. Chem. Tech. Biotechnol.* **29** 515 (1979)
64. A N Nesmeyanov, V A Sazonova, V N Postnov, A M Baran, Ya A Angelyuk, B A Surkov *Dokl. Akad. Nauk SSSR* **241** 1099 (1978)
65. A N Nesmeyanov, V N Postnov, E I Klimova, V A Sazonova *Izv. Akad. Nauk SSSR, Ser. Khim.* **239** (1979)
66. M A El-Maghraby, Kh M Hassan *J. Indian. Chem. Soc.* **53** 1030 (1976)
67. Kh M Hassan, Z H Khalil Z. *Naturforsch. B, Chem. Sci.* **34** 1326 (1979)
68. A N Nesmeyanov, V N Postnov, A M Baran, V A Sazonova *Izv. Akad. Nauk SSSR, Ser. Khim.* **222** (1981)
69. Kh M Hassan *J. Indian Chem. Soc.* **53** 1185 (1976)
70. A M Osman, M S Yousef, Kh M Hassan *J. Prakt. Chem.* **320** 857 (1978)
71. Sh Sh Chen *J. Organomet. Chem.* **202** 183 (1980)
72. D Heydenhauss, C-R Kramer, G Jaenecke Z. *Phys. Chem. (Leipzig)* **267** 33 (1986)
73. I Yu Kozak, G N Yashchenko, A K Sheikman *Khim. Geterotsikl. Soedin.* **996** (1984)
74. V I Ovcharenko, A V Podoplelov *Metallog. Khim.* **2** 1136 (1989)
75. Yo Nakamura, N Koda, H Imamura *Chem. Lett.* **69** (1991)
76. E E Vittal', V I Boev *Zh. Org. Khim.* **13** 2059 (1977)
77. A I Tutubalina, in *Neft' i Gaz i Ikh Produkty (Tr. MINKhGP im. I. M. Gubkina)* [Petroleum and Gas and Their Products (Proceedings of I M Gubkin Moscow Institute of Petroleum Chemistry and Gas Industry)] (Moscow, 1971) p. 178
78. V I Boev, P M Betankourt, L V Popova, V N Babin *Zh. Obshch. Khim.* **61** 1651 (1991)
79. M-G A Shvekhgeimer, V D Tyurin, A I Tutubalina, in *Neft' i Gaz i Ikh Produkty (Tr. MINKhGP im. I. M. Gubkina)* [Petroleum and Gas and Their Products (Proceedings of I M Gubkin Moscow Institute of Petroleum Chemistry and Gas Industry)] (Moscow, 1971) p. 84
80. N S Nametkin, M-G A Shvekhgeimer, V D Tyurin, A I Tutubalina, T N Kosheleva *Izv. Akad. Nauk SSSR, Ser. Khim.* **1657** (1971)
81. N S Nametkin, G A Shvekhgeimer, V D Tyurin, Kh M Hassan, V I Ivanov *Izv. Akad. Nauk SSSR, Ser. Khim.* **1478** (1972)
82. Kh M Hassan, V D Tyurin, N S Nametkin, M-G A Shvekhgeimer *Izv. Akad. Nauk SSSR, Ser. Khim.* **1590** (1971)
83. Kh M Hassan, Candidate Thesis in Chemical Sciences, Moscow Institute of Petroleum Chemistry and Gas Industry, Moscow, 1971
84. A M Osman, Kh M Hassan, Zh H Khalil, V D Turin *J. Appl. Chem. Biotechnol.* **26** 71 (1976)
85. S Kaluz, S Toma *Collect. Czech. Chem. Commun.* **51** 2199 (1986)
86. D Villemijn, M Richard *Synth. Commun.* **17** 283 (1987)
87. H Wu, Yu Zhang, Yo Hu, Sh Wu *Synth. React. Inorg. Met.-Org. Chem.* **24** 1121 (1994)
88. A V Sochivko, V P Tverdokhlebov, I V Tselinskii *Zh. Org. Khim.* **22** 206 (1986)
89. V P Tverdokhlebov, I V Tselinskii, N Yu Vasil'eva *Zh. Org. Khim.* **14** 1056 (1978)
90. V P Tverdokhlebov, I V Tselinskii, N Yu Vasil'eva, B V Polyakov, G M Frolova *Zh. Org. Khim.* **16** 218 (1980)
91. L V Snegur, V I Boev, V N Babin, M Kh Dzhaifarov, A S Batsanov, Yu S Nekrasov, Yu T Struchkov *Izv. Akad. Nauk SSSR, Ser. Khim.* **554** (1995)

92. I Yu Shirobokov, A V Sachivko, V P Tverdokhlebov, V A Ostrovskii, I V Tselinskii, T I Koldobskii *Zh. Org. Khim.* **22** 1763 (1986)
93. A V Sachivko, V P Tverdokhlebov, I V Tselinskii *Zh. Org. Khim.* **22** 1112 (1986)
94. K H Dotz, R Dietz, D Neugenbaer *Chem. Ber.* **112** 1486 (1979)
95. N A Lewis, Bh Patel, P S White *J. Chem. Soc., Dalton Trans.* 1367 (1983)
96. A Ratajczak, B Czech, B Misterkiewicz, A Priorko, H Zyzik *Bull. Akad. Pol. Sci., Ser. Sci. Chem.* **24** 775 (1976)
97. L P Asatiani, I M Gverdtseteli *Soobshch. Akad. Nauk Gruz. SSR* **85** 369 (1977)
98. W E Watts *J. Chem. Soc., Perkin Trans. 1* 804 (1976)
99. M Hisatome, S Koshikawa *Chem. Lett.* 16 789 (1975)
100. M Hisatome, S Koshikawa, K Chimura, H Hasimoto, K Yamakawa *J. Organomet. Chem.* **145** 225 (1978)
101. W P Norris *J. Org. Chem.* **43** 2200 (1976)
102. US P. 3 968 126; *Chem. Abstr.* **85** 124 161 (1978)
103. M Salisova, S Toma, E Solcaniova *J. Organomet. Chem.* **327** 77 (1987)
104. Ch Guillon, P Vierling *J. Organomet. Chem.* **464** C42 (1994)
105. H Uysal, M B Gautheron *C. R. Hebd. Seances Acad. Sci., Ser. C* **278** 1297 (1974)
106. BRD P. 2 453 977; *Chem. Abstr.* **83** 114 640 (1975)
107. A L J Beckwith, R A Jackson, R W Longmore *Austr. J. Chem.* **45** 857 (1992)
108. D Touchard, R Dabard *Bull. Soc. Chim. Fr., Pt. 2* 2567 (1975)
109. V Rasic, L Korontos *J. Organomet. Chem.* **260** 219 (1984)
110. M Lacan, V Rasic *Croat. Chim. Acta* **51** 325 (1978)
111. G Falsone, B Spur, W Peters *Z. Naturforsch., B Chem. Sci.* **38** 493 (1983)
112. E E Vittal', A V Dombrovskii *Zh. Obshch. Khim.* **46** 623 (1976)
113. L Tataru, J Mazilu, M Vata, T Lixandru, C J Simonescu *J. Organomet. Chem.* **214** 107 (1981)
114. Ya M Paushkin, A M Shevchik *Vesti. Akad. Nauk BSSR, Ser. Khim.* 95 (1973)
115. A Ratajczak, B Czech *Rocz. Chem.* **51** 1735 (1977)
116. Ya N Paushkin, A M Shevchik, L P Romanovskaya *Dokl. Akad. Nauk SSSR* **214** 114 (1974)
117. US P. 3 703 771; *Chem. Abstr.* **109** 173 598 (1988)
118. M-G A Shvekhgeimer, M Litim, V I Zvolinskii, V I Shvedov *Metalloorg. Khim.* **3** 933 (1990)
119. M-G A Shvekhgeimer, M Litim, V I Zvolinskii, *Metalloorg. Khim.* **3** 1421 (1990)
120. S Kaluz, S Toma *Gazz. Ital.* **529** (1987)
121. N K Baranetskaya, M A Kondratenko, S M Lukashov, V N Setkina *Metalloorg. Khim.* **3** 83 (1990)
122. R Dabard, H Patin *Bull. Soc. Chim. Fr., Pt. 2* 2158 (1973)
123. A J Moore, P J Skabara, M R Bryce, A S Batsanov, J A K Howard, S T Daley, T K D Stephen *J. Chem. Soc., Chem. Commun.* 417 (1993)
124. V N Postnov, A V Goncharov, I Khakke, D P Krut'ko *Dokl. Akad. Nauk* **331** 196 (1993)
125. M-G A Shvekhgeimer, M Litim *Izv. Akad. Nauk, Ser. Khim.* 139 (1994)
126. BRD P. 3 127 609; *Chem. Abstr.* **98** 179 359 (1983)
127. Yo Nishibayashi, S Uemura *Synlett.* 79 (1995)
128. C J Richard, T Damalidis, D E Hibbs, M B Hursthouse *Synlett.* 74 (1995)
129. E Tauer, K H Grellmann *J. Org. Chem.* **49** 4252 (1984)
130. B H Lipshutz, R W Hugnate *J. Org. Chem.* **46** 1410 (1981)
131. V I Zvolinskii, Candidate Thesis in Chemical Sciences, Moscow Textile Institute, Moscow, 1984
132. M-G A Shvekhgeimer, V I Zvolinskii, K I Kobrakov, A M Krapivin *Dokl. Akad. Nauk SSSR* **252** 636 (1980)
133. V D Tyurin, N S Nametkin, M-G A Shvekhgeimer, Kh M Hassan *Izv. Akad. Nauk SSSR, Ser. Khim.* 2645 (1970)
134. B V Polyakov, V P Tverdokhlebov, I V Tselinskii *Zh. Obshch. Khim.* **60** 2049 (1990)
135. B V Polyakov, V P Tverdokhlebov, I V Tselinskii *Zh. Obshch. Khim.* **56** 1110 (1986)
136. T Kondo, K Yamamoto, H Danda, M Kumata *J. Organomet. Chem.* **61** 361 (1973)
137. Jpn. Appl. 76-128 971; *Chem. Abstr.* **87** 53 307 (1977)
138. A K El-Shafei, Kh M Hassan *J. Indian Chem. Soc.* **54** 743 (1977)
139. M S K Youssef *Rev. Roum. Chim.* **26** 1005 (1981)
140. A Dömling, I Ugi *Angew. Chem., Int. Ed. Engl.* **32** 563 (1993)
141. M Salisova, M Prokesova, M Kubrikanova, S Toma *Chem. Pap./Chem. Zvesti.* **47** 183 (1993); *Chem. Abstr.* **120** 218 053 (1994)
142. R E Bozak, M Murphy, R Rennels *Synth. React. Inorg. Metal.-Org. Chem.* **20** 1395 (1990)
143. V I Boev, A L Pak, M P Perepichko, Yu L Volyanskii *Khim.-Farm. Zh.* **17** 1197 (1983)
144. V I Boev, A V Dombrovskii *Zh. Obshch. Khim.* **54** 1192 (1984)
145. I E Nifant'ev, A A Borisenko, L F Mazhukova, E E Nifant'ev *Phosphorus Sulfur Silicon Relat. Elem.* **68** 99 (1992)
146. V V Krasnikov, G N Dorofeenko *Khim. Geterotsikl. Soedin.* 1376 (1981)
147. G N Dorofeenko, V V Krasnikov, A I Pyshev *Khim. Geterotsikl. Soedin.* 599 (1977)
148. G N Dorofeenko, V V Krasnikov *Zh. Org. Khim.* **8** 2620 (1972)
149. V I Boev, A V Dombrovskii *Zh. Obshch. Khim.* **50** 563 (1980)
150. V V Krasnikov, Yu P Andreichikov, N V Kholodova, G N Dorofeenko *Zh. Org. Khim.* **13** 1566 (1977)
151. Ch Just, R-M Wagner, A Kraatz, H-G Zoebing *Liebigs Ann. Chem.* 874 (1975)
152. Y Omote, T Komatsu, R Kobayashi, N Sugiyama *Tetrahedron Lett.* **13** 93 (1972)
153. K Shibata, I Katsuyama, M Matsui, H Muramatsu *Bull. Chem. Soc. Jpn.* **63** 3710 (1990)
154. K Shibata, I Katsuyama, H Izoe, M Matsui, H Muramatsu *J. Heterocycl. Chem.* **30** 277 (1993)
155. A K Sheinkman, E Yu Nesterova, G N Yashchenko, A I Chernyshov *Khim. Geterotsikl. Soedin.* 1094 (1986)
156. I R Butler *Polyhedron* **11** 3117 (1992)
157. F Gelin, R P Trummel *J. Org. Chem.* **57** 3780 (1992)
158. N J Coville, J A Ramsden, B Staskun *South Afr. J. Chem.* **33** 71 (1980)
159. BRD P. 4 015 250; *Chem. Abstr.* **116** 210 422 (1992)
160. I R Butler, N Burke, L J Hobson, H Findenegg *Polyhedron* **11** 2435 (1992)
161. B Farlow, T A Nile, J L Walsh, A T McPhail *Polyhedron* **12** 2891 (1993)
162. E C Constable, A J Edwards, R Martinez-Manez, P R Raithby *J. Chem. Soc., Dalton Trans.* 645 (1994)
163. USSR P. 3 879 995; *Byull. Izobret.* (28) 74 (1973)
164. N S Kozlov, E A Kalennikov *Zh. Obshch. Khim.* **44** 2490 (1974)
165. V Hedge, Y Jahnk, R D Trummel *Tetrahedron Lett.* **28** 4023 (1987)
166. E C Constable, R Martinez-Manez, T Cargill, M W Aleksander, J V Walker *J. Chem. Soc., Dalton Trans.* **185** (1994)
167. M A Metwally, E E M Kandell, F A Amer *J. Indian Chem. Soc.* **64** 753 (1987)
168. J W Huffman, Z H Keith, R Z Asbury *J. Org. Chem.* **30** 1600 (1965)
169. Sh Kato, T Fukushima, H Ishihara, T Murai *Bull. Chem. Soc. Jpn.* **63** 638 (1990)
170. P D Beer, O Kocian, R J Mortimer *J. Chem. Soc., Perkin Trans. 1* 3283 (1990)
171. I R Butler, Ch Souay-Breau *Can. J. Chem.* **69** 1117 (1991)
172. Ch-F Shu, F C Anson *J. Phys. Chem.* **94** 8345 (1990)
173. V P Tverdokhlebov, I V Tselinskii, B V Gidasov, G Yu Chikisheva *Zh. Org. Khim.* **12** 2335 (1976)
174. A Meyerhans, W Pfau, R Memming, P Margareta *Helv. Chim. Acta* **65** 2603 (1982)
175. A L J Beckwith, G G Vickery *J. Chem. Soc., Perkin Trans. 1* 1818 (1975)
176. E E Vittal', A S Gibin, A V Dombrovskii *Zh. Obshch. Khim.* **45** 1872 (1975)
177. V I Boev, A V Dombrovskii *Zh. Obshch. Khim.* **47** 2215 (1977)
178. R Herrmann, I Ugi *Angew. Chem.* **91** 1023 (1979)
179. A Ratajczak, B Czech, B Misterkiewicz *Bull. Acad. Pol. Sci., Ser. Sci. Chem.* **25** 541 (1977)
180. M Cushman, J K Chem. *J. Org. Chem.* **52** 1517 (1987)
181. M Metwally, F A Amer *J. Indian Chem. Soc.* **65** 51 (1988)
182. V N Postnov, A V Goncharov, I Khokke, D P Krut'ko *Vestn. Mosk. Univ., Ser. 2: Khim.* **34** 497 (1993)
183. S Foma, M Putala, M Salisova *Collect. Czech. Chem. Commun.* **52** 395 (1987)

184. V N Postnov, A V Goncharov, I Khakke, D P Krut'ko *Dokl. Akad. Nauk* **331** 196 (1993)
185. V N Postnov, A V Goncharov, I Hocke, D P Krut'ko *J. Organomet. Chem.* **456** 235 (1993); *Chem. Abstr.* **119** 271 344 (1993)
186. US P. 3 755 311; *Chem. Abstr.* **80** 5 442 (1974)
187. P Meunier, I Ouattara, B Gautheron, J Tiroufflet, D Camboli, J Besançon *Eur. J. Med. Chem.* **26** 351 (1991)
188. R B Meyer, D A Shuman, R K Robins *J. Am. Chem. Soc.* **96** 4962 (1974)
189. R B Meyer, H Uno, R K Robins, L N Simon, J P Miller *Biochemistry* **14** 3315 (1975)
190. US P. 4 397 700; *Ref. Zh. Khim.* **12** N 223P (1984)
191. P E Cassidy, D M Carlton, L Fogle *J. Polym. Sci., Polym. Chem. Ed.* **9** 2419 (1971)
192. US P. 3 577 238; *Chem. Abstr.* **75** 50 436 (1971)
193. K Rehse, W Schinkel, U Siemann *Arch. Pharm. (Weinheim)* **313** 344 (1980)
194. V Rapić, J Lasinger *Croat. Chem. Acta* **58** 315 (1985)
195. M Lacan, V Rapić *Croat. Chem. Acta* **51** 273 (1978)
196. A Ghose, J N Srivastava *Indian J. Heterocycl. Chem.* **1** 241 (1992)
197. R T Jacobs, A D Wright, F X Smith *J. Org. Chem.* **47** 3769 (1982)
198. Sh Marinuzzi-Brozemer, Bh H Patwardhan, K A Greenberg, D C Dittmer *Heterocycles* **26** 969 (1987)
199. O Riant, O Samuel, H B Kagan *J. Am. Chem. Soc.* **115** 5835 (1993)
200. S P Dolgova, M V Galakhov, V I Bakhmutov *Metalloorg. Khim.* **1** 412 (1988)
201. F A Carey, J R Neergaard *J. Chem. Soc.* **36** 2731 (1971)
202. A Ratajczak, A Priorko *Rocz. Chem.* **51** 967 (1977)
203. H Wan, Z Huang *Yinyong Huaxue* **7** 6 (1990); *Chem. Abstr.* **115** 222 033 (1991)
204. P D Beer, A D Keefe, H Sikanyika, Ch Blackburn, J F McAleer *J. Chem. Soc., Dalton Trans.* 3289 (1990)
205. Yu A Volyanskii, V I Boev *Khim.-Farm. Zh.* **13** 68 (1979)
206. G Markl, O Martin, W Weber *Tetrahedron Lett.* **22** 1207 (1981)
207. G E Herberich, B Hessner *J. Organomet. Chem.* **161** C36 (1978)
208. P R Suszko, R R Whittle, H R Allcock *J. Chem. Soc., Chem. Commun.* 960 (1982)
209. H R Allcock, K D Lavin, G H Riding, P R Suszko, R P Whittle *J. Am. Chem. Soc.* **106** 2337 (1984)
210. R Kalish, Th V Steppe, A Walser *J. Med. Chem.* **18** 222 (1975)
211. P D Beer, Ch Blackburn, J F Aleer, H Sikanyika *Inorg. Chem.* **29** 378 (1990)
212. P D Beer, H Sikanyika, Ch Blackburn, J F McAleer, M G B Drew *J. Chem. Soc., Dalton Trans.* 3295 (1990)
213. P D Beer *J. Organomet. Chem.* **297** 313 (1985)
214. P D Beer, D B Crowe, M J Ogden, M G B Drew, B Main *J. Chem. Soc., Dalton Trans.* 2107 (1993)
215. R A Bartsch, B R Czech, B Strzelbicka, R A Hoiwerda, Z Huang *J. Coord. Chem.* **18** 105 (1988)
216. Z Huang, R A Bartsch *Youji Huaxue* **8** 519 (1988); *Chem. Abstr.* **111** 115 493 (1989)
217. H R Allcock, K D Lavin, G H Riding, R P Whittle *Organometallics* **3** 663 (1984)
218. E I Edwards, R Epton, G Marr *J. Organomet. Chem.* **122** C49 (1976)
219. E I Edwards, R Epton, G Marr *J. Organomet. Chem.* **168** 259 (1979)
220. Ch E Carraher, R J Foust *Polym. Prepr., Am. Chem. Soc. Div. Polym. Chem.* **19** 523 (1979); *Chem. Abstr.* **93** 187 077 (1980)
221. Ch U Pittman, P L Grube *J. Appl. Polym. Sci.* **18** 2269 (1974)
222. M-G A Shvekhgeimer, V I Zvolinskii, K I Kobrakov, A M Krapivan, L V Balabanova *Dokl. Akad. Nauk SSSR* **272** 386 (1984)
223. BRD P. 3 346 177; *Chem. Abstr.* **104** 79 157 (1986)
224. US P. 3 951 703; *Chem. Abstr.* **86** 45 340 (1977)
225. US P. 3 789 609; *Chem. Abstr.* **80** 147 449 (1974)
226. US P. 3 745 177; *Chem. Abstr.* **79** 94 199 (1973)
227. US P. 3 437 634; *Chem. Abstr.* **70** 115 727 (1969)
228. US P. 3 371 128; *Chem. Abstr.* **68** 87 752 (1968)
229. G Schuster *Z. Pflanzenkrankheiten Pflanzenschutz* **92** 27 (1985)

The nature and dynamics of nonlinear excitations in conducting polymers. Polyacetylene

V I Krinichnyi

Contents

I. Introduction	81
II. Magnetic parameters of the charge carriers in <i>trans</i> -polyacetylene	83
III. Passage effects and the electronic relaxation of the charge carriers in polyacetylene	86
IV. Dynamics of the soliton and the mechanism of charge transfer in <i>trans</i> -polyacetylene	88
V. Conclusion	91

Abstract. The results of studies on various properties of polyacetylene by the high-resolution EPR method in the 2 mm wavelength range are surveyed and treated systematically. The structures and dynamic properties of the paramagnetic centres as well as the mechanism of charge transfer in the neutral polyacetylene are discussed. The bibliography includes 76 references.

I. Introduction

During recent years, polyacetylene (PA) has attracted considerable attention by investigators because of the uniqueness of its electrodynamic properties, which may prove promising in molecular electronics. Thus when donor or acceptor dopants are introduced, its d.c. conductivity changes by 10–14 orders of magnitude and reaches $\sigma_{dc} \approx 10^5\text{--}10^7 \text{ S m}^{-1}$.^{1–3} PA is the simplest conducting polymer in a large class of organic conducting compounds (polyphenylene, polypyrrole, polythiophene, polyaniline, etc.) with similar magnetic and electrodynamic properties; this led to the most vigorous study of these properties in relation to this particular compound.

The *cis*- and *trans*-conformations of PA are distinguished, the latter being thermodynamically more stable.^{2,3} The morphology of this polymer depends on the method of synthesis, the structure of the initial monomer, and also on the nature and amount of the dopant introduced. The polymer chains of PA are arranged parallel to one another, forming a fibril several tens of nanometres in diameter and several hundreds of nanometres long. The longitudinal axes of the fibrils are usually randomly oriented in space, but they can be partly or fully oriented during synthesis or by stretching the resulting polymer. The polymer chains in such fibrils are close-packed. The PA crystal lattice has the following parameters: $a = 0.761 \text{ nm}$, $b = 0.439 \text{ nm}$, and $c = 0.447 \text{ nm}$ (*cis*-PA) and $a = 0.424 \text{ nm}$, $b = 0.732 \text{ nm}$, and $c = 0.246 \text{ nm}$ (*trans*-PA).^{4,5}

In each monomer unit of PA, three out of four valence electrons are in the hybridised sp^2 orbitals: two electrons

participate in the formation of two σ -bonds responsible for the formation of the quasi-one-dimensional (1D) lattice, while the third is involved in the formation of a bond with a hydrogen atom. The last valence electron is in the $2p_z$ orbital oriented at right angles to the plane in which the remaining three electrons are located. Thus the σ -bonds form a low-lying completely filled valence band, while the π -bonds of the monomer units form a partly filled conduction band. If the lengths of all the C–C bonds were equal, then undoped *trans*-PA could be regarded as a 1D-metal with a half-filled conduction band. In reality, the system represents a set of monomeric CH groups linked by alternating double and longer single bonds, which execute longitudinal vibrations. Such a system is unstable (Peierls instability) and the alternation in it takes place almost without energy expenditure. Calculation has shown⁶ that the degeneracy of the system leads to the generation on the *trans*-PA chains (with an energy expenditure of 0.42 eV) of nonlinear topological excitations — solitons — with a spin $s = \frac{1}{2}$, an effective number of C–C bonds $N \approx 15$, an effective mass m_s^* equal to six times the free electron masses m_e , and a high 1D-mobility. The energy level of the solitons is located at the centre of the energy gap of the polymer. This phenomenon determines to a large extent the fundamental properties of *trans*-PA, including the relatively large width of the energy gap, which is $\sim 1.4 \text{ eV}$. Some experiments (see, for example, Refs 7–9) yield the effective number of C–C bonds $N \approx 50$ and $m_s^* = (0.15 - 0.40)m_e$.

The spin–charge conversion is characteristic of a single soliton in *trans*-PA: the neutral soliton corresponds to a radical with a spin $s = \frac{1}{2}$, whereas a negatively or positively charged soliton lacks spin and becomes diamagnetic. Therefore, in n-type doping, the energy level of the soliton becomes fully occupied, whilst in p-type doping it becomes entirely unoccupied. For a low level of doping, only some of the neutral solitons become charged. With increase in the level of doping, all the solitons become diamagnetic and their individual energy levels merge into the soliton band located in the middle of the energy gap of the polymer. The formation of the soliton band leads to charge transfer by the spin-free carriers after the semiconductor–metal transition. This conduction mechanism, which includes the motion of charged solitons in an occupied or unoccupied band, differs significantly from the charge transfer process in classical semiconductors.

In PA, there is the possibility of the occurrence of various charge transfer processes, which may be arranged in the following sequence in order of their decreasing probability: 1D-conduction along polymer chains; charge transfer in hops between polymer chains; tunnelling of the charge between highly conducting

V I Krinichnyi Laboratory for the Synthesis of Electrically Conducting Compounds, Institute of Chemical Physics in Chernogolovka, 142432 Chernogolovka, Moscow Region, Russian Federation
Fax (7-096) 515 35 88. Tel. (7-096) 524 50 35

Received 6 July 1995

Uspekhi Khimii 65 (1) 84–96 (1996); translated by A K Grzybowski

domains of fibrils separated by regions with a lower conductivity; or fluctuation-induced tunnelling of the charge between fibrils.

It is entirely evident that the contribution of each of these processes depends on the properties of the initial polymer and may change during its doping.

Conjugated polymers are characterised by the presence of a π -electron system and a partly filled band structure, which determines important electronic properties of these systems. In contrast to the classical semiconductors, apart from the activated electron transport,¹⁰ in PA there is also the possibility of phonon-assisted charge tunnelling between the energy levels of solitons¹¹ and of variable range hopping conductivity (VRH)¹² characterised by different frequency and temperature dependences $\sigma(\nu_e, T)$. Such diversity of electron transport is associated with the generation of nonlinear soliton-type excitations and may be associated directly with the evolution of both the crystalline and the electronic structures of the system.

Several theoretical approaches have been put forward for the description of the mobility of the soliton in *trans*-PA. They were developed in terms of the concept of the Brownian 1D-diffusion of solitons interacting with the lattice phonons¹³ and of the scattering of solitons by optical and acoustic phonons in *trans*-PA.¹⁴ One of them predicts a quadratic dependence of the frequency of the 1D-diffusion $\nu_{1D} = D_{1D}c_{||}^{-2}$ (D_{1D} is the 1D-diffusion coefficient and $c_{||}$ is the length of the soliton jump along the polymer chain) on temperature. In the second case, the dependences have the form $\nu_{1D}(T) \sim T^{-1/2}$ and $\nu_{1D}(T) \sim T^{1/2}$ for the optical and acoustic phonons respectively. Calculations showed¹⁵ that the frequency of the 1D-diffusion of the soliton should not exceed the limiting value $\nu_{1D}^F = 3.8 \times 10^{15}$ Hz near the Fermi level.

Many fundamental properties of PA and other conjugated polymers are determined by the existence in them of the localised paramagnetic centres (PC) and/or such centres delocalised along the polymer chains, so that the majority of the investigations of these compounds have been carried out by the EPR method.^{16,17} We shall consider certain possibilities for the study of PA by this method.

At relatively low measuring frequencies ($\nu_e \leq 10$ GHz), PA gives rise, like the classical π electron systems, to a single symmetrical EPR line with $g = 2.002634 \pm 0.000015 \approx g_e$.¹⁸ The g -factor deviates from g_e mainly owing to some contribution by the orbital angular momentum of the unpaired electron to its overall magnetic moment. The EPR line consists of a superposition of individual weakly resolved lines corresponding to the hyperfine interaction of the spin with the carbon nuclei on which the soliton is localised.

According to the model proposed by Su et al.,⁶ the defect-free undoped *cis*-PA contains no paramagnetic centres and should therefore be diamagnetic. In reality, *cis*-PA contains 5%–10% of short segments of *trans*-PA, mainly at the ends of the chains^{3,16} where the trapping of solitons is most likely.¹⁹ Such an isomer therefore gives rise to a relatively weak broad EPR line, in which the distance between the peaks is $\Delta B_{pp} = 0.6$ –1.0 mT ($g = 2.002634$) and the hyperfine interaction tensor constants are $A_{xx} = -1.16$ mT, $A_{yy} = -3.46$ mT, and $A_{zz} = -2.32$ mT²⁰ (the x , y , and z axes are directed along the crystallographic a , c , and b axes respectively). On thermal *cis*–*trans* isomerisation, the concentration of paramagnetic centres increases from $N \sim 10^{18}$ spins g^{-1} (this is equivalent to one spin per $\sim 44\,000$ CH groups) in *cis*-PA to $N \sim 10^{19}$ spins g^{-1} (or one spin per 3000–7000 CH groups) in *trans*-PA.²¹ This is accompanied by a sharp narrowing of the line of 0.03–0.50 mT.^{16,22} The latter quantity depends on the average length of the *trans*-sections and represents a linear function of the concentration of the sp^3 -defects.²³ A dependence of the type $\Delta B_{pp} \sim Z^{2.3}$ has been obtained for PA doped with metal ions having an atomic number Z .²⁴ The line width of *trans*-PA partially ordered by stretching proved sensitive to the direction of stretching c of the specimen in a magnetic field with a strength

B_0 .^{23,25–28} Thus, in the case of the parallel direction of the external magnetic field strength vector relative to the c axis, the line width is 0.48 mT, whilst in the case of the perpendicular direction it is 0.33 mT.²³

The EPR spectrum of *trans*-PA may be represented by a superposition of the contributions of the trapped and highly mobile solitons with concentrations n_1 and n_2 respectively, the ratio of which varies with temperature, and also of the contributions due to other fixed centres, the appearance of which is associated with the presence of traces of catalyst and/or oxygen molecules. In n - and p -doping, the concentration of paramagnetic centres in *trans*-PA changes monotonically for a virtually constant g -factor,^{16,17} which indicates the retention of the nature of the paramagnetic centres responsible for the EPR signal.

Numerous studies on the paramagnetic susceptibility χ of neutral PA have shown¹⁷ that both its conformers exhibit Curie paramagnetism ($\chi \sim T^{-1}$) at $T \leq 300$ K, whereas, according to the data of Tomkiewicz et al.,²⁹ the magnetic susceptibility of *cis*-PA does not obey the Curie law in the temperature range 4–300 K. The reasons for this discrepancy are so far obscure.

High-frequency magnetic field modulation as well as electron spin-echo have been used to investigate the interaction of the unpaired electron with other electrons or with the *trans*-PA lattice. Since a neutral soliton has an electron spin interacting with the spins of the hydrogen nuclei, its dynamics may be investigated by complementary NMR and EPR methods.

The quasi-one-dimensional mobility of the soliton has been investigated by NMR within the framework of the Brownian 1D-diffusion of the soliton.^{30,31} The dependence of the nuclear spin–lattice relaxation time τ_1 on the precession frequency of the nuclear spin $\tau_1 \sim \nu_p^{1/2}$, obtained for undoped and doped *trans*-PA specimens, corresponded to the characteristic spectrum of the spin 1D-diffusion. The frequency of the 1D-diffusion of the soliton in undoped *trans*-PA proved to be 6×10^{14} Hz (at room temperature) and showed a quadratic temperature dependence. Estimates showed³⁰ that the rate of diffusion may increase by more than three orders of magnitude following the introduction of various dopants into the polymer.

However, it must be emphasised that the motion of the soliton influences only indirectly the nuclear spin relaxation time. Since the interaction of the diffusing proton with a fixed electron spin is also characterised by the frequency dependence $\tau_1 \sim \nu_p^{1/2}$,³² this can lead to an incorrect interpretation of the results obtained by NMR spectroscopy. Thus, on the basis of the kinetics of the decay of the ^{13}C NMR signal, it has been concluded³³ that there are no mobile unpaired electrons at all in *trans*-PA. However, according to Ziliox et al.,³⁴ this conclusion may be valid only for the specific specimens investigated by Masin et al.³³

The EPR spectroscopic method is a priori more effective in the study of the dynamics of the soliton in *trans*-PA, since the electronic relaxation times are unambiguously related to the diffusion of the soliton.

The spin dynamics in *trans*-PA has been investigated with the aid of low-frequency steady-state EPR^{26–28,35,36} and the spin-echo method.^{37–39} The relations $\tau_{1,2} \sim \nu_e^{1/2}$ and $\nu_{1D}(T) \sim T^2$ (τ_1 and τ_2 are the spin–lattice and spin–spin relaxation times) were obtained by the first method in the frequency range $\nu_e = 5$ –450 MHz. They indicate the 1D-diffusional spin motion in *trans*-PA with $\nu_{1D} \geq 10^{13}$ Hz and the anisotropy $\nu_{1D}/\nu_{3D} = 10^6$ – 10^7 (at room temperature). A similar frequency dependence of the rate of diffusion has been observed also at higher recording frequencies $\nu_e = 9$ –14 GHz.^{38,40} However, the spin diffusion frequency determined by the spin-echo method is $\nu_{1D} \leq 10^{11}$ Hz (at room temperature) and exhibits a more complex temperature dependence.³⁷

Thus the data obtained by different methods and by different investigators concerning the dynamics of solitons in *trans*-PA are extremely contradictory and do not always find an unambiguous interpretation. EPR spectroscopy is the most promising method

for the investigation of the composition and dynamics of the paramagnetic centres. However, it suffers from considerable limitations owing to the low spectral resolution and the high spin-spin exchange at $\nu_e \leq 40$ GHz. This prevents the separate recording in *trans*-PA of localised and mobile π -radicals with similar magnetic parameters.²²

It had been shown earlier in relation to certain organic radicals^{41,42} that in the 2 mm wavelength range there is a significant increase in the accuracy and the information content of the EPR method in the study of the structure and molecular dynamics of radicals with $g \approx g_e$ in model systems and biological polymers. The high resolving power of the method, attained in this frequency range, converts the g -factor of organic free radicals into an important information parameter. This makes it possible to discover the anisotropic character of the slow molecular motions, to extend the range of the measured correlation times for the rotation of the radical, and also to identify the structure of the radical and of its microenvironment.

The high spectral resolution of the EPR method in the 2 mm range yields important information about the spin and molecular dynamics in organic conducting compounds.⁴³ The present review is devoted to the consideration of the experimental data obtained in the study of the structure and electrodynamic properties of PA by two-millimetre EPR spectroscopy. The theoretical foundations of the method have been described in fair detail in a number of monographs† and will not therefore be considered here.

II. Magnetic parameters of the charge carriers in *trans*-polyacetylene

For a more correct determination of the magnetic resonance parameters of the paramagnetic centres in PA, various films of *cis*- and *trans*-PA were investigated over a wide EPR frequency range.⁴⁴

In the 3 cm EPR range ($\nu_e = 9.8$ GHz), the *cis*- and *trans*-PA specimens are characterised by a single symmetrical line with $g = 2.0026$ and the width between the peaks $\Delta B_{pp} = 0.67$ mT (*cis*-PA) and 0.22 mT (*trans*-PA) (Fig. 1). The latter quantity exceeds the minimum width of the *trans*-PA spectral line,¹⁶ and is apparently associated with the presence in the specimen of oxygen molecules or shorter π -conjugated chains, but is within the limits of the variation of the ΔB_{pp} obtained for different *trans*-PA specimens.²² This line is broadened by 0.05–0.17 mT at 77 K, probably as a consequence of the decrease in the frequency of the librations of the polymer chains and is additionally broadened by 0.1 mT when the polymer comes into contact with atmospheric oxygen, apparently owing to the strengthening of the trapping of the mobile solitons in *trans*-PA.⁴⁵

An increase in the recording frequency to 37.5 GHz results in a slight increase in the width of the lines in the PA spectrum (Table 1) with retention of the symmetry.

In the 3 mm EPR range, the line width of the *cis*-PA spectrum increases to 0.84 mT. This is accompanied by an additional broadening of the high-field spectral peak owing to the manifestation of the anisotropy of the g -factor. *trans*-PA is characterised by a line with $g = 2.00270$, $\Delta B_{pp} = 0.37$ mT, and the asymmetry factor $A:B = 1.1$ (the ratio of the amplitudes of the high-field and low-field spectral peaks).

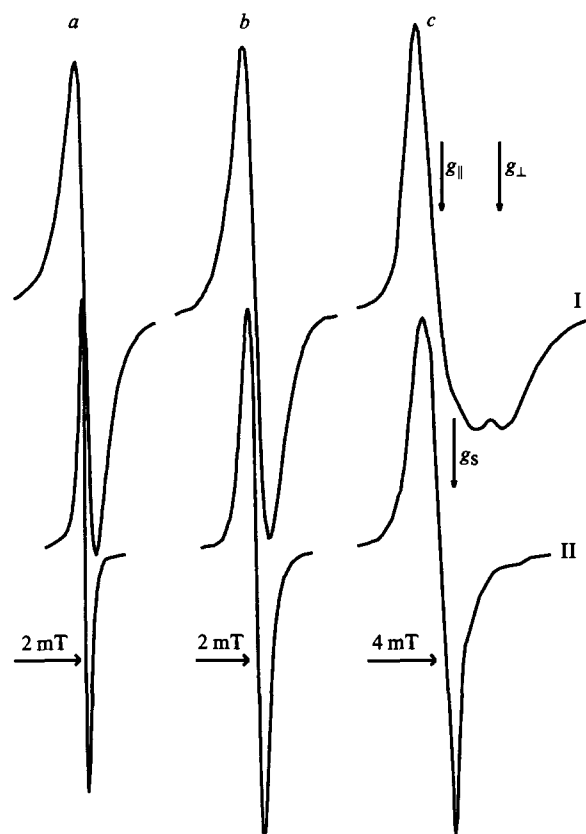


Figure 1. EPR spectra of *cis*-(I) and *trans*-polyacetylene (II) recorded in the 3 cm (a), 2 mm (b), and 0.6 mm (c) ranges at room temperature under an inert atmosphere. The positions of the components of the g -tensor of the localised solitons (g_{\parallel} and g_{\perp}) and the g_s -factor of the delocalised solitons are indicated.

Table 1. The line widths (in mT) and the distances between the spin packets (in Hz) for the paramagnetic centres in neutral polyacetylene at different recording frequencies at 300 K.

ν_e /GHz	ΔB_{pp}			$\Delta\omega_{ij} \times 10^8$		
	I	II	III	I	II	III
9.8	0.70	0.25	0.06 ^a	1.7	1.0	0.8 ^a
37.5	0.75	0.30	0.11 ^a	1.8	1.2	1.3 ^a
94.3	0.85	0.45	0.18	1.9	1.4	1.7
139	0.95	0.61	0.30	2.3	2.2	2.2
250	1.82	1.60	0.50	2.8	2.8	2.9
349	2.42	2.52	0.62	3.2	3.5	3.2
428	2.53	1.91	0.81	3.3	3.1	3.7

Remarks. I—solitons localised in *cis*-PA; II—solitons localised in *trans*-PA; III—solitons delocalised in *trans*-PA.

^a Values obtained by extrapolation.

In the 2 mm range for the recording of the EPR spectrum, there is a further increase in ΔB_{pp} to 1.1 mT (in *cis*-PA) and 0.5 mT (in *trans*-PA) accompanied by a more marked manifestation of the anisotropy of the g -factor in *cis*-PA and a greater asymmetry of the spectral line ($A:B = 1.3$) in *trans*-PA (Fig. 1).

In order to elucidate the possible dependence of the PA spectral line width on the orientation of the magnetic field, a study has been made⁴⁶ of partly oriented *cis*- and *trans*-PA specimens. The investigation showed that the line width in the spectrum of the initial *cis*-PA specimen increases after slight stretching of the film from 1.23 to 1.45 mT ($T = 300$ K).

† J D Memory *Quantum Theory of Magnetic Resonance Parameters* (McGraw-Hill, New York, 1968)

B Ranby, J F Rabek *EPR Spectroscopy in Polymer Research* (Springer, Berlin, 1977)

C P Slichter *Principles of Magnetic Resonance* 2nd Ed. (Springer, Berlin, 1978)

Theoretical Foundations of Electron Spin Resonance Ed. J E Harriman (Academic Press, New York, 1978)

The magnetic parameters of the partly oriented *cis*-PA did not change significantly on varying the angle between the directions of stretching and the external magnetic field, whereas the line width in *trans*-PA changed nonmonotonically from 0.60 to 0.68 mT at room temperature.

With increase in the recording frequency, a further broadening and a further increase in the asymmetry of the EPR spectral lines of both conformers were observed (Fig. 1). Analysis carried out by the method described by Lebedev and Muromtsev⁴⁷ showed that the spectrum of *cis*-PA, presented in Fig. 1, may be assigned to paramagnetic centres with the g -tensor components $g_{\parallel} = 2.00283(5)$ and $g_{\perp} = 2.00236(5)$ (g_{\parallel} and g_{\perp} correspond to the parallel and perpendicular directions of the external magnetic field relative to the crystallographic c axis of the polymer chain). The values of the g -tensor quoted exceed somewhat the values of g_{\parallel} and g_{\perp} determined experimentally⁴⁸ but are close to $g_{\parallel} = 2.0034$ and $g_{\perp} = 2.0028$ calculated in the same study for localised paramagnetic centres. The quantity g_{\parallel} differs from g_e by $\Delta g = 5 \times 10^{-4}$. This deviation corresponds to the excitation of the electron from the bonding σ_{C-C} orbital to the antibonding π^* orbital with $\Delta E_{\sigma\pi^*} = 2\lambda_c \Delta g^{-1} = 14.4$ eV (here $\lambda_c = 3.6$ meV is the constant for the spin-orbital interaction of the unpaired electron with the nucleus of the carbon atom), which is close to the corresponding value calculated for the C-C bond in π -conjugated systems.⁴⁹ Other electronic transitions with a greater ΔE_{ij} do not contribute significantly to Δg . Thus the line form in the *cis*-PA spectrum as well as the agreement between the experimental and theoretical values of $\Delta E_{\sigma\pi^*}$ indicate the existence of localised paramagnetic centres in this isomer.

The transformation of the line shape on *cis-trans* isomerisation of PA evidently indicates the appearance in the PA of mobile paramagnetic centres with $g_s = 2.00268$ (Fig. 1) during the occurrence of this process. The similarity of the isotropic g -factor of the localised paramagnetic centres [$\langle g \rangle = \frac{1}{3}(g_{\perp} + 2g_{\parallel}) = 2.00267$] and the g -factor of the delocalised paramagnetic centres indicates the virtually complete averaging of the components of the g -tensor of the mobile paramagnetic centres owing to their 1D-diffusion at a minimal rate.⁵⁰

$$\nu_{1D}^0 \geq \frac{1}{h} (g_{\parallel} - g_{\perp}) \mu_B B_0 \quad (1)$$

Computer simulation⁴⁴ confirmed this hypothesis. A similar averaging of the components of the anisotropic g -factor was recorded by ourselves also on 'unfreezing' the 1D-diffusion of polarons in other organic conducting polymers.⁴³ Thus two types of paramagnetic centres exist in undoped *trans*-PA, namely the neutral soliton trapped at the ends and/or on short segments of the π -conjugated chain¹⁹ and the soliton moving along the polymer chain with a frequency $\nu_{1D}^0 > 2 \times 10^8$ Hz. The value of ν_{1D}^0 obtained is significantly less than the lower limit of the rate of diffusion of solitons previously predicted.³⁰ The concentrations of the corresponding paramagnetic centres are $n_1 = 1.1 \times 10^{-3}$ and $n_2 = 6 \times 10^{-5}$ spins per carbon atom. It is necessary to note that the latter quantity is almost two orders of magnitude smaller than the value predicted previously.^{18,51}

Analysis of the form of the spectra of *cis*- and *trans*-PA specimens by the method of Tikhomirova and by Voevodskii⁵² showed that, for $\nu_e \geq 140$ GHz, the distribution of the individual spin packets in their low-field sections is described by Lorentzian (at the centre) and Gaussian (on the wings) functions. On the other hand, the high-field parts of the spectra are characterised by a Lorentzian distribution of the spin packets. This made it possible to calculate the frequencies of the spin-spin exchange ν_{ex} between the localised paramagnetic centres in *cis*- and *trans*-PA, which are 3×10^7 and 1.2×10^8 Hz respectively. These quantities are consistent with $\nu_{ex} \geq 10^7$ Hz obtained for *trans*-PA.²² Thus, at a recording frequency $\nu_e \geq 16$ GHz, the distance between the spin packets $\Delta\omega_{ij}$ exceeds ν_{ex} , so that the spin packets may be regarded as virtually noninteracting and the

width of the lines of the localised paramagnetic centres is described by the equation⁵³

$$\Delta B_{PP} = \Delta B_{PP}^0 + \frac{\Delta\omega_{ij}^2}{8\nu_{ex}}, \quad (2)$$

where ΔB_{PP}^0 is the line width in the absence of interaction between the paramagnetic centres. Assuming that the relaxation time τ_2^{mob} of the delocalised paramagnetic centres is 1.8×10^{-7} s for *trans*-PA at room temperature⁵⁴ and taking into account the strong interaction between solitons with different mobilities, it is possible to calculate the line width in the spectrum of the mobile soliton ΔB_{PP} , which proved to be 32 μ T. This quantity agrees well with the line width in the spectrum of the mobile soliton (12–38 μ T) predicted by Holczer et al.²²

The values of $\Delta\omega_{ij}$ calculated for the paramagnetic centres in *cis*- and *trans*-PA by Eqn (2) are presented in Table 1. The table shows that the isomerisation of PA is accompanied by a decrease in $\Delta\omega_{ij}$ for the paramagnetic centres in both conformers. Taking into account the increase in ν_{ex} indicated above, one may conclude that the change of precisely these quantities is the cause of the sharp narrowing of the EPR spectra (for $\nu_e \leq 10^{10}$ Hz) during the *cis-trans* isomerisation of PA. This conflicts with the view current up to the present time that the line narrowing indicated above is possible only by virtue of the 'unfreezing' of the 1D-diffusion of most of the solitons in *trans*-PA.^{13,16,30}

The dependences of the broadening of the lines of the localised and mobile paramagnetic centres on the measuring frequency are illustrated in Fig. 2. The latter shows that the line width in the spectrum of the paramagnetic centres localised in both conformers varies almost quadratically with ν_e , in conformity with Eqn (2), which constitutes additional evidence for the weak interaction of the spin packets in PA. On the other hand, the line width in the spectrum of the delocalised paramagnetic centres increases in accordance with the law $\Delta B_{PP}^{\text{mob}} \sim \nu_e^{3/2}$, which is a consequence of the stronger spin-phonon interaction in *trans*-PA owing to the 1D-motion of the solitons.

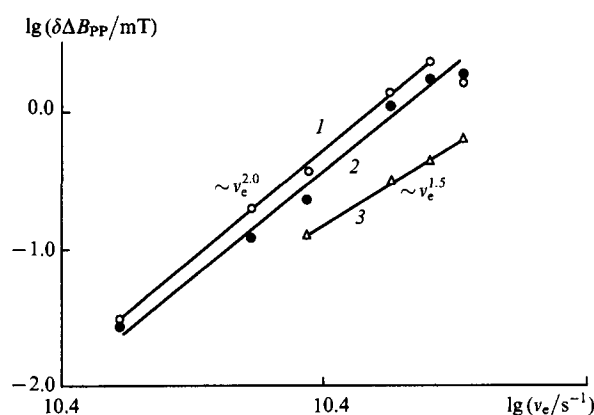


Figure 2. Logarithmic dependences of the broadening ($\delta\Delta B_{PP}$) of the EPR lines of the paramagnetic centres localised in *trans*-polyacetylene (line 1) and *cis*-polyacetylene (line 2) (relative to the quantity ΔB_{PP}^0 measured at 9.8 GHz), as well as the paramagnetic centres delocalised in *trans*-polyacetylene (line 3) (relative to the quantity ΔB_{PP}^0 measured at 94.3 GHz) on the recording frequency at room temperature.

It is seen from the analysis of Table 1 that, at least for $\nu_e \leq 140$ GHz, the following familiar relation holds:⁵⁵

$$(\Delta B_{PP}^{\text{mob}})^3 = \frac{\gamma_e (\Delta B_{\perp}^{\text{loc}})^4}{\nu_{1D}'} \quad (3)$$

where γ_e is the gyromagnetic ratio for the electron. This follows from the theory of random motion and characterises the line narrowing in the EPR spectrum of a semiconductor when spin 1D-diffusion arises in the latter with an effective rate $\nu'_{1D} \approx 2 \times 10^{11}$ Hz.⁵⁶ We may note that another relation is valid for spin 3D-motion:

$$\Delta B_{pp}^{\text{mob}} = \frac{\gamma_e (\Delta B_{\perp}^{\text{loc}})^2}{\nu'_{1D}}.$$

This constitutes additional evidence for the 1D-diffusion of solitons in *trans*-PA. For $\nu_e > 140$ GHz, Eqn (3) does not hold, apparently owing to the similarity of the quantities ν_e and ν'_{1D} .

Fig. 3a presents the temperature dependences of the reduced concentrations of the paramagnetic centres (N) of certain *cis*-PA specimens, which can be fitted by the following function:

$$N(T) = A \exp\left(-\frac{E_a}{kT}\right) + BT^{-n} \quad (1 \leq n \leq 2), \quad (4)$$

where A and B are constants and E_a is the activation energy. The first term of Eqn (4) is determined by the librations of the polymer chains, the activation energies of which for different specimens are 0.035–0.055 eV. A similar manifestation of the electron–phonon interaction (mainly in the form of fluctuations of the electronic polarisation energy of the order of several millielectron volts) has been observed in organic crystalline semiconductors.⁵⁷ As can be seen from the figure, the activated ordering of the magnetic moments of the spins makes the main contribution to the paramagnetic susceptibility only at high temperatures. In the range of temperatures below a critical temperature $T_c \approx 150$ K, this process competes with others, in particular with the process described by the Curie equation ($n = 1$). The contributions of the processes involving the orientation of the magnetic moments of the unpaired electrons are different for different *cis*-PA specimens.

The concentration of the paramagnetic centres in the *trans*-PA specimens is also characterised by an anomalous temperature dependence (Fig. 3b). As in the case of *cis*-PA, the main contribution to the paramagnetic susceptibility of *trans*-PA in the high-temperature region comes from the first term of Eqn (4). The increased value of E_a ($E_a = 0.06 - 0.19$ eV) may be explained by the increase in the rigidity of the polymer chains and in their packing density on *cis*–*trans* isomerisation. This is apparently

also the cause of the shift of the critical temperature into the region $T_c \approx 250$ K.

In contrast to *cis*-PA, *trans*-PA is characterised by a steeper initial section of the $N(T)$ curve at $T < T_c$. [The quantity n in Eqn (4) varies from 1 to 4 for the *trans*-PA specimens obtained] and reaches a plateau at $T \leq 140$ K. The latter fact is analogous to the manifestation of the so called magnetic saturation. However, for the given temperature range, magnetic saturation may occur when the condition $g\mu_B SB_0 > kT$ is fulfilled, i.e. for $B_0 > 100$ T, which greatly exceeds the magnetic field strength $B_0 \leq 5$ T used in our experiments. Most probably, this effect may be induced by the significant increase in the concentration of neutral solitons with an amplitude A and hence by the shortening of the inter-radical distance R and the intensification of the interaction between these charge carriers with the probability $W_R \sim A \exp(-2AR)$.⁵⁸ Furthermore, the ‘unfreezing’ of the 1D-diffusion of a proportion of solitons at a rate ν_{1D} leads to an additional increase in the probability of the intersoliton interaction $W_{ss} \sim \nu_{1D} \sim \nu_{1D}^0 T^{-2}$ (see below). As a consequence of the overlap of the wave functions of the unpaired electrons of neighbouring solitons, their discrete levels, located in the energy gap, are broadened and transformed into a soliton band of finite width. As in the case of *cis*-PA, the constants A , B , and n are determined by the different properties of the *trans*-isomer.

The study of *trans*-PA specimens lightly doped with iodine vapour has shown⁵⁴ that the form of the spectra and the ratio of the concentrations of the mobile and localised paramagnetic centres do not vary. This finding agrees with the earlier hypothesis⁴⁵ of the existence in *trans*-PA of both mobile solitons and solitons trapped in short conjugated sections of the chain. Although the paramagnetic centres indicated do in fact have different mobilities, in the course of the doping process they acquire a charge with equal probabilities and become diamagnetic.

The magnetic properties of PA thus depend significantly both on the conformation of the polymer chains and on the concentration and mobility of the neutral solitons. In the *cis*–*trans* isomerisation of the initial PA specimen, the concentration of the trapped solitons increases appreciably and mobile charge carriers appear. The ‘unfreezing’ of the mobility of a small proportion of the solitons does in fact increase the conductivity of the film by several orders of magnitude. The transition to high fields for the recording of the EPR spectra increases significantly the resolution of the method and diminishes the probability of the

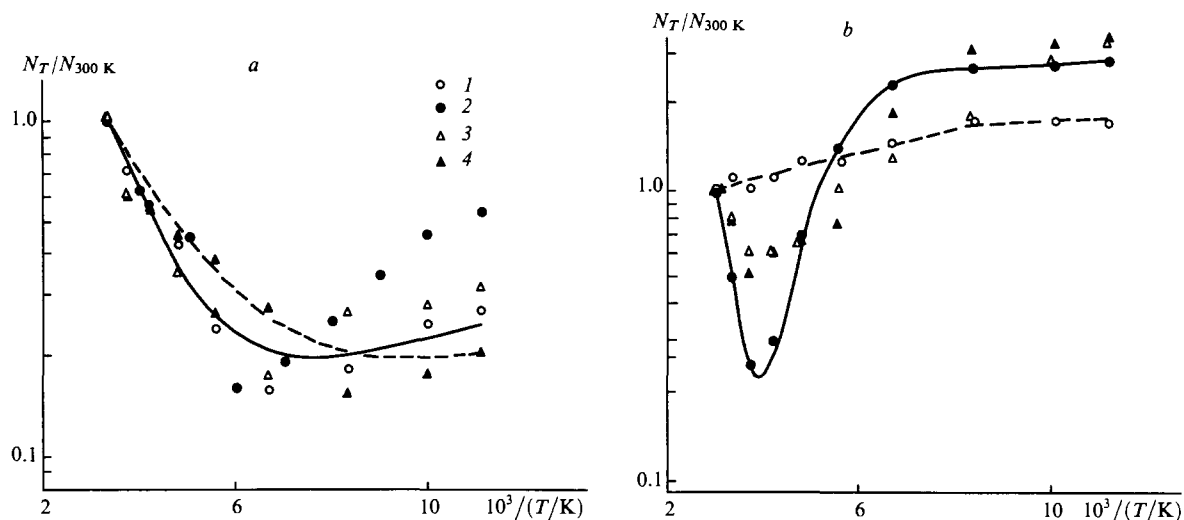


Figure 3. Temperature dependences of the concentrations of the paramagnetic centres in specimens 2 (1), 4 (2), 6 (3), and 5 (4) (Table 2) of (a) *cis*- and (b) *trans*-polyacetylenes relative to values measured at room temperature.

interaction between paramagnetic centres having different mobilities, which makes it possible to analyse more correctly and accurately the magnetic properties of the localised and delocalised solitons in PA.

III. Passage effects and the electronic relaxation of the charge carriers in polyacetylene

With increase of the amplitude of the magnetic component of the UHF field B_1 , dome-shaped components with a Gaussian distribution of the spin packets were recorded in the 2 mm EPR spectra of *cis*- and *trans*-PA (Fig. 4).^{54,59} The intensity and form of these components depend on the amplitude B_m and the frequency ω_m of the HF modulation, the quantity B_1 , and the relaxation times of the paramagnetic centres. The appearance of these signals is associated with the manifestation of the effects of the rapid adiabatic passage of a nonuniformly ordered line.⁶⁰ Such passage effects had not been recorded previously in the study of PA in the frequency range $\nu_e \leq 37$ GHz.¹⁶ The following explanation of this finding can be put forward. The form of an individual spin packet in PA is determined by a set of time characteristics: τ_1 , τ_2 , $(\gamma_e \Delta B_{PP})^{-1}$, ω_m^{-1} , $(\gamma_e B_m)^{-1}$, $(\gamma_e B_1)^{-1}$, and $B_1(dB_0/dt)^{-1}$.

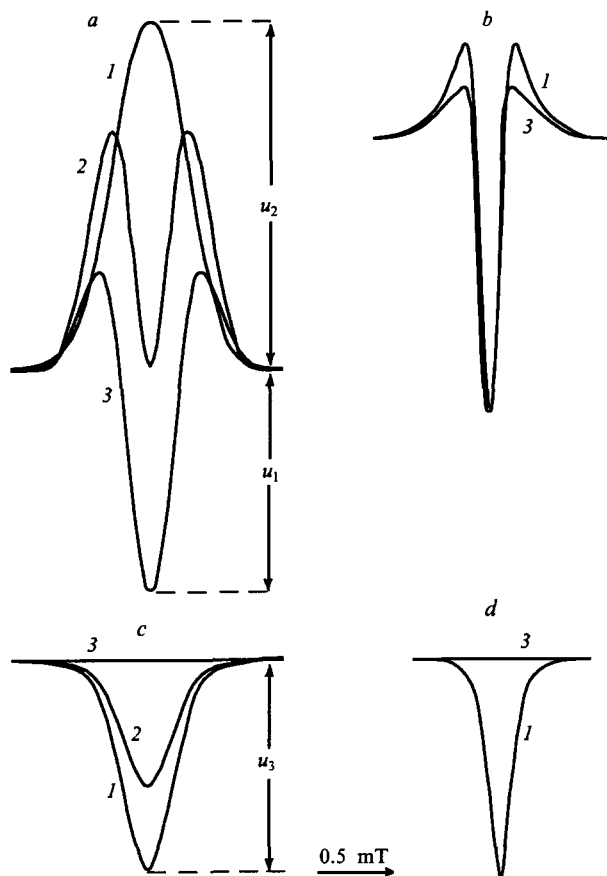


Figure 4. In-phase (a, b) and quadrature (c, d) components of the first derivatives of the dispersion signals of specimens of *cis*-(a, c) and *trans*-PA (b, d) recorded in the two-millimetre EPR range for different values of B_1 (mT): (1) 0.2; (2) 0.2–20; (3) 20.

On transition to high magnetic fields, the probability of the cross-relaxation of the paramagnetic centres with $s = \frac{1}{2}$ and $g \approx 2$, localised at a distance $r_{1,2}$, diminishes in accordance with the law⁶¹

$$W_{cr} \sim r_{1,2}^{-3} \exp(-0.25 B_0^2 r_{1,2}^6 \mu_B^{-2}),$$

as a consequence of which the interaction between the spin packets diminishes and they may be saturated under the usual experimental conditions. When the conditions for the saturation of the signal [$s = \gamma_e B_1(\tau_1 \tau_2)^{1/2} \geq 1$] and for the adiabatic nature of the passage of its envelope ($\gamma_e \omega_m B_m \ll \gamma_e^2 B_1^2$) are fulfilled and also when the signal passage time exceeds the effective relaxation time $\tau = (\tau_1 \tau_2)^{1/2}$, i.e. $B_1(dB_0/dt)^{-1} \gg \tau$, there is insufficient time for the relaxation processes to influence significantly the nature of the motion of the magnetisation vector M of the paramagnetic centres during the period of its precession around the direction B_m . The repeated passage through resonance leads to the establishment of a stationary trajectory of the vector M and to the appearance of three components (u_1, u_2, u_3) of the dispersion signal U with the shape function $g(\nu_e)$.⁶²

$$U = u_1 g'(\nu_e) \sin(\omega_m t) + u_2 g(\nu_e) \sin(\omega_m t - \pi) + u_3 g(\nu_e) \sin(\omega_m t \pm \pi/2), \quad (5)$$

along the z , $-z$, and $-x$ axes respectively. These components can be recorded separately with the appropriate tuning of the phase detector of the instrument. The contribution of each component u_i depends on the ratio of τ to the rate of passage through resonance $B_1(dB_0/dt)^{-1}$. Evidently $u_2 = u_3 = 0$ when $s \ll 1$. In this case, the classical u_1 dispersion signal is recorded. When the inequality $B_1(dB_0/dt)^{-1} \geq \tau$ holds, the vector M has sufficient time to relax to the equilibrium state during each modulation period and the U dispersion signal is determined mainly by the components $u_1 g'(\omega_e)$ and $u_3 g(\omega_e)$ with the intensities at the centre of the spectrum (for $\nu = \nu_e$)

$$u_1 = M_0 \pi \gamma_e^2 B_1 B_m \quad \text{and} \quad u_3 = \frac{1}{2} M_0 \pi \gamma_e^2 B_1 B_m \tau_1 \tau_2.$$

At a low rate of relaxation, the spin 'sees' only an average applied field and the signal is described by the integral terms of Eqn (5) with the central intensities

$$u_2 = \frac{1}{2} M_0 \pi \gamma_e^2 B_1 B_m \tau_2 \quad \text{and} \quad u_3 = M_0 \pi \gamma_e^2 B_1 B_m \tau_2 (4\omega_m \tau_1)^{-1}.$$

The case $\omega_m \tau_1 > 1$ occurs for *cis*-PA, so that the dispersion signal is determined mainly by the last two terms of Eqn (5). Calculations have shown^{54,59} that in this case the relaxation times may be calculated from the ratio of the central amplitudes of these components by means of the following formulae:

$$\tau_1 = \frac{3\omega_m(1+6\Omega)}{\gamma_e^2 B_{10}^2 \Omega(1+\Omega)}, \quad (6a)$$

$$\tau_2 = \frac{\Omega}{\omega_m}, \quad (6b)$$

where $\Omega = u_3 u_2^{-1}$, and B_{10} is the value of the component B_1 for which the condition $u_1 = -u_2$ holds.

In the EPR spectra of *trans*-PA, the passage effects are manifested to a much lesser extent (Fig. 4). The condition $\omega_m \tau_1 < 1$ holds for this substance, so that the relaxation times can be calculated by the formulae^{54,59}

$$\tau_1 = \frac{\pi u_3}{2\omega_m u_1}, \quad (7a)$$

$$\tau_2 = \frac{\pi u_3}{2\omega_m(u_1 + 11u_2)}. \quad (7b)$$

The temperature dependences of the quantities τ_1 and τ_2 , determined from the 2 mm EPR spectra of the specimens of *cis*- and *trans*-PA of different thickness and obtained under different conditions of synthesis, are presented in Table 2 in the functional form $\tau_{1,2} = AT^a$. Fig. 5 presents the functions $\tau_1(T)$ and $\tau_2(T)$ for

Table 2. Temperature dependences of the relaxation times [$\tau_{1,2} = AT^\alpha(s)$] for different *cis*- and *trans*-polyacetylene specimens.

Specimen	τ_1		τ_2		τ_1	τ_2	τ_1	τ_2
	<i>A</i>	α	<i>A</i>	α	<i>A</i>	α	<i>A</i>	α
<i>cis</i> -PA					<i>trans</i> -PA			
1	0.04	-1.6	1.8×10^{-9}	1.2	2.7	-2.6	1.0×10^{-7}	0.5
1 ^a	0.37	-2.0	7.7×10^{-9}	1.0	—	—	—	—
2	0.006	-1.4	1.5×10^{-7}	0.5	0.1	-2.2	7.2×10^{-8}	0.3
2 ^a	0.77	-2.3	1.0×10^{-7}	0.5	—	—	—	—
3	1.4	-2.3	9.5×10^{-8}	0.5	2.0×10^{-3}	-1.7	1.3×10^{-5}	-0.9
3 ^a	290	-3.3	1.7×10^{-8}	0.8	—	—	—	—
3 ^b	52	-2.7	1.2×10^{-8}	0.8	—	—	—	—
3 ^{ab}	6.5	-3.6	4.2×10^{-9}	1.0	—	—	—	—
3 ^c	—	—	—	—	62	-3.5	2.1	-3.0
4	0.65	-2.1	9.6×10^{-9}	0.9	4.0×10^{-3}	-1.5	2.9×10^{-6}	-1.0
4 ^a	10	-2.6	2.8×10^{-9}	1.1	—	—	—	—
5	27	-2.5	2.4×10^{-7}	0.3	4.0×10^{-4}	-1.2	9.1×10^{-6}	-0.7
5 ^d	—	—	—	—	8.3×10^{-4}	-1.3	5.0×10^{-6}	-0.6
6	3125	-3.5	3.4×10^{-8}	0.7	1.7×10^{-4}	-1.1	1.0×10^{-6}	-0.8
7	1587	-2.7	4.2×10^{-9}	1.0	1.1×10^{-2}	-1.9	9.1×10^{-5}	-1.2
8	833	-2.6	9.1×10^{-9}	0.9	2.8×10^{-4}	-1.0	2.2×10^{-5}	-0.7
8 ^c	83	-2.7	3.6×10^{-9}	1.1	—	—	—	—

Remarks. The measurements were performed

^a in the presence of atmospheric oxygen,

^b after storage for 6 months under an inert atmosphere,

^c after doping with iodine vapour up to $\sigma_{dc} \approx 10 \text{ S m}^{-1}$,

^d after annealing under an inert atmosphere. Specimens 1–8 investigated were obtained under different conditions and had different thicknesses.

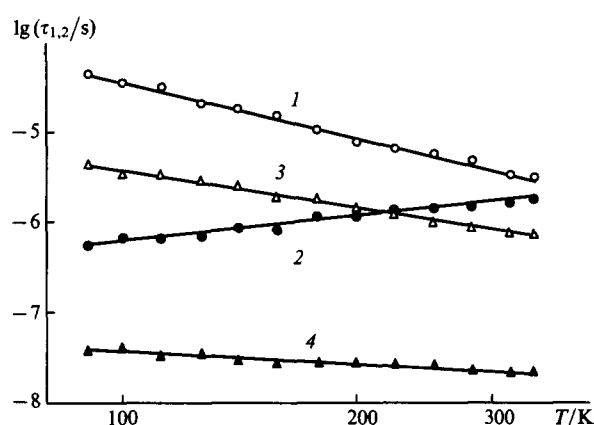


Figure 5. Temperature dependences of the spin–lattice (τ_1) (lines 1 and 3) and spin–spin (τ_2) (lines 2 and 4) relaxation times of *cis*–(lines 1 and 2) and *trans*–polyacetylenes (lines 3 and 4).

the *cis*- and *trans*-isomers of PA (No. 4 in Table 2). It is seen from the data presented that the spin–lattice relaxation times of the paramagnetic centres in both isomers diminish monotonically with increase in temperature, whereas the spin–spin relaxation times exhibit different temperature dependences in the case of *cis*- and *trans*-PA.

It is necessary to note that the PA relaxation times are effective relaxation times of the localised and mobile paramagnetic centres. Therefore, under the conditions where the dipole–dipole interactions of the paramagnetic centres in PA predominate, one can write

$$\left(\frac{1}{\tau_{1,2}}\right)_{cis} \approx \left(\frac{1}{\tau_{1,2}}\right)_{loc}, \quad (8a)$$

$$\left(\frac{n}{\tau_{1,2}}\right)_{trans} \approx \left(\frac{n_1}{\tau_{1,2}}\right)_{loc} + \left(\frac{n_2}{\tau_{1,2}}\right)_{mob}, \quad (8b)$$

where $n = n_1 + n_2$. This makes it possible to determine separately the relaxation times of paramagnetic centres with different mobilities in *trans*-PA, using the experimental quantities τ_1 , τ_2 , n , and n_1/n_2 .

If the spin–lattice relaxation time is formulated as $\tau_1 = An^{-\alpha}v_e^\beta T^{-\gamma}$ (A is a constant), then α varies from 0.7 to 1.0 in the temperature range from 330 to 90 K, β is 3 for *cis*-PA and -0.5 for *trans*-PA, and γ varies from 1.4 to 3.5 for *cis*-PA and from 1.0 to 2.6 for *trans*-PA depending on the thickness of the specimen (Table 2). This shows that mainly Raman two-phonon relaxation processes occur in *cis*-PA,⁶¹ whereas more complex spin–lattice interactions take place in *trans*-PA. The latter factor may be accounted for by the fact that a joint Raman spin–lattice 1D- and 3D-interaction of the immobilised spins with an overall probability⁶³

$$W_R \sim k_1 n_1 v_e^{-1} T^2 + k_2 n_1 v_e^{-1} T,$$

(k_1 and k_2 are constants) and diffusional modulation of the spin–lattice interaction by the 1D-motion of some of the neutral solitons with a probability $W_D \sim v_e^{1/2}$ take place in *trans*-PA.⁶⁴

Table 3 presents the temperature dependences of the relaxation times of *cis*- and *trans*-PA specimens (No. 8, Table 2) partly oriented by stretching. The data presented demonstrate convincingly that the relaxation times $\tau_1(T)$ and $\tau_2(T)$ of the oriented *cis*-PA vary only slightly with the angle ψ between the direction of the external magnetic field and the direction of stretching of the specimen, whereas for the oriented *trans*-PA film the relaxation times are functions of the angle ψ as a result of the 1D-diffusion of a paramagnetic centre of finite extent within the film.

It is essential to note that the relaxation times are important parameters of PA, characterising its structural and conducting properties. Thus it has been shown⁶⁵ that an increase in molecular mass diminishes the electronic spin–lattice relaxation time of the paramagnetic centres in PA. This parameter should therefore be sensitive to the degradation of the polymer. Indeed, the storage of the initial *cis*-PA specimen for six months under an inert atmosphere leads to a significant increase in τ_1 owing to its partial degradation (Fig. 6).^{54,59}

A similar change in τ_1 is observed on irradiation of this specimen with a beam of fast electrons at a dose of 1 MGy.

Table 3. Temperature dependences of the relaxation times [$\tau_{1,2} = AT^2(s)$] of specimens 8 (Table 2) of *cis*- and *trans*-PA, partly oriented by stretching, as a function of the direction of stretching in the external magnetic field.

ψ/deg	τ_1		τ_2		τ_1		τ_2	
	<i>A</i>	α	<i>A</i>	α	<i>A</i>	α	<i>A</i>	α
	<i>cis</i> -PA				<i>trans</i> -PA			
0	0.04	−1.2	4.0×10^{-8}	0.6	2.1×10^{-2}	−2.0	2.4×10^{-3}	−1.7
30	—	—	—	—	5.0×10^{-4}	−1.2	1.0×10^{-5}	−0.5
60	—	—	—	—	2.8×10^{-3}	−1.4	1.5×10^{-5}	−0.5
90	0.16	−1.5	2.7×10^{-8}	0.7	3.5×10^{-5}	−0.5	5.2×10^{-5}	−0.8

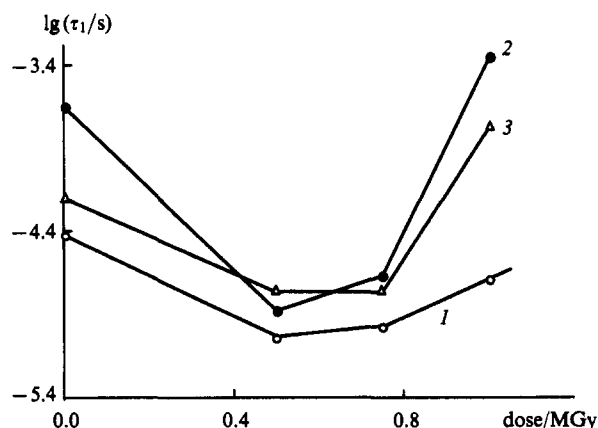


Figure 6. Dependence of the spin-lattice relaxation time τ_1 ($T = 120$ K) for the initial *cis*-PA specimen (specimen 3 in Table 2, curve 1) and after its storage under an inert atmosphere for 6 months (line 2) and 12 months (line 3) as a function of the dose of irradiation by a beam of fast electrons.

However, on irradiation of the specimen with an electron beam at a dose of 0.50–0.75 MGy, the time τ_1 remains virtually constant during the above period of storage (Fig. 6). After more prolonged storage of the initial specimen and the specimen irradiated with a dose of 1 MGy, τ_1 diminishes somewhat, which may be attributed to some increase in the length of the chains and to the *cis*–*trans* isomerisation of PA. This phenomenon demonstrates the possibility of the effective stabilisation and even an improvement of the electrodynamic characteristics of *cis*-PA when the latter is irradiated with the optimum dose.

The increase in the concentration of paramagnetic centres on *cis*–*trans* isomerisation of PA accelerates the spin-lattice relaxation. Since in massive PA films with a low-density of the polymer chains such isomerisation proceeds most readily, longer *trans*-sections with an increased rigidity are formed in them, and is accompanied by an increase in the activation energy for the libration of the chains (E_a). The latter quantity may be determined by analysing the temperature dependence of the width of the spectral line of a trapped soliton.⁵⁴ Since the unpaired electron, delocalised within the limits of a neutral mobile soliton, has a finite density $\rho(n)$ on N hydrogen nuclei, there is a possibility of their hyperfine interaction. In this case the effective width of the delocalisation of the unpaired electron $N = \rho(n)^{-1}$ in *trans*-PA can be found from the equation for the Gaussian component of the line width⁶⁶ $\Delta B_{pp}^G \approx N^{1/2} \rho(n)$ subject to the condition $\sum \rho(n) = 1$.

Figure 7 presents the $\tau_1 - N - E_a$ correlations for *trans*-PA specimens of different thicknesses. It is seen from the figure that, as the specimen becomes more massive, a tendency is observed towards the acceleration of the spin-lattice relaxation processes and towards an increase in the activation energy for the libration of the polymer chains. This constitutes additional evidence for the increase in rigidity, packing density, and length of the *trans* chains with increase in the thickness of the *trans*-PA specimen.

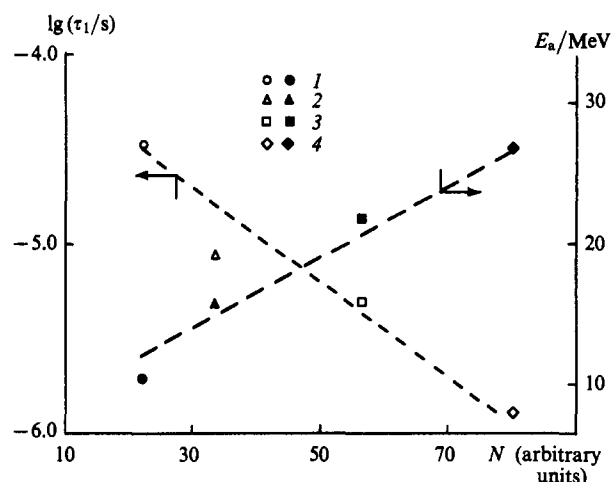


Figure 7. Dependence of the spin-lattice relaxation time τ_1 ($T = 80$ K) and the activation energy for the librations of the chains E_a on the effective spin delocalisation length N in *trans*-PA specimens with different thicknesses (μm): (1) 90; (2) 110; (3) 350; (4) 180.

The correlations presented are useful for the standardisation of *trans*-PA films.

It is essential to note that a light doping of *trans*-PA with iodine vapour (up to $\sigma_{dc} \approx 10 \text{ S m}^{-1}$) leads to a fourfold decrease in the overall spin concentration and to a decrease in τ_2 approximately by an order of magnitude (Table 2). Some change in τ_1 occurs on diffusion of atmospheric oxygen into the *trans*-PA matrix. Taking into account the concentration dependence of this quantity, one may conclude that the introduction of I_2 and O_2 molecules reduces the packing density of the PA chains and increases the number of traps for mobile solitons.

IV. Dynamics of the soliton and the mechanism of charge transfer in *trans*-polyacetylene

The diffusion of the soliton along the polymer chain is characterised by the translational propagator of motion $P_{tr}(r, r_0, \tau)$. If in the initial instant the j th particle is located at a point r_0 relative to the i th particle, then the propagator defines the probability that at the instant $t = \tau$ the i th particle is located in the region $r + dr$ relative to the new position of the j th particle.

For the Brownian model of diffusional motion, the propagator $P_{tr}(r, r_0, \tau)$ constitutes the solution of the familiar equation

$$\frac{\partial P_{tr}(r, r_0, t)}{\partial t} = D_{tr} \Delta P(r, r_0, t), \quad (9)$$

subject to the initial condition $P_{tr}(r, r_0, t) = \delta(r - r_0)$, where $D_{tr} = [D_i]$, $D_i = v_i c_i$ is the diffusion coefficient, v_i is the rate of diffusion, c_i is a constant introduced owing to the discrete nature of the system, and i is a unit vector of the molecular coordinate system. In an explicit form, the above propagator for a 1D-system is given by the following relation:⁶⁷

$$P(r, r_0, \tau)_{1D} = (4\pi v_{\parallel} \tau)^{-1/2} \exp\left[-\frac{(r-r_0)^2}{4v_{\parallel}^2 \tau}\right] \exp(-v_{\perp} \tau), \quad (10)$$

where v_{\parallel} and v_{\perp} are the rates of spin diffusion along the polymer chain and between the chains respectively.

The diffusing soliton induces a local magnetic field $B_{loc}(t)$ at the sites of other electron or nuclear spins, thereby influencing the electronic relaxation times of neighbouring spins. The following general expression may be written for the relaxation time:

$$\tau_{1,2} = f[J(\omega)],$$

where $J(\omega)$ is a function of the spectral density given by

$$J(\omega) = \int_{-\infty}^{+\infty} G(\tau) \exp(-i\omega\tau) d\tau. \quad (11)$$

The autocorrelation function of the oscillating local field $B_{loc}(t)$ for a discrete system is

$$G(\tau) = c_i \sum \sum A(r, t) P(r, r_0, \tau) F(r_0) F^*(r) dr_0 dr, \quad (12)$$

where c_i is the lattice constant for the discrete system, $A(r, t)$ the probability of finding the spin at a distance r at time t , equal to the spin concentration per monomer unit n , and $F(r)$ is the probability of finding two spins at a distance r at time t .

For frequencies $\omega \ll v_{\parallel} c_i^2 (r-r_0)^{-2}$, the spectral density function can assume the following form:

$$J(\omega) = n J_{1D}(\omega) \sum \sum F(r_0) F^*(r) f_{1D}(|r-r_0|), \quad (13)$$

where $n = n_1 + \sqrt{2}n_2$ is the probability of finding the spin in the initial instant in the position r_1 , $J_{1D}(\omega) = (2\pi v_{\parallel} v_e)^{-1/2}$ for $v_{\perp} \ll v_e \ll v_{\parallel}$, and $J_{1D}(\omega) = (2\pi v_{\parallel} v_{\perp})^{-1/2}$ for $v_{\perp} \gg v_e$. The expression under the summation sign[†] can be written in the form

$$F(r_0) F^*(r) f_{1D}(|r-r_0|) = \frac{(3 \cos^2 \vartheta - 1)^2}{r_1^3 r_2^3},$$

where ϑ is the angle between the vectors r_1 and r_2 .

Since PA is characterised mainly by an anisotropic dipolar (and to a lesser extent by an isotropic scalar) hyperfine interaction of the electron (S) and nuclear (I) spins, in the case of the dipolar interaction between equivalent spins ($S=I$), the equations for the rates of electronic relaxation in a polycrystalline specimen can be written in the form⁶⁷

$$\tau_1^{-1} = \langle \Delta\omega^2 \rangle [J(\omega_e) + 4J(2\omega_e)], \quad (14a)$$

$$\tau_2^{-1} = \frac{1}{2} \langle \Delta\omega^2 \rangle [3J(0) + 5J(\omega_e) + 2J(2\omega_e)], \quad (14b)$$

where

$$\langle \Delta\omega^2 \rangle = \frac{1}{5} \left(\frac{\mu_0}{4\pi} \right)^2 \gamma_e^4 \hbar^2 S(S+1) n \sum \sum$$

(here ω_e is the frequency of the precession of the electron spin and m_0 is the magnetic permeability in *vacuo*).

The anisotropic hyperfine interaction accelerates the electronic relaxation by the amounts

$$\begin{aligned} \tau_1^{-1} = & \frac{1}{15} a^2 I(I+1) n \sum \sum [J(\omega_e - \omega_1) + 3J(\omega_e) \\ & + 6J(\omega_e + \omega_1)] + \frac{1}{15} a^2 S(S+1) n \sum \sum [-J(\omega_e - \omega_1) \\ & + 6J(\omega_e + \omega_1)] \frac{\langle I_z \rangle - I_0}{\langle S_z \rangle - S_0}, \end{aligned} \quad (15a)$$

[†] Henceforth double summation will be designated for simplicity by $\sum \sum$.

$$\begin{aligned} \tau_2^{-1} = & \frac{1}{30} a^2 I(I+1) n \sum \sum [4J(0) + J(\omega_e - \omega_1) \\ & + 3J(\omega_e) + 6J(\omega_1) + 6J(\omega_e + \omega_1)], \end{aligned} \quad (15b)$$

(ω_1 is the frequency of the precession of the nuclear spin and $a = \mu_0 \gamma_e \gamma_I \hbar / 8\pi$ is the hyperfine interaction constant), whereas the isotropic interactions of the electron and nuclear spins make an additional contribution to the rate of electronic relaxation:

$$\tau_1^{-1} = \frac{1}{3} n_p a^2 I(I+1) J(\omega_e - \omega_1) \left[1 - \frac{S(S+1)(\langle I_z \rangle - I_0)}{I(I+1)(\langle S_z \rangle - S_0)} \right] \quad (16a)$$

$$\tau_2^{-1} = \frac{1}{6} n_p a^2 I(I+1) [J(0) + J(\omega_e - \omega_1)]. \quad (16b)$$

By setting the expression under the summation sum in Eqn (14) equal to $2 \times 10^{58} \text{ m}^{-6}$ and that in Eqn (15) to $2.8 \times 10^{59} \text{ m}^{-6}$ and also assuming that $(\langle I_z \rangle - I_0)(\langle S_z \rangle - S_0)^{-1} = 0.078$,³⁵ one can formulate simpler expressions for the rate of relaxation of *trans*-PA with randomly oriented polymer chains:⁵⁶

$$\tau_1^{-1} = 1.3 \times 10^{16} (v_e v'_{1D})^{-1/2} (2.7 \times 10^4 n + 1), \quad (17a)$$

$$\begin{aligned} \tau_2^{-1} = & 6.3 \times 10^{15} v_{1D}^{-1/2} [(7.6 \times 10^9 n + 3.4 \times 10^5) v_{3D}^{-1/2} \\ & + (4.3 \times 10^4 n + 1) v_e^{-1/2}]. \end{aligned} \quad (17b)$$

In the case of the predominantly dipole-dipole interaction of the paramagnetic centres, the equations for the rates of relaxation of the partly oriented *trans*-PA with a degree of orientation of the polymer chains A consist of two components:

$$\begin{aligned} \tau_1^{-1} = & A \langle \Delta\omega^2 \rangle [J(\omega_e) P_1 + 4J(2\omega_e) P_2] \\ & + (1-A) \langle \Delta\omega^2 \rangle [J(\omega_e) P'_1 + 4J(2\omega_e) P'_2], \end{aligned} \quad (18a)$$

$$\begin{aligned} \tau_2^{-1} = & \frac{A}{2} \langle \Delta\omega^2 \rangle [3J(0) P_0 + 5J(\omega_e) P_1 + 2J(2\omega_e) P_2] \\ & + \frac{(1-A)}{2} \langle \Delta\omega^2 \rangle [3J(0) P'_0 \\ & + 5J(\omega_e) P'_1 + 2J(2\omega_e) P'_2], \end{aligned} \quad (18b)$$

where the constants P_i and P'_i correspond to the oriented and randomly disposed polymer chains respectively.

If we put $P_0 = 4.3 \times 10^{58} \sin^4 \psi$, $P_1 = 4.8 \times 10^{57} (1 - \cos^4 \psi)$, $P_2 = 4.8 \times 10^{57} (1 + 6 \cos^2 \psi + \cos^4 \psi)$, $P'_0 = 1.6 \times 10^{58}$, $P'_1 = 2.7 \times 10^{57}$, and $P'_2 = 1.1 \times 10^{58} \text{ m}^{-6}$,²⁷ Eqns (18) can be written in a simpler form:

$$\begin{aligned} \tau_1^{-1} = & 5.0 \times 10^{19} n (v_e v'_{1D})^{-1/2} \\ & \times [6.8 - A(1.1 - 14.0 \cos^2 \psi + \cos^4 \psi)], \end{aligned} \quad (19a)$$

$$\begin{aligned} \tau_2^{-1} = & 2.8 \times 10^{20} n v_{1D}^{-1/2} \{ (1-A + A \sin \psi) v_{3D}^{-1/2} \\ & + [2.1 + A(1.1 + 1.3 \cos^2 \psi - 2.9 \cos^4 \psi)] v_e^{-1/2} \}. \end{aligned} \quad (19b)$$

Figure 8 presents the temperature variations of the rates of diffusion v_{1D} and v_{3D} calculated for the initial *trans*-PA specimen ($A=0$) (specimen 8 in Table 2) and for the same specimen with polymer chains partly oriented by stretching ($A=0.07$).

When the unpaired electron is delocalised over 15 carbon nuclei, the rate of 1D-diffusion of the soliton in the initial *trans*-PA specimen is $v_{1D} = 0.25 v'_{1D} N^2 \leq 5.6 \times 10^{11} \text{ Hz}$ at room temperature. The latter quantity is approximately two orders of magnitude smaller than that obtained earlier by magnetic resonance methods.^{22,35} Furthermore, the relation $v'_{1D}(T) \sim T^{-2}$ does not agree with the existing theoretical ideas.^{13,14} The anisotropy of the spin dynamics depends only slightly on

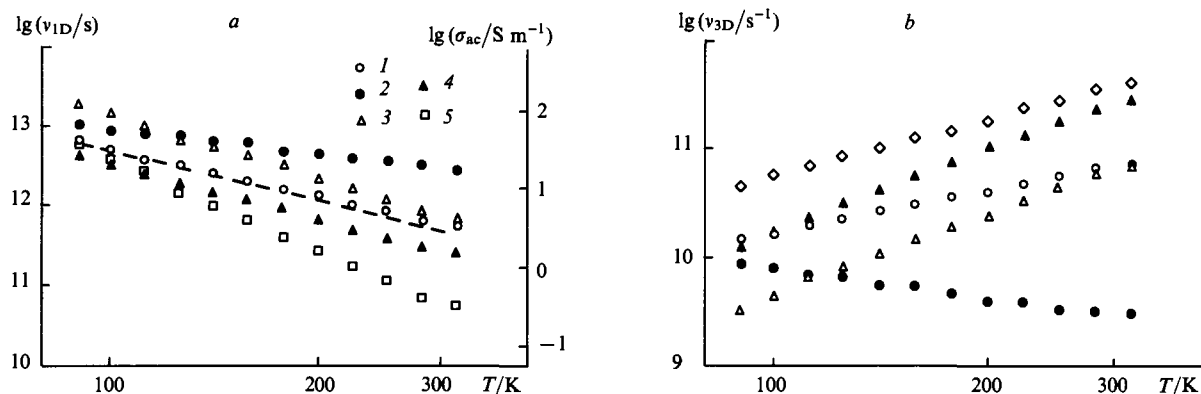


Figure 8. Logarithmic temperature dependences of the quantities v_{1D} (a) and v_{3D} (b) for a neutral soliton in the initial (line 1) and partly oriented ($A = 0.07$) *trans*-PA with the crystallographic c axes oriented at the angles

$\psi = 90^\circ$ (line 2), 60° (line 3), 30° (line 4), and 0° (line 5) relative to the external magnetic field. The temperature dependence of the quantity σ_{ac} , calculated by Eqn (20b) for $\nu_e = 1.4 \times 10^{11}$ Hz, is shown by a dashed line.

temperature and amounts to $v_{1D} v_{3D}^{-1} \geq 30$ in this specimen and to $10 - 10^4$ in other *trans*-PA specimens,⁵⁶ which is significantly less than the values obtained previously.^{22,35}

If the rates of spin diffusion are expressed in the form $v_{1D} = AT^{-\alpha}$ and $v_{3D} = BT^{-\beta}$, then the increase in the anisotropy of the spin diffusion by three orders of magnitude in different specimens is accompanied by the simultaneous increase in the quantities α (from 2 to 5) and β (from 0.4 to 7) at room temperature. When *trans*-PA is doped, it becomes disordered and the Coulombic and confinential trapping of the charge carriers increase.¹⁹ However, if these factors are neglected and it is supposed that all the mobile carriers with the mobility μ participate in the charge transfer process, then the conductivity of *trans*-PA, calculated from the equation $\sigma = Ne\mu = Ne^2 v_{1D} c_{\parallel}^{-1} T^{-1}$ (e is the electronic charge), does not exceed $0.02\ S\ m^{-1}$ at room temperature, which is several orders of magnitude less than the value usually attainable for heavily doped *trans*-PA.¹⁻³ Furthermore, even light doping leads to a significant alteration of the frequencies of spin diffusion in *trans*-PA (Fig. 9). Hence it follows that, in order to attain a high conductivity of the polymer, the condition of the multiple charge transfer by each soliton within a limited section of the polymer chain must be fulfilled.

The dynamic properties of solitons can be described more correctly within the framework of the formal treatment involving the isoenergetic intersoliton charge transfer proposed by Kivelson.¹¹ The essential feature of the method consists of the phonon-assisted interchain tunnelling of the charge between the energy levels of the solitons, based on the Coulombic interaction

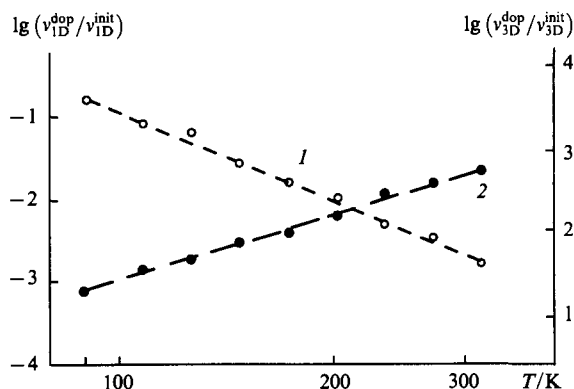


Figure 9. Temperature dependences of the ratios of the quantities v_{1D} (line 1) and v_{3D} (line 2) for a neutral soliton in the initial *trans*-PA to the corresponding values for a soliton in *trans*-PA doped with iodine up to $\sigma_{ac} \approx 10\ S\ m^{-1}$.

of the solitons having a charge q_1 with ions having the opposite charge q_2 present in the undoped and lightly doped *trans*-PA. The excess charge $\Delta q = q_1 - q_2$ may undergo a phonon-assisted transfer, with a finite probability, to a neutral soliton moving along a neighbouring polymer chain. If at the instant of such transfer the neutral soliton is also located close to a charged ion, the energy of the charge carrier before and after charge transfer remains unaltered. In this case, the conductivity of the polymer (the d.c. conductivity σ_{dc} and the a.c. conductivity σ_{ac}) is determined by the probability that the neutral soliton is located near an ion and also by the probability of finding its initial and final energies within the limits of kT .¹¹

$$\sigma_{dc} = k_1 e^2 \frac{\gamma(T) \xi n_n n_{ch}}{k T N R_0^2 (n_n + n_{ch})^2} \exp\left(-\frac{2k_2 R_0}{\xi}\right) = \sigma_0 T^n, \quad (20a)$$

$$\sigma_{ac} = \frac{e^2 n_i^2 n_0 (1 - n_0) \xi_{\parallel}^3 \xi_{\perp}^2 \nu_e}{384 k T} \left[\ln \frac{4\pi \nu_e L_c}{n_0 (1 - n_0) \gamma(T)} \right]^4$$

$$= \frac{\sigma_0 \nu_e}{T} \left[\ln \frac{k_3 \nu_e}{T^{n+1}} \right]^4. \quad (20b)$$

Here $\gamma(T)$ is the hopping frequency of the charge carriers, k_1 , k_2 , and k_3 are constants ($k_1 = 0.45$, $k_2 = 1.39$), $\xi = (\xi_{\parallel} \xi_{\perp}^2)^{1/3}$, ξ_{\parallel} and ξ_{\perp} are the average parallel and perpendicular lengths of the soliton respectively, n_n and n_{ch} are the numbers of neutral and charged solitons per monomer unit, n_0 is the relative content of the charged solitons, $R_0 = (\frac{2}{3} \pi n_i)^{-1/3}$ is the average distance between inhomogeneities with a concentration n_i , and L_c is the degree of polymerisation or the number of monomer units in the polymer chain. A weak bond between the charge carriers and the polymer lattice is characteristic of the case under consideration, which results in the occurrence of hopping charge transfer between relatively remote states of the soliton. The temperature dependences presented above were obtained experimentally in a study of lightly doped *trans*-PA^{10,69} and other conducting polymers.^{70,71} Fig. 8 presents the temperature dependence of σ_{ac} calculated by Eqn (20b) with $\nu_e = 1.4 \times 10^{11}$ Hz, $n = 8.0$, $k_3 = 2.9 \times 10^{23}\ sK^9$, and $\sigma_0 = 9.3 \times 10^{-15}\ S\ s\ K\ m^{-1}$ ($\xi_{\parallel} = 1.0$, $\xi_{\perp} = 0.25$ nm, $n_i = 1.3 \times 10^{25}\ m^{-3}$, and $L_c = 2000$)^{10,11,72,73} for the initial *trans*-PA specimen. As can be seen from the figure, the $v_{1D}(T)$ and $\sigma_{ac}(T)$ relations are quite satisfactorily correlated. Adopting $\sigma_{dc} \sim 10^{-3}\ S\ m^{-1}$ (see, for example, Epstein¹⁰) and $\sigma_{ac} \sim 3\ S\ m^{-1}$ at $T = 300\ K$ (Fig. 8), we obtain $\sigma_{dc}/\sigma_{ac} \approx 3 \times 10^3$, which agrees well with the value calculated¹⁰ within the framework of Kivelson's theory¹¹

$$\frac{\sigma_{ac}(\nu_e \rightarrow \infty)}{\sigma_{ac}(\nu_e \rightarrow 0)} \approx 10^4.$$

This confirms the applicability of the approach used to the interpretation of the transport properties of the soliton in *trans*-PA.

In the initial *trans*-PA specimen, the crystallographic *c* axes of the polymer chains are randomly oriented in space. It follows from Fig. 8 that, under the conditions of the orientational ordering of some of the polymer chains, the rates of the spin 1D- and 3D-diffusion are sensitive to the rotation of the specimen by an angle ψ in the external magnetic field, apparently owing to the finite length of the quasi-particles. The function $v'_{1D}(\psi)$, i.e.

$$\langle v'_{1D}(\psi) \rangle = v_{1D}^{\parallel}(\psi) \sin^2 \psi + v_{1D}^{\perp}(\psi) \cos^2 \psi, \quad (21)$$

where $v_{1D}^{\parallel}(\psi)$ and $v_{1D}^{\perp}(\psi)$ are extrema in the function $v'_{1D}(\psi)$, is in the antiphase relative to $v'_{3D}(\psi)$. We may note that the effective spin diffusion can be described with the aid of a similar relation also in other low-dimensional systems.^{74,75} Thus the inequality $v_{1D}^{\parallel}(\psi) \ll v_{1D}^{\perp}(\psi)$ is evidence for the delocalisation of the unpaired electron along the *c* axis within the limits of the soliton. Bearing in mind the fact that the soliton hops are limited by the interchain lattice constant and that the square of the length of the average diffusional hop along the *c* axis is $0.25(N^2 c^2)$, the width of the soliton N can be calculated with the aid of the following simple equation:⁴⁶

$$N^2 = \frac{4v_{1D}^{\perp}(\psi)}{v_{1D}^{\parallel}(\psi)}. \quad (22)$$

Figure 10 presents the temperature dependence of the width of the soliton calculated by Eqn (22) using the quantities v_{1D}^{\parallel} and v_{1D}^{\perp} , found graphically with the aid of Fig. 8. The value $N = 14.8$ found for room temperature agrees well with the theoretical⁶ and the earlier experimental⁴⁵ values of N . Extrapolation of the $N(T)$ relation to lower temperatures makes it possible to determine the temperature ($T_0 \approx 60$ K) at which the width of the soliton begins to increase. It is important to note that an anomaly in the function $v'_{1D}(T)$ for *trans*-PA,³⁷ accounted for by a change in the mechanism of the electronic relaxation, has been recorded in precisely this temperature range.

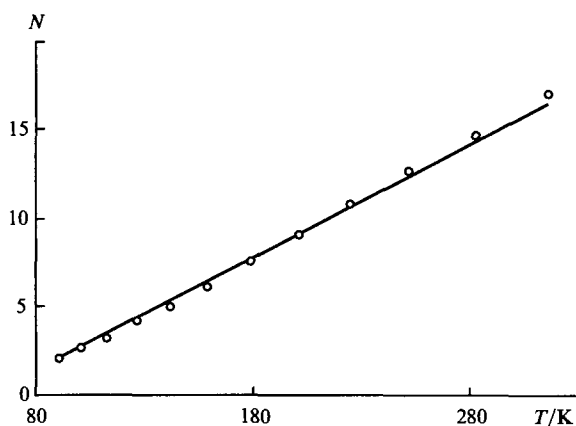


Figure 10. Temperature variation of the effective width N of the soliton in *trans*-PA.

Thus the experimental data indicate the 1D-diffusion of solitons into *trans*-PA at a rate appreciably exceeding the minimum rate v_{1D}^0 calculated above by Eqn (1). This conclusion is confirmed also by the averaging of the components of the *g*-tensor of the mobile paramagnetic centres when condition (1) is fulfilled and by the narrowing of the line in the EPR spectrum of *trans*-PA over a wide frequency range in conformity with Eqn (3).

However, the most obvious evidence in support of the 1D-diffusion of the soliton is the sensitivity of the quantities v_{1D} and v_{3D} to the orientation of the polymer in the magnetic field.

The familiar Burgers–Korteweg–de Vries equation, describing the 1D-motion of unified waves in a nonlinear medium, assumes the form⁷⁶

$$\frac{\partial u}{\partial t} + (v_{1D}^0 + \varepsilon u) \frac{\partial u}{\partial x} - \kappa \frac{\partial^2 u}{\partial x^2} + \beta \frac{\partial^3 u}{\partial x^3} = 0, \quad (23)$$

where ε , κ , and β are the parameters of the nonlinearity, dissipation, and ‘reactive’ dispersion of the medium respectively. In a dissipative system with a low nonlinearity ($\beta \approx 0$), there is a possibility of the formation of a mobile front (kink) with the difference $u_2 - u_1$. For such a quasi-particle, the stationary solution of Eqn (23) assumes the following form:

$$u(x, t) = 0.5(u_1 + u_2) - A \tanh\left(\frac{x - v_{1D}t}{2N}\right), \quad (24)$$

where

$$A = \frac{1}{2}(u_2 - u_1), \quad v_{1D} = v_{1D}^0 + \frac{1}{2}\varepsilon(u_1 + u_2), \quad \text{and} \quad N = \frac{\kappa}{2A\varepsilon},$$

are the amplitude, velocity, and width of the kink respectively. If the dissipation of the system is neglected ($\kappa \approx 0$), then other quasi-particles—solitons—are stabilised in the system. For a family of such solitons, Eqn (23) has another integrable solution:

$$u(x, t) = A \operatorname{sech}^2\left(\frac{x - v_{1D}t}{N}\right), \quad (25)$$

where

$$v_{1D} = v_{1D}^0 + \frac{1}{3}A\varepsilon, \quad \text{and} \quad N^2 = \frac{3\beta}{A\varepsilon} = \frac{\beta}{v_{1D} - v_{1D}^0}.$$

It is essential to note that relations similar to Eqns (24) and (25) have been used⁶ to describe nonlinear deformations of the lattice and electronic states of *trans*-PA.

The experimental⁴⁶ functional relations $v_{1D}(T) \sim T^{-n}$ and $N(T) \sim T^{n/2}$ ($n \approx 2$) yield for *trans*-PA a relation of the type $N^2 \sim v_{1D}^{-1}$. This means that the motion of solitons in the given specimen, subject to the condition $v_{1D} \ll v_{1D}^F = 3.8 \times 10^{15}$ Hz, can also be described by Eqn (23), which is universal for nonlinear systems, with the stationary solution (25). Evidently, different specimens of *trans*-PA may be characterised by different sets of the constants ε , κ , and β in Eqn (23), so that the nature of the motion of the quasi-particles in these polymers may differ somewhat from that described above.

V. Conclusion

It was shown above that the mechanism and rate of charge transfer in PA depend on the conformation, packing density, intramolecular dynamics, and lengths of the polymer chains in the undoped sample. In *cis*-PA, the neutral solitons are trapped in short sections of the *trans*-conformer. As a consequence of this, the probability of the intersoliton charge jump is exceptionally low and $\sigma_{dc} \sim 10^{-11}$ S m⁻¹. In the course of the *cis*–*trans* isomerisation, the length of the *trans*-chains increases, which leads to the ‘unfreezing’ of the mobility of some of the solitons. These quasi-particles acquire a charge and transport it along the chain up to the section where its tunnelling transfer to another soliton, moving along a neighbouring polymer chain, is most probable. As a result of this process, characterised by a fairly strong Raman interaction of the electron spins with the lattice phonons, a sharp increase in the electrical conductivity of the undoped PA actually occurs (up to $\sigma_{dc} \sim 10^{-3}$ S m⁻¹). It must be emphasised that the mobile solitons play an indirect role in the charge transfer in PA, so that the electron transport considered

may operate only in undoped and lightly doped *trans*-PA. On doping, the number of mobile and pinned paramagnetic centres diminishes and the dimensionality of the system increases, which alters the mechanism of the charge transfer.

The data obtained demonstrate the evident advantages of the two-millimetre EPR spectroscopy in the study of different *cis*- and *trans*-PA specimens, which make it possible to analyse more fully and correctly the magnetic and relaxation parameters of paramagnetic centres with different mobilities and to obtain information about the detailed characteristics of the molecular and spin dynamics in PA. Evidently this method can be used successfully also in the study of other organic polymeric semiconductors.

References

1. J L Brédas, R Silbey (Eds) *Conjugated Polymers* (Dordrecht: Kluwer, 1991)
2. H Stubb, E Pankka, J Paloheimo *Mater. Sci. Eng.* **10** 85 (1993)
3. T E Scotheim (Ed.) *Handbook of Conducting Polymers* Vols 1, 2 (New York: Marcel Dekker, 1986)
4. R H Baughmann, S L Hsu, G P Pez, A J Signorelli *J. Chem. Phys.* **68** 5405 (1978)
5. C R Fincher, C-E Chen, A J Heeger, A G MacDiarmid, J B Hastings *Phys. Rev. Lett.* **48** 100 (1982)
6. W P Su, J R Schrieffer, A J Heeger *Phys. Rev. B, Condens. Matter* **22** 2209 (1980)
7. W Markowitsch, G Leising *Synth. Met.* **51** 25 (1992)
8. W Markowitsch, F Kuchar, K Seeger, in *Electronic Properties of Polymers and Related Compounds* (Eds H Kuzmany, M Mehring, S Roth) (Berlin: Springer, 1985) p. 78
9. H Thomann, L R Dalton, in *Handbook of Conducting Polymers* Vol. 2 (Ed. T E Scotheim) (New York: Marcel Dekker, 1986) p. 1157
10. A J Epstein, in *Handbook of Conducting Polymers* Vol. 2 (Ed. T E Scotheim) (New York: Marcel Dekker, 1986) p. 1041
11. S Kivelson *Phys. Rev. B, Condens. Matter* **25** 3798 (1982)
12. N F Mott, E A Davis *Electronic Processes in Non-Crystalline Materials* (Oxford: Clarendon Press, 1979)
13. Y Wada, J R Schrieffer *Phys. Rev. B, Condens. Matter* **18** 3897 (1978)
14. K Maki *Phys. Rev. B, Condens. Matter* **26** 2178; 2181 (1982)
15. A Terai, Y Ono *Synth. Met.* **55-57** 4672 (1993)
16. P Bernier, in *Handbook of Conducting Polymers* Vol. 2 (Ed. T E Scotheim) (New York: Marcel Dekker, 1986) p. 1099
17. T S Zhuravleva *Usp. Khim.* **56** 128 (1987) [*Russ. Chem. Rev.* **56** 69 (1987)]
18. I B Goldberg, H R Crowe, P R Newman, A J Heeger, A G MacDiarmid *J. Chem. Phys.* **70** 1132 (1979)
19. S A Brazovskii *Zh. Eksp. Teor. Fiz.* **78** 677 (1980)
20. A Grupp, P Höfer, H Kass, M Mehring, R Weizenhöfer, G Wegner, in *Electronic Properties of Conjugated Polymers* (Eds H Kuzmany, M Mehring, S Roth) (Berlin: Springer, 1987) p. 156
21. P Bernier, C Linaya, M Disi, I Sledz, I M Fabre, F Schue, L Giral *Polym. J.* **13** 201 (1981)
22. K Holczer, J P Boucher, F Devreux, M Nechtschein *Phys. Rev. B, Condens. Matter* **23** 1051 (1981)
23. A Bartl, J Fröhner, R Zuzok, S Roth *Synth. Met.* **51** 197 (1992)
24. F Rachdi, P Bernier in *Electronic Properties of Conjugated Polymers* (Eds H Kuzmany, M Mehring, S Roth) (Berlin: Springer, 1987) p. 160
25. G Leizing, H Kahlert, O Leitner in *Electronic Properties of Conjugated Polymers* (Eds H Kuzmany, M Mehring, S Roth) (Berlin: Springer, 1987) p. 56
26. K Mizoguchi, K Kume, S Masubuchi, H Shirakawa *Solid State Commun.* **59** 465 (1986)
27. K Mizoguchi, K Kume, S Masubuchi, H Shirakawa *Synth. Met.* **17** 405 (1987)
28. K Mizoguchi, S Komukai, T Tsukamoto, K Kume, M Suezaki, K Akagi, H Shirakawa *Synth. Met.* **28** D393 (1989)
29. Y Tomkiewicz, T D Schultz, H B Broom, T C Clarke, G B Street *Phys. Rev. Lett.* **43** 1532 (1979)
30. M Nechtschein, F Devreux, R G Green, T C Clarke, G B Street *Phys. Rev. Lett.* **44** 356 (1980)
31. Y W Park, A J Heeger, M A Drury, A G MacDiarmid *J. Chem. Phys.* **73** 946 (1980)
32. T C Clarke, J C Scott, in *Handbook of Conducting Polymers* Vol. 2 (Ed. T E Scotheim) (New York: Marcel Dekker, 1986) p. 1127
33. F Masin, G Gusman, R Deltour *Solid State Commun.* **40** 415 (1981)
34. M Ziliox, P Speg, C Mathis, B Francois, G Weill *Solid State Commun.* **51** 393 (1984)
35. K Mizoguchi, K Kume, H Shirakawa *Solid State Commun.* **50** 213 (1984)
36. K Mizoguchi, F Shimizu, K Kume, S Masubuchi *Synth. Met.* **41** 185 (1991)
37. N S Shiren, Y Tomkiewicz, T G Kazyaka, A R Taranko, H Thomann, L Dalton, T C Clarke *Solid State Commun.* **44** 1157 (1982)
38. Y Tomkiewicz, N S Shiren, T D Schultz, H Thomann, L Dalton, A Zettl, G Gruner, T C Clarke *Mol. Cryst. Liq. Cryst.* **83** 1049 (1982)
39. N S Shiren, Y Tomkiewicz, H Thomann, L Dalton, T C Clarke *J. Phys. (France)* **44** C3-223 (1983)
40. J C W Chien, G E Wnek, F E Karasz, J M Warakowski, L C Dickinson, A J Heeger, A G MacDiarmid *Macromolecules* **15** 614 (1982)
41. O Ya Grinberg, A A Dubinskii, Ya S Lebedev *Usp. Khim.* **52** 1490 (1983) [*Russ. Chem. Rev.* **52** 850 (1983)]
42. V I Krinichnyi *Zh. Prikl. Spektrosk.* **52** 887 (1990) [*Appl. Magn. Reson.* **2** 29 (1991)]
43. V I Krinichnyi *2-mm Wave Band EPR Spectroscopy of Condensed Systems* (Boca Raton, FL: CRC Press, 1995)
44. V I Krinichnyi, A E Pelekh, Ya S Lebedev, L I Tkachenko, G I Kozub, A Barrat, L G Brunel, G B Robert *Appl. Magn. Reson.* **7** 459 (1994)
45. M Nechtschein, F Devreux, F Genoud, M Guglielmi, K Holczer *Phys. Rev. B, Condens. Matter* **27** 61 (1983)
46. V I Krinichnyi, A E Pelekh, L I Tkachenko, G I Kozub *Synth. Met.* **46** 13 (1992)
47. Ya S Lebedev, V I Muromtsev *EPR i Relaksatsiya Stabilizirovannykh Radikalov* (EPR and Relaxation of Stabilised Radicals) (Moscow: Khimiya, 1972) p. 255
48. M T Jones, H Thomann, H Kim, L R Dalton, B H Robinson, Y Tomkiewicz *J. Phys. (France)* **44** 455 (1983)
49. V F Traven' *Elektronnaya Struktura i Svoystva Organicheskikh Molekul* (Electronic Structure and Properties of Organic Molecules) (Moscow: Khimiya, 1989)
50. C P Pool *Electron Spin Resonance: A Comprehensive Treatise on Experimental Techniques* (New York: Wiley, 1983)
51. M Mehring, H Weber, W Müller, G Wegner *Solid State Commun.* **45** 1075 (1983)
52. N N Tikhomirova, V V Voevodskii *Opt. Spektrosk.* **7** 829 (1959)
53. A Carrington, A D MacLachlan *Introduction of Magnetic Resonance* (New York: Harper and Row, 1967) (Translated into Russian; Moscow: Mir, 1970)
54. V I Krinichnyi, A E Pelekh, A Yu Brezgunov, L I Tkachenko, G I Kozub *Mater. Sci.* **17** 25 (1991)
55. P D Krasicky, R H Silsbee, J C Scott *Phys. Rev. B, Condens. Matter* **25** 5607 (1981)
56. V I Krinichnyi, A E Pelekh, L I Tkachenko, G I Kozub *Synth. Met.* **46** 1 (1992)
57. E A Silin'sh, M V Kurik, V Chapek, in *Elektronnnye Protssessy v Organicheskikh Molekulyarnykh Kristallakh: Yavleniya Lokalizatsii i Poliarizatsii* (Electronic Processes in Organic Molecular Crystals: Localisation and Polarisation Phenomena) (Riga: Zinatne, 1988) p. 177
58. Yu S Kivshar, B A Malomed *Rev. Mod. Phys.* **61** 763 (1989)
59. A E Pelekh, V I Krinichnyi, A Yu Brezgunov, L I Tkachenko, G I Kozub *Vysokomol. Soedin.* **33** 1731 (1991)
60. A A Bugai *Fiz. Tverd. Tela* **4** 3027 (1962)
61. A A Al'tshuller, B M Kozyrev *Elektronnnye Paramagnitnyi Rezonans Soedinenii Elementov Promezhutochnykh Grupp* (Electron Paramagnetic Resonance of Compounds of Intermediate Group Elements) (Moscow: Nauka, 1972)
62. P R Gullis *J. Magn. Reson.* **21** 397 (1976)

63. S P Kurzin, B G Tarasov, N F Fatkullin, R M Aseeva *Vysokomol. Soedin., Ser. A* **24** 117 (1982)
64. K Mizoguchi *Makromol. Chem. Makromol. Symp.* **37** 53 (1990)
65. J C W Chien, M A Schen *Macromolecules* **19** 1042 (1986)
66. L A Blyumenfel'd, V V Voevodskii, A G Semenov *Primenenie Elektronogo Paramagnitnogo Rezonansa v Khimii* (Applications of Electron Paramagnetic Resonance in Chemistry) (Novosibirsk: Izd. Sib. Otd. Akad. Nauk SSSR, 1962)
67. A Abragam *Principles of Nuclear Magnetism* (London: Oxford University Press, 1961)
68. M A Butler, L R Walker, Z G Soos *J. Chem. Phys.* **64** 3592 (1976)
69. G Paasch *Synth. Met.* **51** 7 (1992)
70. M El Kadiri, J P Parneix, in *Electronic Properties of Conjugated Polymers* (Eds H Kuzmany, M Mehring, S Roth) (Berlin: Springer, 1987) p. 183
71. P Kuivalainen, H Stubb, H Isotalo, L Yli-Lahti, C Holmström *Phys. Rev. B, Condens. Matter* **31** 7900 (1985)
72. A J Epstein, H Rommelmann, M A Druy, A J Heeger, A G MacDiarmid *Solid State Commun.* **38** 683 (1981)
73. B R Weinberger, J Kaufer, A J Heeger, A Pron, A G MacDiarmid *Phys. Rev. B, Condens. Matter* **20** 223 (1979)
74. V V Mank, N I Lebovka *Spektroskopiya Yadernogo Magnitnogo Rezonansa Vody v Geterogennykh Sistemakh* (Nuclear Magnetic Resonance Spectroscopy of Water in Heterogeneous Systems) (Kiev: Naukova Dumka, 1988)
75. G M Bartenev, S Ya Frenkel' *Fizika Polimerov* (The Physics of Polymers) (Leningrad: Khimiya, 1990)
76. Yu S Kivshar, B A Malomed *Rev. Mod. Phys.* **61** 763 (1989)

Nonlinear theory of multicomponent sorption dynamics and chromatography

A I Kalinitchev

Contents

I. Introduction	95
II. Sorption statics	96
III. Theory of nonlinear multicomponent sorption dynamics and chromatography, concentration waves, and velocities	100
IV. A model of ideal equilibrium sorption dynamics and chromatography	101
V. Concentration waves in multicomponent chromatographic systems	101
VI. Coherence	103
VII. Description of the concentration distributions in a multicomponent Langmuir sorption system with the aid of the h -transformation	104
VIII. The equivalence of multicomponent Langmuir systems and multicomponent systems with a nonuniform mobile phase velocity due to the sorption effect	105
IX. Multicomponent chromatographic systems with an invariant affinity sequence of the components	106
X. Chromatographic systems with regions including selectivity reversals of the components	108
XI. Interaction of concentration waves in multicomponent chromatographic systems	110
XII. Stationary concentration waves in multicomponent nonlinear chromatographic systems including dispersion factors	110
XIII. Conclusion	112

Abstract. The results of studies on the nonlinear theory of sorption dynamics and chromatography under conditions of interdependent sorption of the components are surveyed and treated systematically. The principal properties of multicomponent dynamic sorption systems and of the results arising from the nonlinear character of the mass balance equations are analysed in detail. These nonlinear equations describe the propagation and interaction of the multicomponent concentration waves generated in the sorption column during the chromatographic process for a multicomponent mixture of the substances being sorbed. A series of solutions (including those making allowance for dispersion factors in the sorption process), describing the multicomponent concentration waves during their propagation nonlinear multicomponent dynamic sorption systems, are considered. The bibliography includes 224 references.

I. Introduction

Chromatography describes a dynamic process in which at least two phases (one of which is continuous and the other disperse) move relative to one another and mass and/or heat exchange takes place between their interfaces. The general term filtration or percolation processes is frequently applied abroad to such processes.¹ There are phenomenological concepts,¹ potentially common to all filtration processes, which can also be extended to a whole series of other migration phenomena such as sedimentation,² electrophoresis,³ and others.^{1,4–6}

A I Kalinitchev Preparative Chromatography Laboratory, Institute of Physical Chemistry, Russian Academy of Sciences, Leninskii prosp. 31, 117915 Moscow, Russian Federation.
Fax (7-095) 952 53 08. Tel. (7-095) 955 44 05/955 44 10

The increased loadings applied to apparatus and columns in connection with the tendency to intensify modern technological processes leads to the need to separate mixtures of substances at high concentrations (including sorption separations).^{7–19} As a result, in the analysis of percolation processes it is necessary to take into account their nonlinearity and nonstationary nature and also the multicomponent nature of the dynamic systems considered.

Even in one-component sorption systems, the effects of nonlinearity play a major role, since they are responsible for the tendency of the concentration wave generated in the column to be stabilised or, conversely, to undergo progressive spreading.²⁰ If the substances sorbed do not interact in the column, the multicomponent system reduces to a one-component system. This special case makes it possible to regard a multicomponent system as a superposition of independent one-component systems. The hypothesis that there is no sorption interaction between the components usually holds in the case of analytical separations at low concentrations and for small loadings applied to the sorbent or in the elution version where the chromatographic peaks move apart rapidly. For preparative separations, where at high concentrations of the molecules the latter compete for a limited number of accessible sorption centres, this hypothesis becomes inapplicable.

When molecules or ions compete for sorption centres, one may speak of the sorption interaction of species in the disperse phase, i.e. of the mutual influence of the components during the sorption process. This effect has been relevantly called the 'interference of species' in the monograph by Helfferich and Klein²¹ (see also Helfferich's review²²). The same term is used in the thermodynamics of irreversible processes²³ to characterise the mutual influence of coexisting processes — the so-called 'cross effects'.²⁴

There exists yet another aspect of the interference of substances — the interference of concentration waves propagating at different wave velocities during their generation, collision, and interaction in the course of the sorption processes.^{21,22}

Received 27 March 1995

Uspekhi Khimii 65 (2) 103–124 (1996); translated by A K Grzybowski

process is completely analogous to the processes considered in fluid mechanics and in gas dynamics.

In the general case, the interference of substances in a dynamic sorption process can arise as a consequence of various types or forms of interaction. Each of the mixture components may affect the equilibrium interphase distribution of other substances (static interference effects) and also the time required for the establishment of equilibrium between the concentrations in the disperse and continuous phases (kinetic interference effects). The molecules of the substances may be transformed to another state as a result of a chemical reaction (for example, on complex formation) and under these conditions both static and kinetic interference effects may arise.^{21, 22}

The static interference effects can be considered on the basis of the ideal equilibrium model of the sorption system. Numerous studies have been considered by the nonlinear theory of isothermal multicomponent sorption dynamics and chromatography involving the application of the ideal model (see, for example, Refs 20–22 and 25–73). In particular, the results of mathematical investigations included the theory of systems of quasi-linear equations in terms of partial derivatives have been used in such studies.^{4, 39, 46, 47, 74–79}

At the present time, the ideal model has been used successfully for a qualitative explanation of a number of characteristics of the behaviour of multicomponent sorption systems and in many cases also for a quantitative prediction of the results. A further increase in the complexity of the behaviour of multicomponent nonlinear sorption systems is associated with the operation of interference effects together with nonideality factors (a finite rate of establishment of an equilibrium interphase distribution of substances, longitudinal dispersion, etc.). The operation of the static interference effects is fundamentally nonlinear and plays the main role in the behaviour of multicomponent concentration waves generated in the column. The additivity of the factors is impossible under these conditions because of the fundamentally nonlinear character of the multicomponent sorption systems.

The equilibrium properties of sorption systems determine the static interference effects and also sequence, types, forms, and propagation velocities of multicomponent concentration waves. The kinetic and dynamic nonideality factors introduce second-order changes under these conditions into the behaviour of concentration waves. The equilibrium properties of sorption systems determine the first statistical moment of the concentration waves, whereas the nonideality factors determine the second and higher statistical moments.²¹

The successful solution of the problem of the interference of substances and concentration waves together with the description of the behaviour of multicomponent sorption systems in terms of the propagating concentration waves became possible after the introduction of the concept of 'coherence'.^{21, 22, 35, 36} This concept was developed by Helfferich^{22, 35, 36, 80, 81} to facilitate the qualitative understanding and quantitative calculations in the theory of multicomponent nonlinear chromatography under arbitrary initial and boundary conditions. This general concept is fundamental and is applicable to a large class of percolation processes of similar nature.

For a compound multicomponent wave in a nonlinear sorption system, the state of coherence means that the concentration waves for each individual component move jointly without 'splitting', and this implies that their velocities are the same at each point. This leads to the problem of the determination of the eigenvalues and eigenvectors in the mass balance equations for the components.^{22, 25–31, 39, 46, 47, 74–79} The problems of the determination of the eigenvalues for the wave velocities in the theory of multicomponent chromatography, in the fluids and gases mechanic and in nonequilibrium thermodynamics are closely related.

The coherence condition determines the response of the multicomponent system to its perturbation and denotes the state to which it tends. A closed system tends in exactly the same way to

attain a state of equilibrium, while an open system with fixed boundaries and constant conditions imposed on them tends to attain a stationary dynamic state.^{22, 81}

Preparative displacement chromatography, which deals with large concentrations and a strong influence of interference, makes it possible to achieve simultaneously enhancement of concentration and purification of substances. In preparative multicomponent sorption and chromatographic separations, the large loadings applied to the columns and the high concentrations of the components to be separated are responsible for the specific features of the multicomponent dynamic sorption process. These specific features are associated with the interference of the species, which is particularly significant for frontal, displacement, elution, and vacancy versions.^{8, 9, 16}

Nonlinear preparative chromatography, which makes it possible to achieve good results in the separation of substances, has undergone a fresh development recently. It has been applied particularly vigorously in biotechnology.^{7, 10–12, 13, 15, 17–19} Despite the relatively high cost of the separation, it is more than worthwhile because the final bioproduct is more expensive.^{10, 11, 13}

The aim of the present review is to present the state of the art in the field of the theory of multicomponent nonlinear sorption dynamics and chromatography and also to consider the fundamental theoretical features of the behaviour of dynamic sorption systems in the separation of interfering species. In studies on such systems, it is possible to distinguish three main aspects: statics, kinetics, and dynamics of sorption.

II. Sorption statics

The statics of sorption processes is the study of the equilibrium relations between the concentrations of substances in the continuous and disperse phases. Under isothermal conditions, the interaction of the mixture of sorbable species in the continuous phase with the disperse phase determines the sorption isotherms of the components. The sorption isotherms of the mixture characterise the fundamental thermodynamic properties of the system and permit the calculation of the concentration distributions on the basis of the solution of the mass-balance equations.

The chromatographic separation is based on the difference between the equilibrium relations for the mixture of sorbable components. The greater this difference the more effective the separation of the components, other conditions being equal. In the competition of different molecules for available free sites in the sorbent, one may refer to the 'interaction' of the substances in the disperse phase or to their interference,^{21, 22} i.e. to the mutual influence of the substances on one another's sorption.

Interference presupposes that the concentration of any component i in the disperse phase (a_i) depends not only on the concentration of this substance in the continuous phase (c_i), as happens in systems without interference, but also on the concentrations (c_j) of all other substances, i.e.

$$a_i = f_i(c_1, \dots, c_m), \quad i, j = 1, 2, \dots, m. \quad (1)$$

Thus the sorption isotherms for the mixture represent the dependences of the concentrations of the substances in the disperse phase on the mixture composition $\{c_1, \dots, c_j, \dots, c_m\}$ at a constant temperature.

The number of multicomponent concentration waves arising in the column is determined by the parameter which is called the variance of the multicomponent sorption system.^{50, 82} The variance (m), the value of which is determined by the Gibbs phase rule,^{83–86} characterises the number of degrees of freedom of the multicomponent system under isothermal conditions, i.e. it characterises the minimum number of concentration variables which determine the composition of the mixture at equilibrium. In order to calculate the concentration distributions in the sorption system with a variance m , it is necessary to specify m isotherms, each isotherm f_i representing a surface in a multidimensional concentration space $\{c_1, \dots, c_j, \dots, c_m\}$.

Using the concentration distribution ratio a_i/c_i , it is easy to determine the sequence of affinities of the substances for the sorbent or, in other words, the 'affinity sequence' of the components: 1, 2, ..., n . The component i has a greater affinity than the component j provided that the inequality $a_i/c_i > a_j/c_j$ holds. Here it is assumed that $i < j$ for the affinity sequence. The separation factor α_{ij} is defined as the ratio

$$\alpha_{ij} = \frac{a_i/c_i}{a_j/c_j}, \quad i, j = 1, \dots, n, \quad (2)$$

where $\alpha_{ii} = 1$, $\alpha_{ij} = 1/\alpha_{ji}$, and $\alpha_{ij}\alpha_{jk} = \alpha_{ik}$.

In the affinity sequence 1, 2, ..., i , ..., j , ..., n , the components are arranged in the order of decreasing affinity.

When the mixture composition is varied, the positions of the components in the affinity sequence may remain unchanged (we have the so-called 'invariant' affinity sequence²¹) or it may vary. The change in the affinity sequence is called 'inversion'^{33, 87} or selectivity reversal.^{52, 88, 89} It is remarkable that in certain cases the components do not change positions in the affinity sequence for a univariant system (when the mixture composition changes in the binary i/j exchange of heterovalent ions), but in multicomponent systems (for example, in the exchange of more than three ions) inversion is possible.^{21, 38}

An even more complex variant of the inversion arises in nonlinear ion-exchange systems, where the equilibria are complicated by the occurrence of chemical reactions, in particular by complex formation. In such cases, inversion is possible even in systems with a variance $m = 1$, i.e. in two-component i/j systems. Combined concentration waves, in which one region of the wave tends to become sharper whilst the other undergoes progressive spreading, may then be generated in the column.

The equivalence (stoichiometry) conditions

$$\sum_i a_i = a_0, \quad \sum_i c_i = c_0$$

or

$$\sum_i Y_i = 1, \quad \sum_i X_i = 1, \quad i = 1, \dots, n, \quad (3)$$

where $Y_i = a_i/a_0$ and $X_i = c_i/c_0$ are dimensionless (normalised) concentrations, are usually valid for ion exchange. When these conditions are taken into account, the variance m of a stoichiometric system in which n ions undergo exchange, is $n - 1$ and the system must be regarded as an m -component system.

The relations

$$\left(\frac{\partial a_i}{\partial c_k}\right)_{c_s} < 0, \quad j \neq k; \quad \left(\frac{\partial a_j}{\partial c_k}\right)_{c_s} > 0, \quad (4)$$

where $s, j, k = 1, \dots, m$, hold for the sorption of competing substances. Thus, as a result of the competition of the components for available sorption sites, an increase in the concentration c_k leads to a decrease in the concentration a_j for all $j \neq k$. The greater the affinity of the k th component for the sorbent, the stronger this effect.

$$\left(\frac{\partial a_j}{\partial c_k}\right)_{c_s} < \left(\frac{\partial a_j}{\partial c_l}\right)_{c_s} < 0, \quad \text{when } \alpha_{kl} < 1 \quad (5)$$

If the sign of the effect is reversed, then the sorption of substances is called synergistic.

$$\left(\frac{\partial a_j}{\partial c_k}\right)_{c_s} > 0, \quad j \neq k \quad (6)$$

An increase in the sorbability of one component (j) with increase in the concentration of another (k) may arise when the molecules

of these substances tend to form complexes or aggregates in the stationary phase.

Having expressed a_j in terms of c_j with the aid of the Law of Mass Action (LMA) [Eqn (2)] and having substituted this value in Eqn (3), we obtain the Langmuir relations for mixture isotherms reflecting the interference of substances in the m -component system:²¹

$$a_i = f_i(c) = \frac{a_0 c_i}{\sum_j \alpha_{ji} c_j}$$

or

$$Y_i = \frac{X_i}{\sum_j \alpha_{ji} X_j}, \quad i, j = 1, \dots, n. \quad (7)$$

The model of an ideal localised monolayer was introduced by Langmuir⁹⁰ for a single component, but the simplicity of the analytical expression (7) for a mixture of substances⁹¹ makes it possible to employ it widely for calculations in the nonlinear theory of multicomponent sorption dynamics and chromatography (see, for example, Refs 92–132).

The Langmuir relations (7) for physical sorption are written in the form

$$a_i = \frac{(a_0/c_0)\alpha_{ik}c_i}{1 + \sum_j b_j c_j}$$

or

$$Y_i = \frac{\alpha_{ik} X_i}{1 + \sum_j (\alpha_{jk} - 1) X_j}, \quad i, j = 1, \dots, m. \quad (8)$$

Langmuir's adsorption theory¹³³ can be extended to the adsorption of gaseous mixtures^{134, 135} if it is supposed that the molecules are adsorbed at specific sites and do not interact with one another. These equations are referred to as the Langmuir equations for the adsorption of a mixture of gases. Similar equations have also been obtained in other studies^{136, 137} employing the Law of Mass Action.

For constant separation factors α_{jk} , the Langmuir relations (8) for an m -component system with nonstoichiometric sorption can be formally reduced to the Langmuir relations for a stoichiometric system with $m + 1$ components. For this purpose, it is necessary to introduce a k th dummy species with a concentration c_k and one must put²¹

$$\Gamma_i = \frac{a_0}{c_0} \alpha_{ik}, \quad V_i \equiv b_i c_i = (\alpha_{ik} - 1) X_i, \quad i = 1, 2, \dots, k-1, \quad (9)$$

$$\Gamma_j = \frac{a_0}{c_0} \alpha_{j+1k}, \quad V_j \equiv b_j c_j = (\alpha_{j+1k} - 1) X_{j+1}, \quad j = k, \dots, m.$$

Thus the stoichiometric system described by Eqns (2) and (3) for the exchange of n equal-valence ions may be reduced to the Langmuir sorption of a mixture of m components (where $m = n - 1$). The Langmuir equilibrium relations for a mixture have been discussed in detail in a monograph.¹³⁸ Various properties of the mixture isotherms, obtained with the aid of derivatives of types (4) and (5), have been described.²⁶ The Langmuir relations (7) or (8) for the mixture isotherms satisfy all the properties described in the above study.²⁶

Several dynamic methods for the construction of isotherms on the basis of column output curves have been developed for one-component sorption systems, among which the elution^{139, 140} and frontal analysis^{141, 142} methods are the most popular. These methods were updated later for the measurement of isotherms

for binary and multicomponent mixtures.^{62, 143-146} However the frontal chromatographic method is fairly laborious, since it requires a large number of measurements, pure substances, and takes a long time. This method has been compared with one based on the nonlinear wave effects involving a transformation of a hodograph and the optimum experimental conditions for the applicability of both methods have been determined.¹⁴⁷

Analytical expressions for mixtures isotherms which could be derived by the methods of statistical physics are lacking. Phenomenological equations for the mixture isotherms, based on the Law of Mass Action, are most widely used.

We shall consider systems in which sorption is stoichiometric [i.e. Eqns (3) hold]. Any composition of a mixture of species can be represented by a point in the 'composition space' $\{c_i\}$ or $\{a_i\}$. This

term is applied²¹ to an m -dimensional (n -dimensional for a stoichiometric system) space, along the axes of which the concentrations of the mixture components X_i or Y_i are plotted, as shown in Fig. 1a for a three-dimensional ($n = 3$) space.

For the normalised concentrations X_i or Y_i , the space of the possible changes in concentrations is a cube for $n = 3$ and a hypercube for $n > 3$, since the inequalities $1 \geq Y_i$ and $X_i \geq 0$ hold. Eqn (3), defining the stoichiometry of the exchange, reduces the dimensionality of the space of the possible changes in concentration to a hyperplane (for $n > 3$) $P_1 \dots P_n$, where, as can be seen from Fig. 1a, at the points P_i the concentration $X_i(P_i) = 1$, while the concentrations of the remaining components are zero. This hyperplane is usually referred to as a 'simplex'.²¹ Figs 1a and 2 present examples of simplexes for a stoichiometric

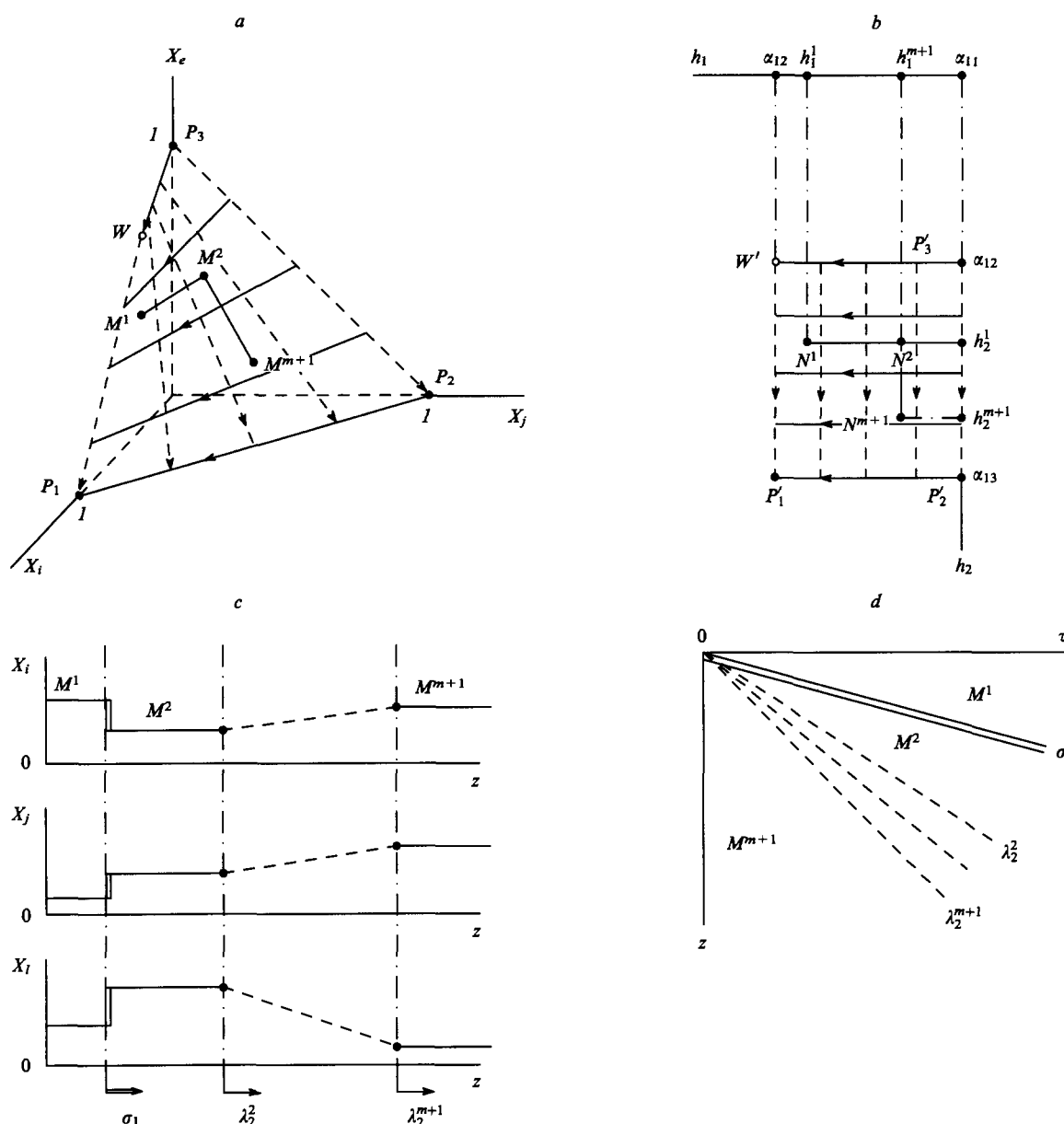


Figure 1. Representations of the characteristics of a three-component stoichiometric system in the composition space and in the physical plane. (a) the simplex $P_1P_2P_3$ for a two-component Langmuir system and the characteristic Γ^k paths corresponding to simple k -waves; (b) the Riemann invariants space $\{h_k\}$ and the h -transformation of the composition space $\{X_i\}$ (a) into the Riemann invariants space $\{h_k\}$ (b). Points M^s represent the concentration plateau in the k -wave; points $N^s\{h_k^s\}$ in the invariants space $\{h_k\}$ correspond to points M^s in the concentration space $\{X_i\}$ in Fig. 1a;

the arrows denote the directions in which the invariants h_k increase along the k -wave; the condition $X_i(P_i) = 1$ holds at points P_i , whilst the condition $h_i = \alpha_{i+1}$ is valid at points P'_i ; (c) the concentration profiles in the shock k -wave M^1M^2 ($k = 1$) and in the spreading k -wave M^2M^{m+1} ($k = 2$) corresponding to the $M^1M^2M^{m+1}$ route in Fig. 1a; σ_1 is the velocity of the first shock wave and $\lambda_2^2, \dots, \lambda_2^{m+1}$ are the velocities of the second spreading wave; (d) is the image on the physical plane (z, τ) of the propagation of the multicomponent concentration k -waves ($k = 1, 2$).

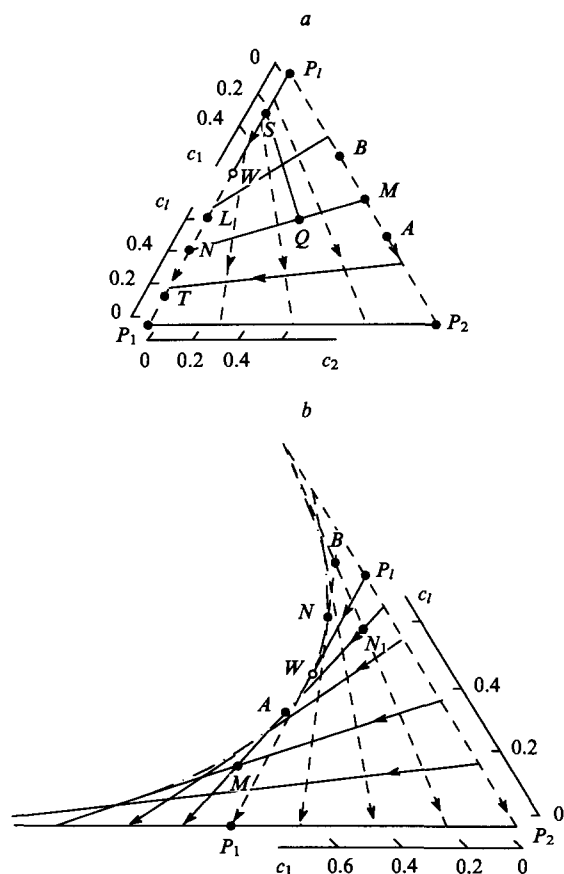


Figure 2. Hodographs for Langmuir two-component sorption systems (8) $\{c_i\}$ and for the equivalent stoichiometric three-component systems (9) $\{X_i\}$. (a) For the competitive sorption of the components ($b_i, b_j > 0$); (b) for the synergistic sorption of the components ($b_i > 0, b_j < 0$). The concentration points A, M, N, etc. correspond to different mixture compositions in the chromatographic process (see text).

Figs 1a and 2 present examples of simplexes for a stoichiometric three-component ($n = 3$) system with a variance of two ($m = 2$). Fig. 2 presents in the same region simplexes for a Langmuir two-component system, which is equivalent [see Eqn (9)] to a stoichiometric three-component system.²¹

The most frequently employed Langmuir multicomponent model lacks thermodynamic rigour, since Eqns (8) expressed in a general form do not satisfy the Gibbs–Duhem relations. Furthermore, the Langmuir model (8) does not yield exact predictions in calculations for elution chromatographic processes involving large loadings^{62, 148} and does not take into account adequately the experimental data for competitive adsorption.^{89, 145, 146} Nevertheless, in many special cases the Langmuir isotherm for a two-component mixture describes experimental data satisfactorily.⁸⁹

Phenomenological bi-Langmuir models for mixture isotherms, represented by the sum of two Langmuir relations, have been proposed:^{121, 149}

$$a_i = \frac{k_{i1}c_i}{1 + \sum_j b_{j1}c_j} + \frac{k_{i2}c_i}{1 + \sum_j b_{j2}c_j}, \quad i, j = 1, 2, \dots, m, \quad (10)$$

where the subscripts $i1$ and $i2$ refer to different adsorption sites¹²¹ or to two different states of the molecules in the sorbent phase (when complex formation takes place in the sorbent phase).¹⁴⁹ Phenomenological equations of the mixture isotherms in the form of the bi-Langmuir relations (10) are frequently used in numerical

calculations of concentration distributions.⁶⁶ It has been shown¹²¹ that type (10) relations describe the sorption isotherms for mixtures of enantiomers, the first term corresponding to selective chiral interactions and the second to nonselective molecular interactions between the enantiomers and the stationary phase.

Generalised phenomenological equations, including Langmuir and Freundlich relations as special cases, have been proposed:^{52, 53}

$$a_i = \frac{k_i c_i^{v_i}}{1 + \sum_j b_j c_j^{v_j}}, \quad i, j = 1, \dots, m. \quad (11)$$

In order to eliminate the thermodynamic inconsistency mentioned above, the Langmuir multicomponent model (8) has been supplemented by the theory of an ideally adsorbed solution proposed by Myers and Prausnitz.¹⁵¹ A thermodynamically consistent model of the competitive adsorption of components has been proposed by LeVan and Vermeulen.¹⁵⁰ The authors introduced into equations (8) of isotherms for two-component systems additional terms taking into account the difference between the column capacities for each component. To a first approximation, subject to the condition that the sorption capacities are the same for both components, the equations which they obtained for the isotherms reduce to the Langmuir equations (8). If the capacities for each component are different, then the LeVan–Vermeulen isotherm¹⁵⁰ can be represented by a rapidly converging series. In practical cases, this series can be restricted to the first two terms

$$a_i = \frac{wb_i c_i}{V} + \left(\frac{a_i}{b_i} - \frac{a_{3-i}}{b_{3-i}} \right) b_1 b_2 c_1 c_2 \ln(V),$$

$$V = 1 + b_1 c_1 + b_2 c_2; \quad w = \frac{a_1 c_1 + a_2 c_2}{V - 1}; \quad i = 1, 2. \quad (12)$$

When two one-component isotherms (for each individual component) are different, then the theory of the ideally adsorbed solution yields a numerical procedure for the determination of the isotherms for the competing components. This approach is based on the normalisation of the spreading pressure.¹⁵¹ It has been shown¹⁵² that the LeVan–Vermeulen model is consistent with the Gibbs adsorption theory. Numerical calculation of two chromatographic peaks with the aid of expansion (12) demonstrates a stronger displacement effect than could be predicted on the basis of the traditional Langmuir adsorption isotherms. For certain experimental systems, the application of isotherms (12) yields a satisfactory approximation.⁸⁹

Analysis of two-component models based on the method of statistical thermodynamics shows that the equations of the isotherms represent the ratio of two polynomials of the same degree.^{153, 154} In the special case of the Langmuir isotherm (8), this is the ratio of first degree polynomials. In another model based on statistical thermodynamics, which yields satisfactory results, the equation of the isotherm has been represented by the ratio of quadratic polynomials of the type.^{148, 153}

$$a_i = \frac{k_i c_i + k_{i(3-i)} c_1 c_2}{1 + b_1 c_1 + b_2 c_2 + b_{i(3-i)} c_1 c_2}, \quad \text{when } i = 1, 2, \quad (13)$$

where $k_{12} = k_{21}$ and the coefficients of this equation are the same as in the equation of a one-component isotherm for an individual i th component. The coefficients k_{ij} and b_{ij} must be determined from experiments on the adsorption of a binary mixture.

Fowler's isotherm

$$\frac{\theta_i}{c_i(1 - \theta_1 - \theta_2)} = b_0 \exp[\chi_i(\theta_1 + \theta_2)], \quad \text{when } i = 1, 2, \quad (14)$$

where θ_i is the ratio of the concentration of the component in the disperse phase to the sorbent capacity and χ_i are numerical coefficients, may be applied to the description of two-component adsorption¹³⁵ taking into account the competitive adsorption of the mixture components. This isotherm is an example of an implicit concentration dependence. The description of the adsorption of a binary mixture with the aid of Eqn (14) requires five parameters: a_{01} , a_{02} , χ_1 , χ_2 , and b_0 .

A binary isotherm model, based on the ion-exchange formalism, has been proposed.¹⁵⁵

Certain models of isotherms for a two-component mixture have been used in the frontal analysis of the output curves for two components^{156–158} for the determination of the constants in the corresponding equations. The simplest model is described by the two-component Langmuir relations (8) (for $i = 1, 2$). In a number of cases, especially when the sorbent capacities are the same for each component, this equation fits satisfactorily the mixture isotherms,¹⁵⁸ but it is more often inconsistent with experimental data.^{146, 157} The binary isotherms have been determined and a comparative study of the four models (presented above) for the description of the sorption of phenylethanols on ODS silica gel has been made with the aid of the two-component frontal analysis of the output curves.¹⁵⁷

We may note that one of the principal problems in the theory of the adsorption of mixtures — the prediction of mixture isotherms based on statistical data obtained for individual isotherms — has still not been solved.

In stoichiometric n -component systems, for which any i/j binary exchange obeys the Law of Mass Action in the form

$$\frac{(Y_i/X_i)^{v_i}}{(Y_j/X_j)^{v_j}} = K_{ij}, \quad \text{when } i, j = 1, \dots, n, \quad (15)$$

(K_{ij} is a concentration constant), the relation between the concentrations Y_i and $\{X_1 \dots X_n\}$ cannot be obtained in an explicit form. The equations of the mixture isotherms can be specified by implicit relations, for example, Eqn (14) or by the combination of Eqns (3) and (15). For systems involving the exchange of heterovalent ions, the quantity $1/v_i$ defines the valence of the i th ion. In nonideal systems obeying the Law of Mass Action, the concentration constants depend on the ratios of the concentrations of the substances undergoing exchange.

The form of the sorption isotherm has a decisive influence on the behaviour of the concentration waves in sorption columns. The criterion of the convexity of the binary i/j exchange isotherm, derived by Samsonov,¹⁵⁹ makes it possible to determine whether a stationary concentration front for the i/j exchange of the components may be established in the column. It is noteworthy that in a binary system, where the equilibrium is described by Eqns (15), the components do not change positions in the affinity sequence [i.e. the f_{ij} binary isotherm is either concave (unfavourable) or convex (favourable)]. In multicomponent systems ($n > 3$) of type (15), there is a possibility of the inversion of the components.^{37, 38}

Inversion takes place also in chromatographic systems with complex formation.^{48, 66, 82} In this case, the selectivity reversal may occur even in a binary system. In other words, the f_{ij} binary isotherm for components i and j can be S -shaped or σ -shaped (with an inflection and an intersection of the diagonal). An inversion of this type influences significantly the form of the chromatograms owing to the appearance of combined concentration waves — partly stationary and partly spreading waves. The occurrence of inversion also influences the form of the chromatographic fronts also in adiabatic sorption columns, where the heat changes may alter the relative affinities of the components for the sorbent. This results in the appearance of combined (stationary-spreading) concentration waves. Their formation may be regarded as the manifestation of 'cross' effects, which are considered in the thermodynamics of nonequilibrium processes.^{23, 24}

III. Theory of nonlinear multicomponent sorption dynamics and chromatography, concentration waves, and velocities

Below we shall speak of the systems investigated as chromatographic systems, emphasising thereby that the behaviour of dynamic systems is considered, although the entire description refers both to multicomponent sorption dynamics and to chromatography.

The nature of the motion, interaction, and spreading of multicomponent concentration waves generated when a mixture of sorbable substances moves through a disperse medium (and hence also the separation of the substances in the mixture) depend on the form of the sorption isotherms for the mixture and on the nonideality factors of the chromatographic process. Such factors include a finite rate of mass exchange between the mixture components in the continuous and disperse phases (kinetic inhibition) and the longitudinal dispersion (usually characterised by the effective dispersion coefficient D_l) of the substances in the continuous phase arising due to various irregularities of the flow in the porous medium of the sorbent (dynamic factor).

In the absence of nonideality factors, when the motion of the mixture of substances is determined solely by the properties of the sorption isotherms for the mixture, the nonlinear theory of sorption dynamics and chromatography is described within the framework of the so-called 'ideal model'.^{1, 20–22, 25–73, 80, 81}

In the general case, the theoretical solution of the problem of the sorption separation of a mixture of interfering substances requires the solution of a system of equations in terms of partial derivatives of concentration functions — a system of nonlinear material balance equations.

Many investigations have been based on a computer-assisted numerical solution of such problems.^{95–103, 106–132, 160–179} An analytical formulation of the mixture isotherms in the form of the Langmuir relations (8) is usually employed in such cases. In these investigations, the numerical simulation of various chromatographic regimes was based on mass balance equations.

Special mention should be made of the theoretical and experimental studies carried out under the overall guidance by Professor Guiochon, which were devoted mainly to the modelling of chromatographic elution regimes for binary mixtures.^{106–122, 156–158, 167–173} In these studies, the numerical calculation was based on the so-called 'semi-ideal model' of sorption dynamics and chromatography in which all the spreading effects are described by a single effective parameter characterising the column (the space integration increment \dagger).^{180, 181}

Theoretical studies based on numerical calculations have shown¹⁰⁶ and experiments have confirmed^{111, 146, 184–187} that two new effects (which do not exist in the linear model of chromatography) arise in nonlinear elution chromatography — displacement and 'tag-along' effects.

Both effects are a consequence of the static effects of the competition between the sorbable molecules of two elutable components for available sorption sites. The displacement effect results in a component with small affinity being 'forced out' ahead, whilst the more effectively sorbed component remains behind. The rear boundary of the first peak on the chromatogram assumes the characteristic L -shape under these conditions.⁶⁰ The second effect is manifested in the form of a plateau of the second component, which arises at the outlet from the column after the completion of the output of the first component (the tag-along effect). It has been shown⁵⁸ that the experimental conditions under which the second effect is significant lead to a decrease in the displacement effect and conversely.⁶⁰ It has been shown on the

[†] Previously a numerical calculation of this type, employing the space integration increment, was described in the Russian literature and was better known under the name 'layer-by-layer calculation'.^{182, 183} This method can be applied only when all the mixture components have the same nonideal parameters.

basis of the ideal model using the Langmuir equation for a two-component mixture¹¹⁵ that the intensities of both effects are determined by the ratios of the loadings factors for each component.‡

In the case of mixtures with large amounts of components having different properties, the numerical calculation is performed by the method of finite differences.^{95–103, 131, 132, 168, 174–179}

Following the ideas of Helfferich and Klein,²¹ we shall consider the propagation of concentration waves and dynamic sorption processes in the sorption column. The velocity of the i th species u_i is the average velocity of the propagation of the molecules of this species in the direction of the flow:

$$u_i = \frac{u_0}{\varepsilon + (1 - \varepsilon)a_i/c_i},$$

or in the dimensionless form

$$U_i = \frac{X_i}{Y_i}. \quad (16)$$

The species velocity u_i is lower than the flow rate u_0 , since the molecules of the i th species, having spent some time in the sorbent, are retarded relative to the flow. As can be seen from Eqn (16), the species velocity is determined solely by the equilibrium properties of the sorption system.

The concentration velocity — the velocity of the k th wave (λ_k) — has a physical significance only in the case where the concentration variables $\{X_i\}$ have a gradient with respect to the column length z (or with respect to the time t when the output curve is considered). Similarly the velocity of the (shock) s th wave σ_s may be determined if the corresponding concentration distributions have a discontinuity which is retained during the propagation along the column. The relations between the concentration velocities λ_k and species velocities are derived from the material balance equations.^{21, 188}

$$\lambda_k = U_k + Y_k \frac{\partial U_k}{\partial Y_k}, \quad k = 1, 2, \dots, m. \quad (17)$$

Eqn (17) represents the formulation of the material balance equations in terms of the velocities. It is completely analogous to the relation known in fluid mechanics.^{4, 189} This expression relates the rate of propagation of a given density to the particle velocity and density. Velocities of the wave (λ_k) and the particle (U_k) have always been distinguished in fluid mechanics and the same difference exists also in the theory of chromatography and sorption dynamics.^{1, 21}

According to Eqns (17), the velocities of the wave and the substances differ both in their significance and in magnitude. Thus the sorbable molecules (or ions) may spread with a velocity U_k greater (or smaller) than the velocity of the wave λ_k moving from the larger to the smaller concentrations or conversely. In conformity with the requirement of continuity of flow, the velocity of the molecules then increases (or diminishes) relative to the velocity in the concentration profile along the wave. This leads to sharpening or spreading effects in the concentration waves, to the instability and abolition of the shock waves (or, conversely to their stabilisation and conservation), and to the accumulation (or depletion) of the species in the region of the concentration plateau.²¹

‡ The loading factor is the ratio of the volume of the injected mixture to the column capacity.^{61, 115}

IV. A model of ideal equilibrium sorption dynamics and chromatography

Within the framework of the ideal model of nonlinear equilibrium sorption dynamics and chromatography (in the absence of kinetic and dynamic effects of nonideality), the principal parameters determining the behaviour of multicomponent concentration waves are the sorption isotherms of the mixture components. Interference of the substances leads to nonlinear effects on the concentration waves. The ideal model has been developed by numerous investigators.^{1, 20–22, 25–73}

The operation of the nonideality factors (kinetic retardation and longitudinal dispersion) leads to the smoothing of the nonlinear effects and to the asymptotic establishment of a stable ('coherent')^{21, 22} state in the system. For example, instead of the shock concentration waves, diffuse stationary waves are formed at the asymptotic stage. However, the nonideality factors cannot alter the fundamentally nonlinear influence of the static effects due to the interference of substances.§

In general mathematical terms, multicomponent nonlinear chromatographic systems are described by a system of nonlinear equations in partial derivatives with respect to functions (concentrations in sorption dynamics and chromatography) which depend on two or more independent variables (time and distance in sorption dynamics and chromatography). The assembly of functions describing the behaviour of the system cannot be obtained by the superposition of the solutions of individual equations in the system for each function separately. Any disturbances in the initial conditions generates a complex response in the system, which is described best on the basis of the theory of propagating multicomponent concentration waves.^{4, 21, 22, 46, 47, 50–73, 80, 81} The term 'wave' is defined for sorption systems as the variation of concentration functions.^{77, 193}

V. Concentration waves in multicomponent chromatographic systems

In terms of the approximation of the ideal equilibrium model, the system of material balance equations for the components being sorbed under isothermal conditions assumes the following form in the case of a stationary disperse phase:^{1, 20–22, 25–74}

$$(1 - \varepsilon) \frac{\partial a_i}{\partial t} + \varepsilon \frac{\partial c_i}{\partial t} + u_0 \frac{\partial c_i}{\partial z} = 0, \quad i = 1, 2, \dots, m. \quad (18)$$

For the adjusted time $\tau = c_0(u_0 t - z)$ and the normalised concentrations $X_i = c_i/c_0$ and $Y_i = a_i/a_0$, these equations are written in the form.^{21, 22}

$$\frac{\partial Y_i}{\partial \tau} + \frac{\partial X_i}{\partial z} = 0. \quad (19)$$

Here ε is the porosity of the bed and u_0 the linear flow rate.

Allowance for the interference of the substances requires the simultaneous solution of Eqns (18) [or (19)], which constitute a system of quasi-linear partial differential equations. The characteristic paths or concentration velocities $\lambda_k = (dz/d\tau)_k$ play a decisive role in the solution of such systems of equations.

§ After the introduction of kinetic equations of specific type or abnormal static relations for multicomponent systems with subsequent solution of characteristic equations, complex values have been obtained^{190–192} for the wave velocities λ_k . This leads to variable-amplitude concentration oscillations within the waves. In practice, however, such theoretical regimes have not been observed hitherto. Furthermore, it has been shown,⁵⁰ on the basis of thermodynamic considerations, that only concentration waves with different wave velocities (the characteristic values of λ_k are real and different) can theoretically be generated in chromatographic systems.

The characteristic equation of system (19), which defines these paths, assumes the form^{21, 74–79}

$$|A - \lambda I| = 0, \quad (20)$$

where $|A|$ is a matrix of the type $|A| = |\partial X_i / \partial Y_j|$ and I is a unit matrix. The characteristic values (or eigenvalues) λ_k ($k = 1, \dots, m$) are solutions of Eqn (20). A multicomponent wave of the k th kind, which will henceforth be designated as the k -wave, corresponds to each eigenvalue of the concentration velocity λ_k . In the general case, the number of characteristic paths (λ_k) is equal to the variance (m) of the chromatographic nonlinear system.

The dynamic behaviour of such nonlinear multicomponent sorption systems is determined by the topology of the characteristic paths in the composition space. These topologies for different nonlinear systems with a variance $m = 2$ are presented as clear examples in Figs 1–4 and will be discussed below.

For multicomponent Langmuir sorption systems (8) [or the equivalent ion exchange system (2), (3)], the characteristic equation corresponding to Eqns (19) has the simple form.^{21, 35, 39}

$$H(h, X) = \sum_i \frac{X_i}{h - \alpha_{1i}} = 0, \quad \text{where } i = 1, \dots, n. \quad (21)$$

The function H describes the transition from the composition space $\{X_i\}$ (Fig. 1a) to the functions space $\{h_i\}$ (Fig. 1b) — the Riemann invariants.²¹ It has been shown²¹ that the reverse transition from the invariants space $\{h_i\}$ to the composition space $\{X_i\}$ or $\{Y_i\}$ is described by the relations

$$X_j = \frac{\prod_i (h_i - \alpha_{1j})}{\prod_i (\alpha_{1i} - \alpha_{1j})},$$

$$Y_j = \frac{\prod_i (1/h_i - 1/\alpha_{1j})}{\prod_i (1/\alpha_{1i} - 1/\alpha_{1j})}, \quad i, j = 1, 2, \dots, n, \quad (22)$$

where the symbol $\prod_i A_i \equiv A_1 A_2 \dots A_n$ denotes the product of all the quantities A_i .

The system of Eqns (18) or (19) is called hyperbolic in a narrow sense — when all the eigenvalues λ_k are real and different:⁴⁷

$$\lambda_1 < \lambda_2 < \dots < \lambda_m. \quad (23)$$

These values define the multicomponent concentration waves propagating different velocities λ_k (Fig. 1c).

Using the principal ideas of thermodynamics and the stability criteria for thermodynamic multicomponent systems, Kvaalen et al.⁵⁰ showed that the roots (eigenvalues) of the characteristic equation (20) are real, positive, and different for physically real sorption systems. The different types of behaviour of multicomponent sorption systems with complex and multiple eigenvalues have been examined theoretically in a number of studies.^{103, 190–192}

The concentration waves formed in a sorption column will be the subject of further exposition and we shall therefore discuss briefly this concept. There is no unique definition of the waves. A wave has been defined in a monograph¹⁹³ as any distinguishable signal propagated from one part of the medium to another at a certain definite velocity. Such a signal may be a perturbation of any kind (for example, a pulse or a step) subject to the condition that the perturbation may be clearly distinguished or its location can be determined at any specified instant. The signal may be distorted or its magnitude may change but it must remain distinguishable. For example, a concentration plateau cannot be a wave. The usual subdivision of waves into two classes — dispersing and hyperbolic waves — is not exhaustive, since there are exceptions which do not correspond to either one of these classes. Mainly hyperbolic concentration waves are formed in the

sorption column. There is a clear definition of hyperbolicity⁴⁷ associated with the difference between the characteristic values λ_k [see Eqn (23)].

One of the most interesting phenomena in nonlinear sorption systems in the absence of nonideality factors is the shock waves, which represent sharp discontinuities (jumps) in concentrations (for example, the $M^1 M^2$ wave in Fig 1a). Shock waves arise in nonlinear systems when waves ‘overlap’^{4, 21, 47, 193} or, in other words, when the characteristics intersect on the physical plane (z, τ). Shock waves may appear and be propagated even when they are not induced by an initial discontinuity. After the appearance of a discontinuity, the shock waves in nonlinear systems are not disrupted on further propagation, except under certain stability conditions.^{21, 39, 74, 78, 79} For essentially nonlinear systems of the hyperbolic type, such conditions have been introduced¹⁹³ and called the entropy conditions. The term ‘Lax’s conditions’ is frequently used in the mathematical literature.⁷⁹ These conditions have a simple physical significance — a shock wave is stable if

(a) the s -wave ‘overlaps’, i.e. the characteristics of the same s th kind intersect on the physical plane (z, t), forming a discontinuity line or a shock line σ (see Fig. 1d) and

(b) the $(s-1)$ -wave cannot catch up with the given s -wave, which in its turn cannot catch up with the next (faster) $(s+1)$ -wave (Figs 1c and 1d).

When applied to sorption dynamics and chromatography, Lax’s conditions are sometimes referred to as ‘convexity conditions’ for the isotherms^{98–103, 163–165} by analogy with a univariant ($m = 1$) system in which a shock sorption boundary of one component arises for a convex $f(c)$ isotherm.²⁰

Chromatographic systems where the equilibrium is described by the Langmuir relations (8) are an example of hyperbolic, truly nonlinear systems. For more complex nonlinear systems, having linearly degenerate regions, the stability conditions are subject to a greater number of limitations.^{78, 79, 98, 99} In these systems, there is a possibility of the appearance of combined concentration waves in which the discontinuity is in contact with a spreading wave of the same family. Contact discontinuities of this type may be formed in chromatographic systems in the presence of regions of selectivity reversals.

On the discontinuity line σ (see Fig. 1d), the material balance differential equations are invalid. They must be replaced by a conservation law expressed in an integral form.^{47, 75, 76, 79} In the integral form, this law does not lose its significance for discontinuous solutions and gives rise to relations between the concentrations on the plateau to the left (X_i^s, Y_i^s) and to the right (X_i^{s+1}, Y_i^{s+1}) of the discontinuity in the shock s -wave (an example of the concentration plateau is presented in Fig. 1c, $M^1 M^2$ wave). These relations are independent of the number (i) of the component, so that for any i and j the following relations are valid:

$$\sigma_s = \frac{\Delta X_i}{\Delta Y_i} = \frac{\Delta X_j}{\Delta Y_j}, \quad (24)$$

$$\Delta X_i = X_i^{s+1} - X_i^s, \quad \Delta Y_i = Y_i^{s+1} - Y_i^s; \quad 1 \leq i, j \leq m,$$

which are called in mathematics the Hugoniot or Rankine–Hugoniot condition,^{4, 47} whilst in the theory of chromatography they are referred to as the compatibility condition^{41, 43} or the integral coherence condition.²¹ These relations form a system of algebraic equations, with the aid of which it is possible to determine the composition $\{X_i^s\}$ on one side of the discontinuity, provided that the velocity of the shock waves σ_s and the composition $\{X_i^{s+1}\}$ on the other side of the discontinuity are known.

For a deeper understanding of the behaviour of concentration waves in multicomponent systems, analysis of the nonideality effects is necessary.

The shock concentration waves are an idealisation. When account is taken of dispersion effects, the shock waves in nonideal models assume the form of a distribution with a finite width.¹⁹⁴ In such models, a stationary regime in the propagation of the wave corresponds to shock waves at the asymptotic stage.^{20, 21, 65, 92–94, 104, 105, 125–128, 195–200}

The special class of solutions, referring to simple waves, is of greatest interest for the solution of the material balance equations (18) or (19) for multicomponent chromatographic systems. Such waves arise in truly nonlinear systems. An example of sorption dynamic systems of this kind is provided by systems with equilibria described by the Langmuir relations (8). The initial and final conditions, corresponding to the frontal-displacement variant of sorption dynamics and chromatography, i.e.

$$X_i(0, z) = X_i^0, 0 \leq z; \quad X_i(t, 0) = X_{i0}H(t), \quad i = 1, 2, \dots, m, \quad (25)$$

[X_i^0 and X_{i0} are constants and $H(t)$ is the Heaviside function] lead to the class of centred simple waves.

The solution of the material balance equations (18) and (19) under these conditions is called the solution of the Riemann problem.^{40, 43, 74, 76, 78, 79} In the Russian literature, this problem is called 'splitting of the initial discontinuity'.⁴⁷

In conformity with the criterion of the stability of shock waves,^{74, 78, 79} the splitting problem has a unique solution in the class of centred spreading and shock waves.^{47, 74, 78} When applied to the theory of sorption dynamics and chromatography, such solutions for different conditions have been considered in a number of studies.^{21, 31–34, 37, 39, 40, 43}

In nonlinear m -component chromatographic systems with an invariant affinity sequence, the initial discontinuity is accompanied by the formation of m concentration waves. This number of waves corresponds to the total number of invariants h which are determined by the characteristic equation (21).

In the m -dimensional composition space $\{X_i\}$, the solution $X_i(h)$ describes the Γ curve with the characteristic parameter h , which varies along this curve. The Γ curve is the geometrical image of the solution (see Figs 1a and 2–4). Sometimes the composition space is referred to as the hodograph space,^{4, 40, 43, 158} although this term is used more frequently in mathematics for the special case with $m = 2$ (Courant and Freidrichs⁴) when the composition space is a plane.

The Γ^k curves have been called the composition paths²¹ and the corresponding concentration waves the coherent^{21, 22} or simple^{46, 47, 77} waves. The term 'coherence' has been defined^{21, 22} as the mutual consistency of the concentrations of the components in the concentration k -wave propagating along the sorption column.

Any changes in the compositions along the composition path grid Γ^k are coherent and all other changes are incoherent. It is important to note that the path grid is determined by the type of the material balance equations and the system parameters — the separation factors in adsorption and ion exchange processes and the relative permeabilities in a multiphase flow in porous media. The topology of the composition path grid is independent of the compositions in the influent and initial flows. Therefore, for given components, the grid of Γ^k paths may be determined and then used to predict the response of the system under arbitrary initial and boundary conditions. The combination of the time–distance diagram with the $M^1M^2M^{m+1}$ route, which corresponds to the composition waves in the composition space, yields a full and compact quantitative description of the behaviour of the system in time and in space. An example of such description is presented in Fig. 1: the $M^1M^2M^{m+1}$ route in Fig. 1a and the corresponding $M^1M^2M^{m+1}$ chromatogram in Fig. 1c as well as the physical plane distance–time (z, τ) with the M^1M^2 shock and the M^2M^{m+1} spreading wave in Fig. 1d. In the presence of the path grid in the composition space, it is easy to predict (at least qualitatively) the response of the multicomponent system to any perturbation.

Any pair of constant compositions in the composition space, the images of which lie on a same Γ^k path, are connected by a simple wave and the solution is given by the one-parameter family $\{X_i(h)\}$. The images of the initial and boundary conditions are presented by two different points M^1 and M^{m+1} respectively. The image of the solution of the Riemann problem [Eqns (19) and (25)] in the composition space represents the $M^1M^2 \dots M^{m+1}$ route consisting of sections of the Γ^k paths; each corresponds to the k th wave M^kM^{k+1} of a different ($k = 1, \dots, m$) kind. The route contains the highest values of m for the different sections, which are disposed consecutively from Γ^1 to Γ^m . Each break point M^k on the route (see Figs 1a and 1c) corresponds to a constant state $\{X_i^k\}$. Thus, together with the terminal points M^1 and M^{m+1} , there are $m+1$ concentration plateaux on a multicomponent chromatogram (see Figs 1a, 1c, and 1d).

The solution represented in the physical plane (z, τ) yields the inverse image of this route (Fig. 1d). The physical significance of the picture considered is that the initial discontinuity in the concentrations [Eqn (25)] splits into m concentration waves. The slowest wave corresponds to the characteristic value λ_1 and the fastest to λ_m value. Any of the waves may be of the spreading or shock type. Each wave of the k th kind is separated from the preceding $(k-1)$ th wave by the $M^k\{X_i^k\}$ concentration plateau (see Fig. 1c). The concentrations $\{X_i^k\}$ on the plateau are independent of the dispersion factors and can therefore be determined by calculations carried out within the framework of the ideal equilibrium model.

VI. Coherence

The coherence conditions define a special regime in the propagation of a multicomponent concentration wave in a chromatographic system in which all the concentrations of the mixture components move synchronously along the k -wave. For a two-component system, this condition has been put forward in the form of a postulate.²⁹ Later the coherence condition was formulated by Glueckauf³⁰ in order to obtain a solution in such nonlinear systems. The study of this problem showed⁴⁶ that the coherence condition holds along the characteristics.⁵⁵

The concept of coherence describes states of chromatographic systems which they tend to attain similarly to the way that closed systems tend to a state of equilibrium, while open systems with fixed boundaries and constant boundary conditions tend to attain stationary states.²²

The concept of coherence was developed by Helfferich and Klein.^{21, 35, 36, 80} It makes it possible to treat qualitatively and to calculate quantitatively the chromatograms in multicomponent chromatographic systems under arbitrary initial and boundary conditions. This concept was generalised by Helfferich.^{22, 81} Subsequently the region of its application was extended to multicomponent multiphase flows in porous media,¹⁹⁵ to multicomponent distillation processes,¹⁹⁶ and to coprecipitation and dissolution processes in multicomponent systems. Up to the present day, the concept of coherence has been justifiably applied to the dynamics of multicomponent nonlinear (sorption) systems.^{21, 22, 55, 80}

This global concept^{22, 80, 81} indicates the direction in which the development of a multicomponent system develops towards the final coherent state, which may be attained after a finite time in the ideal model or asymptotically in the presence of nonideality factors in the system. The equilibrium and stationary states of the system are then regarded as special cases.

Any multicomponent wave may be regarded as a composite one, consisting of the waves of the individual components, but, in contrast to linear systems, the multicomponent wave can not be presented as their superposition. The determination of the velocity of a multicomponent wave reduces to the calculation of the eigenvalues λ_k [from a type (20) equation]. The value λ_k characterises the velocity of a coherent k -wave, while the eigenvectors define the change in the mixture composition along such a wave.

tions coexisting at such a point in space must move in the same direction and with the same velocity.

However, the concept of coherence has a broader application, since it includes the problem of the propagation of arbitrary perturbations in open systems.^{21, 80, 81} It has been shown^{21, 22} that coherence may be defined as the state in which all the independent variables (functions) move in a synchronised regime, i.e. without a shift of their (concentration) profiles relative to one another. In mathematics it is known that 'simple waves' behave in this way.^{46, 47, 77} Thus simple waves are coherent by definition.

The principle of coherence reflects the fact that arbitrary perturbations in the system are 'resolved' (splitted) into a series of simple waves. A mathematical proof of this postulate with the aid of the method of characteristics⁴⁶ has been given by Helfferich^{22, 55} for a system of two equations of the hyperbolic type. However, it had been demonstrated previously in a mathematical study⁷⁵ that the region adjoining the region of constant states is a simple wave.

If the perturbation at the inlet to the system is smooth, then its 'resolution' into coherent waves does not occur instantaneously even in the ideal model. The time of attainment of the coherent state depends on several factors, among which the most important is the difference between the eigenvalues λ_k ($k = 1, 2, \dots$). If the lines for the individual families are almost parallel on the grid of composition paths, the resolution (the transition to the coherent state) requires a longer time interval. Furthermore, when account is taken of the nonideality factors in the system, the state of coherence may be attained only at the asymptotic stage.

VII. Description of the concentration distributions in a multicomponent Langmuir sorption system with the aid of the h -transformation

The solution of the Riemann problem is simplified if certain special functions have been found: the Riemann invariants (designated here by h)^{25, 43} or the generalised Riemann vector-invariants.^{39, 40, 43, 65} Such functions have been found for the Langmuir sorption systems (8) or for the equivalent systems (9) involving the exchange of ions with equal valences.^{21, 39, 40, 43}

The following equation is valid for the invariant h_k changing along the Γ^k path:

$$\frac{\partial h_k}{\partial \tau} + \frac{dX_i}{dY_i} \frac{\partial h_k}{\partial z} = 0 \quad \text{for all } i, j = 1, 2, \dots, m, \quad (26)$$

$$\lambda = \frac{\partial z}{\partial \tau} = \frac{dX_i}{dY_i} = \frac{dX_j}{dY_j} \quad \text{for any component } i, \quad (26a)$$

where d is the symbol of the total differential.

Eqn (26) is the fundamental differential equation of the Riemann problem.^{40, 43, 65} It describes the 'conservation law' from which follows the principal property of these invariants, which facilitates significantly the solution of the problem: only the k th Riemann invariant h_k changes along the shock or spreading wave of the k th kind, while all the remaining invariants h_i ($i \neq k$) are constant. In the monograph of Helfferich and Klein,²¹ Eqn (26a) was called the differential coherence condition.

The solution of the differential equation (26) yields the one-parameter family $X(h)$ or the Γ paths in the m -dimensional composition space $\{X_i\}$ (Fig. 1a), as well as a broken curves in the invariants space $\{h_k\}$ (Fig. 1b).

The relations for the characteristic velocities of the shock s th wave (σ_s) and the spreading k th wave (λ_k) have been derived theoretically²¹ with the aid of the concept of coherence:

$$\sigma_s = h_s^1 h_s^{m+1} Q \left(\prod_{i \neq k} h_i \right),$$

$$\lambda_k = (h_k)^2 Q \left(\prod_{i \neq k} h_i \right), \quad Q \equiv \left(\prod_i \alpha_{i1} \right), \quad (27)$$

where h_s^1 and h_s^{m+1} are the values of the invariant h_s , diminishing along the s th wave, to the left and to the right of the shock s th wave respectively (see, for example, the $M^1 M^2$ wave in Fig. 1a as well as

its image — the $N^1 N^2$ wave in Fig. 1b), $\prod_{i \neq k} h_i$ is the product

of all the cofactors h_i except h_k , h_k are the values of the invariants h_k increasing along the spreading k th wave (see, for example, the $M^2 M^{m+1}$ spreading wave in Fig. 1a and also its image — the

$N^2 N^{m+1}$ wave in Fig. 1b), and $\prod_i \alpha_{i1}$ is the product of all the

cofactors α_{i1} ($i = 1, 2, \dots, n$).

For a clear demonstration of the h -transformation, we shall return to the consideration of the geometrical interpretation of the Riemann problem.

The characteristic equation for multicomponent systems (21) involving the exchange of ions of equal valence describes the transition from the composition space $\{X_i\}$ (Fig. 1a) to the invariants space $\{h_k\}$ (Fig. 1b). The reverse transition is described by Eqn (22).^{21, 35}

The following criteria for the sharpening or spreading of the concentration k th wave, expressed in terms of the invariants h_k , are obtained from Eqns (27): if the value h_k increases along the concentration k -wave, then the velocity λ_k increases and the k -wave spreads (see the $N^2 N^{m+1}$ wave in Fig. 1b and the $M^2 M^{m+1}$ wave in Figs 1a, 1c, and 1d); if the invariant h_s decreases along the s -wave (even if we assume that it is initially diffuse), then this wave tends to become sharpened, becomes a shock wave, and subsequently moves with a velocity σ_s defined by Eqn (27).

The invariant h_k in Eqn (26), changing along the k th wave, can be found by solving Eqn (21), which relates the composition in the wave to the value of this invariant.

The simplification of the solution of the problem on the basis of the function-invariant h consists in the fact that the $M^1 \dots M^m$ in the composition space consisting of sections of the Γ^k paths (see Fig. 1a) corresponds in the invariants space $\{h_k\}$ to the $N^1 \dots N^{m+1}$, the lines in which are orthogonal (see Fig. 1b). Only the invariant h_k out of the assembly $\{h_1 \dots h_k \dots h_m\}$ changes along the k -wave. The linearity of the Γ^k composition paths in the composition space is the property of the Langmuir m -component systems (or the equivalent systems involving the exchange of ions of equal valence) which permits the orthogonalisation of the space, and this simplifies the consideration of the dynamic behaviour of these nonlinear systems. It is noteworthy that the linearity of the Γ paths in the composition space is retained along the stationary concentration waves for multicomponent Langmuir systems even in the presence of dispersion factors identical for each component.^{65, 104, 105, 197–200} This property makes it possible to obtain solutions describing the concentration profiles in the stationary waves for this case.

In the physical plane (z, τ) , the region corresponding to the Γ^k path is covered by a set of lines-characteristics λ_k^l (the dashed line in Fig. 1d) corresponding to the characteristic value λ_k . The direction of the characteristics of the k th kind in the plane (z, τ) is specified by the quantity λ_k . Since the function h_k is constant along each characteristic λ_k^l , each value of $\{X_{iQ}\}$ is represented by a point on the Γ^k path (for example, point Q on the MN line in Fig. 2). Each characteristic λ_k^Q is then a straight line in the physical plane. The family of such straight lines in the plane (z, τ) represents a simple k -wave (see Fig. 1d, the family of the lines $\lambda_2^1 \dots \lambda_2^{m+1}$, $k = 2$). If the inequality $d\lambda_k/dz > 0$ holds in the region of the simple wave, then the characteristics diverge and the k th wave spreads as a function of time. Such a wave is referred to as 'spreading'^{196, 201} or 'nonsharpening'.²¹

It has been noted in a monograph²¹ and a state of the art review²² that in the theory of chromatography the h -transformation (albeit under a different name) was first proposed by Davidson in 1949 for ion exchange but remained unnoticed.²² This transformation was proposed independently by Zhukhovitskii and coworkers^{21, 22, 202, 203} for the theory of the high-concentration gas chromatography, vacancy chromatography, and the chromatography without a carrier gas for constant partition coefficients.

As noted in the above review,²² the polynomial (h) in Eqn (21) is used in differential geometry, but for the description of the behaviour of multicomponent systems in electrodiffusion, electrophoresis, and distillation, this transformation was discovered anew. The transformation (21), based on the h -invariants, has been widely applied to systems in which the interference of the components takes place without any discrimination, i.e. the substances participating in the separation process compete under the conditions of constant relative strengths in the realisation of the function determining the given process.²² The role of such a function may be assumed by the parameter characterising the degree of occupancy of the adsorption sites in chromatography, the fraction of the void space in vacancy chromatography (or distillation), the transport of electric current in electrophoresis,³ etc. Competition between the components in the absence of discrimination then corresponds to constant binary interaction coefficients: the separation factors in chromatography, the relative volatilities in distillation, and the relative electrochemical mobilities in electrophoresis.

A computer program, permitting the calculation of both the h -transformation and of the concentration profiles on the basis of the ideal model, has been developed.⁴⁹

Studies have been performed in which the results obtained in the theory of the chromatography of multicomponent systems have been extended to systems with precipitants and with dissolution of the precipitants.^{201, 204}

A scheme for the solution of the problem of the multicomponent frontal-displacement sorption dynamics and chromatography follows from the foregoing. On the basis of the solution of the characteristic Eqn (21) using the known coordinates of the points M^1 (influent concentrations) and M^{m+1} (initial concentrations in the column) in the concentrations space, the coordinates of the corresponding points N^1 and N^{m+1} in the invariants space $\{h_k\}$ are calculated.

Next, the coordinates $\{h_k^l\}$ ($l = 1, \dots, m$) of the intermediate points N^k on the plateau between the k th and $(k+1)$ th waves are determined in the invariants space. The orthogonality of the representation of the waves in the invariants space is then employed in the calculation. Only one invariant h_k changes (from h_k^l to h_k^{m+1}) along the k th wave ($N^k N^{k+1}$) in this space [all the remaining invariants h_i ($i \neq k$) remain constant], while all the k -waves from point N^1 to point N^{m+1} are arranged in order of increasing index $k = 1, \dots, j, \dots, m$. The coordinates $\{h_k^l\}$ found are then employed to determine the coordinates $\{X_i^k\}$ of points M^k on the concentration plateau between the k th and $(k+1)$ th waves with the aid of Eqns (22).

This scheme for the calculation of concentration plateaux is used in combination with the solutions obtained for stationary waves for multicomponent Langmuir systems.^{104, 105, 198, 204} The above approach made it possible to demonstrate^{105, 198, 200} how a theoretical calculation can be used to correct and test the operation of numerical schemes for computer calculations^{98, 99} concerning problems in the theory of multicomponent sorption dynamics and chromatography.

VIII. The equivalence of multicomponent Langmuir systems and multicomponent systems with a nonuniform mobile phase velocity due to the sorption effect

The flow rate u in the material balance equation cannot remain constant if significant composition variations take place in the column, with involving net sorption and desorption steps in the molecules. This effect was first described^{205, 206} for a single component system. Different aspects of this effect, including the effect in multicomponent systems, have been investigated.^{207–218} Two reviews by Guiochon,^{213, 217} in which the results of the theory of gas chromatography with finite concentrations are discussed, are of great interest. These reviews deal briefly with problems in the solutions of systems of partial differential nonlinear equations by the method of characteristics and discuss the problems of the stability of the shock waves (concentration discontinuities).

In the separation process, net desorption steps at the rear boundary and net sorption steps at the leading boundary of the chromatographic band respectively introduce the molecules of the substance into the mobile phase and remove them from the latter. The flow rate in the region of the chromatographic band is therefore higher of the rear boundary and lower at the leading boundary.

This effect, which is significant for gas chromatography, is sometimes referred to as the 'sorption effect'²¹⁶ and its influence on the profile of the sorption band of one substance has been examined in the theory of chromatography without a carrier gas.^{203, 210, 211} The dependence of the flow rate on the concentration of the substance has been found for a one-component system.²¹⁵ The importance of the sorption effect in chromatographic separation at high concentrations has been emphasised.²¹⁴

The behaviour of the n -component sorption C system, in which account is taken of the influence of sorption effects, has been examined.^{65, 69, 198, 199} In this system the $f_i(c)$ isotherms are linear for each component, while the flow rate u is nonuniform due to the 'sorption effect':

$$f_i(c) = \gamma_i c_i; \quad \sum_{i=1}^n c_i = c_0 = \text{const}, \quad i = 1, 2, \dots, n. \quad (28)$$

It is postulated that the pressure drop in the column may be neglected and that the ideal gas law holds. The sorption effect is taken into account in gas chromatography, while in liquid chromatography it is usually neglected, although in the latter case condition (28) represents incompressibility with retention of the overall concentration c_0 of all the components. In liquid chromatography, this effect may be neglected because of the smallness of the volume changes in the sorption-desorption steps.

The Langmuir system (8) and the C system are united by one common property: in both systems, the separation factors for the i th and m th components are constant, i.e. $\alpha_{mi} = (a_m/c_m)/(a_i/c_i) = \text{const}$. The mixture components $\{c_i\}$ form the affinity sequence 1, 2, ..., n , in which the substances are numbered (and arranged) in order of decreasing affinities of the components for the sorbent:

$$\gamma_1 > \dots > \gamma_i > \dots > \gamma_n \quad \text{or} \quad \alpha_{11} < \dots < \alpha_{1i} \dots < \alpha_{1n},$$

where

$$\alpha_{1i} = \frac{\gamma_1}{\gamma_i}. \quad (29)$$

The existence of the relation (28) makes it possible to eliminate one variable (c_n) from the equations. The system of the mass balance equations then defines only $n-1$ independent functions c_i .

The invariant solutions of the system of quasi-linear material balance equations have been analysed on the basis of the ideal model.^{65, 69, 198} These solutions describe the propagation of the sorption shock and spreading concentration waves at high concentrations of the components in the multicomponent C system.

A relation for a variable flow rate u , reflecting the sorption effect, was derived for the first time for the C system by the present author.^{65, 200}

$$u = \frac{Q}{H - R/c_0} = \frac{Q}{\mu}; \quad \frac{u}{1 + \gamma_i} = \frac{Q_i}{H - R/c_0};$$

$$Q_i = \frac{Q}{1 + \gamma_i}, \quad (30)$$

where $H = \text{const}$, $R = \sum_i^n (f_i)$, and Q is the integration constant determined from the initial conditions.

Eqn (30) thus derived represents the dependence of the flowrate u on the concentrations of a mixture of m components.^{65, 198, 200} When account is taken of Eqn (30), the differential equations for the C system are identical with the mass balance equations describing the multicomponent Langmuir system (8). The relations

$$\frac{ue_i}{1 + \gamma_i} = \frac{Q_i e_i}{H - R/c_0},$$

where $e_i = (\gamma_i - \gamma_n)c_i$, play the role of multicomponent inverse Langmuir isotherms $G_i(a) = f_i^{-1}(c)$ in the mass balance equations for the C system [see Eqn (7)].^{69, 198}

The characteristic equation for the C system is formally identical with the corresponding equation for a multicomponent Langmuir system.^{65, 69, 198, 200} The separation factors (γ_m/γ_i) for the components m and i in the C system are completely analogous to the separation factors $\alpha_{mi} = \gamma_m/\gamma_i$ [see Eqn (29)]^{69, 198} used in the multicomponent theory of chromatography.²¹ The invariants μ_k/γ_1 have the same properties as the invariants $1/h_k$, where h_k are functions introduced for the Langmuir systems.²¹ All the calculations of the chromatograms for the Langmuir system based on the equilibrium model can then be carried out also for the C system using h_k and the ratio $\alpha_{1m} = \gamma_1/\gamma_m$ ($m = 1, 2, \dots, n$), taking into account the agreement between the separation factors for the two multicomponent systems considered. In the Langmuir system (8), the components also form the affinity sequence 1, 2, ..., m , in which they are arranged in order of decreasing affinity for the sorbent, namely $\alpha_{1m} > \alpha_{1i} > 1$ [see Eqn (29), $\alpha_{11} \equiv 1$], where $i < m$.

Only the invariant h_k , as well as the vector-invariant $[J_{kk}]$, varies along the characteristic (Γ^k) k -path (corresponding to a wave of the k th kind), whereas the remaining invariants h_m ($m \neq k$) and $\{J_{mk}\}$ ($m \neq k$) do not vary (Fig. 1b). The corresponding change in the invariant h_k (increase or decrease) determines the type of multicomponent k -wave (spreading or shock) in the chromatogram (see Fig. 1b; decrease of h_1 from h_1^1 to h_1^{m+1} along the M^1M^2 wave and increase of h_2 from h_2^1 to h_2^{m+1} along the M^2M^{m+1} wave).

Relations expressing λ_s (for a spreading wave) or σ_k (for a shock wave) (see Fig. 1d) in terms of the product of the Riemann invariants $h_1 \dots h_m$ (or $\mu_1 \dots \mu_m$) are valid for the characteristic velocities of the multicomponent concentration k -waves in the chromatogram.

For the multicomponent C system, the grid of composition paths in the concentration space has the same properties as for a multicomponent Langmuir system (8). An example for a two-component Langmuir system ($m = 2$) or a system with $n = 3$ is presented in Figs 1a and 2 (the concentrations c_i are then expressed

in terms of an acute-angle coordinate system). The coupling condition (28) reduces the three-dimensional concentrations space $\{c_i\}$ to the $P_1P_2P_3$ plane, where $c_i(P_i) = c_0$ (see Fig. 1a). The shock k -wave (or a stationary wave in the nonideal model) arises in the composition space if the change in the concentrations corresponding to this wave takes place in the direction opposite to that indicated in Figs 1 and 2 (i.e. if the invariant h_k or the corresponding invariant γ_1/μ_k diminishes along the k -wave — see Fig. 1b). The velocities of the shock and spreading k -waves are determined by the magnitude of the h_k -invariant in accordance with Eqn (27).²¹ A large number of examples of composition path grid for multicomponent (m -component) Langmuir systems (or the equivalent systems involving the exchange of n ions of equal valence, where $n = m + 1$) are quoted in the monograph by Helfferich and Klein.²¹ Similar path grids on the $P_1 \dots P_n$ simplex may be obtained also for the C system. The distributions of the concentrations of the components along the shock or spreading k -wave and its velocity are then described with the aid of the h_k -invariant. Examples of such calculations have been published.²⁰⁰

These data indicate the equivalence of the multicomponent sorption systems: C , where there is a sorption effect, and the Langmuir system (8). Naturally, the main result is the possibility of using for such systems a simple procedure for the calculation of the multicomponent (shock and spreading) concentration waves on the basis of the h -invariants.

IX. Multicomponent chromatographic systems with an invariant affinity sequence of the components

The nonlinear theory of sorption dynamics and chromatography may be used also in the calculation for a stoichiometric n -component system consisting of ions with $n = 3$, where all the characteristics lie in one plane (see Fig. 1a). In Figures 1–4 the characteristics of the first kind (Γ^1) are represented by continuous lines and those of the second kind (Γ^2) by dashed lines. In this case, the simplex triangle $P_1P_2P_3$ in the space of the Riemann invariants $\{h_k\}$ is transformed into the rectangle $P'_1P'_2W'P'_3$ (see Figs 1a and 1b).

Points W in Figs 1a and 1b and in Figs 2–4, at which the characteristic velocities of the k -waves coincide, are referred to as the 'watershed' points.^{21, 37, 38} The coordinates of point W for

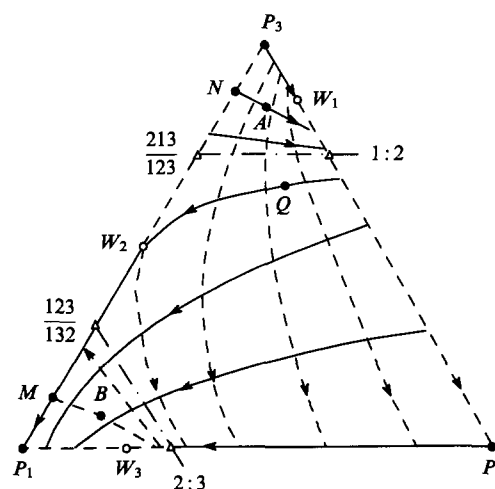


Figure 3. A variant of the hodograph for a stoichiometric three-component system for which the equilibrium relations [of the type of the Law of Mass Action (15) for heterovalent ions] are valid. The ANW_2MB and QW_2MB routes correspond to different variants of the concentration waves (see text).

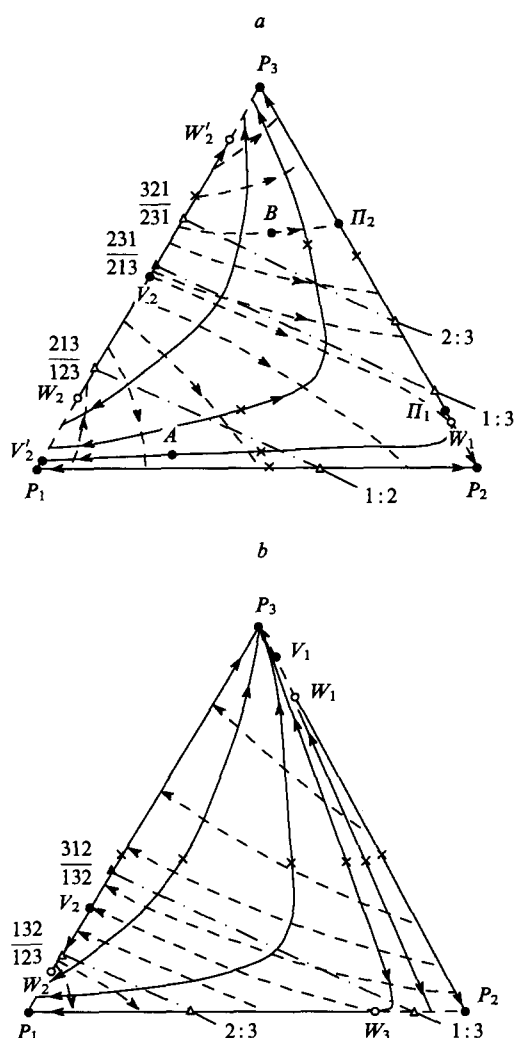


Figure 4. Variants of the hodographs obtained by numerical calculation for a stoichiometric three-component system including selectivity reversals even in a binary exchange (when the binary isotherms f_{ij} are S-shaped). (a) The presence of the inversion $i:j$ (dash-dot lines) for the 1/2, 1/3, and 2/3 components (the corresponding isotherms f_{ij} are S-shaped); (b) the presence of the inversion $i:j$ (dash-dot line) for the 1/2 components (the corresponding isotherm f_{12} is S-shaped); the crosses (x) denote the concentration points at which the wave velocity λ_k on the Γ^k paths is minimal; points V_k correspond to the points of intersection of the borders of the simplex with the Γ^k paths passing through different watershed points W within the composition region; the AP_1P_2B , $P_3V_2W_1P_2$ (a), and $P_3V_2W_3P_2$ (b) routes correspond to different variants of the concentration waves (see text).

systems with constant separation factors (8) are defined by the relation²¹

$$X_W = \frac{\alpha_{12} - 1}{\alpha_{13} - 1}.$$

The characteristics of the first kind (Γ^1) begin on the P_2P_3 side and terminate on the WP_1 segment. All the characteristics of the second kind (Γ^2) begin on the WP_3 segment and terminate on the P_1P_2 side. Each characteristic of the first kind intersects all the characteristics of the second kind and conversely. As a consequence of this, any two composition points, not located on one characteristic, may be connected by a route which initially follows Γ^1 and then Γ^2 paths, i.e. waves of the first kind and then of the second kind are formed in succession in the corresponding chromatogram. The simplex borders P_1P_2 , P_1P_3 , and P_2P_3 are

also characteristics and only they originate from the P_1 , P_2 , and P_3 corner points. There are no characteristics originating from these points within the composition region. Thus two substances cannot be absent on one side of the concentration wave and present on the other. In systems with a variable selectivity of the components, such effects may occur (see Section X).

In the case of an n -component system, the simplex gives rise to an equilateral n -gonal pyramid, but there are no fundamental differences from the case where $n = 3$.²¹

The principal rules governing the behaviour of simple (or coherent) waves may be derived from the compatibility condition (24) (for shock waves) and Eqn (26a) (for spreading waves), and also from properties associated with the continuity of the stream of molecules [see Eqns (16) and (17)]. The same rules may be obtained with the aid of the properties of the Riemann h_i -invariants and Eqn (27). However, these conclusions are valid for systems with constant separation factors α_{ij} . The rules governing the behaviour of simple waves, obtained with the aid of the velocities, are less rigorous: in this, case an invariant selectivity sequence and competitive sorption, reflected by relations (4) and (5), are needed.

In a simple wave, the species velocities u_i differ from the characteristic velocities λ_i , so that the molecules of different species pass through the propagating wave in the direction of flow or in opposition to it. This behaviour gives rise to the following effects.²¹

1. Along the wave the species velocities u_i and the concentrations X_i of all the substances change simultaneously.
2. The existence of the so called 'affinity cut'. This cut subdivides the substances in the affinity sequence $1, \dots, j, k, \dots, n$ into two groups: the high affinity group ($1, \dots, j$) and the low affinity group (k, \dots, n). The cut is designated by $j|k$. The species velocities u_i in the first group are lower and those in the second group are higher than the composition velocity (λ_i for a spreading wave or σ_i for a shock wave). The concentrations of the substances in the wave also vary in the opposite directions (if those of the substances in the first group increase then the species velocities in the second group diminish and conversely).

For an n -component (but m -variant) stoichiometric system (9), there is a possibility of $n-1$ positions of the affinity cut, namely those ranging from $1|2, \dots, n$ to $1, 2, \dots, (n-1)|n$, where the cut $k|(k+1)$ corresponds to a simple wave of the k th kind with a characteristic velocity λ_k . No concentration can vary abruptly if all others vary smoothly. One of the most important corollaries of the rules under discussion is the fact that only the substances j and k , separated by the cut $j|k$, can be present on one side of the wave and absent on the other. All other components are either present on both sides and within the wave or are altogether absent. However, two substances j and k cannot be absent from the same side of the wave, since their concentrations vary in opposite directions.

The transformation of m -component (and m -variant) Langmuir systems (9) into stoichiometric n -component (but m -variant) systems makes it possible to represent hodographs also for Langmuir systems within the space of the simplex. Fig. 2a presents a hodograph for a two-component Langmuir system with competitive sorption ($b_1, b_2 > 0$). The concentrations of the components i and j do not exceed unity and are reckoned in an acute-angle coordinate system.

Complications may arise only in the case where some of the coefficients b_i are negative. For example, the hodograph for systems with synergistic sorption, where the corresponding coefficients for one or more substances are negative ($b_i < 0$), is illustrated in Fig. 2b. As in stoichiometric systems, in such systems the initial discontinuity in concentrations splits into a chain of shock and/or spreading simple waves. Difficulties in the formation of multicomponent waves then arise. Thus Fig. 2b shows that the route along the characteristics in order of their increasing indexes, i.e. $BF^1\Gamma^2M$, is impossible between certain concentration points B (composition at the inlet to the column) and M (initial

composition in the column). In this case, the solution determining the chromatogram tends to the *BNM* route, passing partly along the envelope indicated in Fig. 2b by a dash-dot line. This route does not contain intervening plateaux. Furthermore, routes which may be referred to as metastable (for example, the *ANB* route corresponding to a single, but unstable wave) are likely on this hodograph. Small perturbations lead to the 'switching' of the metastable *ANB* route to the *AN₁B* route corresponding to two simple waves: a wave of the first kind *AN₁* and a wave of the second kind *N₁B*.²¹

In systems with invariant affinity sequence of the components the topology of the characteristics in the composition space (Fig. 3) is similar to that which occurs in systems with constant separation factors α_{ij} (Figs 1 and 2), but the characteristics are not straight lines (Figs 3, middle part of the hodograph). As a result, in systems with variable separation factors α_{ij} the route corresponding to the shock wave does not coincide with the characteristic, although it passes close to it.²¹ The deviations of the shock route are usually small, so that the characteristics may be regarded as a satisfactory approximation also to shock waves.

Problems of frontal and frontal-displacement sorption dynamics in a system with a variance $m = 2$ and with an invariant affinity sequence, in which the first component is always sorbed more effectively than the second, have been examined on the basis of the nonlinear theory of multicomponent sorption dynamics for the ideal model using hodographs with variable factors α_{ij} .²⁰⁰

All the variants of the two-component displacement chromatographs [for both convex (favourable) and concave (unfavourable) isotherms] of the components can be readily obtained with the aid of the hodograph presented in Fig. 2. Both shock and spreading waves are then obtained in the displacement chromatograms in the presence of both enhanced concentration and dilution (deconcentration) of the displaced component.

We shall consider initially the variant where both isotherms $f(c)$, of the displacing agent and the displaced component, are convex (see Fig. 2a).²⁰⁰

1. If the sorbability of the displacing agent is greater than that of the displaced component (i.e. the displacing agent is component 1 and the displaced component is component 2), then the *NMB* and *NMA* routes on the simplex $P_1P_2P_I$ correspond to the displacement regime. The displacement chromatograms corresponding to these routes have been published.²⁰⁰

2. If the sorbability of the displacing agent is lower than that of the displaced component (i.e. the displacing agent is component 2 and the displaced component is component 1), two displacement regimes, corresponding to the *MNL* and *MQS* routes, are possible. It has been noted²⁰ that in this case the displaced first component is concentrated on the plateau (C_1^*) in the intervening zone (the *MNL* and *MQS* routes respectively), but the sharp (shock) displacement wave does not arise under these conditions and two-wave displacement regimes occur: the spreading 1-wave *MN* (or *MQ*) and the shock 2-wave *ML* (or *QS*). The case of the spreading wave *NT* is an exception (see Fig. 2a, *MNT* route).

The overall character of all the types of chromatograms in the case of concave isotherm $f(c)$ consists in the fact that the concentration of the displaced component diminishes on the plateau between the concentration k -waves ($k = 1, 2$). The concentration waves may be both of the spreading and shock types in conformity with the criteria (26).

The possible variants of the calculation of the concentration waves in the displacement sorption dynamics regime for a two-component Langmuir system with different convex and concave isotherms have been examined.²⁰⁰ Tsabek⁹⁸ carried out a numerical computer calculation of two types of displacement chromatograms for two-component Langmuir isotherms. Comparison of the results with those of the present author²⁰⁰ showed that the special cases of the regimes examined in the present author's study²⁰⁰ were obtained in the numerical calculations. For other initial and boundary conditions, it is possible also to obtain other displacement regimes.²⁰⁰ Thus the results of the numerical

calculation do not always yield general conclusions about the behaviour of concentration waves in nonlinear chromatographic systems.

X. Chromatographic systems with regions including selectivity reversals of the components

We shall consider initially a system in which the ion exchange is stoichiometric and is described by the Law of Mass Action. For ideal ion exchange, this variant corresponds to the exchange of heterovalent ions, but in the general case sorption systems can also be assigned to the above systems. The stoichiometric coefficients v_i and v_s for which Eqns (15) hold can then be regarded as empirical.

For systems in which the sorption equilibrium is described by Eqns (15), it has been shown²¹ that the sorption of all the components, other than the two arbitrarily selected components k and l , diminishes if the concentration of component k with a higher affinity for the sorbent increases as a result of the decrease in the concentration of component l having a lower affinity. Thus the sorption in which the equilibrium is described by Eqns (15) is competitive. The condition of competitiveness, obtained for these systems in the monograph by Helfferich and Klein,²¹ refers to differential changes in concentration for a given mixture composition and does not eliminate the selectivity reversals arising in the system, which will be discussed below.

The characteristic equation for such systems yields $n - 1$ real roots λ_k ,²¹ which fall within the range $V_k < \lambda_k < V_{k+1}$, where

$$V_k = \frac{X_k}{Y_k}, \quad k = 1, 2, \dots, (n-1). \quad (31)$$

As in systems with a invariant affinity sequence, in the system under consideration there is an affinity cut. The condition of sorption competitiveness and the existence of the $(n - 1)$ th affinity cut for an arbitrary composition does not eliminate the reversal of selectivity. Within each region with an invariant affinity sequence, the properties of the systems (15) are the same as those of the Langmuir systems but with the difference that here the characteristics are not straight lines (see the example of Figs 3 and 4) and cannot be orthogonalised with the aid of the Riemann invariants (by the h -transformation). In this case, the path grid may be found by the numerical integration of the equation relating the concentrations of the components in the wave.^{21, 66, 200} The separation factor α_{ij} in these systems is variable and depends on the concentrations. When $v_i \neq v_j$, the separation factor varies both as a function of the partition ratio of the components and of mixture composition. If the separation factor α_{ij} varies in the range $\alpha_{ij} < 1$ to $\alpha_{ij} > 1$ course of such variation, then the components i and j change places in the sorption series. This phenomenon is in fact referred to as selectivity reversal or inversion. When the inequality $v_i < v_j$ holds, the separation factor α_{ij} is greater in the concentration range where the partition ratio Y_j/X_j greater, i.e. where there is less competition from the component (i) having a higher affinity for the sorbent. If the composition changes in the direction of a greater proportion of substances with a low affinity, then the affinity of substances with a low stoichiometric coefficient v_i increases relative to the other substances.²¹

The lines in the composition space on which the inversion of components i and j takes place (i.e. the equality $\alpha_{ij} = 1$ holds on this line) have been called^{21, 36, 37} 'reversals' and in the present review are designated by ' $i:j$ ' (the dash-dot lines in Figs 3 and 4). From the standpoint of the appearance of a possible inversion, the specification of the numbering of the substances in the sorption series has been modified.²¹ The substances are numbered in accordance with the rule

$$i < j, \quad \text{if} \quad K_{ij} > 1. \quad (32)$$

In the i/j binary system, for two arbitrary substances, the affinity of the substance with a smaller number is greater. In systems without inversion the definition (32) is equivalent to that

presented above. If inversion takes place in the system, then the composition space is divided by the reversals $i:j$ into regions where $\alpha_{ij} < 1$ and $\alpha_{ij} > 1$ (see Figs 3 and 4). For the systems (15), the reversal $j:k$ in the composition space is described by the equation of a $(n-2)$ -dimensional hyperplane parallel to the P_jP_k edge in the simplex $\{Y_i\}$ or $\{X_i\}$ (for $n = 3$, this is a straight line; see the 1:2 and 2:3 reversal lines in Fig. 3).²¹ For any two substances j and k , such a hyperplane exists $v_j \neq v_k$. There is only one hyperplane j/k of this kind, so that multiple reversal of the selectivities of components j and k does not take place. All these rules can be observed in relation to the hodograph illustrated in Fig. 3.

A sufficient condition for the existence of the reversal $j:k$ is

$$(K_{ij})^{v_k} > (K_{ik})^{v_k} \quad \text{when} \quad j < k, \quad i \neq j, k. \quad (33)$$

The system (15) has at least one reversal $j:k$ or $k:l$ if the coefficients v_i for the three components j , k , and l satisfy the condition

$$v_j, v_l > 2v_k \quad \text{when} \quad j < k < l. \quad (34)$$

It has been noted in the monograph by Helfferich and Klein²¹ that condition (34) contains no coefficients K_{ij} , so that the widely held view that there is no reversal of selectivity when $K_{1n} > K_{2n} > K_{(n-1)n}$ is erroneous. For example, a three-component system ($n = 3$) with $v_1 = 2$, $v_2 = 1$, and $v_3 = 3$ has at least one reversal regardless of the quantity K_{ij} .²¹

The influence of the reversals on the disposition of the characteristics and hence on the dynamic behaviour of chromatographic systems, described by equilibria of type (15), is not very strong owing to the existence of the following rules, which the reversals obey.

1. All the reversals are such that only neighbouring substances change places in the affinity sequence. Thus, for the reversal $j:k$, the affinity sequence changes as follows: $1, \dots, j, k, \dots, n \rightarrow 1, \dots, k, j, \dots, n$ even if j and k do not occupy neighbouring positions.

2. The reversal $j:k$ is not intersected by the characteristic with the cut j/k (for example, the Γ^1 paths in Fig. 3 intersect the reversal 2:3, while the Γ^2 paths intersect the reversal 1:2). Therefore, along any Γ^k path the compositions of groups with high and low affinities do not change. As a result, all the concentrations in the corresponding concentration wave vary monotonically.

3. Sorption remains competitive despite the reversals, so that within the limits of each region between the reversals the orientation of the characteristics and the qualitative dynamic response of the chromatographic system remain the same as in systems with invariant affinity sequence.

However, new features also appear — there is a greater number of watershed points (points W_1 , W_2 , and W_3 in Fig. 3a). Point W_2 on the P_1P_3 segment is unusual because it includes the Γ^1 and Γ^2 paths, which are tangents to the border P_1P_3 of the simplex. This property was first described by Tondeur.³⁷ In addition, the postulate that all the paths of one kind intersect all the paths of another kind, applicable to systems without inversions (cf. the hodographs in Figs 2 and 3), now ceases to be invalid.

The hodographs for systems with inversion have paths along which the velocity λ_s is constant. Such paths coincide with the reversal (the path j/k on the reversal $j:k$). For example, on Fig. 3 the reversal 1:2 coincides with the Γ^1 path and the reversal 2:3 coincides with the Γ^2 path. The concentration changes along the wave corresponding to migration along all these characteristics are not sharpened and do not become diffuse in the ideal model. Evidently, in the presence of dispersion effects in the nonideal model, such waves do become diffuse.

In contrast to systems with invariant affinity sequence in systems where a component participates in more than one reversal (for example, component 2 undergoes inversion in the reversals 1:2 and 2:3 — see Fig. 3), the initial discontinuity in concentrations may split into a larger number of concentration waves, exceeding the variance of the system (m).

Thus in Fig. 3 the ANW_2MB route from the concentration point A via the watershed point W_2 and extending to point B and intersecting two reversals gives rise to three concentration waves: AN , NW_2M , and MB . The component (in the given instance component 2) may be present when the column is filled initially (point B) and may be moved to the inlet (point A), but it is absent from the intervening concentration wave NW_2M .^{21, 200}

This variant may occur also in the case where the route runs along the Γ path, which is tangential to the border of the simplex at the watershed point W (see the concentration wave QW_2M in Fig. 3; point Q corresponds to the mixture composition at the inlet to the column).

We shall consider the properties of nonlinear chromatographic systems in the presence of static complex-formation effects when the inversion $i:j$ may arise even for the i/j binary exchange of a pair of components i and j . In this case, the binary exchange isotherm f_{ij} can have the S - or σ -shape.^{48, 66} A common feature of complex-forming systems in the presence of inversions consists in the fact that the concentration wave may be combined, i.e. may contain both discontinuous and diffuse sections.

Figs 4a and 4b present certain variants of hodographs (among those obtained by numerical integration)⁶⁶ for a system modelling the static complex-formation effects in which the multicomponent isotherms are represented by bi-Langmuir multicomponent isotherms.¹⁴⁹ The nonmonotonic variation of the wave velocity along the wave implies that the corresponding concentration wave may be partly of the shock type and partly of the spreading type — a property which is absent from the sorption systems (9) and (15).

The possible reversals for a three-component system, shown in Fig. 4a, are 1:2, 1:3, and 2:3. A hodograph of this type has been presented in a study⁴⁸ where the exchange of ions of equal valence in the presence of complex formation was considered. In this case, all three binary exchange isotherms $f_{1/2}$, $f_{1/3}$, and $f_{2/3}$ are S -shaped. The same topology of the characteristics, but this time with two reversals, was observed in the above study⁴⁸ and obtained in a theoretical investigation.⁶⁶ The binary isotherms $f_{1/3}$ and $f_{2/3}$ are then S -shaped, while the isotherm $f_{1/2}$ is convex (favourable). Other possible variants of the hodographs for a three-component system in the presence of complex formation have been quoted by the present author.⁶⁶ As for the systems (15), the hodographs for the above systems have several watershed points (cf Figs 3 and 4). There are also characteristics along the tangent to the border of the composition triangle within the composition region (cf the Γ^1 paths passing through the watershed points: through point W_1 in Fig. 4a and through point W_3 in Fig. 4b).

In the previous Section, it was noted that composition lines originating from the corner points of the simplex within the composition region are absent from the hodographs for essentially nonlinear systems. This means that on the chromatogram two components cannot be absent on one side of the wave and present on the other. For complex-forming stoichiometric systems, chromatograms of this kind are possible. For example, on the chromatogram corresponding to the $P_3V_2P_2$ route (Fig. 4b), two components i ($i = 1, 2$) are present only on one (left) side of the shock 2-wave V_2P_2 . In the usual stoichiometric systems, component 3 separates components 1 and 2 on the chromatogram, whereas on the chromatogram corresponding to the $P_3V_2P_2$ route, components 1 and 2 cannot be separated from one another (for further details on this topic, see the present author's earlier communication⁶⁶). The inversion of components 1 and 3 on the isotherm $f_{3/1}$ plays a decisive role in the formation of such a chromatogram.^{66, 200}

For the S -shaped binary isotherm $f_{1/3}$ and the convex (favourable) binary isotherms $f_{1/2}$ and $f_{2/3}$, a study has been made on the basis of qualitative considerations of the possibility of the formation of chromatograms consisting of two shock waves (see Fig. 4b):²¹⁹ the 1-wave P_3V_2 and the 2-wave V_2P_2 . The formation of displacement chromatograms of this type has been demonstrated experimentally.²²⁰

It was stated above that in the general case $n - 1$ concentration waves, separated by $n - 2$ intervening plateaux (Π_k), arise in nonlinear chromatographic n -component stoichiometric systems with invariant affinity sequence of the components. Thus, routes with a single intervening plateau Π_1 (for example, the AP_1V_2 route in Fig. 4a) are possible in three-component stoichiometric systems with complex formation.⁶⁶ Under these conditions, the two concentration waves on the chromatogram may be of the shock or spreading types partly of the shock type and partly of the spreading type. However, in the presence of inversion of the components, the route with a single intervening plateau does not always occur in chromatographic systems.

The postulate that each path of one kind intersects all the paths of another kind is invalid for such systems, so that in a number of instances one cannot move from a certain region of the simplex (the region $P_1V_2W_1P_2$ in Fig. 4a) to another region via a route including consecutively only two paths (Γ^1 and Γ^2). A variant of the route, which passes through a watershed point and contains three concentration waves and two intervening plateaux, has been proposed for such cases.³⁸

A route (for example, the $AP_1\Pi_2B$ route in Fig. 4a), corresponding to a chromatogram with three concentration waves AP_1 , $\Pi_1\Pi_2$, and Π_2B and with two intervening plateaux (Π_1 and Π_2), in which one of the components (component 1) is present during the initial filling (point B) and in the inlet zone (point A) of the chromatogram but is absent from the intervening region (segment $\Pi_1\Pi_2$), arises under these conditions. In individual instances (when the route passes along the characteristic $V_2W_3P_2$ — see Fig. 4b), the concentration of component 1 may become zero on the shock concentration 2-wave (section W_3P_2).⁶⁶

XI. Interaction of concentration waves in multicomponent chromatographic systems

The initial discontinuity in concentrations (from the influent concentration to the concentration during the initial filling of the column) in the frontal displacement multicomponent dynamic sorption problem splits into m concentration waves separated by concentration plateaux. In cyclic chromatographic processes, the column should be regenerated and for this reason yet another discontinuity concentration is created at the inlet. As a result, a further assemble (k) of concentration waves of different kinds ($k = 1, 2, \dots$) arises in the column. Thus there is a possibility of a situation where a fast wave of the k th kind catches up with a slow wave of the s th kind ($k > s$) generated during the preceding break in concentrations, whereupon the interference of two concentration (k, s)-waves of different kinds takes place. In contrast to linear systems, in the interference of waves in nonlinear systems the principle of superposition does not hold, which leads to specific results of the interaction of the waves.

If two waves of different kinds meet, a local noncoherence arises for a time, being resolved by transition to a coherent state, as in the case where a perturbation is introduced into the system. During the interference of waves, the general postulate that the noncoherent state of the wave, defined as a superposition of coherent waves, is resolved during propagation and tends to a coherent state remains valid.²¹

In a calculation for such interaction in ideal systems with constant separation factors, the Riemann invariants have been used.²¹ In the case of variable separation factors, in systems with invariant affinity sequence, the characteristics of the interaction of the concentration waves remain the same, but the Γ^k paths on the hodograph are no longer straight, which significantly complicates the quantitative calculation for the interaction of concentration waves.

It has been shown⁶⁸ that, for a three-component stoichiometric system with invariant affinity sequence of the components but with variable separation factors, there are two special cases of the interaction of concentration waves. If in the interaction of two waves in a three-component stoichiometric system the boundary

concentration plateaux are at the borders of the simplex while one of the interacting waves is of the shock type, the calculation for the interaction is carried out with the aid of only the binary isotherms f_{ij} .⁶⁸ This principle has been applied in a calculation, based on the ideal model, for a cyclic four-stage process involving preparative chromatographic multicomponent separation.⁶⁷

XII. Stationary concentration waves in multicomponent nonlinear chromatographic systems including dispersion factors

The conditions governing the appearance of stationary regimes in multicomponent sorption dynamics for Langmuir mixture isotherms (8) have been analysed^{21, 39, 40} on the basis of both the general theory of quasi-linear equations of the hyperbolic type^{46, 57} and the model of equilibrium ideal sorption dynamics and chromatography. It has been shown³⁹ that, in the case of Langmuir mixture isotherms (8), Lax's stability conditions hold for the shock waves arising under these conditions. Therefore, for certain relations between the assembly of input concentrations and their assembly in the initial stage of the filling of columns in a chromatographic system, various shock S -waves arise (where integral numbers S assume values ranging from 1 to m).

In the presence of dispersion effects in the nonideal models considered, stationary regimes governing the propagation of multicomponent concentration S -waves with a finite width, which depends on the dispersion factors and on the 'curvature' of the multicomponent sorption isotherms, correspond to the shock S -waves.

The conditions governing the attainment of stationary regimes in multicomponent chromatographic systems with invariant affinity sequence of the components are independent of the magnitude of the dispersion factors and are therefore determined on the basis of the ideal model. However, the time required for the attainment of the stationary stage in the propagation of a multicomponent concentration S -wave depends on the values of the nonideality factors. These factors lead to the spreading of the concentration S -wave, the width of which becomes constant after a time. The time needed to establish stationary regimes depends on the height equivalent to the theoretical plate (HETP) and on the 'curvature' of the multicomponent isotherm. The dispersion parameter HETP is well known and is used widely in chromatographic theory and practice. It determines the width of the concentration waves and the effectiveness of the operation of the sorption bed.

After the attainment of the stationary regime (in the asymptotic stage), a multicomponent S -wave with a fixed width propagates at a constant velocity equal to the velocity of the shock wave σ_s . This velocity is independent of dispersion effects and is determined by the concentrations on the plateaux to the left (c_i^S) and to the right (c_i^{S+1}) of the S th wave.^{20, 65, 69, 104, 105, 197–200} The methods for the determination of the concentrations on the plateaux were discussed above and examples of such calculations may be found in a number of communications.^{105, 198, 200}

In the presence of dispersion effects, the material balance equations assume the general form

$$\frac{\partial(a_i + c_i)}{\partial t} + \frac{\partial(c_i u)}{\partial z} = D_i \frac{\partial^2 c_i}{\partial z^2}, \quad i = 1, 2, \dots, m, \quad (35)$$

where D_i are the effective longitudinal dispersion coefficients for m mixture components.

This system must be supplemented by kinetic sorption effects. A reasonable approximation to the kinetic equations is provided by model phenomenological equations based on the concept of linear driving forces. For intraparticle diffusion control, the kinetic equation proposed by Glueckauf^{221, 222} for a one-component system, extended to multicomponent systems, is usually employed:

$$\frac{\partial a_i}{\partial t} = \beta_i [f_i(c) - a_i], \quad i = 1, \dots, m. \quad (36)$$

For film diffusion control, analogous phenomenological equations are employed:^{223, 224}

$$\frac{\partial a_i}{\partial t} = \zeta_i [c_i - \varphi_i(a)], \quad i = 1, 2, \dots, m. \quad (37)$$

Here $f_i(c)$ and $\varphi_i(a)$ are sorption isotherms which are reciprocal relative to one another, i.e. $f_i(c) = \varphi_i^{-1}(a)$.

The solution of the systems of differential equations (35) and (36) and (35) and (37), describing the profiles of stationary k -waves for two special types of nonlinear multicomponent chromatographic systems (L and C), has been considered.^{65, 104, 105, 197–200}

The L system is a multicomponent sorption Langmuir system (8) with constant separation factors for the components and a uniform velocity of the mobile phase u .

The C system is a system of n sorbable components in the presence of the sorption effect with linear isotherms and nonuniform flow rate u .

It has been shown on the basis of the ideal multicomponent model that the L and C systems are equivalent.^{65, 69, 198, 200}

It has been demonstrated for both systems^{65, 69, 104, 105, 197–200} that, in the case of dispersion factors identical for each component, the relation between the concentrations of the components in the stationary multicomponent S -wave is linear: for the L system

$$c_i - c_i^S = A_i^S (V - V^S), \quad \text{where} \quad A_i^S = \frac{c_i^{S+1} - c_i^S}{V^{S+1} - V^S}, \quad (38a)$$

and for the C system

$$c_i - c_i^S = B_i^S (R - R^S), \quad \text{where} \quad B_i^S = \frac{c_i^{S+1} - c_i^S}{R^{S+1} - R^S}, \quad (38b)$$

$i = 1, 2, \dots, m$.

The linear relations (38) describe the dependence of the concentrations of the components along the multicomponent concentration S -wave at the stationary stage with dispersion factors identical for each component. These relations describe a path grid in the concentration space, which coincides with the grid of the Γ^k paths for the ideal model. For a two-component model, examples of path grids of this kind are presented in Figs 1a and 2. The linear relations (38) may serve as reliable tests of the validity, convergence, and accuracy of the numerical schemes developed for the solution of nonlinear problems in multicomponent sorption dynamics (see the examples given in a number of papers^{105, 198, 200}).

In the ideal model, the parameters A_i^S and B_i^S represent the Riemann vector-invariants.^{40, 43, 65, 69, 198} A large number of examples of path grids Γ^k , including those for multicomponent systems, have been presented in the monograph by Helfferich and Klein.²¹

Accurate analytical solutions, describing the stationary multicomponent concentration waves of the S th kind for different combinations of the dispersion factors, have been obtained in the case of the L and C systems in a moving coordinate system (c, Z).^{65, 104, 105, 198–200}

1. The L system^{104, 105, 198, 200}

For equilibrium sorption dynamics, one can write

$$D_i = D \quad \text{and} \quad \frac{1}{\beta_i} = 0 \quad \left(\text{or} \quad \frac{1}{\zeta_i} = 0 \right); \quad \text{HETP} = \frac{2D}{u}.$$

For nonequilibrium (intraparticle diffusion) sorption dynamics, without allowance for longitudinal diffusion, we have

$$D_i = 0 \quad \text{and} \quad \beta_i = \beta; \quad \text{HETP} = \frac{2(1 - \sigma_S/u)\sigma_S}{\beta},$$

$$V^S \ln|E| - V^{S+1} \ln|1 - E| = \frac{2(1 - \sigma_S/u)(V^S - V^{S+1})Z}{\text{HETP}} + K_S,$$

$$V^S = 1 + \sum_i b_i c_i^S, \quad S = 1, 2, \dots, \quad Z = z - \sigma_S t. \quad (39)$$

The following expressions are used for the description of nonequilibrium (film diffusion) sorption dynamics without allowance for longitudinal dispersion:

$$D_i = 0 \quad \text{and} \quad \zeta_i = \zeta; \quad \text{HETP} = \frac{2(1 - \sigma_S/u)^2 u}{\zeta},$$

$$V^{S+1} \ln|E| - V^S \ln|1 - E| = \frac{2(1 - \sigma_S/u)(V^S - V^{S+1})Z}{\text{HETP}} - K_S,$$

$$K_S = V^S - V^{S+1},$$

$$E = E_S = \frac{c_i - c_i^S}{c_i^{S+1} - c_i^S} = \frac{V - V^S}{V^{S+1} - V^S}. \quad (40)$$

Here the distribution of the concentrations E_S along the multicomponent concentration S -wave is independent of the number i of the component ($i = 1, 2, \dots, m$) when account is taken of Eqn (38). The distribution of concentrations has been formulated in a dimensionless form and normalised, since the relation $0 \leq E \leq 1$ is valid.

A widely employed empirical parameter — the effective width Δz_S

$$\Delta z_S = \frac{\text{HETP}(V^S + V^{S+1})}{(V^S - V^{S+1})2(1 - \sigma_S/u)} \ln \left| \frac{1 - \varepsilon}{\varepsilon} \right|, \quad (41)$$

where ε is an arbitrarily selected small dimensionless quantity ($\varepsilon = 0.1$ is usually employed in practice), is applied to the description of the spreading of the wave.

2. The C system^{65, 198–200}

In the case of equilibrium multicomponent sorption dynamics, we have

$$D_i = D \quad \text{and} \quad \frac{1}{\beta_i} = 0 \quad \left(\text{or} \quad \frac{1}{\zeta_i} = 0 \right); \quad \text{HETP} = \frac{2D}{u}$$

$$\ln|E| - \ln|1 - E| = \frac{2(\sigma_S/u)(R^S - R^{S+1})Z}{c_0 \text{HETP}}. \quad (42)$$

The following relation is valid for nonequilibrium intraparticle diffusion multicomponent sorption dynamics without allowance for diffusion:

$$D_i = 0 \quad \text{and} \quad \beta_i = \beta; \quad \text{HETP} = \frac{2(1 - \sigma_S/u)\sigma_S}{\beta},$$

whilst for nonequilibrium film diffusion multicomponent sorption dynamics without allowance for longitudinal dispersion, we have

$$D_i = 0 \quad \text{and} \quad \zeta_i = \zeta; \quad \text{HETP} = \frac{2(1 - \sigma_S/u)^2 u}{\zeta},$$

$$(u^S - \sigma_S) \ln|E| - (\sigma_S - u^{S+1}) \ln|1 - E|$$

$$= \frac{2(1 - \sigma_S/u)(R^S - R^{S+1})\sigma_S Z}{c_0 \text{HETP}} + K_S,$$

$$K_S = u^{S+1} - u^S, \quad (43)$$

where u^S is the velocity on the concentration plateau to the left of the S -wave and u^{S+1} the velocity on the concentration plateau to the right of the S -wave (for the C system, the velocity u is nonuniform).

Relations for estimating the effective width of the multicomponent stationary S -wave are obtained from the distributions (42) and (43):

$$\Delta z_S = \frac{\text{HETP}c_0(u/\sigma_S)}{(R^{S+1} - R^S)} \ln \left| \frac{1 - \varepsilon}{\varepsilon} \right|, \quad (44)$$

$$\Delta z_S = \frac{\text{HETP}c_0[1 - (u^S + u^{S+1})/2\sigma_S]}{(R^{S+1} - R^S)(1 - \sigma_S/u)} \ln \left| \frac{1 - \varepsilon}{\varepsilon} \right|. \quad (45)$$

The integration constants K_S in Eqns (39), (40), (42), and (43) have been obtained from the consideration that the centre of gravity of the S -wave is zero in the moving coordinate system with $Z = z - \sigma_S t$.^{65, 104, 105, 199, 200}

It follows from Eqns (41), (44), and (45), where the denominator includes the difference $V^{S+1} - V^S$ or $R^{S+1} - R^S$, that the smaller the number of concentration jumps in the S -wave the greater its width and diffuseness.

Analytical solutions of Eqns (38) and (45) can be readily used for the analysis of the stationary stage in two-component displacement sorption dynamics of two components (or for the equivalent system involving the exchange of three ions).²⁰⁰ It follows from this analysis that the static effects of the interference of components lead to additional spreading of the concentration wave compared with its spreading in a one-component system. This additional spreading occurs in the concentration profiles of both the displacing agent and of the displaced component and is greater the greater the curvature of the sorption isotherms.

For markedly curved Langmuir isotherms for the displacing agent [large values of b_1 in Eqn (8)], it has been shown^{198, 200} that, in the displacement regime for a two-component system, the additional spreading of the displacing agent wave ($i = 1$) occurs in the region of low concentrations in the 2-wave ($S = 2$) for the intraparticle diffusion kinetic stage and in the region of high concentrations for the film diffusion kinetic stage.

It follows from Eqns (39)–(41) that, in a two-component L system with displacement of component 2 by component 1, the mutual influence of the components leads (owing to the sorption effect) to additional spreading of the concentration waves of both components compared with a one-component system.^{198, 200} In a C system, such operation of the static effect of the interference of substances is analogous to the effect which arises in the Langmuir sorption L systems. This additional spreading is greater the greater the Henry coefficient of the displaced component and the smaller the Henry coefficient of the displacing agent.^{199, 200}

XIII. Conclusion

The above analysis of the nonlinear theory of multicomponent sorption and chromatographic systems yields general conclusions about the current state of this field of study and of the trends in its development.

The application of concepts associated with the description of the behaviour of nonlinear multicomponent chromatographic systems within the framework of multicomponent concentration waves, in particular for the determination of the eigenvalues of the wave velocities, is exceptionally fruitful. Here one should employ the advances achieved in the theory of fluid and gas mechanics and also in the mathematical theory of systems of nonlinear equations of the hyperbolic type.

The theory of multicomponent nonlinear sorption dynamics and chromatography based on the ideal model has been well developed for nonlinear Langmuir systems with constant separation factors for the components.

The Riemann invariants, describing the propagation of the multicomponent concentration waves arising during the separation process, have been found. On this basis, the general characteristics of the behaviour of substances in multicomponent chromatographic systems have been obtained with allowance for interference effects. The application of the Riemann invariants on the basis of the ideal model permits not only calculations of multicomponent shock and spreading concentration waves with allowance for the effects of the interference of substances but also calculation for different forms of the interaction of multicomponent concentration waves.

Such results have been obtained with the aid of both the h -transformation and of the concept of coherence, which is of a general character and is applicable to the vast majority of nonlinear multicomponent chromatographic systems. The results have a simple and visual geometrical interpretation, which is based on the properties of the orthogonalisation of the composition space $\{c_i\}$ on transition to the invariants space $\{h_k\}$.

The application of the h -transformation, based on the properties of the Riemann invariants and developed in detail in the monograph by Helfferich and Klein,²¹ makes it possible to calculate the concentrations $\{c_i^k\}$ on the concentration plateau for the distributions corresponding to the multicomponent waves of the $(k-1)$ th and k th kinds.

The predictive power of these calculations is based on the fact that the calculated values on the concentration plateau between multicomponent waves are independent of the dispersion factors (nonideality factors). Using the criterion of the establishment of stationary regimes in concentration k -waves (defined as the decrease in the invariant h_k along such a wave), it is easy to deduce for Langmuir multicomponent systems whether such a regime is attained for the given k -wave under the specified initial and boundary conditions in the chromatography of a mixture of substances.

The concentration profiles calculated on the basis of the postulates of the ideal model are unrealistic, since they do not take into account the dispersion factors in sorption processes (although these factors always operate). Nevertheless, the ideal model yields a satisfactory first approximation, especially for the concentration distributions of spreading k -waves. In such waves, the nonlinearity factors and the factors associated with the static interference of substances, taken into account in the equations for multicomponent mixture isotherms, play the main role in the spreading of the k -waves.²¹

The solutions presented in Section XII of the present review supplement the approach based on the ideal model of the theory of multicomponent sorption dynamics and chromatography. The solutions obtained describe the stationary distributions of concentrations in a multicomponent k -wave of finite width (Δz) with allowance for the nonideality factors in the dynamic sorption process. According to these solutions, the width (Δz) of a stationary k -wave is proportional both to the HETP and the static factors arising from the interference of substances, which are related to the parameters of multicomponent sorption isotherms. The advantage of these simple analytical solutions consists in the possibility of taking into account the joint influence of the nonideality factors and the factors arising from the interference of the sorbable substances in the stationary stage of the propagation of multicomponent sorption k -waves.

More accurate results have been obtained in the numerical integration of the nonlinear multicomponent equations of sorption dynamics. However, in this case too the analytical solutions presented here [especially the linear relations (38)] can serve as reliable tests of the validity, convergence, and accuracy of the numerical schemes developed for the solution of nonlinear problems of multicomponent sorption dynamics.

Furthermore, the results based on the analytical solutions (in contrast to specific numerical solutions) make it possible to obtain general estimates of the influence of the effects of the interference of substances in nonlinear multicomponent dynamic sorption

systems.^{198–200} It follows from the analytical solutions presented here that the effects of the interference of substances lead to an additional broadening of the concentration distributions along the sorption multicomponent waves generated in the column.

For multicomponent systems with variable separation factors, especially for systems having regions with selectivity reversals of the components, the theory has not so far been adequately developed. For such systems, there is a possibility of a nontrivial chromatogram in which a specific component is present at the inlet and outlet and is absent within the multicomponent concentration distributions in the wave.

The concept of coherence,^{21, 22, 81} used to take into account the effects of the interference of substances, is fundamental in the description of the behaviour of nonlinear multicomponent dynamic systems and plays a major role in the development of a general theory of multicomponent nonlinear sorption dynamics and chromatography for multicomponent systems of a general kind. This concept facilitates the qualitative description and quantitative calculations for multicomponent systems, especially for arbitrary initial and boundary conditions. The fundamental nature of this concept extends to the description of the behaviour of a wide range of multicomponent nonlinear dynamic mass transfer, heterophase systems, such as multiphase flows in porous media,¹⁹⁵ chromatographic reactors, and nonstationary distillation.¹⁹⁶

References

1. A E Rodrigues, D Tondeur (Eds) *Percolation Process: Theory and Applications* (Sijthoff and Nordhoff, The Hague, 1981)
2. G B Wallis *One Dimensional Two-phase Flow* (New York: McGraw-Hill, 1969)
3. V G Babitskii, M Yu Zhukov, V I Yudovich *Matematicheskaya Teoriya Elektroforeza* (Mathematical Theory of Electrophoresis) (Kiev: Naukova Dumka, 1983)
4. R Courant, K O Freidrichs *Supersonic Flow and Shock Waves*
5. D Tondeur, in *Percolation Process: Theory and Applications* (Eds A E Rodrigues, D Tondeur) (Sijthoff and Nordhoff, The Hague, 1981) p. 4
6. I Prigogine, R Herman *Kinetic Theory of Vehicular Traffic* (New York: Elsevier, 1971)
7. *The 8th International Biotechnology Symposium, Société Française de Microbiologie, Paris, 1989*
8. F D Antia, C Horvath *Ber. Bunsenges. Phys. Chem.* **93** 961 (1989)
9. F D Antia, C Horvath *J. Chromatogr.* **590** 119 (1991)
10. S M Cramer, G Subramanian *Sep. Purif. Methods* **19** 31 (1990)
11. G Cretier *Spectra* **2000** **18** 12 (1990)
12. B Bidlingmeyer (Ed.) *Preparative Liquid Chromatography* (Amsterdam: Elsevier, 1987)
13. K Jones *Chromatographia* **32** 469 (1991)
14. S-G Hu, D D Do, M M Hossain *J. Chromatogr.* **605** 175 (1992)
15. N-H L Wang, R D Whitley, in *The 4th International Conference on Fundamentals of Adsorption, Kyoto, 86, 1992 (Extended Abstracts)* p. 66
16. R D Whitby, K E Van Cott, N-H L Wang *Ind. Eng. Chem. Res.* **32** 149 (1993)
17. G Guiochon, in *The 12th International Symposium on Microchemical Technology (ISM'92, Cordoba): Anal. Chem. Acta* **283** 309 (1993)
18. G V Samsonov *Khim. Promst* (7) 292 (1993)
19. J G Dorsey, W T Cooper, J F Wheeler, H G Barth, J P Foley *Anal. Chem.* **66** 500R (1994)
20. V V Rachinskii *Vvedenie v Obshchuyu Teoriyu Dinamiki Sorbtzii i Khromatografii* (Introduction to the General Theory of Dynamics of Sorption and Chromatography) (Moscow: Nauka, 1964)
21. F Helfferich, G Klein *Multicomponent Chromatography. Theory of Interference* (New York: Marcel Dekker, 1970)
22. F Helfferich *J. Chromatogr.* **373** 45 (1986)
23. P Glensdorf, I Prigogine *Thermodynamic Theory of Structure, Stability, and Fluctuations*
24. S R De Groot, P Mazur *Nonequilibrium Thermodynamics*
25. J N Wilson *J. Am. Chem. Soc.* **62** 1583 (1940)
26. D De Vault *J. Am. Chem. Soc.* **65** 532 (1943)
27. J Weiss *J. Am. Chem. Soc.* **145** 297 (1943)
28. A C Offord, J Weiss *Discuss. Faraday Soc.* **7** 25 (1949)
29. A C Offord, J Weiss *Nature (London)* **155** 725 (1945)
30. E Gluekauf *Proc. R. Soc. London, A Math. Phys. Sci.* **186** 35 (1946)
31. E Gluekauf *Discuss. Faraday Soc.* **7** 1247 (1949)
32. S Klaesson *Ark. Mineral Geol.* **A23** 1 (1946)
33. G Klein, D Tondeur, T Vermeulen *Ind. Eng. Chem. Fundam.* **6** 339 (1967)
34. G Klein, D Tondeur *Ind. Eng. Chem., Fundam.* **6** 351 (1967)
35. F Helfferich *Ind. Eng. Chem., Fundam.* **6** 362 (1967)
36. F Helfferich *Adv. Chem. Ser.* **79** 30 (1968)
37. D Tondeur *Chem. Eng. J.* **1** 337 (1970)
38. D Tondeur *J. Chim. Phys. (France)* **68** 311 (1971)
39. N N Kuznetsov, in *Vychislitel'nye Metody i Programirovanie* (Computing Methods and Programming) (Moscow: Izd. Mosk. Gos. Univ., 1967) No 6, p. 242
40. H K Rhee, R Aris, N R Amundson *Philos. Trans. R. Soc. A, Phys. Sci. Eng.* **267** 419 (1970)
41. H K Rhee, R Aris, N R Amundson *Philos. Trans. R. Soc. A, Phys. Sci. Eng.* **269** 187 (1971)
42. H K Rhee, N R Amundson *AIChE J.* **28** 423 (1982)
43. H K Rhee, in *Percolation Process: Theory and Applications* (Eds A E Rodrigues, D Tondeur) (Sijthoff and Nordhoff, The Hague, 1981) p. 295
44. V V Rachinskii, A M Kiyanovskii *Zh. Fiz. Khim.* **48** 964 (1974)
45. V V Rachinskii, A M Kiyanovskii *Zh. Fiz. Khim.* **47** 2855 (1973)
46. R Aris, N R Amundson *Mathematical Methods in Chemical Engineering* Vol. 2 (Englewood Cliffs, NJ: Prentice Hall, 1973)
47. B L Rozhdestvenskii, N N Yanenko *Sistemy Kvazilineinykh Uravnenii i ikh Prilozhenie k Gazovoi Dinamike* (Systems of Quasilinear Equations and Their Application to Gas Dynamics) (Moscow: Nauka, 1978)
48. F M Golden, K I Shiloh, G Klein, T Vermeulen *J. Phys. Chem.* **78** 926 (1974)
49. G Klein, M Nassiri, J M Vislocky *AIChE Symp. Ser.* **80** 14 (1984)
50. E Kvaalen, L Neel, D Tondeur *Chem. Eng. Sci.* **40** 1191 (1985)
51. D Basmadjian, P Coroyannakis *Chem. Eng. Sci.* **42** 1723 (1987)
52. D Basmadjian, P Coroyannakis, C Karayannopoulos *Chem. Eng. Sci.* **42** 1737 (1987)
53. D Basmadjian, P Coroyannakis, C Karayannopoulos *Chem. Eng. Sci.* **42** 1752 (1987)
54. P K DeBorx, P C Baarslag, H P Urbach *J. Chromatogr.* **594** 9 (1992)
55. F Helfferich *Chem. Eng. Commun.* **44** 275 (1986)
56. Y L Hwang, F Helfferich *Chem. Eng. Sci.* **44** 1547 (1989)
57. S Golshan-Shirazi, G Guiochon *J. Chromatogr.* **484** 125 (1989)
58. S Golshan-Shirazi, G Guiochon *J. Phys. Chem.* **93** 4143 (1989)
59. S Golshan-Shirazi, G Guiochon *J. Phys. Chem.* **94** 495 (1990)
60. S Golshan-Shirazi, G Guiochon *Chromatographia* **30** 613 (1990)
61. S Golshan-Shirazi, G Guiochon *Anal. Chem.* **62** 217 (1990)
62. Z Ma, A Katti, B Lin, G Guiochon *J. Phys. Chem.* **94** 6911 (1990)
63. S Golshan-Shirazi, G Guiochon, in *Proceedings of the 9th International Symposium "PREP 92", Nancy, France, 1992* p. 1
64. M Z El Fallah, S Golshan-Shirazi, G Guiochon *J. Chromatogr.* **511** 1 (1990)
65. A I Kalinitchev *Izv. Akad. Nauk SSSR, Mekh. Zhid. Gaz.* **91** (1985)
66. A I Kalinitchev *Teor. Osn. Khim. Tekhnol.* **18** 468 (1984)
67. A I Kalinitchev *Teor. Osn. Khim. Tekhnol.* **19** 768 (1985)
68. A I Kalinitchev *Teor. Osn. Khim. Tekhnol.* **21** 697 (1987)
69. A I Kalinitchev *Teor. Osn. Khim. Tekhnol.* **30** (1996) [*Theor. Farad. Chem. Eng. (Engl. Transl.)* **30** (1996)] (in the press)
70. N H Wang, S Huang *AIChE Symp. Ser.* **79** 26 (1984)
71. S C Jen, N G Pinto *J. Chromatogr.* **590** 3 (1992)
72. H P Urbach *Proc. R. Soc. London, A Math. Phys. Ser.* **437** 403 (1992)
73. H P Urbach *Proc. R. Soc. London, A Math. Phys. Ser.* **440** 303 (1993)
74. P Lax *Comm. Pure Appl. Math.* **10** 537 (1957)
75. B L Rozhdestvenskii *Usp. Mat. Nauk* **15** 95 (1960)
76. R Courant *Partial Differential Equations*
77. A Jeffrey *Quasilinear Hyperbolic Systems and Waves* (London: Pitman, 1976)
78. T P Liu *J. Differ. Equ.* **18** 218 (1975)
79. T P Liu *Mem. Am. Math. Soc.* **30** 1 (1980)
80. F Helfferich *AIChE Symp. Ser.* **80** 1 (1984)
81. F Helfferich, in *New Directions in Adsorption Technology* (Eds G Keller, R Yang) (Boston: Butterworth, 1989) p. 1

82. G Klein, in *Percolation Process: Theory and Applications* (Eds A E Rodrigues, D Tondeur) (Sijthoff and Nordhoff, The Hague, 1981) p. 363
83. B P Nikol'skii, M M Shul'ts, R B Dobrotin *Zh. Fiz. Khim.* **50** 3019 (1976)
84. F M Kuni *Zh. Fiz. Khim.* **50** 3031 (1976)
85. A I Rusanov, D A Fridrikhsberg *Zh. Fiz. Khim.* **50** 3039 (1976)
86. A V Storonkin, V T Zharov, A N Marinichev *Zh. Fiz. Khim.* **50** 3048 (1976)
87. S Yu Elovich *Dokl. Akad. Nauk SSSR* **101** 293 (1955)
88. V I Gorshkov, M S Safonov, N M Voskresenskii *Ionnyi Obmen v Protivotochnykh Kolonnakh* (Ion Exchange in Countercurrent Columns) (Moscow: Nauka, 1982)
89. G Guiochon, M Diack, M Z El-Fallah, S Golshan-Shirazi, P Jandera, in *Pittsburgh Conference Presents (PITTCON'92, New Orleans, LA, 1992)* Book Abstracts No. 337, p. 10
90. I Langmuir *J. Am. Chem. Soc.* **38** 2221 (1916)
91. G M Schwab *Ergebnisse der Exakten Naturwissenschaften* Vol. 7 (Berlin: Springer, 1928)
92. O M Todes *Zh. Prikl. Khim.* **18** 591 (1945)
93. Ya M Bikson *Zh. Fiz. Khim.* **28** 1017 (1954)
94. P P Zolotarev, A I Kalinichev *Zh. Fiz. Khim.* **46** 122 (1972)
95. M L Aleksandrov, N S Reifman, E V Semenenko *Zh. Fiz. Khim.* **49** 207 (1975)
96. L A Rybkina, Yu S Lezin, T G Plachenov, A A Seballo, E I Baranov *Teor. Osn. Khim. Tekhnol.* **9** 600 (1975)
97. A A Seballo, V I Kvasha, Yu S Lezin, T G Plachenov, E I Baranov *Zh. Prikl. Khim.* **50** 63 (1977)
98. L K Tsabek *Zh. Fiz. Khim.* **52** 660 (1978)
99. L K Tsabek *Zh. Fiz. Khim.* **50** 741 3145 (1976)
100. L K Tsabek *Zh. Fiz. Khim.* **54** 689 (1980)
101. L K Tsabek *Zh. Fiz. Khim.* **55** 2176 (1981)
102. L K Tsabek *Zh. Fiz. Khim.* **56** 451 (1982)
103. L K Tsabek *Zh. Fiz. Khim.* **56** 938 (1982)
104. A I Kalinitchev *Zh. Fiz. Khim.* **59** 2000 (1985)
105. A I Kalinitchev *Teor. Osn. Khim. Tekhnol.* **20** 532 (1985)
106. G Guiochon, S Ghodbane *J. Phys. Chem.* **92** 3682 (1988)
107. S Ghodbane, G Guiochon *J. Chromatogr.* **440** 9 (1988)
108. S Ghodbane, G Guiochon *J. Chromatogr.* **444** 275 (1988)
109. S Ghodbane, G Guiochon *J. Chromatogr.* **450** 27 (1988)
110. S Ghodbane, G Guiochon *J. Chromatogr.* **452** 209 (1988)
111. S Ghodbane, G Guiochon *Chromatographia* **24** 53 (1989)
112. M Z El Fallahi, G Guiochon *J. Chromatogr.* **522** 1 (1990)
113. B Lin, Z Ma, S Golshan-Shirazi, G Guiochon *J. Chromatogr.* **500** 185 (1990)
114. Z Ma, G Guiochon *Anal. Chem.* **62** 2330 (1990)
115. S Golshan-Shirazi, G Guiochon *Chromatographia* **30** 613 (1990)
116. S Golshan-Shirazi, G Guiochon *J. Chromatogr.* **517** 229 (1990)
117. M El-Fallah, G Guiochon *J. Chromatogr.* **522** 1 (1990)
118. M El-Fallah, S Golshan-Shirazi, G Guiochon *J. Chromatogr.* **511** 1 (1990)
119. M Czok, G Guiochon *Anal. Chem.* **62** 189 (1990)
120. A M Katti, M Czok, G Guiochon *J. Chromatogr.* **556** 205 S (1991)
121. S Jacobson, S Golshan-Shirazi, G Guiochon *AIChE J.* **37** 836 (1991)
122. S Golshan-Shirazi, J X Huang, G Guiochon *Anal. Chem.* **63** 1147 (1992)
123. Tingyue Gu, Jen Tsai Gow, G T Tsao *AIChE J.* **37** 1333 (1991)
124. H P Urbah, P K DeBorx *Proc. R. Soc. London, A Math. Phys. Sci.* **438** 371 (1992)
125. A S Kamenev *Zh. Fiz. Khim.* **65** 2168 (1991)
126. A S Kamenev *Zh. Fiz. Khim.* **67** 1218, 1225 (1993)
127. A S Kamenev, Yu A Gromov *Izv. Timiryaz. S.-Kh. Akad.* (3) 143 (1992)
128. Yu A Gromov *Zh. Fiz. Khim.* **68** 2183 (1994)
129. A Felinger, G Guiochon *J. Chromatogr.* **590** 31 (1992)
130. H Poppe *J. Chromatogr.* **556** 95 (1991)
131. Tingyue Gu, Jen Tsai Gow, G T Tsao *AIChE J.* **36** 784 (1990)
132. H K S Tan, I H Spinner, in *New Developments in Ion Exchange* (Eds M Abe, T Kataoka, T Suzuki) (Tokyo: Kodansha, 1991) p. 573
133. I Langmuir *J. Am. Chem. Soc.* **40** 1361 (1918)
134. E Huckel *Adsorption and Kapillarkondensation* (Leipzig: Akad. Verlag Ges., 1982)
135. R H Fowler, E A Guggenheim *Statistical Thermodynamics* (Cambridge, 1939)
136. A Boutaric *J. Chim. Phys.* **35** 158 (1938)
137. F Cernuschi C. R. *Hebd. Seances Acad. Sci. (Paris)* **206** 585 (1938)
138. G H de Boer *The Dynamic Character of Adsorption*
139. E Gluekauf *Trans. Faraday Soc.* **A186** 35 (1946)
140. E Cremer, J F K Huber *Angew. Chem.* **73** 461 (1961)
141. D H James, C S G Phillips *J. Chem. Soc.* 1066 (1954)
142. G Schay, G Szekeley *Acta Chim. Hung.* **5** 167 (1954)
143. J M Jacobson, J P Frenz, Cs Horvath *Ind. Eng. Chem. Res.* **26** 43 (1987)
144. J M Jacobson, J P Frenz *J. Chromatogr.* **499** 5 (1990)
145. J-X Huang, G Guiochon *J. Colloid Interface Sci.* **128** 577 (1989)
146. A Katti, G Guiochon *J. Chromatogr.* **499** 21 (1990)
147. Z Ma, G Guiochon *J. Chromatogr.* **603** 13 (1992)
148. A Katti, Z Ma, G Guiochon *AIChE J.* **36** 1722 (1990)
149. A I Kalinitchev *Inzh.-Fiz. Zh.* **42** 488 (1982)
150. M D LeVan, T Vermeulen *J. Phys. Chem.* **85** 3247 (1981)
151. A L Myers, J M Prausnitz *AIChE J.* **11** 121 (1965)
152. S Golshan-Shirazi, G Guiochon *J. Chromatogr.* **545** 1 (1991)
153. B C Lin, S Golshan-Shirazi, Z Ma, G Guiochon *J. Chromatogr.* **475** 1 (1989)
154. M Moreau, P Valentin, C Vidal-Madjar, B S Lin, G Guiochon *J. Colloid Interface Sci.* **141** 127 (1991)
155. A Velayudhan, Cs Horvath *J. Chromatogr.* **443** 13 (1988)
156. S Golshan-Shirazi, J-X Huang, G Guiochon *Anal. Chem.* **63** 1147 (1991)
157. J Zhu, A Katti, G Guiochon *J. Chromatogr.* **552** 71 (1991)
158. S Jacobson, S Golshan-Shirazi, G Guiochon *J. Am. Chem. Soc.* **112** 6492 (1990)
159. G V Samsonov, in *Khromatografiya* (Chromatography) (Ed. N N Nikol'skii) (Leningrad: Izd. Leningradsk. Gos. Univ., 1956) p. 23
160. B I Volkov, V A Nikashina, R N Rubinshtein, M M Senyavin *Zh. Fiz. Khim.* **46** 686 (1972)
161. Yu S Lezin, A A Seballo, V A Kiselev, in *Tez. Dokl. Simpoziuma po Khromatografii, Posvyashchennogo Pamyati M S Tsveta* (Abstracts of Reports at the Symposium on Chromatography, Dedicated to M S Tsvetov) (Leningrad, 1972) p. 52
162. M L Aleksandrov *Zh. Fiz. Khim.* **48** 2292 (1974)
163. L K Tsabek *Zh. Fiz. Khim.* **55** 2173 (1981)
164. L K Tsabek *Zh. Fiz. Khim.* **56** 447 (1982)
165. L K Filippov-Tsabek *Zh. Fiz. Khim.* **56** 933 (1982)
166. P Rouchon, M Schonauer, P Valentin, G Guiochon *Sep. Sci. Technol.* **22** 1793 (1987)
167. A Katti, G Guiochon, *J. Chromatogr.* **449** 25 (1988)
168. S Jacobson, S Golshan-Shirazi, A M Katti, M Czok, Z Ma, G Guiochon *J. Chromatogr.* **484** 103 (1989)
169. B S Lin, G Guiochon *Sep. Sci. Technol.* **24** 31 (1989)
170. S Golshan-Shirazi, G Guiochon *J. Chromatogr.* **506** 495 (1990)
171. Q Yu, N H L Wang *Comput. Chem. Eng.* **13** 915 (1989)
172. A M Katti, E V Dose, G Guiochon *J. Chromatogr.* **540** 1 (1991)
173. S Golshan-Shirazi, G Guiochon *Anal. Chem.* **61** 1368 (1989)
174. J Frenz, C Horvath *AIChE J.* **31** 400 (1985)
175. E B Guglya, G L Aranovich *Teor. Osn. Khim. Tekhnol.* **23** 483 (1989)
176. K S Tan, I H Spinner *AIChE J.* **30** 770 (1984)
177. V Svoboda *J. Chromatogr.* **518** 77 (1990)
178. G Patzay, B Toth, I Szabo *Hung. J. Ind. Chem.* **20** 179 (1992)
179. A V Chanov, I V Lomonosova *Mat. Modelirovanie* **4** 75 (1992)
180. S Golshan-Shirazi, M Z El Fallahi, G Guiochon *J. Chromatogr.* **541** 195 (1991)
181. A M Katti, M Diack, M Z El-Fallahi, S Golshan-Shirazi, S Jacobson, A Seidel-Morgenstern, G Guiochon *Acc. Chem. Res.* **25** 366 (1992)
182. E V Venetsianov, R N Rubinshtein *Dinamika Sorbtitsii iz Zhidkikh Sred* (Dynamics of Sorption from Liquid Mediums) (Moscow: Nauka, 1983)
183. M M Senyavin, R N Rubinshtein, E V Venetsianov, N K Galkina, E M Makhalov *Osnovy Rascheta i Optimizatsii Ionoobmennyykh Protseessov* (Foundations of Calculation and Optimization of Ion Exchange Processes) (Moscow: Nauka, 1972)
184. G Guiochon, A Katti *Chromatographia* **24** 165 (1987)

185. J Newburger, L Liebes, H Colin, G Guiochon *Sep. Sci. Technol.* **22** 1933 (1987)
186. J E Eble, R L Grob, P E Antie, G B Cox, L R Snyder *J. Chromatogr.* **405** 31 (1987)
187. J Newburger, G Guiochon *J. Chromatogr.* **484** 153 (1989)
188. S Mandelsdorf *Anal. Chem.* **38** 1540 (1966)
189. L D Landau, E M Lifshits *Mekhanika Sploshnykh Sred* (Continuum Mechanics) (Moscow: GITTIL, 1953)
190. L K Filippov-Tsabek *Izv. Akad. Nauk SSSR, Mekh. Zhid. Gaz.* **6** 114 (1982)
191. L K Filippov-Tsabek *Dokl. Akad. Nauk SSSR* **254** 1372 (1980)
192. L K Filippov-Tsabek *Dokl. Akad. Nauk SSSR* **260** 557 (1981)
193. G Whitham *Linear and Nonlinear Waves* (New York: Wiley, 1974)
194. Z Ma, G Guiochon *J. Chromatogr.* **609** 19 (1992)
195. F Helfferich *Soc. Pet. Eng., J.* **21** 51 (1981)
196. K Nandakumar, R P Andres *AIChE J.* **27** 450 (1981)
197. A I Kalinichev *Zh. Fiz. Khim.* **68** 1658 (1994)
198. A I Kalinichev *Ind. Eng. Chem. Res.* **34** 2625 (1995)
199. A I Kalinichev *Teor. Osn. Khim. Tekhnol.* **30** (1996) [*Theor. Found. Chem. Eng. (Engl. Transl.)* **30** (1996)] (in the press)
200. A I Kalinichev, Doctoral Thesis in Chemical Sciences, Institute of Physical Chemistry, Academy of Sciences of the USSR, Moscow, 1985
201. G Klein, in *Ion Exchange, Science, and Technology, Troia, Portugal, 1985* (Ed. A Rodrigues) (M Nijhoff, Avon de Rijn, NATO Sci. Division, 1986) p. 199
202. L A Zhukhovitskii, N M Turkel'taub *Dokl. Akad. Nauk SSSR* **143** 646 (1962)
203. L A Zhukhovitskii, M L Sazonov, A F Shlyakhov, A I Karimova *Zavod. Lab.* **31** 1048 (1965)
204. F Helfferich *AIChE J.* **35** 75 (1989)
205. C Bosanquet, G D Morgan, in *Vapor Phase Chromatography* (Ed. D N Desty) (London: Butterworth, 1957)
206. C Bosanquet, in *Gazovaya Khromatografiya* (Gas Chromatography) (Ed. D N Desty) (New York: Academic Press, 1958) p. 102
207. A B Littlewood *Gas Chromatography* Pt 2 (New York: Academic Press, 1962)
208. D L Peterson, F Helfferich *J. Phys. Chem.* **69** 1283 (1965)
209. J R Conder *Progress in Gas Chromatography* (Ed. J H Purnell) (New York: Wiley-Interscience, 1968) p. 209
210. A A Zhukhovitskii, N M Turkel'taub, V P Shvartsman, A F Shlyakhov *Dokl. Akad. Nauk SSSR* **156** 654 (1964)
211. G G Arenkova, M L Sazonov, V I Lozgagev, A A Zhukhovitskii *Zavod. Lab.* **3** 304 (1971)
212. G Shai, in *Uspekhi Khromatografii* (Progress in Chromatography) (Eds K V Chmutov, K I Sakodinskii) (Moscow: Nauka, 1972) p. 179
213. G Guiochon, L Zhakob, in *Uspekhi Khromatografii* (Progress in Chromatography) (Eds K V Chmutov, K I Sakodinskii) (Moscow: Nauka, 1972) p. 170
214. P Valentin, G Guiochon *Sep. Sci. Technol.* **10** 245 (1975)
215. G V Eroshenkova, S A Volkov, K I Sakodinskii *Zh. Fiz. Khim.* **53** 710 (1979)
216. S A Volkov, V Yu Zel'venskii, in *Khromatografiya (Ser. Itogi Nauki i Tekhniki)* [Chromatography (Advances in Science and Engineering Series)] (Moscow: Izd. VINITI, 1983) Vol. 4, p. 46
217. G Guiochon, C Guillemin *Quantitative Gas Chromatography* Pt 1, Ch. 5 (Amsterdam: Elsevier, 1988)
218. K Chihara, N Yanagisawa, N Hasegawa, in *The 4th International Conference on Fundamentals of Adsorption (Extended Abstracts)*, 1992 p. 120
219. V V Belov, A I Kalinichev, P P Nazarov *Zh. Fiz. Khim.* **52** 2116 (1978)
220. V M Gelis, G B Maslova, P P Nazarov, G B Maslova, E A Chuveleva *Zh. Fiz. Khim.* **50** 38 (1977)
221. E Glueckauf *Soc. Chem. Ind. London* **34** (1955)
222. T Vermeulen, G Klein, N K Hiestler, in *Chem. Eng. Handbook* (Eds R H Perry, C H Chilton) (New York: McGraw Hill, 1973) Sec. 16, p. 1
223. F Helfferich *Ionenaustauscher* (Weinheim: Verlag Chemie, 1959)
224. F Helfferich, in *Ion Exchange (A Series of Advances)* Vol. 1 (Ed. Y A Marinsky) Ch. 5

Computer-aided studies of reaction mechanisms

A V Zeigarnik, L G Bruk, O N Temkin, V A Likholobov, L I Maier

Contents

I. A rational strategy for the mechanistic studies of catalytic reactions	117
II. The formulation of hypotheses on the mechanisms of catalytic reactions	119
III. Programs for the formulation of hypotheses on the mechanisms of complex reactions	120
IV. Conclusion	129

Abstract. The principal stages in a rational strategy for the investigation of reaction mechanisms are described, in which the key stage is the formulation of hypotheses at the initial stage of the study. Computer programs are examined in which hypotheses are formulated about the mechanisms of complex reactions with participation of the user. Empirical and formal-logical algorithms and programs as well as various aspects of their application are discussed. The programs are compared with those for computer-aided organic synthesis design, which are similar in their structures and algorithms. The bibliography includes 119 references.

I. A rational strategy for the mechanistic studies of catalytic reactions

Until recently, the dominant approach to the study of the mechanisms of catalytic reactions involved a method which might be called 'inductive'. Its essential feature is that it implies the following stages of the study. Initially an experiment is carried out (mainly a kinetic experiment). A mathematical description is found for the results of this experiment. The reaction mechanism is deduced from the mathematical description. A chemical content is then attributed to this scheme, abstract symbols (such as A, B, C, X, and Y) being replaced by the formulae of specific substances. The reaction mechanism is thus obtained. This approach is so deeply ingrained in the minds of many researchers that, despite the regularly held conferences devoted to the methodological problems of kinetic studies in catalysis, it has been scarcely criticised. On the other hand, the cognitive potentials of this method are extremely limited. Evidently an arbitrary number of models to describe the same experimental data may be proposed, and it is impossible to unambiguously deduce a reaction mechanism from such a description (especially in complex cases).

In practice, investigators studying reaction mechanisms in accordance with the scheme are guided initially by some hypothesis about the mechanism (there is usually only one hypothesis),

justifying and elaborating it when necessary if the experimental data do not fit within the framework of the existing ideas. Doing so, they understand that the interpretation of the kinetic curves does point out how the existing hypothesis should be modified.

Analysis of the literature on philosophy^{1–5} and the applications of computational methods and mathematical statistics in chemical kinetics^{6–10} has clearly shown that the inductive method for the investigation of reaction mechanisms is methodologically unsound. However, the crisis of the inductive method in chemical kinetics did not arise solely as a result of studies by philosophers and mathematicians, who are more skilled in logic than other researchers. The knowledge about reaction mechanisms, including catalytic reaction mechanisms, expanded significantly over several years. As this knowledge accumulated, ideas about the complexity of catalytic processes also changed. Nowadays investigators put forward much more complex mechanisms for the description of catalytic reactions than before. These mechanisms involve intermediates, which have more complex structures, and new types of elementary steps. They include a greater number of intermediates and steps, so that the kinetic models (mathematical equations) corresponding to such mechanisms have become appreciably more complex. It became clear that the path 'from the rate law to a mechanism' is no longer useful for mechanistic studies and kinetic modeling. In general this method is fruitful only in relatively simple cases.

The inductive method was replaced by the deductive method, which can be represented by the following logical sequence:

formulation of hypotheses → experiment design
→ experiment → discrimination between hypotheses
→ mechanisms not in conflict with experiment.

This method is quite natural and has found extensive applications in many branches of science. Interestingly, the American Chemical Society has recommended that papers be written according to a plan that corresponds to the stages of the investigation within the framework of the method.¹⁰ Its undoubted advantage is that the hypotheses are formulated explicitly, making it possible to estimate the width of the 'search space' and to draw conclusions about the value of the 'winning' hypothesis.

Figuratively speaking, the investigator actually addresses questions to nature. According to Polya's apt expression, 'Nature may answer Yes or No, but it whispers one answer and thunders the others; its Yes is provisional and its No is definitive'.¹¹ Thus the difference between the two methods described here is clear: in the case of 'inductive' approach, the investigator is in a search for an arbitrary 'yes', whereas, in the case of the 'deductive' method, the hypotheses for which an unambiguous 'no' is obtained are to be rejected. It is then important to know not only the hypotheses remaining after the

A V Zeigarnik, L G Bruk, O N Temkin Laboratory for Chemical Kinetics and Catalysis, Lomonosov Academy of Fine Chemical Technology, prosp. Vernadskogo 86, 117571 Moscow, Russian Federation. Fax (7-095) 430 79 83

V A Likholobov (Laboratory for Catalysis by Metal Complexes), L I Maier (Laboratory for Information Systems and Computer Programs), Borskov Institute of Catalysis, Siberian Division of the Russian Academy of Sciences, prosp. akad. Lavrent'eva 5, 630090 Novosibirsk, Russian Federation. Fax (7-383) 235 57 76

Received 10 May 1995

Uspekhi Khimii 65 (2) 125–139 (1996); translated by A K Grzybowski

experimental test, but also the entire set of the initial hypotheses. The method works better if the set of hypotheses is more complete.

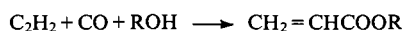
Several papers have been devoted to the popularisation of the deductive method.¹²⁻¹⁴ Comparison of the two strategies allowed us to conclude that the concept of a 'reaction mechanism' combines two types of information, topological and physicochemical, which are interrelated and interdependent.¹⁴

The topological information characterises the structure of the chemical reaction mechanism (the interrelation of the intermediates, reaction paths, and their coupling). The identification of the mechanism structure is based on kinetic and physicochemical methods. The structure of the mechanism can be well represented by graphs, which are widely used in chemistry in general¹⁵⁻²⁰ and in particular the theory of chemical reaction mechanisms.²¹⁻²³

The physicochemical information reflects the specific chemical content of the mechanism — the composition and structure of intermediates, their reactivities (the values of rate constants, the structures of transition states). The topological and physicochemical types of information complement one another and cannot be obtained independently; i.e., 'in general' one cannot first establish the kinetic scheme and then attribute chemical content to it.¹⁴

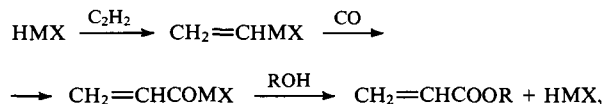
An important argument in favour of the idea that hypotheses must be formulated first is the multiplicity of mechanisms in catalysis. By multiplicity of mechanisms, we understand the possibility for the reaction to occur via several different mechanisms (and different intermediates) and the possibility of several such mechanisms dominating over others depending on the type of catalyst (in the case of metal-complex catalysis, on the nature of metal, its oxidation state, and even on the ligands coordinated to this metal).²⁴

For example, the reaction

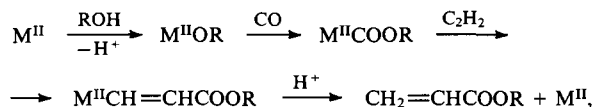


may occur via three mechanisms:^{24, 25}

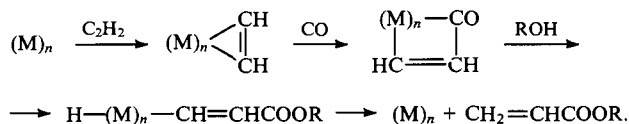
(1) the hydride mechanism:



(2) the alkoxide mechanism:

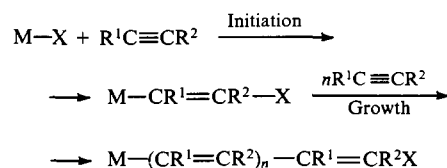


(3) the metallocyclic mechanism:

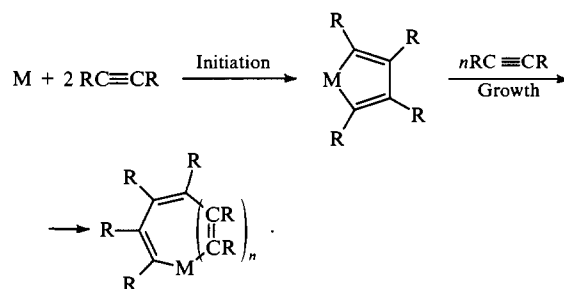


The hydride mechanism is more probable for Pd(0) complexes; the alkoxide mechanism is more probable for Pd(II) complexes; the metallocyclic mechanism is more probable in solutions of Pd(I) clusters.

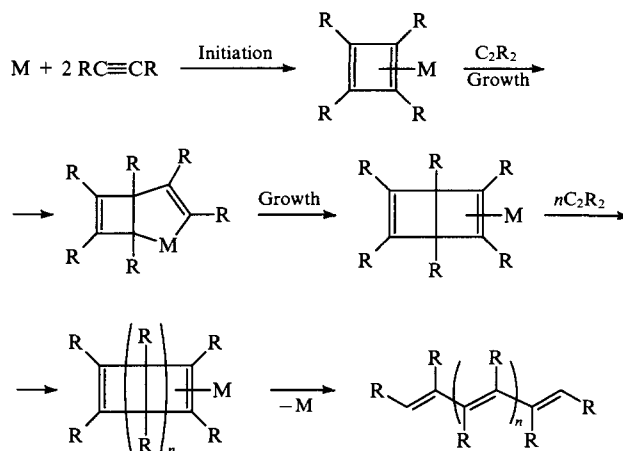
The multiplicity of mechanisms and the increase in their complexity are best manifested in the polymerisation reactions of alkynes.²⁴ The simplest mechanism includes two steps — chain initiation and chain propagation.



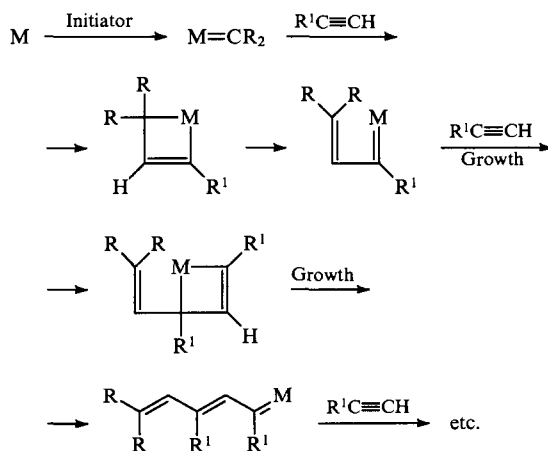
Other alkyne polymerisation mechanisms are the metallocyclic mechanism



and the [2+2]-cycloaddition mechanism.



A mechanism involving several chain propagation and initiation steps is also possible:



As can be seen from the above examples, the same reactions can occur via different mechanisms. The researcher usually knows from the literature some plausible reaction pathways and uses them explicitly or implicitly as hypotheses.

II. The formulation of hypotheses on the mechanisms of catalytic reactions

The formulation of hypotheses is a creative task and cannot be fully formalised either now or in the future. However, certain elements of this procedure can be formalised. Furthermore, it is the investigator's intuition combined with the ability of a computer to execute complex algorithmic procedures that constitutes a good basis for the formulation of mechanistic hypotheses.

Three groups of hypotheses were discussed:¹⁴ (1) hypotheses about the nature of a catalyst, (2) hypotheses about elementary steps, and (3) hypotheses about the conjugation nodes. In addition, a fourth group, which combines the elements of the above three groups, was considered: hypotheses about the reaction mechanism as a whole. Each of these groups of hypotheses can serve as a basis for the design of discriminating experiments (hereafter, we shall use the term 'experiment design' in a broader sense than that adopted by the specialists in statistics).

In the case of homogeneous metal-complex catalysis, the group of hypotheses about the nature of the catalyst includes the following problems: the condition of a catalyst in solution, the existence of complexation equilibria, the specific role of solvent, the degree of nonideality of solution, the influence of the solution components on the solubility of substrates (when the reaction is a heterophase one), and the effect of the reaction medium on metal complexes. In heterogeneous catalysis, the following factors should be considered: the composition and nature of the surface, the phase composition of the catalyst, the degree and the nature of the surface nonuniformity, the adsorption of reactants and products, and the transformations of the active sites under the influence of the reaction medium.

The group of hypotheses about elementary steps of the reaction mechanism permits the discrimination between the mechanisms at the level corresponding to the discrimination between the individual steps. Here it is also essential to have a set of hypotheses which is as complete as possible.

In the complex cases of stoichiometrically ambiguous reactions, the third group of hypotheses proved very useful — the hypotheses about the conjugation nodes in the kinetic scheme of a reaction.¹³ The conjugation node is a fragment of the structure of the reaction mechanism incorporating the intermediate that is transformed by two or more steps. The form of the expression for the ratios between the rates of product formation via different routes having a conjugation node determines the structure of this node. When the reaction is far from equilibrium and the routes via which the products are formed include irreversible stages, the ratios between the product formation rates are far simpler functions of the reactant concentrations than the rates themselves or even the expressions for the selectivity. It is worthwhile analysing the conjugation nodes bearing in mind some hypothesis about the possible reaction mechanism (i.e., at the stage of designing the discriminating experiment). However, even if the general reaction mechanism is unknown, such analysis is all the same useful.¹³ Examples of analysis of conjugation nodes were discussed in several papers.^{13, 26–28}

When *a priori* information about the process is available, it is useful to formulate, before putting forward the hypotheses, the requirements that should be satisfied for all the hypothetical mechanisms. Naturally, the greater the amount of *a priori* information, the smaller the number of hypotheses which should be tested.

In this review, we restrict the consideration to the formal aspect of the problem of the formulation of hypotheses and discuss the methods of computer-aided hypothesis generation.

Numerous publications have been devoted to the problems of computer-assisted synthesis design (CASD). Investigators — users of the CASD program — usually solve the following problems: 'which reactants must be used and which reactions must be carried out to prepare a given substance in the simplest way?' and 'what can be obtained from the specified set of

substances?'.^{29–33} By the most conservative estimate about 500 original papers and several tens of reviews have been devoted to the CASD problem. Here we shall refer only to those reviews that contain a fairly complete list of references.

The CASD methods are in many respects the same as the methods for the computer generation of hypotheses about reaction mechanisms. There is also the resemblance between the algorithms of the programs. Furthermore, problems associated with the complexity of the algorithms for combinatorial search inevitably arise in both cases. In order to avoid a combinatorial explosion, particular attention is devoted to the development of effective selection criteria, which make it possible to shorten the working time of a program. However, computer generation of reaction mechanisms also has its specific features.

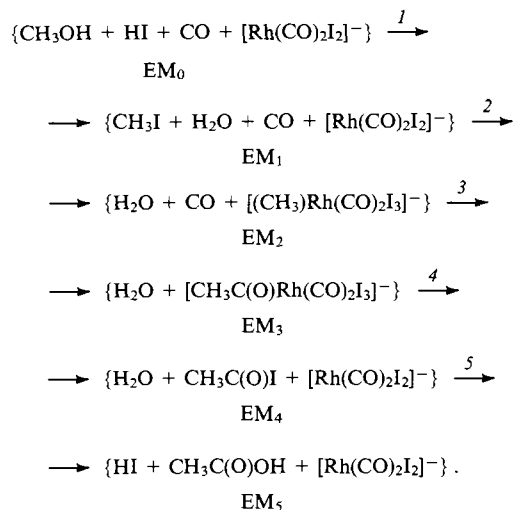
Firstly, in contrast to the majority of CASD algorithms, the programs designed to formulate the mechanistic hypotheses deal with elementary reactions rather than synthetic ones. At any rate, the developers of the programs for mechanism generation devote much more attention to the problem of the reactions being elementary. Secondly, the central problem which then arises is not that of the way in which the multistage synthesis can be carried out but concerns the alternative variants of the behaviour which may be expected from the chemical system when it is 'left alone' (after specifying particular conditions). Thirdly, in the computer-assisted synthesis design, use is also made of the evaluation criteria, which are inapplicable to the reaction mechanisms. These include criteria associated with the choice of a 'synthesis strategy',^{31, 34–36} and with the estimation of the cost of the synthetic steps,³⁷ the criteria characterising the similarity between intermediates and target products,^{29, 38–54} the criteria employing the complexity and similarity information-theoretic indices for the description of the complexity of the synthesis,^{55–57} etc. In certain programs, some of these criteria have been erroneously extended to the study of the mechanisms. Criteria such as the mechanistic complexity indices may be used, in principle, in the study of reaction mechanisms; however, they may not be used as evaluation criteria underlying the program and must be employed for discrimination between hypotheses if it is necessary to choose the simplest mechanism for the description of experimental observations. Otherwise the correct but more complex hypothesis may be neglected whereas sets of simpler but incorrect hypotheses would be subjected to experimental tests.

In the study of a reaction mechanism, the physicochemical criteria come to the fore. These are associated with the estimation of the chemical reactivity and are based, for example, on the calculations of electronegativity, polarisability,⁵⁸ bond energies,^{59–64} thermodynamic functions,^{65, 66} and other physicochemical quantities. In addition, use is made of criteria based on heuristic rules such as Tolman's rules,^{67–69} the restrictions the molecularity of the stages, and others. The choice of the evaluation criteria is a key factor in the development of programs for the study of reaction mechanisms, since they determine in many respects the plausibility of the results and the program execution time.

Yet another difference between the CASD programs and those for the generation of mechanisms is that the completeness of the combinatorially feasible hypotheses concerning the synthetic pathways is less important than the completeness of the hypotheses about the reaction mechanisms.

The computer programs which are being developed for the generation of reaction networks and for the study of the possible reaction routes can manipulate chemical information at a more or less general level. In some cases, the reaction is formulated in a compact form (only the transformation of the molecular fragment is described or it is simply indicated which bonds — and between which atoms — are formed or broken), whilst in others the reaction is specified in greater detail (not only the reacting fragment, but also all the reacting molecules or even the reaction conditions are specified). Depending on how detailed is the description of the reaction, one speaks of a greater or lesser degree of its generality.

For catalytic reactions, the set \mathcal{A} must be supplemented by the atoms entering into the composition of the catalyst. For example, the reaction described above takes place in the presence of the Rh(I)–HI catalytic system.^{70–72} The isomeric ensemble $EM_0 \equiv EM(\mathcal{B})$ must then include the HI and $[Rh(CO)_2I_2]^-$ species. A simplified mechanism of the methanol carbonylation reaction can be written as follows:⁷²



In this example, each of the five stages of the mechanism can be represented in a matrix form:

$$B_i + R_i = E_i, \quad i = 1, 2, \dots, 5,$$

where $B_i = E_{i-1}$ and the overall transformation can be expressed as follows

$$B(EM_0) + R = E(EM_5).$$

$$\text{Here } R = \sum_i R_i.$$

The computer program RAIN was developed for the investigation of reaction mechanisms within the framework of the Munich project.^{29, 30, 73–78} A distinctive feature of this program is the so called 'bilateral' search. The RAIN program inherited from CASD the idea of retrosynthesis,^{79, 80} in which the possibility of searching for possible starting reactants by inspecting the products (retrosearch) is employed. In RAIN, the search is carried out simultaneously in the forward and reverse directions (bilateral search). Reaction generators, which make it possible to find both the reactions and retroractions, are used in the RAIN program.⁷⁷ The reaction generators constitute, in fact, a compilation of logical rules controlling the process of formulation of a specific reaction (or retroraction). These rules are based on the combinatorial enumeration of all possible bond redistributions. The enumeration is constrained by the user's settings. Transition tables should apparently be regarded as the principal constraints. These tables, compiled for atoms of each type, restrict the number of transformations (and retrortransformations) of the valence states of atoms in the course of the generation of elementary steps. No generalised reactions of any kind are thereby used. Therefore, the RAIN program can be categorised as program of the formal-logical type.

The idea of the bilateral search is applied as follows. Isomeric ensembles of the initial species $[EM(\mathcal{B})]$ and final products $[EM(\mathcal{E})]$ are specified. The reactions and retroractions are sought for the ensembles $EM(\mathcal{B})$ and $EM(\mathcal{E})$, respectively. At some step, two (or more) intermediate isomorphous isomeric ensembles are obtained as a result of the search in different directions. In other words, the generation of reaction pathways in the direction of the products and in the direction of the initial

species should lead to isomorphous isomeric ensembles. Methods have been developed for the optimisation of the search for isomeric ensembles of molecules connecting the search tree to the retrosearch tree³⁰ on the basis of the principle of the minimum chemical distance.^{29, 30, 38–43} A chemical distance is regarded as the number of electrons which must be redistributed in order to convert one ensemble of molecules into another.

The action of this principle as an optimising factor is based on the following hypothesis. Let an ensemble of molecules be subjected to various transformations. The processes having smaller chemical distances between the reactants and products are more probable than those having greater distances. According to Ugi et al.⁷⁷ the permissible deviations from this rule are within two units of the chemical distance (one or two electrons); i.e., the reaction can sometimes choose a pathway not corresponding to the minimum structural changes, but these deviations from the general rule are not very large.

The combinatorial search in the RAIN program is limited by the user-defined constraints. In particular, apart from the transition tables, other formal constraints can be introduced: the maximum number of atoms entering into the reacting fragment of the molecule; the maximum change in bond order during the elementary reaction; the maximum number of bonds the order of which changes; the minimum size of the rings in the carbon skeletons of the molecules that contain triple or cumulated double bonds; the maximum number of charged atoms; the maximum number of covalent bonds between heteroatoms; the maximum number of rings; the maximum number of individual molecules in the intermediate ensembles of molecules, etc. (18 rules total).

The bilateral search has several drawbacks. In contrast to CASD, in the study of reaction mechanisms it is necessary to conduct the search in one (preferably forward) direction, since the intermediates formed during the reaction may interact with each other and may participate in reactions with the initial substances. It is then necessary to expand the set \mathcal{A} at each step of the generation of the possible ensemble of molecules (and hence to increase the size of the ensemble). This is impossible within the bilateral search, which, within the framework of the Dugunji–Ugi model, requires the set \mathcal{A} to be fixed and not to change during the execution of the program. According to Barone and Chanon,³² this was first mentioned by Yoneda, but the paper containing a description of his GRACE program⁸¹ does not deal with the problem of the possible expansion of the set \mathcal{A} in the course of its execution.

Like RAIN, the GRACE program belongs to the formal-logical type, but it employs a somewhat different principle of reaction generation. Yoneda put forward the idea of reaction group matrices that describe the transformations of functional groups of the molecules. Upon imposing the constraints, the GRACE program identifies the functional groups within the molecules and generates the reaction group matrices by a combinatorial-logical procedure. Then, it detects all possible combinations of the reaction group matrices from which the elementary reaction matrices may be obtained (the r -matrices of steps). Thus, as in the RAIN program, the GRACE program employs neither the library of functional group transformations nor the library of elementary reactions, which are the combinations of the functional group transformations.

In the GRACE program, the evaluation criteria are formulated by the user according to the standard scheme. The following constraints are possible:

- (1) the number of atoms (reaction centres) the valence state of which changes during the elementary reactions must not exceed 4;
- (2) the number of broken bonds (or bonds the order of which is decreased) and formed bonds (or bonds the order of which is increased) should not be greater than 3;
- (3) the molecularity of each reaction should not exceed 3;
- (4) the number of unpaired electrons on one atom should not be greater than 1;

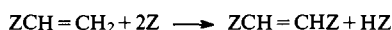
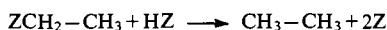
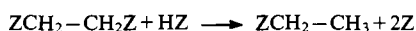
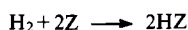
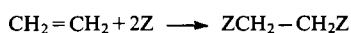
(5) the number of atoms with unpaired electrons in one molecule should not be greater than 4;

(6) the numbers of valence electrons at the carbon and hydrogen atoms should be 4 and 1 respectively;

(7) at least one active centre on the catalyst surface must participate in each step;

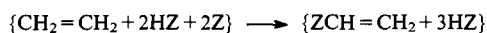
(8) the hydrogen atoms must be adsorbed on the catalyst surface and cannot exist as free radicals.

The program allows the user to change any particular constraints or not use some of them at all. Apart from these constraints, an upper limit to the complexity of the elementary transformation is predefined. The quantity calculated from the r -matrix and equal to half the chemical distance was adopted as a measure of complexity. A network of elementary reactions (the reaction network) is generated in the forward direction only, which makes it possible to expand the set \mathcal{A} in the course of its growth when necessary. The execution of the program may be illustrated by the reaction network generated for the heterogeneous catalytic hydrogenation of ethene:⁸¹



Z is an active site of a catalyst.

It is of interest to note that the same set of reactions, which are formulated as transformations of ensembles of molecules, is somewhat larger by virtue of the identity of certain transformations. For example, the following two transformations constitute essentially the same reaction.



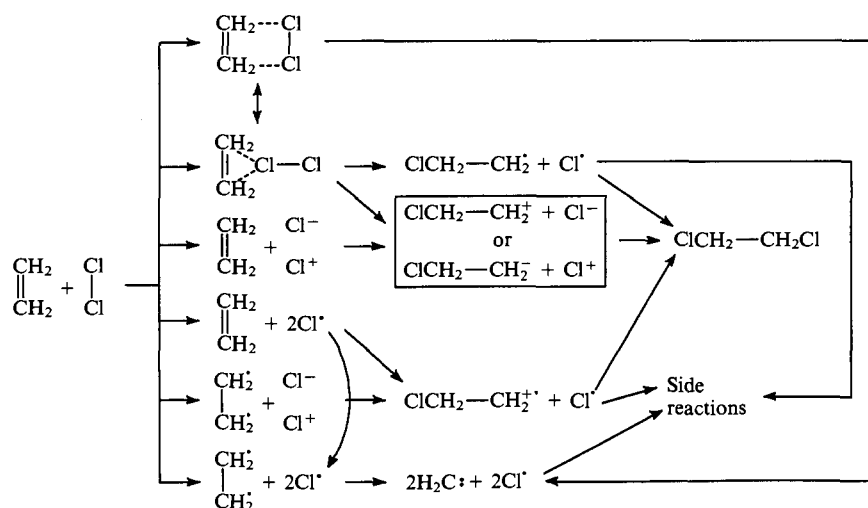
In this sense, the Dugunji-Ugi model is somewhat redundant. Indeed, if the same reaction had not been duplicated, less time would be needed for the program run. When the number of elementary steps is large, this factor plays a significant role. There are seven reactions in the example presented above. If the reactants are represented by an ensemble of molecules, then 11 transformations of such ensembles are required (i.e., 1.5 times more). The time required for the interpretation of the results proportionally increases.

The Dugunji-Ugi model was also used in Dozmorov's program.⁵⁵ Dozmorov proposed a new similarity measure, which made it possible to diminish the number of steps and intermediates generated. This similarity measure is a topological information-theoretic index which involves information components of different nature.⁸² In our opinion, the use of this characteristic as an evaluation criterion has no sufficient physical justification. Dozmorov does not report the details of the algorithm, but it appears that, as in the GRACE program, only the forward search is employed in his program, while the elementary reactions are generated by combinatorial-logical methods (i.e., it also belongs to the formal-logical type). The reaction network of the 'informationally' allowed steps of the ethene chlorination reaction, obtained with the aid of this program, is presented in Scheme 2.

Thus in all the programs of the formal-logical type, based on the Dugunji-Ugi model, similarity characteristics are used to reduce the number of 'false' solutions. In the RAIN program, the criterion is the chemical distance (of all possible transformations of the ensemble of molecules, the program selects only those corresponding to the minimum chemical distance to within an error of 2 units of the chemical distance.) In the GRACE program, the criterion is the complexity of the elementary reaction equal to half the chemical distance (the user specifies the upper limit to this quantity). In Dozmorov's program, the criterion is the information topological index, with the aid of which the program decides whether an elementary reaction is allowed or prohibited from the standpoint of information.

The MECHEM program developed by Valdés-Peréz⁸³⁻⁹² has appeared comparatively recently. Its algorithm is based on the stoichiometry principles. The initial version of the program operated not with the structural formulae of species, but with their compositions. Currently, the program also makes it possible to recognise the structures of substances. The MECHEM program belongs to the type of formal-logical programs because it does not employ any libraries of generalised reactions. The mechanisms are generated by the constrained combinatorial search for possible transformations of hypothetical intermediates. There are no reaction generators as such in the program. The 'skeleton' of the reaction mechanism is formed with further specification of the elementary steps and species. The model for the formulation of hypotheses is based on the following principles:⁸⁵

(1) The program searches for the simplest mechanisms (hypotheses) by a progressive increase in the number of steps and species. If the mechanisms with a smaller number of steps and species do not satisfy all the user-defined constraints or the condition of elemental balance, the number of species is increased or whilst the number of species is held constant the number of



Scheme 2

steps is increased. Thus the complexity of the hypotheses is characterised by the number of species and steps.

(2) The set of reaction mechanisms in which the unknown intermediates are designated by wild cards X, Y, Z, etc., is initially generated. These wild cards are then replaced by the formulae of specific substances. Their empirical formulae are evaluated from the elemental balance (in the latest version of MECHEM, an algorithm for the determination of the structures of species from their formulae is employed;⁹⁰ it is then possible to impose constraints on the species structures⁹³).

(3) The molecularity and the number of products of an elementary reaction do not exceed 2; in the same step, the same species cannot play the role of both the starting material and the product.

(4) The mechanisms are generated in such a way that each step cannot have starting materials that were not generated in the preceding steps or specified by the user as starting materials. (This and several other principles constitute the basis of the canonical representation of mechanisms⁹¹).

The user inputs the starting materials and products, the initial form of the catalyst (if it exists), and the intermediates observed. The user also inputs the constraints on the valence of each atom, the order of the appearance of the intermediates in the steps, the possibility (or impossibility) of the initial species being among the products of particular steps, the number of bonds the order of which changes, etc. A large number of heuristics, which make the algorithm more effective, are used in the program.⁸⁹

Possible mechanisms of ethane hydrogenolysis were generated with the MECHEM program.^{88, 89} The following constraints were used: (1) the overall stoichiometry is $\text{C}_2\text{H}_6 + \text{H}_2 \rightarrow 2\text{CH}_4$; (2) one catalyst active site M can form only one bond (not necessarily a single bond); (3) intermediates with a bridged structure, $\text{MCH}_2-\text{CH}_2\text{M}$ and $\text{MCH}-\text{CHM}$, are present in the reaction; (4) hydrogen is not formed in any of the steps; (5) all intermediates contain at least one catalyst site M; (6) none of the intermediates contain three carbon or metal atoms; (7) no more than three bonds are formed and broken (regardless of their order) in one step; (8) the $\text{MCH}_2-\text{CH}_2\text{M}$ intermediate must appear in the sequence of steps before the $\text{MCH}-\text{CHM}$ intermediate. Apart from these constraints, account was also taken of the need to maintain the elemental balance in each step and the condition that the valences of hydrogen and carbon atoms do not exceed 1 and 4 respectively. Among other mechanisms of the same complexity (i.e., with the same number of steps and species), the following mechanism of ethane hydrogenolysis was generated: §

1. $\text{H}_2 + 2\text{M} \rightarrow 2\text{U}$
2. $2\text{M} + \text{C}_2\text{H}_6 \rightarrow \text{U} + \text{V}$
3. $2\text{M} + \text{V} \rightarrow \text{MCH}_2-\text{CH}_2\text{M} + \text{U}$
4. $\text{M} + \text{MCH}_2-\text{CH}_2\text{M} \rightarrow \text{U} + \text{W}$
5. $2\text{W} \rightarrow \text{MCH}_2-\text{CH}_2\text{M} + \text{MCH}-\text{CHM}$
6. $\text{MCH}-\text{CHM} \rightarrow 2\text{X}$
7. $\text{U} + \text{X} \rightarrow \text{M} + \text{Y}$
8. $2\text{Y} \rightarrow \text{X} + \text{Z}$
9. $\text{U} + \text{Z} \rightarrow 2\text{M} + \text{CH}_4$

Here U, V, W, X, Y, and Z are intermediates which were interpreted by the program as HM, $\text{CH}_3-\text{CH}_2\text{M}$, CH_2-CHM , MCH, CH_2M , and CH_3M respectively. The stoichiometric numbers of steps 1–9 are 1, 1, 1, 2, 1, 1, 4, 2 and 2, respectively, with which all the intermediates vanish in the overall equation.

§ Since the program generates only unimolecular and bimolecular reactions (this is one of the principles inherent in the algorithm for the generation of a step), it is seemingly implied that 2M represents two linked active sites of the heterogeneous catalyst (M_2).

The intermediates MCH and CH_2M may be interpreted as carbyne and carbene complexes (at the time when the above investigation was carried out, the algorithm for the identification of bond orders was introduced into the program).

Generally, the MECHEM program is designed to search for hypotheses invoked to account for the results of observations (i.e., the hypotheses follow the observations). As mentioned above, another formulation of the problem is methodologically more correct: What variants of observations are to be expected? We may note that the weakest feature of this program is the concept of the selection of simplest mechanisms. It is reasonable to employ simplicity criteria at the step involving the discrimination between hypotheses and also at the instant when the experimental tests of the hypotheses have already been completed and the remaining hypotheses explain equally well the observations and agree with the background knowledge about the processes of a given type. In this case, when the future design of experiments is unclear or if it is impossible to experimentally discriminate between the hypotheses by means of the available methods, it is useful to apply criteria characterising the simplicity of the mechanism. These may be criteria based on a simple count of the number of steps and species (as in MECHEM) or more complex criteria.^{94–97}

Apart from the formal-logical methods of generating reaction networks discussed here, in many studies the reaction mechanisms have been generated by the joint application of combinatorial methods and stoichiometry,^{98–100} as well as graph theory.¹⁰¹ Computer programs were not created on the basis of these methods, nor they have been adequately documented in the literature. Methods have also been developed for 'cutting off' the mechanisms from the reaction networks that match a given overall stoichiometry.^{9, 98, 102–112} In these methods, it is postulated that all starting materials, intermediates, and final products and sometimes the equations of the steps are known. For this reason, despite the usefulness of such algorithms and programs for the study of mechanisms, their employment for the generation of hypotheses about the mechanisms of chemical reactions is extremely limited.¹⁴

2. Empirical programs

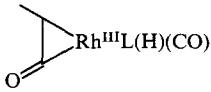
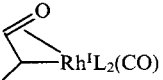
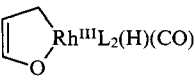
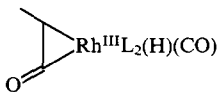
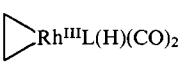
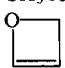
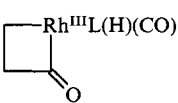
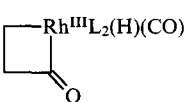
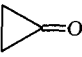
As stated above, all empirical programs are characterized by a general property: generalised reactions (transforms) are employed in them. The method used to describe the generalised reactions can be arbitrary. The general algorithm involves the recognition of molecular fragments to which particular generalised reactions (reaction templates) can be applied with subsequent generation of specific reactions and structures of substances.

One of the first empirical programs is the CAMEO program.¹¹³ At the time of writing the present review, 25 communications have already been published. Here we refer only to the first publication¹¹³ and to a review.¹¹⁴

The CAMEO program is designed to simulate the mechanisms of organic reactions. It is characteristic of the program that the search for each successive fragment to which a particular generalised reaction may be applied is performed in this program solely in the forward direction (side paths are then considered and account is taken of the interaction between the intermediates).

The starting materials and the reaction products, the reaction conditions, and also the list of modules which must be activated are initially specified. The program contains several modules, each of which is designed to describe a particular class of organic reactions. The molecules are represented in the form of special tables in which atoms and bonds are specified.¹⁰⁸ These tables contain the following information: the ordinal number of each atom, the type of each atom (C, H, ...), its coordinates on the graphical display, and the code of the charge (numbers 1, 2, and 3 stand for a cation, anion, or a radical, respectively; if the atom is neutral, then the code 0 is used); it is indicated between which atoms there are bonds and what are their orders. Each bond has a unique number. The location of the bond relative to the conventional plane of the figure is indicated. Furthermore, account is

Table 1. List of substances proposed by the TAMREAC program for the generation of the ethene hydroformylation reaction network.⁶⁸

No. of species	Chemical formula	No. of species	Chemical formula
1	$\text{Rh}^{\text{I}}\text{L}_2(\text{H})(\text{CO})_2$		
2	$(\eta^2\text{-C}_2\text{H}_4)\text{Rh}^{\text{I}}\text{L}_2(\text{H})(\text{CO})_2$	21	
3	$\text{Rh}^{\text{I}}\text{L}(\text{H})(\text{CO})_2$	22	$[\eta^2\text{-C}(\text{O})=\text{CHCH}_3]\text{Rh}^{\text{I}}\text{L}(\text{H})(\text{CO})$
4	$\text{C}_2\text{H}_5\text{Rh}^{\text{I}}\text{L}_2(\text{CO})_2$	23	$\text{O}=\text{CH}-\text{CH}(\text{CH}_3)-\text{Rh}^{\text{III}}\text{L}_2\text{H}_2\text{CO}$
5	$\text{O}=\text{C}(\text{C}_2\text{H}_5)-\text{Rh}^{\text{I}}\text{L}_2(\text{CO})$	24	
6	$\text{O}=\text{C}(\text{C}_2\text{H}_5)-\text{Rh}^{\text{III}}\text{L}_2\text{H}_2(\text{CO})$	25	$\text{CH}_3\text{CH}=\text{CH}-\text{O}-\text{Rh}^{\text{I}}\text{L}_2(\text{CO})$
7	$\text{Rh}^{\text{I}}\text{L}_2(\text{H})(\text{CO})$	26	
8	$\text{CH}_3\text{CH}=\text{Rh}^{\text{I}}\text{L}_2(\text{H})(\text{CO})_2$	27	H_2
9		28	$\text{HO}-\text{CH}=\text{CHCH}_2-\text{Rh}^{\text{I}}\text{L}_2(\text{CO})$
10	$[\eta^2\text{-C}(\text{O})=\text{CHCH}_3]-\text{Rh}^{\text{I}}\text{L}_2(\text{H})(\text{CO})$	29	$\text{HO}-\text{CH}=\text{CHCH}_2-\text{Rh}^{\text{III}}\text{L}_2\text{H}_2(\text{CO})$
11	$\text{O}=\text{CH}-\text{CH}(\text{CH}_3)-\text{Rh}^{\text{I}}\text{L}_2\text{CO}$	30	$\text{CH}_3\text{CH}=\text{CH}-\text{O}-\text{Rh}^{\text{III}}\text{L}_2\text{H}_2(\text{CO})$
12		31	
13		32	$[\eta^2\text{-CH}_2=\text{CH}-\text{C}(\text{O})]\text{Rh}^{\text{I}}\text{L}_2(\text{H})(\text{CO})$
14		33	$\text{CH}_3\text{CH}=\text{CH}-\text{OH}$
15	L	34	$\text{O}=\text{CHCH}_2\text{CH}_2-\text{Rh}^{\text{I}}\text{L}_2(\text{CO})$
16	$(\eta^2\text{-C}_2\text{H}_4)\text{Rh}^{\text{I}}\text{L}(\text{H})(\text{CO})_2$	35	$\text{O}=\text{CHCH}_2\text{CH}_2-\text{Rh}^{\text{III}}\text{L}_2\text{H}_2(\text{CO})$
17	$\text{C}_2\text{H}_5\text{Rh}^{\text{I}}\text{L}(\text{CO})_2$	36	
18	$\text{C}_2\text{H}_5\text{Rh}^{\text{III}}\text{L}(\text{H})_2(\text{CO})_2$	37	C_2H_4
19	CO	38	C_2H_6
20	$\text{CH}_3\text{CH}=\text{Rh}^{\text{I}}\text{L}(\text{H})(\text{CO})_2$	39	$\text{CH}_2=\text{CH}-\text{CH}=\text{O}$
		40	$\text{C}_2\text{H}_5\text{CHO}$

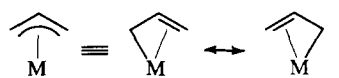
Note. The initial species were $\text{Rh}^{\text{I}}\text{L}_2(\text{H})(\text{CO})_2$ ($\text{L} = \text{PPh}_3$), C_2H_2 , CO , and H_2 .

taken of the evaluation rules, including the rules based on physicochemical principles (estimates of $\text{p}K_{\text{a}}$, ΔH_f , the HOMO–LUMO energies, heats of reaction, etc.).

The following modules were designed: reactions catalysed by bases and acids (reactions involving nucleophilic and electrophilic species) pericyclic reactions, redox reactions, free-radical reactions and chain processes, reactions of carbenoid species, reactions involving reduction by hydrides, and ‘ene’ and ‘retro-ene’ syntheses. With the aid of the CAMEO program, it is possible to determine the most probable sites of attack by active species and to estimate the comparative reactivities.

The TAMREAC program^{67–69} was designed for investigators in the field of organometallic catalysis. Unfortunately, the authors^{67–69} did not publish the details of the algorithm and it is therefore difficult to analyse the real possibilities of the program. Connectivity tables in which each atom is characterised by a number and a symbol (carbon, hydrogen, metal, arbitrary atom, arbitrary electrophilic atom, etc.) are used for the computer representation of the molecules within the framework of this program. In the tables, it is also indicated with which atoms and by what bonds the given element is linked and what is its overall charge (oxidation state). Furthermore, tables of η^2 -bonds have been introduced for the description of the η^2 -bonds with metals,

in which it is indicated between which atoms there is a multiple bond and to which atom it is coordinated. The η^3 -coordination is described with the aid of two isomeric structures:



The TAMREAC program provides for the possibility of generating elementary steps in each of which there is not more than one metal atom. The developers of the TAMREAC program systematically analysed a large number of elementary concerted reactions and constructed a well-organised library of generalised reactions. It includes the following reactions: (1) oxidation of the metal, (2) reduction of the metal, (3) reactions affording occupation of a coordination site, (4) reactions creating a vacant coordination site, (5) reactions without change in the oxidation state or the coordination number of the metal, and (6) radical reactions and one-electron transfers. The library consists of files each containing several generalised reactions, described in the form of a structural transformation of the reaction fragment.

The TAMREAC program contains an algorithm for the recognition of ligands, the number of electrons they can donate

Table 2. The reaction network for the hydroformylation of ethene generated by the TAMREAC program.⁶⁸

No.	Reaction ^a	No.	Reaction ^a	No.	Reaction ^a	No.	Reaction ^a
1	1 → 3+15	23	7+39 → 32	45	13 → 12	67	23 → 7+40
2	1 → 7+19	24	7+40 → 6	46	13+15 → 14	65	23 → 11+27
3	1+37 → 2	25	7+40 → 23	47	14 → 7+36	69	24 → 11
4	2 → 1+37	26	8 → 4	48	14 → 13+15	70	24 → 25
5	2 → 4	27	8 → 9	49	15+16 → 2	71	25+27 → 30
6	2 → 16+15	28	8 → 20+15	50	16 → 3+37	72	25 → 24
7	3+15 → 1	29	9 → 10	51	16 → 9	73	25 → 26
8	3+37 → 16	30	9 → 11	52	16 → 12	74	26 → 7+31
9	4 → 2	31	9 → 16	53	16 → 20	75	26 → 25
10	4 → 5	32	9 → 21+15	54	17+15 → 4	76	26 → 28
11	4 → 8	33	10 → 5	55	17 → 20	77	28 → 26
12	4 → 17+15	34	10 → 9	56	17+27 → 18	78	28+27 → 29
13	5 → 4	35	10 → 11	57	18 → 3+38	79	29 → 7+33
14	5 → 10	36	10 → 22+15	58	18 → 17+27	80	29 → 28+27
15	5+27 → 6	37	11 → 9	59	20+15 → 8	81	30 → 7+33
16	6 → 5+27	38	11 → 10	60	20 → 16	82	30 → 25+27
17	6 → 7+40	39	11 → 24	61	20 → 17	83	32 → 7+39
18	7+19 → 1	40	11 → 32	62	20 → 21	84	32 → 11
19	7+31 → 26	41	11+27 → 23	63	21+15 → 9	85	32 → 34
20	7+33 → 30	42	12 → 9	64	21 → 22	86	34+27 → 35
21	7+33 → 29	43	12 → 13	65	22+15 → 10	87	34 → 32
22	7+36 → 14	44	12 → 16	66	22 → 21	88	35 → 7+40
						89	35 → 34+27

^a The numbers of species are indicated in Table 1.

and the number of sites they can occupy. The number of valence electrons of the metal atom and its oxidation states are calculated from these data. The information obtained is used in the evaluation criteria. For example, it is ensured automatically that the number of valence electrons is within the limits specified by the user. The program also contains an algorithm for the recognition of the geometry of each complex. The developers of TAMREAC created a system of evaluation rules on the basis of which an expert assessment of the reaction plausibility is made using the data on the type of reaction (reductive elimination, migratory insertion, metallocycle formation, etc.), the coordination number of the metal, the number of valence electrons of the metal atom, and the geometry of the complex. This information, formalised in the form of evaluation matrices, is usually very useful to the investigator. However, one should understand that the data on the basis of which a conclusion is made are not sufficient. Therefore, such an estimate can be taken into account, but the possibilities of its employment within the framework of any specific study are extremely limited. Account must also be taken of the fact that the evaluation rules indicated above are usually developed exclusively on the basis of experimental observations which often lack a reliable theoretical justification. These rules are continuously revised and, generally speaking, they lack 'the strength of a law'. By studying a specific system, each investigator has ultimately the right to solve independently the problem of the need to take into account the expert recommendations. For this reason, the most acceptable variant is where the user (the investigator) is himself able to formulate the evaluation rules in accordance with various schemes proposed by the program.

The TAMREAC program was tested on a large number of specific reactions, and in a number of instances extremely inter-

esting results were obtained. For example, this program was used to generate the reaction network for the ethene hydroformylation in the system containing $\text{HRh}(\text{CO})_2\text{L}_2$ ($\text{L} = \text{PPh}_3$).⁶⁸ The starting materials were ethene, H_2 , CO, and $\text{HRh}(\text{CO})_2\text{L}_2$. It is seen from the results presented in Tables 1 and 2 that the program 'synthesised' fairly interesting by products, the search for which in a real catalytic system will help to confirm or reject some of the proposed pathways.

The KOMSIKAT program package for the investigation of the mechanisms of catalytic reactions has been developed at the Institute of Catalysis of the Siberian Division of the Russian Academy of Sciences on the basis of the Dugunji–Ugi model and the group matrix method (similar to that employed in the GRACE program⁸¹).^{59–64} In general, the ideas underlying the KOMSIKAT program are similar to those implemented in the GRACE program, but it does not use all the combinatorially possible group matrices, only those specified by the user. Therefore, this program should be categorised as an empirical program. The authors of the KOMSIKAT project extracted from literature data the characteristic structural types of elementary transformations involving the catalyst. In particular, the authors postulated that the processes occurring in the $\text{CO} + \text{H}_2$ system with participation of a metal M may be described by five basic types of elementary transformations. Table 3 presents the reaction fragments and the corresponding blocks of r -matrices (index group matrices) employed. The diagonal elements of the index group matrices characterise the changes in the number of valence electrons.

In the KOMSIKAT program, the energy criterion was used in the evaluation of reaction pathways. The reaction network was generated as follows. In the first stage, all possible ensembles of

Table 3. The reaction fragments and the index group matrices used in the KOMSIKAT program.⁶⁴

Bond redistribution scheme

Index group matrix

$$M+X-Y \longrightarrow X-M-Y$$

	M	X	Y
M	-2	1	1
X	1	0	-1
Y	1	-1	0

$$X-M-Y \longrightarrow M+X-Y$$

	M	X	Y
M	2	-1	-1
X	-1	0	1
Y	-1	1	0

$$M-X-Y \longrightarrow Y-M-X$$

	M	X	Y
M	-1	0	1
X	0	1	-1
Y	1	-1	0

$$Y-M-X \longrightarrow M-X-Y$$

	M	X	Y
M	-1	0	1
X	0	1	-1
Y	1	-1	0

$$M-Z+X-Y \longrightarrow M-X+Z-Y$$

	M	X	Y	Z
M	0	-1	1	0
X	-1	0	0	1
Y	1	0	0	-1
Z	0	1	-1	0

molecules which may be obtained on the basis of the possible elementary transformations of the initial ensemble of molecules were generated. From the ensemble of molecules obtained in the first stage, only those were selected which corresponded to the maximum atomisation energy (i.e., to the most stable ensembles of molecules)¶ to within some accuracy, while the remaining ones were rejected. For each intermediate ensemble of molecules, remaining after the selection, a new set of ensembles of molecules, obtained by means of allowed elementary transformations, was found. Among them the most stable were also selected. The generation of a 'branch' of the reaction network was terminated in accordance with formal characteristics — after the isolation of the metal-catalyst in a free form (when the ensemble of molecules contained a free metal atom). As a result, the reaction network consisted of intermediate ensembles of molecules, which corresponded to the pathways leading to the transformation of their precursors into the most stable compounds. The atomisation energy was calculated by the method of interacting bonds⁶⁰ using semiempirical parameters of the bond energies of the

¶ The ensemble of molecules for which the sum of the atomisation energies of the species was greatest was regarded as the most stable. Several most stable ensembles of molecules are possible because the metal atom is not known *a priori* and only the range of the possible atomisation energies, obtained by varying the semiempirical parameters of the bond energies, is known.⁶⁰

atoms comprising the molecules in the ensemble. For bonds involving C, H, and O atoms, the parameters obtained from the experimental thermochemical data on the heats of formation of the corresponding compounds were used. Thus, the parameter $E_{C=O}$ was found from the heats of formation of aldehydes and ketones, the parameter E_{C-H} was obtained from the heats of formation of hydrocarbons and alcohols, the parameter E_{O-H} was found from the heats of formation of alcohols, etc.

At the next stage, the optimum catalyst was selected. For this purpose, the parameters E_{M-X} (E_{M-C} , E_{M-H} , E_{M-O}) characterising the metal were varied for each intermediate ensemble and each pathway in the reaction network (in each linear sequence of ensembles of molecules from the starting EM to the final one). Because the variation of the E_{M-X} parameter was organised as step-by-step procedure, the atomisation energy of each intermediate ensemble of each pathway was split into a number of values. The atomisation energy corresponding to the condition of a uniform distribution of energy over the elementary steps of the catalytic process was chosen for each ensemble. In other words, the most smoothed broken line, which corresponds to the atomisation energies of the intermediate ensembles of a pathway, was chosen (Fig. 1). The semiempirical parameters of the bond energies calculated for this broken line were compared to the tabulated values for specific metals. The metal was regarded as optimal when the tabulated parameters of the bond energies for this metal was closest to the calculated values (i.e., values obtained for the most smoothed broken line).

Thus, it follows from a comparison of the calculated parameters of the formation of ethylene glycol in the reaction between CO and H₂ in the presence of a metal catalyst and the tabulated values that the best catalysts for this reaction are Rh, Co, Ir, Ru, and V. The ranges of the optimum E_{M-X} parameters for the formation of each product of the hydrogenation of CO (methane, methanol, ethane, ethanol, acetic acid, methyl formate, and ethylene glycol) were found and the corresponding metals were determined. The optimum parameters E_{M-X} and metals (Mn, Fe, Co, Ni, Ru, and Rh) for the formation of all the C₁ and C₂ products were found from the overlap of these ranges of parameters.

Baltanas and Froment¹¹⁵ developed a program for the generation of reaction networks for the solution of specific

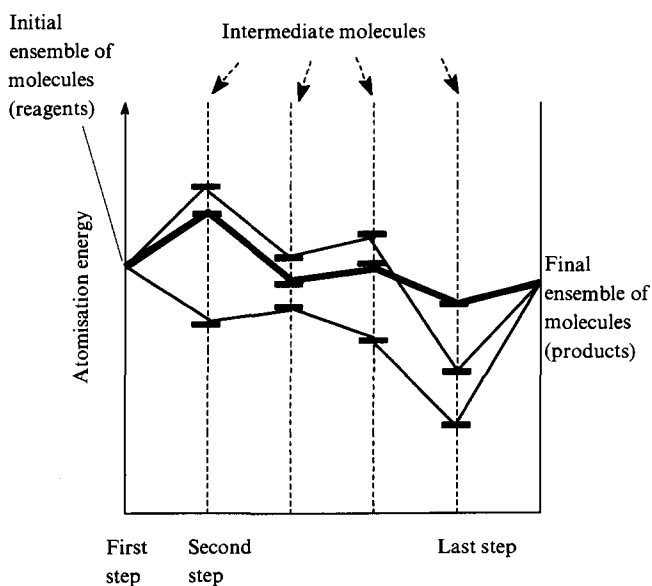


Figure 1. The splitting of the levels upon the variation of the E_{M-X} parameters. The optimum parameters E_{M-X} are those which correspond to the most 'smoothed' broken line, shown in the figure by a heavy line. The split levels of the atomisation energies of ensemble of molecules are shown in the dashed line corresponding to elementary steps.

problems, such as the study of catalytic hydroisomerisation and hydrocracking. Five generalised reactions, which are to be applied in succession to various species, are used in this program. These generalised reactions are designed solely for the investigation of the above catalytic processes. Species and reactions are described in terms of Boolean matrices which do not take into account the bond orders. The kinetic equations for the reaction network obtained were derived by the program. The principal disadvantage of this program is the narrow range of its applications.

Temkin's group (Lomonosov State Academy of Fine Chemical Technology, Moscow) are developing the ChemNet program for the formulation of hypotheses about the mechanisms of catalytic reactions. This program has been discussed in only a few publications, some of which are not readily available.^{14, 116} We shall, therefore, discuss it in more detail.

The first version of the program was written in the mid 1980s in FORTRAN IV, a language which has now become hopelessly obsolete.¹¹⁷ A new version, designed for modern personal computers of the IBM PC type and using the principal ideas of the old program, has been developed recently.

The list of species participating in the reaction as the reactants and system components and the list of the elementary transformations (generalised reactions) are input data. The species are specified by the user in the form of structural formulae and are transformed into records having a special format. Part of the record contains an upper triangular adjacency matrix of the atoms, while another part comprises different characteristics of atoms (charges, oxidation states, etc.), bond orders, as well as multicentre bonds. The elementary transformations are analogues of chemical reactions and describe the characteristic features of the changes occurring. The extent to which the details of the reaction are specified is decided by the user.

The more detailed the description of the elementary transformation, the shorter the list of substances to which this transformation is applicable. For example, the two elementary transformations

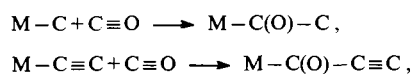


Table 4. List of substances proposed by the ChemNet program for the generation of the reaction network using ten elementary transformations and five initial substances (PdCl₂, CuCl, MeOH, HC≡CMe, CO).

No. of species	Chemical formula	No. of species	Chemical formula	No. of species	Chemical formula
1 ^a	PdCl ₂	17	MeC≡CPdCOOMe	33	MeOPdCH=C(Me)COOMe
2 ^a	CuCl	18	Pd(C≡CMe) ₂	34	MeOPdC(Me)=CHCOOMe
3 ^a	MeOH	19	ClPdCOC≡CMe	35	ClPdCH=C(Me)COC≡CMe
4 ^a	HC≡CMe	20	MeOPdC≡CMe	36	ClPdC(Me)=CHCOC≡CMe
5 ^a	CO	21	MeC≡CC(O)PdCOOMe	37	ClPdH
6	MeOPdCl	22	MeC≡CPdCOC≡CMe	38	MeOPdH
7	HCl	23	Pd(COC≡CMe) ₂	39	MeOC(O)OMe
8	MeOCu	24	MeOC(O)-C(O)OMe	40	HPdCOOMe
9	(MeO) ₂ Pd	25	Pd ⁰	41	HPdC≡CMe
10	ClPdCOOMe	26	MeC≡CCOOMe	42	HPdC(O)C≡CMe
11	CuCOOMe	27	MeC≡C-C≡CMe	43	PdH ₂
12	MeOPdCOOMe	28	MeOC(O)C(O)C≡CMe	44	HPdCH=C(Me)COOMe
13	Pd(COOMe) ₂	29	MeC≡CC(O)C≡CMe	45	HPdC(Me)=CHCOOMe
14	CuC≡CMe	30	MeC≡CC(O)C(O)C≡CMe	46	HPdCH=C(Me)COC≡CMe
15	ClPdC≡CMe	31	ClPdCH=C(Me)COOMe	47	HPdC(Me)=CHCOC≡CMe
16	MeOPdC≡CMe	32	ClPdC(Me)=C(H)COOMe		

^a Initial species.

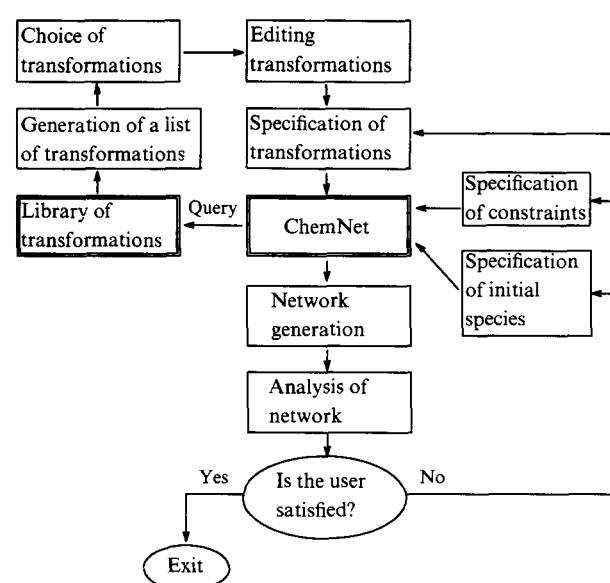


Figure 2. The bookkeeping scheme for the interactive execution of the ChemNet program.

describe the same reaction with specification of details to different extents. The difference consists only in that, in the first case, the program 'inserts' CO into all species containing the M-C bond, whilst, in the second case, it inserts it into metal alkynyl complexes. Note that, in the first case, the program will 'insert' CO also into M-C(O) fragments until the constraints imposed on the number of atoms in the species will begin to work. The elementary transformations can be inputted both in a symbolic form and in the form when standard chemical symbols of atoms are used. If the elementary transformation is formulated in a

Table 5. The reaction network generated by the ChemNet program on the basis of specified ten elementary transformations (ET) and five initial substances (PdCl₂, CuCl, MeOH, HC≡CMe, CO).

ET	Reaction ^a	ET	Reaction ^a	ET	Reaction ^a	ET	Reaction ^a
1	3+1 → 6+7	5	22+5 → 23	9	10+3 → 37+39	10	10+3 → 7+12
1	3+2 → 7+8	5	13 → 24+25	9	12+3 → 38+39	1	15+3 → 7+16
1	6+3 → 7+9	6	17 → 25+26	9	13+3 → 39+40	1	19+3 → 7+20
1	6+5 → 10	6	18 → 25+27	9	17+3 → 39+41	1	31+3 → 7+33
2	8+5 → 11	6	21 → 25+28	9	19+3 → 26+37	1	32+3 → 7+34
2	9+5 → 12	6	22 → 25+29	9	20+3 → 26+38	1	37+3 → 7+38
2	12+5 → 13	6	23 → 25+30	9	21+3 → 26+40	1	16+5 → 17
2	4+2 → 7+14	6	10+4 → 31	9	21+3 → 39+42	2	20+5 → 21
3	14+1 → 2+15	7	10+4 → 32	9	22+3 → 26+41	2	38+5 → 40
4	14+6 → 2+16	7	12+4 → 33	9	23+3 → 26+42	2	37+14 → 2+41
4	14+10 → 2+17	7	12+4 → 34	9	40+3 → 39+43	4	41+5 → 42
4	15+14 → 2+18	7	19+4 → 35	9	42+3 → 26+43	5	40+4 → 44
4	15+5 → 19	7	19+4 → 36	9	11+10 → 2+13	7	40+4 → 45
5	16+5 → 20	7	32 → 26+37	10	15+11 → 2+17	7	42+4 → 46
5	17+5 → 21	8	34 → 26+38	10	19+11 → 2+21	7	42+4 → 47
5	18+5 → 22	8	36 → 29+37	10	19+14 → 2+22	7	45 → 26+43
						8	47 → 29+43

^a The numbers of the species are indicated in Table 1.

symbolic form, it is necessary to determine also the possible substituent of each symbol. For example, the generalised reaction



is formulated in a symbolic form. The symbols M and X must be interpreted, indicating which atoms of the metal M and which atoms X can occur in the reaction.

Upon carrying out a 'rough' generation of the reaction network, the user can alter the degree of specification of detail in the records of steps, thereby excluding the directions of attack by particular species known a priori to be implausible.

A special unique format has been developed for the description of species and elementary transformations.¹¹⁸ The substances and reactions are stored in the computer memory in the form of special codes, the description of which is outside the scope of the present review.

Several evaluation rules are used in the ChemNet program, which are recommended to the user.

1. In an elementary step, the change in the number of valence electrons and in the oxidation state of the metal atom must not exceed 2 in absolute magnitude, which agrees with Tolman's rules.¹¹⁹

2. The molecularity of the elementary reactions must not exceed 2.

3. The user specifies the maximum number of valence electrons, the maximum coordination number, and the range of the possible oxidation states for each metal atom (the quantities stored in a special file are used as default settings).

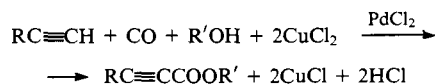
4. The user specifies the maximum number of atoms and/or the maximum numbers of atoms of a particular type (C, H, O, ...) in the products formed.

The generation of the reaction network is also constrained by the transforms which the user specifies himself or selects from the library. Furthermore, the generation of the reaction network is implicitly constrained by the degree of specification of details in the records of the transform.

After the specification of the initial species and elementary transformations (transforms), the program searches for the initial species which are regarded as candidates for participation in each

of the elementary transformations. After finding for each elementary transformation all the combinations of species to which the transformation is applicable and the new species have been stored in the computer memory, the program adds all the new substances to the list of the initial substances and repeats the entire procedure. The combinations of species and steps, tested at the preceding steps, are not examined. The process completes when each species (the starting material or the species obtained in the course of the network generation) was examined with respect to the possibility of its involvement in each elementary transformation, while new substances are not produced owing to the constraints imposed. The overall algorithm for the execution of the program can be represented by the bookkeeping scheme shown in Fig. 2.

One of the tests for the program was the synthesis of an alkynylcarboxylic acid ester in the CuCl₂–CuCl–PdCl₂–R'OH system.



The following elementary transformations were specified:

1. $MCl + ROH \rightarrow MOR + HCl$ (M = Pd, Cu; R = C)
2. $MOR + CO \rightarrow MCOOR$ (M = Pd, Cu; R = C)
3. $MCl + RC\equiv CH \rightarrow MC\equiv CR + HCl$ (M = Cu; R = C)
4. $CuC\equiv CR + Pd-Cl \rightarrow CuCl + PdC\equiv CR$ (R = C)
5. $PdC\equiv CR + CO \rightarrow Pd-C(O)-C\equiv CR$ (R = C)
6. $C-M-C \rightarrow M+C-C$ (M = Pd)
7. $M-C(O)- + C\equiv C \rightarrow M-C=C-C(O)-$ (M = Pd)
8. $M-C=CH \rightarrow C\equiv C+M-H$ (M = Pd)
9. $Pd-C(O)- + ROH \rightarrow PdH + RO-C(O)-$ (R = C)
10. $CuC+C-Pd-X \rightarrow CuX+C-Pd-C$ (X = Cl)

The following constraints were imposed: the maximum number of atoms in the conjectured species must be less than 20, the maximum oxidation state of the metal in the conjectured species is +1 for copper and +2 for palladium, and the maximum coordination numbers of copper and palladium are, respectively, 1 and 2.

The results of the generation of the reaction network are presented in Tables 4 and 5. These results may be used by the experimentalist in the discriminating experimental design.

IV. Conclusion

In conclusion, we may note that there are many computer programs, which make it possible to formulate hypotheses about the mechanisms of complex reactions and to generate reaction networks. Analysis of the programs considered makes it possible to indicate several typical disadvantages of these programs.

1. The impossibility of obtaining complete data on the transformations of the intermediates, side reactions, and by products because of the necessity for a rigid specification of the number of atoms entering into the isomeric ensemble and because of the bilateral nature of the search (RAIN, Dozmorov's program, GRACE).

2. The use of the simplicity criterion as a selection factor (MECHEM).

3. The narrowness of the range of applications (the program of Froment and Baltanas).

A feature common to the majority of the programs considered is that the key factor in the development of methods for the generation of hypotheses is the application of heuristic rules, which are used to different extents and at different stages of the execution of the programs.

1. The use of libraries of transformations (reaction generators) obtained as a result of the generalisation of the available literature data on the reactions (TAMREAC, KOMSIKAT, ChemNet, etc.).

2. The use of the more or less formalised rules for the assessment of the reaction plausibility (TAMREAC, CAMEO).

3. The use of heuristic rules for the optimisation, acceleration, and restriction of the search (RAIN, MECHEM).

4. The estimation of the thermodynamic and other characteristics, obtained by semiempirical or fully empirical methods, which in turn make it possible to assess the plausibility of individual steps or even entire reaction pathways (KOMSIKAT, the program of Froment and Baltanas, CAMEO).

In all cases, it is important for the user to know which heuristic rules are inherent in the program, what are the possibilities for their modification, and whether or not any of them can be abandoned. It is desirable to have such a possibility as regards the constraints as well.

Different levels of generalisation of the elementary reactions are employed in the empirical programs. In some programs, for example, in the ChemNet program, it is possible to apply simultaneously several levels of generalisation (i.e., reactions in which only the transformation of the fragments is characterised and reactions formulated in more detail).

Since different programs are based on different methods and heuristic rules, it is sometimes useful to combine them within the framework of a single program package. In particular, the present authors are working on the creation of a program package combining the ChemNet and KOMSIKAT programs. In our view, such a combination of programs may ensure an additional flexibility in the selection of substances for the formulation of hypotheses.

References

1. K R Popper *The Logic of Scientific Discovery* (London: Hutchinson, 1959)
2. K R Popper *Objective Knowledge* (Oxford: Oxford University Press, 1972)
3. K R Popper *Conjectures and Refutations: The Growth of Scientific Knowledge* (New York: Harper and Row, 1968)
4. L B Bazhenov, L Kh Samorodnitskii *Vopr. Filosofii* **6** 93 (1971)
5. D Hodson *Educ. Chem.* **19** 112 (1982)
6. V V Nalimov *Zavod. Lab.* **44** 325 (1978)
7. L S Polak, V Ya Gol'denberg, A A Levitskii *Vychislitel'nye Metody v Khimicheskoi Kinetike* (Computational Methods in Chemical Kinetics) (Moscow: Nauka, 1988)
8. V N Pisarenko, A G Pogorelov *Planirovanie Kineticheskikh Issledovaniy* (Design of Kinetic Research) (Moscow: Nauka, 1969)
9. V G Gorskii *Planirovanie Kineticheskikh Eksperimentov* (Kinetic Experiment Design) (Moscow: Nauka, 1984)
10. *The ACS Style Guide: A Manual for Authors and Editors* (Ed. V S Dodd) (Washington, DC: American Chemical Society, 1986)
11. G Pólya *Mathematics and Plausible Reasoning* (Princeton: Princeton University Press, 1974)
12. O N Temkin, S M Brailovskii, L G Bruk, in *Khimicheskaya Kinetika v Katalize: Kineticheskie Modeli Zhidkofaznykh Reaktsii* (Chemical Kinetics in Catalysis: Kinetic Models of Liquid-Phase Reactions) (Ed. S L Kiperman) (Chernogolovka: Inst. Chem. Phys. Acad. Sci. of the USSR, Inst. Org. Chem. Acad. Sci. of the USSR, 1985) p. 59
13. O N Temkin, L G Bruk, D Bonchev *Teor. Eksp. Khim.* **24** 282 (1988)
14. O N Temkin, L G Bruk, A V Zeigarnik *Kinet. Katal.* **34** 445 (1993)
15. A T Balaban (Ed.) *Chemical Applications of Graph Theory* (London: Academic Press, 1976)
16. R B King (Ed.) *Chemical Applications of Topology and Graph Theory* (Amsterdam: Elsevier, 1983)
17. N S Zefirov, S I Kuchanov (Eds) *Primenenie Teorii Grafov v Khimii* (Chemical Applications of Graph Theory) (Novosibirsk: Nauka, 1988)
18. N Trinajstić *Chemical Graph Theory* (Boca Raton, FL: CRC Press, 1992)
19. D Bonchev, D H Rouvray (Eds) *Mathematical Chemistry: Graph Theory and Its Applications to Chemistry* Vols 1, 2 (New York: Gordon and Breach, 1991)
20. D H Rouvray (Ed.) *Computational Chemical Graph Theory* (New York: Nova, 1990)
21. A V Zeigarnik, O N Temkin *Kinet. Katal.* **35** 691 (1994)
22. O N Temkin, A V Zeigarnik, D G Bonchev *J. Chem. Inf. Comput. Sci.* **37** 429 (1995)
23. A T Balaban, in *Graph Theoretical Approaches to Chemical Reactivity* (Eds D Bonchev, O Mekenyan) (Dordrecht: Kluwer, 1994) p. 137
24. O N Temkin, G K Shestakov, Yu A Treger *Atsetilen: Khimiya. Mekhanizmy Reaktsii. Tekhnologiya* (Acetylene: Chemistry. Reaction Mechanisms. Technology) (Moscow: Khimiya, 1991)
25. T T Zung, L G Bruk, O N Temkin *Izv. Akad. Nauk, Ser. Khim.* **1806** (1993)
26. T J Katz, J McGinnis *J. Am. Chem. Soc.* **99** 1903 (1977)
27. S M Brailovskii, O N Temkin, A S Kostyushin, K Yu Odintsov *Kinet. Katal.* **31** 1371 (1990)
28. L V Shchel'tsyn, S M Brailovskii, O N Temkin *Kinet. Katal.* **31** 1361 (1990)
29. I Ugi, J Bauer, K Bley, A Dengler, A Dietz, E Fontain, B Gruber, R Herges, M Knauer, K Reitsam, N Stein *Angew. Chem., Int. Ed. Engl.* **32** 201 (1993)
30. I Ugi, J Bauer, C Blomberg, J Brandt, A Dietz, E Fontain, B Gruber, A v Scholley-Pfah, A Senff, N Stein *J. Chem. Inf. Comput. Sci.* **34** 3 (1994)
31. N S Zefirov, E V Gordeeva *Usp. Khim.* **56** 1753 (1987) [*Russ. Chem. Rev.* **56** 1002 (1987)]
32. R Barone, M Chanon, in *Computer Aids to Chemistry* (Eds G Vernin, M Chanon) (Chichester: Ellis Horwood, 1986) p. 19
33. M Bersohn, A Esack *Chem. Rev.* **76** 269 (1976)
34. E J Corey, W T Wipke, R D Crammer, W J Howe *J. Am. Chem. Soc.* **94** 431 (1972)
35. W T Wipke, H Braun, G Smith, F Choplin, W Sieber *ACS Symp. Ser.* **61** 97 (1977)
36. E J Corey, A K Long, S D Rubenstein *Science* **228** 408 (1985)
37. M Bersohn *Bull. Chem. Soc. Jpn.* **45** 1897 (1972)
38. J Dugunji, I Ugi *Top. Curr. Chem.* **39** 19 (1973)

39. C Jochum, J Gasteiger, I Ugi *Angew. Chem., Int. Ed. Engl.* **19** 495 (1980)
40. C Jochum, J Gasteiger, I Ugi *Z. Naturforsch., B Chem. Sci.* **37** 1205 (1982)
41. I Ugi, M Wochner *J. Mol. Struct.* **42** 229 (1988)
42. M Wochner, J Brandt, A v Scholley, I Ugi *Chimia* **42** 217 (1988)
43. I Ugi, M Wochner, E Fontain, J Bauer, B Gruber, R Karl, in *Concepts and Applications of Molecular Similarity* (Eds M A Johnson, G M Maggiora) (New York: Wiley, 1990) p. 239
44. J Koča, M Kratochvil, V Kvasnička, L Matyska, J Pospichal *Synthon Model of Organic Chemistry and Synthesis Design (Lect. Notes Chem.)* Vol. 51 (Berlin: Springer, 1989)
45. V Kvasnička, M Kratochvil, J Koča *Collect. Czech. Chem. Commun.* **48** 2284 (1983)
46. J Koča *Collect. Czech. Chem. Commun.* **53** 1007 (1988)
47. J Koča *Collect. Czech. Chem. Commun.* **53** 3108 (1988)
48. J Koča *Collect. Czech. Chem. Commun.* **53** 3119 (1988)
49. J Koča *J. Math. Chem.* **3** 73 (1989)
50. J Koča *J. Math. Chem.* **3** 91 (1989)
51. V Kvasnička, J Pospichal *J. Math. Chem.* **5** 309 (1990)
52. V Kvasnička, J Pospichal *J. Math. Chem.* **3** 161 (1989)
53. V Kvasnička, J Pospichal *Int. J. Quantum Chem.* **38** 253 (1990)
54. J B Hendrickson, C A Parks *J. Chem. Inf. Comput. Sci.* **32** 209 (1992)
55. S V Dozmozorov *React. Kinet. Catal. Lett.* **19** 289 (1982)
56. S H Bertz, in *Chemical Applications of Topology and Graph Theory* (Ed R B King) (Amsterdam: Elsevier, 1983) p. 206
57. S H Bertz, W C Herndon *ACS Symp. Ser.* **306** 169 (1986)
58. J Gastieger, M G Hutchings, P Löw, H Saller *ACS Symp. Ser.* **306** 258 (1986)
59. V A Likholobov, L I Maier, N N Bulgakov, A V Fedotov, L G Shteingauer, in *Materialy V Mezhdunar. Simp. po Svyazi Mezhd. Gomogennym i Geterogennym Katalizom, Novosibirsk, 1986* (Proceedings of the Fifth International Symposium on the Relation between Homogeneous and Heterogeneous Catalysis, Novosibirsk, 1986) p. 231
60. L I Shtokolo, L G Shteingauer, V A Likholobov, A V Fedotov *React. Kinet. Catal. Lett.* **26** 227 (1984)
61. V A Likholobov, L I Mayer, N N Bulgakov, A V Fedotov, L G Shteingauer, in *Homogeneous and Heterogeneous Catalysis* (Eds Yu Yermakov, V Likholobov) (Novosibirsk: Institute of Catalysis, Siberian Branch of the Russian Academy of Sciences, 1986) p. 229
62. L G Shteingauer, L I Mayer, N N Bulgakov, A V Fedotov, V A Likholobov *React. Kinet. Catal. Lett.* **36** 139 (1988)
63. L G Zabolotnaya, Candidate Thesis in Physicomathematical Sciences, Institute of Catalysis, Siberian Branch of the Russian Academy of Sciences, Novosibirsk, 1989
64. L I Maier, Candidate Thesis in Chemical Sciences, Institute of Catalysis, Siberian Branch of the Russian Academy of Sciences, Novosibirsk, 1990
65. J Gasteiger *Tetrahedron* **35** 1419 (1979)
66. J Gasteiger, P Jacob, U Strauss *Tetrahedron* **35** 139 (1979)
67. R Barone, M Chanon, M L H Green *J. Organomet. Chem.* **185** 85 (1980)
68. I Theodosiou, R Barone, M Chanon *J. Mol. Catal.* **32** 27 (1985)
69. I Theodosiou, R Barone, M Chanon *Adv. Organomet. Chem.* **26** 165 (1986)
70. D Forster *Adv. Organomet. Chem.* **17** 255 (1979)
71. J F Roth, J H Craddock, A Hershman, F E Paulik *Chem. Technol.* **1** 600 (1971)
72. P J Collman, L S Hegedus, J R Norton, P Finke *Principles and Applications of Organotransition Metal Chemistry* (Mill Valley, CA: University Sci. Books, 1987)
73. E Fontain, J Bauer, I Ugi *Chem. Lett.* **37** (1987)
74. E Fontain, K Reitsam *J. Chem. Inf. Comput. Sci.* **31** 97 (1991)
75. E Fontain *Tetrahedron Comput. Method.* **3** 469 (1990)
76. I Ugi, J Bauer, K Bley, A Dengler, E Fontain, M Knauer, S Lohberger *J. Mol. Struct.* **230** 73 (1991)
77. I Ugi, E Fontain, J Bauer *Anal. Chim. Acta* **235** 155 (1990)
78. I Ugi, J Bauer, R Baumgartner, E Fontain, D Forstmeyer, S Lohberger *Pure Appl. Chem.* **60** 1573 (1988)
79. E J Corey, W T Wipke *Science* **166** 178 (1969)
80. E J Corey, X-M Cheng *The Logic of Computer Synthesis* (New York: Wiley, 1989)
81. Y Yoneda *Bull. Chem. Soc. Jpn.* **52** 8 (1979)
82. D Bonchev *Information Theoretic Indices for Characterization of Chemical Structures* (Chichester: Research Studies Press, 1983)
83. R E Valdés-Pérez, Ph. D. Thesis, Carnegie Mellon University, School of Computer Science, 1990
84. R E Valdés-Pérez *Tetrahedron Comput. Method.* **3** 277 (1990)
85. R E Valdés-Pérez *J. Comput. Chem.* **13** 1079 (1992)
86. R E Valdés-Pérez *J. Phys. Chem.* **96** 2394 (1992)
87. R E Valdés-Pérez *J. Comput. Chem.* **14** 1454 (1993)
88. R E Valdés-Pérez *Catal. Lett.* **28** 79 (1994)
89. R E Valdés-Pérez *J. Chem. Inf. Comput. Sci.* **34** 976 (1994)
90. R E Valdés-Pérez *J. Comput. Chem.* **15** 1266 (1994)
91. R E Valdés-Pérez *J. Chem. Inf. Comput. Sci.* **31** 554 (1991)
92. R E Valdés-Pérez *Artif. Intell.* **65** 247 (1994)
93. R E Valdés-Pérez, private communication
94. D Bonchev, O N Temkin, D Kamenski *React. Kinet. Catal. Lett.* **15** 119 (1980)
95. D Bonchev, D Kamenski, O N Temkin *J. Math. Chem.* **1** 345 (1987)
96. E V Gordeeva, D Bonchev, D Kamenski, O N Temkin *Chem. Inf. Comput. Sci.* **34** 436 (1994)
97. A V Zeigarnik, O N Temkin *Kinet. Katal.* **37** (1996) [*Kinet. Catal. (Engl. Transl.)* **37** (1996) (in the press)]
98. G M Ostrovskii, A G Zyskin, Yu S Snagovskii, in *Fizicheskaya Khimiya: Sovremennye Problemy* (Physical Chemistry: Current Problems) (Ed. Ya M Kolotyrkin) (Moscow: Khimiya, 1986) p. 84
99. Yu S Snagovskii, G M Ostrovskii *Modelirovanie Kinetiki Geterogennykh Kataliticheskikh Protessov* (Kinetic Modelling of Heterogeneous Catalytic Processes) (Moscow: Khimiya, 1976)
100. T Morikawa *Match* **13** 7 (1982)
101. D I Kaminski, O N Temkin, D G Bonchev *Appl. Catal.* **88** 1 (1992)
102. J Happel, P H Sellers *Ind. Eng. Chem., Fundam.* **21** 67 (1982)
103. J Happel, P H Sellers *Chem. Eng. Commun.* **83** 221 (1989)
104. P H Sellers, in *Chemical Applications of Topology and Graph Theory* (Ed. R B King) (Amsterdam: Elsevier, 1983) p. 420
105. V I Dimitrov *Prostaya Kinetika* (Simple Kinetics) (Novosibirsk: Nauka, 1982)
106. R H S Mah, R Aris *Ind. Eng. Chem., Fundam.* **2** 90 (1963)
107. V V Kafarov, V N Pisarenko, A V Solokhin *Zh. Fiz. Khim.* **52** 3143 (1978)
108. M L Mavrovouniotis, G Stephanopoulos *Ind. Eng. Chem. Res.* **31** 1625 (1992)
109. M L Mavrovouniotis *Ind. Eng. Chem. Res.* **31** 1637 (1992)
110. M L Mavrovouniotis, G Stephanopoulos, G Stephanopoulos *Biotechnol. Bioeng.* **36** 1119 (1990)
111. M L Mavrovouniotis, G Stephanopoulos, G Stephanopoulos *Comput. Chem. Eng.* **16** 605 (1992)
112. M L Mavrovouniotis, in *Artificial Intelligence Approaches in Product and Process Engineering* (New York: Academic Press, 1995) Ch. 3
113. T D Salatin, W L Jorgensen *J. Org. Chem.* **45** 2043 (1980)
114. W L Jorgensen, E R Laird, A J Gushurts, J M Fleischer, S A Gothe, H E Helson, G D Paderes, S Sinclair *Pure Appl. Chem.* **62** 1921 (1990)
115. M A Baltanas, G F Froment *Comput. Chem. Eng.* **9** 71 (1985)
116. B O Pol'geim, L G Bruk, S I Shalgunov, O N Temkin, in *Tez. Dokl. VII Vsesoyuz. Konf. "Matematicheskie Metody v Khimii"*, Kazan', 1991 (Abstracts of Reports at the Seventh All-Union Conference "Mathematical Methods in Chemistry", Kazan', 1991) p. 220
117. S I Shalgunov, L G Bruk, O N Temkin, unpublished results
118. S I Shalgunov, unpublished results
119. C A Tolman *Chem. Soc. Rev.* **1** 337 (1972)

Chemistry of methylenecyclobutane

M G Vinogradov, A V Zinenkov

Contents

I. Introduction	131
II. Rearrangements	132
III. Formation of complexes with metals	133
IV. Addition to the exocyclic double bond without formation of new C—C bonds	133
V. Addition to the double bond with formation of new C—C bonds	136
VI. Reactions with retention of the C=C bond	139
VII. Cycloaddition	140
VIII. Reactions with ring opening	141
IX. Polymerisation	141

Abstract. Studies devoted to the synthesis, investigation of the properties, and chemical transformations of methylenecyclobutane are surveyed systematically. Data on the reactions of methylenecyclobutane with a broad range of reagents are presented. The bibliography includes 291 references.

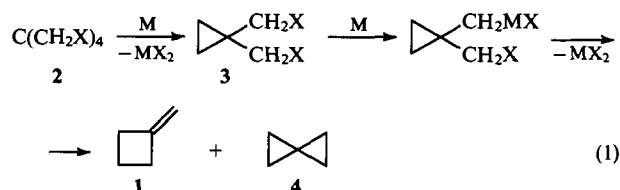
I. Introduction

Methylenecyclobutane (MCB) is a side product in the production of isoprene by the catalytic cleavage of 4,4-dimethyl-1,3-dioxane,^{1,2} which makes it a potential raw material for fine organic synthesis. Due to the presence of two reactive groups, the double bond, and the cyclobutane ring in its molecule, methylenecyclobutane can undergo a variety of chemical transformations, which permits the use of this compound in small-scale chemistry (for example, in the production of pesticides, pheromones, medicinals, and perfumes).

At present, MCB is not produced as a commercial target product in any large quantities. However, it is available as a reagent. For example, 'Aldrich' offers a preparation with a MCB content not less than 92%, and 'EGA-Chemie' supplies methylenecyclobutane of > 97% purity (the remaining 3% is due to spiro(pentane)).

1. Preparation

Methylenecyclobutane **1** was first obtained by Gustavson^{3,4} in 1896 by the treatment of 2,2-di(bromomethyl)-1,3-dibromopropane [tetrabromoneopentane **2**, (X = Br)] with zinc dust in ethanol (the Gustavson method⁵). Gustavson intended to obtain spiropentane **4**, but the resulting hydrocarbon differed in its properties from spiropentane. He studied this compound and mistakenly attributed the structure of vinylcyclopropane to it.



To determine the structure of this hydrocarbon proved fairly difficult. The problem of the structure of the 'Gustavson's hydrocarbon' was ultimately solved as late as 1914 by Filipov,^{6,7} who also presented a detailed list of the papers dealing with the synthesis and properties of MCB published up to that time. The data on the debromination of tetrabromoneopentane published before 1944 are presented in a review.⁸

In subsequent years, researchers paid considerable attention to the reaction of tetrabromoneopentane with zinc.⁹⁻¹⁶ It has been shown that isomerisation occurs during the elimination of the second pair of bromine atoms from the intermediate 1,1-di(bromomethyl)cyclopropane **3**. When Zn^{2+} cations, which catalyse the rearrangement of **3**, are bound into an inactive complex, spirocyclopentane **4** is formed predominantly.¹² The influence of the nature of the halogen atom and the solvent on the reaction of tetrahaloneopentanes **2** with zinc has been studied.¹³⁻¹⁶

Further studies¹⁷⁻²⁰ have shown that the ratio between spiropentane and methylenecyclobutane depends on the nature of the metal used as the reducing agent and the acidity of the medium.

The preparative synthesis of MCB by the reduction of tetrabromoneopentane with zinc dust²¹ is most frequently mentioned in the literature.

It has been suggested that tribromoneopentyl benzenesulfonate, which is more readily available than tetrabromoneopentane, be used in the synthesis of MCB.²²

Methylenecyclobutane is formed, apart from other hydrocarbons, on reduction of trihalo-derivatives of neopentane.^{23,24}

Dehydration of 1-methylcyclobutanol gave a mixture of hydrocarbons consisting of 1-methylcyclobutene (~45%), isoprene (~35%), and MCB (~20%) in a low yield.²⁵

The pyrolysis of cyclobutylmethyl acetate **5a** at 480 °C leads to MCB in 70% yield, and the pyrolysis of the corresponding

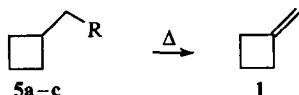
M G Vinogradov N D Zelinskii Institute of Organic Chemistry,
Russian Academy of Sciences, Leninskii prosp. 47, 117913 Moscow,
Russian Federation. Fax (7-095)135 53 28

A V Zinenkov NPO 'Lenneftekhim', Zheleznodorozhnyi proezd 40,
193148 St.-Petersburg, Russian Federation. Fax (7-812)560 95 01

Received 25 April 1995

Uspekhi Khimii **65** (2) 140–155 (1996); translated by Z P Bobkova

S-methyl xanthate **5b** at 380 °C affords MCB in 65% yield.²⁶ In the thermolysis of dimethyl(cyclobutylmethyl)amine oxide **5c**, the yield of MCB reaches 95%.²⁷



R = OAc (**a**), OCS₂Me (**b**), NOME₂ (**c**)

Methylenecyclobutane can also be synthesised starting from 1,4-dibromobutane via cyclobutylidenetriphenylphosphorane²⁸ or by the thermal,²⁹ mercury-photosensitised,³⁰ or laser-induced³¹ isomerisation of spiropentane, but these reactions can hardly be regarded as preparative methods for synthesising MCB.

In the industrial production of isoprene from isobutene and formaldehyde by the Prins reaction,⁵ the still product in the column for the purification of isoprene has been found to contain some MCB.^{1,32} A method for the isolation of MCB from this mixture by fractionation has been suggested.² The specimen thus obtained contained 98.42% of MCB. To identify MCB in the fractions of C₅ hydrocarbons, gas chromatography-mass spectrometry (GCMS) has been used.³³ The liquid-vapour phase equilibria in the systems obtained in the production of isoprene and containing MCB and other hydrocarbons have been considered in a number of papers.³⁴⁻³⁷

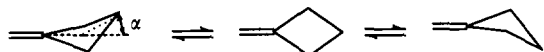
2. Structure and physical properties of methylenecyclobutane

At present, numerous data on the geometric structure of MCB are available. In fact, NMR,³⁸⁻⁴⁹ IR,⁴⁹⁻⁵⁴ UV,^{49,55} photoelectron,⁵⁶⁻⁵⁸ mass,⁵⁹⁻⁶⁴ microwave,⁶⁵⁻⁶⁷ and Raman,^{13-16,68-70} spectra of MCB have been studied in detail. Its physical and thermodynamic characteristics have been determined.^{59,71-76}

Numerous theoretical studies have been devoted to the problems of the geometry and energetics of the MCB molecule.^{50,58,77-100} The authors of these studies used various quantum-chemical computational methods.

According to the computational and experimental data, the MCB molecule possesses conformational mobility. The energy barrier to the transition from the puckered to the planar conformation is fairly low (-0.2 kcal mol⁻¹); it is lower than that for unsubstituted cyclobutane by a factor of 4-5. This distinction is due to the lesser changes in both the angular strain and the torsional interactions which accompany the transition of MCB from the nonplanar to the planar configuration.⁹⁸

Unambiguous data concerning the value of the dihedral angle (α) in the puckered conformation (Scheme 1) are lacking. For example, a dihedral angle of 16° has been found from spin-spin coupling constants.⁴⁸ It follows from electron diffraction, microwave spectra, and quantum-chemical calculations that the angle is 21.6°,¹⁰⁰ which is lower than for unsubstituted cyclobutane, in which the angle α is 30°^{101,102} or 25°.¹⁰⁰

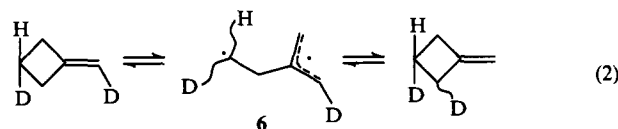


The C=C bond length in MCB is 1.331 Å.⁹¹ It differs little from the length of the double bond in isobutene (1.330 Å) and is shorter than this bond in ethene (1.337 Å).⁹⁰

II. Rearrangements

Whereas at ambient or low temperature MCB undergoes only conformational transformations (Scheme 1), at elevated temperatures (300-350 °C) a reversible process involving a more extensive structural rearrangement of the C-C and C-H bonds is observed. Thus, at a temperature of 332 °C partially deuteriated MCB undergoes a redistribution of deuterium atoms, which is due

to the relative ease of the homolytic cleavage of C-C bonds in the strained four-membered ring, yielding the alkylallyl biradical **6**.¹⁰³



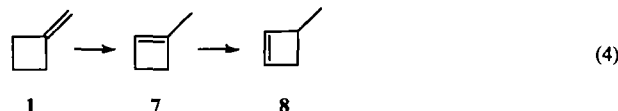
The isomerisation of MCB via a biradical mechanism has been discussed in another study.¹⁰⁴ A quantum-mechanical calculation carried out more recently also provided evidence in support of this mechanism of the thermal rearrangement of MCB.¹⁰⁵

The rearrangement of MCB involving the *exo-endo* migration of the double bond to give 1-methylcyclobutene **7** is of considerable interest.



Like MCB, the latter compound is potentially likely to be useful in organic synthesis. The rearrangement of MCB is energetically the least favourable compared with the corresponding rearrangements of its homologues with larger rings, since the ΔH value for this reaction is fairly small (-0.54 ¹⁰⁶ and -0.9 kcal mol⁻¹¹⁰⁷). For the rearrangements of methylenecyclopentane and methylenecyclohexane, these values are -3.65 and -1.97 kcal mol⁻¹, respectively.¹⁰⁸

MCB rearranges to 1-methylcyclobutene when it is passed over Al₂O₃ at 300 °C,⁶ but, isomerisation under these conditions can also yield isoprene.¹⁰⁹ When MCB is passed over Al₂O₃ at a higher temperature (370-420 °C),¹¹⁰ the ring is cleaved to give isoprene as the main reaction product.^{109,110} The isomerisation of MCB on passing it over various heterogeneous catalysts (aluminosilicates or zeolites) in the temperature ranges 50-400 °C¹¹¹ and 350-500 °C¹¹² has been described. For all the catalysts studied, it was found that the curves for the temperature dependence of the yield of 1-methylcyclobutene pass through a maximum. When the temperature is increased further, migration of the double bond within the four-membered ring occurs, yielding 3-methylcyclobutene **8**.¹¹¹ This compound is the least stable among the three isomers **1**, **7**, and **8**.¹⁰⁹ Isomer **8** was not detected in the products of the isomerisation of MCB over Al₂O₃.¹⁰⁸



It has been shown⁶ that MCB isomerises to 1-methylcyclobutene when heated in aqueous alcohol in the presence of ZnBr₂ and Zn(OH)Br at 140 °C for several days.

Heating of MCB in dimethylacetamide for 10 min at 160 °C gave an equimolar mixture of MCB and 1-methylcyclobutene in 80% yield.¹¹³

When MCB is stirred at room temperature with metallic sodium deposited onto Al₂O₃, an equilibrium between the alkenes with the *exo*- and *endo*-arrangements of the double bond is established after several hours. The equilibrium constant *K* of reaction (3) at 20 °C is equal to 6, which implies that the reaction mixture contains 15% of MCB and 85% of 1-methylcyclobutene.^{109,114-117} As shown in another study,¹¹⁸ this process is not selective, since after its completion the reaction mixture contains 75% of 1-methylcyclobutene, 19% of MCB, 3% of spiropentane, and 3% of unidentified hydrocarbons.

The isomerisation of MCB also takes place in the presence of strong bases. The relative rates of formation of carbanions from

C₄–C₈ methylenecycloalkanes in the presence of potassium *tert*-butoxide in dimethyl sulfoxide have been reported.¹¹⁹ Kinetic studies of the isomerisation of MCB in the presence of potassium or lithium *tert*-butoxide in various solvents have been carried out.¹²⁰ A preparative procedure for the isomerisation of MCB to 1-methylcyclobutene in the Bu^tOK–DMSO catalytic system has been reported;¹²¹ however, the yield of compound **7** per unit volume of the catalyst solution did not exceed 0.1 g cm⁻³ h⁻¹. In the presence of a stronger base, lithium β-aminoethylamide, in ethylenediamine at 10–45 °C, the isomerisation proceeds more effectively (with a productivity of 4.3–4.5 g cm⁻³ h⁻¹). The equilibrium concentrations of MCB and 1-methylcyclobutene (84%–87% MCB¹²²) are virtually attained over a period of several hours.

The isomerisation of MCB [reaction (3)] in the presence of 3 mol % the rhodium hydride complex Rh(H)(CO)(PPh₃)₃ (with benzene as the solvent)¹²³ occurs much less effectively: even after 10 days the composition of the reaction mixture is far from equilibrium (the ratio between isomers **1** and **7** is 0.68 instead of 0.17). In all probability, the reaction proceeds via a π-complex of Rh(I) with MCB (see below). The isomerisation of MCB to 1-methylcyclobutene has also been observed in the presence of PdCl₂ at 100 °C in dioxane and at 22 °C in methanol.^{124, 125}

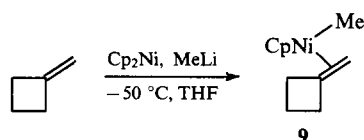
III. Formation of complexes with metals

Like other alkenes, MCB forms complexes with AgNO₃. The stability constants of some complexes of alkenes determined by GLC have been reported.^{126, 127} The formation of complexes with Ag(I) has been used in the analysis of MCB-containing mixtures of light hydrocarbons.¹²⁸

Methylenecyclobutane reacts with Pd(II) chloride or [Rh(CO)₂Cl]₂ to give π-allylic complexes.¹²⁹

The comparative stabilities of Rh(I) complexes with various alkenes have been studied.¹³⁰ The π-complex derived from MCB was found to possess an anomalously high stability, comparable with that of the Rh(I) complex of ethene.

The synthesis of a π-complex of MCB with Ni(II) (yield 61%) has also been reported.¹³¹



A trinuclear cluster-type osmium complex incorporating MCB has been described.¹³² In this complex, MCB forms a bridge between two osmium atoms via the methylenecarbon atom and also forms a π-bond with the third osmium atom.

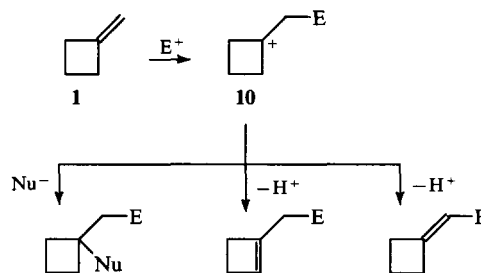
The interaction of MCB with organotitanium,¹³³ organonickel,¹³⁴ organorhodium,¹³⁵ and organopalladium¹³⁶ compounds has also been described in the literature.

IV. Addition to the exocyclic double bond without formation of new C–C bonds

1. Reactivity

a. Cationoid intermediates

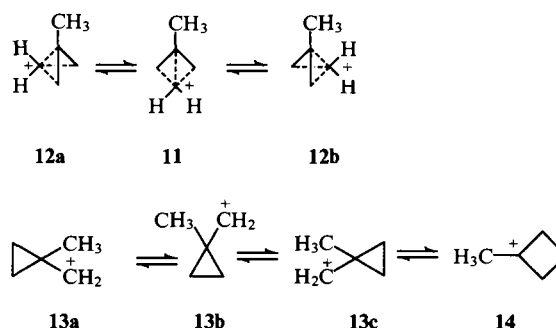
Many known transformations of MCB involve a stage in which active electrophilic species such as protons, acylium cations, etc. add to the double bond. The addition results in the tertiary carbocationic intermediate **10**, which can either combine with a nucleophile or eliminate a proton, and this governs the composition of the final reaction products (Scheme 2).



Scheme 2

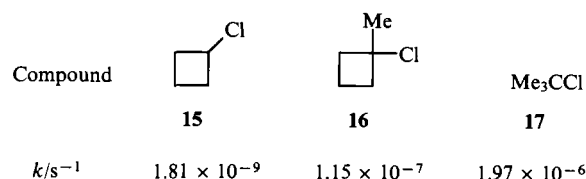
The problem of the structure of the intermediate cation **10** (E = H) has attracted considerable attention and has not yet been solved. According to ¹³C NMR spectroscopy and an isotope study, at –154 °C this cation exists as the symmetrical σ-bridged methylenecyclobutanium structure **11**,^{137, 138} while from –150 to –90 °C it is an equilibrium mixture of three bicyclobutanium ions **11**, **12a**, and **12b** or delocalised 1-methylcyclopropylcarbynyl cations **13a–c** interconverting via the classical planar 1-methylcyclobutyl cation **14** (Scheme 3).

Scheme 3



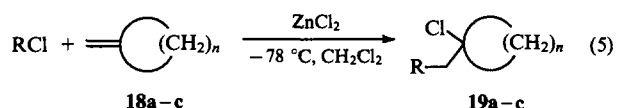
The conformation of the 1-methylcyclobutyl cation **10** (E = H) in an aqueous medium at ambient temperature is unknown. Quantum-chemical calculations referring to the gaseous phase allow the existence of this cation as any of the above structures or as their equilibrium mixture.^{139–141} At the same time, since the tertiary carbocation **14** must be much more stable than the primary rearranged cations **13a–c**, one should expect that the equilibrium would be substantially shifted to the right, that is, toward the formation of the cation **14** (Scheme 3). Therefore, it is the transformations of the nonrearranged cation **10** (Scheme 2) that should determine the composition of the products of electrophilic addition to the double bond of MCB; this is in good agreement with the existing experimental data.

The relative stability of the cation **10** (E = H) can be judged by comparing the rate constants for the solvolysis of the corresponding chlorides **15–17** (80% acetone, 25 °C).¹⁴²



The above data indicate that the cation **10** (E = H) is more stable than the unsubstituted cyclobutyl cation and is less stable than the *tert*-butyl cation.

The reactivity of MCB toward electrophilic addition can be estimated by comparing the rates of the ZnCl₂-catalysed reaction of (*p*-CH₃C₆H₄)₂CHCl with various methylenecycloalkanes **18a–c**.¹⁴³



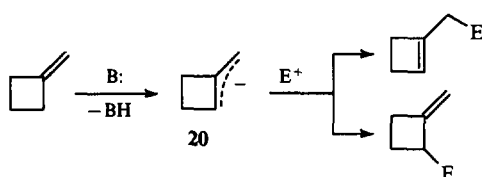
R = (p-CH₃C₆H₄)₂CH

n	3	4	5
k (arbitrary units)	1	51.1	1.03

It follows from these data that the reactivity of MCB in reaction (5) with the above electrophile is close to that of methylenecyclohexane, but is many times lower than that of methylenecyclopentane.

b. Anionoid intermediates

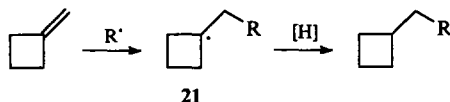
Another important aspect of using MCB in organic synthesis is based on its deprotonation through the action of a strong base and the subsequent transformations of the allylic carbanion **20** thus generated (Scheme 4).



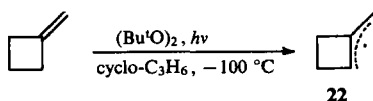
The composition of the products of transformation of the carbanion **20** is determined by the direction of attack by the electrophile (E⁺), which is either on a carbon atom of the side chain or on a ring carbon atom in the allylic system. The predominance of either of these directions depends on the nature of the electrophile and on the conditions under which the reaction is carried out.¹⁴⁴

c. Free-radical intermediates

Another approach to the functionalisation of MCB is based on the radical addition to the double bond. The intermediate adduct formed in this reaction (radical **21**), like the corresponding carbocation **10** produced in the electrophilic addition to MCB (see above), does not undergo fragmentation, and the cyclobutane ring is retained in the products of its transformation.



The radicals **21**, in which R = SiMe₃, SiEt₃,^{145, 146} or MeS,¹⁴⁷ have been detected by EPR at 150–220 K. The formation of the allylic radical **22** upon photolysis of a solution of MCB in cyclopropane containing di-*tert*-butyl peroxide has also been detected by EPR.¹⁴⁸

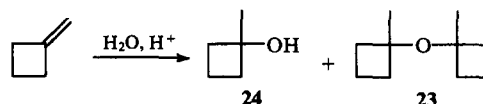


Radical-ion species such as radical cations can also participate in reactions with MCB. The latter are formed, for example, in photoinduced¹⁴⁹ or γ-radiation-induced reactions.¹⁵⁰

2. Addition with formation of the C–O bond

The acid-catalysed hydration of MCB is among the thoroughly studied examples of electrophilic addition to the double bond of

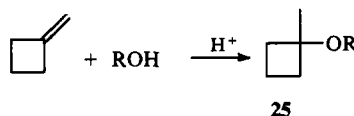
MCB.^{151–154} The mechanism of this reaction has been described by Taft,¹⁵⁵ who has also determined its thermodynamic parameters.¹⁵⁶ The ether **23**, resulting from the addition of 1-methylcyclobutanol **24** to MCB, is formed in this reaction as a side product.



When MCB was hydrated in the presence of the KU-23(10/60) cation-exchange resin at 40 °C with an MCB:H₂O molar ratio of 2:3 and a reaction time of 8 h, the degree of MCB conversion amounted to 87.8% and the selectivity of the formation of compound **24** was 94.4% (the reaction mixture contained 3% of the ether **23**). However, by varying the hydration conditions one can direct the process to the selective formation of the ether **23**. Thus, at 40 °C, for an MCB:H₂O molar ratio of 2:1, and for a reaction time of 3 h, the selectivity of the formation of ether **23** was 96%, the degree of conversion of MCB being 92.1%.¹⁵²

The hydration of MCB under static conditions (without stirring) in the presence of the KU-23(10/60) cation-exchange resin in a batch reactor has been described.¹⁵³

Alcohols or carboxylic acids add to MCB in the presence of an acid catalyst.¹⁵⁷



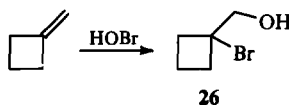
R	Me	Et	Bu ⁿ		MeCO
Yield (%)	90	45	41	63	56

R	ClCH ₂ CO	FCH ₂ CO	Cl ₂ CHCO	CF ₃
Yield (%)	55	60	90	91

The reaction is carried out in hexane with MCB:ROH (or RCOOH):C₆H₁₄ ratios of 1:1:1 in the presence of sulfuric acid or HCl.

Esters derived from 1-methylcyclobutanol have found application as insecticides, acaricides, and fungicides,^{158, 159} and sugar substitutes in foodstuffs.¹⁶⁰ The 1-methylcyclobutoxy-group is incorporated in a metabolism-resistant β-lactam antibiotic possessing a high antibacterial activity.¹⁶¹

The selective addition of HOBr to MCB, affording 1-bromo-1-hydroxymethylcyclobutane in 78% yield, has been described.^{162, 163}

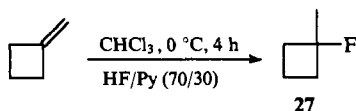


Hypochlorous acid also adds to MCB, but, apart from chlorohydrin, this reaction yields a diol (the ratio between these products is 3:2).¹⁶² The process is carried out in an aqueous suspension of the alkene.

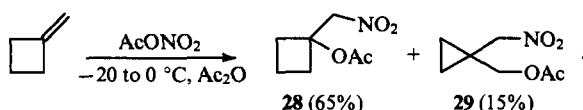
3. Addition with formation of the C–N, C–S, C–Se, or C–Hal bond

The addition of hydrogen halides to MCB has been studied in detail.^{164–168} In polar solvents, hydrogen halides add in conformity with the Markovnikov rule, giving 1-halo-1-methylcyclobutane, while in the presence of a radical source in a nonpolar solvent, anti-Markovnikov addition occurs to yield bromomethylcyclobutane.^{162, 169, 170}

Hittich et al.¹⁷¹ have described the hydrofluorination of MCB, but the yield of 1-fluoro-1-methylcyclobutane **27** isolated by preparative GLC was not reported.

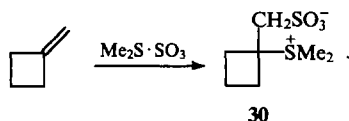


Acetyl nitrate adds to MCB at -20 to 0°C in the presence of acetic anhydride.¹⁷² Apart from the major product, 1-acetoxy-1-nitromethylcyclobutane **28**, the reaction yields the product **29** of the rearrangement of the intermediate cation involving ring contraction:

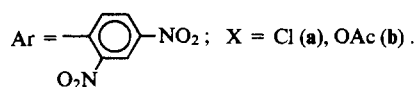
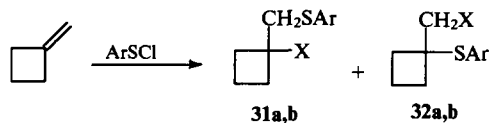


When NO_2BF_4 is used instead of AcONO_2 , the yield of 1,1-disubstituted cyclopropane is twice as high.¹⁷²

The interaction of MCB with the complex $\text{Me}_2\text{S} \cdot \text{SO}_3$ affords the sulfobetaine **30** as the only product in a high yield:^{173, 174}

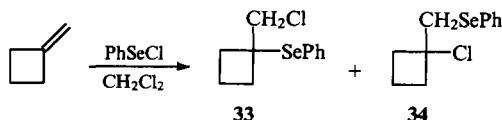


2,4-Dinitrophenylsulfanyl chloride reacts with MCB in acetic acid at 20°C to afford predominantly the arylthiomethyl-substituted cyclobutane **31**. In addition, a small amount of compound **32** was isolated (the **31a**:**32a** ratio was 5.2:1); the overall yield of the products **31** and **32** was 88%.¹⁷⁵ At 40°C , these products are formed in a different ratio (**31a**:**32a** = 2:1):¹⁷⁶

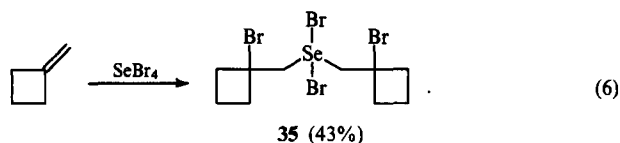


When the reaction is carried out in chloroform, the anti-Markovnikov addition product predominates (**31a**:**32a** = 0.4:1),¹⁷⁶ while the process carried out in acetic acid in the presence of LiClO_4 affords mostly products of the interaction with the solvent (the products **31** and **32** are formed in the following yields: **31a**, 5%; **31b**, 35%; **32a**, 1%; **32b**, 12%).¹⁷⁶

Phenylselenanyl chloride interacts with MCB at -70°C in CH_2Cl_2 to give the chloromethyl derivative of cyclobutane **33** as the major product; at room temperature, compound **33** slowly isomerises to the chloride **34**.¹⁷⁷

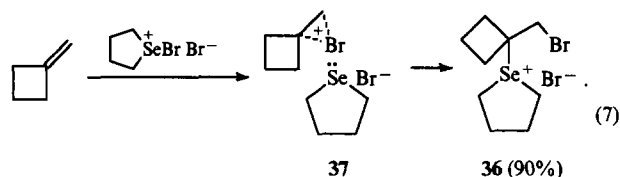


The reaction of MCB with SeBr_4 gives the product **35** incorporating two cyclobutyl groups:¹⁷⁸



At room temperature, compound **35** is gradually dehalogenated and rearranges, affording substituted cyclopropylmethyl bromides.

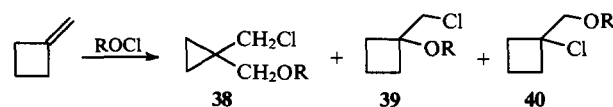
The electrophilic addition of tetramethyleneselenanyl bromide to MCB gives the selenonium salt **36**.¹⁷⁹ In all probability, this reaction occurs via the intermediate bromonium ion **37**.¹⁸⁰



The formation of different products in these reactions (compounds **35** and **36**) may be due to greater steric hindrance in the selenium-containing nucleophile participating in reaction (7), which hampers the attack on the nonterminal carbon atom of the bridged cation **37**.¹⁸⁰

At -60°C , MCB can combine with SO_3 , giving the cyclic β -sultone.¹⁸¹

The chlorosulfamation of MCB yields a mixture of the products **38**–**40**. The addition is nonselective and is accompanied by partial rearrangement:¹⁸²

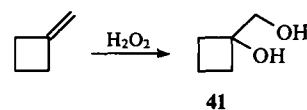


4. Hydrogenation

Hydrogenation under mild conditions involves the addition of hydrogen to the exocyclic double bond. Under more drastic conditions, the cyclobutane ring is cleaved and the reaction yields isopentane as the major product.⁶ The heats of hydrogenation of MCB and 1-methylcyclobutene have been reported by Turner et al.¹⁰⁷ The kinetics of the hydrogenation of MCB over platinum-containing catalysts have been studied.^{183, 184}

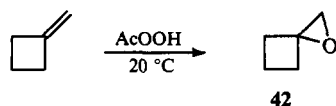
5. Oxidation

When MCB is treated with hydrogen peroxide in the presence of OsO_4 or in formic acid, 1-hydroxy-1-hydroxymethylcyclobutane **41** is formed in 39% and 83% yield, respectively.²¹



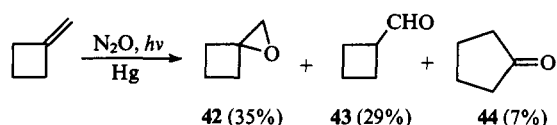
The highly selective dihydroxylation of MCB with hydrogen peroxide occurs in the presence of the osmium catalyst obtained from OsO_4 or $\text{Os}_3(\text{CO})_{12}$ and poly(4-vinylpyridine) or poly(4-vinylpyridine 1-oxide).¹⁸⁵

The epoxidation of MCB with 41% peracetic acid in CH_2Cl_2 in the presence of anhydrous Na_2CO_3 at room temperature gives the oxaspirohexane **42** in 45% yield.^{186, 187}

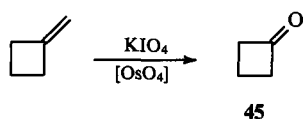


The treatment of MCB with peracetic acid in acetic acid results in a mixture consisting of the monoacetate of the diol **41** and cyclobutanecarboxylic acid, while the use of perbenzoic acid in chloroform yields a mixture of the oxaspirohexane **42** and the monobenzoate of the diol **41**.¹⁸⁸

The kinetics of the epoxidation of MCB with peroxyauric acid have been studied.¹⁸⁹ The epoxidation of MCB with atomic oxygen, generated by the Hg-sensitised photolysis of N_2O , occurs nonselectively: apart from the epoxide **42**, formylcyclobutane **43** and cyclopentanone **44** are produced.¹⁹⁰



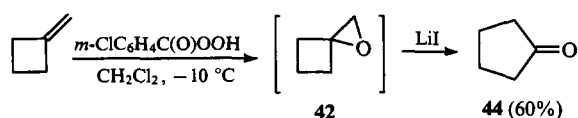
The oxidative cleavage of MCB by potassium periodate in the presence of a catalytic amount of OsO_4 is the simplest of the known ways of preparing cyclopentanone **45**.^{191, 192}



Methylenecyclobutane is ozonised at a temperature of $-70^\circ C$ in pentane. The resulting ozonide decomposes explosively at $-20^\circ C$.¹⁹³

Cyclobutanone has been synthesised in a yield of about 70% by the ozonisation of MCB at -70 to $-80^\circ C$ in CH_2Cl_2 in the presence of pyridine.^{194, 195}

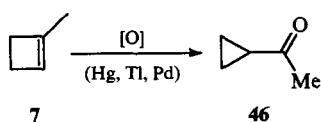
A series of MCB transformations accompanied by ring expansion and resulting finally in cyclopentanone have been described. For example, the oxidation of MCB with nitrous oxide at $300^\circ C$ and 450 atm affords cyclopentanone **44** in a low yield.¹⁹⁶ One of these processes involves the intermediate formation of the epoxide **42**, which is then allowed to react with LiI without isolation from the reaction mixture.^{197, 198}



Methylenecyclobutane can be directly converted into cyclopentanone by oxidation with oxygen in the presence of the $PdCl_2-CuCl_2$ catalytic system. The selectivity of this process depends substantially on the nature of the solvent. It occurs most selectively in benzene, the yield of cyclopentanone being 75%.¹⁹⁹

The oxidation of MCB to cyclopentanone with the complex $(MeCN)_2PdCl(NO_2)$ in CH_2Cl_2 has also been studied.²⁰⁰

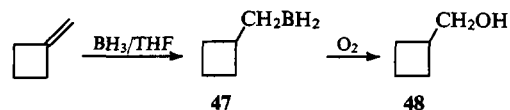
The oxidation of 1-methylcyclobutene with $Tl(III)$ and $Hg(II)$ perchlorates,^{201, 202} as well as with $PdCl_2$,²⁰¹ $PdCl_2L_2$, or $PdCl(NO_2)L_2$ ($L = CD_3CN$)²⁰³ results in cyclopropyl methyl ketone **46**, the chemistry of which has been discussed in a review.²⁰⁴



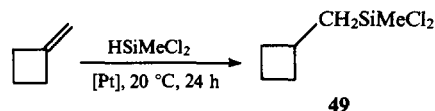
The autooxidation of MCB proceeds more slowly than that of terpenes or other unsaturated alicyclic alkenes, the 2-position of the cyclobutane ring being attacked predominantly.²⁰⁵

6. Hydroboration, hydrosilylation, and hydrophosphorylation

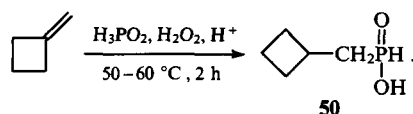
The hydroboration of MCB with the subsequent oxidation of the resulting cyclobutylmethylborane **47** leads to cyclobutylmethanol **48**.²⁰⁶



MCB enters into the hydrosilylation reaction in the presence of a Pt catalyst immobilised on a phosphinated silica gel:²⁰⁷

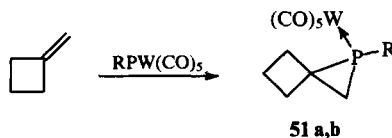


The hydrophosphorylation of MCB with phosphinic acid in the presence of hydrogen peroxide in an acid medium at $50-60^\circ C$ affords cyclobutylmethylphosphinic acid **50**:²⁰⁸



The reaction of MCB with PBr_3 gives the corresponding phosphine as the only product.²⁰⁹ When the reaction is carried out in a stream of O_2 , the yield of the phosphine increases from 49% to 63%. The reaction is regiospecific and occurs via a radical mechanism.

The treatment of the phosphinidene complexes $PhPW(CO)_5$ and $MePW(CO)_5$ with exocyclic olefins affords 1-phosphaspiro[2.n]alkanes ($n = 2-5$).²¹⁰ In the case of MCB, a pentacarbonyl-tungsten complex containing the 1-phosphaspiro[2.3]-hexane ligand **51** is formed.

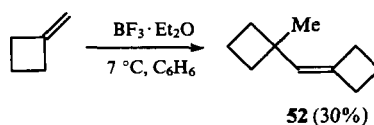


$R = Me$ (a), Ph (b)

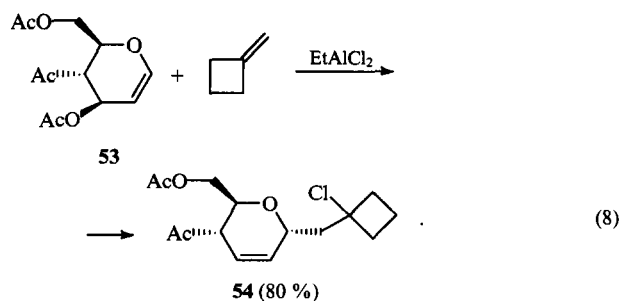
V. Addition to the double bond with formation of new C–C bonds

1. Alkylation

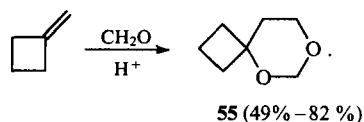
In the presence of 20 mol % $BF_3 \cdot Et_2O$ in benzene at $7^\circ C$, MCB dimerises, giving the bicyclic dimer **52**.²¹¹



A new pathway to the synthesis of C-glycosides, which are of interest for preparing new anticancer preparations, has been suggested by Herscovici et al.^{212, 213} This method is based on the electrophilic addition of the acylated glycals **53** to MCB, catalysed by Lewis acids:

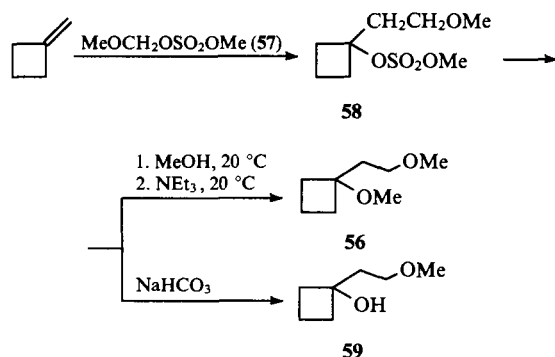


Reaction (8) was carried out at -20°C for 5 min in a $\text{C}_5\text{H}_{12}-\text{Et}_2\text{O}$ (5:1) solvent mixture. A number of workers reported^{157,214,215} the preparation of 5,7-dioxaspiro[3.5]nonane **55** by the reaction of MCB with formaldehyde catalysed by sulfuric acid or *p*-toluenesulfonic acid:



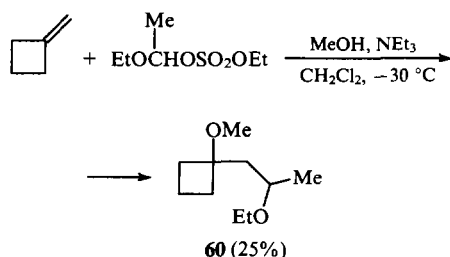
If the above reaction is carried out at 40°C in the presence of 30 mass % H_2SO_4 , the yield of compound **55** is 49%.^{157,214} The yield of 5,7-dioxaspiro[3.5]nonane can be brought to 82% with virtually complete conversion of MCB by conducting this reaction at 90°C and with a $\text{CH}_2\text{O}:\text{MCB}$ molar ratio of 2:1 in the presence of 2.5 mol % sulfuric acid and an equal volume of an extractant (hexane).²¹⁵

The methylated diol **56** has been obtained directly from MCB using methoxymethyl methyl sulfate **57** as the alkylating reagent.²¹⁶

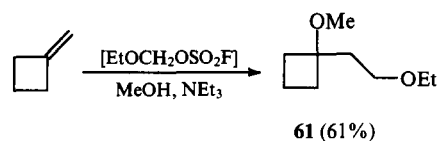


This reaction involves the intermediate formation of the sulfate **58**, which is subjected to methanolysis and then treated with triethylamine without isolation from the solution. When the intermediate **58** is treated with an aqueous solution of NaHCO_3 , the reaction yields the alcohol **59**.²¹⁷

Similarly, 1-ethoxyethyl ethyl sulfate adds to MCB in the presence of methanol to give the adduct **60**.²¹⁸



1-(2-Ethoxyethyl)-1-methoxycyclobutane **61** has been synthesised in a similar way.²¹⁹

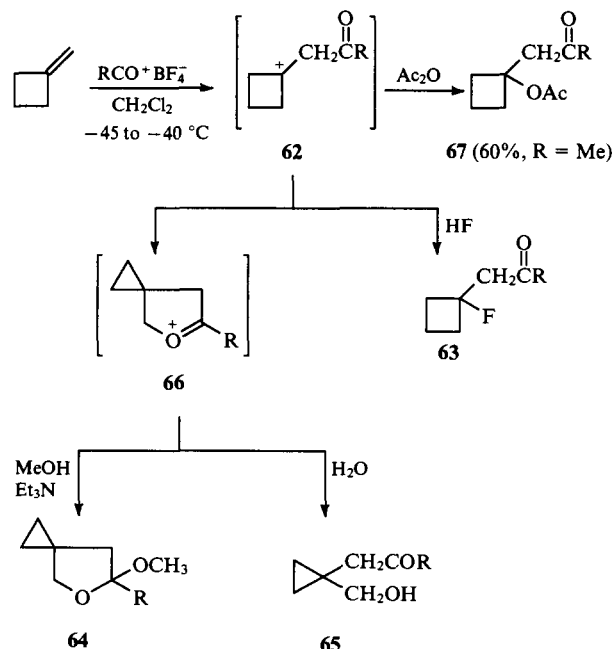


2. Acylation

a. Electrophilic acylation

The known instances of the electrophilic acylation of MCB involved the highly reactive cationoid reagents RCO^+X^- ($\text{X}^- = \text{SO}_3\text{F}^-$, BF_4^- , or SbF_6^-) as electrophiles. The course of the reactions of MCB with acyl tetrafluoroborates $\text{RCO}^+\text{BF}_4^-$ (Scheme 5) depends on the nature of the group R. The bulkier the group R, the larger the contribution of reactions occurring with the rearrangement of the intermediate cation **62**.²²⁰ If R is Me or Et, only the fluorinated ketone **63** is obtained. If R is Bu^t , only the rearranged product, namely, substituted tetrahydrofuran **64**, is formed. When R is Pr^n or Bu^i , mixtures of the products **63** and **64** are isolated. When water is added to the reaction mixture, the hydroxyketone **65** is produced via the hydration of the rearranged cation **66**.²²⁰

Scheme 5



(R = Bu^t , 65%–70%)

R	63 : 64 ratio
Me	100:0
Et	100:0
Pr^n	(85–75):(15–25)
Bu^i	(30–35):(70–65)
Bu^t	0:100

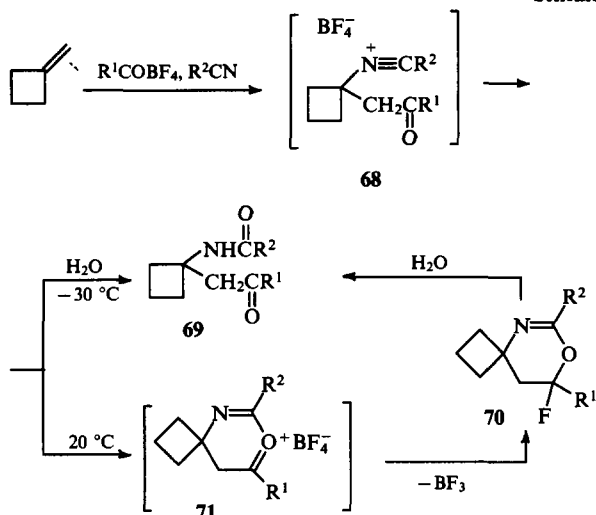
The composition of the products of the acylation of MCB is sensitive not only to the nature of the group R in the cationoid reagent RCO^+X^- , but also to the nature of the anion X. The solvent used also plays an important role.

When the acylation of MCB with acetyl tetrafluoroborate is carried out in the presence of acetic anhydride, 1-acetonyl-1-acetoxycyclobutane **67** is the main reaction product (Scheme 5).^{221,222}

When $\text{RCO}^+\text{BF}_4^-$ is replaced by the harder ionic reagent $\text{RCO}^+\text{SbF}_6^-$, the reaction yields the substituted tetrahydrofuran **64** as the only product, irrespective of the bulk of the group R.²²³

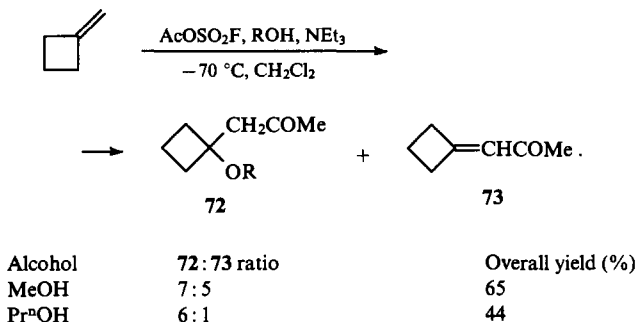
The acylation of MCB with $R^1CO^+BF_4^-$ in the presence of R^2CN proceeds as coupled addition of R^1CO^+ and R^2CN to the $C=C$ bond via the formation of the *N*-alkylnitrilium salt **68** (Scheme 6).²²²

Scheme 6

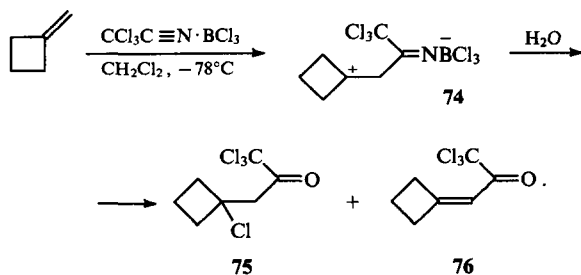


Depending on the reaction temperature, either the amidoketones **69** ($-30^\circ C$) or the 5,6-dihydro-1,3-oxazines **70** ($+20^\circ C$) are formed selectively. The syntheses of a number of amidoketones **69** and oxazines **70** ($R^1 = Me, Et, Pr^i, Pr^i, Bu^i$; $R^2 = Me, CH_2Cl, Ph$) in 34%–100% yields have been reported by Gridnev et al.²²⁴

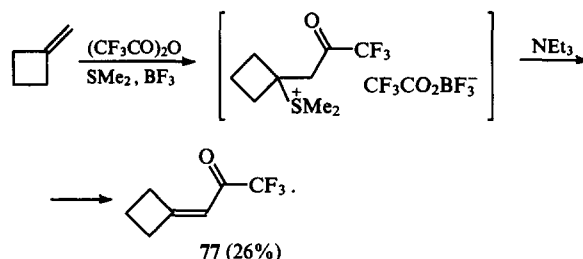
In the case where acetyl fluorosulfonate, prepared in situ from AcF and SO_3 , is used in the acylation of MCB, the composition of the reaction products depends on the nature of the alcohol introduced into the system:²²⁵



It has been reported that the complex of trichloroacetonitrile with boron trichloride can be used as a chemical equivalent of the acylium cation.²²⁶ The first step of the process affords the cation **74**, which is converted in the presence of water mostly into the ketone **75** and, to some extent, into the unsaturated ketone **76**. The overall yield of the products is 91%:²²⁶

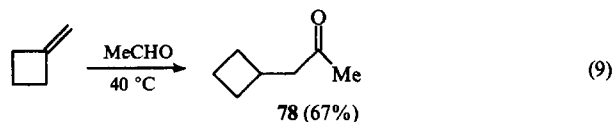


The introduction of a perfluoroacyl group into unsaturated compounds is hampered, because the perfluoroacyl cation is easily decarbonylated and, furthermore, the readily available trifluoroacetic anhydride is insufficiently electrophilic to acylate alkenes. It has been suggested that the perfluoroacylation should be carried out using the complex resulting from the addition of trifluoroacetic anhydride to a solution of dimethyl sulfide in CH_2Cl_2 saturated with BF_3 :²²⁷



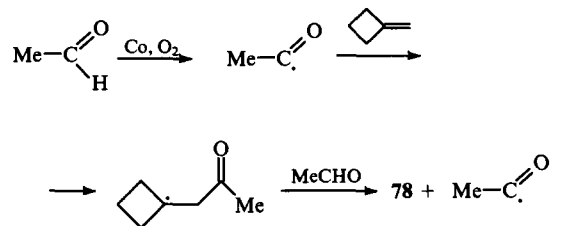
b. Free-radical acylation

Only one example of the free-radical acylation of MCB is known. It is the reaction of MCB with acetaldehyde (with an AcH : MCB molar ratio of 10:1) initiated by atmospheric oxygen (at an air flow rate of $40\ h^{-1}$) in the presence of a catalytic amount of $Co(OAc)_2$ ($1.5 \times 10^{-3}\ mol\ l^{-1}$).²²⁸ Apart from the ketone **78**, acetic acid is also formed.



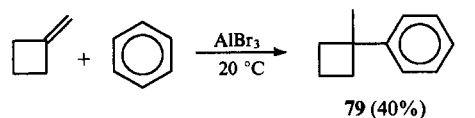
Reaction (9) proceeds by a chain mechanism²²⁹ involving the formation of acyl radicals, their addition to the double bond of MCB, and chain transfer by the intermediate radical adducts:

Scheme 7

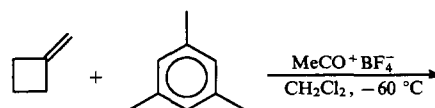


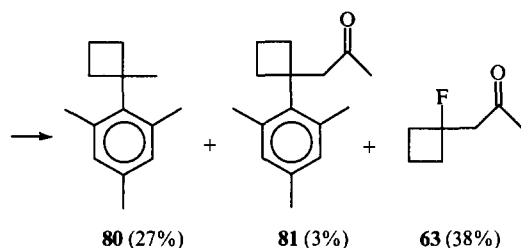
3. Arylation

Only a few examples of the arylation of the MCB double bond are known. For example, in the presence of $AlBr_3$, MCB reacts with benzene, yielding 1-methyl-1-phenylcyclobutane **79**:^{211, 230}



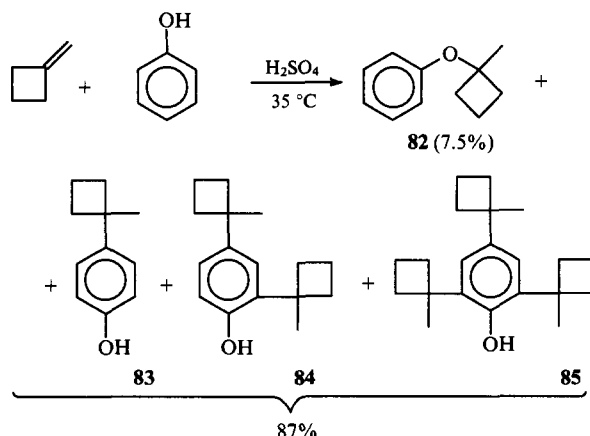
The reaction of MCB with mesitylene in the presence of $MeCO^+BF_4^-$ affords a mixture of arylation (**80**), acylation (**63**), and coupled addition (**81**) products.²³¹





If this reaction is carried out in the presence of BF_3 , the yield of compound **80** is only 5%, and in this case extensive polymerisation of MCB is observed.²³¹

The reaction of MCB with phenol yields mostly a mixture of mono-, di-, and tri(1-methylcyclobutyl)phenols **83–85** and a small amount of the ether **82**.²³²



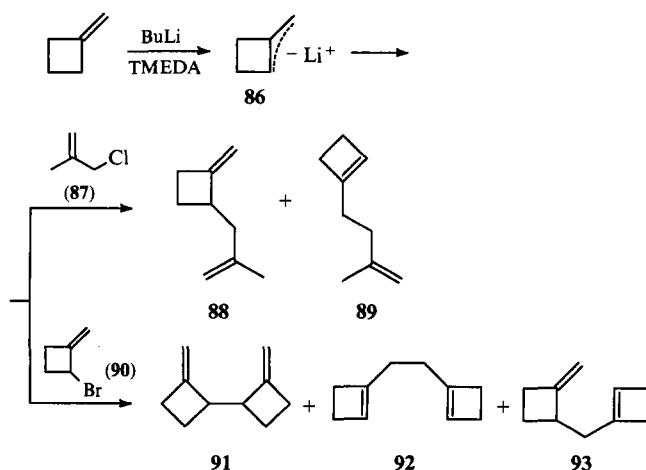
Depending on the reaction conditions, arylation may afford a mono- or disubstituted phenol as the major product (yield 30%–40%).¹⁵⁷

The reactions of MCB and other methylenecycloalkanes with (*p*-anisyl)phenylcarbenium tetrachloroborate have been studied.²³³

VI. Reactions with retention of the C = C bond

1. Allylic alkylation, 'ene' reactions

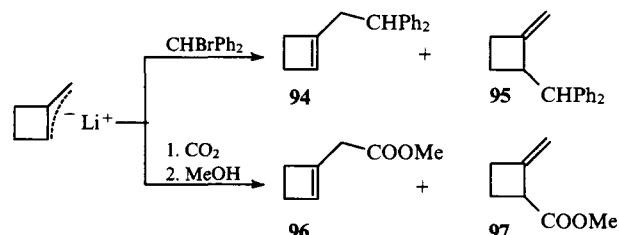
The allylic anion **86** prepared from MCB and butyllithium in tetramethylethylenediamine (TMEDA) reacts with methylallyl chloride **87** to give a mixture of the isomers **88** and **89** usual for allylic systems (**88**:**89** = 85:15, overall yield 90%).²³⁴



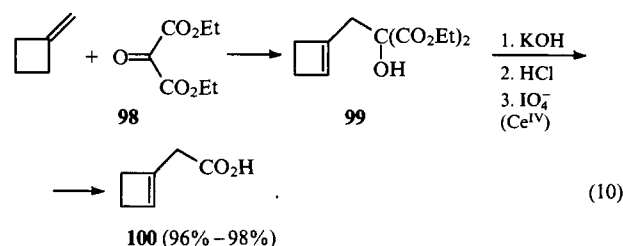
The alkylation of the allylic anion **86** with 2-bromo(methylenecyclobutane) **90** affords a more complex mixture of products,

since in this case not only the anion **86**, but also the bromide **90** are capable of reacting at two centres. The product ratios are **91**:**92**:**93** = 22:46:32, with an overall yield of 85%.

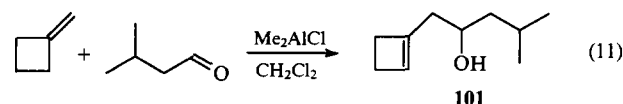
The alkylation of the anion **86** with diphenylmethyl bromide gave compounds **94** and **95** (in a 1:1 ratio) in an unexpectedly low yield (17%).²³⁵ The carboxylation of this anion with carbon dioxide proceeds with an equally low yield.²³⁶



Carbonyl compounds can also be used as the electrophilic component in the alkylation of MCB.^{236–240} Thus, Snider et al.²³⁸ have suggested a method of preparing cyclobutenylmethyl-(hydroxy)malonate from MCB and diethyl oxomalonate **98**. The reaction occurs without a solvent at 80 °C over a period of 170 h. The yield of the alkylation product **99** is 63%. Its hydrolysis followed by oxidation affords 1-cyclobutenylacetic acid **100**.²³⁹

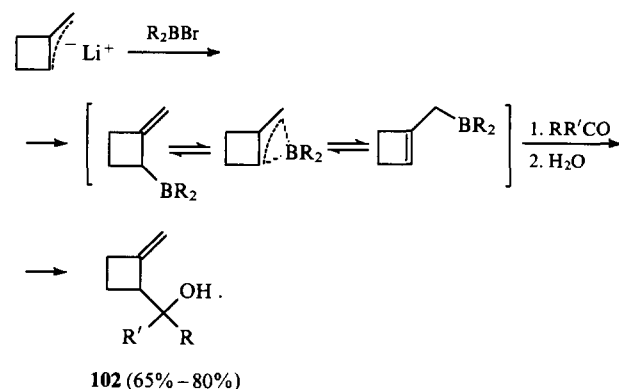


A similar reaction with isovaleraldehyde leads to the alcohol **101** in 43% yield.²³⁸



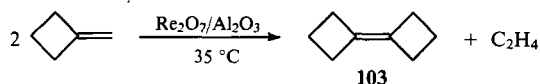
It is noteworthy that the 'ene' reactions (10) and (11) are highly regioselective: in both cases, the addition involves exclusively the *exo*-methylene group of the allylic anion.

The selective alkylation of MCB with ketones (acetone, cyclohexanone, cycloheptanone, or camphor) at the allylic carbon atom of the cyclobutane ring can be carried out by using the novel approach described by Bubnov et al.²⁴¹ A characteristic feature of this approach is that alkylation with an electrophile (in this instance, with a ketone) is preceded by the introduction of a boron-containing group into the allylic anion **86**:



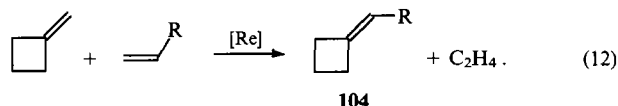
2. Metathesis (disproportionation) and cometathesis

The catalytic disproportionation of MCB in the presence of a heterogeneous rhenium-containing catalyst has been reported in a number of studies carried out mostly in the 1970s.^{242–247}



The yield of bicyclobutylidene **103** in this reaction, carried out in the liquid phase with constant removal of ethene from the reaction zone, reached 70% over a period of 4 h. The disproportionation of MCB can also be carried out in the gaseous phase over the same catalyst in a flow-type setup at 100 °C. The $\text{WCl}_6\text{--EtAlCl}_2\text{--EtOH}$, $\text{WCl}_6\text{--Bu}^n\text{Li}$, and $\text{MoO}_3/\text{Al}_2\text{O}_3$ systems turned out to be virtually inert in this reaction.

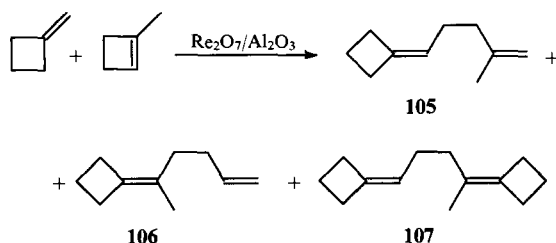
Catalytic processes involving the cometathesis of MCB with other alkenes have also been developed:^{245, 247–249}



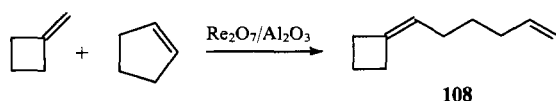
The products of the homometathesis of MCB and $\text{CH}_2=\text{CHR}$ (which are not shown in the scheme) are also formed in reaction (12).

From a mixture of liquid products of the joint disproportionation of MCB and propene in a flow-type setup in the gaseous phase (with $\text{Re}_2\text{O}_7/\text{Al}_2\text{O}_3$ as the catalyst, MCB:propene = 2:1, volume rate of supply of the reactants 500 h^{-1} , 1:1 dilution with nitrogen, 20 °C), ethylenecyclobutane **104** ($\text{R} = \text{Me}$) was isolated in 20% yield.²⁴⁵

The cometathesis of MCB with 1-methylcyclobutene affords a mixture of three diene hydrocarbons (**105–107**), the yield of each depending on the reaction conditions (with $\text{Re}_2\text{O}_7/\text{Al}_2\text{O}_3$ modified by SnBu_4 as the catalyst and benzene as the solvent).²⁴⁸



The cometathesis of MCB and cyclopentene (CP) was carried out at low initial concentrations of the latter (MCB:CP = 9:1) in order to exclude the possibility of its polymerisation, and at temperatures between –65 and 35 °C. At 35 °C, with a CP:catalyst ratio of 10:1 by weight, and for a contact time of 1 h, the reaction gave 6-cyclobutylidenehex-1-ene **108** as the only cometathesis product (the degree of conversion of cyclopentene was 90%).²⁴⁹

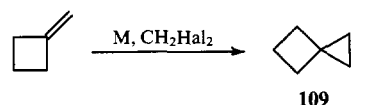


VII. Cycloaddition

1. [2 + 1]-Cycloaddition

The interaction of MCB with dihalomethanes in the presence of metals such as Zn, Cd, or Cu with a CH_2Hal_2 :metal molar ratio of 1:2 in a polar solvent (DMF, dimethylacetamide,

acetonitrile, *N*-methylpyrrolidone, HMPA, formamide) results in the formation of spirohexane **109**.²⁵⁰

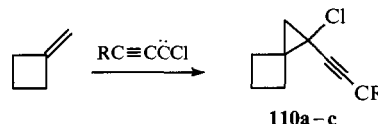


$\text{M} = \text{Zn, Cd, Cu}$.

Spirohexane **109** (yield 48%) has also been obtained by the cyclopropanation of MCB with diazomethane in ether at –10 °C in the presence of palladium acetylacetonate as the catalyst (1 mol% with respect to MCB).²⁵¹

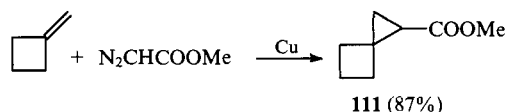
Dichlorocarbene adds to MCB to give 1,1-dichlorospiro[2.3]hexane.²⁵²

Alkynylhalocarbenes also add to MCB, yielding the corresponding substituted spirohexanes **110**.²⁵³

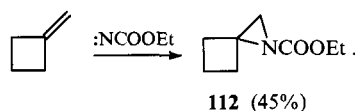


$\text{R} = \text{Me, Pr}^n, \text{Pr}^i$.

The cyclopropanation of MCB with methyl diazoacetate, catalysed by $\text{Cu}(\text{acac})_2$ in CH_2Cl_2 , is a convenient method for preparing esters of spirohexanecarboxylic acid **111**.²⁵⁴

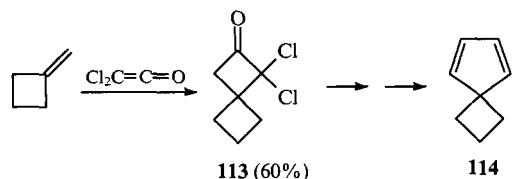


The addition of singlet ethoxycarbonylnitrene to MCB has been described.²⁵⁵ This reaction gives the azaspirane **112** in a moderate yield:

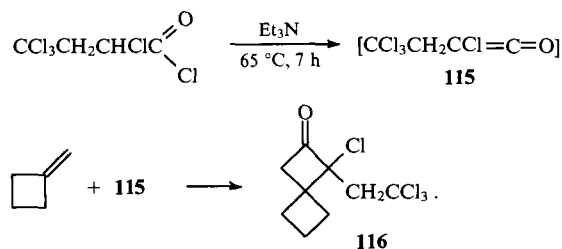


2. [2 + 2]-Cycloaddition

The cycloaddition to MCB of dichloroketene, generated in situ from dichloroacetyl chloride, yielded the adduct **113**.²⁵⁶ This ketone has been used in the synthesis of spiro[3.4]octa-5,7-diene **114**.²⁵⁷

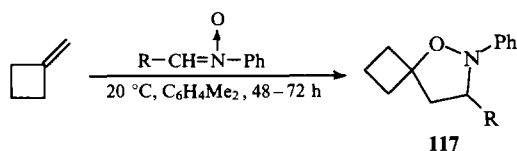


The interaction of MCB with tetrachlorobutanoyl chloride in the presence of Et_3N proceeds in a similar way:²⁵⁸



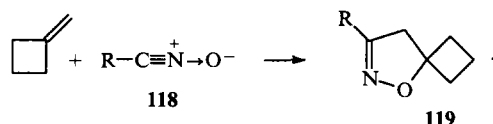
3. [2 + 3]-Cycloaddition

A convenient way of synthesising spirane isoxazolidines **117** incorporating a cyclobutane ring in yields of 70% or more is based on the 1,3-dipolar cycloaddition of *N,C*-disubstituted nitrones to MCB.^{259, 260}

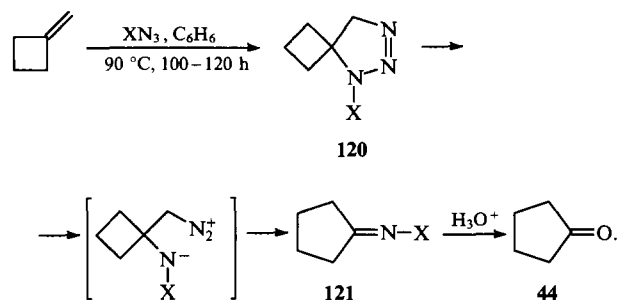


R = Ph, PhCO, PhNHCO, XC₆H₄NHCO (X = Br, Me, Ac, EtO).

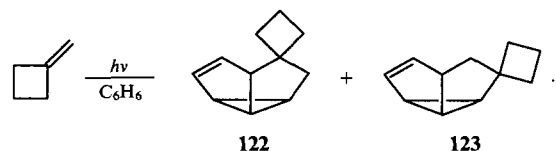
The cycloaddition of the *N*-oxides **118** to MCB is a convenient single-stage method for the synthesis of spiro(4,5-dihydroisoxazole-5,1-cyclobutanes) **119**.^{261–263}



p-Nitrobenzenesulfonyl azide reacts with MCB via a 1,3-dipolar cycloaddition mechanism to give the triazoline intermediate **120**, which undergoes rapid rearrangement with ring expansion, affording the sulfonimide **121**. The latter is hydrolysed to give cyclopentanone:²⁶⁴

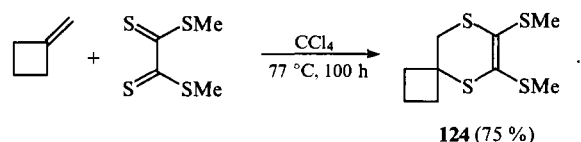


An unusual cycloaddition has been observed on irradiating MCB in benzene; equal amounts of the cyclic adducts **122** and **123** (overall yield 5%) were obtained:²⁶⁵

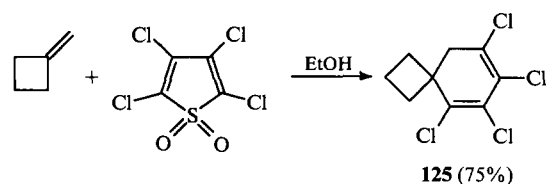


4. [2 + 4]-Cycloaddition

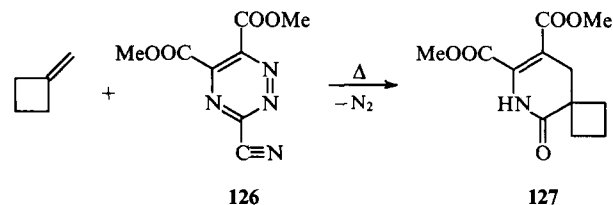
The interaction of MCB with dimethyl tetrathiooxalate occurs similarly to the Diels–Alder reaction in which MCB acts as the dienophile:²⁶⁶



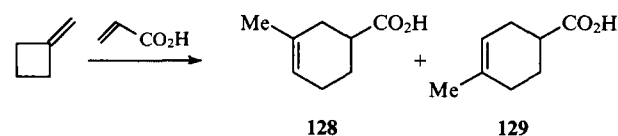
An unusual example of the formation of the cyclic adduct **125** from MCB and tetrachlorothiophene dioxide has been described by Raasch.²⁶⁷



The triazine **126** reacts with MCB in a similar way (with the cleavage of the heterocyclic ring and liberation of nitrogen).²⁶⁸

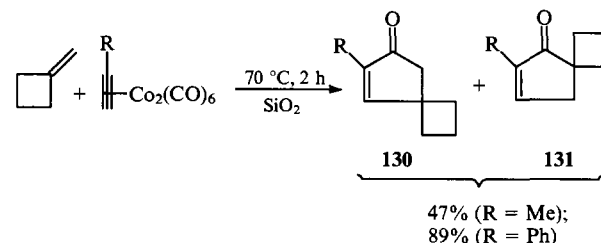


Methylenecyclobutane can enter into the Diels–Alder reaction, acting as the diene.¹⁶⁴



5. [2 + 2 + 1]-Cycloaddition

The cycloaddition to MCB of alkynes bound into a complex with cobalt carbonyl (one of the coordinated CO molecules participates in the reaction) yields a mixture of the spiroketones **130** and **131** in a ratio of 1 : 1.^{269, 270}



VIII. Reactions with ring opening

The opening of the MCB ring has been observed in its reactions with hydroxyl or methyl radicals.^{271, 272}

The thermal decomposition of MCB has been studied.^{273–276} The Arrhenius parameters of this process were determined in the same investigations.

The photolysis of MCB leads to equimolar amounts of ethene and allene.^{277, 278} Vacuum UV photolysis (Xe 147.0 nm and Kr 123.6 nm) occurs less selectively.^{279, 280} Among the photolysis products, H₂, C₂H₂, C₂H₄, allene, methylethyne, vinylthyne, and buta-1,3-diene were detected.

The rearrangements of MCB accompanied by its decomposition have been discussed in a review.²⁸¹

IX. Polymerisation

The possibilities of using MCB for preparing polymers and copolymers have been examined.

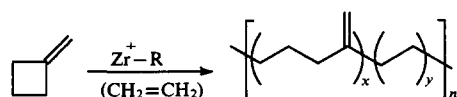
Methylenecyclobutane and some of its derivatives (3-CN, 3-COOH, 3-Me-3-COOH, 3-Ph) do not polymerise in the

presence of radical initiators,^{282, 283} $\text{BF}_3 \cdot \text{Et}_2\text{O}$, or BuLi , but they form copolymers with acrylonitrile, styrene, or methyl methacrylate.²⁸²

The polymerisation of MCB on treatment with Lewis acids (AlCl_3 , TiCl_4 , SnCl_4 , or BF_3) results in a low-molecular-mass polymer (average molecular mass < 2000) having a regular structure with cyclobutane side groups.²⁸⁴

In the presence of Ziegler–Natta catalysts [AlEt_3 – $\text{Ti}(\text{OPr})_4$ or AlEt_3 – TiCl_4 – PPh_3], poly(methylenecyclobutane) is formed, the ozonisation of which yields a linear polyketone.²⁸⁵ When other catalysts were employed, polymerisation occurred with complete or partial opening of the cyclobutane rings.^{286–288}

The regioselective polymerisation of MCB and its regioselective copolymerisation with ethene occur on treatment with $[(1,2\text{-Me}_2\text{C}_5\text{H}_3)_2\text{ZrMe}]^+[\text{MeB}(\text{C}_6\text{F}_5)_3]^-$ ^{289, 290} to yield a linear polymer or copolymer 132 with methylene side groups.



132

The influence of MCB on the polymerisation of isoprene in the presence of the Ziegler–Natta catalyst $\text{Al}(\text{Bu}^i)_3$ – TiCl_4 has been studied by Sire et al.²⁹¹ It was found that an admixture of MCB in the monomer has no effect on the properties of the polymer, but substantially retards the polymerisation.

References

- V P Safronov, V P Vasil'eva *Neftekhimiya* **15** 77 (1975)
- V N Vostrikova, T P Moiseeva, A A Grigor'ev, S P Chernykh, V A Sedlyarov, V I Zavorotov *Promst Sintet. Kauchuka* **11** (1979)
- G G Gustavson *Izv. Imperator. Akad. Nauk* **5** 237 (1896)
- G G Gustavson *J. Prakt. Chem.* **54** (2) 97 (1896)
- K V Vatsuro, G L Mishchenko *Imennye Reaktsii v Organicheskoi Khimii* (Named Reactions in Organic Chemistry) (Moscow: Khimiya, 1976)
- O Filipov *Zh. Russ. Fiz.-Khim. O-va* **46** 1141 (1914)
- O Filipov *J. Prakt. Chem.* **93** 162 (1916)
- S F Marrian *Chem. Rev.* **43** 149 (1948)
- C K Ingold *J. Chem. Soc.* **123** 1706 (1923)
- M J Murray, E H Stevenson *J. Am. Chem. Soc.* **66** 812 (1944)
- V A Slabey *J. Am. Chem. Soc.* **68** 1335 (1946)
- D E Applequist, L F Fanta, B W Henrikson *J. Org. Chem.* **23** 1715 (1958)
- Ya M Slobodin, I N Shokhor *Zh. Obshch. Khim.* **18** 1145 (1948)
- Ya M Slobodin, I N Shokhor *Zh. Obshch. Khim.* **21** 2005 (1951)
- Ya M Slobodin, I N Shokhor *Zh. Obshch. Khim.* **23** 42 (1953)
- Ya M Slobodin, I N Shokhor, in *Sb. Statei po Obshchei Khimii* (Collection of Articles on General Chemistry) (Moscow: Izd. Akad. Nauk SSSR, 1953) Vol. 2, p. 846
- A I D'yachenko, E L Protasova, A I Ioffe, A Ya Shteinshneider, O M Nefedov *Tetrahedron Lett.* **20** 2055 (1979)
- A I D'yachenko, E L Protasova, O M Nefedov *Izv. Akad. Nauk SSSR, Ser. Khim.* **1166** (1979)
- A I D'yachenko, A I Ioffe, E L Protasova, O M Nefedov *Izv. Akad. Nauk SSSR, Ser. Khim.* **1419** (1979)
- A I D'yachenko, E L Protasova, A I Ioffe, O M Nefedov *Dokl. Akad. Nauk. SSSR* **250** 108 (1980)
- J D Roberts, C W Sauer *J. Am. Chem. Soc.* **71** 3925 (1949)
- A I D'yachenko, M Yu Lukina *Izv. Akad. Nauk SSSR, Ser. Khim.* **2237** (1966)
- J M Derfer, K W Greenlee, C E Boord *J. Am. Chem. Soc.* **71** 175 (1949)
- J M Derfer, ThD, Ohio State University, USA, 1946
- P Ries, R W Taft Jr, R H Boyd *J. Am. Chem. Soc.* **79** 3724 (1957)
- J M Conia, J Gore C. R. *Hebd. Seances Acad. Sci.* **254** 3552 (1962)
- J M Conia, J Gore C. R. *Hebd. Seances Acad. Sci.* **254** 3708 (1962)
- L Fitjer, U Quabeck *Synthesis* **299** (1987)
- M C Flowers, H M Frey *J. Chem. Soc.* **5550** (1961)
- G R De Mare, L G Walker, O P Strausz, H E Gunning *Can. J. Chem.* **44** 457 (1966)
- R Fajgar, J Pola *J. Org. Chem.* **58** 7709 (1993)
- R K Belati, S Iglewski *Magy. Asvanyolaj Foldgaz Kiserl. Intez. Kozl.* **29** (1971)
- V E Shefter, L M Aleksandrova, S A Taranenko, S L Skop, A S Rabinovich, G V Syssoeva, O E Batalin *Zh. Anal. Khim.* **43** 700 (1988)
- V A Gil'mutdinova, E I Khrapkova, E M Sire, T M Lesteva *Zh. Prikl. Khim.* **45** 907 (1972)
- V A Gil'mutdinova, E I Khrapkova, T M Lesteva, E M Sire *Zh. Prikl. Khim.* **45** 1138 (1972)
- L S Budantseva, T M Lesteva, M S Nemtsov *Zh. Fiz. Khim.* **49** 1847 (1975)
- L S Budantseva, V A Gil'mutdinova, T M Lesteva, E I Khrapkova, V I Chernaya *Zh. Prikl. Khim.* **48** 2769 (1975)
- A M Krapivin, E Sh Finkel'shtein, V M Vdovin *Izv. Akad. Nauk SSSR, Ser. Khim.* **2697** (1986)
- A M Orendt, J C Facelli, A J Beeler, K Reuter, W J Horton, P W Cutts, D M Grant, J Michl *J. Am. Chem. Soc.* **110** 3386 (1988)
- R Huebers, M Klessinger *Magn. Reson. Chem.* **24** 1016 (1986)
- M Stoecker, M Klessinger, K Wilhelm *Org. Magn. Reson.* **17** 15 (1981)
- M Klessinger, H Van Megen, K Wilhelm *Chem. Ber.* **115** 50 (1982)
- L Knothe, J Werp, H Babsch, H Prinzbach, H Fritz *Liebigs Ann. Chem.* **709** (1977)
- S H Grover, J B Stothers *Can. J. Chem.* **53** 589 (1975)
- G J Abruscato, P D Ellis, T T Tidwell *J. Chem. Soc., Chem. Commun.* **988** (1972)
- H Guenther, W Herrig *Chem. Ber.* **106** 3938 (1973)
- K C Cole, D F R Gilson *Can. J. Chem.* **54** 657 (1976)
- B Lemarie, R Lozach, B Brailion *J. Chim. Phys. Phys.-Chim. Biol.* **72** 1253 (1975)
- K B Wiberg, B J Nist *J. Am. Chem. Soc.* **83** 1226 (1961)
- A Skancke, P N Skancke, M Eckert-Maksic, Z B Maksic *J. Mol. Struct.* **150** 259 (1987)
- A Stoyer-Hansen, E N Svendsen *Spectrochim. Acta, Part A* **36** 359 (1980)
- T B Malloy Jr, F Fisher, R M Hedges *J. Chem. Phys.* **52** 5325 (1970)
- W J Engelbrecht, J M De Vries *J. South Afr. Chem. Inst.* **23** 191 (1970)
- G Chiurdoglu, Th Doehaerd, M Duts *Bull. Soc. Chim. Belg.* **70** 642 (1962)
- B B Loeffler, E Eberlin, L W Pickett *J. Chem. Phys.* **28** 345 (1958)
- G Bieri, F Burger, E Heilbronner, J P Maier *Helv. Chim. Acta* **60** 2213 (1977)
- D A Demeo, A J Yenchu *J. Chem. Phys.* **53** 4536 (1970)
- L L Combs, M Hollman *J. Mol. Struct.* **33** 289 (1976)
- C Dass, D A Peake, M L Gross *Org. Mass. Spectrom.* **21** 741 (1986)
- W Wagner-Redeker, K Levsen, H Schwarz, W Zumack *Org. Mass Spectrom.* **16** 361 (1981)
- C Dass, T M Sack, M L Gross *J. Am. Chem. Soc.* **106** 5780 (1984)
- J L Holmes, J K Terlouw, P C Burgers, R T B Rye *Org. Mass Spectrom.* **15** 149 (1980)
- J P Puttemans, J C Delvaux *Ing. Chim. (Brussels)* **55** (267–8) 7 (1973)
- F L Mohler, E G Bloom, L Williamson, C E Wise, E J Wells Jr *J. Res. Natl. Bur. Stand.* **43** 533 (1949)
- L H Scharpen, V W Laurie *J. Chem. Phys.* **49** 3041 (1968)
- Y S Huang, ThD, 1969; *Diss. Abstr. Int.* **B 30** 4583 (1970)
- M E Charro, J C Lopez, J L Alonso, G Wlodarczak, J Domaison *J. Mol. Spectrosc.* **162** 67 (1993)
- J R Durig, A C Shing, L A Carreira, L A Li *J. Chem. Phys.* **57** 4398 (1972)
- J Goubeau, I Sander *Chem. Ber.* **82** 176 (1949)
- G Chiurdoglu, J Lanne, M Poelmans *Bull. Soc. Chim. Belg.* **65** 257 (1956)
- B V Lebedev, L Ya Tsvetkova, I B Rabinovich, E Sh Finkel'shtein, B S Strel'chik *Termodin. Org. Soedin.* **7** 3 (1978)

72. B V Lebedev, L Ya Tsvetkova, I B Rabinovich *J. Chem. Thermodyn.* **10** 809 (1978)
73. H L Finke, J F Messerly, S H Lee-Bechtold *J. Chem. Thermodyn.* **13** 345 (1981)
74. A G Osborn, D W Scott *J. Chem. Thermodyn.* **12** 429 (1980)
75. W D Good, R T Moore, A G Osborn, D R Douslin *J. Chem. Thermodyn.* **6** 303 (1974)
76. E S Domalski, E D Hearing *J. Phys. Chem., Ref. Data* **19** 881 (1990)
77. S H Bauer, J Y Beach *J. Am. Chem. Soc.* **64** 1142 (1942)
78. F F Cleveland *J. Chem. Phys.* **15** 742 (1947)
79. F F Cleveland *J. Chem. Phys.* **16** 158 (1948)
80. M Eckert-Maksic, Z B Maksic, A Skancke, P N Skancke *Modelling of Structures and Properties of Molecules* (Ed. Z B Maksic) (Chichester, UK: Wiley, 1987)
81. Z B Maksic, M Eckert-Maksic *THEOCHEM* **8** 295 (1983)
82. J Pancir *Collect. Czech. Chem. Commun.* **45** 2452 (1980)
83. V L Lebedev, A A Bagatur'yants, A M Taber, I V Kalechits *Zh. Fiz. Khim.* **52** 1108 (1978)
84. F Baltagi, A Bander, H H Guenthard *J. Mol. Struct.* **62** 275 (1980)
85. N L Allinger, Y Yuh, J T Sprague *J. Comput. Chem.* **1** 30 (1980)
86. W R Roth, O Adamczak, R Breuckmann, H W Lennartz, R Boese *Chem. Ber.* **124** 2499 (1991)
87. H Guo, S R Kass *J. Am. Chem. Soc.* **114** 1244 (1992)
88. V L Lebedev, A A Bagatur'yants, A M Taber, I V Kalechits *Kvantovaya Khim.* **11** (1975)
89. K B Wiberg, G B Ellison, J J Wendoloski, W E Pratt, M D Harmony *J. Am. Chem. Soc.* **100** 7837 (1978)
90. M Eckert-Maksic, A Skancke, P N Skancke *J. Phys. Chem.* **91** 2786 (1987)
91. N L Allinger, V S Mastryukov *Zh. Strukt. Khim.* **24** 172 (1983)
92. K Shimuzi, K Miyamichi, H Kato, T Yonezawa *Nippon Kagaku Zasshi* **91** 206 (1970)
93. H J Koehler, M Scholz *J. Prakt. Chem.* **312** 165 (1970)
94. K Kovacevich, Z B Maksic *J. Org. Chem.* **39** 539 (1974)
95. W W Schoeller *Chem. Ber.* **108** 1285 (1975)
96. L L Combs, M Rossie Jr *J. Mol. Struct.* **32** 1 (1976)
97. E Sh Finkel'shtein, A I Mikaya, V M Vdovin, N S Nametkin *Neftekhimiya* **16** 539 (1976)
98. R L Rosas, C Cooper, J Laane *J. Phys. Chem.* **94** 1830 (1990)
99. O V Dorofeeva, T Jonvik, V S Mastryukov *The Ninth Austin Symposium on Molecular Structure*, Austin, TX, USA, 1982
100. Q Shen, O V Dorofeeva, V S Mastryukov, A Almenningen *J. Mol. Struct.* **246** 237 (1991)
101. J Laane *Pure Appl. Chem.* **59** 1307 (1987)
102. A C Legon *Chem. Rev.* **80** 231 (1980)
103. J J Gajewski *J. Am. Chem. Soc.* **98** 5254 (1976)
104. H E O Neal, S W Benson *J. Phys. Chem.* **72** 1866 (1969)
105. W W Schoeller *J. Am. Chem. Soc.* **99** 5919 (1977)
106. K B Wiberg, D J Wasserman, E J Martin, M A Murcko *J. Am. Chem. Soc.* **107** 6019 (1985)
107. R B Turner, P Goebel, B J Mallon, W von E Doering, J F Coburn Jr, M Pomeranz *J. Am. Chem. Soc.* **90** 4315 (1968)
108. J W Hightower, K W Hall *Trans. Faraday Soc.* **66** 477 (1970)
109. J Shabtai, E Gil-Av *J. Org. Chem.* **28** 2893 (1963)
110. M N Doyarenko *Zh. Russ. Fiz.-Khim. O-va* **58** 29 (1926)
111. Kh I Areshidze, Ya T Eidus, A L Lapidus, A V Dolidze *Dokl. Akad. Nauk. SSSR* **198** 90 (1971)
112. Ya T Eidus, Kh I Areshidze, A L Lapidus, A V Dolidze *Soobshch. Akad. Nauk Gruz. SSR* **63** 81 (1971)
113. W Shubert, S M Leahy Jr *J. Am. Chem. Soc.* **79** 381 (1957)
114. K B Wiberg, S Hao *J. Org. Chem.* **56** 5108 (1991)
115. E Gil-Av, J Herling *Tetrahedron Lett.* **2** 27 (1961)
116. E Gil-Av, J Shabtai *J. Org. Chem.* **29** 257 (1964)
117. J Herling, J Shabtai, E Gil-Av *J. Am. Chem. Soc.* **87** 4107 (1965)
118. M Lajunen, M Himottu *Acta Chem. Scand., Ser. A* **41** 252 (1987)
119. A Schriesheim, R J Muller, C A Rowe Jr *J. Am. Chem. Soc.* **84** 3164 (1962)
120. Yu I Ranneva, G A Kudryavtseva, A V Dolidze, A I Shatenshtein *Zh. Obshch. Khim.* **44** 671 (1974)
121. O E Batalin, G S Idlis, A Yu Vilyatser, A V Zinenkov, T M Morzhakova, L V Fedulova, V E Shefter, *Zh. Prikl. Khim.* **59** 1825 (1986)
122. O E Batalin, A Yu Vilyatser, A V Zinenkov, G S Idlis, T M Morzhakova, L V Fedulova *Zh. Prikl. Khim.* **61** 1934 (1988)
123. R Grigg, G J Reimer, A R Wade *J. Chem. Soc., Perkin Trans. 1* 1929 (1983)
124. N S Nametkin, V M Vdovin, E Sh Finkel'shtein, A M Popov, A Yu Kozhevnik *Dokl. Akad. Nauk SSSR* **211** 1131 (1973)
125. N S Nametkin, V M Vdovin, E Sh Finkel'shtein, A M Popov, A Yu Kozhevnik *Dokl. Akad. Nauk SSSR* **209** 115 (1973)
126. M A Muhs, F T Weiss *J. Am. Chem. Soc.* **84** 4697 (1962)
127. E Gil-Av, J Herling *J. Chem. Phys.* **66** 1208 (1962)
128. J Shabtai, J Herling, E Gil-Av *J. Chromatogr.* **11** 32 (1963)
129. R Rossi, P Diversi, L Porri *J. Organomet. Chem.* **47** C21 (1973)
130. V Schurig *Inorg. Chem.* **25** 945 (1986)
131. H Lehmkuhl, C Naydowsky, F Danowski, M Bellenbaum, R Benn, A Rufinska, G Schroth, R Mynott, S Pasinkewicz *Chem. Ber.* **117** 3231 (1984)
132. A S Batsanov, V G Andrianov, Yu T Struchkov, A A Koridze, O A Kizas, N E Kolobova *J. Organomet. Chem.* **329** 401 (1987)
133. H Lehmkuhl, S Fustero *Liebigs Ann. Chem.* **1361** (1980)
134. H Lehmkuhl, A Rufiriska, R Beun, G Schroth, R Mynott *Liebigs Ann. Chem.* **317** (1981)
135. Ch Ho Jun *Bull. Korean Chem. Soc.* **10** 404 (1989)
136. R C Larock, S Varaprath *J. Org. Chem.* **49** 3432 (1984)
137. H-U Siehl *J. Am. Chem. Soc.* **107** 3390 (1985)
138. G K S Prakash, M Arvanaghi, G A Olah *J. Am. Chem. Soc.* **107** 6017 (1985)
139. R E Davis, A S N Murthy, A Ohno *Tetrahedron Lett.* **9** 1595 (1968)
140. G A Olah, R J Spear, P C Hiberty, W J Herhe *J. Am. Chem. Soc.* **98** 7470 (1976)
141. B A Levi, E S Bluzock, W J Hehre, *J. Am. Chem. Soc.* **101** 5537 (1979)
142. R Ta-Shma, Z Rappoport *J. Am. Chem. Soc.* **105** 6082 (1983)
143. H Mayr, R Pock *Chem. Ber.* **119** 2473 (1986)
144. S R Wilson, L R Phillips, K J Natalie *J. Am. Chem. Soc.* **101** 3340 (1979)
145. V P J Marti, V Paul, B P Roberts *J. Chem. Soc., Perkin Trans. 2* 181 (1986)
146. L Lunazzi, G Placucci, L Grossi *J. Chem. Soc., Perkin Trans. 2* 1761 (1980)
147. L Lunazzi, G Placucci, L Grossi *J. Chem. Soc., Perkin Trans. 2* 703 (1981)
148. L Lunazzi, G Placucci, L Grossi *J. Chem. Soc., Perkin Trans. 2* 1063 (1980)
149. T Miyashi, Y Takahashi, M Kamata, K Yokogawa, H Ohaku, T Mukai *Stud. Org. Chem. (Amsterdam)* **31** 363 (1987); *Chem. Abstr.* **108** 111 537y (1988)
150. K Ushida, T Shida, J C Walton *J. Am. Chem. Soc.* **108** 2805 (1986)
151. USSR P. 666 161; *Byull. Izobret.* (21) 78 (1979)
152. S P Chernykh, L P Putilina, E S Belyaeva, L A Ivanov *Khim. Promst (Moscow)* **148** (1983)
153. S P Chernykh, G V Bakulina, G N Dudnik, L A Ivanov, B P Krymov *Khim. Promst (Moscow)* **716** (1987)
154. I I Moiseev, Ya K Syrkin *Dokl. Akad. Nauk SSSR* **115** 541 (1957)
155. R W Taft *US Dept. Com., Office Tech. Serv. PB Rept.* **1** 520 72 1 (1960)
156. R W Taft *US Dept. Com., Office Tech. Serv. PB Rept.* **15** 207 261 (1960)
157. E Sh Finkel'shtein, M G Eremeshvili, M S Yatsenko, E B Portnykh, V M Vdovin *Neftekhimiya* **25** 48 (1985)
158. Fr. P. 2 526 018; *Chem. Abstr.* **100** 174 330f (1984)
159. Eur. P. 38 271; *Chem. Abstr.* **96** 103 987p (1982)
160. Eur. P. 186 173 (1986)
161. P Brown, S H Calvert, P C A Chapman, S C Cosham, J A Eglinton, R L Elliott, M A Harris, J D Hinks, J Lauther, D J Merrikin, M J Pearson, R J Ponsford, J V Syms *J. Chem. Soc., Perkin Trans. 1* 881 (1991)
162. J G Traynham, O S Pascual *J. Am. Chem. Soc.* **79** 2341 (1957)
163. J G Traynham, O S Pascual *Tetrahedron* **7** 165 (1959)
164. K Alder, H A Dormann *Chem. Ber.* **85** 556 (1952)
165. E F Cox, M C Caserio, M S Silver, J D Roberts *J. Am. Chem. Soc.* **83** 2719 (1961)
166. J C Traynham, O S Pascual *J. Org. Chem.* **21** 1362 (1956)
167. A E Favorskii, V Batalin *Zh. Russ. Fiz.-Khim. O-va* **46** 726 (1914)

168. A Favorsky, V Batalin *Chem. Ber.* **47** 1648 (1914)
169. C E Fry *J. Am. Chem. Soc.* **76** 3222 (1954)
170. K Heyns, K Molge, W Walter *Chem. Ber.* **94** 1015 (1961)
171. R Hittich, H Mach, K Griesbaum *Chem. Ber.* **116** 2738 (1983)
172. A A Borisenko, A V Nikulin, S Wolfe, N S Zefirov, N V Zyk *J. Am. Chem. Soc.* **106** 1074 (1984)
173. A V Shastin, T V Popkova, E S Balenkova, V K Bel'skii, E I Lazhko *Zh. Org. Khim.* **23** 2313 (1987)
174. A V Shastin, V K Bel'skii, N A Bondareva, T V Popkova, E S Balenkova *Dokl. Akad. Nauk. SSSR* **302** 1425 (1988)
175. E V Skorobogatova, E Yu Grudinskaya, P S Afanas'ev, V R Kartashov, N S Zefirov, R Keipl *Zh. Org. Khim.* **23** 2052 (1987)
176. A M Magerramov, L M Gyl'akhmedov, N K Sadovaya, V V Zhdankin, A S Koz'min *Zh. Org. Khim.* **26** 2333 (1990)
177. Pak-Tsun Ho, R J Kolt *Can. J. Chem.* **60** 663 (1982)
178. Yu V Migalina, S V Galla-Bobik, V I Staninets *Zh. Org. Khim.* **18** 2609 (1982)
179. N N Magdesieva, M F Gordeev *Zh. Org. Khim.* **23** 949 (1987)
180. N N Magdesieva, M F Gordeev *Zh. Org. Khim.* **20** 2480 (1984)
181. R M Schonk, C W Meijer, B H Bakker, S Zoellner, H Gerfontain, A de Meijere *Recl. Trav. Chim. Pays-Bas* **112** 457 (1993)
182. N V Zyk, E A Mendeleeva, A V Breev, E E Nesterov, N S Zefirov *Zh. Org. Khim.* **28** 1414 (1992)
183. G C Bond, J Newham *Trans. Faraday Soc.* **56** 1851 (1960)
184. C Zimmerman, K Hayek *Stud. Surf. Sci. Catal.* **75** 2375 (1993)
185. BRD P. 3 920 917 (1991)
186. M Korach, D R Nielson, W H Rideout *J. Am. Chem. Soc.* **82** 4328 (1960)
187. L I Kas'yan, M F Seferova, L G Gorb, M P Kozina, V G Dryuk *Zh. Org. Khim.* **25** 1131 (1989)
188. A Endo, M Saito, Y Okada, Y Fushizaki *Nippon Kagaku Zasshi* **86** 108 (1965)
189. R C Ewins, H B Henbest, M A McKervey *J. Chem. Soc., Chem. Commun.* 1085 (1967)
190. J J Havel *J. Org. Chem.* **43** 762 (1978)
191. E Sh Finkel'shtein, A I Mikaya, V G Zaikin, V M Vdovin *Neftekhimiya* **20** 75 (1980)
192. H Vorbrüggen, C Djerassi *Tetrahedron Lett.* **2** 119 (1961)
193. R Criegee, A Kerckow, H Zinke *Chem. Ber.* **88** 1878 (1955)
194. M Hanack, H Eggensperger *Chem. Ber.* **96** 1341 (1963)
195. J M Conia, J Gore *Bull. Soc. Chim. Fr.* 726 (1963)
196. F S Bridson-Jones, C D Buckley, L H Cross, A D Diver *J. Chem. Soc.* 2999 (1951)
197. M-L Leriverend, P Leriverend *Chem. Ber.* **109** 3492 (1976)
198. M D Taylor, L R Grant *J. Am. Chem. Soc.* **77** 1507 (1955)
199. P Boontanonda, R Grigg *J. Chem. Soc., Chem. Commun.* 583 (1977)
200. I E Beck, E V Gusevskaya, A V Golovin, V A Likhonolobov *J. Mol. Catal.* **83** 301 (1993)
201. J Halpern, J E Byrd, L Cassar, P E Eaton *J. Chem. Soc., D* 40 (1971)
202. P Abley, J E Byrd, J Halpern *J. Am. Chem. Soc.* **95** 2591 (1973)
203. I E Beck, E V Gusevskaya, A V Golovin, V A Likhonolobov *J. Mol. Catal.* **83** 287 (1993)
204. B A Cheskis, N M Ivanova, A M Moiseenkov, O M Nefedov *Usp. Khim.* **62** 365 (1993) [*Russ. Chem. Rev.* **62** 337 (1993)]
205. H Miki, M Saito, K Kayano, Y Fushizaki *Kogyo Nippon Kagaku Zasshi* **68** 948 (1965)
206. E A Hill, P A Nylen, J H Fellinger *J. Organomet. Chem.* **239** 279 (1982)
207. E Sh Finkel'shtein, V E Fedorov, M P Filatova *Izv. Akad. Nauk SSSR, Ser. Khim.* 958 (1991)
208. E E Nifant'ev, R K Magdeeva, N P Shchepet'eva *Zh. Obshch. Khim.* **50** 1744 (1980)
209. N S Zefirov, N V Zyk, A A Borisenko, M Yu Krysin, T G Schestakova *Tetrahedron* **39** 3145 (1983)
210. J T Hung, S W Yang, G M Gray, K Lammertsma *J. Org. Chem.* **58** 6786 (1993)
211. E Sh Finkel'shtein, A I Mikaya, E M Sire, V M Vdovin, N S Nametkin *Dokl. Akad. Nauk SSSR* **228** 1123 (1976)
212. J Herscovici, K Muleka, K Antonakis *Tetrahedron Lett.* **25** 5663 (1984)
213. J Herscovici, K Muleka, L Boumaiza, K Antonakis, *J. Chem. Soc., Perkin Trans. 1* 1995 (1990)
214. E Sh Finkel'shtein, M S Yatsenko V M Vdovin *Izv. Akad. Nauk SSSR, Ser. Khim.* 1665 (1982)
215. O E Batalin, A V Zinenkov, G S Idlis, V V Pinson, E V Fedortsova *Zh. Org. Khim.* **24** 2619 (1988)
216. M Yu Lebedev, E S Balenkova *Zh. Org. Khim.* **25** 434 (1989)
217. M Yu Lebedev, E S Balenkova *Zh. Org. Khim.* **27** 1389 (1991)
218. M Yu Lebedev, I N Koryakina, E S Balenkova *Zh. Org. Khim.* **27** 2517 (1991)
219. M Yu Lebedev, E S Balenkova *Zh. Org. Khim.* **23** 960 (1987)
220. S N Anfilogova, E B Frolov, Yu N Luzikov, E S Balenkova *Zh. Org. Khim.* **15** 1432 (1979)
221. A V Shastin, E S Balenkova *Zh. Org. Khim.* **20** 956 (1984)
222. A V Shastin, E S Balenkova *Zh. Org. Khim.* **20** 1357 (1984)
223. S N Anfilogova, E B Frolov, E S Balenkova *Vestn. Mosk. Univ., Ser. 2, Khim.* 611 (1980)
224. I D Gridnev, A V Shastin, E S Balenkova *Zh. Org. Khim.* **23** 1546 (1987)
225. A V Shastin, E S Balenkova, V D Sorokin, A S Koz'min, N S Zefirov *Zh. Org. Khim.* **22** 1156 (1986)
226. H Hamana, T Sugawara *Chem. Lett.* 571 (1985)
227. V G Nenaidenko, E S Balenkova *Zh. Org. Khim.* **28** 600 (1992)
228. M G Vinogradov, G I Nikishin, S P Verenchikov, O N Petrenko, I P Kovalev, V N Pavlychev, V N Masyutin, V S Markevich, G A Stepanova, B S Strel'chik, M L Gringol'ts *Neftekhimiya* **19** 809 (1979)
229. M G Vinogradov, G I Nikishin *Usp. Khim.* **40** 1960 (1971) [*Russ. Chem. Rev.* **40** 916 (1971)]
230. A I Mikaya, A M Vinogradov in *Novye Aspekty Neftekhimicheskogo Sintez* (New Aspects of Petrochemical Synthesis) (Moscow: A V Topchiev Institute of Petrochemical Synthesis, 1978) p. 12
231. A V Shastin, T V Popkova, E S Balenkova *Zh. Org. Khim.* **22** 664 (1986)
232. V M Vdovin, M G Ereishvili, D M Gabriadze, E Sh Finkel'shtein, A Yu Kozhevnik *Soobshch. Akad. Nauk Gruz. SSR* **112** 545 (1983)
233. M Roth, C Schade, H Mayr *J. Org. Chem.* **59** 169 (1994)
234. K J Shea, S Wise *J. Org. Chem.* **43** 2710 (1978)
235. A Maercker, W Berkulin *Chem. Ber.* **123** 185 (1990)
236. M F Salomon, S N Pardo, R G Salomon *J. Am. Chem. Soc.* **102** 2473 (1980)
237. M F Salomon, S N Pardo, R G Salomon *J. Org. Chem.* **49** 2446 (1984)
238. B B Snider, D J Rodini, T C Kirk, R Cordova *J. Am. Chem. Soc.* **104** 555 (1982)
239. M F Salomon, S N Pardo, R G Salomon *J. Am. Chem. Soc.* **106** 3797 (1984)
240. S R Wilson, L R Phillips *Tetrahedron Lett.* **16** 3047 (1975)
241. Yu N Bubnov, M E Gurskii, L I Lavrinovich *Izv. Akad. Nauk SSSR, Ser. Khim.* 1918 (1986)
242. B S Strel'chik, R A Fridman, E Sh Finkel'shtein, V M Vdovin *Izv. Akad. Nauk SSSR, Ser. Khim.* 579 (1976)
243. A M Popov, R A Fridman, E Sh Finkel'shtein, N S Nametkin, V M Vdovin, A N Bashkirov, Yu B Kryukov, L G Liberov *Izv. Akad. Nauk SSSR, Ser. Khim.* 1429 (1973)
244. E Sh Finkel'shtein, B S Strel'chik, V G Zaikin, V M Vdovin *Neftekhimiya* **15** 667 (1975)
245. E Sh Finkel'shtein, B S Strel'chik, E B Portnykh, V M Vdovin, N S Nametkin *Dokl. Akad. Nauk. SSSR* **232** 1322 (1977)
246. B S Strel'chik, A M Popov, in *Issledovanie v Oblasti Neftekhimii* (Studies in Petrochemistry) (Moscow: A V Topchiev Institute of Petrochemical Synthesis, 1976) p. 40
247. B S Strel'chik, E Sh Finkel'shtein, E B Portnykh, M L Gringol'ts, G V Bakulina *Khim. Promst* **63** (1993)
248. E Sh Finkel'shtein, B S Strel'chik, S V Kotov, E B Portnykh *Neftekhimiya* **25** 41 (1985)
249. V M Vdovin, S V Kotov, E B Portnykh, B S Strel'chik, V D Oppengeim *Neftekhimiya* **28** 61 (1988)
250. USSR P. 1 060 606; *Byull. Izobret.* (46) 89 (1983)
251. U M Dzhemilev, V A Dokichev, S Z Sultanov, R I Khushnutdinov, Yu V Tomilov, O M Nefedov, G A Tolstikov *Izv. Akad. Nauk SSSR, Ser. Khim.* 1861 (1989)
252. E V Couch, J A Landgrebe *J. Org. Chem.* **40** 1636 (1975)

253. K N Shavrin, I V Krylova, I E Dolgii, O M Nefedov *Izv. Akad. Nauk, Ser. Khim.* 1128 (1992)
254. M G Vinogradov, L N Kaigorodova, G S Idlis, A S Dykman, A V Zinenkov *Soobshchenie na Simp. "Sovremennye Problemy Khimii Alifaticeskikh Diazosoidinonii"* (Report at the Symposium on Current Problems in the Chemistry of Aliphatic Diazo-Compounds (St.-Petersburg: St.-Petersburg State Univ., 1993)
255. D S Zhuk, V A Chekrygin, L M Timofeeva, N A Kashcheeva, L I Solnyshkina, V D Oppengeim, E V Portnykh, E Sh Finkel'shtein *Dokl. Akad. Nauk SSSR* 316 1136 (1991)
256. P R Brook, J G Griffiths *J. Chem. Soc., D* 1344 (1970)
257. I Erden, E M Sorenson *Tetrahedron Lett.* 24 2731 (1983)
258. US P. 4 242 278 (1980)
259. F M Cordero, A Goti, F De Sarlo, A Guarna, A Brandi *Tetrahedron* 45 5917 (1989)
260. N A Akmanova, Kh F Sagitdinova, A I Popenova, V N Domrachev, E S Balenkova *Khim. Geterotsikl. Soedin.* 316 (1982)
261. A Goti, A Brandi, F De Sarlo, A Guarna *Tetrahedron Lett.* 27 5271 (1986)
262. N Barbulescu, I Sebe *Rev. Chim. (Bucharest)* 25 695 (1974)
263. A Goti, A Brandi, F De Sarlo, A Guarna *Tetrahedron* 48 5283 (1992)
264. S R McManus, M Ortiz, R A Abramovich *J. Org. Chem.* 46 336 (1981)
265. R Srinivasan *Tetrahedron Lett.* 15 2725 (1974)
266. K Hartke, J Quante, T Kampehn *Liebigs Ann. Chem.* 1482 (1980)
267. M S Raasch *J. Org. Chem.* 45 856 (1980)
268. G Seitz, R Dhar, T Kampehn *Arch. Pharm. (Weinheim, Ger.)* 315 697 (1982)
269. V A Smit, V A Tarasov, E D Daeva, I I Ibragimov *Izv. Akad. Nauk SSSR, Ser. Khim.* 2870 (1987)
270. W A Smit, S L Kireev, O M Nefedov, V A Tarasov *Tetrahedron Lett.* 30 4021 (1989)
271. K Takeda, H Yoshida, K Hayashi, S Okamura *Bull. Inst. Chem. Res., Kyoto Univ.* 45 55 (1967)
272. D H Volman *J. Phys. Chem.* 75 714 (1971)
273. W J Engelbrecht, J M De Vries *J. South Afr. Chem. Inst.* 23 163 (1970)
274. W J Engelbrecht, J M De Vries *J. South Afr. Chem. Inst.* 23 172 (1970)
275. J P Chesick *J. Chem. Phys.* 65 2170 (1961)
276. R L Brandaure, B Short, S M E Kellner *J. Chem. Phys.* 65 2269 (1961)
277. R K Brinton *J. Phys. Chem.* 72 321 (1968)
278. G R De Mare, O P Strausz, H E Gunning *Can. J. Chem.* 44 953 (1966)
279. C-K Tu, R D Doepker *J. Photochem.* 1 271 (1973)
280. C-K Tu, ThD, 1972; *Diss. Abstr. Int. B* 33 4159 (1973)
281. J E Baldwin, R H Fleming *Fortschr. Chem.-Forsch.* 15 281 (1970)
282. K Takemoto, M Izubayashi *Makromol. Chem.* 109 81 (1967)
283. Y Hiraguri, T J Eudo *J. Polym. Sci., Polym. Lett.* 26 381 (1988)
284. C Pinazzi, J Brossas *C. R. Hebd. Seances Acad. Sci.* 261 3410 (1965)
285. C P Pinazzi, J Brossas, G Clouet *Makromol. Chem.* 148 81 (1971)
286. R Rossi, P Diversi, L Porri *Macromolecules* 5 247 (1972)
287. C P Pinazzi, J Brossas *Makromol. Chem.* 122 105 (1969)
288. C P Pinazzi, J Brossas *Makromol. Chem.* 147 15 (1971)
289. X Yang, L Jia, T J Marks *J. Am. Chem. Soc.* 115 3392 (1993)
290. US P. 5 300 598; *Chem. Abstr.* 121 206 266s (1994)
291. E M Sire, L M Popkova, S A Nazarova, Z Kh Evdokimova *Sb. Nauch. Tr. Yaroslav. Tekhnol. Inst.* 22 156 (1972)

Synthesis and properties of sultines, cyclic esters of sulfinic acids

O B Bondarenko, L G Saginova, N V Zyk

Contents

I. Introduction	147
II. Methods for synthesising sultines	147
III. Properties of sultines	160

Abstract. Data on the synthesis and chemical properties of sultines, cyclic esters of sulfinic acids, are reviewed. The known methods for synthesising sultines are considered, the reaction mechanisms and stereochemistry of the compounds obtained are discussed. The chemical transformations of sultines, including photolysis, thermolysis, redox reactions, and interaction with nucleophiles, are described. The bibliography includes 109 references.

I. Introduction

Lactones of sulfinic acids, i.e., sultines, were first mentioned as early as the end of the last century.¹ However, the chemical transformations of sultines long remained little studied due to their inaccessibility. The chemistry of sultines began to develop successfully only in recent decades. Many studies on methods for the synthesis of compounds of this class and their properties were published; the interest both of synthetic chemists and theoreticians in them has grown significantly. From the theoretical viewpoint, sultines are promising as models for studying the stereochemistry of sulfur, since the S atom in them is located at a vertex of a stable pyramid and does not have identical substituents, i.e. it is a chiral centre. The asymmetry of the molecule caused by the S atom can be easily removed by oxidising the sultine to the corresponding sulfoxide.^{2,3} Owing to the existence of a rather high barrier to inversion of the sulfoxide group, the introduction of at least one substituent into the sultine ring results in the appearance of diastereomers differing in the mutual arrangement (*cis* or *trans*) of the sulfoxide group and the substituent relative to the ring plane, i.e., geometric isomerism appears. Sultines are interesting as synthons because they possess hidden (latent) bifunctionality: cleavage of the heterocycle at the S–O bond leads to the simultaneous appearance of two functional groups in the product.

Owing to the increasing interest in studies on sultines and their transformations, we have attempted to systematise the data on the compounds of this class. It is noteworthy that sultines are mentioned in several reviews devoted to sulfinic acids and their derivatives;^{4–6} however, these data are not systematic but very fragmentary and given only in outline.

II. Methods for synthesising sultines

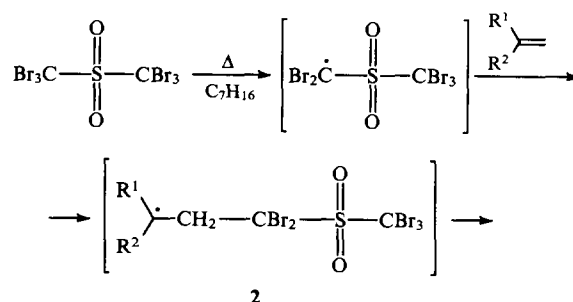
Three main groups can be distinguished among the known methods for sultine synthesis; these groups differ in the approach used to create the sultine structure. One group of reactions involves fragmentation-cyclisation transformations of sulfones. Another group combines cyclisations of bifunctional sulfur-containing compounds, usually thiols, sulfides, or sulfoxides, in which the hydroxyl group serves as the second function. The third group, not the most common but very interesting, involves sultine ring formation reactions with simultaneous introduction of three heteroatoms into the molecule upon addition of sulfur dioxide to unsaturated molecules.

1. Rearrangements of sulfones

A number of studies of both homo- and heterolytic sulfone rearrangements, which result in sultine formation, have been described. The driving force for these reactions frequently originates from a decrease in strain in the starting structure due to an increase in the heterocycle size by one atom, as, for example, in the case of four-membered cyclic sulfones, or from the presence of a good leaving group in the molecule.

a. Reactions of sulfones involving homolytic cleavage of a C–S bond

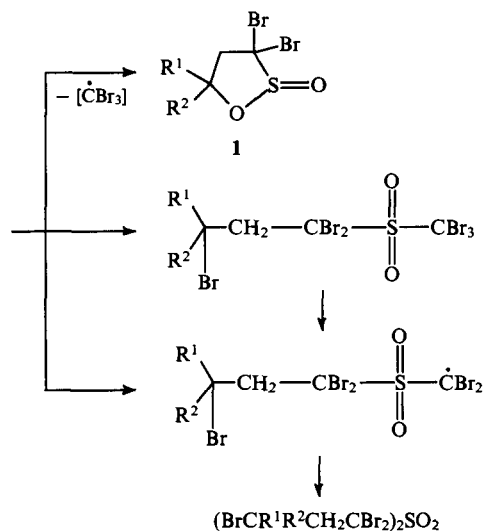
The formation of 5-substituted 3,3-dibromo-1,2-oxathiolane 2-oxides **1** was found to occur in the radical addition of bis(tribromomethyl)sulfone to alkenes.⁷ Most probably, sultine **1** is formed through intramolecular cyclisation of radical **2**. The subsequent elimination of the very stable tribromomethyl radical is the driving force for this unusual cyclisation. Sultine **1** is formed in a low yield, the main processes being chain transfer. However, it cannot be ruled out that a decrease in the concentrations of the sulfone and alkene in solution, i.e., higher dilution, would lead to an increase in the lifetime of radical **2** and, hence, to increased probability of its cyclisation into sultine **1**.



O B Bondarenko, L G Saginova, N V Zyk Chemistry Department,
M V Lomonosov Moscow State University,
Vorob'evy gory, 119899 Moscow, Russian Federation.
Fax (7-095) 939 88 46

Received 30 June, 1995

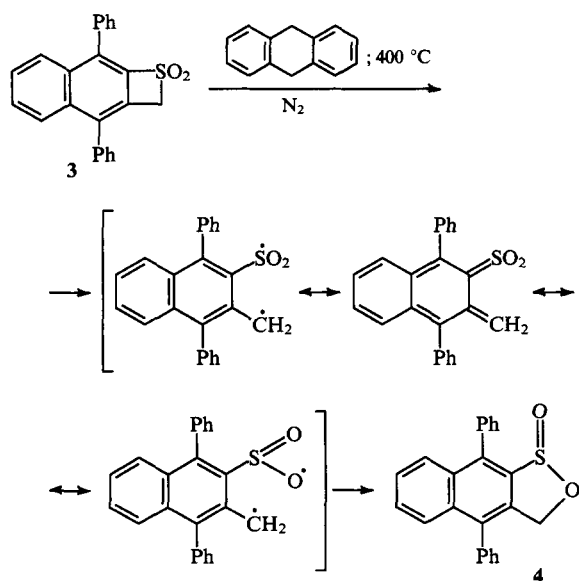
Uspekhi Khimii 65 (2) 156–177 (1996); translated by S S Veselyi



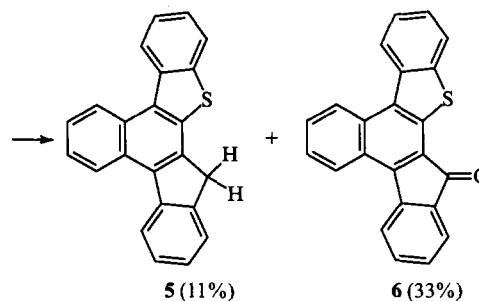
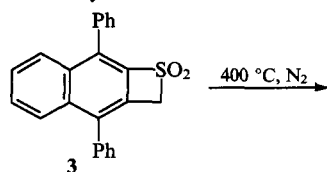
$\text{R}^1 = \text{Ph}, \text{R}^2 = \text{H};$
 $\text{R}^1 = \text{R}^2 = \text{Me}.$

b. Reactions of sulfones and 1,2,3-thiadiazine 1,1-dioxides via a concerted mechanism

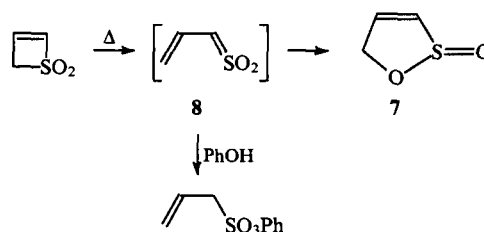
The thermal decomposition of 3,8-diphenylnaphthothiete 1,1-dioxide **3** at 400 °C under nitrogen in the presence of 9,10-dihydroanthracene affords naphthosultine **4** in 78%–81% yield.⁸ The reaction presumably involves a step in which an intermediate (possibly, a dipolar or biradical compound) is formed, which gives sultine **4** upon subsequent cyclisation.



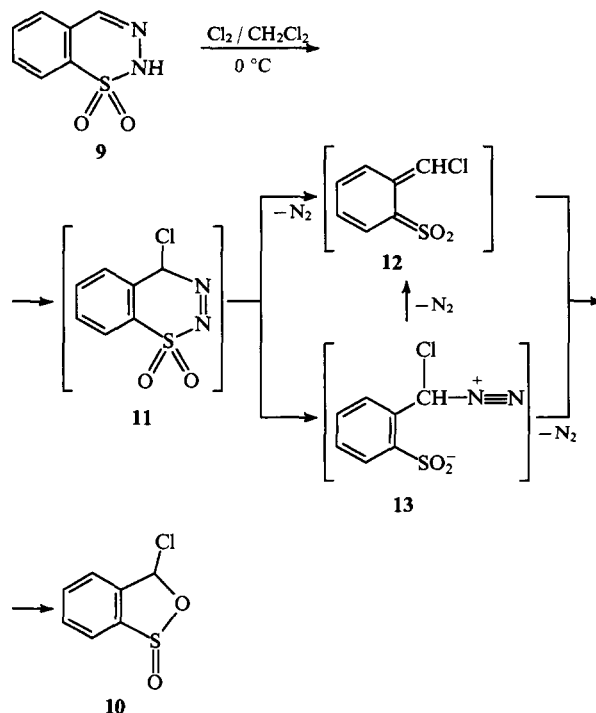
The role of 9,10-dihydroanthracene in this transformation is unclear; however, in its presence the decomposition of sulfone **3** stops at the stage of sultine **4**. In the absence of 9,10-dihydroanthracene, the reaction proceeds further to give the fused-ring fluorene **5** and fluorenone **6**, i.e. the same products as those from the thermolysis of sultine **4**.



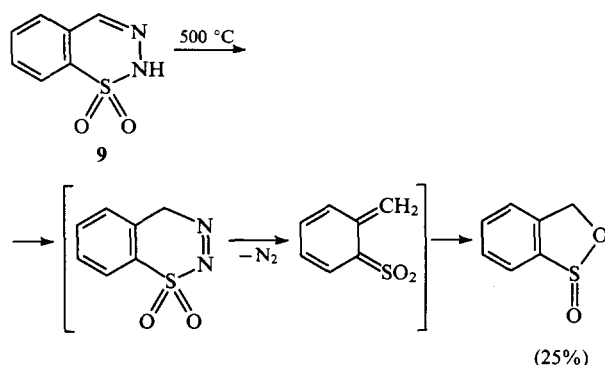
Thermolysis of the unsubstituted thiete 1,1-dioxide in the gas phase at 400 °C or in a degassed benzene or cyclohexane solution at 200 °C also gives the sultine **7** in high yields (up to 90%). It is likely that this transformation involves the vinylsulfene **8** as an intermediate. This is confirmed by the fact that this reaction, in the presence of phenol, gives phenyl allylsulfonate in 15% yield.⁹



The formation of the vinylsulfene **8** and its subsequent transformation into the sultine **7** are believed to occur via a concerted mechanism.⁹ The fact that reaction of 2*H*-1,2,3-benzothiadiazine 1,1-dioxide **9** with chlorine in an anhydrous medium gives the chlorosultine **10** is considered¹⁰ to support this mechanism. It is assumed that in this case the chlorination product **11** initially formed decomposes with elimination of the very stable nitrogen molecule and formation of the vinylsulfene **12**. The latter then cyclises to the chlorosultine **10**. However, it cannot be ruled out that compound **11** gives the diazonium sulfinate **13** by heterolytic cleavage of the S–N bond. Diazo compound **13** can also eliminate a nitrogen molecule to give the same vinylsulfene **12** or be directly transformed into the chlorosultine **10**.

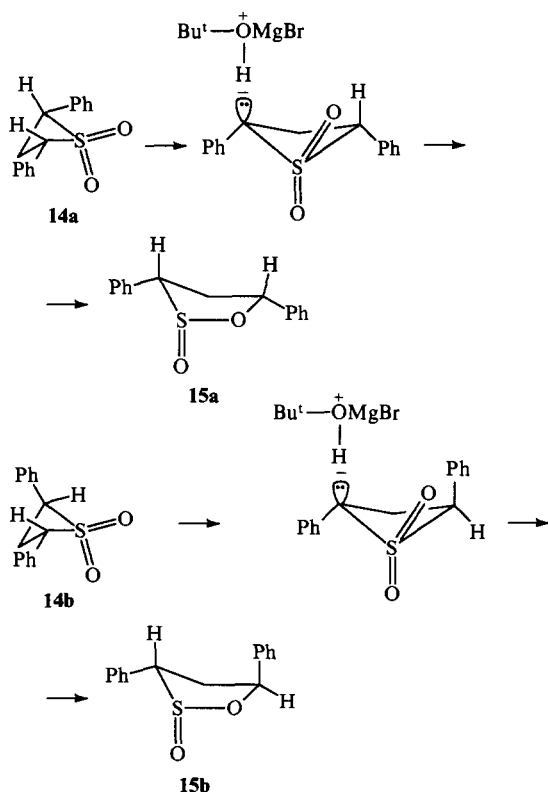


Clearly, the thermal decomposition of compound **9** also follows a similar scheme.¹¹



c. Reactions of sulfones involving heterolytic cleavage of the C–S bond

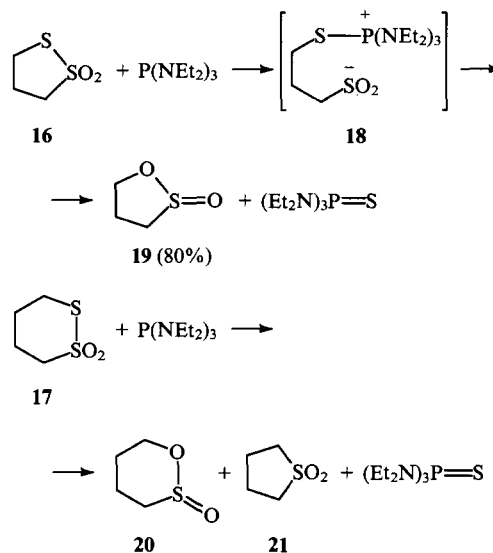
The rearrangement of the four-membered cyclic sulfones **14a,b** on treatment with a base, *tert*-butoxymagnesium bromide, to give the corresponding 3,5-diphenyl-1,2-oxathiolane 2-oxides **15a,b** via an ionic mechanism has been reported.^{12, 13}



Unlike the majority of transformations that result in mixtures of diastereomeric sultines, this reaction is stereospecific with respect to the phenyl substituents and stereoselective with respect to the sulfonyl group oxygen. This is explained^{12, 13} by the unique structure of the reagent, *tert*-butoxymagnesium bromide, which, together with diethyl ether as a solvent, exerts a 'cage' effect around the sulfone. It is assumed that *tert*-butoxymagnesium bromide initially abstracts a proton from the sulfone. The resulting carbanion and *tert*-butyl alcohol appear in close proximity to each other, which permits fast reprotonation of the anion before and after the rearrangement, and hence makes it possible to avoid side reactions. The above scheme reflects the stereochemical features of the reaction. The unusual cleavage of the C–S bond remote from the reaction centre formed initially is explained in terms of molecular orbital theory.

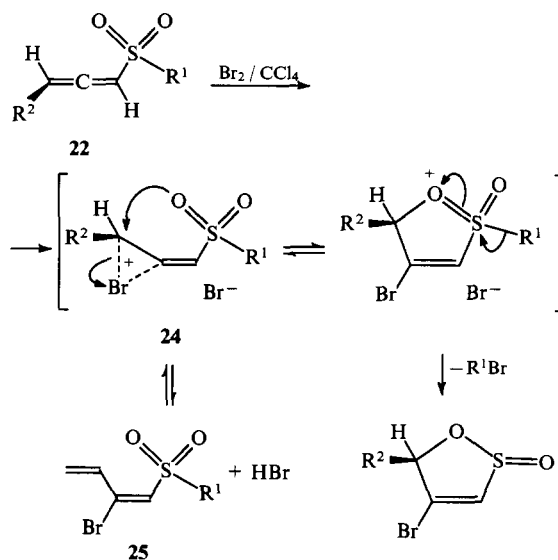
It is also interesting to note that prolonged reaction with sultine **15b**, containing *trans*-oriented phenyl substituents, results in its complete isomerisation to *cis*-3,5-diphenyl-1,2-oxathiolane (2,3-*cis*) 2-oxide **15a**. The latter is probably more thermodynamically stable, since the two bulky phenyl substituents in this compound occupy pseudo-equatorial positions.¹⁴

The synthesis of γ - and δ -sultines by the desulfurisation of the cyclic thiosulfonates **16** and **17** on treatment with tris(diethyl-amino)phosphine has been proposed.¹⁵ According to ³¹P NMR data, the reaction occurs *via* the intermediate phosphonium salt **18**.



The cyclisation of the salt **18** through one of the nucleophilic centres of the sulfinyl group, the O or S atom, accompanied by elimination of the aminophosphine sulfide molecule can give a sultine or a cyclic sulfone, respectively. The determining factor is probably the size of the resulting heterocycle. For example, the reaction with 1,2-dithiolane 1,1-dioxide **16** gives exclusively 1,2-oxathiolane 2-oxide **19**, whereas desulfurisation of 1,2-dithiane 1,1-dioxide **17** gives the sultine **20** and the sulfone **21** in a 9:1 ratio.

Braverman et al.^{2, 3, 16, 17} synthesised unsaturated γ -sultines by cyclisation of the sulfones **22** or sulfinates **23** on treatment with bromine. It is believed that the reaction begins with the electrophilic addition of bromine to the allene moiety with the formation

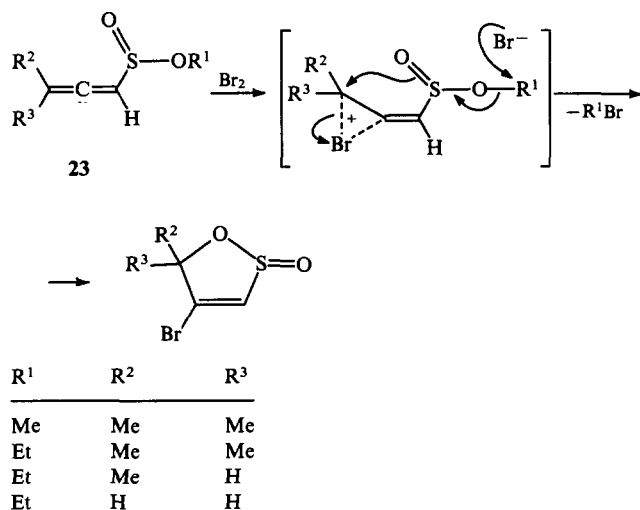


$R^1 = \text{Me}, \text{CH}_2\text{C}\equiv\text{CH}, \text{C}_6\text{H}_4\text{Me}$

$R^2 = \text{Bu}^t, \text{CMe}_2\text{C}\equiv\text{CH}$

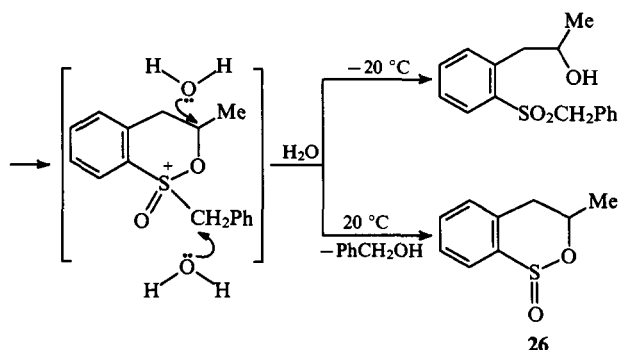
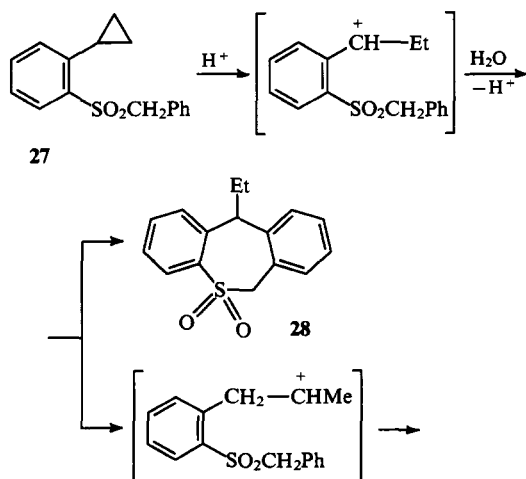
of the bridged bromonium ion **24**. This allows one to explain the retention of chirality at the γ -carbon atom in the optically active sulfones **22** during subsequent nucleophilic attack by the O atom of the sulfonyl group. The subsequent transformation of intermediates **24** into sultines occurs only when the former can eliminate a stable carbocation, such as *tert*-butyl or dimethylpropargyl, and probably proceeds via an S_N1 mechanism. When there is no good leaving group, a proton is eliminated and an acyclic product **25** is formed.

The fragmentation of sulfinates **23**, unlike that of the sulfones **22**, occurs via an S_N2 mechanism in which there is nucleophilic attack by the bromide anion resulting in cyclisation to a sultine with simultaneous elimination of an alkyl bromide molecule.



It is believed that the reactions of a number of sulfones **22**, e.g. with R¹ = Me, cannot occur via the S_N2 mechanism due to steric and electronic effects of the sulfonyl group.^{2, 3, 16, 17}

A six-membered sultine, 3-methylbenzo[*c*][2.1]oxathiine 1-oxide **26**, was obtained along with the usual reaction product, the thiepine **28**, upon isomerisation of benzyl (2-cyclopropylphenyl) sulfone **27** in presence of acid.¹⁸ The formation of sultine **26** is explained by rearrangement of the benzyl α -carbocation formed initially to a β -carbocation followed by its nucleophilic stabilisation by the sulfonyl group and by elimination of the benzyl fragment.



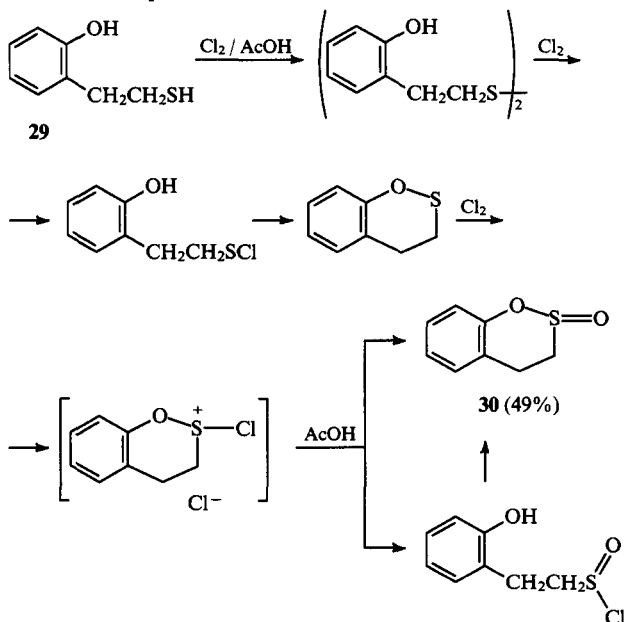
It is to be noted that the ratio of the reaction products strongly depends on the reaction temperature, and at 20 °C one can obtain sultine **26** in up to 84% yield.

2. Cyclisation of bifunctional sulfur-containing compounds

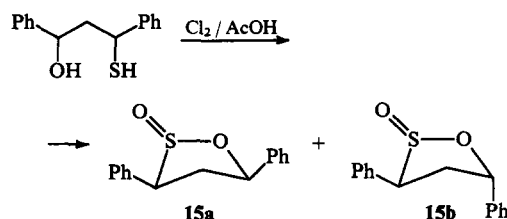
The cyclisation of bifunctional sulfur-containing compounds is the most frequently used method for the synthesis of sultines. This group of reactions is represented by diverse transformations.

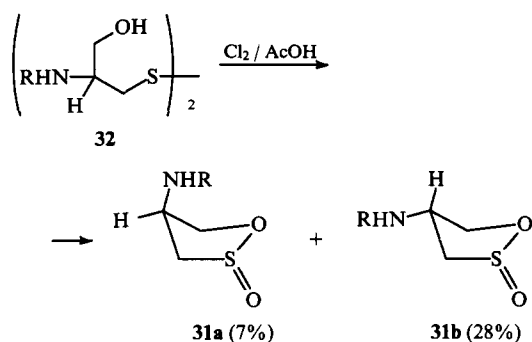
a. Oxidation of α,ω -mercaptoalcohols, disulfides and β -thiolactones

A number of syntheses of sultines by the oxidative chlorination of mercaptoalcohols in various systems have been reported. For example, benzo[*c*][1,2]oxathiine 2-oxide **30** can be obtained by treatment of β -(*o*-hydroxyphenyl)ethanethiol **29** with chlorine in glacial acetic acid.¹⁹ The mechanism of this reaction proposed by the authors is presented below.



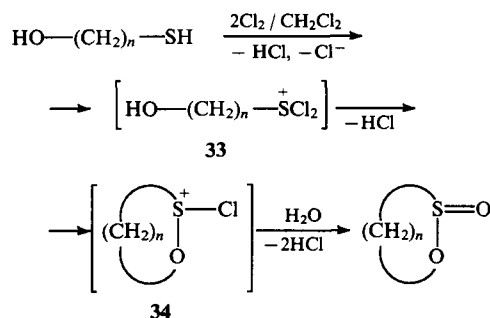
The same method was used to synthesise 3,5-diphenyl-1,2-oxathiolane 2-oxide **15** from 3-hydroxy-1,3-diphenylpropanethiol¹² and 4-[(benzyloxycarbonyl)amino]-1,2-oxathiolane 2-oxide **31** from hydroxypropyl disulfide **32**.²⁰





However, the yields of the isomeric sultines **15a,b** and **31a,b** did not exceed 40%. It is likely that the C—O bonds in compounds **15** and **31** are weaker than the Ar—O bond in the sultine **30** and undergo extensive nucleophilic cleavage by the chloride anions present in excess. This accounts for their considerably lower yields compared with that of sultine **30**. The yield of sultine **31** could be increased to 86%–90% by maintaining the concentration of the halogen at a sufficiently low level, which is possible when *N*-bromosucinimide (NBS) or *N*-chlorosucinimide (NCS) are used as halogenating agents.

A synthesis of the simplest sultines by the cyclisation of α,ω -mercaptoalcohols on treatment with chlorine in nonpolar solvents followed by hydrolysis (see Table I) has been proposed.²¹ The authors suggest that when 2 equiv. chlorine are used in the reaction, the acyclic chlorosulfonium ion **33** is formed; the latter is transformed into the cyclic ion **34**, which then gives the sultine on treatment with 1 equivalent of water.



It should be noted that when the distance between the reacting centres increases, polymerisation prevails over cyclisation, which decreases the yields of sultines.

A preparative method for synthesising cyclic mixed anhydrides of β -sulfino-carboxylic acids **38**²² is based on oxidative chlorination of substituted β -thiolactones **35** (with chlorine or sulfonyl chloride) in acetic anhydride. It was demonstrated that β -(chlorosulfinyl)alkanoyl chlorides **36** are formed in high yields (75%–80%) for a reagent ratio $\mathbf{35} : \text{Cl}_2 : \text{Ac}_2\text{O} = 1 : 2 : 1$, and that the SOCl group is, most probably, formed due to interaction of a trichlorosulfurane intermediate with acetic anhydride. With excess acetic anhydride ($\mathbf{35} : \text{Cl}_2 : \text{Ac}_2\text{O} = 1 : 2 : 2$), sulfinyl chlorides isomerise to the cyclic sulfuranes **37**, which react with acetic anhydride to give 1,2-oxathiolan-5-one 2-oxides **38**.

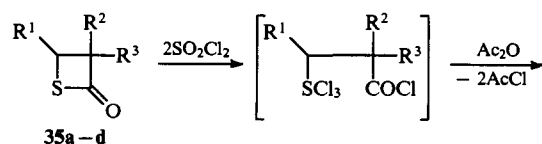
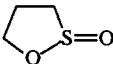
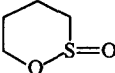
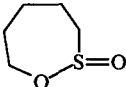
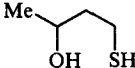
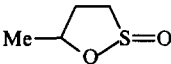
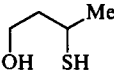
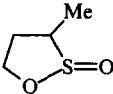
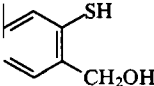
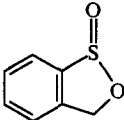
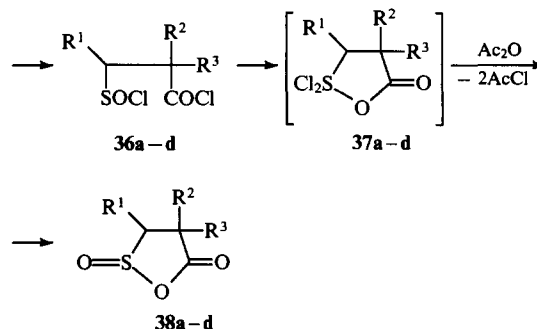


Table 1. Synthesis of the simplest sultines by chlorination of mercaptoalcohols.

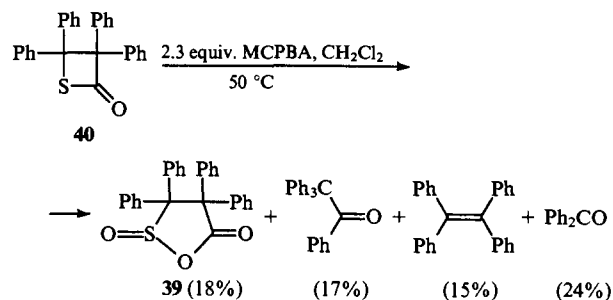
Thiol	Sultone	Yield (%)
$\text{HO}(\text{CH}_2)_3\text{SH}$		90
$\text{HO}(\text{CH}_2)_4\text{SH}$		85
$\text{HO}(\text{CH}_2)_5\text{SH}$		10
		70
		70
		80



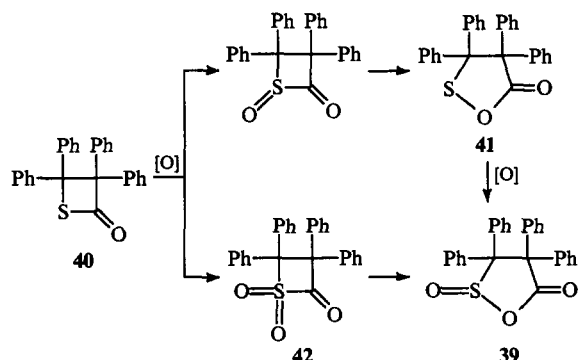
38	R ¹	R ²	R ³	Yield (%)
a	H	H	H	25–40
b	Me	H	H	73–77
c	H	Me	H	87–97
d	H	Me	Cl	100

The cyclic anhydrides **38** are highly reactive and find use in the synthesis of physiologically active compounds.

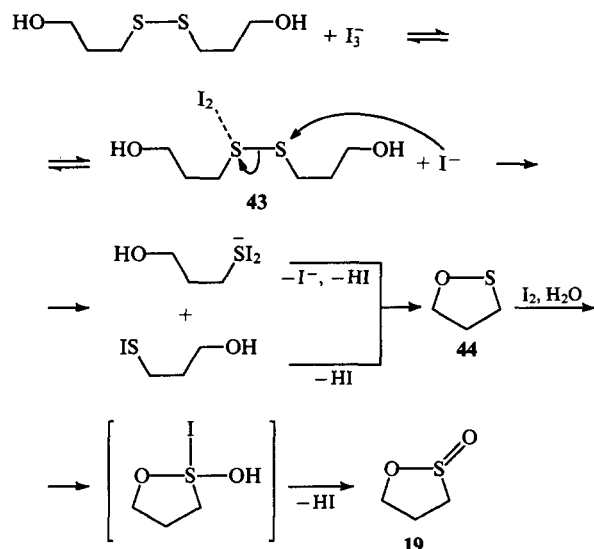
The formation of tetraphenylloxathiolanone **39** by the oxidation of the corresponding β -thiolactone **40** with *m*-chloroperbenzoic acid (MCPBA) has been reported.²³ However, the yield of the sultine obtained by this method did not exceed 18%.



The authors²³ consider that compound **39** could be formed either by the oxidation of the initial thietanone **40** to α -oxo-sulfoxide followed by its isomerisation to the sultene **41** and transformation of the latter into the sultine **39** (cf. Ref. 41) or by the oxidation of the initial thiolactone **40** to the thietanone dioxide **42**, which subsequently rearranges into the sultine **39**.



The oxidative cleavage of 3,3'-dithiodipropanol with aqueous KI-I₂ solution followed by cyclisation gave 1,2-oxathiolane 2-oxide **19** in 77% yield.²⁴ A kinetic study²⁴ allowed the following reaction mechanism to be put forward:

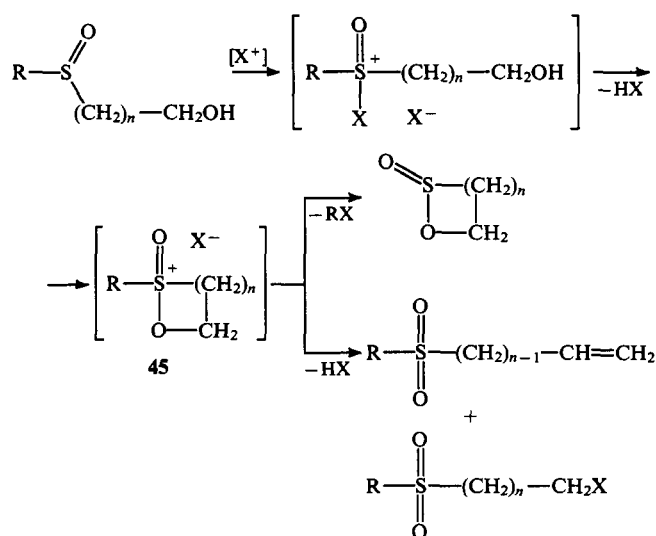


The attack of the disulfide-iodine complex **43** formed initially by an iodide anion cleaves the S-S bond in the disulfide. It was shown that hydroxy groups do not exert nucleophilic assistance in the cleavage, and that the cyclisation of sulfenyl iodide as well as the thiolate-iodine complex occurs in the next step. The resulting sultene **44** undergoes subsequent oxidation and hydrolysis to give 1,2-oxathiolane 2-oxide **19** as the final product. It is noteworthy that this reaction is not general. For example, 4,4'-dithiodibutanol is oxidised by an aqueous solution of iodine to give 4-sulfobutanol, possibly because the distance between the reaction centres involved in the cyclisation increases. Under the same conditions, 3,3'-dithiodipropionic acid is transformed into 3-sulfopropionic acid.

b. Cyclisation of α,ω -hydroxysulfoxides

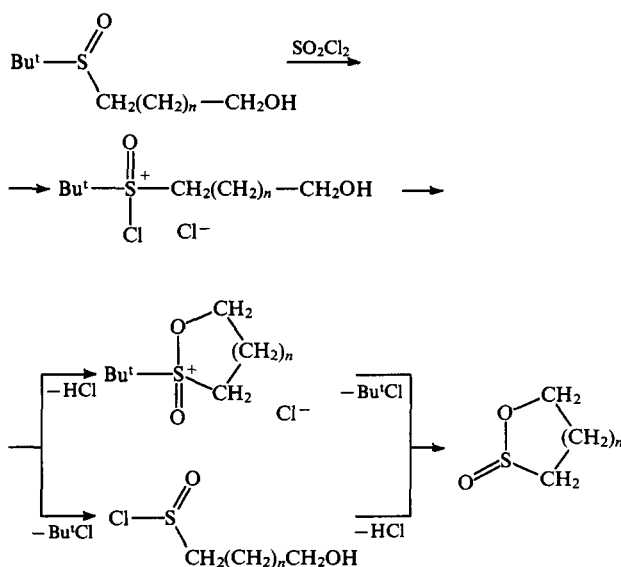
The cyclisation of hydroxyalkyl sulfoxides in the presence of halogenating agents, such as NBS, NCS or SO₂Cl₂, results in the formation of sultines²⁵⁻²⁸ or sulfones,²⁹⁻³⁴ depending on the structure of the starting compound.

In all cases, the existence of a cyclic intermediate of type **45** is assumed,^{33,34} which can be opened at the C-O bond to give sulfones or, when R is a good leaving group, can give the corresponding sultine by cleavage of the R-S bond.



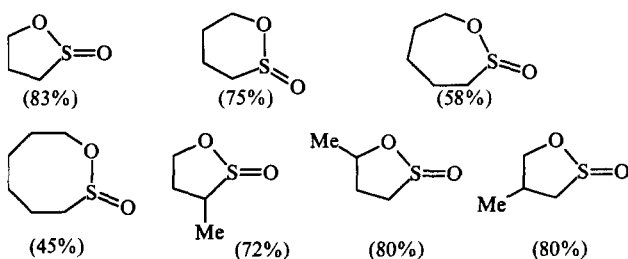
X = Cl, Br; n = 1-4

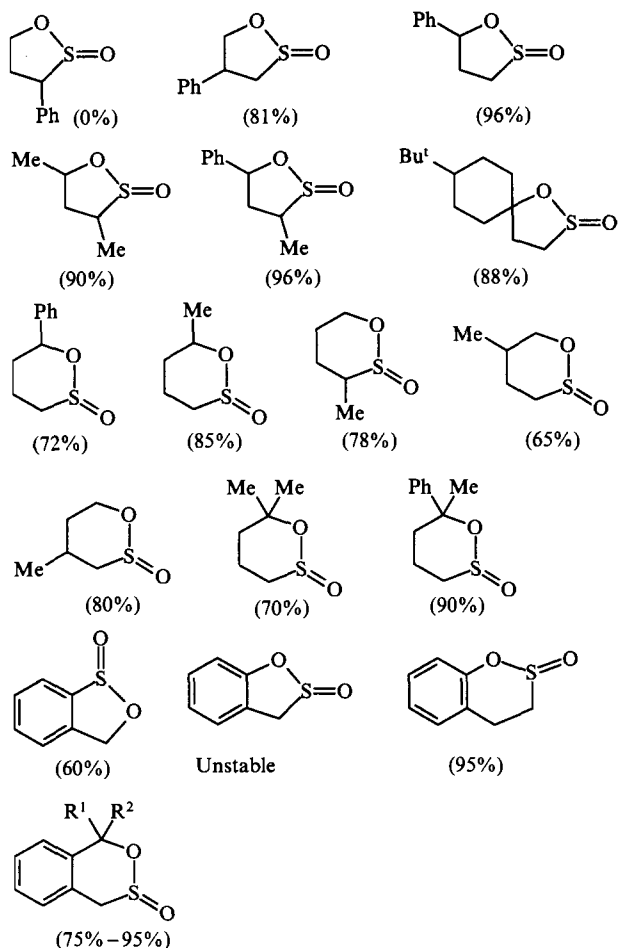
Durst and co-workers²⁶ used this approach to synthesise sultines containing from five to eight atoms in the heterocycle by reactions of *tert*-butyl ω -hydroxyalkyl sulfoxides with sulfuryl chloride.



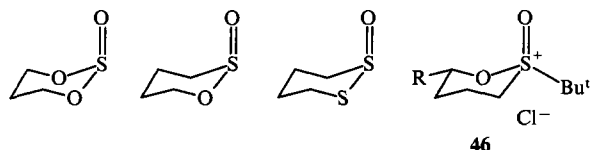
n = 1-4

In this case, the *tert*-butyl group serves as a good leaving group. Sultines are formed in high, nearly quantitative yields for n = 1, 2 (see Table 2). When n increases, i.e., the reaction centres become more distant from each other, the probability of the cyclisation and hence the yields of the sultine decrease. The yields of sultines obtained by the cyclisation of *tert*-butyl hydroxyalkyl sulfoxides in the presence of halogenating agents (NBS, NCS, SO₂Cl₂) are given below.



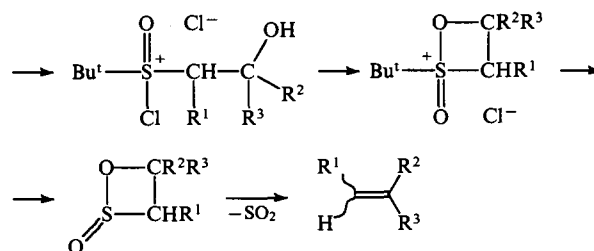
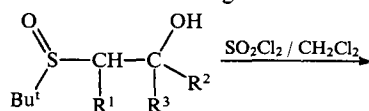


Certain stereochemical features of this reaction are of interest. γ -Sultines with substituents in the ring were isolated as mixtures of diastereomers, whereas the formation of δ -sultines (six-membered heterocycles) occurs stereoselectively and results exclusively, or predominantly, in one isomer having a chair conformation with an axially oriented S=O bond and a substituent in an equatorial position.³⁵ The preference for a conformation with an axially oriented S=O bond for cyclic trimethylene sulfites and their analogues is obviously related to the anomeric effect.^{36,37}

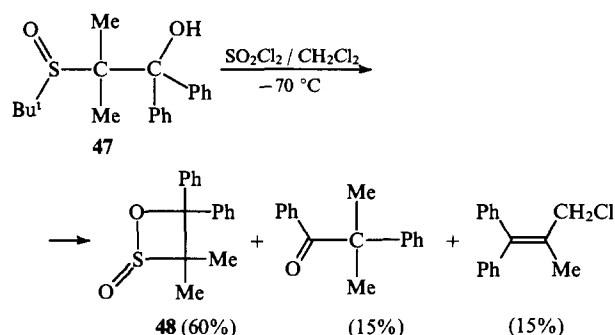


The high selectivity of the transformations in the synthesis of δ -sultines is explained²⁶ by the isomerisation of products under the reaction conditions or during isolation, on the one hand, and by the predominant formation of some of the isomers during the reaction, on the other hand. It cannot be ruled out that this preference manifests itself at the alkoxyoxosulfonium salt formation stage, for which the conformation 46, with both substituents in equatorial positions, is the most favourable.

Attempts to synthesise β -sultines from *tert*-butyl 2-hydroxyalkyl sulfoxides failed due to their instability: at 20 °C, they eliminate sulfur dioxide in several minutes to give unsaturated compounds.^{38,39} This is probably caused by the significant strain in the four-membered ring.

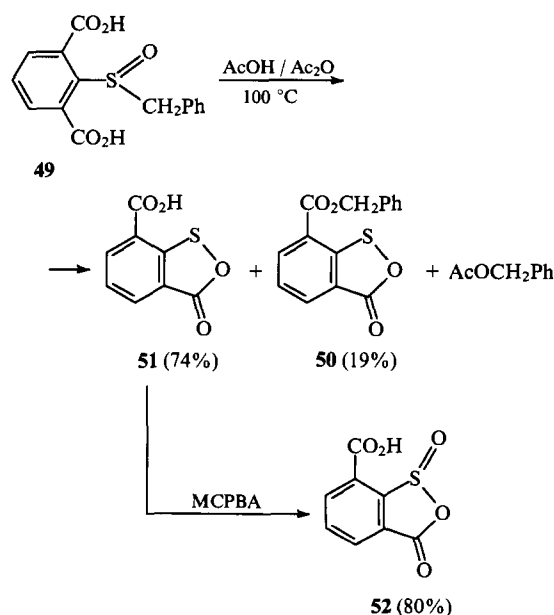


It was only in the case of *tert*-butyl 2-hydroxy-1,1-dimethyl-2,2-diphenylethyl sulfoxide **47** that the corresponding sultine, 3,3-dimethyl-4,4-diphenyl-1,2-oxathietane 2-oxide **48**, which is stable at 20 °C over a period of several days, was isolated and characterised.⁴⁰



However, despite all failures to synthesise β -sultines, the generality of this method leading to heterocycles with 5 to 8 atoms in the ring and the possibility of synthesising various sultines by introducing substituents into the alkyl chain of the initial *tert*-butyl ω -hydroxyalkyl sulfoxide make this reaction a promising preparative method.

The cyclisation of 2-(benzylsulfinyl)isophthalic acid **49** gives the sultenes **50** and **51**. The latter was oxidised with MCPBA to give the corresponding sultine **52**.^{41,42} The reaction mechanism was not discussed in detail; however, it can be assumed that cyclisation of the sulfoxide in an AcOH/Ac₂O mixture probably occurs by an intramolecular Pummerer reaction followed by nucleophilic participation of the neighbouring carboxyl group.

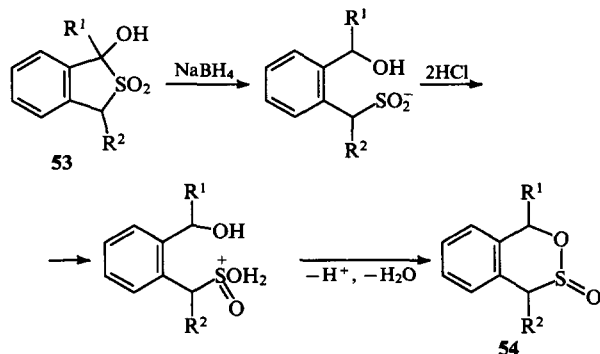


c. Cyclisation of hydroxysulfonates

The sultine ring is also formed through the cyclisation of hydroxysulfonates in acidic media. They can be generated using various methods.

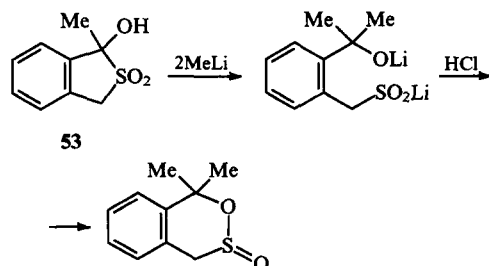
For example, Durst et al.⁴³ suggest that hydroxysulfonates can be obtained by the reduction of 1-hydroxy-1*H*,3*H*-benzo[*c*]-thiophene 2,2-dioxides **53** with sodium tetrahydroborate. Subsequent cyclisation of hydroxysulfonates gave 1*H*,4*H*-benzo-*[d]*[2,3]oxathiane 3-oxides **54**.

It is believed⁴³ that hydroxysulfinate cyclisation in acidic media involves the participation of the protonated form of sulfonic acid. The possibility of this transformation was shown for the acid hydrolysis of methyl toluene-*p*-sulfinate in H₂¹⁸O.⁴⁴

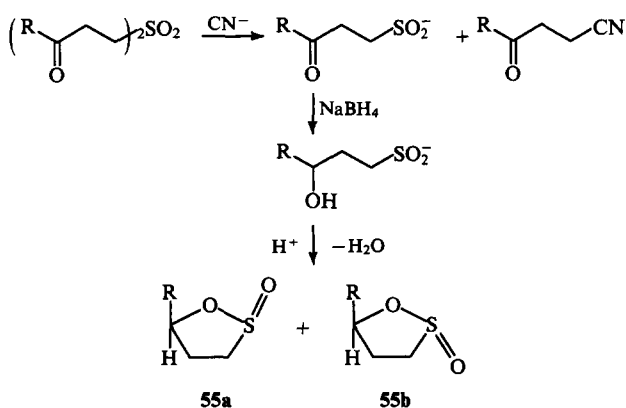


R¹ = R² = H (70%); R¹ = Me, R² = H (55%); R¹ = H, R² = Ph (79%)

The generation of a hydroxysulfinate followed by cyclisation also occurs during the metallation of the cyclic sulfone **53** with organolithium reagents. It was proposed to synthesise various sultines using functionalised lithium derivatives.^{43,45}



Messinger^{46,47} obtained hydroxysulfonates by the cleavage of γ,γ' -dioxosulfones with the cyanide anion followed by their reduction with sodium tetrahydroborate.



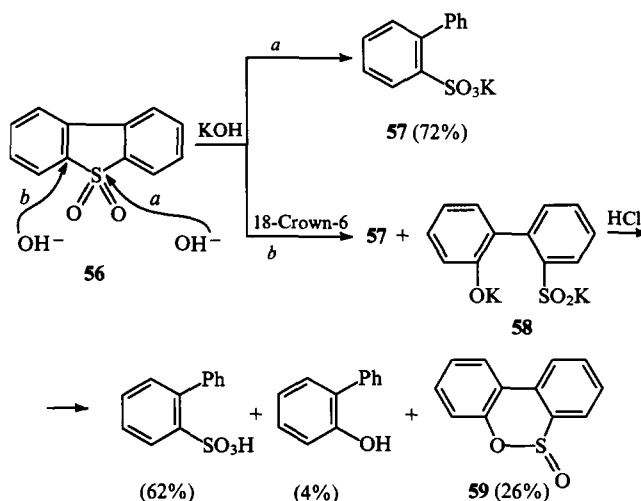
55a: R = *p*-ClC₆H₄ (65%), *p*-MeC₆H₄ (60%), *p*-MeOC₆H₄ (63%);

55a + **55b**: R = Ph₂CH (72%), C₁₀H₇ (42%)

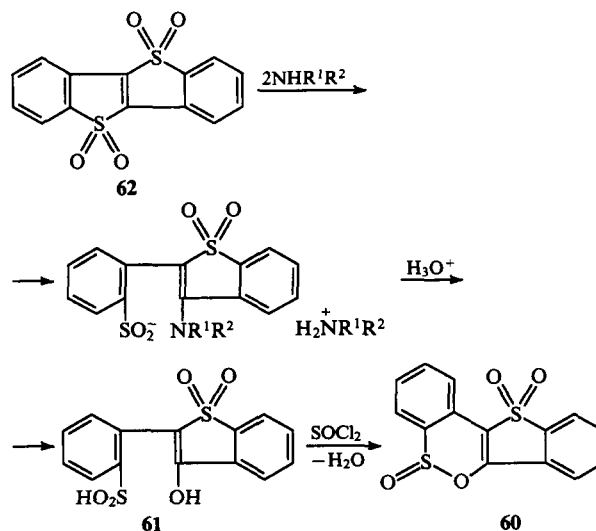
It is interesting to note that upon subsequent acidification of phenyl-substituted hydroxysulfonates (R = *p*-ClC₆H₄, *p*-MeC₆H₄, or *p*-MeOC₆H₄) their cyclisation to sultines occurs stereospecifically and gives exclusively *cis*-diastereomers **55a**. It is likely that this feature of the reaction is due to steric effects of the substituents, since 5-(β -naphthyl)- and 5-(diphenylmethyl)-sultines, obtained under the same conditions, consist of a mixture of isomers **55a** + **55b**.

The alkaline cleavage of dibenzothiophene dioxide **56** in the presence of 18-crown-6 gave potassium biphenyl-2-sulfonate **57** and dipotassium 2'-hydroxybiphenyl-2-sulfinate **58**. Acidification of the mixture gave mainly biphenyl-2-sulfonic acid and the sultine **59**.⁴⁸

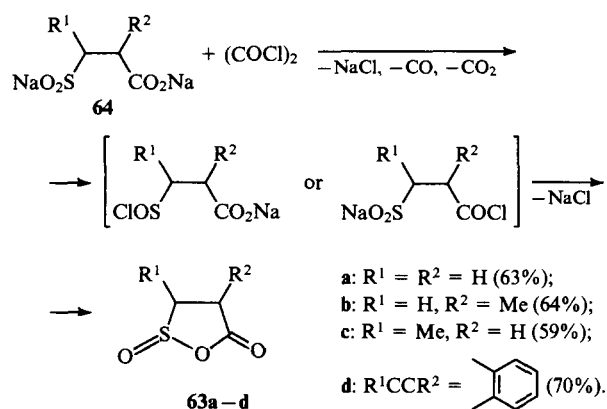
It is remarkable that in the absence of a crown ether, potassium biphenyl-2-sulfonate **57** is formed exclusively, i.e. only the S atom is attacked by the hydroxide ion (pathway *a*). It is assumed that the loss of reaction selectivity in the presence of the crown ether is due to the appearance of free hydroxide ions, which are more reactive than the solvated ions. This allows the hydroxide ions to attack the aromatic ring (pathway *b*) to give the dipotassium salt **58**.



The synthesis of the sultine **60** by the cyclisation of the corresponding hydroxysulfonic acid **61** on treatment with thionyl chloride or acetyl chloride has been reported.⁴⁹ The hydroxysulfonic acid **61** was obtained from benzothienobenzo-thiophenedi-sulfone **62** by nucleophilic cleavage of the C—S bond by the amine and subsequent hydrolysis.



A general method for the synthesis of 1,2-oxathiolane-5-one 2-oxides **63a-c** and 2,1-benzoxathiol-3-one 1-oxide **63d** by treatment of bis-sodium β -(hydroxysulfinyl)carboxylates **64** with oxalyl chloride according to the following scheme has been proposed:⁵⁰

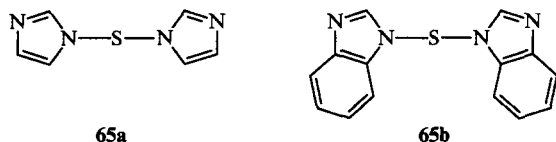


Mixed anhydrides of β -sulfinocarboxylic acids **63** are unstable and can be isolated only if moisture is completely absent.

d. Cyclisation of bifunctional compounds with simultaneous introduction of a sulfur-containing group

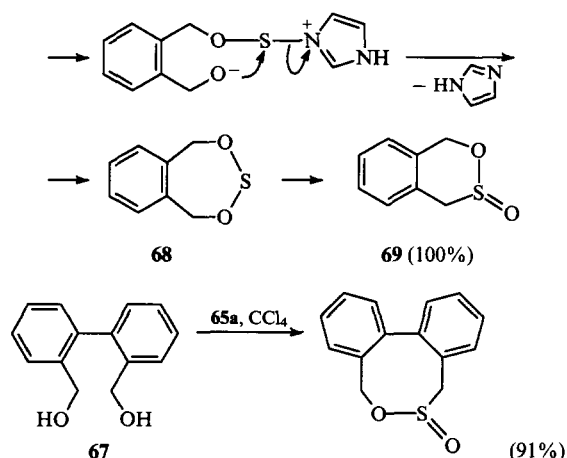
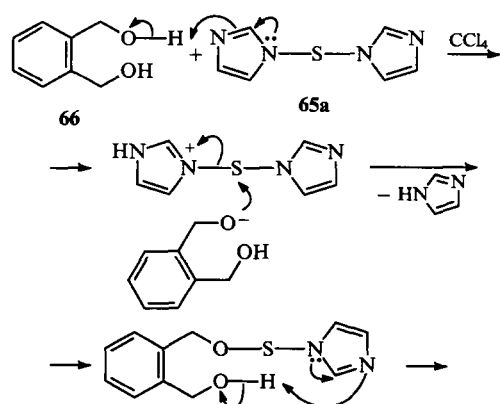
Let us consider several examples demonstrating the syntheses of sultines by the cyclisation of bifunctional compounds involving the introduction of a sulfur-containing group.

In their study of new sulfur transfer reagents, Harpp and coworkers⁵¹ proposed the synthesis of sultines by the reactions of *N,N'*-thiobisimidazole **65a** and *N,N'*-thiobisbenzimidazole **65b** with certain diols.

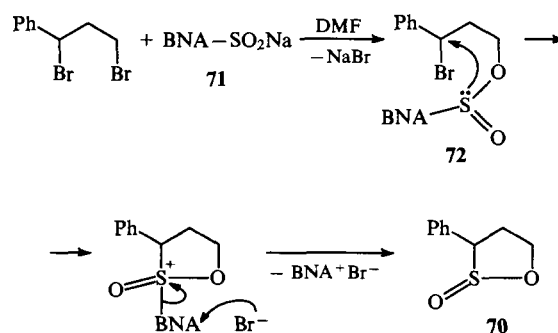


Compounds of type **65a,b** are reactive toward nucleophiles containing an active hydrogen atom (OH, SH, NHR). This is explained by the protonation of the leaving group of the reagent in the first reaction step followed by its nucleophilic substitution (when it is eliminated as a neutral molecule).

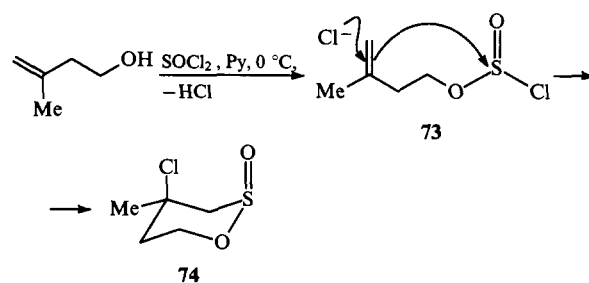
The mechanism of the transformation of the diols **66** and **67** into the corresponding sultines has not been discussed;⁵¹ however, one can assume that formation of the cyclic sulfoxylate **68** occurs initially, and the latter then rearranges to the sultine **69**. Similar rearrangements are known for acyclic allyl and benzyl sulfoxylates.⁵²



The synthesis of 3-phenyl-1,2-oxathiolane 2-oxide **70** by treatment of 1,3-dibromo-1-phenylpropane with sodium 1-benzyl-1,4-dihydronicotinamide-4-sulfonate **71** has been reported.⁵³ The initial step obviously involves the formation of the sulfinic ester **72** with elimination of a bromide anion, the cyclisation of this ester then occurs by nucleophilic attack by the S atom at the C atom of the benzyl fragment. Subsequent elimination of 1-benzyl-1,4-dihydronicotinamide (BNA) yields sultine **70**.

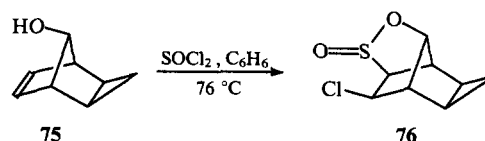


The synthesis of γ -sultines by treatment of γ,δ -unsaturated alcohols with thionyl chloride in the presence of pyridine has been suggested.⁵⁴ In this reaction, the intermediate **73** undergoes cyclisation involving the double bond, which in this case acts as a second functional group.



It should be noted that 4-chloro-4-methyl-1,2-oxathiane 2-oxide **74** was isolated as one diastereomer with *cis*-axial orientation of the S=O group and the Cl atom.

An analogous combination of a double bond and a hydroxyl group is also present in the tricyclic alcohol **75**, which gives the sultine **76** on treatment with thionyl chloride.⁵⁵

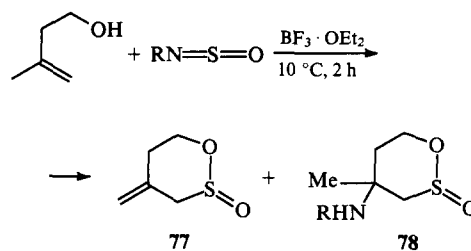


It was shown that the result of the reaction in the rigid structure **75** is largely determined by the mutual orientation of the reaction centres — the hydroxyl group and the double bond — in the molecule and by the distance between them. Another interesting feature of the reaction should be noted: this is an unusual example of an electrophilic *exo-cis*-addition to a double bond. This conclusion was based on the spectral characteristics of the reaction product, the sultine **76**.

The reactions of unsaturated alcohols with *N*-sulfinyltoluene-*p*-sulfonamide in the presence of $\text{BF}_3 \cdot \text{OEt}_2$ gave diverse chiral six- and seven-membered mono- and bi-cyclic sultines (see Table 2).⁵⁶ The high stereoselectivity of the reaction was noted: the stereochemistry of ring annelation is determined by the configuration of the starting alcohol; in each case, the molecules of the resulting sultines contained an axially oriented $\text{S}=\text{O}$ bond and an exocyclic methylene fragment.

Alcohols **A** and **F** (see Table 2) gave the sultine **77** and the product **78**, which retained the amine residue; this did not allow

the authors⁵⁶ to make an unambiguous conclusion about the reaction mechanism.



The synthesis of dibenzoxathiine oxide **59** from *o*-hydroxybiphenyl and thionyl chloride in the presence of Lewis acids⁵⁷ can be formally assigned to the above type of reactions for the aromatic series. In this case, the second reaction step involves typical electrophilic substitution in the aromatic ring.

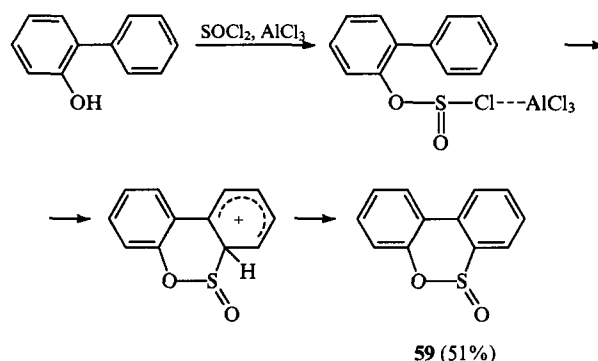


Table 2. Syntheses of sultines by the reaction of unsaturated alcohols with *N*-sulfinyltoluene-*p*-sulfonamide in the presence of $\text{BF}_3 \cdot \text{OEt}_2$.

Alcohol	Formula	Product	Yield (%)
A			32
B			64
C			69
D			55
E			75
F			17
G			46
H			47

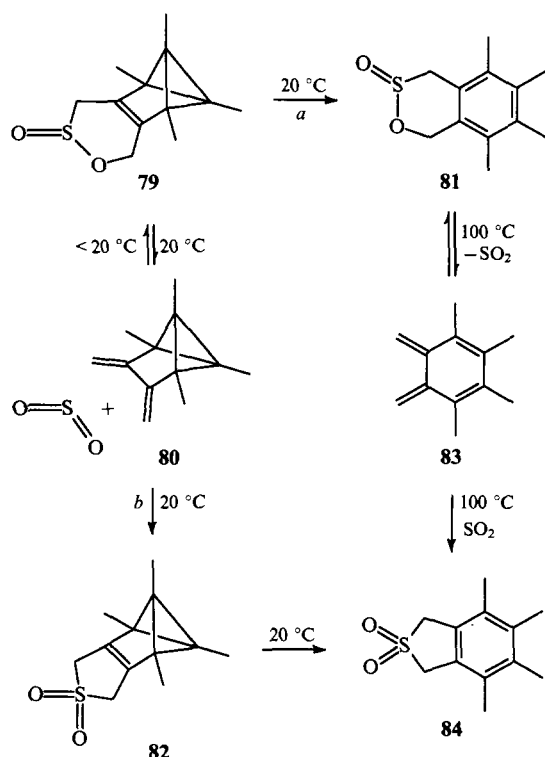
3. Syntheses of sultines with participation of sulfur dioxide

We assigned reactions involving sulfur dioxide as one of the reagents to the third group of transformations resulting in the formation of the sultine ring. When considering these reactions, attention should be paid to particular features of the structure of sulfur dioxide, in the molecule of which the S atom has simultaneously a nonbonding electron pair and vacant *d*-orbitals. It is by virtue of the latter that sulfur dioxide forms charge-transfer complexes with various Lewis bases, namely, amines,⁵⁸ aromatic compounds,^{59–61} ethers, alcohols⁶² and alkenes.⁶³ Sometimes, as in the case of trimethylamine, these complexes are so stable that they can be isolated in the crystalline state.^{64,65}

a. Reactions of sulfur dioxide with 1,3-dienes

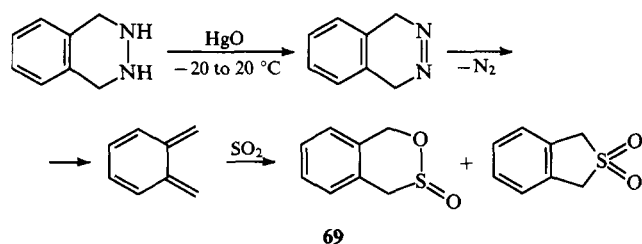
The well-known cheletropic addition of sulfur dioxide to conjugated polyenes in the presence of inhibitors of radical processes involves both the vacant *d*-orbitals and the lone electron pair of the S atom. This transformation occurs as the $[2+4][n+\pi\pi]$ cycloaddition to give five-membered cyclic sulfones, i.e. sulfonenes.⁶⁶ However, it was noted that, in some cases, an atypical mode of addition of sulfur dioxide to dienes involving the $\text{S}=\text{O}$ bond gives unstable unsaturated six-membered sultines, which undergo retrocycloaddition and rapidly decompose into the starting compounds.²⁶

For example, the formation of a kinetically controlled reaction product, the sultine **79**, in the course of $[2+4][\pi+\pi\pi]$ cycloaddition of sulfur dioxide to substituted dimethylene-tricyclohexane **80**, a reactive diene in the Diels–Alder reaction, has been reported.⁶⁷



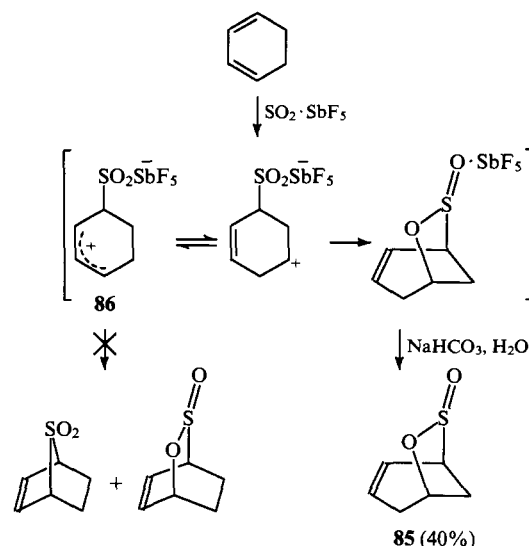
The sultine **79**, which is unstable at room temperature, is transformed into the sultine **81** (up to 90%) by isomerisation of the tricyclic fragment into a benzene ring (pathway *a*), or into the sulfone **82** by retroaddition (pathway *b*). Heating of the sultine **81** in *o*-dichlorobenzene at 80–100 °C results in its dissociation into sulfur dioxide and *o*-quinodimethane **83** with subsequent recombination into the thermodynamically controlled product sulfone **84**, a product of [2 + 4][$n + \pi\pi$] cycloaddition. The same sulfone was obtained by isomerisation of the tricyclic fragment in compound **82**. It was also noted that the addition of diene **80** to liquid sulfur dioxide at -50 °C gave only the aromatic sultine **81**, which is probably due to the isomerisation of the sultine **79** to **81** catalysed by liquid sulfur dioxide.

The preferential formation of the sultine **69**, the product of the [2 + 4][$\pi + \pi\pi$] cycloaddition of sulfur dioxide to *o*-quinodimethane under kinetic control, together with a sulfone (in a 9 : 1 ratio) was noted.⁶⁸



In some cases, the addition of sulfur dioxide to conjugated polyenes is catalysed by Lewis acids.^{69–72} The latter form complexes with sulfur dioxide,⁷³ which then behaves with enhanced electrophilicity. The reactions occur stepwise with intermediate formation of carbocations.

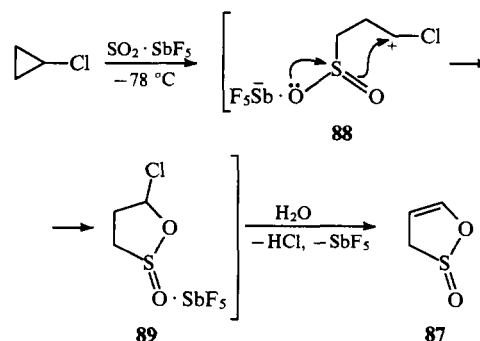
For example, the reaction of cyclohexadiene with the SO₂·SbF₅ complex⁷⁴ gives the bicyclic sultine **85**. The authors⁷⁴ assume that the formation of **85** occurs through a 1,2-hydride shift in the allylic intermediate **86**.



It is interesting that the reaction with 1,3-cyclohexadiene occurs stereospecifically and gives the isomer **85** as the only product; its structure was confirmed by X-ray diffraction analysis. On the other hand, reactions of sulfur dioxide with cyclohepta- or cycloocta-1,3-dienes give complex mixtures of addition products.

b. Reactions of sulfur dioxide with cyclopropanes

The formation of the cyclic sulfinate **87** by the addition of sulfur dioxide to cyclopropyl chloride in the presence of SbF₅ was observed by Olah and co-workers⁷⁵ when attempting to obtain dicyclopropylhalogenonium ions from cyclopropyl halides. The mechanism of this transformation has not been discussed; however, it can be assumed that the first step of the reaction involves electrophilic attack on the cyclopropane ring by the SO₂·SbF₅ complex with the cleavage of the C(1)–C(2) bond to form the carbocation **88**. Subsequent intramolecular cyclisation involving an O atom of sulfur dioxide gives the sultine **89**, which eliminates an HCl molecule to give the cyclic sulfinate **87**.



Several papers^{76–81} have described the addition of sulfur dioxide to arylcyclopropanes in the presence of trifluoroacetic acid. The reaction occurs regioselectively and results exclusively in 5-aryl-1,2-oxathiolane 2-oxides **90** in good yields (Table 3).

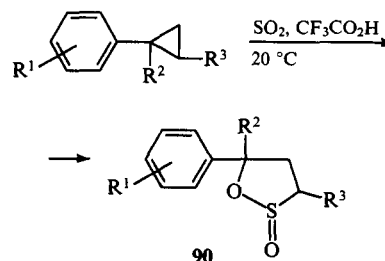


Table 3. Synthesis of sultines by the addition of sulfur dioxide to arylcyclopropanes in the presence of trifluoroacetic acid.⁸¹

Arylcyclopropane			Product yield (%)	Diastereomeric composition of the sultine (%) ^a			
R ¹	R ²	R ³		A	B	C	D
H	H	H	76	60	40	—	—
<i>p</i> -Me	H	H	88	60	40	—	—
<i>p</i> -MeO	H	H	92	60	40	—	—
<i>p</i> -Br	H	H	45	55	45	—	—
<i>p</i> -I	H	H	93	55	45	—	—
<i>o</i> -Cl	H	H	22	65	35	—	—
<i>o</i> -Br	H	H	51	55	45	—	—
<i>o</i> -I	H	H	44	60	40	—	—
H	H	Ph (<i>cis</i>)	70	50	50	—	—
H	H	Ph (<i>trans</i>)	Does not react	—	—	—	—
<i>p</i> -F	H	<i>p</i> -FPh (<i>cis</i>)	80	50	50	—	—
<i>p</i> -Me	H	<i>p</i> -MePh (<i>cis</i>)	84	50	50	—	—
<i>p</i> -MeO	H	<i>p</i> -MeOPh (<i>cis</i>)	95	60	40	—	—
<i>p</i> -Me	H	<i>p</i> -MePh (<i>trans</i>)	65	55	16	16	13
<i>p</i> -MeO	H	<i>p</i> -MeOPh (<i>trans</i>)	94	61	15	13	11
H	Ph	Ph	95	100	—	—	—
H	H	Me	60 ^b	30	5	10	—
H	Me	H	75	50	50	—	—

^a The diastereomers A–D are shown in Scheme 1. ^b In this case 10% of a structural isomer — 4-methyl-5-phenyl-1,2-oxathiolane 2-oxide was isolated.

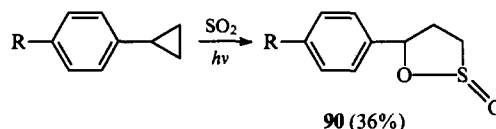
A study of this reaction with a series of arylcyclopropanes substituted in the trimethylene and benzene rings indicated that it is an electrophilic reaction.

The resulting γ -sultines are mixtures of diastereomers (the addition was stereospecific only in the case of 1,1,2-triphenylcyclopropane).

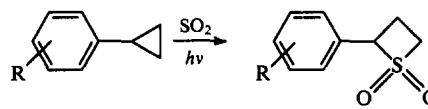
It was suggested that the reaction proceeds through a step involving formation of an open carbocation according to Scheme 1.^{76–81} This is consistent with the steric requirements of the reaction products obtained. The preferential formation of isomer A in the case of *trans*-diarylcyclopropanes is explained by its thermodynamic stability arising from the fact that the bulky phenyl substituents in the latter, which are in a *cis*-position to each other, occupy the most favourable pseudo-equatorial positions in the molecule.¹⁴

The above reaction is a convenient method for obtaining 5-aryl-1,2-oxathiolane 2-oxides, which can be used as synthons in organic syntheses for the bifunctionalisation of hydrocarbons.

The photochemical addition of sulfur dioxide to certain arylcyclopropanes to give 5-aryl-1,2-oxathiolane 2-oxides **90** has also been reported.⁸² In this case, cyclopropanes containing electron-withdrawing groups in the aromatic ring were found to be reactive. *p*-Nitrophenylcyclopropane gives the sultine **90** and the cyclic sulfone **91**; the latter becomes the only reaction product in the case of the *o*-nitro isomer. It is noteworthy that, of the systems studied,⁸² a number of cyclopropanes (phenylcyclopropane, *p*-biphenylcyclopropane, 1-methyl-2-phenylcyclopropane, *p*-halophenylcyclopropanes, cyanocyclopropane, acetylcyclopropane and cyclopropanecarboxylic acid) did not undergo photochemical addition of sulfur dioxide.

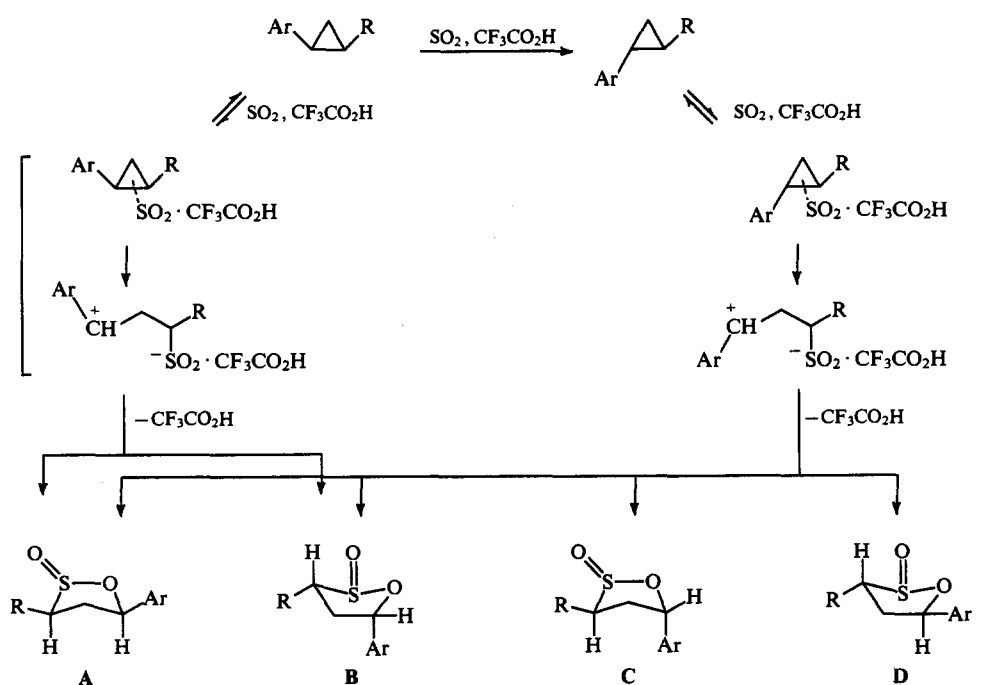


R = CN, NO₂, Ac

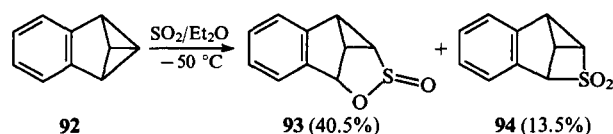


R = *o*-, *p*-NO₂

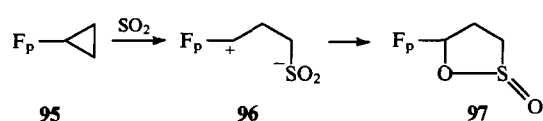
The addition of sulfur dioxide to substituted benzvalenes to give mixtures of isomeric sultines and sulfones has been



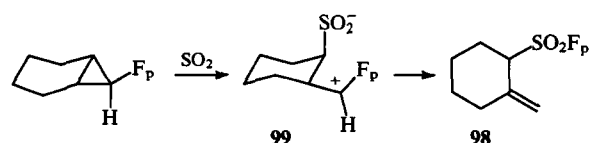
reported.^{83,84} In the case of benzobenzvalene **92**, the sultine **93** is the main reaction product (the product ratio **93**:**94** = 3:1).



The addition of sulfur dioxide to the cyclopropyl- F_p complex **95** [where $\text{F}_p = (\eta^5\text{-C}_5\text{H}_5)\text{Fe}(\text{CO})_2$] has been reported.⁸⁵ Sulfur dioxide is usually inserted into the C–M bond of such compounds, but the reaction involving complex **95** follows a non-standard pathway with opening of the trimethylene ring and formation of the carbocation **96**, which is then transformed into the sultine **97**.

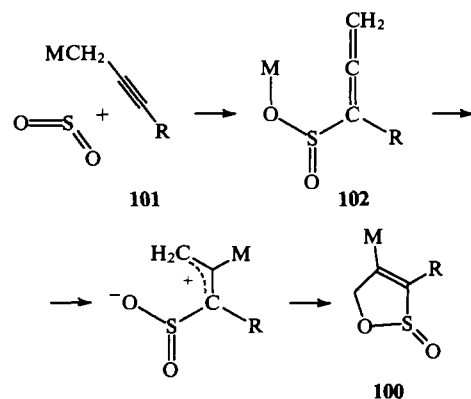


However, the reaction of the norcaradiene- F_p complex with sulfur dioxide results exclusively in the sulfone **98**. It is assumed that the reaction goes through the intermediate ion **99** having a *trans*-configuration, which makes cyclisation impossible.



c. Reactions of sulfur dioxide with organometallic compounds

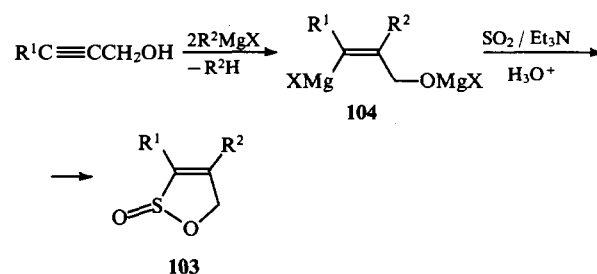
Quite unexpectedly, the sultines **100** were found to be formed in reactions between sulfur dioxide and 2-alkynyl derivatives of transition metals **101**.⁸⁶ The initial electrophilic attack is at the C≡C triple bond. The scheme presented below is supported by the fact that the reaction between sulfur dioxide and the $\text{Ph}_3\text{SnCH}_2\text{C}\equiv\text{CH}$ complex gives the stable sulfinate $\text{Ph}_3\text{Sn}[\text{O}-\text{S}(\text{O})\text{CH}=\text{C}=\text{CH}_2]$, the structure of which is similar to that of intermediate **102**.



M	R	M	R
$\eta^5\text{-C}_5\text{H}_5\text{Fe}(\text{CO})_2$	Me	$\text{Mn}(\text{CO})_5$	Me
$\eta^5\text{-C}_5\text{H}_5\text{Fe}(\text{CO})_2$	Ph	$\eta^5\text{-C}_5\text{H}_5\text{Mo}(\text{CO})_3$	H
$\text{Mn}(\text{CO})_5$	H	$\eta^5\text{-C}_5\text{H}_5\text{Mo}(\text{CO})_3$	Me

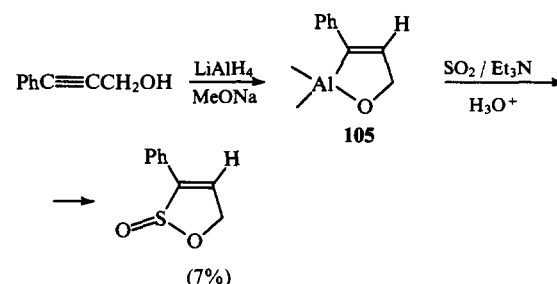
Conversely, the reaction between sulfur dioxide and Grignard reagents or organolithium compounds occurs in the typical way, sulfur dioxide being inserted into the C–M bond. For example, the α,β -unsaturated γ -sultines **103** were synthesised⁸⁷ by the addition of sulfur dioxide to the Grignard reagents **104** obtained from propargyl alcohols. The hydroxysulfinate formed initially

undergoes cyclisation to the sultine **103** upon subsequent hydrolysis (see Section II.2.c).

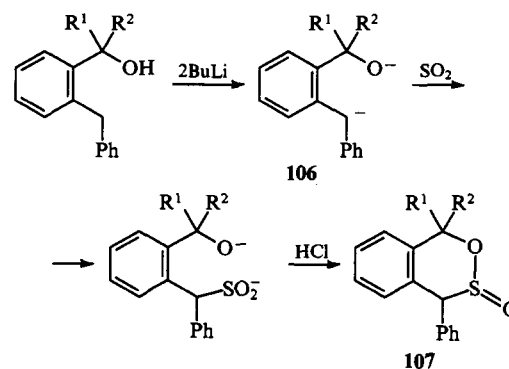


R ¹	R ²	Yield (%)
H	Et	30
H	Ph	60
H	$\text{CH}_2\text{CH}=\text{CH}_2$	32
Ph	Et	40
Ph	Ph	24

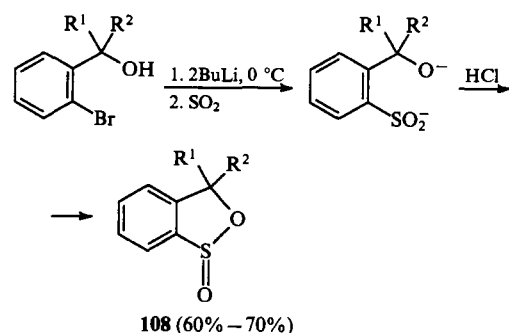
A sultine with $\text{R}^2 = \text{H}$ was isolated in a low yield when the organoaluminium compound **105** containing a vinylic fragment was used instead of the Grignard reagent.



Durst et al.⁴³ proposed that hydroxysulfonates be obtained by adding sulfur dioxide to the previously formed dianion **106**. This approach was used to synthesise benzoxathiine oxides **107** and benzoxathiol oxides **108**.



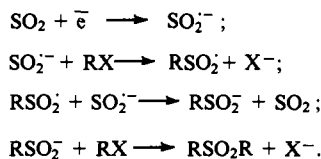
$\text{R}^1 = \text{R}^2 = \text{H}$ (50%–70%); $\text{R}^1 = \text{R}^2 = \text{Me}$ (38%)



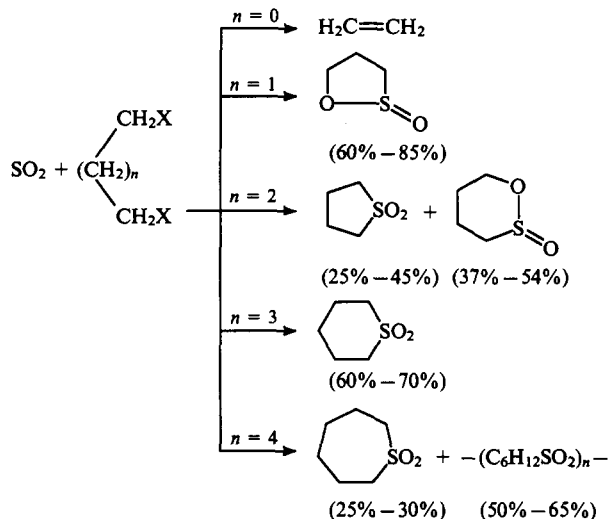
$\text{R}^1 = \text{R}^2 = \text{H}$; $\text{R}^1 = \text{H}, \text{R}^2 = \text{Me}$; $\text{R}^1 = \text{R}^2 = \text{Me}$

d. Electrochemical synthesis of sultines involving sulfur dioxide

In several papers on the cathodic reduction of sulfur dioxide in aprotic solvents (DMF, acetonitrile),⁸⁸⁻⁹⁰ a synthesis of five- and six-membered sultines by treatment of alkylene dihalides with the SO_2^- anion radical was proposed. The following mechanism of reaction of the latter in the presence of alkylene dihalides was assumed:



The yields of sultines or cyclic sulfones depend on the distance between the reaction centres in the alkylene dihalide. This can be demonstrated by the scheme below.



X = Cl, Br, OTs

III. Properties of sultines

The limited number of convenient methods for the synthesis of sultines has meant that their chemistry has been studied inadequately, and data on their reactions are rather fragmentary. The thermal and photochemical decomposition of sultines as well as the oxidation, reduction, and cleavage of the sultine ring by nucleophiles have been studied in more detail.

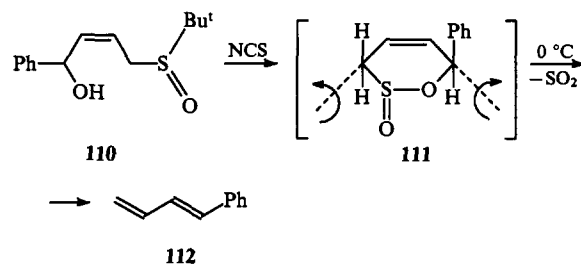
1. Thermolysis and photolysis of sultines

The thermal stability of sultines is primarily determined by the size of the heterocyclic ring, the nature and position of substituents in the ring, and to a lesser extent by other features of their structure.

For example, with rare exceptions, β -sultines are very unstable and decompose even at room temperature in several minutes with the evolution of sulfur dioxide and formation of unsaturated compounds³⁸⁻⁴⁰ (see Section II.2). This is probably a consequence of the considerable strain in the four-membered

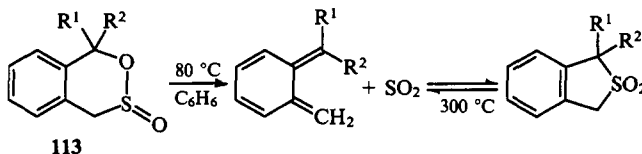
heterocycle. The loss of sulfur dioxide occurs stereospecifically by *cis*-elimination, which was demonstrated in the formation of *cis*-stilbene **109** (> 99%).

β , γ -Unsaturated six-membered sultines — 3,6-dihydro-1,2-oxathiine 2-oxides — are unstable at temperatures above 0 °C and decompose into 1,3-dienes and sulfur dioxide.^{25, 67} The stereospecific nature of this reaction was shown for the *cis*-hydroxy-sulfoxide **110**, which gave exclusively *trans*-1-phenylbuta-1,3-diene **112** (> 99.5%) by fragmentation of the intermediate sultine **111**.



This process is characterised by extremely easy sulfur dioxide elimination: the decomposition of 3,6-dihydro-1,2-oxathiine 2-oxide into the corresponding 1,3-diene and sulfur dioxide occurs at a temperature lower by 125 °C than that required for the similar decomposition of 2,5-dihydrothiophene 1,1-dioxide.

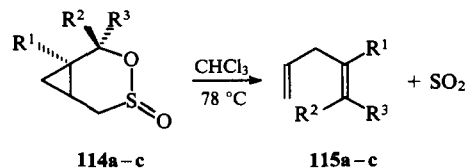
Unlike the 3,6-dihydro-1,2-oxathiine 2-oxides already considered, benzoxathiine oxides **113** are more stable and decompose into the corresponding *o*-quinodimethanes and sulfur dioxide only at 80 °C, whereas the elimination of sulfur dioxide from the corresponding sulfones occurs only at 300 °C.^{25, 45, 67} In the absence of other dienophiles, the resulting diene once again traps the sulfur dioxide molecule to give a cyclic sulfone isomeric with the original sultine **113**.



$\text{R}^1 = \text{H}; \text{R}^2 = \text{H, Ph, Me}; \text{R}^1 = \text{R}^2 = \text{Me}.$

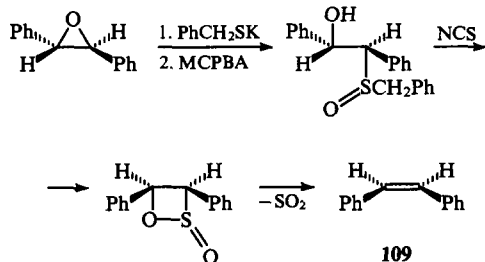
The ease of sulfur dioxide elimination allows one to use this reaction for generating such reactive dienes as *o*-quinodimethanes by cycloaddition in situ under mild conditions.

The fragmentation of 3,4-oxathiabicyclo[4.1.0]heptane 4-oxides **114** in boiling chloroform into a 1,4-diene and sulfur dioxide occurs stereospecifically.⁹¹ This reaction produces *cis*- and *trans*-4-phenylhexa-1,4-dienes **115a** and **115b** from sultines **114a** and **114b** with > 99.5% isomeric purity.



a: $\text{R}^1 = \text{Ph}, \text{R}^2 = \text{H}, \text{R}^3 = \text{Me};$
 b: $\text{R}^1 = \text{Ph}, \text{R}^2 = \text{Me}, \text{R}^3 = \text{H};$
 c: $\text{R}^1 = \text{R}^2 = \text{R}^3 = \text{H}$

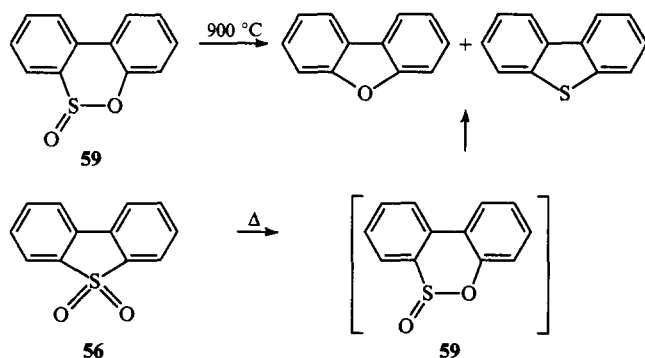
The stereochemistry of the sulfinyl group and the mutual arrangement of substituents considerably affect the decomposition rate. It should be noted that the decomposition of sultines again occurs at a temperature 100 °C lower than that required for the decomposition of the isomeric sulfone, 3-thia-bicyclo[3.1.0]-hexane 3,3-dioxide.



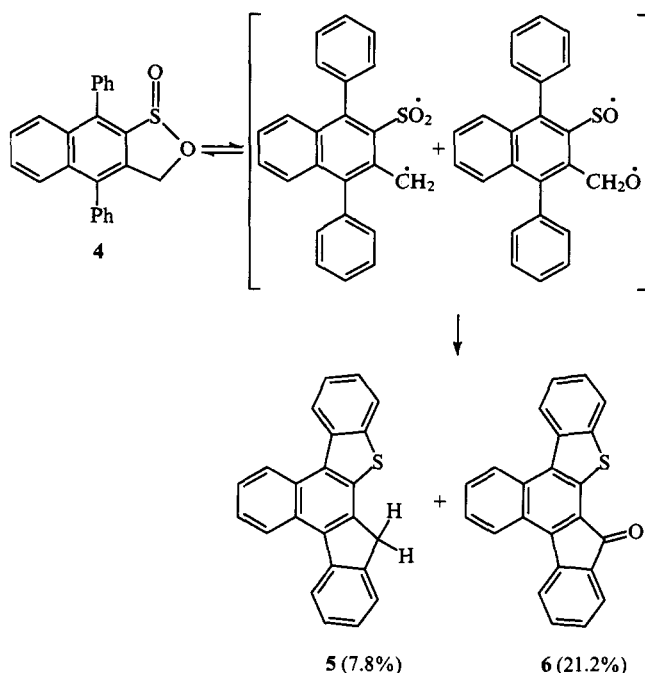
All the above examples of the thermal decomposition of sultines occur apparently as concerted processes, which is suggested by the stereospecificity of the transformations and the ease (low temperatures) of sulfur dioxide elimination.

The examples of the thermal and photochemical degradation of six- and five-membered sultines described below are likely to be radical processes. The reactions occur at very high temperatures (400–900 °C), and their course significantly depends on the structure of the initial sultine and on the nature of the substituents.

For example, the thermolysis of dibenzoxathiine oxide **59** yields a mixture of dibenzofuran and dibenzothiophene in a 6 : 1 ratio.⁴⁸ The pyrolysis of dibenzothiophene 1,1-dioxide **56** gives the same products and in the same ratio, which makes it possible to assume the intermediate formation of the sultine **59**.⁹²

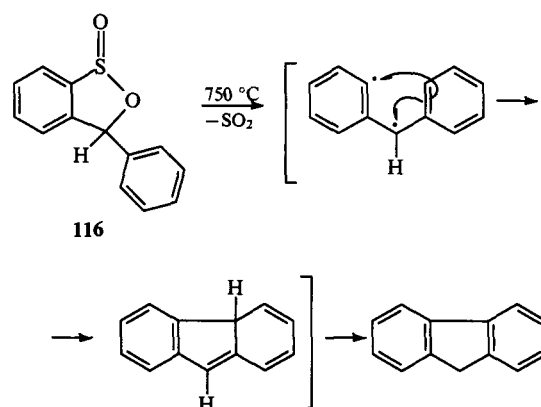


The thermolysis of diphenylnaphthoxathiole oxide **4** results in two cyclisation products, compounds **5** and **6**, which are formed by the interaction of radical centres with the neighbouring phenyl groups.⁷

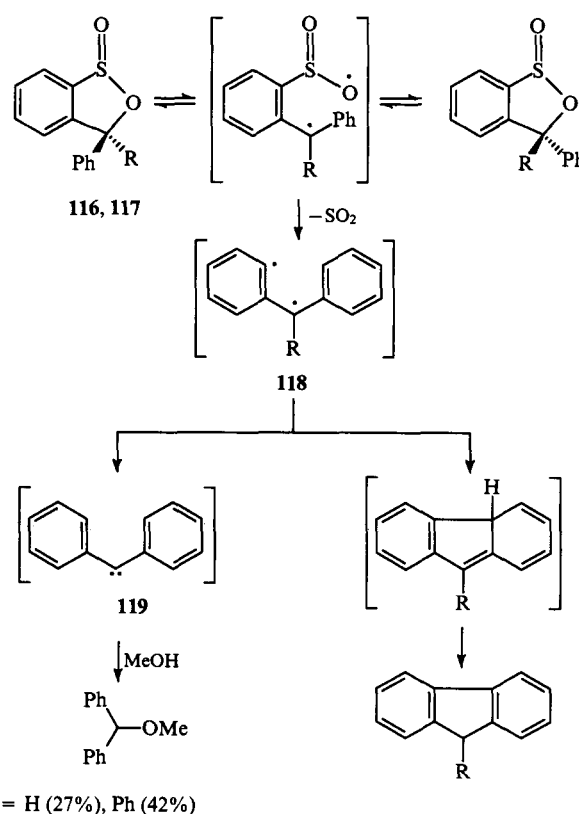


In general, the presence of stabilising phenyl groups adjacent to the reaction centres in the molecule has a decisive effect on the thermal and photolytic transformations of sultines.

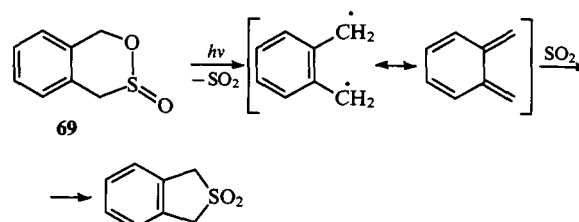
For example, the thermal decomposition of phenyl-benzoxathiol oxide **116** at 750 °C occurs by the elimination of a sulfur dioxide molecule to give a 1,3-biradical, which then rearranges to fluorene. However, the thermolysis of the unsubstituted analogue under the same conditions results in an uncharacterised mixture of degradation products.⁹³

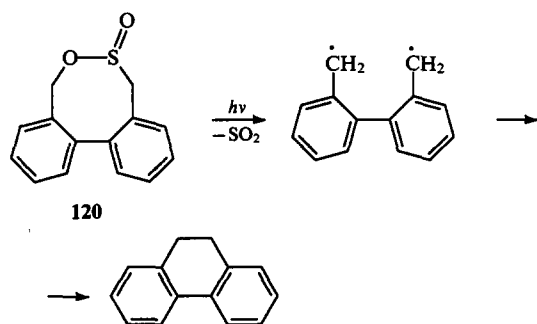


A complete analogy between the reactions was also observed in the photolytic decomposition of the sultines **116** and **117**.⁹⁴ It was shown that the resulting 1,3-biradical **118** can also rearrange to the carbene **119**, which was identified by its reaction with methanol.

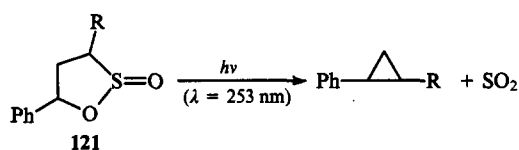


The photolysis of six-membered (**69**) and eight-membered (**120**) sultines in methanol gave a sulfone and 9,10-dihydrophe-nanthrene, respectively.

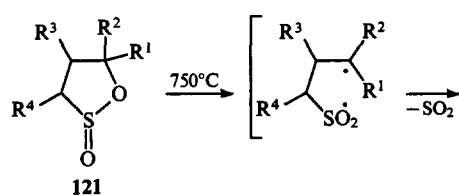




The thermolysis and photolysis of 5-phenyl-1,2-oxathiolane 2-oxides **121** are accompanied by the formation of a 1,3-biradical, in which one centre is located on the C atom of the benzyl group. This radical then recombines to give the corresponding cyclopropane. If other substituents are attached at the C(5) atom, stabilisation of the 1,3-biradical leads predominantly to isomeric alkenes.^{93, 94}

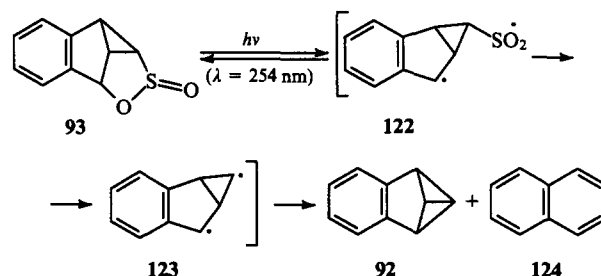


R = H (95%), Me (98%)



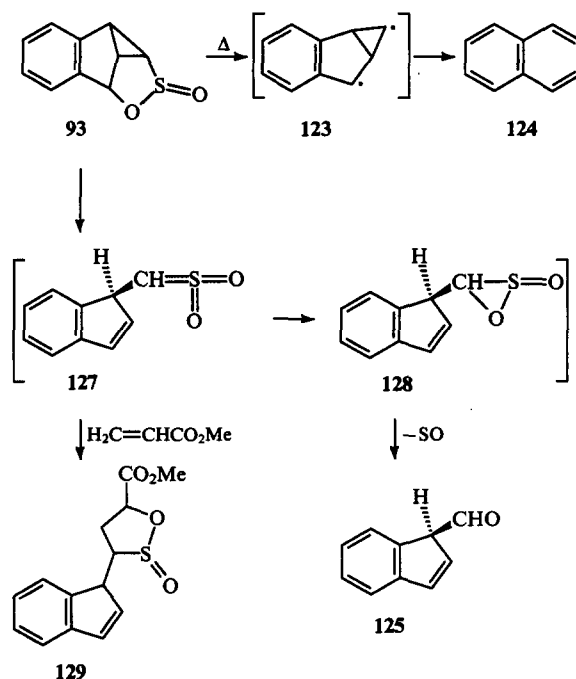
				Product yield (%)	
				A	B
R ¹	R ²	R ³	R ⁴		
Ph	H	H	H	100	—
Ph	Me	H	H	100	—
H	H	Me	H	37	62
H	H	Ph	H	—	†
Me	H	H	H	45	35

The addition of sulfur dioxide to benzobenzvalene, like the addition to arylcyclopropanes (see Section II.3.b), was found to be photochemically reversible. When the sultine **93** was irradiated with UV light, it evolved sulfur dioxide with the regeneration of the original benzobenzvalene **92** and formation of naphthalene in a 1 : 3 ratio.⁸⁴



This reaction is believed⁸⁴ to occur by reversible homolytic cleavage of the sultine to give the biradicals **122** and **123**. The latter, which is in a singlet state, gives benzobenzvalene **92**; alternatively, naphthalene **124** is formed by bond cleavage in the cyclopropane fragment.

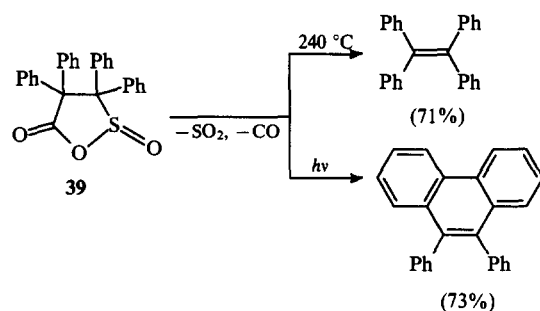
The pyrolysis of the sultine **93** gives a complex mixture of products; 1*H*-indene-1-carboxaldehyde **125** and 1*H*-indene-3-carboxaldehyde **126** together with naphthalene were isolated from it in the proportion **124** : **125** : **126** : **92** = 52 : 22 : 16 : 9.5.⁹⁵ It is assumed that naphthalene is also formed due to the cleavage of the C—C bond in the intermediate biradical **123**. The formation of aldehydes in the reaction mixture was explained⁹⁵ by the generation of sulfene **127** and its subsequent cyclisation to the oxathiirane *S*-oxide **128**. In the final step, the oxathiirane *S*-oxide **128** loses a sulfur monoxide molecule to give the aldehyde **125**.



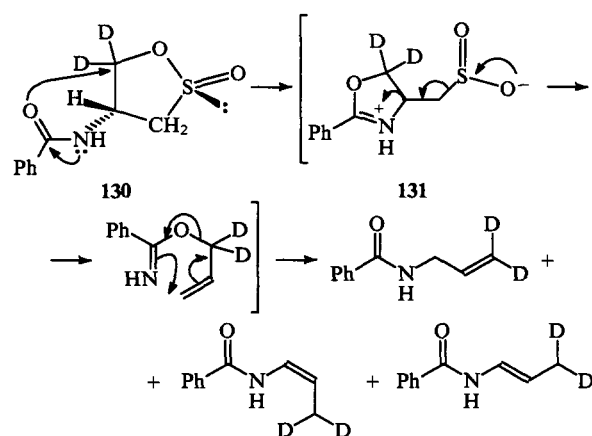
The presence of the sulfene **127** in the reaction mixture was proved by performing the pyrolysis with a tenfold excess of methyl methacrylate. This gave naphthalene (22%) and the sultine **129** (58%), the product of the 1,3-dipolar cycloaddition of the sulfene. The formation of aldehydes was not observed in this case.

The thermolysis and photolysis of the γ -sultine **39** give different products.²³ In the former case, the elimination of sulfur dioxide and carbon monoxide molecules gives tetraphenylethene, while in the latter, the intermediate is stabilised by participation of the neighbouring phenyl groups to give 9,10-diphenylphenanthrene.

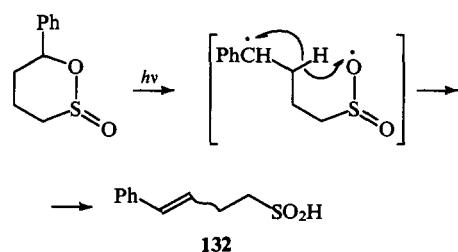
† Compound **B** is the only product; yield is not reported.⁹³



The thermal transformation of the functionally-substituted γ -sultine 130 considered below leads to a mixture of *N*-allylamide and enamides owing to heterolytic bond cleavage with participation of neighbouring functional groups.⁹⁶ This decomposition is considered to involve most probably the formation of oxazolinium species 131 due to intramolecular nucleophilic attack by the amide oxygen atom at the C–O bond in the sultine ring.⁹⁶

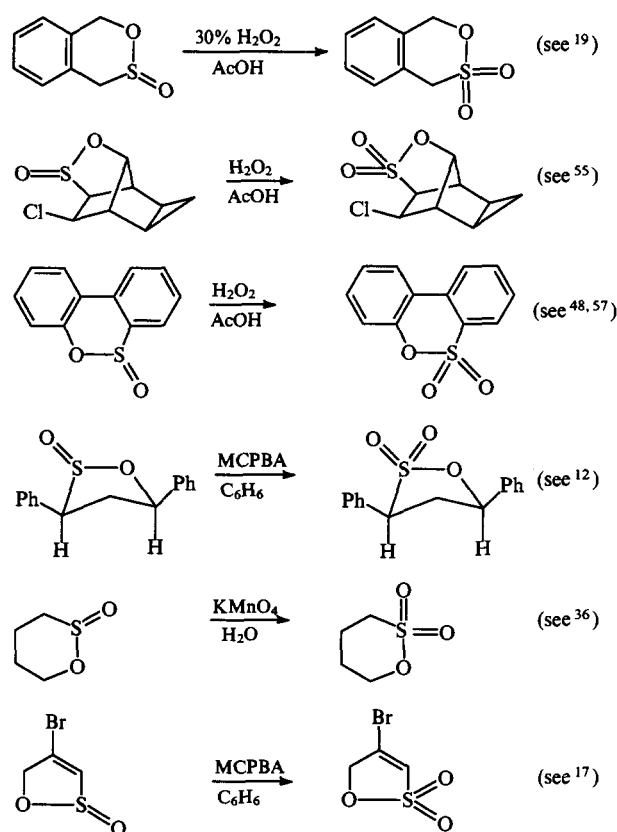


The thermal and photolytic decomposition of six-membered saturated sultines has scarcely been studied. Only the photolysis of 6-phenyl-1,2-oxathiane 2-oxide to give the unsaturated sulfinic acid 132 has been reported.⁹⁴

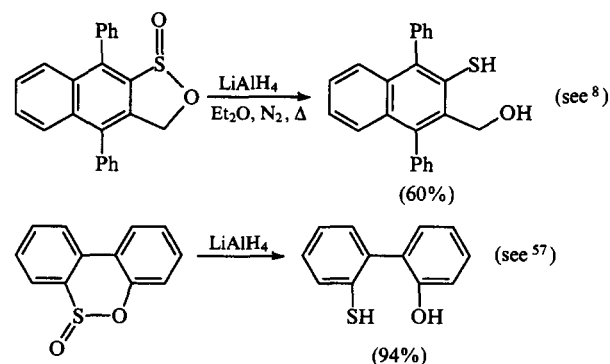


2. Redox reactions of sultines

One of the most typical reactions, which is often used to prove the presence of a sulfinyl group in the compound under investigation, is the oxidation of sultines. The reaction gives sultones, cyclic esters of sulfonic acid, with characteristic frequencies at 1300–1360 cm^{-1} in their IR spectra. This distinguishes them from sultines, which unlike sultones, do not have this characteristic band in their IR spectra, and absorption is observed only at 1100–1150 cm^{-1} . (For the methods of preparation and reactions of sultones, see Ref. 97). As a rule, a 30% solution of hydrogen peroxide in glacial acetic acid^{9, 19, 48, 55, 57, 82} or MCPBA^{12, 17, 24, 26} are used as oxidants; the latter permits oxidation under mild conditions. In addition, potassium permanganate,³⁶ chromic acid⁹⁸ and potassium hydropersulfate⁸⁷ are also used for the oxidation of sultines. A few typical reactions are given below:

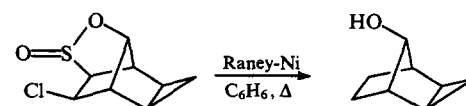


Unlike the oxidation of heterocycles containing an SO fragment in the ring, which can be carried out in stages, passing from sulfinyl to sulfinyl group⁴¹ and then to the sulfonyl group, the known sultine reduction reactions proceed exhaustively omitting the sultene formation stage. In this case, cleavage of the sultine ring at the S–O bond occurs leading, as a rule, to mercaptoalcohols.

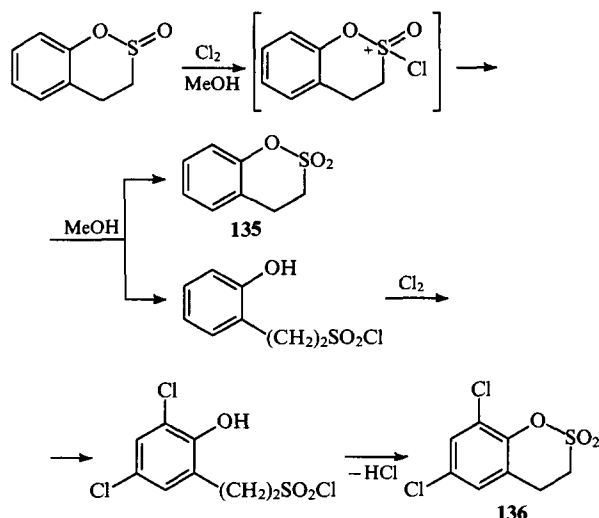


The latter reaction is of interest because this is a convenient method for the bifunctionalisation of biphenyl.⁵⁷

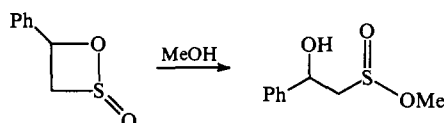
The reduction of sultines in the presence of Raney nickel or with a great excess of lithium tetrahydroaluminate results in the total desulfurization of the compound to give the corresponding alcohol.⁵⁵



The reduction of γ - and δ -sultines with trichlorosilane in the presence of tri(*n*-propyl)amine affords symmetrical dihydroxydisulfides in high yields.⁹⁹ The reduction mechanism is unclear;

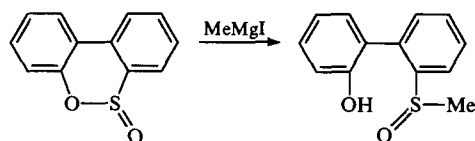


In the case of the alcoholysis of a four-membered sultone, 4-phenyl-1,2-oxathietane 2-oxide, nucleophilic attack is directed at the S atom giving hydroxysulfonate esters.³⁸

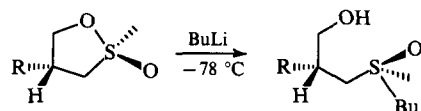


Thus, nucleophilic attack can be directed to both the C and S atoms, probably depending on the structure of the starting compounds. These data are consistent with the results obtained for sultones: the decomposition of sultones with fused aromatic rings occurs both through the cleavage of the C—O bond^{104, 105} and the S—O bond,^{106, 107} depending on their structure and reaction conditions, but, as a rule, β -sultones react with nucleophiles through the sulfur atom, while the reactions of larger-ring sultones involve the carbon atom.

The cleavage of sulfonate esters with organomagnesium compounds to give sulfoxides is well known. In the case of the cyclic esters, i.e. sultines, this cleavage results in the corresponding hydroxysulfoxides.^{48, 108}



The reactions of sultines with alkyllithium compounds proceeds in a similar way; hydroxyalkyl sulfoxides are also formed as a result of nucleophilic attack at the S atom.²⁰



R = Bu⁺CONH

Interesting data on the ability of sultines to form crystalline molecular complexes with organotin compounds (of the composition $\text{RSnCl}_3 \cdot \text{L} = 1:2$ where L is 3,5-diaryl-1,2-oxathiolane 2-oxide), which may possess biological activity, have been published.¹⁰⁹

As already mentioned, the chemistry of the sultines has not yet been adequately studied, although their presently known reactions make them rather promising reagents for use in organic synthesis. This inadequacy is partly related to the lack of convenient methods for the synthesis of sultines. Therefore, the development of new methods of synthesis of sultines and the study of their properties remain of great current interest.

This study was financially supported by the Russian Fundamental Research Fund (Grant No. 94-03-09592).

References

1. E Baumann, G Walter *Chem. Ber.* **26** 1124 (1893)
2. S Braverman, Y Duar *J. Am. Chem. Soc.* **105** 1061 (1983)
3. S Braverman *Phosphorus Sulfur* **23** 297 (1985)
4. T P Vasil'eva, in *Organicheskaya Khimiya (Ser. Itogi Nauki i Tekhniki)* T. 13 [Organic Chemistry (Advances in Science and Engineering Series) Vol. 13] (Moscow: Izd. VINITI, 1988) p. 99
5. D C Dittmer, M D Hoey, in *The Chemistry of Functional Groups* (Ed. S Patai) (Chichester: Wiley, 1990) p. 239
6. K Hiroi, S Sato, R Kitayama *Annu. Rep. Tohoku Coll. Pharm.* **30** 1 (1983)
7. C J Kelley, M Carmack *Tetrahedron Lett.* **16** 3605 (1975)
8. D C Dittmer, R S Henion, N Takashina *J. Org. Chem.* **34** 1310 (1969)
9. J F King, P de Mayo, C L McIntosh, K Piers, D J H Smith *Can. J. Chem.* **48** 3704 (1970)
10. J F King, A Hawson, B L Huston, L J Danks, J Komery *Can. J. Chem.* **49** 943 (1971)
11. J F King, B L Huston, A Hawson, J Komery, D M Deaken, D R K Harding *Can. J. Chem.* **49** 936 (1971)
12. R M Dodson, P D Hammen, R A Davis *J. Org. Chem.* **36** 2693 (1971)
13. R M Dodson, P D Hammen, J U Fan *J. Org. Chem.* **36** 2703 (1971)
14. E L Eliel, N L Allinger, S J Angyal, G A Morrison, in *Conformational Analysis* (New York: Interscience, 1965) (Translated into Russian; Moscow: Mir, 1969, p. 247)
15. D N Harpp, J G Gleason, D K Ash *J. Org. Chem.* **36** 322 (1971)
16. S Braverman, D Reisman *J. Am. Chem. Soc.* **99** 605 (1977)
17. S Braverman, D Reisman *Tetrahedron Lett.* **18** 1753 (1977)
18. S V Veselovskaya, L G Saginova, Yu S Shabarov *Zh. Org. Khim.* **23** 129 (1987)
19. E N Givens, L A Hamilton *J. Org. Chem.* **32** 2857 (1967)
20. R M J Liskamp, H J M Zeegers, H C J Ottenheijm *J. Org. Chem.* **46** 5408 (1981)
21. J P King, R Rathore *Tetrahedron Lett.* **30** 2763 (1989)
22. T P Vasil'eva *Izv. Akad. Nauk, Ser. Khim.* 2153 (1992)
23. H Kohn, P Charumilind, S H Simonsen *J. Am. Chem. Soc.* **101** 5431 (1979)
24. J T Doi, G W Luehr, W K Musker *J. Org. Chem.* **50** 5716 (1985)
25. F Jung, M Molin, R Van Den Elzen, T Durst *J. Am. Chem. Soc.* **96** 935 (1974)
26. N K Sharma, F de Reinach-Hirtzbach, T Durst *Can. J. Chem.* **54** 3012 (1976)
27. L Breau, N K Sharma, J R Butler, T Durst *Can. J. Chem.* **69** 185 (1991)
28. M Casey, A C Manage, P J Murphy *Tetrahedron Lett.* **33** 965 (1992)
29. T Durst, K-C Tin, M J V Marcil *Can. J. Chem.* **51** 1704 (1973)
30. H Taguchi, H Yamamoto, H Nozaki *Tetrahedron Lett.* **14** 2463 (1973)
31. A R Derzhinskii, O S Chizhov, E N Prilezhaeva *Izv. Akad. Nauk SSSR, Ser. Khim.* 850 (1977)
32. A R Derzhinskii, L D Konyushkin, E N Prilezhaeva *Izv. Akad. Nauk SSSR, Ser. Khim.* 2070 (1978)
33. P J R Nederlof, M J Moolenaar, E R de Waard, H O Huisman *Tetrahedron* **34** 447 (1978)
34. T Durst, K-C Tin *Can. J. Chem.* **49** 2374 (1971)
35. G W Buchanan, N K Sharma, F de Reinach-Hirtzbach, T Durst *Can. J. Chem.* **55** 44 (1977)
36. D N Harpp, J G Gleason *J. Org. Chem.* **36** 1314 (1971)
37. O Exner, D N Harpp, J G Gleason *Can. J. Chem.* **50** 548 (1972)

38. F Jung, N K Sharma, T Durst *J. Am. Chem. Soc.* **95** 3420 (1973)
39. J Nokami, N Kunieda, M Kinoshita *Tetrahedron Lett.* **16** 2179 (1975)
40. T Durst, B P Gimbarzevsky *J. Chem. Soc., Chem. Commun.* 724 (1975)
41. W Walter, B Krische, G Adiwidjaja, J Vob *Chem. Ber.* **111** 1685 (1978)
42. W Walter, B Krische, G Adiwidjaja *Liebigs Ann. Chem.* **1** 14 (1980)
43. T Durst, J L Charlton, D B Mount *Can. J. Chem.* **64** 246 (1986)
44. C A Bunton, B N Hendy *J. Chem. Soc.* 2562 (1962)
45. J L Charlton, T Durst *Tetrahedron Lett.* **25** 5287 (1984)
46. P Messinger, Von R Vietinghoff-Scheel *Arch. Pharm. (Weinheim)* **318** 813 (1985)
47. P Messinger *Arch. Pharm. (Weinheim)* **318** 950 (1985)
48. T G Squires, C G Venier, B A Hodgson, L W Chang, F A Davis, T W Panunto *J. Org. Chem.* **46** 2373 (1981)
49. V E Udre, E Ya Lukevits, A A Kemme, Ya Ya Bleidelis *Khim. Geterotsikl. Soedin.* 320 (1980)
50. M G Lin'kova, T P Vasil'eva, V M Bystrova, N V Kalyuzhnaya, O V Kil'disheva, I L Knunyants *Izv. Akad. Nauk SSSR, Ser. Khim.* 617 (1984)
51. D N Harpp, K Steliou, T H Chan *J. Am. Chem. Soc.* **100** 1222 (1978)
52. Q E Thompson *J. Org. Chem.* **30** 2703 (1965)
53. H Inoue, N Inogushi, E Imoto *Bull. Chem. Soc. Jpn.* **5** 197 (1977)
54. K S Dhami *Chem. Ind. (London)* 1004 (1968)
55. K Henrick, B L Jonson *Aust. J. Chem.* **25** 2263 (1972)
56. C M Marson, P R Giles, H Adams, N A Bailey *J. Chem. Soc., Chem. Commun.* 1195 (1993)
57. G Hanson, D S Kemp *J. Org. Chem.* **46** 5441 (1981)
58. J Grundnes, S D Christian *J. Am. Chem. Soc.* **90** 2239 (1968)
59. L J Andrews, R M Keefer *J. Am. Chem. Soc.* **73** 4169 (1951)
60. L J Andrews *Chem. Rev.* **54** 713 (1954)
61. N N Lichtin, R E Weston Jr, J D White *J. Am. Chem. Soc.* **74** 4715 (1952)
62. P A D Maine *J. Chem. Phys.* **26** 1036 (1957)
63. D Booth, F S Dainton, K J Ivin *Trans. Faraday Soc.* **55** 1293 (1959)
64. S D Christian, J Grundnes *Nature (London)* **214** 1111 (1967)
65. D van der Helm, J D Childs, S D Christian *J. Chem. Soc., Chem. Commun.* 887 (1969)
66. S D Turk, R L Cobb, in *1,4-Cycloaddition Reactions* (Ed. J Hamer) (New York: Academic Press, 1967) Vol. 8, Pt 2
67. R F Heldeweg, H Hogeveen *J. Am. Chem. Soc.* **98** 2341 (1976)
68. T Durst, L Tetreault-Ryan *Tetrahedron Lett.* **19** 2353 (1978)
69. H Hogeveen, H Jorritsma, P W Kwant *Tetrahedron Lett.* **16** 1795 (1975)
70. J Gasteiger, R Huisgen *J. Am. Chem. Soc.* **94** 6541 (1972)
71. L A Paquette, U Jacobsson, M Oku *J. Chem. Soc., Chem. Commun.* 115 (1975)
72. R-L Fan, J I Dickstien, S I Miller *J. Org. Chem.* **47** 2466 (1982)
73. J W Moore, H W Baird, H B Miller *J. Am. Chem. Soc.* **90** 1358 (1968)
74. K S Fongers, H Hogeveen *Tetrahedron Lett.* **20** 275 (1979)
75. G A Olah, G K S Prakash, M R Bruce *J. Am. Chem. Soc.* **101** 6463 (1979)
76. O B Bondarenko, L G Saginova, Yu S Shabarov *Zh. Org. Khim.* **23** 1114 (1987)
77. O B Bondarenko, T I Voevodskaya, L G Saginova, V A Tafeenko, Yu S Shabarov *Zh. Org. Khim.* **23** 1736 (1987)
78. O B Bondarenko, A V Buevich, T I Voevodskaya, L G Saginova, Yu S Shabarov *Zh. Org. Khim.* **24** 1937 (1988)
79. O B Bondarenko, L G Saginova, T I Voevodskaya, A V Buevich, D S Yufit, Yu T Struchkov, Yu S Shabarov *Zh. Org. Khim.* **26** 281 (1990)
80. O B Bondarenko, L G Saginova, T I Voevodskaya, Yu S Shabarov *Zh. Org. Khim.* **26** 553 (1990)
81. O B Bondarenko, Candidate Thesis in Chemical Sciences, Moscow State University, Moscow, 1987
82. D E Applequist, L F McKenzie *J. Org. Chem.* **42** 1251 (1977)
83. H Hogeveen, L Zwart *J. Am. Chem. Soc.* **104** 4889 (1982)
84. U Burger, C Gmunder, S Schmidlin, G Bernardinelli *Helv. Chim. Acta* **73** 1724 (1990)
85. A Cutler, R W Fish, W R Giering, M Rosenblum *J. Am. Chem. Soc.* **94** 4354 (1972)
86. J E Thomasson, P W Robinson, D A Poss, A Wojcicki *Inorg. Chem.* **10** 2130 (1971)
87. E Thoumazeau, B Jousseau, F Tiffon, J-G Duboudin *Heterocycles* **19** 2247 (1982)
88. D Knittel, B Kastening *J. Appl. Electrochem.* **3** 291 (1973)
89. B Kastening, B Gostisa-Mihelcic *J. Electroanal. Chem.* **100** 801 (1979)
90. D Knittel *Monatsch. Chem.* **113** 37 (1982)
91. F Jung *J. Chem. Soc., Chem. Commun.* 525 (1976)
92. E K Fields, S Meyerson *J. Am. Chem. Soc.* **88** 2836 (1966)
93. T Durst, J D Finlay, D J H Smith *J. Chem. Soc. Perkin Trans. 1* 950 (1979)
94. T Durst, J C Huang, N K Sharma *Can. J. Chem.* **56** 512 (1978)
95. U Burger, D Erner-Lellweger, A W Sledeski, S Schmidlin *Tetrahedron Lett.* **30** 2797 (1989)
96. R M J Liskamp, H J Blom, R J F Nivard, H C J Ottenheim *J. Org. Chem.* **48** 2733 (1983)
97. D W Roberts, D L Williams *Tetrahedron* **43** 1027 (1987)
98. J Wolinsky, R L Marhenke *J. Org. Chem.* **40** 1766 (1975)
99. T H Chan, J P Montillier, W F van Horn, D N Harpp *J. Am. Chem. Soc.* **92** 7224 (1970)
100. T Okuyama, H Takano, K Ohnishi, S Nagase *J. Org. Chem.* **59** 472 (1994)
101. T P Vasil'eva, V M Bystrova, O V Kil'disheva *Izv. Akad. Nauk SSSR, Ser. Khim.* 1633 (1988)
102. V V Znamenskii, A D Efremov, V M Bystrova, T P Vasil'eva, O V Kil'disheva *Khim.-Farm. Zh.* **20** 843 (1986)
103. T P Vasil'eva, V V Znamenskii *Khim.-Farm. Zh.* **28** 33 (1994)
104. E E Gilbert, in *Sulfonation and Related Reactions* (Translated into Russian; Moscow: Khimiya, 1969, p. 249)
105. A Mori, M Nagayama, H Mandai *Bull. Chem. Soc. Jpn.* **44** 1669 (1971)
106. A Mustafa *Chem. Rev.* **54** 195 (1954)
107. A Laleh, R Ranson, J G Tillett *J. Chem. Soc., Perkin Trans. 2* 610 (1980)
108. D N Harpp, S M Vines, J P Montillier, T H Chan *J. Org. Chem.* **41** 3987 (1976)
109. N V Novozhilov, L G Saginova, E V Grigor'ev, V S Petrosyan *Vestn. Mosk. Univ., Ser. 2, Khim.* **35** 273 (1994)

Synthesis of monodisperse functional polymeric microspheres for immunoassay

NI Prokopov, I A Gritskova, V R Cherkasov, A E Chalykh

Contents

I. Introduction	167
II. Synthesis of polymeric suspensions with functional groups on the particle surface	168
III. Activation of functional groups on the surface of particles of a polymeric suspension	172

Abstract. Methods for the synthesis of functional polymeric suspensions with narrow particle size distribution are analysed. Attention is concentrated on the conditions of the preparation of polymeric microspheres with aldehyde, carboxyl, epoxy, or amino groups on the surface, which possess a set of properties enabling their use for biochemical studies. Methods of modification of functional groups of the polymeric suspensions that make it possible to accomplish covalent binding of the surface groups to bioligands are considered. The bibliography includes 218 references.

I. Introduction

Aqueous suspensions containing strictly spherical polymer particles of identical diameters are usually referred to as polymeric suspensions with narrow particle size distribution (PSD).¹ Typical magnitudes of the variation coefficient (a measure of the deviation of the particle diameters from the mean value) are 1%–3% (for particles 0.1–10 μm in diameter)^{2–4} or 10%–30% (for particles with diameters smaller than 0.06 or greater than 10 μm).^{2,5}

Polymeric microspheres with a narrow PSD are used in various fields of science and engineering, for example, as calibration standards in the electron and optical microscopy and light-scattering, for counting aerosol particles, in small-angle X-ray diffraction, for counting viral particles, for determining pore sizes in filters or biological membranes, for stimulating cellular production of antibodies and their purification,^{6–9} as model colloid systems for studying their rheology,^{10,11} stability, or sedimentation¹¹ etc. In recent years, monodisperse functional suspension particles have found wide application as protein carriers in development of immunodiagnostic assays.²

The function of these assays is based on the immunochemical reaction between an antigen (a substance carrying signs of genetic information alien for a particular type of organism) and antibodies (proteins belonging to the class of immunoglobulins and produced by the cells of the organism's immune system as a

response to the appearance of the antigen) yielding an 'antigen–antibody' complex.¹² The reaction in which this complex is formed is highly immunospecific, i.e. in response to the appearance of a particular antigen, the immune system generates antibodies of a strictly specified structure capable of interacting only with this antigen. Since both an antigen and an antibody can react simultaneously with several molecules, spatial networks are produced with the antigen molecules as nodes.

The formation of network agglomerates and, therefore, the appearance of one or another type of antigens can be detected by various methods, for example, by spectrophotometry, turbidimetry, nephelometry, laser self-correlation spectroscopy, etc. The need to use special expensive equipment for the detection of 'antigen–antibody' complexes hampers wide employment of the above methods in the diagnosis of diseases. However, when antigens (or antibodies) are bound to a polymeric carrier serving only as an indicator, the complexes can be detected even by the naked eye as crowding of agglomerates of the carrier particles.

The first communication on successful use of polyvinyltoluene and polystyrene microspheres with a narrow PSD in the diagnosis of rheumatoid arthritis was published in 1956.¹³ It was reported that the interaction of antigens present in the blood serum of a patient with gamma-globulin adsorbed on the microsphere surface of a suspension resulted in the agglutination of the polymeric particles affording large agglomerates, easily discernible by the naked eye. Later, publications appeared^{14–24} dealing with the use of polystyrene and poly(methyl methacrylate) suspension particles as protein carriers for preparing diagnostic test-systems for other types of diseases.

However, the use of particles of polymeric suspensions in the development of immunodiagnostic tests has been limited by irreproducibility of the results of analysis, which is caused, as has been suggested by Yen et al.,²⁴ by the fact that on slight variations of the conditions (pH, ionic strength of the medium, temperature, etc.), the protein adsorbed on the surface of particles is desorbed to the aqueous phase; and this lowers the sensitivity of the tests and leads to nonspecific reactions with other biological objects.

Polymeric suspensions containing hydrophilic particles with surface functional groups capable of forming covalent bonds with bioligands have proved to be free of these drawbacks. Polymeric suspensions based on copolymers of methyl methacrylate (MMA), 2-hydroxyethyl methacrylate, acrylic and methacrylic (MAA) acids, acrylamide, vinylpyridine, etc. have been synthesised and used successfully for developing immuno-diagnostic tests.^{24–29}

NI Prokopov, I A Gritskova, V R Cherkasov M V Lomonosov Moscow State Academy of Fine Chemical Technology, prosp. Vernadskogo 86, 117571 Moscow, Russian Federation. Fax (7-095) 430 79 83
A E Chalykh Institute of Physical Chemistry, Russian Academy of Sciences, Leninskii prosp. 31, 117915 Moscow, Russian Federation. Fax (7-095) 952 07 14

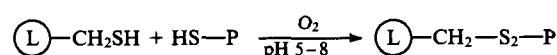
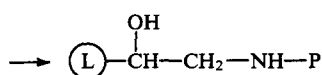
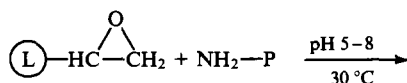
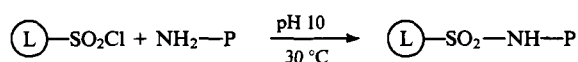
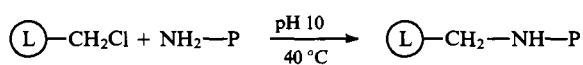
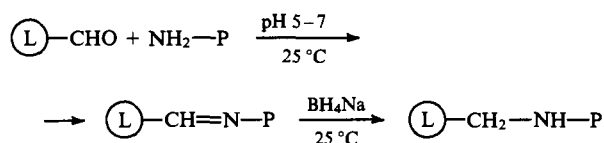
Received 14 July 1995

Uspekhi Khimii 65 (2) 178–192 (1996); translated by Z P Bobkova

The advantages of these suspensions over hydrophobic ones are the following:

- the absence of nonspecific adsorption of bioligands due to the high hydrophilicity of the surface of particles;
- the absence of desorption of protein molecules from the surface of microsphere due to the covalent bonding between a bioligand and functional groups of a polymeric particle;
- the possibility of covalent bonding of antigens and antibodies that are poorly sorbed on hydrophobic suspension surfaces;
- the possibility of the appearance of conditions ensuring the optimal orientation of biomolecules on microsphere surfaces, which would provide the maximum sensitivity and high specificity of the diagnostica synthesised.

The polymeric suspensions used in immunodiagnostics are classified in terms of the type of functional groups present on the surface. According to this criterion, they can be divided into two types. Suspensions, whose particles contain surface groups capable of direct interaction with amino, carboxyl, or mercapto groups of biomolecules, belong to the first type. These are, for example, chloromethyl,^{30–34} chlorosulfonyl,³¹ aldehyde,^{35–38} epoxy,³⁹ and mercapto^{40,41} groups, which react with biomolecules in an aqueous medium at moderate temperatures.



$\textcircled{\text{L}}$ — polymeric particle; P — protein

Suspensions with functional groups, which are not able to interact directly with proteins, but can form chemical bonds with them after a fairly simple activation reaction, belong to the second group. These are, for example, polymeric suspensions with carboxyl,^{2, 26, 27, 42–45} hydroxyl,^{24, 46} amino,^{24, 27} amide,^{27, 47–50} glycol,^{51, 52} and other groups. Methods of activation of these groups are considered below.

At present, numerous methods of preparation of polymeric microspheres with various functional groups on the surface have been reported (these are emulsion, suspension, dispersion, precipitation, emulsifier-free, seed, and other types of polymerisations). The choice of the method of synthesis is determined by the necessity of obtaining suspensions with a specified set of properties: particle diameter and structure, narrow size distribution, stability in physiological solutions and during storage, the presence of functional groups of a particular nature at a specified concentration on the surface of the particles. Below we survey the methods of the synthesis of functional polymeric suspensions with definite functional groups on the particle surface.

II. Synthesis of polymeric suspensions with functional groups on the particle surface

1. Synthesis of polymeric suspensions with aldehyde groups on the particle surface

Polymeric suspensions with aldehyde groups on the particle surface are obtained by homopolymerisation of unsaturated aldehydes (acrolein, formylstyrene) or by their copolymerisation with monomers of various natures.

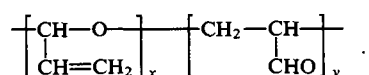
Polymerisation of acrolein has been studied most comprehensively. Two routes of preparing polyacrolein microspheres with narrow PSD's have been reported, namely, the anionic precipitation polymerisation in an alkaline medium³⁹ and the radical emulsion polymerisation induced by γ -radiation or a redox system.⁵³

The radical emulsion polymerisation of acrolein has been carried out in an aqueous solution at a monomer concentration of 10 vol.% in the presence of poly(ethylene oxide) as an emulsifier. The process was initiated by the potassium persulfate–silver nitrate redox system and conducted in the dark at room temperature and varying acrolein concentrations. Polyacrolein microspheres 0.01–0.2 μm in diameter (depending on the acrolein concentration in the system) with a variation coefficient of less than 10% were obtained in this way. It was noted that kinetic features of the acrolein polymerisation differ substantially from those observed for hydrophobic monomers, which was accounted for⁵³ both by the high solubility of the monomer in water ($\sim 20\%$) and by intermolecular cross-linking processes occurring in polymer-monomeric particles (PMP).

The γ -radiation induced radical polymerisation was carried out in an aqueous solution containing a mixture of ionogenic (sodium dodecyl sulfate) and nonionic [poly(ethylene oxide) with a molecular weight of 100,000] surfactants at concentrations of 0%–20% and 0%–15% relative to the monomer concentration, respectively and a radiation dose of 0.4 Mrad at room temperature for 4 h. It was noted that the initial polymerisation rate obeys the first-order kinetics with respect to the monomer. The size of the particles and their PSD depend considerably on the monomer and surfactant concentrations: the particle size increases with the increase in the monomer concentration and with the decrease in the surfactant concentration. By varying the above-mentioned parameters, the authors obtained polyacrolein microspheres of a broad range of sizes (from 0.01–0.02 to 5.0 μm). Stable monodisperse microspheres were formed only when the monomer concentration did not exceed 15%.

Schlund et al.³⁹ managed to obtain polyacrolein suspensions with particle sizes ranging from 0.04 to 8.0 μm and variation coefficients of less than 10% by the precipitation homopolymerisation of acrolein in alkaline medium ($\text{pH} > 11.0$) with solution of an alkali being gradually added to an aqueous solution of acrolein, only in the presence of a specially synthesised emulsifier produced by the interaction of polyglutaraldehyde oligomers with sodium hydrogensulfite. The polymerisation was carried out for 10 h at room temperature.

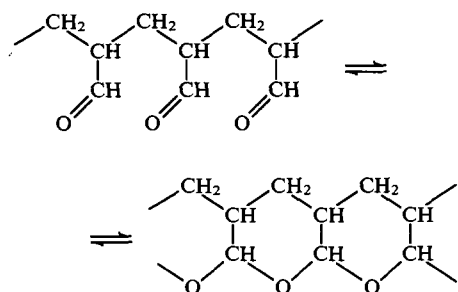
It has been shown that the structure of polyacrolein depends significantly on the conditions in which the microspheres are synthesised. For example, it has been reported⁴⁰ that polymerisation of acrolein can involve both the double bond and the aldehyde group. Therefore, polyacrolein incorporates two types of repeating units:



The $x:y$ ratio depends on the method and conditions of preparation of the microspheres and varies from 4:1 for 'anionic' microspheres to 1:7 for 'emulsion' microspheres. It has been noted that the conditions in which polyacrolein suspensions are synthesised determine the concentration of functional aldehyde

groups on the surface of particles and, hence, the number of covalently bound protein molecules.

Based on spectrophotometric studies, Rembaum et al.⁴⁰ have suggested that the polyacrolein molecules synthesised by γ -radiation induced polymerisation incorporate the following structural fragments:



Due to the bifunctional character of acrolein, the polymeric chains are formed by a fairly complex mechanism and their structure is a combination of the above-presented fragments. Thus, the structure of the macromolecules and, consequently, the properties of the polymeric suspensions (particle size, PSD, concentration of aldehyde groups on the particle surface, etc.) vary over a wide range depending on the polymerisation conditions, and, hence, the process is poorly reproducible. This is especially pronounced in the case of precipitation polymerisation. Radiation-induced polymerisation has a number of advantages over the precipitation polymerisation, namely, it is better controlled and reproducible, and it yields particles with higher concentrations of reactive groups on the surface.

Poor reproducibility of the precipitation polymerisation of acrolein has also been reported in other papers.^{39,53} In addition, it was reported that particles of polyacrolein suspensions always contain a certain amount of an oligomeric product, associated with characteristic features of the precipitation polymerisation mechanism. In the course of time, these oligomeric molecules can diffuse from the particle bulk to the surface; therefore, the properties of the microspheres can change noticeably during storage.

A number of methods have been suggested to eliminate the above drawbacks which make it possible to increase considerably the chemical stability of polyacrolein microspheres, to decrease the physical adsorption of protein molecules on their surface, and to increase the yield of the target product.^{54–57} For example, the synthesis of polyacrolein suspensions in an aqueous alkaline solution in the presence of 3%–6% radical initiators with respect to the monomer, has been reported.⁵⁶ The polymerisation was carried out in two temperature regimes: at 5–35 °C for 1.5–2.5 h or at 40–90 °C for 2–3 h. The resulting polyacrolein microspheres had diameters of 0.2–6.0 μm and a narrow PSD (variation coefficient $\sim 10\%$); they were chemically more stable than the microspheres obtained by the conventional anionic precipitation polymerisation, apparently due to additional cross-linking of the polymer by radical initiators.

A similar effect has been achieved when the anionic precipitation polymerisation of acrolein has been carried out in an aqueous alkaline medium in the presence of water-soluble crown-ethers⁵⁷ at 2–38 °C and the reaction system has been kept in the presence of radical initiators [potassium persulfate, benzoyl peroxide, or azobis(isobutyronitrile) (AIBN)] at 40–90 °C. The polyacrolein suspension particles had a diameter of 0.04–6.0 μm and a variation coefficient of 14%–18%.

Polystyrene-acrolein suspensions obtained by the emulsifier-free copolymerisation of acrolein and styrene are more stable.^{35,58} The copolymerisation was carried out at various proportions of comonomers in the presence of potassium persulfate at 55 °C for 8 h in an atmosphere of nitrogen.

The copolymerisation rate has been shown to depend on the molar concentration of acrolein and is optimal at 1 : 1 molar ratio between the comonomers. The copolymeric polystyrene-acrolein particles had an average diameter of 0.25 to 0.30 μm and a variation coefficient of less than 3%. The concentration of the aldehyde groups on the surface of these microspheres exhibited linear dependence on the molar concentration of acrolein and varied from 0.08 (at 20 mol.% acrolein) to 0.17 $\mu\text{mol g}^{-1}$ (at 90 mol.% acrolein).

A similar picture has been observed in the case of the γ -radiation-induced copolymerisation of acrolein with 2-hydroxyethyl methacrylate (HEMA).³⁶ A mixture of acrolein and HEMA was dispersed in a 1% aqueous solution of polyvinyl alcohol, then the emulsion of monomers was rapidly frozen, and the radiation-induced copolymerisation was carried out at –78 °C applying a radiation dose of 1 Mrad over a period of 1 h. The resulting microspheres were thawed and purified from the remaining monomer. Depending on the copolymerisation conditions, the concentration of the comonomers, and the ratio between them, the copolymeric polyacrolein–2-hydroxyethyl methacrylate microspheres had a diameter ranging from 0.6 to 4.0 μm and a narrow PSD.

A method for preparing polymeric microspheres with aldehyde groups on the surface by the post-radiation graft polymerisation of acrolein from the gaseous phase onto stable polystyrene or poly(methyl methacrylate) particles of identical sizes serving as matrices has been described.⁵⁹

Since the conditions of the synthesis of a polymeric suspension (PS) influence essentially the properties of the modification product, the suspension particles obtained both in the presence and in the absence of an emulsifier have been used as matrices for the radiation-chemical graft polymerisation of acrolein.

Water-soluble hydroxyethylated poly(propylene glycol) [PS(F-68)] and di-*p*-tolyl-*o*-alkoxycarbonylphenylmethanol soluble in the monomer phase [PS(DTC)] were used as surfactants. In all cases, the polymerisation was initiated by potassium persulfate and conducted until the complete conversion of the monomers was achieved, which took 24 h. The particles of these polymeric suspensions proved to be stable in physiological salt solutions or during storage and had a narrow size distribution and diameters of 0.2 and 0.45 μm , respectively. The resulting polymeric suspensions were freeze-dried, and the polymer powders were used as matrices.

To determine the irradiation dose necessary for the graft copolymerisation of acrolein, the accumulation of radicals in the supporting polymer was studied by EPR. An irradiation dose of 15 Mrad was chosen at which the radical growth curves flatten out, i.e. a steady-state concentration of radicals is established.

A study of the sorption of acrolein vapour by the support particles at various acrolein vapour pressures showed that the concentration of acrolein in the particles depends appreciably on the nature of the polymer serving as the support and the surfactant used.

From the kinetic curves of acrolein sorption on the support particles, the rate constants for this process have been determined, and it has been shown that the yield of grafted polyacrolein as a function of time depends on the nature of the polymer.

An analysis of the IR spectra of the initial polymers and of those modified by polyacrolein showed that they all exhibit an absorption band in the region of 1725 cm^{-1} corresponding to vibrations of the carbonyl groups in aliphatic aldehydes. An increase in the degree of polyacrolein grafting on the polymeric matrix leads to an increase in the intensity of absorption in this region of the spectrum.

The spectra of polyacrolein-modified polymers contain an absorption band at 1100 cm^{-1} corresponding to vibrations of C–O bonds in acetals. These bonds can be formed either via polymerisation of acrolein with involvement of the carbonyl group or due to the interaction of the aldehyde groups existing in the hydrated form in the polymer produced. The latter is possible,

because free aldehyde groups exist in equilibrium with the corresponding hydrated groups, since acrolein polymers, even being dried in a high vacuum, contain certain amount of water.

To elucidate the manner in which the C—O bonds in the synthesised polymers are produced, the polymers were subjected to reaction with hydroxylamine hydrochloride. It was suggested that if the polymer incorporated free or hydrated aldehyde groups, this reaction would yield the corresponding polymeric oxime. Otherwise, if the C—O bonds are incorporated in the backbone, this reaction will not occur.

An analysis of the IR spectra showed that the reaction resulted in a decrease in the absorption intensity not only in the region of 1725 cm^{-1} , but also at 1100 cm^{-1} . The latter indicates that the C—O bonds result from the formation of cyclic acetals, which can be opened to give free aldehyde groups.

Based on the results obtained by IR spectroscopy, Bastos et al.⁵⁹ concluded that the radical polymerisation of acrolein involves mostly the vinyl group.

The amounts of free and bound CHO groups in polyacrolein are mainly determined by the conditions in which it is synthesised.

For example, the microspheres prepared by the ionic polymerisation of acrolein contain 2.9 mmol of aldehyde per g of microspheres, whereas those obtained by the radical polymerisation, for example, under the action of a radical redox system contain 12.0 mmol of aldehyde groups per g.

Calculations have shown that polyacrolein-modified microspheres obtained by the emulsifier-free polymerisation, PS(DTC) microspheres, and microspheres of the MMA—MAA copolymer contain on their surface 5.39, 4.80, and 9.34 and 8.07 mmol of aldehyde per g of grafted polyacrolein, respectively. Comparison of these results with the published data indicates that the content of aldehyde groups in the microspheres prepared by postradiation polymerisation of acrolein is twice as high as that in the microspheres prepared under conditions of basic catalysis, even in the sample with the lowest acrolein content.

Polymeric suspensions with aldehyde groups on the surface can also be synthesised by dispersion polymerisation of formylstyrene in aqueous ethanol using AIBN as the initiator and polyvinylbenzoic acid as the stabiliser.^{31, 60} The polymerisation was conducted for 24 h at 70°C . Depending on the monomer concentration, the resulting particles had a diameter of 0.5 to $2.0\text{ }\mu\text{m}$, the variation coefficient was 8%–10%, and the concentration of aldehyde groups on the particle surface was $0.1\text{--}0.2\text{ }\mu\text{mol g}^{-1}$.

A method of preparing particles with aldehyde groups on the surface involving polymerisation of glutaraldehyde has been reported.^{38, 61, 62} Polyglutaraldehyde suspensions are unstable (especially in strongly alkaline media) and have no apparent advantages over the suspensions considered above. Therefore, they have found only a limited application for marking cellular receptors.

2. Synthesis of polymeric suspensions with chloromethyl groups on the particle surface

Polymeric suspensions with chloromethyl groups on the particle surface can be obtained by precipitation^{30, 31, 63} or seeded³³ polymerisation of chloromethylstyrene and chloromethyl methacrylate. A serious drawback of this method is the high toxicity of the monomers.

The precipitation polymerisation is induced by AIBN and conducted in ethanol in the presence of a stabiliser (polyvinylbenzoic acid) at 70°C . Polymeric particles were from 0.5 to $2.0\text{ }\mu\text{m}$ in diameter (depending on the monomer concentration), with the variation coefficient being about 10%. During storage of polychloromethyl suspensions, reactive chloromethyl groups are partially hydrolysed, and, hence, properties of the suspensions changed.

The polymeric suspensions obtained by the seeded copolymerisation of chloromethylstyrene with styrene were more stable on

storage.³³ Seed polystyrene particles were obtained by the dispersion polymerisation of styrene initiated by AIBN (1 mol l^{-1}) in aqueous ethanol, 1:4 by volume, in the presence of polyacrylic acid (1 g l^{-1}) as a stabiliser. The reaction yielded seed particles with a diameter of $1.9\text{ }\mu\text{m}$ and a variation coefficient of less than 3%. The polymerisation was conducted for $\sim 10\text{ h}$ at 70°C . After that, the seed latex, styrene, chloromethylstyrene, and AIBN were mixed in a specified ratio and stirred for 24 h at 0°C , to allow the particles of seed suspension to swell, and then the polymerisation was carried out for 24 h at 70°C .

The resulting suspension particles had a diameter of $2.1\text{ }\mu\text{m}$, a variation coefficient of less than 3%, and a 'core-shell' structure. Virtually all the chloromethyl groups were located on the surface of the suspension particles.

Data concerning the use of styrene-chloromethylstyrene copolymeric suspensions in immunodiagnostics have been reported.^{64, 65}

3. Synthesis of polymeric suspensions with epoxy groups on the particle surface

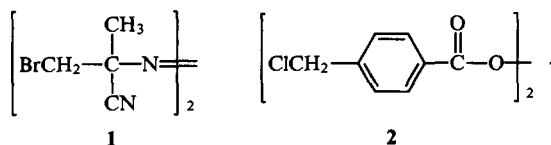
Polymeric suspensions, whose particles contain epoxy groups on the surface, are mostly prepared by the emulsifier-free copolymerisation of styrene with glycidyl methacrylate. According to published data,^{66–77} the optimal conditions of the styrene copolymerisation with glycidyl methacrylate are as follows: ionic strength of the aqueous phase $0\text{--}0.02\text{ mol l}^{-1}$, concentration of potassium persulfate $0.011\text{--}0.02\text{ mol l}^{-1}$, and overall concentration of monomers $3.7 \times 10^{-3}\text{ mol l}^{-1}$. The process is carried out for 5–10 h at 65°C . Under these conditions, microspheres having an average diameter of 220–400 nm and a variation coefficient of 2%–6% are produced. During the synthesis of styrene-glycidyl methacrylate copolymeric suspensions some of the epoxy groups located on the surface of particles are lost due to hydrolysis. Nevertheless, the number of these groups on the particle surface remains sufficient for ensuring a required concentration of a bioligand by its covalent bonding.

To suppress the hydrolysis of epoxy groups during the synthesis of the suspension, it has been advised that the polymerisation be carried out with gradual introduction of the functional monomer into the polymerising system.^{39, 76} This procedure makes it possible to obtain particles with a structure of the 'core-shell' type. This is exemplified by the synthesis of particles containing a copolymer of n-butyl acrylate with butyl methacrylate as the 'core'. These particles were obtained by the emulsion copolymerisation of the monomers in the presence of sodium dodecyl sulfate and a redox system consisting of potassium persulfate and sodium thiosulfate. The process was carried out at 20°C for 20 min, after which a mixture of monomers with glycidyl methacrylate was introduced.

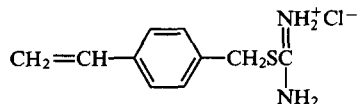
The resulting microspheres had diameters of 150–300 nm and a variation coefficient of $< 10\%$. According to the data obtained by Schlund et al.,³⁹ under these conditions, up to 90% of the epoxy groups are preserved and virtually all of them are distributed within a thin layer (about $150\text{ }\text{\AA}$) on the surface of the particles.

4. Synthesis of polymeric suspensions in the presence of surface active functional initiators and surfactants

The use of polyfunctional initiators and surfactants in the synthesis of polymeric suspensions with narrow PSD to be employed in immunodiagnostics has been reported. However, the use of these substances is restricted by their high prices and by the absence of a technology for their production. Azobis(bromoisocyanonitrile) 1 and di(4-chloromethylbenzoyl) peroxide 2 can be mentioned among the polyfunctional initiators which make it possible to obtain reactive functional groups, capable of forming covalent bonds with biomolecules, on the surface of suspension particles.⁷⁸



Isothiuronium salts, in particular (4-vinylphenyl)methylisothiurea hydrochloride, are used as polyfunctional emulsifiers.⁴¹



The latter compound is a cation-active emulsifier, able to copolymerise with vinylic monomers. For example, in the presence of this compound, polystyrene microspheres 0.15–0.19 μm in diameter with a variation coefficient of 2.7%, containing isothiuronium groups on the surface, have been prepared. Hydrolysis of these groups under mild conditions (pH 10–11, 25 °C, 10 min) gave mercaptogroups on the particle surface.⁴¹ It was found that the average diameter of particles or their PSD are almost constant throughout the hydrolysis.

Polymeric suspensions, whose particles contain aldehyde groups on the surface, can be prepared by modifying other functional groups. For example, the particles of polystyrene suspensions obtained in the presence of the polysaccharide dextran or ammonium glycyrrhizate as a stabiliser contain carbohydrate groups on the surface.⁷⁹ The periodate oxidation under mild conditions leads to the cleavage of the α -glycol groups and formation of reactive groups that can directly interact with the amino groups of proteins.

In both cases, the conditions for the synthesis are chosen in which polymeric suspensions with narrow PSD stable in physiological salt solutions and during storage are formed. The concentration of aldehyde groups on the surface of suspension particles is in turn determined by the concentration of the stabilising agent and the oxidation conditions.

5. Synthesis of polymeric suspensions with carboxyl groups on the particle surface

The main and most studied method for synthesis of polymeric suspensions with carboxyl groups on the surface of particles is the copolymerisation of hydrophobic monomers with various unsaturated acids (acrylic, methacrylic, itaconic, etc.) in the presence or in the absence of an emulsifier. The presence of readily dissociating carboxyl groups imparts an additional stability to the suspension particles, therefore, these microspheres are resistant to mechanical action or low temperatures (freezing).^{11, 80–83}

The distribution of the carboxyl groups between the aqueous phase, the surface, and the bulk of polymeric particles is a rather important question in the synthesis of carboxyl-containing polymeric suspensions. In a study of the emulsifier-free copolymerisation of styrene with three unsaturated acids possessing different hydrophilicities, namely, acrylic (AA), methacrylic (MAA), and itaconic (IA) acid, it has been found^{84, 85} that AA concentrates in the surface area of the particles, the more hydrophobic MAA is distributed between the bulk of microspheres and their surface, and the most hydrophilic IA mainly homopolymerises in the aqueous phase. These features of the distribution of the acrylic monomers among the phases of an emulsion system determine the properties of the suspensions obtained.

Similar information has been presented in other papers^{86, 87} devoted to the study of the distribution of carboxyl groups in the suspension particles obtained by the copolymerisation of acrylic monomers with styrene or butadiene. It was found that the functional groups are distributed between the aqueous phase, the

microsphere surface, and the microsphere bulk in a ratio of 2 : 3 : 1 in the case of acrylic acid or 0.1 : 1 : 1 when methacrylic acid is used.

Thus, it is obvious that the conventional way of conducting copolymerisation of hydrophobic monomers with unsaturated acids affords polymeric suspensions in which functional groups are distributed among various phases of the polymerisation system.

The distribution of the carboxyl groups between the surface and the bulk of the particles can be changed by gradual introduction of the functional monomer into the reaction system. It has been shown^{88, 89} that in the case where itaconic acid is added in the initial stages of the polymerisation of styrene, only 12% of itaconic acid units are located on the surface of copolymer particles, while introducing the acid at the stage where the degree of styrene conversion has already reached 80% or 95% leads to an increase in the concentration of the functional monomer on the surface to 60% or 80%, respectively.

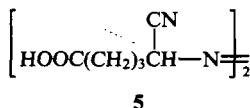
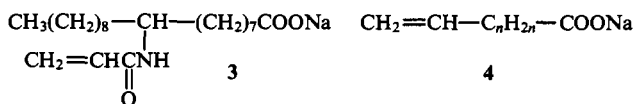
Another method of preparing a polymeric suspension with a high concentration of a carboxyl-containing comonomer on the surface of particles consists in the seeded emulsifier-free copolymerisation of styrene and butadiene with unsaturated acids (AA, MAA, or IA),⁹⁰ with pH of the medium being varied in the course of the synthesis. In the first stage of the process carried out at low pH, all the components (including the acid), but only a portion of the main monomers, are added to the reaction system. Then the pH of the seed latex is increased, and, consequently, the carboxyl groups located near the surface of particles are ionised. In the second stage, seeded copolymerisation of the rest of the monomers is carried out.

Some authors believe that the concentration of carboxyl groups on the surface of polymeric microspheres can be increased by heating the suspension at high pH values, which ensures the migration of the ionised carboxyl groups from the particle bulk to the interface with the aqueous phase (see, for example, the paper by Okubo et al.⁹¹).

The presence of MAA or AA in the monomeric mixture leads to the formation of emulsions characterised by a higher dispersity than emulsions of hydrophobic monomers, due to a lower interfacial tension (σ_{12}). A study carried out by Okubo et al.⁹² has shown that MAA, present at a concentration of 2% with respect to styrene, diminishes the surface tension at the interface between a styrene solution of MAA and water to 22 mN m⁻¹. A dispersion analysis of styrene-methacrylate emulsions obtained with MAA concentrations being 0.2% or 3.0% with respect to styrene showed that in the former case, the emulsion of the monomers consists of drops, whose size is 1–5 μm , and in the latter case, the size of the drops varies from 0.2 to 1.0 μm .

The dispersity of the initial monomer emulsion influences the size distribution of the polymer-monomeric particles (PMP). In fact, the copolymerisation of styrene with MAA, induced by potassium persulfate and carried out at an MAA concentration in an emulsion of 0.2% with respect to styrene gives a polymeric suspension, in which 90% of the particles have an average diameter of 0.6 μm , while in the case where the MAA concentration is 3% with respect to styrene, 85% of the particles have an average diameter of 0.3 μm . When copolymerisation of styrene with MAA is carried out under the same conditions, but in the presence di-*p*-tolylalkoxycarbonylphenylmethanol (DTC), which is a water-insoluble stabiliser, polymeric suspensions with a narrower distribution of the particles of the same size were formed. These suspensions were stable in physiological salt solutions or on six-months storage.

Functional microspheres with carboxyl groups on the surface can also be synthesised by the polymerisation or copolymerisation of surface active monomers,^{93–103} for example, sodium acrylamidostearate **3**⁹³ or salts of vinylalkylcarboxylic acids **4**,⁷⁸ or surface active initiators, such as 5,5'-azobis-5-cyanopentanoic acid **5**.⁷⁸



However, these compounds have not found wide application owing to their high costs.

A new interesting method of synthesis of polymeric suspensions with carboxyl groups on the particle surface is the polymerisation of styrene in the presence of water-insoluble surfactants, whose molecules incorporate carboxyl groups. These are, for example, DTC, oligomeric peroxy esters,⁹⁴ and α -(ethoxycarbonyl)- ω -(trimethylsilyloxy)polydimethylsiloxane (PDS).⁹⁵

In the papers considered above,^{94,95} a hypothesis was put forward that the PMP are formed from drops of the monomer and that their structure is similar to that observed in the 'core-shell' type particles, whose shell is a surfactant displaced by the polymer to the interface. It was shown that the strength of the interfacial layer depends on the molecular mass of the resulting polymer, the concentration of the initiator (in this particular case, potassium persulfate), and the concentration of the surfactant.⁹⁵

The particle size distribution of particles in polymeric suspensions obtained in the presence of water-insoluble surfactants are much narrower than those observed in the presence of water-soluble surfactants. First of all, this precludes the possibility of the formation of PMP from emulsifier micelles or globules of surfactant molecules in the aqueous phase of the emulsion.

Polystyrene, poly(methyl methacrylate), polychloroprene, and polystyrene-methacrylate suspensions with narrow particle size distributions have been obtained in the presence of water-insoluble surfactants. For example, polystyrene microspheres with diameters varying from 0.2 to 0.9 μm and the content of dry substance from 8% to 33% were prepared at surfactant and potassium persulfate concentrations of 1%–4% and 0.5%–1.0% with respect to styrene, respectively. These polymeric suspensions exhibited high stabilities in physiological salt solutions during storage and have found wide application in immunochemical studies.⁹⁶

6. Synthesis of polymeric suspensions with amide groups on the surface of particles

Amide-containing polymeric suspensions are synthesised most frequently by emulsifier-free copolymerisation of styrene with amides of acrylic or methacrylic acid.^{2, 25, 104–106}

The emulsifier-free copolymerisation of styrene with acrylamide (AAM, 0.1%–0.5% with respect to styrene) at pH 9 has been studied most comprehensively.¹⁰⁶ Three stages can be distinguished in the copolymerisation process: (1) copolymerisation of the monomers in the aqueous phase yielding oligomers; (2) polymerisation of styrene within the particles formed by these oligomers; (3) copolymerisation of AAM with styrene dissolved in the aqueous phase.

Special attention in the studies of styrene copolymerisation with AAM is paid to the distribution of amide groups between the aqueous and polymeric phases (owing to the high hydrophilicity of AAM, the aqueous phase always contains a substantial quantity of the water-soluble homopolymer).^{107, 108} The particle diameters in the resulting polymeric suspensions vary from 0.2 to 0.5 μm , and the variation coefficient is less than 3%.

7. Synthesis of polymeric suspensions with hydroxyl groups on the particle surface

Polymeric suspensions with hydroxyl groups on the particle surface are synthesised by the emulsifier-free copolymerisation of

styrene with HEMA or 2-hydroxyethyl acrylate.^{106–108} An essential feature of these monomers is the absence of ionising groups in their molecules, which allows one to change hydrophilic properties of the surface of the polymeric microspheres without changing its charge. This is particularly convenient for selecting the optimal conditions for binding biomolecules.^{109–111}

Polymeric microspheres with high concentrations of surface functional groups are obtained by seeded copolymerisation with gradual introduction of a mixture of styrene and HEMA taken in a certain ratio.^{112–114} The polystyrene particles with diameters of 0.3–0.9 μm and a narrow PSD are used as the seed suspension. Polymeric suspensions with a particle size of 0.6–1.1 μm and a polydispersity coefficient of 1.0003–1.0006 are obtained in this way.

8. Synthesis of polymeric suspensions with amino groups on the particle surface

Polymerisation of functional monomers such as aminostyrene,¹¹⁵ 2-aminoethyl acrylate, 2-dimethylaminoethyl methacrylate, or allylamine⁶⁶ is a rather uncommon method for the synthesis of amine-containing polymeric suspensions. This is caused by the high cost of these monomers and by the low stability of the polymeric microspheres based on them as well as by the fact that a narrow particle size distribution is difficult to achieve due to the high hydrophilicity of the monomers.^{116–124}

Amine-containing polymeric suspensions are much more readily prepared by modifying available suspensions containing hydroxyl, chloromethyl, amide, or other groups. As an example, let us consider the synthesis of polymeric suspensions with surface amino groups by the dispersion catalytic polymerisation of *p*-aminostyrene. The polymerisation of *p*-aminostyrene is carried out in the presence of a mineral or organic acid (with pK_a below 4.76) and an organic solvent (10%–80% with respect to water), which is miscible with water and whose dielectric permeability is lower than that of water.¹¹⁵ This process yields polyaminostyrene microspheres with diameters varying from 0.6 to 10.0 μm and a narrow particle size distribution.

Polymeric microspheres with diameters of 0.2–3.5 μm and polydispersity coefficients of no more than 1.08 have also been obtained by dispersion cationic polymerisation of *p*-aminostyrene in aqueous methanol at 60 °C with a monomer:water ratio of 1:9, a concentration of cetylpyridinium bromide of 1% with respect to the monomer, and a catalyst (hydrogen chloride) concentration of 10% with respect to the monomer.

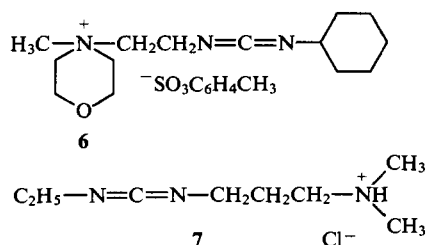
III. Activation of functional groups on the surface of particles of a polymeric suspension

The methods for activation of functional groups on the surface of particles of a polymeric suspension considered in this Section are widely applied in biochemistry and biology, in particular, to prepare sorbents for affinity chromatography.^{89, 90} However, to be suitable for preparing a highly sensitive diagnostic, these methods should comply with the following requirements:²

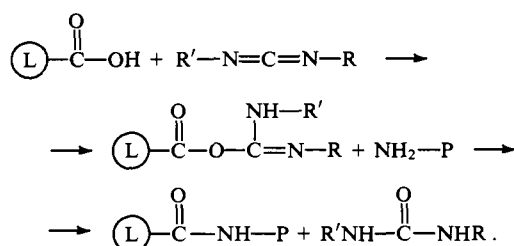
- to proceed quantitatively and irreversibly under as mild conditions as possible;
- not to decrease the stability of suspensions and not to influence noticeably the particle diameter and PSD;
- to have no influence on the biochemical activity of the bioligand molecules covalently bound to the functional groups on the surface of the suspension particles.

1. Methods for the activation of carboxyl groups on the particle surface

The carboxyl groups on the surface of suspension particles can react with amino groups of a biopolymer in the presence of water-soluble carbodiimides (WSC).⁸⁰ The most frequently used WSC are 1-cyclohexyl-3-[2-(*N*-methylmorpholinio)ethyl]carbodiimide toluenesulfonate **6** and 3-ethyl-1-(3-dimethylaminopropyl)carbodiimide hydrochloride **7**.



The activation reaction occurs via the following scheme:

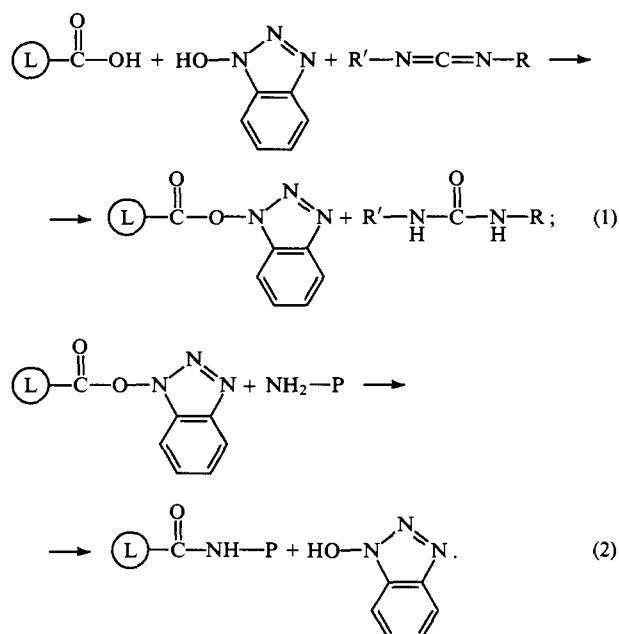


It is carried out at a temperature of 4–6 °C and pH 6–7 for 2–4 h in the presence or absence of an inert buffer like 4-(2-hydroxyethyl)piperazin-1-yl(ethane-2-sulfonic) acid.

One of the advantages of this method for activating functional groups is its simplicity. However, since protein molecules contain both carboxyl and amino groups, inter- or intramolecular cross-linking is possible, which reduces the immunochemical activity of the bioligand.^{26, 104, 125–128}

This problem can be solved to a substantial extent by using two-stage activation: in the first stage, the carboxyl groups are converted into an active (but stable) form and the microspheres are separated from the dispersion medium containing the unchanged components, and in the second stage, the covalent binding to a bioligand is carried out.

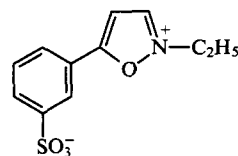
The so-called method of 'activated esters' is among the most generally used two-stage methods for the activation of functional groups.^{2, 48, 129} In this case, the activation occurs according to the following scheme:



Apart from *N*-hydroxybenzotriazole, *N,N*-dialkylhydroxylamines and some other compounds can be used. The conditions in which the first stage of the process is conducted are similar to those described above for the 'carbodiimide' method. Following the first

stage, the suspension is purified from side products. The second step proceeds at 4 °C and pH 7–7.5 for 2–3 days, and after that, the obtained diagnostic is completely freed from impurities.

Yet another possible version of two-stage activation is the use of the Woodward reagent, namely, *N*-ethyl-5-phenylisoxazoline-3'-sulfonate.¹³⁰



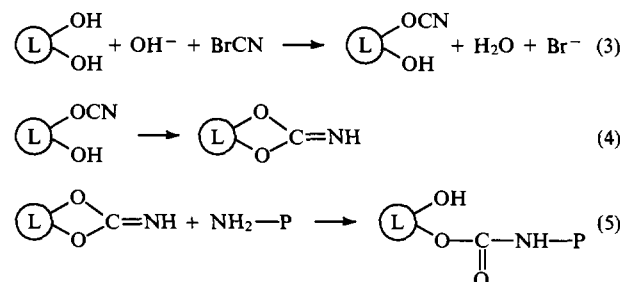
In this case, the first stage is carried out at pH 8.5 and a temperature of 3 °C for 3 h, the resulting suspensions with the activated carboxyl groups on the particle surface are purified from side products and then bound to bioligands at pH 7 and a temperature of 5 °C over a period of 3 h.

Common drawbacks of the above methods are their high costs and the low stabilities during storage of the reagents used, which makes the process of binding biomolecules to the functional groups of microspheres poorly reproducible. Moreover, the biomolecules bound by these methods are arranged near the surface of polymeric particles, which may result in changes in their conformations and may decrease their biochemical activity.

Therefore, the method involving the introduction of a spacer by the reaction of carboxyl groups on suspension particles with various diamines (1,6-diaminohexane, 1,7-diaminoheptane) has gained acceptance.^{47, 131–133} In the first stage, the carboxyl groups on the microsphere surface are bound to diamine in the presence of WSC, and after that the resulting amino groups are activated by one of the methods described below.

2. Methods for the activation of hydroxyl groups

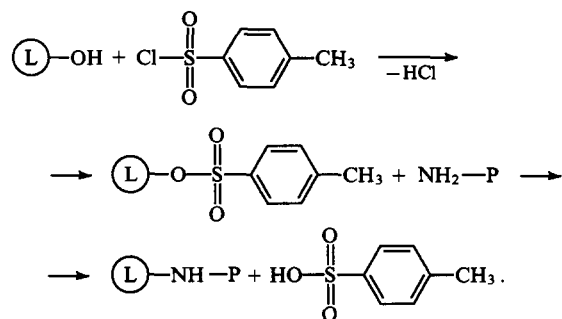
The 'cyanogen-bromide' method for the activation of hydroxyl groups consists in their interaction with cyanogen bromide in strongly alkaline media (pH 10–11) followed by the formation of bonds with amino groups of protein molecules.¹³⁴



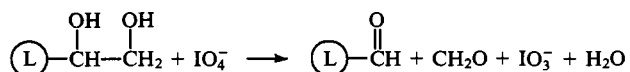
The first two stages, (3) and (4), proceed at 25 °C over a period of 15 min, alkaline pH being maintained by the periodical addition of 2 M sodium hydroxide. Then the suspension is purified from side products, and stage (5) is carried out in a 0.1 M borate buffer at pH 8.0–8.5 and a temperature of 4 °C for 4 h. The unaffected activated hydroxyl groups are bound by adding 0.1 M glycine buffer with pH 8.5, and then the suspension is extensively purified.

This activation method is applicable only to the covalent binding of biomolecules stable in strongly alkaline media. The high toxicity of cyanogen bromide and the noticeable aggregation of polymeric microspheres during binding bioligands to the functional groups are among the drawbacks of this method.

Activation of hydroxyl groups can be carried out by using some other reagents such as tosyl chloride,² 2,2,2-trifluoroethanesulfonyl chloride^{135, 136} and carbonyldiimidazole.^{137, 138} Overleaf we present the scheme of the activation of hydroxyl groups by tosyl chloride as an example:



A fairly convenient method for the activation of hydroxyl groups is the oxidation of glycol groups, which can be readily obtained by the hydrolysis of epoxy-groups or oxidation of double bonds in polydienes (see below). Microspheres with glycol groups on the surface are obtained, as has been mentioned above, by the polymerisation of styrene in the presence of dextrans as functional surfactants.¹³⁹ The oxidation is carried out by periodic acid or periodates at room temperature at neutral pH for 30–60 min in the dark.^{50, 140, 141} Only glycols with primary or secondary hydroxyl groups enter into this reaction, which involves the cleavage of the C–C bond yielding two aldehyde groups.

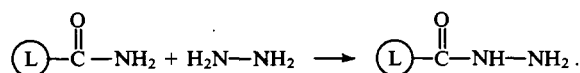


The side products are removed during purification of the polymeric microspheres.

3. Methods for the activation of amide groups

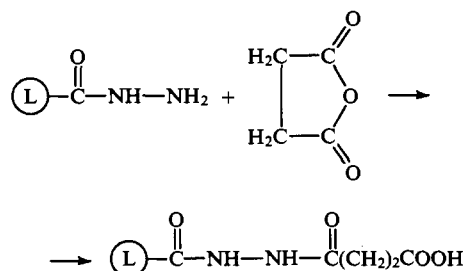
Although amide groups do not interact directly with protein molecules, there are a number of methods involving polymer-analogous transformations that make it possible to convert amide-containing polymeric suspensions into microspheres with some other groups that can be easily activated.

For example, the modification of amide groups to hydrazide groups is widely used.^{27, 46} The reaction occurs at 50–80 °C in 7–10 h according to the following scheme:

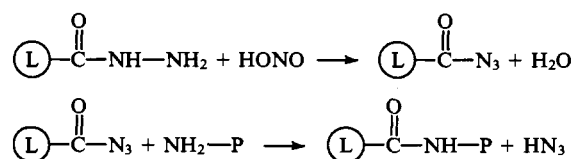


The hydrazide groups formed in this reaction can be transformed either into the carboxyl groups, which need to be further activated, or into azide groups, which can directly interact with biomolecules.

The former process can be accomplished by treating the hydrazide groups with succinic anhydride.^{142, 143}



Azide-containing polymeric suspensions are obtained by diazotisation in the presence of nitrous acid at a low temperature (2–5 °C);²⁷ after that, the direct interaction of biomolecules with azide groups on the microsphere surface is possible (pH 7.0 to 9.5, duration 4 h).



It should be noted that hydrazide groups can be activated by virtue of the same methods as amino groups.

Another possible way of modification of amide-containing polymeric suspensions is the transformation of amide groups into primary amino groups under the action of sodium hypochlorite in an alkaline medium (the Hoffmann reaction^{139, 140}). The factors influencing the course of this process have been studied.^{143, 144} It was shown that, apart from the transformation of amide groups into amino groups, hydrolysis yielding carboxyl groups occurs to a substantial extent, the degree of hydrolysis increasing with increase in the temperature and decrease in the NaOCl:polyamide ratio. The following optimal conditions under which the maximum quantity of amino groups is obtained on the surface of the suspension particles were found: a ratio between the concentrations of hypochlorite and amide groups of 0.6 to 0.9, a temperature of 5–10 °C, and a duration of the process of 1–2 h. It was shown that under these conditions, the diameter of suspension particles or their PSD are virtually unchanged during modification. This method has been used for the covalent binding of enzymes to the amide groups located on the particle surface in acrylamide-styrene copolymeric suspensions (glutaraldehyde was used to activate the resulting amino groups).¹⁰⁴

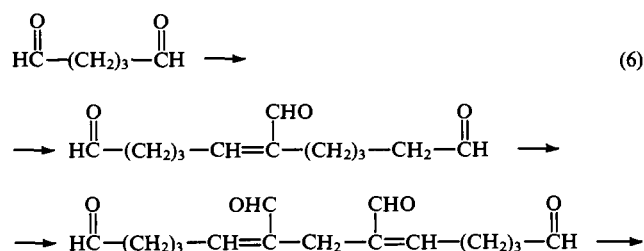
The transformation of amide groups into carboxyl groups, which is frequently required for increasing the stability of microspheres, can be performed by alkaline hydrolysis under mild conditions (30 °C, 3–4 h).¹⁴⁴ The degree of hydrolysis and, consequently, the concentration of carboxyl groups on the surface of suspension particles, can vary depending on the duration of the process, and this allows one to obtain particles with various concentrations of carboxyl groups on the surface.

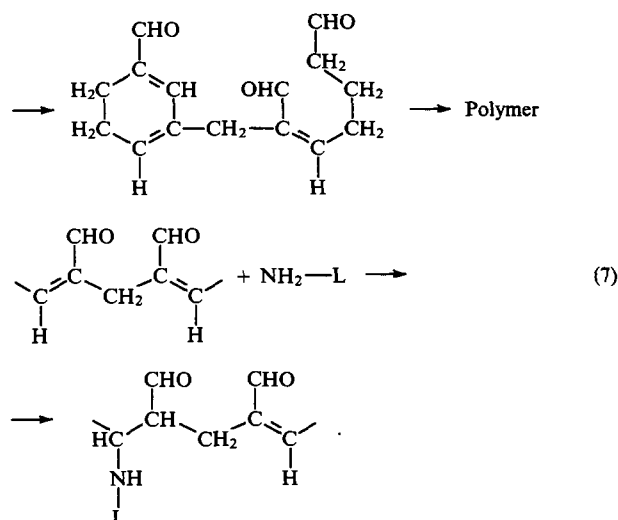
Finally, polymeric suspensions with hydroxyl groups on the surface can be obtained from amide-containing suspensions by hydroxymethylation. The reaction proceeds for 1 h at 50 °C and pH ≥ 12.0. In relation to the emulsifier-free copolymerisation of styrene and AAm taken in a ratio of 9:1 followed by the modification of the amide groups to the hydroxyl groups, it has been shown that this process yields stable monodisperse microspheres 220 nm in diameter containing 4.58 OH groups per nm² of the surface of particles.¹⁴⁴

4. Methods for the activation of amino groups

Since primary amino groups are highly reactive, polymeric suspensions containing these groups on the surface of microspheres are readily activated via reactions with various bifunctional compounds.

The most commonly used activation method involves reaction with glutaraldehyde, which is due to both the ease of conducting this reaction and the availability of the reagent itself. The primary amino groups react with glutaraldehyde by the following scheme:^{145, 146}





The activation can be accomplished in one or in two stages.¹⁴⁷ According to the one-stage procedure, linking a bioligand to the amino groups on the particles is carried out in the presence of an excess of glutaraldehyde. Although this method is rather simple, appreciable aggregation of polymeric microspheres due to their cross-linking is observed in the course of activation.

Preference is given to the two-stage activation. The first stage (6) involves oligomerisation of glutaric aldehyde and the reaction of the resulting oligomer with the amino groups on the surface of polymeric microspheres (7). After liberation of the suspension from side reaction products, covalent binding to bioligands is performed. The first stage is carried out at 20–25 °C in 0.01 M phosphate buffer (pH 7.0) for 1 h.²⁴ After removal of the excess of glutaraldehyde by dialysis (24 h, against a system consisting of 0.01 M phosphate buffer and 0.01 M salt buffer, pH 7.0), the molecules of a bioligand are bound to the microsphere functional groups for 5 h at 25 °C. Then the unaffected aldehyde groups on the microsphere surface are blocked with a 0.1 M solution of glycine at pH 7.0, and the resulting test-system is purified. This activation method makes it possible to avoid inter- or intramolecular cross-linking of bioligands and to prevent the functional microspheres from aggregation.²⁴

Other bifunctional compounds, for example, 1,5-difluoro-2,4-dinitrobenzene, 4,4'-difluoro-3,3'-dinitrophenyl sulfone, or 2,4-dichloro-6-methoxycarbonylmethyl sulfone, can also be used in place of glutaraldehyde.^{148, 149} Drawbacks of these methods are the high costs of the reagents and the prolonged period (4–7 days) required for covalent binding of functional groups to biomolecules.² However, the properties of the test-systems obtained by these methods are more reproducible than those of the test-systems prepared using glutaraldehyde; in the latter case, the properties of the test-systems are determined by the conditions and duration of the storage of glutaraldehyde (polymerisation is possible).

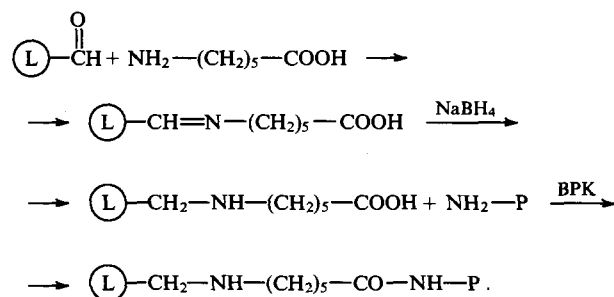
It is noteworthy that one of the possible ways of binding antibodies and enzymes incorporating polysaccharide residues to amino groups on the surface of a polymeric suspension is the treatment of the bioligand itself with periodic acid or periodates, rather than the activation of the amino groups.¹⁰⁴ The oxidation of the glycol groups of the polysaccharides incorporated in biomolecules affords reactive aldehyde groups, which can react with the amino groups on the surface of polymeric microspheres. The use of this method for binding glucose oxidase and glucose peroxidase makes it possible to retain up to 40% of their activities (compared with 10% of the activity retained when other methods, in particular the carbodiimide method, are used).¹⁰⁴

5. Methods for the modification of chloromethyl, epoxy, and aldehyde groups

In this section we consider polymer-analogous transformations involving functional groups capable of direct interaction with bioligands. These reactions are often required either to introduce an additional spacer group between a polymeric particle and a biomolecule in order to retain the biological activity of the latter, or to generate chemical groups on the surface of the suspension particles, whose reactivity is retained during the preparation and storage of microspheres (the transformation of epoxy or chloromethyl groups into aldehyde groups is an example).

Aldehyde groups are most frequently modified in order to introduce a spacer. This is achieved by conducting the reaction with diamines and the subsequent activation of the NH₂ groups with glutaraldehyde. It should be noted that the Schiff's base resulting from the interaction of a primary amino group with an aldehyde group and containing a CH=N fragment is unstable at low pH values. Therefore, it is often reduced to CH₂NH with mild reducing agents like sodium tetrahydroborate (25 °C, 30 min).^{37, 38}

Aldehyde-containing suspensions can also be modified using the reaction of aldehyde groups with amino acids (for example, with 6-amino-n-caproic acid).^{35, 150} This reaction affords carboxyl groups on the surface of the polymeric microspheres:



Chloromethyl groups are modified both in order to introduce a spacer and to suppress hydrolysis, which occurs to a substantial degree at high pH values.³¹ In the former case, the same methods as for aldehyde groups can be applied.^{28, 29, 34} The reaction is carried out in neutral or weakly alkaline media at 30–40 °C for 1–2 h.

Chloromethyl groups are rather reactive and possess pronounced electrophilic properties,³² which makes it possible to perform various polymer-analogous transformations to impart additional valuable properties to the functional microspheres, such as storage stability, hydrophilicity of the surface, etc.¹⁵¹ For this purpose, chloromethyl groups are most frequently converted into aldehyde groups. The functional groups located on the surface of the particles of a polymeric suspension are modified by treatment with iodates in an aqueous solution of chromic acid,^{117, 151–153} or by the oxidative alkylation with the sodium salt of 2-nitropropane.^{154–156}

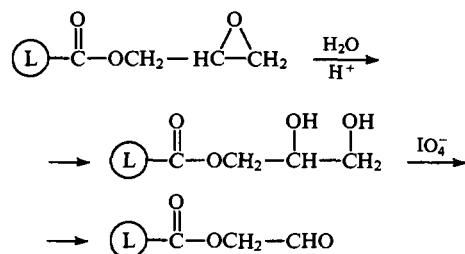
In the latter case, sodium methoxide and 2-nitropropane are gradually added to a poly(styrene-chloromethyl) copolymeric suspension. The reaction proceeds at room temperature over a period of 2 h, and after that, the modified copolymeric microspheres are purified from the unchanged components and side products. It was shown that under these conditions almost all the chloromethyl groups are oxidised to aldehyde groups, the modification having virtually no effect on the diameter or PSD of the resulting polymeric particles. A comparison of the reactivities of the initial chloromethyl groups and the resulting aldehyde groups toward human immunoglobulin G has shown that the latter are better in binding this antibody and provide higher sensitivity of the diagnostic.

As has already been mentioned, epoxy groups can be hydrolysed, especially at low pH values. Therefore, epoxy groups are subjected to further modification with the aim of obtaining more

stable groups on the particle surface or to introduce an additional spacer group.

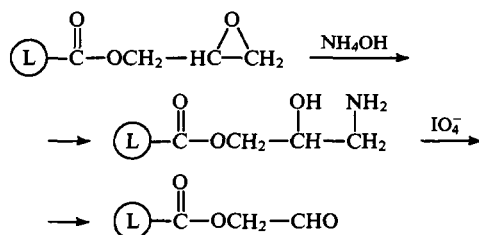
Owing to the high reactivity of epoxy groups, they participate in various polymer-analogous transformations.⁴⁰

For example, the hydrolysis of surface epoxy groups at 50 °C and pH 2 gives particles with glycol groups, which are readily converted thereafter into aldehyde groups by treatment with periodic acid.

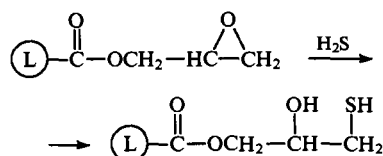


It is noteworthy that up to 60% of the theoretically possible (based on the concentration of the epoxy groups on the surface of the suspension particles) number of glycol groups can be obtained by the hydrolysis, and the particle, diameter, or PSD, virtually do not change during the process: these are 440 nm and a variation coefficient of 3.9% for the starting suspension and 475 nm and a variation coefficient of 5.8% for the modified particles.

The reaction of epoxy groups with ammonium hydroxide (ammonolysis) occurs even more readily at 20 °C.



Epoxy groups on the surface of suspension particles can be converted into thiol groups by the reaction with an aqueous solution of hydrogen sulfide, which proceeds under mild conditions (20 °C, 2–4 h).



However, in this case, it was noted that the modified particles undergo substantial agglomeration (variation coefficient 15.5%).

Epoxy groups on a microsphere surface can also be modified by introducing a spacer via the reaction with diamines or amino acids (see above).

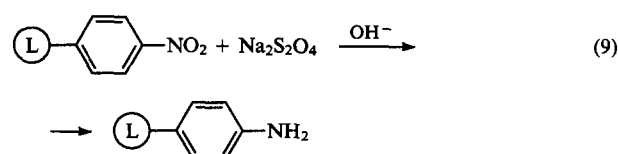
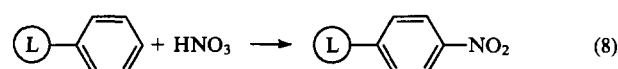
6. Methods for the preparation of polystyrene suspensions with a narrow particle-size distribution containing functional groups on the particle surface

Polystyrene suspensions have found the most extensive application in immunodiagnostic studies. This is caused by the fact that polymerisation of styrene has been most thoroughly studied and it is easy to obtain microspheres with the required diameter and a narrow PSD.^{3–5, 157–175} Here, it is expedient to consider methods for the synthesis of functional polystyrene suspensions consisting of particles with a specified diameter and a narrow PSD.

Polystyrene microspheres with hydroxyl groups on the surface are obtained in two stages: the first stage involves emulsifier-free

polymerisation of styrene initiated by potassium persulfate giving monodisperse suspensions, whose particles contain sulfate groups on the surface and which are stable in physiological salt solutions. In the second stage, the sulfate groups are converted into hydroxyl groups by the hydrolysis in alkaline media (pH 9–10, 50–70 °C, 2–5 h).^{176, 177} The resulting hydroxyl groups can be either modified further by virtue of the cyanogen-bromide method or oxidised in the presence of Ag⁺ ions (50 °C, 5 h)¹²⁷ to carboxyl groups, which are then activated. It should be noted that the hydrolysis of ionogenic sulfate groups to yield non-dissociating hydroxyl groups is accompanied by a sharp reduction in the stability of the modified microspheres due to the decrease in the electrostatic repulsion between the particles. Therefore, to prevent coagulation, non-hydrolysing sulfonate groups should be introduced.^{32, 175, 178}

The preparation of polystyrene particles with amino groups on the surface is an even more complex and cumbersome procedure.^{179, 180}



The first stage [reaction (8)] is carried out in glacial acetic acid at room temperature for 4 h, concentrated nitric acid being gradually added to the reaction mixture. The polymeric particles are then separated from the nitrating reagent by decantation and washed. The second stage (9) is carried out in ethanol; it involves the treatment with sodium dithionite at 40 °C for 2 h. The resulting polystyrene microspheres with amino groups on the surface can be activated thereafter by any of the procedures considered above. It is obvious that to be subjected to all the stages of the process, polystyrene suspensions should meet very stringent requirements for their stability, therefore, the above way of modification is applicable only to particles with cross-linked structures (copolymer of styrene with 2%–5% divinylbenzene) and diameters of no less than 0.8 μm (they can be redispersed fairly easily).²

An original method for binding bioligands to polystyrene microspheres has been suggested by Berge et al.¹³⁸ This method makes it possible to avoid any chemical effect on the surface of polystyrene particles and thus to maintain their stability. The first step of this process involves the adsorption of bovine serum albumin (BSA) onto polystyrene particles of a specified diameter with a narrow PSD; then the suspension is treated with a bifunctional compound (glutaraldehyde, diethyl adipinimidate, etc.) for the cross-linking of protein molecules and their fixation on the microsphere surface. After that, further binding of biomolecules is possible via amino or carboxyl groups of BSA.

7. Methods for the activation of polydiene microspheres

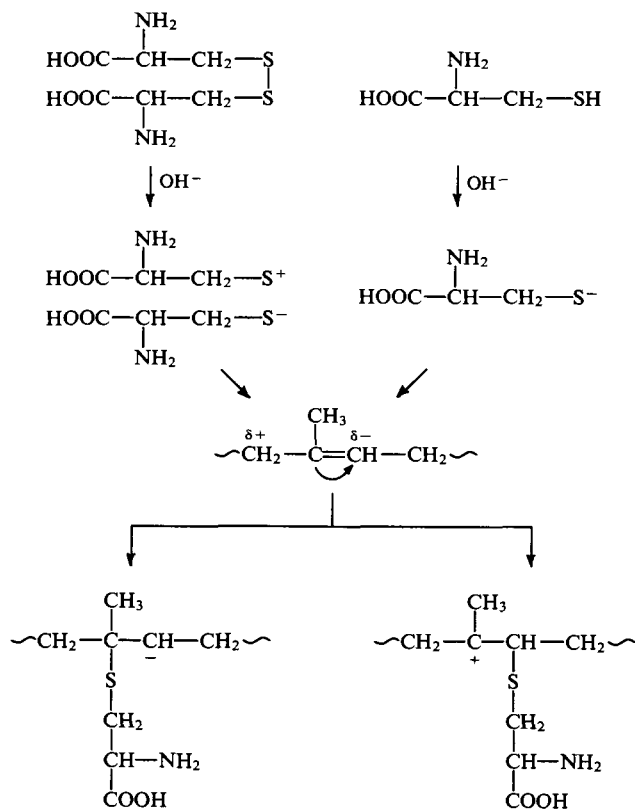
The main characteristic feature of polydiene microspheres is the presence of double bonds, which can undergo further modification.^{139, 140} However, good film-forming ability of diene polymers is responsible for the low stability of microspheres during their purification by ultrafiltration, microfiltration, or centrifugation.² Therefore, the functional polymeric suspensions are synthesised by copolymerisation of dienes (butadiene, isoprene, etc.) with various proportions of styrene.

A possible method of introducing hydroxyl groups into polydiene-styrene microspheres (for example, polyisoprene-styrene microspheres) is the oxidation of the double bonds of the polydiene by such oxidising reagents as potassium permanganate

or hydrogen peroxide.^{181, 187} The oxidation proceeds under mild conditions (pH 3–7, 5–10 °C, 30 min). The resulting glycol groups can be subjected to further activation.

The oxidation of the polybutadiene or polyisoprene double bonds to epoxy groups by their interaction with peracetic acid at reduced temperatures is of great interest.^{188, 189} It was shown that the rate and degree of epoxidation depend to a substantial extent on the polymer content in the suspension and on the concentration of peracetic acid, and does not depend on the nature of the surfactant present in the reaction system, the size of polymeric particles, or the rate of stirring. The following optimal conditions of the oxidation were found: a concentration of the polymer in the suspension of 15%–30%, a concentration of peracetic acid of 2%–3%, and a duration of the reaction of 2–3 h. Data on epoxidation of unsaturated polymers with a mixture of hydrogen peroxide and formic acid has also been reported.¹⁸⁹

Regarding the modification of polydiene microspheres, the use of thio-compounds containing mercapto groups which readily react with double bonds of polydiene microspheres, is of considerable interest. Thioglycols or thioamines are known¹⁹⁰ to be used for enhancing plastic properties of polybutadiene rubbers. In this respect, attention is attracted by the possibility of modifying polydiene microspheres by thiol compounds containing various functional groups, for example, by sulfur-containing amino acids. The modification of an artificial dispersion of SKI-3 polyisoprene by sulfur-containing amino acids has been reported.¹⁹¹ It was shown that amino acids such as cystine or cysteine, due to the presence of reactive disulfide and mercapto groups in their molecules, are capable of direct binding to partially polarised double bonds of 1,4-*cis*-polyisoprene, which occurs by an ionic mechanism.



The preparation of polymeric suspensions with amino groups on the particle surface with the aid of modification with sulfur-containing amino acids has been reported by Gritskova et al.¹⁹² They suggested a method for synthesising modified suspensions that consisted of three independent stages: the first stage involved the synthesis of seed polystyrene particles with a specified diameter and a narrow PSD, the second stage was the seed

polymerisation of isoprene, ensuring a high concentration of polyisoprene units on the surface of the particles, and in the third stage, the resulting isoprene-styrene polymeric suspensions having the 'core-shell' structure were modified by cysteine.

If all the stages of this process are conducted under controlled conditions, it is possible to obtain polymeric suspensions with diameter of particles varying over a wide range (0.1–2.0 µm), a narrow PSD (1%–5%), and a high concentration of amino groups on the particle surface.

It was shown that by varying conditions in which modification is carried out, one can control the properties of the suspensions obtained, which is particularly significant for choosing the optimal conditions for the immobilisation of protein molecules and for further application of modified suspensions in immuno-diagnostics.

* * *

Thus, the data considered above indicate that the main stage in the synthesis of functional polymeric suspensions suitable for immuno-diagnostic studies is the heterophase polymerisation. The choice of polymerisation conditions determines the stability of the suspensions, the particle diameter, and their size distribution. Functional groups on the surface of microspheres can be obtained either during the synthesis or by modifying the resulting polymeric suspensions.

Despite the fact that numerous methods for the synthesis of functional suspensions have been suggested, studies in this field are being intensely carried out.^{193–218} The purpose of the studies is to find conditions of a technologically facile method for preparing suspensions with the use of available reagents.

The work was carried out with financial support from the Russian Fundamental Research Fund (Grant No. 94-03-08987).

References

1. R E Wachtel, V R La Mer *J. Colloid Interface Sci.* **17** 531 (1962)
2. L B Bang (Ed.) *Uniform Latex Particles* (Indianapolis: Seradyn, 1984)
3. J Ugelstad, H R Mfutakamba, P C Mork, T Ellingsen, R Berge, L Holm, R Schinid, A Jorgedal, F K Hansen, K Nustad *J. Polym. Sci., Polym. Symp.* **72** 225 (1985)
4. S K Ober, K P Lok, M L Hair *J. Polym. Sci., Polym. Lett. Ed.* **23** 103 (1985)
5. W M Brouwer *J. Appl. Polym. Sci.* **38** 1335 (1989)
6. A Rembaum, Z Tokes (Eds) *Microspheres: Medical and Biological Applications* (Boca Raton, FL: CRC Press, 1988)
7. P Guioot, P Couvreur (Eds) *Polymeric Nanoparticles and Microspheres* (Boca Raton, FL: CRC Press, 1986)
8. L Illum, S D Davis *J. Parent. Sci. Technol.* **36** 242 (1982)
9. S D Davis, L Illum *Br. Polym. J.* **15** 160 (1983)
10. H Zecha *Makromol. Chem. Makromol. Symp.* **31** 169 (1990)
11. J Hearn, M C Wilkinson, A R Goodall *Adv. Colloid Interface Sci.* **14** 173 (1981)
12. N P Elinov *Khimicheskaya Mikrobiologiya* (Chemical Microbiology) (Moscow: Vysshaya Shkola, 1984)
13. J M Singer, C M Plotz *Am. J. Med.* **21** 888 (1956)
14. US P. 3 234 096 (1966)
15. W P L Severin *J. Clin. Path.* **25** 1079 (1972)
16. M Leinonen, E Herva *Scand. J. Infect. Dis.* **26** 187 (1977)
17. A Bernard, J Vyskogil, R Lauwerys *J. Clin. Chem.* **27** 832 (1982)
18. L De Coster, S Cambiaso, J R Masson *The Riogenology* **13** 433 (1980)
19. J M Singer *Am. J. Med.* **31** 766 (1961)
20. D Collet-Cassard, M Mareschall, R Sindic, P Tomassy, J R Masson *Clin. Chem.* **29** 1127 (1983)
21. J M Singer, I Oreskes, F Hutterer, J Ernst *Ann. Rheumatic Dis.* **22** 424 (1963)
22. L Bonacker, J Staerk *Prog. Immunol. Stand.* **5** 70 (1972)
23. US P. 3 992 517 (1976)

24. S P S Yen, A Rembaum, R W Molday, W Dreyer *Emulsion Polym.* 236 (1976)
25. A Rembaum, S P S Yen, R S Molday *J. Macromol. Sci. Chem.* 13 603 (1979)
26. US P. 3 857 931 (1974)
27. US P. 4 046 723 (1977)
28. US P. 4 060 597 (1977)
29. US P. 4 226 747 (1980)
30. S Margel, E Nov, I Fisher *J. Polym. Sci. Part A, Polym. Chem.* 29 347 (1991)
31. M Shahar, H Meshylam, S Margel *J. Polym. Sci. Part A, Polym. Chem.* 24 203 (1986)
32. D A Upson *J. Polym. Sci., Polym. Symp.* 72 45 (1985)
33. M Okubo, K Ikegami, Y Yamamoto *Colloid Polym. Sci.* 267 193 (1989)
34. C H Suen, H Moravetz *Macromolecules* 17 1800 (1984)
35. Y Changhong, X Zhang, Z Sun, H Kitano, N Ise *J. Appl. Polym. Sci.* 40 89 (1990)
36. M Kumakura, I Kaetsu *Colloid Polym. Sci.* 262 450 (1984)
37. S Margel *J. Polym. Sci., Polym. Chem. Ed.* 22 3521 (1984)
38. S Margel, A Rembaum *Macromolecules* 13 19 (1980)
39. B Schlund, T Pith, M Lambla *Macromol. Chem. Suppl.* 10/11 419 (1985)
40. A Rembaum, M Chang, J Richards, M Li *J. Polym. Sci., Polym. Chem. Ed.* 22 609 (1984)
41. E Zurkova, K Bouchal, D Zdenkova, Z Pelzbayer, F Svec, J Kalal, H G Batz *J. Polym. Sci., Polym. Chem. Ed.* 21 2949 (1983)
42. K Yamaguchi, S Watanabe, S Nakahama *Macromol. Chem., Rapid Commun.* 10 397 (1989)
43. US P. 4 140 662 (1979)
44. Eur. P. 15 841 (1980)
45. Fr. P. 2 363 459 (1981)
46. Fr. P. 2 378 094 (1982)
47. L Johansen, K Nustad, T B Orstavik, J Ugelstad, A Berge, T Ellengsen *J. Immunol. Methods* 59 255 (1983)
48. R S Molday, W J Dreyer *J. Cell. Biol.* 64 75 (1975)
49. US P. 4 045 384 (1976)
50. C Pichot *Bull. Soc. Chim. Fr.* 4 725 (1987)
51. US P. 3 847 745 (1974)
52. Br. P. 2 004 892 (1974)
53. S Margel *J. Eng. Chem., Prod. Res.* 21 343 (1982)
54. E A Dorokhova, Candidate Thesis in Chemical Sciences, Moscow Institute of Fine Chemical Technology, Moscow, 1991
55. Yu V Lukin, I A Gritskova, A N Pravednikov, V I Bakharev *Dokl. Akad. Nauk SSSR* 285 159 (1985)
56. USSR P. 1 565 845 (1990); *Byull. Izobret.* (19) 108 (1990)
57. USSR P. 1 565 846 (1990); *Byull. Izobret.* (19) 108 (1990)
58. USSR P. 1 685 955 (1991); *Byull. Izobret.* (39) 100 (1991)
59. D Bastos, R Santos, J Forcada, R Hidalgoalvarez, F J Delasnieves *Colloid. Surf. A, Physicochem. Eng. Aspects* 92 137 (1994)
60. I A Gritskova, S A Gusev, E Grzywa, E N Teleshov, S M Shumanskii, S M Grzywa-Niksinska *Polymer* 36 229 (1991)
61. B Charleux, P Fanget, C Pichot *Makromol. Chem., Makromol. Chem. Phys.* 193 205 (1992)
62. M Okubo, Y Kondo, M Takahashi *Colloid Polym. Sci.* 271 109 (1993)
63. M D B Oenick, A Warshawsky *Colloid Polym. Sci.* 269 139 (1991)
64. S Margel, E Nov, I Fisher *J. Polym. Sci. Part A, Polym. Chem.* 29 347 (1991)
65. Y H Huang, Z M Li, H Moravetz *J. Polym. Sci., Polym. Chem. Ed.* 23 795 (1985)
66. C H Suen, H Moravetz *Makromol. Chem.* 186 255 (1985)
67. W Funke *Br. Polym. J.* 21 107 (1989)
68. W Funke *J. Coat. Technol.* 60 68 (1988)
69. S Magnet, J Guillot, A Guyot, C Pichot *Prog. Org. Coat.* 20 73 (1992)
70. C Moberg, L Rakos *React. Polym.* 16 171 (1992)
71. P D Verweij, D C Sherrington *J. Mater. Chem.* 1 371 (1991)
72. R Arshady *J. Chromatogr.* 586 199 (1991)
73. D Horak, F Svec, T B Tennikova, M Nahuneck *Angew. Makromol. Chem.* 195 139 (1992)
74. M Walenius, L I Kulin, P Flodin *React. Polym.* 17 309 (1992)
75. S M Jovanovic, A Nastasovic, N N Jovanovic, K Jeremic, Z Savic *Angew. Makromol. Chem.* 219 161 (1994)
76. T Maehara, Y Eda, K Mitani, S Matsuzawa *Biomaterials* 11 122 (1990)
77. A Tuncel, R Kahraman, E Piskin *J. Appl. Polym. Sci.* 51 1485 (1994)
78. D Horak, J Straka, B Schneider, F Lednický, J Pilar *Polymer* 35 1195 (1994)
79. S S Ivanchev *Usp. Khim.* 60 1368 (1991) [*Russ. Chem. Rev.* 60 701 (1991)]
80. I A Gritskova, P V Nuss, E V Dorokhova, D A Al'-Khavarin *Kolloidn. Zh.* 56 487 (1991)
81. V I Eliseeva, T R Aslamazova *Usp. Khim.* 60 398 (1991) [*Russ. Chem. Rev.* 60 206 (1991)]
82. V I Eliseeva *Polimernye Suspenzii* (Polymer Suspensions) (Moscow: Khimiya, 1980)
83. S Muroi *J. Appl. Polym. Sci.* 10 713 (1966)
84. S Muroi, K Hosoi, T Ishikawa *J. Appl. Polym. Sci.* 11 1963 (1967)
85. B R Vizayendran *J. Appl. Polym. Sci.* 23 893 (1979)
86. G W Ceska *J. Appl. Polym. Sci.* 18 427 (1974)
87. B W Greene *J. Colloid Interface Sci.* 43 449 (1973)
88. B W Greene *J. Colloid Interface Sci.* 43 462 (1973)
89. K Sakota, T Okaya *J. Appl. Polym. Sci.* 20 1235 (1976)
90. K Sakota, T Okaya *J. Appl. Polym. Sci.* 20 2583 (1976)
91. M Okubo, K Kanaida, T Matsumoto *J. Appl. Polym. Sci.* 33 1511 (1987)
92. M Okubo, D H Xu, K Kanaida *Colloid Polym. Sci.* 265 246 (1987)
93. I A Gritskova, E G Grzywa *Polymer* 36 418 (1991)
94. B W Greene, D P Sheetz, T D Filer *J. Colloid Interface Sci.* 32 90 (1970)
95. Pol. P. 163 091 (1994)
96. I A Gritskova, O V Chirikova, O I Shchegolikhina, A A Zhdanov *Dokl. Akad. Nauk* 334 57 (1994)
97. O V Chirikova, Candidate Thesis in Chemical Sciences, Moscow Academy of Fine Chemical Technology, Moscow, 1994
98. L Rios, M Hidalgo, J Y Cavaille, J Guillot, A Guyot, C Pichot *Colloid Polym. Sci.* 269 812 (1991)
99. A Kondo, S Uchimura, K Higashitani *J. Ferment. Bioeng.* 78 164 (1994)
100. J Snuparek, P Bradna, L Mrkvickova, F Lednický, O Quadrat *Collect. Czech. Chem. Commun.* 58 2451 (1993)
101. P Bajaj, M Goyal, R B Chavan *J. Appl. Polym. Sci.* 53 1771 (1994)
102. M C Davies, R A P Lynn, S S Davis, J Hearn, J F Watts, J C Vickerman, D Johnson *Langmuir* 10 1399 (1994)
103. A Kondo, K Yoshioka, K Higashitani *Kagaku Kogaku Ronbunshu* 18 353 (1992)
104. K Kjellqvist *Prog. Org. Coat.* 24 209 (1994)
105. H Kawagushi, N Koiwai, Y Ohtsuka *J. Appl. Polym. Sci.* 35 743 (1988)
106. H Kawagushi, N Koiwai, T Mita, Y Ohtsuka, T Takeuchi, S Kobayashi *J. Colloid Polym. Sci.* 268 1167 (1990)
107. Y Ohtsuka, H Kawagushi, Y Sugi *J. Appl. Polym. Sci.* 26 1637 (1981)
108. H Tamai, A Iida, T Suzava *J. Colloid Polym. Sci.* 262 77 (1984)
109. H Tamai, T Murukami, T Suzava *J. Appl. Polym. Sci.* 30 3857 (1985)
110. S Kamei, M Okubo, T Matsuda, T Matsumoto *J. Colloid Polym. Sci.* 264 743 (1986)
111. S Kamei, M Okubo, T Matsumoto *J. Polym. Sci., Polym. Chem. Ed.* 24 3109 (1986)
112. M Okubo, Y Yamamoto, M Uno, S Kamei *J. Colloid Polym. Sci.* 265 1061 (1987)
113. H Shirahama, T Suzava *J. Appl. Polym. Sci.* 29 3651 (1984)
114. T Suzava, H Shirahama, T Fuimoto *J. Colloid Interface Sci.* 86 144 (1982)
115. H Shirahama, T Suzava *J. Colloid Interface Sci.* 104 416 (1985)
116. USSR P. 1 616 927 (1990); *Byull. Izobret.* (48) 85 (1990)
117. F Twigt, P Piet, A L German *Eur. Polym. J.* 27 939 (1991)
118. B Verriercharleux, C Graillat, Y Chevalier, C Pichot, A Revillon *J. Colloid Polym. Sci.* 269 398 (1991)
119. F Twigt, J Broekman, P Piet, A L German *Eur. Polym. J.* 29 745 (1993)
120. J J Lee, W T Ford *J. Org. Chem.* 58 4070 (1993)
121. W T Ford, H Yu, J J Lee, H Elhamshary *Langmuir* 9 1698 (1993)

122. T Delair, V Marguet, C Pichot, B Mandrand *J. Colloid Polym. Sci.* **272** 962 (1994)
123. T Delair, C Pichot, B Mandrand *J. Colloid Polym. Sci.* **272** 72 (1994)
124. J J Lee, W T Ford *J. Am. Chem. Soc.* **116** 3753 (1994)
125. P Cousin, P Smith *J. Appl. Polym. Sci.* **54** 1631 (1994)
126. O Zaborsky (Ed.) *Immobilized Enzymes* (Cleveland: CRS Press, 1978)
127. I Chaiken, V Wilchek, I Pakikh (Eds) *Affinity Chromatography and Biological Recognition* (New York: Academic Press, 1984)
128. H Kitano, Z H Sun, N Ise *Macromolecules* **16** 1306 (1983)
129. R L Schuur *Anal. Biochem.* **143** 1 (1984)
130. Yu A Ovchinnikov *Bioorganicheskaya Khimiya* (Bioorganic Chemistry) (Moscow: Prosveshchenie, 1987)
131. T Wagner, C J Hsu, G Kelleher *Biochem. J.* **108** 892 (1968)
132. G Quash, A-M Roch, A Nivelian, J Grange, T Keolonangkhot, J Huppert *J. Immunol. Methods* **22** 165 (1978)
133. R P Patel, S Price *Biopolymers* **5** 583 (1967)
134. P V Sundaram *Biochem. Biophys. Res. Commun.* **61** 667 (1974)
135. P Cuatrecasas *J. Biol. Chem.* **245** 3059 (1970)
136. K Nilsson, K Mosbach *Eur. J. Biochem.* **12** 397 (1980)
137. K Nilsson, K Mosbach *Biochem. Biophys. Res. Commun.* **102** 449 (1981)
138. K Nustad, L Johansen, R Schmid, J Ugelstad, T Ellingsen, A Berge *Agents Actions Suppl.* **9** 207 (1982)
139. G S Bethell, J S Ayers, W S Hancock, M T W Hearn *J. Biol. Chem.* **254** 2572 (1979)
140. L Yu Basyreva, Candidate Thesis in Chemical Sciences, Moscow Academy of Fine Chemical Technology, Moscow, 1994
141. N S Vul'fson (Ed.) *Preparativnaya Organicheskaya Khimiya* (Preparative Organic Chemistry) (Moscow: Khim. Lit., 1959)
142. Weygand-Higetag *Organisch-chemische Experimentierkunst* (Translated into Russian; Moscow: Khimiya, 1968)
143. H Kawaguchi, H Hochino, Y Ohtsuka *J. Appl. Polym. Sci.* **26** 2015 (1981)
144. H Tanaka *J. Polym. Sci., Polym. Chem. Ed.* **17** 1239 (1979)
145. H Kawaguchi, H Hochino, H Amagasa, Y Ohtsuka *J. Colloid Interface Sci.* **97** 465 (1984)
146. L Stenberger (Ed.) *Electron Microscopy of Enzymes: Principles and Methods* (New York: Elsevier, 1973)
147. F Richards, J Knowles *J. Mol. Biol.* **37** 231 (1968)
148. H Otto, H Takamiya, A Vogt *J. Immunol. Methods* **3** 137 (1973)
149. J K Inman, H M Dintzis *Biochemistry* **8** 4074 (1969)
150. US P. 4 419 543 (1984)
151. H Kitano, C Yan, Y Maeda, N Ise *Biopolymers* **28** 693 (1989)
152. M Fedtke *Reaktionen an Polymeren* (Leipzig: VEB Deutscher Verlag, 1985)
153. R Gopalan, K Subbarayan *J. Indian Chem. Soc.* **56** 669 (1979)
154. P Ferrabochi, M N Azandi, E Santaniella, S Trave *Synth. Commun.* **16** 43 (1986)
155. R C Kerber, G W Urry, N Kornblum *J. Am. Chem. Soc.* **87** 4520 (1965)
156. M D B Oenick, A Warshawsky *Colloid Polym. Sci.* **269** 139 (1991)
157. M D Bale, S J Danielson, R E Goppert, R C Sutton *J. Colloid Interface Sci.* **132** 176 (1989)
158. Z Song, G W Poehlein *J. Polym. Sci. Part A, Polym. Chem.* **28** 2365 (1989)
159. J W Goodwin, J Hearn, C C Ho, R H Ottewill *Colloid Polym. Sci.* **252** 464 (1974)
160. Y Chung-li, J W Goodwin, R H Ottewill *Prog. Colloid Polym. Sci.* **60** 163 (1976)
161. J W Goodwin, R H Ottewill, R Pelton *Colloid Polym. Sci.* **257** 62 (1979)
162. R H Ottewill, R Satgurunathan *Colloid Polym. Sci.* **265** 845 (1987)
163. D Zou, V Derlich, K Gandhi, M Park, L Sun, D Kriz, Y D Lee, G Kim, J J Aklonis, R Salovey *J. Polym. Sci. Part A, Polym. Chem.* **28** 1909 (1990)
164. Y Almong, S Reich, M Levy *Br. Polym. J.* **12** 131 (1982)
165. C M Tseng, Y Y Lu, M S El-Aasser, J W Vanderhoff *J. Polym. Sci. Part A, Polym. Chem.* **24** 2995 (1986)
166. M Okubo, M Shiozaki, M Tsujihiro, Y Tsukuda *Colloid Polym. Sci.* **269** 222 (1991)
167. T J J Van der Hoven, B H Bijsterboch *J. Colloid Interface Sci.* **115** 559 (1987)
168. W M Brouwer, R L J Zsom *Colloids Surf. (Netherlands)* **24** 195 (1987)
169. J H Kim, M S El-Aasser, A Klein, J W Vanderhoff *J. Appl. Polym. Sci.* **35** 2117 (1988)
170. B R Paulke, W Hartig, G Bruckner *Acta Polym.* **43** 288 (1992)
171. M Antonietti, S Lohmann, C Vanniel *Macromolecules* **25** 1139 (1992)
172. W T Ford, R D Badley, R S Chandran, S H Babu, M Hassanein, S Srinivasan, H Turk, H Yu, W M Zhu, in *Polymer Latexes* (Eds E S Daniels, E D Sudol, M S El-Aasser) (Washington, DC: American Chemical Society, 1992) p. 422
173. E Piskin, A Tuncel, A Denizli, H Ayhan *J. Biomater. Sci., Polym. Ed.* **5** 451 (1994)
174. E Piskin, A Tuncel, A Denizli, H Ayhan, E B Denkbaz, H Cicek, K T Xu *ACS Symp. Ser.* **556** 222 (1994)
175. J M Vanderhoff *Chem. Eng. Sci.* **48** 203 (1993)
176. D Hunkeler, F Candau, C Pichot, A E Hemielec, T Y Xie, J Barton, V Vaskova, J Guillot, M V Dimonie, K H Reichert *Adv. Polym. Sci.* **112** 115 (1994)
177. A A Kamel, Ph D Thesis, Lehigh University, Bethlehem, 1981
178. Y C Chen, V Dimonie, M S El-Aasser *Macromolecules* **24** 3779 (1991)
179. Eur. P. 158 443 (1985)
180. H J Tenoso, D B Smith (Eds) *Covalent Bonding of Antibodies to Polystyrene Latex Beads: a Concept* (Washington, DC: NASA Tech. Brief., 1972)
181. US P. 493 992 (1974)
182. L M Kogan, V A Krol', in *Khimicheskaya Modifikatsiya Polimer-nykh Dienov* (Chemical Modification of Polymer Dienes) (Moscow: TsNIITeftekhim, 1976) p. 73
183. L M Kogan, V A Krol' *Zh. Vses. Khim. O-va im. D I Mendeleeva* **26** 272 (1981)
184. P Reinholdsson, T Hargitai, R Isaksson, B Tornell *Angew. Makromol. Chem.* **192** 113 (1991)
185. Y Yamamoto, M Okubo, Y Iwasaki *Colloid Polym. Sci.* **269** 1126 (1991)
186. A Guyot, P Hodge, D C Sherrington, H Widdecke *React. Polym.* **16** 233 (1992)
187. K Li, H D H Stover *J. Polym. Sci. Part A, Polym. Chem.* **31** 3257 (1993)
188. T B Gonsovskaya, F G Ponomarev, P T Poluektov, L K Khvatova *Kauchuk Rezina* **1** 23 (1971)
189. P T Poluektov, T B Gonsovskaya, F G Ponomarev, Yu K Gusev *Vysokomol. Soedin., Ser. A* **15** 606 (1973)
190. A D Roberts (Ed.) *Natural Rubber Science and Technology* Vol. 2 (London: Oxford University Press, 1988)
191. E G Imnadze, Candidate Thesis in Chemical Sciences, Moscow Institute of Fine Chemical Technology, Moscow, 1987
192. I A Gritskova, N I Prokopov, V R Cherkasov *Vysokomol. Soedin., Ser. A* **37** 683 (1995)
193. V R Cherkasov, Candidate Thesis in Chemical Sciences, Moscow Institute of Fine Chemical Technology, Moscow, 1992
194. H Tamai, T Oyanagi, T Suzawa *Colloids Surf. (Netherlands)* **57** 115 (1991)
195. I Noda *Nature (London)* **350** 143 (1991)
196. B Vincent *Chem. Eng. Sci.* **48** 429 (1993)
197. C Graillat, B Dumont, P Depraetere, V Vintenon, C Pichot *Langmuir* **7** 872 (1991)
198. J S Tan, D E Butterfield, C L Voycheck, K D Caldwell, J T Li *Biomaterials* **14** 823 (1993)
199. M Shiozaki, T Tokuno *Polym. Int.* **30** 217 (1993)
200. S Rudt, H Wesemeyer, R H Muller *J. Control. Release* **25** 123 (1993)
201. S Stolnik, S E Dunn, M C Garnett, M C Davies *Pharm. Res.* **11** 1800 (1994)
202. S Rudt, R H Muller *Eur. J. Pharm. Sci.* **1** 31 (1993)
203. N Privitera, R Naon, J G Riess *Int. J. Pharm.* **104** 41 (1994)
204. A Guyot, K Tauer *Adv. Polym. Sci.* **111** 43 (1994)
205. J H Kim, M Chainey, M S El-Aasser, J W Vanderhoff *J. Polym. Sci. Part A, Polym. Chem.* **30** 171 (1992)
206. F J Delasnieves, E S Daniels, M S El-Aasser *Colloids Surf. (Netherlands)* **60** 107 (1991)
207. C Graillat, C Pichot, A Guyot *Colloids Surf. (Netherlands)* **56** 189 (1991)
208. M Okubo, I Azuma, H Hattori *J. Appl. Polym. Sci.* **45** 245 (1992)

209. D Bastos, F J D Nieves *Colloid Polym. Sci.* **271** 860 (1993)
210. S Watanabe, S Nakahama, K Yamaguchi *Makromol. Chem., Makromol. Chem. Phys.* **192** 1891 (1992)
211. S Watanabe, H Ozaki, K Mitsuhashi, S Nakahama, K Yamaguchi *Makromol. Chem., Makromol. Chem. Phys.* **193** 2781 (1992)
212. E Ruckenstein, X Wang *Biotechnol. Bioeng.* **42** 821 (1993)
213. M T Charreyre, P Boullanger, T Delair, B Mandrand, C Pichot *Colloid Polym. Sci.* **271** 668 (1993)
214. M C Davies, R A P Lynn, S S Davis, J Hearn, J F Watts, J C Vickerman, A J Paul *Langmuir* **9** 1637 (1993)
215. K Sugiyama, K Shiraishi, K Ohga, H Shirahama, H Tamai, K Kikukawa, H Yasuda *Polym. J.* **25** 521 (1993)
216. C Li, D J Yang, L R Kuang, S Wallace *Int. J. Pharm.* **94** 143 (1993)
217. K Sugiyama, H Aoki *Polym. J.* **26** 561 (1994)
218. K Sugiyama, K Ohga, K Kikukawa *Makromol. Chem., Makromol. Chem. Phys.* **195** 1341 (1994)

Electrochemistry of hydride-forming intermetallic compounds and alloys

O A Petrii, S Ya Vasina, I I Korobov

Contents

I. Introduction	181
II. Brief history of the discovery and use of hydride-forming intermetallic compounds	181
III. The main types of metal hydride electrodes	182
IV. The technology of the manufacture and activation of metal hydride electrodes	187
V. Hydrogen evolution reaction on metal hydride electrodes	188
VI. Charge–discharge processes on metal hydride electrodes	189
VII. Corrosion of metal hydride electrodes	191
VIII. Conclusion	193

Abstract. The present review covers studies published over the past 15 years on the electrochemistry of hydride-forming intermetallic compounds (IMC) and alloys. Data on the discharge capacity and stability of electrode materials based on IMC and AB, AB₂, AB₃ and AB₅ type alloys and their substituted derivatives during potential cycling are classified and generalised. The problems concerning the optimisation of the elemental composition of IMC and alloys, their production and activation as well as the reasons for the degradation of electrodes based on these materials are discussed. The mathematical models suggested for describing the processes of discharge and degradation of metal hydride electrodes are analysed. The bibliography includes 149 references.

I. Introduction

It was found in the 1960s that a series of intermetallic compounds (IMC) possess the unique capability to absorb reversibly an anomalously large amount of hydrogen (up to 1.5%–2%)[†] at moderate pressures and temperatures.¹ This led to the appearance of several new fields of scientific investigations directly related to the solution of problems of hydrogen energetics and technology. The results of these studies show the possibility of developing methods, new in principle, for the preparation, storage, purification, compression and application of hydrogen in different technological processes and energy-transforming systems.^{1,2}

The present review deals with electrode materials based on hydride-forming IMC and alloys with a high sorption capacity for hydrogen. These materials are primarily intended for use in nickel–metal hydride batteries. Palladium was the first hydride-

forming element to attract the particular attention of electrochemists after studies by Nilen³ and Frumkin.^{4,5} Palladium has since been extensively used as a classical model in hydride electrochemistry, since processes of hydrogen sorption–desorption, reversible at ambient temperature but not complicated by corrosion phenomena, can be implemented only with this material. The recent commercial use of hydrides was preceded by extensive studies of a wide range of new materials, which makes it urgent to analyse and generalise the data obtained to date.

In this review we consider the main aspects of the electrochemistry of hydride-forming materials that have attracted most research attention in recent years and that we believe to be of interest to a wide circle of chemists.

II. Brief history of the discovery and use of hydride-forming intermetallic compounds

The first studies on the use of hydride-forming IMC as reversible electrodes carried out by Justi et al.⁶ for individual compounds of the Ti_{1–x}Ni_x system, and by Gutjahr et al.⁷ for a mixture of intermetallic compounds Ti₂Ni–TiNi, have demonstrated, in principle, the possibility of the cathodic storage of hydrogen using these IMC.

In 1973, the results of a study on the electrochemical behaviour of LaNi₅ were reported.⁸ This compound was found to have a discharge capacity of 200 mA h g^{–1}, which, however, was much lower than the value expected from the pressure–composition isotherm for the LaNi₅–H₂ system (360 mA h g^{–1}). In 1975, the first battery with LaNi₅ as a metal hydride cathode was patented.⁹

During the following years, the main attention of researchers was devoted to increasing the electrochemical capacity of metal hydride (MH) electrodes and to decreasing the loss of capacity in storage (self-discharge). With this purpose, IMC of the LaNi₅ type with partial replacement of lanthanum and nickel by other metals, whose electrochemical charging results in hydride phases with lower equilibrium dissociation pressures, have been studied.^{10–12}

It was found that the main difficulty in the use of such IMC as TiNi, Ti₂Ni, LaNi₅, MmNi₅ (Mm is ‘mischmetal’, i.e., a technical mixture of rare-earth metals) and their substituted derivatives as MH electrodes in batteries was the low stability of the IMC under electrochemical charge–discharge cycling conditions due to degradation processes.

[†] The content of hydrogen in these materials (v/v) is 1.5 to 2 times higher than in liquid hydrogen.

O A Petrii, S Ya Vasina M V Lomonosov Moscow State University, Chemistry Department, 119899 Moscow, Russian Federation.
Fax (7-095) 939 27 42. Tel. (7-095) 939 13 21, (7-095) 939 53 75.

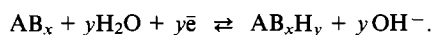
I I Korobov Institute of New Chemical Problems, Russian Academy of Sciences, 142432 Chernogolovka, Russian Federation.
Fax (7-095) 524 50 24.

Since the early '80s, studies in the field of MH electrodes have been directed at increasing the stability of AB₃ type IMC under cycling conditions (requiring the development of multicomponent alloys maintaining the initial hexagonal structure of the CaCu₅ type),¹³ on the one hand, and at the search for electrochemically new species, i.e., IMC of the AB₃ type and the substituted derivatives,^{14,15} multicomponent Laves phases of AB₂ stoichiometry,^{16,17} hyperstoichiometric compounds of AB_{5+x},^{18,19} and AB_{2+x} types,^{17,20–22} IMC in amorphous, nanocrystalline forms and IMC films.^{23–26}

III. The main types of metal hydride electrodes

The adsorption and desorption of gaseous hydrogen on IMC are described by P – T – c diagrams, while those on MH electrodes are described by charge-discharge curves, i.e., plots of electrode potential versus the quantity of electricity passed (Q).

The charging of MH electrodes in alkaline electrolytes occurs because the electrochemical reduction of water gives hydrogen, which is then absorbed by the IMC. During discharge, hydrogen diffuses from the bulk of the IMC to the electrode surface and is oxidised. The electrochemical adsorption-desorption of hydrogen by AB_x compounds can therefore be represented by the following general equation:



A charge of one electron corresponds to each absorbed hydrogen atom, and the charge-discharge capacity (C) per unit mass (m) is determined by the equation:

$$C = \frac{Q}{m}.$$

The charge-discharge curves used for the determination of the full hydrogen capacity of electrodes (C_{eq}^0) should be recorded under equilibrium conditions, i.e., at very low charge or discharge currents. In practice, after passing a certain amount of electricity, it is necessary to disconnect the circuit and record the currentless (equilibrium) potential, and then plot graphically the dependence of the amount of electricity passed on the currentless potential. This procedure makes it possible to avoid errors related to the retardation of hydrogen diffusion into the bulk of the electrode and of other steps. In most studies, the full capacity values (C^0) were obtained under nonequilibrium conditions: first, the capacity was determined at high discharge currents (C_h), then the current was diminished (usually, tenfold), and the capacity was determined at low current (C_l). The full capacity is calculated as $C_h + C_l$.

The equilibrium potential of an MH electrode is related to the equilibrium pressure in the adsorption and desorption of hydrogen (p_{H_2}) by the Nernst equation

$$E_r = -\frac{RT}{2F} \ln p_{\text{H}_2}, \quad (1)$$

where E_r is the potential of the MH electrode relative to the reversible hydrogen electrode in the same solution. Thus, the equilibrium hydrogen pressure over the hydride phase that characterises the stability of the latter can be calculated from the potential corresponding to a plateau on equilibrium charge-discharge curves. The main requirements that should be met by MH electrodes used in current sources are high discharge capacity and cyclic stability during electrochemical charge and discharge, $S(N)$

$$S(N) = \frac{C(N)}{C^0} 100 (\%), \quad (2)$$

where $C(N)$ is the discharge capacity at the N th cycle.

Table 1 presents the currently available literature data on the studies of IMC and various alloys, i.e., AB, AB₂, AB₃, AB₅ and their substituted derivatives, as MH electrodes.

1. LaNi₅ and its substituted derivatives

LaNi₅ is an intermetallic compound which has been the most frequently studied electrochemically as an MH electrode. It is characterised by a high discharge capacity (in closed electrochemical cells), electrocatalytic activity and corrosion resistance in alkaline electrolytes. However, despite all of these advantages, LaNi₅ has a significant drawback, viz. low cyclic charge-discharge stability due to degradation processes, the mechanism of which will be considered below.

The partial replacement of Ni in LaNi₅ by Mn, Cu, Cr, Al or Co, which have higher atomic radii than that of nickel, enables the synthesis of IMC with lower equilibrium dissociation pressures of the hydride phases (< 0.098 MPa) with retention of the hexagonal type of the lattice. For example, the replacement of one nickel atom by one aluminium atom decreases p_{H_2} by almost three orders of magnitude.²⁷ Hence, MH electrodes based on such IMC have lower self-discharge due to the desorption of hydrogen as a gas under atmospheric pressure.

A comparison of $S(N)$ values and relative increases in the unit cell volume upon hydrogenation ($\Delta V/V$) showed^{13,27} that alloys, the hydrogenation of which results in insignificant volume increase, have the highest stability. Unfortunately, such alloys normally have low discharge capacity, while both of these parameters should be taken into account in the selection of MH electrode composition.

The considerable increase in the cyclic stability of LaNi₅ when alloyed with cobalt was first noted by Willems.¹³ The effect of the replacement of nickel by cobalt is enhanced when a small amount of silicon or aluminium is added^{13,34} due to the formation of a protective oxide layer on the surface. The presence of this layer, which hinders hydrogen diffusion into the bulk of the metal, increases the overvoltage of the electrochemical charge-discharge of the electrode. The addition of titanium increases the cyclic stability, but simultaneously decreases markedly the electrochemical capacity, unlike neodymium, which increases this parameter. According to the data of Sakai and co-workers³⁴, an alloy in which there is partial replacement of lanthanum by neodymium and of cobalt by aluminium, viz. La_{0.8}Nd_{0.2}Ni_{2.5}Co_{2.4}Al_{0.1}, is the most suitable MH electrode [$C^0 = 241$ mA h g⁻¹, $S(300) = 85\%$].

The partial replacement of lanthanum by zirconium and of nickel by aluminium in LaNi₅ considerably prolongs the operation time of MH electrodes. The optimum compositions correspond to the formula La_{1-x}Zr_xNi_{4.5}Al_{0.5}, where $x = 0.1 - 0.2$.³⁷

2. MmNi₅ and its substituted derivatives

The price of industrially manufactured LaNi₅ on the world market is ~\$30 US per kg.³⁹ The cost of MH electrodes can be reduced considerably if the lanthanum in the IMC is completely or partly replaced by 'mischmetal'. However, this replacement increases the dissociation pressure of the hydride phases. For example, this value is ~1.5 MPa at 298 K for MmNi₅.⁴⁰

To decrease the equilibrium pressure over the hydride phase in MmNi₅, as in the case of LaNi₅, it is necessary to partly replace nickel by such metals as aluminium or manganese.^{28,41} It was found that MmNi₅ should be alloyed not only with aluminium or manganese, but also with cobalt in order to enhance the cyclic stability of MH electrodes.^{41,43} It is remarkable that a profound effect is observed upon replacement of as little as one nickel atom by a cobalt atom, whereas the optimum replacement number for LaNi₅ is from 2 to 2.5 nickel atoms. This may be connected with the presence of Ce in the Mm.

The general criteria for selection of the IMC composition of the MmNi₅ type are the same as in the case of LaNi₅, and the optimum compositions differ only in the quantity of components added (see Table 1).

Table 1. The main types of MH electrodes based on hydride-forming intermetallic compounds (IMC) and alloys.

IMC	$C^0 / \text{mA h g}^{-1}$	$S(N) (\%)$	Ref.
LaNi ₅ and its substituted derivatives			
LaNi ₅	350 – 372	12 – 15 (400)	12, 13, 19, 28, 29
	250 – 275	26 (150)	27, 91
LaNi _{4.5} Mn _{0.5}	318	17 (150)	27
	315	40 – 60 (100)	30
LaNi ₄ Mn	220	31 (150)	27
LaNi _{4.5} Cu _{0.5}	250	36 (150)	27
LaNi ₄ Cu	260 – 270	27 (150)	12, 27
	342 – 373	16 (400)	19, 28, 29
LaNi _{4.5} Cr _{0.5}	286	41 (150)	27
LaNi ₄ Cr	174; 280	67 (150)	12, 27
LaNi _{5-x} Al _x $x = 0.1 - 1.0$	355 – 185	16 (400) ($x = 0.1$) 56 (150) ($x = 0.5$) 100 (150) ($x = 1$)	13, 27, 28, 31 32 27
LaNi _{5-x} Co _x $x = 1.0 - 3.3$	372 – 273	25 – 64 (400)	13
LaNi _{2.5} Co _{2.5}	230	90 (150)	27
	244 – 264	57 (300)	33, 34
LaNi _{4.5} Fe _{0.5}	320	40 (200)	35
LaNi _{4.9-x} Co _x Al _{0.1} $x = 2.5 - 3.0$	365 – 289	30 – 94 (400)	13
LaNi _{2.5} Co _{2.4} Al _{0.1}	231	83 (300)	34
LaNi _{4.7} Si _{0.3}	270		36
LaNi _{4.9-x} Co _x Si _{0.1} $x = 1.0 - 3.0$	350 – 280	33 – 96 (400)	13
LaNi _{2.5} Co _{2.4} Si _{0.1}	230	76 (300)	34
LaNi _{2.5} Co _{2.4} Mn _{0.1}	244		33
LaNi _{4.4} Al _{0.3} Si _{0.3}	270		36
La _{0.8} Nd _{0.2} Ni ₂ Co ₃	302	48 (400)	13
La _{0.7} Nd _{0.3} Ni _{2.5} Co _{2.4} Al _{0.1}	293	87 (400)	13
La _{0.8} Nd _{0.2} Ni _{2.5} Co _{2.4} Al _{0.1}	241	85 (300)	34
La _{0.8} Nd _{0.2} Ni _{2.5} Co _{2.4} Si _{0.1}	293	88 (400)	13
	280	30 (1000)	29
La _{0.7} Nd _{0.2} Ti _{0.1} Ni _{2.5} Co _{2.5}	178	90 (300)	34
La _{0.7} Nd _{0.2} Ti _{0.1} Ni _{2.5} Co _{2.4} Al _{0.1}	175	94 (300)	34
La _{0.7} Nd _{0.2} Ti _{0.1} Ni _{2.5} Co ₂ Al _{0.5}	254	90 (400)	13
La _{0.7} Nb _{0.3} Ni _{2.5} Co _{2.4} Cr _{0.1}	186		33
La _{0.9} Zr _{0.1} Ni ₅	137	50 (440)	37
La _{0.8} Zr _{0.2} Ni ₅	140	50 (540)	37
La _{0.9} Zr _{0.1} Ni _{4.5} Al _{0.5}	300 – 350	75 (300)	38
	280	50 (580)	37
La _{0.85} Zr _{0.15} Ni _{4.5} Al _{0.5}	271	50 (690)	37
La _{0.8} Zr _{0.2} Ni _{4.5} Al _{0.5}	254	50 (810)	37
La _{0.8} Ce _{0.2} Ni ₂ Co ₃	267	84 (265)	33
MmNi ₅ and its substituted derivatives			
MmNi ₅	170		40
MmNi ₄ Mn	350	30 (700)	41
MmNi ₄ Al	214; 280		28, 41
MmNi ₄ Co _{0.7} Al _{0.3}	300		41
	200 – 300		42
MmNi _{3.5} Co _{0.7} Al _{0.8}	240; 200; 183; 250	95 (1000) 92 (2000)	43, 44 33, 45
Mm _{1.1} Ni _{3.25} CoAl _{0.75}	220	65 (600)	41
MmNi _{3.25} (CoMn) _{1.75}	220	65 (700)	41
MmNi _{3.45} (CoMnTi) _{1.55}	300	87 (540) 77 (1000)	41
MmNi _{3.55} Co _{0.75} Al _{0.3} Mn _{0.4}	240		46
Mm(Ni _{3.6} Co _{0.7} Al _{0.3} Mn _{0.4}) _{0.92}	210		28
MmNi _{4.49} Co _{0.1} Al _{0.205} Mn _{0.205}	330		47
MmNi _{4.2} Mo _{0.6} Al _{0.2}		80 (150)	48
MmNi _{3.7} Al _{0.5} Fe _{0.7} Cu _{0.1}	220	Reserve of 60 cycles ($N = 60$)	49
MmNi _x Cu _a Mn _b Al _c $3.5 < x < 4.3$; $0.2 < a < 1.2$; $0.15 < b < 0.85$; $0.05 < c < 0.5$	250 – 300	Reserve of 200 cycles ($N > 200$)	50
Mm _{0.5} La _{0.5} Ni ₂ Co ₃	156		33

Table 1 (continued).

IMC	$C^0 / \text{mAh g}^{-1}$	$S(N) (\%)$	Ref.
$\text{Mm}_{0.8}\text{Ti}_{0.1}\text{Zr}_{0.1}\text{Ni}_{4.8}\text{Si}_{0.2}$	298	Reserve of 300 cycles ($N = 300$)	51
$\text{Mm}_{0.8}\text{Zr}_{0.2}\text{Ni}_4\text{Al}$	240	40 (700)	41
$\text{Mm}_{0.9}\text{Ti}_{0.1}\text{Ni}_{3.9}\text{Co}_{0.4}\text{Al}_{0.3}\text{Mn}_{0.4}$	259	65 (200)	52
$\text{Ln}_{1-x}\text{M}_x\text{Ni}_{5-y}\text{M}'_y$ Ln = La or Mm; M = Ti, Y, Zr, Nb, Mo, Hf, Ta, Th, Ba, Ca; M' = Si, V, Fe, Co, Zn, Mg, Ca, Ba, Cu, Mn, Al, Mo, Cr, Sn, Sb	250 – 300	Reserve of 160 – 200 cycles ($N = 160 - 200$)	51 – 55
$\text{MmNi}_{3.7}\text{Al}_{0.8}\text{Si}_{0.5}$	100		36
$\text{Mm}_{0.5}\text{La}_{0.5}\text{Mn}_{0.2}\text{Ni}_{4.2}\text{Al}_{0.3}\text{Si}_{0.3}$	270		36
$\text{ML}_{0.6}\text{La}_{0.4}(\text{NiAlCu})_{4.2}\text{Co}_{0.8}$ ML — Mm, enriched with La	270	97.5 (100)	56
$\text{ML}_{0.5}\text{Mm}_{0.5}\text{Ni}_4\text{Mn}_{0.2}\text{Al}_{0.5}\text{Si}_{0.3}$	200		36
Hyperstoichiometric IMC of $\text{AB}_{(5+x)}$ type			
$\text{LaNi}_{5.4}$	360	25 (400)	19
$\text{LaNi}_{4.2}\text{Cu}$	360	62 (400)	19
$\text{LaNi}_{4.4}\text{Cu}$	285	90 (400)	19
LaNi_5Cu	198	98 (400)	19
$\text{LaNi}_{4.9}\text{Cu}_{0.5}$	306	63 (400)	19
$\text{LaNi}_{4.6}\text{Cu}_{0.5}$	282	81 (400)	19
$\text{LaNi}_{3.9}\text{Cu}_{1.5}$	281	83 (400)	19
$\text{LaNi}_{3.4}\text{Cu}_2$	245	89 (400)	19
$\text{LaNi}_{2.9}\text{Cu}_{2.5}$	230	87 (400)	19
$\text{LaNi}_{2.4}\text{Cu}_3$	230	73 (400)	19
$\text{La}_{0.8}\text{Nd}_{0.2}\text{Ni}_3\text{Co}_{2.4}\text{Si}_{0.1}$	276	84 (400)	18
$\text{La}_{0.8}\text{Nd}_{0.2}\text{Ni}_{2.9}\text{Co}_{2.4}\text{Mo}_{0.1}\text{Si}_{0.1}$	285	73 (400)	18
Intermetallic compounds of AB_3 type and their substituted derivatives			
$\text{CeNi}_{3-x}\text{Co}_x$; $x = 0, 1, 2$	160		14
$\text{YNi}_{2.5}\text{M}_{0.5}$ M = Ni, Al, Fe, Cr, Cu, Co, Mn	150 – 200		15
(Ti, Zr) – Ni alloys			
TiNi	250		6
Ti_2Ni	250		6
$\text{TiNi} + \text{Ti}_2\text{Ni}$	320		7
$\text{Ti}_{1-x}\text{Zr}_x\text{Ni}_y$ $x = 0.2 - 0.8$; $y = 0.5 - 1$	450 – 250		60
$\text{Ti}_{0.6}\text{Zr}_{0.4}\text{Ni}_{0.75}$	180 – 200	50 (120)	61
$\text{Ti}_{0.5}\text{Zr}_{0.5}\text{Ni}$	180 – 200	50 (240)	61
$\text{Ti}_{0.5}\text{Zr}_{0.5}\text{Ni}_{0.95}\text{Cu}_{0.05}$	180 – 200	50 (360)	61
$\text{Ti}_{0.5}\text{Zr}_{0.5}\text{Ni}_{0.9}\text{Cu}_{0.1}$	180 – 200	50 (630)	61
$\text{Ti}_{0.2}\text{Zr}_{0.8}\text{Ni}_{1.25}$	180 – 200	50 (1200)	61
$\text{ZrNi}_{1.45}$	180 – 200	50 (2230)	61
$\text{ZrNi}_{1.43}$	285		62
ZrNi_2	182		63
Laves phases with AB_2 stoichiometry and with hyperstoichiometric composition			
$\text{TiV}_3\text{Ni}_{0.56}$	420		64
$\text{ZrNi}_{2-x}\text{V}_x$ $x = 0.1 - 0.8$	113 – 345		63
$\text{ZrNi}_{1.5}\text{V}_{0.5}$	345	60 (300)	63
	240	75 (180)	59
	300 – 600		65
$\text{Zr}(\text{Ni}_{0.67}\text{V}_{0.33})_2$	218 – 297	57 (100)	17
$\text{Zr}_{1.6-1.7}\text{Ti}_{2-1}\text{V}_{2.6-5.4}\text{Ni}_{4.7-2.3}$	350 – 265		16
$\text{Zr}_{0.9}\text{Ti}_{0.1}(\text{V}_{0.33}\text{Ni}_{0.67})_2$	273	57 (100)	17
$\text{Zr}(\text{V}_{0.33}\text{Ni}_{0.67})_{2.4}$	304 – 311	57 (100)	17
	200		21
$\text{Zr}_{0.9}\text{Ti}_{0.1}(\text{V}_{0.33}\text{Ni}_{0.67})_{2.4}$	262 – 264	57 (100)	17
$\text{Zr}(\text{V}_{0.33}\text{Ni}_{0.59}\text{Co}_{0.08})_{2.4}$	326	57 (100)	17
$\text{Zr}(\text{V}_{0.33}\text{Ni}_{0.5}\text{Co}_{0.17})_{2.4}$	328	57 (100)	17
$\text{Zr}(\text{V}_{0.33}\text{Ni}_{0.59}\text{Fe}_{0.08})_{2.4}$	332	57 (100)	17
$\text{Zr}(\text{V}_{0.33}\text{Ni}_{0.59}\text{Mn}_{0.08})_{2.4}$	363	57 (100)	17
$\text{Zr}(\text{V}_{0.33}\text{Ni}_{0.5}\text{Mn}_{0.17})_{2.4}$	366	57 (100)	17
$\text{Zr}_{0.9}\text{Ti}_{0.1}(\text{V}_{0.33}\text{Ni}_{0.59}\text{Co}_{0.08})_{2.4}$	314 – 316	57 (100)	17
$\text{ZrNi}_{1.2}\text{Mn}_{0.8-x}\text{Cr}_x$ $x = 0.2 - 0.8$	200 – 300		57, 58

Table 1 (continued).

IMC	$C^0/\text{mA h g}^{-1}$	$S(N)\%$	Ref.
Zr _{1-y} Ni _{1.2} Mn _{0.4} Cr _{0.4} $y = 0.8 - 1.2$	200		57
ZrNi _{1.2} Mn _{0.5} Cr _{0.2} V _{0.1}	340		57
ZrNi _{1.2} Mn _{0.3} Cr _{0.2} V _{0.3}	360		57
ZrNi _{1.2} Mn _{0.4} Cr _{0.4}	250		57
ZrNi _{1.2} Cr _{0.8}	330		57
Zr _{0.5} Ti _{0.5} NiV	350	50 (10)	59
Zr _{0.5} Ti _{0.5} Ni _{1.25} V _{0.75}	270	50 (120)	59
Zr _{0.5} Ti _{0.5} Ni _{1.3} V _{0.7}	280	28 (70)	59
Zr _{0.5} Ti _{0.5} Ni _{1.5} V _{0.5}	250	72 (170)	59
Zr _{0.6} Ti _{0.4} Ni _{1.5} V _{0.5}	260	58 (140)	59
Zr _{0.5} Ti _{0.5} Ni _{1.1} V _{0.75} Fe _{0.15}	250	88 (70)	59
Zr _{0.5} Ti _{0.5} Ni _{1.1} V _{0.75} Cr _{0.15}	210	100 (70)	59
Zr _{0.5} Ti _{0.3} Ni _{1.1} V _{0.75} Cr _{0.3}	330		66
TiNi _{0.6-0} V _{0.64} Mn _{0.61-1.21} Fe _{0.15}	137–160		67
Ti _{0.8} Zr _{0.2} Ni _{0.6} V _{0.64} Mn _{0.61} Fe _{0.15}	154		67
ZrCr _{0.8} Mo _{0.2} NiMm _{0.05} $M = \text{V, Mn, Fe, Co}$	300–370		22
Zr(V–Mn–Ni–Mo) _{2.4}	300		20
Zr _{0.5} Ti _{0.5} Ni _{1.3} V _{0.7} Mo _{0.2} $M = \text{Fe, Cr, Mn}$	200–300		24
Zr _{0.5} Ti _{0.5} V _{0.75} Ni _{1.5}	294	85 (1000)	68
Zr _{0.9} Ti _{0.1} (Ni _{0.51} V _{0.33} Co _{0.08} Mn _{0.08}) ₂	240		21
CeNi ₂	81	91 (500)	69
PrNi ₂	71	84 (500)	69
LaNi ₂	70	100 (500)	69
MmNi ₂	61	79 (500)	69

3. Nonstoichiometric intermetallic compounds AB_{5+x}

In the early 1990s, the first reports appeared^{18, 70–73} on the electrochemical behaviour of hydrogen-absorbing nonstoichiometric alloys. It was assumed^{72, 73} that a portion of the La atoms in the crystal lattice of LaNi₅ can be replaced by B atoms (one La atom is replaced by two B atoms) to form a new class of nonstoichiometric compounds AB_x, where $x > 5$.

The first compounds studied were two-phase.^{20, 74} In addition to the AB₅ phase, they contained a second, electrochemically highly reactive phase homogeneously distributed at the grain boundaries of the main alloy. This second phase contained transition metals; it was difficult to predict its composition, although it was undoubtedly determined by the thermodynamic stability of the corresponding compounds.

A detailed study¹⁸ of AB_{5.5} type IMC, such as La_{0.8}Nd_{0.2}Ni₃Co_{2.4}Si_{0.1} and La_{0.8}Nd_{0.2}Ni_{2.9}Mo_{0.1}Co_{2.4}Si_{0.1}, using scanning electron microscopy, optical microscopy, and electron microanalysis showed that cooling of homogeneous alloys resulted in the formation of grains of an AB₅ type of hydride-forming alloy, NiCo₃ (in the former case) or MoCo₃ (in the latter case) being distributed at the grain boundaries. It is likely that it is the

presence of these phases that results in a two- to threefold increase in the exchange current density of the hydrogen evolution reaction, since, according to the Brewer–Engel⁷⁵ valence bond theory, the simultaneous presence of Ni and Co or Mo and Co can cause a synergistic effect.

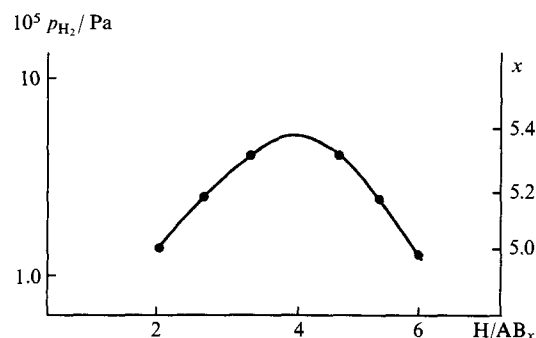
Such properties as the capacity and the cycling stability of two-phase and of the corresponding single-phase systems are similar, since they are determined by the main alloy. However, the discharge properties of two-phase systems are significantly better.

Later, single-phase nonstoichiometric alloys were obtained by the homogenising annealing of La(NiCu)_x alloys, where $5 \leq x \leq 6$, and their electrochemical characteristics were studied.¹⁹ It was found that an increase in x increases the annealing temperature required for obtaining single-phase samples, decreases the discharge capacity, and lengthens the activation process. However, the cyclic stability of electrodes is improved considerably: the residual discharge capacities of LaNi₄Cu and LaNi₅Cu after 400 charge-discharge cycles are 16% and 98%, respectively.

Based on measurements of the adsorption isotherms of gaseous hydrogen, a phase diagram of Cu-containing AB_x–H₂ ternary systems was plotted (Fig. 1).¹⁹ The region of coexistence of α - and β -hydride phases rapidly narrows as x increases and completely disappears at a certain 'critical' composition that approximately corresponds to the formula LaNi_{4.4}Cu. The isotherm of hydrogen sorption by this compound contains almost no horizontal plateau corresponding to the $\alpha \rightleftharpoons \beta$ transition.

4. Intermetallic compounds of AB₃ type and their substituted derivatives

The electrochemical behaviour of the IMC of the composition AB₃ has so far been studied only for the CeNi_{3–x}Co_x and YNi_{3–x}M_x systems, where $M = \text{Al, Fe, Co, Cu, Mn}$ and Cr.^{14, 15, 76–78} Increase in the cobalt content of CeNi_{3–x}Co_x increases the thermodynamic stability of the corresponding hydride phases and decreases the equilibrium dissociation pressure from 0.5×10^3 Pa for CeNi₃ to 0.2×10^3 Pa for

Figure 1. Phase diagram for Cu-containing AB_x–H₂ ternary systems.¹⁹

CeNiCo₂ at 293 K.¹⁴ The electrochemical charge–discharge processes of the IMC of this system follow the equation



Because a stable monohydride of the IMC is formed, the reversible electrochemical capacity of these MH electrodes is lower than that of LaNi₅ and MmNi₅ electrodes.

The partial replacement of Ni in YNi₃ by Al, Co, Fe, Mn, Cr, or Cu has almost no effect on the reversible electrochemical capacity but increases (except for Cr) the equilibrium dissociation pressure of the corresponding hydride phases.¹⁵

5. Ti–Ni alloys and their substituted derivatives

Ti–Ni alloys were the first materials studied as MH electrodes.^{6,7} The electrochemical charging capacity of the Ti₂Ni alloy is 425 mA h g^{−1}, which corresponds to the formation of the hydride Ti₂NiH_{2.5}. On the other hand, the discharge capacity is considerably lower (250 mA h g^{−1}), i.e. part of the hydrogen (~1 mol) is not available electrochemically. Unlike Ti₂Ni, the intermetallic compound TiNi is a totally reversible electrode with a discharge capacity of 250 mA h g^{−1}.

When equimolar amounts of TiNi and Ti₂Ni are present simultaneously, the reversible electrochemical capacity of the system increases to 320 mA h g^{−1}, which corresponds to the oxidation of ~85% of the hydrogen; the final composition of the system is Ti₂NiH_{0.5} + TiNi. It was assumed⁷ that the complete discharge of TiNiH into TiNi with simultaneous partial discharge of the Ti₂NiH_{2.5} phase occurs in the first step, and then redistribution of hydrogen between the Ti₂NiH_x phase and TiNi takes place along with its further electrochemical oxidation, i.e. the TiNi phase has a specific 'catalytic' effect on the completeness of the electrochemical discharge.

The introduction of zirconium to Ti–Ni alloys decreases the discharge capacity due to the formation of ZrNi and Zr₂Ni intermetallic compounds, which have very low discharge capacity because of the formation of hydride phases with strongly bound hydrogen states.⁶⁰ The capacity of Ti_{0.8}Zr_{0.2}Ni_x alloys is considerably higher at $x > 1$. This may be due to the formation of a hydride phase based on Zr₇Ni₁₀, whose enthalpy of formation is lower than that of a hydride phase based on ZrNi. An increase in the zirconium content in the Ti–Zr–Ni alloy results in a noticeable increase in the cyclic stability, but a greater number of activation cycles is then required for attaining the appropriate discharge capacity.

6. Metal hydride electrodes based on multicomponent Laves phases

Titanium and zirconium do not form two-component Laves phases with nickel. These phases can exist only in ternary systems with partial substitution of nickel for other metals.⁷⁹

Of two-component alloys with the AB₂ stoichiometry, ZrV₂, ZrCr₂, ZrMn₂, TiCr₂, and TiMn₂ have attracted most attention. They are characterised by the high stability of hydride phases that can be considerably decreased by replacing part of the zirconium by titanium and of the second metal by iron, cobalt, copper, nickel, or by addition of a hyperstoichiometric amount of a B-type element, or by a combination of these methods.

Alloys based on ZrV₂ with partial replacement of vanadium by nickel and of zirconium by titanium were first proposed for use in MH electrodes in a patent¹⁶ and were then studied more thoroughly by several workers.^{17,80} It was found that the content of vanadium and nickel should lie within the limits Zr._{0.1–0.6}Ni_{1.9–1.4} in order to provide optimum discharge and cyclic characteristics. The high discharge capacity of hyperstoichiometric alloys of the composition Zr(V_{0.33}Ni_{0.67})_{2.4} predetermined their choice as a base material for developing multicomponent MH electrodes with improved characteristics.¹⁷

The replacement of 12.5% to 25% of the nickel by manganese results in an increase in the discharge capacity, which is ~370 mA h g^{−1} for the Zr(V_{0.33}Ni_{0.50}Mn_{0.17})_{2.4} alloy. The partial replacement of zirconium by titanium decreases the discharge capacity, whereas the replacement of nickel by cobalt or iron somewhat increases the discharge capacity. The introduction of a small amount of aluminium to Zr–V–Ni alloys noticeably increases the cyclic stability of MH electrodes. For example, the Zr(V_{0.33}Ni_{0.67})_{2.4} alloy loses ~43% of the original capacity after 100 charge–discharge cycles, whereas the Zr(V_{0.33}Ni_{0.67})_{2.4}Al_x alloys, where $x = 0.05–0.1$, lose as little as 12–15%.

It has been shown⁵⁷ that the partial replacement of manganese by vanadium in multicomponent alloys based on a ZrNi_{1.2}Mn_{0.6}Cr_{0.2} Laves phase considerably increases the discharge capacity: from 240 mA h g^{−1} for ZrNi_{1.2}Mn_{0.6}Cr_{0.2} to 360 mA h g^{−1} for ZrNi_{1.2}Mn_{0.3}Cr_{0.2}V_{0.3}.

At present, the number of studies and patents dealing with MH electrodes based on multicomponent Laves phases of the AB₂ stoichiometry approaches that concerning multicomponent alloys of the AB₅ type based on lanthanum or the 'mischmetal' (see Table 1); this is a result not only of the acceptable exploitation characteristics of these materials but also of their lower cost.

7. Thin-film, nanocrystalline and amorphous MH electrodes

In the early 1990s, Adachi et al.⁸¹ used flash evaporation–deposition of a LaNi₅ powder onto a support to synthesise a thin, highly porous film that was stable under conditions of repeated sorption–desorption of gaseous hydrogen but possessed poor adhesion and lower sorption capacity than the bulk alloy.

Later, denser thin LaNi₅ and LaNi_{2.5}Co_{2.5} films were obtained by high-frequency spraying.^{82,83} Depending on the nature of the target and support and on spraying conditions (beam power, spraying time and support temperature), the films were either amorphous or crystalline. In the authors' opinion, the absence of a plateau on the discharge curves in alkaline solutions suggested that the adsorption of hydrogen gave only a solid solution without the formation of a new hydride phase.

The discharge characteristics listed in Table 2 for MH electrodes of this type show that a decrease in the absorption capacity occurs on passing from bulk alloy to crystalline, and further to amorphous, film. This can be ascribed to the change in the distribution of crystallographic cavities suitable for hydrogen sorption and to an increase in the strength of the crystal lattice in thin films. The cyclic electrochemical stability of LaNi_{2.5}Co_{2.5} films was found to be much higher than that of LaNi₅ films. The stability of films obtained in an atmosphere of hydrogen was higher than that of films obtained in argon, but their maximum capacity was twice as low because of the formation of a more stable protective layer on the surface.

Table 2. Discharge capacity and cyclic stability of powder and film MH electrodes.^{83,84}

Form	$C^0/\text{mA h g}^{-1}$	$S(N)\%$
LaNi₅		
Powder	320	50 (160)
Crystalline film	160	50 (100)
	250 ^a	40 (500)
Amorphous film	60	50 (15)
	160 ^a	60 (500)
LaNi_{2.5}Co_{2.5}		
Powder	240	50 (400)
Crystalline film	120	75 (500)
Amorphous film	80	75 (200)

^a Data from Ref. 84.

Thin-film LaNi_5 and $\text{LaNi}_{2.5}\text{Co}_{2.5}$ electrodes are highly active in the hydrogen evolution reaction, and the exchange currents on these electrodes are of the same order as those on the corresponding compact alloys ($\sim 10^{-4} \text{ A cm}^{-2}$).^{83,84}

Crystalline and amorphous LaNi_5 films obtained by electron-beam evaporation of lanthanum and nickel in an ultrahigh vacuum⁸⁵ have higher capacity and cyclic stability than the films obtained by high-frequency spraying.⁸³

It is unlikely that thin films would find practical use, at least in the near future. However, they are of particular interest in fundamental studies of hydrogen absorption by IMC and alloys.

It was reported recently that the structure of IMC affects the characteristics of MH electrodes.^{23–25} It was found that, as in the case of thin-film electrodes, the amorphisation of the structure of a bulk alloy decreases the discharge capacity of the MH electrodes.²⁴ Of considerable interest are nanocrystalline IMC obtained by the fusion together of the components.^{23,25} With LaNi_5 , it was found²⁵ that these electrodes possess higher discharge capacity, lower equilibrium pressure of hydride dissociation and higher cyclic stability than macrocrystalline IMC. This effect of the size of the IMC particles on the characteristics of hydrogen absorption seems unexpected, since the solubility of hydrogen in Pd-electrodes has been found to decrease with increasing dispersity of Pd when particle sizes are $\leq 10 \text{ nm}$.^{86–89} When the palladium particles are smaller than 2.5 nm, hydrogen is no longer soluble in them.

IV. The technology of the manufacture and activation of metal hydride electrodes

The successful application of compact electrode materials requires their mechanical strength against destruction during charge-discharge and their corrosion stability in electrolyte solutions to be ensured. It is also necessary to solve the problems of electrical conductivity (the contact between the IMC grains), hydrophilicity (wetting) and porosity (accessibility of the whole bulk of an electrode material to the electrolyte). Various technological approaches are used to attain the necessary characteristics.

The mechanical destruction of electrodes due to hydrogen absorption-desorption is prevented by the use of binders, viz., powders of metals (most often Cu, more rarely Ni and Co, and sometimes Au and Pt) or of polymeric organic compounds such as polytetrafluoroethylene (PTFE), polyethylene, polyvinyl alcohol, polystyrene, polyurethane, polyacrylic acid and silicones^{47,90} or combinations of metal and polymeric powders.

The fraction of metal binder in electrode materials usually ranges from 60% to 80%. It has been found for a Cu binder⁶⁵ that increasing the mass ratio, alloy:binder, increases the internal resistance of the electrode material although the discharge characteristics remain almost unchanged.

The content of a polymeric binder is normally 15%–20%. Electron microscopic studies¹⁴ of electrode materials containing polymeric binders showed that in these materials the IMC particles are enclosed in a three-dimensional framework, which, however, does not form a continuous and uniform film of the polymeric binder.

The introduction of acetylene black (up to 10%) is also recommended to improve the electric characteristics of electrode materials containing a polymeric binder,^{46,48} and the hydrophilicity should be controlled by adding hydrophilisers.⁴⁶

Electrode materials containing metal binders are activated more readily and have higher capacity and better charge-discharge reversibility^{15,33} than electrodes with polymeric binders. However, in some cases the metal binder can be oxidised at electrode discharge potentials.

At present, a technological procedure of microcapsulation of the IMC particles with copper, nickel, cobalt, iron and palladium is widely used.^{27,34,52,91–94} The metal coating (up to 20%) is applied by chemical or electrochemical deposition from solutions of the corresponding salts. A compact electrode material is then

produced from the microcapsulated IMC powder with the addition of a polymeric binder (5%–10%). These electrodes have improved discharge characteristics and longer service life.^{52,92}

It has been proposed⁹⁵ to cover the particles of IMC or a binder (coal, acetylene black) with a polymeric film by adsorption from a dilute emulsion of, for example, Teflon. The highest mechanical stability and cycling stability were shown by electrodes with 'teflonated' coal because an elastic, electrically conducting coal-Teflon framework provided a good contact between IMC grains.

A new method for modifying the surface of V-Ti alloys by sintering them with a nickel powder has been proposed.⁹⁶ The VNi_3 phase formed upon sintering is inert with respect to hydrogen, but catalytically affects hydrogen absorption-desorption in alkaline solutions and hence makes it possible to discharge an MH electrode.

All of the procedures for the manufacture of MH electrodes involve the introduction of additional components that decrease the specific capacity of an electrode material; hence, a decrease in the amount of a binder or the manufacture of binder-free electrodes are problems of current interest. In this respect, a noteworthy paper⁹⁷ reports the manufacture of electrodes that maintain their shape by the usual rolling of Zr-V-Ti-Ni-Cr alloys into the active compound without any binders or other additives, possibly due to unique physicochemical properties of these alloys.

Of particular interest are MH electrodes of amorphous alloys. They can be obtained in the form of a ribbon by very fast cooling of a melt and then used without any additional technological treatment.^{47,61,98} However, it is still unclear, for how long the properties of such materials remain unchanged.

When working with MH electrodes, it is important to obtain as high a discharge capacity as possible for the IMC used. This goal is accomplished by activating the electrodes, that is, by repeating charge-discharge cycles, the number of which depends on many factors, primarily, on the IMC composition. However, in most cases the attainable discharge capacity of an MH electrode remains lower than the sorption capacity of the corresponding IMC from the gas phase, and in some cases, satisfactory discharge curves cannot be obtained at all (e.g., for LaCo_5 ,^{84,99} CeCo_3 ,¹⁴ YCo_3 ,¹⁵ and V-Ti.⁹⁶

The following processes occur during the activation of the electrode materials: (i) the alloy particles are dispersed during the absorption-desorption of hydrogen, hence a larger area of fresh, nonoxidized surface of the material is exposed to the electrolyte; (ii) the surface oxides are reduced, dissolved, or become electrically conducting; (iii) a catalytically active metal (e.g., nickel) is accumulated on the surface; (iv) the porosity of the structure increases and access of the electrolyte to an IMC surface becomes easier.

The latter phenomenon has been investigated in several studies^{100,101} by the method of standard porosimetry of the electrode materials prepared from CeNi_3 , CeNi_2Co and ZrNi with a polymeric binder, using two measuring liquids, decane and water.

Fig. 2 presents the integral distribution curves of pore volume vs. their radii (porograms) in an initial electrode material based on ZrNi and PTFE and in the same material after prolonged cathodic polarisation in the region of hydrogen evolution. The total bulk porosity of a nonactivated Zr-Ni electrode is as low as $\sim 13\%$ and is little affected by activation. (For example, activation increases the total bulk porosity of a CeNi_3 electrode (6%–8%) by a factor of 2.5–3.¹⁰⁰) The volume of hydrophilic pores in a Zr-Ni sample is $\sim 50\%$ of the total pore volume; mixed pores occupy a considerable volume (curve 2'). The pore radii in the materials analysed varied from 10^2 to 10^4 nm and almost did not change during activation.

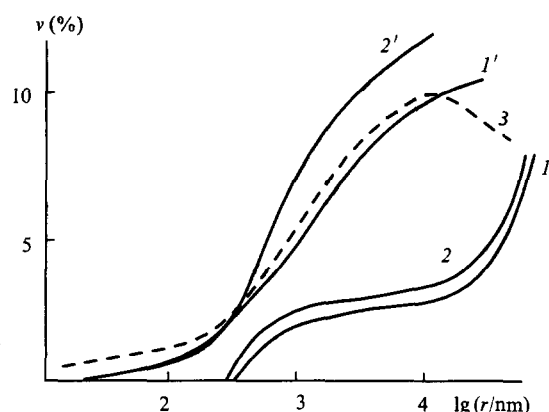


Figure 2. Integral distribution curves of pore volume vs. pore radius for a nonactivated (1, 1') and activated (2, 2', 3) Zr-Ni electrode plotted by measuring the evaporation of water (1, 2, 3) and decane (1', 2').¹⁰¹

Of particular interest in Fig. 2 is curve 3 obtained by measuring the evaporation of water from a Zr-Ni electrode immediately after cathodic polarisation without preliminary drying. In this case, the porosity is almost the same as that measured from decane evaporation. It is likely that during cathodic polarisation, a pressure drop arises in the bulk of the material due to intense liberation of hydrogen. As a result, the electrolyte fills even the hydrophobic pores, and this should increase the effective electrical conductivity of the material.

To decrease the number of activation cycles, IMC powders are sometimes pretreated with reducing reagents (H_3PO_2 , KBH_4)^{61,102} or with solutions of fluorides in order to convert the oxide layer into a fluoride layer.^{31,103} An unexpected enhancement of the activity of Ti-Zr-V-Ni alloys was observed upon their oxidative treatment with oxygen or after anodic polarisation in an alkali.^{17,104} This effect was explained by a change in the structure of the superficial zirconium oxide: a dense hydrogen-impermeable layer of a monoclinic modification of ZrO_2 is transformed into a tetragonal, hydrogen-permeable modification.

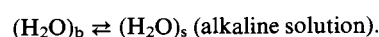
When Ti-Zr-V-Ni alloys are treated with a hot concentrated solution of alkali (6 M KOH or 10 M NaOH, 65–70 °C), activation occurs as a result of the modification of the surface layer (accumulation of nickel metal) and of the surface cracking due to the absorption of evolved hydrogen.⁶⁸

The modification of the surface of MH electrodes with palladium and cobalt⁹¹ facilitates activation by acceleration of the hydrogen discharge reaction, and the introduction of small amounts of rare-earth elements (La, Mm, Nd)¹⁰⁵ into ZrCrNi alloys facilitates activation due to the formation of a second, catalytically more active phase, or to a change in the structure of the surface layer.

V. Hydrogen evolution reaction on metal hydride electrodes

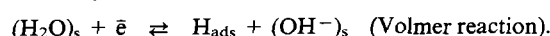
The cathodic polarisation of MH electrodes in electrolyte solutions results in the evolution of gaseous hydrogen along with the accumulation of dissolved hydrogen in the bulk of the electrode. The overall cathodic process includes the following steps.

1. Diffusion (convection) of the reacting species from the bulk of the solution to the electrode/solution interface

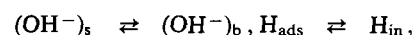


The 'b' index refers to the solution bulk, and 's' refers to the electrode/solution interface.

2. Charge transfer

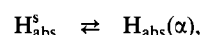
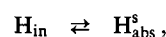


3. Diffusion of the reaction products from the surface of the electrode

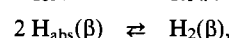
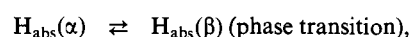


where H_{in} indicates an intermediate position of H atoms directly below the superficial atomic layer of the metal (near-surface hydrogen).

4. Diffusion of hydrogen into the bulk of the IMC particles

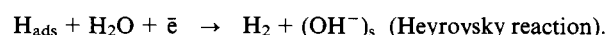


where $\text{H}_{\text{abs}}(\alpha)$ indicates hydrogen dissolved in the α -phase,



where $\text{H}_2(\beta)$ is hydrogen dissolved in the β -phase.

5. Desorption of adsorbed hydrogen



The problem of finding the slow step in such a complex process and determining the rates of separate steps is an independent current problem of electrochemical kinetics and electrocatalysis which still continues to attract attention.

The activity of MH electrodes in the hydrogen evolution reaction (HER) is mostly determined by the elemental composition of the IMC;^{14,84,106–110} it also depends on the composition and properties of the electrode material as a whole (in particular, on the nature and amount of the binder^{95,107}) and on the methods for the manufacture and pretreatment of MH electrodes.^{108,111}

The observation of the low overvoltage of hydrogen evolution on TiNi and LaNi₅ was first made by Miles¹¹² and was confirmed in several studies,^{84,106} in which the exchange currents of the HER on beads of the LaNi₅ and LaCo₅ alloys comparable to those for palladium¹¹³ were observed. The synergistic effect on passing from pure metals to IMC was rationalised in terms of the sharply defined changes in the electronic properties of the alloys when lanthanum, containing 5d-electrons, is introduced.

The electrocatalytic activity of the HER on various electrode materials prepared under similar conditions using Cu and PTFE as binders was the subject of several studies^{14,107} (Table 3). The synergistic effect was not observed, i.e., electrodes based on LaNi₅ and Raney nickel had equal activity. The partial replacement of La by Mm and of Ni by Co decreased, while alloying the IMC with Ce increased, the activity of the electrode. The addition of Nb to LaNi₅ did not result in a noticeable enhancement of its electrocatalytic activity, whereas the addition of Nb to the TiFe alloy accelerated the HER by a factor of ~30.¹¹⁰

Table 3. Electrocatalytic activity of MH electrodes in the HER.^{14,107}

IMC	Binder	$-\log(i_0/\text{A cm}^{-2})$
Ni	PTFE	5.0
LaNi ₅	PTFE	5.0
LaNi ₅	Cu	5.4
La _{0.8} Ce _{0.2} Ni ₂ Co ₃	Cu	5.4
La _{0.7} Nb _{0.3} Ni _{2.5} Co _{2.4} Cr _{0.1}	Cu	5.8
LaNi _{2.5} Co _{2.5}	Cu	5.9
MmNi _{3.5} Co _{0.7} Al _{0.8}	Cu	5.9
LaNi _{2.5} Co _{2.4} Mn _{0.1}	Cu	6.1
Mm _{0.5} La _{0.5} Ni ₂ Co ₃	Cu	6.1
CeCo ₃	PTFE	4.6
CeCo ₂ Ni	PTFE	4.0
CeCoNi ₂	PTFE	3.7
CeNi ₃	PTFE	3.2

The activity of $\text{CeNi}_{3-x}\text{Co}_x$ electrodes increased¹⁴ on increasing the Ni content of the alloy, and the exchange current density on CeNi_3 was found to be close to that on Pd.

The decrease in activity of LaNi_5 on passing from a PTFE binder to a Cu binder has not been rationalised.¹⁰⁷ This seems to be partially related to the difficulties in the determination of the actual electrode surface on which the HER occurs. For example, it was found for Ni electrodes prepared by different procedures¹¹⁴ that hydrogen overvoltage is simultaneously affected by the inherent activity of the electrode material and by the change in the area of the real surface. To separate these effects it is necessary to compare the results obtained from polarisation curves and from impedance spectroscopy.

Hydrogen evolution on palladium, its alloys and hydrogen-sorbing materials occurs according to the Volmer–Tafel scheme. The overall overvoltage of the reaction (η) is a sum of overvoltages of the Volmer reaction (η_1) and the Tafel reaction (η_2) determined from the curves of decay (or rise) of potential after switching off (or on) the polarising current (η , t -curves). The kinetics of hydrogen evolution on palladium was considered taking several rate-determining steps into account,¹¹⁵ which made it possible to describe completely the experimental polarisation η , $\log i$ -curves.

Information on the mechanism and kinetics of the HER in alkaline solutions on LaNi_5 and Ti–Ni alloys was obtained using electrodes as thin amorphous films that are more stable mechanically during hydrogen sorption-desorption than the corresponding bulk alloys.¹¹⁶ The results of quantitative processing of the η , t -curves presented in Table 4 showed that hydrogen evolution on LaNi_5 and Ti–Ni alloys occurs according to the Volmer–Tafel mechanism with comparable exchange currents of both steps. The slope of the straight regions on the η , $\log i$ -curves was 120 mV, hence, at high η the overall reaction rate is determined by the charge transfer step. The exchange current ($i_{0,\text{exp}}$) obtained by extrapolating the η , $\log i$ -dependence to $\eta = 0$ differed from that obtained by the formula

$$\frac{1}{i_0} = \frac{1}{i_{0,\text{V}}} + \frac{1}{i_{0,\text{T}}},$$

where $i_{0,\text{V}}$ and $i_{0,\text{T}}$ are the exchange currents of the Volmer and Tafel reactions, respectively.

Table 4. Kinetic parameters of the HER on various cathodes in 1 M NaOH at 303 K.¹¹⁶

Sample	Thickness /Å	Exchange current density / $\mu\text{A cm}^{-2}$			
		$i_{0,\text{V}}$	$i_{0,\text{T}}$	i_0	$i_{0,\text{exp}}$
LaNi_5	2000	3.22	0.70	0.58	1.7
	2000	3.86	0.68	0.57	
Ni	1000	—			1.4
Ni (wire)					0.45
$\text{Ni}_{0.11}\text{Ti}_{0.89}$	2000				2.1
$\text{Ni}_{0.5}\text{Ti}_{0.5}$	1500	2.46	0.93	0.67	1.7
$\text{Ni}_{0.76}\text{Ti}_{0.24}$	1500	2.76	0.15	0.81	2.6

It is evident from Table 4 that the $i_{0,\text{exp}}$ values on thin-film alloys are similar to those on a nickel film and nickel wire as well as to the values previously obtained on amorphous NiTi .¹¹⁷ Thus, the electrocatalytic activity of thin-film electrodes studied is determined by nickel, while synergism between lanthanum and nickel or titanium and nickel is not observed.

Results supporting the Volmer–Tafel mechanism for the hydrogen evolution reaction were also obtained for MH electrodes based on LaNi_5 , MmNi_5 , and $\text{MmNi}_{3.6}\text{Mn}_{0.4}\text{Al}_{0.3}\text{Co}_{0.7}$ powders.^{99,118} The $i_{0,\text{V}}/i_{0,\text{T}}$ value is, for example, ~ 9 for the $\text{MmNi}_{3.6}\text{Mn}_{0.4}\text{Al}_{0.3}\text{Co}_{0.7}$ system, which suggests a mixed character for the rate-determining step. The addition of oxides such as Co_2O_4 or RuO_2 to an electrode material markedly

accelerates the Volmer reaction and only slightly changes the rate of the Tafel reaction.

On the whole, however, the problem of the relation between the activity of IMC and its components with respect to the hydrogen evolution reaction cannot be regarded as completely solved. Solution of this problem requires the development of a procedure for the measurement and consideration of the real electrode surface area. On the other hand, the gradual change in the electronic properties of these materials on changing their composition affords a unique opportunity to reveal the fundamental problems of the nature of electrocatalytic activity.

VI. Charge-discharge processes on metal hydride electrodes

The electrochemical method of saturation of IMC with hydrogen requires much simpler equipment than that for saturation with gaseous hydrogen. However, electrochemical saturation at potentials corresponding to effective pressures above 0.098 MPa ($E_r < 0$ V) cannot be performed under equilibrium conditions due to concurrent hydrogen evolution. Thus, the effectiveness of MH electrode charging is determined by the ratio between the rates of hydrogen diffusion into the bulk of IMC particles and its desorption into the electrolyte bulk. The driving force of the sorption process is the difference between the chemical potentials of hydrogen on the surface, which is determined by the surface coverage by hydrogen, and in the bulk, which is determined by the overall fraction of occupied absorption sites.

Hydrogen sorbed by metals can exist in three different forms, namely, adsorbed hydrogen, hydrogen in a near-surface layer and dissolved hydrogen. An equilibrium is established between these forms. The quantity of near-surface hydrogen does not depend, while that of adsorbed hydrogen does depend, on the nature of the surface.¹¹⁹ The sorption of hydrogen can be accompanied by phase transitions such as the formation of hydride phases (e.g. the $\alpha \rightleftharpoons \beta$ transition in the case of the Pd electrode). No data are available on the type of isotherms of hydrogen electrochemical sorption on IMC, while the sorption isotherms on the Pd electrode differ in the α , $\alpha \rightleftharpoons \beta$, and β regions.^{1,120}

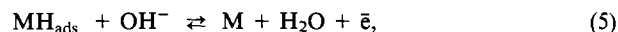
Under equilibrium conditions, the relation between the pressure of sorbed hydrogen (p_{H_2}) and the electrode potential is determined by the Nernst equation. At a cathodic polarisation, the dependence of p_{H_2} on η deviates from the Nernst equation and is determined by the mechanism of hydrogen evolution and the ratio of exchange currents of its different steps. In the case of the Volmer–Tafel mechanism, the relation between the hydrogen pressure at a certain polarisation (\bar{p}) and that at the equilibrium potential (\bar{p}_0) depends on the contribution of the overvoltage η_2 for the Tafel step by the equation¹¹³

$$\eta_2 = \frac{RT}{2F} \ln \frac{\bar{p}}{\bar{p}_0}.$$

It was found¹⁰⁸ that, after cathodic polarisation of a ZrNi electrode at potentials of hydrogen evolution followed by circuit disconnection, stationary potentials are established and maintained in the region from -0.04 to -0.008 V, depending on the polarisation potential and the composition of the solution. In addition, the passage from $\eta < -0.1$ to the -0.08 to -0.006 V range resulted in a considerable anodic current, which gradually decreased over a long period (hundreds of seconds), until converted into a cathodic current and attained the values corresponding to the rate of hydrogen evolution at the corresponding potential. An additional study showed that this does not result in dissolution of IMC components. The effects observed are evidently related to prolonged retention of hydrogen in the bulk of IMC due to hindrance of the recombination step or interphase transfer of hydrogen.^{115,121}

The amount of the hydrogen sorbed can be determined by recording the discharge curves under galvanostatic conditions, i.e., by measuring the potential versus time at constant I , or under potentiostatic conditions, by measuring the current versus time at constant E .

The process of electrochemical discharge involves the following steps:



Each of these can be the rate-determining step under certain conditions.

Metal hydride electrodes based on IMC and a binder are porous and differ considerably both from gas-diffusion porous electrodes^{136,137} and from liquid-containing porous electrodes.¹³⁸ Gas-diffusion electrodes contain pores flooded with the electrolyte and gas-filled pores, through which the gaseous reagent is transported into the bulk of the electrode to the active catalyst surface. Porous electrodes made of hydrogen-sorbing IMC do not require gas porosity. These electrodes differ from liquid-containing electrodes by the continuous supply of the reagent by diffusion from inside material particles to their outer surfaces where the electrochemical reaction occurs. Thus, porous MH electrodes should be regarded as systems with parameters distributed over the electrode thickness and over the IMC particle radius (Fig. 3).

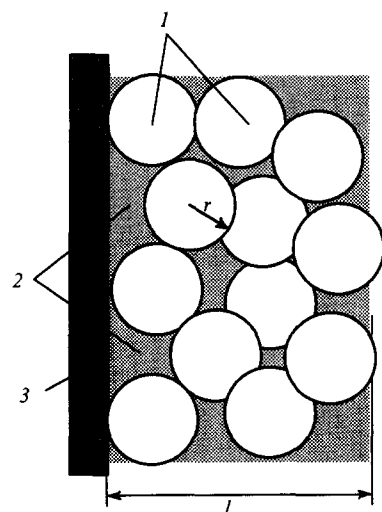


Figure 3. A model of a porous hydrogen-sorbing electrode:¹²⁶ (1) IMC particles; (2) solution-containing pores; (3) metal current collector; (l) electrode thickness; (r) radius of an IMC particle.

Several mathematical models have been suggested for the description of experimental discharge curves. These models can be divided into two groups: in one group, the models consider hydrogen diffusion only within IMC particles (along the radius r , see Fig. 3),^{31,122–125} while in the other, models also take into account diffusion across the electrode thickness (along the coordinate l).^{126,127}

Pshenichnikov and co-workers^{122,123} proposed a model for calculating galvanostatic charge-discharge curves on an isolated spherical grain of a hydrogen-absorbing metal. Assuming that potential E is a single-valued function of the degree of surface coverage by adsorbed hydrogen, which is related to the hydrogen concentration in the bulk by the Frumkin isotherm, the authors took the nonstationary mass transfer in a unit grain into account and obtained a relation between E and the amount of electricity

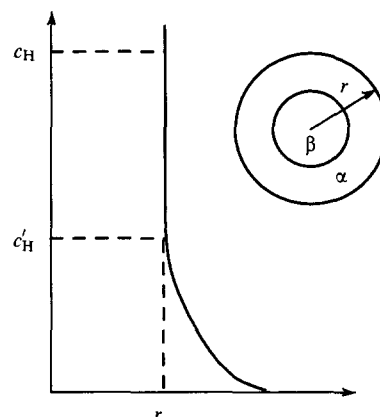


Figure 4. A scheme for the variation of the hydrogen concentration in a spherical particle during discharge:³¹ (c_H) hydrogen concentration in the β -phase; (c'_H) hydrogen concentration at the interface between the α - and β -phases.

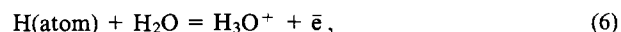
passed. By adjusting the adsorption equilibrium constant within this model, they managed to obtain qualitative agreement between the experimental and calculated data. If one assumes that the electrode consists of particles with two different radii, charge-discharge curves with two delays can be obtained. Based on this model, it was concluded that the total charging and discharging of a grain are impossible if the diffusion current is commensurate with the charging current.

It was believed^{31,124} that the quantity of ionised hydrogen is proportional to the thickness of the surface α -layer (Fig. 4) and that the rate of discharge at low discharge currents is determined by hydrogen diffusion in the α -phase. Under these conditions, the dependence of the discharge capacity (C) on the discharge current (I) has the following form:

$$C = C^0 \left\{ 1 - \left(1 + \frac{C^0 k_5}{I} \right)^{-3} \right\},$$

where C^0 is the discharge capacity (at $I \rightarrow 0$) and k_5 is the rate constant of the discharge step (5).

At high discharge currents, the rate-determining step is the electrochemical reaction occurring on the Ni-centres



and the dependence of the discharge capacity on the discharge current acquires the form

$$C = C^0 \left\{ 1 - \exp \left[-k_6 \left(\frac{C}{I} \right)^n \right] \right\}, \quad (7)$$

where n is an empirical constant and k_6 is the rate constant of reaction (6).

The model proposed was tested for a $\text{LaNi}_{4.7}\text{Al}_{0.3}$ electrode. The dependences of $\log \log [1/(1 - C/C^0)]$ on $\log(C/I)$ contained a break point at currents of ca. 1000 mA g^{-1} , which indicated a change in the discharge mechanism. The experimentally determined discharge capacities coincided with those calculated by equation (7); the k_6 value depended on the duration of the treatment of the electrode surface with a potassium fluoride solution due to changes in the composition of the surface layer.

The basic feature of yet another model¹²⁵ is the possibility of quantitative processing of step (4) as a heterogeneous chemical reaction. The authors derived equations for hydrogen diffusion in the bulk of electrodes of various shapes (plate, cylinder, sphere), which coincide with the equations obtained previously by Bucur et al.^{128,129} who theoretically described the ionisation of hydrogen dissolved in a Pd electrode. The concentration of hydrogen in the

near-surface layer (c_H^s) at low D/l^2 (where D is the diffusion coefficient of hydrogen and l is a parameter determined by the electrode size) and low discharge currents decreases linearly with increase in the discharge time (t). At high D/l^2 and/or higher discharge currents, the c_H^s value linearly depends on t only within a narrow time range. In this case, when c_H^s reaches zero (i.e., the discharge is effectively finished), the bulk of the electrode still contains a fraction (f) of the dissolved hydrogen that cannot be ionised because of the limited rate of hydrogen diffusion. The value

$$f \approx \frac{Il}{c^0 D}$$

(where c^0 is the initial concentration of the dissolved hydrogen) characterises the effectiveness of discharge. It depends on the electrode geometry and decreases in the series: plate > cylinder > sphere.

Based on the theoretically derived equation for the dependence of the electrode potential on t under galvanostatic discharge conditions, experimental discharge curves for MH electrodes made of $ZrNi_2$, $Zr(V_{0.33}Ni_{0.67})_{2.4}$ and $Zr(CrFe)_2$ were analysed and the kinetic parameters of steps (3)–(5) were calculated. They were found to depend not only on the electrode composition but also on the surface structure or the phase composition of the hydride phase.

The discharge capacity at low discharge currents is obtained by subtracting two quantities linearly dependent on the current, the first one being related to the limiting rate of hydrogen diffusion in the electrode bulk and the other to the limiting rate of hydrogen transfer from the adsorbed state, from the equilibrium capacity C ,

$$C = C^0 - \frac{Il}{aD} - C_0 \frac{I}{Fk_4 c_H^0},$$

where a is a constant depending on the electrode geometry, and k_4 is the rate constant of reaction (4). Thus, the linear C/I dependences observed at low discharge currents are analogous to those found in a previous study.¹²⁸

At high discharge currents

$$C = (C^0)^2 \frac{\pi D}{bISl^2} \left(1 - \frac{ISl}{cFk_4 c_H^0} \right)^2$$

where b and c are constants depending on the electrode geometry, and S is the surface area of the electrode.

The model described above is applicable only when the chemical potential of hydrogen (μ_H) changes continuously with changes in the concentration (c_H) in the bulk of the electrode; in particular, this is the case for amorphous films. In the case of crystalline alloys, for which the μ_H, c_H -dependences contain a plateau due to a phase transition, the model describes only single-phase regions (the starting and terminal regions) of the discharge curves.

Models based on the macrokinetics of the ionisation of the dissolved hydrogen in porous MH electrodes have also been proposed.

A theory was proposed¹²⁶ that considered a porous planar electrode of thickness l consisting of spherical IMC particles of radius r . The joint application Fick's second law and theories of slow discharge and charge-discharge of the electric double layer gave a system of equations with four dimensionless parameters determined by the characteristic times of the following processes: hydrogen diffusion in a particle; charging of the electric double layer of a porous electrode; charging of the electric double layer of a smooth electrode; and reactions of hydrogen ionisation. In the general case, an analytical solution of this system is difficult; however, numeric modelling is possible by variation of three parameters: the diffusion coefficient of hydrogen, the capacity of the electric double layer and the exchange current density.

By choice of the parameters, one can obtain the distribution of hydrogen concentration in the bulk of the particle and across the electrode thickness. When diffusion limitations prevail over ohmic limitations, the hydrogen distribution in the bulk of the electrode should play the major role. This dependence can be obtained by analytical methods.

A model was proposed¹²⁶ for the description of the discharge process by comparing the calculated and experimental potentiostatic discharge curves for an MH electrode compressed from a $CeNi_3$ powder with 20% PTFE. This model is applicable to any systems containing a phase of a reducible or oxidisable component; in particular, it was used for describing the charge-discharge behaviour of porous polyaniline electrodes under galvanostatic conditions.¹³⁰

The following drawbacks of the model proposed by Volfkovich et al.¹²⁶ should be noted: first, electrode charging is complicated by a phase transition, which can be taken into account formally only by varying the double layer capacity; second, the step of interphase transfer of hydrogen (4) is not taken into account.

Another treatment of porous systems has been proposed¹²⁷ for a cylindrical electrode consisting of spherical IMC particles. The model takes into account the diffusion of hydrogen in the bulk of IMC particles (based on Fick's second law), the charge transfer and the potential drop in the IMC particles and in the electrolyte that fills the pores. For the majority of metals the potential drop in the metal phase is low: cycling of the electrode can decrease the electrical conductivity of the powder, e.g. due to the oxidation of the surface or impairment of contacts between the particles. Because the equations obtained¹²⁷ are very complex and the model uses a great number of parameters, it is difficult to apply this model to the analysis of experimental discharge curves. Furthermore, it does not permit calculation of the kinetic parameters of reactions (3)–(5).

Thus, none of the mathematical models proposed for describing the discharge process is general, since they do not take into account all the steps of the process. The models assume that the diffusion coefficient of hydrogen (D) does not depend on its concentration in the alloy, whereas the existence of this dependence has been established experimentally.^{131,132} In addition, the models proposed do not take into account the specific nature of the $\alpha \rightleftharpoons \beta$ transition, except for the formal introduction of an infinitely large capacity corresponding to this transition.¹²⁶

VII. Corrosion of metal hydride electrodes

One of the main properties of MH electrodes required for their practical application is a sufficiently high stability during repeated electrochemical charge-discharge cycles in electrolyte solutions. As has been noted, the measure of the cyclic stability is the $S(N)$ value, which is primarily determined by the nature of the IMC and the binder, the manufacturing method, and the pretreatment of the electrode.

The high stability of AB_5 type IMC containing Al, Si, Ti and Zr is determined by a superficial oxide film formed during electrode cycling in alkaline solutions.^{13, 29, 34, 37, 117, 133, 134}

The addition of manganese to alloys, often used for decreasing the hydride dissociation pressure, impairs the corrosion stability of IMC. This is caused by the diffusion of manganese from the bulk to the surface and degradation of the alloy to give hydroxides of manganese and rare-earth elements as well as metallic nickel.^{27,33}

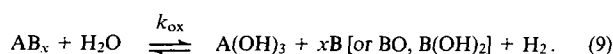
The increase in the plasticity of alloys on alloying $LaNi_5$ with Co decreases the rate of its dispersal and, as a consequence, decreases the newly formed surface prone to oxidation, imparting high stability to the alloy during cycling.^{135–138}

It has been shown that the corrosion stability of the intermetallic compound $LaNi_{4.5}Mn_{0.5}$ produced under diverse conditions is affected by the disruption of the atomic order within the same AB_5 crystalline system: homogenisation of the structure increases the stability of the material.³⁰

The effect of homogenising annealing or rapid cooling on the cyclic stability of $\text{MmNi}_{1.5}\text{Co}_{0.7}\text{Al}_{0.8}$ is explained⁴³ by the difference in size of IMC grains formed ($\sim 50 \mu\text{m}$ in the former case and $\sim 10 \mu\text{m}$ in the latter), assuming that a protective oxide layer can be formed not only on the particle surface, but also at the grain boundaries. In the case of the quenched alloy, the cyclic stability was found experimentally to increase with decreasing grain size.

The spectrophotometric analysis of 1 M NaOH solutions after prolonged potentiostatic polarisation of YNi_3 and YCo_3 electrodes in these solutions showed¹⁵ that the rate of yttrium dissolution from the IMC is lower by at least an order of magnitude than that from the pure metal, even at potentials much higher than the potential of the anodic boundary for total IMC dehydrogenation. Nickel and cobalt were found not to pass into solution over the whole range of potentials studied.

When an IMC of an AB_x type contacts an electrolyte, corrosion can be represented as follows:



As a result of this heterogeneous reaction, the amount of the hydrogen-sorbing compound decreases in proportion to the specific surface. Thus, the larger the IMC particles, the weaker should be the trend to decreasing capacity. The validity of this hypothesis was confirmed for $\text{LaNi}_{4.4}\text{Cu}$ electrodes produced from powders with different specific surfaces.²²

As follows from the above considerations, the disintegration of IMC grains into smaller particles during the charge-discharge process stimulates corrosion. The comminution of IMC grains is caused by the coexistence of various hydrides on the surface. These hydrides increase the volume of the unit cell to different extents; as a result, mechanical stress appears at the boundaries of hydride grains, leading to brittleness of the system and to increased local mobility of metal atoms contained in the IMC.^{13, 29}

These concepts were further developed in a study of the effect of electrode cycling on: the in situ X-ray diffraction spectra; the hydrogen concentration; the variation of the unit cell volume upon formation of α - and β -phases ($V_\beta - V_\alpha$); the variation of the overall unit cell volume upon hydride formation ($V - V_0$); and the electrode stability (Table 5).¹⁹

The ($V_\beta - V_\alpha$) and ($V - V_0$) values for the LaNi_x and $\text{LaNi}_{x-1}\text{Cu}$ electrodes decrease with an increase in the non-stoichiometry of a system, the ($V_\beta - V_\alpha$) value decreasing much more quickly. The introduction of copper into the alloy primarily affects the ($V_\beta - V_\alpha$) value. The stability of the alloys is determined by the changes in the volume of the unit cell upon formation of the β - and α -phases. An increase in ($V_\beta - V_\alpha$) enhances mechanical strain and the desintegration of the alloy particles in agreement with the results of microscopic studies.

A mathematical model of the degradation of MH electrodes has been developed²² based on the assumption that the specific surface is the main factor determining the rate of particle oxidation.

Table 5. Stability of MH electrodes and changes in unit cell volume upon hydride formation.¹⁹

Alloy	AB_x	$(V_\beta - V_\alpha)/V_0$ (%)	$(V - V_0)/V_0$ (%)	$S(400)$, (%)
LaNi_5	AB_5	21.5	22.5	15
$\text{LaNi}_{5.4}$	$\text{AB}_{5.4}$	19.9	22.0	25
LaNi_4Cu	AB_5	17.0	21.2	16
$\text{LaNi}_{4.2}\text{Cu}$	$\text{AB}_{5.2}$	13.2	19.7	62
$\text{LaNi}_{4.4}\text{Cu}$	$\text{AB}_{5.4}$	2.8	18.2	90
LaNi_3Cu	AB_6	0.0	8.5	98

For spherical particles with initial radii r_0 , the electrode capacity after cycling for a period t is

$$C_t^{1/3} = C_t(0)^{1/3} - t \left[\frac{1}{3} C_t(0)^{1/3} S_0 k_9 a_{\text{H}_2\text{O}} M_{\text{AB}_x} \right] t \quad (10)$$

where $C_t(0)$ is the electrode capacity before cycling, S_0 is the initial specific surface of the powder, $a_{\text{H}_2\text{O}}$ is the activity of water, M_{AB_x} is the IMC mass, and k_9 is the rate constant of reaction (9). If the diffusion of the water molecules is not the rate-determining step, then a linear dependence of $C_t^{1/3}$ on t should be observed. Such dependence was obtained for $\text{LaNi}_{4.4}\text{Cu}$ electrodes with three different S_0 values.²² The increase in the slope of the straight lines correlated well with the size of the alloy particles. All three straight lines intersected at one point but not at $t = 0$.

Equation (10) can be transformed into

$$C_t = C_t(0) \exp(-S_0 k_9 a_{\text{H}_2\text{O}} M_{\text{AB}_x} t) \quad (11)$$

Since $t = bN$, where b is a proportionality factor, relation (11) is analogous to the empirical equation¹³

$$C(N) = C_0 \exp\left(-\frac{N}{N^*}\right), \quad (12)$$

where C_0 is the maximum capacity, $C(N)$ is the capacity in the N th cycle, and parameter N^* reflects the rate of capacity decrease and is regarded as a stability constant. It follows from equations (11) and (12) that

$$N^* = \frac{1}{S_0 k_9 M_{\text{AB}_x}}.$$

One of the drawbacks of the model is that it does not account for the dependence of the oxidation rate on the surface state (oxidised or reduced) and on the potential. In addition, cycling gradually changes the composition of the surface layer and, hence, its protective properties.

A model including the changing discharge capacity of MH electrodes caused during cycling proposed in another study³¹ simultaneously accounts for the discharge and degradation processes. During low-current cycling, the decrease in the capacity over time should obey the following equation:

$$C(I, N) = C(0, 0) \left\{ 1 - \left[1 + \frac{C(0, 0) k_1}{I} \right]^{-3} \right\} \times \\ \times [1 - P \exp(-FN)] \exp(-K_N N), \quad (13)$$

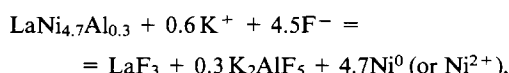
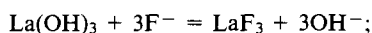
while during high-current cycling, the following equation is obeyed:

$$C(I, N) = C(I, 0) [1 - P \exp(-kN) \exp(-k_1 N)] \\ C(I, 0) = C(0, 0) \left\{ 1 - \exp\left[-\frac{v_1 C(I, 0)^n}{I^n}\right] \right\}, \quad (14)$$

where $C(0, 0)$ is the capacity at the zeroth cycle, I is the discharge current, N is the number of galvanostatic cycles, k_1 is the rate constant of the electrochemical discharge reaction, P is the fraction of the hydrogenated alloy particles active in the cycling, k is the rate constant of the MH electrode activation, K_N is the factor of degradation of the capacity of the MH electrode equal to $S_c L \gamma^2 \Delta t$ (S_c is the fraction of corroded specific surface, L is the number of hydride particles per unit area, γ is the rate of hydride growth, and Δt is the time of corrosion during each charge-discharge cycle), v_1 is the rate of the electrochemical reaction, and n is an empirical constant.

The dependence of the discharge capacity of untreated and fluoride-treated $\text{LaNi}_{4.7}\text{Al}_{0.3}$ electrodes on the discharge current and the number of cycles were plotted, the constants were calculated by use of equations (13) and (14), and three-dimensional C, I, N -diagrams were plotted.³¹ The dependence of kinetic and corrosion characteristics on the time of treatment of

the electrodes with fluoride ions was explained by the following reactions:



leading to the accumulation of catalytically active nickel and of LaF_3 , which has better protective properties than $\text{La}(\text{OH})_3$, on the surface.

Up to the present, almost no systematic data are available on the cyclic stability of AB_3 -type IMC, where A is Ce or Y, and B is Ni or Co. For MH electrodes based on multicomponent Laves phases, only the results of electrochemical charge-discharge cycling tests have been reported (see Table 1). However, the mechanism and the nature of the accompanying degradation processes have not been considered, although, because of the different elemental composition, they would probably differ from those in the rather well-studied IMC of AB_5 type and their substituted derivatives.^{139–148}

VIII. Conclusion

To date, several countries have set up the production of nickel-metal hydride accumulators. For example, the number of such accumulators in Japan is as high as 25% of the number of nickel-cadmium current sources, and there exists a trend for a gradual displacement of the latter. This is caused both by environmental considerations and by the good specific characteristics of MH-accumulators as well as by the possibility of manufacturing them without considerable investment and with almost the same equipment. Along with small-scale MH-accumulators for portable computers, video cameras and home electronic appliances, large MH-accumulators are being developed, in particular, for electric cars.

As has been shown above, the properties of hydride-forming materials depend very strongly on their composition and change considerably on adding apparently insignificant quantities of several elements or on small changes in stoichiometry. For example, the addition of less than 2 at.% Li¹⁴⁹ or a decrease in the stoichiometric coefficient to 4.5–4.8¹⁴⁷ increases the capacity of the $\text{Mm}(\text{NiCoAlMn})_5$ electrode with respect to hydrogen, and the service life of the MH battery reaches 1000 cycles with loss of less than 10% of the initial capacity. Therefore, the problem of optimising the composition of hydride electrodes is still of current interest. From the fundamental scientific aspect, a theoretical analysis of the effect of the composition and of concentrations of particular components on the sorption properties of IMC is required. Some approaches to the problem have been reported; however, they have not been developed and generalised because primary attention was paid to extensive empirical studies aiming at the solution of applied problems.

The facts set forth above suggest that active electrochemical investigations of hydride-forming IMC have in fact led to the appearance of a new field, i.e., electrochemistry of hydrides. The particular features of these materials are the strong dependence of their properties on the amount of hydrogen sorbed and their specific electrochemical behaviour. Unfortunately, the latter has been studied insufficiently, although, judging by certain theoretical considerations and preliminary data, one can anticipate that these materials would have unusually high electrocatalytic activity and selectivity in electrochemical hydrogenation and reduction.^{78, 111, 140–142}

A detailed study of the pronounced degradation processes occurring upon hydrogen sorption can lead to a deeper insight into the nature of hydrogen embrittlement of materials, which is particularly important for the prediction of the corrosion behaviour of certain metals and alloys, for hydride materials science and electrochemical technology. Possibly cheap hydrogen-sorbing materials will be found in the future and used as gas-

separating membranes in various systems, including electrochemical ones. As yet, such membranes are most frequently made of palladium and its alloys. It has been found that when palladium is alloyed with rare-earth metals its properties as a membrane are improved.^{143, 144} It is not known at present whether similar membranes can be created using the typical IMC representatives considered above. The realisation of this possibility would drastically expand the field of use of hydrogen-sorbing IMC.

Intermetallic compounds sorbing hydrogen are interesting and promising subjects for revealing the nature of fine interactions in hydride phases. These investigations performed over a broad temperature range and using deuterium as a sorbate^{145, 146} show the most promise. It can be expected that investigations in this field will lead to the appearance of new concepts in hydride chemistry.

References

1. G Alefeld, J Völkl (Eds) *Hydrogen in Metals* Vol. 2 (Berlin: Springer, 1978)
2. T V Geld, R A Ryabov, L P Mokhracheva *Vodorod i Fizicheskie Svoystva Metallov i Splavov* (Hydrogen and Physical Properties of Metals and Alloys) (Moscow: Nauka, 1982)
3. P Nylen *Z. Elektrochem.* **43** 915 (1937)
4. A N Frumkin, in *Advances in Electrochemistry and Electrochemical Engineering* Vol. 3 (Ed. P Delahay) (New York: Interscience, 1963) p. 287
5. A N Frumkin, N A Alajalova *Acta Physicochim. USSR* **18** 1 (1944)
6. E W Justi, H H Ewe, A W Kalberlah, N M Saridakis, M H Schaefer *Energy Convers.* **10** 183 (1970)
7. M A Gutjahr, H Buchner, K D Beccu, H Saufferer, in *Power Sources* Vol. 4 (Ed. D H Collins) (Newcastle upon Tyne: Oriel Press, 1973) p. 79
8. H H Ewe, E W Justi, K Stephan *Energy Convers.* **13** 109 (1973)
9. USP 3 874 928; *Ref. Zh. Khim.* **5** L 327P (1976)
10. A Percheron-Guegan, F Briaucourt, H Diaz, J C Achard, J Sarradin, G Bronoel, in *The 12th Rare Earth Research Conference (Proceedings)* (Ed. C E Lundin) (Denver, CO: Univ. Denver, 1976) p. 300
11. A Percheron-Guegan, J C Achard, J Sarradin, G Bronoel, in *Hydrides for Energy Storage* (Eds A F Andresen, A J Maeland) (Oxford: Pergamon Press, 1978) p. 485
12. M H J Van Rijswijk in *Hydrides for Energy Storage* (Eds A F Andresen, A J Maeland) (Oxford: Pergamon Press, 1978) p. 261
13. J J G Willems *Philips J. Res.* **39** 1 (1984)
14. O A Petrii, K N Semenenko, I I Korobov, S Ya Vasina, I V Kovrigina, V V Burnasheva *J. Less-Common Met.* **136** 121 (1987)
15. I I Korobov, S Ya Vasina, O A Petrii, G A Tsirlina, M Yu Rusanova *Elektrokhimiya* **31** 652 (1995)
16. USP 4 551 400; *Chem. Abstr.* **104** 53 682w (1988)
17. S Wakao, H Sawa, J J Furukawa *J. Less-Common Met.* **172** – **174** 1219 (1991)
18. P H L Notten, R E F Einerhand *Adv. Mater.* **3** 343 (1991)
19. P H L Notten, R E F Einerhand, J L C Daams *J. Alloys Compd.* **210** 221; 233 (1994)
20. X Gao, D Song, Z Zhou, H Yang, Y Zhang, P Shen, in *The International Symposium on Metal-Hydrogen Systems (Abstracts of Reports)* (Fujiyoshida, Japan, 1994) Mo.B7
21. H Sawa, S Wakao, J Furukawa *Denki Kagaku* **59** 945 (1991)
22. S-R Kim, J Y Lee *J. Alloys Compd.* **210** 109 (1994)
23. L Varga, A Lovas, K Tompa, J Joubert, A Percheron-Guegan, in *The International Symposium on Metal-Hydrogen Systems (Abstracts of Reports)* (Fujiyoshida, Japan, 1994) Fr.A1
24. H Miyamura, T Sakai, N Kuriyama, I Uehara, N Shiraishi, T Iwasaki, in *The International Symposium on Metal-Hydrogen Systems (Abstracts of Reports)* (Fujiyoshida, Japan, 1994) Mo.P40
25. Z Chen, M Lü, Z Hu, in *The International Symposium on Metal-Hydrogen Systems (Abstracts of Reports)* (Fujiyoshida, Japan, 1994) Th.B7
26. W Hu, Y Zhang, D Song, J Huang, Y Wang, X Gao, in *The International Symposium on Metal-Hydrogen Systems (Abstracts of Reports)* (Fujiyoshida, Japan, 1994) Mo.P21

27. T Sakai, K Oguro, H Miyamura, N Kuriyama, A Kato, H Ishikawa *J. Less-Common Met.* **161**193 (1990)
28. S Wakao, Y Yonemura *J. Less-Common Met.* **89**481 (1983)
29. J J G Willems, K H J Buschow *J. Less-Common Met.* **129**13 (1987)
30. W Tang, G Sun *J. Alloys Compd.* **203**195 (1994)
31. Z Li, D Yan, S Suda *Res. Rep. of Kagakuin Univ.* **75**113 (1993)
32. T Sakai, H Ishikawa, K Oguro, C Iwakura *Prog. Batt. Solar Cells* **6**221 (1987)
33. S Ya Vasina, Kh M Shao, I I Korobov, O A Petrii *Elektrokhimiya* **32** (1996) (in the press)
34. T Sakai, H Miyamura, N Kuriyama, A Kato, K Oguro, H Ishikawa *J. Less-Common Met.* **159**127 (1990)
35. F Meli, A Züttel, L Schlapbach, in *The International Symposium on Metal-Hydrogen Systems (Abstracts of Reports)* (Fujiyoshida, Japan, 1994) Tu.B4
36. F Meli, A Züttel, L Schlapbach *J. Alloys Compd.* **190**17 (1992); **202**81 (1993)
37. T Sakai, H Miyamura, N Kuriyama, A Kato, K Oguro, H Ishikawa *J. Electrochem. Soc.* **137**795 (1990)
38. T Sakai, H Miyamura, K Oguro, A Kato, H Kuriyama, H Ishikawa *Denki Kagaku* **57**612 (1989)
39. D C Magnuson, H F Gibbres *Mater. Lett.* **211** (1994)
40. C Folonari, F Iemmi, F Manfredi, A Rolle *J. Less-Common Met.* **74**371 (1980)
41. Z-P Li, Y-Q Lei, C-P Chen, J Wu, Q-D Wang *J. Less-Common Met.* **172**–174 1265 (1991)
42. M Ohnishi, Y Matsumura, K Hasegawa, M Oshitani, K Takeshima *Yuasa Yiho* **75**4 (1993)
43. T Sakai, T Hazama, H Miyamura, N Kuriyama, A Kato, H Ishikawa *J. Less-Common Met.* **172**–174 172; 1175 (1991)
44. T Hara, N Yasucha, Y Takeuchi, T Sakai, A Uchiyama *J. Electrochem. Soc.* **140**2450 (1993)
45. T Sakai, H Yashinaga, H Miyamura, N Kuriyama, H Ishikawa *J. Alloys Compd.* **180**37 (1992)
46. M Yamashita, H Higuchi, H Takemura, K Okuno *Denki Kagaku* **61**729 (1993)
47. J Choi, C-N Park *J. Alloys Compd.* **217**25 (1995)
48. M Kanda, M Yamamoto, K Kanno, Y Satoh, H Hayashida, M Suzuki *J. Less-Common Met.* **172**–174 1227 (1991)
49. K Hasegawa, H Mori, M Oshitani *Yuasa Yiho* **71**13 (1991)
50. Jpn. P.62/119 863 [871 119 863]; *Chem. Abstr.* **107**99770p (1987)
51. Jpn. P.61/168 871 [86 168 871]; *Chem. Abstr.* **106**7556b (1987)
52. M Geng *J. Alloys Compd.* **206**L.3 (1994)
53. Jpn. P. 62/119 864 [87 119 864]; *Chem. Abstr.* **107**99769v (1987)
54. Jpn. P.61/214 361 [86 214 361]; *Chem. Abstr.* **106**105 440d (1987)
55. Jpn. P.61/233 969 [86 233 969]; *Chem. Abstr.* **106**87709s (1987)
56. L Jiang, F Zhan, D Bao, G Ging, Y Li, X Wei, in *The International Symposium on Metal-Hydrogen Systems (Abstracts of Reports)* (Fujiyoshida, Japan, 1994) Mo.P22
57. Y Moriwaki, T Gamo, H Seri, T Iwaki *J. Less-Common Met.* **172**–174 1211 (1991)
58. M Sugawara, T Endo, K Matsuki *Denki Kagaku* **57**488 (1989)
59. H Sawa, S Wakao, J Furukawa *Denki Kagaku* **58**862 (1990)
60. S Wakao, Y Yonemura, H Nakano, H Shimada *J. Less-Common Met.* **104**365 (1984)
61. M Matsuoka, K Asai, K Asai, Y Fukumoto, C Iwakura *J. Alloys Compd.* **192**149 (1993)
62. H Sawa, K Ohzeki, M Ohta, H Nakao, S Wakao *Z. Phys. Chem. N.F.* **164**1521 (1989)
63. A Züttel, F Meli, L Schlapbach *J. Alloys Compd.* **203**235 (1994)
64. M Tsukahara, K Takahashi, T Mishima, H Miyamura, N Kuriyama, T Sakai, I Uehara, in *The International Symposium on Metal-Hydrogen Systems (Abstracts of Reports)* (Fujiyoshida, Japan, 1994) We.B5
65. A Züttel, F Meli, L Schlapbach *J. Alloys Compd.* **206**31 (1994)
66. USP.4 849 205; *Chem. Abstr.* **111**8 1436g (1989)
67. D Song, X Gao, Y Zhang, J Yan, P Shen *J. Alloys Compd.* **206**43 (1994)
68. D-Y Yan, G Sandrock, S Suda, in *The International Symposium on Metal-Hydrogen Systems (Abstracts of Reports)* (Fujiyoshida, Japan, 1994) Mo.P43; *J. Alloys Compd.* **216**237 (1994)
69. H Miyamura, N Kuriyama, T Sakai, K Oguro, A Kato, H Ishikawa, T Iwasaki *J. Less-Common Met.* **172**–174 1205 (1991)
70. T Sakai, A Takagi, T Hasama, H Miyamura, N Kuriyama, H Ishikawa, C Iwakura, in *The III International Conference on Batteries for Utility Energy Storage (Proceedings)* (Kobe, Japan, 1991) p.499
71. C Iwakura, M Matsuoka *Prog. Batt. Solar Cells* **10**81 (1991)
72. P H L Notten, P Hokkeling, in *The 178th Electrochemical Society Meeting (Ext. Abstracts)* (Seattle, USA, 1990) No.75
73. P H L Notten, J L C Daams, R E F Einerhand *Ber. Bunsenges Phys. Chem.* **96**656 (1992)
74. P H L Notten, P Hokkeling *J. Electrochem. Soc.* **138**1877 (1991)
75. M M Jaksic *High Temp. Sci.* **30**19 (1990)
76. K N Semenenko, O A Petrii, S Ya Vasina, I I Korobov, I V Kovrigina *Dokl. Akad. Nauk SSSR* **276**1424 (1984)
77. I V Kovrigina, S Ya Vasina, I I Korobov, O A Petrii, K N Semenenko *Elektrokhimiya* **22**1143 (1986)
78. O A Petrii, I V Kovrigina, S Ya Vasina *Mater. Chem. Phys.* **22**51 (1989)
79. D G Ivey, D O Northwood *Z. Phys. Chem. N.F.* **147**191 (1986)
80. USP.4 728 586; *Chem. Abstr.* **109**76 599s (1988)
81. G Adachi, K Niki, J Shiokawa *J. Less-Common Met.* **81**345 (1981)
82. T Sakai, H Miyamura, K Oguro, T Iwasaki, H Ishikawa *Z. Phys. Chem. N.F.* **164**1539 (1989)
83. T Sakai, H Ishikawa, H Miyamura, N Kuriyama, S Yamada, T Iwasaki *J. Electrochem. Soc.* **138**908 (1991)
84. H Tamura, C Iwakura, T Kitamura *J. Less-Common Met.* **89**567 (1983)
85. Y Li, Y-T Cheng, M A Habib *J. Alloys Compd.* **209**7 (1994)
86. N A Zakarina, G D Zakumbaeva, N F Toktabaeva *Elektrokhimiya* **19**938 (1983)
87. R P Petukhova, G Garson Valensiya, B I Podlovchenko *Vestn. Mosk. Univ., Ser. 2, Khim.* **28**62 (1987)
88. N Tateishi, K Yahikozawa, K Nishimura, M Suzuki, Y Iwanaga, M Watanabe, E Enami, Y Matsuda, Y Takasu *Electrochim. Acta* **36**1235 (1991)
89. M Baldauf, D M Kolb *Electrochim. Acta* **38**2145 (1993)
90. I Matsumura, L Sogiura, H Uchida *Z. Phys. Chem. N.F.* **164**1545 (1989)
91. M Matsuoka, T Kohno, C Iwakura *Electrochim. Acta* **38**787 (1993)
92. T Sakai, H Ishikawa, K Oguro, C Iwakura, H Yoneyama *J. Electrochem. Soc.* **134**558 (1987)
93. C-N Park, M-H Chang, in *The International Symposium on Metal-Hydrogen Systems (Abstracts of Reports)* (Fujiyoshida, Japan, 1994) Mo.B6
94. M Geng *J. Alloys Compd.* **217**90 (1995)
95. K Petrov, A A Rostami, A Visintin, S Srinivasan *J. Electrochem. Soc.* **141**1747 (1994)
96. D-M Lee, J-Y Lu, in *The International Symposium on Metal-Hydrogen Systems (Abstracts of Reports)* (Fujiyoshida, Japan, 1994) Mo.P25
97. M Fetencen, S Venkatesan, S Ovshinsky, in *Proceedings of the 34th International Power Sources Symposium* (New York: Cherry Hill, 1990) p.305
98. H H Van Mal, K H J Buschow, A R Miedema *J. Less-Common Met.* **35**65 (1974)
99. T Kitamura, C Iwakura, H Tamura *Electrochim. Acta* **27**1723 (1982)
100. I V Kovrigina, E I Shkol'nikov, S Ya Vasina, Yu M Vol'fkovich *Vestn. Mosk. Univ., Ser. 2, Khim.* **26**473 (1985)
101. I V Kovrigina, I L Gogichadze, S Ya Vasina, O A Petrii, E I Shkol'nikov, Yu M Vol'fkovich, in *Problemy Termodinamiki, Kinetiki i Massoperenosa v Elektrokhimicheskoi Energetike* (The Problems of Thermodynamics, Kinetics, and Mass Transfer in Electrochemical Energetics) (Moscow: Izd. Mosk. Energetich. Inst., 1986) No.95, p.84
102. M Matsuoka, M Terashima, C Iwakura *Electrochim. Acta* **38**1087 (1993)
103. A Züttel, F Meli, L Schlapbach *J. Alloys Compd.* **209**99 (1994)
104. H Sawa, M Ohta, H Nakano, S Wakao *Z. Phys. Chem. N.F.* **164**1527 (1989)
105. S-R Kim, J-Y Lu *J. Alloys Compd.* **185**L.1 (1992)
106. T Kitamura, C Iwakura, H Tamura *Chem. Lett.* 965 (1981)
107. Kh B Shao, S Ya Vasina, I I Korobov, O A Petrii *Elektrokhimiya* **32** (1996) (in the press)

108. O A Petrii, S Ya Vasina, I L Gogichadze, in *The Xth International Congress of Metallic Corrosion (Ext. Abstracts)* (Madras, India, 1987) p. 335
109. H Sawa, M Ohta, M Hiroaki, S Wakao *Z. Phys. Chem. N. F.* **164**1527 (1989)
110. S Fukushima, H Tanabe *Int. J. Hydrog. Energy* **8** 33 (1983)
111. O A Petrii, I L Gogichadze, S Ya Vasina, in *Dvoynoi Sloi i Adsorbsiya na Tverdykh Elektrodakh (Tez. Dokl.)* [Double Layer and Adsorption on Solid Electrodes] (Abstracts of Reports) (Tartu: Izd. Tartusk. Univ., 1985) Vol. 7, p. 263
112. M H Miles *J. Electroanal. Chem. Interfacial Electrochem.* **60** 89 (1975)
113. T Maoka, M Enyo *Electrochim. Acta* **26** 607 615 (1981)
114. P Los, A Lasia, *J. Electroanal. Chem. Interfacial Electrochem.* **333** 115 (1992)
115. M Enyo *Electrochim. Acta* **39** 1715 (1994)
116. K Machida, M Enyo, G Adachi, J Shiokawa *Electrochim. Acta* **29** 807 (1984)
117. K Machida, M Enyo, I Toyoshima, K Miyahara, K Kai, K Suzuki *Bull. Chem. Soc. Jpn.* **56** 3393 (1983)
118. C Iwakura, M Matsuoka, T Kohno *J. Electrochem. Soc.* **141** 2306 (1994)
119. R V Bucur, V Mecea, T Flanagan *Surf. Sci.* **54** 77 (1976)
120. A I Fedorova, A N Frumkin *Zh. Fiz. Khim.* **27** 247 (1953)
121. L Gao, B E Conway *Electrochim. Acta* **39** 1681 (1994)
122. Yu G Chirkov, V N Zhuravleva, K V Shnepelev, A G Pshenichnikov *Elektrokhimiya* **24** 1305 (1988)
123. Yu G Chirkov, A G Pshenichnikov *Elektrokhimiya* **26** 864 (1990)
124. Z-P Li, Y-Q Lei, C-P Chen, J Wu, Q-D Wang *J. Less-Common Met.* **172** – **174** 1260 (1991)
125. Q M Yang, M Ciureanu, D H Ryan, J O Strom-Olsen *J. Electrochem. Soc.* **141** 2108 2113 (1994)
126. Yu M Vol'fkovich, O A Petrii, A A Zaitsev, I V Kovrigina *Vestn. Mosk. Univ., Ser. 2, Khim.* **29** 173 (1988)
127. M Viitanen *J. Electrochem. Soc.* **140** 936 (1993)
128. R V Bucur, I Covaci *Electrochim. Acta* **24** 1213 (1979)
129. R V Bucur, F Bota *Electrochim. Acta* **27** 521 (1982)
130. Yu M Vol'fkovich, T K Zolotova, S L Bobe, A V Shlepakov *Elektrokhimiya* **29** 897 (1992)
131. R Kirchheim, F Sommer, G Schluckebier *Acta Metall.* **30** 105 (1982)
132. J O Strom-Olsen, Y Zhao, D H Ryan *J. Less-Common Met.* **172** – **174** 982 (1991)
133. J H Weaver, A Franciosi, W E Wallace, S H Kevin *J. Appl. Phys.* **51** 5847 (1980)
134. K Machida, M Enyo *J. Res. Inst. Catal. Hokkaido Univ.* **32** 737 (1984)
135. D-Y Yan, G Sandroch, S Suda, in *The 46th Annual Meeting of the International Society of Electrochemistry (Extended Abstracts)* (Xiamen, China: Xiamen University Press, 1995) Abstr. 6 – 52
136. Yu A Chizmadzhev, V S Markin, M R Tarasevich, Yu G Chirkov *Makrokinetika Protsessov v Poristyykh Sredakh* (Macrokineitics of Processes in Porous Media) (Moscow: Nauka, 1971)
137. Yu M Vol'fkovich, E I Shkol'nikov *Elektrokhimiya* **19** 656; 757; 1199; 1312 (1983)
138. I G Gurevich, Yu M Vol'fkovich, V S Bagotskii *Zhidkostnye Poristye Elektrody* (Liquid Porous Electrodes) (Minsk: Nauka i Tekhnika, 1974)
139. C Iwakura, I Kim, N Matsui, H Inoue, M Matsuoka *Electrochim. Acta* **40** 561 (1995)
140. S Ya Vasina, S A Stuken, O A Petrii, I L Gogichadze, V A Mukhin *Elektrokhimiya* **23** 1127 (1987)
141. D E Hall, J M Sarver, D O Goothard *Int. J. Hydrog. Energy* **13** 547 (1988)
142. V S Bagotskii, N V Osetrova *Elektrokhimiya* **31** 453 (1995)
143. D T Hughes, I R Harris *J. Less-Common Met.* **61** 9 (1978)
144. M L Doyle, I R Harris *Platinum Metals Rev.* **32** 130 (1988)
145. C J Lihn, C C Wan, T P Perng *J. Appl. Electrochem.* **25** 61 (1995)
146. G A Tsirlina, M Yu Rusanova-Berdonosova, V A Roznyatovskii, O A Petrii *Elektrokhimiya* **31** 25 (1995)
147. M Nogami, M Tadokoro, M Kimoto, Y Chikano, I Ise, N Furukawa *Denki Kagaku* **61** 1088 (1993)
148. S Srinivasan, W Zhang, M P Kumar, A Visintin, in *The 46th Annual Meeting of the International Society of Electrochemistry (Extended Abstracts)* (Xiamen, China: Xiamen University Press, 1995) Abstr. 5 – 44
149. J Chen, in *The 46th Annual Meeting of the International Society of Electrochemistry (Extended Abstracts)* (Xiamen, China: Xiamen University Press, 1995) Abstr. 5 – 38

Direct high-pressure gas-phase oxidation of natural gas to methanol and other oxygenates

V S Arutyunov, V Ya Basevich, V I Vedenev

Contents

I. Introduction	197
II. The current state of natural gas processing technology	197
III. The main experimental data on the direct high-pressure oxidation of methane	198
IV. High-pressure oxidation of methane homologues	205
V. The mechanism of the high-pressure oxidation of methane	207
VI. Analysis of the results of kinetic modelling of the high-pressure oxidation of methane	211
VII. Technical and economic aspects of the direct oxidation of natural gas to methanol	219
VIII. Promising aspects of the scientific research dealing with direct oxidation of natural gas to methanol	221
IX. Conclusion	222

Abstract. The published experimental data on the direct gas-phase oxidation of natural gas (methane) to methanol are surveyed. The results of kinetic modelling of the process, its mechanism, and its most characteristic features are considered. Prospects of the industrial use of the process and the most important directions for further studies are discussed. The bibliography includes 146 references.

I. Introduction

Direct oxidation of natural gas (methane) to methanol (DMTM) is a promising way of solving the problem of conversion of natural gas into more easily transportable fuels and chemicals. This process can be carried out both in the presence of a heterogeneous catalyst and under homogeneous conditions. In the latter case, pressures higher than 50 atm are needed to achieve a sufficiently high yield of the target products. The extensive literature devoted to the high-pressure gas-phase oxidation of methane,^{1–65} including numerous papers published in recent years, makes it possible to speak of a branch of science dealing with the study of the chemical fundamentals of this process and having a long-term task of developing a competitive method for the direct processing of natural gas.

Since the possibility, in principle, of obtaining valuable oxygen-containing chemical products (oxygenates) by the direct oxidation of methane had been established,^{1–3} it was reported^{4–7} that direct gas-phase oxidation of methane at high pressures can yield methanol with a high selectivity. Efforts were made to increase the yields of these products and to develop industrial processes for their production. As early as 1905, one of the first patents⁸ dealing with the catalytic oxidation of methane to oxygenates (formaldehyde, methanol, formic acid, etc) was obtained, and in 1929 and 1930 the first catalytic process carried

out at high pressures was patented.^{9, 10} At present, there are no operating industrial units for the direct oxidation of natural gas to methanol; however, during World War II more than one fourth of the annual output of formaldehyde and methanol in the USA was produced in this way.^{11, 12}

Currently, interest in this process has revived because the role of natural gas in the world energy balance has increased, because of the urgent need for environmentally clean motor fuels in leading industrial countries, and, the publication of experimental data⁶⁶ indicating the possibility of achieving a very high selectivity in the formation of methanol.⁶⁵

The problem of partial gas-phase oxidation of methane to methanol at high pressure has been considered in a number of reviews, beginning with a monograph²⁰ that summarised more than fifty years of research on the mechanism of the oxidation of hydrocarbons and ending with more up-to-date, though not fully comprehensive, reviews.^{65–67} A detailed and competent survey of the studies dealing with the DMTM problem and published before 1991 is given in a difficultly accessible publication.⁶⁸ However, the time is ripe for the analysis of all the accumulated results in terms of the modern views on the kinetics of this process in order to identify the most significant lines for further research.

We shall not consider here the numerous studies dealing with the oxidation of hydrocarbons at low pressures and with the catalytic oxidation of methane to methanol and other oxygenates, particularly since a number of detailed up-to-date reviews devoted to this problem have been published.^{69–75} The conclusions concerning the technological prospects of the direct gas-phase oxidation made in the present review retain their validity for the heterogeneous catalytic oxidation of methane, which does not afford higher yields of valuable oxygen-containing compounds than the gas-phase oxidation.

II. The current state of natural gas processing technology

The high strength of the C–H bonds in a molecule of methane, which is the main component of natural gas, substantially hampers its use in technological processes. As a rule, these processes require rather high pressures and temperatures. Therefore, until recently, only a few processes involved natural gas as a raw material. The proportions of natural gas used as a raw

V S Arutyunov, V Ya Basevich, V I Vedenev Laboratory for the Oxidation of Hydrocarbons, Semenov Institute of Chemical Physics, Russian Academy of Sciences, ul. Kosygina 4, 117977 Moscow, Russian Federation. Fax (7-095) 938 21 56. E-mail: kinet@glas.apc.org

Received 28 March 1995

Uspekhi Khimii 65 (3) 211–241 (1996); translated by ZP Bobkova

material and a motor fuel in Russia are extremely low (2.0%–2.5% and 0.5%, respectively).⁷⁶

Natural gas is used mainly in the production of synthesis gas or hydrogen. It is the possibility of producing these valuable intermediate materials that makes natural gas a very important source of various organic compounds. Among other processes, the production of chlorinated derivatives of methane, hydrogen cyanide, and ethyne are noteworthy.⁷⁷

Liquefiable components of natural gas find much more extensive applications. At present, approximately 750000 m³ of liquefied hydrocarbons per day is obtained from natural gas in the world, which constitutes about 7.3% of the overall world production of liquid hydrocarbons. In the USA, the gas condensate and other liquefied components of natural gas account for 18% of the overall production of liquid hydrocarbons and 70% of the raw material for the production of ethene and other basic petro-chemical products. In view of the current trends in the development of oil and natural gas production, liquid components of natural gas will amount to 25%–30% of the total quantity of liquid hydrocarbons produced in the USA by the late 90s.⁷⁸

Apart from liquefied hydrocarbons, motor fuels, methanol, and other oxygenates including high-octane components of motor fuels, are the target products of gas processing. However, at present there are only a few operating industrial processes in the world for the conversion of natural gas into motor fuels, based on its initial transformation into synthesis gas. It is at present the most advanced technology for producing chemicals from natural gas. However, optimistic views on the conversion of methane into synthesis gas and then into methanol or the products of the Fischer–Tropsch synthesis are difficult to justify, since synthesis gas can also be obtained from cheaper carbon-containing materials. Moreover, the high cost of these processes and a number of technological problems do not promote the maintenance of a wide interest in such conversion.

The uncertainty as regards future sources of petroleum-based raw materials and the introduction of more severe laws concerning environmental protection create a real prospect of using the enormous natural gas resources for producing traditional petro-chemical products. It would be desirable to learn how to convert this gas, which is relatively difficult to handle, into a more versatile raw material. Methanol is the most probable candidate for a raw material of this kind. Therefore, the preparation and utilization of methanol is now one of the main aspects of the research in the field of industrial chemical synthesis.⁷⁹

Despite the predicted vigorous increase in the consumption of methanol for the synthesis of *tert*-butyl methyl ether and other ethers, industrial companies still refrain from building new large plants for the production of methanol. This is mostly caused by the fear of creating excess capacities and financial stringency.⁸⁰ In our opinion, this restraint of the manufacturers is to a large extent explained by the complexity of the existing technological processes,⁸¹ by their large capital requirements, and by the fact that they are highly power-consuming and have low profitability; this results in the obvious disinclination of the manufacturers to risk large investments, taking into account the possible underemployment of industrial capacities, as was already the case in 1988–1990. This actually reflects the already existing and clearly perceptible demand for a change in the basic technological processes.

At present, substantial efforts are concentrated on the perfection of technological processes for the catalytic synthesis of hydrocarbons and alcohols from synthesis gas. However, even a breakthrough in this field can hardly change the situation fundamentally, since the energy-consuming steam reforming of methane to synthesis gas accounts for approximately 75% of the prime cost in the production of methanol.⁸² Only an increase in the degree of conversion of synthesis gas into methanol from the present-day ~25% to a level close to 100%, the abandonment of the circulation of synthesis gas, and the use of much cheaper air

instead of oxygen, could influence strongly the economic parameters of the process.⁸³ Therefore, the possibility of achieving large-scale processes based on natural gas and competitive with petroleum processing, apparently depends to a large extent on the success in the development of a technology for the direct conversion of methane without the prior production of synthesis gas.

Three promising methods for the direct conversion of natural gas into chemical products have been outlined:⁸⁴

(1) direct partial oxidation of natural gas into methanol and other oxygenates,

(2) oxidative condensation of natural gas to ethane and ethene,

(3) oxyhydrochlorination of natural gas.

Each of these methods has its own attractive features and their combination allows the production of a broad range of the most important chemical intermediate products. Hence, they supplement one another, rather than compete, though at present, the first route is certainly the most thoroughly developed and is close to practical implementation.

The development of a profitable process for producing methanol from natural gas would permit the solution of three important world-wide problems, namely, the problem of transportation, the problem of providing the chemical industry with a very valuable intermediate compound, and the problem of the mass production of environmentally clean high-octane motor fuels.

III. The main experimental data on the direct high-pressure oxidation of methane

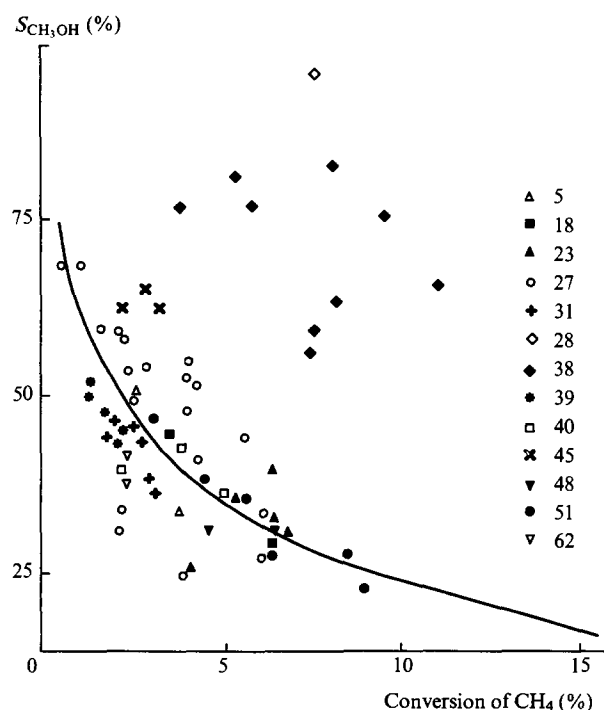
Studies of the high-pressure gas-phase oxidation of methane and other hydrocarbons, carried out in the 1930s in order to elucidate the role of alcohols in the mechanism of the oxidation of hydrocarbons,^{4–6} which was of fundamental importance in the scientific views of that time, showed for the first time that alcohols and aldehydes can be obtained in fairly high yields directly from alkanes. It was found that methanol is formed also at atmospheric pressure under conditions including the induction period of the oxidation reaction.⁸⁵ Although under these conditions the selectivity of the formation of methanol in individual stages of the oxidation of methane can reach 20%, the overall selectivity apparently does not exceed 5%.⁸⁶ Therefore, high pressure is a prerequisite for producing methanol by the direct oxidation of methane.

In fact, the range of conditions necessary for the DMTM to be accomplished had already been roughly outlined in the 1930s. They are: high pressures (100–135 atm),^{4,5,15} moderate temperatures (400–450 °C),¹⁴ and low oxygen concentrations.^{13,14} The practically attainable selectivity of the formation of methanol (up to 60%) was determined,^{4,5} and the main kinetic features of the process, namely the decrease in the selectivity of the formation of methanol with increase in the oxygen concentration^{13,14} and high CO/CO₂ ratios in the products,³ were identified. Until now, the main aim of the studies has been to find the conditions that would permit stable high-output production of valuable compounds in sufficiently high yields, so that the process under consideration could compete successfully with other technological processes. According to estimates,⁸⁷ this requires that the selectivity of the formation of methanol (or the sum of organic products) be higher than 75%. In the majority of studies,^{4,5,19,23–26,31,39,40,46,48,60,62} for methane conversions of more than 2%, the selectivity of the formation of methanol ($S_{\text{CH}_3\text{OH}}$) did not exceed 50% (Table 1, Fig. 1). Some workers reported higher values up to 60%–65%^{27,45} or even 95%.^{28,38,41,43,66} However, an attempt to reproduce the latter results was unsuccessful,⁴⁰ and the reasons for so great a difference are still unclear.

We shall not go into the experimental details of the investigations considered. As a rule, the researchers, who carried out this process at very high pressures (thousands of atmospheres),^{23–26} used static reactors. Later, flow reactors, which are more suitable

Table 1. The selectivity of the formation of methanol and formaldehyde in the conversion of methane.

P/atm	$T/^\circ\text{C}$	$[\text{O}_2]$ (%)	Conversion of CH_4 (%)	$S_{\text{CH}_3\text{OH}}$ (%)	$S_{\text{CH}_2\text{O}}$ (%)	Yield of CH_3OH (%)	t_r/s	Ref.
106.4	341	11.0		22.3	0.75		720	4
50	430	3.0		51.0	4.1		5	5
50	410	5.0		29.0	1.4		5	5
141	475	4.5	2.51	45.0	3.66	1.13	48	18
141	475	8.7	5.30	29.6	2.48	1.57	48	18
3500	264	7.9	6.29	40.1	0.64	2.52	600	23
40	455	2.04	2.10	59.6	17.04	1.25	~0.08	27
40	461	3.2	2.90	54.4	17.0	1.58	~0.08	27
40	483	7.2	6.10	34.6	13.83	2.11	~0.08	27
65	310	3.85	7.5	95		6	2–1000	28
65	410	7	21	80		17	2–1000	28
100	410–450	2.8		46.0	9.1	~2.8 ^a	~1 ^a	31
100	410–450	4.0		37.0	11.1	~3.4 ^a	~1 ^a	31
65.3	456	5.1	8.0	83.0		6.6	~150 ^a	38
65.4	456	7.4	11.0	66.5		7.3	~150 ^a	38
40	474–498	2.35–3.14	1.3–2.2	43.6–52.1	6.4–13.8	0.73–1.0 ^a	1.2–2.1	39
50	425	4.9		43			100–300	40
70	448	3.3	3.9	67.5	1.8	2.56 ^a	~2 ^a	45
20	400	5.0	>4.6	~32			10–100	48
20	440	10.0	>6.5	~32			10–100	48
30	401	2.5	3.1	47.0		1.3–1.5		51
30	407	5.0	4.5	37.7		1.5–1.7		51
30	447	9.5	9.0	23.5		1.9–2.1		51
21–41	300–500	1–5		~30		0.5–0.8	3–15	59
50	350–550	1.5		44		1.1	>10	60
50	350–550	3		32		1.26	>10	60
50	350–550	6		22		1.8	>10	60
50	350–550	12		15.5			>10	60
100	400	2.8		38–42	6.3–7.4		~100	62

^a Estimated by the authors.**Figure 1.** Dependence of the selectivity of the formation of methanol on the degree of conversion of methane. The symbols correspond to experimental data and the curve is the calculated plot ($P = 100$ atm, $T = 420$ °C).⁶⁴ The numerals denote the corresponding references.

for the practical realisation of the process, were mostly used. The experiments were carried out in broad pressure (1–230 atm) and temperature (300–500 °C and higher) ranges, with the reaction time t_r varying from fractions of a second to tens of minutes. More exotic cases can also be found. For example, the possibility of using the cylinder of an internal-combustion engine with a high compression ratio, operated by an electric motor, as a reactor for the DMTM has been investigated.²¹

1. The influence of pressure on the yields of the products of partial oxidation of methane

The high selectivity of the formation of methanol is the main characteristic feature of the high-pressure oxidation of rich mixtures of methane with oxygen. Water and formaldehyde are the two other main liquid products. The reaction always yields minor quantities of liquids such as ethanol (up to 1.5%–2%), acetone (up to 1%), and formic acid (up to 0.8%) (Table 2).⁶² Small amounts of higher alcohols,^{29,31,62} aldehydes,^{31,68} and organic acids^{25,29,31,68} have also been detected. When gases with high concentrations of ethane or other alkanes are oxidised, the yield of C_2 – C_3 alcohols, aldehydes, and acids may increase considerably (see Section IV). There is some evidence that the oxidation of methane also gives methyl formate.^{23,25} A GC/MS analysis of the liquid products of the partial oxidation of methane in a pilot plant³¹ has shown the presence of minor quantities (fractions per cent) of dimethyl formal, dimethyl acetal, and dimethyl ether; however, it was not established whether these compounds were formed directly in the reaction or resulted from the interaction of primary liquid products after cooling. In any case, a special attempt to detect them was unsuccessful.⁴ Repeated attempts to find hydrogen peroxide or organic peroxides in the reaction products have also given no positive results.^{4,22} Traces of these products have been found only at atmospheric pressure.⁸⁸

Table 2. Side products of the high-pressure gas-phase oxidation of methane.

P/atm	$T/^{\circ}\text{C}$	$[\text{O}_2] (\%)$	H_2	$\text{C}_2\text{H}_5\text{OH}$	C_2H_6^b	CH_3OCH_3	CH_3COCH_3	Ref.
				HCOOH	CH_3CHO	C_2H_4^b	CH_3COOH	
48–150	335–393	11.0	+			—		4
50	400–430	3.0–5.0	—					5
135	300–500	3.0–8.6	+	+				15
141–231	350–500	2.8–8.7	+	+				18
172–200	450	5.5–6.3	+	+	—	—		19
105	350	2–8	+		+	+		22
100–750	250–363	10	+		+		+	25
1700–3400	270–480	8.0	—	+			+	26
100	430	2.8	+	$+$ ^a		$+$ ^a	+	29
100	410–450	2–4	+	$+$ ^a	+	$+$ ^a	+	31
40	474–498	2.35–3.14	+	+	+			39
20–50	425–500	3–10	+		+	+		46
15–50	384–476	2.5–9.5			+	+		51
21–41	300–500	1–5		+	+	+		59
30–230	400	2.8	+	+	$+$ ^a		+	62
25–53	< 535	2.0–4.7	+	+	+	+	+	68

^a Higher homologues of these compounds have also been detected. ^b Relates to those cases where the initial gases contain no ethane or ethene or their concentration in the products is higher than the initial concentration.

The main gaseous products are carbon oxides and hydrogen, the yield of carbon monoxide at high pressures being several times larger than that of the dioxide,⁶² although carbon dioxide appears earlier than carbon monoxide.²² The yield of ethane and ethene increases with increase in temperature.

An increase in pressure intensifies the oxidation of methane by decreasing its duration or the initial temperature. For example, the pressure dependence of the delay of the self-ignition of the 8.8:1.2 methane–air mixture in the 60–113 atm range is described by the relation $\tau_1 \sim P^{-1.4}$ (Fig. 2),²² and the ten-fold increase in pressure from 5 to 50 atm in a flow reactor leads to the decrease in temperature corresponding to the complete conversion of oxygen from 500 to 400 °C⁴⁰ (Fig. 3). However, the main consequence of the application of high pressures in the oxidation of rich methane mixtures is high selectivity of the formation of methanol. The increase of pressure from 10 to 106 atm increased $S_{\text{CH}_3\text{OH}}$ by a factor of 20,⁶ and when the pressure increased from 5 to 50 atm, the temperature at which methanol begins to be detected decreased from 450 to 375 °C.⁴⁰

The results obtained by Arutyunov et al.⁶² indicate that the overall yield of liquid products of the partial oxidation of methane increases monotonically as the pressure increases up to 200 atm (Fig. 4). However, the concentrations of alcohols and acetone pass through a maximum near 150 atm (Fig. 5). Consequently, the pressure dependence of the yield of methanol has a weakly

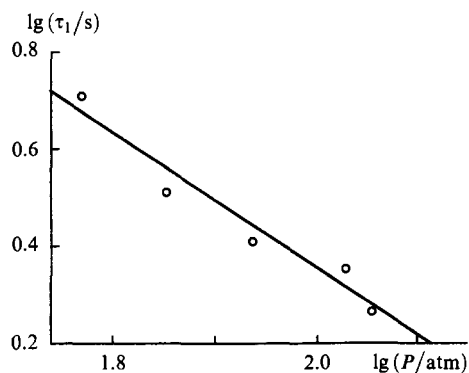


Figure 2. Pressure dependence of the delay of self-ignition of the mixture containing 88% of methane and 12% of air ($T = 406^\circ\text{C}$).²²

defined maximum at these pressures (Fig. 6). Other data also indicate that the yield of methanol diminishes at pressures above 180 atm¹⁸ or that the selectivity of its formation decreases at pressures above 100 atm.⁶⁵

Despite the fact that the concentration of formaldehyde in the liquid oxidation products decreases monotonically with increase in pressure (Fig. 5), its yield remains approximately constant, since the overall yield of liquid products increases (Fig. 6). Thus, pressure is the crucial factor influencing the composition of liquid oxidation products, including the ratio of methanol to formaldehyde (Fig. 7).⁶² The partial oxidation of methane under very high pressures, up to 3400 atm²⁶ or higher,²³ provides no real advantages. The pressure range between 75 atm (the standard pressure in gas mains) and 100 atm may apparently be considered optimal. Since the cost of gas compression is one of the major constituents of the prime costs of the products obtained by the DMTM,⁸⁷ this conclusion is important practically.

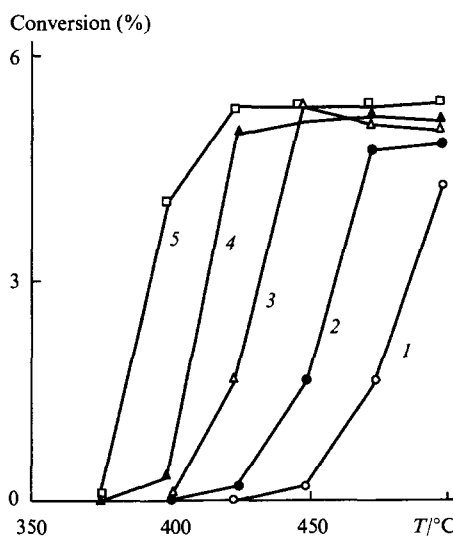


Figure 3. Temperature dependence of the conversion of methane at different pressures (atm): (1) 5, (2) 10, (3) 20, (4) 30, (5) 50 (reported by Burch et al.⁴⁰).

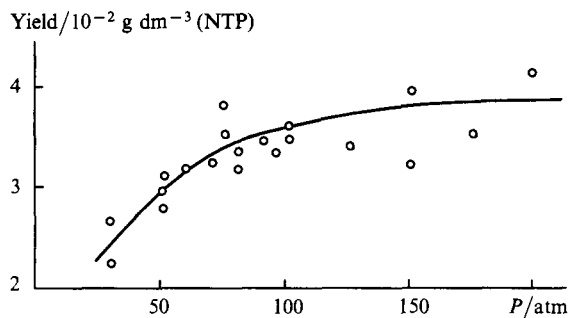


Figure 4. Pressure dependence of the overall specific yield of liquid products of the oxidation of methane ($T = 400^\circ\text{C}$).⁶² Gas volumes are referred to the normal temperature and pressure (NTP).

The concentration of the main gaseous product, carbon monoxide, in the gases leaving the reactor reaches $\sim 1.5\%$ for an initial oxygen concentration of $\sim 3\%$, and remains approximately constant in the pressure range from 30 to 230 atm (Fig. 8). The concentration of carbon dioxide is several times lower and increases with pressure, which results in the corresponding decrease in the CO/CO_2 ratio.⁶² The increase in the CO_2 concentration with pressure may be partially due to the formation and subsequent decomposition of formic acid by the mechanism suggested by Vedenev et al.⁴⁷

At higher temperatures of $515\text{--}630^\circ\text{C}$, when the yield of ethane and ethene is fairly high, a pressure increase from 31 to

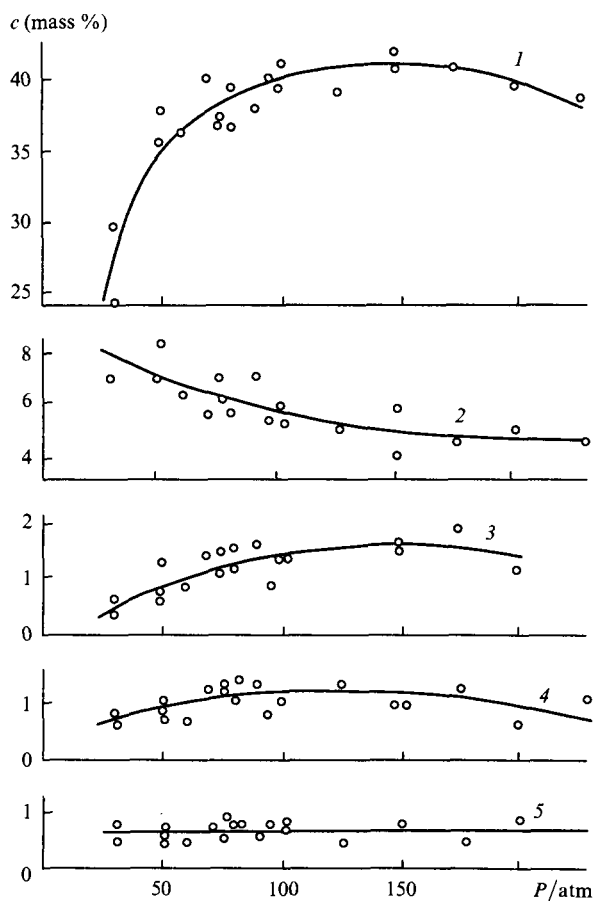


Figure 5. Pressure dependences of current concentrations of the main liquid products of the oxidation of methane ($T = 400^\circ\text{C}$):⁶² (1) methanol; (2) formaldehyde; (3) ethanol; (4) acetone; (5) organic acids.

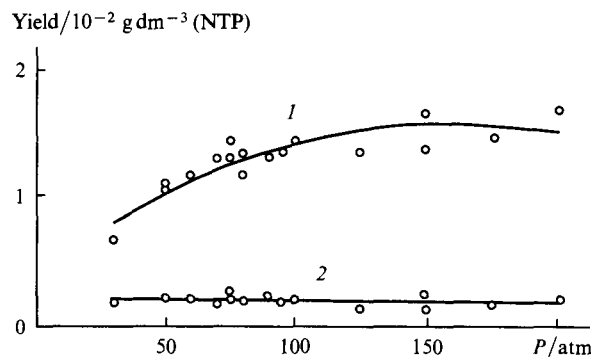


Figure 6. Pressure dependences of the yields of methanol (1) and formaldehyde (2) ($T = 400^\circ\text{C}$).⁶²

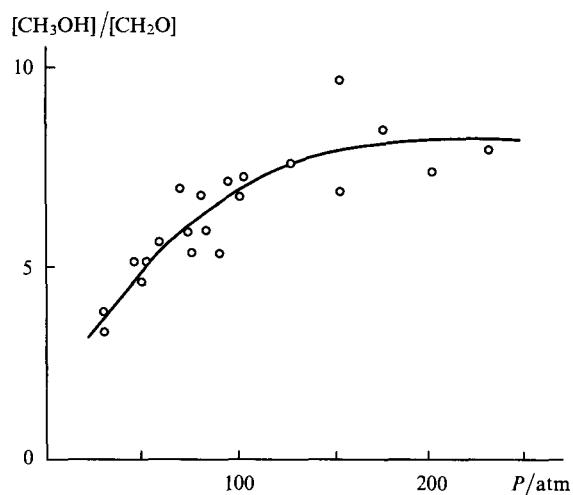


Figure 7. Pressure dependence of the ratio of the methanol and formaldehyde concentrations in the liquid product of oxidation ($T = 400^\circ\text{C}$).⁶²

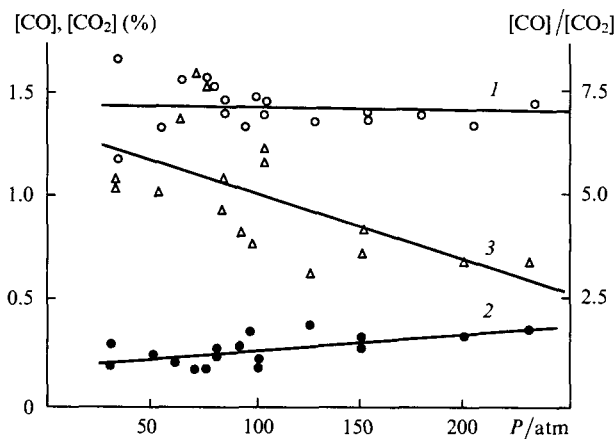


Figure 8. Pressure dependences of the yields of CO (1), CO_2 (2), and of their ratio (3) ($T = 400^\circ\text{C}$).⁶²

102 atm leads to an increase in the yield of C_2 hydrocarbons from 8% to 36%; in addition, the temperature at which complete conversion of oxygen is achieved decreases by 100°C .⁵⁰

2. The influence of temperature and contact time

An increase in temperature leads to a diminution of the induction period of the reaction. As shown by Melvin,²² $\lg \tau_1$ (τ_1 is the self-ignition delay) depends linearly on $1/T$. The activation energy for

the oxidation of methane with air in mixtures having compositions from 60 : 40 to 90 : 10 at a pressure of 105 atm lies in the range of 163–188 kJ mol⁻¹.²² However, the temperature dependence of the degree of conversion of methane for a fixed length of the reactor (see Fig. 3) is clearly S-shaped, whereupon the transition from negligibly small to maximum conversion occurs within a range of not more than 20 °C,^{40,51} which reflects the critical character of the process.⁵⁸ When the temperature of the reactor walls decreases, hystereses are observed in the temperature dependences of the process parameters (heating of the mixture, conversion of methane).⁵¹

Once oxygen is entirely converted, further increase in the temperature within a certain range has apparently little influence on the yield of methanol.¹⁸ Some workers have observed^{40,51} that, at a pressure of 50 atm and above 425 °C (which is the temperature of the complete conversion of oxygen⁴⁰), the value of $S_{\text{CH}_3\text{OH}}$ already decreases monotonically (from 40% to 32% at 500 °C⁴⁰); however, according to other data,⁴⁵ the selectivity remained practically constant between 420 and 460 °C ($P = 40$ atm) or passed through a maximum at ~450 °C.^{18,59} (Fig. 9). Further increase in temperature may lead to a diminution of the yield of methanol due to both a decrease in the selectivity of its formation and the decomposition of a portion of the product already formed on contact with the reactor surface.⁴⁰ For the same reason, it is undesirable to increase the residence time of the mixture in the reactor for a longer period than is necessary for the complete conversion of oxygen at the given temperature.^{40,59} However, if the surface of the reactor is relatively inert (quartz, Pyrex, stainless steel), the variation of the residence time of the unreacted reaction mixtures within fairly broad limits has little influence on the final yield of methanol and even on the yield of formaldehyde, although the latter is less stable under these conditions.^{40,62} Attempts to increase the yield of methanol by rapid cooling of the mixture as it leaves the reactor³⁹ have given no significant advantage over the results of most other studies (Table 1).

When the temperature is increased to 500 °C or more, the composition of reaction products changes toward ethane, ethene, and small quantities of ethyne, the overall selectivity of their formation being as high as 37% at 515 °C and 100 atm.^{49,50}

The combination of high temperatures and relatively low pressures is favourable for an increased yield of formaldehyde. When the reaction was carried out at 625 °C and 5 atm, with a methane : air ratio of 1 : 5 and a contact time of 2.3 s, the yield of formaldehyde in the gas-phase oxidation of methane was raised to 3.5% ($S_{\text{CH}_2\text{O}} \approx 50\%$ for a degree of conversion of ~7%), which is even greater than in the presence of oxide catalysts.⁴⁴

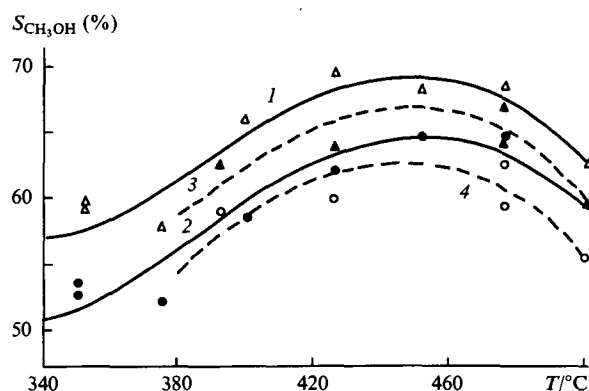


Figure 9. Temperature dependences of the selectivity of the formation of the sum of useful oxygen-containing products (1, 3) and methanol (2, 4) at pressures of 184 (1, 2) and 231 atm (3, 4).¹⁸

3. The conversion of methane and oxygen in the oxidation of methane to methanol

A low concentration of oxygen in the DMTM predetermines a low degree of conversion of methane after its single passage through the reactor. In virtually all experimental studies (see Table 1, Fig. 1), the degree of conversion of methane was lower than the initial percentage of oxygen. Only Gesser et al.²⁸ and Yarlagaadda et al.,³⁸ who have achieved very high selectivities in the formation of methanol, reported methane conversions substantially higher than the initial oxygen contents. The reasons for this discrepancy are still unclear.

It has been noted⁶² that the gas-phase reaction products always contain a small amount of oxygen {~5% of its initial concentration $[\text{O}_2]_0$ on average}. Special studies made it possible to rule out trivial explanations of this fact such as that oxygen entered the system after it had left the reactor or unreliability of the analysis. The fact that the oxidation of methane stops before the oxygen is entirely consumed is difficult to explain from the theoretical viewpoint.

In one of the early studies, Newitt and Huffner⁴ stated that oxygen was fully consumed in this reaction. On the other hand, a careful analysis carried out in the study by Boomer and Thomas¹⁷ indicated that the gases leaving the reactor contain oxygen almost in all cases. The authors emphasised that the material balance of this reaction with respect to oxygen is difficult or even impossible to reconcile. A review⁶⁵ cites data⁸⁹ which state that 95% of the oxygen present in the system enters into the reaction, i.e. 5% of the oxygen remains unchanged. Finally, Bauerle et al.²⁵ presented reliable data indicating that at 100–750 atm, 250–363 °C, for reaction times of up to 900 min, and $[\text{O}_2]_0 = 10\%$, the process stops when the residual oxygen content is $(0.3–0.5)[\text{O}_2]_0$. Perhaps, the most remarkable relevant data are concerned with the existence of a limiting oxygen concentration in the oxidation of butane.⁹⁰ Appreciable amounts of unchanged oxygen have also been observed in experiments on the oxidation of methane at very high pressures of 1700–3400 atm.²⁶ In other papers, either there is no special mention of the presence of noticeable quantities of oxygen in the gas after the reaction or complete consumption of oxygen has been reported. Nevertheless, the question why the oxidation stops before all the oxygen is consumed requires an additional analysis.

4. The influence of mixture composition on the kinetics of the process and the yield of products

The kinetics and the yield of products of the DMTM are very sensitive to the composition of the mixture, especially, to the methane : oxygen ratio. As the oxygen concentration increases, the degree of methane conversion also increases, but at the same time, the selectivity of the formation of methanol rapidly diminishes.^{5,13,18,31,38,39,45,60} (Table 1, Fig. 10). Since $S_{\text{CH}_3\text{OH}}$ is governed by the methane : oxygen ratio,⁶⁰ the decrease in $[\text{CH}_4]/[\text{O}_2]$ at a constant oxygen concentration leads to diminished yields of methanol and other liquid oxidation products (Fig. 11).⁶³ The optimal proportion of oxygen in methane is about 3%–5%; however, at this concentration, the degree of conversion of methane in a single pass through the reactor is inevitably low.

An increase in the oxygen concentration has an inhibitory effect on the reaction rate. For example, the delay of the self-ignition of mixtures of methane with air at 72 or 83 atm increases with increase in the oxygen concentration²² (Fig. 12).

Dilution of the reaction mixture with nitrogen,^{40,63} helium,⁶⁰ or other inert gases does not influence the proportions of the products, if the methane : oxygen ratio remains constant. Therefore, the results are identical no matter whether oxygen or air is used as the oxidant.

Carbon dioxide and water vapour cannot apparently be regarded as being absolutely inert during the DMTM. In all probability, the oxygen incorporated in these compounds can participate in the formation of methanol or other oxygen-

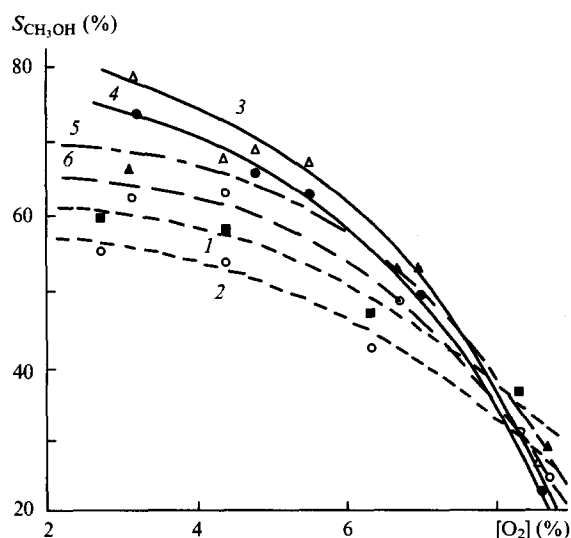


Figure 10. Dependences of the selectivity of the formation of the sum of useful oxygen-containing products (1, 3, 5) and methanol (2, 4, 6) on the oxygen concentration at pressures of 141 (1, 2), 184 (3, 4), and 231 atm (5, 6).¹⁸

containing products, thus increasing their yields.¹³ However, no reliable experimental data concerning this problem have been reported. When about 75% of the methane in a $8.5CH_4 + O_2$ mixture was replaced by N_2 , CO_2 , or H_2O (at 50 atm), apart from the reduction of the reaction rate caused by the decrease in the methane concentration, the yield of methanol also diminished (by approximately 40%).⁵ This is most probably due to the decrease in the methane: oxygen ratio. The yield of formaldehyde was almost unchanged on dilution of methane with nitrogen or carbon

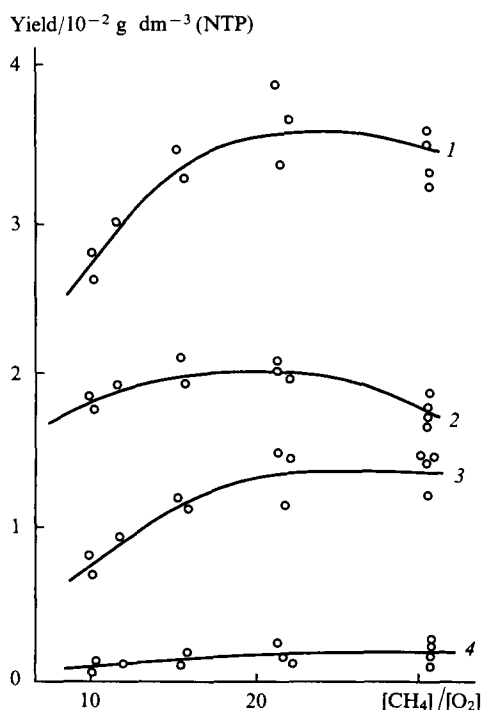


Figure 11. Dependences of the yields of liquid products of the partial oxidation of methane on the $[CH_4]/[O_2]$ ratio ($P = 100 \text{ atm}$, $T = 400^\circ\text{C}$):⁶³ (1) the sum of liquid oxidation products; (2) water; (3) methanol; (4) formaldehyde.

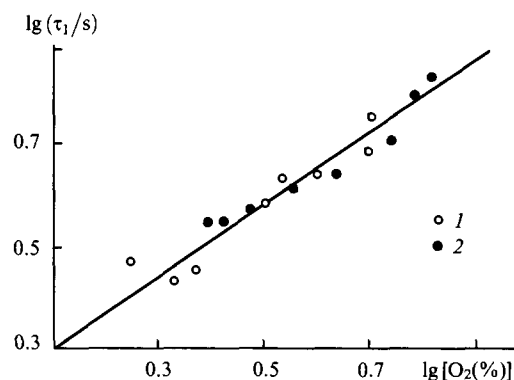


Figure 12. Dependence of the delay of the self-ignition of the mixture of methane with air at 406°C on the oxygen concentration²² at different methane pressures (atm): (1) 83.3, (2) 71.8.

dioxide; on dilution with water vapour, it increased almost two-fold, which confirms the suggestion that water plays an active role in this process.

In a study of the possibility of realising a recirculation scheme for the DMTM process, Arutyunov et al.⁶³ investigated the influence of the addition of the two main reactive gaseous products, namely, carbon monoxide and hydrogen, to the reaction system on the yield of liquid products. It was found that, if the initial concentration of these compounds does not exceed 5%, they virtually do not influence the methanol yield. However, at higher concentrations, the methanol yield may decrease by more than one half.

The influence of the addition of minor quantities of carbon dioxide (10%) or hydrogen (4%) on the DMTM process in the temperature range $400\text{--}500^\circ\text{C}$ at $P = 41 \text{ atm}$, for $CH_4:O_2:N_2 = 30:1:4$, and for a contact time of 1 s has also been investigated.⁵⁹ The addition of either of these gases caused a slight (by $\sim 10^\circ\text{C}$) decrease in the temperature of the onset of the process, but the maximum yield of methanol almost did not change.

5. Homogeneous promotion of the process

Attempts to promote the DMTM process were undertaken as early as 1921, when a number of methods for the preparation of methanol and formaldehyde from natural gas were studied. These methods are: (1) oxidation over various catalysts; (2) oxidation with ozone; (3) iodination followed by hydrolysis; (4) interaction of methane with CO_2 ; (5) synthesis of C_2H_4 from natural gas and its subsequent oxidation; (6) oxidation of methane in solution and with liquid oxidising agents.⁶⁸

In a study of the oxidation of a mixture of methane with air (3:1) at 25 atm and $300\text{--}400^\circ\text{C}$, it was found that minor quantities of HNO_3 accelerate the reaction significantly, while small amounts of $PbEt_4$ retard it.⁷ However, these additives have little influence on the composition of the products.

The possibility of initiating the partial oxidation of methane with ozone under flow conditions at $P = 1 \text{ atm}$ has been considered.⁹¹ Although ozone appreciably promotes the reaction and increases the yield of methanol, a selectivity $> 42\%$ was achieved only when the degree of conversion of methane was no more than 1%. The use of high pressures, more favourable for the formation of methanol, requires the development of effective methods for the production of ozone under these conditions.

The presence of even minor admixtures of heavier hydrocarbons in methane is well known to decrease the reaction temperature with no substantial effect on the yields of the main products. In fact, the replacement of natural gas by methane necessitated that the temperature at the beginning of the process be increased from 350 to $425\text{--}475^\circ\text{C}$,¹⁸ and the addition of 5% ethane to methane led to a 50°C decrease in the temperature.⁴⁰

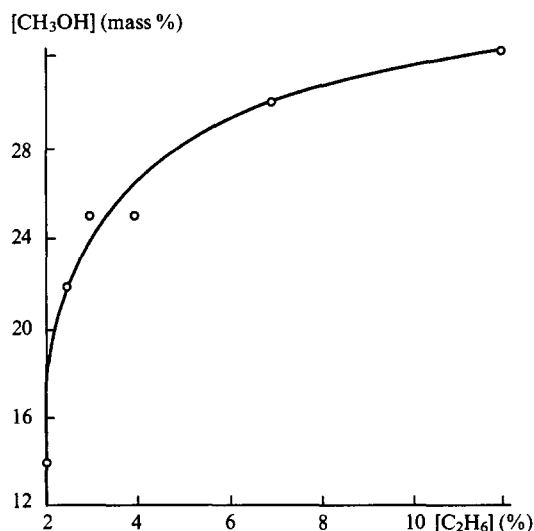


Figure 13. Influence of the addition to natural gas on the concentration of methanol in the liquid oxidation products at $P = 140.6$ atm and $[O_2] = 6\%$.¹⁵

Some data indicate that the yield of methanol increases substantially in the presence of large quantities of ethane (Fig. 13).¹⁵ Unfortunately, no systematic studies on the influence of other hydrocarbons on the DMTM process have been carried out.

A decrease in the temperature of the process and an increase in the conversion of methane and the yield of methanol following the addition of 3% of ethane, propane, or isobutane have been reported ($P = 41$ atm, $CH_4:O_2:N_2 = 30:1:4$, contact time 1 s).⁵⁹ However, in view of the magnitude of this effect, it is difficult to determine unambiguously whether or not the added hydrocarbon itself acts as a source of the additionally formed methanol.

The most systematic study of the influence of promoters on the DMTM process has been carried out by Hunter et al.⁴¹ at a pressure of 10 atm. About 30 different compounds, including saturated, unsaturated, cyclic, and aromatic hydrocarbons, ethers, alcohols, ketones, aldehydes, water, peroxides, sulfur-containing compounds, and amines, were tested as promoters. Many of these promoters decrease noticeably the temperature of the process. Diethyl ether exerts the greatest influence; the addition of 3.9% of diethyl ether decreases the reaction temperature from 402 to 225 °C. Another obvious consequence of the action of some promoters is a significant increase in the yield of formaldehyde, probably at the expense of the corresponding decrease in the yield of methanol. In some cases, the selectivity of the formation of methanol or/and formaldehyde increases, compared with a system containing no promoters. However, this requires the addition of fairly large amounts of promoters, which cancels the economic prospects of thus increasing the yield of methanol in a real technological process.

6. The influence of catalysts and the material of the reactor surface

The question whether the effectiveness of the DMTM process can be significantly increased by using catalysts has remained unsolved throughout the period of its study. An investigation of the influence of certain metals and alloys on this process¹⁹ did not reveal any significant advantages of the catalytic reaction over the purely gas-phase transformation. The use of metallic reactors or catalysts at relatively low pressures favours the formation of products of the complete oxidation of methane.⁴⁰ However, at higher pressures catalysts exert no significant influence on the

selectivity of the formation of methanol. Similar conclusions were based on other data.^{41, 56}

Analysis of the results of the reactions conducted under catalytic conditions^{69–75} and in a series of recent comparative studies^{40, 41, 56} makes it possible to conclude almost unambiguously that the catalytic process has no real advantages over the gas-phase reaction carried out at high pressures.^{40, 71} The same conclusion follows from the kinetic analysis of the reaction mechanism (Section V). The only obvious positive result of using catalysts in the DMTM is the possibility of lowering the reaction temperature.

The question how the material of the reactor surface influences the stability of the products of the partial oxidation of methane is of great importance. A study of the stability of methanol in reactors made of Pyrex, stainless steel, and copper⁴⁰ has shown that, in the case of copper, methanol decomposes almost completely even at 375 °C. Stainless steel is much more inert. In a Pyrex reactor, decomposition of methanol cannot be observed even at 500 °C; nevertheless, up to 15%–18% of the methanol added to the reaction mixture decomposes, probably through being involved in the reaction.⁴⁰ Quartz and Teflon are also among the best materials for reactors used for the DMTM.⁴¹ When light paraffins are oxidised in copper or steel reactors, especially at atmospheric pressure, the yields of both alcohols and aldehydes decrease.⁹² The decomposition of methanol on some surfaces affords dimethyl ether.⁹³ Ultimately, the reactor material exerts no crucial effect on the selectivity of the formation of methanol and other organic products, because the reaction is homogeneous and the rate of diffusion of radicals to the surface at high pressures is low. The results of pilot tests indicate³¹ that the relatively low temperature of the process, which does not exceed 600 °C at the reactor outlet for an initial oxygen content of ~3%, and the low concentration of the organic acids formed can hardly create serious problems in the choice of the material of the reactor.

7. Physical initiation of the process

Attempts to use various physical methods for controlling the rate and selectivity of the DMTM have been undertaken since the 1920s. The effects of an electric discharge, radiation, and ultraviolet light on this process were then studied.¹⁵

In the 1980s, studies on the initiation of the DMTM by laser radiation were carried out in the Los Alamos National Laboratory (USA).^{94, 95} From the results obtained, one can judge that, at 450 °C, 2.04 atm, and an oxygen concentration of 11%, only the rate of the reaction could be really increased, while S_{CH_3OH} and the proportions of products do not change noticeably. However, kinetic analysis of the system showed that at elevated temperatures (530–730 °C), a pressure of 60 atm, and for the $CH_4:O_2 = 2:1$ ratio one may expect a 50% selectivity of the formation of methanol with a degree of conversion of about 25%. The time scale of the reaction (3 ms) dictated the use of a reactor with a supersonic nozzle.⁹⁴ Nevertheless, the authors were apparently unable to solve the problem of the quick removal of the heat of reaction and to achieve quick 'quenching' of the reaction products, without which a high selectivity of the formation of methanol at a relatively high oxygen concentration cannot be ensured.

Among the physical methods for stimulating the oxidation of methane, the use of an ultra-high frequency, glow discharge and thermal initiation by a heated wire have also been considered.⁹⁶ It has been shown⁹⁷ that, in a methane plasma, methane dimerises to C_2 hydrocarbons with a selectivity of more than 95% for a degree of conversion from 30% to 90%. However, the energy efficiency of this thermodynamically unfavourable process is only 0.2%–3.3%. An attempt to use an ultra-high frequency discharge for oxidising methane to methanol⁹⁸ has shown that the features of the reactor design are also significant. The introduction of methane behind the area of plasma induction allowed the yield of C_2 hydrocarbons to be significantly diminished, but the selectivity of the formation of methanol was still extremely low.

8. Cool-flame and periodic phenomena in the oxidation of methane

The existence of cool-flame and related periodic and critical phenomena has been observed in the oxidation of many hydrocarbons with various structures, including alkanes up to propane and ethane.^{20,99,100} In the vast majority of studies, cool flames have not been detected in the oxidation of methane. However, the authors of some studies have noticed phenomena that could have been interpreted as cool-flame phenomena. These situations have also been found in the high-pressure oxidation of methane to methanol.^{23,42,45} Only Vanpee¹⁰¹ and Egret et al.,¹⁰² who worked at atmospheric pressure, obtained fairly convincing experimental evidence for this phenomenon. Recently it was confirmed once again:¹⁰³ cool flames were detected in a $2\text{CH}_4 + \text{O}_2$ mixture at 650–740 Torr and about 500 °C. The dependence on time of the temperature of the reaction mixture exhibited two maxima, the temperature rise in the first one being 100–120 °C. A region of a negative temperature coefficient of the rate of oxidation of methane has been found.¹⁰⁴

Since there is a theoretical possibility of the appearance of cool-flame regimes in the high-pressure oxidation of methane,^{61,105} which may lead to the yields of products, differing fundamentally from those reached in other known oxidation regimes, we present here the published experimental data.

In a process carried out at a pressure of 3360 atm, an oxygen concentration of 8%, and an initial temperature of 262 °C in a static reactor, two temperature peaks with amplitudes of 6 and 14 °C, accompanied by corresponding pressure increases, have been observed against the background of a slow temperature rise.²³

Temperature oscillations typical of the cool-flame phenomena have been observed during the oxidation of methane in a flow reactor at 25–35 atm and an oxygen concentration not less than 5%.⁴² At oxygen concentrations of 8% or more and temperatures of about 410 °C, these oscillations were steady. An increase in the temperature to 450 °C led to a decrease in the amplitude of the oscillations and an increase in their frequency. At 475 °C, the oscillations disappeared. The amplitudes and the frequencies of the oscillations at various points along the reactor axis were very different. The maximum $S_{\text{CH}_3\text{OH}}$ was achieved at the lowest temperatures at which oscillations no longer occurred; however, the selectivity remained lower than that observed at the optimal oxygen concentrations ($\leq 3\%$). It was suggested that, under the conditions in which these oscillations occur, the process in the reactor can be controlled in order to achieve the highest selectivity.

9. The role of other factors

Among other factors which can, in principle, influence the kinetics and the yield of products of the partial oxidation of methane, one should mention the rate at which the reagents are introduced into the reactor, the conditions in their mixing, the heat transfer conditions, and features of the reactor design.

The fact that the yield of products depends substantially on the ratio between the diameter of the reactor, through which a slow (1.6 m s^{-1}) stream of methane is passed, and the diameter of the coaxial nozzle, through which oxygen is passed at a high velocity (60–300 m s^{-1}), and on the velocity of the oxygen supply through the nozzle has been reported in a patent.²⁷

There is evidence that it is necessary to ensure the maximum homogeneity of the mixture entering the reactor. For this purpose, a premixing chamber filled with Teflon turnings has been mounted before the reactor.²⁸ However, an attempt⁴⁰ to reproduce the high yields of methanol obtained by Gesser et al.²⁸ by using the same premixing device gave no noticeable positive results. The composition of the gas, the mixing conditions, as well as the reactor size and the constructional materials used^{28,40} were approximately the same and could not account for the large difference between the selectivities of the formation of methanol ($\sim 80\%$ and $\sim 40\%$, respectively). It was concluded⁴⁰ that some

slight, but perhaps significant, differences in the reactor design may account for this difference, and that the essential influence of this factor is due to the cool-flame reaction regime.

The influence of the reactor design (the way in which oxygen is supplied into the stream of methane) on the process has been studied.⁶⁰ The improvement of the conditions in the mixing of the reactants by introducing oxygen through a spiral nozzle or into a narrow zone of the reactor did not lead to a substantial increase in the yield of methanol. The best results were achieved by distributing the oxygen supply along the whole reactor.^{30,60} In this connection, it was suggested⁶⁰ that the high yields attained in some experiments reported in a patent²⁷ were due to the great distance of the flow of oxygen, before it was mixed with methane, the oxygen being injected into the reactor through a narrow coaxial nozzle, which is equivalent to a distributed supply. The best results were achieved at moderate rates of supply of oxygen. At high rates, the degree of turbulence might increase, and, hence, the mixing area might diminish, which could cause a decrease in the yield of methanol.

Theoretical calculations predict the possibility of increasing the yield of methanol by an order of magnitude by using a fundamentally different scheme for conducting the process.^{95,106} In conformity with these calculations, conducting the reaction at 730 °C with rapid quenching of the products may ensure $S_{\text{CH}_3\text{OH}} = 57\%$ with an oxygen concentration of 25%, which corresponds to a methanol yield of about 13%.¹⁰⁶

IV. High-pressure oxidation of methane homologues

Data on the oxidation of rich mixtures of methane homologues with air or oxygen at high pressures are quite scarce and are presented in a very small number of papers.^{5,6,13,15,90,107–109} Most of these papers have been considered in detail in a review.²⁰

When gases containing large proportions of higher hydrocarbons are used, the process parameters such as the pressure and the temperature needed decrease sharply. As the concentration of higher hydrocarbons grows, there is an increase in the degree of conversion of natural gas, for which the selectivity of the formation of alcohols still remains high; in addition, higher alcohols, including iso-alcohols, aldehydes, and some other compounds, are also formed.

1. Ethane

Since ethane is oxidised much more readily than methane, it follows that, as mentioned in Section III, even a slight increase in the proportion of the ethane admixture in methane (natural gas) decreases the reaction temperature by approximately 100 °C and increases the yield of alcohols (Fig. 13). The most comprehensive studies of the oxidation of ethane have been carried out by Newitt and coworkers.^{5,6,107} The oxidation of mixtures with the approximate composition $\text{C}_2\text{H}_6:\text{O}_2 = 9:1$ under static conditions at 15–100 atm,^{6,107} afforded methanol, ethanol, formaldehyde, acetaldehyde, formic acid, and acetic acid apart from carbon oxides, methane, and water. On the basis of the results obtained, it has been concluded⁶ that an increase in pressure, with approximately the same reaction time (2.5–4.5 min), leads to an increase in the yield of C_2 products (ethanol, acetaldehyde, and acetic acid) and to a decrease in the yields of methanol and formaldehyde. However, maintenance of a constant reaction time does not ensure the maximum yield of alcohols. In any case, examination of the full set of experimental data¹⁰⁷ shows (Table 3) that the maximum yields of alcohols and acetaldehyde depend only slightly on pressure, at least in the range above 50 atm. The role of pressure is more clearly manifested by an increase in the yield of acetic acid, the maximum selectivity of its formation reaching 27.2% at 100 atm, and a monotonic decrease in the yield of formaldehyde. Apparently, one can also conclude that the selectivities of the formation of ethanol and acetic acid increase as the oxygen concentration in the mixture decreases. In the oxidation of a

Table 3. Pressure dependence of the selectivity of the formation of the products of the oxidation of ethane.¹⁰⁷

<i>P</i> /atm	<i>T</i> /°C	Selectivity of the formation (%) ^a											CO/CO ₂	<i>t_r</i> /min
		EtOH	CH ₃ OH	CH ₃ CHO	HCHO	AcOH	HCOOH	CO	CO ₂	CH ₄	Σ _l	Σ _g		
15 ^b	315	16.0	19.4	1.9	4.5	0	0	—	—	—	41.8	—	—	3.0
50 ^{c,d}	286	24.4	14.1	8.3	2.0	1.7	0.9	34.8	10.0	0	51.4	44.8	3.48	10.7
75 ^b	279	18.0	16.6	6.8	0.4	3.6	0.6	—	—	—	46.0	—	—	2.5
100 ^{c,d}	266.5	23.7	11.2	6.0	0.05	23.8	0.6	9.3	14.2	8.6	65.3	32.1	0.65	34.5

^a Based on the combusted ethane. ^b Initial mixture composition: 88.2% C₂H₆ + 11.8% O₂. ^c Initial mixture composition: 88.4% C₂H₆ + 11.6% O₂.

^d The results of the experiments in which the highest ethanol yields were achieved. Σ_l and Σ_g are the sums of liquid and gaseous products respectively.

mixture with the composition C₂H₆:O₂:N₂ = 90:3:7 in a flow reactor at *P* = 50 atm, *T* = 360 °C, and for a contact time of 4 s, the selectivity of the formation of ethanol was 63%.⁵ When the contact time increased to 20 s, the selectivity of the formation of ethanol decreased to 14.5%, while *S*_{CH₃OH} increased from trace amounts to 7.8%. When portions of oxygen were successively added to the mixture which had already reacted, the quantities of ethanol, aldehydes, and acids formed and the quantity of methane remained virtually constant, and only the contents of methanol and carbon oxides increased monotonically.¹⁰⁷

In a more recent study,¹⁰⁸ in which the process was carried out under flow conditions at 27–37 atm, a high selectivity of the formation of alcohols (more than 70%) was also observed. However, whereas at the relatively low pressures mentioned above the ethanol:methanol ratio in the reaction products was less than unity, with increase in pressure to 90 atm this ratio increased to 6. In the experiments under consideration, the time the mixture spent in the reactor also increased from ~1 min at 15 atm to 7 min at 90 atm. Therefore, it is difficult to distinguish the influence of the linear velocity of the reactant flow in the reactor from the influence of the pressure itself. It should be noted that in another study,⁵ the opposite influence of the residence time of the mixture in the reactor has been observed: at 50 atm, the increase in the residence time from 7 to 20 s reduced the ethanol:methanol ratio from 19 to 2. It has also been reported¹⁰⁹ that this ratio increases as the oxygen concentration decreases.

2. Propane

Data on oxidation of propane at high pressures have been reported by Newitt and coworkers^{6,109} (static conditions) and Wiezevich and Frolich¹⁵ (flow conditions). These data are partly presented in Tables 4 and 5. Qualitative analysis showed that, among aldehydes, propanal and acetaldehyde are formed, among normal alcohols, methanol, ethanol, and propanol are produced, while carboxylic acids are mostly represented by acetic acid with minor amounts of propionic and formic acids.¹⁰⁹ An increase in pressure results in a substantial increase in the yields of

2-propanol, acetone, and organic acids, some reduction of the yields of aldehydes and normal alcohols, an increase in the yield of CO₂, and a decrease in the yield of CO; when the pressure is 20 atm or more, propene is no longer present in the reaction products. In addition, increase pressure appreciably diminishes the temperature of the process (Table 4) and leads to a change in the content of normal alcohols in the reaction products. The proportions of methanol and ethanol decrease with increasing pressure, while the proportion of propanol increases (Table 5). From the data presented, one can see that the most significant changes in almost all the process characteristics occur when the pressure increases to 20 atm. Further increase to 100 atm¹⁰⁹ or 200 atm¹⁵ gives no fundamental advantages, except for an increase in the yield of 2-propanol.

It is necessary to take into account the fact that the data¹⁰⁹ concerning the pressure dependences of the yields of the propane oxidation products, presented in Tables 4 and 5, have been obtained at temperatures ensuring an approximately constant rate of the process rather than under the conditions ensuring the optimal yields of the alcohols. Since according to the same study an increase in temperature increases the overall yield of normal alcohols (at 30 atm, it increases from 21% to 40% as the temperature increases from 260 to 286 °C), one should expect that, under the optimal conditions, the yield of the alcohols would be appreciably higher. As in the oxidation of methane or ethane, a decrease in the oxygen concentration in the mixture leads to an increase in the selectivity of the formation of the alcohols.¹⁰⁹ However, in the oxidation of propane, a relatively high selectivity of the formation of the alcohols (more than 30%–40%) can be achieved even for the propane:oxygen ≈ 1:1 ratio. The optimal conditions for the formation of the alcohols are ensured by the highest possible safe oxygen concentration.¹⁵

3. Butane, pentane, and heptane

There are only scattered data on the gas-phase oxidation of butane, pentane, and heptane at high pressures,^{15,90} permitting only a general idea about the expected yield of the alcohols and their proportions. The oxidation of *n*-butane, pentanes, and heptanes was studied¹⁵ using the same equipment and under approximately the same flow conditions as were used for the oxidation of propane. The following conditions are optimal for the formation of higher alcohols from alkanes: pressure from 130 to 200 atm, the lowest possible temperature, a reaction time less

Table 4. Selectivity of the formation of the products of the oxidation of the propane: air = 1:3.6 mixture (according to Newitt^{6,109}).

Products	Selectivity (%) ^a			
	A	B	C	D
The sum of aldehydes	20.5	21.8	13.5	13.7
The sum of normal alcohols	19.7	21.0	17.5	15.2
Isopropyl alcohol	1.3	2.8	6.2	16.0
Acetone	0.5	4.3	12.5	7.9
The sum of acids	4.3	17.0	19.0	18.9
Carbon dioxide	7.3	17.1	21.4	20.6
Carbon monoxide	21.3	16.0	9.9	7.7
Propene	25.1	0	0	0

^a Reaction conditions: A — 1 atm, 373 °C; B — 20 atm, 281 °C; C — 60 atm, 252 °C; D — 100 atm, 250 °C.

Table 5. Relative yields of alcohols in the oxidation of the mixture propane: air = 1:3.6 (according to Newitt^{6,109}).

Alcohol	Yield (%)			
	5 atm	30 atm	65 atm	
CH ₃ OH	76.3	58.0	55.3	50.1
C ₂ H ₅ OH	19.1	17.6	13.2	9.8
<i>n</i> -C ₃ H ₇ OH	4.6	4.3	7.3	12.2
iso-C ₃ H ₇ OH	—	20.0	24.2	27.9

than 10 s in a heated reactor, and the highest possible safe concentration of oxygen.

Apart from the compounds found also in the products of the oxidation of propane, the oxidation of n-butane with oxygen at a pressure of 33–160 atm yields also butanols, their proportion increasing with increase in pressure. In general, low pressures during the oxidation of alkanes are likely to be favourable for the formation of lower alcohols and organic acids, while high pressures promote the formation of higher alcohols and aldehydes.¹⁵ In addition, increasing the pressure decreases the temperature of the process: the temperature of the oxidation of n-butane decreases from 255 to 210 °C as the pressure increases from 33 to 160 atm. The composition of the products of the gas-phase oxidation of butane differs greatly from that in its liquid-phase oxidation at high pressures, the latter yielding mostly acetic acid and ethyl methyl ketone with minor amounts of alcohols.¹¹⁰

The oxidation of a mixture of 60% n-pentane and 40% isopentane, saturated beforehand with oxygen up to its concentration of 5%–6%, gives mostly alcohols, aldehydes, acetone, and acids containing 2–3 carbon atoms. Conversely, the products of the oxidation of heptane (the fraction boiling at 70 to 97 °C and containing almost all of the heptane isomers present in the head of the petrol fraction) contained mainly hexanols and heptanols with boiling points from 140 to 180 °C. The fact that these results differ from those obtained with pentane has been tentatively attributed to the occurrence of the reaction in the liquid phase.

In another study,⁹⁰ the oxidation of n-butane, carried out at 385 °C, 3.5–12.5 atm, with reaction times from 1.0 to 4.5 s, and under turbulent flow conditions in order to minimise the transverse concentration and temperature gradients, was rapidly quenched by cooling with water. The butane and oxygen concentrations varied between 1.5 mol % and 6 mol % each, and the rest was nitrogen. The pressure dependence of the yield of useful products (alcohols, aldehydes, acetone, and acids) passed through a maximum at $P = 8.8$ atm. No appreciable variations of the ratios between various products were observed. The most surprising finding was that there are limiting oxygen concentrations for the onset and termination of the process. The reaction did not proceed if the starting oxygen concentration was less than 1.5% and stopped when the concentration of O₂ fell below this value. Although incomplete conversion of oxygen has also been noted in other studies (Section III, 3), the existence of concentration limits in the high-pressure oxidation of alkanes was pointed out in none of them. The maximum yield of useful products was achieved for an oxygen concentration of 4.5%.⁹⁰

Under the optimal conditions ($P = 8.4$ – 9.8 atm, reaction time 1.2–1.8 s, concentrations of n-butane and oxygen mixed with nitrogen 4–5% each), 20% of the hydrocarbon taken was converted into useful products. The selectivity of the formation of these products was about 50%.

4. General features of the high-pressure oxidation of alkanes

On the basis of the experimental data considered in Sections III and IV, some general conclusions concerning the features of the oxidation of methane homologues at high pressures can be drawn (Table 6).

1. In the oxidation of all the C₁–C₅ alkanes under optimal conditions, a selectivity of the formation of liquid organic products not less than 50% can be achieved.

2. An increase in the oxygen concentration reduces the selectivity of the formation of liquid organic products, but, on passing from methane to pentane, the hydrocarbon : oxygen ratio for which a high selectivity is still achieved decreases sharply (~30 for methane, ~10 for ethane, and ~1 for propane, butane, and pentane). The degree of conversion of hydrocarbons into useful products increases in the same series (up to ~2% for methane, ~5% for ethane, and ~20% for propane, butane, and pentane).

3. The pressure and the temperature optimal for the production of liquid hydrocarbons decrease monotonically in the methane–pentane series (100 atm and 450 °C for methane,

Table 6. The optimal parameters of the high-pressure oxidation of alkanes for the formation of liquid organic products (averaged published data).

Hydro-carbon	P/atm	$T/^\circ\text{C}$	$[\text{C}_n\text{H}_{2n+2}]/[\text{O}_2]$	Degree of conversion into useful products (%) ^a
CH ₄	100	450	30	2
C ₂ H ₆	50	360	10	5
C ₃ H ₈	20	280	1	20
C ₄ H ₁₀	9	260	1	20

^a The maximum overall selectivity of the formation of liquid organic products from all the alkanes exceeds 50%.

50 atm and 360 °C for ethane, 20 atm and 280 °C for propane, and 9 atm and 260 °C for butane). As a rule, these data correspond to a process conducted under flow conditions with a reaction time of several seconds.

4. The influence of pressure on the product composition decreases in the methane–pentane series.

V. The mechanism of the high-pressure oxidation of methane

The understanding of the mechanism and, consequently, the optimisation of the conditions in a process as complex as the oxidation of methane, which has been one of classical objects of study in chemical kinetics for decades,¹¹¹ are impossible without the creation of an adequate kinetic model. Several theories which make it possible to explain the experimentally observed characteristic features have been suggested,²⁰ however, at present, the radical-chain mechanism of the gas-phase oxidation of alkanes is generally accepted.¹¹² In view of the complexity of the methane oxidation process, one can hardly expect that a universal model, suitable for the quantitative analysis of all cases of practical interest, will be developed in the near future. Therefore, the existing quantitative models have as a rule limited applicability. In conformity with the subject of our review, we shall consider only those models which involve the modelling of the oxidation of methane at high pressures and moderate temperatures.

1. The principles of the construction of quantitative kinetic models of complex gas-phase processes

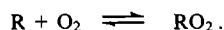
One can hardly expect that a mathematical description (kinetic model) of a complex chemical reaction will be in complete quantitative agreement with the real process. This is due to both the unavoidable inaccuracy of the kinetic parameters of a model and the errors of the real experiment. The kinetic parameters of complex models are mainly selected using the experimental rate constants for the elementary reactions, and it is desirable to have available also the results of theoretical calculations or empirical or semiempirical estimates for all the key elementary stages as well as those elementary stages, which have not been studied or have been poorly studied. The experience in modelling complex gas-phase reactions indicates that, if there is no confidence in the reliability of the available experimental rate constants for any elementary reactions or if these data deviate significantly from the theoretical estimates or calculations, the latter should be preferred.⁶⁴

Models adequately describing a whole set of reliable and noncontradictory experimental data are the most valuable. The adjustment of a model to make it describe accurately a group of results by manipulating the rate constants for individual reactions is not very promising. Kinetic analysis indicates³⁶ that the yields of products often depend strongly on the parameters of those elementary reactions in which these products are neither formed nor consumed. Moreover, a rather complex kinetic model possesses certain 'internal stability'. In some cases, several parallel pathways to the formation of particular products exist, and

attempts to attain a specified change of their yield by varying the parameters of 'obvious' reactions may fail.

2. Characteristic features of the oxidation of methane at high pressures and moderate temperatures

The rise in pressure influences the course of gas-phase reactions for several reasons. As the pressure grows, the frequency of intermolecular collisions and hence the rate of the process increase, which decreases the reaction temperature. This, in turn, leads to the possibility of the 'survival' of certain intermediates, which would decompose or undergo further transformations at a higher temperature. Pressure can also shift the equilibria of reversible reactions, and in the oxidation of hydrocarbons at moderate temperatures the most important are reactions of the type^{113, 114}



Pressure changes can also result in a redistribution of the contributions of various paths in multipath reactions (for example, in the reactions of biradicals with unsaturated hydrocarbons),¹¹⁵ in an increase in the yields of the products of radical recombination, and in the deactivation of excited molecules.¹¹¹ Finally, pressure is a critical factor for chain reactions.¹¹²

The possibility that, even at pressures of several hundreds of atmospheres, fundamentally new reaction paths may appear, due to the manifestation of the cage effect, when a short-lived molecular complex formed during the process has time to react with other reactants before it decomposes, has been discussed.¹¹⁶

At the same time, modelling of kinetic processes occurring at pressures of tens of atmospheres is facilitated in the vast majority of cases by the possibility of neglecting the pressure dependences of the rate constants for unimolecular and termolecular reactions and of using their values obtained for the infinite pressure limit.¹¹¹ The heterogeneous destruction of radicals and intermediates at these pressures is limited by the rate of their diffusion to the

surface and plays a relatively small role, which also facilitates the modelling.

Since the DMTM process occurs at moderate temperatures, its modelling is simplified, because a large number of elementary reactions requiring high activation energies as well as processes involving CH, C, C₂, and other species, formed only at high temperatures, can be excluded from the kinetic scheme. Moreover, when rich mixtures are employed, some reactions that are significant only at relatively high oxygen concentrations can also be ignored.

3. The model of the high-pressure oxidation of methane

The development of a quantitative model of the high-pressure oxidation of methane is a complicated problem in spite of the above possibilities of simplifying the kinetic scheme. Models developed for other conditions cannot be applied directly to the DMTM process; at best, they can serve as the starting point for such work. The most logical and comprehensive programme for the modelling of the DMTM has been reported by Vedenev and coworkers.^{33–37, 64} An extensive study on the modelling of the DMTM has been carried out at Trondheim University and the Norwegian Technological Institute.^{39, 68} Several other research groups have also presented their results.^{45, 54, 61, 94} Unfortunately, these publications are either difficult to obtain^{68, 94} or give no detailed description or justification.^{45, 54}

Detailed analysis and comparison of various models is beyond the scope of our review. We shall consider only the first model suggested for the DMTM process,³⁴ since it has been most fully described and tested in the modelling of a wide range of experimental results by the same workers and by other research groups.^{48, 60} In addition, the base model³⁴ and its modifications^{37, 64, 117, 118} have proved suitable for describing various processes ranging from the DMTM^{34, 37, 64} to the oxidative condensation of methane¹¹⁸ or the oxidation of methane below atmospheric pressure.¹¹⁷

The base model³⁴ (Table 7) takes into account all the main reliably established elementary reactions that play a significant

Table 7. The mechanism of the oxidation of methane³⁴ and the parameters of the equation $k = AT^n \exp(-E/RT)$.

Reaction	A^a	n	$E/\text{kJ mol}^{-1}$
1. $\text{CH}_4 + \text{O}_2 = \text{CH}_3 + \text{HO}_2$	1.00×10^{-10}	0	234.30
2. $\text{CH}_3 + \text{HO}_2 = \text{CH}_4 + \text{O}_2$	1.00×10^{-12}	0	0
3. $\text{CH}_3 + \text{O}_2 = \text{CH}_3\text{OO}^\bullet$	2.00×10^{-12}	0	0
4. $\text{CH}_3\text{OO}^\bullet = \text{CH}_3 + \text{O}_2$	8.90×10^{13}	0	130.96
5. $\text{OH}^\bullet + \text{CH}_4 = \text{H}_2\text{O} + \text{CH}_3$	1.32×10^{-17}	1.9	11.25
6. $\text{CH}_3\text{OO}^\bullet + \text{CH}_3\text{OO}^\bullet = \text{CH}_3\text{O}^\bullet + \text{CH}_3\text{O}^\bullet + \text{O}_2$	1.71×10^{-13}	0	0
7. $\text{CH}_3\text{OO}^\bullet + \text{CH}_3\text{OO}^\bullet = \text{CH}_2\text{O} + \text{CH}_3\text{OH} + \text{O}_2$	0.74×10^{-13}	0	0
8. $\text{CH}_3\text{OO}^\bullet + \text{CH}_3 = \text{CH}_3\text{O}^\bullet + \text{CH}_3\text{O}^\bullet$	4.50×10^{-11}	0	0
9. $\text{CH}_3\text{OO}^\bullet + \text{HO}_2 = \text{CH}_3\text{OOH} + \text{O}_2$	7.70×10^{-14}	0	-10.88
10. $\text{CH}_3 + \text{HO}_2 = \text{CH}_3\text{O}^\bullet + \text{OH}^\bullet$	3.00×10^{-11}	0	0
11. $\text{HO}_2 + \text{HO}_2 = \text{H}_2\text{O}_2 + \text{O}_2$	2.20×10^{-13}	0	-5.15
12. $\text{CH}_3 + \text{CH}_3 = \text{C}_2\text{H}_6$	4.00×10^{-11}	0	0
13. $\text{CH}_3\text{O}^\bullet + \text{HO}_2 = \text{CH}_3\text{OH} + \text{O}_2$	1.70×10^{-11}	0	0
14. $\text{CH}_3\text{O}^\bullet + \text{CH}_4 = \text{CH}_3\text{OH} + \text{CH}_3$	1.00×10^{-12}	0	46.02
15. $\text{CH}_3\text{O}^\bullet + \text{O}_2 = \text{CH}_2\text{O} + \text{HO}_2$	1.00×10^{-13}	0	10.88
16. $\text{CH}_3\text{O}^\bullet = \text{CH}_2\text{O} + \text{H}^\bullet$	1.00×10^{14}	0	125.52
17. $\text{CH}_3\text{OO}^\bullet + \text{CH}_4 = \text{CH}_3\text{OOH} + \text{CH}_3$	1.00×10^{-12}	0	89.96
18. $\text{CH}_3\text{OO}^\bullet + \text{CH}_2\text{O} = \text{CH}_3\text{OOH} + \text{CHO}^\bullet$	4.70×10^{-13}	0	50.21
19. $\text{HO}_2 + \text{CH}_2\text{O} = \text{H}_2\text{O}_2 + \text{CHO}^\bullet$	2.00×10^{-12}	0	46.02
20. $\text{CH}_3 + \text{CH}_2\text{O} = \text{CH}_4 + \text{CHO}^\bullet$	1.40×10^{-12}	0	29.10
21. $\text{CH}_3\text{O}^\bullet + \text{CH}_2\text{O} = \text{CH}_3\text{OH} + \text{CHO}^\bullet$	1.00×10^{-12}	0	15.06
22. $\text{OH}^\bullet + \text{CH}_2\text{O} = \text{H}_2\text{O} + \text{CHO}^\bullet$	1.25×10^{-11}	0	0.73
23. $\text{H}^\bullet + \text{CH}_4 = \text{H}_2 + \text{CH}_3$	1.30×10^{-10}	0	49.90
24. $\text{H}^\bullet + \text{O}_2 + \text{M} = \text{HO}_2 + \text{M}$	1.00×10^{-32}	0	-4.18
25. $\text{H}^\bullet + \text{CH}_2\text{O} = \text{H}_2 + \text{CHO}^\bullet$	3.27×10^{-11}	0	15.35
26. $\text{CHO}^\bullet + \text{O}_2 = \text{CO} + \text{HO}_2$	5.50×10^{-11}	-0.4	0
27. $\text{CHO}^\bullet + \text{M} = \text{CO} + \text{H}^\bullet + \text{M}$	4.00×10^{-10}	0	71.13
28. $\text{CH}_3\text{OOH} = \text{CH}_3\text{O}^\bullet + \text{OH}^\bullet$	4.00×10^{15}	0	179.91

Table 7 (continued).

Reaction	A^a	n	$E/\text{kJ mol}^{-1}$
29. $\text{H}_2\text{O}_2 = \text{OH}^\cdot + \text{OH}^\cdot$	3.00×10^{14}	0	207.94
30. $\text{OH}^\cdot + \text{H}_2 = \text{H}_2\text{O} + \text{H}^\cdot$	1.06×10^{-17}	2.0	6.23
31. $\text{HO}_2^\cdot + \text{H}_2 = \text{H}_2\text{O}_2 + \text{H}^\cdot$	5.60×10^{-12}	0	93.30
32. $\text{CH}_3\text{OO}^\cdot + \text{H}_2 = \text{CH}_3\text{OOH} + \text{H}^\cdot$	3.60×10^{-12}	0	93.30
33. $\text{CH}_3\text{O}^\cdot + \text{H}_2 = \text{CH}_3\text{OH} + \text{H}^\cdot$	3.60×10^{-12}	0	41.80
34. $\text{CH}_3^\cdot + \text{H}_2 = \text{CH}_4 + \text{H}^\cdot$	3.60×10^{-12}	0	45.20
35. $\text{CH}_3\text{OO}^\cdot + \text{CH}_3\text{O}^\cdot = \text{CH}_3\text{OOH} + \text{CH}_2\text{O}$	1.50×10^{-12}	0	0
36. $\text{CH}_4 + \text{HO}_2^\cdot = \text{CH}_3^\cdot + \text{H}_2\text{O}_2$	3.00×10^{-12}	0	89.96
37. $\text{CH}_3^\cdot + \text{CH}_3\text{OH} = \text{CH}_4 + \text{CH}_2\text{OH}^\cdot$	3.30×10^{-13}	0	41.00
38. $\text{CH}_3\text{OO}^\cdot + \text{CH}_3\text{OH} = \text{CH}_3\text{OOH} + \text{CH}_2\text{OH}^\cdot$	5.00×10^{-13}	0	60.25
39. $\text{CH}_2\text{OH}^\cdot + \text{O}_2 = \text{CH}_2\text{O} + \text{HO}_2^\cdot$	2.00×10^{-12}	0	0
40. $\text{HO}_2^\cdot + \text{CH}_3\text{OH} = \text{H}_2\text{O}_2 + \text{CH}_2\text{OH}^\cdot$	1.50×10^{-12}	0	60.25
41. $\text{OH}^\cdot + \text{CH}_3\text{OH} = \text{H}_2\text{O} + \text{CH}_2\text{OH}^\cdot$	5.70×10^{-12}	0	5.86
42. $\text{OH}^\cdot + \text{CH}_3\text{OH} = \text{H}_2\text{O} + \text{CH}_3\text{O}^\cdot$	1.70×10^{-11}	0	13.81
43. $\text{CH}_3\text{O}^\cdot + \text{CH}_3\text{OH} = \text{CH}_3\text{OH} + \text{CH}_2\text{OH}^\cdot$	6.60×10^{-13}	0	22.17
44. $\text{H}^\cdot + \text{CH}_3\text{OH} = \text{H}_2 + \text{CH}_2\text{OH}^\cdot$	2.16×10^{-11}	0	22.00
45. $\text{H}^\cdot + \text{H}_2\text{O}_2 = \text{OH}^\cdot + \text{H}_2\text{O}$	3.00×10^{-10}	0	26.36
46. $\text{OH}^\cdot + \text{H}_2\text{O}_2 = \text{H}_2\text{O} + \text{HO}_2^\cdot$	3.70×10^{-12}	0	2.16
47. $\text{H}^\cdot + \text{H}_2\text{O}_2 = \text{H}_2 + \text{HO}_2^\cdot$	1.70×10^{-11}	0	20.92
48. $\text{CH}_3\text{OO}^\cdot + \text{H}_2\text{O}_2 = \text{CH}_3\text{OOH} + \text{HO}_2^\cdot$	2.50×10^{-13}	0	54.39
49. $\text{CH}_3\text{O}^\cdot + \text{H}_2\text{O}_2 = \text{CH}_3\text{OH} + \text{HO}_2^\cdot$	2.50×10^{-13}	0	16.74
50. $\text{CH}_3^\cdot + \text{H}_2\text{O}_2 = \text{CH}_4 + \text{HO}_2^\cdot$	2.50×10^{-13}	0	11.71
51. $\text{OH}^\cdot + \text{CO} = \text{H}^\cdot + \text{CO}_2$	2.50×10^{-17}	1.3	-3.20
52. $\text{HO}_2^\cdot + \text{CO} = \text{OH}^\cdot + \text{CO}_2$	1.70×10^{-10}	0	96.20
53. $\text{CH}_3\text{O}^\cdot + \text{CO} = \text{CH}_3^\cdot + \text{CO}_2$	2.60×10^{-11}	0	49.37
54. $\text{CH}_3\text{O}^\cdot + \text{CH}_3\text{O}^\cdot = \text{CH}_3\text{OH} + \text{CH}_2\text{O}$	3.00×10^{-11}	0	0
55. $\text{CH}_3^\cdot + \text{CH}_3\text{O}^\cdot = \text{CH}_4 + \text{CH}_2\text{O}$	2.80×10^{-11}	0	0
56. $\text{CH}_3^\cdot \xrightarrow{\text{heter.}} \text{radical destruction}$	5.00×10^{-3}	0	0
57. $\text{CH}_3\text{OO}^\cdot \xrightarrow{\text{heter.}} \text{radical destruction}$	5.00×10^{-3}	0	0
58. $\text{HO}_2^\cdot \xrightarrow{\text{heter.}} \text{radical destruction}$	5.00×10^{-3}	0	0
59. $\text{CH}_3\text{OOH} \xrightarrow{\text{heter.}} \text{radical destruction}$	5.00×10^{-3}	0	0
60. $\text{H}_2\text{O}_2 \xrightarrow{\text{heter.}} \text{H}_2\text{O}$	1.50×10^{-3}	0	0
61. $\text{H}_2\text{O}_2 \xrightarrow{\text{heter.}} \text{H}_2\text{O} + \text{O}_2$	1.50×10^{-3}	0	0

^a Preexponential factors are expressed in s^{-1} for unimolecular reactions, $\text{cm}^3 \text{ molecule}^{-1} \text{ s}^{-1}$ for bimolecular reactions, or $\text{cm}^6 \text{ molecule}^{-2} \text{ s}^{-1}$ for the termolecular reaction 24.

role at high pressures and moderate temperatures, including heterogeneous destruction of radicals and peroxides on the reactor surface. Some reactions, discussed in the literature but not properly justified, have not been included in the model.

a. The main stages of the process

In a kinetic analysis of a complex process, the possibility of identifying the minimum number of elementary stages necessary and sufficient to describe the process and also the identification of the elementary stages the variation of the rate constants for which influences most appreciably the process kinetics or the product composition (the rate-limiting stages), are of prime importance. This problem is solved by analysing the sensitivity of the process kinetics, the rate of product accumulation, and other characteristic features to the variation of the rate constants for individual reactions.³⁵

Analysis of the process kinetics indicates³⁵ that the rate-determining stages include the decomposition of methyl hydro-

peroxide (stage 28 in Table 7) and of hydrogen peroxide (29) and also the formation of methyl hydroperoxide (17, 18, 38, 48) and hydrogen peroxide (36, 40). All the above stages of the peroxide formation and decomposition reactions belong to the group of reactions responsible for degenerate branching. The hydrogen peroxide formation (stage 19) is not included in the set of rate-determining stages, since at low temperatures the effectiveness of branching associated with the decomposition of hydrogen peroxide is low and the effective consumption of formaldehyde, one of the main degenerate-branching agents, exerts a greater influence.

The most important quadratic chain termination reactions are stages 6, 7, and 11. Although in stage 6 two relatively inactive $\text{CH}_3\text{O}_2^\cdot$ radicals are converted into two reactive $\text{CH}_3\text{O}^\cdot$ radicals, the latter are partly converted into HO_2^\cdot radicals (the competing stages 14 and 15), which are effectively destroyed in stage 11.

Due to the rapid decomposition of methyl hydroperoxide, stage 9 is a chain propagation reaction, though formally two

other reactions also cannot be ignored. The main contribution to the formation of formaldehyde is made by stages 15 and 39, while its consumption occurs mostly via stage 19. Formaldehyde is mostly produced via independent parallel processes, primarily stage 15, rather than via a path involving the oxidation of methanol (stage 39), and the rate of its formation exceeds that of methanol. The fact that the final yield of formaldehyde in the DMTM is almost an order of magnitude lower than that of methanol (see Section III) is determined only by the higher rate of the further transformation of formaldehyde. This is properly illustrated by the experimental data,¹¹⁹ indicating that in the initial stage of the process, when the degree of conversion of methane is less than 1%, the selectivity of the formation of formaldehyde (~54%) exceeds appreciably the selectivity of the formation of methanol (~36%) but falls very rapidly as the degree of conversion of methane increases to 4%–6%, which occurs in the final stage of the DMTM process.

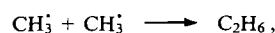
Hydrogen peroxide plays an important role in the process kinetics and, in particular, in the self-acceleration mechanism, despite the fact that it has not been experimentally detected in the studies on the high-pressure oxidation of methane. Hydrogen peroxide is formed mostly in stages 11, 19, 36, and 40. Carbon monoxide is formed in stages 26 and 27 and carbon dioxide is produced in stages 51–53. Certain other reactions in which CO and CO₂ are formed, in particular, the addition of HO₂ radicals to H₂CO and the addition of HCO radicals to O₂, should probably also be taken into account, although their mechanisms have not yet been reliably elucidated.

The model discussed above³⁴ has been supplemented⁶⁴ by two heterogeneous termination reactions and a set of reactions describing in more detail the kinetics of the formation and decomposition of carbon monoxide and a significant side product — formic acid. A mechanism of the formation of the latter has been suggested.⁴⁷ However, analysis has shown that allowance for this set of reactions has no appreciable influence on the kinetics of the consumption of the reactants and the formation of the remaining products.

d. Modelling of the high-pressure oxidation of ethane and methane–ethane mixtures

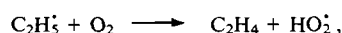
The quantitative models of the oxidation of the closest methane homologues suggested by various groups of researchers do not cover the region of relatively high pressures and hence they unfortunately cannot be applied directly to the analysis of the partial oxidation of methane homologues to alcohols. Therefore, Vedenev et al.¹¹⁸ have developed a preliminary model of the high-pressure oxidation of ethane based on the model of the oxidation of methane at high pressures.³⁴

The recombination of the methyl radicals



has been regarded as the main reaction yielding ethane. At pressures above 10 atm, the values corresponding to the infinite-pressure limit were used for the pressure-dependent rate constants. The reactions of all the reactive species, namely H[•], O[•], OH[•], HO₂[•], CH₃[•], CH₃O[•], and CH₃OO[•], with ethane were taken into account. The numerical values of the rate constants for these reactions were taken from the published data, except for the reactions of ethane with HO₂[•] and CH₃OO[•], the rate constants for which were calculated from the rate constants for similar reactions involving methane with allowance for the 8.4 kJ mol⁻¹ decrease in the activation energy, in conformity with the Polanyi–Semenov rule.

The formation of ethene was described by the reactions



although the latter is probably not an elementary stage. This model includes both the forward and the corresponding reverse reactions related by equilibrium constants (altogether 188 elementary stages). The model does not take into account the formation of C₃ or higher hydrocarbons.

The model under consideration¹¹⁸ makes it possible to describe quantitatively a wide range of processes, from the oxidation of methane to methanol (20–100 atm, 650–750 K) to its oxidative condensation to ethane and ethene (1–5 atm, 900–1200 K), as well as flame propagation at not very high temperatures and cool-flame phenomena during the oxidation of methane. This model was used for the kinetic analysis of the oxidation of ethane and methane–ethane mixtures at high pressures. Preliminary results indicate that, when mixtures are used, the total selectivity of the formation of alcohols (methanol and ethanol) increases substantially and reaches a maximum when the ethane concentration in methane is 30%–40%, that it is possible to retain high selectivities for high degrees of conversion of the hydrocarbon (more than 8%), and that at $P > 20$ atm the selectivity depends only slightly on pressure.

VI. Analysis of the results of kinetic modelling of the high-pressure oxidation of methane

The present-day level of experimental studies on the DMTM process is deficient in systematic combined investigations carried out within the framework of a unified programme and there are significant discrepancies between the results which are difficult to explain. Therefore theoretical analysis of the process is of particular importance. Such analysis should certainly be based on models, which describe adequately the most reliable experimental data, but, unfortunately, experimental details which would allow a direct comparison of these data with the results of kinetic analysis are not always known. In this section, we present the results of the kinetic modelling of the DMTM process based on the model developed by Vedenev et al.³⁴ (Table 7) or its modification.⁶⁴

1. Modelling of the product yields and the process time

The kinetic modelling of the consumption of oxygen and product (methanol, formaldehyde, and carbon oxides) accumulation³⁴ was performed for the experimental conditions adopted in two previous studies^{4,25} (Figs 14 and 15). The model reflects correctly

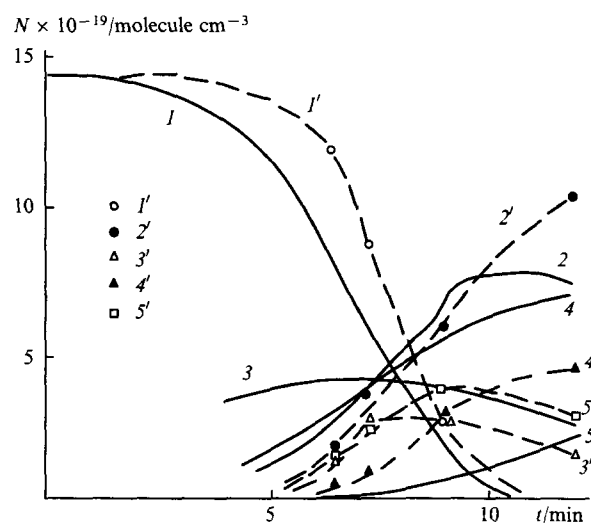


Figure 14. Kinetic curves for the consumption of oxygen (I , I') and the accumulation of methanol (2 , $2'$), formaldehyde (3 , $3'$), CO (4 , $4'$), and CO₂ (5 , $5'$) during the oxidation of methane at $T = 614$ K, $P = 100$ atm, and for $[\text{CH}_4]:[\text{O}_2] = 8.1:1.0$. Dashed lines correspond to experimental data⁴ and the continuous lines to calculations.³⁴

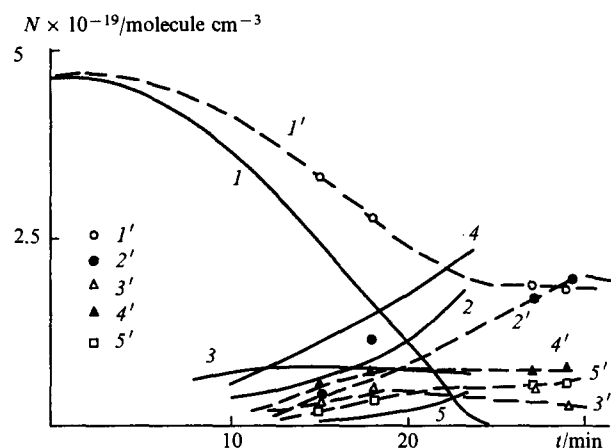


Figure 15. Kinetic curves for the oxidation of methane at $T = 585$ K, $P = 367$ atm, and for $[\text{CH}_4]:[\text{O}_2] = 9:1$. The designations are the same as in Fig. 14. Dashed lines correspond to experimental data,²⁵ and continuous lines to calculations.³⁴

the main features of the process: the occurrence of self-acceleration, the duration of induction periods and of the whole process, the characteristic features of the product accumulation, and their dependences on temperature, pressure, and composition of the mixture. The fact that the appreciable concentrations of hydrogen peroxide (comparable to those of methanol) predicted by the model³⁴ were not detected in the high-pressure experiments^{4,22} may be explained by its rapid decomposition on metallic surfaces.

On the basis of an extended version of the model under consideration,³⁴ the delay period of the self-ignition of methane under the conditions reported by Melvin²² has been calculated.³⁷ The resulting self-ignition delay periods exceed the experimental values by a factor of only ~ 1.5 , which must be regarded as a very close agreement. In the same study,³⁷ the experimentally observed²² increase in the delay of self-ignition with increase in the oxygen concentration in the mixture²² (see Fig. 12) was theoretically interpreted for the first time. It was shown that during the self-ignition delay period, oxygen inhibits the process, because the reaction of the alkoxyl radicals with molecular oxygen is virtually a chain termination reaction, since the reactive chain-propagating $\text{CH}_3\text{O}^\bullet$ radical is converted via this reaction into the less reactive HO_2^\bullet radical, which is destroyed rapidly.

Figs 16–18 present the main results of the modelling of the DMTM process⁶⁴ based on the extended version of the model developed by Vedenev et al.³⁴ The variation of temperature within rather wide limits, for the optimal pressure and mixture composition and virtually complete oxygen conversion $\{[\text{O}_2]/[\text{O}_2]_0 < 5\%\}$, does not influence substantially the yields of the products (Fig. 16). The selectivity of the formation and the yield of methanol pass through a weak maximum in the region of 480°C . Conversely, the selectivity of the formation of formaldehyde increases monotonically over the whole temperature range, its increase accelerating with rise in temperature. A redistribution of the reaction paths favouring the formation of formaldehyde, ethane, and ethene^{49,50} is known to occur exactly in the temperature range above 500°C .^{49,50} Since at $P > 30$ atm and $T < 500^\circ\text{C}$, the target products, that is, methanol and formaldehyde, virtually do not decompose in the reactor after the complete conversion of oxygen,⁴⁰ the temperature range $420\text{--}480^\circ\text{C}$ may be considered optimal. The significant decrease in temperature (by up to 100°C) known from the literature and due to the promoting action of higher hydrocarbons (on passing to natural gas) or to the use of catalysts does not lead to a substantial change in the proportions of the products.

An increase in the temperature is naturally accompanied by a sharp decrease in the reaction time t_r (here t_r is the time required for 95% oxygen conversion). According to an estimate, the

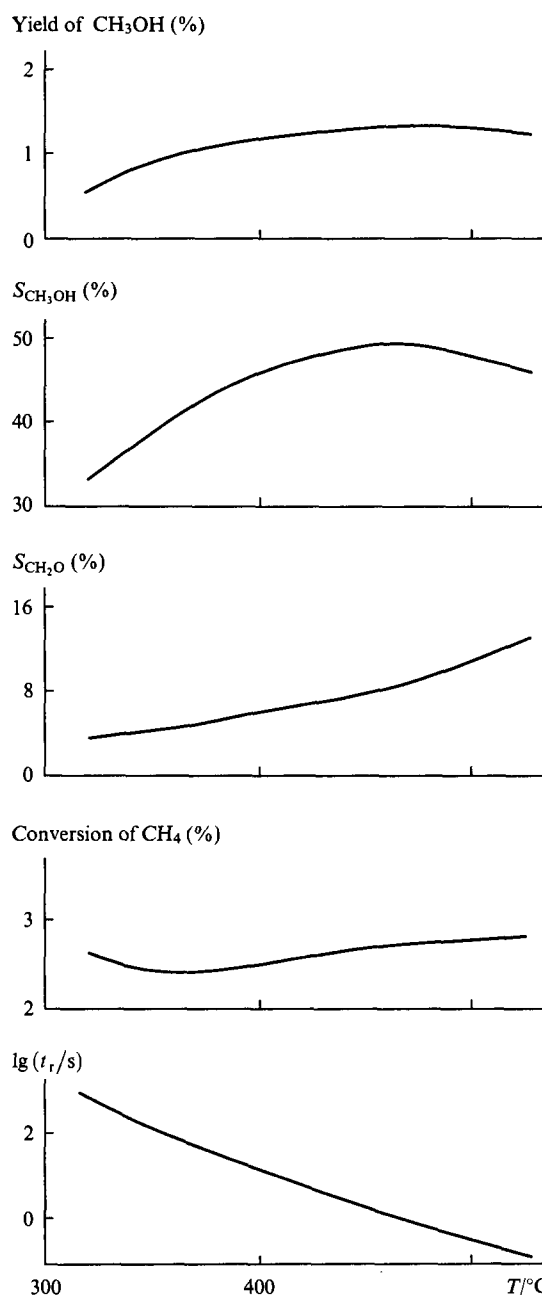


Figure 16. Calculated temperature dependences of some parameters of the DMTM process at $P = 100$ atm and $[\text{O}_2] = 3\%$.⁶⁴

effective activation energy $E_{\text{eff}} \approx 167$ kJ mol⁻¹. This is in good agreement with the experimental value found from the temperature dependence of the self-ignition delays (from 163 to 188 kJ mol⁻¹).²²

An increase in the oxygen concentration results primarily in an increase in the degree of conversion of methane (Fig. 17) and in heating of the mixture. The calculations were carried out for two extreme process regimes, namely isothermal and adiabatic regimes. Although significant difficulties are associated with the practical realisation of an isothermal regime at high pressures, these calculations are of undoubted interest, since they demonstrate the possibility, in principle, of improving a number of characteristics of the process, primarily, the yield of methanol, relative to the process conducted under nonisothermal conditions. At $[\text{O}_2] \leq 3\%$, when the real temperature rise does not exceed 120°C , virtually identical results are achieved in both regimes. Allowance for nonisothermal conditions affects only the

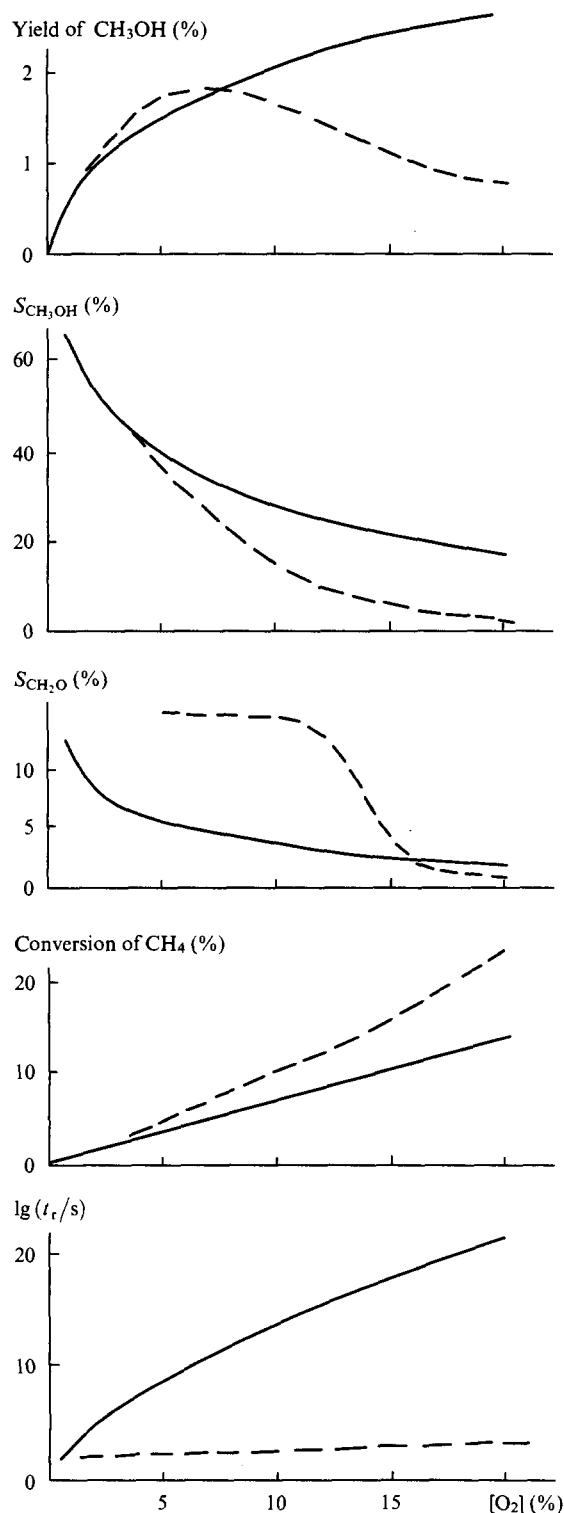


Figure 17. Calculated dependences of some parameters of the DMTM process on the initial oxygen concentration ($P = 100$ atm, $T = 420$ °C). Continuous lines correspond to the isothermal regime and dashed lines to the adiabatic regime.⁶⁴

selectivity of the formation of formaldehyde and the reaction time (Fig. 17). Both versions of the calculation confirm the experimentally observed sharp decrease in the selectivity of the formation of methanol with increase in the oxygen concentration. At the same time, the isothermal calculation indicates that the yield of methanol grows slowly and monotonically as the oxygen concentration increases. The adiabatic calculation gives a qualitatively different picture. In this case, the selectivity of the

formation of methanol drops so sharply that at $[O_2] > 5\%$ its yield also decreases. Thus, the use of mixtures with a higher concentration of oxygen to increase the yield of methanol is not expedient unless the problem of heat removal has been fully solved.

It is noteworthy that, according to the calculations, one of the initial reactants, namely oxygen, is virtually an inhibitor, since an increase in its concentration leads to a decrease in the rate of reaction (an increase in its duration). Even a substantial increase in the temperature of the gas mixture by its adiabatic heating does not balance entirely the inhibitory effect of oxygen.

The calculated pressure dependences of the yields of the main products are in good agreement with the experimental results

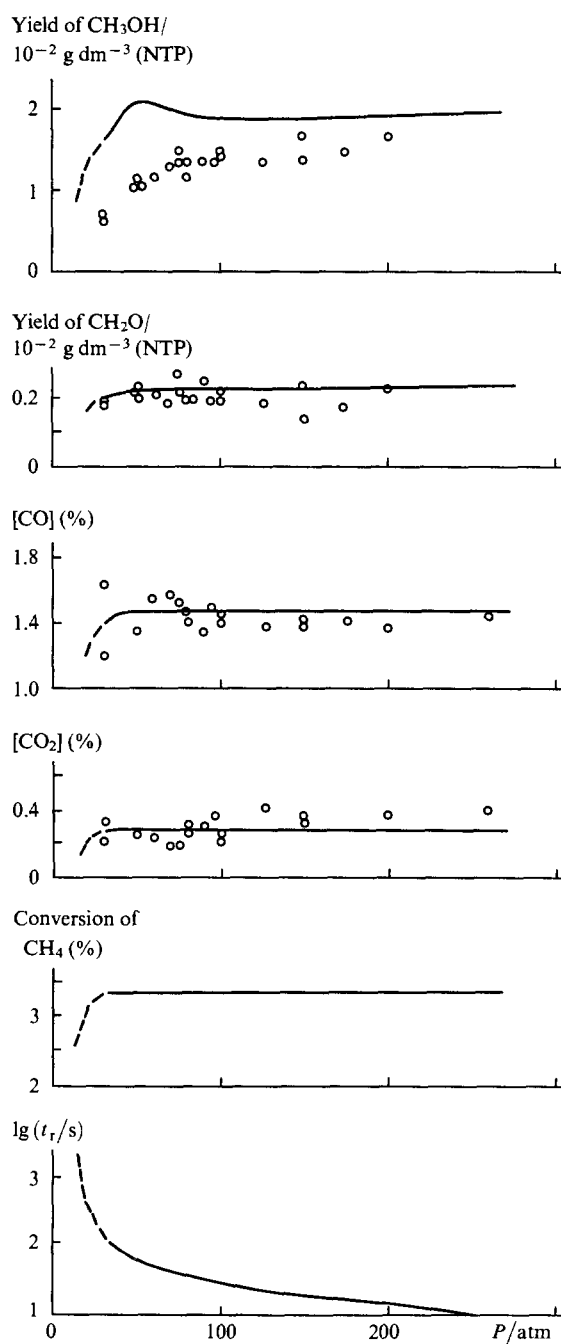


Figure 18. Calculated and experimental pressure dependences of some parameters of the DMTM process ($T = 420$ °C, $[O_2] = 3\%$). Continuous lines correspond to calculations⁶⁴ and circles correspond to experimental data.⁶²

obtained in a pilot plant⁶² (Fig. 18). According to the authors, the lower (by ~20%) yield of methanol is caused to a large extent by the imperfect separation unit, which does not exclude up to 10%–20% of the methanol formed being carried away with the gas phase.

Since the version of the model³⁴ used by Arutyunov et al.⁶⁴ (Table 7) is meant for describing processes occurring at pressures not less than 30 atm, the calculations carried out for pressures of 20 atm and especially 10 atm yield only qualitative results. Nevertheless, they reflect correctly the tendency towards a sharp decrease in the conversion of methane and in the product yields at pressures below 30 atm (see the dashed lines in Fig. 18). The sharp increase in the reaction time implies that, in this pressure region, there is a critical transition from the fast branched-chain reaction to a much slower chain-radical process.⁵⁷

Together with the experimental results, Fig. 1 presents a calculated plot of the selectivity of the formation of methanol in the DMTM against the degree of conversion of methane.⁶⁴ It is clearly seen that the vast majority of the experimental points lie near the theoretical plot.

2. The role of pressure in the critical transitions between the steady-state regimes in the oxidation of methane

As shown in the previous section, the high-pressure oxidation of methane generally occurs by a branched-chain mechanism. In the present section, we consider the results of a theoretical study of the influence of pressure on the regime in which the reaction proceeds.⁵⁷

The calculations were carried out for a mixture with the composition $\text{CH}_4 : \text{O}_2 = 9 : 1$ in the temperature range 600–750 K and the pressure range 1–100 atm. Fig. 19 shows the calculated pressure dependence of the reaction time (the time required for 95% oxygen conversion). It is clearly seen that there exists a narrow pressure range (the critical pressure P_{cr}) in which the process rate changes by several orders of magnitude. This can be caused only by a change in the reaction mechanism. The critical pressure is temperature dependent: it decreases from 6.2 atm at 600 K to 1.4 atm at 750 K (Fig. 20).

A change in the reaction mechanism should be manifested primarily by a change in the reaction kinetics. At pressures below P_{cr} , the shape of the kinetic curves is typical for nonbranched-chain reactions (more precisely, for reactions with weakly degenerate branching) (Fig. 21a). At pressures above P_{cr} , the self-acceleration of the reaction becomes much more clear-cut and the initial rate increases by a factor of approximately 10^3 (Fig. 21b).

The appearance of the critical phenomena discovered by calculations may be explained by analysing the initial stage of

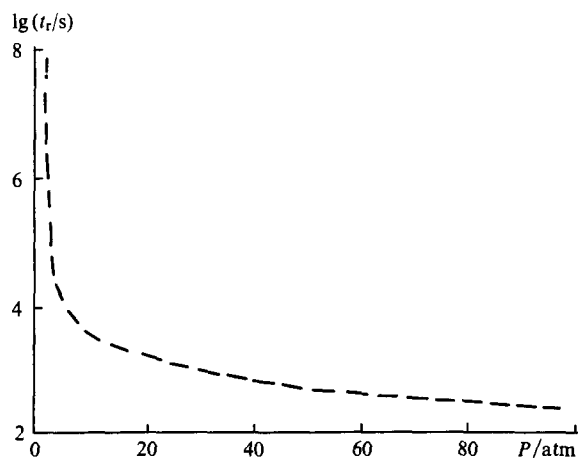


Figure 19. Pressure dependence of the reaction time at $T = 650$ K.⁵⁷

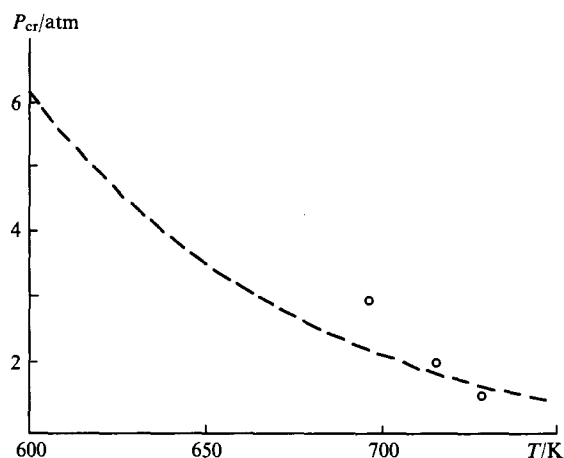


Figure 20. Temperature dependence of the critical pressure.⁵⁷ The circles represent experimental¹¹⁹ temperatures of the onset of the reaction at $P = 1.5, 2$, and 3 atm.

the process³³ (Section V, 3b), where a steady-state branched-chain reaction occurs and the increase in the concentration of radicals is limited by the quadratic recombination of active centres.

In the one-centre approximation, one can easily obtain the expression

$$\frac{d[\text{CH}_3\text{OO}']}{dt} = 2k_1[\text{CH}_4]_0[\text{O}_2]_0 + \varphi[\text{CH}_3\text{OO}'] - 2k_7[\text{CH}_3\text{OO}']^2,$$

which implies that the character of the process is determined by the branching factor

$$\varphi = 2k_{17}[\text{CH}_4]_0 - k_{57},$$

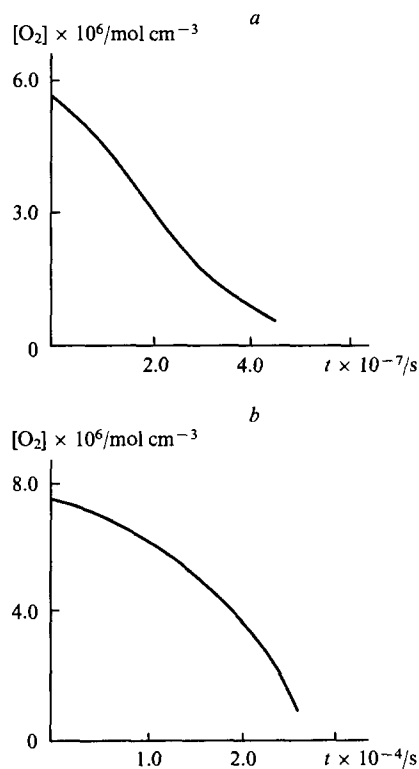


Figure 21. Kinetics of the consumption of oxygen at $T = 650$ K:⁵⁷ (a) $P = 3$ atm; (b) $P = 4$ atm.

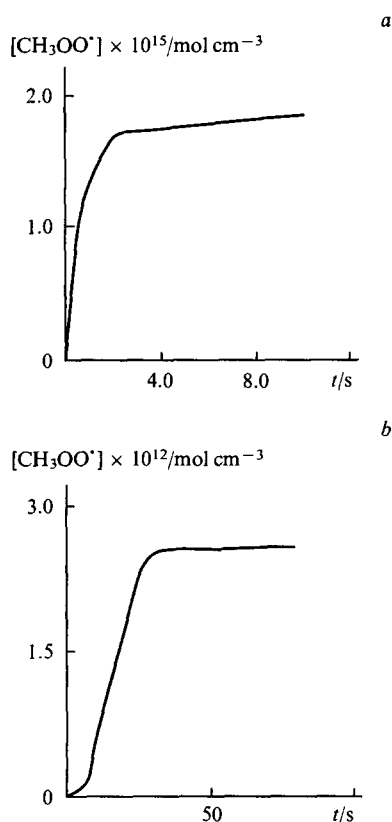


Figure 22. Kinetics of the accumulation of the methylperoxy radicals at $T = 650\text{ K}$: ⁵⁷ (a) $P = 3\text{ atm}$; (b) $P = 4\text{ atm}$.

(the numbers of the reactions and of the corresponding constants are given in Table 7).

At low pressures, $\varphi < 0$ and the concentration of the chain-propagating radicals is governed by the ratio of the rates of their generation and heterogeneous destruction. As the pressure increases, there is a transition to the region in which $\varphi > 0$, and the concentration of the propagating $\text{CH}_3\text{OO}^\bullet$ radicals is determined by the ratio of the rate of branching to the rate of their quadratic destruction. Since the rate of branching is several orders of magnitude higher than the rate of generation, the concentrations of the $\text{CH}_3\text{OO}^\bullet$ radicals at $\varphi > 0$ and $\varphi < 0$ differ from each other by approximately the same factor (Fig. 22). Figure 22 illustrates the calculations carried out using the full process scheme; however, the one-centre approximation for the initial stage of the DMTM gives the critical pressures $P_{\text{cr}}(600\text{ K}) = 6\text{ atm}$ and $P_{\text{cr}}(700\text{ K}) = 2\text{ atm}$, which are in good agreement with the values found by calculations based on the full model.⁵⁷

The calculated critical pressures correspond to the experimental plot of the temperature of the onset of reaction in the pressure range of 1.5–3 atm¹¹⁹ (Fig. 20), despite the fact that the precise value of the critical pressure may depend on certain parameters that are difficult to take into account, for example, the reactor design. From the calculations performed, it is clear that the experimental conditions influence very strongly the initial stage and, consequently, the whole oxidation process. For example, whereas at $T = 650\text{ K}$ and $P = 3\text{ atm}$ the presence of a catalyst or a change in the reactor design has a substantial influence on the process, when the pressure is increased to 4 atm (this leads to an increase in the quasi-steady-state concentration of radicals by a factor of 10^3 – 10^4) this influence can disappear almost entirely.

The results presented by Vedenev et al.⁵⁷ account for the fact that the introduction of catalysts, or homogeneous promoters, or other initiation methods (Section III) does not influence appreciably the DMTM process, carried out at sufficiently high

pressures. In fact, at $\varphi > 0$, an additional generation of radicals, even in much larger quantities than in the thermal process, cannot compete with their generation in the branched-chain reaction itself. Apparently, the fact that the use of catalysts becomes unnecessary when the oxidation of methane to formaldehyde is carried out at $P > 3\text{ atm}$ in the temperature range 873–923 K can be explained in a similar way.⁴⁴

3. Theoretical study of the possibility of the occurrence of cool-flame phenomena during the high-pressure oxidation of methane

As stated in Section V, the mechanism of the oxidation of methane is highly nonlinear, because virtually all the main chain initiation, chain propagation, chain termination, and branching reactions are nonlinear. Experimental results also indicate that, during the oxidation of methane, nonlinear phenomena can arise. These phenomena include the temperature oscillations at high pressures,⁴² the appearance of cool flames,^{101–103} and the existence of a region where the reaction rate has a negative temperature coefficient.¹⁰⁴ It is natural to assume that similar regimes may also arise in the oxidation of methane under other conditions that have not yet been studied, for example, at high pressures.

The main sign of the existence of cool flames in the oxidation of hydrocarbons is that a rapid increase in temperature is replaced by the retardation of the process before the reactants have undergone complete chemical conversion. The attainment of the peak conversion rate is usually accompanied by the luminescence of excited formaldehyde. Then the reaction either stops or, conversely accelerates again, up to the hot ignition of the mixture. Two or more cool-flame flashes can occur. In those cases where the appearance of cool flame is followed by the self-ignition of the mixture, the process includes at least two stages, namely, the cool-flame stage and the hot-ignition stage.^{99, 100}

Basevich et al.¹⁰⁵ carried out mathematical modelling of the homogeneous oxidation of methane under nonisothermal conditions, with heat removal from the reactor surface, based on the kinetic scheme for the oxidation of methane to methanol suggested previously³⁴ (Table 7).

The calculations were first carried out for conditions under which successive cool-flame oxidation and ignition have been observed experimentally in methane–oxygen mixtures.¹⁰¹ At initial temperatures $T_0 < 710\text{ K}$, the reaction does not occur for up to 700 s. In the temperature range $T_0 = 728$ – 753 K , flashes with incomplete heat evolution are observed and are followed by retardation of the reaction, which is accompanied by a temperature drop caused by the cooling of the reaction mixture by the reactor walls (Fig. 23). At $T_0 > 758\text{ K}$, ignition occurs (the arrows

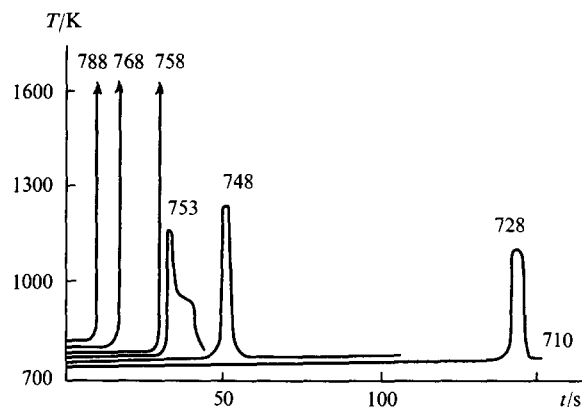


Figure 23. Calculated reaction time dependences of the reaction temperature for methane–oxygen mixtures¹⁰⁵ under the following experimental conditions: $[\text{CH}_4]_0 = 67\%$, $[\text{O}_2]_0 = 33\%$, $P = 0.92\text{ atm}$. The numerals denote the initial temperatures (K).

at the ends of the curves denote a further increase in the temperature). The calculations are in fairly good agreement with the experimental results.¹⁰¹

There are almost no experimental data dealing with cool-flame phenomena under the conditions of the high-pressure oxidation of methane. Therefore, a series of calculations involving gradual transition to high pressures were performed in the modelling, so that signs of the appearance of a cool flame could be detected in each stage.¹⁰⁵ The calculations were carried out for the pressures $P_0 = 1, 1.8, 4.6, 9.2, 18.4, 70$, and 100 atm, at the constant initial temperature $T_0 = 710$ K, and at the initial concentrations $[\text{CH}_4]_0 = 67\%$ and $[\text{O}_2]_0 = 33\%$.

In the analysis of the results of modelling, a general rule was discovered: an increase in pressure leads to the self-ignition of the mixture, the ignition being achieved after progressively shorter periods. Even intense heat transfer (within the limits of reasonable heat-transfer coefficients) from the gas to the reactor walls cannot stop ignition and cause a reverse temperature variation, although it does increase the induction periods (the times required for the development of the reaction before self-ignition). However, the increase in temperature is accompanied by explicit signs of the cool-flame stage. Fig. 24 shows a typical dependence of the temperature of the mixture on reaction time. When the time scale is expressed in seconds, there are no signs of the appearance of a cool flame, and the curve can seemingly be referred to a normal self-ignition process. However, on the microsecond time scale one can see that, after $t = 4.65$ s, the increase in the temperature to 1400 K is followed by retardation of the reaction, and the next flash occurs only ~ 10 μs later. Thus, in the present case, the duration of the first stage is 4.65 s and that of the second is ~ 10 μs . Of course, it is extremely difficult to detect these two stages experimentally. The calculated kinetic curves and the time dependences of the reaction temperature under the conditions of the self-ignition of methane-oxygen mixtures at 70 atm are presented in Fig. 25. A similar $T(t)$ plot is also obtained in the absence of heat losses. Further analysis showed that similar features are also observed at low pressures, for example, under the conditions indicated in the caption to Fig. 23 (at $T \geq 750$ K), when the ignition on the time scale expressed in seconds seems to be a one-stage process.

The calculations were also carried out for $P_0 = 100$ atm and the temperatures $T_0 = 683\text{--}710$ K, but for lower oxygen contents, which is typical for the direct homogeneous oxidation of methane to methanol. It turned out that, as the oxygen content decreases, the signs of a cool flame become increasingly less clear-cut and for $[\text{O}_2] \leq 5\%$ they disappear entirely.

The elucidation of the mechanism of the appearance of cool flames and the subsequent retardation of the reaction remains the

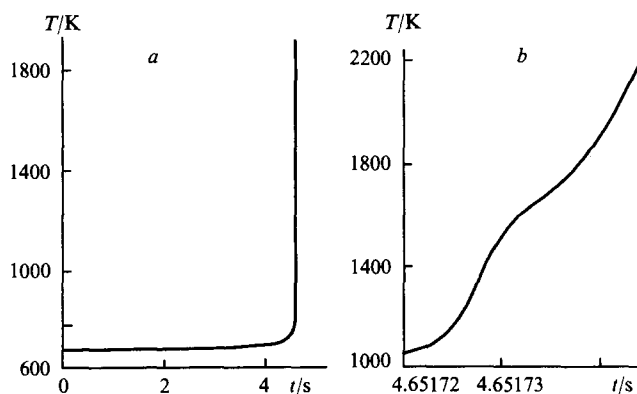


Figure 24. Calculated reaction time dependences of the reaction temperature on time scales in terms of seconds (a) and microseconds (b) for methane-oxygen mixtures at a high pressure.¹⁰⁵ $[\text{CH}_4]_0 = 67\%$, $[\text{O}_2]_0 = 33\%$, $P = 70$ atm, $T_0 = 710$ K.

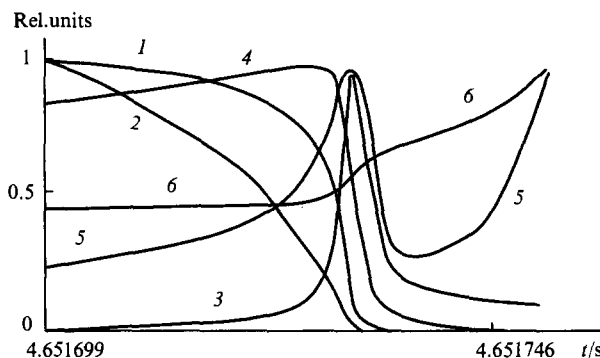


Figure 25. Calculated kinetic curves (1–5) and reaction time dependence of the reaction temperature (6) under the conditions of the self-ignition of methane-oxygen mixtures at a high pressure.¹⁰⁵ $[\text{CH}_4]_0 = 67\%$, $[\text{O}_2]_0 = 33\%$, $P = 70$ atm, $T_0 = 710$ K. The maximum concentrations corresponding to 1 on the ordinate axis (mol cm^{-3}): (1) $[\text{H}_2\text{O}_2] = 2.279 \times 10^{-6}$; (2) $[\text{CH}_3\text{OOH}] = 1.412 \times 10^{-8}$; (3) $[\text{HO}_2] = 1.619 \times 10^{-6}$; (4) $[\text{CH}_3\text{O}_2] = 2.156 \times 10^{-7}$; (5) $[\text{H}] = 1.420 \times 10^{-8}$. The maximum temperature T_{max} on curve 6 is 2273 K.

most important problem. This is a very complex nonlinear process involving critical phenomena, which is not amenable to a simple interpretation. For example, it cannot be explained by the mere shift of the equilibrium



to the left with increase in temperature, although the decomposition of the methylperoxyl radical certainly leads to a decrease in its concentration and to a change in the reaction mechanism, because in the first stage, prior to the appearance of a cool flame, branching is accomplished primarily via methyl hydroperoxide, whereas after the appearance of a cool flame, in the high-temperature region, it occurs mostly via hydrogen peroxide. Other reactions of methylperoxyl radicals are also significant in the mechanism by which a cool flame arises.

It should be emphasised that a qualitative agreement between the calculations¹⁰⁵ and the experimental results¹⁰¹ was achieved without any adjustment of the kinetic parameters of the model, except that the pressure dependences of the rate constants for some reactions were taken into account.³⁴ No attempts to attain a closer agreement with the experimental values were undertaken, because the main task was to discover whether a kinetic description of phenomena of this type is possible in principle.

4. The influence of mixing of the reactants on the product yield

In the kinetic modelling of the homogeneous oxidation of methane to methanol, the transverse and axial diffusion processes are usually neglected, for the sake of simplicity, even in the most commonly encountered case where the initial reactants, methane and an oxidant (oxygen or air), are mixed directly in the reactor. However, some workers, for example, Gesser et al.,²⁸ have noted that it is very important to achieve the homogeneity of the mixture in order to obtain a high yield of methanol. Therefore, the need arose to find out whether or not the influence of mixing on the main chemical reaction may be ignored and to identify the conditions under which this influence is insignificant. This problem has been analysed by Basevich et al.¹²⁰

A very simple flow reactor was considered in which air is supplied along an axial channel and methane is supplied along an outer coaxial channel. Then the reactants are mixed and interact to afford methanol. To simplify the complex two-dimensional problem arising during the joint consideration of the transverse (along the y axis) and axial (along the x axis) diffusion, these two types of diffusion were considered independently of each other.

In addition, the process was assumed to be isothermal, which is fairly close to the actual conditions during the oxidation of methane to methanol.

In the calculations with allowance for the transverse diffusion, two further assumptions were made:

(1) the rates of entry of the reactants via both channels are identical (isokinetic flow) and coincide with the flow rate in the reactor;

(2) the concentration gradients along the x axis are small compared with those along the y axis and may be ignored.

The initial distribution of the methane and oxygen concentrations was specified as power functions taking into account the position of the initial point in the reactor. The location of the boundary between methane and oxygen corresponded to the chosen ratio of $[\text{CH}_4]$ and $[\text{O}_2]$, and the time t determined the position x of the cross-section being considered: $x = vt$, where v is the flow rate of the gas in the reactor.

The modelling was based on the mechanism suggested by Vedenev et al.³⁴ (Table 7) with some refinements.¹²⁰ The problem under consideration is much more complex than the simple kinetic problem for a homogeneous mixture, since in this case one should take into account not only the chemical reaction but also the diffusion of all the components. Hence, a space coordinate is added to the time coordinate and the kinetic problem is solved simultaneously at all the points in space specified by the plotting step. Therefore, a number of additional expedients were used in the calculations in order to reduce the size of the kinetic scheme being processed and diminish the scale of the calculations.¹²⁰

Two extreme gas flow regimes in the reactor were considered separately. These are laminar flow (Reynolds numbers $R < 2000$), which corresponds to the normal conditions in laboratory experiments, and turbulent flow ($R > 2000$), which is more typical for industrial large-scale reactors. This large difference between the conditions in the flow of the gas mixture and hence between the mixing conditions in laboratory reactors and industrial units permanently poses the question whether data obtained in laboratory studies may be legitimately transferred to industrial plants.

The calculations were carried out for the methane–air system at a pressure of 100 atm and a temperature of 683 K in a reactor 4 cm in diameter with a central channel of variable cross-section for the air supply. Typical results of the calculation carried out for a laminar flow are presented in Fig. 26, which gives an estimate of the spatial distribution of the methane, oxygen, and methanol concentrations at various times.

In the initial moment, $t = 0$, the reactants are not mixed, the concentration of the oxidant at the reactor axis $[\text{O}_2]_0 = 20.9\%$, and the concentration of methane at the periphery $[\text{CH}_4]_0 = 100\%$. For the chosen reactor size, this corresponds to the $[\text{CH}_4]:[\text{O}_2] = 33.6:1$ ratio, typical for the DMTM process. At consecutive times of 0.93, 2.40, and 3.90 s, the concentrations of the components are affected by the diffusion of oxygen to the periphery, by the diffusion of methane to the reactor axis, and by the simultaneous chemical reaction producing methanol. The distribution of the concentrations of all the other intermediate and final products was also calculated.

From Fig. 26, it can be seen that the concentrations of the reactants do not level off over the reactor cross-section in the time interval under consideration: the methane concentration on the reactor axis ($y = 0$) at the end of the process is only 58%, and that of free oxygen is 12%. The time required for the reaction in the homogeneous mixture to be completed (that is, the time required for the consumption of 99% of the oxygen $t_r = 4.45$ s) is insufficient for the complete mixing of the reactants, i.e. $t_r < t_{\text{mix}}$, where t_{mix} is the mixing time. This accounts for the low degree of conversion η , which proved to be only 0.32%. The selectivity with respect to methanol, $S_{\text{CH}_3\text{OH}} = 47.6\%$, is also lower than that in the homogeneous mixture, in which $S_{\text{CH}_3\text{OH}} = 50.2\%$ (Table 8). In addition, during the oxidation of methane with slow molecular mixing along the whole length of the

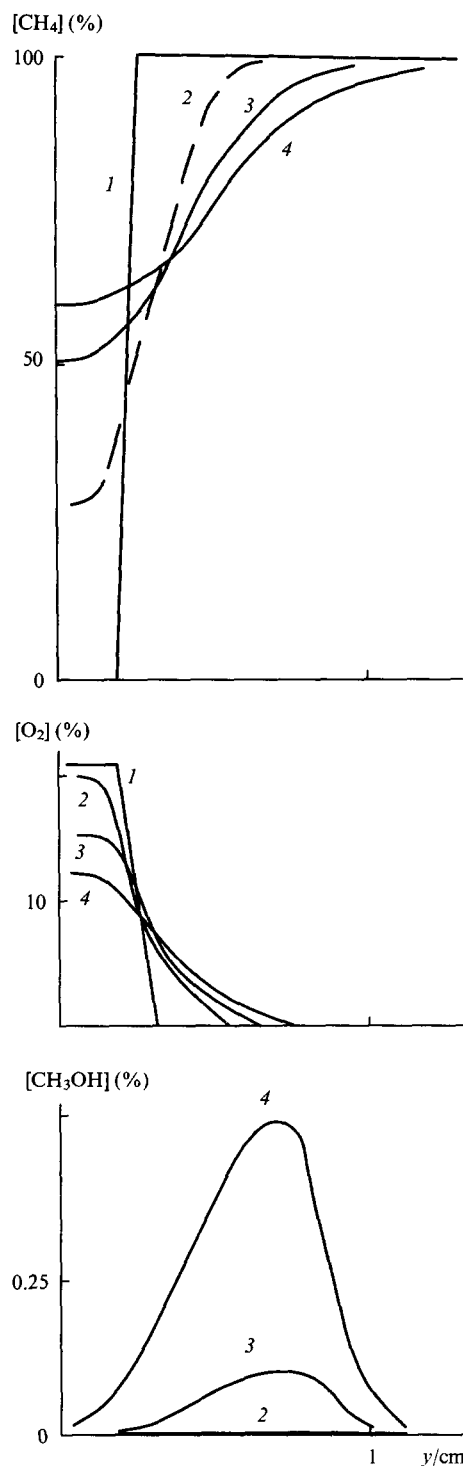


Figure 26. Concentration profiles for some components of the methane oxidation reaction in the transverse cross-section of a reactor with molecular diffusion.¹²⁰ $P = 100$ atm, $T = 683$ K, $[\text{CH}_4]:[\text{O}_2] = 33.6:1$, air as the oxidant. Time (s): (1) 0; (2) 0.93; (3) 2.40; (4) 3.90.

reactor, large volumes of the mixture with an oxygen content more than 5%, capable of self-ignition, are formed (Fig. 26), which makes the process less stable.

In the case of turbulent flow, the diffusion coefficient, which is the same for all the components, was calculated from the equation¹²¹

$$D = \varepsilon v L,$$

Table 8. Influence of the transverse diffusion of the reactants and of the conditions in the flow of gas mixture on the degree of conversion of methane and the selectivity of the formation of methanol.¹²⁰

Flow	<i>t</i> /s	[O ₂] ₀ (%)	η (%) ^a		S _{CH₃OH} (%) ^a	
			A	B	A	B
Laminar	2.27	0.52	0.86	0.19	68.2	63.0
	4.45	2.61	2.87	0.32	50.2	47.6
	6.87	4.7	5.14	2.5	39.6	33.6
Turbulent	2.27	0.52	0.86	0.89	68.2	68.7
	4.45	2.61	2.87	2.66	50.2	54.0
	6.87	4.7	5.14	5.0	39.6	41.5

^a Supply of the reactants: A — joint, B — separate.

adopting the recommended values for the degree of turbulence $\varepsilon = 0.03$ and the scale of turbulence $L = 0.35d$ (d is the reactor diameter). The calculations for a pilot unit³¹ ($d = 4.0$ cm, flow rate $v = 3$ m s⁻¹) yielded $D = 12$ cm² s⁻¹, which is greater than the molecular diffusion coefficients by three orders of magnitude.

The distribution of the concentrations in the case of turbulent diffusion at various times is shown in Fig. 27 under the same conditions as in Fig. 26. In this case, the mixing is very rapid and is

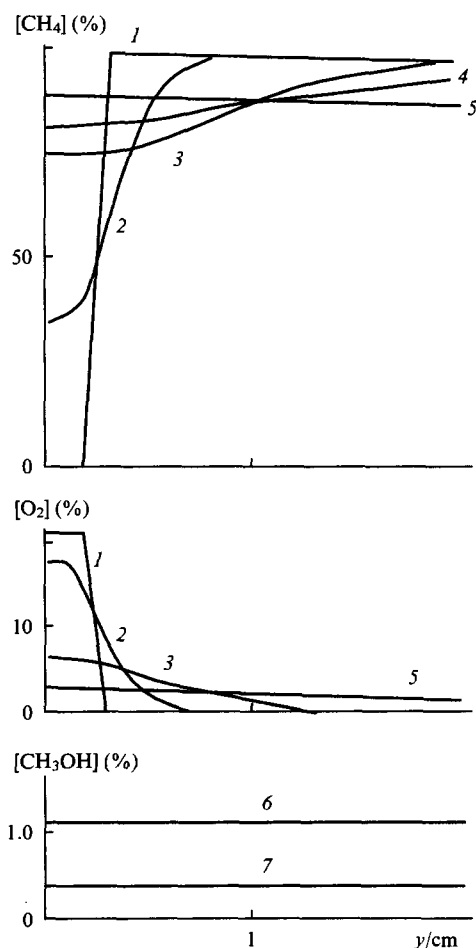


Figure 27. Concentration profiles for some components of the oxidation of methane in the transverse cross-section of a reactor with turbulent diffusion.¹²⁰ $P = 100$ atm, $T = 683$ K, $[\text{CH}_4]:[\text{O}_2] = 33.6:1$, air as the oxidant. Time (s): (1) 0; (2) 0.0015; (3) 0.014; (4) 0.029; (5) 0.9; (6) 6.3; (7) 90.

completed in less than 0.9 s. During this time, less than 1% of the final quantity of methanol is formed. After that, the reactions proceed in the resulting homogeneous mixture. In the example shown in Fig. 27, the degree of conversion is practically the same as in a homogeneous mixture (2.66%), and the selectivity with respect to methanol $S_{\text{CH}_3\text{OH}} = 54\%$ (Table 8), i.e. the case where $t_{\text{mix}} < t_r$ is realised. Thus, for turbulent diffusion, the degree of conversion is similar to the corresponding value attained in a homogeneous mixture and the selectivity is even somewhat higher. This is natural, because the duration of the chemical reaction is much greater than the characteristic time of the turbulence (frequencies from 10 to 1000 Hz). Hence, the turbulence does not influence the course of the reaction. The results obtained are in agreement with the experimental data indicating that good characteristics of the process are achieved when the reactants are quickly mixed by jets, the velocity of which is close to the velocity of sound.²⁷ For rapid turbulent mixing, mixtures capable of self-ignition exist only in the initial section of the reactor (Fig. 27); in other words, the process is more stable than that involving slow molecular mixing.

Calculations¹²⁰ have shown that, for molecular diffusion coefficients, axial diffusion has no influence on the DMTM process. When the diffusion coefficients correspond to a turbulent regime, the observed influence of axial diffusion is slight: the concentration profiles shift somewhat along the axis to the left, that is, to the entry to the reactor, and the yields of all the main products virtually do not change.

Thus, the following conclusions can be drawn:

- kinetic modelling with no allowance for diffusion under the conditions of rapid mixing provides a qualitatively correct description of the chemical process and evaluation of the product yields;
- when methane and oxygen are supplied separately, their rapid mixing ensuring that the $t_{\text{mix}} \ll t_r$ relation holds is a necessary condition for a high degree of conversion of methane and high selectivity of the formation of methanol;
- in the case of slow mixing, the process is less stable.

5. Modelling of circulation regimes in the oxidation of methane

To make the DMTM process suitable for the industrial production of methanol, one should increase the degree of conversion of natural gas, while maintaining the high selectivity of the formation of methanol. In reality, this can be achieved by conducting the process according to a circulation scheme. In this process, reactive gas-phase products (carbon monoxide and hydrogen and also nitrogen, in the case where oxidation is carried out with air) can accumulate in the circulating gases. This naturally influences the characteristics of the DMTM technological process. To elucidate the possibility of improving the characteristics of the process by using a circulation scheme, the corresponding theoretical analysis has been carried out with the aid of a special kinetic programme.¹²² The kinetic model developed by Vedenev et al.³⁴ supplemented by reactions that take more precise account of the interaction between the products formed, was used in the calculations.

The methane oxidation process with product recirculation includes three stages.

1. Methane and an oxidising agent (air or oxygen) enter the reactor, where methane is oxidised.

2. The gases leaving the reactor are cooled and the liquid phase containing the target product (methanol) is separated. As this takes place, all the unstable intermediates decompose.

3. The gaseous products are partly discarded, and the rest is mixed with fresh methane (which makes up for the lost liquid phase and for the discarded part of the gas phase) compressed to the operating pressure, heated, and injected into the reactor once again, together with the oxidising agent.

The calculations were carried out for conditions close to the optimal conditions for a flow-type process: a temperature of

713 K, a pressure of 100 atm, a reaction time corresponding to the consumption of oxygen (several seconds), and a constant oxygen concentration at the reactor inlet of 2.2%.

The relative quantity of the gas being recycled λ has the greatest influence on the course of the process involving circulation ($\lambda = 0$ means that all the gas is discarded, which corresponds to a flow regime; $\lambda = 1$ means that no gas is discarded, and stable gaseous products are accumulated in the circulating gas, while the methane concentration at the reactor inlet continuously decreases). If oxygen is used as the oxidant, even a considerable number of cycles N carried out at $\lambda = 1$ influences only slightly the initial methane concentration $[\text{CH}_4]_0$ (Fig. 28). Accordingly, the quantity of methanol formed in each cycle decreases equally slowly. The total amount of the methanol collected continuously increases, so that at $N = 30$ its overall yield $\Sigma[\text{CH}_3\text{OH}]$ reaches $\sim 30\%$. The only component that is also accumulated continuously in the circulating gas is carbon dioxide (Fig. 29); its concentration reaches 17%. The other gaseous products (carbon monoxide, hydrogen, and ethane) are accumulated much more slowly, because they are consumed during the reaction. The concentrations of these compounds after 30 cycles are 2.4, 1.2, and 0.17%, respectively.

The selectivity of the formation of methanol in the first pass under these conditions is 57.2%. As the number of cycles increases, $S_{\text{CH}_3\text{OH}}$ decreases somewhat, but for $N = 30$ it is still fairly high and amounts to 50%, so that on average $S_{\text{CH}_3\text{OH}} = 52\%$. The results obtained for $0 < \lambda < 1$ are intermediate between those observed in the flow and closed-loop (without discard) regimes.

Thus, when the circulation scheme is used, the degree of conversion in one pass virtually does not decrease, the selectivity decreases only slightly, but, in return, the overall quantities of methane being converted and methanol formed increase sharply. At $\lambda < 1$, after a fairly large number of cycles have been carried out, the system approaches a steady state in which the concentrations of the reaction products at the end of each step remain virtually constant. This corresponds to the realisation of the circulation scheme in the steady-state regime. The higher the rate of accumulation of the nonconsumable inert gases (carbon dioxide and nitrogen), the larger the proportion of the gas, which needs to be discarded (that is, the smaller the value of λ) and the smaller the number of cycles required for a steady-state to be achieved. However, the degree of conversion of the initial

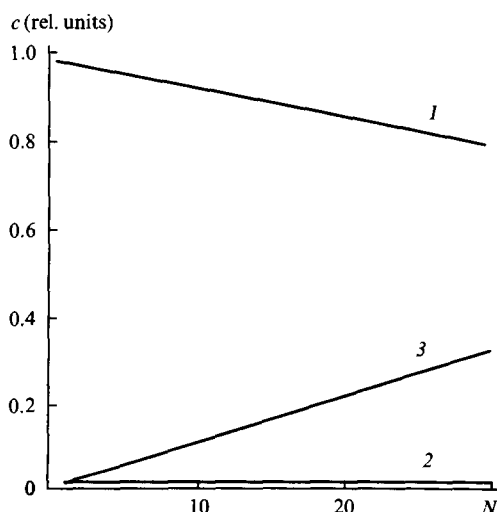


Figure 28. Dependences of the initial methane concentration (1), the final current methanol concentration (2), and the overall yield of methanol (3) on the number of cycles (N) at $P = 100$ atm, $T_0 = 713$ K, $[\text{O}_2]_0 = 2.2\%$, $[\text{CH}_4]_0 = 97.8\%$.¹²²

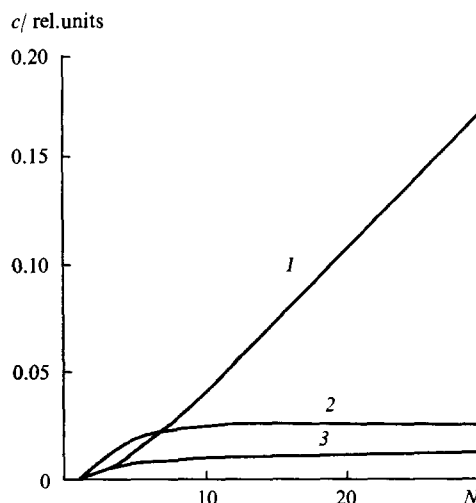


Figure 29. Dependences of the final concentrations of CO_2 (1), CO (2), and H_2 (3) on the number of cycles (N) at $P = 100$ atm, $T_0 = 713$ K, $[\text{O}_2]_0 = 2.2\%$, $[\text{CH}_4]_0 = 97.8\%$.¹²²

methane diminishes correspondingly. The selectivity at steady-state depends on the ratio between the steady-state concentrations of methane and oxygen, which is determined by the value of λ , chosen from the standpoint of attaining the optimal yields of the products.

The DMTM circulation scheme has also been modelled for the case where air is used as the oxidising agent.¹²² The λ parameter was varied within limits ensuring a steady-state proportion of nitrogen in the working medium (up to 60%).

It may be assumed that when the circulation scheme is used, the energy expenditure is lower than in the flow regime, because in the former case the quantity of mains gas that has to be brought to the operating pressure is much smaller. However, the productivity of the reactor diminishes due to the lowering of the steady-state initial methane concentration and the decrease in the selectivity of the formation of methanol. Therefore, the optimal version of the circulation scheme should be chosen with allowance for particular technical and economic conditions including the possibility of utilising the discarded gases, for example, for heating the operating mixture, etc.

Thus, the modelling has demonstrated the possibility of implementing the circulation scheme for the oxidation of methane, in which the degree of conversion of methane increases by more than an order of magnitude with no substantial decrease in the selectivity of its formation.

VII. Technical and economic aspects of the direct oxidation of natural gas to methanol

1. Prospects for the increase in the use of methanol and other oxygenates

Methanol is among the main products of organic synthesis. The constant intense development of its production is due to the continuous extension of its applications, the main ones being the production of formaldehyde, acetic acid, solvents, ethers, and other chemicals.^{81,123} In the future, methanol may form a universal basis for organic synthesis. It is finding an increasing use in the production of high-octane components of motor fuels, primarily, of methyl *tert*-butyl ether (MTBE).¹²⁴ In the overall world consumption of methanol in 1990 (19.6 million tonnes), 40% was due to the production of formaldehyde, 45% was due to other chemical products, and 14% was accounted for by fuel components.

From 1990 to 1995, the annual increase in the demand for methanol in North America should reach 6.6%, while in the

previous five years it was only 4.3%. The major part of this increase is accounted for by the production of MTBE, necessary to meet demands associated with protection of the atmosphere against the pollutants arising during the combustion of automobile fuels. The USA demand for MTBE in 1995 should be from 15 to 30 million tonnes. However, the production of oxygenates may delay the introduction of clean fuels. Without new plants for the synthesis of methanol, North America will experience a deficit in the capacity for the production of methanol estimated as 4.7 million tonnes a year already by 1995.¹²⁵

Whereas in 1990 the producers of formaldehyde were the main users of methanol in the USA, already by 1995 from 38% to 55% of methanol will be consumed for the production of MTBE.¹²⁵ The boom in the consumption of MTBE in the USA cannot but influence the world production of MTBE and methanol, since the USA import not only MTBE but also the methanol and butane necessary for its production.⁸⁰ It is expected that in 1991–2000 the annual increase in the world consumption of methanol will be 5.6% and the increase in the consumption of MTBE will be 20%.⁸⁰ Forecasts predict that by 2001 the overall consumption of oxygenates will increase by a factor of 10 with respect to its current level¹²⁶ and the cost of their production will amount to 50 billion dollars by 2000.¹²⁷ In view of the fact that since 1995 more than 85% of the petrol used in the USA should contain oxygenates, a global deficit of oxygenates, including methanol, and a rise in their prices have been predicted.¹²⁷

Methanol is an alternative to an oil distillate fuel. There are examples of its use in power plants as a fuel for gas turbines. Boilers can also run on methanol. The main advantage of methanol over distillate fuels is that it contains no sulfur. The possible consumers of methanol are power plants, transport, food industry, metallurgy (reducing gas), and some other industries. In certain cases, it is economically favourable to produce hydrogen from methanol.¹²³

The significance of methanol as one of the most promising alternative fuels for transport has long been discussed in the literature^{128–130} [see also the proceedings of the international symposia on alcohol fuels IX ISAF, Florence (Italy), 1991; X ISAF Colorado-Springs (USA), 1993]. If full advantage is taken of the beneficial motor-fuel properties, primarily the high octane numbers, of methanol, mixtures of alcohols and petrol–methanol mixtures, these fuels become quite competitive with modern petrols.^{128, 131} Since automobiles can run on mixtures containing about 20% of methanol or other alcohols, the use of these mixtures may become an important source of the energy for transport.¹²³

The energetic efficiency of the engine specially developed to run on methanol is 30% higher than that of the analogous petrol engine.¹³¹ Its environmental advantages are particularly attractive. However, the large-scale use of methanol is impossible without a reconstruction of both the methanol-producing and oil refining industries and, most of all, of the system of distribution of automobile fuels.

As a response to the need to improve the environmental characteristics of motor fuels, the so called 'reformulated gasoline' has been developed. This fuel contains additives such as methanol, ethanol, MTBE, ETBE, mixtures of alcohols, etc., which has made it possible to increase the oxygen content in a fuel to 3.7%.¹³² Large-capacity production of MTBE already exists in many countries and its world output in 1990 amounted to 8 million tonnes (13 million tonnes has been predicted for 1995 and 25 million tonnes for 2000).¹³³ However, an important place in the concept of ecologically clean fuels is occupied by the 'fuel alcohols', that is, by mixtures of alcohols used either by themselves or as high-octane additives to motor fuels.^{132, 134} The fuel alcohols consisting of methanol to which 20%–30% of higher alcohols has been added make it possible to increase the octane number and to reduce the amount of harmful exhaust gases; their mixtures with petrols do not separate into layers in the presence of water and they are a real alternative to ethers.^{132, 134} The production of these

fuels, unlike the production of MTBE and other ethers, does not require the corresponding alkenes, which are themselves valuable products and in limited supply.¹³²

Methanol can be used to fuel an engine in a pure state, as an emulsion in hydrocarbons, or as one of the components in a separate fuel supply system. It can be preliminarily converted into CO and H₂ and into highly inflammable compounds (like dimethyl ether). Finally, it can be converted in the presence of catalysts (to obtain heat) or in fuel cells (to obtain electric energy). At present, one of the most feasible schemes for the operation of electric cars involves the catalytic conversion of methanol into hydrogen, which supplies the vehicle-borne fuel cells.¹²⁵

All the promising aspects of the development of environmentally clean transport are associated in one way or another with the use of alcohols, either directly in fuel mixtures or as intermediate compounds in the synthesis of MTBE and other ethers. This raises the problem of lowering the cost of methanol, which has so far been neglected within the framework of the traditional technology for its production via synthesis gas.⁸³

Natural gas is almost unreservedly considered to be the main raw material source for meeting the increasing demand for methanol, although a sharp increase in the use of natural gas for the production of methanol requires a thorough economic analysis.¹³⁵

2. Technical and economic estimates of the technological process for the direct oxidation of natural gas to methanol

Extensive application of a new technology for the production of methanol is impossible without serious economic prerequisites. Some economic estimates of the effectiveness of this process have been reported.^{67, 87, 136–138}

Edwards and Foster⁸⁷ have reported an economic assessment of the production of methanol by the direct catalytic partial oxidation of natural gas with an output of 2000 tonnes per day. If the selectivity of the formation of methanol is more than 77%, the direct process undoubtedly proves to be more economically viable than the traditional method. With regard to consumption of heat and hydrocarbons, the effectiveness of the direct partial oxidation of methane is also higher.¹³⁶ It has been reported⁶⁷ that methanol obtained by the direct oxidation would be 20%–30% cheaper than the product obtained by the existing methods. Some economic aspects have been discussed by Renesme et al.¹³⁸ and Crocco.¹³⁹

According to economic calculations, the cost of raw materials accounts for ~50% of the operating costs, however there exist vast reserves including the casing-head gas, oil refinery gases, and de-ethanisation gases, which now have no commercial value and are burned in flares, thus polluting the environment.

The use of gases containing substantial amounts of higher hydrocarbons would make it possible to decrease sharply the pressure and the temperature of the process. The degree of conversion of these gases in one pass can be as high as 20%, instead of 3%–4% obtained in the oxidation of methane; the efficiency may be increased further by using the circulation oxidation scheme. In addition, this process may yield valuable products, for example, iso-alcohols or aldehydes, in fairly high yields, and the isolation of these products would recoup a considerable part of the production costs.

The currently available technical solutions allow the selectivity of the formation of methanol in this process to be increased to 60% or more, and the process may therefore become nearly profitable.

3. Technological scheme for the direct oxidation of methane to methanol

The technological scheme for the DMTM is fairly simple, and this is one of its main advantages. The catalytic version of the process has been described in a paper cited above.⁸⁷ A basic scheme for a plant producing methanol by the direct gas-phase oxidation of natural gas with a productivity of 10 000 tonnes of methanol per

year, developed within the framework of the Russian state programme 'Environmentally Clean Power Engineering' has been reported.⁵⁵ The plant is meant to satisfy the local needs of the gas-industry for methanol and motor fuels. The project involves the development and the subsequent commercial production of self-contained modular units for the direct homogeneous conversion of natural gas into methanol and provides for the possibility of further transformation of methanol into a high-octane petrol.

The process makes it possible to avoid the intermediate formation of the synthesis gas, which is unfavourable from the thermodynamic standpoint, and the equipment involved is relatively simple. The project is based on a kinetic analysis^{33–37} and on the results of pilot tests on a unit with a production capacity of 100 tonnes of methanol per year.³¹ The main parameters of the process are: pressure 5–10 MPa, temperature 380–480 °C (depending on the composition of the gas), oxygen concentration 2.8%, degree of conversion of oxygen 95%–98%, yield of crude methanol 20 kg per 1000 m³ of the input gas or 0.63 kg per 1 kg of the converted gas.⁵⁵

After being compressed to an operating pressure of 5–10 MPa and heated to 380–480 °C, natural gas enters a gas-phase mixer, which also serves as the reactor. Oxygen (or air) is conveyed to the same reactor at a pressure of 10 MPa. After the reaction, the mixture is cooled in a heat exchanger and then conveyed to a condenser, in which liquid products are condensed. It then goes to an apparatus for the neutralisation of acids. After that, the liquid phase is separated from the unreacted gas in a separator. The resulting liquid product is concentrated in a fractionating column. Simultaneously, the formaldehyde formed is separated as an aqueous solution (formalin). The unchanged gases are either discharged to a gas pipeline or reenter the unit inlet. If there is an additional catalytic unit for producing petrol, the crude methanol obtained is supplied directly to the inlet of this unit. The degree of conversion of natural gas in one pass is less than 3%. Since the process yields no significant amounts of incombustible side products, the natural gas may be returned to the gas pipeline or recycled.⁵⁵

The unit is meant for the independent conversion of natural gases into crude methanol, containing more than 90% methanol, in remote gas fields where there is no developed infrastructure. It does not require a complex repair base or highly qualified personnel. The methanol produced is supposed to be consumed at site as an inhibitor of hydrate formation in the extraction and transport of natural gas and also for its direct conversion in a second unit into petrol with an octane number of 93 (3300 tonnes per year) and for other purposes. The formalin obtained as a side product also finds application in the gas fields.

In the course of the implementation of this project, a number of novel technological approaches were developed which allowed the yield of methanol to be increased by approximately 30%. The use of this technology (with the parameters already attained) in remote or relatively inaccessible oil and gas fields is at least 30% more profitable than the traditional method for the production of methanol.

As noted above, when oxygen is used as the oxidising agent, the content of incombustible impurities in the outgoing gases hardly increases and the gas can therefore be returned to the pipeline. In the case where this process is carried out just before the gas is dispensed to the consumer, the best way is to use the cheaper air as the oxidising agent.

The most significant drawback of the homogeneous partial oxidation of natural gas to methanol at high pressures is the need to maintain a low initial oxygen concentration (~3%) in order to achieve a satisfactory selectivity of the conversion of methane to methanol, and this precludes the possibility of attaining a sufficiently high degree of conversion of natural gas in a single pass through the reactor. It is therefore desirable to use a circulation scheme to increase the overall degree of conversion of natural gas.

4. The concept of small-capacity processes to meet the regional and related industrial requirements for oxygenates

At present, there are reasons for establishing a new 'sub-branch' within the structure of the gas-production industry, namely, small-capacity gas-processing chemistry, based largely on the production of methanol as the main intermediate compound. The small-capacity technological plant designed as a set of units (modular small-scale units, MSU) should be located in particular gas fields taking into account the locally available raw materials and the local needs for the hydrocarbon-based products.¹⁴⁰

Estimates indicate that the operation over a period of 10–15 years of a MSU with a production capacity of ~3000 tonnes of products per year requires that the natural gas resources in the particular deposit be at least 0.3–0.5 billion m³ and ensure a gas output of 30000 m³ per day over the whole exploitation period. The vast majority of gas fields and newly found deposits comply with these requirements.¹⁴⁰

Of the 1195 deposits of hydrocarbon gases in the C.I.S., 880 are small, their weighted average gas reserves being ~1.5 billion m³ per deposit.¹⁴¹ Connecting them to the main pipelines is unprofitable, and they also cannot be used as a source of raw materials for large-capacity chemical production. The only means of the industrial exploitation of these deposits is the processing at site of the extracted hydrocarbon raw materials by using MSU. The MSU can also be applied at condensed gas deposits, coal basins, which contain huge methane reserves, and any other hydrocarbon reserves that can be converted into the initial gaseous raw material, including biomass, the annual reproducible world resources of which are estimated as 200 billion tonnes.¹⁴⁰

The undoubted simplicity of the DMTM technological scheme,⁵⁵ compared with the traditional schemes for the production of methanol or synthetic motor fuels via synthesis gas,⁸¹ the weak dependence of the prime cost of the product on the production output, and modest demands on raw material sources are good prerequisites for the implementation of this scheme on MSU. Up to 7% of the methanol produced in our country is used to prevent the formation of gas hydrates during natural gas extraction and transportation; the expected annual demand by the gas industry for methanol in 2000 is 500 000 tonnes. The high cost of the delivery of methanol to the main gas fields, far exceeding its selling price, makes the conversion of natural gas into methanol directly in the gas fields very attractive. At the same time, these regions may be provided with motor fuels and with formaldehyde — a side product of the process.^{55, 140}

Thus, the use of MSU for the direct processing of natural gas in gas fields in order to provide the corresponding regions with methanol and motor fuels proves to be intimately connected with the technological implementation of the DMTM process. The DMTM process realised as MSU may manifest its technical and economical advantages well before it finds an application in the large-capacity chemical industry.

VIII. Promising aspects of the scientific research dealing with direct oxidation of natural gas to methanol

In many countries, large investments are made in state and private research aimed at the effective use of the abundant natural gas resources.¹⁴² The main purpose of these studies is to increase the effectiveness of the most promising processes for the production of methanol and higher hydrocarbons, which are potentially competitive with the traditional petroleum refining.

The research activity was greatly promoted by the discovery made in 1982 of catalysts ensuring high yields of ethane and ethene in the oxidative condensation of methane. In recent years, studies on the catalytic conversion of natural gas have been mostly concerned with the overcoming of kinetic barriers, which

apparently restrict the yields of C_2 hydrocarbons in the oxidative condensation of methane to $\sim 25\%$.^{75,118} This is sufficient to maintain interest in the scientific research but too low for the practical realisation of the process.

Regarding the direct gas-phase oxidation of methane to methanol, the challenge now is to reproduce on the pilot scale the high (up to 70%–80%) selectivity of the process for the fairly high (more than 5%) degrees of conversion, which have been achieved in some laboratory studies.^{28,38,41,43,45} These results, if obtained on the industrial scale, would permit the development of an undoubtedly profitable process.

Therefore, clear identification of the conditions or search for process regimes, which may lead, in principle, to such results, is a fundamental goal of the studies. In our opinion, this can be done by investigating periodic and cool-flame regimes in the oxidation of methane, in which the product yields may differ fundamentally from those obtained in other known regimes. The high degree of nonlinearity of the mechanism of the oxidation of methane (Section V) and the known data concerning the appearance of periodic phenomena, hysteresis, and cool flames during its oxidation (Section III, 8) make it possible to rely on the possibility of achieving in open reaction systems (among which are flow-type reactors¹⁴³) steady-state oxidation regimes that have not yet been investigated, or those regimes which can be stabilised artificially by means of additional physical or chemical effects. This assumption is supported by the existence of several steady-state and oscillatory regimes in the oxidation of the near homologues of methane,²⁰ including ethane.¹⁴⁴ Since in such a complex system (the oxidation of hydrocarbons is apparently among the most complex systems, if biological processes are excluded¹⁴³), a fortuitous experimental discovery of new regimes can hardly be expected, the main efforts should be concentrated on the analysis of the most realistic models (in the first place, on the stability of the regime).

The above problem is closely connected with the practically important task of analysing the stabilities of the known steady-state regimes in the case where the process is carried out in industrial-scale reactors. There are lots of reasons for the instability of a chemical process in an open system, for the appearance of non-steady-state regimes, pulsations, and oscillations, which may become dangerous. Therefore, conditions should be found in which the process would be so stable that any random fluctuation of the composition, temperature, and pressure would decay rapidly.

Yet another promising line of research is the study of the high-pressure oxidation of methane homologues, their mixtures, and the real natural gases, because the direct oxidation of gaseous hydrocarbons containing high proportions of methane homologues may provide appreciable technological and economic advantages. In our country, there are huge resources of these gases of both natural and industrial origin (ethane-containing natural gases, casing-head gases, refinery gases, de-ethanisation gases, etc.). The proportion of ethane-containing gases in the total explored gas resources is 30.5%,¹⁴⁵ and the amount of petroleum gas with high proportions of ethane, propane, and butane burned in flares every year reaches 12–15 billion m^3 .¹⁴⁶ Since raw materials account for more than 50% of the production cost,⁸⁷ the use of gases of low value with high proportions of methane homologues can enhance sharply the economic effectiveness of the process and extend the range of its feedstock.

Evidently, the study of the influence of external parameters and gas composition on the detailed composition of the products as well as the search for various methods for its correction, including the subsequent additional catalytic treatment and partial isolation of products in order to obtain mixtures of standard composition and commercial products, will be of great importance.

The development of sufficiently predictive quantitative kinetic models of the high-pressure oxidation of methane homologues

and the development of a model of the oxidation of the real natural gases based on them are also very important scientific tasks.

IX. Conclusion

Through the experimental and theoretical studies carried out for many years on the partial oxidation of methane and its homologues at high pressures, the chemical fundamentals of the direct synthesis of methanol and other oxygenates have been developed. The current level to which the technological process has been developed, its relative simplicity, its flexibility regarding production output, and its low power and capital requirements give this process in some cases real advantages over the traditional methods for the synthesis of methanol. The rapidly increasing demand of the world market for cheap methanol and other oxygenates and hence for flexible and highly-profitable methods for their production dictate the need to intensify the scientific research designed to discover the fundamental paths leading to the enhancement of the selectivity of the formation of methanol and of its yield in this process to the level of absolute profitability, to extend the range of raw materials by involving poorly utilised sources of gaseous hydrocarbons, and to develop optimal schemes for the organisation of the process.

This review was written with the financial support from the Scientific Council of Russian SSTP "Novel Principles and Methods of Preparation of Chemical Compounds and Materials".

References

- W A Bone, R V Wheeler *J. Chem. Soc.* **81** 535 (1902)
- W A Bone, R V Wheeler *J. Chem. Soc.* **83** 1074 (1903)
- W A Bone, R E Allum *Proc. R. Soc. London, A Math. Phys. Sci.* **134** 578 (1932)
- D M Newitt, A E Huffner *Proc. R. Soc. London, A Math. Phys. Sci.* **134** 591 (1932)
- D M Newitt, P Szego *Proc. R. Soc. London, A Math. Phys. Sci.* **147** 555 (1934)
- D M Newitt *Chem. Rev.* **21** 299 (1937)
- K Yoshikawa *Bull. Inst. Phys. Chem. Res. (Jpn.)* **10** 305 (1931); *Chem. Abstr.* **25** 4 842 (1931)
- Fr. P. 352 687 (1905)
- Can. P. 291 411 (1929)
- US P. 1 776 771 (1930)
- A D Petrov *Khim. Promst* **11** (1945)
- V G Fastovskii *Metan (Methane)* (Moscow: Gostoptekhizdat, 1947)
- H Pichler, D R Reder *Angew. Chem.* **46** 161 (1933)
- A Paris *Chim. Ind., Special No 411-20* (April 1934); *Chem. Abstr.* **28** 5 806 (1934)]
- P J Wiezevich, P K Frolich *Ind. Eng. Chem.* **26** 267 (1934)
- E H Boomer, J W Broughton *Can. J. Res., Sect. B* **15** 375 (1937)
- E H Boomer, V Thomas *Can. J. Res., Sect. B* **15** 401 (1937)
- E H Boomer, V Thomas *Can. J. Res., Sect. B* **15** 414 (1937)
- E H Boomer, N Naldrett *Can. J. Res., Sect. B* **25** 495 (1947)
- V Ya Shtern *Mekhanizm Okisleniya Uglevodorodov* (Moscow: Izd. Akad. Nauk SSSR, 1960) [*Gas Phase Oxidation of Hydrocarbons* (Oxford: Pergamon Press, 1964)]
- P E Oberdorfer, R F Winch *Ind. Eng. Chem.* **53** 41 (1961)
- A Melvin *Combust. Flame* **10** 120 (1966)
- J L Lott, C M Sliepcevich *Ind. Eng. Chem., Process. Des. Dev.* **6** 67 (1967)
- N L Hardwicke, J L Lott, C M Sliepcevich *Ind. Eng. Chem., Process. Des. Dev.* **8** 133 (1969)
- G L Bauerle, J L Lott, C M Sliepcevich *J. Fire Flammability* **5** 190 (1974)
- N Tripathy *Isr. J. Chem.* **13** 190 (1975)
- Br. P. 2 006 757 (1979)
- US P. 4 618 732 (1986)
- USSR P. 1 145 014; *Byull. Izobret.* (10) 78 (1985)
- Russ. P. (1994) based on Appl. 5 028 053/04 (1992)

31. V F Budymka, S A Egorov, N A Gavrya, A S Mochaev, G A Khomenko, V E Leonov *Khim. Promst* 330 (1987)
32. V V Bak, A D Bondar', V I Vedeneev, S A Egorov, P M Shcherbakov *Khim. Promst* 272 (1988)
33. V I Vedeneev, M Ya Gol'denberg, N I Gorban', M A Teitel'boim *Khim. Fiz.* 6 626 (1987)
34. V I Vedeneev, M Ya Gol'denberg, N I Gorban', M A Teitel'boim *Kinet. Katal.* 29 7 (1988)
35. V I Vedeneev, M Ya Gol'denberg, N I Gorban', M A Teitel'boim *Kinet. Katal.* 29 14 (1988)
36. V I Vedeneev, M Ya Gol'denberg, N I Gorban', M A Teitel'boim *Kinet. Katal.* 29 1291 (1988)
37. V I Vedeneev, M Ya Gol'denberg, N I Gorban', M A Teitel'boim *Kinet. Katal.* 29 1297 (1988)
38. P S Yarlagadda, L Morton, N R Hunter, H D Gesser *Ind. Eng. Chem. Res.* 27 252 (1988)
39. O T Onsager, P Soraker, R Lodeng, in *Methane Activation Symposium on Pacificchem. (Preprints)* (Honolulu, Hawaii, 1989) p. 113
40. R Burch, G D Squire, S C Tsang *J. Chem. Soc., Faraday Trans. 1* 85 3561 (1989)
41. N R Hunter, H D Gesser, L A Morton, P S Yarlagadda, D P C Fung *Appl. Catal.* 57 45 (1990)
42. P S Yarlagadda, L A Morton, N R Hunter, H D Gesser *Combust. Flame* 79 216 (1990)
43. L A Morton, H D Gesser, N R Hunter *Fuel Sci. Technol. Int.* 9 913 (1991)
44. T R Baldwin, R Burch, G D Squire, S C Tsang *Appl. Catal.* 74 137 (1991)
45. M Bistolfi, M Dente, E Ranzi, in *The IX International Symposium on Alcohol Fuels, Firenze, Italy, 1991* Vol. 1, p. 105
46. D W Rytz, A Baiker *Ind. Eng. Chem. Res.* 30 2287 (1991)
47. V I Vedeneev, V S Arutyunov, N Yu Krymov, P M Cherbakov, A D Sedykh *Catal. Today* 13 613 (1992)
48. D J Thomas, R Willi, A Baiker *Ind. Eng. Chem. Res.* 31 2272 (1992)
49. D E Walsh, D J Martenak, S Han, R E Palermo *Ind. Eng. Chem. Res.* 31 1259 (1992)
50. D E Walsh, D J Martenak, S Han, R E Palermo, J N Michaels, D L Stern *Ind. Eng. Chem. Res.* 31 2422 (1992)
51. G A Foulds, B F Gray, S A Miller, G S Walker *Ind. Eng. Chem. Res.* 32 780 (1993)
52. J-W Chun, R G Anthony *Ind. Eng. Chem. Res.* 32 259 (1993)
53. J-W Chun, R G Anthony *Ind. Eng. Chem. Res.* 32 788 (1993)
54. J-W Chun, R G Anthony *Ind. Eng. Chem. Res.* 32 796 (1993)
55. V S Arutyunov, V I Vedeneev, V R Grunval'd, N Yu Krymov, V E Leonov, A D Sedykh *Khim. Promst* 543 (1993)
56. G S Walker, J Lapszewicz, G A Foulds, in *The 4th European Workshop on Methane Activation (Book of Abstracts)* (Eindhoven, Netherlands, 1994)
57. V I Vedeneev, V S Arutyunov, V Ya Basevich, M Ya Gol'denberg, M A Teitel'boim, N Yu Krymov *Catal. Today* 21 527 (1994)
58. V I Vedeneev, V S Arutyunov, V Ya Basevich, L B Romanovich, in *The Second Workshop Meeting on C₁-C₃ Hydrocarbon Conversion (Abstracts)* (Krasnoyarsk: Institute of Chemistry of Natural Organic Materials, 1994) p. 111; V S Arutyunov, V I Vedeneev, V Ya Basevich, S V Sokolov *Izv. Akad. Nauk, Ser. Khim.* 53 1996 (1994)
59. K Omata, N Fukuoka, K Fujimoto *Ind. Eng. Chem. Res.* 33 784 (1994)
60. P S Casey, T McAllister, K Foger *Ind. Eng. Chem. Res.* 33 1120 (1994)
61. B F Gray, J F Griffiths, G A Foulds, B G Charlton, G S Walker *Ind. Eng. Chem. Res.* 33 1126 (1994)
62. V S Arutyunov, V I Vedeneev, S Yu Klimovetskaya, V E Leonov, L V Pavlii *Teor. Osn. Khim. Tekhnol.* 28 627 (1994)
63. V S Arutyunov, V I Vedeneev, S Yu Klimovetskaya, V E Leonov, L V Pavlii *Teor. Osn. Khim. Tekhnol.* 29 71 (1995)
64. V S Arutyunov, V Ya Basevich, V I Vedeneev, L B Romanovich *Kinet. Katal.* (1996) (in the press)
65. E Y Garcia, D A Loffer *Lat. Am. J. Chem., Eng. Appl. Chem.* 14 267 (1984)
66. H D Gesser, N R Hunter, C B Prakash *Chem. Rev.* 85 235 (1985)
67. H D Gesser, N R Hunter, in *Direct Methane Conversion by Oxidative Processes. Fundamentals and Engineering* (Ed. E E Wolf) (New York: Van Nostrand, 1992) p. 402
68. R Lodeng, PhD Thesis, Institute for Industriell Kjemi, Trondheim, 1991
69. N R Foster *Appl. Catal.* 19 1 (1985)
70. R Pitchai, K Klier *Catal. Rev.* 28 13 (1986)
71. M Yu Sinev, V N Korchak, O V Krylov *Usp. Khim.* 58 38 (1989) [*Russ. Chem. Rev.* 58 22 (1989)]
72. J C Mackie *Catal. Rev. Sci. Eng.* 33 169 (1991)
73. M J Brown, N D Parkyns *Catal. Today* 8 305 (1991)
74. O V Krylov *Usp. Khim.* 61 2040 (1992) [*Russ. Chem. Rev.* 61 1118 (1992)]
75. O V Krylov *Catal. Today* 18 209 (1993)
76. A I Gritsenko *Gazovaya Promst* (10) 19 (1993)
77. N Ya Usachev, Kh M Minachev *Neftekhimiya* 33 387 (1993)
78. A Tarbatton, M Salazar *Nefi', Gaz i Neftekhimiya za Rubezhom* (4) 115 (1992)
79. V P Pereushanu, M Koroby, G Muska *Proizvodstvo i Ispol'zovanie Uglevodorodov* (Production and Use of Hydrocarbons) (Moscow: Khimiya, 1987)
80. *Nefi', Gaz i Neftekhimiya za Rubezhom* (10) 96 (1992)
81. M M Karavaev, V E Leonov, I G Popov, E T Shepelev *Tekhnologiya Sinteticheskogo Metanola* (Technology of Synthetic Methanol) (Moscow: Khimiya, 1984)
82. D L Trim, M S Wainwright *Catal. Today* 6 261 (1990)
83. M Marchionna, A Aragno, L Basini, M Lami, F Ancillotti, in *The IXth International Symposium on Alcohol Fuels, Firenze, Italy, 1991* Vol. 1, p. 88
84. J M Fox, T-P Chen, B D Degen *Chem. Eng. Progr.* 86 (4) 42 (1990)
85. D M Newitt, J B Gardner *Proc. R. Soc. London, A Math. Phys. Sci.* 154 329 (1936)
86. G A Luckett, B Mile *Combust. Flame* 26 299 (1976)
87. J H Edwards, N R Foster *Fuel Sci. Technol. Int.* 4 365 (1986)
88. T C Chou, L F Albright *Ind. Eng. Chem., Process Des. Dev.* 17 454 (1978)
89. J L Lott, PhD Thesis, Oklahoma University, 1965
90. D Quon, Dalla Lana, G W Govier *Can. J. Chem.* 32 880 (1954)
91. G Zhu, H D Gesser, N R Morton *Proceedings of the Natural Gas Conversion Symposium, Sydney, Australia, July 4-9, 1993*
92. S Mahajan, W R Menzies, L F Albright *Ind. Eng. Chem., Process Des. Dev.* 16 271 (1977)
93. S Mahajan, D M Nickolas, F Sherwood, W R Menzies, L F Albright *Ind. Eng. Chem., Process Des. Dev.* 16 275 (1977)
94. I Tepermeister, J Smith, J Streit, R Oldenborg, F Finch, W Danen, R Rauenzahn, C Rofer *Methane to Methanol: Reactor Design and Process Evaluation* LA-11396-MS DE89 003 381
95. S L Baughum, R C Oldenborg, W C Danen, G E Streit, C Rofer, in *Proceedings of the 1986 Quebec International Symposium on Optical and Optoelectric Applied Sciences and Engineering, Quebec, Canada, 1986*
96. H D Gesser, L A Morton *Catal. Lett.* 11 357 (1991)
97. J Huang, S L Suib *J. Phys. Chem.* 97 9403 (1993)
98. J Huang, M V Badani, S L Suib, J B Harrison, M Kablauoi *J. Phys. Chem.* 98 206 (1994)
99. A S Sokolik *Samovosplamnenie, Plamya i Detonatsiya v Gazakh* (Self-ignition, Flames, and Explosions in Gases) (Moscow: Izd. Akad. Nauk SSSR, 1960)
100. B Lewis, G Elbe *Combustion, Flames, and Explosions of Gases* (Orlando: Academic Press, 1987)
101. M Vanpee C. R. *Hebd. Seances Acad. Sci.* 243 804 (1956)
102. J Egret, L R Sochet, M Lucquin *Bull. Soc. Chim. Fr.* 2205 (1965)
103. O V Sokolov, V S Arutyunov, V Ya Basevich, V I Vedeneev *Kinet. Katal.* 36 317 (1995)
104. V S Arutyunov, V Ya Basevich, V I Vedeneev, O V Sokolov *Kinet. Katal.* 36 501 (1995)
105. V Ya Basevich, V I Vedeneev, V S Arutyunov *Khim. Fiz.* 13 (8-9) 157 (1994)
106. W C Danen, M J Ferris, J L Lyman, R C Oldenborg, C K Rofer, G E Steit, in *Abstracts of Papers, Symposium on Methane Upgrading, Division of Petroleum Chemistry, the 201st National Meeting of the American Chemical Society, Atlanta, 1991* p. 166
107. D M Newitt, A M Bloch *Proc. R. Soc. London, A Math. Phys. Sci.* 140 426 (1933)

108. H D Gesser, N R Hunter, L A Morton, P S Yarlagadda, in *The IX International Symposium on Alcohol Fuels, Firenze, Italy, 1991* Vol. 1, p. 99
109. D M Newitt, W G Schmidt *J. Chem. Soc.* 1665 (1937)
110. N M Emanuel', E T Denisov, Z K Maizus *Tsepnye Reaktsii Okisleniya Uglevodorodov v Zhidkoi Faze* (Chain Oxidation Reactions of Hydrocarbons in the Liquid Phase) (Moscow: Nauka, 1965)
111. V N Kondrat'ev, E E Nikitin *Kinetika i Mekhanizm Gazofaznykh Reaktsii* (Kinetics and Mechanisms of Gas-Phase Reactions) (Moscow: Nauka, 1974)
112. N N Semenov *O Nekotorykh Problemakh Khimicheskoi Kinetiki i Reaktsionnoi Sposobnosti* (Some Problems of Chemical Kinetics and Reactivity) (Moscow: Izd. Akad. Nauk SSSR, 1958)
113. L A Khachatryan, O M Niazryan, A A Mantashyan, V I Vedeneev, M A Teitel'boim *Int. J. Chem. Kinet.* **14** 1231 (1982)
114. I R Slagle, D Gutman *J. Am. Chem. Soc.* **107** 5342 (1985)
115. V D Knyazev, V S Arutyunov, V I Vedeneev *Int. J. Chem. Kinet.* **24** 545 (1992)
116. B C Wu, M T Klein, S I Sandler *Ind. Eng. Chem. Res.* **30** 822 (1991)
117. V I Vedeneev, A A Karnaukh, A A Mantashyan, M A Teitel'boim *Kinet. Katal.* **31** 7 (1990)
118. V I Vedeneev, O V Krylov, V S Arutyunov, V Ya Basevich, M Ya Gol'denberg, M A Teitel'boim *Appl. Catal. A* **127** 51 (1995)
119. Li-Biao Han, S Tsubota, T Kobayashi, M Haruta *J. Chem. Soc., Chem. Commun.* 93 (1995)
120. V Ya Basevich, V I Vedeneev, V S Arutyunov *Teor. Osn. Khim. Tekhnol.* **30** (1996) (in the press)
121. I O Khintse *Turbulentnost', ee Mekhanizm i Teoriya* (Turbulence, Its Mechanism and Theory) (Moscow: Fizmatgiz, 1963)
122. V Ya Basevich, V I Vedeneev, V S Arutyunov *Teor. Osn. Khim. Tekhnol.* **30** (1996) (in the press)
123. E B Bukhgalter *Metanol i ego Ispol'zovanie v Gazovoi Promyshlennosti* (Methanol and its Use in the Gas Industry) (Moscow: Nedra, 1986)
124. Rezkii Rost Mirovogo Potrebleniya Metanola na Proizvodstvo MTBE (Rapid Growth in the World Consumption of Methanol for the Production of MTBE) *Nefi', Gaz i Neftekhimiya za Rubezhom* (11/12) 125 (1992)
125. *The Clean Fuel Report* Vol. 4, No. 1 (Hiwot, CO: J E Sinor Consultant Inc., 1992)
126. Burnyi Rost Potrebleniya Oksigenatov (Rapid Growth of the Use of Oxygenates) *Nefi', Gaz i Neftekhimiya za Rubezhom* (11/12) 122 (1992)
127. Perspektivy Global'nogo Potrebleniya Oksigenatov (Prospects for the Global Use of Oxygenates) *Nefi', Gaz i Neftekhimiya za Rubezhom* (11/12) 125 (1992)
128. F V Smal', E E Arsenov *Perspektivnye Topliva dlya Avtomobilei* (Possible Future of Fuels for Cars) (Moscow: Transport, 1979)
129. Ya B Chertkov *Motornye Topliva* (Motor Fuels) (Novosibirsk: Nauka, 1987)
130. G A Terent'ev, V M Tyukov, F V Smal' *Motornye Topliva iz Al'ternativnykh Syr'evykh Resursov* (Motor Fuels from Alternative Raw Material Resources) (Moscow: Khimiya, 1989)
131. L V MacDougall *Catal. Today* **8** 337 (1991)
132. B Hohlein, D Mausbeck, E Supp, P Konig, in *The IXth International Symposium on Alcohol Fuels, Firenze, Italy, 1991* Vol. 1, p. 43
133. A Forestiere, J L Nocca, B Torck, P Leprince, in *The IXth International Symposium on Alcohol Fuels, Firenze, Italy, 1991* Vol. 1, p. 292
134. P Comotti, S Marengo, S Martinengo, L Zanderighi, in *The IXth International Symposium on Alcohol Fuels, Firenze, Italy, 1991* Vol. 1, p. 73
135. J T Jensen, in *The IXth International Symposium on Alcohol Fuels, Firenze, Italy, 1991* Vol. 1, p. 9
136. J C W Kuo, C K Kresge, R E Palermo *Catal. Today* **4** 463 (1989)
137. J W M H Geerts, J H B J Hoebink, K van der Wiele *Catal. Today* **6** 613 (1990)
138. G Renesme, J Saint-Just, Y Muller *Catal. Today* **13** 371 (1992)
139. J Crocco *Chem. Ind.* (2) 97 (1990)
140. V S Arutyunov, V I Vedeneev, N Yu Krymov, M N Radchenko, A D Sedykh *Gazovaya Promst* (7) 19 (1992)
141. A D Sedykh, in *The IXth International Symposium on Alcohol Fuels, Firenze, Italy, 1991* Vol. 1, p. 29
142. J Haggin *Chem. Eng. News* **70** (17) 33 (1992)
143. P Gray *Ber. Bunsenges. Phys. Chem.* **84** 309 (1980)
144. P Gray, J F Griffiths, S M Hasco *Proc. R. Soc. London, A Math. Phys. Sci.* **396** 227 (1984)
145. V I Starosel'skii *Miner. Resursy Rossii* (6) 13 (1992)
146. F Salmanov, A Zolotov *Izvestiya* 23rd March (1992)

Coordination chemistry of hydrophosphorane compounds

K N Gavrilov, I S Mikhel'

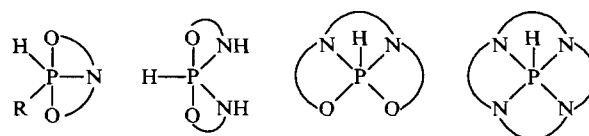
Contents

I. Introduction	225
II. The formation of complexes by bicyclic hydrophosphoranes	226
III. The formation of complexes by tricyclic hydrophosphoranes	235
IV. The formation of complexes by tetracyclic hydrophosphoranes	236
V. Conclusion	245

Abstract. The overall results of the study of hydrophosphorane compounds as ligands for metal complex synthesis and catalysis are summarised and discussed. The principal types of coordination of hydrophosphoranes, the structure of their metallo-derivatives, and the possible mechanism of the complex formation reaction are examined. The prospects for the employment of hydrophosphoranes in modern coordination design are demonstrated. The bibliography includes 102 references.

I. Introduction

The current range of phosphorus-containing ligands is exceptionally varied and in many respects determines the progress in the field of metal complex design. Many phosphorus-containing ligands are involved in the construction of tens and perhaps hundreds of coordination compounds. Thus the Cambridge Structural Database contains information about the structures of 720 complexes based on one of the simplest organophosphorus compounds—triphenylphosphine,¹ and this does not constitute the maximum information available since new studies are being regularly published. After all, there has been no flagging of interest for more than 30 years in perhaps the most popular P, N-bidentate ligand—2-diphenylphosphinopyridine. We may also point to the outstanding range of complex chiral systems which have found application in asymmetric catalysis.^{2,3} Overall, the stream of information about the coordination compounds of phosphorus has recently assumed an avalanche-like character. Nevertheless, the notable event which occurred towards the end of the 1970s is outstanding even against this background—the introduction into practical metal complex synthesis of a fundamentally new class of phosphorus-containing ligands—hydrophosphoranes.



At first sight, the structure of hydrophosphoranes contains no potential donor centres—their phosphorus atom has no lone pair (LP) and those of the nitrogen and oxygen atoms should be involved in $p\pi-d\pi$ conjugation with the d orbitals of the phosphorus atoms. However, these compounds are in fact the most variable phosphorus-containing ligands capable of P-, N-, P,N-, P,O-, and N,N-coordination. Furthermore, many new metal complexes have been obtained precisely in the study of the reactivities of hydrophosphoranes (HP), whereupon a whole series of unusual coordination polyhedra were synthesised. Any complex reaction involving hydrophosphoranes is a nontrivial phenomenon in coordination chemistry from the standpoint both of its products and of the initial compounds. Indeed hydrophosphoranes can quite justifiably be called paradoxical ligands: they are formally incapable of binding Lewis acids but exhibit an extremely wide range of coordination possibilities.

Nowadays hydrophosphoranes constitute an independent, unique class of phosphorus-containing ligands. They have occupied this position as a result of deliberate efforts by two leading research teams: the French school under the leadership of Professor Riess, who were involved in the initiation of the coordination chemistry of hydrophosphoranes, and the American school led by Professor Lattman.

The reactivity of hydrophosphoranes has been investigated in considerable detail from the standpoint of organophosphorus chemistry and several thorough reviews have been published on this topic (see, for example, Nifant'ev and Kukhareva⁴). However, many new data concerning the formation of complexes by hydrophosphoranes have appeared since their publication and, furthermore, the data on the chemistry of hydrophosphoranes presented in these reviews are either very scanty^{5,6} or are invoked merely to illustrate certain fundamental concepts: the relation between organometallic and coordination chemistry,⁷ the characteristics of phosphoranide coordination,⁸ the characteristics of complex formation in systems with a phosphorus–nitrogen bond,⁹ and the structural characteristics of metallated phosphoranes.¹⁰ The present review is the first attempt at a systematic consideration of the coordination properties of hydrophosphoranes and of their role and position in the series of phosphorus-containing ligands. We have tried to compare the reactivities of various groups of

K N Gavrilov Department of Chemistry, Esenin Ryazan State Pedagogic [Teacher Training] University, ul. Svobody 46, 390000 Ryazan', Russian Federation. Fax (7-091) 244 43 90

I S Mikhel' Laboratory for Asymmetric Catalysis, Zelinskii Institute of Organic Chemistry, Russian Academy of Sciences, Leninskii prosp. 47, 117913 Moscow, Russian Federation. Fax (7-095) 135 53 28

Received 28 July 1995

Uspekhi Khimii 65 (3) 242–265 (1996); translated by A K Grzybowski

hydrophosphoranes, to differentiate within each group the principal types of bonding to the central atom, to discuss certain spectroscopic features (primarily ^{31}P NMR and IR spectroscopic data concerning metallo-derivatives of hydro-phosphoranes), and to indicate the prospects for the use of hydrophosphoranes in modern coordination design.

The data presented in this review have been divided into sections in accordance with the number of phosphorus-containing rings in the initial hydrophosphoranes and the nature of the junctions between them: bicyclic systems (condensed and spiro-systems) were examined initially and then tricyclic and tetracyclic systems.

II. The formation of complexes by bicyclic hydrophosphoranes

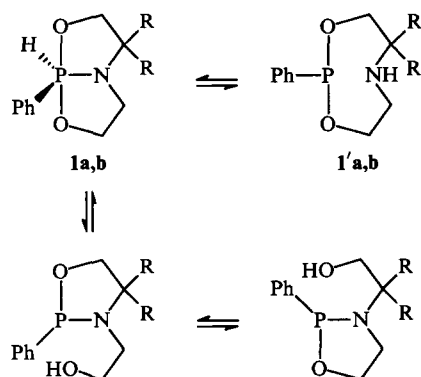
1. Processes involving bicyclic aminophosphoranes with condensed rings

Complexes of bicyclic aminophosphoranes (BAP) with condensed rings containing Rh, Pd, Ru, Mo, W, Fe, and Co are known at present. In the arrangement of the data for this part of the review, account was taken primarily of the nature of the central metal atom. An attempt was made to demonstrate strikingly the principal types of coordination of the ligands under discussion and as far as possible to reflect the history of the development of the branch of the chemistry of hydrophosphoranes considered. In view of the last factor, the discussion is initiated by considering compounds of platinum metals.

a. Rhodium complexes of bicyclic aminophosphoranes

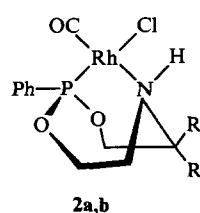
A communication¹¹ concerning the coordination of BAP, which in historical terms proved to be the first group of ligands of a fundamentally new class, was published in 1978.

A general scheme for a possible tautomeric equilibrium involving BAP was presented¹¹ and, although only forms with pentacoordinate phosphorus **1a,b** were detected spectroscopically in solution, the presence of two donor centres — the phosphorus and nitrogen atoms in the potential phosphocane tautomers **1'a,b** — led the authors to carry out complex formation reactions with BAP.



R = H (a) (Phoran), Me (b)

It was found that compounds **1a,b** react rapidly under mild conditions with $[\text{Rh}(\text{CO})_2\text{Cl}]_2$ (P:Rh = 1:1), forming compounds **2a,b** in yields exceeding 95%.



Parameter	Compound	
	2a	2b
$\nu(\text{NH})/\text{cm}^{-1}$	3195	3178
$\nu(\text{CO})/\text{cm}^{-1}$	1991	1985
$\nu(\text{RhCl})/\text{cm}^{-1}$	290	285
$\delta_{\text{P}}/\text{ppm}$	162.0	160.8
$^1J(\text{P,Rh})/\text{Hz}$	190.5	197

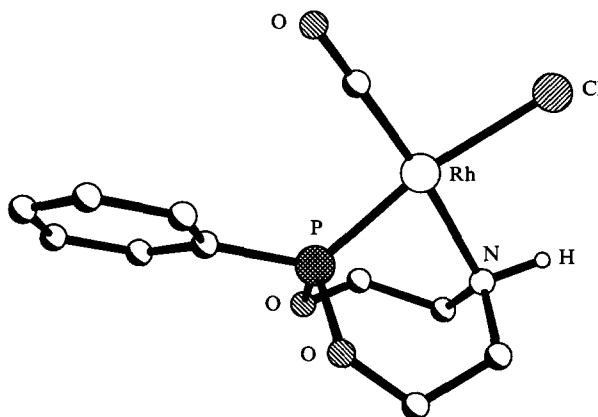


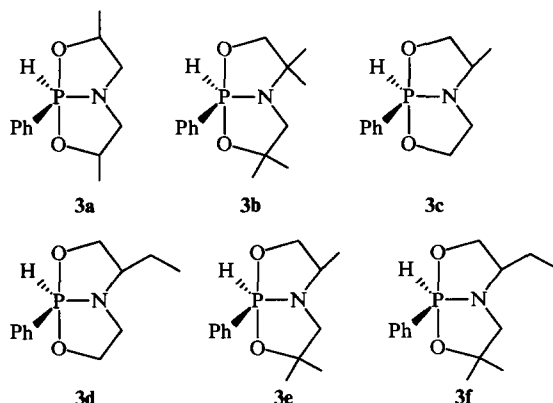
Figure 1. The structure of complex **2a**.

We may note that the IR and ^{31}P NMR spectroscopic parameters [especially $\nu(\text{CO})$, $\nu(\text{RhCl})$, and the spin-spin coupling constants (SSCC) $^1J(\text{P,Rh})$] quoted for complexes **2a,b** are typical (taking into account the nature of the phosphorus centre) for mononuclear chlororhodium(I) carbonyl compounds with various chelating P,N-bidentate ligands.¹²⁻¹⁴ On the other hand, the chemical behaviour of complexes **2a,b** differs appreciably from that of the rhodium complexes with trivial phosphorus-containing ligands. Thus the formation of a 2:1 complex is not observed on interaction of compounds **1a,b** with $[\text{Rh}(\text{CO})_2\text{Cl}]_2$ in the molar proportions P:Rh = 2:1. The reactions of compound **2b** with an excess of triphenylphosphine affords *trans*- $[\text{RhCl}(\text{CO})(\text{PPh}_3)_2]$ with displacement of the P,N-bidentate ligand, but this time in the form of the initial pentacoordinate structure **1b** and not the phosphocane form **1'b**.

X-Ray diffraction study of complexes **2a,b** (Fig. 1)¹⁵ revealed distances between the rhodium atom and its nearest neighbours typical of those for chelate chlororhodium carbonyl compounds with P,N-bidentate ligands as well as normal intramolecular $\text{Cl}\cdots\text{H}-\text{N}$ hydrogen bonds. The phosphorus-nitrogen atom distances of 2.793 and 2.788 Å (for compounds **2a** and **2b** respectively), are much less than the sum of the van der Waals radii (3.4 Å). This indicates the occurrence of the intramolecular $\text{P}\cdots\text{N}$ attractive interaction.

Ethene-containing analogues of compounds **2a,b**, formed by the reaction of compounds **1a,b** with $[\text{Rh}(\text{C}_2\text{H}_4)_2\text{Cl}]_2$ in the molar proportions P:Rh = 1:1, are also known. The same reaction, but with a molar ratio of P:Rh = 2:1, leads to the cationic complexes $[\text{RhL}_2]^+\text{Cl}^-$ (L = bicyclic aminophosphorane) with a *cis*-configuration of the phosphorus atoms. We may note the presence of the $\text{N}-\text{H}\cdots\text{Cl}\cdots\text{H}-\text{N}$ hydrogen bonds between the nitrogen centres of the coordinated phosphocyclanes and the counterion.

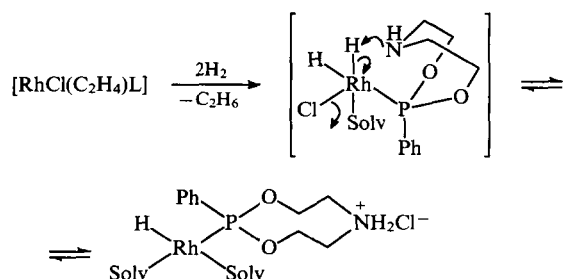
The interaction of $[\text{Rh}(\text{CO})_2\text{Cl}]_2$ with a series of new BAP (compounds **3a-f**) was investigated subsequently.^{16,17}



Compounds **3c–f** were synthesised in a homochiral form from L-alaninol or D-ethylalaninol. The rhodium complexes $[\text{RhCl}(\text{CO})\text{L}]$ obtained from compounds **3a–f** have the same structures as complexes **2a,b** mentioned above, which follows from their ^{31}P NMR and IR spectra: $\delta_{\text{P}} = 147\text{--}161$ ppm, $^1J(\text{P,Rh}) = 180\text{--}190$ Hz; $\nu(\text{CO}) = 1995\text{--}2003$ cm^{-1} , $\nu(\text{RhCl}) = 280\text{--}300$ cm^{-1} , $\nu(\text{NH}) = 3190\text{--}3203$ cm^{-1} . One of the possible diastereoisomers of the complex based on the phosphorane **3c**, used as the catalyst of the enantioselective hydrogenation of (*Z*)- α -acetamidocinnamic acid with a chemical yield of 92% and an optical yield of 18%, has been isolated by fractional crystallisation from solution in acetonitrile.

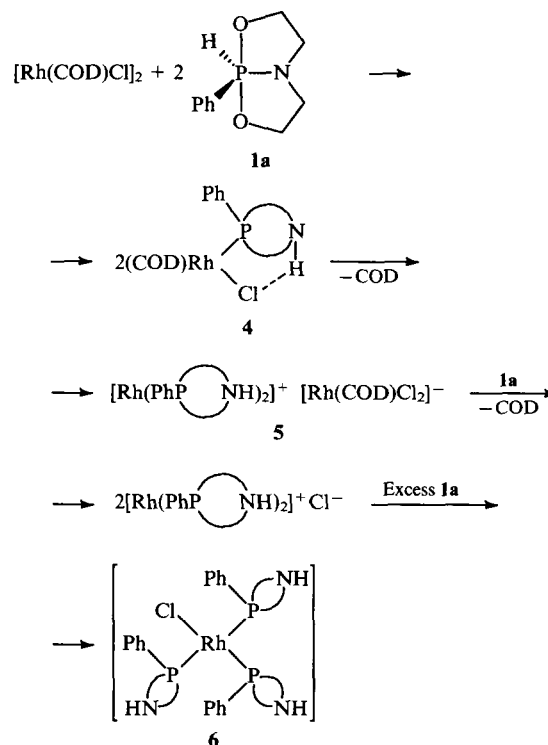
Catalysis involving rhodium complexes of BAP merits special consideration. They are all coordination systems of the metal in a 'cradle' type, formed by the phosphocane bound as a P,N-bidentate species. The more labile nitrogen centre under these conditions is the hydrophilic NH group, capable of binding a proton in the course of the catalytic cycle. The binding of a proton is accompanied by the freeing of a coordination vacancy at the central atom. These structural features make it possible to regard the rhodium derivatives of BAP as promising metal complex catalysts. Several attempts have been made to use such compounds as catalysts. In particular, in the hydroformylation of hex-1-ene, complex **2b** ensures under comparable conditions a higher degree of conversion than $\text{RhCl}(\text{CO})(\text{PPh}_3)_2$ (85% and 52% respectively).¹⁶ The cationic systems $[\text{Rh}(\text{CO})\text{L}(\text{MeCN})]^+ \text{PF}_6^-$, obtained from compounds **2a,b** and AgPF_6 in acetonitrile, catalyse the hydrogenation of (*Z*)- α -acetamidocinnamic acid to *N*-acetylphenylalanine.¹⁸ The yield of the product was not indicated.

The hydrogenation of hex-1-ene in the presence of the ethene complex $[\text{RhCl}(\text{C}_2\text{H}_4)\text{L}]$ has been investigated in detail.¹⁹ It was shown that its activity in hydrogenation and isomerisation is somewhat superior to that of the familiar Wilkinson catalyst $\text{RhCl}(\text{PPh}_3)_3$. This applies particularly to the isomerisation process. The above feature is due to the role played by the nitrogen centre in the catalytic cycle, since the monohydride complex formed with its participation is in fact the true catalyst of the isomerisation of the alkene.



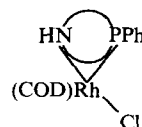
Overall, the study of the catalytic properties of the rhodium derivatives of BAP has been fragmentary and limited. Thus, in the light of the latest advances in asymmetric catalysis,³ it is evident that the hydrogenation of the prochiral precursors of aminoacids is by no means the only field where rhodium complexes with P,N-bidentate optically active ligands can be used. Apparently, this catalyst may be expected to exhibit a much higher asymmetrising activity in, for example, hydroformylation and isomerisation processes. One thing is clear, the search for a due place for BAP in modern metal complex catalysis (especially enantioselective) has only just begun and requires further efforts.

The study of the interaction of compound **1a** (Phoran) with $[\text{Rh}(\text{COD})\text{Cl}]_2$ (COD = cycloocta-1,5-diene)—a familiar precursor of active catalytic systems—is of special interest in this connection.²⁰ The reaction is monitored by IR, ^{31}P NMR, and UV spectroscopic methods.



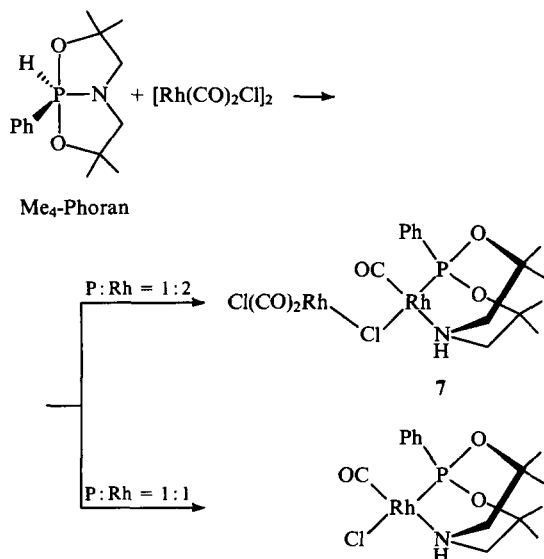
Complex **4**, formed initially with the phosphocane coordinated as a P-monodentate species, is subsequently transformed into the unusual ionic adduct **5** with a *cis*-disposition of the phosphorus atoms in the cation, which has been characterised by X-ray diffraction. The $\nu(\text{NH})$ absorption band of a single crystal of complex **5** is in the region of 3190 cm^{-1} . Only one $\text{N}\cdots\text{H}\cdots\text{Cl}$ hydrogen bond was detected under these conditions. It is of interest that a further two forms of compound **5**, characterised by $\nu(\text{NH})$ frequencies of 3205 and 3215 cm^{-1} , have been isolated. According to the authors, the difference between the $\nu(\text{NH})$ absorption frequencies is due to the different orientations of the cation and the anion in the crystals of these forms.

The indication of the P-monodentate binding of the phosphocane in complexes **4** and **6** is of fundamental importance. However, this important conclusion appears inadequately justified. Firstly, these compounds were not isolated from the reaction mixture. Secondly, the spectroscopic data presented are clearly insufficient for a rigorous demonstration of their structure. Thus the structure of compound **6** was postulated solely on the basis of UV spectroscopic data. For complex **4**, it is possible to put forward a structure in which the coordination number (CN) of rhodium is five with a consequent apical coordination of the amino-group. Such a structure does not conflict with the spectroscopic parameters of this complex: $\delta_{\text{P}} = 140.0$ ppm, $^1J(\text{P,Rh}) = 210$ Hz; $\nu(\text{NH}) = 3140$ cm^{-1} , and $\lambda_{\text{max}} = 404$ nm. Indeed such a low $\nu(\text{NH})$ frequency is more likely to indicate direct coordination of the nitrogen centre to rhodium than the presence of the $\text{N}\cdots\text{H}\cdots\text{Cl}$ bond involving a noncoordinated amino-group.



Considerable attention has been devoted to the detailed study of the reaction of BAP with another rhodium catalyst popular in metal complex synthesis and catalysis— $[\text{Rh}(\text{CO})_2\text{Cl}]_2$. A series of chelate chlororhodium carbonyl complexes, obtained by the interaction of various BAP with this precursor, have already

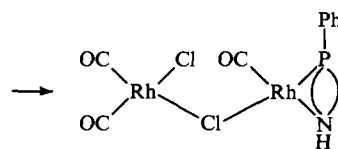
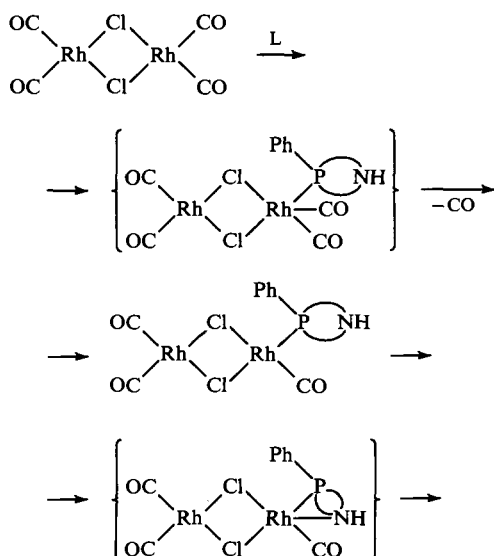
been mentioned. An important discovery was made in the course of a detailed study of this process with participation of BAP such as Phoran²¹ and especially Me₄-Phoran:²² the stable dinuclear rhodium(I) complexes **7** with one chloride bridge were obtained unexpectedly.



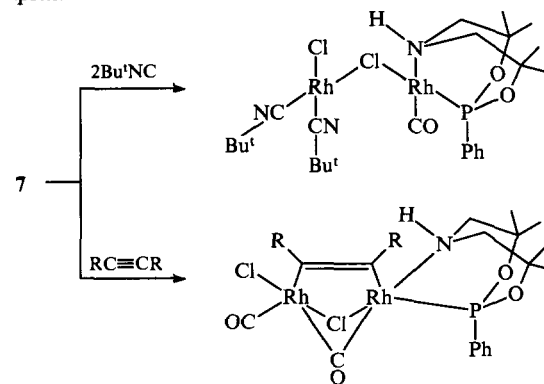
Compound **7** was characterised by ¹H and ³¹P NMR and IR spectroscopic methods, by field desorption mass spectrometry, and by X-ray diffraction. The N—H...Cl intramolecular hydrogen bond between the nitrogen centre and the chloride ligand of the [Cl(CO)₂Rh] fragment was detected. The distance between the phosphorus and nitrogen atoms (2.705 Å) is appreciably shorter than in complexes **2a,b**, which indicates a more pronounced attractive N...P interaction in the case of complex **7**. The further reaction between complex **7** and Me₄-Phoran leads to a mononuclear complex. It is of interest that the coordination of unsubstituted Phoran is not quite so selective, since for the molar ratio P : Rh = 1 : 2 a mixture of products is formed: compound **2a**, already known, and an analogue of compound **7**, namely [Cl(CO)₂Rh(μ-Cl)Rh(CO)(Phoran)]. Attempts at a preparative separation of the latter product were unsuccessful.

A general mechanism of the interaction of BAP (L) with [Rh(CO)₂Cl]₂ has been proposed.

The dirhodium complex with one chloride bridge is a stable intermediate in this process on the way to chelate mononuclear compounds.



Study of the reactivity of complex **7** revealed an appreciable stability of the chloride bridge:²³ reactive compounds such as O₂, CO, CO₂, CS₂, CH₃I, CH₂=CH₂, and HC≡CH do not interact with compound **7** even under conditions of thermal or photochemical activation. Only Bu^tNC or activated alkynes are capable of modifying the structure of this unusual dinuclear complex.



R = CO₂Me, CO₂Bu, CF₃

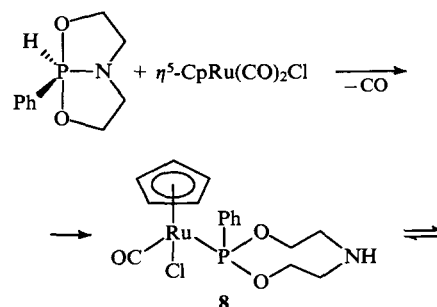
In considering the structures of new rhodium compounds ¹H, ¹³C, and ³¹P NMR and IR spectroscopy and, in the case of the *tert*-butyl isocyanide derivative, ¹⁵N NMR spectroscopy were used. In the last case, direct binding of the nitrogen centre of the phosphocane to the metal was demonstrated by use of the naturally abundant ¹⁵N isotope and the INEPT method [$\delta_N = -370.0$ ppm, $^1J(N, Rh) \approx ^2J(N, P) \approx 11.8$ Hz]. This is an extremely rare and elegant experiment involving the application of ¹⁵N NMR spectroscopy to determine the nature of the coordination of the P,N-containing ligand. We may note that the study of Brun et al.²³ is the latest of a series of studies carried out over a decade and devoted to the rhodium derivatives of BAP.

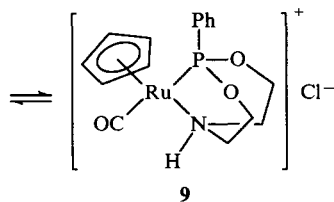
Summarising, we may note that chelate P,N-bidentate coordination of BAP in the phosphocane form is characteristic of rhodium. There exists indirect evidence for the possibility of their P-monodentate binding, but this type of coordination has been established reliably only in relation to complexes of other transition metals.

b. Ruthenium and palladium compounds

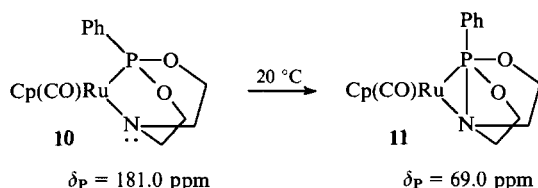
We are aware of only one study²⁴ devoted to the interaction of BAP (specifically Phoran) with the ruthenium complex CpRu(CO)₂Cl.

The ionic complex **9**, which according to ¹H and ³¹P NMR spectroscopic data is in equilibrium with the neutral complex **8**, was isolated from the reaction mixture in an almost quantitative yield. The ion-exchange reaction between NaBPh₄ and compound

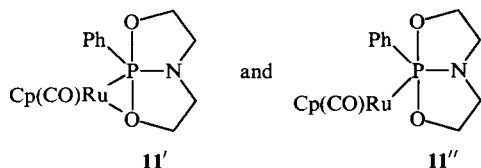




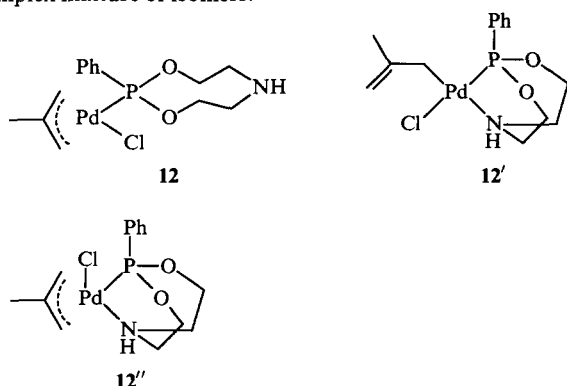
9 afforded an analogue of the latter complex, containing tetraphenylborate as the anion. Its deprotonation by treatment with MeLi at $-100\text{ }^{\circ}\text{C}$ leads to the amide adduct **10**, which is stable only at low temperatures, being transformed gradually at $20\text{ }^{\circ}\text{C}$ into the phosphoranide complex **11**.



The structures of complexes **8–11** have been established by means of ^1H and ^{31}P NMR and IR spectroscopy and, in the case of compounds **10** and **11**, by comparing their ^{31}P NMR spectroscopic parameters with those of the Mo- and W-containing analogues, which have been investigated in detail by X-ray diffraction. Later in this review we shall discuss further the characteristics of the phosphoranide type of binding of BAP to metals. For the moment, we may note that Vierling et al.²⁴ postulated the existence of equilibrium (even at $-100\text{ }^{\circ}\text{C}$) between complex **11** and its isomers **11'** and **11''** with P,O-bidentate or P-monodentate phosphoranide coordination.



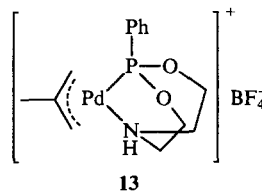
Like ruthenium and rhodium, palladium is capable of P-monodentate and P,N-bidentate binding of BAP in the phosphocane form. In particular, the reaction between $[\text{CH}_2\text{CMeCH}_2\text{PdCl}]_2$ and Phoran (P: Pd = 1:1) affords a complex mixture of isomers.²⁵



The IR spectrum of the reaction solution contains three absorption bands at 3400 , 3280 , and 3200 cm^{-1} , corresponding to the NH group, the highest frequency band referring to the noncoordinated amino-group of complex **12**. It has been suggested that complexes **12'** and **12''** are stabilised by the formation of intramolecular hydrogen bonds. There is apparently a dynamic equilibrium between the three isomers, as a consequence of which

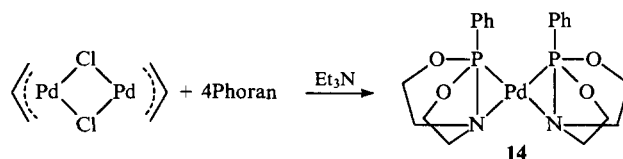
a poor resolution is observed in the ^{31}P NMR spectrum. On the whole, one may agree with Agbossou et al.²⁵ that a more correct description of the reaction under consideration requires additional studies.

Apart from complexes **12**, **12'**, and **12''**, the chelate cationic complex **13** is also known.



According to conductimetric data, complex **13** is an electrolyte of a type intermediate between 1:1 and 1:2. This is apparently associated with the existence of equilibrium between complex **13** and the dimer $[\text{CH}_2\text{CMeCH}_2\text{Pd}(\mu\text{-L})_2\text{PdCH}_2\text{CMeCH}_2](\text{BF}_4)_2$, in which the phosphocane ligands are of the bridging P,N-bidentate type. The high activity of complex **13** in the catalysis of the oligomerisation of butadiene is noteworthy (a mixture of C_8 , C_{12} , and C_{16} products with 100% conversion was obtained).

It has been stated²⁶ that an unstable palladium phosphoranide derivative **14** is formed.²⁶

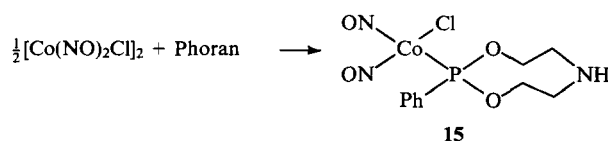


Since the structure of complex **14** was postulated solely on the basis of ^{31}P NMR spectroscopic data, further experimental data for its confirmation appear necessary.

Summarising, we may note that the ruthenium and especially the palladium derivatives of BAP are represented by few examples and have been investigated fairly superficially. This field of BAP coordination chemistry still awaits its investigators.

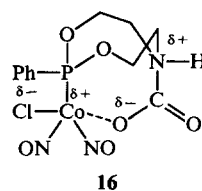
c. Cobalt and iron complexes

We are aware of only one complex formation reaction between BAP and a cobalt compound, namely $[\text{Co}(\text{NO})_2\text{Cl}]_2$.^{27, 28}



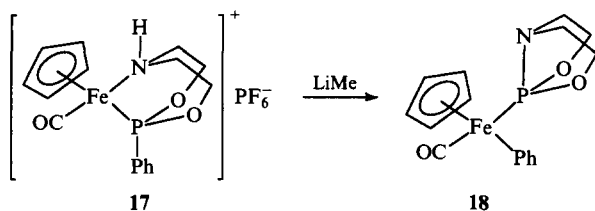
According to X-ray diffraction data, although the distance between the P and N atoms in the phosphocane ring (2.978 \AA) in complex **15** is greater than in the case of the chelate rhodium complexes **2a,b**, it is again appreciably less than the sum of the van der Waals radii. By virtue of the noncoordinated peripheral amino-group, compound **15** enters into an interesting reaction with carbon dioxide, leading to the formation of the carbamate-like adduct **16**.²⁸

During storage under an argon atmosphere, complex **16** gradually loses the CO_2 group with regeneration of the initial

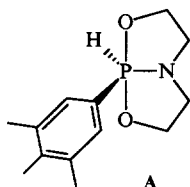


compound **15**. The reversible binding of CO₂ observed here models to some extent biosynthetic carboxylation processes with participation of biotin.

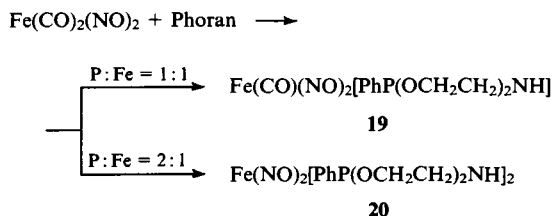
In contrast to the cobalt-containing complexes, the iron-containing BAP complexes have been investigated fairly widely. The first step in the study of their chemical properties already led to the discovery of the unique reversible migration of the phenyl group from phosphorus to the metal without change in the oxidation state and the coordination number of the latter.²⁹ The deprotonation of complex **17** [obtained from CpFe(CO)₂Br and Phoran], carried out for the synthesis of a phosphoranide derivative, led to the formation of complex **18** with a bicycloposphoramidite ligand.



The structure of complex **18** has been demonstrated by X-ray diffraction. The deprotonation process is reversible: the passage of gaseous HCl through a solution of complex **18** in tetrahydrofuran (THF) in the presence of NH₄PF₆ regenerates complex **17** with a 60% yield. It has been suggested that the transannular N → P interaction in the structure of complex **17** facilitates the 1,2-shift of the phenyl group attached to the P–Fe bond. Subsequently a similar reversible migration was observed²⁴ also for a homologue of Phoran (compound A), where precisely the carbon atom which had been previously linked to phosphorus was found to be bound to iron, which agrees well with the concept of a 1,2-sigmatropic shift of the aryl group.

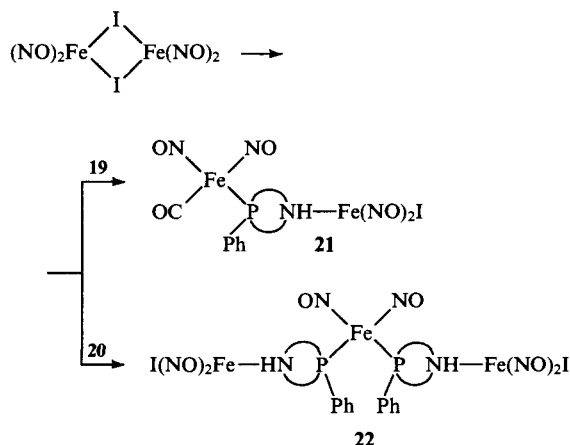


As a result of the successful choice of the initial iron compounds, it proved possible to obtain, via a two-stage synthesis, systems with bridging P,N-bidentate binding of the phosphocane ring.^{30,31} We may note that this type of unusual coordination of BAP was observed for the first time. Complexes with the P-monodentate coordination of the ligand were obtained initially.



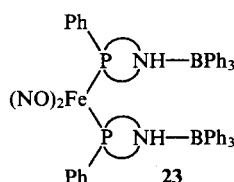
A weak broad ν(NH) absorption band at 3400 cm⁻¹, characteristic of a noncoordinated secondary amino-group, was observed in the IR spectrum of compound **19**. Two weak, narrow, ν(NH) bands at 3400 and 3300 cm⁻¹ were recorded for complex **20**, the presence of the latter band being tentatively attributed to the existence of intermolecular hydrogen bonds. Subsequently the

dinuclear and trinuclear iron complexes **21** and **22** were obtained from complexes **19** and **20**.

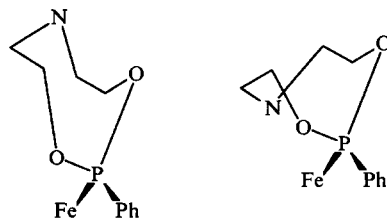


Unfortunately compounds **21** and **22** have been studied inadequately. Thus only fragment peaks were detected in their mass spectra, although an extremely mild method (chemical ionisation) was used. Nothing is said in the communication of Mordenti et al.³¹ about attempts to determine the molecular structures of compounds **21** and **22** by independent methods.

The peripheral amino-groups in complex **20** are capable of coordinating various Lewis acids, for example the proton (in the HCl–NaBPh₄–EtOH system) or BPh₃.³² In the latter case, an interesting three-centre adduct of the P–Fe–P type (compound **23**) was obtained from BAP.

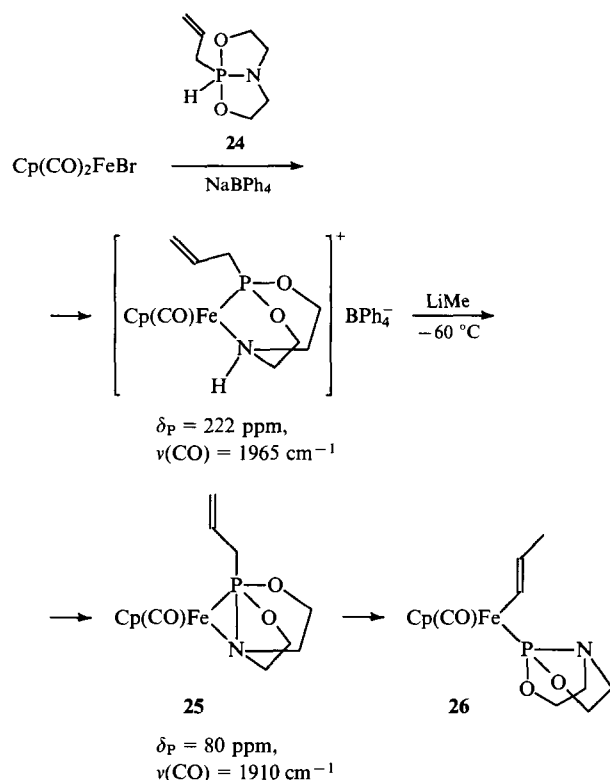


The structures of compounds **20** and **23** were established by X-ray diffraction. A tetrahedral coordination of the iron atom was observed in both cases. The distances between the phosphorus and nitrogen atoms in the phosphorus-containing rings are 3.647 and 3.616 Å for compound **20** and 3.590 Å for compound **23**, which appreciably exceeds the sum of the van der Waals radii. The conformations of the phosphocane rings in compounds **20** and **23** can be described as 'chair-boat'.



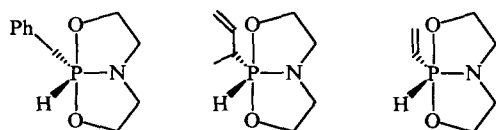
The O...H–N hydrogen bond involving the amino-group of one molecule and the nitrosyl oxygen atom of another was detected in complex **20**. It had been postulated previously on the basis of IR spectroscopic data. A weak N–H...N contact was also found. These hydrogen bonds apparently actually stabilise the novel ligand conformations.

Iron phosphoranide complexes are also known. In particular, such an adduct has been detected by ³¹P NMR spectroscopy as an intermediate in the unprecedented process involving the reorganisation and migration of the allyl group from phosphorus to iron.^{34,35}

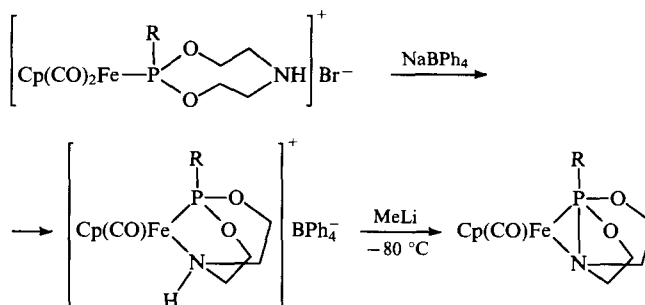


The coordination of the allyl-substituted BAP (compound **24**) leads not to a σ -allyliron complex, which might be formed as a result of the direct migration of the allyl group from phosphorus to iron, but to the σ -vinyliron compound **26** as a result of the isomerisation of this substituent accompanying the transfer process. The phosphoranide adduct **25** is stable in solution only at temperatures below 0°C . At 60°C , it is fully converted into compound **26** in 1 h. The structure of complex **26** was established by ^1H , ^{13}C , and ^{31}P NMR and IR spectroscopy. Whereas the migration of the phenyl group is known to be a reversible process, the reverse transfer of the vinyl group from iron to phosphorus is not observed even when complex **26** is treated with hydrogen chloride. It has been suggested that the phosphoranide coordination of compound **25** increases the electron density on the metal and hence its basicity, activating the insertion of iron into an allyl or vinyl C–H bond with the subsequent 1,3-shift of a proton and dissociation of the P–C bond. In fact the decrease in the $\nu(\text{CO})$ frequency by 55 cm^{-1} on passing from the cationic complex to the phosphoranide adduct **25** agrees well with an increase in electron density on the iron atom in the adduct. Thus the migration of the allyl group differs radically both from the transfer of the phenyl group (accompanied by dissociation of the P–C bond alone) and from the known *ortho*-metallation reactions (involving only the insertion of the metal in a C–H bond).

Apart from the allylphosphorane **24**, several further related BAP were used to investigate the fine details of the migration of organo groups from phosphorus to iron.³⁵



The interaction of these compounds with $\text{Cp}(\text{CO})_2\text{FeBr}$ leads in the first stage to ionic complexes and then to phosphoranide complexes.



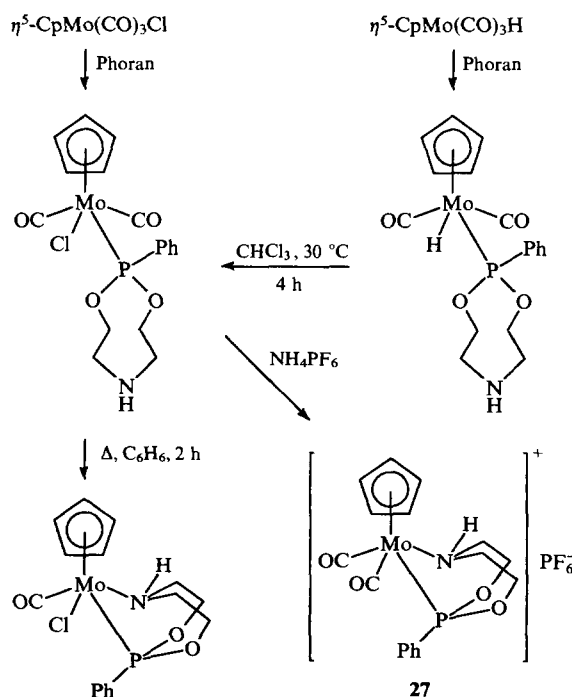
The phosphoranide complexes exist in solution only at temperatures below 0°C . It is of interest that the iron-containing analogue of the ruthenium amide intermediate **10** has not been detected spectroscopically even at -100°C , apparently as a consequence of its short lifetime. Since the structures of the phosphoranide complexes have been discussed only on the basis of ^{31}P NMR and IR spectroscopic data, one cannot rule out the possibility of the existence in solution of their isomers with P-monodentate and P,O-bidentate coordination, analogous to the ruthenium derivatives **11** and **11'**.

An attempt to isolate the iron phosphoranide compounds led to their further reactions. The complex with a methylallyl group rearranges smoothly after refluxing in THF for 1 h into the σ -vinyliron compound (like compound **25**), while the remaining compounds form complex mixtures of products under these conditions.

Thus the study of the iron complexes has been an important stage in the development of the coordination chemistry of BAP: the P-monodentate and P,N-bidentate bridging types of binding of the phosphocane forms have been clearly demonstrated and a series of phosphoranide adducts have been characterised spectroscopically.

d. Molybdenum and tungsten compounds

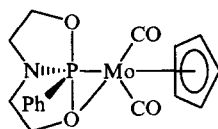
Virtually all the data obtained on the formation of complexes by BAP with molybdenum and tungsten compounds refer to molybdenum complexes. There are very few tungsten adducts of BAP. In particular, the interaction of compound **3c** with $\text{M}(\text{CO})_6$ ($\text{M} = \text{Mo}, \text{W}$) at $120\text{--}150^\circ\text{C}$ for 24 h leads to the products $\text{M}(\text{CO})_5\text{L}$ with P-monodentate coordination of the phosphocane.¹⁶ The use in this process of the sterically less



hindered ligand Phoran made it possible to obtain the disubstituted compounds $M(CO)_4L_2$, but complexes of the type $M(CO)_4L$ in which the phosphocane is bound as a P,N-bidentate species have not been obtained.

Both P-monodentate and P,N-bidentate coordination has been achieved by employing more reactive molybdenum compounds initially.³⁶ All these complexes were investigated by IR and 1H , ^{13}C , and ^{31}P NMR spectroscopy, mass spectrometry, and by vapour phase osmometry.

The deprotonation of compound **27** by treatment with LiMe (ether/THF, 60 °C) leads to a molybdenum compound with P,O-bidentate phosphoranide coordination of the ligand.³⁷



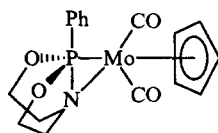
28

$\delta_P = 23.8$ ppm,
 $\nu(CO) = 1925$ and 1835 cm^{-1}

This is the first example not only of the phosphoranide type coordination of BAP but also of the synthesis of a metallated phosphorane.¹⁰

It has been shown by X-ray diffraction that the P—O bond involved in the formation of a three-membered metallocycle is significantly lengthened compared with the second P—O bond (1.893 and 1.653 Å). We may note that the usual BAP geometry is retained in complex **28**: the oxygen atoms being axial and the nitrogen atoms and the phenyl group equatorial.

The first transition metal complex containing the $\overline{N-P-M}$ cyclic fragment was synthesised by the deprotonation of compound **27** with methyl lithium under mild conditions (THF, -20 °C).³⁸

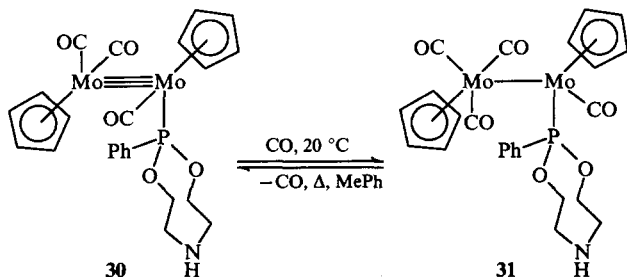


29

$\delta_P = 43.9$ ppm,
 $\nu(CO) = 1945$ and 1855 cm^{-1}

According to X-ray diffraction data, the P—N bond in complex **29** is one of the longest (1.91 Å) of this type. The equatorial orientation of the oxygen atoms, unusual for trigonal-bipyramidal phosphorus, and the axial orientation of the phenyl group are also noteworthy. It is of interest that complex **29** isomerises readily to complex **28** (on heating in solution in THF to 60 °C). When hydrogen chloride was passed through a THF solution of complex **29**, an analogue of complex **27** was obtained in a quantitative yield (the counterion is the chloride anion). The tungsten analogue of compound **29** has also been obtained.

The dimeric molybdenum complex $Cp(CO)_2Mo \equiv Mo(CO)_2Cp$ has also been resorted to in order to investigate the coordination of BAP. In this case, the lack of information about its interaction with potentially chelating ligands and also the presence of the highly reactive $Mo \equiv Mo$ bond are of interest. It has been found that the reaction of this complex with Phoran leads to two main products — **30** and **31**.^{39,40}



30

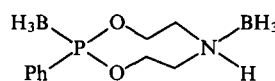
31

Both substances were characterised by 1H , ^{13}C , and ^{31}P NMR and IR spectroscopy and by field desorption mass spectrometry, while complex **30** was characterised in addition by X-ray diffraction. Compound **30** was the first example of the direct substitution of a CO ligand in $Cp_2Mo_2(CO)_4$ with retention of the $Mo \equiv Mo$ bond and at the same time it was the first BAP complex where the P-monodentate coordination of the phosphocane form was confirmed by X-ray diffraction.

A methylated analogue of compound **30** — the complex $(C_5Me_5)Mo_2(CO)_3L$ — has been synthesised and investigated⁴¹ by X-ray diffraction. Its synthesis requires more severe conditions and the yield is much lower than that of compound **30**. This is associated with the large steric factor for the $\eta^5-C_5Me_5$ ligand compared with $\eta^5-C_5H_5$. The special importance of molybdenum in the coordination chemistry of BAP is noteworthy because unique phosphoranide complexes with three-membered metallocycles have in fact been obtained precisely with this metal and characterised by X-ray diffraction.

e. The adducts of BAP with BH_3

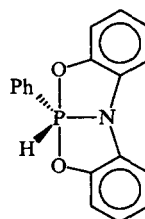
Apart from the formation of complexes between BAP and transition metal compounds, the interaction of the former with certain borane complexes has been investigated. Thus the reaction of Phoran with $BH_3 \cdot SMe_2$ affords compound **32** as the main product (for the molar ratio B : P = 2 : 1).⁴²



32

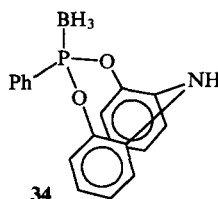
The adduct **32** was characterised reliably by spectroscopic methods: 1H , ^{11}B , and ^{31}P NMR and IR spectroscopic, as well as mass-spectrometric data have been published. The stereospecificity of the above reaction has been demonstrated because compound **32** is characterised by a *cis*-disposition of the BH_3 fragments relative to the phosphocane ring.

Special mention should be made of an unusual BAP, the bicyclic skeleton of which contains condensed benzene rings.⁴³



33

In contrast to Phoran, compound **33** exhibits a high chemical stability: it does not hydrolyse, it does not undergo deuterium exchange with D_2O in the presence of either triethylamine or toluene-*p*-sulfonic acid, and it does not react with the NaH/MeI system. The phosphorane **33** hardly interacts with $BH_3 \cdot SMe_2$. Its reaction with $BH_3 \cdot THF$ takes place in the course of a week and leads to a complex mixture of products, among which compound **34** was identified by the ^{31}P and ^{11}B NMR methods.



34

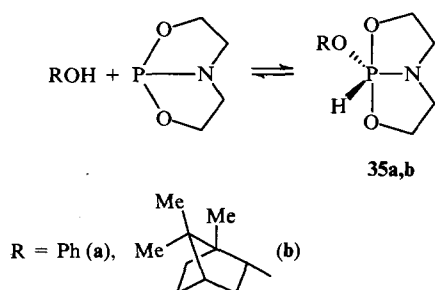
The attempt to isolate compound **34** was unsuccessful: the initial BAP was isolated in ~90% yield. Such a low reactivity of compound **33** can be accounted for by the marked delocalisation

of the lone pair of nitrogen through interaction with phosphorus and the benzene rings (all four rings are coplanar). This stabilises additionally the phosphorane structure in relation to the possible phosphocane tautomer and is also responsible for the absence of donor centres. Unfortunately we do not possess literature data on the formation of complexes between compound **33** and transition metals. In our view, it would be interesting in this instance to compare the reactivities of compound **33** and other BAP, in the first place Phoran, which would assist in a better understanding of the mechanism of the coordination of hydrophosphorane compounds.

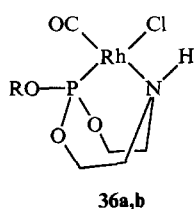
f. The formation of BAP complexes *in situ*

There exists a nonstandard approach to the synthesis of BAP involving the interaction, under mild conditions, of the corresponding proton-donor reagent (ROH, ArOH, R₂NH) with bicyclo[3.3.0]-1-phospha-2,8-dioxa-5-azaocane in an organic solvent.^{44,45} The BAP is then characterised *in situ* without isolation from the solution.

It is surprising that this very convenient method of synthesis of a wide variety of BAP as potential ligands has been introduced only quite recently into practice in coordination synthesis. Compounds **35a,b** have been synthesised by this method in CH₂Cl₂.⁴⁶



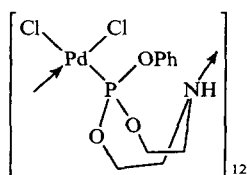
The addition of solutions containing compounds **35a,b** to [Rh(CO)₂Cl]₂ (P/Rh = 1) led to the formation of the chelate mononuclear rhodium complexes **36a,b**.



Parameter	Compound	
	36a	36b
$\nu(\text{NH})/\text{cm}^{-1}$	3230	3148
$\nu(\text{CO})/\text{cm}^{-1}$	2012	1996
$\nu(\text{RhCl})/\text{cm}^{-1}$	294	300
$\delta_{\text{P}}/\text{ppm}$	128.3	133.5
$^1J(\text{P,Rh})/\text{Hz}$	291	262

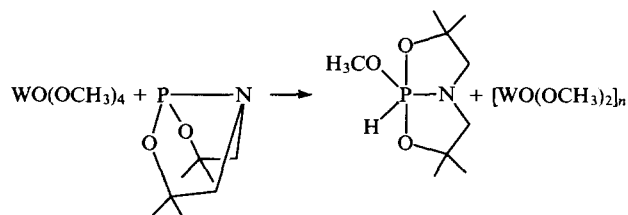
Compounds **36a,b** are insoluble in organic solvents, except DMSO, but at 80 °C they undergo vigorous solvation followed by degradation. For this reason, the final confirmation of the structure of compounds **36a,b** was achieved by ¹³C solid-state NMR spectroscopic and ESCA methods.

The complex formation reaction between compound **35a** and Pd(COD)Cl₂ resulted in the formation of a polynuclear palladium complex with a bridging phosphocane ligand.⁴⁷



The complex was characterised in detail by IR and ³¹P and ¹³C NMR spectroscopy, ESCA, and ultracentrifugation; its nonstereoregular structure was established.

We may note an important feature—in contrast to other BAP, the coordination of compounds **35a,b** leads to complexes with a phosphite, and not phosphonite, phosphorus centre.



It is of interest that a reaction formally the reverse of the processes mentioned above had been achieved earlier.⁴⁸

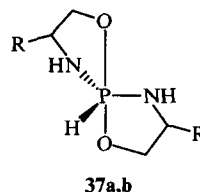
The formation of the free phosphorane is treated as a result of the intracomplex oxidative addition of methanol to the N-coordinated phosphoramidite catalysed by the traces of H⁺ present in the reaction medium.

It follows from the foregoing that the BAP function either as precursors of the phosphocanes (chelating or bridging) bound via P-monodentate or P,N-bidentate linkages or as P,N- or P,O-bidentate phosphoranide ligands. In the coordination of BAP in the phosphocane form, the differentiation of P-monodentate and P,N-bidentate binding is made feasible by a reliable criterion—the absorption frequency of the NH group in the IR spectra of these complexes. Thus a wide range of vibrational frequencies (3050–3320 cm⁻¹) is characteristic of the coordinated amino-group, but the unusually high values of $\nu(\text{NH}) = 3280\text{--}3320\text{ cm}^{-1}$ are observed only in the spectra of the cationic compounds and are associated with the presence of a positive charge on the metal atom, while the anomalously low frequencies 3050–3080 cm⁻¹ are known only for [RhL₂]⁺Cl⁻, which contains strong hydrogen bonds with the counterion. On the other hand, the typical values of $\nu(\text{NH})$ are in the range 3140–3260 cm⁻¹. The free peripheral amino-group is characterised by the frequency range 3340–3400 cm⁻¹. Occasionally a decrease to 3300 cm⁻¹ is observed owing to the participation of this group in hydrogen bonds.

2. Processes with participation of hydrospirophosphoranes

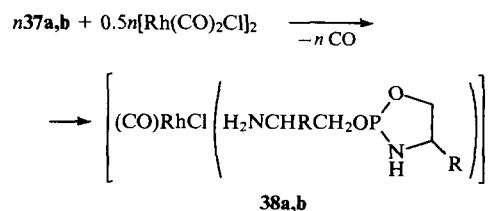
a. Rhodium complexes of hydrospirophosphoranes

Hydrospirophosphoranes (HSP) constitute the most thoroughly investigated group of hydrophosphoranes,⁴⁹ but their coordination chemistry began to develop comparatively recently.^{50,51}



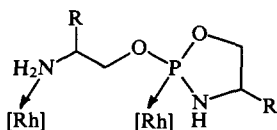
R = H (a), Et (b)

As in the case of BAP, the first transition metal complexes with HSP ligands were those of rhodium.



n = 4 (a), 6 (b)

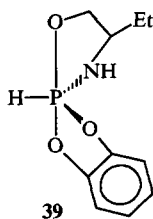
It has been established that processes involving HSP are much slower than those involving organic phosphorus(III) ligands. Thus, in complex formation with the oxazahydrospirophosphorane **37a**, the residual signal of this ligand persists in the ^{31}P NMR spectrum of the reaction solution for 30 min even at 20 °C, whereas in complex formation with the aminophosphite under the same conditions the free ligand signal is recorded only at -70 °C.⁵² It follows from the ^{31}P and ^{15}N NMR data (compound **37a** with 96.4% enrichment in the ^{15}N isotope) and IR spectroscopy that the key factor in the coordination of HSP is the opening of the oxazaphospholane ring with liberation of the peripheral amino-group bound to the metal.



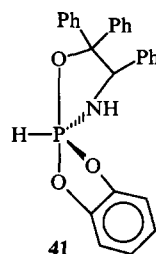
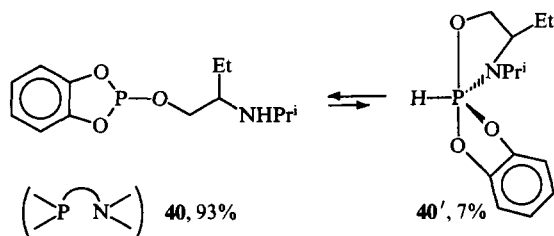
The polynuclear nature of these complexes, where the phosphorus-containing ligand functions as a bridging P,N-bidentate species, has been established by sedimentation analysis of solutions of compounds **38a,b** in DMSO. The elementary units of compounds **38a,b** have *trans*-orientation of the phosphorus and nitrogen centres in the coordination sphere of rhodium. This is yet another distinctive feature of the complexes based on HSP: the chlororhodium carbonyl complexes of aminophosphites and aminophosphoramidites are as a rule mononuclear with a *cis*-disposition of the phosphorus and nitrogen atoms.⁵²⁻⁵⁴

Despite thorough investigation of complexes **38a,b**, the driving force of the formation of the polynuclear structures remained unelucidated. It is also not known whether these compounds are linear or cyclic oligomers. At the present time, we are inclined to regard them as cyclooligomers, since signals due to the noncoordinated phosphorus or nitrogen centres have not been detected in the ^{31}P and ^{15}N NMR spectra.

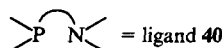
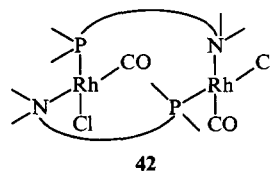
The use of the chiral HSP **37b** and **39** in the asymmetric hydrosilylation of acetophenone by diphenylsilane [both ligands were obtained from (*R*)-2-aminobutanol] has been reported.⁵⁵



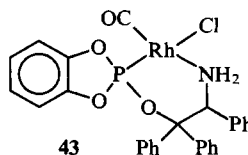
The 2L/[Rh(CO)₂Cl]₂ (L = compound **39**) catalytic system ensures an optical yield of the reaction product of 9%. Unfortunately, the use of chiral HSP in asymmetric catalysis has not received due development and only the studies concerned with the synthesis and coordination of optically active HSP with a catechol fragment have been continued.⁵⁶ This concerns the synthesis of the aminophosphite **40**, which is in equilibrium with its P(V) tautomer **40'** (this is typical for aminophosphites and aminophosphoramidites with a secondary peripheral amino-group), and also of the hydrophosphorane **41**.



The complex formation reaction between compound **40** and [Rh(CO)₂Cl]₂ (P:Rh = 1:1) leads to the formation of the dinuclear rhodium compound **42**.

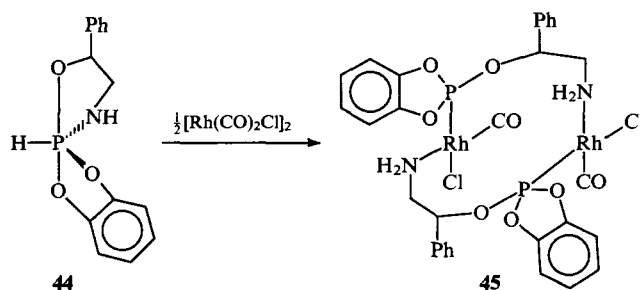


It was shown that the structure of compound **42** contains the N-H...Cl intramolecular hydrogen bonds. Under the same conditions, the ligand **41** forms the mononuclear chelate complex **43**.

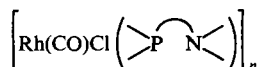


It exists in the form of two conformers: pseudotetrahedral and pseudosquare, which follows from ^{13}C NMR and IR spectroscopic data. The tendency of compound **43** to isomerise to the form with a *cis*-disposition of the carbonyl and amino-groups in the coordination sphere of the rhodium has been discovered.

In contrast to compound **41**, the sterically less hindered HSP **44** forms a dinuclear, and no longer a mononuclear, rhodium complex.⁵⁷



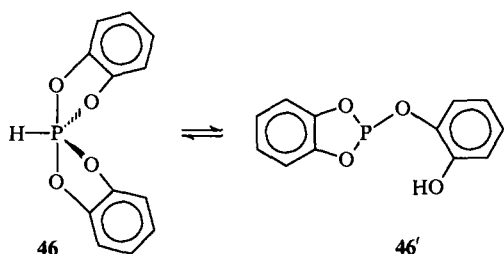
We may note that compound **45** is perhaps the most thoroughly investigated complex based on HSP: ^{31}P NMR (including the low-temperature version), ^1H NMR, ^{13}C NMR (including the version in the solid state), ^{14}N NMR, and ^{103}Rh NMR spectroscopy, IR spectroscopy, ESCA, and desorption mass spectrometry were resorted to in the consideration of its structure. The dissolution of compound **45** in acetone is accompanied by its reorganisation; fragments with a *cis*-orientation of the carbonyl and amino-groups at the rhodium atom appear in solution and ultimately a polynuclear compound with $n = 12$



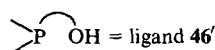
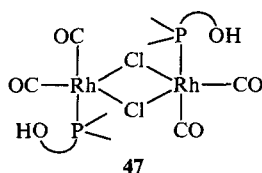
(according to ultracentrifugation data) is formed.

In all probability, for the rhodium derivatives of HSP with a catechol fragment there is a definite relation between the steric factor associated with the ligand and the nature of the coordination compound: less sterically hindered ligands give rise to metal complexes with a larger number of rhodium centres.

The study⁵⁸ of the interaction of 2,2'-spirobis(1,3,2-benzodioxaphosphole) **46** with $[\text{Rh}(\text{CO})_2\text{Cl}]_2$ is of special interest because this is the only example of complex formation involving tetraoxohydrospirophosphoranes. The HSP **46** is known⁴⁹ to be in equilibrium with its tricoordinate tautomer **46'**.

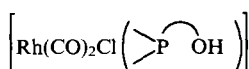


The rhodium complex formed with the ligand **46'** in CH_2Cl_2 is a dimer with a rhodium coordination number of five (the rhodium coordination polyhedron is a trigonal bipyramid with an apical phosphorus atom).



The peripheral OH group is not then bound to the metal.

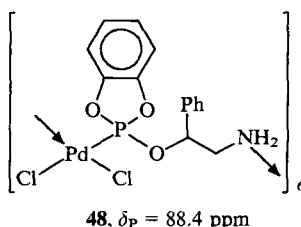
In the crystalline complex **47**, the phosphorus-containing ligands function as P-monodentate and P,O-bidentate species, the phosphorus centre now occupying an equatorial position. It has been suggested that the fragments



can combine into a polynuclear aggregate as a result of the bridging function of both the chloride ligands and the ligands coordinated as P,O-bidentate species.

b. Palladium and platinum derivatives of hydrospirophosphoranes

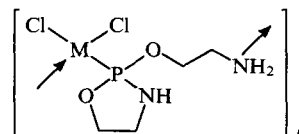
At the present time, we know of only three metal complexes of hydrospirophosphoranes. In particular, the reaction between $\text{Pd}(\text{COD})\text{Cl}_2$ and the HSP **44** gave compound **48**, which was initially described as mononuclear.⁵⁹ However, measurement of the molecular mass of this complex by ultracentrifugation revealed its hexanuclear nature.⁶⁰



The terminal positions of the chloride ligands in the structure of compound **48** have been reliably established by three independent physical methods—ESCA, IR, and X-ray emission

spectroscopy. Hence it follows that the bridging ligands in the polynuclear complex **48** are in fact the phosphorus—containing ligands.

The polynuclear metal complexes **49** and **50** have been synthesised by the reaction of the HSP **37a** with $\text{M}(\text{COD})\text{Cl}_2$ ($\text{M} = \text{Pd}, \text{Pt}$).^{47, 61}



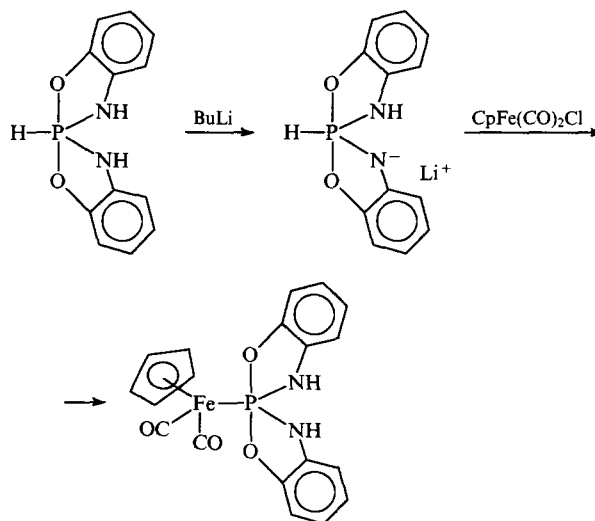
49, 50

49: $\text{M} = \text{Pd}, n = 4$

50: $\text{M} = \text{Pt}, n = 6$

Their structures were established from ^{31}P , ^{13}C , and IR spectroscopic, ESCA, and flame-desorption mass-spectrometric data and by sedimentation analysis.

Instead of the initial hydrospirophosphorane, its amide derivative has been used⁶² in the complex formation reaction, which led unexpectedly to the formation of a phosphoramide adduct.

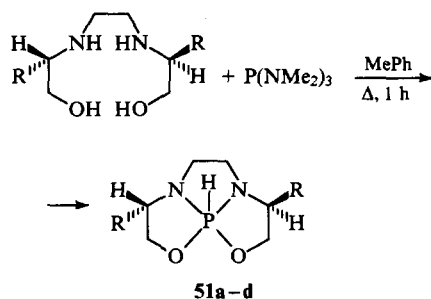


The information accumulated hitherto on the coordination behaviour of HSP permits the following conclusions: (1) these ligands do not tend to undergo coordination of the phosphoramide type and hence the spectroscopic parameters of their metal complexes are close to those for compounds based on organophosphorus(III) P,N-bidentate ligands—aminophosphites and aminophosphoramidites; (2) the majority of HSP complexes are polynuclear, but the available data on the molecular masses of the metal derivatives of HSP have been obtained mainly in the study of their solutions, so that direct structural investigations of solid-state specimens of these substances are needed.

III. The formation of complexes by tricyclic hydrophosphoranes

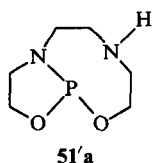
There are as yet few publications on this topic, but we are devoting to it a separate section of the present review because it is one of the most rapidly developing fields of modern coordination chemistry of hydrophosphorane compounds.

In 1990 Vannoorenberghe and Buono⁶³ reported the synthesis of the first representatives of a new group of hydrophosphoranes—tricyclic hydrophosphoranes which they called 'triquinphosphoranes'.

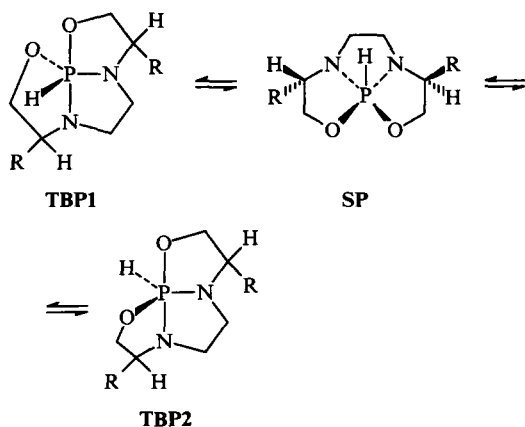


R = H (a), Me (b), Prⁱ (c), CH₂Ph (d)

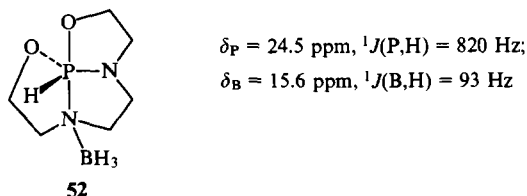
The ³¹P NMR spectrum of a solution of compound **51a** in deuterated DMSO in the temperature range 20 to 80 °C did not reveal the presence of the potential P(III)-tautomer **51'a**.



It was shown that rapid pseudorotation is characteristic of the 'triquinphosphoranes', the difference between the conformational energies of the trigonal bipyramid (TBP) and the square pyramid (SP) being small — 2.0 ± 1.5 kcal mol⁻¹.



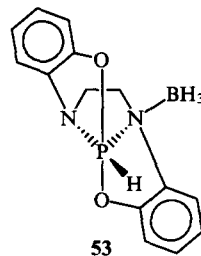
It is extremely significant that one nitrogen atom in the TBP is in the unusual apical position, so that it is displaced from the *pπ*-*dπ* conjugation with the phosphorus atom and is an independent donor centre. Indeed, the interaction of compound **51a** with BH₃·SMe₂ in the molar proportions P : B = 1 : 1 leads to the formation of the stable crystalline adduct **52** in 90% yield.



We may recall that the P,N-bidentate phosphoranide coordination of the BAP is also characterised by an apical nitrogen atom.

The synthesis of tricyclic hydrophosphoranes from ephedrine and compounds with condensed benzene rings has also been reported.⁶⁴ The latter hydrophosphorane is known in the form

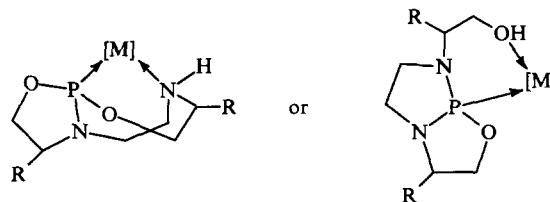
of a stable monoborane complex, for which the structure **53** has been proposed.



However, this structure is surprising, since no hydrophosphoranes in which an equatorial nitrogen atom functions as a donor centre are known. Since the above communication⁶⁴ contains no rigorous evidence for the structure **53**, one may suppose that the compound is more likely to have a structure similar to that of the boron-containing adduct, mentioned above, with an axial orientation of the P—N—B fragment.†

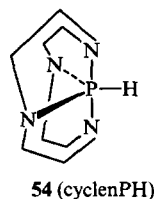
Subsequently the synthesis of yet another chiral 'triquinphosphorane' **51e** (R = Et) was described.⁶⁵ Despite the use of the less reactive phosphorylating agent P(NEt₂)₃ and the fact that the reaction was carried out without a solvent, the yield of compound **51e** proved to be not less than that of compounds **51a-d**. The first transition metal complex with a tricyclic phosphorane was obtained from compound **51e**. The reaction of compound **51e** with Pd(COD)Cl₂ (P : Pd = 1 : 1) proceeds under mild conditions. According to ³¹P NMR data, phosphoranide coordination of the ligand takes place in this complex.

There is no doubt that there are satisfactory prospects for the coordination chemistry of 'triquinphosphoranes'. One can postulate that, by varying the metallic matrix and (or) the reaction conditions, it is possible to control the complex formation process involving tricyclic hydrophosphoranes and achieve not only phosphoranide coordination but also other types, for example,

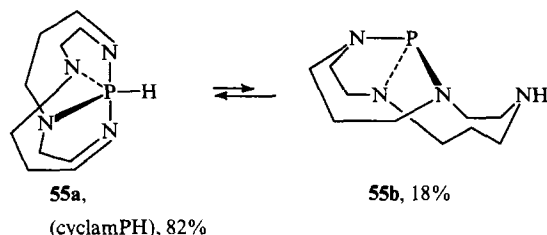


IV. The formation of complexes by tetracyclic hydrophosphoranes

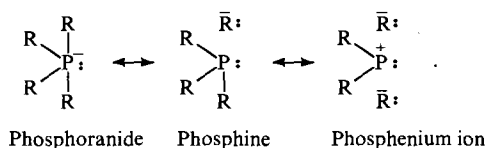
The synthesis of a series of polycyclic and tetraamino-substituted phosphorus compounds, two of which (cyclenPH and cyclamPH) have found applications in coordination chemistry, was reported in 1978.^{66,67}



† The P—N—B fragment in compound **53** does indeed occupy an axial position, which has been demonstrated by X-ray diffraction (personal communication by Dr Contreras).



Several years later, the structure of the hydrophosphorane cyclenPH was refined with the aid of X-ray and electron diffraction.⁶⁸ This compound has the structure of a distorted trigonal bipyramid with a large equatorial N–P–N angle (137.9° according to X-ray diffraction data) as a consequence of the small steric effect of the hydrogen atom. The anion of **54** with Li⁺ as the counterion was described in the same study, while the polymeric complex [Li(THF)cyclenP]_n was investigated by X-ray diffraction. The structure of this unusual compound merits a detailed discussion because the coordination of compound **54** to transition metals is achieved as a rule in the phosphoranide form. Furthermore cyclenPH is the first hydrophosphorane for which a direct structural comparison with the phosphoranide anion has been carried out. We may note that the linking units between the fragments in the polymer [Li(THF)cyclenP]_n are lithium cations. Despite the presence of a formal negative charge on the phosphorus atom, lithium is bound directly to the axial nitrogen atoms of two neighbouring fragments in this instance. This indicates the greater nucleophilicity of the axial nitrogen atoms compared with phosphorus. Furthermore, the axial bonds are lengthened by 0.21 Å compared with the initial cyclenPH and exceed by 0.1 Å the sum of the covalent radii. Overall, the phosphoranide ion may be described as resonance hybrid of three canonical forms:



The contribution of each of these forms is determined by the specific ligand environment at the phosphorus atom.

Although the study of the complex formation reactions of tetracyclic tetraazahydrophosphoranes (TTP) was initiated somewhat later than that of the BAP, at the present time two representatives of this group of ligands (compounds **54** and **55**) proved to be the most thoroughly investigated among hydrophosphorane ligands. The complexes of the ligands **54** and **55** will be considered simultaneously. The order in which they are described is based on the structure of the product of the coordination of the phosphorane and the type of complex-forming atom. Reactions involving the simultaneous occurrence of processes in which the hydrophosphorane structure is preserved and transformed will be discussed in one section.

1. Coordination with retention of the hydrophosphorane structure

a. Boron complexes

The pioneering communication concerning the coordination possibilities of the hydrophosphorane **54** appeared in 1983. It was found that the hydrophosphorane **54** readily reacts with diborane to form complex **56** in an almost quantitative yield.⁶⁹

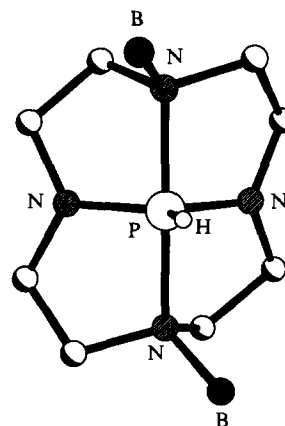
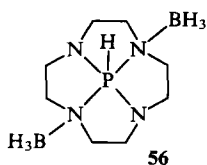
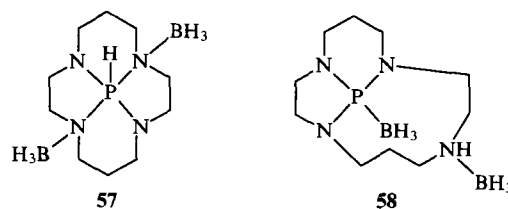


Figure 2. The structure of compound **56**.

Compound **56** has a high decomposition temperature and a high stability in air, which distinguishes it favourably from the few other borane adducts constructed from the usually unstable strained phosphorus-containing structures. The monoborane complex has not even been detected: when 0.5 mol of B₂H₆ is added, the same compound (compound **56**) is formed, whilst half of the initial compound **54** remains unreacted. The difference in the behaviour of the phosphoranes cyclenPH and Phoran in relation to BH₃ is determined both by the strong macrocyclic effect, which in the case of compound **54** favours the formation of the 'closed' form, and by the presence in compound **54** of the more basic axial nitrogen atoms.

The interaction of cyclamPH with B₂H₆ was described in the same study. It proceeds less unambiguously and leads to a mixture of products, from which only two were isolated and identified: compounds **57** and **58** (in 40% and 15% yields respectively).



Both compounds can be stored in the solid state for several months without appreciable changes, but, when compound **57** is allowed to stand at room temperature in a sealed tube in solution in CD₂Cl₂, it is fully converted into compound **58** in several weeks.

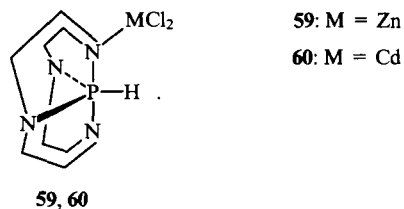
The structures of complexes **56** and **58** have been demonstrated by X-ray diffraction.^{70,71} The molecule of compound **56** (Fig. 2) can be regarded as a trigonal bipyramid with a slight deviation towards a square pyramid. Lengthening of the apical P–N bonds and the shortening of the equatorial P–H and P–N bonds compared with the initial cyclenPH is observed. Although both BH₃ groups are coordinated to the apical nitrogen atoms, the B–N bonds are not located in a single plane owing to the slight helical distortion of the molecule. It was established that compound **58** exists in the form of only one of the two possible diastereoisomers, in which the P–B and N–B bonds are in the *trans*-positions relative to one another.

b. Transition metal complexes

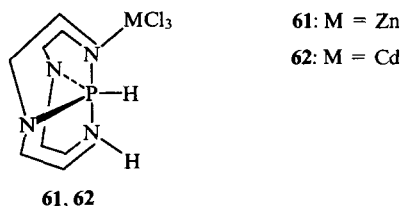
Before beginning the consideration of transition metal complexes of cyclenPH, we may note that one or both apical nitrogen centres in the molecule of compound **54** can be easily protonated by strong acids (for example, CF₃CO₂H or HBF₄).

On the other hand, the quaternisation reaction leads only to the monoalkylated product even on treatment with an excess of MeI.⁷²

In order to synthesise N-linked metallo-derivatives of cyclenPH, a study has been made⁷³ of its interaction with ZnCl₂ and CdCl₂. On the basis of spectroscopic data, similar to those obtained for the monoprotonated and monoalkylated adducts, the following structure was attributed to the zinc (compound **59**) and cadmium (compound **60**) complexes of cyclenPH:

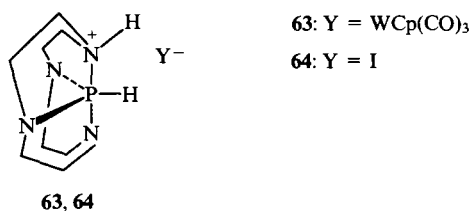


Attempts to isolate 1:2 compounds by treatment with an excess of zinc or cadmium chloride were unsuccessful. Both complexes give rise to derivatives on treatment with strong acids. Thus treatment of compounds **59** and **60** with one equivalent of HCl led to the formation of compounds **61** and **62**.



X-Ray diffraction of complex **61** showed that it exists in the form of a 'head to tail' dimer stabilised by two N—H...Cl hydrogen bonds.

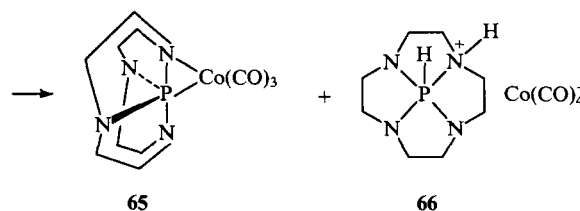
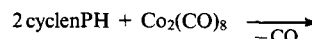
The interaction of compound **54** with cobalt, molybdenum, manganese, iron and tungsten carbonyls and hydrides has been examined in an extensive investigation.⁷⁴ The reaction of compound **54** with HW Cp(CO)₃ proceeds as an acid-base process with formation of the salt **63**.



Its treatment with MeI leads to the replacement of the anion: MeWCp(CO)₃ and compound **64** are formed. Similarly to the reaction involving compound **54**, only fairly strong nitrogen-containing bases (in particular NEt₃) react with HW Cp(CO)₃, whereas weaker bases, for example pyridine, do not react.

Here it is appropriate to mention that all the monoprotonated nitrogen-monocoordinated cyclenPH adducts give rise to a single signal in the ¹³C NMR spectra (at room temperature) in the range 42.8–45.0 ppm. However, the low-temperature (at –76 °C) ¹³C NMR spectrum of compound **64** contains five signals. These spectroscopic features can be explained, according to Lattman et al.⁷⁴, by two different exchange processes: pseudorotation with proton transfer between the nitrogen atoms and the dissociation of the P—N bond in the P—N—H fragment accompanied by the transfer of a proton and the reduction of the P—N bond. However, the available data are insufficient for the identification of these two mechanisms, although it has been stated⁶⁶ that compound **54** undergoes pseudorotation.

The interaction of compound **54** with metal carbonyl dimers proceeds in a much more complex manner.



The salt **66** is stable in solution in THF at room temperature under an inert atmosphere, but an increase in temperature to 55 °C leads to the spontaneous loss of H₂ and CO molecules by the salt and the formation of the covalent derivative **65**. The corresponding reaction of compound **54** with [MoCp(CO)₃]₂ affords analogous products: (cyclenP)MoCp(CO)₂ **67** and (cyclenPH₂)⁺[MoCp(CO)₃][–] **68**. However, in this case even prolonged refluxing of a mixture of compounds **67** and **68** in THF does not lead to the transformation of the salt into the covalent derivative. The only product of the reaction of compound **54** with Mn₂(CO)₁₀ (refluxing in THF) which was isolated proved to be the salt (cyclenPH₂) [Mn(CO)₅].

The covalent derivative of manganese analogous to compounds **65** and **67** is apparently unstable under the reaction conditions and decomposes, while the reaction of cyclenPH with [FeCp(CO)₂]₂ does not occur at all even after prolonged refluxing in THF or dioxane.

According to Lattman et al.⁷⁴, the behaviour of compound **54** in the reaction with dinuclear transition metal carbonyls is very similar to the behaviour of phosphines under the same conditions. For example, the interaction of PR₃ with Co₂(CO)₈ leads to the initial formation of the salt [Co(CO)₃(PR₃)₂]⁺[Co(CO)₄][–], which then loses a CO molecule and is converted into Co₂(CO)₆(PR₃)₂. The structures of compounds **67**, and later⁷⁵ also of **65**, were confirmed by X-ray diffraction. Their principal feature is the presence of the three-membered ring



with a greatly lengthened P—N bond. Such compounds will be examined in greater detail in the next section.

Thus the TTP are capable of both N-monodentate and N,N-bidentate coordination to the corresponding Lewis acids. Coordination of this structural type is reflected in the length of the apical and equatorial bonds in the hydrophosphorane (the former are lengthened and the latter are shortened) and is manifested spectroscopically by a downfield shift of δ_P and an increase in the spin-spin coupling constants ¹J(P,H) in the ³¹P NMR spectra.

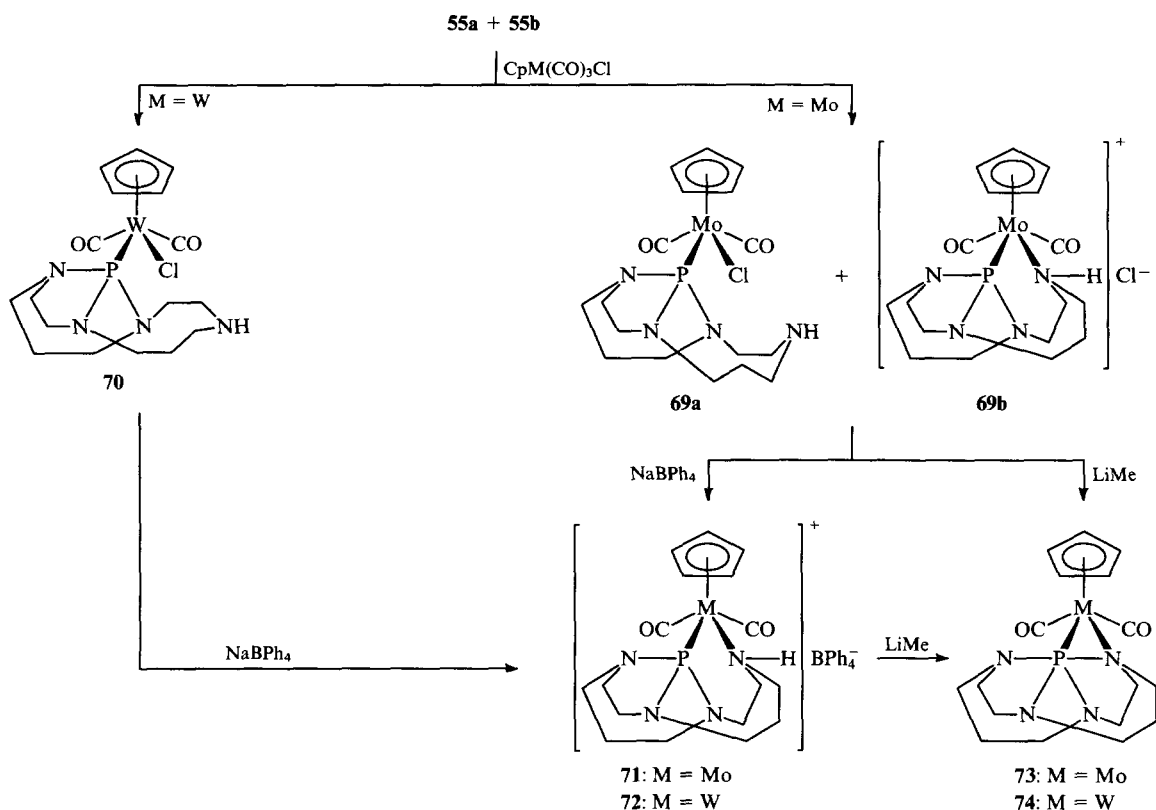
In a number of instances, N-monodentate and N,N-bidentate binding is accompanied by the occurrence of parallel processes leading to P,N-bidentate coordination. This is caused either by the existence of a tautomeric equilibrium (as in the case of cyclamPH) or by the nature of the initial metal complex.

2. Coordination with transformation of the hydrophosphorane structure

a. Molybdenum and tungsten complexes

The first communication concerning the use of tetracyclic hydrophosphoranes in coordination chemistry dates back to 1982.⁷⁶ A series of molybdenum and tungsten complexes obtained from cyclamPH are described in this paper and X-ray diffraction data are presented for one of them. An extensive study, in which all the aspects of the synthesis, reactivity, and structural features of these compounds are analysed in detail, was published much later (Scheme 1).⁷⁷

As stated above, cyclamPH exists as an equilibrium mixture of the closed and open forms. On addition of this mixture of the molybdenum and tungsten complexes, the equilibrium is



quantitatively displaced to the right and compounds **69** and **70** are formed respectively. According to ^{31}P NMR and conductimetric data, complex **69** exists in solution as a mixture of the covalent form **69a** (75%) and the ionic form **69b** (25%).

Only complex **69a** is present in the solid phase, which is indicated by the $\nu(\text{NH}) = 3297 \text{ cm}^{-1}$ absorption band, characteristic of a noncoordinated secondary amino-group. The conductimetric data obtained for compound **70** also indicate the absence of any appreciable amounts of the ionic product. On treatment with NaBPh_4 , complexes **69** and **70** are readily converted into compounds **71** and **72** respectively. Unfortunately, compounds **71** and **72** have been less fully characterised spectroscopically than compounds **69** and **70**. Thus, in the description of their IR spectra, the frequencies $\nu(\text{NH})$ are not indicated. Furthermore, only $\delta_{\text{P}} = 118 \text{ ppm}$ is quoted for complex **72** without an indication of the value of the spin-spin coupling constant $^1J(\text{P}, \text{W})$. The reactions of compounds **71** and **72** with MeLi lead to compounds **73** and **74** with P,N-bidentate phosphoranide coordination. Complex **73** can also be obtained

from compound **69**, but its yield is then low (20%), since in this case mainly unidentified decomposition products are formed. The transition to phosphoranide coordination is accompanied by an appreciable upfield shift of δ_P in the ^{31}P NMR spectra (by more than 170 ppm). In the IR spectra of complexes **73** and **74**, the frequencies $\nu(\text{CO})$ are reduced by $\sim 50\text{ cm}^{-1}$ compared with compounds **71** and **72** as a consequence of the decrease in the positive charge on the metal atom. The structure of compound **73** has been demonstrated by X-ray diffraction (Fig. 3). The environment of the phosphorus atom constitutes an almost regular trigonal bipyramid. Thus the N(1), P, and N(3) atoms lie virtually on a single straight line (176°), while the angles in the equatorial plane are close to 120° . The greater length of the P–N(1) bond (1.85 Å) and, conversely, the small lengths of the remaining three P–N bonds are striking. The P–Mo and N–Mo bonds have the usual lengths.

It is of interest that the structure of compound **73** shown an unusual 'negative' distortion of the trigonal-bipyramidal configuration, which means that it is not intermediate between the ideal trigonal bipyramidal and square pyramidal configurations.⁷⁷

Several studies have been devoted to the complex of cyclenPH with $\text{Mo}(\text{CO})_6$ and its reactivity.^{78–81} It was established⁷⁸ that treatment of compound **54** with the complex $\text{Mo}(\text{CO})_6$ in boiling toluene affords $\text{HcyclenPMo}(\text{CO})_5$ **75**, in which cyclenPH is linked to the metal only via the phosphorus atom.

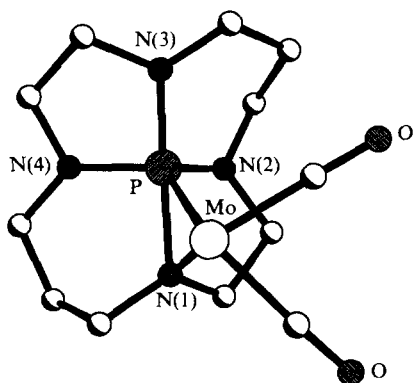
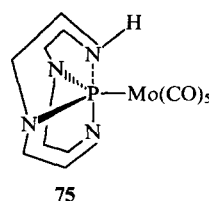


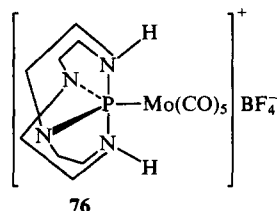
Figure 3. The structure of complex **73** (the η^5 -C₅H₅ ring has been omitted for clarity).


$$\delta_P = 116 \text{ ppm},$$

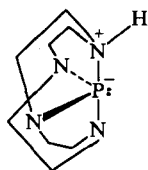
$$\nu(\text{NH}) = 3400 \text{ cm}^{-1}$$

NMR and IR spectroscopic data indicate unambiguously the presence of a noncoordinated secondary amino-group in the structure of compound **75**. However, treatment of it with HBF_4 leads to the formation of a product with a pentacoordinate

phosphorus atom, where both axial nitrogen atoms are protonated, and not a simple ammonium salt.



The cause of such unusual reactivity was deduced with the aid of X-ray diffraction. The geometry of the phosphorus atom in compound **75** is unique: instead of the tetrahedral configuration, a distorted trigonal bipyramidal coordination obtains (Fig. 4). The Mo, N(2), and N(4) atoms are in the equatorial positions, whilst the N(1) atom is in one of the axial positions. The other axial position is occupied by the N(3) atom, which interacts with phosphorus via the lone pair. Although $P-N(3) = 2.356 \text{ \AA}$, a distance which exceeds by $\sim 0.4 \text{ \AA}$ the lengths of the axial $P-N$ bonds in other cyclenPH derivatives, it is nevertheless less than the sum of the van der Waals radii. A more important feature is that the phosphorus atom is almost in the plane of the Mo, N(2), and N(4) atoms, while the equatorial and axial $N-P-N$ angles are typical of those for other trigonal-bipyramidal derivatives of cyclenPH, in which all four nitrogen atoms form with the phosphorus atom bonds having 'normal' lengths. It is more correct to regard the 'cyclenPH' fragment as a phosphoranide zwitterion.



The reactions of compounds **75** with Lewis acids are unusually sensitive to the nature of the acid. It has been reported⁷⁹ that the interaction of compound **75** with $\text{THF} \cdot \text{BH}_3$ affords the product **77**, in which the coordination number of phosphorus is four and there is an unusual conformation of the cyclenP ring.

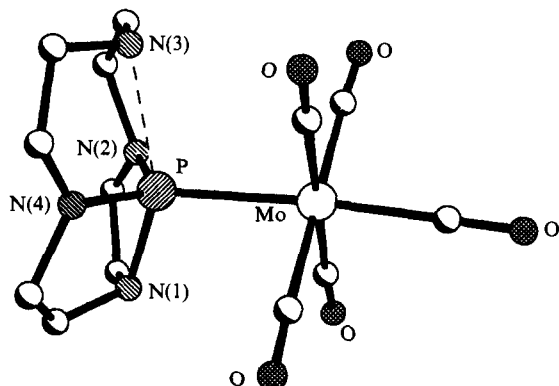
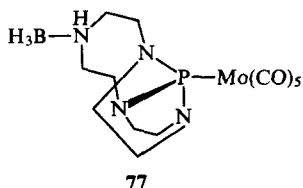
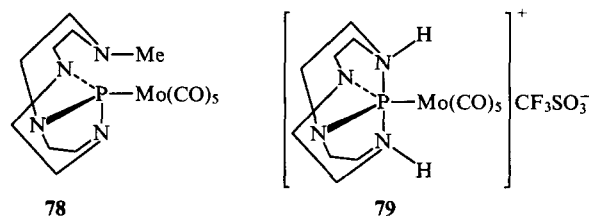


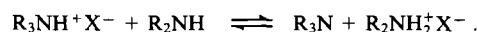
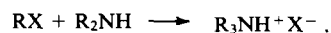
Figure 4. The structure of compound **75**.

The structure of compound **77** was established from ^{31}P , ^{13}C , ^{11}B , and ^1H NMR and IR spectroscopic data and was confirmed by X-ray diffraction. Treatment of complex **75** with $\text{Me}_3\text{O}^+ \text{BF}_4^-$ leads to the analogue **76**, where one of the apical nitrogen atoms is not protonated but methylated. Unfortunately, this structure has been discussed only on the basis of ^{31}P NMR spectroscopic data.

The interaction of compound **75** with $\text{CF}_3\text{SO}_3\text{Me}$ led to the formation of two products—**78** and **79**.⁸⁰

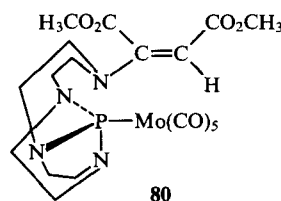


The same compounds, **78** and **79**, were isolated also after carrying out the reaction with the molar ratio $\text{75} : \text{CF}_3\text{SO}_3\text{Me} = 2 : 1$. The authors put forward two different mechanisms of the interaction of compound **75** with HBF_4 , methyl triflate, and $\text{THF} \cdot \text{BH}_3$. According to the first mechanism, the Lewis acid reacts initially with the lone pair of the second amino-group, which is followed by proton transfer. This process is analogous to the addition of alkyl halides to secondary amines.



In the case of the complex with borane, the proton transfer is unfavourable and the corresponding structure may be isolated.

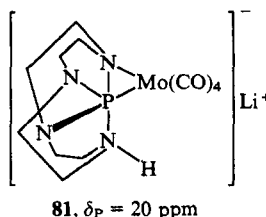
The other mechanism involves the initial protonation of the second axial nitrogen atom in the *trans*-position relative to NH . This results in the immediate formation of the salt **76**.



The similarity of compound **75** to a secondary amine is also indicated by its interaction with $\text{CH}_3\text{O}_2\text{CC} \equiv \text{CCO}_2\text{CH}_3$ giving rise to compound **80**.

The structure of compound **80** was established by X-ray diffraction. Overall, the complex formation reaction between cyclenPH and Mo(CO)_6 demonstrates the ability of the 'cyclen' fragment to stabilise the trigonal bipyramidal geometry around the phosphorus atom as a result of a transannular interaction. This interaction is fairly weak and in subsequent reactions the complex may behave as a secondary amine.

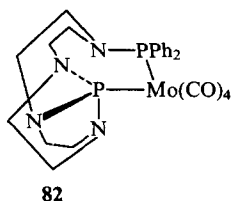
The deprotonation of compound **75** by BuLi led to the formation of a phosphoranide adduct.⁸¹



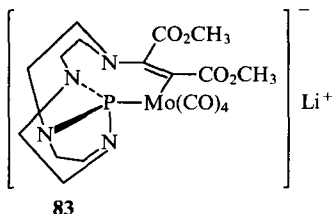
We may note that the transition from the transannular $P \cdots \text{NH}$ contact in compound **75** to the direct $P-N$ bond in compound **81** is accompanied by a pronounced (96 ppm) upfield shift of the δ_P resonance signal of compound **81** compared with the

signal of complex **75**. The presence of both carbonyl ligands and of a secondary amino-group in complex **75** makes it necessary to think about the mechanism of the formation of complex **81**. It is well known that the reactions of metal carbonyls with alkyl lithium compounds lead to acyl complexes. If this reaction path is followed, the acyl complex should split off pentanal with formation of compound **81**. However, if compound **75** undergoes direct deprotonation by butyllithium with subsequent attack by the nitrogen on the metal, butane and CO are formed. Since butane was in fact isolated from the reaction mixture, the occurrence of the process via the second path was confirmed.

We have frequently noted a fundamental feature of the three-membered phosphoranide rings $P-N-M$, namely the presence in the latter of a lengthened $P-N$ bond, which, together with the negative charge of the complex ion of compound **81**, increases significantly the reactivity of the compound. Thus the addition of $ClPPh_2$ to the latter leads to a derivative with two different phosphorus atoms.



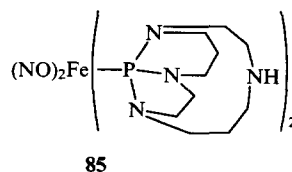
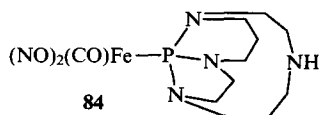
The structure of compound **82** was confirmed by IR and ^{31}P , ^{13}C and 1H NMR spectroscopic data and X-ray diffraction. Treatment of compound **81** with $H_3CO_2CC\equiv CCO_2CH_3$ also induces the dissociation of the $Mo-N$ bond, which results in the formation of the metallated enamine **83**.



Thus the reactions of tricyclic hydrophosphoranes with molybdenum and tungsten complexes take place with dissociation of the $P-H$ and $P-N$ bonds accompanied by the P -monodentate binding of the ligand in the open form. The products obtained may undergo further reactions accompanied by the transition to the P,N -bidentate (including phosphoranide) and the P -monodentate phosphoranide coordination of the ligand.

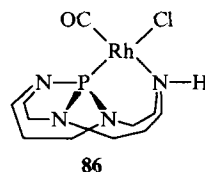
b. Iron and rhodium complexes

In contrast to the bicyclic hydrophosphoranes, TTP have not been widely employed in the coordination chemistry of iron and rhodium. Only four iron and rhodium complexes with the cyclamPH and cyclenPH ligands are known at present. The interaction of cyclamPH with $Fe(NO)_2(CO)_2$ for different ligand: metal molar ratios was investigated in the study⁷⁷ already mentioned above. It was established that the reaction proceeds with formation of monosubstituted or disubstituted products (**84** and **85**), in which the ligand is bound exclusively via the phosphorus atom.



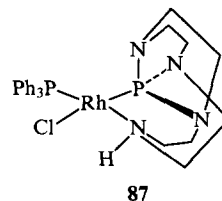
The structures of these substances were confirmed by ^{31}P NMR and IR spectroscopic data as well as mass-spectrometric data (chemical ionisation method). Compared with the initial complex $Fe(NO)_2(CO)_2$, the IR spectra of complexes **84** and **85** exhibit a bathochromic shift of $\nu(CO)$ (for compound **84**) and $\nu(NO)$ (for compounds **84** and **85**). This finding indicates that the aminophosphoramidite ligand is a pronounced σ -donor and a weak π -acceptor, apparently owing to the strong $p\pi-d\pi$ interaction characteristic of this compound. The presence of two $\nu(NH)$ bands in the spectrum of compound **85** (3120 and 3340 cm^{-1}) may be caused, according to the authors, by intermolecular hydrogen bonds.

The synthesis of the chlororhodium carbonyl complex **86** from $[Rh(CO)_2Cl]_2$ and cyclamPH was described in the same study.

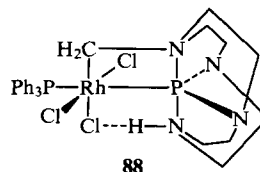


The ^{31}P NMR and IR spectroscopic characteristics of compound **86** are analogous to those of the rhodium(I) carbonyl-containing complexes with P,N -bidentate ligands already mentioned.

An attempt has been made⁷⁰ to initiate the tautomeric rearrangement of the phosphorane by treating cyclenPH with the complex $[Rh(CO)_2Cl]_2$, which was unsuccessful. However, the authors do not state what the particular result of this interaction was, so that such a claim can be treated in extremely broad terms, for example, as one implying the complete absence of the occurrence of any reaction. Nevertheless, the latter appears most improbable, since one is dealing with contact between a reactive phosphorane and a reactive rhodium substrate, particularly since cyclenPH interacts readily⁸² with $[Rh(PPh_3)_3Cl]$ with formation of compound **87**.



It was found that complex **87** reacts slowly (in two days) with methylene chloride, affording the unique rhodium complex **88** with pentacoordinate phosphorus atom and the four-membered ring $P-N-C-Rh$.



The structures of compounds **87** and **88** were established by use the ^{31}P and 1H NMR methods, while that of compound **88** was further confirmed by X-ray diffraction. The coordination

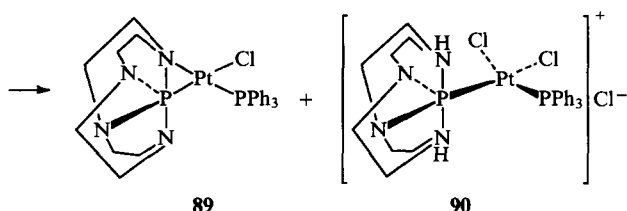
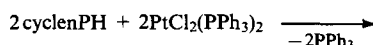
polyhedra in complex **88** are a distorted octahedron for the rhodium atom and a distorted trigonal bipyramid for the phosphorus atom. The formation of compound **88** apparently includes the oxidative addition of CH_2Cl_2 to rhodium and a subsequent rearrangement of the 'cyclenP' fragment accompanied by a change in the coordination number of phosphorus from 4 to 5 and attack by the nitrogen atom on a carbon atom with displacement of a chloride anion. It is of interest that a compound similar to compound **88** is formed in CDCl_3 immediately after the dissolution of complex **87**.

Thus the coordination of the tetracyclic hydrophosphoranes to iron and rhodium proceeds with decomposition of the hydrophosphorane structure of the ligand and by their P-monodentate (in the case of iron) or P,N-bidentate (in the case of rhodium) binding.

c. Platinum complexes

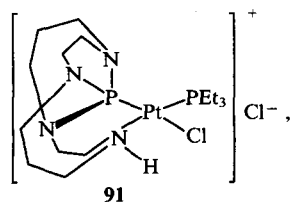
Platinum complexes are in fact most widely used in the study of the coordination possibilities of tetracyclic hydrophosphoranes. An impressive diversity of interconversions of complexes of one kind into others has been observed for these complexes. However, only cyclenPH has been used in most of these complexes; only one compound with cyclamPH is known.

The pioneering communication⁸³ published in 1987 discusses an unusual reaction between cyclenPH and *cis*- $\text{PtCl}_2(\text{PPh}_3)_2$.

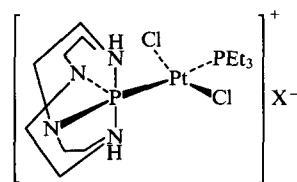


The very high value of the spin-spin coupling constant $^1J(\text{P}, \text{Pt}) = 5567 \text{ Hz}$ for compound **90** (for compound **89**, it is 3672 Hz) and the anomalously low frequency $\nu(\text{Pt}-\text{Cl}) = 249 \text{ cm}^{-1}$ for complex **89** (for complex **90**, its values are 275 and 300 cm^{-1}) are noteworthy. Such a low frequency $\nu(\text{Pt}-\text{Cl})$ corresponds as a rule to a considerable lengthening of the $\text{Pt}-\text{Cl}$ bond. Indeed, X-ray diffraction of compound **89** showed that the $\text{Pt}-\text{Cl}$ distance in this compound is 2.44 \AA . The geometry of the 'cyclenP' ligand in complex **89** is of the 'usual' type: the distance from the phosphorus to the nitrogen atom in this three-membered ring is very large (1.872 \AA), whereas the length of the three other $\text{P}-\text{N}$ bonds are in the range $1.68-1.70 \text{ \AA}$. Owing to the strain in the metallocycle, all four bond angles in the plane of the platinum square deviate appreciably from 90° . We may note that lengthening of the $\text{Pt}-\text{Cl}$ bond is as a rule caused by the strong *trans*-influence of the corresponding substituent. However, the authors did not decide to account for this anomaly by the pentacoordinate state of the phosphorus atom, because the frequencies $\nu(\text{Pt}-\text{Cl})$ in complex **90** and *cis*- $\text{PtCl}_2(\text{PPh}_3)_2$ are fairly close. In their view, long $\text{Pt}-\text{Cl}$ bond and the low frequency $\nu(\text{Pt}-\text{Cl})$ may be dictated to a large extent by steric and/or electronic requirements of the three-membered metallocycle. We shall return later to the analysis of this problem.

The reaction between cyclamPH and the dinuclear compound $[\text{Pt}_2\text{Cl}_4(\text{PEt}_3)_2]$ leads to the cationic complex **91**.⁸⁴



whereas the only product of the reaction of the same platinum dimer with cyclenPH which has been isolated proved to be complex **92**.

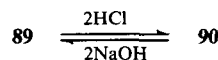


92: $\text{X} = \text{Cl}^-$

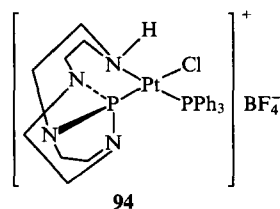
93: $\text{X} = \text{PF}_6^-$

Analogue **93** of compound **92** was obtained by ion exchange of the latter with KPF_6 . The structures of the salts **92** and **93** are similar to the structure of complex **90**, but in the latter the chloride ligands have the *cis*-configuration. In the determination of the structures of compounds **91-93**, the ^1H , ^{13}C , ^{31}P , and ^{195}Pt NMR methods and conductimetry were used, whilst in the case of compound **91** X-ray diffraction was also employed. All the bond lengths in the first coordination sphere of the platinum atom in compound **91** are within the standard ranges of values. Unfortunately, the comparison of the complex formation reactions of cyclenPH and cyclamPH with the same metallic substrate was not developed further.

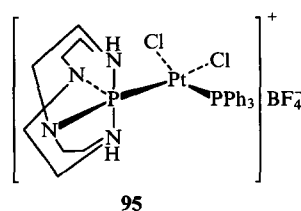
Subsequent studies were devoted to further reactions of compounds **89** and **90**. Thus their tendency towards the interconversion has been demonstrated.⁸⁵



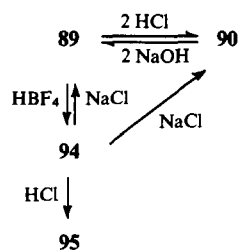
It is noteworthy that the monoprotonated intermediate was not isolated or even detected in this reaction. Thus the interaction of compound **89** with less than two equivalents of HCl nevertheless leads to the product **90** and part of the initial complex does not react. This is apparently associated with the fact that the chloride anion is a strongly coordinating ligand, which may displace the mode of reaction towards double protonation. Consequently the use of a noncoordinating anion can ensure the isolation of the monoprotonated derivative. Indeed, the reaction of compound **89** with one equivalent of HBF_4 affords compound **94**.



The cation of compound **94** is apparently a key intermediate in the conversion of compound **89** into compound **90**. In fact, treatment of compound **94** with HCl results in the immediate formation of the diprotonated adduct **95**.



Furthermore, when a source of chloride ions (NaCl) is added to compound **94**, compounds **89** and **90** are formed. Taken all together, the interconversions of complexes **89**, **90**, **94**, and **95** can be represented by the following scheme:



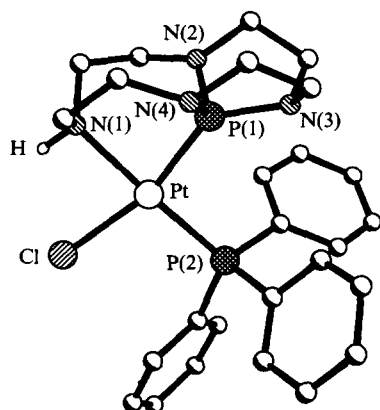
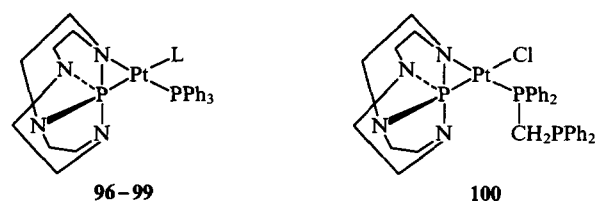
Scheme 2

The structures of compounds **90** and **94** were confirmed by X-ray diffraction. The phosphorus centre in complex **90** has the configuration of a distorted trigonal bipyramid with lengthened axial P–N bonds, while that in compound **94** has a distorted tetrahedral configuration (Fig. 5). The dissociation of the P–N bond increases the phosphorus–nitrogen distance to 2.775 Å and the P(1)–Pt–N(1) angle by 28.2° compared with the analogous angle in compound **89**. The appreciable similarity of the ligand structures in compounds **89**, **90**, and **94** indicates the tendency of the 'cyclenPH' fragment to retain the trigonal bipyramidal geometry.

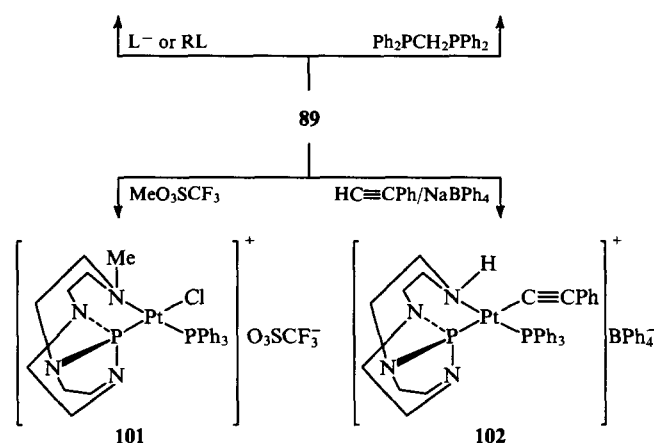
Systematic studies of the reactivity of compound **89** towards various nucleophiles and electrophiles were carried out subsequently.^{86,87} The results are presented in Scheme 2.

The reactions of compound **89** with Na[Co(CO)₄], NaSMe, KI, and KBr afford the substitution products **96–99** respectively. The NMR spectra of compounds **89**, **98**, and **99** are virtually identical with the exception of small differences in δ_P and $^1J(P, Pt)$. The $\nu(CO)$ frequencies in the spectrum of compound **96** are significantly lower than in those of other compounds of the type LCo(CO)₄. This indicates a markedly ionic character of the Pt–Co bond and the presence of a partial negative charge on the Co(CO)₄ group. In fact, the interaction of compound **96** with Me₃SiI leads to the formation of complex **98** and Me₃SiCo(CO)₄.

On the other hand, the reaction of compound **89** with Ph₂PCH₂PPh₂ leads to the substitution of a triphenylphosphine ligand and the attempts to displace the chloride ligand outside the coordination sphere of platinum by treatment with NaBPh₄ were unsuccessful. Treatment of compound **89** with electrophiles such as MeI and BuⁿBr also leads to compounds **98** and **99**. The exchange reactions between platinum complexes and RHal (Hal = Br, I), involving the exchange of chlorine at the platinum atom, usually proceed via oxidative addition and reductive elimination with participation of the metal atom. However, no evidence in support of this reaction mechanism was found even in a low-temperature experiment. An alternative to this mechanism may be the formation of a *N*-alkylated derivative with subsequent substitution of the halogen and the elimination of an alkyl halide. Indeed, metallation of compound **89** by MeO₃SCF₃ leads to the salt **101**, whilst its treatment with KI affords compound **98**.

Figure 5. The structure of the cation of compound **94**.

L = Co(CO)₄ (**96**),
SMe (**97**), I (**98**), Br (**99**)



Very weak electrophiles do not react with compound **89**. For example, the interaction of compound **89** and HC≡CPh does not take place even in boiling THF. However, after the addition of NaBPh₄ to the reaction mixture, compound **102** is formed. Various possible mechanisms of the formation of compound **102** have been compared.⁸⁷ According to the authors *N*-protonation takes place and is followed by the coordination of the alkyne with substitution of the chloride ion.

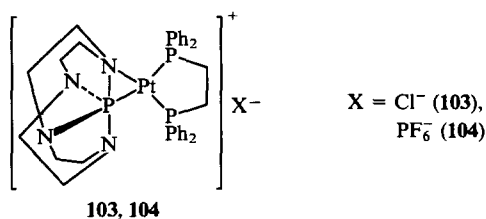
It follows from the scheme presented above that anionic nucleophiles substitute Cl[−], whilst neutral nucleophiles substitute PPh₃. Cationic electrophiles with noncoordinating anions attack the nitrogen atom, which leads to the dissociation of the P–N bond, whereas electrophiles with coordinating anions induce the dissociation of the Pt–N bond.

The structures of compounds **96**, **98**, and **99** have been demonstrated by X-ray diffraction.⁸⁸ The cause of the lengthening of the Pt–Cl bond and of the low $\nu(Pt-Cl)$ frequency was again discussed in this connection. The cause may not be solely the strain in the three-membered ring or solely the strong *trans*-effect of the pentacoordinate phosphorus. According to the authors, the principal difference between the structures of compounds **89** and **90** consists in the orientation of the N–P–N axis with participation of the axial nitrogen atoms: in the plane of the platinum square in compound **89** and at right angles to this square in compound **90**. It may be that in the former case the trigonal-bipyramidal phosphorus atom exerts a stronger *trans*-influence. However, the question arises of the legitimacy of such comparison, since in fact one is dealing with completely different ligands: one nitrogen centre is coordinated in compound **89**, whereas in compound **90** both axial nitrogen atoms are protonated. For this reason, the limited *trans*-influence of 'H₂cyclenP' in complex **90** does not permit conclusions concerning such influence of 'cyclenP' in compound **89**. Furthermore, in compound **90** 'H₂cyclenP' exhibits a fairly strong *trans*-influence, although not as strong as in complex **89**. Indeed, the length of the Pt–Cl bond in the *trans*-position relative to the phosphorus atom of 'H₂cyclenP' in compound **90** is 2.386 Å, whereas in compound **94** it is 2.353 Å. The Pt–Cl bond in the *trans*-position relative to the triphenyl phosphine ligand in compound **90** is shorter still (2.343 Å). The conclusion that the *trans*-influence of the pentacoordinate phosphorus atom is

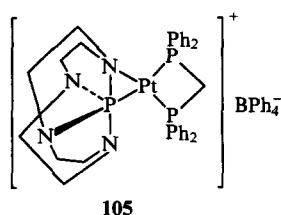
greater than that of the tetracoordinate phosphorus atom follows from these data. Whereas the Pt—Cl distance in compound **94** may be regarded as 'normal' on the basis of the nature of the phosphorus centre, in compound **90** the distance is anomalously large.

It is also scarcely possible to agree with the treatment of the unusually high spin-spin coupling constant $^1J(\text{P}, \text{Pt})$ in complex **90** by Siriwardane et al.⁸⁸ In their view, the bonding σ orbital used by phosphorus to form a bond with platinum is approximately sp^2 -hybridised. It was then concluded that the high level of s character leads to a high value of $^1J(\text{P}, \text{Pt})$. However, increase in the s character of the σ -bond should inevitably lead to the shortening of the Pt—P bond. However, the Pt—P bond in compound **90** is very long (2.289 Å). Complexes of platinum with phosphites are also characterised by high spin-spin coupling constants $^1J(\text{P}, \text{Pt})$ (from 5600 to 6000 Hz) and short Pt—P bonds (~ 2.20 Å).^{89–92} Thus metallated phosphoranes exhibit a whole series of spectroscopic and structural anomalies. The characteristics established for complexes with trivial organophosphorus(III) ligands are not always confirmed in the case of pentacoordinate phosphorus. Specific syntheses of a whole series of homologous structures and a thorough spectroscopic and structural study are apparently needed for the determination of the mutual correlations.

In the latest experimental study⁹³ devoted to platinum complexes, investigation of the reactions of compound **89** with various phosphines was continued. Thus the interaction of compound **89** with $\text{Ph}_2\text{P}(\text{CH}_2)_2\text{PPh}_2$ afforded the ionic product **103**.

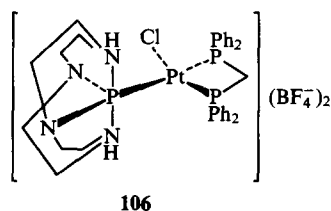


The ionic nature of compound **103** was established both spectroscopically and chemically: the exchange of the chloride ion for PF_6^- with formation of compound **104**, which has ^{31}P NMR characteristics almost identical with those of complex **103**, was carried out. The structure of complex **103** differs sharply from that of compound **100**. It is extremely likely that the monodentate coordination of the ligand $\text{Ph}_2\text{PCH}_2\text{PPh}_2$ is associated with its small chelate angle (73°), whereas in $\text{Ph}_2\text{P}(\text{CH}_2)_2\text{PPh}_2$ the angle is 85° . In most cases, this difference is of no fundamental importance. However, the presence of the three-membered phosphorane ring in compound **100** apparently inhibits the formation of the second small ring. As already mentioned, the attempts to coordinate the free phosphorus centre in compound **100** by treatment with NaPF_6 or NaBPh_4 were on the whole unsuccessful. This results in the formation of a mixture of adducts, which could not be separated, but the authors⁹³ nevertheless postulated the formation of complex **105**.



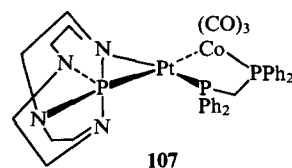
In support of their view, they quote only the values of δ_P for the three different phosphorus atoms and the spin-spin coupling constant $^2J(\text{P}, \text{P})$. The spin-spin coupling constant $^1J(\text{P}, \text{Pt})$ could not be determined owing to the presence of numerous signals due to impurities.

It was found that the free phosphorus centre in compound **100** can be coordinated via another path—the decomposition of the three-membered ring. This aim was achieved by a procedure already tested, by treatment with HBF_4 .



Again, as in the synthesis of compound **90**, the monoprotonated adduct could not be obtained.

The presence of the noncoordinated phosphorus atom in the structure of compound **100** raised the possibility that interaction with another metal complex would yield a heterobinuclear compound. In fact, the reaction of compound **100** with $\text{Na}[\text{Co}(\text{CO})_4]$ led to the formation of the bimetallic complex **107** with a Pt—Co bond.



The structures of compounds **106** and **107** were established by X-ray diffraction. The geometry around the phosphorus atom in compound **106** can be described as distorted trigonal bipyramidal (Fig. 6). The lengths of the axial P—N bonds not only exceed by 0.25–0.30 Å the lengths of the equatorial bonds, but they are also greater than the sum of the covalent radii. Apparently only the unusual geometry of the 'cyclenP' ring prevents the dissociation of these bonds. Both N—H groups form hydrogen bonds with the counterion.

The facts mentioned above indicate that platinum can be readily incorporated in both three- and five-membered rings simultaneously, whereas the inclusion of the metal in three- and four-membered rings is very difficult to achieve.

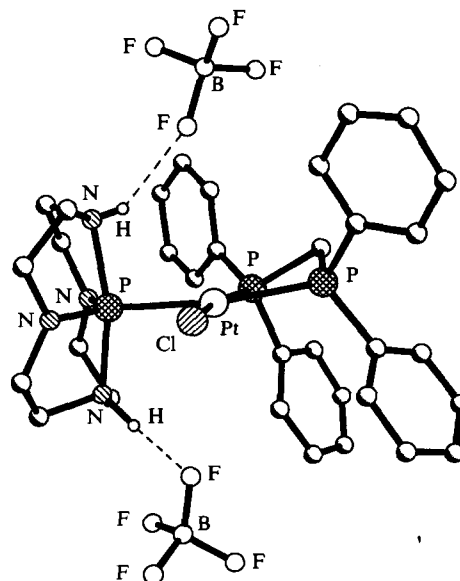


Figure 6. The structure of compound **106**.

On the whole, the coordination of cyclenPH to platinum leads to metallated phosphoranes with P-monodentate or P,N-bidentate binding of the ligand. On treatment with appropriate reagents, the compounds obtained can be interconverted or they can be converted into a multiplicity of different metal complexes with P,N-bidentate coordination, in which the coordination number of phosphorus is smaller. The interaction of cyclamPH and platinum has been clearly inadequately investigated. Nevertheless, the available data indicate the displacement of the $55a \rightleftharpoons 55b$ equilibrium towards the open form with P,N-bidentate binding of the ligand.

Evidently TTP are the most versatile ligands in the coordination chemistry of hydrophosphoranes. They are capable of N- and P-monodentate and N,N- and P,N-bidentate coordination, including coordination of the phosphoranide type.

The tetracyclic hydrophosphoranes can behave as amines, phosphoramidites, aminophosphoramidites, or as hydrophosphoranes proper depending on the type of Lewis acid, forming at the same time unique metal complexes. When bound to a metal, they sometimes assume the functions of the latter, interacting with reagents of different nature. However, reactions in which TTP are coordinated solely in the P-monodentate or the P,N-bidentate phosphorane form, without the occurrence of parallel reactions or without treatment by deprotonating agents, are so far unknown. The search for processes of this kind is still to be carried out.

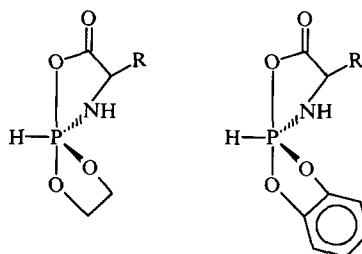
V. Conclusion

It is seen from the data presented that considerable advances have been made in the chemistry of metallo-derivatives of hydrophosphoranes. The bicyclic and tetracyclic hydrophosphoranes were found to be the most thoroughly investigated groups of compounds, whilst a new aspect—the study of a complex formation reaction by ‘triquinphosphoranes’—has only just become outlined but promises to be continued on a duly impressive scale. At the same time the extensive coordination possibilities of hydrophosphoranes have not yet been utilised to the extent that they deserve. We may point to certain fundamental problems the solution of which we believe to be of current interest.

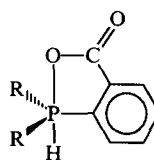
1. Comparison of the reactivities of various groups of hydrophosphoranes employing a specific metallic substrate and standard complex formation conditions. So far, there have been few such studies—only $[\text{Rh}(\text{CO})_2\text{Cl}]_2$ is known as a general partner in the complex formation reactions involving BAP, HSP, and TTP. The remaining platinum metals have been used to a lesser extent. Rhodium complexes have been thoroughly investigated for the BAP, while the palladium complexes have been studied very superficially and there are no examples whatever of platinum adducts. On the other hand, the platinum derivatives of the tetracyclic hydrophosphoranes have been investigated in detail, while the studies on the rhodium complexes have been fragmentary and the palladium complexes are unknown. So far, the chemistry of the HSP is in many respects the chemistry of one metal, namely of rhodium. Palladium and especially platinum have clearly not been employed adequately. Furthermore, it would be useful to investigate the interaction of a specific phosphorane with a series of analogous metal complexes, for example $\text{M}(\text{COD})\text{Cl}_2$ ($\text{M} = \text{Pd}, \text{Pt}$), $\text{M}(\text{CO})_n$, etc. This would assist in a better understanding of the mechanism of the coordination of the hydrophosphoranes. Such studies are also extremely few in number.

2. The extensive employment of all groups of hydrophosphoranes in catalysis, especially asymmetric catalysis. Nowadays this field has already been outlined—certain BAP and HSP have been involved in catalytic processes, whereas the tetracyclic hydrophosphoranes have been completely ignored by specialists in catalysis. Clearly extraordinary results may be expected for ligands with superior coordination and stereochemical properties of the kind possessed by hydrophosphoranes.

HSP with aminoacid residues,^{94,95} i.e.

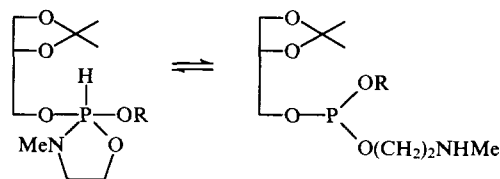


may be of special interest primarily for metal complex asymmetric catalysis because these stable compounds are obtained in satisfactory yields by the direct phosphorylation of readily available chiral precursors—natural aminoacids. The authors of the present review have begun studies on the employment of such HSP in coordination design. We may also mention a novel hydrophosphorane with an unusual axial orientation of the P–H bond.⁹⁶



It is significant that an active catalyst of the oligomerisation of ethene has been obtained from this compound by treatment with KOH, NiCl_2 , and NaBH_4 .

3. The expansion of the range of hydrophosphorane ligands by resorting to new systems, for example, monocyclic hydrophosphoranes.⁹⁷



$\text{R} = \text{Me}, \text{CH}_2\text{Ph}$

Tetraoxohydrophosphoranes, on the coordination chemistry of which only one study has been published, merit more constant attention.

It is essential to state that the field of synthesis of a wide variety of BAP with additional coordination centres by the interaction of proton-donating reagents with derivatives of bicyclo[3.3.0]-1-phospha-2,8-dioxo-5-azaoctane has been developing vigorously in recent times.⁹⁸ These systems can also be regarded as promising polyfunctional ligands.

4. The study of the mechanism of complex formation reactions of hydrophosphoranes. The interaction of the tautomer having a tricoordinate phosphorus atom with a metal-containing substrate has been traditionally postulated. However, in a whole series of cases the existence of such a tautomer is doubtful. Thus NMR and IR spectroscopic studies of solutions of oxazahydrospirophosphoranes did not reveal the presence of the phosphorus(III) form.^{51,99,100} Furthermore, these HSP do not react under mild conditions with $(\text{acac})\text{Rh}(\text{CO})_2$ and $\text{BF}_3 \cdot \text{Et}_2\text{O}$, atypical of organophosphorus(III) compounds. The tautomeric equilibrium postulated for Phoran has also not been detected spectroscopically¹¹ [the phosphorus(III) isomer has been found only in the gas phase]. Finally, cyclenPH exists in the phosphorus(V) form in solution, in the solid state, and in the gas phase,⁷⁸ although a whole series of metallo-derivatives are known

where it is coordinated in the open form. On the other hand, the interaction of cyclenPH with B_2H_6 leads to a bisborane adduct with pentacoordinate phosphorus. All these facts indicate the active role of the transition metal in the complex formation reaction involving the hydrophosphorane and hence the existence of a mechanism involving the formation of a metal hydride intermediate (in accordance with the same principle as in the reactions of silanes, secondary phosphines, or hydrophosphoryl compounds).^{51, 101} At the same time, one cannot exclude from discussion the mechanism with participation of the phosphorus(III) tautomers of hydrophosphoranes. We may recall that a bisborane adduct has been obtained for Phoran, in which the latter exists in an open form let alone the fact that phosphorus(III) isomers have been detected spectroscopically for many hydrophosphoranes. Both mechanisms apparently operate, their contributions depending on the nature of the hydrophosphorane, the Lewis acid, and the reaction conditions. However, additional studies are needed to justify this view.

The interest in the employment of hydrophosphoranes in metal complex design has not weakened. A review by Lattman and co-workers, containing a brief survey of the ligand properties of cyclenPH, has been published recently.¹⁰² We believe that the current achievements in the coordination chemistry of hydrophosphoranes constitute merely a prologue to its further development.

In the preparation of the figures, the facilities of the Cambridge Structural Database (1995 release) were employed. These permit a graphical representation of molecules on the basis of the atomic coordinates of the crystals of the test compounds deposited in the Database.

References

- M J Baker, K N Harrison, A G Orpen, P G Pringle, G Shaw *J. Chem. Soc., Dalton Trans.* 2607 (1992)
- M Nogradi *Stereoselective Synthesis* (Weinheim: VCH, 1987)
- V V Dunina, I P Beletskaya *Zh. Org. Khim.* 28 1929 (1992)
- E E Nifant'ev, T S Kukhareva, in *Obzor Monografi i Obzorov po Khimii Fosfororganicheskikh Soedinenii* (Review of Monographs and Reviews on the Chemistry of Organophosphorus Compounds) (Moscow: Nauka, 1989) p. 45
- J G Riess, F Jeanneaux, P Vierling, J Wachter, A Grand *ACS Symp. Ser.* 171 469 (1981)
- M Lattman, S Chopra, E Burns *Phosphorus Sulfur Relat. Elem.* 30 185 (1987)
- J G Riess *J. Organomet. Chem.* 281 1 (1985)
- J G Riess *Methods Stereochem. Anal.* 8 695 (1987)
- J G Riess *Phosphorus Sulfur Relat. Elem.* 27 93 (1986)
- C D Montgomery *Phosphorus Sulfur Silicon Relat. Elem.* 84 23 (1993)
- D Bondoux, I Tkatchenko, D Houalla, R Wolf, C Pradat, J Riess, B F Mentzen *J. Chem. Soc., Chem. Commun.* 1022 (1978)
- A J Deeming, J P Rothwell, M B Hursthouse, K M Malik *J. Chem. Soc., Dalton Trans.* 1974 (1980)
- B A Boyce, A Garroy, S M Lehn, D Parker *J. Chem. Soc., Chem. Commun.* 1546 (1984)
- J M Kittaneh, H A Hodali, H A Tagim *Inorg. Chem. Acta* 60 223 (1982)
- D Bondoux, B F Mentzen, I Tkatchenko *Inorg. Chem.* 20 839 (1981)
- C Pradat, J G Riess, D Bondoux, B F Mentzen, I Tkatchenko, D Houalla *J. Am. Chem. Soc.* 101 2234 (1979)
- F Jeanneaux, J G Riess, J Wachter *Inorg. Chem.* 23 3036 (1984)
- D Bondoux, D Houalla, C Pradat, J G Riess, I Tkatchenko, R Wolf *Fundam. Res. Homogeneous Catal.* 3 969 (1979)
- M C Bonnet, B Stitou, I Tkatchenko *J. Organomet. Chem.* 279 C1 (1985)
- M C Bonnet, I Tkatchenko, R Fauré, H Loiseleur *Nouv. J. Chim.* 7 601 (1983)
- J Wachter, F Jeanneaux, P Brun, J G Riess *Phosphorus Sulfur Relat. Elem.* 18 476 (1983)
- J Wachter, F Jeanneaux, G Le Borgne, J G Riess *Organometallics* 3 1034 (1984)
- P Brun, P Vierling, J G Riess *Inorg. Chem.* 26 1451 (1987)
- P Vierling, J G Riess, A Grand *Inorg. Chem.* 25 4144 (1986)
- S Agbossou, M C Bonnet, I Tkatchenko *Nouv. J. Chim.* 9 311 (1985)
- I Tkatchenko *Phosphorus Sulfur Relat. Elem.* 18 311 (1983)
- D Ballivet-Tkatchenko, M Bonnet, R Fauré, H Loiseleur *Phosphorus Sulfur Relat. Elem.* 18 468 (1983)
- M Aresta, D Ballivet-Tkatchenko, M Bonnet, R Fauré, H Loiseleur *J. Am. Chem. Soc.* 107 2994 (1985)
- P Vierling, J G Riess, A Grand *J. Am. Chem. Soc.* 103 2466 (1981)
- L Mordenti, J L Roustau, F Tomi, M Postel, J G Riess *Phosphorus Sulfur Relat. Elem.* 18 473 (1983)
- L Mordenti, J L Roustau, J G Riess *Organometallics* 2 843 (1983)
- L Mordenti, J L Roustau, J G Riess *Inorg. Chem.* 23 4503 (1984)
- G Le Borgne, L Mordenti, J G Riess, J L Roustau *Nouv. J. Chim.* 10 97 (1986)
- P Vierling, J G Riess *J. Am. Chem. Soc.* 106 2432 (1984)
- P Vierling, J G Riess *Organometallics* 5 2543 (1986)
- J Wachter, F Jeanneaux, J G Riess *Inorg. Chem.* 19 2169 (1980)
- J Wachter, B F Mentzen, J G Riess *Angew. Chem.* 93 299 (1981)
- F Jeanneaux, A Grand, J G Riess *J. Am. Chem. Soc.* 103 4272 (1981)
- J Wachter, A Mitschler, J G Riess *J. Am. Chem. Soc.* 103 2121 (1981)
- J Wachter, J G Riess, A Mitschler *Organometallics* 3 714 (1984)
- J G Riess, U Klement, J Wachter *J. Organomet. Chem.* 280 215 (1985)
- R Contreras, D Houalla, A Kläbe, R Wolf *Tetrahedron Lett.* 22 3953 (1981)
- R Contreras, A Murillo, G Uribe, A Kläbe *Heterocycles* 23 2187 (1985)
- D Houalla, F H Osman, M Sanchez, R Wolf *Tetrahedron Lett.* 3041 (1977)
- D Houalla, M Sanchez, R Wolf *Tetrahedron Lett.* 4675 (1978)
- K Gavrilov, I Michel, A Teleshev, E Nifant'ev *J. Organomet. Chem.* 461 229 (1993)
- K N Gavrilov, I S Mikhel' *Zh. Neorg. Khim.* 39 1364 (1994)
- L G Hubert-Pfalzgraf *Inorg. Chim. Acta* 88 89 (1984)
- N A Polezhaeva, R A Cherkasov *Usp. Khim.* 54 1899 (1985) [*Russ. Chem. Rev.* 54 1126 (1985)]
- K N Gavrilov, E Yu Zhorov, A T Teleshev, V A Pavlov, L S Gorshkova, E I Klabunovskii, E E Nifant'ev, in *Tez. Dokl. 2-go Resp. Soveshch. po Asimmetricheskimi Reaktsiyam, Telavi, 1989* (Abstracts of Reports of the Second Meeting on Asymmetric Reactions, Telavi, 1989) p. 32
- E Nifant'ev, K Gavrilov, G Timofeeva, A Teleshev, S Krasnokutsky, E Zhorov, V Pavlov, E Klabunovskiy *J. Organomet. Chem.* 397 245 (1990)
- A T Teleshev, K N Gavrilov, A R Bekker, N N Nevskii, E E Nifant'ev *Zh. Obshch. Khim.* 62 2470 (1992)
- K N Gavrilov, A T Teleshev, A R Bekker, N N Nevskii, E E Nifant'ev *Zh. Obshch. Khim.* 63 2791 (1993)
- K N Gavrilov, A I Rebrov, S V Rykov *Zh. Neorg. Khim.* 39 99 (1994)
- E Yu Zhorov, K N Gavrilov, V A Pavlov, A T Teleshev, Yu D Koreskov, L S Gorshkova, E E Nifant'ev, E I Klabunovskii, in *Tez. Dokl. 2-go Resp. Soveshch. po Asimmetricheskimi Reaktsiyam, Telavi, 1989* (Abstracts of Reports of the Second Meeting on Asymmetric Reactions, Telavi, 1989) p. 33
- K Gavrilov, A Teleshev, E Nifant'ev *J. Organomet. Chem.* 461 233 (1993)
- K N Gavrilov, A T Teleshev *Koord. Khim.* 20 786 (1994)
- K N Gavrilov *Zh. Neorg. Khim.* 39 1660 (1994)
- K N Gavrilov, I S Mikhel', E G Orlova, A T Shuvaev, A V Kozinkin *Koord. Khim.* 19 326 (1993)
- I S Mikhel', K N Gavrilov *Koord. Khim.* 20 54 (1994)
- K N Gavrilov, I S Mikhel' *Zh. Neorg. Khim.* 38 643 (1993)
- H Hakazawa, K Kubo, K Migoshi *J. Am. Chem. Soc.* 115 5863 (1993)
- Y Vannooenenbergh, G Buono *J. Am. Chem. Soc.* 112 6142 (1990)
- R Contreras *Phosphorus Sulfur Relat. Elem.* 87 49 (1994)
- K N Gavrilov, D V Lechkin *Koord. Khim.* 21 432 (1995)
- J E Richman, T J Atkins *Tetrahedron Lett.* 4333 (1978)
- T J Atkins, J E Richman *Tetrahedron Lett.* 5149 (1978)
- M Lattman, M M Olmstead, P P Power, D W H Rankin, H E Robertson *Inorg. Chem.* 27 3012 (1988)
- J-M Dupart, S Pace, J G Riess *J. Am. Chem. Soc.* 105 1051 (1983)
- J-M Dupart, G Le Borgne, S Pace, J G Riess *J. Am. Chem. Soc.* 107 1202 (1985)

71. J-M Dupart, A Grand, S Pace, J G Riess *Inorg. Chem.* **23** 3776 (1984)
72. F Bouvier, J-M Dupart, J G Riess *Inorg. Chem.* **27** 427 (1988)
73. D V Khasnis, M Lattman, U Siriwardane *Inorg. Chem.* **29** 271 (1990)
74. M Lattman, S K Chopra, A H Cowley, A M Arif *Organometallics* **5** 677 (1986)
75. P de Meester, M Lattman, S S C Chu *Acta Crystallogr., Sect. C, Cryst. Struct. Crystallogr.* **43** 162 (1987)
76. J-M Dupart, A Grand, S Pace, J G Riess *J. Am. Chem. Soc.* **104** 2316 (1982)
77. J-M Dupart, A Grand, J G Riess *J. Am. Chem. Soc.* **108** 1167 (1986)
78. D V Khasnis, M Lattman, U Siriwardane, S K Chopra *J. Am. Chem. Soc.* **111** 3103 (1989)
79. D V Khasnis, M Lattman, U Siriwardane *J. Chem. Soc., Chem. Commun.* **20** 1538 (1989)
80. D V Khasnis, M Lattman, U Siriwardane *Organometallics* **10** 1326 (1991)
81. D V Khasnis, J M Burton, H Zhang, M Lattman *Organometallics* **11** 3745 (1992)
82. E G Burns, S S C Chu, P de Meester, M Lattman *Organometallics* **5** 2383 (1986)
83. M Lattman, E G Burns, S K Chopra, A H Cowley, A M Arif *Inorg. Chem.* **26** 1926 (1987)
84. D E Berry, J Browning, G W Bushnell, K R Dixon, A Pidcock *Can. J. Chem.* **67** 48 (1989)
85. D V Khasnis, M Lattman, U Siriwardane *Inorg. Chem.* **28** 681 (1989)
86. D V Khasnis, M Lattman, U Siriwardane *Inorg. Chem.* **28** 2594 (1989)
87. D V Khasnis, M Lattman, U Siriwardane *Phosphorus Sulfur, Silicon Relat. Elem.* **49-50** 459 (1990)
88. U Siriwardane, D V Khasnis, M Lattman *Acta Crystallogr., Sect. C, Cryst. Struct. Crystallogr.* **45** 1628 (1989)
89. A Pidcock, R E Richards, L M Venanzi *Proc. Chem. Soc.* 184 (1962)
90. N Ahmad, E W Ainscough, T A James, S D Robinson *J. Chem. Soc., Dalton Trans.* **11** 1148 (1973)
91. K N Gavrilov, I S Mikhel', F M Ovsyannikov, A T Shuvaev, T A Lyubeznova *Zh. Neorg. Khim.* **39** 933 (1994)
92. E N Rasadkina, N S Magomedova, V K Bel'skii, E E Nifant'ev *Zh. Obshch. Khim.* **65** 214 (1995)
93. D V Khasnis, M Lattman, U Siriwardane, H Zhang *Organometallics* **11** 2074 (1992)
94. B Garrigues, A Munoz, M Koenig, M Sanchez, R Wolf *Tetrahedron* **33** 635 (1977)
95. B Garrigues, A Munoz, M Mulliez *Phosphorus Sulfur Relat. Elem.* **9** 183 (1980)
96. R A Kemp *Phosphorus Sulfur Relat. Elem.* **87** 83 (1994)
97. D A Predvoditelev, G A Urvantseva, E E Nifant'ev *Zh. Obshch. Khim.* **43** 1801 (1973)
98. D Houalla, Z Bounja, M-C Monje, S Skouta *Phosphorus Sulfur Relat. Elem.* **81** 1 (1993)
99. M Sanchez, J Ferekn, J Brazier, A Munoz, R Wolf *Rocz. Chem.* **45** 131 (1971)
100. N P Grechkin, R R Shagidullin, L N Grishina *Dokl. Akad. Nauk SSSR* **161** 115 (1965)
101. R Schunn *Inorg. Chem.* **12** 1573 (1973)
102. D V Khasnis, J M Burton, J D McNeil, H Zhang, M Lattman *Phosphorus Sulfur Relat. Elem.* **87** 93 (1994)

Cardo polyheteroarylenes. Synthesis, properties, and characteristic features

S V Vinogradova, V A Vasnev, Ya S Vygodskii

Contents

I. Introduction	249
II. Polyarylates	249
III. Aromatic polyethers	253
IV. Aromatic polyketones	255
V. Epoxide polymers	256
VI. Polyarylenephthalides	257
VII. Aromatic polyamides	258
VIII. Polyimides	261
IX. Poly-1,3,4-oxadiazoles	269

Abstract. The characteristic features of the synthesis and properties of cardo polyheteroarylenes (polyarylates, aromatic polyethers, polyamides, polyimides, polyoxadiazoles, and others) are examined and surveyed. It is shown that cardo polymers containing bulky side-groups, linked via cyclic groups to the polymer main chain, have enhanced thermal characteristics combined with a satisfactory solubility. Certain aspects of the practical applications of polymers of this kind are considered. The bibliography includes 309 references.

I. Introduction

Among polymers with an enhanced thermal stability, cardo polymers occupy a special place; the term cardo polymers is applied to those containing at least one element in the repeating group which is included in the cyclic side group. The term arose from the Latin word 'cardo', meaning loop, because such cyclic side groups can be regarded as loops in relation to the backbone of the macromolecule.^{1–4}

Many years of study of the influence of chemical structure on the properties of polymers led to the idea that the asymmetry of the macromolecules, the incorporation of bridging units in the polymer chain, and the presence of bulky side substituents in the polymer chain may impart solubility in organic solvents to heat-resistant polymers, thereby facilitating their processing. An important factor in this connection is that the modification of the polymers in order to increase their solubility should not be accompanied by a decrease in their heat resistance. As will be shown in the present review, cardo polymers satisfy these requirements.

Data on the use of phenolphthalein for the synthesis of polyesters and alkyd, epoxide, phenolformaldehyde, and other polymers began to appear in patents and publications in the 1940s.^{3,5} A characteristic

feature of these polymers was that phenolphthalein was used simply as one of the diols without taking into account its specific influence on the properties of the polymers. The synthesis of high-molecular-mass polyarylates derived from phenolphthalein and various dicarboxylic acids, achieved in 1961, when attention was first directed to the specific contribution of the phthalide cardo group to the properties of the polymers, should be regarded as the start of systematic and deliberate studies on cardo polymers.^{6,7}

In subsequent years, the studies on cardo polymers developed widely.

II. Polyarylates

Data on the syntheses and the results of studies on cardo polyarylates have been published in a series of communications.^{2–4,6–89} The most useful method for their synthesis is the polycondensation of dicarboxylic acid chlorides with dihydric phenols which contain cardo groups. Depending on the structure of the initial monomers, the polycondensation process can occur under high-temperature conditions in solution, under acceptor-catalytic conditions, or by the interfacial method.^{8,10–12,14,15,49,50,55–58}

Scheme 1 presents examples of certain structures of cardo polyarylates.

Many cardo polyarylates have been synthesised successfully by the high-temperature polycondensation of the starting materials in solution in ditolylmethane, α -chloronaphthalene, Sovol (chlorinated biphenyl), nitrobenzene, etc. in the temperature range from 100 to 220 °C for ~10 h. The amount of starting materials used was 0.6–5 mol l⁻¹.^{6,7,22,23,44,59,60} The polymers were obtained in nearly quantitative yields and had high molecular masses (for example, molecular masses of the order of 60 000–100 000 are attained in the case of polyarylates derived from phenolphthalein and aromatic dicarboxylic acids).

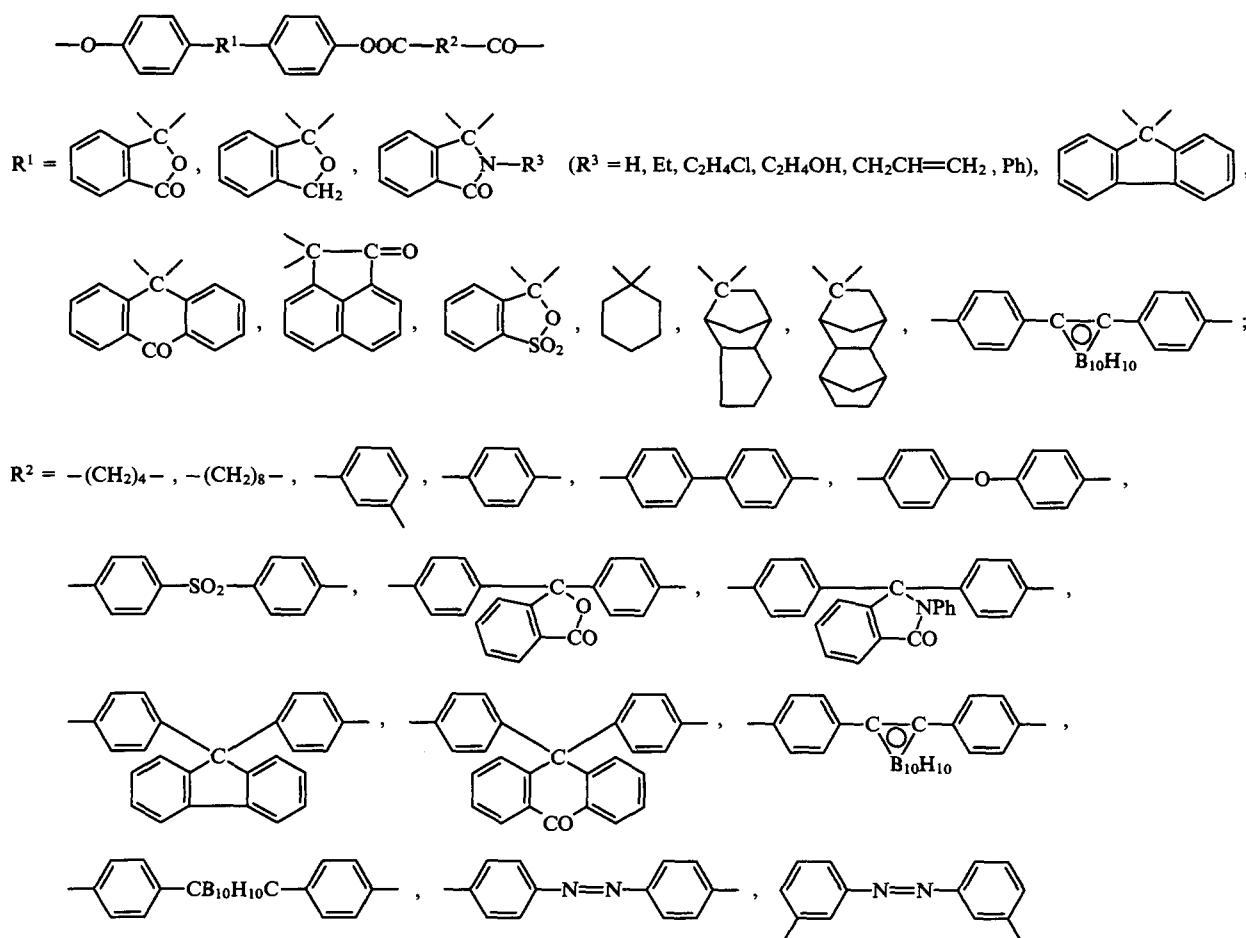
The kinetics of the process in the temperature range from 150 to 200 °C have been investigated in relation to the high-temperature polycondensation of 9,9-bis(4-hydroxyphenyl)fluorene (phenol-fluorene) and bisphenols of the norbornane type with the chlorides of terephthalic and isophthalic acids in ditolylmethane. It was concluded that these reactions proceed in accordance with an ionic mechanism via an acylium ion.^{54,61,62} The study of the influence of the nature of the reaction medium on the results of the polycondensation of phenolphthalein and its derivatives with the chlorides of aromatic dicarboxylic acid revealed an

S V Vinogradova, V A Vasnev Heterochain Polymer Laboratory, Nesmeyanov Institute of Organoelement Compounds, Russian Academy of Sciences, ul. Vavilova 28, 117813 Moscow, Russian Federation. Fax (7-095) 135 50 85. Tel. (7-095) 135 61 78 (S V Vinogradova).
Ya S Vygodskii Condensation Polymer Laboratory of the same Institute.

Received 11 September 1995

Uspekhi Khimii 65 (3) 266–295 (1996); translated by A K Grzybowski

Scheme 1



interesting feature. It was found that the reaction medium influences significantly the formation of the supermolecular structure and the properties of the amorphous vitreous polymers of this type.^{59,60} The solvent power of the medium directs the process involving the formation of rigid macromolecules in the direction of either coiled or uncoiled conformations, as a consequence of which globular or fibrillar forms of supermolecular structures are produced. Thus, in the synthesis of the polyarylate derived from phenolphthalein and isophthalic acid in ditolylmethane, the polymer precipitates and has a globular supermolecular structure, whereas in the synthesis in solvents such as Sovol, α -chloronaphthalene, and nitrobenzene the polymer remains in solution throughout the reaction and a product with a predominantly fibrillar supermolecular structure and a better set of physicomechanical properties is formed.^{50, 59,60}

In the interfacial polycondensation of phenolphthalein anilide with terephthalic acid chloride (organic medium — benzene), where the polymer is formed at the interface between two liquid phases (the polymer is not soluble in either), the polyarylate has a distinct globular structure, whereas the polyarylate synthesised by the high-temperature polycondensation in a homogeneous medium (in α -chloronaphthalene) has a fibrillar supermolecular structure. Whereas the first polymer has a softening point of 280–285 °C, a tensile strength of 960 kgf cm⁻², a relative elongation at break of 13%, and a specific impact strength (*A*) of ~ 1 kgf cm cm⁻², the fibrillar specimen has a softening point of 315–320 °C, a tensile strength of 1000 kgf cm⁻², a relative elongation at break of 40%–50%, and a specific impact strength of 7–9 kgf cm cm⁻².⁶⁰

In the synthesis of crystallising cardo polyarylates,^{19,20,52} for example the polyarylate obtained from 9,9-bis(4-hydroxyphenyl)-10-anthrone (phenolanthrone) and terephthalic acid, the process conditions (reaction temperature, rate of heating and cooling of the reaction mass, concentration, etc.) influence not only the molecular mass of the polymer obtained but also its structure. This polymer is obtained with the highest percentage of the crystalline form

when the polycondensation is carried out at 220 °C (in Sovol, α -chloronaphthalene, and nitrobenzene). When the process is carried out at a temperature above 220 °C, polyarylates with a lower degree of order are produced. An amorphous polyarylate is obtained when the reaction is performed in Sovol at 330 °C (with rapid heating and cooling of the reaction mass). The concentration of the initial monomers should be of the order of 0.6 M under these conditions; when the concentration is raised, an amorphous polymer cannot be obtained.

A series of studies^{8,63–68} have been devoted to the characteristic features of the formation of phenolphthalein polyarylates by acceptor-catalytic polycondensation. One should note in the first place that the synthesis of polyarylates by this method is faster and proceeds under milder conditions than the synthesis by high-temperature polycondensation in solution. For example, the polycondensation of phenolphthalein with the terephthaloyl chloride in the presence of triethylamine in dichloroethane at 50 °C leads to the formation of a polymer after 5 min in a nearly quantitative yield, having a reduced (intrinsic) viscosity in tetrachloroethane of ~ 0.9 dl g⁻¹.⁶⁵ The study of the reaction of phenolphthalein with terephthaloyl chloride in the presence of triethylamine revealed the influence of the nature of the reaction medium on the acceptor-catalytic polycondensation.^{66,67} It was established that the lack of the complete solubility of the initial compounds in the reaction medium is a significant obstacle to the formation of a high-molecular-mass polymer. The molecular mass of the polymer formed is greatly influenced by the properties of the reaction medium such as its polarity and its ability to dissolve the initial reactants and the polymer. In the study of the dependence of the molecular mass of the polymer formed on the composition of the binary reaction mixture (a mixture of acetone and benzene), it was found that the polyarylate with the highest molecular mass is obtained when the reaction mixture contains 30–40 vol% of acetone.⁶⁷ In this medium, it was possible to synthesise a polyarylate

with a very high molecular mass (250 000) and with a reduced viscosity in tetrachloroethane of 10 dl g^{-1} . In general, the optimum conditions for the synthesis of polyarylates by acceptor-catalytic polyesterification in heterogeneous systems are as follows: a high solubility of the initial compounds in the reaction medium and an appreciable swellability of the polymer in a weakly polar medium, or a high polarity of the medium where the swellability of the polymer in the solvent is insignificant.^{58, 66–70}

The cardo polyarylates based on trifunctional monomers such as 2- β -hydroxyethyl-3,3-bis(4-hydroxyphenyl)phthalimidine or phenolphthalein imide can be usefully synthesised by interfacial polycondensation because it is then possible to obtain linear high-molecular-mass polyarylates with free ethoxy- or imide groups when appropriate conditions are selected.^{16, 17, 50, 70} The synthesis of the same polyarylates by high-temperature polycondensation affords insoluble three-dimensional polymers owing to the reaction of the chlorocarbonyl groups with the ethoxy- or imino-group of the lactam at high temperatures.

Oligoarylates with a branched structure and an average functionality of 2, having terminal and side alcoholic hydroxy-groups, have been obtained by the acceptor-catalytic polyesterification reaction of terephthaloyl chloride with phenolphthalein, 2- β -hydroxyethyl-3,3-bis(4-hydroxyphenyl)phthalimidine, and ethylene glycol in dioxane at 30°C in the presence of triethylamine.⁶⁴ It was shown that branched oligoarylates soluble in organic solvents may be obtained when 2- β -hydroxyethyl-3,3-bis(4-hydroxyphenyl)phthalimidine is introduced into their composition in an amount not exceeding 50 mol % of the sum of the bisphenols. An increase in the degree of branching of polyarylates entails an increase in their softening temperature. Thus, when the content of 2- β -hydroxyethyl-3,3-bis(4-hydroxyphenyl)phthalimidine in a mixture with phenolphthalein is increased from 3 to 25 mol %, the softening temperature increases from 280 to 340°C . On the other hand, when the content of the first bisphenol is up to 50 mol %, the product does not soften up to 410°C .⁶⁴

The properties of cardo polyarylates depend significantly on their chemical structure. The amorphous nature of the polyarylates with asymmetric cardo groups (for example, phthalide and acenaphthene groups) can be explained by the statistical nature of the polycondensation and the asymmetric form of the cardo groups, which lead to their different positions relative to the macromolecule.^{21, 49–51} The ability of cardo polyarylates to crystallise increases following the introduction of symmetrical cardo groups (the fluorene and anthrone groups) and when the cardo groups contain polar groups (for example, the anthrone group) and groups capable of forming hydrogen bonds [polyarylates derived from phenolphthalein imide and 2- β -hydroxyethyl-3,3-bis(4-hydroxyphenyl)phthalimidine].

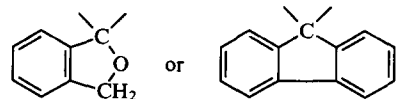
Polyarylates containing cardo groups in both the bisphenol and acid fragments exhibit explicit signs of ordering. It has also been noted that the ability to crystallise is influenced significantly by the disposition of the cardo groups relative to the ester bond. Thus the phenolanthrone polyterephthalate, synthesised by high-temperature polycondensation at 220°C , is crystalline to the extent of approximately 40%, while the isomeric polyarylate derived from hydroquinone and 9,9-bis(4-carboxyphenyl)-10-anthrone and obtained under similar conditions is amorphous.^{33, 51}

The softening temperatures of a series of amorphous cardo polyarylates and, for comparison, of certain polyarylates of the noncardo type are presented in Table 1.^{29, 51, 52, 54, 72, 73} It is seen from the data presented that the cardo polyarylates have significantly higher softening temperatures (compare, for example, polymers Nos 1–3, 5, and 6 with polymers Nos 12 and 13, etc.). Comparison of polymers Nos 7 and 8 with polymer No. 19 permits the conclusion that polyarylates with a cyclic acid fragment have appreciably higher softening temperatures than polyarylates with an acyclic, 'open-chain', structure of the isomeric acid fragment.^{29, 51} Thus the softening temperatures of the polyarylates obtained from bis(4-carboxyphenyl)phthalide and acyclic dihydric phenols [1,3- and 1,4-di(4-hydroxybenzyl)benzenes] are 250 and 270°C respectively,

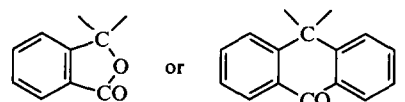
whereas the softening temperature of the polyarylate obtained from phenolphthalein and bis(4-carboxyphenyl)phthalide is 340°C .^{29, 51, 62}

A high heat resistance is characteristic also of carborane-containing cardo polyarylates.^{74–78} Thus the softening temperatures of the polyarylates obtained by the reaction of 1,2- and 1,7-bis(4-carboxyphenyl)carboranes with phenolphthalein, phenolfluorene, and phenolanthrone are $340–360^\circ\text{C}$. It is noteworthy that, according to X-ray diffraction data, these polyarylates have crystalline structures with low or moderate degrees of order. One can only note a tendency towards the formation of an amorphous structure on transition to polyarylates based on the *m*-carborane-containing isomer. The softening temperature of the amorphous cardo polyarylate derived from 1,2-bis(4-hydroxyphenyl)carborane and bis(4-carboxyphenyl)phthalide is also high, being 330°C .

There is no doubt that the high heat resistance of the cardo polyarylates and, incidentally, of other cardo polymers (see below) is due to the increased rigidity of the polymer chain. The cardo groups not only increase the rigidity of the main polymer chain but also loosen the structure of the polymer, diminishing thereby the interchain interaction, which ensures a high solubility of such polyarylates in many organic solvents. The majority of amorphous cardo polyarylates are readily soluble in methylene chloride, dichloroethane, chloroform, tetrachloroethane, trichloroethane, tetrahydrofuran, dioxane, cyclohexanone, nitrobenzene, and dimethylformamide, frequently with formation of highly concentrated solutions.^{3, 4, 6, 7, 51} The chemical structure of polyarylates also influences their solubility. Thus polyarylates containing groups capable of forming hydrogen bonds, for example phenolphthalein imide polyarylates, do not dissolve in chlorinated solvents but are readily soluble in dioxane, tetrahydrofuran, trichloroethane, and dimethylformamide. In contrast to polyarylates with phthalide and anthrone cardo groups, i.e.



those with cardo groups not containing the CO group, i.e.

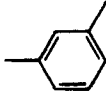
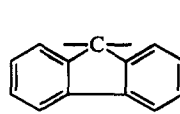
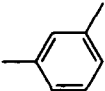
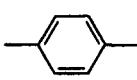
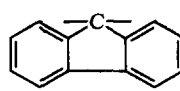
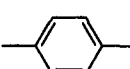
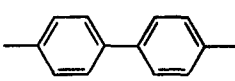
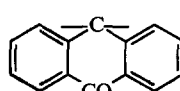
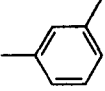
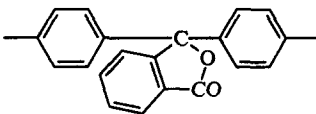
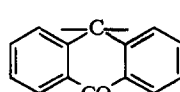
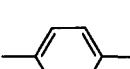
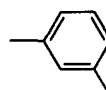
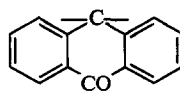
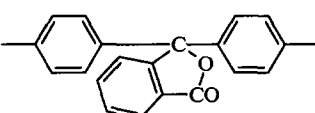
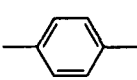
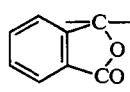
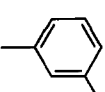
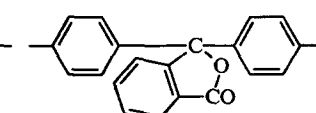
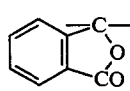
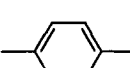
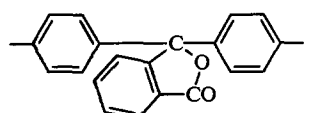
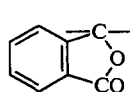
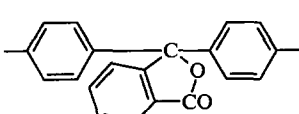
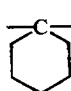
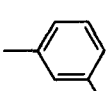
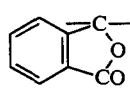
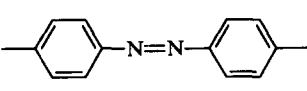
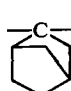
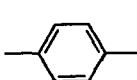
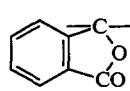
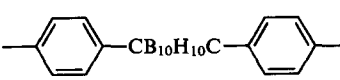
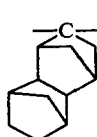
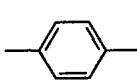
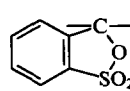
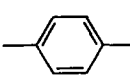


are soluble in chlorobenzene, toluene, and *o*- and *m*-xylenes.⁵¹ Carborane-containing polyarylates derived from 1,2- and 1,7-bis(4-carboxyphenyl)carboranes and 1,2-bis(4-hydroxyphenyl)carborane are readily soluble in aromatic hydrocarbons.^{76, 78} Amorphous phenolphthalein, phenolacenaphthene, and phenolanthrone polyarylates give rise to 35% solutions in chloroform, whereas phenolfluorene polyterephthalate gives only 5% solutions.⁵²

The heat resistance and solubility of cardo polyarylates are also greatly influenced by their physical state. In particular, this has been clearly established for phenolanthrone polyterephthalate, the structure of which can be deliberately altered from amorphous to crystalline by changing the conditions of its synthesis or the subsequent treatment of the finished polymer.^{21, 51, 52} Whereas the amorphous polyarylate softens at $335–365^\circ\text{C}$ and dissolves in a wide range of organic solvents, with increase in the degree of order in the structure of the polyarylate the range of solvents becomes narrower and the heat resistance increases. The crystalline polymer dissolves only in the phenol–tetrachloroethane mixture and is highly heat resistant (it does not melt before decomposition). Thus the heat resistance and solubility of cardo polyarylates can be varied specifically by varying their chemical and physical structures.

High thermal stability is characteristic of cardo polyarylates.^{36, 50, 52} Under an inert atmosphere, the temperature of the onset of decrease in the mass of phenolphthalein, phenolfluorene,

Table 1. The softening temperatures of the polyarylates

$\text{---O---}\langle\text{benzene ring}\rangle\text{---R}^1\text{---}\langle\text{benzene ring}\rangle\text{---O(O)CR}^2\text{CO---}$							
No	R ¹	R ²	T/ °C	No	R ¹	R ²	T/ °C
1	$\text{---C(CH}_3)_2\text{---}$		180	12			295
2	$\text{---C(CH}_3)_2\text{---}$		215	13			340
3	$\text{---C(CH}_3)_2\text{---}$		230	14			325
4	$\text{---C(CH}_3)_2\text{---}$		315	15			365
5	$\text{---C(C}_6\text{H}_5)_2\text{---}$		235	16			390
6	$\text{---C(C}_6\text{H}_5)_2\text{---}$		280	17			280
7	$\text{---OC---}\langle\text{benzene ring}\rangle\text{---CO---}$		270	18			340
8	$\text{---OC---}\langle\text{benzene ring}\rangle\text{---CO---}$		250	19			340
9			240	20			295
10			290	21			340
11			310	22			265

and phenolanthrone polyterephthalates is about 350–360 °C. The polymers decompose at a low rate, losing only 2%–3% of their mass before the onset of vigorous decomposition (at 460–470 °C). The chemical structure of the bisphenol does not influence significantly the temperature of the onset of the thermal decomposition of these polyarylates, which is determined mainly by the presence of the ester bond. The carborane-containing cardo polyarylates obtained by the reaction of 1,2- and 1,7-bis(4-carboxyphenyl)carboranes with phenolphthalein, phenol-fluorene, and phenolanthrone, as well as the polyarylates obtained from 1,2-bis(4-hydroxyphenyl)-carborane

and bis(4-carboxyphenyl)phthalide have the best thermal characteristics.^{74–79} The temperature of the onset of the change in their mass under an inert atmosphere and in air is 400–420 °C. After heat treatment for 3 h in air at 400 °C, these polymers give rise to large amounts of coke residues (86%–98%), whereas phenolfluorene polyterephthalate decomposes to an extent of 35% under these conditions.

The phenolphthalein, phenolfluorene, and phenolanthrone polyarylates are thermoplastic polymers. They can be processed by usual method for thermoplastic materials, which, combined with

their high thermal stability, give rise to extensive possibilities for their employment as constructional materials. By virtue of their effective dielectric properties, they can be used successfully in radio and electrical engineering. Filled materials, including antifriction materials with a low coefficient of friction and capable of working for a long time without a lubricant at high temperatures (250 °C) in a vacuum and under the conditions of high velocity gradients between the friction surfaces (sliding and roller bearings), are obtained from polyarylates.

The satisfactory solubility of cardo polyarylates in organic solvents and their compatibility with many polymers (in particular with epoxide polymers) makes it possible to convert them readily, both from solution and from mixtures, into coating films, fibrous materials, heat-resistant composite materials, and potting compounds and also permits their use as binders for reinforced plastics.^{4, 10, 14, 49–51, 80–82} In particular, a promising procedure for the conversion of cardo polyarylates, for example phenolphthalein polyterephthalate, into monolithic articles involves its combination with a reactive epoxide oligomer and subsequent moderate heating. The chemical interaction of the epoxyoligomer with the polyarylate (via a mechanism involving the 'insertion' of an oxirane ring in the ester bond⁸⁰) results in the formation of a network system having a specific set of properties and the region of mechanical usability of such compositions extends to more elevated temperatures compared with the traditional compositions based on oligoepoxides.⁸² The part of the chemically reactive heat-resistant polymer in the composition with oligoepoxides which has not reacted serves as a filler. The presence of such a high-molecular-mass chemically reactive filler reduces significantly the density of the composition and improves its strength characteristics compared with compositions containing a usual mineral filler.³⁷

The high glass points of cardo polyarylates ensure the retention at high temperatures of the effective mechanical and dielectric properties of articles made from these polymers. For example, nonoriented phenolanthrone polyterephthalate films have at 25 °C a tensile strength (σ_t) of 940 kgf cm⁻², and an elongation at break (ϵ) of 10%, whereas at 250 °C $\sigma = 470$ kgf cm⁻² and $\epsilon \leq 5\%$. After heating for 100 h at 300 °C or 500 h at 250 °C, the film retains about 50% of its initial strength. The tangent of the dielectric loss angle for this polymer hardly changes up to 250 °C; high specific volume resistivities ($\geq 1 \times 10^{15}$ Ω cm) are retained up to this temperature.^{51, 52}

At 300 °C, phenolfluorene polyterephthalate films retain more than 50% of their initial strength. The tangent of the dielectric loss angle for this polymer is 0.0025 at 220 °C.^{44, 45} Fibrous filtering materials based on phenolphthalein polyterephthalate, employed successfully for the purification of gases and liquids and for trapping aerosols, may be used up to 300 °C.^{10, 14}

Cardo polyarylates can be converted also into heat-resistant strong monolithic articles. The bending strength (σ_b) of monolithic phenolanthrone polyterephthalate reaches 1700 kgf cm⁻².⁵² The specific impact strengths of test specimens of phenolphthalein, phenolfluorene, and phenolanthrone polyterephthalates are 15–20 kgf cm cm⁻².⁴ Monolithic articles made from the polyarylates of phenolphthalein and isophthalic acid, obtained by casting under pressure, have effective physicochemical parameters (both in the initial state and after prolonged heat treatment).

Characteristic	Initial specimen	Heat-treated specimen (1000 h, 200 °C)
σ_t / kgf cm ⁻²	940	800
A / kgf cm cm ⁻²	30	70
σ_b / kgf cm ⁻²	1300	1200
H / kgf cm ⁻² ^a	1280	1250
$\tan \delta$ ^b	2×10^{-2}	2×10^{-2}

^a H is hardness. ^b $\tan \delta$ is tangent of dielectric loss angle.

Articles made from phenolphthalein polyterephthalate, filled with talc or powdered quartz, exhibit a high resistance to repeated temperature changes from –60 to 250 °C and possess satisfactory electrical insulating properties.⁸³

Cardo polyarylates are satisfactorily resistant to the action of ultraviolet and ionising radiations, retaining, for example, effective physicochemical parameters after prolonged exposure to ⁶⁰Co γ -rays in air. Cardo polyarylates with fluorene groups are more stable than polymers with phthalide groups.⁴ The partial or complete replacement of the lactone ring by a lactam ring in phenolphthalein polyarylates as well as the presence of fluorene groups in the bisphenol residues increase appreciably the resistance of the polyarylate to the action of light. The inclusion in the polymer chain of phenolphthalein polyarylates of small amounts ($\sim 1\%$) of sulfur, phosphorus, and hydroxy-groups by employing, for example, monomers such as phenolsulfophthalein, phloroglucinol, bis(4-carboxyphenyl)methylphosphine oxide, etc. promotes the formation of polyarylates with increased resistance to light-induced ageing.^{72, 84–87}

The employment of chromophore-containing monomers (the chlorides of azobenzene-3,3'-dicarboxylic and azobenzene-4,4'-dicarboxylic acids, quinizarine, alizarine, Alizarine Blue, and others) in the synthesis of cardo polyarylates led to the possibility of obtaining coloured polyarylates with different colours, the colours exhibiting a high photostability. Colours with a high photostability can be achieved even in the presence of only a small amount (0.05 mol %) of the chromophore-containing monomer in the polyarylate chain.^{49, 50, 88–91} It is also noteworthy that the introduction of even a small amount of a chromophore-containing monomer into mixed polyarylates derived from terephthalic acid and phenolphthalein greatly increases the resistance of the polymer to ultraviolet radiation.⁸⁰

Thus cardo polyarylates have enhanced thermal characteristics, satisfactory solubilities, and effective physicochemical properties.

III. Aromatic polyethers

Since the 1960s, aromatic polyethers have attracted the attention of investigators because of their high thermal stability and a number of other valuable properties.^{92–94} However, their comparatively low heat resistance is a significant disadvantage of these polymers.

The positive influence of the cardo groups on the heat resistance of polyarylates stimulated the synthesis and study of aromatic cardo polyethers.^{49, 51, 95–108}

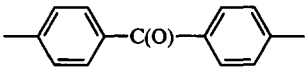
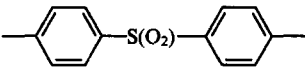
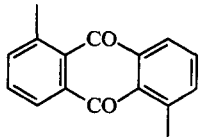
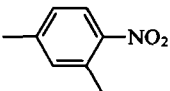
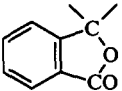
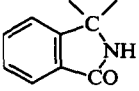
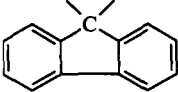
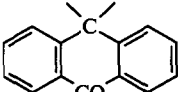

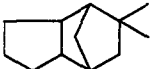
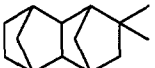
Aromatic cardo polyethers are obtained by the nucleophilic substitution reaction between phenoxides derived from bisphenols and activated aromatic dihalides (usually in dimethyl sulfoxide at 160–180 °C). Scheme 2 presents some of the structures of the polymers of this type which have been synthesised.

In the polycondensation of dihalo-derivatives with phenoxides derived from cardo bisphenols (with the exception of adamantane-containing bisphenols), only the difluoro-derivatives proved to be sufficiently reactive (for the formation of polymers with a high molecular mass). It has been suggested that the lower reactivity of the phenoxides obtained from cardo bisphenols compared with the phenoxide derived from 2,2-bis(4-hydroxyphenyl)propane is due in some cases to the greater acidity of the cardo bisphenols or the poorer solubility of the initial phenoxide in the reaction medium.^{51, 95, 99} Polyethers based on phenolphthalein contain a phthalide ring,⁹⁷ although the lactone ring of phenolphthalein is opened in alkaline media.

It has been noted that, in the polycondensation of phenolphthalein imide with bis(4-fluorophenyl) sulfone, not only the phenoxide groups but also the mobile hydrogen atom at the nitrogen atom of the lactam ring can participate in the reaction, which leads to the formation of a structured fraction.⁹⁹

A series of characteristics of the formation of cardo polyethers by the reactions of phenolphthalein and phenolfluorene with dihalobenzophenones in dimethylacetamide in the presence of potassium carbonate have been investigated.⁹⁷ It was established

Table 2. The softening temperatures (°C) of the polyethers $\text{—O—C}_6\text{H}_4\text{—R}^1\text{—C}_6\text{H}_4\text{—O—R}^2\text{—}$.

R ¹	R ²			
				
$\text{—C(CH}_3)_2\text{—}$	170	190	220	155
	230	260	280	—
	—	295	—	—
	240	270	285	—
	240	265	300	—
	240	250	—	210
	245	260	—	220
	265	270	—	235

Chemical modification of polyarylene ether-ketones and polyarylene ether sulfones, including those of the cardo type, has been achieved by treating them with chromium, molybdenum, and tungsten hexacarbonyls. Polymers containing 0.7–12 mass % of the metal (0.1–1.5 of a metal atom per polymer unit) were obtained. It was noted that the polymers containing arenemetal tricarbonyl fragments in the polymer chain can be worked into articles by employing a solution (for films and coatings) and a melt (for monolithic specimens). Such polymers have effective mechanical, optical, and adhesion properties.^{109, 110}

IV. Aromatic polyketones

The use for the synthesis of polymers of cardo monomers such as bis(4-carboxyphenyl)phthalide and 2-bis(4-carboxyphenyl)-*N*-phenylphthalimide led to the possibility of synthesising cardo polyketones.^{49, 111, 112}

The study of the process characteristics showed that the polycondensation of the dicarboxylic acid with an aromatic hydrocarbon can be usefully carried out in polyphosphoric acid containing 85 mass % of phosphorus pentoxide at a concentration of the starting materials of ~0.5 M, a reaction temperature of 120–160 °C, and for a reaction time of 8–20 h. A series of polyketones of the noncardo type have also been synthesised

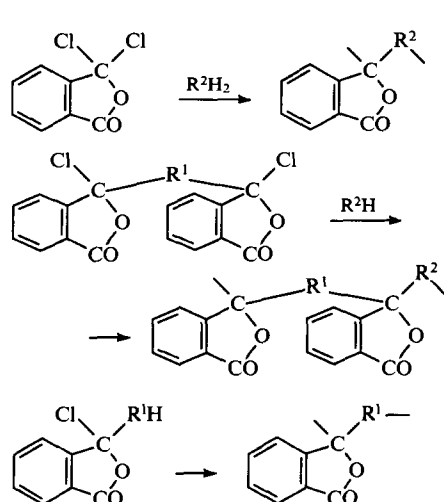
for comparison. Scheme 3 presents examples of the structures of the polymers obtained.

In most cases, the polyketones were obtained in high yields (the reduced viscosity in sulfuric acid was 0.40–1.60 dl g⁻¹). The molecular mass of the polyketone based on bis(4-carboxyphenyl)phthalide and diphenyl ether and having a reduced viscosity of 0.68 dl g⁻¹ was 44 000.

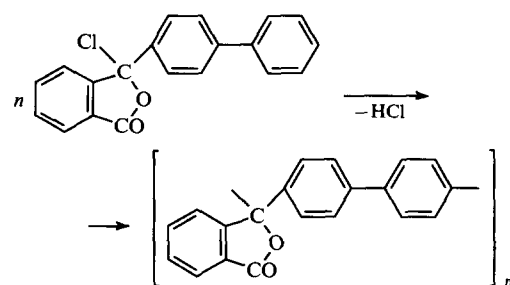
All the polyketones obtained were amorphous. The polyketones without cardo groups crystallise on heating above the softening temperature. The softening temperatures of the polyketones with phthalide and 2-(*N*-phenylphthalimidine) groups exceed by 60–80 °C those of the noncardo polyketones. Thus, whereas the softening temperatures of the polyketones based on diphenyl ether and bis(4-carboxyphenyl)phthalide and 2-bis(4-carboxyphenyl)-*N*-phenylphthalimide are 250 and 270 °C, the softening temperatures of the polymers based on terephthalic acid and bis(4-carboxyphenyl) ether are 190 and 185 °C respectively.

The cardo polyketones dissolve readily in organic solvents (tetrachloroethane, chloroform, methylene chloride, dimethylacetamide, *N*-methylpyrrolidone, benzyl alcohol, etc.) to form 30%–50% solutions, whereas the polyketones without cardo groups dissolve only in sulfuric acid. Colourless transparent films with a tensile strength of 690 kgf cm⁻² and an elongation at break of ~10% were obtained from 30% solutions of the cardo polyketones

Polyaryleneephthalides are also cardo polymers.¹²⁸⁻¹⁴² Polymers of this type have been synthesised by electrophilic substitution with the aid of carboxylic acid pseudochlorides (Scheme 5).¹²⁸ The polycondensation was carried out in solution in chlorinated hydrocarbons (methylene chloride, dichloroethane, etc.) or in nitrobenzene at temperatures from -70 to 140°C in the presence of Group III – V and VIII metal halides as catalysts (for example, AlCl_3 , FeCl_3 , and SbCl_5) in amounts ranging from 0.01 to 1.5 moles per acid chloride group. Certain properties of the polymers obtained in this way are presented in Table 3.¹²⁸



Scheme 5



Scheme 6

All the polymers presented in Table 3 are amorphous and readily soluble in methylene chloride, chloroform, tetrachloroethane, dimethylformamide, and other solvents. Nonoriented films with a tensile strength of 800–900 kgf cm⁻² and a relative elongation at break of 10–20% have been obtained from the first three polymers by casting from solution. Table 3 shows that polyarylenephthalides have high heat resistances and thermal stabilities.

It is noteworthy that in a number of instances the synthesis of polyarylenephthalides may be accompanied by the formation of a gel.¹²⁹

Special studies have been carried out to investigate the characteristic features of the formation of polydiphenylene-

phthalide by the polycondensation of 4-(3-chloro-3-phthalyl)-biphenyl (Scheme 6).^{130,131}

The influence of the type of solvent (chlorinated aliphatic hydrocarbons, aliphatic and aromatic nitro-compounds), temperature, reaction time, and the concentrations of the monomer and the catalyst has also been investigated. It has been noted that the polycondensation in nitro-compounds (especially in nitrobenzene) proved to be more universal and effective than in halo-derivatives, because it proceeds under the influence of catalysts of different types (ZnCl₂, AlCl₃, AlBr₃, InCl₃, SnCl₄, TiCl₄, SbCl₅, SbCl₃, SbF₃, FeCl₃) and leads to polymers with a higher molecular mass. The following are the most favourable conditions for the synthesis of polydiphenylenephthalide: monomer concentration 2–3 M, reaction temperature 100–110 °C, and SbCl₃ (7–10 mol %) or InCl₃ (3–10 mol %) as the catalyst. These ensure the selective formation of a polymer with a high molecular mass (46 000–60 000) and an intrinsic viscosity of 0.65–0.78 dl g⁻¹ (in tetrachloroethane).¹³⁰ When the polycondensation is carried out under severe conditions (in the presence of large amounts of the catalyst and at high temperatures), in some cases the quality of the polymer and the process selectivity decrease and anomalous units, for example fragments with keto-groups, arise in the macromolecules.¹³⁰

Polydiphenylenephthalide can also be obtained by precipitation polycondensation. In this case, the synthesis of the polymer proceeds in the initial stage in a homogeneous solution with subsequent segregation of the polymer in a separate phase.¹³¹ For comparison, polydiphenylenephthalide has been synthesised in two variants: by polycondensation in solution in nitrobenzene (80 °C, 10 h) and by precipitation polycondensation in dichloroethane (20 °C, 24 h) with anhydrous aluminium chloride as the catalyst. It was found that the precipitation polycondensation affords a polymer with a higher molecular mass: its η_{red} in sulfuric acid was 1.02 dl g⁻¹, whereas in the case of the polymer obtained in nitrobenzene η_{red} was 0.64 dl g⁻¹. It has also been noted that nonoriented films of the 'precipitation' polydiphenylenephthalide, obtained by moulding from a solution of the polymer in chloroform, exhibit a higher optical anisotropy than the films of the 'solution' polymer and have a degree of crystallinity of 25%–30%. The films of the 'solution' polymer are amorphous.¹³¹

The molecular mass characteristics of polydiphenylenephthalide have been investigated and the equilibrium rigidity of its macromolecules has been estimated. The length of the Kuhn segment of this polymer is 24 Å. It has been established¹³² that, in order to obtain strong films, a polymer with a molecular mass $>3 \times 10^4$ is needed. The study of the chemical stability of polyarylenephthalides showed that they exhibit a satisfactory resistance to the action of corrosive media at elevated temperatures.¹³³ The thermal stability of the phthalide ring in polyarylenephthalide is determined by the nature of the groups joining the benzene rings in the main chain. The thermal stability of polydiphenylenephthalide is higher than that of poly(oxydiphenylene)phthalide.¹³⁴

The thermal transformations of polydiphenylenephthalide and poly(diphenylene oxide)phthalide have been investigated over a wide temperature range (400–650 °C).¹³⁵ It was shown that the degradation of the polymers proceeds both via the end groups and via the phthalide ring and the hetero-bonds when such are present. The phthalide ring probably decomposes in three ways: without the evolution of carbon oxides (the formation of anthraquinone

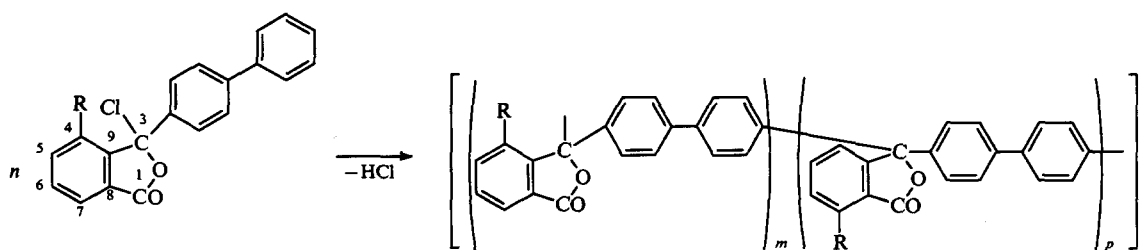
Table 3. The properties of the polyarylenephthalides

R	η_{red} / dl g ⁻¹ (tetrachloroethane)	T / °C	
		softening	onset of decomposition
Bond ^a	0.65	420	440
O	1.50	310	390
	0.55	> 300	380
S	0.50	> 250	380
	0.86	> 450	> 450
	0.72	> 400	> 450

Note. The softening temperature was determined from the thermomechanical curve obtained with a 1 kgf cm⁻² load applied to the specimen and for a heating rate of 3 K min⁻¹. The temperature of the onset of decomposition was determined from the thermogravimetric curve at a heating rate in air of 5 K min⁻¹.

^a The molecular mass of the polymer obtained by the light scattering method is 46 000.

Scheme 7



structures), with evolution of CO (the formation of compounds of the type of fluorenone), and with evolution of CO₂ (the formation of fragments of the anthracene, phenanthrene, and fluorene types), the last type of decomposition predominating. The first two reactions are accompanied by the rupture of the polymer chain, whilst the third leads to the formation of cross-linked structures.¹³⁵

Certain electrophysical properties of polyarylenephthalides have been investigated and the possibility of the thermal initiation of conduction in aromatic polymers containing readily polarisable phthalide side groups has been demonstrated.¹³⁶

Halo-substituted polyarylenephthalides have been synthesised by the Friedel-Crafts polycondensation of 3-aryl-3-chlorophthalides containing substituents in the 4-position relative to the phthalide ring. It was found that polymers containing two types of isomeric units in the polymer chain in the 4- and 7-positions can be obtained from such monomers (Scheme 7).¹³⁷

Effective thermal and physicochemical parameters are characteristic of these polymers. Thus chloro-substituted polyarylenephthalides with a characteristic viscosity in tetrachloroethane of 1.52 dl g⁻¹ have a softening temperature >450 °C, a temperature for the onset of decomposition of 450 °C, a degree of crystallinity of 30%, a tensile strength of the film of 900 kgf cm⁻², and an elongation at break of 85%.

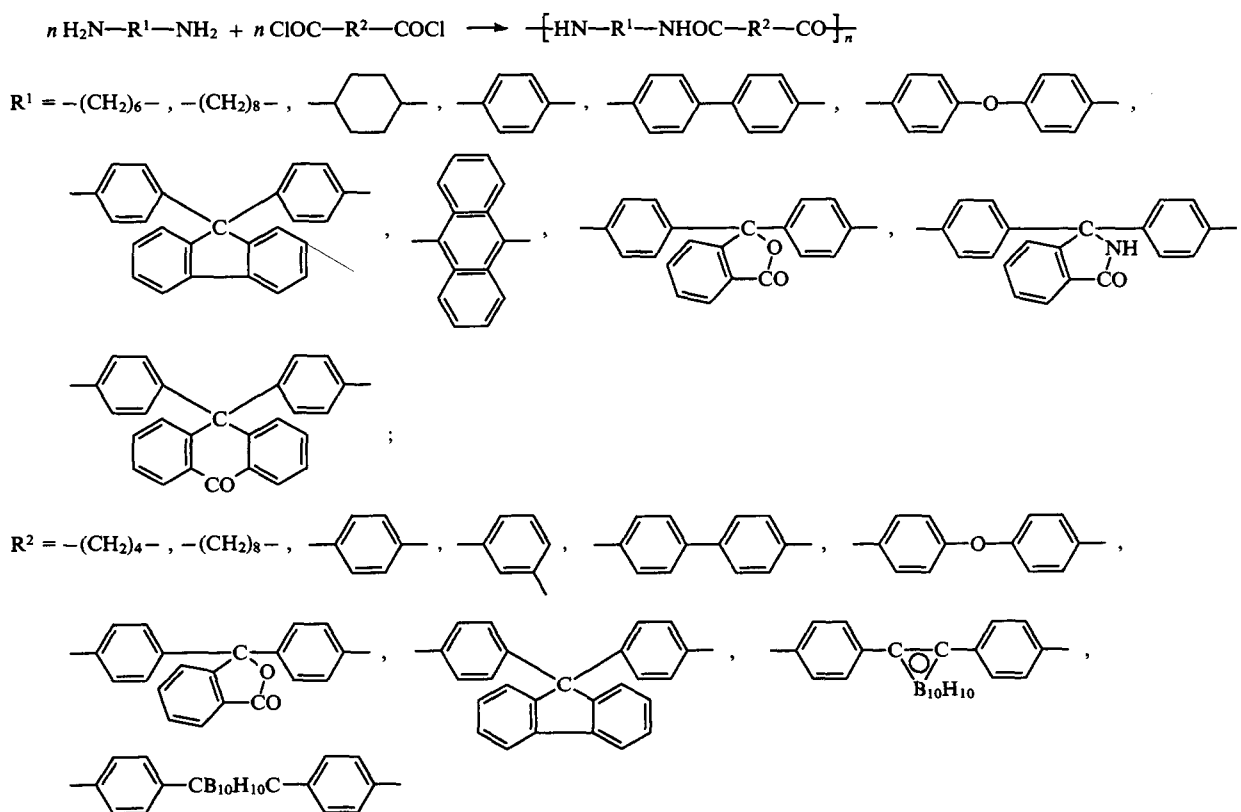
Nitro-derivatives containing a controllable number of nitro-groups in the repeat unit (0.2–3.0 nitro-groups) have been obtained by nitrating polydiphenylenephthalide with potassium nitrate in

nitric acid or with nitric acid in sulfuric acid.^{138–140} It was found that the trinitro derivatives of polydiphenylenephthalide contain nitro-groups in the 6-position in the phthalide ring and in the 2- and 2'-positions in the biphenylene unit. They are soluble in nitrobenzene, dimethylformamide, dimethylacetamide, *N*-methylpyrrolidone, and cyclohexanone. The nitro-derivatives containing less than one nitro-group per repeat unit of the monomer are soluble in tetrachloroethane, aniline, and benzonitrile. The polymers containing more than one nitro-group per repeat unit are soluble in tetrahydrofuran, 1-chloro-2,3-epoxypropane, and dimethyl sulfoxide, in contrast to the initial polymer. Strong elastic films may be obtained from solutions of the polymers containing up to two nitro-groups in the repeat unit. The decomposition temperatures in air of nitro-substituted polyphenylenephthalides containing 0.2–2.6 nitro-groups in the repeat unit are in the range 320–340 °C. These polymers do not soften before they decompose.¹⁴⁰

VII. Aromatic polyamides

The use of aromatic diamines and dicarboxylic acid chlorides with cardo groups for the synthesis of polyamides made it possible to obtain cardo polyamides.^{2–4, 12, 27, 37, 38, 49, 76, 77, 127, 143–169} Scheme 8 presents examples of such polymers. The study of the characteristic features of the formation of cardo polyamides showed that satisfactory results are obtained when the low-temperature polycondensation is carried out in aprotic solvents

Scheme 8



(dimethylacetamide, *N*-methylpyrrolidone) at -10 to -30 °C for 15–60 min and at reactant concentrations of 0.6–0.7 M. The reaction is carried out by adding the solid acid chloride to a solution of the diamine.^{27, 143–147, 154} The optimum polycondensation conditions for the polyamide based on 9,10-bis-(4-aminophenyl)-anthracene are as follows: temperature 20 °C, reaction time 2 h, solvent — 2:1 (vol %) *N*-methylpyrrolidone–hexamethylphosphoramide mixture, concentration of monomers 0.25 M, and concentration of LiCl 5% (relative to the solvent).¹⁵²

Electron microscope study of the films and pressed anilinephthalein polyamides, obtained by low-temperature polycondensation in solution, showed that such polymers contain supramolecular 500–1000 Å globular formations.¹⁴⁶ The majority of the cardo polyamides synthesised have an amorphous structure, although some of them exhibit a tendency towards ordered structures. This is characteristic of, for example, the polyamide based on anilinephthalein and terephthalic acid or bis(4-carboxyphenyl)phthalide and anilinefluorene polyterephthalamides and polyisophthalamides.^{146, 147, 154}

When the fluorene cardo group with a dicarboxylic acid residue is introduced into the polyamide, the products are polyamides which show no tendency to crystallise.¹⁵⁴ According to the results of thermomechanical tests, the cardo polyamides derived from aliphatic dicarboxylic acids have comparatively low softening temperatures (210–240 °C),^{147, 154} exceeding somewhat the melting points of the widely familiar crystalline polyamides based on hexamethylenediamine and adipic and sebacic acids. Table 4 presents the softening temperatures (determined by the thermomechanical method) of a series of aromatic cardo polyamides.^{27, 147, 152, 155, 161, 162, 164}

These polymers have a high heat resistance, which changes little on passing from isophthalic polyamides to the polyamides of terephthalic, biphenyl-4,4'-dicarboxylic, and carborane-dicarboxylic acids, or on replacement of the anilinephthalein residues in the repeat unit by anilinephthalein imide. An appreciable decrease in heat resistance is observed when bis(4-carboxyphenyl) ether residues are introduced into the polyamide, which is apparently due to the decreased rigidity of the main polymer chain owing to the presence of bridging units (oxygen atoms) in the hinge positions. The polyamide derived from 9,10-bis(4-amino-phenyl)anthracene and bis(4-carboxyphenyl)phthalide as well as the copolymers of terephthalamide with diphenylanthracene and anilinefluorene, which do not soften up to the decomposition point, have exceptionally high heat resistances.¹⁵² It is noteworthy that the softening temperature of cardo polyamides are always higher than those of the corresponding cardo polyarylates.^{148, 151}

The thermal and thermooxidative degradation of cardo polyamides has been investigated.^{146, 147, 149, 150, 164} The temperature of the onset of mass decrease of these polymers is in the range 360–450 °C. It has been shown that the thermal stabilities of the cardo polyamides depend to some extent on the nature of the cardo group, whereas those of the polyarylates are limited mainly by the stability of the ester bond. Polyterephthalamides with anthrone and fluorene groups exhibit a higher stability than the polymers with phthalide groups. The study of the thermal degradation of anilinephthalein and anilinefluorene polyterephthalamides showed that the decomposition of these polymers begins at temperatures above 350 °C; the hydrolytic decomposition predominates at 350–400 °C, whereas the contribution of the homolytic decomposition increases above 400 °C. The homolytic

Table 4. The softening temperatures of the aromatic cardo polyamides $\text{—NH—C}_6\text{H}_4\text{—R}^1\text{—C}_6\text{H}_4\text{—NHOC—R}^2\text{—CO—}$.

R ¹	R ²	T/ °C	R ¹	R ²	T/ °C
		385			Above decomposition temperature
		390			
		395			
		340			405
		385			430
		380			320
		390			420
		395			370
		400			380

decomposition of the amide bond is accompanied mainly by cross-linking processes in the polymers, which lead to the formation of tertiary amide and amine fragments in the polymeric structures.¹⁴⁹ The thermal oxidation of these polymers hardly differs from their thermal decomposition.¹⁴⁹ At temperatures preceding the decrease in the mass of the polymers (up to 350 °C), branching and cross-linking processes develop. During the isothermal heating of aromatic cardo polyamides at 300 °C in air and in vacuo for 3 h, no decrease in the mass and no appreciable impairment of the properties of these materials are observed.¹⁴⁷ According to the results of dynamic thermogravimetric analysis in air at a heating rate of 4–4.5 K min⁻¹, the temperatures of the onset of mass loss for a polyterephthalamide of anilinephthalein, anilinephthalimidine, and anilinefluorene and the polyamide obtained from anilinefluorene and 9,9-bis(4-carboxyphenyl)fluorene are 400, 390, 405, and 410 °C respectively.^{147, 154}

Thermogravimetric study of the carborane-containing polyamides obtained from 1,2- and 1,7-bis(4-carboxyphenyl)-carboranes, anilinefluorene, and anilinephthalein showed that the principal difference in the nature of the degradation of these polymers and of the usual aromatic cardo polyamides consists in a lower rate of decomposition, while the temperature ranges of vigorous decomposition are comparatively the same. At the same temperature, the decrease in the mass of carborane-containing polyamides is 3–5 times less than for the usual aromatic polyamides.¹⁶³

The use of cardo monomers for the synthesis of polyamides not only leads to the formation of heat-resistant and thermostable polymers but also greatly improves their solubility. In contrast to the majority of aromatic polyamides, sparingly soluble in organic solvents and soluble predominantly in solutions of inorganic salts in amide solvents,¹⁷⁰ cardo polyamides dissolve readily in dimethylformamide, dimethylacetamide, methylpyrrolidone, dimethyl sulfoxide, benzyl alcohol, and cresol with formation of highly concentrated solutions (in excess of 400 g l⁻¹).^{4, 147} Cardo polyamides dissolve in an unusual manner in cyclohexanone.¹⁵⁴ Whereas cardo polyamides with phthalide groups dissolve readily in cyclohexanone (this applies even to polyterephthalamide), anilinefluorene polyterephthalamide is almost insoluble in this solvent, while solutions of anilinefluorene polyisophthalamide are unstable, which is believed to be caused by the tendency of this amide to acquire an ordered structure. Anilinefluorene polyterephthalamide, which precipitates from solution in dimethylformamide, also exhibits a tendency towards ordering on standing at room temperature. This property of the chains can be suppressed by synthesising mixed polyamides derived from anilinefluorene and terephthalic and isophthalic acids with a molar ratio of the latter of 85:15. When the fluorene cardo group with a dicarboxylic acid residue is introduced into the polyamide, the products are also polyamides which do not exhibit a tendency towards ordering and which are readily soluble in cyclohexanone.¹⁵⁴ The study of solutions of anilinephthalein polyterephthalamide in dimethylformamide showed that such solutions are stable over a wide range of temperatures and compositions.¹⁶⁷

Films with satisfactory strength parameters (tensile strength of 800–1500 kgf cm⁻², elongation at break 20%–70%) are obtained by moulding cardo polyamides from solutions.^{4, 27, 49, 147, 154} Polyamide films, for example, anilinefluorene polyterephthalamide films, exhibit a high resistance to ultraviolet light and radiation. Thus the strength of a film made from this polyamide remains unchanged after exposure to ⁶⁰Co γ-rays in vacuo at a dose of 20 000 Mrad; 60% of the strength is retained on irradiation in air at a dose of 3500 Mrad.^{154, 166} The strength characteristics of the anilinefluorene polyterephthalamide film remain unchanged also after subsequent irradiation with UV light and electrons (50 MGy), while the relative elongation and the heat resistance increase.¹⁵⁸

Aromatic cardo polyamides exhibit a satisfactory chemical stability.^{146, 147} Thus the molecular mass of anilinephthalein polyisophthalamide hardly changes after being kept for 40 h at room temperature in concentrated sulfuric acid or in a 40% sodium

hydroxide solution. Films of this polyamide retain their strength and elasticity after heating in water for 4 h at 200 °C. The polymer is resistant to the action of boiling dimethylformamide and dimethylacetamide.

Cardo polyamides have satisfactory electrical characteristics, similar to those of other polyamides. Their stability is much higher by virtue of their high heat resistance.⁴ Highly heat-resistant monolithic articles with effective mechanical and antifriction properties can be obtained by pressing filled and unfilled cardo polyamides.^{4, 147}

A number of studies^{153, 156, 157} of the matrix polycondensation of the cardo polyanilinephthalein- and cardo polyanilinefluorene-terephthalamides with less rigid chains in a medium comprising the macromolecules of rigid-chain poly-*p*-phenyleneterephthalamide or polyphenylenebenzimidazoleterephthalamide have been carried out in order to be able to regulate the structures of cardo polyamides and hence their properties and to obtain polymer–polymer compositions. Thus blends of aromatic polyamides obtained by low-temperature polycondensation in solution of terephthaloyl chloride with anilinefluorene (cardo polyamide 1) on a rigid-chain poly-*p*-phenyleneterephthalamide matrix (matrix 2) and by the retrosynthesis of poly-*p*-phenyleneterephthalamide (polyamide 2) on a polyanilineterephthalamide matrix (matrix 1) have been investigated.^{156, 157} Interesting results have been obtained in the synthesis of polyamide 1 on matrix 2. The matrix polyanilinefluorene-terephthalamide has the highest coefficient of friction at elevated temperatures and the lowest intensity of linear wear of its specimens (obtained by compression pressing), amounting to 2 × 10⁻¹⁰, which is five times smaller than for specimens of matrix poly-*p*-phenyleneterephthalamide (retrosynthesis) and is smaller by a factor of two than for a mechanical mixture of polyamides 1 and 2. In contrast to polymer blends, obtained by retrosynthesis or by mechanical mixing of polyamides 1 and 2, this polymer blend could not be separated quantitatively into the corresponding homopolymers by extraction with *N*-methylpyrrolidone. The content of polyamide 1, which is as it were 'encapsulated' in matrix 2, is 55%. These data indicate a definite influence of the method of synthesis of the polymer systems on their properties and also the possibility of employing such aromatic polyamides for the creation of antifriction materials with improved properties.¹⁵⁷

The regulation of the properties of the polymers by varying the previous history of their synthesis, carried out in the presence of a matrix comprising one of the blend components, has also been demonstrated in relation to polymer blends of polyphenylenebenzimidazoleterephthalamide and polyanilinefluorene-terephthalamide.¹⁵³ It was found that, depending on the structure of the polymer, the structure of the matrix can exert both disordering and ordering effects on the other polymer. This makes it possible not only to alter the mechanical properties of the films but also to obtain films from blends containing a large amount of the polymer which does not itself form films (in the given instance, this is polyphenylenebenzimidazoleterephthalamide, which is insoluble in organic solvents and has a high softening temperature).

The possibility of the formation of linear-network polymer systems based on a cardo polyamide and unsaturated cardo amides in which the linear cardo polyamide is enclosed in a network polymer matrix has been demonstrated.¹⁶⁸ In particular, the possibility of the polymerisation of amorphous and high-melting ($T_m > 350$ °C) crystalline unsaturated cardo amides (for example, anilinefluorene bisacrylamide) in a matrix comprising the amorphous heat-resistant anilinefluorene polyterephthalamide has been investigated. Films were cast from solutions in dimethylformamide containing both the unsaturated bisamides and the polyamide. It was found that anilinefluorene and anilinephthalein bisacrylamides can be satisfactorily blended with the polyamide and that, when the crystalline anilinefluorene bisacrylamide is blended with the cardo polyamide, it becomes amorphous. The crystalline anilinefluorene bisacrylamide does not itself polymerise in bulk up to 350 °C, but, when it is introduced into a matrix comprising a heat-resistant cardo polyamide in an amount of 10–100 mass %, it passes

to the amorphous state and polymerises effectively with formation of a network polymer in air at 250 °C in the course of 5 h. Such network systems, filled with amorphous cardo polymers, exhibit a high strength and heat resistance.¹⁶⁸

Heat-resistant compositions based on cardo polyamides and oligoepoxides have also been described. It has been observed that at elevated temperatures epoxide compounds interact with aromatic cardo polyamides via a mechanism involving the 'insertion' of a fragment of an oxirane ring in the amide bond,^{80, 81, 126, 127, 169} giving rise to three-dimensional polymer systems.

VIII. Polyimides

The cardo principle has been used successfully also for the synthesis of polymers with a cyclochain structure. In particular, cardo polyimides are the first representatives of heterocyclic cardo polymers. Numerous studies have been devoted to their synthesis and investigation (see, for example, Refs 2–4, 49, 146, and 171–269). Cardo diamines such as anilinephthalide, anilinephthalimide, anilinefluorene, anilineanthrone, anilinecyclohexane, and also the dianhydride of bis(3,4-dicarboxyphenyl)phthalide combined with various aromatic, aliphatic, and aliphatic-aromatic diamines as well as the dianhydrides of tetracarboxylic acids have been used as the starting materials for the synthesis of cardo polyimides.

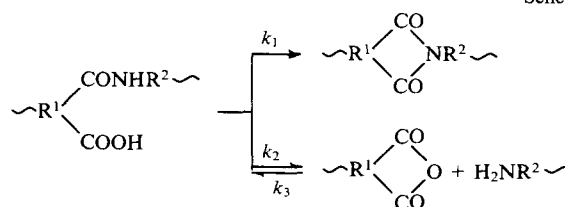
It is noteworthy that the ready solubility of cardo polyimides has led to the possibility of their synthesis by different procedures: by the two-stage polycyclisation of tetracarboxylic acid dianhydrides and diamines^{2–4, 49, 146, 174–177, 201, 210–213, 218–220, 223, 228, 250, 258, 262, 263, 265} with thermal and catalytic imidisation of polyamidoacids, by a single-stage polycyclisation in solution both in the presence of catalysts and without them (see, for example, Refs 2–4, 49, 146, 171–173, 178–183, 211–214, 217, 222, 223, 225, 250, 258, 261, 263), by the reaction of tetracarboxylic acid dichloride diesters and diamines,^{2–4, 49, 183–185, 200, 211, 261} and by the polycyclisation of tetracarboxylic acid dianhydrides and trimethylsilyl derivatives of diamines.^{211, 216, 258}

In the two-stage polycondensation, the first stage (the formation of polyamidoacids) is carried out under the conditions of low-temperature polycondensation in solution of solvents such as dimethylacetamide, dimethyl sulfoxide, *N*-methylpyrrolidone, etc. The study of the kinetics of the formation of cardo polyamidoacids from anilinefluorene and a number of dianhydrides in *N*-methylpyrrolidone^{201, 262} showed that, in terms of decreasing reactivity, the dianhydrides can be arranged in the series presented in Scheme 9, the most reactive dianhydride being to a large extent involved in side reactions with the solvent or the impurities present in it. The rate of reaction increases on passing from a less polar solvent (dioxane) to a more polar one (methylpyrrolidone).²⁰¹ The formation of polyamidoacids involving the carboxy-groups arising on opening of the anhydride ring was found to be autocatalytic.^{211, 262} This made it possible to develop catalytic procedures for the synthesis of polyamidoacids and polyimides in the presence of carboxylic acids.

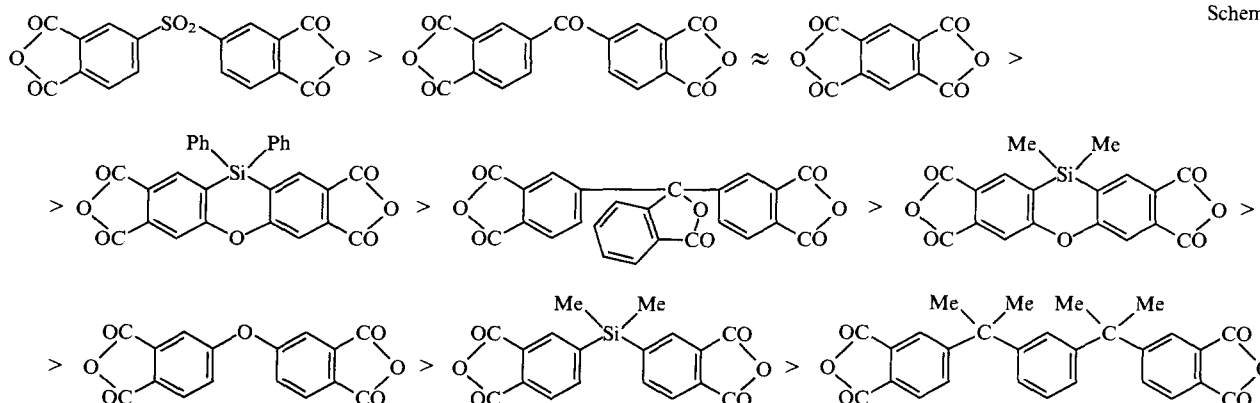
The catalytic method is extremely effective in the reactions of relatively unreactive diamines [for example bis(4-aminophenyl) sulfone] and tetracarboxylic acid dianhydrides [for example, bis(3,4-dicarboxyphenyl) ether].

In the synthesis of polyimides, account must be taken of the reversibility of the formation of polyamidoacids.^{69, 70, 211, 217–219} The reversibility is manifested particularly strongly in the thermal cyclisation of polyamidoacids, which leads to a sharp decrease in the molecular mass of the polymer in the initial instant of the cyclisation process. However, as the end groups accumulate, the resynthesis of the polyimides as a result of the condensation of the fragments formed via the terminal anhydride and amino-groups assumes an increasing importance. A mechanism has been proposed for the thermal imidisation of polyamidoacids (Scheme 10), taking into account the occurrence of consecutive-parallel cyclisation reactions of the *o*-carboxyamido units, their decomposition, and the condensation of the resulting fragments, i.e. this process must be described not by one but by at least three rate constants. The difficulties in the synthesis of polyimides associated with the instability of polyamidoacids and the reversibility of the imidisation stage can to some extent be overcome by carrying out the polycyclisation in the presence of catalytic systems^{174, 211, 262} such as mixtures of acetic anhydride with various tertiary amines, alkali metal acetates, silazanes, mixtures of chlorotrimethylsilane with tertiary amines, etc. By virtue of the mild temperatures (20–100 °C) at which the catalytic cyclisation takes place, it is possible to obtain linear soluble polyimides with a reactive group, for example the cardo polyimides derived from benzophenone-3,3',4,4'-tetracarboxylic acid, which are cross-linked via the ketogroup if synthesised by other methods. One should also note that polymers with extremely high molecular masses (up to 200 000) can be obtained by the chemical cyclisation of polyamidoacids, whereas thermal cyclodehydration affords polyimides with a molecular mass of ~20 000.

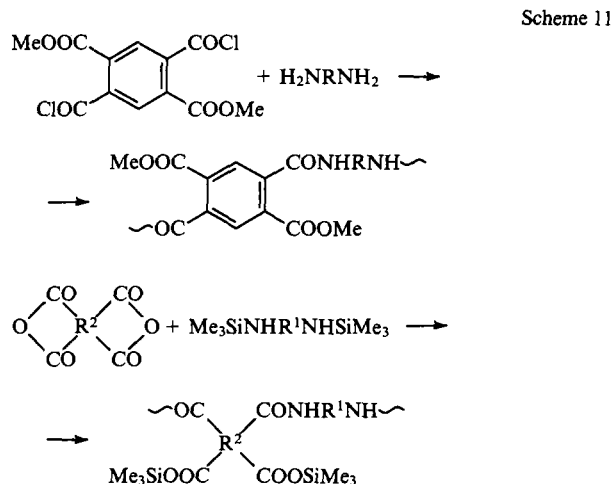
Scheme 10



The formation of polyamidoacids may be avoided by employing as starting materials tetracarboxylic acid dichloride diesters and diamines or tetracarboxylic acid dianhydrides and bis-(trimethylsilyl) derivatives of diamines. Stable alkyl and silyl esters of polyamidoacids are then obtained at an intermediate stage, as shown in Scheme 11.



Scheme 9



The cyclisation of polyamidoesters, which are hydrolytically more stable than polyamidoacids, leads to polyimides with higher molecular masses than those obtained by the cyclodehydration of the corresponding polyamidoacids. High-molecular-mass polyimides (molecular mass in the range 100 000–140 000) are formed on cyclisation of polyamidoesters in solution (for example, in nitrobenzene and sulfolane) at 210 °C and also on chemical cyclisation, which can be achieved directly in the film.

The solubility of cardo polyimides was a precondition for the development of a fundamentally new method of their synthesis — one-step high-temperature polycyclisation in an organic solvent (nitrobenzene, sulfolane, *p*-nitrotoluene, α -chloronaphthalene, cresol, etc.).^{2–4, 49, 171–173, 178–182, 211, 217, 222} An equimolecular mixture of the starting materials in a solvent is heated rapidly to 200–210 °C in an inert gas stream and is maintained at this temperature for a specified time (3–10 h). The growth of the polymer chain (the formation of the polyamidoacid) and intramolecular cyclisation take place almost simultaneously. The one-step polycyclisation in the presence of acid catalysts proved extremely successful.^{49, 181, 182, 211–214} In this case, it is possible either to decrease significantly the reaction time (down to 1–3 h), with formation of polymers with extremely high molecular masses under these conditions, or to carry out the process at lower temperatures (140–160 °C).

Carboxylic acids (for example benzoic acid) are effective catalysts also in the synthesis of high-molecular-mass polyimides from monomers with a reduced reactivity such as the dianhydride of naphthalene-1,4,5,8-tetracarboxylic acid.²¹⁴

Since, as mentioned above, the formation reaction of polyimides is reversible, it follows that in order to obtain high-molecular-mass polyimides, it is necessary to remove from the reaction sphere, as fully as possible, the water evolved during cyclisation, which is achieved by raising the reaction temperature, by carrying out the reaction in an inert gas stream, by binding the water with chemical reagents, etc. The simplicity of the one-step polycyclisation, its ready reproducibility, and the possibility of obtaining polyimides with a high molecular mass, which contain virtually no defective *o*-carboxamide units, makes it possible to regard this method as promising for the synthesis of a wide variety of polyimides.²¹¹

In the synthesis of copolyimides, one must not forget that their formation reaction is reversible. There is also no doubt that one must take into account the involvement of polyimides in exchange reactions at elevated temperatures, in the first place aminolysis.^{70, 216, 223–225, 244, 246, 247, 258} It has been shown that the formation of the microstructures of copolyimides may depend on three factors: the ratio of the reactivities of the comonomers, the rate of introduction of the intermonomer into the reaction vessel, and the occurrence or nonoccurrence of exchange reactions.

In the two-stage method of synthesis, the foundation of the microstructure of copolyimides is laid in the stage involving the formation of copolyamidoacids. Such a microstructure may be

retained or damaged in the subsequent cyclisation. Since in the two-stage method of synthesis the polyamidoacids are formed close to room temperature, the exchange reactions are then virtually ruled out. For this reason, the formation of the copolyamidoacid microstructure is determined by the ratio of the rates of the interactions of the intermonomer with the comonomers, which depend on their reactivities and on the rate at which the intermonomer is introduced into the reaction. The formation of block copolyamidoacids when there is a significant difference between the reactivities of the comonomers is observed when the intermonomer is introduced into the reaction zone comparatively slowly, for example when it is added in the solid state (frequently in portions). On the other hand, in the synthesis of the copolyamidoacid by the rapid mixing of dianhydrides and diamines, statistical copolymers are produced.

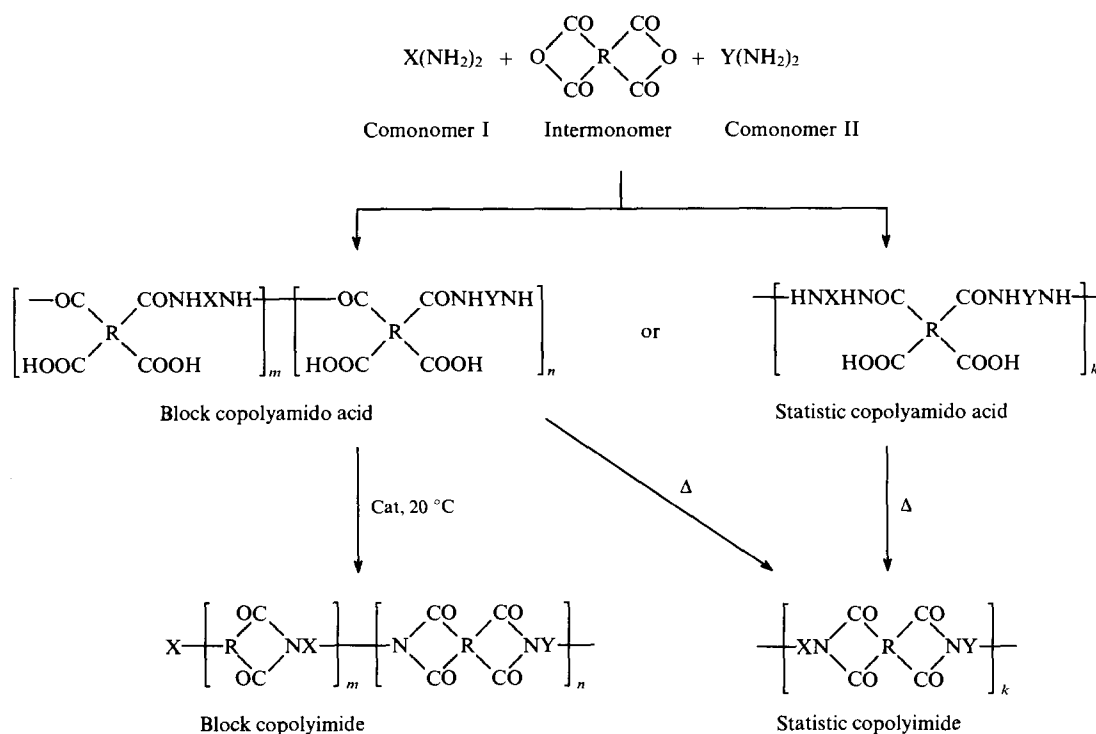
The microstructure of the copolyimides based on copolyamidoacids may be regulated by varying the cyclisation conditions. In the cyclisation under the influence of chemical reagents, occurring under mild conditions and not complicated by degradative or exchange reactions, the microstructure of the copolymer formed is identical with that of the corresponding copolyamidoacid. In thermal cyclisation, accompanied by exchange reactions, predominantly statistical copolyimides are formed from both block copolyamidoacids and from statistical copolyamidoacids.

A detailed study of the one-step copolycondensation showed that in this method of synthesis the copolymer microstructure depends on the relative reactivities of the comonomers, the differences between the reactivities of the functional groups of the intermonomer, the rate at which the intermonomer is introduced into the reaction, and the resistance of the imide rings to destructive exchange reactions and is in many respects determined by the ratio of the rates of the main polymer formation reaction and the exchange reactions, in the first place aminolysis.^{70, 216, 223, 225, 258} When aliphatic and aromatic diamines (for example, hexamethylenediamine and anilinefluorene) are used as the comonomers, while the intermonomer is the dianhydride of bis(3,4-dicarboxyphenyl) ether, statistical copolyimides are obtained owing to the occurrence of effective aminolysis. The increase in the rate of formation of the polymer when the much more reactive pyromellitic dianhydride is used permits the formation of a copolyimide with a block structure. The microstructure of copoly(naphthoylene imide), which is more resistant to aminolysis, can be altered deliberately by varying the reaction conditions. Statistical copolyimides are obtained when the starting materials and the catalyst (benzoic acid) are introduced simultaneously into the reaction, whilst in the case where the intermonomer is added slowly together with the catalyst to a solution of a mixture of diamines, the product is a copolyimide with a block structure. Scheme 12 presents the overall mechanism of the formation of copolyimides by the one-step and two-stage methods.

The use of siloxane-containing diamines, together with cardo diamines, for the synthesis of copolyimides makes it possible to obtain high-molecular-mass siloxane-containing copolyimides with different numbers of dimethylsiloxane fragments in the repeat unit (Scheme 13). Such copolyimides have been synthesised by the low-temperature polycondensation of tetracarboxylic acid dianhydrides and diamines in solution with subsequent cyclodehydration of the copolyamidoacids in the presence of chemical reagents under conditions promoting the initial formation of siloxane-amidoacid and then arylene-amidoacid fragments.¹⁹⁸

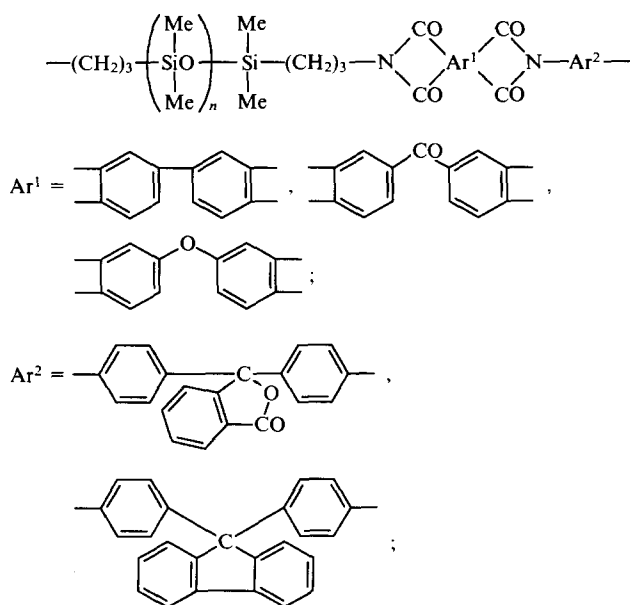
The presence of a cardo group in rigid-chain polymers such as polyimides affects primarily their solubility.^{2–4, 46, 49, 173, 175, 176, 179, 186, 187, 211, 263, 270} Many cardo polyimides are readily soluble in organic solvents: dimethylformamide, dimethylacetamide, methylpyrrolidone, dimethyl sulfoxide, hexafluoroisopropyl alcohol, sulfolane, chloroform, methylene chloride, tetrachloroethane, phenol, *m*-cresol, nitrobenzene, etc., while individual polyimides are soluble in dioxane and cyclohexanone. Among the cardo groups investigated, the asymmetric phthalide and phthalimidine groups impart the highest solubility to polymers. Their introduction

Scheme 12



X = alkylene or arylene, Y = arylene (cardo)

Scheme 13



$n = 1, 29, 39, 99$

increases the solubility of even the polyimides with a most rigid chain such as polypyromellitimide and poly(1,4,5,8-naphthoylene imide). The solubility of cardo polyimides is influenced appreciably also by the structure of the tetracarboxylic acid dianhydride. It has been found that the different groups entering into the composition of the main chain of the polymer can be arranged in a sequence, in terms of their influence on solubility, in which each successive group expands the range of the solvents for the polymer (Scheme 14).²¹¹ Polyimides containing cardo groups in both the dianhydride and diamine components, (for example, phthalide or phthalide and fluorene) are more soluble than the polyimides containing only one such group in the elementary unit. (In particular,

the former acquire solubility in cyclohexanone.¹⁸⁶) The presence of the phthalide cardo group solubilises adamantane-containing polyimides based on the dianhydride of bis(3,4-dicarboxyphenyl)-phthalide, while their analogues based on the dianhydrides of pyromellitic and benzophenone-3,3',4,4'-tetracarboxylic acids are insoluble.²³⁴ The synthesis of cardo copolyimides has led to extensive possibilities for the variation of solubility. In particular, the formation of copolyimides is an effective method of imparting solubility to polyimides derived from naphthalenetetracarboxylic acid.^{70, 225}

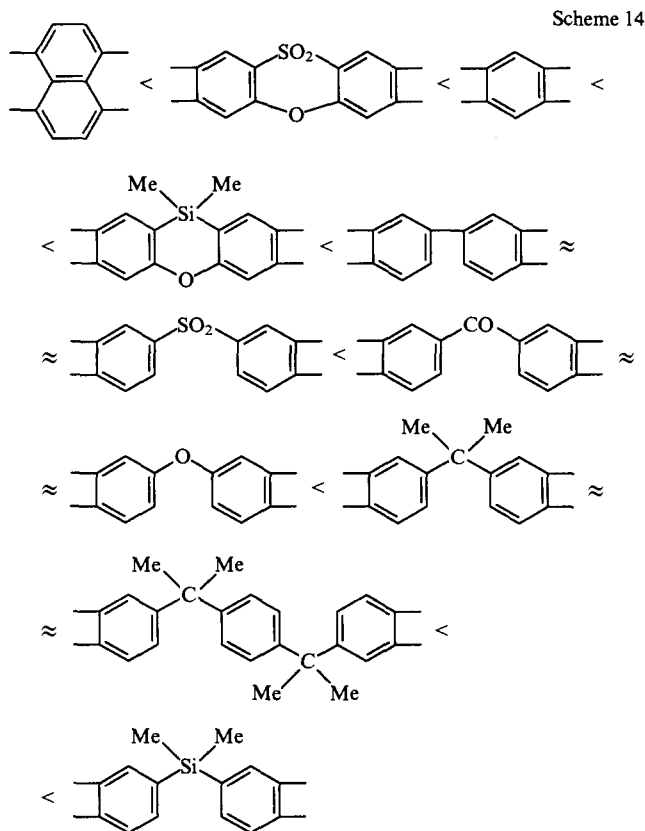
The effect of solvent antagonism has been observed for certain cardo polyimides. Such antagonists are dimethylformamide, dimethyl sulfoxide, dimethylacetamide, and methylpyrrolidone, on the one hand, and methylene chloride, chloroform, and tetrachloroethane, on the other.^{211, 263} Thus the polyimide derived from anilinefluorene and bis(3,4-dicarboxyphenyl) ether does not dissolve in a 1:1 (vol %) dimethylformamide–chloroform mixture, but is readily soluble in each of these solvents. This effect is manifested even more strikingly in anilinephthalene poly(naphthoylene imide), which is insoluble in nitrobenzene–methylpyrrolidone mixtures with different proportions of the individual solvents.

The majority of cardo polyimides are amorphous, but some of them tend to crystallise, which exerts a considerable influence on their solubility. Thus anilinefluorene and anilineanthrone polypyromellitimides and poly(naphthoylene imides) are weakly crystallising polymers which are insoluble in organic solvents (in contrast to the corresponding polyimides with phthalide groups).²¹¹

The ready solubility of cardo polyimides in organic solvents has led to the possibility of investigating their molecular mass characteristics and the determination of their constants in the Mark–Kuhn–Houwink equation (Table 5).^{195, 202, 205, 211, 230, 263, 268}

$$[\eta] = KM_w^\alpha$$

A number of studies^{167, 233, 235} have been devoted to the investigation of solutions of cardo polyimides in greater depth. Thus the study of solutions and gels of anilinephthalene polypyromellitimide in dimethylformamide showed that solutions of the polyimide lose their stability after a time, become turbid, and



are converted into a gel, which can be explained by the poor thermodynamic affinity of the polyimide for dimethylformamide. It follows from X-ray diffraction and polarised light scattering data that the polyimide gels contain both isotropic and anisotropic regions having approximately the same dimensions ($\sim 400 - 600$ nm).¹⁶⁷ The second virial coefficients of solutions of the polyimide derived from anilinephthalein and bis(3,4-dicarboxyphenyl) ether in *N*-methylpyrrolidone, dimethyl sulfoxide, chloroform, THF, and dimethylformamide have been determined.

It has been shown that the molecular masses of this polymer in various solvents are virtually identical, which indicates the absence of association.²³³ The phase diagram for solutions of cardo polypyromellitimides and poly(naphthoylene imides) with fluorene, phthalide, and anthrone groups in fused antimony trichloride has been investigated. The formation of spherulites of anilinefluorene polypyromellitimide and anilinefluorene poly(naphthoylene imide) solutions and of nonordered anisotropic rods has been established for the anilinephthalein pyromellitimide system in antimony trichloride. The results indicate the possibility of the crystallisation of cardo polypyromellitimides and cardo poly(naphthoylene imides) in antimony trichloride on phase separation of their solutions, which leads to new possibilities for the regulation of the properties of these polymers.²³⁵

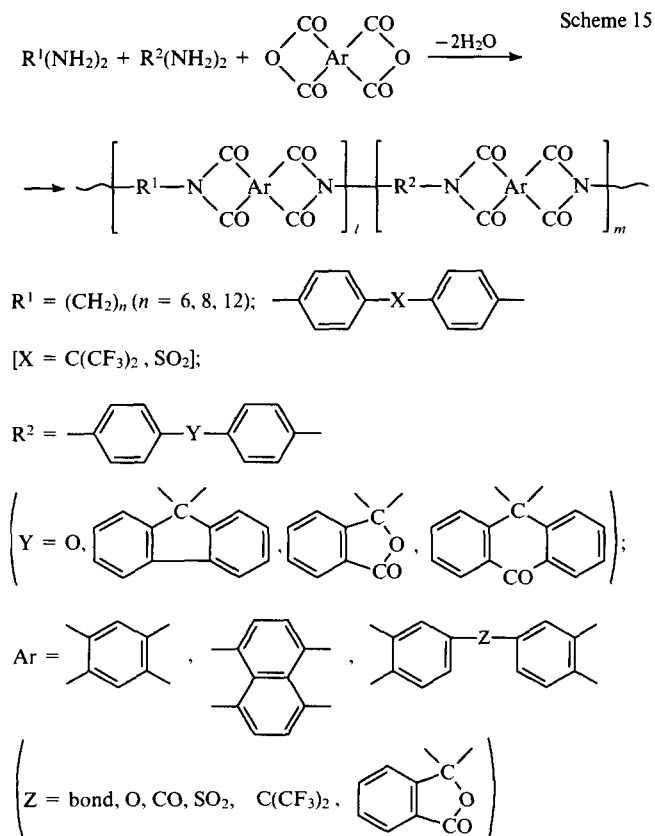
Table 6 (see over) presents the softening temperatures of a series of cardo polyimides.^{211, 265} It is seen from these data that polymers with three and five condensed rings in the dianhydride residue have the highest heat resistance, which is significantly higher than that of the polyimides with phthalimidine groups having similar chemical structures (cf, for example, polymers Nos 1 and 10, 5 and 4, or 6, 7, and 8).

Scheme 15 presents examples of the structures of aliphatic-aromatic and aromatic cardo copolyimides.^{49, 214, 216, 223, 225, 258} Their heat resistance may be varied within wide limits ($160 - 500$ °C) by varying the chemical structures and microstructures of the copolymers. The softening temperatures of the aliphatic-aromatic polyimides increase consistently with increase in the cardo diamine proportion in the macromolecule and on passing to polyimides with six-membered imide rings.

Like other aromatic polyimides, aromatic cardo polyimides have high thermal stability.^{164, 179, 187, 191 - 193, 211, 250, 265} Polyimides with anthrone and fluorene groups are the most thermostable, the onset of decrease in their mass being observed at $500 - 520$ °C. They retain 70% of their mass on heating to 900 °C under an inert atmosphere. The cardo groups in polyimides with anthrone and fluorene groups are stable virtually up to the same temperatures as the imide ring, whereas in the polyimides with phthalide and especially with cyclohexylidene groups, destruction affects primarily the cardo groups. According to the results of dynamic thermogravimetric analysis (heating rate 4.5 K min⁻¹), the polyimides with phthalide groups begin to decompose in air at

Table 5. The constants in the Mark - Kuhn - Houwink equation for the cardo polyimides

		$\begin{array}{c} \text{OC} \quad \text{CO} \\ \diagdown \quad \diagup \\ \text{N} \quad \text{Ar}^1 \quad \text{N} \\ \diagup \quad \diagdown \\ \text{OC} \quad \text{CO} \end{array}$		
Ar ¹	Ar ²	Solvent	$K \times 10^{-4}$	α
		Dimethylformamide	0.71	0.88
		<i>N</i> -Methylpyrrolidone	1.28	0.77
		Dimethylformamide	8.91	0.56
		Dimethylacetamide	3.33	0.64



450–490 °C. Saturation of the polymer chain by fragments with a large number of condensed rings in the system and replacement of the five-membered phthalimide groups by the six-membered naphthoylene imide groups increase the thermal stability of the cardo polyimides. On heating in helium (heating rate 5 K min⁻¹), the 'coke' residues from carborane-containing anilinefluorene cardo polyimides with 1,7- and 1,2-bis(3,4-dicarboxyphenyl)-carboranes amount to 92% and 80% respectively.²⁶⁵

The pyrolysis of the cardo polyimide obtained from anilinefluorene and the dianhydride of benzophenone-3,3',4,4'-tetracarboxylic acid has been investigated in the temperature range from 450 to 3000 °C.^{249, 253, 266} It was noted that thermochemical transformations begin in the polymer at a temperature above 450 °C. In argon, destructive processes take place most vigorously at 550–650 °C (with a 20–22% mass loss). At 700–750 °C, the formation of the polyimide coke residue, containing 92.5% carbon, is largely complete. It was of interest to note that, in contrast to a series of the usual polypyromellitimides, heat treatment of the cardo polyimide up to 3000 °C leaves a residue of up to 0.75% of the nitrogen forming part of the composition of condensed six-membered rings. As a result of pyrolysis, the electrical resistance of the system decreases by 12–13 orders of magnitude. The carbon materials thus obtained have a high mechanical strength, a low coefficient of friction, and, in contrast to graphite, a very low porosity. It was established that the electrical conductivity of the polyimide-based carbon materials may be increased still further by their thermal decomposition in various metal (copper, nickel, zinc, and iron) formates.²⁵¹

The ability of soluble cardo polyimides to form charge-transfer complexes with low-molecular-mass (*N*-methylcarbazole) and high-molecular-mass (poly-*N*-vinylcarbazole) electron donors has been noted; in the latter case, a very distinct cooperative polymeric effect is observed.²⁵²

The radiolysis of anilinephthalein polypyromellitimide on prolonged γ -irradiation in vacuo has been investigated.²⁵⁴ The high radiation stability of this polymer was demonstrated. The radiation-induced electrical conductivities of certain copolyimides have been studied in the course of their irradiation in vacuo by electron pulses

with an energy of 65 keV. It was established that the macrostructure (block or statistical) of the copolyimide exerts a definite influence on the electrical conductivity.²⁵⁶

The high heat resistance, thermal stability, radiation resistance, and chemical stability of cardo polyimides, as well as the possibility of working many of them in the 'cyclised' form makes them promising for practical use in the manufacture of various articles designed for prolonged use at temperatures above 200 °C.

Virtually colourless strong films (tensile strength 1000–1100 kgf cm⁻², elongation at break 40%–70%), the electrical properties of which in the temperature range 20–300 °C are not inferior to the familiar Kapton H film, are obtained from solutions of cardo polyimides by casting.²¹¹ The study of the optical properties of polyimide films obtained from anilinefluorene and bis(3,4-dicarboxyphenyl) ether showed that they exhibit a high optical transmittance at 500 nm (81%–87%) and are thermophotoradiation-resistant. After heat treatment at temperatures up to 300 °C or after UV irradiation at a dose equivalent to a 300 h exposure to sunlight, the optical transmittance of the film diminishes by only 1%–3%.¹⁵⁸

The cardo polyimide based on anilinefluorene and bis(3,4-dicarboxyphenyl) ether (PIR-2 brand) has been used successfully for the preparation and attachment by adhesive at room temperature of resistance strain gauges for the measurement of static deformations, operating over a wide temperature range (from –190 to 300 °C). A series of cardo polyimides can be worked in the fused state into strong plastics for various purposes. Thus the compressive strength of PIR-2 plastics is 1800 kgf cm⁻² and their modulus of elasticity is 2.2×10^4 kgf cm⁻².²¹¹ The strengths and moduli of elasticity on compression of plastics made from a series of cardo copolyimides reach 1400–2100 and $(1.7 \text{ to } 2.2) \times 10^4$ kgf cm⁻² respectively, the strength characteristics remaining virtually unimpaired after preliminary heating of the plastics to 200–240 °C.²²³ Monolithic plastics with an impact strength of 15 kgf cm cm⁻² and a bending strength of 700–1000 kgf cm⁻² have been moulded from cardo copoly(naphthoylene imides) by the hot pressing method.²²⁵

The satisfactory solubility of cardo polyimides and their compatibility with many polymers and oligomers, for example, with phenolformaldehyde and epoxide polymers, ensured their approval as heat-resistant fibre-forming materials, as binders for reinforced plastics, as coatings, and as adhesives.^{126, 127, 211, 264} In particular, the modification of epoxide oligomers by cardo polyimides leads to the formation of cross-linked polymer systems superior as regards heat resistance, strength, and other properties to materials obtained with the aid of the usual hardening agents for epoxide oligomers. For example, the use of polyimide–epoxide compositions as binders for reinforced carbon plastics proved successful. The compressive strength of such plastics is 2900–4200 kgf cm⁻² at 20 °C and remains virtually unchanged up to 250 °C.²⁶⁴

A linear-network system, in which the linear amorphous cardo polyimide is enclosed in a network polymer matrix, has been obtained by the polymerisation at 200–250 °C of anilinefluorene bisacrylamide in a matrix comprising a cardo polyimide based on anilinefluorene and bis(3,4-dicarboxyphenyl) ether. This system has a high strength and heat resistance.¹⁶⁸

The high thermal stability of the imide rings combined with the valuable physicomechanical properties of the materials based on linear polyimides made it desirable to develop methods of synthesis of thermoreactive polyimides based on reactive oligomers having comparatively low softening temperatures. By imparting thermoreactive properties to polyimides, the possibilities for their processing into various materials are expanded. In particular, thermoreactive polymers containing imide rings have been synthesised from the dianhydrides of tetracarboxylic acids and the corresponding diamines with subsequent blocking of the terminal amino-groups by the acrylic or methacrylic acid chlorides in the oligomeric amidoacid stage (Scheme 16a) or the oligoimide stage (Scheme 16b).²⁰⁶ A series of studies have been devoted to the preparation and study of certain oligomeric cardo imides with terminal unsaturated acrylamide and methacrylamide

Table 6. The softening temperatures of some polyimides —N—Ar¹—N—Ar²—.

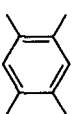
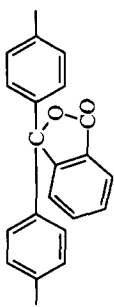
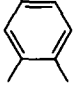
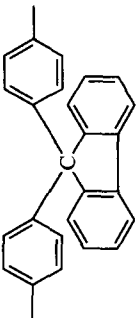
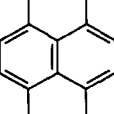
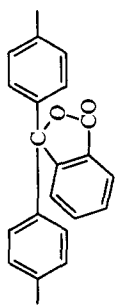
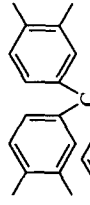
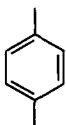
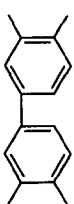
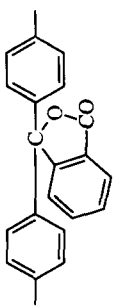
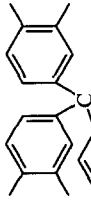
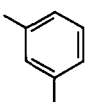
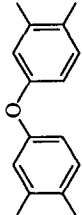
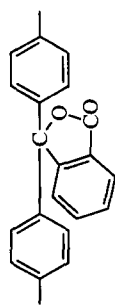
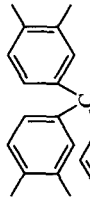
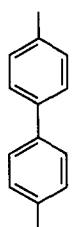
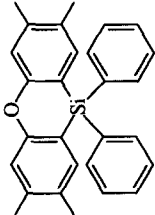
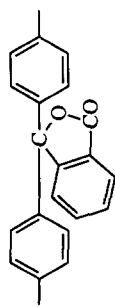
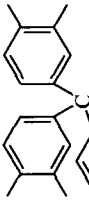
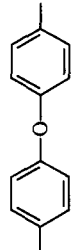
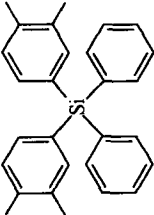
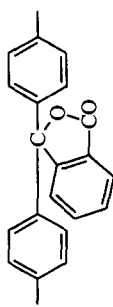
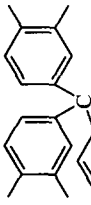
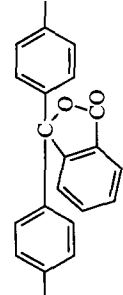
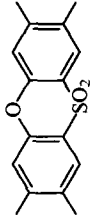
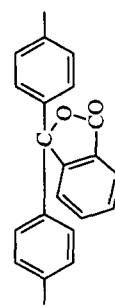
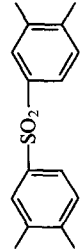
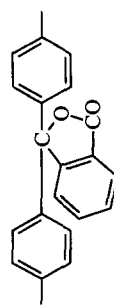
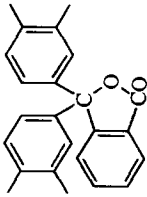
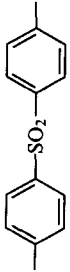
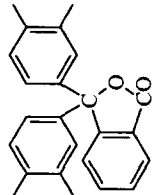

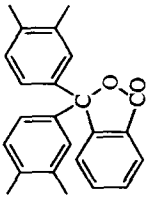

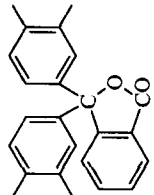
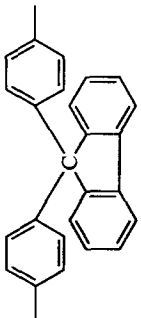
No	Ar ¹	Ar ²	T/°C	No	Ar ¹	Ar ²	T/°C
1			480	9			380
2			540	10			410
3			415	11			360
4			375	12			415
5			460	13			345
6			330	14			415
7			Above decomposition temperatures				
8			400				

Table 6 (continued)

No	Ar ¹	Ar ²	T/°C	No	Ar ¹	Ar ²	T/°C
15			370	17			380
16			315	18			425

groups.^{49, 168, 203, 204, 206, 207, 211, 245, 259} They have been obtained in quantitative yields and with a specified degree of polymerisation.

Unsaturated oligoimides obtained from cardo diamines and having terminal acrylamide and methacrylamide groups are amorphous substances readily soluble in dimethylformamide, dimethylacetamide, and tetrachloroethane with formation of concentrated solutions. Their softening temperatures can be regulated by varying the nature of the cardo group and the degree of polymerisation of the oligomer. Thus, when the degree of polymerisation of the oligoimide obtained from anilinephthalein and benzophenone-3,3',4,4'-tetracarboxylic acid and having terminal acrylamide groups is increased from 3 to 10, its softening temperature increases from 210 to 280 °C, remaining at the same time appreciably lower than the softening temperature of the corresponding high-molecular-mass linear polyimide (380 °C).

Cross-linked insoluble polymers which do not soften up to the onset of thermal destruction have been obtained by the thermal polymerisation in bulk of unsaturated cardo oligoimides in air at 250–310 °C. The thermal destruction develops vigorously only at temperatures above 400 °C.²⁰⁶ Glass fibre-reinforced plastics with a low porosity and a high bending strength (4000–5000 kgf cm⁻²) both at room and elevated temperatures have been prepared from solutions of unsaturated anilinefluorene- and anilineanthrone-benzophenone-3,3',4,4'-tetracarboxylic acid oligoimides in *N*-methylpyrrolidone.²⁵⁹

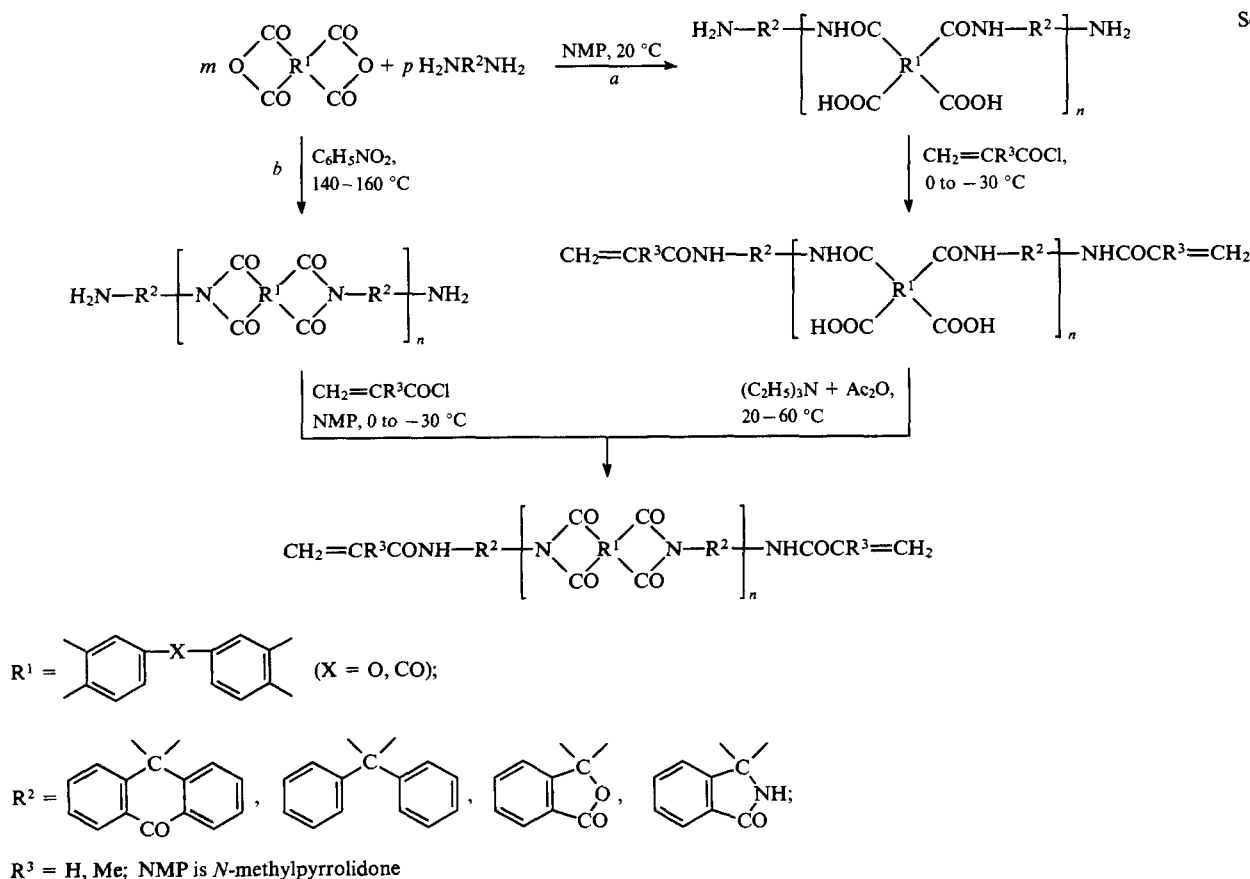
The above unsaturated oligoimides have been used successfully to prepare copolymers with monomers such as *N*-vinylpyrrolidone, *N*-phenylmaleimide, and the bismaleimides obtained from various aliphatic diamines, the oligomers being readily soluble in such monomers.^{49, 207, 211, 259} It was established that the cross-linked copolymers are formed at lower temperatures than the corresponding cross-linked homopolyimides. Thus the use of *N*-vinylpyrrolidone makes it possible to reduce the polymerisation temperature by 50–80 °C.²⁰⁷ The cross-linked copolymers obtained in up to 90% yields by thermal polymerisation at 200–250 °C have high heat resistances and chemical and thermal

stabilities.^{207, 211, 259} Such copolymers begin to undergo deformation only at temperatures above 300 °C, and, according to dynamic thermogravimetric data, the onset of decrease in their mass in air is in the temperature range from 350 to 400 °C. The cross-linked copolymers of unsaturated polyoligoimides as well as the corresponding network homopolyimides undergo hardly any change in their mass on being kept for a week in sulfuric and nitric acids, 25% ammonia, and 10, 20, and 40% solutions of sodium hydroxide. In this respect, they are superior to their linear analogues, which undergo appreciable destruction under the conditions indicated.

The satisfactory solubility of the unsaturated cardo oligoimides in a monomer such as *N*-phenylmaleimide makes it possible to obtain from them (without using an inert solvent as a binder) reinforced plastics (using organic and glass fibres) having a high mechanical strength both in the initial state and after prolonged maintenance at elevated temperatures. For example, the glass fibre-reinforced plastic based on the cross-linked copolymers of *N*-phenylmaleimide and the anilinefluorene-benzophenone-3,3',4,4'-tetracarboxylic acid cardo oligoimide with terminal acrylamide groups and $n = 5$ (Scheme 16) has tensile strengths of 15500 and 15000 kgf cm⁻² and bending strengths of 8500 and 14000 kgf cm⁻² at room temperature and 250 °C.²¹¹

The cross-linked copolymers based on the unsaturated oligoimides considered and the bismaleimides obtained from aliphatic diamines have interesting properties. These are solid, transparent, heat-resistant substances which do not undergo deformation up to the onset of thermal decomposition (the temperature of which in air is 400–450 °C according to thermogravimetric data). They have effective mechanical properties. At room temperature, the above substances have a compressive strength of 2000 kgf cm⁻² and a modulus of elasticity on compression in the temperature range from 180 to 300 °C of $(4-7) \times 10^3$ kgf cm⁻² which shows that such copolymers exhibit properties similar to those of leather over a wide range of elevated

Scheme 16



temperatures. This makes it possible to regard them as promising materials for high-temperature hermetic seals.^{211, 259, 260}

Network cardo polymers of the polyaminoimide type^{49, 208, 209, 260} have been synthesised by the interaction of *N,N'*-hexa-, octa-, nona-, deca-, and dodecamethylenebismaleimides with cardo diamines (anilinefluorene, anilinephthalein). The process may be regulated by varying the conditions under which it is carried out (temperature, reaction time, proportions of starting materials, addition of a catalyst and initiator) and by regulating the contribution of each of the two main reactions: migration polymerisation (addition of amino-groups to double bonds) and three-dimensional copolymerisation (via carbon-carbon double bonds). The density of the three-dimensional polymer network and the length of the fragments between its nodes change under these conditions. Network cardo polyimides of this type are solid monolithic materials insoluble in organic solvents and characterised by a valuable set of physicochemical properties: high heat resistances and chemical and thermal stabilities, and effective physicomechanical parameters.

We shall deal with yet another type of cardo polyimides, the so called functional cardo polyimides containing in their polymer chains free functional groups, which in a number of instances impart specific properties to the polyimides and give rise to the possibility of their further chemical modification.²⁶⁹

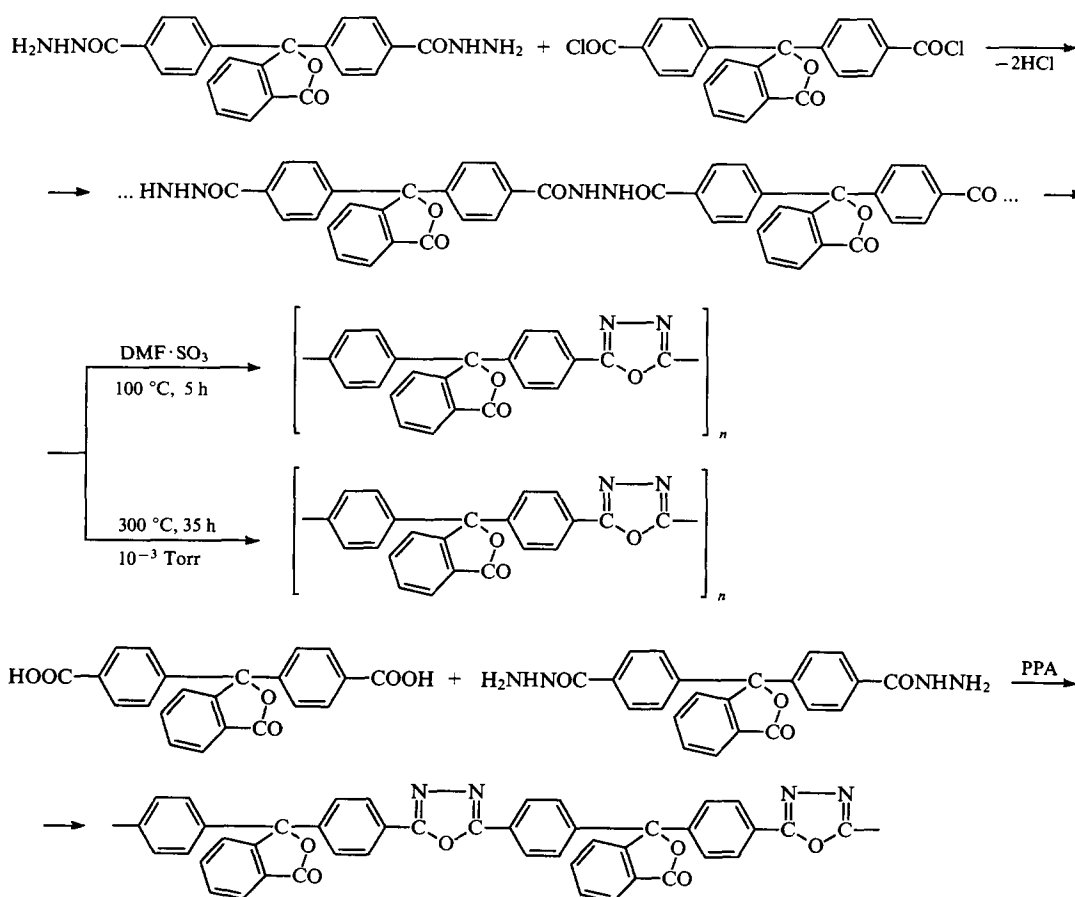
Thus the synthesis of cardo polyimides with free hydroxy-groups [the dianhydrides of bis(3,4-dicarboxyphenyl)methanol and cardo diamines were used as the starting materials] has been achieved. Copolyimides with benzimidazole rings, containing a free reactive NH group, in the main chain have been obtained by the polycondensation of various tetracarboxylic acid dianhydrides with a mixture of a cardo diamine and 5(6)-amino-2(4-aminophenyl)benzimidazole. Aromatic polyimides with reactive quinuclidine cardo groups have been synthesised by the reaction of various tetracarboxylic acid dianhydrides with 3,3-bis(4-

aminophenyl)quinuclidine. Polyimides with functional groups are readily soluble in organic solvents and have satisfactory heat resistances, thermal stabilities, and dielectric characteristics as well as enhanced adhesive properties and they form strong transparent films. The possibility of modifying epoxide oligomers by polyimides derived from bis(3,4-dicarboxyphenyl)methanol has been demonstrated. Such modification afforded cross-linked polymer systems with heat resistances and mechanical strengths superior to those of the epoxide oligomers hardened by the traditional methods. The presence of quinuclidine fragments in the polyimides gives rise to prospects for their employment as catalytic systems and for their further chemical modification at the tertiary nitrogen atoms of the quinuclidine ring system.

IX. Poly-1,3,4-oxadiazoles

The introduction of cardo groups also into polymers with a cyclochain structure such as poly-1,3,4-oxadiazoles has been successful.^{2-4, 12, 49, 76, 77, 186, 270-296} The high heat resistances and thermal stabilities of aromatic polyoxadiazoles together with the comparatively ready availability of the initial compounds (dicarboxylic acids and their derivatives) used for their synthesis are responsible for the interest in these polymers.²⁹⁷⁻³⁰⁰ However, aromatic polyoxadiazoles are in the main high-melting polymers insoluble in organic solvents. This limits the possibilities for the comprehensive investigation of such polymers and in many cases their practical applications.

Bis(4-carboxyphenyl)phthalide and its derivatives (the acid chloride and dihydrazide) containing a central carbon atom in the polar cyclic side group²⁷⁰⁻²⁷⁵ and also 2-[3,3-bis(4-carboxyphenyl)]-*N*-phenylphthalimidine and its derivatives containing *N*-phenyl-2-phthalimidine cardo groups²⁹³ were selected as the starting materials for the synthesis of cardo polyoxadiazoles.



The polymers were synthesised by a two-stage polycyclisation method in which low-temperature polycondensation was employed in the first stage in order to produce a polyhydrazide with its subsequent cyclisation and by one-step polycyclisation in polyphosphoric acid (Scheme 17).

The ready solubility of the polyhydrazides based on bis(4-carboxyphenyl)phthalide and its derivatives owing to the presence of phthalide cardo groups permits their successful synthesis by low-temperature polycondensation not only in hexamethylphosphoramide, normally employed in the synthesis of aromatic polyhydrazides, but also in other organic solvents (*N*-methylpyrrolidone, dimethylacetamide).²⁷¹ Admittedly, polyhydrazides with a high molecular mass ($\eta_{\text{red}} = 2 \times 10 \text{ dl g}^{-1}$ in dimethylformamide) are obtained only in hexamethylphosphoramide apparently as a result of the much smaller tendency of this solvent (compared with dimethylacetamide and *N*-methylpyrrolidone) to undergo side reactions with acid chlorides.

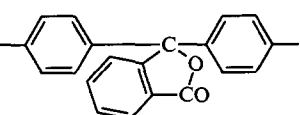
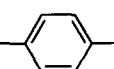
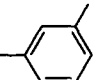
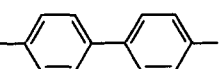
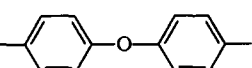
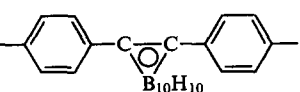
The thermal cyclodehydration of the polyhydrazide based on bis(4-carboxyphenyl)phthalide, like that of the polyhydrazides of aromatic dicarboxylic acids, requires extremely severe conditions as regards temperature in order to attain high degrees of cyclisation: prolonged (of the order of 30 h) heat treatment of the polymer at 300 °C *in vacuo* is needed. If the cyclodehydration of cardo polyhydrazides is carried out by treatment with the dimethylformamide-sulfur trioxide or dimethylacetamide-sulfur trioxide complex, it is possible to reduce the temperature (to 100 °C) and the reaction time (to 5 h).^{49, 270, 271, 275}

The characteristic features of the formation of cardo polyoxadiazoles by one-step polycondensation in polyphosphoric acid have been investigated in detail.^{49, 271, 275, 281} It was found that a side reaction involving the lactone ring takes place, leading to the

formation of an insoluble cross-linked polymer, together with the growth of the polymer chain, in the one-step polycyclisation of the dihydrazide of bis(4-carboxyphenyl)phthalide in polyphosphoric acid and also in the interaction of bis(4-carboxyphenyl)phthalide with hydrazine sulfate. The side reaction may be avoided if the polyoxadiazole is synthesised from bis(4-carboxyphenyl)phthalide and its dihydrazide or the dihydrazides of other aromatic dicarboxylic acids, or from the dihydrazide of bis(4-carboxyphenyl)phthalide and various aromatic dicarboxylic acids.

A series of characteristics of the formation of polyoxadiazoles have been investigated in relation to the reaction of bis(4-carboxyphenyl)phthalide with its dihydrazide. It was established that the results of the polycondensation (yield and molecular mass of the polymer) and the possibility of the occurrence of side reactions are greatly influenced by the ratio of the starting materials, the reaction temperature, the reaction time, the concentration of the starting materials, and the content of phosphorus pentoxide in polyphosphoric acid. Thus a soluble polymer with a high molecular mass is obtained for the equimolecular ratio of the starting materials. An excess of the acid gives rise to a decrease in molecular mass, while an excess of the dihydrazide leads to the formation of an insoluble polymer as a result of the side reaction involving the lactone ring. When the process is carried out at 140 °C, it is desirable to continue it over a period of 5 h. Polymers with the highest molecular mass are obtained when the concentration of the starting materials is approximately 0.3 mole per kilogram of phosphoric acid. The molecular mass of polyoxadiazole depends greatly on the concentration of phosphorus pentoxide in polyphosphoric acid, increasing significantly with increase in the content of the pentoxide from 82% to 86%. However, polycondensation in polyphosphoric acid containing about 84% of

Table 7. The properties of the cardo polyoxadiazoles

R	Temperature/ °C		Mechanical properties of nonoriented films	
	softening	onset of decomposition	$\sigma_t/\text{kgf cm}^{-2}$ ^a	ε (%) ^b
	390	400	1200	8
	390	430	2200	80
	360	400	1200	10
	400	430	2400	75
	340	430	1400	100
	335	420	—	—

^a σ_t is tensile strength of the film. ^b ε is relative elongation at break.

phosphorus pentoxide is preferable on technological grounds. Mixed polyhydrazides and polyoxadiazoles were obtained when one of the initial components was replaced by the corresponding derivative of an aromatic dicarboxylic acid such as isophthalic, terephthalic, and biphenyl-4,4'-dicarboxylic acids, bis(4-carboxyphenyl) ether, benzophenone-4,4'-dicarboxylic acid, or 1,2- and 1,7-bis(4-carboxyphenyl)carboranes.

All three methods of synthesis (thermal dehydration, chemical dehydration in the presence of the dimethylformamide-sulfur trioxide complex, and one-step polycyclisation in polyphosphoric acid) can be used successfully for the synthesis of cardo polyoxadiazoles. However, polymers with a high molecular mass (up to 300 000) are obtained when the process is carried out in polyphosphoric acid.^{49, 271, 275}

The homopolymers and copolymers of 1,3,4-oxadiazoles with *N*-phenyl-2,2-phthalimidine cardo groups have been synthesised successfully by one-step polycondensation in polyphosphoric acid.²⁹³ In this case, the polyoxadiazoles were obtained by the interaction of salts of hydrazine or dicarboxylic acid dihydrazides with 2-[3,3'-bis(4-carboxyphenyl)]-*N*-phenylphthalimidine. The presence of the *N*-phenyl-2,2-phthalimidine group in the initial monomer (in contrast to the phthalide group) rules out the occurrence of undesirable side reactions during synthesis. The synthesis of polyoxadiazoles from hydrazine sulfate involves the formation of polymeric adducts with sulfuric acid having high heat resistances and thermal stabilities and satisfactory solubilities even in solvents such as acetone, THF, ethyl methyl ketone, dioxane, and cyclohexanone.

Table 7 presents some properties of a series of cardo polyoxadiazoles with phthalide groups which have been obtained.^{49, 271, 275} These polymers have high heat resistances and thermal stabilities. Thus the softening temperatures of polyoxadiazoles are from 340 to 400 °C. According to thermogravimetric data (heating rate 5 K min⁻¹), these polymers begin to decompose in air at 400–430 °C. Cardo polyoxadiazoles are resistant to the action of water and corrosive media at room temperature and to the action of water at 100 °C.^{271, 291} Comparison of the thermomechanical curves for the polyoxadiazole derived from bis(4-carboxyphenyl)phthalide and the noncardo poly-2,5-(4,4'-diphenylene oxide)-1,3,4-oxadiazole in the amorphous state revealed the influence of the cardo group on the heat resistance of polymers of this type: the softening temperature of the cardo polymer exceeds by approximately 150 °C that for the noncardo polyoxadiazole.^{49, 271}

Among various polyoxadiazoles with phthalide groups, poly 2,5-(4,4'-diphenylphthalide)-1,3,4-oxadiazole has the highest solubility. It is soluble in methylene chloride, tetrachloroethane, dimethylacetamide, hexamethylphosphoramide, pyridine, benzyl alcohol, methylpyrrolidone, etc. The solubility of cardo polyoxadiazoles gives rise to the possibility of obtaining different articles from them by moulding from solution. Strong transparent films, with effective physicochemical and dielectric properties both at room and elevated temperatures, are formed from solutions of cardo polyoxadiazoles.^{271, 275} Thus the strength of films of the homopolyoxadiazole obtained from bis(4-carboxyphenyl)phthalide is 1000 kgf cm⁻² after heating at 250 °C for 500 h and 400 kgf cm⁻² after heating at 300 °C for 1000 h (the initial strength is 1200 kgf cm⁻²). At 20 °C and a frequency of 5000 Hz, the specific volume resistivity of this polymer is 6×10^{15} Ω cm, while the tangent of the dielectric loss angle is 3.2×10^{-2} ; at 300 °C, these parameters are respectively 10^{13} Ω cm and 2.0×10^{-2} .

The solubility of cardo polyoxadiazoles made it possible to investigate for the first time the hydrodynamic properties, polydispersity, and the molecular mass characteristics of cyclochain polymers of this type.^{178, 179, 270, 271, 282, 287} For the cardo polyoxadiazole obtained from bis(4-carboxyphenyl)phthalide in dimethylacetamide and THF, the Mark-Houwink equations are $[\eta] = 7.74 \times 10^{-4} M^{0.57}$ and $[\eta] = 4.00 \times 10^{-4} M^{0.66}$ respectively. The polydispersity coefficient for this polymer, synthesised by one-step polycyclisation in polyphosphoric acid, is 3.0–3.1.^{270, 278, 279}

Polyoxadiazoles containing phthalide rings in the side chain have an amorphous structure regardless of the method of synthesis, whereas the familiar poly-1,3,4-oxadiazoles, synthesised in two stages, have a crystalline structure.²⁷⁵ The radiation stability of the polyoxadiazole based on bis(4-carboxyphenyl)phthalide is fairly high and is superior to that of poly(ethylene terephthalate) and polycarbonate.²⁸⁸

The use in the synthesis of cardo polyoxadiazoles of phosphorus-containing monomers such as bis(4-carboxyphenoxymethyl)-methylphosphine oxide, bis(4-carboxyphenyl)methylphosphine oxide, and bis(1-carboxy-3,5-dichloro-4-phenoxy-methyl)methylphosphine oxide together with bis(4-carboxyphenyl)phthalide and its hydrazide made it possible to obtain phosphorus-containing cardo polyoxadiazoles with a satisfactory solubility, high heat resistance and thermal stability, effective adhesive properties, and an enhanced resistance to combustion.^{285, 294, 295}

Cardo polyoxadiazoles may be of interest for the electrical engineering industry, machine building, aircraft construction, and other industries employing materials in units and constructions designed for prolonged use at 200–300 °C. They have been used in the form of powders and solutions for the preparation of glass fibre-reinforced and carbon plastics, moulding materials, films, coatings, adhesives, filtering materials, including materials of the membrane type, and heat- and atmosphere-resistant anticorrosion coatings. Table 8 presents certain data on the properties of the moulding

Table 8. The properties of the 'Niplon 1' polyoxadiazole.

Parameter	Moulding material	Glass fibre-reinforced plastic	Carbon plastic
Density/g cm ⁻³	1.34	1.8	1.3
Tensile strength /kgf cm ⁻²			
at 20 °C	600	—	3500
at 325 °C	100	—	—
Young's modulus /kgf cm ⁻²	—	3×10^5	9×10^5
Bending strength /kgf cm ⁻²			
in the initial state			
at 20 °C	600	4000	5000
at 300 °C	400	3500	3700
after thermal ageing for 2000 h at 300 °C	—	1200	3000
Compressive strength /kgf cm ⁻²			
in the initial state			
at 20 °C	1900	—	—
at 300 °C	600	—	—
after thermal ageing for 200 h at 300 °C	700	—	—
Specific impact strength /kgf cm cm ⁻²	12	—	35
Brinell hardness /kgf cm ⁻²	1900	3300	3700
Vicat's temperature resistance / °C	330–340	—	—
Specific volume resistivity /Ω cm	10^{15}	2×10^{14}	—
Tangent of dielectric loss angle at 10 ⁶ Hz	0.01	0.015	—
Dielectric constant at 10 ⁶ Hz	3.7	4.0	—
Dielectric strength /kV mm ⁻¹	18	—	—
Water absorption			
after 24 h (%)	1.2	—	—
after 1 month (%)	—	0.70	—

materials and glass fibre-reinforced and carbon plastics based on the 'Niplon 1' cardo poly-1,3,4-oxadiazole.^{301, 302}

The data presented above show that cardo polyoxadiazoles have a set of valuable properties and are promising for practical employment.

* * *

Summarising the foregoing, one should note that the 'cardo' principle has been justified in a series of different types of polymers: polyarylates, aromatic polyethers, polyamides, polyarylene-phthalides, epoxide polymers, polyheteroarylenes with a cyclochain structure (polyimides, polyoxadiazoles, polybenzoxazoles,³⁰³⁻³⁰⁸ polybenzimidazoles³⁰⁹) etc. A characteristic feature of the cardo polymers, distinguishing them from their noncardo analogues, is a combination of an enhanced heat resistance with a satisfactory solubility in organic solvents whilst retaining other valuable properties characteristic of the particular type of polymer to which they belong. This makes the employment of such polymers for practical purposes undoubtedly promising.

As shown above, the properties of cardo polymers depend on their chemical and physical structures and can be altered deliberately by varying the latter, including a transition from polymers of one class to another. For example, the heat resistances and the operating temperatures of cardo polymers and the materials based on them increase on passing from aromatic polyethers to polyarylates and aromatic polyamides and polyimides.

The solubility of cardo polymers in readily available organic solvents made it possible to investigate a series of common features of the formation of polymers with a cyclochain structure, which had not been possible previously owing to the insolubility of these polymers. The solubility of cardo polymers and their satisfactory compatibility with various monomers, oligomers, and polymers has also led to unlimited possibilities for the creation of new polymers in a matrix comprising cardo polymers and hence the creation of new valuable polymer systems.

References

1. S V Vinogradova, S N Salazkin, G Sh Chelidze, G L Slonimskii, A A Askadskii, K A Bychko, L I Komarova, I V Zhuravleva, V V Korshak *Plast. Massy* (8) 10 (1971)
2. S V Vinogradova, Ya S Vygodskii *Usp. Khim.* **42** 1225 (1973) [*Russ. Chem. Rev.* **42** 551 (1973)]
3. V V Korshak, S V Vinogradova, Ya S Vygodskii *J. Macromol. Sci., Rev. Macromol. Chem.* **C11** 45 (1974)
4. Ya S Vygodskii, S V Vinogradova, in *Khimiya i Tekhnologiya Vysokomolekulyarnykh Soedinenii*, T. 7 (*Ser. Itogi Nauki i Tekhniki*) [Chemistry and Technology of High-Molecular-Mass Compounds, Vol. 7 (Advances in Science and Engineering Series)] (Moscow: Izd. VINITI, 1975) p. 14
5. US P. 2 035 578; *Chem. Abstr.* **30** 3 542 (1936)
6. USSR P. 140 990; *Byull. Izobret.* (17) 51 (1961)
7. V V Korshak, S V Vinogradova, S N Salazkin *Vysokomol. Soedin.* **4** 339 (1962)
8. V V Korshak, S V Vinogradova *Neravnovesnaya Polikondensatsiya* (Nonequilibrium Polycondensation) (Moscow: Nauka, 1972)
9. V V Korshak, S V Vinogradova *Usp. Khim.* **39** 679 (1970) [*Russ. Chem. Rev.* **39** 308 (1970)]
10. V V Korshak, S V Vinogradova *Poliarilaty* (Polyarylates) (Moscow: Nauka, 1964)
11. A A Askadskii *Fiziko-Khimiya Poliarilatov* (Physical Chemistry of Polyarylates) (Moscow: Khimiya, 1968)
12. S V Vinogradova, in *Polymer Science Contemporary Themes* Vol. 2. (New Delhi: Tata McGraw-Hill, 1991) p. 658
13. V V Korshak, S V Vinogradova *Usp. Khim.* **37** 2024 (1968) [*Russ. Chem. Rev.* **37** 885 (1968)]
14. S V Vinogradova, in *Tekhnologiya Plasticheskikh Mass* (Technology of Plastics) (Moscow: Khimiya, 1985) p. 344
15. P W Morgan *Condensation Polymers by Interfacial and Solution Methods* (New York: Interscience, 1965)
16. S V Vinogradova, S N Salazkin, V V Korshak, S V Bereza, B V Lokshin, L I Komarova *Vysokomol. Soedin.* **9** 1792 (1967)
17. V V Korshak, S V Vinogradova, S N Salazkin, L I Komarova *Eur. Polym. J.* **10** 976 (1974)
18. V V Korshak *Termostoikiye Polimery* (Heat-Resistant Polymers) (Moscow: Nauka, 1969)
19. USSR P. 203 891; *Byull. Izobret.* (21) 81 (1966)
20. S V Vinogradova, S N Salazkin, L A Beridze, A I Mzhel'skii, G L Slonimskii, A A Askadskii, V V Korshak *Izv. Akad. Nauk SSSR, Ser. Khim.* 931 (1969)
21. V V Korshak, S N Salazkin, L A Beridze, S V Vinogradova *Vysokomol. Soedin., Ser. A* **15** 841 (1973)
22. S V Vinogradova, V V Korshak, G Sh Papava, N A Maisuradze, P D Tsikarishvili *Izv. Akad. Nauk SSSR, Ser. Khim.* 434 (1969)
23. V V Korshak, S V Vinogradova, G Sh Papava, N A Maisuradze, P D Tsikarishvili *Soobshch. Akad. Nauk Gruz. SSR* **51** 301 (1968)
24. USSR P. 507 595; *Byull. Izobret.* (11) 77 (1976)
25. USSR P. 241 013; *Byull. Izobret.* (13) 91 (1969); US P. 3 480 597 (1969); BRD P. 1 620 929 (1970); Jpn. P. 620 275 (1971); Br. P. 1 196 128 (1970)
26. USSR P. 172 492; *Byull. Izobret.* (13) 70 (1965)
27. V V Korshak, S V Vinogradova, G L Slonimskii, Ya S Vygodskii, S N Salazkin, A A Askadskii, A I Mzhel'skii *Vysokomol. Soedin., Ser. A* **10** 2058 (1968)
28. S V Vinogradova, S N Salazkin, L A Bereza, A I Mzhel'skii, A A Askadskii, G L Slonimskii, V V Korshak *Vysokomol. Soedin., Ser. A* **11** 27 (1969)
29. S V Vinogradova, V V Korshak, S N Salazkin, L A Beridze, G L Slonimskii, A A Askadskii *Izv. Akad. Nauk SSSR, Ser. Khim.* 2554 (1969)
30. S V Vinogradova, S N Salazkin, L A Beridze, A I Mzhel'skii, A A Askadskii, G L Slonimskii, V V Korshak *Izv. Akad. Nauk SSSR, Ser. Khim.* 931 (1969)
31. G L Slonimskii, A A Askadskii, A I Mzhel'skii, V V Korshak, S V Vinogradova, S N Salazkin, L A Beridze *Vysokomol. Soedin., Ser. A* **11** 2265 (1969)
32. V V Korshak, S V Vinogradova, V G Danilov, L A Beridze, S N Salazkin *Vysokomol. Soedin., Ser. B* **12** 129 (1970)
33. S V Vinogradova, L A Beridze, T M Pavlova, S N Salazkin, V V Korshak *Vysokomol. Soedin., Ser. B* **13** 681 (1971)
34. V V Korshak, S N Salazkin, L A Beridze, S V Vinogradova *Vysokomol. Soedin., Ser. A* **15** 841 (1973)
35. V V Korshak, S V Vinogradova, V G Danilov, S N Salazkin *Dokl. Akad. Nauk SSSR* **202** 1076 (1972)
36. S A Pavlova, L V Dubrovina, N B Klimanova, S N Salazkin *Vysokomol. Soedin., Ser. B* **19** 175 (1977)
37. A A Askadskii *Struktura i Svoistva Teplostoikikh Polimerov* (The Structure and Properties of Heat-Resistant Polymers) (Moscow: Khimiya, 1981)
38. A A Askadskii, Yu I Matveev *Khimicheskoe Stroenie i Fizicheskie Svoistva Polimerov* (Chemical Structure and Physical Properties of Polymers) (Moscow: Khimiya, 1983)
39. USSR P. 159 030; *Byull. Izobret.* (23) 54 (1963)
40. USSR P. 176 401; *Byull. Izobret.* (22) 58 (1965)
41. S V Vinogradova, V V Korshak, S N Salazkin, S B Bereza *Vysokomol. Soedin.* **6** 1403 (1964)
42. P W Morgan *J. Polym. Sci., Part A* **2** 437 (1964)
43. USSR P. 231 120; *Byull. Izobret.* (35) 87 (1968)
44. V V Korshak, S V Vinogradova, V A Pankratov *Dokl. Akad. Nauk SSSR* **181** 1393 (1968)
45. V V Korshak, S V Vinogradova, V A Pankratov *Plast. Massy* (5) 21 (1967)
46. V V Rode, I V Zhuravleva, S R Rafikov, V V Korshak, S V Vinogradova, V A Pankratov *Vysokomol. Soedin.* **7** 1614 (1965)
47. Z Jedlinski (Ed.) *Advances in the Chemistry of Thermally Stable Polymers* (Warsaw: Pol. Sci. Publ., 1977)
48. Z Jedlinski *Thermal Stability of Polymers Containing Naphthalene Units in the Chain* (Warsaw: Pol. Sci. Publ., 1977)
49. S V Vinogradova, V A Vasnev *Chem. Rev. Harwood Acad. Publ., Part 2* **21** 1 (1996)
50. S V Vinogradova, V A Vasnev, P M Valetskii *Usp. Khim.* **63** 885 (1994) [*Russ. Chem. Rev.* **63** 833 (1994)]

51. S N Salazkin, Doctoral Thesis in Chemical Sciences, Institute of Organoelement Compounds, Academy of Sciences of the USSR, Moscow, 1979
52. L A Beridze, Candidate Thesis in Chemical Sciences, Institute of Organoelement Compounds, Academy of Sciences of the USSR, Moscow, 1970
53. V V Korshak *Khimicheskoe Stroenie i Temperaturnye Kharakteristiki Polimerov* (Chemical Structure and Temperature Characteristics of Polymers) (Moscow: Nauka, 1970)
54. N A Maisuradze, Candidate Thesis in Chemical Sciences, Institute of Physical Organic Chemistry, Academy of Sciences of the Georgia SSR, Tbilisi, 1970
55. S V Vinogradova *J. Prakt. Chem.* **313B** 359 (1971)
56. S V Vinogradova, in *Progress Polimernoj Khimii* (Progress in Polymer Chemistry) (Moscow: Nauka, 1969) p. 113
57. P W Morgan *Macromolecules* **3** 536 (1970)
58. V A Vasnev, S V Vinogradova *Usp. Khim.* **48** 30 (1979) [*Russ. Chem. Rev.* **48** 16 (1979)]
59. G L Slonimskii, V V Korshak, S V Vinogradova, A I Kitaigorodskii, A A Askadskii, S N Salazkin, E M Belavtseva *Dokl. Akad. Nauk SSSR* **156** 924 (1964); *Vysokomol. Soedin., Ser. A* **9** 402 (1967)
60. G L Slonimskii, V V Korshak, S V Vinogradova, A I Kitaigorodskii, A A Askadskii, S N Salazkin, E M Belavtseva *Dokl. Akad. Nauk SSSR* **165** 1323 (1965)
61. R S Velichkova, V V Korshak, S V Vinogradova, V V Ivanov, A T Ponomarenko, N S Enikolopyan *Izv. Akad. Nauk SSSR, Ser. Khim.* 858 (1969)
62. S V Vinogradova, V V Korshak, G Sh Papava, N A Maisuradze, R S Velichkova *Izv. Akad. Nauk SSSR, Ser. Khim.* 820 (1970)
63. V V Korshak, S V Vinogradova, V A Vasnev *Vysokomol. Soedin., Ser. A* **10** 1329 (1968)
64. S V Vinogradova, V A Vasnev, T S Simonenko, A M Tartakovskaya, V V Korshak *Vysokomol. Soedin., Ser. A* **23** 619 (1981)
65. S V Vinogradova, V A Vasnev, V V Korshak *Vysokomol. Soedin., Ser. B* **9** 522 (1967)
66. V V Korshak, S V Vinogradova, V A Vasnev, T I Mitaishvili *Vysokomol. Soedin., Ser. A* **11** 81 (1969)
67. T I Mitaishvili, Candidate Thesis in Chemical Sciences, Institute of Organoelement Compounds, Academy of Sciences of the USSR, Moscow, 1970
68. V A Vasnev, Doctoral Thesis in Chemical Sciences, Institute of Organoelement Compounds, Academy of Sciences of the USSR, Moscow, 1975
69. S V Vinogradova, in *Advances in Polymer Chemistry* (Moscow: Mir, 1986) p. 75
70. S V Vinogradova, V A Vasnev *Chem. Rev. Harwood Acad. Publ., Part I* **21** 1 (1996)
71. S R Rafikov, S V Vinogradova, V V Korshak, Z Ya Fomina, B V Lokshin, V V Rode *Vysokomol. Soedin.* **8** 2189 (1966)
72. V V Korshak, S V Vinogradova, S A Siling, S R Rafikov, Z Ya Fomina, V V Rode *J. Polym. Sci. Part A, Polym. Chem.* **7** 157 (1969)
73. V V Korshak, S V Vinogradova, G L Slonimskii, S N Salazkin, A A Askadskii *Vysokomol. Soedin.* **8** 548 (1966)
74. V V Korshak, S V Vinogradova, A I Kalachev, P M Valetskii, N S Titova, V I Stanko *Vysokomol. Soedin., Ser. A* **14** 1306 (1972)
75. V V Korshak, S V Vinogradova, A I Kalachev, P M Valetskii, V I Stanko *Vysokomol. Soedin., Ser. A* **13** 848 (1971)
76. S V Vinogradova, P M Valetskii, N I Bekasova *Chem. Rev.* **18** 1 (1993)
77. S V Vinogradova, P M Valetskii, Yu A Kabachii *Usp. Khim.* **64** 390 (1995) [*Russ. Chem. Rev.* **64** 365 (1995)]
78. P M Valetskii, E K Lamenkova, S V Vinogradova *Vysokomol. Soedin., Ser. A* **16** 305 (1974)
79. P M Valetskii *Karbotsepnnye i Geterotsepnnye Polimery s Karboranovymi Gruppami v Tsepi* (Carbon-Chain and Heterochain Polymers with Carbaborane Groups in the Chain) (Gomel', 1972)
80. L I Komarova, S N Salazkin, Ya S Vygodskii, S V Vinogradova *Vysokomol. Soedin., Ser. A* **32** 1571 (1990)
81. V V Korshak, S V Vinogradova, I A Bulgakova, L I Komarova, Ya S Vygodskii, M A Yusufov, E E Zaborovskaya *Plast. Massy* (6) 47 (1986)
82. A A Askadskii, L N Belkina, K A Bychko, S N Salazkin, I A Bulgakova, L I Komarova, S V Vinogradova, G L Slonimskii, V V Korshak *Vysokomol. Soedin., Ser. A* **22** 1338 (1980)
83. S V Vinogradova, V V Korshak, E I Fridman, M A Andreeva, L N Baraboshkina *Plast. Massy* (9) 16 (1965)
84. Z Ya Fomina, Candidate Thesis in Chemical Sciences, Mendeleev Moscow Chemical Technological Institute, Moscow, 1967
85. S R Rafikov, V V Korshak, S V Vinogradova, Z Ya Fomina, V A Pankratov *Vysokomol. Soedin., Ser. A* **9** 1903 (1967)
86. S R Rafikov, S V Vinogradova, V V Korshak, Z Ya Fomina *Vysokomol. Soedin., Ser. A* **9** 98 (1967)
87. S V Vinogradova, S R Rafikov, V V Korshak, Z Ya Fomina *Vysokomol. Soedin., Ser. A* **9** 1797 (1967)
88. I P Antonova-Antipova, Candidate Thesis in Chemical Sciences, Mendeleev Moscow Chemical Technological Institute, Moscow, 1966
89. S V Vinogradova, V V Korshak, I P Antonova-Antipova *Vysokomol. Soedin.* **7** 2052 (1965)
90. S V Vinogradova, I P Antonova-Antipova, in *Progress Polimernoj Khimii* (Progress in Polymer Chemistry) (Moscow: Nauka, 1969) p. 375
91. V V Korshak, S V Vinogradova, I P Antonova-Antipova, A Plakhov *Dokl. Akad. Nauk SSSR* **177** 120 (1967)
92. D M White, in *Comprehensive Polymer Science. The Synthesis, Characterization, Reactions, and Applications of Polymers* Vol. 5 (Oxford: Pergamon Press, 1989) p. 473
93. P A Staniland, in *Comprehensive Polymer Science. The Synthesis, Characterization, Reactions, and Application of Polymers* Vol. 5 (Oxford: Pergamon Press, 1989) p. 483
94. F Parodi, in *Comprehensive Polymer Science. The Synthesis, Characterization, Reactions, and Application of Polymers* Vol. 5 (Oxford: Pergamon Press, 1989) p. 561
95. A A Kul'kov, Candidate Thesis in Chemical Sciences, Mendeleev Moscow Chemical Technological Institute, Moscow, 1972
96. M K Kutateladze, Candidate Thesis in Chemical Sciences, Tbilisi State University, Tbilisi, 1981
97. V V Shaposhnikova, Candidate Thesis in Chemical Sciences, Institute of Organoelement Compounds, Russian Academy of Sciences, Moscow, 1993
98. V V Korshak, S V Vinogradova, S N Salazkin, A A Kul'kov *Dokl. Akad. Nauk SSSR* **208** 360 (1973)
99. S V Vinogradova, V V Korshak, S N Salazkin, A A Kul'kov *Vysokomol. Soedin., Ser. A* **14** 2545 (1972)
100. USSR P. 372 234; *Byull. Izobret.* (13) 77 (1973)
101. A A Kul'kov, S N Salazkin, G L Slonimskii, A A Askadskii, K A Bychko, S V Vinogradova, V V Korshak *Vysokomol. Soedin., Ser. A* **16** 1543 (1974)
102. V M Laktionov, I V Zhuravleva, S A Pavlova, S R Rafikov, S N Salazkin, S V Vinogradova, A A Kul'kov, V V Korshak *Vysokomol. Soedin., Ser. A* **18** 330 (1976)
103. G Sh Papava, S V Vinogradova, M K Kutateladze, K R Papava, G Borisov, S Verbanov *Acta Polymer.* **42** 74 (1991)
104. USSR P. 503 859; *Byull. Izobret.* (7) 67 (1976)
105. L A Beridze, G Sh Papava, M K Kutateladze, P D Tsiskarishvili *Izv. Akad. Nauk Gruz. SSR, Ser. Khim.* **2** 226 (1976)
106. L A Beridze, M K Kutateladze, G Sh Papava, P D Tsiskarishvili *Soobshch. Akad. Nauk Gruz. SSR* **83** 269 (1976)
107. L A Beridze, M K Kutateladze, G Sh Papava, P D Tsiskarishvili *Soobshch. Akad. Nauk Gruz. SSR* **84** 401 (1976)
108. L A Beridze, M K Kutateladze, G Sh Papava *Izv. Akad. Nauk Gruz. SSR, Ser. Khim.* **6** 232 (1980)
109. V M Agapov, S N Salazkin, V A Sergeev, L I Komarova, P V Petrovskii *Dokl. Akad. Nauk SSSR* **316** 126 (1991)
110. V M Agapov, S N Salazkin, V A Sergeev, L I Komarova, P V Petrovskii, G I Timofeeva *Vysokomol. Soedin., Ser. A* **34** 3 (1992)
111. USSR P. 403 705; *Byull. Izobret.* (43) 73 (1973)
112. V V Korshak, S V Vinogradova, D R Tur *Faserforsch. Textiltech.* **28** 339 (1977)
113. L K Solov'eva, Candidate Thesis in Chemical Sciences, Mendeleev Moscow Chemical Technological Institute, Moscow, 1969
114. N S Dokhturashvili, Candidate Thesis in Chemical Sciences, Tbilisi State University, Tbilisi, 1980

115. S N Salazkin, S V Vinogradova, L I Komarova *Izv. Akad. Nauk SSSR, Ser. Khim.* 144 (1973)
116. V V Korshak, L K Solov'eva, I V Kamenskii *Vysokomol. Soedin., Ser. A* 13 150 (1971)
117. V V Korshak, L K Solov'eva *Vysokomol. Soedin., Ser. B* 13 714 (1971)
118. V V Korshak, S V Vinogradova, L K Solov'eva, N S Dokhturashvili, G Sh Papava, P D Tsiskarishvili, L B Makina *Plast. Massy* (3) 74 (1975)
119. V V Korshak, G Sh Papava, N S Dokhturashvili, L K Solov'eva, L B Makina *Plast. Massy* (2) 17 (1974)
120. G Sh Papava, N S Dokhturashvili, N A Maisuradze, P D Tsiskarishvili, S V Vinogradova, V V Korshak, in *Sintez i Svoistva Nekotorykh Novykh Polimernykh Materialov* (Synthesis and Properties of Some New Polymeric Materials) (Tbilisi: Metsniereba, 1974) p. 51
121. N S Dokhturashvili, G Sh Papava, P D Tsiskarishvili, L K Solov'eva, S V Vinogradova, V V Korshak, in *Sintez i Svoistva Nekotorykh Polimernykh Materialov* (Synthesis and Properties of Some New Polymeric Materials) (Tbilisi: Metsniereba, 1974) p. 66
122. USSR P. 454 228; *Byull. Izobret.* (47) 48 (1974)
123. G Sh Papava, N S Dokhturashvili, N A Maisuradze, P D Tsiskarishvili, B M Mgeladze, K S Kvashvadze *Izv. Akad. Nauk Gruz. SSR, Ser. Khim.* 3 121 (1977)
124. G Sh Papava, N S Dokhturashvili, N A Maisuradze, P D Tsiskarishvili, V V Korshak, S V Vinogradova *Izv. Akad. Nauk Gruz. SSR, Ser. Khim.* 3 249 (1977)
125. G Sh Papava, N A Maisuradze, N S Dokhturashvili, G G Andronikashvili *Soobshch. Akad. Nauk Gruz. SSR* 91 349 (1978)
126. V V Korshak, S V Vinogradova, S N Salazkin, I A Bulgakova, L I Komarova, Ya S Vygodskii, M A Yusufov, E E Zaborovskaya *Issledovanie Vliyaniya Khimicheskogo Stroeniya Epoksidnykh Oligomerov Kardovykh Poligeteroarilenov na Ikh Sovmestimost' i Svoistva Poluchaemykh Kompozitsii* (Investigation of the Influence of the Chemical Structure of Epoxy-Oligomers of Cardo-Polyheteroarylenes on Their Compatibility and on the Properties of the Compositions Obtained) Article deposited at the All-Union Institute of Scientific and Technical Information (VINITI) No 7855, Moscow, 1984
127. I A Bulgakova, Candidate Thesis in Chemical Sciences, Institute of Organoelement Compounds, Academy of Sciences of the USSR, Moscow, 1983
128. S N Salazkin, S R Rafikov, G A Tolstikov, M G Zolotukhin *Dokl. Akad. Nauk SSSR* 262 355 (1982)
129. M G Zolotukhin, V D Skirda, V I Sundukov, S N Salazkin, E A Sedova, Kh G Mindiyarov, S R Rafikov *Vysokomol. Soedin., Ser. B* 29 378 (1987)
130. M G Zolotukhin, V A Kovardakov, S N Salazkin, S R Rafikov *Vysokomol. Soedin., Ser. A* 26 1212 (1984)
131. M G Zavarukhin, N G Gileva, E A Sedova, A E Egorov, Yu A Sangalov, S N Salazkin, Yu A Lebedev *Dokl. Akad. Nauk SSSR* 304 378 (1989)
132. S N Salazkin, M G Zolotukhin, V A Kovardakov, S R Rafikov, L V Dubrovina, E A Gladkova, S A Pavlova *Vysokomol. Soedin., Ser. A* 29 1437 (1987)
133. S R Rafikov, S N Salazkin, M G Zolotukhin *Plast. Massy* (10) 36 (1986)
134. V A Kraikin, S N Salazkin, V D Komissarov, M G Zolotukhin, S R Rafikov *Vysokomol. Soedin., Ser. B* 28 264 (1986)
135. V A Kraikin, V A Kovardakov, A A Panasenکو, R R Maslakhov, S N Salazkin, S R Rafikov *Vysokomol. Soedin., Ser. A* 34 28 (1992)
136. S N Salazkin, M G Zolotukhin, A N Lachinov, Yu A Sangalov, G I Nikiforova, A A Panasenکو, F A Valyamova *Dokl. Akad. Nauk SSSR* 302 365 (1988)
137. S N Salazkin, M G Zolotukhin, E A Sedova, Yu L Sorokina, Yu A Sangalov, V S Sultanova, A A Panasenکو, L M Khalilov, R M Muslakhov *Makromol. Chem.* 191 1477 (1990)
138. A V Shitikov, M G Zolotukhin, S N Salazkin, S R Rafikov, V S Sultanova *Khimicheskaya Modifikatsiya Polidifenilnftalida* (Chemical Modification of Polydiphenylenephthalide) Article deposited at the All-Union Institute of Scientific and Technical Information (VINITI) No 6632, Moscow, 1985
139. V S Sultanova, L M Khalilov, A V Shitikov, M G Zolotukhin, A A Panasenکو, S N Salazkin, S R Rafikov *Vysokomol. Soedin., Ser. B* 30 659 (1988)
140. A V Shitikov, M G Zolotukhin, V S Sultanova, A A Panasenکو, S N Salazkin, S R Rafikov *Makromol. Chem.* 190 1837 (1989)
141. M G Zolotukhin, E A Egorov, E A Sedova, Yu L Sorokina, V A Kovardakov, S N Salazkin, Yu A Sangalov *Dokl. Akad. Nauk SSSR* 311 127 (1990)
142. M G Zolotukhin, E A Sedova, Yu L Sorokina, S N Salazkin, Yu A Sangalov, V S Sultanov *Dokl. Akad. Nauk SSSR* 307 617 (1989)
143. USSR P. 195 100; *Byull. Izobret.* (9) 120 (1967)
144. USSR P. 191 119; *Byull. Izobret.* (3) 93 (1967)
145. USSR P. 198 644; *Byull. Izobret.* (14) 95 (1967)
146. Ya S Vygodskii, Candidate Thesis in Chemical Sciences, Institute of Organoelement Compounds, Academy of Sciences of the USSR, Moscow, 1968
147. S V Vinogradova, V V Korshak, Ya S Vygodskii, V I Zaitsev *Vysokomol. Soedin., Ser. A* 9 658 (1967)
148. A A Askadskii, G L Slonimskii, Ya S Vygodskii, V V Korshak, S V Vinogradova, Ya S Vygodskii, S N Salazkin, V I Zaitsev *Vysokomol. Soedin.* 8 2131 (1966)
149. V V Rode, P N Gribkova, Ya S Vygodskii, S V Vinogradova, V V Korshak *Vysokomol. Soedin., Ser. A* 10 2550 (1968); *Izv. Akad. Nauk SSSR, Ser. Khim.* 85 (1969)
150. K A Reddy, M Srinivasan *Br. Polym. J.* 22 333 (1990)
151. G L Slonimskii, A A Askadskii, V V Korshak, S V Vinogradova, Ya S Vygodskii, S N Salazkin *Vysokomol. Soedin., Ser. A* 9 1706 (1967)
152. S V Vinogradova, Ya S Vygodskii, N A Churochkina, L B Tunik, V V Korshak, V I Berendyaev *Vysokomol. Soedin., Ser. A* 31 45 (1989)
153. S V Vinogradova, Ya S Vygodskii, V V Korshak, G L Slonimskii, A A Askadskii, N A Churochkina, V V Kazanceva, H Raubach, B Falk *Acta Polymer* 41 489 (1990)
154. S V Vinogradova, Ya S Vygodskii, G S Gurbich, V V Korshak, G Reinisch, U Gohlke *Faserforsch. Textiltech.* 29 613 (1978)
155. USSR P. 513 051; *Byull. Izobret.* (47) 198 (1977)
156. V V Korshak, S V Vinogradova, Ya S Vygodskii, N A Churochkina *Issledovanie Obrazovaniya Kardovykh Poliamidov v Rastvore Poli-4-fenilenteretefalamida* (Investigation of the Formation of Cardo Polyamides in Poly-4-phenyleneterephthalamide Solution) Article deposited at the All-Union Institute of Scientific and Technical Information (VINITI) No 837, Moscow, 1984
157. V V Korshak, S V Vinogradova, I A Gribova, Ya S Vygodskii, N A Churochkina, G I Gureeva, N Yu Krainova *Trenie Iznos* 10 566 (1989)
158. N N Rukhlyada, N A Churochkina, Ya S Vygodskii, S V Vinogradova, T A Magula, E R Klinshpont, V K Milinchuk *Vysokomol. Soedin., Ser. A* 34 94 (1992)
159. S N Salazkin, L I Komarova, I A Bulgakova, M I Melaniya, V I Nikolaichik, E E Zaborovskaya *Tezisy Mezhdunarodnogo Simpoziuma po Makromolekulyarnoi Khimii, Tashkent, 1978* (Abstracts of the International Symposium on Macromolecular Chemistry, Tashkent, 1978) Vol. 6, p. 56
160. A P Khardin, I A Novakov, S S Radchenko, N A Brel', O A Kuznechikov, Ya S Vygodskii *Vysokomol. Soedin., Ser. B* 25 433 (1983)
161. V V Korshak, P M Valetskii, L A Glivka, S V Vinogradova, N S Titova, V I Stanko *Vysokomol. Soedin., Ser. A* 14 1043 (1972)
162. T N Balykova, P N Gribkova, L A Glivka, P M Valetskii, V V Korshak, S V Vinogradova *Vysokomol. Soedin., Ser. A* 15 2441 (1973)
163. P M Valetskii, L A Glivka, L V Dubrovina, S V Vinogradova, V G Danilov, V I Stanko, V V Korshak *Vysokomol. Soedin., Ser. A* 15 1227 (1973)

164. E P Krasnov, V P Aksenova, S N Khar'kov, in *Proizvodstvo Sinteticheskikh Volokon* (Production of Synthetic Fibres) (Moscow: Khimiya, 1971) p. 255
165. V V Rode, P N Gribkova, V V Korshak *Vysokomol. Soedin., Ser. A* **11** 57 (1969)
166. V V Lyashevich, V V Korshak, V V Rode, Ya S Vygodskii *Vysokomol. Soedin., Ser. A* **19** 581 (1977)
167. V M Andreeva, V I Konevets, A A Tager, Ya S Vygodskii, S V Vinogradova *Vysokomol. Soedin., Ser. A* **24** 1285 (1982)
168. Ya S Vygodskii, A A Askadskii, G S Gurbich, Yu S Kochergin, G L Slonimskii, V V Korshak, S V Vinogradova *Vysokomol. Soedin., Ser. A* **21** 161 (1979)
169. L I Komarova, Doctoral Thesis in Chemical Sciences, Institute of Organoelement Compounds, Russian Academy of Sciences, Moscow, 1992
170. L Vollbracht, in *Comprehensive Polymer Science. The Synthesis, Characterization, Reactions, and Application of Polymers* Vol. 5 (Oxford: Pergamon Press, 1989) p. 375
171. Ya S Vygodskii, Z V Gerashchenko, S V Vinogradova, in *Preprints of the International Symposium Macromolecules, Helsinki, 1972* Vol. 2, p. 889
172. V V Korshak, S V Vinogradova, Ya S Vygodskii, B N Yudin *Izv. Akad. Nauk SSSR, Ser. Khim.* **1405** (1968)
173. S V Vinogradova, N A Churochkina, Ya S Vygodskii, G V Zhdanova, V V Korshak *Vysokomol. Soedin., Ser. A* **13** 1146 (1971)
174. S V Vinogradova, Ya S Vygodskii, V D Vorob'ev, N A Churochkina, T N Spirina, L I Chudina *Vysokomol. Soedin., Ser. A* **16** 506 (1974)
175. USSR P. 171 552; *Byull. Izobret.* (11) 76 (1965)
176. S V Vinogradova, V V Korshak, Ya S Vygodskii *Vysokomol. Soedin., Ser. A* **8** 809 (1966)
177. Ya S Vygodskii, S V Vinogradova, V V Korshak *Vysokomol. Soedin., Ser. B* **9** 587 (1967)
178. USSR P. 215 493; *Byull. Izobret.* (13) 80 (1968)
179. V V Korshak, S V Vinogradova, Ya S Vygodskii, S A Pavlova, L V Boiko *Izv. Akad. Nauk SSSR, Ser. Khim.* **2267** (1967)
180. S V Vinogradova, Ya S Vygodskii, V V Korshak *Vysokomol. Soedin., Ser. A* **12** 1987 (1970)
181. US P. 3 988 303 (1976); Fr. P. 7 442 536 (1977); Can. P. 1 043 940 (1978); Austral. P. 486 453 (1977); Aust. P. 340 685; Br. P. 1 489 933 (1977); Ital. P. 1 026 948 (1977); Jpn. P. 1 159 664 (1983); BRD P. 2 461 350 (1977)
182. *Vysokoteplostoiкие Rastvorimye Kardovye Poliimidy* (Soluble Highly Heat-Resistant Cardo Polyimides) (Moscow: Nauka, 1977)
183. V V Korshak, S V Vinogradova, Ya S Vygodskii, Z V Gerashchenko *Vysokomol. Soedin., Ser. A* **13** 1190 (1971)
184. S N Khar'kov, E P Krasnov, Z N Lavrova *Vysokomol. Soedin., Ser. A* **13** 833 (1971)
185. V V Korshak, S V Vinogradova, Z V Gerashchenko, Ya S Vygodskii *Tr. Mosk. Khim.-Tekhnol. Int.* **70** 168 (1972)
186. S V Vinogradova, Ya S Vygodskii, V V Korshak, N A Churochkina, D R Tur, V G Danilov *Vysokomol. Soedin., Ser. A* **13** 1507 (1971)
187. S V Vinogradova, G L Slonimskii, Ya S Vygodskii, A A Askadskii, A I Mzhel'skii, N A Churochkina, V V Korshak *Vysokomol. Soedin., Ser. A* **11** 2725 (1969)
188. S V Vinogradova, S A Pavlova, V V Korshak, Ya S Vygodskii, L V Boiko, N A Golubeva *Vysokomol. Soedin., Ser. B* **10** 398 (1968)
189. V V Korshak, S A Pavlova, L V Boiko, T M Babchinitser, S V Vinogradova, Ya S Vygodskii, N A Golubeva *Vysokomol. Soedin., Ser. A* **12** 56 (1970)
190. G L Slonimskii, V V Korshak, A I Mzhel'skii, A A Askadskii, Ya S Vygodskii, S V Vinogradova *Dokl. Akad. Nauk SSSR* **182** 851 (1968)
191. USSR P. 257 010; *Byull. Izobret.* (35) 74 (1969)
192. E P Krasnov, V P Aksenova, S N Khar'kov, S A Baranova *Vysokomol. Soedin., Ser. A* **12** 873 (1970)
193. P N Gribkova, V V Rode, Ya S Vygodskii, S V Vinogradova, V V Korshak *Vysokomol. Soedin., Ser. A* **12** 220 (1970)
194. V V Korshak, S V Vinogradova, Ya S Vygodskii, Z V Gerashchenko, N I Lushkina *Vysokomol. Soedin., Ser. A* **14** 1924 (1972)
195. S A Pavlova, G I Timofeeva, V V Korshak, Ya S Vygodskii, S V Vinogradova, N A Churochkina *Vysokomol. Soedin., Ser. A* **15** 2650 (1973)
196. USSR P. 295 785; *Byull. Izobret.* (8) 69 (1971)
197. USSR P. 310924 SSSR; *Byull. Izobret.* (24) 89 (1971)
198. Ya S Vygodskii, N A Churochkina, L V Dubrovina, T P Bragina, S A Pavlova, S V Vinogradova, A E Travkin, V M Kopylov, M I Shkol'nik *Vysokomol. Soedin., Ser. A* **32** 2372 (1990)
199. S V Vinogradova, N A Churochkina, Ya S Vygodskii, V V Korshak *Vysokomol. Soedin., Ser. A* **15** 1713 (1973)
200. G L Slonimskii, Ya S Vygodskii, Z V Gerashchenko, F N Nurmukhametov, A A Askadskii, V V Korshak, S V Vinogradova, E M Belavtseva *Vysokomol. Soedin., Ser. A* **16** 2249 (1974)
201. Ya S Vygodskii, T N Spirina, P P Nechaev, L I Chudina, G E Zaikov, V V Korshak, S V Vinogradova *Vysokomol. Soedin., Ser. A* **19** 1516 (1977)
202. Ya S Vygodskii, E D Molodtsova, G I Timofeeva, S V Vinogradova, S A Pavlova, V V Korshak *Vysokomol. Soedin., Ser. B* **21** 100 (1979)
203. USSR P. 644 783; *Byull. Izobret.* (4) 86 (1979)
204. T Szekeley, V V Korshak, S V Vinogradova, M Lengyel, Ya S Vygodskii, G S Gurbich *Acta Chim. Acad. Sci. Hung.* **100** 121 (1979)
205. E D Molodtsova, S A Pavlova, G I Timofeeva, Ya S Vygodskii, S V Vinogradova, V V Korshak *Vysokomol. Soedin., Ser. A* **16** 2183 (1974)
206. V V Korshak, S V Vinogradova, Ya S Vygodskii, G S Gurbich, I F Davydov, B A Kiselev *Vysokomol. Soedin., Ser. A* **22** 52 (1980)
207. V V Korshak, Ya S Vygodskii, G S Gurbich, S V Vinogradova *Vysokomol. Soedin., Ser. A* **23** 1023 (1981)
208. Ya S Vygodskii, V A Adigezalov, A A Askadskii, G L Slonimskii, Sh T Bagirov, V V Korshak, S V Vinogradova, Z M Nagiev *Vysokomol. Soedin., Ser. A* **21** 2672 (1979)
209. S V Vinogradova, Ya S Vygodskii, V A Adigezalov, V S Papkov, I I Dubovik, G L Slonimskii, Ya G Urman, S G Alekseeva, Sh T Bagirov, V V Korshak *Vysokomol. Soedin., Ser. A* **23** 1761 (1981)
210. S V Vinogradova, Ya S Vygodskii, T N Spirina, L I Chudina, V V Korshak *Vysokomol. Soedin., Ser. A* **21** 1064 (1979)
211. Ya S Vygodskii, Doctoral Thesis in Chemical Sciences, Institute of Organoelement Compounds, Academy of Sciences of the USSR, Moscow, 1980
212. S V Vinogradova, Ya S Vygodskii, N A Churochkina, V V Korshak *Vysokomol. Soedin., Ser. B* **19** 93 (1977)
213. S V Vinogradova, Ya S Vygodskii *Faserforsch. Textiltech.* **28** 581 (1977)
214. V V Korshak, S V Vinogradova, Ya S Vygodskii *Faserforsch. Textiltech.* **28** 439 (1977)
215. S V Vinogradova, V V Korshak, Ya S Vygodskii, B V Lokshin *Vysokomol. Soedin., Ser. A* **9** 1091 (1967)
216. V V Korshak, S V Vinogradova, Ya S Vygodskii, Z M Nagiev, Ya G Urman, S G Alekseeva, I Ya Slonim *Makromol. Chem.* **184** 235 (1983)
217. S V Vinogradova, Z V Gerashchenko, Ya S Vygodskii, F B Sherman, V V Korshak *Dokl. Akad. Nauk SSSR* **203** 821 (1972)
218. P P Nechaev, Ya S Vygodskii, G E Zaikov, S V Vinogradova *Vysokomol. Soedin., Ser. A* **18** 1667 (1976)
219. E V Kamzolkina, P P Nechaev, V S Markin, Ya S Vygodskii, T V Grigor'ev, G E Zaikov *Dokl. Akad. Nauk SSSR* **213** 650 (1974)
220. S G Alekseeva, S V Vinogradova, V D Vorob'ev, Ya S Vygodskii, V V Korshak, I Ya Slonim, T N Spirina, Ya G Urman, L I Chudina *Vysokomol. Soedin., Ser. A* **21** 2207 (1979)
221. P P Nechaev, Yu V Moiseev, S V Vinogradova, Ya S Vygodskii, G E Zaikov, V V Korshak *Vysokomol. Soedin., Ser. A* **15** 702 (1973)
222. Z V Gerashchenko, Ya S Vygodskii, G L Slonimskii, A A Askadskii, V S Papkov, S V Vinogradova, V G Dashevskii, V A Klimova, F B Sherman, V V Korshak *Vysokomol. Soedin., Ser. A* **15** 1718 (1973)
223. Ya S Vygodskii, S V Vinogradova, Z M Nagiev, V V Korshak, Ya G Urman, G Reinisch, G Rafler *Acta Polymer* **33** 131 (1982)

224. G S Alekseeva, S V Vinogradova, V D Vorob'ev, Ya S Vygodskii, E I Efimova, V V Korshak, I Ya Slonim, P M Tanunina, Ya G Urman *Vysokomol. Soedin., Ser. B* **21** 883 (1979)
225. Ya S Vygodskii, Z M Nagiev, V V Korshak, S V Vinogradova, Ya G Urman, S G Alekseeva, I Ya Slonim, G Reinisch, E Bonatz, E Yakab, F Till, G Rafler *Acta Polymer* **35** 690 (1984)
226. P P Nechaev, Yu V Moiseev, G E Zaikov, Ya S Vygodskii, Z V Gerashchenko *J. Polym. Sci.* **42** 1425 (1973)
227. Ya S Vygodskii, in *Tekhnologiya Plasticheskikh Mass* (Technology of Plastics) (Moscow: Khimiya, 1985) p. 408
228. S G Alekseeva, S V Vinogradova, V D Vorob'ev, Ya S Vygodskii, V V Korshak, I Ya Slonim, T N Spirina, Ya G Urman, L I Chudina *Vysokomol. Soedin., Ser. B* **18** 803 (1976)
229. P P Nechaev, T N Simakina, Yu V Moiseev, Ya S Vygodskii, G E Zaikov *Izv. Akad. Nauk SSSR, Ser. Khim.* 2809 (1976)
230. E D Molodtsova, G I Timofeeva, S A Pavlova, Ya S Vygodskii, S V Vinogradova, V V Korshak *Vysokomol. Soedin., Ser. A* **19** 346 (1977)
231. E V Kamzolkina, P P Nechaev, Ya S Vygodskii, G E Zaikov *Dokl. Akad. Nauk SSSR* **233** 156 (1977)
232. S V Vinogradova, Ya S Vygodskii, V V Korshak, T N Spirina *Acta Polymer* **30** 3 (1979)
233. A A Tager, L K Kolmakova, S A Vshivkov, E V Kremlyakova, Ya S Vygodskii, S N Salazkin, S V Vinogradova *Vysokomol. Soedin., Ser. B* **19** 738 (1977)
234. V V Korshak, S S Novikov, S V Vinogradova, A P Khardin, I A Novakov, B S Orlinson, S S Radchenko *Vysokomol. Soedin., Ser. B* **21** 248 (1979)
235. S G Andreeva, A A Tager, V I Konevets, O V Glukhikh, Ya S Vygodskii, V V Korshak, S V Vinogradova *Vysokomol. Soedin., Ser. A* **21** 2229 (1979)
236. USSR P. 250 454; *Ref. Zh. Khim.* 19 S 309P (1970)
237. USSR P. 267 893; *Ref. Zh. Khim.* 5 S 338P (1971)
238. USSR P. 410 057; *Byull. Izobret.* (1) 89 (1974)
239. USSR P. 412 212; *Byull. Izobret.* (3) 100 (1974)
240. USSR P. 526 641; *Byull. Izobret.* (32) 78 (1976)
241. USSR P. 531 819; *Byull. Izobret.* (38) 77 (1976)
242. USSR P. 565 045; *Byull. Izobret.* (26) 50 (1977)
243. USSR P. 615 100; *Byull. Izobret.* (26) 81 (1978)
244. USSR P. 790 725; *Byull. Izobret.* (3) 279 (1983)
245. USSR P. 696 759; *Byull. Izobret.* (20) 259 (1981)
246. Ya S Vygodskii, S V Vinogradova, V V Korshak, Z M Nagiev, G Reinisch, G Rafler, Ya G Urman, in *Tezisy 8-go Mezhdunar. Simpoziuma po Polikondensatsii, Alma-Ata, 1981* (Abstracts of the Eighth International Symposium on Polycondensation, Alma-Ata, 1981) p. 91
247. Ya S Vygodskii, Z M Nagiev, V A Adigezalov, Sh T Bagirov, Ya M Nagiev, in *Tezisy 22-i Vsesoyuznoi Konferentsii po Vysokomolekulyarnym Soedineniyam, Alma-Ata, 1985* (Abstracts of the 22nd All-Union Conference on High-Molecular-Mass Compounds, Alma-Ata, 1985) p. 70
248. E M Belavtseva, L G Radchenko, Ya S Vygodskii, N A Churochkina *Vysokomol. Soedin., Ser. B* **24** 374 (1982)
249. L G Gladkova, E F Kolpikova, Ya S Vygodskii, A S Fialkov *Usp. Khim.* **57** 1742 (1988) [*Russ. Chem. Rev.* **57** 999 (1988)]
250. S N Khar'kov, Z N Lavrova, G A Tintsova, E P Krasnov, A S Chegolya, in *Proizvodstvo Sinteticheskikh Volokon* (Production of Synthetic Fibres) (Moscow: Khimiya, 1971) p. 289
251. L G Gladkova, E F Kolpikova, A S Fialkov, Ya S Vygodskii *Plast. Massy* (8) 70 (1989)
252. E V Lyamskaya, D V Pebak, B V Kotov, Ya S Vygodskii, A N Pravednikov *Vysokomol. Soedin., Ser. B* **29** 228 (1987)
253. A S Fialkov, E F Kolpikova, L G Gladkova, D S Konstantinova, Ya S Vygodskii, S V Vinogradova, V V Korshak *Vysokomol. Soedin., Ser. B* **27** 818 (1985)
254. V V Korshak, V V Lyashevich, V V Rode, Ya S Vygodskii *Vysokomol. Soedin., Ser. A* **22** 2559 (1980)
255. Ya S Vygodskii, L I Komarova, Yu V Antipov, V V Kazantseva, A V Davydov *Izucheniye Vzaimodeistviya Epoksidnykh Oligomerov s Poliimidami* (Investigation of the Interaction of Epoxy-Oligomers with Polyimides) Article deposited at the All-Union Institute of Scientific and Technical Information (VINITI) No 2342, Moscow, 1990
256. L I Titova, Z M Nagiev, A P Tyutnev, V S Saenko, Ya S Vygodskii *Acta Polymer* **35** 247 (1984)
257. V M Andreeva, A A Tager, B I Lirova, V I Konovets, O V Glukhikh, Ya S Vygodskii, S V Vinogradova, V V Korshak *Acta Polymer* **31** 727 (1980)
258. Z M Nagiev, Candidate Thesis in Chemical Sciences, Institute of Organoelement Compounds, Academy of Sciences of the USSR, Moscow, 1983
259. G S Gurbich, Candidate Thesis in Chemical Sciences, Institute of Organoelement Compounds, Academy of Sciences of the USSR, Moscow, 1981
260. V A Adigezalov, Candidate Thesis in Chemical Sciences, Institute of Organoelement Compounds, Academy of Sciences of the USSR, Moscow, 1981
261. Z V Gerashchenko, Candidate Thesis in Chemical Sciences, Mendeleev Moscow Chemical Technological Institute, Moscow, 1972
262. T N Spirina, Candidate Thesis in Chemical Sciences, Institute of Organoelement Compounds, Academy of Sciences of the USSR, Moscow, 1978
263. N A Churochkina, Candidate Thesis in Chemical Sciences, Institute of Organoelement Compounds, Academy of Sciences of the USSR, Moscow, 1972
264. Yu V Antipov, Candidate Thesis in Chemical Sciences, Institute of Organoelement Compounds, Academy of Sciences of the USSR, Moscow, 1990; Ya S Vygodskii, L I Komarova, Yu V Antipov *Vysokomol. Soedin., Ser. A* **37** 197 (1995)
265. V V Korshak, S V Vinogradova, T A Burtseva, P M Valetskii, V I Stanko, M S Klebanov *Vysokomol. Soedin., Ser. A* **17** 959 (1975)
266. Ya S Vygodskii, L G Gladkova, E F Kolpikova, in *Abstracts of the Fifth International Conference on Polyimides. New Trends in Polyimide Science and Technology* (New York, 1994) p. 116
267. A A Askadskii, in *Abstracts of the Fifth International Conference on Polyimides. New Trends in Polyimide Science and Technology* (New York, 1994) p. 105
268. E D Molodtsova, Candidate Thesis in Chemical Sciences, Institute of Organoelement Compounds, Academy of Sciences of the USSR, Moscow, 1982
269. Ya S Vygodskii, T N Panova, S V Vinogradova *Vysokomol. Soedin.* **38** (1996) (in the press)
270. A L Rusanov, in *Advances in Polymer Chemistry* (Moscow: Mir, 1986) p. 159
271. D R Tur, Candidate Thesis in Chemical Sciences, Institute of Organoelement Compounds, Academy of Sciences of the USSR, Moscow, 1970; USSR P. 221 276; *Byull. Izobret.* (21) 92 (1968)
272. S V Vinogradova, D R Tur *Vysokomol. Soedin., Ser. A* **15** 284 (1973)
273. S V Vinogradova, V V Korshak, D R Tur *Vysokomol. Soedin., Ser. B* **10** 396 (1968)
274. S V Vinogradova, D R Tur, V V Korshak, E S Krongauz *Izv. Akad. Nauk SSSR, Ser. Khim.* 2827 (1968)
275. V V Korshak, S V Vinogradova, D R Tur *Izv. Akad. Nauk SSSR, Ser. Khim.* 439 (1969)
276. V V Rodez, E M Bondarenko, V V Korshak, S V Vinogradova, D R Tur *Izv. Akad. Nauk SSSR, Ser. Khim.* 1509 (1969)
277. V V Korshak, V M Mamedov, G E Golubkov, D R Tur *Vysokomol. Soedin., Ser. B* **12** 57 (1970)
278. G I Timofeeva, S A Pavlova, S V Vinogradova, D R Tur *Vysokomol. Soedin., Ser. A* **13** 2653 (1971)
279. S A Pavlova, G I Timofeeva, V V Korshak, S V Vinogradova, D R Tur, D Sharoshi *Vysokomol. Soedin., Ser. A* **13** 2643 (1971)
280. V V Korshak, G L Berestneva, S V Vinogradova, M S Gergaya, D R Tur *Khim. Geterotsikl. Soedin.* 1457 (1971)
281. S V Vinogradova, V V Korshak, D R Tur *Vysokomol. Soedin., Ser. A* **14** 915 (1972)
282. L A Pankratova, G I Timofeeva, V V Korshak, S A Pavlova, D R Tur, S V Vinogradova *Vysokomol. Soedin., Ser. A* **16** 2666 (1974)
283. V V Korshak, S A Pavlova, D R Tur, G I Timofeeva, L A Pankratova, S V Vinogradova *Vysokomol. Soedin., Ser. A* **17** 486 (1975)
284. I P Bragina, V V Korshak, G L Berestneva, S V Vinogradova, D R Tur, V A Khomutov, V V Krylov *Vysokomol. Soedin., Ser. A* **18** 2318 (1976)

285. G Borisov, S Sivriev, V V Korshak, S V Vinogradova, D R Tur *Faserforsch. Textiltech.* **28** 601 (1977)
286. P V Karyakin, V N Sapozhnikov, G P Kamelova, V V Korshak, G L Berestneva, D R Tur *Vysokomol. Soedin., Ser. A* **21** 18 (1979)
287. V V Korshak, G I Timofeeva, I A Ronova, D R Tur, S V Vinogradova *Vysokomol. Soedin., Ser. A* **21** 74 (1979)
288. V V Lyashevich, V V Korshak, D R Tur, V V Rode *Vysokomol. Soedin., Ser. A* **22** 2211 (1980)
289. I A Gribova, V V Korshak, L S Fedorova, L I Komarova, G E Morozova, D R Tur, N E Kolobova, Ya V Genin *Vysokomol. Soedin., Ser. A* **23** 2294 (1981)
290. V V Korshak, S A Pavlova, P N Gribkova, I A Gribova, O V Vinogradova, L L Chatova, S V Vinogradova, D R Tur, I V Zarubina *Vysokomol. Soedin., Ser. A* **27** 161 (1985)
291. V V Korshak, S V Vinogradova, D R Tur, V A Khomutov *Izv. Akad. Nauk SSSR, Ser. Khim.* 2721 (1969)
292. V V Korshak, S A Pavlova, D R Tur, G I Timofeeva, L A Pankratova, S V Vinogradova *Issledovanie Nekotorykh Zakonomernostei Obrazovaniya Poligidrazidov na Primere Poli-(4,4'-difenilnftalid) digidrazida* [Investigation of Certain Characteristic Features of the Formation of Polyhydrazides in Relation to Poly(4,4'-diphenylenephthalide) Dihydrazide] Article deposited at the All-Union Institute of Scientific and Technical Information (VINITI) No 5876, Moscow, 1973
293. USSR P. 389 118; *Byull. Izobret.* (29) 95 (1973)
294. USSR P. 513 053; *Byull. Izobret.* (17) 86 (1976)
295. Bulg. P. 25 013; *Byull. Izobret.* (7) (1978); *Ref. Zh. Khim.* 18 S 370P (1979)
296. V V Korshak, S V Vinogradova, L A Glivka, P M Valetskii, V I Stanko *Vysokomol. Soedin., Ser. A* **15** 1495 (1973)
297. A N Frazer, F T Wallenberger, W G Sweeny *J. Polym. Sci., Part A* **2** 1157 (1964)
298. Y Iwakura, K Uno, S Hara *J. Polym. Sci., Part A* **3** 45 (1965)
299. A L Rusanov, V V Korshak, E S Krongauz, I B Nemirovskaya *Vysokomol. Soedin.* **8** 804 (1966)
300. E S Krongauz, V V Korshak, A L Rusanov, B V Lokshin *Vysokomol. Soedin., Ser. A* **9** 87 (1967)
301. *Novye Termostoikiye Materialy "Niplon-1" i "Niplon-2"* (The New Heat-Resistant Materials 'Niplon-1' and 'Niplon-2') Exhibition of National Economic Achievement, USSR, Moscow, 1977
302. *Termostoikiye Materialy "Niplon-1" i "Niplon-2"* (The Heat-Resistant Materials 'Niplon-1' and 'Niplon-2') (Moscow: Soyuzkhimeksport Vneshtorgizdat)
303. USSR P. 448 205; *Byull. Izobret.* (40) 50 (1974)
304. USSR P. 413 162; *Byull. Izobret.* (4) 67 (1974)
305. USSR P. 361 185; *Byull. Izobret.* (1) 59 (1973)
306. USSR P. 398 580; *Byull. Izobret.* (38) 77 (1973)
307. G I Timofeeva, V V Korshak, S A Pavlova, G M Tseitlin, N S Zabel'nikov, K A Krishtul *Vysokomol. Soedin., Ser. B* **15** 428 (1973)
308. V V Korshak, V A Khomutov, N S Zabel'nikov, V G Danilov, Yu E Doroshenko, G M Tseitlin *Vysokomol. Soedin., Ser. A* **16** 2671 (1974)
309. A A Izyneev, V P Mazurevskii, A D Markov, V V Korshak *Dokl. Akad. Nauk SSSR* **231** 1126 (1976)

Titanium compounds as catalysts for esterification and transesterification

M I Siling, T N Laricheva

Contents

I. Introduction	279
II. The main groups of titanium-containing catalysts	279
III. The activity of titanium-containing catalysts	280
IV. The selectivity of titanium-containing catalysts	283
V. The activity and the selectivity of titanium-containing catalysts from the viewpoint of the theory of information transmission	284

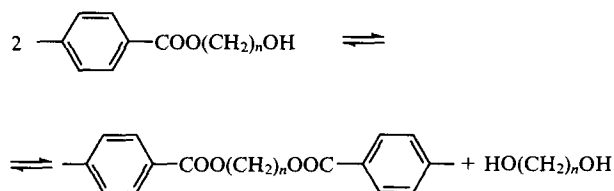
Abstract. Published data on the activity and selectivity of titanium-containing catalysts of esterification and transesterification reactions are surveyed. The influence of the nature of ligands and of the composition of the medium on the activity of catalysts is shown. The selectivity of the catalysis is considered from the viewpoint of information transmission theory. The bibliography includes 61 references.

I. Introduction

The esterification of carboxylic acids has been studied for 130 years. This reaction may be considered to be a classical topic of physical organic chemistry. Its investigation is associated with such names as Berthelot, Ostwald, Menshutkin, Guldberg, Waage, and others.¹ Esterification and transesterification reactions occupy an important place in industrial organic synthesis; they are widely used for the production of solvents, perfumes, polymers, and plasticisers.

Esterification reactions are traditionally catalysed by strong protic acids, which are active and cheap catalysts, although not free from certain drawbacks. Among these drawbacks one should note the low selectivity of protic acids caused by their ability to accelerate many side reactions, the necessity to neutralize the catalyst and to purify substantial amounts of effluent, and corrosion of the equipment.^{2,3} This has stimulated the search for new catalysts for esterification and transesterification; a broad range of organic and inorganic compounds of various metals have been proposed as these catalysts, and titanium compounds occupy a special place among them. The high activity and selectivity of titanium-containing catalysts, their good solubility, and the absence of acidic effluent, which causes corrosion, are the reasons why these catalysts are frequently used in industry. Titanium compounds are used as catalysts for the synthesis of ester-based plasticisers, mostly dioctyl phthalate^{3–5} and poly(alkylene terephthalates) — the polymers that have found application in the production of synthetic fibres, films, and structural materials.^{5–8}

In the present review, attention is concentrated on the titanium-containing catalysts used in the preparation of poly(alkylene terephthalates) (PATP) by the esterification of terephthalic acid with ethylene glycol, butane-1,4-diol, and other diols, by the transesterification of dimethyl terephthalate (DMT) with diols, and by the so-called polycondensation.



The latter reaction can also be regarded as transesterification in which one polymeric molecule acts as the ester and another one acts as the alcohol. It should be noted that the general rules of catalysis with titanium compounds manifested in these reactions are also valid for many other esterification and transesterification reactions.

Our review mostly deals with the activity and selectivity of titanium-containing catalysts. The problems of kinetics and mechanisms of the reactions are considered only in relation to the discussion of particular data on activity and selectivity. We also present nontraditional approaches to the mechanism of the catalytic action of titanium compounds based on the use of control and information theories.

II. The main groups of titanium-containing catalysts

It has not been our aim to consider the numerous patents in which the application of various titanium compounds as catalysts for esterification and transesterification is described. These data have been reported previously.^{2–7,9} We shall restrict ourselves to the classification of the catalysts according to their chemical composition. In conformity with this principle, titanium-containing catalysts can be divided into organic, inorganic, mixed, and complex catalysts.

Compounds containing a Ti—OR bond (R is an organic radical) are usually referred to as organic catalysts. Among them, tetraalkyl titanates (alkyl orthotitanates or titanium alkoxides) Ti(OR)₄, where R = Et, Prⁱ, Bu, are most frequently used. Some other titanium compounds have also been suggested as catalysts. For example, titanium salts of aromatic or aliphatic

M I Siling, T N Laricheva Research Institute of Plastics,
Perovskii proezd 35, 111024 Moscow, Russian Federation.
Fax (7-095) 273 29 58

Received 1 August 1995
Uspekhi Khimii 65 (3) 296–304 (1996); translated by Z P Bobkova

carboxylic or dicarboxylic acids (formates, benzoates, oxalates), titanium polyacrylates and polymethacrylates, titanates of the general formula $Ti[O(CH_2CH_2O)_nH]_4$, where $n = 2, 3, 4$, obtained by the interaction of butyl orthotitanate with the corresponding diol, bis(chelate)bis(hydroxyalkoxy)titanates, and bis(chelate)bis-(oligoether)titanates, where the chelate is the residue of a chelating compound such as acetylacetone, dibenzoylmethane, 8-hydroxyquinoline, or ethyl salicylate. It has been shown that various oligotitanates, for example, compounds of the formula $RO[Ti(OR)_2O]_nR$, where $n = 2-20$, $R = H$, Et and/or Pr^i and/or Bu, can also be used.

Among inorganic titanium-containing catalysts, hexafluorotitanates $M_x(TiF_6)_y$, where M is an alkali metal, alkaline earth metal, zinc, antimony, or ammonium, are noteworthy. Data concerning the use of titanium oxides and hydroxides, orthotitanium acid and its salts have also been reported.

Organic compounds that incorporate, apart from oxygen (the Ti—O bond), atoms of other metals or other elements, such as halogens, Si, S, P, or N, belong to mixed titanium-containing catalysts. Metal hexaalkyl orthotitanates $MH[Ti(OR)_6]$ and $M'[Ti(OR)_6]$, where M is an alkali metal, M' is an alkaline earth metal, and R is C_1-C_6 alkyl residue, are examples of this type of compounds. The use of titanium salts of aromatic thiols (thioxine, dimercaptobenzene, etc.) and compounds of the formula $M_x[TiO_2 \cdot (C_2O_4)_2]_y$, where M is an alkali metal, alkaline earth metal, Sb, Sn, Zn, Pb, or Co has also been reported.

In recent years, complex catalytic systems consisting of several catalysts or containing one catalyst with functional additives have found wide application. This direction is very promising, since it appreciably widens the possibility of controlling the activity and selectivity of catalysts. Both organic and inorganic titanium compounds can serve as the main components of the complex catalysts for esterification and transesterification reactions. For example, catalytic systems based on tetraalkyl titanates and containing carboxylic acids, their salts, alkoxides of Group 3, 4, and 5 elements, organic compounds of sulfur, tin, bismuth, and antimony have been suggested.

Among inorganic titanium-containing catalysts with additives, mixtures of titanium metal with titanium hydrides and zinc acetate, mixtures of alkali and alkaline earth metal hexafluorotitanates with Li, Ca, Pb, Zn, and Mn salts of aliphatic carboxylic acids are noteworthy.

The above data illustrate the great diversity of titanium-containing catalysts for esterification and transesterification

III. The activity of titanium-containing catalysts

1. Comparison of the activities of titanium-containing and other catalysts

The higher catalytic activity of titanium compounds compared with similar compounds of other metals is manifested, for example, in the alcoholysis of alkyl benzoates.^{10,11} Some of the results obtained are presented in Table 1.

As can be seen from Table 1, compounds of transition metals of the titanium and vanadium subgroups are the most active. The activation energy of the alcoholysis in the presence of Ti compounds (46.9 kJ mol^{-1}) is lower than that in the presence of other metal derivatives by a factor of almost two ($84-105 \text{ kJ mol}^{-1}$).

Tetrabutyl titanate (TBT), as a catalyst of the reactions of heptanol with benzoic acid and methyl benzoate, i.e. esterification and transesterification reactions, is superior to Zn, Mn, and Co compounds.¹²

The catalytic activity of dibutyl tin dilaurate, dibutyltin diphenoxide, dibutyltin oxide, and tetraphenyltin in the transesterification of 4-hydroxybutyl benzoate at 167°C , was two orders of magnitude lower than that of TBT,¹³ the composition of organotin compounds having only slight influence on their catalytic activity.

Table 1. The activity of various catalysts in the alcoholysis of methyl benzoate with heptanol at 200°C .¹⁰

Catalyst	Concentration of the catalyst (mol %)	Rate constant/ min^{-1}
$Ti(OBu)_4$	0.0190	1.0×10^{-2}
$Zr(Pr^iO)_4$	0.0200	3.0×10^{-3}
$Nb(OEt)_5$	0.0189	2.4×10^{-3}
$Ta(OEt)_5$	0.0203	5.7×10^{-3}
$B(OBu)_3$	0.0231	3.0×10^{-4}
$Al(Pr^iO)_3$	0.0193	2.0×10^{-4}
$Sb(OBu)_3$	0.0220	0.9×10^{-4}
$As(OBu)_3$	0.0203	0.8×10^{-4}

The influence of the nature of catalyst on the kinetics of the reaction of dimethyl terephthalate with butane-1,4-diol at a temperature of $175-225^\circ\text{C}$ and a catalyst content of $0.16\%-0.17\%$ has been studied.¹⁴ The rate of transesterification was monitored by following the liberation of methanol. In the series of catalysts $Co(OAc)_2$, $Mn(OAc)_2$, and $Ti(OPr^i)_4$, the latter exhibited the highest activity.

The kinetics of this reaction were studied at a DMT: butane-1,4-diol molar ratio of $1:2.2$, a catalyst content of 5×10^{-4} moles per mole of DMT, and temperatures of $160-240^\circ\text{C}$ in the presence of zinc acetate, lead oxide, and TBT.¹⁵ The highest degree of conversion, 98% after 4 h, was achieved with the titanium catalyst, while in the presence of PbO , it was 83% and with zinc acetate it was 75%.

It is known^{7,16} that in the transesterification of DMT with ethylene glycol, titanium compounds exhibit lower catalytic activity than zinc, manganese, and cobalt acetates, which are usually employed in industrial processes.

The data presented imply that the activity of a catalyst in transesterification depends on the number of methylene units in the diol.

A number of papers have been devoted to the comparison of catalytic activities of various metal compounds in polycondensation in relation to the synthesis of poly(ethylene terephthalate) (PETP). Refler et al.¹⁷ have studied the catalytic activity of metal butoxides in polycondensation in a thin layer of the polymer melt. At 280°C and a catalyst content of 3×10^{-4} moles per mole of bis(hydroxyethyl) terephthalate, metals can be arranged in the following series in terms of their catalytic activities (rate constants, $\text{g mmol}^{-1} \text{s}^{-1}$, and degrees of polymerisation are given in parentheses): $Zn (2.5, 105) < Al (2.6, 99) < Ge (4.6, 114) \ll Ti (6.4, 175) < Sn (7.9, 202)$. In the polycondensation of oligo(ethylene terephthalates), titanium derivatives are also more active catalysts than manganese or antimony compounds.

While analysing the data on the activity of catalysts for esterification and transesterification, one should take into account the fact that equilibrium constants of the reactions under consideration are low and are of the order of unity.¹⁸ Therefore, the reverse reaction can substantially influence the rates of esterification and transesterification. In order to obtain data on the catalytic activity, independent of the reverse reaction, initial reaction rates should be measured or the process be conducted under conditions in which the reaction is virtually irreversible owing to the quick removal of the reaction products from the reaction zone. When esterification or transesterification reactions involve low-molecular-mass compounds, the realisation of these conditions is not difficult. A different situation occurs in the syntheses of polymers, especially when they are conducted in highly viscous media. For example, melt polycondensation of oligo(butylene terephthalate) used in the production of poly(butylene terephthalate) proceeds in a system in which the viscosity increases during the reaction to $5000-10000 \text{ Pa s}$.

The rate of the removal of the low-molecular-mass product, namely, butane-1,4-diol, from the reaction mixture in such systems may be low and comparable with the rate of the chemical transformation.

Thus, to compare the activities of polycondensation catalysts, one should take into account that the observed rate of the process may be determined not only by the rate of the chemical reaction, which is influenced by the catalyst, but also by the velocity of mass transfer. The latter depends on the thickness of the melt layer or on the interfacial area, which is a function of the intensity of stirring, composition of the reaction mixture, the temperature, and the degree of bubble-formation. Correct determination of the catalytic activity, based on the kinetics of polycondensation, requires that the above factors be taken into account in the mathematical model used for the calculations. The problems of mathematical modelling of the processes of the production of poly(alkylene terephthalates) have been considered by Adorova and Kuznetsov.¹⁸

In collaboration with Kuznetsov, we developed a procedure for studying the kinetics of polycondensation of oligo(alkylene terephthalates) convenient for the determination of the activity and the selectivity of a catalyst. In this case, the viscosity of the reaction medium is the most sensitive indication of the occurrence of polycondensation; it sharply increases in the course of the process. The change in the viscosity can be conveniently monitored by the increase in the power consumed in stirring the reaction melt. The power of an electric motor with mild [responsive] characteristics is directly related to the speed of the stirrer rotation, which can be easily measured. During the reaction the number of revolutions [per unit time] of the stirrer diminishes, the dependence of this value on the number-average degree of polymerisation of the product formed being nearly linear. It is notable that the rotation speed of a stirrer depends appreciably on the material of the reactor, in this particular case, on the kind of glass. This effect, which has been noted previously,¹⁹ is probably due to the fact that the properties of the reactor material influence the adhesion of the polymer melt to the reactor walls and, hence, the processes of bubble and foam formation. These processes determine to a large degree the liquid-to-vapour interfacial area, through which the low-molecular-mass product of polycondensation is transferred. The effect observed indicates once again that mass transfer contributes significantly to the macrokinetic features of the polycondensation in the synthesis of poly(alkylene terephthalates).

The experimentally observed dependence of the number-average degree of polymerisation on the reaction time was treated using a mathematical model that took into account the following processes: (1) the formation of the ester bond via interaction of two terminal hydroxyalkoxycarbonyl groups or hydroxyalkoxycarbonyl and carboxyl groups; (2) side reactions yielding tetrahydrofuran and carboxyl groups (see below); and (3) the mass transfer of the diol and water liberated during the formation of the ester bond. The calculated rate constants for reactions (1) served as a measure of the activity of the catalysts studied, and the rate constants for reactions (2) served as a measure of their selectivity.

2. Catalytic activities of various titanium compounds.

The effect of the medium

Several studies have been devoted to the influence of the nature of ligands (fragments) on the catalytic activity of titanium compounds. An evaluation of the activity of various titanium compounds in the esterification of 2-ethylhexyl hydrogen phthalate with an excess of 2-ethylhexanol at 170–175 °C and at a catalyst concentration of 0.01 mol kg⁻¹ has shown that there is no substantial difference between the catalytic activities of the following compounds: titanium sulfate, titanium acetate, titanium dichlorodiacetate, titanium tetrachloride, TBT, tetra-2-ethylhexyl titanate, poly(butyl titanate), triethanolamine titanate, tributoxo titanium butyl hydrogen phthalate, and a complex of butyl levulinate with TBT.²⁰ Ortho- and metatitanic acids were found

Table 2. Catalytic activity of titanium compounds in the alcoholysis of methyl benzoate with heptanol at 200 °C.¹⁰

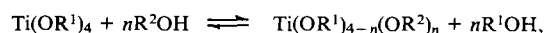
Catalyst	Concentration of catalyst (mol %)	Initial heptanol : methyl benzoate ratio/mol mol ⁻¹	Rate constant/10 ⁻² min ⁻¹
Ti(C ₇ H ₁₅ O) ₄	0.020	21.50	0.96
Ti(CF ₃ CH ₂ O) ₄	0.021	20.30	1.01
Ti(C ₂ H ₅ OC ₂ H ₄ O) ₄	0.021	20.26	1.04
Ti(C ₄ H ₉ O) ₄	0.020	20.17	0.83
Ti(C ₆ H ₅ O) ₄	0.019	20.18	1.03
Ti(Cl-C ₆ H ₃ Cl-O) ₄	0.019	19.47	1.06

to be somewhat less active, and the catalytic action of titanium dioxide was much weaker. It is natural to attribute the low activities of the latter titanium-containing catalysts to their poor solubilities in the reaction medium.

The catalytic activities of various alkoxy and aryloxy titanium derivatives of the general formula Ti(OR)₄ in the transesterification of methyl benzoate with heptanol have been compared (Table 2).^{10, 21}

One can see that the nature of the organic radical does not influence significantly the reaction rate constant, which remains almost invariable even when twelve electronegative fluorine atoms or an aryl group are introduced into the catalyst molecule. Judging from the ability of alkoxy and aryloxy titanium derivatives to undergo quick radical exchange reactions, the results obtained were rationalised¹⁰ in the following way: in the presence of excess heptanol, the alcohol and the catalyst undergo a quick exchange reaction giving tetraheptyl titanate. This was confirmed by NMR data. Therefore, alcoholysis reactions conducted in the presence of various titanium-containing compounds are characterised by nearly identical rate constants.

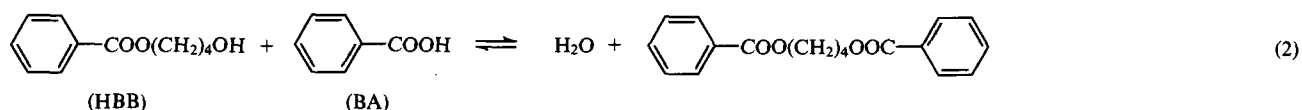
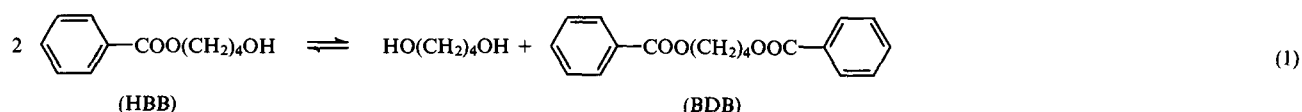
The formation of complexes and the radical exchange during the interaction of tetraalkyl titanates with esters and alcohols, as well as the formation of various complexes, have been reported.^{22, 23} It should be noted that in the general case, exchange reactions of the type



do not necessarily proceed up to the complete conversion of the initial tetraalkyl titanate to Ti(OR²)₄. The position of the equilibrium is determined by the composition of the reaction mixture and by the equilibrium constant of the reaction. For example, in the TBT–*n*-heptanol system at 20 °C, the degree of conversion is 0.65, which corresponds to an equilibrium constant of 3.4.²³ In conformity with our data obtained by gas chromatography, in the transesterification of DMT with butanediol, 1.5–2 moles of butanol per mole of the catalyst (TBT) is liberated. These data imply that there is in principle the possibility of a substantial influence of the nature of the ligands in titanium-containing catalysts on their activities. Obviously, this effect should be most pronounced in the case of bulky and/or chelate-forming ligands, whose exchange may be hampered due to thermodynamic or kinetic restrictions. This is in agreement with published data.^{24–26}

The catalytic activities of TBT and chelated titanium derivatives in the esterification of phthalic anhydride can differ by an order of magnitude.^{25, 26} Bis(acetylacetonato)dibutoxytitanium exhibited the highest esterification catalytic activity in a 2-ethylhexanol medium, and TBT was the most active when the process was carried out in di(2-ethylhexyl) phthalate.

In general, the rates of esterification and trans-esterification reactions, accelerated by titanium-containing catalysts, are appreciably influenced by the composition of the



reaction medium.^{12, 26–28} This effect cannot be reduced to nonspecific solvation, which is measured in terms of the dielectric permeability of the medium. It is likely that the influence of the medium is mostly determined by the ability of titanium-containing catalysts to enter into various reactions with the components of the medium including the reagents.

For example, in a study of the esterification of 2-ethylhexyl hydrogen phthalate (monoester) to dioctyl phthalate (diester), it has been found²⁸ that in the medium of the monoester, TBT exhibits virtually no catalytic activity. In fact, in the beginning of the process, when the concentration of the monoester in the reaction medium is high and the concentration of the diester is low, an increase in the TBT concentration does not lead to any noticeable increase in reaction rate, which almost does not differ from the rate of esterification in the absence of the catalyst. As the reaction proceeds and the monoester content in the mixture decreases, the influence of TBT on the rate of the process increases appreciably. These data are supported by the results of Lemman et al.,^{27, 29} who found that when 2-ethylhexyl hydrogen phthalate or dioctyl phthalate instead of 2-ethylhexanol are used as solvents, the rate of the catalytic esterification of phthalic anhydride decreases in the following sequence: diester > 2-ethylhexanol > monoester. These experimental data were interpreted with a mathematical model, which made allowance for the reactions of TBT with the carboxyl group of the monoester, the hydroxyl group of the alcohol, and the ester group of the diester, that is, with all the main components of the reaction medium.²⁸ In addition, the effects of interaction between neighbouring ligands and the ligands of the inner and outer coordination spheres were taken into account.

3. The influence of additives and impurities on the catalytic activities of titanium-containing catalysts

The synthesis of PATP and other esterification and transesterification reactions are often carried out in the presence of titanium-containing catalysts mixed with other compounds. The question of how these additives influence the activity of titanium-containing catalysts is of interest both for the practice and for the theory of catalysis. Very little information concerning this problem has been published in the literature; therefore, the information provided by patent descriptions merits attention. An analysis of the latter has shown⁹ that the use of complex titanium-containing catalytic systems may be favourable for both increase in the catalytic activity and improvement of the properties of the products obtained, for example, complex polyesters.

Ca, La, Zr, Co, Zn, Cd, Mg, Hg, Ge, Sn, and Sb derivatives, silver carboxylates, aromatic thiols, aliphatic and aromatic sulfonic acids, and their salts have been suggested as additives that increase the activity of titanium-containing catalysts.⁹

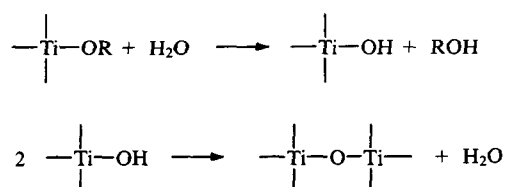
The problem of the influence of free carboxyl groups and water deserves particular attention, since they are virtually always present in the reaction mixtures. It should be noted that published data on this problem are somewhat contradictory. Despite the fact that carboxylic acids themselves are catalysts of alcoholysis, their influence on the activity of titanium-containing catalysts in esterification and transesterification is ambiguous. The addition of a small amount of adipic acid to TBT accelerates transesterification of its dimethyl ester with diethylene glycol.³⁰

The maximum rate constant was achieved at a concentration of COOH groups of 0.96 mol % with respect to dimethyl adipate. In some patents, carboxylic and dicarboxylic acids have been offered as activators for titanium-containing catalysts in the synthesis of PATP.⁹ This made it possible to obtain polyesters with increased molecular weights.

However, a study of the synthesis of poly(butylene terephthalate) using model compounds in the presence of TBT at 150 and 167 °C has shown that benzoic acid deactivates the catalyst.³¹ 4-Hydroxybutyl benzoate (HBB) was used as a model compound with a terminal hydroxyl group, benzoic acid (BA) was taken as a model compound with a terminal carboxyl group, and 1,4-butylene dibenzoate (BDB) was used as a model polymer. Attention was concentrated on the reactions modelling the polymer chain growth, namely, polycondensation (1) and direct esterification (2).

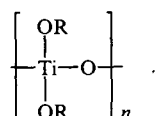
The results obtained in the experiments with various concentrations of the reactants and TBT led the authors to the following conclusions. Benzoic acid behaves as an inhibitor, if it is introduced in the reaction mixture together with TBT, or as a catalyst in the absence of TBT. In conformity with the coordination mechanism suggested for the catalytic reaction involving TBT, the inhibiting action of BA is caused by the formation of its adduct with the titanium-containing catalyst; this adduct is more stable than the adducts of titanium-containing catalysts with HBB or BDB. The existence of a stable Ti–BA adduct at room temperature in chloroform was confirmed by IR spectroscopy. However, the spectroscopic study provided no evidence supporting the existence of a product of addition of HBB to TBT under the experimental conditions. Based on the suggested mechanism, kinetic equations for calculating the rates of the formation of BDB and consumption of BA were derived. The calculated data proved to be close to the experimental results. It was also found that the stability of the BA–TBT adduct decreases appreciably with an increase in the temperature (the equilibrium constant for the adduct formation decreases by a factor of more than three as the temperature increases from 150 to 167 °C). Consequently, the inhibitory influence of BA is weaker at higher temperatures. The inhibitory effect of carboxyl groups on catalytic transesterification in the presence of titanium-containing catalysts is much less pronounced than that in the case of zinc-, manganese-, and cobalt-containing catalysts.¹²

The influence of water on the activity of titanium-containing catalysts has not been fully elucidated. Many organic compounds of titanium are known³² to be rapidly hydrolysed in the presence of even traces of water to give oligotitanates.



In a study of the kinetics of the transesterification of DMT with ethylene glycol,³³ it has been found that the activity of titanium-containing catalysts depends only slightly on the

added water. This is due to the low stability of aqueous complexes of titanium compounds, which are converted to polymeric derivatives of the following structure:



Ioda³³ managed to show experimentally that the catalytic activity of these compounds is nearly identical to that of the initial TBT.

An attempt has been made³⁴ to study the influence of the degree of preliminary hydrolysis of TBT on its catalytic activity in the esterification of phthalic anhydride with octanol. When the water:TBT molar ratio increased to 1.22:1 (which corresponded to a degree of TBT hydrolysis of 60%), the activity of the compound resulting from the hydrolysis became somewhat higher than the activity of the initial TBT. Further increase in the water:TBT molar ratio and in the degree of hydrolysis led to a monotonic diminution of the reaction rate, due to the decrease in the solubility of the TBT hydrolysis products. An analysis of the TBT hydrolysis products by IR and NMR spectroscopy and a comparison of their catalytic activities have shown that the products of TBT hydrolysis having a mainly linear structure are the most active. The increased catalytic activity of linear polytitanates is believed to be caused by the fact that they are more stable in the reaction medium than TBT, which incorporates reactive alkoxy groups.³⁴

There are patents describing the use of oligotitanates as effective catalysts for the synthesis of PATP.⁹ However, a study of the reversible reactions (1) and (2) has shown that water exerts an inhibiting influence on transesterification in the presence of TBT.³⁵ It was suggested that interaction of the catalyst with water and butane-1,4-diol affords catalytically inactive titanium derivatives. It was assumed that the active catalyst, water, and the inactive form of the titanium-containing catalyst exist in an equilibrium. Assuming that TBT is not capable of self-association under the reaction conditions and that most of the butoxy groups in its molecule have been substituted by alkoxy groups, Pilati et al.³⁵ has derived an equation for calculating the initial reaction rates at various initial ratios of the reactants. The results of these calculations are in good agreement with experimental data.

The above information indicates that the contradictory character of the data on the influence of carboxylic acids and water on the activity of titanium-containing catalysts is associated with the ability of the latter to enter into various reactions with these compounds.

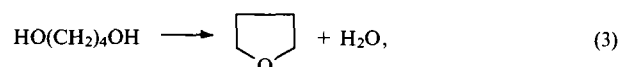
IV. The selectivity of titanium-containing catalysts

The esterification and transesterification processes are accompanied, as a rule, by side reactions. First of all, there are various reactions of dehydration of alcohols and diols yielding ethers, including cyclic ones, aldehydes, and unsaturated compounds.³⁻⁷ For example, usual products of the synthesis of PETP are diethylene glycol, 1,4-dioxane, formaldehyde, acetaldehyde, cyclic compounds, and some other compounds.⁷ The major contributions are made by processes giving acetaldehyde and diethylene glycol and by the thermal degradation of the polymer.

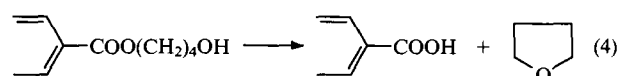
The major side products in the synthesis of poly(butylene terephthalate) are tetrahydrofuran, water, and acids. A TLC analysis of the products of the transesterification of DMT with 1,4-butanediol has shown that when titanium-containing catalysts or acetates of certain metals are used, no di(4-hydroxybutyl) ether is detected among the reaction products.³⁶ This was confirmed by NMR spectroscopy. Since THF is the main side product in the

synthesis of poly(butylene terephthalate), the extent of its formation can serve as a measure of catalyst selectivity. Let us consider this problem in more detail.

Studies of a number of reactions involving model compounds and the real process³⁷⁻⁴¹ led to the conclusion that during the esterification of terephthalic acid or transesterification of DMT with butane-1,4-diol at 160–225 °C, THF can result from the dehydration of butane-1,4-diol



or from the cyclisation of the terminal hydroxybutylene groups.



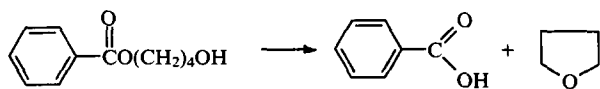
THF has also been detected by thin-layer chromatography among the products formed in the synthesis of poly(butylene terephthalate) without a catalyst.⁴² In addition, as shown by IR spectroscopy, the polymeric product incorporates carboxyl groups. Based on these data, it was suggested that THF is produced via reaction (4). The same conclusion was drawn by Radas and Hall,³⁷ who have found THF in the products of polycondensation of bis-hydroxybutyl terephthalate in the presence of various titanium- or tin-containing catalysts.

In a kinetic study,¹⁴ it has been shown that in the transesterification of DMT with butane-1,4-diol at a diol:DMT molar ratio > 2 in the presence of titanium isopropoxide at 175–225 °C, THF is formed mainly via reaction (3). The rate of the accumulation of THF varies only slightly with increase in the degree of the conversion of the monomers, because the number of terminal carboxyl groups, which catalyse dehydration of butane-1,4-diol, increases simultaneously with the decrease in the diol concentration. In the late stages of the polycondensation, the formation of THF from the terminal hydroxybutylene groups is likely to prevail.

It is logical to raise the question of the role of titanium-containing catalysts in the formation of THF via reactions (3) and (4). Analysis of the published data provides no unambiguous answer to the question whether or not titanium-containing catalysts accelerate the dehydration of butane-1,4-diol. It has been reported³⁷ that the heating of butane-1,4-diol at 210 °C for 8 h without a catalyst does not produce THF. According to another study,³⁸ butane-1,4-diol is dehydrated over a period of 4–5 h at 180–190 °C, THF being formed both without any added compounds and in the presence of TBT, benzoic acid, THF itself, or water. The reaction has a clear-cut induction period, which allowed it to be described as an autocatalytic reaction.³⁸ However, in our opinion, the attempt to attribute a catalytic influence to water or THF is dubious, especially in view of the fact that no substantial influence of added water or THF on the rate of dehydration of butane-1,4-diol was observed. The formation of THF on prolonged heating of butane-1,4-diol at 180 °C in the presence of various esterification and transesterification catalysts, including TBT, has been found by Moller et al.⁴³

The general consensus of researchers on the influence of acidic additives is that acids are active catalysts of this reaction. For example, butane-1,4-diol is easily converted to THF on heating to 160–185 °C in the presence of orthophosphoric, benzoic, terephthalic, or hydrochloric acid.^{9, 37, 38}

There are virtually no published data on the acceleration of reaction (4) by titanium-containing catalysts. Only Pilati et al.,³⁸ who have studied cyclisation of a model compound, namely, 4-hydroxybutyl benzoate, at 160–190 °C,



have shown that this reaction is not accelerated by acids and that catalysts used in the synthesis of PATP, including TBT, exert no influence on it.

The data presented indicate that there is no clear-cut catalytic influence of titanium-containing catalysts on the side reactions proceeding during the synthesis of poly(butylene terephthalate), which points to high selectivity of these catalysts. As regards their selectivity, titanium-containing catalysts of many esterification and transesterification reactions are superior not only to strong protic acids, but also to other metal-containing catalysts. This conclusion is in agreement with the results of a kinetic study¹⁵ of the transesterification of DMT with butane-1,4-diol in the presence of various metal-containing catalysts in which TBT proved to be the most selective. A similar conclusion has been drawn by Suvaram et al.,⁴⁵ who have studied this reaction carried out at 220 °C and at a catalyst content of 0.1% by mass with respect to DMT. Titanium isopropoxide, phenoxide, diisopropoxyacetate, and triethanolamine, calcium acetate, and antimony(III) oxide were used as the catalysts. It was found that in the presence of traditional catalysts for transesterification, for example calcium acetate, THF is formed in a high yield. Titanium-containing catalysts were much more selective, the best results being achieved with titanium isopropoxide. It has been shown⁴⁶ that the rate of the formation of a side product, namely diethylene glycol, during the synthesis of PETP in the presence of titanium-containing catalysts is lower than in the presence of antimony trioxide, which is frequently used as the catalyst.

In the patent literature, there is much information concerning highly selective catalysts for the synthesis of PATP based on titanium derivatives with added tin, antimony, germanium, lead, calcium, zinc, and manganese derivatives or amides of monocarboxylic acids, sulfonic acids, and phosphoric acid.⁹ There are data concerning high selectivity of titanium-containing catalysts in other esterification and transesterification reactions. For example, TBT does not catalyze the side reaction of octanol dehydration during the esterification of phthalic anhydride with this alcohol.⁴⁷

V. The activity and the selectivity of titanium-containing catalysts from the viewpoint of the theory of information transmission

The optimal catalyst should possess high activity and selectivity. The experimental data that refer mainly to enzymes, as well as to some chemical catalysts, indicate that it is possible to combine these characteristics in a single catalytic system. This possibility has been theoretically justified based on a cybernetic approach to catalysis developed in a number of studies.^{8,9,48} The use of this approach made it possible to explain the remarkable activity and selectivity of titanium-containing catalysts for esterification and transesterification reactions.

According to the concept outlined by Siling,⁸ a reaction system is regarded as being an object under control, a catalyst is considered to be a control device, and the rate of the reaction is taken to be a controlled parameter. The catalyst points to a reaction pathway that differs substantially from the noncatalytic one or, more precisely, it 'pilots' the reaction system along this pathway.

Any control is based on information transmission. In this case, one may speak of the information transmission from the catalyst to the reactants. The catalyst-reactant interactions serve here as the material basis for the information transmission. From the standpoint of statistical information theory,⁸ the activity of a catalyst is largely determined by the diversity of these interactions.

To accomplish the main reaction, a catalyst should transmit particular information to the reactants. The information is transmitted along a communication channel as signals with the use of a certain code. In this particular case, the reaction system itself serves as the communication channel, a separate interaction of the catalyst with a reactant acts as a signal, and the space and time sequence of the interactions, which ensures the occurrence of the main reaction, is the code.

The information transmission along a communication channel is almost inevitably accompanied by errors (noise). This may be manifested, for example, as the omission of a necessary interaction, as the replacement of a necessary interaction by another one, or as the appearance of an 'excessive' interaction. Whereas the transmission of the nonperturbed information ensures the occurrence of the main reaction, the noise can be responsible for the side reactions. Thus, the problem of selectivity can be solved by using the theory of the information transmission along a channel with noise.⁴⁹ It should be noted that such a consideration will refer to the selectivity of the catalytic reaction, which does not always coincide with the selectivity of the overall process, first of all, due to the contribution of noncatalytic reactions.

The rate of the information transmission along channels with noise can be represented as jV , where V is the rate of the signal transmission, and j is the average information content of one signal. The latter value is a function of the probability of the appearance of errors in the signal transmission. The appearance of noise leads to the loss of information, and consequently j diminishes. As the probability of the appearance of errors decreases, j increases, and so does the rate of the information transmission. The highest possible rate of the information transmission for a particular channel with noise is referred to as the capacity of a communication channel.

If the amount of information transmitted in a unit time (I) is smaller than the channel capacity (C), then, in conformity with the Shannon theorem, there exists a way of presenting the information (coding), which makes it possible to transmit a message without delay and with a minor error. In the case where $I > C$, no way of coding that would provide high reliability and transmission of the message without delay can be chosen; however, as the coding becomes more perfect, the unreliability of the information transmission would decrease approaching the $I = C$ value, and the transmission rate would tend to C .

The Shannon theorem, as applied to catalysis, makes it possible to identify some general features concerning the reaction selectivity. First, it follows from the theorem that a selectivity as high as desired can in principle be achieved. It is known that this possibility is most fully realised in enzymic catalysis, though chemical catalysts that ensure the selective course of certain reactions also exist. One may believe that in these cases, the condition $I < C$ is met.

Regarding the relationship between activity and selectivity in a series of catalysts of the same type, one may assume from general considerations that the selectivity and the activity would vary, as a rule, in opposite directions, because transmission of a large amount of information is associated with a larger probability of an error. However, from the theorem it follows that this is not always true, and the relationship between activity and selectivity is determined by the manner in which the $I - C$ value varies over the given series of catalysts. In a series of catalysts for which $I < C$, there exists in principle the possibility of coding which ensures that high selectivity of the catalysts is retained as their activity increases. In a series of catalysts with $I > C$, limiting selectivity decreases as the $I - C$ difference increases. If, in this series, the channel capacity varies slightly and the activity grows with an increase in the amount of information transmitted, then selectivity and activity of the catalysts will vary in the opposing directions.

Thus, theoretical consideration indicates that different relationships between activity and selectivity in a series of single-type

catalysts are possible. This is consistent with experimental data (see, for example, the books by Golodets⁵⁰ and Gates et al.⁵¹).

In the context of information theory, the selectivity of a catalyst can be increased in the following ways.

(1) By increasing the capacity of the communication channel. With the average information content of one catalyst-reactant interaction being constant, the C value is determined by the number of the interactions in unit time. Therefore, high selectivity can be reached in those systems in which many fast interactions occur. Such situations are observed in enzymic catalysis,⁵²⁻⁵⁴ which is one of the reasons why in this case the condition $I < C$ is satisfied. It is believed that it is the set of adsorption or other additional interactions of an enzyme with substrates that predetermines the high substrate specificity observed in the enzymic catalysis.

(2) By a decrease in the bulk of the information transmitted. The amount of information can be relatively small in the case where the reaction involves the cleavage and formation of a small number of bonds, and consequently, a great diversity of the catalyst-reactant interactions is not required. It has been noted⁵⁵ that one enzyme does not catalyse, as a rule, complex transformations involving cleavage and formation of many bonds. This requires a set of enzymes, each of them accelerating a relatively simple chemical transformation.

(3) By perfecting the coding procedure. According to information theory, correct transmission of messages along a channel with noise is favoured by connecting signals in long blocks. This way of coding is manifested in the catalysis as synchronous (concerted) reaction mechanisms, where the cleavage and the formation of bonds occur synchronously in a single activation complex.⁵⁶⁻⁵⁸ Mechanisms of this type are frequently realised in enzymic catalysis.

It can be seen that all the main factors contributing to the selectivity of catalysis from the viewpoint of information transmission are manifested in enzymic reactions. For our purposes, it is necessary to note the important role of the diversity of fast catalyst-reactant interactions, which ensures high channel capacity and effectiveness of coding.

Considering titanium-containing compounds in this context, one may suggest that the high activity and the high selectivity of these catalysts in esterification and transesterification reactions are caused by two main factors.

The first of them is the great diversity of the catalyst-reactant interactions. In fact, titanium is known to be capable of interacting with various oxygen-containing ligands.^{32, 59, 60} Furthermore, tetraalkyl titanates tend to undergo exchange reactions at the Ti-O bond in which one oxygen-containing ligand is substituted by another. For example, in a tetraalkyl titanate-DMT-diols-oligo(alkylene terephthalate) system, a large number of coordination and exchange interactions occur leading to the appearance of the fifth and the sixth ligands at the titanium atom and to the complete or partial substitution of the OR groups by the molecules of the reactants and giving a wide range of mixed complexes and chelate-type derivatives. It is noteworthy that in the systems under consideration, information is transmitted not only via the interaction of titanium with the reactants or the components of the medium, but also via the formation of hydrogen bonds between these compounds and inner-sphere ligands (the interaction of ligands of the inner and outer coordination spheres and its role in catalysis have been considered in a number of studies.^{8, 23, 28, 58, 61}). Of course, not all these interactions are stages of the catalytic process; moreover, some of them may retard the reaction (see for example, the paper by Siling et al.²⁸). Nevertheless, it is the great diversity of the catalyst-reactant interactions that ensures the transmission of a large bulk of information from titanium-containing catalysts to the reactants. This diversity is a characteristic feature of complex catalytic systems based on titanium compounds.

High rates of the coordination and exchange reactions are the second factor. In fact, the high rate of exchange of alkoxyl radicals

in the case of titanium alkoxides has been confirmed by NMR.^{10, 22, 23} In terms of the rate of these reactions, metals can be arranged in the following sequence $Ti > Sb > As$.

The concept developed above is consistent with the fact that virtually all the titanium-containing catalysts suggested for esterification and transesterification are compounds with Ti-O bonds, which are prone to undergo a variety of fast reactions with the reactants, rather than compounds with Ti-C bonds.

As can be seen from the presented data, the application of information transmission theory to the problem of catalyst selectivity gives results consistent with the experimental data. In our opinion, the informational approach to catalysis has also a predictive ability. For example, one can speak of the design of an effective catalytic system, in which primary importance is assigned to the diversity and the rate of the interactions of the catalyst with the reactants. These interactions can be not only direct, but also indirect (with the participation of ligands of the outer coordination sphere).

* * *

This review covers studies published in the last 10-15 years and demonstrates the prospects of using complex catalytic systems based on titanium derivatives for esterification and transesterification reactions. Study of these catalysts may also prove to be fruitful in elucidating the general features of the homogeneous catalysis.

References

1. C K Ingold *Structure and Mechanism in Organic Chemistry* (Ithaca: Cornell University Press, 1969)
2. E G Maksimenko, V I Kirilovich, A I Kutsenko *Katalizatory Protsessa Proizvodstva Slozhnoefirnykh Plastifikatorov Polivinilkhlorda* (Catalysts of the Production of Ester Plasticisers of Polyvinyl Chloride) (Moscow: NIITEKhim, 1981)
3. R S Barshtein, I A Sorokina, V G Gorbunova, in *Khimiya i Tekhnologiya Vysokomolekulyarnykh Soedinenii* (Ser. Itogi Nauki i Tekhniki) [Chemistry and Technology of High-Molecular-Weight Compounds (Advances in Science and Engineering Series)] (Moscow: Izd. VINITI, 1982) Vol. 17, p. 190
4. R S Barshtein, V I Kirilovich, Yu E Nosovskii *Plastifikatory dlya Polimerov* (Plasticisers for Polymers) (Moscow: Khimiya, 1982)
5. A Fradet, E Marechal *Adv. Polym. Sci.* **43** 51 (1982)
6. R S Barshtein, I A Sorokina *Kataliticheskaya Polikondensatsiya* (Catalytic Polycondensation) (Moscow: Khimiya, 1988)
7. B V Petukhov *Poliefirnye Volokna* (Polyester Fibres) (Moscow: Khimiya, 1976)
8. M I Siling *Polikondensatsiya. Fiziko-Khimicheskie Osnovy i Matematicheskoe Modelirovanie* (Polycondensation. Physicochemical Fundamentals and Mathematical Modelling) (Moscow: Khimiya, 1988)
9. T N Laricheva, I G Raskina, M I Siling *Katalizatory Sinteza Polialkilentereftalatov* [Catalysts of the Synthesis of Poly(alkylene terephthalates)] (Moscow: NIITEKhim, 1989)
10. J Otton, S Ratton, V A Vasnev, G D Markova, K M Nametov, V I Bakhmutov, L I Komarova, S V Vinogradova, V V Korshak *J. Polym. Sci., Polym. Chem. Ed.* **26** 2199 (1988)
11. J Otton, S Ratton *J. Polym. Sci., Polym. Chem. Ed.* **26** 2183 (1988)
12. J Otton, S Ratton, V A Vasnev, G D Markova, K M Nametov, V I Bakhmutov, S V Vinogradova, V V Korshak *J. Polym. Sci., Polym. Chem. Ed.* **27** 3535 (1989)
13. F Pilati *Polym. Commun.* **25** 187 (1984)
14. L Yurramendi, M Barandiaran, J Asua *J. Macromol. Sci.-Chem., Part A* **24** 1357 (1987)
15. E Tucek, H Dinse *Acta Polymer* **31** 429 (1980)
16. K Wolf, B Kuster, H Herlinger *Angew. Makromol. Chem.* **68** 133 (1978)
17. G Rafler, F Tesch, D Kunath *Acta Polymer* **39** 315 (1988)

18. I V Adorova, V V Kuznetsov *Matematicheskoe Modelirovanie Protsessa Sinteza Polialkilentereftalatov* [Mathematical Modelling of the Synthesis of Poly(alkylene Terephthalates)] (Moscow: NIITEKhim, 1987)
19. E Bonatz, G Rafler, G Reinisch *Faserforsch. Textiltech.* **24** 118, 309 (1973)
20. L M Bolotina, A I Kutsenko, E G Maksimenko *Plast. Massy* (7) 13 (1973)
21. G D Markova, K M Nametov, in *Polikondensatsionnye Protsessy i Polimery* (Polycondensation Processes and Polymers) (Nal'chik: Kabardino-Balkariya State University, 1986) p. 88
22. L I Komarova, N N Lapina, B V Lokshin, V I Bakhmutov, G D Markova, V A Vasnev *Izv. Akad. Nauk SSSR, Ser. Khim.* 1991 (1990)
23. L I Komarova, N N Lapina, B V Lokshin, V I Bakhmutov, G D Markova, V A Vasnev *Izv. Akad. Nauk SSSR, Ser. Khim.* 2001 (1991)
24. K Tomita *Kobunshi Ronbunshu* **33** 417 (1976)
25. E A Khrustaleva, M A Kochneva, L I Fridman, V G Lundina, A L Suvorov, A I Tarasov, V D Alekhina, L I Kurinkova *Plast. Massy* (10) 6 (1984)
26. E A Khrustaleva, Yu G Yatluk, A L Suvorov *Izv. Akad. Nauk SSSR, Ser. Khim.* 1247 (1989)
27. V N Sapunov, G M Lemman, N N Lebedev *Izv. Vyssh. Uchebn. Zaved., Khim. Khim. Technol.* **19** 696 (1976)
28. M I Siling, V V Kuznetsov, Yu E Nosovskii, S A Osintseva, A N Kharrasova *Kinet. Katal.* **27** 98 (1986)
29. G M Lemman, Candidate Thesis in Chemical Sciences, Moscow Chemical Technology Institute, Moscow, 1974
30. Yu P Kudyukov, V Z Maslosh, I A Popova, E E Neskoredeva, T V Alekseeva *Plast. Massy* (12) 28 (1988)
31. F Pilati, P Manaresi, B Fortunato, A Munari, P Monari *Polymer* **24** 1479 (1983)
32. R Feld, P L Cowe *The Organic Chemistry of Titanium* (London: Butterworths, 1965)
33. K Ioda *Chem. Soc. Jpn., Ind. Chem. Sect.* **74** 1476 (1971)
34. S I Chervina, E G Maksimenko, R S Barshtein *Plast. Massy* (7) 31 (1987)
35. F Pilati, A Munari, P Manaresi, V Bonora *Polymer* **26** 1745 (1985)
36. T N Laricheva, I V Adorova, A Kh Bulai, M I Siling *Proizvodstvo i Pererabotka Plastmass i Sinteticheskikh Smol (Ekspress-Informatsiya)* [Production and Reprocessing, Plastics and Synthetic Resins (Express Information)] (5) 1 (1985)
37. A Radas, H Hall *J. Polym. Sci., Polym. Chem. Ed.* **19** 1021 (1981)
38. F Pilati, P Manaresi, B Fortunato, A Munari, V Passalacqua *Polymer* **22** 1566 (1981)
39. I V Adorova, A E Raver, T N Laricheva, in *Protsessy i Apparaty Proizvodstva Polimernykh Materialov, Metody i Oborudovanie dlya Pererabotki ikh v Izdeliya (Tez. Dokl. Vsesoyuz. Konf.)* (Abstracts of Reports of the All-Union Conference on Processes and Apparatus for Production of Polymer Materials, Methods and Equipment for Their Processing to Products) (Moscow: Moscow Institute of Chemical Machine Building, 1986) Vol. 2, p. 83
40. V Stah, E Poterasu, C Moisa, in *Abstracts of Reports of the Second National Congress on Chemistry, Bucharest, 1981* Vol. 1, Part 1, p. 64
41. M Tanaka, H Iida, H Ikeuchi *J. Soc. Fiber Sci. Technol.* **43** 35 (1987)
42. Yu Tong-yin, Fu Shon-kuan, Ch Chuan-yn, Ch Wei-zhung, Xu Rui-yun *Polymer* **27** 1111 (1986)
43. B Moller, J Blaesch, M Mudrick, G Rafler, H Zimmerman, H Stromeyer *Acta Polymer* **33** 38 (1982)
44. F Pilati, P Manaresi, B Fortunato, A Munari, V Passalacqua, in *IUPAC Macro Mainz [The 26th International Symposium on Macromolecules, 1979 (Short Communication Preprints)]* Vol. 1, p. 231
45. S Suvaram, V Upadhyay, K Phardway *Polym. Bull.* **5** 159 (1981)
46. T Yamada *J. Appl. Polym. Sci.* **37** 1821 (1989)
47. S I Chervina, E G Maksimenko, R S Barshtein, L M Vorob'eva *Kinet. Katal.* **32** 1157 (1991)
48. A Ya Malkin, M I Siling *Vysokomol. Soedin., Ser. A* **33** 2275 (1991)
49. V I Dmitriev *Prikladnaya Teoriya Informatsii* (Applied Information Theory) (Moscow: Vysshaya Shkola, 1989)
50. G I Golodets *Geterogenno-Kataliticheskie Reaktsii s Uchastiem Molekulyarnogo Kisloroda* (Heterogeneous Catalytic Reactions involving Molecular Oxygen) (Kiev: Naukova Dumka, 1977)
51. B C Gates, J R Katzer, G C A Schuit *Chemistry of Catalytic Processes* (New York: McGraw-Hill, 1979)
52. A D Klesov, I V Berezin *Fermentativnyi Kataliz* (Enzymatic Catalysis) Part 1 (Moscow: Izd. Mosk. Gos. Univ., 1980)
53. M L Bender, R J Bergeron, M Komiyama *The Bioorganic Chemistry of Enzymatic Catalysis* (New York: Wiley, 1984)
54. V K Antonov *Khimiya Proteoliza* (Chemistry of Proteolysis) (Moscow: Nauka, 1991)
55. L A Nikolaev *Osnovy Fizicheskoi Khimii Biologicheskikh Protsessov* (Fundamentals of the Physical Chemistry of Biological Processes) (Moscow: Vysshaya Shkola, 1976)
56. G K Borekov *Zh. Vses. Khim. O-va im. D I Mendeleeva* **22** 495 (1977)
57. O M Poltorak, in *Kataliz. Fundamental'nye i Prikladnye Issledovaniya* (Catalysis. Fundamentals and Applied Investigations) (Moscow: Izd. Mosk. Gos. Univ., 1987) p. 7
58. K I Zamaraev *Usp. Khim.* **62** 1051 (1993)
59. I Shihara, W T Schwartz Jr, H W Post *Chem. Rev.* **61** 1 (1961)
60. A A Grinberg *Vvedenie v Khimiyu Kompleksnykh Soedinenii* (Introduction to the Chemistry of Complex Compounds) (Leningrad: Khimiya, 1971)
61. V M Nekipelov, K I Zamaraev *Zh. Strukt. Khim.* **24** 133 (1983)

Design of inorganic compounds with tetrahedral anions

B I Lazoryak

Contents

I. Introduction	287
II. The use of crystal-chemical data for the construction of compounds with specified structures and properties	288
III. Construction of compounds with a new composition	289
IV. The structures and physicochemical properties of the materials	300
V. Conclusion	302

Abstract. The review deals with aspects of the modelling of the compositions and properties of inorganic compounds with tetrahedral anions on the basis of crystal-chemical information. One of the possible algorithms employing crystal-chemical data for the modelling of the compositions, structures, and properties of new compounds is proposed on the basis of the structures of six structural types (glaserite, β - K_2SO_4 , bredigite, palmierite, NASICON, and whitlockite). The likely usefulness of such data for the solution of various problems in materials science is demonstrated. The bibliography includes 208 references.

I. Introduction

Solid state chemistry is the science of chemical phenomena in solid materials observed during their preparation, heat treatment, use, ageing, and regeneration. This branch of chemistry is also concerned with the development of theoretical foundations for the synthesis of solid materials. Progress in many branches of science and engineering is determined by the development of new materials with a set of special properties. The methods of solid state chemistry have been devised to accelerate fundamental research involving the search for and development of new materials.

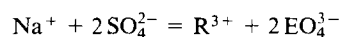
At the present stage of development, solid state chemistry faces a task concerned with the transition from the consideration of individual aspects of the structures, reactivities, and properties of materials with specified structures, properties, and compositions to the determination of the dependences of their properties on structure and the development of procedures for the construction of such materials based on scientific principles. This problem can be partly solved on the basis of crystal-chemical data and the theory of the electronic structure of solids and crystal lattice defects.

The employment of crystal-chemical data is of interest both for fundamental research — the understanding of the relations between the chemical compositions, structures, and properties of

compounds — and for applied studies — the search for new materials with special and practically important properties (phosphors, chemical sensors, superconductors, catalysts, semiconductors, piezo- and ferro-electric materials, solid electrolytes, materials for the storage of information, etc.). The consideration of problems in materials science from the structure–property–composition standpoint makes it possible to achieve the specific syntheses of compounds and materials having specified physicochemical characteristics. However, problems in materials science have hitherto been usually solved by empirical methods. Such an approach retards the development of procedures for the synthesis of compounds possessing a set of predetermined parameters.

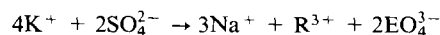
The structures of a large number of inorganic compounds (more than 15000) have now been established. New studies concerned with the determination of the crystal structures of inorganic phases have mainly refined the assignment of a particular compound to a structural type already known. When the chemical composition of a compound becomes more complex, its subcell usually increases or becomes distorted, but the overall order in the alternation of cations and anions remains unchanged.

As an example, we shall consider the ideal structure of the natural mineral glaserite $\text{K}_3\text{Na}(\text{SO}_4)_2$ [space group (sp.gr.) $P\bar{3}m1$, $a = 5.680 \text{ \AA}$, $c = 7.309 \text{ \AA}$].¹ Following substitution in accordance with the scheme



the compounds $\text{K}_3\text{R}(\text{EO}_4)_2$ ($\text{R}^{3+} = \text{rare earth, Y; E}^{5+} = \text{P, As, V}$) with a glaserite-like structure are formed.^{2–4} Depending on the set of cations, different distortions of the ideal structure arise in the crystals — from trigonal in $\text{K}_3\text{R}(\text{PO}_4)_2$ ($\text{R} = \text{Sc, Lu}$)^{5,6} to monoclinic in $\text{R}_3\text{Nd}(\text{PO}_4)_2$.⁷ The characteristic features of such distortions have been discussed in a review.⁸ Here we shall only note that the unit cell in lutetium and scandium compounds increases by a factor of 3 and in neodymium compounds by a factor of 2. A twofold increase in the size of the unit cell has been observed also in $\text{K}_2\text{MR}(\text{PO}_4)_2$ ($\text{M} = \text{Rb, Cs}$).⁹

Within the framework of the β - K_2SO_4 structural type ($Pnam$, $a = 7.456 \text{ \AA}$, $b = 10.08 \text{ \AA}$, $c = 5.776 \text{ \AA}$),¹⁰ substitutions also occur, for example in accordance with the scheme



with formation of the compounds $\text{NaR}(\text{EO}_4)_2$.^{11–15} They are subdivided into nine structural types,¹⁶ each of them characterised by a different volume of the unit cell and a different space group. On passing from the ideal β - K_2SO_4

B I Lazoryak. Chemical Technology Cathedra, Department of Chemistry, M V Lomonosov Moscow State University, Vorob'evy Gory, 119899 Moscow, Russian Federation.
Fax (7-095) 939 21 38.
E-mail: lazoryak@eng.chem.msu.su.

Received 28 July 1995

Uspekhi Khimii 65 (4) 307–325 (1996); translated by A K Grzybowski

structure to structures of the type $\text{Na}_3\text{R}(\text{EO}_4)_2$, the volume of the unit cell increases by a factor of 1–6.¹⁶ For other types of substitution, for example



the size of the unit cell remains unchanged, as in KBaPO_4 ($Pnam$, $a = 7.709 \text{ \AA}$, $b = 5.663 \text{ \AA}$, $c = 9.972 \text{ \AA}$),¹⁷ or increases, as in $\beta\text{-CaNaPO}_4$ ($Pn2_1a$, $a = 20.397 \text{ \AA}$, $b = 5.412 \text{ \AA}$, $c = 9.161 \text{ \AA}$),¹⁸ depending on the radii of the cations forming part of the composition of the compounds.

In the examples quoted, the number of atoms in the subcell does not change and all the cationic sites are fully occupied, but it is possible to quote examples of structures in which some of the cationic sites may be vacant. For example, in the structures of $\text{Ca}_5(\text{PO}_4)_2\text{SiO}_4$,¹⁹ $\text{Cd}_5(\text{PO}_4)_2\text{EO}_4$ ($\text{E} = \text{Ge}, \text{Si}$),²⁰ $\text{NaCd}_4(\text{PO}_4)_3$,²¹ and $\alpha\text{-Ca}_3(\text{EO}_4)_2$,²² which are similar to that of $\beta\text{-K}_2\text{SO}_4$, one of the sites is partly occupied. The vacant sites in the crystal lattice may be occupied by additionally introduced cations and it is then possible to calculate theoretically the limiting compositions of the phases.

The stability of a structure with a partly occupied site (or sites) permits the existence of a lattice with a fully vacant site, i.e. it is possible to 'remove' from the lattice a calculated number of cations at non structure-forming sites and predict the limiting composition of the new phases. Consequently the formation and occupation of vacancies in the crystal lattice make it possible to model new compounds within wide composition ranges.

The arsenates, vanadates, and phosphates having the general formula $\text{M}_3(\text{EO}_4)_2$ ($\text{M} = \text{Sr}, \text{Ba}; \text{E} = \text{As}, \text{V}, \text{P}$)^{24–27} and the molybdates $\text{M}_5\text{R}(\text{MoO}_4)_4$ ($\text{M} = \text{Rb}, \text{K}, \text{R} = \text{rare earth}$)^{28–32} crystallise in the structural type of the natural mineral palmierite $\text{K}_2\text{Pb}(\text{SO}_4)_2$ ($R\bar{3}m$, $a = 5.49 \text{ \AA}$, $c = 20.83 \text{ \AA}$).²³ In most cases, these compounds retain the trigonal palmierite-like unit cell. A decrease of symmetry to monoclinic has been observed for some of them.³¹ We emphasise that, among the numerous palmierite-like structures, there are no representatives with vacancies in the cationic sublattice.

As regards the modelling of new compounds with specified structures and properties, the NASICON (Na Super Ionic Conductor) structural type is of undoubted interest.³³ Compounds having the general formula $\text{A}_x\text{M}_2(\text{EO}_4)_3$, where A is a monovalent or divalent cation (Li^+ , Na^+ , K^+ , Ag^+ , Cu^+ , Ca^{2+} , Sr^{2+} , Ba^{2+} , Cu^{2+}), M is a divalent (Mg), trivalent ($\text{Sc}, \text{V}, \text{In}, \text{Cr}, \text{Fe}$), tetravalent (Ti, Zr), or pentavalent (Nb, Ta) cation, and $\text{E} = \text{Si}, \text{Ge}, \text{P}, \text{or As}$, and $0 \leq x \leq 4$, belong to this structural type.^{34–38} In compounds of this class, the occupation of some of the cationic sites may vary from 1 [$x = 4$, $\text{Na}_4\text{Zr}_2(\text{EO}_4)_3$, $\text{E} = \text{Ge}, \text{Si}$]^{39,40} to 0 [$x = 0$, $\text{Sc}_2(\text{MoO}_4)_3$].⁴¹ Depending on the set of cations, the symmetry of the unit cell varies from trigonal to monoclinic. It is also possible to quote examples of other isostructural classes of compounds with garnet,⁴² perovskite,⁴³ bredigite,⁴⁴ eulythine,⁴⁵ and whitlockite⁴⁶ structures, in which some cations are substituted by others with retention of the overall architecture of the structure.

Many of the phases listed above were initially synthesised and only then assigned to a particular structural type, but most of them could be predicted within the framework of a definite structural type. All the necessary preconditions required for this purpose were in fact available, namely the crystal structures and radii of the cations were known^{47,48} (in the present review the cationic radii quoted by Shannon⁴⁸ are used).

II. The use of crystal-chemical data for the construction of compounds with specified structures and properties

One example of the use of crystal-chemical data for the preparation of compounds in which the metal atoms would be in an unusual valence state is the synthesis of the $\text{La}_2\text{LiFeO}_6$ oxide phase containing Fe(V) cations.⁴⁹ The synthesis of this

compound became possible by the creation of the necessary structural preconditions promoting the existence of the $t_{2g}^3e_g^0$ electronic configuration of the iron atoms. Demazeau et al.⁴⁹ stabilised the 'unusual' iron(V) valence state by introducing lithium cations, which strengthen the $\text{Fe}-\text{O}$ bond by means of the six weakly competing $\text{Li}-\text{O}$ bonds in the octahedron of the perovskite structural type.

Another example is the synthesis of the K_2NaPdF_6 fluoride phase.⁵⁰ The authors stabilised the palladium (III) ion in the $t_{2g}^6e_g^1$ electronic configuration, which is intermediate between the stable $t_{2g}^6e_g^0$ [Pd(IV)] and $t_{2g}^5e_g^2$ [Pd(II)] configurations, by the deformation of the elpasolite (K_2NaAlF_6) structural type. In the K_2NaPdF_6 lattice, the [PdF_6] octahedra are extended compared with the [AlF_6] octahedra, which also promotes stabilisation of the $t_{2g}^6e_g^1$ state.

After the discovery by Bednorz and Muller⁵¹ of high-temperature superconductivity (HTSC) in the compounds $\text{La}_{2-x}\text{Ba}_x\text{CuO}_4$ with a perovskite-like structure, crystal-chemical data became the basis of the search for subsequent generations of materials with higher critical temperatures (T_c) of the transition to the superconducting state. The structures of the superconducting phases have been examined in detail in a number of reviews.^{52–54} By selecting the ionic radii and the oxidation states of the cations within the framework of the perovskite structural type, the copper-containing superconducting oxide materials $\text{Bi}_2\text{Sr}_2\text{Ca}_{n-1}\text{Cu}_n\text{O}_{2n+4}$,^{55,56} $\text{Ti}_2\text{Ba}_2\text{Ca}_{n-1}\text{Cu}_n\text{O}_{2n+4+\delta}$,^{57,58} $\text{Pb}_2\text{Sr}_2\text{R}_x\text{Cu}_3\text{O}_{8+\delta}$ ($\text{R} = \text{rare earth}, \text{Y}; \text{M} = \text{Ca}, \text{Sr}$),⁵⁹ and $\text{HgBa}_2\text{CuO}_{4+\delta}$ (see Ref. 60) were in fact synthesised. The conductivity in these phases is ensured by the two-dimensional (CuO_2) layers.

Many superconducting compounds have the composition $\text{A}_m\text{M}_2\text{R}_{n-1}\text{Cu}_n\text{O}_x$, where $\text{A} = \text{Bi}, \text{Ti}, \text{Pb}, \text{or Hg}$, $\text{M} = \text{Ba or Sr}$, $\text{R} = \text{Ca or rare earth}$, and $m = 1$ or 2 . They are made up of (AO), (MO), (BO), and (CuO_2) layers alternating along the c axis of the unit cell. An increase in the number of (CuO_2) layers in one block of the structure (usually to three) leads to an increase in the critical temperature T_c . The problem of the synthesis of multilayered structures of the 'puff pastry' type arose in this connection. This can be achieved by means of a layer-by-layer arrangement of the 'dielectric' blocks and CuO_2 layers. However, a necessary condition for the formation of such structures is that the distances in different layers are commensurate. This is particularly important for the (CuO_2) and (MO) layers, where the ratio $d_{\text{M-O}}:d_{\text{Cu-O}}$ must be approximately equal to $\sqrt{2}$.⁷⁴ In the layered HTSC cuprates, where the distance $d_{\text{Cu-O}}$ varies from 1.9 to 1.98 \AA , the distance $d_{\text{M-O}}$ should be 2.69–2.80 \AA , i.e. the cations M may be Ba^{2+} , Sr^{2+} , and La^{3+} . Such crystal-chemical preconditions served as a basis for the construction of the mercury-containing compounds $\text{HgBaRCu}_2\text{O}_{6+\delta}$ ($\text{R} = \text{rare earth}$)⁶¹ and of superconductors of a new class⁶⁰ with the record-breaking critical temperatures $T_c = 135\text{--}164 \text{ K}$.

The dimensions of the polyhedra in the structure make it possible to predict the positions of the cations in the lattice and their mobilities. Thus, in the case of superionic conductors with the NASICON structure,^{33,62–64} it is possible to show on the basis of structural information that decrease in the size of the structure-forming cation (M) hinders the migration of the mobile sodium ions within the channels of the structural framework. The corresponding weakening of ionic conductivity has been observed experimentally on passing from $\text{Na}_3\text{Zr}_2(\text{SiO}_4)_2\text{PO}_4$ ($\sigma_{300^\circ\text{C}} = 0.2 \Omega^{-1} \text{ cm}^{-1}$)^{33,62} to $\text{Na}_3\text{MgZr}(\text{PO}_4)_3$ ($\sigma_{300^\circ\text{C}} = 0.16 \Omega^{-1} \text{ cm}^{-1}$) and $\text{Na}_3\text{MnZr}(\text{PO}_4)_3$ ($\sigma_{300^\circ\text{C}} = 5.5 \times 10^{-4} \Omega^{-1} \text{ cm}^{-1}$).³⁸ The radii of the structure-forming cations with $\text{CN} = 6(r_{\text{VI}})$ are 0.72 \AA for Zr^{4+} , 0.83 \AA for Mn^{2+} , and 0.72 \AA for Mg^{2+} . On substitution of the tetravalent cation by a divalent one, the channels within the structure decrease with a corresponding diminution of conductivity. An analogous increase in conductivity is observed in $\text{Na}_3\text{M}_2(\text{PO}_4)_3$ on increase in the radius of the cation M .

Cation	$r_{VI}/\text{\AA}$	$\sigma_{570} \text{ } ^\circ\text{C}/\Omega^{-1} \text{ cm}^{-1}$	Ref.
Cr^{3+}	0.615	7.8×10^{-3}	65
Fe^{3+}	0.645	9.8×10^{-3}	65
Sc^{3+}	0.745	5.0×10^{-2}	66

It follows from the examples presented that information about the dimensions of the channels makes it possible to alter deliberately the conductivity in structures of the NASICON type. Thus the analysis of vacancies made it possible to discover channels in which the sodium cations migrated from their narrowest sites.^{67–69} Later a similar scheme was also proposed in other investigations.^{70–72}

A structure of the NASICON type has a high capacity in relation to metal cations. This promotes the formation of a large number of compounds of this structural type having different compositions but identical structures. In the lattice of the NASICON type with the crystal-chemical formula $A'M_2(EO)_4$ ($E = \text{P, As, Si, Ge}$), heterovalent and isovalent substitutions can be carried out at the A' , A , M , and E sites. The occupations of the A' and A sites may vary from 1 [in $\text{Na}_4\text{Zr}_2(\text{EO}_4)_3$]^{39, 40} to 0 [in $\text{Sc}_2(\text{MoO}_4)_3$].⁴¹ Monovalent [Li, Na, K, Cu ; $A'M_2(\text{PO}_4)_3$],^{35–38, 73–78} divalent [Ca, Sr, Ba, Cu ; $A_{0.5}M_2(\text{PO}_4)_3$],^{79–82} and trivalent [Ln ; $A_{1/3}M_2(\text{PO}_4)_3$]⁸³ cations can enter these positions. Tetravalent ($\text{Zr, Hf, Ti, Ge, Sn}$)^{39, 40, 74–86} and trivalent [$\text{Sc, Cr, Fe, Ga, V, In}$; $A_1M(\text{PO}_4)_3$]^{65, 67, 68, 80, 87–89} cations can enter the M positions. These positions can also be occupied by cations with different valences, for example divalent and trivalent [$M^{II} = \text{Mg, Zn}$; $M^{III} = \text{Sc, Cr}$; $\text{Na}_{2x}M_{2x}\text{Sc}_{2-2x}(\text{PO}_4)_3$, $\text{Na}_{3+x}\text{Cr}_{2-x}\text{Mg}_x(\text{PO}_4)_3$],^{37, 90} trivalent and tetravalent [$M^{III} = \text{Cr, Fe, Ga, In, Ti}$; $M^{IV} = \text{Ti, Zr}$; $A^{II}M^{III}M^{IV}(\text{PO}_4)_3$],^{79, 80} as well as tetravalent and pentavalent [$\text{Nb}^V\text{Ti}^{IV}(\text{PO}_4)_3$ and $\text{Nb}^V\text{Nb}^{IV}(\text{PO}_4)_3$]^{34, 91} cations. The compositions of the compounds listed above have been modelled on the basis of crystal-chemical data. The introduction of cations with different sizes and in different oxidation states influences appreciably the mobility of the type A cations in the three-dimensional cavity framework.^{65, 66, 92} The latter fact is important for the preparation of solid electrolytes with specified electrophysical characteristics.

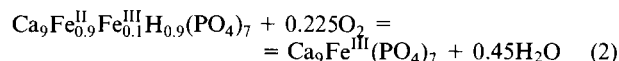
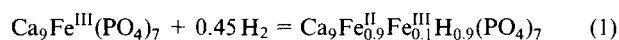
The ability of the $\{[M_2(\text{EO}_4)]^p\}_{3\infty}$ framework to retain the cations of one element in different oxidation states at an A site (for example Cu^+ (see Refs 93–95) and Cu^{2+} (see Ref. 82)) promotes the occurrence of reversible redox reactions ($\text{Cu}^{2+} + e \rightleftharpoons \text{Cu}^+$),⁹⁶ which is a precondition for the application of these materials as catalysts, for example in the dehydrogenation of butanol.⁹⁷

Yet another example of the synthesis of compounds with a specified structure by means of isovalent substitution based on crystal-chemical data is the synthesis of the compounds $M_2M'R(\text{PO}_4)_2$ having structures analogous to that of glaserite with $M-M'$ combinations: potassium–rubidium, potassium–cesium, and rubidium–cesium.^{6, 9, 98} In conformity with the crystal-chemical formula of the glaserite-like structure $X^{[12]}Y_2^{[10]}M^{[6]}(\text{EO}_4)_2$, the chemical composition of the compounds was chosen in such a way that the number of alkali metal cations with a larger radius is two times smaller than that of the alkali metal cations with a smaller radius. This relation was established on the basis of the number of $X^{[12]}$ and $2Y^{[10]}$ sites in the glaserite type structure.¹ According to the results of structural analysis, the alkali metal cation with the larger radius in the glaserite-type structure occupies the more capacious $X^{[12]}$ site. Depending on the set of alkali metal cations, different types of distortions of the glaserite structure occur in the compounds under discussion.

Analysis of the dimensions of the polyhedra and of their number in the $\beta\text{-Ca}_3(\text{PO}_4)_2$ structure,⁹⁹ which belongs to the structural type of the mineral whitlockite $\text{Ca}_{18.19}\text{Mg}_{1.17}\text{Fe}_{0.83}\text{H}_{1.62}(\text{PO}_4)_{14}$,⁴⁶ made it possible to model the new compounds $\text{Ca}_9(\text{PO}_4)_7$ ($R^{3+} = \text{Ln, Y, Bi, Sc, Cr, Fe, In}$),^{100–103}

$\text{Ca}_{10}\text{M}(\text{PO}_4)_7$ ($M = \text{Li, Na, K, Cu}$),^{104, 105} and $\text{Ca}_9\text{MgM}(\text{PO}_4)_7$ ($M = \text{Li, Na, K}$)¹⁰⁶ and to predict a wide region corresponding to the ternary phosphates in the $\text{Ca}_3(\text{PO}_4)_2\text{--RPO}_4\text{--M}_3\text{PO}_4$ systems.¹⁰⁷ Cations with different dimensions and oxidation states (from +1 to +4) form part of the composition of the whitlockite-type crystal lattice.

Analysis of whitlockite like structures made it possible to predict the occurrence of reversible redox reactions. Such reactions proceed without the destruction of the crystal lattice but with a change in the oxidation state of the transition metal cation. The reduction reaction is accompanied by the incorporation of a proton in the crystal lattice, while the oxidation reaction involves its elimination.^{108–110} The corresponding reactions proceed in accordance with the following schemes:



The materials in the crystal lattice of which reversible redox reactions take place may be used as catalysts,^{111–115} intermediates for the two-stage oxidation of hydrogen,^{116, 117} and sensors.¹¹⁸

Crystal chemistry makes it possible to interpret successfully and to predict the formation of different phases in oxide systems exhibiting a complex polymorphism. Such compounds have valuable practical properties (luminescent, magnetic, ferro-elastic, piezo- and ferro-electric, and catalytic), which are often successfully combined in a single material. The properties of such complex systems cannot be always predicted, but the use of crystal-chemical data makes it possible to solve successfully certain controversial problems.¹¹⁹

The $\text{Ca}_3(\text{PO}_4)_2\text{--Ca}_2\text{SiO}_4$ system is important in the processing of natural phosphate raw material and in the metallurgy of converter slags. The experimental data obtained by different authors^{120–124} concerning the regions of existence of individual phases in the system are extremely contradictory and it has been possible to interpret them correctly only by employing data on the structures of the individual phases of the system.¹²⁵ Furthermore, crystal-chemical data made it possible to justify on a scientific basis the use of various additives in the formation of a charge for the preparation of phosphate fertilisers with the maximum solubility in 2% citric acid solution^{110, 125–130} and hence to avoid additional studies concerning the search for the optimum charge composition.

The examples quoted demonstrate that crystal-chemical data can be used effectively for the prediction of the compositions of new compounds with specified physicochemical properties.

III. Construction of compounds with a new composition

In the modelling of new phases on the basis of crystal-chemical data, analysis of the dimensions of the occupied and vacant polyhedra and of their number is important in the first stage. The outcome of such analysis is the crystal-chemical formula of an individual structure or structural type on the basis of which the composition of the possible phases may be predicted by means of iso- or hetero-valent substitutions, taking into account the formal valences and dimensions of the cations. In addition, the dimensions of the ions and polyhedra in this structure make it possible to predict the positions of the atoms in the lattices.

The characteristic features of the structures of a series of structural types with tetrahedral anions, which will be used for the modelling of the compositions of compounds with specified structures and properties, are discussed below. The generalised data, obtained as a result of such analysis, provide an algorithm for the modelling of new compounds and their properties.

1. The glaserite $K_3Na(SO_4)_2$ structural type

The glaserite structural type is common among inorganic salts with tetrahedral anions. Two types of columns directed along the $\bar{3}$ axis are differentiated in the glaserite crystal lattice (Figs 1 and 2): cationic (C) and mixed cationic-anionic (A). The A column is made up of alternating (EO_4) tetrahedra and YO_{10} polyhedra: $\dots - YO_{10} - EO_4 - YO_{10} - \dots$ (Fig. 1). The cation in the Y position is surrounded by ten oxygen atoms: four of these are close (three belong to the face of a single tetrahedron, the fourth apical oxygen — on the $\bar{3}$ axis — belongs to another tetrahedron), while six are remote (the edges of three tetrahedra are disposed along the equator) (Fig. 3b). The coordination number of this site can be formulated as $Y^{[4+6]}$.

The C columns in the glaserite-like structures are made up of octahedra and dodecahedra: $\dots - MO_6 - XO_{12} - MO_6 - \dots$. The atom at the M site is surrounded by six oxygen atoms (one atom each from the six tetrahedra) and its coordination number can be formulated as $M^{[6]}$ (Fig. 3d). The atom at the X site is surrounded by six nearest oxygen atoms (one oxygen atom each from the six tetrahedra) and six more remote apical oxygen atoms and its coordination number can be specified as $X^{[6+6]}$ (Fig. 3a). The crystal-chemical formula for glaserite-like structures can be written as $X^{[6+6]}Y_2^{[4+6]}M^{[6]}(EO_4)_2$. The cations K^+ in the $K_3Na(SO_4)_2$ structure occupy the large $X^{[6+6]}$

and $Y^{[4+6]}$ polyhedra, whilst the cations Na occupy the $M^{[6]}$ polyhedra.

The two neighbouring cationic-anionic type A columns in the glaserite-like structures have different orientations of the EO_4 tetrahedra along the $\bar{3}$ axis [with the apical oxygen atoms pointing downwards or upwards (Fig. 1)]. Each type C column is surrounded by three type A columns, in which the tetrahedra are oriented in such a way that the apical oxygen atoms are directed downwards, and by three columns with tetrahedra in which the apical oxygen atoms are directed upwards (Fig. 2). The greatest amount of information about the positions of the tetrahedra and the cations is contained in the projection of the glaserite-like structure on to the $(1\bar{1}1)$ plane. Henceforth we shall compare layers which are arranged around this plane. The glaserite structure can be constructed from such layers, two neighbouring layers being displaced relative to one another by $1/2$ of a translation along the c axis, while two neighbouring A columns in the layer have the opposite orientations of the tetrahedra (Fig. 1).

It follows from the analysis of the surroundings of the $X^{[12]}$, $Y^{[10]}$, and $M^{[6]}$ sites that in a glaserite-like structure¹ with the composition $M_3M'(EO_4)_2$ there are three large polyhedra ($X^{[12]} + 2Y^{[10]}$) and one small polyhedron ($M^{[6]}$). This structural type is characteristic of salts in which the large cation:small cation ratio is 3:1. This ratio as well as the dimensions of the cations

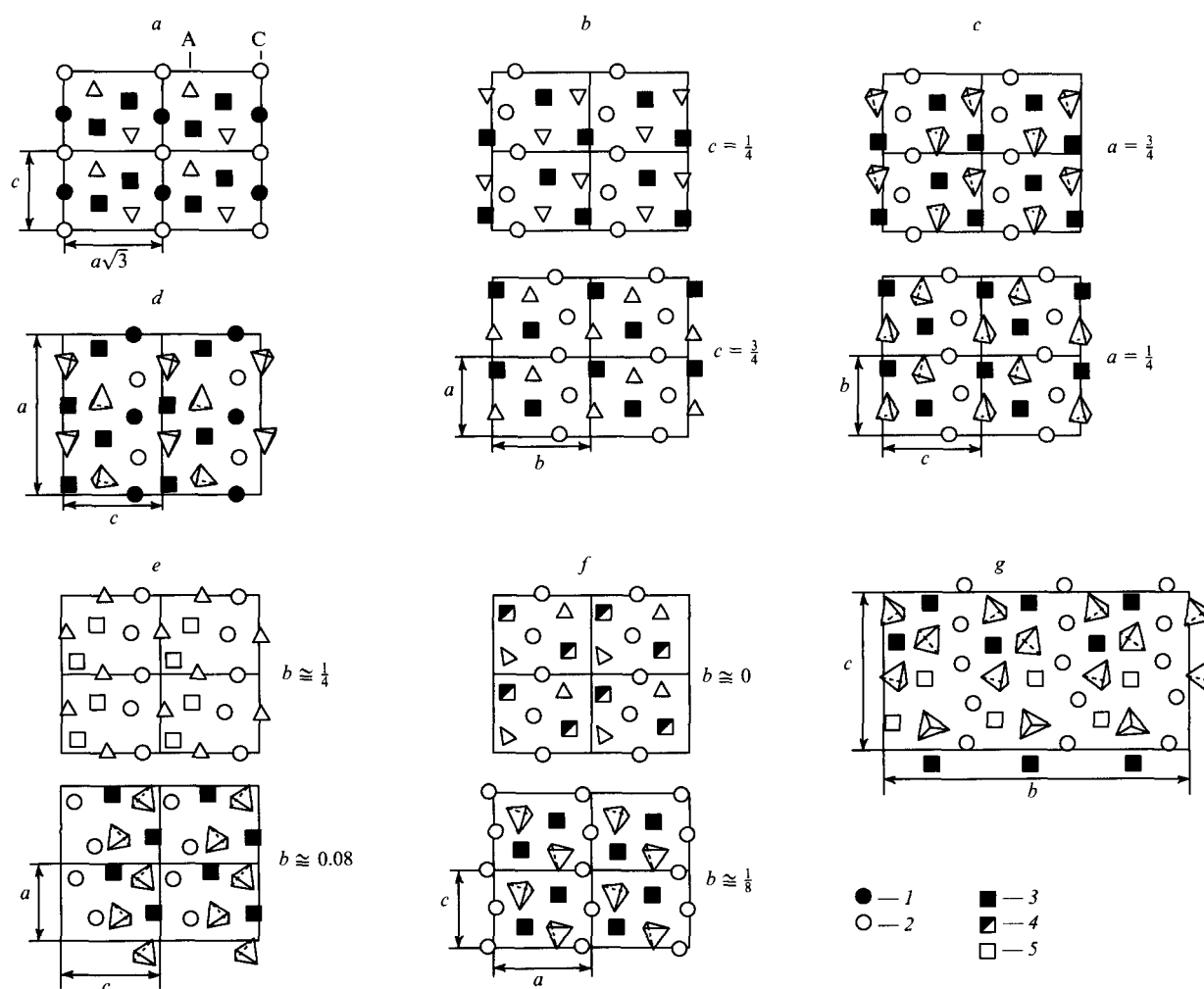


Figure 1. The layers in the $K_3Na(SO_4)_2$ and $\beta-K_2SO_4$ structural types.

(a) $K_3Na(SO_4)_2$; (b) $\beta-K_2SO_4$; (c) $\beta-Ca_2SiO_4$; (d) $Ca_3Mg(SiO_4)_2$; (e) $Ca_5(PO_4)_2SiO_4$; (f) $6Ca_2SiO_4 \cdot Ca_3(PO_4)_2$; (g) $\alpha-Ca_3(PO_4)_2$.

Sites: (1) $M = Na^+$ or Mg^{2+} cations; (2) $X = Ca^{2+}$ or K^+ cations; (3) and (4) $Y = Ca^{2+}$ or K^+ cations.

(3) fully occupied site; (4) half-occupied site; (5) vacancy. The unit cells are differentiated. The triangles and tetrahedra represent anions.¹²⁵

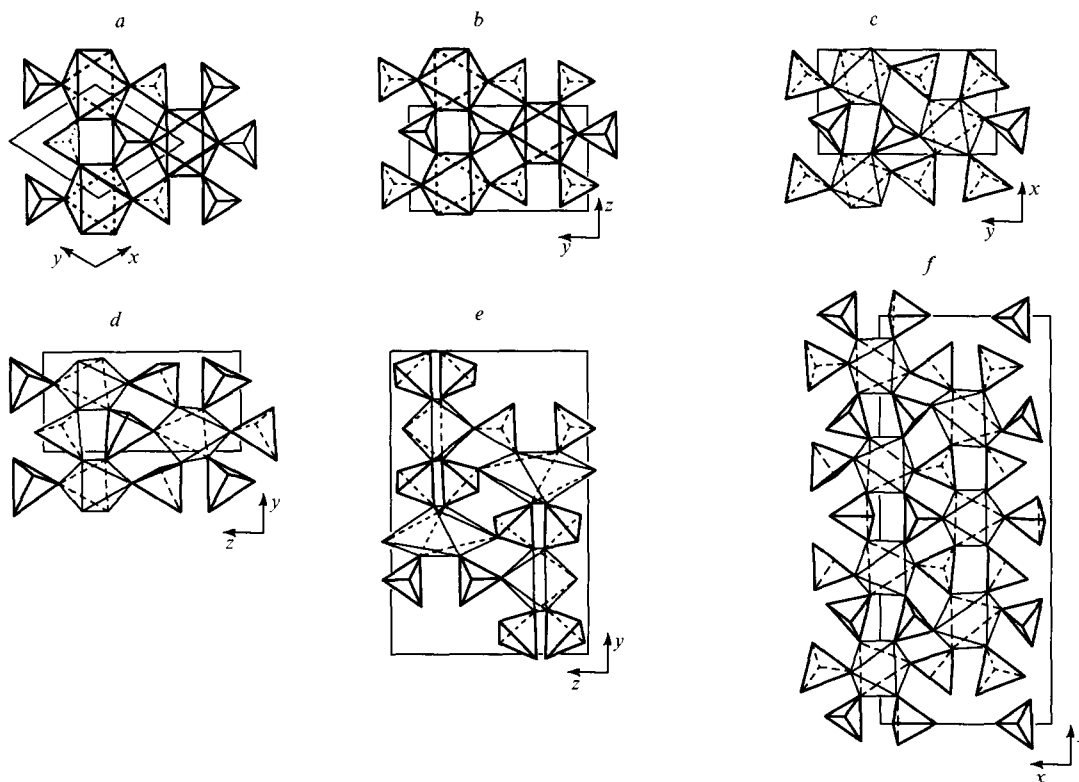


Figure 2. The alteration of polyhedra in the $K_3Na(SO_4)_2$ and $\beta-K_2SO_4$ structural types.

(a) $K_3Na(SO_4)_2$; (b) $\beta-K_2SO_4$; (c) $\beta-Ca_2SiO_4$; (d) $Ca_3Mg(SiO_4)_2$; (e) $Ca_5(PO_4)_2SiO_4$; (f) $6Ca_2SiO_4 \cdot Ca_3(PO_4)_2$. The unit cells are differentiated.¹²⁵

are of fundamental importance in the formation of a glaserite-like structure. If the $K_3Na(SO_4)_2$ structure is adopted as a basis, then the difference Δr between the radii of potassium [$r_{XII}(K) = 1.64 \text{ \AA}$] and sodium [$r_{VI}(Na) = 1.02 \text{ \AA}$] is approximately 0.6 \AA . In this case, an ideal arrangement is achieved. When this difference is altered (a set of other cations is adopted), the structure is distorted (Table 1). It may be metastable ($\Delta r = 0$) when the radii of the cations at the X, Y, and M sites are identical, as happens, for example, in $\alpha-Ca_2SiO_4$ (see Ref. 131) and $\alpha'-Ca_3(PO_4)_2$.¹³² These two phases crystallise in the glaserite-like structural type and exist only at high temperatures. Under the usual conditions, they crystallise in the $\beta-K_2SO_4$ structural type,¹⁰ which will be described below.

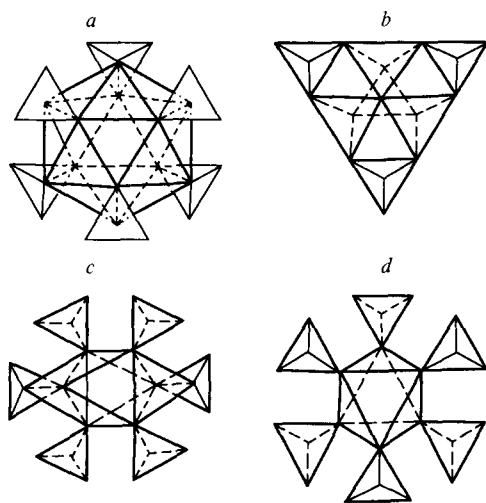


Figure 3. The $X^{[6+6]}$ (a), $Y^{[4+6]}$ (b), $X^{[6+3]}$ (c), and $M^{[6]}$ (d) polyhedra in the glaserite, palmierite, and $\beta-K_2SO_4$ structural types.¹¹⁰

With increase in the difference Δr , the symmetry of the cell may be reduced to monoclinic,² as happens, for example, in $Rb_3Sc(PO_4)_2$ [$r_{XII}(Rb^+) = 1.72 \text{ \AA}$, $r_{IX}(Sc^{3+}) = 0.745 \text{ \AA}$]. In this case, Δr has the maximum value of 0.97 \AA among those known for glaserite-like phases. The minimum value $\Delta r = 0.59 \text{ \AA}$ is observed for $BaNaPO_4$.¹³⁴ In the $Ca_3Mg(SiO_4)_2$ (merwinite) crystal lattice,¹³³ the positions of the tetrahedra are the same, apart from small rotations, as in the glaserite-like structure (Fig. 1). The Mg^{2+} cations occupy the M site, while the Ca^{2+} cations occupy the X and Y sites. Thus the partial replacement of Ca^{2+} by Mg^{2+} in calcium α -silicate leads to the formation of a stable glaserite-like structure.

The glaserite structural type is stable for compounds in which the difference between the radii of the cations occupying the M and X(Y) sites is in the range $0.59 \leq \Delta r \leq 0.89 \text{ \AA}$. With decrease in this difference, metastable glaserite-like structures or compounds crystallising in the $\beta-K_2SO_4$ structural type are formed.¹⁰ The upper limit can apparently reach 0.98 \AA . However, these data are unreliable, since the $Rb_3Sc(PO_4)_2$ structure, for which $\Delta r = 0.98 \text{ \AA}$, has not been investigated. In the case of cations with a small radius, characterised by an octahedral environment, the above difference Δr gives rise to the formation of the glaserite structural type. With increase in its radius, the small cation tends to increase the size of its coordination polyhedron and hence to alter the structural type. This conclusion can be well illustrated for compounds of the $K_3R(PO_4)_2$ series. Thus $K_3Lu(PO_4)_2$ (see Ref. 5) belongs to the glaserite structural type, whilst $K_3Nd(PO_4)_2$ (see Ref. 7) belongs to the $\beta-K_2SO_4$ structural type. According to Kalinin's data,² the glaserite structural type is stable for compounds with $R = Gd - Lu$.

It follows from the analysis of the distances in the polyhedra of the glaserite-like phases that the large cation:small cation ratio may also be 1:1. Thus a small cation, for example, sodium can also enter the $X^{[6+6]}$ position. Such a position of sodium (at the X and M sites) has been found in the crystal structures of $KNaSO_4$ (see Ref. 1) and $BaNaPO_4$.¹³⁴ Compounds with a

Table 1. X-Ray diffraction characteristics of certain glaserite-like phases.

Compound	<i>a</i> / Å	<i>b</i> / Å	<i>c</i> / Å	β / °	Space group	Δ <i>r</i> / Å	Ref.
K ₃ Na(SO ₄) ₂ ^a	5.68	5.68	7.305		<i>P</i> $\bar{3}$ <i>m</i> 1	0.62	1
α-Ca ₂ SiO ₄	5.529	5.529	7.311		<i>P</i> $\bar{3}$ <i>m</i> 1	0.0	131
Ca ₃ Mg(SiO ₄) ₂ ^a	13.254	5.293	9.328	91.90	<i>P</i> 2 ₁ / <i>a</i>	0.62	133
K ₃ Sc(PO ₄) ₂ ^a	9.430	9.430	7.629		<i>P</i> $\bar{3}$ <i>m</i> 1	0.89	6
K ₃ Lu(PO ₄) ₂ ^a	9.601	9.601	7.725		<i>P</i> $\bar{3}$ <i>m</i> 1	0.78	5
Rb ₃ Sc(PO ₄) ₂	10.51	10.07	9.813	104.6	—	0.97	2
Rb ₃ Gd(PO ₄) ₂	19.53	34.45	7.725	90.8	—	0.70	2
Rb ₃ Ho(PO ₄) ₂	9.879	9.879	8.118		<i>P</i> $\bar{3}$ <i>m</i> 1	0.70	2
KNaSO ₄ ^a	5.607	5.607	7.177		<i>P</i> $\bar{3}$ <i>m</i> 1	0.62	1
BaNaPO ₄ ^a	5.622	5.622	7.259		<i>P</i> $\bar{3}$ <i>m</i> 1	0.59	134

^a The crystal structure has been determined.

similar composition have been found among tungstates and molybdates, for example MR(EO₄)₂ with M^I = K or Rb and R^{III} = Al, Sc, Fe, Cr, or In.¹³⁵ Thus the formation of the crystal lattice in the structural type under discussion depends both on the ratio of the radii of the cations and on their number.

Having at one's disposal data on the structure of K₃Na(SO₄)₂ and knowing the radii of the cations, it is possible to predict the compositions of a series of compounds which may crystallise in the glaserite structural type. Thus, the substitution of SO₄²⁻ by MoO₄²⁻, EO₄³⁻ (E = P, V, As), and EO₄⁴⁻ (E = Si, Ge) and the selection of the corresponding cations in order to maintain electroneutrality may be expected to result in the formation of the compounds M₃Na(MoO₄)₂, M₃R(EO₄)₂ (M' = K, Rb; R = Ln, Y, Sc; E = P, V, As), M₃M(SiO₄)₂ (M' = Ba, Sr, Pb; M = Mg, Cu) and BaCa₂Mg(SiO₄)₂. Some of them have been described above. The characteristic features of the structures and the physicochemical properties of some of the glaserite-like phases have been described in detail.^{2-6, 8, 9, 79, 135}

2. The β-K₂SO₄ structural type

The β-K₂SO₄ structure is made up of cationic (C) and anionic (A) columns (Fig. 1)¹⁰ similar to the columns in the glaserite structure. In the type A column (...-EO₄-YO₁₀-EO₄-...), the coordination polyhedra are retained, whilst in the type C column (...-XO₉-XO₉-...) they are changed.

The cationic column in β-K₂SO₄ (see Ref. 10) is surrounded by four type A columns with a single orientation of the tetrahedron and by two such columns with a different orientation (Fig. 2). This results in the formation of a structure in which layers with a single orientation of the tetrahedra alternate with layers having tetrahedra with the opposite orientation (Fig. 1). In contrast to glaserite, in the structure of which two neighbouring tetrahedra from two type A columns always have the opposite orientations, in the β-K₂SO₄ structure the two neighbouring tetrahedra can have both identical or opposite orientations of the tetrahedra along the *c* axis of the unit cell (Fig. 1), i.e. on passing from glaserite to β-K₂SO₄ the orientation of some of the tetrahedra is reversed. As a result of the rotation of the tetrahedra, the unit cell symmetry is reduced from trigonal to orthorhombic, while the environment of the Y site in the A column is retained (Fig. 3*b*). The rotation of the tetrahedra in no way affects the positions of the E and Y sites on the threefold 'pseudoaxis', while the X site is displaced from this 'pseudoaxis'. The coordination numbers of the X and M sites in the C column are changed. These sites in the β-K₂SO₄ structure become equivalent and the immediate octahedral (as in glaserite) arrangement of the surrounding oxygen atoms from six tetrahedra is retained for these sites. When account is taken of the three more remote apical oxygen atoms, the coordination number of these sites (X and M) becomes nine — X^[6+3] (Fig. 3*c*). The crystal-chemical formula of the β-K₂SO₄ structural type is X^[6+3]Y^[4+6]EO₄.

It follows from the analysis of the X—O and Y—O distances in the XO₉ and YO₁₀ polyhedra that the β-K₂SO₄ structural type is more stable for cations with similar radii. Iso- and hetero-valent substitutions in the cationic and anionic sublattices of the β-K₂SO₄ structure may lead to compounds having different compositions. After the substitution of SO₄²⁻ by EO₄²⁻ (E^{VI} = Mo, W), EO₄³⁻ (E^V = P, V, As), and EO₄⁴⁻ (E = Si, Ge), it is necessary to select cations such that the ratio of their radii differs little from unity (Table 2). The formation of the β-K₂SO₄ structural type is promoted by cations tending to achieve an octahedral environment. The latter is associated with the fact that the X site in the most immediate environment must have six oxygen atoms (a distorted octahedron) and the long X—O distances in this octahedron promote the incorporation in the latter of cations with a radius greater than 0.9 Å.

β-Ca₂SiO₄ is constructed similarly to β-K₂SO₄.¹³⁶ The substitution of potassium by calcium and of SO₄²⁻ by SiO₄⁴⁻ is accompanied by a monoclinic distortion of the ideal β-K₂SO₄ structure. As can be seen from Fig. 2, on passing from β-K₂SO₄ to β-Ca₂SiO₄, the tetrahedra rotate and the reflection plane disappears. Owing to the rotation of the tetrahedra, eight oxygen atoms (one each from the six tetrahedra and two apical oxygen atoms) located at a distance of 2.36–2.80 Å, and a further one oxygen atom, separated by a distance of 3.25 Å, enter the first coordination spheres of the Ca²⁺ ions occupying the X sites. The coordination number of this site can be formulated as X^[8+1]. Furthermore, the rotation of the tetrahedra alters the immediate environment of the metal atom at the Y site: six oxygen atoms are accommodated in the first coordination sphere at distances of 2.30–2.75 Å, whilst the other four oxygen atoms, which build up the Y polyhedron to a decahedron, form the second coordination sphere with distances *d*_{Y-O} = 2.98–3.30 Å. The rotations of the tetrahedra also bring the two apical oxygen atoms closer to the Y site (*d*_{Ca-O} = 3.48 and 3.56 Å). In β-K₂SO₄ they are separated by more than 4 Å. The coordination polyhedron of the Ca²⁺ cations at the Y site in the β-Ca₂SiO₄ structure can be formulated as Y^[6+4+2], whereupon the crystal-chemical formula assumes the form X^[8+1]Y^[6+4+2]EO₄. The idealised formula is X^[9]Y^[10]EO₄, as in the β-K₂SO₄ structure. The layers in the two structures are similar (Fig. 1).

The γ-, β-, α_L-, α_H- and α-polymorphic modifications have been observed for Ca₂SiO₄.¹³⁷ The characteristic features of the structures of the polymorphic calcium orthosilicate modifications have been described in detail.^{131, 138, 139} The α_H-Ca₂SiO₄ phase is isostructural with α'-Sr₂SiO₃¹³⁹ and α'-Sr_{1.9}Ba_{0.1}SiO₄.¹⁴⁰ and has a structure of the undistorted β-K₂SO₄ type. The α_L-Ca₂SiO₄ structure is intermediate between β-Ca₂SiO₄ and β-K₂SO₄ and is apparently constructed similarly to the calcium silicophosphate 6Ca₂SiO₄·Ca₃(PO₄)₂ with partially ordered layers.¹⁴¹ The α_H-Ca₂SiO₄ structure is similar to the undistorted β-K₂SO₄ structure. According to

Table 2. X-Ray diffraction characteristics of certain phases based on the β -K₂SO₄ structure.

Compound	<i>a</i> /Å	<i>b</i> /Å	<i>c</i> /Å	β /°	Space group	Δr /Å	Ref.
β -K ₂ SO ₄ ^a	7.456	10.08	5.776		<i>Pnam</i>	0	10
β -Ca ₂ SiO ₄ ^a	5.502	6.745	9.297	94.59	<i>P2₁/n</i>	0	136
β -Sr ₂ SiO ₄ ^a	5.663	7.084	9.767	92.67	<i>P2₁/n</i>	0	140
α'_L -Ca ₂ SiO ₄	11.18	18.92	6.832		<i>Pmcn</i>	0	131
α'_H -Ca ₂ SiO ₄	5.63	9.52	6.85		<i>Pmcn</i>	0	139
α' -Sr ₂ SiO ₄	5.682	7.09	9.773		<i>Pmnb</i>	0	131
α' -Sr _{1.9} Ba _{0.1} SiO ₄ ^a	5.674	7.08	9.745		<i>Pmnb</i>	0	140
6Ca ₂ SiO ₄ ·Ca ₃ (PO ₄) ₂ ^a	9.40	21.71	6.83		<i>Pnm2₁</i>	0	141
Ca ₅ (PO ₄) ₂ SiO ₄ ^a	6.737	15.508	10.132		<i>Pnma</i>	0	19
α -Ca ₃ (PO ₄) ₂ ^a	12.887	27.280	15.219	126.2	<i>P2₁/a</i>	0	22
β -K ₂ PO ₃ F ^a	7.543	10.16	5.933		<i>Pnam</i>	0	10
Cd ₄ Na(PO ₄) ₃ ^a	6.67	15.10	10.04		<i>Pnam</i>	0.05	21
Cd ₅ (PO ₄) ₂ SiO ₄ ^a	6.692	14.99	10.140		<i>Pnam</i>	0	20
Cd ₅ (PO ₄) ₂ GeO ₄ ^a	6.734	15.107	10.210		<i>Pnam</i>	0	20
KBaPO ₄ ^a	7.709	5.663	9.972		<i>Pnam</i>	0.06	17
β -CaNa(PO ₄) ₂ ^a	20.397	5.412	9.161		<i>Pn2₁a</i>	0.16	18
Na ₃ La(VO ₄) ₂ ^a	5.582	14.240	19.42		<i>Pbc2₁</i>	0.196	11
Na ₃ Nd(PO ₄) ₂ ^a	15.874	13.952	18.470		<i>Pbc2₁</i>	0.143	13
Na ₃ Er(VO ₄) ₂ ^a	5.490	9.739	7.215	93.1	<i>P2₁/n</i>	0.04	14
K ₃ Nd(PO ₄) ₂ ^a	9.532	5.631	14.22	90.95	<i>P2₁/m</i>	0.387	7
Na ₃ Nd(VO ₄) ₂ ^a	29.14	5.574	14.22	91.4	<i>Cc</i>	0.143	12

^a The crystal structure has been determined.

Kozak et al.¹³¹ the $\alpha'_H \rightarrow \alpha$ polymorphic transition can occur as a result of the jump of the 'small' Si⁴⁺ cation from its tetrahedron to a neighbouring vacant tetrahedron, which ultimately appears as rotation of the tetrahedra. As a result of such a jump, the structure of α -Ca₂SiO₄ corresponds to that of the ideal glaserite. The cationic positions are fully occupied in the crystal lattices of all the polymorphic modifications of calcium silicates.

In the β -K₂SO₄ structural type, substitutions in both cationic and anionic components are possible. For example, the compound β -K₂PO₃F, isostructural with β -K₂SO₄, has been synthesised.¹⁰ The structures of compounds with vacancies in the cationic sublattice, for example the calcium silicophosphates formed in the Ca₂SiO₄-Ca₃(PO₄)₂ system, have been described.^{19, 22, 141}

Two crystal structures have been determined for calcium silicophosphates: 6Ca₂SiO₄·Ca₃(EO₄)₂ (see Ref. 141) and Ca₅(PO₄)₂SiO₄.¹⁹ The 6Ca₂SiO₄·Ca₃(PO₄)₂ structure belongs to the β -K₂SO₄ structural type. Four-layer fragments along the [010] direction can be differentiated in it (Figs 1 and 2). Three layers are the same as in the β -Ca₂SiO₄ structure, whilst the fourth layer differs little from the layer in β -K₂SO₄. A similar alternation of distorted and undistorted (weakly distorted) layers has been found in Cd₅(PO₄)₂EO₄ (E = Si, Ge),²⁰ Cd₄Na(PO₄)₃,²¹ and α -Ca₃(PO₄)₂.²² We may note that the Y sites in the undistorted layer of these structures are vacant. Taking into account the latter factor, one may claim that the Y sites in the 6Ca₂SiO₄·Ca₃(PO₄)₂ structure are half-occupied in one layer (Fig. 1), while in the remaining layers they are still fully occupied (Fig. 2). This structure can be obtained by the alternation of the three occupied layers and one layer with a half-occupied site. The coordination numbers of the Y site vary from 7 to 10, whilst those of the X site are 7 and 8.

The structure of silicocamotite Ca₅(PO₄)₂SiO₄ can also be built up by alternating the layers (two with a occupied Y site and one with an vacant Y site) (Figs 1 and 2).¹⁹ The two occupied layers resemble in this instance the analogous layers in β -Ca₂SiO₄, while the layer with an vacant Y site corresponds to the layer in the β -K₂SO₄ structure. Appreciable rotation and shifts of the tetrahedra from the ideal sites are observed in the occupied layers, whereas in the vacant layer the vacancies in the

type A column promote the 'ideal' arrangement of the tetrahedra.

The maximum distortion of the type β -K₂SO₄ lattice is observed in α -Ca₃(PO₄)₂.²² An ordered occupation of the Y sites in type A columns occurs in this structure (Fig. 2). The tetrahedra in this structure are intermediate between the ideal positions in the β -K₂SO₄ and the glaserite structures. This is manifested also in the coordination numbers of calcium, which vary from 6 to 10. The intermediate structure α -Ca₃(PO₄)₂ has also been confirmed by the arrangement of the cations in the type C column, where some of the calcium cations are located virtually on the threefold 'pseudoaxis', whilst the others are arranged as in β -K₂SO₄ (Fig. 1).

At a temperature above 1723 K, the α -Ca₃(PO₄)₂ phase undergoes a transition to the α' -modification.¹³² One may postulate that this modification is built up on the basis of the glaserite and not the β -K₂SO₄ structure. This conclusion was confirmed by the fact that a continuous series of solid solutions is formed at high temperatures (>1723 K) between α -Ca₂SiO₄ and α' -Ca₃(PO₄)₂,¹²⁰⁻¹²³ which is possible only when the components of the system are isostructural.

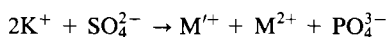
It follows from the data presented that the β -K₂SO₄ structural type is more stable also in the presence of vacancies in the cationic sublattice. These vacancies are present only in the mixed anionic-cationic column (the Y site).^{22, 141} The maximum number of vacancies occurs in α -Ca₃(PO₄)₂.²² In the α -Ca₃(PO₄)₂ lattice, the Y site is half-occupied. In the compounds Cd₄Na(PO₄)₃ (see Ref. 21) and Cd₅(PO₄)₂EO₄ (E = Si, Ge),²⁰ there is an intermediate occupation of the Y site, as in the case of Ca₅(PO₄)₂SiO₄.¹⁹ The different degrees of occupation of the Y sites in these phases are clearly reflected by their crystal-chemical formulae: X₂Y□(PO₄)₂ and X₃Y₂□(EO₄)₃.

With increase in the number of vacancies in the crystal lattice, the distortion of the type β -K₂SO₄ structure increases and in the silicophosphates the following features are observed: (1) the layers in which the Y sites are vacant or are partly occupied correspond to the ideal layers in β -K₂SO₄ (Figs 1 and 2); (2) neighbouring layers with fully occupied Y sites are distorted owing to the rotation of the tetrahedra. The individuality of the cation exerts a lesser influence on the crystal lattice. Thus Cd₄Na(PO₄)₃ (see Ref. 21) and Ca₅(PO₄)₂SiO₄ (see Ref. 19) have identical structures although they have different

sets of cations, but the degree of occupation of the Y sites is the same.

The distortion of the type β -K₂SO₄ structure is mainly associated with the rotation of the tetrahedra, which has been confirmed by luminescence spectroscopic studies of solid solutions in the MNaPO–Na₂Eu(PO₄)₂ (M = Ca, Sr) systems.^{142, 143} The authors note that the broadening of the lines in the luminescence spectra is associated with the rotation of the PO₄^{3–} tetrahedra without change in the cationic sublattice. The X-ray diffraction patterns of solid solutions in the MNaPO–Na₂Eu(PO₄)₂ (M = Ca, Sr) system are identical. On the other hand, three (for M = Ca) and two (for M = Sr) composition ranges with identical spectra have been differentiated in the luminescence spectra of these solid solutions.

Heterovalent substitution in accordance with the scheme



leads to the formation of the compounds M'MPO₄ (rhenanites). There are data on the crystal structures of the compounds γ -, β -, and α -NaSrVO₄,¹⁴⁴ NaBaPO₄,^{134, 135} KBaPO₄,^{17, 146} TlBePO₄,¹⁴⁷ and β -CaNaPO₄.¹⁸ Only the crystal structures of KBaPO₄ and β -CaNaPO₄ are of the β -K₂SO₄ type. In these structures, the alkali metal cations occupy the Y site, while the alkaline earth metal cations occupy the X site (Fig. 4). In the β -CaNaPO₄ structure, the type A column contains three different PO₄^{3–} tetrahedra. This increases the parameter *a* by a factor of three compared with that in β -K₂SO₄. As a result of the rotations of the tetrahedra in this structure, the coordination numbers of the Y and X sites change. In the β -CaNaPO₄ structure, the sodium cation is surrounded by six oxygen atoms in the immediate vicinity (up to 2.8 Å) or by ten oxygen atoms when more remote ones (up to 3.3 Å) are taken into account. The *d*_{Ca–O} distances in the cationic C column are 2.39–2.79 Å. The coordination polyhedron consists of eight oxygen atoms.

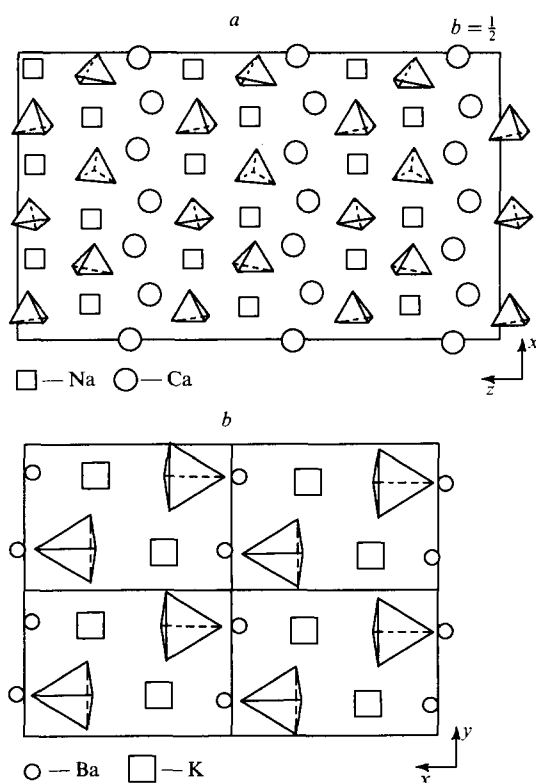


Figure 4. The layers in the β -CaNaPO₄ (a)¹⁸ and BaKPO₄ (b)¹⁷ structures.

As noted above, a large group of compounds with the composition Na₃R(EO₄)₂ (R = rare earth; E = P, V, As) crystallises in the β -K₂SO₄ structural type. Eight varieties of this structural family are distinguished (Fig. 5).¹⁶

The cations alternate in the same sequence in the compounds Na₃R(EO₄)₂. The lanthanide and sodium cations occupy the X site in an ordered manner (...–Na–R–Na–...). The Y site is occupied by sodium cations. Depending on the set of elements in the compounds, the crystal lattice is subjected to different distortions induced by the rotation of the EO₄ tetrahedra. The coordination polyhedra of the cations change as a result of the rotation of the tetrahedra (6–7 for Na, 6–8 for R). The rotation of the tetrahedra is induced by the tendency of sodium and lanthanide cations to assume smaller and larger coordination numbers respectively than those 'inherent' in the ideal β -K₂SO₄ structure.

It is noteworthy that the distortions of the crystal lattice in the compounds Na₃R(EO₄)₂ become more pronounced with increase in Δr (Table 2). For Na₃R(PO₄)₂ with R = Tm, Yb, or Lu, the structural type under discussion does not occur owing to the tendency of the lanthanide cations at the end of the series to acquire an environment comprising six oxygen atoms. The high-temperature modifications of Na₃R(PO₄)₂ (R = Tm–Lu)¹⁴⁸ crystallise similarly to the NASICON structural type.⁷³

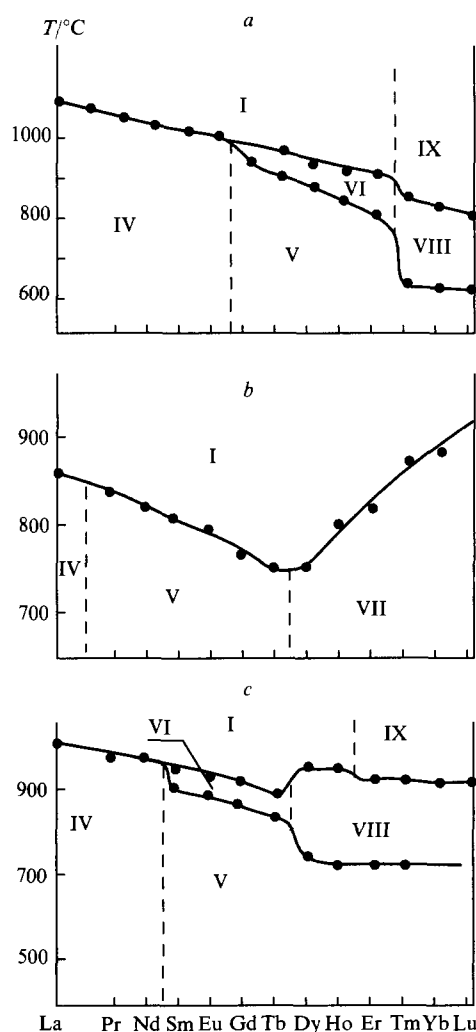


Figure 5. The regions of existence of the Na₃R(EO₄)₂ modifications, where E = P (a), V (b), As (c).¹⁶

The β - K_2SO_4 structural type is very common among phosphates, silicates, arsenates, and vanadates. The existence of a β - K_2SO_4 type structure with and without vacancies gives rise to extensive possibilities for substitution in the cationic and anionic groups without a reconstructive rearrangement of the structure. The compositions of compounds with the β - K_2SO_4 structure may include monovalent, divalent, and trivalent cations. Thus, one may expect the formation of the silicates $MRSiO_4$ ($M = Na, K$), the phosphates $MCa_4(PO_4)_3$ ($M = Na, K$), and other phases. Laborious studies on phase diagrams are not needed in this instance. For example, the existence of the compounds $NaPbPO_4$, $NaPb_4(PO_4)_3$, $AgPbPO_4$, and $AgPb_4(PO_4)_3$ could have been postulated also without studying the phase diagrams for the Na_3PO_4 - $Pb_3(PO_4)_2$ and Ag_3PO_4 - $Pb_3(PO_4)_2$ system.¹⁴⁹ Querton et al.¹⁴⁹ assigned the compounds $MPbPO_4$ ($M = Na, Ag$) and $MPb_4(PO_4)_3$ which they synthesised, to the β - K_2SO_4 and apatite structural types with vacancies respectively, but the unit cell parameters of all the compounds synthesised do not differ from the analogous parameters for potassium sulfate. Apparently the assignment of the compounds $MPb_4(PO_4)_3$ to the apatite and not the β - K_2SO_4 structural type should be regarded as erroneous, since, in view of the lack of $MPb_4(PO_4)_3$ single crystals, it was impossible to carry out a full X-ray diffraction study of these compounds.

As mentioned above, the β - K_2SO_4 structural type is stable for the compounds in which heterotypical cations (two or more) have similar radii. Such a structure obtains for the compounds $Na_3R(PO_4)_2$ ($R = La-Ho$),^{13,14} $CaNaPO_4$,¹⁸ and $KBaPO_4$.¹⁷ With increase in the difference between the radii of heterotypical cations, the glaserite-like structure, of the kind occurring, for example, in $BaNaPO_4$ (see Ref. 134) and $KNaSO_4$,¹ or the olivine structure, as in $NaMnPO_4$ (see Ref. 150) and $NaB^{II}PO_4$ ($B^{II} = Co, Fe, Mn, Gd$),¹⁵¹ becomes more stable. The features noted above, must be taken into account in modelling the compounds within the framework of the β - K_2SO_4 structural type.

3. The bredigite structural type

In the analysis of the structures of various modifications of $Na_3R(EO_4)_2$, there are difficulties in the assignment of the compounds to the β - E_2SO_4 or glaserite structural types. This applies particularly to compounds with large unit cells (Table 2). In such compounds, the tetrahedra have appreciably rotated away compared with the ideal arrangement. Some of them occupy, as it were, an intermediate position between their positions in glaserite and β - K_2SO_4 . For an appropriate selection of the cations, one can apparently expect the formation of a phase with a 'mixed' (glaserite and β - K_2SO_4) arrangement of the tetrahedra. The compositions of such compounds should include small ($<0.8 \text{ \AA}$), medium ($\sim 1 \text{ \AA}$), and large ($>1.2 \text{ \AA}$) cations.

Analysis of the literature data showed that such a compound does indeed exist and its composition corresponds to the general formula $(Ca, Ba, Mn)Ca_{13}Mg_2(SiO_4)_8$ (the mineral bredigite). The crystal structure of $Ca_{26.9}Ba_{0.6}Mg_{3.6}Mn_{0.9}(SiO_4)_{16}$ has been determined (space group $Pmch$, $a = 10.909 \text{ \AA}$, $b = 18.34 \text{ \AA}$, $c = 6.739 \text{ \AA}$, $Z = 2$).⁴⁴ The projections of the ideal and real structures of bredigite are presented in Fig. 6. This structure is made up of type A and C columns, as in β - K_2SO_4 and glaserite discussed above. The ideal crystal-chemical formula of the bredigite structural type, i.e. $X^{[12]}X_2^{[9]}Y_4^{[10]}M^{[6]}(EO_4)_4$ includes the polyhedra of the glaserite and β - K_2SO_4 structures in proportions of 1:2.

In the $Ca_{26.9}Ba_{0.6}Mg_{3.6}Mn_{0.9}(SiO_4)_{16}$ structure, there are two sets of independent sites, two sites in each set, namely $X^{[12]}$ and $X^{[9]}$ in one set and $Y^{[10]}$ and $M^{[6]}$ in the other. The cations are distributed among the sites in the following manner:⁴⁴ $X(1) = 0.707Ca^{2+} + 0.293Ba^{2+}$; $M(1) = 0.93Mg^{2+} + 0.07Mn^{2+}$; $Y(1) = 0.88Ca^{2+} + 0.12Mg^{2+}$. The remaining sites are occupied by calcium cations only. Owing to the rotations of the tetrahedra (Fig. 6), in the real structure the coordination

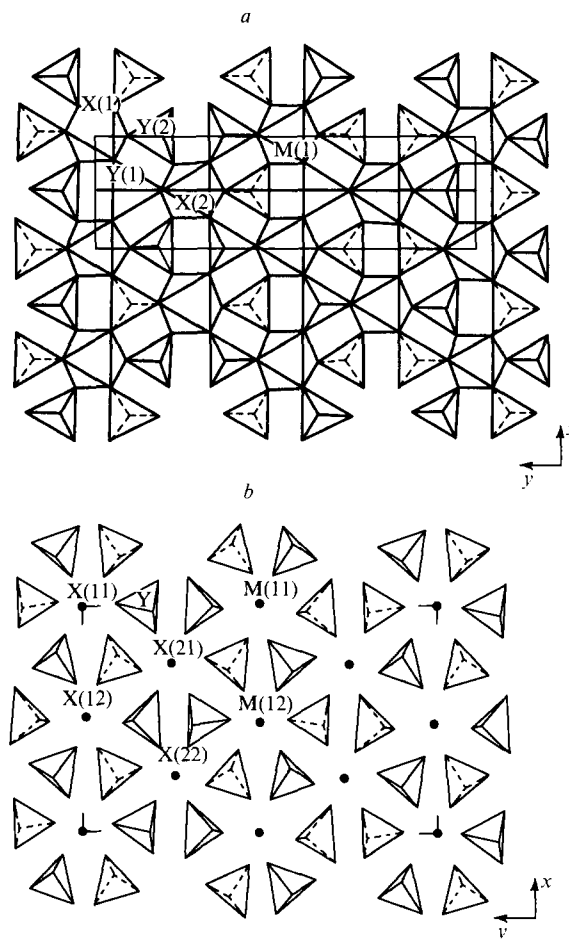


Figure 6. Projections of the bredigite structure on to the xy plane. Ideal (a) and real (b) arrangements.⁴⁴

numbers of the sites are smaller than in the ideal structure. However, when account is taken of the longer distances, they correspond to the coordination numbers of the sites in the ideal structure.

It has been established that the bredigite structure occurs also for the solid solutions in the range $(Ca_{1.8}Mg_{0.2})SiO_4$ - $(Ca_{1.7}Mg_{0.3})SiO_4$.^{19,152} If the formulae of the compounds $(Ca_{1.8}Mg_{0.2})SiO_4$ ¹⁹ and $(Ca_{1.7}Mg_{0.3})SiO_4$ (see Ref. 152) are adjusted to the composition reflecting the ideal crystal-chemical formula, they become $Ca_{7.2}Mg_{0.8}(SiO_4)_4$ and $Ca_{6.8}Mg_{1.2}(SiO_4)_4$. In the solid solutions between these phases, the $M^{[6]}$ site and one of the $Y^{[9]}$ sites are statistically occupied by magnesium and calcium cations. The remaining sites, $X^{[12]}$ and $Y^{[10]}$, are occupied by calcium cations only. The compound $Ca_7Mg(SiO_4)_4$ corresponds to the ideal formula of the bredigite structure (without a statistical occupation of the sites).

When account is taken of the dimensions of the X, Y, and M polyhedra, one may expect the formation of the compound $BaCa_6Mg(SiO_4)_4$, in which the cations occupy the following sites: $X^{[12]}$ by Ba^{2+} , $Y^{[10]}$ and $X^{[9]}$ by Ca^{2+} , and $M^{[6]}$ by Mg^{2+} . Apparently the ideal structure is not produced in this case. In order to obtain the ideal structure of the bredigite type, it is more likely to be useful to employ the compounds $K_3R(PO_4)_2$ (the compounds with $R = Sc$ or Lu have the ideal glaserite structure)^{5,6} and $KBaPO_4$ (with a structure of the β - K_2SO_4 type)⁷ or $BaNaPO_4$ (glaserite structural type)¹³⁴ and $KBaPO_4$ (type β - K_2SO_4 structure).¹⁷ In this case, one may expect the formation of the $Ba_2K_5R(PO_4)_4$ ($R = Lu, Sc$) and $Ba_4K_2Na_2(PO_4)_4$ phases respectively. In the latter compound,

the second sodium cation may occupy one of the Y sites together with Ba, as in the case of BaNaPO₄.¹³⁴

The modelling of the phases based on the bredigite structure examined above is important for the synthesis of compounds with the required physicochemical properties. Firstly, the combination of two structures with different coordination polyhedra into one structure makes it possible to introduce various cations into a lattice of this kind. The problem of the synthesis of multifunctional materials is thus solved. Secondly, the successive alternation of polyhedra of different structures makes it possible to increase the distances between like cations, preventing thereby their interaction, which may improve the physicochemical characteristics of the materials. The latter is important in the synthesis of phosphors and diamagnetic materials with cations having magnetic properties.

4. The palmierite K₂Pb(SO₄)₂ structural type

In contrast to α -Ca₃(PO₄)₂ (β -K₂SO₄ structural type), the phosphates of divalent elements with large radii, namely M₃(PO₄)₂ (M = Sr, Ba, Pb),^{26,153} Pb₄(PO₄)₂CrO₄,¹⁵⁴ and also the molybdate K₂Pb(MoO₄)¹⁵⁵ crystallise in the structural type corresponding to the natural mineral palmierite K₂Pb(SO₄)₂.²³ Barium and strontium vanadates and arsenates also belong to this structural type.^{25–27}

In the K₂Pb(SO₄)₂ structure, the potassium cation occupies the YO₁₀ decahedron, while the lead cation occupies the XO₁₂ dodecahedron. The XO₁₂ coordination polyhedron is formed by the edges of six tetrahedra (Fig. 3a). The X–O distances are divided into two types: six short distances (2.83–2.85 Å) form an appreciably extended (along the $\bar{3}$ axis) trigonal antiprism, while six long ones (3.4–3.5 Å to the apical oxygen atoms) are located in the equatorial plane of the antiprism. The symmetry of this polyhedron is $\bar{3}2/m$. XO₁₂ is adjoined below and above (along the $\bar{3}$ axis) by two YO₁₀ polyhedra (Fig. 7). They have triangular faces in common with the antiprism. The YO₁₀ polyhedron is formed by three edges of three tetrahedra (equatorial plane), three oxygen atoms in three other tetrahedra (at distances of ~ 3 Å), and one (apical) oxygen atom on the threefold axis (Figs 3b and 7).

Overall, the palmierite structure is made up of ...–YO₁₀–XO₁₂–YO₁₀–EO₄–EO₄–... columns and its crystal-chemical formula is X^[12]Y₂^[10](EO₄)₂. The Sr²⁺, Ba²⁺, and Pb³⁺ ions occupy the large XO₁₂ and YO₁₀ polyhedra.

At first sight, the existence of the double molybdates M₅R(MoO₄)₄ (M = K, Rb; R = rare earth, Bi, Y, Al, Fe), crystallising in the palmierite structural type, appears unusual. Such compounds have been found in the study of the M₂MoO₄–R₂(MoO₄)₃ systems.^{28,29} It follows from crystal-chemical data that the X sites may be occupied also by small cations. To a first approximation, their coordination number is then six (the nearest six oxygen atoms). As a result of the ease of the rotation of the tetrahedra, coordination numbers different from those in the ideal structure may occur in the palmierite-like structure. For example, the phase transition in Pb₃(PO₄)₂ is accompanied by an increase in the symmetry from monoclinic to trigonal at 473 K.¹⁵⁴

The mobility of the tetrahedra in the palmierite-like structure promotes the formation of coordination polyhedra characteristic of the given trivalent cation. For this reason, the compounds M₅R(MoO₄)₄ are formed for the entire series of lanthanide, bismuth, iron, and aluminum cations.^{28–32,155–161} Analogous tungstates are formed only for M = K or Rb and R = Bi, La, or In.^{162–165} An intrinsic distortion of the ideal palmierite structure, precisely characteristic of the given compound, occurs in each case (Table 3).

With the aid of the crystal-chemical formula X^[6+6]Y₂^[9+1](EO₄)₂ and the characteristics of the environment of the X site, one may predict the compositions of the M₅R(MoO₄)₄ phases, bypassing the laborious investigation of phase diagrams. Taking into account the fact that palmierite-like structures include large and small cations or only large cations, one may expect that isovalent or heterovalent substitutions would entail the formation of the following phases: M'₄NaR(MoO₄)₄ (M' = K, Rb); SrBa₂(PO₄)₂; BaSr₂(PO₄)₂; M'MR(PO₄)₂ (M' = K, Rb; M = Sr, Ba; R = Ln, Y, Bi, Fe, Al); M₂R(SiO₄)₂ (M = Sr, Ba; R = Ce, Zr, Hf); M₂RPO₄SiO₄ (M = Sr, Ba; R = Ln, Fe, Al, Bi, Y); M'MRPO₄SiO₄ (M' = Sr, Ba; M = K, Rb; R = Ce, Zr, Hf). A series of compounds having similar compositions and structures had been synthesised earlier, for example, Sr₄(PO₄)₂CrO₄,¹⁶⁶ Ba₃(TaO₄)₂,¹⁶⁷ M₂M(EO₄)₂

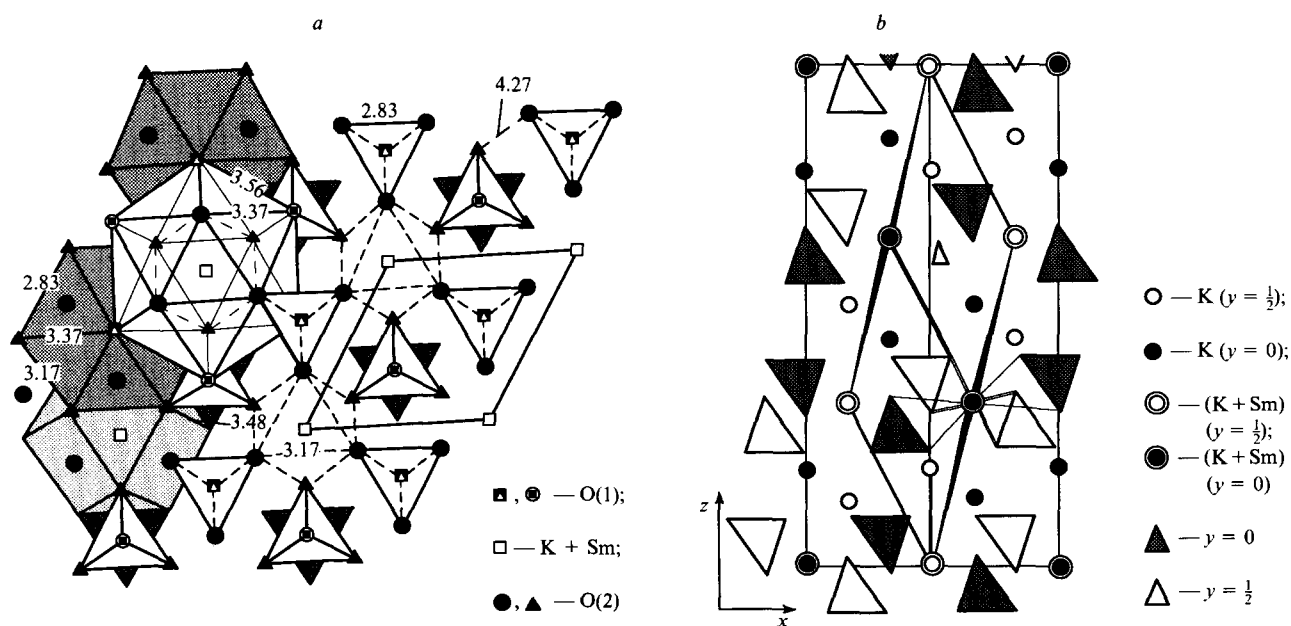


Figure 7. Projection of the structure of palmierite K₅Sm(MoO₄)₄ on to the xy plane: (a) 0.10 ≤ z ≤ 0.44, (b) xz.¹⁵⁶

Table 3. X-Ray diffraction characteristics of certain palmierite-like phases.

Compound	$a/\text{\AA}$	$b/\text{\AA}$	$c/\text{\AA}$	Angle /°			Space group	Ref.
				α	β	γ		
$\text{K}_2\text{Pb}(\text{SO}_4)_2^a$	5.50	5.50	20.863				$R\bar{3}m$	23
$\text{K}_2\text{Pb}(\text{MoO}_4)_2^a$	10.38	7.81	11.98		115.9		$P2$	155
$\text{Sr}_3(\text{PO}_4)_2^a$	5.621	5.621	20.14				$R\bar{3}m$	26
$\text{Ba}_3(\text{PO}_4)_2^a$	5.783	5.783	21.34				$R\bar{3}m$	26
$\text{Sr}_3(\text{VO}_4)_2$	5.621	5.621	20.14				$R\bar{3}m$	27
$\text{Ba}_3(\text{VO}_4)_2^a$	5.762	5.762	21.29				$R\bar{3}m$	27
$\text{Sr}_3(\text{AsO}_4)_2$	5.581	5.581	19.98				$R\bar{3}m$	27
$\text{Ba}_3(\text{AsO}_4)_2$	5.753	5.753	21.18				$R\bar{3}m$	27
$\alpha\text{-Pb}_3(\text{PO}_4)_2^a$	5.53	5.53	20.30				$R\bar{3}m$	154
$\beta\text{-Pb}_3(\text{PO}_4)_2^a$	13.816	5.692	9.429		102.4		$C2c$	154
$\text{K}_5\text{Nd}(\text{MoO}_4)_4^a$	10.360	17.943	14.301		103.98		$P2/m$	32
$\alpha\text{-K}_5\text{Y}(\text{MoO}_4)_4^a$	10.453	10.453	41.04				$R\bar{3}m$	157
$\beta\text{-K}_5\text{Y}(\text{MoO}_4)_4$	10.478	6.034	7.736		118.0		$C2/m$	159
$\alpha\text{-K}_5\text{In}(\text{MoO}_4)_4$	10.30	18.21	14.99	90.97	106.61	89.58	$P1$	158
$\beta\text{-K}_5\text{In}(\text{MoO}_4)_4^a$	10.46	12.092	14.625		114.0		Aa	158
$\text{K}_5\text{Bi}(\text{MoO}_4)_4^a$	6.019	6.019	41.761				$P\bar{3}1m$	32
$\text{Rb}_5\text{Gd}(\text{MoO}_4)_4^a$	10.604	18.349	14.725	90.11	104.41	89.99	$P1$	32
$\alpha\text{-Rb}_5\text{Al}(\text{MoO}_4)_4^a$	10.520	6.078	8.470		114.5		Cc	161
$\beta\text{-Rb}_5\text{Er}(\text{MoO}_4)_4$	11.44	7.99	11.19		113.0		$P2/c$	160
$\text{K}_5\text{Sm}(\text{MoO}_4)_4^a$	5.978	5.978	20.79				$R\bar{3}m$	156

^a The crystal structure has been determined.

($E = \text{S, Cr}$),^{168–170} $\text{K}_5\text{R}(\text{SO}_4)_4$ ($R = \text{Ln}$),¹⁷¹ $\text{M}_8\text{Th}(\text{MoO}_4)_6$,¹⁷² and $\text{K}_3(\text{MoO}_4)(\text{ReO}_4)$.¹⁷³

In the case of both palmierite and other structural types, an important factor in the prediction of such phases is the estimation of their crystal lattice energies. An estimate of this kind can be achieved provided that the coordinates and the 'effective' charges of the atoms are known.

5. The NASICON structural type

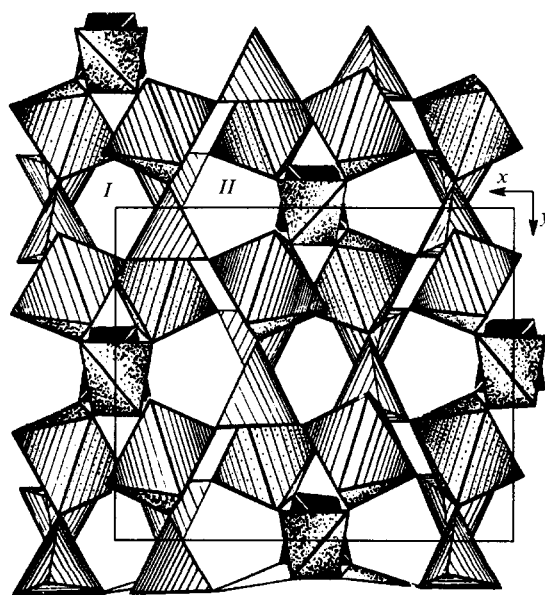
The NASICON structural type occurs for cations with small radii (Sc^{3+} , Fe^{3+} , Cr^{3+} , V^{3+} , Mg^{2+} , Zr^{4+} , Ti^{4+} , Nb^{4+} , Nb^{5+}) accommodated in the (RO_6) octahedra. A three-dimensional skeletal composition made up of RO_6 octahedra, sharing their vertices with the EO_4 tetrahedra, is characteristic of structures of this class (Fig. 8). A framework of this kind was first described by Abrahams and Bernstein.¹⁷⁴ Subsequently, as the structures of other representatives of this family were determined, the characteristic features of its structure were refined.^{33–41, 62, 68–73, 95} At present, there are more than 400 publications on the structures and properties of compounds of this class. Many of them are devoted to the elucidation of the mechanism of ionic conduction on the basis of crystal-chemical data.

The formula $\text{M}_n\text{R}_2(\text{EO}_4)_3$, where $0 \leq n \leq 4$, describes all the possible compounds with the NASICON structure.⁴¹ The NASICON-like phases are based on the three-dimensional framework $\{[\text{R}_2(\text{EO}_4)_3]^{p-}\}_{3\infty}$ where $E = \text{P, Si, S, Mo, As, W, Se, or Ge}$. The sodium cation is usually employed as the vacancy-filling cation (M), but it can be replaced by Li^+ and Cu^+ or by Cu^{2+} , Ca^{2+} , Sr^{2+} , and Ba^{2+} .

The structural framework is threaded by channels of two types, *I* and *II*, along the c axis of the unit cell (Fig. 8). The zigzag network of type *III* channels passes at right angles to them along the $[010]$ direction. Channels *III* intersect channels *I* and *II*, forming a three-dimensional cavity framework. The channels have variable widths, the cross-sections of the narrowest sites being 1.0 Å for type *I* channels, 1.1 Å for type *II* channels, and 0.9 Å for type *III* channels. Cations with radii of 1.2–1.4 Å can be placed in the wide spaces within the channels (at the intersection of channels *III* with channels *I* and of channels *II* with channels *III*). In the above cavities, it was possible to differentiate two sites — $M(1)$ and $M(2)$ (Fig. 9).

If the space group $R\bar{3}c$ is adopted as the basis (the highest symmetry for the compounds under discussion), then in this case the sixfold $M(1)$ site is an extended antiprism with distances of ~ 2.6 Å to the nearest six oxygen atoms (the other six oxygen atoms are separated by long distances of ~ 3.7 Å). The eightfold $M(2)$ site is surrounded by eight oxygen atoms at distances of ~ 2.47 – 2.89 Å and two oxygen atoms at distances of ~ 3.25 Å.

It follows from the analysis of the cross-sections of the channels that a cation with a radius of ~ 1 Å (for example, Na) can migrate through them. During the migration of sodium cations from the $M(1)$ site to the $M(2)$ site, the narrowest places are at the $A-B-C$ and $A-B-D$ faces (Fig. 9b).¹⁷⁵ When account is taken of the thermal displacements of the oxygen

**Figure 8.** The framework of the $\text{Sc}_2(\text{MoO}_4)_3$ structure.⁴¹

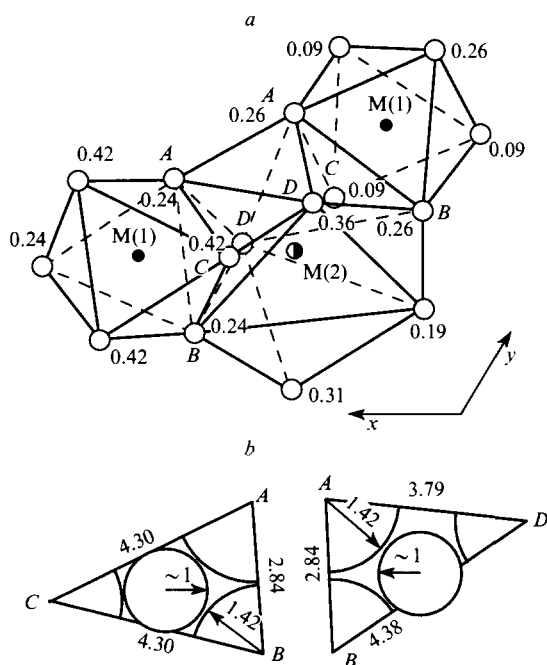


Figure 9. The NASICON structural type: (a) surroundings of the M(1) and M(2) sites; (b) the free space bounded by the common faces of the M(1)O₆ and M(2)O₈ polyhedra in the α -Na₃Sc₂(PO₄)₃ structure.¹⁷⁵

atoms, particularly with increase in temperature, the sodium cations ($r_{V1} = 1.02 \text{ \AA}$) can migrate from one site to the other without any obstacles. This fact is indeed the reason for the appearance of superionic conduction in compounds of this class.^{33, 38, 65, 66} The mobility of sodium cations has been confirmed experimentally by the distribution of their electron density within the conduction channels observed even at 60 °C in α -Na₃Sc₂(PO₄)₃ (Fig. 10).⁶⁷

It follows from the analysis of the number of polyhedra and their surroundings that the crystal-chemical formula of the NASICON structural type is $M(1)^{[6]}M(2)^{[8]}R_2^{[6]}(EO_4)_3$. A necessary condition for the occurrence of the structural type under discussion is the small size ($<0.8 \text{ \AA}$) of the cations R. Their valence should be in the range $2 \leq p \leq 5$. Phases with valences of 2 and 5 have not been described in the literature.

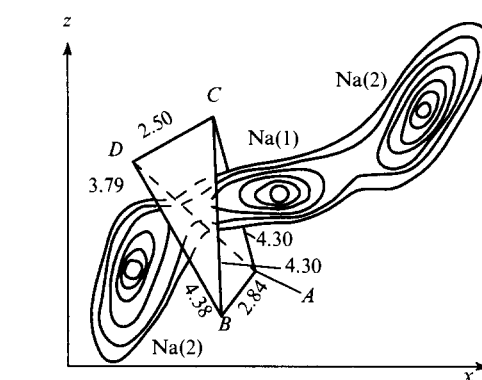


Figure 10. Distribution of the electron density of the sodium atoms in the conduction channels of the α -Na₃Sc₂(PO₄)₃ structure (60 °C).⁶⁷

However, phases with 'formal' valences of 2.5 ($2R = Cr^{3+} + Mg^{2+}$)³⁷ and 4.5 ($2R = Nb^{5+} + Ti^{4+}$)³⁴ are known. The additional atoms M can be accommodated at the M(1) and M(2) sites. Structures with fully occupied M(1) and M(2) sites [Na₄Zr₂(EO₄)₃ (E = Si, Ge),^{39, 40} Na_{4.5}R_{1.5}(PO₄)₃ or Na₃R(PO₄)₂ (R = Tm, Yb, Lu)¹⁴⁸], structures in which only the M(1) sites are occupied [NaR₂(PO₄)₃, R = Ti, Zr]^{62, 73}, structures in which only the M(2) sites are occupied (jointly with the vacancies) [Cu^ITi₂(PO₄)₃ (see Ref. 95)] and the low-temperature Na₃Sc₂(PO₄)₃ (see Ref. 68)], structures with a statistical occupation of the M(1) and M(2) sites (jointly with the vacancies) [the high-temperature Na₃Sc₂(PO₄)₃ (see Ref. 67)], and structures with fully vacant M(1) and M(2) sites [R₂(EO₄)₃ (R = Sc, Fe; E = Mo, S),^{41, 176, 178} MM'(PO₄)₃ (M = Mo, Nb; M' = Ti, Zr),¹⁷⁹ and NbTi(PO₄)₃ (see Ref. 34)] have been found.

Depending on the set of cations, the ideal trigonal unit cell may be distorted to an orthorhombic or monoclinic cell. Examples of certain compounds of the structural type under consideration are presented in Table 4. As can be seen from the Table 4, different distortions of the unit cell occur even for a set of the same cations. The symmetry of the cell is appreciably influenced by the distribution of the cations among the structural sites. A highly symmetrical cell is characteristic of compounds with an occupied M(1) site. In this case, an appreciable cationic conductivity occurs at a temperature above 500 K. When the M(2) site is fully occupied, the cationic conductivity even appears at room temperature.⁶²

Table 4. X-Ray diffraction characteristics of certain NASICON-like phases.

Compound	$a/\text{\AA}$	$b/\text{\AA}$	$c/\text{\AA}$	$\beta/^\circ$	Space group	Ref.
Sc ₂ (MoO ₄) ₃ ^a	13.242	9.544	9.637		<i>Pbcn</i>	41
<i>m</i> -Fe ₂ (SO ₄) ₃ ^a	8.29	8.53	11.63	90.8	<i>P2₁/n</i>	177
Fe ₂ (MoO ₄) ₃ ^a	15.7	9.23	18.2	125.3	<i>P2₁/n</i>	176
NaZr ₂ (PO ₄) ₃ ^a	8.80	8.80	22.76		<i>R3c</i>	73
KZr ₂ (PO ₄) ₃	8.71	8.71	23.89		<i>R3c</i>	181
RbZr ₂ (PO ₄) ₃	8.66	8.66	24.38		<i>R3c</i>	181
CsZr ₂ (PO ₄) ₃	8.62	8.62	24.86		<i>R3c</i>	181
Na ₃ Zr ₂ Si ₂ PO ₁₂ ^a	15.128	8.722	8.793	125.76	<i>C2/c</i>	62
β -Na ₃ Sc ₂ (PO ₄) ₃ ^a	16.10	9.11	8.93	127.2	<i>Bb</i>	68
α -Na ₃ Sc ₂ (PO ₄) ₃ ^a	8.927	8.927	22.34		<i>R3c</i>	67
Na ₄ Zr ₂ (SiO ₄) ₃ ^a	9.10	9.10	22.07		<i>R3c</i>	39
Na ₄ Zr ₂ (GeO ₄) ₃ ^a	9.429	9.429	22.53		<i>R3c</i>	40
CuTi ₂ (PO ₄) ₃ ^a	8.523	8.523	21.303		<i>R3c</i>	95
Cu _{0.5} Ti ₂ (PO ₄) ₃	8.84	8.84	22.77		<i>R3c</i>	82
H _{0.5} Cu _{0.5} Zr ₂ (PO ₄) ₃	8.84	8.84	22.75		<i>R3c</i>	96
HZr ₂ (PO ₄) ₃	8.80	8.80	23.23		<i>R3c</i>	180

^a The crystal structure has been determined.

Detailed information about the structure of compounds of the NASICON type made it possible to synthesise, with the aid of isovalent and heterovalent substitutions in the cationic and anionic sublattices, new superionic materials with low temperatures of the onset of ionic conduction, for example, $\text{Na}_{3+x}\text{Cr}_{2-y}\text{Mg}_z(\text{PO}_4)_3$,³⁷ $\text{Na}_{1+x}\text{Zr}_2\text{Si}_x\text{P}_{3-x}\text{O}_{12}$,⁶² $\text{NbTi}(\text{PO}_4)_3$,³⁴ $\text{Na}_{1+x}\text{Zr}_{2-x}\text{In}_x(\text{PO}_4)_3$,⁷² $\text{HZr}_2(\text{PO}_4)_3$,¹⁸⁰ $\text{Cu}_{0.5}^{\text{II}}\text{Ti}_2(\text{PO}_4)_3$,⁸² $\text{Na}_{2x}\text{M}_{2-x}\text{Sc}_{2-2x}(\text{MoO}_4)_3$ ($\text{M} = \text{Zn}, \text{Cd}, \text{Mg}$),⁹⁰ $\text{Cu}^{\text{I}}\text{Zr}_2(\text{PO}_4)_3$,⁹³ $\text{H}_{0.5}\text{Cu}_{0.5}^{\text{I}}\text{Zr}_2(\text{PO}_4)_3$,⁹⁶ and many others.

It follows from the data presented above that the NASICON structural type is based on the $\{[\text{R}_2(\text{EO}_4)_3]^{p-}\}_{3\infty}$ three-dimensional framework. Other atoms can be introduced into such a framework by means of substitution or insertion with formation of new phases. A framework of a similar kind has been encountered also in compounds of other classes belonging to the garnet $\text{Ca}_3\text{Zr}_2(\text{Si},\text{AlO}_{12})$ ⁴² and langbeinite $\text{K}_2\text{Mg}_2(\text{SO}_4)_3$ (see Ref. 182) structural types. The crystal-chemical analysis of the $\{[\text{R}_2(\text{EO}_4)_3]^{p-}\}_{3\infty}$ framework for these structural types has been described in detail.¹⁸³

6. The whitlockite structural type

The low-temperature β -modification of calcium orthophosphate is isostructural with the natural mineral whitlockite ($R3c$, $Z = 3$) $\text{Ca}_{18.19}\text{Mg}_{1.17}\text{Fe}_{0.83}\text{H}_{1.62}(\text{PO}_4)_{14}$.⁴⁶ Projections of this $\beta\text{-Ca}_3(\text{PO}_4)_2$ structure with the highest information content are presented in Fig. 11. This structure is made up of isolated EO_4^{3-} tetrahedra, which bind the MO_n polyhedra into a three-dimensional framework via common vertices. Along the c axis in the structure, it is possible to differentiate two types of columns — A and B. In the type B column, the MO_8 polyhedra, containing calcium cations at the M(1), M(2), and M(3) sites and two tetrahedra alternate consecutively $[\text{M}(1)\text{O}_8 - \text{M}(3)\text{O}_8 - \text{M}(2)\text{O}_8 - \text{PO}_4 - \text{PO}_4 - \dots]$. The type A column (along the 3 axis) consists of a sequence of polyhedra and cavities $\dots - \text{PO}_4 - \text{M}(4)\text{O}_{15} - \text{M}(5)\text{O}_6 - \text{M}(6)\text{O}_{10} - \dots$ (Fig. 12). The M(4) site in this column is vacant or partly occupied, while the M(6) site is always vacant.

The unit cell of $\beta\text{-Ca}_3(\text{PO}_4)_2$ contains 21 formula units.⁹⁹ In conformity with the stoichiometric formula of the compound, there are 63Ca^{2+} cations and 42PO_4^{3-} tetrahedra per unit cell. The $R3c$ symmetry presupposes the occupation of 66 sites (three 18-fold and two sixfold) by calcium cations. Consequently three cationic vacancies (\square) are present in the unit cell.

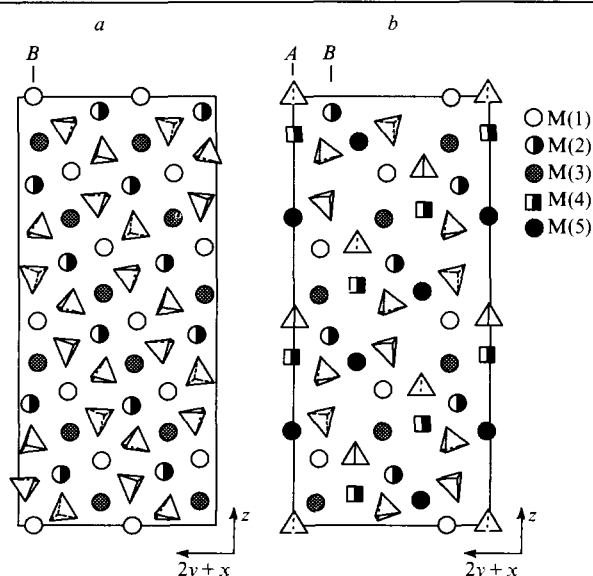


Figure 11. The layers in the $\beta\text{-Ca}_3(\text{PO}_4)_2$ structure: (a) layer with type B columns ($y = -0.25$); (b) layer with type A and B columns ($y = 0$).¹⁰³

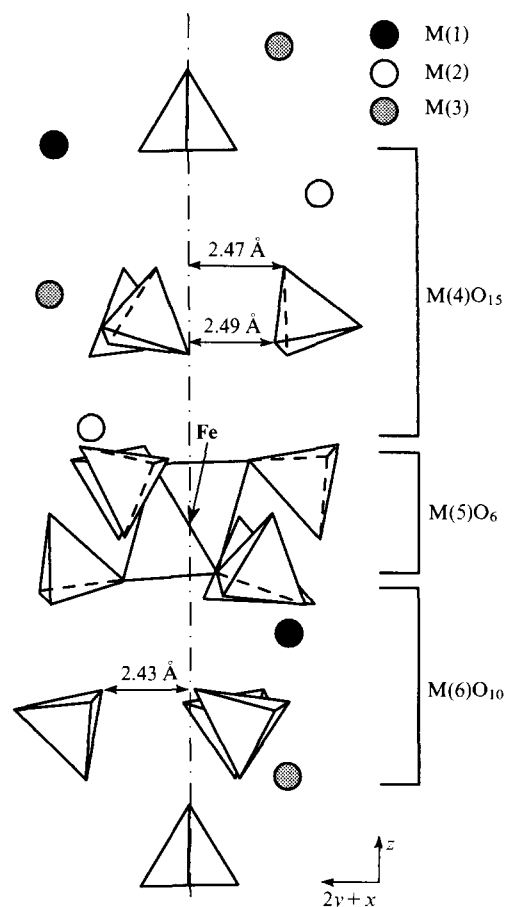


Figure 12. Fragment of a type B column in the $\text{Ca}_9\text{Fe}(\text{PO}_4)_7$ structure. Certain interatomic distances are indicated.¹⁰⁹

The composition of the unit cell is reflected by the formula $\text{Ca}_3\square_3(\text{PO}_4)_{42}$ ($Z = 1$) and its crystal-chemical analogue $\text{Ca}(1)_{18}^{[8]}\text{Ca}(2)_{18}^{[8]}\text{Ca}(3)_{18}^{[8]}\text{Ca}(4)_{18}^{[9]}\square_3^{[9]}\text{Ca}(5)_{18}^{[6]}(\text{PO}_4)_{42}$ where \square is a vacancy at the M(4) site. Having differentiated the calcium atoms with similar environments at the 18-fold M(1), M(2), and M(3) sites, we obtain the formula $\text{Ca}_{54}\text{Ca}_6\text{Ca}_3\square_3(\text{PO}_4)_{42}$ ($Z = 1$) or, in an abbreviated form $\text{Ca}_9\text{CaCa}_{0.5}\square_{0.5}(\text{PO}_4)_7$ ($Z = 6$).

The M(4) site is half-filled by calcium cations in $\beta\text{-Ca}_3(\text{PO}_4)_2$.⁹⁹ It is not structure-forming and theoretically may be both entirely free ($6\square$) or fully occupied (6M). The boundary conditions (number of vacancies) make it possible to model phases with specified compositions.

The postulated compositions of the new compounds have been calculated taking into account the heterovalent substitutions of the Ca^{2+} cations by M^+ , R^{3+} , and R^{4+} .^{100–106, 108, 110} Different substitution schemes with formation or population of vacancies were used for the modelling of the compositions of the compounds:

- (1) $9\text{Ca}^{2+} + 3\square = 6\text{R}^{3+} + 6\square$, $\text{Ca}_3(\text{PO}_4)_2\text{-RPO}_4$ section, limiting composition $\text{Ca}_9\text{R}\square(\text{PO}_4)_7$ ($Z = 6$);^{100–103, 108}
- (2) $3\text{Ca}^{2+} + 3\square = 6\text{M}^+$, $\text{Ca}_3(\text{PO}_4)_2\text{-M}_3\text{PO}_4$ section, limiting composition $\text{Ca}_{10}\text{M}(\text{PO}_4)_7$ ($\text{M} = \text{Si}, \text{Na}, \text{K}, \text{Cu}^{105}$) ($Z = 6$); (3) $9\text{Ca}^{2+} + 3\square = 6\text{Mg}^{2+} + 6\text{M}^+$, limiting composition $\text{Ca}_9\text{MgM}(\text{PO}_4)_7$ ($\text{M} = \text{Li}, \text{Na}, \text{K}$) ($Z = 6$);¹⁰⁶
- (4) $9\text{Ca}^{2+} + 3\square = 3\text{R}^{3+} + 9\text{Na}^+$, $\text{Ca}_3(\text{PO}_4)_2\text{-Na}_3\text{R}(\text{PO}_4)_2$ section, limiting composition $\text{C}_{18}\text{Na}_3\text{R}(\text{PO}_4)_{14}$ ($Z = 3$);^{107, 184, 185}
- (5) $6\text{Ca}^{2+} + 3\square = 3\text{R}^{4+} + 6\square$, $\text{Ca}_3(\text{PO}_4)_2\text{-R}_3(\text{PO}_4)_4$ section, limiting composition $\text{Ca}_{19}\text{R}\square_2(\text{PO}_4)_{14}$ ($\text{R} = \text{Ce}$) ($Z = 3$).¹⁰⁸

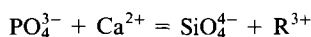
Variable-composition phases with whitlockite-like structures are formed between $\text{Ca}_3(\text{PO}_4)_2$ and the limiting compositions.^{101, 103, 104, 107, 108, 160, 161} This predetermines the existence of phases within the $\text{Ca}_3(\text{PO}_4)_2$ – $\text{Ca}_{10}\text{Na}(\text{PO}_4)_7$ – $\text{Ca}_{18}\text{Na}_3\text{R}(\text{PO}_4)_{14}$ – $\text{Ca}_9\text{R}(\text{PO}_4)_7$ tetragon.¹⁰⁷

It follows from the analysis of the interatomic distances in the polyhedra of the whitlockite-type structure that the lanthanide elements should occupy the M(1)–M(3) sites, whilst the cations with $r < 0.8 \text{ \AA}$ should occupy the octahedral M(5) site.¹¹⁰ There is sufficient space within the M(4)O₁₅ cavity to accommodate cations with a radius of $\sim 1.5 \text{ \AA}$ (Na, K) but not enough to accommodate rubidium and caesium cations (Fig. 12). The Na and K cations can occupy different sites along the threefold axis in the M(4)O₁₅ cavity which are restricted by the distances to the O(12) and O(33) oxygen atoms.

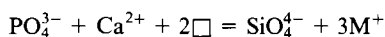
The choice of the most suitable distribution of cations among the structural sites in the model compounds has been made taking into account the calculated Madelung constants.¹⁸⁶ Trivalent and tetravalent cations are most probably accommodated at the M(1) and M(2) sites, while monovalent cations are at the M(4) sites. Subsequent studies on the structures of $\text{Ca}_{10}\text{Na}(\text{PO}_4)_7$,¹⁰⁴ $\text{Ca}_9\text{Fe}(\text{PO}_4)_7$,^{109†} and $\text{Ca}_9\text{Eu}(\text{PO}_4)_7$ (see Refs 188, 189) confirmed these calculations.

It is noteworthy that, in contrast to the glaserite, palmierite, β -K₂SO₄, and NASICON structural types examined above, the whitlockite-like crystal structure is not distorted after the insertion or substitution of cations in it (Table 5). The architecture of the whitlockite-type structure remains unchanged after the introduction into the lattice of cations having different dimensions and oxidation states. The stability of this structure predetermines the occurrence of reversible redox reactions without the destruction of the structure.^{108–110}

Together with substitutions in the cationic lattice of a whitlockite-like structure, one can achieve substitution also in the anionic component, for example in accordance with the scheme



with retention of the number of vacancies, or in accordance with the scheme



with occupation of the vacancies in the structure. For trivalent cations with $r < 0.8 \text{ \AA}$, the formula describing the limiting composition with six cations at the M(5) site is $\text{Ca}_{19}\text{R}_2(\text{PO}_4)_{12}(\text{SiO}_4)_2$, whilst for cations with $r > 0.8 \text{ \AA}$ the formula is $\text{Ca}_7\text{R}_4(\text{SiO}_4)_{14}$; intermediate compounds have the compositions $\text{Ca}_{15}\text{R}_6(\text{PO}_4)_8(\text{SiO}_4)_6$ and $\text{Ca}_9\text{R}_{12}(\text{PO}_4)_2(\text{SiO}_4)_{12}$ with full occupation of one or two 18-fold sites by the cations of the trivalent element. The limiting composition of compounds with a small trivalent cation (R') at the M(5) site and a large cation (R) at the M(1)–M(3) sites is described by the formula $\text{Ca}_4\text{R}'_2\text{R}_{14}(\text{SiO}_4)_{14}$. In this case, when the M(5) site is occupied by the Mg^{2+} cation, the limiting composition is $\text{Ca}_5\text{Mg}_2\text{R}_{14}(\text{SiO}_4)_{14}$. The possibility of the existence of silicates and silicophosphates with a whitlockite-type structure is confirmed indirectly by the mineral cerite $(\text{Ce, La, Nd, Ca})_9(\text{Fe, Mg, Al})(\text{SiO}_4)_6(\text{SiO}_3\text{OH})(\text{OH})_3$,¹⁸⁷ which is isostructural with whitlockite.

Thus the data on the whitlockite structural type made it possible to calculate theoretically for the first time a wide range corresponding to the existence of variable-composition phases in the $\text{Ca}_3(\text{PO}_4)_2$ – Na_3PO_4 – RPO_4 ternary system¹⁰⁷ and the compositions of the individual compounds. This region is located within the $\text{Ca}_3(\text{PO}_4)_2$ – $\text{Ca}_{10}\text{Na}(\text{PO}_4)_7$ – $\text{Ca}_{18}\text{Na}_3\text{R}(\text{PO}_4)_{14}$ – $\text{Ca}_9\text{R}(\text{PO}_4)_7$ tetragon.

†The full structural data have been published by B I Lazoryak, V A Morozov, A A Belik, S S Krasnov, V Sh Shekhtman. *J. Solid State Chem.*, **121**, 1(1966).

Table 5. X-Ray diffraction characteristics of certain whitlockite-like phases (space group $R\bar{3}c$).

Compound	$a/\text{\AA}$	$c/\text{\AA}$	Ref.
$\text{Ca}_{18.19}(\text{Mg}_{1.17}\text{Fe}_{0.83})\text{H}_{1.62}(\text{PO}_4)_{14}^a$	10.330	37.103	46
$\beta\text{-Ca}_3(\text{PO}_4)_2^a$	10.439	37.375	99
$\text{Ca}_3(\text{AsO}_4)_2^a$	10.77	37.81	190
$\text{Ca}_3(\text{VO}_4)_2^a$	10.809	38.028	191
$\text{Ca}_{18}\text{Mg}_2\text{H}_2(\text{PO}_4)_{14}^a$	10.350	37.085	192
$\text{Ca}_{18}\text{Mn}_2\text{H}_2(\text{PO}_4)_{14}^a$	10.438	37.15	193
$\text{Ca}_{20.23}\text{Mg}_{0.77}(\text{PO}_4)_{14}^a$	10.401	37.316	194
$\text{Ca}_{18.97}\text{Mg}_{2.03}(\text{PO}_4)_{14}^a$	10.337	37.068	194
$(\text{Ce, La, Nd, Ca})_9(\text{Fe}^{\text{III}}, \text{Mg, Al}) \times (\text{SiO}_4)_6(\text{SiO}_3\text{OH})(\text{OH})_3$	10.779	38.061	187
$\text{Ca}_9\text{Fe}(\text{PO}_4)_7^a$	10.3391	37.130	109
$\text{Ca}_9\text{FeH}_{0.9}(\text{PO}_4)_7^a$	10.354	37.165	109
$\text{Ca}_9\text{La}(\text{PO}_4)_7$	10.492	38.55	101
$\text{Ca}_{10}\text{Cu}(\text{PO}_4)_7$	10.442	37.39	105
$\text{Ca}_{10}\text{Li}(\text{PO}_4)_7$	10.421	37.38	104
$\text{Ca}_{10}\text{Na}(\text{PO}_4)_7$	10.442	37.31	104
$\text{Ca}_{10}\text{K}(\text{PO}_4)_7$	10.471	37.29	104
$\text{Ca}_9\text{MgLi}(\text{PO}_4)_7$	10.321	37.06	106
$\text{Ca}_9\text{MgNa}(\text{PO}_4)_7$	10.346	37.04	106
$\text{Ca}_9\text{MgK}(\text{PO}_4)_7$	10.398	36.96	106
$\text{Ca}_{18}\text{Na}_3\text{Fe}(\text{PO}_4)_{14}$	10.373	37.18	107
$\text{Ca}_{18}\text{Na}_3\text{Nd}(\text{PO}_4)_{14}$	10.458	37.39	107
$\text{Ca}_{19}\text{Cu}_2(\text{PO}_4)_{14}$	10.3638	37.219	110
$\text{Ca}_{19}\text{Cu}_2\text{H}_2(\text{PO}_4)_{14}$	10.3982	37.298	110

^a The crystal structure has been determined

IV. The structures and physicochemical properties of the materials

In the search for new or improved known materials with specified properties, synthetic chemists must either estimate theoretically or postulate the properties which the newly formed compounds will have. Known prototypes are most often used for such purposes and more rarely, data on the structure of the solid material. Certain possibilities for the prediction of properties on the basis of crystal-chemical data will be considered in this section. We shall deal with certain approaches to the solution of problems of this kind.

Since the 1960s, a vigorous search for laser materials and phosphors has been prosecuted. Some of them have found applications in engineering. One of the most important characteristics of such materials is the lifetime (τ) of the excited state and the quantum yield. These two characteristics are interrelated. An increase in the concentration of the activator in the matrix is usually accompanied by a decrease in the lifetime and an increase in the quantum yield. According to the data of Hong and Chinn,⁷ the optimum ratio of these parameters is observed for materials containing isolated NdO_x polyhedra, which prevent the Nd–Nd interaction and hence the concentration-induced quenching, and in which the polyhedron surrounding Nd^{3+} has no centre of inversion, since the intensity of the emission is largely associated with electric dipole transitions.

In laser materials with a high Nd^{3+} concentration ($> 10^{21} \text{ cm}^{-3}$, when the condition of 'localness' does not hold),¹⁹⁵ the Nd^{3+} – Nd^{3+} distances are 4.65–6.66 Å. As can be seen from the data presented in Table 6, the lifetime of the metastable levels for isostructural compounds, for example for $\text{M}_2\text{B}(\text{MoO}_4)_4$, increases with increasing Nd^{3+} – Nd^{3+} distance. However, such a dependence cannot be traced for the entire series of compounds presented in Table 6 because the symmetry of the surroundings of the activator ion changes in these phases. Thus the Nd^{3+} – Nd^{3+} distances in the $\text{K}_3\text{Nd}(\text{PO}_4)_2$ (see Ref. 7) and $\text{Na}_3\text{Nd}(\text{PO}_4)_2$ (see Ref. 13) structures, based on β -K₂SO₄,

Table 6. The lifetimes of the excited state (τ) and the Nd–Nd distances in certain laser materials.

Compound	$d_{\text{Nd-Nd}}/\text{\AA}$	$\tau/\mu\text{s}^a$		Ref.
		max	min	
NdP ₅ O ₁₄	5.194	115	320	196
KNdP ₄ O ₁₂	6.661	100	275	197
LiNdP ₄ O ₁₂	5.62	135	325	198
Na ₅ Nd(WO ₄) ₄	6.45	85	220	196
K ₅ Nd(MoO ₄) ₄	5.98	70	290	199
Rb ₅ Nd(MoO ₄) ₄	6.08	79	350	199
K ₃ Nd(PO ₄) ₂	4.873	21	460	7
Al ₃ Nd(BO ₃) ₄	5.917	19	50	200
Na ₃ Nd(PO ₄) ₂	4.65	see ^b	see ^b	13

^a The values τ for the maximum (max) and minimum (min) Nd³⁺ concentrations are quoted; ^b the lifetime of the metastable level has not been quoted ¹³ for Na₃Nd(PO₄)₂.

differ little (Table 6) and the lifetime of the metastable Na₃Nd(PO₄)₂ level is probably the same as for K₃Nd(PO₄)₂.

Crystal-chemical analysis makes it possible to estimate the laser characteristics of the compounds postulated. The structural type of bredigite, the structure of which contains fragments of the glaserite and β -K₂SO₄ structural types, should be promising in this connection. The insertion of glaserite columns between type β -K₂SO₄ columns would increase the Nd³⁺–Nd³⁺ distance by a factor of 2 and the latter, would amount to 9 Å on average. The neodymium concentration would diminish by a factor of 2 and would be $2 \times 10^{21} \text{ cm}^{-3}$ [in Na₃Nd(PO₄)₂, the Nd³⁺ concentration is $4 \times 10^{21} \text{ cm}^{-3}$]. In the postulated compound M₃Na₃NdR(PO₄)₄ (M = K, Rb; R = Lu, Sc), the minimum distance between the Nd atoms (5.4 Å) may be achieved only in the C column (Fig. 1). The lifetime of this compound would be $\sim 100 \mu\text{s}$, as for NdP₅O₁₄.¹⁹⁶ This conclusion is based on the fact that, as in NdP₅O₁₄, the two neighbouring Nd polyhedra in M₃Na₃NdR(PO₄)₄ do not have a common tetrahedron linking them and are separated by two tetrahedra or the NaO_x polyhedron.

The lifetimes of glaserite-like phases containing neodymium atoms may be estimated similarly. For example, the compound K₂NaNd(PO₄)₂ [obtainable by the heterovalent substitution $\text{K}^+ + 2\text{SO}_4^{2-} = \text{Nd}^{3+} + 2\text{PO}_4^{3-}$ in K₃Na(SO₄)₂] may serve as a laser material. Regardless of which of the polyhedra (X^[6+6] or Y^[4+6]) is occupied by Nd³⁺ cations, the minimum Nd³⁺–Nd³⁺ distances in the postulated phase would be determined by the X–X or Y–Y distances. These distances are the same and amount to 5.68 Å in glaserite itself. Two neighbouring (X or Y) polyhedra in K₂NaNd(PO₄)₂ are linked together by an edge of the tetrahedron, as in M₅Nd(MoO₄)₄. These data suggest that the lifetime of the metastable level in the compound K₂NaNd(PO₄)₂ would be of the same order of magnitude as in M₅Nd(MoO₄)₄. It follows from the data presented that, by using crystal-chemical ideas, it is possible to estimate to a first approximation the characteristics of laser materials.

In optical materials, the luminescence (lasing) line width depends on the number of activator cations, their surroundings, and the quality of the crystals. The smaller the difference between the surroundings of the activator cations, the smaller the half-width of the emission lines. Despite this, dilution is used to diminish the concentration-induced quenching in laser materials. For this purpose, Nd³⁺ cations are substituted by La³⁺, Lu³⁺, Y³⁺, or Bi³⁺ cations. The correct choice of the diluent cation can be achieved only by taking into account crystal-chemical data. For example, in order to reduce the concentration-induced quenching in M₅Nd(MoO₄)₄, it is more promising to substitute Nd³⁺ by La³⁺ and not by Y³⁺, Lu³⁺,

or Bi³⁺, which have surroundings in the palmierite-like matrix different from those of Nd³⁺.³¹

The luminescence line width of the lanthanide cation in M₅R(MoO₄)₄ (R = rare earth) is appreciably increased owing to the presence of several RO_x polyhedra in close proximity.³² When a second trivalent element (diluent) is introduced into such a material, the line width increases appreciably, which impairs the optical characteristics of the material. A similar effect is observed also in the Na₃Nd_{1-x}R_x(PO₄)₂ (R³⁺ = Gd, Lu, Y) solid solutions. The surroundings of Nd³⁺ and R³⁺ in these phases are different.¹⁶

Apart from crystal-chemical data, in selecting diluent cations it is useful to employ in certain cases other structure-sensitive methods, for example optical data may be employed. This extremely sensitive method makes it possible to determine the number of active centres and the limits of existence of the phases of two structurally similar compounds. In certain cases this method is the only one suitable for the elucidation of the regions of homogeneity. For example, in the study of the solid solutions in the Na₃Eu(PO₄)₂–K₃Eu(PO₄)₂, Na₃Gd(PO₄)₂–R₃Gd(PO₄)₂,²⁰¹ NaCaPO₄–Na₃Eu(PO₄)₂, NaSrPO₄–Na₃Eu(PO₄)₂,¹⁴² and Ca₃(PO₄)₂–Na₃R(PO₄)₂ (R = Nd, Eu, Er) solid solutions,¹⁸⁵ only the luminescence method made it possible to discover the limits of existence of the solid solutions. The X-ray powder diffraction analysis of a mixture of compounds with similar structures entails a large error in this case or altogether fails to distinguish them.

It has been established that the number of nonequivalent Eu³⁺ sites in the Na₃Eu(PO₄)₂–K₃Eu(PO₄) solid solutions²⁰¹ is the same as in the corresponding initial compounds. There are six such nonequivalent sites in Na₃Eu(PO₄)₂ and one in E₃Eu(PO₄)₂ (Fig. 13). It follows from the experimental determinations of the regions of homogeneity^{142,185,201} that the substitution of cations in the crystal lattice is accompanied by slight changes in the surroundings of the R³⁺ ions, which cannot be predicted solely on the basis of crystal-chemical data or be determined by X-ray diffraction.

Analysis of the geometry of the polyhedra and of their relative positions in the β -K₂SO₄ and glaserite structures made it possible to postulate initially the composition and then also to synthesise effective phosphors with lanthanide elements^{141,202–206} characterised by a long lifetime and a high luminescence intensity. In the search for such materials, various structural types were considered and the compositions of the compounds were modelled within the framework of a single structural type. For example, the introduction of Ce³⁺ and Tb³⁺ cations into a type β -K₂SO₄ matrix increased the quantum yield as a result of energy transfer from Ce³⁺ to Tb³⁺.^{203–205}

The ability of the tetrahedra to rotate readily, noted in the β -K₂SO₄ structural type, and the occurrence of low-temperature phase transitions in compounds of this type have been used by Elouadi et al.²⁰⁷ to predict the possible ferroelectric and piezoelectric transitions in the compounds MM'PO₄ (M = Na⁺, K⁺; M' = Ca²⁺, Zn²⁺, Sr²⁺, Ba²⁺, Pb²⁺). It has been established experimentally that such transitions occur in the temperature range 585–1470 K.²⁰⁷

In a study of the structure of the low-temperature modification of Na₃Sc₂(PO₄)₃, it has been found⁶⁸ that sodium occupies two close sites in the M(2) polyhedron with an 'effective' distance of 1.28 Å. The occupations of these sites differ by a factor of 1.7. Such non equivalence of the site occupations in the M(2) polyhedron is equivalent to the existence in the structure of a system of uncompensated dipoles,⁶⁸ the presence of which suggests ferroelectric properties [it has been established experimentally⁶⁶ that α -Na₃Sc₂(PO₄)₃ is a ferroelectric substance up to 333 K].

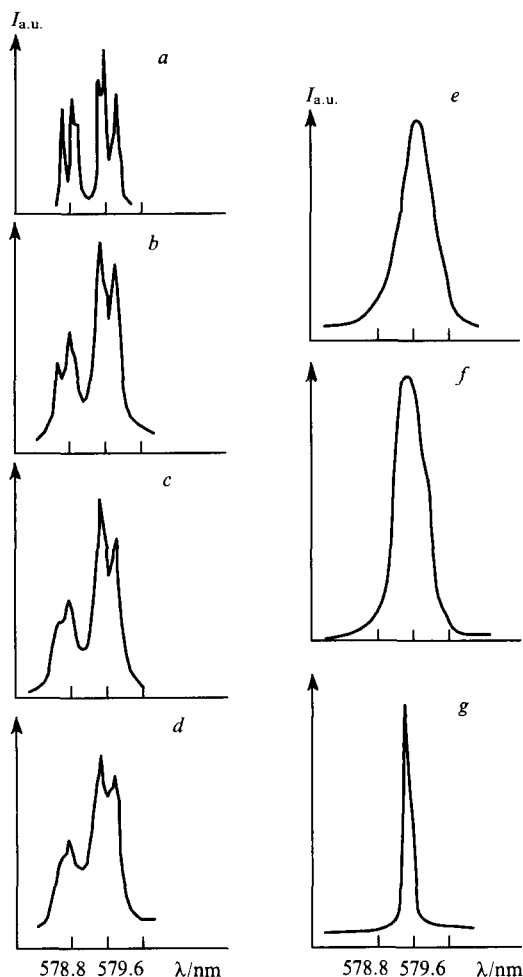


Figure 13. Luminescence spectra of Eu^{3+} in the region of the transition $^5D_0 \rightarrow ^7F_0$ in $\text{Na}_{3-x}\text{K}_x\text{Eu}(\text{PO}_4)_2$: (a) $x = 0$; (b) $x = 0.15$; (c) $x = 0.4$; (d) $x = 0.6$; (e) $x = 1$; (f) $x = 1.5$; (g) $x = 3$.²⁰¹

V. Conclusion

It follows from the data presented in this review that crystal chemistry constitutes an effective instrument for the modelling of the compositions of new compounds with a specified structure, for the prediction of new materials with specified properties, for the modification and improvement of the properties of materials, and for the correct interpretation of experimental data concerning the regions of existence of the initial phases and their polymorphic transitions.

Furthermore, reliable information about the structure of a solid makes it possible to estimate the crystal lattice energies of known and model phases, to establish the symmetry and the coordination environment of the cations in the compounds, to determine the geometrical characteristics of the polyhedra in the structure and their relative positions, to determine or estimate the cation-cation and cation-anion distances in the model phases, to introduce chemical elements with different dimensions and oxidation states into the crystal lattice of the structure in order to obtain materials with the required properties, and to deform the structure in order to improve the properties or obtain materials with unusual properties (for example, oxide superconductors).

However, at the present time crystal-chemical data are used effectively only for the interpretation of experimental data and to only a very slight extent (excluding the search for superconducting materials) for the prediction of the compositions of materials and their properties. The reason

for this is the lack of a well-founded algorithm for the application of the crystal-chemical data accumulated hitherto (due to the fact that the relevant studies have been shared between synthetic and structural chemists).

At the present time, problems in materials science are mainly considered from the composition-structure-property standpoint. Such a scheme includes the following components: (1) empirical search for the compound; (2) the study of its structure; (3) the study of its properties. On the other hand, the structure-property-composition scheme proposed in the present review includes the following components: (1) analysis of the structures of the compounds or classes of compounds; (2) prediction of the possible properties; (3) prediction of the compositions of the compounds with the necessary properties; (4) synthesis of the predicted compounds; (5) test of the properties; (6) refinement of the structure (if necessary). At the present level of development of solid state chemistry and information science, this approach is quite realistic. It makes it possible to shorten the time required to search for the necessary compositions of the compounds or phases and also to reduce the extent to which the equipment is used and to diminish the expenditure on the search stages. The structures of a large number of inorganic compounds have now been established; there exists a data bank for the structures of many inorganic phases; the radii of the cations in fluoride and oxide phases have been determined fairly reliably.^{47, 48}

On the basis of the crystal-chemical analysis of structures belonging to different structural types and containing tetrahedral anions described above, the following algorithm may be proposed for the search for compounds with specified structures and properties.

1. Determination of the projections, layers, or fragments of the structure with the greatest information content for the differentiation of the occupied and free polyhedra and channels.
2. Analysis of the symmetry and the geometrical characteristics of the differentiated polyhedra in the structure (structural types) in order to introduce into the latter new cations by means of isovalent or heterovalent substitution.
3. Establishment of a general crystal-chemical formula taking into account the occupied, free, and partly occupied sites.
4. Modelling of the compositions of the possible compounds by means of isovalent or heterovalent substitutions in the cationic or anionic sublattice taking into account the formal valences and dimensions of the atoms and polyhedra.
5. Comparison of blocks of different structural types in order to achieve their arrangement for the formation of a new structural type (made up of two or several fragments of different structural types) in which the distances between the cations are specified.

6. Estimation of the crystal lattice energy change following the introduction of additional atoms into the basic structure or structural type.

7. Prediction and estimation of the possible properties taking into account the characteristics of the structure.

Depending on the tasks faced by the synthetic chemist, some of the items may be omitted or they may change places, but items 1-4 and 7 are in all cases fundamental for the specific design of new compounds based on crystal-chemical data.

Only one of the possible aspects of the construction of compounds (geometrical and spatial factors) has been considered in the present review. Problems concerning the distortion of crystal lattices, the changes in symmetry, the distribution of cations and electron density in the structure, energetic aspects, and others have been considered only occasionally, mainly for the understanding of the transition from the model to a specific compound. There is no doubt that, in the solution of a problem as complex as the modelling of the compositions, structures, and properties of new phases, many approaches exist which have not been mentioned in this review, for example the methods of energetic crystal chemistry.²⁰⁸

References

1. K Okada, U Ossaka *Acta Crystallogr., Sect. B, Struct. Crystallogr.* **36** 919 (1980)
2. V B Kalinin, Candidate Thesis in Chemical Sciences, Moscow State University, Moscow, 1974
3. V B Kalinin, G Ya Pushkina, V A Efremov, P P Mel'nikov, L N Komissarova *Zh. Neorg. Khim.* **23** 943 (1978)
4. P P Mel'nikov, L N Komissarova *Dokl. Akad. Nauk SSSR* **256** 878 (1981)
5. V A Efremov, P P Mel'nikov, L N Komissarova *Koord. Khim.* **7** 467 (1981)
6. V A Efremov, P P Melnikov, L N Komissarova *Rev. Chim. Miner.* **22** 666 (1985)
7. H Y-P Hong, S R Chinn *Mater. Res. Bull.* **11** 421 (1976)
8. P P Mel'nikov, L N Komissarova *Koord. Khim.* **12** 1299 (1986)
9. P P Melnikov, V A Efremov, H Quiroga, L N Komissarova *J. Less-Common. Met.* **91** 21 (1983)
10. M T Robinson *J. Phys. Chem.* **62** 925 (1958)
11. M Vlasse, R Salmon, C Parent *Inorg. Chem.* **15** 1440 (1976)
12. C Parent, J Fava, R Salmon, M Vlasse, G Le Flem, P Hagenmuller, E Antic-Fidancev, M Lemaitre-Blaise, P Caro *Nouv. J. Chim.* **3** 523 (1979)
13. R Salmon, C Parent, M Vlasse, G Le Flem *Mater. Res. Bull.* **13** 439 (1978)
14. R Salmon, C Parent, G Le Flem, M Vlasse *Acta Crystallogr., Sect. B, Struct. Crystallogr.* **32** 2799 (1976)
15. C Parent, G Demazeau, R Salmon, G Le Flem *Rev. Chim. Miner.* **16** 548 (1979)
16. M Vlasse, C Parent, R Salmon, G Le Flem, P Hagenmuller *J. Solid State Chem.* **35** 318 (1980)
17. R Masse, A Durif *J. Solid State Chem.* **71** 574 (1987)
18. M Ben Amara, M Vlasse, G Le Flem, P Hagenmuller *Acta Crystallogr., Sect. C, Cryst. Struct. Commun.* **39** 1483 (1983)
19. B Dickens, W E Brown *Tschermaks Mineral. Petrog. Mitt.* **16** 1 (1971)
20. G Engle G, U Fisher *Z. Kristallogr.* **173** 101 (1991)
21. M Ben Amara, R Olazcuaga, G Le Flem, M Vlasse *Acta Crystallogr., Sect. B, Struct. Crystallogr.* **35** 1567 (1979)
22. M Mathew, L W Schroeder, B Dickens, W E Brown *Acta Crystallogr., Sect. B, Struct. Crystallogr.* **33** 1325 (1977)
23. C K Moller *Acta Chem. Scand.* **8** 81 (1954)
24. Y Schwarz *Angew. Chem.* **75** 1112 (1963)
25. P Susse, M Buerger, J Martin *Z. Kristallogr.* **131** 161 (1970)
26. W H Zachariasen *Acta Crystallogr.* **1** 263 (1948)
27. A Durif *Acta Crystallogr.* **12** 420 (1959)
28. V K Trunov, T P Rybakova *Zh. Neorg. Khim.* **15** 3028 (1970)
29. T P Rybakova, V K Trunov *Zh. Neorg. Khim.* **16** 277 (1971)
30. V A Efremov, V K Trunov *Kristallografiya* **19** 989 (1974)
31. B I Lazoryak, V A Efremov *Kristallografiya* **32** 378 (1987)
32. B I Lazoryak, V A Efremov *Kristallografiya* **31** 237 (1986)
33. J B Goodenough, H-P Hong, J A Kafalas *Mater. Res. Bull.* **11** 203 (1976)
34. G V Subba Rao, U V Varadaraju, K A Thomas, B Sivasankar *J. Solid State Chem.* **70** 101 (1987)
35. D Tran Qui, S Hamdoune, J L Soubeyroux, E Prince *J. Solid State Chem.* **72** 309 (1988)
36. U Warhus, J Maier, A Rabenau *J. Solid State Chem.* **72** 113 (1988)
37. C Delmas, F Cherkaoui, P Hagenmuller *Mater. Res. Bull.* **21** 469 (1986)
38. A Feltz, St Barth, M Andratschke, Ch Jager *J. Less-Common. Met.* **137** 43 (1988)
39. R G Sizova, A A Voronkov, N G Shumyatskaya, V V Ilyukhin *Dokl. Akad. Nauk SSSR* **205** 90 (1972)
40. R G Sizova, V A Blinov, V A Kuznetsov, A A Voronkov, V V Ilyukhin, N V Belov *Dokl. Akad. Nauk SSSR* **238** 855 (1978)
41. V A Efremov, B I Lazoryak, V K Trunov *Kristallografiya* **26** 72 (1981)
42. C Milton, B L Ingram, L V Blade *Am. Mineral.* **46** 533 (1961)
43. P Granguly, C N R Rao *J. Solid State Chem.* **53** 193 (1984)
44. P B Moore, T Araki *Am. Mineral.* **61** 74 (1976)
45. R Perret, M Damak *J. Less-Common. Met.* **108** 23 (1985)
46. C Calvo, R Gopal *Am. Mineral.* **60** 120 (1975)
47. R D Shannon, C T Prewitt *Acta Crystallogr., Sect. B, Struct. Crystallogr.* **25** 925 (1969)
48. R D Shannon *Acta Crystallogr., Sect. A, Fund. Crystallogr.* **32** 751 (1976)
49. G Demazeau, B Buffat, F Menil, L Fournes, M Pouchard, J M Dance, P B Fabritchnyi, P Hagenmuller *Mater. Res. Bull.* **16** 1465 (1981)
50. S Khairoun, J M Dance, J Grannec, G Demazeau, A Tressaud *Rev. Chim. Miner.* **20** 871 (1983)
51. J G Bednorz, K A Muller *Z. Phys. B, Condens. Matter* **64** 189 (1986)
52. C N R Rao *J. Solid State Chem.* **74** 147 (1988)
53. E V Antipov, L N Lykova, L N Kovba *Zh. Vses. Khim. O-va im. D. I. Mendeleeva* **34** 458 (1989)
54. E V Antipov, S N Putilin *Priroda (Moscow)* **10** 3 (1994)
55. H Maeda, A Koizumi, N Bamba, E Takayama-Muromachi, F Izumi, M Onoda, Y Kuroda, H Maruyama, Y Yoshikawa *Jpn. J. Appl. Phys. 2, Lett.* **27** 807 (1988)
56. H Maeda, Y Tanaka, M Fukutomi, T Asano *Jpn. J. Appl. Phys.* **27** 209 (1988)
57. Z Z Sheng, A M Hermann *Nature (London)* **332** 55 (1988)
58. Z Z Sheng, A M Hermann *Nature (London)* **332** 138 (1988)
59. R I Cava, B Batlogg, J Krajewski, L W Rupp, L F Schneemeyer, T Siegrist, R B Van Dover, P Marsh, W F Peck *Nature (London)* **336** 211 (1988)
60. S N Putilin, E V Antipov, O Chmaissem, M Marezio *Nature (London)* **362** 226 (1993)
61. S N Putilin, I Brunse, E V Antipov *Mater. Res. Bull.* **26** 1299 (1991)
62. H Y-P Hong *Mater. Res. Bull.* **11** 173 (1976)
63. N B Desai, K Byrappa, A B Kulkarni, G S Gopalkrishana *Bull. Mater. Sci.* **9** 117 (1987)
64. S Ikeda, M Takahashi, J Ishikawa, K Ito *Solid State Ion.* **23** 125 (1987)
65. F D'Yvoire, M Pintard-Screpel, E Bretey *C.R. Seances Acad. Sci., Ser. C* **290** 185 (1980)
66. S Yu Stefanovich, V B Kalinin *Fiz. Tverd. Tela* **23** 3509 (1981)
67. B I Lazoryak, V B Kalinin, S Yu Stefanovich, V A Efremov *Dokl. Akad. Nauk SSSR* **250** 861 (1980)
68. V A Efremov, V B Kalinin *Kristallografiya* **23** 703 (1978)
69. V B Kalinin, B I Lazoryak, S Yu Stefanovich *Kristallografiya* **25** 264 (1983)
70. H Kohler, H Schulz *Mater. Res. Bull.* **20** 1461 (1985)
71. H Kohler, H Schulz *Mater. Res. Bull.* **21** 23 (1986)
72. F Cherkaoui, G Villeneuve, C Demals, P Hagenmuller *J. Solid State Chem.* **65** 293 (1986)
73. L O Hagman, P Kierkegaard *Acta Chem. Scand.* **22** 1822 (1968)
74. J-M Winand, A Rulmoot, P Tarte *J. Solid State Chem.* **107** 351 (1993)
75. J-M Winand, A Rulmoot, P Tarte *J. Solid State Chem.* **93** 341 (1991)
76. J Gapalakrishnan, K Kasturirangan *Chem. Mater.* **4** 745 (1992)
77. S Krimi, I Mansouri, A El Jazouli, J P Chaminade, P Gravereau, G Le Flem *J. Solid State Chem.* **105** 561 (1993)
78. E Fargin, I Bussereau, R Olazcuaga, G Le Flem *J. Solid State Chem.*, **112** 176 (1994)
79. R Masse *Bull. Soc Fr. Mineral. Crystallogr.* **95** 405 (1972)
80. M Sugantha, U V Varadaraju, G V Subba Rao *J. Solid State Chem.* **111** 33 (1994)
81. A Boudjada, R Parret *C. R. Hebd. Seances Acad. Sci., Ser. C* **281** 31 (1975)
82. A El Jazouli, J L Soubeyroux, J M Dance, G Le Flem *J. Solid State Chem.* **65** 351 (1986)
83. M Alami Talbi, R Brochu, C Parent, L Robardel, G Le Flem *J. Solid State Chem.* **110** 350 (1994)
84. D K Agrawal, V S Stubichn *Mater. Res. Bull.* **20** 99 (1985)
85. S Y Li Mage, D K Agrawal, H A McKinstry *J. Am. Ceram. Soc.* **70** 232 (1987)
86. M Alami Talbi, R Brochu, C Parent, L Robardel, G Le Flem *J. Solid State Chem.* **118** 117 (1992)
87. M Pintard-Screpel, F D Yvoire, F Remy *C. R. Hebd. Seances Acad. Sci., Ser. C* **286** 381 (1978)
88. A Nogai, V B Kalinin, S Yu Stefanovich, R R Shifrina, Yu N Venevtsev *Zh. Neorg. Khim.* **31** 181 (1986)
89. C Delmas, R Olazcuaga, F Cherkaoui, R Brochu, G Le Flem *C. R. Hebd. Seances Acad. Sci., Ser. C* **287** 169 (1978)
90. B I Lazoryak, V A Efremov *Zh. Neorg. Khim.* **32** 652 (1987)
91. A Benmoussa, M M Borel, A Grandin, A Leclaire, R Raveau *Ann. Chim.* **14** 181 (1989)

92. A Nogai, V B Kalinin, S Yu Stefanovich, Yu N Venevtsev *Zh. Neorg. Khim.* **30** 2939 (1985)
93. P C Yao, D J Fray *Solid State Ion.* **8** 35 (1983)
94. A Mbandza, E Bordes, P Courtine *Mater. Res. Bull.* **20** 251 (1985)
95. E M MacCarron, J C Calabrese, M A Subramanian *Mater. Res. Bull.* **22** 1421 (1987)
96. G Le Polles, A El Jazouli, R Olazcuaga, J M Dance *Mater. Res. Bull.* **22** 1171 (1987)
97. L Monceaux, P Courtine *Eur. J. Solid State Inorg. Chem.* **28** 233 (1991)
98. P P Mel'nikov, E Kiroga Karri'l'o, Kh D Karri'l'o Egedero, V A Efremov, L N Komissarova *Dokl. Akad. Nauk SSSR* **285** 1134 (1985)
99. B Dickens, L W Schroeder, W E Brown *J. Solid State Chem.* **10** 232 (1974)
100. B I Lazoryak, S Yu Oralkov, V N Golubev, A N Zhdanova *Zh. Neorg. Khim.* **34** 1710 (1989)
101. V N Golubev, B I Lazoryak *Izv. Akad. Nauk SSSR, Neorg. Mater.* **27** 576 (1991)
102. V N Golubev, B N Viting, O B Dogadin, B I Lazoryak, R G Aziev *Zh. Neorg. Khim.* **35** 3037 (1990)
103. B I Lazoryak, V N Golubev, R Salmon, C Parent, P Hagenmuller *Eur. J. Solid State Inorg. Chem.* **26** 455 (1989)
104. S Yu Oralkov, B I Lazoryak, R G Aziev *Zh. Neorg. Khim.* **33** 73 (1987)
105. O V Yanov, V A Morozov, B N Vieting, L N Ivanov, B I Lazoryak *Mater. Res. Bull.* **29** 1307 (1994)
106. B I Lazoryak, S V Khoina, V N Golubev, R G Aziev *Zh. Neorg. Khim.* **35** 1374 (1990)
107. B I Lazoryak, T V Strunenkov, V N Golubev, E A Vovk, L N Ivanov *Mater. Res. Bull.* **31** 207 (1996)
108. B I Lazoryak, R Sal'mon, K Parent, P Khagenmyuller, B N Viting, A B Yaroslavtsev *Vest. Mosk. Univ., Ser. 2, Khim.* **31** 406 (1990)
109. B I Lazoryak, V A Morozov, M S Safonov *Mater. Res. Bull.* **30** 1269 (1995)
110. B I Lazoryak, Doctoral Thesis in Chemical Sciences, Moscow State University, Moscow, 1992
111. S Attaly, B Vigouroux, M Lenzi, J Persia *J. Catal.* **63** 456 (1980)
112. R Guardia-Useche, J Lenzi, M Lenzi *Bull. Soc. Chim. Fr.* (1-2) I-25 (1982)
113. M M Andrushkevich, V V Molchanov, G N Kustova, L M Plyasova, G S Litvak, R A Buyanov, G R Kotel'nikov, L V Strunnikova *Kinet. Katal.* **21** 1034 (1980)
114. M M Andrushkevich, G R Kotel'nikov, V V Molchanov, G N Kustova, A V Golovin, R A Buyanov, L V Strunnikova *Kinet. Katal.* **21** 1041 (1980)
115. J-P Bourgeois, M Lenzi *C. R. Hebd. Seances Acad. Sci., Ser. C* **277** 375 (1973)
116. M S Safonov, B I Lazoryak, S B Pozharskii, S B Dashkov *Dokl. Akad. Nauk* **338** 633 (1994)
117. M Ishida, D Zheng, T Akehata *Energy* **12** 147 (1987)
118. B I Lazoryak, in *Fundamental'nye Issledovaniya Materialov i Protsessov v Veshchestve* (Fundamental Investigations of Materials and Processes in Matter) (Ed. Yu D Tret'yakov) (Moscow: Izd. Mosk. Gos. Univ., 1994) p. 54
119. V A Efremov *Usp. Khim.* **59** 1085 (1990) [*Russ. Chem. Rev.* **59** 627 (1990)]
120. R W Nurse, J H Welch, W Gutt *J. Chem. Soc.* 1077 (1959)
121. W Gutt *Silicat. Ind.* **27** 285 (1962)
122. W Fix, H Heymann, R Heinke *J. Am. Ceram. Soc.* **52** 346 (1969)
123. M A Bredig *Am. Mineral.* **28** 594 (1942)
124. R L Barrett, W J McCaughey *Am. Mineral.* **27** 680 (1942)
125. B I Lazoryak, V N Golubev, R G Aziev *Kristallografiya* **33** 1113 (1988)
126. B I Lazoryak, B Baatarsukh, V N Golubev, R G Aziev *Khim. Promst* (10) 604 (1991)
127. B Baatarsukh, V N Golubev, B I Lazoryak, R G Aziev *Khim. Promst* (11) 663 (1991)
128. B Baatarsukh, B I Lazoryak, R G Aziev *Vest. Mosk. Univ., Ser. 2, Khim.* **29** 418 (1988)
129. B Baatarsukh, Candidate Thesis in Chemical Sciences, Moscow State University, Moscow, 1988
130. V N Golubev, Candidate Thesis in Chemical Sciences, Moscow State University, Moscow, 1988
131. V F Kozak, V I Domanskii, A I Boikova, V V Ilyukhin, N V Belov *Kristallografiya* **19** 1179 (1974)
132. R W Nurse, J H Welch, W A Gutt *Nature (London)* **182** 1230 (1958)
133. P B Moore, T Araki *Am. Mineral.* **57** 1355 (1972)
134. C Calvo, R Faggiani *Can J. Chem.* **53** 1849 (1975)
135. V K Trunov, V A Efremov, Yu A Velikodnyi *Kristalloghimiya i Svoistva Dvoynykh Molibdatov i Vol'framatov* (Crystal Chemistry and Properties of Double Molybdates and Tungstates) (Leningrad: Nauka, 1986)
136. K H Jost, B Ziemer, R Seydel *Acta Crystallogr., Sect. B., Struct. Crystallogr.* **33** 1696 (1977)
137. W Eysel, T Wahn *Z. Kristallogr.* **131** 322 (1970)
138. J Barbier, B G Hyde *Acta Crystallogr., Sect. B, Struct. Sci.* **41** 383 (1985)
139. M Catti, G Gazzoni, G Ivaldi, G Zanian *Acta Crystallogr., Sect. B, Struct. Sci.* **39** 674 (1983)
140. M Catti, G Gazzoni, P Ivaldi *Acta Crystallogr., Sect. C, Cryst Struct. Commun.* **39** 29 (1983)
141. H Saalfeld, K H Klaska *Z. Kristallogr.* **155** 65 (1981)
142. M Ben Amara, C Parent, M Vlasse, G Le Flem *J. Solid State Chem.* **46** 321 (1983)
143. M Ben Amara, C Parent, M Vlasse, E Antic-Fidancev, B Pirou, P Caro *J. Less-Common. Met.* **93** 425 (1983)
144. S Draï, R Olazcuaga, G Le Flem *J. Solid State Chem.* **10** 95 (1974)
145. A W Kolsi, M Querton, W Freundlich *J. Solid State Chem.* **36** 107 (1981)
146. C W By Struc, J G White *Acta Crystallogr.* **15** 290 (1962)
147. G Waliez, S Jaulmes, A Elfakir, M Querton *J. Solid State Chem.* **114** 123 (1995)
148. R Salmon, C Parent, G Le Flem *Mater. Res. Bull.* **14** 85 (1979)
149. M Querton, M T Oumba, W Freundlich, A W Kolsi *Mater. Res. Bull.* **19** 1063 (1984)
150. J Moring, E Kostiner *J. Solid State Chem.* **61** 379 (1986)
151. M-Th Paques-Ledent *Rev. Chim. Miner.* **10** 785 (1973)
152. G M Biggar *Cement Concrete Res.* **1** 493 (1971)
153. U Keppler *Z. Kristallogr.* **132** 228 (1970)
154. J Barbier, D Maxin *J. Solid State Chem.* **116** 179 (1995)
155. V A Efremov, V K Trunov *Dokl. Akad. Nauk SSSR* **235** 820 (1977)
156. P V Klevtsov, L P Kozeeva, V I Protasova, V Yu Kharchenko, L A Glinskaya, R F Klevtsova, V V Bakakin *Kristallografiya* **20** 57 (1975)
157. B I Lazoryak, V A Efremov *Kristallografiya* **26** 464 (1981)
158. O V Kudin, V A Efremov, V K Trunov *Zh. Neorg. Khim.* **26** 2734 (1981)
159. V A Efremov, Candidate Thesis in Chemical Sciences, Moscow State University, Moscow, 1976
160. R F Klevtsova, L P Glinskaya *Dokl. Akad. Nauk SSSR* **230** 1337 (1976)
161. B I Lazoryak, V A Efremov, P B Fabricnyi, A R Gizhinskii *Dokl. Akad. Nauk SSSR* **237** 1354 (1977)
162. P V Klevtsov, L P Kozeeva, R F Klevtsova *Izv. Akad. Nauk SSSR, Neorg. Mater.* **10** 2234 (1974)
163. P V Klevtsov, V A Vinokurov *Izv. Akad. Nauk SSSR, Neorg. Mater.* **11** 387 (1975)
164. L P Kozeeva, I G Konstanchuk, P V Klevtsov *Izv. Akad. Nauk SSSR, Neorg. Mater.* **11** 2096 (1975)
165. V K Trunov, Yu A Velikodnyi *Izv. Akad. Nauk SSSR, Neorg. Mater.* **8** 881 (1972)
166. K Hartl, R Braumgart *Z. Naturforsch., B Chem. Sci.* **33** 954 (1978)
167. M V Paromova, L N Lykova, Z Ya Kulikova, L M Kovba *Vest. Mosk. Univ., Ser. 2, Khim.* **18** 79 (1977)
168. H Schwarz *Z. Anorg. Allg. Chem.* **345** 230 (1966)
169. L D Iskhakova, V E Plyushchev, L A Perezhogina *Zh. Neorg. Khim.* **16** 1836 (1971)
170. H Schwarz *Z. Anorg. Allg. Chem.* **344** 41 (1966)
171. V K Trunov, L D Iskhakova, N N Solov'eva *Zh. Neorg. Khim.* **22** 2005 (1977)
172. N N Bushuev, V K Trunov *Dokl. Akad. Nauk SSSR* **217** 827 (1974)
173. I P Silvestre, A Durif *J. Solid State Chem.* **24** 97 (1978)
174. S C Abrahams, J L Bernstein *J. Chem. Phys.* **45** 2745 (1966)
175. B I Lazoryak, Candidate Thesis in Chemical Sciences, Moscow State University, Moscow, 1982

176. L M Plyasova, R F Klevtsova, S V Borisov, L M Kefeli *Dokl. Akad. Nauk SSSR* **167** 84 (1966)
177. P C Christidis, P J Rentzeperis *Z. Kristallogr.* **141** 233 (1975)
178. R Perret, B Rosso, J Loriers *Bull. Soc. Chim. Fr.* **7** 2698 (1968)
179. L Bennouna, S Arsalane, R Brochu, M R Lee, J Chassaing, M Quarton *J. Solid State Chem.* **114** 224 (1995)
180. A Clearfield, B D Roberts, M A Subramanian *Mater. Res. Bull.* **19** 219 (1984)
181. M Sljukic, B Matkovic, B Prodic, D Anderson *Z. Kristallogr.* **130** 148 (1969)
182. A Zemman, J Zemman *Acta Crystallogr.* **10** 409 (1957)
183. R G Sizova, V A Blinov, A A Voronkov, V V Ilyukhin, N N Belov *Kristallografiya* **26** 293 (1981)
184. B I Lazoryak, T V Strunenkov, S Yu Oralkov, B N Viting *Zh. Neorg. Khim.* **34** 2044 (1989)
185. B I Lazoryak, L N Ivanov, T V Strunenkov, V N Golubev, B N Viting *Izv. Akad. Nauk SSSR, Neorg. Mater.* **26** 341 (1990)
186. B N Viting, Candidate Thesis in Chemical Sciences, Moscow State University, Moscow, 1990
187. P B Moore, J Shen *Am. Mineral.* **68** 996 (1983)
188. B I Lazoryak, B N Viting, P B Fabrichnyi, L Furnes, R Sal'mon, P Khagenmyuller *Kristallografiya* **35** 837 (1990)
189. B I Lazoryak, B N Viting, P B Fabrichnyi, L Furnes, R Sal'mon, P Khagenmyuller *Kristallografiya* **35** 1403 (1990)
190. R Gopal, C Calvo *Can. J. Chem.* **49** 1036 (1971)
191. R Gopal, C Calvo *Z. Kristallogr.* **137** 67 (1971)
192. R Gopal, C Calvo, J Ito, W K Sabine *Can. J. Chem.* **52** 1155 (1974)
193. E Kostiner, J R Rea *Acta Crystallogr., Sect. B, Struct. Crystallogr.* **32** 250 (1976)
194. L W Schroeder, B Dickens, W E Brown *J. Solid State Chem.* **22** 253 (1977)
195. A A Kaminskii *Lazernye Kristally* (Laser Crystals) (Moscow: Nauka, 1975)
196. H Y-P Hong, K Dwight *Mater. Res. Bull.* **9** 775 (1974)
197. H Y-P Hong *Mater. Res. Bull.* **10** 1105 (1975)
198. T Yamada, K Otsuka, J Nakano *J. Appl. Phys.* **45** 5096 (1974)
199. E V Vasil'ev, A A Evdokimov, V A Efremov, B I Lazoryak, V F Populovskii, R K Sviridova, A F Solokha, V K Trunov *Zh. Prikl. Spektrosk.* **29** 846 (1978)
200. H Y-P Hong, K Dwight *Mater. Res. Bull.* **9** 1661 (1974)
201. M Mesnaoui, M Maazaz, Zhang Jin Chao, C Parent, R Olazcuage, G Le Flem, P Hagenmuller *Rev. Chim. Miner.* **24** 338 (1987)
202. C Parent ThD L'Universite de Bordeaux, France, 1980
203. C Parent, P Bochu, A Daoudi, G Le Flem *J. Solid State Chem.* **43** 190 (1982)
204. J Fava, A Perrin, J C Bourcet, R Salmon, C Parent, G Le Flem *J. Lumin.* **18/19** 389 (1979)
205. C Parent, G Le Flem, M Et-Tabirou, A Daoudi *Solid State Commun.* **37** 857 (1981)
206. C Parent, J Fava, R Salmon, G Le Flem, P Hagenmuller *Solid State Commun.* **35** 451 (1980)
207. B Elouadi, L Elammari, J Ravez *Ferroelectrics* **56** 17 (1984)
208. V S Urusov, L S Dubrovskii *EVM-Modelirovanie Struktury i Svoistv Mineralov* (Computer Modelling of the Structure and Properties of Minerals) (Moscow: Izd. Mosk. Gos. Univ., 1989)

The tautomerism of heterocyclic thiols. Five-membered heterocycles

E D Shtefan, V Yu Vvedenskii

Contents

I. Introduction	307
II. Furan-, thiophene- and selenophene-thiols	307
III. 5-Mercaptopyrazoles	307
IV. Imidazolethiones and 1,3-oxazole-2-thiones	308
V. Thiazole-2-thiones	308
VI. 1,3,4-Oxadiazolethiones and 1,3,4-thia(selena)diazolethiones	308
VII. 5-Mercapto-1,3,4-thiadiazole-2-thiones and 1,2,4-thiadiazole-3,5-dithione	309
VIII. 1,2,4-Triazolethiones	310
IX. Tetrazolethiones	311

Abstract. Data on the tautomerism of five-membered heterocyclic thiols and its effect on the behaviour of these compounds in different chemical reactions are surveyed. The bibliography includes 113 references.

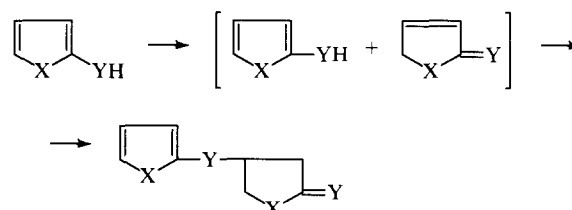
I. Introduction

The tautomerism possible in heterocyclic thiols imparts a considerable diversity to their properties compared with those of aromatic thiols. Consequently, the investigation of the effect of tautomerism on the mechanism of the reactions of these compounds is interesting. In the present review, we attempted to combine the results of spectroscopic studies with selected data on the reactivity of five-membered heterocyclic thiols, namely, data directly concerned with the tautomeric nature of the latter. It is to be noted that there is a series of reviews and general monographs on the tautomerism itself,¹ as well as on the chemistry of certain classes of heterocyclic compounds,^{2–7} which to a certain extent deal with the problems under consideration. However, new experimental data have been published recently and need to be surveyed. The new data have served as a basis for the consideration of particular types of thiols in this review.

II. Furan-, thiophene- and selenophene-thiols

Unlike the hydroxy derivatives that mostly occur as oxo-forms, furan- and thiophene-thiols exist, according to all spectroscopic and other physicochemical characteristics, as mercapto-compounds.^{5,6,8–12} The only report¹³ that 2-mercaptoselenophene occurs in the thione form has been disproved.¹⁴

At the same time, the tautomeric nature of these compounds was never doubted. Besides the thione structure of mercapto-aldehydes (see the review of Litvinov et al.¹⁵) and the ketonic structure of the corresponding heterocyclic hydroxy derivatives (see, for example, Gronovitz's review¹⁶), the most important evidence for the tautomeric nature of heterocyclic thiols was the extreme lability of the thiols of the thiophene and, particularly, the furan series. The corresponding selenols are even more labile. Some of them have only recently been characterised by spectroscopic methods.^{17,18} A common reason for the lability of the heterocyclic thiols and selenols proved to be associated with their tautomerism. Analysis of the auto-transformation products has shown these compounds to be dimers, which are most probably formed by the addition of the chalcogenols to their own tautomeric forms.^{14,16,17–22}

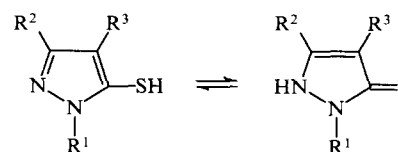


X = O, S, Se; Y = S, Se

This reaction is catalysed by triethylamine and phenylhydrazine (in the latter case, the hydrazones Y = N–NHPh of the dimeric products are formed).

III. 5-Mercaptopyrazoles

Mercaptopyrazoles represent an unusual example of compounds where tautomerism can be detected directly by spectroscopic methods.²³



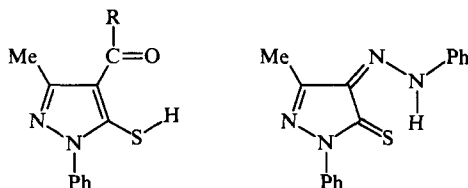
R¹, R² = Me, Ph; R³ = H, Me

E D Shtefan, V Yu Vvedenskii Irkutsk Institute of Organic Chemistry, Siberian Division of the Russian Academy of Sciences, ul. Favorskogo 1, 664033 Irkutsk, Russian Federation. Fax (7-395) 246 03 31. E-mail: vlad@iochem.irkutsk.su

Received 23 June 1995

Uspekhi Khimii 65 (4) 326–333 (1996); translated by A V Geiderikh

The equilibrium position depends strongly on the solvent. In aprotic media, the $[NH]:[SH]$ ratio increases with increase in the polarity of the medium. For example, the concentration of the NH-form of 5-mercapto-1,4-dimethyl-pyrazole in dioxane is close to zero, in THF it is about 5%, and in DMSO it is as high as 70%. In alcohols, the amount of the NH-form increases with increase in their ability to form hydrogen bonds. Depending on the nature of the substituent in the 4-position, intramolecular hydrogen bonds stabilise one or the other tautomer. It is the thiol form in the case of the carbonyl group, and the thione in the case of the phenylazo group.



R = H, Me, Ph

It is interesting to note that no traces of the possible third tautomer (C—H) have been found.

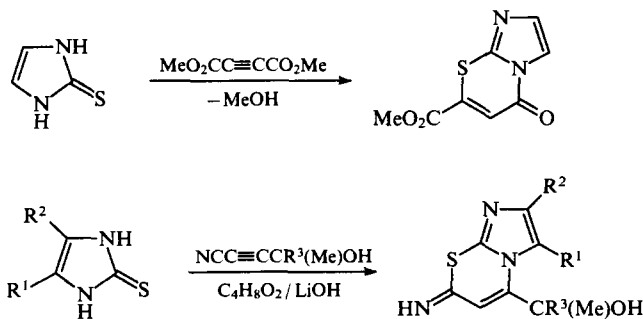
Only the SH-forms of 3-mercapto-1-methyl- and 5-mercapto-1-methyl-pyrazoles have been detected in their photoelectron spectra in nonpolar solvents.²⁴

IV. Imidazolethiones and 1,3-oxazole-2-thiones

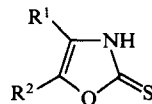
The ^{15}N NMR spectra of 2-mercapto-1-methyl-imidazole indicate that in a polar solvent (DMSO) this compound exists only in the thioamide form, while in chloroform the presence of a small amount (2%) of iminothiol form is observed.^{25,26} The additional stabilisation of the thioamide form in DMSO is caused presumably by formation of hydrogen bonds with the solvent. The prevalence of the thioamide form is also corroborated by UV,²⁷ ^{13}C NMR,²⁸ and photoelectron spectroscopy,²⁹ quadrupole resonance,³⁰ and acidity constant measurements.³¹ Polarographic studies have shown that 2-mercapto-1-methylimidazole occurs in the thione form in aqueous solution at $pH < 6$, while at $pH > 6$ it forms thiolates.³²

The IR spectrum of 1-methylimidazole-2-thione, obtained by Ettlinger as early as 1950,³³ is identical with that of the corresponding imidazolone; this is convincing evidence in favour of the thione structure.³⁴ An unexpected result was obtained by Spanish investigators.³⁵ According to their IR and Raman spectroscopic data, in the crystalline phase imidazolethione actually exists as the pure thiol. This conclusion probably requires additional proof.

Both the sulfur and nitrogen atoms can serve as the reaction centres in the nucleophilic addition of imidazolethiones to an activated acetylenic bond.^{36,37}



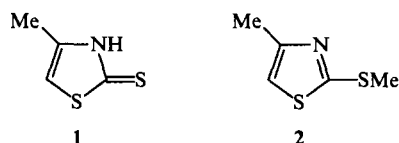
Data obtained by several investigators^{29,31,38-41} have shown that the IR spectra of a series of oxazole-2-thiones provide no grounds for doubts about their thione nature.



An MNDO calculation also confirms that the thione form predominates over the thiol form. The difference between the enthalpies of formation of these two forms is 43.96 kJ mol⁻¹ when $R^1 = R^2 = H$.⁴²

V. Thiazole-2-thiones

The first evidence for the thione structure of thiazolethione and its methyl derivatives was obtained by Ettlinger from IR spectra which were indistinguishable from those of thiazolones.³³ These data were confirmed in later studies.^{29,31,35,43-46} Sheinker, Postovskii, and Voronina supposed⁴³ that the thione form predominates both in the condensed phase and in solution (dioxane). This was confirmed by the comparison of the spectra of compounds 1 and 2.

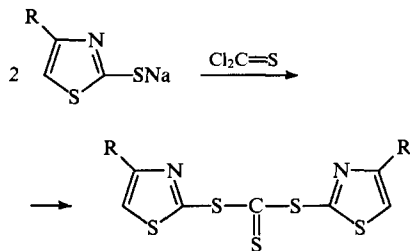


In addition, Flett has noted⁴⁴ that the NH vibration bands in the 3430 cm⁻¹ region in the spectrum of a solid sample disappeared in a CCl₄ solution. Hence it was concluded that 4-methylthiazole-2-thione exists in the crystalline form as thioamide complexes with hydrogen bonds.

The evidence for the thione structure of 4-indolyl-2-mercaptothiazole is, firstly, the absence of SH-group absorption bands in the IR spectra, and, secondly, the presence of a maximum at 332 nm in the UV spectrum, disappearing in an alkaline medium.⁴⁵

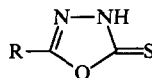
According to the MNDO calculation, the difference between the enthalpies of formation of the thione and thiol forms of the unsubstituted potential mercaptothiazole is 56.82 kJ mol⁻¹, which is evidence in favour of the thione form.⁴²

In an alkaline medium, the nucleophilic centre in the mercaptothiazole molecule is the exocyclic sulfur atom. For example, sodium thiazolethiolates react with thiophosgene to give trithiocarbonates.⁴⁷



VI. 1,3,4-Oxadiazolethiones and 1,3,4-thia(selena)diazolethiones

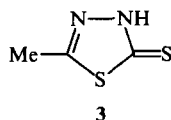
In 1956, Ainsworth obtained a series of substituted oxadiazolethiones.⁴⁸



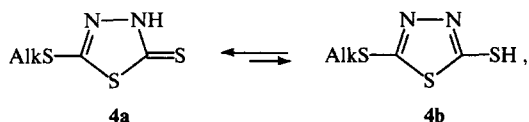
R = Alk, Ar, Het.

Their thione structures were confirmed by IR spectroscopic data.⁴⁸ Later studies^{49,50} gave the same result.

In 1958, Ainsworth⁵¹ found that the IR spectrum of 2-mercapto-5-phenyl-1,3,4-thiadiazole was identical with that of the corresponding oxadiazolethione; hence, this compound also exists in the thione form. A similar conclusion was also reached recently by Indian investigators⁵² who studied 5-substituted 2-mercapto-1,3,4-thiadiazoles. In the ¹H NMR spectra of these compounds, the chemical shift (δ) of the NH proton is about 5.2–5.5 ppm. There are no SH absorption bands (2500 to 2600 cm⁻¹) in the IR spectrum of the thione **3** in the condensed state.⁵³

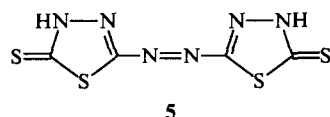


In the system

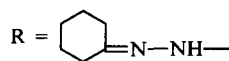
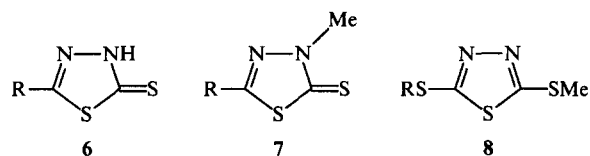


the equilibrium is significantly shifted towards the thione form, which has been confirmed by spectroscopic methods: IR (the absence of the SH-group absorption band), ¹H NMR [δ (NH) = 12–14 ppm], and ¹³C NMR spectroscopy [δ (C=S) = 188 ppm].^{54,55} Only in the IR spectrum of a concentrated chloroform solution, has a weak absorption of the SH group (2560 cm⁻¹) been detected, which may indicate the coexistence of two tautomeric forms.

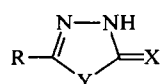
The absorption bands corresponding to the SH group were not found in the IR spectrum of 2,2'-azo-1,3,4-thiadiazole-5-thione **5**.⁵⁶



According to the data of Arvidsson and Sandström,⁵⁷ the hydrazones **6** and **7** have very similar UV spectra, differing markedly from that of the *S*-methylated compound **8**; this fact undoubtedly proves the thione structure of these compounds.



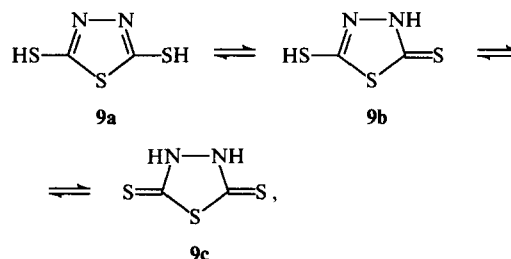
The structures of some potential thiols and selenols of thia- and selenodiazoles were studied by ¹³C NMR spectroscopy.⁵⁸ It was found that, on oxidation of these compounds to disulfides and diselenides respectively, the chemical shifts of the carbon atoms change significantly: the C(2) signal is shifted upfield (by about 30 ppm) and the C(5) signal is shifted downfield (by 10 ppm).



Bearing in mind that disulfides and diselenides should be good models for thiol and selenol tautomerism, these data suggest that the thione and selenone structures are preferred.

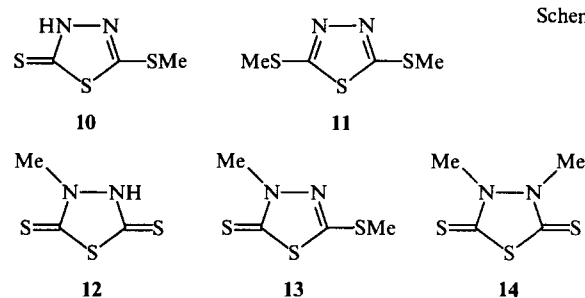
VII. 5-Mercapto-1,3,4-thiadiazole-2-thiones and 1,2,4-thiadiazole-3,5-dithione

The IR spectra of 2,5-dimercapto-1,3,4-thiadiazole **9**⁴³



contain a distinct absorption band in the region of 2489 cm⁻¹ (corresponding to the SH group) and intense bands in the range 2860–3067 cm⁻¹, indicating the presence of the NH group. Hence it was concluded that compound **9** has a mixed thione-thiol structure, i.e. form **9b** predominates.

Later, Thorn⁵⁹ undertook a detailed study of the absorption spectra of compound **9** and a series of its methyl derivatives **10**–**14** (Scheme 1).

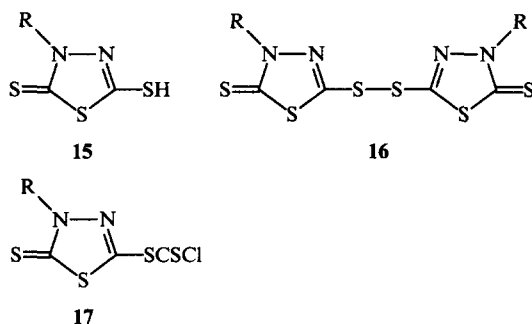


Compound	9	10	11	12	13	14
λ_{\max} /nm	335	318	288	333	320	324
	260	235	—	260	243	268

Analysis of the UV spectra revealed a striking similarity of the absorption maxima of compounds **9**, **12**, and **14** that appeared to show unambiguously that they have the dithione structure. However, this conclusion was not confirmed by IR spectra. In all the spectra except that of compound **11**, there is a band at 1475–1508 cm⁻¹, which has been assigned to the thioamide fragment. However, for all the compounds except compound **14**, the band at 1415–1435 cm⁻¹, which should be assigned to the iminothiol group, is also detected. Furthermore, in the spectra of compounds **9** and **12** bands in the thiol region (2590 cm⁻¹ and 2555 cm⁻¹ respectively) were detected. To account for this discrepancy between the IR and UV spectroscopic data, Thorn assumed⁵⁹ that compounds **9** and **12** exist in a mixed form in a concentrated chloroform solution (i.e. under the conditions of the recording of the IR spectra) while the dithione form prevails in dilute alcoholic solution used for UV spectroscopy. Stanovnik and Tišler⁶⁰ suggested a 'monomercapto-monodipolar' structure for compound **9**. Later, the presence of at least one thiol group was established⁶¹ by IR spectroscopy, this group being deprotonated on formation of complexes with metals.

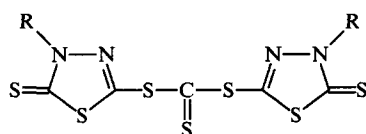
Zaidi et al.⁶² have noted the presence of a 'weak' absorption band (at about 2490 cm⁻¹) due to the thiol group, in contrast to the 'medium' bands at 3060 cm⁻¹ and 2875 cm⁻¹ corresponding to the N–H bond. They suggested that structure **9b** should be discounted, because the band due to the SH group is too weak compared with that of the NH group; thus, 2,5-dimercapto-1,3,4-thiadiazole exists mainly in the dithione form, which is in equilibrium with a small amount of the thiol form. However, in the next paper⁶³ a modified view was expressed: here the SH

bands were classified as 'medium', and the NH bands — as 'strong'. This has two possible explanations. Firstly, the authors⁶³ may have been influenced by their own results on the structures of complexes of compound **9** with transition metals, where the ligand is in the thione-thiolate form **9b**. Secondly, the important study by Anthony et al.⁶⁴ was published a year earlier. They used for the first time ¹³C NMR spectroscopy of chloroform solutions in order to solve this problem. The chemical shifts of the two carbon atoms in the rings of compounds **15**–**17** were found to differ significantly (186–188 ppm and 144–154 ppm), while in the symmetrical dithione **14** the shift is 180 ppm. This fact proves reliably the presence of structure **9b**. In the IR spectra of compound **15**, bands at 2560 cm⁻¹ and 930–933 cm⁻¹ were detected, disappearing on its oxidation with iodine to the disulfide **16**. They were assigned to S–H stretching and C–S–H deformation vibrations.



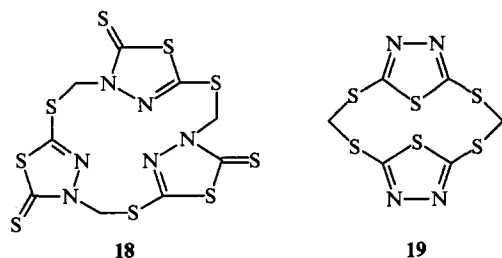
R = Ph, Me

Mercaptothiones do not yield N-adducts in the reaction with thiophosgene, but form trithiocarbonates.^{47,64}

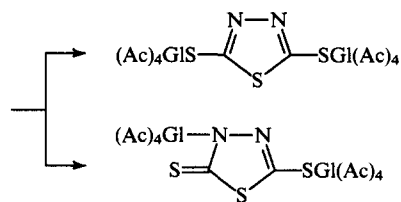
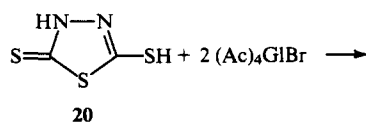


R = Me, Ar

Unsubstituted mercaptothiadiazolethione reacts with dibromoalkanes in the presence of bases to form various macroheterocyclic compounds.⁶⁵ The final product composition depends strongly on the reaction conditions and the selection of the initial reactants. For example, by using dibromomethane with one equivalent of alkali (KOH), it is possible to obtain trithiathiadiazolinophanetrithione **18**, i.e. the product of the reaction at both S and N atoms. With two equivalents of alkali, tetrathiathiadiazolophane **19** can be produced.

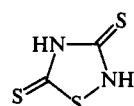


Depending on the conditions, the reaction with 2,3,4,6-tetra-O-acetyl-α-D-glucopyranosyl bromide [α-acetobromoglucose, (Ac)₄GlBr] leads to S,S'- or S,N-bisglycosides.⁶⁶



The S,N-adduct is formed either *via* the stepwise glycosidation of compound **20** by one and then by another mole of (Ac)₄GlBr, or by the glycosidation of the mercury salt of **20**, or by the transglycosidation of the S,S'-adduct in the presence of HgBr₂.

In the case of 1,2,4-thiadiazole-3,5-dithione, the IR spectroscopic data seem to be in favour of the dithione structure.⁶⁷



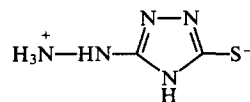
The intense absorption at 3010 cm⁻¹ and 2830 cm⁻¹ is due to the NH group, while the SH band in the 2600 cm⁻¹ region is absent.

VIII. 1,2,4-Triazolethiones

In 1959, Reynolds and VanAllan⁶⁸ compared the UV spectra of potential mercaptotriazoles and their S-methyl and S-acyl-derivatives and concluded that the thione form predominates. This conclusion was confirmed^{29, 69–71} by means of the IR and NMR spectroscopy of 3-mercapto-1,2,4-triazoles having various substituents in the 4- and 5-positions. In the IR spectrum of 4-amino-1,2,4-triazole-3,5-dithione, SH bands are absent, but there are bands at 1333 cm⁻¹ and 1519 cm⁻¹, which can be assigned to the C=S and HN–C=S fragments respectively. The latter two bands disappear on alkylation of the dithione with methyl iodide.⁷² According to X-ray diffraction data,⁷³ 4-amino-3-hydrazino-5-mercapto-1,2,4-triazole crystallises in the thione form.

At the same time, the IR and ¹H NMR spectra of 5-ferrocenyl-4-phenyl-1,2,4-triazole-3-thiol indicate that it is more likely to exist as a mixture of tautomers.⁷⁴ The same conclusion has been made for 4-amino-5-mercaptotriazoles and the Schiff's bases derived from them. In the IR spectra of these compounds, there is a weak absorption in the 2480–2550 cm⁻¹ region, which can be assigned to the thiol group. In addition, the thiol proton with a chemical shift of about 8.5–8.8 ppm was detected in the ¹H NMR spectra, together with the NH-group protons.^{75,76} Furthermore, the bold hypothesis has been put forward⁷⁷ that the absence of signals in the thiol region of the IR spectra of 4-amino-5-mercaptotriazoles does not necessarily indicate the absence of the thiol form, since the S–H bond usually has a very weak absorption.

A zwitter-ionic structure has been proposed for 3-hydrazino-5-mercapto-1,2,4-triazole on the basis of crystallographic data.⁷⁸

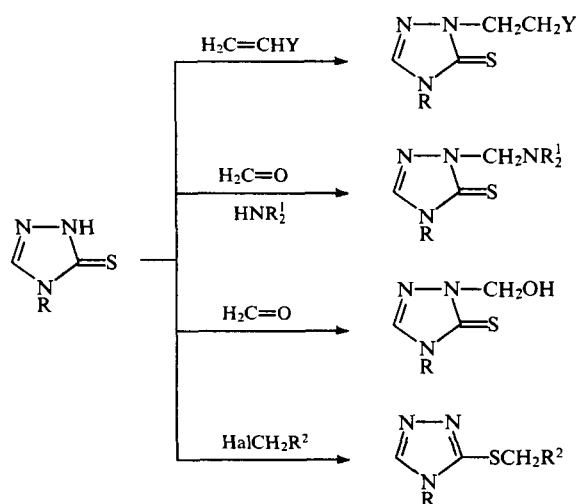


Thus, the C–S bond length is 0.174 nm, which is, of course, closer to that of the single bond and not the double bond.

In 1,2,4-triazolethiones, both the sulfur and nitrogen atoms can act as nucleophilic centres, depending on the nature of the attacking reagent and on the reaction conditions (Scheme 2).^{79–83}

The introduction of an arylamino group into the 5-position does not change the mode of nucleophilic substitution reactions.⁸⁴

Scheme 2



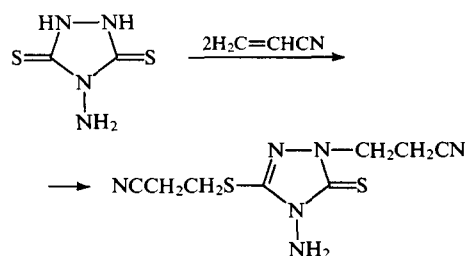
$R = p\text{-XC}_6\text{H}_4$, $X = \text{H, Cl, OEt}$;

$Y = \text{CN, } \alpha\text{-Py}$;

$\text{NR}_2^1 = \text{N} \begin{array}{c} \diagup \diagdown \\ \text{C} \quad \text{O} \end{array}$, etc.;

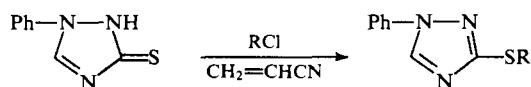
$R^2 = \text{H, Ph, C}_6\text{H}_4\text{NO}_2\text{-}p, \text{CONH}_2, \text{COOH, CH}_2\text{COOH}$

Regardless of the nature of the substituents in the 4- and 5-positions, cyanoethylation occurs at the nitrogen atom^{72, 85–87} with one exception:⁷²

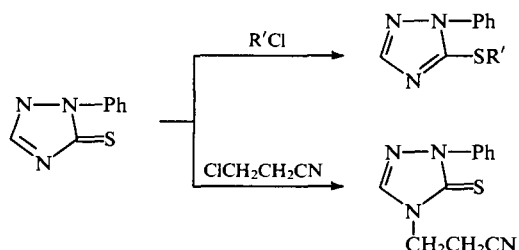


On the other hand, compounds of the HalCH_2R type usually react at the sulfur atom.^{79, 81–85, 87–89}

The situation is changed if the aryl substituent is present in the 1- or 2-position. In the case of 1-phenyl-1,2,4-triazole-3-thione, cyanoethylation at the sulfur atom takes place, while alkylation of 2-phenyl-1,2,4-triazole-3-thione by β -chloropropionitrile can occur at a nitrogen atom.⁹⁰



$R = \text{CH}_2\text{CH}_2\text{CN, CH}_2\text{CH}_2\text{COOH, CH}_2\text{Ph}$

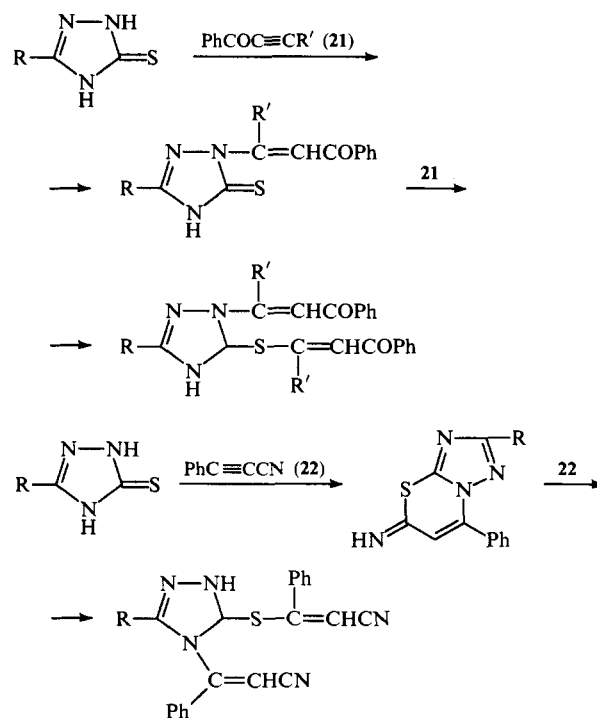


$R' = \text{CH}_2\text{CH}_2\text{COOH, CH}_2\text{Ph}$

The mechanism of the cyanoethylation reaction is believed to begin (in all cases) with the attack of the reagent on the sulfur atom, since it carries a greater negative charge. However, this is followed by transcyanoethylation with the participation of a second reagent molecule. This is based on quantum-chemical calculations of the charge distribution in the triazolethione molecules by Hückel's MO method.⁹⁰

The acylation of 4,5-disubstituted triazole-3-thiones with benzoyl and cinnamoyl chlorides yields ultimately C–N-products; however, when phenyl substituents are present in both positions and the reaction is carried out in an alkaline medium, it is possible to isolate C–S-derivatives, which are, however, readily transacylated on heating.^{86, 87}

Under ethyne pressure in the presence of alkali, 1,2,4-triazolethiones give S-vinyl derivatives. Further vinylation at the nitrogen is possible when catalysts (cuprous chloride, cadmium acetate) are used.^{91–93} The formation of divinyl products also occurs in the case of various substituted ethynes.^{94, 95}

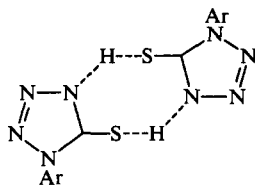


However, initial N-vinylation takes place in this case.

IX. Tetrazolethiones

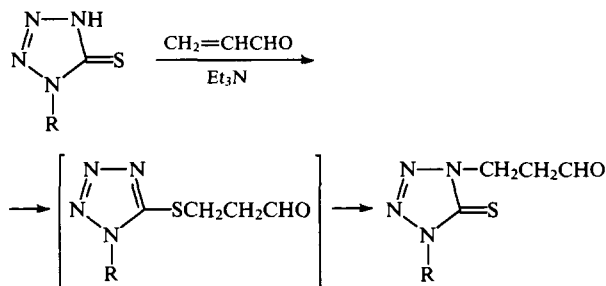
In 1958, Lieber et al.⁹⁶ reported the absence of bands corresponding to SH groups in the IR spectra of aryltetrazolethiones. The absorptions in the $1470\text{--}1500\text{ cm}^{-1}$ and $1338\text{--}1359\text{ cm}^{-1}$ regions were assigned to the N=C=S and C=S fragments respectively. The UV spectra of methyl- and benzyl-thiotetrazoles differed from those of mercapto-derivatives, resembling more closely the spectra of non-tautomeric tetrazoles,⁹⁷ which also constituted evidence in favour of the thione structure.

Kauer and Sheppard concluded that the UV and IR spectra of arylmercaptotetrazoles did not correspond to those of aryltetrazole systems.⁹⁸ However, the question of the position of the proton remained unsolved, and it was suggested that arylmercaptotetrazoles may exist (at least in the solid state or in weakly polar solvents) as hydrogen-bonded dimers.

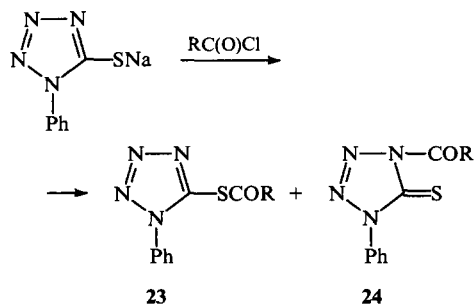


Fairly definite results have been obtained by means of ^{13}C NMR spectroscopy.^{29, 58, 99–101} The chemical shift of the carbon atom in substituted tetrazolethiones was shown to be 163–165 ppm (depending on the substituent and the solvent), while in the *S*-derivatives (sulfides, disulfides, etc.) this value is lower by 8–18 ppm. Thus, the thione structure of the compounds under consideration is confirmed. According to ^{15}N NMR spectra,¹⁰² most tetrazolethiones have the 2H-structure; however, Stefaniak¹⁰³ believes 4*H*-tetrazole-5-thione to be the dominant structure.

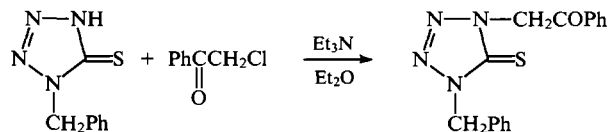
From the chemical viewpoint, the properties of tetrazolethiones are similar to those of triazolethiones. For example, they undergo pyridylethylation⁸⁰ and aminomethylation¹⁰⁴ at the nitrogen atom adjacent to the thione group. At the same time, tetrazolethiones are more prone to form sulfides than triazolethiones in reactions with α,β -unsaturated carbonyl compounds and in the cyanoethylation reaction.^{99, 105, 106} Addition occurs at the nitrogen atom in presence of triethylamine and at the sulfur atom in an alkaline medium. The sulfides formed can rearrange into C–N-adducts. Moreover, a special experiment involving the use of ^1H NMR spectroscopy showed the C–S-adduct to be the intermediate in the reaction catalysed by triethylamine.



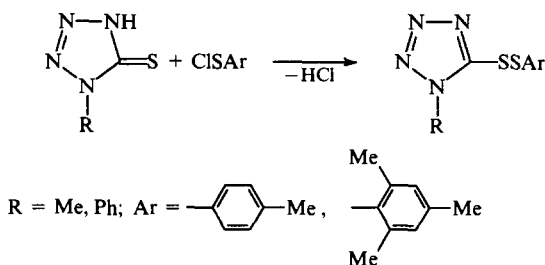
The mode of acylation depends on both the nature of the substituent in the ring and on the acyl halide structure.^{100, 107, 108} For example, sodium 1-phenyltetrazole-5-thiolate gives a mixture of products of the acylation at the sulfur atom and the nitrogen atom in the 4-position, the fraction of the latter decreasing with increase in the bulk of the substituent R.



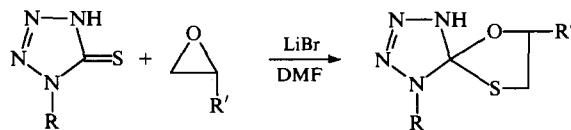
The yields of compounds **23** and **24** are equal for $\text{R} = \text{Me}$, while for $\text{R} = \text{Bu}^t$ the C–N-adduct is not formed. In 1-alkyltetrazolethiones not only the nitrogen atom at the 4-position but also the nitrogen atom at the 2-position undergoes acylation, and a mixture of three products is formed. Arenesulfonyl chlorides, benzoyl chloride, and compounds containing the $\text{Hal}-\text{C}(\text{sp}^3)$ bond react at the sulfur atom. Only one exception is known.



Arylsulfonyl chlorides react with tetrazolethiones in ether in the presence of pyridine to give disulfides.¹⁰⁹



Diazomethane reacts with 1-methyltetrazole-5-thione to give a mixture of *S*-methyl- and 4-*N*-methyl-derivatives,¹⁰¹ while oxiranes give spirocyclic 1,3-oxathiolanes.¹¹⁰

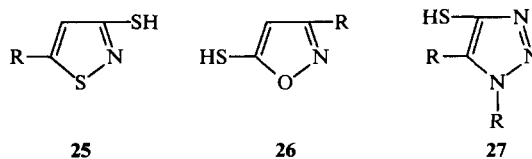


The thione structure was assigned¹¹¹ to 1,2,3,4-tetrazole-5-thione on the basis of the absence of absorption at $2500-2600\text{ cm}^{-1}$ in the IR spectrum.

In alkaline medium, this compound is alkylated and acylated at the sulfur atom.^{100, 111–113}

* * *

Comparative analysis of the structures of tautomeric five-membered heterocyclic thiols leads to the following conclusions. The thione form predominates in all azoles having the mercapto-group between two heteroatoms, as happens, for instance, in imidazole-2-thione, thiadiazole-2-thione, and tetrazolethione. 5-Mercaptothiadiazole-2-thione is an exception; it contains a thiol group, unlike, for example, 1,2,4-thiadiazole-3,5-dithione. On the other hand, if the above condition is not fulfilled and at least one of the 'neighbours' of the mercapto group is a carbon atom, the predominance of the thiol form may be expected. Among such compounds are furan-, thiophene-, and selenophene-thiols, mercaptopyrazoles, as well as 3-mercaptoisothiazoles **25**, 5-mercaptoisoxazoles **26**, and 4-mercapto-1,2,3-triazoles **27**, which have not been considered here (see the review of Elguero et al.¹).



As to the characteristic features of the chemical properties of the compounds considered, one may note that the predominance of one or another tautomeric form does not often determine the regioselectivity of the reaction. The alkylation of azolethiones with alkyl halides at the sulfur atom and the autothiolation of furan-, thiophene-, and selenophene-thiols may be given as examples.

References

1. J Elguero, C Marzin, A R Katritzky, P Linda *The Tautomerism of Heterocyclic Compounds* (New York: Academic Press, 1976)
2. J Sandström *Adv. Heterocycl. Chem.* **9** 165 (1968)
3. A R Katritzky, J M Lagowsky *Adv. Heterocycl. Chem.* **2** 3 (1963)
4. F Kurzer *Adv. Heterocycl. Chem.* **5** 119 (1965)
5. S Gronowitz, A-B Hörnfeldt, in *Thiophene and Its Derivatives* (New York: Interscience, 1986) p. 136
6. M V Ulev, E D Shtefan, V Yu Vvedenskii *Usp. Khim.* **60** 2528 (1991) [*Russ. Chem. Rev.* **60** 1309 (1991)]
7. B V Trzhtsinskaya, N A Abramova *Sulfur Rep.* **10** 389 (1991)
8. E Niwa, H Aoki, H Tanaka, K Munakata, M Namiki *Chem. Ber.* **99** 3215 (1966)
9. A V Anisimov, V S Babaitsev, E A Viktorova *Khim. Geterotsikl. Soedin.* 1313 (1980)
10. J J Peron, P Saumagne, J M Lebas *Spectrochim. Acta, Part A* **26** 1651 (1970)
11. H Lumbroso, D M Bertin, P Cagniant *Bull. Soc. Chim. Fr.* 1720 (1970)
12. B Cederlund, R Lantz, A-B Hörnfeldt, O Thorstad, K Undheim *Acta Chem. Scand. Ser. B* **31** 198 (1977)
13. J Morel, C Paulmier, D Semard, P Pastour *Bull. Soc. Chim. Fr.* 3547 (1971)
14. V Yu Vvedenskii, E D Shtefan, R N Malyushenko, E N Deryagina *Khim. Geterotsikl. Soedin.* (1996) (in the press)
15. V P Litvinov, A F Vaisburg, V Yu Mortikov *Sulfur Rep.* **11** 321 (1992)
16. S Gronowitz *Khim. Geterotsikl. Soedin.* 1445 (1994)
17. V Yu Vvedenskii, S V Zinchenko, E D Shtefan, M V Ulyev, A R Zhnikin, T A Shkarupa, E N Deryagina *Sulfur Lett.* **14** 129 (1992)
18. V Yu Vvedenskii, E D Shtefan, R N Malyushenko, E N Deryagina *Khim. Geterotsikl. Soedin.* 891 (1994)
19. V Yu Vvedenskii, S V Zinchenko, T A Shkarupa, N A Korchevin, E N Deryagina, M G Voronkov *Dokl. Akad. Nauk SSSR* **305** 624 (1989)
20. G S Ponticello, C N Habecker, S L Varga, S M Pitzenberger *J. Org. Chem.* **54** 3223 (1989)
21. V Yu Vvedenskii, E D Shtefan, M V Ulyev, E N Deryagina, M G Voronkov *Sulfur Lett.* **17** 257 (1994)
22. V Yu Vvedenskii, T A Shkarupa, S V Zinchenko, A R Zhnikin, E N Deryagina, M G Voronkov *Zh. Org. Khim.* **26** 2237 (1990)
23. A Maquestiau, Y Van Haverbeke, J-C Vanoververlt *Bull. Soc. Chim. Belg.* **86** 949 (1977)
24. C Guimon, G Pfister-Guillouzo, M Begtrup *Can. J. Chem.* **61** 1197 (1983)
25. E Bojarska-Olejnik, L Stefaniak, M Witanowski, B T Hamdi, G A Webb *Magn. Reson. Chem.* **23** 166 (1985)
26. R S Balestrero, D M Forkey, J G Russell *Magn. Reson. Chem.* **24** 651 (1986)
27. P Bouin-Roubaud, J Kister, M Rajzmann, L Bouscasse *Can. J. Chem.* **59** 2883 (1981)
28. E Bojarska-Olejnik, L Stefaniak, M Witanowski, G A Webb *Bull. Pol. Acad. Sci., Chem.* **34** 295 (1986)
29. C Guimon, G Pfister-Guillouzo *Tetrahedron* **30** 3831 (1974)
30. M L S Garsia, J A S Smith, P M G Bavin, C R Ganellin *J. Chem. Soc., Perkin Trans. 2* 1391 (1983)
31. G Kjellin, J Sandström *Acta Chem. Scand.* **23** 2888 (1969)
32. Z Fijalek, P Zuman *Anal. Lett.* **23** 1213 (1990)
33. M Ettlinger *J. Am. Chem. Soc.* **72** 4699 (1950)
34. P Karagiannidis, P Aslanidis, S Papastefanou *Polyhedron* **9** 981 (1990)
35. J Perez-Peña, M Gonzalez-Davila, M Suarez-Tangil, J Hernandez-Brito *Collect. Czech. Chem. Commun.* **54** 2045 (1989)
36. R M Acheson, J D Wallis *J. Chem. Soc., Perkin Trans. 1* 415 (1981)
37. USSR P. 1 121 265; *Byull. Izobret.* (40) 65 (1984); *Chem. Abstr.* **102** 203 978 (1985)
38. J F Willems, A Vandenberghe *Bull. Soc. Chim. Belg.* **70** 745 (1961)
39. R Gompper, H Herlinger *Chem. Ber.* **89** 2816 (1956)
40. R Gompper, H Herlinger *Chem. Ber.* **89** 2825 (1956)
41. F Weygand, H J Bestmann, F Steden *Chem. Ber.* **91** 2537 (1958)
42. G S Kapsomenos, P P Akrivos *Can. J. Chem.* **66** 2835 (1988)
43. Yu N Sheinker, I Ya Postovskii, N M Voronina *Zh. Fiz. Khim.* **33** 302 (1959)
44. M St C Flett *J. Chem. Soc.* 347 (1953)
45. Yu I Smushkevich, Ts M Babueva, N N Suvorov *Khim. Geterotsikl. Soedin.* 91 (1969)
46. W O Foye, N Abood, J M Kauffman, Y-H Kim, B R Patel *Phosphorus Sulfur* **8** 205 (1980)
47. F Runge, Z El-Hewehi, E Taeger *J. Prakt. Chem.* **18** 262 (1962)
48. C Ainsworth *J. Am. Chem. Soc.* **78** 4475 (1956)
49. W R Sherman *J. Org. Chem.* **26** 88 (1961)
50. S Misra, B L Dubey, S C Bahel *Synth. React. Inorg. Metal.-Org. Chem.* **24** 1027 (1994)
51. C Ainsworth *J. Am. Chem. Soc.* **78** 5201 (1958)
52. S Misra, B L Dubey, S C Bahel *Synth. React. Inorg. Metal.-Org. Chem.* **21** 637 (1991)
53. A C Fabretti, G C Franchini, G Peyronel *Spectrochim. Acta, Part A* **36** 517 (1980)
54. P Umapathy, A R Budhkar *Synth. React. Inorg. Metal.-Org. Chem.* **16** 1289 (1986)
55. A R Katritzky, Z Wang, R J Offerman *J. Heterocycl. Chem.* **27** 139 (1990)
56. N Petri, O Glemser *Chem. Ber.* **94** 553 (1961)
57. K Arvidsson, J Sandström *Acta Chem. Scand.* **15** 1179 (1961)
58. J R Bartels-Keith, M T Burgess, J M Stevenson *J. Org. Chem.* **42** 3725 (1977)
59. G D Thorn *Can. J. Chem.* **38** 1439 (1960)
60. B Stanovnik, H Tišler *Croat. Chem. Acta* **37** 17 (1965); *Chem. Abstr.* **63** 2967b (1965)
61. M R Gajendragad, U Agarwala *Aust. J. Chem.* **28** 763 (1975)
62. S A A Zaidi, D K Varshney *J. Inorg. Nucl. Chem.* **37** 1804 (1975)
63. S A A Zaidi, D K Varshney *J. Inorg. Nucl. Chem.* **39** 581 (1977)
64. U Anthony, B M Dahl, H Eggert, C Larsen, P H Nielsen *Acta Chem. Scand., Ser. B* **30** 71 (1976)
65. S Pappalardo, F Bottino, C Tringali *J. Org. Chem.* **52** 405 (1987)
66. G Wagner, B Dietzsch *J. Prakt. Chem.* **315** 915 (1973)
67. H J Emeleus, A Haas, N Sheppard *J. Chem. Soc.* 3168 (1963)
68. G A Reynolds, J A VanAllan *J. Org. Chem.* **24** 1478 (1959)
69. F Malbec, R Milcent, G Barbier *J. Heterocycl. Chem.* **21** 1689 (1984)
70. V I Kelarev, G A Shvekhgheimer, A F Lunin *Khim. Geterotsikl. Soedin.* 1271 (1984)
71. S Gopinathan, S A Pardhy, A P Budhkar, C Gopinathan *Synth. React. Inorg. Metal.-Org. Chem.* **18** 823 (1988)
72. A D Sinegibskaya, E G Kovalev, I Ya Postovskii *Khim. Geterotsikl. Soedin.* 562 (1973)
73. R G Dickinson, N W Jacobsen *Anal. Chem.* **41** 1324 (1969)
74. W Hui, Z Yulan, H Youhong, W Shaozu *Synth. React. Inorg. Metal.-Org. Chem.* **24** 1121 (1994)
75. K Chaturvedi, O P Pandey, S K Sengupta *Synth. React. Inorg. Metal.-Org. Chem.* **24** 1487 (1994)
76. S Goel, O P Pandey, S K Sengupta *Bull. Soc. Chim. Fr.* 771 (1989)
77. B S Garg, P C Gupta, S K Garg *Synth. React. Inorg. Metal.-Org. Chem.* **18** 643 (1988)
78. M E Senko, D H Templeton *Acta Crystallogr.* **11** 808 (1958)
79. I L Shegal, I Ya Postovskii *Khim. Geterotsikl. Soedin.* 133 (1965)
80. I Ya Postovskii, V L Nirenburg *Khim. Geterotsikl. Soedin.* 161 (1965)
81. I Ya Postovskii, I L Shegal *Khim. Geterotsikl. Soedin.* 443 (1965)
82. I L Shegal, I Ya Postovskii *Khim. Geterotsikl. Soedin.* 449 (1965)
83. I Ya Postovskii, I L Shegal *Khim. Geterotsikl. Soedin.* 443 (1966)
84. R G Dubenko, I M Bazavova, P S Pel'kis *Khim. Geterotsikl. Soedin.* 129 (1971)
85. M M Tsitsika, S M Khripak, I V Smolanka *Khim. Geterotsikl. Soedin.* 1425 (1974)
86. M M Tsitsika, S M Khripak, I V Smolanka *Khim. Geterotsikl. Soedin.* 851 (1974)
87. M M Tsitsika, S M Khripak, I V Smolanka *Khim. Geterotsikl. Soedin.* 844 (1975)
88. H M Eisa *Sulfur Lett.* **10** 239 (1990)
89. A A Hassan, N K Mohamed, Yu R Ibrahim, K U Sadek, A-F E Mourad *Bull. Chem. Soc. Jpn.* **66** 2612 (1993)
90. E G Kovalev, I Ya Postovskii *Khim. Geterotsikl. Soedin.* 1138 (1970)
91. G G Skvortsova, B V Trzhtsinskaya, L F Teterina, V K Voronov, M N Popova *Khim. Geterotsikl. Soedin.* 1561 (1977)
92. B V Trzhtsinskaya, G G Skvortsova, Yu A Mansurov, P I Buchin, M G Viderker *Khim.-Farm. Zh.* **16** 1466 (1982)

93. B V Trzhtsinskaya, E V Rudakova, A V Afonin, B Z Pertsikov, Yu A Mansurov, V P Aksenov *Izv. Akad. Nauk SSSR, Ser. Khim.* 1674 (1986)
94. L I Vereshchagin, R L Bol'shedvorskaya, G A Pavlova, N V Alekseeva *Khim. Geterotsikl. Soedin.* 1552 (1979)
95. N D Abramova, B V Trzhtsinskaya, Yu M Skvortsov, A G Mal'kina, A I Albanov, G G Skvortsova *Khim. Geterotsikl. Soedin.* 1051 (1982)
96. E Lieber, C N R Rao, C N Pillai, J Ramachandran, R D Hites *Can. J. Chem.* **36** 801 (1958)
97. E Lieber, J Ramachandran, C N R Rao, C N Pillai *Can. J. Chem.* **37** 563 (1959)
98. J C Kauer, W A Sheppard *J. Org. Chem.* 3580 (1967)
99. G L'Abbe, G Vermeulen, J Flemal, S Toppet *J. Org. Chem.* **41** 1875 (1976)
100. G L'Abbe, S Toppet, G Verhelst, C Martens *J. Org. Chem.* **39** 3770 (1974)
101. M Narisada, Y Terui, M Yamakawa, F Watanabe, M Ohtani, M Miyazaki *J. Org. Chem.* **50** 2794 (1985)
102. E Bojarska-Olejniki, L Stefanyak, M Witanowski, G A Webb *Bull. Chem. Soc. Jpn.* **59** 3263 (1986)
103. L Stefaniak, Private communication
104. I Ya Postovskii, V L Nirenburg *Zh. Obshch. Khim.* **34** 2517 (1964)
105. I Ya Postovskii, V L Nirenburg *Zh. Obshch. Khim.* **34** 3200 (1964)
106. E Lippmann, D Reifegerste *Z. Chem.* **15** 146 (1975)
107. E Lippmann, D Reifegerste, E Kleinpeter *Z. Chem.* **13** 134 (1973)
108. E Lippmann, D Reifegerste, E Kleinpeter *Z. Chem.* **14** 16 (1974)
109. G Stajer, E A Szabo, J Pintye, F Klivenyi, P Sohar *Chem. Ber.* **107** 299 (1974)
110. P-C Tromm, H Heimgartner *Helv. Chim. Acta* **73** 2287 (1990)
111. E Lieber, C N Pillai, J Ramachandran, R D Hites *J. Org. Chem.* **22** 1750 (1957)
112. C Christophersen, A Holm *Acta Chem. Scand.* **25** 2015 (1971)
113. E Lieber, E Oftedahl, C N R Rao *J. Org. Chem.* **28** 194 (1963)

The reactivity of metal β -diketonates in the thermal decomposition reaction

E I Tsyganova, L M Dyagileva

Contents

I. Introduction	315
II. The influence of the nature of the metal and the ligand on the volatility of metal β -diketonates	315
III. Kinetics of the thermal decomposition of metal β -diketonates	319
IV. Conclusion	325

Abstract. Characteristic features of the thermal decomposition of Group I–IV metal β -diketonates are surveyed and analysed. A systematic account is given of data concerning the influence of the nature of the metal and of the substituent in the β -diketone on the volatility of the metal β -diketonates and the kinetics and mechanism of their thermal decomposition. The bibliography includes 95 references.

I. Introduction

Metal β -diketonates are a class of compounds which have been quite adequately investigated.^{1–5} The syntheses and properties of the β -diketonates of virtually all the metals in the Periodic System and the structures of the complexes^{6–8} have been described in the literature and the nature of the bond in the chelate ring has been examined.^{9, 10}

Metal β -diketonates constitute a convenient model for the study of theoretical problems in the chemistry of coordination compounds and possess a series of properties of practical value which are responsible for their wide-ranging application as catalysts in oxidation, addition, and polymerisation processes,^{11, 12} for the separation of mixtures of lanthanides,^{13, 14} and for the preparation of metallic and oxide coatings.^{15–26} Interest in the β -diketonates has again grown in recent years because, by virtue of their volatility and resistance to oxidation, they proved convenient starting compounds for the introduction of metals into high-temperature superconducting films by deposition from the gas phase.^{27–36}

The volatility and thermal stability of the β -diketonates are fundamental factors in their use in the technology of the preparation of films. However, there are no data in the literature on the analysis of the thermal stability of these compounds.

The aim of the present review is to give a systematic account of the literature data and the authors own studies on the volatility and kinetics of the thermal decomposition of Group I–VIII metal β -diketonates, to discover the common features of the influence of

the nature of the metal and the ligand on the volatility and on the kinetic and activation parameters of the thermal decomposition and on its mechanism.

II. The influence of the nature of the metal and the ligand on the volatility of metal β -diketonates

Vapour pressure is one of the most important physicochemical characteristics of pure compounds. Metal β -diketonates exhibit an enhanced volatility at temperatures in the range 373–573 K. Various methods are used nowadays to measure the vapour pressures of metal β -diketonates: the isotenoscope, membrane, and spectrophotometric methods, the flow method, and the Knudsen effusion method. The advantages and disadvantages of each of the above methods have been analysed in monographs.^{37–39}

There have been fairly numerous studies on the vapour pressures of metal β -diketonates.^{40–70} However, their results are contradictory. The establishment of the general characteristics of the influence of the nature of the metal and the ligand on the volatility of metal β -diketonates is therefore of undoubted interest.

There are quantitative data on the vapour pressures of metal β -diketonates mainly for Group II–IV and VIII metals, metals of the 3d series, and also the lanthanides and actinides.^{41–65}

The results of vapour pressure measurements on metal β -diketonates obtained by the isotenoscope,^{40–42, 51–55} spectrophotometric,^{56, 57} membrane,^{58, 59} effusion,⁶⁰ and flow⁶¹ methods have been analysed in a review by Igumenov et al.⁴³ Appreciable discrepancies between the experimental vapour pressures obtained by different methods have been noted.^{41, 52, 57, 61} It has been concluded that, in the study of fairly volatile and thermally stable β -diketonates, the static method with a membrane null-manometer is the most reliable.⁴³

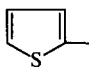
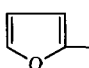
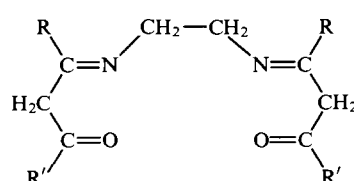
Table 1 presents the conventional designations of the metal β -diketonates investigated and Table 2 lists the thermodynamic parameters of their evaporation process obtained by the static method. All the compounds investigated exist in the gas phase as monomers and the thermodynamic parameters obtained refer to heterogeneous processes of the type $A(\text{solid, liq.}) \rightleftharpoons A(\text{gas})$. The authors of the above review⁴³ believe that the enthalpies of sublimation of the β -diketonates in the range 83.6 to 104.5 kJ mol^{–1}^{58, 59} are more reliable than the values in the range 12.5–58.5 kJ mol^{–1} established by Berg and his coworkers.^{40–42}

E I Tsyganova, L M Dyagileva The Kinetics Laboratory, Institute of Chemistry at the Lobachevskii Nizhnii Novgorod State University, prosp. Gagarina 23, korp. 5, 603600 Nizhnii Novgorod, Russian Federation.
Fax (7-831) 235 64 80 Tel. (7-831) 265 74 12 (E I Tsyganova)

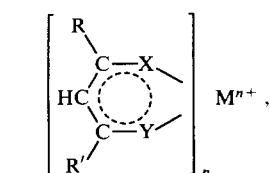
Received 27 April 1995

Uspekhi Khimii 65 (4) 334–349 (1996); translated by A K Grzybowski

Table 1. Conventional designations of β -diketones.

Name based on IUPAC nomenclature	Traditional name	Abbreviation	R	R'
$R-CO-CH_2-CO-R'$				
Pentane-2,4-dione	Acetylacetone	Hacac	Me	Me
1,1,1-Trifluoropentane-2,4-dione	Trifluoroacetylacetone	Htfacac	Me	CF ₃
5,5-Dimethylhexane-2,4-dione	Pivaloylacetone	Hpacac	Me	Bu ^t
2,2,6,6-Tetramethylheptane-3,5-dione	Dipivaloylmethane	Hdpm	Bu ^t	Bu ^t
1,1,1,5,5,5-Hexafluoropentane-2,4-dione	Hexafluoroacetylacetone	Hhfacac	CF ₃	CF ₃
6,6,7,7,8,8,8-Heptafluoro-2,2-dimethyloctane-3,5-dione	—	Hfod	C ₃ F ₇	Bu ^t
1,1,1-Trifluoro-5,5-dimethylhexane-2,4-dione	Pivaloyltrifluoroacetone	Hptfacac	CF ₃	Bu ^t
1-Benzoylbutane-1,3-dione	Benzoylacylacetone	Hbenacac	Me	PhCO
1-Benzoyl-4,4,4-trifluorobutane-1,3-dione	Benzoyltrifluoroacetylacetone	Hbentfacac	CF ₃	PhCO
4,4,4-Trifluoro-1-thienylbutane-1,3-dione	Thenoyltrifluoroacetone	Htentfacac	CF ₃	
4,4,4-Trifluoro-1-furylbutane-1,3-dione	Furoyltrifluoroacetone	Hfurfacac	CF ₃	
5-Oxaheptane-2,4-dione	Ethyl acetoacetate	Hetoxacac	CH ₃	OEt
1,5-Diphenylpentane-2,4-dione	Dibenzoylmethane	Hdibenm	PhCH ₂	PhCH ₂
5,5,6,6,7,7,7-Heptafluoroheptane-2,4-dione	—	Hhfh	Me	C ₃ F ₇
7-Ethyl-1,1,1,2,2,3,3-heptafluoro-nonane-4,6-dione	Isopentylheptafluoroacetylacetone	Hhfen	Et ₂ CH	C ₃ F ₇
1,1,1,2,2,3,3,7,7,7-Decafluoroheptane-2,4-dione	Decafluoroacetylacetone	Hdfh	CF ₃	C ₃ F ₇
Heptane-3,5-dione	Dipropionylmethane	Hdprm	Et	Et
Nonane-4,6-dione	Di-n-butylmethane	Hdbtm	Pr	Pr
2,6-Dimethylheptane-3,5-dione	Diisobutylmethane	Hdibtm	Pr ⁱ	Pr ⁱ
3,8-Dimethylnonane-4,6-dione	Diisovalerylmethane	Hdivm	Bu ⁱ	Bu ⁱ
Tridecane-6,8-dione	Dicaproylmethane	Hdkm	CH ₃ (CH ₂) ₄	CH ₃ (CH ₂) ₄
$R-C(NH)-CH_2-CO-R'$				
4-Iminopentan-2-one	Acetylacetone imine	HAcim	Me	Me
1,1,1-Trifluoro-4-iminopentan-2-one	Trifluoroacetylacetone imine	Htfacim	Me	CF ₃
1,1,1-Trifluoro-4-imino-5,5-dimethylhexan-2-one	Pivaloyltrifluoroacetone imine	Hptfim	Bu ^t	CF ₃
				
5,8-Diaza-4,9-dimethyldodeca-4,8-diene-2,11-dione	Ethylenediaminebisacetylacetone	H ₂ etdmacac	Me	Me
5,8-Diaza-1,1,1-trifluoro-4,9-dimethyldodeca-4,8-diene-2,11-dione	Ethylenediaminebistrifluoroacetylacetone	H ₂ etdmtfacac	Me	CF ₃

The volatility of chelates of the type



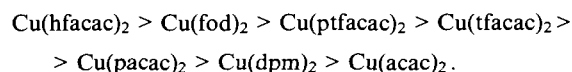
n = oxidation state of the metal,

may be influenced by the end groups R and R', the nature of the metal and of the donor atoms X and Y, the stoichiometry of the complexes, and the crystal lattice structure.⁴³

It has been noted⁶⁷ that the replacement of a hydrogen atom by alkyl groups diminishes the volatility of the complexes.

Among the Group I metal complexes, the volatility of copper(II) β -diketonates with fixed donor atoms (X = Y = O; X = O, Y = N) but different groups R and R' has been investigated (Table 2).^{2, 48, 68, 69}

The following series based on the variation of the volatility of copper(II) complexes was obtained:



It was shown that the introduction of the CF₃ and C₃F₇ groups into the ligand increases the volatility of the copper complexes. The replacement of both groups R and R' in Cu(acac)₂ by *tert*-butyl groups increases the volatility slightly, but the thermal stability of the complex rises sharply.⁴⁸ The presence of aromatic, heterocyclic, and ether groups lowers the volatility of the complexes drastically.² Comparison of the

Table 2. The coefficients in the equation for the temperature variation of the vapour pressure, $\lg P = B - A/T$ (at $P \times 1.33$ GPa), and the thermodynamic parameters of the vaporisation of metal β -diketonates.

Compound	A	B	$\Delta H_T^\circ /$ kJ mol^{-1}	$\Delta S_T^\circ /$ $\text{J mol}^{-1} \text{K}^{-1}$	T / K	Ref.
Al(acac) ₂	4055.3 \pm 41.5	6.89 \pm 0.08	69.2 \pm 0.3	131.6 \pm 0.7	471–536	43
Al(tfacac) ₃	3636.2 \pm 56.7	6.83 \pm 0.13	69.6 \pm 0.5	130.6 \pm 1.2	392–484	43
Al(ptfacac) ₃	3621 \pm 56.3	6.55 \pm 0.13	69.3 \pm 0.5	100.2 \pm 1.2	378–488	43
Al(dpm) ₃	3598.3 \pm 35.9	5.37 \pm 0.06	65.0 \pm 1.0	102.7 \pm 0.2	537–607	43
Sc(tfacac) ₃	4294.6 \pm 90.1	7.86 \pm 0.21	82.1 \pm 0.8	152.3 \pm 1.6	397–457	43
Ga(tfacac) ₃	3949.1 \pm 61.8	7.23 \pm 0.14	75.5 \pm 0.5	138.3 \pm 1.2	401–476	43
In(tfacac) ₃	4044.8 \pm 72.0	7.30 \pm 0.16	77.4 \pm 0.6	139.3 \pm 1.4	398–478	43
Cr(tfacac) ₃	4004.2 \pm 68.5	7.24 \pm 0.15	76.6 \pm 0.6	138.5 \pm 1.2	424–486	43
Cr(acac) ₃	4280.4 \pm 63.6	6.86 \pm 0.12	81.8 \pm 0.4	131.2 \pm 1.1	491–563	43
Fe(tfacac) ₃	4545.6 \pm 135.8	8.47 \pm 0.33	86.9 \pm 1.2	162.0 \pm 2.8	392–428	43
Ir(tfacac) ₃	3972.0 \pm 88.1	6.91 \pm 0.20	76.0 \pm 0.8	132.2 \pm 1.6	402–476	43
Ni(dpm) ₂ ^a	3854.5 \pm 110.9	6.20 \pm 0.21	73.7 \pm 0.8	118.5 \pm 1.6	515–536	43
V(tfacac) ₃	3722.2 \pm 85.1	6.61 \pm 2.01	71.2 \pm 7.8	126.4 \pm 4.2	402–467	43
Cu(acac) ₂	5579.6 \pm 89.0	9.82 \pm 1.9	106.7 \pm 16.7	187.9 \pm 3.6	424–454	48
Cu(tfacac) ₂	6047.4 \pm 80.8	11.78 \pm 0.18	115.7 \pm 1.6	225.3 \pm 0.9	392–475	48
Cu(hfacac) ₂	3216.0 \pm 49.2	6.62 \pm 0.12	61.5 \pm 0.4	126.7 \pm 1.2	377–423	43
Cu(pacac) ₂	6513.5 \pm 165.0	12.12 \pm 0.37	124.56 \pm 3.2	231.74 \pm 6.9	426–465	48
Cu(dpm) ₂	5843.2 \pm 89.1	10.45 \pm 0.21	111.73 \pm 1.7	200.0 \pm 3.6	434–468	48
Cu(dpm) ₂ ^b	4069.5 \pm 37.6	6.68 \pm 0.08	77.83 \pm 0.7	127.7 \pm 1.46	468–519	48
Cu(ptfacac) ₂ ^b	3703.9 \pm 53.2	6.63 \pm 0.12	70.9 \pm 1.0	126.8 \pm 2.26	385–505	48
Cu(acim) ₂	5356.3 \pm 172.1	9.64 \pm 0.39	102.4 \pm 3.3	78.5 \pm 7.4	418–454	48
Cu(tfacim) ₂	5519.7 \pm 158.5	10.38 \pm 0.49	105.6 \pm 3.1	198.6 \pm 8.8	426–460	48
Cu(ptfim) ₂	6265.2 \pm 598.1	10.11 \pm 1.39	119.8 \pm 11.5	231.3 \pm 26.6	421–435	48
Cu(etdmacac) ₂	4921.1 \pm 145.6	7.41 \pm 0.29	94.1 \pm 2.8	141.7 \pm 5.5	478–520	48
Ca(acac) ₂	2877 \pm 387	7.92 \pm 0.8	—	—	410–430	44
Ca(tfacac) ₂	1180 \pm 120	4.12 \pm 0.3	—	—	380–420	44
Ca(dpm) ₂	4060 \pm 450	11.5 \pm 2.2	—	—	400–427	44
Ca(ptfacac) ₂	8140 \pm 500	21.9 \pm 2.7	—	—	373–400	44
Sr(tfacac) ₂	3250 \pm 360	9.12 \pm 0.7	—	—	410–450	44
Sr(ptfacac) ₂	8600 \pm 500	22.42 \pm 2.9	—	—	400–420	44
Ba(dpm) ₂	4750 \pm 500	12.82 \pm 2.6	—	—	397–421	45
Ba(ptfacac) ₂	3100 \pm 300	8.82 \pm 0.6	—	—	406–450	45
Ba(tfacac) ₂	1977 \pm 496	6.82 \pm 1.2	—	—	380–404	45
Ba(hfacac) ₂	4740 \pm 550	13.6 \pm 1.3	—	—	378–401	45
Y(dpm) ₃	4145 \pm 260	11.82 \pm 0.6	—	—	430–500	46
Y(ptfacac) ₃	4060 \pm 400	10.32 \pm 0.8	—	—	426–463	46
Y(tfacac) ₃	9400 \pm 500	24.02 \pm 5.9	—	—	412–434	46
Y(hfacac) ₃	22100 \pm 900	56.32 \pm 0.8	—	—	403–416	46
Pr(tpfacac) ₃	422.19 \pm 21.42	3.32 \pm 0.4	—	—	388–505	47
Pt(hfacac) ₂ ^a	6670	12.88	55.2 \pm 3.3	107 \pm 7.9	419–439	49
Pt(dpm) ₂ ^a	9820	16.16	81.5 \pm 2.9	134.2 \pm 6.7	447–467	49
Ir(tfacac) ₃ ^a	9462	16.29	78.6 \pm 2.51	136.7 \pm 5.4	458–488	49
Ir(hfacac) ₃ ^a	6793	13.79	56.4 \pm 0.4	114.1 \pm 0.8	401–443	49
Rh(hfacac) ₃ ^a	7442	15.35	61.9 \pm 0.4	127.7 \pm 0.8	388–421	49
Ir(ptfacac) ₃ ^a	8259	13.88	68.6 \pm 0.4	111.6 \pm 0.8	413–518	49
Ir(dpm) ₃ ^a	8927	13.94	73.99 \pm 0.8	115.8 \pm 0.8	418–522	49
Sc(dpm) ₃	3988 \pm 54	9.24 \pm 0.11	76.1 \pm 0.8	121.8 \pm 2.1	458–558	50
Y(dpm) ₃	3977 \pm 65	9.13 \pm 0.13	76.1 \pm 1.2	119.7 \pm 2.5	463–574	50
La(dpm) ₃	5630 \pm 237	11.55 \pm 0.44	107.9 \pm 4.6	116.1 \pm 8.4	530–567	50
Pr(dpm) ₃	5449 \pm 135	11.56 \pm 0.26	104.3 \pm 2.6	166.2 \pm 5.0	496–550	50
Nd(dpm) ₃	4850 \pm 130	10.51 \pm 0.26	92.9 \pm 2.5	146.1 \pm 5.0	492–546	50
Eu(dpm) ₃	4253 \pm 52	9.47 \pm 0.10	81.4 \pm 1.0	126.2 \pm 2.0	467–625	50
Gd(dpm) ₃	4117 \pm 77	9.26 \pm 0.14	78.8 \pm 1.5	122.2 \pm 2.7	480–600	50
Yb(dpm) ₃	3981 \pm 26	9.13 \pm 0.05	76.2 \pm 0.5	119.7 \pm 10	477–588	50
Lu(dpm) ₃	3938 \pm 49	9.03 \pm 1.0	75.4 \pm 0.9	117.6 \pm 1.7	457–591	50
Sc(acac) ₃	5199.9	11.61	—	—	383–403	56
Zr(acac) ₄	6050 \pm 2000	13.2 \pm 2.5	—	—	423–443	66
Hf(acac) ₄	7240 \pm 820	16.1 \pm 1.9	—	—	423–443	66
Th(dpm) ₄ ^a	18304 \pm 371	36.92 \pm 0.94	—	—	391–409	63
U(dpm) ₄ ^a	17932 \pm 184	35.83 \pm 0.32	—	—	392–409	63
La(fod) ₃ ^a	17479 \pm 941	32.33 \pm 0.87	—	—	387–403	64
Gd(fod) ₃ ^a	18613 \pm 101	40.25 \pm 0.27	—	—	362–385	64
Yb(fod) ₃ ^a	18608 \pm 424	44.5 \pm 1.2	—	—	339–355	64

continued over

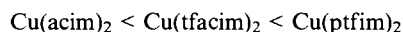
Table 2 (continued)

Compound	A	B	$\Delta H_T^\circ /$ kJ mol ⁻¹	$\Delta S_T^\circ /$ J mol ⁻¹ K ⁻¹	T/K	Ref.
Th(fod) ₄ ^a	17238 ± 173	39.88 ± 0.48	—	—	343–367	63
U(fod) ₄ ^a	16654 ± 382	38.74 ± 1.07	—	—	344–367	63
Np(fod) ₄ ^a	17779 ± 354	41.42 ± 0.98	—	—	350–368	63
Pu(fod) ₄ ^a	18455 ± 947	43.60 ± 0.27	—	—	349–363	63

^a Refers to the equation $\ln P = B - A/T$. ^b The substance is in the liquid phase.

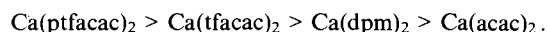
volatilities of Cu(tfacac)₂ and Cu(fod)₂ shows that an increase in the length of the fluorinated chain hardly affects the volatility of the complexes.⁴⁸

In the case of the N and O donor atoms, the dependence of the volatility on the nature of R and R' remains the same as before.

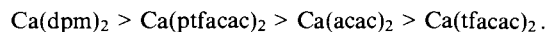


It is essential to note the conventional nature of the series presented, since, depending on the temperature range in which the comparison is carried out, the relative volatilities of adjacent complexes may change. Only comparison of experimental $P-T$ curves can yield a concrete answer to the question of the greater or lower volatility of a complex in a particular temperature range.

Among Group II metal β -diketonates, the volatility of calcium,⁴⁴ strontium,⁴⁴ and barium⁴⁵ β -diketonates has been investigated. It was established that the volatility of the calcium compounds at temperatures below 400 K varies as follows:⁴⁴



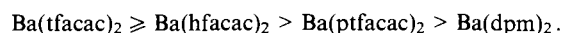
In the temperature range 430–520 K, the series assumes a different form:



Thus the introduction of the *tert*-butyl group into the calcium compounds increases the volatility of the complexes to a greater extent than the introduction of the trifluoromethyl group.

For the strontium compounds⁴⁴ in the temperature range from 430 to 500 K, the change in the volatility of Sr(tfacac)₂ is greater than for Sr(ptfacac)₂. At temperatures below 430 K and above 500 K, the opposite relation holds.

In terms of their volatilities, the β -diketonates can be arranged in the following series:⁴⁵



As in the case of copper β -diketonates, the volatility of the barium compounds increases following the introduction of the trifluoromethyl group into the ligand molecule. The introduction of the *tert*-butyl group lowers the volatility of these compounds. The lowest volatility is that of Ba(dpm)₂, which contains two *tert*-butyl groups. Here it was noted that the volatilities of Ba(dpm)₂ synthesised at different times differ significantly. A decrease in the volatility of Ba(dpm)₂ during its storage has been observed.⁴⁵

It has been shown⁷⁰ that, according to mass-spectrometric data, Ba(dpm)₂ exists as a trimer in the gas phase and that its thermolysis is preceded by its depolymerisation. During the storage of Ba(dpm)₂ or Ba(dpm)₂ · 2H₂O, the complex decomposes slowly with formation of Hdpm or the diketone Bu'-CO-CH=CH-CO-Bu'. It is therefore recommended that Ba(dpm)₂ be stored in vacuo.

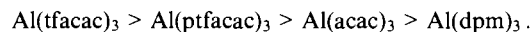
We shall consider how the nature of the metal influences the volatility of the isotypical calcium, strontium, and barium β -diketonates.

The volatility of the complexes M(tfacac)₂ (M = Ca, Sr, Ba) increases with increase in the atomic number of the metal: Ca < Sr < Ba. For the complexes M(ptfacac)₂, the above series is reversed: Ca > Sr ≈ Ba. The same trend has been observed for M(dpm)₂: Ca > Ba.

Thus in the series of Group II metal β -diketonates we see no common trends in the variation of the volatility with the atomic number of the metal for different ligands.

Among the Group III metal diketones, the variation of the volatility of the aluminium,⁴³ gallium,⁴³ indium,⁴³ scandium,^{43, 50} yttrium,⁴⁶ and the lanthanide and actinide^{50, 56, 60–64, 66} β -diketonates has been investigated.

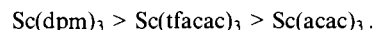
For aluminium β -diketonates, the series based on increasing volatility has the following form:⁴³



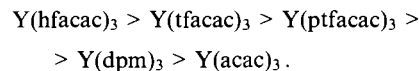
The influence of the end groups has been clearly traced for the aluminium compounds. The introduction of the CF₃ group into the ligand of the chelate increases sharply the volatility of the complex. The joint presence of the *tert*-butyl and trifluoromethyl groups reduces the volatility of the complex compared with Al(tfacac)₃. Thus, in the case of the aluminium complexes, as for the copper and barium complexes, the trifluoromethyl group increases while the *tert*-butyl group diminishes the vapour pressure of the chelate.

A successive decrease in volatility with increase in the atomic number of the metal has been observed for the compounds M(tfacac)₃ (M = Al, Ga, In).⁴³

In terms of their volatilities, scandium β -diketonates can be arranged in the following sequence:^{43, 50, 56}

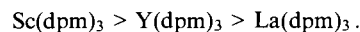


The chelates with *tert*-butyl substituents proved to be more volatile than those with the trifluoromethyl substituents (although one should bear in mind that data obtained by different workers were compared). The following dependence of the volatility of the β -diketonates on the nature of the ligand has been established for yttrium β -diketonates:⁴⁶



The volatility of yttrium β -diketonates increases in proportion to the number of fluorine atoms introduced into the ligand molecule: in the series of fluorine-substituted acetylacetonates, the hexafluoroacetylacetonates have the highest vapour pressure. The greater volatility of the complexes with fluorine-containing ligands compared with their analogues without fluorine has been attributed to the mutual repulsion of the strongly electronegative terminal fluorine atoms and the corresponding decrease in the extent of van der Waals interactions.

The following series based on the variation of volatility has been observed for M(dpm)₃ (M = Sc, Y, La):⁵⁰



Evidently, the volatility of the chelate diminishes with increase in the atomic number of the metal, as in the aluminium subgroup.⁴³

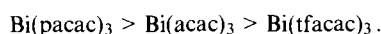
The variation of the volatility of lanthanide β -diketonates Ln(dpm)₃ (Ln = La, Ce, Pr, Nd, Pm, Sm, Eu, Gd, Tb, Dy, Ho, Er, Tm, Yb, Lu) has been investigated.^{50, 62} A monotonic increase in the volatility of Ln(dpm)₃ with increase in molecular mass and with some decrease in the size of the molecule has been observed.

Konstantinov et al.⁵⁰ attribute this to the different degrees of association of the compounds in the condensed phase. It is suggested that, on passing to lighter elements, the concentration of the involatile dimeric molecules in the melt increases and the vapour pressure of the monomeric molecules over the melt diminishes. With increase in the temperature of the melt and hence with increase in the degree of dissociation of the dimeric molecules in the melt, the volatilities of different $\text{Ln}(\text{dpm})_3$ are similar and they become indistinguishable as regards their ability to evaporate.

It has been shown for the actinides⁶² that the compounds $\text{M}(\text{fod})_3$ are more volatile than $\text{M}(\text{dpm})_3$, the nature of the metal having a greater influence than that of the radicals.

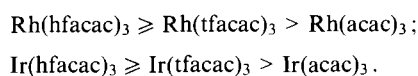
The influence of the nature of the metal on the volatility of Group IV metal acetylacetonates is insignificant.⁶⁶

The influence of the nature of the ligand substituent on the volatility of Group V metal β -diketonates has been investigated for bismuth.⁷¹ It was shown that, depending on the type of substituent, the volatility of the complexes diminishes in the sequence

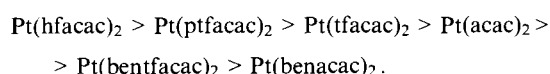


We observe a rare instance of a decrease in volatility following the introduction of the trifluoromethyl group into the ligand.

Factual data on the volatility of Group VIII metal (Pt, Pd, Ir, Rh) β -diketonates have been treated systematically by Igumenov et al.⁴⁹ The usual sequence based on the variation of volatility was observed for rhodium and iridium:



A greater volatility of the iridium complexes compared with the rhodium complexes was observed.⁴⁹ The following sequence based on the variation of volatility was established for platinum(II) chelates:



Igumenov et al.⁴⁹ note that all the octahedral platinum(IV) chelates, even dimeric ones, have appreciably higher vapour pressures than the isoligand pseudosquare platinum(II) chelates. It was shown that *trans*- $\text{Pt}(\text{tfacac})_2$ occupies a special place among platinum(II) β -diketonates. Its volatility is lower than that of *cis*- $\text{Pt}(\text{tfacac})_2$ and even that of $\text{Pt}(\text{dpm})_2$. This is one of the few experimental confirmations of a decrease in volatility after the introduction of the CF_3 group into the ligand.

The introduction of the trifluoromethyl group into the ligand in nickel(II) complexes led to a significant increase in the vapour pressure.⁷²

The study of the volatility of the trifluoroacetylacetonates of the metals in the first transition series (Sc, V, Cr, Fe, Co) led to the conclusion that the volatility decreases with increase in the atomic number of the element. It was noted in this connection that the influence of the nature of the metal on the volatility of the complexes for fixed groups R and R' is insignificant.^{43, 68}

Igumenov et al.⁴⁹ observed a decrease in the thermodynamic parameters characterising the sublimation and evaporation of the β -diketonates after the introduction of the CF_3 group into the ligand. The decrease in ΔH°_f , which should entail a sharp increase in the vapour pressure, is compensated by the corresponding decrease in ΔS°_f . Analysis of the data for compounds belonging to one group in the Periodic System shows a decrease in the absolute values of the thermodynamic parameters with increase in the atomic number of the metal.

Analysis of the data presented above for metal β -diketonates shows that the decisive factor in the volatility of the chelates is the nature of the ligand. In terms of their influence on the volatility, the factors considered can be arranged as follows:⁴³

(1) the influence of the nature of the terminal R and R' groups of the ligand;

(2) the influence of the nature of the metal within the groups of the Periodic System;

(3) the influence of the nature of the metal within the periods of the Periodic System.

The fact that the volatility of copper, calcium, strontium, barium, yttrium, aluminium, gallium, indium, nickel, palladium, iridium, and platinum β -diketonates increases following the introduction of trifluoromethyl groups into the β -diketone and diminishes after the introduction of *tert*-butyl groups into the latter may be regarded as established. A decrease in the volatility after the introduction of CF_3 groups has been observed only for calcium (at 430–520 K), scandium, and bismuth β -diketonates and the *trans*-isomer of $\text{Pt}(\text{tfacac})_2$.

General trends in the variation of the volatility of the β -diketonates as a function of the atomic number of the metal have not been noted. A decrease in volatility with increase in the atomic number of the metal has been observed in the calcium subgroup for the complexes $\text{M}(\text{ptfacac})_2$ and $\text{M}(\text{dpm})_2$ (M = Ca, Sr, Ba), in the aluminium subgroup for the complexes $\text{M}(\text{tfacac})_3$ (M = Al, Ga, In), in the scandium subgroup for the complexes $\text{M}(\text{dpm})_3$ (M = Sc, V, La), and in the group of metals of the first transition series (Sc, V, Cr, Fe, Co) for the $\text{M}(\text{tfacac})_n$ complexes. On the other hand, an increase in volatility with increase in the atomic number of the metal has been observed for the compounds $\text{M}(\text{tfacac})_2$ (M = Ca, Sr, Ba) and $\text{M}(\text{dpm})_3$ (M = lanthanides).

It is at present impossible to establish an unambiguous correlation between the thermodynamic data and the structural parameters of metal β -diketonates because these compounds have been little investigated.⁴³

III. Kinetics of the thermal decomposition of metal β -diketonates

In the present review an attempt is made to treat systematically the available literature data concerning the influence of the nature of the metal and the substituent on the kinetics and mechanism of the gas-phase pyrolysis of substituted metal β -diketonates. The thermal decomposition of the β -diketonates can occur both in the gas and solid phases. In the case of the gas-phase thermal decomposition of metal β -diketonates, the rate constant for the thermal decomposition serves as a measure of reactivity. In the solid-phase decomposition investigated by differential thermal analysis (DTA), the comparison of the reactivities was based on the temperatures of the onset of decomposition, while in the case of the solid-phase decomposition, investigated by the kinetic method, it was based on the initial rates of thermal decomposition.

1. Thermal decomposition of Group I metal β -diketonates

Among Group I metal β -diketonates, the kinetics of the thermal decomposition of copper(II) β -diketonates have been described in greatest detail.^{73–78} The kinetics of the thermal decomposition of copper(II) complexes have been studied by static,⁷³ flow,⁷⁴ and mass-spectrometric⁷⁵ methods. The experimental conditions and the activation parameters for the thermal decomposition are presented in Table 3.

The gas-phase pyrolysis of $\text{Cu}(\text{acac})_2$ under static conditions in vacuo is homogeneous-heterogeneous in character and is described satisfactorily by a first-order kinetic equation.⁷³ The acceleration of the thermal decomposition in the presence of oxygen has been noted.

Mass-spectrometric analysis led to the detection of the following components in the products of the total thermal decomposition at 573 K (in mol %): acetone (22.3), ethene (carbon monoxide) (38.0), ethyl methyl ketone (0.3), CO_2 (36.2), and H_2O (3.2). This product composition indicates appreciable degradation of acetylacetone, which is formed in the initial stages of the thermal decomposition. The splitting off of the ligand is observed at temperatures close to that of the onset of

Table 3. Kinetic parameters of the gas-phase pyrolysis of copper(II) β -diketonates obtained by a flow method ⁷⁴ (A — pro-exponential factor).

Compound	Temperature range/K	lg A	$E/\text{kJ mol}^{-1}$
Cu(acac) ₂ ^a	536–613	7.48 ± 0.98	115.4 ± 10.8
Cu(acac) ₂	553–723	7.16 ± 0.65	58.7 ± 6.2
Cu(tfacac) ₂	473–673	7.15 ± 0.48	46.9 ± 4.5
Cu(hfen) ₂	473–723	7.07 ± 0.35	45.9 ± 5.4
Cu(hfh) ₂	473–653	6.55 ± 0.52	39.3 ± 4.16
Cu(hfacac) ₂	453–523	6.32 ± 0.32	33.5 ± 3.8
Cu(dfh) ₂	453–593	6.28 ± 0.45	31.8 ± 8.2
Cu(dpm) ₂ ^b	423–823	13.176	155.5 ± 7.1

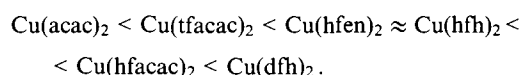
^a Data obtained by a static method.⁷³ ^b Data obtained by the mass-spectrometric method.⁷⁵

decomposition.⁷⁷ The ligand Hdpm is also formed in the initial stages of the pyrolysis of Cu(dpm)₂.

It has been established⁷⁹ that acetylacetone has a higher thermal stability than that of the chelate complexes based on it. The M–O bond energy in acetylacetonates is 160–280 kJ mol^{−1}. The M–O bond is the least stable in the chelate molecule.⁷⁹

The kinetics of the thermal decomposition of fluorine-substituted copper β -diketonates in an open system have been investigated in a stream of helium at temperatures in the range 453–723 K in a reactor the walls of which were lined with metallic copper having a constant catalytic activity (Table 3).⁷⁴

Analysis of the dependence of the maximum rate of growth of the metallic copper film under dynamic deposition conditions enabled Mazurenko et al.⁷⁴ to conclude that the rate-limiting stage of the thermal decomposition of fluorine-substituted copper(II) β -diketonates is the decomposition of the adsorption complex. A linear dependence of the energy characteristics of the thermal dissociation process on the electronic structure of the coordination unit of the β -diketonate complexes has been observed. Thus, following the enhancement of the electron-accepting properties of the α -substituent, a decrease in the activation energy and an increase in the rate constants for the thermal decomposition of copper(II) β -diketonates have been observed in the sequence



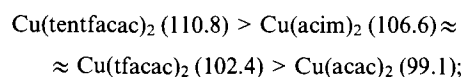
Cu(acac)₂ has the highest kinetic stability in the thermal decomposition reaction. An increase in the number of fluorine atoms in the β -diketone leads to a successive increase in the thermal decomposition rate constant. Thus at 553 K the rate constant for the thermal decomposition of Cu(acac)₂ is accordingly smaller than those for the thermal decomposition of the fluorine-substituted analogues.

The greater thermal stability of Cu(acac)₂ compared with the substituted β -diketonates has been attributed⁷⁸ to the fact that the contribution of ring conjugation in copper(II) β -diketonates is greater than in the chelates of other metals by virtue of the π -bonding ($p\pi-d\pi$) nature of the Cu–O bond. The alkyl substituents in these chelates exhibit a hyperconjugation effect, which disrupts the resonance in ring-conjugated systems.

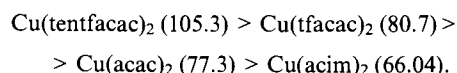
It was not possible to reach a conclusion about the comparative stabilities of Cu(acac)₂ and Cu(dpm)₂, since the thermal decomposition rate constants were obtained under different experimental conditions^{73,75} and may refer to different rate-limiting stages.

A kinetic analysis of the thermal decomposition of copper(II) β -diketonates in vacuo and under an inert atmosphere, based on the results of thermogravimetric analysis, has been published.⁷⁶ In terms of the apparent activation energies, the compounds can be arranged in the following sequences [the values of E (kJ mol^{−1}) are given in brackets]:

(a) under an inert atmosphere:

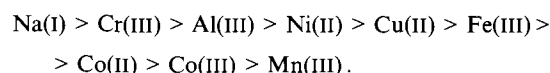


(b) in vacuo:



However, no conclusions concerning the comparative thermal stabilities of the copper(II) β -diketonates can be reached on the basis of these series, since the pre-exponential factor in the rate constant equation is unknown.

The thermal stability of Na(acac) has been investigated by the DTA method⁷⁸ relative to the thermal stabilities of the acetylacetonates of divalent and trivalent metals: Cu(II), Ni(II), Co(II), Cr(III), Fe(III), Co(III), and Mn(III). It was shown that all the compounds M(acac)_n investigated decompose in the temperature range from 423 to 673 K. In terms of the thermal stabilities of their acetylacetonates, the metals can be arranged in the following sequence:



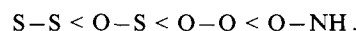
The principal gaseous products of the decomposition of M(acac)_n [M = Co(II), Co(III), Al(III), Fe(III)] are acetone and carbon dioxide. In the case of Na(I) and Cr(III), methane appears in the thermal decomposition products on raising the temperature. The principal product of the thermal decomposition of copper(II) and manganese(III) acetylacetonates is acetylacetone over the entire temperature range.

The thermal decomposition of three types of chelate complexes of dimethylgold(III) having the general formula Me₂Au(R–CX–CH–CO–R'), where X = O, NH, or S and R and R' = Me, Bu^t, or CF₃ in various combinations, has been investigated by the DTA method⁷⁹ in the solid and gaseous states. Thermolysis of all types of chelates proceeds in the same way regardless of the nature of the donor atoms and the type of substituents R and R' in the ligand.

The complexes containing the *tert*-butyl group exhibit the highest thermal stability. The introduction of the CF₃ group into the β -diketonate complexes leads to an appreciable decrease in their thermal stability, while, conversely, the introduction of CF₃ groups into the β -iminoketonates increases the thermal stability of the complex.

The decisive factor governing the variation of the thermal stability of the complexes in the condensed state is not the type of substituents R and R' but the nature of the donor atoms in the ligand. The introduction of sulfur atoms into the chelate ring leads to a sharp decrease in the thermal stability of the dimethylgold(III) complexes.

It has been established that, in the series of dimethylgold(III) chelates investigated, the thermal stability increases as a function of the chelate unit in the following sequence:



The thermal stability of the β -diketonate complexes in the gas-phase decomposition is analogous to their stability in the solid-phase decomposition.

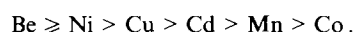
When the CF₃ group is introduced into the chelate ligand, the series of the thermal stabilities of the gaseous β -iminoketonates is reversed.

The principal volatile products of the thermal decomposition of the compounds investigated are the free β -diketonates, β -iminoketonates, HL, CH₄, C₂H₆, and MeL (L = ligand). The presence of this set of products indicates the occurrence of competing rearrangements of the thermally excited species with opening of the chelate ring.

In the interaction of the β -diketonates with deuterium, the ketones $R-CO-CDMe-CO-R'$ and monosubstituted deuteriated β -diketonates were detected in the reaction products. Deuteriated metal-containing products were not found. Appreciable temperature-dependent deuteriation of the molecules of the complexes has been observed for the β -iminoketonates. Mainly monosubstituted deuteriated metal-containing products are formed, whereas in the case of the free β -iminoketonates, disubstituted molecules were detected, which confirms the above hypothesis of the initial opening of the chelate ring in the thermally excited molecule with subsequent decomposition via different paths.

2. Thermal decomposition of Group II metal β -diketonates

The following thermal stability series has been obtained from the results of the study of the relative reactivities of divalent Group II metal acetylacetonates:⁸⁰



The size of the alkyl substituent in beryllium β -diketonates has little effect of the stability of the complexes. Among Group II metal compounds fluorine-substituted calcium and strontium β -diketonates have been investigated in greatest detail.⁴⁴ The thermal decomposition of these compounds takes place in the gas phase and is described by a first-order kinetic equation (Table 4). From 1.5 to 6.0 moles of gaseous products are evolved per mole of the decomposed chelate. The complexes $Ca(dpm)_2$ and $Ca(acac)_2$ undergo the greatest and smallest degradation respectively. The main product of the thermal decomposition of calcium acetylacetonate is acetone, the content of which diminishes with increasing degree of conversion of the reactant. The first decomposition stage is the opening of the chelate ring with subsequent dissociation of the C-C bonds.⁴⁴ In terms of their kinetic stabilities, the calcium compounds can be arranged in the following sequence:

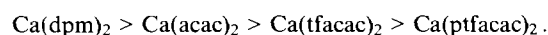


Table 4. Kinetic and activation parameters for the gas-phase pyrolysis of Group II–V metal β -diketonates (the initial pressures of the reactants were 50–200 GPa).

Compound	Temperature/K	lgA	E/ kJ mol ⁻¹	Ref.
Ca(acac) ₂	613–693	3.19 ± 0.83	74.9 ± 5.8	44
a(tfacac) ₂	553–633	5.26 ± 0.33	92.0 ± 3.6	44
Ca(dpm) ₂	673–798	5.71 ± 0.34	117.5 ± 4.9	44
Ca(ptfacac) ₂	533–613	5.77 ± 0.82	97.6 ± 9.1	44
Sr(tfacac) ₂	533–573	12.06 ± 0.72	159.0 ± 7.6	44
Sr(ptfacac) ₂	483–523	7.64 ± 1.31	99.6 ± 12.5	44
Ba(acac) ₂ ^a	536–633	6.50 ± 0.48	81.1 ± 5.1	73
Ba(ptfacac) ₂	525–625	2.23 ± 0.34	53.1 ± 3.7	45
Ba(hfacac) ₂	539–630	1.73 ± 0.63	52.0 ± 2.1	45
Ba(tfacac) ₂	475–623	0.88 ± 0.19	35.6 ± 3.2	45
Ba(dpm) ₂ ^b	623–773	0.42 ± 0.15	38.9 ± 2.0	45
Y(acac) ₃ ^a	513–593	4.77 ± 0.43	50.6 ± 3.8	73
Y(dpm) ₃	523–633	4.31 ± 0.14	76.5 ± 1.6	46
Y(ptfacac) ₃	493–533	13.88 ± 0.9	166.6 ± 8.9	46
Y(tfacac) ₃	453–523	1.93 ± 0.38	44.5 ± 3.5	46
Y(hfacac) ₃	403–478	4.08 ± 0.77	53.3 ± 6.4	46
Pr(ptfacac) ₃	553–613	2.90 ± 0.72	63.4 ± 7.8	47
Ti(acac) ₃	573–633	5.32 ± 0.85	90.7 ± 9.6	82, 83
V(acac) ₃	683–743	5.02 ± 0.56	102.4 ± 7.5	82, 83
VO(acac) ₂	638–723	8.32 ± 0.44	143.0 ± 5.8	82, 83

^a Pyrolysis in the solid phase. ^b Calculated from the initial rates of pyrolysis.

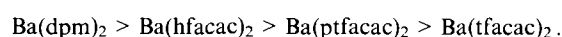
The thermal stability of the compound $Ca(dpm)_2$ is highest. The introduction of trifluoromethyl groups diminishes significantly the thermal stability of the calcium chelates.

Comparison of the kinetic parameters of the thermal decomposition of the strontium compounds shows that the complex $Sr(tfacac)_2$ is much more stable than $Sr(ptfacac)_2$. A considerable amount of trifluoromethane is present in the products of the decomposition of fluorinated strontium chelates.

Comparison of calcium and strontium β -diketonates containing isotypical ligands shows that the calcium compounds have a higher thermal stability than the corresponding strontium compounds. The difference between the thermal stabilities of the β -diketonates $M(tfacac)_2$ is smaller than in the case of $M(ptfacac)_2$. The thermal decomposition of the strontium compounds is retarded in the presence of oxygen, whereas the decomposition of the calcium chelates is accelerated under these conditions.⁴⁴ The rate constant for the thermal decomposition process diminishes with increase in the heterogeneous factor S/V (S is the surface area of the reactor and V its volume). This indicates a complex homogeneous-heterogeneous character of the thermal decomposition of the chelates, the main products of which are carbon oxides (for both low and high degrees of conversion) (Table 5).

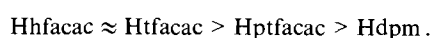
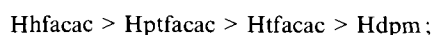
The decomposition of barium β -diketonates takes place both in the solid and gas phases (Table 4).^{45, 73} The pyrolysis of barium acetylacetonate proceeds topochemically in the solid phase and is accompanied by the formation of both solid and gaseous products.⁷³ The composition of the solid phase has the empirical formula $BaC_{3.6}H_{6.06}O_{1.91}$. More extensive degradation of barium acetylacetonate to the carbide BaC_2 takes place in the presence of oxygen, the initial rate of thermal decomposition remaining unchanged. The following substances were detected among the products of the total pyrolysis of barium acetylacetonate at 573 K (mol %): acetone (86.6), ethanol (0.8), ethene (carbon monoxide) (9.3), ethyl methyl ketone (0.2), carbon dioxide (1.0), water (2.1).

The thermal decomposition of the fluorine-substituted barium β -diketonates takes place in the gas phase and is described satisfactorily by the kinetic equation for a first-order reaction.⁴⁵ The kinetic stability of barium β -diketonates in the thermal decomposition reaction varies in the following series:



The influence of oxygen on the rate of the thermal decomposition of fluorine-substituted barium β -diketonates is specific and is determined by the nature of the ligand.⁴⁵ In the thermal decomposition of $Ba(ptfacac)_2$ and $Ba(dpm)_2$, a decrease in the rate constant to a minimum value in the presence of 30%–50% of added oxygen is observed. In the case of $Ba(hfacac)_2$, the addition of oxygen hardly affects the rate, whereas an appreciable increase in the rate constant is observed for $Ba(tfacac)_2$. As in the case of the analogous calcium and strontium compounds, a decrease in the decomposition rate constant with an increase in the heterogeneous factor is likewise observed for the barium chelates.⁴⁵

The main products of the thermal decomposition of all the barium compounds investigated, in both the initial and final decomposition stages, were CO and CO₂, the content of which decreases on passing from the $Ba(hfacac)_2$ to the $Ba(dpm)_2$ complexes in the following series of ligands:



The amount of the main ligand in the total pyrolysis products does not exceed 0.2%–1.4% for all the compounds investigated, which indicates its far-reaching degradation (Table 6). The trends in the variation of the contents of other products are determined by the nature of the initial ligand and by the degree of decomposition.

Comparison of the thermal stabilities of the Group II metal β -diketonates $M(tfacac)_2$ ($M = Ca, Sr, Ba$) shows that the kinetic

Table 5. Compositions (in mol %) of the volatile products of the thermal decomposition of calcium and strontium β -diketonates.⁴⁴

Compound	Temperature/K	Degree of decomposition	CO	CO ₂	Methyl pivaloyl ketone	iso-C ₄ H ₈ (iso-C ₄ H ₁₀)	C ₃ H ₈ (C ₃ H ₆)	CH ₄ (CF ₄)	CF ₃ H (CF ₂ H ₂)	L ^a (trifluoroacetone)	C ₃ H ₇ F (acetone)	H ₂ (N ₂)	C ₂ H ₄ (C ₂ H ₆)
Ca(acac) ₂	673	0.3	16.0	2.6	—	—	—	12.2	—	0.08	(54.2)	2.2	11.9 (0.8)
Ca(acac) ₂	673	1.0	23.5	2.7	—	—	—	21.0	—	0.2	(37.3)	3.3	11.1 (0.9)
Ca(tfacac) ₂	573	0.3	54.6	23.8	—	—	—	5.1 (0.9)	3.5 (0.3)	0.01 (9.5)	1.8	—	(0.5)
Ca(tfacac) ₂	573	1.0	54.6	22.6	—	—	—	5.1 (2.1)	4.7 (0.3)	0.05 (8.8)	1.3	—	(0.4)
Ca(dpm) ₂	738	0.2	36.5	0.9	3.4	11.3	(12.8)	30.3	—	2.9 ^b	—	1.2	(0.7)
Ca(dpm) ₂	738	1.0	32.3	4.3	12.6	16.2	(16.0)	13.7	—	2.4 ^b	—	1.6	(0.9)
Ca(ptfacac) ₂	573	0.2	30.7	18.0	5.5	3.3 (1.0)	0.9 (1.4)	0.2 (4.3)	0.1 (0.2)	0.2	0.02	—	(0.4)
Ca(ptfacac) ₂	573	0.6	18.8	7.3	3.8	1.6 (0.4)	2.3 (0.7)	0.6 (0.2)	0.2	0.2	0.1	0.08 (31.7)	(0.5)
Sr(tfacac) ₂	573	0.3	49.6	29.1	—	—	—	5.6 (0.7)	11.5 (0.2)	0.05 (2.4)	(0.5)	—	(0.4)
Sr(tfacac) ₂	573	1.0	38.4	32.9	—	—	—	5.2 (2.3)	13.7 (0.3)	0.02 (4.8)	(0.8)	—	(1.6)
Sr(ptfacac) ₂	523	0.1	23.6	48.6	0.05	0.8	0.9 (0.2)	5.4	19.2 (0.4)	0.5	—	—	(0.4)
Sr(ptfacac) ₂	523	1.0	35.2	34.4	0.3	0.9 (0.1)	0.4 (0.2)	2.4	25.6 (0.1)	0.2	—	0.02	(0.2)

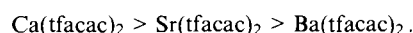
^a L = initial ligand. ^b Dimethylpropionaldehyde.

Table 6. Compositions (in mol %) of the volatile products of the thermal decomposition of metal β -diketonates (degree of decomposition 0.3).^{45–47}

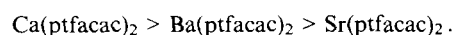
Compound	Temperature/K	CO	CO ₂	H ₂	CH ₄ (CF ₄)	CF ₃ H (CF ₂ H ₂)	C ₂ H ₆ (C ₂ F ₆)	C ₃ H ₂ F (C ₂ F ₄)	C ₃ H ₆ (C ₃ H ₈)	iso-C ₄ H ₈ (iso-C ₄ H ₁₀)	Methyl pivaloyl ketone	L ^a
Ba(ptfacac) ₂	623	35.7	33.6	0.2	4.3	4.5 (0.2)	0.5	—	2.5 (7.5)	4.2 (0.2)	6.4	0.2
Ba(hfacac) ₂	630	46.2	29.1	—	(2.0)	15.6 (0.2)	(0.2)	0.2 (1.3)	—	—	3.8 ^b	1.4
Ba(dpm) ₂	623	33.2	1.5	4.3	6.2	—	0.9	—	23.8	13.3	5.8	0.4
Ba(tfacac) ₂	623	38.9	22.8	—	4.7 (10.3)	3.0	0.5	0.8	—	—	—	0.1
Y(dpm) ₃	623	20.7	7.8	0.04	0.4	—	3.1	—	10.0	3.7	13.4	0.1
Y(ptfacac) ₃	623	30.3	13.7	0.1	3.0 (11.3)	0.9 (0.4)	10.3	(0.8)	2.6 (1.1)	4.2 (1.6)	10.3	0.4
Y(tfacac) ₃	623	42.9	18.8	—	2.4 (7.7)	0.01 (0.7)	4.1	—	—	—	—	0.2
Y(tfacac) ₃	630	39.3	25.3	—	(5.2)	7.0 (1.5)	(0.2)	0.6	—	—	—	0.2
Pr(ptfacac) ₃	573	40.5	20.0	0.2	0.15	12.2	0.2	—	—	14.0	4.6	—
											8.1 ^b	

^a Initial ligand. ^b Trifluoroacetone.

stability of these compounds in the thermal decomposition reaction falls with increase in the atomic number of the metal:^{44, 45}



For the complexes $\text{M}(\text{ptfacac})_2$ ($\text{M} = \text{Ca}, \text{Sr}, \text{Ba}$), the kinetic stability series assumes the following form:



A study has been devoted to the radiation-induced thermal decomposition of zinc and cadmium acetylacetonates.⁸¹ Zinc acetylacetonate is thermally less stable than cadmium acetylacetonate. The decomposition curves are S-shaped and, after the sigmoid section, there are long linear sections on the curves. The activation energies corresponding to the sigmoid and linear sections of the decomposition curves have been found.

3. Thermal decomposition of Group III metal β -diketonates

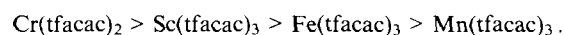
The thermal stability of aluminium β -diketonates, investigated by the DTA method, decreases in the following series:⁴³



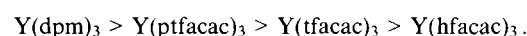
As for copper,⁷⁴ calcium,⁴⁴ strontium,⁴⁴ and barium⁴⁵ β -diketonates, the introduction of the trifluoromethyl group into the ligand decreases and the introduction of the *tert*-butyl group increases the thermal stability of the aluminium complexes. In the Al, Ga, and In group, a successive decrease in the thermal stability of the trifluoroacetylacetonate complexes with increase in the atomic number of the element is observed.⁴³

The study of the thermal decomposition of aluminium acetylacetonate in the gas phase, which we carried out by the manometric method, showed that, at temperatures in the range 657–723 K, the degree of decomposition of the reactant is independent of the initial pressure in the range from 130 to 200 GPa. The kinetic decomposition curves at low temperatures are autocatalytic in character, which is induced by the aluminium oxide formed. With increase in the decomposition temperature, the autocatalytic character of the curves vanishes as a consequence of the high rates of decomposition. The first-order rate constant calculated for 723 K is $4.1 \times 10^{-1} \text{ s}^{-1}$. The activation energy for the overall process, calculated by the method involving the transformation of the kinetic curve, is 68.1 kJ mol^{-1} . The primary product of the gas-phase decomposition is acetylacetone, which decomposes to acetone and carbon dioxide. The following substances have been found (mol%) among the products of the total pyrolysis of aluminium acetylacetonate at 673 K: acetylacetone (0.3), diacetyl (0.17), carbon dioxide (33.81), butane (9.54), methane (1.49), dimethylfuran (0.35), acetone (44.67), carbon monoxide (6.90), ketene (0.84), hydrogen (1.54), and unidentified products (0.7). The addition of oxygen accelerates the decomposition.

The trifluoroacetylacetonate chelates of other trivalent metals can be arranged in the following sequence in terms of their thermal stability:⁶⁸



The thermal decomposition of yttrium acetylacetonate takes place in the solid phase similarly to that of the barium analogue.⁷³ The gaseous products of the total pyrolysis of yttrium acetylacetonate at 573 K have the following composition (mol %): acetone (80.0), ethanol (0.4), ethene (carbon monoxide) (8.7), ethyl methyl ketone (0.2), carbon dioxide (1.0), water (0.4). On the other hand, the decomposition of the fluorine-substituted yttrium β -diketonates takes place in the gas phase in accordance with the kinetic law for a first-order reaction (Table 4).⁴⁶ From 2 to 8 moles of volatile products are evolved per mole of the compound decomposed depending on the temperature and the nature of the ligand. The ligand in the complex $\text{Y}(\text{tfacac})_3$ undergoes degradation to the greatest extent, whilst those in the complexes $\text{Y}(\text{dpm})_3$ and $\text{Y}(\text{tfacac})_3$ are least degraded. The kinetic stability of yttrium β -diketonates diminishes in the sequence



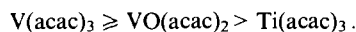
This sequence agrees well with the inductive influence of the *tert*-butyl and trifluoromethyl groups on the reaction centre. The electron-donating *tert*-butyl groups strengthen the Y–O bond, which leads to a greater thermal stability of the compounds $\text{Y}(\text{dpm})_3$ and $\text{Y}(\text{ptfacac})_3$ compared with the fluorine-substituted analogues $\text{Y}(\text{tfacac})_3$ and $\text{Y}(\text{hfacac})_3$, in which the strongly electron-accepting CF_3 groups weaken the Y–O bond. Thus the introduction of fluorine atoms into the ligands of the yttrium chelates not only increases the volatility but also diminishes the thermal stability of the complexes.

Evidence indicating a homogeneous-heterogeneous thermal decomposition of yttrium complexes as well as the accelerating effect of oxygen on the rate of thermal decomposition has been observed. The thermal decomposition of yttrium complexes is accompanied by far-reaching degradation of the ligands with formation of a wide range of products, including fluorine-containing hydrocarbons (Table 6).

Among the lanthanide derivatives, the kinetics of the thermal decomposition have been investigated only for the complex $\text{Pr}(\text{ptfacac})_3$ (Table 4).⁴⁷ The thermal decomposition of the praseodymium complex in vacuo takes place in the gas phase and is described satisfactorily by the kinetic equation for a first-order reaction. About 4 moles of gaseous products are evolved per mole of the compound decomposed, the main products being CO and CO₂, which indicates a far-reaching degradation of the ligand (Table 6).

4. Thermal decomposition of Group IV – VII metal β -diketonates

The kinetic and activation parameters of the gas-phase thermal decomposition of titanium, vanadium, and vanadyl acetylacetonates in vacuo have been investigated.^{82,83} The acetylacetonate derivatives of trivalent and tetravalent vanadium have comparable reactivities (Table 4). On the other hand, the replacement of the central metal atom has a much greater influence on the thermal stability of the acetylacetonates than the oxidation state of the metal. The thermal stabilities of the compounds investigated diminish in the sequence



The complex homogeneous-heterogeneous character of the decomposition reactions of these compounds has been demonstrated. As in the case of the barium,⁴⁵ calcium,⁴⁴ and strontium⁴⁴ chelates, a decrease in the rate constant for the thermal decomposition of vanadium acetylacetonate is observed with increase in the surface area, whereas the nature of the surface does not influence the rate of the process. The principal volatile products of the thermal decomposition of vanadium acetylacetonate at 703 K and for low degrees of decomposition were (in moles per mole of the reactant decomposed): acetone (2.0), carbon dioxide (2.5), carbon monoxide (1.2), xylene (0.14), hydrogen (0.11), butene (0.29), and an unidentified product (with m/e 86) (0.02). Similar products have been detected also in the decomposition of vanadyl acetylacetonate. The set of kinetic and analytical data indicates the preferential operation of an intramolecular pathway leading to the decomposition of these compounds. However, the influence of the addition of substances which might serve as initiators of a radical process (acetone, oxygen) indicates indirectly a small contribution of the radical decomposition path. Thus the addition of acetone and oxygen increases the rate constants for the decomposition of vanadium and vanadyl acetylacetonates. The same trends have been observed in the pyrolysis of the copper,^{73–75} yttrium,⁴⁶ barium,⁴⁵ calcium,⁴⁴ strontium,⁴⁴ and aluminium⁴³ chelates. The formation of the acetylacetonyl radical has also been postulated in the pyrolysis of the metal chelates.⁸⁴

The thermal decomposition of zirconium acetylacetonate has been investigated by the DTA method under an inert atmosphere at temperatures from 293 to 773 K.²¹ The process takes place in two stages. In the first stage (453 K), the displacement of two chelate ligands as a result of coordination polymerisation and the formation of an intermediate polymeric product are observed; in the second stage (623 K), zirconium dioxide in the cubic modification is formed. In contrast to the acetylacetonate derivative, the decomposition of the complex $\text{Zr}(\text{ptfacac})_4$ takes place in one stage. It involves the dissociation of the bonds within the chelate ligand with formation of volatile low-molecular-mass products. This decomposition path is associated with the absence of α -hydrogen atoms from the side chains, which would lead to the possibility of the radical recombination of the carbon chains. On further heating, zirconium dioxide passes from the cubic to the pure monoclinic form.

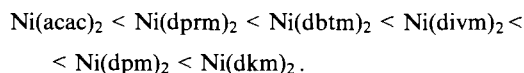
The thermal decomposition of the bismuth chelates $\text{Bi}(\text{tfacac})_3$, $\text{Bi}(\text{hfacac})_3$, and $\text{Bi}(\text{ptfacac})_3$ in the vapour and solid phase has been investigated in helium and oxygen streams.⁷¹ The most characteristic gas-phase products of the thermolysis of the bismuth chelate vapours were the β -diketonates and their fragments. The complex $\text{Bi}(\text{ptfacac})_3$ decomposing at a temperature above 573 K, showed the highest thermal stability. This complex shows a smaller tendency to form oligomers owing to the steric hindrance generated by the bulky substituents in the ligands within the octahedral bismuth complex. The increase in the steric factor as a result of the replacement of the Bu^t groups by MeOCMe_2 rules out almost completely the possibility of dimerisation of the molecules.

Comparison of the thermal stabilities of chromium(III) and manganese(III) acetylacetonates and their alkyl and fluorine-

substituted derivatives, carried out by the DTA method in terms of the initial decomposition temperatures, shows that the chromium chelates are more stable than the manganese chelates.⁸⁰ The pyrolytic decomposition of the β -diketonates of manganese(III) in an unstable oxidation state is accompanied by the transition of the central metal ion from the trivalent to the divalent state and the liberation of the ligand. It has been suggested that this process proceeds via a radical mechanism.⁸⁰

5. Thermal decomposition of Group VIII metal β -diketonates

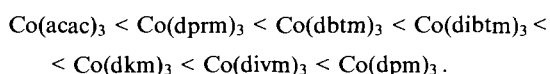
The thermal stability of iron(III), cobalt(II), cobalt(III), and nickel(II) β -diketonates in the solid phase has been investigated by the DTA method.⁸⁰ The thermal stability of divalent metal acetylacetonates increases on passing from cobalt to nickel: $\text{Co}(\text{acac})_2 < \text{Ni}(\text{acac})_2$. The thermal stability of the chelate nickel acetylacetonate complexes with bulky alkyl substituents increases in the sequence



This agrees with the increase in the number of carbon atoms in the alkyl substituents. A similar sequence has been observed also for cobalt(II) chelates. The thermal stability of these chelates depends on the electron-donating effect of the alkyl group, which increases the basicity of the ligand oxygen atom and this increases the strength of the $\text{M}-\text{O}$ bond. At room temperature, the alkyl derivatives of cobalt(II) and nickel(II) have a polymeric octahedral structure. An increase in temperature favours the formation of chelates with a square planar structure in the liquid phase. This tendency intensifies with increase in the bulk of the alkyl substituents owing to steric hindrance. Near the temperature of the onset of decomposition, the axial $\text{M}-\text{O}$ bond in cobalt(II) and nickel(II) β -diketonates is weakened, whilst the equatorial bond is strengthened. If one considers the decomposition of metal β -diketonates with the dissociation of the equatorial $\text{M}-\text{O}$ bond, then the β -diketonates with less bulky alkyl substituents, which favour the formation of a polymeric hexacoordinate structure, should be less stable.

The influence of the structure of the compound on the thermal properties of the nickel complexes $\text{Ni}(\text{acac})_2$, $\text{Ni}(\text{dpm})_2$, $\text{Ni}(\text{acim})_2$, and $\text{Ni}(\text{tfacim})_2$ has been traced.⁷² The introduction of the trifluoromethyl group into the ligand instead of the methyl group increases the thermal stability of the nickel acetylacetonate complexes and decreases the stability of the imino-derivatives. The thermal decomposition of the β -diketonate derivatives of nickel proceeds via a mechanism involving an intramolecular rearrangement with evolution of the free β -diketonates into the gas phase. A second decomposition path with formation of a ligand radical operates for the ketoiminate complexes, the contribution of this path increasing with temperature. In the presence of hydrogen, the main products of the decomposition of all the nickel(II) complexes investigated are the free ligands.

Iron(III) acetylacetonates and alkylacetylacetonates are more stable than the analogous cobalt(III) compounds. The thermal stability of cobalt(III) β -diketonates increases in the sequence



A similar trend has also been observed for iron(III) β -diketonates, which is consistent with the increasing bulk of the alkyl substituent. The pyrolytic decomposition of cobalt(III) and iron(III) (an unstable oxidation state of the metal) β -diketonates is accompanied by the transition of the central metal ion from the trivalent to the divalent state and the liberation of the ligand. It has been suggested that the decomposition of these compounds proceeds via a radical path.

The characteristic features of the thermal decomposition of palladium, iridium, rhodium, and platinum β -diketonates have

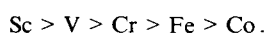
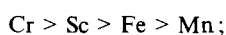
been examined.^{49, 80, 85} The dependence of the thermal stability of the β -diketonates of these metals on the type of substituents in the ligand is weak.⁴⁹ One can only confirm fairly unambiguously the ability, frequently noted above, of the *tert*-butyl group to increase somewhat the thermal stability of the complex. It has been noted for palladium(II) β -diketonates that the unsubstituted acetylacetonates have a higher thermal stability than the acetylacetonates with bulky alkyl groups.⁸⁰ The palladium complexes are characterised by a larger contribution of the ring conjugation than other metal chelates by virtue of the π -bonding ($p\pi-d\pi$) nature of the M—O bond. The alkyl substituents in these ligands exhibit hyperconjugation, which disrupts the resonance in the ring-conjugated systems and this increases the contribution of π -bonding in the M—O bond. Problems concerning the influence of substituents in the *cis*- and *trans*-positions in rhodium complexes with asymmetric substitution in a planar chelate ring have been examined on the basis of IR and NMR spectroscopic data.^{86, 87} The inductive effect of the alkyl substituents on the free energy of the gas-phase oxidation of ruthenium β -diketonates has been studied: $\text{Ru}(\text{acac})_3$, $\text{Ru}(\text{dprm})_3$, $\text{Ru}(\text{dbtm})_3$, $\text{Ru}(\text{dibtm})_3$, and $\text{Ru}(\text{divm})_3$.⁸⁸ It was shown that it varies from $-200.6 \text{ kJ mol}^{-1}$ for the complexes with methyl substituents to $-150.5 \text{ kJ mol}^{-1}$ for the complexes with *tert*-butyl substituents. The one-electron oxidation energy varies from -79.4 to $-66.9 \text{ kJ mol}^{-1}$ and is not correlated with the size of the alkyl substituent.⁸⁸ The replacement of one of the donor oxygen atoms by nitrogen in the palladium, iridium, rhodium, and platinum complexes leads to an increase in the gas-phase thermal stability of the complexes. The products of the thermal decomposition of these compounds contain considerable amounts of the noncoordinated ligand molecules.⁸⁵

IV. Conclusion

The above analysis of the literature data concerning the influence of the nature of the metal and the substituents in the β -diketone on the volatility and thermal stability of metal β -diketonates shows that the volatility of the complexes depends to a large extent on the nature of the substituent in the β -diketone, while their thermal stability is determined both by the nature of the metal and that of the substituent in the ligand.

Unambiguous rules governing the variation of volatility and thermal stability as a function of the atomic number of the metal have not been established. The kinetic stability of the metal β -diketonate complexes $\text{M}(\text{tfacac})_n$ [$\text{M} = \text{Ca}, \text{Sr}$ or Ba ($n = 2$) and Al, Ga , or In ($n = 3$)] decreases successively in the thermal decomposition reaction with increase in the atomic number of the metal: $\text{Ca} > \text{Sr} > \text{Ba}$, $\text{Al} > \text{Ga} > \text{In}$.

The parallel variation of the volatility and thermal stability of the complexes $\text{M}(\text{tfacac})_3$ ($\text{M} = \text{Al}, \text{Ga}, \text{In}$) has been observed. The volatility of these compounds diminishes with increase in the atomic number of the element, which is associated with the characteristic features of the electronic structures of these compounds.⁸⁹ For $\text{M}(\text{tfacac})_2$ ($\text{M} = \text{Ca}, \text{Sr}, \text{Ba}$), the opposite variation of this kind is observed: the volatility of the complexes increases with increase in the atomic number of the metal. The variation of the thermal stability with increasing atomic number of the metal presented above does not hold for the complexes $\text{M}(\text{tfacac})_3$ ($\text{M} = \text{Sr}, \text{Cr}, \text{Mn}, \text{Fe}$). Their thermal stability and volatility vary in the following series of metals respectively:



A clear-cut dependence of the thermal stability on the atomic number also does not occur for the acetylacetonate complexes of monovalent, divalent, and trivalent metals. The thermal stability of the complexes is influenced not only by the energy of the M—O bond, determined by the nature of the metal, but also by the steric structure of the complexes, the possibility of the formation of

oligomers, and the phase in which the thermal decomposition takes place. The rate of the gas-phase pyrolysis is determined by the type of reaction — homogeneous, heterogeneous, and homogeneous–heterogeneous — and also by the type of the rate-limiting stage.

In the study of the kinetics of the thermal decomposition of fluorine-substituted calcium, strontium, and barium β -diketonates, the decrease in the rate constant for the thermal decomposition of the chelate with increase in the surface area of the reactor can be clearly traced, whilst in other cases it is rarely manifested. This may be associated with the retardation of the rate-limiting stage of the thermal decomposition — the conversion of the bidentate ligand into a monodentate one with subsequent splitting off of the free ligand.

A general rule is the increase, frequently emphasised in the literature, in volatility and the decrease in the thermal stability of the metal β -diketonates after the introduction of the trifluoromethyl group into the ligand. On the other hand, the introduction of the *tert*-butyl group decreases the volatility of the complex and increases its thermal stability.

The influence of chain length of the alkyl substituents in the β -diketone on the thermal stability of the chelates is determined by the structure of the complexes. The thermal stability of the cobalt(II), cobalt(III), iron(III), and nickel(II) complexes, which have polymeric octahedral structure at room temperature, increases with increase in the length of the alkyl group. This is associated with the electron-donating effect of the alkyl group, which strengthens the M—O bond. Among the palladium(II) and copper(II) complexes, which have a square planar structure, the acetylacetonate derivatives are more stable than the derivatives with alkyl substituents. This has been attributed to the hyperconjugation effect of the alkyl substituents, which disrupts the resonance in the ring-conjugated system of the chelate. A common feature of the thermal decomposition of the metal β -diketonates investigated is its acceleration in oxygen and also the complex and homogeneous–heterogeneous character of the process.⁹⁰

The principal aspects of the gas-phase thermal decomposition of metal β -diketonates have been examined.^{91–95}

The characteristic features of the mechanism of the thermal decomposition of the chelates are determined by the presence of two reaction centres — the M—O bond and the γ -CH proton. It has been suggested that the first stage of the thermal decomposition of the β -diketonates is the opening of the ring and the conversion of the bidentate ligand into a monodentate one. This is followed by decomposition via different paths:

(a) intramolecular decomposition with formation of the free ligand and low molecular mass products:

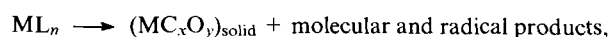


$n > m$;

(b) decomposition with homolytic dissociation of the metal–ligand bonds and the formation of the ligand radical L^\cdot :



(c) decomposition with far-reaching degradation of the organic component of the complex, which results in the formation of both low molecular mass and radical products:



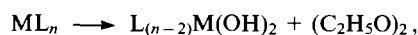
$x, y \geq 0$;

(d) decomposition with dissociation of the C—O bonds and the formation of gaseous products having the general formula $\text{R}^1\text{C}(\text{O})\text{CH}_k\text{CR}^2$ (where $k = 0, 2$):



$k = 0; n > m$;

(e) decomposition with formation of a cyclic diketone as a result of the intramolecular interaction of the opened chelate rings of two ligands:



$L = \text{Hacac}$, $n = 3, 4$.

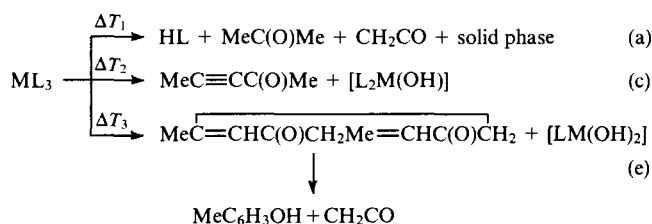
Depending on the type of terminal substituents in the ligand and on the nature of the central metal atom, a particular decomposition path operates. The thermal decomposition can proceed via one of the paths enumerated or simultaneously via several.

Path (a) is the main one in the thermal decomposition of the complexes $\text{Cu}(\text{dpm})_2$, $\text{Ru}(\text{acac})_2$, and $\text{Zr}(\text{tfacac})_4$. Thermolysis of the vapours of palladium β -diketonates takes place simultaneously via paths (a) and (b). With increase in temperature, path (b) becomes dominant. Path (c) operates in the thermolysis of the vapours of the complexes $\text{Ru}(\text{tfacac})_3$ and $\text{Y}(\text{dpm})_3$. Both the free ligand and its radical are absent from the products of the thermal decomposition of the $\text{Ru}(\text{tfacac})_3$ vapour, the main bulk of the latter comprising the CO , CO_2 , H_2O , and HF molecules and the CF_3 radical. Complexes for which the thermal stability is higher than that of the ligand decompose via path (c).⁹⁵ The threshold decomposition temperature of these complexes is $763 \pm 283 \text{ K}$.

The thermolysis of $\text{Ba}(\text{dpm})_2$ takes place simultaneously via paths (a), (c), and (d) and includes in addition the depolymerisation reaction of the molecules and the oligomeric composition of the gas phase does not then correspond to the composition of the condensed phase. Thus the complex exists in the form $\text{Ba}_4(\text{dpm})_3$ in the condensed phase, whilst in the gas phase it is present as a mixture of trimers, dimers, and monomers.

The thermal decomposition of the complexes $\text{Al}(\text{acac})_3$, $\text{Sc}(\text{acac})_3$, and $\text{Hf}(\text{acac})_3$ proceeds simultaneously via paths (a), (c), and (d) near the threshold temperature, whereas the thermal decomposition of $\text{Mg}(\text{acac})_2$ takes place via paths (a) and (c).⁹⁵

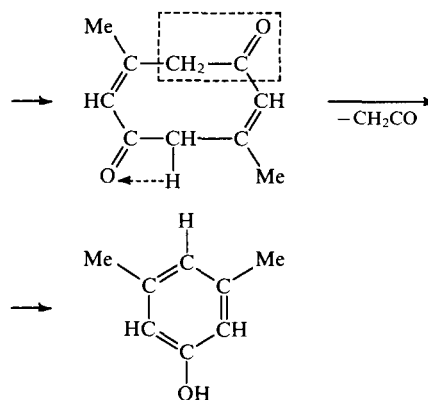
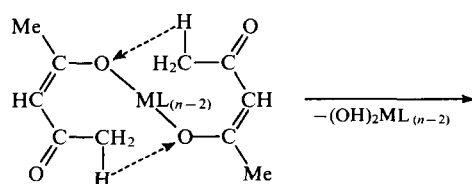
A scheme for the thermal decomposition of the $\text{Al}(\text{acac})_3$ and $\text{Sc}(\text{acac})_3$ vapours is presented below (the postulated species are indicated in square brackets).



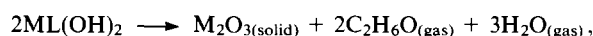
$M = \text{Sc, Al}$; $L = \text{C}_5\text{H}_7\text{O}_2$.

Each of the thermal decomposition paths operates in a particular temperature range ΔT .

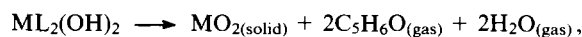
The path leading to the formation of the $(\text{C}_5\text{H}_6\text{O})_2$ species as a result of the cyclic dimerisation of two ligands coordinated as monodentate species on dissociation of the carbon-oxygen (enolic) bonds with migration of a hydrogen atom from the methyl group to the enolic oxygen atom of a neighbouring ligand has been demonstrated. The cyclic diketone formed eliminates ketene CH_2CO and is converted into the more stable 3,5-dimethylphenol.



On the basis of this scheme, one can postulate a path leading to the formation of metal oxides in the condensed phase.



$M = \text{Al, Sc}$;



$M = \text{Hf}$, $L = \text{C}_5\text{H}_7\text{O}_2$.

The existence of path (c) for aluminium and scandium acetylacetonates constitutes experimental confirmation that the thermal decomposition is preceded by a stage involving the thermal excitation of the molecules, in which the coordination of the ligands changes from bidentate to monodentate (in terms of the isolated molecules approximation).⁹⁵

Paths (d) and (e) are characteristic of thermal decomposition processes leading to the formation of oxides in the condensed phase as a result of intramolecular reactions.

In virtually all cases, the presence of oxygen diminishes the threshold decomposition temperature of the β -diketonates and increases the rate of reaction.^{90, 95} Under these conditions, there is an appreciable increase in the fraction of simple molecular thermolysis products such as CO_2 , CO , and H_2O . The influence of oxygen on the thermal decomposition process can be exerted in two ways.⁹⁵ If the reaction proceeds via path (a) with formation of the free ligand, then oxygen participates quantitatively in the reaction at the stage involving the oxidation of the free ligand. As a rule, this occurs at a higher temperature than the temperature of the onset of decomposition of the complex. On the other hand, if the thermal decomposition takes place via path (b) or (d), virtually all the gaseous products are oxidised immediately after the threshold temperature has been exceeded. Paths (c) and (e) do not then operate in the presence of oxygen. A similar situation is observed also on path (c).

The influence of hydrogen on the thermal decomposition of the metal β -diketonate vapours depends on the nature of the metal and the ligand.⁹⁵ In the case of the $\text{Ru}(\text{acac})_3$, $\text{Zr}(\text{tfacac})_4$, $\text{Sc}(\text{acac})_3$, and $\text{Al}(\text{acac})_3$ vapours, the threshold temperature increases by 283–353 K and the rate of thermal decomposition falls, whereas the threshold temperature decreases for $\text{Ru}(\text{tfacac})_3$. Such different effects of hydrogen on the kinetics of the thermal decomposition process can be accounted for by the specific interaction of the hydrogen adsorbed on the surface with the molecules of the complex. Hydrogen does not influence appreciably the composition of the gaseous products and the path followed in the thermal decomposition of metal β -diketonates.

Thus the kinetics, the thermal decomposition path, and the composition of the condensed phase are determined by the nature of the metal and the ligand in the complex and by the decomposition temperature.

References

1. M Knell, in *Advances in Chemistry Series* Vol. 23 (Washington, DC: American Chemical Society, 1959) p. 37
2. R W Moshier, R E Sievers *Gas Chromatography of Metal Chelates* (Translated into Russian; Moscow: Mir, 1967)
3. N N Korneev, A F Popov, B A Krentsel' *Kompleksnye Metalloorganicheskie Katalizatory* (Complex Organometallic Catalysts) (Leningrad: Khimiya, 1969)
4. K C Jishi, V N Pathak *Coord. Chem. Rev.* **22** 37 (1977)
5. D F Graddon *Coord. Chem. Rev.* **4** 1 (1969)
6. M A Porai-Koshits *Dokl. Akad. Nauk SSSR* **134** 1104 (1960)
7. E C Lingafelter *Coord. Chem. Rev.* **1** 151 (1966)
8. L M Shkol'nikova, M A Porai-Koshits, in *Teoreticheskaya i Prikladnaya Khimiya β -Diketonatov Metallov* (Theoretical and Applied Chemistry of Metal β -Diketonates) (Ed. V I Spitsin) (Moscow: Nauka, 1985) p. 11
9. E Bayer *Angew. Chem.* **76** 76 (1964)
10. J P Collman *Angew. Chem.* **77** 154 (1965)
11. M I Siling, A I Gel'bshtein *Usp. Khim.* **48** 479 (1969) [*Russ. Chem. Rev.* **48** 249 (1969)]
12. Yu N Nizel'skii, S S Tishchenko, T E Lipatova, in *Teoreticheskaya i Prikladnaya Khimiya β -Diketonatov Metallov* (Theoretical and Applied Chemistry of Metal β -Diketonates) (Ed. V I Spitsin) (Moscow: Nauka, 1985) p. 236
13. V Yu Golubtsova, I A Murav'eva, L I Martynenko, in *Teoreticheskaya i Prikladnaya Khimiya β -Diketonatov Metallov* (Theoretical and Applied Chemistry of Metal β -Diketonates) (Ed. V I Spitsin) (Moscow: Nauka, 1985) p. 173
14. S S Travnikov, E V Fedoseev, A V Davydov, B F Myasoedov, in *Teoreticheskaya i Prikladnaya Khimiya β -Diketonatov Metallov* (Theoretical and Applied Chemistry of Metal β -Diketonates) (Ed. V I Spitsin) (Moscow: Nauka, 1985) p. 224
15. G A Razuvaev, B G Gribov, G A Domrachev, B A Salamatin *Metalloorganicheskie Soedineniya v Elektronike* (Organometallic Compounds in Electronics) (Moscow: Nauka, 1972)
16. G A Domrachev, O N Suvorova, V A Varyukhin, V V Kutyreva, in *Teoreticheskaya i Prikladnaya Khimiya β -Diketonatov Metallov* (Theoretical and Applied Chemistry of Metal β -Diketonates) (Ed. V I Spitsin) (Moscow: Nauka, 1985) p. 228
17. V A Varyukhin, V Yu Vodinskii, G A Domrachev, in *Teoreticheskaya i Prikladnaya Khimiya β -Diketonatov Metallov* (Theoretical and Applied Chemistry of Metal β -Diketonates) (Ed. V I Spitsin) (Moscow: Nauka, 1985) p. 178
18. G A Domrachev, O N Suvorova *Usp. Khim.* **49** 1671 (1980) [*Russ. Chem. Rev.* **49** 810 (1980)]
19. B G Gribov, G A Domrachev, B V Zhuk, B S Kaverin, B I Kozyrkin, V V Mel'nikov, O N Suvorova *Osazhdenie Plenok i Pokrytii Razlozheniem Metalloorganicheskikh Soedinenii* (Deposition of Films and Coatings by the Decomposition of Organometallic Compounds) (Moscow: Nauka, 1981)
20. O N Mittov, G A Chislova, E D Novikova *Metalloorg. Khim.* **1** 610 (1988)
21. O N Suvorova, V V Kutyreva, V A Varyukhin, G A Domrachev, in *Stroenie, Svoistva i Primenenie β -Diketonatov Metallov* (Structure, Properties, and Applications of Metal β -Diketonates) (Ed. V I Spitsin) (Moscow: Nauka, 1978) p. 116
22. O N Suvorova, V A Varyukhin, V V Kutyreva, in *Primenenie Metalloorganicheskikh Pokrytii i Materialov* (Applications of Organometallic Coatings and Materials) (Ed. G A Razuvaev) (Moscow: Nauka, 1986) p. 68
23. G A Domrachev, E V Shitova, V Yu Vodinskii *Dokl. Akad. Nauk SSSR* **226** 1080 (1976)
24. D N Suglobov, G V Sidorenko, E K Legin, in *Letuchie Organicheskie Kompleksnye Soedineniya f -Elementov* (Volatile Organic Complex Compounds of f -Elements) (Moscow: Energoatomizdat, 1987)
25. L A Ryabova, V U Antokhina, I P Serbinov *Zh. Prikl. Khim.* **45** 2103 (1972)
26. V A Titov, V A Dodonov, L G Sedova *Metalloorg. Khim.* **1** 616 (1988)
27. A F Kaul' *Zh. Vses. Khim. O-va im D I Mendeleeva* **34** 492 (1989)
28. T Nakamori, H Abe, T Kanomori, S Shibata *Jpn. J. Appl. Phys.* **27** 1265 (1988)
29. H Abe, T Tsuruoka, T Nakamori *Jpn. J. Appl. Phys.* **27** 1473 (1988)
30. H Yamane, H Kurosawa, H Iwasaki, H Masumoto, T Hirai, N Kaayashi *Jpn. J. Appl. Phys.* **27** 1275 (1988)
31. J Zhao, K H Dahmen, H O Marcy, L M Tonge, T J Marks, B W Wessels, C R Kannewurf *Appl. Phys. Lett.* **53** 1750 (1988)
32. A D Berry, D K Gaskill, R T Holm, E J Cukauskas, R Kaplan, R I Herry *Appl. Phys. Lett.* **52** 1743 (1988)
33. T Tsuruoka, H Takahaki, R Kawasaki, T Kanamori *Appl. Phys. Lett.* **54** 1808 (1989)
34. J Zhao, H O Marcy, L M Tonge, B W Wessels, T J Marks, C R Kannewurf *Physica* **159** 710 (1989)
35. J Zhao, K H Dahmen, H O Marcy, L M Tonge, C R Kannewurf *Solid State Commun.* **69** 187 (1989)
36. A D Barry, R T Holm, E J Cukauskas, M Fatemi, D K Gaskill, R Kaplan, W B Fox *J. Cryst. Growth* **92** 344 (1988)
37. A N Nesmeyanov *Davlenie Para Khimicheskikh Elementov* (Vapour Pressures of Chemical Elements) (Moscow: Izd. Akad. Nauk SSSR, 1961)
38. A V Suvorov *Termodinamicheskaya Khimiya Paroobraznogo Sostoyaniya* (Thermodynamic Chemistry of the Vapour State) (Leningrad: Khimiya, 1970)
39. A V Novoselova, A S Pashinkin *Davlenie Para Letuchikh Khal'kogenidov Metallov* (Vapour Pressures of Volatile Metal Chalcogenides) (Moscow: Nauka, 1978)
40. E W Berg, J T Truemper *J. Phys. Chem.* **64** 487 (1960)
41. E W Berg, H W Dowling *J. Chem. Eng. Data* **6** 556 (1961)
42. E W Berg, J T Truemper *Anal. Chim. Acta* **32** 245 (1965)
43. I K Igumenov, Yu V Chumachenko, S V Zemskov, in *Problemy Khimii i Primeneniya β -Diketonatov Metallov* (Problems of the Chemistry and Applications of Metal β -Diketonates) (Ed. V I Spitsin) (Moscow: Nauka, 1982) p. 100
44. E I Tsyganova, O M Titova, V I Faerman, L V Stepanova, Yu A Aleksandrov *Zh. Obshch. Khim.* **63** 271 (1993)
45. E I Tsyganova, G I Mazurenko, O M Titova, N N Kaloshina, V I Faerman, Yu A Aleksandrov *Zh. Obshch. Khim.* **62** 2422 (1992)
46. E I Tsyganova, G A Mazurenko, O M Titova, V I Faerman, Yu A Aleksandrov *Zh. Obshch. Khim.* **62** 1947 (1992)
47. O M Titova, E I Tsyganova, V I Faerman, V N Drobotenko, Yu A Aleksandrov *Zh. Obshch. Khim.* **62** 2419 (1992)
48. I K Igumenov, Yu V Chumachenko, S V Zemskov, in *Stroenie, Svoistva i Primenenie β -Diketonatov Metallov* (The Structure, Properties, and Applications of Metal β -Diketonates) (Ed. V I Spitsin) (Moscow: Nauka, 1978) p. 105
49. I K Igumenov, G I Zharkova, V G Isakova, S V Zemskov, in *Teoreticheskaya i Prikladnaya Khimiya β -Diketonatov Metallov* (Theoretical and Applied Chemistry of Metal β -Diketonates) (Ed. V I Spitsin) (Moscow: Nauka, 1985) p. 36
50. S G Konstantinov, G P Dudchik, O G Polyachenok, in *Teoreticheskaya i Prikladnaya Khimiya β -Diketonatov Metallov* (Theoretical and Applied Chemistry of Metal β -Diketonates) (Ed. V I Spitsin) (Moscow: Nauka, 1985) p. 148
51. R Fontaine, C Pommier, G Guiochon *Bull. Soc. Chim. Fr.* 3011 (1972)
52. M M Jones, J L Wood *Inorg. Chem.* **3** 1553 (1964)
53. M Z Gurevich, Candidate Thesis in Chemical Sciences, Institute of Very Pure Materials, Moscow, 1973
54. D T Farrar, M M Jones *J. Phys. Chem.* **67** 1049 (1963)
55. J L Wood, M M Jones *J. Inorg. Nucl. Chem.* **29** 113 (1967)
56. T R Melia, R Merrifield *J. Inorg. Nucl. Chem.* **32** 1489 (1970)
57. T R Melia, R Merrifield *J. Inorg. Nucl. Chem.* **32** 2573 (1970)
58. S G Konstantinov, G P Dudchik, V P Bochinn, O G Polyachenok, in *Termodinamika Organicheskikh Soedinenii (Tez. Dokl.)* [Thermodynamics of Organic Compounds (Abstracts of Reports)] (Moscow: Nauka, 1976) p. 22
59. W R Wolf, R E Sievers, G H Brown *Inorg. Chem.* **11** 1995 (1992)
60. H R Brunner, B J Curtis *J. Therm. Anal.* **5** 111 (1973)
61. H J Gotze, K Bloss, H Molketin *Z. Phys. Chem.* **64** 487 (1960)
62. J E Sicre, J T Dubois, K J Eisentraut, R E Sievers *J. Am. Chem. Soc.* **91** 3476 (1969)
63. H A Swain, D G Karraker *Inorg. Chem.* **9** 1766 (1970)
64. H A Swain, D G Karraker *Inorg. Nucl. Chem.* **33** 2851 (1971)
65. G B Ray, B E Huss *J. Chem. Eng. Data* **22** 239 (1977)

66. E M Rubtsov, V Ya Mishin, in *Problemy Khimii i Primeneniya β -Diketonatov Metallov* (Problems of the Chemistry and Applications of Metal β -Diketonates) (Ed. V I Spitsin) (Moscow: Nauka, 1982) p. 136
67. D N Sokolov *Usp. Khim.* **46** 740 (1977) [*Russ. Chem. Rev.* **46** 388 (1977)]
68. I K Igumenov, Yu V Chumachenko, S V Zemskov *Zh. Fiz. Khim.* **52** 2416 (1978)
69. Yu V Chumachenko, I K Igumenov, S V Zemskov *Koord. Khim.* **5** 1625 (1979)
70. N E Nefedova, I K Igumenov, A F Bykov, in *Primenenie Metalloorganicheskikh Soedinenii dlya Polucheniya Neorganicheskikh Pokrytii i Materialov (Tez. Dokl.)* [Application of Organometallic Compounds in the Preparation of Inorganic Coatings and Materials (Abstracts of Reports)] (N Novgorod: Institute of Organometallic Chemistry of the Academy of Sciences of the USSR, 1991) p. 153
71. P P Semyanikov, V M Grankin, I I Zharkova, I K Igumenov, in *Primenenie Metalloorganicheskikh Soedinenii dlya Polucheniya Neorganicheskikh Pokrytii i Materialov (Tez. Dokl.)* [Application of Organometallic Compounds in the Preparation of Inorganic Coatings and Materials (Abstracts of Reports)] (N Novgorod: Institute of Organometallic Chemistry of the Academy of Sciences of the USSR, 1991) p. 127
72. P P Semyanikov, V M Grankin, V V Pervukhin, I K Igumenov, in *Primenenie Metalloorganicheskikh Soedinenii dlya Polucheniya Neorganicheskikh Pokrytii i Materialov (Tez. Dokl.)* [Application of Organometallic Compounds in the Preparation of Inorganic Coatings and Materials (Abstracts of Reports)] (Moscow: Nauka, 1987) p. 176
73. E I Tsyganova, G A Mazurenko, V N Drobotenko, L M Dyagileva, Yu A Aleksandrov *Zh. Obshch. Khim.* **62** 499 (1992)
74. E A Mazurenko, V Ya Zub, S L Voroginskii, S V Volkov *Ukr. Khim. Zh.* **54** 1235 (1988)
75. A F Bykov, P P Semyanikov, I K Igumenov, in *Primenenie Metalloorganicheskikh Soedinenii dlya Polucheniya Neorganicheskikh Pokrytii i Materialov (Tez. Dokl.)* [Application of Organometallic Compounds in the Preparation of Inorganic Coatings and Materials (Abstracts of Reports)] (N Novgorod: Institute of Organometallic Chemistry of the Academy of Sciences of the USSR, 1991) p. 157
76. N N Kostyuk, G N Klavut', I I Vinogradov, A A Erdman, L G Sedova, V L Shirokii, in *Primenenie Metalloorganicheskikh Soedinenii dlya Polucheniya Neorganicheskikh Pokrytii i Materialov (Tez. Dokl.)* [Application of Organometallic Compounds in the Preparation of Inorganic Coatings and Materials (Abstracts of Reports)] (N Novgorod: Institute of Organometallic Chemistry of the Academy of Sciences of the USSR, 1991) p. 150
77. O N Druzhkov, A V Gushchin, T K Postnikova, A M Rabinovich, V L Shirokii, Yu A Andrianov, in *Primenenie Metalloorganicheskikh Soedinenii dlya Polucheniya Neorganicheskikh Pokrytii i Materialov (Tez. Dokl.)* [Application of Organometallic Compounds in the Preparation of Inorganic Coatings and Materials (Abstracts of Reports)] (N Novgorod: Institute of Organometallic Chemistry of the Academy of Sciences of the USSR, 1991) p. 149
78. J V Hoene, R G Charles, W M Hickam *J. Phys. Chem.* **62** 1098 (1958)
79. G I Zharkova, P P Semyanikov, V M Grankin, T M Tyukalevskaya, I K Igumenov, S V Zemskov, in *Primenenie Metalloorganicheskikh Soedinenii dlya Polucheniya Neorganicheskikh Pokrytii i Materialov (Tez. Dokl.)* [Application of Organometallic Compounds in the Preparation of Inorganic Coatings and Materials (Abstracts of Reports)] (Gor'kii, 1987) p. 184
80. K Ueno, H Kobayashi, J Yoshida *Mem. Fac. Eng. Kyushu Univ.* **38** 83 (1978)
81. S K Patnaik, P K Maharana, S N Sanu, G S Murty *J. Radioanal. Nucl. Chem. Lett.* **128** 283 (1988)
82. L M Dyagileva, E I Tsyganova, V P Mar'in, Yu A Aleksandrov *Zh. Obshch. Khim.* **52** 2024 (1982)
83. L M Dyagileva, E I Tsyganova, V P Mar'in, Yu A Aleksandrov, in *Teoreticheskaya i Prikladnaya Khimiya β -Diketonatov Metallov* (Theoretical and Applied Chemistry of Metal β -Diketonates) (Ed. V I Spitsin) (Moscow: Nauka, 1985) p. 69
84. N M Uvarova, V B Polikarpov, O N Druzhkov, T K Postnikova, in *Stroenie, Svoistva i Primenenie β -Diketonatov Metallov* (The Structure, Properties, and Applications of Metal β -Diketonates) (Ed. V I Spitsin) (Moscow: Nauka, 1978) p. 14
85. P P Semyanikov, V M Grankin, I K Igumenov, in *Primenenie Metalloorganicheskikh Soedinenii dlya Polucheniya Neorganicheskikh Pokrytii i Materialov (Tez. Dokl.)* [Application of Organometallic Compounds in the Preparation of Inorganic Coatings and Materials (Abstracts of Reports)] (Gor'kii, 1987) p. 164
86. Yu S Varshavskii, T G Cherkasova, I S Podkorytov, in *VI Vserossiiskaya Konf. po Metalloorganicheskoi Khimii (Tez. Dokl.)* [The Sixth All-Russian Conference on Organometallic Chemistry (Abstracts of Reports)] (N Novgorod: Institute of Organometallic Chemistry of the Russian Academy of Sciences, 1995) p. 312
87. Yu S Varshavskii, T G Cherkasova, N I Pavlenko, A I Rubailo, in *VI Vserossiiskaya Konf. po Metalloorganicheskoi Khimii (Tez. Dokl.)* [The Sixth All-Russian Conference on Organometallic Chemistry (Abstracts of Reports)] (N Novgorod: Institute of Organometallic Chemistry of the Russian Academy of Sciences, 1995) p. 313
88. P Sharpe, N G Alameddine, D E Richardson *J. Am. Chem. Soc.* **116** 11098 (1994)
89. V I Vovna, A Yu Ustinov, O M Ustinova *Zh. Neorg. Khim.* **40** 290 (1995)
90. E I Tsyganova, L M Dyagileva, in *VI Vserossiiskaya Konf. po Metalloorganicheskoi Khimii (Tez. Dokl.)* [The Sixth All-Russian Conference on Organometallic Chemistry (Abstracts of Reports)] (N Novgorod: Institute of Organometallic Chemistry of the Russian Academy of Sciences, 1995) p. 246
91. M George, A Carol, L Kigsmill, K Johan, L Holmes *J. Am. Chem. Soc.* **116** 7807 (1994)
92. A F Bykov, P P Semyanikov, I K Igumenov *J. Therm. Anal.* **38** 1463 (1992)
93. A F Bykov, P P Semyanikov, I K Igumenov *J. Therm. Anal.* **38** 1477 (1992)
94. A F Bykov, I K Igumenov, V I Lisoivan, I P Asanov, I V Yushina, B M Ayupov *Zh. Neorg. Khim.* **39** 2053 (1993)
95. A F Bykov, Candidate Thesis in Physicomathematical Sciences, Institute of Inorganic Chemistry of the Siberian Division of the Russian Academy of Sciences, Novosibirsk, 1995

Catalytic asymmetric synthesis of β -hydroxyacids and their esters

E I Klabunovskii

Contents

I. Introduction	329
II. Optically active biodegradable polymers based on β -hydroxyesters	329
III. β -Hydroxyacid esters as chiral synthons	331
IV. Enzymic synthesis of β -hydroxyacids and β -hydroxyesters	331
V. Synthesis of β -hydroxyesters by the hydrogenation of ketoesters on heterogeneous dissymmetric catalysts	333
VI. Synthesis of optically active β -hydroxyesters by the hydrogenation of ketoesters on metal complex catalysts with chiral ligands	342
VII. Conclusion	342

Abstract. Data on the catalytic methods for the reduction of β -ketoacids and their esters to the corresponding optically active hydroxyacids and hydroxyesters with the aid of enzymes and chiral heterogeneous and metal complex catalysts are surveyed. The application of optically active hydroxyesters as chiral synthons and monomers for the synthesis of biodegradable polymers is examined. Procedures for increasing the optical purity of the products are outlined on the basis of an analysis of the literature data and the author's own results. The bibliography includes 151 references.

I. Introduction

Optically active carboxylic hydroxyacids and their esters are key intermediates in the biosynthesis and metabolism of aliphatic acids, which are widely distributed in biological systems. A number of chiral lower homologues of hydroxyacids are used as chiral synthons in asymmetric syntheses of natural products and medicinal preparations. The efforts of many investigators have therefore been directed towards the search for new effective methods of synthesis of the most important α - and β -hydroxyacids and their esters and to the improvement of the already known procedures for their synthesis by the enzymic reduction of ketoacids^{1,2} or by the hydrogenation of the keto-group with the aid of chiral heterogeneous and homogeneous catalysts.^{3,4}

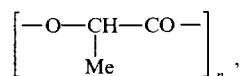
Optically active hydroxyacid esters have also attracted special attention as promising chiral monomers for the synthesis on an industrial scale of biodegradable polymers, for example of the type Biopol (Zeneca Company, Great Britain).

Despite the interest shown in the development of methods of synthesis of chiral β -hydroxyacids and their esters, publications giving a compilation of data on the methods of synthesis of these compounds together with their critical assessment are so far lacking in the literature, although the increasing number of

publications has led to an urgent need for such a survey. In the present review, an attempt is made to fill this gap. Studies carried out during the last ten years are mainly analysed. The analysis considers principally the most thoroughly developed methods: the reduction of ketoacids and their esters by the enzymic procedure and with the aid of heterogeneous metallic catalysts modified by optically active compounds. Less attention has been devoted in the literature to the application of highly effective chiral metal complex hydrogenation catalysts and one can only hope for a development of this aspect in the future.

II. Optically active biodegradable polymers based on β -hydroxyesters

Optically active polycondensation polymers are known to have higher melting points (softening temperatures), higher degrees of crystallinity, and better mechanical properties than racemic polymers by virtue of the stereoregularity of their structure. For example, the optically active polylactide



is significantly superior to the corresponding polymer based on the racemate as regards characteristics such as crystallinity, melting point (< 449 K), and insolubility in a number of solvents, these characteristics improving with increase in the optical purity of the polymer.^{5,6}

Polycondensation polymers based on carboxylic β -hydroxyacids and their esters, which participate in the metabolism of a number of microorganisms and decompose when acted upon by soil bacteria, have aroused particular interest. These polymers constitute an ideal environmentally clean material for the manufacture of polymeric articles because they decompose biologically in waste after use.

An optically active polycondensation polymer is formed from (*R*)-(-)- β -hydroxybutyric acid (HBA) or its esters when they are acted upon by a number of microorganisms. It can also be obtained by reducing ketoacids or the corresponding esters in the presence of enzymes and heterogeneous or metal complex catalysts.^{7,8} In a number of papers published after the first communication about the synthesis of poly(hydroxybutyric acids) (PHBA) from HBA,⁹ the properties of this lipid-like

E I Klabunovskii Laboratory for Asymmetric Catalysis,
N D Zelinskii Institute of Organic Chemistry, Russian Academy of
Sciences, Leninskii prosp. 47, 117913 Moscow, Russian Federation.
Fax (7-095) 135 53 28. Tel. (7-095) 135 53 02

Received 26 October 1995

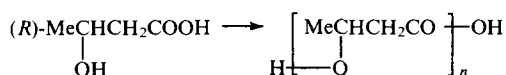
Uspekhi Khimii 65 (4) 350–366 (1996); translated by A K Grzybowski

polymer are examined¹⁰ (the microbiological preparation of PHBA has been surveyed¹¹).

The polymer PHBA, accumulating in the cells of bacteria of a particular species, serves as an energy storage material and plays the same role as starch in plants.^{12,13} The polymer, containing on average 138 000 units, can be isolated from the bacterial mass in the form of hydrophobic 0.5 μm grains. A polymer with a molecular mass from 60 000 to 1 000 000 (100–10 000 HBA units) can be formed, for example, when the system is acted upon by hydroxybutanolate-Co-A-polymerase. The PHBA–PHVA copolymer is formed from a mixture of HBA and β -hydroxyvaleric acid (HVA).

PHBA can be obtained by the usual fermentation methods using laboratory equipment.¹⁴ Cell material containing up to 70% of PHBA is obtained by the fermentation of a 24% aqueous solution of fructose acted upon by *Bacto Nutrient Broth* (Difco). Pure PHBA is isolated by extracting the biomass in a Soxhlet extractor with chloroform and is precipitated by adding ether. This laborious procedure involves filtration for many hours and treatment of the solutions, which requires the consumption of large amounts of solvents. For example, 5 litres of acetone has to be consumed in order to obtain 35 g of PHBA.

The polymer obtained, consisting of (R)-(–)-HBA units, has a 'head to tail' linear structure.¹²



The polyester, namely poly(ethyl β -hydroxybutyrate) (PEHB), is a crystalline substance with a right-handed helical structure^{15,16} and weak optical activity. This polymer exhibits a positive Cotton effect at a wavelength of 215 nm (in ethanol).^{13,14}

In solution in chloroform and dichloroacetic acid, the PEHB structure is analogous to that of proteins (helix–coil). For certain proportions of the solvents, maintaining or loosening the helical structure of the polymer (dichloroacetic acid and ethylene dichloride), there is a sharp jump in optical activity. A similar jump, corresponding to the helix–coil transition at 351 K, is also observed as the temperature is increased (Fig. 1). With increase in molecular mass, the melting point rises from 350 to 473 K. The polymer is insoluble in water, methanol, and dimethylformamide (DMF).

Thermal instability and sensitivity to the action of acids and bases are characteristic of PEHB. It is thermoplastic and may be used in the form of films, fibres, etc. A valuable property of this polymer is its susceptibility to biodegradation. The PEHB–PEHV copolymers, which began to be produced by British companies (ICI, Zeneca, Marlborough Biopolymers Ltd) in 1986, are of considerable interest.⁷

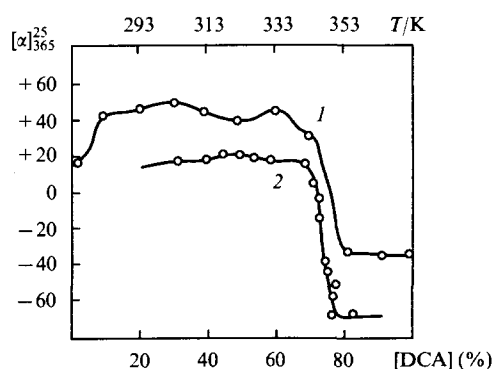
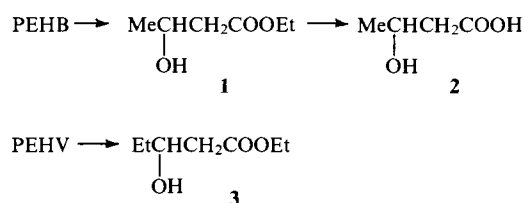


Figure 1. Dependence of the specific rotation $[\alpha]_{365}^{25}$ of the PEHB polymer on the solvent composition in the dichloroacetic acid (DCA)–methylene dichloride (EDC) system (1) and on temperature in the 76:24 DCA:EDC mixture (2) according to the data of Marchesault et al.¹²

Publicity announcements in the scientific and popular chemical literature of the 1980s convey the sensational nature of the discovery of these new polymers: 'Artificial polymeric materials from bacteria',¹⁷ 'A new procedure for the development of polymers based on bacteria',¹⁸ 'Back to nature — the beginning of a new era of biopolymers',¹⁸ etc. The (R)-EHB–(R)-EHV copolymer with different monomer ratios can be obtained in yields up to 80% by the controlled fermentation of glucose or fructose by the bacteria *Alcaligenes eutrophus*,^{19,20} *Hydrogenomonas eutropha*,²⁰ or *Bacto Nutrient Broth*.¹⁴

By depolymerising the copolymer produced, for example, by ICI under the name Biopol TM, it is possible to obtain in a high chemical yield (γ) the corresponding monomeric optically pure esters and, after their hydrolysis, also the optically pure β -hydroxyacids.^{20–22} For this purpose, the crude cell material, containing up to 70% of PEHB, is treated with $\text{Ti}(\text{OEt})_4$ in ethanol and heated for 2 h at 388–433 K. The mixture is filtered, the solvent eliminated, and the product, (R)-(–)-EHB 1, is distilled. The yield is 75%. The acid (R)-(–)-HBA 2 is obtained by the hydrolysis of EHB with 1 M KOH at 273 K.



The chemical yields and specific rotations of the optically pure β -hydroxyacids and their esters obtained in this way are presented below in Table 1.

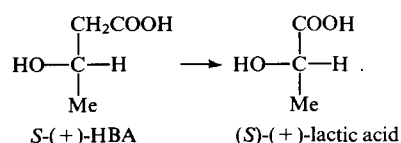
Table 1. Optical characteristics of certain β -hydroxyacids and their esters.

Com-pound	T_b /K (P /Pa)	T_m /K	$[\alpha]_D^{25}$ a/deg	γ (%) (OY) ^b	Ref.
1	353 (2100)	—	–43.2 (c 5, chloroform)	90	20–22
2	358–360 (10)	315–317	–24.5 (c 5, chloroform)	93	20–22
5	—	316–319	–25.0 (c 6, water)	(98)	19, 28
3	363 (2000)	—	–34.5 (c 5, chloroform)	65	20–22
4	333 (20)	—	–19.0 (c 2.7, chloroform)	94	1

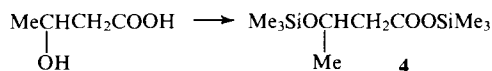
^a Here and henceforth this formulation means that the specific rotation $[\alpha]_D^{25}$ has been measured at the given temperature and wavelength (589 nm, Na D-line) in the solvent indicated (chloroform, water, etc.) at a concentration c expressed as the number of grams of the compound under consideration (1 g of EHB, 5 g of HBA, etc.) in 100 ml of the solution in a layer 1 dm thick. ^b OY is the optical yield (%) defined as

$$\text{OY} = \frac{[R] - [S]}{[R] + [S]} 100.$$

Optically pure (R)-(–)- and (S)-(+)-HBA have been obtained by the resolution of the racemic acid via the quinine and strychnine salts.²¹ The configuration of the acid (S)-(+)-HBA is genetically linked to that of (S)-(+)-lactic acid:



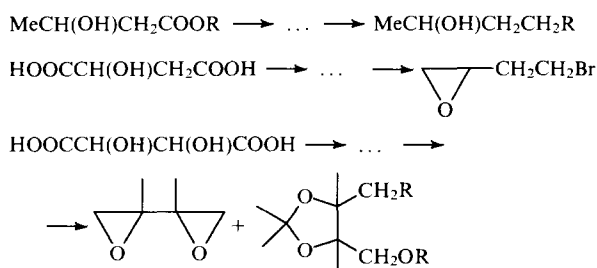
β -Hydroxyacid esters are unstable: during storage at room temperature, they give rise to oligomers, this tendency increasing in the series of esters $\text{Pr}^i < \text{Et} < \text{Me}$. Since the oligomerisation is catalysed by alkalies and acids, the ester to be stored must be carefully purified. The usual acetoacetic ester contains admixtures of dehydroacetic acid, methyl 3-acetoxypropionate, and diketene, which influence significantly the catalytic asymmetric hydrogenation of the ester.²³ For this reason, it is best to store EHB specimens in the form of the PEHB polymer or to convert HBA into the silyl ester **4**:^{1, 14, 24–28}



The Fluka Company has suggested that the polymer (*R*)-PHBA be used as the starting material for the preparation of (*R*)-HBA **5** (Table 1)^{19, 28} and (*R*)- β -butyrolactone.^{14, 25, 26}

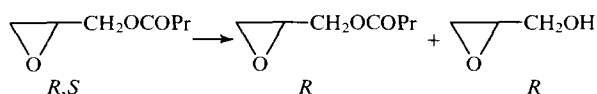
III. β -Hydroxyacid esters as chiral synthons

The molecules of β -hydroxyacids are extremely reactive, which makes it possible to obtain from them a wide variety of optically active derivatives and chiral synthons used in the synthesis of a number of medicinal preparations.^{29, 30} Certain examples of the successful use of optically active hydroxyacids as chiral synthons for the preparation of a number of chiral initial compounds are presented below.³¹

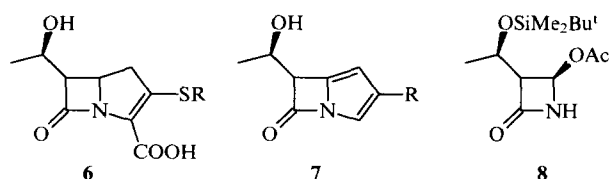


R = OTs, Br

The Andeno Company used PPL lipase for the kinetic resolution of the racemic glycidyl butyrate:³²

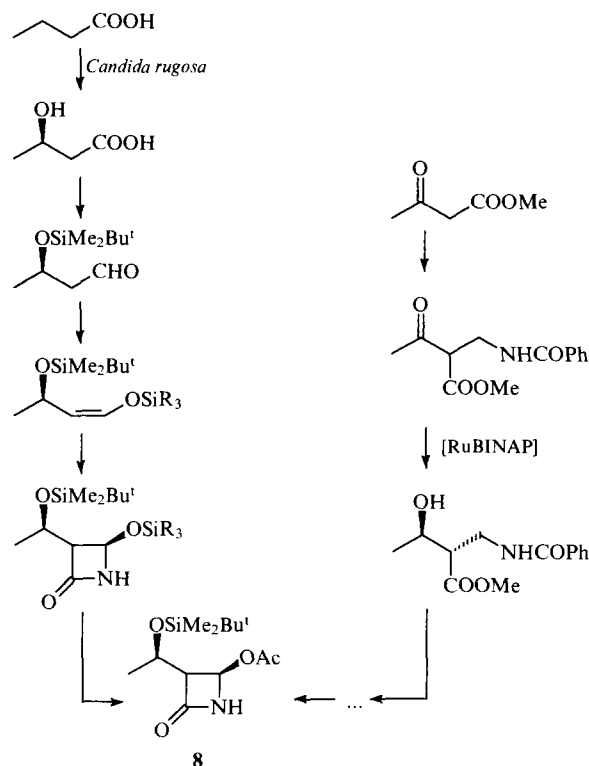


Antibiotics containing the β -lactam group belong to an important class of medicinal preparations. In the synthesis of carbapenem **6** and penem **7**, the key intermediate is the azetidinone **8**, which is synthesised in two ways.



Thus the Kanegafuchi Company (Japan)³³ uses enzymic reduction in the synthesis of β -EHB, while the Tagasago Company (Japan)³² employs the chiral ruthenium complex [Ru-BINAP] [BINAP = 2,2'-bis(diphenylphosphino)-1,1'-binaphthyl]³⁴ in the reduction stage. In the latter case the azetidinone is obtained with $OY = 98\%$ and $de = 95\%$.†

† The symbol de denotes an excess of the diastereoisomer and ee denotes an excess of the enantiomer, both expressed as percentages.



The acid (*R*)-HBA is used to synthesise a number of medicinal preparations. The depolymerisation of PHBA opens an easy path to the formation of the chiral synthon EHB, HBA, and a PHBA degradation product — the diol (*R*)-MeCH(OH)CH₂CH₂OH.¹⁴ (*R*)- and (*S*)-2-Hydroxyglutaric acids have also become readily available. (*R*)-Isobutyl lactate is produced by the BASF Company. Carbomycin B,³⁵ (*R,R*)-pyrenophorin,³⁶ gramimycin A₁,³⁷ sulcatol,² lavandulol,³⁸ colletodiol,³⁷ and recifeiolid³⁹ belong to the class of medicinal preparations the structures of which contain a fragment of the chiral (*R*)-EHB molecule. (*R*)- β -Hydroxyiso-butyric acid, produced by the Kanegafuchi Company by the microbiological oxidation of isobutyric acid, can be used to synthesise the inhibitor captopril⁴⁰ via (*R*)- β -acetylmercaptoisobutyric acid, produced by the Andeno Company,⁴¹ while its enantiomer, (*S*)- β -hydroxyisobutyric acid, is used in the synthesis of phytol — a fragment of the vitamin E molecule.^{42, 43}

IV. Enzymic synthesis of β -hydroxyacids and β -hydroxyesters

The bank of chiral natural optically active hydroxyacids consists of an extremely limited number of compounds: (*R*)- and (*S*)-lactic, (*R,R*)-(+)-tartaric, (*S*)-malic, and (*S*)-mandelic acids and their esters. The enzymic and catalytic asymmetric syntheses of these compounds therefore constitute an important source of chiral β -hydroxyesters. β -Hydroxyacids and β -hydroxyesters in the enantiomeric form are synthesised as follows:

by the kinetic resolution of the racemate with participation of a chiral auxiliary compound;⁴⁴

by the depolymerisation of polyhydroxyesters or polyhydroxyacids;^{14, 45}

by the microbiological reduction of ketoesters with the aid of enzymes;¹⁴

by the catalytic hydrogenation of ketoesters on modified metallic catalysts;^{3, 4, 46}

by the catalytic hydrogenation of ketoesters on chiral complex catalysts.⁴⁷

The last three methods are of greatest interest.

The enzymic reduction of ketoesters to optically active hydroxyesters was first achieved with the aid of baker's yeast in 1918.⁴⁸ Although data^{2,49} indicating a high effectiveness of this method were not subsequently confirmed,⁵⁰ its improvement made it possible to achieve an optical yield of EHB up to 85% and above,⁴⁵ while in a bioreactor (with continuous introduction of the substrate and aeration) the yield was up to 96%.⁵¹ The method was developed further^{52,53} and acquired preparative value mainly as a result of the studies by Seebach.^{45,54} It proved possible to employ the reduction of ketoesters with the aid of baker's yeast (*Saccharomyces cerevisiae*) in practical organic synthesis.^{32,51,54,55}

High OY values for the products are usually attained when the concentration of the substrate in the fermenting solution does not exceed 0.1%,⁵¹ while the reaction time is 30–130 h. Under these conditions, the productivity of the process is 20–70 mg dm⁻³ h⁻¹. However, the need to employ large volumes of solutions, the long reaction time, the high consumption of sucrose (or another organic reducing agent — a hydrogen donor), the instability of the bacterial strain, the impossibility of the repeated employment of the reducing system, as well as the complexity of the isolation of the product prevent the wide scale employment of this method.^{56,57} Furthermore, the selectivity of the enzymic reaction depends on a number of factors, such as the nature of the enzyme, the structure of the substrate molecule, and the reaction conditions.^{58,59} For example, ketovalerate is reduced less effectively than ketobutyrate.^{58,59}

According to the standard method for the reduction of acetoacetic ester [ethyl acetoacetate (EAA)] with the aid of baker's yeast,⁴⁵ the synthesis of 24 g of EHB from 40 g of EAA requires the consumption of 600 g of sucrose and 200 g of yeast and a vessel with a volume up to 5 litres has to be used. The reaction time is 134 h with a process productivity of 0.068 g dm⁻³ h⁻¹. The final product, (S)-(+)-EHB, is obtained in 59%–71% yield with OY = 85%. A similar method is used to obtain BuHB (OY = 90%).¹⁴ The optical yield of HBA may be increased to 97% after several recrystallisations of the derivative EHB 3,5-dinitrobenzoate.⁶⁰ The optically pure EHB obtained had $[\alpha]_D = +43.5^\circ$ (c 1, chloroform). The optical purity of EHB can be determined from the ¹⁹F NMR spectrum of the ester comprising the Mosher reagent.⁶¹

An improvement in the method for the reduction of EAA also makes it possible to increase the optical yield of EHB to 95%. This is attained by the slow introduction of EAA into the fermenting solution under aerobic conditions.⁵¹ The replacement of 5%–15% of sucrose in the fermenting solution by ethanol, glucose, fructose, glycerol, or mannitol⁶² also helps to increase the OY of the hydroxyester.

Keeping the yeast in 5% aqueous ethanol for four days before use in the reaction helps to activate it and to raise the optical yield of the product to 95.9%.^{63–65} According to the method of Ehrler et al.,⁶⁶ a suspension of 125 g of baker's yeast in 1 litre of 5% aqueous ethanol is stirred at 303 K for 4 days,

after which 5 g of EAA is added. After 2–3 days, the reaction comes to an end (it is monitored with the aid of gas–liquid chromatography). The mixture is centrifuged and the filtrate is repeatedly extracted with ether for 4 days and the extract is vacuum distilled. EHB is obtained in 70% yield with OY = 94% and $[\alpha]_D = +40.9^\circ$ (c 1, chloroform). Unfortunately this method does not yield satisfactory results when applied to other substrates, such as ketovalerate and fluorine-containing ketoesters. Only 2-formylbutanoate could be reduced to (S)-2-hydroxymethylbutanoate HOCH₂CH(Et)COOEt in 70% yield with OY = 95.5%. This product is an important chiral synthon analogous to the Roche acid HOCH₂CH(Me)COOH.⁶⁷ According to the data published by the Hoffmann La Roche Company, the latter product can be obtained with the aid of *Streptomyces griseus* with OY not exceeding 86.3%.⁶⁸

A strain of the *Halobacterium halobium* bacteria reduces EAA to (S)-(+)-EHB with OY = 44%–76%, but the chemical yield of the product is low and the reduction is accompanied by hydrolysis of the ester to the acid. Hydrolysis of the racemic ester EHB with the aid of the above strain leads to (R)-(-)-EHB with OY = 88%.⁶⁹

The reduction of ketoesters with the aid of the thermophilic bacteria *Thermoanaerobium brockii* (*Th.b.*) is carried out in the usual laboratory apparatus or in a bioreactor⁷⁰ by a procedure similar to that used in the case of yeast. However, this strain is sensitive to atmospheric oxygen and the reduction must be carried out under an argon atmosphere. In contrast to yeast, the strain reduces ethyl ketovalerate effectively to the β-hydroxyester (OY = 93%–97%).

Depending on the nature of the microorganism and the structure of the substrate molecule, products with the (R)- or (S)-configuration can be obtained by reduction of the ketoesters. Table 2 presents comparative data obtained for different substrates with the aid of baker's yeast and a strain of *Th.b.*⁷¹ As can be seen, in certain cases the *Th.b.* strain is more effective than baker's yeast and, furthermore, it is possible to obtain the other enantiomer of the hydroxyester.

Both enantiomers of the hydroxyacid may be obtained by reducing the ketoacid in the presence of NADH (reduced β-nicotinamide-adenine dinucleotide), bound to poly(ethylene glycol) in a membrane reactor.^{72,73} The reduction of ketoesters in a nonaqueous medium (in solution in isopropyl hexadecanoate) by a suspension of a mixture of Asolectine phospholipids produced by the Fluka Company and yeast proceeds rather effectively (Table 3).⁷⁴

Other examples of the influence of the structure of the substrate molecule and of the introduction of aromatic substituents or aromatic hexahydro-substituents into the ketoester XCOCH₂COOR on the configuration of the enantiomers and diastereoisomers obtained⁷⁵ are presented in Table 4.

Apart from the asymmetric enzymic reduction of ketoesters to obtain optically active hydroxyesters from hydroxyacids, it is also possible to employ the enantioselective kinetic conversion of the hydroxyester racemate by the enzyme. Thus the DSM

Table 2. The influence of the structure of the β-ketoester and of the source of the enzyme on the optical yield and the absolute configuration of the β-hydroxyester formed.^{70,71}

Initial ketoester	Hydroxyester obtained	Baker's yeast, 303 K		<i>Th.b.</i> strain, 345 K	
		configuration of product	OY (%)	configuration of product	OY (%)
EAA	EHB	S	97	S	80
EtCOCH ₂ COOEt	EtCH(OH)CH ₂ COOEt	R	40	S	84
ClCH ₂ COCH ₂ COOMe	ClCH ₂ CH(OH)CH ₂ COOEt	S	36	R	89
PrCOCH ₂ COOEt	PrCH(OH)CH ₂ COOEt	R	90	S	25
HCOCH(Me)COOEt	HOCH ₂ CH(Me)COOEt	R	60	R	72

Table 3. Reduction of β -ketoesters in solution in isopropyl hexadecanoate by a mixture of phospholipids and baker's yeast.⁷⁴

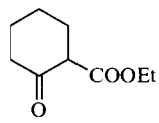
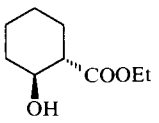
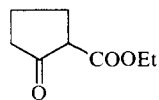
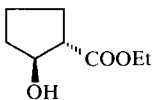
Ketoester	Hydroxyester	OY (%)	Reaction time /h	Enzyme : substrate mass ratio
MeCOCH ₂ COOBu ^t	MeCH(OH)CH ₂ COOBu ^t	91	96	10.6
F ₃ CCOCH ₂ COOEt	F ₃ CCH(OH)CH ₂ COOEt	58	120	11.8
		99	24	46.6
		99	19	14.0

Table 4. The influence of the substituents in the ketoester XCOCH₂COOR molecule on the absolute configuration of the hydroxyester formed.

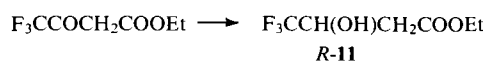
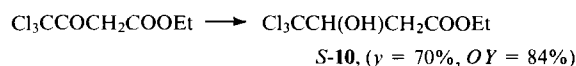
R	X	Configuration of hydroxyester	OY (%)	Micro-organism	Ref.
Et	Me	S	97	yeast	51, 65
Et	Me	S	95	<i>C. Kluyveri</i>	50
Et	Ph	S	99	yeast	53
Et	CF ₃	R	98	"	76
Et	CCl ₃	S	98	"	76
Et	ClCH ₂	R	99	<i>C. Kluyveri</i>	50
C ₈ H ₁₇	ClCH ₂	R	98	yeast	63
Et	BrCH ₂	S	98	"	77
PhCH ₂	N ₃ CH ₂	R	95	"	77
K	CH ₂ OCH ₂ Ph	S	99	"	78
K	Me	S	100	"	52

Andeno Company has used successfully the lipase from *Pseudomonas fluorescens* for the kinetic resolution of the ester.²⁴ The product PhOCH(Et)COOEt is formed with OY = 99% and a conversion of 57%.²⁸

Examples of the effective enantioselective resolution of other racemic hydroxyacids and hydroxyesters are known: thus, on treatment with *Candida rugosa*, the acid HOCH₂CH(Me)COOH affords the (*R*)-product;⁷⁹ on treatment with chymotrypsin, the (*R*)-product is formed from PhCH(OH)CH₂COOEt with OY = 98%;⁸⁰ EtC(Me)(OH)COOMe is hydrolysed by esterase with formation of the (*S*)-product (OY = 98%);⁸¹ the product of the conversion of MeCH(OH)CH(Me)COOEt by yeast has the (2*R*,3*S*)-configuration (*de* = 86% and OY = 96%);⁸² the asymmetric resolution of the PhCH₂CH(OH)CH(Me)COOEt racemate on treatment with *P. farinosa* leads to the (2*R*,3*S*)-product with OY = 99%.⁸³

β -Hydroxyesters can be obtained by reversible transesterification. The acid anhydride is used as the reversible acylating agent. When acted upon by PS lipase, it gives rise to the (*R*)-acid PhCH₂CH₂CH(OH)COOH **9** in 39% yield and with OY = 99%.³²

The synthesis of chlorine- and fluorine-containing hydroxyesters by the reduction of the corresponding ketoesters effected by baker's yeast is of interest.⁷⁶



Crystallisation of the product **9** from methylcyclohexane increases OY to 98%. The optical yield of the (*R*)-(+)-ester **11** on crystallisation from a pentane-ether mixture can be raised to 98%. The ester **11** has a configuration which is the opposite of that of the product **10**, whence it follows that, in conformity with Prelog's rule, the CF₃ group should have the same seniority as the methyl group.

In conclusion, one should note that a number of companies have achieved the enzymic synthesis of optically active hydroxyesters. Thus the Kanegafuchi Company produces (*R*)- β -hydroxyisobutyric acid by the microbiological oxidation of *n*-butyric acid³² or by the fermentation of isobutyric and methacrylic acids by a strain of *C. rugosa*. The cost of (*S*)-(+)-MHB and (*R*)-(-)-MHB is US\$ 2.5 per gram. According to the catalogue of the Aldrich Company, (*R*)-(-)-EHB with $[\alpha]_D = -46^\circ$ (*c* 1, chloroform) is sold at a price of US\$ 9 per gram, whilst the price of the racemate is smaller by a factor of 20.⁸⁴

The synthesis of β -hydroxyacids and β -hydroxyesters by the depolymerisation of PHBA and PEHB was examined above in Section III.

V. Synthesis of β -hydroxyesters by the hydrogenation of ketoesters on heterogeneous dissymmetric catalysts

The asymmetrising activity of copper, nickel, and platinum catalysts deposited on crystals of optically active quartz in the asymmetric decomposition of racemic butan-2-ol was first observed by Schwab and coworkers.^{85,86} Terent'ev and Klabunovskii⁸⁷ extended the studies on catalysts of this type to other reactions. The enantioselectivity of such catalysts was low, the optical yield not exceeding 1%. Akabori and Izumi³ suggested that palladium based on the fibroin of natural silk fibres be used as the catalyst for the asymmetric hydrogenation of the C=C bond in the prochiral precursors of amino acids. Its effectiveness was fairly high (for example, OY = 35.5% in the hydrogenation of azlactone), but there are no literature data on the reproducibility of these results. Nevertheless, the studies carried out have demonstrated the important role of complex formation in asymmetric catalysis and served as a stimulus for the development of dissymmetric metallic catalysts of new types. Among the latter, we may mention the skeletal Raney nickel catalyst and catalysts modified by optically active amino acids or hydroxyacids, which readily form complexes on the surface of the metal. As a result of the modification, centres for enantioselective hydrogenation arise on the surface of the metallic catalysts.

The choice of acetoacetic acid esters [methyl acetoacetate (MAA)³ and ethyl acetoacetate (EAA)⁴] proved successful. Methods for the preparation of effective catalysts have been developed in relation to these substrates and the characteristic

features of asymmetric hydrogenation have been investigated. Almost 20 years of research were required to increase the *OY* in this reaction from 10%–15% to 90%–94%.

The achievements in this field have been surveyed in a series of monographs^{3,4,87,88} and reviews.^{89–93} Factors influencing the enantioselectivity of catalysts for the hydrogenation of β -ketoesters will be examined below and procedures for increasing the optical purity of the hydroxyesters formed will be outlined.

The effectiveness of the modified metallic catalysts[†] depends significantly not only on the stereochemical properties of the modifying agent and the substrate but also on the state of the catalyst surface, its genesis, the nature of the salts used to prepare the initial catalyst mass, the conditions in its reduction, the degree of crystallinity of the catalyst, the size of the crystallites, the nature of their size distribution, and the adsorption and complex-forming capacities of the metallic catalyst in relation to the molecules of the modifying agent and the substrate (product).

According to Balandin's theory of hydrogenation,⁹⁴ the effectiveness of the hydrogenation depends significantly on the hydrogen pressure. Since the modification of the catalyst alters its activity usually by diminishing it, the reaction has to be carried out at elevated temperatures and pressures. The complexity of the dependence of *OY* in the MAA and EAA hydrogenation reactions on the hydrogen pressure (*P*) has been examined.⁹⁵ In the hydrogenation of EAA on Ru–SiO₂–TA, the optical yield *OY* increases with increase in *P*, but, after the attainment of a pressure of 7 MPa, it ceases to vary.⁹⁶ On the RCo–TA catalyst, the optical yield initially increases with increase in *P* to 2 MPa and then remains constant up to *P* = 8 MPa.⁹⁷ On RNi–TA, the optical yield is independent of hydrogen pressure in the range 5–10 MPa.⁹⁸ When EAA is hydrogenated in the vapour phase on HNi–TA,^{99,100} a zero order of the reaction with respect to hydrogen is observed in the pressure range 10–14 MPa (*OY* = 17.8%).

The enantioselectivity of the hydrogenation of MAA on deposited Ni–SiO₂–TA and Ni–SiO₂–TA–NaBr catalysts depends significantly on the reaction conditions (hydrogen pressure, MAA concentration, nature of the solvent). The experiments have been performed¹⁰¹ both in the kinetic region (stirring rate 500–800 revolutions per minute), where the rate of reaction and *OY* are independent of the stirring rate and are proportional to the amount of the catalyst, and in the diffusion region in a rocking autoclave with a MAA:Ni = 8 ratio. When the experiments were carried out in the kinetic region on Ni–SiO₂–TA, the optical yield of the (–)-MHB formed fell from 50% to 30%–35% with increase in hydrogen pressure, while on Ni–SiO₂–TA–NaBr it hardly changed. Evidently, treatment of the catalyst with NaBr imparts to it an increased enantioselectivity and stability. In the diffusion region, *OY* was 38%–40% and hardly changed as the pressure increased from 1.0 to 8.0 MPa, which agrees with the data of Lippart et al.⁹⁸ An increase in *OY* when the reaction is carried out in the kinetic region can be achieved by reducing *P* and by increasing the MAA concentration in EtOAc (Fig. 2). A similar picture is also observed when MeOH and THF are used as the solvent.

It is noteworthy that such effectiveness is attained only at low pressures (0.2–1.0 MPa) and only in the initial stages of the reaction (for degrees of conversion up to 15%). It is not stated in the above communication¹⁰¹ whether a similar variation is retained at higher conversions. Data concerning the variation of

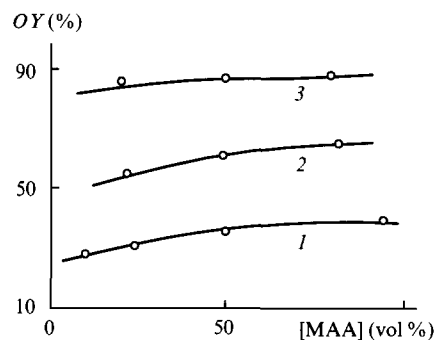


Figure 2. The influence of the MAA concentration in EtOAc on *OY* in the MAA hydrogenation reaction on the Ni–SiO₂–TA catalyst at pressures of 6.0 MPa (1) and 1.0 MPa (2) and on the Ni–SiO₂–TA–NaBr catalyst at a pressure of 1.0 MPa (3). Degree of conversion 15%.¹⁰¹

OY during the reaction are also lacking. Nevertheless the practical value of the proposed methods for increasing the enantioselectivity of the process depends precisely on this factor.

The substrate:catalyst ratio is also important. The maximum optical yield in the hydrogenation of EAA at pressures of 0.1 and 10 MPa has been achieved⁹⁸ for the ratio EAA:Ni = 10–20. The independence of *OY* on the degree of conversion was also noted. This shows that, under the given conditions, the reaction is a kinetically controlled process and the product does not racemise during its occurrence.

In certain cases, *OY* varied as a function of the degree of conversion and the nature of the solvent simultaneously with the variation of the overall rate of reaction *w* due to the inhibition of the latter by its product.

The antiparallel variation of *OY* and *w* during the reaction has been noted.^{95,102} Thus *OY* decreased with increase in the rate of hydrogenation of MAA on RNi–TA.¹⁰² The optical yield also changed with increase in the degree of conversion:¹⁰³ it reached 56.4% for a conversion of 10% and then fell.

According to Balandin's theory of hydrogenation,⁹⁴ the product may inhibit the reaction if the adsorption coefficients of the substrate and the product differ greatly. Chernysheva and coworkers^{104,105} showed for the first time that the addition of (–)-EHB to a solution of EAA inhibits the enantioselective hydrogenation of the latter on RNi–TA and lowers *OY* as a result of the preferential adsorption of (–)-EHB on the selective centres. According to the data of Chernysheva and coworkers,^{104,105} the ratio of the adsorption coefficients of (–)-EHB and EAA is 3:2. As a consequence of this, *OY* decreases, as can be seen from Fig. 3, where the results of Chernysheva et al.¹⁰⁴ are compared with those of Nitta et al.¹⁰⁶

The relative adsorption coefficients were calculated¹⁰⁴ by the equation⁹⁴

$$\frac{1}{w} = \frac{b_2/b_1}{kC_2/C_1} + \frac{1}{k},$$

where *b*₁ and *b*₂ are the relative adsorption coefficients and *C*₁ and *C*₂ are the concentrations of EAA and EHB respectively.

When the reaction is inhibited by the EHB racemate, *b*₂:*b*₁ = 1:2. It follows from the data of Chernysheva et al.¹⁰⁴ that the degree of adsorption of (–)-EHB on the selective centres exceeds that of (+)-EHB. The introduction into the EAA solution of other strongly adsorbed substances, for example catalyst poisons such as pyridine, thiophene, or amines, exerts a strong inhibiting effect on the enantioselective reaction, the effectiveness of the additives increasing in the sequence (+)-EHB < (–)-EHB < pyridine < thiophene.¹⁰⁴

For example, the addition of pyridine in the initial stage of the hydrogenation of EAA (for degrees of conversion up to

†The following notation has been adopted in the literature: RM = skeletal metallic catalyst of the Raney type; M–TA = catalyst modified by (*R,R*)-tartaric acid (TA); M–SiO₂–TA = deposited metallic catalyst modified by TA; M–SiO₂–TA–NaBr = catalyst modified by TA with added NaBr; HM = catalyst obtained by reducing the metal oxide in a stream of hydrogen.

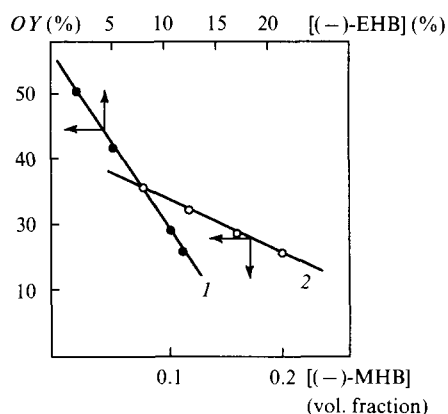


Figure 3. Dependence of OY on the concentrations of the additives in the hydrogenation reactions of EAA on $RNi-TA$ (1)¹⁰⁴ and of MAA on $Ni-SiO_2-TA$ (2)¹⁰⁶. The additives are $(-)$ -EHB in the first case and $(-)$ -MHB in the second.

5%–10%) increases OY as a result of the preferential adsorption of this inhibitor on the nonselective centres which were not protected in the modification by the adsorbed TA. Afterwards, as the degree of conversion increases, OY falls almost to zero. In the hydrogenation of EAA on the $HNi-TA$ catalysts, the addition of pyridine and butylamine increases OY in the initial stage of the reaction from 11% to 17% and 50% respectively.⁹⁹ After the introduction of pyridine or thiophene, the optical yield for $y = 10\%$ increased from 7% to 12% and from 2.5% to 11.5% respectively.¹⁰⁵ Chernysheva and coworkers^{104,105} determined the optical yields polarimetrically, taking into account the change in the specific rotation of EHB for low degrees of conversion ($y \leq 7\%$):

$$\lg [\alpha]_D = 1.55 - 0.2 \lg y.$$

A significant increase in OY in the hydrogenation of MAA¹⁰¹ was achieved by adding unsaturated compounds, which are hydrogenated preferentially on nonselective centres. The fraction of enantioselective centres on which MAA is hydrogenated increases under these conditions (Fig. 4).

The addition of benzene, which is not hydrogenated under these conditions, also ensures an appreciable increase in OY .

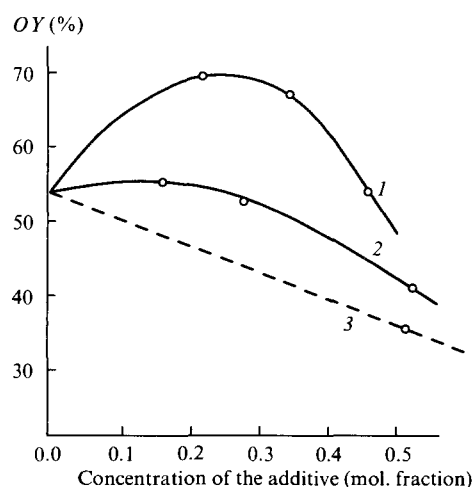


Figure 4. The influence of added benzene (1), cyclohexene (2), and ethyl acetate (3) on the optical yield of $(-)$ -MHB in the hydrogenation of MAA on $Ni-SiO_2-TA$ (pressure 1.0 MPa, degree of conversion 15%).¹⁰¹

However, its use as a solvent in the hydrogenation of MAA lowers OY , apparently as a result of the displacement of TA from the modified centres of nickel.

A complex pattern in the variation of OY in the hydrogenation of MAA on $RNi-TA$ catalysts prepared by different procedures (the 1:1 $Ni-Al$ alloy was leached with a 20% $NaOH$ solution at different temperatures in the range 278–353 K) has been noted.¹⁰³ When the reaction was carried out on the most active catalyst, a flat maximum ($OY = 18\%$) was observed on the curve relating OY to the degree of conversion at $y = 70\%$, whereas in the case where less active catalysts were employed the maximum optical yield (45%–50%) was attained at $y = 25\%$.

Table 5. Chemical and phase composition of the $RNi-TA$ catalysts.¹⁰⁵

Composition (%)	Alloy specimen			Catalyst specimen	
	1	2	3	2	3
Chemical					
Ni	50.0	45.2	38.3	79.1	91.4
Al	50.0	51.2	59.7	17.7	8.5
Cr	—	3.6 ^a	2.0 ^a	1.0	0.10
Ti	—	—	—	2.1	0.03
Phase					
$NiAl_3$	—	25.1	51.2		
Ni_2Al_3	90.0	74.9	48.8		
Bayerite				3.0	2.1
Ni				91.5	97.9
Al				5.4	0.0

^a Cr + Ti.

The variation of OY with y is influenced by the chemical and phase compositions of the initial $Ni-Al$ alloys (Table 5).¹⁰⁵ A decrease in the nickel content, i.e. an increase in the content of the intermetallic compound $NiAl_3$ in the alloy, promotes a more complete removal of aluminium in the leaching of the alloy (cf. the catalyst specimens 1–3 in Fig. 5), which should apparently increase OY in the hydrogenation of EAA for low degrees of conversion ($y = 10\%$ –30%). However, as can be seen from Fig. 5, the dependence of OY on y is complex and for this reason comparison of the enantioselectivities of different catalysts only for low degrees of conversion, as was done,

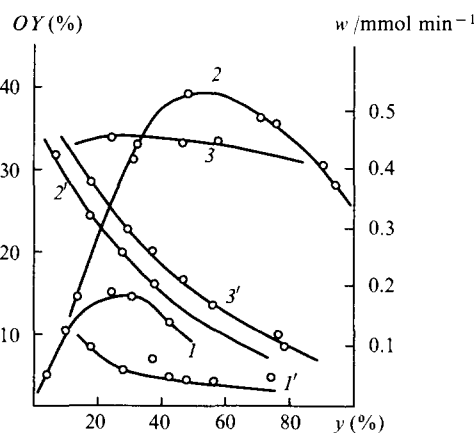


Figure 5. Dependence of the optical yield OY (1, 2, 3) and of the rate of hydrogenation of EAA w (1', 2', 3') on the degree of conversion y on specimens of the $RNi-TA$ catalyst obtained from alloys with different initial compositions¹⁰⁵ (Table 4): (1, 1') specimen 1; (2, 2') specimen 2; (3, 3') specimen 3.

for example, by Nitta et al.,¹⁰¹ is clearly inadequate: it is necessary to follow the variation of OY over the entire range of y .

The nature of the dependence of OY on y is also influenced by the strength of the bond between hydrogen and the catalyst surface. Catalysts obtained from $NiAl_3$ are known to contain a greater amount of weakly bound hydrogen than catalysts prepared from alloys in which the intermetallic compound Ni_2Al_3 predominates (specimen 3).^{104, 105} A higher optical yield is attained on the latter.

Another way of increasing OY is by controlling the degree of dispersion of the catalyst metal on the carrier surface. As was shown for the first time by Klabunovskii and coworkers,^{4, 107} the quantity OY in the hydrogenation of EAA on the $Ru-SiO_2-TA$ catalysts depends significantly on the degree of crystallinity of ruthenium. The optical yield increases with increase in the catalyst reduction time and attains its maximum value for an average size of the crystallites of 4.5 nm. On the catalyst with 8.0 nm crystallites, the enantioselectivity of the hydrogenation reaction diminishes (Fig. 6).

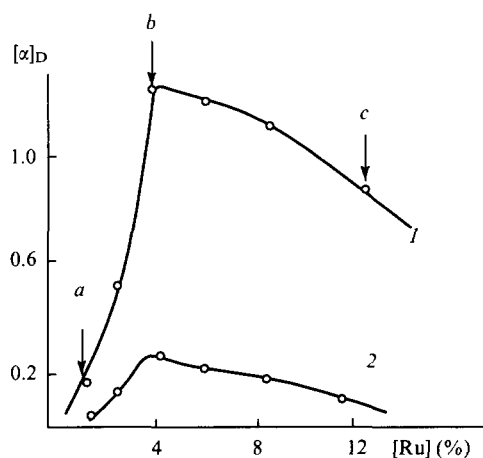


Figure 6. The influence of the metal content in the $Ru-SiO_2-TA$ catalyst on its asymmetrising capacity — on $[\alpha]_D$ for the product — in the EAA hydrogenation reaction. The preliminary catalyst reduction times were 0.5 h (1) and 5 h (2). Points *a*, *b*, and *c* on curve 1 correspond to ruthenium crystallite sizes of 1.6, 4.5, and 8.0 nm respectively.⁴

The important role of the size of the crystallites and of their size distribution was confirmed in a study of the enantioselective hydrogenation of MAA on the $Ni-SiO_2-TA$ catalyst.¹⁰⁸ By varying the conditions in the preparation of the catalyst, it was possible to achieve a narrow peak in the size distribution of nickel crystallites on the surface. $Ni-TA$ catalysts (without a carrier) of different composition were investigated:¹⁰⁹ nickel boride ($Ni-B$), nickel phosphide ($Ni-P$), Raney nickel (RNi), and nickel black obtained by the decomposition of nickel formate (DNi) or by the reduction of NiO (HNi). The $HNi-TA$ ($OY = 56.2\%$), $DNi-TA$ (42.3%), and $RNi-TA$ (26.7%) catalysts exhibited the highest enantioselectivity. On the $Ni-B$ and $Ni-P$ catalysts, the optical yield did not exceed 3–5%. Their low enantioselectivity was attributed to the cryptocrystallinity of the Ni phase (it is X-ray amorphous) and also to the strong adsorption of TA .¹¹⁰ After the modification of the $Ni-B$ catalyst by tartaric acid, the latter was adsorbed in an amount of $4.9 \times 10^{-3} \text{ mmol g}^{-1}$, which is 9 times greater than on RNi . Careful washing of the $Ni-B-TA$ catalyst and its treatment with a solution of alkali led to the removal of boron from the surface and to a decrease in the TA content on the surface to $0.5 \times 10^{-3} \text{ mmol g}^{-1}$. As a result, the optical yield in the hydrogenation of MAA increased to 26.7%, while the $Ni-B-TA$ catalyst was virtually converted into $HNi-TA$ as a result of the liberation of part of the surface.

According to the data of Nitta et al.,¹⁰⁹ the adsorption of tartaric acid on the catalyst surface in an amount exceeding that required for the specific modification of the surface does not influence significantly the enantioselectivity. This conclusion conflicts with data^{99, 100} indicating a linear increase in OY with increase in the fraction of the TA dianion on the DNi surface.

The increase in the size of the nickel crystallites from 6 to 20 nm increases OY from 36.1% to 54.9%.¹¹¹ This can be accounted for with the aid of a stereochemical model of the catalytically active centre,⁴ according to which the accommodation of the catalytic complex on the surface of the enantioselective catalyst requires fairly large crystalline formations (faces, planes). This view is confirmed also by data¹¹⁰ according to which the reduction of NiO leads to the formation of cryptocrystalline, almost amorphous, nickel, which does not exhibit enantioselectivity after modification.

The high effectiveness of the coarsely crystalline $TNi-TA$ specimens¹⁰⁹ is attributed to the presence in this catalyst of impurities remaining after the decomposition of the formate. These data also agree with the previously proposed model⁴ and confirm the influence of the crystallinity of the metal on its enantioselectivity. Since cryptocrystalline nickel catalysts are ineffective in asymmetric hydrogenation, in order to increase the enantioselectivity of the MAA hydrogenation reaction it is desirable to produce a catalyst with relatively large crystallites having uniform dimensions.^{108, 110–115}

It had been noted earlier⁴ that aluminium oxide is relatively unsuitable as a carrier for asymmetric hydrogenation. Thus the $Ru-Al_2O_3-TA$ catalyst did not exhibit enantioselectivity in the hydrogenation of EAA, whereas $Ru-SiO_2-TA$ had a weak activity. This can be explained by the fact that ruthenium interacts much more strongly with Al_2O_3 than with SiO_2 . However, by varying the conditions in the formation of the catalyst, it was also possible to obtain enantioselective catalytic systems when Al_2O_3 was used as the carrier, for example $Ni-Al_2O_3-TA$ and $Ni-Co-Al_2O_3-TA$ with a metal content of 20%.¹¹⁶ These catalysts were reduced at 773 K and EAA was hydrogenated at 393–408 K and a pressure of 10–12 MPa. The optical yield on the first catalyst was 76.0% and that on the second was 62.6%. Such relatively high values of OY can be due to the presence on the nickel surface of incompletely reduced residues of the metal salts, which decrease the fraction of the small crystallites. The reduction of the catalyst under mild conditions (for example at a reduced partial pressure of hydrogen) increases the ratio of large crystallites and their enantioselectivity.

The formation of small nickel crystallites can be prevented by introducing into the catalyst mass (nickel and aluminium hydroxides), before its deposition, a certain number of Fe^{3+} ions, which weaken the interaction between nickel and the carrier.¹¹⁷ Thus the introduction of up to 10% of Fe^{3+} increases the enantioselectivity of the $Ni-Al_2O_3-TA$ catalyst in the hydrogenation of MAA, increasing OY from 18% to 38%, i.e. making the effectiveness of the catalyst comparable to that of $Ni-SiO_2-TA$. On the other hand, the addition of Fe^{3+} in the preparation of $Ni-SiO_2$ lowers both the optical and the chemical yields of the MAA hydrogenation product (Fig. 7). The introduction of a palladium salt has a similar effect.¹¹¹ It is noteworthy that the promoting effect of Fe^{3+} is manifested only when Al_2O_3 is used as the carrier: in this case, the increase in the $Fe:(Fe + Ni)$ ratio to 10% increases OY from 16% to 38%, whereas the addition of iron in the preparation of the $Ni-SiO_2-TA$ catalyst lowers OY from 30% to 10%.¹¹⁷

The use of a mixed carrier instead of silica gel (the $Ni-Al_2O_3-SiO_2-TA$ catalyst) lowers OY from 49.7% to 18.3%, although the size of the crystallites increases under these conditions from 8 to 24 nm. One should note in this connection that the nickel catalyst on a zeolite (1:5), obtained by impregnation, is less effective in the hydrogenation of MAA. The optical yield attained on this catalyst is 7.3%, whereas on the

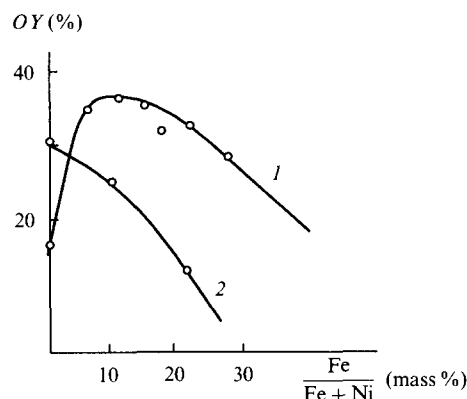


Figure 7. Dependence of *OY* in the MAA hydrogenation reaction on the iron content in the Ni-Fe-Al₂O₃-TA (1) and Ni-Fe-SiO₂-TA (2) catalysts.¹¹⁷

Ni-zeolite-TA catalyst, obtained by joint deposition, *OY* = 45.6%.¹⁰⁸

In order to investigate the role of the size of the crystallites at a constant surface coverage,¹¹⁸ the Ni₃(OH)₄Si₂O₅ system was prepared on the basis of chrysotile — a layered silicate.¹¹⁹ Its reduction in a stream of hydrogen afforded the 59.4% Ni-SiO₂ catalyst with a constant degree of surface coverage and a uniform dispersity, which could be regulated by varying the reduction conditions. An increase in the temperature of the reduction of Ni-chrysotile helped to increase the size of the crystallites (\bar{D}) and in the temperature range 673–973 K \bar{D} varied from 4 to 11 nm, while *OY* in the hydrogenation of MAA reached 40% (Fig. 8). The nature of the initial nickel salt, used in the preparation of Ni-chrysotile, influenced significantly the size of the crystallites and *OY*.¹²⁰

Vedenyapin et al.¹²¹ investigated the influence of platinum metals, introduced into various metallic catalysts, on the enantioselectivity of the latter. The TA-modified palladium catalyst did not exhibit an activity in the enantioselective hydrogenation of EAA. The introduction of even 5% of palladium into the RCu-TA catalyst, capable of promoting enantioselective hydrogenation albeit with a low effectiveness, led to a decrease in *OY* from 9% to 1%.¹²¹

The 10% (Ni-Pd)-aerosil and 10% (Ni-Pd)-Al₂O₃ catalysts were obtained by impregnating the carriers with solutions of the appropriate salts.¹²² The catalysts were dried and reduced at 630 K in a H₂-He stream. Catalysts of another

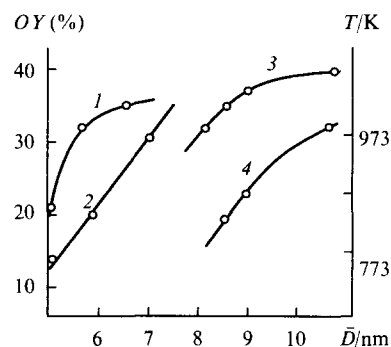


Figure 8. Dependence of the enantioselectivity of the Ni-SiO₂-TA catalyst, obtained from Ni-chrysotile, in the MAA hydrogenation reaction (333 K, 10 MPa) on the average size of the crystallites (\bar{D}) (1, 3) and the influence of the temperature of the reduction of the catalysts on \bar{D} (2, 4): (1, 2) initial salt Ni(NO₃)₂·6H₂O; (3, 4) initial salt NiCl₂·6H₂O (according to the data of Nitta and coworkers^{119, 120}).

series were prepared by impregnating Ni-SiO₂ with a PdCl₂ solution. The modification was carried out with a 5% TA solution at pH 5. Similar results in the hydrogenation of EAA were obtained on the catalysts of both series: the optical yield was 7%–9% for an overall rate of reaction of 0.1 mmol min⁻¹ (g catalyst)⁻¹.

The modification of the RNi-Ru catalyst obtained by leaching ternary Ni-Ru-Al alloys containing 70% of aluminium was achieved by employing a 2% solution of TA at pH 4.5.¹²³ With increase in the ruthenium content, *OY* decreased. According to the data of Vedenyapin et al.,¹²³ the introduction of palladium or ruthenium as additives into nickel or copper catalysts does not promote the enantioselective hydrogenation of EAA. A similar picture was observed when the DNi-TA catalyst, obtained by decomposing nickel formate, was employed.¹¹⁰ The addition of 15% of palladium lowered the optical yield in the MAA hydrogenation reaction from 50% to zero. After the introduction of palladium, the amount of TA adsorbed by the catalyst during its modification diminished from 0.01 to 0.001 mmol (g Ni)⁻¹ as a consequence of the displacement of TA from the surface by palladium. Thus, in conformity with the data of Nitta et al.,¹¹¹ the high effectiveness of nickel catalysts alloyed with 1% of platinum metals, observed by Orito and coworkers,^{124–128} can be accounted for by the influence of these additives on the formation of the catalyst surface and primarily on the crystallinity of nickel.

Orito and coworkers^{124–128} showed that the 1:1 nickel catalyst on kieselguhr (Kg), alloyed with 1% of noble metals and modified with (*R,R*)-TA, exhibits an exceptionally high enantioselectivity in the hydrogenation of MAA to MHB. The optical yield of MHB reached¹²⁷ 99.4% on the Ni-Pd-Kg catalyst. However, Orito and coworkers^{124–128} determined the values of *OY* polarimetrically and adopted $[\alpha]_D = +20.9^\circ$ for the optically pure MHB. Since it was later established⁴⁶ that the specific rotation of MHB is 22.95° and not 20.9°, the highest values of *OY* in the above investigations should have been 79.0%–90.5%, which are also extremely high parameters. The importance of the results obtained led us to describe here the methods for the preparation of the catalyst and for carrying out experiments on the hydrogenation of MAA.¹²⁴

Kieselguhr [manufactured by the National Chemical Laboratory for Industry (Japan)] was introduced, without additional purification,§ into a solution of nickel nitrate and a platinum metal salt in an amount such that the ratios Ni:Pt:Kg = 100:1:100 were attained. The mixture was allowed to stand for 1 h and was then treated with a solution of sodium carbonate. The precipitate was thoroughly washed and dried for 24 h at 383 K. The 3 g catalyst specimen was heated by a quartz lamp in a stream of H₂ (7 dm³ h⁻¹) up to 573 K for 1 h, after which it was cooled and added to a 100 ml of a 1.5% aqueous solution of (*R,R*)-TA at pH 4.1 bubbled with nitrogen, reducing the temperature of the solution gradually to 358 K. The catalyst was then centrifuged and washed initially twice with water (with 25 ml in each case) and then with methanol and the solvent in which the hydrogenation was to be carried out. The reaction was performed in an autoclave with stirring at a pressure of 6–8 MPa and with a substrate:catalyst \approx 14:1 ratio. The reaction temperature was raised from 293 K to the specified level at a rate of 0.7 K min⁻¹. When the absorption of hydrogen was completed, the catalyst was filtered off and the product distilled.

The compilation in Table 6 presents the maximum optical yields of MHB under different conditions.¶ By carrying out the reaction in THF and by adding small amounts of carboxylic

§Personal communication by Prof. Orito.

¶The optical yields obtained by Orito and coworkers^{124–128} and presented in Table 6 were corrected in accordance with the new value of the specific rotation of MHB $[\alpha]_D = 22.95^\circ$.

Table 6. Enantioselective hydrogenation of MAA on deposited nickel catalysts alloyed with added platinum metals and modified by (*R,R*)-tartaric acid (according to the data of Orito and coworkers^{124–128}).

Number of experiment	Catalyst	Solvent	$w / \text{mmol h}^{-1} (\text{g catalyst})^{-1}$ ^a	$[\alpha]_D^{20}$	OY (%)
1 ^b	Ni–Kg	without solvent	5.9	12.20	53.2
2	Ni–Rh–Kg	"	7.8	13.75	59.9
3	Ni–Pt–Kg	"	9.7	14.20	61.9
4 ^c	Ni–Pt–Kg	THF	4.7	15.00	65.4
5 ^d	Ni–Pt–Kg	THF	7.2	18.05	78.6
6 ^e	Ni–Pd	without solvent	3.8	9.15	39.8
7	Ni–Pd–Kg	"	8.7	14.65	63.8
8 ^d	Ni–Pd–Kg	THF	6.9	18.22	79.4
9 ^d	Ni–Pd–Kg	THF	2.8	20.10	87.6
10 ^d	Ni–Pd–Kg	THF	2.5	20.44	89.1
11 ^f	Ni–Pd–Kg	THF	2.5	20.79	90.6
12 ^g	Ni–Pd–Kg	THF	2.6	20.49	89.3
13	Ni–Pd–C	without solvent	5.6	13.02	56.7
14	Ni–Pd–Al ₂ O ₃	"	5.2	11.13	48.5
15	Ni–Ir–Kg	THF	4.9	16.50	71.9
16 ^c	Ni–Ru–Kg	without solvent	8.8	11.35	49.5
17	Ni–Ru–Kg	"	7.8	12.35	53.8
18 ^h	Ni–Ru–Kg	"	9.3	12.05	52.5
19 ^d	Ni–Ru–Kg	THF	6.7	16.75	73.0
20 ⁱ	Ni–Ru	without solvent	1.6	4.1	17.0

Note. Composition of catalyst: nickel:platinum metal:kieselguhr = 100:1:100. Samples: 2.3 g of catalyst, 2.3 g of MAA, and 44 ml of the solvent. Catalyst modification conditions: 1.5% aqueous TA solution, pH 4.3, 357 K. Hydrogenation conditions: pressure 5.5 MPa, temperature 294–403 K.

^a Rate of formation of the (*R*)-(-)-MHB enantiomer. ^b Catalyst composition Ni:Kg = 1:1. ^c The catalyst was modified at 293 K. ^d 1 ml of AcOH

was added. ^e Catalyst composition Ni:Ru = 100:1. ^f 0.05 g of HCOOH was added. ^g 0.5 g of benzoic acid was added. ^h Catalyst composition Ni:Ru:Kg = 100:3:100. ⁱ Catalyst composition Ni:Ru = 100:1. Modification conditions: pH 4.5, 293 K. Samples: 0.2 g of the catalyst, 41 ml of EAA. The hydrogenation was carried out at 333 K (according to the data of Klabunovskii and Vedenyapin⁴).

acids into the reaction mixture, the OY for the product is increased by 6%–10%.

The method of synthesis of MHB with OY up to 90.6%, in which the modification with tartaric acid is carried out at pH 4.3–4.5 (0.68–0.72 g of NaOH on 1.5 g of TA) at 357 K, was developed for the Ni–Pd–Kg catalyst. Before the reaction, the catalyst (2.3 g sample) must be heated for 4 h in THF without stirring, having added 1.5% of acetic acid, at 382 K and a pressure of 5.5 MPa (experiment No. 10). The reaction mixture (MAA in 44 ml of THF to which 1 ml of AcOH has been added) is kept initially without stirring for 1 h at the same temperature and pressure and is then stirred for 10–20 h. The optical yield of the MHB thus obtained reaches a maximum value of 90.6% (experiment No. 11). Instead of acetic acid, formic or benzoic acid may be added. The optical yield of the product increases if the added monocarboxylic acid has a pK_1 lower than that of the modifying agent — tartaric acid ($pK_1 = 2.89$).

It follows from Table 6 that the alloying of the nickel catalyst with platinum metals increases significantly the enantioselectivity and the overall rate of the reaction. The deposited Ni–Ru–Kg catalyst is more effective (OY = 50%) than the Raney RNi–Ru catalyst without a carrier, on which OY is 4% and 17% respectively in the MAA and EAA hydrogenation reactions.⁴

An increase in the temperature of the modifying TA solution from 293 to 353–363 K helps to increase the optical yield of MHB. When the reaction is carried out in alcohols, OY diminishes but the overall rate of reaction increases. The best solvent has proved to be THF and ethyl acetate with added acids (acetic, formic, or benzoic). The antiparallel variation of OY and the overall rate of reaction, observed earlier by Orito and coworkers,^{124–128} was confirmed.⁴ Among the carriers investigated (activated charcoal, aluminium oxide, silica gel, kieselguhr), best results were obtained with kieselguhr.

Unfortunately there are no literature data on the reproducibility of the results of the studies by Orito and coworkers.^{124–128} Nevertheless, a question arises concerning the reason for the high enantioselectivity of nickel catalysts alloyed with other metals and especially concerning the role of kieselguhr as the carrier. Bimetallic catalysts based on nickel and copper with added platinum metals (ruthenium and palladium) did not exhibit an appreciable enantioselectivity in the EAA hydrogenation reaction.^{4,123}

Nitta et al.¹¹¹ investigated in detail modified nickel catalysts on carriers, including kieselguhr. They exhibited a high enantioselectivity, but kieselguhr as a carrier had no special properties. Apparently the addition of platinum or palladium at the nickel catalyst preparation stage promotes a more complete reduction of nickel and the formation at nickel crystallites of optimum size.¹¹¹ The NiO reduction process is influenced significantly by Cl[−] and Br[−] anions. The addition of PdCl₂ to the initial NiO–SiO₂ system promotes the reduction of NiO but has little influence on the enantioselectivity.¹¹¹

Contrary to the data of Orito and coworkers,^{124–128} the deposition of nickel on kieselguhr of the Shimalite brand or on Al₂O₃ with subsequent modification by (*R,R*)-tartaric acid did not make it possible to attain a value of OY in the MAA hydrogenation reaction in excess of 54–68% even in the presence of a high metal content on the carrier.¹²⁹ Similar optical yields were also obtained when nickel was deposited on TiO₂ (70%) and ZrO₂ (68%). The reactions were carried out at a pressure of 9 MPa and a temperature of 393 K.¹²⁹

The higher values of OY attained by Orito and coworkers^{124–128} can apparently be partly accounted for by the high nickel content on the carrier (50%), which actually converts the deposited catalyst into nickel black, and also by the specially favourable conditions in the formation of the catalyst created by the addition of platinum metals. It is also possible

Table 7. Conditions in the preparation of the Ni–SiO₂–TA catalysts for the hydrogenation of MAA (Ni : SiO₂ = 1 : 1).

Conditions	Methods adopted by Nitta et al. ¹¹¹			Method adopted by Orito et al. ¹²⁴
	A	B	C	
Ni(NO ₃) ₂ : Na ₂ CO ₃	1	1.2	0.83	1
Deposition temperature / K	348	358	273	298
Ageing time / min	15	30	5	60
Drying temperature / K	383	393	323	383
Drying time / h	24	45	20	24
NiCO ₃ content in deposit (%)	35–40	7–10 ^a	60–65	—

^a Ni(OH)₂ content.

that the kieselguhr employed in the above studies contained promoting admixtures.

Nitta et al.¹¹¹ concluded that the high effectiveness of the nickel catalysts under discussion^{124–128} may be accounted for by the special conditions in their formation. According to Nitta et al.,¹¹¹ the introduction of 1% of palladium into the Ni–SiO₂ catalyst in the stage involving the reduction of the NiCO₃–SiO₂ system promotes the reduction of the salt, a decrease in the process temperature, and the formation of larger nickel crystallites. Nitta et al.¹¹¹ attempted to reproduce the data of Orito and coworkers.^{124–128} The Ni–SiO₂ catalytic systems were prepared by three methods differing in the conditions in the deposition of the catalyst and its reduction. The influence of the introduction of palladium into the catalysts on the formation and enantioselectivity of the catalysts and the role of kieselguhr as the carrier were also investigated.

Table 7 presents the conditions for the preparation of the nickel catalysts described by Nitta et al.¹¹¹ and for comparison the conditions quoted by Orito et al.¹²⁴ Nitta et al.¹¹¹ used silica gel (60–200 mesh) with a specific surface of 600 m² g^{−1} and kieselguhr with a specific surface of 5.7 m² g^{−1} supplied by the Yoneyama Yakuhin Company. The suspension of the carrier was impregnated with a solution of nickel nitrate and precipitated with a solution of sodium carbonate at 348 K. After drying (383 K), the catalysts were reduced in a stream of hydrogen for 1 h at 773 K. In order to obtain the Ni–Pd–SiO₂ system, PdCl₂ was added to the catalyst mass before its reduction (Ni : Pd : carrier = 100 : 1 : 100).¹¹¹ As can be seen from Table 7, methods A, B, and C differ in the severity of the conditions during the deposition and treatment of the catalyst mass. The catalyst obtained by method C contained an excess of NiCO₃. Method A is distinguished by milder conditions, similar to those adopted by Orito and coworkers.^{124–128} Method B affords a deposit containing less effectively reducible Ni(OH)₂, the reduction of which even in the presence of palladium gives rise to larger crystallites.¹¹⁵ Depending on the composition of the initial mixture, the catalysts differ significantly in their enantioselectivity in the MAA hydrogenation reaction in EtOAc at 333 K and a pressure of 1 MPa. It was shown¹¹¹ that nickel catalysts with added palladium, deposited on silica gel or kieselguhr, are usually less effective than the catalysts without such an additive, which conflicts with the data of Orito et al.¹²⁴ Admittedly, the introduction of palladium into the catalyst obtained by method A promoted some increase in enantioselectivity as a consequence of the increase in the average size of the nickel crystallites (Table 8).

The use of kieselguhr did not increase but actually somewhat diminished *OY* even when the modification was carried out by the method of Orito et al.¹²⁴ at pH 4.1. The reaction rates on all the Ni–SiO₂–TA catalysts were similar and amounted to 0.4–0.8 mmol min^{−1} (g Ni)^{−1}. The introduction of palladium decreased somewhat the average size of the crystallites, which increased the rate of reaction but did not increase *OY*, whereas, according to the data of Orito et al.,¹²⁴ the catalysts on kieselguhr with added palladium are more active [the rate of

reaction is 2.5–8.7 mmol min^{−1} (g Ni)^{−1}] and enantioselective (*OY* = 63.8%–89.1%). Thus, contrary to the data of Orito and coworkers,^{124–128} the introduction of palladium and the use of kieselguhr as the carrier did not lead to the formation of specially effective catalysts.¹¹¹

Table 8. The influence of the method of preparation of the catalyst, the nature of the carrier, the reduction temperature (*T_r*), and added palladium on the enantioselectivity of the catalysts for the hydrogenation of MAA to (−)-MHB (according to the data of Nitta et al.¹¹¹).

Method of preparation ^a	Catalyst ^b	<i>T_r</i> / K	\bar{D} / nm	<i>OY</i> (%)
A	Ni–Kg	523	31	32.5
A	Ni–Pd–Kg	523	16	26.3
A	Ni–Kg ^c	573	31	12.1
A	Ni–SiO ₂	573	—	23.8
		673	9	50.6
A	Ni–Pd–SiO ₂	573	—	27.8
		673	12	41.6
B	Ni–SiO ₂	673	4	29.8
B	Ni–Pd–SiO ₂	673	5	20.1
C	Ni–SiO ₂	573	13	43.4
C	Ni–Pd–SiO ₂	573	13	30.1
C	Ni–SiO ₂ ^c	573	13	36.8
C	Ni–Pd–SiO ₂ ^c	573	13	34.6
C	Ni–Pd–Kg	573	12	27.7
	Ni–Pd–Kg ^c	573	—	63.8 ^d
	Ni–Pd–Kg	573	—	89.1 ^e

^a See Table 7. ^b Ni : Pd : carrier = 100 : 1 : 100; modification by (R,R)-tartaric acid at pH 5.1. ^c Modification carried out at pH 4.1. ^d Experiment No. 7 in Table 6. ^e Experiment No. 10 in Table 6.

With increase in the fraction of NiCO₃ in the catalyst mass above 25% there is an increase in the specific surface and in the average size of the nickel crystallites (from 5 to 18 nm). *OY* passes through a maximum corresponding to the catalyst obtained from the catalyst mass containing 37% of NiCO₃ and reduced at 773 K. The increase in the fraction of NiCO₃ to 58% makes it possible to lower the reduction temperature to 573 K. This leads to an increase in \bar{D} to 15 nm, which promotes an increase in *OY*. Hence it follows that the enantioselective hydrogenation is a structure-sensitive reaction and may be used as a method for the monitoring of the size distribution of the nickel crystallites. Fig. 9 presents the variations of the catalytic activity and the optical yield in the MAA hydrogenation reaction on Ni–SiO₂ with the fraction of NiCO₃ in the catalyst mass. The size of the nickel crystallites is related, in its turn, to this quantity.

Studies have shown^{114,115} that the formation of the catalyst is greatly influenced by the additives, the nature of the initial salts, and the reduction conditions. The high effectiveness of the bimetallic catalysts deposited on kieselguhr may therefore be

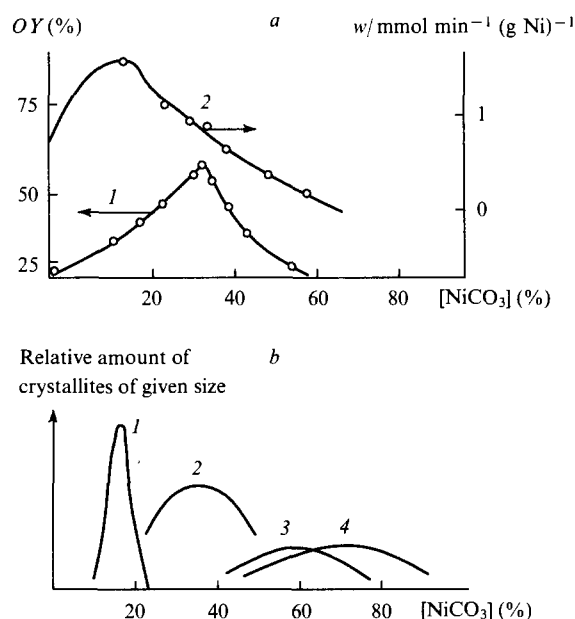


Figure 9. The influence of the NiCO_3 content in the initial catalyst mass (catalyst reduction temperature 673 K) on the optical yield of MHB (1) and the catalytic activity (w) of $\text{Ni-SiO}_2\text{-TA}$ (2) in the MAA hydrogenation reaction (a) and also on the average size of the nickel crystallites (b). Curves 1–4 (b) correspond to $\bar{D} = 3.5, 8.0, 16.0$, and 18.0 nm respectively (according to the data of Nitta et al.^{114, 115}).

caused by the precise influence of these factors on the formation of the structure of the catalyst surfaces and primarily on the size of the nickel crystallites.^{106, 108, 109, 113–115}

The introduction of palladium into the catalyst apparently affects the degree of reduction of nickel, which occurs in this case at lower temperatures. This influence depends greatly on the nature of the initial salts: the presence of palladium promotes the reduction of NiCO_3 , formed on precipitation with sodium carbonate, but has little effect on the reduction of Ni(OH)_2 . The presence of the carrier accelerates the conversion of part of NiCO_3 into Ni(OH)_2 , but the reduction of the hydroxide requires more severe conditions.

As already mentioned,^{124–128} the addition of AcOH increases significantly OY in the hydrogenation of MAA on Ni-Pd-Kg . The addition of certain salts into the modifying TA solution also helps to increase OY, the nature of the anion playing an important role. NaBr proved to be the most effective modifying additive to RNi-TA .⁴⁶

High concentrations of halide salts in the modifying TA solution have a negative effect on the rate of reaction and on OY,¹¹⁸ but the addition of NaI (or KI) at very low concentrations tends to increase the optical yield. It has been found that NaI reduces OY sharply at a concentration of just 0.002%, whereas NaBr is effective even at concentrations higher by a factor of 100. This is associated with the fact that the iodide is adsorbed on nickel much more strongly than the bromide. Thus the anion affects OY no less strongly than the cation.⁴⁶

The nature of the cation is important in the leaching of the Ni-Al alloy and in the establishment of a suitable pH of the modifying tartaric acid solution. Best results were achieved when Na^+ ions were employed: at a NaBr concentration of 8% and a TA concentration of 1%, the optical yield in the hydrogenation of MAA was 70.2%. Li^+ and Rb^+ ions hardly affect OY. The cations are coordinated to the oxygen in TA and MAA adsorbed on nickel, sodium and potassium participating in the octahedral coordination, which intensifies the template effect in the stereochemical interaction of TA with MAA (and MHB). The anions are by themselves incapable of showing the

template effect, particularly at high salt concentrations, their function consisting in fixing the appropriate amounts of the cation on the catalyst surface, needed for coordination to the TA–MAA (MHB) complex. The influence of NaBr is also manifested by the fact that the salt is a weak poison for the nickel catalysts. It blocks the most active centres on the nickel surface, intensifying thereby the enantioselective effect of the modified centres.

According to Nitta et al.,¹¹¹ the introduction of chlorides or bromides into the catalyst mass during the formation of deposited catalysts promotes an increase in OY by virtue of the increase in \bar{D} , but the overall rate of reaction decreases under these conditions. The addition of the salts NiCl_2 , NaCl , FeCl_2 , and NaBr or of the acids HCl or HBr to the catalyst mass prepared by method A increases OY from 36.1% to 49.7%–57.5%. With increase in \bar{D} (from 13 to 20–30 nm), a narrower size distribution of the nickel crystallites is obtained.¹¹¹

The increase in OY after the addition of NiCl_2 is of interest. The introduction of 29.8% of this salt into the catalyst mass, prepared by methods A, B, or C, diminishes sharply the specific surface of the reduced nickel (the reduction was carried out at 623 K for 1 h), which indicates an increase in \bar{D} . Depending on the method employed, OY increases from 36.1% to 54.9% (A), from 19.3% to 51.0% (B), and from 39.4% to 53.2% (C) respectively. The sharp diminution in the specific surface indicates not only the growth of \bar{D} but also the presence on the surface of chloride residues, which hinder the adsorption of hydrogen. At the same time, the Cl^- ions remaining on the catalyst after its reduction may act as a promoting additive, i.e. may behave similarly to NaBr in the modifying solution.⁴⁶

The RNi-TA-NaBr catalyst was obtained by leaching the 42:58 Na-Al alloy at 373 K.⁴⁶ The catalyst was washed 15 times with portions of deionised water and was modified in 1% (*R,R*)-TA solution containing 10 g of NaBr at 373 K in the course of 1 h. After the modification, the catalyst was again washed with water and methanol. MAA was hydrogenated in an $\text{EtCOOMe} + 0.2$ ml AcOH solution at a pressure of 9 MPa and a temperature of 373 K. The rate of reaction was $0.2 \text{ mmol min}^{-1} (\text{g Ni})^{-1}$. A threefold repetition of the modification procedure increased OY from 83.1% to 88.6%. Under the same conditions but without the addition of NaBr and AcOH, OY was 31.2%. The introduction of NaBr at a concentration of $0.01\text{--}0.04 \text{ mmol (g Ni)}^{-1}$ did not affect the degree of adsorption of TA on nickel and the optical yield increased in proportion to the NaBr concentration. This has been attributed⁴⁶ to the presence on the surface of the modified catalyst of two types of centres:⁴ selective centres, modified by TA, on which the (–)-enantiomer is formed, and nonselective centres on which the MHB racemate is produced.

This method also has its negative aspects: as stated above, NaBr diminishes the activity of the nonselective centres and lowers the overall rate of reaction. In order to compensate for this negative effect, it is necessary to increase the reaction pressure and temperature and this entails a decrease in regioselectivity and the appearance of side products, in particular the ester $\text{MeCH(CH}_2\text{COOMe)OCOCH}_2\text{CH(OH)Me}$. The behaviour of the deposited nickel catalyst is somewhat different from that of the Raney catalysts. The presence of residual amounts of Cl^- ions in the Ni-SiO_2 catalyst imparts stability to the latter in repeated hydrogenation. On the other hand, the Ni-SiO_2 (1:1) catalyst modified by TA with added NaBr is not quite so effective¹¹¹ as RNi .⁴⁶ The modification by NaBr increases OY in the MAA hydrogenation reaction from 36.1% to 46.0%, but, after repeated hydrogenation on the same portion of the catalyst, OY fell to 11.0%, while the catalyst promoted by the addition of NiCl_2 to the catalyst mass before reduction retained its stability in three consecutive experiments ($y = 90\%$, 79%, and 81% for $\text{OY} = 52.7\%$, 55.0%, and 54.9% respectively). This can be explained not only by the presence of

residual amounts of the halogen on the nickel surface but also by a more uniform size distribution of the nickel crystallites. Promotion by halides (nickel chloride) of the initial catalyst mass increases the degree of reduction of NiO to the metal.¹¹¹ This effect is manifested to a particularly notable extent in the reduction of the catalyst mass obtained by method B and containing Ni(OH)₂, which is reduced with difficulty as a consequence of the strong interaction with the carrier.¹¹⁷ As a result of this, the catalyst obtained has a higher activity but a lower enantioselectivity.

The low enantioselectivity of the Ni–Al₂O₃ catalysts, in the preparation of which NaOH is used to precipitate the hydroxides, can be accounted for by the strong interaction of the metal with the carrier and the formation of Ni–Al compounds on the surface. However, similar catalysts formed under mild conditions, which rule out the formation of small nickel crystallites, have the same enantioselectivity as Ni–SiO₂.¹¹⁶

A series of studies by Izumi and coworkers^{3, 46, 92} were devoted to the development of methods for increasing the enantioselectivity of the RNi–TA catalysts in the MAA hydrogenation reaction. With increase in the temperature of the leaching of the Ni–Al alloy, the optical activity of the product increases as a result of the decrease in the residual amount of aluminium present in the catalyst as aluminium hydroxide. The OH groups present in TA and Al(OH)₃ compete with one another for the formation of hydrogen bonds with MAA, reducing thereby OY. The elimination or blocking of the aluminium-enriched nickel centres increases the fraction of dissymmetric centres and increases OY. This view is confirmed by the fact that the nickel catalyst, obtained by the reduction of NiO in a stream of hydrogen at 523 K and modified with a 1% solution of TA at 358 K and pH 4.1, exhibits a higher enantioselectivity than the RNi–TA Raney catalyst. The hydrogenation of MAA in solution in EtCOOMe at a pressure of 1 MPa and a temperature of 393 K leads to the formation of (R)-(–)-MHB with OY = 81.7%, whereas the optical yield on RNi–TA under the same conditions is only 44%.⁴⁶

The fraction of nonselective centres on the nickel surface may be diminished by the ultrasonic treatment of the catalyst, which induces the selective disruption of the more active centres not protected by the modifying agent, tartaric acid.¹³⁰ Such treatment makes it possible to increase not only OY but also the overall activity of the catalyst, i.e. to eliminate the disadvantage characteristic of RNi catalyst modified by TA in the presence of NaBr (as already stated, the adsorption of this salt increases OY, but decreases significantly the overall catalytic activity).

Table 9. Hydrogenation of the methyl esters of ketoacids on the RNi–TA–NaBr catalyst treated with ultrasound and the untreated catalyst (according to the data of Tai et al.¹³⁰).

Compound hydrogenated	Treatment of a catalyst ^a	$w/\text{mmol min}^{-1}$ (g catalyst) ^{–1}	OY (%)
MeCOCH ₂ COOMe	+	18.0	86
	–	9.0	80
n-C ₇ H ₁₅ COCH ₂ COOMe	+	1.3	89
	–	0.3	83
n-C ₉ H ₁₉ COCH ₂ COOMe	+	0.9	91
	–	0.2	86
n-C ₁₁ H ₂₃ COCH ₂ COOMe	+	0.9	94
	–	0.2	86

Note. Reaction conditions: solvent — EtCOOMe, pressure 1 MPa, temperature 373 K.

^a + — with treatment by ultrasound, – — without treatment by ultrasound.

The overall rate of hydrogenation after the ultrasonic treatment of the catalyst increases by a factor of 2–4, while OY increases to 86%–94% (Table 9). This is the maximum optical yield attained hitherto on modified RNi–TA–NaBr catalysts. After such treatment, the catalyst becomes stable and can be used to obtain the optically active (R)-(–)-MHB on a large scale. Thus it has been possible to hydrogenate 10 kg of MAA, dissolved in 100 dm³ of EtCOOMe, on 190 g of the ultrasonically treated RNi–TA–NaBr catalyst after 18 h. The optical yield of (–)-MHB in this reaction, carried out at a pressure of 10 MPa and a temperature of 373 K, was 81%.

Optically pure 100% MHB can be obtained by crystallising a MHB derivative — the dibenzylammonium salt of HBA.¹³⁰ For this purpose, (–)-MHB with an excess of the enantiomer (OY = 83%) is hydrolysed in a 1:1 MeOH–H₂O mixture. The sodium salt is passed through a column with Amberlite IR-120 and the resulting acid (–)-HBA is converted into the dicyclohexylammonium¹³¹ or dibenzylammonium salt,¹³⁰ which is then crystallised. This leads to the formation of the optically pure (OY = 98%–100%) acid (R)-(–)-HBA in a high yield (Table 10).

Table 10. Preparation of optically pure carboxylic β -hydroxyacids by the hydrogenation of the methyl esters of the β -ketoacids Me(CH₂)_nCOCH₂COOMe on the RNi–TA–NaBr catalyst after three crystallisations of the dicyclohexylammonium salts of the acids from acetonitrile (according to the data of Tai and coworkers^{131, 135, 136}).

<i>n</i>	OY for hydroxyester (%) ^a	Consumption of acetonitrile /ml (gram salt) ^{–1}	β -Hydroxyacid	
			yield (%)	OY (%) ^b
0	86	7.0	52	98
6	87	11.5	50.5	98
8	88	18.0	73.5	100
10	85	19.0	72.1	100
12	87	24.5	75.1	98

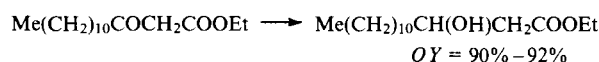
^a Before crystallisation. ^b After crystallisation.

An important practical problem concerns the possibility of the repeated use of the RNi–TA–NaBr catalysts. It has been shown that RNi–TA–NaBr introduced into a solid matrix of vulcanised silicone rubber containing oxime groups (KE-441 produced by the Shin Etsu Chemical Company) can be used repeatedly, up to 30 times, in the hydrogenation of MAA to (–)-MHB.^{132, 133} The optical yield on a single catalyst specimen (9 MPa, 373 K) is maintained at the level of 58%–62% and there is no significant decrease in enantioselectivity.¹³⁴ The usual catalyst without a matrix is somewhat more enantioselective but is less stable and OY has already decreased from 76% to 28% by the third experiment. The stability of the catalyst inserted into a silicone matrix is ensured by the binding of the nickel to the oxime groups of the polymer, which are converted into amino-groups during the reaction.¹³⁴ Treatment with a solution of pyridine or MePrNH^{100, 104} therefore also makes it possible to obtain a stable catalyst on one portion of which up to 10 consecutive hydrogenations can be performed with only a slight decrease in OY (from 80% to 73%).¹³⁴

Processes in which the optical yield is not less than 80% while the preparation of the catalyst and the process technology are fairly simple are of practical interest. These requirements are satisfied by modified metallic catalysts. The industrial production of chiral hydroxyesters and glycols with OY up to 90% can be achieved on modified nickel catalysts.

The high effectiveness of the RNi–TA–NaBr catalysts has been used to synthesise practically important optically active β -hydroxyacids, which are common in biological systems. (R)-(–)-3-Hydroxydecanoic acid forms part of the composition

of growth factors, 3-hydroxytetradecanoic acid is the principal aliphatic acid in 'lipid A' in endotoxin,¹³⁵ the choline ester of 3-acetoxyhexadecanoic acid, known as pahutoxin, is one of the components of fish poison,^{131,136} while 3-hydroxyoctadecanoic acid is a component of the antitumour preparation emposatin. All these compounds have been obtained in high optical yields by the hydrogenation of the corresponding ketoacids on RNi-TA-NaBr at a pressure of 9.5 MPa and a temperature of 373 K in solution in $\text{EtCOOMe} + \text{AcOH}$. After 2–3 recrystallisations of the dicyclohexylammonium or dibenzylammonium salts, obtained from the esters of the corresponding hydroxyacids,^{131,137} it is possible to obtain the optically pure acids in high yields. The nickel catalyst is also used in the synthesis of the hydroxyester which is an intermediate in the synthesis of tetrahydrolipostatin produced by the Hoffmann-LaRoche Company.¹³⁸



β -Hydroxyesters and β -glycols, for example ethyl β -hydroxybutyrate and pentane-(2*R*,4*R*)- and -(2*S*,4*S*)-diols, are produced industrially on the RNi-TA-NaBr catalysts. The optical yield of the diol reaches 87%, while after the crystallisation of its derivative it becomes 100%.¹³⁹ This is used in the synthesis of the chiral diphosphine Skewphos [(*R,R*)-2,4-bis(diphenylphosphino)pentane].¹⁴⁰

Modified nickel catalysts for asymmetric hydrogenation are produced by the Wako Pure Chemistry,¹⁴¹ Kawaken Pure Chemistry, and Degussa Companies (RNi-TA-NiBr)¹³⁸ and by the Heraeus Company (HNi-TA-NaBr).^{138,142}

VI. Synthesis of optically active β -hydroxyesters by the hydrogenation of ketoesters on metal complex catalysts with chiral ligands

Chiral rhodium–diphosphine complexes are highly effective chiral catalysts on which it is possible to hydrogenate dehydroamino acids to optically active amino acids with OY close to 100%.¹⁴³ Under certain conditions, ketones can also be reduced on these catalysts.^{143,144} The presence of the COOR group in the molecule facilitates reduction and hydroxyesters are formed from α - and β -ketoesters with high values of OY .¹⁴⁵ The ketoesters are particularly effectively reduced on chiral rhodium and ruthenium complexes.¹⁴⁶ The methyl acetoacetate is reduced

to MHB with $OY = 71\%$ when acted upon by the complex $[\text{Rh-CAMP}]$ [$\text{CAMP} = (R)$ -cyclohexyl-*o*-methoxyphenylmethylphosphine].¹⁴⁷ The rhodium complex with the chiral diphosphine BINAP,^{47,148} produced by the method of Takaya et al.,¹⁴⁹ exhibits a very high enantioselectivity. MAA is hydrogenated at pressures of 1.0 or 1.12 MPa and a temperature of 298 K for 48 h.^{150,151} The (*R*)-(-)- β -hydroxyester with $OY = 99\%$ is formed from methyl β -ketovalerate in solution in 1:1 $\text{MeOH-CH}_2\text{Cl}_2$ in the presence of the complex $[\text{Rh-BINAP}]$, and the optically pure (*R*)-(-)-hydroxyvaleric acid can be obtained by its hydrolysis.

The use of phospholanes as chiral ligands in rhodium complexes proved to be relatively ineffective: the optical yield did not exceed 27% in the reduction of MAA at a pressure of 2 MPa and a temperature of 298 K.¹⁵¹

VII. Conclusion

In conclusion, the three methods of synthesis of β -hydroxyesters examined above should be compared from the standpoint of their practical applicability. Table 11 presents the main characteristics of the processes involving the reduction of β -ketobutyrate, acted upon by baker's yeast, on a Raney nickel catalyst modified by (*R,R*)-tartaric acid with added NaBr, and in the presence of a chiral ruthenium complex containing a chiral ligand, the diphosphine BINAP.³² As can be seen, all three methods ensure a high effectiveness of the process. The optical yield is 85%–99%. We shall now consider their disadvantages.

Despite the high enantioselectivity (in the best instances), the possibilities for wide scale application of the enzymic reduction of ketoesters are limited by the low productivity of the process, by the need to employ large volumes of solutions, by the low concentration of the product in solution, by the need for additional purification (filtration, extraction), by the long duration of the process, and by the instability of the enzyme. This is a single-use process which cannot be carried out under flow or cyclic conditions and the reducing agents are not regenerated.

The employment of a metal complex catalyst ensures an extremely high effectiveness and productivity, the turnover number for the reaction on such a catalyst being very high. The process can be performed at room temperature. However, the cost of the catalyst and of the chiral ligand is high and they cannot be regenerated.

Table 11. Comparative characteristics of various methods for the synthesis of β -hydroxybutyrate by the reduction of β -ketoesters.

Characteristic	Enzymic reduction ^a	Heterogeneous-catalytic process RNi-TA-NaBr	Metal complex catalysis Ru-BINAP
Substrate and its sample/g	EAA, 40	MAA, 40	MAA, 40
Solvent and its volume/ml	water, 2600	none	methanol, 40
Catalyst and its sample/g	baker's yeast, 200	Ni-TA-NaBr , 2	Ru-BINAP , 0.14
Reductant	sucrose (600 g)	hydrogen (75 atm)	hydrogen (20–100 atm)
Process temperature/K	293	373	293
Reaction time/h	134	20	40
Method for isolation of product	filtration, extraction, distillation	filtration, distillation	distillation
Chemical yield (%)	59–76	94	99
Chemical yield/g	24–30	38	39
Optical yield (%)	85	90	99
Configuration of molecule	<i>S</i> only	<i>S</i> or <i>R</i>	<i>S</i> or <i>R</i>
Productivity/g (litre solution) ⁻¹ h ⁻¹	0.07	40	12
Possibility of repeated use of catalyst	none	5–30 times	none

^a Standard method.⁴⁵

The somewhat reduced enantioselectivity of the heterogeneous catalyst modified by tartaric acid (the maximum optical yield attained so far is 94%) is compensated by the high productivity of the process, the possibility of the repeated employment of the catalyst (up to 30 times in certain cases), the ease of its separation from the product, and the low cost and ease of preparation of the catalyst. The heterogeneous catalyst can be readily prepared in large amounts and it can be usefully employed in the large-scale production of the chiral β -hydroxybutyrate with an optical yield of about 90%, particularly if it is proposed to carry out further purification of the product by the crystallisation of its derivatives.

Overall, chemical methods have clear advantages over enzymic procedures, which constitutes an important stimulus for the improvement of the latter. There is no doubt that further search for effective catalytic systems, both heterogeneous and metal complex, is needed.

References

1. D Seebach, S Roggo, J Zimmermann, in *Stereochemistry of Organic and Bioorganic Transformations* Vol. 17 (Eds W Bartmann, K Sharpless) (Weinheim: VCH, 1987) p. 85
2. K Mori, in *Studies in Natural Products Chemistry* Vol. 1 (Ed. Atta-ur-Rahman) (Amsterdam: Elsevier, 1988) Part A, p. 677
3. Y Izumi, A Tai *Stereo-differentiating Reactions; the Nature of Asymmetric Reactions* (New York: Academic Press, 1977)
4. E I Klabunovskii, A A Vedenyapin *Asimmetricheskii Kataliz. Gidrogenizatsiya na Metallakh* (Asymmetric Catalysis. Hydrogenation on Metals) (Moscow: Nauka, 1980)
5. J Kleine, H H Kleine *Makromol. Chem.* **30** 23 (1954)
6. R Schulz, J Schwab *Makromol. Chem.* **87** 90 (1965)
7. D Seebach, in *Stereochemistry of Organic and Bioorganic Transformations* Vol. 17 (Eds W Bartmann, K Sharpless) (Weinheim: VCH, 1987) p. 92
8. Jpn. P. 24, 289-(64); *Chem. Abstr.* **62** P9 311g (1965)
9. M Lemoigne C. R. *Hebd. Seance. Soc. Biol.* **94** 1291 (1926)
10. P J Senior, E A Dawes *Biochem. J.* **134** 225 (1973)
11. E A Dawes *Adv. Microbiol. Physiol.* **10** 203 (1973)
12. R H Marchesault, K Okamura, C J Su *Macromolecules* **3** 735 (1970)
13. K Okamura *Dis. Abstr. Int. B* (68-4418) 4968 (1968)
14. D Seebach, M Züger *Helv. Chim. Acta* **65** 495 (1982)
15. K Okamura, R H Marchesault, in *Conformational Aspects of Biopolymers* Vol. 2 (New York: Academic Press, 1967) p. 709
16. J Cornibert *Macromolecules* **8** 296 (1975)
17. J H Mannon *Chem. Eng. (USA)* **88** 723 (1981)
18. S Yanchinski *New Scientist* **89** 723 (1981)
19. H G Schlegel, H Kaltwasser, G Gottschalk *Arch. Microbiol.* **38** 209 (1961)
20. R M Lafferty, B Korsatko, in *Biotechnology* (Ed. G Rem) (Weinheim: Verlag Chemie, 1987) p. 135
21. W P McCann, in *Biochemical Preparations* Vol. 9 (Ed. M J Coon) (New York: Wiley, 1962) p. 63
22. D Seebach *Helv. Chim. Acta* **67** 2747 (1984)
23. T Ninomiya *Bull. Chem. Soc. Jpn.* **45** 2555 (1972)
24. D Seebach, J Zimmermann *Helv. Chim. Acta* **69** 1147 (1986)
25. D Seebach *Helv. Chim. Acta* **70** 448 (1987)
26. P Schnurrenberger *Helv. Chim. Acta* **65** 1127 (1982)
27. *Catalog Fluka Chemika (Chiral Compounds)* Buchs, 1989 p. 90
28. D Seebach, in *Modern Synthetic Methods* Vol. 4 (Ed. R Sheffold) (Heidelberg: Springer, 1986) p. 125
29. D Seebach, H-O Kalinowski *Nachr. Chem. Tech. Lab.* **24** 415 (1976)
30. R D Ridley, M Strawlaw *J. Chem. Soc., Chem. Commun.* 400 (1975)
31. H Meyer, D Seebach *Liebigs Ann. Chem.* 2261 (1975)
32. R A Sheldon, in *Chirotechnology. Industrial Synthesis of Optically Active Compounds* (New York: Marcel Dekker, 1993) p. 245
33. T Okashi, J Hasegawa *J. Synth. Org. Chem. Jpn.* **45** 331 (1987)
34. R Noyori, T Ikeda, T Ohkuma, M Kitamura, H Takaya, S Akutagawa *J. Am. Chem. Soc.* **111** 9134 (1989)
35. R C Nicolaou, M R Pavia, S P Seitz *J. Am. Chem. Soc.* **103** 1224 (1981)
36. B Seuring, D Seebach *Liebigs Ann. Chem.* 2044 (1978)
37. R Amstutz, E Hungerbühler, D Seebach *Helv. Chim. Acta* **64** 1796 (1981)
38. A Kramer, H Pfander *Helv. Chim. Acta* **65** 293 (1982)
39. H Gerlach, K Oertel, A Thalmann *Helv. Chim. Acta* **59** 755 (1976)
40. M Shimazaki, J Hasegawa, K Kan, K Nomura, Y Nose, H Kondo, T Ohashi, K Watanabe *Chem. Pharm. Bull.* **30** 3139 (1982)
41. R A Sheldon, P A Porskam, W Ten Hoeve, in *Biocatalysis in Organic Synthesis* (Ed. J Tramper) (Amsterdam: Elsevier, 1985) p. 59
42. H G Leuenberger, in *Biocatalysis in Organic Synthesis* (Ed. J Tramper) (Amsterdam: Elsevier, 1985) p. 99
43. N Cohen, W F Eickel, R Lopresti, C Neukom *J. Org. Chem.* **41** 3505 (1976)
44. H T Clarke *J. Org. Chem.* **24** 1610 (1959)
45. D Seebach, M A Sutter, R H Weber, M F Züger *Org. Synth.* **63** (1985)
46. T Harada, Y Izumi *Chem. Lett.* 1195 (1978)
47. S Akutagawa, M Kitamura, H Kumabayashi, R Noyori *J. Am. Chem. Soc.* **109** 5856 (1987)
48. C Neuberg, A Lewite *Biochem. Z.* **91** 257 (1918)
49. A I Meyer, R A Amos *J. Am. Chem. Soc.* **102** 870 (1980)
50. H Simon, J Bader, H Günther, S Neumann, J Thanos *Angew. Chem., Int. Ed. Engl.* **24** 539 (1985)
51. B Wipf, E Kupfer, R Bertozzi, H Leuenberger *Helv. Chim. Acta* **66** 485 (1983)
52. R V Lemieux, J Giguere *Can. J. Chem.* **29** 678 (1951)
53. B S Deol, D D Ridley, G W Simpson *Aust. J. Chem.* **29** 2459 (1976)
54. D Seebach, E Hungerbühler, in *Modern Synthetic Methods* (Ed. R Sheffold) (Frankfurt - Aarau: Salle und Sauerländer Verlag, 1980) p. 91
55. S Servi *Synthesis* 1 (1990)
56. A S Gopalan, W R Sieh, C J Sih *J. Am. Chem. Soc.* **107** 2993 (1985)
57. B Wipf, B Zhou, C J Sih *Angew. Chem.* **96** 556 (1984)
58. D Seebach, M A Sutter, K H Weber, M F Züger *Org. Synth. Coll.* **VII** 215 (1990)
59. G Frater *Helv. Chim. Acta* **62** 2829 (1979)
60. E Hungerbühler, D Seebach, D Wasmuth *Helv. Chim. Acta* **64** 1467 (1981)
61. J A Dale, D L Dull, H S Mosher *J. Org. Chem.* **34** 2543 (1969)
62. M Bucciarelli, A Forni, I Moretti, G Torre *Synthesis* 897 (1983)
63. B N Zhou, A S Gopalan, F van Middlesworth, W-R Sieh, C J Sih *J. Am. Chem. Soc.* **105** 5925 (1983)
64. C J Sih, C Chen *Angew. Chem., Int. Ed. Engl.* **23** 570 (1984)
65. K Nakamura, M Higaki, K Ushio, S Oka, A Ohno *Tetrahedron Lett.* **26** 4213 (1985)
66. J Ehrler, F Giovannini, B Lamatsch, D Seebach *Chimia* **40** 172 (1986)
67. J W Scott, in *Asymmetric Synthesis* Vol. 4 (Eds J Morrison, J Scott) (New York: Academic Press, 1984) p. 1
68. P K Matzinger, H C Leuenberger *Appl. Microbiol. Biotechnol.* **22** 208 (1985)
69. J Ehrler, D Seebach *Helv. Chim. Acta* **72** 793 (1989)
70. D Seebach, F Giovannini, B Lamatsch *Helv. Chim. Acta* **68** 958 (1985)
71. D Seebach, M F Züger, F Giovannini, B Sonleitner, A Flechter *Angew. Chem., Int. Ed. Engl.* **23** 151 (1984)
72. US P. 4 326 031 (1982)
73. H Schütte, W Himmel, M R Kuls *Eur. J. Appl. Microbiol. Biotechnol.* **19** 167 (1984)
74. T Haag, T Arslan, D Seebach *Chimia* **43** 351 (1989)
75. H G Leuenberger, W Boguth, R Barker, M Schmid, R Zell *Helv. Chim. Acta* **62** 455 (1979)
76. D Seebach, P Renaud, W B Schweizer, M F Züger, M J Brienne *Helv. Chim. Acta* **67** 1843 (1984)
77. C Fugatti, P Grasselli, P Casati, M Carmeno *Tetrahedron Lett.* **26** 101 (1985)
78. M Hirama, M Shimizu, M Iwashita *J. Chem. Soc., Chem. Commun.* 599 (1983)
79. Jpn. P. 8 239 787; *Chem. Abstr.* **97P** 37 534f (1982)
80. S G Cohen, E Khedouri *J. Am. Chem. Soc.* **83** 4228 (1961)
81. W K Wilson, S B Baca, Y J Barber, C J Soallen, W J Morrow *J. Org. Chem.* **48** 3960 (1983)

82. R W Hoffmann, W Ladner, K Steinbach, W Massa, R Schmidt, G Snatzke *Chem. Ber.* **114** 2786 (1981)
83. H Akita, A Furuichi, H Koshiji *Chem. Pharm. Bull.* **37** 4376 (1983)
84. *Catalog Handbook of Fine Chemicals* (Milwaukee: Aldrich Chem. Co. Inc., 1990–1991) p. 614
85. G M Schwab, L Rudolph *Naturwissenschaften* **20** 363 (1932)
86. G M Schwab, F Rost, L Rudolph *Kolloid Z.* **68** 157 (1934)
87. E I Klabunovskii *Stereospetsificheskii Kataliz* (Stereospecific Catalysis) (Moscow: Nauka, 1968)
88. M Bartok, in *Stereochemistry in Heterogeneous Metal Catalysis* (New York: Wiley, 1985) p. 511
89. A Tai, T Harada, in *Tailored Metal Catalysts* (Ed. Y Iwasawa) (Dordrecht: Reidel, 1986)
90. E I Klabunovskii *Usp. Khim.* **60** 1920 (1991) [*Russ. Chem. Rev.* **60** 980 (1991)]
91. E I Klabunovskii *Izv. Akad. Nauk SSSR, Ser. Khim.* **85** (1984)
92. Y Izumi *Adv. Catal.* **32** 215 (1983)
93. M J Fish, D F Ollis *Catal. Rev. Sci. Eng.* **18** 259 (1973)
94. A A Balandin *Mul'tipletnaya Teoriya Kataliza* (The Multiplet Theory of Catalysis) Part III (Moscow: Izd. Mosk. Gos. Univ., 1970)
95. E I Klabunovskii *Zh. Fiz. Khim.* **47** 1353 (1973)
96. A A Vedenyapin, E I Klabunovskii, Yu M Talanov, N P Sokolova *Kinet. Katal.* **16** 1101 (1975)
97. V I Neupokoev, E I Klabunovskii, Yu I Petrov *Kinet. Katal.* **14** 447 (1973)
98. E N Lipgart, Yu I Petrov, E I Klabunovskii *Kinet. Katal.* **12** 1491 (1971)
99. I Yasumori *Pure Appl. Chem.* **50** 971 (1978)
100. I Yasumori, Y Inoue, K Okabe, in *Relations Between Heterogeneous and Homogeneous Catalytic Reactions. Colloque Int. Brussels, 1974 (Preprints)* A2
101. Y Nitta, T Imanaka, S Teranishi *J. Catal.* **80** 31 (1983)
102. D O Hubbell, P Rys *Chimia* **24** 442 (1970)
103. L H Gross, P Rys *J. Org. Chem.* **39** 2429 (1974)
104. V V Chernysheva, I P Murina, E I Klabunovskii *Izv. Akad. Nauk SSSR, Ser. Khim.* **757** (1983)
105. V V Chernysheva, Candidate Thesis in Chemical Sciences, Institute of Organic Chemistry, Academy of Sciences of the USSR, Moscow, 1984
106. Y Nitta, F Sekine, J Sasaki, T Imanaka, S Teranishi *J. Catal.* **79** 211 (1983)
107. A A Vedenyapin, E I Klabunovskii, Yu M Talanov, G Kh Areshidze *Izv. Akad. Nauk SSSR, Ser. Khim.* **2628** (1976)
108. Y Nitta, F Sekine, T Imanaka, S Teranishi *J. Catal.* **74** 382 (1982)
109. Y Nitta, F Sekine, T Imanaka, S Teranishi *Bull. Chem. Soc. Jpn.* **54** 980 (1981)
110. T Harada, Y Imachi, A Tai, Y Izumi *Stud. Surf. Sci. Catal.* **11** 377 (1982)
111. Y Nitta, T Utsumi, T Imanaka, S Teranishi *J. Catal.* **101** 376 (1986)
112. I Yasumori, Y Inoue, K Okabe, in *Catalysis: Heterogeneous and Homogeneous* (Eds B Dalmon, G Jannes) (Amsterdam: Elsevier, 1975) p. 41
113. Y Nitta, O Yamanishi, T Imanaka, S Teranishi *J. Catal.* **79** 475 (1983)
114. Y Nitta, T Utsumi, T Imanaka, S Teranishi *Chem. Lett.* **1339** (1984)
115. Y Nitta, T Imanaka, S Teranishi *J. Catal.* **96** 429 (1985)
116. E I Klabunovskii, N D Zubareva, G V Dorokhin *Izv. Akad. Nauk SSSR, Ser. Khim.* **1769** (1991)
117. Y Nitta, M Kawabe, T Imanaka *Appl. Catal.* **30** 141 (1987)
118. W M H Sachtler, in *Catalysis of Organic Reactions* (New York: Marcel Dekker, 1988) p. 189
119. Y Nitta, M Kawabe, H Kajita, T Imanaka *Chem. Express* **1** 631 (1986)
120. Y Nitta, M Kawabe, Lu Sun, Y Ohmachi, T Imanaka *Appl. Catal.* **53** 15 (1989)
121. A A Vedenyapin, T I Kuznetsova, E I Klabunovskii, V M Akimov, N B Gorina, V P Polyakova, E V Zykina *Izv. Akad. Nauk SSSR, Ser. Khim.* **2206** (1983)
122. T I Kuznetsova, I P Murina, A A Vedenyapin, V M Akimov, E I Klabunovskii *React. Kinet. Catal. Lett.* **37** 363 (1988)
123. A A Vedenyapin, E I Klabunovskii, N P Sokolova, in *Splavy Blagorodnykh Metallov* (Alloys of Noble Metals) (Moscow: Nauka, 1977) p. 187
124. Y Orito, S Niwa, S Imai *J. Synth. Org. Chem. Jpn.* **34** 236 (1976)
125. Y Orito, S Niwa, S Imai *J. Synth. Org. Chem. Jpn.* **34** 672 (1976)
126. Y Orito, S Niwa, S Imai *J. Synth. Org. Chem. Jpn.* **35** 672 (1977)
127. Y Orito, S Niwa, S Imai *J. Synth. Org. Chem. Jpn.* **35** 753 (1977)
128. *Jpn. P.* **7** 705 692; *Chem. Abstr.* **86** P146 521f (1977)
129. T Harada, M Yamamoto, S Onaka, M Imaida, H Ozaki, A Tai, Y Izumi *Bull. Chem. Soc. Jpn.* **54** 2323 (1981)
130. A Tai, T Kikukawa, T Sugimura, Y Inoue, T Ozawa, S Fujii *J. Chem. Soc., Chem. Commun.* **795** (1991)
131. M Nakahata, M Imaida, H Ozaki, T Harada, A Tai *Bull. Chem. Soc. Jpn.* **55** 2186 (1982)
132. A Tai, Y Imachi, T Harada, Y Izumi *Chem. Lett.* **1651** (1981)
133. A Tai, K Tsukioka, Y Imachi, Y Inoue, H Ozaki, T Harada, Y Izumi, in *Proceedings of the VIII International Congress on Catalysis* (Berlin-West: Verlag Chemie, 1984) p. V-531
134. A Tai, K Tsukioka, H Ozaki, T Harada, Y Izumi *Chem. Lett.* **2083** (1984)
135. A Tai, M Nakahata, T Harada, Y Izumi, S Kusumoto, M Inage, T Shiba *Chem. Lett.* **1125** (1980)
136. M Yoshikawa, T Sugimura, A Tai *Agric. Biol. Chem.* **53** 37 (1989)
137. T Kikukawa, Y Iizuka, T Sugimura, T Harada, A Tai *Chem. Lett.* **1267** (1987)
138. H U Blaser, M Müller, in *Heterogeneous Catalysis and Fine Chemicals II* (Ed. M Guisnet) (Amsterdam: Elsevier, 1991) p. 73
139. K Ito, T Harada, A Tai *Bull. Chem. Soc. Jpn.* **53** 3367 (1980)
140. J Bakos, I Toth, L Marko *J. Org. Chem.* **46** 5427 (1981)
141. *Catalog Wako Pure Chem.* (Osaka: Wako Pure Chemicals Inc.) p. 471, 547
142. H Brunner, M Muschiol, T Wischert, J Wiehl *Tetrahedron Asymmetry* **1** 159 (1990)
143. H B Kagan, in *Comprehensive Organometallic Chemistry* Vol. 8, Part 53 (Ed. G Wilkinson) (Oxford: Pergamon Press, 1982) p. 463
144. R Noyori *Science* **248** 1194 (1990)
145. I Ojima, T Kogure, K Achiwa *J. Chem. Soc., Chem. Commun.* **428** (1977)
146. R Spindler, V Pittelkow, H U Blaser *Chirality* **3** 370 (1991)
147. J Solodar *CHEMTECH* **421** (1975)
148. S Akutagawa *Appl. Catal. (A)* **128** 171 (1995)
149. H Takaya, K Mashima, K Koyano, M Yagi, H Kumobayashi, T Taketomi, S Akutagawa, R Noyori *J. Org. Chem.* **51** 629 (1986)
150. M Kitamura, T Ohkuma, M Takunaga, R Noyori *Tetrahedron Asymmetry* **1** 1 (1990)
151. M J Burk, J E Feaster, R L Harlow *Tetrahedron Asymmetry* **2** 569 (1991)

Gradient interpenetrating polymer networks: formation and properties

L M Sergeeva, L A Gorbach

Contents

I. Introduction	345
II. Methods of preparation and layer-by-layer analysis of the compositions of gradient interpenetrating polymer networks	345
III. Thermodynamic compatibility of the components in layers of gradient interpenetrating polymer networks	347
IV. Relaxation properties and transition temperatures	348
V. Mechanical properties of gradient interpenetrating polymer networks	350
VI. The use of the principle governing the formation of gradient interpenetrating polymer networks for the preparation of gradient lenses and other polymeric materials	351
VII. Conclusion	352

Abstracts. The methods of preparation and physicochemical and mechanical properties of gradient interpenetrating polymer networks (IPN) are examined. The results of studies on the viscoelastic properties as well as the strength and other mechanical characteristics in layers of gradient IPN are presented. The properties of the usual and gradient IPN of the same chemical nature are compared. Data are presented on the layer-by-layer variation of the thermodynamic compatibility of the components in gradient IPN. The bibliography includes 64 references.

I. Introduction

One aspect of the chemistry of macromolecular compounds which is of current interest is the modification of finished polymers and preparation of materials based on them. From this standpoint, the study of mixtures and blends of linear polymers (interpenetrating polymer networks) is promising, since one can vary indefinitely the structures and properties of polymeric materials obtained on the basis of such systems. Interpenetrating polymer networks (IPN) are polymer–polymer compositions consisting of two or more three-dimensional polymers (or of network and linear polymers) in which the individual networks are not chemically linked but are indistinguishable owing to the mechanical intertwining of the chains determined by the conditions of the synthesis.

Interpenetrating polymer networks are obtained by modifying polymers with a three-dimensional structure. Since the appearance of the term ‘interpenetrating polymer network’¹ much time has elapsed, but the principal studies in this field began in the 1980s^{13–17} and have continued up to the present time.

L M Sergeeva, L A Gorbach Division of Thermoreactive and Thermoplastic Polymers, Institute of the Chemistry of Macromolecular Compounds, National Academy of Sciences of Ukraine, Khar'kovskoe shosse, 48, 253160 Kiev, Ukraine. Fax (7-044) 552 40 64. Tel. (7-044) 559 47 95 (L M Sergeeva).

There are two monographs and several review articles^{2–12} in which the methods of preparation, the nomenclature, and the structure and properties of IPN of different types are considered. Analysis of the literature shows that gradient IPN are some of the most interesting and promising polymers. Sperling,⁴ Sergeeva and Lipatov,¹⁰ and Sergeeva¹¹ have considered gradient IPN very briefly.

Gradient IPN are mixtures of three-dimensional polymers (or mixtures of a three-dimensional and a linear polymer), the concentrations of the components in which vary along the cross-section of the specimen. Gradient IPN constitute the basis for the synthesis of promising polymeric materials used, for example, in medicine, optoelectronics, wave optics, and instrument making, for vibration- and sound-proofing, and in other fields. The volume characteristics of polymeric materials based on IPN may remain unchanged. However, the overall characteristics of the composite are improved.

II. Methods of preparation and layer-by-layer analysis of the compositions of gradient interpenetrating polymer networks

The first studies involving the preparation and investigation of gradient IPN were associated with the search for and development of materials for medicine.^{13–17} The interpenetrating polymer networks used for such purposes can be obtained only by the successive hardening method. This method consists of the following procedures: in the first stage, the preformed polymer (the first component) is kept in a monomer, which subsequently polymerises with formation of a second polymer. Swelling is interrupted at a certain stage, before the attainment of equilibrium, after which the second polymer is obtained, its concentration in the matrix polymer varying perpendicular to the surface as a consequence of the slowness of the swelling and diffusion processes in the matrix network. This results in the formation of an IPN, the properties of which differ both from those of the individual polymers and from the properties of the IPN of the same chemical nature but obtained by the successive hardening method under equilibrium conditions.

Since in the preparation of gradient IPN there is a stage involving the nonequilibrium swelling of the matrix network in the monomers, problems arise, associated with the influence of various factors on the rate of diffusion of the monomers into the matrix network and hence with the distribution of the second

Received 27 March 1995

Uspekhi Khimii 65 (4) 367–376 (1996); translated by A K Grzybowski

polymer through the thickness of the matrix. In order to investigate the nature of the distribution of the polymers entering into the composition of the IPN as a function of thickness, use is made as a rule of the layer-by-layer elemental analysis. In the gradient IPN based on polystyrene (PS) and polyacrylonitrile (PAN) (with ethylene dimethacrylate as the cross-linking agent),¹³ PS served as the matrix network and PAN was concentrated in the surface layer of PS with a definite concentration gradient. In order to establish the nature of the distribution of PAN in PS, layers 0.05 mm thick were removed and their nitrogen content assayed chemically. It was shown that the highest content of PAN (~50%) occurs near the surface of the specimen of the gradient IPN. The concentration of PAN near the surface is also confirmed by the finding that the specimens of the test IPN are more resistant to the action of hydrocarbons, for example benzene, in contrast to pure PS.¹³ It has been suggested that the diffusion of the monomer into the matrix network in the test specimen generally obeys Fick's law, although there are certain deviations.¹⁴ For systems such as poly(methyl methacrylate)–polymethacrylate, the layer-by-layer methods of chemical analysis proved unsuitable, since both polymers contain the same elements.

The rate of diffusion of the monomers during the preparation of gradient IPN and the subsequent distribution of the polymers probably depend on the monomer concentration in the solvent (if such is used), on the concentration of the cross-linking agent, and other factors. These problems have been examined in detail in a study of the gradient IPN based on polyester urethanes (PU) and cross-linked polyacrylamide (PAA).¹⁵ The polyester urethanes were obtained by a two-stage method from diphenylmethane diisocyanate and poly(propylene glycol) using diaminoethane as the lengthening agent. The polyester urethane contained rigid domains — physical cross-links forming a network. The IPN specimens were obtained by swelling PU plates in a solution containing acrylamide (AA), a cross-linking agent (tetraethylene glycol dimethacrylate), and an initiator. This was followed by the polymerisation of the AA. The overall amount of the PAA was determined from the difference between the masses of the initial PU film and that obtained after its saturation by the PAA. It has been shown for this system that an increase in the monomer concentration in the swelling mixture leads to a steady increase in the PAA concentration in the IPN, although the dependence of its content on the AA concentration in solution is nonlinear. Naturally, an increase in the PAA content in the IPN leads subsequently to an increase in the degree of swelling of the specimen in water. An increase in the initiator concentration in the AA solution also leads to an increase in the PAA content in the IPN, but only up to a certain limit, beyond which the influence of the initiator concentration is insignificant. The change in the concentration of the cross-linking agent influences non-monotonically the PAA content in the IPN: there is an optimum concentration ensuring the maximum PAA content, but the capacity of the IPN for swelling in water decreases monotonically under these conditions.

The concentration of the monomer and its distribution in the matrix network are naturally to a large extent determined by the duration of the swelling of the initial network in the monomer. Thus, the influence of the swelling time (from 5 to 30 min) on the PAA content in the IPN has been investigated for the PU–PAA system.¹⁶

It has been established that the dependence of the fraction of PAA in the IPN ($\omega = W_{\text{PAA}}/W_{\text{IPN}}$) on the swelling time is described by the equation

$$\omega_t = \omega_\infty(1 - e^{-kt}),$$

where ω_t and ω_∞ are respectively the fractions of PAA in the IPN during polymerisation after swelling for a time t and after equilibrium swelling.

Apart from varying the swelling time, other procedures may be used to set up a concentration gradient along the thickness of the IPN layer, for example one can employ cross-linking agents with a higher molecular mass or the diffusion of the cross-linking agent.¹⁶ The latter method can be described as follows: the matrix network is kept in the monomer solution with the initiator until the attainment of equilibrium, after which the swollen matrix network is placed for a time in a solution of the cross-linking agent. It was found that, when this procedure is employed, the fraction of PAA in the IPN based on PU and PAA is independent of the time during which the swollen PU is kept in the solution of the cross-linking agent.

The Fourier transform IR spectroscopic method¹⁶ makes it possible to obtain more accurate information about the nature of the distribution of polymers in gradient IPN based on PU and PAA compared with chemical analysis.^{14,15} It has been established¹⁶ that, when the partial swelling method is employed (the method involving different exposure times), PAA concentrates mainly at the surface of the specimen (the depth of penetration by PAA does not exceed 10 μm). The PAA concentration gradient along the thickness has also been observed in the preparation of IPN after the attainment of the equilibrium swelling of the matrix network in the monomer, but it is not quite so distinct as in the previous case. Finally, the diffusion of the cross-linking agent and the variation of its molecular mass have virtually the same influence on the PAA concentration gradient in PU.

Like the usual IPN, 'direct' and 'reverse' gradient IPN may be synthesised. The system based on poly(methyl methacrylate) (PMMA) and poly(chloroethyl acrylate) (PCEA) have been obtained in two ways.¹⁷ In the first case, the PMMA obtained beforehand was swollen in chloroethyl acrylate (CEA) and the CEA was then polymerised. The initiator was fluorobutyl ether from petrol and the cross-linking agent was ethylene glycol dimethacrylate. In the second case, PCEA was swollen in methyl methacrylate (MMA) and the latter was subsequently polymerised. Gradient IPN containing 30 mass % of PCA in a PMMA matrix and up to 50 mass % of PMMA in a PCEA matrix were obtained in this way. In order to determine the profile of the concentration gradient (in the present instance of chlorine) in the test system, chemical analysis was employed, as in certain other gradient IPN.

Fig. 1 presents the gradient in the distribution of PCEA in specimens obtained by the first method. Evidently the PCEA content decreases sharply on moving away from the surface, particularly when its concentration in the gradient IPN is low whereupon the main bulk of PCEA concentrates at the surface of the specimen.

It is noteworthy that in the usual IPN (Fig. 1, curve 4) i.e. those obtained by the successive hardening method under the conditions of the equilibrium swelling of the matrix network in the monomer, the PCEA concentration does not change on moving away from the surface of the specimen. This conflicts with data obtained for the PU–PAA system,¹⁴ where a concentration gradient with respect to the thickness was established even for the usual IPN. It is most likely that this may be induced by the time during which the PU specimens are kept in PAA, before the start of the polymerisation, being insufficient.

For specimens of the second series, the PMMA content does not diminish quite so sharply (judging from the growth in the PCEA content with increasing thickness) on moving away from the specimen surface.

Gradient IPN based on PU and polyacrylate copolymers have been obtained^{18,19} by a method involving the swelling of a preformed network PU without attaining the equilibrium distribution of the diffusants and subsequent photopolymerisation of the reactants. The composition of the components in the layers was determined by comparing the glass points (T_g) of the

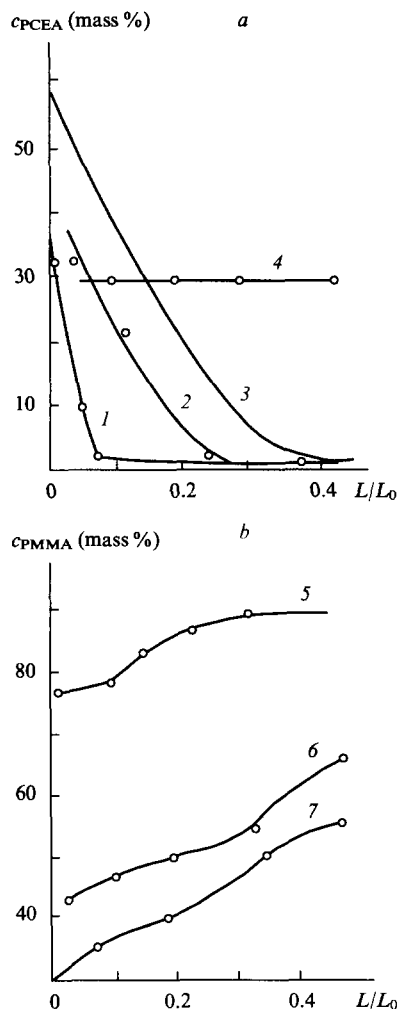


Figure 1. Distribution of PCEA and PMMA in specimens of gradient polymers (1–3) and IPN (4–7) with a PMMA matrix (a) and a PCEA matrix (b) for different PCEA and PMMA contents. c_{PCEA} (mass %): (1) 10; (2) 20; (3) and (4) 30; c_{PMMA} (mass %): (5) 10; (6) 30; (7) 50; L/L_0 = relative thickness of the specimen.

usual IPN and gradient IPN of the same nature and also by elemental analysis.^{20–33}

Free-radical initiation was used in the studies described above to obtain the second polymer with a concentration gradient in the first polymer-matrix. The use of polycondensation appears at first sight impractical, since the reaction can occur during the swelling process. After the attainment of equilibrium, the reactants must then be present in the matrix in almost equivalent proportions for the formation of a high-molecular-mass condensation polymer. Nevertheless, it has been shown³⁴ that polycondensation can be used extremely successfully for the preparation of gradient IPN. For this purpose, one of the reactants is initially kept in the preformed polymer-matrix and the matrix is then placed in the second reactant or its solution. Diffusion and the polycondensation reaction between the reactants take place simultaneously under these conditions. Such a process may be referred to as diffusion-controlled polycondensation occurring in the matrix in the mixing zone of the two components.

A gradient IPN, the matrix of which consisted of the 2-hydroxyethyl methacrylate–*N*-vinylpyrrolidone copolymer while the polymer with a concentration gradient was polyurethane based on a diol or a triol and 1,6-diisocyanato-2,4,4(2,2,4)-trimethylhexane, was obtained in this way.

III. Thermodynamic compatibility of the components in layers of gradient interpenetrating polymer networks

At a certain stage during the formation of the IPN, a microphase separation of the components begins as a consequence of thermodynamic incompatibility caused by the formation of heterogeneous three-dimensional structures.^{3,20–22} The phase separation conditions are determined both by the composition of the IPN and by the rate of formation of the two networks. Apparently, the separation in each layer of the gradient IPN occurs to different extents, since the component ratio undergoes continuous layer-by-layer variation. It is noteworthy that the microphase separation is not completed in the IPN formed, which results in the formation of nonequilibrium 'frozen structures', which are nevertheless kinetically stable.^{3,10}

The thermodynamic parameters which make it possible to infer the compatibility of the components in layers at different distances from the surface of the specimens have been estimated²³ in relation to the gradient IPN based on polyurethane and cross-linked poly(butyl methacrylate). The changes in the free energy of mixing of the network components Δg_x were estimated by analysing the isotherms for the sorption of benzene vapour by the IPN specimens. Fig. 2 presents the variation of Δg_x in IPN layers on moving away from the specimen surface (from the first to the fourth layer). Evidently, Δg_x is positive, so that the components are incompatible, as in the majority of the usual IPN.^{3,24,31–36} The absolute value of Δg_x depends on the depth of the layer in the specimen. This fact is due not only to changes in the composition of the networks as the core of the specimen is approached but also to changes in the phase separation conditions in each layer of the IPN produced.

The different degrees of compatibility of the components in the IPN layers influence the structure formed and at the same time the properties of the component as a whole. Each layer in a gradient IPN can be regarded as an independent two-phase IPN with a different phase composition.²³ By considering each phase arising during the incomplete phase separation as an independent quasi-equilibrium IPN,²⁴ the authors²³ estimated the compositions and ratio for these phases. For this purpose, they used Fox's equation,²⁵ proposed for compatible polymer blends, and the glass points obtained by the dilatometric method both for the individual networks and for the networks in the layers of the gradient IPN. In the gradient IPN based on polyurethane, T_g refers to one of the phases enriched in PU or the copolymer. The volume fractions of PU in the PU-enriched phase and of the copolymer in the copolymer-enriched phase were calculated from the corresponding glass points in the IPN and in the layers of the gradient IPN.

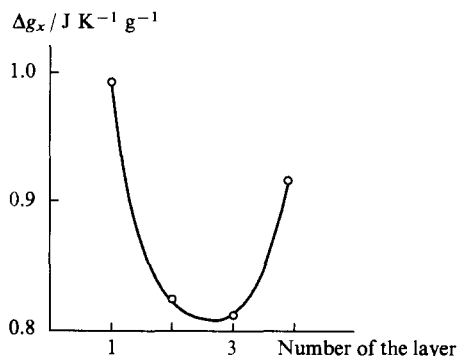


Figure 2. Variation of the free energy of mixing of the components in the layers of gradient IPN.

Analysis of the data obtained led to the conclusion that, as a consequence of the incomplete separation, two phases are formed in the layers of the gradient IPN, the composition of which depends on the phase separation conditions in each layer. As a result of the variation of the composition (and hence of the thermodynamic compatibility of both networks), the degree of segregation in each layer is different from that for the usual IPN having the same composition.²³

Thus gradient IPN are multicomponent systems, the properties of which are determined by the presence not only of the composition gradient but also of the phase composition gradient and the phase ratio in the microphase systems.

IV. Relaxation properties and transition temperatures

A considerable proportion of the studies on gradient IPN have been devoted to dynamic mechanical properties. Information about the transition temperatures and the compatibility of the components in the test systems can be obtained from these data. Thus two transition temperatures have been observed for the IPN based on PMMA and PCEA (PMMA matrix)¹⁷ in a study of the temperature dependence of the modulus of dynamic losses: one at 263 K, corresponding to PCEA, and the other at 383 K, corresponding to PMMA. This indicates unambiguously the occurrence of phase separation and the incompatibility of the components in the IPN.

However, a single transition in the region between the glass points T_g of the corresponding homopolymers has been observed for the same IPN but with a PCEA matrix. The transition temperature shifts to 323 K at a PMMA concentration up to 50%, which constitutes evidence, according to Martin et al.,¹⁷ in favour of the absence of phase separation. As will be shown below, the latter conclusion is hardly legitimate.

The mechanical relaxation properties of a polymer with a composition gradient have been modelled for a qualitative estimation of the influence of the change in composition on the viscoelastic properties of a polymeric specimen with a glass

point gradient.²⁶ A system consisting of eleven plates, differing in the glass points by a known number of degrees determined by the gradient, was adopted as the model gradient material for this purpose.

Fig. 3 presents the calculated temperature variations of the real component of the complex modulus of shear ($\lg G'$) of the model gradient material, the layers of the material being deformed in parallel. The presence of a glass point gradient leads to the appearance of characteristic temperature variations, which are less steep the higher the gradient. At the same time, with increase in the temperature gradient, the height of the maximum of the tangent of the angle of mechanical losses ($\tan \delta$) decreases, becomes broader, and shifts by 8–10° into the low-temperature region compared with the position of the $\tan \delta$ maximum corresponding to a high glass point. It was also established that, in the formation of the specimen in the direction coinciding with the direction of the gradient (i.e. for the consecutive deformation of the layers), the nature of the temperature dependences of $\lg G'$ and $\tan \delta$ is predetermined by the properties of the components having low glass points. However, the $\tan \delta$ maxima for the gradient materials are shifted towards higher temperatures by 5–7° relative to the $\tan \delta$ maximum corresponding to the 'lowest temperature' component and the changes in the height of the maxima are slight.

The theoretical data obtained led to the conclusion²⁶ that the temperature range of the transition state of the gradient materials expands significantly, increasing with increase in the temperature gradient. An important feature of materials of this kind is the anisotropy of the properties in different directions, which is manifested most strikingly in limiting cases where the direction of the deformation is parallel or perpendicular to the direction of the gradient.

Experimental studies^{18,19} have confirmed to some extent the above theoretical conclusions. Gradient IPN based on PU with a network structure and the copolymer of butyl methacrylate with triethylene glycol dimethacrylate¹⁸ or oligo(carbonate-methacrylate)¹⁹ were obtained. The usual IPN having the same composition were also obtained for comparison.

Fig. 4 presents the temperature variations of $\tan \delta$ for the usual IPN based on PU and the butyl methacrylate-oligo(carbonate-methacrylate) copolymer and also for their components.¹⁹ Similar variations have also been obtained for another IPN of a similar chemical nature.¹⁸ Evidently the $\tan \delta$ maximum is observed at 248 K for PU and at 366 K for the copolymer. For the IPN with 10 mass % of the copolymer, the temperature dependence is characterised by the occurrence of the relaxation α -transition, corresponding to the acrylate

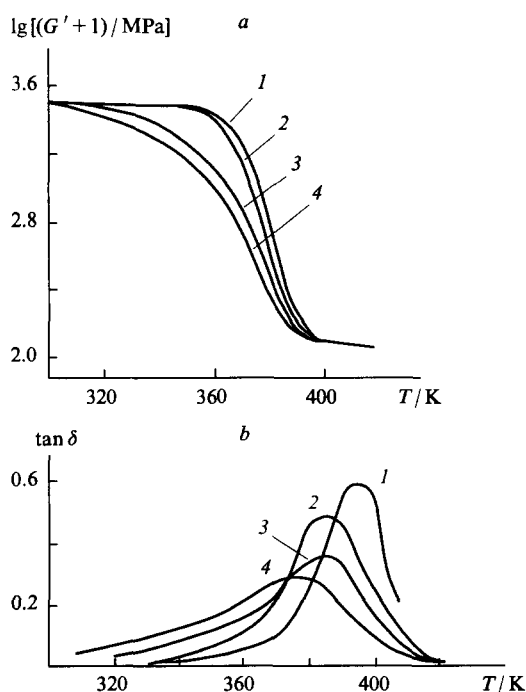


Figure 3. Calculated temperature variation of $\lg G'$ (a) and $\tan \delta$ (b) for a gradient model ($n = 11$) with different T_g gradients $[(dT_g/dx)/K]$: (1) <20; (2) 20; (3) 50; (4) 70 with parallel deformation of the components.

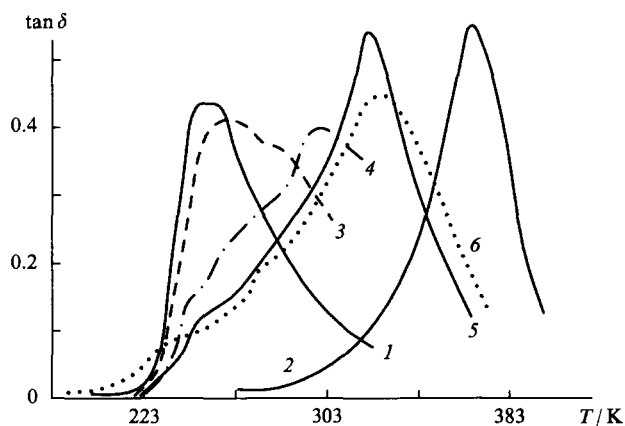


Figure 4. Temperature variations of $\tan \delta$ for PU, the copolymer, and the IPN based on them with different component ratios: (1) PU; (2) copolymer; (3)–(6) IPN containing 10, 20, 30, and 40 mass % of the copolymer respectively.

component, and is manifested by a distinct shoulder on the descending branch of the curve in the temperature range 273–303 K (Fig. 4, curve 3). With increase in the fraction of the copolymer in the IPN, the relaxation maximum corresponding to the copolymer is manifested more distinctly and the temperature range where this transition occurs shifts, with increase in the copolymer concentration in the IPN, towards the temperature range of the relaxation α -transition of the initial copolymer (Fig. 4, curves 2–6).

The nature of curves 3–6 in Fig. 4 shows that the IPN are two-phase systems in which both components form continuous phases.²⁷ The expansion of the temperature range of the α -transition of the copolymer indicates the generation of an extensive interfacial region in the IPN during the formation of the acrylate network under these conditions.

Calculation of the segregation coefficients of the components (α) by the method proposed by Rosovitskii and Lipatov²⁸ showed that α for all the IPN is in the range from 0.3 to 0.5 and tends to fall with increase in the fraction of the copolymer in the IPN, i.e. the degree of segregation of the components diminishes.

Thus the usual IPN are two-phase systems. However, the observed shift of the $\tan \delta$ maximum along the temperature scale for the copolymer in the IPN compared with its position in the individual network and also its broadening indicate an incomplete phase separation of the components in the formation of the IPN. This confirms data indicating the thermodynamic incompatibility of the components in the IPN of the same chemical nature.

The gradient IPN-1 IPN-2 with different copolymer contents, 30% and 15% respectively, have been investigated layer-by-layer, both along the copolymer concentration gradient and at right angles to it.¹⁹ Fig. 5 presents the temperature variations of $\tan \delta$ for specimens obtained sections at right angles to the concentration gradient. Analysis of the family of curves and their shape as well as the intensity and relative positions on the temperature scale of the maxima corresponding to PU and the copolymer led the authors¹⁹ to the conclusion that, firstly, a copolymer distribution gradient is indeed observed as one moves away from the surface of the specimen and, secondly, the continuity of both phases in the gradient IPN-1 containing a greater amount of the copolymer is observed at a greater distance from the specimen surface than for IPN-2.

The average concentrations of the copolymer in the layers of the gradient IPN were calculated from the observed linear dependence of the glass point of the copolymer (T_g is the temperature corresponding to the high-temperature $\tan \delta$ maximum) on composition for the usual IPN. Thus the first three layers in IPN-1 contained 38.6, 26.9, and 15.3% of the copolymer, while the contents of the copolymer in the first and second layers in IPN-2 were respectively 38.6 and 10.6 mass %, i.e., for a greater average concentration of the copolymer in the specimen, a more uniform distribution with respect to the depth in the specimen is observed.

The study of the viscoelastic properties of sections obtained along the copolymer concentration gradient revealed certain differences (Fig. 6).^{18,19} For specimens representing a complete section through the gradient system (Fig. 6, curves 2), a

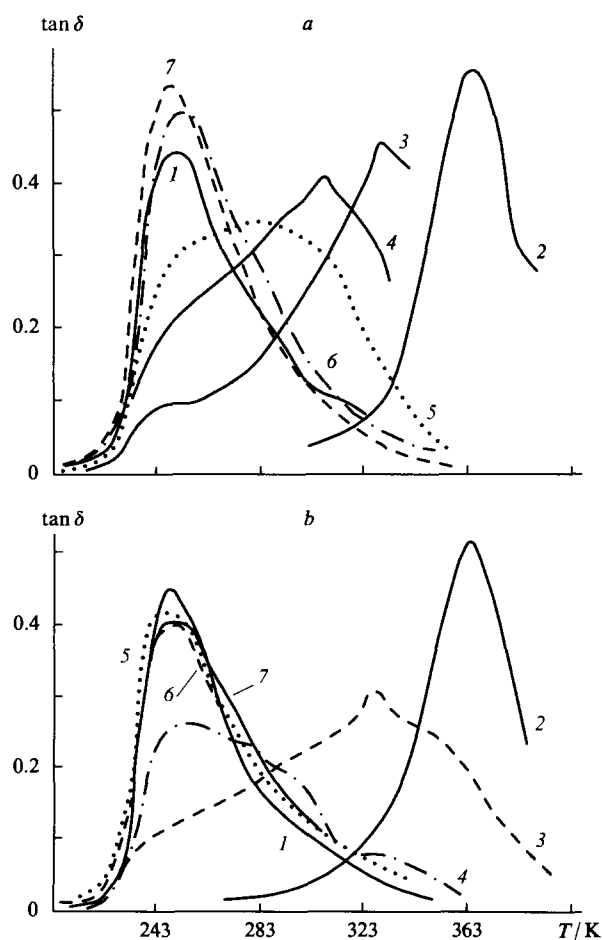


Figure 5. Temperature variations of $\tan \delta$ obtained for perpendicular sections through gradient IPN-1 (a) and IPN-2 (b): (1) PU; (2) copolymer; (3)–(7) the first, second, third, fourth, and fifth sections respectively.

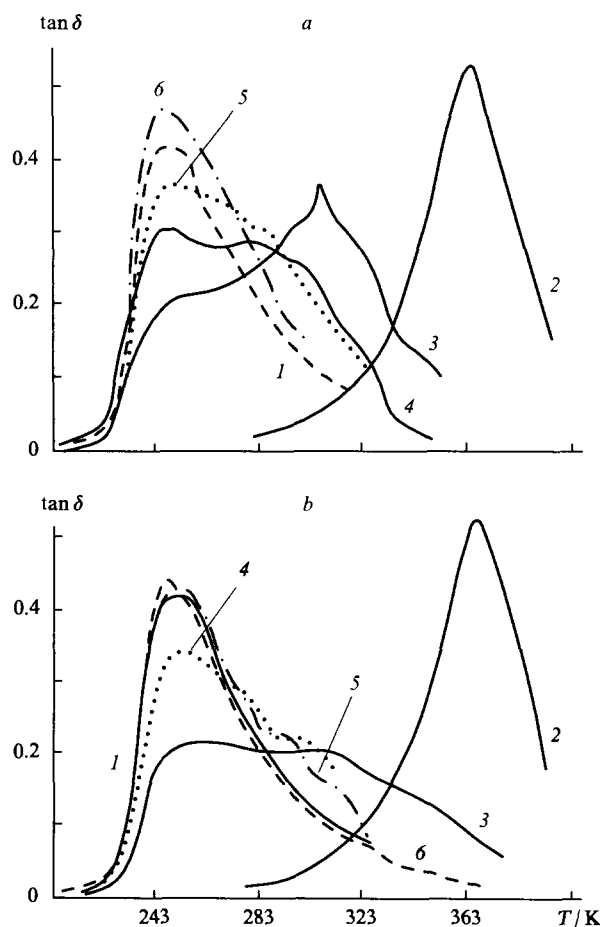


Figure 6. Temperature variations of $\tan \delta$ for specimens obtained from longitudinal sections of gradient IPN-1 (a) and IPN-2 (b): (1) PU; (2) copolymer; (3)–(6) the first, second, third, and fourth sections respectively.

maximum is observed in the range 233–363 K. For IPN-1, the maximum is observed at 308 K in the region corresponding to the transition in the copolymer, while in the region of the relaxation α -transition in PU there is a distinct shoulder. A single broad maximum in the form of a plateau, overlapping the region of the relaxation transitions in both components, is observed for IPN-2.

The presence of broad maxima on the $\tan \delta$ – T curves is probably not a result of the compatibility of the components in the IPN but indicates a superposition of a large number of relaxation maxima in layers with gradually varying compositions.¹⁸ These data agree with the results of modelling²⁶ and also account for the appearance of a single but broad transition for the PMMA–PCEA system, which has been erroneously regarded¹⁷ as evidence for the compatibility of the components.

The damping properties of the gradient and the usual IPN based on PU and the butyl methacrylate–oligo(carbonate-methacrylate) copolymer have been compared¹⁹ on the basis of the analysis of dynamic mechanical spectroscopic data for these systems. One of the integral parameters characterising the ability of a material to scatter mechanical energy is known^{29,30} to be the area under the curve describing the temperature variation of the imaginary component of the complex modulus of elasticity ($S_{E''-T}$), which is determined by the intensity and width of the temperature range of the relaxation transition. For all the test specimens, this parameter has been calculated by the method of trapezia on a computer. For specimens of the usual IPN, the values of this parameter have been calculated assuming additivity.¹⁹

Examination of the results revealed that in general the damping properties of the IPN investigated are superior to those of the initial components (the $S_{E''-T}$ for the IPN are higher). For gradient IPN specimens sliced at right angles to the copolymer concentration gradient, $S_{E''-T}$ diminishes with decrease in the concentration of the copolymer, whereas for sections along the $S_{E''-T}$ gradient the values of $S_{E''-T}$ actually increase with decrease in the copolymer concentration, i.e. the anisotropy of the properties is observed, which confirms the conclusions reached by Lipatov et al.²⁶

Furthermore, it was found that the variation of the damping properties of the usual and gradient IPN is not the same for chemically similar IPN specimens: thus the damping characteristics of the gradient IPN based on PU and the butyl methacrylate–ethylene glycol dimethacrylate copolymer¹⁸ are superior to those of the usual IPN, whereas the opposite picture is observed for the IPN based on the same PU and the butyl methacrylate–oligo(carbonate-methacrylate) copolymer.¹⁹

Thus analysis of the results of the study of the relaxation characteristics of the usual and gradient IPN indicates a significant difference between their viscoelastic properties. Furthermore, the results of the modelling agree satisfactorily with the experimental data.

V. Mechanical properties of gradient interpenetrating polymer networks

The strength characteristics of gradient IPN have been investigated in some studies. Thus, in a study of the IPN based on PMMA and PCEA, Martin et al.¹⁷ established that the gradient IPN differ from the usual IPN and the homopolymers by a higher decomposition energy and that the deformation of gradient IPN with a PMMA matrix and 30 mass % of PCEA increased by an order of magnitude on decomposition compared with the pure PMMA, while the strength of the IPN with a PCEA matrix and 50 mass % of PMMA is 10–15 times higher than that of PCEA.

The study of the mechanical characteristics of gradient IPN based on PMMA and methyl methacrylate (MMA) showed¹³ that, whereas pure PMMA decomposes (at 373 K) on 2% extension, the gradient IPN containing ~10 mass % of MMA

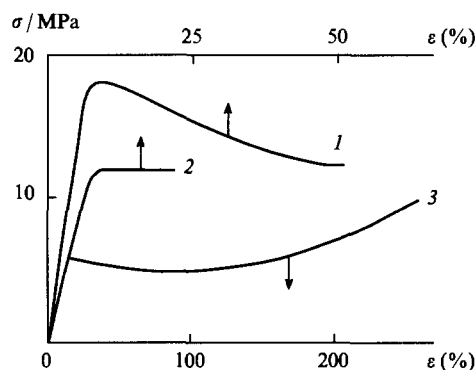


Figure 7. Stress–deformation curves for a gradient polymer (1), IPN (2), and a statistical methyl methacrylate–methyl acrylate copolymer (3).

breaks after 10% extension. The introduction of 19 mass % of MMA leads to the disruption of the IPN specimen only after 80% extension. Fig. 7 presents the stress–deformation relations for PMMA–MMA specimens obtained in the form of a gradient polymer, an IPN obtained by successive hardening, and a statistical copolymer.¹³ Evidently, the gradient polymer is subjected to the highest stress at rupture and the area under the stress–deformation curve is greatest for this polymer.

Comparative study of the mechanical properties of the usual and gradient PU-based IPN and the butyl methacrylate–triethylene glycol dimethacrylate copolymer (for the same component ratios) showed (Fig. 8) that the highest strength parameters are observed for the gradient IPN:¹⁸ the area under the stress–deformation curve increases and so does Young's modulus (the slope of the initial section of curve 3 is greater than that of curve 2).

Thus when a gradient of the concentrations of the components is established in a polymeric material, there is a tendency towards an improvement in its mechanical properties. Several hypotheses have been put forward to account for these phenomena.^{13,17} According to one of them, a gradient IPN is regarded as an assembly of an infinite multiplicity of layers, the compositions and moduli of elasticity of which vary monotonically on moving away from the surface the bulk of the specimen. On deformation of the specimen, all the layers are stretched to the same extent and the stress in each layer corresponds to its modulus. Such distribution of stresses promotes the development of plastic deformation, and not brittle rupture, and leads to an increase in the elongations at rupture and rupture energies.

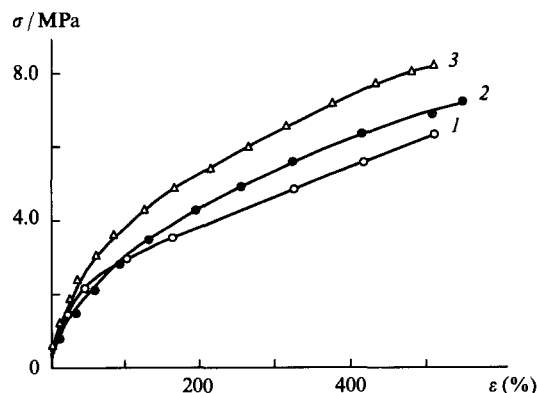


Figure 8. Stress–deformation curves for polyurethane (1), a usual IPN containing 33.7 mass % of the butyl methacrylate–triethylene glycol dimethacrylate copolymer (2), and a gradient IPN containing 33.7 mass % of the copolymer (3).

Another hypothesis attributes the increase in the strength of gradient IPN to a decrease in the defectiveness of the surface layers. One can postulate that the introduction of an elastomer into the surface layer of a 'rigid' matrix inhibits the growth of cracks and increases thereby the stress necessary to initiate cracks. The study of the morphology of the specimens confirmed that the presence of an elastic shell can increase the stress corresponding to the formation of 'cracks'.¹⁷ The near-surface layers (after the rupture of the specimen) proved to be smoother than the internal regions of the specimen.

In order to confirm or reject the hypotheses proposed, further studies involving the use of a wider range of gradient IPN are needed.

VI. The use of the principle governing the formation of gradient interpenetrating polymer networks for the preparation of gradient lenses and other polymeric materials

Polymers with nonlinear optical properties have found extensive application in engineering at the present time,^{35,36} in particular a series of polymeric materials based on IPN with nonlinear optical characteristics have been obtained.^{37–39} These have definite advantages over both inorganic materials and polymers of other classes.^{38,39} Studies on the creation of gradient or graded-index lenses — light-focussing elements based on transparent materials with a parabolic distribution of the refractive index — are of interest in this connection.^{40–51} Such lenses have been used successfully in optoelectronics and wave optics (adjusting devices, light beam dividers), in instrument making, and medical engineering.

In most of the studies, the synthesis of graded-index lenses is accompanied by the formation of gradient IPN. The possibility of obtaining graded-index lenses from gradient polymers was first pointed out by Ohtsuka.⁴⁰ For this purpose, methyl methacrylate was allowed to diffuse into a cylindrical gel matrix consisting of a diallyl isophthalate (DAIP) prepolymer (70 mass % of the monomer + a mixture of linear and cross-linked polymers), the refractive index of methyl methacrylate being lower than that of DAIP. The distribution of the refractive index generated during the diffusion process was 'fixed' by additional polymerisation. Refractive index differences $\Delta n_D \approx \pm 0.04$ were then obtained, which is appreciably beyond the possibilities of the diffusion technology in inorganic glasses.⁴²

A similar polymer system has been used^{41,42,44} to obtain light-focussing elements (LFE). The physicochemical processes constituting the basis of the preparation of such elements were investigated in detail. Exchange diffusion processes in the DAIP–MMA system were examined using Fick's equation. The influence of various parameters (diffusion time, temperature, diffusant concentration, etc.) on the variation of the refractive index in the LFE was analysed.

Thus it has been established⁴¹ that the variation of the diffusion coefficient with the diffusant concentration does not alter significantly the optimum diffusion conditions and in many instances impairs the distribution of n_D compared with the case in which there is a constant diffusion coefficient. In order to create the maximum change in n_D along the LFE cross-section, it has been suggested⁴⁰ that a polymerisation initiator (benzoyl peroxide) be added to the diffusant (MMA). Bearing in mind that Fick's equation cannot be used to calculate the n_D profile under conditions where polymerisation reactions take place, the authors⁴¹ suggested that account be taken of the cessation of the diffusion of some of the MMA and DAIP molecules. They modified a series of equations for the calculation of the diffusion coefficient and calculated the changes in the MMA and DAIP concentrations during the preparation of the LFE and also the variation of the n_D profile along the specimen cross-section.

It was noted⁴¹ that the use of monomers capable of forming a network in the early stages of the polymerisation is very important from the standpoint of the n_D distribution obtained. In the study of the influence of temperature on the variation of the n_D distribution along the LFE cross-section, it was shown that, up to certain temperatures, the polymerisation reaction has an insignificant influence on the n_D profile, but at high temperatures, for example at 353 K, the influence of polymerisation is reflected in a change in the distribution of n_D after only 20 min. In the preparation of polymeric LFE, account must also be taken of the disappearance of the n_D gradient along the LFE cross-section and its subsequent restoration.⁴¹

An important conclusion reached by Marturunkakul et al.³⁹ and Ohtsuka⁴⁰ is that it is essential to select systems capable of increasing sharply the rate of polymerisation after the attainment of a specified degree of conversion. This property, called the gel effect, is characteristic of many vinyl monomers during their radical block polymerisation. The gel effect plays an important role in the formation of gradient lenses from gradient IPN based on DAIP and MMA⁴⁴ and on styrene–triethylene glycol dimethacrylate (TGDM)–MMA.^{43,45,50} A characteristic feature of the latter system is that, at a certain instant after the beginning of the diffusion of MMA into the polymerised matrix consisting of styrene and TGDM, rapid spontaneous copolymerisation of the matrix monomers and the diffusant up to virtually complete conversion takes place. After the diffusion process has ceased, the n_D profile generated at the given instant is fixed.

The problem is how to make sure that the fixation of the distribution of n_D should occur at the instant when it is closest to the ideal form^{43,48} because one then rules out the separate stage involving the fixation of the distribution of the refractive index established during the diffusion process (characteristic of other systems⁴⁸), in which it is difficult to avoid the diffusion-induced impairment of the distribution of n_D .

A mathematical model has been proposed^{43,45} for the establishment of the n_D distribution profile and the following conclusion was reached on the basis of the analysis of the results of the modelling of the diffusion and copolymerisation processes in the styrene–TGDM–MMA system: if the chosen amount of initiator and the temperature are such that the gel effect begins for a distribution n_D close to that given by the expression

$$n_D(r) = n_0 \operatorname{sech}(\alpha r) \simeq n_0 \left(1 - \frac{\alpha^2 r^2}{2} \right),$$

where n_0 is the refractive index along the axis of the lens, r is the radius of the graded-index lens and α is the distribution constant, then the distribution is preserved and the gradient lens obtained is of good optical quality. The results of the modelling have been confirmed experimentally and the optimum conditions for the preparation of polymeric gradient elements based on the copolymer of styrene with TGDM and MMA have been proposed.^{43,45}

Further study of the molecular diffusional exchange in the DAIP–maleic anhydride (matrix)–MMA (penetrant) system established the occurrence of diffusional anomalies⁵² when specimens having different diameters are employed. It was established that a disk model for the description of the molecular diffusional exchange in the system investigated is applicable to specimens having diameters between 5 and 12 mm. On the other hand, for specimens with larger diameters (from 12 to 30 mm), a sharpening of the diffusion was, as it were, observed and in addition the experimental refractive index distribution (RID) curves differed from the Fick RID.^{53,54} Hui et al.⁵⁴ put forward ideas according to which the volume fraction of the penetrant on the surface may increase to an equilibrium value, the rate of change of the volume fraction of the penetrant (at any point on the surface) being determined by

the rate of deformation of the creep, which depends on the osmotic pressure arising in the polymer during swelling. Here it has been suggested that the longitudinal viscosity diminishes exponentially with increase in the concentration of the penetrant. Bukhbinder et al.⁵² suggested that the concentration of the penetrant at the boundary increases fairly slowly, so that for short times (diffusion into specimens having small diameters) conditions are not attained under which there is a sharp decrease in viscosity accompanied by an abrupt increase in the diffusion coefficient. Thus the mechanism of the diffusion in specimens with small diameters is close to the Fick mechanism, whereas, on passing to specimens with a large diameter (an increase in the diffusion time), the equilibrium concentration reaches the threshold value. After the attainment of the threshold value, there is a sharp jump in the diffusion coefficient and a front begins to be formed on the RID curves. This front can be regarded as the moving boundary of the penetrant, which is equivalent to a decrease in the effective diameter of the specimen as a function of time. The proposed explanation for the diffusional anomaly is supported by the fact that a large change in n_D along the cross-section, virtually equal to the theoretical change, can be attained in large-diameter specimens, in contrast to specimens with a small diameter. Thus a reasonable explanation of the observed diffusional anomaly has been found and an interesting conclusion has been reached: the geometrical factor (the change in the dimensions of the specimens) is important in the preparation of graded-index lenses with a specified RID.

The possibility of using gradient IPN of different nature for the preparation of polymers with hard external, soft internal, and intermediate zones and with a continuously varying composition has been demonstrated.⁵⁵

In order to obtain materials with a surface susceptible to hydration, which can replace protective coatings in arteriovenous shunts, a gradient IPN based on oxyethylene methacrylate monomers and a silicone rubber has been employed.⁵⁶

The possibility of forming grains from hydrogels, the surface layer of which consists of a gradient IPN acting as a membrane permitting the regulation of the migration of the water-soluble medicinal substances absorbed by the grains, has been demonstrated in relation to gradient IPN based on polyurethane and cross-linked polymers consisting of 2-hydroxyethyl methacrylate and *N*-vinylpyrrolidone.^{34, 57–59} This makes it possible to create new forms of long-acting medicinal preparations.

Gradient IPN are promising for the preparation of vibration- and sound-proofing materials.^{4, 18} It is possible to apply the principle governing the formation of gradient IPN in other fields as well. Thus, the use of IPN as adhesives, especially for polymeric substrates, is promising. It has been shown⁵⁹ that in this instance an adhesion junction consisting of a gradient IPN is formed. The authors used the IPN based on polyurethane and the MMA–triethylene glycol dimethacrylate (TEGDM) copolymer for glueing vulcanised natural rubber (NR) to poly(vinyl chloride) (PVC). It was established that, as a consequence of the diffusion of the MMA and TEGDM monomers into the polymeric materials and subsequent hardening of the composition, two gradient IPN are formed: a three-component gradient IPN consisting of natural rubber, PU, and the copolymer is produced at the interface with natural rubber, whilst a three-component IPN, consisting of PVC, PU, and the copolymer, is formed at the interface with PVC. The thickness of the transitional layer at the interface with natural rubber reaches 30 μm , while that at the interface with PVC reaches 20 μm . The thickness of the transitional layers as well as the adhesive strength can be regulated by varying the duration of contact between the unhardened composition with natural rubber and PVC and also by employing different procedures for the preparation of the IPN-adhesive, namely by employing the

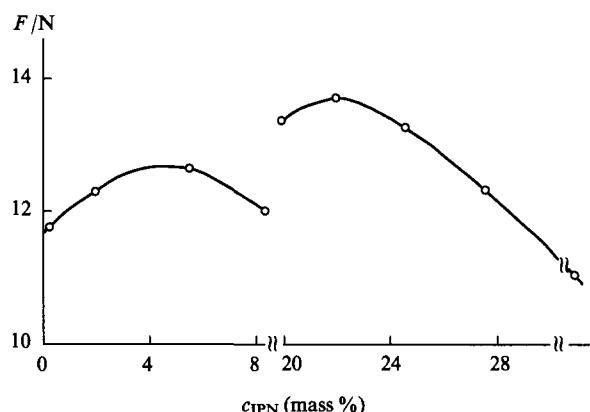


Figure 9. Dependence of the strength of a complex capron filament in the presence of an IPN in its surface layer at 373 K.

prepolymerisation MMA or the simultaneous mixing of the components and subsequent hardening of the composition.

It has been shown⁶⁰ that the method for the preparation of gradient IPN for the improvement of the physicochemical characteristics of synthetic fibres and organic plastics based on the latter is promising. This has been demonstrated in relation to polyamide fibres, which were swollen for different times in an alcoholic solution of a phenol-formaldehyde oligomer containing a hardening agent with subsequent hardening of the binder. This resulted in the formation in the surface layer of the fibre of a gradient IPN, the matrix of which is the polyamide, while the hardened phenol-formaldehyde layer is distributed in it with a certain concentration gradient. Physicochemical study of the fibres obtained showed that the modified fibres are more effectively wetted by solutions of the phenolic oligomer and that their heat resistance is improved: the temperature of the onset of degradation increases to 373 K and the mass loss in the temperature range 373–473 K is smaller by a factor of 2 than for the initial fibres. The strength properties of the fibres at room and elevated temperatures also increase under these conditions. The strength of the hardened oligomer in the surface layer of the fibres (Fig. 9) varies non-monotonically. The curve has two maxima in the regions where the contents of the IPN are 1.8–4.5 and 22 mass%. The breaking stress on compression of organic phenoplastics, obtained from the modified fibres, is 50% greater than for the plastics obtained from the initial fibres, i.e. the application of the method for the preparation of gradient IPN is promising for the preparation of organic plastics with improved physicochemical characteristics.

VII. Conclusion

The preparation of gradient IPN is a promising procedure for the specific modification of the surface layers of monomers with a three-dimensional structure, which makes it possible to impart to them new characteristics — to improve the optical and mechanical properties of composites based on them, to alter the relaxation behaviour, etc.

Variation of the degree of thermodynamic compatibility of the matrix network with the monomer or polymer diffusing in it and the conditions governing the diffusion process (diffusion time and temperature) makes it possible to regulate specifically the thickness of the layer with a composition gradient and at the same time to obtain polymeric composites with specified characteristics.

The number of gradient IPN obtained and investigated hitherto is unfortunately small. However, a series of materials based on IPN of this type have already found quite definite applications in various branches of engineering and biomedicine.

As is frequently the case, the studies on the preparation and practical employment of the gradient IPN have outstripped those on the mechanism of their formation, structure, and the relation between structure and physicochemical properties. Furthermore, during the formation of gradient IPN, there is a change not only in the ratio of the components in the layers but also in the formation conditions, in particular phase separation conditions in the layers of gradient IPN, which should alter the morphological characteristics and the properties of these layers compared with the IPN obtained by the usual methods.

Studies along these lines have only just begun. The available information about the layer-by-layer variation of the morphology in gradient IPN is limited. It is of interest to obtain multicomponent IPN with a composition gradient and to investigate their formation and properties. Analysis of the available data on gradient IPN does not as yet permit definite conclusions about the causes of their different properties. It may be that, for a certain change in the formation conditions, it is possible to obtain a particular gradient for the same polymer system. All the problems noted here and others listed above require further investigations in order to be able to create new gradient systems. The synthesis of gradient IPN leads to new prospects for the preparation of polymeric materials and it is so far difficult to predict what diverse combinations of properties these systems will possess. In addition, further studies on gradient IPN as well as other types of IPN are extremely important from the standpoint of the theory of the formation of multicomponent polymer systems and the principles governing the preparation of composite polymeric materials from them.

In conclusion, one should note that the synthesis of gradient IPN is only one of the ways of obtaining gradient polymeric materials. There are also other procedures. Recent investigations,⁶¹⁻⁶⁴ in which a fundamentally new aspect of the creation of gradient polymeric materials from network copolymers has been developed, are particularly interesting. In order to obtain other polymeric materials, in which the modulus of elasticity varies smoothly within the boundaries of one specimen in a specified direction (in the absence of transitional layers and interfaces), an approach based on the creation of dense-network structures containing bulky rigid nodes connected by flexible linear chains with a controllable length has been employed. The creation of such structures has been demonstrated experimentally in the synthesis of network polyisocyanurates, in which the role of the node was assumed by isocyanurate rings with the aromatic rings adjoining them and the role of the internodal fragment was assumed by fairly short but flexible organosilicon chains^{61,62} or short chains based on the oligomeric tetrahydrofuran-epoxypropane copolymer.⁶⁴ This resulted in the formation of materials in which the modulus of elasticity varies smoothly within a single specimen in the specified direction from 4.5 MPa to 2.0 GPa, i.e. a smooth transition from a rubber to a plastic has been achieved. The following conclusion is of fundamental importance: despite the fact that the range of moduli for the materials synthesised overlaps the values characteristic of the region corresponding to the transition from the vitreous to the highly elastic state, the materials obtained exhibit elastic and not viscoelastic properties, behaving, for example, as glasses or rubbers.⁶⁴ Studies on these lines are being vigorously prosecuted.

This review has been written in the course of studies carried out with the support of the International Scientific Fund (grant UAZ 000).

References

1. J R Millar *J. Chem. Soc.* 1311 (1960)
2. D R Paul, S Newman (Ed.) *Polymer Blends* (Translated into Russian; Moscow: Mir, 1981)
3. Yu S Lipatov, L M Sergeeva, in *Vzaimopronikayushchie Polimernye Setki* (Interpenetrating Polymer Networks) (Kiev: Naukova Dumka, 1978) p. 160
4. L H Sperling, in *Interpenetrating Polymer Networks and Related Materials* (New York: Plenum, 1981) p. 260
5. H L Frisch *Br. Polym. J.* **17** 149 (1985)
6. L H Sperling, in *Polymer Blends: Processes, Morphology and Properties. Polish-Italian Joint Seminar of Multicomponent Polymer Systems, Lodz, 1982* Vol. 2 (New York: Plenum, 1984) p. 1
7. L H Sperling *Polym. Eng. Sci.* **25** 17 (1985)
8. Yu S Lipatov, L M Sergeeva *Usp. Khim.* **55** 2086 (1986) [*Russ. Chem. Rev.* **55** 1186 (1986)]
9. Yu S Lipatov, T G Alekseeva *Usp. Khim.* **61** 2187 (1992) [*Russ. Chem. Rev.* **61** 1203 (1992)]
10. L M Sergeeva, Yu S Lipatov, in *Fizikokhimiya Mnogokomponentnykh Polimernykh Sistem* T. 2 (Physical Chemistry of Multi-component Polymer Systems) Vol. 2 (Kiev: Naukova Dumka, 1986)
11. L M Sergeeva, in *Fizikokhimiya i Modifikatsiya Polimerov* (Physical Chemistry and Modification of Polymers) (Kiev: Naukova Dumka, 1987) p. 55
12. Nidhi Gupta, A K Srivastava *Polym. Int.* **35** 109 (1994)
13. G Akovali, K Biliyar, M Shen *J. Appl. Polym. Sci.* **20** 2419 (1976)
14. G Akovali, A Labban *IUPAC Macro, Florence, 1980* (*International Symposium on Macromolecules*) Vol. 3, p. 264
15. M Dror, M Z Elsbabee, G C Berry *J. Appl. Polym. Sci.* **26** 1741 (1981)
16. M Z Elsbabee, M Dror, G C Berry *J. Appl. Polym. Sci.* **28** 2151 (1983)
17. G C Martin, E Enssani, M Shen *J. Appl. Polym. Sci.* **26** 1465 (1981)
18. Yu S Lipatov, L M Sergeeva, L V Karabanova, V F Rosovitskii, L A Gorbach, N V Babkina *Mekh. Kompozit. Mater.* **6** 1028 (1988)
19. A A Brovko, L M Sergeeva, L V Karabanova, L A Gorbach *Ukr. Khim. Zh.* **61** 7 (1995)
20. L M Sergeeva, G M Semenov, L V Karabanova, T E Lipatova, Yu S Lipatov *Dokl. Akad. Nauk SSSR* **288** 1134 (1986)
21. Yu S Lipatov, O P Grigoryeva, G P Kovernik, V V Shilov, L M Sergeeva *Makromol. Chem.* **186** 1401 (1985)
22. Yu S Lipatov, O P Grigor'eva, L M Sergeeva, V V Shilov *Vysokomol. Soedin., Ser. A* **28** 335 (1986)
23. Yu S Lipatov, L V Karabanova, L A Gorbach, E D Lutsyk, L M Sergeeva *Polym. Int.* **28** 99 (1992)
24. Yu S Lipatov *J. Macromol. Sci., Rev. Macromol. Chem. Phys.* **C30** 209 (1990)
25. T G Fox *Bull. Am. Phys. Soc.* **2** 123 (1956)
26. Yu S Lipatov, L N Perepelitsina, V F Babich *Mekh. Kompozit. Mater.* **4** 585 (1986)
27. J A Manson, L H Sperling, in *Polymer Blends and Composites* (New York: Plenum, 1976) p. 440
28. V F Rosovitskii, Yu S Lipatov *Dokl. Akad. Nauk SSSR* **283** 910 (1985)
29. J D Ferry *Viscoelastic Properties of Polymers* (New York: Wiley, 1980)
30. L H Sperling, J J Fay, C J Murphy, D A Thomas *Makromol. Chem., Makromol. Symp.* **38** 99 (1990)
31. H L Frisch, A Yu Grosberg *Macromol. Theory Simul.* **2** 517 (1993)
32. D J Hourston, M G Huson *J. Appl. Polym. Sci.* **45** 1753 (1992)
33. A Mathew, P C Deb *J. Appl. Polym. Sci.* **45** 2145 (1992)
34. K F Mueller, S J Heiber *J. Appl. Polym. Sci.* **27** 4043 (1982)
35. S Esmer, J F Valley, R Lytel, F Lipscomb, T E Van Eck, D G Garton *Appl. Phys. Lett.* **61** 2272 (1992)
36. P N Prasad, D J Williams, in *Introduction to Nonlinear Optical Effects in Molecules and Polymers* (New York: Wiley, 1991) p. 59
37. S Marturunkakul, J I Chen, L Li, R J Jeng, J Kumar, S K Tripathy *Chem. Mater.* **5** 592 (1993)
38. J I Chen, S Marturunkakul, L Li, R J Jeng, J Kumar, S K Tripathy *Macromolecules* **26** 7379 (1993)
39. S Marturunkakul, J I Chen, L Li, X L Jiang, R J Jeng, S K Sengupta, J Kumar, S K Tripathy *Polymer Preprint. Am. Chem. Soc. Div. Polym. Chem. Meeting, Washington, DC, 1994*
40. Y Ohtsuka *Appl. Phys. Lett.* **23** 247 (1973)
41. N B Galimov, V I Kosyakov, R M Minkova, I K Mosevich, A N Ramazanov, L Yu Tikhonova, A Sh Tukhvatulin, M L Shevchenko *Zh. Prikl. Khim.* **54** 1552 (1981)
42. V I Kosyakov, L I Ginzburg, in *Diffuzionnye Yavleniya v Polimerakh* (Diffusion Effects in Polymers) (Chernogolovka: Institute of Chemical Physics, 1985) p. 86.

43. E I Krivchenko, L I Ginzburg, L N Nabatova, A Sh Tukhvatulin, V I Kosyakov, S N Sadikov, in *Sintez i Svoystva Polimerov i Sopolimerov Stirola* (The Synthesis and Properties of Polymers and Copolymers of Styrene) (Leningrad: Leningrad Polytechnic Institute, 1985) p. 54
44. T L Bukhbinder, V I Kosyakov *Vysokomol. Soedin., Ser. B* **28** 625 (1986)
45. E I Krivchenko, R V Matvienko, V P Pavlova, V P Budtov, M I Gandel'sman, E I Egorova, L I Ginzburg *Plast. Massy* **4** 26 (1988)
46. Y Ohtsuka, J Nakamoto *Appl. Phys. Lett.* **29** 559 (1976)
47. F B Bronfin, V G Il'in, G O Karapetyan, G Ya Livshits, V M Maksimov, D K Sattarov *Zh. Prikl. Spektrosk.* **18** 523 (1973)
48. K Jga, N Yamamoto *Appl. Opt.* **16** 1305 (1977)
49. N Yamamoto, K Jga *Jpn. J. Appl. Phys.* **17** 1437 (1978)
50. USSR P. 722 128; *Byull. Izobret.* (31) 35 (1980)
51. V R Duflo, Yu A Chikin, L Yu Tikhonov, V I Kosyakov, in *Pyataya Konferentsiya po Khimii i Fizikokhimii Oligomerov (Tez. Dokl.)* (Abstracts of Reports at the Fifth Conference on the Chemistry and Physical Chemistry of Oligomers) (Chernogolovka: Institute of Chemical Physics, 1994) p. 123
52. T L Bukhbinder, V I Kosyakov, A Sh Tukhvatulin *Vysokomol. Soedin., Ser. B* **33** 246 (1991)
53. G Camera-Roda, G C Sarti *Transp. Theory Stat. Phys.* **15** 1023 (1986)
54. C-Y Hui, K-C Wu, R C Lasky, J Kramer *J. Appl. Phys.* **61** 5129 (1987)
55. US P. 3 833 404 (1974)
56. P Predecki *J. Biomed. Mater. Res.* **8** 487 (1974)
57. G C Berry, M Dror, in *Am. Chem. Soc. Div. Org. Coat. Plast. (Preprints)* 1978 Vol. 38, p. 465
58. M Dror, M Z Elsabee, G C Berry *Biomater. Med. Devices Artif. Organs.* **7** 31 (1979)
59. D Jia, Y Pang, Xi Liang *J. Polym. Sci. Part B, Polym. Phys.* **32** 817 (1994)
60. Yu S Lipatov, L M Sergeeva, O M Novikova, M I Glukhovskaya *Khim. Volokna* **4** 14 (1983)
61. A A Askadskii, G I Surov, V A Pankratov, Ts M Frenkel', A A Zhdanov, L I Makarova, A S Marshalkovich, L G Radchenko *Vysokomol. Soedin., Ser. A* **32** 1517 (1990)
62. A A Askadskii, G I Surov, V A Pankratov, Ts M Frenkel', L I Makarova, A A Zhdanov, I V Blagodatskikh, A V Pastukhov *Vysokomol. Soedin., Ser. A* **32** 1528 (1990)
63. RF Appl. 5 054 649 (1993); Positive Decision No 05 (034 193)
64. A A Askadskii, L M Goleneva, K A Bychko *Vysokomol. Soedin., Ser. A* **37** 829 (1995)

Interaction of bleomycin and its oligonucleotide derivatives with nucleic acids

D S Sergeev, V F Zarytova

Contents

I. Introduction	355
II. Binding of bleomycin to nucleic acids	356
III. Cleavage of nucleic acids by bleomycin	363
IV. Bleomycin derivatives of oligonucleotides. Synthesis and site-specific cleavage of DNA	369

Abstract. Various aspects of interaction of the antitumour glycopeptide antibiotic bleomycin with nucleic acids are considered. Data on equilibrium binding parameters obtained by various physicochemical methods have been collected and compared. The contribution of N- and C-terminal domains of the glycopeptide molecule to the binding with DNA and sequence specificity of DNA cleavage are discussed. Data on a recently created new class of compounds — bleomycin–oligonucleotide conjugates — are presented. These compounds, like antibiotics, possess DNA-cleaving activity (also in a catalytic manner) together with high selectivity towards a selected nucleotide sequence. The bibliography includes 267 references.

I. Introduction

1. A brief review of the bleomycin antibiotics family

The discovery and pioneering studies on the family of bleomycin antibiotics date back to 1963 when a group of Japanese investigators headed by Umezawa detected a substance possessing a high antibiotic activity in the culture fluid of the mutant strain of the soil bacterium *Streptomyces verticillus*. Just three years later, in 1966, a wide range of structurally related compounds, given common name of bleomycins, were isolated.^{1,2} Owing to their beneficial therapeutic effects, these compounds have found wide use in the clinical practice as valuable pharmaceutical drugs endowed with both antibacterial and, even more important, antitumour activities.^{3–8} The major area for clinical application of bleomycins is in the chemotherapy of malignant tumours, particularly of lymphomas and squamous carcinomas.^{9–12} Along with their high antitumour activity, bleomycins are characterized by relatively low toxicity and lack of immunodepressive action which makes them helpful tools in combined chemotherapy.^{13,14} Applications of bleomycins in clinical oncology have been described in numerous reviews and special publications.^{13–20}

Simultaneously with practical applications of bleomycin antibiotics, in-depth studies into their actions on the cell were

under way. It turned out that the main target for bleomycin antibiotic action in the cell is DNA.^{21,22} Bleomycin has a number of actions coupled to DNA degradation, namely, the loss by animal and bacterial cells of their ability to form colonies,⁵ inhibition of DNA synthesis,^{6,23} chromosomal aberrations,²⁴ intracellular DNA degradation to acid-soluble products,²⁵ and DNA dissociation from the membrane complex.²⁶ These findings prompted extensive research concerned with bleomycin interactions with DNA with special emphasis on its binding to DNA, action mechanisms, cofactors required, etc. Recent studies have demonstrated that bleomycin can also cleave RNA. This important discovery gave a strong impetus to further studies into the action mechanisms of bleomycin and the basis for its biological activities.

To date, a great body of information on this antibiotic has been accumulated in the literature. Some of the data concerning the nature of bleomycin interactions with DNA are presented in this review.

2. Functional domains of bleomycin

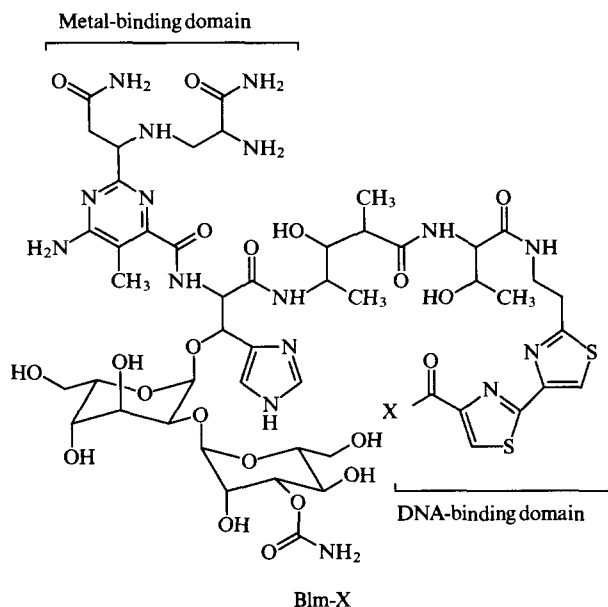
Since the initial isolation of individual bleomycins, intensive studies have taken place with the aim of establishing the structure, the elucidation of which required a vast variety of chemical and physicochemical methods including NMR spectroscopy and X-ray analysis. For general features, this work was completed by 1972.²⁷ In 1978, the bleomycin structure was finally elucidated;²⁸ total chemical synthesis of bleomycin A₂ was carried out in 1982.²⁹

Bleomycins are glycopeptides with a molecular mass of about 1500 Da. The fragment of the molecule (termed as bleomycinic acid) common to all bleomycins consists of pyrimidoblamincic acid, β -hydroxyhistidine, 4-amino-3-hydroxy-2-methylpentanoic acid, threonine, 2'-(2-aminoethyl)-2,4'-bithiazole-4-carboxylic acid linked by peptide bonds, and a carbohydrate moiety containing 3-(O-carbamoyl)-D-mannose and L-gulose attached to the hydroxyl group of β -hydroxyhistidine. The structures of bleomycin (Blm) and C-terminal amines of the most commonly occurring bleomycins are given below. Individual bleomycins differ from one another by the terminal amine bound to the carboxyl group of the bithiazole residue. Bleomycinic acid (Blm–OH) represents a compound with OH instead of NHX. Depending on the composition of their terminal amines, bleomycins are divided into two subgroups: A and B. Group A bleomycins carry in their terminal amine both primary and secondary amino groups with the exception of bleomycins A₁ and A₂; group B bleomycins have guanidinium groups. Studies on bleomycin carried out abroad were largely performed on bleomycin A₂ and bleomycin B₂, a mixture of bleomycins A₂ (60%–65%), bleomycin B₂ (30%) and minor components (B₄, A₅, etc.). In our country, bleomycin A₅ is routinely used in clinical practice and in laboratory studies.

D S Sergeev, V F Zarytova Division of Chemistry of Nucleic Acids, Novosibirsk Institute of Bioorganic Chemistry, Siberian Branch of the Russian Academy of Sciences, prosp. Akad. Lavrent'eva 8, 630090 Novosibirsk, Russian Federation. Fax: (7-383) 235 16 65, tel: (7-383) 239 62 24, E-mail: zarytova@modul.bioch.nsk.su

Received 28 August 1995

Uspekhi Khimii 65 (4) 377–402 (1996); translated by R L Birnova



X	Name	Designation
$\text{NH}(\text{CH}_2)_3\text{S}^+(\text{CH}_3)_2$	Bleomycin A ₂	(Blm-A ₂)
$\text{NH}(\text{CH}_2)_3\text{NH}(\text{CH}_2)_4\text{NH}_2$	Bleomycin A ₅	(Blm-A ₅)
$\text{NH}(\text{CH}_2)_3\text{SCH}_3$	Demethylbleomycin A ₂	(DMBlm-A ₂)
NH_2	Bleomycin B ₂	(Blm-B ₂)
$\text{NH}(\text{CH}_2)_4\text{NHC}(\text{NH})\text{NH}_2$	Bleomycin B ₂	(Blm-B ₂)
$\text{NH}(\text{CH}_2)_3\text{NH}(\text{CH}_2)_3\text{N}(\text{CH}_2)_4$	Bleomycin BAPP	(Blm-BAPP)

In parallel with the determination of the bleomycin structure, general concepts of molecular mechanisms of their biological activity were developed. It was found, in particular, that bleomycin can interact with DNA and form strong noncovalent complexes with it.^{30–34} Bleomycin can also form complexes with metal ions and cause DNA degradation in the presence of Fe(II) ions and molecular oxygen.^{35–37} Based on these findings, the bleomycin molecule was conventionally divided into domains in accordance with their specific function.^{38–40} Pyrimidinobis(2-aminopropyl)amine and β-hydroxyhistidine are involved in the metal-binding domain. The primary and secondary amino groups present in this domain provide for the formation of a tight complex with many transient metals.^{41–44} The bithiazole residue and the C-terminal amine responsible for the binding to DNA are termed 'the DNA-binding domain'. 4-Amino-3-hydroxy-2-methylpentanoic acid and threonine determine the reciprocal arrangement of these two domains needed for the tight binding and effective cleavage of DNA. Finally, the disaccharide favours the binding of molecular oxygen which, in turn, is necessary for oxidative cleavage of DNA.^{45,46}

II. Binding of bleomycin to nucleic acids

1. Parameters of equilibrium binding

An assumption that bleomycin binds to DNA was made as long ago as 1969^{30,33} and the first evidence for the binding of tritium-labelled bleomycin A₂ to *E. coli* DNA was obtained a year thereafter.³⁴ However, systematic studies of this process employing physicochemical methods were begun only in the late 1970s. The discovery of quenching of bleomycin fluorescence in the binding of the antibiotic to DNA was a boon for experimenters.³⁸ Being light-excited at the wavelength of 300 nm, bleomycins produce two emission bands with maxima at 353 and 405 nm. Light with a wavelength of 353 nm is emitted by the bithiazole residue and exceeds in intensity the emission of the 4-aminopyrimidine ring at 405 nm. Addition of calf thymus DNA to bleomycin solutions

results in significant (up to 50%) quenching of the fluorescence at 353 nm. This finding made it possible to quantify both bound and free bleomycin and to calculate, at variable concentrations of DNA, the apparent equilibrium binding constant, K_{app} , and the number of DNA nucleotides per bound molecule of the antibiotic, n . The K_{app} and n values were also determined using equilibrium dialysis,^{47–49} gel filtration⁴⁹ and circular dichroism spectroscopy (CD).^{50–52} The values of K_{app} and n determined by different methods are summarized in Table 1.

As can be seen from Table 1, the binding constants determined by different authors for metal-free bleomycin A₂ vary from 10^5 to $10^6 \text{ dm}^3 \text{ mol}^{-1}$. The number of DNA base pairs per bound antibiotic molecule also varies significantly in different studies, being equal, on average, to 3–10 pairs. The lower values cited in the most recent papers^{52,55} appear to be far more reliable. An increase in ionic strength does not affect the K_{app} values but increases the n value, thereby decreasing the number of accessible binding sites.^{38,54} Interestingly, bleomycin binding to homogenous DNA of poly(dG)·poly(dC) and poly(dA)·poly(dT) appears to be stronger than that to heterogeneous DNA, and parameter n ⁴⁹ is greater in the former case. The binding of bleomycin to the bivalent copper ion slightly decreases the binding constant but increases the number of accessible binding sites.^{49,57} At the same time, the binding constant for the bleomycin–Fe(III) complex is twice as high as that for bleomycin itself, while the number of accessible binding sites is the same in both cases.⁵⁶ Bleomycin complexes with Co(III) are characterized by K_{app} of 10^5 to $10^7 \text{ dm}^3 \text{ mol}^{-1}$ depending on the nature of the chelated ligand.^{50,59} An increase in ionic strength strongly decreases the constant of binding of bleomycin–copper and cobalt complexes to DNA without any change in the number of base pairs per bound molecule,^{48,59} thus suggesting that electrostatic interactions have a role in this process.

Evidence concerning the parameters of bleomycin binding to RNA is very sparse in the current literature except for a study,⁶¹ in which K_{app} and n values for bleomycin binding to yeast phenylalanine tRNA were determined by the fluorescence quenching method. The parameters of binding to this tRNA are close to those for DNA ($K_{\text{app}} = 0.86 \times 10^5 \text{ dm}^3 \text{ mol}^{-1}$ and $n = 25$ in 5 mmol dm^{-3} phosphate buffer pH 7.0).

Most of the data listed in Table 1 were obtained using the method of quenching the fluorescence of bithiazole rings. This widely used procedure, which has a number of indisputable advantages (simplicity, rapidity, etc.), also has some limitations. Firstly, the quantum yield of this fluorescence is rather low (ca. 0.01).³⁸ Chelation of the metal ion leads to a further decrease in bleomycin fluorescence,^{54,57} which imposes certain restrictions on the accuracy of the experimental results. Secondly, according to recent data,⁵⁵ upon excitation by light with a wavelength of 300 nm, the intensity of bleomycin fluorescence decreases significantly with time due to the decay or phototransformation of the bithiazole residue that has been neglected in earlier studies. Finally, bleomycin fluorescence is effectively quenched not only by double-stranded DNA (binding data are given in Table 1) but also by single-stranded DNA and RNA.^{54,57} However, it is known that neither single-stranded DNA nor RNA protect double-stranded DNA from bleomycin action.^{62–65} Apparently, the mode of bleomycin fluorescence quenching by these substrates depends on the binding type and affinity. The fact that, after incubation under identical conditions and subsequent dialysis,³⁴ the amount of tritium-labelled bleomycin on double-stranded *E. coli* DNA exceeds 30-fold that on ribosomal RNA, provides additional evidence that fluorescence quenching does not indicate strong binding. Moreover, the fluorescence quenching itself depends, in turn, on the composition of DNA: poly(dG)- and poly(dG)·poly(dC) sequences quench the fluorescence to a greater extent.^{54,57} Presumably, the K_{app} and n values listed in Table 1 are mean values for different binding sites displaying different affinity.

Table 1. Parameters for equilibrium binding of bleomycins, metal-containing bleomycins, and bleomycin A₂ C-terminal fragments to DNA.

Compound	$10^5 K_b/\text{dm}^3 \text{ mol}^{-1}$ ^a	n ^a	Buffer conditions	DNA	Method ^b	Ref.
Heterogeneous DNA at low ionic strength						
Blm-A ₂	1.2 ± 0.2	11 ± 1	1.2 mmol dm ⁻³ NaCl, 2.5 mmol dm ⁻³ Tris – HCl (pH 8.4)	Calf thymus	F	38
	0.34 ± 0.04	3.4 ± 0.5	1.2 mmol dm ⁻³ NaCl, 2.5 mmol dm ⁻³ Tris – HCl (pH 8.4)	Salmon sperm	F	53
	7.8 ± 0.5	25 ± 3	1.2 mmol dm ⁻³ NaCl, 2.5 mmol dm ⁻³ Tris – HCl (pH 8.4)	Calf thymus	F	54
	1.0	7.6	1.2 mmol dm ⁻³ NaCl, 2.5 mmol dm ⁻³ Tris – HCl (pH 8.4)	"	F	55
Blenoxane ^a	9.3	6	0.8 mmol dm ⁻³ sodium citrate (pH 5.5)	<i>Col E1</i>	E	47
	4.1	10	1.0 mmol dm ⁻³ Tris – HCl (pH 8.0)	Calf thymus	F	56
Heterogeneous DNA at ionic strength of 25 – 50 mmol dm ⁻³						
Blm-A ₂	0.92 ± 0.01	52 ± 4	1.2 mmol dm ⁻³ NaCl, 25 mmol dm ⁻³ Tris – HCl (pH 8.4)	Calf thymus	F	38
	3.2	417	15 mmol dm ⁻³ NaCl, 15 mmol dm ⁻³ Tris – HCl (pH 8.4), 1.5 mmol dm ⁻³ EDTA	"	F	57
	8.1	36	50 mmol dm ⁻³ NaCl, 1.5 mmol dm ⁻³ Tris – HCl (pH 8.4)	"	F	54
	5.7 ± 0.5	7.4 ± 0.6	25 mmol dm ⁻³ Na ₂ HPO ₄ (pH 7.0)	"	G	49
	6.8 ± 0.4 2.5 ± 0.1	7.8 ± 0.4 6.6 ± 0.6	25 mmol dm ⁻³ Na ₂ HPO ₄ (pH 7.0)	"	E	49
Homogeneous DNA						
Blm-A ₂	26 ± 1 3.9 ± 0.2	22.8 ± 0.8 9.0 ± 0.6	25 mmol dm ⁻³ Na ₂ HPO ₄ (pH 7.0)	poly(dG) · poly(dC)	E	49
	19 ± 1 2.7 ± 0.1	29.4 ± 0.6 13.2 ± 0.4	25 mmol dm ⁻³ Na ₂ HPO ₄ (pH 7.0)	poly(dA) · poly(dT)	E	49
	69.5 0.51	19.2 2.7	25 mmol dm ⁻³ NaCl 10 mmol dm ⁻³ Na ₂ HPO ₄ (pH 6.8)	poly(dA) · poly(dT)	F	58
	87.0 0.50	20.4 2.6	100 mmol dm ⁻³ NaCl, 10 mmol dm ⁻³ Na ₂ HPO ₄ (pH 6.8)	poly(dA) · poly(dT)	F	58
Heterogeneous DNA						
Cu(II)Blm-A ₂	2.3	77	15 mmol dm ⁻³ NaCl, 15 mmol dm ⁻³ Tris – HCl (pH 8.4), 1.5 mmol dm ⁻³ EDTA	Calf thymus	F	57
	3.9 ± 0.3	5.6 ± 0.4	25 mmol dm ⁻³ Na ₂ HPO ₄ (pH 7.0)	"	G	49
	4.4 ± 0.4 1.7 ± 0.1	5.6 ± 0.4 4.2 ± 0.2	25 mmol dm ⁻³ Na ₂ HPO ₄ (pH 7.0)	"	E	49
	18 ± 1 2.6 ± 0.1	20.2 ± 0.4 8.2 ± 0.6	25 mmol dm ⁻³ Na ₂ HPO ₄ (pH 7.0)	poly(dG) · poly(dC)	E	49
	10 ± 1 1.7 ± 0.1	22.0 ± 0.6 12.0 ± 0.6	25 mmol dm ⁻³ Na ₂ HPO ₄ (pH 7.0)	poly(dA) · poly(dT)	E	49

Table 1 (continued).

Compound	$10^5 K_b/\text{dm}^3 \text{mol}^{-1}$ ^a	n ^a	Buffer conditions	DNA	Method ^b	Ref.
Cu(II)Blenoxane	0.2	8	25 mmol dm ⁻³ Tris-HCl (pH 7.0)	Calf thymus	F	48
	0.01	8	50 mmol dm ⁻³ NaCl, 20 mmol dm ⁻³ Tris-HCl (pH 8.0)	"	F	48
	0.012	8	50 mmol dm ⁻³ NaCl, 20 mmol dm ⁻³ Tris-HCl (pH 8.0)	"	E	48
Fe(III)Blenoxane	9.6	10	1 mmol dm ⁻³ Tris-HCl (pH 8.0)	"	F	56
Fe(III)Blm-A ₂	3.5 (pH 7.4)	5.2	50 mmol dm ⁻³ Hepes	"	CD	51
Co(III)Blm-A ₂	4.7 ± 0.4	10 ± 2	1 mmol dm ⁻³ NaCl, 20 mmol dm ⁻³ Tris-HCl (pH 8.0), 1 mmol dm ⁻³ EDTA	"	F	59
	1.5 ± 0.2	10 ± 2	20 mmol dm ⁻³ NaCl, 20 mmol dm ⁻³ Tris-HCl (pH 8.0), 1 mmol dm ⁻³ EDTA	"	F	59
HO ₂ ⁻ - Co(III)Blm-A ₂	130 ± 30	8 ± 2	20 mmol dm ⁻³ NaCl, 20 mmol dm ⁻³ Tris-HCl (pH 8.0), 1 mmol dm ⁻³ EDTA	"	F	59
H ₂ O - Co(III)Blenoxane	500 ± 100	6 ± 2	1 mmol dm ⁻³ NaCl, 20 mmol dm ⁻³ Tris-HCl (pH 8.0), 1 mmol dm ⁻³ EDTA	"	F	59
	19 ± 3	26 ± 2	140 mmol dm ⁻³ NaCl, 20 mmol dm ⁻³ Tris-HCl (pH 8.0), 1 mmol dm ⁻³ EDTA	"	F	59
Cu(II)Blm-A ₅	3	14	15 mmol dm ⁻³ NaCl, 15 mmol dm ⁻³ Tris-HCl (pH 8.4), 1.5 mmol dm ⁻³ EDTA	"	F	57
Ni(II)Blm-B ₂	4	—	100 mmol dm ⁻³ NaCl, 10 mmol dm ⁻³ Na ₂ HPO ₄ (pH 7.5)	12-Meric duplex	CD	52
Tripeptide S ^d	1.95 ± 0.04	8 ± 1	1.2 mmol dm ⁻³ NaCl, 2.5 mmol dm ⁻³ Tris-HCl (pH 8.4)	Calf thymus	F	38
	0.59 ± 0.01	35 ± 4	1.2 mmol dm ⁻³ NaCl, 25 mmol dm ⁻³ Tris-HCl (pH 8.4)	"	F	38
	4.5	5	1.25 mmol dm ⁻³ NaCl, 2.5 mmol dm ⁻³ Tris-HCl (pH 8.4)	"	F	55
	10	5	0.8 mmol dm ⁻³ sodium citrate (pH 5.5)	Col E1	F	47
	1.5	5	2 mmol dm ⁻³ Tris-HCl (pH 8.0), 1 mmol dm ⁻³ EDTA	"	F	47
Acetyldipeptide ^e	7.5	16	0.1 mmol dm ⁻³ EDTA, 10 mmol dm ⁻³ sodium cacodylate (pH 7.0)	Calf thymus	F	60
	5	16	0.1 mmol dm ⁻³ EDTA, 10 mmol dm ⁻³ sodium cacodylate (pH 7.0)	poly(dA) · poly(dT)	F	60

Table 1 (continued).

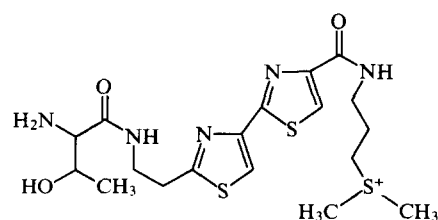
Compound	$10^5 K_b/\text{dm}^3 \text{ mol}^{-1}$ ^a	n ^a	Buffer conditions	DNA	Method ^b	Ref.
Acetyldipeptide ^c	27.0	20.8	25 mmol dm ⁻³ NaCl, 10 mmol dm ⁻³ Na ₂ HPO ₄ (pH 6.8)	poly(dA) · poly(dT)	F	58
	0.66	4.8				
	74.9	41.7	100 mmol dm ⁻³ NaCl, 10 mmol dm ⁻³ Na ₂ HPO ₄ (pH 6.8)	poly(dA) · poly(dT)	F	58
	0.28	5.0				

^a Where two values are indicated, the former corresponds to strong binding, and the latter to weak binding.

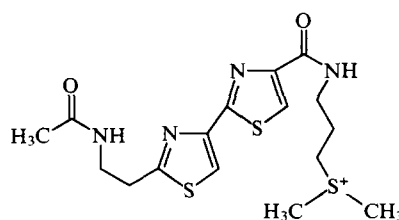
^b F is fluorescence quenching; E is equilibrium dialysis; G is gel filtration; CD is circular dichroism spectroscopy.

^c Bleomycin is a mixture of bleomycin A₂ (60%–70%), bleomycin B₂ (30%) and minor components (bleomycin A₅, bleomycin B₄, demethylbleomycin A₂, etc.) used as a chemotherapeutic drug.

^d Tripeptide S:



^e Acetyldipeptide:



Another method of using the fluorescence quenching technique for a determination of the parameters of bleomycin binding to DNA has been described by Sakai et al.⁵⁸ In this study, the fluorescence was excited at a wavelength of 260 nm (not 300 nm) as usual. This made it possible to increase the difference between the fluorescence of DNA-bound and free bleomycin and thus to increase the sensitivity of the method, as a result of which two binding constants could be obtained for bleomycin binding to poly(dA) · poly(dT). One of them, which reflects the binding of one molecule of the antibiotic per 10 base pairs, corresponds to stronger binding and is equal to $(7-9) \times 10^6 \text{ dm}^3 \text{ mol}^{-1}$, whereas the other one, which reflects the binding of one bleomycin molecule per 1.5 base pairs, is $5 \times 10^4 \text{ dm}^3 \text{ mol}^{-1}$. The existence of different binding sites was also demonstrated by applying the method of equilibrium dialysis to tritium-labelled bleomycin A₂ and its copper complex.⁴⁹ The difference between K_{app}^1 and K_{app}^2 determined for calf thymus DNA appeared to be insignificant (6.8×10^5 and $2.5 \times 10^5 \text{ dm}^3 \text{ mol}^{-1}$). A greater difference between the binding constants was observed when bleomycin A₂ was bound to the homopolynucleotides poly(dG) · poly(dC) and poly(dA) · poly(dT) (Table 1).

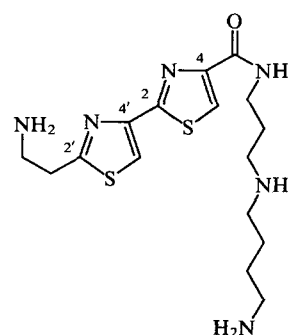
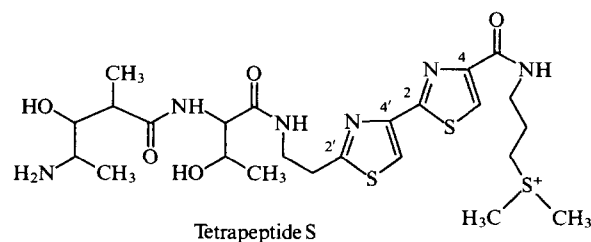
Hence, the parameters of equilibrium binding obtained by various methods suggest a significant affinity of bleomycin and its metal complexes for double-stranded DNA. Strong binding of the antibiotic to the double helix precedes a cascade of events resulting in oxidative degradation of the DNA chain.^{41,66}

2. The role of domains in binding

a. The role of the bithiazole residue and C-terminal amine in bleomycin binding to DNA

Historically, NMR spectroscopy was the first and the most informative method to shed some light on the involvement of certain parts of the bleomycin molecule in the binding to DNA. Bleomycin interaction with calf thymus DNA was accompanied, first of all, by broadening and changes in the intensity of the signals in the ¹H NMR spectrum of the bithiazole residue and the dimethylsulfonium group, thus suggesting the strongest binding of these fragments of the bleomycin A₂ molecule to DNA.³⁸ The phenomenon of quenching bithiazole ring fluorescence detected by Horwitz et al. also argues for the interaction of the bithiazole residue with DNA. This pioneering study was followed by a vast series of NMR investigations into interactions of bleomycin A₂ and its derivatives with poly(dA) · poly(dT).^{40,58,60,67-71} It was

found that significant spectral changes were observed only in the binding of bleomycin to double-stranded DNA, being maximal for the signals for the aromatic protons of the bithiazole residue, which upon interaction with poly(dA) · poly(dT) broadened and shifted upfield. An upfield shift was also noted for adjacent protons: CH₃–S⁺ and CH₂–S⁺ of the terminal amine, CH₂–N of the 2'-substituent of the bithiazole residue, and CH(CH₃)CO of methylpentanoic acid.⁶⁷

C-Terminal fragment Blm-A₅

Similar results were obtained in the study of binding of bleomycin and its metal complexes to short duplex fragments of DNA.^{52,72-75}

The use of the nuclear Overhauser effect (NOE technique) made it possible to detect complex formation between bleomycin containing a Zn(II) or Fe(II) ion in the metal-binding domain, and DNA.⁶⁸ In this case, bleomycin acts as a spacer between DNA and the metal ion. The general changes in the chemical shifts for the protons of bleomycin during the formation of such a complex virtually represent overall changes produced by chelation of the

metal ion and its binding to DNA.⁴⁰ The signals for the protons of the N-terminal fragment of the molecule comprising β -hydroxy-histidine and disaccharide change only upon their interaction with the metal; those in the C-terminal dipeptide, only during the binding to DNA, whereas the signals for the protons of 4-amino-3-hydroxy-2-methylpentanoic acid and threonine are equally sensitive to the both interactions.

The same research group studied the binding of C-terminal fragment of bleomycin A₂, C-terminal fragments of Blm-A₂ (acetyldipeptide, tripeptide S, tetrapeptide S) and Blm-A₅, to DNA. The nature of changes in the signals for bithiazole ring and terminal amine protons was identical for both the entire bleomycin molecule and its C-terminal fragments.^{58,60,67,69} Thus, the NMR spectroscopy data suggest that the C-terminal fragment of the bleomycin molecule containing 2'-(2-aminoethyl)-2,4'-bithiazole-4-carboxylic acid and the terminal amine binds to DNA to a greater degree and apparently determines the strength of binding.

This conclusion was supported by the data obtained by equilibrium methods. The parameters of binding of tripeptide S and acetyldipeptide to DNA practically coincide with those for bleomycin A₂ (Table 1).^{38,47,55,58,60} An attempt was made⁵⁵ to establish a correlation between the values of binding constants for the C-terminal fragments of bleomycin A₂ and their increasing lengths, beginning with the dipeptide fragment. The latter plays a crucial role in the binding; L-threonine increases the binding constant by a factor of 2, while 4-amino-3-hydroxy-3-methylpentanoic acid and β -hydroxyhistidine have no effect on the magnitude of the binding constant.

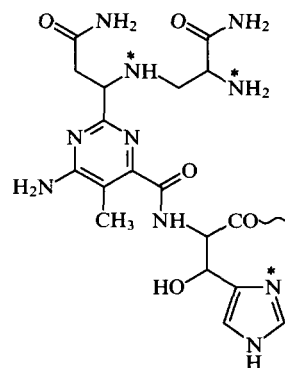
This finding is consistent with the ability of bleomycin C-terminal fragments to inhibit DNA cleavage by the complete antibiotic.^{76,77} Unlike other inhibitors, C-terminal fragments diminish the cleavage proportionally to each cleavage site, i.e., the inhibition is competitive.⁷⁶ It is necessary to mention in this connection that bleomycin analogues devoid of the bithiazole residue or C-terminal amine cleave DNA far less effectively than the bleomycin itself.^{78–81} At the same time, they can chelate the iron ion and effectively oxidise some organic substrates, e.g., *cis*-olefins.⁷⁸

b. The role of electrostatic interactions in bleomycin binding to DNA As can be seen from Table 1, the parameters of bleomycin binding to DNA depend on ionic strength, thus implicating electrostatic interactions between bleomycin and DNA. An increase in ionic strength also leads to a loss of the upper threshold of fluorescence quenching.⁵⁴ Similarly, an increase in ionic strength from 10 to 150 mmol dm⁻³ strongly attenuates the changes in the chemical shift of the aromatic protons H(5) and H(5') of the bithiazole residue and methyl CH₃-S⁺ protons of bleomycin A₂ interacting with poly(dA)·poly(dT). Under these conditions, the changes in the chemical shifts of protons CH₂-N of the substituent at position 2', of bithiazole and CH₂-S⁺ of the C-terminal amine, are completely suppressed. No changes in the ¹H NMR spectrum of bleomycin added to DNA are observed at an ionic strength of 1.0 mol dm⁻³.⁷¹

It should be noted that the bleomycin molecule (devoid of the terminal amine) has several ionogenic groups at its N-terminus: a secondary NH group of β -aminoalanine within the structure of the pyrimidoblaminc acid ($pK_a = 2.7–2.9$), an N(1) atom of the imidazole ring of β -hydroxyhistidine ($pK_a = 4.7–4.9$) and a primary NH₂ group of β -aminoalanine ($pK_a = 7.3–7.7$).^{27,82,83}

The structure of the N-terminal fragment of Blm is given below (the ionogenic groups within the pH range of 2–8 are marked with asterisks).

This indicates that the positive charge of the bleomycin molecule at pH 7.5 is mainly localised at the C-terminal amine which provides for electrostatic interactions with the negatively charged DNA backbone.



Evidence for this assumption can be derived from the following data.

1. Bleomycinic acid bearing a negative charge at its C-end only weakly cleaves DNA.^{57,63,84}

2. The extent of fluorescence quenching upon binding to DNA increases in the following order: bleomycinic acid (negatively charged C-end), bleomycin B₁ (neutral C-end), bleomycin A₂ (positively charged C-end).^{54,57}

3. Demethylbleomycin A₂ and deglycobleomycin A₁ with neutral C-terminal fragments cleave DNA much more weakly than does bleomycin A₂.^{69,70,81,84} No changes in the NMR spectrum of demethylbleomycin A₂ were found upon its interaction with DNA.^{69,70}

4. The copper complex of demethylbleomycin A₂ (1×10^{-4} mol dm⁻³) does not cause any unfolding of the supercoiled plasmid DNA, whereas the copper complex of bleomycin A₂ provides its effective unfolding.⁸⁵

At the same time, there is evidence that the positive charge at the N-end of the bleomycin molecule influences the binding of bleomycin to DNA. Acetylation of the primary amino group of β -aminoalanine gives acetylbleomycin A₂, whose N-end is neutral at pH 6.8. Virtually no changes in the NMR spectrum of this derivative occur in its interaction with poly(dA)·poly(dT).⁶⁹ The appearance of a positive charge at the N-end of the bleomycin A₂ molecule at pH < 7 (6.8 and 4.5) results in a higher upfield shift of bithiazole proton signals; however, this does not affect the shift of proton signals in the N-terminal fragment of the bleomycin molecule upon its interaction with DNA.⁷¹ Chelation of the metal ion, e.g., Cu(II) or Fe(III), which also provokes the appearance of a positive charge in the N-terminal fragment of the antibiotic molecule,⁸³ only weakly reflects on the value of the binding constant.^{49,56,57} However, the appearance of an extra charge at the C-end of the bleomycin A₅ molecule increases the degree of fluorescence quenching and affinity of the antibiotic for DNA.^{54,57}

The results presented above testify to the fact that electrostatic interactions are a necessary prerequisite for bleomycin binding to DNA. A crucial role in providing strong binding to DNA is played by the positive charge at the C-terminal amine.

c. Interaction of the N-terminal fragment of the bleomycin molecule with DNA

In late 1970s, a definite concept was formed concerning the relationship between the structure of the bleomycin molecule and its biological activity, namely, that the C-terminal fragment of the antibiotic binds to DNA, while its N-end chelates the metal (iron) ion which interacts with molecular oxygen, eventually resulting in DNA decay.^{38–40} According to this concept, the interaction between the metal-binding domain and DNA was thought to be very weak. However, the ¹H NMR spectra of the bleomycin N-terminal fragment and the Zn(II)-bleomycin complex reveal small, though persistent changes upon their interaction with poly(dA)·poly(dT).⁴⁰ These changes are even more pronounced in the case of the CO-Fe(II)Blm-A₂ complex binding to DNA. In parallel with the broadening and upfield shift of signals for the protons of the bithiazole residue and the terminal amine, the signals for the aromatic protons of β -hydroxyhistidine also tend to

broaden considerably with a small shift towards the higher field. The fact that the signals for the pyrimidine methyl protons also shift upfield (by 0.08 ppm)⁸⁶ is also suggestive of interactions between the N-terminal fragment of the bleomycin molecule and the DNA backbone.

¹H NMR data on the binding of bleomycin to short oligonucleotide duplexes provide support for the interaction of the metal-binding domain with the double helix.^{52,73–75} The most interesting results were obtained in the study in which the binding of bleomycin A₅ to the 8-meric duplex d(CGCTAGGCG)₂ was analysed⁷⁵ using the NOE technique. The authors succeeded in establishing intermolecular interactions between the protons of the α -CH₂-group of β -hydroxyhistidine and H(4') of the deoxyribose C(7) residue. The formation of a hydrogen bond between the NH₂ group of β -aminoalanine and the oxygen atom of the ribose–phosphate backbone in the oligonucleotide chain was also postulated in this study.

EPR data provide additional support in favour of the metal-binding domain interaction with DNA. Thus, the interaction of the NO–Fe(II)Blm complex with calf thymus DNA was accompanied by marked spectral shifts indicating changes in the Fe(II) microenvironment.^{45,87,88} Evidence for direct interaction of the metal-binding domain with DNA can be derived from changes in the EPR spectrum of 'activated bleomycin' [HOO–Fe(III)Blm] upon its binding to the double helix.⁸⁹ The binding to DNA converts the Fe(III)Blm complex from the high spin ($g = 4.3$) to the low spin state ($g = 2.45, 2.18, 1.89$). In this case, native double-stranded DNA stabilises the low spin state with a greater efficiency than the denatured one.⁸⁹

Characteristic changes in EPR spectra are produced upon addition of DNA to the O₂–Co(II)Blm–A₂ complex which mimics the active O₂–Fe(II)Blm–A₂ complex.^{90,91} This may be due to the alteration of the oxygen molecule orientation relative to the plane containing the cobalt ion. Recent studies⁹² on this complex revealed significant restrictions in the orientation of the O–O bond, which is almost perpendicular to the main axis of the DNA helix.

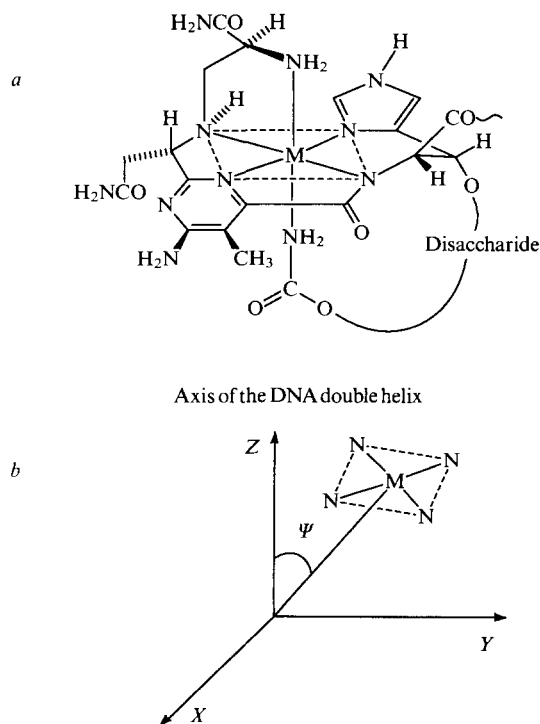


Figure 1. The structure of the site of the bleomycin molecule that chelates the copper ion (a)^{93,94} and the hypothetical position of the plane containing a metal ion relative to the axis of the DNA helix (b).^{96,97}

Conclusive evidence in favour of tight contacts of the metal-binding domain and DNA is the displacement of ligand L from the coordination sphere of the L–Fe(III)Blm complex (where L is the ligand of the N₃[–], S₂O₃^{2–} or SCN[–] type).⁵¹

The influence of the positive charge of the bleomycin N-terminal fragment on its binding to DNA can also be regarded as evidence of interaction of the metal-binding domain with DNA. In this context, mention should be made of the study⁸⁵ in which chelation of the Cu(II) ion by bleomycin A₂ produced qualitative changes in the binding of the antibiotic to supercoiled plasmid DNA. Whereas metal-free bleomycin A₂ is practically incapable of unfolding such DNA under conditions excluding DNA cleavage, its copper-containing counterpart effectively eliminates the coils in the DNA superhelix. It should be noted also that Cu(II) and Fe(III) complexes of bleomycin bind to DNA at different rates which also points to the involvement of the bleomycin N-terminal fragment in the binding to the polymer.⁴⁸

The application of the EPR method to oriented DNA fibres provides valuable information on the position of the metal-binding domain relative to the axis of the DNA double helix. As is known, the nitrogen atoms in the N-terminal moiety of the bleomycin molecule which chelate copper or iron ions, viz., the nitrogen atom of the secondary amino group of β -aminoalanine, the N(1) atom of pyrimidine, the N(1) atom of imidazole, and the nitrogen atom of β -hydroxyhistidine forming a peptide bond,^{39,93,94} lie in one plane with the metal ion (Fig. 1). For the bleomycin molecule bound to DNA, the angle Ψ between the normal (perpendicular) to this plane and the axis of the DNA helix has been found to be 15° for the Cu(II)Blm complex, with rotational freedom of the normal around one of the axes lying in the plane of base pairs of $\pm 80^\circ$.⁹⁵ However, recent studies using the same model gave different results, namely, the angle between the normal and the axis of the DNA helix is 25° with deviations in the range of $\pm 30^\circ$.⁹⁶ This is consistent with the earlier data for the Fe(III)Blm complex bound to oriented DNA fibres (the Ψ value for this model is 15–30° with variations of $\pm 26^\circ$).⁹⁷

Thus, the great body of experimental evidence testifies to tight contacts of the bleomycin N-terminal fragment with DNA. These contacts are manifested also in the influence of the metal-binding domain on the specificity of DNA cleavage (see below).

3. Models of bleomycin binding to DNA

The data obtained by physicochemical methods suggest that the interaction of bleomycin with DNA involves both the metal-binding domain and the C-terminal fragment of the antibiotic molecule. It is the latter, which contains the bithiazole residue and the terminal amine and is especially tightly bound to DNA, that is responsible for the binding to the polymer. We have already noted that electrostatic interactions between the positively charged terminal amine and the negatively charged sugar–phosphate backbone contribute to the binding of bleomycin to DNA. However, there exist other interactions that can also play a role in the binding of bithiazole rings to DNA. The three hypotheses postulating the nature of this binding are as follows: the intercalation model, the partial intercalation model and binding in the minor groove of DNA.

Both heterocyclic rings of the bleomycin bithiazole fragment lie in the same plane⁹⁸ and can theoretically intercalate between the base pairs of DNA. First experimental evidence for intercalation binding of bleomycin was obtained in 1979.⁴⁷ It was found that bleomycin A₂ and its C-terminal fragment, tripeptide S, cause the unfolding of covalently closed circular double-stranded DNA and increase the length of short rod-like DNA molecules as determined by their orientation time in an electric field. Moreover, they favour parallel arrangement of the bithiazole rings and base pairs as evidenced by linear dichroism data.⁴⁷ Changes of this kind usually occur in intercalation binding.⁹⁹ Metal complexes of bleomycin reveal a similar capacity upon their binding to DNA.

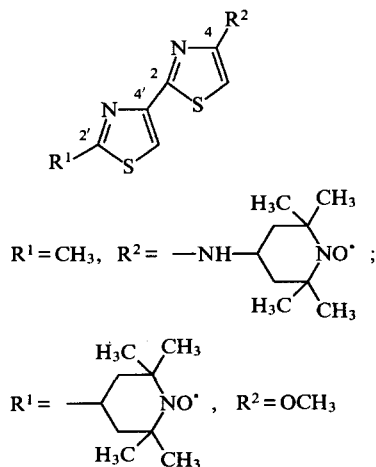
It has already been mentioned that the copper-containing complex of bleomycin A₂ can produce the relaxation of supercoiled DNA.⁸⁵ According to Povirk et al.,⁴⁸ the length of short-chain DNA (150 base pairs) increases by 0.46 nm upon binding to the Cu(II)Blm molecule. For the Fe(III)Blm complex, this value is equal to 0.32 nm, and for Blm, 0.31 nm;⁴⁷ such elongation is characteristic of typical intercalators.^{99,100} At the same time, the copper-containing complex of the bleomycin analogue phleomycin, whose thiazole ring is partially reduced,¹⁰¹ does not produce any elongation of DNA upon binding.⁴⁸ It follows, therefore, that DNA elongation can only be achieved in the case of a planar chromophore.

In 1981, Lin and Grollman¹⁰² proposed, on the basis of NMR data, a model for complete intercalation binding of the bleomycin C-terminal fragment to dinucleotides. In this study, the greatest changes in the chemical shift (0.4 ppm) were observed for aromatic protons of the bithiazole residue upon binding to pdG-dC. According to this model, the bithiazole residue is 'stacked' to base pairs in such a way that its aromatic protons appear to be oriented towards the minor groove of DNA. Theoretical calculations confirmed the indisputable energetic superiority of the proposed intercalation model for binding of the terminal positively charged amine in the minor groove of DNA.¹⁰³

In a recent work by Wu et al.,⁷⁴ two-dimensional NMR was used to study the interaction of the cobalt-containing bleomycin A₂ complex with the 10-meric DNA-duplex d(CCAGGCCTGG)₂. It was found that the bithiazole residue intercalate between GC pairs corresponding to positions C(6) and C(7). In this case, the upfield shifts of the signals for bithiazole protons were 0.9 and 0.61 ppm for H(5') and H(5''), respectively.

However, the model of complete intercalation binding does not agree with numerous experimental data. Thus, the angle of unfolding of supercoiled DNA upon its binding to the bleomycin molecule is 12°,⁴⁷ whereas for the majority of intercalators it constitutes 17–26°.¹⁰⁰ Bleomycin interaction with sonicated DNA did not increase significantly the solution viscosity and, correspondingly, the length of the DNA chain,³⁸ which is in conflict with the results reported by Povirk et al.⁴⁷ Moreover, viscosimetric data for the binding of the bleomycin C-terminal fragment to calf thymus DNA suggest that the length of the DNA molecules decreases slightly.¹⁰⁴ Laser scattering data point to the length reduction of short rod-like DNAs upon their interaction with the antibiotic.¹⁰⁵

Incorporation of spin labels into bleomycin molecules is a convenient tool for determining the parameters of their binding to DNA.^{106,107} The EPR spectrum of such a label (2,2,6,6-tetramethyl-1-piperidine-*N*-oxide) incorporated at position 4 or 2' of bithiazole, practically did not change upon its interaction with DNA which is hardly likely in the case of complete intercalation binding.¹⁰⁴



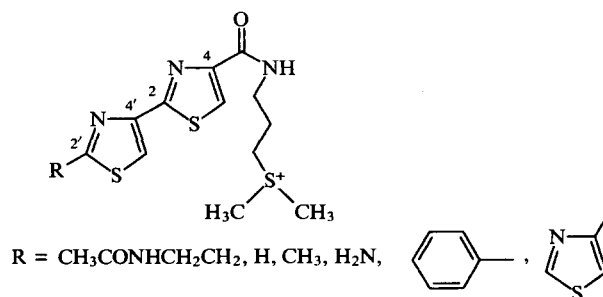
Changes in the ¹H NMR spectrum of bleomycin upon its binding to poly(dA)·poly(dT) are also incompatible with the

complete intercalation model. Although the most pronounced changes are observed for the signals of bithiazole ring protons (their maximum upfield shift is 0.1–0.2 ppm),^{38,40,67,69–71} for typical intercalators this varies from 0.4 to 1.0 ppm.^{108,109} It should be noted also that the shift strongly depends on temperature, ranging from 0.02 to 0.05 ppm at 20 °C up to 0.1–0.2 ppm at temperatures just below the melting temperature for poly(dA)·poly(dT) (50–60 °C)^{67,69,71} and thus cannot be explained within the framework of the complete intercalation model.

There are a number of publications dedicated to the analysis of interactions of bleomycin and its metal complexes with oligonucleotide duplexes using the NMR method.^{52,72–75} Most of the data obtained are also contrary to the complete intercalation model. Hiroaki et al.⁵² studied the binding of bleomycin to the duplex d(CCCCAGCTGGGG)₂ possessing a single site for the antibiotic-induced cleavage (underlined). The signals from non-exchangeable protons of the bithiazole residue and the bleomycin terminal amine displayed a characteristic shift towards higher field (0.15 to 0.2 ppm), however, without any changes in the chemical shifts of signals for imino protons and phosphorus nuclei of the oligonucleotide in the vicinity to the binding site. On the other hand, it is known that intercalating molecules produce significant changes in the chemical shifts of signals for these nuclei.^{110,111} A somewhat greater upfield shift of the signals for bithiazole protons (0.2–0.4 ppm) was observed upon the interaction of the antibiotic with the duplex d(CGCGCG)₂.^{72,73} In this case the temperature dependence of the chemical shifts characteristic for poly(dA)·poly(dT) was not observed, apparently, due to the stronger binding of bleomycin to GC sequences. The use of the NOE technique makes it possible to establish the intercalation type of binding.¹¹² The presence of cross-peaks along the whole length of the 8-meric duplex d(CGCTAGCG)₂ chain upon its interaction with bleomycin A₅ is suggestive of the non-intercalating type of antibiotic binding.⁷⁵

In order to rationalise the experimental data in favour of intercalation and against it, an attempt was made to interpret them in terms of the hypothesis of partial intercalation of bithiazole rings proposed as early as in 1976.¹¹³ According to this hypothesis, one of the bithiazole rings is inserted between the DNA bases, thereby producing a local bending in the helix. Its effect on the length and, correspondingly, hydrodynamic properties of DNA may be very different¹¹⁴ as evidenced by viscosimetric^{38,104} and laser scattering data.¹⁰⁵ This model provides an explanation for relatively small changes in the chemical shift of bithiazole proton signals as well as for temperature dependence of the chemical shift magnitude. A rise in temperature up to values just below the melting temperature for DNA chains causes local denaturation of the helix, thereby facilitating the incorporation of the bithiazole residue between the base pairs and enhancing the upfield shift of the signals for the protons.⁷¹ A decrease in ionic strength, which causes destabilisation of the double helix, would also favour partial intercalation of the bithiazole residue and, as a consequence, more intensive fluorescence quenching and changes in the chemical shift.^{54,71}

Evidence for the improbability of complete intercalation of bithiazole rings into the DNA double helix can be derived from experiments with analogues of the C-terminal fragment of bleomycin A₂.



According to ^1H NMR data, the removal of the aliphatic substituent from position 2' of the 2,4'-bithiazole derivative enhances the ability of bithiazole rings to intercalate and increases the binding constants for poly(dA)·poly(dT).^{58,69} At the same time, the substitution of the aliphatic chain at position 2' by an aromatic ring (thiazole or benzene) strongly changes the characteristics of bithiazole analogue binding to DNA, thus permitting their intercalation. Changes in the chemical shifts (by 0.5–0.8 ppm) produced by such analogues upon their binding to DNA are far more pronounced than those for bleomycin.^{58,69,115,116} In contrast to bleomycin, its analogues increase the viscosity of DNA solutions¹¹⁶ and cause effective unfolding and folding (positive supercoiling) of covalently bound circular DNA.⁷⁷ Moreover, they display a far greater affinity for DNA and are more potent competitive inhibitors of DNA cleavage.⁷⁷ Thus, despite its inability to undergo complete intercalation binding to DNA, the bithiazole residue can partly incorporate between the base pairs, the most accessible loci for such binding being the sites of local injuries to the double-helical structure (transition regions between denatured and native states of the DNA helix, bends and breaks on the helix, protrusions formed by an extra base, etc.).

Yet another model for bleomycin binding to DNA also provides a satisfactory explanation for the available experimental data. According to this model, the terminal amine and bithiazole rings of bleomycin bind in the minor groove of DNA. This model, which was first proposed in 1986,¹¹⁷ is based on the structural similarity of the bleomycin C-terminal fragment and netropsin and the fluorescent dye Hoechst 33258, both of which bind in the minor groove of DNA. In favour of this model are experiments in which changes in site-specificity and efficiency of DNA cleavage by bleomycin were studied in the presence of ligands tightly bound to DNA. Thus, distamycin A, which binds to the sites enriched with AT sequences in the minor groove of DNA, can inhibit DNA cleavage at sequences GT and GA by increasing the cleavage selectivity at GC sequences.^{118–120} By contrast, actinomycin D binding to GC sequences and blocking the minor groove of DNA by its peptide rings around the binding sites (by 5–6 base pairs)¹²¹ produces an opposite effect: cleavage at GT and GA sequences increases, while that at sequences GC decreases. Covalent attachment of aflatoxin B to the N(7) atom of guanine or of mitomycin C to the O(6) atom of guanine in the major groove of DNA has practically no influence on the specificity or efficiency of DNA cleavage by bleomycin.¹²² The presence of bulky glycosyloxy-methyl residues in the major groove of DNA of the wild-type phage T4 also has insignificant effect on the specificity and efficiency of cleavage.¹²³ In addition, bleomycin displays a similar affinity for both glycosylated and nonglycosylated DNA of phage T4.¹²⁴ A crucial role in the antibiotic affinity for DNA is played by the nucleotide composition of DNA, particularly by the presence of guanine and the 5'-guanine–pyrimidine-3' sequence. Thus, G- and GC-enriched DNA sequences quench bithiazole ring fluorescence far more effectively,^{54,57} whereas poly- and oligonucleotides carrying sequences GC and GT appear to be the most effective inhibitors of the SV40 DNA cleavage by the antibiotic.^{63,64} The value of the constant for bleomycin binding to poly(dG)·poly(dC) exceeds those for binding to poly(dI)·poly(dC) and poly(dA)·poly(dT) (3- and 5-fold, respectively).¹²⁴ It should be noted that the minor groove of the double helix of poly(dG)·poly(dC) contains a 2-amino group of guanine which is absent in inosine or adenine. The crucial role of this amino group in strong binding of bleomycin was confirmed by experiments with anthramycin-modified DNA. This antibiotic, being localised in the minor groove, can form a covalent bond with the 2-amino group of guanine without any appreciable effect on the B-form of DNA.¹²⁵ Treatment of DNA with anthramycin results in strong inhibition of DNA cleavage by bleomycin at sequences GC and GT.¹²⁴ On the basis of these data, Kuwahara and Suguira¹²⁴ proposed a model for bleomycin binding to the 6-meric duplex d(ATGCCA)·d(TGGCAT) possessing a site for effective cleavage (underlined). The terminal amine and the bithiazole residue are arranged along

the DNA minor groove in the direction from the 5'- to the 3'-end relative to the chain to be cleaved. The binding occurs owing to electrostatic interactions and hydrogen bond formation between the 2-amino group of guanine and the nitrogen of the thiazole ring and/or oxygen of the carboxamide group. The bleomycin binding site comprises two to three base pairs which is in keeping with the data on DNA protection from cleavage by DNase I.¹²⁶

Two-dimensional NMR data also testify to the possibility of bleomycin binding in the minor groove of the double helix. Of particular interest in this respect are the results⁷⁵ which in many features provide support for the earlier hypothesis.¹²⁶ In this study, the NOE technique was used to establish the interactions between the protons of the zinc-containing bleomycin A₅ complex and the protons of the 8-meric duplex d(CGCTAGCG)₂ localised in the minor groove of the double helix. On the basis of the data obtained by molecular dynamics methods, a hypothetical spatial model of the complex was calculated. According to the calculations, the bleomycin A₅ molecule is localised in the minor groove, overlapping 4–5 base pairs. The complex is stabilised by hydrogen bonds between the amino groups of the C-terminal fragment of spermidine and the oxygen atoms of the phosphate group and the deoxyribose cycle, between the nitrogen atom of the thiazole ring and the 2-amino group of guanine as well as between the primary amino group of β -aminoalanine and the oxygen atom of the sugar–phosphate backbone. The authors of this model state, however, that this structural model is not unique: a considerable upfield shift of the signals for bithiazole protons by 0.18 ppm [H(5)] and 0.52 ppm [H(5')] and for the imino protons of GC- and AT-pairs corresponding to positions G(2) and T(4) suggests partial intercalation of the bithiazole rings.⁷⁵

Thus, there is no experimental evidence thus far allowing an unequivocal identification of the binding mode (complete or partial intercalation or binding in the minor groove) characteristic of bleomycin. It is quite probable that these binding modes are characteristic of different structures in the DNA double helix. Nevertheless, it is certain that the C-terminal fragment of the bleomycin molecule provides the binding of the antibiotic to DNA by 'anchoring' the rest of the molecule which interacts with the polymer upon oxidative cleavage of the sugar–phosphate backbone. Whatever the mode of C-terminal fragment binding, the mechanism of DNA oxidation (see below) implies the closest approximation of the bleomycin metal-binding domain to the minor groove of the DNA double helix.

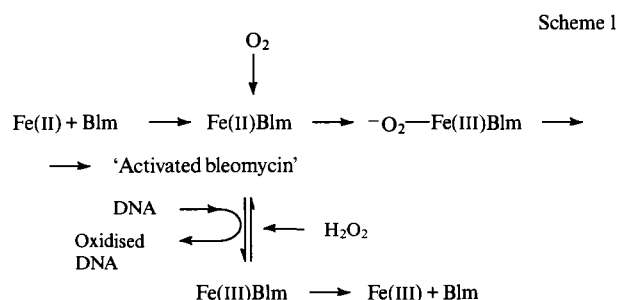
III. Cleavage of nucleic acids by bleomycin

1. The mechanism of DNA cleavage

Degradation of DNA by treatment with bleomycin eventually resulting in the cleavage of the sugar–phosphate backbone was discovered as early as 1969;^{30–33} however, the mechanism of action underlying this process has long remained obscure. The first theoretical speculations on the putative mechanism of DNA cleavage were made in 1973, and bleomycin was considered to be a hydrolytic enzyme.^{113,127} Shortly thereafter, cofactors essential for the antibiotic activity were identified. In 1975, it was found that molecular oxygen favours the DNA degradation by bleomycin.¹²⁸ In the same period it was shown that Fe(II) and Fe(III) ions stimulate the DNA cleavage by bleomycin in the presence of 2-mercaptoethanol;^{129,130} these two cofactors favouring DNA degradation were distinguished as being the most essential ones.^{35–37} According to nuclear absorption data,¹³⁰ the previously observed degradation of DNA upon treatment with bleomycin was due to the constant presence of trace amounts of iron ions in the reaction mixture. The discovery that iron atoms and molecular oxygen are essential for DNA degradation was immediately followed by a hypothesis suggesting a free radical mechanism for this process.^{37,56,130–132} Indeed, the Fe(II)Blm complex can generate $\cdot\text{OH}$ radicals^{133,134} that can interact with DNA. The enzyme superoxide dismutase converting the $\text{O}_2^{\cdot-}$ ion into O_2 and H_2O_2 inhibits DNA cleavage under the action of

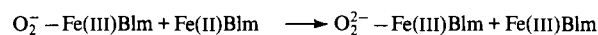
bleomycin.^{37,135,136} A correlation exists between the biological activity of bleomycin analogues and the amount of 'OH radicals generated by them.¹³² However, it turned out soon afterwards that *tert*-butylphenylnitron and dimethylsulfoxide, which act as 'traps' for 'OH radicals, do not inhibit the cleavage of DNA. Moreover, the efficiency of 'OH radical production by the Fe(II)Blm complex is 40 times lower than in the Fe(II)-H₂O₂ system.¹³⁷ Another group of investigators¹³⁶ succeeded in demonstrating that inhibition of DNA cleavage by superoxide dismutase is not related to the reduced amount of O₂^{•-} ions but is rather due to the association of the enzyme with DNA.

An alternative explanation for the bleomycin action mechanism is the formation of the so-called 'activated bleomycin' which causes direct oxidative degradation of DNA.^{89,138,139} Electron spectroscopy and EPR data as well as the use of the Mössbauer effect made it possible to propose the following scheme for DNA cleavage by bleomycin with participation of the iron ion and molecular oxygen (Scheme 1).⁸⁹



The Fe(II)Blm complex formed in the first stage rapidly interacts with molecular oxygen. In this complex the bivalent iron atom undergoes oxidation, giving rise to the O₂^{•-}-Fe(III)Blm complex. The formation of 'activated bleomycin' requires an extra

electron which is provided either by the reducing agent present in the solution or by an additional Fe(II)Blm molecule undergoing disproportionation.¹³⁹



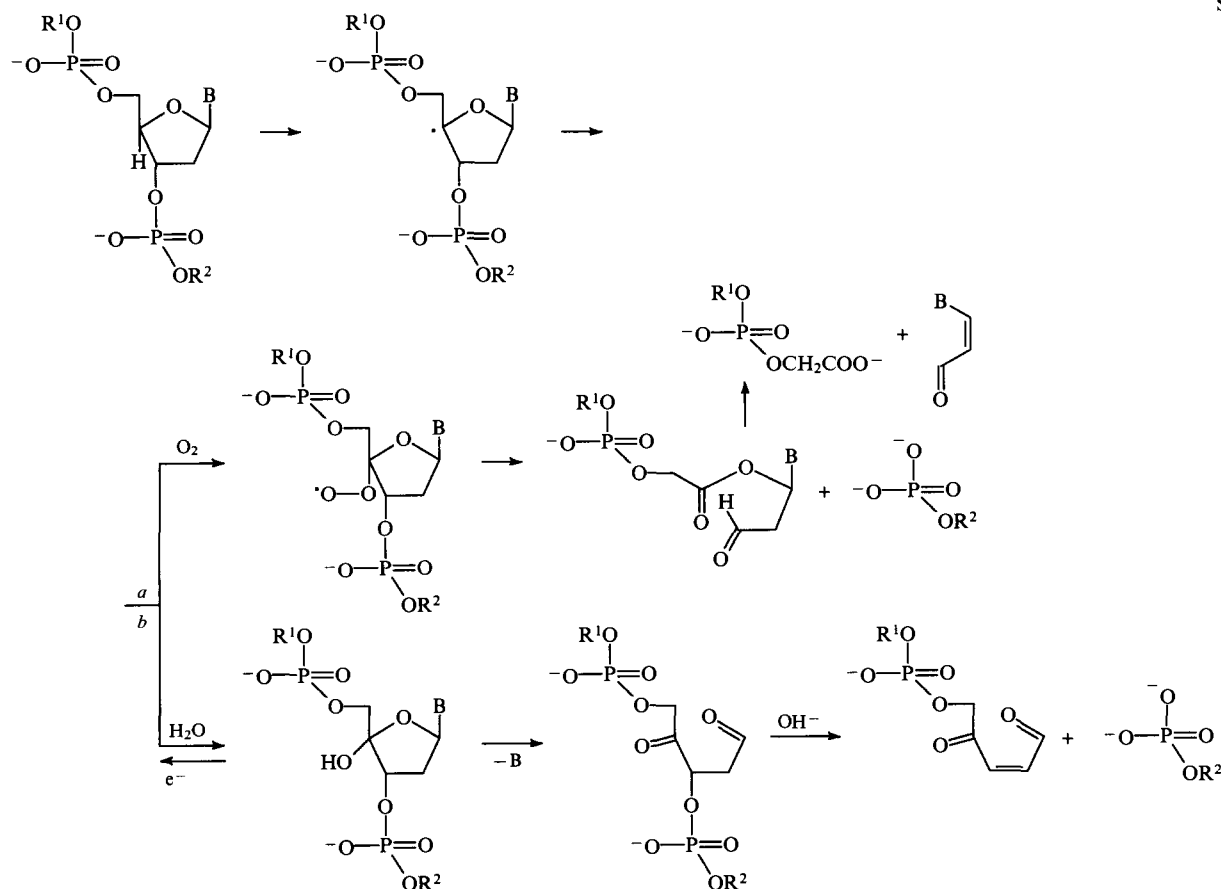
'Activated bleomycin' can oxidise organic substrates and DNA to form a Fe(III)Blm complex which can be reactivated by peroxy compounds.^{89,138-142}

According to recent mass-spectrometry data, the structure of 'activated bleomycin' corresponds to the peroxy complex of the ferric ion, HOO-Fe(III)Blm.¹⁴³ This scheme, which depicts the bleomycin activity in the presence of iron ions and molecular oxygen, was confirmed experimentally and developed further.

Intensive studies of the mechanism of action of bleomycin led by late 1980s to the establishment of all the main stages of bleomycin activation and pathways of oxidative degradation of DNA. These were documented in detail in reviews and publications.^{41,66,144,145} Therefore, in this review we give only a brief description of the main pathways of DNA oxidation by bleomycin.

Activated bleomycin induces oxidation at position 4' of a carbon atom of the deoxyribose ring¹⁴⁶⁻¹⁴⁸ which is accompanied by the splitting of the H(4') atom and the formation of a 4'-radical (Scheme 2). The oxidation is the limiting step in the chain of subsequent conversions as unequivocally follows from the isotope effect produced by substitution of the hydrogen atom for deuterium or tritium (the rate of the end product formation is 2-7 and 7-12 times less, respectively).¹⁴⁸⁻¹⁵⁰

Further conversions of the 4'-radical proceed in two different ways (*a* and *b* in Scheme 2).⁶⁶ Under aerobic conditions (pathway *a*), an addition of molecular oxygen may occur, resulting in the formation of a 4'-peroxy radical.¹⁴⁶ The subsequent scission of the C(3')-C(4') bond results in the elimination of the base-substituted propenal and cleavage of the sugar-phosphate backbone of DNA, 5'-phosphate and 3'-phosphoglycollate being formed at the site of the chain scission.^{146,151,152}



Pathway *b* is associated with hydroxylation at position 4',¹⁴⁷ apparently as a result of oxidation of the 4'-radical to a carbocation and subsequent attachment of water.¹⁵³ Under physiological conditions, the hydroxylation results in the elimination of the free base without any scission of the DNA chain.^{119, 147, 153–157} Under alkaline conditions β -elimination occurs, which results in the cleavage of the sugar–phosphate backbone and the formation of 5'-phosphate at the cleavage site. The oxidised deoxyribose residue is further converted into 2,4-dihydroxycyclopentenone which remains covalently bound to the 3'-phosphate group. If alkaline treatment is carried out in the presence of hydrazine, 3'-pyridazine is formed; treatment with alkylamines yields 3'-phosphate.¹⁵⁶

Under normal conditions (e.g., at atmospheric pressure of O₂) DNA oxidation by bleomycin results in the formation of approximately equal amounts of free bases and their propenal derivatives,¹⁵⁸ i.e., both pathways of the 4'-radical conversion are possible. Under anaerobic conditions only free bases are formed.^{148, 158} Under O₂ pressure of 3 atm, the ratio of base-propenal derivatives to free bases is 7;¹⁴⁸ at 4 atm this is equal to 10.¹⁵⁹

The high selectivity of bleomycin action with respect to oxidation of deoxyribose is worth noting. As it has been mentioned above, bleomycin can only slowly generate OH radicals.¹³⁷ Chromatomass-spectrometry data¹⁶⁰ demonstrate that treatment of DNA with the Fe(II)Blm complex in the presence of molecular oxygen and a reducing agent is practically unaccompanied by the formation of side products of DNA oxidation (as distinct from the products of the 4'-radical conversion). In particular, the major side product, 8-hydroxyguanine, constitutes only 2%–3% of the total amount of the bases and their propenal derivatives formed in the process.^{160, 161}

2. Specificity and efficiency of DNA cleavage by bleomycin

a. Effect of the primary sequence

Elaboration by Maxam and Gilbert in 1977¹⁶² of a convenient method for identifying the sequences of long-chain DNAs gave a strong impetus to a series of investigations of the sequence specificity of DNA cleavage by bleomycin and related compounds. It turned out that bleomycin displays marked specificity towards dinucleotide sequences carrying guanine at the 5'-end.^{163, 164} In this case deoxyribose of the second nucleotide undergoes oxidative degradation. The most preferred sequences for the cleavage are GT and GC; sequences GA, AT and GG are less susceptible to degradation. This finding correlates with the amount of liberated free bases: T > C \gg A > G.^{37, 164, 165} Soon it was noted, however, that identical dinucleotide sequences are cleaved to a different degree. It was hypothesised that the specificity of DNA cleavage by bleomycin is determined by DNA sequences larger than dinucleotides.^{166, 167} Mirabelli et al.¹⁶⁸ found that pyrimidine present at the 5'-end of the GC sequence enhances the cleavage.¹⁶⁸ Statistical analysis of the sequence specificity of the bleomycin-induced cleavage confirmed that the base preceding the purine–pyrimidine sequence has a certain influence on the extent of cleavage.¹⁶⁹ Thymine enhances, whereas adenine diminishes, the cleavage in the sequences GT, GC, AT, and AC.

b. Effect of the double helix structure on bleomycin-induced cleavage

Despite the conclusions of Mirabelli et al.¹⁶⁸ (which further received experimental support) one cannot explain the difference in the DNA cleavage at different sites by the effect of the primary sequence alone. Lloyd et al.¹⁷⁰ demonstrated that bleomycin induces single- and double-strand scissions at a limited number of sites in bacteriophage PM2 DNA. Some of these sites, if present in DNA in a supercoiled form, were cleaved to a greater extent.^{171, 172} The specificity of cleavage of the linear pBR 322 DNA differed from that of the supercoiled DNA, the extent of cleavage being greater for the latter.¹⁷³ It is known that the supercoiled DNA of plasmid *ColE1* is cleaved 1.5 times more

effectively than the relaxed form.⁴⁷ It was noted also that SV40 DNA contained regions which, by virtue of their secondary structure, were preferentially cleaved by bleomycin.¹⁷⁴ Interestingly, the intracellular DNA is cleaved by the antibiotic at the same preferential cleavage sites as the purified DNA.

The influence of structure on the cleavage efficiency manifests itself in the interaction of bleomycin with the modified DNA. Thus, covalent attachment of mitomycin C¹²² or *cis*-diaminodichloroplatinum(II)¹⁷⁵ in the major groove of DNA enhances the bleomycin-induced cleavage. *cis*-Diaminodichloroplatinum(II) also influences the specificity of cleavage,^{175, 176} apparently due to alterations in the structure of the DNA double helix resulting from intrastrand cross-links. Of special interest are recent findings testifying to the enhancement of the bleomycin effect:¹²⁰ distamycin A strongly (about 100-fold) enhances the bleomycin-induced cleavage of DNA at certain GC-rich sequences. Other compounds bound in the minor groove, such as Hoechst 33258, berenyl, 4',6'-diamidino-2-phenylindol, only slightly increase the efficiency of DNA cleavage by the antibiotic. Presumably, the significant enhancement of DNA cleavage is associated with structural changes in the double helix upon binding of distamycin A.¹²⁰

The presence of a protruding base has a strong effect on the specificity of the bleomycin-induced cleavage by directing its action to nucleotides located in close proximity to the given base.¹⁷⁷ It is quite probable that this effect is due to the ability of bithiazole rings to intercalate into sites with a distorted secondary structure.⁷¹

Convincing evidence for the sensitivity of the antibiotic to even minor changes in the target DNA structure was obtained in the studies by Murray et al.¹⁷⁸ when the cleavage of two virtually identical sequences in the human genome was compared. Substitution of 11 bases in a 340-meric double-stranded fragment produced significant changes in the mode of cleavage. Statistical analysis revealed that some of these changes may be attributed to the direct effect of the substituting base, whereas the changes in the cleavage at other sites located at a distance of 2–12 nucleotides from the substitution site result from structural changes in the substituted DNA.

The effect of the double helix structure on the bleomycin-induced cleavage of DNA is also manifested in DNA methylation. Enzymatic methylation of cytosine residues at position 5 diminishes the extent of cleavage in the vicinity of such sites. The protective effect is observed even at a distance of 14 nucleotides from the methylation site for DNA duplexes having the lengths from 100 to 400 base pairs.¹⁷⁹ This may be associated with local changes in the DNA structure, since it is known that methylation of cytidine facilitates the B–Z transition, the major conformational change in DNA.¹⁸⁰ Further studies with poly(dG)·poly(dC) and poly(dG)·poly(dC^{Me}) revealed that the B–Z transition induced by increasing the salt concentration strongly inhibited the cleavage of these polynucleotides by bleomycin. This finding indicates that the Z-form of DNA is conformationally unprofitable for the manifestation of the antibiotic activity. Additional evidence can be derived from circular dichroism data. In the presence of bleomycin, the B–Z transition needs a far greater ionic strength for its realisation which indicates that bleomycin predominantly binds to and stabilises the B-form of DNA.¹²³

Methylation of cytidine has a different inhibiting action on DNA cleavage by various bleomycins. Demethylbleomycin A₂ and bleomycin B₂ are less sensitive to the presence of 5-methylcytidine than bleomycin A₂ and bleomycin BAPP. At the same time, methylation of adenosine at the N(6) atom diminishes the DNA cleavage by the above-mentioned bleomycins.¹²³ In another study, a self-complementary dodecanucleotide methylated at one of its cytidine residues was used as a target. Long et al.¹⁸¹ showed that the efficiency of oxidation of methylated and nonmethylated oligonucleotides appeared to be the same, but the ratio of liberated free bases and their propenal derivatives was different. In case of the methylated dodecanucleotide, the amount of

liberated free bases was 1.5 times as great as that with the nonmethylated one; hence, the 4'-radical tended to be more susceptible to hydroxylation than to the interaction with molecular oxygen.

The effect of the polynucleotide secondary structure on the efficiency and specificity of the bleomycin-induced cleavage is especially pronounced in the case of cleavage of RNA.

3. Cleavage of RNA by bleomycin

Early studies dating back to the mid 1970s repeatedly demonstrated that RNA was resistant to the action of bleomycin.^{34, 182, 183} In RNA-DNA hybrids, the cleavage affected only the DNA chain.^{159, 184, 185} Cleavage of DNA by bleomycin was not inhibited even by a great excess of RNA.^{62-65, 186}

This generally accepted viewpoint was dispelled in 1989 when it was demonstrated that approximately three molecules of Fe(III)Blm bind to one molecule of yeast phenylalanine tRNA with an equilibrium binding constant of $0.86 \times 10^5 \text{ dm}^3 \text{ mol}^{-1}$. The cleavage occurred at three separate sites with low efficiency [5%–10% for 0.3 mmol dm^{-3} Fe(II)Blm and 3 mmol dm^{-3} tRNA as calculated per nucleotide] and resulted in the formation of free adenine and uracyl.⁶¹ This pioneering study was followed by a number of publications^{65, 187-195} dealing with various aspects of bleomycin interaction with RNA, particularly with a comparison of RNA and DNA cleavage patterns. In both cases the cleavage occurs due to oxidation of the sugar-phosphate backbone¹⁹¹ with iron ions and molecular oxygen (or peroxy compounds) as necessary cofactors.^{191, 194} The presence of reducing agents, such as ascorbate or 2-mercaptoethanol favours the RNA cleavage. A chromatographic analysis of oligonucleotide degradation products and data on electrophoretic mobility in polyacrylamide gel of degradation products of long-chain RNA testify to the formation, at the cleavage site, of 3'-phosphoglycollate and 5'-phosphate.^{191, 194} However, in contrast with DNA, the cleavage of RNA results in the liberation of free bases alone.^{61, 65, 191, 194} In all probability, the detachment of the H(4') atom of ribose triggers a chain of events resulting in the cleavage of the RNA chain.^{190, 192, 194}

The specificity and efficiency of RNA cleavage by bleomycin differ essentially from those for DNA. Firstly, RNA cleavage is more selective at a lesser number of sites. Secondly, the efficiency of the bleomycin-induced cleavage varies considerably for different RNA molecules. Some RNAs are cleaved even by micromolar concentrations of bleomycin, whereas other RNAs are resistant to even very high (0.3 mmol dm^{-3}) concentrations of the antibiotic.^{61, 194}

Bleomycin splits both single- and double-stranded fragments in RNA. However, the cleavage is especially efficient in those parts of the RNA molecule where the single-stranded structure transforms into the double-stranded one and vice versa. Interestingly, the sequence specificity typical of DNA cleavage is not observed in this case. The available data suggest that the bleomycin molecule predominantly cleaves GU sites in RNA,^{65, 188-190, 191, 193, 194} however, by no means all these sites undergo cleavage, while the intensity of cleavage for each GU site may vary considerably. It may thus be concluded that the specificity of RNA cleavage by bleomycin depends not so much on the primary sequence but is rather determined by peculiarities of the secondary or tertiary structure of the polymer molecule. The resistance of some RNA molecules to the effect of bleomycin and the lability of other molecules indicate a crucial role of certain spatial structures in the realization of effective cleavage.

The sensitivity of bleomycin to the structure of the substrate to be cleaved is likely to be manifested in its interaction with RNA. As has been mentioned, bleomycin preferentially cleaves the B-form of DNA. It is known also that the A-form of the double helix exists in RNA. The difference in sizes between the major and minor grooves and the conformation of the carbohydrate residue may be the reason for 'non-recognition' and, as a consequence, of 'non-cleavage' of RNA. Nevertheless, at definite sites, e.g., at the sites of the helix transition from the double-stranded to the single-stranded

structure and vice versa, structures may be formed that represent suitable targets for the cleavage by bleomycin. These structures may resemble the B-form of DNA. An important role in this process is played by the size of the minor groove and the position of the 4' hydrogen atom in it. It may also be assumed that such sites favour stronger binding of the antibiotic, presumably due to the possibility of intercalation of the bithiazole residue.^{71, 177} The low incidence of such sites accounts for the low number of RNA cleavage sites, which results in higher selectivity in RNA cleavage, than for DNA.¹⁹⁴

A spectacular proof of the significance of the spatial structure in effective cleavage of the double helix is given in the study by Holmes and Hecht.¹⁹³ These authors showed that DNA, which represented a copy of histidine tRNA of *Bacillus subtilis*, had one major cleavage site that coincided with the single cleavage site for this tRNA.

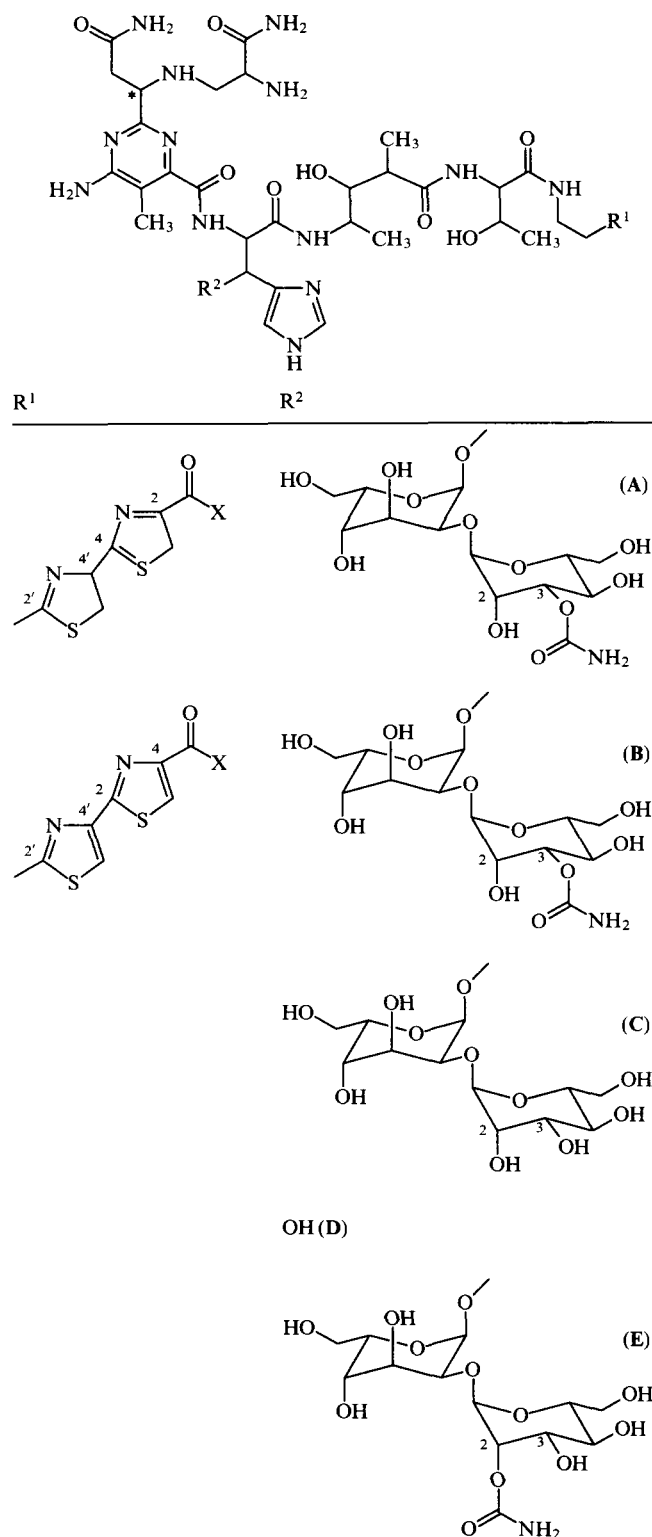
4. The role of domains in determining the specificity of bleomycin action in DNA cleavage

Immediately after the discovery of sequence-specific DNA cleavage by bleomycin, a question arose as to the nature of this specificity. By then, it had already been established that the C-terminal fragment of the antibiotic molecule is responsible for the binding to DNA.^{38, 39, 47} The fact that various bleomycins cleave DNA in a similar way^{196, 197} suggests that the terminal amine does not contribute at all to the specificity of bleomycin action. For this reason, the preferential cleavage of certain DNA sequences was attributed to the specificity of bithiazole residue binding, particularly during intercalation.¹⁶⁴ However, an increasing body of experimental evidence argues against this hypothesis.

Thus, phleomycin (B) having one reduced bond in the bithiazole residue¹⁰¹ and, correspondingly, incapable of intercalation, displays the same site specificity.^{48, 167, 197} Bleomycin with a phototransformed bithiazole residue (the 4,4' bond between the thiazole rings instead of the 2,4' bond) (A) has a site specificity that is practically identical with that of natural bleomycin.^{198, 199}

On the other hand, according to the most recent data, a certain role in sequence specificity of DNA cleavage is played by the metal-binding domain. Thus, cleavage of the self-complementary dodecanucleotide CGCTTTAAAGCG by bleomycin occurs at GC sequences (underlined), the C(3) residue being cleaved to the greatest extent.¹¹⁹ Removal of the disaccharide residue (deglycobleomycin, D) or the carbamoyl group of D-mannose (decarbamoylbleomycin, C) from the bleomycin molecule does not influence the sequence specificity of cleavage of this oligonucleotide. However, the predominant site for such cleavage is residue C(11).^{200, 201} According to the data reported by Oppenheimer et al.,²⁰² the carbamoyl group of D-mannose may become involved in the chelation of the iron ion in the metal-binding domain of bleomycin. Its removal may affect the coordination sphere of the metal as follows from NMR data.²⁰³ Hence, the change of the site of preferential cleavage of the dodecanucleotide seems to be due to the alterations in the metal-binding domains of deglyco- and decarbamoylbleomycin.

Experimental proof for the dependence of the geometry of the metal-binding domain on the sequence specificity of DNA cleavage has been presented.²⁰⁴ The degradation of three restriction fragments of DNA under the action of various bleomycin derivatives has been studied. Bleomycin B₂, deglycobleomycin A₂ (D), and isobleomycin A₂ (E) having a carbamoyl group at position 2 of D-mannose²⁰⁵ (in the case of natural bleomycin this group is at position 3) displayed a sequence specificity identical with that of bleomycin A₂. At the same time, in the case of epibleomycin A₂, which differs from bleomycin A₂ in the configuration at the chiral carbon atom of the substituent at position 2 of the pyrimidine ring (marked with an asterisk) and, consequently, in the orientation of the propionamide residue relative to the metal-binding domain,²⁰⁶ the mode of DNA cleavage changed significantly. Epibleomycin A₂ effectively cleaved guanosine at sequence TG, this cleavage mode being



non-typical of natural bleomycin. The percentage of cleaved CT and GG sequences was also higher in this case; sequences AT, TT, TC, and GC were cleaved to a lesser extent. Decarbamoylbleomycin A₂ (C) did not cleave sequences AA, AC, or CT at all, though they are weakly cleaved by bleomycin A₂. With bleomycinic acid, not only the cleavage of DNA was by 35% weaker than with bleomycin A₂ but the sequence specificity of the cleavage also changed. The main cleavable sequences were GT and GA (but not GT and GC); for CT, the percentage of cleavage was also relatively high.²⁰⁴

The nature of the chelated metal (Cu, Co, Mn) has also certain influence on the specificity of the antibiotic action.^{59, 207–209} In the presence of dithiothreitol, the Cu(II)Bln complex can effectively

cleave DNA, the site specificity for such cleavage being different from that for Fe(II)Bln. The difference in the specificity of DNA cleavage by the Fe(II)- and Cu(II)-complexes of bleomycin was especially apparent when the 127-meric double-stranded fragment of SV40 DNA was used.²⁰⁷ Unfortunately, no data on the efficiency of cleavage of specific dinucleotide sequences were given. It is interesting to note that the cleavage of DNA by the Cu(II)-deglycobleomycin complex is more effective than by the Cu(II)-decarbamoylbleomycin complex, whereas for Fe(II)-dependent cleavage an inverse dependence is observed.²⁰⁰ Noteworthy, the isobleomycin A₂-Fe(II) complex effectively cleaves DNA,²⁰⁴ whereas the isobleomycin A₂-Cu(II) complex is fully inactive.²⁰⁷

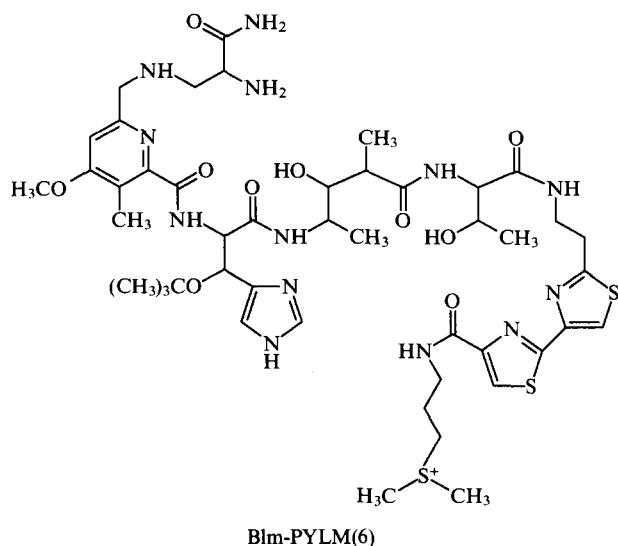
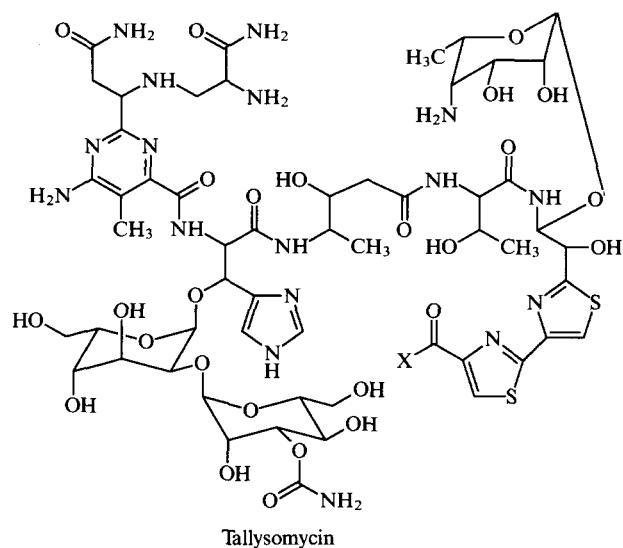
Upon irradiation with UV-light, the specificity of DNA cleavage by bleomycin complexes containing trivalent cobalt differs from that by Fe-containing bleomycin complexes.^{59, 208} A statistical analysis of sequence specificity of Co(III)-bleomycin complexes is also absent in these studies. What is evident from these experiments, is that sequences GT and GA are preferably cleaved, while sequence GC is cleaved less effectively.

Valuable information on the nature of sequence specificity of the bleomycin action can be derived from the studies of bleomycins with a significantly modified structure. One such work²¹⁰ describes the synthesis of deglycodemethylbleomycin A₂ analogues (see below) carrying glycine residues (Gly)_n (where $n=0-2$ and 4) instead of threonine, and gives an analysis of their cleaving capacity. It turned out that the sequence specificity of such analogues differs only slightly from that of the natural antibiotic. However, the efficiency of cleavage was much lower than with the natural deglycodemethylbleomycin A₂. Thus, the analogue with $n=0$ hardly cleaved DNA, whereas the level of DNA degradation by the analogues with $n=1$ and 2 possessing the maximum efficiency was comparable with that characteristic of the natural antibiotic at 10–20-fold higher concentrations.^{188, 210}

It was thus concluded that the metal-binding domain plays a decisive role in the sequence specificity of DNA cleavage. However, this definite conclusion is appropriate only in case of a mechanistic approach to the consideration of the bleomycin molecule as was the case in the late 1970s: the C-terminal fragment specifically binds to DNA and the change in the length of the spacer between this fragment and the cleaving (metal-binding) domain would alter the specificity of cleavage. If this does not take place, the situation is reversed, namely, the metal-binding domain determines the specificity of cleavage, and the C-terminal fragment defines the affinity for DNA.

As noted above, bleomycin is highly sensitive to the structure of the substrate to be cleaved. High selectivity of oxidation of C(4') of deoxyribose evidences the fine adjustment of the bleomycin molecule to the double helix conformation. It may thus be assumed that any alteration in the spacer leads to an unprofitable (with regard to cleavage) positioning of the metal-binding domain, resulting in self-degradation (but not oxidation) of DNA. Alternatively, instead of additional stabilisation of binding due to electrostatic interactions, the unfavourable localisation of the metal-binding domain may decrease the affinity of the modified antibiotic for the polymer which can also be the reason for the low cleavage efficiency. And, finally, in all previous speculations the threonine residue was regarded only as a constitutive component of the spacer, which does not take part in binding or determining the sequence specificity of the cleavage. However, one must not rule out the possibility that the free OH group can form intra- or intermolecular hydrogen bonds and thus contribute to the sequence specificity of the bleomycin action.

It is known that the bleomycin analogue tallysomycin²¹¹ having additional OH groups in the aliphatic chain at position 2' of the bithiazole residue and the aminosugar tallose attached to one of those OH groups induce the formation of single-strand scissions less effectively than bleomycin and differ from the latter in sequence specificity.^{173, 212, 213} Thus, the cleavage of supercoiled DNA of bacteriophage PM2 by tallysomycin proceeds 5–10 times

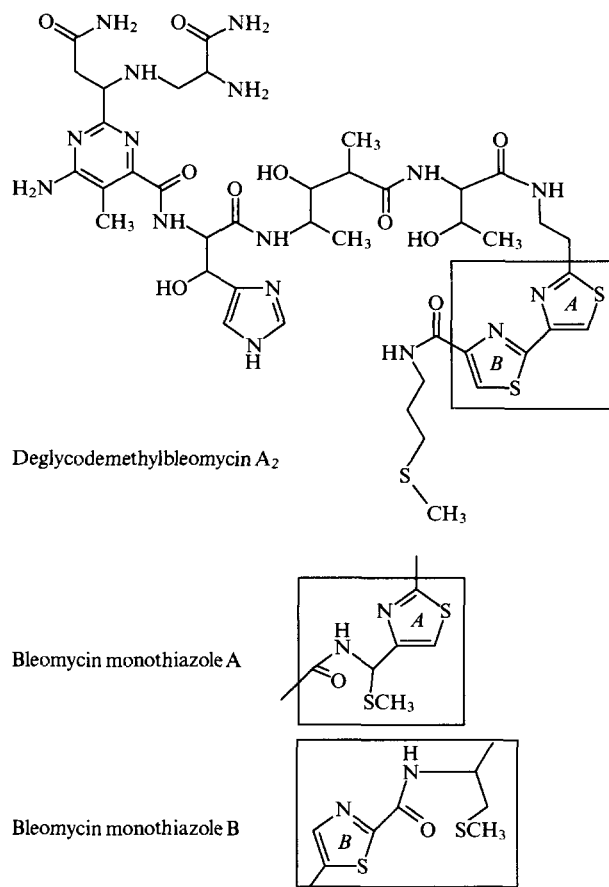


less effectively than that by bleomycin.^{53, 214} Furthermore, tallysomylin cleaves GA sequences far more effectively,^{166, 167, 197} GT and GA sequences being preferential for this antibiotic.¹⁶⁸ This finding points to the role of the bleomycin C-terminal fragment in determining the specificity and efficiency of DNA cleavage.

Convincing evidence of the ability of the bleomycin C-terminal fragment to determine sequence specificity has been given in the studies carried out by Japanese investigators.^{215, 216} These authors performed the chemical synthesis of a bleomycin metal-binding domain analogue, in which the 4-aminopyrimidine ring was substituted by methoxypyridine, the disaccharide residue was substituted by a *tert*-butyl group, and the carbamoylmethyl residue in the 2-substituent of pyrimidine was missing. In the presence of iron ions, this compound activated molecular oxygen and oxidised low molecular weight organic substrates with an efficiency comparable with that of the natural antibiotic.^{215, 216} Attachment to this compound of the C-terminal fragment of bleomycin A₂ [Blm-PYLM(6)] was accompanied by the appearance of the DNA-cleaving activity^{217, 218} despite significant changes in the metal-binding domain. These studies received further development, culminating in the synthesis of a molecule comprising the metal-binding domain, 4-aminopentanoic acid as a spacer and a distamycin A residue instead of the C-terminal tripeptide S.²¹⁹ This synthetic molecule effectively cleaved DNA (relative to natural bleomycin), the maximum degree of cleavage being observed in the regions enriched with AT sequences, to which distamycin A binds especially strongly.²²⁰ No specificity to GT and

GC sequences was observed, which is characteristic of bleomycin-induced cleavage.

Studies by Hamamichi et al.²²¹ provided valuable information as to whether the C- or the N-terminal fragment of the antibiotic molecule determines the sequence specificity of bleomycin action. To this end, the authors synthesised and assayed DNA-cleaving agents (analogues of natural deglycodemethylbleomycin A₂) containing, instead of one of the thiazole rings (A or B), its biosynthetic precursor, *S*-methyl-L-cysteine).²²²



It turned out that such analogues cleave supercoiled covalently closed and linear double-stranded DNA less effectively than natural deglycobleomycin A₂. No discernible sequence specificity was observed in the cleavage of 5'- or 3'-labelled linear double-stranded DNA. Thus, the synthetic analogues cleave DNA statistically in contrast with sequence-specific cleavage by the natural antibiotic. This study is a sound argument in favour of the determining role of the bithiazole residue in sequence specificity of the bleomycin action, the bi- (but not mono-) thiazole fragment being the crucial factor.²²²

Another recent study of the role of bleomycin N- and C-terminal fragments in the recognition of definite DNA sequences²²³ concerned the synthesis of molecules containing both DNA-binding and DNA-cleaving groups. As the DNA-binding group the C-terminal fragment of bleomycin A₂, or demethylbleomycin A₂ carrying a bithiazole residue and a terminal amine, was used. The DNA-cleaving group, EDTA (ethylenediaminetetraacetic acid), was attached to the bithiazole residue by an amide bond. If the bithiazole fragment in the bleomycin molecule is the critical factor determining the direction of the antibiotic action, such molecules will cleave DNA in the vicinity of guanine-pyrimidine sequences. However, no appreciable sequence specificity of DNA cleavage characteristic of bleomycin was noted in these model compounds.²²³ One serious pitfall of this study is that its authors did not provide any experimental proof for the binding of their synthetic model

compounds to DNA. This is an important circumstance if one takes into consideration that synthetic compounds cleave DNA far less effectively (approximately 10-fold) than natural bleomycin. The efficiency of DNA cleavage by EDTA-containing compounds is comparable with that for EDTA. It can thus be assumed that at the concentration of the analogues of $100 \mu\text{mol dm}^{-3}$ that had been used to demonstrate the sequence specificity of the antibiotic action, the degradation of DNA is predominantly effected by diffusing $\cdot\text{OH}$ radicals generated by the reagent molecules not bound to DNA. In this case, the conclusion made by the authors in favour of the determining role of the bleomycin N-terminal fragment in sequence specificity appears to lack sufficient experimental justification.

Yet another detail worth noting is important for the correct understanding of the nature of sequence specificity. According to Otsuka et al.,²¹⁹ cleavage by a bleomycin analogue containing distamycin A occurred at sites enriched with AT sequences, i.e., at sites responsible for the binding of distamycin A. This provides evidence of the spatial proximity of the metal-binding domain to the DNA-binding fragment in the bleomycin molecule. Molecular models for this compound suggest the existence of a bend in the residue linking distamycin A and a metal-binding site providing for such cleavage. Presumably, a similar situation takes place in the binding and cleavage of DNA by natural bleomycin; in this case, site-specific recognition of DNA may be effected by both C- and N-terminal fragments of the antibiotic molecule.

However, the data available do not provide any unambiguous conclusion on the nature of the sequence-specific effect of bleomycin. Many of these data and, particularly, the model of binding in the minor groove of DNA, point to the important role of the bleomycin C-terminal fragment in the specific recognition of DNA. Nevertheless, one should not rule out that the C-terminal fragment alone cannot induce either the sequence-specific binding or cleavage of DNA. There are strong grounds for believing that the metal-binding domain plays an important role in preferential recognition of the dinucleotide sequence to be cleaved. It is not excluded that an important role in this process is played by the matching of the sizes of the metal-binding domain and the minor groove. Apparently, the residues of threonine and 4-amino-3-oxy-2-methylpentanoic acid providing correct spatial orientation of N- and C-terminal fragments, also contribute to the specificity of the bleomycin action. It follows from these data that adequate interpretation of the nature of such site specificity is possible if one takes into consideration all the three structural elements, such as affinity for the cleavage site provided predominantly by the C-terminal fragment, microvariations in DNA structure determining the size of the minor groove and the optimal position of the deoxyribose C(4')–H bond for oxidation by the iron hydroperoxide complex as well as the possibility of fixing the orientation of the metal-binding domain needed for the attack through the connecting group and/or due to the interaction of the bleomycin N-terminal fragment with the double helix of DNA. To this can be added the necessity of penetration of the oxygen molecule to the chelated iron ion provided by the disaccharide which may form a hydrophobic pocket and the important role of the reducing agent in generating 'activated bleomycin'. The elucidation of these factors will undoubtedly shed more light on the nature of site specificity of bleomycin.

5. Correlation between the affinity and efficiency of cleavage

Cleavage of DNA by bleomycin is preceded by the binding of the antibiotic to the polymer. This raises the following questions: Do cleavage and binding sites coincide? How many base pairs does bleomycin cover upon binding? Is the cleavage efficiency determined exclusively by the bleomycin affinity for the given site or are other factors also involved? Some recent results provide answers to these questions. In particular, studies^{126, 224–226} describe DNA cleavage by different endonucleases in the absence and in the presence of bleomycin and phleomycin complexes with Co(III). The mode of DNA cleavage by DNAase I and micrococcal

nuclease changed considerably in the presence of bleomycin, showing a distinct protective effect at definite regions on the radiograms. These regions comprised, as a rule, a site for the cleavage by the Fe(II)Blm complex. In this case, one bleomycin molecule 'covered' from 3 to 5 adjacent base pairs from the endonuclease action^{126, 225} which agreed well the earlier observations.¹²⁴ Nightingale and Fox¹²⁶ even made an attempt to validate, on the basis of nuclease hydrolysis inhibition data, the orientation of arrangement of the bleomycin molecule at the binding-cleavage site 5'...ACGT...3', stipulating that one antibiotic molecule 'covers' three base pairs. The authors assumed that bleomycin encompasses sequence 5'-CGT-3', i.e., its molecule is positioned at the 5'-end of the chain relative to the base to be cleaved. Another interesting finding of this study is that the sites with alternating (AT)_n sequences, where $n = 3$, are cleaved by bleomycin with almost the same efficiency as GT sequences. At the same time, the Co(III)Blm complex does not protect these sites from the DNAase I action. In other words, these sites are characterized by efficient cleavage at a relatively weak binding. At the (AT)_n sites, the cleavage affected only the AT (but not TA) sequences. (AAT)_n, (ATT)_n, (TTA)_n, (TAA)_n, A_n·T_n and some individual AT sites did not practically undergo cleavage. It was assumed that the observed phenomenon is due to an unusual alternating conformation of the B-form in sequences (AT)_n, where the turn of the helix at 5'-TA-3' is greater than at 5'-AT-3'.²²⁷ It is probable also that changes in the normal B-form of DNA are due to the low ionic strength of the buffer solution used for the cleavage.^{126, 225, 226}

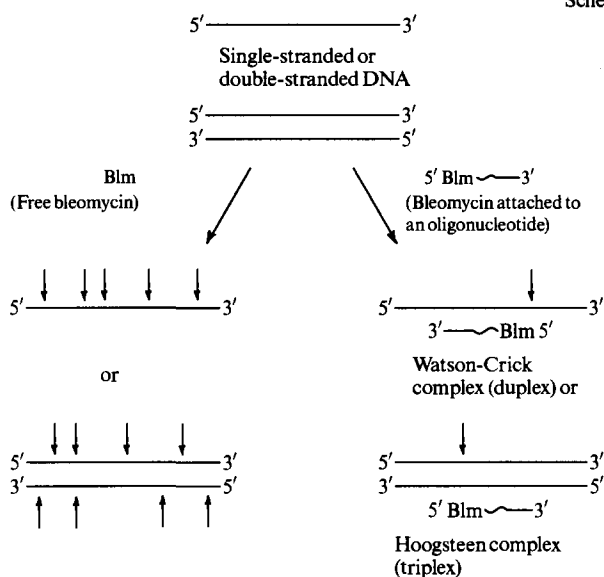
Thus, there exists a certain dependence between the strong binding of bleomycin to DNA and the efficient cleavage of the latter. An important factor is the presence of guanine in the nucleotide sequence. The efficiency of cleavage depends, to a large extent, on the local structure of the double helix which must be in conformation B (but not Z or A). Obviously, the cleavage is more efficient in alternating purine–pyrimidine sequences as can be evidenced from preferential cleavage of guanine–pyrimidine (relative to guanine–purine) and thymine–purine–pyrimidine (relative to adenine–purine–pyrimidine) sequences, and efficient cleavage of (AT)_n. Summing up, one may conclude that the efficiency of cleavage depends not only on the strength of binding but also on DNA structure. Therefore, the cleavage of DNA by bleomycin can be used as a sensitive method for determining microvariations in the double helix structure.

IV. Bleomycin derivatives of oligonucleotides. Synthesis and site-specific cleavage of DNA

As noted above (see Section I), owing to its relatively low toxicity, bleomycin has found wide use in treating squamous tumours both separately or in combination with other chemotherapeutic drugs. Nevertheless, the application of this antibiotic is restricted due to its damaging action on certain tissues, in which the content of a bleomycin-inactivating enzyme is low. One of the most common side effects produced by this antibiotic is pulmonary fibrosis.^{13, 15, 228} Among other ways to enhance the specificity of therapeutic actions of this drug is to increase its selectivity towards specific nucleic acids. The inherent specificity of natural bleomycin towards dinucleotide sequences prevents it from distinguishing various nucleic acid molecules or different sites of the same macromolecule. The enhancement of specificity of the bleomycin action can be achieved through its attachment to the oligonucleotide exemplified in Scheme 3. In this scheme, the sites of hypothetical cleavage of the DNA chain are marked by arrows. This approach, which was first suggested in the 1960s^{229, 230} and is widely used now^{231–235} permits spatial approximation of bleomycin and the preselected nucleic acid region and thus ensures its directed chemical modification. Such an approach is now widely used in routine studies.^{231–235}

A broad spectrum of reactive oligonucleotide derivatives have been created by now that carry alkylating or photoreactive groups, platinum complexes capable of coordinating target heterocycles,

Scheme 3



and groups catalysing oxidative degradation of target nucleic acids.^{231, 235} The latter can chelate transient metals; their interaction with molecular oxygen can catalytically generate active oxygen-containing species which degrade DNA. There exist natural compounds (among those is the antitumour antibiotic bleomycin) which cause destruction of DNA in the same way. From the data presented in Sections I–III, one may conclude that oligonucleotides carrying the residue of this antibiotic should be effective site-specific reagents able to 'switch-off' the function of definite genes. However, taking into account the complex nature of bleomycin, which has several nucleophilic centres, special efforts will be necessary in order to obtain its oligonucleotide derivatives.

1. Synthesis and properties of bleomycin derivatives of mono- and oligonucleotides

When constructing bleomycin derivatives of oligonucleotides suitable for site-specific degradation of target DNA, it is necessary to preserve both the ability of the antibiotic to cleave the DNA of an oligonucleotide fragment to form complementary complexes.

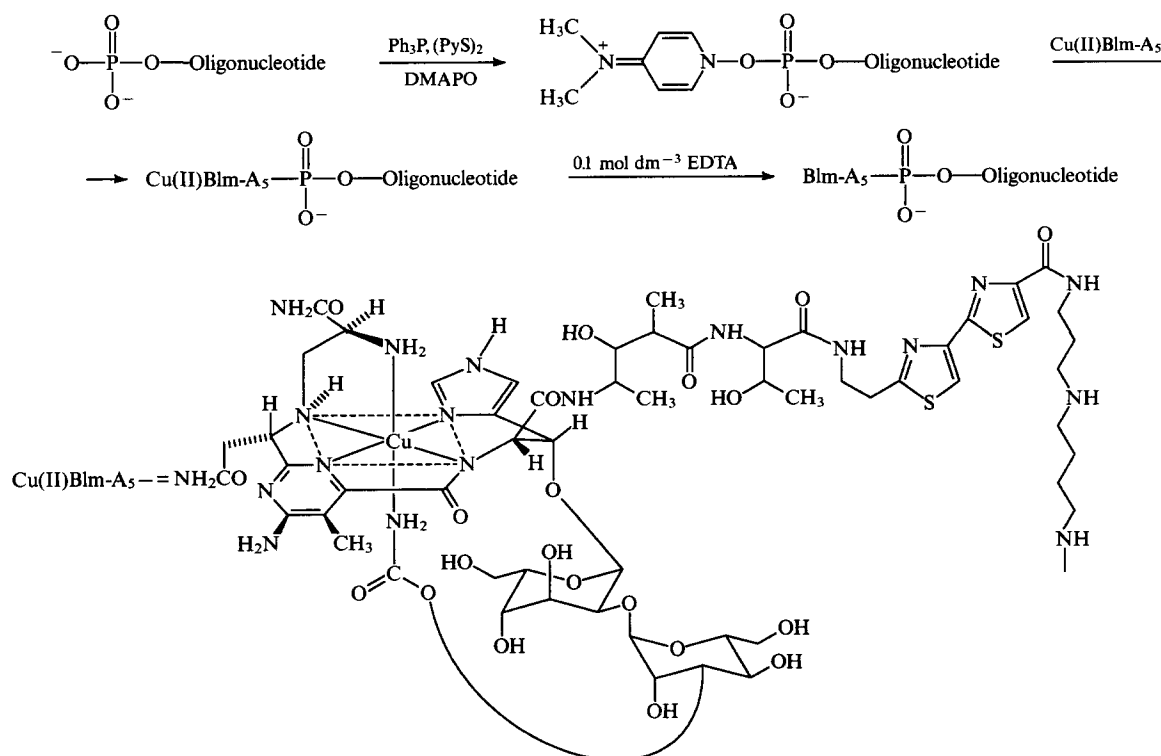
To meet these requirements, the antibiotic was attached to an oligonucleotide at the 5'- or 3'-terminal phosphate group preactivated with triphenylphosphine-2,2'-dipyridyl disulfide in the presence of 4-*N,N*-dimethylaminopyridine-1-oxide (DMAPO) (Scheme 4). It is known that the phosphate group in the thus obtained zwitterion derivative readily reacts with aliphatic amino groups.²³⁶ Bleomycin A₅ contains several such groups. The amino groups in the metal-binding domain essential for the DNA-cleaving activity of the antibiotic were protected by chelation with the copper ion, thus directing the attachment to the amino groups of the spermidine residue at the C-terminal fragment of the bleomycin molecule. The successful use of the copper-containing bleomycin complex for selective acylation of the C-terminal amine was documented in earlier studies.²³⁷ In order to avoid the attachment of two oligonucleotide molecules to one antibiotic molecule, the latter was taken in a 10-fold excess.

Analysis of electronic absorption spectra revealed the presence in the synthetic compounds of both the oligonucleotide fragment and the bleomycin residue, the contribution of each component to the total spectrum being commensurate with the binding of one antibiotic molecule to one oligonucleotide molecule.^{238, 239}

The structure of bleomycin-oligonucleotide derivatives was finally established in ¹³C NMR studies.²⁴⁰ It was found that the linkage of the terminal phosphate group of the oligonucleotide involves the spermidine primary amino group in bleomycin A₅ (see Scheme 4).

As has been mentioned above (see Table 1), bleomycin can form relatively stable complexes ($K_b = 10^5 \text{ dm}^3 \text{ mol}^{-1}$) with double-stranded DNA. Moreover, being bound to DNA, this antibiotic stabilises the structure of the double helix. Thus, the melting temperature for calf thymus DNA in the presence of bleomycin

Scheme 4

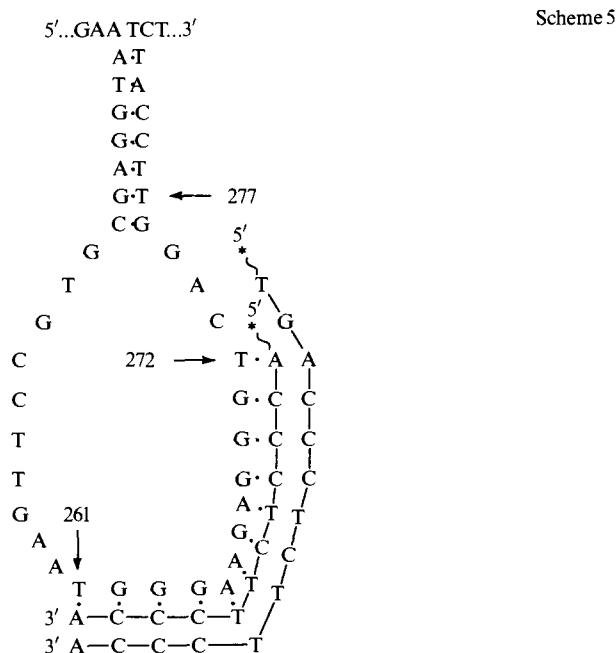


risers by 4 °C.¹⁰⁴ Attachment of bleomycin to an oligonucleotide should stabilise the complementary complex formed thereby. Indeed, the melting temperature for a complex of tetradecanucleotide pd(TGTTTGGCGAAGGA) with the bleomycin derivative of the complementary heptanucleotide, Blm-A₅-pd(CCAAACA), is 33 °C which is 11 °C higher than that for the analogous complex formed by the original heptanucleotide.^{238, 239} This is an important point in the realisation of the targeted complementary action, since the efficiency of this action on DNA depends, in a large measure, on the stability of the complementary complex formed by target DNA and the reagent.²⁴¹

The next step in this direction was to investigate the DNA-cleaving activity of bleomycin derivatives of oligonucleotides.

2. Site-specific cleavage of a single-stranded fragment of DNA by bleomycin derivatives of oligonucleotides

In a study by Sergeev et al.,²⁴² a 302-meric DNA fragment representing a copy of the RNA fragment of the tick-borne encephalitis virus was used to examine the site specificity of oligonucleotide derivatives of bleomycin. Two oligonucleotide reagents carrying a bleomycin A₅ residue at their 5'-ends were complementary to sequence 261–274 which is predominantly located in the single-stranded hairpin (the Blm-A₅ residue attached to 5'-phosphate is marked by an asterisk) (Scheme 5).^{243, 244}



Cleavage of the 302-meric DNA target was studied using polyacrylamide gel electrophoresis. This approach allows one to separate the degradation products from the original DNA target and to determine (with an accuracy of one base) the site where the target has been cleaved. The latter is achieved by comparing electrophoretic mobilities of degradation products of the target by the reagent with electrophoretic mobilities of the products of statistical degradation of the target at one or two types of bases using the procedure described by Maxam and Gilbert in 1979.¹⁶²

The results of electrophoretic analysis suggest that under conditions of complementary complex formation, both oligonucleotide reagents induce scissions at the GT sequences of the target closest to the antibiotic residue, i.e., at T(272) and T(277) (Fig. 2). The cleavage proceeds with high efficiency and selectivity. By illustration, when the shorter, 12-meric reagent is used at a concentration of 1×10^{-5} mol dm⁻³, direct breaks (without an additional alkaline treatment, Scheme 2, pathway *a*) occur at sequences T(272) and T(277) in 70% of the DNA target.

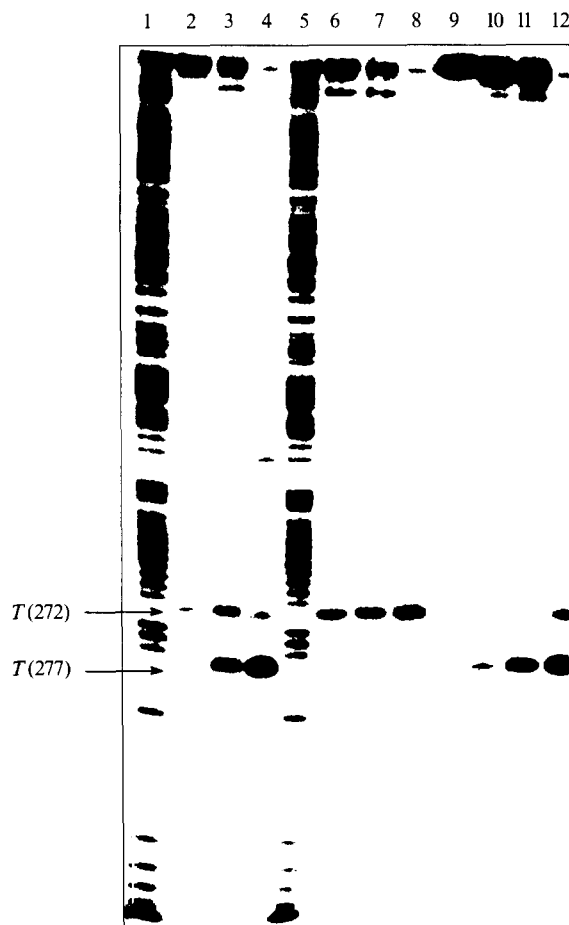
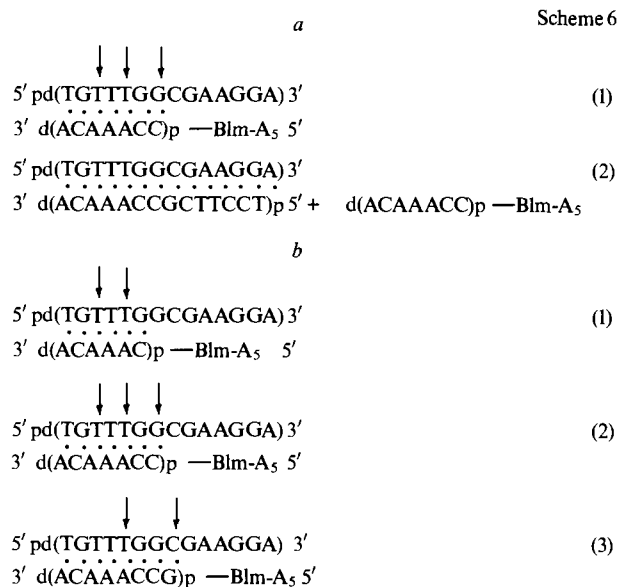


Figure 2. The results of analysis of degradation products of a 302-meric 3'-³²P-labelled DNA target by 12- and 14-meric oligonucleotide reagents. Lanes 1 and 5, is statistical cleavage of the DNA target at purine residues;¹⁶² lanes 2–4, is the 12-meric reagent (1×10^{-7} , 1×10^{-6} and 1×10^{-5} mol dm⁻³, respectively); lanes 6–8, is cleavage by a 14-meric reagent (5×10^{-6} mol dm⁻³) for 1, 3 and 6 h, respectively; lane 9, is the DNA target incubated in the absence of the reagents; lanes 10–12, is cleavage by a 12-meric reagent (5×10^{-6} mol dm⁻³) for 1, 3 and 6 h, respectively.

This cleavage is determined by site-specific binding of the oligonucleotide fragment of the reagents to the complementary sequence of the DNA fragment. This becomes obvious when analysing the DNA cleavage by bleomycin and its oligonucleotide derivative whose nucleotide sequence is devoid of the complementary binding site at the preselected fragment. It was shown that (i) both reagents cleave the DNA target with lower efficiency than do complementary reagents and at multiple positions and (ii) T(272) and T(277) are not the preferential sites for the cleavage.²⁴²

Evidence for the necessity of complementary complex formation for effective degradation of the DNA target is presented in Scheme 6 (the main cleavage sites are marked by arrows).²³⁹ The 14-meric DNA target is effectively cleaved by the 7-meric oligonucleotide reagent Blm-A₅-pd(CCAAACA) [Scheme 6 *a* (1)]. In the presence of a tetranucleotide complementary to the target, this reagent loses its ability to form a complementary complex with the target and does not practically cleave it [Scheme 6 *a* (2)].

Complementary oligonucleotide reagents of various lengths are characterised by different positional directionality of cleavage. Thus, for a 6-meric reagent, the main cleavage sites are T(5) and T(3) [Scheme 6 *b* (1)]; those for a 7-meric reagent are G(7), T(5), and T(3) [Scheme 6 *b* (2)], while those for a 8-meric reagent are C(8) and T(5) [Scheme 6 *b* (3)]. It is interesting to note that when 7- and 8-meric reagents are used, the target is directly cleaved at the



nucleotide closest to bleomycin which is involved in the formation of a complementary complex with the reagent (at residues G(7) and C(8), respectively). In the case of a 6-meric reagent, the adjacent nucleotide [residue G(6)] does not undergo cleavage, while residue T(5) is cleaved. Nucleotide G(6) remains intact both when 7- and 8-meric reagents are used (Scheme 6b).²³⁹ Apparently, under these conditions, the specificity determined by the moiety of the oligonucleotide reagents is superimposed on the specificity of the antibiotic itself, for which the cleavage at sequence TG is not typical (see Section III).

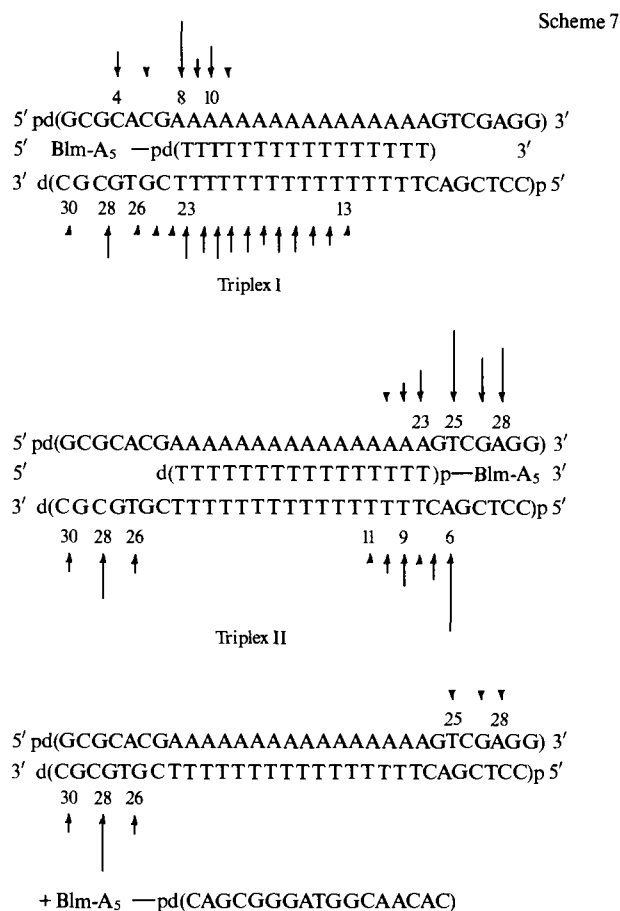
Thus, the alteration in the length of the oligonucleotide moiety of the reagent changes the site-direction of the DNA cleavage, indicating a site-specific mode of action of the covalently attached bleomycin residue.

3. Degradation of a double-stranded DNA target by bleomycin derivatives of oligonucleotides within the triplex structure

One of the versions of the complementary targeted modification is the use of reactive oligonucleotide derivatives capable of attacking selected sites of a double-stranded DNA by forming a ternary complex.^{235, 247} Oligonucleotides containing alkylating^{246, 247} or photoreactive groups,²⁴⁸ as well as groups with a redox mechanism of action,^{249, 250} have been used. The bleomycin A₅ residue, which has demonstrated effective cleavage of a DNA target within a duplex structure was assayed as the reactive group.²⁵¹

The DNA target for the study of the oligonucleotide reagent action within the ternary complex was selected in accordance with the following demands. First, the target had to contain a region of homopurine and homopyrimidine sequences necessary for the ternary complex formation. Second, a stable ternary complex should be formed at neutral pH values, since bleomycin effectively cleaves DNA in the pH range of 7–9.^{37, 62, 63} If these conditions are fulfilled, stable ternary T·AT complexes are formed.^{252, 253} Third, the fragment involved in the formation of the complex with the reagent must be flanked by sequences which could serve as targets for the action of the bleomycin residue during the complex formation. Since bleomycin predominantly cleaves DNA at sequences GT, GC, AT, and GA at deoxyribose, the second nucleotide (Section III), a 30-meric double-stranded target (Scheme 7) was selected (the cleavage sites are marked by arrows whose length is proportional to the cleavage intensity).

Under conditions of ternary complex formation, 5'- and 3'-bleomycin derivatives of the 16-meric oligothymidylate induce the cleavage of the target. Both reagents cleave DNA at both chains in the vicinity of the antibiotic residue upon binding of the third chain



(reagent), which is parallel to purine-rich (triplex I) and antiparallel to pyrimidine-rich (triplex II) sequences. This is in agreement with the literature data^{249, 250} for the cleavage of double-stranded DNA by EDTA- and 1,10-phenanthroline-containing oligonucleotide reagents which form a ternary complex with DNA.

Cleavage of a pyrimidine-rich chain by a 3'-bleomycin derivative of hexadecathymidylate occurs both in the vicinity of the 5'-end of the oligo(T)-track due to the formation of a ternary complex and around the 3'-end of the chain (Scheme 7). The latter cleavage occurs at sites C(30), C(28) and T(26) of the GC and GT sequences that are preferential for the binding and cleavage by the bleomycin itself (Section III). At a 5-fold excess of the reagent (relative to the target), this cleavage may be due to the ability of the bleomycin residue to bind to a double-stranded DNA without the formation of a triplex by the oligonucleotide moiety of the reagent. To check this hypothesis, a DNA target was cleaved by a 5'-bleomycin derivative of a 16-meric oligonucleotide, Blm-A₅—pd(CAGCGGGATGGAACAC), which a priori is incapable to form a ternary complex with the target. In this case, the purine-rich chain is cleaved only insignificantly (by 6%), whereas the pyrimidine-rich chain, as in the case of bleomycin derivatives of hexadecathymidylate, is cleaved at the 3'-end at sites C(30), C(28), and T(26) (16%). This suggests that the action of a 5-fold excess of 5'- and 3'-bleomycin derivatives of hexadecathymidylate on the double-stranded DNA target can be both site-specific due to the targeted attachment of the oligonucleotide in the ternary complex formation and nonspecific when the bleomycin residue binds to double-stranded DNA.

Comparing the total extent of cleavage of the double-stranded DNA target by bleomycin-containing reagents (Table 2), one may conclude that for both 5'- and 3'-bleomycin derivatives of hexadecathymidylate, site-specific cleavage associated with the ternary complex formation prevails over nonspecific ones.

Table 2. Total extent of cleavage of a 30-meric double-stranded DNA target by bleomycin derivatives of oligonucleotides.

Reagent	Total extent of cleavage (%)	
	Purine-rich chain	Pyrimidine-rich chain
Blm-A ₅ –p(dT) ₁₆	25	47
(dT) ₁₆ p–Blm-A ₅	35	36
Blm-A ₅ –pd(CAGCGGGATGCAACAC) ^a	6	16

^a Does not form a ternary complex with the DNA target.

4. Catalytic degradation of a DNA target by an oligonucleotide derivative of bleomycin

The advantage of applying groups with a redox-type mechanism of action [Fe(III)–EDTA, metalloporphyrins or Cu(II)–1,10-phenanthroline] over alkylating or photoreactive groups for the site-specific DNA modification is their ability to produce catalytically active oxygen-containing species and thus exert manifold action on the DNA target.^{254–256} The glycopeptide antibiotic bleomycin is an illustrious representative of compounds with a redox mechanism of action. Cyclic oxidation–reduction of the iron ion chelated in the metal-binding domain of bleomycin by molecular oxygen and some reducing agent results in multiple production of ‘activated bleomycin’ and, as a consequence, in catalytic oxidation of organic substrates.^{56, 257, 258} In the process of oxygen reduction, bleomycin acts as an enzyme with the iron ion as a cofactor.^{56, 259} Recent studies²⁶⁰ provide evidence that in the presence of ascorbate one molecule of bleomycin can catalyse the reduction of 4.7 molecules of oxygen. The main advantage of bleomycin as a reactive group for the site-specific cleavage of DNA is its ability to oxidise catalytically not only low molecular weight substrates but also DNA.^{201, 261}

It has already been noted that all the redox groups used for site-specific modification of DNA can reduce molecular oxygen catalytically. However, the capability of these groups to cause multiple degradation of DNA within the structure of the oligonucleotide reagent has not yet been realised. One of the reasons for this is an accidental damage to nucleotide residues by reactive oxygen-containing species generated by these reagents. The analysis by chromatomass spectrometry revealed the presence of a greater number of modified bases (compared to the number of direct cleavages) after treatment of DNA with Fe(III)–EDTA and Cu(II)–1,10-phenanthroline complexes.^{262, 263} Similarly, a great deal of modified bases (primarily, guanine) are formed upon treatment of DNA with metalloporphyrins.²⁵⁶

Modification of bases does not lead to direct cleavage of the DNA chain. Moreover, many modified bases, particularly 8-hydroxyguanine and 8-hydroxyadenine, the major products of ·OH radical interaction with purine heterocycles, are stable under alkaline conditions and even treatment with piperidine does not result in the cleavage of the sugar–phosphate backbone at these sites. Such hidden modifications mask the catalytic activity of the above-mentioned reagents.

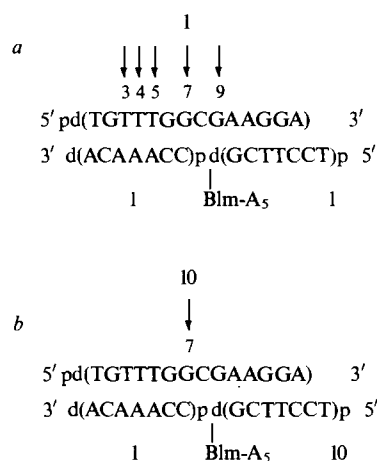
The mechanism of effective degradation of DNA by bleomycin differs essentially from that by redox groups. Under physiological conditions, bleomycin-induced selective oxidation of the C(4′) atom of deoxyribose leads with equal probability either to direct cleavage of the DNA chain or to the formation of a base-labile site (Section III). For this antibiotic, modification of nucleotides is only a minor reaction.^{160, 161} Thus, the yield of the major side product of the reaction, 8-hydroxyguanosine, constitutes 2%–5% of the amount of oxidised deoxyribose.¹⁶⁰ Thus, bleomycin oxidises nucleotide residues with a far greater selectivity than its redox analogues.

Bleomycin does not form covalent linkages with DNA following oxidation of deoxyribose but it can bind to a new site in DNA, and after reduction of the iron ion in the active centre it

can again oxidise the sugar–phosphate backbone. Analysis of extended DNA revealed that one antibiotic molecule stimulates the formation of several molecules of free heterocyclic bases or propenal derivatives.²⁶¹ The ability of one bleomycin molecule to induce degradation of several DNA molecules has been demonstrated for oligonucleotides used as targets.²⁰¹

In order to examine the ability of the bleomycin residue within the structure of the oligonucleotide conjugate to cleave DNA catalytically, a model with an equimolar target: reagent ratio (Scheme 8 *a*) and 10-fold excess of the target relative to the reagent (Scheme 8 *b*) was used. The cleavage sites in the scheme are marked by arrows.²⁶⁴

Scheme 8



It is known that bleomycin more effectively cleaves double-stranded DNA than single-stranded DNA.^{167, 265–267} This circumstance considered, a model comprising a 14-meric DNA target, a 5′-bleomycin derivative of a heptanucleotide, and a heptanucleotide complementary to the 3′-end of the target was chosen.

The catalytic activity of the bleomycin residue covalently bound to the oligonucleotide, can be manifested (depending on the experimental conditions) in a damage to several DNA target molecules by one reagent molecule or in repeated attacks on the same target by the complementary complex.

a. Repeated cleavage of a 14-meric DNA target by an oligonucleotide derivative of bleomycin

Interaction of an oligonucleotide derivative of bleomycin with the tetradecanucleotide at their equimolar ratio (Scheme 8 *a*) results in a practically complete (80%) degradation of the target. This is accompanied by the formation of a broad range of degradation products and modification of sites T(3)–T(5) remote from the site of covalent attachment of the antibiotic. At the same time, with a 10-fold excess of the target, the modification predominantly occurs at G(7) (Scheme 8 *b*). This result can be interpreted in terms of catalytic properties of the bleomycin residue, which under conditions of an equimolar reagent: target ratio can be manifested in repeated action on the DNA target. Analysis of the time dependence of the tetradecanucleotide degradation at 20 °C revealed that the target is primarily attacked at position G(7) (Fig. 3). This is followed by accumulation of shorter fragments formed upon the destruction of sites T(5), T(4) and T(3). The amount of the degradation product at position G(7) does not increase any longer but decreases with time. A similar situation is observed when the cleavage occurs at position G(9). These findings provide direct evidence in favour of repeated exposure of the DNA target to the antibiotic action.

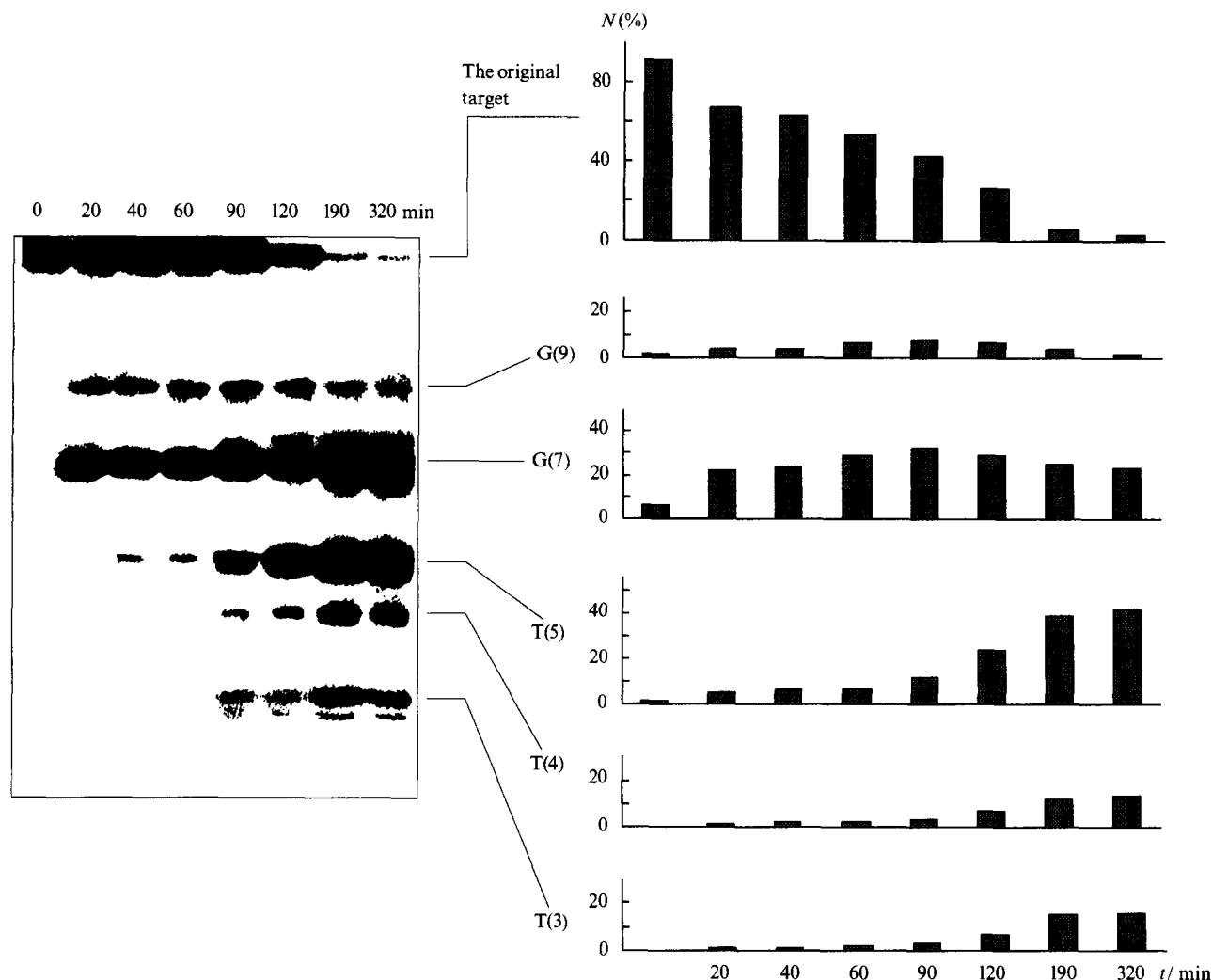


Figure 3. Time dependence of the cleavage of the 14-meric DNA target by the oligonucleotide reagent (see Scheme 8 a) (electrophoretic and densitometric data). Oligonucleotide concentration is 1×10^{-5} mol dm $^{-3}$; N is the concentration of the product in the reaction mixture.

b. Degradation of several target molecules by one reagent molecule

In order to manifest the catalytic activity, the oligonucleotide derivative of bleomycin has to attack one target molecule after another. This will require an excess of the target and selection of conditions enabling both ready dissociation of the complementary reagent–target complex and, simultaneously, the stability needed for efficient modification. Fig. 4 illustrates the cleavage of the DNA target by the reagent at different temperatures and under conditions when the reagent concentration is 10 times less than that of the target and the heptanucleotide. The cleavage of the target is a maximum in the temperature range of 25–35 °C which includes the melting temperature for the reagent–target complex ($T_{m.p.} = 33$ °C). Under these conditions, the reagent readily dissociates from the complementary complex, thereby enabling its transfer from one target molecule to another. At the same time, about half of the reagent molecules remain within the complementary complex. An increase in temperature sharply decreases the degree of cleavage, apparently, due to the decrease in the concentration of the complementary reagent–target complex. Lowering of temperature also diminishes the degree of the target cleavage, which can be attributed to nonoptimal conditions for the manifestation by the reagent of its catalytic activity. It has been established that at temperatures around 30 °C, about 20% of the target undergoes direct cleavage, while subsequent treatment with piperidine reveal an additional 10% of sites that are labile under alkaline conditions.²⁶⁴

Degradation of about 30% of the tetradecanucleotide by the oligonucleotide reagent and in the presence of a 10-fold excess of the target testifies to the fact that one reagent molecule can attack, on average, three target molecules. Restricted efficiency of the reagent action in the presence of a sufficient amount of iron ions,

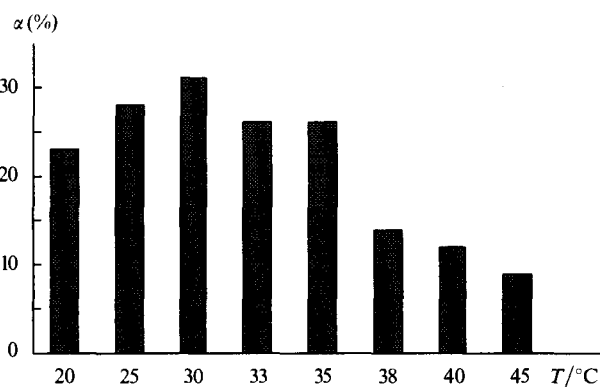


Figure 4. The total extent of cleavage (α) of 14-meric target DNA (1×10^{-5} mol dm $^{-3}$) by the oligonucleotide reagent (1×10^{-6} mol dm $^{-3}$) in the presence of heptanucleotide (1×10^{-5} mol dm $^{-3}$) (see Scheme 8 b) at different temperatures, according to densitometric analytical data.

reducing agents, and molecular oxygen may be attributed either to the degradation of its oligonucleotide moiety or to the degradation of the antibiotic itself. To elucidate possible reasons for the restriction of the catalytic activity, synthesis of the 5'-³²P-labelled reagent and cleavage of the nonlabelled target DNA were carried out under conditions of 10-fold target excess (Scheme 8b). Electrophoretic analysis data indicate that catalytic degradation of the target is accompanied by significant degradation of the oligonucleotide reagent.²⁶⁴ Removal of the bleomycin residue from the reagent after termination of the reaction gave rise to a nonmodified oligonucleotide. Hence, the restriction of the reagent catalytic activity is associated with the destruction of bleomycin itself.

Thus, chemical attachment of the antibiotic to the oligonucleotide makes it possible to direct it to a preselected site of one of nucleic acids and thus to increase markedly the selectivity of its action on all these acids. The method described of covalent attachment of bleomycin to the oligonucleotide^{238,239} makes it possible to preserve not only the ability of the antibiotic to cleave DNA, but also its capacity for catalytic cleavage characteristic of free bleomycin.

References

1. H Umezawa, K Maeda, T Takeushi, Y Okami *J. Antibiot.* **19** 200 (1966)
2. H Umezawa, Y Suhora, T Takita, K Maeda *J. Antibiot.* **19** 210 (1966)
3. M Ishizuka, H Takayama, T Takeushi, H Umezawa *J. Antibiot.* **20** 15 (1967)
4. T Ishikawa, A Matsuda, K Yamamoto, M Tsubosaki, T Kaihara, K Sakamoto, H Umezawa *J. Antibiot.* **20** 149 (1967)
5. H Umezawa, M Ishizuka, K Maeda, T Takeushi *Cancer* **20** 891 (1967)
6. M Suzuki, K Nagai, H Yamaki, N Tanaka, H Umezawa *J. Antibiot.* **21** 379 (1968)
7. H Umezawa, M Ishizuka, K Kimura, J Iwanaga, T Takeushi *J. Antibiot.* **21** 592 (1968)
8. M Takeushi, T Yamamoto *J. Antibiot.* **21** 631 (1968)
9. T Ichikawa, in *Progress in Antimicrobial and Anticancer Chemotherapy (Proceedings of the 6th International Congress of Chemotherapy)* (Tokyo: University of Tokyo Press, 1970) Vol. 2, p. 288
10. M B Mosher, R C DeConti, J R Bertino *Cancer* **30** 56 (1972)
11. R A Rudders *Blood* **40** 317 (1972)
12. B I Sikis, M Rozenzweig, S K Carter (Eds) *Bleomycin Chemotherapy* (Orlando: Academic Press, 1985)
13. R H Blum, S K Carter, K Agre *Cancer* **31** 903 (1973)
14. S S Cohen, in *Bleomycin: Chemical, Biochemical, and Biological Aspects* (Ed. S M Hecht) (New York: Springer, 1979) p. 267
15. S T Crooke, W T Bradner *J. Med.* **7** 333 (1976)
16. H Umezawa, in *Antibiotics. Mechanism of Action of Antimicrobial and Antitumor Agents* Vol. 3 (Eds J W Corcoran, F E Hahn) (Berlin: Springer, 1975) p. 21
17. W E G Muller, R K Zahn, in *Progress in Nucleic Acid Research and Molecular Biology* Vol. 20 (Ed. W E Cohn) (London: Academic Press, 1977) p. 21
18. H Umezawa *Lloydia* **40** 67 (1977)
19. S M Hecht, in *Bleomycin: Chemical, Biochemical, and Biological Aspects* (Ed. S M Hecht) (New York: Springer, 1979) p. 1
20. H Umezawa *Cancer Treat. Rep.*, **68** 137 (1984)
21. M Watanabe, Y Takabe, T Katsumata *J. Antibiot.* **26** 417 (1973)
22. Z I Yamazaki, W E G Muller, R K Zahn *Biochim. Biophys. Acta* **308** 412 (1973)
23. G P Sartiano, A Winkelstein, W Lynch, S S Boggs *J. Antibiot.* **26** 437 (1973)
24. R S Bornstein, D A Hungerford, G Haller, P F Engstrom, J W Yarbro *Cancer Res.* **31** 2004 (1971)
25. T Onishi, K Shimada, Y Takagi *Biochim. Biophys. Acta* **312** 248 (1973)
26. M Miyaki, T Kitayama, T Ono *J. Antibiot.* **27** 647 (1974)
27. T Takita, Y Myraoka, T Yoshioka, A Fujii, K Maeda, H Umezawa *J. Antibiot.* **25** 755 (1972)
28. T Takita, Y Myraoka, T Nakatani, A Fujii, Y Umezawa, H Naganawa, H Umezawa *J. Antibiot.* **31** 801 (1978)
29. T Takita, Y Umezawa, S-I Saito, H Morishima, H Naganawa, H Umezawa, T Tsuchiya, T Miyake, S Kageyama, S Umezawa, Y Myraoka, M Suzuki, M Otsuka, M Narita, S Kobayashi, M Ohno *Tetrahedron Lett.* **23** 521 (1982)
30. K Nagai, H Yamaki, H Suzuki, N Tanaka, H Umezawa *Biochim. Biophys. Acta* **179** 165 (1969)
31. K Nagai, H Suzuki, N Tanaka, H Umezawa *J. Antibiot.* **22** 569 (1969)
32. K Nagai, H Suzuki, N Tanaka, H Umezawa *J. Antibiot.* **22** 624 (1969)
33. H Suzuki, K Nagai, H Yamaki, N Tanaka, H Umezawa *J. Antibiot.* **22** 446 (1969)
34. H Suzuki, K Nagai, E Akutsu, H Yamaki, N Tanaka, H Umezawa *J. Antibiot.* **23** 473 (1970)
35. E A Sausville, J Peisach, S B Horwitz *Biochem. Biophys. Res. Commun.* **73** 814 (1976)
36. E A Sausville, J Peisach, S B Horwitz *Biochemistry* **17** 2740 (1978)
37. E A Sausville, R W Stein, J Peisach, S B Horwitz *Biochemistry* **17** 2746 (1978)
38. M Chien, A P Grollman, S B Horwitz *Biochemistry* **16** 3641 (1977)
39. T Takita, Y Myraoka, T Nakatani, A Fujii, Y Iitaka, H Umezawa *J. Antibiot.* **31** 1073 (1978)
40. J D Glickson, R P Pillai, T T Sakai *Proc. Natl. Acad. Sci. USA* **78** 2967 (1981)
41. D H Petering, R W Byrnes, W E Antholine *Chem.-Biol. Interact.* **73** 133 (1990)
42. J C Dabrowiak, F T Greenaway, W E Longo, M van Husen, S T Crooke *Biochim. Biophys. Acta* **517** 517 (1978)
43. J C Dabrowiak, F T Greenaway, F S Santillo, in *Bleomycin: Chemical, Biochemical, and Biological Aspects* (Ed. S M Hecht) (New York: Springer, 1979) p. 137
44. J C Dabrowiak *J. Inorg. Biochem.* **13** 317 (1980)
45. Y Sugiura, T Suzuki, M Otsuka, S Kobayashi, M Ohno, T Takita, H Umezawa *J. Biol. Chem.* **258** 1328 (1983)
46. A Kittaka, Y Sugano, M Otsuka, S Kobayashi, M Ohno, Y Sugiura, H Umezawa *Tetrahedron Lett.* **27** 3631 (1986)
47. L F Povirk, M Hogan, N Dattagupta *Biochemistry* **18** 96 (1979)
48. L F Povirk, M Hogan, N Dattagupta, M Buechner *Biochemistry* **20** 665 (1981)
49. S N Roy, G A Orr, C F Brewer, S B Horwitz *Cancer Res.* **41** 4471 (1981)
50. J P Albertini, A Garnier-Suillerot *Biochemistry* **21** 6777 (1982)
51. J P Albertini, A Garnier-Suillerot *Biochemistry* **23** 47 (1984)
52. H Hiroaki, T Nakayama, M Ikehara, S Uesugi *Chem. Pharm. Bull.* **39** 2780 (1991)
53. J E Strong, S T Crooke *Cancer Res.* **38** 3322 (1978)
54. C-H Huang, L Galvan, S T Crooke *Biochemistry* **19** 1761 (1980)
55. D L Boger, S L Colletti, T Honda, R F Menezes *J. Am. Chem. Soc.* **116** 5607 (1994)
56. W J Caspary, D A Lanzo, C Nizak *Biochemistry* **21** 334 (1982)
57. H Kasai, H Naganawa, T Takita, H Umezawa *J. Antibiot.* **31** 1316 (1978)
58. T T Sakai, J M Riordan, J D Glickson *Biochemistry* **21** 805 (1982)
59. C-H Chang, C F Meares *Biochemistry* **23** 2268 (1984)
60. T T Sakai, J M Riordan, T E Booth, J D Glickson *J. Med. Chem.* **24** 279 (1981)
61. R S Magliozzo, S Peisach, M R Ciriolo *Mol. Pharmacol.* **35** 428 (1989)
62. H Umezawa, H Asakura, K Oda, S Hori *J. Antibiot.* **26** 521 (1973)
63. H Asakura, S Hori, H Umezawa *J. Antibiot.* **28** 537 (1975)
64. M Hori, in *Bleomycin: Chemical, Biochemical, and Biological Aspects* (Ed. S M Hecht) (New York: Springer, 1979) p. 195
65. B J Carter, E de Vroom, E S Long, G A van der Marel, I H van Boom, S M Hecht *Proc. Natl. Acad. Sci. USA* **87** 9373 (1990)
66. J Stubbe, J W Kozarich *Chem. Rev.* **87** 1107 (1987)
67. D M Chen, T T Sakai, J D Glickson, D J Patel *Biochem. Biophys. Res. Commun.* **92** 197 (1980)
68. R P Pillai, N R Krishna, T T Sakai, J D Glickson *Biochem. Biophys. Res. Commun.* **97** 270 (1980)

69. T T Sakai, J M Riordan, N G Kumar, F J Haberle, G A Elgavish, J D Glickson, A Levy *J. Biomol. Struct. Dyn.* **1** 809 (1983)
70. T T Sakai, J M Riordan, J D Glickson *Biochim. Biophys. Acta* **758** 176 (1983)
71. T E Booth, T T Sakai, J D Glickson *Biochemistry* **22** 4211 (1983)
72. M P Gamcsik, J D Glickson, G Zon *J. Biomol. Struct. Dyn.* **7** 1117 (1990)
73. H Urata, Y Ueda, Y Usami, M Akagi *J. Am. Chem. Soc.* **115** 7135 (1993)
74. W Wu, D E Vanderwall, J Stubbe, J W Kozarich, C J Turner *J. Am. Chem. Soc.* **116** 10843 (1994)
75. R A Manderville, J F Ellena, S M Hecht *J. Am. Chem. Soc.* **116** 10851 (1994)
76. J Kross, W D Henner, W A Haseltine, L Rodriguez, M D Levin, S M Hecht *Biochemistry* **21** 3711 (1982)
77. L M Fisher, R Kuroda, T T Sakai *Biochemistry* **24** 3199 (1985)
78. R E Kilkuskie, H Suguna, B Yellin, N Murugesan, S M Hecht *J. Am. Chem. Soc.* **107** 260 (1985)
79. E Farinas, J D Tan, N Baidya, P K Mascharak *J. Am. Chem. Soc.* **115** 2996 (1993)
80. R J Guajardo, S E Hudson, S J Brown, P K Mascharak *J. Am. Chem. Soc.* **115** 7971 (1993)
81. D L Boger, T Honda, R F Menezes, S L Colletti *J. Am. Chem. Soc.* **116** 5631 (1994)
82. Y Muraoka, A Fujii, T Yoshioka, T Takita, H Umezawa *J. Antibiot.* **30** 178 (1977)
83. Y Sugiura, K Ishizu, K Miyoshi *J. Antibiot.* **32** 453 (1979)
84. D E Berry, L-H Chang, S M Hecht *Biochemistry* **24** 3207 (1985)
85. M J Levy, S M Hecht *Biochemistry* **27** 2647 (1988)
86. W E Antholine, D H Petering, L A Saryan, C E Brown *Proc. Natl. Acad. Sci. USA* **78** 7517 (1981)
87. W E Antholine, D H Petering *Biochem. Biophys. Res. Commun.* **91** 528 (1979)
88. Y Sugiura, K Ishizu *J. Inorg. Biochem.* **11** 171 (1979)
89. R M Burger, J Peisach, S B Horwitz *J. Biol. Chem.* **256** 11636 (1981)
90. Y Sugiura *J. Antibiot.* **31** 1206 (1978)
91. Y Sugiura *J. Am. Chem. Soc.* **102** 5216 (1980)
92. M Chikara, W E Antholine, D H Petering *J. Biol. Chem.* **264** 21478 (1989)
93. Y Iitaka, H Nakamura, T Nakatani, Y Myraoka, A Fujii, T Takita, H Umezawa *J. Antibiot.* **31** 1070 (1978)
94. M A J Akkerman, E W J F Neijman, S S Wijmenga, C W Hilbers, W Bermel *J. Am. Chem. Soc.* **112** 7462 (1990)
95. H Shields, C McGlumphy, P J Hamrick *Biochim. Biophys. Acta* **697** 113 (1982)
96. M Chikira, T Sato, W E Antholine, D H Petering *J. Biol. Chem.* **266** 2859 (1991)
97. H Shields, C McGlumphy *Biochim. Biophys. Acta* **800** 277 (1984)
98. G Koyama, H Nakamura, Y Myraoka, T Takita, K Maeda, H Umezawa, Y Iitaka *Tetrahedron Lett.* 4635 (1968)
99. S Neidle, Z Abraham *CRC Crit. Rev. Biochem.* **17** 73 (1984)
100. M J Waring *Annu. Rev. Biochem.* **50** 159 (1981)
101. T Takita, Y Myraoka, A Fujii, H Itoh, K Maeda, H Umezawa *J. Antibiot.* **25** 197 (1972)
102. S Y Lin, A P Grollman *Biochemistry* **20** 7589 (1981)
103. K J Miller, M Lauer, W Calocchia *Biopolymer* **24** 913 (1985)
104. J-P Henichart, J-L Bernier, N Helbecque, R Houssin *Nucleic Acids Res.* **13** 6703 (1985)
105. K H Langley, M R Patel, M J Fournier, in *Biomedical Application of Laser Light Scattering* (Eds D B Sattelle, W I Lee, B R Ware) (Amsterdam: Elsevier, Biomedical Press, 1982) p. 37
106. S-J Hong, L H Piette *Cancer Res.* **36** 1159 (1976)
107. J-L Bernier, J-P Henichart, J P Catteau *Anal. Biochem.* **117** 12 (1981)
108. T R Krugh, F N Wittlin, S P Cramer *Biopolymers* **14** 197 (1975)
109. D J Patel *Acc. Chem. Res.* **12** 118 (1979)
110. J Feigon, W A Denny, W Leupin, D R Kearns *J. Med. Chem.* **27** 450 (1984)
111. W D Wilson, R L Jones *Nucleic Acids Res.* **10** 1399 (1982)
112. K Wuthrich, in *NMR of Proteins and Nucleic Acids* (New York: Wiley, 1986) p. 3
113. H Murakami, H Mori, S Taira *J. Theor. Biol.* **59** 1 (1976)
114. E J Gabbay, P D Adawadkar, W D Wilson *Biochemistry* **15** 146 (1976)
115. R Kuroda, S Neidle, J M Riordan, T T Sakai *Nucleic Acids Res.* **10** 4753 (1982)
116. J M Riordan, T T Sakai *J. Med. Chem.* **26** 884 (1983)
117. R E Dickerson, in *Implication for Carcinogenesis and Risk Assessment in Basic Life Sciences* Vol. 38 (Eds M G Simic, L Grossman, A C Upton) (New York: Plenum, 1986) p. 245
118. Y Sugiura, T Suzuki *J. Biol. Chem.* **257** 10544 (1982)
119. H Sugiama, R E Kilkuskie, S M Hecht, G A van der Marel, J H van Boom *J. Am. Chem. Soc.* **107** 7765 (1985)
120. K Yamamoto, S Kawanishi *Biochem. Biophys. Res. Commun.* **183** 292 (1992)
121. H M Sobell, S C Jain *J. Mol. Biol.* **68** 21 (1972)
122. T Suzuki, J Kuwahara, Y Sugiura *Biochem. Biophys. Res. Commun.* **117** 916 (1983)
123. R P Hertzberg, M J Caranfa, S M Hecht *Biochemistry* **27** 3164 (1988)
124. J Kuwahara, Y Sugiura *Proc. Natl. Acad. Sci. USA* **85** 2459 (1988)
125. R L Petrusek, G L Anderson, T F Garner, Q L Fannin, D J Kaplan, S G Zimmer, L H Hurley *Biochemistry* **20** 1111 (1981)
126. K P Nightingale, K R Fox *Nucleic Acids Res.* **21** 2549 (1993)
127. H Murakami, H Mori, S Taira *J. Theor. Biol.* **42** 443 (1973)
128. T Onishi, H Iwata, Y Takagi *J. Biochem.* **77** 745 (1975)
129. R Ishida, T Takahashi *Biochem. Biophys. Res. Commun.* **66** 1432 (1975)
130. J W Lown, S-K Sim *Biochem. Biophys. Res. Commun.* **77** 1150 (1977)
131. J W Lown, in *Bleomycin: Chemical, Biochemical, and Biological Aspects* (Ed. S M Hecht) (New York: Springer, 1979) p. 184
132. Y Sugiura *J. Am. Chem. Soc.* **102** 5208 (1980)
133. Y Sugiura, T Kikushi *J. Antibiot.* **31** 1310 (1978)
134. L W Oberley, G R Buettner *FEBS Lett.* **97** 47 (1979)
135. J W Lown, A V Joashua *Biochem. Pharmacol.* **29** 521 (1979)
136. L Galvan, C-H Huang, A W Prestayko, J T Stout, J E Evans, S T Crooke *Cancer Res.* **41** 5103 (1981)
137. L O Rodriguez, S M Hecht *Biochem. Biophys. Res. Commun.* **104** 1470 (1982)
138. R M Burger, J Peisach, W E Blumberg, S B Horwitz *J. Biol. Chem.* **254** 10906 (1979)
139. H Kurososhi, K Takahashi, T Takita, H Umezawa *J. Antibiot.* **34** 576 (1981)
140. G Pratiavel, J Bernadou, B Meunier *Biochem. Pharmacol.* **38** 133 (1989)
141. A Natrajan, S M Hecht, G A van der Marel, J H van Boom *J. Am. Chem. Soc.* **112** 3397 (1990)
142. A Natrajan, S M Hecht, G A van der Marel, J H van Boom *J. Am. Chem. Soc.* **112** 4532 (1990)
143. J W Sam, X-J Tang, J Peisach *J. Am. Chem. Soc.* **116** 5250 (1994)
144. S M Hecht *Acc. Chem. Res.* **19** 383 (1986)
145. D G Knorre, O S Fedorova, E I Frolova *Usp. Khim.* **62** 70 (1993) [*Russ. Chem. Rev.* **62** 65 (1993)]
146. L Giloni, M Takeshita, F Johnson, C Iden, A P Grollman *J. Biol. Chem.* **256** 8608 (1981)
147. J C Wu, J W Kozarich, J Stubbe *J. Biol. Chem.* **258** 4694 (1983)
148. J C Wu, J W Kozarich, J Stubbe *Biochemistry* **24** 7562 (1985)
149. J W Kozarich, L J Worth, B L Frank, D A Christner, D E Vanderwall, J Stubbe *Science* **245** 1396 (1989)
150. L J Worth, B L Frank, D A Christner, M J Absalon, J Stubbe, J W Kozarich *Biochemistry* **32** 2601 (1993)
151. S Uesugi, T Shida, M Ikehara, Y Kobayashi, Y Kyogoku *Nucleic Acids Res.* **12** 1581 (1984)
152. N Murugesan, C Xu, G M Ehrenfeld, H Sugiama, R E Kilkuskie, L O Rodriguez, L-H Chang, S M Hecht *Biochemistry* **24** 5735 (1985)
153. L E Rabow, G H McGall, J Stubbe, J W Kozarich *J. Am. Chem. Soc.* **112** 3203 (1990)
154. J C Wu, J W Kozarich, J Stubbe *Biochemistry* **24** 7569 (1985)
155. H Sugiama, C Xu, N Murugesan, S M Hecht *J. Am. Chem. Soc.* **107** 4104 (1985)
156. H Sugiama, C Xu, N Murugesan, S M Hecht *Biochemistry* **27** 58 (1988)

157. L E Rabow, J Stubbe, J W Kozarich *J. Am. Chem. Soc.* **112** 3196 (1990)
158. R M Burger, J Peisach, S B Horwitz *J. Biol. Chem.* **257** 3372 (1982)
159. M J Absalon, C R Krishnamoorthy, J W Kozarich, J Stubbe *Nucleic Acids Res.* **20** 4179 (1992)
160. E Gajewski, O I Aruoma, M Dizdaroglu, B Halliwell *Biochemistry* **30** 2444 (1991)
161. K Kohda, H Kasai, T Ogawa, T Suzuki, Y Kawazoe *Chem. Pharm. Bull.* **37** 1028 (1989)
162. A M Maxam, W Gilbert *Proc. Natl. Acad. Sci. USA* **74** 560 (1977)
163. A D D'Andrea, W A Haseltine *Proc. Natl. Acad. Sci. USA* **76** 3608 (1979)
164. M Takeshita, A P Grollman, E Ohtsubo, H Ohtsubo *Proc. Natl. Acad. Sci. USA* **76** 5983 (1979)
165. L F Povirk, W Kohnlein, F Hutchinson *Biochim. Biophys. Acta* **521** 126 (1978)
166. C K Mirabelli, W G Beattie, C-H Huang, A W Prestayko, S T Crooke *Cancer Res.* **42** 1399 (1982)
167. J Kross, D W Henner, S M Hecht, W A Haseltine *Biochemistry* **21** 4310 (1982)
168. C K Mirabelli, A Ting, C-H Huang, S Mong, S T Crooke *Cancer Res.* **42** 2779 (1982)
169. V Murray, R F Martin *Nucleic Acids Res.* **13** 1467 (1985)
170. R S Lloyd, C W Haidle, D L Robberson *Biochemistry* **17** 1890 (1978)
171. R S Lloyd, C W Haidle, D L Robberson *Gene* **7** 289 (1979)
172. R S Lloyd, C W Haidle, D L Robberson, in *Bleomycin: Chemical, Biochemical, and Biological Aspects* (Ed. S M Hecht) (New York: Springer, 1979) p. 222
173. C K Mirabelli, C-H Huang, S T Crooke *Biochemistry* **22** 300 (1983)
174. J E Grimwade, E B Cason, T A Beerman *Nucleic Acids Res.* **15** 6315 (1987)
175. P K Mascharak, Y Sugiura, J Kuwahara, T Suzuki, S J Lippard *Proc. Natl. Acad. Sci. USA* **80** 6795 (1983)
176. B Gold, V Dange, M A Moore, A Eastman, G A van der Marel, J H van Boom, S M Hecht *J. Am. Chem. Soc.* **110** 2347 (1988)
177. L D Williams, I H Goldberg *Biochemistry* **27** 3004 (1988)
178. V Murray, L Tan, J Matthews, R F Martin *J. Biol. Chem.* **263** 12854 (1988)
179. R P Hertzberg, M J Caranfa, S M Hecht *Biochemistry* **24** 5285 (1985)
180. M Bene, G Felsenfeld *Proc. Natl. Acad. Sci. USA* **78** 1619 (1981)
181. E C Long, S M Hecht, G A van der Marel, J H van Boom *J. Am. Chem. Soc.* **112** 5272 (1990)
182. W E G Muller, Z-I Yamazaki, H J Breter, R K Zahn *Eur. J. Biochem.* **31** 518 (1972)
183. M T Kuo, L T Auger, G F Saunders, C W Haidle *Cancer Res.* **37** 1345 (1977)
184. C W Haidle, J Bearden, Jr *Biochem. Biophys. Res. Commun.* **65** 815 (1975)
185. C R Krishnamoorthy, D E Vanderwall, J W Kozarich, J Stubbe *J. Am. Chem. Soc.* **110** 2008 (1988)
186. C W Haidle, M T Kuo, K K Weiss *Biochem. Pharmacol.* **21** 3308 (1972)
187. B J Carter, K S Reddy, S M Hecht *Tetrahedron* **47** 2463 (1991)
188. B J Carter, C E Holmes, R B van Atta, V Dange, S M Hecht *Nucleosides Nucleotides* **10** 215 (1991)
189. A Huttenhofer, S Hudson, H F Noller, P K Mascharak *J. Biol. Chem.* **267** 24471 (1992)
190. M J Absalon, C R Krishnamoorthy, G McGall, J W Kozarich, J Stubbe *Nucleic Acids Res.* **20** 4179 (1992)
191. C E Holmes, B J Carter, S M Hecht *Biochemistry* **32** 4293 (1993)
192. R J Duff, E de Vroom, A Geluk, S M Hecht *J. Am. Chem. Soc.* **115** 3350 (1993)
193. C E Holmes, S M Hecht *J. Biol. Chem.* **268** 25909 (1993)
194. S M Hecht *Bioconjugate Chem.* **5** 513 (1994)
195. M A Morgan, S M Hecht *Biochemistry* **33** 10286 (1994)
196. M Takeshita, A P Grollman, in *Bleomycin: Chemical, Biochemical, and Biological Aspects* (Ed. S M Hecht) (New York: Springer, 1979) p. 207
197. M Takeshita, L S Kappen, A P Grollman, M Eisenberg, I H Goldberg *Biochemistry* **20** 7599 (1981)
198. T Morii, T Matsuura, I Saito, T Suzuki, J Kuwahara, Y Sugiura *J. Am. Chem. Soc.* **108** 7089 (1986)
199. T Morii, I Saito, T Matsuura, J Kuwahara, Y Sugiura *J. Am. Chem. Soc.* **109** 938 (1987)
200. H Sugiyama, G M Ehrenfeld, J B Shipley, R E Kilkuskie, L-H Chang, S M Hecht *J. Nat. Prod.* **48** 869 (1985)
201. H Sugiyama, R E Kilkuskie, L-H Chang, L-T Ma, S M Hecht *J. Am. Chem. Soc.* **108** 3852 (1986)
202. N J Oppenheimer, L O Rodrigues, S M Hecht *Proc. Natl. Acad. Sci. USA* **76** 5616 (1979)
203. N J Oppenheimer, C Chang, L-H Chang, G Ehrenfeld, L O Rodrigues, S M Hecht *J. Biol. Chem.* **257** 1606 (1982)
204. J B Shipley, S M Hecht *Chem. Res. Toxicol.* **1** 25 (1988)
205. Y Nakayama, M Kunishima, S Omoto, T Takita, H Umezawa *J. Antibiot.* **29** 400 (1973)
206. M Kunishima, T Fujii, Y Nakayama, T Takita, H Umezawa *J. Antibiot.* **29** 853 (1976)
207. G M Ehrenfeld, J B Shipley, D S Heimbrook, H Sugiyama, E C Long, J H van Boom, G A van der Marel, N J Oppenheimer, S M Hecht *Biochemistry* **26** 931 (1987)
208. M J McLean, A Dar, M J Waring *J. Mol. Recognit.* **1** 184 (1989)
209. T Suzuki, J Kuwahara, M Goto, Y Sugiura *Biochim. Biophys. Acta* **824** 330 (1985)
210. B J Carter, V S Murty, K S Reddy, S-N Wang, S M Hecht *J. Biol. Chem.* **265** 4193 (1990)
211. M Konishi, K Saito, K Numata, T Tsuno, K Asama, H Tsukura, T Naito, H Kawaguchi *J. Antibiot.* **30** 789 (1977)
212. C K Mirabelli, S Mong, C-H Huang, S T Crooke *Biochem. Biophys. Res. Commun.* **91** 871 (1979)
213. C K Mirabelli, C-H Huang, A W Prestayko, S T Crooke *Cancer Chemother. Pharmacol.* **8** 57 (1982)
214. C K Mirabelli, S Mong, C-H Huang, S T Crooke *Cancer Res.* **40** 4173 (1980)
215. Y Sugano, A Kittaka, M Otsuka, M Ohno, Y Sugiura, H Umezawa *Tetrahedron Lett.* **27** 3635 (1986)
216. A Kittaka, Y Sugano, M Otsuka, M Ohno *Tetrahedron* **44** 2811 (1988)
217. M Otsuka, A Kittaka, M Ohno, T Suzuki, J Kuwahara, Y Sugiura, H Umezawa *Tetrahedron Lett.* **27** 3639 (1986)
218. A Kittaka, Y Sugano, M Otsuka, M Ohno *Tetrahedron* **44** 2821 (1988)
219. M Otsuka, T Masuda, A Haupt, M Ohno, T Shiraki, Y Sugiura, K Maeda *J. Am. Chem. Soc.* **112** 838 (1990)
220. M L Kopka, C Yoon, D Goodsell, P Pjura, R E Dickerson *Proc. Natl. Acad. Sci. USA* **82** 1376 (1985)
221. N Hamamichi, A Natrajan, S M Hecht *J. Am. Chem. Soc.* **114** 6278 (1992)
222. A Fujii, in *Bleomycin: Chemical, Biochemical, and Biological Aspects* (Ed. S M Hecht) (New York: Springer, 1979) p. 75
223. S A Kane, A Natrajan, S M Hecht *J. Biol. Chem.* **269** 10899 (1994)
224. K R Fox, G W Grigg, M J Waring *Biochem. J.* **243** 847 (1987)
225. K R Fox *Anti-Cancer Drug Des.* **5** 99 (1990)
226. K P Nightingale, K R Fox *Biochem. J.* **284** 929 (1992)
227. A Klug, A Jack, O Kennard, Z Shakked, T Steitz *J. Mol. Biol.* **131** 669 (1979)
228. I H Raisfeld, in *Bleomycin: Chemical, Biochemical, and Biological Aspects* (Ed. S M Hecht) (New York: Springer, 1979) p. 324
229. A M Belikova, V F Zarytova, N I Grineva *Tetrahedron Lett.* 3557 (1967)
230. N I Grineva, in *Afinnaya Modifikatsiya Biopolimerov* (Affine Modification of Biopolymers) (Novosibirsk: Nauka, 1983) p. 187
231. D G Knorre, V V Vlassov, V F Zarytova, A V Lebedev *Sov. Sci. Rev.* **12** 271 (1989)
232. J Goodchild *Bioconjugate Chem.* **1** 165 (1990)
233. C Helene, J-J Toulme *Biochim. Biophys. Acta.* **1049** 99 (1990)
234. E Wickstrom (Ed.) *Prospects for Antisense Nucleic Acid Therapy of Cancer and AIDS* (New York: Wiley-Liss, 1991)
235. D G Knorre, V V Vlassov, V F Zarytova, A V Lebedev, O S Fedorova, in *Design and Targeted Reactions of Oligonucleotide Derivatives* (Boca Raton, FL: CRC Press, 1994)
236. T S Godovikova, V F Zarytova, T V Mal'tseva, L M Khalinskaya *Bioorg. Khim.* **15** 1246 (1989)

237. T Takita, A Fujii, T Fukuoka, H Umezawa *J. Antibiot.* **26** 252 (1973)
238. T S Godovikova, V F Zarytova, D S Sergeev *Bioorg. Khim.* **17** 1193 (1991)
239. V F Zarytova, D S Sergeyev, T S Godovikova *Bioconjugate Chem.* **4** 189 (1993)
240. D S Sergeev, A Yu Denisov, V F Zarytova *Bioorg. Khim.* **22** 695 (1996)
241. G G Karpova, L O Kozlova, N P Pichko *Izv. Sib. Otd. Akad. Nauk, Ser. Khim. Nauk* (3) 96 (1983)
242. D S Sergeyev, V F Zarytova, S V Mamaev, T S Godovikova, V V Vlassov *Antisense Res. Dev.* **2** 235 (1992)
243. V V Vlassov, V F Zarytova, I V Kutiaev, S V Mamaev, M A Podyminogin *Nucleic Acids Res.* **14** 4065 (1986)
244. E B Brosalina, V V Vlasov, I V Kutiaev, S V Mamaev, A G Pletnev *Bioorg. Khim.* **12** 240 (1986)
245. C Helene *Curr. Opin. Biotechnol.* **4** 29 (1993)
246. O S Fedorova, D G Knorre, L M Podust, V F Zarytova *FEBS Lett.* **228** 273 (1988)
247. T J Povsic, S A Strobel, P B Dervan *J. Am. Chem. Soc.* **114** 5941 (1992)
248. M Takasugi, A Guendouz, M Chassignol, J L Decout, J Lhomme, N T Thuong, C Helene *Proc. Natl. Acad. Sci. USA* **88** 5602 (1991)
249. S A Strobel, P B Dervan *Science* **249** 73 (1990)
250. J-C Francois, T Saison-Behmoaras, C Barbier, M Chassignol, N T Thuong, C Helene *Proc. Natl. Acad. Sci. USA* **86** 9702 (1989)
251. D S Sergeev, T S Godovikova, V F Zarytova *Bioorg. Khim.* **21** 188 (1995)
252. S Arnott, E Selsing *J. Mol. Biol.* **88** 509 (1974)
253. D S Pilch, C Levenson, R H Shafer *Proc. Natl. Acad. Sci. USA* **87** 1942 (1990)
254. L A Basile, J K Barton, in *Metal Ions in Biological System* Vol. 25 (Eds H Sigel, A Sigel) (New York: Marcel Dekker, 1989) p. 31
255. P Hertzberg, P B Dervan *Biochemistry* **23** 3934 (1984)
256. R B van Atta, J Bernadou, B Meunier, S M Hecht *Biochemistry* **29** 4783 (1990)
257. N Murugesan, G M Ehrenfeld, S M Hecht *J. Biol. Chem.* **257** 8600 (1982)
258. N Murugesan, S M Hecht *J. Am. Chem. Soc.* **107** 493 (1985)
259. W J Caspary, C Niziak, D A Lanzo, R Friedman, N R Bachur *Mol. Pharmacol.* **16** 256 (1979)
260. G R Buettner, P L Moseley *Biochemistry* **31** 9784 (1992)
261. L F Povirk *Biochemistry* **18** 3989 (1979)
262. O I Aruoma, B Halliwell, E Gajewski, M Dizdaroglu *J. Biol. Chem.* **264** 20509 (1989)
263. M Dizdaroglu, O I Aruoma, B Halliwell *Biochemistry* **29** 8447 (1990)
264. D S Sergeev, T S Godovikova, V F Zarytova *Bioorg. Khim.* **22** 55 (1996)
265. H Umezawa, in *Bleomycin: Chemical, Biochemical, and Biological Aspects* (Ed. S M Hecht) (New York: Springer, 1979) p. 15
266. K Ueda, S Kobayashi, H Sakai, T Komano *J. Biol. Chem.* **260** 5804 (1985)
267. H Sugiyama, T Sera, Y Dannoue, R Marumoto, I Saito *J. Am. Chem. Soc.* **113** 2290 (1991)

Phase equilibria in $M-X-X'$ and $M-Al-X$ ternary systems (M = transition metal; $X, X' = B, C, N, Si$) and the crystal chemistry of ternary compounds

A I Gusev

Contents

I. Introduction	379
II. Phase equilibria in $M-B-C$ borocarbide systems	382
III. $M-B-N$ ternary boronitride systems	388
IV. Phase relationships in the Si-containing $M-B-Si$, $M-Si-C$, and $Me-Si-N$ systems	390
V. Phase equilibria in $M-Al-X$ ternary systems ($X = C, N, Si$)	402
VI. Phase equilibria in $X-X'-X''$ ternary systems ($X, X', X'' = B, C, N, Si, Al$)	414
VII. Conclusion	415

Abstract. The published data on phase equilibria in the $M-X-X'$ and $M-Al-X$ ternary systems (M is a Group III–VIII transition metal, X, X' are B, C, N, Si) are surveyed. These systems provide a basis for the directed search for oxygen-free ceramic materials for various purposes. The phase diagrams for the ternary systems are presented; more than two hundred ternary phases formed in these systems are systematised and described for the first time. The typical crystal structures of the ternary compounds and of the phases are considered, the general and distinguishing features of these structures are analysed. It is shown that ternary compounds containing the XM_6 octahedral groups possess homogeneity regions. The bibliography includes 240 references.

I. Introduction

Ceramics are materials which have been in use for a very long time. Products of fired clay, faience, and porcelain have been traditionally referred to as ceramics. However, the range of ceramic materials has now considerably widened, and the term 'ceramics' is used in relation to polycrystalline materials based on compounds of Group III–VI nonmetals with one another and/or with metals, obtained by various methods such as sintering, pressing, precipitation from the gas phase or from the liquid colloidal state, etc. Borides, carbides, nitrides, oxides, and silicides are the initial compounds for the preparation of ceramics.

The interest in ceramic materials has substantially grown in the last few decades. In the developed countries, the amount of the manufactured ceramic products is rapidly increasing, new technologies appear, and the ceramic products have found wide application in industry, transport, energetics, electronics, and medicine. The new ceramics have revolutionised materials science. At present, ceramics are the third industrial material, regarding the tonnage of use, after metals and polymers, and it occupies a key position in the field of high technologies.

An evaluation of the dynamics of the increase in the manufacture of ceramics over the period between 1990 and 1995 and up to 2000 indicates that the output volume is doubling every five years (Table 1). This is caused by the demand for the materials meant for performing new functions (for example, in force lasers, memory cells, superconducting devices, catalysts, electrodes, and heat- or radiation-resistant devices). Actually, the new ceramics often prove to be stronger than metals, though they are lighter; they may be elastic enough to be suitable for the manufacture of elastic units; ceramics withstand high temperatures and thermal shocks; they are highly resistant to corrosion and to wear.

The perfection of the existing ceramic materials and the development of new materials involves both the synthesis of complex compounds and heterogeneous compositions and the preparation of finely dispersed materials (with a particle size of $\sim 1-10$ nm) from these compounds and compositions, which ensures the stability and the high level of performance.

The new ceramic materials and the relevant technologies are extremely science-dependent. This accounts for the intense fundamental research in the field of physical chemistry, physics and chemistry of solids, and physical material technology. All the studies on physical chemistry and material technology dealing with the search for new solid-phase compounds and compositions for ceramics are based on phase equilibria and phase diagrams presented in many publications.

The aim of the present review is to generalise and systematise the data on the phase equilibria in the oxygen-free $M-X-X'$ and $M-Al-X$ ternary systems (where M is a Group III–VIII

Table 1. Production of new ceramics and ceramic composite materials (in millions of US dollars) in developed countries over the period from 1990 to 1995 and a forecast for the production in 2000.

Field of application	1990	1995	2000
Electronics	3740	6565	11360
Aviation and astronautics	80	200	445
Motor-construction	81	310	820
Medicine and biology	15	34	60
Metal working, cutting tools	92	246	500
Industrial heat and power engineering	15	50	100
Other fields of application	150	320	720
Overall	4173	7725	14005

A I Gusev Laboratory of High-Melting Compounds, Institute of Solid State Chemistry, Ural Division of the Russian Academy of Sciences, ul. Pervomaiskaya 91, 620219 Ekaterinburg, Russian Federation.
Fax (7-343) 244 44 95. Tel. (7-343) 249 35 23.
E-mail: aig@gusev.e-burg.su.

Received July 6 1995

Uspekhi Khimii 65 (5) 407–451 (1996); translated by Z P Bobkova

transition metal, X and X' are B, C, N, Si) and on the crystal structure of the ternary compounds formed in these systems. These ternary systems serve as the constituents of more complex 4- and 5-component systems and cover largely the systems that are used or can be used for preparing new ceramic materials.

Before we discuss ternary systems, let us consider briefly some characteristic features of the structures of the binary compounds that are permanently involved in the phase equilibria in the M–X–X' systems, namely, transition metal carbides, nitrides, borides, and silicides, and of binary high-melting compounds of nonmetals.

The cubic (with the *B1* structure) and hexagonal (with the *L'3* structure) carbides and nitrides of Group IV and V transition metals MC_y , M_2C_y , MN_y , and M_2N_y ($0.4 \leq y \leq 1.0$) belong to the group of nonstoichiometric interstitial compounds^{1,2} and possess (in contrast to other compounds considered here) metallic electrical conductivity. The atomic radius of carbon is fairly small and is equal to ~ 0.077 nm, therefore, in compounds with transition metals carbon always acts as the interstitial element and is located in the interstices of the metal sublattice. The interstitial nonmetal atoms (carbon or nitrogen) in the cubic carbides and nitrides MC_y and MN_y occupy the octahedral interstices of the face-centred cubic (Fcc) metal sublattice and can populate either all of the interstices or only some of them. The octahedral interstices free from these atoms are referred to as structural vacancies. In hexagonal lower carbides and nitrides M_2C_y and M_2N_y , the interstitial atoms occupy half the octahedral interstices of the hexagonal close-packed metal sublattice. The interstitial atoms and the structural vacancies may be arranged in a crystal lattice either statistically (irregularly) or regularly.

The nonstoichiometric carbides and nitrides with the *B1* and *L'3* structures belong to the class of the so-called octahedral structures, that is to the structures in which each six transition metal atoms constitute the octahedral environment of an interstitial atom X or of a vacancy. These structures are built of the XM_6 octahedra joined with one another in various ways. For example, in the NaCl type structure (*B1*) the octahedra are joined through their edges (Fig. 1). Many of the ternary compounds considered below also incorporate regular or distorted XM_6 octahedra as the main structural motif.

Carbides and nitrides of Group VI–VIII transition metals have virtually no homogeneity regions and can have various crystal structures with a relatively high symmetry, namely, orthorhombic, tetragonal, hexagonal, or cubic.

A detailed description of the structures and properties of binary carbides and nitrides of transition metals with allowance for the short-range and long-range effects of nonstoichiometry has been published.^{1–6}

Transition metal compounds with boron are built in a different manner. The boron atoms are larger than the carbon or

nitrogen atoms; therefore, B–B bonds can arise in the crystal lattice of borides. In the borides M_2B , the boron atoms are separated from one another, and the M–B interactions are the most significant. With the increase in the boron content, changes occur from the structure with the separated boron atoms in M_2B to the ...–B–B–... zigzag-like chains in MB and to hexagonal chains in M_3B_4 , and then to a two-dimensional hexagonal network of boron atoms bound to one another in the diborides MB_2 and to cage structures built of boron atoms in the borides MB_4 , MB_6 , and MB_{12} , which contain interpenetrating lattices of the metal and boron atoms.⁷

The atom radius of silicon, an analogue of carbon, is much larger, being equal to ~ 0.117 nm. In compounds with Group IV and V transition metals, whose atoms are sufficiently large, silicon still acts as an interstitial element; the silicides of other transition metals occupy an intermediate position between interstitial compounds and intermetallics. Thus, silicon can be incorporated in a metallic lattice as an interstitial element or as a substituting element. In lower silicides (for example, in M_3Si), the silicon atoms are separated from one another, and only M–Si bonds exist. As the content of silicon atoms increases, isolated Si–Si pairs are formed initially; the further increase in the silicon content results in one-dimensional zigzag-shaped chains of the silicon atoms (in compounds of the M_5Si_3 type), two-dimensional close-packed networks (in MSi_2), and, finally, three-dimensional spatial frameworks of silicon atoms (for example, in lanthanide disilicides⁸). The crystal structures of borides and silicides are quite diverse.

Aluminium forms numerous intermetallic compounds with transition metals, many of which have homogeneity regions.

The great difference between the crystal structures of carbides and nitrides, on the one hand, and borides, silicides, and aluminides, on the other hand, result in their low mutual solubility.

Boron, carbon, nitrogen, silicon, and aluminium form solid solutions not only with metals, but also with one another, for example, in the X–X' binary systems (B–C, B–N, Si–B, Al–B, C–N, Si–C, Al–C, Si–N, and Al–N). Let us discuss briefly the characteristic features of the crystal chemistry of these high-melting carbides, nitrides, and borides of nonmetals. The structural characteristics of the high-melting compounds are listed in Table 2.

The B–C system. The main phase in the B–C system is boron carbide B_4C ($B_{12}C_3$); the carbide $B_{13}C_2$ is also formed (see Table 2).

The twelve boron atoms in $B_{12}C_3$ are located at the vertices of an icosahedron. The B_{12} icosahedra constitute an Fcc-lattice, the three carbon atoms being located as the C–C–C chain in the large octahedral interstices. The terminal carbon atoms in this chain are linked to four boron atoms from the two nearest icosahedra (the B–C distance is 0.164 nm); and the central carbon atom of the carbon chain is bound only to the other carbon atoms of this chain, which are located at a distance of 0.139 nm from it.

The carbide $B_{13}C_2$ has a structure derived from that of B_4C ($B_{12}C_3$). This compound can be represented as $(B_{12})BC_2$, i.e., it may be regarded as $B_{12}C_3$ in which one of the C atoms has been substituted by boron. The boron atom and the two carbon atoms are located in the octahedral interstices of the B_{12} icosahedra as C–B–C chains.

The similarity of the crystal lattices of the carbides B_4C ($B_{12}C_3$) and $B_{13}C_2$ led some authors to suppose that there exists one phase with a broad homogeneity region. However, the dependence of the properties of boron carbide on the carbon content exhibits two extrema at the compositions $B_{12}C_3$ and $B_{13}C_2$, which attests to the existence of two different phases.

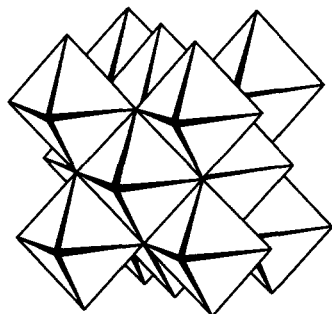


Figure 1. Crystal structure of the NaCl (*B1*) type of the cubic (space group *Fm3m*) monocarbides and mononitrides MX (X = C, N) represented by XM_6 octahedra.

Table 2. Crystal-chemical characteristics of high-melting compounds of nonmetals.

Compound	Symmetry and type of structure	Space group	Z ^a	Unit cell parameters / nm			Ref.
				<i>a</i>	<i>b</i>	<i>c</i>	
B ₄ C (B ₁₂ C ₃)	Hexagonal	<i>R</i> $\bar{3}m$	9	0.561	—	1.214	9
B ₁₃ C ₂ (B ₁₂ BC ₂)	"	<i>R</i> $\bar{3}m$	9	0.5633	—	1.2164	10
α -BN	"	<i>P</i> 6 ₃ / <i>mmc</i>	4	0.2504	—	0.6661	11
β -BN	Cubic, sphalerite ZnS (<i>B3</i>) type	<i>F</i> $\bar{4}3m$	8	0.3615	—	—	12
γ -BN	Hexagonal, wurtzite ZnS (<i>B4</i>) type	<i>P</i> 6 ₃ <i>mc</i>	4	0.255	—	0.423	13
SiB ₄	Hexagonal	<i>R</i> $\bar{3}m$	9	0.635	—	1.269	7
SiB ₆	Orthorhombic	<i>Pnnm</i>	40	1.4392	1.8267	0.9885	14
SiB ₁₄ (SiB _{12+x})	Hexagonal	<i>R</i> $\bar{3}m$	7	1.113	—	2.383	15
AlB ₂	Hexagonal, C32 type	<i>P</i> 6/ <i>mmm</i>	1	0.3009	—	0.3262	16
α -AlB ₁₂	Tetragonal	—	14	1.016	—	1.428	1
α -AlB ₁₂	"	<i>P</i> 4 ₁ 2 ₁ 2	4	1.0158	—	1.4270	18
γ -AlB ₁₂	Orthorhombic	<i>P</i> 2 ₁ 2 ₁ 2 ₁	4	1.6573	1.7510	1.0144	19
β -C ₃ N ₄	Hexagonal, β -Si ₃ N ₄ type	<i>P</i> 6 ₃ / <i>m</i>	2	0.63	—	0.246	20
α -SiC (2 <i>H</i>)	Hexagonal	<i>P</i> 6 ₃ <i>mc</i>	2	0.3073	—	0.5028	21
α -SiC (4 <i>H</i>)	"	<i>P</i> 6 ₃ <i>mc</i>	4	0.3073	—	1.0053	21
α -SiC (6 <i>H</i>)	"	<i>P</i> 6 ₃ <i>mc</i>	6	0.3073	—	1.5079	21
α -SiC (15 <i>R</i>)	Rhombohedral	<i>R</i> 3 <i>m</i>	5	0.3073	—	3.770	21
β -SiC (3 <i>C</i>)	Cubic, sphalerite ZnS (<i>B3</i>) type	<i>F</i> $\bar{4}3m$	4	0.4349	—	—	21
Al ₄ C ₃	Hexagonal, <i>D</i> 7 ₁ type	<i>R</i> $\bar{3}m$	3	0.3330	—	2.489	22
α -Si ₃ N ₄	Hexagonal, phenacite Be ₂ SiO ₄ type	<i>P</i> 31 <i>c</i>	4	0.767	—	0.564	23
β -Si ₃ N ₄	"	<i>P</i> 6 ₃ / <i>m</i>	2	0.759	—	0.292	23
AlN	Hexagonal, wurtzite ZnS (<i>B4</i>) type	<i>P</i> 6 ₃ <i>mc</i>	4	0.3113	—	0.4982	24
AlN	"	<i>P</i> 6 ₃ <i>mc</i>	4	0.3111	—	0.4978	22

^a From here on, Z is the number of formula units in the unit cell.

The B–N system. In the B–N system only one compound is formed, namely, boron nitride BN, which exists in α , β , and γ modifications.

The nitride α -BN has a hexagonal graphite-like structure. The boron and nitrogen atoms in this ideal structure are regularly distributed in hexagonal networks; the networks are arranged one above the other in such a way that the boron and nitrogen atoms alternate along the *c* axis of the crystal. The distance between the layers in α -BN is larger than the interatomic distances in the networks by a factor of 2.5. This causes substantial anisotropy of the properties of α -BN. The α -BN modification can have various degrees of ordering ranging from an amorphous structure to a completely ordered structure. The resistance of α -BN to oxidation increases with an increase in the degree of ordering.

The cubic modification β -BN has a sphalerite-type structure (ZnS, *B3*), and γ -BN has a wurtzite-type structure (ZnS, *B4*). The structures of β - and γ -BN are very similar, and they may be regarded as polytypes. The cubic boron nitride β -BN is stable to attrition and possesses an extremely high hardness close to that of diamond. Only α - and β -BN are thermodynamically stable.¹³

The Si–B system. Three compounds, SiB₄, SiB₆, and SiB_{12+x} (SiB₁₄), are formed in this system (see Table 2).

The structure of the boride SiB₄ is similar to that of B₄C (B₁₂C₃): B₁₂ icosahedra form an Fcc-lattice, the silicon atoms being located in its octahedral interstices; some of the silicon atoms can substitute the boron atoms in the B₁₂ groups. The boride SiB₄ is stable at *T* ≤ 1640 K; at higher temperatures it decomposes peritectically to give the orthorhombic boride SiB₆ and silicon.

The compound SiB_{12+x} (SiB₁₄), which also exists in the Si–B system, is sometimes regarded as being a solid solution of silicon in β -B (the groups of boron atoms in the β -B structure constitute a rhombohedrally distorted cubic close packing, the interstices of

which may contain silicon and aluminium atoms, together with the boron atoms²⁵).

The Al–B system. In the Al–B system, the existence of borides AlB₂ and α - and γ -AlB₁₂ has been established reliably.

The boride AlB₂ has a hexagonal structure (space group *P*6/*mmm*) of the C32 type. In this structure, the aluminium atoms form trigonal prisms joined through all faces; the axes of the prisms are parallel to the *c* direction. The boron atoms are located at the centres of these prisms, therefore the structure of AlB₂ may be regarded as a filled structure of the WC type.

The borides α -AlB₁₂ and γ -AlB₁₂ have tetragonal and monoclinic structures of their own types (see Table 2). The orthorhombic boride β -AlB₁₂, which has been repeatedly described in the literature, is in fact the borocarbide Al₃B₄₈C₂.²⁵

The C–N system. Gaseous cyanogen C₂N₂ exists in this system under equilibrium conditions. On heating to 870 K cyanogen polymerises to give a dark-brown solid (amorphous) and insoluble paracyanogen. When paracyanogen is heated to 1130 K in the absence of air, it is again converted to cyanogen.

In the system under consideration, the existence of a solid phase resembling a diamond-like solid solution of nitrogen in carbon C(N) cannot be ruled out. Furthermore, in recent years, information on crystalline carbon nitride has been reported. Liu and Cohen^{26,27} who have used a model suggested previously²⁸ for the calculation of the crystal and electronic structures of solid phases, predicted the possible existence of crystalline β -C₃N₄. Later, this compound has been found as particles with a size of ~0.5 μ m in a ~1 mm thick C,N-containing film obtained on a silicon support by atomisation of graphite (*T* = 673–873 K) under a nitrogen atmosphere (*P*_{N₂} = 2.3 Pa).²⁰ The carbon nitride β -C₃N₄ has a hexagonal structure of the β -Si₃N₄ type (see Table 2).

The Si—C system. In this system only one phase exists, namely, silicon carbide SiC having α - and β -modifications.

The structure of α -SiC consists of close-packed layers of silicon atoms and close-packed layers of carbon atoms, which are arranged between the silicon layers at a height equal to $\frac{3}{4}$ of the distance between them; the carbon atoms occupy the same crystallographic positions as the silicon atoms. Consequently, all the atoms of one kind in the carbide α -SiC are located in the tetrahedral environment of atoms of the other kind (SiC₄ and CSi₄). The number of the layers in the structure of α -SiC may differ, which accounts for the polytypism of silicon carbide. The carbide α -SiC forms more than 100 hexagonal and rhombohedral polytypes. More than 70 polytypes of α -SiC differing in the number of the layers have been described in a review.²¹ The most commonly encountered structures are 4-, 6-, and 15-layered polytypes denoted as 4H, 6H, and 15R (the letters H and R correspond to hexagonal and rhombohedral polytypes and the digits correspond to the numbers of the layers in the polytypes; the cubic close-packed structure is designated as 3C).

The cubic modification β -SiC crystallises with the sphalerite ZnS (*B3*) structural type; its formation is probably promoted by a slight excess of silicon.

The temperature of the peritectic decomposition of silicon carbide is 3030–3100 K.

The Al—C system. Al₄C₃ is formed as the only hexagonal carbide in the Al—C system (see Table 2). In this compound, the aluminium atoms constitute close-packed planes, with $\frac{2}{3}$ and $\frac{1}{3}$ of all the carbon atoms being located between these planes in the tetrahedral and octahedral interstices, respectively. Consequently, the Al₂C₂ and Al₂C layers alternate along the *c* axis (a rhombohedral unit cell contains 12 close-packed planes of aluminium atoms).

The Si—N system. The silicon nitride Si₃N₄ is the only stable silicon compound with nitrogen. It exists in two modifications: α -Si₃N₄ (trigonal) and β -Si₃N₄ (hexagonal) (see Table 2).

The nitride α -Si₃N₄ has a layered structure in which each silicon atom is in the tetrahedral environment of four nitrogen atoms, and three silicon atoms constitute the nearest environment of each nitrogen atom.

The structure of β -Si₃N₄ also consists of SiN₄ tetrahedra in which each nitrogen atom is shared by three tetrahedra. The nitride β -Si₃N₄ is stable up to 1700 K in the absence of nitrogen. The intercalation of admixtures into the lattice of β -Si₃N₄ can lead to the formation of the α -modification (for example, the structure of α -Si₃N₄ is stabilised by elemental silicon).

The Al—N system. In the Al—N system, too, only one compound is known, namely, the nitride AlN with a hexagonal structure of the wurtzite ZnS (*B4*) type. The nitrogen atoms in AlN occupy tetrahedral vacancies between the hexagonal close-packed layers of aluminium atoms. The sintering of an aluminium nitride powder prepared by the plasmachemical method yields a multi-layer sphalerite polytype of AlN.¹³ In all probability, this modification arises due to the presence of an admixture of oxygen.

Aluminium nitride possesses high hardness, heat conductivity, and thermal stability and low thermal expansion coefficient; it is resistant to oxidation up to 1000 K.

The Al—Si system. In this system no compounds have been detected.

II. Phase equilibria in M—B—C borocarbide systems

The transition metal borocarbide systems are among the ternary systems of transition metals with boron, carbon, nitrogen, and silicon studied most thoroughly. Nevertheless, virtually no survey papers devoted to them have been published. Some of the M—B—C systems have been described in monographs.^{8, 29–31}

1. Borocarbides of Group III transition metals

Borocarbides of scandium, yttrium, and lanthanides have not been studied adequately, though it is in these systems that most of the known ternary compounds M_xB_yC_z (Table 3) have been found. In particular, scandium, yttrium, and all the lanthanides (except for Pm) form ternary borocarbides of the formula MB₂C₂.^{33, 34, 36, 37, 41, 44–46} For the lanthanide borocarbides LnB₂C₂, a small tetragonal unit cell containing one LnB₂C₂ formula unit and having similar *a*₀ and *c*₀ parameters was initially suggested.^{36, 41} The boron and carbon atoms in this structure are arranged randomly. Using YB₂C₂ as an example, Bauer and Nowotny have shown³⁴ that the crystal structure with disordered distribution of the B and C atoms is described by the *P4/mmm* space group, the small cell being regarded as only the first approximation to the structure of the borocarbides LnB₂C₂. Judging from the general views about bond lengths and directions, a tetragonal structure with a regular arrangement of B and C atoms (space group *P4/mbm* with *a* = *a*₀ $\sqrt{2}$ and *c* = *c*₀) has been suggested for the compounds MB₂C₂. Bauer and Nowotny³⁴ have suggested a more plausible model for the ordering of the boron and carbon atoms in the compounds MB₂C₂ under consideration in relation to yttrium borocarbide YB₂C₂. According to this model, the small tetragonal unit cell with a statistical distribution of the atoms is doubled along the *c* axis, i.e. *a* = *a*₀ and *c* = 2*c*₀. In the unit cell thus obtained (space group *P42c*), the metal atoms occupy the 2(*e*) sites, the four boron atoms occupy the 4(*i*) sites with *y* = 0.232, and the four carbon atoms are at the 4(*h*) sites with *x* = 0.168 (Fig. 2).

A study of the crystal structure of LaB₂C₂ carried out by Bauer and Bars³⁷ has confirmed the validity of the ordering model described above.³⁴ The diffraction pattern of LaB₂C₂ was interpreted³⁷ in terms of several models: a small tetragonal unit cell with a disordered distribution of boron and carbon atoms [space group *P422*, *Z* = 1, the B and C atoms occupy the 4(*m*) sites with *x* = 0.203]; a small unit cell with an ordered distribution of nonmetal atoms [space group *Pmmm*, *Z* = 1, the B and C atoms occupy the 2(*p*) and 2(*l*) sites, respectively]; an ordered tetragonal structure with *a* = *a*₀ $\sqrt{2}$ and *c* = *c*₀ (space group *P4/mbm*, *Z* = 2); and an ordered tetragonal structure (space group *P42c*, *Z* = 2). The latter model proved to be the most successful. This made it possible to conclude that all the borocarbides LnB₂C₂ crystallise with a tetragonal structure (space group *P42c*) with an ordered distribution of the carbon and boron atoms in the lattice. The unit cell parameters of the yttrium and lanthanide borocarbides MB₂C₂ with ordered and disordered distributions of the boron and carbon atoms are listed in Table 3.

Another common structure of scandium, yttrium, and heavy lanthanide borocarbides is MB₂C.^{32, 34, 35} In the case of disordered distribution of the B and C atoms in the borocarbide YB₂C (space group *P4/mbm*), four Y atoms occupy the 4(*g*) sites, and twelve boron and carbon atoms are distributed statistically

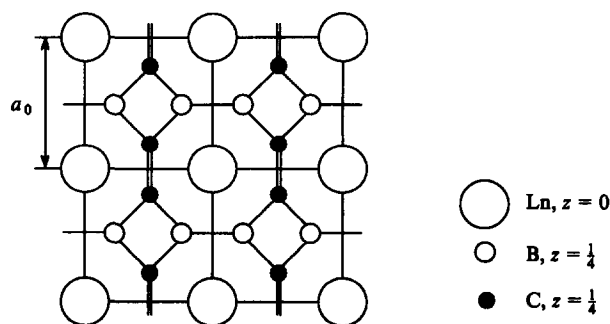


Figure 2. Projection along the [001] axis of the ordered crystal structure of the borocarbides MB₂C₂ of the YB₂C₂ type (space group *P42c*).³⁴ Only one half of the unit cell is shown; for *z* = $\frac{1}{4}$, the B—C network is rotated by 90°.

Table 3. Some ternary compounds in borocarbide systems of Group III transition metals and lanthanides.

Compound	Symmetry and type of structure	Space group	Z	Unit cell parameters / nm			Ref.
				<i>a</i>	<i>b</i>	<i>c</i>	
ScB ₂ C	Tetragonal, the YB ₂ C type	<i>P4₂/mbc</i>	8	0.6651	—	0.6763	32
ScB ₂ C ₂	Orthorhombic	<i>Pham</i>	4	0.5175	1.0075	0.3340	33
YBC	"	<i>Cmmm</i>	4	0.3388	1.3693	0.3627	34
Y ₂ BC ₂	Isostructural to Y ₁₅ C ₁₉ (?)	—	—	—	—	—	34
YB ₂ C	Tetragonal (disordered)	<i>P4/mbm</i>	4	0.6769	—	0.3715	34
YB ₂ C	Tetragonal (ordered)	<i>P4₂/mbc</i>	8	0.6769	—	0.7430	34
YB ₂ C	"	<i>P4₂/mbc</i>	8	0.6793	—	0.7438	34
YB ₂ C ₂	Tetragonal (disordered)	<i>P4/mmm</i>	1	0.3796	—	0.3562	34
YB ₂ C ₂	Tetragonal (ordered)	<i>P4₂c</i>	2	0.3796	—	0.7224	34
YB ₂ C ₂	Tetragonal	—	—	0.3788	—	0.3551	36
CeB ₂ C ₂	"	—	—	0.3817	—	0.3852	36
CeB ₂ C ₂	"	<i>P4₂c</i>	2	0.3817	—	0.7704	37
CeB ₂ C ₄	—	—	—	—	—	—	38
Ce ₅ B ₂ C ₆	Tetragonal	<i>P4</i>	4	0.8418	—	1.2077	39
LaBC	—	—	—	—	—	—	40
LaB ₂ C ₂	Tetragonal	<i>P4₂c</i>	2	0.3822	—	0.7924	37
LaB ₂ C ₄	—	—	—	—	—	—	38
La ₅ B ₂ C ₆	Tetragonal	<i>P4</i>	4	0.8585	—	1.2313	42
PrB ₂ C ₂	"	—	—	0.382	—	0.381	41
PrB ₂ C ₂	"	<i>P4₂c</i>	2	0.381	7	0.762	37
NdB ₂ C ₂	"	—	—	0.3803	—	0.3794	41
NdB ₂ C ₂	"	<i>P4₂c</i>	2	0.3803	—	0.7588	37
SmB ₂ C ₂	"	—	—	0.3796	—	0.3696	36
SmB ₂ C ₂	"	<i>P4₂c</i>	2	0.3796	—	0.7392	37
EuB ₂ C ₂	"	<i>P4₂c</i>	2	0.3801	—	0.7602	37
GdB ₂ C ₂	"	—	—	0.3792	—	0.3640	36, 41
GdB ₂ C ₂	"	<i>P4₂c</i>	2	0.3792	—	0.7280	37
GdBc	Orthorhombic	<i>Cmmm</i>	4	0.4356	0.3796	0.3697	43
Gd _{0.35} B _{0.45} C _{0.20} (~ Gd ₇ B ₉ C ₄)	—	—	—	—	—	—	41
Gd _{0.3} B _{0.4} C _{0.3} (~ GdBC)	—	—	—	—	—	—	41
Gd _{0.4} B _{0.35} C _{0.25} (~ Gd ₈ B ₇ C ₅)	—	—	—	—	—	—	41
Gd _{0.35} B _{0.19} C _{0.46} (~ Gd ₂ BC ₂)	Orthorhombic (?)	—	—	0.609	≥ 0.8	0.856	41
TbB ₂ C	Tetragonal, the YB ₂ C type	<i>P4₂/mbc</i>	8	0.6791	—	0.7522	35
TbB ₂ C ₂	Tetragonal	—	—	0.3784	—	0.3591	41
TbB ₂ C ₂	"	<i>P4₂c</i>	2	0.3784	—	0.7182	37
DyBC	Orthorhombic	<i>Cmmm</i>	4	0.3384	1.3727	0.3647	43
DyB ₂ C	Tetragonal, the YB ₂ C type	<i>P4₂/mbc</i>	8	0.6788	—	0.7452	35
DyB ₂ C ₂	Tetragonal	—	—	0.3782	—	0.3560	41
DyB ₂ C ₂	"	<i>P4₂c</i>	2	0.3781	—	0.7118	37
HoB ₂ C	Tetragonal, the YB ₂ C type	<i>P4₂/mbc</i>	8	0.6773	—	0.7399	35, 44
HoB ₂ C ₂	Tetragonal	—	—	0.3780	—	0.3537	41
HoB ₂ C ₂	"	<i>P4₂c</i>	2	0.3780	—	0.7074	37, 44
HoBC	Orthorhombic (high-temperature the YBC type)	<i>Cmmm</i>	4	0.3384	1.3697	0.3594	44
HoBc	Tetragonal (long-period)	—	—	0.3546	—	4.640	44
Ho ₂ BC ₃	Centred tetragonal (high-temperature)	—	—	0.3561	—	1.2455	44

Table 3 (continued).

Compound	Symmetry and type of structure	Space group	Z	Unit cell parameters / nm			Ref.
				a	b	c	
LaB ₂ C ₂	Tetragonal	—	—	0.3816	—	0.3975	36, 41
Ho ₂ BC ₃	Primitive tetragonal	—	—	0.3567	—	2.4515	44
Ho ₃ B ₂ C ₃	—	—	—	—	—	—	44
Ho ₅ B ₂ C ₆	Tetragonal, the La ₅ B ₂ C ₆ type	P4	4	0.7981	—	1.1561	44
Ho ₅ B ₂ C ₅	Tetragonal	—	—	0.8033	—	1.0812	44
Ho ₁₅ B ₂ C ₁₇	Tetragonal (substitution of ² in Ho ₁₅ C ₁₉ by B)	P4 ₂ 1c	2	0.8004	—	1.5984	44
ErB ₂ C	Tetragonal	P4 ₂ /mbc	8	0.6753	—	0.7321	35
ErB ₂ C ₂	"	—	—	0.3778	—	0.3508	41
ErB ₂ C ₂	"	P4 ₂ c	2	0.3778	—	0.7016	37
TmB ₂ C	Tetragonal, the YB ₂ C type	P4 ₂ /mbc	8	0.6735	—	0.7284	35
TmB ₂ C ₂	Tetragonal	—	—	0.3776	—	0.3477	36
TmB ₂ C ₂	"	P4 ₂ c	2	0.3776	—	0.6954	37
YbB ₂ C	Tetragonal, the YB ₂ C type	P4 ₂ /mbc	8	0.6724	—	0.7240	35
YbB ₂ C ₂	Tetragonal	—	—	0.3775	—	0.3560	36, 41
YbB ₂ C ₂	"	P4 ₂ c	2	0.3775	—	0.7120	37
LuB ₂ C	Tetragonal, the YB ₂ C type	P4 ₂ /mbc	8	0.6755	—	0.7178	32
LuB ₂ C ₂	Tetragonal	—	—	0.3762	—	0.3453	36
LuB ₂ C ₂	"	P4 ₂ c	2	0.3762	—	0.7102	37

between the 8(*j*) and 4(*h*) sites. In the case of the borocarbides MB₂C with an ordered distribution of the B and C atoms (space group *P4₂/mbc*), the unit cell parameter *c* is twice as large as that for the disordered unit cell; the Y atoms occupy the 8(*g*) sites, sixteen boron atoms are arranged at the 8(*h*) sites of two types, and eight carbon atoms occupy the 8(*h*) sites.

Phase equilibria in the Y–B–C,³⁴ Eu–B–C,³¹ Gd–B–C,⁴¹ and Ho–B–C⁴⁴ systems have been studied; in these systems, four, two, five, and eight ternary compounds, respectively, have been found (Fig. 3). The state diagram for the Y–B–C system has been constructed using the data of an X-ray structural study of samples quenched from a melt. A phase

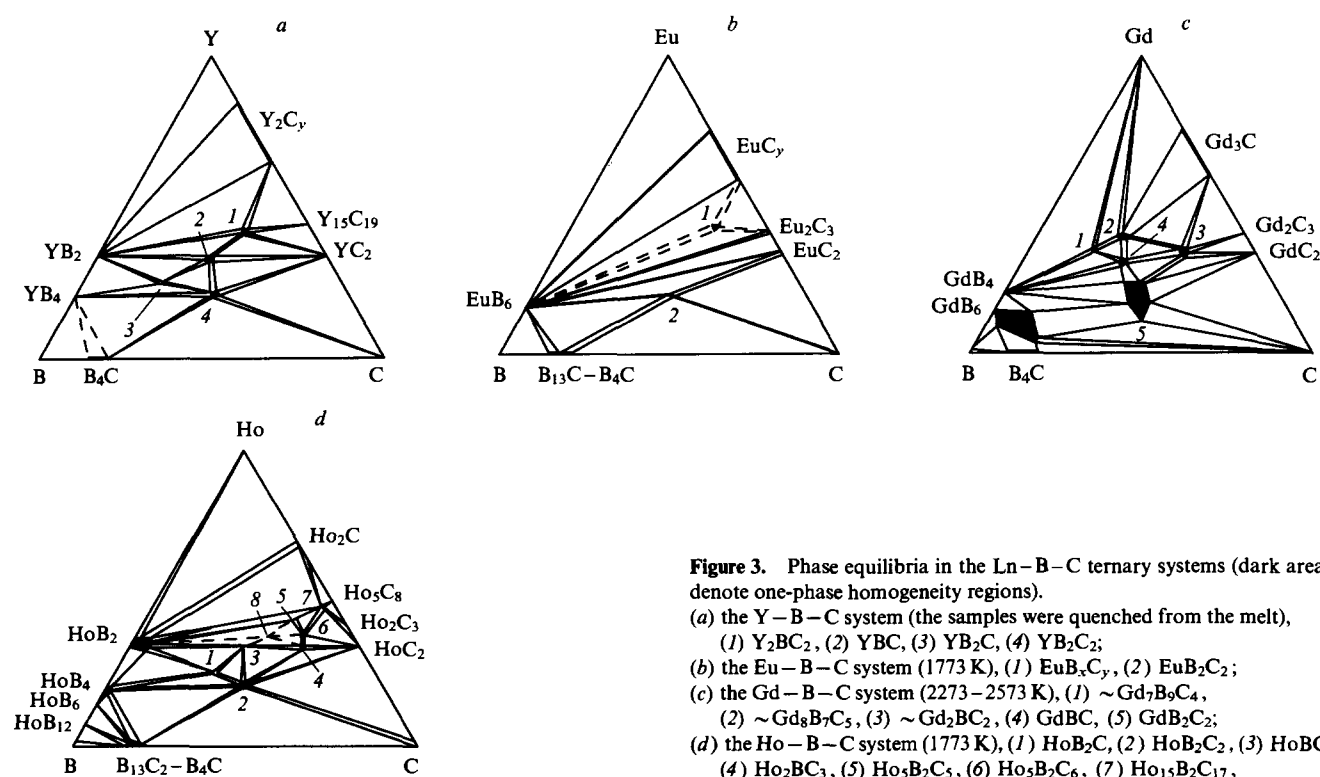


Figure 3. Phase equilibria in the Ln–B–C ternary systems (dark areas denote one-phase homogeneity regions).

- (a) the Y–B–C system (the samples were quenched from the melt), (1) Y₂BC₂, (2) YBC, (3) YB₂C, (4) YB₂C₂;
 (b) the Eu–B–C system (1773 K), (1) EuB_xC_y, (2) EuB₂C₂;
 (c) the Gd–B–C system (2273–2573 K), (1) ~Gd₇B₉C₄, (2) ~Gd₈B₇C₅, (3) ~Gd₂BC₂, (4) GdB₂C₂, (5) GdB₂C₂;
 (d) the Ho–B–C system (1773 K), (1) HoB₂C, (2) HoB₂C₂, (3) HoBC, (4) Ho₂BC₃, (5) Ho₅B₂C₅, (6) Ho₅B₂C₆, (7) Ho₁₅B₂C₁₇, (8) Ho₃B₂C₃.

diagram for the Ce–B–C system has been suggested⁴⁷ based on thermodynamic estimates; however, only one ternary compound, which was known at that time, was taken into account in this study.

2. Borocarbides of Group IV transition metals

Due to their high stability borides of Group IV transition metals exist in equilibrium with carbon, boron carbide B_4C , and non-stoichiometric monocarbides $M^{IV}C_y$. The mutual solubility of borides and carbides is very low.

The Ti–B–C system. The first version of the state diagram for this system was suggested by Brewer and Haraldsen.⁴⁷ According to the thermodynamic calculations made by them, four titanium borides, namely, Ti_2B , TiB , TiB_2 , and Ti_2B_3 , are formed in this system. The existence of the Ti_2B and Ti_2B_3 phases has not been confirmed reliably in experimental studies. The phase diagram for the Ti–B–C system, commonly accepted at present, has been constructed using the results of a detailed study⁴⁸ and has been refined later in another study;⁴⁹ this variant has also been presented in a paper by Schouler et al.⁵⁰ (Fig. 4). The isothermal cross-section through the Ti–B–C system at 2273 K⁵¹ coincides almost exactly with that presented in Fig. 4a.

There is almost no mutual solubility of titanium carbide $TiC_{1.0}$ and titanium diboride TiB_2 at temperatures below 2273 K. When the stoichiometric composition of titanium carbide is disturbed, the solubility of TiB_2 in it increases. In fact, at 1873 K,

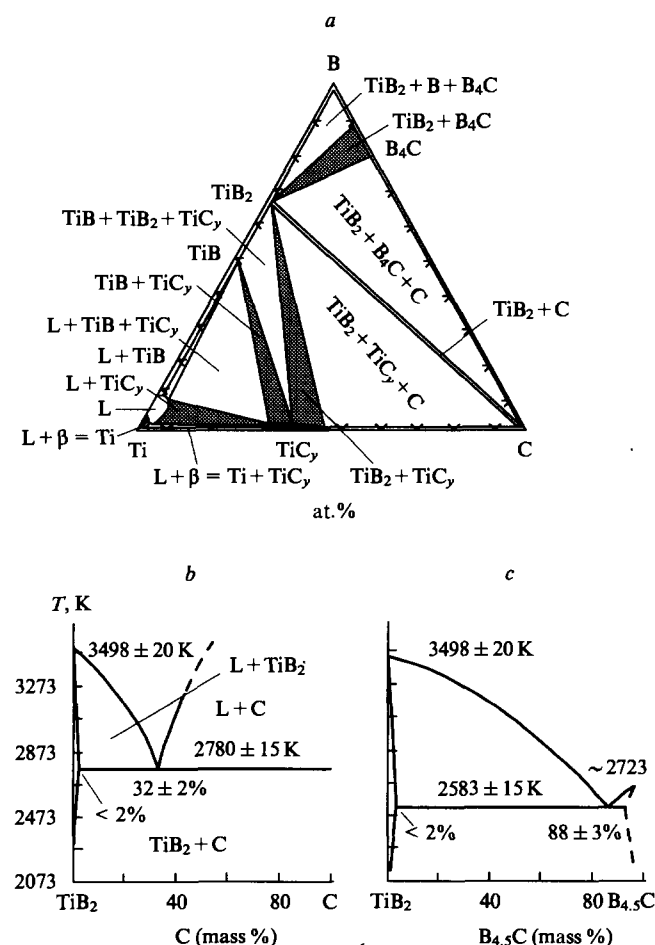


Figure 4. State diagram for the Ti–B–C ternary system and its pseudobinary cross-sections.^{49, 50}

(a) the isothermal cross-section through the Ti–B–C system at 1873 K (dark areas denote one-phase homogeneity regions); (b) polythermal pseudobinary TiB_2 –C cross-section; (c) polythermal pseudobinary TiB_2 – $B_{4.5}C$ cross-section.

~3 mol % of TiB_2 is dissolved in the carbide $TiC_{0.95}$, whereas $TiC_{0.68}$ dissolves ~7 mol % of TiB_2 . The increase in the solubility of TiB_2 is in good agreement with the conclusion made by Gusev² that an increase in the concentration of structural vacancies creates new interstitial positions and is favourable for the increase in the solubility. Note that the hardness of titanium carbide increases on the addition of TiB_2 .

In the TiC_y – TiB_2 , TiB_2 –C, and TiB_2 – B_4C pseudobinary cross-sections, ordinary eutectics at 2900, 2780, and 2600 K, respectively, are formed. The mutual solubility of titanium boride and titanium carbide along the TiC_y – TiB_2 pseudobinary cross-section should most likely be unlimited, if these compounds have identical structures of the $B1$ type, and their unit cells have similar sizes. In the TiC_y – TiB system, there is a possibility of the formation of solid solutions, but it is prevented by the decomposition of TiB at temperatures above 2200 K.⁵²

The Zr–B–C system. The state diagram of this system has been studied in a number of papers.^{47, 53, 54} The ZrC_y – ZrB_2 , ZrB_2 –C, and ZrB_2 – B_4C pseudobinary equilibria were found in the Zr–B–C ternary system; later, their existence has been confirmed experimentally. In addition, the ZrC_y – ZrB equilibrium exists at $T \leq 1523$ K and the ZrB_{12} – B_4C equilibrium exists at $T > 1923$ K.⁴⁷ ZrB has not been detected.⁵³ The solubility of ZrB_2 in the carbide ZrC_y increases with an increase in the concentration of structural vacancies in the carbon sublattice of the carbide.

The Hf–B–C system. The phase diagram for the Hf–B–C ternary system was constructed for the first time by Nowotny et al.⁵³ It proved to be fairly similar to the state diagram of the Ti–B–C system. The HfB – HfC_y , HfB_2 – HfC_y , HfB_2 –C, and ZrB_2 – B_4C pseudobinary equilibria exist in the Hf–B–C system. In the HfB_2 – HfC_y , HfB_2 –C, and ZrB_2 – B_4C pseudobinary cross-sections, ordinary eutectics at temperatures of 3410, 2790, and 2600 K, respectively, are formed. The solubility of HfB_2 in HfC_y increases with an increase in the defectiveness of the carbon sublattice of the carbide.

A general feature of the interaction of boron with titanium, zirconium, and hafnium carbides is the formation of limited MB_xC_{1-x} borocarbide solid solutions. The solubility of boron in carbides increases in the sequence $TiC_y \rightarrow ZrC_y \rightarrow HfC_y$ and with a decrease in the carbon content. Hafnium carbide dissolves up to 6 at.% of boron.

No ternary compounds are formed in the titanium, zirconium, and hafnium borocarbide systems.^{47–50, 53–55}

The Th–B–C system. Only binary carbides ThC , ThC_2 , and B_4C and borides ThB_4 and ThB_6 exist in this system. There are four pseudobinary phase equilibria in the Th–B–C ternary system, namely, ThC – ThB_4 , ThC_2 – ThB_6 , ThB_6 –C, and ThB_6 – B_4C .⁴⁷ It has been shown by experimental studies that in this system (in contrast to the titanium, zirconium, and hafnium borocarbide systems), four ternary compounds $Th_3B_2C_3$, $ThBC$, ThB_2C , and $ThBC_2$, are formed (Table 4). They all have homogeneity regions, the homogeneity region of $ThBC$ being fairly large. A state diagram for the Th–B–C system has been reported.⁵⁶ Five ternary compounds, namely, $ThBC$, ThB_2C , $ThBC_2$, Th_2BC , and Th_2BC_2 , were found in this diagram (the ternary monoclinic thorium borocarbide $Th_3B_2C_2$ reported in another paper⁵⁸ was not taken into account in this diagram). The compounds $ThBC$ and ThB_2C melt congruently at 2370 and 2310 K, respectively.

A characteristic feature of the Th–B–C system is that carbon is almost insoluble in borides, and boron is almost insoluble in carbides.

3. Borocarbides of Group V–VIII transition metals

The ternary systems of Group V transition metals with boron and carbon differ from the analogous systems containing Group IV transition metals in that new binary borides, M_3B_4 and M_3B_2 , arise in these systems. No ternary borocarbides of Group V transition metals were detected in the M^V –B–C systems.

Chromium, molybdenum, and uranium form borocarbides with boron and carbon, whereas in the W–B–C system no ternary compounds were detected.

The V–B–C system. The state diagram for the V–B–C system has been constructed by Markovsky et al.⁶⁹ In this system, all the carbides and borides are in equilibria with one another: V_2C_y – V_3B_2 , V_2C_y –VB, VC_y –VB, VC_y – V_3B_4 , VC_y – VB_2 , and VB_2 – B_4C . The VB_2 –C pseudobinary equilibrium also exists. The solubility of boron in vanadium carbides is low, but it is somewhat higher than the solubility of carbon in vanadium borides.

The Nb–B–C system. This system involves the same phase equilibria as the V–B–C system.⁶⁹ The NbC_y – NbB_2 pseudobinary cross-section is eutectic with an eutectic temperature of ~2900 K. The solubility of boron in the carbide NbC_y increases with a decrease in y and can reach 5 at.%. The hardness of the niobium carbide NbC_y increases noticeably on the dissolution of boron.

The Ta–B–C system. In this system, the existence of borides Ta_2B and Ta_3B , in addition to the borides TaB_2 , Ta_3B_4 , and TaB , which are also characteristic of the V–B–C and Nb–B–C systems, has been reported.⁴⁷ Later, the existence of Ta_2B has been confirmed, and the boride Ta_3B_2 has also been found. The existence of Ta_3B has not been confirmed. The Ta–B–C system, unlike the V–B–C and Nb–B–C systems, involves one more pseudobinary equilibrium, namely, Ta_2C_y – Ta_2B . The TaC_y – TaB_2 pseudobinary cross-section has a eutectic at a temperature of ~3000 K. The solubility of boron in TaC_y increases with an increase in the concentration of carbon vacancies and can reach 6 at.%. The solubility of carbon in TaB_2 is no more than 2 at.%. The dissolution of boron in TaC_y leads to a substantial increase in the microhardness.

The Cr–B–C system. Chromium carbides, in contrast to carbides of other transition metals, can dissolve substantial quantities of boron. This is caused by the significant differences between the crystal structures of chromium carbides and carbides

of other transition metals. For example, at 1723 K, about 30% of the carbon can be substituted by boron in the carbide $Cr_{23}C_6$, about 36% in Cr_7C_3 , and about 5% in Cr_3C_2 .²⁹ The state diagram for the Cr–B–C ternary system has been constructed;⁷⁰ however, the phase relationships in the region rich in carbon and boron have been studied inadequately. Chromium forms four ternary phases with boron and carbon, namely, the $Cr_3(B,C)_2$, $Cr_7(B,C)_3$, and $Cr_{23}(B,C)_6$ solid solutions and the compound Cr_7BC_4 (see Table 4).

The boron atoms and some of the carbon atoms in Cr_7BC_4 fill the trigonal prismatic interstices and the rest are arranged in the octahedral vacancies of the metal sublattice.⁶⁰ This compound is stable in the temperature range 1820 K–1980 K. A neutron-diffraction study has shown that the borocarbide Cr_7BC_4 has a filled structure of the Re_3B type (space group $Cmcm$) (Fig. 5), which is also peculiar to other ternary compounds (for example, zirconium and hafnium aluminidoborides).⁶¹ In the borocarbide

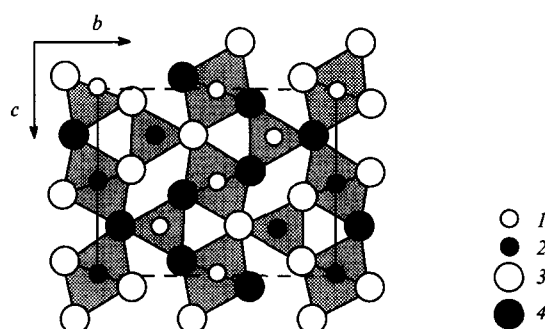


Figure 5. Projection along the [001] axis of the crystal structure of the Re_3B type (space group $Cmcm$).

(1, 2) nonmetal atoms located at heights $x = 0$ and $x = \frac{1}{2}$, respectively; (3, 4) metal atoms located at heights $x = 0$ and $x = \frac{1}{2}$, respectively.

Table 4. Some ternary compounds in borocarbide systems of Group IV and Group VI–VIII transition metals.

Compound	Symmetry and type of structure	Space group	Z	Unit cell parameters/ nm			Ref.
				a	b	c	
ThBC	Tetragonal	$P4_122$	8	0.3762	—	2.5246	56, 57
$Th_3B_2C_3$	Monoclinic	$P2_1/m$	1	0.3703	0.9146	0.3773 ^a	58
ThB_2C	Hexagonal	$P6/mmm$	3	0.3868	—	0.3810	56
ThB_2C	Trigonal (rhombohedral)	$R\bar{3}m$	9	0.6676	—	1.1376	59
$ThBC_2$	—	—	—	—	—	—	56
Cr_7BC_4	Orthorhombic filled structure of the Re_3B type	$Cmcm$	4	0.2870	0.9260	0.6982	60
$Cr_3(B_{0.44}C_{0.56})C_{0.85}$	"	$Cmcm$	4	0.2857	0.9233	0.6967	61
Mo_2BC	Orthorhombic	$Cmcm$	4	0.3086	1.735	0.3047	62
UBC	Monoclinic	$C2_1/m$	4	0.3591	1.195	0.3372	57
UBC	Orthorhombic	$Cmcm$	4	0.3591	1.195	0.3372	63
UBC	"	$Cmcm$	4	0.3591	1.1985	0.3348	64
UB_2C	Trigonal, the ThB_2C type (high-temperature modification)	$R\bar{3}m$	9	0.6535	—	1.0781	64
$U_5B_2C_7$	Tetragonal, the $La_5B_2C_6$ type (?)	—	—	—	—	—	64
$Mn_{23}C_3B_3$	Cubic, the $Cr_{23}C_6$ (D_{8h}) type, a solid solution of boron in $Mn_{23}C_6$	$Fm\bar{3}m$	4	1.071	—	—	65
Mn_7BC_2	Orthorhombic, a solid solution of boron in Mn_7C_3	$Pnma$	4	0.4521	0.6986	1.2099	31
$Fe_{23}C_3B_3$	Cubic, the $Cr_{23}C_6$ (D_{8h}) type	$Fm\bar{3}m$	4	1.0594	—	—	67
$Fe_3(B,C)$	Orthorhombic, the cementite Fe_3C (D_{011}) type	$Pnma$	4	—	—	—	68
$Co_{11}B_2C$	Cubic, the $Cr_{23}C_6$ (D_{8h}) type	$Fm\bar{3}m$	8	1.047	—	—	69

^a In the unit cell $\beta = 100.06^\circ$.

Cr_7BC_4 with the Re_3B type of structure, the carbon atoms at the 4(b) sites populate 85% of the octahedral interstices, and the rest of the carbon atoms together with the boron atoms share the 4(c) sites at the centres of trigonal prisms. Thus, the more exact structural formula of this compound should be written as $Cr_3(B_{0.44}C_{0.56})C_{0.85}$.

The Mo-B-C system. The possible phase equilibria in the Mo-B-C system were first estimated by a thermodynamic calculation.⁴⁷ According to this estimate, six pseudobinary phase interactions exist in this system, and ternary compounds are absent. More recently,⁶⁹ the Mo-B-C phase diagram has been made substantially more precise.

One ternary compound Mo_2BC with a small homogeneity region and an orthorhombic structure (space group $Cmcm$) of its own type (see Table 4), typical also of a number of other ternary compounds discussed in this review, is formed in this system. The structure of Mo_2BC is a combination of the boride and carbide sublattices (Fig. 6). The carbon atoms are located at the centres of the octahedra formed by the molybdenum atoms. The CMo_6 octahedra are connected to one another by eight edges and form double-stranded octahedral layers. The boron atoms in Mo_2BC linked in zigzag-shaped chains are arranged between the octahedral layers. Each boron atom is located at the centre of a trigonal prism, molybdenum atoms serving as the vertices of the prism. This distribution of boron atoms is specific and typical of transition metal monoborides. This gives grounds for regarding the borocarbide Mo_2BC as a derivative of β -MoB in which the octahedral interstices of the molybdenum sublattice are occupied by carbon atoms.

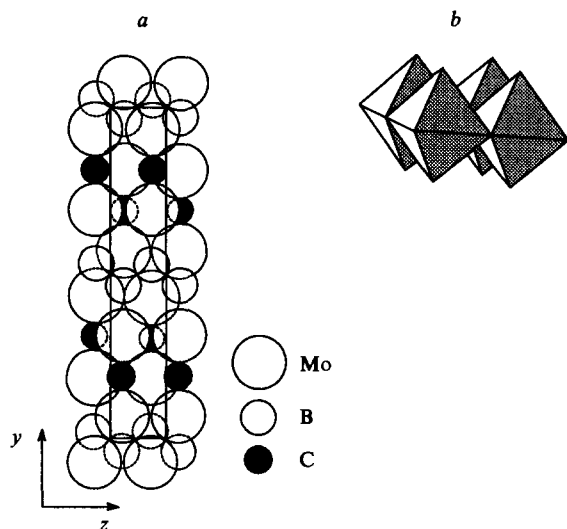


Figure 6. Crystal structure of Mo_2BC (space group $Cmcm$).

(a) projection along the [100] axis (the wholly visible atoms are located at height $x = 0$; the atoms that are partly seen are located at height $x = \frac{1}{2}$); (b) the layer of the CMo_6 octahedra joined through their edges, parallel to the (010) plane; in Mo_2BC , these layers are joined in pairs in such a way that each octahedron is linked to the neighbouring octahedra via its eight edges.

At 1573 K, three borides Mo_2B , MoB , and Mo_2B_5 , molybdenum carbide Mo_2C , boron carbide B_4C , and ternary compound Mo_2BC exist in the Mo-B-C system. The following equilibria are established between these compounds: Mo_2B-Mo_2C , $MoB-Mo_2C$, $MoB-Mo_2BC$, $MoB-C$, Mo_2BC-Mo_2C , Mo_2BC-C , $Mo_2B_5-B_4C$, and Mo_2B_5-C . At 2073 K, the Mo_2B_5-C equilibrium disappears, since the boride MoB_2 arises, and the MoB_2-C equilibrium is established; in addition, carbide Mo_3C_2 arises distinct from Mo_2C ; 1–2 at. % of boron dissolves in

both carbides. Boron stabilizes the high-temperature carbide phases of molybdenum. The MoB_2-C and $MoB-C$ pseudobinary cross-sections are eutectic systems.

The W-B-C system. This system contains only binary tungsten carbides W_2C and WC , tungsten borides W_2B , WB , and W_2B_5 , and boron carbide B_4C .⁴⁷ Tungsten borides WB_{12} ⁶⁹ and WB_4 ^{49,50} have also been detected. The existence of the boride WB_4 is more probable. Six pseudobinary cross-sections, namely, W_2B-W_2C , W_2B-WC , $WB-WC$, $WB-C$, W_2B_5-C , and $W_2B_5-B_4C$ contain ordinary eutectics with temperatures 2640, 2560, 2600, 2630, 2550, and 2500 K, respectively.⁴⁹ In all probability the WB_4-B_4C pseudobinary cross-section is also an eutectic system.

The U-B-C system. The phase equilibria in this system have been studied.^{63,64} It was originally believed that the U-B-C system contains one ternary compound UBC (see Table 4) with an extended homogeneity region, which exists at 1573 K in equilibrium with UC, UC_2 , C, UB_2 , and UB_4 . In addition, there are $UC-UB_2$, UB_4-C , UB_4-B_4C , and $UB_{12}-B_4C$ pseudobinary equilibria. The ternary borocarbide UBC lies at the UC_2-UB_2 pseudobinary cross-section. The distribution of the carbon and boron atoms in this orthorhombic phase is intermediate between those in the tetragonal carbide UC_2 and the hexagonal boride UB_2 .

In a more recent study of the U-B-C system, two other ternary compounds UB_2C and $U_5B_2C_7$ have been detected, apart from UBC (see Table 4). The isothermal cross-section through the U-B-C system at 1873 K at an argon pressure of 1×10^5 Pa has been constructed by Rogl et al.⁶⁴ The phase equilibria at 1273, 1673, 1873, and 2073 K are virtually identical. The high-temperature modification of UB_2C has a structure of the ThB_2C type and has a narrow homogeneity region; with an increase in carbon content the unit cell volume of U_2BC somewhat decreases. At temperatures below 1900 K, the low-temperature modification of UB_2C is formed; its structure is unknown. The compound $U_5B_2C_7$ probably has a tetragonal structure similar to that of $La_5B_2C_6$.⁴² The temperatures of the congruent melting of UBC and UB_2C are 2420 ± 25 K and 2550 ± 30 K, respectively. The borocarbide UB_2C exists in equilibrium with UBC, UB_4 , and C, and $U_5B_2C_7$ is in equilibrium with UBC, UC, and UC_2 .

The Mn-B-C system. Among the ternary systems formed by boron and carbon with manganese, technetium, and rhenium, only the Mn-B-C system has been studied fairly extensively. An isothermal cross-section through the manganese-rich part of the phase diagram of this system at 1073 K has been reported.⁶⁵ At 1073 K the borocarbide formed on the dissolution of boron in the cubic carbide $Mn_{23}C_6$ has the composition $Mn_{23}C_{4.6}B_{1.4}$ ($a = 1.064$ nm), and at 1273 K, its composition is $Mn_{23}C_3B_3$. The dissolution of boron in the carbide Mn_7C_3 at 1273 K yields the Mn_7BC_2 ternary phase (see Table 4).^{65,66} At 1273 K the boride Mn_4B exists in equilibrium with $Mn_{23}C_3B_3$ and Mn_7BC_2 , MnB is in equilibrium with Mn_7BC_2 and C; two other equilibria, namely, Mn_3B_4-C and $Mn_3B_4-B_4C$, also exist in the system.⁷¹

The borocarbide $Mn_{23}C_3B_3$ has a structure of the $Cr_{23}C_6$ type, which is also typical of the iron borocarbide $Fe_{23}B_3C_3$, the cobalt borocarbide $Co_{11}B_2C$, and some other ternary compounds.

The unit cell of the carbide $Cr_{23}C_6$ and the borocarbid $Mn_{23}C_3B_3$ and $Fe_{23}B_3C_3$ (space group $Fm\bar{3}m$) is a cube including 4 formula units, i.e. 92 metal atoms and 24 atoms of the nonmetals. Each metal atom occupies a cube vertex and is surrounded by 12 metal atoms constituting a cubooctahedron. Similar cubooctahedra formed by 12 metal atoms surround the centre of each face of the cube. Eight metal atoms occupy the 8(c) and equivalent sites and the remaining metal atoms are at the 32(f) sites and form simple cubes surrounding the middle of each unit cell edge. Each nonmetal atom in compounds with the $Cr_{23}C_6$ type of structure is surrounded by eight metal atoms located at the vertices of a tetragonal antiprism.

Among ternary systems of boron and carbon with Group VIII transition metal, only the Fe–B–C system has been studied in detail. In the Co–B–C system, a ternary compound $\text{Co}_{11}\text{B}_2\text{C}$ has been found (see Table 4).⁶⁹

The Fe–B–C system. Iron forms a carbide Fe_3C (cementite) and borides Fe_2B and FeB . Up to 80 at. % of the carbon in Fe_3C can be substituted by boron; carbon is markedly soluble in both borides. Two ternary compounds $\text{Fe}_{23}\text{C}_3\text{B}_3$ and $\text{Fe}_3(\text{B,C})$ have been found in this system (see Table 4). Boron introduced to the cementite Fe_3C can replace not only the carbon atoms, but also the iron atoms, the boron atoms being predominantly distributed over the crystallographic planes of cementite.⁶⁸ The borocarbide $\text{Fe}_{23}\text{C}_3\text{B}_3$ (the τ -phase) having fairly extended homogeneity regions both for boron and carbon has been studied most thoroughly. The borocarbide $\text{Fe}_{23}\text{C}_3\text{B}_3$ melts congruently. As the temperature increases, the homogeneity region of the τ -phase decreases, and at 1240 K, the τ -phase decomposes to give the γ -phase (austenite) and $\text{Fe}_3(\text{B,C})$.⁷³

III. M–B–N ternary boronitride systems

The properties of the boronitride systems of transition metals are largely similar to those of the borocarbide systems. For a long time, no ternary compounds were found in the M–B–N systems; however, since 1983, several boronitrides of lanthanides and also a ternary compound in the Nb–B–N system were detected (Table 5). The phase equilibria in the M–B–N ternary systems have been analysed in a number of studies.^{80–83}

Rogl et al.,⁷⁴ who have studied ternary systems containing lanthanides, boron, and nitrogen, have found a family of new ternary lanthanum, cerium, praseodymium, and neodymium boronitrides $\text{M}_3\text{B}_2\text{N}_4$ with the orthorhombic structure of the W_2CoB_2 type. In the M–B–N-systems ($\text{M} = \text{Sc}, \text{Y}, \text{Gd} \rightarrow \text{Lu}$), the $\text{M}_3\text{B}_2\text{N}_4$ ternary phases are not formed. The boronitride $\text{Nd}_3\text{B}_2\text{N}_4$ is unstable at temperatures above 1673 K. The structure of boronitrides $\text{M}_3\text{B}_2\text{N}_4$ can be regarded as a variant of the $(\text{W}_2\text{Co})\text{B}_2\Box_4$ filled structure. The boron atoms in this structure are located in trigonal prisms consisting of six metal atoms and form B–B pairs; in addition, each boron atom is bound to two nitrogen atoms (Fig. 7). In turn, the nitrogen atoms of $\text{M}_3\text{B}_2\text{N}_4$

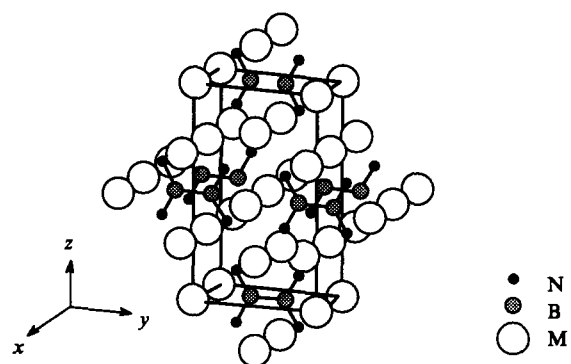


Figure 7. Orthorhombic structure of the lanthanide boronitrides $\text{M}_3\text{B}_2\text{N}_4$ ($\text{M} = \text{La}, \text{Ce}, \text{Pr}, \text{Nd}$) of the $(\text{W}_2\text{Co})\text{B}_2\Box_4$ type (space group Immm).⁷⁴

occupy the 8(*l*) sites, which are vacant in $(\text{W}_2\text{Co})\text{B}_2\Box_4$. In other words, the nitrogen atoms are located in the distorted octahedral interstices and are surrounded by five metal atoms (the M atoms are in the vertices of a rectangular pyramid) and by one boron atom, i.e. NM_5B groups are formed. There are no direct N–N interactions in the structure of the boronitrides $\text{M}_3\text{B}_2\text{N}_4$.

Ternary compounds MBN_2 of the same type have been found in the M–B–N systems ($\text{M} = \text{Pr}, \text{Nd}, \text{Sm}, \text{Gd}$) (see Table 5). The boronitride GdBN_2 is stable only at $T > 1763 \text{ K}$.⁷⁶ The boronitride $\text{Ce}_{15}\text{B}_8\text{N}_{25}$ has been detected in the Ce–B–N system.⁷⁵ Scandium, yttrium, and lanthanides from Tb to Lu do not form compounds MBN_2 .⁸¹ In the M–B–N systems ($\text{M} = \text{Tb} \rightarrow \text{Lu}, \text{Y}$), the boron nitride BN exists in equilibrium with a metal nitride MN and with all the existing borides beginning with MB_4 and ending with MB_{66} , and MN coexists with borides MB_2 and MB_4 ; in the Sc–B–N system, there are only two borides, ScB_2 and ScB_{12} , existing in equilibrium with BN; and ScN is in equilibrium with ScB and BN.⁶³ The mutual solubilities of boron nitride and lanthanide borides and nitrides are extremely limited.⁸¹

Table 5. Some ternary compounds in boronitride systems of transition metals.

Compound	Symmetry and type of structure	Space group	Z	Unit cell parameters / nm			Ref.
				a	b	c	
$\text{La}_3\text{B}_2\text{N}_4$	Orthorhombic, filled structure of the W_2CoB_2 type	Immm	2	0.3634	0.6414	1.0974	74
$\text{Ce}_3\text{B}_2\text{N}_4$	"	Immm	2	0.3565	0.6316	1.0713	74
$\text{Ce}_{15}\text{B}_8\text{N}_{25}$	Trigonal (rhombohedral)	$R\bar{3}c$	2	1.0946 ^a	—	—	75
$\text{Pr}_3\text{B}_2\text{N}_4$	Orthorhombic, filled structure of the W_2CoB_2 type	Immm	2	0.3540	0.6310	1.0795	74
PrBN_2	Trigonal (rhombohedral)	$R3c$	18	1.2114	—	0.7013	76
$\text{Nd}_3\text{B}_2\text{N}_4$	Orthorhombic, filled structure of the W_2CoB_2 type	Immm	2	0.3520	0.6278	1.0756	74
NdBN_2	Trigonal (rhombohedral)	$R3c$	18	—	—	—	76
NdBN_2	Monoclinic	$P2_1/m$ or $P2_1/c$	10	0.6950	1.2077	0.5856 ^b	77
SmBN_2	"	$P2_1/m$ or $P2_1/c$	10	0.6897	1.1928	0.5783 ^c	77
SmBN_2	Trigonal (rhombohedral)	$R3c$	18	—	—	—	76
GdBN_2	"	$R3c$	18	—	—	—	76
Nb_2BN	Orthorhombic	Cmcm	4	0.3172	1.7841	0.3114	78, 79
$\text{Nb}_{2-x}\text{V}_x\text{BN}$	"	Cmcm	4	0.3172	1.7841	0.3113	78
$\text{Nb}_{2-x}\text{Ta}_x\text{BN}$	"	Cmcm	4	0.3171	1.7846	0.3114	78

^a In the unit cell $\alpha = 82.96^\circ$. ^b In the unit cell $\beta = 99.32^\circ$. ^c In the unit cell $\beta = 99.84^\circ$.

The Ti–B–N system. Studies of the phase equilibria in ternary systems containing Group IV transition metals, boron, and nitrogen have shown that no ternary compounds are formed in these systems. According to thermodynamic data,⁴⁷ six pseudobinary equilibria are possible in the Ti–B–N system, namely, TiN_y-Ti_2B , TiN_y-TiB , TiN_y-TiB_2 , TiB_2-N , TiB_2-BN , and Ti_2B_5-BN . There are no reliable experimental data supporting the existence of the borides Ti_2B and Ti_2B_5 . The phase diagram for the Ti–B–N system has been constructed by Nowotny et al.⁴⁸ Four binary compounds, namely, TiB , TiB_2 , TiN_y , and BN , exist in this system; ternary compounds are absent. The titanium nitride TiN_y exists in equilibrium with the borides TiB and TiB_2 and with BN . The lower boride TiB is in equilibrium with the solid solution of nitrogen in α -Ti and the higher boride TiB_2 is in equilibrium with BN . The solubility of boron in the titanium nitride is low, but it is higher than that in the carbide TiC_y . When the composition of nitride TiN_y deviates from the stoichiometric composition, the solubility of boron in it increases. The solubility of nitrogen in titanium borides is negligibly small. The TiN_y-BN equilibrium at a nitrogen pressure of 0.05 MPa exists only below 1900 K, and at $T > 1900$ K, the boride TiB_2 exists in equilibrium with nitrogen.⁴⁷

The Zr–B–N system. The phase equilibria in this system have been investigated in a number of studies.^{47, 54, 84} Brewer and Haraldsen⁴⁷ suggested the existence of three zirconium borides, ZrB , ZrB_2 , and ZrB_{12} , therefore, five possible pseudobinary equilibria, ZrN_y-ZrB , ZrN_y-ZrB_2 , ZrB_2-N , ZrB_2-BN , and $ZrB_{12}-BN$, were considered in the Zr–B–N system. ZrB_2 is the main boride phase of zirconium. In this system, four binary equilibria exist: zirconium diboride exists in equilibrium with the solid solution of nitrogen and boron in α -Zr and with the nitrides ZrN_y and BN ; and the nitride ZrN_y is in equilibrium with BN . The latter equilibrium can exist at a pressure of nitrogen of 0.05 MPa (0.5 atm) up to a temperature of 1820 K; at $T > 1820$ K, the zirconium diboride ZrB_2 exists in equilibrium with nitrogen.⁴⁷ The solubility of boron in zirconium nitride ZrN_y is much higher than that in TiN_y , and it increases from 8 at.% to 25 at.% as the composition of the zirconium nitride varies from $ZrN_{1.00}$ to $ZrN_{0.55}$.

The Hf–B–N system. In the state diagram of the Hf–B–N ternary system, the borides HfB and HfB_2 exist in an equilibrium with the solid solution of nitrogen and boron in α -Hf. The HfB_2-HfN_y , HfB_2-BN , and HfB_2-N equilibria exist in this system [the latter exists at a nitrogen pressure of more than 0.1 MPa (1 atm)].⁸⁴ The solubility of boron in the nitride HfN_y at the lower boundary of the homogeneity region reaches 40–50 at.%. The solubility of nitrogen in HfB and HfB_2 is low, but it is higher than that in the titanium and zirconium borides.

The V–B–N system. The phase equilibria in the V–B–N ternary system have been studied by Spear et al.⁸⁵ (Fig. 8a). No ternary compounds exist in this system, but there are eight binary compounds including five borides (V_3B_2 , VB , V_3B_4 , V_2B_3 , and VB_2), two vanadium nitrides (V_2N_y and VN_y), and one boron nitride (BN). At a pressure of nitrogen of 0.1 MPa (1 atm), eight pseudobinary equilibria are possible in the V–B–N system depending on the temperature, namely, $VB-BN$, $V_3B_2-V_2N_y$, $VB-V_2N_y$, $VB-VN_y$, V_3B_4-BN , V_2B_3-BN , VB_2-BN , and VN_y-BN . The central three-phase $VB + BN + VN_y$ field exists at $T < 2010$ K, the $VB + BN + V_3B_4$ field exists at $T < 2180$ K, and the $V_3B_4 + BN + V_2B_3$ and $V_2B_3 + BN + VB_2$ fields exist at $T < 2290$ K.⁸⁴ Boron is hardly soluble in vanadium nitrides, and nitrogen is almost insoluble in vanadium borides.

The Nb–B–N system. The phase equilibria in this system have been studied in a number of works.^{78, 79, 86} The Nb–B–N system is the only one among the boronitride systems of Group V–VIII transition metals in which ternary compounds have been found. Rogl et al.⁷⁹ have constructed an isothermal cross-section through the Nb–B–N system at 1473 K and a pressure of argon of 1×10^5 Pa (Fig. 8b). The phase equilibria in this system involve three ternary compounds, among which Nb_2BN is formed most

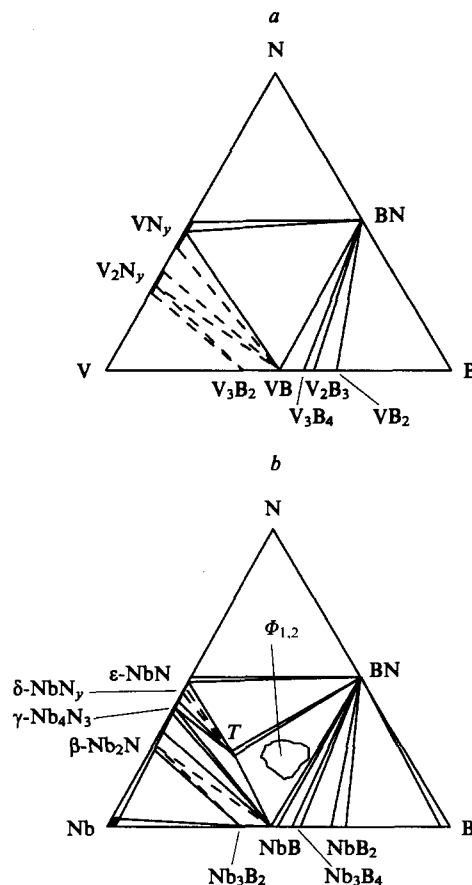


Figure 8. Isothermal cross-sections through the $M-B-N$ ($M = V, Nb$) ternary systems at 1473 K.

(a) the V–B–N system at a nitrogen pressure of 1×10^5 Pa (dark areas denote one-phase homogeneity regions);⁸⁵ (b) the Nb–B–N system at an argon pressure of 1×10^5 Pa [$T = Nb_2BN$, $\phi_{1,2}$ is the designation for two (or more) unknown ternary phases, observed in the $BN + Nb_2BN + NbB$ region].⁷⁹

easily (at 1473 K). The other two ternary compounds were observed in the $NbB-Nb_2BN-BN$ region. The boronitride Nb_2BN exists in equilibrium with ϵ -NbN, δ -NbN, γ -Nb₄N₃, BN , and NbB ; besides, the niobium nitride β -Nb₂N coexists with Nb_3B_2 and NbB ; γ -Nb₄N₃ coexists with the boride NbB , and boron nitride is in equilibrium with ϵ -NbN, Nb_3B_4 , and NbB_2 .

The crystal structure of only one of the ternary compounds, Nb_2BN_{1-x} , has been determined.^{78, 79} This compound has a very narrow homogeneity region and the orthorhombic structure of the Mo_2BC type (space group $Cmcm$).⁷⁸ The structure of the boronitride Nb_2BN is shown in Fig. 9. The boron atoms are located at the centres of trigonal prisms formed by six niobium atoms, and

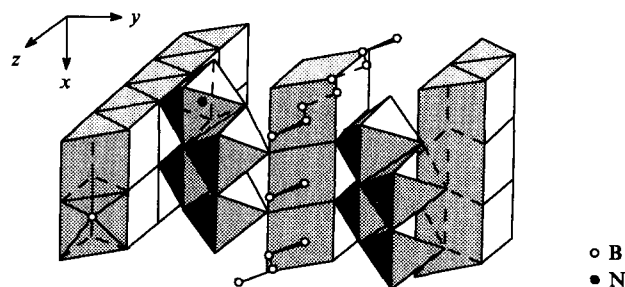


Figure 9. Crystal structure of Nb_2BN (the Mo_2BC type, space group $Cmcm$).⁷⁸

the seventh niobium atom is located at the centre of one of the square faces of the prism. The nitrogen atoms in Nb_2BN occupy the octahedral interstices of the niobium sublattice. The boron atoms are joined in zigzag-shaped chains parallel to the c axis; the N–N and N–B bonds are missing. Similar compounds V_2BN and Ta_2BN could not be obtained even by the thermobaric treatment (pressure 65×10^8 Pa, temperature 1273 K). The boronitride Nb_2BN forms limited solid solutions with V and Ta, $\text{Nb}_{2-x}\text{V}_x\text{BN}$ ($x \approx 0.1$) and $\text{Nb}_{2-x}\text{Ta}_x\text{BN}$ ($x \approx 0.2$). The substitution of niobium by vanadium or tantalum is accompanied by a slight decrease in the unit cell volume.

The Ta–B–N system. In this system, boron is insoluble in nitrides and nitrogen is insoluble in borides.⁸⁶

The Cr–B–N system. The phase equilibria in ternary systems of Group VI–VIII transition metals with boron and nitrogen have not been adequately studied. The Cr–B–N system involves eight pseudobinary equilibria:⁴⁷ $\text{Cr}_4\text{B–N}$, $\text{Cr}_2\text{B–N}$, $\text{Cr}_5\text{B}_3\text{–N}$, CrB–N , $\text{Cr}_3\text{B}_4\text{–N}$, $\text{CrB}_2\text{–N}$, $\text{CrB}_2\text{–BN}$, and $\text{Cr}_2\text{B}_5\text{–BN}$. Three additional pseudobinary equilibria are possible at a nitrogen pressure of 0.05 MPa. The CrN–BN equilibrium can exist at temperatures below 1300 K, $\text{Cr}_2\text{N–BN}$ exists from 1300 K to 1500 K, and the Cr–BN equilibrium exists from 1500 K to 2000 K. An experimental study has confirmed the absence of ternary compounds in the Cr–B–N system and has shown the existence of one more chromium nitride, Cr_3N .⁸⁷ Later it was shown that at 1873 K and a nitrogen pressure of 0.1 MPa, the $\text{Cr}_2\text{B–Cr}_2\text{N}$, $\text{Cr}_2\text{B–N}$, $\text{Cr}_5\text{B}_3\text{–N}$, and $\text{Cr}_5\text{B}_3\text{–BN}$ pseudobinary equilibria are observed in the Cr–B–N system.²⁹

The W–B–N system. In this system, at a nitrogen pressure of 0.05 MPa, the tungsten borides W_2B (at $T > 1600$ K), WB , and W_2B_5 exist in equilibrium with nitrogen; a $\text{W}_2\text{B}_5\text{–BN}$ pseudobinary equilibrium also exists.⁴⁷ At the same nitrogen pressure, the $\text{W}_2\text{B–BN}$ and WB–BN equilibria as well as the W–BN equilibrium (at $T < 1600$ K) are also possible. Only binary compounds are formed in the W–B–N system.⁸⁷ Boron is virtually insoluble in tungsten nitrides, and nitrogen is virtually insoluble in tungsten borides.

The Fe–B–N system. Studies of the phase equilibria in the Fe–B–N system^{87,88} have shown the presence of binary compounds Fe_2B , FeB , Fe_2N (ζ), Fe_3N (ϵ), Fe_4N (γ'), and BN . Nitrogen is insoluble in iron borides, and boron is insoluble in iron nitrides.

IV. Phase relationships in the Si-containing M–B–Si, M–Si–C, and Me–Si–N systems

1. The common type of structures of ternary Si-containing compounds

The ternary systems of transition metals with boron and silicon are of interest as refractory materials resistant to the oxidation at high temperatures. The similarity of the structures of silicides and borides facilitates their mutual solubility and the formation of ternary compounds. The phase equilibria in the M–B–Si systems have been studied.^{89–100}

An investigation of doping of high-melting silicides with boron, carbon, nitrogen, and oxygen⁸⁹ and some more recent studies^{90–92} have shown that in all the M–Si–X systems (M is a transition metal, X = B, C, N, O) a number of ternary phases are formed on the basis of the silicides M_5Si_3 , namely, $\text{M}_5\text{Si}_3\text{X}$ or $\text{M}_5\text{Si}_3\text{X}_2$ with hexagonal structure of the Mn_5Si_3 type (D_{8h}) and/or M_5SiX_2 [the Cr_5B_3 type ($\alpha\text{-Nb}_5\text{Si}_3$) ($T_2 - D_{8h}$)], and $\text{M}_5\text{Si}_2\text{X}$ [the W_5Si_3 type ($\beta\text{-Nb}_5\text{Si}_3$) ($T_1 - D_{8h}$)].

The hexagonal filled structure of the Mn_5Si_3 type (the D_{8h} structural type, space group $P6_3/mcm$) (Fig. 10) is characteristic of many transition metal silicoborides, carbosilicides, and siliconitrides $\text{M}_5\text{Si}_3\text{X}$ as well as for aluminocarbides and aluminonitrides. It is likely to be the commonest structure of ternary compounds in the M–X–X' systems being considered. Its unit cell incorporates two $\text{M}_5\text{Si}_3\text{X}$ formula units. The transition atom metals M occupy the 4(d) and 6(g) sites in this structure.

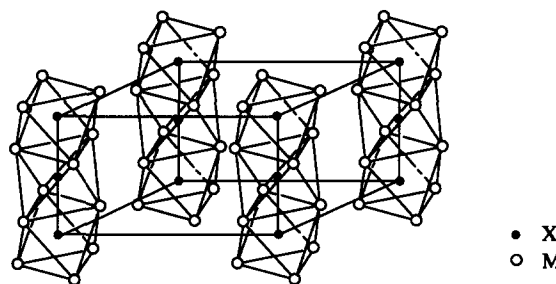


Figure 10. Filled crystal structure of the Mn_5Si_3 (D_{8h}) type of the ternary compounds $\text{M}_5\text{Si}_3\text{X}$ (space group $P6_3/mcm$). Only the transition metal atoms M at the 6(g) sites and the interstitial nonmetal atoms X at the 2(b) sites forming the XM_6 octahedra are shown. The XM_6 octahedra are linked to one another through two faces and form columns directed along the $[001]$ axis.

The silicon atoms also occupy the 6(g) sites, but with other coordinates, and are located within distorted trigonal prisms constituted by two metal atoms at the (d) sites and four metal atoms at the (g) sites. The M atoms located at the 6(g) sites form octahedra; the nonmetal atoms X (C, N, O) can be arranged inside these octahedra at the 2(b) sites (see Fig. 10). Each XM_6 octahedron is joined with two neighbouring octahedra through its opposite faces; thus, parallel chains of octahedra are formed along the c axis. An important characteristic feature of the phases with the D_{8h} structure is the presence of a broad homogeneity region, since the interstitial atoms can occupy not all the octahedra, but only some of them.

The $\text{M}_5\text{Si}_2\text{X}$ tetragonal phases of the W_5Si_3 type [$\beta\text{-Nb}_5\text{Si}_3$, the D_{8h} (T_1) structural type] and M_5SiX_2 of the Cr_5B_3 type [$\alpha\text{-Nb}_5\text{Si}_3$, the D_{8h} (T_2) structural type] belong to the same space group $I4/mcm$ (D_{4h}^{18}) and have very similar structures. Their unit cells incorporate 4 formula units each, i.e. 20 metal atoms and 12 nonmetal atoms. A characteristic feature of the structure of these phases is that the silicon atoms at the 8(h) sites are isolated and form the localised Si–Si pairs. These phases may be regarded as resulting from the substitution of silicon in the silicides M_5Si_3 by the X atoms.

It is of interest that the tetragonal silicides M_5Si_3 are very sensitive to admixtures of the C, B, N, and O nonmetal atoms; their introduction leads to the transition to ternary phases with the Mn_5Si_3 (D_{8h}) type of structure. When this transformation takes place, the X nonmetal atoms occupy the octahedral interstices of the metal sublattice, whereas the displaced silicon atoms occupy the points in the metal sublattice. In the tetragonal silicoborides $\text{M}_5\text{Si}_2\text{B}$ (T_1), the boron atoms occupy the vacant positions in the silicon sublattice, whereas the silicon atoms replace some of the metal atoms in the metal sublattice.

Phases with the D_{8h} structure are stabilised most effectively by carbon and somewhat less effectively by boron, they are very slightly stabilised by nitrogen and not at all by oxygen.

2. The ternary M–B–Si silicoboride systems

The ternary phases formed in the M–B–Si systems are presented in Table 6. Typically, boron possesses substantial initial solubility in all the M_5Si_3 phases with the D_{8h} , D_{8h} , and D_{8h} structures. The addition of boron to pure silicides leads to an expansion of the D_{8h} lattice caused by the intercalation of boron to the vacant points of the silicon sublattice and to the compression of the T_1 and T_2 lattices due to the direct substitution of the silicon atoms by boron.

The Ti–B–Si system. This system involves four titanium borides Ti_2B , TiB , TiB_2 , and Ti_2B_5 and three titanium silicides Ti_5Si_3 , TiSi , and TiSi_2 .⁸ No reliable experimental data on the temperature-dependent concentration ranges for the existence of the borides Ti_2B and Ti_2B_5 have been reported. In all probability, the TiB–TiSi , $\text{TiB}_2\text{–TiSi}_2$, and $\text{TiB}_2\text{–Si}$ (or $\text{Ti}_2\text{B}_5\text{–Si}$)

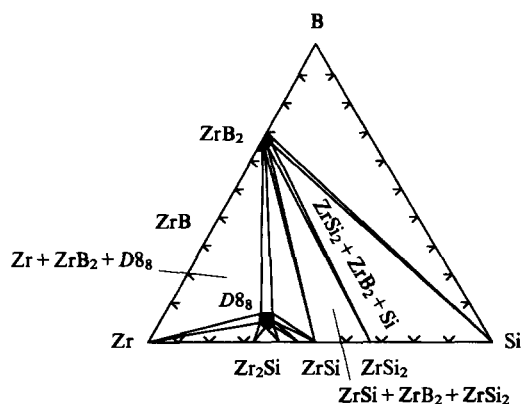
Table 6. Some ternary compounds in silicoboride systems of Group IV–VIII transition metals.^{89–100}

Compound	Symmetry	Type of structure ^a	Unit cell parameters / nm		
			<i>a</i>	<i>b</i>	<i>c</i>
Ti ₅ Si ₃ (B)	Hexagonal	<i>D</i> 8 ₈	—	—	—
Zr ₅ Si ₃ (B)	"	<i>D</i> 8 ₈	0.7788	—	0.5558
Hf ₅ Si ₃ (B)	"	<i>D</i> 8 ₈	0.789	—	0.556
V ₅ Si ₃ B _{0.45}	"	<i>D</i> 8 ₈	0.718	—	0.489
V ₅ SiB ₂	Tetragonal	<i>D</i> 8 ₁ (<i>T</i> ₂)	0.581	—	1.079
Nb ₅ Si ₃ B ₂	Hexagonal	<i>D</i> 8 ₈	0.754	—	0.525
Ta ₅ Si ₃ B ₂	"	<i>D</i> 8 ₈	0.747	—	0.523
Cr ₅ Si ₃ B	"	<i>D</i> 8 ₈	0.706	—	0.473
Mo ₅ SiB ₂	Tetragonal	<i>D</i> 8 ₁ (<i>T</i> ₂)	0.601	—	1.103
W ₅ (Si ₃ B) ₃	"	<i>D</i> 8 ₁ (<i>T</i> ₂)	0.6047	—	1.009
Mn ₅ SiB ₂	"	<i>D</i> 8 ₁ (<i>T</i> ₂)	0.561	—	1.044
Fe ₅ SiB ₂	"	<i>D</i> 8 ₁ (<i>T</i> ₂)	0.554	—	1.032
Fe ₃ Si _{0.2} B _{0.8}	Orthorhombic	<i>D</i> 0 ₁₁	0.446	0.536	0.666
Fe _{4.8} Si ₂ B	Tetragonal	<i>D</i> 8 _m (<i>T</i> ₁)	0.882	—	0.434
Co _{4.7} Si ₂ B	"	<i>D</i> 8 _m (<i>T</i> ₁)	0.862	—	0.425
Ni ₆ Si ₂ B	Hexagonal	<i>C</i> 22	0.6105	—	0.2895

^a *D*8₈ is a filled structure of the Mn₅Si₃ type (space group *P*6₃/*mcm*), *Z* = 2; *D*8₁(*T*₂) is a structure of the Cr₅B₃–α-Nb₅Si₃ type (space group *I*4/*mcm*), *Z* = 4; *D*0₁₁ is a structure of the Fe₃C type (space group *Pnma*), *Z* = 4; *D*8_m(*T*₁) is a structure of the W₅Si₃–β-Nb₅Si₃ type (space group *I*4/*mcm*), *Z* = 4; *C*22 is a structure of the Fe₂P type (space group *P*6̄2*m*), *Z* = 3.

pseudobinary equilibria exist in the Ti–B–Si system. The existence of the ternary hexagonal silicoboride Ti₅Si₃B formed from Ti₅Si₃ via the substitution of a minor portion (~1–2 at.%) of the silicon atoms by the boron atoms is also quite probable.

The Zr–B–Si system. The state diagram of the Zr–B–Si ternary system (Fig. 11) shows eight binary zirconium compounds.⁹³ They include three borides ZrB, ZrB₂, and ZrB₁₂ and five silicides Zr₂Si, Zr₅Si₃ (Zr₃Si₂), Zr₄Si₃, ZrSi, and ZrSi₂. The existence of the boride ZrB at 1623 K is doubtful, because it is stable only within a narrow temperature range and decomposes already at 1500 K. In addition, the silicon borides SiB₃, SiB₄, and SiB₆ are not shown in the diagram. In the zirconium diboride ZrB₂ up to 20 at.% of boron can be substituted by silicon, i.e. a limited solid solution of ZrSi₂ in ZrB₂, namely Zr(B,Si)₂, is formed. An important characteristic feature of the Zr–B–Si system is the presence of the ternary hexagonal compound Zr₅Si₃(B) containing from 5 to 8 at.% of boron. The phase diagram of this system (see Fig. 11) exhibits ten pseudobinary equilibria, namely, Zr(B,Si)₂–Zr, Zr(B,Si)₂–

**Figure 11.** Isothermal cross-section through the Zr–B–Si system at 1623 K (dark areas denote one-phase homogeneity regions).⁹³

ZrSi, Zr(B,Si)₂–Zr₅Si₃(B), Zr(B,Si)₂–ZrSi₂, Zr(B,Si)₂–Si, Zr₅Si₃(B)–Zr, Zr₅Si₃(B)–Zr₂Si, Zr₅Si₃(B)–Zr₃Si₂, Zr₅Si₃(B)–Zr₄Si₃, and Zr₅Si₃(B)–ZrSi. In all probability, three more pseudobinary equilibria of Z(B,Si)₂ with the silicon borides SiB₃, SiB₄, and SiB₆ also exist.

The Hf–B–Si system. This system includes the borides HfB and HfB₂, the silicides Hf₅Si₃, HfSi, and HfSi₂, and compound Hf₅Si₃(B) with a minor (2–3 at.%) content of boron, which substitutes silicon.⁸

The V–B–Si system. The V–B–Si ternary system has been studied.^{90,91} Kudielka et al.⁹⁰ suggested a scheme for the triangulation of the V angle (V–VB–VSi) of the state diagram of the V–B–Si system, which incorporates two ternary compounds, namely, V₅Si₃B_{0.45} with a hexagonal lattice and V₅SiB₂ (the *T*₂ type) with a tetragonal lattice (see Table 6). The former of these compounds crystallises with the *D*8₈ structural type and is formed via partial substitution of the silicon atoms in the silicide V₅Si₃ by boron atoms. Six pseudobinary equilibria exist in the system, namely, V₂B–V₅SiB₂, VB–V₅SiB₂, V₃Si–V₅SiB₂, V₅Si₃B_{0.45}–V₅SiB₂, V₃Si–V₅Si₃B_{0.45}, and V₅Si–V₅Si₃B_{0.45}. One may expect that six more pseudobinary equilibria, VB–V₅Si₃B_{0.45}, VSi₂–V₅Si₃B_{0.45}, VB–VSi₂, V₃B₄–VSi₂, VB₂–VSi₂, and VB₂–Si, will be found.

The Nb–B–Si system. The state diagram of the Nb–B–Si system has been studied rather comprehensively.⁹² This system incorporates ten binary compounds (the niobium borides Nb₃B₂, NbB, Nb₃B₄, and NbB₂, the niobium silicides Nb₄Si, Nb₅Si₃, and NbSi₂, and the silicon borides SiB₃, SiB₄, and SiB₆) and two ternary compounds based on Nb₅Si₃, namely, Nb₅Si₃B with the *D*8₈ structure and Nb₅SiB₂ with the *D*8₁ structure. Both ternary compounds have fairly extended homogeneity regions, and the nonmetal sublattice of these silicoborides can contain a substantial number of vacancies, apart from the boron and silicon atoms. The boride NbB₂ which has a homogeneity region can dissolve up to 2 at.% of silicon.

The Ta–B–Si system. The phase diagram of state of the Ta–B–Si ternary system has been studied.^{90,94} It is very similar to the state diagram of the Nb–B–Si system, but differs from it by the greater numbers of binary compounds (twelve) and ternary compounds (three). Two ternary phases (of the *D*8₈ and *T*₂ types) are based on the silicide Ta₅Si₃ and the third one is based on Ta₂Si.

The Cr–B–Si system. This system contains six chromium borides, four chromium silicides, and two ternary phases with the *D*8₈ and *T*₁ structures; the phase with the *T*₂ structure is a limited solid solution of silicon in the boride Cr₅B₃.⁹⁵ The Cr₅Si₃B ternary phase (the *D*8₈ type) (see Table 6) has virtually no homogeneity region.

The Mo–B–Si system. The phase equilibria in this system (Fig. 12a) have been studied in a number of works.^{91,96,97} The state diagram of the Mo–B–Si system is simpler than the analogous diagram for the system containing chromium, since it incorporates a smaller number of binary compounds. There are two ternary phases with structures of the *T*₁ and *T*₂ types, but the ternary phase with the *D*8₈ type of structure is missing. It has been shown that silicon is insoluble in the molybdenum borides Mo₂B, MoB, Mo₂B₅, and boron does not dissolve in MoSi₂.⁹⁷

The W–B–Si system. Two ternary phases exist in this system: W₁₀Si₃B₃ [W₅(Si₃B)₃] with the *T*₂ type of structure and W₅Si₂B with the *T*₁ type of structure (Fig. 12b).⁹¹

The Mn–B–Si system. In the Mn–B–Si system, the ternary compound Mn₅SiB₂ with the tetragonal structure of the *T*₂ type (see Table 6) existing in an equilibrium with the hexagonal silicide Mn₅Si₃ has been found.⁹⁹

The Fe–B–Si system. The phase equilibria in this system have been studied in detail in the Fe–angle of the state diagram.^{98,99} Four ternary phases were discovered, namely, Fe₅SiB₂ with the structure of the *T*₂ type and with a small homogeneity region formed on the B ↔ Si mutual substitution; Fe_{4.8}Si₂B with the *T*₁ type of structure; Fe₃(Si₃B) (with the composition Fe₃Si_{0.2}B_{0.8}) with the cementite Fe₃C structure and with a small homogeneity

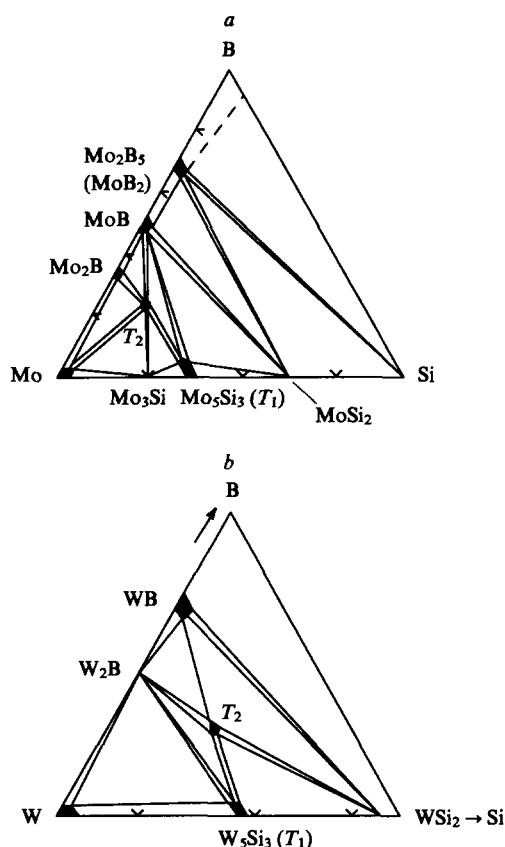


Figure 12. Isothermal cross-sections through the Mo-B-Si system at 1873 K (a) and through the W-B-Si system at 2073 K (b); dark areas denote one-phase homogeneity regions.⁹¹

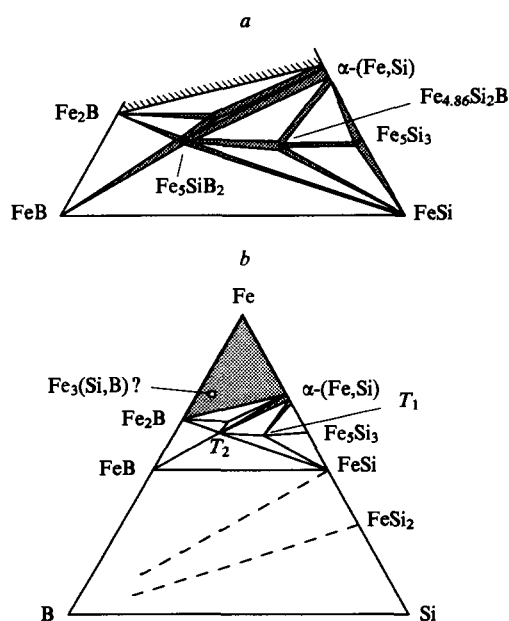


Figure 13. State diagram and isothermal cross-section for the Fe-B-Si system at 1273 K; dark spots denote one-phase regions, two-phase regions are cross-hatched).⁹⁹

(a) a cross-section in the silicoboride region with iron contents ranging from 50 to 70 at.%; (b) the contours of the state diagram for the whole Fe-B-Si ternary system.

region; and $\text{Fe}_2(\text{Si,B})$ (with the composition $\text{Fe}_2\text{Si}_{0.4}\text{B}_{0.6}$), the structure of which is unknown (Fig. 13). It was found that a minor amount of boron can be dissolved in Fe_5Si_3 . The other binary iron borides and silicides are absolutely insoluble in one another.

The Co-B-Si system. Only one ternary phase $\text{Co}_{4.7}\text{Si}_2\text{B}$ with the T_1 type of structure and a small homogeneity region is formed in this system. It exists in an equilibrium with the cobalt borides CoB and Co_2B and with the cobalt silicides CoSi and Co_2Si ; in addition, there are the CoB-CoSi and $\text{Co}_2\text{B}-\text{Co}_2\text{Si}$ pseudobinary equilibria.⁹⁸

The Ni-B-Si system. The ternary compound $\text{Ni}_6\text{Si}_2\text{B}$ with a hexagonal structure of the C22 type, isomorphous to the phosphides Mn_2P , Fe_2P , and Ni_2P , has been found in this system (see Table 6).

3. The M-Si-C ternary carbosilicide systems

The atomic radius of carbon is small (~ 0.077 nm); therefore, carbon always acts as the interstitial element in compounds with transition metals and is located in the interstices of the metal sublattice. Silicon, which is an analogue of carbon in the Periodic System, has a substantially larger atomic radius, equal to ~ 0.117 nm. In compounds with Group IV and V transition metals, the atoms of which are fairly large, silicon can act as an interstitial element; silicides of other transition metals occupy an intermediate position between interstitial compounds and intermetallic compounds. Thus, silicon can enter into the metal lattice either as an interstitial element or as a substituting element. The same dual behaviour of silicon is exhibited in transition metal carbosilicides.

The ternary hexagonal phases of the $\text{M}_5\text{Si}_3(\text{C})$ type, similar to the $\text{M}_5\text{Si}_3(\text{B})$ silicoboride ternary phases with the filled structure of the Mn_5Si_3 type (D_{8h}) are characteristic of the majority of the M-Si-C systems. The main ternary carbosilicide phases are

Table 7. Some ternary compounds in carbosilicide systems of Group IV-VIII transition metals.

Compound	Unit cell parameters / nm			Ref.
	a	b	c	
$\text{Ti}_5\text{Si}_3\text{C}_x$	—	—	—	89, 101–103
Ti_3SiC_2 ^a	0.3064–0.3068	—	1.7646–1.7669	104–106
$\text{Zr}_5\text{Si}_3\text{C}_x$	0.7914–0.7909	—	0.5559–0.5579	89, 107
$\text{V}_5\text{Si}_3\text{C}_x$	0.7135	—	0.4842	107
$\text{Nb}_5\text{Si}_3\text{C}_x$	0.7536	—	0.5249	107
$\text{Ta}_{4.8}\text{Si}_3\text{C}_{0.5}$	0.7494	—	0.5242	108
$\text{Cr}_{5-x}\text{Si}_{3-y}\text{C}_{x+y}$	0.6993	—	0.4726	109
$\text{Cr}_{5 \pm 0.2}\text{Si}_{3 \pm 0.1}\text{C}_x$ ($0.25 < x < 1.05$)	0.6980–0.6983	—	0.4726–0.4737	110
$\text{Mo}_{5-x}\text{Si}_{3-y}\text{C}_{x+y}$	0.7285	—	0.5030	109
$\text{Mo}_{4.8}\text{Si}_3\text{C}_{0.6}$	0.7286	—	0.5046	111
$\text{Mo}_5\text{Si}_3\text{C}$	0.7303	—	0.5057	112
$\text{W}_{5-x}\text{Si}_{3-y}\text{R}^b$	0.7205	—	0.4850	109
$\text{U}_3\text{Si}_2\text{C}_3$ ^c	0.3598	0.3535	1.896	113, 114
$\text{U}_{20}\text{Si}_{16}\text{C}_3$ ^c	1.0385	—	0.8013	113, 115
$\text{U}_3\text{Si}_2\text{C}_x$ ^c	0.7306	—	0.3901–0.3942	116
$\text{Mn}_5\text{Si}_3\text{C}_x$	0.6915	—	0.4823	117
$\text{Mn}_8\text{Si}_2\text{C}$	—	—	—	117
Mn_5SiC	—	—	—	117

Note. All the ternary compounds listed in the Table, except for $\text{Mn}_8\text{Si}_2\text{C}$ and Mn_5SiC (the structures of which are unknown), Ti_3SiC_2 , and uranium ternary phases, have hexagonal filled structure of the Mn_5Si_3 (D_{8h}) type with space group $P6_3/mcm$, $Z = 2$. ^a This compound crystallises with a hexagonal structure and with space group $P6_3/mmc$, $Z = 2$. ^b $\text{R} = (\text{C,N,O})_{x+y}$. ^c $\text{U}_3\text{Si}_2\text{C}_3$ has the orthorhombic symmetry, $Z = 2$; $\text{U}_{20}\text{Si}_{16}\text{Si}_3$ crystallises with the hexagonal symmetry, $Z = 1$; $\text{U}_3\text{Si}_2\text{C}_x$ is a tetragonal (space group $P4/mbm$) solid solution of carbon in U_3Si_2 , $Z = 2$.

listed in Table 7. The phase diagrams for a number of M–Si–C ternary systems have been surveyed.^{101–103}

a. Carbonsilicides of Group IV–VI transition metals

The Ti–Si–C system. The kinetics and thermodynamics of the reactions of titanium silicides with carbon were studied for the first time by Kudielka et al.⁹⁰ They found that the titanium carbide TiC_y exists in equilibrium with the silicon carbide SiC and the titanium silicides Ti_5Si_3 , TiSi, and TiSi_2 , whereas SiC is in equilibrium with TiSi_2 . It has been shown⁸⁹ that the addition of carbon stabilizes the Ti_5Si_3 hexagonal phase and leads to the formation of a ternary phase $\text{Ti}_5\text{Si}_3\text{C}_x$, which contains¹⁰¹ up to 11 at.% of carbon. The $\text{Ti}_5\text{Si}_3\text{C}$ phase belongs to the group of ternary silicoborides and carbosilicides $\text{M}_5\text{Si}_3\text{X}$ with the hexagonal structure of the $D8_8$ type. The Ti–Si–C system includes one more ternary compound, Ti_3SiC_2 , with a hexagonal structure (space group $P6_3/mmc$) (Fig. 14).^{101–103} In this compound, the carbon atoms occupy the octahedral vacancies in the octahedra formed by the titanium atoms. Each CTi_6 octahedron is joined to the neighbouring octahedra through its nine edges in such a way that one octahedral layer is superimposed onto another (see Fig. 14b). A half of all the titanium atoms are located in the middle of the double octahedral layer and each of these atoms is shared by six octahedra. The remaining titanium atoms are located on the upper and lower surfaces of the double octahedral layer, and each of them is shared by three neighbouring octahedra. The chemical formula of the double octahedral layer is Ti_3C_2 . The octahedral layers contain open and closed tetragonal interstices, the open tetragonal vacancies of one double octahedral layer being located over the same vacancies of another double octahedral layer. The silicon atoms are arranged halfway between the centres of the tetrahedral vacancies of the neighbouring double octahedral layers and also constitute a layer.

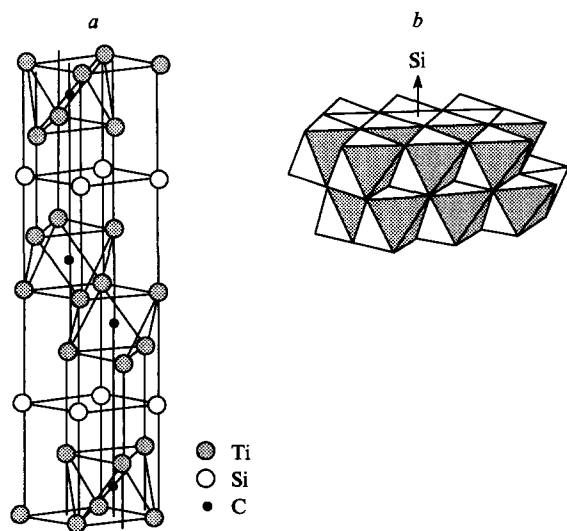


Figure 14. Crystal structure of the titanium carbosilicide Ti_3SiC_2 . (a) unit cell (space group $P6_3/mmc$) with distinct CTi_6 octahedra; (b) the double layer of the CTi_6 octahedra joined via nine edges; the silicon atoms are arranged over the centres of the open tetrahedral vacancies.

The carbosilicide Ti_3SiC_2 exists in equilibrium with the carbides TiC_y and SiC, with the disilicide TiSi_2 , and with the $\text{Ti}_5\text{Si}_3\text{C}$ ternary phase. The phase equilibria in the Ti–Si–C system at 1373 K and 1523 K have been studied.^{118, 119} The ternary compounds and multiphase materials present in the Ti–Si–C system have been investigated by Auger spectroscopy.¹²⁰ The isothermal cross-sections through the Ti–Si–C system at 1473 K¹²¹ and 1523 K^{118, 119} are very similar. At a lower temperature of 1373 K, titanium silicide Ti_3Si appears. It exists

in equilibrium with $\text{Ti}_5\text{Si}_3\text{C}$ and with the solid solution of Si and C in $\beta\text{-Ti}$.

A schematic phase diagram for the Ti–Si–C system, which does not take into account the actual existing ternary phases has been reported.¹²²

The compatibility of phases in the Ti–Si–C system at 1473–1773 K has been studied under the conditions of confining compression at a pressure of $(1-2) \times 10^8$ Pa.¹²³ At high pressures, the titanium silicide Ti_3Si becomes stable and dissolves up to 9 at.% of carbon (without external pressure, Ti_3Si decomposes at the same temperatures to give TiC_y , Ti_5Si_3 , and a solid solution of silicon and carbon in titanium). It is of interest that at high pressures carbon is insoluble in the silicide Ti_5Si_3 , although under ambient conditions the solubility of carbon in this compound reaches 11 at.%.

The Zr–Si–C system. The first scheme for the triangulation of the phase diagram for the Zr–Si–C ternary system has been suggested by Brewer and Krikorian.¹⁰⁸ According to the data obtained by Nowotny et al.,⁸⁹ the silicide Zr_5Si_3 dissolves a substantial amount of carbon to give the $\text{Zr}_5\text{Si}_3\text{C}_x$ ternary phase. The Zr–Si–C system incorporates seven binary compounds (the carbides ZrC_y and SiC and the silicides Zr_2Si , Zr_5Si_3 (Zr_3Si_2), Zr_5Si_4 , ZrSi, and ZrSi_2) and one ternary phase $\text{Zr}_5\text{Si}_3\text{C}_x$. The silicon carbide exists in equilibrium with ZrC_y , ZrSi_2 , and ZrSi, whereas the zirconium carbide ZrC_y is in equilibrium with SiC, ZrSi, Zr_2Si , and $\text{Zr}_5\text{Si}_3\text{C}_x$.¹⁰¹ Pseudobinary equilibria connect the ternary phase also to the silicides Zr_2Si , Zr_5Si_3 (Zr_3Si_2), Zr_5Si_4 , and ZrSi. The isothermal cross-section at 1573 K through the Zr–Si–C ternary system has been studied.¹²⁴

The Hf–Si–C system. According to a number of studies,^{101–103} the phase diagrams for this system and for the system discussed above are similar. The existing differences are due to the fact that the hafnium carbide HfC_y is in equilibrium with HfSi_2 ; therefore, the SiC–HfSi pseudobinary equilibrium is missing. Taking into account the data on the stabilisation by carbon of hexagonal phases with the Mn_5Si_3 type of structure ($D8_8$) and also the similarity of the phase diagrams for Hf–Si–C and Zr–Si–C, one may assume that the Hf–Si–C system contains a $\text{Hf}_5\text{Si}_3\text{C}_x$ ternary phase.

The V–Si–C system. In the V–C, Nb–C, and Ta–C binary systems, rhombohedral ζ -phases of the composition M_4C_3 are formed in narrow concentration and temperature intervals ($1200 \text{ K} < T < 1800 \text{ K}$).^{125, 126} The carbides $\zeta\text{-M}_4\text{C}_3$ cannot be isolated as individual phases, therefore equilibria involving these compounds are not discussed in the ternary carbosilicide systems of vanadium, niobium, and tantalum. Vanadium forms three silicides, namely, V_3Si , V_5Si_3 , and VSi_2 . The dissolution of up to 10 at.% of carbon in V_5Si_3 leads to the formation of the $\text{V}_5\text{Si}_3\text{C}_x$ ternary phase.^{101, 107} It exists in an equilibrium with the carbides SiC and VC_y and with the silicides V_5Si_3 and VSi_2 . In addition, five pseudobinary equilibria, $\text{SiV} - \text{VS}_2$, $\text{SiV} - \text{VC}_y$, $\text{VC}_y - \text{V}_5\text{Si}_3$, $\text{V}_2\text{C}_y - \text{V}_5\text{Si}_3$, and $\text{V}_2\text{C}_y - \text{V}_3\text{Si}$, exist in the V–Si–C system. The phase diagrams for the V–Si–C ternary system have been reported.^{122, 127}

The Nb–Si–C system. In this system, the carbide NbC_y is in equilibrium with two silicides NbSi_2 and Nb_5Si_3 , with the silicon carbide SiC,^{101, 108} and with the $\text{Nb}_5\text{Si}_3\text{C}_x$ ternary phase.¹⁰⁷ The quantity of carbon dissolved in the $\text{Nb}_5\text{Si}_3\text{C}_x$ phase is likely to be less than that dissolved in the analogous $\text{V}_5\text{Si}_3\text{C}_x$ phase. The $\text{Nb}_5\text{Si}_3\text{C}_x$ ternary phase is in equilibrium with NbC_y and with the niobium silicides NbSi_2 and Nb_5Si_3 , whereas the carbides SiC and Nb_2C_y are in equilibrium with NbSi_2 and Nb_5Si_3 , respectively. The phase diagram for the Nb–Si–C ternary system has been reported by Brukl.¹²¹

The Ta–Si–C system. The phase equilibria in this system have been studied repeatedly.^{89, 101, 108, 127} The isothermal cross-sections through the phase diagram of the Ta–Si–C system at 1273 K,¹²⁷ 1823 K,⁸⁹ and 1873 K⁸⁹ are virtually identical. All the workers noted that the $\text{Ta}_5\text{Si}_3\text{C}_x$ ($\text{Ta}_{4.8}\text{Si}_3\text{C}_{0.5}$) ternary phase with the hexagonal structure of the Mn_5Si_3 type ($D8_8$) exists in this

system.¹⁰⁸ This phase is isomorphous to the hexagonal silicide Ta_5Si_3 stabilised by carbon (the pure silicide Ta_5Si_3 has a tetragonal structure) and forms a continuous series of solid solutions with it. The $Ta_5Si_3C_x$ phase is in an equilibrium with the carbides TaC_y and Ta_2C_y and with the silicides Ta_2Si , Ta_5Si_3 , and $TaSi_2$. The system also includes five pseudobinary equilibria: $SiC-TaSi_2$, $SiC-TaC_y$, TaC_y-TaSi_2 , $Ta_2C_y-Ta_2Si$, and $Ta_2C_y-Ta_3Si$.

The Cr-Si-C system. At 1673 K, eight binary compounds (SiC , Cr_3C_2 , Cr_7C_3 , $Cr_{23}C_6$, $CrSi_2$, $CrSi$, Cr_5Si_3 , and Cr_3Si),¹¹⁰ the $Cr_5Si_3C_x$ ternary phase having a homogeneity region,^{109,110} a solid solution of silicon in chromium $Cr(Si)$, and a substitution solid solution based on the silicide Cr_3Si exist in this system. The $Cr_5Si_3C_x$ ternary phase has the hexagonal structure of the $D8_8$ type and exists in an equilibrium with silicon carbide SiC , chromium carbides Cr_3C_2 and Cr_7C_3 , chromium silicides $CrSi$ and Cr_5Si_3 , and the substitution solid solution based on Cr_3Si . The solid solution based on Cr_3Si exists in equilibrium with the carbides Cr_7C_3 and $Cr_{23}C_6$ and with the solid solution of silicon in chromium $Cr(Si)$. In addition, there are four equilibria, namely, $SiC-CrSi_2$, $SiC-CrSi$, $SiC-Cr_3C_2$, and $Cr_{23}C_6-Cr(Si)$. The diagram of the phase equilibria in the Cr-Si-C system has been reported.¹²²

Parthe et al.¹⁰⁹ believed that the $Cr_5Si_3C_x$ ternary phase results from the substitution of chromium and silicon atoms by carbon. However, later it was shown¹¹⁰ that the unit cell parameters and the unit cell volume of the $Cr_{5\pm0.2}Si_{3\pm0.1}C_x$ ternary phase ($0.25 < x < 1.05$) increase with an increase in x . This means that the carbon atoms do not replace Cr or Si atoms, as was believed previously,¹⁰⁹ but are located in the vacant octahedral interstices of the structure of the $D8_8$ type of this compound. Evidence that the carbon atoms fill the octahedral interstices of the metallic sublattice of the $M_5Si_3C_x$ phases with the $D8_8$ type of structure has also been obtained in another study.¹¹¹

The Mo-Si-C system. The first variant of the phase diagram for the Mo-Si-C ternary system has been suggested by Brewer and Krikorian.¹⁰⁸ This diagram reflects fairly adequately all the characteristic features of this system including the existence of a stable ternary hexagonal compound with an extended homogeneity region and a temperature of congruent melting of ~ 2340 K. The composition Mo_4Si_3C has been suggested for this compound. This ternary compound exists in equilibrium with carbon, with the carbides SiC , MoC_y (Mo_3C_2), and Mo_2C , and with the silicides $MoSi_2$ and Mo_5Si_3 (Mo_3Si_2); SiC is in equilibrium with $MoSi_2$, and Mo_2C is in equilibrium with Mo_5Si_3 (Mo_3C_2) and Mo_3Si .¹²⁸

It has been shown¹¹² that the ternary molybdenum carbosilicide has the stoichiometric composition Mo_5Si_3C and belongs to the M_5Si_3X type of ternary hexagonal phases common for the M-Si-X systems ($X = B, C, N$); the homogeneity region of Mo_5Si_3C is much narrower than has been found by Nowotny et al.¹²⁸ The isothermal cross-section through the Mo-Si-C system at 1473 K has been reported.¹¹² According to this study, at 1473 K, the silicon carbide SiC exists in equilibrium with Mo_5Si_3 , and the $MoSi_2-Mo_5Si_3C_x$ pseudobinary equilibrium is absent.

The reason for the discrepancies between the results obtained by Van Loo et al.¹¹² and Nowotny et al.¹²⁸ concerning these pseudobinary equilibria can be elucidated by additional investigations of the phase relationships in the Mo-Si-C system. The isothermal cross-section through the Mo-Si-C system at 1873 K¹²⁸ virtually coincides with the cross-section at 1673 K reported by Spear et al.⁸⁵

It has been suggested¹⁰⁹ that the carbon atoms in the ternary molybdenum carbosilicide $Mo_{5-x}Si_{3-y}C_{x+y}$ substitute the molybdenum and silicon atoms; however, it has been shown in another study¹¹¹ that such a substitution does not occur, and the carbon atoms are located in the octahedral interstices formed by the molybdenum atoms.

The W-Si-C system. In this system, no ternary compounds exist,¹⁰⁸ however, when a minor amount of nitrogen or oxygen is present, a quasi-ternary hexagonal phase $W_{5-x}Si_{3-y}(C,N,O)_{x+y}$

arises.¹⁰⁹ In the absence of nitrogen or oxygen admixtures, the pseudobinary equilibria existing in the W-Si-C system at 2073 K involve only binary compounds: $SiC-WSi_2$, $SiC-W_5Si_3$, $SiC-WC$, $WC-W_5Si_3$, and $W_2C-W_5Si_3$.⁴⁹ The conclusion reached by Parthe et al.¹⁰⁹ that the tungsten and silicon atoms in the ternary phase have been substituted by interstitial atoms (C, N, O) was erroneous, since the carbon and nitrogen atoms in the compounds M_5Si_3X with the $D8_8$ structure behave as interstitial elements and are arranged in octahedral interstices formed by the metal atoms.^{110,111}

The U-Si-C system. The phase equilibria in this system at 1000–1773 K under an argon atmosphere have been investigated.¹¹³ Two ternary compounds $U_3Si_2C_3$ and $U_{20}Si_{16}C_3$ with orthorhombic and hexagonal crystal lattices, respectively, have been found in the U-Si-C system (see Table 7).^{114,115} It has also been shown^{113,116} that the silicide U_3Si_2 dissolves up to 4 at.% of carbon thus forming the $U_3Si_2C_x$ interstitial solid solution. At 1100 K (Fig. 15) the ternary compound $U_3Si_2C_3$ exists in the U-Si-C system in equilibrium with UC, SiC , and U_3Si_5 ; SiC is in equilibrium with U_2C_3 , UC, U_3Si_5 , USi_2 , and USi_3 ; UC coexists with U_3Si , $U_3Si_2C_x$, $U_{20}Si_{16}C_3$, and U_3Si_5 ; the carbosilicide $U_{20}Si_{16}C_3$ coexists with $U_3Si_2C_x$, USi , and U_3Si_5 ; and U_3Si exists in equilibrium with $U_3Si_2C_x$.

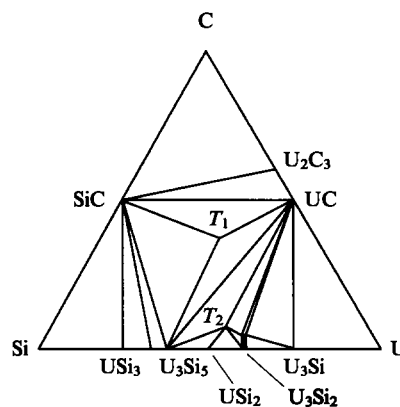


Figure 15. Isothermal cross-section through the U-Si-C system at 1100 K (the dark area denotes the homogeneity region of the $U_3Si_2C_x$ solid solution).¹¹³

$T_1 = U_3Si_2C_3$, $T_2 = U_{20}Si_{16}C_3$.

Later the phase equilibria in the alloys with large proportions of uranium have been studied at 1023–1223 K.¹¹⁶ At temperatures below 1090 K, the phase equilibria in the U-UC-USi region were the same as those in the diagram shown in Fig. 15. At 1100–1150 K, the UC- U_3Si pseudobinary equilibrium disappears and the U- $U_3Si_2C_x$ equilibrium appears instead and, at temperatures above 1200 K, the silicide U_3Si and the $U_3Si-U_3Si_2C_x$ equilibrium do not exist.^{116,129} According to the data obtained by Guinet et al.,¹¹⁶ the solubility of carbon in U_3Si_2 reaches 4 at.%. On the dissolution of carbon, the c parameter of the unit cell of U_3Si_2 increases by 0.0042 nm thus becoming equal to 0.3942 nm. The maximum solubility of carbon in the U_3Si silicide at 1083 K is 0.15 at.%.¹³⁰

b. Carbosilicides of Group VII and VIII transition metals

The Mn-Si-C system. The phase diagram for this system (Fig. 16a), in addition to eight binary compounds, contains the $Mn_5Si_3C_x$ ternary phase (a solid solution of carbon in Mn_5Si_3), Mn_8Si_2C , and Mn_5SiC .^{101–103} Silicon carbide exists in equilibrium with the silicides $Mn_{15}Si_{26}$ and $MnSi$, with the $Mn_5Si_3C_x$ and Mn_8Si_2C ternary phases, and perhaps with Mn_5SiC . The unit cell parameters of the $Mn_5Si_3C_x$ ternary phase are larger than the corresponding unit cell parameters of Mn_5Si_3 ;¹⁰⁷ this implies that

the carbon atoms are located in the octahedral interstices formed by the manganese atoms. The $\text{Mn}_5\text{Si}_3\text{C}_x$ hexagonal phase with a structure of the $D8_8$ type is in equilibrium with MnSi , Mn_3Si_3 , Mn_3Si , Mn_9Si_2 , and $\text{Mn}_8\text{Si}_2\text{C}$; and the $\text{Mn}_8\text{Si}_2\text{C}$ phase coexists with Mn_9Si_2 . The pseudobinary equilibria involving the Mn_5SiC ternary phase are given hypothetically. The scheme of phase equilibria in the Mn–Si–C system have been reported by Lyakishev et al.¹²²

The Re–Si–C system. This system contains no ternary phases.^{101–103, 131} The scheme of triangulation of the phase diagram of the Re–Si–C system at 1873 K suggested by Searcy and Finnie¹³¹ involves four pseudobinary equilibria of the silicon carbide SiC with rhenium and three rhenium silicides. Figure 16b presents the isothermal cross-section through this system at 1273 K constructed using published data;^{101–103} rhenium silicides are in equilibrium with carbon, and SiC coexists with ReSi_2 .

Jeitschko et al.,¹¹⁷ who have studied the phase equilibria in the M–Ga–C and M–Ge–C systems, also have paid attention to the M–Si–C systems (M = Mn, Re, Fe). In the Re–Si–C system they discovered a ternary phase containing 45 at.% Re, 40 at.% Si, and 15 at.% C; the structure of this phase was not determined. There is no other evidence in support of the existence of a ternary phase in this system.

The Fe–Si–C system. The phase relationships in the Fe–Si–C system have been considered in many studies, because they are related to the problems of the production of cast iron, steel, various iron-based alloys, and refractory materials. The equilibrium and nonequilibrium phase transformations in the Fe–C system become substantially more complicated on the addition of silicon, since the silicon atom is much larger than the carbon atom.

When silicon substitutes iron, the ferrite solid solution is stabilised and the γ -region (solid solution of C and Si in Fe) narrows. At the same time this substitution promotes decomposition and graphitisation of the cementite Fe_3C . In all probability, the Fe–Si–C system contains no stable ternary phase. The information concerning ternary iron carbosilicides (for example, a ternary phase of an unknown composition of the type of the Nowotny phase with the $D8_8$ structure has been observed in this system;¹¹⁷ and the carbosilicide $\text{Fe}_{10}\text{Si}_2\text{C}_3$ containing about 9 mass % of silicon has been mentioned in a monograph⁸) refers most probably to a metastable phase. It is even possible that there are several metastable phases in which silicon substitutes either iron $[(\text{Fe},\text{Si})_3\text{C}]$ or carbon $[\text{Fe}_3(\text{C},\text{Si})]$. The formation of a ternary metastable phase based on austenite also cannot be ruled out.

No stable ternary phases have also been found in the recent studies of the phase diagram of the Fe–Si–C ternary system at 1123 K¹³² and 1243 K.^{101–103} At temperatures below 1100 K (the temperature of the decomposition of the Fe_5Si_3 high-temperature phase) silicon carbide exists in equilibrium with the silicides FeSi_2 , FeSi , and Fe_3Si . Above this temperature the equilibrium silicide Fe_5Si_3 with a hexagonal structure of the $D8_8$ type appears in this system, and silicon carbide is in equilibrium with the disilicide FeSi_{2+x} having a homogeneity region and with the silicides FeSi and Fe_5Si_3 [according to a study by Schuster,¹⁰¹ instead of the SiC – FeSi_{2+x} equilibrium, two equilibria exist, SiC – Fe_2Si_5 and SiC – $\text{FeSi}_2(\text{h})$]. The silicides Fe_5Si_3 and Fe_3Si as well as α -Fe and γ -Fe are in equilibrium with carbon. The isothermal cross-section through the Fe–Si–C system at 1243 K is presented in Fig. 16c. The scheme of the main phase equilibria in this system have been reported by Lyakishev et al.¹²²

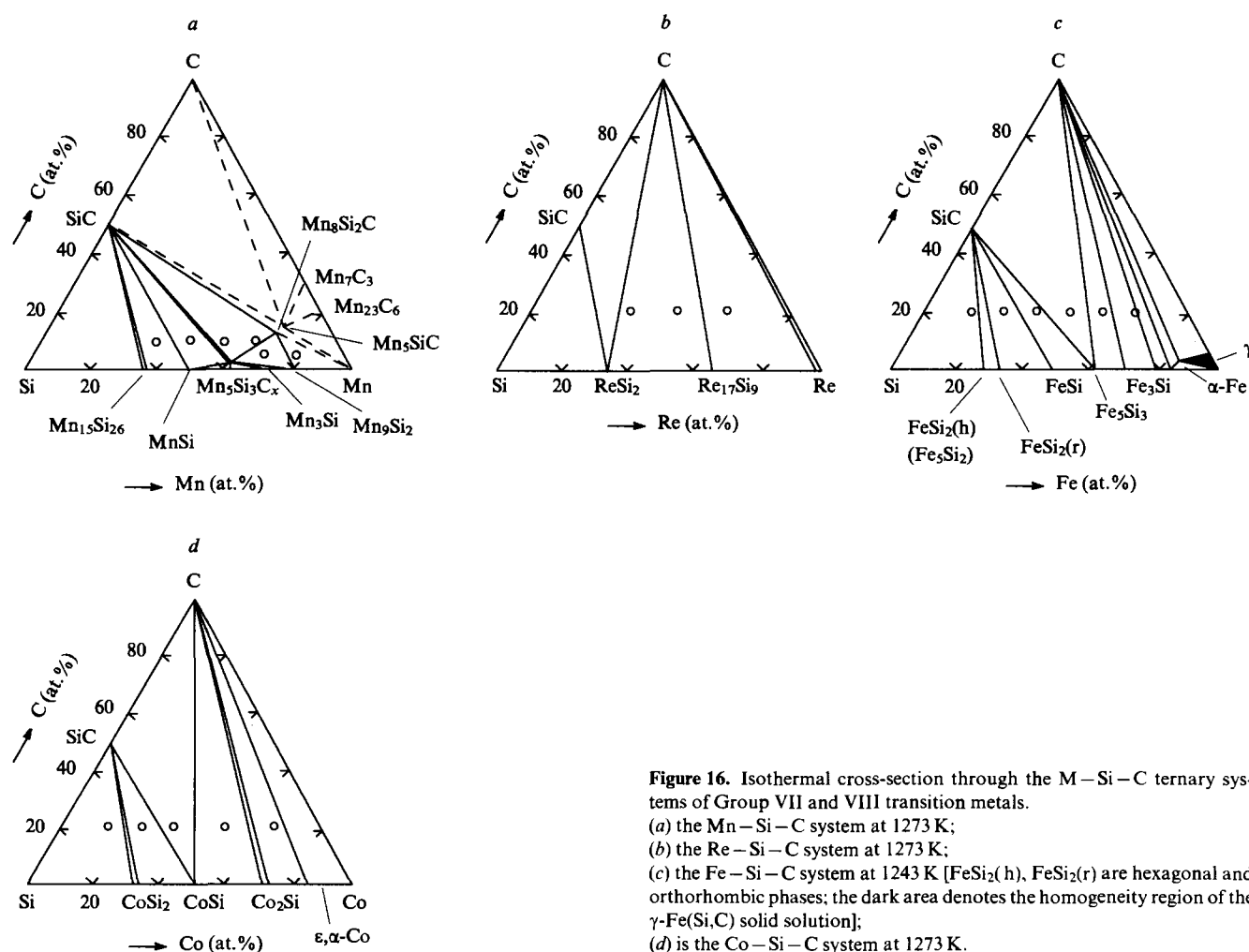


Figure 16. Isothermal cross-section through the M–Si–C ternary systems of Group VII and VIII transition metals.
(a) the Mn–Si–C system at 1273 K;
(b) the Re–Si–C system at 1273 K;
(c) the Fe–Si–C system at 1243 K [$\text{FeSi}_2(\text{h})$, $\text{FeSi}_2(\text{r})$ are hexagonal and orthorhombic phases; the dark area denotes the homogeneity region of the γ -Fe(Si,C) solid solution];
(d) the Co–Si–C system at 1273 K.

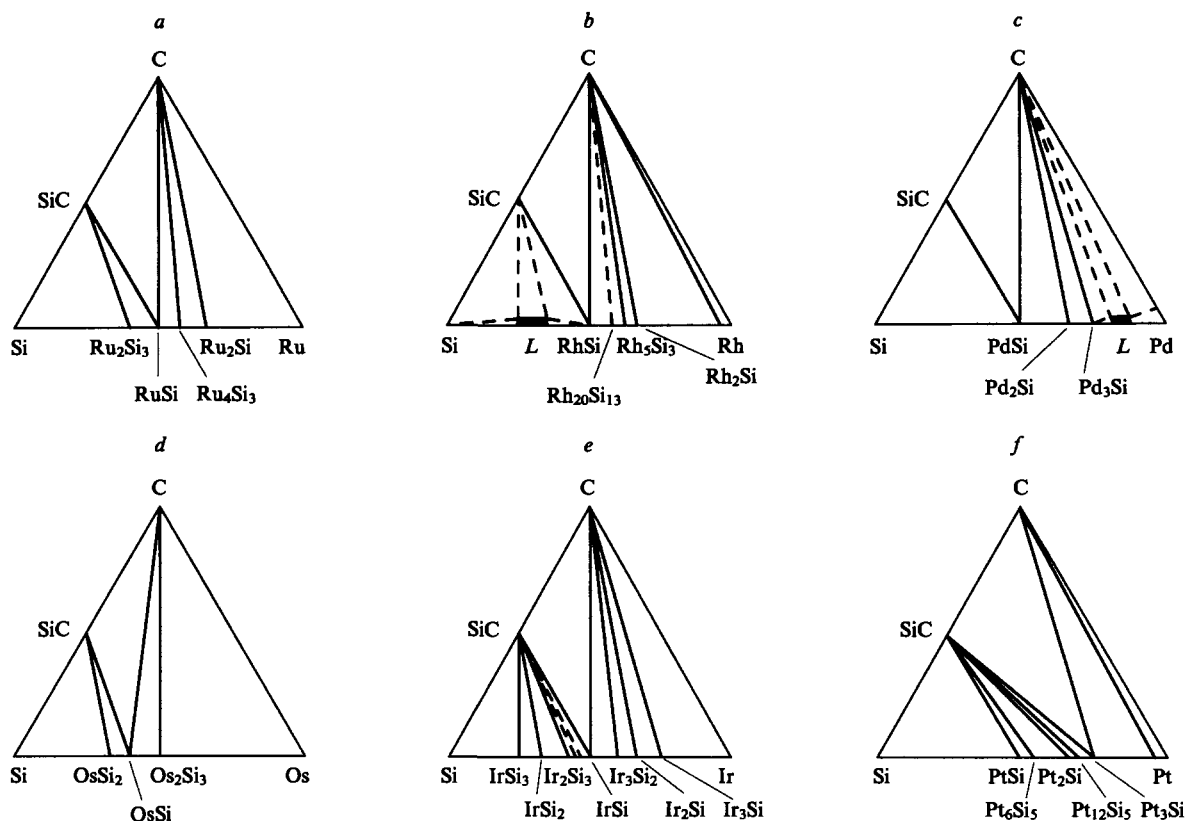


Figure 17. State diagrams for platinum group metal-silicon-carbon ternary systems, dark areas denote the regions of the existence of a liquid phase.^{103, 131}

Two metastable cubic phases of an unknown composition have been discovered in the Fe-Si-C system under the conditions of rapid cooling; the unit cell of one of these phases belongs to the $P4_132$ or $P4_332$ space group and has the period $a = 0.63$ nm, and the second metastable phase has a body-centred cubic (Bcc) lattice with the period $a = 0.89$ nm.¹³³

The Co-Si-C system. There are hardly any stable ternary phases in the Co-Si-C system. The silicon carbide SiC is in an equilibrium with the silicides CoSi₂ and CoSi, whereas carbon coexists with CoSi, Co₂Si, and with the extended solid solution of silicon in cobalt (Fig. 16d).¹⁰¹⁻¹⁰³

The Ni-Si-C system. The phase diagram for the Ni-Si-C system has been studied and constructed at 1123 K¹³² and 1423 K.¹³⁴ No ternary compounds were found. At 1123 K, the silicon carbide SiC is in equilibrium with four silicides: NiSi₂, NiSi, Ni₃Si₂, and Ni₂Si, whereas Ni₂Si, Ni₅Si₂ (Ni₃₁Si₁₂), Ni₃Si, and the solid solution of silicon and carbon in nickel Ni(Si,C) are in equilibrium with carbon. At 1423 K the SiC-Ni₂Si-C three-phase region is still retained. At higher temperatures the silicides Ni₅Si₂ and Ni₃Si no longer exist, and Ni₂Si coexists directly with the Ni(Si,C) solid solution and also with carbon and SiC.

On rapid cooling, the Ni_{67.5}Si_{17.5}C₁₅ nonequilibrium ordered Bcc phase with the period $a = 0.2744$ nm containing 4 at.% of carbon and 15-21 at.% of silicon is formed in the Ni-Si-C system.¹³⁵

(Ru,Rh,Pd,Os,Ir,Pt)-Si-C systems. The phase equilibria in the M-Si-C systems (M = Ru, Rh, Pd, Os, Ir, Pt) have been studied by Searcy and Finnie¹³¹ and have been refined later by Schuster¹⁰³ (Fig. 17). The platinum-group metals do not form carbides, and no stable ternary compounds of these metals with silicon and carbon exist; thus, only equilibria between carbon and silicon carbide on the one hand, and platinum metal silicides on the other hand, are possible in the (Ru, Rh, Pd, Os, Ir, Pt)-Si-C systems.

The SiC-MSi-C three-phase regions exist at 1613 K in the Ru-Si-C system, at 1443 K in the Rh-Si-C system, at 1100 K in the Pd-Si-C system, and at 1613 K in the Ir-Si-C system. The silicides with the highest proportions of silicon are in equilibrium with SiC, and the silicides with high proportions of metal coexist with carbon. In the Rh-Si-C system, the Rh₂SiC unstable ternary phase can be formed in the temperature range 1770-1870 K, whereas in the Pt-Si-C system, the formation of the Pt₃(Si_{2-x}C_x) phase is possible. In more recent papers these phases have not been mentioned. According to the data reported by Chou,¹³⁶ in the Pt-Si-C system at 1073 K silicon carbide SiC exists in an equilibrium with all the platinum silicides, and carbon coexists with Pt₃Si, i.e. the phase equilibria differ from those reported by Searcy and Finnie¹³¹ (see Fig. 17).

4. The M-Si-N ternary siliconitride systems

The ceramics based on silicon nitride Si₃N₄ preserve their high hardness, wear resistance, and strength up to high temperatures, which accounts for its wide industrial application. The composite ceramic materials based on silicon nitride usually also contain a metallic component. This has necessitated the investigation of the phase equilibria in the M-Si-N ternary systems formed by the transition metal M, silicon, and nitrogen. The studies on the M-Si-N ternary systems have been surveyed in a monograph.⁸⁰

The ternary phases formed in the M-Si-N systems are few in number, as in the M-Si-C carbosilicide systems. As a rule, these are M₅Si₃N₈ phases with a filled structure of the Mn₅Si₃ type (D_{8h}). Ternary phases with a different crystal structure are present in the siliconitride systems of some lanthanides and manganese. The structural characteristics of the ternary phases formed in the M-Si-N systems are presented in Table 8.

a. Siliconitrides of Group III transition metals

Based on the classification of the M-Si binary systems (M = Sc, Y, La → Lu) in terms of their composition and the crystal

Table 8. Some ternary phases in siliconitride systems of Group III–VII transition metals.

Compound	Symmetry and type of structure	Space group	Z	Unit cell parameters/ nm			Ref.
				a	b	c	
LaSi ₃ N ₅	Orthorhombic	P2 ₁ 2 ₁ 2 ₁	4	0.7838	1.1236	0.4807	137, 138
Sm ₃ Si ₆ N ₁₁	Tetragonal	—	4	0.9993	—	0.4836	139
Ho ₅ Si ₃ N _x (0 ≤ x ≤ 0.4)	Hexagonal ^a (a solid solution of nitrogen in Ho ₅ Si ₃)	P6 ₃ /mcm	2	0.8356–0.8324	—	0.6273–0.6477	140
Ti ₅ Si ₃ N _x (0 ≤ x ≤ 1.0)	Hexagonal ^a (a solid solution of nitrogen in Ti ₅ Si ₃)	P6 ₃ /mcm	2	—	—	—	119
Zr ₅ Si ₃ N _x (0.1 ≤ x ≤ 0.3)	Hexagonal ^a	P6 ₃ /mcm	2	0.7949	—	0.5573	89, 141
Hf ₅ Si ₃ N _x (x ≤ 0.1)	Hexagonal phase ^a , stabilised by nitrogen	P6 ₃ /mcm	2	0.7801	—	0.5523	141, 142
V ₅ Si ₃ N _x (0.2 ≤ x ≤ 1.0)	Hexagonal ^a	P6 ₃ /mcm	2	0.7121	—	0.4847	89, 141
Nb ₅ Si ₃ N _x (x < 0.3)	"	P6 ₃ /mcm	2	0.7517	—	0.5249–0.5310	89, 108, 141
Ta ₅ Si ₃ N _x (0.3 ≤ x ≤ 1.2)	"	P6 ₃ /mcm	2	0.7501	—	0.5229–0.5246	89, 108, 141
MnSiN ₂	Orthorhombic	Pna2 ₁	4	0.5248	0.6511	0.5070	143, 144
MnSiN ₂	"	Pna2 ₁	4	0.5266–0.5268	0.6522–0.6521	0.5074–0.5069	145

^a Hexagonal (space group *P6₃/mcm*) M₅Si₃N_x phases, among which there are ternary compounds (M = Zr, Hf, V, Nb, Ta) and solid solutions (M = Ho, Ti), have the filled structure of the Mn₅Si₃ (*D8₈*) type, Z = 2.

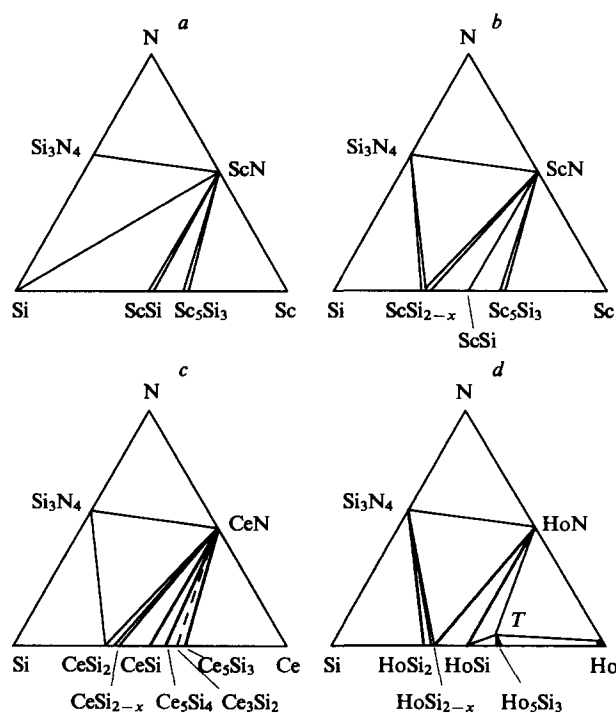
structure of the silicides formed, Weitzer et al.¹⁴⁰ have divided the M–Si–N ternary siliconitride systems into three groups: (1) (La,Ce,Pr,Nd)–Si–N; (2) (Sm,Gd,Tb,Dy,Ho,Er,Y)–Si–N; and (3) (Tm,Yb,Lu,Sc)–Si–N. They chose one M–Si–N ternary system from each group and studied the phase equilibria in it assuming that the phase equilibria in all the siliconitride systems of the same group are similar. This assumption is true only within certain limits: for example, no ternary compounds were found in the Ce–Si–N system (the first group) or in the Ho–Si–N system (the second group), but ternary compounds LaSi₃N₅ and Sm₃Si₆N₁₁ were discovered in the La–Si–N and Sm–Si–N systems, which belong to the same groups (see Table 8).¹³⁹ Thus, the phase equilibria in the M–Si–N ternary systems of the same group are not entirely similar.

The Sc–Si–N system. The isothermal cross-sections through this system at 1073 K and 1273 K have been reported¹⁴⁰ (Fig. 18a,b). No ternary compounds were found in this system. At 1073 K only two scandium silicides ScSi and Sc₅Si₃ are stable. The scandium silicides, silicon, and the silicon nitride Si₃N₄ exist in equilibrium with the scandium nitride ScN. At 1273 K one more stable silicide appears, namely, ScSi_{2–x} (Sc₃Si₅), which coexists with silicon nitride and scandium nitride; ScN is also in equilibrium with Si₃N₄, ScSi, and Sc₅Si₃.

The Ce–Si–N system. In the absence of external nitrogen pressure the Ce–Si–N system contains no ternary compounds at 1273 K.¹⁴⁰ The cerium nitride CeN exists in equilibrium with Si₃N₄ and six cerium silicides — CeSi₂, CeSi_{2–x}, CeSi, Ce₅Si₄, Ce₃Si₂, and Ce₅Si₃; the silicon nitride Si₃N₄ exists in equilibrium with CeSi₂ (Fig. 18c). The solubility of a third component in the binary phases is negligibly small.

The Ho–Si–N system. Based on an X-ray diffraction study and a metallographic study and on the determination of the melting points, Weitzer et al.¹⁴⁰ have constructed the phase diagram of the Ho–Si binary system. In this system, they detected all of the six known holmium silicides. The holmium disilicide HoSi₂ melts incongruently at 2153 K, whereas HoSi_{2–x} and HoSi melt congruently at temperatures above 2260 K. In the Ho–Si alloys containing less than 50 at.% Ho, HoSi has a structure of the FeB (*B27*) type; in the alloys containing more than 50 at.% Ho, the

HoSi modification with a structure of the CrB (*B_f*, *B33*) type predominates. The Ho₅Si₄ phase melts incongruently at *T* > 2120 K, and in the 1870 K > *T* > 1270 K range it decom-

**Figure 18.** Isothermal cross-section through the M–Si–N ternary systems of Group III transition metals.¹⁴⁰

(a) the Sc–Si–N system at 1073 K; (b) the Sc–Si–N system at 1273 K; (c) the Ce–Si–N system at 1273 K; (d) the Ho–Si–N system at 1273 K (dark areas denote the homogeneity regions of the Ho₅Si₃N_x solid solution and of the solid solution of silicon and nitrogen in holmium), *T* = Ho₅Si₃N_x.

poses to HoSi (the CrB structural type) and Ho₅Si₃. The temperature of the congruent melting of Ho₅Si₃ is 1983 K.

The Ho–Si–N system incorporates no ternary compounds at 1273 K (Fig. 18d); however, up to 4 at.% of nitrogen is dissolved in Ho₅Si₃ to form the Ho₅Si₃N_x limited solid solution having a filled structure of the Mn₅Si₃ (D8₈) type (see Table 8). The holmium nitride HoN is in equilibrium with Si₃N₄, HoSi_{2–x}, HoSi, and Ho₅Si₃N_x; in addition, there exist Si₃N₄–HoSi₂, HoSi–Ho₅Si₃N_x, and Ho–Ho₅Si₃N_x equilibria. Metallic holmium dissolves up to 2 at.% of nitrogen. The holmium silicide HoSi coexisting with HoN and Ho₅Si₃N_x has a structure of the CrB type.

b. Siliconitrides of Group IV and V transition metals

The Ti–Si–N system. According to thermodynamic estimates,^{146,147} the interaction of metallic titanium with silicon nitride Si₃N₄ in the 300 K < *T* ≤ 1800 K temperature range most probably yields the silicide Ti₅Si₃ and the nitride TiN_y. This type of interaction is retained up to 2300 K. Taking into account these data and also the results of a study^{148,149} of the interaction between silicon nitride and titanium nitride under an atmosphere of NH₃ and H₂ [at a total pressure in the gas phase of (1.33–10.7) × 10⁵ Pa] at 1323–1723 K, Schuster and Nowotny¹⁴¹ concluded that under these conditions, Si₃N₄ exists in equilibrium with TiN_y and with the silicide TiSi₂, whereas TiN_y coexists with all the titanium silicides. The study of the phase equilibria in the Ti–Si–N ternary system at 1273 K (in vacuo) and at 1573 K (under an argon atmosphere) has shown that the above phase equilibria are retained under these conditions (Fig. 19a). From the authors' viewpoint,¹⁴¹ the phase equilibria in the Ti–Si–N system are insensitive to the variations of the temperature or nitrogen pressure. No ternary compounds were found in the Ti–Si–N system; no solubility of nitrogen in the silicide Ti₅Si₃ with the structure of the Mn₅Si₃ type or in other binary phases was observed.

The isothermal cross-section through the Ti–Si–N system at 973–1273 K has been constructed by Beyers et al.,¹⁵⁰ who have studied phase equilibria in thin films. These researchers¹⁵⁰ (in contrast to Schuster and Nowotny¹⁴¹) did not note the equilibrium between Si₃N₄ and TiSi₂, because there exists an equilibrium between TiN_y and silicon. The other equilibria reported in these two papers^{141,150} are the same. Thermodynamic calculations^{119,151} have shown that the TiN_y–Si equilibrium exists most likely up to 1573 K; in particular, the variation in the Gibbs energy for the reaction 4TiSi₂ + Si₃N₄ → 4TiN + 11Si at 1373 K is –11.1 kJ (g-at)^{–1}.

The most recent studies^{119,151} of the phase equilibria in the Ti–Si–N system at 1373 K have been carried out in relation to the diffusion pairs of the Ti–Si₃N₄, Ti_{1–x}Si_x–Si₃N₄, and Ti_{1–x}Si_x–TiN types. A study involving the nitriding of Ti₃Si alloys proved to be impossible due to the formation of a thin film of titanium nitride on the surface of the samples, which prevents further diffusion of nitrogen. The isothermal cross-section through the Ti–Si–N system at 1373 K (Fig. 19b) largely coincides with the cross-section obtained by Beyers et al.¹⁵⁰ The titanium nitride TiN_y coexists with Si, Si₃N₄, TiSi₂, and the Ti₅Si₃N_x ternary phase, which is a solid solution of nitrogen in Ti₅Si₃. The solubility of nitrogen in Ti₅Si₃ reaches 11 at.%.^{119,151} The silicide Ti₃Si decomposes to β-Ti and Ti₅Si₃N_x at 1373 K on the addition of even small amounts of nitrogen. Similar effects (substantial solubility of carbon or oxygen in Ti₅Si₃ and decomposition of Ti₃Si on the addition of a third element) have also been observed in the Ti–Si–C and Ti–Si–O systems.^{118,119,151}

In all probability, the disagreement between the results of Schuster and Nowotny¹⁴¹ and those obtained by other workers^{119,150,151} is caused by the experimental procedure: Schuster and Nowotny¹⁴¹ studied the phase equilibria in the Ti–Si–N system using massive samples, Beyers et al.¹⁵⁰ used thin films, whereas in the other two studies^{119,151} diffusion pairs were employed. The phases formed in thin films due to diffusion are

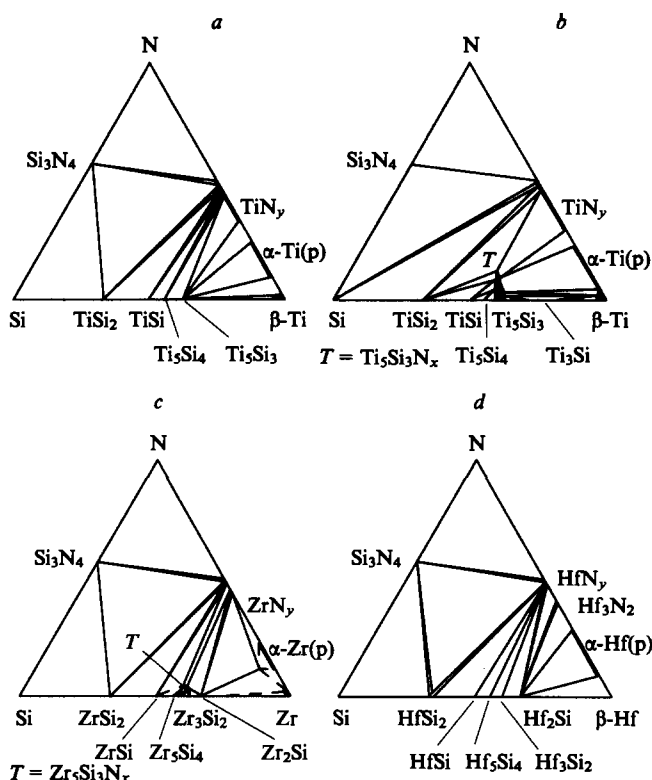


Figure 19. Isothermal cross-sections through M–Si–N ternary systems of Group IV transition metals (dark areas denote one-phase homogeneity regions).

(a) the Ti–Si–N system at 1573 K; (b) the Ti–Si–N system at 1373 K, *T* = Ti₅Si₃N_x; (c) the Zr–Si–N system at 1573 K, *T* = Zr₅Si₃N_x; (d) the Hf–Si–N system at 1573 K.

The cross-sections *a*, *c*, and *d* were constructed using the results of a study of samples sintered under an argon atmosphere at 1573 K; the cross-section *b* was constructed by a layer-by-layer study of the samples obtained by sintering diffusion pairs at 1373 K.

not always reproduced in massive samples and are probably nonequilibrium phases. Also in massive samples the real equilibrium is not always reached due to the short durations of the annealing (sometimes, annealing requires hundreds or even thousands of hours).

The Zr–Si–N system. In the first investigation of this system,⁸⁹ a ternary zirconium siliconitride with a structure of the Mn₅Si₃ (D8₈) type has been detected. This compound contains up to 10 at.% of nitrogen and its chemical formula and crystal structure are similar to those of the zirconium carbosilicide Zr₅Si₃C_x. The distribution of phase fields in the Zr–Si–N system was reported⁸⁹ to be identical to that in the Zr–Si–C system at 1873 K. The experimental results obtained with the samples sintered at 1573 K under argon¹⁴¹ have confirmed the views⁸⁹ of the phase equilibria in the Zr–Si–N system.

The isothermal cross-section through the Zr–Si–N system at 1573 K is shown in Fig. 19c.¹⁴¹ The nitride ZrN_y is in equilibrium with Si₃N₄, with the ternary compound Zr₅Si₃N_x, with the silicides ZrSi₂, ZrSi, and Zr₂Si, and with the α-Zr(N) solid solution; Si₃N₄ is in equilibrium with ZrSi₂, and Zr₅Si₃N_x also coexists with ZrSi, Zr₅Si₄, Zr₃Si₂, Zr₂Si, and with the solid solution of nitrogen in α-Zr.

At a lower temperature, namely at 1273 K, all the phases existing in the Zr–Si–N system at 1573 K are retained, but the content of nitrogen in Zr₅Si₃N_x noticeably decreases (*x* ≤ 0.2), and the Si₃N₄–ZrSi, ZrN_y–Zr₅Si₄, and ZrN_y–Zr₃Si₂ equilibria arise instead of Zr₅Si₃N_x–Zr₅Si₄ and ZrN_y–ZrSi₂.

The Hf–Si–N system. The phase equilibria in this system at 1273 and 1573 K are virtually identical and are similar to those in the

Zr–Si–N system at these temperatures.¹⁴¹ The main distinction between the isothermal cross-section through the Hf–Si–N system at 1273 K and the corresponding cross-section through the Zr–Si–N system is the existence of the $\text{Si}_3\text{N}_4 + \text{HfSi}_2 + \text{HfN}$ three-phase field. The ternary compound $\text{Hf}_5\text{Si}_3\text{N}_x$ with a very low content of nitrogen ($x \leq 0.1$) is formed in the Hf–Si–N system. It has a structure of the Mn_5Si_3 (D_{8h}) type and exists in an equilibrium with HfN_y and Hf_2Si . The isothermal cross-section through the Hf–Si–N system at 1573 K is presented in Fig. 19d (the position of the ternary compound $\text{Hf}_5\text{Si}_3\text{N}_x$ is not shown).¹²⁴

The V–Si–N system. The heating of V_5Si_3 to 1673 K under an NH_3 atmosphere leads to the formation of the ternary compound $\text{V}_5\text{Si}_3\text{N}_x$ with a filled structure of the Mn_5Si_3 (D_{8h}) type and the nitride VN_y .⁸⁹ The phase equilibria in the V–Si–N system at 1273 K (in vacuo) and at 1773 K (under an argon atmosphere) (Fig. 20a,b) have been studied.¹⁴¹ At 1273 K the ternary compound is in equilibrium with Si_3N_4 , VSi_2 , V_6Si_5 , V_5Si_3 , V_3Si , and V_9N_4 ; the silicon nitride Si_3N_4 coexists with VSi_2 , VN_y , and V_9N_4 ; and the silicide V_3Si coexists with V_9N_4 and with the solid solution of nitrogen in vanadium.

As the temperature increases, the nitrogen content in $\text{V}_5\text{Si}_3\text{N}_x$ increases substantially, as indicated by the increase in the unit cell parameters from $a = 0.7121$ nm and $c = 0.4847$ nm at 1273 K to $a = 0.7155$ nm and $c = 0.4852$ nm at 1773 K. The nitrides Si_3N_4 and VN_y are unstable under an argon atmosphere at 1773 K. Thus, the ternary compound $\text{V}_5\text{Si}_3\text{N}_x$ and the silicide VSi_2 in the V–Si–N system coexist directly with nitrogen, whereas the other equilibria are retained (Fig. 20b). The solubility of a third component in the binary phases is negligibly small.¹⁴¹

The compound V_9N_4 crystallises with a hexagonal ordered structure with the periods $a = a_V \sqrt{3}$ and $c = c_V$ (a_V and c_V are the parameters of the hexagonal close-packed vanadium sublattice). According to the data obtained by Onozuka,¹⁵² the nitrides stable in the V–N binary system at temperatures above 900 K are VN_y and V_9N_4 (rather than V_2N_3 , as has been believed

previously), whereas at $T < 900$ K, the $\text{V}_{32}\text{N}_{26}$ (space group $P4_2/nmc$) and V_9N_4 (space group $P6_322$) ordered phases are stable. The VN_y ($y = 0.78$) $\rightarrow \text{V}_{32}\text{N}_{26}$ ordering occurs at 793 K as a first-order phase transition.

The Nb–Si–N system. A thermodynamic calculation¹⁴⁶ implies that the reaction between the silicon nitride Si_3N_4 and metallic niobium at 1300 K most probably yields the silicide Nb_5Si_3 and the nitride Nb_2N . This is in agreement with the experimental data.¹⁴¹ The isothermal cross-section through the Nb–Si–N system at 1273 K (in vacuo) is shown in Fig. 20c.¹⁴¹ There are no ternary phases in the Nb–Si–N system at this temperature, the nitride Si_3N_4 coexists with all the binary niobium silicides and nitrides, whereas the silicide Nb_5Si_3 exists in equilibrium with Nb_2N .

The annealing of the alloys existing in the Nb–Si–N system at 1773 K led to the appearance of the ternary compound $\text{Nb}_5\text{Si}_3\text{N}_x$ with a filled structure of the Mn_5Si_3 (D_{8h}) type.¹⁴¹ This compound exists in equilibrium with NbSi_2 , Nb_5Si_3 , Nb_2N , $\delta\text{-NbN}$, and probably with nitrogen. The equilibria of $\text{Nb}_5\text{Si}_3\text{N}_x$ ($\text{Nb}_{5-x}\text{Si}_{3-y}\text{N}_z$) with N_2 and NbSi_2 have been reported.¹⁰⁸ The assumption that in the ternary compound, nitrogen substitutes niobium and silicon¹⁰⁸ have not been confirmed: the interstitial atoms X in the compounds $\text{M}_5\text{M}'_3\text{X}$ with the Mn_5Si_3 (D_{8h}) type of structure fill the octahedral vacancies formed by the M atoms. The $\text{Nb}_5\text{Si}_3\text{N}_x$ ternary phase has been obtained by heating Nb_5Si_3 under an atmosphere of NH_3 at 1673 K.⁸⁹ The parameter c of the crystal lattice of $\text{Nb}_5\text{Si}_3\text{N}_x$ has been reported^{89,141} to increase from 0.5249 nm to 0.5310 nm with an increase in the nitrogen content, with the invariable parameter $a = 0.7517$ nm. The invariability of the parameters of the crystal lattices of the binary phases in the Nb–Si–N system indicates that the solubility of the third component in these phases is negligibly small.

The Ta–Si–N system. This system has been the most comprehensively studied among the siliconitride systems of group IV and V transition metals (except for titanium). The first investigation of the phase equilibria in this system was carried out by Kudielka et

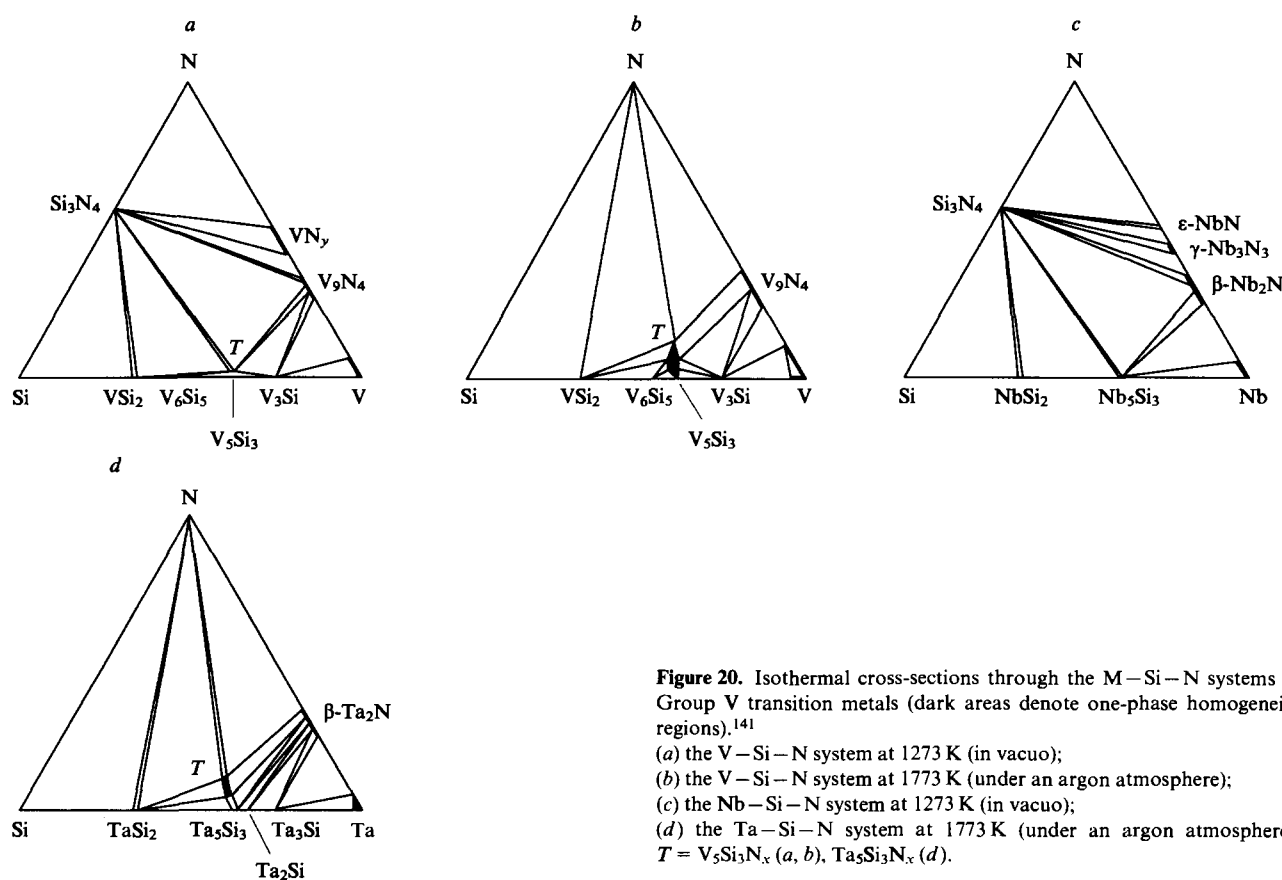


Figure 20. Isothermal cross-sections through the M–Si–N systems of Group V transition metals (dark areas denote one-phase homogeneity regions).¹⁴¹

(a) the V–Si–N system at 1273 K (in vacuo);
(b) the V–Si–N system at 1773 K (under an argon atmosphere);
(c) the Nb–Si–N system at 1273 K (in vacuo);
(d) the Ta–Si–N system at 1773 K (under an argon atmosphere);
 $T = \text{V}_5\text{Si}_3\text{N}_x$ (a, b), $\text{Ta}_5\text{Si}_3\text{N}_x$ (d).

al.⁹⁰ They constructed the isothermal cross-section through the Ta–Si–N system at 1600 K and a nitrogen pressure of 0.75×10^5 Pa. The ternary compound $Ta_{5-x}Si_{3-y}N_z$ with a broad homogeneity region exists in this system; it exists in equilibrium with nitrogen, the silicon nitride Si_3N_4 and with the tantalum nitrides and silicides TaN_y , Ta_2N , Ta_5Si_3 , and $TaSi_2$.¹⁰⁸ The formation of the $Ta_5Si_3N_x$ ternary phase on nitriding the silicide Ta_5Si_3 at 1673 K by various methods and on the interaction of Si_3N_4 with tantalum at 1873 K has also been observed in another study.⁸⁹ The ternary compound $Ta_5Si_3N_x$ has a filled structure of the Mn_5Si_3 ($D8_8$) type common to the $M_5Si_3N_x$ phases. The phase equilibria in the Ta–Si–N system have been studied at 1273 K (in vacuo) and at 1773 K (under an argon atmosphere).¹⁴¹ It was found that at 1273 K, no ternary phase exists, and the silicon nitride is in equilibrium with $TaSi_2$, Ta_5Si_3 , TaN_y , and Ta_2N , whereas the nitride Ta_2N coexists also with Ta_5Si_3 , Ta_2Si , and Ta_3Si . At 1773 K, the ternary compound $Ta_5Si_3N_x$ exists in the Ta–Si–N system. It is in equilibrium with nitrogen, Ta_2N , Ta_2Si , and Ta_5Si_3 (Fig. 20d). When the content of nitrogen in $Ta_5Si_3N_x$ increases, the parameter c of the crystal lattice increases from 0.5229 nm to 0.5246 nm with the parameter $a = 0.7501$ nm being constant. The solubility of the third component in the binary phases of the Ta–Si–N system is negligibly small.¹⁴¹

c. Siliconitrides of Group VI–VIII transition metals

The Cr–Si–N system. The interaction of the silicon nitride Si_3N_4 with chromium can yield Cr_3Si , Cr_5Si_3 , $CrSi$, $CrSi_2$, Cr_2N , Si, and gaseous nitrogen, depending on the amount of chromium.¹⁴⁶ Heating a mixture of Cr, Si, and Si_3N_4 to 1673 K in a moist atmosphere leads to the formation of Cr_5Si_3 (structure of the W_5Si_3 type), containing up to 10 at.% of nitrogen, and Cr_3Si , containing up to 20 at.% of nitrogen; chromium nitrides are not formed in the absence of an external nitrogen pressure.⁸⁹

A detailed study of the phase equilibria in the Cr–Si–N system¹⁵³ has shown that at 1273 K and under an argon atmosphere, the nitride Si_3N_4 coexists in this system with all the chromium silicides, namely, $CrSi_2$, $CrSi$, Cr_5Si_3 , and Cr_3Si , whereas Cr_3Si and the solid solution of silicon in chromium are in equilibrium directly with nitrogen. However, at 1273 K, even a low nitrogen pressure is sufficient to stabilise Cr_2N existing in equilibrium with Cr_3Si and with the solid solution of silicon in chromium; the other equilibria in the Cr–Si–N system under a low nitrogen pressure are the same as the equilibria under argon. At a higher temperature of 1673 K under an argon atmosphere, the silicides Cr_5Si_3 and Cr_3Si are in equilibrium with nitrogen, whereas Si_3N_4 coexists with Cr_5Si_3 . Nitrogen is insoluble in chromium silicides.¹⁵³

The isothermal cross-section through the Cr–Si–N system at 1873 K and at a nitrogen pressure of 1×10^5 Pa has been constructed¹⁵³ with the aid of the results obtained in another study.¹⁵⁴ The equilibria existing at 1673 K under argon are retained under these conditions; in addition, new equilibria arise, due to the stabilisation of the chromium nitride Cr_2N and the appearance of the liquid phase of chromium.

The Mo–Si–N system. The nitriding of Mo_5Si_3 at 1673 K gives Mo and Mo_3Si , whereas the nitriding of $MoSi_2$ under the same conditions is accompanied by the appearance of Mo_5Si_3 .⁸⁹ The annealing of a mixture of Mo, Si, and Si_3N_4 powders at 1973 K affords Mo_5Si_3 and nitrogen.⁸⁹ The reaction between Mo and Si_3N_4 at 1273 K proceeds very slowly; in the absence of an external pressure of nitrogen, Si_3N_4 coexists with $MoSi_2$ and Mo_5Si_3 , whereas the silicides Mo_5Si_3 and Mo_3Si exist in equilibrium with nitrogen.¹⁵³ The same phase equilibria are retained in the Mo–Si–N system at 1673 K under argon. At 1850 K, the silicon nitride Si_3N_4 is unstable, and all the molybdenum silicides are in equilibrium with nitrogen. No ternary compounds have been found in the Mo–Si–N system.

The phase equilibria in the Mo–Si–N system have been studied at 1573 K and at various nitrogen pressures (Fig. 21).¹³⁷

At $p_{N_2} < 18$ Pa, the Mo–Si–N system incorporates only the silicides $MoSi_2$, Mo_5Si_3 , and Mo_3Si existing in equilibrium with nitrogen. At $18 \text{ Pa} < p_{N_2} < 3000$ Pa all the molybdenum silicides are still in equilibrium with nitrogen, and $MoSi_2$ coexists with Si_3N_4 . The phase equilibria in the Mo–Si–N system at higher nitrogen pressures ($3 \times 10^3 \text{ Pa} \leq p_{N_2} < 7 \times 10^5 \text{ Pa}$) are the same as shown in Fig. 21c. At a nitrogen pressure of $7 \times 10^5 \text{ Pa} \leq p_{N_2} < 88 \times 10^5 \text{ Pa}$, the silicon nitride Si_3N_4 exists in equilibrium with all the molybdenum silicides, and Mo_3Si coexists with nitrogen. When the nitrogen pressure is $(88-98) \times 10^5 \text{ Pa}$, the nitride Mo_2N becomes stable, and one more equilibrium appears, namely, Mo_2N – Mo_3Si . At $p_{N_2} > 98 \times 10^5 \text{ Pa}$, the Mo_3Si –N equilibrium disappears, and the Si_3N_4 – Mo_2N equilibrium arises instead; silicon nitride coexists also with all the molybdenum silicides, and Mo_2N is in equilibrium with Mo_3Si (Fig. 21f).

The W–Si–N system. The nitriding of W_5Si_3 at 1673–2073 K under an NH_3 atmosphere does not lead to the formation of a phase with the structure of the Mn_5Si_3 ($D8_8$) type observed in the M–Si–N systems of Group V transition metals.⁸⁹ It has been shown¹⁵³ that silicon nitride does not react with tungsten or with the silicides WSi_2 and W_5Si_3 at 1273 K, but exists in equilibrium with them. The Si_3N_4 –W equilibrium is retained up to 1400 K. At higher temperatures, Si_3N_4 and tungsten interact to give W_5Si_3 and nitrogen that exist in equilibrium with each other. At 1773 K, the silicides WSi_2 and W_5Si_3 are in equilibrium with nitrogen.

The Re–Si–N system. The phase equilibria in this system have been studied at 1273 K and 1673 K under argon.¹⁵³ At 1273 K, the silicon nitride Si_3N_4 coexists with rhenium and with its silicides $ReSi_2$ and $Re_{17}Si_9$. At a higher temperature Si_3N_4 reacts with rhenium, and thus the $Re_{17}Si_9$ –N equilibrium arises instead of Si_3N_4 –Re. No ternary phases in the Re–Si–N system have been found.

The Mn–Si–N system. The interaction of liquid manganese with the silicon nitride Si_3N_4 in vacuo, under an inert gas, or under nitrogen is accompanied, in particular, by the formation of the ternary compound $MnSiN_2$.¹⁵⁶ The nitrogen atoms in the siliconitride $MnSiN_2$ are located at the centres of the distorted tetrahedra comprising two manganese atoms and two silicon atoms.^{143, 144} The decomposition of $MnSiN_2$ to the silicide $MnSi$ and gaseous nitrogen begins at 1570 K (at a nitrogen pressure of 1×10^5 Pa) or at 1070 K (under argon).

The study of the phase equilibria in the Mn–Si–N system carried out by Weitzer and Schuster¹⁴⁵ has confirmed the presence of only one ternary compound $MnSiN_2$ with an orthorhombic lattice (see Table 8). It has a narrow homogeneity region. In the absence of an external nitrogen pressure at 1273 K the siliconitride $MnSiN_2$ is in equilibrium with nitrogen, with the silicon nitride Si_3N_4 , with β -Mn (the solid solution of silicon in manganese), and with the silicide Mn_3Si ; Si_3N_4 also coexists with $MnSi_2$, $MnSi$, Mn_5Si_3 , and Mn_3Si . Nitrogen is insoluble in manganese silicides.

In the presence of an external nitrogen pressure, γ -Mn (the solid solution of nitrogen in manganese) arises in the system. This leads to the appearance of β -Mn– γ -Mn and $MnSiN_2$ – γ -Mn phase equilibria. With an increase in the external pressure of nitrogen, manganese nitrides (in particular, ϵ - Mn_4N) appear in the system and equilibria between them and $MnSiN_2$ are established.

The Fe–Si–N system. The combined influence of the nitrogen and silicon admixtures in iron and its alloys on the properties of the latter have been studied in connection with the development of siliceous sheet transformer steel. In steels with high silicon contents (up to 4 at.%), the nitride Si_3N_4 can segregate from the solid solution of silicon in iron. The silicon nitride is also formed in the nitriding of steels with low contents of silicon.

The phase equilibria in the Fe–Si–N system have been studied at 1173 K and 1423 K.¹⁴⁵ In the absence of an external nitrogen pressure at 1173 K, Si_3N_4 coexists with all the iron silicides stable at this temperature and with α -Fe (the solid

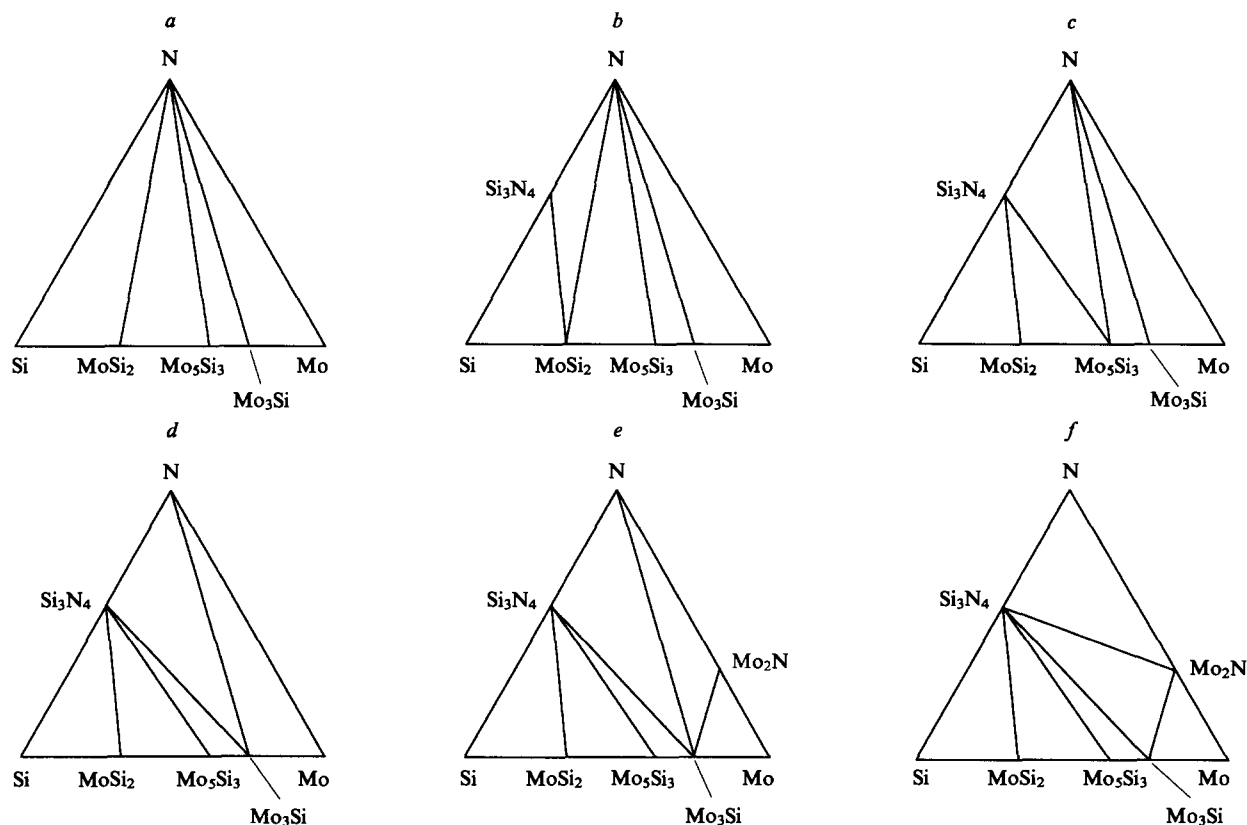


Figure 21. The influence of nitrogen pressure p_{N_2} on phase equilibria in the Mo–Si–N system at 1573 K.¹⁵⁵

(a) < 18 Pa, (b) $18 \leq p_{N_2} < 3 \times 10^3$ Pa, (c) $3 \times 10^3 \leq p_{N_2} < 7 \times 10^5$ Pa, (d) $7 \times 10^5 \leq p_{N_2} < 88 \times 10^5$ Pa, (e) $88 \times 10^5 \leq p_{N_2} < 98 \times 10^5$ Pa, (f) $p_{N_2} \geq 98 \times 10^5$ Pa.

solution of silicon in iron). In the presence of pure iron at 1390 ± 10 K Si_3N_4 starts to decompose yielding the solid solution of α -Fe containing 6–8 at.% of silicon.

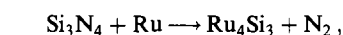
At 1423 K the nitride Si_3N_4 coexists with silicides Fe_2Si_5 , $FeSi$, Fe_2Si , and Fe_3Si , and also with α -Fe (the solid solution of silicon in iron). No ternary phases have been detected in the Fe–Si–N system.

The Co–Si–N system. When Si_3N_4 reacts with liquid cobalt, it decomposes to give cobalt silicides and gaseous nitrogen. In the absence of an external nitrogen pressure at 1273 K, the silicon nitride is in an equilibrium with $CoSi_2$, $CoSi$, the low-temperature silicide Co_2Si , α -Co and ϵ -Co (the solid solutions of silicon in cobalt), and cobalt.¹⁴⁵ The reaction between Co and Si_3N_4 with the decomposition of the latter starts at 1440 K. Nitrogen is insoluble in cobalt silicides. No ternary compounds have been found in the Co–Si–N system.

The Ni–Si–N system. The interaction of molten nickel with the silicon nitride Si_3N_4 is accompanied by the decomposition of the latter. At temperatures above 1440 K, the decomposition occurs very rapidly. Without an external nitrogen pressure at 1173 K, the silicon nitride Si_3N_4 coexists with nickel and with all the nickel silicides stable at this temperature. Nickel silicides do not dissolve nitrogen. No ternary compounds have been detected in this system.

The phase equilibria in the Ni–Si–N system have been studied at 1373 K and at a nitrogen pressure of 1×10^5 Pa.¹⁵⁵ Under these conditions, the silicides Ni_2Si , Ni_5Si_2 ($Ni_{31}Si_{12}$), and Ni_3Si and the solid solution of silicon in nickel exist in equilibrium with the silicon nitride Si_3N_4 . Nickel dissolves up to 15 at.% of silicon.

The Ru–Si–N system. There are no ternary phases in the Ru–Si–N system at temperatures from 1270 K to 1520 K and at an argon pressure of 1×10^5 Pa.¹⁵⁷ At 1273 K the nitride Si_3N_4 coexists with ruthenium and with its silicides Ru_2Si_3 , $RuSi$, and Ru_4Si_3 (Fig. 22a). At 1480 K, decomposition of Si_3N_4 begins



and the appearance of the phase diagram changes. At 1520 K, the nitride Si_3N_4 exists in equilibrium with Ru_2Si_3 and $RuSi$, and the silicides $RuSi$, Ru_4Si_3 , and Ru_2Si are in equilibrium with nitrogen (Fig. 22b).

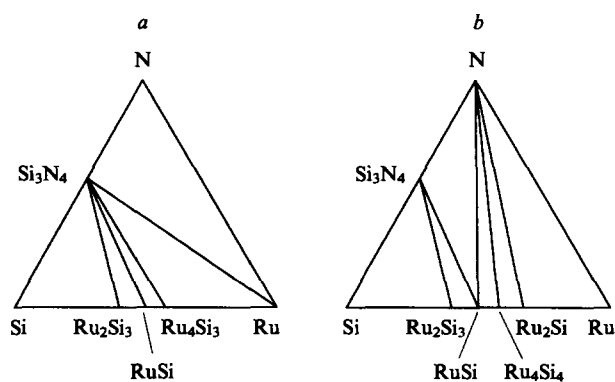


Figure 22. Isothermal cross-sections through the Ru–Si–N system at 1273 K (a) and 1520 K (b) under an argon atmosphere.¹⁵⁷

V. Phase equilibria in M–Al–X ternary systems (X = C, N, Si)

1. The common types of the crystal structures of ternary compounds in the M–Al–X systems

Aluminidocarbides and aluminidonitrides of transition metals have, as a rule, one of several specific crystal structures peculiar to these compounds.

The cubic structure [space group $Pm\bar{3}m(O_h^h)$] of the perovskite CaTiO_3 ($E2_1$) type, which is usually found in double oxides, for example, in barium titanate BaTiO_3 , is the most common among these structures. The M and Al atoms in the aluminidocarbides and aluminidonitrides M_3AlX with the perovskite type of structure form an ordered metallic Fcc-sublattice: the aluminium atoms occupy the vertices of a cube, whilst the transition metal atoms M are located at the centres of the faces of the cube; the M atoms constitute octahedra in the centres of which the interstitial atoms X are located (Fig. 23). The interstitial atoms X (C, N) occupy all or some of the octahedral interstices formed by the transition metal atoms M; this accounts for the fact that most of aluminidocarbides and aluminidonitrides with the perovskite type of structure have fairly extensive homogeneity regions. The presence of the metallic Fcc-lattice, with interstitial atoms located in its octahedral interstices, and the existence of the homogeneity regions make these compounds very similar to the classical nonstoichiometric interstitial compounds, namely, carbides and nitrides MX_y with the structure of the B1 (NaCl) type. In addition, in some cases the X atoms in the aluminidocarbides and aluminidonitrides M_3AlX with the perovskite type of structure can not only fill the octahedral interstices, but can also substitute aluminium.

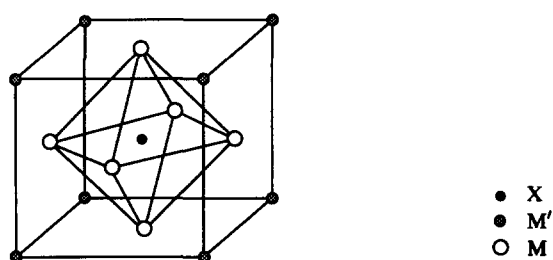


Figure 23. Unit cell of the ternary compounds $\text{M}_3\text{M}'\text{X}$ with the ideal cubic structure (space group $Pm\bar{3}m$) of the perovskite CaTiO_3 type.

Another group of transition metal aluminidocarbides and aluminidonitrides $\text{M}_2\text{M}'\text{X}$ (H -phases) have the hexagonal structure (space group $P6_3/mmc$) of the Cr_2AlC type (Fig. 24). A significant element of this structure, as well as of the previous one, is the octahedron XM_6 formed by six transition metal atoms M with the nonmetal atom X located at the centre of it. In the $\text{M}_2\text{M}'\text{X}$ H -phases, each XM_6 octahedron is joined with the adjacent octahedra via its six edges; thus layers with tetrahedral vacancies between the octahedra are formed (Fig. 24b). The nontransition metal atoms M' are located over these tetrahedral vacancies in the trigonal prisms formed by six M atoms. The octahedral layers separated by the layer of the M' atoms are packed in such a way that the tetrahedral interstices are located above one another. The unit cell of the H -phases incorporates two $\text{M}_2\text{M}'\text{X}$ formula units.

The frequently occurring aluminidocarbides and aluminidonitrides of the composition $\text{M}_3\text{M}_2'\text{X}$ have a cubic structure [space group $P4_132(O_h^7)$] of the $\beta\text{-Mn}$ type ($A13$) in which twenty atoms of the transition and nontransition metals occupy the 12(d) and 8(c) sites, respectively. The transition metal atoms M constitute slightly distorted octahedra that are connected to one another via their vertices; the octahedral interstices correspond to the 4(a) sites in the structures of the $\beta\text{-Mn}$ type, and in the compounds $\text{M}_3\text{M}_2'\text{X}$

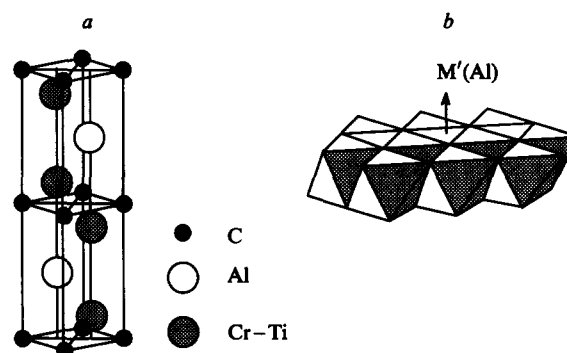


Figure 24. Crystal structure of the Nowotny phase (H -phase) of the Cr_2AlC type ($\text{M}_2\text{M}'\text{X}$).

(a) unit cell (space group $P6_3/mmc$); (b) the layer of the XM_6 octahedra joined via six edges; nontransition metal atoms in compounds with the Cr_2AlC type of structure are arranged over tetrahedral vacancies.

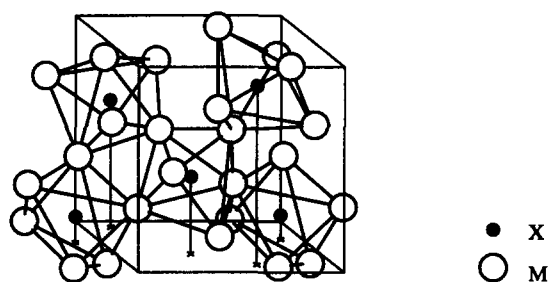


Figure 25. Filled crystal structure of the $\beta\text{-Mn}(A13)$ type of the ternary cubic (space group $P4_132$) compounds $\text{M}_3\text{M}'_2\text{X}$.

Only the transition metal atoms M at the 12(d) sites and interstitial nonmetal atoms X (C, N) at the 4(a) sites are shown; these atoms form distorted XM_6 octahedra joined via all the vertices.

of the stoichiometric composition they are occupied by the nonmetallic interstitial atoms X, that is, carbon or nitrogen atoms (Fig. 25). In the case where the composition of a ternary carbide or nitride with the structure of the $\beta\text{-Mn}$ type deviates from the stoichiometry, some of the octahedral interstices remain vacant.

A filled structure of the Mn_5Si_3 type ($D8_8$) (see Fig. 10), which is common for the transition metal silicoborides, carbosilicides, and siliconitrides $\text{M}_5\text{Si}_3\text{B}_x$, $\text{M}_5\text{Si}_3\text{C}_x$, and $\text{M}_5\text{Si}_3\text{N}_x$ considered above, is also a frequently encountered type of the structure of the ternary compounds in the M–Al–C and M–Al–N systems. It is of interest that this structure is hardly found among the transition metal aluminosilicides.

2. The M–Al–C ternary aluminidocarbide systems

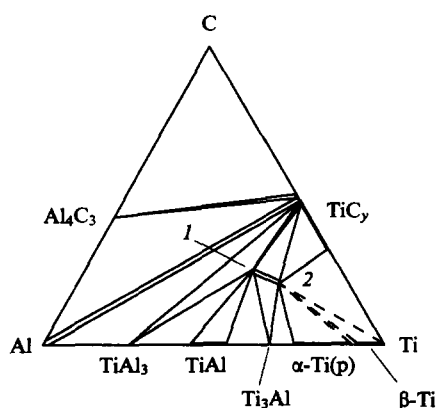
The structural characteristics of the ternary phases formed in the M–Al–C aluminidocarbide systems are presented in Table 9.

Some lanthanides form aluminium and carbon cubic ternary compounds Ln_3AlC ($\text{Ln} = \text{Tb}, \text{Er}, \text{Tm}$) with the perovskite type of structure.¹⁵⁸

The Ti–Al–C system. In a study of the phase equilibria in the Ti–Al–C system,¹⁷⁹ the existence of the ternary cubic compound Ti_3AlC with the perovskite structure¹⁵⁹ and of the ternary hexagonal compound Ti_2AlC (the H -phase) with the Cr_2AlC type of structure^{169–172} has been confirmed (Table 9). The following pseudobinary equilibria occur in the Ti–Al–C system under equilibrium conditions at 1273 K (Fig. 26): $\text{Al}_4\text{C}_3\text{–TiC}_y$, $\text{TiAl}_3\text{–TiC}_y$, $\text{Ti}_2\text{AlC–TiAl}_3$, $\text{Ti}_2\text{AlC–TiAl}$, $\text{Ti}_2\text{AlC–Ti}_3\text{Al}$, $\text{Ti}_2\text{AlC–Ti}_3\text{AlC}$, $\text{Ti}_2\text{AlC–TiC}_y$, $\text{Ti}_3\text{AlC–TiC}_y$, $\text{Ti}_3\text{AlC–Ti}_3\text{Al}$, $\text{Al}(\text{liq})\text{–TiC}_y$, $\text{Ti}_3\text{AlC–}\alpha\text{-Ti}(\text{sol})$ and $\text{Ti}_3\text{AlC–}\beta\text{-Ti}(\text{sol})$ [$\text{Al}(\text{liq})$ is molten aluminium, and $\alpha\text{-Ti}(\text{sol})$ and $\beta\text{-Ti}(\text{sol})$ are solid solutions of aluminium in $\alpha\text{-Ti}$ and $\beta\text{-Ti}$, respectively]. Titanium is

Table 9. Some ternary phases in the M–Al–C systems.

Compound	Symmetry and type of structure	Space group	Z	Unit cell parameters / nm		Ref.
				<i>a</i>	<i>c</i>	
Tb ₃ AlC	Cubic, the perovskite CaTiO ₃ (<i>E</i> ₂₁) type	<i>Pm</i> 3 <i>m</i>	1	0.4876	—	158
Er ₃ AlC	"	<i>Pm</i> 3 <i>m</i>	1	0.4792	—	158
Tm ₃ AlC	"	<i>Pm</i> 3 <i>m</i>	1	0.4776	—	158
Ti ₃ AlC _{<i>x</i>} (<i>x</i> = 1.0)	"	<i>Pm</i> 3 <i>m</i>	1	0.4156	—	159
Cr ₃ AlC _{<i>x</i>}	—	—	—	—	—	160
Mn ₃ AlC _{<i>x</i>} (<i>x</i> = 1.0–1.2)	Cubic, the perovskite CaTiO ₃ (<i>E</i> ₂₁) type	<i>Pm</i> 3 <i>m</i>	1	0.3869	—	161–165
Fe ₃ AlC _{<i>x</i>} (<i>x</i> ≈ 0.66)	"	<i>Pm</i> 3 <i>m</i>	1	0.3728–0.3788	—	163, 164
Co ₃ AlC _{<i>x</i>} (<i>x</i> ≈ 0.59)	"	<i>Pm</i> 3 <i>m</i>	1	0.3697	—	163, 164, 166
Ni ₃ AlC _{<i>x</i>} (<i>x</i> ≈ 0.3)	Cubic (a solid solution of carbon in Ni ₃ Al)	<i>Pm</i> 3 <i>m</i>	1	0.3617	—	163, 164, 167, 168
Ni ₃ AlC _{<i>x</i>} (<i>x</i> ≈ 0.3)	"	<i>Pm</i> 3 <i>m</i>	1	0.3583	—	168
Ti ₂ AlC	Hexagonal (<i>H</i> -phase of the Cr ₂ AlC type)	<i>P</i> 6 ₃ / <i>mmc</i>	2	0.304	1.360	169–172
V ₂ AlC	"	<i>P</i> 6 ₃ / <i>mmc</i>	2	0.2913	1.314	169–172
Nb ₂ AlC	"	<i>P</i> 6 ₃ / <i>mmc</i>	2	0.3103	1.383	169–172
Ta ₂ AlC	"	<i>P</i> 6 ₃ / <i>mmc</i>	2	0.3075	1.383	169–172
Cr ₂ AlC	"	<i>P</i> 6 ₃ / <i>mmc</i>	2	0.286	1.282	169–172
Nb ₃ Al ₂ C	Cubic, the β-Mn (<i>A</i> 13) type	<i>P</i> 4 ₁ 32	4	0.7065–0.7079	—	172–174
Ta ₃ Al ₂ C	"	<i>P</i> 4 ₁ 32	4	0.7038	—	172–174
Mo ₃ Al ₂ C	"	<i>P</i> 4 ₁ 32	4	0.6860–0.6866	—	172, 174–176
Zr ₂ Al ₃ C ₅	Hexagonal	<i>P</i> 31 <i>c</i>	2	0.3345	2.2231	177
Hf ₂ Al ₃ C ₅	"	<i>P</i> 31 <i>c</i>	2	0.3319	2.209	177
ZrAlC ₂	"	<i>P</i> 6 ₃ / <i>mcm</i>	6	0.3345	2.761	177
HfAlC ₂	"	<i>P</i> 6 ₃ / <i>mcm</i>	6	0.3319	2.742	177
Zr ₅ Al ₃ C	Hexagonal, filled structure of the Mn ₅ Si ₃ type (<i>D</i> 8 ₈)	<i>P</i> 6 ₃ / <i>mcm</i>	2	0.822	0.568	177
Hf ₅ Al ₃ C	"	<i>P</i> 6 ₃ / <i>mmc</i>	2	0.812	0.5679	172, 177
Ta ₅ Al ₃ C	"	<i>P</i> 6 ₃ / <i>mmc</i>	2	0.7734	0.5245	177
Th ₄ Al ₂ C ₅	—	—	—	—	—	178
ThAlC ₂	—	—	—	—	—	178
ThAl ₄ C ₄	Hexagonal	—	—	0.823	0.334	178

**Figure 26.** Isothermal cross-section through the Ti–Al–C system at 1273 K (the dark areas denote one-phase regions).¹⁷⁹ (1) Ti₂AlC; (2) Ti₃AlC.

insoluble in Al₄C₃, carbon is insoluble in titanium aluminides, and aluminium is insoluble in TiC_γ. α-Ti dissolves up to 10 at.% of aluminium. The Ti₂AlC *H*-phase annealed at 973 K has no homogeneity region. The variation of the unit cell parameters on the substitution of titanium by aluminium in the ternary phases is relatively greater than the variation caused by a similar change in the carbon content.¹⁷⁹ Thus, the lattice period of the Ti₃AlC annealed at 1273 K decreases on the substitution of titanium by aluminium and increases with an increase in the concentration of carbon. The unit cell parameters of the Ti₂AlC *H*-phase annealed at 1273 K vary in the ranges *a* = 0.3045 to 0.3065 nm and *c* = 1.3636 to 1.3671 nm. The variation of the unit cell parameters points to the existence of small homogeneity regions of the ternary phases annealed at 1273 K.

While considering the phase equilibria in the Ti–Al–C system, one should mention a study¹⁸⁰ published in 1988, when the ternary compounds Ti₂AlC and Ti₃AlC were already known, in which a wrong variant of the phase diagram with no allowance for the existence of the ternary phases was suggested for the Ti–Al–C system.

The Zr–Al–C system. All the known zirconium aluminides except for Zr₂Al, Zr₅Al₄, and Zr₅Al₃, have been found in the Zr–Al–C system.¹⁷⁷ The Zr₂Al phase may be stabilised only in the presence of silicon.¹⁸¹ The aluminide Zr₅Al₄ decomposes at a

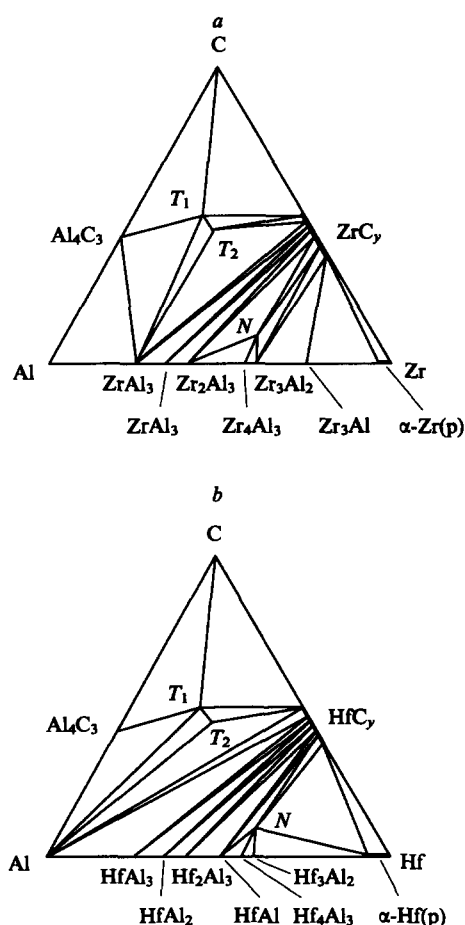


Figure 27. Isothermal cross-sections through the Zr–Al–C (a) and Hf–Al–C (b) systems at 973 K (dark sections denote single-phase homogeneity regions of carbides and of solid solutions of aluminium in transition metals).¹⁷⁷

$T_1 = M_2Al_3C_{5-x}$, $T_2 = MAlC_{2-x}$, $N = M_5Al_3C$ ($M = Zr, Hf$).

temperature of ~ 1250 K, and Zr_5Al_3 almost coincides in its composition with Zr_3Al_2 .

Three ternary phases have been found in the Zr–Al–C system: $Zr_2Al_3C_{5-x}$, $ZrAlC_{2-x}$, and Zr_5Al_3C (see Table 9). The new ternary compound with the ideal formula $Zr_2Al_3C_5$ has a hexagonal structure [space group $P31c$ (C_{3v}^4)] with the unit cell parameters $a = 0.3345$ nm and $c = 2.2230$ nm; carbon atoms are located in the octahedral interstices. The $ZrAlC_2$ phase also crystallises with a hexagonal structure [space group $P6_3/mmc$ (D_{6h}^4)], carbon being located in the octahedral interstices. The Zr_5Al_3C phase has a structure of the Mn_5Si_3 type the octahedral interstices of which are filled with carbon.

The greatest number of pseudobinary equilibria in the Zr–Al–C system are formed by the very stable zirconium carbide ZrC_γ (Fig. 27a). However, in contrast to the Ti–Al–C system, ZrC_γ does not form pseudobinary equilibria with aluminium at temperatures below ~ 1300 K. Carbon is soluble only in the aluminide Zr_3Al_2 (Zr_5Al_3), thus stabilising its structure (Mn_5Si_3 type); aluminium is insoluble in ZrC_γ . The distribution of the phase fields near the ternary compound Zr_5Al_3C at 1273 K differs from that at 973 K, namely, the ZrC_γ – Zr_3Al_2 and ZrC_γ – Zr_3Al equilibria disappear, the Zr_5Al_3C – Zr_3Al and Zr_5Al_3C – β -Zr(sol) appearing instead [β -Zr(sol) is the solid solution of aluminium in β -Zr].

The Hf–Al–C system. Three ternary compounds exist in the Hf–Al–C system, their structures and compositions (see Table 9) being similar to those of the corresponding ternary compounds formed in the Zr–Al–C system.¹⁷⁷ However, in

contrast to the zirconium-containing system, there is no Al_4C_3 – $HfAl_3$ equilibrium in the system under consideration, and aluminium coexists with $Hf_2Al_3C_5$, $HfAlC_2$, and HfC_γ (Fig. 27b). Carbon is insoluble in the hafnium aluminides and aluminium is insoluble in hafnium carbide. The phase equilibria in the Hf–Al–C system at 973 K and 1273 K are virtually identical, differing only in that the solubility of aluminium in α -Hf increases (up to 12 at.% of Al at 1273 K) and some solubility of carbon in α -Hf appears.

The V–Al–C system. One ternary compound, namely V_2AlC with a hexagonal structure of the Cr_2AlC type, is formed in the V–Al–C system (see Table 9).^{169–172} At 1273 K this compound coexists with molten aluminium, the carbides Al_4C_3 , VC_γ , ζ - V_4C_3 , and V_2C , and with V(sol) [V(sol) is the solid solution of aluminium in vanadium]; Al_4C_3 exists in an equilibrium with VC_γ (V_8C_7), and V_2C is in an equilibrium with V(sol).¹⁷⁹ The solid solution V(sol) coexisting with V_2AlC and V_2C contains up to 23 at.% of Al. Note that both the disordered carbide VC_γ and the ordered phase V_8C_7 have been observed in this system at 1273 K.¹⁷⁹ The V_2AlC ternary phase has no homogeneity region, binary phases do not dissolve the third component.¹⁷⁹

The Nb–Al–C system. The data^{169–172} concerning the existence of the Nb_2AlC ternary *H*-phase in this system (see Table 9) have been confirmed by Schuster et al.¹⁷⁷ At 973 K this phase exists in equilibrium with $NbAl_3$, Nb_2Al , Nb_3Al , NbC_γ , and Nb_2C ; NbC_γ coexists with Al_4C_3 and $NbAl_3$, and Al_4C_3 coexists with $NbAl_3$ (Fig. 28a). The carbide Nb_3Al_2C with the β -Mn type of structure (see Table 9) is unstable at 973 K and is not shown in Fig. 28a.

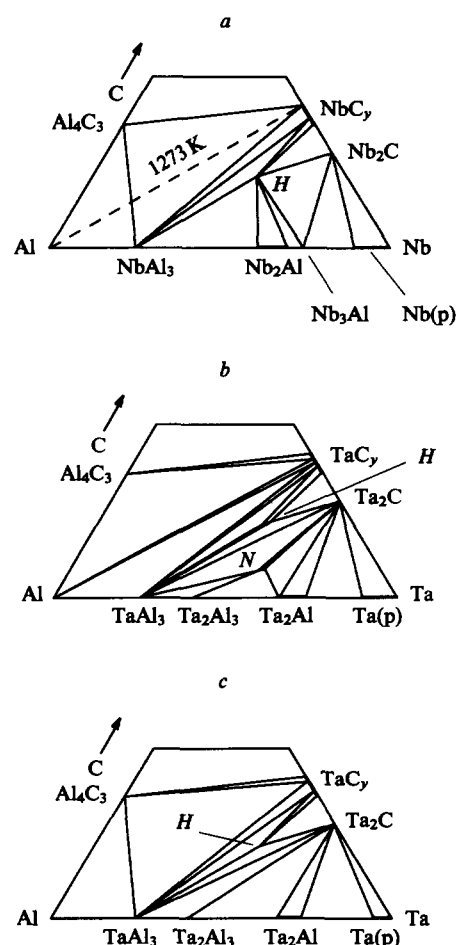


Figure 28. Isothermal cross-sections through the Nb–Al–C system at 973–1273 K (a) and through the Ta–Al–C system at 1273 K (b) and 973 K (c).¹⁷⁷

$H = Nb_2AlC$ (a), Ta_2AlC (b, c), $N = Ta_5Al_3C$.

At a higher temperature of 1273 K the Al_4C_3 – NbAl_3 equilibrium disappears, and the carbide NbC_y coexists directly with liquid aluminium (similarly to the Ti–Al–C system in which the carbide TiC_y is in an equilibrium with liquid aluminium). In all other aspects, the isothermal cross-sections through the Nb–Al–C system at 973 K and 1273 K are similar.

The variation of the parameters of the *H*-phase (*a* varies from 0.3105 nm to 0.3115 nm and *c* varies from 1.3860 nm to 1.3921 nm) indicates the existence of a small homogeneity region corresponding to the formula $\text{Nb}_{2-x}\text{Al}_{1+x}\text{C}_{1-x/2}$, which was suggested in a previous study.¹⁶⁹ Carbon is insoluble in the niobium aluminides, and aluminium is insoluble in the niobium carbides.

The Ta–Al–C system. The isothermal cross-sections through the Ta–Al–C system at 973 K and 1273 K are shown in Fig. 28*b,c*. At 973 K one ternary compound with the formula Ta_2AlC exists in this system, and at 1273 K the second ternary compound appears, namely, $\text{Ta}_5\text{Al}_3\text{C}_x$ with a filled structure of the Mn_5Si_3 type (see Table 9). The ternary compound $\text{Ta}_3\text{Al}_2\text{C}$ is unstable at these temperatures and is not shown in Fig. 28*b,c*. At 1273 K carbon populates only some of the octahedral interstices of the tantalum sublattice in $\text{Ta}_5\text{Al}_3\text{C}_x$ ($x < 1.0$), and the occupation of all the interstices can be achieved at a higher temperature.

As the temperature increases, carbon stabilises the $\text{Ta}_5\text{Al}_3\text{C}$ phase with the $D8_8$ type of structure; as this takes place an equilibrium arises between the carbide TaC_y and liquid aluminium, and the Al_4C_3 – TaAl_3 equilibrium disappears (see Fig. 28*b,c*).

The Cr–Al–C system. There is one ternary compound in this system: Cr_2AlC (see Table 9), which is more stable at 1073 K than the carbides Al_4C_3 and Cr_3C_2 and exists in an equilibrium directly with carbon (graphite); with an increase in the temperature, the *H*-phase becomes less stable than Al_4C_3 and Cr_3C_2 , and the Cr_2AlC –C equilibrium disappears (Fig. 29). According to the data obtained by Schuster et al.,¹⁷⁹ the compound Cr_2AlC has no homogeneity region. There is no solubility of the third component in the binary phases of the Cr–Al–C system. The existence of the Cr_3AlC carbide phase with an unknown structure has been reported;¹⁶⁰ however, these data have not been confirmed subsequently.

The Mo–Al–C system. One ternary compound has been detected in this system, namely, the compound $\text{Mo}_3\text{Al}_2\text{C}$ with a cubic structure of the β -Mn type, similar to the analogous compounds formed in the Nb–Al–C and Ta–Al–C systems. The aluminidocarbide $\text{Mo}_3\text{Al}_2\text{C}$ exists in equilibrium with the carbides Al_4C_3 and Mo_2C and with the aluminides Mo_3Al_8 and Mo_3Al ; Al_4C_3 coexists with Mo_2C , MoAl_3 , and Mo_3Al_8 ; the carbide Mo_2C is in equilibrium with Mo_3Al and with the solid solution of aluminium and carbon in molybdenum $\text{Mo}(\text{Al,C})$.¹⁷⁶ The ternary compound $\text{Mo}_3\text{Al}_2\text{C}$ has a small homogeneity region and is formed via a peritectic reaction between the carbide Mo_2C and the aluminium melt. A ternary eutectic ($\text{Mo}_3\text{Al}_2\text{C} + \text{Mo}_3\text{Al} + \text{Mo}_3\text{Al}_8$) with a melting point of ~ 1823 K exists in the system. The compound $\text{Mo}_3\text{Al}_2\text{C}$ has a small homogeneity region: as the content of molybdenum increases from 47 to 51 at.%, the content of carbon being constant and equal to 16.7 at.%, the cubic lattice period increases from 0.6860 nm to 0.6866 nm.^{171,172} A small amount of carbon can be dissolved in all the molybdenum aluminides, whereas molybdenum (up to 3 at.%) is soluble in Al_4C_3 . In all probability, the Al_4C_3 – MoC_y (Mo_3C_2) pseudo-binary equilibrium should exist in the Mo–Al–C system at $T > 1750$ K.

The W–Al–C system. There are no ternary compounds in the W–Al–C system at 1173 K.¹⁷⁶ The intermetallide WAl_2 exists in equilibrium with the carbides Al_4C_3 , WC, and W_3C , whereas Al_4C_3 is in equilibrium with the hexagonal carbide WC (the WC_y high-temperature cubic phase was not taken into account). It should be kept in mind that the designation of the intermetallide WAl_2 , which is formed from tungsten and aluminium melt via the

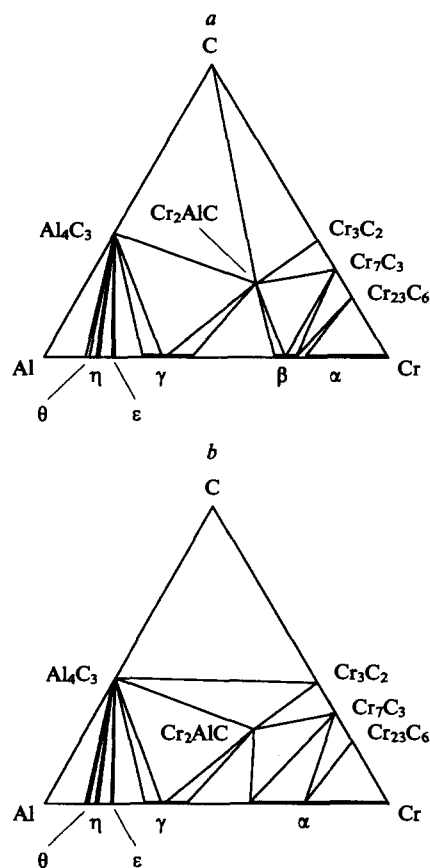


Figure 29. Isothermal cross-sections through the Cr–Al–C system at 1073 K (a) and 1273 K (b) (dark sections denote single-phase regions).¹⁷⁹

peritectic reaction and is stable in the narrow temperature range from 1600 K to 1830 K, is somewhat arbitrary.¹⁸²

The Mn–Al–C system. A study of the phase equilibria in the Mn–Al–C system has provided evidence for the existence of the ternary compound Mn_3AlC with the perovskite type of structure¹⁸³ (see Table 9). At 973 K this compound is in equilibrium with Al_4C_3 and with solid solutions of aluminium in α -Mn(sol) and β -Mn(sol) as well as with the carbides Mn_7C_3 , Mn_5C_2 , and Mn_{23}C_6 and with carbon, whereas Al_4C_3 is in equilibrium with all the manganese aluminides (Fig. 30a). The period of the lattice of Mn_3AlC annealed at 973 K varies from 0.3856 nm to 0.3873 nm. This apparently reflects the variation of the carbon content in the compound rather than the alteration of the ratio between the manganese and aluminium. A similar conclusion can be drawn from the results of another study.¹⁶³

At 1273 K γ -Mn dissolves ~ 5 at.% of carbon and 25 at.% of aluminium thus forming a broad one-phase region; the high-temperature ϵ -MnAl phase dissolves up to 5 at.% of carbon (Fig. 30b). The parameters of the cubic lattice in the compounds Mn_3AlC thus formed differ from each other and are equal to 0.3840 nm and 0.3874 nm. It should be noted that two phases (apart from the γ -Mn Fcc structure) with the perovskite structure and different parameters, $a = 0.384$ nm and $a = 0.387$ nm, have been also observed in the $\text{Mn}_7\text{Al}_2\text{C}$ alloy.

The temperature of the congruent melting of Mn_3AlC is 2000 K.

The Fe–Al–C system. Figure 31 presents a fragment of the Fe–Al–C ternary system at 1273 K.¹⁸⁴ The carbide Fe_3AlC_x with the perovskite type of structure is formed in this system (see Table 9); the metal atoms in this compound form an ordered Fcc-lattice. The corresponding aluminide Fe_3Al has a cubic structure (space group $Fm\bar{3}m$) of the BiLi_3 or BiF_3 ($D0_3$) type. This structure consists of four interpenetrating Fcc sublattices.

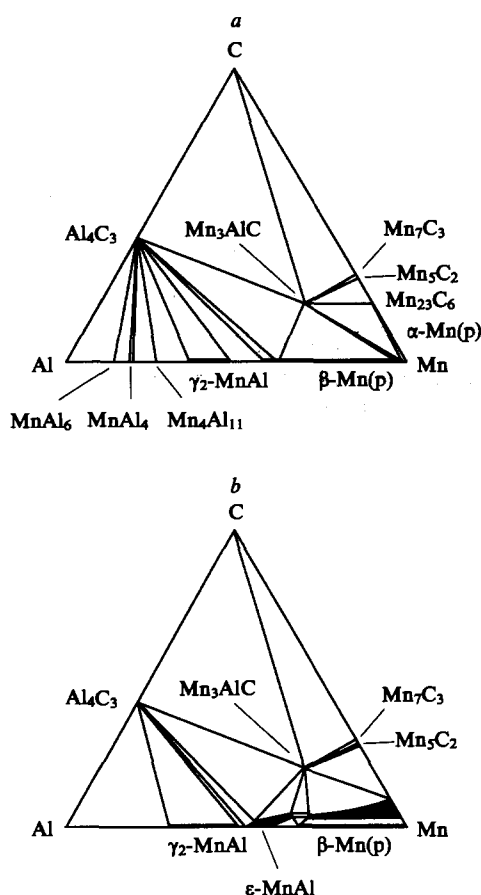


Figure 30. Isothermal cross-sections through the Mn-Al-C system at 973 K (a) and 1273 K (b) (dark sections denote single-phase regions).¹⁸³

The aluminium atoms are located at the unit cell vertices and at the centres of faces, whereas iron atoms occupy the centres of octahedral and tetrahedral interstices of the aluminium fcc-sublattice. As a whole, the atoms in Fe_3Al populate the same positions as do the atoms in the eight cells of a body-centred cubic (Bcc) lattice of the $\text{CsCl}(B2)$ type. This permits Fe_3Al to be regarded as a superstructure based on a Bcc lattice. The

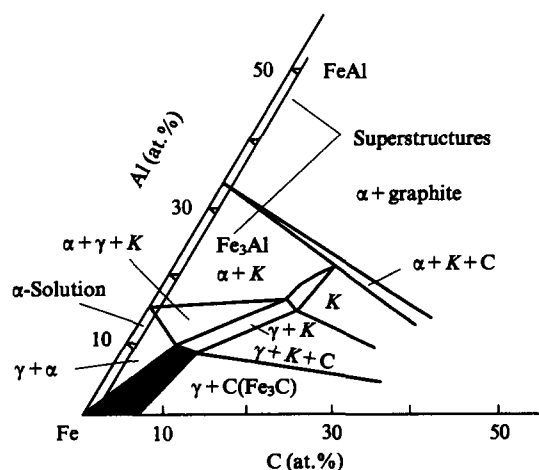


Figure 31. Fragment of the isothermal cross-section through the Fe-Al-C system at 1273 K.¹⁸⁴ K is the ternary compound Fe_3AlC_x with the perovskite type of structure; dark area indicates the region of austenite $\gamma\text{-Fe}(\text{C})$.

introduction of carbon into Fe_3Al leads to the formation of the ternary carbide Fe_3AlC with the perovskite type of structure. The carbide Fe_3AlC has an extended homogeneity region that is connected to the homogeneity region of austenite $\gamma\text{-Fe}(\text{C})$ via a two-phase region. The ternary compound Fe_3AlC_x exists in equilibrium with Fe_3Al , FeAl , the solid solution of aluminium in $\alpha\text{-Fe}$, $\gamma\text{-Fe}(\text{C})$, carbon, and possibly with the cementite Fe_3C .

The Co-Al-C system. One ternary compound Co_3AlC_x with the perovskite type of structure is formed in the Co-Al-C system.^{163, 164, 166} The proportions of carbon in Co_3AlC_x and Fe_3AlC_x are approximately equal ($x \approx 0.6$).^{163, 164} The carbide Co_3AlC_x is formed via a peritectic reaction of CoAl with carbon and aluminium melt. The ternary compound Co_3AlC_x forms pseudobinary equilibria with $\alpha\text{-Co}$ (more precisely, with the limited solid solution of aluminium and carbon in cobalt), CoAl , C, and probably with Al_4C_3 .

The Ni-Al-C system. In the Ni-Al-C system, the nickel aluminide Ni_3Al [Cu_3Au ($L1_2$) structural type, space group $Pm\bar{3}m(O_h^1)$] has an ordered cubic lattice and dissolves up to 7 at.% of carbon, the symmetry of the metallic lattice being retained and the period of the lattice increasing from 0.3587 nm to 0.3617 nm.^{163, 164} Thus, the Ni_3AlC_x phase is an interstitial solid solution of carbon in Ni_3Al . The structure of this solid solution is characterised by the same distribution of atoms as in the carbides M_3AlC_x with the perovskite structure, which has been confirmed in a special study.¹⁶⁸ The method of forming the Ni_3AlC_x solid solution and its crystal structure (the $L1_2$ type with some of the octahedral interstices being filled with carbon atoms) indicate that the compounds M_3AlC_x with the perovskite structure are interstitial compounds, like the cubic [with the structure of the $\text{NaCl}(B1)$ type] carbides and nitrides MX_y ($y \leq 1.00$).

It has been found¹⁶⁸ that carbon is markedly soluble not only in Ni_3Al , but also in NiAl . According to this study, on passing from Ni_3Al to $\text{Ni}_3\text{Al}(\text{C}_{1.0})$, the period of the metallic lattice increases from 0.3557 nm to 0.3583 nm.

3. The ternary M-Al-N aluminidonitride systems

The interest in the use of the compounds and heterophase compositions formed in the M-Al-N systems as abrasives is due to their high chemical stability and hardness. In addition, the ability of the aluminium nitride AlN to retain its high mechanical properties at elevated temperatures $T > 1000$ K makes the development of construction materials based on it particularly attractive, since these materials can be used under drastic conditions, for example, in aggressive media, at high temperatures, and under great loads.

The structural characteristics of the ternary phases formed in the M-Al-N systems are listed in Table 10.

The Sc-Al-N system. All the alloys formed in the Sc-Al-N systems in which the concentration of scandium is more than 50 at.% contain the Sc_3AlN_x ternary cubic phase with the perovskite structure.¹⁸⁵ The ternary compound Sc_3AlN_x is in equilibrium with ScAl , Sc_2Al , ScN , and $\text{Sc}(\text{sol})$ (the solid solution of Al and N in scandium). In addition, the following pseudobinary equilibria exist in the Sc-Al-N system: $\text{AlN}-\text{ScAl}_3$, $\text{AlN}-\text{ScAl}_2$, $\text{AlN}-\text{ScN}$, $\text{ScN}-\text{ScAl}_2$, $\text{ScN}-\text{ScAl}$, $\text{ScN}-\text{Sc}(\text{sol})$, and $\text{Sc}_2\text{Al}-\text{Sc}(\text{sol})$ (Fig. 32a). The lattice period of Sc_3AlN_x is 0.4396 nm (in equilibrium with ScAl and Sc_2Al), 0.4405 nm [in equilibrium with $\text{Sc}(\text{sol})$ and ScN], and 0.4435 nm (in equilibrium with ScN and ScAl). Scandium dissolves up to 15 at.% of nitrogen and more than 5 at.% of aluminium.

The Yl-Al-N system. According to Schuster and Bauer,¹⁸⁵ there are no ternary phases in this system at temperatures from 1073 K to 1573 K. At 1273 K the yttrium nitride YN coexists with AlN , YAl_2 , YAl , and Y_3Al_2 , whereas the aluminium nitride AlN coexists with YAl_2 (Fig. 32b). At 1573 K the aluminides YAl and Y_3Al_2 disappear from the Y-Al-N system, the $\text{AlN} + \text{YN} + \text{YAl}_2$ region being retained as the only solid three-phase region.

Table 10. Some ternary phases in M–Al–N systems.

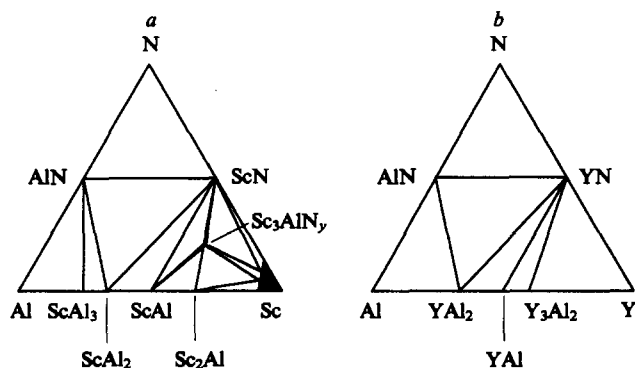
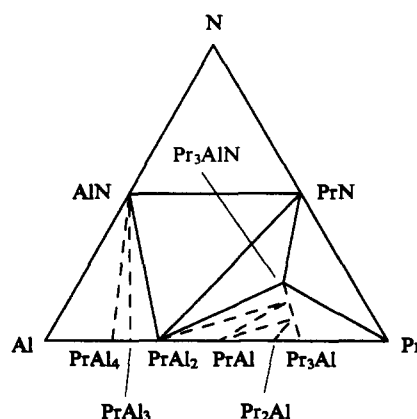
Compound	Symmetry and type of structure	Space group	Z	Unit cell parameters / nm			Ref.
				a	b	c	
Sc ₃ AlN _x	Cubic, the perovskite CaTiO ₃ (<i>E2₁</i>) type	<i>Pm3m</i>	1	0.4396–0.4435	—	—	185
La ₃ AlN _x	"	<i>Pm3m</i>	1	0.507	—	—	186
Nd ₃ AlN _x	"	<i>Pm3m</i>	1	0.4910	—	—	187
Nd ₃ AlN _x	"	<i>Pm3m</i>	1	0.4939	—	—	186
Sm ₃ AlN _x	"	<i>Pm3m</i>	1	0.4862	—	—	186
Ce ₃ Al(N)	Cubic, a solid solution of nitrogen in Ce ₃ Al [the Cu ₃ Au (<i>L1₂</i>) type]	<i>Pm3m</i>	1	0.5008	—	—	186
Pr ₃ Al(N)	Cubic, a solid solution of nitrogen in Pr ₃ Al [the Cu ₃ Au (<i>L1₂</i>) type]	<i>Pm3m</i>	1	0.4977	—	—	186
Ti ₃ AlN	Cubic, the perovskite CaTiO ₃ (<i>E2₁</i>) type	<i>Pm3m</i>	1	0.4120	—	—	188
Fe ₄ N(Al) (Fe ₃ AlN)	Cubic, a solid solution of aluminium in γ -Fe ₄ N (<i>L'</i> 1)	—	1	0.380	—	—	189
Ni ₃ Al(N)	Cubic (a solid solution of nitrogen in Ni ₃ Al (the Cu ₃ Au (<i>L1₂</i>) type)	<i>Pm3m</i>	1	0.380	—	—	189
Ti ₂ AlN _x	Hexagonal (<i>H</i> -phase the Cr ₂ AlC type)	<i>P6₃/mmc</i>	2	0.2991–0.304	—	1.361–1.369	188, 190–192
Ti ₃ Al ₂ N ₂	Trigonal	<i>P31c</i>	2	0.2988	—	2.335	188
Zr ₃ AlN	Monoclinic	—	—	0.5988	0.8966	0.3367 ^a	193
Hf ₃ AlN	"	—	—	0.5901	0.8865	0.3319 ^b	194
Zr ₃ AlN	Orthorhombic, the type of filled Re ₃ B	<i>Cmcm</i>	4	0.3369	1.1498	0.8983	195
Hf ₃ AlN	"	<i>Cmcm</i>	4	0.3319	1.1326	0.8865	195
Zr ₅ Al ₃ N _x (0.1 ≤ x ≤ 0.9)	Hexagonal, the type of filled Mn ₅ Si ₃ (<i>D8₈</i>)	<i>P6₃/mcm</i>	2	0.8170–0.8240	—	0.5655–0.5694	193, 194
Hf ₅ Al ₃ N _x	"	<i>P6₃/mcm</i>	2	0.8062	—	0.5603	194
Ta ₅ Al ₃ N _x	Tetragonal, the Cr ₅ B ₃ (<i>D8₁</i>) type	<i>I4/mcm</i>	4	—	—	—	196
Nb ₃ Al ₂ N	Cubic, the β -Mn type	<i>P4₁32</i>	4	0.7031–0.7039	—	—	174, 196, 197

^a In the unit cell $\beta = 106.39^\circ$. ^b In the unit cell $\beta = 106.33^\circ$.

The Ln–Al–N systems. A study has shown¹⁸⁶ that there are no ternary phases in the Ln–Al–N systems with Ln = Gd, Tb, Dy, Ho, Er, Tm, Yb, and Lu. In the La–Al–N, Nd–Al–N, and Sm–Al–N systems, the Ln₃AlN_x ternary phases with the perovskite type of structure are formed, whereas in the Ce–Al–N and Pr–Al–N systems, the Ce₃AlN_x and Pr₃AlN_x ternary phases based on the aluminides Ce₃Al and Pr₃Al with

structures of the Cu₃Al (*L1₂*) type are formed. The latter result from filling of the octahedral interstices of the lanthanide sublattice with nitrogen atoms.

Figure 33 presents the isothermal cross-section through the Pr–Al–N system at 873 K.¹⁸⁶ The ternary compound Pr₃AlN coexists with PrAl₂, PrAl₃, PrN, and Pr, the aluminium nitride

**Figure 32.** Isothermal cross-sections through the Sc–Al–N (a) and Y–Al–N (b) systems at 1273 K (dark areas indicate single-phase regions).¹⁸⁵**Figure 33.** Isothermal cross-section through the Pr–Al–N system at 873 K (pseudobinary equilibria marked by dashed lines are shown conventionally).¹⁸⁶

AlN coexists with PrAl_4 , PrAl_3 , PrAl_2 , and PrN , and PrAl_2 is in an equilibrium with PrN . The $\text{Pr}_3\text{Al}-\text{Pr}_3\text{AlN}_x$ pseudobinary equilibrium is shown with a dashed line, because the ternary phase is actually a solid solution of nitrogen in the aluminide Pr_3Al . The equilibria in the $\text{PrAl}_4-\text{AlN}-\text{PrAl}_3$ and $\text{PrAl}_2-\text{Pr}_3\text{AlN}_x-\text{Pr}_3\text{Al}$ regions are shown arbitrarily and require additional investigation.

The Ti–Al–N system. Numerous studies of the phase relationships in the Ti–Al–N ternary system have shown that depending on the temperature, two or three ternary compounds can exist in it under equilibrium conditions. At 1273 K there are two ternary phases Ti_3AlN and Ti_2AlN .¹⁸⁸ The cubic phase Ti_3AlN with the perovskite structure (see Table 10) is iso-structural to the carbide Ti_3AlC ¹⁵⁹ and has a negligibly small homogeneity region. The hexagonal Ti_2AlN *H*-phase has been detected for the first time by Jeitschklo et al.¹⁹⁰ Its existence has been confirmed in other studies.^{188,191,192} This phase is isostructural to the analogous Ti_2AlC phase^{169–172} crystallising with the Cr_2AlC type of structure and, judging from the difference in the lattice parameters determined in a number of studies,^{188,190,191} it possesses a certain homogeneity region, which is defective with respect to nitrogen. At 1273 K, the ternary cubic Ti_3AlN phase coexists with Ti_3Al , TiN_y , and Ti_2AlN , whereas the Ti_2AlN *H*-phase is in an equilibrium with TiAl , Ti_3Al , Ti_3AlN , TiN_y , and AlN . In addition, the $\text{AlN}-\text{TiAl}$, $\text{AlN}-\text{TiN}_y$, and $\text{TiN}_y-\text{Ti}_3\text{Al}$ pseudobinary equilibria exist in the Ti–Al–N system. The solubility of aluminium in TiN_y is less than 2 at.%. The lower hexagonal titanium nitride $\epsilon\text{-Ti}_2\text{N}$ does not form any equilibria with ternary compounds or titanium aluminides; it coexists only with TiN_y and with the solid solution of aluminium and nitrogen in $\alpha\text{-Ti}$.

Apart from Ti_2AlN and Ti_3AlN , the $\text{Ti}_3\text{Al}_2\text{N}_2$ ternary phase with a layered trigonal structure (see Table 10) arises in the Ti–Al–N system at 1573 K. It coexists with AlN , TiN_y , TiAl , TiAl_3 , and Ti_2AlN (Fig. 34) and exists in the narrow temperature range 1473–1573 K.

The Zr–Al–N system. The phase equilibria in this system have been studied.^{193,195} The ternary compound Zr_3AlN exists in the Zr–Al–N system at 1273 K (see Table 10). Initially this compound was believed to crystallise with a monoclinic symmetry,¹⁹³ however, an X-ray diffraction structural study of its single crystal¹⁹⁵ has shown that Zr_3AlN has an orthorhombic structure of the Re_3B type. The aluminium atoms in the compound Zr_3AlN are located at the centres of trigonal prisms formed by six

zirconium atoms, whereas the nitrogen atoms are arranged in the weakly distorted octahedral interstices of the zirconium sublattice. The formation of the second ternary phase $\text{Zr}_5\text{Al}_3\text{N}_x$ is associated with the stabilisation of the hexagonal structure of the Mn_5Si_3 type with nitrogen; at 1273 K the nitrogen content in $\text{Zr}_5\text{Al}_3\text{N}_x$ is low ($x < 0.2$).

At a temperature of 1273 K the compound Zr_3AlN exists in equilibrium with AlN , Zr_2Al_3 , ZrAl , $\text{Zr}_5\text{Al}_3\text{N}_x$ ($x < 0.2$), ZrN_y , and $\alpha\text{-Zr(sol)}$ (the solid solution of aluminium and nitrogen in $\alpha\text{-Zr}$); the aluminium nitride coexists with ZrAl_3 , ZrAl_2 , Zr_2Al_3 , and ZrN_y ; the $\text{Zr}_5\text{Al}_3\text{N}_x$ phase exists in equilibrium with ZrAl , Zr_5Al_4 , Zr_3Al_2 , Zr_5Al_3 , Zr_2Al , and $\alpha\text{-Zr(sol)}$; and ZrN_y is in equilibrium with $\alpha\text{-Zr(sol)}$ (Fig. 35a). Note that in a study of the Zr–Al–C system, Schuster and Nowotny¹⁷⁷ did not find such zirconium aluminides as Zr_2Al , Zr_5Al_4 , and Zr_5Al_3 , which have been observed in the related Zr–Al–N ternary system.¹⁹³

An increase in the temperature to 1573 K leads to a substantial extension of the homogeneity region of the $\text{Zr}_5\text{Al}_3\text{N}$ ternary phase, which contains up to 10 at.% of nitrogen under these conditions. At 1573 K the appearance of the phase diagram of the Zr–Al–N system (Fig. 35b) changes somewhat, since the $\text{ZrN}_y-\text{ZrAl}_2$, $\text{ZrN}_y-\text{Zr}_2\text{Al}_3$, $\text{ZrN}_y-\text{Zr}_5\text{Al}_3\text{N}$, $\text{Zr}_2\text{Al}_3-\text{Zr}_5\text{Al}_3\text{N}$, $\text{ZrAl}-\text{Zr}_5\text{Al}_3\text{N}$, and $\text{Zr}_5\text{Al}_3\text{N}-\beta\text{-Zr(sol)}$ pseudobinary equilibria arise [$\beta\text{-Zr(sol)}$ is the solid solution of aluminium in $\beta\text{-Zr}$].

The Hf–Al–N system. Only one stable ternary phase exists in this system at 1273 K, namely, the Hf_3AlN phase with a monoclinic structure determined using a powder.¹⁹⁴ A single-crystal X-ray diffraction study¹⁹⁵ has shown that Hf_3AlN has an orthorhombic structure of the Re_3B type. The Hf_3AlN phase coexists with HfN_y , AlN , Hf_2Al_3 , HfAl , Hf_4Al_3 , Hf_3Al_2 , and $\alpha\text{-Hf(sol)}$ (the solid solution of aluminium and nitrogen in hafnium, Fig. 35c). The line connecting HfN_y and $\alpha\text{-Hf(sol)}$ confines the possible area of the existence of the nitrides $\text{Hf}_4\text{N}_{3-x}$ and $\text{Hf}_3\text{N}_{2-x}$, which are unstable at 1273 K.

The X-ray diffraction patterns of the samples, the compositions of which corresponded to the $\text{Hf}_2\text{Al}_3-\text{Hf}_3\text{AlN}-\text{HfAl}$ region, exhibited an additional set of reflections due to a fourth phase.¹⁹⁴ In all probability, this phase exists in the equilibrium state only at lower temperatures or is stabilised by admixtures.

Two ternary phases Hf_3AlN and $\text{Hf}_5\text{Al}_3\text{N}$ exist in the Hf–Al–N system at 1673 K (Fig. 35d). The $\text{Hf}_5\text{Al}_3\text{N}$ phase has a structure of the Mn_5Si_3 type; its unit cell parameters ($a = 0.8062$ nm, $c = 0.5603$ nm) are smaller than those of the analogous carbide phase $\text{Hf}_5\text{Al}_3\text{C}$ ($a = 0.8120$ nm, $c = 0.5679$ nm). It follows from the comparison of the unit cell dimensions of $\text{Zr}_5\text{Al}_3\text{C}$ and $\text{Zr}_5\text{Al}_3\text{N}$, $\text{Hf}_5\text{Al}_3\text{C}$ and $\text{Hf}_5\text{Al}_3\text{N}$ that nitrogen occupies only some of the octahedral interstices of the transition metal sublattice. It should be noted that the $\text{Hf}_5\text{Al}_3\text{N}$ and Hf_3AlN ternary phases have no homogeneity regions.

The V–Al–N system. In the temperature range from 1273 to 1773 K no ternary compounds exist in this system, although the attempts to synthesise the nitride V_2AlN with a structure of the *H*-phase have resulted in some cases in multiphase samples, the X-ray diffraction patterns of which contained lines due to the *H*-phase.¹⁹⁸ However, the observed lattice parameters were close to those of the carbide V_2AlC *H*-phase. In addition, the sample containing the *H*-phase was nonequilibrium and incorporated more than three phases. The $\text{V}_{0.50}\text{Al}_{0.25}\text{N}_{0.25}$ alloy corresponding to the ideal stoichiometric composition of the *H*-phase contained only the nitrides VN_y and AlN even at a nitrogen pressure of 3×10^6 Pa. Thus, no ternary phases were detected in the V–Al–N system in the experiment described above.¹⁹⁸

At $T = 1273$ K the aluminium nitride AlN is in equilibrium with VAl_3 , V_5Al_8 , VN_y , and V(sol) [V(sol) is the solid solution of aluminium and nitrogen in vanadium]; VN_y and V_9N_4 exist in equilibrium with V(sol) . At 1573 K the cubic nitride VN_y does not exist, therefore the $\text{AlN}-\text{V}_9\text{N}_4$ equilibrium arises. The V(sol) solid solution existing in equilibrium with AlN and V_9N_4 has the

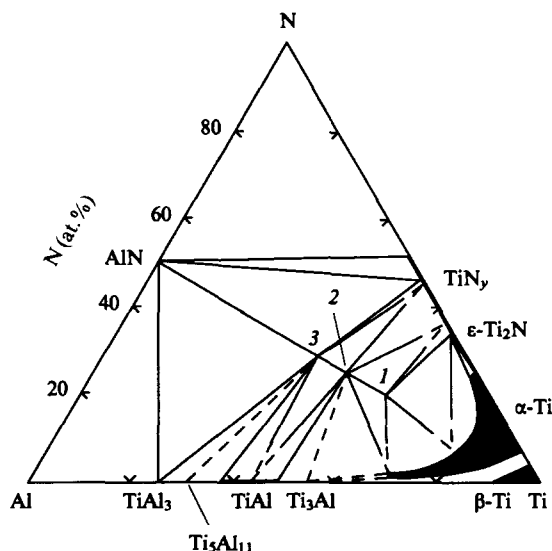


Figure 34. Isothermal cross-section through the Ti–Al–N system at 1573 K (dark areas denote single-phase regions).¹⁸⁸
(1) Ti_3AlN , (2) Ti_2AlN , (3) $\text{Ti}_3\text{Al}_2\text{N}_2$.

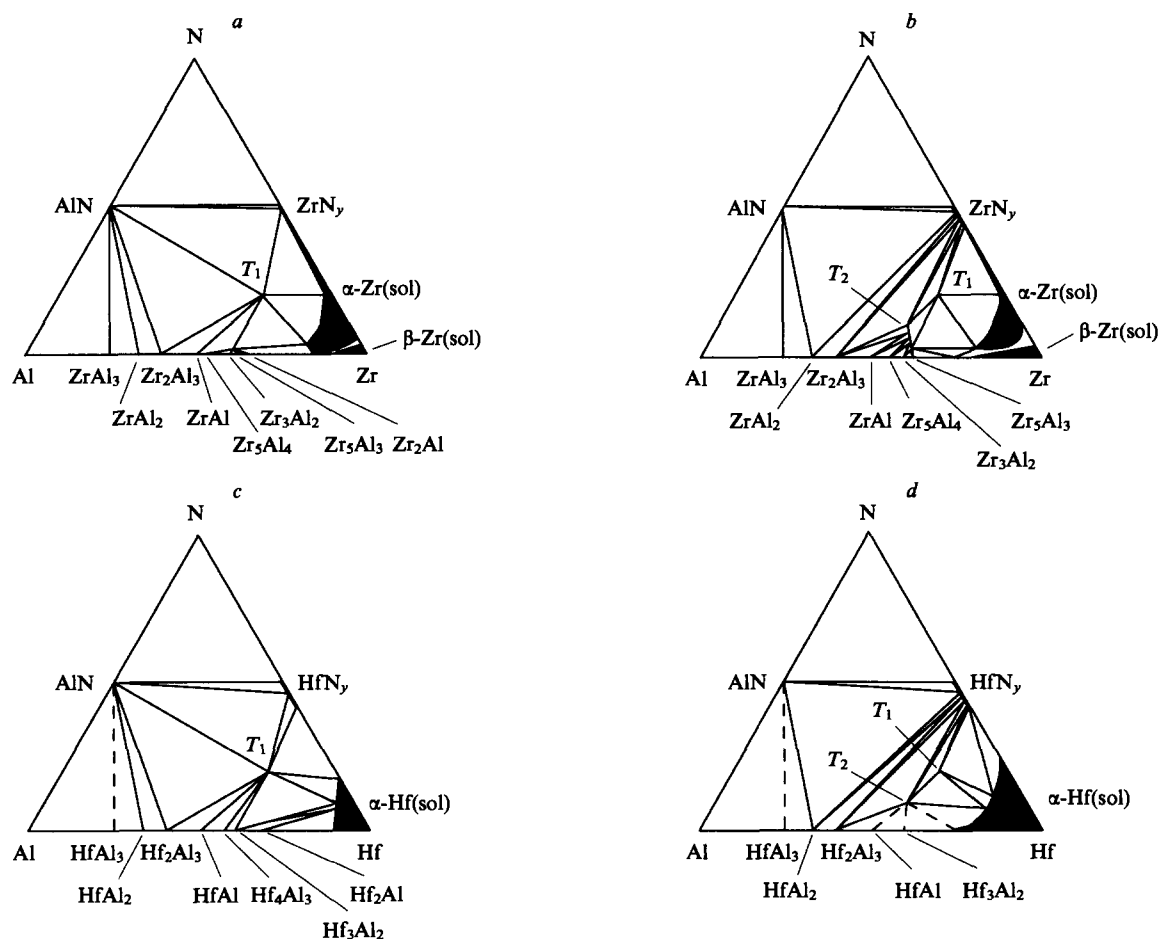


Figure 35. Isothermal cross-sections of the Zr–Al–N system at 1273 K (a) and 1573 K (b) and of the Hf–Al–N system at 1273 K (c) and 1673 K (d).^{193, 194} Dark areas denote single-phase regions; pseudobinary

equilibria marked by dashed lines are shown conventionally; $T_1 = M_3AlN$, $T_2 = M_5Al_3N$ ($M = Zr, Hf$).

composition $V_{0.67}Al_{0.33}$. At 1773 K the $AlN + V_9N_4 + V(sol)$ field is the main region where ternary phase equilibria exist. The solubility of nitrogen in the $V(sol)$ solid solution with high aluminium proportions is low, but it increases markedly with the decrease in the amount of aluminium. The homogeneity region of the $V(sol)$ solid solution expands with an increase in the temperature.

The Nb–Al–N system. The phase equilibria in the Nb–Al–N system have been studied by Schuster and Nowotny.¹⁹⁷ The samples for the investigation were prepared by sintering Nb–Al alloys with the nitrides AlN and NbN under an argon atmosphere. Previously the ternary compound Nb_3Al_2N with a structure of the β -Mn type has been found in this system.^{174, 196} According to Schuster and Nowotny,¹⁹⁷ this compound is stable in the temperature range from 1273 to 1773 K studied and melts congruently. The compound Nb_3Al_2N exists in equilibrium with AlN , Nb_2N , $NbAl_3$, and Nb_2Al ; the nitride AlN is in equilibrium with $NbAl_3$ and with the niobium nitrides Nb_4N_3 and Nb_2N ; and Nb_2N also coexists with Nb_2Al , Nb_3Al , and the solid solution of aluminium and nitrogen in niobium (Fig. 36a). The solubility of Nb or Nb-containing compounds in AlN is negligibly small. The compound Nb_3Al_2N has apparently a narrow homogeneity region, since the period of its lattice varies from 0.70314 nm (in equilibrium with Nb_2Al and Nb_2N) to 0.70387 nm (in equilibrium with $NbAl_3$ and Nb_2Al).

The nitride NbN_y becomes stable at 1273 K, and the $AlN-NbN_y$ equilibrium arises instead of $AlN-Nb_4N_3$. In all other aspects, the phase diagram for the Nb–Al–N system at 1273 K is identical to that at 1773 K.

The Ta–Al–N system. The ternary compound $Ta_5Al_3N_x$ with a structure of the Cr_5B_3 type having vacancies in the nitrogen sublattice has been found in the Ta–Al–N system.¹⁹⁶ However, in another study¹⁹⁷ no ternary compounds have been observed in this system at temperatures from 1273 to 1773 K. The following pseudobinary phase equilibria occur in this system at 1273 K and 1523 K: $AlN-TaAl_3$, $AlN-Ta_2Al_3$ (as the low-temperature modification at 1273 K and as the high-temperature modification at 1573 K), $AlN-Ta_2Al$, $AlN-Ta_2N$, and $AlN-\epsilon-TaN$ (Fig. 36b).

At low temperatures AlN coexists with tantalum, but the reaction between AlN and Ta slowly yields Ta_2N and Ta_2Al . At 1773 K the major part of the ternary system is liquid, and the melt is in an equilibrium with all the binary solid phases.

The Cr–Al–N system. This system contains no ternary phases under the equilibrium conditions in the temperature range 1273–1773 K.¹⁹⁸ The X-ray diffraction patterns of the samples, the composition of which was close to Cr_2AlN , exhibited reflections corresponding to a ternary compound of this composition with a structure of the H -phase. Nevertheless, an equilibrium H -phase could not be detected in the Cr–Al–N system even at a nitrogen pressure of 3×10^6 Pa. Four solid-phase equilibria exist in this system at 1273 K, namely, $AlN-CrAl_4$, $AlN-Cr_4Al_9$, $AlN-Cr_5Al_8$, and $AlN-\alpha-Cr$ ($\alpha-Cr$ is the solid solution of aluminium in chromium having the composition $Cr_{0.58}Al_{0.42}-Cr_{0.98}Al_{0.02}$). Chromium is insoluble in AlN .

The Mo–Al–N system. Two solid three-phase fields ($Mo_3Al_8 + AlN + Mo_3Al$) and ($Mo_3Al + AlN + Mo$) exist in the Mo–Al–N system in the temperature range 1273–1773 K.¹⁹⁸ Molybdenum is insoluble in AlN , and nitrogen

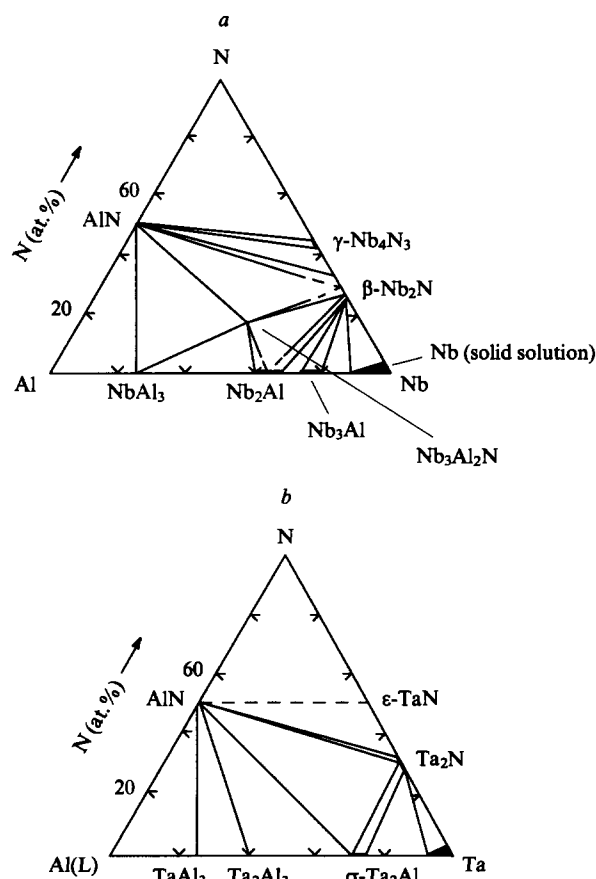


Figure 36. Isothermal cross-sections of the Nb–Al–N system (a) at 1773 K and the Ta–Al–N system (b) at 1523 K (dark areas denote homogeneity regions of binary phases and of solid solutions).¹⁹⁷

is insoluble in the molybdenum aluminides. The molybdenum nitride Mo_2N becomes stable at low temperatures or at high partial pressures of nitrogen (for example, at 1273 K and 1×10^6 Pa). The molybdenum nitride Mo_2N apparently exists in equilibrium with AlN. No ternary phases have been found in the Mo–Al–N system.

The W–Al–N system. There are two pseudobinary solid-phase equilibria, namely, $\text{AlN} - \text{WAl}_4$ and $\text{AlN} - \text{W(sol)}$ [W(sol) is the solid solution of aluminium in tungsten], and no ternary compounds in the W–Al–N system at temperatures from 1273 K to 1773 K. The solubility of tungsten in AlN and the solubility of nitrogen in WAl_4 and W(sol) are negligibly small.

The Mn–Al–N system. No ternary phases exist in the Mn–Al–N system at 873 K; the $\text{Mn}_{88.4}\text{Al}_{9.8}\text{N}_{1.8}$ and $\text{Mn}_{68.1}\text{Al}_{29.2}\text{N}_{2.7}$ alloys studied have a cubic structure of the β -Mn type with the periods a equal to 0.637 nm and 0.643 nm, respectively, and the $\text{Mn}_{75.9}\text{Al}_{8.3}\text{N}_{15.8}$ alloy incorporates two cubic phases, one of which has $a = 0.900$ nm and a structure of the β -Mn type, and the other is characterised by $a = 0.637$ nm and the α -Mn type of structure (the $A12$ structural type, space group $I\bar{4}3m$).¹⁸⁹

Schuster and Nowotny¹⁹⁸ also have not found any ternary phases in the Mn–Al–N system at temperatures of up to 1273 K. At 1073 K the nitride AlN coexists with MnAl_4 , $\text{Mn}_4\text{Al}_{11}$, MnAl, β -Mn (the solid solution of aluminium in manganese), γ -Mn (the solid solution of aluminium and nitrogen in manganese), and with the hexagonal nitride ζ - Mn_2N . Neither solubility of manganese in AlN or solubility of nitrogen in manganese aluminides was observed, while γ -Mn dissolves up to 10 at.% of aluminium and 8 at.% of nitrogen. The only solid-phase equilibrium existing at 1273 K is the equilibrium between AlN and β -Mn.

The Re–Al–N system. There are no ternary phases in the Re–Al–N system in the temperature range from 1273 to 1773 K at a nitrogen pressure of 2×10^7 Pa.¹⁹⁸ At 1273 K aluminium nitride exists in an equilibrium with ReAl_4 , ReAl_3 , ReAl, Re_2Al , and Re. Only two aluminides ReAl_3 and Re_2Al coexisting with AlN are stable at 1773 K.

The Fe–Al–N system. No ternary compounds were found in this system after nitriding the metal alloys at 873 K.¹⁸⁹ The $\text{Fe}_{57}\text{Al}_{19}\text{N}_{24}$ ($\text{Fe}_3\text{AlN}_{1+x}$) alloy contains only the hexagonal iron nitride ϵ - Fe_3N with the parameters $a = 0.276$ nm and $c = 0.442$ nm and contains no aluminium nitride AlN. The alloy of the composition $\text{Fe}_{63.9}\text{Al}_{21.3}\text{N}_{14.8}$ ($\text{Fe}_3\text{AlN}_{1-x}$), apart from ϵ - Fe_3N ($a = 0.273$ nm, $c = 0.438$ nm), incorporates also the cubic austenite γ -Fe (the $A1$ structural type, space group $Fm\bar{3}m$) with $a = 0.356$ nm. The main phases in the $\text{Fe}_{35.8}\text{Al}_{35.8}\text{N}_{28.4}$ (FeAlN_{1-x}) alloy are the hexagonal nitrides ϵ - Fe_3N ($a = 0.273$ nm, $c = 0.439$ nm) and AlN. Finally, the cubic iron nitride γ' - Fe_4N (the $L'1$ structural type) with the unit cell period $a = 0.380$ nm and the hexagonal aluminium nitride AlN [the wurtzite ZnS ($B4$) structural type, space group $P6_3mc$] are present in the alloy of composition $\text{Fe}_{43.1}\text{Al}_{43.1}\text{N}_{13.8}$ ($\text{FeAlN}_{0.32}$). The results obtained by Stadelmaier and Yun¹⁸⁹ indicate that γ' - Fe_4N dissolves substantial amounts of aluminium, and the homogeneity region is extended forming a ternary system.

The Co–Al–N system. There are no ternary compounds in this system.¹⁸⁹ The aluminium nitride is in an equilibrium with α -Co and with the only stable cobalt aluminide β -CoAl.

The Ni–Al–N system. In this system, the dissolution of up to 8 at.% of nitrogen in the cubic nickel aluminide Ni_3Al (the $L1_2$ structural type, $a = 0.358$ nm) leads to the formation of the ternary cubic phase Ni_3AlN_x (the $L'1_2$ structural type) with the lattice period $a = 0.380$ nm.¹⁸⁹

4. The ternary M–Al–Si aluminidosilicide systems

The ternary systems of transition metals with silicon and aluminium have been studied with regard to their resistance to oxidation at high temperatures and the possibility of using them for protective coatings. A characteristic feature of M–Al–Si systems is the ability of aluminium and silicon atoms to substitute each other, which leads to continued solid solutions (or limited solid solutions with high mutual solubilities) of silicides and aluminides. In particular, continued or limited solid solutions arise in those systems where the silicides MSi_2 and M_5Si_3 are formed. Virtually no ternary phases with filled structures of the Mn_5Si_3 type, which are highly typical of the M–B–Si, M–Si–C, M–Si–N, M–Al–C, and M–Al–N systems, are produced in the M–Al–Si systems. Nevertheless, ternary phases with the Mn_5Si_3 type of structure and with vacant octahedral interstices appear in the Zr–Si and Hf–Si systems in the presence of aluminium.

The structural characteristics of the ternary phases formed in the M–Al–Si systems are listed in Table 11.

The Ti–Al–Si system. The phase equilibria and the crystal structures of the compounds formed in this system have been studied in a number of works.^{199–201} The alloys were prepared by sintering the powders and were annealed at 1473 K. The $(\text{Ti},\text{Si})_{2-3}\text{Al}$ ternary phase with a structure of the Mg_3Gd (BiF_3) type was found in the Ti–Al–Si system. The homogeneity region of this phase is located from Ti_2Al to Ti_3Al , and it dissolves up to 5 at.% of silicon. A slight amount of silicon (no more than 2 at.%) is also dissolved in the γ -TiAl solid solution [the $\text{CuAu}(L1_0)$ structural type, space group $P4/mmm$]. A limited substitution solid solution containing up to 12 at.% of silicon is also formed based on the tetragonal aluminide TiAl_3 (the $D0_{22}$ structural type, space group $I4/mmm$). The orthorhombic disilicide TiSi_2 (the $C54$ structural type, space group $Fddd$) dissolves up to 5 at.% of aluminium. The hexagonal disilicide Ti_5Si_3 with the Mn_5Si_3 type of structure also dissolves up to 5 at.% of aluminium, some of the aluminium atoms substituting the silicon atoms and the rest filling the octahedral interstices. The ternary

Table 11. Some ternary phases in M–Al–Si systems.

Compound	Symmetry and type of structure	Space group	Z	Unit cell parameters / nm			Ref.
				a	b	c	
TiAl _x Si _{2-x} (<i>x</i> = 0.3–0.6) [Ti(Si, Al) ₂]	Orthorhombic (pseudo-tetragonal), the ZrSi ₂ (C49) type	<i>Cmcm</i>	4	0.3590–0.3618	0.3590–0.3618	1.3517	199, 200
Ti ₂ AlSi ₃	Orthorhombic, the ZrSi ₂ (C49) type	<i>Cmcm</i>	4	0.3635	1.419	0.3613	201
Ti ₂ AlSi ₃	Tetragonal, the ZrSi ₂ (C49) type	—	4	0.360	0.360	1.353	201
Ti ₇ Al ₅ Si ₁₂	—	—	—	0.3570–0.3645	—	2.715–2.865	201
Ti ₂₋₃ Al(Si)	Cubic, the BiLi ₃ [BiF ₃ (D0 ₃)] type	<i>Fm3m</i>	4	—	—	—	199, 200
Zr(Si, Al) (ZrAl _{0.3} Si _{0.7})	Orthorhombic, the CrB [<i>B</i> ₇ (B33)] type, high-temperature	<i>Cmcm</i>	4	0.3762–0.3788	0.9912–1.007	0.3754–0.3788	200, 202
	Orthorhombic, the FeB (<i>B</i> 27) type, low-temperature	<i>Pnma</i>	4	—	—	—	200, 202
Zr(Al, Si) ₃	Tetragonal, the TiAl ₃ (D0 ₂₂) type	<i>I4/mmm</i>	2	0.5520	—	0.9008	200, 202
Zr ₂ Al ₅ Si	"	<i>I4/mmm</i>	2	0.392–0.400	—	0.8938–0.8960	201
Zr ₃ Al ₄ Si ₅	Tetragonal	<i>I4₁/amd</i>	2	0.371	—	2.935	201
Zr ₂ Al–Zr ₂ Si	Tetragonal, the CuAl ₂ (C16) type, CSSS ^a	<i>I4/mcm</i>	4	—	—	—	201
Zr ₅ Al ₃ –Zr ₅ Si ₃	Hexagonal, the Mn ₅ Si ₃ (D8 ₈) type	<i>P6₃/mcm</i>	2	—	—	—	200, 201
Zr(Al)Si ₂	Orthorhombic, the ZrSi ₂ (C49) type, LSS ^a of Al in ZrSi ₂	<i>Cmcm</i>	4	0.372	1.473	0.3663	201
HfAl _{0.35} Si _{0.65}	Orthorhombic, the CrB [<i>B</i> ₇ (B33)] type	<i>Cmcm</i>	4	0.3714	0.9890	0.3754	200, 202
Hf ₅ (Si, Al) ₃	Hexagonal, the Mn ₅ Si ₃ (D8 ₈) type	<i>P6₃/mcm</i>	2	—	—	—	200
Hf ₂ Al–Hf ₂ Si	Tetragonal, the CuAl ₂ (C16) type, CSSS ^a	<i>I4/mcm</i>	4	—	—	—	200, 202
VAl _x Si _{2-x} (<i>x</i> = 0–0.7)	Hexagonal, the CrSi ₂ (C40) type, LSS ^a of Al in VSi ₂	<i>P6₂22</i>	3	0.4566–0.4608	—	0.6372–0.6439	203, 204
NbAl _{0.6} Si _{1.4} [Nb(Si, Al) ₂]	Orthorhombic, the TiSi ₂ (C54) type	<i>Fddd</i>	8	0.8402	0.4901	0.8794	204, 205
Nb ₅ Al _x Si _{3-x} (<i>x</i> = 1.8–1.4) [Nb ₅ (Si, Al) ₃]	Tetragonal, the W ₅ Si ₃ (D8 _m) type	<i>I4/mcm</i>	4	1.016–1.021	—	0.508	204, 205
TaAl _x Si _{2-x} (<i>x</i> = 0–0.9) [Ta(Si, Al) ₂]	Hexagonal, the CrSi ₂ (C40) type	<i>P6₂22</i>	3	0.4773–0.4800	—	0.6558–0.6635	206
Cr ₄ Al ₁₃ Si ₄	Hexagonal, the Mn ₃ Al ₉ Si type	—	—	—	—	—	207
MoAl _{1.3} Si _{0.7}	Orthorhombic, the TiSi ₂ (C54) type	<i>Fddd</i>	8	0.8239	0.4783	0.8758	199
MoAl _x Si _{2-x} (<i>x</i> = 0.3–1.0) [Mo(Si, Al) ₂]	Hexagonal, the CrSi ₂ (C40) type	<i>P6₂22</i>	3	0.4618–0.4722	—	0.6563	208, 209
MoAlSi	—	—	—	0.4709	—	0.6556	210
Mo(Si, Al) ₂	Tetragonal, the α-MoSi ₂ (C11 _b) type, LSS ^a of Al in MoSi ₂	<i>I4/mmm</i>	2	0.3199	—	0.7847	209, 210
Mo ₃ Al–Mo ₃ Si	Cubic, the W ₃ O (A15) type, CSSS	<i>Pm3n</i>	2	—	—	—	210
Mo ₃ Al _{0.77} Si _{0.23} [Mo ₃ (Al, Si)]	Cubic, the W ₃ O (A15) type	<i>Pm3n</i>	2	0.4923	—	—	210
WAl _x Si _{2-x} (<i>x</i> = 0.6–1.4) [W(Al, Si) ₂]	Hexagonal, the CrSi ₂ (C40) type	<i>P6₂22</i>	3	0.4696–0.4741	—	0.6556–0.6615	206

Table 11 (continued).

Compound	Symmetry and type of structure	Space group	Z	Unit cell parameters / nm			Ref.
				a	b	c	
Mn ₃ Al ₂ Si ₄ (MnAl _{0.75} Si _{0.25})	Hexagonal, the CrSi ₂ (C40) type	P6 ₂ 22	3	0.4475	—	0.6427	201, 211
Mn ₃ Al ₄ Si ₂ (MnAl _{1.3} Si _{0.7})	Orthorhombic, the TiSi ₂ (C54) type	Fddd	8	0.7889	0.4570	0.8506	201, 211
β-Mn ₃ Al ₉ Si	Hexagonal	—	2	0.7513	—	0.7745	201, 211
Mn ₃ Al ₉ Si	"	C6/mmc	2	0.7519	0.7500	0.7768–0.7722	212
Mn ₃ AlSi ₅	—	—	—	—	—	—	201
α-Mn ₃ Al ₂ Si ₅	—	—	—	—	—	—	211
γ-Mn ₂ Al ₂ Si	—	—	—	—	—	—	211
δ-Mn(Si,Al) ₄	—	—	—	—	—	—	211
Fe ₂ Al ₉ Si ₂ (FeAl ₅ Si, m-AlFeSi)	Monoclinic	—	—	0.6122	0.6122	4.1484 ^b	213
Fe ₅ Al ₂₀ Si ₂ (Fe ₃ Al ₁₂ Si, c-AlFeSi)	Cubic ^c	—	—	1.2548	—	—	213
Fe ₅ Al ₂₀ Si ₂ (α-AlFeSi)	"	Im3	—	1.256	—	—	214
α-AlFeSi (Fe ₅ Al ₁₉ Si ₂)	Hexagonal	—	—	1.23	—	2.62	215
γ-AlFeSi (Fe ₁₈ Al ₆₀ Si ₂₂)	Monoclinic	—	—	1.78	1.0.25	0.89 ^d	215
Fe ₃ (Al,Si)	Cubic, the Fe ₃ Al type with ordering of aluminium and silicon	—	—	0.5685	—	—	216
FeAl ₄ Si ₂ (t-AlFeSi)	Tetragonal	—	—	0.6122	0.6122	0.9479	213
FeAl ₃ Si ₂ (FeAl _{2.7} Si _{2.3})	Orthorhombic, isostructural to PdGa ₅ , but is a superstructure	Pbcn	4	0.6011	—	0.9525	217
Co ₃ Al ₃ Si ₄	Cubic, the Ir ₃ Ge ₇ (D8 ₇) type	Im3m	4	0.8091	—	—	218
Co ₂ AlSi ₂	Hexagonal, the Ni ₂ Al ₃ (D5 ₁₃) type	P3m1	1	0.387–0.391	—	0.4750–0.4791	218
NiAl _{0.5} Si _{0.5}	Cubic, the FeSi (B20) type	P2 ₁ 3	4	0.4537	—	—	219
Ni ₃ (Al,Si) ₇	Cubic, the Ir ₃ Ge ₇ (D8 ₇) type	Im3m	4	0.8291	—	—	219

^a The following designations are used: CSSS is a continuous series of solid solutions; LSS is a limited solid solution. ^b In the unit cell $\alpha = 91^\circ$. ^c The unit cell of the aluminosilicide Fe₅Al₂₀Si₂ incorporates 138 atoms (100 aluminium atoms, 24 iron atoms and 14 silicon atoms). ^d In the unit cell $\alpha = 132^\circ$.

pseudotetragonal (orthorhombic) TiAl_{0.3–0.6}Si_{1.7–1.4} phase [Ti(Si,Al)₂] has a structure of the ZrSi₂ type and possesses a significant homogeneity region.

A titanium silicide containing ~45 at.% of silicon and dissolving considerable amounts of aluminium has also been found. This compound has been reported to be a solution of aluminium in Ti₅Si₄.²⁰¹ The same authors²⁰¹ also showed that the orthorhombic silicide TiSi [the FeB (B27) structural type, space group *Pnma*] dissolves up to 8 at.% of aluminium. One more unknown ternary compound has been detected near the Ti(Si,Al)₂ ternary phase;²⁰⁰ its composition has been determined as Ti₇Al₅Si₁₂.²⁰¹ This compound is stable at least up to 1173 K; with allowance for the data of Schob et al.,²⁰⁰ it is stable up to 1473 K.

The Zr–Al–Si system. The phase equilibria in the Zr–Al–Si system have been studied at 973 K²⁰¹ and at 1273–1473 K.^{200, 202} Two ternary phases exist in this system at 1473 K, namely, the orthorhombic Zr(Si,Al) phase and the tetragonal Zr(Al,Si)₃ phase. The ideal composition of the ternary tetragonal phase was determined²⁰¹ to be Zr₂Al₃Si. One more ternary compound

Zr₃Al₄Si₅ with a narrow homogeneity region was found in this system at 973 K.

Continued solid solutions are formed in this system over the Zr₂Al–Zr₂Si pseudobinary cross-section. It has been reported²⁰⁰ that the mutual solubility of the components over the Zr₅Al₃–Zr₅Si₃ cross-section is absent only in a narrow region near Zr₅Si₃; according to another study,²⁰¹ the mutual solubility is infinite. Limited solid solutions of silicon in ZrAl₃ (up to 5 at.%) and of aluminium in ZrSi₂ (up to 8 at.%²⁰⁰ or up to 24 at.%²⁰¹) are also formed in the Zr–Al–Si system.

At 973 K aluminium is highly soluble in the silicide ZrSi substituting both zirconium and silicon up to the composition Zr_{0.33}Al_{0.33}Si_{0.34}. The high-temperature modification of this solution has the CrB type of structure, whereas the low-temperature modification crystallises with the FeB type of structure.

The Hf–Al–Si system. The isothermal cross-section through the Hf–Al–Si system at 1473 K has been constructed.²⁰⁰ The ternary compound Hf(Si,Al) (HfAl_{0.35}Si_{0.65}) with the orthorhombic structure of the CrB type was found in this system. A continuous series of solid solutions is formed over the Hf₂Al–Hf₂Si pseudobinary cross-section. The Hf₅(Al,Si)₃

ternary phase with a structure of the Mn_5Si_3 ($D8_8$) type possesses an extended homogeneity region, although there are no compounds M_5X_3 with the Mn_5Si_3 type of structure in the $Hf-Al$ and $Hf-Si$ binary systems. Thus, in the presence of aluminium, there is no need for boron, carbon, or nitrogen admixtures to stabilise the $D8_8$ structural type. The silicide Hf_3Si_2 dissolves aluminium yielding a solid solution of the composition $Hf_3Al_{0.5}Si_{1.5}$. Limited solid solutions of silicon (up to 10 at.%) in $HfAl_3$ and of aluminium (up to 10 at.%) in $HfSi_2$ are also formed. The $Hf(Si,Al)$ ternary phase with a structure of the CrB type is in an equilibrium with $HfAl_3$ (the $ZrAl_3$ type) and with the silicides Hf_3Si_2 and $HfSi$.

The V-Al-Si system. No ternary compounds have been found in the $V-Al-Si$ system.^{203,204} Vanadium disilicide VSi_2 dissolves substantial amounts of aluminium, which substitutes silicon thus yielding a limited solid solution with the $CrSi_2$ ($C40$) type of structure. The composition of the solid solution with the highest aluminium content can be written as $V(Si_{0.67}Al_{0.33})_2$. The unit cell parameters of the solid solution increase with an increase in the content of aluminium.

The Nb-Al-Si system. There are two ternary phases in the $Nb-Al-Si$ system at 1673 K, namely, $Nb_5(Al,Si)_3$ with a tetragonal structure of the W_5Si_3 ($D8_m$) type and $Nb(Si,Al)_2$ with an orthorhombic structure of the $TiSi_2$ ($C54$) type.^{204,205} These phases are in equilibrium with each other and have homogeneity regions in which silicon is substituted by aluminium. The tetragonal silicide Nb_5Si_3 with the Cr_5B_3 ($D8_7$) type of structure dissolves up to 18 at.% of aluminium; further increase in the aluminium content leads to the transition from the $Nb_5(Si,Al)_3$ substitution solid solution with the Cr_5B_3 type of structure to the $Nb_5(Al,Si)_3$ ternary phase with the W_5Si_3 structure. A substitution solid solution containing up to 10 at.% of aluminium is also formed based on the silicide $NbSi_2$ with the $CrSi_2$ ($C40$) structure. The aluminide Nb_3Al [the W_3O ($A15$) structural type, space group $Pm\bar{3}n$] dissolves up to 7 at.% of silicon thus yielding a substitution solid solution. The ternary σ -phase containing up to 2 at.% of silicon may be regarded as a solid solution of silicon in niobium aluminide in the region between Nb_2Al and Nb_3Al .

The Ta-Al-Si system. The isothermal cross-section through the $Ta-Al-Si$ system at 1673 K has been constructed.²⁰⁶ No ternary compounds were found in this system. On the basis of tantalum silicides, limited solid solutions are formed in which silicon is substituted by aluminium: Ta_2Si dissolves 9 at.% of Al; Ta_5Si_3 with the W_5Si_3 structure dissolves up to 20 at.% of Al (as a consequence, the unit cell parameters of Ta_5Si_3 increase somewhat); and $TaSi_2$ with a structure of the $CrSi_2$ ($C40$) type dissolves more than 20 at.% of aluminium. A solid solution with a low silicon content (up to 2 at.%) is formed on the basis of the σ -phase having the homogeneity region from Ta_2Al to Ta_3Al .

The Cr-Al-Si system. The phase equilibria in the $Cr-Al-Si$ system have been studied at 1573 K.²⁰⁴ There are no ternary compounds in this system, but the silicides Cr_3Si [the W_3O ($A15$) structural type], Cr_5Si_3 [the W_5Si_3 ($D8_m$) structural type], and $CrSi_2$ dissolve 12, 7, and 22 at.% of aluminium, respectively. The solid solutions resulting from the substitution of silicon by aluminium retain the crystal structures of the chromium silicides. The extended solid solution of aluminium in chromium also dissolves up to 4 at.% of Si. It has been reported²⁰⁷ that the ternary cubic compound $Cr_4Al_3Si_4$ having a homogeneity region is formed from the $Cr-Al-Si$ melt (see Table 11). This compound is stable at temperatures below 870 K, and at 870 K it melts incongruently.

The Mo-Al-Si system. The phase equilibria and the ternary phases existing in the $Mo-Al-Si$ system have been studied by a number of authors.^{199,204,208-210} Two ternary compounds were found: $Mo(Si,Al)_2$ with the hexagonal structure of the $CrSi_2$ ($C40$) type, having a broad homogeneity region from $MoAl_{0.3}Si_{1.7}$ to $MoAlSi$, and $Mo(Si,Al)_2$ with a rhombic structure of the $TiSi_2$ ($C54$) type and a narrow homogeneity region (see Table 11). A continuous series of cubic solid solutions with the $A15$ type of

structure are formed over the Mo_3Al-Mo_3Si pseudobinary cross-section. The silicide Mo_5Si_3 dissolves up to 12 at.% of aluminium, which substitutes silicon. The limited solid solution of aluminium in Mo_5Si_3 with the highest content of aluminium (Mo_5Si_2Al) exists in equilibrium with a solid solution of the composition $Mo_3Al_{0.77}Si_{0.23}$ from the Mo_3Al-Mo_3Si continuous series of solid solutions.

The W-Al-Si system. The isothermal cross-section through the $W-Al-Si$ system at 1773 K has been reported.²⁰⁶ The tetragonal silicides W_5Si_3 and WSi_2 dissolve 4 at.% and 15 at.% of aluminium, respectively, thus forming the $W_5(Si,Al)_3$ and $W(Si,Al)_2$ limited solid solutions; a limited solid solution of aluminium and silicon in tungsten also exists in the $W-Al-Si$ system. In addition, there exists the $W(Al,Si)_2$ hexagonal ternary phase with the $CrSi_2$ ($C40$) structure. It possesses a broad homogeneity region from $WAl_{0.6}Si_{1.4}$ to $WAl_{1.4}Si_{0.6}$, the unit cell parameters increasing as the content of silicon decreases (see Table 11). The $W(Al,Si)_2$ hexagonal ternary phase is in equilibrium with aluminium and silicon, with the $W_5(Si,Al)_3$ and $W(Si,Al)_2$ limited tetragonal solid solutions [the α - $MoSi_2$ ($C11_b$) structural type], and also with WAl_2 and with tungsten [more precisely, with the limited solid solution of aluminium (~ 2 at.%) and silicon (~ 8 at.%) in tungsten].

The Mn-Al-Si system. Six ternary phases exist in this system at 1073 K,²¹¹ namely, γ - Mn_2Al_2Si , $MnAl_{1.3}Si_{0.7}$ (near γ - Mn_2Al_2Si), $MnAl_{0.75}Si_{1.25}$ ($Mn_3Al_2Si_4$) with the $CrSi_2$ ($C40$) type of structure, α - $Mn_3Al_{21}Si_5$, δ - $Mn(Si,Al)_4$, and Mn_3Al_9Si with a hexagonal structure (see Table 11). The Mn_3Al_9Si ternary phase results from the dissolution of silicon in Mn_3Al_{10} and is apparently an ordered solid solution of silicon in this compound [silicon atoms replace only those aluminium atoms, which occupy the $2(a)$ sites]. It has been shown²¹¹ that $MnSi$ dissolves up to 3 at.% of aluminium; however, in another study,²⁰¹ the solubility of aluminium in $MnSi$ has been found to reach 20 at.%. The silicide Mn_3Al_9Si exists in an equilibrium with γ - Mn_2Al_2Si , $Mn_3Al_2Si_4$, and δ - $Mn(Si,Al)_4$. The $Mn_3Al_2Si_4$ ternary phase forms pseudobinary equilibria with γ - Mn_2Al_2Si and δ - $Mn(Si,Al)_4$, whereas δ - $Mn(Si,Al)_4$ is in an equilibrium with α - $Mn_3Al_{21}Si_5$.

The Fe-Al-Si system. The $Fe-Al-Si$ system has been studied repeatedly. The superstructure $Fe_3(Al,Si)$ has been discovered in the homogeneity region of the solid solution of aluminium and silicon in iron.²¹⁶ The solid solution of iron and silicon in aluminium is in equilibrium with two ternary phases: $Fe_5Al_{20}Si_2$ (which has also been written as $Fe_5Al_{19}Si_2$, $Fe_3Al_{12}Si$, and α - $AlFeSi$) with a cubic^{213,214} or hexagonal²¹⁵ structure and the monoclinic²¹³ $Fe_2Al_9Si_2$. Other ternary phases are also known (see Table 11).

The compounds $FeAl_4Si_2$ and $FeAl_3Si_2$ ought to be identical, in view of the similarity of their unit cell dimensions. However, it has been found²¹⁷ that the lattice of $FeAl_3Si_2$ is a superstructure with respect to the tetragonal disordered phase of the same composition isostructural to $PdGa_5$.

The great number of ternary compounds with similar compositions and close unit cell dimensions indicates that the majority of the ternary phases in the $Fe-Al-Si$ system possess homogeneity regions. It is of interest that most of the ternary phases contain from 14 at.% to 25 at.% of iron.

The Co-Al-Si system. Two ternary phases have been found in this system:²¹⁸ $Co_3Al_3Si_4$ with a cubic structure of the Ir_3Ge_7 ($D8_7$) type and Co_2AlSi_2 with a hexagonal structure (see Table 11). In all probability, the Co_2AlSi_2 ternary phase exists in equilibrium with $CoSi$ and $Co_3Al_3Si_4$. Judging by the substantial alteration of unit cell parameters, Co_2AlSi_2 possesses a noticeable homogeneity region. The cobalt atoms in the $Co_3Al_3Si_4$ cubic ternary phase occupy the $12(e)$ sites, while the aluminium and silicon atoms are likely to be statistically distributed among the $12(d)$ and $16(f)$ sites; the predominant location of the aluminium atoms at the $12(d)$ sites, with the silicon atoms filling predominantly the $16(f)$ sites, should lead to a superstructure based on the Ir_3Ge_7 structural type.

The Ni–Al–Si system. Three ternary phases exist in this system at 1000 K:^{219, 220} Ni_4AlSi (there is no information concerning its structure), $\text{NiAl}_{0.5}\text{Si}_{0.5}$, and $\text{Ni}_3(\text{Al},\text{Si})_7$ with a high content of aluminium (see Table 11). The $\text{NiAl}_{0.5}\text{Si}_{0.5}$ ternary phase is in equilibrium with all the nickel silicides, with the aluminide NiAl , and with the $\text{Ni}_3(\text{Al},\text{Si})_7$ and Ni_4AlSi ternary phases; Ni_4AlSi is in equilibrium with the aluminides NiAl and Ni_3Al and with the silicide Ni_3Si , and $\text{Ni}_3(\text{Al},\text{Si})_7$ coexists with silicon, aluminium, NiAl_3 , Ni_2Al_3 , and NiSi_2 . At temperatures above 1370 K all the alloys in the Ni–Al–Si system containing less than 50 at. % of Ni are in the molten state.

VI. Phase equilibria in $X-X'-X''$ ternary systems ($X, X', X'' = \text{B, C, N, Si, Al}$)

The overwhelming majority of the currently existing oxygen-free ceramic materials are multicomponent systems and, apart from metals, they contain such elements as B, C, N, Si, or Al. Therefore, for understanding the equilibria in complex multicomponent systems, it is important to know what compounds and phase equilibria exist in simpler ternary systems formed by boron, carbon, nitrogen, silicon, and aluminium. The $X-X'-X''$ ternary systems ($X, X', X'' = \text{B, C, N, Si, Al}$) are constituents of $M-X-X'-X''$ four-component systems containing transition metals M . The $X-X'-X''$ ternary systems have not been adequately studied so far, and phase diagrams have not been constructed for all of them. The crystal-chemical characteristics of the ternary compounds found in these systems are listed in Table 12.

The Si–B–C system. The phase equilibria in the Si–B–C system have been studied at temperatures of 1973 K and 2173 K.²²⁹ At these temperatures, the silicon carbide SiC exists in an equilibrium with the silicon melt, with the boride SiB_6 , and with the carbides B_4C and B_{13}C_2 ; and the boron carbides coexist with SiB_6 and SiB_{12+x} (Fig. 37a). The $\text{SiC}-\text{B}_4\text{C}$ pseudobinary cross-section is an eutectic system. The composition of the eutectics is close to SiB_5C_2 and its melting point is ~ 2530 K. These data are in good agreement with the results obtained by Dokukina et al.²³⁰ As the temperature increases to 2273 K, the $\text{SiC}-\text{SiB}_6$ equilibrium disappears, and the carbide B_{13}C_2 coexists with the silicon and boron melt (Fig. 37b).

The authors of a number of studies^{51, 229, 230} of the Si–B–C system have not found the ternary compounds SiB_5C_2 and $\text{Si}_2\text{B}_3\text{C}_2$, which have been reported by Portnoi et al.²³¹

The Si–C–N system. The phase equilibria in the Si–C–N system have been studied at 1900 K and 2000 K at a nitrogen pressure of 1×10^5 Pa.^{232, 233} At 1900 K the silicon nitride Si_3N_4 exists in equilibrium with the silicon carbide SiC , cyanogen C_2N_2 , and carbon (Fig. 37c). As the temperature increases, the nitride Si_3N_4 reacts with carbon yielding the carbide SiC ; therefore, the $\text{SiC}-\text{C}_2\text{N}_2$ equilibrium arises instead of $\text{Si}_3\text{N}_4-\text{C}$ (Fig. 37d). The carbide $\beta\text{-SiC}$ forms the nitride Si_3N_4 on heating in nitrogen [$T = 2273$ K, $p_{\text{N}_2} = (1-30) \times 10^5$ Pa].²³²

The possible phase equilibria involving the carbon nitride $\beta\text{-C}_3\text{N}_4$ are shown by the dashed lines in the isothermal cross-sections through the Si–C–N system (Fig. 37c,d). This compound, the existence of which had been predicted,^{26-28, 234} has been recently discovered experimentally.²⁰

Data concerning the existence of the ternary compounds $\text{Si}_2\text{C}_2\text{N}$ and $\text{Si}_3\text{C}_3\text{N}$ have found no support. A number of researchers, who have studied this system, have not found any silicon carbonitrides.^{232, 233, 235}

The Al–Si–C system. Several ternary compounds have been found in this system (see Table 12). However, these data are very contradictory. For example, the existence of two modifications α - and $\beta\text{-Al}_4\text{SiC}_4$ has been reported.²³⁶ Later the existence of $\alpha\text{-Al}_4\text{SiC}_4$ has been confirmed;^{225, 228, 237} however, the β -modification was not found. The ternary compound $\text{Al}_4\text{Si}_2\text{C}_5$ has been reported by Inoue et al.,^{225, 226} however, it was not detected in another study.²²⁸ The hexagonal carborosilicide Al_8SiC_7 has been observed.^{227, 228} The aluminium carborosilicides Al_4SiC_4 and Al_8SiC_7 were found to decompose incongruently at 2353 and at 2358 K, respectively.²²⁸ Both ternary compounds are formed with great difficulty at relatively low temperatures (below 1800 K).

The isothermal cross-sections through the Al–Si–C system at 900 and 2273 K are presented in Fig. 37e,f. At 900 K (below the melting point of aluminium), silicon carbide exists in equilibrium with Al_4SiC_4 and Al, Al_4C_3 coexists with Al_8SiC_7 , and the ternary compounds are in equilibrium with each other, and also with carbon and aluminium (see Fig. 37e). When the liquid phase appears, silicon carbide and aluminium carborosilicides coexist with the aluminium melt (Fig. 37f).

Table 12. Some ternary compounds in the Al–B–C, Al–C–N, and Al–Si–C systems.

Compound	Symmetry and type of structure	Space group	Z	Unit cell parameters / nm			Ref.
				a	b	c	
$\text{Al}_3\text{B}_{48}\text{C}_2$	Orthorhombic	<i>Cmma</i>	2	1.234	1.263	0.508	28
$\text{Al}_3\text{B}_{48}\text{C}_2$	"	<i>Ammm</i>	2	0.617	1.263	1.016	28
$\text{Al}_3\text{B}_{48}\text{C}_2$	Tetragonal, high-temperature	<i>P4/mmm</i>	1	0.882	—	0.509	28
$\text{AlB}_{24}\text{C}_4$	Orthorhombic	<i>Bbmm</i>	2	0.888	0.910	0.569	221
$\text{Al}_{2.1}\text{B}_{51}\text{C}_8$	"	<i>Cmcm</i>	2	0.5690	0.8881	0.9100	222
$\text{AlB}_{40}\text{C}_4$	Hexagonal	<i>R3m</i>	1	0.5642	—	1.2367	223
$\text{Al}_8\text{B}_4\text{C}_7$	"	<i>P6_3cm</i>	3	0.5906	—	1.5901	224
$\text{Al}_5\text{C}_3\text{N}$	Hexagonal	<i>P6_3mc</i>	2	0.3281	—	2.167	25
$\text{Al}_6\text{C}_3\text{N}_2$	Trigonal	<i>R3m</i>	3	0.3248	—	4.003	25
$\text{Al}_7\text{C}_3\text{N}_3$	Hexagonal	<i>P6_3mc</i>	2	0.3226	—	3.170	25
$\text{Al}_8\text{C}_3\text{N}_4$	Trigonal	<i>R3m</i>	3	0.3211	—	5.508	25
$\text{Al}_9\text{C}_3\text{N}_5^a$	Hexagonal	<i>P6_3mc</i>	2	0.3197	—	4.169	25
$\text{Al}_{10}\text{C}_3\text{N}_6^a$	Trigonal	<i>R3m</i>	3	0.3186	—	7.000	25
$\alpha\text{-Al}_4\text{SiC}_4$	Hexagonal	<i>P6_3mc</i>	2	0.3277	—	2.1676	225
$\text{Al}_4\text{Si}_2\text{C}_5$	"	<i>R3m</i>	3	0.3251	—	4.0108	225, 226
Al_8SiC_7	"	—	1	0.3313	—	1.9242	227, 228

^a The carbonitrides $\text{Al}_9\text{C}_3\text{N}_5$ and $\text{Al}_{10}\text{C}_3\text{N}_6$ have not been observed experimentally, their hypothetical structural characteristics have been reported.²⁵

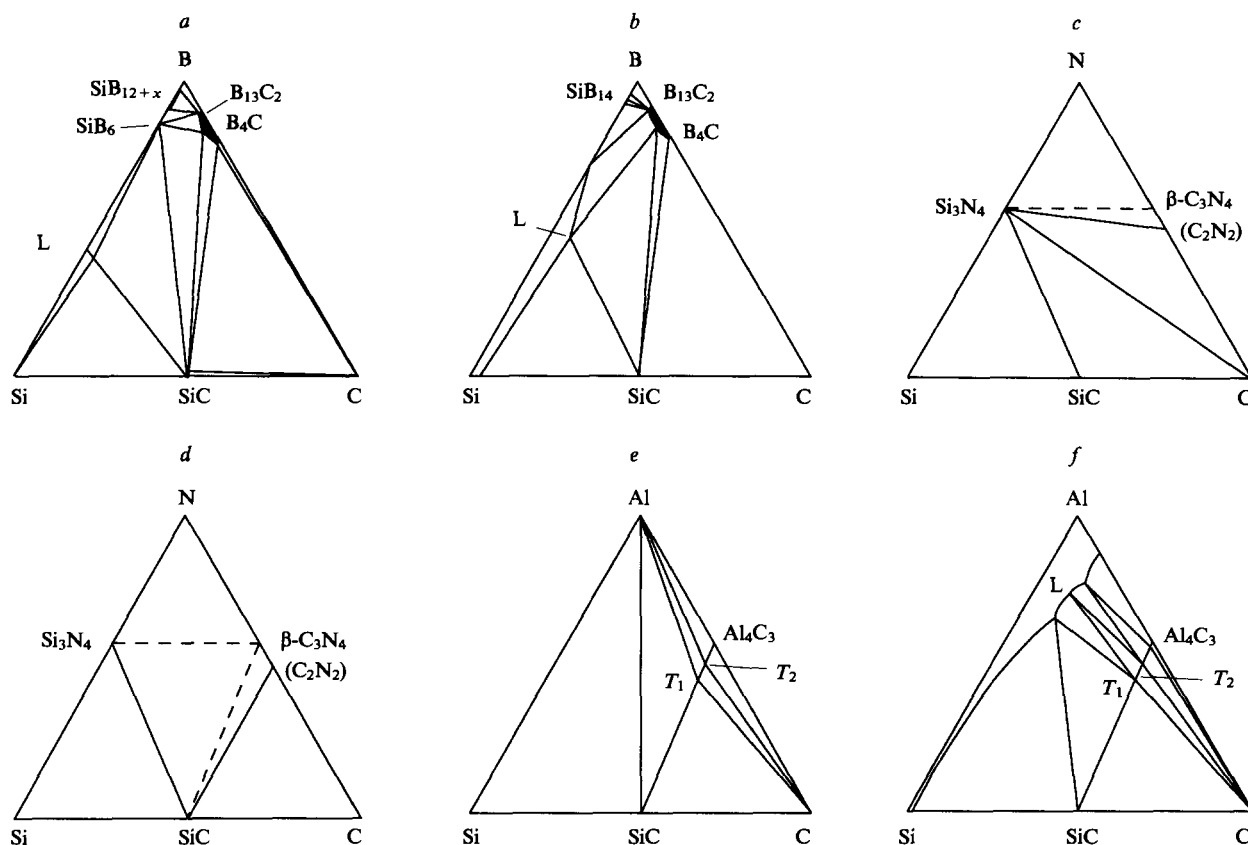


Figure 37. Isothermal cross-sections of ternary systems of silicon with boron, carbon, nitrogen, and aluminium (dark areas denote single-phase homogeneity regions). (a) the Si–B–C system at 1973 K; (b) the Si–B–C system at 2273 K; (c) the Si–C–N system at 1900 K;

$p_{N_2} = 1 \times 10^5$ Pa; (d) the Si–C–N system at 2000 K, $p_{N_2} = 1 \times 10^5$ Pa; (e) the Al–Si–C system at 900 K; (f) the Al–Si–C system at 2273 K; $T_1 = Al_4SiC_4$, $T_2 = Al_8SiC_7$.

The Si–B–N system. The silicon nitride Si_3N_4 in the Si–B–N system at temperatures below 1700 K coexists with the boron nitride BN and the boride SiB_6 ; the BN– SiB_{12+x} (SiB_{14}) pseudobinary equilibrium also exists (Fig. 38a).

The Al–Si–N system. The isothermal cross-section through the Al–Si–N system at 873 K is presented in Fig. 38b.²³⁸ The aluminium nitride AlN exists in equilibrium with Si and Si_3N_4 ; however, the Si_3N_4 –Al metastable equilibrium should also be taken into account. Its existence is caused by the following: the interaction of Si_3N_4 with aluminium leads to the appearance on the surface of aluminium grains of an AlN film, which acts as a diffusion barrier and prevents further occurrence of the reaction

even during prolonged annealing. No ternary compounds have been found in the Al–Si–N system.

The Al–B–C system. Several aluminium borocarbides have been found in this system (see Table 12). In all probability, the ternary compound $Al_8B_4C_7$ exists in equilibrium with the carbide Al_4C_3 and also with aluminium and carbon. The $AlB_{24}C_4$ phase observed by Will,²²¹ has the composition $Al_{2.1}B_{51}C_8$, according to Perotta et al.²²² The $Al_3B_{48}C_2$ phase exists at high temperatures as a tetragonal modification, which decomposes to two related orthorhombic phases of the same composition at $T < 800$ K (see Table 12).

The Al–C–N system. The carbide Al_4C_3 and the aluminium nitride AlN in the Al–C–N system form several ternary compounds, namely, aluminium carbonitrides $(Al_4C_3)(AlN)_n$, where $n = 1-4$ (see Table 12). The structures of aluminium carbonitrides have been studied.²⁵ The aluminium atoms in these ternary compounds form close-packed planes, the carbon and nitrogen atoms being arranged between these planes (the carbon atoms occupy the tetrahedral or octahedral interstices, while the nitrogen atoms populate only tetrahedral interstices). Thus, the Al_2C_2 , Al_2C , and AlN layers can be distinguished in the structure of aluminium carbonitrides. It has been suggested²⁵ that two other ternary compounds $Al_9C_3N_5$ and $Al_{10}C_3N_6$ also exist (see Table 12).

Aluminium carbonitrides are in equilibrium with aluminium and carbon as well as with the carbonitrides closest to them; Al_5C_3N is also in equilibrium with Al_4C_3 , and $Al_8C_3N_4$ coexists with AlN.

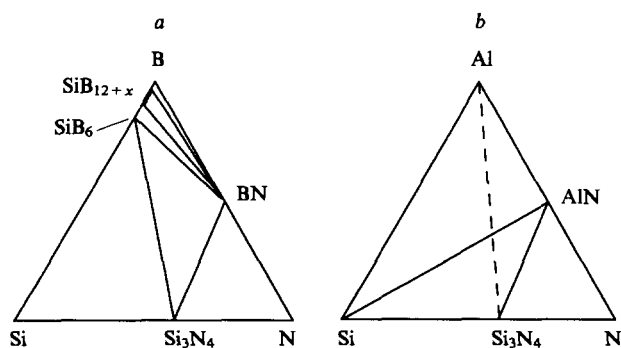


Figure 38. Isothermal cross-sections through the Si–B–N system (a) at 1700 K (the dark area denotes the single-phase homogeneity region of SiB_{12+x}) and through the Al–Si–N system at 873 K (b) (the dashed line marks a metastable equilibrium).

VII. Conclusion

The thermodynamic state of a multicomponent system containing several phases is described by a set of equations of state $\varphi(c, p, T)$ characterising each of the phases. The numerical values of the c , p , and T parameters unambiguously determine the state of the system, which is represented graphically as a point in the three-dimensional c , p , T system of coordinates. If two of these parameters are known, the third one can be found from the equation of state. This means that to determine the state of the system, it is sufficient to find the position of the figurative point in a two-dimensional system of coordinates, usually in the c, T -coordinates. This graphical representation of the equation of state of a system is its state diagram.

The real equations of state of multicomponent systems are unknown; therefore, the state diagrams are of great importance. By virtue of these diagrams, the actual relationship between the physical and chemical parameters determining the state of the system can be clearly represented on the basis of experimental data. Each characteristic of the system varies continuously as a function of one or several parameters within the limits of a particular phase region. The boundaries of phase regions are represented by singular points (inflection, break, or discontinuity points, cusps, etc.). Hence it is obvious, how important it is to know the positions of phase boundaries, which are the main information provided by state diagrams.

The problem of constructing state diagrams has been solved at present to a very small extent. In particular, no more than 5% of the state diagrams of ternary systems are known. In the present review, the author has attempted to generalise and to make available the results of experimental studies of the phase equilibria in the $M-X-X'$ and $M-Al-X$ ternary oxygen-free systems (M is a transition metal, X, X' are B, C, N, Si), which provide a basis for the development of new ceramic materials.

The greatest contribution to the systematic studies of phase diagrams of the ternary systems considered was made by scientists of the Austrian school: H Nowotny, W Jeitschko, F Benesovsky, E Rudy, P Rogl, J Schuster, and their colleagues.

It follows from the analysis performed that the interaction of a transition metal with the two other components of a $M-X-X'$ or $M-Al-X$ ternary system is often accompanied by the formation

of one or several ternary phases. This leads to a substantial complication of the phase equilibria, to the appearance of a large number of phase boundaries, and to the splitting of the state diagram into many phase fields. The allowance for these data will permit researchers to carry out the target-directed synthesis of compounds and heterogeneous compositions with specified properties.

The analysis of the crystal structures of the ternary compounds formed in the $M-X-X'$ or $M-Al-X$ systems considered has shown that an ideal or a distorted octahedron built of six transition metal atoms M is the main structural unit of the majority of these compounds. The octahedral interstice can be either occupied by an interstitial nonmetal atom X (B, C, N) or vacant. The possibility of the complete or partial population of the octahedral interstices causes the existence of the homogeneity regions (fairly broad or narrow) for many ternary compounds. Those of the considered ternary compounds, which incorporate the XM_6 octahedral units and possess homogeneity regions, constitute an extensive group of ternary nonstoichiometric interstitial compounds, which are related to the binary nonstoichiometric interstitial compounds MX_y and M_2X_y ($X = C, N$) with structures of the NaCl ($B1$) and W_2C ($L'3$) types. The ternary nonstoichiometric interstitial compounds have looser structures than the binary compounds, due to the presence of the third element, i.e. the V/n volume, which corresponds to one atom in the ternary compounds, is greater than in the binary compounds (V is the unit cell volume and n is the number of atoms in the unit cell).

In this connection, it is of interest to compare various carbide and nitride phases of the same transition metal differing in the X/M ratio of the atomic concentrations of the interstitial element and the metal. The titanium compounds, namely, the cubic Ti_3AlC and Ti_3AlN with the perovskite type of structure; the hexagonal Ti_2AlC and Ti_2AlN with a structure of the Cr_2AlC type; the hexagonal carbosilicide Ti_3SiC_2 and the trigonal aluminonitride $Ti_3Al_2N_2$; the cubic carbide $TiC_{1.0}$ and the cubic nitride $TiN_{1.0}$ with the NaCl ($B1$) type of structure (Table 13) can be considered as typical examples. Each pair of these compounds (except for Ti_3SiC_2 and $Ti_3Al_2N_2$) have the same structure. The structure of $Ti_3Al_2N_2$ differs from that of Ti_3SiC_2 in that in the former case, the double-stranded layers of the XTi_6 octahedra are separated by two layers of nontransition metal

Table 13. Interatomic distances in carbide and nitride phases of titanium with different degrees of filling of the titanium sublattice with interstitial atoms.

Stoichiometric composition	Symmetry and type of structure, space group	Unit cell parameters / nm		Interatomic distances / nm			V / nm^3	$V n^{-1} / \text{nm}^3$ (see ^a)
		a	c	Ti-C	Ti-Ti	Ti-N		
Ti_3AlC	Cubic, perovskite $CaTiO_3$ type, space group $Pm\bar{3}m$	0.4156	—	0.208	0.294	—	0.0718	0.0144
Ti_2AlC	Hexagonal H -phase, the Cr_2AlC type, space group $P6_3/mmc$	0.304	1.360	0.212	0.292	—	0.1088	0.0136
Ti_3SiC_2	Hexagonal, space group $P6_3/mmc$	0.3068	1.7669	0.215	0.297	—	0.1440	0.0120
$TiC_{1.0}$	Cubic, the NaCl ($B1$), type, space group $Fm\bar{3}m$	0.4328	—	0.216	0.306	—	0.0811	0.0101
Ti_3AlN	Cubic, the perovskite $CaTiO_3$ type ($E2_1$), space group $Pm\bar{3}m$	0.4120	—	—	0.291	0.206	0.0699	0.0140
Ti_2AlN	Hexagonal H -phase, the Cr_2AlC type, space group $P6_3/mmc$	0.2991	1.3621	—	0.290	0.208	0.1055	0.0132
$Ti_3Al_2N_2$	Trigonal, space group $P31c$	0.2988	2.3350	—	0.297	0.209	0.1805	0.0129
$TiN_{1.0}$	Cubic, the NaCl ($B1$), type, space group $Fm\bar{3}m$	0.4244	—	—	0.300	0.213	0.0764	0.0096

^a V is the unit cell volume, n is the number of atoms in the unit cell.

atoms, whereas in Ti_3SiC_2 , they are separated by one layer of nontransition element atoms.

A general feature of the structures of all these compounds is that the interstitial atoms (carbon or nitrogen) are located at the octahedral interstices formed by six transition metal atoms. In the compounds with an ideal stoichiometric composition, all the octahedral vacancies are filled with the interstitial atoms. The structures of the compounds under consideration differ in the manner in which the XM_6 octahedra are linked to one another. In the compounds $\text{M}_3\text{M}'\text{X}$ the octahedra are joined via all their six vertices (see Fig. 23); in the $\text{M}_2\text{M}'\text{X}$ *H*-phases, each octahedron is linked to the adjacent octahedra via six edges thus forming an octahedral layer of the composition M_2X (see Fig. 24); in the next pair of compounds, namely, Ti_3SiC_2 and $\text{Ti}_3\text{Al}_2\text{N}_2$, the XM_6 octahedra are joined with one another via nine edges thus forming a double octahedral layer of the composition M_3X_2 (see Fig. 14); finally, the XM_6 octahedra in the cubic carbides and nitrides $\text{MX}_{1.0}$ are joined via all their twelve edges and form the closest packing (see Fig. 1).

In the sequence $\text{M}_3\text{M}'\text{X} \rightarrow \text{M}_2\text{M}'\text{X} \rightarrow \text{M}_3\text{M}'\text{X}_2$ ($\text{M}_3\text{M}'_2\text{X}_2$) $\rightarrow \text{MX}$ the X/M ratio increases in the following way: $\frac{1}{3} \rightarrow \frac{1}{2} \rightarrow \frac{2}{3} \rightarrow 1$, which indicates an increase of the degree of filling of the transition metal sublattice with the interstitial atoms. For the cubic carbides and nitrides MX_y , the increase in the degree of filling of the octahedral vacancies of the metallic sublattice (i.e. the increase in the content of interstitial atoms) is accompanied by an increase in the period of the crystal lattice and by an increase in the interatomic distances. By analogy with the cubic carbides and nitrides MX_y , one may expect a similar variation of the interatomic distances and a similar decrease in the V/n volume corresponding to one atom in the sequence $\text{M}_3\text{M}'\text{X} \rightarrow \text{M}_2\text{M}'\text{X} \rightarrow \text{M}_3\text{M}'_2\text{X}_2$ ($\text{M}_3\text{M}'_2\text{X}_2$) $\rightarrow \text{MX}$.

Table 13 presents the Ti–X and Ti–Ti interatomic distances and the V/n volume for the binary and ternary titanium compounds considered as examples. With an increase in the X/M ratio the Ti–C interatomic distances in the series of carbide phases and the Ti–N distances in the series of nitride phases increase monotonically, whereas the V/n volume decreases. A similar increase is observed for the Ti–Ti interatomic distances, except for those in the *H*-phases.

Thus, the majority of the compounds of transition metals with B, C, N, Si, and Al retain the octahedral fragment consisting of six transition metal atoms M as the main structural unit; this fragment is either vacant or filled with interstitial nonmetal atoms. The atoms of the third element make the structure of the ternary compound more complex and more loose than the structure of the corresponding binary compound of the transition metal.

The ternary compounds with the homogeneity regions discussed in this review can exist in two structural states, namely, the disordered and the ordered state. In the former case, the interstitial atoms are randomly distributed among the octahedral interstices, and in the latter case, they are regularly distributed. The ordering phenomenon in the binary nonstoichiometric interstitial compounds has been studied fairly extensively^{1,2,6,239,240} however, ordering in the ternary nonstoichiometric compounds and its influence on the properties of these compounds are scarcely known. It may be expected that the investigation of the ordering effects will become one of the major directions in the research on ternary nonstoichiometric compounds of transition metals with boron, carbon, nitrogen, silicon, and aluminium.

The work was supported by the Russian Foundation for Basic Research (project 95-02-03549a) and the State scientific and technical programme 'New materials' (project 07.02.0103m).

References

1. A I Gusev, A A Rempel' *Strukturnye Fazovye Perekhody v Nestekhiometricheskikh Soedineniyakh* (Structural Phase Transitions in Nonstoichiometric Compounds) (Moscow: Nauka, 1988)
2. A I Gusev *Fizicheskaya Khimiya Nestekhiometricheskikh Tugoplavkikh Soedinenii* (Physical Chemistry of Nonstoichiometric High-Melting Compounds) (Moscow: Nauka, 1991)
3. A I Gusev, S I Alyamovskii, Yu G Zainulin, G P Shveikin *Usp. Khim.* **55** 2067 (1986) [*Russ. Chem. Rev.* **55** 1175 (1986)]
4. A I Gusev *Usp. Khim.* **57** 1595 (1988) [*Russ. Chem. Rev.* **57** 913 (1988)]
5. A I Gusev *Phys. Status Solidi, B* **156** 11 (1989)
6. A I Gusev *Phys. Status Solidi, B* **163** 17 (1991)
7. V I Matkovich (Ed.) *Boron and Refractory Borides* (Berlin: Springer, 1977)
8. H J Goldschmidt *Interstitial Alloys* (London: Butterworth, 1967) (Translated into Russian; Moscow: Mir, 1971)
9. W B Pearson *The Crystal Chemistry and Physics of Metals and Alloys* (New York: Wiley, 1972)
10. A Kirfel, A Gupta, G Will *Acta Crystallogr., Sect. B, Struct. Crystallogr.* **35** 1052 (1979)
11. R S Pease *Acta Crystallogr.* **5** 356 (1952)
12. R H Wentorf *J. Chem. Phys.* **26** 956 (1957)
13. V A Kurdyumov, A N Pilyankevich *Fazovye Prevrashcheniya v Uglerode i Nitride Bora* (Phase Transformations in Carbon and in Boron Nitride) (Kiev: Naukova Dumka, 1979)
14. R F Adamsky *Acta Crystallogr.* **11** 744 (1958)
15. R F Giese, J J Economy, V I Matkovich *Z. Kristallogr.* **122** 144 (1965)
16. E J Felten *J. Am. Ceram. Soc.* **78** 5977 (1956)
17. V I Matkovich, R F Giese, J J Economy *Z. Kristallogr.* **122** 116 (1965)
18. I Higashi, T Sakurai, T Atoda *J. Solid State Chem.* **20** 67 (1977)
19. I Higashi *J. Solid State Chem.* **47** 333 (1983)
20. K M Yu, M L Cohen, E E Haller, W L Hansen, A Y Liu, I C Wu *Phys. Rev. B* **49** 5034 (1994)
21. P T B Schaffer *Acta Crystallogr., Sect. B, Struct. Crystallogr.* **25** 477 (1969)
22. G A Jeffrey, V Y Wu *Acta Crystallogr.* **16** 559 (1963)
23. A J Moulson *J. Mater. Sci.* **14** 1017 (1979)
24. G A Slack *J. Phys. Chem. Solids* **34** 321 (1973)
25. V I Matkovich, R F Giese, J J Economy *Z. Kristallogr.* **122** 108 (1965)
26. A Y Liu, M L Cohen *Science* **245** 841 (1989)
27. A Y Liu, M L Cohen *Phys. Rev. B* **41** 10727 (1990)
28. M L Cohen *Phys. Rev. B* **32** 7988 (1985)
29. H Holleck *Binäre und Ternäre Carbide- und Nitridsysteme der Übergangsmetalle* (Berlin: Gebrüder Borntraeger, 1984) (Translated into Russian; Chelyabinsk: Metallurgiya, 1988)
30. R A Andrievskii, I I Spivak *Prochnost' Tugoplavkikh Soedinenii i Materialov na Ikh Osnove* (The Strength of High-Melting Compounds and of Materials Based on Them) (Chelyabinsk: Metallurgiya, 1989)
31. Yu B Kuz'ma, N F Chaban *Dvoynye i Troynye Sistemy. Soderzhashchie Bor* (Binary and Ternary Boron-containing Systems) (Moscow: Metallurgiya, 1990)
32. J Bauer *J. Less-Common Met.* **87** 45 (1982)
33. G S Smith, Q Johnson, P C Nordine *Acta Crystallogr.* **19** 668 (1965)
34. J Bauer, H Nowotny *Monatsh. Chem.* **102** 1129 (1971)
35. J Bauer, J Debuigne *J. Inorg. Nucl. Chem.* **37** 2473 (1975)
36. N A Fishel, H A Eick *J. Inorg. Nucl. Chem.* **31** 891 (1969)
37. J Bauer, O Bars *Acta Crystallogr., Sect. B, Struct. Crystallogr.* **36** 1540 (1980)
38. L Ya Markovskii, N V Vekshina, G F Pron' *Zh. Prikl. Khim.* **35** 2090 (1962)
39. J Bauer, O Bars *J. Less-Common Met.* **83** 17 (1982)
40. R W Johnson, A H Daane *J. Phys. Chem.* **65** 909 (1961)
41. P K Smith, P W Gilles *J. Inorg. Nucl. Chem.* **29** 375 (1967)
42. J Bauer, C Politis *J. Less-Common Met.* **88** L1 (1982)
43. J Bauer, J Debuigne *C. R. Hebd. Seances. Acad. Sci., Ser. C, Sci. Chim.* **274** 1271 (1972)
44. J Bauer, P Vennegues, J L Vergneau *J. Less-Common Met.* **110** 295 (1985)
45. E T Bezruk, L Ya Markovskii *Zh. Prikl. Khim.* **45** 3 (1972)
46. L Ya Markovskii, N V Vekshina, Yu D Kondrashev *Zh. Prikl. Khim.* **45** 1183 (1972)
47. L Brewer, H Haraldsen *J. Electrochem. Soc.* **102** 399 (1955)
48. H Nowotny, F Benesovsky, C Brukl, O Schob *Monatsh. Chem.* **92** 403 (1961)

49. E Rudy *Compendium of Phase Diagram Data. Final Report AFML TR-65-2 Part V* (Ohio, USA: Metals and Ceramics Division, Air Force Materials Laboratory, Wright-Patterson Air Force Base, 1969)
50. M Schouler, M Dicarroi, C Bernard *Rev. Int. Hautes Temp. Refract.* **20** 261 (1983)
51. R Telle, R J Brook, G Petzow *J. Hard Mater.* **2** 79 (1991)
52. A I Gusev, G P Shveikin *Izv. Akad. Nauk SSSR, Neorg. Mater.* **10** 2144 (1974)
53. H Nowotny, E Rudy, F Benesovsky *Monatsh. Chem.* **92** 394 (1961)
54. H Nowotny, E Rudy, F Benesovsky *Monatsh. Chem.* **91** 963 (1960)
55. F W Glaser *J. Met.* **4** 391 (1952)
56. L E Toth, F Benesovsky, H Nowotny, E Rudy *Monatsh. Chem.* **92** 956 (1961)
57. P Rogl *J. Nucl. Mater.* **80** 187 (1979)
58. P Rogl *J. Nucl. Mater.* **79** 154 (1979)
59. P Rogl, P Fischer *J. Solid State Chem.* **78** 294 (1989)
60. Yu D Kondrashev *Kristallografiya* **11** 559 (1966)
61. H Nowotny, P Rogl, J C Schuster *J. Solid State Chem.* **44** 126 (1982)
62. W Jeitschko, H Nowotny, F Benesovsky *Monatsh. Chem.* **94** 565 (1963)
63. L E Toth, H Nowotny, F Benesovsky, E Rudy *Monatsh. Chem.* **92** 794 (1961)
64. P Rogl, J Bauer, J Debuigne *J. Nucl. Mater.* **165** 74 (1989)
65. H H Stadelmaier, J B Ballance *Z. Metallkd.* **58** 449 (1967)
66. L Ya Markovskii, E T Bezruk *Zh. Prikl. Khim.* **39** 258 (1966)
67. H H Stadelmaier *Metall* **17** 412 (1963)
68. M E Nicholson *J. Met.* **9** 1 (1957)
69. L Ya Markovskii, E T Bezruk, G E Berlova *Izv. Akad. Nauk SSSR, Neorg. Mater.* **7** 56 (1971)
70. E Rudy, F Benesovsky, L E Toth *Z. Metallkd.* **54** 345 (1963)
71. G Papesch, H Nowotny, F Benesovsky *Monatsh. Chem.* **104** 933 (1973)
72. M Lucco Borlera, G Pradelli *Met. Ital.* **59** 907 (1967)
73. M Lucco Borlera, G Pradelli *Met. Ital.* **60** 140 (1968)
74. P Rogl, H Klesnar, P Fischer *J. Am. Ceram. Soc.* **73** 2634 (1990)
75. J Gaude, P L Haridon, J Guyader, J Lang *J. Solid State Chem.* **59** 143 (1985)
76. P Rogl, H Klesnar *J. Solid State Chem.* **98** 99 (1992)
77. J Gaude *C. R. Hebd. Seances Acad. Sci., Ser. 2* **297** 717 (1983)
78. P Rogl, H Klesnar, P Fischer *J. Am. Ceram. Soc.* **71** C450 (1988)
79. P Rogl, H Klesnar, P Fischer, B Chevalier, B Buffat, G Demazeau, J Etourneau *J. Mater. Sci. Lett.* **7** 1229 (1988)
80. P Rogl, J C Schuster *Phase Diagrams of Ternary Boron Nitride and Silicon Nitride Systems* (Materials Park, OH: American Society of Material Science, 1992)
81. H P Klesnar, P Rogl *High Temp.-High Press.* **22** 453 (1990)
82. I Šmid, P Rogl, F Weitzer, in *Proceedings of the 12th International Plansee Seminar Vol. 2* (Eds H Bildstein, H M Ortner) (Reutte, Austria: Metallwerk Plansee, 1989) p. 577
83. H Klesnar, P Rogl, in *Proceedings of the 12th International Plansee Seminar Vol. 2* (Eds H Bildstein, H M Ortner) (Reutte, Austria: Metallwerk Plansee, 1989) p. 599
84. E Rudy, F Benesovsky *Monatsh. Chem.* **92** 415 (1961)
85. K E Spear, H Schäfer, P W Gilles *J. Less-Common Met.* **14** 449 (1968)
86. M P Asanova, A F Gerasimov, V N Konev *Fiz. Met. Metalloved.* **9** 689 (1960)
87. R Kiessling, Y H Liu *J. Met.* **3** 639 (1951)
88. R W Fountain, J Chipman *Trans. Metall. Soc. AIME* **224** 599 (1962)
89. H Nowotny, B Lux, H Kudielka *Monatsh. Chem.* **87** 447 (1956)
90. H Kudielka, H Nowotny, G Findeisen *Monatsh. Chem.* **88** 1048 (1957)
91. H Nowotny, R Kieffer, F Benesovsky *Planseeber. Pulvermetall.* **5** 86 (1957)
92. H Nowotny, F Benesovsky, E Rudy, A Wittman *Monatsh. Chem.* **91** 975 (1960)
93. E Parthe, J T Norton *Monatsh. Chem.* **91** 1127 (1960)
94. R Kieffer, F Benesovsky *Hartstoffe* (Wien: Springer, 1963)
95. H Nowotny, E Piegger, R Kieffer, F Benesovsky *Monatsh. Chem.* **89** 611 (1958)
96. B Aronsson *Acta Chem. Scand.* **12** 31 (1958)
97. V N Konev, A F Nesterov, I P Glazkova *Fiz. Met. Metalloved.* **16** 86 (1963)
98. B Aronsson, G Lundgren *Acta Chem. Scand.* **13** 433 (1959)
99. B Aronsson, I Engström *Acta Chem. Scand.* **14** 1403 (1960)
100. S Rundqvist, F Jellinek *Acta Chem. Scand.* **13** 425 (1959)
101. J C Schuster, in *Proceedings of the 13th International Plansee Seminar Vol. 2* (Eds H Bildstein, R Eck) (Reutte, Austria: Metallwerk Plansee, 1993) p. 571
102. J C Schuster *Int. J. Refract. Hard Met.* **12** 173 (1993–1994)
103. J C Schuster *Ceram. Trans.* **35** 43 (1993)
104. W Jeitschko, H Nowotny *Monatsh. Chem.* **98** 329 (1967)
105. J J Nickl, K K Schweitzer, P Luxenberg *J. Less-Common Met.* **26** 335 (1972)
106. T Goto, T Hirai *Mater. Res. Bull.* **22** 1195 (1987)
107. E Parthe, H Nowotny, H Schmid *Monatsh. Chem.* **86** 385 (1955)
108. L Brewer, O Krikorian *J. Electrochem. Soc.* **103** 38 (1956); **103** 701 (1956)
109. E Parthe, H Schachner, H Nowotny *Monatsh. Chem.* **86** 182 (1955)
110. P W Pellegrini, B C Giessen, J M Feldman *J. Electrochem. Soc.* **119** 535 (1972)
111. E Parthe, W Jeitschko, V Sadagopan *Acta Crystallogr.* **19** 1031 (1965)
112. F J J Van Loo, F M Smet, G D Rieck, G Verspui *High Temp.-High Press.* **14** 25 (1982)
113. P Guinet, H Vaugoyeau *C. R. Hebd. Seances Acad. Sci., Ser. C, Sci. Chim.* **262** 1856 (1966)
114. P L Blum, P Guinet, G Silvestre *C. R. Hebd. Seances Acad. Sci.* **260** 1911 (1965)
115. P L Blum, G Silvestre *C. R. Hebd. Seances Acad. Sci., Ser. B, Sci. Phys.* **263** 709 (1966)
116. P Guinet, H Vaugoyeau, J Laugier, P L Blum *J. Nucl. Mater.* **21** 21 (1967)
117. W Jeitschko, H Nowotny, F Benesovsky *Monatsh. Chem.* **94** 844 (1963)
118. W J J Wakelkamp, F J J Van Loo, R Metselaar *J. Eur. Ceram. Soc.* **8** 135 (1991)
119. W Wakelkamp *Tijdschr. Klei. Glas Keram.* **13** 18 (1992)
120. M Maline, M Ducarroir, F Teyssandier, R Hillel, R Berjoan, F J J Van Loo, W Wakelkamp *Surf. Sci.* **286** 82 (1993)
121. C E Brukl, in *Ternary Phase Equilibria in Transition Metal–Boron–Carbon–Silicon Systems. Technical Report AFML TR-65-2 Part II, Vol. VII* (Ohio, USA: Metals and Ceramics Division, Air Force Materials Laboratory, Wright-Patterson Air Force Base, 1966) p. 35
122. N P Lyakishev, M I Gasik, O I Polyakov *Izv. Akad. Nauk SSSR, Metall* **5** (1991)
123. S Sambasivan, W T Petuskey *J. Mater. Res.* **7** 1473 (1992)
124. C E Brukl, in *Technical Report AD 489752* (US Clearinghouse Federal Scientific Technical Information, 1966) p. 37
125. K Yvon, E Parthe *Acta Crystallogr., Sect. B. Struct. Crystallogr.* **26** 149 (1970)
126. B V Khaenko, V G Fak *Izv. Akad. Nauk SSSR, Neorg. Mater.* **14** 1294 (1978)
127. J C Schuster *J. Chim. Phys. Phys.-Chim. Biol.* **90** 373 (1993)
128. H Nowotny, E Parthe, R Kieffer, F Benesovsky *Monatsh. Chem.* **85** 255 (1954)
129. Z M Alekseeva *Izv. Akad. Nauk SSSR, Metall* **212** (1990)
130. P Guinet, H Vaugoyeau, J Jolivet *J. Nucl. Mater.* **36** 94 (1970)
131. A W Searcy, L N Finnie *J. Am. Ceram. Soc.* **45** 268 (1962)
132. R C J Schiepers, F J J Van Loo, G de With *J. Am. Ceram. Soc.* **71** C284 (1988)
133. Y C Chen, C M Chen, K C Su, K Yang *Mater. Sci. Eng. A, Struct. Mater.* **133** 596 (1991)
134. M R Jackson, R L Mehan, A M Davies, E L Hall *Metall. Trans. A, Phys. Metall. Mater. Sci.* **14** 355 (1983)
135. A Inoue, S Furukawa, T Masumoto *J. Mater. Sci.* **22** 1670 (1987)
136. T C Chou *J. Mater. Sci.* **26** 1412 (1991)
137. Z Inoue, M Mitomo, N Il J. *Mater. Sci.* **15** 2915 (1980)
138. C E Holcombe, L Kovach *Am. Ceram. Soc. Bull.* **60** 546 (1981)
139. J Gaude, J Lang, D Louër *Rev. Chim. Miner.* **20** 523 (1983)
140. F Weitzer, J C Schuster, J Bauer, B Jounel *J. Mater. Sci.* **26** 2076 (1991)
141. J C Schuster, H Nowotny, in *Proceedings of the 11th International Plansee Seminar Vol. 1* (Eds H Bildstein, H M Ortner) (Reutte, Austria: Metallwerk Plansee, 1985) p. 899
142. J C Schuster, F Weitzer, J Bauer, H Nowotny *Mater. Sci. Eng. A, Struct. Mater.* **105/106** 201 (1988)

143. R Marchand, M Maunaye, J Lang C. R. *Hebd. Seances Acad. Sci., Ser. C* **272** 1654 (1991)
144. M Maunaye, R Marchand, J Guyader, Y Laurent, J Lang *Bull. Soc. Fr. Mineral. Cristallogr.* **94** 561 (1972)
145. F Weitzer, J C Schuster *J. Solid State Chem.* **70** 178 (1987)
146. Yu I Krylov, V A Bronnikov *Poroshk. Metall.* (1) 52 (1976)
147. Yu S Borisov, A L Borisova, Yu A Kocherzhinskii, E A Shishkin *Poroshk. Metall.* (3) 63 (1978)
148. T Hirai, S Hayashi *J. Mater. Sci.* **17** 1320 (1982)
149. S Hayashi, T Hirai, K Hiraga, M Hirabayashi *J. Mater. Sci.* **17** 3336 (1982)
150. R Beyers, R Sinclair, M E Thomas *J. Vac. Sci. Technol. B* **2** 781 (1984)
151. W Wakelkamp, PhD, Technische Universiteit Eindhoven, Eindhoven, Netherlands, 1991
152. T Onozuka *Trans. Jpn. Inst. Met.* **23** 315 (1982)
153. J C Schuster *J. Mater. Sci.* **23** 2792 (1988)
154. T Kato, M Yoshimura, S Somiya *Yogyo-Kyokai-Shi* **89** 221 (1981)
155. E Heikinheimo, A Kodentsov, J A Van Beek, J T Klomp, F J J Van Loo *Acta Metall. Mater.* **40** S111 (1992)
156. R Pompe *Thermochim. Acta* **34** 245 (1979)
157. F Weitzer, P Rogl, J C Schuster *Z. Metallkd.* **79** 154 (1988)
158. H Haschke, H Nowotny, F Benesovsky *Monatsch. Chem.* **98** 273 (1967)
159. W Jeitschko, H Nowotny, F Benesovsky *Monatsch. Chem.* **95** 319 (1964)
160. D S Bloom, N J Grant *J. Met.* **2** 41 (1950)
161. E R Morgan *J. Met.* **6** 983 (1954)
162. R G Butters, H P Myers *Philos. Mag.* **46** 895 (1955)
163. L J Hütter, H H Stadelmaier *Acta Metall.* **6** 367 (1958)
164. L J Hütter, H H Stadelmaier *Z. Metallkd.* **50** 199 (1959)
165. M L Swanson *Can. J. Phys.* **40** 719 (1962)
166. L J Hütter, H H Stadelmaier, A C Fraker *Metall* **14** 113 (1960)
167. H H Stadelmaier *Z. Metallkd.* **52** 758 (1961)
168. J C Schuster, H Nowotny *Monatsch. Chem.* **113** 163 (1982)
169. W Jeitschko, H Nowotny, F Benesovsky *Monatsch. Chem.* **94** 672 (1963)
170. W Jeitschko, H Nowotny, F Benesovsky *J. Less-Common Met.* **7** 133 (1964)
171. H Nowotny, W Jeitschko, F Benesovsky *Planseeber. Pulvermetall.* **12** 31 (1964)
172. H Nowotny *Angew. Chem.* **84** 973 (1972)
173. W Jeitschko, H Nowotny, F Benesovsky *Monatsch. Chem.* **94** 332 (1963)
174. W Jeitschko, H Nowotny, F Benesovsky *Monatsch. Chem.* **95** 1212 (1964)
175. W Jeitschko, H Nowotny, F Benesovsky *Monatsch. Chem.* **94** 245 (1963)
176. W Jeitschko, H Nowotny, F Benesovsky *Monatsch. Chem.* **95** 30 (1964)
177. J C Schuster, H Nowotny *Z. Metallkd.* **71** 341 (1980)
178. C Brisi, F Abbatista *Ann. Chim. (Roma)* **51** 452 (1961)
179. J C Schuster, H Nowotny, C Vaccaro *J. Solid State Chem.* **32** 213 (1980)
180. T Lundström, M M Korsukova, V N Gurin *Prog. Cryst. Growth Charact.* **16** 143 (1988)
181. H Nowotny, O Schob, F Benesovsky *Monatsch. Chem.* **92** 1300 (1961)
182. A E Vol *Stroenie i Svoystva Dvoynykh Metallicheskich Sistem T. 1* (The Structure and Properties of Binary Metal Systems, Vol. 1) (Moscow: Fizmatgiz, 1959)
183. J C Schuster, H Nowotny *Z. Metallkd.* **72** 63 (1981)
184. F R Morral *J. Iron Steel Inst.* **130** 419 (1934)
185. J C Schuster, J Bauer *J. Less-Common Met.* **109** 345 (1985)
186. J C Schuster *J. Less-Common Met.* **105** 327 (1985)
187. H Haschke, H Nowotny, F Benesovsky *Monatsch. Chem.* **98** 2157 (1967)
188. J C Schuster, J Bauer *J. Solid State Chem.* **53** 260 (1984)
189. H H Stadelmaier, T S Yun *Z. Metallkd.* **52** 477 (1961)
190. W Jeitschko, H Nowotny, F Benesovsky *Monatsch. Chem.* **94** 1198 (1963)
191. M J Kaufman, D G Konitzer, R D Shull, H L Fraser *Scr. Metall.* **20** 103 (1986)
192. F Ueda, M Yageta, I Tajima *J. Hard Mater.* **2** 233 (1991)
193. J C Schuster, J Bauer, J Debuigne *J. Nucl. Mater.* **116** 131 (1983)
194. J C Schuster *J. Nucl. Mater.* **120** 133 (1984)
195. J C Schuster *Z. Kristallogr.* **175** 211 (1986)
196. W Jeitschko, H Nowotny, F Benesovsky *Monatsch. Chem.* **95** 156 (1964)
197. J C Schuster, H Nowotny *Z. Metallkd.* **76** 728 (1985)
198. J C Schuster, H Nowotny *J. Mater. Sci.* **20** 2787 (1985)
199. C Brukl, H Nowotny, O Schob, F Benesovsky *Monatsch. Chem.* **92** 781 (1961)
200. O Schob, H Nowotny, F Benesovsky *Planseeber. Pulvermetall.* **10** 65 (1962)
201. A Raman, K Schubert *Z. Metallkd.* **56** 40 (1965)
202. O Schob, H Nowotny, F Benesovsky *Monatsch. Chem.* **92** 1218 (1961)
203. E Gerhardt, G Joseph *Z. Metallkd.* **52** 310 (1961)
204. C Brukl, H Nowotny, F Benesovsky *Monatsch. Chem.* **92** 967 (1961)
205. H Nowotny, F Benesovsky, C Brukl *Monatsch. Chem.* **92** 193 (1961)
206. H Nowotny, C Brukl, F Benesovsky *Monatsch. Chem.* **92** 116 (1961)
207. K Robinson *Acta Crystallogr.* **6** 854 (1953)
208. H Nowotny, C Brukl *Monatsch. Chem.* **91** 313 (1960)
209. C Brukl, F Benesovsky, H Nowotny *Planseeber. Pulvermetall.* **11** 20 (1963)
210. H Holleck, F Benesovsky, E Laube, H Nowotny *Monatsch. Chem.* **93** 1075 (1962)
211. J B Kusma, H Nowotny *Monatsch. Chem.* **95** 1266 (1964)
212. K Robinson *Acta Crystallogr.* **5** 397 (1952)
213. G L Phragmen *J. Inst. Met.* **77** 489 (1950)
214. M Cooper *Acta Crystallogr.* **23** 1106 (1967)
215. D Munson *J. Inst. Met.* **95** 217 (1967)
216. R I Garrod, L M Hogen *Acta Metall.* **2** 887 (1954)
217. C Gueneau, C Servant, F d'Yvoire, N Rodier *Acta Crystallogr. Sect. C, Cryst. Struct. Commun.* **51** 177 (1995)
218. K O Burger, A Wittmann, H Nowotny *Monatsch. Chem.* **93** 9 (1962)
219. A Wittmann, K O Burger, H Nowotny *Monatsch. Chem.* **93** 674 (1962)
220. R W Guard, E A Smith *J. Inst. Met.* **88** 369 (1960)
221. G Will *Acta Crystallogr., Sect. B, Struct. Crystallogr.* **25** 1219 (1969)
222. A J Perrotta, W D Townes, J A Potenza *Acta Crystallogr., Sect. B, Struct. Crystallogr.* **25** 1223 (1969)
223. H Neidhard, R Mattes, H J Becher *Acta Crystallogr., Sect. B, Struct. Crystallogr.* **26** 315 (1970)
224. Z Inoue, H Tanaka, Y Inomata *J. Mater. Sci.* **15** 3036 (1980)
225. Z Inoue, Y Inomata, H Tanaka, H Kawabata *J. Mater. Sci.* **15** 575 (1980)
226. Z Inoue, Y Inomata, H Tanaka, H Kawabata *J. Mater. Sci.* **15** 255 (1980)
227. B L Kidwell, L L Oden, R A McCune *J. Appl. Crystallogr.* **17** 481 (1984)
228. L L Oden, R A McCune *Metall. Trans. A, Phys. Metall. Mater. Sci.* **18** 2005 (1987)
229. R Kieffer, E Gugel, G Leimer, P Ettmayer *Ber. Deutsch. Keram. Ges.* **49** 41 (1972)
230. N V Dokukina, A A Kalinina, M I Sokhor, F I Shamrai *Izv. Akad. Nauk SSSR, Neorg. Mater.* **3** 630 (1967)
231. K I Portnoi, G V Samsonov, L A Solonnikova *Zh. Neorg. Khim.* **5** 2032 (1960)
232. R Kieffer, E Gugel, P Ettmayer, A Schmidt *Ber. Deutsch. Keram. Ges.* **43** 621 (1966)
233. E Gugel, P Ettmayer, A Schmidt *Ber. Deutsch. Keram. Ges.* **45** 395 (1968)
234. M L Cohen *J. Hard Mater.* **2** 13 (1991)
235. M Billy, F Colombeau C. R. *Hebd. Seances Acad. Sci., Ser. C, Sci. Chim.* **264** 392 (1967)
236. V J Barczak *J. Am. Ceram. Soc.* **44** 299 (1961)
237. G Schneider, L J Gauckler, G Petzow, A Zangvil *J. Am. Ceram. Soc.* **62** 574 (1979)
238. F Weitzer, K Remsching, J C Schuster, P Rogl *J. Mater. Res.* **5** 2152 (1990)
239. A A Rempel' *Effekty Uporyadocheniya v Nestekhiometricheskikh Soedineniyakh Vnedreniya* (Ordering Effects in Nonstoichiometric Interstitial Compounds) (Ekaterinburg: Nauka, 1992)
240. A I Gusev, A A Rempel *Phys. Status Solidi A* **135** 15 (1993)

Synthesis and application of sulfenamides

I V Koval'

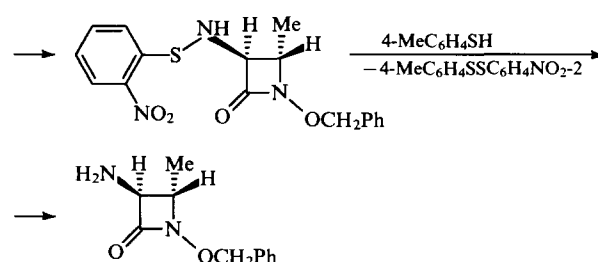
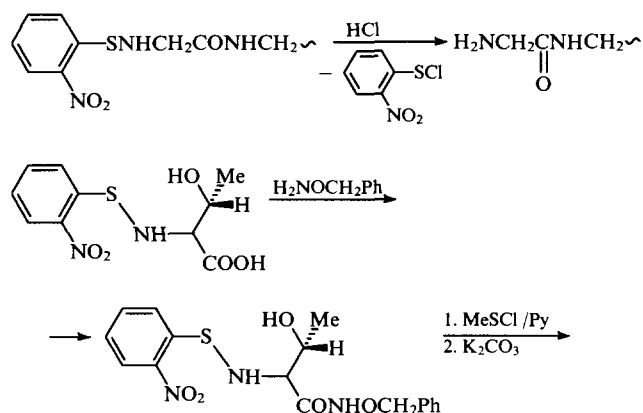
Contents

I. Introduction	421
II. Methods of sulfenylamide synthesis	422
III. The application of sulfenamides in organic synthesis	427
IV. Practical application of sulfenamides	435

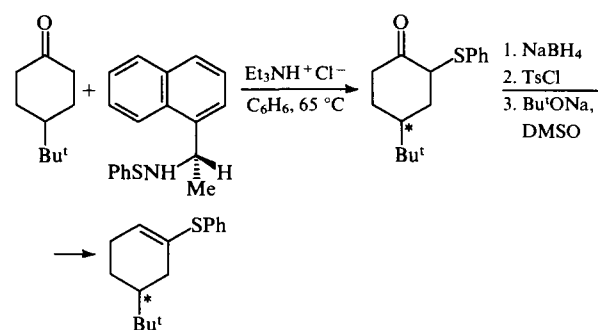
Abstract. The results of studies on the use of sulfenamides in organic synthesis are systematised and generalised. The fields of industrial application of sulfenamides are considered. The bibliography includes 220 references.

I. Introduction

The wide application of sulfenamides in fine organic synthesis is due to the specific features of their structure and reactivity, namely, to the existence of two active reaction centres (S and N), one of them having variable valence, and to the instability of the S–N bond which can rather readily be cleaved by both nucleophiles and electrophiles. High lability of this bond allows one to remove the sulfenyl moiety of the sulfenamide function, which is frequently used as a protective group in peptide synthesis,^{1,2} and in natural product syntheses,^{3,4} at a certain stage of synthesis. Elimination of the sulfenyl moiety occurs under sufficiently mild conditions by hydrochlorolysis or thiolysis of the S–N bond.



On the other hand, the high lability of the S–N bond enables the sulfenamide function to be used for the introduction of a sulfenyl fragment into organic compounds under relatively mild conditions in multistep organic syntheses. Thus, the sulfenylation of 4-*tert*-butylcyclohexanone with chiral *N*-phenylthio- α -naphthylethylamine gives 62% of a diastereomeric mixture of the corresponding sulfides.⁵ The reduction of this mixture with NaBH₄, subsequent tosylation and elimination of toluene-*p*-sulfonic acid gives a mixture of unsaturated sulfides with an isomer of *S*-configuration being predominant.



Yet another specific feature of sulfenamides is their tendency to generate both relatively stable and highly reactive intermediates (aminyl and sulfenyl radicals, radical cations, nitrenes, etc.) that participate in the transfer of sulfenyl and aminyl groups and in some other processes. The ability of the sulfur atom in sulfenamides to pass relatively readily from one valence state to another, as well as to increase its electron density at the expense of its shift from the adjacent *N*-anionic centre, is often used for the synthesis of compounds possessing four- and six-valent sulfur, for example, sulfur-containing imino compounds.

Bifunctional sulfenamides, i.e., sulfenamides containing both sulfenamide and other functional groups (Cl, Br, CCl₃, CF₂Cl, etc.) are synthetically very important. Based on such

I V Koval' Ukrainian Chemico-Technological University,
prosp. Gagarina 8, 320005 Dnepropetrovsk, Ukraine,
Fax (7-056) 247 33 16

Received 15 August 1995

Uspekhi Khimii 65 (5) 452–473 (1996); translated by A V Geiderikh

sulfenamides, many preparative methods for the synthesis of various sulfur and nitrogen-containing heterocyclic compounds have been developed.

The primary products of sulfenamide transformations, such as aminosulfonium, thioammonium and sodium salts, are also widely used in organic synthesis, and numerous synthetic routes involve the conversion of sulfenamides to these products with their subsequent transformation without isolation from the reaction mixture.

In addition to fine organic synthesis, some sulfenamides are widely used in polymer chemistry, in agriculture, in the rubber industry, etc. These aspects are also considered in the present review.

II. Methods of sulfenylamide synthesis

1. Syntheses based on elemental sulfur

Elemental sulfur is not often used directly in the synthesis of sulfenamides because it has to be preactivated,⁶ or highly reactive reagents have to be used. Probably only one example of the direct use of sulfur in sulfenamide synthesis, involving the interaction of elemental sulfur with various nitrobenzenes in liquid ammonia, has been described.⁷ The reaction is accompanied by formation of the corresponding disulfides and sulfides, which is a drawback of the method.

2. Syntheses based on sulfenyl chlorides

The use of sulfenyl chlorides in the synthesis of sulfenamides is based on three main reactions:

(a) the sulfenylation of compounds containing N—H or N—X bonds (X = Li, Na, K, Ag, Me₃Si);

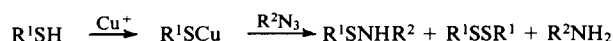
(b) the sulfenylation of inorganic isocyanates and the subsequent interaction of sulfenyl isocyanates with amines and alcohols;

(c) the addition of sulfenyl chlorides to the C=N or C≡N bond.

Based on these reactions, various preparative methods of sulfenamide synthesis have been developed. They are described in the published reviews,^{8,9} and in the references cited in them. Later publications^{10–21} are mostly devoted to the perfection of these methods and to the expansion of the scope of their application.

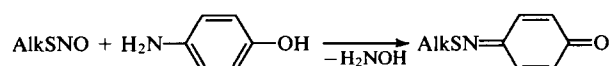
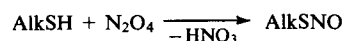
3. Syntheses based on thiols

Amination of thiols with *N*-halo compounds, amines in the presence of oxidising reagents, sodium hydroxylaminosulfonate, and with other iminating reagents is the basis for a series of preparative methods of synthesis of unsubstituted and *N*-substituted sulfenamides (see review²² and the references cited therein). The amination of thiols can also be performed using azides²³ in the presence of cuprous salts. The formation of disulfides and amines as side products is a drawback of the method.



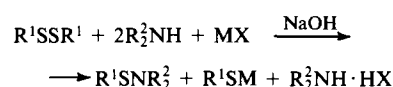
$R^1 = \text{Bu, Bz}; R^2 = \text{BuCO, HCO}$

A two-step synthesis of sulfenamides from thiols, *p*-aminophenol, and nitrogen dioxide has been described.²⁴ The first step involves the interaction of thiols with N₂O₄ to yield alkylsulfenyl nitrenes which then react with *p*-aminophenol (the second step).



4. Syntheses based on disulfides

There are several methods of sulfenamide synthesis based on disulfides. One of them involves the interaction of disulfides with ammonia or amines in the presence of silver acetate or nitrate, or mercuric chloride in alkaline medium.^{25, 26}

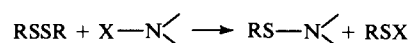


$R^1 = \text{Alk, Ar, Het}; R^2 = \text{H, Alk, Ar};$

$MX = \text{AgNO}_3, \text{AgOAc, HgCl}_2$

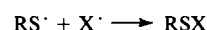
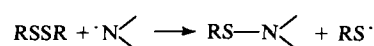
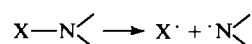
It is supposed²⁶ that a complex of disulfide with a metal is formed initially, which then undergoes nucleophilic attack by ammonia or amines to produce the sulfenamide and other products. The reaction is performed in methanol or ethyl acetate by treating equimolar amounts of disulfide and a metal salt with an excess of ammonia or the amine. The best yields of sulfenamides (60%–80%) were obtained with aromatic disulfides.

The second method of sulfenamide synthesis from disulfides is based on their reaction with *N*-halo compounds.



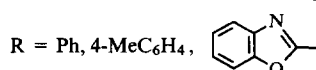
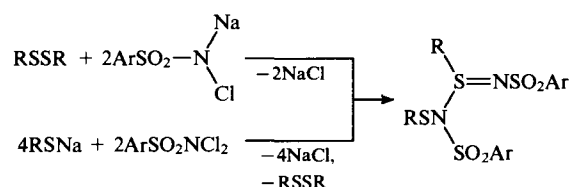
$R = \text{Alk, Ar}; X = \text{Cl, Br}$

The reaction occurs by a radical mechanism, which involves the homolysis of the N—X bond and the interaction of the N·-radical formed with the disulfide.



$X = \text{Cl, Br}$

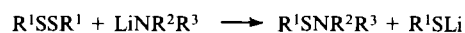
To bind sulfenyl halides, pyridine, triethylamine, and other reagents are used. *N*-Chloro- and *N*-bromosuccinimide,²⁷ *N*-chlorophthalimide,²⁷ *N*-chloroformamidoyl chloride,²⁷ alkyl *N*-chlorobenzenecarboximidates,²⁸ *N*-chloroimino-carbonates,²⁸ *N*-chlorobenzamide,²⁹ and *N*-chlorodialkylamines³⁰ react with disulfides according to this scheme. Sodium *N*-chlorosulfonamides react with disulfides in non-aqueous media to give sulfenamides of the general formula RSN(SO₂Ar)X [$X = \text{S(R)}=\text{NSO}_2\text{Ar}$]³¹ which can also be obtained by the reaction of sodium thiolates with dichlorosulfon-



$\text{Ar} = \text{Ph, 4-MeC}_6\text{H}_4$

amides.³²

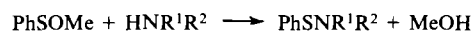
The third method of sulfenamide synthesis from disulfides is their decomposition in the presence of lithium amides,³³ the yield of sulfenamides being as high as 62%–96%. As side products, Li thiolates are formed, which sometimes hinder the isolation of the target sulfenamides.



$R^1 = Pr^n, Ph; R^2 = H, Et, Pr^n, Pr^i, Bu^i;$
 $R^3 = Et, Pr^n, Pr^i, Bu$

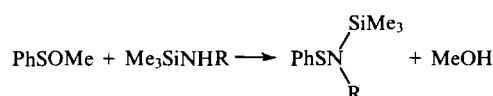
5. Syntheses based on arylsulfenates, sulfonyl thiocyanates, and thiosulfonates

Sulfenamides are obtained in high yields by the sulfonylation of primary and secondary amines with esters of sulfenic acids.^{23, 34}

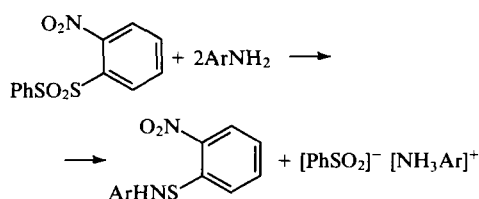


$R^1 = Pr, Ph; R^2 = H, Me, Et, Pr, Bu, Ph$

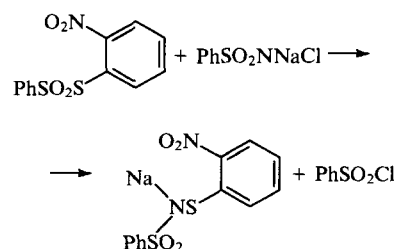
The use of sulfenates instead of sulfonyl chlorides as sulfonylation agents is sometimes preferable, in particular, if a substrate contains other highly reactive functional groups which are unstable toward sulfonyl chlorides. For example, trimethylsilyl derivatives of amines preserve the trimethylsilyl group upon interaction with sulfenates.³⁴



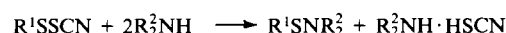
The possibility of using thiosulfonates for sulfenamide synthesis was first demonstrated by the sulfonylation of aromatic amines with *S*-(2-nitrophenyl) benzenethiosulfonate.^{23, 34} In this case the corresponding *N*-aryl-2-nitrobenzenesulfenamides were obtained in relatively good yields.



The reaction of *S*-(2-nitrophenyl) benzenethiosulfonate with sodium *N*-chlorobenzenesulfonamide to give *N*-(2-nitrophenylthio)benzenesulfonamide has been described.³⁵

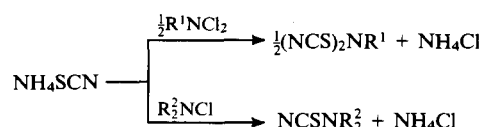


A series of *N,N*-dialkylsulfenamides have been obtained by the interaction of sulfonyl thiocyanates with a twofold excess of dialkylamine in ether.³⁶



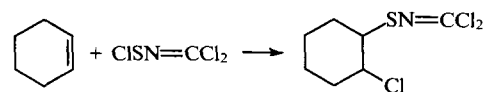
$R^1 = Ph, Et, Pr, Bu; R^2 = Et, Bu^i$

The possibility of using inorganic thiocyanates for the synthesis of sulfenamides has been demonstrated.³⁷ In particular, ammonium thiocyanate gives the corresponding sulfenamides on treatment with alkyl- and dialkylchloroamines.

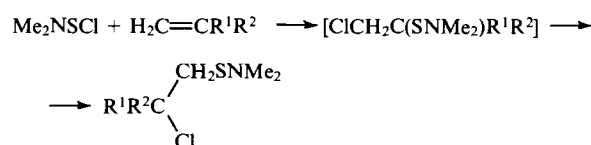


6. Syntheses based on *N*-chlorothio-compounds

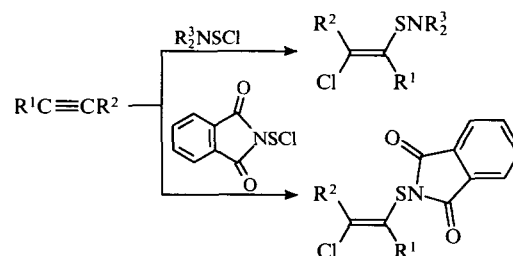
Two main routes of sulfenamide synthesis based on *N*-chlorothio-compounds have been developed. The first one involves the addition of *N*-chlorothio-compounds to C=C and C≡C multiple bonds. For example, *N*-(chlorothio)dichloroketimine adds to the C=C bond of cyclohexene to give 80% of the corresponding sulfenamide.³⁸



The addition of *N*-(chlorothio)dimethylamine to unsymmetrical alkenes in the presence of iodine was shown³⁹ to be anti-Markovnikov with subsequent isomerisation of the adducts formed to more stable sulfenamides.

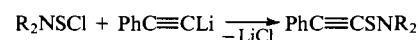


A series of *N,N*-disubstituted vinylsulfenamides was obtained by the addition of *N*-(chlorothio)dialkylamines⁴⁰ and *N*-(chlorothio)phthalimide^{41–43} at the C≡C bond of alkynes.



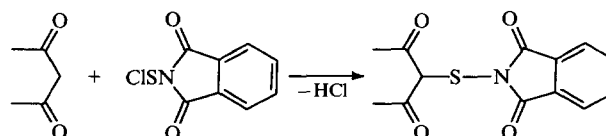
$R^1 = Me, Et, Bu^i, Ph; R^2 = H, Me, Ph; R^3 = Me, Et$

The second method of sulfenamide synthesis based on *N*-chlorothio-compounds is the treatment of CH-acids or their salts with *N*-chlorothio-compounds. For example, a series of *N,N*-(dialkyl)phenylacetylenesulfenamides has been synthesised by the interaction of *N*-(chlorothio)dialkylamines with lithium phenylacetylide.⁴⁰

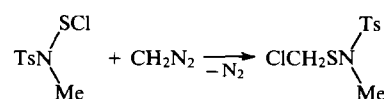


$R = Me, Et$

In the reaction of *N*-(chlorothio)phthalimide with dicarbonyl compounds containing activated C–H bonds sulfenamides are formed relatively readily and in high yields.^{44, 45}



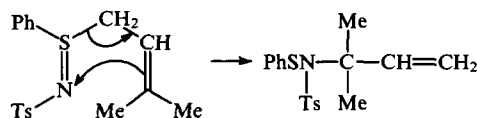
The synthesis of *N*-methyl-*N*-tosylchloromethanesulfenamide from *N*-(chlorothio)methyltosylamine and diazomethane has been reported.³⁸



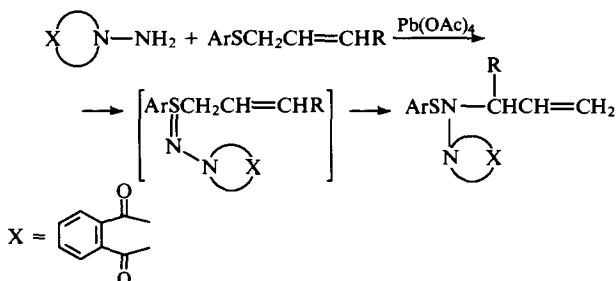
7. Syntheses based on sulfur imino compounds

a. Syntheses based on sulfinimines

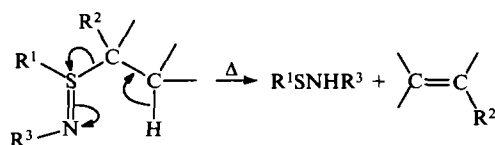
The ability of the S^{IV} atom in sulfinimines to undergo rather easy conversion to the bivalent state can be used in the syntheses of sulfenamides. Several synthetic routes have been developed depending on the structure of the initial sulfinimines. One of them is based on the [2,3]-sigmatropic rearrangement of *S*-allylsulfinimines, which involves migration of the allyl group from the sulfur to the nitrogen atom to produce the *N*-substituted sulfenamides.^{32, 46}



The tendency of *S*-allylsulfinimines to rearrange into more stable *N*-substituted sulfenamides is so pronounced that sometimes they cannot be isolated. For example, the reaction of nitrenes, obtained on treatment of *N*-amino-compounds with lead tetraacetate, with allyl aryl sulfides gave not *S*-allyl-*S*-arylsulfinimines, but the corresponding *N*-substituted sulfenamides.⁴⁷⁻⁵⁰



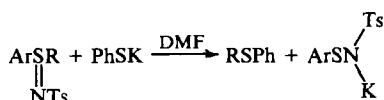
The second route for the synthesis of sulfenamides based on sulfinimines is the thermal rearrangement of *S*-alkylsulfinimines which contain a β -H-atom^{46, 51} (a thermal cycloelimination of alkenes from sulfinimines).



$R^1 = \text{Ar, Alk}; R^2 = \text{H, Me}; R^3 = \text{Ar, MeCO}$

The reaction occurs under relatively mild conditions and leads to sulfenamides in good yields. One shortcoming of this method is the possible formation of a mixture of two sulfenamides from sulfinimines containing two different alkyl groups at the sulfur atom, as, for example, in the thermolysis of *N*-tosyl-*S*-*tert*-butyl-*S*-isopropylsulfinimines.⁵² *N*-Unsubstituted alkane- and arene-sulfenamides,⁵² as well as a series of *N*-substituted sulfenamides with aryl,^{53, 54} tosyl,⁵¹ ethoxycarbonyl,⁴⁶ and carbamoyl⁴⁶ substituents were obtained by thermal cycloelimination of alkenes from sulfinimines.

The third method of sulfenamide synthesis from sulfinimines is their reductive decomposition in the presence of thiolate anions. This reaction occurs on heating in DMF.⁵⁵

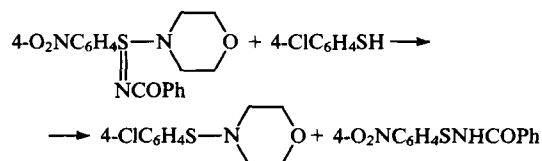


One drawback of this method is the formation of sulfides as side products, which complicates the isolation of the sulfenamides.

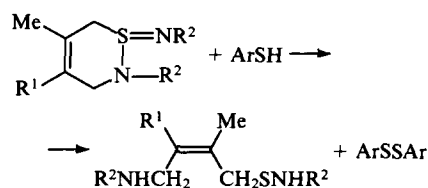
On the other hand, an excess of thiolate can favour the decomposition of the sulfenamide formed.

b. Syntheses based on derivatives of sulfinimide acids

Some amides of sulfinimide acids undergo reductive cleavage in the presence of thiophenols to give sulfenamides. For example, the reductive cleavage of *p*-nitrobenzenesulfinimido amide in the presence of *p*-chlorothiophenol gives a mixture of two sulfenamides.⁵⁶

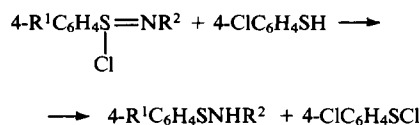


The reductive cleavage of imidodihydrothiazine, which can be considered as a cyclic amide of sulfinimide acid, leads to amino-butenesulfenamides in 65%–95% yields.⁵⁷



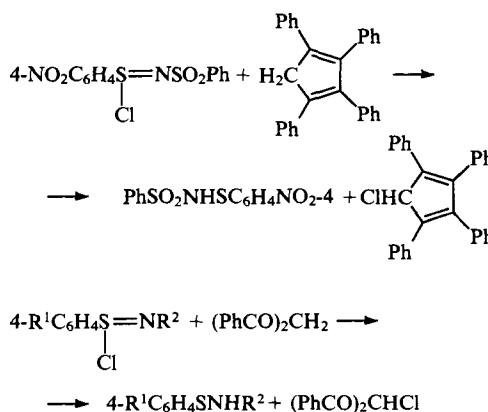
$\text{Ar} = 4\text{-ClC}_6\text{H}_4, 4\text{-MeC}_6\text{H}_4$

Sulfinimido chlorides react in a similar manner in the presence of thiophenols.⁵⁷



$R^1 = \text{NO}_2; R^2 = \text{PhSO}_2, \text{PhCO}$

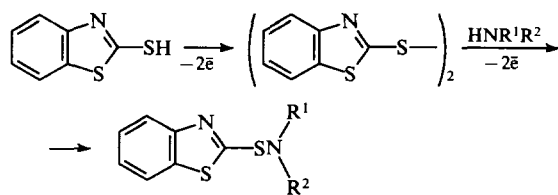
The reductive cleavage of sulfinimido chlorides to yield sulfenamides occurs also on treatment with some CH-acids.⁵⁸



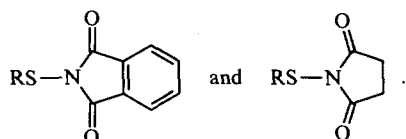
$R^1 = \text{Me, NO}_2; R^2 = \text{PhSO}_2, \text{PhCO, EtOCO}$

8. Electrochemical methods of synthesis of sulfenamides

N,N-Disubstituted benzothiazolesulfenamides were obtained by electrolysis of a 2-mercaptobenzothiazole-amine or bisbenzothiazol-2-yl disulfide-amine system in 70%–98% yield.⁵⁹



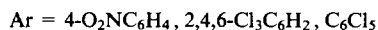
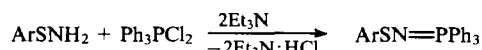
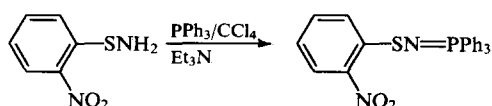
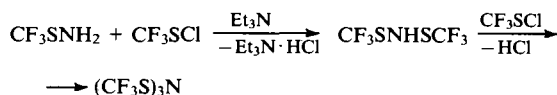
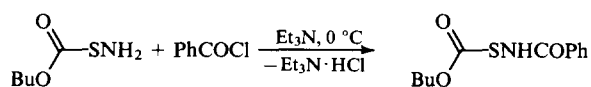
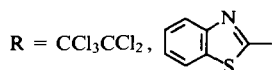
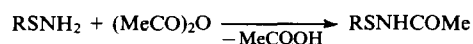
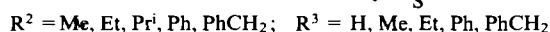
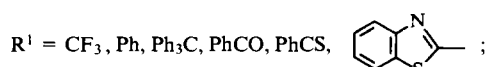
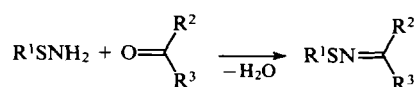
The electrolysis was performed with platinum electrodes in DMF in the presence of triethylammonium perchlorate. Under similar conditions, sulfenamides are formed from tetraalkylthiuramdisulfide, diphenyldisulfide, di-*tert*-butyl-disulfide, and dibenzyl-disulfide.⁶⁰ The electrolysis of a disulfide-phthalimide and disulfide-succinimide system in the presence of NaBr in acetonitrile⁶⁰ gives the corresponding sulfenamides



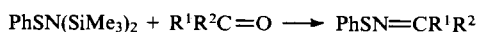
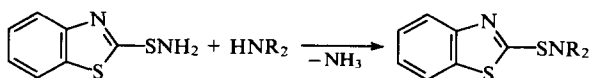
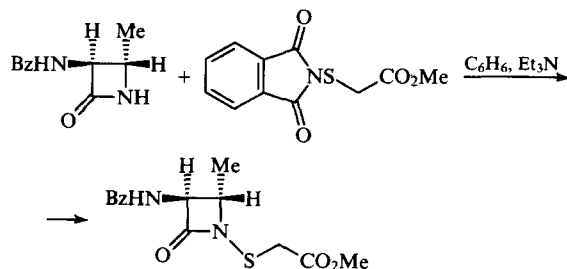
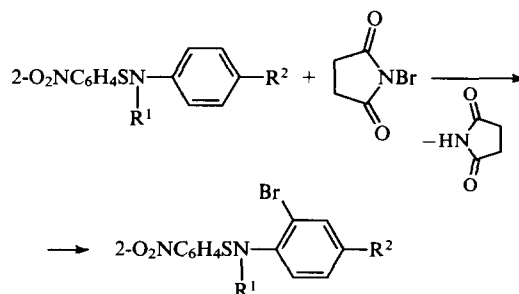
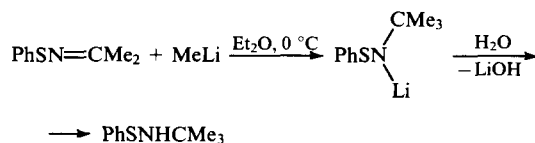
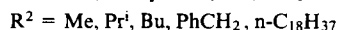
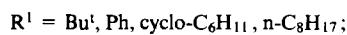
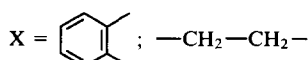
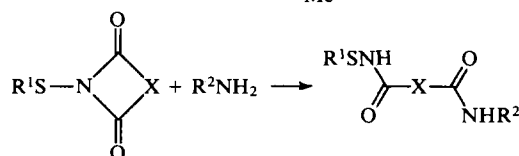
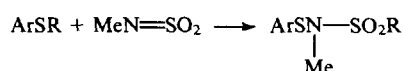
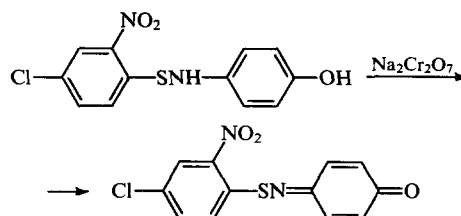
The mechanism of formation of these sulfenamides is believed⁶⁰ to involve a nucleophilic attack of the disulfide on the intermediate *N*-bromoisimide.

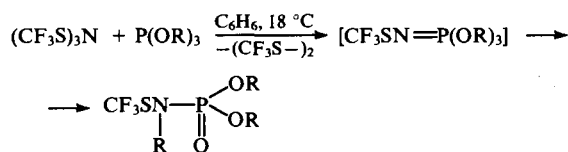
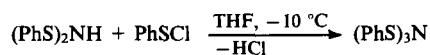
9. Modification of sulfenamides

The change of sulfenamide structures by chemical modification of substituents at the sulfur and nitrogen atoms, as well as by the complete replacement of the amide or sulfonyl moieties, is the basis of methods for synthesising new types of sulfenamides. Chemical modification of the amide group of *N*-unsubstituted sulfenamides is the most common. The relatively high nucleophilicity of the nitrogen atom of the NH₂ group, as well as the availability of two active H atoms permit various chemical transformations. They are based on condensation with carbonyl compounds,⁶¹⁻⁶³ acylation,^{23,64,65} sulfonylation,⁸ phosphorylation,^{23,66} etc.³⁴ Some examples of such reactions are given below.



The modification of substituents at the nitrogen atom of sulfenamides,^{34,67-70} or their complete substitution by other substituents^{34,71-74} are also often used in the synthesis of new sulfenamides.

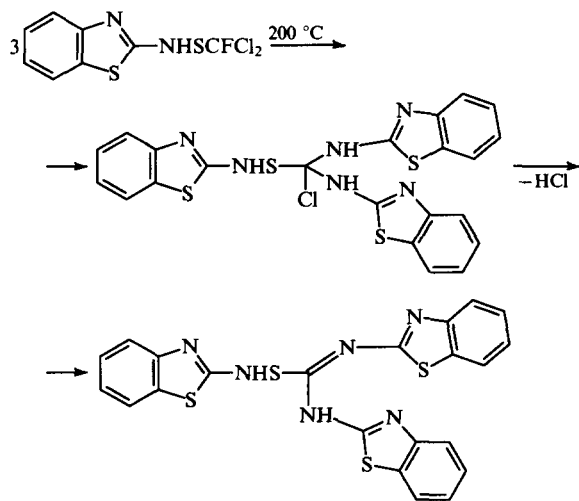




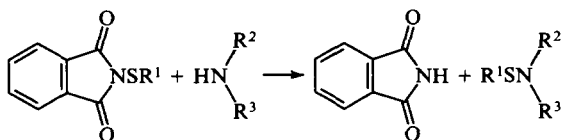
The chemical modification of radicals at the sulfur atom is not so frequently used for the synthesis of new sulfenamides. The substitution of one or two chlorine atoms by fluorine in *N,N*-(diethyl)trichloromethanesulfenamide using antimony trifluoride is an example of such modification.⁸



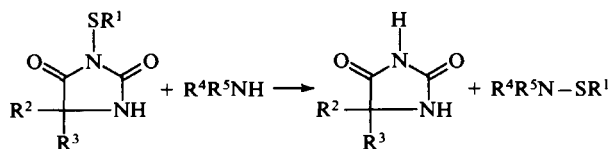
The thermolytic modification of the dichlorofluoromethyl group in *N*-(benzothiazole-2-yl)dichlorofluoromethanesulfenamide has been described.³⁸



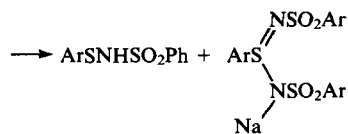
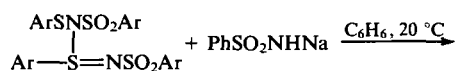
The complete substitution of the amide moiety can be performed on transamidation of sulfenamides in their interaction with *N*-nucleophiles whose nucleophilicity is higher than that of the amide moiety.^{23, 32, 34}



$\text{R}^1 = \text{Me, Et, Ph}; \text{R}^2 = \text{Me, Et}; \text{R}^3 = \text{Et, Pr}^i$



$\text{R}^1 = \text{CCl}_3, \text{Ph}; \text{R}^2 = \text{R}^3 = \text{Me}; \text{R}^4 = \text{H, Ph};$
 $\text{R}^5 = \text{PhCH}_2; \text{R}^4 + \text{R}^5 = -(\text{CH}_2)_3-$

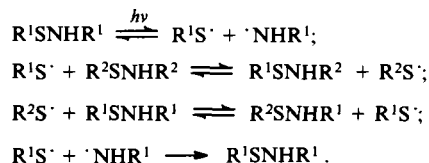


$\text{Ar} = \text{Ph, 4-MeC}_6\text{H}_4$

The replacement of the sulfenyl fragment in sulfenamides can result from the so called 'transsulfenylation', which involves the mutual exchange of sulfenyl groups between sulfenamides and other compounds containing these groups. For example, transsulfenylation of sulfenamides by esters of thiosulfonic acids has been described.⁷⁵

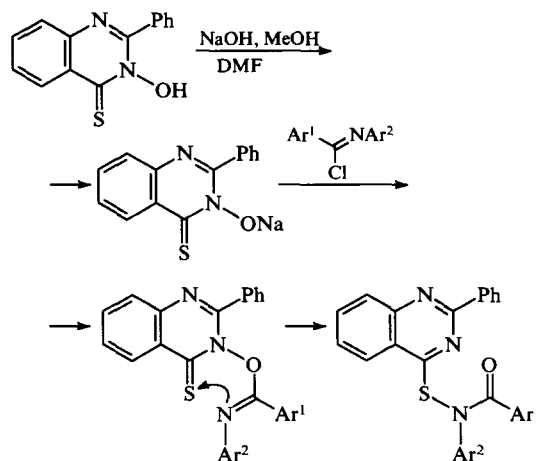


The mutual exchange of sulfenyl groups was observed upon photolysis of a mixture of two sulfenamides.⁷⁶ The photolysis is a radical process and involves the following transformations:

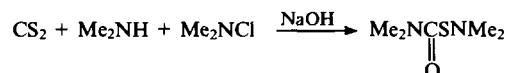


10. Other methods

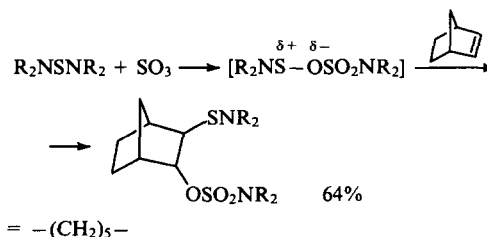
a. The sigmatropic rearrangement of the products of the reaction of 3-hydroxy-2-phenyl-4-thioxo-3,4-dihydroquinazoline with diarylimidoyl chlorides.⁷⁷



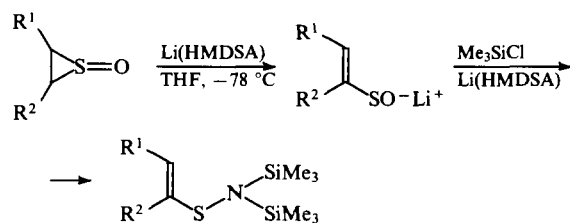
b. The reaction of carbon disulfide with amines and *N*-chloroamines.⁷⁸



c. The addition of the products of sulfur trioxide insertion at the S-N bond of diaminosulfides to alkenes.⁷⁹



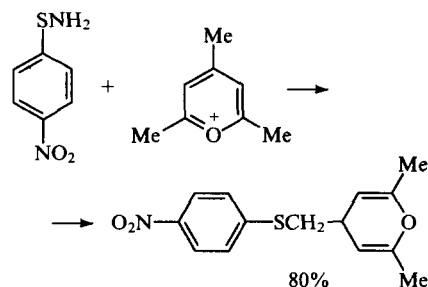
d. The interaction of alkylthiirane-S-oxides with lithium hexamethyldisilazide [Li(HMDSA)] and trimethylsilyl chloride.⁸⁰



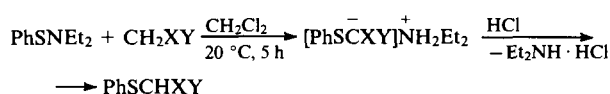
III. The application of sulfenamides in organic synthesis

1. Synthesis of sulfides

Several basic methods of synthesis of sulfides from sulfenamides have been developed. One of them is based on the sulfonylation of CH-acids or their salts with both substituted and *N*-unsubstituted sulfenamides. The sulfenamides are milder sulfonylating agents than sulfonyl halides; this fact allows their use in reactions with CH-acids which contain multiple bonds or functional groups which are vulnerable to sulfonyl halides. For example, the reaction of *p*-nitrobenzenesulfenamide with a 2,4,6-trimethylpyrylium salt produces the corresponding sulfide.⁸¹

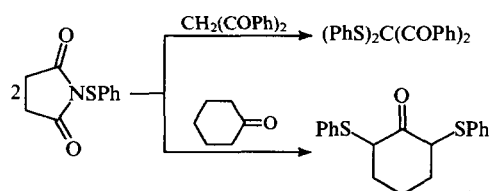


Sulfides are also obtained relatively smoothly and in good yields in the reaction of *N,N*-(dialkyl)arenesulfenamides with disubstituted methanes containing strong electron-withdrawing groups, such as CN, PhCO, MeCO, EtOCO, etc.⁸²

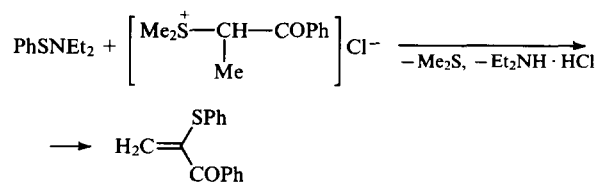


X	Y
CN	CN
PhCO	PhCO
MeCO	MeCO
MeCO	EtOCO
EtOCO	EtOCO

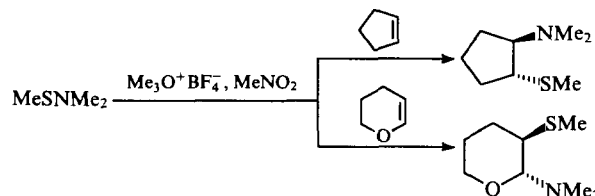
Excess of the sulfenamide can induce substitution of the second hydrogen atom of the CH-acid by the arylthio group.²³



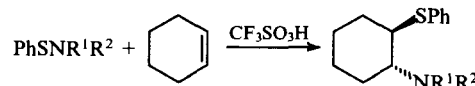
The synthesis of unsaturated sulfides by the sulfonylation of chlorosulfonium salts containing activated CH-bonds with sulfenamides has been described.⁸³



The second method of sulfide synthesis from sulfenamides involves the addition of sulfenamides at the C=C bond of unsaturated compounds. This method is widely used for the synthesis of functionally substituted sulfides; several modifications of the method are known. The first one is the interaction of sulfenamides with alkenes in the presence of activating agents (Me₃O⁺BF₄⁻, Et₂O·BF₃, CF₃SO₃H, etc.). The role of the activating agents is to increase the electrophilic properties of the sulfur atom in the initial sulfenamide, and to stabilise the intermediates formed. For example, the aminosulfonylation of cyclopentene and 3,4-dihydro-2*H*-pyran with *N,N*-(dimethyl)methanesulfenamide occurs rather smoothly in nitromethane in the presence of trimethyloxonium tetrafluoroborate.^{84, 85}

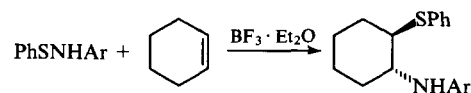


The addition of *N*-substituted benzenesulfenamides at the C=C bond of cyclohexene in the presence of trifluoromethanesulfonic acid has been described.⁸⁶



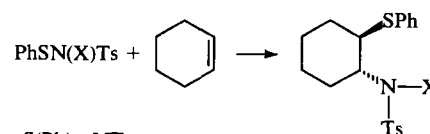
R¹ = H, R² = Bu^t; R¹ + R² = -(CH₂)₅-, -(CH₂)₂O(CH₂)₂-

Under analogous conditions, these sulfenamides add at the C=C bond of octene and indene.⁸⁶ *N*-(Aryl)benzenesulfenamides readily react with cyclohexene in the presence of boron trifluoride etherate to give the corresponding aminosulfides in 50%–90% yields.⁸⁷



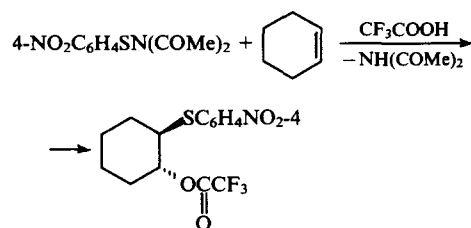
Ar = 4-NO₂C₆H₄, 4-ClC₆H₄, 4-MeC₆H₄, 4-MeOC₆H₄, 3-MeOC₆H₄

The sulfenamides PhSN(X)Ts [X = S(Ph)=NTs] add at the C=C bond of cyclohexene under acidic activation conditions to yield *N*-disubstituted aminosulfides.⁸⁸

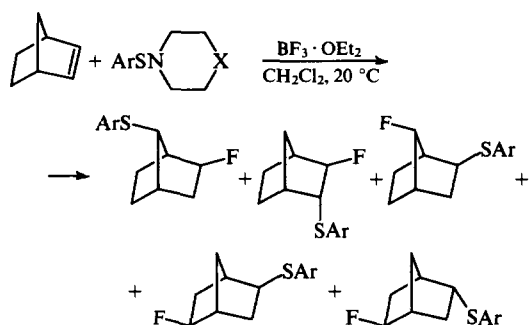


X = S(Ph)=NTs

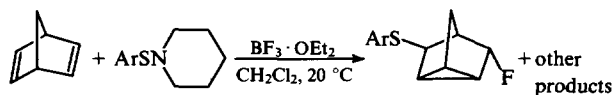
According to the second route, the participation of an external nucleophile in the reaction is envisaged, which provides a fragment substituting the amino group in the adduct. This route was first realised in the reaction of *N,N*-diacetyl-*p*-nitrobenzenesulfenamide with cyclohexene in the presence of trifluoroacetic acid.⁸⁸



Apparently, in this case, an episulfonium intermediate is formed initially⁸⁴ in which ring-opening by trifluoroacetate anion leads to a *trans*-adduct. Thus, trifluoroacetic acid acts as both the activator and the external nucleophile. Likewise, boron trifluoride etherate has a double function in reactions of arene-sulfenamides with norbornene⁸⁹ and norbornadiene.⁹⁰ The addition is accompanied by the rearrangement of the carbon skeleton resulting in a mixture of several products.

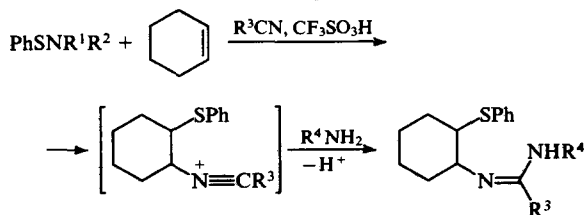


Ar = 2-O₂NC₆H₄; 2,4-(O₂N)₂C₆H₃; X = O, CH₂



Ar = 2,4-(O₂N)₂C₆H₃

Two reagents are generally used to accomplish the addition of sulfenamides to unsaturated compounds, one of them being an activator, and the other an external nucleophile. For example, the addition of *N*-substituted benzenesulfenamides to cyclohexene in the presence of trifluoromethanesulfonic acid and nitriles has been reported^{91,92} to give sulfides with the amidine fragments. In this case, nitriles act as external nucleophiles.



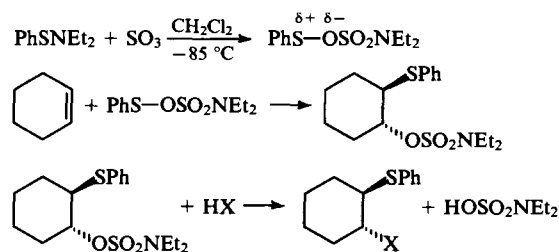
R¹ = R² = cyclo-C₆H₁₁; R¹ + R² = -(CH₂)₂O(CH₂)₂-;
R¹ = H, R² = Bu; R³ = Me, Et; R⁴ = Ph

The synthesis of sulfides of general formula R¹HN.C(Me)=NC(R²)=C(R³)SPh with an acetamidine fragment (R¹ = Ph, 4-O₂NC₆H₄, 4-ClC₆H₄, 4-MeC₆H₄, 4-MeOC₆H₄; R² = H, Me, Et; R³ = Me, Et, Pr, Bu) using the addition of *N*-(aryl)benzenesulfenamides to the corresponding alkynes in acetonitrile in the presence of boron trifluoride etherate has been described.⁹³

The addition of *N*-(*p*-nitrophenyl)benzenesulfenamide to alkynes R¹C≡CR² (R¹ = H, R² = Me; R¹ = H, R² = Bu^t; R¹ = H, R² = Pr; R¹ = H, R² = Bu; R¹ = Me, R² = Pr; R¹ = R² = Me;

R¹ = R² = Et; R¹ = R² = Pr; R¹ = H, R² = Ph; R¹ = Me, R² = Ph; R¹ = Et, R² = Ph; R¹ = R² = Ph) in acetic acid in the presence of boron trifluoride etherate is a stereospecific reaction, which results in a mixture of two products, (*E*)-R²C(OAc)=C(R¹)SPh and (*E*)-R¹C(OAc)=C(R²)SPh, in total yields of 30%–80%.^{94,95}

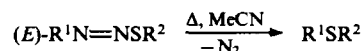
The third route to sulfides by the addition of sulfenamides at multiple bonds involves enhancement of the sulfur atom electrophilicity by insertion of sulfur trioxide into the S–N bond of sulfenamides with the subsequent addition of the insertion product to the C=C bond of alkenes (that is, sulfamatosulfonylation of alkenes).⁹⁶ For example, the addition of *N,N*-(diethyl)benzenesulfenamide to cyclohexene in the presence of sulfur trioxide in chloroform yields a *trans*-1,2-adduct, which is converted to the corresponding functionally substituted sulfide upon treatment with acid.⁹⁷



X = Br, MeCOO, CF₃COO, HCOO

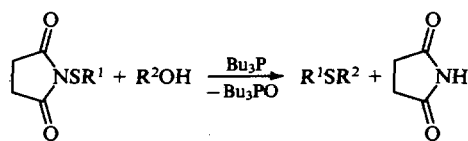
The sulfamatosulfonylation of norbornene and norbornadiene⁹⁸ is accompanied by rearrangement of the carbon skeleton and results in a mixture of different sulfides that are difficult to separate. The use of pyridine–sulfur trioxide as a donor of SO₃ allows one to perform the sulfamatosulfonylation of alkenes at ambient temperature.⁹⁹ The addition of sulfenamides to alkenes in the presence of sulfamic acid^{100,101} and potassium persulfate¹⁰² has also been studied.

Yet another method of sulfide synthesis from sulfenamides which should be mentioned involves thermal decomposition of arylthioazo compounds.¹⁰³



R¹ = 4-NCC₆H₄, 4-O₂NC₆H₄; R² = Bu^t, Ph

The thermolysis is believed¹⁰³ to occur by aromatic nucleophilic substitution (*S_{NR}1*) through the intermediate radical anion [R¹N=NSR²]^{·-}. The formation of sulfides, together with other products, was observed¹⁰⁴ in the reaction of sulfenamides with alcohols in the presence of trialkylphosphites.



2. Synthesis of sulfonyl halides

The treatment of sulfenamides with hydrogen halides in anhydrous organic solvents yields the corresponding sulfonyl halides.

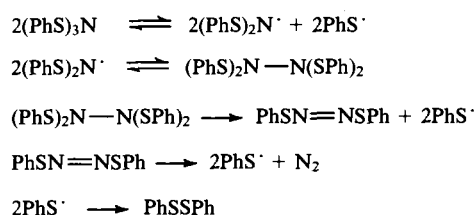


The reaction has preparative value, but it is not often used for the synthesis of sulfonyl halides, because the starting sulfenamides are usually synthesised from the same sulfonyl halides, to which they are then converted. The transformation of a sulfonyl halide function to sulfenamide followed by cleavage of the S–N bond with gaseous hydrogen halide is used as a synthetic method in the modification of a sulfonyl halide aimed at protecting the sulfonyl

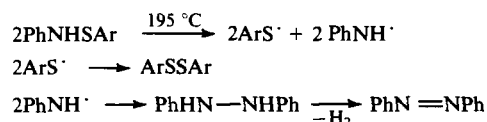
halide function,⁸ as well as in peptide synthesis, in which the sulfenyl fragment acts as a protective group. 2-Nitrobenzenesulfenyl chloride forms crystalline sulfenamide derivatives with amino acids, which can rather readily be cleaved in the presence of hydrogen chloride; this appeared to be of particular value in peptide synthesis.¹⁰⁵ The triphenylmethanesulfenyl group is also successfully used as a protective group in the synthesis of alkaloids.³⁴

3. Synthesis of disulfides

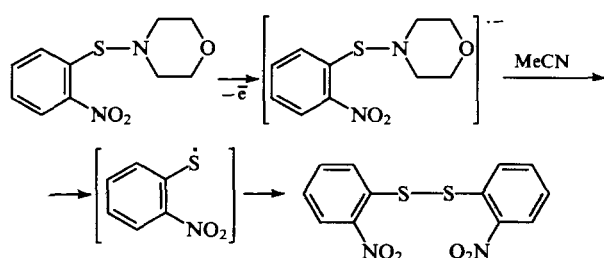
Thermolysis, thiolysis, and hydrolysis of sulfenamides are the most common processes for the practical synthesis of disulfides among a wide range of reactions of sulfenamides that give disulfides. The homolytic cleavage of the S–N bond upon the heating of sulfenamides gives thiyl radicals which recombine to disulfides. The choice of thermolysis conditions depends both on the basicity and the structure of the initial sulfenamides. For example, the thermolysis of tri(phenylsulfenyl)amine occurs under rather mild conditions at ~50 °C to yield diphenyldisulfide.¹⁰⁶



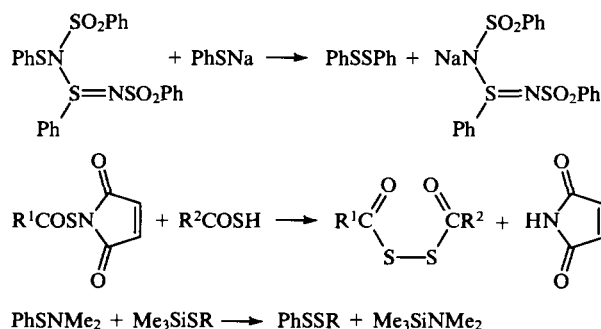
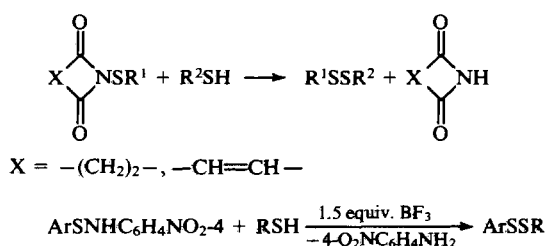
The thermolysis of *N*-(aryl)benzenesulfenamides requires more severe conditions, the products being diaryldisulfides and azobenzene.¹⁰⁷



The homolytic cleavage of the S–N bond with the subsequent recombination of the thiyl radicals formed was observed during the anodic oxidation of *N*-(2-nitrophenylthio)morpholine in acetonitrile in the presence of NaClO.¹⁰⁸

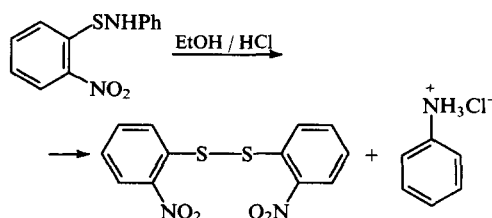


The thiolysis of sulfenamides is used in the synthesis of both symmetrical and unsymmetrical disulfides. Nucleophilic substitution of the amide group at the sulfur atom of sulfenamides by an alkyl- or arylthio group occurs upon their interaction with thiols^{34, 109} or thiolates,¹¹⁰ thioacids,¹¹¹ alkyl- or arylthiosilanes.¹¹²

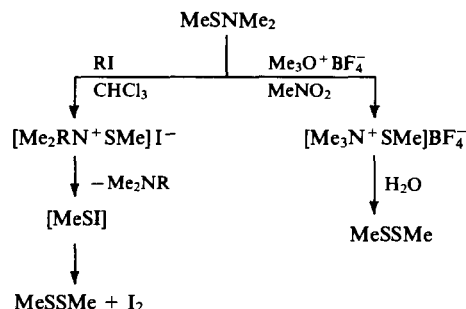


However, the synthesis of unsymmetrical disulfides is accompanied by the formation of a small amount of symmetrical ones,¹⁰⁹ this being the drawback of the method.

The hydrolysis of sulfenamides in acid-alcoholic media results in the formation of symmetrical disulfides.²³ They are, apparently, disproportionation products of sulfenic acids that are formed at the first stage of the hydrolysis.

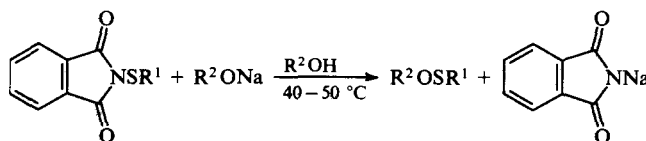


Symmetrical disulfides are also formed upon decomposition of thioammonium salts resulting from the alkylation of sulfenamides with alkyl halides or trialkyloxonium salts.¹¹³

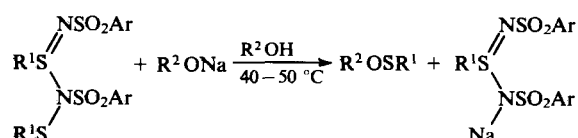


4. Synthesis of sulfenic esters

N,N-Disubstituted sulfenamides having strong electron withdrawing substituents relatively readily undergo alcoholysis in the presence of alkoxides. Alkyl sulfenates are produced in this way. For this purpose, *N*-(alkylthio)phthalimides^{114, 115} are most frequently used. They react with alkoxides in alcoholic media to form the corresponding sulfenates.



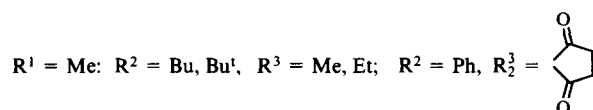
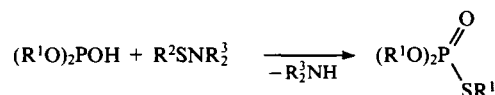
N-Arylsulfenyl-*N,N'*-bis(arylsulfonyl)arenesulfonamides undergo even easier alcoholysis.^{32, 116, 117}



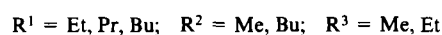
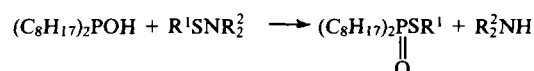
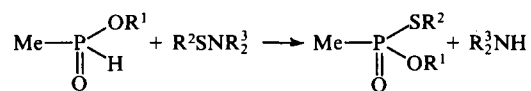
The use of sulfenamides for the synthesis of sulfenates is preferable to that of sulfonyl chlorides, because the latter often induces undesirable side processes.¹⁰⁴

5. Synthesis of compounds with a P—S bond

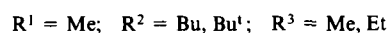
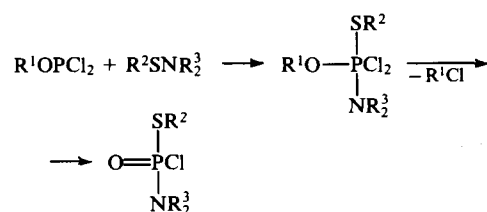
The use of sulfenamides for the synthesis of various phosphor-sulfur-containing compounds is based on phosphorolysis of the S—N bond with phosphorylating reagents. The synthesis of thiolphosphates using the interaction of *N,N*-disubstituted sulfenamides with dialkyl phosphites has been described.^{118, 119}



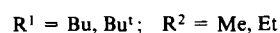
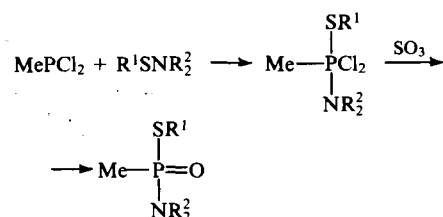
The syntheses of thiolphosphonates and thiolphosphinates were performed in a similar manner.¹¹⁹



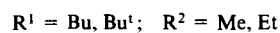
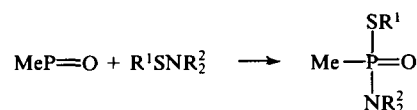
The reaction of sulfenamides with alkyl phosphodichloridites yields alkyl (amido)thiophosphochloridates.¹¹⁹



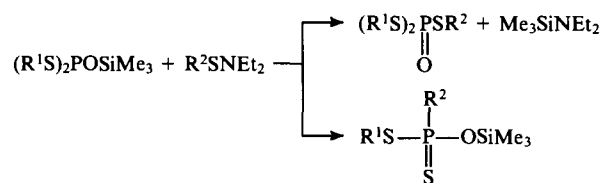
The reaction of sulfenamides with methyldichlorophosphine gives phosphoranes, which may be converted to *S*-alkyl dialkylamidothiophosphonates upon treatment with sulfur trioxide.²³



Similar compounds are formed when sulfenamides react with methylphosphonous anhydride.²³

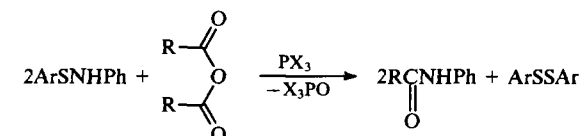
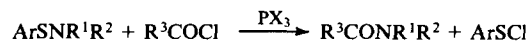
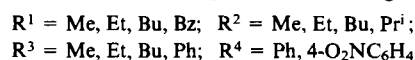
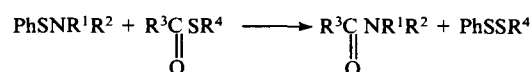


Sulfenamides react with *S,S*-dialkyl-*O*-trimethylsilyl dithiophosphites to yield trithiophosphates.¹²⁰ In this case, a part of the initial *O*-trimethylsilyl dithiophosphite is transformed to *S*-alkyl-*O*-trimethylsilyl dithiophosphonate.



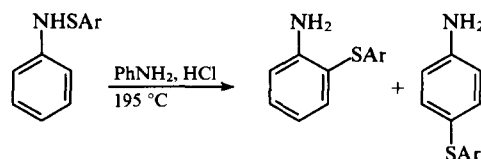
6. Synthesis of nitrogen-containing compounds

Sulfenamides are good amidating reagents with respect to *S*-esters of thiocarboxylic acids, carboxylic anhydrides, and acyl chlorides. This feature is often used in syntheses of various *N*-substituted carboxamides. The corresponding reactions occur in the presence of trivalent phosphorus compounds under rather mild conditions to give the target products in high yields.^{23, 121-123}



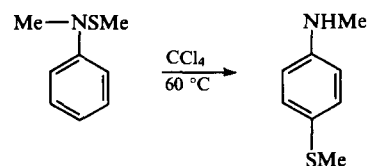
The role of the catalyst is to form the intermediate phosphonium salts with sulfenamides having a highly polarised S—N bond.¹²⁴

Different rearrangements of sulfenamides are often used in the syntheses of functionally substituted aromatic amines. For example, the heating of *N*-(phenyl)arenesulfenamides in aniline in the presence of hydrochloric acid results in a mixture of ortho- and para-substituted aniline derivatives.¹²⁵



Under similar conditions, *N*-phenyl-2-nitrobenzenesulfenamide gives a mixture of 2- and 4-aminodiphenyldisulfides, phenothiazine, and 2-aminobenzenesulfenamide.¹²⁶

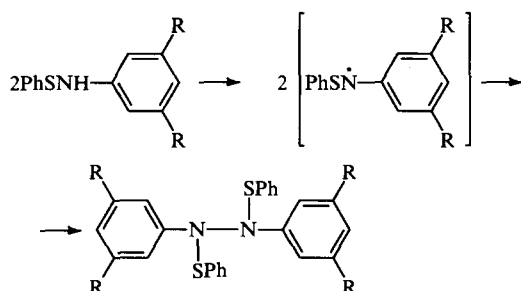
When heated in CCl_4 , *N*-methyl-*N*-phenylmethanesulfenamide rearranges into 4-methylthio-*N*-methylaniline.¹²⁷



When 4-nitrobenzenesulfenamide reacts with liquid ammonia in an autoclave, a mixture of 4-nitroaniline, 4,4'-dinitrodiphenyl-disulfide, and 4-nitrothiophenol is formed.¹²⁸ In addition to various rearrangements, other transformations of sulfenamides are used in the syntheses of functionally substituted aromatic amines. For example, the treatment of *N*-(4-nitrophenyl)-benzenesulfenamide with di-*tert*-butyl hyponitrite at 40 °C in *tert*-butyl alcohol has been reported¹²⁹ to yield a radical

$4\text{-O}_2\text{NC}_6\text{H}_4\text{NSPh}$, which transforms to the *N*-nitroaniline under the action of Bu_3SnH . Vicarious nucleophilic substitution of the hydrogen atom in the aromatic nucleus of nitroarenes using *N*-unsubstituted sulfenamides has been described.¹³⁰ For example, the amination of nitrobenzene with 1-pyrrolidino-carbonylsulfenamide in DMF in the presence of potassium *tert*-butoxide produces a mixture of 2-nitro- and 4-nitroanilines in yields of 34% and 41.5%, respectively. The amination of 1-nitronaphthalene with benzothiazole-2-sulfenamide in DMSO in the presence of potassium *tert*-butoxide gives a mixture of 2-amino-1-nitro- and 4-amino-1-nitronaphthalenes in 11% and 75% yield, respectively.

Among other nitrogen containing compounds that have been synthesised from sulfenamides, tetrasubstituted hydrazines should be noted; they are formed by dimerisation of thioaminy radicals generated from sulfenamides.^{131, 132}

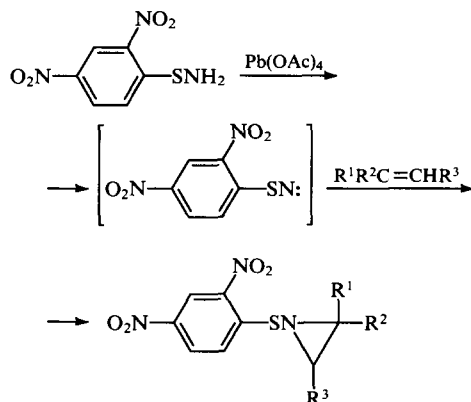


7. Synthesis of heterocyclic compounds

The use of sulfenamides in the synthesis of heterocyclic compounds is mainly based on the following transformations: a) generation of highly reactive intermediates and their reactions with unsaturated compounds; b) thermal rearrangements of sulfenamides; and c) various cyclisation reactions of sulfenamides.

a. Generation of highly reactive intermediates and their reactions with unsaturated compounds

Generation of nitrenes. The generation of nitrenes from *N*-unsubstituted sulfenamides followed by their reactions with alkenes is one method for the synthesis of *N*-aryltioaziridines.^{133–135} Nitrenes are generated in situ by the action of lead tetraacetate on *N*-unsubstituted sulfenamides that contain strong electron-acceptor groups at the sulfur atom, such as 2,4-dinitrophenyl.

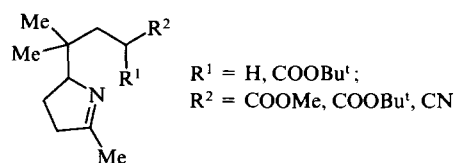


$\text{R}^1 = \text{H, Me, Ph, H}_2\text{C}=\text{CH}_2$; $\text{R}^2 = \text{H, Me, Ph}$; $\text{R}^3 = \text{H, Me}$

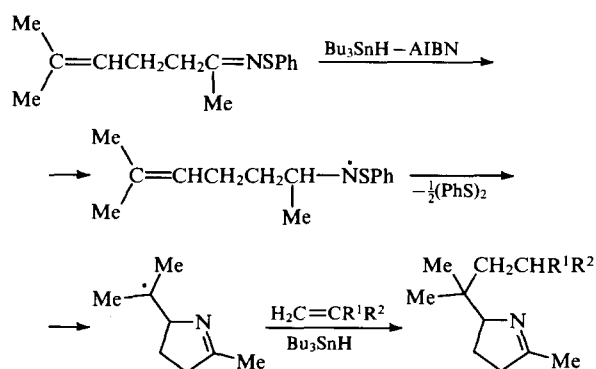
It is noted^{133, 135} that 2,4-dinitrobenzenesulfenamide is oxidised by lead tetraacetate in the presence of (*Z*)-phenylpropene to give a mixture of *trans*- and *cis*-1-(2,4-dinitrophenylsulfenyl)-2-methyl-3-phenylaziridines, their ratio being dependent on the nature of solvent, on the ratio of the reactants, and on the order of mixing the reagents.^{133, 135} For example, in benzene, the ratio of

trans- and *cis*-isomers is 1 : 1, while in chloroform and dichloromethane it is 3 : 1. In more polar solvents (MeCN, MeOH), the overall yield of both isomers decreases. If lead tetraacetate is added to a mixture of 2,4-dinitrobenzenesulfenamide and (*Z*)-phenylpropene, *N*-(2,4-dinitrophenyl)-2,4-dinitrobenzenesulfenamide is formed together with aziridines, and partial isomerization of (*Z*)-phenylpropene to (*E*)-phenylpropene is observed. However, the addition of a mixture of 2,4-dinitrobenzenesulfenamide and lead tetraacetate in chloroform to (*Z*)-phenylpropene results only in high yields of aziridines. The oxidation of 2,4-dinitrophenylsulfenamides is assumed¹³³ to produce initially a triplet nitrene in equilibrium with the singlet one, both of which react with (*Z*)-phenylpropene. This concept is supported by the fact that the introduction of $4\text{-ClC}_6\text{H}_4\text{SCH}_2\text{CH}=\text{CH}_2$, which is an efficient trap for singlet nitrenes, into the reaction mixture changes both the overall yield of aziridines and the ratio of isomers, while in the presence of efficient traps for triplet nitrenes, e.g. alkenes, $\text{PhC(R)}=\text{CH}_2$ ($\text{R} = \text{Ph, Me}$), the ratio of *cis*- and *trans*-isomers does not change, while the overall yield of aziridines decreases.

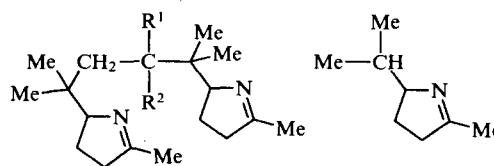
Generation of iminyl radicals. The generation of iminyl radicals from sulfenamides containing $\text{C}=\text{N}$ and $\text{C}=\text{C}$ bonds, and their subsequent addition to alkenes, is the basis for the synthesis of various pyrrolines. For example, a preparative method of synthesis of the pyrroline system is described¹³⁶ which involves the interaction of sulfenamide $\text{Me}_2\text{C}=\text{CHCH}_2-\text{CH}_2\text{C(Me)}=\text{NSPh}$ with the alkenes $\text{H}_2\text{C}=\text{CR}^1\text{R}^2$ ($\text{R}^1 = \text{H, COOBu}^t$; $\text{R}^2 = \text{COOMe, COOBu}^t, \text{CN}$) in the presence of Bu_3SnH –azobis(isobutyronitrile) (AIBN).



It is supposed¹³⁶ that the iminyl radical generated from the sulfenamide is transformed, via cyclisation, to the carbon-centred pyrrolinyl radical whose addition to the alkenes gives the final product.

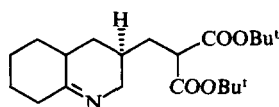


In this case, inconsiderable amounts of the products of the double addition of the primary pyrroline system to alkenes are formed, as well as the products of its stabilisation without subsequent addition.

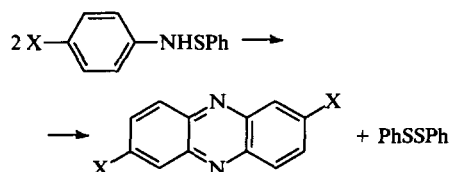


Similarly, when the sulfenamide $\text{H}_2\text{C}=\text{CHCH}_2-\text{CH}(\text{CH}_2)_4\text{C}=\text{NSPh}$ reacted with $\text{H}_2\text{C}=\text{C}(\text{COOBu}^t)_2$ in the

presence of $\text{Bu}_3\text{SnH} - \text{AIBN}$,¹³⁶ the heterocyclic ester was isolated as the main product.

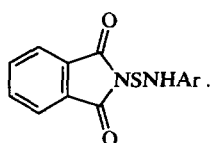


The transformation of 4-substituted *N*-(aryl)benzenesulfenamides into phenazine derivatives in the presence of lead tetraacetate or upon electrolysis is also assumed to occur via iminyl radicals.³⁴

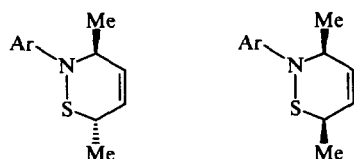


$\text{X} = \text{Me}, \text{Cl}, \text{OMe}$

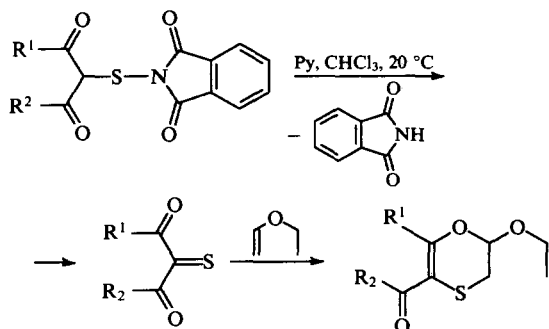
Generation of thionitroso compounds. A method for the synthesis of *N*-substituted derivatives of 1,2-thiazine has been described,¹³⁷ which involves the cycloaddition of dienes, (*E,E*)- and (*E,Z*)- $\text{MeCH}=\text{CH}-\text{CH}=\text{CHMe}$, to arylthionitroso compounds $\text{ArN}=\text{S}$ ($\text{Ar} = 4\text{-MeOC}_6\text{H}_4$, $4\text{-BrC}_6\text{H}_4$, $4\text{-MeC}_6\text{H}_4$, $4\text{-ClC}_6\text{H}_4$), obtained upon the action of triethylamine in acetone on sulfenamides



The cycloaddition occurs with retention of configuration of the initial dienes, and the following products are obtained, respectively:



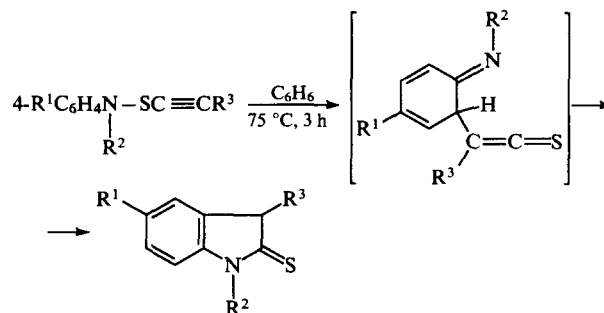
Generation of thiones. In the presence of organic bases, sulfenamides with β,β' -dicarbonyl fragments at the sulfur atom relatively readily transform into α,α' -dioxothiones. The latter undergo Diels-Alder type reactions with unsaturated compounds to yield various cyclic products.¹³⁸ A convenient preparative method for the synthesis of some 5,6-dihydro-1,4-oxathiine derivatives has been developed taking into account these features.^{44, 138}



$\text{R}^1 = \text{Me}, \text{R}^2 = \text{MeO}$ (70%); $\text{R}^1 = 4\text{-MeOC}_6\text{H}_4, \text{R}^2 = \text{SPh}$ (87%)

b. Thermal rearrangements of sulfenamides

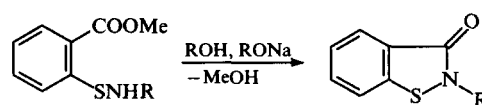
Sulfenamides containing ethenyl and ethynyl fragments at the sulfur atom are usually prone to thermal rearrangement resulting in heterocyclic systems. For example, heating of the sulfenamide $\text{Ph(Me)C}=\text{NSCH}=\text{CH}_2$ for 40 h in 1,2-diethoxyethane under nitrogen flow gives a 40% yield of 2-phenyl-pyrrole.¹² Under similar conditions, the sulfenamide $\text{cyclo-C}_6\text{H}_{10}=\text{NSCH}=\text{CH}_2$ gives 4,5,6,7-tetrahydroindole in 60% yield.¹² Upon heating in toluene, *N*-(1-naphthyl)-ethenesulfenamides undergo a [3,3]-sigmatropic rearrangement with subsequent elimination of hydrogen sulfide and formation of 1-*R*-1*H*-benz[g]indoles ($\text{R} = \text{H}, \text{Me}$).¹³⁹ Similar rearrangement with subsequent cyclisation occurs upon heating *N*-aryl-1-alkynesulfenamides in anhydrous benzene in an argon atmosphere.¹⁴⁰



$\text{R}^1 = \text{H}, \text{Me}; \text{R}^2 = \text{Me}; \text{R}^3 = \text{Me}, \text{Me}_3\text{Si}$

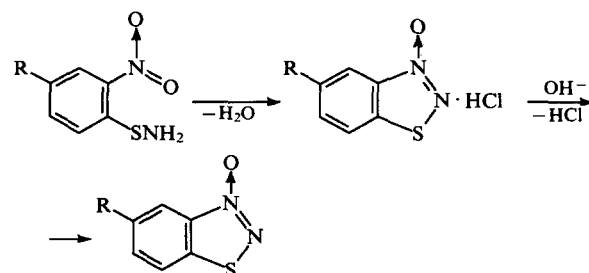
c. Cyclisation reactions of sulfenamides

The possibility of cyclisation of sulfenamides to heterocyclic systems depends on several factors, and mainly on the nature and the structure of substituents at the sulfur and nitrogen atoms, their mutual arrangement, as well as the lability of the S-N and of other bonds in the molecule. Taking into account these factors, preparative synthetic methods for various heterocyclic systems have been developed. For example, *N*-monosubstituted arenesulfenamides containing the alkoxycarbonyl group in the ortho position have successfully been used for the synthesis of 1,2-benzothiazole derivatives. Intramolecular cyclisation of such sulfenamides occurs relatively readily in alcoholic media in the presence of alkoxides.¹⁴¹



$\text{R} = \text{Me}, \text{Et}, \text{Pr}, \text{PhCH}_2, 4\text{-MeOC}_6\text{H}_4$

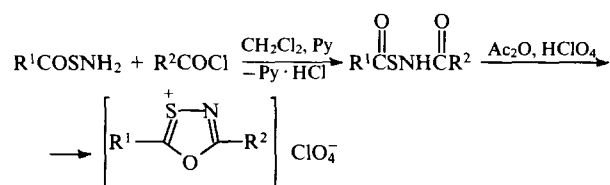
Intramolecular cyclisation of *N*-unsubstituted arenesulfenamides containing the nitro group in the ortho-position occurs in the presence of phosphorus acid chlorides [POCl_3 , PhOP(O)Cl_2 , $(\text{PhO})_2\text{P(O)Cl}$] and organic bases to give benzo-1,2,3-thiadiazole 3-oxide hydrochlorides.¹⁴²



$\text{R} = \text{H}, \text{NO}_2$

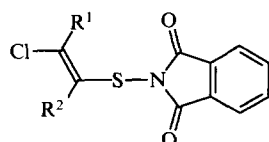
A simple and efficient method for the synthesis of 1,3,4-oxathiazolium perchlorates has been described¹⁴³ that involves the

cyclisation of *N*-(acyl)arenecarbonylsulfenamides in acetic anhydride in the presence of 70% HClO_4 .

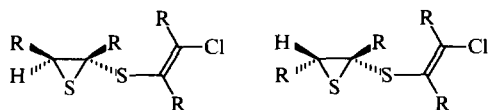


$\text{R}^1 = 4\text{-MeOC}_6\text{H}_4$; $\text{R}^2 = \text{Me}, \text{Ph}, 4\text{-MeOC}_6\text{H}_4$

Sulfenamides

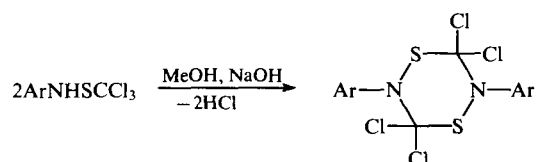


($\text{R}^1 = \text{H}, \text{Me}, \text{Et}, \text{R}^2 = \text{Me}, \text{Et}, \text{Bu}^t$) form ¹⁴⁴ a diastereomeric mixture (93:7) of thiirane derivatives when treated with 2 equiv. of LiEt_3BH , NaBH_4 , or LiAlH_4 in THF at -78°C .



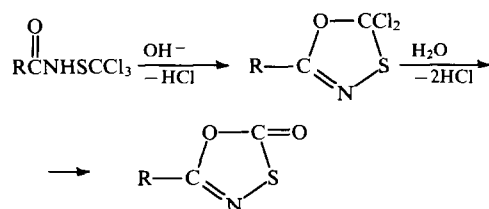
$\text{R} = \text{Me}, \text{Et}$

Owing to the high reactivity of the trichloromethyl group a rather wide range of methods for the synthesis of various heterocycles has been developed based on *N*-substituted trichloromethanesulfenamides. For example, *N*-(aryl)trichloromethanesulfenamides cyclise in the presence of alcoholic alkali to give 2,5-diaryl-3,3,6,6-tetrachloro-2,3,5,6-tetrahydro-1,4,2,5-dithiadiazines.^{8, 38}



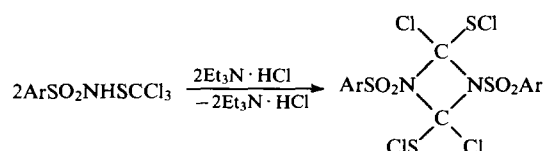
$\text{Ar} = \text{Ph}, 4\text{-MeC}_6\text{H}_4, 4\text{-MeOC}_6\text{H}_4$

Under the action of bases (NaOH , EtONa , Et_3N , Py), *N*-(acyl)trichloromethanesulfenamides cyclise to form 5-*R*-1,3,4-oxathiazol-2-ones.^{145, 146}

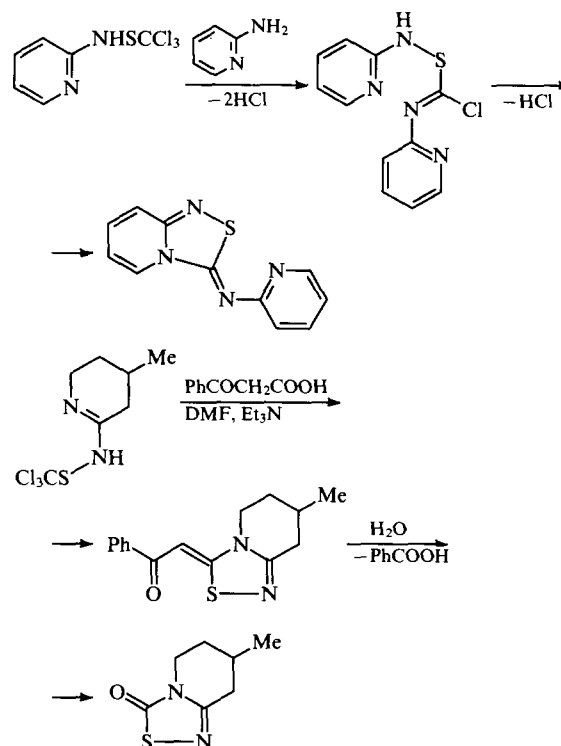


$\text{R} = \text{Ph}, 4\text{-MeC}_6\text{H}_4, 4\text{-MeOC}_6\text{H}_4, 3\text{-MeOC}_6\text{H}_4, 3,5\text{-Me}_2\text{C}_6\text{H}_3$

In the presence of triethylamine, *N*-(trichloromethylthio)arenesulfenamides are converted into 2,4-dichloro-2,4-bis(chlorothio)-1,3-bis(arylsulfonyl)-1,3-diazetidines.⁸



A series of 1,2,4-thiadiazole derivatives have been synthesised by the reaction of *N*-(pyrid-2-yl)- and *N*-(tetrahydropyrid-2-yl)trichloromethanesulfenamides with 2-aminopyridine^{147, 148} or benzoylacetic acid.¹⁴⁹

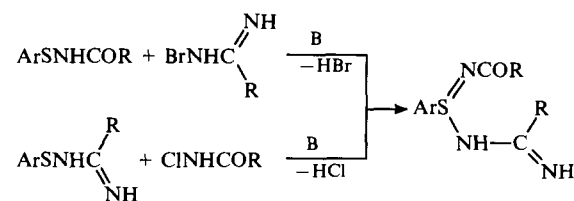


A considerable number of sulfur-nitrogen-containing heterocyclic compounds were obtained by reactions of trichloromethanesulfenyl chloride with various nitrogen-containing compounds, without isolating the intermediate *N*-substituted trichloromethanesulfenamides. Methods for the synthesis of these heterocycles are described in detail in a review⁸ and in the literature cited therein.

8. Synthesis of iminosulfur compounds

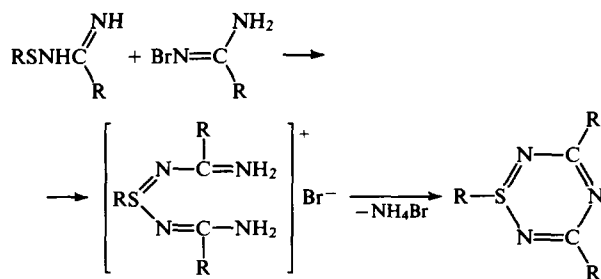
a. Synthesis of amides of sulfinimidic acid

Several methods for the synthesis of amides of sulfinimidic acids based on sulfenamides have been developed. One of the most common methods is based on oxidative imination of sulfenamides with *N*-halo compounds. The main advantage of this method is its one-step character, as well as the possibility of synthesising amides of sulfinimidic acids of varying structure by altering the nature of both the sulfenamide and the iminating reagent. For example, the amides of arenesulfinimidic acids containing acyl and carboximidoyl groups at the nitrogen atoms can be obtained by oxidative imination of *N*-(acyl)arenesulfenamides with *N*-bromoamidines, or by oxidative imination of *N*-(carboximidoyl)arenesulfenamides with *N*-chlorocarboxamides.¹⁵⁰



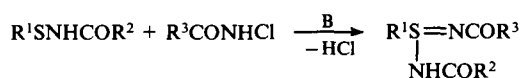
$\text{Ar} = 4\text{-O}_2\text{NC}_6\text{H}_4$; $\text{R} = \text{Me}, \text{Ph}$

N-Bromoamidines also react relatively readily with *N*-(carboximidoyl)sulfenamides to give salts of *N,N'*-bis-(carboximidoyl)amides of sulfinimidic acids which form triazines upon heating.^{151, 152}



R = Alk, Ar

A series of amides of sulfinimidic acids containing the same or different acyl groups at the nitrogen atoms was obtained by the oxidative imination of *N*-(acyl)sulfenamides with *N*-chlorocarbonylamides in the presence of organic bases (RONa, Py, Et₃N).^{153, 154}

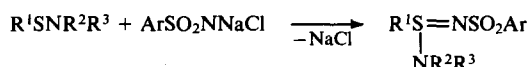


R¹ = 4-O₂NC₆H₄, CCl₃;

R² = Me, Et, Ph, 4-MeC₆H₄, PhCH₂, NH₂, PhNH;

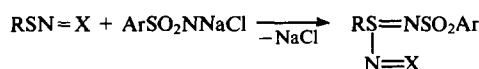
R³ = Me, Ph

Several amides of sulfinimidic acids containing arylsulfonyl groups were synthesised from sulfenamides and sodium *N*-chlorosulfonamides.^{19, 20, 35, 65, 146, 155-163}



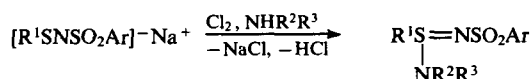
R¹ = Ar, Me, CH₂Cl, EtOCCl₂, CCl₃, CCl₂F, CF₂Cl;

R² = H, Alk, Ar, Ac, ArSO₂, CN; R³ = H, Alk, Ar

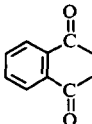


R = Ar; X = S(O)Ph₂, C(OMe)NH₂, C(OEt)NH₂, C(SeEt)NH₂, C(NH₂)NH₂

Yet another method of synthesis of amides of sulfinimidic acids from sulfenamides involves chlorination of sodium *N*-(arylthio)arenesulfonamides with chlorine in the presence of *N*-nucleophiles.¹⁶⁴⁻¹⁶⁶



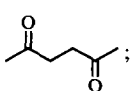
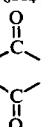
R¹ = 2-O₂NC₆H₄, 2,4-(O₂N)₂C₆H₃;

R², R³ = Et, C₅H₁₁, iso-C₅H₁₁; R² + R³ = 

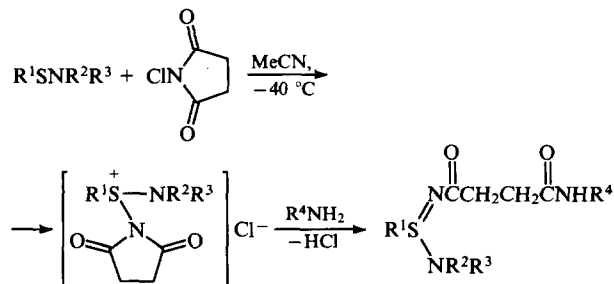
The reaction of sodium *N*-(arylthio)arenesulfonamides with *N*-haloimides is one of the modifications of this method.^{166, 167}



R = 2-O₂NC₆H₄, 4-O₂NC₆H₄; X = Cl, Br;

Y = ; 

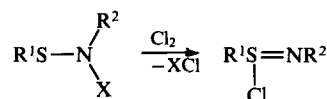
The reaction of *N,N*-dialkylsulfenamides with *N*-chlorosuccinimide gives sulfonium salts which form amides of sulfinimidic acids in the presence of amines.¹⁶⁸



R¹ = Alk, Ar; R² = R³ = R⁴ = Alk

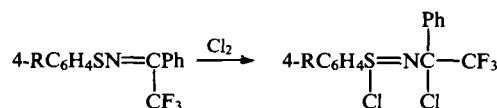
b. Synthesis of sulfinimidoyl chlorides

Sulfinimidoyl chlorides are obtained by oxidative chlorination of sulfenamides containing N-H, N=C, N-Si, and N-Na groups, usually in anhydrous aprotic organic solvents.¹⁶⁹⁻¹⁷⁴



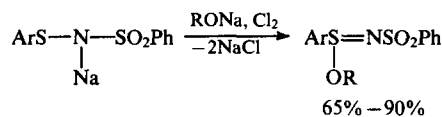
R¹ = Ar, CF₃; R² = ArSO₂, ArCO, CF₃S, Me₃Si, Bu^t;

X = H, Na, Me₃Si



c. Synthesis of alkyl sulfinimidoates

A simple and efficient method of synthesis of alkyl *N*-(arylsulfonyl)sulfinimidoates has been developed, which involves the chlorination of sodium *N*-(arylthio)arenesulfonamides with *tert*-butyl hypochlorite or chlorine in alcoholic media.¹⁷⁵⁻¹⁷⁷

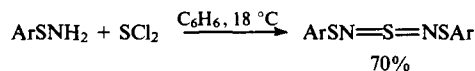


65% - 90%

R = Me, Et, Pr, Prⁱ, Bu, Buⁱ

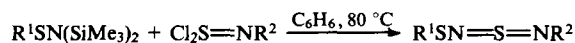
d. Synthesis of sulfurdiimines

N-Unsubstituted arenesulfenamides react with sulfur dichloride in anhydrous benzene to yield *N,N'*-bis(arylsulfonyl)sulfurdiimines.¹⁷⁸



Ar = 4-O₂NC₆H₄

Sulfurdiimines are obtained in the reaction of *N,N*-bis(trimethylsilyl)sulfenamides with *N*-substituted *S,S*-dichlorosulfonimides.¹⁷⁹

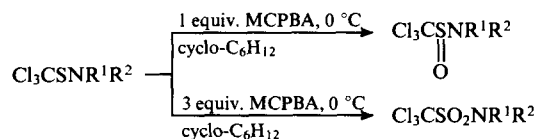


R¹ = Et, Ph; R² = Ts, 4-O₂NC₆H₄, 2,4,6-Cl₃C₆H₂, 2,4,6-Br₃C₆H₂

N,N'-Bis(2,4,6-*tert*-butylphenyl)sulfurdiimine resulted from the reaction of 2,4,6-tri-*tert*-butylbenzenesulfenamide with lead tetraacetate.¹⁸⁰

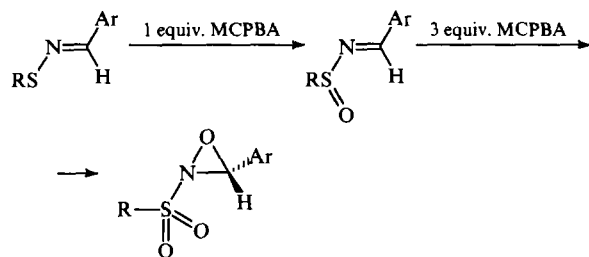
9. Synthesis of sulfin- and sulfonamides

The oxidation of sulfenamides can yield either sulfin- or sulfonamides, depending on the nature of the sulfenamide and the oxidant, on their ratio, and on the oxidation conditions. Manganese dioxide,¹⁸¹ *m*-chloroperbenzoic acid (MCPBA),^{182–184} *N*-chlorosuccinimide,¹⁸⁵ *N*-chlorobenzotriazole,¹⁸⁶ and other reagents¹⁸⁴ are generally used as the oxidants. MCPBA is the most common oxidising reagent for the synthesis of sulfin- and sulfonamides from sulfenamides. The use of 1 equiv. of MCPBA yields sulfinamides, while three or more equivalents of the oxidising reagent are required for the preparation of sulfonamides, as exemplified by the oxidation of *N,N*-disubstituted trichloromethanesulfenamides.



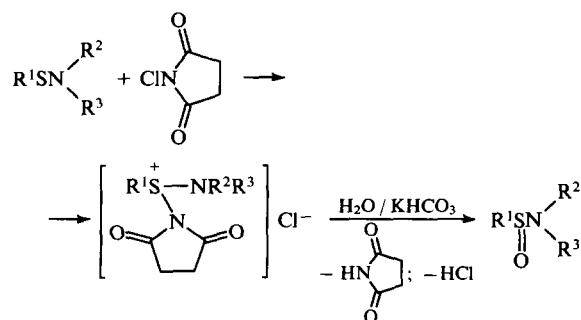
R¹ = Alk; R² = Alk, Ar

The oxidation of *N*-arylsulfinamides with 1 equiv. of MCPBA results in *N*-sulfinylimines, while a large excess of MCPBA leads to *N*-alkylsulfonylaziridines of (*E*)-configuration.³⁴



R = Me, Bu, PhCH₂

The oxidation of 6-ethoxybenzothiazole-2-sulfenamide to the corresponding sulfonamide has been shown¹⁸⁴ to occur smoothly in the presence of MCPBA, while the use of hydrogen peroxide or *tert*-butyl hypochlorite is accompanied by oxidation of the heterocycle. The reaction of sulfenamides with *N*-chlorosuccinimide proceeds via the intermediate succinimidiosulfonium salt.¹⁸⁵



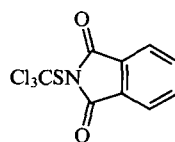
Optically active sulfinamides are obtained by oxidation of the corresponding sulfenamides with *N*-chlorobenzotriazole in the presence of L-menthol or D-tartrate.¹⁸⁶

IV. Practical application of sulfenamides

1. Biological activity of sulfenamides

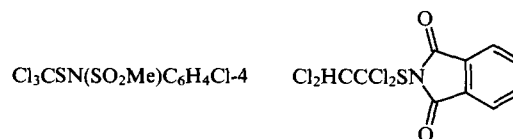
After the first reports on the biological activity of sulfenamides,¹⁸⁷ investigations in this area began to develop intensely. Many patents and scientific papers devoted to this problem have been

published. An analysis of the results obtained has been partially reviewed.^{8, 23, 24, 188, 189} The main achievements involve: the discovery of the fungicidal activity of some sulfenamides, the development of technology for the manufacture of highly effective sulfenamide-based fungicides, and their application in agriculture. The *N*-(trichloromethyl)thiophthalimide, Phthalan, is one of the most valuable fungicides of this series.^{190, 191}

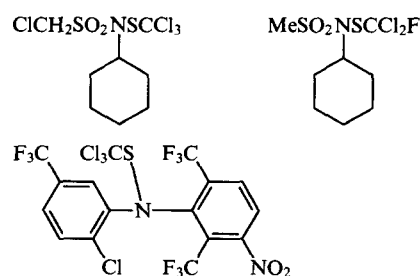


This sulfenamide is widely used as a standard fungicide, against the diseases of apples and pears (tetter), stone-fruits (leaf spots), grapes (mould, anthracnose, red-rot, black, white, and grey rot), gooseberries and currants (anthracnose), tomatoes and potatoes (phytophthora infection).

N-Trichloromethylthio-1,2,5,6-tetrahydrophthalimide (commercial name Kaptan) is also a very valuable fungicide.^{190, 191} It is widely used against diseases of apples, pears, stone-fruits, strawberries, berry bushes, grapes, tomatoes and potatoes. Mesulfan¹⁹⁰ and Difolathan¹⁹⁰ are characterised by the same fungicidal properties.

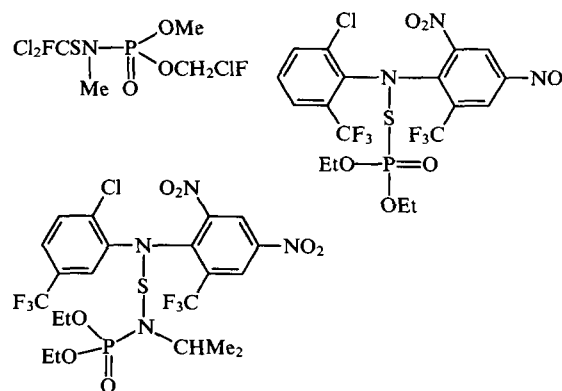


The sulfenamides FCl₂CSN(Ph)SO₂NMe₂ (Euparen) and FCl₂CSN(SO₂NMe₂)C₆H₄Me-4 (Euparen-M) are also effective fungicides.^{191, 192} They are used against the diseases of apples, currants, and grapes. The sulfenamides

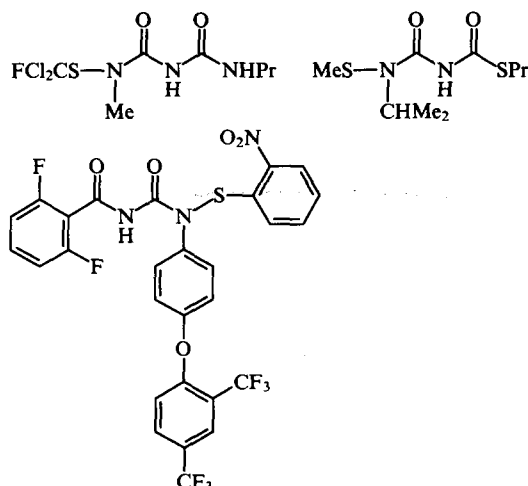


appear to have similar fungicidal properties.^{34, 193, 194}

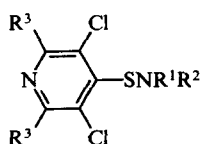
Some phosphorus-containing sulfenamides also exhibit rather high fungicidal activity.^{34, 195–197}



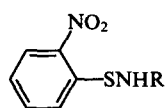
as well as some derivatives of sulfonylurea^{198, 199} which in addition display insecticidal activity.²⁰⁰



Some *N*-substituted 4-pyridinesulfenamides²⁰¹ and 2-nitrobenzenesulfenamides²⁰² exhibit herbicidal, insecticidal, and nematocidal activity.

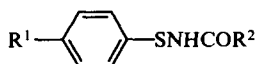


$R^1 = R^2 = \text{H, Me, Et, etc.};$
 $R^3 = \text{F, Cl}$



$R = \text{H, 2-O}_2\text{NC}_6\text{H}_4\text{S, PhCO, PhSO}_2$

The sulfenamides of the general formula



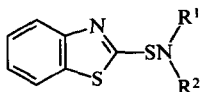
$R^1 = \text{H, Cl, NO}_2; \quad R^2 = \text{Me, EtO, Ph.}$

are plant growth regulators.²⁰³

2. Sulfenamides in the rubber industry

In the rubber industry, sulfenamides are mainly used to accelerate the process of rubber vulcanisation^{34, 204, 205} owing to the high lability of the S—N bond and to its relatively easy homolysis to yield sulfenyl radicals that participate in the vulcanisation processes. Sulfenamides meet all the main requirements for industrial vulcanisation accelerators. In addition to intensification of the process, sulfenamides affect the structure of the resulting cross-linked structures, thus largely predetermining the mechanical properties of the rubber.

2-Benzothiazolesulfenamides are efficient accelerators of rubber vulcanisation;^{204, 205} they have found wide industrial application.



For example, *N,N*-(diethyl)benzothiazole-2-sulfenamide ($R^1 = R^2 = \text{Et}$) is an efficient delayed action accelerator at the beginning of vulcanisation. It provides the rubber with strong resistance to ageing and good elasticity. In particular, it is very efficient for rubber working under hard, dynamic conditions.

N-(*tert*-Butyl)benzothiazole-2-sulfenamide ($R^1 = \text{H, } R^2 = \text{Bu}^t$) is also an efficient delayed action accelerator. It results in rubber with strong resistance to ageing, and is used for the production of protectors and carcass rubber.

N,N-(Diisopropyl)benzothiazole-2-sulfenamide ($R^1 = R^2 = \text{Pr}^i$) is used as markedly delayed action accelerator which

increases the resistance of rubber mixtures to prevulcanisation as well as to ageing.

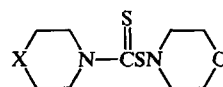
N-(*tert*-Octyl)benzothiazole-2-sulfenamide ($R^1 = \text{H, } R^2 = \text{Me}_3\text{CCH}_2\text{CMe}_2$) is characterised by distinct delayed action at the beginning of vulcanisation. It prevents rubber mixtures undergoing premature vulcanisation.

N-(Cyclohexyl)benzothiazole-2-sulfenamide ($R^1 = \text{H, } R^2 = \text{cyclo-C}_6\text{H}_{11}$) is a very efficient delayed action accelerator at the beginning of vulcanisation. It provides rubber of high elasticity and increased tensile strength as well as good durability. This accelerator is used for the manufacture of protectors and tyre carcasses.

N-(Hexamethylene)benzothiazole-2-sulfenamide [$R^1 + R^2 = -(\text{CH}_2)_6-$], as well as benzothiazole-2-sulfenomorpholide and -(2,6-dimethylmorpholide) [$R^1 + R^2 = (\text{CH}_2\text{CH}_2)_2\text{O}$ and $(\text{CH}_2\text{CHMe})_2\text{O}$, respectively], display analogous functional activity.

N,N-(Dicyclohexyl)benzothiazole-2-sulfenamide ($R^1 = R^2 = \text{cyclo-C}_6\text{H}_{11}$) is also a pronounced delayed action accelerator at the initial stage of vulcanisation and provides rubber mixtures of high elasticity and strong resistance to ageing. This accelerator is used in the manufacture of tyres, transporters, shock absorbers, etc.

The thiocarbonylsulfenamides of the general formula



$X = \text{O, CH}_2.$

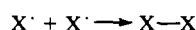
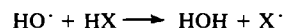
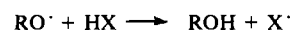
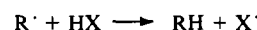
are even more efficient vulcanisation accelerators than the benzothiazole-2-sulfenamides.^{206, 207}

The sulfenamides $\text{RSN}(X)\text{SO}_2\text{Ph}$ [$X = \text{S(R)} = \text{NSO}_2\text{Ph}$; $R = \text{Ph, 4-MeC}_6\text{H}_4, \text{benzoxazolyl}$] have proved to be efficient accelerators of vulcanisation of butadiene–nitrile rubber 'SKN-26'.^{208, 209}

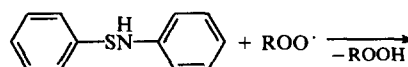
Sulfenamides are also used, but not so often, as vulcanisation inhibitors to prolong the prevulcanisation period.^{210–213} Usually, *N*-substituted sulfenamides with acyl, arylsulfonyl, and other substituents display these properties.

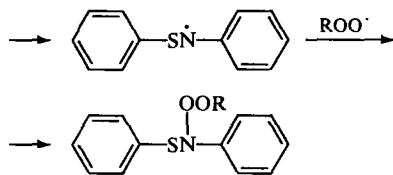
3. Sulfenamides in the chemistry of polymers

To protect polymers from oxidative degradation specific anti-oxidants are introduced into polymers. They not only prevent oxidation, but often suppress other undesirable processes favoured by oxygen or peroxides. According to the generally accepted mechanism of oxidant activity,²¹⁴ their main role is to bind the active radicals $R^\cdot, \text{RO}^\cdot, \text{ROO}^\cdot, \text{HO}^\cdot$ formed under the action of oxygen. This results in stable substances or stabilised radicals, X^\cdot , that cannot attack a new polymeric chain.



If we take these criteria into account, sulfenamides can be considered as potential polymer antioxidants. Similar to the secondary amines used as industrial antioxidants,²¹⁴ *N*-mono-substituted sulfenamides are prone to eliminate a hydrogen atom from the nitrogen atom to produce aminyl radicals; this process can occur in the presence of peroxide radicals.

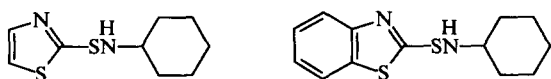




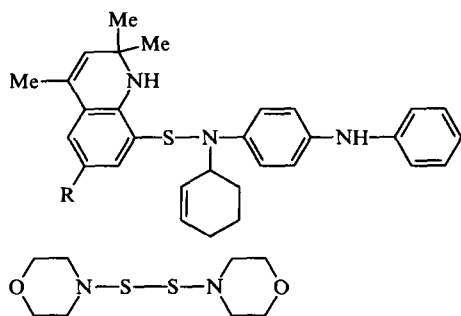
On the other hand, the presence of bivalent sulfur in the sulfenamide molecule, which is able to pass to a higher valence state in the presence of oxidants, should favour the antioxidative properties. Hence, *N*-(cyclohexyl)pentachlorobenzene sulfenamide has been proposed as an antioxidant for polyolefins.²¹⁵

One serious problem hindering the processing of poly(vinyl chloride) is its thermal instability. Thermal destruction of poly(vinyl chloride) occurs in a temperature range of 130–170°C, while the plastic state which is necessary for processing is reached at a temperature higher than 200°C.²¹⁶ The processing of poly(vinyl chloride) is therefore performed after it has been stabilised. The destruction process of this polymer is rather complicated and has not yet been entirely studied. However, radicals are assumed to play the main role in this process.^{214, 215} The destruction is initiated by the R· radical, which is formed from admixtures or from the polymer itself upon heating.

During degradation, the initially colourless poly(vinyl chloride) first turns yellow, then orange, brown, and black depending on the concentration of conjugated double bonds, which, in turn, depends on the extent of the degradation. It is supposed²¹⁴ that HCl liberated is a catalyst of this process, and the role of thermostabilisers is to bind it. However, another mechanism of action of thermostabilisers involving a capture of R· radicals and their transformation into inactive products at the beginning of the initiation, should not be excluded. Apparently, the thermostabilisation of poly(vinyl chloride) in the presence of some *N*-substituted sulfenamides occurs according to this scheme. Thus, high thermostabilising activity of *N*-(cyclohexyl)thiazole-2- and benzothiazole-2-sulfenamides towards poly(vinyl chloride) has been reported.²¹⁵

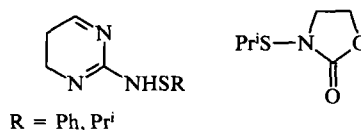


The following sulfenamides have been proposed to thermostabilise halogenated butyl rubber.²¹⁵



4. Sulfenamides as pharmaceuticals

Some sulfenamides are potential pharmaceuticals. Thus, sulfenamides of the pyrimidine series have proved to be antihemorrhagic inhibitors of lipoxygenase and hinder leukocyte migration.^{217, 218} The oxazolidinone sulfenamide has been described²¹⁹ which, in addition to the above mentioned properties, also displays antiasthmatic activity.



3-Nitropyridine-2-sulfenamide and its analogues display anti-tumour activity.

5. Sulfenamides as electrolytic additives

The application of *N*-phenylthio-*N,N'*-bis(phenylsulfonyl)benzenesulfenamide as an additive to the electrolyte for silver plating of metals was shown to improve the coating quality.²²⁰ The use of this electrolyte provides coatings with fine crystal structure, lustre, and good adhesion to a support.

* * *

Thus, application of sulfenamides in fine organic synthesis is based on the specific features of their structure and reactivity, namely the presence of two active centres (S and N) and the high lability of the S–N bond. The capability of this bond to be relatively easily cleaved in the presence of both nucleophilic and electrophilic reagents, as well as to be homolysed, enables sulfenamides to be used as carriers of the sulfonyl group in syntheses of sulfides, disulfides, esters of sulfenic acids, and other sulfur-containing compounds, and to be used as a protective function in syntheses of peptides and alkaloids. The ability of sulfenamides to generate various highly reactive intermediates is a property of synthetic importance, which is widely used in syntheses of heterocyclic compounds and various sulfur-imino compounds. The practical application of sulfenamides in the rubber industry, macromolecular chemistry, agriculture, and other areas is of no less importance.

The search for, and development of, unusual methods of sulfenamide synthesis, such as the chlorosulfonylamidation of alkenes and alkynes, sulfonylamidation of CH-acids, etc., seem in the immediate future to be the main directions of research in this field of organic synthesis. The study of the reactions of sulfenamides involving the generation of various highly reactive intermediates should progress considerably. Their employment in organic synthesis will prompt the emergence of new polyfunctional compounds, including potentially valuable ones.

References

1. A Fontana, E Scoffone *Mech. React. Sulfur Compd.* **4** 14 (1969)
2. R E Vegner, I K Perkone, G I Chipens, in *IX Mezhdunar. Simp. po Khimii Organicheskikh Soedinenii (Tez. Dokl.)* [The Ninth International Symposium on the Chemistry of Organic Compounds (Abstracts of Reports)] (Riga: Zinatne, 1980) p. 60
3. E M Gordon, M A Ondetti, J Pluscek, C M Cimarusti, D P Bonner, R B Sykes *J. Am. Chem. Soc.* **104** 6053 (1982)
4. B P Branchaud *J. Org. Chem.* **48** 3538 (1983)
5. K Hiroi, M Nishida, A Nakayama, K Nakazawa *Chem. Lett.* 969 (1979)
6. L I Belen'kii (Ed.) *Khimiya Organicheskikh Soedinenii Sery* (Chemistry of Organic Compounds of Sulfur) (Moscow: Khimiya, 1988)
7. R Sato, Y Hoshi, M Sasaki, M Nakayama, T Goto, M Saito *Chem. Express* **3** 355 (1988)
8. I V Koval' *Usp. Khim.* **60** 1645 (1991) [*Russ. Chem. Rev.* **60** 830 (1991)]
9. I V Koval' *Usp. Khim.* **64** 781 (1995) [*Russ. Chem. Rev.* **64** 731 (1995)]
10. B T Christensen, I Thomson, A Senning *Sulfur Lett.* **10** 193 (1990)
11. A Senning, A Bouregghda, M F Abdel-Megeed, B Jensen, B Nielsen, A K Jensen *Sulfur Lett.* **13** 187 (1991)
12. O Ruel, J B Baudin, A S Julia *Synth. Commun.* **20** 2151 (1990)
13. W R Bowman, D N Clark, J R Marmon *Tetrahedron Lett.* **32** 6441 (1991)

14. Y C Sutaria, P B Patel *J. Inst. Chem. (India)* **62** 121 (1990)
15. C V Christov, T V Vasilev, C M Angelow, in *The XVth International Symposium on the Organic Chemistry of Sulfur (Abstracts of Papers)* (Caen: University of Caen, 1992) p. 142
16. C V Christov, I J Tackeva, T V Vasilev, M C Angelov *Phosphorus Sulfur Silicon Relat. Elem.* **78** 199 (1993)
17. D H R Barton, H R Hease, C A O'Sullivan, M M Pechet *J. Org. Chem.* **56** 6702 (1991)
18. B V Kunshenko, V O Omarov, N N Muratov, L M Yagupol'skii *Zh. Org. Khim.* **28** 892 (1992)
19. I V Koval', T G Oleinik, L B Novikova *Zh. Org. Khim.* **29** 1822 (1993)
20. I V Koval', V N Goncharuk, T G Oleinik *Zh. Org. Khim.* **29** 2002 (1993)
21. I V Alabugin, V K Brel', in *Materialy Simpoziuma po Organicheskoi Khimii* (Proceedings of a Symposium on Organic Chemistry) (St. Petersburg: Nauka, 1995) p. 99
22. I V Koval' *Usp. Khim.* **62** 813 (1993) [*Russ. Chem. Rev.* **62** 769 (1993)]
23. K A Petrov, G V Rudnev, V D Sorokin *Usp. Khim.* **59** 1431 (1990) [*Russ. Chem. Rev.* **59** 832 (1990)]
24. S Oae, K Shinhasse, J H Kim *Chem. Lett.* 1077 (1979)
25. F A Davis, W A R Siegeir, S Evans, A Schwartz, D L Goff, R Palmer *J. Org. Chem.* **38** 2809 (1973)
26. F A Davis, A T Friedman, E W Kluger, E B Skibo, E R Fretz, A P Milicia, W C Le Masters *J. Org. Chem.* **42** 967 (1977)
27. I V Koval' *Usp. Khim.* **63** 776 (1994) [*Russ. Chem. Rev.* **63** 735 (1994)]
28. E S Levchenko, T N Dubinina, S V Sereda, M Yu Antipin, Yu T Struchkov, I E Boldeskul *Zh. Org. Khim.* **23** 86 (1987)
29. E S Levchenko, T N Dubinina, L V Budnik *Zh. Org. Khim.* **19** 2158 (1983)
30. Europ. P. 10 477; *Chem. Abstr.* **93** 220 730y (1980)
31. E S Levchenko *Ukr. Khim. Zh.* **55** 929 (1989)
32. I V Koval' *Sulfur Rep.* **14** 149 (1993)
33. H Ikehira, S Tanimoto *Synthesis* 716 (1983)
34. L Craine, M Raban *Chem. Rev.* **89** 689 (1989)
35. I V Koval', T G Oleinik, M M Kremlev *Zh. Org. Khim.* **16** 633 (1980)
36. H Bock, K L Kompa *Z. Anorg. Allg. Chem.* **332** 238 (1964)
37. P Kovacic, M K Lowery, K W Field *Chem. Rev.* **70** 639 (1970)
38. E Kühle *Synthesis* 617 (1971)
39. W H Mueller, P E Butler *J. Org. Chem.* **33** 2111 (1968)
40. A G Kutateladze, O V Denisenko, N V Zyk, N S Zefirov, in *XVIII Konf. po Khimii i Tekhnologii Organicheskikh Soedinenii Sery* (Tez. Dokl.) [The XVIIIth Conference on the Chemistry and Technology of Organic Compounds of Sulfur (Abstracts of Reports)] (Kazan': Izd. Kazansk. Univ., 1992) p. 177
41. G Capozzi, L Gori, S Menichetti, C Nativi *J. Chem. Soc., Perkin Trans. 1* 1923 (1992)
42. E Busi, G Capozzi, S Menichetti, C Nativi *Synthesis* 643 (1992)
43. E Busi, G Capozzi, S Menichetti, C Nativi, A Rosi, G Valle *Tetrahedron* **48** 9023 (1992)
44. G Capozzi, S Menichetti, C Nativi, A Rosi, in *The XVth International Symposium on the Organic Chemistry of Sulfur (Abstracts of Papers)* (Caen: University of Caen, 1992) p. 31
45. G Capozzi, S Menichetti, C Nativi, A Rosi, R W G Franck *Tetrahedron Lett.* **34** 4253 (1993)
46. I V Koval' *Usp. Khim.* **59** 1409 (1990) [*Russ. Chem. Rev.* **59** 819 (1990)]
47. R S Atkinson, B D Judkins, B Patwardhan *J. Chem. Soc., Perkin Trans. 2* 1490 (1979)
48. R S Atkinson, S B Awad *J. Chem. Soc., Chem. Commun.* 651 (1975)
49. R S Atkinson, S B Awad, J M Barlow, D R Russell *J. Chem. Res.* 331 (1978)
50. R S Atkinson, S B Awad *J. Chem. Soc., Perkin Trans. 1* 346 (1977)
51. T Yamamoto, M Kakimoto, T Macjima, M Okawara *Bull. Chem. Soc. Jpn.* **56** 1249 (1983)
52. W Franck, P K Claus *Monatsch. Chem.* **121** 539 (1990)
53. P K Claus, W Silbernagel, W Franck, W Rieder *Monatsch. Chem.* **116** 841 (1985)
54. A R Katritzky, I Takahashi, C M Marson *J. Org. Chem.* **51** 4914 (1986)
55. S Oae, A Tetsuo, N Masachi, N Furukawa *Tetrahedron* **30** 947 (1974)
56. N P Pel'kis, E S Levchenko *Zh. Org. Khim.* **22** 387 (1986)
57. E S Levchenko, N P Pel'kis *Zh. Org. Khim.* **20** 672 (1984)
58. T N Dubinina, E S Levchenko *Zh. Org. Khim.* **15** 743 (1979)
59. S Toru, H Tanaka, M Ukida *J. Org. Chem.* **43** 3223 (1978)
60. S Toru, H Tanaka, M Ukida *J. Org. Chem.* **44** 1554 (1979)
61. F A Davis, U K Nadir *Org. Prep. Proced. Int.* **11** 33 (1979)
62. B P Branchaud *J. Org. Chem.* **48** 3531 (1983)
63. I Shibuya, K Yonemoto, A Oishi, M Yasumoto, Y Taguchi, T Tsuchiya *J. Chem. Soc. Jpn., Chem. Ind. Chem.* **7** 857 (1993)
64. A Bouregda, M F Abdel-Megeed, A G A B Chattas, B Jensen, A Senning *Sulfur Lett.* **5** 159 (1987)
65. I V Koval', A I Tarasenko, T G Oleinik, M M Kremlev *Zh. Org. Khim.* **15** 1004 (1979)
66. J-L Zhang, X-B Ma, in *The International Conference on Phosphorus Chemistry (Abstracts of Reports)* (Tallin: Zinatne, 1989) Vol. 1, p. 1
67. N S Zefirov, N V Zyk, A G Kutateladze, E S Ignatenko, O V Denisenko, in *Vsesoyuz. Simp. po Organicheskomu Sintezu* (Tez. Dokl.) [The Fifth All-Union Symposium on Organic Synthesis (Abstracts of Reports)] (Moscow: Nauka, 1988) p. 51
68. K Boustany, J P V Kool *Tetrahedron Lett.* 4983 (1970)
69. F A Davis, P A Mancinelli *J. Org. Chem.* **42** 398 (1977)
70. T Mishida, M Mizuhara, H Sayo *Chem. Pharm. Bull.* **39** 1857 (1991)
71. V A Ignatov, R A Akshurina, P A Pirogov, R S Bairakova *Zh. Obshch. Khim.* **51** 609 (1981)
72. T Morimoto, Y Nezu, K Achiwa, M Sekiya *J. Chem. Soc., Chem. Commun.* 1584 (1985)
73. J Almog, D H R Barton, P D Magnus, R K Norris *J. Chem. Soc., Perkin Trans. 1* 853 (1974)
74. A Haas, J Hahne *Z. Anorg. Allg. Chem.* **490** 230 (1982)
75. B G Boldyrev, T K Bilozor *Zh. Org. Khim.* **22** 458 (1986)
76. R F Bayfield, E R Cole *Phosphorus Sulfur* **1** 19 (1976)
77. P Molina, A Arques, L Cartagena, M V Valcarcel *Synth. Commun.* **15** 643 (1985)
78. US P. 3 985 743; *Chem. Abstr.* **86** 30 837w (1977)
79. S Z Vatsadze, N S Zefirov, N V Zyk, A G Kutateladze, in *The XVth International Symposium on the Organic Chemistry of Sulfur (Abstracts of Reports)* (Merseburg: Gordon and Breach, 1994) p. 333
80. A L Schwan, M D Refvik, in *The XVIth International Symposium on the Organic Chemistry of Sulfur (Abstracts of Reports)* (Merseburg: Gordon and Breach, 1994) p. 327
81. I N Zhmurova, A P Martynyuk, A V Kirsanov *Zh. Obshch. Khim.* **37** 1879 (1967)
82. T Kumamoto, S Kabayashi, T Mukaiyama *Bull. Chem. Soc. Jpn.* **45** 866 (1972)
83. T Mukaiyama, K Hoso'i, S Inokuma, T Kumamoto *Bull. Chem. Soc. Jpn.* **44** 2453 (1971)
84. R A Abramovitch, J Pilski *J. Chem. Soc., Chem. Commun.* 704 (1981)
85. M C Caserio, J K Kim *J. Am. Chem. Soc.* **104** 3231 (1982)
86. P Brownbridge *Tetrahedron Lett.* **25** 3579 (1984)
87. L Benati, P C Montevecchi, P Spagnolo *Tetrahedron Lett.* **25** 2039 (1984)
88. D H R Barton, M R Britten-Kelly, D Ferreira *J. Chem. Soc., Perkin Trans. 1* 1682 (1978)
89. V D Sorokin, I G Plokhikh, M Yu Berlin, Yu K Grishin, K A Potekhin, A S Koz'min, N S Zefirov *Dokl. Akad. Nauk* **332** 730 (1993)
90. V D Sorokin, I G Plokhikh, M Yu Berlin, K A Potekhin, A S Koz'min, Yu T Struchkov, N S Zefirov *Dokl. Akad. Nauk* **333** 734 (1993)
91. N A Smith, N S Zefirov, I V Bodrikov, N Z Krimer *Acc. Chem. Res.* **12** 282 (1979)
92. W M Grizmadia, G M Schmid, P G Merey *J. Chem. Soc., Perkin Trans. 2* 1019 (1977)
93. L Benati, P C Montevecchi, P Spagnolo *J. Chem. Soc., Perkin Trans. 1* 1105 (1989)
94. L Benati, D Casarini, P C Montevecchi, P Spagnolo *J. Chem. Soc., Perkin Trans. 1* 1113 (1989)
95. L Benati, P C Montevecchi, P Spagnolo *Gazz. Chim. Ital.* **121** 387 (1991)
96. N S Zefirov, N V Zyk, A G Kutateladze, S I Kolbasenko, Yu A Lapin *Zh. Org. Khim.* **22** 214 (1986)
97. N S Zefirov, N V Zyk, A G Kutateladze, Yu A Lapin, A O Chizhov *Zh. Org. Khim.* **22** 2462 (1986)

98. N S Zefirov, N V Zyk, A G Kutateladze, Yu A Lapin, A O Chizhov *Zh. Org. Khim.* **23** 392 (1987)
99. N S Zefirov, N V Zyk, A G Kutateladze, B I Ugrak, Yu T Struchkov, K A Potekhin, A V Malcev *Dokl. Akad. Nauk SSSR* **301** 1385 (1988)
100. N S Zefirov, N V Zyk, A G Kutateladze, E K Butina, S Z Vatsadze *Izv. Akad. Nauk SSSR, Ser. Khim.* 2870 (1989)
101. N S Zefirov, N V Zyk, A G Kutateladze, E K Butina *Zh. Org. Khim.* **26** 671 (1990)
102. N S Zefirov, N V Zyk, A G Kutateladze, E S Ignatenko *Zh. Org. Khim.* **26** 670 (1990)
103. M Novi, G Petrillo, J Pinson *J. Org. Chem.* **58** 2670 (1993)
104. D H Barton, W D Ollis (Eds), in *Comprehensive Organic Chemistry* Vol. 5
105. J Goerdeler, A Holat *Angew. Chem.* **71** 775 (1959)
106. D H R Barton, I A Blair, P D Magnus, R K Norris *J. Chem. Soc., Perkin Trans. 1* 1031 (1973)
107. F A Davis, E R Freetz, C J Horner *J. Org. Chem.* **38** 690 (1973)
108. H Sayo, Y Yamada, T Michida *Chem. Pharm. Bull.* **31** 4530 (1983)
109. L Benati, P C Montevicchi, P Spagnolo *Tetrahedron Lett.* **27** 1739 (1986)
110. M M Kremlev, I V Koval' *Zh. Org. Khim.* **6** 1457 (1970)
111. M Mizuta, T Katada, E Itoh, S Kato, S Miyagawa *Synthesis* 721 (1980)
112. D V Armitage, M J Clark, C C Tso *J. Chem. Soc., Perkin Trans. 1* 680 (1972)
113. I K Kim, Y Souma, N Bentow, M C Casserio *J. Org. Chem.* **54** 1714 (1989)
114. D H R Barton, G Page, D A Widdowson *Chem. Commun.* 1466 (1970)
115. R D Allan, D H R Barton, M Girijavallabhan, P G Sammes *J. Chem. Soc., Perkin Trans. 1* 1456 (1974)
116. E S Levchenko, N P Pel'kis, V N Kalinin, A A Duzhak *Zh. Org. Khim.* **18** 1191 (1982)
117. E S Levchenko, N P Pel'kis, V N Kalinin *Zh. Org. Khim.* **18** 1197 (1982)
118. S Torii, N Sayo, H Tanaka *Chem. Lett.* 695 (1980)
119. K A Petrov, N K Bliznyuk, V A Savostenok *Zh. Obshch. Khim.* **31** 1361 (1961)
120. V A Al'fonsov, A G Trusenev, E S Batyeva, A N Pudovik *Izv. Akad. Nauk SSSR, Ser. Khim.* 2146 (1990)
121. D Barton, in *Protective Groups in Organic Chemistry* (Ed. J F W McOmie) (New York: Plenum, 1973)
122. D N Harpp, B A Orving *Tetrahedron Lett.* 2691 (1970)
123. E A Parfenov, V A Fomin *Zh. Obshch. Khim.* **51** 1144 (1981)
124. E A Parfenov, V A Fomin *Zh. Obshch. Khim.* **51** 1129 (1981)
125. F A Davis, R P Johnson *J. Org. Chem.* **37** 859 (1972)
126. F A Davis, R B Wetzel, T J Devon, J E Stackhouse *J. Org. Chem.* **36** 799 (1971)
127. P Ainpour, N E Heimer *J. Org. Chem.* **43** 2061 (1978)
128. R Sato, K Araga, Y Takikana, I Takizawa, S Oae *Phosphorus Sulfur* **5** 245 (1978)
129. L Grossi, C P Montevicchi *Tetrahedron Lett.* **32** 5621 (1991)
130. M Makosza, M Biatacki *J. Org. Chem.* **57** 4784 (1992)
131. Y Morimoto, T Yokogama, Y Higuchi, T Ohnishi, Y Miura, N Yasuoka *Chem. Express* 6 387 (1991)
132. Y Morimoto, S Sugiyama, Y Higuchi, A Tanaka, Y Miura, N Yasuoka *Chem. Express* 6 391 (1991)
133. R S Atkinson, B D Judkins *J. Chem. Soc., Chem. Commun.* 833 (1979)
134. R S Atkinson, B D Judkins *J. Chem. Soc., Perkin Trans. 1* 2615 (1981)
135. R S Atkinson, B D Judkins, N Khan *J. Chem. Soc., Perkin Trans. 1* 2491 (1982)
136. J Boivin, E Fouquet, S Z Zard *Tetrahedron Lett.* **31** 3545 (1990)
137. R M Bryce, C P Taylor *Tetrahedron Lett.* **30** 3835 (1989)
138. G Capozzi, S Menichetti, C Nativi, in *Collect. Lect. XVIth International Symposium on the Organic Chemistry of Sulfur* (Merseburg: Gordon and Breach, 1994) p. 359
139. J B Baudin, S A Julia, O Ruel *Tetrahedron* **43** 881 (1987)
140. J B Baudin, M Bekhazi, S A Julia, O Ruel, R L P de Jong, L Brandsma *Synthesis* 956 (1985)
141. J C Grivas *J. Org. Chem.* **40** 2029 (1975)
142. I V Koval', A I Tarasenko, M M Kremlev, R P Naumenko *Zh. Org. Khim.* **22** 1178 (1986)
143. W T Yung, P M Sammes *Tetrahedron Lett.* **31** 5935 (1990)
144. G Capozzi, L Gori, S Menichetti *Tetrahedron* **47** 7185 (1991)
145. A Senning, P Kelly *Acta Chem. Scand.* **21** 1871 (1967)
146. I V Koval', A I Tarasenko, M M Kremlev, N R Molchanova *Zh. Org. Khim.* **17** 533 (1981)
147. K T Potts, R Armbruster *J. Org. Chem.* **35** 1965 (1970)
148. K T Potts, R Armbruster *J. Org. Chem.* **36** 1846 (1971)
149. J A Mitchell, D H Reid *J. Chem. Soc., Perkin Trans. 1* 490 (1982)
150. J Goerdeler, K Doerk *Chem. Ber.* **95** 389 (1962)
151. J Goerdeler, B Wedekind *Chem. Ber.* **95** 147 (1962)
152. J Goerdeler, K Doerk *Chem. Ber.* **95** 154 (1962)
153. J Goerdeler, W Roose *Chem. Ber.* **95** 394 (1962)
154. I V Koval', A I Tarasenko, I S Panchenko, N R Molchanova *Zh. Org. Khim.* **22** 1712 (1986)
155. J Goerdeler, B Redies *Chem. Ber.* **92** 1 (1959)
156. K Akutagawa, N Furukawa, S Oae *Bull. Chem. Soc. Jpn.* **57** 518 (1984)
157. I V Koval', T G Oleinik, M M Kremlev *Zh. Org. Khim.* **17** 2174 (1981)
158. M M Kremlev, A I Tarasenko, I V Koval', V V Ryabenko *Zh. Org. Khim.* **10** 2320 (1974)
159. I V Koval', A I Tarasenko, M M Kremlev *Zh. Org. Khim.* **14** 111 (1978)
160. I V Koval', T G Oleinik, A I Tarasenko, M M Kremlev *Zh. Org. Khim.* **21** 2578 (1985)
161. E S Levchenko, I N Berzin *Zh. Org. Khim.* **6** 2273 (1970)
162. I V Koval', T G Oleinik, M M Kremlev *Zh. Org. Khim.* **15** 2319 (1979)
163. I V Koval', T G Oleinik, M M Kremlev *Zh. Org. Khim.* **17** 565 (1981)
164. I V Koval', V D Zinukhov *Zh. Org. Khim.* **24** 1784 (1988)
165. I V Koval', T G Oleinik, M Yu Timoshin *Zh. Org. Khim.* **30** 726 (1994)
166. I V Koval', T G Oleinik, M Yu Timoshin *Zh. Org. Khim.* **30** 389 (1994)
167. I V Koval', T G Panasenko *Zh. Org. Khim.* **26** 678 (1990)
168. M Haake, H Benack *Synthesis* 308 (1976)
169. L N Markovskii, T N Dubinina, E S Levchenko, S V Pen'kovskii *Zh. Org. Khim.* **12** 1049 (1976)
170. Yu G Shermolovich, V S Talanov, G N Dolenko, L N Markovskii *Zh. Org. Khim.* **16** 964 (1980)
171. Yu G Shermolovich, V S Talanov, V V Pirozhenko, L N Markovskii *Zh. Org. Khim.* **18** 2539 (1982)
172. A Haas, R Walz *Chem. Ber.* **118** 3248 (1985)
173. I V Koval', A Yu Romanenko *Zh. Org. Khim.* **24** 457 (1988)
174. I V Koval' *Zh. Org. Khim.* **24** 665 (1988)
175. I V Koval', L B Novikova, T G Oleinik *Zh. Org. Khim.* **28** 1718 (1992)
176. I V Koval', T G Oleinik, L B Novikova *Ukr. Khim. Zh.* **59** 1082 (1993)
177. I V Koval', in *Materialy Simpoziuma po Organicheskoi Khimii* (Proceedings of a Symposium on Organic Chemistry) (St. Petersburg: Nauka, 1995) p. 50
178. H C Buchholt, A Senning *Acta Chem. Scand.* **24** 1279 (1969)
179. R Mayer, D Decker *Z. Chem.* **28** 361 (1988)
180. R Mayer, D Decker, S Bleisch, C Domschke *J. Prakt. Chem.* **329** 81 (1987)
181. J Glander, A Golloch *J. Fluorine Chem.* **5** 83 (1975)
182. R S Glass, R J Swedo *Synthesis* 798 (1977)
183. F A Davis, A J Friedman, U K Nadir *J. Am. Chem. Soc.* **100** 2844 (1978)
184. R D Larsen, F E Roberts *Synth. Commun.* **18** 809 (1986)
185. M Haake, H Gebbing, H Benack *Synthesis* 97 (1979)
186. K Okuma, T Dorkawa, H Ohta, M Kobayashi, F D R Shuno *Fukuoka Daigaku Rigaku Shuno* **12** 105 (1982); *Chem. Abstr.* **98** 197 702h (1983)
187. Swiss P. 255 886; *Chem. Abstr.* **48** 7 633d (1944)
188. E Riesz *Bull. Soc. Chim. Fr.* 1449 (1966)
189. C Hennart *Bull. Soc. Chim. Fr.* 4395 (1967)
190. N N Mel'nikov *Khimiya Pestitsidov* (Chemistry of Pesticides) (Moscow: Khimiya, 1968)

191. N N Mel'nikov, K V Novozhilov, T N Pylova *Khimicheskie Sredstva Zashchity Rastenii* (Chemical Agents for the Protection of Plants) (Moscow: Khimiya, 1980)
192. L M Yagupol'skii *Aromaticheskie i Geterotsiklicheskie Soedineniya s Florsoderzhashchimi Zamestitelyami* (Aromatic and Heterocyclic Compounds with Fluorine-containing Substituents) (Kiev: Naukova Dumka, 1988)
193. US P. 4 323 580; *Chem. Abstr.* **97** 5 979p (1982)
194. Europ. P. 12 036; *Chem. Abstr.* **93** 239 032u (1980)
195. Europ. P. 60 464 A1; *Chem. Abstr.* **98** 143 640r (1983)
196. US P. 4 341 772 A; *Chem. Abstr.* **98** 16 845p (1983)
197. US P. 430 2451 A; *Chem. Abstr.* **96** 99 434m (1982)
198. Europ. P. 55 442 A2; *Chem. Abstr.* **97** 215 593 (1982)
199. Europ. P. 55 429 A1; *Chem. Abstr.* **97** 162 622 (1982)
200. German P. 3 314 383 A1; *Chem. Abstr.* **100** 68 028d (1984)
201. V K Promononkov, K I Kobrakov, M A Shvekhgeimer, V A Rudenko, M V Shatanskaya, L Ya Leitis, in *Aktual'nye Napravleniya Issledovaniya i Primeneniya Khimicheskikh Sredstv Zashchity Rastenii* (Present Direction of Investigation and Application of Chemical Agents for the Protection of Plants) (Ed. M I Kabachnik) (Moscow: Nauka, 1990) p. 327
202. I V Koval', V A Martyushenko *Vopr. Khim. Khim. Tekhnol.* **96** 60 (1991)
203. N P Pel'kis, Yu V Karabanov, V P Borisenko, E S Levchenko *Fiziol. Akt. Veshchestva* **16** 47 (1984)
204. G N Shalygina, G F Shalygin, Z N Nudel'man, in *Spravochnik Rezinshchika* (Rubber Specialist's Handbook) (Moscow: Khimiya, 1971) p. 277
205. G A Blokh, in *Organicheskie Uskoriteli Vulkanizatsii i Vulkaniziruyushchie Sistemy dlya Elastomerov* (Organic Accelerants of Vulcanisation and Vulcanising Systems of Elastomers) (Leningrad: Khimiya, 1973)
206. R W Layer *Rubber Chem. Technol.* **59** 274 (1986)
207. R N Datta, D K Basu *Rubber Chem. Technol.* **59** 27 (1986)
208. V I Kolesnik, M M Kremlev, I V Koval', Yu B Mar'yaskin *Vopr. Khim. Khim. Tekhnol.* **26** 79 (1971)
209. USSR P. 384 823; *Byull. Izobret.* (25) 81 (1973)
210. German P. 2 824 630; *Chem. Abstr.* **92** 95 141h (1980)
211. German P. 2 551 504; *Chem. Abstr.* **87** 86 217g (1977)
212. R Anand, D S Blackley, K S Lee *Plast. Rubber. Mater. Appl.* **4** 8 (1979)
213. Europ. P. 27 622; *Chem. Abstr.* **95** 132 359v (1981)
214. V R Govariker, N V Visvanatkhan, Dzh Shridkhar, in *Polimery* (Polymers) (Moscow: Nauka, 1990) p. 230
215. J Voigt, in *Stabilisation of Plastics against Light and Heat*, Monographs on the Chemistry, Physics, and Technology of Plastics, No. 10 (Berlin: Springer, 1966)
216. V V Korshak (Ed.) *Tekhnologiya Plasticheskikh Mass* (Technology of Plastics) (Moscow: Khimiya, 1985)
217. German P. 3 118 126; *Chem. Abstr.* **98** 143 447k (1983)
218. German P. 3 118 127; *Chem. Abstr.* **98** 143 446j (1983)
219. Europ. P. 64 657 A1; *Chem. Abstr.* **98** 143 405v (1983)
220. USSR P. 295 824; *Byull. Izobret.* (8) 78 (1971)

Natural aliphatic oxygenated unsaturated acids. Synthesis and biological activity

A G Tolstikov, G A Tolstikov

Contents

I. Introduction	441
II. Linear unsaturated hydroxy and epoxy acids and their derivatives	441
III. Branched-chain unsaturated acids	446
IV. Unsaturated di- and tricarboxylic acids and their derivatives	448
V. Acids with oxygen-containing heterocyclic fragments	449
VI. Total synthesis of natural unsaturated acids with oxygen-containing functions	451

Abstract. The review is devoted to natural unsaturated acyclic acids containing oxygen functions. Compounds of the aceto-genin and propiogenin types containing hydroxy, oxo, and epoxy groups as well as ether, hydrofuran, and hydropyran fragments are considered. Data are given on the biological activities of the acids themselves or of natural compounds whose structural elements are unsaturated acids. The methodology and strategy of the synthesis of both linear unsaturated hydroxy and alkoxy acids and those containing a heterocyclic fragment are discussed. The bibliography includes 172 references.

I. Introduction

The unique biological role of oxygen-containing unsaturated acids is generally acknowledged. By now, a unified theory for the arachidonic acid cascade has been elaborated, which provides, together with offering a deeper insight into the mechanism of oxidative metabolism, a means to important discoveries in bio-organic chemistry and medicine. More and more attention is being given to hydroxy unsaturated acids as promising tools in the self-defence of plants against fungal diseases. The development in the foreseeable future of radically new fungicides, which are active even when used at nanogram concentrations, is becoming ever more realistic. Of significant interest are unsaturated acids that possess the ability to control the biosynthesis of cholesterol. A striking diversity of biological activities has been found among the unsaturated acids and compounds containing their fragments, isolated from marine organisms.

Thus, the importance of biological screening, however modest are the means it employs, is in no doubt. At present, biotesting is becoming a more and more sophisticated procedure, which reflects the increasing interest in naturally occurring acids shown by numerous laboratories and firms engaged in the design of medicinal drugs and means for raising agricultural yields.

A G Tolstikov Boreskov Institute of Catalysis, Siberian Branch of the Russian Academy of Sciences, prosp. akad. Lavrent'eva 5, 630090 Novosibirsk, Russian Federation. Fax (7-383) 235 57 66. Tel (7-383) 239 73 50

G A Tolstikov Novosibirsk Institute of Organic Chemistry, Siberian Branch of the Russian Academy of Sciences, prosp. akad. Lavrent'eva 9, 630090 Novosibirsk, Russian Federation. Fax (7-383) 235 47 52

Received 12 May 1995

Uspekhi Khimii 65(5) 474–495 (1996); translated by R L Birnova

Nevertheless, the chemistry and biochemistry of oxygen-containing unsaturated acids discussed herein needs further extensive research. It can be said with confidence that this class of natural compounds is of interest both to synthetic chemists and specialists dealing with the development of technological methods for the synthesis of natural compounds and their analogues with predetermined biological activity.

While preparing the present review, the authors were faced with the necessity to restrict its remit and exclude from the consideration:

lactones of hydroxy unsaturated acids meriting special attention;

macrolide antibiotics that are regularly covered in reviews and monographs;

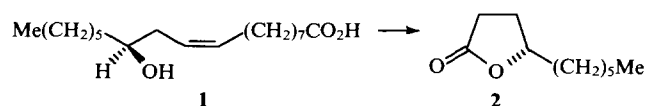
compounds of the arachidonic acid cascade with the exception of certain metabolites;

polyester toxins of the ocaidaic acid type.

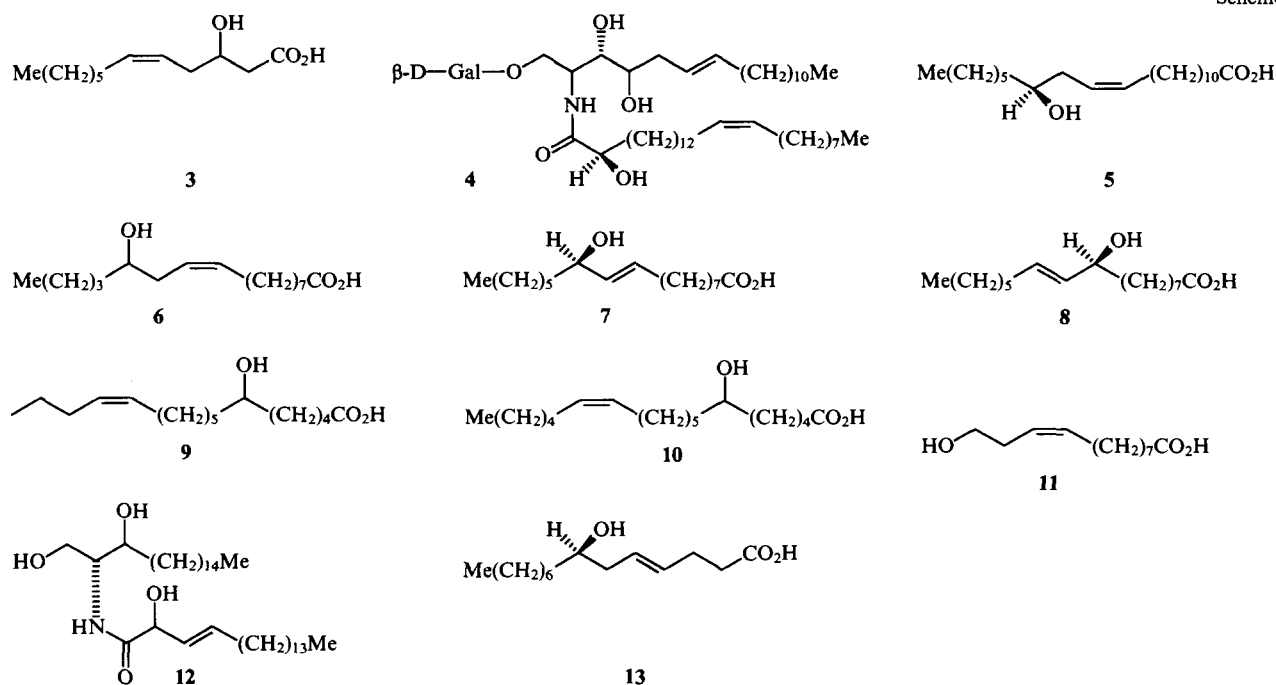
The review is concerned with the acids and their derivatives, in the structure of which a continuous carbon chain can be traced providing for the formation of oxygen-containing heterocycles of the hydrogenated furan and pyran type. In some cases, metabolites of unsaturated acids are considered that have an ether group, which interrupts the continuous carbon chain, as well as halogen-containing acids. Special attention is given to the biological activities and physiological functions of the compounds under discussion.

II. Linear unsaturated hydroxy and epoxy acids and their derivatives

Many unsaturated monohydroxy acids are related to the group of widely occurring natural compounds. Thus, in 1985 the worldwide production of castor oil containing ricinoleic acid **1** as the major acid component, amounted to 400 000 tons.¹ The technical significance of castor oil is great. This includes polymeric compounds and the production of sebacic and undecenoic acids, as well as enanthal. Of great practical utility is the microbial degradation of ricinoleic acid into the optically active decanolate **2**.



Scheme 1

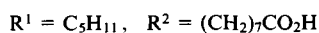
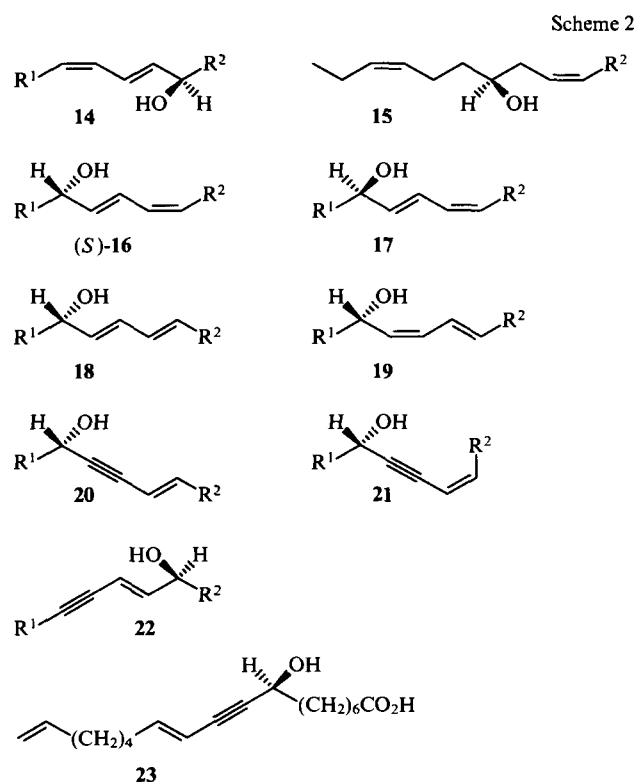


The isolation of several monohydroxy monoenoic acids has been described. Thus, 3-hydroxy-(5*Z*)-dodecenoic acid **3** has been obtained from the lipids of the plant *Serratia marcescens*.² (2*R*)-Hydroxy-(15*Z*)-tetracosenoic acid is a constituent of the galactosphingolipid **4** isolated from marine organisms.³ Lesquerolic acid **5**⁴ and the acid **6**⁵ have been isolated from plants of the *Lesquerella* genus. Internodes of the timothy (*Phleum*) infested with the fungus *Epichloe typhii* have been found to contain the acids **7** and **8**; the enhanced resistance of the infested plants against some pathogenic fungi has been noted.⁶ The plant *Acanthopanax sessilifloria* contains the acids **9** and **10** with an unestablished configuration of the asymmetric centre.⁷ The physiologically active 12-hydroxy-(9*Z*)-dodecenoic acid **11** has been isolated from homogenates of pea leaves;⁸ the synthesis of this acid has been described.⁹ The sphingolipid **12** containing (2*R*)-hydroxy-(3*E*)-octadecenoic acid possesses antileukemic activity.¹⁰ The structure of the antibiotic malingamide A isolated from the marine alga *Lyngbya majuscula* involves (7*R*)-hydroxy-(4*E*)-tetradecenoic acid **13**¹¹ (Scheme 1).

An important role in the vital activity of plants is played by monohydroxy dienoic acids. Thus, dimorphecolic acid **14** isolated from rice stems,¹² from seed oils of *Dimorphotheca* and *Osteospermum*,¹³ as well as from sea buckthorn oil,¹⁴ belongs to the class of acids that provide defence against diseases in some rice varieties known for their high productivity and resistance against pathogenic fungi. Esters of the acid **14** also exhibit insecticidal activity.¹⁵ The synthesis of four geometric isomers of dimorphecolic acid **16** has been performed. Densipolic acid **15** has been isolated from the lipids of *Lesquerella densipila*.¹⁷

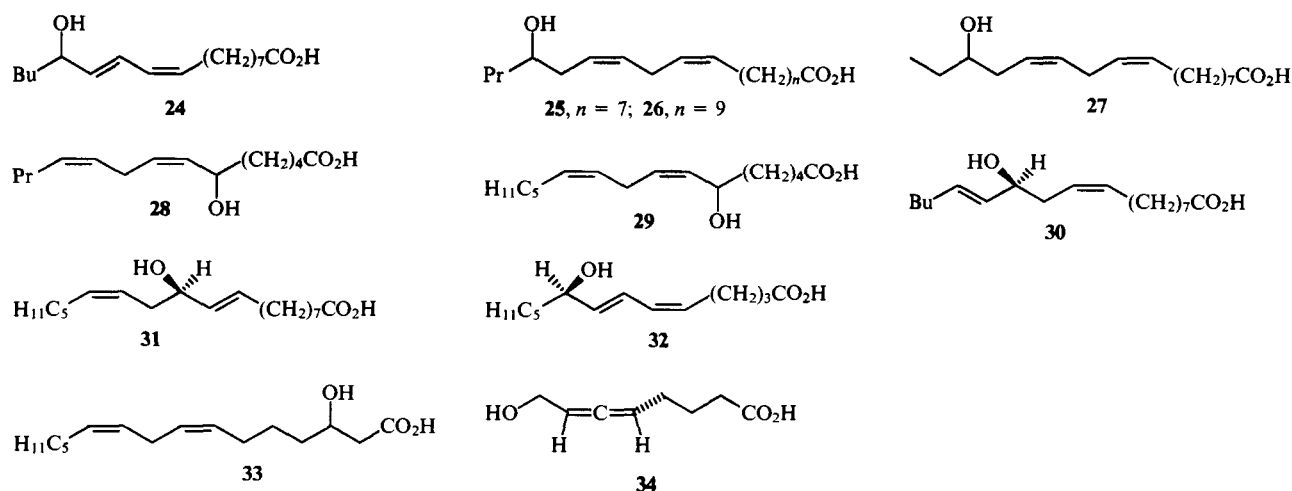
Much attention in the current literature is being given to coriolic acid **16** detected as a component of sea buckthorn lipids¹⁴ and isolated as the (13*S*) isomer from the roots of the rice plant.¹⁸ This compound can influence Ca^{2+} transport in the cell system of some pathogens of rice diseases, which accounts for its role in self-defence of the plant. Its (13*R*)-isomer **17** and the geometric isomers **18** and **19** exhibit similar fungicidal activity. The synthetic dehydrocoriolic acids **20** and **21** display potent antifungal activity.¹⁸

The natural enynic acids **22**¹⁹ and **23**²⁰ possessing antibacterial and antifungal properties are also worth noting in this context (Scheme 2).



Of particular interest is the detection of coriolic acid in heart tissue mitochondria of patients with Mediterranean fever. Highlighted is the role of (*R*)-coriolic acid in the control of thrombosis, which is associated with its ability to block Ca^{2+} transport.²¹ The synthesis of coriolic acid has been described in Refs 22 and 23.

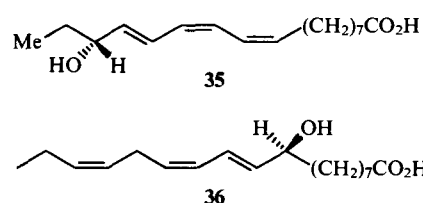
Hydroxydienoic acids **24**–**27** of unknown configuration have been isolated from the seeds of the plant *Galeopsis bifida*.²⁴ The configuration of the asymmetric centres of the acids **28** and **29** detected in some plants of the *Acanthopanax* genus is



also unknown.⁷ The fungistatic activity of the fungus *Epichloe*, which infests the timothy, is ascribed to the presence of the acids **30** and **31**; the latter has been obtained synthetically.²⁵

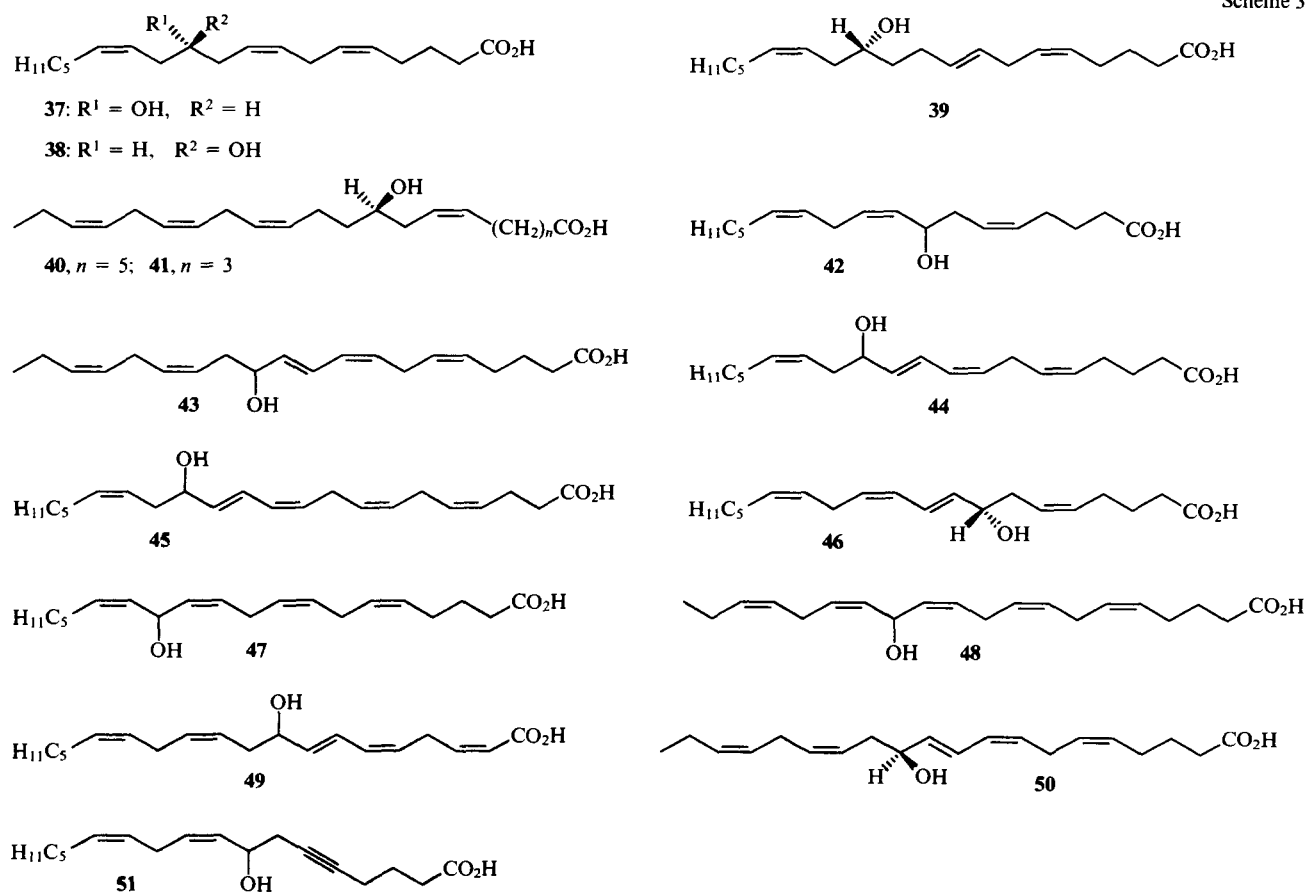
The seed oil of *Securidaca longipedunculata* contains (9*R*)-hydroxy-(5*Z*,7*E*)-tetradecadienoic acid **32**.²⁶ The acid **33** is the structural component of the nucleoside antibiotic produced by *Streptomyces griseosporus*.²⁷ The optically active allenic acid **34** isolated from the plant *Sapium japonicum* has a potent antifungal action.²⁸

High biological activity has been detected in some monohydroxy tri- and monohydroxy polyenoic acids. The disease-resistant rice variety Fukuyuki contains the C₁₈-trienoic acids **35** and **36** endowed with strong fungicidal activity.²⁹ Their structures have been confirmed by total synthesis.³⁰



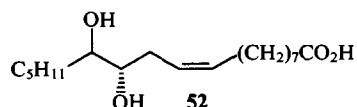
The acid **37** isolated from wheat epithelium turned out to be a strong vasodilator that stimulates the protein inflow into the ocular fluid. Noteworthy, its enantiomer **38** is fully devoid of activity, while the (8*E*)-isomer **39** displays only 10% of the activity of the natural acid (Scheme 3).³¹ The lipids of the Indian Ocean

Scheme 3



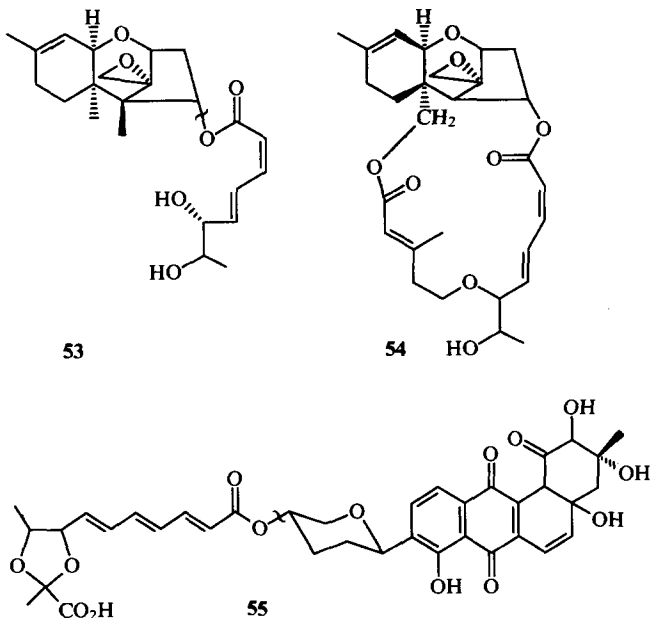
black coral *Leiopathes* contain leiopathic acid **40** as well as the acids **41** and **42**.³² The sponge *Echinochalina mollis* inhabiting the Coral Sea produces three hydroxypolyenoic acids, **43–45**.³³ The eicosanoid **46** has been isolated from the starfish *Patiria miniata*.³⁴ Biologically active acids have been detected in red algae. Thus, *Litotamnion corallioides* and *Litotamnion calcareum* produce the acids **47** and **48**;³⁵ pentaenoic acid **49** exhibiting antimicrobial activity has been isolated from the alga *Laurensia hybrida*.³⁶ The high content of the acid **50** which inhibits platelet aggregation has been found in the alga *Murrayella pericladus*.^{36,37} The acid **51** isolated from the lipids of the alga *Liagora farinosa* is ichthiotoxic.³⁸

Only a few unsaturated dihydroxy acids have been described, and among them there are *threo*-12,13-dihydroxyoleic **52**,³⁹ 6,7-dihydroxy-(2*Z*,4*E*)-octadienoic, and 8,9-dihydroxy-(2*E*,4*E*,6*E*)-decatrienoic acids.

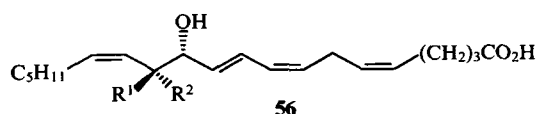


Dihydroxyoctadienoic acids are structural components of the trichotecenoid toxins produced by the fungi *Fusarium*, *Myrothecium*, *Trichoderma*, and *Cylindrocarpon*. Trichotecenes are strong poisons inhibiting such vital processes as protein and DNA biosynthesis. Also known are mycotoxins, e.g., the vomiting factor of *Fusarium* and toxic aleukia of pigs and cattle fed on a pathogenic fungi-infested forage. Two types of toxins, **53** and **54**, exist that contain dihydroxyoctadienoic acids. The antibiotic dioxamycin **55** comprises a fragment of decatrienoic acid.⁴⁰

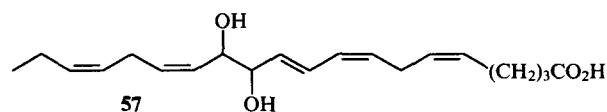
The extensive literature on trichotecenoid toxins has been generalised in various monographs.^{41–43}



The dihydroxytetra- and pentaenoic acids **56** and **57** have been isolated from the lipids of the red alga *Farlowia mollis*.⁴⁴

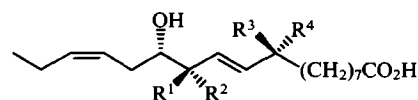


$R^1 = H, R^2 = OH; R^1 = OH, R^2 = H$

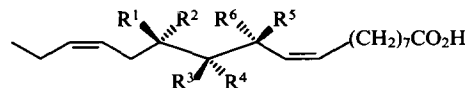


A group of trihydroxy acids **58–62** has been isolated from the stems of some rice varieties resistant to fungal diseases.^{45,46} It has been demonstrated that wetting of rice seedlings in aqueous solutions of these acids increases the resistance of the plant against fungal diseases throughout the whole vegetation period.⁴⁷ The pharmacologically promising trihydroxy acids **63–66** are contained in the lipids of the medicinal plant *Brionia alba*.^{48–50} Like prostaglandins, the complex of these lipids increases smooth muscle tonicity, lowers the glucose level in the blood, normalises the lipid composition in liver and brain of experimental animals, and produces stimulating and tonic effects. These acids are formed by lipoxygenase oxidation of α -linolenic acid.

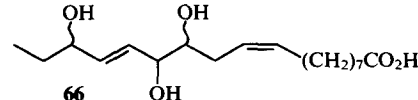
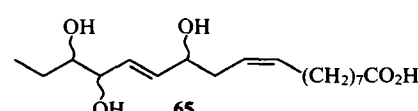
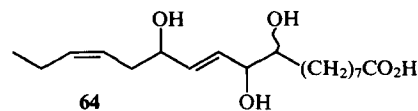
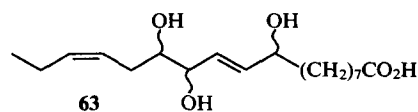
The sea alga *Lyngbya majusculus* contains malyngic acid **67**,⁵¹ whereas the cyanobacteria (blue-green algae) produce its stereoisomer **68**.⁵²



	R ¹	R ²	R ³	R ⁴
58	OH	H	H	OH
59	OH	H	OH	H
67	H	OH	H	OH
68	H	OH	OH	H



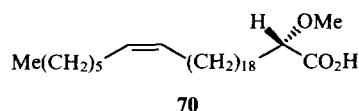
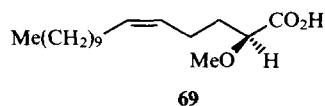
	R ¹	R ²	R ³	R ⁴	R ⁵	R ⁶
60	H	OH	OH	H	H	OH
61	OH	H	H	OH	OH	H
62	OH	H	H	OH	OH	H



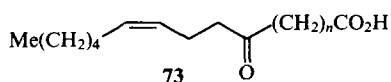
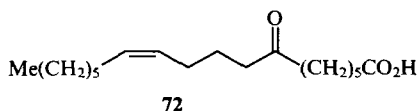
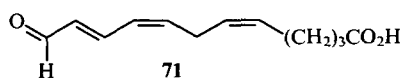
Syntheses of some of these acids have been described in Refs 47, 51–55.

Natural unsaturated acids are known that contain alkoxy, oxo, and epoxy groups. The structural element of the malyngamides isolated from the alga *Lyngbya majuscula* is (7*R*)-methoxy-(4*E*)-tetradecenoic acid.⁵⁶ Nontoxic stylocheiamides have been isolated from the tissues of the ugrug *Stylocheilus longicanela*, which feeds on this alga.⁵⁷

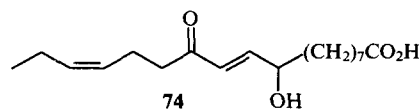
Malyngamide G contains (7*R*)-methoxy-(4*E*)-tridecenoic acid.⁵⁸ (2*S*)-Methoxy-(5*Z*)-hexadecenoic acid **69**, a tentative structural component of sphingolipids, has been isolated from the sea sponge *Amphimedon compressa*.⁵⁹ The lipids of the green sea alga *Higginsia tethyoides* contain the unique C₂₈-acid **70**.⁶⁰



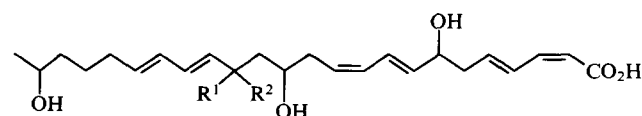
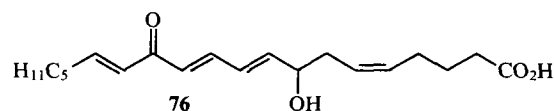
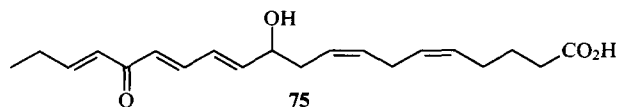
The aldehydo acid **71** with antimicrobial action is present in the lipids of the red alga *Laurensia hybrida*.³⁶ The C₁₈-oxo acid **72** has been found in the seed oil of *Gardenia lucida*.⁶¹ The acids **73** isolated from the lipid fraction of *Cuspidaria pterocarpa* seeds have a longer chain.^{62,63} The hydroxyoxo acid **74** is formed in the potato plant as a result of lipoxygenase oxidation of linolenic acid.⁶³



$n = 13, 15, 17$



The red alga *Ptilota filicina* produces the oxo acid **75** manifesting antimicrobial activity and the ability to inhibit 5-lipoxygenase and Na⁺/K⁺-ATPase.⁶⁴ The oxo acid **76** has been isolated from the alga *Lithotomnion corallioides*.⁶⁵ Gram-positive bacteria of the deep-sea sediment core produce macrolides and open-chain acids exhibiting antiviral activity. Among them, macrolactinic **77** and isomacrolactinic **78** acids have been identified; however, their absolute configurations have not been established.⁶⁶

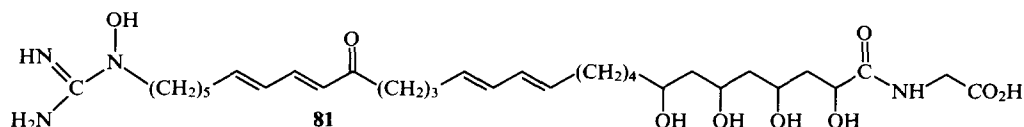
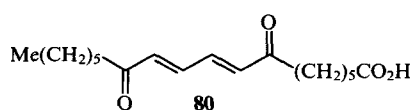
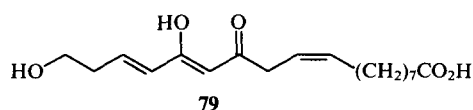
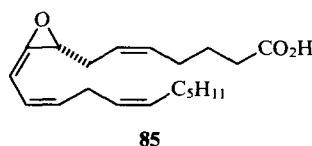
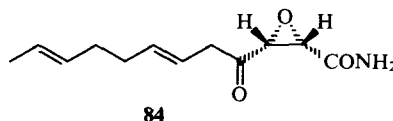
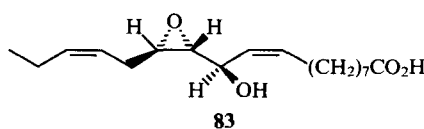
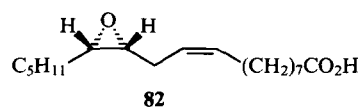


The *Cantharellus cibarius* (chanterelle) is one of the most widespread edible mushrooms. Its resistance against parasites, insects, and snails is due to the high content of cibacic acid **79**.⁶⁷ The dioxoacid **80**, which has been named ostopanonic acid, has been isolated from the stems and fruits of the plant *Ostodes paniculata*. Its ability to inhibit the growth of lymphocytic leukemia cells has been reported.⁶⁸

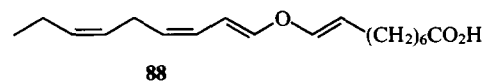
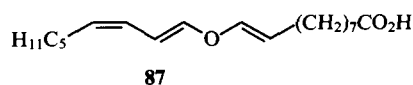
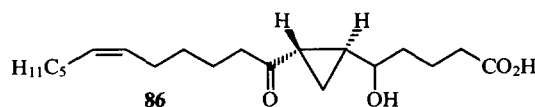
The antibiotic MG 398HF9A **81** with a unique structure isolated from the culture of *Pseudomonas azurea*, has been recommended for the treatment of fungal diseases⁶⁹ (Scheme 4).

Vernolic acid **82**, which has an epoxy group in its structure, has been detected in the seeds of *Euphorbia lagascea*.^{1,21} The epoxy acid **83**, whose structure was confirmed by total synthesis, had been isolated from rice.⁷⁰ Like coriolic and vernolic acids, this compound has been attributed to the factors that ensure self-defence of the rice plant against pathogenic fungi. The fungus *Cephalosporium caerulens* produces cerulenin **84**, which inhibits the biosynthesis of steroids and lipids. Its inhibition index for fatty acid synthetase is very high ($JC = 1 \mu\text{g ml}^{-1}$).⁷¹ As stated in Ref. 13, sea buckthorn oil contains more than twenty epoxy acids which have been identified by chromatomass spectrometry; their major component is the 15,16-epoxy-octadeca-9,12-dienoic acid of an unestablished stereochemistry.

Incubation of (8*R*)-hydroperoxyeicosatetraenoic acid with homogenates of the coral *Plexaura nomomalea* affords the allenic epoxide **85**, an intermediate in the biosynthesis of the cyclopropane eicosanoid **86** isolated from the coral.⁷²



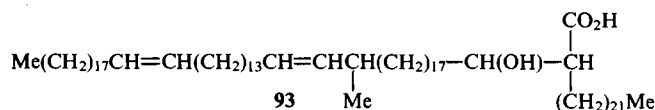
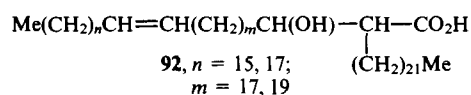
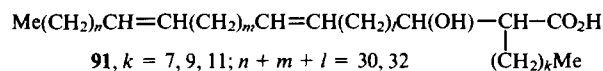
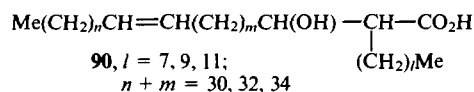
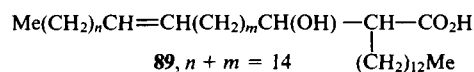
Scheme 4



Colnelic **87** and colnelenic **88** acids from potato have a unique structure.⁷³⁻⁷⁵ It is assumed that these acids are formed due to enzymatic rearrangements of the hydroperoxides produced by lipoxygenase oxidation of linoleic and linolenic acids. It is remarkable that the above compounds have a strong inhibiting action on potato lipoxygenase.

III. Branched-chain unsaturated acids

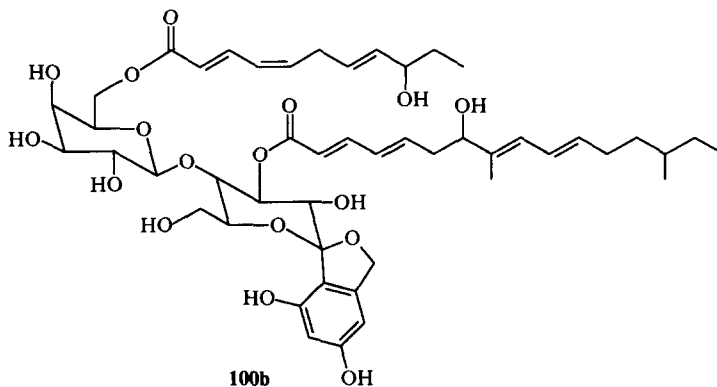
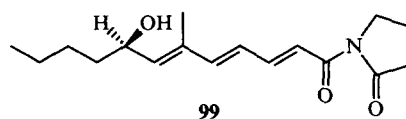
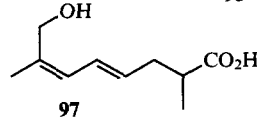
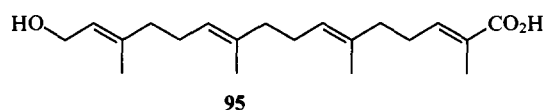
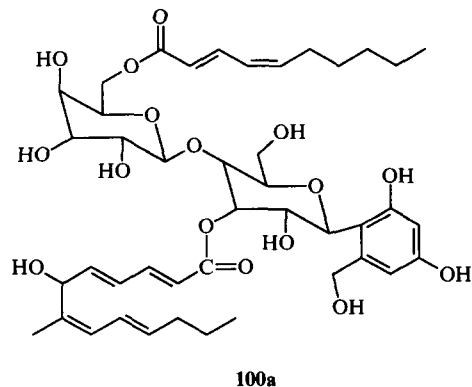
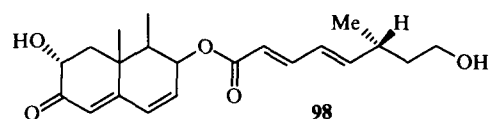
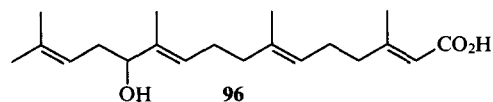
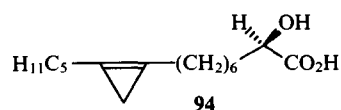
Several α -branched mono- and dioenoic acids have been isolated from the lipids produced by mycobacteria and actinomycetes. They involve corinomycolenic **89**,⁷⁶ nocardenoic **90**,⁷⁷ nocardienoic **91**, α' -smegmamycolic **92**, and α -smegmamycolic **93** acids.⁷⁸



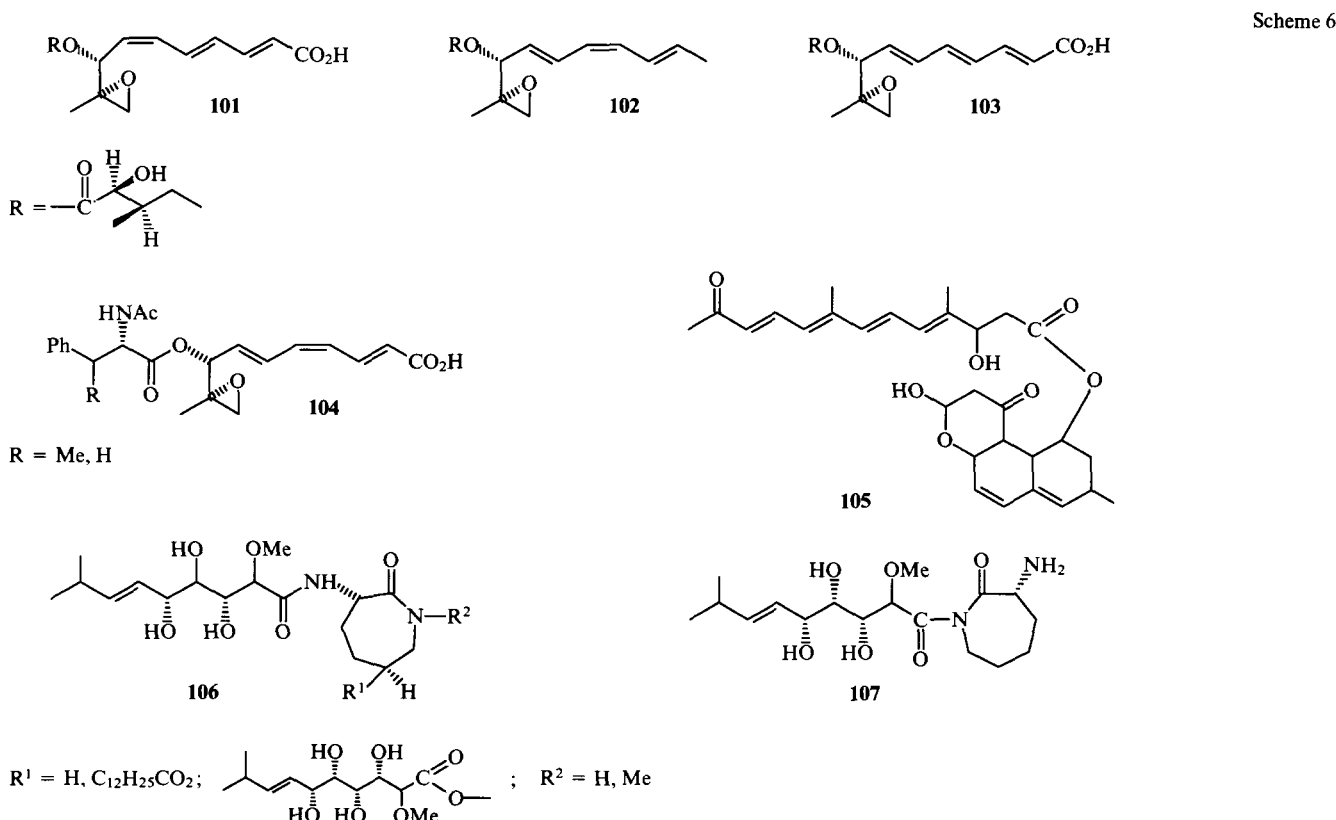
Hydroxysterculic acid **94** is contained in the roots of the plant *Hibiscus rosa*.^{79,80} The fungus *Nocardia* produces the acid **95** possessing antiulcerous activity.⁸¹ The green alga *Bifurcaria bifurcata* contains isoprenoid acid **96**.⁸² The acid **97** has been isolated from the fruits of *Cydonia oblonga*.⁸³ Some hydroxy acids containing methyl substituents are structural fragments of the molecules of natural compounds. Thus, dendriphiellin **98** isolated from the sea sponge *Dendriphiella salina* contains a fragment of 8-hydroxy-(6*R*)-methylocta-(2*E*,4*E*)-dienoic acid⁸⁴ and variotin **99**, a potent inhibitor of fatty acid synthetase, is an amide of 6-methyltrienoic acid.⁷¹ The fungus *Papularia sphaerosperma* produces the glycolipids, xanthicandin **100a** and papulacandins, e.g., papulacandin B **100b** possessing strong fungicidal activity.⁸⁵⁻⁸⁷ Structurally related fungicides have been isolated from cell cultures of the fungi *Pialophora cyclaminis*⁸⁸ and *Dictyochaeta simplex*⁸⁹ (Scheme 5).

The pathogenic fungus *Alternaria kikuchiana*, the agent of the black spot disease in strawberry, produces the toxins AF-II a, b, c **101-103**, AK-I, and AK-II **104**,^{90,91} whose structures have been confirmed by total synthesis.^{92,93} The ester of the oxotetraenoic acid **105** isolated from the culture of *Aspergillus versicolor* has been patented as a means for reducing the cholesterol level in the blood.⁹⁴ The sea sponges of *Choristid* sp.⁹⁵ and *Jaspidae*⁹⁶ contain the antibiotics bengamides A-F **106** and isobengamide **107**, which are highly active against the parasites *Nippostrongyls brasiliensis*, streptococci, and fungi^{97,98} (Scheme 6).

The isolation of amides of the polyenoic acid with a more complex structure has been described. Thus, *Myxococcus xanthus* produces the antibiotics myxalamides **108**, which demonstrate high activity against gram-positive bacteria and yeasts.⁹⁹ The fungus *Myxococcus stipitatus* is a source of phenalamides **109** and



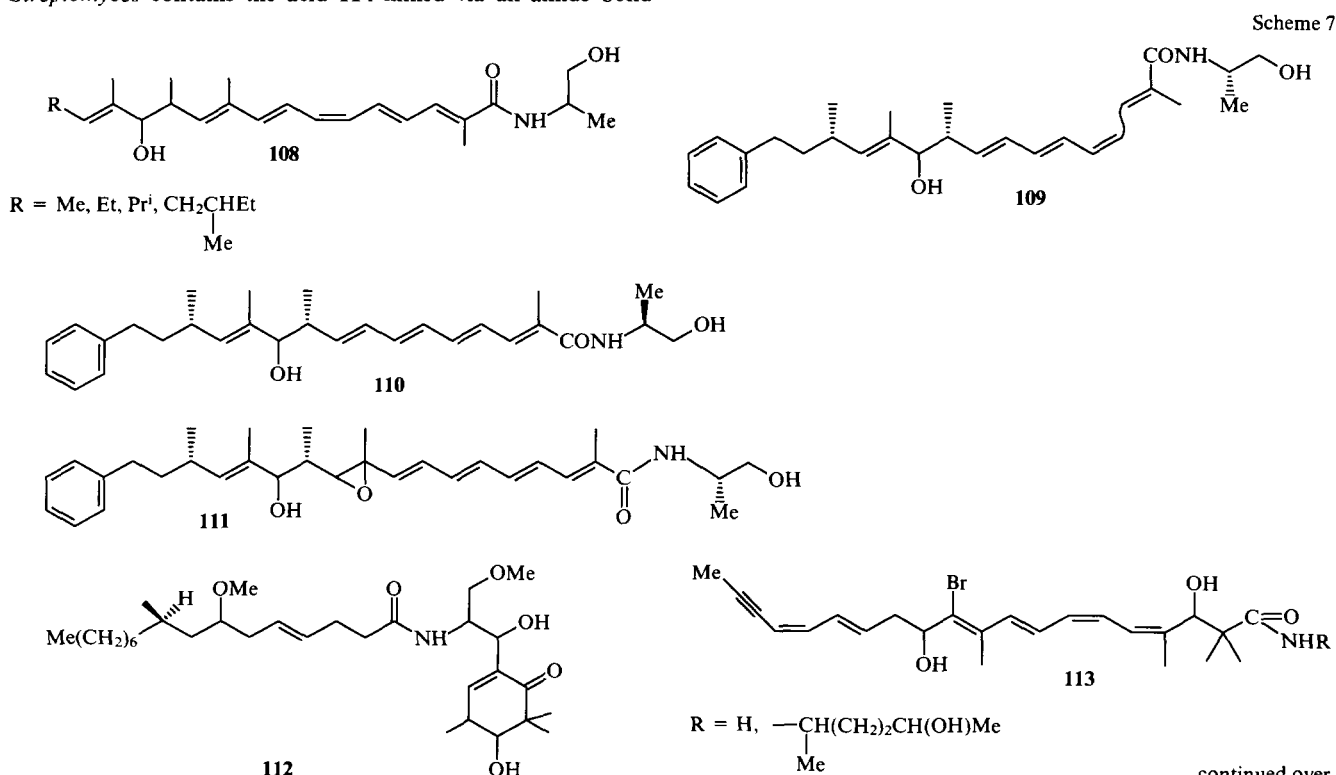
Scheme 5



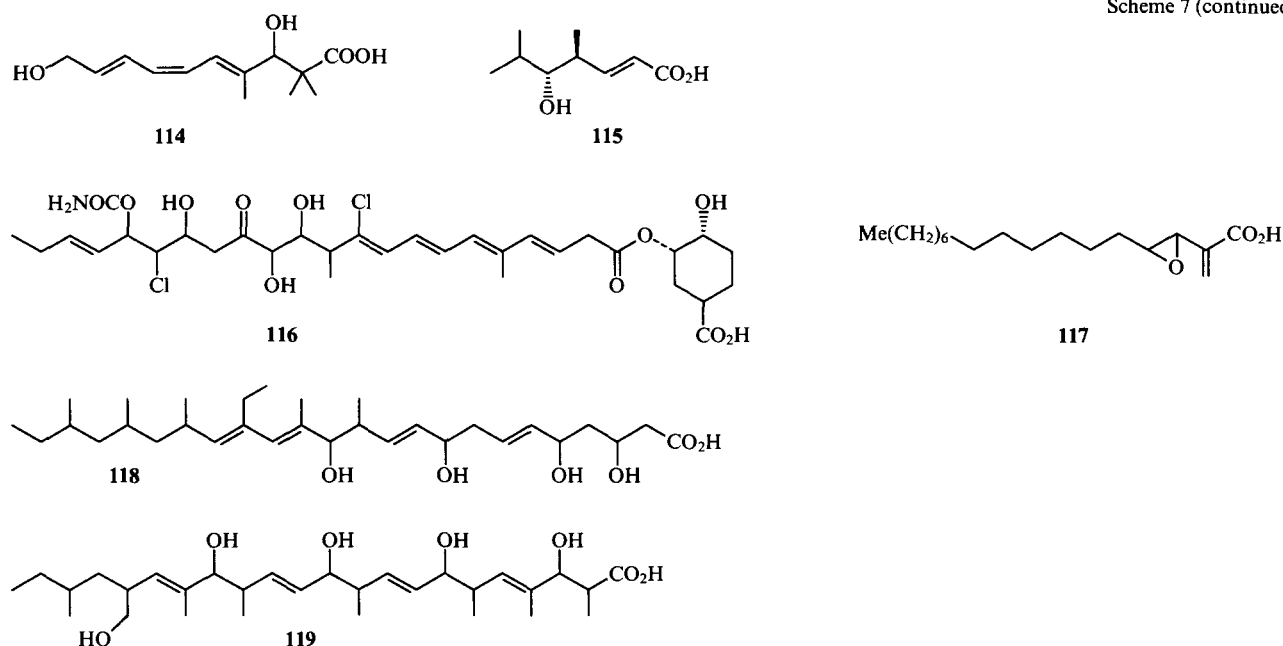
110, which have been patented as a basis for medicinal drugs designed for the treatment of fungal and parasitic diseases.¹⁰⁰⁻¹⁰³ Phenalamide **C 111** has been noticed to inhibit strongly the reproduction of the human immunodeficiency virus. Malingamide **E** isolated from algae is the amide of 7-methoxy-9-methyl-hexa-(4*E*)-decenoic acid **112**.¹⁰⁴ The sea sponge *Clathria* contains clathrinamides **113** capable of inhibiting cell division, as has been established in experiments with starfish eggs.¹⁰⁵ The molecule of the antitumour antibiotic **AJL** produced by *Streptomyces* contains the acid **114** linked via an amide bond

with the fragment of a complex structure.¹⁰⁶ The structurally simple hydroxy acid **115** is a constituent of the molecule of oxazole macrolides (virginiamycins), which have found wide use as antibiotic drugs.¹⁰⁷ The antibiotic enacyloxin **116**, which is active against gram-positive bacteria and influences protein synthesis, has a unique structure.¹⁰⁸

The antibiotic conocandin **117**¹⁰⁹ and the compound **118**¹¹⁰ are free acids. The fungus *Xylaria cubensis* produces the antibiotic, cubenic acid **119**¹¹¹ (Scheme 7).



Scheme 7 (continued)



IV. Unsaturated di- and tricarboxylic acids and their derivatives

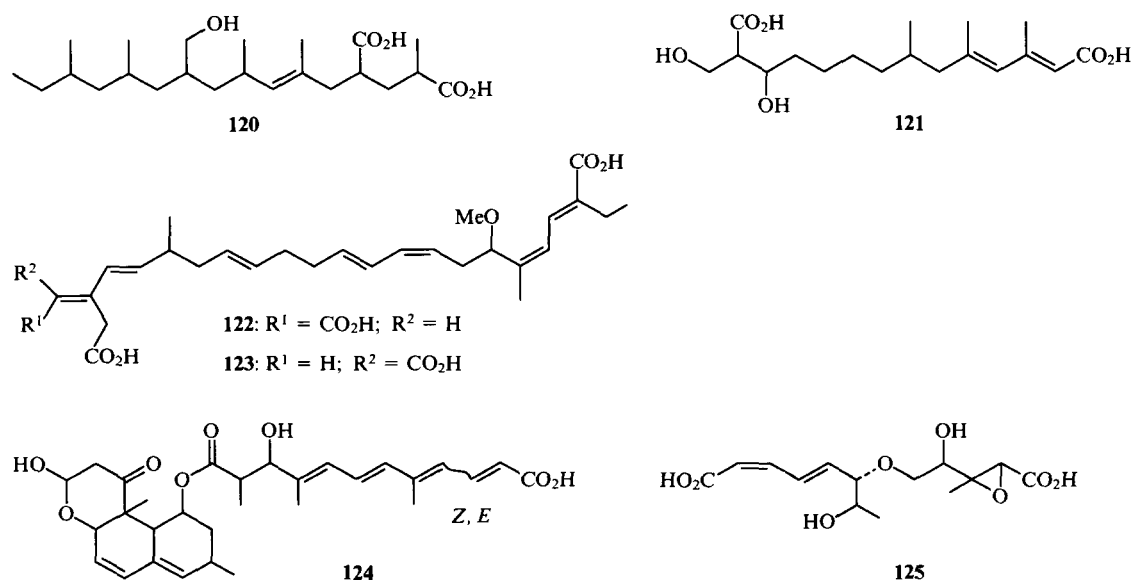
The group of unsaturated dicarboxylic acids is not too numerous but diverse as regards their structural elements. The ability to control plant growth is characteristic of radiclonic acid **120** isolated from *Penicillium* sp.¹¹² The antibiotic 123313 **121** has been obtained from *Cephalosporium*.¹¹³ Bongkreic acid **122** produced by the fungus *Pseudomonas cocoreneaus* causes severe (sometimes, lethal) food poisoning. 'Bongkreik' coconuts, commonly used as a dietary product in Indonesia, are infested with a culture of *Pseudomonas*. The high toxicity of the acid **122** produced by this culture is due to its effect on ATP/ADP translocation in mitochondrial membranes and blocking of oxidative phosphorylation.¹¹⁴ Isobongkreic acid **123** isolated from an unidentified strain of *Eubacterium* strongly inhibits the activity of phytopathogenic fungi when used at concentrations of

7–125 $\mu\text{g ml}^{-1}$. The antibiotic activity of compound **123** is lower than that of bongkreic acid. Both compounds are characterised by high toxicity: LD_{50} is 4.5 mg kg^{-1} . Tetraenedioic acid is a structural element of the molecule of the calbistrin antibiotic **124** produced by *Penicillium restrictum*.¹¹⁵

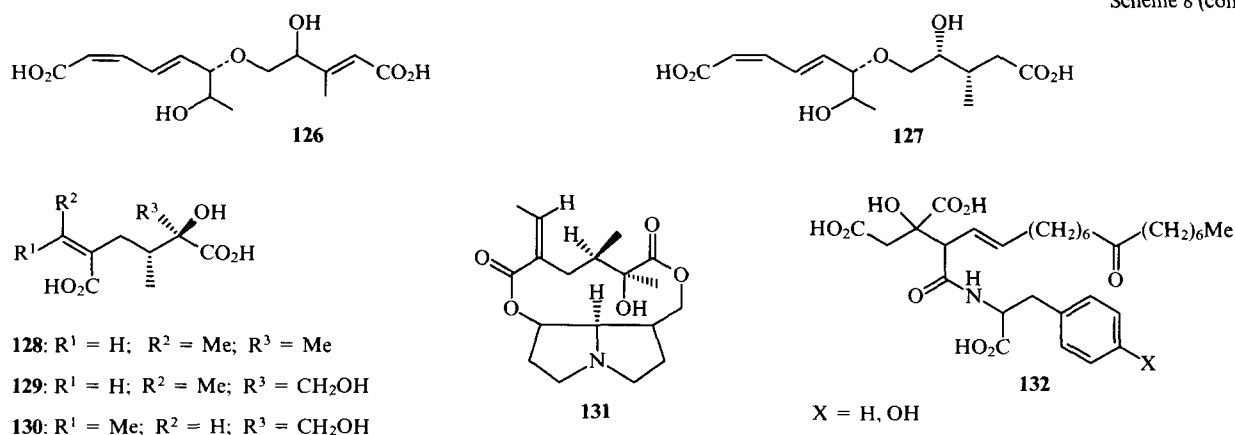
Baccharinoids related to toxins of the trichotecenoid series and produced by the fungus *Baccharis megapota mica* are cyclic esters of the dicarboxylic acids **125–127**.^{116,117} The alkaloids of the groundsel *Senecio* possessing valuable biological properties contain dicarboxylic acids, of which intergerrineic acid **128** as well as the acids **129** and **130**, are especially widespread.^{118,119} Platyphilline **131** has found use in medicine as a cholinolytic agent.

The oxotricarboxylic acid peptide derivatives, viridifungins A and C **132**, produced by *Trichoderma viride*, exert a strong antifungal action against *Candida*, *Aspergillus*, and *Cryptococcus*. Their ability to inhibit squalene synthetase has also been reported¹²⁰ (Scheme 8).

Scheme 8



Scheme 8 (continued)



V. Acids with oxygen-containing heterocyclic fragments

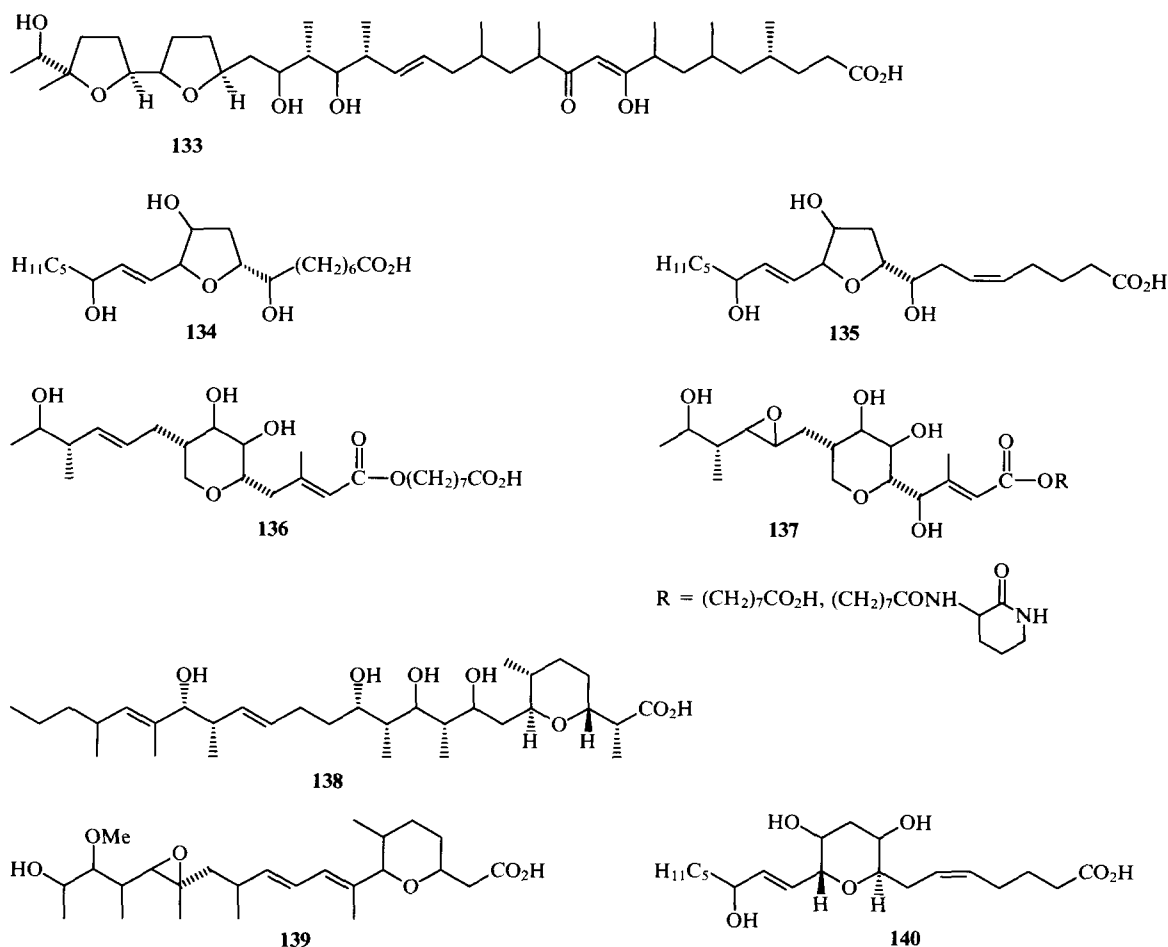
The formation of tetrahydrofuran or tetrahydropyran cycles is rather typical of linear polyhydroxy compounds. Polyhydroxy-unsaturated acids are not exceptional in this respect. If their molecules contain oxo groups, appropriate arrangement of the hydroxyl groups gives rise to heterocyclic systems containing two oxygen atoms which represent internal ketals.

Among the variety of acids containing the tetrahydrofuran fragment, we shall note the antibiotic ionomycin **133** possessing the properties of an ionophore selective towards calcium ions.¹²¹ The cycloecosanoids **134** and **135** isolated from ram seminal fluid are the metabolites of arachidonic acid.^{122, 123}

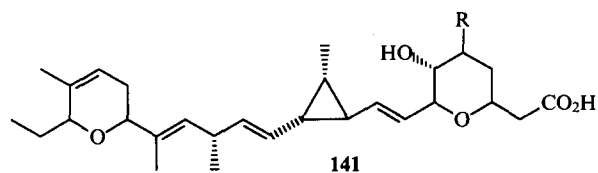
Of practical significance is pseudomonic acid **136** and its structural analogues containing the tetrahydropyran fragment **137**.^{124–126}

The antibiotic zincoforin **138** produced by *Streptomyces griseus* selectively binds Mg^{2+} and Zn^{2+} ions which accounts for its ability to stimulate the growth and development of ruminant animals.^{127, 128} Some strains of *Streptomyces* produce the antibiotic gerboxydiene **139**, which has a strong antimicrobial action.¹²⁹ The 8,12-epoxy-9,11,15-trihydroxy-(5*Z*,13*E*)-eicosadienoic acid with an unestablished configuration of the asymmetric centres is the product of enzymatic conversion of arachidonic acid in humans.¹³⁰ The synthesis of its (8*R*,9*R*,11*S*,12*R*)-diastereoisomer **140** has been carried out¹³¹ (Scheme 9).

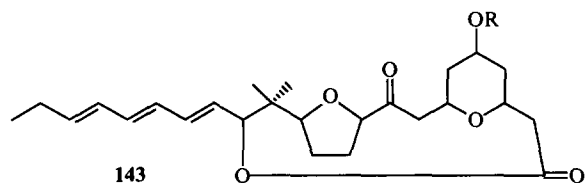
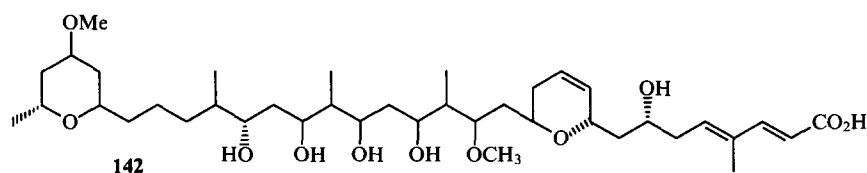
Scheme 9



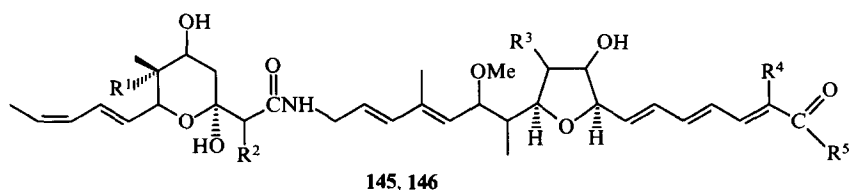
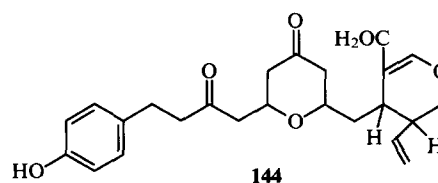
Scheme 10



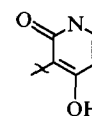
R = OH, NH₂, NHMe, NMe₂, ONMe₂, NMe₃⁺



R = trisaccharide



	R ¹	R ²	R ³	R ⁴	R ⁵
145	OH	Et	H	H	H
146	H	Me	OH	Me	

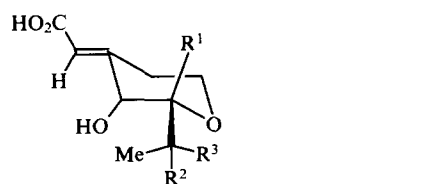


The acids of this series, which contain two heterocyclic fragments, possess valuable biological activity. For example, ambruticin¹³² **141** (R = OH) and its amino derivatives¹³³ are active against many pathogenic fungi. A potent cytostatic action is exerted by swincholide D **142** isolated from the sea sponge *Theonella*.¹³⁴ The alga *Polycavernosa tsudai* contains the antibiotic polycavernoside A **143**.¹³⁵ Hydrangenoside A **144** detected in the plant *Hydrangea macrophylla* is a glycoside.¹³⁶ Some strains of *Streptomyces* produce antibiotics L 681.217 **145**¹³⁷ and SB 22.484 **146**¹³⁸ (Scheme 10).

The di- and tricarboxylic acids of this type are structurally very diverse. Some trichotenes comprise dicarboxylic acids carrying the tetrahydropyran fragment,¹³⁹ e.g., the acids **147–150** are present in satratoxin H, roritoxin A, mitoxin B, and vertisporin, respectively. The epoxy acids **151–155** are the structural components of myratoxin, satratoxin F, roritoxins D and C, and of mitoxin C (Scheme 11).

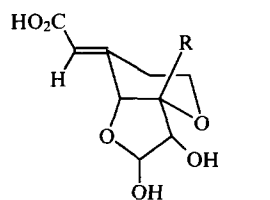
Some acids are of the ketal type. For example, the potent antibiotics, reversomycins F, C, D **156**, and B **157**, have been

Scheme 11



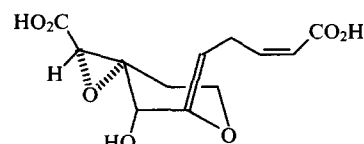
147: R¹ = $\text{CH}_2\text{CH}=\text{CHCO}_2\text{H}$; R² + R³ = O

149: R¹ = $(\text{CH}_2)_2\text{CH}=\text{CHCO}_2\text{H}$; R² = H, R³ = H

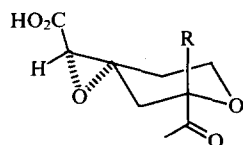


148: R = $\text{CH}_2\text{CH}=\text{CHCO}_2\text{H}$

150: R = $(\text{CH}_2)_6\text{CH}=\text{CHCO}_2\text{H}$

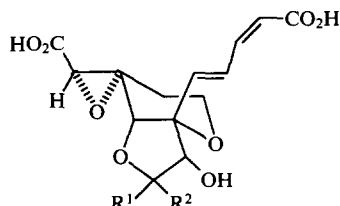


151



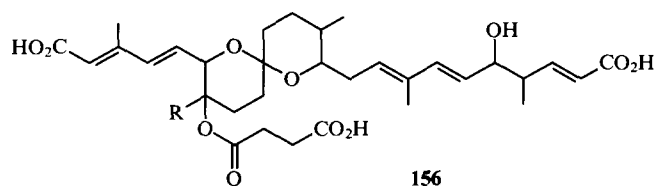
152: R = $\text{CH}_2\text{CH}=\text{CHCO}_2\text{H}$

155: R = $(\text{CH}_2)_2\text{CH}=\text{CHCO}_2\text{H}$

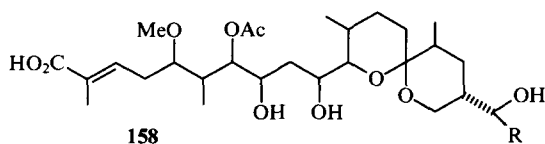
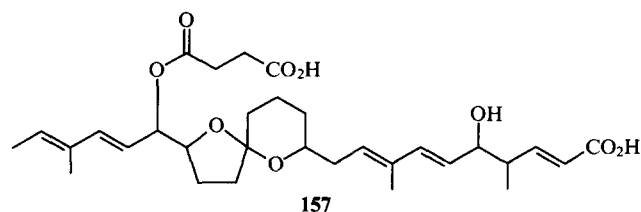


153: R¹ = H, R² = OH; 154: R¹ + R² = O

isolated from some strains of *Streptomyces*.¹⁴⁰ The ionophore antibiotics, didemnoketals A and B **158**, possess high antimicrobial activity.¹⁴¹

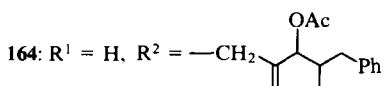
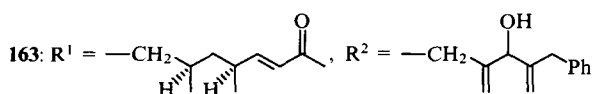
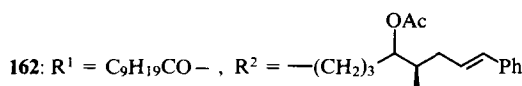
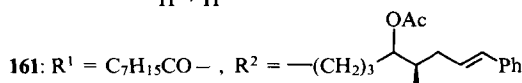
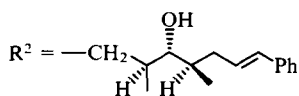
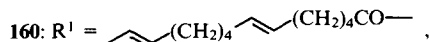
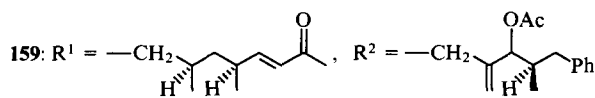
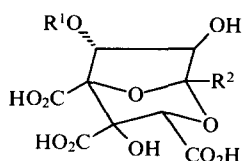


R = Bu, C₅H₁₁, (CH₂)₂CHMe₂



R = COMe, —CH₂—C(CH₃)=CH—CH₂—CH₂—CO₂H

Considerable attention has recently been focussed on the tricarboxylic acids of the ketal type, which can effectively reduce the cholesterol level. These extremely active farnesyl transferase inhibitors produced by the cultures of *Sporomielia intermedia*, and *Leptodontium elatius*¹⁴² as well as by the fungi of *Phoma* species,^{143, 144} have been named zaragozic acids A, B, C, D₁, and D₂, and squalostatins S₁, S₂, and H₁. The identity of the zaragozic acid A with squalostatin S₁ has been established. These metabolites are of particular importance for cardiology, since it has been



reported that they have a number of advantages over clinically widespread hypocholesterolinemic drugs, such as lovastatin mevinoids.^{145, 146} The structures **159–162** are considered to be correct for the zaragozic acids A, B, D₁, and D₂, and structures **163** and **164**, for squalostatins S₂ and H₂.^{147–150}

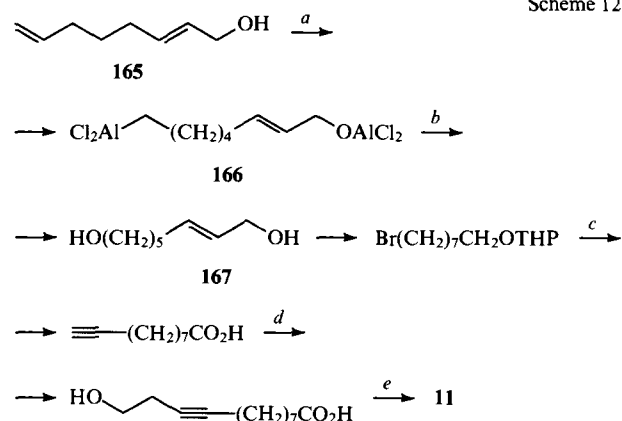
VI. Total synthesis of natural unsaturated acids with oxygen-containing functions

Total synthesis of natural acids of the above type has received much attention. Its significance is growing with increasing frequency far beyond the scope of the laboratory studies aimed at confirming a structure or elaborating a methodology. Many synthetic schemes are of technological value and suitable for obtaining the target products in amounts having practical significance.

An exhaustive discussion of papers dealing with the complete synthesis of unsaturated acids with oxygen-containing functions is not the specific goal of the present review. It seemed more reasonable to trace the strategy and methodology of the synthesis; therefore, our attention was focussed not only on enantiospecific approaches but on the syntheses of achiral compounds as well.

The first stage in the synthesis of a 12-hydroxy-dodec-(9Z)-enoic acid metabolite **11**⁹ is particularly remarkable, for it makes use of a novel procedure of hydroalumination with AlHCl₂.¹⁵¹ Hydroalumination of octa-2,7-dien-1-ol **165** followed by oxidation of the organoaluminium compound **166** affords oct-2-en-1,8-

Scheme 12

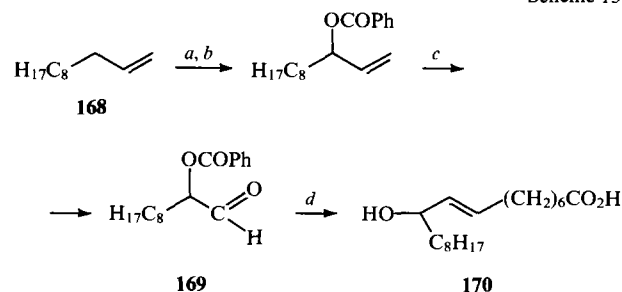


THP = tetrahydropyran-2-yl; (a) AlHCl₂; (b) O₂, H₃⁺O; (c) HC≡CNa, H₃⁺O, H₂CrO₄; (d) LiN(Pr)₂, CH₂=CH₂-O; (e) H₂, Pd-BaSO₄

diol **167**; its further conversions are depicted in Scheme 12.

The racemic 10-hydroxy-octadec-(8E)-enoic acid **170** isolated from rice stems, which provides self-defence in the plant against fungal diseases, has been synthesised from undecene **168**

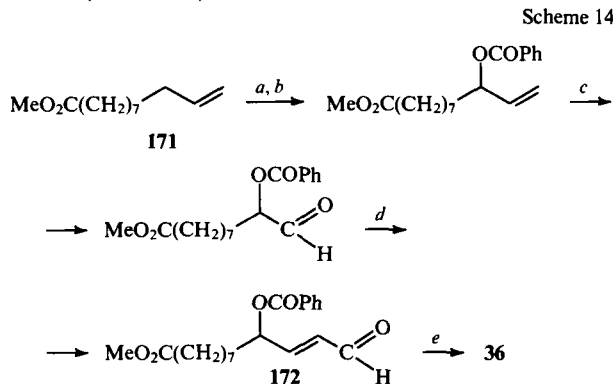
Scheme 13



(a) Bu^tO₂H—SeO₂; (b) PhCOCl—Py; (c) OsO₄, NaIO₄; (d) HO₂C(CH₂)₆CH=PPh₃

(Scheme 13).¹⁵² Allylic oxidation, benzylation, and periodate cleavage of the double bond results in 2-benzoyl oxydecanal **169** which, after Wittig olefination and hydrolysis, gives the target product.

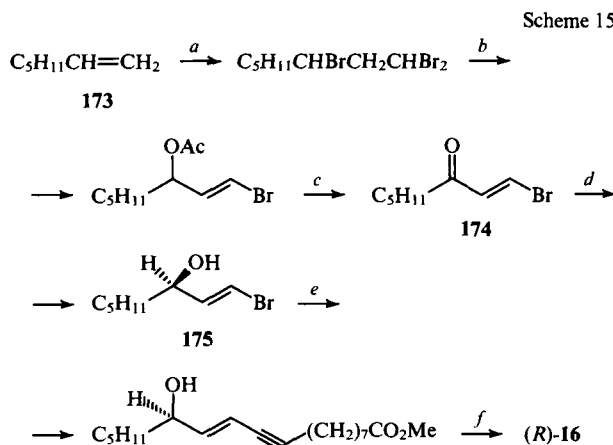
The preparation of the C₁₂-synthon **172** used in the synthesis of the optically inactive 9-hydroxy-(10*E*,12*Z*,15*Z*)-octadecatrienoic acid **36** is based on the allylic oxidation of methyl undec-10-enoate **171** (Scheme 14).¹⁵²



- (a) Bu^tO₂H – SeO₂; (b) PhCOCl – Py; (c) O₃; (d) Ph₃P=CHC(=O)H;
(e) $\text{CH}_2=\text{CH}-\text{PPh}_3\text{Br}$, Bu^tOK

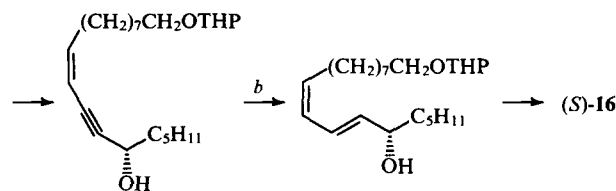
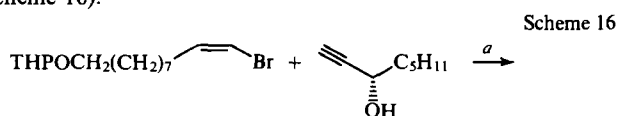
The syntheses of biologically active C₁₈-acids employ a wide variety of approaches, from metal complex catalysis to enantio-specific methods based on the use of the initial chiral compounds.

The palladium phosphine complex-catalysed coupling of vinyl halides with alkynes has been used in the synthesis of (13*R*)-coriolic acid **16**. One of the key synthons, 1-bromo-oct-1-en-(3*R*)-ol **175**, has been obtained from hept-1-ene **173** as shown in Scheme 15, which involves the asymmetric reduction of 1-bromo-oct-1-en-3-one **174** in the presence of baker's yeast (Scheme 15).¹⁵³



- (a) CHBr₃; (b) AcOK, 18-crown-6;
(c) NaOH, PCC (pyridinium chlorochromate); (d) baker's yeast;
(e) HC≡C(CH₂)₇CO₂Me, Pd(PPh₃)₄, CuI; (f) H₂, Pd – CaCO₃

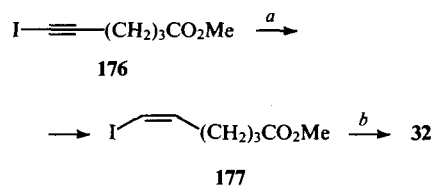
This approach, in a slightly modified form, has been used in the synthesis of the *S*-enantiomer of coriolic acid **16** (Scheme 16).¹⁵⁴



- (a) Pd(PPh₃)₄, CuI; (b) LiAlH₄

Interesting procedures have been employed in the synthesis of (9*R*)-hydroxytetradeca-(5*Z*,7*E*)-dienoic acid **32**.¹⁵⁵ The stages of stereospecific reduction of methyl 6-iodo-hept-5-ynoate **176** in the presence of dipotassium azodicarboxylate and the Pd(OAc)₂-catalysed oxidative coupling of methyl-6-iodohex-5-enoate **177** with oct-1-en-(3*R*)-ol **178** (Scheme 17) have attracted our attention.

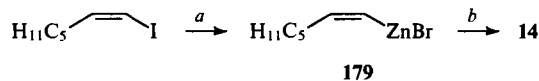
Scheme 17



- (a) KO₂CN=NCO₂K, BuNH₂;
(b) $\text{C}_5\text{H}_{11}\text{CH}(\text{OH})\text{CH}_2\text{C}\equiv\text{CH}$ (**178**); 5 Pd(OAc)₂ – AgOAc

The formation of the carbon – carbon bond at the key stage of the synthesis of dimorphecolic acid **14** is effected by cross-coupling of the *Z*-vinylzinc intermediate **179** with the vinylic iodide **180** catalysed by Pd(PPh₃)₄ (Scheme 18).¹⁵⁶

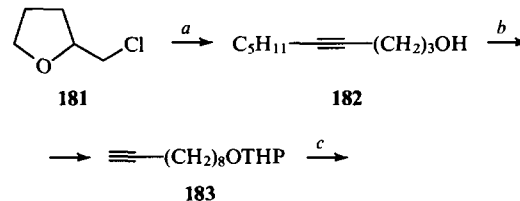
Scheme 18

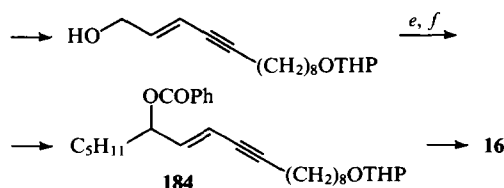


- (a) Bu^tLi, ZnBr₂; (b) I-CH=CH-(CH₂)₇CO₂Me (**180**), Pd(PPh₃)₄

An interesting procedure involved in the synthesis of coriolic acid **16** which has been developed by Indian investigators¹⁵⁷ is the preparation of the acetylenic precursor **184**. Tetrahydroxyfurfuryl chloride **181** gives dec-4-yn-1-ol **182** under the action of lithium bromide and bromopentane; this is further isomerised into dec-9-yn-1-ol **183** in the presence of sodium amide and propane-1,3-diamine. Further synthesis is depicted in Scheme 19.

Scheme 19



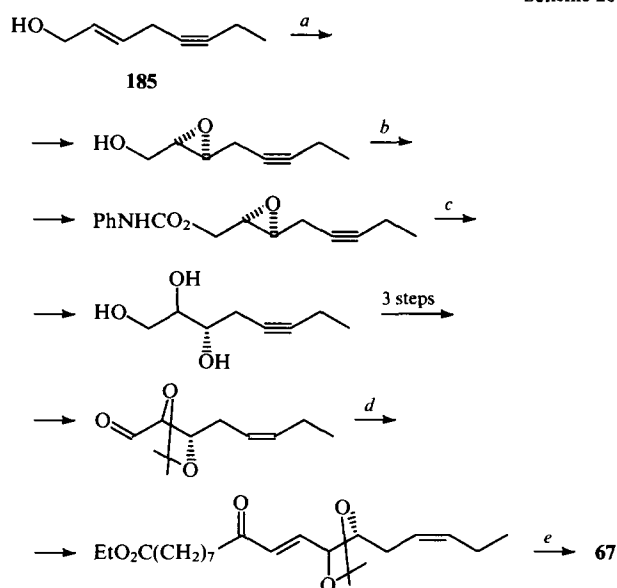


(a) LiNH_2 , $\text{C}_5\text{H}_{11}\text{Br}$; (b) NaNH_2 , $(\text{CH}_2)_3(\text{NH}_2)_2$; DHP (dihydropyran);

(c) $\text{BrC}\equiv\text{CCH}_2\text{OH}$, CuCl , NH_2OH , Pr^iNH_2 ; (d) LiAlH_4 ;

(e) MnO_2 ; (f) $\text{C}_5\text{H}_{11}\text{MgBr}$, $\text{PhCOCl}-\text{Py}$

The Sharpless asymmetric epoxidation has been widely used to obtain optically active hydroxy- and epoxyunsaturated acids. For example, the first stage in the enantioselective synthesis of malingic acid **67** is the epoxidation of the initial oct-(2*E*)-en-5-yn-1-ol **185** (Scheme 20).¹⁵⁸



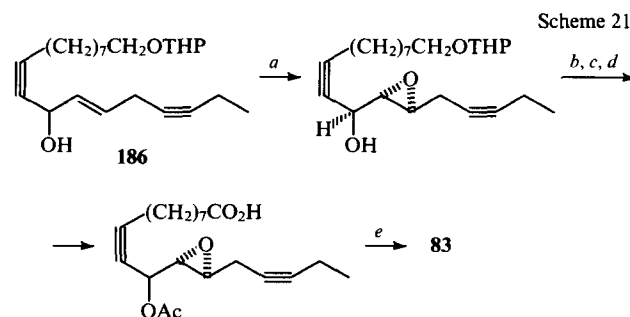
(a) $\text{Bu}^t\text{O}_2\text{H}$, $\text{Ti}(\text{OPr}^i)_4$, (+)DIPT (diisopropyl tartrate); (b) PhNCO ;

(c) $\text{BF}_3 \cdot \text{OEt}_2$, NaOH ; (d) $\text{EtO}_2\text{C}(\text{CH}_2)_7\text{COCH}=\text{PPh}_3$;

(e) NaBH_4 , NaOH

The asymmetric epoxidation of the compound **186** containing the fragment of allylic alcohol, has been used in the synthesis of (12*S*,13*S*)-epoxy-(11*R*)-hydroxyoctadeca-(9*Z*,15*Z*)-dienoic acid **83** possessing antifungal activity.¹⁵⁹ The two-step oxidation of the

primary hydroxyl group into the carboxyl group (Scheme 21) is noteworthy. It is based on the use of pyridinium chlorochromate and then of NaClO_2 in the presence of 2-methylbut-2-ene.

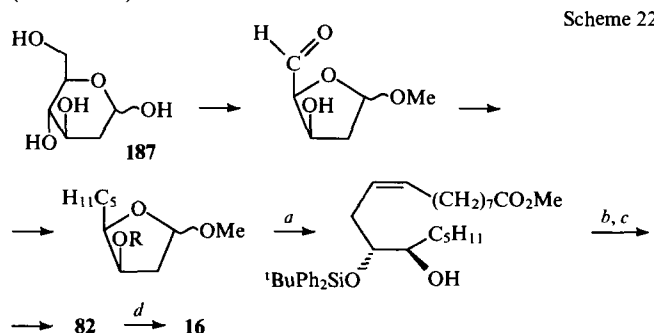


(a) $\text{Bu}^t\text{O}_2\text{H}$, $\text{Ti}(\text{OPr}^i)_4$, (+)DIPT; (b) Ac_2O , Py, H^+O ;

(c) PCC; (d) NaClO_2 , NaHPO_4 , $\text{Me}_2\text{C}=\text{CHMe}$;

(e) H_2 , Pd - CaCO_3

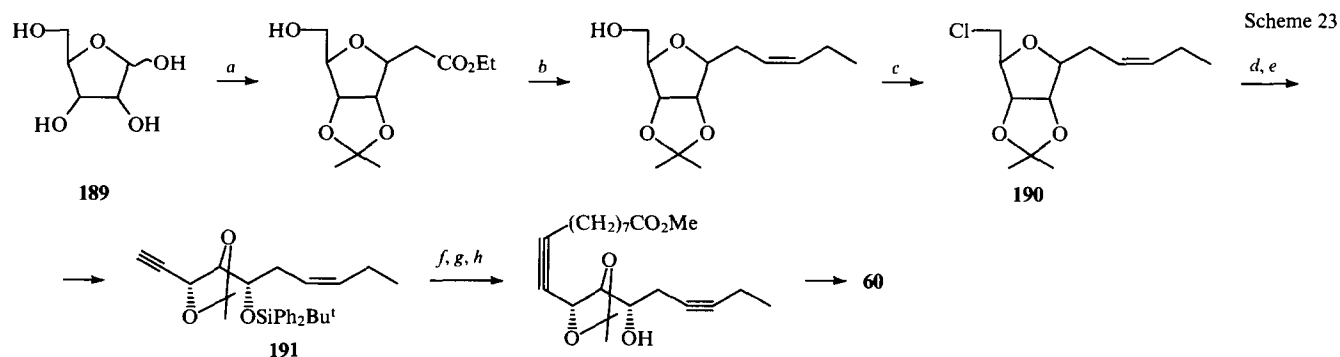
Monosaccharides have been widely employed in the past decade for enantiospecific syntheses of low molecular weight bioregulators, including hydroxyunsaturated acids as the starting chiral compounds. Thus, the scheme of synthesis of vernolic **82** and coriolic **16** acids is based on the transformations of 2-deoxy-D-glucose **187**. A noteworthy step in this chain of conversions is the allyl isomerisation of the epoxy group in the acid **82** under the action of cyclohexyl(isopropyl)methylmagnesium amide **188** (Scheme 22).¹⁶⁰



(a) $\text{HO}_2\text{C}(\text{CH}_2)_8\text{PPh}_3\text{Br}$, $\text{LiN}(\text{SiMe}_3)_2$, CH_2N_2 ; (b) $\text{TsCl}-\text{Py}$;

(c) Bu_4NF ; (d) $\text{C}_6\text{H}_{11}(\text{Pr}^i)\text{NMgMe}$ (188)

The synthesis of (11*S*,12*S*,13*R*)-trihydroxy-(9*Z*,15*Z*)-octadienoic acid **60** has been performed on the basis of D-ribose **189** (Scheme 23).¹⁶¹ In this series of transformations, the conversion

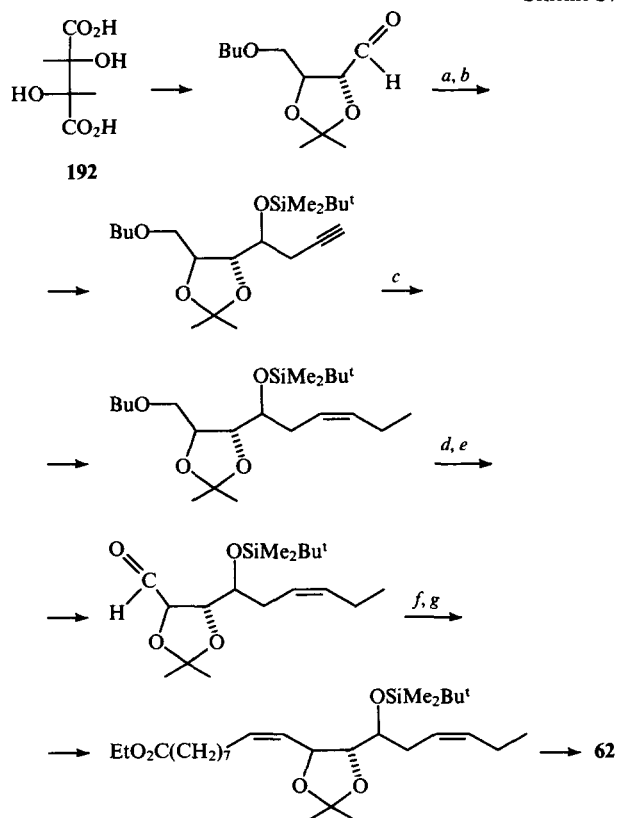


(a) $\text{Ph}_3\text{P}=\text{CHCO}_2\text{Et}$; (b) Bu^i_2AlH , $\text{C}_2\text{H}_2\text{CH}=\text{PPh}_3$; (c) $\text{CCl}_4-\text{PPh}_3$; (d) LiNH_2 ; (e) $\text{Bu}^i\text{Ph}_2\text{SiCl}$; (f) $\text{Br}(\text{CH}_2)_7\text{CO}_2\text{Li}$, BuLi ; (g) CH_2N_2 ; (h) $\text{C}_5\text{H}_5\text{N}\cdot\text{HF}$

(h) $C_5H_5N \cdot HF$

of the chloro derivative **190** into the acetylenic compound **191** deserves special notice.

L-(+)-Tartaric acid **192** has been used as the starting compound in the synthesis of (1*S*,12*R*,13*R*)-trihydroxyocta-deca-(9*Z*,15*Z*)-dienoic acid **62** (Scheme 24).¹⁶²

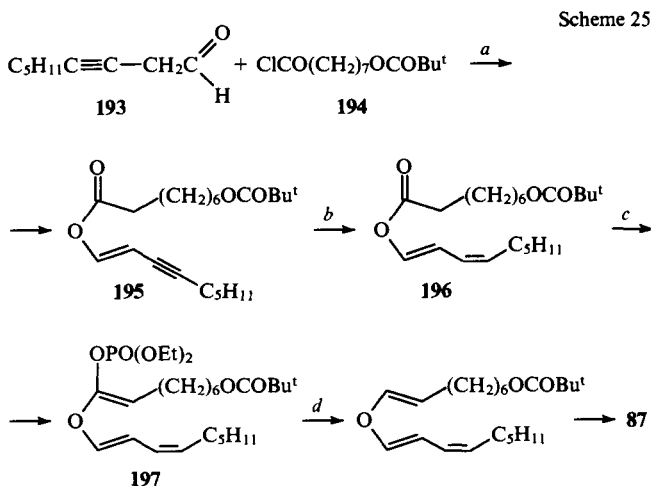


(a) $\text{CH}\equiv\text{CCH}_2\text{Br}$, Zn; (b) $\text{Bu}^t\text{Me}_2\text{SiCl}$;

(c) BuLi , $\text{C}_2\text{H}_5\text{Br}$, Pd, Pb – CaCO_3 ; (d) $\text{Li} - \text{NH}_3$; (e) $(\text{COCl})_2$,

DMSO; (f) $\text{EtO}_2\text{C}(\text{CH}_2)_7\text{CH} = \text{PPh}_3$; (g) Bu_4NF

The synthesis of colnelic acid **87** having in its structure a rather rare fragment of divinyl ether also presents certain interest.¹⁶³ The key step in the synthesis of this compound is the acylation of non-3-ynal **193** with 8-pivaloyloxyoctanoyl chloride **194** in the

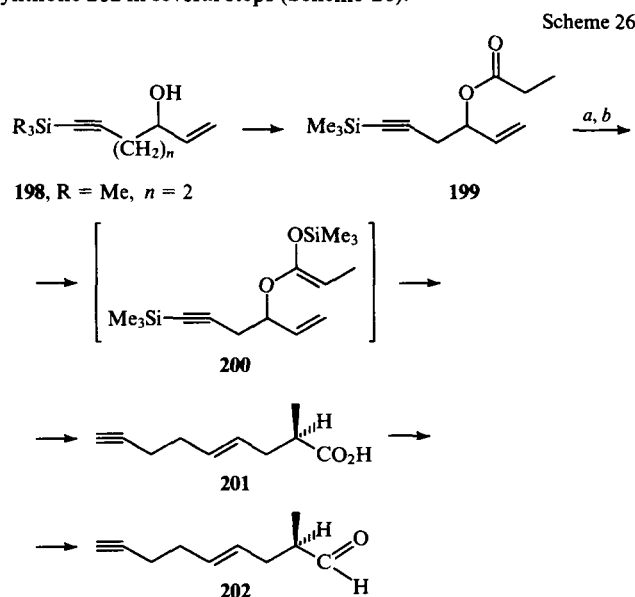


(a) $(\text{Me}_3\text{Si})_2\text{NNa}$; (b) H_2 , Pd – CaCO_3 ; (c) LDA, $(\text{EtO})_2\text{POBr}$;

(d) Et_3Al , $\text{Pd}(\text{PPh}_3)_4$

presence of bis(trimethylsilyl)sodium amide to form the enynyl ester **195**. The creation of the divinyl ether fragment has required the phosphorylation of the diene ester **196** in the presence of lithium diisopropylamide (LDA) and triethylaluminum-mediated hydrogenolysis of phosphate **197** in the presence of $\text{Pd}(\text{PPh}_3)_4$ (Scheme 25).

The synthesis of bongkreic acid **122** is related to syntheses of higher complexity.¹⁶⁴ Hydroxysylans **198** were the starting compounds for the preparation of bongkreic acid. Thus, in the synthesis of the synthon **201**, hydroxysylane **198** ($n = 2$) was converted into propionate **199**, which after silylation was subjected to Klaisen–Ireland rearrangement. The necessary (*S*)-enantiomer was isolated from the racemic mixture of 2-methyl-non-4-nonen-8-ynoic acid **201**, using HPLC on a column with a chiral adsorbent. The latter was transformed into the key synthon **202** in several steps (Scheme 26).

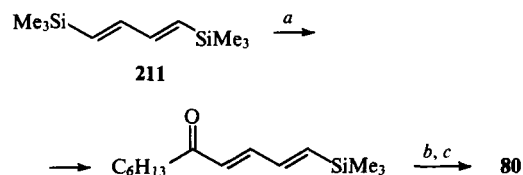


(a) Me_3SiCl , LDA; (b) HF

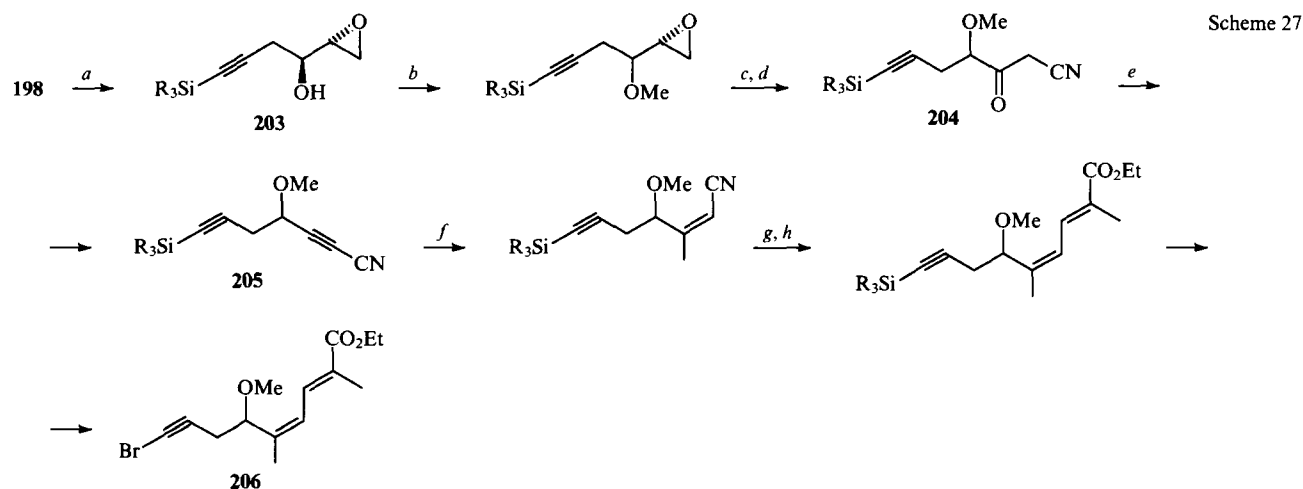
A parallel scheme for the conversion of C_6 -hydroxysylane **198** ($n = 1$) involves its asymmetric epoxidation to form the optically active epoxide **203**. An important step in these transformations is the preparation of cyanodiyne **205** from α -cyanoketone **204** with elimination of trifluoromethanesulfonic acid by NaH. Further conversions resulting in the block **206** are shown in Scheme 27.

The final step in the synthesis of the acid **122** involved interaction of the dilithium derivative of methyl 3-methylglutamate **207** with the aldehyde **202**. This was followed by hydroboration of acetylene **208** with diisoamylborane, preparation of the cuprate reagent **209**, and its stereoselective coupling with the bromide **206**. Hydrogenation of the triple bond in the precursor **210** and alkaline hydrolysis gave bongkreic acid **122**, whose characteristics were identical with those of the natural toxin (Scheme 28).

The high reactivity of vinylsilanes has been employed in the synthesis of ostopanoic acid **80**.¹⁶⁵ The interaction of 1,4-bis(trimethylsilyl)buta-1,3-diene **211** first with heptanoyl chloride and then with pimeloyl chloride made it possible to obtain the target dioxocarboxylic acid.



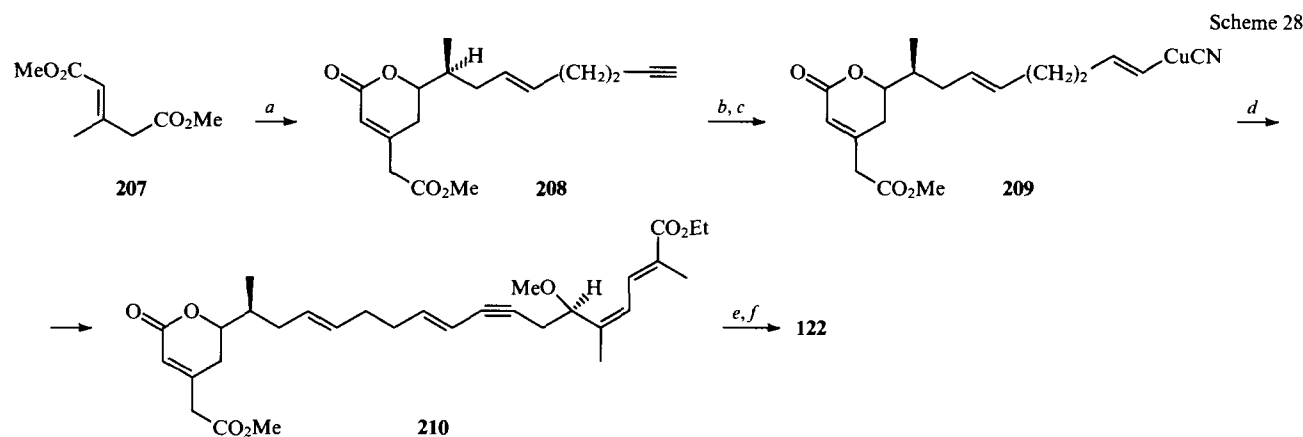
(a) $\text{C}_6\text{H}_{13}\text{COCl}$, AlCl_3 ; (b) $\text{ClOC}(\text{CH}_2)_5\text{COCl}$; (c) NaOH



$R = \text{Pr}^i, n = 1$

(a) $\text{Bu}^t\text{O}_2\text{H}$, $\text{Ti}(\text{OPr}^i)_4$, (+)DIPT; (b) NaH , MeI ; (c) NaCN ; (d) PCC ; (e) $(\text{CF}_3\text{SO}_2)_2\text{O}$, NaH ; (f) Me_2CuLi ; (g) $(\text{Bu}^t)_2\text{AlH}$;

(h) $\text{Ph}_3\text{P}=\text{C}(\text{Me})\text{CO}_2\text{Et}$

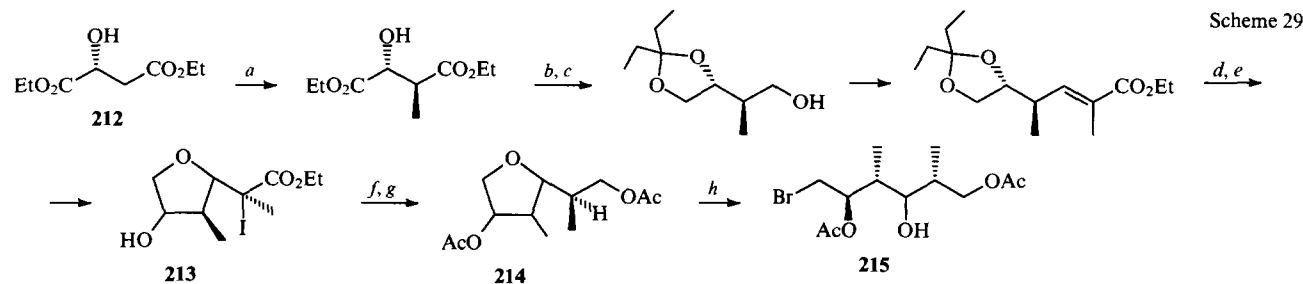


(a) LDA , **202**; (b) $(\text{Me}_2\text{CHCHMe})_2\text{BH}$; (c) CuCN ; (d) **206**; (e) Pd , $\text{Pb}-\text{CaCO}_3$; (f) KOH , MeOH

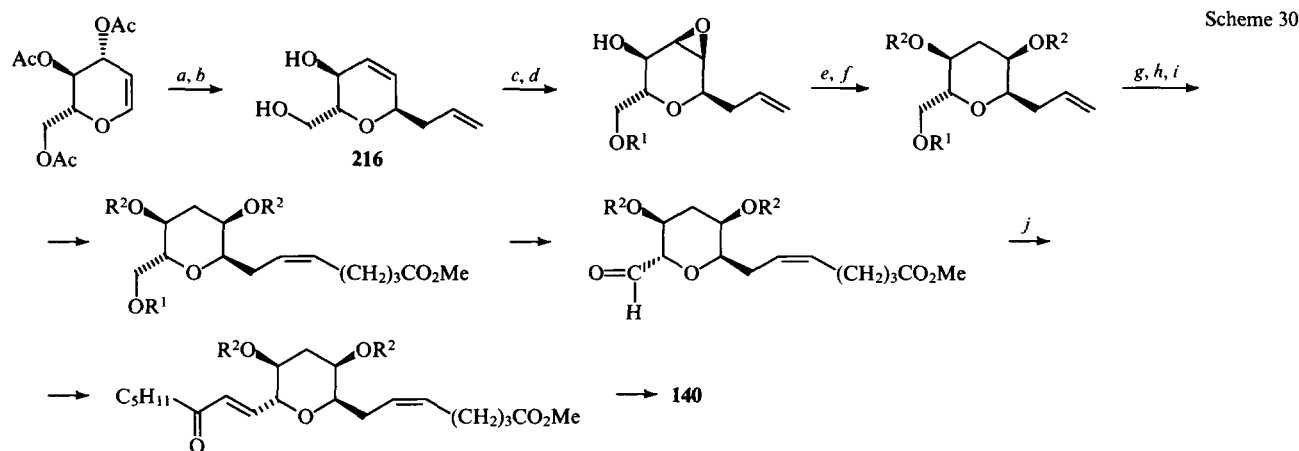
The synthesis of unsaturated acids carrying a heterocyclic fragment is acknowledged to be rather difficult to realise. This is the reason for the appearance of a large number of publications dealing with the problems of stepwise synthesis of these structures. For example, the synthesis of the C_{22} -fragment of ionomycin **133** has been carried out on the basis of (*S*)-malic acid **212** via compound **215** (Scheme 29).¹⁶⁶

In this sequence of conversions, the formation of the tetrahydrofuran derivative **213** and the heterocycle ring-opening in the product **214** by dimethylbromoborane are of interest.

Triacetyl-D-glucal has been used as the starting compound in the enantioselective synthesis of the arachidonic acid metabolite **140**.¹³¹ Its interaction with trimethylallylsilane accompanied by Ferrier rearrangement gives the diol **216**, the subsequent conversions of which are shown in Scheme 30.



(a) MeI , LDA ; (b) $\text{BH}_3 \cdot \text{Me}_2\text{S}$; (c) $\text{Et}_2\text{C}(\text{OMe})_2$; (d) H^+O ; (e) I_2 , NaHCO_3 ; (f) $\text{Ac}_2\text{O}-\text{Py}$; (g) Bu_3SnH ; (h) Me_2BBr , Et_3N .



$R^1 = \text{Bu}^t\text{Me}_2\text{Si}$; $R^2 = \text{MeO}(\text{CH}_2)_2\text{OCH}_2$

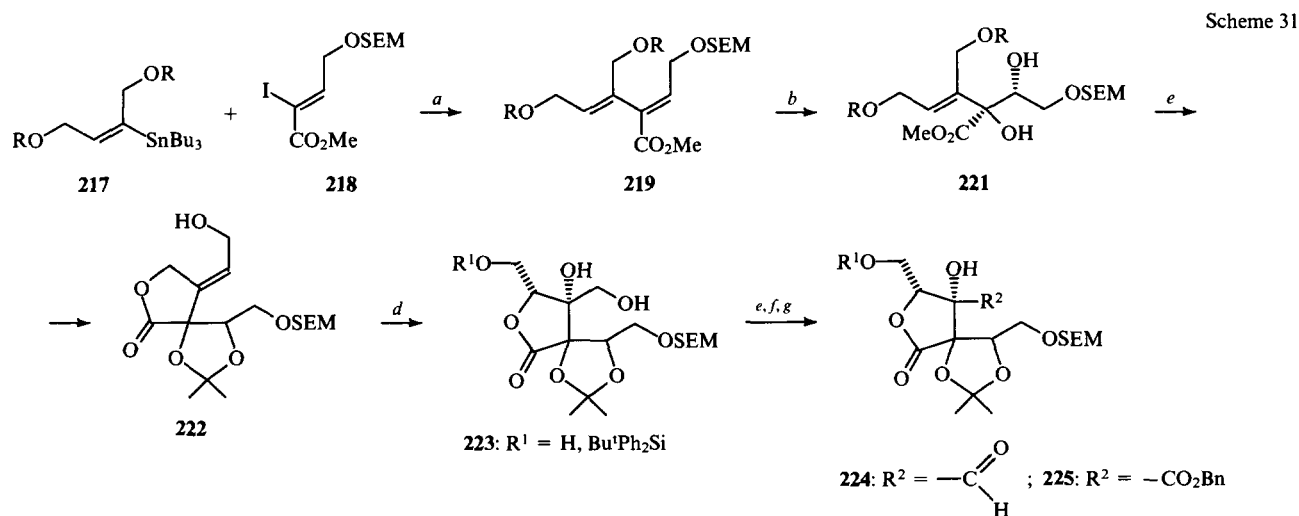
(a) $\text{Me}_3\text{SiCH}_2\text{CH}=\text{CH}_2$, $\text{BF}_3 \cdot \text{Et}_2\text{O}$; (b) KOH , MeOH ; (c) $m\text{-ClC}_6\text{H}_4\text{CO}_3\text{H}$; (d) $\text{Bu}^t\text{Me}_2\text{SiCl}$; (e) LiAlH_4 ; (f) $\text{MeOCH}_2\text{CH}_2\text{OCH}_2\text{Cl}$; (g) O_3 ; (h) $\text{Ph}_3\text{P}=\text{CH}(\text{CH}_2)_3\text{CO}_2\text{Na}$; (i) CH_2N_2 ; (j) $(\text{MeO})_2\text{POCH}_2\text{COC}_5\text{H}_{11}$, K_2CO_3

In the scheme of synthesis of the zaragozic acid **A 159** (squalstatin **S₁**) published recently, the synthesis of the key synthon **228** merits attention.^{167, 168} This synthesis begins with coupling of the vinylstannane **217** with the iodide **218** catalysed by a palladium complex. This is followed by chiral Sharpless hydroxylation of the diene ester **219** with the $\text{K}_3\text{Fe}(\text{CN})_6\text{-K}_2\text{OsO}_2(\text{OH})_4$ complex in the presence of the bidentate ligand, $(\text{DHQD})_2\text{PHAL}$ responsible for the stereodifferentiating effect (Scheme 31).¹⁶⁹

The thus formed optically active ester **221** is lactonised by 2,3-dichloro-5,6-dicyano-1,4-benzoquinone (DDQ) to give the lactone **222**, which is further converted into the diol **223**. The latter undergoes a series of conversions aimed at differentiated

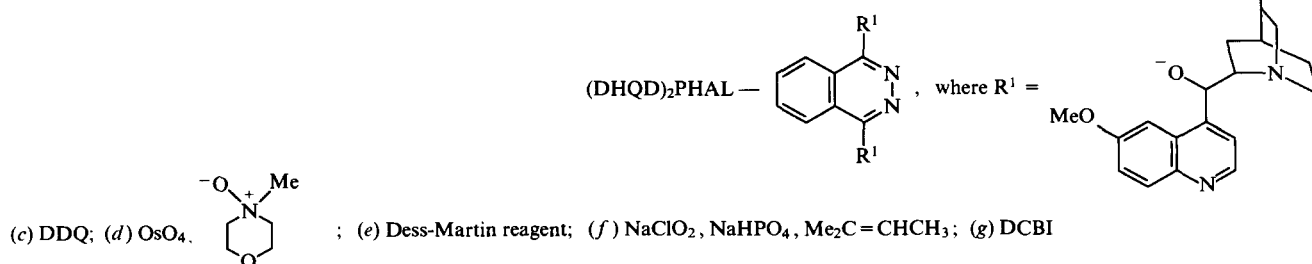
protection of the hydroxyl groups and is further oxidised with the Dess–Martin reagent.¹⁷⁰ The resulting aldehyde **224** is oxidised with NaClO_2 to the corresponding acid, which was benzylated with N,N' -dicyclohexyl-*O*-benzylisourea (DCBI) into the ester **225** (Scheme 31).

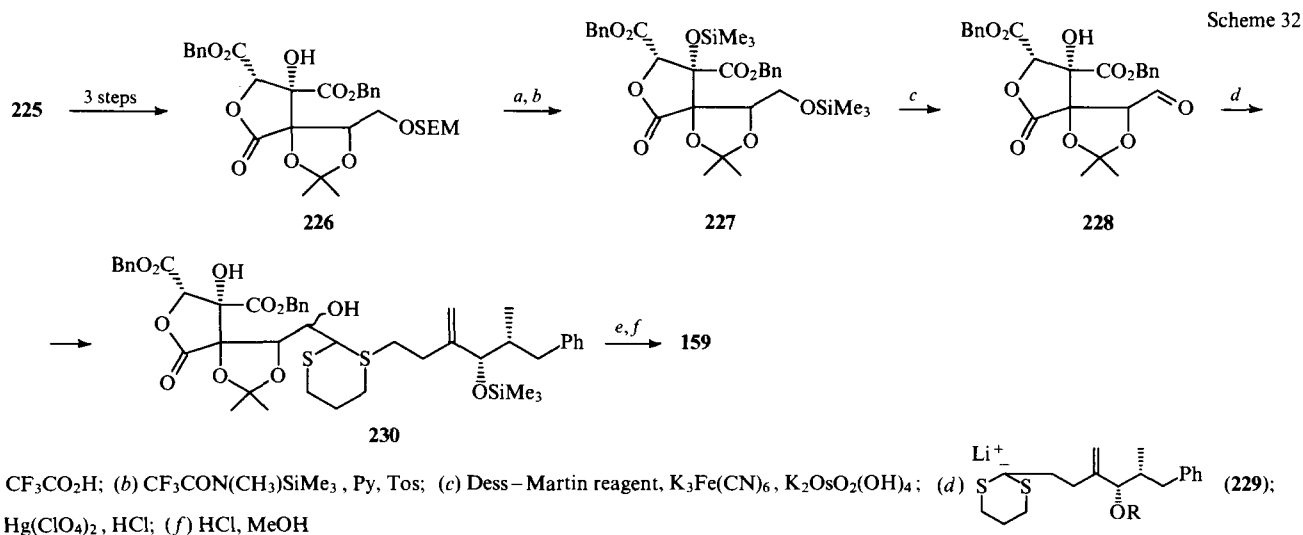
After removal of the protecting silyl group, the benzyl ester **225** is converted into the ester **226** in three steps. Its hydrolysis with trifluoroacetic acid and treatment of the reaction product with $\text{CF}_3\text{CON}(\text{CH}_3)\text{SiMe}_3$ in the presence of toluene-*n*-sulfonic acid in pyridine results in the bisilyl ether **227**. The oxidation of compound **227** with the Dess–Martin reagent is regiospecific and does not involve the tertiary Me_3SiO group, giving the key aldehyde **228**.



$R = \text{COC}_6\text{H}_4\text{OMe}$; $\text{SEM} = \text{Me}_3\text{Si}(\text{CH}_2)\text{OCH}_2$

(a) $\text{PdCl}_2(\text{MeCN})_2$; (b) $(\text{DHQD})_2\text{PHAL}$ (**220**), $\text{K}_3\text{Fe}(\text{CN})_6$, $\text{K}_2\text{OsO}_2(\text{OH})_4$;

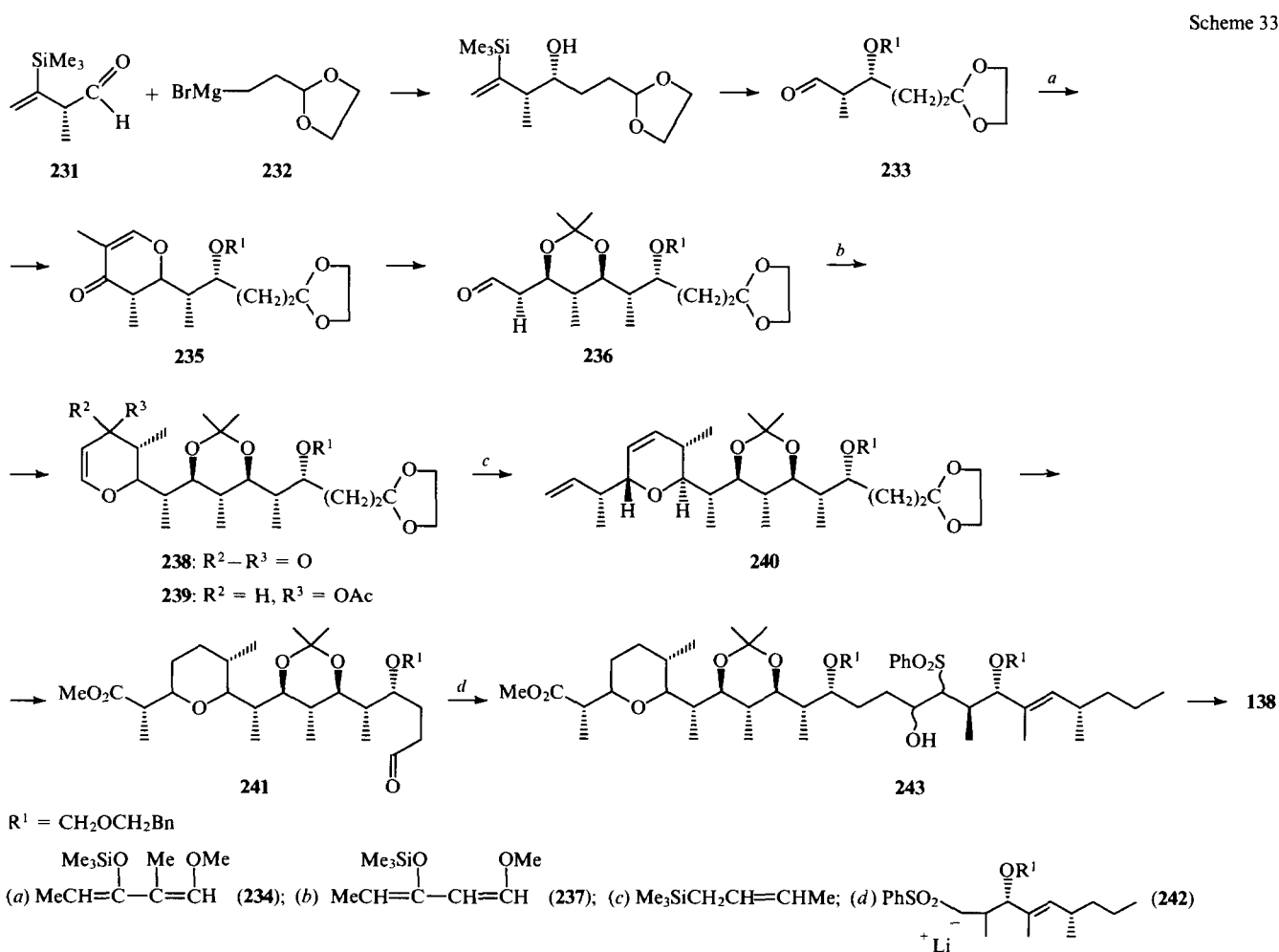




Similar conversions of bissilyl ethers under the action of a $(\text{COCl})_2$ –DMSO system has been used to obtain synthons for prostaglandins.¹⁷¹ The aldehyde **228** reacts with the lithium derivative of the dithiane **229**, giving the compound **230**, and is then converted into zaragozic acid A in two steps **159** (Scheme 32).

The total synthesis of zincoforin **138** is marked by multiple application of organosilicon reagents.¹⁷² For example, the role of the Me_3Si group in the reaction of the aldehyde **231** consists in stereodifferentiation of the attachment of the Grignard reagent **232**; the aldehyde-acetal **233** obtained upon desilylation and

ozonolysis reacts with siloxy-1,3-diene **234** to form dihydropyran **235**. The latter undergoes a series of conversions to give the aldehyde **236** which, after an analogous reaction with siloxy-1,3-diene **237**, affords the ketone **238**; the latter is further converted into the acetate **239**. This is followed by $\text{BF}_3 \cdot \text{Et}_2\text{O}$ -catalysed cross-coupling with trimethylcrotylsilane, eventually resulting in the compound **240**. The conventional procedures gave the methylformylcarboxylate **241**, which was then introduced in the reaction with the sulfone anion **242**. The obvious conversions of the hydroxysulfone **243** afforded zincoforin **138** (Scheme 33).



The authors of the present review would like to call the reader's attention to the prospects that emerge from synthetic studies in the area of unsaturated acids. For example, polyhydroxy acids present interest as potential immunizing agents capable of protecting plants from pathogenic fungi even when used in nanogram quantities. Metabolites of the zaragozic acid type are of prime interest for large pharmaceutical firms involved in the solution of vital problems of cardiology, such as regulation of cholesterol biosynthesis. Bengamides, the technological synthesis of which is quite feasible, are also of substantial interest.

The authors express the hope that synthetic chemists will not only further advance the problems discussed in this review but will also proceed along interesting and promising paths.

This review has been written with the financial support of the Russian Fundamental Research Fund (Grant Nos 94-03-08009 and 95-03-08517).

References

1. H Baumann, M Bühler, H Fochem, F Hirsinger, J Falbe *Angew. Chem.* **100** 46 (1988) [*Angew. Chem., Int. Ed. Engl.* **27** 42 (1988)]
2. D Bishop *J. Lipid Res.* **4** 81 (1963)
3. P Ishida, H Shirahama, T Matsumoto *Chem. Lett.* **9** (1993)
4. C R Smith, T L Wilson, T K Miwa, H Zobel, R Lohmar, J A Wolff *J. Org. Chem.* **26** 2903 (1961)
5. R Biuder, A Lee *J. Org. Chem.* **31** 1477 (1966)
6. H Koshina, S Togija, T Ioshihara, S Sakamura *Tetrahedron Lett.* **28** 73 (1987)
7. D T Asil'bekova, S D Gusakova, A I Glushenkova *Khim. Prir. Soedin.* **616** (1991)
8. A N Grechkin, O S Korolev, R A Kuramshin, I A Tarchevskii *Dokl. Akad. Nauk SSSR* **297** 1257 (1987)
9. A V Kuchin, A G Tolstikov, E V Gorobets, V N Odionokov, A N Grechkin, G A Tolstikov *Dokl. Akad. Nauk SSSR* **308** 384 (1989)
10. J Joshida, M Nakagama, H Seki, T Hino *J. Chem. Soc., Perkin Trans. I* **343** (1992)
11. C Fryhle, P Willard, C Rybak *Tetrahedron Lett.* **33** 2327 (1992)
12. S Tsuboi, Han Wu, S Malda, S Ono, A Kuroda *Bull. Chem. Soc. Jpn.* **60** 1103 (1987)
13. C Smith, T Wilson *J. Am. Chem. Soc.* **82** 1417 (1960)
14. T G Nemyrko, Ya V Rashkes, A I Glushenkova, in *Novoe v Biologicheskoi Khimii i Farmakologii Oblepikhi* (Advances in the Biochemistry and Pharmacology of Sea Buckthorn) (Novosibirsk: Siberian Branch of the Academy of Sciences of the USSR, 1991) p. 85
15. A Verneugli *Can. J. Bot.* **64** 973 (1986)
16. J-M Duffarlt, J Einhorn, A Alexakis *Tetrahedron Lett.* **32** 3701 (1991)
17. C Smith, T Wilson *J. Org. Chem.* **27** 3112 (1962)
18. J Kobayashi, S Okamoto, T Shimazari, J Ochiai, F Sato *Tetrahedron Lett.* **30** 3959 (1987)
19. W Karrer, in *Konstitution und Vorkommen der Organischen Pflanzstoffe* Vol. 2 (Wien: Ergänzungsband,) p. 1037
20. R Rowell, C Smith *J. Org. Chem.* **31** 528 (1966)
21. C Chan, P Cox, S Roberts *J. Chem. Soc., Chem. Commun.* **971** (1988)
22. G Moustakis, O Weerasinghe, J Falk *Tetrahedron Lett.* **27** 303 (1986)
23. A Rama Rao, S Reddy, R Reddy *J. Org. Chem.* **51** 4158 (1986)
24. S D Gusakova, D T Esil'bekova *Khim. Prir. Soedin.* **744** (1991)
25. A Rama Rao, V Varaprasad, E Reddy *Synth. Commun.* **21** 1143 (1991)
26. T Jeffery *Tetrahedron Lett.* **34** 1133 (1993)
27. M Ubukata, K Kimura, K Isono, J McCloskey *J. Org. Chem.* **57** 6392 (1992)
28. J Huguet, M del Carmen Reges *Tetrahedron Lett.* **31** 4279 (1990)
29. T Kato, J Jamaguchi, T Hitano, N Harada *Chem. Lett.* **409** (1984)
30. A Rama Rao, R Reddy *Tetrahedron Lett.* **27** 2279 (1986)
31. D Shiwi, D Jadagiri, J Falk, J Masferrer, M Schwartzman *Tetrahedron Lett.* **30** 3923 (1989)
32. A Guerriero, M D'Ambrosio, F Pietra *Helv. Chim. Acta* **71** 1094 (1988)
33. A Guerriero, M D'Ambrosio, F Pietra, O Ribes *J. Nat. Prod.* **53** 57 (1990)
34. M D'Auria, L Minale, K Riccio *Experientia* **44** 719 (1988)
35. A Guerriero, M D'Ambrosio, F Pietra *Helv. Chim. Acta* **73** 2183 (1990)
36. M Higgs, J Mulheim *Tetrahedron* **37** 4259 (1981)
37. M Bernart, W Gerwick *Tetrahedron Lett.* **29** 2015 (1988)
38. V Paul, W Fenical *Tetrahedron Lett.* **21** 3327 (1980)
39. F Gunstone *J. Chem. Soc.* **1611** (1954)
40. R Sawa, N Matsuda, T Uchida, T Ikeda *J. Antibiot.* **44** 396 (1991)
41. S Kadis, A Ciegler, S Aji, in *Microbial Toxins* Vol. 7 (New York: Academic Press, 1971) p. 207
42. Y Ueno *Trichotecenes — Chemical, Biological, and Toxicological Aspects* Vol. 4 (Elsevier, New York, 1983)
43. W Herz, in *Fortschritte Chem. Org. Natur-Stoffe* Vol. 47 (New York: Springer, 1953) p. 153
44. M Solem, Z Jiang, W Gerwick *Lipids* **24** 256 (1989)
45. T Kato, J Jamaguchi, T Hirakawa, N Hoshino *Agr. Biol. Chem.* **55** 1349 (1991)
46. T Kato, J Jamaguchi, M Abe, T Ueyhara, T Namai, M Kodama, J Shiobara *Tetrahedron Lett.* **26** 2357 (1985)
47. B Cosse-Kobo, P Mosset, R Gree *Tetrahedron Lett.* **30** 4235 (1989)
48. A Panossian, G Avetissian, S Batrakov, S Varbanian, E Gabrielian *Planta Medica* **47** 17 (1983)
49. A G Panosyan *Bioorg. Khim.* **11** 126 (1985)
50. A Panossian *Prostaglandins* **33** 363 (1987)
51. G Sharma, S Rao *Tetrahedron Lett.* **33** 2305 (1992)
52. J Cardellina, H Dahetos, F Marneri *Phytochemistry* **17** 2091 (1978)
53. J Jadav, M Chander *Tetrahedron Lett.* **31** 4349 (1990)
54. P Quinton, T Le Gall *Tetrahedron Lett.* **32** 4909 (1991)
55. H Suemune, T Harabe, K Sakai *Chem. Pharm. Bull.* **36** 3632 (1988)
56. P Schener, in *Marine Natural Products* Vol. 4 (New York: Academic Press, 1981) p. 40
57. P Schener, in *Marine Natural Products* Vol. 1 (New York: Academic Press, 1978) p. 85
58. A Prand, R Valls, L Piovetti, B Banaigs *Tetrahedron Lett.* **34** 5437 (1993)
59. N Carballerio, V Negrou *J. Nat. Prod.* **55** 333 (1992)
60. E Aganoglu, J Kornbobst, A Abou-Bichara, C Djerassi *Tetrahedron Lett.* **24** 1111 (1983)
61. Ch Mahmood, J Daulatabad, M Mohaddin *Phytochemistry* **30** 2399 (1991)
62. C Smith *Lipids* **1** 268 (1966)
63. L Crombie, D Morgan *J. Chem. Soc., Chem. Commun.* **558** (1988)
64. A Lopez, W Gerwick *Tetrahedron Lett.* **29** 1505 (1988)
65. A Guerriero, M D'Ambrosio, F Pietra *Helv. Chim. Acta* **73** 2183 (1990)
66. K Gustafson, M Roman, W Fenical *J. Am. Chem. Soc.* **111** 7519 (1989)
67. Z Pang, O Sterner *J. Org. Chem.* **56** 1233 (1991)
68. M Hamburger, S Handa, G Cordell *J. Nat. Prod.* **50** 281 (1987)
69. Jpn. P. 63 159 390; *Ref. Zh. Khim.* **37** 17 O 120P (1989)
70. T Kato, J Jamaguchi, S Ohnuma, M Kodama *Chem. Lett.* **577** (1986)
71. J Nagao, T Miyasaka, K Seno, E Fujita, D Shibata, E Doi *J. Chem. Soc., Perkin Trans. I* **2439** (1984)
72. S Baertschi, A Brash, T Harris *J. Am. Chem. Soc.* **111** 5003 (1989)
73. E Corey, S Wright *J. Org. Chem.* **55** 1670 (1990)
74. E Corey, R Nagata, S Wright *Tetrahedron Lett.* **28** 4917 (1987)
75. C McIntyre, F Scott, T Simpson, L Trimble *J. Chem. Soc., Chem. Commun.* **501** (1986)
76. A Etemadi, J Gasche *Bull. Soc. Chim. Biol.* **47** 631 (1965)
77. A Etemadi *C. R. Hebd. Seances Acad. Sci., Sec. D* **263** 835 (1966)
78. A Etemadi, E Lederer *Bull. Soc. Chim. Fr.* **868** (1964)
79. M Nakanishi, T Hase *Bull. Chem. Soc. Jpn.* **64** 3084 (1991)
80. M Nakanishi, T Hase *Chem. Lett.* **47** (1991)
81. US P. 4 386 227; *Ref. Zh. Khim.* **9** 3 O 33P (1984)
82. L Semmak, A Zerzout, P Valls *Phytochemistry* **27** 2347 (1988)
83. R Näf, A Velluz *Tetrahedron Lett.* **32** 4487 (1991)
84. A Guerriero, M D'Ambrosio, V Guomo, F Pietra *Helv. Chim. Acta* **71** 57 (1988)
85. D Traxler, H Fritz, W Richter *Helv. Chim. Acta* **60** 578 (1977)
86. G Rihs, D Traxler *Helv. Chim. Acta* **64** 1533 (1981)
87. F Van Middlesworth, M Omstead, D Schmatz, K Bartizal, K A Fromtling, G Bills, K H Nollstadt, S Honeycutt, M M Zweriuk *J. Antibiot.* **44** 45 (1991)

88. H Chiba, R Kanebo, H Agematu, R Okamoto *J. Antibiot.* **46** 356 (1993)
89. F Van Middlesworth, C Dufresne, J Smith, K Wilson *Tetrahedron* **47** 7563 (1991)
90. L Crombie, M Horsham, S Jarrett *Tetrahedron Lett.* **30** 4299 (1989)
91. S Nakatsuka, K Ueda, T Goto, M Jamamoto, S Nishimura, K Kohmoto *Tetrahedron Lett.* **27** 2753 (1986)
92. T Kitagawa, M Miyashita, Zhang Jang *Chem. Pharm. Bull.* **39** 2445 (1991)
93. H Jrie, K Matsumoto, T Kitagawa *Chem. Pharm. Bull.* **38** 1451 (1990)
94. US P. 5 182 298; *Ref. Zh. Khim.* **36** 9 O 139P (1994)
95. M Adamczeski, E Quinoa, P Crews *J. Org. Chem.* **55** 240 (1990)
96. M Adamczeski, E Quinoa, P Crews *J. Am. Chem. Soc.* **111** 647 (1989)
97. N Chida, T Tobe, Sh Okada *J. Chem. Soc., Chem. Commun.* 1064 (1992)
98. J Marshall, G Luke *J. Org. Chem.* **58** 6229 (1993)
99. R Jansen, G Reifenshane, K Gerth, H Reichenbach, G Holfe *Liebigs Ann. Chem.* 1081 (1983)
100. W Trowitsch-Kinnst, E Forsche, H Reichenbach, V Wray *Liebigs Ann. Chem.* 659 (1992)
101. J Kim, F Furinata, Sh Jamanaka *J. Antibiot.* **44** 553 (1991)
102. BRD P. 4 041 686; *Ref. Zh. Khim.* **4** 7 O 28P (1993)
103. BRD P. 4 041 688; *Ref. Zh. Khim.* **38** 10 O 144P (1993)
104. A Wright, J Coll, J Price *J. Nat. Prod.* **53** 845 (1990)
105. Sh Ohta, H Okada, H Kobayashi, J Oclarit, S Ikegami *Tetrahedron Lett.* **33** 5935 (1993)
106. Jpn. P. 58-150 595; *Ref. Zh. Khim.* **30** 23 O 216P (1994)
107. A Gangloff, B Akemark, P Hequist *J. Org. Chem.* **57** 4797 (1992)
108. T Watanabe, T Suzuki, K Uzaki *J. Antibiot.* **44** 1457 (1991)
109. L Banfi, W Carbi, G Poli, D Potenza, C Scolastico *J. Org. Chem.* **52** 5452 (1987)
110. M Devys, J-P Ferezoy, R Topgi, M Barbier, J -E Bousqret, A Kollman *J. Chem. Soc., Perkin Trans. I* 2133 (1984)
111. D O'Hagan, S Rogers, G Diffiu, R Edwards *Tetrahedron Lett.* **33** 5585 (1993)
112. H Seto, T Sasaki, H Jonehara *Tetrahedron Lett.* **28** 4083 (1977)
113. D Aldridge, D Giles, W Turner *J. Chem. Soc., C* 3888 (1971)
114. S Chatterjee, E Vijayakumar, K Roy, R Rupp, B Ganguli *J. Org. Chem.* **53** 4883 (1988)
115. G Bill, R Chen, R Rasmussen, J McAlpine *J. Antibiot.* **46** 39 (1993)
116. B Jarvis, S N Cómezoglu, M Rao, B Pena, F E Boettner, T M Williams, G Forsyth, B Epling *J. Org. Chem.* **52** 45 (1987)
117. B Jarvis, S Comezogu, H Anmon, S Kupchan *J. Nat. Prod.* **50** 815 (1987)
118. S Yu Yunusov, *Alkaloidy* (Alkaloids) (Tashkent: FAN, 1981) p. 354
119. A Mattocks *Chemistry and Toxicology of Pyrrolizidine Alkaloids* (London: Academic Press, 1986)
120. J Harris, J Turner, M Meinz, M Nallin-Omstead, G Helms, G Bills, D Zink, K Wilson *Tetrahedron Lett.* **34** 5235 (1993)
121. C Spino, L Weiler *Tetrahedron Lett.* **28** 731 (1987)
122. C Pace-Asciac, L Wolfe *J. Chem. Soc., Chem. Commun.* 1235 (1980)
123. G Just, D Crosilla *Can. J. Chem.* **58** 2349 (1980)
124. E Chain, G Mellows *J. Chem. Soc., Perkin Trans. I* 294 (1977)
125. G Keck, A Tafesh *J. Org. Chem.* **54** 5845 (1989)
126. D Stierle, A Stierle *Experientia* **48** 1165 (1992)
127. M Balestra, M Wittman, J Kallmerben *Tetrahedron Lett.* **29** 6905 (1988)
128. S Danishefsky, C Selnick, M DeNinno, R Zelle *J. Am. Chem. Soc.* **109** 1572 (1987)
129. B Isaak, S Ager, R Elliot, R Stonard *J. Org. Chem.* **57** 7220 (1992)
130. C Pace-Asciac *Biochemistry* **10** 3664 (1971)
131. A G Tolstikov, O F Prokopenko, L V Spirikhin, G A Tolstikov *Bioorg. Khim.* **19** 262 (1993)
132. G Just, P Povin *Can. J. Chem.* **58** 2173 (1980)
133. G Hofle, H Steinmetz, K Gerth, H Reichenbach *Liebigs Ann. Chem.* 941 (1991)
134. S Tsukamoto, M Ishibashi, T Sasaki, J Kobayashi *J. Chem. Soc., Perkin Trans. I* 3185 (1991)
135. M Yofsu-Yamashita, R Haddock, T Yasumoto *J. Am. Chem. Soc.* **115** 1147 (1993)
136. H Inouye, Y Takaeda, S Uesato, K Uobe, T Hashimoto *Tetrahedron Lett.* **21** 1059 (1980)
137. A Kempf, K Wilson, O Hensens, R Monahan *J. Antibiot.* **39** 1361 (1986)
138. E Selva, G Beretta, R Pallanza *J. Antibiot.* **43** 1349 (1990)
139. J Grove *Nat. Prod. Rep.* **10** 429 (1993)
140. H Koshino, H Takahashi, H Osaka, K Isono *J. Antibiot.* **45** 1420 (1992)
141. B Potts, D Faulkner *J. Am. Chem. Soc.* **113** 6321 (1991)
142. O Hensens, C Dufresne, J Liesch, D Zink, R Reamer, F VanMiddlesworth *Tetrahedron Lett.* **34** 349 (1993)
143. M Dawson, J Farthing, P Marshall, M O'Neil, R Tait, H Wildman, M Hages *J. Antibiot.* **45** 639 (1992)
144. P Sidebothom, R Hitchcock, S Lane, N Watson *J. Antibiot.* **45** 648 (1992)
145. S Grundy *New England J. Med.* **319** 24 (1988)
146. A Baxter, B Fitzgerald, M Sapra, C Wright *J. Biol. Chem.* **267** 11705 (1992)
147. M Lester, G Giblin, G English, P Procopin, B Ross, N Watson *Tetrahedron Lett.* **34** 4357 (1993)
148. A Robichand, G Berger, D Evans *Tetrahedron Lett.* **34** 8403 (1993)
149. Chuen Chan, G Guglis, P Procopin, B Ross, N Watson, A Srikantha *Tetrahedron Lett.* **34** 6143 (1993)
150. C Dufresne, K Wilson, S Singh, D Zink *J. Nat. Prod.* **56** 1923 (1993)
151. E B Gorobets, A V Kuchin, G A Tolstikov *Metalorg. Khim.* **4** 198 (1991)
152. A Rama Rao, E Reddy, A Purandare *Tetrahedron* **43** 4385 (1987)
153. U Balerao, L Dasaradhi, C Muralikrishna, N Fadnavis *Tetrahedron Lett.* **34** 2359 (1993)
154. J Kobayashi, S Okamoto, F Sato *Tetrahedron Lett.* **28** 3959 (1987)
155. T Jeffrey *Tetrahedron Lett.* **34** 1133 (1993)
156. J M Duffault, J Einhorn, A Alexakis *Tetrahedron Lett.* **32** 3701 (1991)
157. A Rama Rao, E Reddy, J Jadav *Tetrahedron* **42** 4523 (1986)
158. M Gurjar, E Reddy *Tetrahedron Lett.* **31** 1783 (1990)
159. J Jadav, P Radhakrishna *Tetrahedron* **46** 5825 (1990)
160. Ch Moustakis, D Weerasinghe, J Falk *Tetrahedron Lett.* **27** 303 (1986)
161. J Jadav, M Chander *Tetrahedron Lett.* **31** 4349 (1990)
162. Wen-Lian Wu, Ju-Lin Wu *Tetrahedron Lett.* **33** 3887 (1992)
163. E Corey, S Wright *J. Org. Chem.* **55** 1670 (1990)
164. E Corey, A Tramontano *J. Am. Chem. Soc.* **106** 462 (1984)
165. F Naso *J. Org. Chem.* **56** 6245 (1991)
166. Y Guindon, C Yoakim, V Gorys, W W Ogilvie, D Delorme, J Renaud, G Robinson, J-F Lavallée, A Slassi, G Jung, J Rancourt, K Durkin, D Liotta *J. Org. Chem.* **59** 1166 (1994)
167. K Nicolaou, E Jue, J Naniwa, Zhen Jang *Angew. Chem., Int. Ed. Engl.* **33/21** 2184 (1994)
168. K Nicolaou, A Nadin, J Lereche, E Jue *Angew. Chem., Int. Ed. Engl.* **33/21** 2190 (1994)
169. R Johnson, K Sharpless, in *Catalytic Asymmetric Synthesis* (Ed. A Ojima) (New York: VCH, 1993) p. 227
170. D Dess, J Martin *J. Org. Chem.* **48** 4156 (1983)
171. G A Tolstikov, M S Miftakov, M E Adler *Zh. Org. Khim.* **24** 224 (1988)
172. S Danishefsky, H Selnick, M De Ninno, R Zelle *J. Am. Chem. Soc.* **109** 1572 (1987)

Ternary carbides and nitrides based on transition metals and subgroup IIIB and IVB elements: electronic structure and chemical bonding

A L Ivanovskii

Contents

I. Introduction	461
II. Chemical bonding and electronic structures of <i>d</i> -metal aluminonitrides and aluminocarbides	461
III. Electronic properties of transition metal siliconitrides and silicocarbides	469
IV. Chemical bonding in ternary carbides and nitrides based on subgroup VIIA and VIIIA transition metals	474

Abstract. Data obtained in theoretical and experimental studies on the electronic structures, the nature of chemical bonding, and certain physicochemical properties of ternary carbides and nitrides involving transition metals and subgroup IIIB and IVB elements are surveyed. The possibilities and prospects for the application of computational quantum-chemical methods for the modelling of new complex solid solutions based on metal-like carbides and nitrides and also for the description of their fundamental properties are discussed. The bibliography includes 168 references.

I. Introduction

The high-temperature refractory transition metal (TM) carbides and nitrides and their reciprocal solid solutions (SS) constitute an extensive class of compounds which are interstitial phases.^{1–3} By virtue of a unique combination of a series of physicochemical properties, these compounds are exceptionally important.^{3–6} Studies on the electronic properties and on the nature of the chemistry bonding in such compounds have made a significant contribution to the development of the quantum chemistry of the solid state. They are being continued vigorously also at the present time. The results obtained in the course of these investigations have been described in numerous publications.^{7–12}

The current state of the chemistry and materials science of refractory transition metal carbides and nitrides involves vigorous investigations directed to the improvement of their properties. The properties can be altered by introducing into the composition 'non-traditional' interstitial elements, mainly subgroup IIIB and IVB elements (Al, Si, etc.). The compounds of these elements with carbon and nitrogen are nonisostructural with *d* metal carbides and nitrides, involving predominantly covalent bonding. Such compounds have found a wide variety of application as chemically stable, ultrahard, semiconducting materials^{13–15} and they are also convenient objects for the investigation of the electronic structures of solids by computational quantum-chemical methods.^{16–21}

The interest in the study of ternary systems of the type $M-M'-(C,N)$, where *M* is a transition metal and *M'* a non-

transition subgroup IIIB or IVB element, is associated primarily with the search for new ceramic materials, which are likely to be useful in the development of protective coatings, materials for the manufacture of instruments, and constructional materials and with the creation of new composites and the determination of the possibilities for their employment in microelectronics, and optics, as catalysts, and as elements in reinforced composite materials for space technology.

Studies on the equilibrium phase relations in the $M-M'-(C,N)$ systems have demonstrated^{1–5} the existence of an extremely large set of ternary phases. The thin-film technologies,^{22–29} which make it possible to produce equilibrium metastable or crystalline and amorphous phases and to vary their microstructure and the content of atomic components over a wide range of concentrations, have therefore assumed a special importance in the creation of new materials. The combination of thin-film technologies with various procedures for the activation of processes involving the preparation of the compositions has led to the possibility of a flexible modification of their physicochemical properties. The problem of the description of the electronic properties of the above multicomponent systems (both mono- and hetero-phase) has become of current interest in this connection. An important place has also been assigned to the determination of specific features of the electronic structure (ES) and the chemical bonding in the individual ternary phases formed in the $M-M'-(C,N)$ systems. The groups of carbides and nitrides having the composition $M_3M'(C,N)$ are of considerable interest in this respect.

The magnetic properties of these carbides and nitrides, in particular the magnetic (and structural) phase transitions, which are of technological importance, have attracted the greatest attention of investigators.^{29–32}

In the present review, an attempt has been made to survey available data on the electronic structures and the chemical bonding in the solid solutions and in the ternary carbide and nitride phases based on transition metals and subgroup IIIB and IVB elements, obtained within the framework of computational approaches to solid state quantum chemistry and also with the aid of X-ray emission and X-ray photoelectron spectroscopy.

II. Chemical bonding and electronic structures of *d*-metal aluminonitrides and aluminocarbides

The aluminium-containing phases formed in the $M-Al-C$, $M-Al-N$, $M-Al-C-N$, etc. systems have been most thoroughly investigated among complex carbides and nitrides. A representative group of solid compounds of the type $M_3Al(C,N)$ and $M_2Al(C,N)$, having individual crystal structures^{1–4} and

A L Ivanovskii Institute of Solid State Chemistry, The Ural Division of the Russian Academy of Sciences, Pervomaiskaya ul. 91, 620219 Ekaterinburg, Russian Federation. Fax (7-343) 244 44 95.

between the octahedra. According to estimates,^{1,60} the compositions of Ti_2AlC_x and Ti_3AlC_x may vary in the range $0.2 \leq x \leq 1.2$.

The initial ideas about the possible types of interatomic interactions in the Ti_2AlC_x and Ti_3AlC_x phases were based on the analysis of their crystal-chemical parameters. Thus the Ti–C distance in Ti_3AlC is close to the sum of the covalent radii of titanium and carbon, which makes it possible to postulate⁶¹ the existence of a strong covalent Ti–C bond. On the other hand, the Al–Al distance is much greater than the sum of the covalent radii of aluminium, which discounts the occurrence of direct Al–Al interactions. Similar comparisons of the atomic radii and the interatomic distances for the Ti–Ti, Al–Ti, and Al–C pairs of atoms lead to the conclusion that there is a possibility of the formation of bonds between titanium and aluminium atoms (Ti–Ti, Al–Ti) and that there are no bonds between aluminium and carbon atoms.⁶¹

A more detailed analysis of the nature of the interatomic interactions in the aluminocarbides Ti_2AlC_x and Ti_3AlC_x has become possible by virtue of the results of studies of their X-ray emission and absorption spectra.⁶² It was found that the Ti L_α band in the emission spectrum, reflecting the energy distribution of the d states of the metal, becomes appreciably broadened in the sequence $\text{TiC}_x \rightarrow \text{Ti}_2\text{AlC}_x \rightarrow \text{Ti}_3\text{AlC}_x$, the main maximum shifting towards the long-wavelength region of the spectrum with simultaneous increase in the intensity of the short-wavelength maximum, which has the same energy as the Al $L_{2,3}$ peak, i.e. the $d(t_{2g})$ states of titanium are filled as a result of the partial transfer of electron density in the Al \rightarrow Ti direction. This may indicate the hybridisation of the near-Fermi Ti $3d, 4s$ –Al $3s, 3d$ states. The identity of the energies of the long-wavelength Ti L_α and Al $L_{2,3}$ maxima in the emission spectra indicates the appearance of covalent Ti–Al bonds.⁶²

With increase in the number of carbon vacancies, the intensity of the low-energy maximum of the Ti L_α band also increases, which is due to the transfer of part of the electron density to the near-Fermi region. Overall, the variable-composition transition metal aluminocarbides may be regarded as phases involving the insertion of carbon into the hypothetical titanium aluminides Ti_2Al and Ti_3Al , the system of interatomic interactions which results in the formation of the Ti–C, Ti–Ti, and Ti–Al bonds.⁶² The ionic components of the Ti–C and Ti–Al bonds are due to partial charge transfer in the Ti \rightarrow C and Al \rightarrow Ti directions.

More detailed information about the nature of the interatomic structure and the chemical bonding in aluminium-containing carbides and nitrides has been provided by the results of quantum-chemical calculations.^{10, 12, 63–65}

The initial ideas about the specific features of the rearrangement of the electronic state in MC and MN ($M = \text{Ti, V, Zr, Nb}$), associated with the insertion of isolated aluminium atoms in the sublattices of these binary phases (similar systems evidently occur in the initial stage of the syntheses of aluminocarbide and aluminonitride solid solutions and compounds) have been considered,⁶³ resorting to band and cluster approaches.

The linearised muffin-tin-orbital Green's functions method (LMTO GF) has been used^{63, 65} to calculate the electronic structures of the MC:Al and MN:Al systems in which single aluminium impurities are inserted at sites within the metallic or nonmetallic sublattices of the matrix with formation of 'micro-clusters' of the type AlC_6 , AlN_6 or AlM_6 (when account is taken of the size factor, this appears most likely) in the bulk of the initial crystal.

In particular, it has been found for the TiC:Al system in the case of Al \rightarrow Ti substitution that there is now an admixture of the Al $3s$ states at the bottom of the valence band of the monocarbide. The Al $3p$ states form an intense peak near the Fermi energy (E_F) in the region of the minimum of the density of states (DOS) of titanium carbide, i.e. in this instance the impurity–crystal interaction takes place mainly with participation of the Al $3s$ –C $2p$ functions with an additional contribution by the hybrid Al $3p$ –C $2p$ orbitals.

The pattern in the distribution of the local density of states (LDOS) of the impurity inserted at a C-sublattice site, whereupon the Al $3s$ states are localised near the lower edge of the p – d band of the carbide and their overlap with the valence states of the latter is significant, becomes markedly different. In their turn, the Al $3p$ functions give rise to distinct atom-like resonances in the region of the local DOS minima of the carbide.

A similar pattern in the distribution of impurity states occurs in the TiN:Al system.⁶⁵

Thus an appreciable difference in the energy distributions of the impurity states of the aluminium and the states of the component atoms of the matrix is observed in the MC:Al and MN:Al systems, which indicates significant differences in the nature of the bonds formed by Al with the matrix component atoms and the M–C (or M–N) bonds.^{7–12} This is one of the causes of the limited solubility of aluminium in TiC and TiN (in contrast to transition metals).^{1, 60}

Evidently the presence of local impurity peaks near the edge of the TiC and TiN energy bands, reflecting the states of the aluminium atoms not participating in the formation of the Al–carbide (Al–nitride) bonds, promotes an increase in the number of direct Al–Al interactions with increase in the concentration of aluminium in the bulk of the crystals. Such interactions compete with the system of bonds in carbides and nitrides. As a result, the structural type of the initial matrix changes because of the formation of phases with an individual type of crystal structure, which has in fact been observed experimentally.⁶⁰

The partial interatomic interactions in the TiN:Al system have been analysed⁶⁶ within the framework of the nonempirical discrete variation method.^{67, 68} The parameters of the photoelectron spectrum and the populations of the interatomic bonds of the $\text{TiN}_6\text{Ti}_{12}\text{N}_8$ and $\text{AlN}_6\text{Ti}_{12}\text{N}_8$ fragments, modelling $\text{TiN}_{1.0}$ and TiN:Al respectively, have been compared. The overlap integrals (OI) of the atomic wave functions obtained for the above fragments indicate that the interatomic bonds are based on the Ti $d(e_g, t_{2g})$ –N $2p_{x,y,z}$ interactions (of the σ and π types). The introduction of aluminium atoms diminishes somewhat the maximum values of the Ti–N overlap integrals (c ranges from approximately 0.300e to 0.296e for the $\text{TiN}_6\text{Ti}_{12}\text{N}_8$ and $\text{AlN}_6\text{Ti}_{12}\text{N}_8$ groups respectively), the Al–N interaction occurring as a result of the overlap of the Al $3s, 3p$ –N $2p$ functions.

The electronic properties of a series of hypothetical ordered $\text{Ti}_x\text{Al}_{1-x}\text{N}$ ($x = 0.75, 0.50$) cubic solid solutions have been investigated by the self-consistent linearised augmented plane waves (LAPW) method.^{69, 70} The unit cell of the model structure of the $\text{Ti}_{0.75}\text{Al}_{0.25}\text{N}$ ($\text{Ti}_3\text{AlN}_3^{[4]}\text{N}^{[6]}$) phase contained a nitrogen atom ($\text{N}^{[6]}$) involved in a regular Ti_6 octahedral coordination and $\text{N}^{[4]}$ type atoms with a Ti_4Al_2 in closest proximity. The cell used for the description of the $\text{Ti}_{0.5}\text{Al}_{0.5}\text{N}$ ($\text{TiAlN}^{[2]}\text{N}^{[4]}$) composition is formed on the basis of the cubic cell by the displacement of the titanium atoms in its upper and lower planes by aluminium atoms.

The principal characteristics of the electron spectra of both phases are presented in Fig. 3 and Table 3. Comparison with the data obtained with the $\text{TiN}_{1.0}$ electron spectrum^{71–74} shows that the aluminonitride alloys on the whole retain the principal features of the spectrum characteristic of titanium mononitride: the $\text{Ti}_x\text{Al}_y\text{N}$ valence band contains an isolated low-energy band made up predominantly of the nitrogen $2s$ states (the s band) and separated by the forbidden gap (FG) from the main valence-bonding band (the p – d band). Partial Ti \rightarrow Al replacement leads to a narrowing of the s band (by 0.08 Ry for $\text{Ti}_{0.5}\text{Al}_{0.5}\text{N}$ compared with $\text{TiN}_{1.0}$) and of FG (by 0.18 Ry); on the other hand, the p – d band, partially overlapping the bands of the near-Fermi Ti d states, is broadened (as a consequence of the admixture of the aluminium s, p valence states).

Compared with $\text{TiN}_{1.0}$,^{71–74} the DOS distribution for aluminonitrides^{60, 70} does not exhibit significant differences in the region of the s and d subbands. The most notable DOS rearrangement, arising due to the appearance of new DOS peaks near the

Table 3. The results of LMPW calculations for the $\text{Ti}_{0.75}\text{Al}_{0.25}\text{N}$ and $\text{Ti}_{0.50}\text{Al}_{0.50}\text{N}$ ordered cubic phases.

Parameter	$\text{Ti}_{0.75}\text{Al}_{0.25}\text{N}$	$\text{Ti}_{0.50}\text{Al}_{0.50}\text{N}$
Lattice constant / a.u.		
a	7.9841	5.5988
c	—	7.9179
Radii of atomic spheres / a.u.		
Ti, Al	2.1206	2.1031
N	1.8714	1.8559
Band width / Ry		
s	0.224	0.265
p	0.576	0.600
d (occupied)	0.166	0.162
Width of the $s-p$ interband gap / Ry	0.282	0.279
E_F (relative to bottom of s band) / Ry	1.247	1.305
E_F (relative to muffin-tin zero) / Ry	0.841	0.871

upper and lower edges of the given subband, is observed in the region of the $p-d$ band of the nitride.

The densities of states of the $\text{N}^{[6]}$ atoms, having the Ti_6 environment, are similar to those for nitrogen in $\text{TiN}_{1.0}$ ⁷⁴ and are determined by the σ -bonds ($p-d_{z^2}$ overlap) and π -bonds (overlap of $p-d_{xz}$, d_{yz} orbitals). The $\text{N}^{[4]}$ p_z orbitals are oriented towards the aluminium atoms and form DOS peaks in the region of the localisation of the energies of the Al 3s,3p states, which indicates the occurrence of the $\text{N}^{[4]}-\text{Al}(p_z-s,p)$ interactions. The highest-energy peak of the $\text{N}^{[4]}$ p_z states is due to the partial

Table 4. The effective atomic charges (e) for $\text{TiN}_{1.0}$, $\text{Ti}_{0.75}\text{Al}_{0.25}\text{N}$, and $\text{Ti}_{0.50}\text{Al}_{0.50}\text{N}$.

Phase	Ti	$\text{N}^{[6]*}$	$\text{N}^{[4]}$	$\text{N}^{[2]}$	Al
$\text{TiN}_{1.0}$	-0.33	0.38	—	—	—
$\text{Ti}_{0.75}\text{Al}_{0.25}\text{N}$	-0.27	0.36	0.38	—	-0.43
$\text{Ti}_{0.50}\text{Al}_{0.50}\text{N}$	-0.24	—	0.39	0.41	-0.39

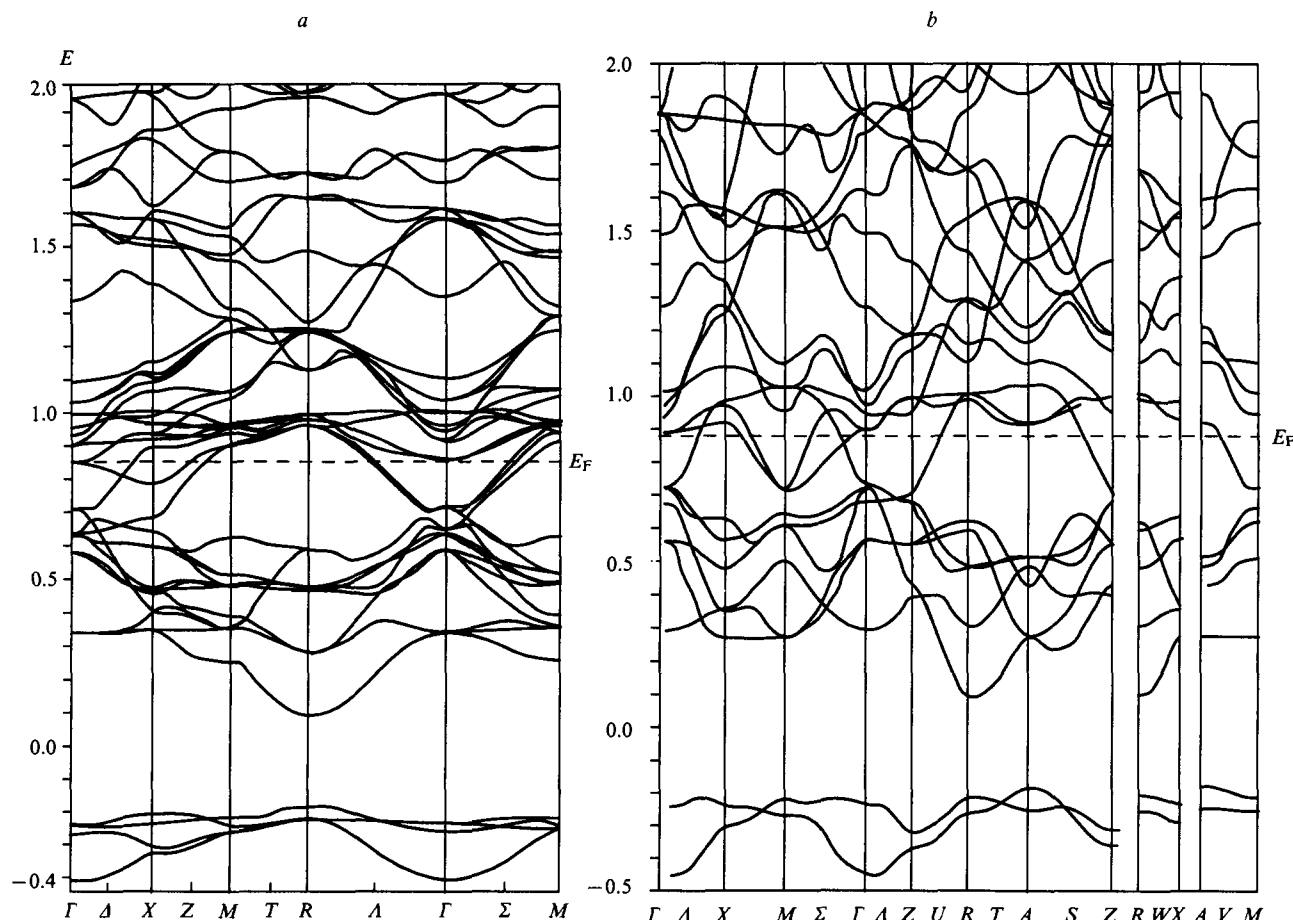
Note. The effective atomic charges were determined as the differences between the charges in the atomic spheres according to the LAPW calculations and the superposition of the charge densities of the atoms in the crystal.

transfer of electron density from the nearest surrounding nitrogen atoms to the atomic sphere of the aluminium.

The distribution of the local density of states of $\text{Ti}_{0.50}\text{Al}_{0.50}\text{N}$ repeats overall the situation examined above with the exception of certain features⁷⁰ associated with the decrease in the symmetry of the system as a consequence of the increase in the Al:Ti ratio.

Analysis of the partial charges in the atomic spheres presented in Table 4 shows that the charge polarisation in aluminonitrides leads to a partial shift of electron density (ED) in the (Ti,Al) \rightarrow N direction, which agrees with the XPES data and the results of cluster calculations by the discrete variation method.^{35, 54, 66}

The features noted above in the distribution of the charge densities and interatomic interactions are clearly illustrated by the maps of the electron density distribution (Fig. 4). Comparison of Figs 4a and 4b shows that the $\sigma(\text{Ti}-\text{N})$ -bond in the $\text{Ti}_{0.50}\text{Al}_{0.50}\text{N}$ phase is somewhat stronger than in the $\text{Ti}_{0.75}\text{Al}_{0.25}\text{N}$ phase. This is also true of the π -type Ti-Ti bonds. Furthermore, the distribution

**Figure 3.** The energy bands of the hypothetical ordered aluminonitrides $\text{Ti}_{0.75}\text{Al}_{0.25}\text{N}$ (a) and $\text{Ti}_{0.50}\text{Al}_{0.50}\text{N}$ (b); calculation by the LAPW method.

of the maxima in the contours of the $d(e_g)$ orbitals indicates the possibility of Ti–Al bond formation and the appreciable density of the lines around the atomic nuclei of aluminium indicates the presence of an ionic component of the bond.

It was noted previously that the cubic aluminonitride alloys synthesised are characterised by configurational disorder in the metallic sublattice. An attempt has been made^{69,75} to take this factor into account. The calculation was performed within the framework of the Korringa–Kohn–Rostocker coherent potential approximation (KKR CPA) method; the concept of an effective medium, simulating the average configuration of the system, has been introduced for the description of disordered systems.⁷⁶ Since the calculations^{69,75} were nonself-consistent, the potentials of the atoms of the disordered $\text{Ti}_x\text{Al}_{1-x}\text{N}$ ($x = 0.75, 0.50$) alloys were taken from calculations of regular structures by the LAPW method⁷⁰ and were averaged for atoms of one kind.

Fig. 5 presents as an example the local densities of states for aluminium in the ordered and disordered aluminonitrides. Evidently, allowance for disorder in the metallic sublattice is manifested mainly (with retention of the overall sequence in the energy distributions of the s, p, d functions of aluminium in the spectrum) by the ‘spreading’ of a series of peaks in the LDOS spectrum of the regular structure. Furthermore, the noncoincidence of the maxima of the Al 3s subband, calculated by the KKR CPA and LAPW methods, has been noted,⁷⁵ while the bottom of the band for the ordered alloy is ~ 1 eV deeper than for the disordered alloy with a statistical distribution of the Ti and Al atoms at the corresponding sublattice sites.

The specific features of the fitting of the coherent potential approximation are known⁷⁷ to preclude a detailed consideration of the mechanism of chemical bonding. The LDOS obtained were therefore used⁷⁵ for the theoretical calculation of the form of the X-ray emission, photoelectron, and Auger electron spectra. The Al $K\alpha$ emission lines plotted (within the framework of the formalism of the dipolar approximation^{77,78}) for $\text{Ti}_{0.75}\text{Al}_{0.25}\text{N}$ and

$\text{Ti}_{0.50}\text{Al}_{0.50}\text{N}$ are presented in Fig. 5. Estimates⁶⁹ of the transition matrix elements make it possible to interpret the form of the L spectrum of aluminium as a superposition of its s and d states. The L band in the aluminium spectrum (as for the wurtzite-like AlN)⁷⁹ contains three maxima, but the ratios of their intensities are markedly different, while the energy gaps between the maxima for $\text{Ti}_{0.75}\text{Al}_{0.25}\text{N}$ are greater than those for AlN by ~ 0.9 eV. Furthermore, in contrast to aluminium nitride,⁷⁹ the Al N and Al K line maxima do not have the same energies. The aluminium K bands undergo the greatest changes (with a relative stability of Al L line) associated with the variation of the Al/Ti ratio.

The photoelectron spectra of $\text{Ti}_x\text{Al}_y\text{N}$ have been calculated^{77,80,81} by a standard method for the photon energies $E = 1487$ and 150 eV. The theoretical integral Auger spectra were also plotted (Fig. 5) as convolutions of the corresponding partial states of the aluminonitrides.^{82,83} In particular, it was noted that the form of the Ti $L_2M_{23}V$ line is determined by the distribution of the p and d states of titanium.

Comparative analysis of the stability of the cubic titanium aluminocarbides and aluminonitrides as a function of the site of substitution (Al \rightarrow Ti or Al \rightarrow C, N) and also of the aluminium content in the initial TiC and TiN has been carried out^{84–86} within the framework of the LMTO method in terms of the atomic sphere approximation (ASA).⁸⁷

Using the Ti_4X_4 ($X = \text{C}, \text{N}$) supercell, the Ti–Al–N and Ti–Al–C solid solutions having the following compositions have been modelled with the aid of the successive substitution of titanium or nonmetal atoms by aluminium atoms: TiN, $\text{Ti}_{0.75}\text{Al}_{0.25}\text{N}$, $\text{Ti}_{0.50}\text{Al}_{0.50}\text{N}$, $\text{TiAl}_{0.25}\text{N}_{0.75}$; TiC, $\text{Ti}_{0.75}\text{Al}_{0.25}\text{C}$, $\text{Ti}_{0.50}\text{Al}_{0.50}\text{C}$, $\text{TiAl}_{0.25}\text{C}_{0.75}$.

The results of the calculations of the electronic structure of $\text{Ti}_x\text{Al}_{1-x}\text{N}$ by the LMTO^{84–86} and LAPW⁷⁰ methods agree satisfactorily. A significantly different type of DOS and LDOS has been obtained^{84,86} for the $\text{TiAl}_{0.25}\text{N}_{0.75}$ solid solution, where

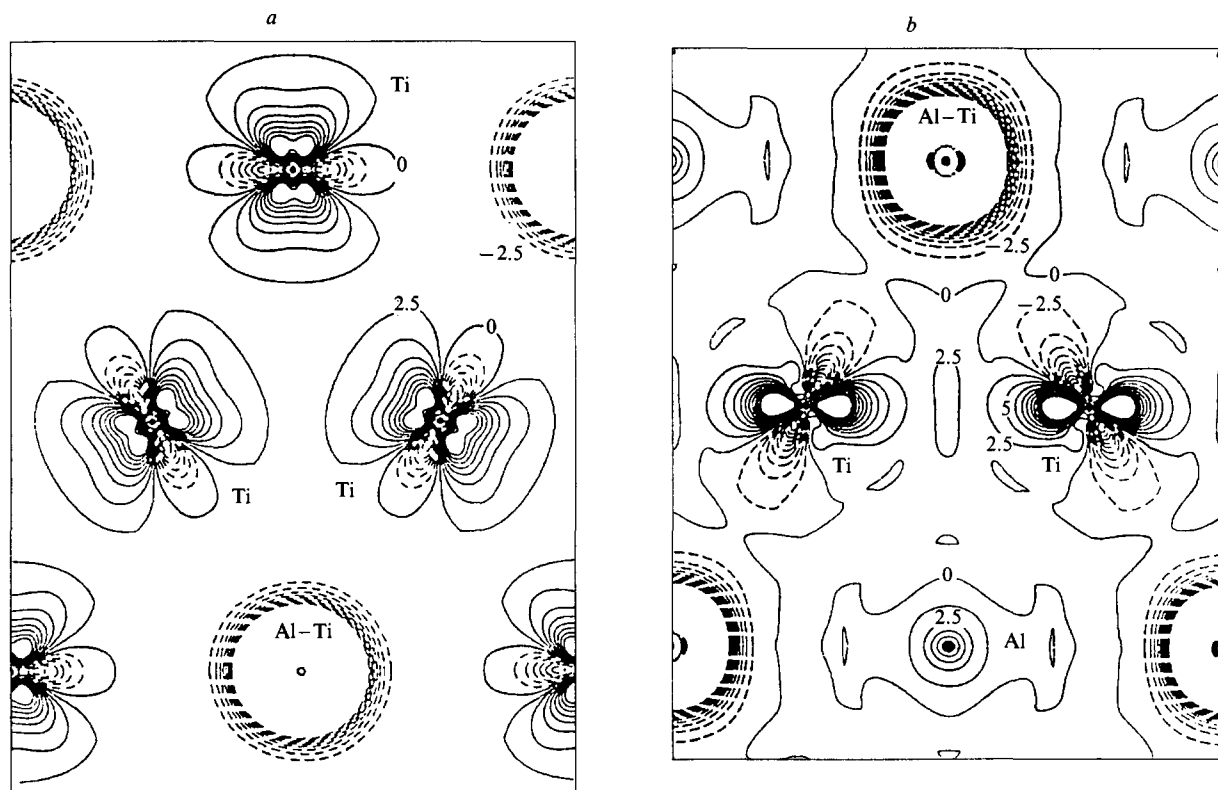


Figure 4. Maps of the differential electron density in the (111) plane of the $\text{Ti}_{0.75}\text{Al}_{0.25}\text{N}$ and $\text{TiN}_{1.0}$ phases (a) and of the $\text{Ti}_{0.50}\text{Al}_{0.50}\text{N}$ and $\text{Ti}_{0.75}\text{Al}_{0.25}\text{N}$ phases (b). The numerals on the curves denote the electron densities; the electron density between the contours is $0.01 \text{ e } \text{\AA}^{-3}$; calculation by the LAPW method.

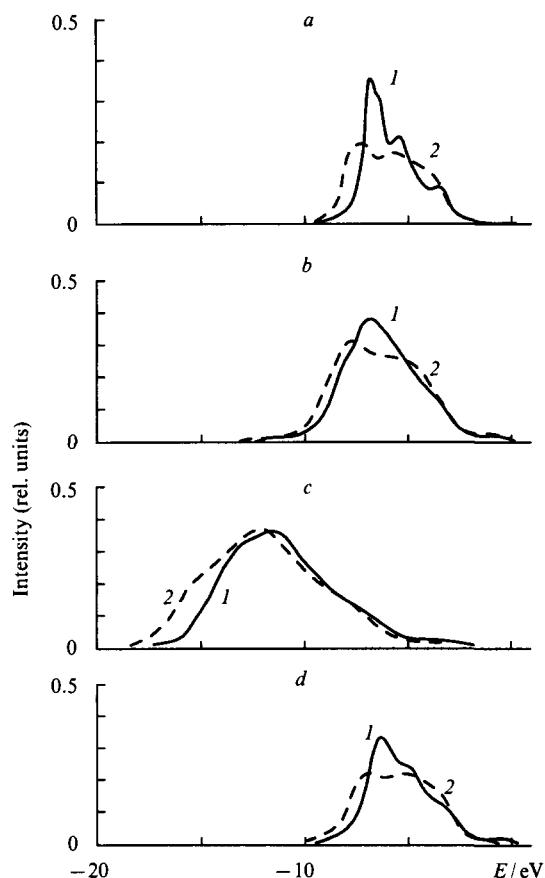


Figure 5. The distribution of the Al 3p states (a), the theoretical forms of the Al $KL_{2,3}V$ (b) and Al KVV (c) Auger electron spectra, and the form of the Al $K\alpha$ line (d) in the X-ray emission spectra for the $Ti_{0.75}Al_{0.25}N$ (1) and $Ti_{0.50}Al_{0.50}N$ (2) phases. Calculation by the KKR CPA method.

the insertion of the aluminium atoms at the N-sublattice sites was postulated (Fig. 6).

The most characteristic difference between the $TiAl_{0.25}N_{0.75}$ and $Ti_xAl_{1-x}N$ spectra is the sharp increase in the energies of the Al 3s and Al 3p states: the energies of the Al 3s state range from -0.55 to -0.52 Ry (peak A in Fig. 6; the lower edge of the $p-d$ band), giving rise to an intense atom-like resonance, while the energies of the Al 3p states (peak B in Fig. 6) correspond to the region of the DOS minimum for the nitride between the $p-d$ and d bands. The forms of the N 2s and N 2p local densities of states remain similar to those in the nitride under these conditions (the immediate environment of aluminium in the given solid solution is $AlTi_6$), which may be attributed to the local character of the interatomic interactions occurring in the solid solutions under discussion.

The dissociation of some of the Ti–N bonds in $TiAl_{0.25}N_{0.75}$ (on replacement of N atoms by Al) results in the transition of a series of titanium states to a higher-energy region [between the $p-d$ and d bands, the LDOS peak of titanium (Fig. 6) has the same energy as peak B of the density of states of $TiAl_{0.25}N_{0.75}$] where the Al 3p,3d states are also located. As a result, in contrast to the solid solutions $Ti_xAl_{1-x}N$, in which the bonding of the aluminium atoms is achieved via the Al 3s,3p–N 2p hybridisation, in the hypothetical solid solution $TiAl_yN_{1-y}$ the bonding of aluminium takes place primarily as a result of the mixing of the Al 3p,3d–Ti 3d,4s functions.

The LMTO calculations^{84,86} for the electronic states of the cubic (B1) solid solutions $Ti_xAl_{1-x}C$ and $TiAl_xC_{1-x}$ show that, as for the aluminonitride alloys, the LDOS distributions for the component atoms in these solutions differ markedly depending on the sites occupied by the aluminium atoms. Thus, for the

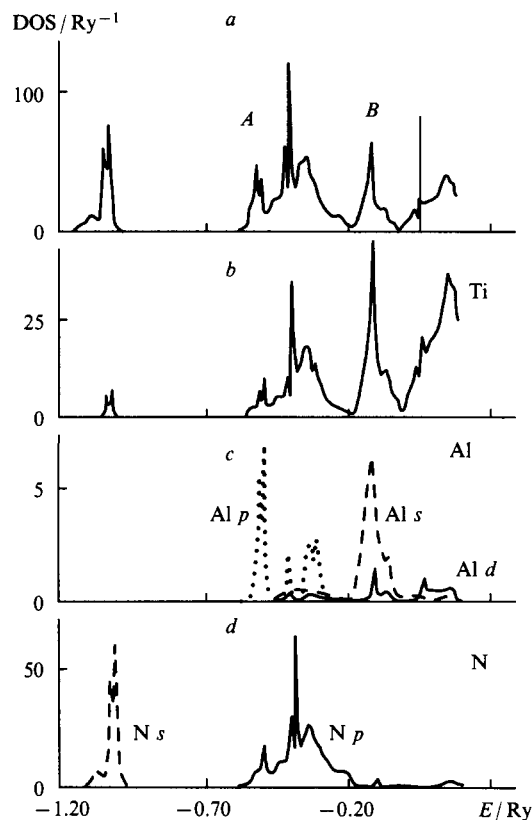


Figure 6. The total (a) and partial (b–d) DOS for the cubic $TiAl_{0.25}N_{0.75}$. Calculation by the LMTO method.

substitution of the Ti → Al type, the impurity states are located in the region of the C 2s and $p-d$ bands of the carbide; the occurrence of impurity resonances in the region of the local minima in the density of states in the $p-d$ band of $TiC_{1.0}$ and between the $p-d$ and d bands is characteristic of the $AlTi_6$ coordination.

Furthermore, with increase in the aluminium content (with decrease in the concentration of the valence electrons), E_F for $Ti_xAl_{1-x}C$ shifts, as for $Ti_xAl_{1-x}N$, to the region of low energies. However, the nature of the change in the filling of the valence band for these two groups of solid solutions is fundamentally different: in the case of $Ti_xAl_{1-x}N$ the band of the antibonding delocalised Ti d,s,p states is 'emptied', whereas in the case of $Ti_xAl_{1-x}C$ the filling of the band of the bonding $p-d$ states diminishes.

The above effect as well as the energy required to 'dissociate' the Ti–(N,C) bonds (for the Ti → Al substitution mechanism) can be attributed⁶⁵ to the relative stability of the cubic titanium aluminonitrides and aluminocarbides. Numerous calculations have shown^{8–11} that the Ti–C bond energy is much higher than the Ti–N bond energy. Taking into account the nature of the variation of the filling of bands of different nature noted above for the carbide and nitride phases and also the smaller energy expenditure required for the dissociation of the Ti–N bonds, it was concluded qualitatively^{64,65} that the probability of the formation of single-phase cubic alloys is higher in the Ti–Al–N system than in the Ti–Al–C system.

In order to confirm this hypothesis, calculations of the cohesion energy (E_{coh}) (i.e. the atomisation energy), of the energy of the substitution (E_{sub}) of titanium (or C, N) by aluminium, and the partial pressures of the electronic-nuclear system of the crystals (p_i) were carried out by the LMTO method.^{64,66} The energies E_{coh} and E_{sub} are presented in Table 5. Evidently the absolute value of the cohesion energy for the $Ti_xAl_{1-x}N$ solid solutions diminishes with increasing aluminium content; in the presence of identical aluminium concentrations, $|E_{coh}|$ for

$\text{Ti}_{0.75}\text{Al}_{0.25}\text{N}$ is greater than that for $\text{TiAl}_{0.25}\text{N}_{0.75}$. Similar relations have been obtained also for substitution energies. From the foregoing, one may conclude that, firstly, the synthesis of homogeneous cubic aluminium-containing solid solutions under equilibrium conditions is difficult (the solutions have been obtained mainly in a metastable state — in the form of films^{35–48}); secondly, the probability of the formation of solid solutions diminishes with increasing aluminium content; thirdly, for equal concentrations of aluminium, the substitution by the latter of Ti sublattice sites is energetically more favourable.

Table 5. The cohesion and substitution energies for the aluminium-containing solid solutions based on TiC and TiN.

Compound	$-E_{\text{coh}}/\text{Ry}$	E_{sub}/Ry
TiC	1.588	—
$\text{Ti}_{0.75}\text{Al}_{0.25}\text{C}$	1.452	0.136
$\text{Ti}_{0.50}\text{Al}_{0.50}\text{C}$	1.316	0.272
$\text{TiAl}_{0.25}\text{C}_{0.75}$	1.379	0.209
TiN	1.327	—
$\text{Ti}_{0.75}\text{Al}_{0.25}\text{N}$	1.224	0.103
$\text{Ti}_{0.50}\text{Al}_{0.50}\text{N}$	1.062	0.265
$\text{TiAl}_{0.25}\text{N}_{0.75}$	1.185	0.142

Similar conclusions^{65,66} follow also from the analysis of the energies E_{coh} and E_{sub} for the Ti–Al–C system (Table 5). By comparing the above quantities for the aluminocarbides and aluminonitrides having the same compositions and structures, one may claim that, since $|E_{\text{coh}}|$ for Ti–Al–C is greater than that for Ti–Al–N whereas E_{sub} for Ti–Al–N is greater than that for Ti–Al–C, the formation of stable cubic titanium aluminonitrides is more probable.

These conclusions have been confirmed⁶⁴ also by the comparison of the pressures p_1 . The highest values of $|p_1|$ for TiC and TiN correspond to the (C,N) 2*p* and Ti 3*d* states, the hybridisation of which determines the nature of the chemical bonding in the binary phases.^{8–11} When aluminium atoms are inserted at the Ti sites the Ti–(C,N) bonds are somewhat weakened [the quantities $|p_1(\text{Ti})|$ diminish], but some new bonds of the type (N,C)–Al arise as a result of the interaction of the (C,N) 2*p*–Al *s,p,d* states. Such bonds proved to be much stronger than the Ti–Al bonds formed when aluminium is inserted at nonmetallic sublattice sites. Finally the bonding (negative) pressure of the aluminium states is higher for the nitride alloys than for the carbide-based solid solutions, which again indicates a greater stability of the cubic aluminonitride solid solutions.

The synthesis of aluminium-containing solid solutions involving IVA–VIA subgroup *d* metals, for example, $(\text{TiAlZr})\text{N}_x$, $(\text{ZrAl})\text{N}_x$, and $(\text{TiAlV})\text{N}_x$, has been reported.^{23,36,37} However, there is at present no information about their electronic-energy spectra.

In conclusion of this section, we shall mention again those studies^{64,65} in which the cluster semiempirical LCAO method was used to analyse the energies of the molecular orbitals (MO) of the clusters, simulating the nonstoichiometric (with respect to the nonmetallic sublattice) *H*- and perovskite-like titanium aluminocarbides and aluminonitrides. In conformity with the available X-ray emission data (see above), it has been established, in particular, that, in the overall system of the Ti_2AlC_x molecular orbitals, it is possible to distinguish four groups, consisting predominantly of the contributions of the C 2*s*, Al 3*s*, C 2*p*–Ti 3*d*–Al 1*s,p*, and Al *s,p*–Ti 3*d* states. The differences between the formula compositions and the crystal structures of the aluminocarbide phases determine the relative change in the line widths and energies of the individual subbands of the Ti_3AlC and Ti_2AlC valence spectra.

The formation of carbon vacancies leads⁶⁵ to the progressive filling of the delocalised near-Fermi Ti 3*d* and Al 1*s,p* states and

also to some decrease in the contribution of the C 2*p* orbitals to the hybrid band of the Ti 3*d*–C 2*p*–Al 3*s,3p* type and to a narrowing of the quasi-core C 2*s* band. Similar relations are observed also in the transition $\text{Ti}_2\text{AlN} \rightarrow \text{Ti}_2\text{AlN}_x$ ($x < 1$).

Narrowing and low-energy shifts of the metalloid *s,p* sub-bands are characteristic of aluminonitrides (compared with aluminocarbides). The energy separation of the Ti *d*–N *p* states leads to the virtually complete absence of contributions by the latter to the subband of the Ti–Al states, the population of which increases (as a consequence of the increase in the electron concentration per unit cell of the compound).

The overlap populations (OP) of the atomic orbitals and the bond indices [bond populations (BP)] in the case of the fragments for which calculations have been made indicate that the chemical bonding in the *H*-phases is based on Ti–(C,N), Ti–Al, Ti–Ti-type interactions, comparable in terms of BP, and on the interactions of nontransition metals with one another, whereas the bonds between the atoms of nontransition metals and metalloids are virtually absent (Table 6). The Ti–C and Ti–N bond populations in Ti_2AlC and Ti_2AlN are much smaller than in titanium carbides and nitrides, which is evidently the main reason for the reduced hardness and thermal stability of the aluminocarbides compared with titanium carbides.^{1,61,62}

The relative bond populations depend on the number of vacancies: when nonmetal defects are introduced, the interlayer interactions are weakened and the bonds in the aluminium layer are strengthened. Individual Ti–(C,N) bonds are weakened (in contrast to the bonds in the cubic TiC_x and TiN_x ,^{9,10} where the formation of vacancies strengthens some of the remaining metal–nonmetal bonds). An appreciable anisotropy of the individual interactions in the layers near the defect arises; the occurrence of a weak direct Ti–Ti interaction through the carbon or nitrogen layer is observed.

Table 6. Results of calculations by the LCAO MO method of the overlap populations of the valence atomic orbitals (e) for the clusters in the structures of titanium aluminocarbides and aluminonitrides.

Orbital	Al <i>s</i>	Al <i>p</i>	(C, N) <i>s</i>	(C, N) <i>p</i>
Compound Ti_2AlC , cluster $\text{TiAl}_3\text{C}_6\text{Ti}_9$				
Ti <i>s</i>	0.06	0	0.11	0.03
Ti <i>p</i>	0.08	0.02	0.06	0.02
Ti <i>d</i>	0.06	0.02	0.04	0.34
Compound Ti_2AlC_x , cluster $\text{TiAl}_3\text{C}_4\Box_2\text{Ti}_9^a$				
Ti <i>s</i>	0.05	0.02	0.11	0.05
Ti <i>p</i>	0.06	0.01	0.05	0.05
Ti <i>d</i>	0.07	0.03	0.04	0.22
Compound $\text{Ti}_2\text{Al}_2\text{N}$, cluster $\text{TiAl}_3\text{N}_6\text{Ti}_9$				
Ti <i>s</i>	0.08	0	0.09	0.03
Ti <i>p</i>	0.14	0.01	0.05	0.04
Ti <i>d</i>	0.09	0	0.03	0.23
Compound Ti_2AlN_x , cluster $\text{TiAl}_3\text{N}_4\Box_2\text{Ti}_9^a$				
Ti <i>s</i>	0.11	0	0.09	0.04
Ti <i>p</i>	0.05	0.04	0.03	0.05
Ti <i>d</i>	0.11	0.02	0.03	0.20
Compound Ti_3AlC , cluster $\text{TiAl}_4\text{C}_2\text{Ti}_8$				
Ti <i>s</i>	0.03	0.02	0.05	0.06
Ti <i>p</i>	0	0	0	0
Ti <i>d</i>	0.05	0.03	0.03	0.11
Compound Ti_3AlC_x , cluster $\text{TiAl}_4\text{C}\Box\text{Ti}_8^a$				
Ti <i>s</i>	0.02	0.06	0.04	0.06
Ti <i>p</i>	0	0	0	0
Ti <i>d</i>	0.02	0.06	0.03	0.10

^a The symbol \Box denotes vacancies in the C or N sublattices.

On passing from the carbon-containing to the nitrogen-containing phases, the Ti–nontransition metal bonds and the bonds in the aluminium layers are strengthened, primarily as a result of the weakening of the Ti–nonmetal bonds.

It follows from the data^{64,65} that the transition metal atoms have an effective positive charge in all the phases considered, which increases on passing from the carbide to the nitride phases. Finally analysis of the overlap integrals between the atomic orbitals shows⁶⁵ that the Ti–(C,N) interaction in the *H*-phases takes place, as in the binary carbides and nitrides mainly as a result of the hybridisation of the Ti *3d*–(C,N) *p* states. The Ti–Al bonds are of a mixed character, involving predominantly the Al *s, p* states hybridised with all the valence orbitals of titanium.

III. Electronic properties of transition metal siliconitrides and silicocarbides

Yet another class of objects, for which quantum-chemical studies of the electronic-energy spectra and of the nature of the chemical bonds have been initiated and are developing vigorously, comprises transition metal siliconitrides and silicocarbides. Together with aluminium-containing compounds, these substances are of great interest for the manufacture of new ceramic materials, including constructional ceramics. Preliminary investigations^{88–94} of ceramics based on transition metal and silicon carbides and nitrides have demonstrated particularly their potential suitability in manufacturing technology at high temperatures.

The first information about the electronic states of the atomic components in phases based on the M–Si–C systems was obtained⁹⁵ by the LMTO GF method. This method has been used to calculate the LDOS for isolated atoms of aluminium and

the entire series of *3d* metals which are incorporated at the Si sublattice sites of cubic silicon carbide. These objects were regarded as models and the process involving the incorporation of the atoms M was considered to be a stage leading to the formation of hypothetical solid solutions in the M–Si–C systems, which retain the initial sphalerite-like structure of silicon carbides. In addition, they can simulate one of the probable mechanisms of the formation of intermediate layers in complex silicon-containing ceramics at the contact boundary between a solid grain (SiC) and the elements of the plasticiser, which consist as a rule of *d, p* metals or their alloys.

The results obtained are presented in Fig. 7. Taking into account the data obtained by band calculations for the ideal 3C–SiC carbide,^{96–101} it was found that the form of the LDOS for the transition metals at the beginning of the *3d* series is determined by the nature of the overlap of their outer states with the valence band of the matrix. As the orbital energies of the impurity decrease (Sc → Cu), the filled part of the LDOS undergoes a low-energy shift. For M = Mn, the impurity states are concentrated in the region of the local minimum in the density of states in the *pp* band of SiC, whereas for M = Fe, Co or Ni atom-like (nonbonding) LDOS resonances arise in the forbidden gap between the *ss* and *pp* bands of silicon carbide.

The distributions of the lowest free states of the doping *d* atoms are also found to be significantly different. Their concentration near the upper boundary of the forbidden gap of the carbide increases sharply with increase in the atomic number of the impurity. The nickel impurity exerts the most 'dramatic' effect on the conducting properties of SiC, its presence being responsible for the appearance of resonance peaks in the forbidden gap of silicon carbide.⁹⁵

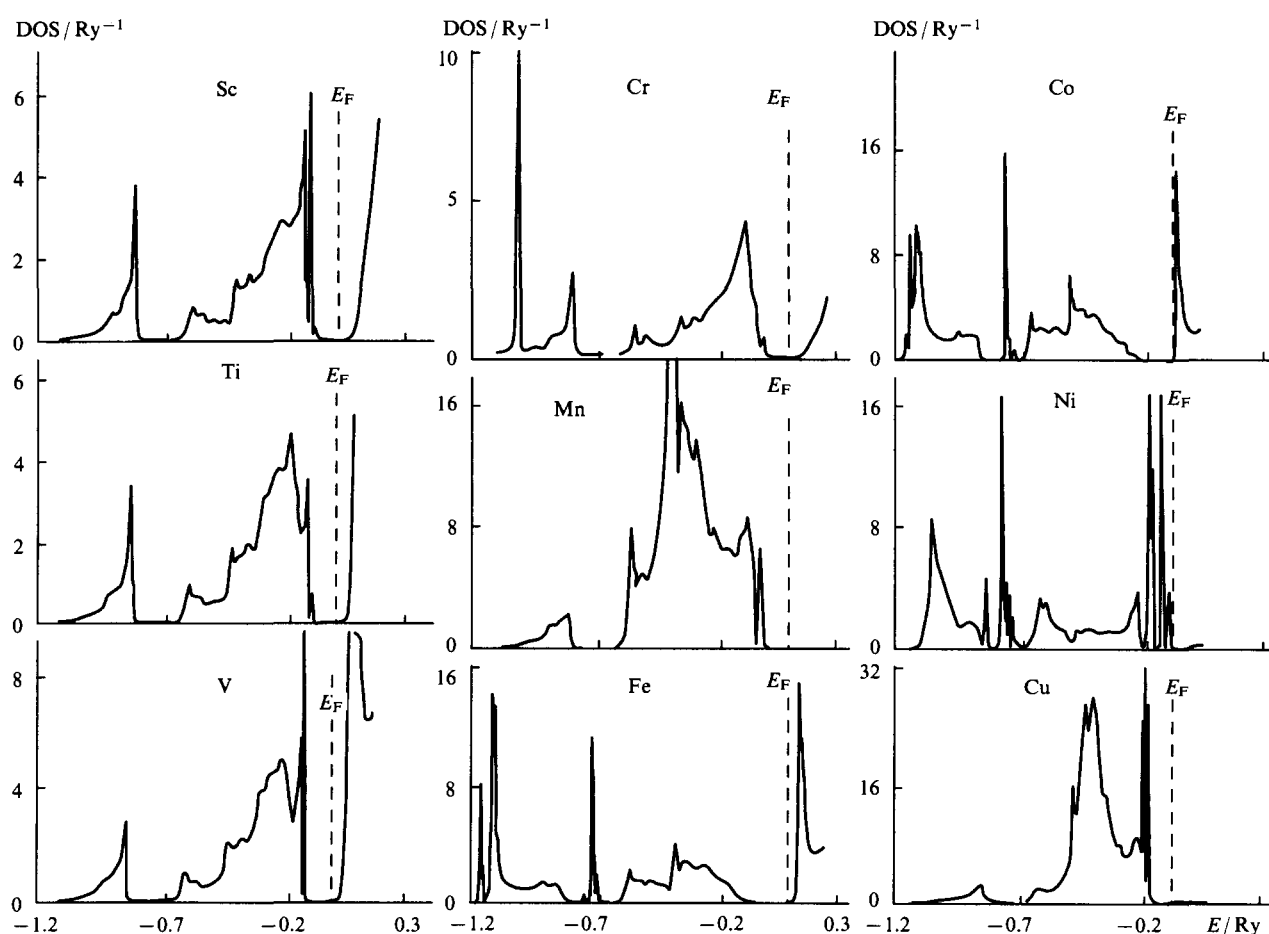


Figure 7. Local DOS of the *3d* metal impurities in cubic 3C–SiC. Calculation by the LMTO GF method.

Estimation of the energy characteristics of the rearrangement of the interatomic interactions under the influence of the impurity (by the method proposed in the study of Anisimov et al.¹⁰²) indicates that in all cases the change in the total energy of the initial crystal is positive ($\Delta E > 0$), i.e. the 'rupture' of the stronger Si–C bonds is not compensated by the newly formed M–C bonds and in this respect the systems under consideration proved to be unstable. Minimal destabilisation occurs when the atoms of aluminium and of the 3d metals at the beginning and end of the series are introduced into the bulk of silicon carbide. It follows from the foregoing that the formation of the modelled homogeneous solid solutions, retaining the SiC structure, is more difficult⁹⁵ than, for example, the formation of reciprocal solid solutions of transition metal carbides and nitrides.^{1–7}

The study of M → Si substitution for a 25% concentration of titanium and vanadium impurities in 3C-SiC, which exert the least destabilising effect on the energetics of the system under consideration, has been continued^{103,104} by the LMTO method. The initial carbide was described using the Si₄C₄ supercell in which the silicon atoms were replaced by titanium or vanadium atoms. This made it possible to calculate the electronic properties of the Si_{0.75}Ti_{0.25}C and Si_{0.75}V_{0.25}C ternary systems. It has been noted that the titanium and vanadium impurities lead to the appearance of sharp DOS peaks in the region of the top of the valence band and alter significantly the form of the DOS of the conductivity band of silicon carbide. These changes are caused by the 3d orbitals of the metal, to which corresponds a large negative pressure of the electronic-nuclear system (p_1), i.e. they are bonding in character. For Si_{0.75}Ti_{0.25}C, the energy of the substitution of 25% of the silicon atoms by titanium (E_{sub}) is negative, which indicates the possibility of the formation of a stable structure in the Si–Ti–C system, where the titanium atoms occupy silicon sites.

For Si_{0.75}V_{0.25}C, the substitution energy is positive. This may be associated both with the differences in the energetics of the formation of bonds by vanadium and titanium with the environment [$|p_1|(\text{Ti}) > |p_1|(\text{V})$] and with the overall decrease in the cohesion energy of the carbide crystal with the vanadium impurity as a result of the increase in the overall electron concentration.

The possibility of the partial substitution by titanium atoms of the silicon carbide C-sublattice sites has been considered.¹⁰⁴ It was established that the doping of the nonstoichiometric (with respect to carbon) SiC_x with titanium has a negative effect on the overall stability of the system.

The nitrogen impurity has a significantly different effect in this respect. LMTO calculations for the silicon carbonitride SiC_{0.75}N_{0.25} have shown¹⁰⁴ that, on partial C → N substitution, the substitution energy is 0.09 Ry, whereas after application of corrections for dissociation (0.10 Ry) the substitution energy becomes negative.^{105,106} Consequently such substitution may be energetically favourable. We may note that a similar small deviation from the linear variation of E_{sub} has been found also for titanium carbonitride.¹⁰⁶

The results obtained in the syntheses and in the study of the electronic states of yet another group of silicon-containing solid solutions with a different (cubic, of the NaCl type) structure of titanium siliconitrides and silicocarbides have been published in a series of communications.^{85,107–109} Films of Ti_xSi_yN_z solid solutions were deposited on a molybdenum foil substrate and on the (100) surface of a NaCl crystal.¹⁰⁹ The composition of the solid solution and the structure and chemical state of the component atoms were investigated as a function of the pressure of the working gas (N₂), temperature, and the potential of the substrate and the cathodic current. With increase in p_{N_2} the nitrogen content in the film increases up to saturation, while the oxygen concentration actually diminishes. The observed type of variation of the N:Ti and O:Ti ratios with nitrogen pressure (Fig. 8) is typical for MN films (M is a transition d metal). At lower nitrogen pressures, the variation of the Si:Ti ratio is

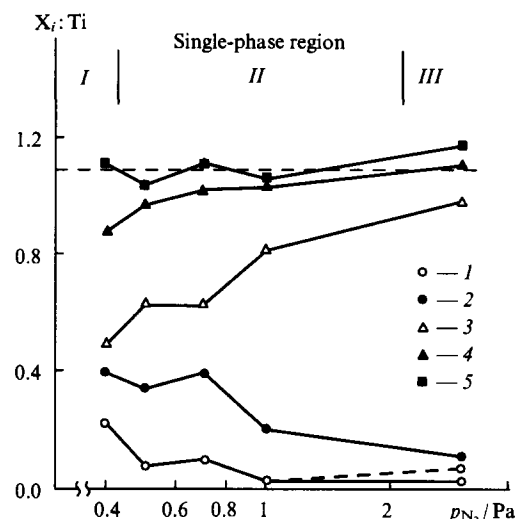


Figure 8. Dependence of the composition of the Ti_xSi_yN_z(O) films on the nitrogen pressure. X: (1) Si; (2) O; (3) N; (4) O + N; (5) O + N + Si.

unexpected — it increases in parallel with increase in the oxygen content up to 0.3, which is much greater than the Si:Ti ratio in the target employed (~0.1).

It was established that, within the narrow range of nitrogen pressures $p_{\text{N}_2} = 6 \times 10^{-2} - 1 \times 10^{-1}$ Pa (region II in Fig. 8), the Ti_xSi_yN_zO₂ films have a single-phase cubic structure. X-Ray photoelectron spectra indicate¹¹⁰ identical energetics of the core states (Ti 2p, N 1s, O 1s) of these films and cubic titanium nitride and oxide nitride films.^{53,54} The Si 2p silicon line is recorded distinctly in the region of the 99.1 eV binding energy. An estimate of the Si:Ti ratio based on XPES yielded ~0.04–0.12 depending on the film deposition conditions.^{109,110} X-Ray probe microanalysis confirmed the presence of silicon and its uniform distribution in the cubic phase.

An increase in the lattice parameter of the siliconitride (from 4.16 to 4.28 Å) with increase in the silicon content was observed, which has been attributed to the differences between the atomic radii of silicon and nitrogen (1.71 and 0.71 Å respectively).¹⁰⁹

The question of the sites occupied by the silicon atoms in the single-phase (of the NaCl type) Ti_xSi_yN_z solid solutions, which was investigated by XPES, is of independent interest.¹¹⁰ The binding energies of the Si 2p, Ti 2p_{3/2} N 1s, and O 1s core levels for a TiSi_{0.1}N_{0.9}(O) film with a cubic structure and certain chemical compounds containing silicon and titanium are presented in Table 7. Evidently, in the specimens where silicon is the electron donor, oxygen or nitrogen atoms are disposed in its immediate environment and the maximum of the Si 2p level is displaced towards higher binding energies relative to the 'pure' silicon. On the other hand, if the first coordination sphere of silicon contains titanium atoms, the Si 2p line shifts towards lower binding energies.

Table 7. The binding energies (eV) for certain core levels in Ti_xSi_yN_z(O) cubic (B1) films and certain titanium- and silicon-containing compounds according to X-ray photoelectron spectroscopy studies.

Compound	Ti 2p _{3/2}	Si 2p	N 1s	O 1s
Ti ₅ Si ₃ (O)	454.1	98.8	—	530.9
Ti _{0.7} Si _{0.25} O _{0.02} (target)	454.1	99.0	—	531.6
Ti _x Si _y N _z (O)	455.0	99.1	397.3	531.4
TiN(O)	455.1	—	397.3	531.5
Si	—	99.5	—	—
Si ₃ N ₄ (O)	—	101.7	397.5	531.3
SiO ₂	—	103.1	—	532.4

The energy of the Si 2*p* level in the Ti–Si–N(O) film (99.1 eV) indicates the existence of a negative charge on the silicon atom and hence the disposition of these atoms in the nonmetallic sublattice of titanium oxynitrides.

A correlation between the content of silicon, nitrogen, and oxygen atoms and the degree of defectiveness has been observed^{109, 110} for all the Ti_xSi_yN_z films investigated: in the region of the existence of the single-phase structure, the silicon content in the films increases simultaneously with increase in the oxygen concentration with retention of a virtually constant overall concentration of oxygen and nitrogen [(N + O)/Ti ≈ 1.0]. The decrease in the quantity (N + O)/Ti leads to an increase in the silicon concentration in the cubic B1 phase and one can therefore postulate that, as the degree of defectiveness of the nonmetallic sublattice and its oxygen content increase, the incorporation of silicon atoms into the TiN(TiN_xO_y) structure becomes more favourable.

A synthesis of metastable cubic single-phase SS (as a coating) of the composition Ti_{0.5}Si_{0.5}C by the magnetron sputtering method using a hot-pressed two-phase TiC/SiC target has been reported.⁹⁴ The preparation of single-phase SS based on TiC and including silicon was noted to be substantially more energy consuming (ion bombardment, heating of the substrate) than the preparation of aluminium-containing alloys like Ti_{0.5}Al_{0.5}N. This was attributed⁹⁴ to the lower mobility of atoms in the near-surface layer of TiC/SiC, which is due to the presence of strong covalent bonds. The localisation of the silicon atoms in the cubic structure of the Ti_xSi_yC_z films has not been specially studied (it has been assumed implicitly that the silicon atoms substitute the metal atoms in TiC by analogy with the Al→Ti substitution). In our opinion, this problem needs to be further considered.

Simultaneously with the synthesis and the study of the structure and properties of films of the cubic TiSi_xN_y phase, the computer simulation of the electronic characteristics of a series of cubic (of the NaCl type) alloys with a variable content of component atoms in the unit cell of the crystals was undertaken.^{107, 108} The relative stabilities of the hypothetical cubic solid solutions were investigated as a function of their composition and the possible mechanism of the substitution by silicon of different kinds of sites in the initial TiC and TiN matrices.

The following series of solid solutions were examined:

I. TiC–TiSi_{0.25}C_{0.75}–TiSi_{0.50}C_{0.50}; TiN–TiSi_{0.25}N_{0.75}–TiSi_{0.50}N_{0.50}–TiSi_{0.75}N_{0.25}.

II. TiC–Ti_{0.75}Si_{0.25}C–Ti_{0.50}Si_{0.50}C; TiN–Ti_{0.75}Si_{0.25}N–Ti_{0.50}Si_{0.50}N.

The process involving the formation of a solid solution on Si→(C,N) substitution was simulated for the series I solid solutions (by the LMTO method adopting TiC and TiN as the bases), whereas the substitution of silicon atoms by titanium atoms was simulated for the series II solutions.

Certain results of such simulation^{107, 108} are presented in Table 8 and in Fig. 9. Evidently, when silicon atoms are introduced into the bulk of the initial TiN, its spectrum is significantly transformed. On Si→N substitution, two intense DOS peaks arise near the upper and lower edges of the *p*–*d* band and broaden markedly with increase in the silicon concentration, which diminishes the forbidden gap between the *s* and *p*–*d* bands of TiN. A decrease in the intensity of the peak of the density of the N 2*s* states, as well as the partial emptying (as a consequence of the decrease in the concentration of valence electrons) of the antibonding (relative to the *p*–*d* band) subband of the delocalised metallic states, a decrease in the density of states at the Fermi level *N*(*E*_F), are observed at the same time.

On the other hand, on Ti→Si substitution the concentration of valence electrons in the cell does not change (9 e) and the Fermi energy does not actually shift; however, the perturbation of the TiN spectrum as a result of the introduction of the impurity is accompanied by an appreciable increase in *N*(*E*_F).

A series of significant differences in the distribution of the LDOS of the elements comprising the solid solution have also

Table 8. The cohesion and substitution energies for solid solutions in the Ti–Si–C–N–O system.

Compound	– <i>E</i> _{coh} / Ry	<i>E</i> _{sub} / Ry
TiN	1.32	–
Ti _{0.75} Si _{0.25} N	1.03	0.23
Ti _{0.50} Si _{0.50} N	0.72	0.53
TiSi _{0.25} N _{0.75}	1.13	0.18
TiSi _{0.50} N _{0.50}	1.05	0.21
TiSi _{0.75} N _{0.25}	1.01	0.25
TiSi _{0.25} N _{0.50}	0.92	0.37
TiSi _{0.25} N _{0.50} O _{0.25}	1.05	0.24
TiSi _{0.25} N _{0.50} C _{0.25}	1.21	0.08
TiC	1.59	–
Ti _{0.75} Si _{0.25} C	1.31	0.28
Ti _{0.50} Si _{0.50} C	1.05	1.54
TiSi _{0.25} C _{0.75}	1.42	0.17
TiSi _{0.50} C _{0.50}	1.28	0.31

been noted as a function of the type of sites occupied by silicon. These are caused primarily by the fundamentally different nature of the hybridisation of the valence states of silicon and the atoms coordinating it (SiN₆ or SiTi₆).¹⁰⁷ One may assume that fairly simple X-ray emission experiments (for example the study of the nitrogen and silicon *K* lines and the titanium *L*_α lines) may provide unambiguous evidence in support of one of the possible mechanisms of the incorporation of silicon in the crystal.

The incorporation of silicon in TiC exerts an even greater influence on the electronic structure of the matrix (Fig. 9). In the completed state, the carbide may be classified as a semimetal.^{1–4} Thus, whereas on substitution of silicon by carbon the Si 3*p* states are concentrated in the region of the *p*–*d* subband and peak *A* corresponds to the atom-like nonbonding Si 3*s* resonance in the region of the forbidden gap between the C 2*s* and *p* subbands of the carbide (i.e. the bonding in TiSi_xC_{1–x} is of the Ti 3*d*–Si 3*p* hybrid type), in the Ti_{1–x}Si_xC spectrum one can trace distinctly, apart from the additional Si 3*s*-like maximum (in the vicinity of the lower edge of the C 2*s*-type band) and the DOS peak (in the region of the forbidden gap of TiC of the mixed Si 3*s*, 3*p* type), a progressive increase in the Si 3*s*, 3*p* and C 2*p* local density of states (giving rise to the *p*–*p* bonding) in the near-Fermi region of the crystal characterised by a deep DOS maximum for the ideal TiC_{1.0}.

The introduction of silicon at both N and Ti sites of the TiN lattice reduces appreciably the cohesion energy of the crystal, while the substitution energy is positive (Table 8). This should hinder the synthesis of homogeneous silicon-containing cubic solid solutions under equilibrium conditions, i.e. these solutions may be obtained predominantly in a metastable state.

On Si→N substitution (for solid solutions with identical silicon concentrations) |*E*_{coh}| is greater and *E*_{sub} is smaller than the corresponding values calculated for the alloys where silicon is inserted at Ti sublattice sites (solid solutions containing identical silicon concentrations are compared), which indicates unambiguously that the substitution of nitrogen by silicon is preferable. With increase in the silicon concentration, |*E*_{coh}| diminishes and there is a corresponding sharp increase in the positive *E*_{sub}, which indicates that the preparation of cubic solid solutions with a high silicon content becomes more difficult.

Comparison of the energy parameters of the silicon-containing nitride and carbide alloys shows^{107, 108} that the trends in the variation of *E*_{coh} and *E*_{sub} for the Ti_xSi_yC_z solid solutions are the same as for titanium siliconitrides.

(1) The insertion of silicon at both Ti and C sites is an energetically unfavourable process, the Si→C substitution occurring more readily than Si→Ti.

(2) With increase in the silicon concentration, there is an appreciable decrease in |*E*_{coh}| and an increase in *E*_{sub}, which is the

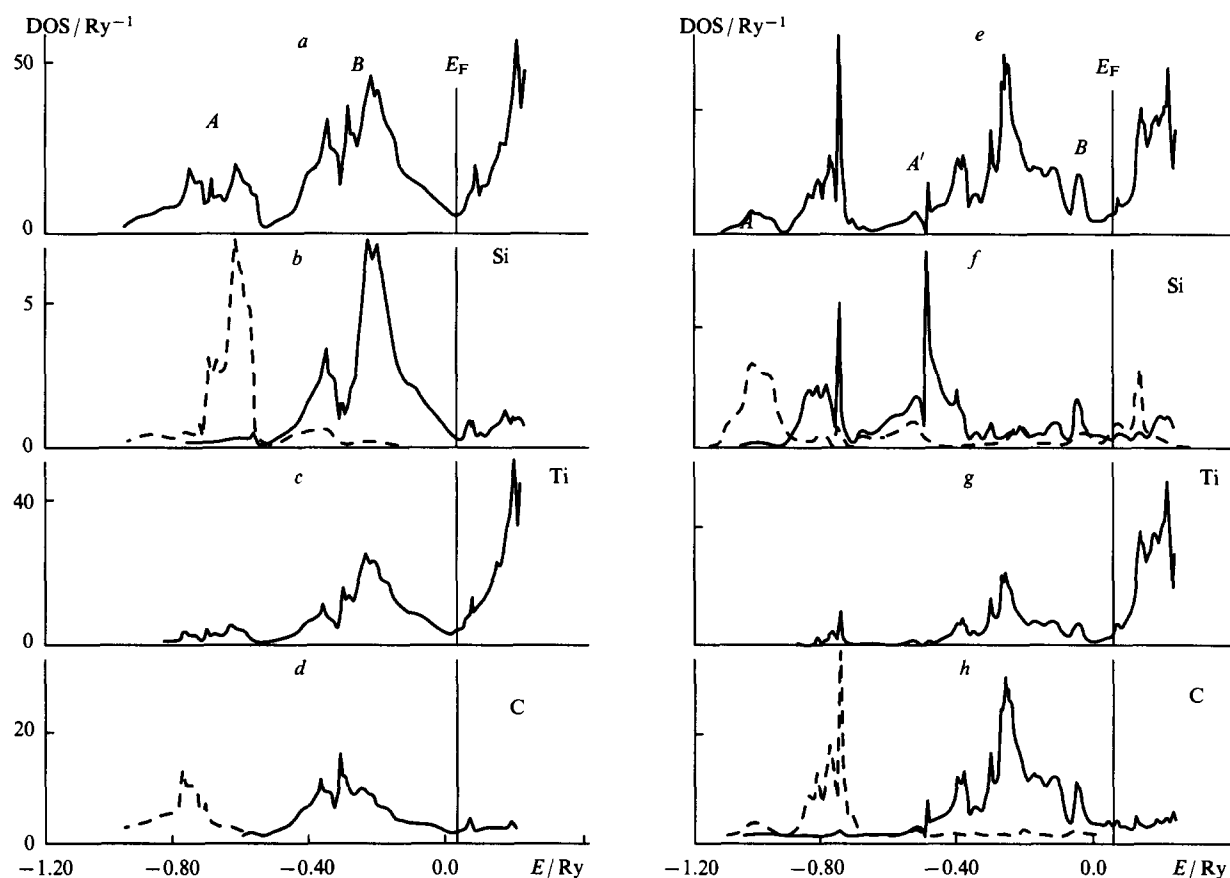


Figure 9. The total (a, e) and partial (b–d, f–h) DOS for the $\text{TiSi}_{0.25}\text{C}_{0.75}$ (a–d) and $\text{Ti}_{0.75}\text{Si}_{0.25}\text{C}$ (e–h) solid solutions.

reason for the instability of the silicon-enriched cubic solid solutions.

(3) In the $\text{Si} \rightarrow \text{C}$ substitution, silicon becomes involved in a p – d hybrid bond with the metal, whereas in the $\text{Si} \rightarrow \text{Ti}$ substitution the type of bond is determined by the mixing of the p – p functions.

The influence of impurities and N vacancies on the electron spectra and the stability of the cubic TiSi_xN_y solid solution have been investigated within the framework of the LMTO method. The following compositions were examined:¹⁰⁸ $\text{TiN}_{1.0}$, $\text{TiSi}_{0.25}\text{N}_{0.75}$, $\text{TiSi}_{0.25}\text{N}_{0.50}$, and $\text{TiSi}_{0.25}\text{N}_{0.50}\text{O}_{0.25}$. In addition, the dependence of the equilibrium lattice parameter R of the TiSi_xN_y alloys on the composition of the metalloid sublattice was determined.¹⁰⁸ Fig. 10 presents the dependence of the total energy of the alloys E_{tot} on R . Evidently, for the completed nitride $\text{TiN}_{1.0}$, the calculated parameter $R = 4.22 \text{ \AA}$ agrees with the experimental value.^{4,5} The incorporation of silicon atoms in the N sublattice leads to an appreciable increase in R (from 4.22 \AA in $\text{TiN}_{1.0}$ to 4.32 \AA in $\text{TiSi}_{0.25}\text{N}_{0.75}$). The presence of oxygen impurities or vacancies promotes a further increase in R ($\sim 4.34 \text{ \AA}$ for $\text{TiSi}_{0.25}\text{N}_{0.50}$ and $\text{TiSi}_{0.25}\text{N}_{0.50}\text{O}_{0.25}$), which agrees with experiment.^{109, 110}

Comparison of the DOS and LDOS distributions for the $\text{TiN}_{1.0}$, $\text{TiSi}_{0.25}\text{N}_{0.75}$, $\text{TiSi}_{0.25}\text{N}_{0.50}$, and $\text{TiSi}_{0.25}\text{N}_{0.50}\text{O}_{0.25}$ phases, obtained for equilibrium values of R , shows that the introduction of N defects is accompanied by a steady decrease in the contributions of the N $2s, 2p$ states to the region of the occupied states of the spectrum and also by a significant redistribution of the valence states of titanium with the appearance of distinct d resonances, one of which is in the immediate vicinity and the other has the same energy as E_F (Fig. 11). The distribution of the ‘vacancy’ states is similar. The above features are due to the reorganisation of the states of the metallic centres coordinating the vacancy and reflect the partial ‘elimination’ of the splitting of the Ti states into bonding and antibonding. (This occurs for the completed TiX_6

immediate environment.) The Ti states pass to the region of nonbonding states (in the vicinity of E_F), giving rise to the ‘vacancy’ peaks in the DOS for titanium noted above. Some of the latter are ‘trapped’ by the sphere of the defect, giving rise to DOS vacancies.^{9, 10, 102, 108, 111–114}

A different type of DOS distribution is observed for the $\text{TiSi}_{0.25}\text{N}_{0.50}\text{O}_{0.25}$ alloy (Fig. 11). The most notable changes in the electronic structures of the solid solutions, associated with the incorporation of oxygen atoms in their sublattices, consist^{86, 108} in the appearance of additional ‘impurity’ subbands of the O $2s$ and O $2p$ types, the former being of the quasi-core type and being located in the energy gap below the bottom of the valence band of

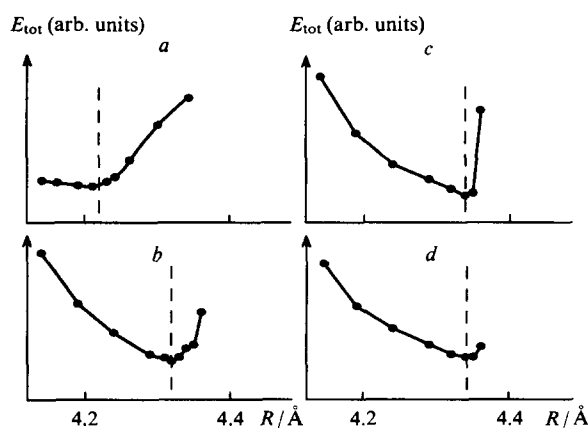


Figure 10. Dependence of the total energy of the crystal (E_{tot}) on the lattice constant for the $\text{TiN}_{1.0}$ (a), $\text{TiSi}_{0.25}\text{N}_{0.75}$ (b), $\text{TiSi}_{0.25}\text{N}_{0.50}$ (c), and $\text{TiSi}_{0.25}\text{N}_{0.50}\text{O}_{0.25}$ (d) cubic phases. Calculations by the LMTO method.

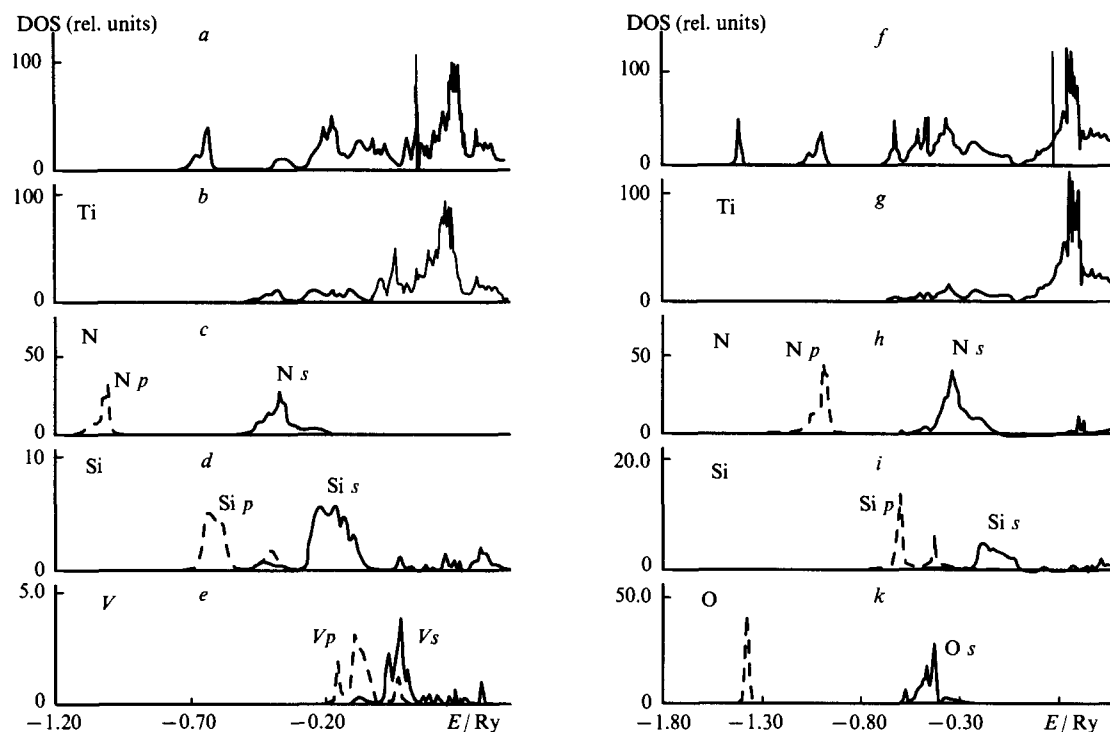


Figure 11. The energy distributions of the total (*a, f*) and partial (*b–d, g–k*) DOS for the nonstoichiometric (with respect to the N sublattice) $\text{TiSi}_{0.25}\text{N}_{0.50}$ (*a–c*) and $\text{TiSi}_{0.25}\text{N}_{0.50}\text{O}_{0.25}$ (*f–k*) cubic solid solutions. Calculation by the LMTO method. (*e*) Resolution of the 'vacancy' states into states with the V_s and V_p symmetries.

the siliconitride. The latter subband (of the O 2*p* type) is localised near the DOS minimum between Si 3*s* band and the hybrid *p–d* band of the matrix.

The influence of the defects considered on the energy state of the Ti–Si–N system has been discussed^{86, 108} using the cohesion energies of the crystals and the substitution energies. It was established that the presence of the oxygen impurity or of lattice vacancies in the structure of the TiSi_xN_y phase leads to a decrease in $|E_{\text{coh}}|$ and an increase in $|E_{\text{sub}}|$, indicating a progressive destabilisation of the system in the series $\text{TiSi}_{0.25}\text{N}_{0.75} \rightarrow \text{TiSi}_{0.25}\text{N}_{0.50}\text{O}_{0.25} \rightarrow \text{TiSi}_{0.25}\text{N}_{0.50}$. These data indicate a greater energy stability of the siliconitride with an oxygen impurity compared with the solid solution containing N vacancies.^{109, 110}

The results of studies on the electronic properties of silicon-containing solid solutions retaining the basic structure of the initial binary phases — sphalerite (SiC) or rock salt (TiC, TiN) — have been considered hitherto.

The study of the phase equilibria in the Ti–Si–C system made it possible to establish the existence of at least two ordered silicocarbide phases — $\text{Ti}_5\text{Si}_3\text{C}_x$ and Ti_3SiC_2 .^{1–3, 88, 92, 115–117} Among these phases, the Ti_3SiC_2 phase with a hexagonal structure (P6₃/mmc space group, unit cell parameters $a = 3.066 \text{ \AA}$, and $c = 17.646 \text{ \AA}$), in which the metal atoms occupy two structurally nonequivalent sites with and without silicon atoms in their immediate environment (Fig. 12), has attracted the greatest attention recently.^{93, 94, 116, 117} It plays a significant role in the formation of the microstructure of the contact band of ceramics of the type TiC/SiC and Ti/SiC.^{92–94} The development of ceramic polycrystalline materials based on titanium silicocarbide has been reported.^{88–93}

The band structure of Ti_3SiC_2 has been calculated by the full-potential self-consistent LMTO method.¹¹⁸

In contrast to the electron structure of the binary titanium carbide,^{7–10} E_F for the electronic structure of the silicocarbide coincides with the peak of the density of the *d* states of titanium (Fig. 13), which should give rise to the metal-like properties of this phase. The contributions to $N(E_F)$ by the states of the structurally

nonequivalent titanium atoms are significantly different, the Ti(1) states playing a decisive role [$N(E_F)_{\text{Ti}(1)} : N(E_F)_{\text{Ti}(2)} \approx 3.76$].

The form and energy distribution of the DOS for the Ti(1) and Ti(2) atoms are also different (Fig. 13). Thus, whereas the DOS for the Ti(1) atoms, having both Si and C centres in its environment, contains two maxima with energies identical with those of the DOS peaks for carbon and silicon, the valence states of the Ti(2) atoms, containing only carbon atoms in the first coordination sphere, are displaced downwards on the energy scale [relative to the density of states of the Ti(1) type], whereas the form of the density of states for the Ti(2) centres repeats in many respects the form of the C 2*p* states.

An estimate of the effective charges on the atoms [$+0.614 e$ for Ti(1); $+0.641 e$ for Ti(2); $-0.304 e$ for Si; $-0.384 e$ for C] indicates partial charge transfers in the Ti(1,2) → Si direction, which ensures the existence of an ionic component in the overall chemical bonding system in Ti_3SiC_2 . Consequently a combined ionic-covalent-metallic type of chemical bonding arises in Ti_3SiC_2 . It is determined by the charge polarisation between the

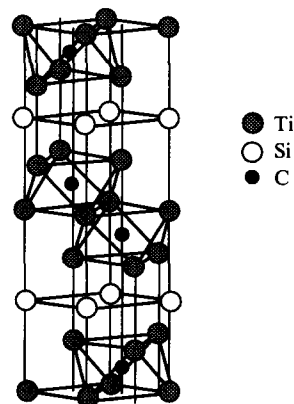


Figure 12. A fragment of the Ti_3SiC_2 crystal structure.

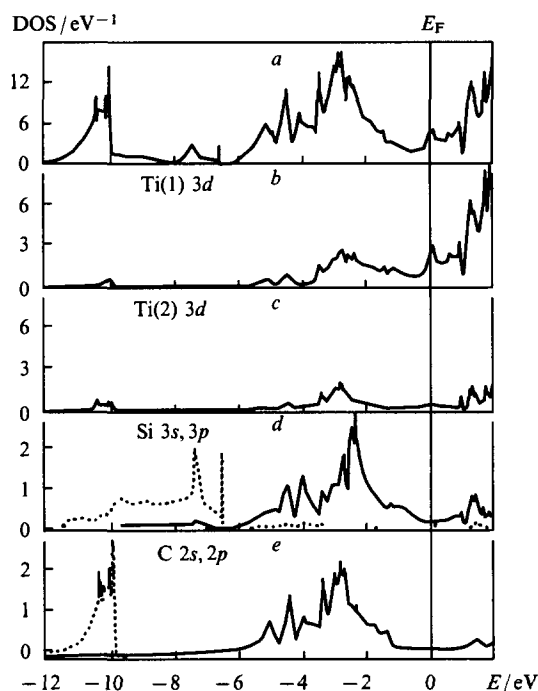


Figure 13. The total (a) and partial (b–e) DOS for Ti_3SiC_2 . For the significance of Ti(1) and Ti(2), see text.

atoms of the metal and the metalloids, the hybridisation of the valence states [of the Ti(1) $3d$ –Si $3p$, Ti(1) $3d$ –C $2p$, Ti(2) $3d$ –C $2p$, and Si $3p$ –Si $3p$ types], and the delocalisation of the near-Fermi d states of titanium [mainly of the Ti(1) atoms].¹¹⁸

The next stage in the study of the electronic properties of titanium silicocarbides (as well as the silicocarbides of other transition metals) should include a more detailed description of the chemical bonding, its anisotropy, and its influence on the properties of the silicon-containing phases.

IV. Chemical bonding in ternary carbides and nitrides based on subgroup VIIA and VIIIA transition metals

The compounds based on subgroup VIIA and VIIIA transition metals constitute a representative class of ternary carbides and nitrides.^{1–3, 29–32} The carbides $\text{M}_3\text{M}'\text{C}$ (M is a transition metal and M' are subgroup IIIB and IVB nontransition elements) have been most thoroughly investigated. The magnetic characteristics of these compounds as well as the magnetic and structural phase transitions, observed in the temperature range 200–500 K, have attracted the greatest attention of investigators.^{29–32} In the high-temperature region, these compounds have a cubic structure of the antiperovskite type^{1–3, 119–128} and are paramagnetic materials of the Pauli type; at lower temperatures, tetragonal lattice distortions as well as second-order magnetic phase transitions with formation of several possible types of ordered magnetic structures have been discovered for the series of carbides.^{29–32, 129–142}

The first model of the interatomic interactions and the electronic states in the $\text{M}_3\text{M}'\text{C}$ phases was proposed by Jardin and Labbe.^{143–145} According to this model, the carbides have an extended conductivity band, which overlaps with a narrow band of hybrid states made up of contributions by the M d and C $2p$ orbitals. The distribution of the DOS for this band has been estimated with the aid of the approximate tight-binding scheme.¹⁴⁵ A logarithmic singularity has been observed in the DDS near its energy centre. Postulating that the Fermi level E_F is located near the peak of the antibonding p – d subband, Jardin and

Labbe^{143–145} explained the instability of the crystal and magnetic structures of $\text{M}_3\text{M}'\text{C}$ on the basis of the characteristics of the electronic structure which they postulated.

We may note that this model was not confirmed in subsequent numerical calculations for the series of perovskite-like carbides.

The first self-consistent LAPW calculations for $\text{Mn}_3\text{M}'\text{C}$ ($\text{M}' = \text{Zn, Ga, In, Sn}$) in a nonmagnetic high-temperature state (cubic structure) established^{146, 147} that the near-Fermi region of the carbide is made up mainly of the d states of the transition metal, whereas the valence bonding (antibonding) subbands for the other component atoms are located somewhat below (above) the Fermi level. Estimates of the local magnetic moments (LMM), carried out with the aid of spin-polarised calculations for the ferromagnetic states of Mn_3GaC , showed¹⁴⁶ that the Mn $3d$ states undergo the maximum spin splitting; the LMM on the atoms are $1.35 \mu_B$ (Mn), $-0.12 \mu_B$ (C), and $-0.008 \mu_B$ (Ga), the estimates being quite reasonably correlated with experiment (the LMM on Mn is $1.3 \pm 0.1 \mu_B$ at 193 K).³²

Systematic LMTO calculations for the cubic carbides $\text{M}_3\text{M}'\text{C}$ ($\text{M} = \text{Mn, Fe}$; $\text{M}' = \text{Zn, Al, Sn, Ga}$) made it possible to discover^{148, 149} the rules governing the variation of the electronic structures of the compounds as a function of the composition of the M and M' lattices. Fig. 14 presents as an example the electronic states of Mn_3ZnC . Evidently the valence band contains four distinct subbands. The lower subband is of the quasi-core type and is made up mainly of the contributions of the C $2s$ states with slight additional contributions of the Zn $3d$, Mn $3d$, and Zn $4s$ states. The next bonding band includes the hybrid C $2p$ –Mn $3d$ functions as well as the pseudoatomic resonances of the Zn $3d$ and Zn $4s$ states. The nonbonding, partly filled near-Fermi subband is determined by the dispersion of the Mn $3d$

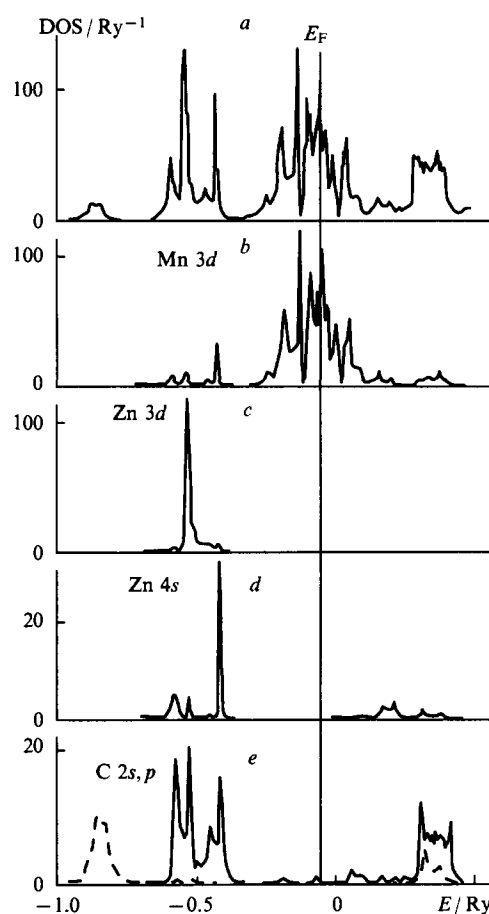


Figure 14. The total (a) and partial (b–e) DOS for the nonmagnetic Mn_3ZnC . Calculations by the LMTO method.

Table 9. The partial charges in the atomic spheres (q/e) and the differences between the charges in the atomic spheres in the crystal and in the free state ($\Delta q/e$) in manganese and iron carbides.

Charge	Mn ₃ ZnC	Mn ₃ AlC	Mn ₃ SnC	Mn ₃ GaC	Charge	Fe ₃ ZnC	Fe ₃ AlC	Fe ₃ SnC
$q(\text{Mn}, s)$	1.616	1.670	1.645	1.598	$q(\text{Fe}, s)$	1.682	1.704	1.698
$q(\text{Mn}, p)$	1.844	1.974	2.065	1.916	$q(\text{Fe}, p)$	1.856	1.964	2.058
$q(\text{Mn}, d)$	3.207	3.153	3.175	3.218	$q(\text{Fe}, d)$	4.207	4.158	4.178
$\Delta q(\text{Mn})$	+0.333	+0.221	+0.115	+0.268	$\Delta q(\text{Fe})$	+0.255	+0.174	+0.066
$q(\text{M}', s)^a$	1.122	1.238	1.480	1.472	$q(\text{M}', s)$	1.060	1.242	1.500
$q(\text{M}', p)$	0.650	1.392	1.973	1.521	$q(\text{M}', p)$	0.928	1.280	1.848
$q(\text{M}', d)$	10.030	0.226	0.	0.	$q(\text{M}', d)$	9.886	0.226	0.0
$\Delta q(\text{M}')$	+0.198	+0.144	+0.547	+0.007	$\Delta q(\text{M}')$	+0.126	+0.252	+0.652
$q(\text{C}, s)$	1.426	1.420	1.396	1.428	$q(\text{C}, s)$	1.430	1.424	1.382
$q(\text{C}, p)$	3.374	3.388	3.494	3.384	$q(\text{C}, p)$	3.458	3.348	3.466
$\Delta q(\text{C})$	-0.800	-0.808	-0.890	-0.812	$\Delta q(\text{C})$	-0.888	-0.772	-0.848

^a $\text{M}' = \text{Zn, Al, Sn, or Ga}$.

states, with a lower vacant antibonding band including the C 2*p* and Mn 3*d* states. The above four-band structure is characteristic of all the carbides examined^{146–149} and the changes in the composition of the M' sublattice influence only the energetics of the 'centre of gravity' of the M' subband and the degree of their splitting (into bonding and antibonding components). Furthermore, the change in the concentration of valence electrons on replacement of the nontransition metal by elements of a different kind determines the position of E_F relative to the near-Fermi resonance of the M 3*d* type. Thus the Fermi level for Mn₃SnC coincides with the DOS peak, as a result of which $N(E_F)$ is a maximum in the above series of compounds. This can be treated as the factor responsible for the minimal stability of the cubic structure of the given carbide, which undergoes lattice distortions or variations in composition.^{1, 2, 119–122}

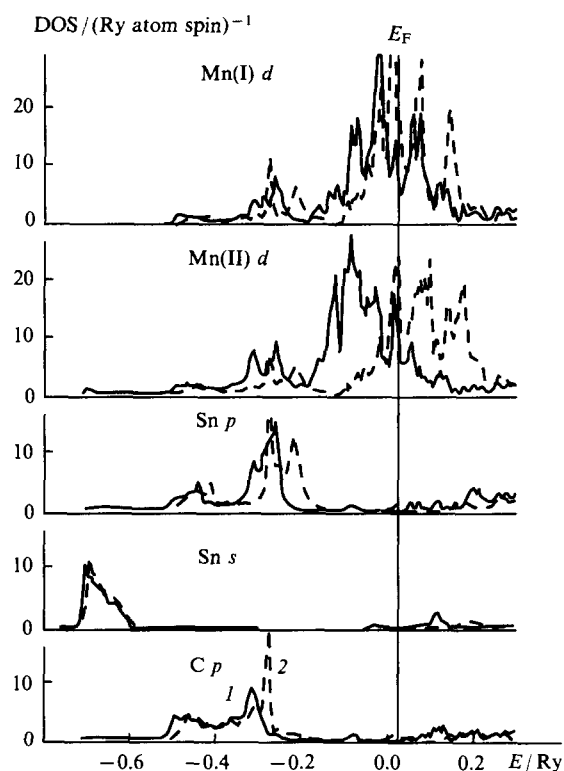
The Mn → Fe replacement in the above phase leads (as a consequence of the decrease in the lattice parameter) to a somewhat greater splitting of the bonding and antibonding sub-bands^{148, 149} and also to the filling of the nonbonding states, whereupon $N(E_F)$ reaches a maximum value for Fe₃AlC.

As regards the nature of the interatomic interactions, analysis shows^{148, 149} that, apart from the direct bonds linking transition and nontransition metals to one another and covalent M–C interactions of the *p*–*d* type, the chemical bonding system in crystals is supplemented by interactions of the *s*–*s*, *s*–*p*, and *p*–*p* types between nontransition metals and carbon. In addition, it follows from Table 9 that partial transfer of charge density from metals (transition and nontransition) to the sphere of the carbon atom is observed, but in the case of compounds with the same M' sublattice [for example, Mn₃M'C and Fe₃M'C (Table 9)] the effective positive charges are found to be higher for manganese than for iron. We may note that in this respect the situation repeats the familiar tendency in binary carbides, where the ionic component of the bond diminishes with increase in the atomic number of the carbide-forming metal.^{7–12}

The band structures and magnetic properties of individual representatives of the carbides $\text{M}_3\text{M}'\text{C}$, in the first place the relative stabilities of the possible types of ordering of the spin subsystem, have been investigated.^{150–153}

The total energy has been estimated by the LAPW method for the nonmagnetic, ferromagnetic, and antiferromagnetic states of Mn₃GaC as a function of the volume of the unit cell.¹⁵⁰ It was established that the ferromagnetic spin ordering is energetically most preferred for the equilibrium volume, since with increase in the lattice constant a transition from the ferromagnetic to the antiferromagnetic state (FM → AFM) should be observed. This finding conflicts with experiments^{153, 154} according to which the AFM state is established at $T < 165$ K. The authors¹⁵⁰ attribute this discrepancy to the use of the spherically-symmetrical approximation to the potential.

An attempt to take into account the influence of the tetragonal lattice distortion on the photoelectron spectra of the Mn₃M'C ($\text{M}' = \text{In, Sn}$) has been undertaken¹⁵¹ within the framework of the LMTO ASA method wherein the manganese atoms are at two structurally nonequivalent sites [Mn(I) and Mn(II)], which is significantly reflected both in the distribution of their DOS (Fig. 15) and in the local magnetic moments localised on the given atoms, the difference between which amounts to $\sim 1.59 \mu_B$ for Mn₃SnC (in the ferromagnetic state) and to $\sim 1.17 \mu_B$ for Mn₃InC. Together with the ferromagnetic spin ordering, ferromagnetic spin ordering as well as the possibility of their coexistence were investigated. An estimate of the total energy for the above cases made it possible to claim¹⁵¹ that a 'mixed' state of the spin subsystem is most probable.

**Figure 15.** The partial DOS for the Mn₃SnC ferromagnetic phase with a tetragonal structure. The DOS for the structurally nonequivalent manganese atoms [Mn(I) and Mn(II)] with 'upward' (1) and 'downward' (2) spin directions. Calculation by the LMTO method.

The type of transition (FM \rightleftharpoons AFM) has been determined¹⁵¹ in relation to Mn_3GaX ($X = \text{C}, \text{N}$) as a function of the composition of the metalloid sublattice and the lattice constant (the LMTO ASA method). In contrast to the preceding data,¹⁵¹ it was established that, for the equilibrium value of the lattice constant, the AFM state is the most stable for Mn_3GaC , the maximum local magnetic moment corresponding to it (the local magnetic moment on the manganese atom is $1.63 \mu_B$ for AFM and $1.39 \mu_B$ for FM); the local magnetic moment increases with increase in the lattice constant. The local magnetic moment on the manganese atom in Mn_3GaN is $1.52 \mu_B$,¹⁵² which exceeds somewhat the experimental value of $1.17 \mu_B$.³²

In contrast to carbides, the available information about the electronic properties of the ternary nitrides belonging to the class under discussion is extremely limited. With the exception of the study already mentioned,¹⁵² we are aware only of calculations for the nitride Fe_3SnN ¹⁵⁵ and also for Fe_3MnN and Fe_3PdN ,¹⁵⁶ carried out by the LMTO method. The main task of the above investigations^{155, 156} was to determine the influence of partial substitution of the iron atoms in the face-centred cubic crystal structure of $\gamma\text{-Fe}_4\text{N}$ by elements of a different kind on the parameters of the band structure and on the stability and magnetic properties of the latter.

The magnetic characteristics of the cubic Fe_4N have now been investigated in fair detail both experimentally^{157–159} and theoretically (by the quantum-chemical computational method).^{160–162}

In the series of ternary nitrides listed above, the electronic structure of the Fe_3SnN alloy is of greatest interest in the context of this review.¹⁵⁵ According to Mössbauer spectroscopic data,^{158, 163} the tin atoms are inserted predominantly at the sites occupied by the Fe(1) atoms located at the vertices of the $\gamma\text{-Fe}_4\text{N}$ unit cell [in contrast to the Fe(2) atoms, which are at the centres of its lateral faces].

In order to take into account the influence of the size factor [in the $\text{Sn} \rightarrow \text{Fe}(1)$ substitution], calculations were made of the DOS with the lattice constant varied in the range $\sim 7.17\text{--}7.46$ a.u. It was established¹⁵⁵ that the energy bands close to E_F are made up mainly of the Fe d states, which make the maximum contribution to $N(E_F)$, with only slight additional contributions by the Sn d and N p states. The introduction of the tin impurity into the perovskite-like $\gamma\text{-Fe}_4\text{N}$ diminishes appreciably the overall magnetisation of the system from 9.40 to $6.00 \mu_B$ (per formula unit) respectively. The contributions of iron to $N(E_F)$ and the local magnetic moments on the given centres in Fe_3SnN exceed in their turn the corresponding values for Fe(2) in $\gamma\text{-Fe}_4\text{N}$.

The dependence of the local magnetic moments on the Fe(1) and Fe(2) atoms in $\gamma\text{-Fe}_4\text{N}$ and on the iron atoms in Fe_3SnN on the lattice parameter is extremely interesting (Fig. 16). It shows that the 'contraction' of the crystals (by 10% of the volume) has the most 'dramatic' effect on the local magnetic moments on the Fe(2) and Fe centres: as a result of the contraction, they diminish sharply up to the disappearance of the local magnetism on the Fe(2) atoms of the γ -nitride. A similar phenomenon had been observed earlier for iron^{164–167} in a series of Fe–Pd and Fe–Ni invar alloys with a face-centred cubic structure.¹⁶⁸ The above 'magnetic collapse' effect on decrease in volume can be accounted for by the appearance of several magnetic phases. The wide scale employment of this model for the interpretation of the nature of the variation of the local magnetic moments on the Fe centres of the nitrides requires correct calculations of the total energies of these objects for different types of spin ordering.

Finally, the results of Kuhn and dos Santos¹⁵⁵ make it possible to describe the charge transport and the nature of the interatomic bonds in Fe_3SnN . The effective atomic charges [$-1.415 e$ (Sn), $+0.658 e$ (Fe), and $-0.560 e$ (N)] indicate the transfer of charge density into the sphere of the iron atoms. As regards the nature of the chemical bonding, analysis of the form of the LDOS for the component atoms permits the conclusion that the nitrogen atoms are mainly involved in covalent $p\text{--}d$ bonds with the iron atoms to which they are coordinated, the outer states

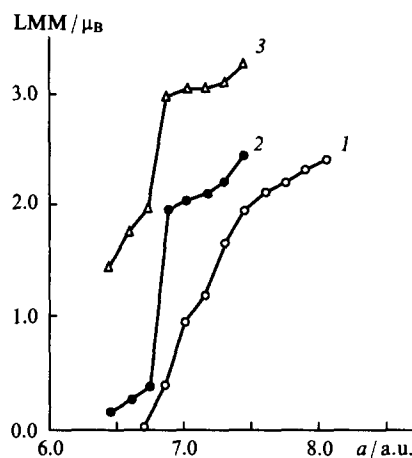


Figure 16. Dependence of the local magnetic moments of iron [Fe(1) and Fe(2), see text] for $\gamma\text{-Fe}_4\text{N}$ and of the iron atoms in Fe_3SnN on the lattice parameter: (1) Fe; (2) Fe(2); (3) Fe(1).

of the latter becoming mixed with the s, p functions of the Sn centres and the s, p, d states of the neighbouring (in the Fe_6N octahedron) iron atoms, whereas the Sn–N interaction is assumed¹⁵⁵ to be negligible. Finally, the determination of the types of interatomic interactions, predominating in the organisation of the overall chemical bonding system in the crystal and responsible for its structural and physicochemical properties, requires more detailed calculations, including the estimation of pair (and multicentre) bonds of different nature as regards energy.

* * *

In conclusion we may note that, despite the fact that the studies on the electronic properties of complex carbides and nitrides of transition metals and subgroup IIIB and IVB elements began fairly recently, the results obtained hitherto constitute a fairly promising basis for a correct interpretation of the fundamental features of the electronic structure, the nature of the chemical bonding, the charge distributions, and certain properties (in the first place spectroscopic and magnetic) of the groups of the above substances which are of greatest interest and practical significance.

Priorities in further research are formulated taking into account the results obtained. Among such priorities, one may include the determination of the characteristics of the transformation of the properties of ideal three-component systems under the influence of impurities, defects (in the ordered and disordered states), and crystal distortions as well as under the influence of their combined action. The mechanical, thermal, strength, and catalytic properties, which determine the technological aspects of the employment of the phases under discussion, have been virtually uninvestigated (from the theoretical standpoint). The development of models and numerical calculations of the above properties (which may also be predictive in nature) should constitute the next stage in the study of such phases. Investigations designed to achieve a theoretical description and modelling of the heterophase (in the structural and magnetic respects) materials based on the substances considered will be of undoubted importance.

References

1. H J Goldschmidt *Interstitial Alloys* (London: Butterworths, 1967)
2. G V Samsonov, G Sh Upadkhaya, V S Neshpor *Fizicheskoe Materialovedenie Karbidov* (Physical Materials Science of Carbides) (Kiev: Naukova Dumka, 1974)
3. L E Toth *Transition Metal Carbides and Nitrides* (New York: Academic Press, 1971)

4. G V Samsonov, I M Vinitskii *Tugoplavkie Soedineniya* (High-Melting Compounds) (Moscow: Mir, 1976)
5. G V Samsonov, O P Kulik, V S Polishchuk *Poluchenie i Metody Analiza Nitridov* (Synthesis and Methods of Analysis of Nitrides) (Kiev: Naukova Dumka, 1978)
6. T Ya Kosolapova (Ed.) *Svoistva, Poluchenie i Primenenie Tugoplavkikh Soedinenii. Spravochnik* (Properties, Synthesis, and Application of High-Melting Compounds. Handbook) (Moscow: Metallurgiya, 1986)
7. J Calais *Adv. Phys.* **26** 847 (1977)
8. A Neckel *Int. J. Quantum Chem.* **23** 1317 (1983)
9. A L Ivanovskii, V A Gubanov, G P Shveikin, E Z Kurmaev *Usp. Khim.* **52** 705 (1983) [*Russ. Chem. Rev.* **52** 395 (1983)]
10. A L Ivanovskii, V P Zhukov, V A Gubanov *Elektronnoe Stroenie Tugoplavkikh Karbidov i Nitridov Perekhodnykh Metallov* (Electronic Structure of Refractory Carbides and Nitrides of Transition Metals) (Moscow: Nauka, 1990)
11. R Freer (Ed.) *The Physics and Chemistry of Carbides, Nitrides, and Borides* (Dordrecht: Kluwer, 1990)
12. A L Ivanovsky, G P Shveikin *Phys. Status Solidi B* **181** 251 (1994)
13. G V Samsonov *Nemetallicheskie Nitridy* (Nonmetallic Nitrides) (Moscow: Metallurgiya, 1969)
14. T Lundstrom, S Rundqvist (Eds) *Borides, Silicides, and Phosphides* (London: Methuen, 1965)
15. T Ya Kosolapova, T V Andreeva, T B Bartnitskaya, G G Gnesin, G N Makarenko, I I Osipova, E V Prilutskii *Nemetallicheskie Tugoplavkie Soedineniya* (Nonmetallic High-Melting Compounds) (Moscow: Metallurgiya, 1985)
16. J Kallwait *Theory of Energy Band Structure* (Translated into Russian; Moscow: Mir, 1969)
17. W A Harrison *Electronic Structure and the Properties of Solids* (Translated into Russian; Moscow: Mir, 1983)
18. E A Zhurakovskii, I N Frantsevich *Rentgenovskie Spektry i Elektronnaya Struktura Silitsidov i Germanidov* (X-Ray Spectra and Electronic Structure of Silicides and Germanides) (Kiev: Naukova Dumka, 1981)
19. V V Sobolev, V V Nemoshkalenko *Metody Vychislitel'noi Fiziki v Teorii Tverdogo Tela. Elektronnaya Struktura Poluprovodnikov* (Methods of Computational Physics in the Theory of Solids. Electronic Structure of Semiconductors) (Kiev: Naukova Dumka, 1988)
20. A Katz (Ed.) *Indium Phosphide and Related Materials: Processing, Technology, and Devices* (Boston: Artech House, 1992)
21. S Adachi *Physical Properties of III-V Semiconductor Compounds: InP, InAs, GaAs, InGaAs, and InGaAsP* (New York: Wiley, 1992)
22. J E Sundgren, B O Johansson, S E Carlsson *Thin Solid Films* **105** 353 (1983)
23. O Knotec, T Leyendecker *J. Vac. Sci. Technol.* **5** 2173 (1986)
24. O Knotec, T Leyendecker *J. Solid State Chem.* **70** 318 (1987)
25. L Hultman, G Hakansson, U Wahlstrom, J Sundgren *Thin Solid Films* **205** 133 (1991)
26. R Strydom, S Hoffmann *J. Electron Spectrosc. Relat. Phenom.* **56** 85 (1991)
27. P J Martin *Thin Solid Films* **153** 91 (1987)
28. K Upadhyaya *JOM* (5) 15 (1992)
29. Le Dang Khoi, E Fruchart, D Fruchart *Solid State Commun.* **8** 49 (1970)
30. D Fruchart, E F Bertaut, F Sayetat, G Lorthioir, R Madar, A Ronault *Solid State Commun.* **8** 91 (1970)
31. A Kenmotsu, T Shinohara, H Watanabe *J. Phys. Soc. Jpn.* **32** 377 (1972)
32. D Fruchart, E F Bertaut *J. Phys. Soc. Jpn.* **44** 781 (1978)
33. G Hakansson, J E Sundgren *Thin Solid Films* **153** 55 (1987)
34. M V Kuznetsov, S V Borisov, Yu F Zhuravlev, R S Baryshev, O F Denisov, B V Mitrofanov, V A Gubanov *Poverkhnost'* (12) 141 (1989)
35. M V Kuznetsov, E V Shalaeva, V A Gubanov *Poverkhnost'* (2) 95 (1994)
36. D T Quinto *Thin Solid Films* **153** 37 (1987)
37. A J Herman, S Hoffman *Thin Solid Films* **153** 45 (1987)
38. R Luthier, F Levy *J. Vac. Sci. Technol. A, Vac. Surf. Films* **9** 102 (1991)
39. S Inomura, K Nobugai, F Kanamura *J. Solid State Chem.* **68** 124 (1987)
40. H A Jehn, S Hoffmann, V E Ruckborn, D W Munz *J. Vac. Sci. Technol. A, Vac. Surf. Films* **4** 2701 (1986)
41. O Knotec, M Boehmer, T Leyendecker *J. Vac. Sci. Technol. A, Vac. Surf. Films* **4** 2695 (1986)
42. H Freller, H Haessler *Thin Solid Films* **153** 67 (1987)
43. D W Muenz *J. Vac. Sci. Technol. A, Vac. Surf. Films* **4** 2717 (1987)
44. G Hakansson, J E Sundgren, D McIntyre, J E Greene, D W Munz *Thin Solid Films* **153** 55 (1987)
45. D McIntyre, J E Greene, G Hakansson, J E Sundgren, D W Munz *J. Appl. Phys.* **67** 1542 (1990)
46. I Penttinen, J M Molatius, A S Korhonen, R Lappalainen *J. Vac. Sci. Technol. A, Vac. Surf. Films* **6** 2158 (1988)
47. D Zlatanovic, P Stosic *Vacuum* **39** 557 (1989)
48. H Randhawa, P C Johnson, R Cunningham *J. Vac. Sci. Technol. A, Vac. Surf. Films* **6** 2136 (1988)
49. A M Dorodnov, V A Potrossov *Zh. Tekh. Fiz.* **51** 504 (1981)
50. G Lemperiere, J M Poltvin *Thin Solid Films* **111** 353 (1984)
51. M V Kuznetsov, J F Zhuravlev, E V Shalaeva *Thin Solid Films* **215** 1 (1992)
52. M V Kuznetsov, Yu F Zhuravlev, V A Gubanov *Zashch. Met.* **28** (1992)
53. M V Kuznetsov, Yu F Zhuravlev, D L Novikov, V A Gubanov *Poverkhnost'* (1) 131 (1990)
54. M V Kuznetsov, Candidate Thesis in Physicomathematical Sciences, Institute of Chemistry, Ural Branch of the Academy of Sciences of the USSR, Sverdlovsk, 1989
55. D Briggs, M P Seah *Practical Surface Analysis by Auger and X-Ray Photoelectron Spectroscopy* (New York: Wiley, 1983)
56. U Gelius *Electron Spectroscopy* (Amsterdam: North-Holland, 1972)
57. H Hochst, R D Bringans, P Steiner, T Wolf *Phys. Rev. B, Condens. Matter* **25** 7183 (1982)
58. L Porte, L Roux, J Hanus *Phys. Rev. B, Condens. Matter* **28** 3214 (1983)
59. R D Bringans, H Hochst *Phys. Rev. B, Condens. Matter* **30** 5416 (1984)
60. H Nowotny, P Ettmayer *J. Inst. Met.* **97** 180 (1969)
61. V I Ivchenko, M I Lesnaya, V F Nemchenko, T Ya Kosolapova *Poroshk. Metall.* (5) 45 (1976)
62. I A Brytov, V S Neshpor, Yu N Romashchenko, E A Ivchenko *Fiz. Met. Metalloved.* **56** 253 (1983)
63. A L Ivanovskii, Doctoral Thesis in Chemical Sciences, Institute of Chemistry, Ural Scientific Centre of the Academy of Sciences of the USSR, Sverdlovsk, 1988
64. A L Ivanovskii, I V Solov'ev, V A Gubanov *Zh. Neorg. Khim.* **32** 1754 (1987)
65. A L Ivanovskii, V I Anisimov, I V Solov'ev, V A Gubanov *Izv. Akad. Nauk SSSR, Neorg. Mater.* **24** 1311 (1988)
66. A L Ivanovsky, R F Sabiryanov *J. Phys. Chem. Solids* **54** 1061 (1993)
67. D E Ellis, G S Painter *Phys. Rev. B, Condens. Matter* **9** 2887 (1970)
68. V A Gubanov, A L Ivanovsky, G P Shveikin, D E Ellis *J. Phys. Chem. Solids* **45** 719 (1984)
69. J Petru, J Klima, P Herzig *Z. Phys. B, Condens. Matter* **76** 483 (1989)
70. D Vogtenhuber-Pawelczak, P Herzig, J Klima *Z. Phys. B, Condens. Matter* **84** 211 (1991)
71. P Herzig, J Redinger, R Eibler, A Neckel *J. Solid State Chem.* **70** 281 (1987)
72. J Redinger, R Eibler, P Herzig, A Neckel, R Podlousky, E Wimmer *J. Phys. Chem. Solids* **47** 387 (1986)
73. A Neckel *Int. J. Quantum Chem.* **23** 1317 (1983)
74. A Neckel, K Schwarz, R Eibler, P Weinberger *Ber. Bunsenges. Phys. Chem.* **79** 1053 (1975)
75. L Szunyogh, J Klima, D Vogtenhuber-Pawelczak, P Herzig, P Weinberger *Z. Phys. B, Condens. Matter* **85** 281 (1991)
76. B Gyorffy, M J Stott, in *Band Structure Spectroscopy of Metals and Alloys* (Eds F J Fabian, L M Watson) (New York: Academic Press, 1968) p. 385
77. P Weinberger *Electron Scattering Theory for Ordered and Disordered Matter* (Oxford: Clarendon Press, 1990)
78. E Beaupres, C F Hagne, J M Mariot, P Weinberger *Phys. Rev. B, Condens. Matter* **34** 886 (1986)
79. G Wiech, E Zoepf *J. Phys. (France)* **32** C4-200 (1971)
80. J Redinger, P Marksteiner, P Weinberger *Z. Phys. B, Condens. Matter* **63** 321 (1986)
81. H Winter, P I Durham, G M Stocks *J. Phys. F, Met. Phys.* **14** 1047 (1984)
82. G Hoermandinger, P Weinberger, P Marksteiner, J Redinger *Phys. Rev. B, Condens. Matter* **38** 1040 (1988)

83. G Hoernander, P Weinberger, J Redinger *Phys. Rev. B, Condens. Matter* **40** 7989 (1989)
84. A L Ivanovsky, N I Medvedeva, G P Shveikin *Mendeleev Commun.* 176 (1994)
85. N I Medvedeva, A L Ivanovskii *Zh. Neorg. Khim.* **40** 1195 (1995)
86. A L Ivanovsky, N I Medvedeva, G P Shveikin, V M Zhukovsky *Phys. Status Solidi* (1996) (in the press)
87. H L Skriver *The LMTO Method* (London: Springer, 1984)
88. J J Nickl, K K Schweitzer *Z. Met.kd.* **6** 54 (1970)
89. J Lis, R Pampuch, J Piekarczyk, L Stobierski *Ceram. Int.* **19** 219 (1993)
90. B Gottselig, E Gyarmati, A Naoumidis, H Nickel *J. Eur. Ceram. Soc.* **6** 153 (1990)
91. J Lis, R Pampuch, L Stobierski *Int. J. Self-Propag. High-Temp. Synth.* **1** 401 (1992)
92. R Pampuch, J Lis, L Stobierski, M Tymkiewicz *J. Eur. Ceram. Soc.* **5** 283 (1989)
93. H Holleck *Surf. Coat. Technol.* **36** 151 (1988)
94. R Fella, H Holleck *Mater. Sci. Eng.* **A140** 676 (1991)
95. R F Sabiryanov, A L Ivanovskii, G P Shveikin *Zh. Neorg. Khim.* **38** 1572 (1993)
96. F Herman, J P van Dyke, R L Kortum *Mater. Res. Bull.* **14** 167 (1969)
97. F Bassani, M Yashimine *Phys. Rev.* **130** 20 (1964)
98. L A Hemstreet, C Y Fong *Solid State Commun.* **9** 643 (1971)
99. A R Lubinsky, D E Ellis, G S Painter *Phys. Rev. B, Condens. Matter* **11** 1537 (1975)
100. K J Chang, M L Cohen *Phys. Rev. B, Condens. Matter* **35** 8196 (1987)
101. M Causa, R Dovesi, C Roetti *Phys. Rev. B, Condens. Matter* **43** 937 (1991)
102. V I Anisimov, V P Antropov, V A Gubanov, A L Ivanovskii, A V Postnikov, E Z Kurmaev *Elektronnaya Struktura Defektov i Primesei v Metallakh, Splavakh i Soedineniyakh* (Electronic Structure of Defects and Impurity in Metals, Alloys, and Compounds) (Moscow: Nauka, 1989)
103. Zh V Gertner, N I Medvedeva, V M Zhukovskii, A L Ivanovskii, G P Shveikin *Metallofiz. Noveishie Tekhnol.* **16** 78 (1994)
104. N I Medvedeva, Zh V Gertner, V V Kraskovskaya, A L Ivanovskii, G P Shveikin *Neorg. Mater.* **31** 55 (1995)
105. V P Zhukov, V A Gubanov, O Jepsen, N E Christensen, O K Andersen *Philos. Mag.* **58B** 139 (1988)
106. V P Zhukov, N I Medvedeva, V A Gubanov *Phys. Status Solidi B* **151** 407 (1989)
107. G G Shveikin, N I Medvedeva, A L Ivanovskii *Neorg. Mater.* **32** 52 (1996)
108. N I Medvedeva, A L Ivanovskii *Zh. Neorg. Khim.* **41** (1996) (in the press)
109. M V Kuznetsov, E V Shalaeva, S V Borisov, B V Mitrofanov, A L Ivanovsky, G P Shveikin *Mendeleev Commun.* **94** (1995)
110. M V Kuznetsov, S V Borisov, E V Shalaeva *Thin Solid Films* (1996) (in the press)
111. J Redinger, P Marksteiner, P Weinberger *Z. Phys. B, Condens. Matter* **63** 321 (1986)
112. P Marksteiner, P Weinberger, A Neckel, R Zeller, H Dederichs *J. Phys. F, Met. Phys.* **16** 1495 (1986)
113. P Pecheur, G Toussaint, E Kauffer *Phys. Rev. B, Condens. Matter* **29** 6606 (1984)
114. W E Pickett, B M Klein, R Zeller *Phys. Rev. B, Condens. Matter* **34** 2517 (1986)
115. W Jeitschko, H Nowotny *Monatsh. Chem.* **98** 329 (1967)
116. J J Nickl, K K Schweitzer, P Luxenberg *J. Less-Common Met.* **26** 335 (1972)
117. T Goto, T Hirai *Mater. Res. Bull.* **22** 1195 (1987)
118. A L Ivanovsky, D L Novikov, G P Shveikin *Mendeleev Commun.* **90** (1995)
119. L T Huetter, H H Stadelmaier *Z. Met.kd.* **41** 230 (1950)
120. R Butters, H P Myers *Philos. Mag.* **46** 895 (1955)
121. M L Swanson *Can. J. Phys.* **40** 719 (1962)
122. H H Stadelmaier, L J Huetter *Acta Metall.* **7** 415 (1959)
123. D Fruchart, E F Bertaut, B Le Clere *J. Solid State Chem.* **8** 182 (1973)
124. J Schoebel, H H Stadelmaier, G Lorthioir, E Fruchart, R Fruchart *Z. Met.kd.* **55** 378 (1964)
125. M Haschke, H Nowotny, F Benesovsky *Monatsh. Chem.* **98** 273 (1967)
126. W Jeitschko, H Nowotny, F Benesovsky *Monatsh. Chem.* **95** 436 (1964)
127. H H Stadelmaier, A Fraeker *Z. Met.kd.* **53** 48 (1962)
128. H H Stadelmaier, T Yun *Z. Met.kd.* **52** 477 (1961)
129. D Fruchart, E F Bertaut, R Madar, G Lorthioir, R Fruchart *Solid State Commun.* **9** 1793 (1971)
130. E F Bertaut, D Fruchart *Int. J. Magn.* **2** 259 (1972)
131. D Fruchart, E F Bertaut, J P Senateur, R Fruchart *J. Phys. Lett.* **38** 21 (1977)
132. D Fruchart, E F Bertaut *J. Phys. Soc. Jpn.* **44** 781 (1978)
133. D Fruchart, J P Bouchand, E Fruchart, G Lorthioir, R Madar, A Ronault *Mater. Res. Bull.* **2** 1009 (1967)
134. E F Bertaut, D Fruchart, J P Bouchand, R Fruchart *Solid State Commun.* **6** 251 (1968)
135. M Barberon, E Fruchart, R Fruchart, G Lorthioir, R Madar, M Nardin *Mater. Res. Bull.* **7** 109 (1972)
136. M Barberon, R Madar, E Fruchart, G Lorthioir, R Fruchart *Mater. Res. Bull.* **5** 1; 903 (1970)
137. S Nagakura, K Tanehoski *J. Phys. Soc. Jpn.* **25** 840 (1968)
138. R Fruchart, R Madar, M Barberon, E Fruchart, G Lorthioir *J. Phys. Colloq.* **32** 982 (1971)
139. T Kaneko, T T Kanomata, K Shirakawa *J. Phys. Soc. Jpn.* **56** 4047 (1987)
140. E Kren, G Kadar, L Pal, J Solyon, P Szabo, T Tarnorzi *Phys. Rev.* **171** 574 (1968)
141. T Kaneko, T Kanomata, S Hiura, G Kido, Y Nakagawa *J. Magn. Magn. Mater.* **70** 261 (1987)
142. T Kanomata, T Kaneko, Y Nakagawa *J. Solid State Chem.* **96** 451 (1992)
143. J P Jardin, J Labbe *J. Phys.* **36** 1317 (1975)
144. J P Jardin, J Labbe *J. Appl. Phys.* **52** 3 (1981)
145. J P Jardin, J Labbe *J. Solid State Chem.* **46** 275 (1983)
146. K Motizuki, H Nagai *J. Phys. C, Solid State Phys.* **21** 5251 (1988)
147. K Motizuki, H Nagai, T Tanimoto *J. Phys. (France)* **49** 161 (1988)
148. A L Ivanovskii, I S Elfimov, A N Skazkin, V M Zhukovskii, G P Shveikin *Fiz. Tverd. Tela* **37** 3738 (1995)
149. A L Ivanovskii *Zh. Neorg. Khim.* **41** (1996) (in the press)
150. M Shirai, Y Ohata, N Suzuki, K Motizuki *Jpn. J. Appl. Phys.* **32** 250 (1993)
151. S Ishida, S Fujii, M Maeda, S Asano *Jpn. J. Appl. Phys.* **32** 248 (1993)
152. S Ishida, S Fujii, A Sawabe, S Asano *Jpn. J. Appl. Phys.* **32** 282 (1993)
153. T Kaneko, T Kanomata, in *Recent Advances in Magnetism of Transition Metal Compounds* (Eds A Kotani, N Suzuki) (Singapore: World Scientific, 1993) p. 103
154. T Kaneko, T Kanomata, K Shirakawa *J. Phys. Soc. Jpn.* **44** 781 (1978)
155. C A Kuhnen, A V dos Santos *Solid State Commun.* **85** 273 (1993)
156. C A Kuhnen, A V dos Santos *J. Magn. Magn. Mater.* **130** 353 (1994)
157. K Tagowa, E Kita, A Tasaki *J. Phys. Soc.* **21** 1596 (1982)
158. D Andriamandroso, L Fefilatiev, G Demazeau, L Fournes, M Pouchard *Mater. Res. Bull.* **19** 1187 (1984)
159. G Ertl, M Nuber, N Thiele *Z. Naturforsch. A, Phys. Sci.* **34** 30 (1979)
160. S Matar, P Mohn, G Demazeau, B Siberchicot *J. Phys. (France)* **49** 1761 (1988)
161. Wei Zhou, Li-jia Qu, Q Zhang, D Wang *Phys. Rev. B, Condens. Matter* **40** 6392 (1989)
162. C A Kuhnen, R S de Figueiredo, V Drago, E Z da Silva *J. Magn. Magn. Mater.* **111** 95 (1992)
163. G Demazeau, D Andriamandroso, M Pouchard, B Tanguy, P Hagenmuller *C. R. Seances Acad. Sci. II, Mech.-Phys. Chim. Sci.* **297** 843 (1983)
164. U K Poulsen, J Kollar, O K Andersen *J. Phys. F, Met. Phys.* **6** L241 (1976)
165. O K Andersen, S Madsen, U K Poulsen, O Jepsen, J Kollar *Physica B* **86-87** 249 (1977)
166. D M Roy, D G Pettifor *J. Phys. F, Met. Phys.* **7** L183 (1977)
167. J Kubler *Phys. Rev. Lett.* **81A** 81 (1981)
168. C A Kuhnen, E Z da Silva *Phys. Rev. B, Solid State* (1996) (in the press)

Stabilisation of metal ions in unusual oxidation states and electron dynamics in oxide glasses

A I Aleksandrov, A I Prokof'ev, N N Bubnov

Contents

I. Introduction	479
II. Ions in unusual oxidation states in oxide glasses	479
III. Electron dynamics in oxide glasses	489
IV. Conclusion	

Abstract. The results of studies on the stabilisation of metal ions in unusual oxidation states in oxide glasses are surveyed. Attention is concentrated on the relation between the stabilisation of these ions and redistribution of the electron density, and on the disproportionation reactions accompanying it. The effect of reversible low-temperature disproportionation on niobium, titanium, vanadium, molybdenum, tungsten, and other ions is considered. The formation of metal clusters in oxide glasses is shown also to be associated with disproportionation. The bibliography includes 108 references.

I. Introduction

Current developmental chemistry is addressing the problems of producing new compounds and materials possessing valuable practical properties.

Metal ions in unusual oxidation states (UOS) arise in intermediate stages of redox processes including radiation-induced, catalytic, biochemical, mechanochemical, and other processes. Ions of this type have short lifetimes, and their steady-state concentrations are low. The fact that these ions are formed and their role in physicochemical processes have long remained obscure and their existence has been supported only by indirect data. Therefore, the physicochemical properties of these species could be inferred only from theoretical considerations. The appearance of matrix isolation methods in combination with various spectroscopic methods and techniques for the investigation of fast chemical processes have made it possible to begin an investigation of the properties of ions of various elements in UOS.

By the early 70s, studies devoted to the preparation of compounds containing metal ions in UOS in liquid or glassy aqueous media were published.^{1,2} The UOS of metals were generated by radiation. Glassy media have been studied at 77 K by stationary methods, namely, EPR and optical spectroscopy.^{3–6} The aqueous solutions at room temperature have been studied by

pulse radiolysis using fast optical recording.^{7,8} The information obtained made it possible to identify the regular variation of the physicochemical properties of metal ions in UOS as a function of their position in the Periodic Table and to embark upon solving the problem of their long-term stabilisation in inorganic glasses at 300 K.

It turned out that the solution of this problem is primarily associated with the elucidation of the role of the ligand environment of the metal ion, namely, the influence of the nature of ligands on the distribution of the electron density in the atomic orbital (AO) containing the electron that imparts to the ion the properties typical of ions in UOS. In the second place, solution of this problem is associated with the study of the physical properties of the solid glassy matrix itself, which contains modifying ions passing into UOS under various physical influences. Despite the great structural diversity of inorganic glasses, the problem actually reduces to the solution of a single fundamental problem, namely, to the study of localisation and delocalisation of electrons in the outer orbitals of atoms or ions as a function of the structure and properties of the solid matrix. Our review is devoted to this problem in relation to low-temperature glasses and inorganic oxide glasses (silicate, germanate, borate, and phosphate).

II. Ions in unusual oxidation states in oxide glasses

1. Frozen (glassy) solutions

In the late 1970s and the early 1980s, a series of studies was carried out at the Institute of Physical Chemistry of the RAS dealing with UOS of Period 4–6 metals obtained by low-temperature radiolysis in aqueous solutions of acids (HClO₄, HCl, H₂SO₄) or bases (NaOH, KOH) containing salts of these metals.^{3–6,9–14} The choice of metals was determined by the fact that ions with the electron configuration $d^{10}s^1$, i.e. ions existing in a $^2S_{1/2}$ electronic state, are conveniently studied by the highly sensitive EPR method. These ions contain an unpaired electron in the outer ns -AO and arise upon single-electron reduction or oxidation of the central metal atom of an aqua, chloride, or other complex induced by γ -irradiation of frozen glassy solutions. The ions in UOS can be stabilised in glassy matrices at 77 K for an infinitely long period.

It has been shown^{3–6,9–14} that the reactions of the initial ions with thermalised electrons (e^-) and HO \cdot radicals in low-temperature glasses make it possible to obtain Zn¹⁺, Cd¹⁺, Hg¹⁺, Ga²⁺, In²⁺, Tl²⁺, Ge³⁺, Sn³⁺, Pb³⁺, Sb⁴⁺, and Bi⁴⁺ ions in the $^2S_{1/2}$ electronic state as well as Sn¹⁺ and Pb¹⁺ ions, which contain an unpaired electron in the outer p -orbital. The ions in a $^2S_{1/2}$ electronic state were shown to arise in the competing reactions of e^- with metal ions or with the hydroxonium ion. The Sn¹⁺ and Pb¹⁺ ions are also formed via the reduction of Sn²⁺ and Pb²⁺

A I Aleksandrov Institute of Synthetic Polymer Materials, Russian Academy of Sciences, ul. Profsoyuznaya 70, 117393 Moscow, Russian Federation. Fax (7-095) 420 22 29

A I Prokof'ev, N N Bubnov A N Nesmeyanov Institute of Organoelement Compounds, Russian Academy of Sciences, ul. Vavilova 28, 117813 Moscow, Russian Federation. Fax (7-095) 135 50 85

Received 3 October 1995

Uspekhi Khimii 65 (6) 519–537 (1996); translated by Z P Bobkova

with thermalised electrons. The relative rate constants for the reactions of e^- with Group IB–VB metal ions were determined.



For the ions in a $^2S_{1/2}$ electronic state and for the Sn^{1+} and Pb^{1+} ions, g -factors, constants A_i of the isotropic hyperfine coupling (HFC), optical absorption bands, and the extinction coefficients were determined from EPR data and optical spectroscopy at 77 K (Table 1).

To study metal ions in a $^2S_{1/2}$ electronic state by EPR, it is important to know the isotropic HFC constants for these species in the free state, $A_i^{(0)}$. Ershov and Aleksandrov¹⁵ have suggested a semiempirical method for the calculation of the $A_i^{(0)}$ HFC constants for series of isoelectronic ions of Periods 4–6 of the Periodic Table existing in the $^2S_{1/2}$ electronic state. Comparison of these $A_i^{(0)}$ values obtained with the HFC constants A_i of these ions in a real medium permits determination of the character of their interaction with ligands. In fact, for a 'free' ion, $A_i^{(0)} = |\Psi_{ns}(0)|^2$, where $|\Psi_{ns}(0)|^2$ is the electron density at the nucleus caused by the electron in the outer ns -AO, while for the M^{Z+} ion in a real medium, $A_i \sim \Psi_{ns}$, where Ψ_{ns} is the electron density in the presence of a certain ligand environment. Thus, the $A_i/A_i^{(0)}$ ratio is the electron occupancy of the outer ns -AO that forms the chemical bond with the ligands of the complex.

It has been shown that the density of the unpaired electron at IIB–IVB Group metal ions, existing in the $^2S_{1/2}$ electronic state, in aqua and chloride complexes decreases with an increase in the charge of the metal ion within the same period.^{9, 12, 14}

In a study of optical characteristics of these ions, it has been found that the energy of optical transitions at the maxima of absorption bands ($E_{\lambda_{\text{max}}}$) for the aqua complexes of IIB–IVB Group metal ions existing in UOS and in the $^2S_{1/2}$ electronic state increases regularly with an increase in the charge of the metal ion within the same period, while for the chloride complexes, this energy decreases. Semiempirical calculations of the energies of the a_{1g}^* and t_{1u}^* molecular orbitals for aqua complexes have shown that experimental $E_{\lambda_{\text{max}}}$ values are in agreement with $\Delta E = E(t_{1u}^*) - E(a_{1g}^*)$; this confirms the fact that the optical absorption bands are due to the $a_{1g}^* \longrightarrow t_{1u}^*$ transition.

It has been shown that in the case of chloride complexes, optical absorption bands are due to the $1t_{1u} \longrightarrow a_{1g}^*$, $2t_{1u} \longrightarrow a_{1g}^*$, and $3t_{1u} \longrightarrow a_{1g}^*$ electron transitions. The energies of these transitions decrease with increase in the charge on the central metal ion in isoelectronic series.¹² The antiparallel courses of the variation of the energies of optical transitions in aqua and chloride complexes of metal ions in an isoelectronic series are accounted for by the crucial role of the ligand environment. Unlike the optical transition in aqua complexes, which is caused by the transfer of an electron from the central ion to the ligands (H_2O molecules), the optical transition in the chloride complexes

Table 1. Spectroscopic parameters of metal ions in unusual oxidation states in aqueous solutions of their salts at 77 K (low-temperature glasses).

Ion in UOS (J) ^a	Solution	g -factor of the ion in UOS	$A_i/A_i^{(0)}$	$\lambda_{\text{max}}/\text{nm}$	$\epsilon/10^3 \text{ dm}^6 \text{ mol}^{-1} \text{ cm}^{-1}$	Ion in UOS (J) ^a	Solution	g -factor of the ion in UOS	$A_i/A_i^{(0)}$	$\lambda_{\text{max}}/\text{nm}$	$\epsilon/10^3 \text{ dm}^6 \text{ mol}^{-1} \text{ cm}^{-1}$
Zn^{1+} ($\frac{3}{2}$)	8 M HCl	1.997		230	7.0	Hg^{1+} ($\frac{1}{2}$)	5 M H_2SO_4	1.986	0.750		
	6 M HClO_4			290	6.5		5 M D_2SO_4	1.996			
Ga^{2+} ($\frac{3}{2}$)	9–10 M HCl	2.001	0.391	260			5 M H_3PO_4	1.979 (1.987) ^b	0.765		
	7 M HClO_4	2.001	0.562	245	9.2						
Ge^{3+} ($\frac{9}{2}$)	8–10 M HCl	2.003		270	5.0	Tl^{2+} ($\frac{1}{2}$)	8 M HCl	2.002	0.398	210	
Cd^{1+} ($\frac{1}{2}$)	6–10 M HCl	1.987	0.697	220	9.0					280	
				300	6.0		7 M HClO_4	2.002	0.594	225	13.6
	6 M HClO_4	1.989	0.633	270	13.6			2.002	0.477		
	5 M H_2SO_4	1.989	0.650			Pb^{3+} ($\frac{1}{2}$)	6–10 M HCl	2.005	0.359	220	
	5 M D_2SO_4	1.997	0.617							300	13.0
	5 M H_3PO_4	1.980	0.650							430	9.0
		(1.986) ^b	(0.622) ^b				5–8.5 M HClO_4	1.999	0.533	200	
In^{2+} ($\frac{9}{2}$)	6–10 M HCl			245			10 M NaOH	1.991 (g_{\perp}), 2.004 (g_{\parallel})	0.274		
	6 M HClO_4			310		Sn^{1+} (see c)	6–10 M HCl	1.993 (g_{aver})			
				235	14.3		5–8 M HClO_4	1.824 (g_1), 2.196 (g_3)		210	
Sn^{3+} ($\frac{1}{2}$)	6–10 M HCl	2.005	0.413	275			5 M H_2SO_4	1.812 (g_1), 2.174 (g_3)			
	5–8 M HClO_4	1.995	0.428	215			10 M NaOH	1.989 (g_{aver})			
	5 M H_2SO_4	1.996	0.516			Pb^{1+}	6 M HClO_4			300	
	10 M NaOH	1.989 (g_{\perp}), 2.001 (g_{\parallel})	0.267	310			6–10 M NaOH			275	2.3
Hg^{1+} ($\frac{1}{2}$)	6–10 M HCl	1.981	0.660	200						360	1.8
				270	12.0						
	6 M HClO_4	1.982	0.785	240	17.6						
		(1.991) ^b	(0.840) ^b								

^a The nuclear spin for the odd isotope of an ion in a $^2S_{1/2}$ electronic state is given in parentheses. ^b The g -factor of the ion at another stabilisation site.

^c For Sn^{1+} ion, $g_{\text{aver}} = (g_1 + g_2 + g_3)/3$ or those values of g -factors that could be determined in the experiment, for example, g_1 and g_3 , are given.

is due to the electron transfer from the ligand (Cl^- ion) to the central ion.

A regular variation of the $E^0[\text{M}^{(Z+1)+}/\text{M}^{Z+}]$ redox potentials as a function of the charge on the cation existing in an unusual oxidation state has been found:^{14, 16} the $E^0[\text{M}^{(Z+1)+}/\text{M}^{Z+}]$ values increase as the charge on the cation increases within one Period, whereas within one Group, i.e. for ions having the same charge, they increase with increase in the number of the Period. The theoretical grounds for these regularities have been reported.¹⁷

The above results reflect a fundamental feature of metals (in particular, of metals in UOS having the $d^{10}s^1$ electron configuration), namely, that their physicochemical properties vary monotonically with the atomic number.

These conclusions refer also to the ions in UOS arising at room temperature. At 300 K in aqueous solutions, these species disappear over periods of 10^{-6} – 10^{-4} s, the time for their destruction being determined by the diffusion mobility. Their properties can be conveniently studied by pulse radiolysis with fast optical recording,^{18–22} which makes it possible to determine the positions of optical absorption bands and the extinction coefficients and to measure the rate constants for the reactions of these ions with short-lived species such as hydrated electron (e^-), the CO_2^- radical anion, the HO^\cdot radical, and the $\text{O}^{\cdot-}$ radical anion in aqueous solutions. Based on the characteristics of the optical spectra recorded in the initial stages of chemical transformations over various time intervals (up to 10^{-4} s), the formation of monosubstituted hydroxo- and chloride complexes of IB–IVB Group metals in UOS and in a $^2\text{S}_{1/2}$ electronic state was established, and the instability constants for these complexes were determined; these constants were found to vary monotonically in the series of isoelectronic ions in UOS as a function of the position of the metal in the Periodic Table.

When low-temperature glasses are defrosted, the ions in UOS disappear irreversibly due to the intensification of the diffusion of cations and anions in the matrix. This is why the authors cited above did not answer the question of how hydrogen-like ions with the $d^{10}s^1$ electron configuration form stable chemical compounds. However, the results of studies on the influence of the ligand environment on the properties of metal ions in UOS suggest the possibility of preparing solid glasses in which metal ions in UOS will be stable over periods of time from microseconds to months and even longer. The physicochemical parameters of these glasses should vary as functions of the properties of the stabilised ion.

2. Stabilisation of metals in unusual oxidation states in oxide glasses

As noted above, ions in UOS can exist over extended periods in low-temperature glasses at 77 K. However, it is obvious that these frozen aqueous solutions containing ions in UOS are of no practical interest, since the unusual properties imparted to them by metals in UOS disappear irreversibly when the temperature is slightly raised. Therefore, the logical pathway to the development of new materials with new unusual properties caused by the presence of ions in UOS is the preparation of solid-state materials based on 'true' molten glasses, which are capable of stabilising these species in their matrices.

In fact, the absence of symmetry in their structure and their isotropic properties make glasses identical to liquids, whereas the elasticity of shape makes glasses similar to solids. A glass is considered to be a true solution in which a relationship exists between the composition, the structure, and the properties. At present, articles of glass and glassy materials are used in virtually all branches of industry.²³ Therefore, to confer on these objects new properties specified beforehand is a significant and urgent problem.

In recent years, investigations of glassy media have been vigorously pursued, although the background for these studies was laid long ago by D I Mendeleev,²⁴ who suggested the polymeric concept of the structure of glass, and by Lebedev and

Zakhariasen,^{25, 26} who developed the ideas of microheterogeneity and network structure of glass. Even now these works stimulate studies aimed at controlling the properties of glasses both by varying the structure of glass with a particular elemental composition²⁷ and by introducing ions to modify its properties.²⁸ The modifying ions can alter the properties of a glass both during its synthesis (glass melting) and when a finished (solid) glass is exposed to a certain influence (heat, light, radiation).^{29, 30} Oxide glasses have found the widest practical application.

Oxide glasses can be divided conventionally into four main classes (according to the main glass-forming compound), namely, borate, silicate, germanate, and phosphate glasses. These groups of glasses differ in microstructure and, consequently, their physicochemical properties are also dissimilar. The introduction of modifying ions into these glasses extends considerably the range of existing properties.³¹ Stabilisation of these ions in a glass matrix is associated with redistribution of the electron density of the ligands surrounding the ions and with local variations of the glass structure.

Since the 1970s, studies have been carried out dealing with chemically active species generated by various kinds of treatment and stabilised in glassy matrices as colour centres (CC), paramagnetic centres (PMC), and luminescence centres.^{27–31} The physicochemical properties of these centres have been studied by stationary and pulse methods.^{27–31} However, all the information obtained at that time referred to the matrix centres of the main classes of glasses. The studies were concerned with the optical and kinetic properties of these centres, i.e., they reduced to utilitarian investigation of the radiation sensitivity of glasses by a trial-and-error method. This approach did not conform completely to the modern state of development of the physical chemistry of the glassy state. Therefore, systematic studies are needed that would take into account the properties of elements incorporated in glasses, depending on their position in the Periodic Table.

Apparently, glasses capable of stabilising the modifying ions as well as ions in UOS should contain a wide range of valence states of atoms and ions, which would permit the glassy system to reach an equilibrium after the introduction of ions in metastable states. Borate, silicate, germanate, and phosphate glasses have been studied.^{32–47} Particular attention was focused on three-component alkali glasses: lithium, sodium, and potassium borate, germanate, phosphate, and silicate glasses as well as on the barium aluminophosphate glasses (BAPG). The content of metal oxide in these glasses varied from 3 to 30 mol %. Other glass-forming systems have also been studied; they are mentioned below.

As a rule, after irradiation at 77 and at 300 K, the systems under study containing admixtures of metal oxides exhibited EPR signals and optical absorption bands (AB) differing from those typical of the known electron and hole sites in borate, silicate, and germanate glasses and also from those exhibited by PO_4^{2-} and PO_3^{2-} radical anions in the phosphate glasses.^{32–43} The intensity of these additional EPR signals and of the absorption bands depends on the amount of the oxide introduced, on the ratio of all the glass components, and on the method used for the synthesis of the glass.

For glasses containing cadmium, mercury, gallium, thallium, and lead oxides, it has been found that the increase in the intensity of the additional EPR signals in the magnetic field region corresponding to the g -factor for the free electron (g_e) is accompanied by an increase in the intensity of the high-field (450–700 mT) EPR signals. The latter signals are due to the hyperfine coupling of the electron spins in the outer ns -AO with the $J \neq 0$ nuclear spins of the odd isotopes of the metals added.³⁶ The ratio of the normalised surface of the high-field signals to the surface of the signals in the g_e region corresponds to the ratio of the percentage of metal isotopes with $J = \frac{1}{2}$ or $\frac{3}{2}$ to the percentage of isotopes with $J = 0$. This indicates that the additional EPR signals in question are associated with the metals introduced and proves unambiguously that these signals refer to UOS of metals in

the $^2S_{1/2}$ electronic state, namely, Cd^{1+} , Hg^{1+} , Ga^{2+} , Tl^{2+} , Sn^{3+} , and Pb^{3+} . The spectral parameters for these species are listed in Table 2.

In the case of glasses containing zinc, antimony, and germanium oxides (for odd isotopes of these metals, $J = \frac{5}{2}$, $\frac{7}{2}$ and $\frac{9}{2}$, respectively), additional signals typical of Zn^{1+} , Ge^{3+} , and Sb^{4+} , have also been detected in the EPR spectra after γ -irradiation. The parameters of these signals are also presented in Table 2. All the above metals in UOS in a phosphate matrix exhibit symmetrical EPR lines, the difference between the widths of the high-field and low-field signals being smaller than that in the case of borate, germanate, and silicate glasses.^{37,38} This suggests that in phosphate glasses the ligand environment of the metal ions in UOS is more symmetrical than in other glasses.

Studies³²⁻³⁶ of the optical characteristics of glasses irradiated at 77 and 300 K have shown that, in addition to the well known AB corresponding to the 'matrix' colour centres, additional AB are observed due to the introduction of various metal oxides. For example, it has been shown that on γ -irradiation of sodium borate glasses, the intensity of the absorption bands that appear after the introduction of metal oxides increases in parallel with the concentration of the oxides, whereas the intensities of the absorption bands with $\lambda = 350$ and 500 nm associated with BO_4^{4-} decrease correspondingly, until these bands disappear completely.³³ The spectra of borate glasses containing Zn, Cd, Ga, and Pb oxides and irradiated at 300 K, apart from the AB caused by BO_4^{4-} , contain broad absorption bands possessing a

Table 2. Characteristics of ions in unusual oxidation states in the glasses: 20% of $\text{Li}_2\text{O}(\text{Na}_2\text{O}, \text{K}_2\text{O})$ –70% of $\text{B}_2\text{O}_3(\text{GeO}_2, \text{SiO}_2, \text{P}_2\text{O}_5)$ –10% of M_xO_y (M_xO_y — metal oxide).

Ion in UOS (J) ^a	Glass ^b	g -factor	$A_i/A_i^{(0)}$	$\lambda_{\text{max}}/\text{nm}$	Ion in UOS (J) ^a	Glass ^b	g -factor	$A_i/A_i^{(0)}$	$\lambda_{\text{max}}/\text{nm}$
Zn^{1+} ($\frac{5}{2}$)	LBG	1.998	0.66		Sb^{4+} ($\frac{7}{2}$)	LPG		0.028	
	SBG	1.998		310, 550		SPG		0.023	
	SSG	1.988		320		PPG		0.038	
	BAPG			510		BAPG		0.025	
Ga^{2+} ($\frac{3}{2}$)	LBG		0.36		Hg^{1+} ($\frac{1}{2}$)	LBG	2.00	0.79	
	SBG		0.50	380, 470		SBG	1.998	0.92	
	KBG					SGG			350
	SSG		0.22		Tl^{2+} ($\frac{1}{2}$)	BAPG		0.83	505
	LSG		0.29	256		LBG	2.00	0.650	
Ge^{3+} ($\frac{9}{2}$)	LPG		0.55	500		SBG		0.653	420, 500
	LBG	1.996	0.31	300					640, 740
	SBG	1.997	0.33	300		PBG		0.60	
				(310)		LGG		0.52	
	LSG	1.996	0.78	275		SGG		0.54	413
Cd^{1+} ($\frac{1}{2}$)	LPG		0.75	290		PGG		0.536	
	LBG	1.999	0.81			LSG		0.26	357, 610,
	SBG	1.998	0.86	330, 440					714
				(375, 480)		SSG		0.29	357, 633,
	PBG	1.996	0.88						730
	LGG	2.01	0.839		Pb^{3+} ($\frac{1}{2}$)	PSG		0.41	
	SGG	2.01	0.835	400		SPG		0.50	
	PGG	2.01	0.830			BAPG		0.56	340, 625,
	LSG	1.995	0.68						750, 1100
	SSG	1.993	0.59			LBG	1.995	0.46	
	PSG	1.989	0.54			SBG		0.47	325, 500
	LPG		0.86	320, 420					(340, 530)
	SPG		0.76			PBG		0.44	
	BAPG		0.80	520		LGG	1.996	0.36	
						SGG	1.992	0.41	465
Sn^{3+} ($\frac{1}{2}$)	LBG	1.995	0.56			PGS	1.992	0.39	
	PBG	1.989	0.58			LSG	1.985	0.37	
	LGG	1.993	0.36			SSG	1.988	0.39	330, 440
	SGG	1.992	0.39			PSG	1.993	0.41	
	PGG	1.992	0.38						
Sb^{4+} ($\frac{7}{2}$)	LSG	1.989		290		LPG		0.49	330, 410,
	SBG		0.029	460, 500					730
				(380, 520)		SPG		0.46	
	SGG	1.950	0.053	380		PPG		0.50	750, 900
	SSG	2.050		290		BAPG		0.41	760, 900

^a The value of the nuclear spin of the odd isotope is given in parentheses. ^b Notation: LBG, SBG, and PBG — lithium, sodium, and potassium borate glasses, respectively; LSG, SSG, and PSG — lithium, sodium, and potassium silicate glasses; LGG, SGG, and PGG — lithium, sodium, and potassium germanate glasses; LPG, SPG, and PPG — lithium, sodium and potassium phosphate glasses; BAPG — barium aluminophosphate glasses.

low-intensity 'satellite' peak. These AB can be assigned to the Zn^{1+} , Cd^{1+} , Ga^{2+} , and Pb^{3+} ions as follows:

Ion	Zn^{1+}	Cd^{1+}	Ga^{2+}	Pb^{3+}
$\lambda_{\text{max}}/\text{nm}$	310	330	380	325
	550	440	470	500

The presence of the 'satellite' line indicates that the energy levels responsible for the optical transition are split due to the asymmetrical environment of the ions in sodium borate glasses. This is consistent with the EPR spectroscopic data, namely, with the anisotropy observed for the g -factor of the EPR signals corresponding to the ions in UOS in the region $g_e = 2.0023$.

The absorption spectra recorded at 77 K for ions in UOS in sodium borate glasses irradiated at 77 K are shifted to the long-wavelength region with respect to the spectra recorded at 300 K. For example, the following AB are observed for the Cd^{1+} , Pd^{3+} , Ge^{3+} , and Sb^{4+} ions at 77 K:

Ion	Cd^{1+}	Pb^{3+}	Ge^{3+}	Sb^{4+}
$\lambda_{\text{max}}/\text{nm}$	375	340	310	380
	480	530	—	520

The EPR spectra exhibit additional signals due to these ions, the signals corresponding to BO_4^{4-} being virtually absent.^{33, 34}

The absorption spectra of sodium borate glasses containing thallium oxide, measured after γ -irradiation at 300 K, exhibit AB with maxima at 420, 500, 640, and 740 nm. The intensity of the AB with a maximum at 420 nm varies in parallel with that of the 20 mT-wide EPR signal observed in the region of 580 mT and corresponding to Ti^{2+} ions.^{33, 34} In addition, this is the only band that undergoes temperature displacement (at 77 K, the maximum absorption is observed at 430 nm); therefore it is assigned to the Ti^{2+} ion.

Of special note is the observation³⁶ that, in the $\text{Ti}_2\text{O}-\text{Na}_2\text{O}-\text{SiO}_2$ ($\text{Ti}_2\text{O}-\text{Na}_2\text{O}-\text{B}_2\text{O}_3-\text{SiO}_2$) and $\text{PbO}-\text{Na}_2\text{O}-\text{SiO}_2$ ($\text{PbO}-\text{Na}_2\text{O}-\text{B}_2\text{O}_3-\text{SiO}_2$) systems, there is no correlation between the increase in the intensity of some additional AB and the increase in the intensity of the EPR signals corresponding to Ti^{2+} and Pb^{3+} ions. This may be due to the fact that during the synthesis of these glasses under specific redox conditions, metallic clusters of the Pb_m^{n+} and Ti_m^{n+} type (where $n, m = 1, 2, 3 \dots$) are formed. These clusters capture the electrons knocked out by γ -irradiation and thus give additional AB. Clusters of this type are also formed during the post-radiation annealing of glasses, when the following processes occur: $\text{Ti}^{1+} + \text{Ti}^{2+} \rightarrow \text{Ti}_2^{3+}$; $\text{Ti}_2^{3+} + \text{Ti}^0 \rightarrow \text{Ti}_3^{3+}$, etc. In place of thallium ions, these reactions can involve cadmium, lead, bismuth, and other ions. The cluster formation is induced by metal ions in UOS.

In the case of other kinds of glasses, it has also been found that the additional AB arise in parallel with the EPR signals corresponding to the UOS of metals. One intense bell-shaped AB is typical of glasses containing zinc, gallium, germanium, indium, tin, and antimony oxides, whereas in the case of glasses with cadmium, mercury, thallium, lead, and bismuth oxides, two or more optical absorption bands are recorded. The parameters of these bands are presented in Table 2.

It should be noted that for identical matrices with equal contents of oxides of Group IB–VB metals, the energy of the optical transitions $E_{\lambda_{\text{max}}}$ (the energy of the optical transition at the maximum λ_{max} of the optical absorption band corresponding to the metal in UOS was taken as $E_{\lambda_{\text{max}}}$) and the electron density in the ns -AO (which is characterised by the $A_i/A_i^{(0)}$ ratio) in the isoelectronic series $\text{Cd}^{1+} - \text{In}^{2+} - \text{Sn}^{3+} - \text{Sb}^{4+}$ and $\text{Hg}^{1+} - \text{Ti}^{2+} - \text{Pb}^{3+} - \text{Bi}^{4+}$ have been found to decrease with an increase in the formal oxidation number Z . An exception is provided by the $\text{Zn}^{1+} - \text{Ga}^{2+} - \text{Ge}^{3+}$ series, for which the reverse correlation has been established in lithium, sodium, and potassium phosphate glasses, i.e. the $E_{\lambda_{\text{max}}}$ and $A_i/A_i^{(0)}$ values increase with an increase in

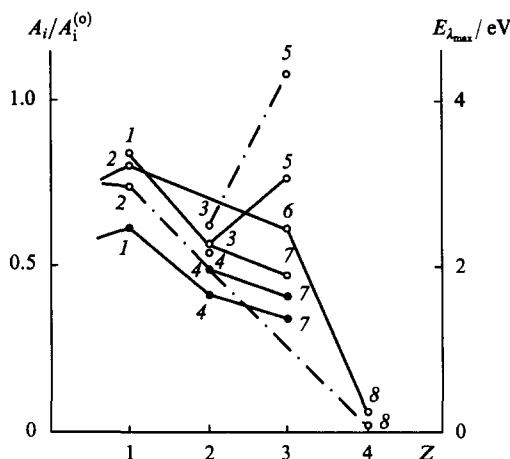


Figure 1. Dependence of the electron density in ns -AO (light circles) and of the energies of optical transitions at λ_{max} (dark circles) on Z for ions in UOS in barium aluminophosphate glasses (continuous line) and in lithium phosphate glasses (dot-and-dash line). (1) Hg^{1+} , (2) Cd^{1+} , (3) Ga^{2+} , (4) Ti^{2+} , (5) Ge^{3+} , (6) Sn^{3+} , (7) Pb^{3+} , (8) Sb^{4+} .

Z (Fig. 1). These results indicate both that the physicochemical properties of metals in UOS vary regularly as a function of their positions in the Periodic Table and that there is a possibility of controlling the course of the above dependences by changing the glass matrix, for example, by replacing one glass-forming oxide by another (SiO_2 by P_2O_5).^{32–36}

The spectral characteristics of metal ions in UOS also depend on the alkali metal cation incorporated in the glass. In other words, for glasses of the same class with equal percentages of oxides, the parameters of metal ions in UOS change when the alkali metal oxide present is replaced by another one. It is seen from Table 2 that the $A_i/A_i^{(0)}$ ratios and other parameters for the same ions in UOS incorporated in glasses, containing equal proportions of oxides but different cations (Li^+ , Na^+ , K^+), are distinct. However, there is no general well-defined rule for the variation of the properties of metals in UOS in the series of alkali metal cations (Li^+ , Na^+ , and K^+).

When the temperature of the irradiation changes from 77 to 300 K, the absorption bands corresponding to metal ions in UOS in all matrices undergo a hypsochromic shift, the magnitude of which depends on the alkali metal cation introduced into the glass. It has been found that the more stable the metal ion in UOS, the greater this shift. Thus, the framework of alkali metal cations participates in the stabilisation of UOS. It can be suggested that the alkali metal cations participate in the rearrangement of the ligand environment of the metal during stabilisation of its UOS. This conclusion has also been confirmed by EPR data. The magnitude of the shift of the high-field component of the EPR spectrum, occurring when the irradiation temperature changes from 77 to 300 K, depends on the nature of the alkali metal cation. The nature of the alkali metal cation also influences the magnitude of the g -factor and the width of lines in high and low fields (the corresponding g_e).

It has been noted^{32–38} that by choosing appropriately the composition of glasses, one can achieve stabilisation of metal ions in UOS at 300 K for a period of a month or even longer; in other words, stable compounds of metals in UOS can be obtained in glasses. By varying the elemental composition of a glass or by creating particular redox conditions during its synthesis, one can enhance or reduce the ability of the glass to stabilise or destabilise UOS of metals, colour centres (CC), and paramagnetic centres (PMC).

The kinetic curves for the thermal annealing of ions in UOS have a stepped shape for all types of glasses and are linearised in the coordinates n/n_0 against $\lg(t/t_0)$ at a fixed temperature [here n and n_0 are the concentrations of ions in UOS at current (t) and

initial (t_0) instants of time, respectively]. The kinetic curves for photoannealing can also be linearised in the coordinates n/n_0 against $\lg(t/t_0)$ and depend both on the intensity and on the spectral composition of the incident light.^{37, 38} The above characteristic features imply that there is a discrete set of activation energy values for these processes and that there exist sites for the stabilisation of metals in UOS, which are nonequivalent in their energy and structural parameters.

For glasses of the same composition synthesised under identical conditions but containing various metal oxides, the rates of the thermal annealing or photoannealing of PMC and CC (carried out at the same temperature or with light of the same spectral composition) are different. This refers both to the matrix PMC and CC (PO_4^{4-} , PO_3^{3-} , BO_4^{4-} , $>\text{SiO}^*$, $>\text{GeO}^*$, SiO_3^{3-}) and to metals in UOS in all the glasses considered above. If we assume that the rate (the efficiency) of the photodestruction of metals in UOS is proportional to the tangent of the slope ξ of the curve describing the kinetics of the destruction in the coordinates mentioned above, then the following rule is fulfilled: in the isoelectronic series of ions Cd^{1+} – Sn^{3+} – Sb^{4+} and Hg^{1+} – Tl^{2+} – Pb^{3+} – Bi^{4+} , the efficiency of the thermo- (ξ_t) and photo- (ξ_{ph}) destruction decreases as the oxidation number of ions increases (Figs 2 and 3). In the case of the Zn^{1+} – Ga^{2+} series of ions, the order of this correlation differs depending of the type of glass. For example, the efficiency of photodestruction of these ions in phosphate glasses varies in the reverse order.

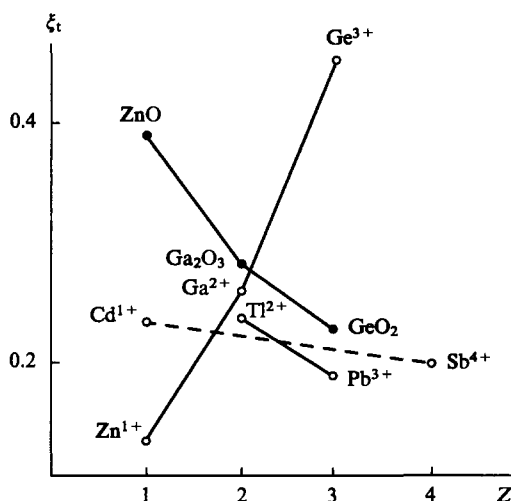


Figure 2. Dependence of ξ_t on Z in lithium borate glasses for ions in UOS (light circles) and for BO_4^{4-} ions (dark circles). All the glasses contain 10 mol % of the metal oxide, which gives rise to the ions in UOS.

The efficiency of the destruction of matrix PMC and CC in glasses with various oxides in the presence of various metals in UOS also depends linearly on Z . However, the course of these dependences can be opposite to the analogous dependence for the UOS. It is seen from Fig. 2 that in the Zn^{1+} – Ga^{2+} – Ge^{3+} series, the ξ_t value for the cations in UOS increases with an increase in Z , while this value for the matrix BO_4^{4-} centre decreases. Thus, the ξ_t and ξ_{ph} values for the matrix centres PO_4^{4-} , PO_3^{3-} , BO_4^{4-} , $>\text{SiO}^*$, and $>\text{GeO}^*$ are influenced by the nature of the modifying metal introduced into the glass. The strength of this influence depends both on the position of this metal in the periodic system of elements and on its state in the glass, namely, whether the metal exists as a modifying cation or is incorporated into the glass-forming network.

Certainly, the structural features of the glass matrix have an influence on the course of the A_i – Z and $E_{i_{\max}}$ – Z dependences and determine the photo and thermal stability of ion ensembles.

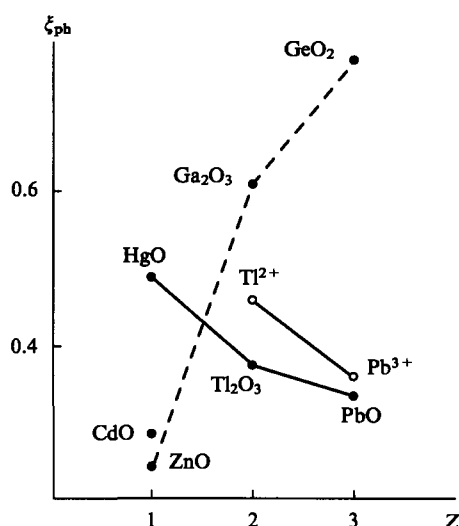


Figure 3. Dependence of ξ_{ph} on Z for ions in UOS (light circles) and for PO_4^{3-} ions (dark circles) in barium aluminophosphate glasses, containing 10 mol % of the metal oxide, which gives rise to the ions in UOS.

In fact, ions in UOS can be formed both in reactions with thermalised electrons (2) or in reactions with hole sites (3)



The Zn^{1+} , Cd^{1+} , Hg^{1+} , Ga^{2+} , In^{2+} , Tl^{2+} , Ge^{3+} , Sn^{3+} , Pb^{3+} , Sb^{4+} , and Bi^{4+} ions are formed via reaction (2), and only the Tl^{2+} , Sn^{3+} , Pb^{3+} , Sb^{4+} , and Bi^{4+} ions are formed via reaction (3). Both reactions can occur simultaneously in the same glass if it contains pairs of ions, for example, Sn^{2+} – Sn^{4+} , Tl^{1+} – Tl^{3+} , Pb^{2+} – Pb^{4+} , Sb^{3+} – Sb^{5+} , or Bi^{3+} – Bi^{5+} .

These suggestions have been confirmed in a study of the kinetic behaviour of ions in UOS at various stages of formation and destruction, carried out by pulse radiolysis with optical recording. Such studies were reported for the first time by Aleksandrov et al.^{45–47} The measurements were carried out using a setup with optical recording, designed based on a 'U-12F' accelerator and operating on the microsecond time scale ($t = 2.3 \mu\text{s}$, $E = 5 \text{ MeV}$, $I = 0.2 \text{ A}$).^{7, 8} The radiation colour centres (RCC) arising due to a pulse of accelerated electrons were annealed in the light beam of a DKSSH-150 xenon lamp focused to a diameter of 3 mm. The absorption spectra were recorded within intervals from 2 μs to several minutes. The amount of metal oxides added ranged from 1 to 10 mol %. Simultaneously, optical characteristics of glasses of the same composition exposed to γ -irradiation at 77 and 300 K were measured.

In the case of pulse irradiation of sodium borate glasses with various metal oxides added, rapidly diminishing absorption was detected, the λ_{\max} of which lay at 360 and 520 nm (without metal oxides), 350 nm (with ZnO added), 380 and 440 nm (CdO), 390 and 440 nm (Ga_2O_3), 430, 500, 550, 620, and 750 nm (Tl_2O_3), 360 and 430 nm (PbO), and 460 and 500 nm (Sb_2O_3). The λ_{\max} values of the absorption bands corresponding to ions in a $^2\text{S}_{1/2}$ electronic state observed immediately after a pulse of fast electrons differ only slightly from those obtained in the case of γ -radiolysis at 77 K (see Table 2 and the data given in the text). However, 140–200 μs after the pulse, the absorption maxima start to shift toward the position at which they are observed in the case where the irradiation is carried out at 300 K. Since the EPR parameters (g -factors, A_i , intensities of EPR lines) of ions in a $^2\text{S}_{1/2}$ electronic state at 77 K and at 300 K are different,^{33, 34} it is obvious that the changes in the optical spectra following the temperature rise or the photoannealing are due not only to the variation of the geometry of the nearest atom environment but also to the disappearance of some of the least photo- and thermostable ions in UOS. In fact, at

77 K the overall spectrum is recorded, whereas the spectrum obtained at 300 K corresponds only to those ions which are stable at this temperature.

The diminution of the absorption in glasses of the same composition corresponds to a linear dependence of D/D_0 on $\lg(t/t_0)$ (D and D_0 are optical densities at times t and t_0 , respectively, $t_0 = 1 \mu\text{s}$). The kinetics of the destruction of an individual ion in a glass of a particular composition depend on the intensity of the light acting on the sample. When ions in a $^2S_{1/2}$ electronic state are photoannealed with unfiltered light within a broad time interval (from microseconds to minutes), the slope of the straight lines depends on the nature of the metal ion. The tangent of the slope ξ_{ph} characterises the efficiency of the photoannealing of a particular ion in an UOS. The higher the intensity of light, the more efficient the photoannealing. This follows from the dependences obtained with the light beam attenuated by 55% with a reticulated filter. Experiments on the photoannealing also confirm the fact that only ions in a $^2S_{1/2}$ electronic state, rather than cluster groups incorporating these ions, are formed in the glasses under consideration containing zinc, cadmium, gallium, germanium, and antimony oxides, because under various conditions of light treatment, all the optical absorption bands assigned to these ions disappear in parallel.

In glasses containing lead oxide, two types of species with dissimilar kinetic parameters exist, which account for the AB with $\lambda_{max} = 360$ and 430 nm, whereas glasses with thallium oxide contain at least three types of species, which absorb light at 430, 500 and 550, and 620 and 750 nm, respectively. Evidently, all the CC in these glasses belong to ions and clusters of thallium and are destroyed in parallel by the influence of light.

The energies of optical transitions at the maxima of the AB ($E_{\lambda_{max}}$) for the ions in a $^2S_{1/2}$ electronic state (Ag^0 , Cd^{1+} , Ga^{2+} , Tl^{2+} , Ge^{3+} , Pb^{3+} , and Sb^{4+}), obtained on exposure to pulse radiation, depend on both the oxidation number Z of the metal and its position in the Periodic Table. In the isoelectronic series $\text{Zn}^{1+} - \text{Ga}^{2+}$, $\text{Cd}^{1+} - \text{Sb}^{4+}$, and $\text{Tl}^{2+} - \text{Pb}^{3+}$, the $E_{\lambda_{max}}$ values decrease as Z increases. A similar correlation has also been observed for the efficiency of the photoannealing of the above ions with unfiltered light. This is in agreement with the dependences found previously for the optical parameters and for the density of the unpaired electron in the outer ns -AO for ions in UOS in isoelectronic series.^{33, 34}

The method of pulse radiolysis has also been used to study the fast processes occurring in sodium silicate glasses (SSG), containing 10 mol % of Zn, Cd, In, Ga, Ge, Sn, Pb, and Sb oxides, exposed to ionising radiation.⁴⁷ It was found that in these glasses, apart from the known AB (with maxima at 460, 580, and 620 nm) typical of glasses containing no metal oxides,⁴⁸ additional AB corresponding to the long-lived products of radiolysis arise after irradiation. Simultaneously, the absorption bands associated with the sodium silicate matrix disappear. For example, for glasses with zinc, cadmium, gallium, germanium, tin, indium, and antimony oxides irradiated with a pulse of accelerated electrons at 300 K, the following absorption bands were observed:

Oxides	Zn	Cd	Ga	Ge	In	Sn	Sb
λ_{max}/nm	370	390	375	430	360	470	480
	—	460	435	—	490	—	—

The intensity of these bands depends on the concentration of the metal oxide added. The positions of the AB maxima corresponding to the products of the pulse radiolysis are in good agreement with the λ_{max} values of the AB obtained by γ -radiolysis at 77 K of the SSG containing the same compounds.³⁶ The absorption spectra of glasses containing cadmium, gallium, indium, and lead oxides recorded immediately after a pulse of accelerated

electrons are broad AB accompanied by satellite lines of low intensity. Since no other AB arise upon irradiation of glasses with the above metal oxides, and the intensities of the main and the satellite lines vary in parallel, these AB can be attributed to the Zn^{1+} , Cd^{1+} , Ga^{2+} , In^{2+} , Pb^{3+} , Sn^{3+} , and Sb^{4+} ions in the $^2S_{1/2}$ electronic state. The presence of the satellite line indicates that the energy levels responsible for the optical transition are split due to the asymmetrical environment of the ions in UOS.

The kinetic curves for the photodestruction of the Zn^{1+} , Cd^{1+} , and Pb^{3+} ions are similar in appearance: they have no inflection points. The kinetic curves for the SSG with gallium, germanium, tin, and antimony oxides contain two sections, namely, a section where the absorption falls quickly (up to 100 μs) and a section where it diminishes slowly (up to several minutes). This implies that there are two pathways to the disappearance of the Ga^{2+} , Ge^{3+} , Sn^{3+} , and Sb^{4+} ions. In the case of indium, the kinetic curve for the diminution of the absorption in the coordinates mentioned above has a flat section (up to 0.1 s), which is followed by a steeper section. Thus, in terms of destruction kinetics, metal ions can be divided into three main groups: the first group includes Cd^{1+} , Zn^{1+} , and Pb^{3+} ions, the second group consists of Ga^{2+} , Ge^{3+} , Sn^{3+} , and Sb^{4+} ions, and In^{2+} belongs to the third group. Evidently, the difference between the kinetic behaviour of the ions is due to the specific structural features of the glass matrix that arise during the synthesis of glasses containing the corresponding metal oxides.

In fact, cadmium, zinc, and lead oxides are capable of being incorporated into the glass network formed by the main oxide, which constitutes the glass structure. Gallium, germanium, tin, and antimony oxides exhibit dual properties: they can act both as modifying compounds and as glass-forming compounds. A part of the ensemble corresponding to the modifying ions is responsible for the fast-diminution section on the kinetic curves. Indium oxides act as modifying ions existing both as free ions and as ions linked to bridging and nonbridging oxygen atoms. Under certain conditions the modifiers of the former type are fairly free to move in the matrix and react with the electrons knocked out of the glass matrix, similarly to ions in solution. This accounts for the fact that the kinetic curve for the photodestruction of In^{2+} ions consists of two components, one of which (for the free modifying ions) obeys formally second-order kinetics, i.e. it is linearised in the $1/D - t$ coordinates, and is most clear-cut for periods of time of the order of seconds. The other component follows the normal disappearance kinetics typical of solids, which has been observed for other ions (the initial more gently sloping section of the curve). Thus it is obvious that in the initial stage, the In^{2+} ions connected to the glass network through oxygen atoms predominantly disappear, and then the free modifying In^{2+} ions are destroyed. These ions vanish completely, i.e. the glass is completely 'photobleached' over a period of several seconds. This has also been observed for Zn^{1+} and Tl^{2+} ions in sodium borate glasses.⁴⁶

The pulse radiolysis studies also permitted the following characteristic features to be elucidated. The course of the dependences of $E_{\lambda_{max}}$ and ξ_{ph} on Z coincides with the course of the kinetic curves for the destruction of the Zn^{1+} , Cd^{1+} , Ga^{2+} , In^{2+} , Ge^{3+} , Sn^{3+} , Pb^{3+} , and Sb^{4+} ions, plotted as $D/D_0 - \lg(t/t_0)$ coordinates and obtained for the 'steady-state' variant in the analysis of the gently sloping sections. In contrast, the initial (steep) sections of the curves for the destruction of the Ga^{2+} , Ge^{3+} , Sn^{3+} , and Sb^{4+} ions show an inverted profile (Fig. 4). This fact is of fundamental importance, since it thus becomes obvious that there are several structurally different sites for the stabilisation of the same ion in an unusual oxidation state. However, despite the above distinctions, the general rule of the regular variation of physicochemical properties of ions in UOS as functions of the positions of these elements in the Periodic Table is retained.

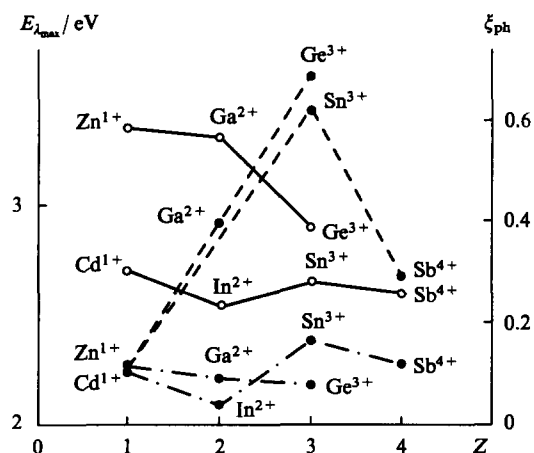


Figure 4. Dependence of $E_{\lambda_{\max}}$ (continuous line) and of ζ_{ph} on the steep (dashed line) and gently sloping (dot-and-dash line) sections of the kinetic curves for the destruction of metal ions in UOS on the oxidation number Z in sodium silicate glasses.

3. Formation of unusual oxidation states of transition metals Ti, Ni, Mo, W, and Nb

When glasses containing transition metal oxides are exposed to radiation, ions in UOS are also formed. For example, Ni^{1+} ions have been detected in BAPG with nickel oxide. The EPR parameters of these ions depend substantially on the composition of the glass. When 10 mol % of nickel oxide is added, an EPR signal with triaxial anisotropy is observed, $g_1 = 2.355$, $g_2 = 2.229$, and $g_3 = 2.074$, and when the oxide concentration is increased to 30 mol %, a broad singlet with $g_{\text{aver}} = 2.327$ arises.

In alkali glasses and in BAPG, Ti^{3+} , Nb^{4+} , Mo^{5+} , and W^{5+} ions exhibiting characteristic EPR spectra have been detected following γ -irradiation at 77 K. For example, the Ti^{3+} ion in SPG is characterised by a line with biaxial anisotropy with $g_{\perp} = 1.876$ and $g_{\parallel} = 1.991$. In alkali phosphate glasses with high concentrations of tungsten oxide (more than 35 mol %), an EPR signal with $g_{\text{aver}} = 2.018$ and a line width ΔH of 2.25 mT arises. This signal differs from the known signals typical of W^{5+} ($g_{\perp} = 1.81$ and $g_{\parallel} = 1.66$).

In the case of LPG, SPG, and PPG (lithium, sodium, and potassium phosphate glasses) containing niobium oxide (Nb_2O_5 concentration not exceeding 20 mol %), the formation of niobium ions in UOS has been observed after γ -irradiation at 77 and 300 K. In fact, in addition to the doublet signals corresponding to the $PO_4^{\cdot-}$ radical anion, the EPR spectrum exhibited ten main lines extending by 252 mT, the distance between them being 28 mT. Since only Nb possesses a nuclear spin of $\frac{9}{2}$, this spectrum consisting of ten lines is unambiguously associated with the Nb^{4+} ion, for which $g_{\perp} = 1.91$, $g_{\parallel} = 1.88$, $A_{\perp} = 28.0$, $A_{\parallel} = 13.0$ mT, and $A_{\parallel}/A_{\perp}^{(0)} = 0.12$. Apart from the signal due to Nb^{4+} , a 19.0 mT-wide singlet with $g_{\text{aver}} = 2.017$ arises in these glasses, when the concentration of Nb_2O_5 exceeds 20 mol %. As this signal appears, the signal due to Nb^{4+} disappears. The new signal has been attributed to a hole site.³²

In view of the fact that the spectra of glasses with large amounts of WO_3 , MoO_3 , and Nb_2O_5 contain broad singlets, one may assume that an increase in the concentration of the oxides and, consequently, in the intensity of the EPR signals associated with the corresponding ions leads to the appearance of isotropic exchange interaction. Blurring of the HFS resulting in the appearance of broad lines (100.0 and 140.0 mT, respectively) has also been observed in glasses containing manganese oxides with an increase in the oxide concentration. In the EPR spectra of glasses with iron oxide a set of lines is recorded, the intensities of which depend on the redox conditions of the synthesis.

Short-lived radiation-induced defects have been studied by pulse radiolysis in the $M_2O-P_2O_5-Nb_2O_5$ glass systems ($M = Na, K, Li$) that exhibited no initial ('glass melting') absorption bands.³⁹ At low concentrations of Nb_2O_5 , an AB with $\lambda_{\max} = 500$ nm, typical of $PO_4^{\cdot-}$, was observed. With an increase in the concentration of Nb_2O_5 the intensity of the absorption band corresponding to the $PO_4^{\cdot-}$ ion decreased, and an AB with $\lambda_{\max} = 650$ nm appeared instead, its intensity increasing with increase in the concentration of Nb_2O_5 . The lifetime of this AB, which was assigned to Nb^{4+} , is tens of microseconds at 300 K.

The $Na_2O-SiO_2-CeO_2$ (Eu_2O_3) glasses have been studied.⁴⁰ The spectra of these glasses exhibit at least two broad AB in the region of 500–700 nm. The kinetic parameters of the species responsible for these AB are influenced by the Na_2O/SiO_2 ratio and by the amount of the oxides CeO_2 and Eu_2O_3 added.

* * *

Thus, the studies of alkali glasses of four main classes described above permit the following conclusions to be made:

- the properties of ions in UOS vary regularly with the position of the element in the Periodic Table;
- the order of these dependences can be controlled by varying the ligand environment;
- formation of metal clusters in glasses is possible and is initiated by metal ions in UOS;
- the UOS of metals influence regularly the photo- and thermal stability of the matrix CC and PMC in glasses, the kinetic curves for the photoannealing and thermoannealing being linearised in the $n/n_0 - \lg(t/t_0)$ coordinates;
- the possibility of the long-term stabilisation of UOS of metals in alkali glasses was established, and the influence on it of the cationic framework was found.

All the above properties depend on the elemental composition of glasses and on the redox conditions of their synthesis. Evidently, it is these factors that are favourable for the stabilisation of the UOS and for the appearance of certain integral properties against the background of the topological disordering of the spatial structure of glass. Thus, the following causal relationship arises: composition–synthesis–structure–stabilisation or destabilisation of the UOS of a metal. From this it follows that by choosing the composition of a glass and the method for its synthesis under appropriate redox conditions one may impart desired properties to the glass by means of ions in UOS or by means of other species that arise with their participation.

4. Oxide glasses containing no alkali metals

We have considered above the processes of stabilisation of ions in UOS in glasses of four main classes (borate, silicate, germanate, and phosphate glasses) containing alkali metal cations. The role of alkali metal cations in the stabilisation of transition metal ions in UOS has been repeatedly emphasised. However, the role of the ligand environment, i.e. of the oxygen-containing network formed in the glass during its synthesis, has not been considered separately. The structure of the glass network is known to depend on the redox conditions under which it has been formed. These conditions account for a wide range of various matrix defects in a glass and ensure the formation of various types of coordination of ions in the glass network. These effects are most clear-cut in borate glasses in which boron can exist both in tricoordinated and tetracoordinated states.²³

Studies carried out with $CdO-B_2O_3$, $CdO-SiO_2$, and $CdO-B_2O_3-SiO_2$ glasses^{42, 49, 50} have shown that, if the synthesis is carried out under reducing conditions, the proportion of tricoordinated boron increases. This was found by comparison of the intensities of IR absorption bands at $1500-1150\text{ cm}^{-1}$ and at $1100-800\text{ cm}^{-1}$ corresponding to $BO_3^{\cdot-}$ and $BO_4^{\cdot-}$, respectively.

In addition, glasses obtained under these conditions exhibit a photochromic effect, which becomes more pronounced as the proportion of tricoordinated boron atoms increases.^{49, 50}

It has been shown by EPR⁴² that following the photo- and γ -irradiation of cadmium-containing glasses, Cd^{1+} ions are formed, and it is these ions that account for the colour of the glasses. The maximum optical absorption of the Cd^{1+} ion is observed at 400–420 nm for both types of treatment, but the concentration of the Cd^{1+} ions arising upon γ -irradiation is higher than that arising upon UV irradiation by 1–2 orders of magnitude.⁴² It is therefore obvious that any ion in an UOS can also be stabilised in the absence of alkali metal cations. Fig. 5 shows the plots for the accumulation of the hole ($\text{BO}_4^{\cdot-}$) and electron (Cd^{1+}) sites in glasses exposed to equal doses of γ -radiation but synthesised under different conditions, namely, under normal and reducing conditions. The accumulation of hole sites in these glasses occurs similarly, whereas the accumulation of the electron sites depends essentially on the conditions of the synthesis. The amount of Cd^{1+} formed in the glasses synthesised under reducing conditions is several times greater than that formed in glasses synthesised under normal conditions. Apparently, the synthesis of glasses under oxygen-deficient conditions leads to greater instability of the system, to the rupture of chemical bonds, and to the displacement of the Cd^{1+} ions to the cationic part of the glass network.

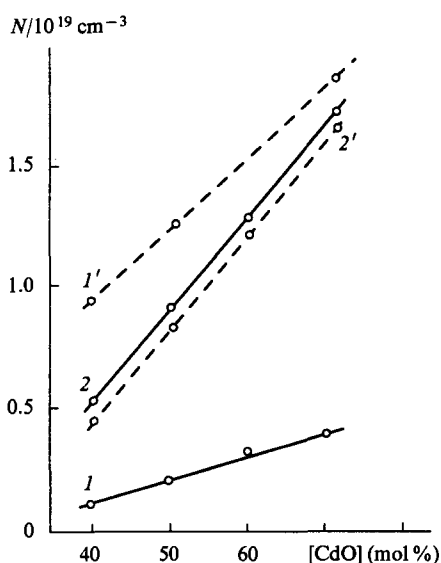


Figure 5. Accumulation of paramagnetic centres in cadmium borate glasses synthesised under normal (1, 2) and reducing (1', 2') conditions: (1, 1') Cd^{1+} ; (2, 2') $\text{BO}_4^{\cdot-}$.

Bismuth-containing glasses are also fairly sensitive to the conditions of the synthesis and are readily reduced as far as the liberation of metallic bismuth. By introducing transition metal oxides into these glasses, one may influence the occurrence of redox processes even during glass melting. This effect of added compounds is due to their influence on the glass structure. Data on the structure of bismuth borate glasses as well as on the influence of transition metal oxides on their structure are scarce, whereas data on the stabilisation of ions in UOS in these glasses are totally lacking. This problem has been investigated in relation to glasses melted on the basis of the $\text{ZnO}-\text{Bi}_2\text{O}_3-\text{B}_2\text{O}_3$ system and to the same glasses containing added tungsten oxide.⁵¹

An IR-spectroscopic study of bismuth-containing glasses showed that the initial glass exhibits AB in the region of 1300–1400 cm^{-1} and a band at 1250 cm^{-1} corresponding to the stretching vibrations in the $\text{B}^{3+}-\text{O}-\text{B}^{3+}$ and $\text{B}^{3+}-\text{O}-\text{B}^{4+}$ groups, respectively, and a weak band in the range

900–1000 cm^{-1} associated with the vibrations in the $\text{B}^{4+}-\text{O}-\text{B}^{4+}$ group. The EPR spectrum of the initial glass, containing no additives, recorded after γ -irradiation is a broad singlet with a g -factor of 2.022 ($\Delta H = 3.3$ mT) due to Bi^{4+} ions, which can result both from localisation of electrons by Bi^{5+} ions and from capture of holes by Bi^{3+} ions. The strong broadening of the signal and the absence of a hyperfine structure in Bi (the nuclear spin J of Bi is $\frac{9}{2}$) suggest that bismuth exists in the glass as clusters, because under oxygen deficiency, a Bi–Bi bond is formed.

The introduction of tungsten oxide into bismuth-containing glasses leads to the appearance of an AB at 870 cm^{-1} in its IR spectrum, corresponding to the stretching vibrations of tungsten in the WO_6 octahedra. The intensity of this band increases with an increase in the content of tungsten oxide in the glass. The EPR spectra of these glasses contain an additional anisotropic line with $g_{\text{aver}} = 1.607$ ($\Delta H = 46$ mT) corresponding to the W^{5+} ions and caused by the localisation of electrons at W^{6+} ions. The intensity of the signal due to Bi^{4+} simultaneously decreases. The relationship between the intensities of lines of Bi^{4+} and W^{5+} suggests that the tungsten ions are incorporated into the bismuth network of the glass. When bismuth and tungsten ions are located close to each other, the localisation of the free electrons during γ -irradiation occurs mainly at the W^{6+} ions, which possess stronger acceptor properties.⁷ This conclusion has been supported by the results of X-ray phase analysis of thermally treated glasses: bismuth tungstates were detected as one of the phases in the products of crystallisation.⁵¹ Thus, in bismuth-containing glasses modified by tungsten oxides, bismuth tungstate complexes are formed; they bind the bismuth ions strongly and prevent them from liberation as metallic macroparticles during the glass melting. This change in the glass structure favours the occurrence of single-electron processes accompanied by the formation of W^{5+} and Bi^{4+} ions under the influence of ionising radiation.

* * *

Thus, ions in UOS can also arise under the action of radiation in glasses containing no alkali metal cations. The fact that these ions are stabilised in the matrices of the glasses considered above implies that the set of various oxidation states of ions forming the glass network (for borate glasses, these are B^{3+} and B^{4+} ions) permit the processes of stabilisation to be accomplished also in the absence of alkali metal cations.

5. Sulfate-containing glasses

The studies described above have shown unambiguously that the stabilisation of UOS of metal ions is related to the structure of a glass. Since the stabilisation of UOS of metals is caused in some cases by mobile cations, the stabilisation of these cations, in its turn, can be due to the formation of ions in UOS. The latter, being present in the glass as modifying ions or being incorporated into the glass-forming network, can stabilise the cationic framework to different extents, since the Na^+ , K^+ , Li^+ , and Cs^+ cations are incorporated into the 'ligand' environment of ions in UOS in different ways.

These considerations are related directly to the problem of neutralisation of radioactive wastes with medium activity level.⁵² In fact, a glass matrix consisting of a continuous irregular network of coordination polyhedra of glass-forming units accumulates various radionuclides, which can either enter into the composition of the crystalline framework (Na_2O , Cs_2O , SrO , etc.) or be accumulated in the cavities of the structural network as discrete species (RuO_2 , UO_2 , PuO_2 , etc.); a glass matrix can also accumulate inactive salts often containing sulfur. Therefore, the solution of the problem of stabilisation of radionuclide ions and sulfur-containing ions accompanying them can be linked to the stabilisation of ion metals in UOS, for example, Pb^{3+} and VO^{2+} , in sulfate-containing glasses of three main classes, namely, borate, phosphate, and silicate glasses.

Any information on the structure and the nature of radiation-induced defects, on the mechanism of damage arising under the action of radionuclide radiation, and on the radiation resistance of glasses during prolonged storage is of scientific and practical interest. For example, the possibility of stabilising ions of different natures in glasses of various compositions in the $\text{Na}_2\text{O}(\text{PbO}, \text{V}_2\text{O}_5) - \text{EO}_x(\text{SiO}_2, \text{B}_2\text{O}_3, \text{P}_2\text{O}_5) - \text{SO}_3$ systems has been studied by EPR.⁵³⁻⁶⁰ It was found^{53, 56-59} that the regions of glass formation in the $\text{Na}_2\text{O}(\text{PbO}) - \text{EO}_x(\text{SiO}_2, \text{B}_2\text{O}_3, \text{P}_2\text{O}_5) - \text{SO}_3$ systems are broadened on passing from silicate glasses to borate and phosphate glasses and also on passing from sodium to lead glasses (Fig. 6 *a, b*). The largest region of glass formation was observed in the $\text{PbO} - \text{P}_2\text{O}_5 - \text{SO}_3$ system (the maximum content of SO_3 being 33 mol %).

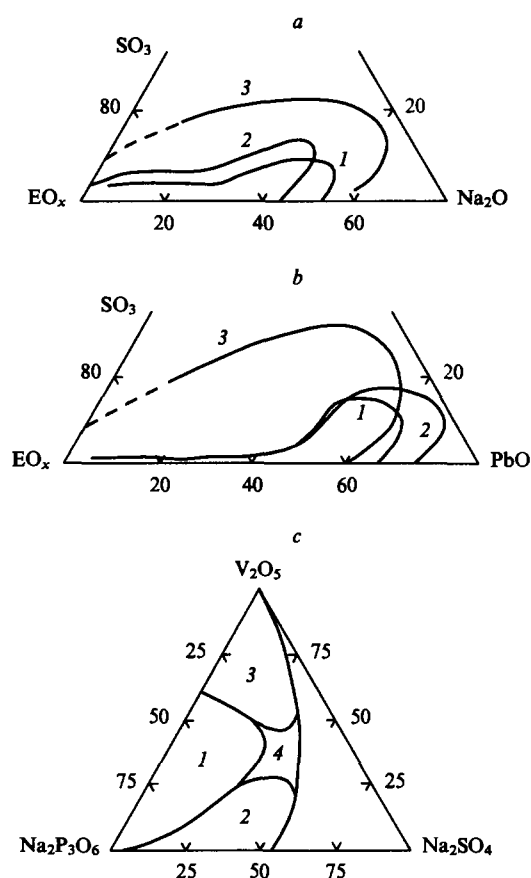


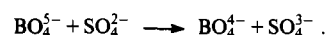
Figure 6. Regions of glass formation in the $\text{Na}_2\text{O} - \text{EO}_x - \text{SO}_3$ (*a*), $\text{PbO} - \text{EO}_x - \text{SO}_3$ (*b*), and $\text{Na}_2\text{P}_2\text{O}_7 - \text{V}_2\text{O}_5 - \text{Na}_2\text{SO}_4$ (*c*) systems. $\text{EO}_x = \text{SiO}_2$ (1), B_2O_3 (2), and P_2O_5 (3).

In order to study the structure in each system, two series of glasses were chosen, with the following concentrations of the initial components: $[\text{SO}_3]/([\text{SO}_3] + [\text{EO}_x]) = \text{const.}$ in the first series and $[\text{M}_y\text{O}]/([\text{SO}_3] + [\text{EO}_x]) = \text{const.}$ in the second series, where EO_x and M_yO are glass-forming oxides and modifying oxides, respectively.

Glasses based on the $\text{Na}_2\text{O} - \text{SiO}_2 - \text{SO}_3$ system, in which the region of glass formation is the smallest among the glasses studied and the content of SO_3 does not exceed 7 mol %, give no EPR signals due to sulfur-and-oxygen-containing PMC; only signals corresponding to the silicon-and-oxygen PMC are observed.⁵⁸ The EPR spectra of sulfate-containing borate and sulfate-containing phosphate glasses, in addition to the signals corresponding to boron-and-oxygen and phosphorus-and-oxygen PMC, exhibit signals due to the sulfate constituent of the anionic character of the glass.^{54, 55, 58}

The EPR spectra of binary alkali borate and sulfate-containing alkali borate glasses,⁵⁵ the compositions of which fall in the centre of the glass-formation region, exhibit signals characteristic of irradiated alkali borate glasses: BO_3^{2-} ($g_1 = 2.002$; $g_2 = 2.011$; $g_3 = 2.034$) and BO_4^{3-} ($g_{\text{aver}} = 2.012$ for glasses containing more than 20 mol % of Na_2O). In the spectra of sulfate-containing borate glasses (the compositions of which are at the boundary of the glass-formation region), in addition to the signals mentioned above, a signal due to the (SO_4^-) PMC has also been detected (a similar signal has been observed in irradiated solutions of H_2SO_4).³ The formation of the (SO_4^-) PMC in this composition region can be associated with the processes of chemical differentiation leading to the formation of microregions enriched in sodium sulfate. This inference has been confirmed in a study of thermally treated glasses by electron microscopy.⁵⁵

In the magnetic field region corresponding to $g < g_e$, for sulfate-containing borate glasses⁵⁷ with compositions lying at the centre of the glass-formation region, an electron site signal has been detected, the thermal behaviour of which differs from that of (BO_4^{3-}) or (SO_4^{2-}) PMC. This PMC was assigned to a sulfur-containing ion in UOS, namely, to the S^{5+} ion. This may arise when an electron is trapped by an SO_4 tetrahedron incorporated into the glass-forming chains (trapping of an electron is not typical of isolated SO_4^{2-} ions). Apparently, in this case, redistribution of the electron density occurs among mixed boron-sulfur-and-oxygen chains between the boron- and sulfur-and-oxygen fragments in the following way:



This process accounts for the increase in the concentration of the S^{5+} ion. This assumption is supported by the fact that the (SO_4^{3-}) PMC is not found in the irradiated glasses, the compositions of which lie near the boundary of the glass-formation region, because chemical differentiation in these glasses leads to the destruction of the chains containing SO_4 polyhedra.

The EPR spectra of sulfate-containing borate glasses with compositions corresponding to the metaphosphate region, together with the known signals due to the (PO_4^{3-}) and (PO_3^{2-}) PMC, also exhibit a signal associated with SO_4^- .⁵⁵ As the proportion of the sulfur-and-oxygen-containing constituent in the anionic character of the glass increases, the concentration of phosphorus-and-oxygen PMC decreases, while that of SO_4^- increases. The irradiation of glasses with compositions lying in the ultraphosphate region⁵⁴ also results in the formation of PMC associated with branched units and ring structures like $\text{P}_4\text{O}_{12}^{3-}$. Simultaneously, the (SO_3^-) PMC with $g = 2.004$ are formed upon rupture of phosphorus-sulfur-oxygen chains under the action of γ -radiation ($-\text{O}-\text{PO}_2-\text{O}-\text{SO}_2-\text{O} \longrightarrow -\text{O}-\text{PO}_2-\text{O} + -\text{SO}_2-\text{O}$). On passing from the ultraphosphate region to the metaphosphate region of composition, the concentrations of SO_3^- and $\text{P}_4\text{O}_{12}^{3-}$ decrease, whereas those of SO_4^- and PO_4^{3-} increase. This is associated with the depolymerisation of the sulfate-phosphate network. Evidently, ultraphosphate glasses incorporate a common phosphorus-sulfur-oxygen network, while metaphosphate glasses contain phosphorus-oxygen chains and isolated sulfate ions. This interpretation of the EPR spectra is not inconsistent with the van Wazer rearrangement theory.⁶¹

The EPR spectra of irradiated sulfate-containing lead silicate, borate, and phosphate glasses with a PbO concentration of more than 30 mol % exhibit only one well-known singlet due to Pb^{3+} in the g_e region and at high fields.^{53, 56, 58, 59} Glasses containing ≤ 30 mol % of PbO can be synthesised only in the sulfate-phosphate system. The EPR spectra of glasses containing not less than 20 mol % of SO_3 or Na_2SO_4 are complex in appearance, being a superposition of the singlets corresponding to Pb^{3+} and SO_4^- .

For glasses based on the $\text{PbO} - \text{SiO}_2(\text{B}_2\text{O}_3) - \text{SO}_3(\text{Na}_2\text{SO}_4)$ systems, no signals corresponding to sulfur-oxygen PMC have been recorded. However, with an increase in the content of sulfate

ions, the shape of the Pb^{3+} line changes; in particular, anisotropy of the g -factor increases ($g_{\perp} = 2.004$, $g_{\parallel} = 1.955$), which is associated with a change in the glass structure. This is also indicated by the presence of maxima in the curves of the dependence of the concentration (the width of the EPR line) of the Pb^{3+} ion on the composition of the glass (Fig. 7). However, the fact that only the signal for SO_4^- ions is recorded in the EPR spectra indicates that sulfate ions, responsible for their formation in the networks of lead glasses, are mainly isolated.

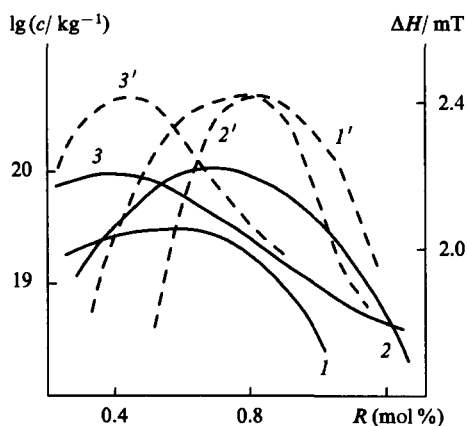


Figure 7. Dependences of the concentration of Pb^{3+} (curves 1–3) and of the line width $\Delta H(\text{Pb}^{3+})$ (curves 1'–3') on the composition of the glass $\text{PbO}-\text{P}_2\text{O}_5-\text{SO}_3$ $\{R = [\text{PbO}]/([\text{P}_2\text{O}_5] + [\text{SO}_3])$, mol % $\}$. Content of SO_3 , mol %: 0 (1), 10 (2), 20 (3).

The influence of sulfate ions on the radiation resistance of vanadate glasses has been studied in relation to the pseudoternary $\text{Na}_2\text{P}_2\text{O}_6-\text{V}_2\text{O}_5-\text{Na}_2\text{SO}_4$ system.⁶⁰ Fig. 6,c shows the region of glass formation in this system. It was found⁶⁰ that this region can be divided into four areas, according to the character and behaviour of the PMC formed in them. In the first area the HFS, due to VO^{2+} with $g_{\perp} = 1.994$, $g_{\parallel} = 1.932$; $A_{\perp} = 9.0$ and $A_{\parallel} = 21.2$ mT, is observed at 77 and 300 K. In the second area, the HFS due to VO^{2+} is also observed at 77 K; however, at 300 K in nonirradiated glasses and at 77 and 300 K in the case of γ -irradiated glasses, a symmetrical singlet with $g_{\text{aver}} = 1.957$ and $\Delta H = 2.5$ mT is recorded. The EPR spectra recorded for the third area at 77 K are characterised by poorly resolved HFS, while at 300 K, they exhibit a broad line with $\Delta H = 28$ mT and $g_{\text{aver}} = 1.970$, which narrows as the content of V_2O_5 increases from 50%–60% to 90%–100% and turns into a narrow asymmetrical line with $g_{\text{eff}} = 1.975$. For γ -irradiated glasses corresponding to this area, only an asymmetrical singlet is recorded at 77 and 300 K. In the fourth area, well resolved HFS corresponding to VO^{2+} is observed at 77 K, while at 300 K a low-intensity symmetrical singlet line with $g_{\text{aver}} = 1.960$ and $\Delta H = 2.0$ mT is recorded. The spectra of glasses γ -irradiated at 77 and 295 K contain no singlet with $g_{\text{aver}} = 1.960$; an anisotropic singlet with $g_{\text{eff}} = 1.975$ appears instead. All these changes were attributed to variations in the glass structure. The structure of the glass in the first area is based on the phosphorus–oxygen network, which may incorporate vanadium–oxygen tetrahedra, and the cavities in the network are occupied by Na^+ , SO_4^- , and VO^{2+} ions. The network consisting of vanadium–oxygen chains with tetrahedrally coordinated vanadium predominates in the third area. In the second area, the glass contains a fairly large amount of VO^{2+} ions present in an octahedral coordination with tetragonal constriction as well as VO^{2+} ions arranged in the cavities of the structural network as modifying ions. In the fourth area glasses have an intermediate structure: they consist of phosphorus–oxygen, vanadium–oxygen, and mixed chains as well as of sulfate ions.

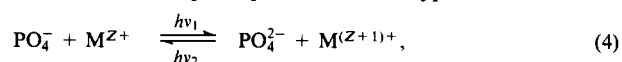
The studies considered in this Section reflect most clearly the principle of construction of a glassy matrix based on the composition–structure dependence and the possibility of investigating the glass structure by EPR. When various glasses are compared, one can note that the course of the composition–property dependence for sulfate-containing phosphate glasses varies more smoothly than that for silicate or borate glasses. This difference may be attributed to the higher homogeneity of sulfate-containing phosphate glasses. Sulfate ions increase the radiation resistance of glasses. Some chemically inert and radiation-resistant lead-containing glasses may incorporate up to 25 mol % of sulfate-containing wastes.

III. Electron dynamics in oxide glasses

1. Reactions of reversible electron transfer occurring under the action of light

We have described above the processes of destruction of ions in UOS on exposure to light. It was noted that photoannealing with boundary filters leads to partial destruction of both CC and PMC. As the region of transmission of the boundary filter used moves to the UV region, energetically more stable CC and PMC (i.e. centres for which the activation energies for the photodestruction are higher) are annealed, the photoannealing curves being linearised in the $n/n_0 - \lg(t/t_0)$ coordinates. By now it has been established that if CC with nonoverlapping AB arise in a γ -irradiated glass, reversible phototransfer of an electron between the species responsible for these AB is possible. From this standpoint, lithium, sodium, potassium, and barium aluminophosphate glasses proved most promising, since γ -irradiation of these glasses leads to the appearance of $\text{PO}_4^{2-}-\text{M}^{Z+}$ pairs of species ($Z+$ is an unusual oxidation number), which are responsible for nonoverlapping AB. In fact, an AB with $\lambda_{\text{max}} = 500$ nm corresponds to the PO_4^{2-} ion, while, for example, Ti^{2+} and Nb^{4+} ions account for AB with $\lambda_{\text{max}} = 420$ and 650 nm, respectively.

It has been shown that these ions arising on irradiation can be involved in reversible photoprocesses of the type



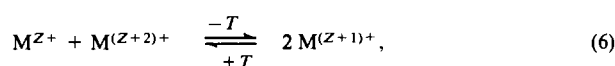
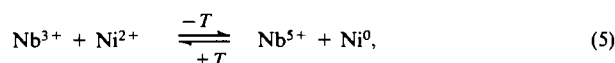
and the unpaired electron can thus be transferred from the ion in UOS to the PO_4^- ion by phototreatment (in the region of the AB corresponding to the ion in UOS). The reverse process is carried out by treating the PO_4^{2-} ion with light (in the region of the AB with $\lambda_{\text{max}} = 500$ nm). In this case, the kinetic curves are also linearised in the $n/n_0 - \lg(t/t_0)$ coordinates. The concentration of the PO_4^{2-} ions being destroyed decreases in parallel with an increase in the concentration of the ions in UOS being formed (for example, Ti^{2+} and Nb^{4+} ions); this can be written as $|\Delta[\text{PO}_4^{2-}]| = |\Delta[\text{Ti}^{2+}]| \{|\Delta[\text{Nb}^{4+}]]|\}$. The paramagnetic species PO_4^{2-} , Ti^{2+} , and Nb^{4+} are especially convenient, because the reversible processes involving these species can be monitored both by optical spectroscopy and by EPR.

The number of cycles in such reversible processes is influenced by the structure of the glass as well as by the degree of overlap of an edge of the AB corresponding to the ion in UOS with an edge of the AB due to the phosphorus-containing radical ion resulting from the light treatment. The formation in the glass of cluster species of the M_m^{n+} type (where m and n are 1, 2, 3, ...), together with the ions in UOS, prevents the realisation of a large number of cycles; the clusters also participate in the electron dynamics thus creating additional reaction pathways and blurring the pattern of 'ideal' photoreversible transitions between the radiation-induced CC and PMC. In the case of phosphate glasses with added Nb_2O_5 the pattern of reversible photoreactions is also blurred because niobium oxide forms its own niobium–oxygen network, along which the electron, knocked out from PO_4^{2-} by the phototreatment, can migrate. Apparently, this electron no longer participates in the reverse reactions. This may be why the number of cycles for the $\text{PO}_4^{2-}-\text{Nb}^{4+}$ pair is much smaller than for the $\text{PO}_4^{2-}-\text{Ti}^{2+}$ pair.

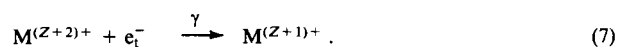
2. Temperature-dependent reactions of reversible electron transfer

An attempt has been made⁶² to obtain metal ions in UOS without the action of ionising radiation. For this purpose, lithium tungstate-, lithium niobate-, and lithium molybdate-phosphate glasses (LTPG, LNPG, and LMPG) with added tin, titanium, vanadium, molybdenum, tungsten, and nickel oxides have been synthesised under reducing conditions. The completed glasses were intensely coloured (the 'glass melting' colour). The following PMC were found in these glasses by EPR:⁶² Nb^{4+} , Mo^{5+} , W^{5+} , Ti^{3+} , VO^{2+} , and Ni^0 . The integral intensity of the EPR signals corresponding to the above PMC in these glasses increased by several orders of magnitude as the temperature decreased from 300 to 6 K. It was also found that as the temperature decreased, the EPR parameters of the PMC already present altered, which points to structural changes in the glass network, at least in the local environment of the ions in UOS. As the temperature decreased, the edge of the fundamental absorption for all the above glasses shifted to the UV region of the optical spectrum by 5–10 nm. For the matrix LNPG, the intensity of the AB with $\lambda_{\text{max}} = 800$ nm decreased, whereas the intensity of the AB with $\lambda_{\text{max}} = 600$ nm increased with a decrease in the temperature, i.e. a low-temperature thermochromic effect was observed. All the processes and parameters are temperature-reversible, i.e. the parameters return with time to the values corresponding to a given temperature.

Aleksandrov et al.⁶² believe that these variations are due to the stabilisation–destabilisation (localisation–delocalisation) of electron pairs caused by slight local variations of the structural network of the glass. A decrease or an increase in the temperature leads to the transfer of an electron pair and to disproportionation reactions of the type:



where Z is the oxidation number; M^{Z+} are Nb^{3+} , Sn^{2+} , Ti^{2+} , V^{3+} , Mo^{4+} , and W^{4+} ions at which a pair of electrons with opposite spins is localised due to structural features of the glasses obtained. The existence of $\text{M}^{(Z+2)+}$ ions in the glasses synthesised is indicated unambiguously by the fact that the γ -irradiation of these glasses at 300 K leads to reduction reactions of the following type



The continuous increase in the concentration of ions in UOS as the temperature decreases down to 6 K (Fig. 8) is evidence in favour of the disproportionation of electron pairs [according to reaction (6)].

Thus, Aleksandrov et al.⁶² showed for the first time the possibility of temperature-dependent reversible transfer and disproportionation of a pair of electrons in oxide glasses, i.e. the so-called P_e -processes and D^2 -disproportionation reactions, the existence of which in solids had already been suggested in theoretical papers.^{63–65}

Aleksandrov et al.⁶⁶ have also proved unambiguously the possibility that during the synthesis of glasses, D^+ and D^- sites arise on transition metal ions, i.e. pairs of negatively and positively charged defective sites existing in charge equilibrium. The quantum level of the D^- site is occupied by two electrons, while that of the D^+ site contains no electrons. The reason why these sites are defective was considered by Street and Mott in their model of glassy media.⁶⁵ The quantum levels of the D^+ and D^- sites are located near the conduction band and near the valence band, respectively. According to Street and Mott, the metastable D^0 site, which is a level singly occupied by an unpaired electron, is

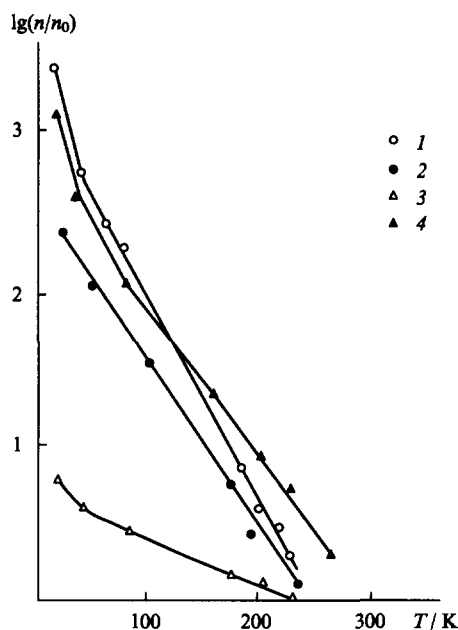


Figure 8. Dependences of the concentration of (Nb^{4+}) PMC on temperature in the 'matrix' LNPG (1) and in LNPG with added tin (2), vanadium (3), or titanium (4) oxide. Curve 4 shows the overall concentration $\text{Nb}^{4+} + \text{Ti}^{3+}$.

located in the middle of the forbidden gap; this site results from an external action on the glassy medium during reduction or oxidation reactions involving D^+ and D^- sites. In the examples described above, ions in UOS act as D^0 sites. Aleksandrov et al.⁶² were the first to find experimentally the D^+ , D^- , and D^0 defects at transition metal ions in oxide glasses.

It is noteworthy that in the LNPG doped with tin oxide, additional PMC have been observed only on Nb^{4+} ; when the glass is doped with titanium oxide, PMC can be detected either on both Nb^{4+} and Ti^{3+} or only on Ti^{3+} , depending on the composition of the glass and on the glass melting conditions; in the case where vanadium, molybdenum, and tungsten oxides act as dopants, only PMC caused by VO^{2+} , Mo^{5+} , and W^{5+} are observed. In the LMPG system doped with tungsten oxide, (Mo^{5+}) and (W^{5+}) PMC have been observed, the ratio between the concentrations of Mo^{5+} and W^{5+} depending on the composition of the glass and on the glass melting conditions. The yields of all ions on decreasing the temperature are strongly dependent on these conditions. Thus, it is obvious that under certain conditions the D^2 -disproportionation reactions are preceded by the P_e -process involving the transfer of an electron pair from Nb^{3+} to V^{5+} , Mo^{6+} , W^{6+} , and Ti^{4+} yielding V^{3+} , Mo^{4+} , W^{4+} , and Ti^{2+} and then V^{4+} , Mo^{5+} , W^{5+} , and Ti^{3+} . The Nb^{4+} ion is not formed in these glasses, i.e. the separated electrons do not react with the dopant. Apparently, this is an example of accepting an electron pair and subsequent accepting of the separated electrons by a stronger acceptor.

If glasses contain dopants leading to the formation of metal ions with weaker accepting properties compared with those of the V^{5+} , Mo^{5+} , W^{5+} , and Ti^{4+} ions, only Nb^{4+} is formed. However, the influence of the compounds added on the trapping of the electrons resulting from the dissociation of electron pairs can be judged from the increase in the concentration of the Nb^{4+} ion with a decrease in the temperature. Fig. 9 shows the dependence of the concentration of the Nb^{4+} ions at 77 K in LNPG on the kind of dopant (silver, zinc, indium, tin, antimony, gallium, or germanium oxide), which can lead to the formation of ions in UOS with the corresponding oxidation number Z . The dopants were introduced during the glass melting in a concentration of 3 mol %. The pattern of the $\Delta[\text{Nb}^{4+}] - Z$ plot coincides with those

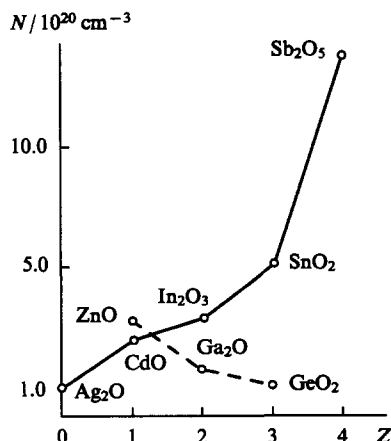


Figure 9. Dependence of the yield of Nb^{4+} ions at 77 K in LNPG containing metals, forming the corresponding ions in UOS, added as dopants (introduced as oxides in an amount of 3 mol %).

of the $A_i/A_i^{(0)} - Z$ and $E_{\lambda_{\text{max}}} - Z$ plots obtained for γ -irradiated alkali phosphate glasses. Evidently, after the decomposition of species with paired electrons to single-electron species, doping metals enter into redox reactions with them yielding ions in UOS, as with the action of γ -radiation.

Since niobium oxide acts in LNPG as the glass-forming compound, forming a glass network possessing microcavities, channels, and pores peculiar to it, one can assume that surface disproportionation reactions occur, which are accompanied by surface transport of electron pairs to stronger acceptors affording ions in UOS. Naturally, the disproportionation reactions proceeding within the structural units of the glass also contribute to this process.

To elucidate the mechanism of the reversible low-temperature disproportionation (RLD) and the reasons for stabilisation of particular concentrations of elements in UOS at a fixed temperature, the following experiments have been carried out. LNPG (this glass is subsequently referred to as the 'matrix LNPG') with added titanium, tin, and vanadium oxides, containing Nb, Li, P, and M (Sn, Ti, V) atoms in concentrations of $(1-4) \times 10^{21}$, $(4-8) \times 10^{21}$, $(1-3) \times 10^{22}$, and $2 \times 10^{20} \text{ cm}^{-3}$, respectively, were taken as model objects. These glasses had an intense ('glass melting') colour, resulting from the reducing conditions used in their synthesis. The number of PMC was determined from the EPR spectra recorded in the integration regime.⁶⁶ In this case, up to 10^{21} PMC per cm^3 arise.

It is seen from Fig. 8 that the activation energy for the increase in the concentration of elements in UOS depends on temperature, $E = f(T)$. The increase in the concentration of ions in UOS (Nb^{4+} , Ti^{3+} , etc.) is caused by several processes for which a spread in energy parameters is possible due to the statistical distribution of the initial transition metal ions in the glass matrix. These processes include: decomposition of species with electron pairs (denoted formally by Nb^{3+} , Ti^{2+} , Mo^{4+} , W^{4+} , etc); and stabilisation of 'separate' electrons (subsequently, this term refers to 'exchange' electrons participating in exchange processes and to the free electrons in the glass matrix). These processes end with the formation of ions in UOS: Nb^{4+} , Ti^{3+} , etc., which are stable at a given temperature.

In order to evaluate the contributions of the stabilisation of 'separate' electrons, and of those electrons resulting from the decomposition of species with electron pairs, to the RLD effect (to the formation of the Nb^{4+} , Ti^{3+} , etc. UOS), the temperature dependences of the electrical conductivity at direct current have been recorded (by the four-electron method) for the matrix LNPG and for the LNPG doped with vanadium, titanium, and tin oxides (Fig. 10). In fact, since the electrical conductivity varies down to

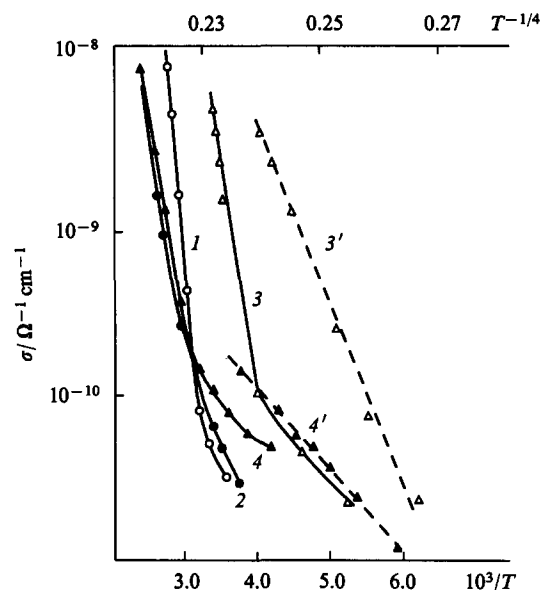


Figure 10. Temperature dependence of electrical conductivity in the $\sigma - 10^3/T$ coordinates (curves 1-4) and in the $\sigma - T^{-1/4}$ coordinates (curves 3'-4') in the 'matrix' LNPG (1) and in LNPG with added tin (2), vanadium (3, 3'), or titanium (4, 4') oxide.

low temperatures (200 K), the hopping mechanism of conductivity is valid, as well as the thermostimulated conductivity of electrons and holes, described by the dependence $\sigma = \sigma_0 \exp(\Delta E/kT)$, where $\Delta E = E_c - E_F$ for electrons and $\Delta E = E_F - E_v$ for holes (E_c , E_v , and E_F are the energies of the edge of the conduction band, the edge of the valence band, and the Fermi level, respectively). The hopping conductivity involves tunnelling of thermoactivated charge carriers from one trap to another over the energy levels at the edges of the bands (in the energy ranges $E_c - E_a$ and $E_b - E_v$), occurring in accordance with the geometrical and energy distances between the individual traps (see Fig. 11).

Apparently, one more charge transfer mechanism occurs. It involves 'jumps' of various distances over localised states near the Fermi level. For this type of conductivity, Mott⁶⁷ has found the relation $\sigma = \sigma_1 \exp[-(T_0/T)^{1/4}]$. It is the Mott's temperature dependence of the conductivity that is obeyed at low temperatures in the glasses under consideration (Fig. 10). Tentative values for the number of conduction electrons (numerically equal to the

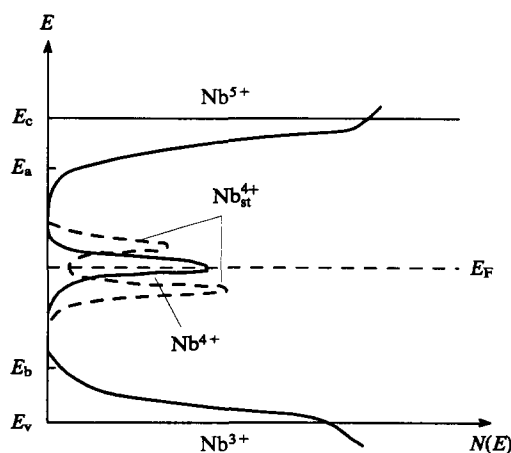
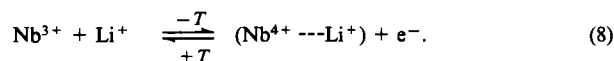


Figure 11. Scheme for the density of the electron states on ions in LNPG at low temperatures (the dashed line shows the possible energy spectrum of niobium ions intercalated with Li^+ cations).

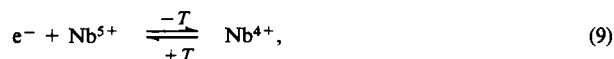
concentration of 'separate' electrons) in these glasses are 10^6 – 10^{12} cm $^{-3}$. This is less by many orders of magnitude than the number of Nb $^{4+}$ and Ti $^{3+}$ UOS arising by the RLD mechanism in the same glasses on decreasing the temperature. Thus, it is obvious that the contribution of the stabilisation processes of the exchange and free electrons to the formation of UOS is quite insignificant. The UOS observed arise largely via the type (6) disproportionation of species with paired electrons. In addition, the conductivity of the glasses increases by several orders of magnitude following the introduction of transition metal oxides (Fig. 10); and the conductivity determined for direct current is time-dependent. Hence, it can be claimed that there is a contribution of the cationic framework to the conductivity of this class of glasses; in other words, these glasses incorporate a mobile cationic framework.

It has been found⁶⁶ that the yields of Nb $^{4+}$ and Ti $^{3+}$ in LNPG with a constant Nb $_2$ O $_5$ /P $_2$ O $_5$ ratio depend on the number of lithium cations, since the concentrations of Nb $^{4+}$ and Ti $^{3+}$ pass through a maximum at a particular Li $^+$ concentration and fall to undetectable values as the latter decreases. This suggests that the mobile cation ensemble has an influence on the dissociation of the electron pairs at Nb $^{3+}$ and on the subsequent stabilisation of the UOS of niobium ion, Nb $^{4+}$. Evidently the cationic ensemble stimulates the reaction (6) and stabilises the resulting UOS by the following multistage mechanism.

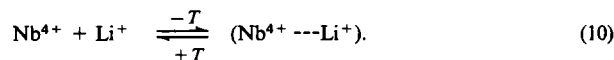
In the first stage, the electron pair at Nb $^{3+}$ dissociates, and Nb $^{4+}$ is stabilised by a lithium cation.



The unpaired electron thus liberated reacts with Nb $^{5+}$



and the resulting Nb $^{4+}$, in its turn, is stabilised by a lithium cation



Thus, if we refer the designations Nb $^{3+}$, Nb $^{4+}$, Nb $^{5+}$, Ti $^{2+}$, etc. to oxygen-containing cluster species incorporating a particular ion in the corresponding oxidation state and consider that the lithium ions are located within the sphere of this cluster and are probably bound to the metal (titanium, niobium, etc.) ions via oxygen bridges, then formally Nb $^{4+}_{\text{st}} = (\text{Nb}^{4+} \cdots \text{Li}^+)$. The stable Nb $^{4+}_{\text{st}}$ ion is now detectable by the EPR method (strictly speaking, only Nb $^{4+}_{\text{st}}$ can be detected 'directly' by EPR). Thus, the temperature-dependent reversible liberation–capture of the cations from shallow to deep energy traps stabilises the forming UOS and promotes the disproportionation reaction (6). This is certainly accompanied by variations of the charge density in the local space in the vicinity of the ion in UOS.

Obviously, the cationic ensemble also influences the conductivity of glasses, since intercalation of a glass with lithium changes (splits, shifts, etc.; see Fig. 11) the energy levels of all the ions present. The transfer of electrons and holes at low temperatures occurs along the system of the lithium-intercalated glass, i.e. the glass in which energy levels and quantitative ratios of ions have changed.

Thus the RLD effect can be considered to be associated with the crucial role of the cationic framework in the stabilisation of UOS and, consequently, with the occurrence of the disproportionation processes (6). The cationic framework determines the Nb $^{3+}$ /Nb $^{4+}$ /Nb $^{5+}$ ratio of ion concentrations. However, at the concentrations found [Nb $^{4+}$] = $N = 10^{21}$ cm $^{-3}$, the value $NZ_B < 0.25$ (Z_B is the Bohr radius of Nb), i.e. according to the Mott criterion,⁶⁷ metallisation of this glassy system has still not been achieved.

3. Formation of ions in UOS as a result of mechanochemical treatment

It follows from the above that the unpaired electrons arising due to various kinds of treatment of a solid (γ -radiation, phototreatment, heat treatment) are characterised by similar chemical behaviour: they give rise to ions in UOS in the glass matrix. It should be expected that mechanical treatment of the glasses described above will also lead to the appearance of ions in UOS. It has been noted⁶⁸ that when a LiF crystal is cracked, F atoms are liberated. One of the hypotheses put forward for the explanation of the emission of F atoms states that the following electron transfer reactions occur during the cracking: $\text{F}_v^- \longrightarrow \text{F} + \text{e}^-$, $\text{Li}^+ + \text{e}^- \longrightarrow \text{Li}$, where F_v^- is a vibrating F $^-$ ion which has undergone vibrational excitation immediately after the cleavage of bonds in the mouth of the mechanical crack. If the amplitude of these vibrations reaches 0.75 of the magnitude of the lattice parameter, rupture of the chemical bond occurs according to the above scheme. The mechanisms of dislocation-induced excitation of the electron subsystem of a solid, according to which electron-hole pairs are formed upon collision of dislocations or upon their exposure at the surface of a pore (or a crack) in a solid, have also been reported.^{69,70} The collision or surface exposure of dislocations is accompanied by intense acoustic emission, i.e. vibrational excitation of atoms. If the amplitude of vibrations of the atoms exceeds the limit mentioned above, an electron-hole pair is formed. Obviously, the subsequent scheme of elementary chemical steps following the mechanical destruction of a solid should include reaction (2) (formation of ions in UOS).

We carried out experiments on mechanical treatment in a ball mill of sodium silicate (SSG) and sodium borate (SBG) glasses at 77 K. It was found by EPR that in the SSG doped with cadmium, tin, thallium, and lead oxides, Cd $^{1+}$, Sn $^{3+}$, Tl $^{2+}$, and Pb $^{3+}$ ions are formed. The $A_i/A_i^{(0)}$ ratios for these ions are 0.64, 0.35, 0.55, and 0.48, respectively. It is seen that the $A_i/A_i^{(0)} - Z$ dependences for the ions in UOS obtained by mechanical treatment and by γ -irradiation at 77 K are similar.

After the mechanical treatment of SBG in a ball mill at 77 K, only weak signals corresponding to BO $_4^{4-}$ PMC were observed. Apparently, the number of ions in UOS in these glasses is so small that they cannot be detected by EPR.

These data are in good agreement with the views on the structure of inorganic glasses presented above and with the model of the vibrational formation of electron-hole pairs in a glass after mechanical treatment. In fact, boron oxide usually forms linear chains in glasses with low resistance to deformation, whereas silicate glasses consist of highly rigid three-dimensional networks.⁷¹ Naturally, the stronger the glass, the higher is the mechanical stress needed for its destruction, and the more intense in amplitude and frequency are the vibrational processes arising in it. Hence, it is clear that the formation of electron-hole pairs and, consequently, of ions in UOS, should be more intense in silicate glasses. This is in good agreement with the above experimental results.

4. The role of metals in UOS in the nucleation in a glass

The formation of the crystalline phase from glasses and melts is an important problem in the theory and practice of the glassy state. This process plays a key role in the preparation of crystalline enamels and glazes, in the directed colloidal colouring of glasses, and in the production of glass ceramics, photo glass ceramics, and photochromic glasses existing in both the amorphous and crystalline states. The theoretical foundations for these processes have been formulated by Kolmogorov⁷² and developed further by other researchers.^{73–81} However, stage-by-stage molecular chemical investigation of the mechanism of the formation of the crystalline phase has hardly been developed. In all these studies, only the initial and final substances were examined. Nothing was said about the role of disproportionation reactions.

The formation of the colloidal and crystalline phases can be divided conventionally into three stages: (1) the formation of atomic centres; (2) the appearance of molecular aggregates; and (3) the formation of colloidal and crystalline inclusions. The first two stages are often combined into a single stage — nucleation, the growth of crystals and colloids being regarded as the second stage.

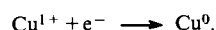
To obtain the nuclei, photosensitisers, thermosensitisers and photosensitive metals are introduced into photo glass ceramics and in photochromic glasses. Ce, Sm, and Pr compounds, i.e. compounds of elements that readily release electrons on exposure to light, for example, by the reaction



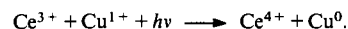
act as photosensitisers.

The wavelength of the active light depends on the nature and properties of both the photosensitiser and the matrix glass. The metals Sn, Sb, Pb, etc., small amounts of which (0.02%–1.5%) increase the capability of a photosensitive metal to form nuclei during heat treatment of the glass and thus decrease the irradiation time, are referred to as thermoreducing sensitizers.

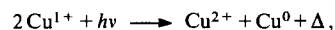
Photosensitive metals are mainly Cu, Ag, Au, and Pt. Thermosensitisers can reduce the ions of photosensitive metals even during glass melting. In this case, the following reactions occur on exposure to light:



The atomic copper, gold, silver, etc. form colloidal and crystalline phases when heated to a certain temperature. Cerium added to the glass permits the yields of Cu^0 , Ag^0 , and Au^0 to be increased, due to the occurrence of reactions of the type



Photosensitive materials can act as self-sensitisers



where Δ is the excess energy liberated. Hard radiation exerts a similar influence on these glasses, i.e. γ -irradiation also creates prerequisites for the nucleation.

Spontaneous (homogeneous) crystallisation can proceed in a glass melt. The process of nucleation in this case has been rationalised at the microquantitative level by Weyl,^{77,78} who relates the nucleation to defects or asymmetric fragments. In his opinion, the 'asymmetry' is caused by disproportionation (not electronic) of the bonding forces, which lowers the energy barrier to the formation of crystallisation centres. Berezhnoi⁷⁹ believes that the 'appearance of the centres for spontaneous crystallisation in complex glasses is associated with the diffuse chemical differentiation of atoms and structural groups forming aggregates as zones, the composition of which is close to that of the segregating crystals.' Thermodynamic description of the homogeneous crystallisation has also been reported.⁷³

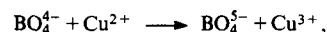
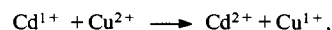
An important role in the theory of heterogeneous (or catalytic) crystallisation is played by metastable zones, the necessity of wetting the catalyst with the crystalline phase, and the similarity of crystal structures and interatomic distances in the catalyst and in the crystalline phase. This process is greatly influenced by stirring or vibration of the supercooled melt or by the action of ultrasound, electrical and magnetic fields, and γ -irradiation. The oxides TiO_2 , ZrO_2 , P_2O_5 , ZnO , Cr_2O_3 , V_2O_5 , NiO , Nb_2O_5 , WO_3 , and MoO_3 are used as catalysts. The choice of the catalyst in each particular case depends on the composition and properties of the glass melt.

Turnbull⁸⁰ has derived equations for calculating the rate of formation of crystallisation centres for heterogeneous crystallisation. After that, the rules for the selection of the catalyst have been established:⁸¹ the catalyst should be readily soluble in the glass blend at the temperature of glass melting (and manufacture) and

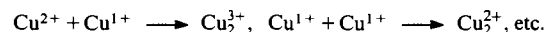
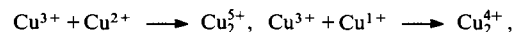
be sparingly soluble at low temperatures; the free activation energy for the formation of homogeneous crystallisation centres from the melt at low temperatures should be low, which is favoured by a low surface energy of the dissolved and crystalline phases and by a high degree of supersaturation on cooling; the free activation energy for the diffusion process should be low; the surface energy at the interface between the glass and the catalyst crystal should be low; the parameters of the crystal lattice of the catalyst should be close to those of the segregating crystalline phase. However, Weyl^{77,78} has noted that the distribution of chemical bonds within the system is also important.

It is clear from the foregoing that the processes of nucleation and segregation of the crystalline and colloidal phases from glasses have mainly been described at a macroscopic level. The role of transition metal ions and ions in UOS as well as concepts at the molecular level, similar to those considered above in relation to the formation of metal clusters M_m^{n+} ($\text{M} = \text{Pb}, \text{Tl}, \text{Bi}$), was not mentioned in any of these studies. In none of the papers surveyed in relevant monographs^{79,82,83} is mention made of the fact that only the presence of atoms capable of disproportionating, such as $\text{Bi}^{3+} - \text{Bi}^{5+}$, $\text{Tl}^{1+} - \text{Tl}^{3+}$, $\text{Cu}^{1+} - \text{Cu}^{3+}$, $\text{Pt}^{2+} - \text{Pt}^{4+}$, $\text{Ti}^{2+} - \text{Ti}^{4+}$, in combination with ions in UOS acting as sensitizers, is the crucial factor for the beginning of the nucleation process.

The above is confirmed by the reversible formation and decomposition of Cu_m^{n+} colloidal particles, induced by ions in UOS obtained by irradiation, such as Zn^{1+} , Cd^{1+} , Hg^{1+} , In^{2+} , Tl^{2+} , Sn^{3+} , Pb^{3+} , Sb^{4+} , and Bi^{4+} .⁸⁴ Let us consider a sodium aluminoborosilicate glass with added cadmium and copper oxides. It has been shown by EPR that irradiation of this glass leads to the formation of Cd^{1+} and BO_4^{4-} ions. On heating to 150–200 °C these ions virtually disappear. Further heating to 800 °C leads to the formation and destruction of particles of colloidal copper Cu_m^{n+} . This indicates that the Cd^{1+} and BO_4^{4-} ions are not merely annihilated, but enter into redox reactions with Cu^{2+}



which afford the D^- , D^+ defects, i.e. the Cu^{1+} and Cu^{3+} ions. It is pairs of these ions, identified based on the AB with $\lambda_{\text{max}} = 570$ nm, that act as the precursors of the nuclei of colloidal copper. In fact, the lattice around the D^+ defect should be substantially stressed, whereas the D^- defect interacts with the environment only weakly but possesses a higher mobility. This leads to the possible occurrence of the following reactions:



The species Cu_2^{5+} , Cu_2^{4+} , Cu_2^{3+} , and Cu_2^{2+} can also be regarded formally as D^- and D^+ defects. Some of them are more mobile than others. Reactions then proceed in which the number of copper atoms in one nucleus increases to give Cu_m^{n+} particles.

The decomposition of the colloidal particles Cu_m^{n+} following further increase in the temperature occurs stepwise. This is indicated by the decrease in the intensity of the AB with $\lambda_{\text{max}} = 570$ nm and by the appearance of an AB with $\lambda_{\text{max}} = 455$ nm, which also disappears as the temperature is further increased. The latter AB corresponds apparently to species with lower numbers of copper atoms or to small colloidal particles of copper incorporating cadmium atoms. It can be assumed that the decomposition of Cu_m^{n+} is related to the high-temperature disproportionation reactions. The diagram for this process is shown in Fig. 12. This process can be repeated many times, beginning with the radiation-induced generation of the Cd^{1+} and BO_4^{4-} ions at 300 K.

Thus, the following sequence of transformations occurs: low-temperature defects \longrightarrow disproportionation reactions \longrightarrow high-temperature products \longrightarrow disproportionation reactions \longrightarrow

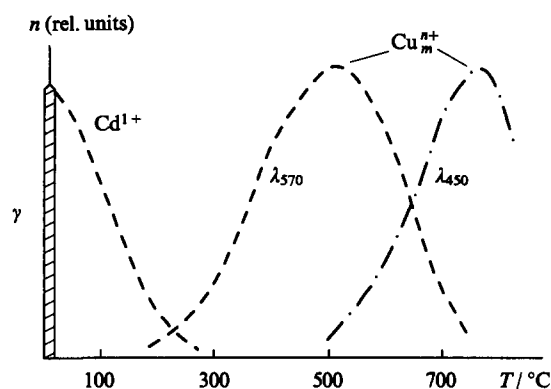
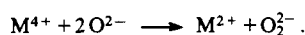


Figure 12. Processes in the accumulation and disappearance of Cd^{1+} ions and Cu_m^{n+} clusters after γ -irradiation followed by thermoannealing.

return to the initial state. To control the formation of the nuclei of crystalline and colloidal phases in glasses, in glass-like materials, and, possibly, in ceramics, one should elucidate the relationships in this sequence. The problem of elucidating these relationships can be solved only by detailed investigation of the whole set of ions present in the glass and of the electron dynamics of their interactions,⁸⁵ which, in the presence of disproportionation reactions, may be complex and involve in oxide glasses both the metal and oxygen. For example, the following disproportionation reactions of the D^{2-} type may occur



Oxygen ions and clusters should promote the disproportionation reactions.^{86–90} Obviously, studies along these lines will be continued.

IV. Conclusion

The data presented in our review imply that the stabilisation and reversible stabilisation–destabilisation of metal ions in UOS with the localisation of one or two electrons are complex processes involving the whole glass or the glass-like solid. These processes are associated with the electron-vibrational and conformational rearrangements, electron density transfer, shifts of atoms, and with variations (reversible or irreversible) of the local structure of the glass. The processes of electron disproportionation are accompanied by redox chemical reactions. Specific features of these processes are determined by the structure of the glass (the network geometry and the characteristic features of the electronic structure).

Currently the most common view on the structure of glasses is that the borate, germanate, silicate, and phosphate glasses are built of the main structural units $\text{BO}_{3/2}$, $\text{BO}_{4/2}$, $\text{GeO}_{4/2}$, $\text{SiO}_{4/2}$, and $\text{PO}_{4/2}$ (the indices 3/2 and 4/2 point to the fact that the B, Ge, Si, and P atoms are linked to the glass network via three or four bridging oxygen atoms), which are transformed during the synthesis into progressively more complex structures,^{91–98} i.e. mono-, di-, and oligomeric anions. The latter are converted, in their turn, into diverse macroanions (MA) of linear $(\text{SiO}_3^{2-})_n$, layered (philo) $[\text{BO}_{3/2}(\text{O}^-)]_m^{2mn}$, or network (texto) $(\text{Si}_2\text{O}_5^{2-})_n$ type or into clusters with any number of atoms. Thus, glass can be treated as a solid, porous at the molecular level, with an immense inner surface, the channels and pores of which are occupied by modifying cations, and dangling bonds also emerge there.^{38, 84}

The dangling chemical bonds and modified structural groups give rise to a set of various defects of donor or acceptor character. The frequency of origination of these sites (defects) is determined by the free energy of formation of each of them. At the same time, if a glass contains no paramagnetic ions introduced during the synthesis, it is a diamagnetic material. If singly charged positive and negative defects could arise during the synthesis of glasses,

they would correspond to high concentrations of unpaired electrons. However, EPR studies indicate unambiguously that their concentration is lower than 10^{15} cm^{-3} and can be brought to $10^{17} - 10^{19} \text{ cm}^{-3}$ in amorphous Si and Ge only by various external factors.^{99, 100} The presence of singly charged positive and negative defective sites would also cause substantial conductivity at low temperatures, but no contribution of this conductivity has been found so far.⁸³

These contradictions have been resolved in terms of the theory of chemical bonding describing the characteristic features of the electronic structure of glass. A great contribution to the development of this theory has been made by Anderson.¹⁰¹ He noted that in amorphous semiconductors and glasses, electrons tend to be combined in pairs thus forming stable states. The stability of the states with paired electrons is due to the fact that the energy of the Coulomb repulsion is lower than the energy of the electron-phonon interaction; the polarisability of the solid lattice surrounding the electrons should also be taken into account. Later Street and Mott⁶⁵ and Kastner, Adler, and Fritzche¹⁰² developed (almost contemporaneously) the theory of localised states in a glass, which are positively and negatively charged defects (D^+ and D^- , respectively). These authors claim that a half of the defects remain unoccupied with electrons and acquire a positive charge (D^+ site), and the rest of the defects are occupied by electron pairs and have a negative charge (D^- site). These studies made it possible to explain the diamagnetism of glass and the linearity of the variation of the molecular heat capacity of glasses at low temperature.

Lucovsky¹⁰³ and Greaves¹⁰⁴ have developed these views in relation to glassy SiO_2 . They proved that the abstraction of an electron from a D^- site or the addition of an excited electron from the valence band to a D^+ site result in the formation of a paramagnetic neutral D^0 site. Within the framework of quantum chemistry, all these models are based on the fact that the heterolytic rupture of chemical bonds yielding D^+ and D^- sites is energetically more favourable than the homolytic rupture of bonds leading to the formation of sites with unpaired spins. The antibonding state has an electronic configuration that is described by the D^+ state located in the forbidden gap below the conduction band, while the D^- state has a completely filled valence electronic shell, forms no additional bonds, and is located in the forbidden gap above the valence band. The smaller the polarisation of the lattice caused by the D^- site, the stronger the polarisation effect caused by the D^+ site.

All the models considered above describe the same effect; they go under the general name of the model of charged defective sites, which is valid only for fairly simple structures in the glass.⁸³ A more adequate model, namely, the model of quasimolecular defects, has been suggested by Popov.¹⁰⁵ This model involves the realisation of multicentre multielectron bonds in glasses. This model shares a number of traits with the Dembovskii model, which develops the theory of 'soft' three-centre bonds (arising due to the fact that the bonds are formed by antibonding electrons).¹⁰⁶ It is clear that the extension of the above concepts to the description of the geometric and electronic structure of glass has not yet been completed.

If we suggest, from general chemical knowledge, that an analogy between the processes of structural disordering in glass and dissociation reactions like $2\text{H}_2\text{O} \rightleftharpoons \text{H}_3\text{O}^+ + \text{OH}^-$ in aqueous media can be drawn legitimately,^{55, 101–105} then the acid–base concept applied to oxide melts and glasses correlates quite well with views on the redox disproportionation yielding D^+ and D^- sites. According to this concept, the heterolytic rupture of bonds leads to the formation of a D^+ hole site on the oxygen atom bound to three silicon atoms [$^+\text{O}(\text{SiO}_{3/2})_3$] and of a D^- two-electron site on the oxygen atom bound to one silicon atom [$\text{SiO}_{3/2}\text{O}^-$]. In the presence of foreign metal oxides, the scheme by which the defective sites arise changes: metal cations act as the D^+ sites instead of $^+\text{O}(\text{SiO}_{3/2})_3$. This refers also to three other main types of oxide glasses: borate, germanate, and phosphate glasses.^{83, 107}

The modelling of the formation and stabilisation of ions in UOS at the level of local reactions, with allowance for the disproportionation of the electron density between the selected atomic centres, makes it possible to explain completely the processes of stabilisation of ions and switching of bonds both during the synthesis of glasses and following various kinds of physical treatment of them.¹⁰⁸ Moreover, it follows from the data presented in our review that a key role in the stabilisation of ions in UOS in low-temperature glasses is played by hydrogen bonds, due to which a glass-like network is formed. In this case, protons act as the mobile cationic framework; after the addition of an unpaired electron to a metal cation, protons occupy energetically favourable positions in its environment and lead to the redistribution of the electron density due to local disproportionation reactions.

Thus, allowance for the structural features of glass, the presence of dangling and multicentre bonds leading to the initial localisation of the electron pairs, and the presence of a mobile cationic ensemble determine the subsequent cooperative processes based on redox reactions, which are similar as regards the nature of the elementary step and lead to the formation and stabilisation of ions in UOS.

References

1. A K Pikaev *Sol'vatirovannyi Elektron v Radiatsionnoi Khimii* (The Solvated Electron in Radiation Chemistry) (Moscow: Nauka, 1969)
2. B G Ershov, A K Pikaev *Khim. Vys. Energ.* (1) 29 (1967)
3. A I Aleksandrov, B G Ershov, A K Pikaev, V I Spitsyn *Izv. Akad. Nauk SSSR, Ser. Khim.* 249 (1976)
4. A I Aleksandrov, in *Tez. Dokl. II Vsesoyuz. Konf. Molodykh Uchenykh po Radiatsionnoi Khimii* (Abstracts of Reports of the Second All-Union Young Scientists Conference on Radiation Chemistry) (Obninsk: Karpov NIFKhI, 1975) p. 62
5. B G Ershov, A I Aleksandrov, V I Spitsyn *Dokl. Akad. Nauk SSSR* 279 1120 (1976)
6. B G Ershov, A I Aleksandrov *Int. J. Radiat. Phys. Chem.* 10 327 (1977)
7. A K Pikaev *Sovremennaya Radiatsionnaya Khimiya* T. 1–3 (Modern Radiation Chemistry, Vols 1–3) (Moscow: Nauka, 1985–1987)
8. A K Pikaev, S A Kabakchi, I E Makarov, B G Ershov *Metod Impul'snogo Radioliza i ego Primenenie* (The Method of Pulse Radiolysis and its Applications) (Moscow: Atomizdat, 1980)
9. A I Aleksandrov, G V Ionova, B G Ershov *Radiat. Phys. Chem.* 13 199 (1979)
10. B G Ershov, A I Aleksandrov *Izv. Akad. Nauk SSSR, Ser. Khim.* 743 (1978)
11. B G Ershov, A I Aleksandrov, N L Sukhov, V I Spitsyn *Dokl. Akad. Nauk SSSR* 242 1086 (1978)
12. A I Aleksandrov, B G Ershov, V I Spitsyn *Dokl. Akad. Nauk SSSR* 254 907 (1980)
13. A I Aleksandrov, B G Ershov *Izv. Akad. Nauk SSSR, Ser. Khim.* 1187 (1982)
14. B G Ershov, A I Aleksandrov, V I Spitsyn *Izv. Akad. Nauk SSSR, Ser. Khim.* 768 (1982)
15. B G Ershov, A I Aleksandrov *Teor. Eksp. Khim.* 14 679 (1978)
16. B G Ershov *Usp. Khim.* 50 2137 (1981) [*Russ. Chem. Rev.* 50 1119 (1981)]
17. G V Ionova, B G Ershov, V I Spitsyn *Dokl. Akad. Nauk SSSR* 288 1400 (1986)
18. N L Sukhov, I E Makarov, B G Ershov *Khim. Vys. Energ.* 12 375 (1978)
19. N L Sukhov, B G Ershov *Khim. Vys. Energ.* 13 55 (1979)
20. N L Sukhov, B G Ershov, A V Akinshin *Izv. Akad. Nauk SSSR, Ser. Khim.* 1440 (1984)
21. A V Gogolev, I E Makarov, A K Pikaev *Khim. Vys. Energ.* 15 109 (1981)
22. A I Aleksandrov, I E Makarov *Izv. Akad. Nauk SSSR, Ser. Khim.* 249 (1987)
23. N M Pavlushkin (Ed.) *Khimiya i Tekhnologiya Stekla i Sitallov* (The Chemistry and Technology of Glass and Glass Ceramics) (Moscow: Stroiizdat, 1983)
24. D I Mendelev *Osnovy Khimii* (Foundations of Chemistry) (St.-Petersburg, 1895) p. 780
25. A A Lebedev, in *Proceedings of the State Optical Institute, Petrograd, 1921* Vol. 8, No. 10
26. W H Zachariasen *J. Am. Chem. Soc.* 54 3841 (1932)
27. G T Petrovskii *Vestn. Akad. Nauk SSSR* 3 89 (1984)
28. A A Bukharev, D G Galimov, K D Tarzimanov, N R Yafaev *Fiz. Khim. Stekla* 8 200 (1982)
29. E I Abdrashidova, M V Artamonova *Fiz. Khim. Stekla* 5 369 (1979)
30. S M Brekhovskikh, Yu N Viktorova, L M Landa *Radiatsionnye Effekty v Steklakh* (Radiation Effects in Glasses) (Moscow: Energoizdat, 1982)
31. A A Appen *Khimiya Stekla* (The Chemistry of Glass) (Leningrad: Khimiya, 1970)
32. A I Aleksandrov, A I Prokof'ev, E V Shishmentseva, T F Evdokimova, S L Kraevskii, N N Bubnov, V F Solinov *Dokl. Akad. Nauk SSSR* 284 1382 (1985)
33. A I Aleksandrov, A I Prokof'ev, Z I Raspertova, N N Bubnov, S L Kraevskii, V F Solinov *Dokl. Akad. Nauk SSSR* 284 886 (1985)
34. A I Aleksandrov, A I Prokof'ev, Z I Raspertova, V F Solinov, N N Bubnov *Dokl. Akad. Nauk SSSR* 289 900 (1986)
35. A I Aleksandrov, A I Prokof'ev, N N Bubnov, Z I Raspertova, V F Solinov *Dokl. Akad. Nauk SSSR* 289 1144 (1986)
36. A I Aleksandrov, A I Prokof'ev, N N Bubnov, V F Solinov *Dokl. Akad. Nauk SSSR* 292 1414 (1987)
37. A I Aleksandrov, A I Prokof'ev, N N Bubnov, V F Solinov *Dokl. Akad. Nauk SSSR* 298 624 (1988)
38. A I Aleksandrov, N N Bubnov, A I Prokof'ev, V F Solinov *Khim. Fiz.* 7 1114 (1988)
39. V F Solinov, A I Aleksandrov, E V Shishmentseva, I E Makarov, A K Pikaev, in *Sb. Tezisev 'Soveshchanie-Seminar po Radiatsionnoi Khimii'* (Abstracts of Reports from a Conference-Seminar on Radiation Chemistry) (Tbilisi: Metsniereba, 1985) p. 72
40. V F Solinov, A I Aleksandrov, E V Shishmentseva, A K Pikaev, I E Makarov, A V Bludenko, in *VI Simpozium po Opticheskim i Spekttral'nym Svoistvam Stekol* (The Sixth Symposium on the Optical and Spectroscopic Properties of Glasses) (Riga: Stuchka Latv. Gos. Univ., 1986) p. 168
41. A I Aleksandrov, A I Prokof'ev, N N Bubnov, V F Solinov, in *Abstracts of the 6th 'Tihany' Symposium on Radiation Chemistry, Balatons Zeplak, Hungary, 1986* p. 1
42. O S Makedontseva, A I Aleksandrov, A M Zyabnev, in *VIII Vsesoyuz. Soveshchanie po Stekloobraznomu Sostoyaniyu* (The Eighth All-Union Conference on the Vitreous State) (Leningrad: Nauka, 1986) p. 281
43. A I Aleksandrov, in *VIII Vsesoyuz. Soveshchanie po Stekloobraznomu Sostoyaniyu* (The Eighth All-Union Conference on the Vitreous State) (Leningrad: Nauka, 1986) p. 49
44. A I Aleksandrov, A I Prokof'ev, N N Bubnov, S A Zelentsova, N A Paramonova, V F Solinov, in *VI Vsesoyuz. Konf. po Radiatsionnoi Fizike i Khimii Ionnykh Kristallov* (The Sixth All-Union Conference on the Radiation Physics and Chemistry of Ionic Crystals) (Riga: Institute of Physics, Academy of Sciences of Latvia SSR, 1986) Pt I, p. 111
45. A I Aleksandrov, I E Makarov, A V Bludenko, A K Pikaev, V F Solinov, in *VI Vsesoyuz. Konf. po Radiatsionnoi Fizike i Khimii Ionnykh Kristallov* (The Sixth All-Union Conference on the Radiation Physics and Chemistry of Ionic Crystals) (Riga: Institute of Physics, Academy of Sciences of Latvia SSR, 1986) Pt II, p. 350
46. A I Aleksandrov, A V Bludenko, I E Makarov, A K Pikaev, V F Solinov *Khim. Vys. Energ.* 23 146 (1989)
47. A V Bludenko, A I Aleksandrov, I E Makarov, A K Pikaev *Khim. Vys. Energ.* 26 499 (1992)
48. A Bishay *J. Non-Crist. Solids* 3 54 (1970)
49. G S Meiling *Phys. Chem. Glasses* 14 118 (1973)
50. K Kumata, K Yamamoto, H Namikawa *J. Ceram. Soc. Jpn.* 85 359 (1977)
51. T D Donskaya, A I Aleksandrov, V M Tovmasyan, R Ya Khodakovskaya, S A Petrosyan, V F Solinov, in *VII Vsesoyuz. Simpozium po Opticheskim i Spekttral'nym Svoistvam Stekol* (The Seventh All-Union Symposium on the Optical and Spectroscopic Properties of Glasses) (Leningrad: State Optical Institute, 1989) p. 181

52. A S Nikiforov, V V Kulichenko, M I Zhikharev *Obezvrezhivanie Zhidkikh Radioaktivnykh Otkhodov* (Neutralisation of Liquid Radioactive Wastes) (Moscow: Energoatomizdat, 1984)
53. S V Stefanovskii, A I Aleksandrov *Fiz. Khim. Stekla* **16** 308 (1990)
54. S V Stefanovskii, A I Aleksandrov, A K Pikaev *Fiz. Khim. Stekla* **16** 48 (1990)
55. S V Stefanovskii, A I Aleksandrov, A K Pikaev *Fiz. Khim. Stekla* **16** 635 (1990)
56. S V Stefanovskii, A I Aleksandrov *Fiz. Khim. Stekla* **16** 53 (1990)
57. S V Stefanovskii, A I Aleksandrov *Zh. Prikl. Spektrosk.* **54** 242 (1991)
58. S V Stefanovskii, A I Aleksandrov *Zh. Prikl. Spektrosk.* **51** 267 (1989)
59. S V Stefanovskii, A I Aleksandrov *Zh. Prikl. Spektrosk.* **53** 121 (1990)
60. S V Stefanovskii, A I Aleksandrov *Zh. Prikl. Spektrosk.* **56** 59 (1992)
61. J van Wazer *Phosphorus and Its Compounds* (Translated into Russian; Moscow: Izd. Inostr. Lit., 1962)
62. A I Aleksandrov, S P Ionov, N N Bubnov, A I Prokof'ev, V F Solinov, E V Shishmentseva *Dokl. Akad. Nauk SSSR* **302** 1130 (1988)
63. B Ya Moizhes, S G Suprun *Fiz. Tverd. Tela* **24** 550 (1982)
64. S P Ionov, V A Kondrat'ev, V S Lyubimov *Dokl. Akad. Nauk SSSR* **227** 329
65. R A Street, N F Mott *Phys. Rev. Lett.* **35** 1293 (1975)
66. A I Aleksandrov, N N Bubnov, S P Ionov, A I Prokof'ev *Dokl. Akad. Nauk SSSR* **311** 1401 (1990)
67. N Mott, E Davis *Electron Processes in Non-Crystalline Materials* Vols 1, 2 (Oxford: Clarendon Press, 1979)
68. P Yu Butyagin *Usp. Khim.* **63** 1031 (1994) [*Russ. Chem. Rev.* **63** 965 (1994)]
69. V S Boiko, R I Garber, A M Kosevich *Obratimaya Plastichnost' Kristallov* (Reversible Plasticity of Crystals) (Moscow: Nauka, 1991)
70. V D Natsik *Pis'ma Zh. Eksp. Teor. Fiz.* **8** 324 (1968)
71. G M Bartenev *Sverkhprochnye i Vysokoprochnye Stekla* (Super-Strength and High-Strength Glasses) (Moscow: Stroiizdat, 1974)
72. A N Kolmogorov *Izv. Akad. Nauk SSSR, Ser. Mat.* 355 (1937)
73. V Z Belen'kii *Geometriko-Veroyatnye Modeli Kristallizatsii* (Geometrically Probable Crystallisation Models) (Moscow: Nauka, 1980)
74. M D Bal'makov *Fiz. Khim. Stekla* **14** 19 (1988)
75. V B Bochkarev, M P Shipilov *Fiz. Khim. Stekla* **14** 284 (1988)
76. V N Filippovich, T A Zhukovskaya *Fiz. Khim. Stekla* **14** 300 (1988)
77. W A Weyl *J. Phys. Chem.* **19** 147 (1955)
78. W A Weyl, E Q Marboe *Glass Ind.* **4** 549 (1962)
79. A I Berezhnoi *Sitally i Fotositally* (Glass Ceramics and Photo Glass Ceramics) (Moscow: Mashinostroenie, 1966)
80. D Turnbull *J. Chem. Phys.* **20** 411 (1950)
81. I Guttsov *Fiz. Khim. Stekla* **1** 431 (1980)
82. R Ya Khodakovskaya *Khimiya Titansoderzhashchikh Stekol i Sitallov* (The Chemistry of Titanium-Containing Glasses and Glass Ceramics) (Moscow: Khimiya, 1978)
83. A Feltz *Amophe und Glassartige Unorganische Festkerper* (Berlin: Akademie-Verlag, 1983)
84. S P Ionov, A I Aleksandrov *Peremennaya Valentnost' i Elektronnaya Dinamika v Oksidnykh Steklakh* (Preprint IAE-4788/9) [Variable Valence and Electron Dynamics in Oxide Glasses (Preprint of Institute of Atomic Energy No. 4788/9)] (Moscow: TsNIIAtominform, 1989)
85. S P Ionov, V S Lyubimov, in *Kinetika Dvukheletronnogo Perenosa v Kondensirovannykh Sredakh* (Preprint IAE-4684/9) [Kinetics of Two-Electron Transfer in Condensed Media (Preprint of Institute of Atomic Energy No. 4684/9)] (Moscow: TsNIIAtominform, 1988)
86. S Ram *Phys. Status Solidi A* **107** 55 (1988)
87. P Ganguly, M S Hende *Phys. Rev. B, Condens. Matter* **37** 5107 (1988)
88. T Gerber, B Himmel, Z Wiss Rostock. *Naturwiss. R., Wilhelm-Pieck-Univ.* **36** 14 (1987)
89. U Koster *Mater. Sci. Eng.* **97** 233 (1988)
90. S Budurov, T Spassov *Mater. Sci. Eng.* **97** 361 (1988)
91. S M Brekhovskikh, V A Tyul'nin *Radiatsionnye Tsentry v Neorganicheskikh Steklakh* (Radiation Centres in Inorganic Glasses) (Moscow: Energoatomizdat, 1988)
92. D H Griscom *J. Non-Cryst. Solids* **13** 251 (1973/74)
93. N H Ray *Inorganic Polymers* (New York; London: Academic Press, 1978)
94. V V Tarasov *Problemy Fiziki Stekla* (Problems in the Physics of Glass) (Moscow: Stroiizdat, 1979)
95. D S Sanditov, G M Bartenev *Fizicheskie Svoistva Neuporyadochennykh Struktur* (Physical Properties of Disordered Structures) (Novosibirsk: Nauka, 1982)
96. B P Tarasevich, E V Kuznetsov *Usp. Khim.* **56** 353 (1987) [*Russ. Chem. Rev.* **56** 203 (1987)]
97. *Stekloobraznoe Sostoyanie* (Tr. III Vsesoyuz. Soveshchaniya) (Proceedings of the Third All-Union Conference on the Vitreous State) (Moscow; Leningrad: Izd. Akad. Nauk SSSR, 1960)
98. L I Tatarinova *Struktura Tverdykh, Amorfnnykh i Zhidkikh Veshchestv* (Structure of Solids, Amorphous Substances and Liquids) (Moscow: Nauka, 1983)
99. S G Agarwal *Phys. Rev.* **B7** 685 (1973)
100. S G Bishop, U Strom, P C Taylor *Phys. Rev. Lett.* **34** 1346 (1975); **36** 543 (1976)
101. P W Anderson *Phys. Rev. Lett.* **34** 953 (1975)
102. M Kastner, D Adler, H Fritzsche *Phys. Rev. Lett.* **37** 1504 (1976)
103. G Lucovsky *Philos. Mag. B* **39** 513 (1979); **41** 457 (1980)
104. G N Greaves *Philos. Mag. B* **37** 437 (1978); *J. Non-Cryst. Solids* **32** 295 (1979)
105. N A Popov *Pis'ma v Zh. Eksp. Teor. Fiz.* **31** 437 (1980)
106. S A Dembovskii *Novye Idei v Fizike Stekla* (New Ideas in the Physics of Glass) (Moscow: VNIIESM, 1987)
107. M M Shul'ts *Fiz. Khim. Stekla* **10** 129 (1984)
108. A I Aleksandrov, in *IV Vsesoyuz. Soveshch. 'Mekhanizmy Dvukheletronnnoi Dinamiki v Neorganicheskikh Materialakh'* (The Fourth All-Union Conference on the Mechanisms of the Two-Electron Dynamics in Inorganic Materials) (Moscow, Chernogolovka: VNIIFTRI, 1989) p. 10

Reactivity of hydrocarbons and their individual C–H bonds with peroxy radicals

W W Pritzkow, V Ya Suprun

Contents

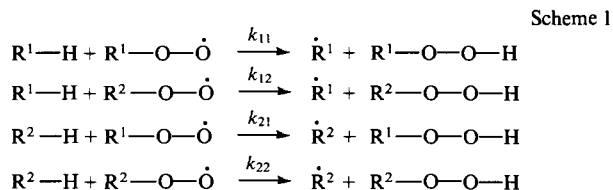
I. Introduction	497
II. Reactivities of alkylbenzenes and their activated α -C–H bonds	498
III. Relative reactivities of aliphatic C–H bonds	500
IV. Ring strain effects in the oxidation of cycloalkanes and their derivatives	501
V. Reactivities of the equatorial and axial C–H bonds in cyclohexane derivatives	501
VI. Reactivities of cycloalkenes	502
VII. Reactivities of styrene derivatives	502
VIII. Conclusion	502

Abstract. The possibility of determining relative rates of oxidation of hydrocarbons and of their individual C–H bonds by competitive oxidation has been demonstrated. Data on the reactivities of C–H bonds of various hydrocarbons are discussed. Information about relative reactivities of the C=C double bonds of cyclic alkenes and of some styrene derivatives is presented. The bibliography includes 42 references.

I. Introduction

Competitive reactions have been widely used to obtain data concerning the relative rates of chlorination of various hydrocarbons.^{1–6} If these data and also the compositions of the isomeric chloro-derivatives formed from the individual hydrocarbons are known, it is possible to calculate the relative reactivities of individual C–H bonds with chlorine atoms.

In the chlorination of mixtures of hydrocarbons only one radical capable of attacking C–H bonds is present, namely the chlorine atom. In the liquid-phase oxidation of a mixture of two hydrocarbons, individual C–H bonds may be attacked by at least two different peroxy radicals, each derived from one of the starting hydrocarbons (Scheme 1). It has been assumed that

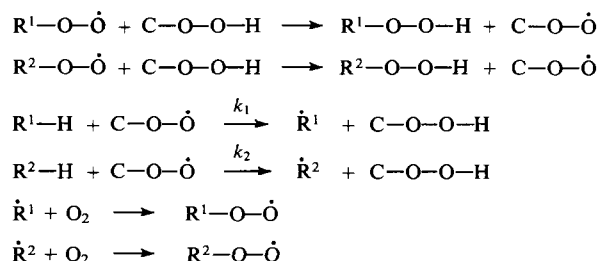


Scheme 1

$k_{11} : k_{12} = k_{21} : k_{22} = k_1 : k_2$. Here k_1 and k_2 are the rate constants for the oxidation of the hydrocarbons R^1H and R^2H , respectively. In competitive oxidation correct data for k_1/k_2 can be obtained only if the relative reaction rates of peroxy radicals with different

C–H bonds are independent of the nature of the attacking radical.⁷ If the cooxidation is accomplished in the presence of a large excess of an individual hydroperoxide then all peroxy radicals formed from the starting hydrocarbons will react with it (Scheme 2).⁸

Scheme 2



In this case the relative reactivities of hydrocarbons and their individual C–H bonds with respect to the peroxy radical derived from the added hydroperoxide can be calculated by the methods used in chlorination.^{8,9}

Table 1 presents the relative rates of oxidation of certain aromatic hydrocarbons in the presence of different individual

Table 1. The relative rates of reaction of various peroxy radicals with aromatic alkyl-substituted hydrocarbons.

Radical	Hydrocarbon			
	toluene	ethylbenzene	cumene	tetralin
$\text{Bu}^t\text{—O—O}^\bullet$	0.23	0.91	1	9.1
$\text{Pr}^i\text{C}_6\text{H}_4\text{—O—O}^\bullet$	0.17	1.00	1	9.2
$\text{C}_2\text{H}_5\text{—C}(\text{CH}_3)_2\text{—O—O}^\bullet$	0.33	1.47	1	8.7
$\text{Bu}^n\text{—O—O}^\bullet$	0.25	1.25	1	16.0
$\text{Bu}^s\text{—O—O}^\bullet$	0.25	1.25	1	10.5
$\alpha\text{-C}_{10}\text{H}_{12}\text{—O—O}^\bullet$ ^a	0.20	1.00	1	12.5

^a The α -tetralinylperoxy radical.

W W Pritzkow, V Ya Suprun Institut für Technische und Makromolekulare Chemie der Martin-Luther-Universität, Geusaer Strasse, D-06217 Merseburg, Germany. Fax (49-3461) 46 20 73

Received 14 December 1995

Uspekhi Khimii 65 (6) 538–546 (1996); translated by A K Grzybowski

Table 2. The relative rates of oxidation of the R¹H and R²H pairs of hydrocarbons as a function of their initial molar ratio.

R ¹ H	R ² H	k_1/k_2 for different molar ratios R ¹ H : R ² H				
		25 : 75	30 : 70	40 : 60	50 : 50	60 : 40
Cyclodecane	Cumene	0.60	0.62	0.60	0.59	0.48
Cyclooctane	"	0.79	0.75	0.74	0.72	0.72
	Cycloheptane	1.80	2.05	2.14	1.94	2.41
<i>cis</i> -Decalin	Cumene	0.67	0.72	0.67	0.66	0.63
<i>cis</i> -Pinane	"	1.55	1.52	1.62	1.49	1.64
	Cycloheptane	6.27	6.18	7.48	7.52	7.98
	Cyclooctane	3.94	3.58	3.25	3.29	3.39
Diphenylmethane	Cumene	1.86	1.97	1.69	1.97	1.82
1,2-Diphenylethane	"	0.68	0.58	0.73	0.76	0.74
Tetralin	"	4.44	5.14	6.19	5.06	5.31
<i>p</i> -Xylene	"	0.43	0.47	0.53	0.46	0.42
<i>p</i> -Di(<i>tert</i> -butyl)benzene	"	0.19	0.18	0.20	0.19	0.18
1,1-Diphenylethane	"	1.39	1.35	1.30	1.42	1.39

hydroperoxides. The data confirm the assumption that the relative rates do not depend strongly on the nature of the attacking peroxy radical.⁸

The ratios of oxidation rates of hydrocarbons R¹H and R²H (i.e. their relative reactivities with peroxy radicals) were calculated from the equation

$$\frac{k_1}{k_2} = \frac{\Sigma[R^1OH][R^2H]}{\Sigma[R^2OH][R^1H]}.$$

Binary mixtures of hydrocarbons were oxidised at molar ratios ranging from 25 : 75 to 60 : 40, temperatures of 90–110 °C, and oxygen absorptions up to 10 mmol per 100 mmol of the sum of both hydrocarbons. After oxidation was complete, the reaction mixture was reduced with lithium aluminium hydride, and the alcohols formed were analysed gas chromatographically. For all the mixtures investigated k_1/k_2 ratios identical within the limits of error were obtained (Table 2). This demonstrates the validity of the assumption that the relative rates of reaction of peroxy radicals with hydrocarbons are independent of the nature of the radical. One must take into account the fact that at high concentrations of R¹H the fraction of its peroxy radical R¹OO[•] in the reaction mixture must be higher than at low concentrations.

The independence of the relative rates of oxidation of a mixture of two hydrocarbons of a given initial ratio demonstrates that the relative rates of the individual C—H bonds with attacking peroxy radicals are independent of the nature of the latter. If this is the case, the rates of oxidation relative to any other partner can be calculated indirectly by employing the oxidation of two pairs of hydrocarbons (e.g. R¹H + R³H and R²H + R³H) in accordance with the equation

$$\frac{k_1}{k_2} = \frac{k_1/k_3}{k_2/k_3}.$$

The results of such calculations do agree with data obtained by direct cooxidations (of R¹H and R²H) (Table 3). This constitutes yet another confirmation of the independence of the relative rates of oxidation of various hydrocarbons (or different C—H bonds) of the nature of the attacking peroxy radicals.

Evidently, it is necessary to select a certain hydrocarbon as a standard and to refer to its oxidation rate the oxidation rates (reactivities) of all other compounds. In the present review, the highly reactive tertiary C—H bond of cumene was chosen as the standard. This means that in most cases cumene was used as the second component of the starting mixture in the cooxidation experiments. Cyclooctane can also be used as a convenient reference hydrocarbon; its reactivity is relatively high, and only

one alcohol (cyclooctanol) is formed from its oxidation products on reduction with lithium aluminium hydride.

Table 3. A test of the possibility of the indirect determination of the relative rates of oxidation of the R¹H + R²H pairs of hydrocarbons under the conditions of their cooxidation.

R ¹ H + R ² H	k_1/k_2	
	directly determined	indirectly determined
<i>cis</i> -Pinane + cycloheptane	7.09	—
Cumene + cycloheptane	2.24	—
<i>cis</i> -Pinane + cumene	2.29	2.29
<i>cis</i> -Pinane + cyclooctane	3.52	—
Cumene + cyclooctane	1.40	—
<i>cis</i> -Pinane + cumene	2.29	2.51
Ethylbenzene + indane	0.18	—
Cumene + indane	0.25	—
Ethylbenzene + cumene	0.84	0.72
3-Phenylbutane + cumene	0.18	—
<i>n</i> -Butylbenzene + cumene	0.44	—
3-Phenylbutane + <i>n</i> -butylbenzene	0.35	0.41
2-Phenylbutane + cumene	0.51	—
<i>n</i> -Propylbenzene + cumene	0.57	—
2-Phenylbutane + <i>n</i> -propylbenzene	0.85	0.89

II. Reactivities of alkylbenzenes and their activated α -C—H bonds

The reactivities of activated (α -position to the benzene ring) and nonactivated C—H bonds of alkylbenzenes have been investigated in detail.^{7, 10–12} Table 4 presents data on the relative rates of oxidation of alkyl-substituted benzene and also on the relative reactivities of their individual C—H bonds. Evidently, the reactivities of both the primary and secondary C—H bonds at the α -position in most cases do not depend significantly on the presence of additional alkyl substituents in the benzene ring. A similar conclusion can also be reached concerning the reactivities of tertiary α -C—H bonds. Table 4 shows that the reactivities of the α -C—H bonds increase in the sequence primary (0.08) < secondary (0.29) < tertiary (0.82) in the ratio of approximately 1 : 3 : 10 (Table 5). The mean deviation of the reactivity data increases in the same sequence. The reason for this is obviously the steric hindrance caused by the alkyl groups linked to the α -carbon atoms.

Table 4. The relative rates of oxidation of aromatic alkyl-substituted hydrocarbons and the relative reactivities of their α -C–H bonds.

Hydrocarbon	Rate of oxidation (rel. units)	Reactivity of C–H bonds (rel. units) ^a		
		primary	secondary	tertiary
Toluene	0.189 ± 0.012	0.06	—	—
<i>p</i> -(<i>tert</i> -Butyl)-toluene	0.189 ± 0.003	0.06	—	—
<i>o</i> -Xylene	0.509 ± 0.009	0.08	—	—
<i>m</i> -Xylene	0.411 ± 0.020	0.07	—	—
<i>p</i> -Xylene	0.460 ± 0.019	0.08	—	—
Mesitylene	0.674 ± 0.043	0.07	—	—
Durene	1.472 ± 0.080	0.12	—	—
Ethylbenzene	0.805 ± 0.014	—	0.42	—
<i>p</i> -Ethyltoluene	1.89 ± 0.07	0.13	0.75	—
<i>n</i> -Propylbenzene	0.573 ± 0.047	—	0.29	—
<i>n</i> -Butylbenzene	0.436 ± 0.030	—	0.22	—
Isobutylbenzene	0.494 ± 0.027	—	0.16	—
3-Methyl-1-phenylbutane	0.618 ± 0.021	—	0.26	—
3-Methyl-1- <i>p</i> -tolylbutane	0.866 ± 0.045	0.06	0.32	—
Cumene	1	—	—	1
<i>p</i> -Isopropyltoluene	1.875 ± 0.015	0.13	—	1.50
<i>p</i> -Isobutyltoluene	0.81 ± 0.02	0.08	0.23	—
2-Phenylbutane	0.507 ± 0.003	—	—	0.51
3-Phenylpentane	0.184 ± 0.003	—	—	0.18
Diphenylmethane	1.861 ± 0.052	—	—	—
2- <i>p</i> -Tolylbutane	1.316 ± 0.086	0.13	—	0.93
Phenyl- <i>p</i> -tolylmethane	2.06 ± 0.14	0.05	—	—
Bis(<i>p</i> -tolyl)methane	2.235 ± 0.067	0.06	—	—
Fluorene	4.35 ± 0.13	—	—	—
1,2-Diphenylethane	0.695 ± 0.033	—	0.17	—
1,2-Bis(<i>p</i> -tolyl)ethane	1.367 ± 0.078	0.06	0.25	—
1,3-Diphenylpropane	0.645 ± 0.022	—	0.17	—
1,1-Diphenylethane	1.370 ± 0.021	—	—	—
1,1-Diphenylpropane	0.626 ± 0.015	—	—	—
1,1-Diphenylbutane	0.524 ± 0.022	—	—	—
Indane	3.973 ± 0.087	—	—	—
Tetralin	5.23 ± 0.28	—	—	—

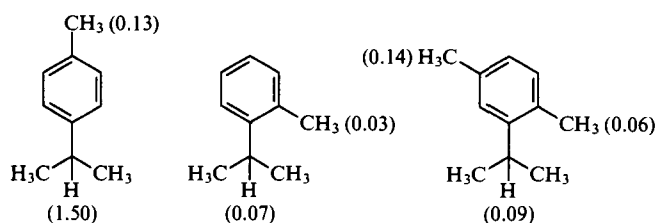
^a The average reactivities of the C–H bonds are 0.083 ± 0.008 for the primary bond, 0.294 ± 0.051 for the secondary bond, and 0.82 ± 0.23 relative units for the tertiary bond.

Table 5. Relative reactivities of the C–H bonds^a nonactivated and activated by one phenyl group.

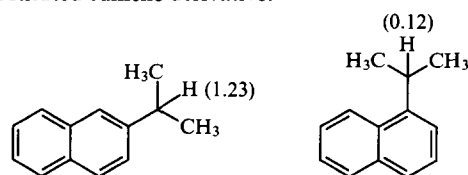
C–H bond	Nonactivated	Activated	Activation factor
Primary	0.00133	0.083	64
Secondary	0.011	0.29	26
Tertiary	0.10	0.82	8

^a With respect to the tertiary C–H bond of cumene.

It is known from the literature^{13–15} that *ortho*-substituted cumene derivatives are very difficult to oxidise; this is caused by steric hindrance of the coplanar arrangement of the methyl groups of the intermediate 2-arylisopropyl radical and the *ortho*-substituted benzene ring. Our data on the relative reactivities of the tertiary C–H bonds of two cumene derivatives containing *ortho*-methyl groups confirm this qualitative conclusion (the relative reactivities of the C–H bonds are indicated in brackets in the formulae presented).¹²



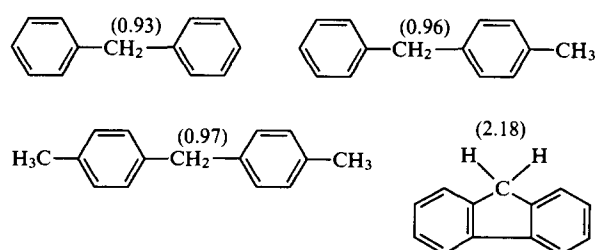
A similar decrease in reactivity is also observed in the case of α -isopropyl naphthalene,¹² which can be regarded as an *ortho*-substituted cumene derivative.

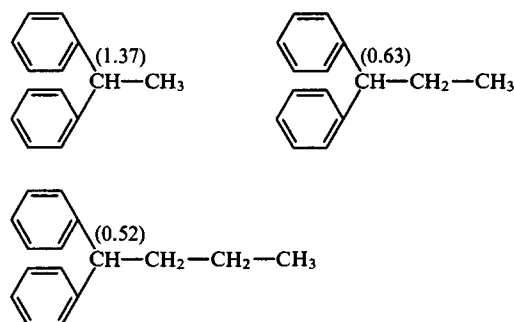


The tertiary C–H bonds in *ortho*-substituted cumenes and the inactivated tertiary C–H bonds have approximately the same reactivities in relation to the tertiary C–H bond of cumene (on average 0.10 ± 0.03):

Compound	Relative reactivity of the tertiary C–H bond
Isobutylbenzene	0.17
<i>p</i> -Isobutyltoluene	0.12
3-Methyl-1-phenylbutane	0.07
3-Methyl-1- <i>p</i> -tolylbutane	0.04

Only the question of the reactivities of the C–H bonds activated by a single benzene ring has been discussed hitherto, but Table 4 also contains data on diphenylmethane derivatives and 1,1-diphenylalkanes, i.e. hydrocarbons possessing C–H groups activated by two phenyl groups.





From the data presented in the formulae shown above, it follows that the second phenyl group induces only a small additional activation of the secondary C—H bonds and influences even less the reactivity of the tertiary C—H bonds. The cause of the influence of the phenyl groups on the reactivities of α -C—H groups is known to be the stabilisation of the corresponding carbon radicals and of the transition states during their formation. A prerequisite to such mesomeric stabilisation is the coplanar arrangement of the benzene rings with all the substituents at the α -carbon atom. Since two benzene rings at one radical (sp^2) carbon atom cannot be located in one plane, it follows that the second phenyl group is unable to induce a significant additional activation of the α -C—H bonds. On the other hand, if both benzene rings are forcibly accommodated in one plane, as in the case of fluorene, then the reactivity of α -C—H bonds is indeed increased (2.18).

III. Relative reactivities of aliphatic C—H bonds

Numerous studies of the cooxidation of n-alkanes with cumene carried out in our laboratory made it possible to determine their relative oxidation rates and also the reactivities of their individual C—H bonds (Table 6).¹⁶ The secondary C—H bonds of n-alkanes are appreciably more reactive than the primary bonds in oxidation as well as in other radical substitution reactions.⁵ The reactivity of the secondary C—H bond is lower the more remote its position from the end of the hydrocarbon chain. In the oxidation of normal paraffins a side reaction takes place, the intramolecular hydrogen transfer in the intermediate peroxy radicals, which results in the formation of up to 20% of bifunctional products.^{16–18} In the case of branched paraffins, the contribution of the intramolecular H-transfer is much higher, so that the determination of relative reactivities of such hydrocarbons and their C—H bonds is difficult. In the oxidation of aromatic compounds containing bulky alkyl groups, the non-

Table 6. Relative rates of oxidation of n-alkanes and relative reactivities of their C—H bonds.

n-Alkane	Rate of oxidation ^b	x^a	Reactivity ^b of one C—H group (rel. units) in position:			
			1	2	3	4— x^c
n-Nonane	0.181±0.005	5	0.0016	0.015	0.012	0.010
n-Decane	0.181±0.002	5	0.0014	0.014	0.011	0.009
n-Undecane	0.179±0.004	6	0.0010	0.013	0.010	0.008
n-Dodecane	0.200±0.011	6	0.0015	0.013	0.010	0.008
n-Tridecane	0.183±0.010	7	0.0006	0.011	0.009	0.007
n-Tetradecane	0.194±0.010	7	0.0009	0.011	0.009	0.007
n-Pentadecane	0.202±0.003	8	0.0008	0.010	0.008	0.007
n-Hexadecane	0.207±0.011	8	0.0007	0.009	0.007	0.007

^a Position most remote from the chain end. ^b With respect to the tertiary C—H bond of cumene. ^c Mean value for the positions 4 to x . The corresponding secondary alcohols could not be separated by capillary gas chromatography.

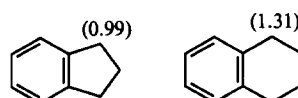
Table 7. The relative reactivities of the nonactivated C—H bonds in n-alkanes and in aromatic alkyl-substituted compounds.

Hydrocarbon	Relative reactivity of one C—H bond ^{a, b} (rel. units)			
	primary	secondary		tertiary
		position	value	
n-Nonane	0.0016	2	0.015	—
		3	0.012	
n-Decane	0.0014	2	0.014	—
		3	0.011	
n-Undecane	0.0010	2	0.013	—
		3	0.010	
n-Dodecane	0.0015	2	0.013	—
		3	0.010	
n-Tridecane	0.0006	2	0.011	—
		3	0.009	
n-Tetradecane	0.0009	2	0.010	—
		3	0.009	
n-Pentadecane	0.0008	2	0.010	—
		3	0.008	
n-Hexadecane	0.0007	2	0.009	—
		3	0.007	
1-Phenylpropane	—	2	0.011	—
1-Phenylbutane	—	2	0.009	—
		3	0.011	
2-Phenylbutane	—	3	0.011	—
2- <i>p</i> -Tolylbutane	—	3	0.013	—
3-Phenylpentane	—	2	0.013	—
3-Methyl-1-phenylbutane	—	2	0.023	0.07
3-Methyl-1- <i>p</i> -tolylbutane	—	2	0.010	0.04
Ethylbenzene	0.0020	—	—	—
n-Propylbenzene	0.0015	—	—	—
n-Butylbenzene	0.0018	—	—	—
Isobutylbenzene	—	—	—	0.17
<i>p</i> -Isobutyltoluene	—	—	—	0.12

^a With respect to the tertiary C—H bond of cumene. ^b The average reactivities of one C—H bond are 0.00125±0.00014 for the primary bond, 0.011±0.001 for the secondary bond, and 0.10±0.03 relative units for the tertiary bond.

activated C—H bonds are also attacked by peroxy radicals. It follows from Table 7 that the ratios of the reactivities of the primary, secondary, and tertiary aliphatic C—H bonds in alkanes and alkylaromatic hydrocarbons are 0.0013:0.011:0.10 ≈ 1:8.5:80. This was in fact to be expected, since the reactivities of aliphatic C—H bonds increase in precisely this sequence in all radical substitution reactions.

The reactivities of activated and nonactivated C—H bonds are collated in Table 5. The ratio of these quantities constitutes the activation factor. The data presented in Table 5 show that the activating effect of the phenyl group at the α -position decreases in the sequence primary > secondary > tertiary C—H bond. The cause is probably steric hindrance of the coplanar arrangement of the alkyl groups linked to the α -carbon atom with the atoms of the benzene ring. The coplanar arrangement gives rise to strain which increases with the increase in the number and the size of the alkyl groups. In indane and tetralin the groups linked to the α -carbon atoms are located in approximately the same plane as the benzene ring, and this causes an increase in the reactivities of their α -C—H bonds.



IV. Ring strain effects in the oxidation of cycloalkanes and their derivatives

The change in the hybridisation of one carbon atom of a carbocyclic compound from sp^3 to sp^2 is always associated with a change of the ring strain, which depends on the size of the ring.¹⁹ Therefore the rates of the reactions in which cycloalkyl radicals are formed are determined to a large extent by the ring size.²⁰ A similar dependence is characteristic also for the radical bromination (but not for the chlorination) of cycloalkanes.⁴

The cooxidation of cycloalkanes and their methyl-, ethyl-, and phenyl-substituted derivatives with cumene made the determination of the relative reactivities of their individual C—H bonds possible (Table 8).^{21, 22} As is to be expected,^{4, 19, 20} the reactivities of the C—H bonds in six-membered rings are especially low, whilst those in five-, seven-, and eight-membered rings are much higher. In cyclododecane, the C—H bonds have about the same reactivity as the secondary C—H bonds in normal paraffins (Table 6).

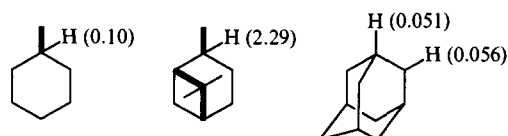
Table 8. Dependence of the reactivities of the C—H bonds of cycloalkane derivatives on ring size.

Number of carbon atoms in the ring	Relative reactivity ^a of one C—H bond (rel. units)			
	secondary C—H bond in cycloalkanes	tertiary C—H bond in methylcycloalkanes	tertiary C—H bond in ethylcycloalkanes	tertiary C—H bond in phenylcycloalkanes
4	—	—	—	1.1
5	—	—	0.128	5.3
6	—	0.102	0.072	0.8
7	0.032	0.261	0.122	1.5
8	0.045	0.258	0.148	2.6
9	0.038	0.115	0.128	—
10	0.029	—	—	—
11	0.028	—	—	—
12	0.011	—	—	—

^a With respect to the tertiary C—H bond of cumene.

It must be expected that ring strain effects observed in saturated carbocyclic compounds also occur in cycloalkenes and benzocycloalkenes and that the reactivity of the C—H bonds at the α -position to the double bond in cycloalkenes and benzocycloalkenes depends on the ring size. Such dependence has indeed been observed in the oxidation of cycloalkenes.²³ This also gives an explanation for the particularly high reactivity of indane and tetralin.⁷

Ring strain effects should also determine their reactivities in the oxidation of bicyclic and tricyclic compounds. The cooxidation of *cis*-pinane and cumene yields an unexpected result: the tertiary C—H bond in position 2 is 22 times more reactive than the analogous tertiary C—H bond of methylcyclohexane.²⁴ It is even more reactive than the tertiary C—H bond of cumene.



The tertiary C—H bonds at the bridgehead carbon atoms of *cis*-pinane do not react with peroxy radicals in accordance with Bredt's rule.^{24, 25} In adamantane both the secondary and the tertiary C—H bonds have approximately the same reactivities as the corresponding bonds in *n*-paraffins and in alkylaromatic hydrocarbons (Table 7).

V. Reactivities of the equatorial and axial C—H bonds in cyclohexane derivatives

The rates of oxidation of the *cis*- and *trans*-isomers of decalin²⁶ and dimethyl cyclohexanes²⁷ are substantially different. Obviously, tertiary C—H bonds in the equatorial position react more readily with peroxy radicals than similar C—H bonds in the axial position.²⁸ The cooxidation of the isomeric dimethyl cyclohexanes and of the decalins made it possible to determine the relative reactivities of the tertiary and secondary C—H bonds in these hydrocarbons (Table 9).²⁹ We were able to calculate separately the reactivities of the equatorial and axial C—H bonds from the overall reactivities of the tertiary C—H bonds (Table 10).

Table 9. Reactivities of the *cis*- and *trans*-isomers of dimethylcyclohexane and decalin and of their individual C—H bonds relative to cumene.

Compound	Relative reactivity (rel. units)		
	overall	tertiary C—H bond	secondary C—H bond ^a
<i>cis</i> -1,2-Dimethylcyclohexane	0.541	0.227	0.0087
<i>trans</i> -1,2-Dimethylcyclohexane	0.217	0.064	0.0113
<i>cis</i> -1,3-Dimethylcyclohexane	0.344	0.150	0.0059
<i>trans</i> -1,3-Dimethylcyclohexane	0.545	0.239	0.0085
<i>cis</i> -1,4-Dimethylcyclohexane	0.556	0.245	0.0082
<i>trans</i> -1,4-Dimethylcyclohexane	0.267	0.108	0.0065
<i>cis</i> -Decalin	0.671	0.262	0.0094
<i>trans</i> -Decalin	0.235	0.056	0.0078

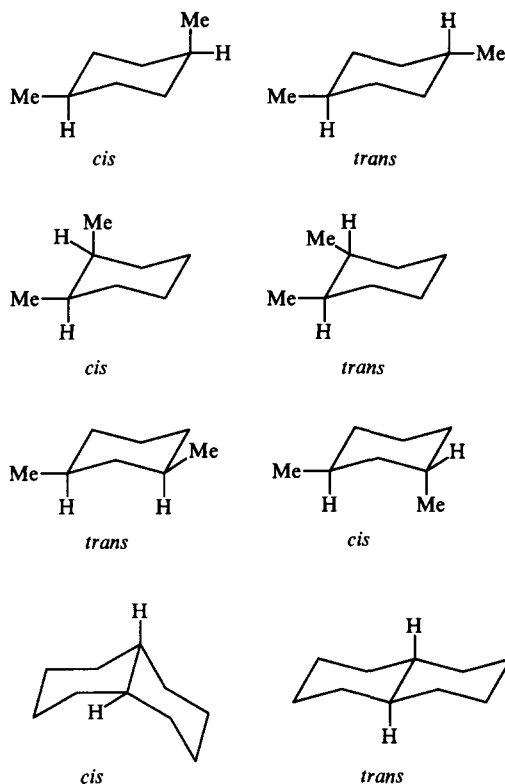
^a The average reactivity is 0.0083 ± 0.0006 rel. units.

Table 10. Relative reactivities of axial and equatorial C—H bonds in cyclohexane derivatives.

Compound	Overall reactivity of tertiary C—H bond	Equation for the calculation of the reactivity of an individual C—H bond ^a	Reactivity of one tertiary C—H bond (rel. units) ^b	
			a	e
<i>cis</i> -1,2-Dimethylcyclohexane	0.227	$a + e = 0.454$	0.064	0.390
<i>trans</i> -1,2-Dimethylcyclohexane	0.064	$2a = 0.128$		
<i>cis</i> -1,3-Dimethylcyclohexane	0.150	$2a = 0.300$		
<i>trans</i> -1,3-Dimethylcyclohexane	0.239	$a + e = 0.478$	0.150	0.328
<i>cis</i> -1,4-Dimethylcyclohexane	0.245	$a + e = 0.490$	0.108	0.382
<i>trans</i> -1,4-Dimethylcyclohexane	0.108	$2a = 0.216$		
<i>cis</i> -Decalin	0.262	$a + e = 0.524$	0.056	0.468
<i>trans</i> -Decalin	0.056	$2a = 0.112$		

^a Designations: (a) reactivity of axial tertiary C—H bond; (e) reactivity of equatorial C—H bond. ^b The average reactivities are 0.095 ± 0.022 for the axial bond and 0.392 ± 0.029 relative units for the equatorial bond.

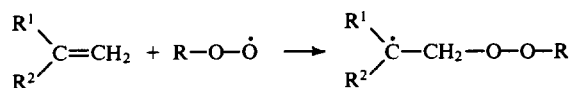
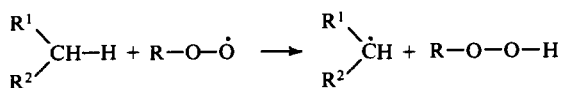
This was possible because one of the tertiary C—H bonds in *cis*-1,2- and *cis*-1,4-disubstituted cyclohexanes is in an equatorial whilst the other is in an axial position. In the corresponding *trans*-isomers, both tertiary C—H bonds are in axial positions. In *cis*-1,3-dimethylcyclohexane, both tertiary C—H bonds are axial, in *trans*-1,3-dimethylcyclohexane one of the tertiary C—H bonds is axial, the other is equatorial.



The reactivities of the secondary C—H bonds of disubstituted cyclohexane derivatives (Table 9) are similar to those of the secondary C—H bonds in acyclic hydrocarbons (Table 7). The equatorial tertiary C—H bond is approximately four times more reactive than the tertiary C—H bond in an axial position (Table 10). The reason for this difference is still not quite clear.²⁹ On the one hand, attack by peroxy radicals on the axial C—H bond is more hindered than on the equatorial bond. On the other hand, the internal strain in compounds with axial C—alkyl bonds is greater than in compounds with analogous equatorial bonds. It must be expected that the internal strain of cyclohexane derivatives diminishes if one H-atom is abstracted from a tertiary C—H bond and that the decrease of strain is higher if the geminal alkyl group is axial than if it is equatorial.

VI. Reactivities of cycloalkenes

In the oxidation of cycloalkenes, peroxy radicals do not only attack C—H bonds but also the C=C double bond.



We studied the cooxidation of certain cyclic alkenes with cumene and determined their relative reactivities (Table 11).²³ The reactivity of the allylic C—H bonds diminishes in the cyclopentene–cyclooctene sequence. The reactivity of these bonds is particularly high in the case of five- and six-membered rings. The reactivities of cyclopentene and cyclohexene are comparable with the reactivities of the corresponding indane and tetralin bonds. The reactivity of the C=C double bond also depends on the ring size and increases from cyclopentene to cyclooctene. The data presented in Table 11 make it possible to explain the results obtained previously in the oxidation of individual cycloalkenes.³⁰

Table 11. The reactivities of certain cycloalkenes and their individual bonds relative to cumene.

Alkene	Overall reactivity (rel. units)	Reactivity (rel. units)	
		of C=C bond	of allylic C—H bond
Cyclopentene	8.2	0.24	1.98
Cyclohexene	6.6	0.56	1.62
Cycloheptene	4.9	1.02	0.97
Cyclooctene	1.6	1.16	0.10
Norbornene	6.5	6.5	0.00

The bicyclic olefin norbornene has an unusually high reactivity³¹ and is attacked by peroxy radicals exclusively at the C=C double bond.^{32,33} It is noteworthy that in the cooxidation of cycloalkenes and norbornene with cumene, the only products from the interaction of the peroxy radicals with the C=C double bond are the corresponding epoxy compounds.

VII. Reactivities of styrene derivatives

The study of the cooxidation of certain styrene derivatives with cumene made the estimation of relative reactivities of their double bonds possible (Table 12). The C=C bond of styrene is much more reactive than the double bonds in monocyclic alkenes, and its reactivity is comparable to that of the C=C bond of norbornene. A methyl group at the α -position increases the reactivity of the double bond and the effect induced by it is only slightly weaker than the effect of the α -phenyl group. The introduction of a phenyl group at the α -position increases only insignificantly the reactivity of the double bond in comparison with α -methylstyrene because a coplanar arrangement of two phenyl groups linked with one radical carbon atom is not possible. A *tert*-butyl group at the α -position diminishes the reactivity of styrene since in this case it is not possible to achieve a planar structure of the intermediate carbon radical. Further studies showed that the reactivity of the double bond in styrene derivatives usually increases if an electron-donating substituent is introduced in the α - or *para*-position.^{34,35}

Table 12. The relative rates of oxidation of certain styrene derivatives.

Substituents in styrene molecule		Reactivity of the C=C bond (rel. units)
α -position	<i>para</i> -position	
H	H	6.98 \pm 0.40
Me	H	12.78 \pm 0.54
Bu ^t	H	0.75 \pm 0.05
Ph	H	15.6 \pm 0.9
Me	Bu ^t	14.0 \pm 0.2

In the cooxidation of styrene and its derivatives with cumene, not only the corresponding epoxides but also oligomeric peroxides and products of an oxidative degradation are formed.^{34–36} The proportion of the particular product depends on the nature of the substituent and on the reaction conditions.

VIII. Conclusion

Thus the oxidation of binary hydrocarbon–cumene mixtures makes it possible to determine both the relative overall rates of interaction of hydrocarbons with peroxy radicals and the relative reactivities of their individual C—H bonds without the addition of an individual hydroperoxide. For this purpose, the oxidation products are subjected to total quantitative analysis after preliminary reduction of the oxidation products by lithium aluminium hydride. Reproducible and mutually consistent

relative reactivities of hydrocarbons, which in most cases agree with the theoretical predictions, can be obtained in this way.

In the studies^{37–42} the absorption of oxygen was followed during liquid-phase cooxidations. Relative and absolute rate constants for the interaction of peroxy radicals with hydrocarbons were determined with the aid of the copolymerisation equation without taking into account the formation of various isomeric peroxy radicals from each hydrocarbon. For this reason, in all the studies it was assumed that the rates of reaction of isomeric peroxy radicals with various hydrocarbons are equal. It is noteworthy that in most cases the data obtained in the studies^{37–42} for the relative rates of interaction of hydrocarbons with peroxy radicals agree well with our results.⁷ It must be stressed, however, that relative reactivities of individual C—H bonds cannot be determined by the methods described in Refs 37–42.

The authors thank the 'Fonds der Chemischen Industrie' and the 'Deutsche Forschungsgemeinschaft' for financial support.

References

1. N Coleburn, E S Stern *J. Chem. Soc.* 3599 (1965)
2. E M Hodnett, P S Juneja *J. Org. Chem.* **32** 4114 (1967)
3. E M Hodnett, P S Juneja *J. Org. Chem.* **33** 1231 (1968)
4. N J Bunce, M Hadley *J. Org. Chem.* **39** 2271 (1974)
5. H Berthold, Ch Braeunig, S Grosse, M Hampel, F D Kopinke, W Pritzkow, G Stachowski *J. Prakt. Chem.* **318** 1019 (1976)
6. A S Dneprovskii *Zh. Vses. Khim. O-va im D I Mendeleeva* **30** 315 (1985)
7. V A Belyakov, G Lauterbach, W Pritzkow, V Voerckel *J. Prakt. Chem.* **334** 373 (1992)
8. J A Howard, K U Ingold *Can. J. Chem.* **46** 2655; 2661 (1968)
9. J A Howard *Isr. J. Chem.* **24** 33 (1984)
10. W Pritzkow, G Thomas, L Willecke *J. Prakt. Chem.* **327** 847 (1985)
11. W Pritzkow, G Thomas, L Willecke *J. Prakt. Chem.* **327** 945 (1985)
12. A Heinze, G Lauterbach, W Pritzkow, W Schmidt-Renner, V Voerckel, N Zewegsuren *J. Prakt. Chem.* **329** 439 (1987)
13. M I Farberov, A V Bondarenko, V M Obukhov, G I Karakulev *Dokl. Akad. Nauk SSSR* **179** 1359 (1968)
14. M I Farberov, A V Bondarenko, G N Shustovskaya *Dokl. Akad. Nauk SSSR* **187** 831 (1969)
15. A V Bondarenko, M I Farberov, G N Shustovskaya *Zh. Org. Khim.* **5** 651 (1969)
16. G Lauterbach, F Karabet, M Makhoul, W Pritzkow *J. Prakt. Chem.* **336** 712 (1994)
17. R K Jensen, S Korcek, L R Mahoney, M Zinbo *J. Am. Chem. Soc.* **101** 7574 (1979)
18. L Chaly, R Peitzsch, W Pritzkow, V Voerckel, N Zewegsuren *J. Prakt. Chem.* **336** 545 (1987)
19. H C Brown *J. Chem. Educ.* **36** 424 (1959)
20. C Rüchardt *Usp. Khim.* **47** 2014 (1978) (Translated into Russian from *Forschungsberichte des Landes Nordrhein-Westfalen* No. 2471, Westdeutscher Verlag, 1975)
21. R Harnisch, G Lauterbach, W Pritzkow *J. Prakt. Chem.* **337** 60 (1995)
22. B Batke, G Lauterbach, W Pritzkow, V Voerckel *J. Prakt. Chem.* **331** 424 (1989)
23. G Lauterbach, W Pritzkow *J. Prakt. Chem.* **337** 237 (1995)
24. G Lauterbach, W Pritzkow *J. Prakt. Chem.* **337** 416 (1995)
25. Th Brose, W Pritzkow, G Thomas *J. Prakt. Chem.* **334** 403 (1992)
26. R Criegee *Ber. Dtsch. Chem. Ges.* **77** 22 (1944)
27. R Criegee, P Ludwig *Erdoel Kohle, Erdgas Petrochem.* **15** 523 (1962)
28. C E Doering, H G Hauthal, Y Noglik, W Pritzkow *J. Prakt. Chem.* **24** (4) 183 (1964)
29. G Lauterbach, W Pritzkow *J. Prakt. Chem.* **336** 83 (1994)
30. K Blau, U Mueller, W Pritzkow, W Schmidt-Renner, Z Sedshaw *J. Prakt. Chem.* **322** 915 (1980)
31. C E Doering, H Gross, I Hahn, H G Hauthal, W Pritzkow, U Szalajko *J. Prakt. Chem.* **35** (4) 236 (1967)
32. D E Van Sickle, F R Mayo, R M Arluck *J. Org. Chem.* **32** 3680 (1967)
33. Ch Duschek, W Grimm, M Hampel, R Jauch, W Pritzkow, H Rosner *J. Prakt. Chem.* **317** 1027 (1975)
34. W Suprun, K Blau, K Reinker *J. Prakt. Chem.* **337** 496 (1995)
35. W Suprun *J. Prakt. Chem.* **338** 231 (1996)
36. W Suprun, F Vogt *J. Prakt. Chem.* **337** 601 (1995)
37. J Alagy, G Clement, J-C Balaceanu *Bull. Soc. Chim. Fr.* 1325 (1959)
38. J Alagy, G Clement, J-C Balaceanu *Bull. Soc. Chim. Fr.* 1459 (1960)
39. J Alagy, G Clement, J-C Balaceanu *Bull. Soc. Chim. Fr.* 1303 (1961)
40. J Alagy, G Clement, J-C Balaceanu *Bull. Soc. Chim. Fr.* 1792 (1961)
41. R V Kucher, I A Opeida *Usp. Khim.* **54** 765 (1985) [*Russ. Chem. Rev.* **54** 452 (1985)]
42. R V Kucher, I A Opeida *Sookislenie Organicheskikh Soedinenii* (Cooxidation of Organic Compounds) (Kiev: Naukova Dumka, 1989)

Cyclic mechanisms of chain termination in the oxidation of organic compounds

E T Denisov

Contents

I. Introduction	505
II. Chain termination with phenols and aromatic amines in the oxidation of hydrocarbons	505
III. Cyclic chain termination in the oxidation of alcohols, alkenes, and amines	507
IV. Cyclic chain termination with quinones in the oxidation of alcohols and polymers	510
V. Cyclic chain termination mechanisms involving nitroxyl radicals	512
VI. Cyclic chain termination mechanisms involving acid catalysis	515
VII. Ions and complexes of variable-valence metals as catalysts for chain termination in the oxidation of alcohols, amines, and alkenes	516
VIII. Conclusion	516

Abstract. All the mechanisms known at present for cyclic (repeated) chain termination involving aromatic amines, quinones, nitroxyl radicals, and variable-valence metal complexes in the oxidation of hydrocarbons, polymers, alcohols, and aliphatic amines are surveyed. The mechanisms are classified and the factors needed for the realisation of a particular mechanism are analysed. The reasons for the limitation of the number of cycles in the cyclic chain termination mechanism are considered. The bibliography includes 84 references.

I. Introduction

Inhibitors of oxidation (antioxidants) play an important role in modern technology for the production of polymers,^{1–4} lubricants,⁵ hydrocarbon fuel,⁶ solvents, intermediate products in organic synthesis,⁷ and foodstuffs.⁸ They also perform the function of protecting living organisms from the harmful influence of oxygen, light, and radiation. Studies in the fields of synthesis and physicochemical and biochemical properties of antioxidants and intermediate products formed from them have been developed intensely during the last three decades. An important place among these studies is occupied by the studies of elementary reactions of inhibitors and of the radicals derived from them.^{9–11}

The oxidation of organic compounds with oxygen in the liquid phase proceeds as a rule by a chain mechanism involving participation of peroxy radicals in the chain propagation. Therefore, compounds that are able to react rapidly with peroxy radicals and thus cause chain termination occupy a prominent place among antioxidants. Phenols, thiophenols, and aromatic amines are effective oxidation inhibitors and are irreversibly consumed in reactions with peroxy radicals. When the oxidation is propagating rapidly at a sufficiently high temperature or under the action of very intense light, these inhibitors permit the process to be decelerated for only a short period.

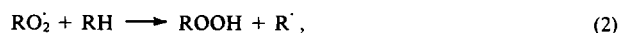
In this connection, the inhibiting systems that ensure the possibility of regenerating the inhibitor consumed in the chain termination steps are of interest. This permits the oxidation to be retarded effectively by adding a relatively small amount of an inhibitor.

The cyclic mechanism of chain termination was discovered in a study of oxidation of alcohols^{12–14} in which aromatic amines have been used as inhibitors. A short time later, the ability of copper ions to terminate repeatedly the chains during oxidation of cyclohexanol was found.¹⁵ The cyclic mechanisms of chain termination are due to the dual reactivity of the hydroxyperoxy radicals formed in the oxidation of an alcohol. This has been confirmed in relation to *p*-benzoquinone,¹⁶ which terminates the chains in the oxidation of alcohols by the cyclic mechanism, but has virtually no influence on the oxidation of hydrocarbons.

The possibility of the repeated chain termination with stable nitroxyl radicals in the oxidation of polymers was discovered in 1972.¹⁷ Later, a fundamentally new three-component system ensuring the cyclic chain termination in the oxidation of hydrocarbons was suggested. Apart from nitroxyl radicals, an important role in this system is played by an alcohol (primary or secondary) and an organic (citric) acid, which are responsible for the acid catalysis.¹⁸ Certain aspects of the cyclic chain termination during oxidation have been considered in a number of reviews.^{19–23} However, in the present review all the currently known systems and mechanisms for the cyclic chain termination in the oxidation of organic compounds are considered comprehensively for the first time, and the reasons enabling the realisation of these mechanisms are also analysed.

II. Chain termination with phenols and aromatic amines in the oxidation of hydrocarbons

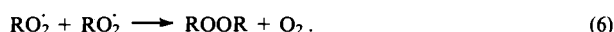
Oxidation of hydrocarbons⁹ and of many other organic compounds^{24,25} involves alkyl (R^\cdot) and peroxy (RO_2^\cdot) radicals and proceeds by a chain mechanism that includes the following elementary stages:



E T Denisov Laboratory of the Kinetics of Liquid-Phase Radical Reactions, Institute of Chemical Physics in Chernogolovka, Russian Academy of Sciences, 142432 Chernogolovka, Moscow Region, Russian Federation. Fax (7-096) 515 35 88.

Received 10 November 1995

Uspekhi Khimii 65 (6) 547–563 (1996); translated by Z P Bobkova



At a partial pressure of oxygen of 10–100 kPa and with sufficiently intense stirring of the liquid phase (which facilitates the diffusion of oxygen into the compound being oxidised) alkyl radicals are converted very rapidly (over a period of 10^{-6} – 10^{-4} s) into peroxy radicals. Chain termination occurs via reaction (6), which accounts for the limitation of the chain length.

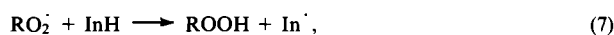
$$v = \frac{k_2[RH]}{(2k_6v_i)^{0.5}},$$

where v_i is the rate of initiation and k_2 and k_6 are rate constants of the corresponding stages. The lower the rate of reaction (6), the longer the chain. The chain regime is realised when

$$k_2^2[RH]^2 > 2k_6v_i.$$

As the hydroperoxide is accumulated, the initiation rate increases and the oxidation accelerates.

The introduction of an inhibitor InH (phenol or amine) accelerates the chain termination due to the occurrence of the following reactions:^{9–11}



(Mol are molecular products).

If the concentration of the inhibitor is sufficiently high, so that

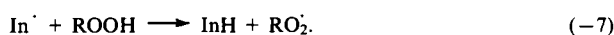
$$k_7[InH] > (2k_6v_i)^{0.5},$$

then the chain termination will proceed via reactions (7)–(9) and the chain length will be equal to

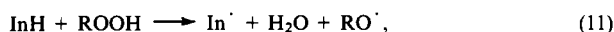
$$v = \frac{k_2[RH]}{fk_7[InH]},$$

where f is the stoichiometric coefficient of inhibition. The reactions (8) and (9) occur very rapidly (their rate constants are 10^8 – 10^9 dm³ mol⁻¹ s⁻¹), the rate of the chain termination being limited by the reaction (7). Within the framework of this scheme, which is typical of oxidation of hydrocarbons, $f \cong 2$ in the case where reaction (8) predominates or $f \cong 1$ if the reaction (9) predominates. The f values determined experimentally fall in this range.²⁶

The In^{\cdot} radicals can react with ROOH and RH to give the RO_2^{\cdot} and R^{\cdot} radicals,²³ which are then involved in the chain propagation:



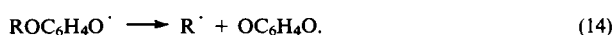
When the temperature is fairly high (>400 K), the inhibitor starts to react with the hydroperoxide and with oxygen at a noticeable rate thus initiating chains:²³



The quinolide peroxides InOOR, resulting from the recombination of phenolic and peroxy radicals, redissociate into radicals, which initiate oxidation at fairly high temperatures:¹¹



The decomposition of *p*-alkoxy-substituted phenoxyl radicals affords alkyl radicals, which continue the oxidation chain.¹¹



The semiquinone radicals continue the chain by reacting with oxygen.²⁷



Thus, the kinetics of the inhibited oxidation depend, on the one hand, on a number of reactions involving ROOH, RO_2^{\cdot} , and O_2 and, on the other hand, on the reactions involving the inhibitor and the radicals derived from it.

The duration of the retarding action of an inhibitor is determined by its concentration and reactivity, and also by the conditions and the regime of the chain oxidation. At a constant initiation rate and with intense chain termination by the inhibitor [$fk_7[InH]_0 > (k_6v_i)^{0.5}$], the induction period τ is equal to $f[InH]_0v_i^{-1}$, i.e. it is directly proportional to the concentration of the added inhibitor and to the inhibition coefficient. Under the conditions of autooxidation, when the hydroperoxide formed acts as an initiator, a feedback appears between the efficiency of the chain termination with the inhibitor and the induction period τ . Problems of the mechanism and the efficiency of oxidation inhibitors have been considered in detail in a number of monographs and reviews.^{3,6,9–11} It is noteworthy that the induction period of the inhibited oxidation depends in all cases on the coefficient f and on the concentration of the inhibitor. The reactions (7)–(15) associated with the participation of the inhibitor may be divided into two groups: reactions having no influence on the coefficient f [reactions (7), (–7), and (10)], and reactions, the occurrence of which influences the f value [reactions (8), (9), (11)–(15)].

It seems that oxidation could be retarded if a large amount of an inhibitor is added. However, both theory and experience indicate that the use of high concentrations of an inhibitor reduces its efficiency and leads sometimes to a shortening rather than to an extension of the induction period. This is accounted for by the following reasons. An increase in the concentration of an inhibitor leads to an increase in the quasi-steady concentration of the In^{\cdot} radicals, and, consequently, the chain propagation reactions involving these radicals [reactions (10), (–7), (14), and (15)] proceed more intensely. The rate of the initiation reactions [(11) and (12)] involving the inhibitor is directly proportional to its concentration. Therefore, it is expedient to increase the concentration of the inhibitor only up to a value at which initiation involving it is insignificant.

There are also other reasons why high antioxidant concentrations are undesirable. First, the evaporation of the inhibitor from the polymer sample or its washing-out in the case where it is in contact with a liquid accelerates at high concentrations. Second, high concentrations of an antioxidant may be toxic for a human organism. Third, antioxidants deteriorate the mechanical properties of polymeric articles. Fourth, the introduction of large quantities of a fairly expensive antioxidant increases substantially the cost of an article or a product. In some cases, this contradictory situation can be resolved by using antioxidants that provide repeated chain termination per one initial molecule of the inhibitor, owing to the realisation of the cyclic chain termination mechanism. In these cases, prolonged retardation of the oxidation can be achieved with a small amount of an inhibitor.

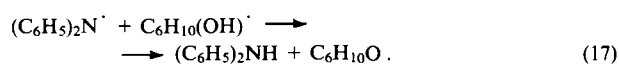
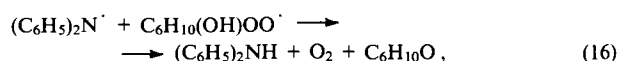
An important role in the identification and investigation of cyclic mechanisms of chain termination has been played by experiments dealing with the measurement of the coefficient f . It should be noted that this coefficient is stoichiometric only when it is determined by the reactions (7)–(9). In the case where cyclic chain termination occurs, the coefficient f is influenced by the competition between the irreversible destruction of the In^{\cdot} radicals on the one hand, and the conversion of In^{\cdot} into the initial InH on the other hand. In these systems, f should be considered and said to be the inhibition coefficient.

The coefficient f has been measured by various methods. When aromatic amines were used as inhibitors, f was defined as the ratio v_i/v_{InH} , where v_{InH} is the rate of consumption of the amine in an experiment with a constant rate of initiation.

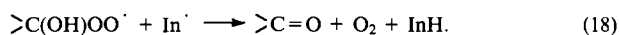
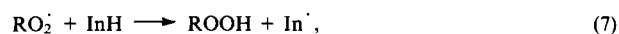
The concentration of the amine was determined by colorimetry after its conversion into a brightly coloured compound.^{12–14} When stable nitroxyl radicals were used as inhibitors, the variation of their concentration during the experiment has been monitored by EPR.^{17,18} The consumption of a quinone has been evaluated from the increase in the rate of the initiated oxidation during the experiment.¹⁶ In the case where variable-valence metals were used as inhibitors, the evaluation was based on the induction period.

III. Cyclic chain termination in the oxidation of alcohols, alkenes, and amines

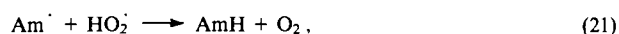
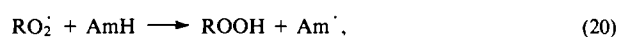
A high value of the inhibition coefficient ($f = 28$) was detected for the first time in the oxidation of cyclohexanol in the presence of α -naphthylamine (393 K, *tert*-butyl peroxide as the initiator, $P_{O_2} = 10^5$ kPa).¹² For the oxidation of *n*-decane under the same conditions, $f = 2.5$. In the case of the oxidation of *n*-decane–cyclohexanol mixtures, the coefficient f increased with increase in the cyclohexanol concentration, from 2.5 (in pure *n*-decane) to 28 (in pure alcohol).¹² When the oxidation of cyclohexanol was carried out in the presence of tetraphenylhydrazine, the diphenylamino radicals produced from tetraphenylhydrazine were reduced to diphenylamine.¹⁴ This conclusion has been confirmed in another study.²⁸ Diphenylamine was formed only in the presence of the initiator, no matter whether the process was conducted under an oxygen atmosphere or under an inert atmosphere. In the former case, the amino radical was reduced by the hydroperoxyl radical derived from the alcohol, and in the latter case, it was reduced by the hydroxyalkyl radical:



On the basis of these results the following mechanism was suggested for the cyclic chain termination:¹⁴



The oxidation of primary and secondary alcohols in the presence of α -naphthylamine, β -naphthylamine, or phenyl- α -naphthylamine is characterised by high values of the inhibition coefficient ($f \gg 2$).^{12–14} Alkylperoxyl and α -ketoperoxyl radicals, like the peroxyl radicals derived from tertiary alcohols, are incapable of reducing the amino radicals. For example, when oxidation of *tert*-butanol is inhibited by α -naphthylamine, f is equal to 2, which coincides with the value found in the oxidation of alkanes.¹⁴ However, the addition of hydrogen peroxide to the *tert*-butanol being oxidised leads to the realisation of the cyclic chain termination mechanism (α -naphthylamine as the inhibitor, 393 K, cumyl peroxide as the initiator, $P_{O_2} = 100$ kPa).²⁹ This is due to the participation of the HO_2^\cdot radicals formed in the chain termination:

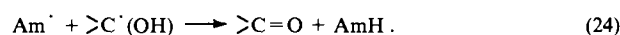
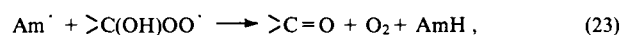
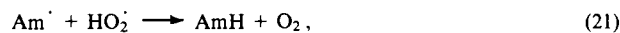


where AmH is an amine (in this particular case, it is α -naphthylamine).

Since the peroxyl radicals derived from the alcohol dissociate to a carbonyl compound and HO_2^\cdot

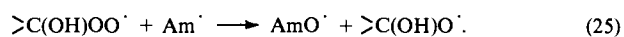


three reactions, in which the amino radicals formed from the amine are reduced, proceed in parallel under the conditions of the oxidation of the alcohol:

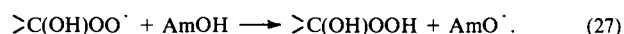
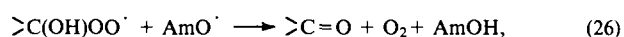


In the presence of dissolved oxygen, the hydroxyalkyl radicals are converted very rapidly into the hydroxyperoxyl radicals, therefore, only $>C(OH)OO^\cdot$ and HO_2^\cdot participate in the reduction of the amino radicals. The higher is the temperature, the more effectively the decomposition of the hydroxyperoxyl radicals proceeds and the higher is the proportion of the HO_2^\cdot radicals participating in the regeneration of the amine.

Our investigation has shown³⁰ that in the case of repeated chain termination with aromatic amines in the oxidation of alcohols, the situation is more complicated. In parallel with the reaction (23), the following reaction proceeds:



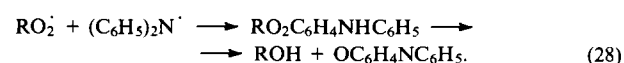
The nitroxyl radical, in its turn, gives rise to a new cyclic mechanism of chain termination according to reactions:



The intermediate formation of nitroxyl radical has been detected in the oxidation of isopropanol retarded by diphenylamine; chain termination occurs by cyclic mechanisms involving both Am^\cdot and AmO^\cdot .³⁰ In the case where the oxidation of isopropanol is decelerated by bis(*p*-methoxyphenyl)amine, only the cycle involving nitroxyl radicals is realised.³⁰

Organic acids retard the formation of nitroxyl radicals via reaction (25).³¹ Apparently, the formation of a hydrogen bond of the $N \cdots HOC(O)R$ type leads to shielding of nitrogen, which precludes the addition of oxygen to it, yielding the nitroxyl radical. Thus, the products of the oxidation of hydrocarbons (acids) have an influence on the mechanism of the cyclic chain termination.

As noted above, the duration of the retarding action of an inhibitor is directly proportional to the f value. In systems with a cyclic chain termination mechanism, the coefficient f depends on the ratio of the rate constants for the two reactions, in which the inhibitor is regenerated and irreversibly consumed. In the oxidation of alcohols, amino radicals are consumed irreversibly via reaction (25) and via the following reaction:



The formation of the nitroxyl radical [reaction (25)] and of quinone imine [reaction (28)] precludes the possibility of the recovery of amine and, hence, either of the above reactions interrupts the cycle at the amino radical

$$f = 1 + \frac{k_{23}}{k_{25} + k_{28}}.$$

Table 1 presents the inhibition coefficients and the termination rate constants in systems with a cyclic mechanism of chain termination with aromatic amines. Naturally, these are effective rate constants, which characterise primarily the rate-limiting stage of the chain termination process.

The question of why the amino radicals ensure cyclic chain termination in those systems in which the HO_2^\cdot and $>C(OH)OO^\cdot$ radicals are formed, but not in the oxidation of hydrocarbons where alkylperoxyl radicals RO_2^\cdot are the chain-propagating species, deserves special attention.⁴²

Disproportionation of the amino and peroxyl radicals that involves both the O–H and C–H bonds is, in principle, possible:

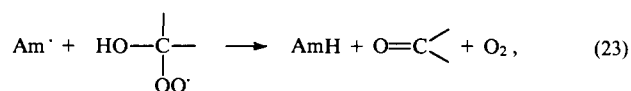
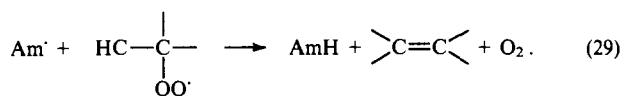


Table 1. Inhibition coefficients and rate constants for the reactions of peroxy radicals with aromatic amines in systems with a cyclic mechanism of chain termination.

Amine	Substrate	Peroxy radical	<i>T</i> / K	<i>f</i>	<i>k</i> / 10 ⁴ dm ³ mol ⁻¹ s ⁻¹	Ref.
(C ₆ H ₅) ₂ NH	(CH ₃) ₂ CHOH	RO ₂ [•]	343	> 23	—	30
(C ₆ H ₅) ₂ NH	CH = CHCH = CHCH ₂ CH ₂	HO ₂ [•]	348	200	—	32
(C ₆ H ₅) ₂ NH	<i>trans</i> -C ₆ H ₅ CH = CHCOOC ₂ H ₅	HO ₂ [•]	323	20	36.0	33
(C ₆ H ₅) ₂ NH	<i>trans</i> -C ₆ H ₅ CH = CHCOOCH ₃	HO ₂ [•]	323	20	28.0	33
(C ₆ H ₅) ₂ NH	<i>trans</i> -C ₆ H ₅ CH = CHCOOC ₆ H ₅	HO ₂ [•]	323	20	1.1	33
(C ₆ H ₅) ₂ NH	cyclo-C ₆ H ₁₁ OH	RO ₂ [•]	393	56	0.5	34
(C ₆ H ₅) ₂ NH	(CH ₃) ₂ N(CH ₂) ₂ OCO(CH ₃)C = CH ₂	RO ₂ [•]	323	10	0.6	35
(4-CH ₃ OC ₆ H ₄) ₂ NH	(CH ₃) ₂ NCH ₂ CH ₂ N(CH ₃) ₂	RO ₂ [•]	313	26	6.5	36
(4-CH ₃ OC ₆ H ₄) ₂ NH	(CH ₃) ₂ CHOH	RO ₂ [•]	343	22	—	30
(4-CH ₃ OC ₆ H ₄) ₂ NH	cyclo-[N(CH ₃)(CH ₂) ₅]	RO ₂ [•]	323	52	7.3	37
(4-CH ₃ OC ₆ H ₄) ₂ NH	N(CH ₂ CH ₃) ₃	RO ₂ [•]	313	80	44.0	38
(4-CH ₃ OC ₆ H ₄) ₂ NH	cyclo-C ₆ H ₁₁ N(CH ₃) ₂	RO ₂ [•]	323	70	150	38
(4-CH ₃ OC ₆ H ₄) ₂ NH	CH ₃ CON(CH ₂ CH ₃) ₂	RO ₂ [•]	348	30	> 10	39
(4-CH ₃ OC ₆ H ₄) ₂ NH	cyclo-C ₆ H ₁₁ NH ₂	RO ₂ [•]	348	18	2.2	40
(4-CH ₃ OC ₆ H ₄) ₂ NH	(C ₄ H ₉) ₂ NH	RO ₂ [•]	348	29	4.2	40
(4-CH ₃ OC ₆ H ₄) ₂ NH	C ₆ H ₅ CH ₂ NH ₂	RO ₂ [•]	338	25	0.82	40
(4-CH ₃ OC ₆ H ₄) ₂ NH	C ₆ H ₅ CH ₂ NHCH ₃	RO ₂ [•]	333	> 10	3.7	38
(4-CH ₃ OC ₆ H ₄) ₂ NH	(CH ₃) ₂ N(CH ₂) ₂ OCO(CH ₃)C = CH ₂	RO ₂ [•]	323	18	1.2	35
(4-CH ₃ OC ₆ H ₄) ₂ NH	(CH ₃) ₂ NC ₄ H ₉	RO ₂ [•]	323	16	10.6	41
(4-CH ₃ OC ₆ H ₄) ₂ NH	(CH ₃) ₂ N(CH ₂) ₂ OCOCH ₂ CH ₃	RO ₂ [•]	323	26	8.0	41
1-C ₁₀ H ₇ NH ₂	(CH ₃) ₂ N(CH ₂) ₂ OCO(CH ₃)C = CH ₂	RO ₂ [•]	323	10	0.6	35
1-C ₁₀ H ₇ NH ₂	cyclo-C ₆ H ₁₁ NH ₂	RO ₂ [•]	348	16	0.08	40
1-C ₁₀ H ₇ NH ₂	cyclo-C ₆ H ₁₁ OH	RO ₂ [•]	393	56	0.13	34
1-C ₁₀ H ₇ NH ₂	CH = CHCH = CHCH ₂ CH ₂	HO ₂ [•]	348	28	—	32
1-C ₁₀ H ₇ NH ₂	cyclo-C ₆ H ₁₁ OH	RO ₂ [•]	393	28	3.2	12
1-C ₁₀ H ₇ NH ₂	cyclo-C ₆ H ₁₁ OH	RO ₂ [•]	413	30	—	12
1-C ₁₀ H ₇ NH ₂	cyclo-C ₆ H ₁₁ OH	RO ₂ [•]	393	28	—	13
1-C ₁₀ H ₇ NH ₂	cyclo-C ₆ H ₁₁ OH	RO ₂ [•]	348	15	—	14
1-C ₁₀ H ₇ NH ₂	cyclo-C ₆ H ₁₁ OH	RO ₂ [•]	348	90	—	29
1-C ₁₀ H ₇ NH ₂	(CH ₃) ₂ CHOH	RO ₂ [•]	348	90	—	29
1-C ₁₀ H ₇ NH ₂	cyclo-C ₆ H ₁₁ OH + H ₂ O ₂	HO ₂ [•]	398	22	—	29
1-C ₁₀ H ₇ NH ₂	cyclo-C ₆ H ₁₁ N(CH ₃) ₂	RO ₂ [•]	323	> 4	4.2	38
1-C ₁₀ H ₇ NH ₂	CH ₃ (CH ₂) ₃ OH	RO ₂ [•]	347	12	—	13
1-C ₁₀ H ₇ NH ₂	CH ₃ (CH ₂) ₃ OH	RO ₂ [•]	383	17	—	13
1-C ₁₀ H ₇ NH ₂	CH ₃ (CH ₂) ₃ OH	RO ₂ [•]	347	12	—	13
1-C ₁₀ H ₇ NH ₂	CH ₃ CH(OH)CH ₂ CH ₃	RO ₂ [•]	347	12	—	13
1-C ₁₀ N ₇ NH ₂	(CH ₃) ₃ COH + H ₂ O ₂	RO ₂ [•]	358	9	—	13
1-C ₁₀ H ₇ NH ₂	(CH ₃) ₃ COH + H ₂ O ₂	HO ₂ [•]	348	22	—	29
1-C ₁₀ H ₇ NH ₂	(CH ₃) ₂ CHOH	RO ₂ [•]	348	90	—	29
1-C ₁₀ H ₇ NH ₂	(CH ₃) ₂ NCH ₂ CH ₂ N(CH ₃) ₂	RO ₂ [•]	313	—	0.16	36
1-C ₁₀ H ₇ NH ₂	cyclo-[N(CH ₃)(CH ₂) ₅]	RO ₂ [•]	323	—	0.20	37
1-C ₁₀ H ₇ NH ₂	N(CH ₂ CH ₃) ₃	RO ₂ [•]	313	—	1.3	38
1-C ₁₀ H ₇ NH ₂	(C ₄ H ₉) ₂ NH	RO ₂ [•]	348	26	0.15	40
1-C ₁₀ H ₇ NH ₂	C ₆ H ₅ CH ₂ NH ₂	RO ₂ [•]	338	30	0.16	40
2-C ₁₀ H ₇ NH ₂	CH ₃ (CH ₂) ₃ OH	RO ₂ [•]	347	6	—	13
2-C ₁₀ H ₇ NH ₂	cyclo-C ₆ H ₁₁ OH	RO ₂ [•]	393	28	0.2	34
2-C ₁₀ H ₇ NHC ₆ H ₄ NH-2'-C ₁₀ H ₇	(CH ₃) ₂ N(CH ₂) ₂ OCO(CH ₃)C = CH ₂	RO ₂ [•]	323	26	12.0	35
2-C ₁₀ H ₇ NHC ₆ H ₄ NH-2'-C ₁₀ H ₇	CH = CHCH = CHCH ₂ CH ₂	HO ₂ [•]	348	6.5	—	32
2-C ₁₀ H ₇ NHC ₆ H ₄ NH-2'-C ₁₀ H ₇	CH = CHCH = CHCH ₂ CH ₂	HO ₂ [•]	313	22	—	32
2-C ₁₀ H ₇ NHC ₆ H ₄ NH-2'-C ₁₀ H ₇	cyclo-[N(CH ₃)(CH ₂) ₅]	RO ₂ [•]	323	43	8.2	37
2-C ₁₀ H ₇ NHC ₆ H ₄ NH-2'-C ₁₀ H ₇	cyclo-C ₆ H ₁₁ N(CH ₃) ₂	RO ₂ [•]	323	17	21.0	38
2-C ₁₀ H ₇ NHC ₆ H ₄ NH-2'-C ₁₀ H ₇	<i>trans</i> -C ₆ H ₅ CH = CHCOOC ₂ H ₅	HO ₂ [•]	323	40	26.0	33
2-C ₁₀ H ₇ NHC ₆ H ₄ NH-2'-C ₁₀ H ₇	<i>trans</i> -C ₆ H ₅ CH = CHC ₆ H ₅	HO ₂ [•]	323	40	17.0	33
2-C ₁₀ H ₇ NHC ₆ H ₄ NH-2'-C ₁₀ H ₇	(CH ₃) ₂ NCH ₂ CH ₂ N(CH ₃) ₂	RO ₂ [•]	313	22	4.0	36
4-C ₆ H ₅ NHC ₆ H ₄ NHCH(CH ₃) ₂	cyclo-C ₆ H ₁₁ OH	RO ₂ [•]	393	200	—	34
1-C ₁₀ H ₇ NHC ₆ H ₅	cyclo-C ₆ H ₁₁ OH	RO ₂ [•]	393	15	—	34
2-C ₁₀ H ₇ NHC ₆ H ₅	cyclo-C ₆ H ₁₁ OH	RO ₂ [•]	393	26	0.9	34
2-C ₁₀ H ₇ NHC ₆ H ₅	cyclo-C ₆ H ₁₁ NH ₂	RO ₂ [•]	348	36	1.2	40
(4-C ₆ H ₅ NH-4'-C ₆ H ₄ O) ₂ Si(CH ₃) ₂	(CH ₃) ₂ CHOH	RO ₂ [•]	343	18	—	30
2-C ₁₀ H ₇ NHC ₆ H ₅	C ₆ H ₅ CH ₂ NH ₂	RO ₂ [•]	338	52	1.2	40
2-C ₁₀ H ₇ NHC ₆ H ₅	cyclo-C ₆ H ₁₁ N(CH ₃) ₂	RO ₂ [•]	323	20	1.0	38



We present below the heats (ΔH) of disproportionation of the diphenylamino radicals both with hydroxyl radicals and with alkyl-containing peroxy radicals:⁴²

Peroxy radical	$-\Delta H / \text{kJ mol}^{-1}$
HO_2^\cdot	161
$(\text{CH}_3)_2\text{C}(\text{OH})\text{O}_2^\cdot$	145
cyclo- $\text{C}_6\text{H}_{10}(\text{OH})\text{O}_2^\cdot$	135
$\text{C}_6\text{H}_5\text{C}(\text{CH}_3)_2\text{O}_2^\cdot$	95
cyclo- $\text{C}_6\text{H}_{11}\text{O}_2^\cdot$	84

It can be seen that all these reactions are exothermic, and the ΔH values are fairly close to one another. All these reactions should seemingly proceed equally rapidly. The question as to how easily the amino radicals react with the O—H and C—H bonds of the peroxy radicals can be answered by analysing these reactions in terms of the parabolic model of transition state.^{43–45} This model treats the transition state in a radical abstraction reaction as the point of intersection of two nonperturbed parabolic terms, one of which describes the potential energy of the bond being attacked, whereas the other describes the potential energy of the bond being formed. The model makes it possible to calculate, using experimental data (activation energy, rate constant), an important characteristic of the elementary step, namely the distance by which the hydrogen atom being attacked shifts. This permits, in turn, the calculation of the activation energy for a thermally neutral reaction of this class. By a class of reactions is meant a set of all structurally similar reactions, characterised by the same distance of the displacement of an atom in the elementary step. For example, all the $\text{RO}_2^\cdot + \text{RH}$ reactions, in which an aliphatic hydrogen atom is attacked, belong to the same class.

Each elementary reaction is characterised in this model by enthalpy ΔH_e , which incorporates the difference between the zero point energies of the reacting bonds, and also by activation energy E_a , which is the sum of the activation energy E measured experimentally and the zero point vibration energy of the bond being attacked (in the case of the O—H bond, the latter is 21 kJ mol^{−1}). The activation energies for all the thermally neutral reactions of radical abstraction ($E_{e,0}$) and the coefficients α of reactions of this class are identical.⁴⁵

Analysis of experimental data has shown that, when amino radicals react with hydrocarbons, phenols, and hydroperoxides, they are extremely reactive toward specifically the O—H bonds.⁴⁶ The $E_{e,0}$ values for the reactions of amino radicals with various compounds are presented below:⁴⁶

Compound	$E_{e,0} / \text{kJ mol}^{-1}$
ROOH	39.0
ArOH	41.8
AmOH	32.2
AlkH	69.7
AralkH	81.7

The reactions of amino radicals with the O—H bonds ($E_{e,0}$ varies from 32 kJ mol^{−1} to 42 kJ mol^{−1}) and their reactions with the C—H bonds ($E_{e,0}$ varies from 70 kJ mol^{−1} to 82 kJ mol^{−1}) are very different, which leads to the following significant fact.

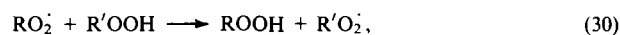
The activation energies for reactions are known to decrease as ΔH decreases. According to the parabolic model,⁴⁵ for highly exothermic reactions with fairly high ΔH_e values the activation energy $E = 0.5 RT$. The transition from higher activation energies to $E = 0.5 RT$ occurs at a certain minimum value of ΔH_e ($\Delta H_{e,\min}$), which depends on $E_{e,0}$ for the class of reactions being considered. The higher $E_{e,0}$, the higher $\Delta H_{e,\min}$ and the broader the ΔH range, in which $E > 0.5 RT$.

For the reaction of amino radicals with the O—H bond in ROOH, $\Delta H_{e,\min} = -39.4 \text{ kJ mol}^{-1}$, which is substantially smaller in magnitude than $\Delta H_{e,\min}$ for the reactions of diphenylamino radicals with HO_2^\cdot and $(\text{CH}_3)_2\text{C}(\text{OH})\text{O}_2^\cdot$ (−161 to −135 kJ mol^{−1}, see above). Thus all these reactions require virtually no activation energy, i.e. proceed fairly rapidly. The $E_{e,0}$ value for the reactions of Am^\cdot with the C—H bond is markedly higher,⁴⁶ and the $\Delta H_{e,\min}$ value corresponding to it is −141.1 kJ mol^{−1}. In the case of the reactions of diphenylamino radicals with $\beta\text{-C-H}$ bonds in the alkylperoxy radicals, $\Delta H = 84\text{--}95 \text{ kJ mol}^{-1}$, which is smaller than $\Delta H_{e,\min}$. Hence, these reactions should proceed with activation energies $E > 0.5 RT$, i.e. their rates are much lower than the rate of interaction of Am^\cdot with the O—H bond in the corresponding peroxy radical.

To give the ultimate answer to the question of why the cyclic chain termination mechanism is realised in those systems where HO_2^\cdot and $\text{>C}(\text{OH})\text{OO}^\cdot$ radicals act as the chain-propagating species but is not realised during the oxidation of hydrocarbons, one should compare the rate constants for the disproportionation reactions in which Am^\cdot affords the starting AmH [reactions (23) and (27)] with the rate constant for the irreversible destruction of Am^\cdot [reaction (28)]. The diphenylamino radical reacts with RO_2^\cdot via two parallel routes (25) and (28) at approximately identical rates.³⁰ The rate constant for the overall reaction k is known to be $6 \times 10^8 \text{ dm}^3 \text{ mol}^{-1} \text{ s}^{-1}$.⁴⁷ This implies that the rate constant for the addition of the peroxy radical to the aromatic ring of the diphenylamino radical k_{28} is $3 \times 10^8 \text{ dm}^3 \text{ mol}^{-1} \text{ s}^{-1}$. The cyclic mechanism is realised if the inequality $k_{21} > k_{28}$ or $k_{23} > k_{28}$ inequality holds. Therefore, it is necessary to evaluate the rate constants for the disproportionation of Am^\cdot and RO_2^\cdot and for the regeneration of AmH . It should be noted that, according to the parabolic model, in the case of highly exothermic reactions the pre-exponential factor A is related to the enthalpy of the reaction at $\Delta H_e > \Delta H_{e,\min}$ by the following relationship:⁴⁸

$$\left(\frac{A}{A_0}\right)^{0.5} = 1 - \beta[|\Delta H_e|^{0.5} - |\Delta H_{e,\min}|^{0.5}]$$

For this class of reactions, $A_0 = A$ at $\Delta H_e < \Delta H_{e,\min}$, and the coefficient β for the reactions



is $1.6 \text{ kJ}^{-0.5} \text{ mol}^{-0.5}$.⁴² The activation energy, which is equal to $0.5 RT$ for exothermic reactions with $\Delta H_e > \Delta H_{e,\min}$ and is greater than $0.5 RT$ for reactions with $\Delta H_e < \Delta H_{e,\min}$, can be calculated from the equations of the parabolic model.⁴⁵

The activation energies and rate constants for the reactions (21), (23), and (29) of the diphenylamino radical with various RO_2^\cdot calculated in this way are presented below:⁴²

Peroxy radical	$E / \text{kJ mol}^{-1}$	$k / \text{dm}^3 \text{ mol}^{-1} \text{ s}^{-1}$
$\text{C}_6\text{H}_5\text{C}(\text{CH}_3)_2\text{O}_2^\cdot$	16.6	1.5×10^7
cyclo- $\text{C}_6\text{H}_{11}\text{O}_2^\cdot$	19.8	3.1×10^6
HO_2^\cdot	1.4	8.4×10^9

One can see that the rate constants for the disproportionation of the amino and peroxy radicals (k_{29}) involving the C—H bond are substantially lower than the rate constants for the addition of RO_2^\cdot to the aromatic ring of the amino radical ($k_{28} = 3 \times 10^8 \text{ dm}^3 \text{ mol}^{-1} \text{ s}^{-1}$). Conversely, the reaction of Am^\cdot with HO_2^\cdot proceeds very rapidly and can compete successfully with the addition reaction. Thus, the result obtained in terms of the parabolic model is in good agreement with the experiment.

The reason for the different reactivities of Am^\cdot with respect to alkyl- and hydroxyl-containing peroxy radicals lies in the energy characteristics of the transition states of the C...H...N and O...H...N types. In the former case, the triplet repulsion makes a substantial contribution to the energy of the transition state, because the C—N bond is fairly strong, and the energy of its nonbonding orbital is high.⁴⁵ In the latter case, the hypothetical

compound ROOAm incorporates a weak N—O bond, and the contribution of the triplet repulsion to $E_{e,o}$ is slight. Apart from the triplet repulsion, the electronegativities of the atoms forming the reaction centre of the transition state are also significant:⁴⁵ the higher the difference between the electronegativities of the atoms, the lower the $E_{e,o}$ activation barrier. In this respect, too, the relationship between the C...H...N and O...H...N reaction centres counts in favour of the latter: the electron affinities of the C and N atoms are close to each other, whereas the electronegativities of the O and N atoms are substantially different.

An evaluation based on the equations of the parabolic model⁴⁵ indicates that a reaction of the type (18) involving phenoxyl radicals also requires no activation energy (in this case, $\Delta H_e > \Delta H_{e,min} = 57 \text{ kJ mol}^{-1}$). However, the addition of RO_2^\cdot to the aromatic ring of the phenoxyl radical occurs very rapidly, so that the rate constant for this reaction is determined by diffusion processes.¹¹ The data on the $E_{e,o}$ values are also consistent with this: for $\text{ArO}^\cdot + \text{HOOR}$ reactions (the O...H...O reaction centre and for $\text{Am}^\cdot + \text{HOOR}$ reactions (the N...H...O reaction centre), these values are 45.3 kJ mol^{-1} and 39.0 kJ mol^{-1} , respectively.⁴⁶ At the same time, calculation of the pre-exponential factor in terms of the parabolic model indicates that the rate constant k_{-7} for the reaction of ROOH with the participation of amino radical is several times higher than that for the reaction involving phenoxyl radical, the enthalpies of these reactions being identical. Thus, the irreversible destruction of ArO^\cdot in its reactions with HO_2^\cdot and $>\text{C}(\text{OH})\text{O}_2^\cdot$ occurs more rapidly than the conversion of ArO^\cdot into ArOH , and the cyclic mechanism of chain termination is not realised with phenols. An exception is provided by hydroquinones, which are considered below.

Aromatic amines also cause cyclic chain termination in the oxidation of primary and secondary aliphatic amines (Table 1). AmH is recovered from Am^\cdot via the reaction of Am^\cdot with the N—H bond of the $\text{RCH}(\text{NHR}')\text{O}_2^\cdot$ peroxy radical. Together with AmH , the reaction yields the imine $\text{RCH}=\text{NR}'$ and O_2 , i.e. a process similar to reaction (23) occurs. The rapid occurrence of this reaction involving primary and secondary amines is apparently due to the fact that the triplet repulsion in this case is weak, because a transition state of the N...H...N type is formed and the energy of the dissociation of the N—N bond is substantially lower than that for the N—C and C—C bonds. This can be seen from a comparison of the $D_{\text{C}-\text{C}}$, $D_{\text{N}-\text{N}}$ and $D_{\text{N}-\text{C}}$ dissociation energies (see handbooks^{26,49}):

Compound	$D/\text{kJ mol}^{-1}$
CH_3-CH_3	376
$\text{H}_2\text{N}-\text{NH}_2$	275
$\text{H}_2\text{N}-\text{NHC}_6\text{H}_5$	219
$\text{CH}_3-\text{NHC}_6\text{H}_5$	299
$(\text{C}_6\text{H}_5)_2\text{N}-\text{N}(\text{C}_6\text{H}_5)_2$	119

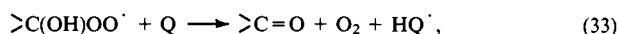
Cyclic chain termination with aromatic amines also occurs in the oxidation of tertiary aliphatic amines (see Table 1). To explain this fact, a mechanism of the conversion of Am^\cdot into AmH involving the $\beta\text{-C}-\text{H}$ bonds [reaction (29)] has been suggested;³⁹ however, its realisation is hampered by its high activation energy. Since tertiary amines have low ionisation potentials and readily participate in reactions with electron transfer, the cyclic mechanism in systems of this type is realised apparently as a sequence of such reactions, similar to what occurs in the systems containing complexes of variable-valence metals (see below).

IV. Cyclic chain termination with quinones in the oxidation of alcohols and polymers

Quinones (Q) are well known as inhibitors of radical polymerisation; they terminate chains by adding alkyl radicals via the following reactions⁵⁰



At the same time, quinones do not retard oxidation of hydrocarbons, since alkyl radicals react very rapidly with oxygen (see Section II) to give alkylperoxy radicals, which scarcely react with quinones. Quinones exhibit their inhibiting properties only in the oxidation of polymers; the chain termination results from their interaction with alkyl macroradicals,⁵¹ which is due to the specific features of the oxidation of polymers in the solid phase and also due to the fact that alkyl macroradicals react with O_2 in a polymeric matrix relatively slowly.³ Quinones decelerate the oxidation of alcohols very effectively and for long periods by ensuring cyclic chain termination via the following reactions¹⁶



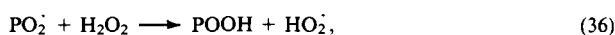
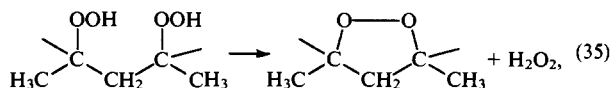
The processes of oxidation of cyclohexadiene, 1,2-substituted ethenes, and aliphatic amines are decelerated by quinone or hydroquinone by a similar mechanism. The values of the stoichiometric inhibition coefficients and of the rate constants (f and k) for the corresponding reactions involving peroxy radicals [HO_2^\cdot , $>\text{C}(\text{OH})\text{OO}^\cdot$, and $>\text{C}(\text{NHR})\text{O}_2^\cdot$] are presented in Table 2. The f coefficients in these reactions are relatively high, varying from 8 to 70. Evidently, the irreversible consumption of quinone in these systems is due to the addition of RO_2^\cdot to the aromatic ring of the quinone followed by the decomposition of the resulting adduct.

The data on the deceleration of the oxidation of polymers (polyethylene, polypropylene) by quinones deserve particular attention.⁵¹ It has been noted above that benzoquinone, which retards the initiated oxidation of polymers, behaves as a typical acceptor of alkyl radicals. It decreases the rate of chain oxidation, which obeys the following dependence:

$$v \sim v_i P_{\text{O}_2} [\text{Q}]^{-1}$$

In this case, the chain termination occurs stoichiometrically: one quinone molecule terminates two chains.

However, when stilbenequinone is introduced into a preliminarily oxidised polymer containing hydroperoxy-groups, a totally different picture is observed.⁵² In this case, quinone acquires the ability to repeatedly terminate the chains ($f = 20$ in the oxidation of polypropylene with a concentration of the hydroperoxy-groups $[\text{POOH}] = 0.13 \text{ mol kg}^{-1}$, $T = 356 \text{ K}$). The chain termination at $P_{\text{O}_2} = 10^5 \text{ Pa}$ occurs predominantly via the reaction with peroxy radicals. The increase in the efficiency of the retarding action of the quinone is due to the fact that in the oxidised polypropylene containing associated $\beta\text{-OOH}$ groups, the latter decompose to give hydrogen peroxide, which serves as the source of the HO_2^\cdot radicals and these radicals ensure cyclic chain termination via interaction with quinones:⁵²



(PO_2^\cdot is the peroxy macroradical).

It is evident from Table 2 that quinones react rapidly with the hydroperoxy radicals. Calculation shows that the change in the enthalpy in the reaction (33) is relatively small. The calculation was based on the ΔH_f data for quinone and hydroquinone⁴⁹ and on the $D_{\text{O}-\text{H}}$ value for hydroquinone⁵³ ($350.3 \text{ kJ mol}^{-1}$). The dissociation energy of the O—H bond in the 4- $\text{HOC}_6\text{H}_4\text{O}^\cdot$ semiquinone radical is $228.1 \text{ kJ mol}^{-1}$. The dissociation energies

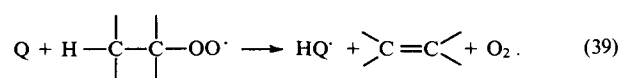
Table 2. Inhibition coefficients and rate constants for the reactions of quinones and hydroquinones with RO₂[•] in systems with a cyclic mechanism of chain termination.

InH	RH	RO ₂ [•]	T/K	f	k/10 ⁴ dm ³ mol ⁻¹ s ⁻¹	Ref.
4-HOC ₆ H ₄ OH	cyclo-[N(CH ₃)(CH ₂) ₅]	RO ₂ [•]	323	14	3.2	38
4-HOC ₆ H ₄ OH	N(CH ₂ CH ₃) ₃	RO ₂ [•]	313	>20	14.0	38
4-HOC ₆ H ₄ OH	cyclo-C ₆ H ₁₁ N(CH ₃) ₂	RO ₂ [•]	323	20	7.2	38
4-HOC ₆ H ₄ OH	(CH ₃) ₂ NCH ₂ CH ₂ N(CH ₃) ₂	RO ₂ [•]	313	—	0.7	36
4-HOC ₆ H ₄ OH	CH ₃ CON(CH ₂ CH ₃) ₂	HO ₂ [•]	348	10	0.94	39
4-HOC ₆ H ₄ OH	<i>trans</i> -C ₆ H ₅ CH=CHCOOC ₂ H ₅	HO ₂ [•]	323	15	14.0	33
4-HOC ₆ H ₄ OH	<i>trans</i> -C ₆ H ₅ CH=CHC ₆ H ₅	RO ₂ [•]	323	15	0.3	33
4-OC ₆ H ₄ O	cyclo-[N(CH ₃)(CH ₂) ₅]	RO ₂ [•]	323	8	4.0	38
4-OC ₆ H ₄ O	N(CH ₂ CH ₃) ₃	RO ₂ [•]	313	>10	29.0	38
4-OC ₆ H ₄ O	cyclo-C ₆ H ₁₁ N(CH ₃) ₂	RO ₂ [•]	323	16	2.7	38
4-OC ₆ H ₄ O	(CH ₃) ₂ CHOH	RO ₂ [•]	344	23	29.0	16
4-OC ₆ H ₄ O	cyclo-[(CH=CH) ₂ CH ₂ CH ₂]	HO ₂ [•]	348	70	—	32
4-OC ₆ H ₄ O	(CH ₃) ₂ NCH ₂ CH ₂ N(CH ₃) ₂	RO ₂ [•]	313	—	1.0	36
4-OC ₆ H ₄ O	(CH ₃) ₂ N(CH ₂) ₃ CH ₃	RO ₂ [•]	323	12	4.2	41
4-OC ₆ H ₄ O	(CH ₃) ₂ N(CH ₂) ₂ OCOC(CH ₃) ₃ =CH ₂	HO ₂ [•]	323	34	1.6	35
C ₆ H ₅ NC ₆ H ₄ O	(CH ₃) ₂ CHOH	RO ₂ [•]	343	12	20.0	30
Stilbenequinone	Polypropylene	HO ₂ [•]	365	20	—	42

of the O—H and C—H bonds in the corresponding peroxy radicals⁴² and enthalpies of the reaction (33) are presented in Table 3. It can be seen from this Table that the ΔH_f value for reaction (33) varies from -25 kJ mol⁻¹ in the case of HO₂[•] to 1.7 kJ mol⁻¹ in the case of hydroxycyclohexylperoxy radical. The activation energies for this reaction were calculated from the equations of the parabolic model;⁴⁵ parameters of a similar reaction of phenoxyl radicals with hydroperoxide ($E_{e,o} = 45.3$ kJ mol⁻¹, $\alpha = 1$) were used for the calculation. The activation energies of these reactions were found to be relatively low and equal to 14 – 26 kJ mol⁻¹. The low activation barriers to these reactions are accounted for by the fact that the transition state of the O...H...O type arising in the reaction (33) is characterised by the absence of the triplet repulsion, which makes a substantial contribution to the activation energy in other reactions. For the ArO[•] + ROOH reaction, the pre-exponential factor A is equal to 10^8 dm³ mol⁻¹ s⁻¹. Therefore, with allowance for the fact that benzoquinone incorporates two reaction centres, we may take $A = 2 \times 10^8$ dm³ mol⁻¹ s⁻¹ for the reaction (33).

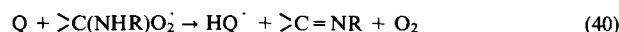
Table 3 presents the results of the calculations of the rate constants for reactions (33) involving HO₂[•] and two hydroperoxy radicals. Comparison of the calculated and experimental values of k_{33} can be carried out using the reaction of benzoquinone with the peroxy radical derived from isopropanol as an example. According to the data of Denisov,¹⁶ the $k_{33}/2k_t$ ratio in this case at 344 K is 9.4 litre^{0.5} mol^{-0.5} s^{-0.5}, whereas the rate constant for the disproportionation of two RO₂[•] radicals is 1.1×10^9 dm³ mol⁻¹ s⁻¹.²⁶ Hence we obtain $k_{33} = 3.1 \times 10^5$ dm³ mol⁻¹ s⁻¹. The theoretical calculation from the equations of the parabolic model gives $k_{33} = 2 \times 10^8 \exp(-21.2/RT) = 1.2 \times 10^5$ dm³ mol⁻¹ s⁻¹ (344 K), i.e. a closely similar value. Thus, the calculation permits the rate constants for reaction (33) to be evaluated with sufficient accuracy.

The question arises as to why quinones terminate chains via reaction (33) and not via reaction with the β -C—H bond of the alkylperoxy radical:



The cleavage of the C—H and C—O bonds in the reaction (39) is compensated to a substantial degree by the formation of the π -C=C and O—H bonds of the semiquinone radical. Table 3 presents the ΔH values for the reaction (39) involving two hydrocarbon peroxy radicals C₆H₅(CH₃)₂CO₂[•] and cyclo-C₆H₁₁O₂[•]. The reaction is endothermic in both cases

($\Delta H = 40$ – 50 kJ mol⁻¹). However, the fact that such reactions proceeding via a transition state of the C...H...O type are characterised by high thermally neutral activation energies $E_{e,o}$ is more significant. The difference between the $E_{e,o}$ values for reactions involving an ArO[•]...H...R transition state [an analogue of reaction (39)] and an ArO[•]...H...OOR transition state [an analogue of reaction (33)] amounts to 69.8 – $45.3 = 24.5$ kJ mol⁻¹. This accounts for the high activation energy for reaction (39) involving the C₆H₅(CH₃)₂CO₂[•] and cyclo-C₆H₁₁O₂[•] radicals (~ 74 and ~ 79 kJ mol⁻¹, respectively). If we take the pre-exponential factor A to be equal to 2×10^9 dm³ mol⁻¹ s⁻¹, then the rate constants for the reaction (39) will assume the values given in Table 3. With the rate constants being so small, reaction (39) cannot influence the oxidative chain termination via the interaction of two RO₂[•] radicals {the rate constant for the latter is 10^5 – 10^7 dm³ mol⁻¹ s⁻¹;²⁶ in these cases, the inequality $(2k_{60})^{0.5} \ll 2k_{39}[Q]$ always holds}. What is the reason for such high $E_{e,o}$ values and, hence, for the high activation energies characteristic of the reactions involving transition states of the O...H...C type? Comparison of reactions of various types has shown that this is the strong triplet repulsion.⁴⁵ It is this repulsion that precludes rapid occurrence of reaction (39), as also in the reactions involving amino radicals. In the case of aminoperoxy radicals (primary and secondary amines), the high rate of the reaction



is due to the low activation barrier $E_{e,o}$, which is only 39 kJ mol⁻¹ for the N...H...O type transition state.⁴⁶ This is explained by weak triplet repulsion in compounds AmOOR and by an additional attraction between the N and O atoms owing to their different

Table 3. Some energy and kinetic parameters of the reactions of benzoquinone with the O—H [reaction (33)] and C—H bonds [reaction (39)] of peroxy radicals.

Peroxy radical	$D_{\text{O-H}}$ or $D_{\text{C-H}}$, ^a	ΔH , ^a	E , ^a	$k(333\text{ K})$ ^b
HO ₂ [•]	203.4	-24.7	13.7	1.4×10^6
(CH ₃) ₂ C(OH)O ₂ [•]	219.9	-8.9	21.2	9.5×10^4
cyclo-C ₆ H ₁₀ (OH)O ₂ [•]	229.8	1.7	26.0	1.7×10^4
C ₆ H ₅ (CH ₃) ₂ CO ₂ [•]	270.0	41.9	73.6	3.4×10^{-2}
cyclo-C ₆ H ₁₁ O ₂ [•]	280.3	52.9	78.9	3.4×10^{-3}

^a kJ mol⁻¹; ^b dm³ mol⁻¹ s⁻¹

Table 4. Rate constants for the reactions of alkylperoxyl radicals with alcohols (the method of selective inhibition).⁵⁴

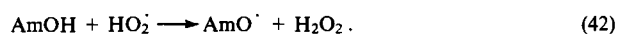
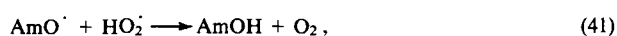
Hydrocarbon	Alcohol	<i>T</i> / K	<i>k</i> / dm ³ mol ⁻¹ s ⁻¹	Ref.
cyclo-C ₆ H ₁₀	CH ₃ OH	313	0.3	53
cyclo-C ₆ H ₁₀	C ₂ H ₅ OH	333	1.9	53
cyclo-C ₆ H ₁₀	(CH ₃) ₂ CHOH	333	2.0	53
cyclo-C ₆ H ₁₀	CH ₃ (CH ₂) ₃ OH	333	1.2	53
cyclo-C ₆ H ₁₀	cyclo-C ₆ H ₁₁ OH	333	2.5	53
cyclo-C ₆ H ₁₀	C ₆ H ₅ CH ₂ OH	333	5.6	53
CH ₃ (CH ₂) ₁₄ CH ₃	CH ₃ (CH ₂) ₈ CH ₂ OH	404	1.8 × 10 ²	54
CH ₃ (CH ₂) ₁₄ CH ₃	CH ₃ CH(OH)(CH ₂) ₅ CH ₃	404	2.3 × 10 ²	54
CH ₃ (CH ₂) ₁₄ CH ₃	CH ₂ (OH)CH ₂ (OH)	404	78	54
CH ₃ (CH ₂) ₁₄ CH ₃	[CH ₂ (OH)CH ₂] ₂	404	87	54
CH ₃ (CH ₂) ₁₄ CH ₃	CH ₂ (OH)CH ₂ CH(OH)CH ₃	404	1.2 × 10 ²	54
CH ₃ (CH ₂) ₁₄ CH ₃	CH ₂ (OH)C(CH ₃) ₂ CH ₂ OH	404	3.4 × 10 ³	54
CH ₃ (CH ₂) ₁₄ CH ₃	CH ₃ CH ₂ C(CH ₂ OH) ₃	404	9.4 × 10 ²	54
CH ₃ (CH ₂) ₁₄ CH ₃	O[CH ₂ CH(OH)CH ₂ OH] ₂	404	1.6 × 10 ³	54
[CH ₃ (CH ₂) ₄ COO(CH ₂) ₂ OCH ₂] ₂	CH ₃ (CH ₂) ₈ CH ₂ OH	404	22.5	54
[CH ₃ (CH ₂) ₄ COO(CH ₂) ₂ OCH ₂] ₂	CH ₃ (CH ₂) ₇ CH ₂ OH	404	23.0	54
[CH ₃ (CH ₂) ₄ COO(CH ₂) ₂ OCH ₂] ₂	CH ₃ CH(OH)(CH ₂) ₅ CH ₃	404	22.5	54
[CH ₃ (CH ₂) ₄ COO(CH ₂) ₂ OCH ₂] ₂	CH ₂ (OH)(CH ₂) ₂ CH ₂ OH	404	14.0	54
[CH ₃ (CH ₂) ₄ COO(CH ₂) ₂ OCH ₂] ₂	CH ₂ (OH)CH ₂ CH(OH)CH ₃	404	15.6	54
[CH ₃ (CH ₂) ₄ COO(CH ₂) ₂ OCH ₂] ₂	CH ₂ (OH)C(CH ₃) ₂ CH ₂ OH	404	1.2 × 10 ²	54
[CH ₃ (CH ₂) ₄ COO(CH ₂) ₂ OCH ₂] ₂	CH ₃ CH ₂ C(CH ₂ OH) ₃	404	1.2 × 10 ²	54
[CH ₃ (CH ₂) ₄ COO(CH ₂) ₂ OCH ₂] ₂	O[CH ₂ CH(OH)CH ₂ OH] ₂	404	71	54
[CH ₃ (CH ₂) ₄ COO(CH ₂) ₂ OCH ₂] ₂	CH ₃ [CH(OH)] ₂ CH ₃	404	27	54

electron affinities (as also in the case of reactions of amino radicals with the O—H groups of the peroxy radicals). (Apparently, quinones react with the peroxy radicals derived from tertiary amines with transfer of an electron).

The selectivity of the reaction of benzoquinone with hydroxyperoxy radicals and its inertness with respect to alkylperoxy radicals has been used for the development of an original method for measuring the rate constants for the reactions of alkylperoxy radicals with alcohols.⁵⁴ For this purpose, the initiated oxidation of a mixture of a hydrocarbon and an alcohol is carried out in the presence of benzoquinone. The latter is added in a concentration that is high enough to ensure that all the hydroxyperoxy radicals derived from the alcohol react with it (are destroyed) and is low enough to cause no noticeable chain termination via the reaction of quinone with the alkyl radicals. This 'operating' range of the benzoquinone concentrations is $(1-10) \times 10^{-3}$ mol dm⁻³. The rate constants for the reactions of a number of alkylperoxy radicals with alcohols found by this method are presented in Table 4.

V. Cyclic chain termination mechanisms involving nitroxyl radicals

Nitroxyl radicals react rapidly with alkyl radicals⁵³ and efficiently retard the radical polymerisation of hydrocarbons. At the same time, only aromatic nitroxyls are capable of reacting with alkylperoxy radicals,⁵³ and in this case the chain termination in the oxidation of saturated hydrocarbons occurs stoichiometrically. However, in the processes of oxidation of alcohols, alkenes, and primary and secondary aliphatic amines in which the chain reaction involves the HO₂[•], >C(OH)O₂[•], and >C(NHR)O₂[•] radicals, respectively, nitroxyl radicals are capable of terminating the chains repeatedly by a cyclic mechanism.^{30,32,40} For example, chain termination in the oxidation of alcohols occurs via the following reactions



Reaction (41) is the rate-determining stage. During the oxidation a kinetic equilibrium is established between the two forms of the

inhibitor — AmO[•] and AmOH.³⁸ The kinetic characteristics of this mechanism are presented in Table 5.

Let us try to account for the rapidity of reactions (41) and (42). The disproportionation of radicals (41) is an exothermic reaction. For example, the enthalpies of disproportionation of 2,2,6,6-tetramethylpiperidinoxyl with HO₂[•], (CH₃)₂C(OH)O₂[•], and cyclo-C₆H₁₀(OH)O₂[•] are -109, -92, and -82 kJ mol⁻¹, respectively. The *E*_{e,o} value for the abstraction of an H atom from the O—H bond in ROOH by a nitroxyl radical is 45.6 kJ mol⁻¹ and is matched by the value Δ*H*_{e,min} = -58 kJ mol⁻¹. Since Δ*H* < Δ*H*_{e,min}, the activation energy *E* ≈ 0.5 *RT* for these reactions is low,⁴⁸ and the rate constant is correspondingly high. Therefore, in the systems in which hydroperoxy and hydroxyperoxy radicals participate in the chain propagation, the cyclic chain termination mechanism is realised.

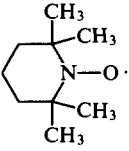
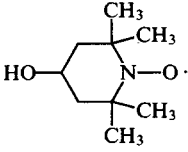
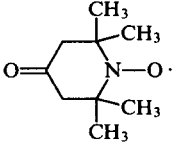
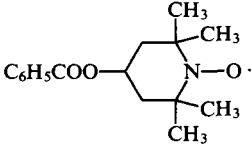
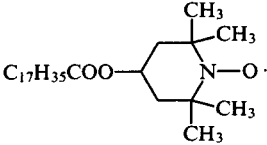
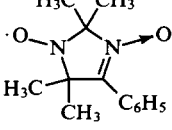
The reactions of disproportionation of nitroxyl and alkylperoxy radicals are also exothermic. For example, 2,2,6,6-tetramethylpiperidinoxyl abstracts an H atom from the β-C—H bond of cumylperoxy and cyclohexylperoxy radicals. The enthalpies of these reactions are -42 and -32 kJ mol⁻¹. The activation energy for the radical abstraction (*E*_{e,o}) for the AmO[•] + RH reaction is 58 kJ mol⁻¹, and the corresponding Δ*H*_{e,min} value is -125 kJ mol⁻¹,⁴² that is, Δ*H*_{e,min} substantially exceeds Δ*H* in magnitude. Thus, both reactions under consideration



should require appreciable activation energies. According to a calculation,⁴² for the reaction of AmO[•] with C₆H₅(CH₃)₂CO₂[•], *E* = 23.7 kJ mol⁻¹ and *k* = 1.1 × 10⁶ dm³ mol⁻¹ s⁻¹, and for the reaction of AmO[•] with cyclo-C₆H₁₁O₂[•], *E* = 27.4 kJ mol⁻¹ and *k* = 2.0 × 10⁵ dm³ mol⁻¹ s⁻¹. The recombination of nitroxyl radicals with alkyl radicals proceeds as a rule much more rapidly.⁵³

Why are the *E*_{e,o} values in the reactions of nitroxyl radicals with O—H bonds lower than those in their reactions with C—H bonds? As in the case of disproportionation of RO₂[•] with amino radicals, the low *E*_{e,o} values are accounted for by triplet repulsion.⁵⁷ When a transition state of the O...H...O type is formed (the AmO[•] + HO₂[•] reaction), the triplet repulsion is close to zero, because the O—O bond in the labile compound AmOOH is very weak. Conversely, the triplet repulsion in the reaction of AmO[•]

Table 5. Some kinetic characteristics of the cyclic mechanism of the chain termination on nitroxyl radicals in the oxidation of alcohols and amines.

Inhibitor	Substrate	RO ₂	T/K	f	k/10 ⁴ dm ³ mol ⁻¹ s ⁻¹	Ref.
(4-CH ₃ OC ₆ H ₄) ₂ NO [•]	(CH ₃) ₂ CHOH	RO ₂	343	50	—	30
	CH ₃ CON(CH ₂ CH ₃) ₂	RO ₂	348	30	3.5	39
	[CH ₃ (CH ₂) ₃] ₂ NH	RO ₂	348	100	21.0	39
	cyclo-C ₆ H ₁₁ NH ₂	RO ₂	348	100	8.1	39
	cyclo-C ₆ H ₁₁ OH	RO ₂	348	50	8.4	39
	C ₆ H ₅ CH ₂ NH ₂	RO ₂	338	140	34.0	39
	C ₆ H ₅ CH ₂ NHCH ₃	RO ₂	323	16	4.2	39
	<i>trans</i> -C ₆ H ₅ CH = CHCOOC ₂ H ₅	HO ₂	323	> 100	19.0	33
	<i>trans</i> -C ₆ H ₅ CH = CHCOOCH ₃	HO ₂	323	> 100	12.0	33
	CH ₃ CON(C ₂ H ₅) ₂	RO ₂	348	50	1.3	39
	<i>trans</i> -C ₆ H ₅ CH = CHC ₆ H ₅	HO ₂	323	> 100	3.2	33
	cyclo-C ₆ H ₁₁ NH ₂	RO ₂	348	200	2.4	39
	(CH ₃) ₂ C = CHC(O)CH ₃	HO ₂	323	> 100	2.2	33
	[CH ₃ (CH ₂) ₃] ₂ NH	RO ₂	348	160	14.0	39
	C ₂ H ₅ OCOCH = CHCOOC ₂ H ₅	HO ₂	323	> 100	1.2	7
	CH ₂ = C(CH ₃)COOCH ₂ CH ₂ N(CH ₃) ₂	RO ₂	323	30	2.6	35
	CH ₃ CH ₂ COOCH ₂ CH ₂ N(CH ₃) ₂	RO ₂	323	10	0.2	7
	cyclo-[(CH ₂) ₅ NCH ₃]	RO ₂	323	90	7.2	39
	(CH ₃ CH ₂) ₃ N	RO ₂	313	25	57.0	39
	cyclo-C ₆ H ₁₁ N(CH ₃) ₂	RO ₂	323	92	18.0	39
	C ₆ H ₅ CH ₂ NHCH ₃	RO ₂	323	16	4.2	39
	<i>trans</i> -C ₆ H ₅ CH = CHCOOC ₂ H ₅	HO ₂	323	> 100	14.0	33
	cyclo-C ₆ H ₁₁ NH ₂	RO ₂	348	100	2.8	39
	[CH ₃ (CH ₂) ₃] ₂ NH	RO ₂	348	100	15.2	39
	(CH ₃) ₂ NCH ₂ CH ₂ N(CH ₃) ₂	RO ₂	313	> 4	1.3	36
	C ₆ H ₅ CH ₂ NH ₂	RO ₂	338	100	7.9	39
	CH ₂ = C(CH ₃)CO ₂ CH ₂ CH ₂ N(CH ₃) ₂	RO ₂	323	70	0.8	35
	CH ₃ (CH ₂) ₃ N(CH ₃) ₂	RO ₂	323	80	5.6	39
	CH ₃ CH ₂ CO ₂ CH ₂ CH ₂ N(CH ₃) ₂	RO ₂	323	10	0.3	7
	cyclo-C ₆ H ₁₁ OH	RO ₂	348	120	21	40
	cyclo-C ₆ H ₁₁ NH ₂	RO ₂	348	—	3.0	40
	[CH ₃ (CH ₂) ₃] ₂ NH	RO ₂	348	—	12.6	40
	C ₆ H ₅ CH ₂ NH ₂	RO ₂	338	—	19.0	40
	cyclo-C ₆ H ₁₁ NH ₂	RO ₂	348	—	—	40
	[CH ₃ (CH ₂) ₃] ₂ NH	RO ₂	348	—	—	40
	Polypropylene	RO ₂ , R [•]	387	14	—	17
	cyclo-C ₆ H ₁₁ NH ₂	RO ₂	348	—	2.5	40
	[CH ₃ (CH ₂) ₃] ₂ NH	RO ₂	348	—	16.6	40
	Oxidized polypropylene	HO ₂	388	> 40	—	56
	cyclo-C ₆ H ₁₁ NH ₂	RO ₂	348	—	0.7	40
	[CH ₃ (CH ₂) ₃] ₂ NH	RO ₂	348	—	6.6	40
	C ₆ H ₅ CH ₂ NH ₂	RO ₂	338	—	7.2	40
	cyclo-C ₆ H ₁₁ OH	RO ₂	348	—	5.9	40
	cyclo-C ₆ H ₁₁ NH ₂	RO ₂	348	—	0.9	40
	[CH ₃ (CH ₂) ₃] ₂ NH	RO ₂	348	—	9.4	40

with the C—H bond is fairly great, due to the high dissociation energy of the AmO—R bond. This accounts for the difference between the activation energies and between the rate constants for the reactions considered above. Thus, the possibility of the realisation of a cyclic chain termination mechanism in the reactions of Am \cdot and AmO \cdot with peroxy radicals, incorporating O—H groups, is caused by the weak triplet repulsion in the disproportionation reactions in which the corresponding inhibitor (AmH or AmOH) is recovered.

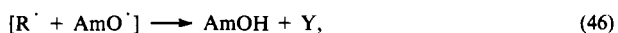
HO $_2\cdot$ radicals are also generated in the oxidation of polymers, in particular, in the oxidation of polypropylene,⁵⁸ when intramolecular chain transfer affords associated hydroperoxy-groups.³ The thermal decomposition of the latter yields H $_2$ O $_2$, which reacts with peroxy macroradicals and thus generates the HO $_2\cdot$ radicals, which are responsible for the cyclic chain termination via reactions (41) and (42).^{52,58}

The nitroxyl radicals also participate in other cyclic mechanisms of chain termination. One of these mechanisms involves alternation of reactions involving the R \cdot and RO $_2\cdot$ radicals. This mechanism has been discovered in a study of the retarding effect of 2,2,6,6-tetramethyl-4-benzoylpiperidin-*N*-oxyl on the initiated oxidation of polypropylene.¹⁷ It has been shown^{17,59,60} that the nitroxyl radical terminates the oxidation chain by reacting with the alkyl macroradical of polypropylene being oxidised. The resulting compound AmOR is fairly reactive with respect to the peroxy radicals AmO \cdot being regenerated in this reaction. Thus, the cycle includes the following two reactions (mechanism I):^{59–62}



where Y is a polypropylene macromolecule with a double bond formed by the abstraction of the H atom from the β -C—H bond and by the cleavage of the O—N bond in ROAm. This conclusion was confirmed later in a study of radiation-induced chemical oxidation of octane;⁶³ in this work, AmOR was identified as a reaction product.

The ether AmOR is thermally unstable. At elevated temperatures it dissociates with cleavage of the R—O bond, which leads to the appearance of an [Am \cdot + R \cdot] radical pair in the cage of the polymer or of the hydrocarbon being oxidised; disproportionation of this radical pair gives hydroxylamine and an alkene. The peroxy radical reacts rapidly with hydroxylamine thus regenerating the nitroxyl radical. This scheme was suggested and justified in a number of papers.^{64–68} The cyclic mechanism (II) includes the following stages:



The fact that hydroxylamine has been found among the products of the transformations of nitroxyl during the oxidation of hydrocarbons is evidence in support of this mechanism. Both mechanisms described above are realised in parallel and supplement each other. The result of the competition between them depends primarily on the temperature, since the thermal decomposition of the product ROAm requires a fairly high activation energy. The problem of the competition between the mechanisms I and II of cyclic chain termination has been considered by Denisov.²¹ In the case of the oxidation of polypropylene at the initiation rate $v_i = 10^{-7}$ mol kg $^{-1}$ s $^{-1}$ and for $[O_2] = [AmO\cdot] = 10^{-3}$ mol kg $^{-1}$, the ratio of the rates of chain termination via reactions (44) and (46) varies as a function of the temperature in the following way:⁶²

T/K	350	365	380	388	400	420
v_I/v_{II}	50.0	9.55	2.14	1.00	0.33	0.029

It is obvious that when the temperature is not very high and the ether AmOR is stable, the mechanism I predominates, that is, the regeneration of AmO \cdot from AmOR is ensured by the reaction of AmOH with the peroxy radical. At higher temperatures, when AmOR becomes unstable, the mechanism II predominates. It should be taken into account that only some of the radical pairs formed upon decomposition of ROAm disproportionate giving AmOH and an alkene. The remaining radical pairs pass into the bulk, and the radical R \cdot reacts with O $_2$ to give RO $_2\cdot$ and thus initiate a new oxidation chain. Hence, the regeneration of AmO \cdot from AmOH is inevitably accompanied by the initiation of the process, which certainly decreases the efficiency of the inhibition.

As the oxidation of the polymer proceeds and hydroperoxy groups which decompose to give H $_2$ O $_2$ accumulate, the cyclic chain termination mechanisms involving the HO $_2\cdot$ radical [reactions (41) and (42)] become more significant. Below we present the results illustrating the relative efficiency of the chain termination mechanisms involving the R \cdot and RO $_2\cdot$ radicals (mechanisms I and II), on the one hand, and the mechanism involving the HO $_2\cdot$ radicals, on the other hand, obtained for the oxidation of polypropylene.⁶² Polypropylene was oxidised at 388 K and $P_{O_2} = 10^5$ Pa in the presence of an initiator (cumyl peroxide) and with an inhibitor (2,2,6,6-tetramethyl-4-stearyl piperidin-*N*-oxyl),⁵⁶ the consumption of which was monitored by EPR. The inhibiting activity was characterised by the coefficient

$$f = \frac{v_i}{v_{AmO\cdot}},$$

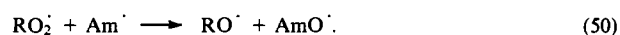
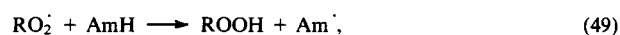
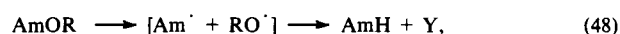
where v_i and $v_{AmO\cdot}$ are the initiation rate and the rate of consumption of the nitroxyl radical, respectively, and by the parameter F :

$$F = \frac{v_i}{v} \left(1 - \frac{v^2}{v_0^2} \right) [AmO\cdot]^{-1},$$

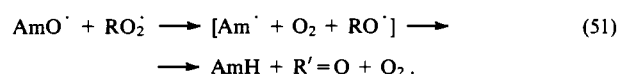
where v_0 and v are the rates of oxidation of the polymer without an inhibitor and with the inhibitor AmO \cdot , respectively. The parameter F characterises the efficiency of AmO \cdot as an inhibitor terminating the chains. In experiments on the oxidation of polypropylene containing no hydroperoxy-groups the following values were found: $f = 4$ and $F = 7$ kg mol $^{-1}$, whereas for the oxidation of polypropylene that had been preliminarily oxidised and contained 4.12×10^{-2} mol kg $^{-1}$ of hydroperoxy-groups, these parameters were: $f = 40$ and $F = 1060$ kg mol $^{-1}$.

Thus, there is a clear dissimilarity between the cyclic chain termination mechanism involving only R \cdot and RO $_2\cdot$ radicals and the mechanism involving HO $_2\cdot$ radicals produced from H $_2$ O $_2$.

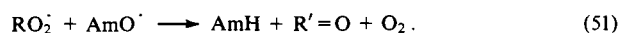
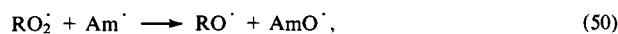
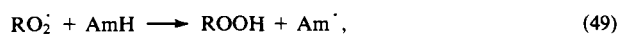
Recently, a new cyclic mechanism of chain termination by nitroxyl radicals, including the formation of amino radicals as intermediate species, has been found.^{69,70} It was shown that the addition of 4,4'-dioctyldiphenylnitroxyl radical to hexadecane being oxidised ($T = 433$ K) leads to the formation of the corresponding diphenylamine as an intermediate compound during its transformations. The following cyclic mechanism of chain termination was suggested:



A specific feature of this mechanism is the reaction (48), in which AmOR cleaves at the N—O bond rather than at the C—O bond as observed for the inhibition by alicyclic nitroxyl radicals. An alternative mechanism of the regeneration of the amino radical from the nitroxyl radical is also possible:



In this case, the cyclic chain termination mechanism can be realised only with participation of peroxy radicals.



Thus, nitroxyl radicals can participate in various cyclic mechanisms of chain termination. In the oxidation of alcohols, peroxides, and amines, when peroxy radicals possess both oxidising and reducing ability, the cyclic mechanism of chain termination includes reactions of peroxy radicals with AmO^\cdot and AmOH . The cyclic mechanism occurring under the conditions of polymer oxidation includes the $\text{R}^\cdot + \text{AmO}^\cdot$ and $\text{RO}_2^\cdot + \text{AmOR}$ reactions. At elevated temperatures AmOR becomes thermally unstable, and the mechanism that includes homolysis of AmOR at the C—O or N—O bonds with the generation of AmO^\cdot (AmOH) or Am^\cdot (AmH) radicals is realised.

VI. Cyclic chain termination mechanisms involving acid catalysis

We have by no means described all the cyclic mechanisms of chain termination involving nitroxyl radicals. A new interesting branch of modern antioxidant chemistry deals with cyclic mechanisms involving acid catalysis. The first inhibiting system of this type was discovered in 1988.¹⁸ It consisted of an alcohol (primary or secondary), a stable nitroxyl radical (2,2,6,6-tetramethylpiperidin-*N*-oxyl), and an organic (citric acid). This three-component system effectively retarded the initiated oxidation of ethylbenzene. Each component taken by itself and binary combinations of these components did not retard oxidation of ethylbenzene or retarded it only slightly. Intense chain termination was ensured only by the presence of all three components of this system.

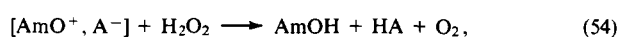
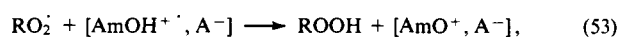
The important role of the acid was established in experiments on the oxidation of ethylbenzene containing an alcohol and nitroxyl radicals, when air or air mixed with gaseous HCl was passed through the reactor. The concentration of the peroxy radicals in the hydrocarbon being oxidised was determined by the chemiluminescence method. The intensity of chemiluminescence was evaluated in terms of $I \sim [\text{RO}_2^\cdot]^2 \sim v_i^2/2k_t$, where k_t is the rate constant for the disproportionation of RO_2^\cdot . When a mixture of air with HCl was used, the intensity of the chemiluminescence decreased by approximately two orders of magnitude.¹⁸

The $\text{H}_2\text{O}_2 + \text{AmO}^\cdot$ (2,2,6,6-tetramethylpiperidin-*N*-oxyl) + HA (citric acid) system also exhibits an extremely high inhibiting effect. The data presented below demonstrate how the individual components of this system and the whole system influence the rate of the chain oxidation of ethylbenzene (343 K, $P_{\text{O}_2} = 10^5$ Pa, $v_i = 5.21 \times 10^{-7}$ mol dm⁻³ s⁻¹):⁷¹

$[\text{AmO}^\cdot]/10^{-4}$ mol dm ⁻³	$[\text{HA}]/10^{-4}$ mol dm ⁻³	$[\text{H}_2\text{O}_2]/10^{-3}$ mol dm ⁻³	$v/10^{-6}$ mol dm ⁻³ s ⁻¹
0	0	0	4.92
5	0	0	3.78
5	5	0	3.00
5	5	2.5	0.22

It can be seen that complete termination of the chain process is ensured only by the three-component system.

The very effective retardation of the oxidation of the hydrocarbon by this system can be explained in terms of the following mechanism:^{71,72}



According to this mechanism, H_2O_2 is consumed during oxidation of hydrocarbons at a rate of $\frac{1}{2}v_i$, whereas the rate at which nitroxyl radicals are consumed via the reaction (46) is much lower. Only a small portion of the R^\cdot radicals react with AmO^\cdot , since the latter react very rapidly with oxygen. The kinetic characteristics of the inhibited oxidation are fully consistent with the suggested scheme for the cyclic chain termination. When the concentration of H_2O_2 is relatively low, the chain termination rate is limited by the stage (54), and then the function F assumes the following form:⁷¹

$$F = 2 \frac{k_{36} + k_{54}K_{52}[\text{AmO}^\cdot][\text{HA}]}{(2k_1v_i)^{0.5}} [\text{H}_2\text{O}_2].$$

If the concentration of H_2O_2 is large, the stage (54) occurs rapidly and the reaction (53) becomes the rate-limiting stage of the cyclic chain termination. Under these conditions

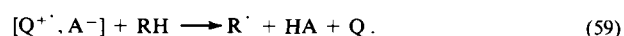
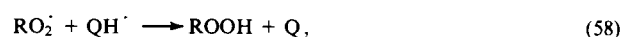
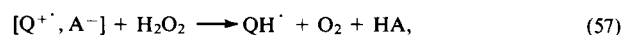
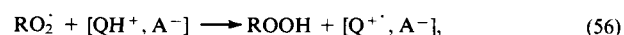
$$F = 2 \frac{k_{53}K_{52}[\text{AmO}^\cdot][\text{HA}] + k_{36}[\text{H}_2\text{O}_2]}{(2k_6v_i)^{0.5}}.$$

The mechanism of chain termination consisting of the reactions (47), (52), (53), and (54) is notable because the acid protonates nitroxyl and thus converts it into a donor of hydrogen atom for the peroxy radical, while hydrogen peroxide reduces the AmO^+ cation to hydroxylamine, which reacts rapidly with RO_2^\cdot . Thus, the acid and hydrogen peroxide transform AmO^\cdot , which is unreactive with respect to RO_2^\cdot , into AmOH^+ and AmOH , and the latter inhibit effectively the oxidation of hydrocarbons.

Recently an analogous mechanism for cyclic chain termination has been proposed for quinones.⁷³ Quinones, which can act as acceptors of alkyl radicals, do not decelerate the oxidation of hydrocarbons at concentrations of up to 5×10^3 mol dm⁻³, because the R^\cdot radicals react very rapidly with oxygen. However, the ternary quinonemonoanilide (Q) + H_2O_2 + acid (HA) system effectively retards the initiated oxidation of methyl oleate and ethylbenzene.⁷³ This is indicated by the following results obtained for the oxidation of ethylbenzene (343 K, $P_{\text{O}_2} = 10^5$ Pa, $v_i = 5.21 \times 10^{-7}$ mol dm⁻³ s⁻¹).

$[\text{Q}]/10^{-4}$ mol dm ⁻³	$[\text{H}_2\text{O}_2]/10^{-3}$ mol dm ⁻³	$[\text{HA}]/10^4$ mol dm ⁻³	$v/10^{-7}$ mol dm ⁻³ s ⁻¹
0	0	0	4.92
5.0	0.0	0	3.01
0.0	1.25	0	3.27
0.0	0.0	5.0	3.93
5.0	1.25	5.0	2.39
5.0	12.5	5.0	0.69

The following mechanism, analogous to the mechanism involving nitroxyl radicals, has been suggested for the retarding influence of this system:



In conformity with this mechanism, the function F depends on the concentrations of the components of the inhibiting mixture in the following way:

$$F = \frac{2K_{55}k_{56}k_{57}[\text{Q}][\text{H}_2\text{O}_2][\text{HA}]}{(k_{57}[\text{H}_2\text{O}_2] + k_{59}[\text{RH}])(2k_6v_i)^{0.5}}.$$

Experimental data on the kinetics of oxidation of methyl oleate and ethylbenzene are in good agreement with the scheme consisting of the reactions (55)–(59).

The cyclic mechanism of chain termination with quinone imines involving acid catalysis is very important for an understanding of the retarding influence of aromatic amines on the oxidation of hydrocarbons and of other organic compounds via the reaction (28). Hydrogen peroxide arises during the oxidation of alcohols due to the decomposition of RO_2^\cdot to yield HO_2^\cdot and ketone and due to the decomposition of $>\text{C}(\text{OH})\text{OOH}$ giving ketone and H_2O_2 . In addition, H_2O_2 is formed in the hydrolysis of alkyl hydroperoxide through the action of water or acids, which also arise in the system during oxidation of hydrocarbons. Thus, two of the three components needed for the realisation of the cyclic chain termination mechanism involving acid catalysis result from the oxidation of the hydrocarbon, while the third component — quinone imine — results from the oxidation of the starting inhibitor (amine). It is possibly owing to this mechanism that aromatic amines exhibit high inhibiting capacity during oxidation at elevated temperatures ($>400\text{ K}$).

VII. Ions and complexes of variable-valence metals as catalysts for chain termination in the oxidation of alcohols, amines, and alkenes

Compounds of variable-valence metals (Mn, Fe, Co, Ce) are well known as catalysts for oxidation of hydrocarbons and aldehydes. They accelerate oxidation by destroying hydroperoxides and initiating the formation of free radicals.⁹ Salts and complexes containing transition metals in a lower valence state react rapidly with peroxy radicals and so when these compounds are added to a hydrocarbon prior to its oxidation an induction period arises.⁹ The chain termination occurs stoichiometrically ($f \approx 1$) and stops when the metal passes to a higher valence state due to oxidation. On the addition of an initiator or hydroperoxide the induction period disappears.

Another situation is observed when salts or complexes of metals with variable valence states are added to an alcohol (primary or secondary) subjected to oxidation: in this case, a prolonged deceleration of the initiated oxidation occurs, owing to repeated chain termination. This was discovered for the first time in relation to the oxidation of cyclohexanol in the presence of a copper salt.¹⁵ Copper and manganese ions also exert a decelerating influence on the initiated oxidation of cyclohexadiene,³²

aliphatic amines,⁴⁹ and 1,2-disubstituted ethenes.³³ This is accounted for by the dual redox nature of the peroxy radicals HO_2^\cdot , $>\text{C}(\text{OH})\text{O}_2^\cdot$, and $>\text{C}(\text{NHR})\text{O}_2^\cdot$, and by the ability of ions (complexes) of heavy metals to accept an electron when they are in a higher valence state, and to release an electron when they are in a lower valence state, for example:

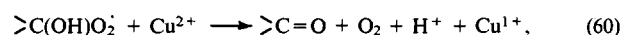
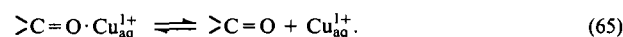
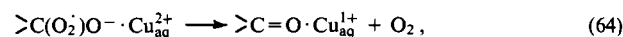
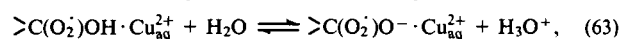
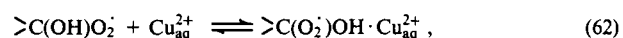


Table 6 presents the results of a kinetic study of the reactions (60) and (61). Copper and manganese compounds exhibit the highest inhibiting activity. The chain termination on variable-valence metals in the systems in which hydroperoxyl and hydroxy-peroxyl radicals act as the chain-propagating species is characterised by very large coefficients: $f \approx 10^4 - 10^6$.

Both reactions (60) and (61) may include several stages. If an aqueous solution of a copper salt, for example sulfate, is used, the following mechanism involving the incorporation of RO_2^\cdot into the inner coordination sphere of the metal ion is possible for the reaction (60):



In the case of metal complexes with strongly bound ligands, the outer-sphere transfer of an electron from the radical to the ion and back is more probable.

When variable-valence metals are used as catalysts in the oxidation of hydrocarbons, the chain termination via reactions (60) and (61) manifests itself late in the process. This case has been specially studied in relation to the oxidation of paraffins to fatty acids in the presence of a K–Mn catalyst,⁸⁰ which ensures a high oxidation rate and a high selectivity of formation of the target product. As the reaction proceeds, alcohols are accumulated in the reaction mixture, their oxidation being accompanied by the formation of hydroxyperoxyl radicals. The more extensively has the oxidation proceeded, the higher is the concentration of alcohols in the oxidised paraffin, and, hence, the higher is the kinetically equilibrium concentration of these radicals. The latter enter into reactions resembling the reactions (60) and (61) with Mn^{2+} and Mn^{3+} ions and thus cause chain termination. When

Table 6. Rate constants for the reactions of metal salts and complexes with peroxy radicals in systems with a cyclic mechanism of chain termination.

Metal complex ^a	Substrate	<i>T</i> / K	<i>k</i> / dm ³ mol ^{−1} s ^{−1}	Ref.
Mn(CO ₂ CH ₃) ₂	(C ₄ H ₉) ₂ NH	348	2.5 × 10 ⁶	39
Mn(CO ₂ CH ₃) ₂	(CH ₃) ₂ NCH ₂ CH ₂ N(CH ₃) ₂	313	1.1 × 10 ⁶	36
Mn(CO ₂ CH ₃) ₂	cyclo-C ₆ H ₁₁ NH ₂	348	7.3 × 10 ⁷	40,74
Mn(CO ₂ CH ₃) ₂	C ₆ H ₅ CH ₂ NH ₂	338	2.8 × 10 ⁸	40
Mn(CO ₂ CH ₃) ₂	CH ₂ =C(CH ₃)C(O)OC ₂ H ₄ N(CH ₃) ₂	323	1.2 × 10 ⁷	35
Mn(CO ₂ CH ₃) ₂	C ₃ H ₇ OCOC ₂ H ₄ N(CH ₃) ₂	323	1.5 × 10 ⁷	7
Mn(CO ₂ CH ₃) ₃	CH ₂ =CHCOOC ₂ H ₄ N(CH ₃) ₂	323	1.2 × 10 ⁷	35
MnSt ₂	cyclo-C ₆ H ₈	348	1.9 × 10 ⁶	32
MnSt ₂	cyclo-C ₆ H ₁₁ OH	348	6.8 × 10 ⁶	75
MnSt ₂	(C ₄ H ₉) ₂ NH	348	3.5 × 10 ⁶	40,74
MnSt ₂	cyclo-C ₆ H ₁₁ NH ₂	348	1.6 × 10 ⁸	40,74
MnSt ₂	CH ₃ CON(C ₂ H ₅) ₂	348	7.8 × 10 ⁵	39
Mn(Acac) ₂	cyclo-C ₆ H ₁₁ NH ₂	363	9.8 × 10 ⁷	76
MnEN(Sal) ₂	cyclo-C ₆ H ₁₁ NH ₂	348	3.1 × 10 ⁸	76
FeSt ₃	cyclo-C ₆ H ₁₁ OH	348	1.3 × 10 ⁴	75
FeSt ₃	cyclo-C ₆ H ₁₁ NH ₂	348	1.2 × 10 ⁶	39,40
Fe(Acac) ₃	cyclo-C ₆ H ₁₁ NH ₂	348	1.0 × 10 ⁵	39,40
Fe(DMG) ₂ Py ₂	cyclo-C ₆ H ₈	348	2.3 × 10 ³	77
Fe(DMG) ₂ Py ₂	(CH ₃) ₂ CHOH	344	1.0 × 10 ³	78
CoCl ₂	cyclo-C ₆ H ₁₁ OH	348	6.1 × 10 ⁴	39

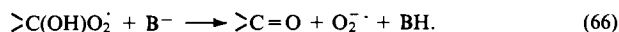
Table 6 (continued)

Metal complex	Substrate	T/K	k / dm ³ mol ⁻¹ s ⁻¹	Ref.
Co(CO ₂ CH ₃) ₂	cyclo-C ₆ H ₁₁ NH ₂	348	1.2 × 10 ⁵	39,40
CoSt ₂	cyclo-C ₆ H ₁₁ OH	348	2.8 × 10 ⁵	75
CoSt ₂	cyclo-C ₆ H ₁₁ NH ₂	348	3.2 × 10 ⁴	40
Co(III)(Acac) ₃	(CH ₃) ₂ CHOH	344	2.9 × 10 ²	78
Co(Acac) ₂	cyclo-C ₆ H ₁₁ OH	348	6.4 × 10 ⁶	40
Co(Acac) ₂	cyclo-C ₆ H ₁₁ NH ₂	348	6.4 × 10 ⁴	40
Co(Acac) ₃	cyclo-C ₆ H ₁₁ NH ₂	348	6.3 × 10 ⁴	40
Co(C ₆ H ₁₁ CO ₂) ₂	cyclo-C ₆ H ₁₁ OH	348	8.7 × 10 ⁴	39
Co(II)(DMG) ₂ NH ₃ Cl	cyclo-C ₆ H ₈	348	8.4 × 10 ²	77
Co(II)(DMG) ₂ NH ₃ Cl	(CH ₃) ₂ CHOH	344	5.0 × 10 ³	78
Co(II)(DMG) ₂ NH ₃ I	cyclo-C ₆ H ₈	348	2.3 × 10 ⁴	77
Co(II)(DMG) ₂ NH ₃ I	(CH ₃) ₂ CHOH	344	3.1 × 10 ²	78
Co(II)(DMG) ₂ PyI	(CH ₃) ₂ CHOH	344	7.0 × 10 ⁴	78
Co(II)(DMG) ₂ Py ₂	(CH ₃) ₂ CHOH	344	1.2 × 10 ⁴	78
Co(EN)(Slm) ₂	cyclo-C ₆ H ₁₁ OH	348	3.3 × 10 ⁵	76
Co(II)Prf	cyclo-C ₆ H ₁₁ OH	348	3.6 × 10 ⁴	76
Ni(Sal) ₂	C ₈ H ₁₇ OH	363	1.6 × 10 ⁴	76
Ni(Sal) ₂	cyclo-C ₆ H ₁₁ NH ₂	353	2.8 × 10 ⁴	76
NiEN(Slm) ₂	C ₈ H ₁₇ OH	363	7.9 × 10 ³	76
NiEN(Slm) ₂	cyclo-C ₆ H ₁₁ NH ₂	353	1.5 × 10 ⁴	76
NiEN(Slm) ₂	C ₈ H ₁₇ OH	363	3.5 × 10 ⁴	76
NiEN(Slm) ₂	cyclo-C ₆ H ₁₁ NH ₂	353	6.6 × 10 ⁴	76
NiENSlmTln	cyclo-C ₆ H ₁₁ NH ₂	353	1.7 × 10 ⁵	76
CuSO ₄	cyclo-C ₆ H ₁₁ OH	348	8.8 × 10 ⁶	15
CuCl ₂	<i>trans</i> -C ₆ H ₅ CH = CHCOOC ₂ H ₅	323	5.9 × 10 ⁵	33
CuCl ₂	<i>trans</i> -C ₆ H ₅ CH = CH = CHCOOCH ₃	323	5.6 × 10 ⁵	33
CuCl ₂	<i>trans</i> -C ₆ H ₅ CH = CHC ₆ H ₅	323	2.6 × 10 ⁵	33
Cu(CO ₂ CH ₃) ₂	C ₆ H ₅ CH ₂ NH ₂	338	1.5 × 10 ⁸	39
Cu(CO ₂ CH ₃) ₂	C ₃ H ₇ COOC ₂ H ₄ N(CH ₃) ₂	323	1.3 × 10 ⁷	79
Cu(CO ₂ CH ₃) ₂	C ₄ H ₉ N(CH ₃) ₂	323	1.0 × 10 ⁷	79
Cu(CO ₂ CH ₃) ₂	C ₆ H ₅ CH = CHCOOC ₂ H ₅	323	2.2 × 10 ⁵	33
Cu(CO ₂ CH ₃) ₂	C ₆ H ₅ CH = CHCOOCH ₃	323	4.5 × 10 ⁵	33
Cu(CO ₂ CH ₃) ₂	C ₆ H ₅ CH = CHC ₆ H ₅	323	5.3 × 10 ⁵	33
CuSt ₂	cyclo-C ₆ H ₈	348	1.9 × 10 ⁶	77
CuSt ₂	cyclo-C ₆ H ₁₁ OH	348	2.9 × 10 ⁶	75
CuSt ₂	(C ₄ H ₉) ₂ NH	348	4.1 × 10 ⁶	40
CuSt ₂	cyclo-C ₆ H ₁₁ NH ₂	348	9.5 × 10 ⁷	39
CuSt ₂	cyclo-C ₆ H ₁₁ NH ₂	348	1.0 × 10 ⁷	76
CuSt ₂	(CH ₃) ₂ NCH ₂ CH ₂ N(CH ₃) ₂	313	2.7 × 10 ⁵	36
Cu(Acac) ₂	C ₆ H ₅ CH ₂ NH ₂	338	1.3 × 10 ⁶	39
Cu(Acac) ₂	cyclo-C ₆ H ₁₁ NH ₂	348	7.2 × 10 ⁵	39
Cu(DMG) ₂	cyclo-C ₆ H ₈	348	1.3 × 10 ⁵	77
Cu(DMG) ₂	cyclo-C ₆ H ₈	348	1.5 × 10 ⁵	77
Cu(DMG) ₂	(CH ₃) ₂ CHOH	344	5.0 × 10 ⁵	78
Cu(Sal) ₂	cyclo-C ₆ H ₈	348	1.7 × 10 ⁵	77
Cu(Sal) ₂	(CH ₃) ₂ CHOH	344	1.2 × 10 ⁵	78
Cu(DPG) ₂	(CH ₃) ₂ CHOH	344	5.9 × 10 ⁴	78
Cu(DMG) ₂	(CH ₃) ₂ CHOH	344	3.7 × 10 ⁴	78
Cu(4-NO ₂ -Slm) ₂	cyclo-C ₆ H ₁₁ NH ₂	363	2.8 × 10 ⁸	76
Cu(Slm) ₂	cyclo-C ₆ H ₁₁ NH ₂	363	1.4 × 10 ⁸	76
Cu(4-HO-Slm) ₂	cyclo-C ₆ H ₁₁ NH ₂	363	9.2 × 10 ⁷	76
Cu(4-CH ₃ O-Slm) ₂	cyclo-C ₆ H ₁₁ NH ₂	363	1.1 × 10 ⁸	76
CuEN(Slm) ₂	cyclo-C ₆ H ₁₁ NH ₂	348	7.5 × 10 ⁷	76
CuEN(Slm) ₂	cyclo-C ₆ H ₁₁ NH ₂	363	3.6 × 10 ⁷	76
Cu(EN) ₂ (Slm) ₂	cyclo-C ₆ H ₁₁ NH ₂	348	4.7 × 10 ⁶	76
Cu(EN) ₃ (Slm) ₂	cyclo-C ₆ H ₁₁ NH ₂	348	7.9 × 10 ⁵	76
CuC ₆ H ₄ (Slm) ₂	cyclo-C ₆ H ₁₁ NH ₂	348	7.9 × 10 ⁶	76
CuC ₆ H ₄ -C ₆ H ₄ (Slm) ₂	cyclo-C ₆ H ₁₁ NH ₂	348	2.6 × 10 ⁶	76
Cu(II)Prf	cyclo-C ₆ H ₁₁ NH ₂	348	7.3 × 10 ⁵	39
CuPrf	C ₆ H ₅ CH ₂ NH ₂	338	1.5 × 10 ⁶	39
CeSt ₃	cyclo-C ₆ H ₁₁ OH	348	1.1 × 10 ⁵	75
CeSt ₃	cyclo-C ₆ H ₁₁ NH ₂	348	8.6 × 10 ⁵	39

^a Notation: AcacH — acetylacetone, StH — stearic acid, DMGH — dimethylglyoxime, SlmH — salicylaldehyde, 4-X-SlmH — 4-X-salicylanilide, ENSlm — o-salicylaldehydeneimine, ENH₂ — ethylene diamine, TlnH — toluidine, SalH — salicylic acid, Prf — porphyrin, DPGH — diphenylglyoxime.

the rate of chain termination with the hydroxyperoxyl radicals becomes equal to the rate of generation of the chain-propagating radicals, the oxidation virtually ceases.

The oxidation of alcohols is also retarded by bases,⁸¹⁻⁸³ which is apparently due to the decomposition of the hydroxyperoxyl radical giving ketone and superoxide ion $O_2^{\cdot-}$:



The superoxide ion cannot continue the chain and is destroyed via disproportionation with RO_2^{\cdot} .

VIII. Conclusion

Studies of the mechanisms of cyclic chain termination in oxidation processes carried out for three decades have demonstrated on the one hand that they are extremely diverse and, on the other hand, that they are highly structurally selective. The 19 currently known mechanisms, which are presented in Table 7, can be divided into three groups.

The first group includes mechanisms with the participation of such inhibitors as aromatic amines, nitroxyl radicals, quinones, and compounds of variable-valence metals (Mn, Fe, Co, Cu, Ce). These inhibitors or, more precisely, the inhibiting pairs (AmH and Am^{\cdot} , Q and QH^{\cdot} , AmO^{\cdot} and $AmOH$, and M^{n+} and M^{n+1})

retard oxidation only provided that the chain is continued by the HO_2^{\cdot} , $>C(OH)O_2^{\cdot}$, or $>CH(NHR)O_2^{\cdot}$ radicals. The latter disproportionate very rapidly with hydrogen atom acceptors such as Am^{\cdot} , AmO^{\cdot} , or Q . This leads to the recovery of the reduced form of the inhibitor, which again reacts rapidly with a peroxy radical; this ensures the effective chain termination. The number of cycles is determined by the ratio of the rate of the reaction of the peroxy radical, in which the inhibitor is recovered, to the rate of its irreversible consumption. The direction of the transformation of RO_2^{\cdot} is largely determined by the nature of the reaction centre of disproportionation. Analysis has shown that the triplet repulsion in the transition state of an elementary step of the regeneration of the inhibitor by the peroxy radical needs to be very weak. It is also essential that the atoms between which the electron transfer occurs (for example, N and O) should differ in electron affinity. Thus, the structure of the peroxy radical is the crucial factor for the mechanisms of the first group.

The second group of mechanisms, by which the inhibitors (nitroxyl radicals) are recovered, involves successive participation of the R^{\cdot} and RO_2^{\cdot} radicals in the reactions with AmO^{\cdot} and $AmOH$. The possibility of the realisation of these mechanisms depends on the conditions of the oxidation, which should ensure fairly rapid interaction of the alkyl radicals with AmO^{\cdot} , and this requires that the reaction of R^{\cdot} with oxygen does not occur very rapidly. This requirement is fulfilled in the oxidation of solid

Table 7. Cyclic mechanisms of chain termination in the liquid-phase oxidation of organic compounds.

Inhibiting system	Radical	Mechanism	Ref.
AmH , Am^{\cdot}	HO_2^{\cdot}	$HO_2^{\cdot} + AmH \longrightarrow H_2O_2 + Am^{\cdot}$, $Am^{\cdot} + HO_2^{\cdot} \longrightarrow AmH + O_2$	29, 32, 33
AmH , Am^{\cdot}	$>C(OH)O_2^{\cdot}$	$>C(OH)OO^{\cdot} + AmH \longrightarrow >C(OH)OOH + Am^{\cdot}$ $>C(OH)OO^{\cdot} + Am^{\cdot} \longrightarrow >C=O + O_2 + AmH$	14, 18, 19, 28, 29, 30, 34
AmH , Am^{\cdot}	$>C(NHR)O_2^{\cdot}$	$>C(NHR)OO^{\cdot} + AmH \longrightarrow >C(NHR)OOH + Am^{\cdot}$ $>C(NHR)OO^{\cdot} + Am^{\cdot} \longrightarrow >C=NR + O_2 + AmH$	35-41
AmO^{\cdot} , $AmOH$	HO_2^{\cdot}	$AmO^{\cdot} + HO_2^{\cdot} \longrightarrow AmOH + O_2$ $AmOH + HO_2^{\cdot} \longrightarrow AmO^{\cdot} + H_2O_2$	32, 33, 56
AmO^{\cdot} , $AmOH$	$>C(OH)O_2^{\cdot}$	$>C(OH)OO^{\cdot} + AmO^{\cdot} \longrightarrow >C=O + O_2 + AmOH$ $>C(OH)OO^{\cdot} + AmOH \longrightarrow >C(OH)OOH + AmO^{\cdot}$	30
AmO^{\cdot} , $AmOH$	$>C(NHR)O_2^{\cdot}$	$>C(NHR)OO^{\cdot} + AmO^{\cdot} \longrightarrow >C=NR + AmOH$ $>C(NHR)OO^{\cdot} + AmOH \longrightarrow >C(NHR)OOH + AmO^{\cdot}$	35, 36, 39, 40
Q , HQ^{\cdot}	HO_2^{\cdot}	$Q + HO_2^{\cdot} \longrightarrow HQ^{\cdot} + O_2$ $HQ^{\cdot} + HO_2^{\cdot} \longrightarrow Q + H_2O_2$	30, 32, 33, 42, 58
Q , HQ^{\cdot}	$>C(OH)O_2^{\cdot}$	$>C(OH)OO^{\cdot} + Q \longrightarrow >C=O + O_2 + HQ^{\cdot}$ $>C(OH)OO^{\cdot} + HQ^{\cdot} \longrightarrow >C(OH)OOH + Q$	16, 52-54
Q , HQ^{\cdot}	$>C(NHR)O_2^{\cdot}$	$>CC(NHR)OO^{\cdot} + Q \longrightarrow >C=NR + O_2 + HQ^{\cdot}$ $>CC(NHR)OO^{\cdot} + HQ^{\cdot} \longrightarrow >C(NHR)OOH + Q$	36, 38-41
M^{n+} , M^{n+1}	HO_2^{\cdot}	$M^{n+} + HO_2^{\cdot} \longrightarrow M^{n+1} + HO_2^{\cdot}$ $M^{n+1} + HO_2^{\cdot} \longrightarrow H^+ + O_2 + M^{n+}$	32, 33, 77
M^{n+} , M^{n+1}	$>C(OH)O_2^{\cdot}$	$>C(OH)OO^{\cdot} + M^{n+} \longrightarrow >C(OH)O_2^{\cdot} + M^{n+1}$ $>C(OH)OO^{\cdot} + M^{n+1} \longrightarrow >C=O + O_2 + H^+ + M^{n+}$	15, 39, 40, 75-79
M^{n+} , M^{n+1}	$>C(NHR)O_2^{\cdot}$	$>C(NHR)OO^{\cdot} + M^{n+} \longrightarrow >C(NHR)O_2^{\cdot} + M^{n+1}$ $>C(NHR)OO^{\cdot} + HQ^{\cdot} \longrightarrow >C=NR + O_2 + H^+ + M^{n+}$	35, 39, 40, 74, 77, 79
AmO^{\cdot} , $AmOR$	R^{\cdot} , RO_2^{\cdot}	$AmO^{\cdot} + R^{\cdot} \longrightarrow AmOR$ $AmOR + RO_2^{\cdot} \longrightarrow ROOH + Alkene + AmO^{\cdot}$	

Table 7. (continued)

Inhibiting system	Radical	Mechanism	Ref.
AmO \cdot , AmOR	R \cdot , RO $_2\cdot$	$\text{AmO}\cdot + \text{R}\cdot \longrightarrow \text{AmOR}$ $\text{AmOR} \longrightarrow [\text{AmO}\cdot + \text{R}\cdot] \longrightarrow \text{AmOH} + \text{Alkene}$ $\text{AmOH} + \text{RO}_2\cdot \longrightarrow \text{ROOH} + \text{AmO}\cdot$	64–68
AmO \cdot , AmOR	R \cdot , RO $_2\cdot$	$\text{AmO}\cdot + \text{R}\cdot \longrightarrow \text{AmOR}$ $\text{AmOR} \longrightarrow [\text{Am}\cdot + \text{RO}\cdot] \longrightarrow \text{AmH} + \text{Alkene}$ $\text{AmH} + \text{RO}_2\cdot \longrightarrow \text{ROOH} + \text{Am}\cdot$ $\text{Am}\cdot + \text{RO}_2\cdot \longrightarrow \text{AmO}\cdot + \text{RO}\cdot$	69, 70
I $_2$	R \cdot , RO $_2\cdot$	$\text{R}\cdot + \text{I}_2 \longrightarrow \text{RI} + \text{I}\cdot$ $\text{RI} + \text{RO}_2\cdot \longrightarrow \text{R}\cdot + \text{ROOI}$ $2 \text{ROOI} \longrightarrow \text{I}_2 + \text{O}_2 + \text{ROOR}$	84
AmO \cdot	RO $_2\cdot$	$\text{AmO}\cdot + \text{HA} \rightleftharpoons [\text{AmOH}^{+\cdot}, \text{A}^-],$ $\text{RO}_2\cdot + [\text{AmOH}^{+\cdot}, \text{A}^-] \longrightarrow \text{ROOH} + [\text{AmO}^+, \text{A}^-],$ $[\text{AmO}^+, \text{A}^-] + \text{H}_2\text{O}_2 \longrightarrow \text{AmOH} + \text{HA} + \text{O}_2,$ $\text{RO}_2\cdot + \text{AmOH} \longrightarrow \text{ROOH} + \text{AmO}\cdot.$	30, 71, 72
Q, H $_2$ O $_2$, HA	RO $_2\cdot$	$\text{Q} + \text{HA} \rightleftharpoons (\text{QH}^+, \text{A}^-),$ $(\text{QH}^+, \text{A}^-) + \text{RO}_2\cdot \longrightarrow (\text{Q}^{+\cdot}, \text{A}^-) + \text{ROOH},$ $(\text{Q}^{+\cdot}, \text{A}^-) + \text{H}_2\text{O}_2 \longrightarrow \text{HQ}\cdot + \text{HA} + \text{O}_2,$ $\text{RO}_2\cdot + \text{HQ}\cdot \longrightarrow \text{ROOH} + \text{Q}$	73
B	>C(OH)O $_2\cdot$	$>\text{C}(\text{OH})\text{O}_2\cdot + \text{B}^- \longrightarrow >\text{C}=\text{O} + \text{O}_2^{2-} + \text{BH}$	81–83

polymers, since in this case, the solubility of O $_2$ and the rate of its reaction with R \cdot are lower than those in a liquid under similar conditions. Mechanism of this sort can also occur in the liquid phase, when the concentration of the dissolved oxygen is relatively low ([O $_2$] \ll [ArO \cdot]). For the dissociation of the intermediate product at the O–C or N–O bond, a sufficiently high temperature is needed.

The third group of mechanisms includes acid catalysis as a necessary stage of the cycle. An acid protonates an inhibitor in the oxidised form (AmO \cdot , Q) and thus transforms the corresponding species into a potential hydrogen donor. The cycle begins with attack by RO $_2\cdot$ on the protonated inhibitor. Of course, the reduction of the cationic form of the inhibitor with hydrogen peroxide also plays an important role. Mechanisms of this sort should be characteristic of the oxidation in the systems in which hydrogen peroxide and an acid are generated, and this refers to many organic compounds.

Evidently, catalysis with bases is characteristic of systems in which the HO $_2\cdot$ or >C(OH)O $_2\cdot$ radicals act as the chain-propagating species in the oxidation. Repeated chain termination has also been observed in the presence of sulfur-containing inhibitors,²³ but the exact mechanism of these processes is still unknown.

References

- V Ya Shlyapintokh *Fotokhimicheskie Prevrashcheniya i Stabilizatsiya Polimerov* (Photochemical Transformations and Stabilisation of Polymers) (Moscow: Khimiya, 1979)
- N M Emanuel', A L Buchachenko *Khimicheskaya Fizika Molekulyarnogo Razrusheniya i Stabilizatsii Polimerov* (Chemical Physics of Molecular Degradation and Stabilisation of Polymers) (Moscow: Nauka, 1988)
- E T Denisov *Okislenie i Destruktsiya Karbotsepykh Polimerov* (Oxidation and Degradation of Carbon-Chain Polymers) (Leningrad: Khimiya, 1990)
- G Scott (Ed.) *Mechanism of Polymer Degradation and Stabilisation* (London: Elsevier Applied Science, 1990)
- A M Kuliev *Khimiya i Tekhnologiya Prisadok k Maslam i Toplivam* (The Chemistry and Technology of Additives to Oils and Fuels) (Moscow: Khimiya, 1972)
- E T Denisov, G I Kovalev *Okislenie i Stabilizatsiya Reaktivnykh Topliv* (Oxidation and Stabilisation of Jet Fuels) (Moscow: Khimiya, 1983)
- M M Mogilevich, E M Pliss *Okislenie i Okislitel'naya Polimerizatsiya Nepredel'nykh Soedinenii* (Oxidation and Oxidative Polymerisation of Unsaturated Compounds) (Moscow: Khimiya, 1990)
- N M Emanuel', Yu N Lyaskovskaya *Tormozhenie Protsesov Okisleniya Zhirov* (Inhibition of Oxidation Processes in Fats) (Moscow: Pishchepromizdat, 1961)
- N M Emanuel', E T Denisov, Z K Maizus *Tsepnye Reaktsii Okisleniya Uglevodorodov v Zhidkoi Faze* (Chain Reactions in the Oxidation of Hydrocarbons in the Liquid Phase) (Moscow: Nauka, 1965)
- E T Denisov, I V Khudyakov *Chem. Rev.* **87** 1313 (1987)
- V A Roginskii *Fenol'nye Antioksidanty* (Phenolic Antioxidants) (Moscow: Nauka, 1988)
- E T Denisov, V V Kharitonov *Izv. Akad. Nauk SSSR, Ser. Khim.* 2222 (1963)
- E T Denisov, V P Shcheredin *Izv. Akad. Nauk SSSR, Ser. Khim.* 919 (1964)
- V V Kharitonov, E T Denisov *Izv. Akad. Nauk SSSR, Ser. Khim.* 2764 (1967)
- A L Aleksandrov, E T Denisov *Izv. Akad. Nauk SSSR, Ser. Khim.* 1652 (1969)
- E T Denisov *Izv. Akad. Nauk SSSR, Ser. Khim.* 328 (1969)
- Yu B Shilov, R T Battalova, E T Denisov *Dokl. Akad. Nauk SSSR* **207** 388 (1972)

18. V I Gol'denberg, N V Katkova, E T Denisov *Izv. Akad. Nauk SSSR, Ser. Khim.* 287 (1988)
19. E T Denisov *Kinet. Katal.* 11 312 (1970)
20. E T Denisov, in *Teoriya i Praktika Zhidkofaznogo Okisleniya* (Theory and Practice of Liquid-Phase Oxidation) (Ed. N M Emanuel') (Moscow: Nauka, 1974) p. 237
21. E T Denisov, in *Developments in Polymer Stabilisation* Vol. 3 (Ed. G Scott) (London: Elsevier Applied Science, 1980) p. 1
22. V Ya Shlyapintoch, V B Ivanov, in *Developments in Polymer Stabilisation* Vol. 5 (Ed. G Scott) (London: Elsevier Applied Science, 1982) p. 41
23. E T Denisov, in *Kinetika i Kataliz (Ser. Itogi Nauki i Tekhniki)* T. 17 [Kinetics and Catalysis (Advances in Science and Engineering Ser.) Vol. 17] (Moscow: Izd. VINITI, 1987)
24. E T Denisov, N I Mitskevich, V E Agabekov *Mekhanizm Zhidkofaznogo Okisleniya Kislorodsoderzhashchikh Soedinenii* (The Mechanism of the Liquid-Phase Oxidation of Oxygen-Containing Compounds) (Minsk: Nauka i Tekhnika, 1975) Vol. 16 (Amsterdam: Elsevier, 1980)
26. E T Denisov *Konstanty Skorosti Gomoliticheskikh Zhidkofaznykh Reaktsii* (Rate Constants for Homolytic Liquid-Phase Reactions) (Moscow: Nauka, 1971)
27. N N Pozdeeva, I K Yakushchenko, A L Aleksandrov, E T Denisov *Kinet. Katal.* 32 1302 (1991)
28. V V Shalya, B I Kolotusha, F A Yampol'skaya, Ya B Gorokhovatskii *Kinet. Katal.* 10 1090 (1969)
29. R L Vardanyan, V V Kharitonov, E T Denisov *Izv. Akad. Nauk SSSR, Ser. Khim.* 1536 (1970)
30. E T Denisov, V I Gol'denberg, L G Verba *Izv. Akad. Nauk SSSR, Ser. Khim.* 2217 (1988)
31. V I Gol'denberg, E T Denisov, L G Verba *Izv. Akad. Nauk SSSR, Ser. Khim.* 2223 (1988)
32. R L Vardanyan, E T Denisov *Izv. Akad. Nauk SSSR, Ser. Khim.* 2818 (1971)
33. E M Pliss, Doctoral Thesis in Chemical Sciences, Institute of Chemical Physics, Academy of Sciences of the USSR, Chernogolovka, 1990
34. R L Vardanyan, V V Kharitonov, E T Denisov *Neftekhimiya* 11 247 (1971)
35. E M Pliss, A L Aleksandrov, M M Mogilevich *Izv. Akad. Nauk SSSR, Ser. Khim.* 1441 (1977)
36. U Ya Samatov, A L Aleksandrov, I R Akhunov *Izv. Akad. Nauk SSSR, Ser. Khim.* 2254 (1978)
37. A L Aleksandrov, L D Krisanova *Izv. Akad. Nauk SSSR, Ser. Khim.* 2469 (1980)
38. G A Kovtun, A L Aleksandrov *Izv. Akad. Nauk SSSR, Ser. Khim.* 1274 (1974)
39. A L Aleksandrov, Doctoral Thesis in Chemical Sciences, Institute of Chemical Physics, Academy of Sciences of the USSR, Chernogolovka, 1987
40. G A Kovtun, Candidate's Thesis in Chemical Sciences, Institute of Chemical Physics, Academy of Sciences of the USSR, Chernogolovka, 1974
41. E M Pliss, A L Aleksandrov, V S Mikhlin, M M Mogilevich *Izv. Akad. Nauk SSSR, Ser. Khim.* 2259 (1978)
42. E T Denisov *Izv. Akad. Nauk SSSR, Ser. Khim.* (1996) (in the press)
43. E T Denisov *Kinet. Katal.* 32 461 (1991)
44. E T Denisov *Mendeleev Commun.* 1 (1992)
45. E T Denisov *Kinet. Katal.* 35 671 (1994)
46. E T Denisov *Polym. Deg. Stabil.* 49 71 (1995)
47. V T Varlamov, R L Safiullin, E T Denisov *Khim. Fiz.* 408 (1983)
48. E T Denisov *Kinet. Katal.* 37 (1996) (in the press)
49. D Lide (Ed.) *Handbook of Chemistry and Physics* (Boca Raton, FL: CRC Press, 1991–1992)
50. C H Bamford, C F H Tipper (Eds) *Comprehensive Chemical Kinetics* Vol. 14 (Amsterdam: Elsevier, 1976)
51. Yu B Shilov, E T Denisov *Vysokomol. Soedin., Ser. A* 16 1736 (1974)
52. Yu B Shilov, E T Denisov *Vysokomol. Soedin., Ser. A* 26 1753 (1984)
53. R L Vardanyan, E T Denisov, V I Zozulya *Izv. Akad. Nauk SSSR, Ser. Khim.* 611 (1972)
54. T G Degtyareva, E T Denisov, V S Martem'yanov, L Ya Badretidinova *Izv. Akad. Nauk SSSR, Ser. Khim.* 1219 (1979)
55. E T Denisov *Handbook of Antioxidants* (Boca Raton, FL: CRC Press, 1995)
56. A V Kirgin, Yu B Shilov, E B Krisyuk, A A Efimov, V V Pavlikov *Kinet. Katal.* 31 58 (1990)
57. E T Denisov *Kinet. Katal.* 36 387 (1995)
58. Yu B Shilov, E T Denisov *Vysokomol. Soedin., Ser. A* 29 1359 (1987)
59. Yu B Shilov, E T Denisov *Vysokomol. Soedin., Ser. A* 16 2313 (1974)
60. Yu B Shilov, Candidate's Thesis in Chemical Sciences, Institute of Chemical Physics, Academy of Sciences of the USSR, Chernogolovka, 1979
61. E T Denisov *Polym. Deg. Stabil.* 25 209 (1989)
62. E T Denisov *Polym. Deg. Stabil.* 34 325 (1991)
63. M V Sudnik, M F Romantsev, A B Shapiro, E G Rozantsev *Izv. Akad. Nauk SSSR, Ser. Khim.* 2813 (1975)
64. D J Carlsson, A Garton, D M Wiles *Dev. Polym. Stabil.* 1 219 (1979)
65. K B Chakraborty, G Scott *Polymer* 21 252 (1980)
66. H Berger, T A Bolsman, D M Brower *Dev. Polym. Stabil.* 6 1 (1983)
67. G Scott *J. Polym. Sci. Polym. Lett. Ed.* 22 553 (1984)
68. D J Carlsson *Pure Appl. Chem.* 55 1651 (1983)
69. S Korcek, R K Jensen, M Zinbo, J L Gerlock, in *Regeneration of Amine in the Catalytic Inhibition of Oxidation in Organic Free Radicals*. (Ed. H Fischer) (Berlin: Springer, 1988) p. 95
70. R K Jensen, S Korcek, M Zinbo, J L Gerlock *J. Org. Chem.* 61 (1996) (in the press)
71. V I Gol'denberg, E T Denisov, N A Ermakova *Izv. Akad. Nauk SSSR, Ser. Khim.* 738 (1990)
72. E T Denisov, in *12th International Conference on Advances in the Stabilization and Controlled Degradation of Polymers, Luzerne, Switzerland, 1990* p. 77
73. V I Gol'denberg, N A Ermakova, E T Denisov *Izv. Akad. Nauk SSSR, Ser. Khim.* 79 (1995)
74. G A Kovtun, A L Aleksandrov, E T Denisov *Izv. Akad. Nauk SSSR, Ser. Khim.* 2611 (1973)
75. A L Aleksandrov, G I Solov'ev, E T Denisov *Izv. Akad. Nauk SSSR, Ser. Khim.* 1527 (1972)
76. G A Kovtun, Doctoral Thesis in Chemical Sciences, Institute of Organic and Inorganic Chemistry, Academy of Sciences of the USSR, Moscow, 1984
77. N G Zubareva, E T Denisov, A V Ablov *Kinet. Katal.* 14 579 (1973)
78. N G Zubareva, E T Denisov, A V Ablov *Kinet. Katal.* 14 346 (1973)
79. E M Pliss, A L Aleksandrov *Izv. Akad. Nauk SSSR, Ser. Khim.* 214 (1978)
80. A V Oberemko, A A Perchenko, E T Denisov, A L Aleksandrov *Neftekhimiya* 11 229 (1971)
81. E T Denisov, V M Solyanikov, A L Alexandrov *Adv. Chem. Ser.* 75 (1) 112 (1968)
82. A L Aleksandrov, E T Denisov *Dokl. Akad. Nauk SSSR* 178 379 (1968)
83. A L Aleksandrov, E T Denisov *Izv. Akad. Nauk SSSR, Ser. Khim.* 2322 (1969)
84. A L Aleksandrov, T I Sapacheva, E T Denisov *Neftekhimiya* 10 711 (1970)

The nature and dynamics of nonlinear excitations in conducting polymers. Heteroaromatic polymers

V A Krinichnyi

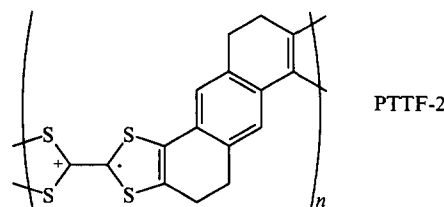
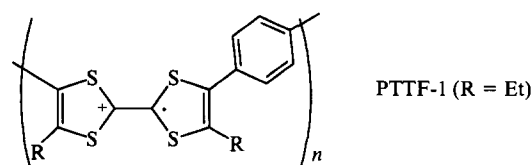
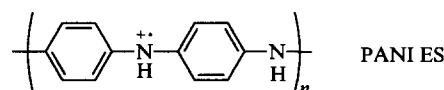
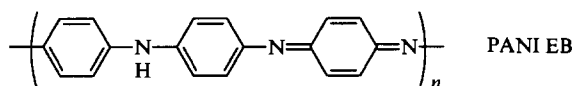
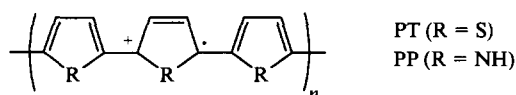
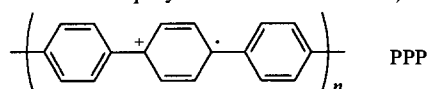
Contents

I. Introduction	521
II. Polyparaphenylene	522
III. Polythiophene	523
IV. Polypyrrole	525
V. Polyaniline	526
VI. Polytetrathiafulvalene	532
VII. Conclusion	535

Abstract. The results of studies on the structural, conformational, and dynamic properties of organic conducting polymers by 2 mm EPR spectroscopy are treated systematically and surveyed. The structural and dynamic features of the paramagnetic centres as well as the mechanism of charge transfer in the conducting polymers are discussed. The bibliography includes 73 references.

I. Introduction

Various organic conducting compounds are known at the present time: charge-transfer complexes and radical-ion salts, platinum complexes with cyanide ligands, phthalocyanines, dyes, metal-filled polymers, etc.^{1–4} These compounds are of interest from the standpoint of a study of the fundamental principles of charge transfer. Among them, one should distinguish particularly organic conducting polymers such as polyparaphenylene (PPP), polythiophene (PT), polypyrrole (PP), the emeraldine base (EB) and emeraldine salt (ES) form of polyaniline (PANI), polytetra-thiafulvalene (PTTF), polyacetylene (PA), etc., which may prove promising in molecular electronics (the spin charge carriers stabilised in the polymers are shown below).^{5–7}



These compounds are characterised by an anisotropic quasi-one-dimensional (1D) π -conjugated structure and, in contrast to classical polymers, exhibit an electrical conductivity which varies by more than 10 orders of magnitude when the polymer is doped with various counterions.⁵ The introduction of BF_4^- , ClO_4^- , AsF_6^- , I_3^- , FeCl_4^- , MnO_4^- , etc. anions induces a positive charge on its chains, i.e. leads to a *p*-type conductivity, whereas *n*-type conductivity is achieved by doping the polymer with various alkali metals, for example Li^+ , K^+ , and Na^+ .

The electrodynamic properties of conducting polymers are significantly influenced by their structure, conformation, and the packing of their chains. The globular structure of the polymers is made up of fibrils with a typical diameter of 100 nm, the fibrils consisting in their turn of crystallites. The parameters of the corresponding unit cells of such crystallites are listed in Table 1. The dihedral angle θ between the planes of the monomer units in the polymer, for example in PPP, is $\sim 23^\circ$.¹² The value of this angle is a result of a compromise balance between the conjugation effect, tending to bring the system to a planar conformation, and the steric repulsion of the hydrogen atoms in the *ortho*-positions, which rules out a planar conformation. The electron density transfer integral I between the monomer units is given by $I \sim \cos \theta$,¹³ so that the probability of the 1D-charge transfer in the polymer increases with increase in the planarity of the chain.

V I Krinichnyi. Laboratory for Electrically Conducting Compounds, Institute of Chemical Physics in Chernogolovka, Russian Academy of Sciences, 142432 Chernogolovka, Moscow Region, Russian Federation. Fax (7-096) 515 35 88. Tel. (7-096) 524 50 35

Received 6 July 1995

Uspekhi Khimii 65 (6) 564–580 (1996); translated by A K Grzybowski

Table 1. The unit cell parameters of conducting polymers.

Polymer	System	Parameter / nm			Ref.
		<i>a</i>	<i>b</i>	<i>c</i>	
PPP	Monoclinic	0.779	0.562	0.426	8
	Orthorhombic	0.781	0.553	0.420	8
PT	Hexagonal	0.950	0.620	1.220	9
PP	Monoclinic	—	0.341	0.718	10
PANI	Monoclinic	0.705	0.860	0.950	11

The overlap of the π orbitals of the monomer rings results in the formation of a band structure of the polymer with gap widths of 3.5 eV (PPP), 2.2 eV (PT), 3.0 eV (PP), 4.0 eV (undoped PANI), and 1.5 eV (ES form of PANI).^{10,14} The resonance interaction of the energetically nonequivalent benzenoid and quinonoid forms of the monomers is the cause of the nonlinear topological excitation — the formation of a polaron with a spin of $\frac{1}{2}$, delocalised over 4–5 monomer units of the polymer.⁸ The energy levels of such a polaron are located in the forbidden band at a distance Δ_1 below the conductivity band and at a distance Δ_2 above the valence band. $\Delta_1 = \Delta_2 = 0.7$ eV for PPP, $\Delta_1 = 0.9$ eV and $\Delta_2 = 0.45$ eV for PP, and $\Delta_1 = 0.7$ – 0.9 eV and $\Delta_2 = 0.5$ – 0.6 eV for the other conducting polymers.¹⁴ For sufficiently high levels of doping, pairs of polarons may recombine with formation of longer spin-less bipolarons.

Conducting polymers contain paramagnetic centres (PC) at a concentration $N = 10^{16}$ – 10^{21} spins g^{-1} ,^{15,16} so that one of the most promising methods for their investigation is EPR spectroscopy, which makes it possible to obtain varied and unique information about the structure of the polymer and about the nature and properties of the paramagnetic centres (their concentration, mobility, relaxation, etc.). Such studies are as a rule carried out at relatively low recording frequencies ($\nu_e \leq 10$ GHz). In these bands, conducting polymers, like other π -electron systems, usually give rise to a single symmetrical line with a width between the peaks $\Delta B_{\text{PP}} = 0.02$ – 1.70 mT and a g -factor close to that for a free electron ($g_e = 2.00232$).^{15,16} The deviation from g_e can occur on interaction of an unpaired electron with heteroatoms or the alkali metals of the dopants.^{17,18} For a sufficiently high level of doping, the so called Dyson line,^{15,19} leading to the asymmetry of the spectrum, is manifested as a consequence of the increase in the electrical conductivity of the sample. However, in the study of conducting polymers with $\nu_e \leq 10$ GHz, investigators have encountered fundamental difficulties associated mainly with the low spectral resolution and a strong spin–spin exchange in this EPR frequency range.

It was shown previously in relation to various organic radicals^{20–23} that the information content and the accuracy of the method increase significantly on passing to the 2 mm band for the recording of the EPR spectra. In this range, it is possible to achieve the separate detection of paramagnetic centres with similar magnetic parameters, which permits a more accurate determination of the components of their anisotropic g -factor and also makes it possible to investigate the anisotropic dynamics of the radicals and of their microenvironment. The method makes it possible to study in fair detail different properties of *cis*- and *trans*-polyacetylenes as well as the relaxation and dynamic features of nonlinear charge carriers (solitons) in *trans*-polyacetylene.²⁴

The present review is devoted to the consideration of the principal results of the study at the 2 mm EPR band of the structural and conformational properties of certain other conducting polymers as well as the charge carriers present in them, the dynamics of which is described by the universal nonlinear Korteweg-de Vries equations of motion.

II. Polyparaphenylene

The concentration of unpaired electrons in PPP depends significantly on the polymerisation methods and may vary within the range 10^{17} – 10^{19} spins g^{-1} .^{15,16} The line width increases on doping and such broadening may depend both on the degree of doping and on the atomic number of the alkali metal of the dopant. The latter finding indicates an appreciable spin–orbital interaction between the dopant molecule and the unpaired electron. As in other conducting polymers, the charge transfer is effected mainly by polarons in lightly doped PPP and by bipolarons in a quasi-metallic sample.^{8,12,14}

Various PPP samples (in the form of films), synthesised by the electrochemical oxidation of benzene in a $\text{C}_3\text{H}_7\text{C}_5\text{H}_4\text{NCl} - \text{AlCl}_3$ melt, have been investigated by the EPR method: the initial evacuated PPP sample doped with Cl^{3-} anions (PPP-1); the same sample after storage over four days (PPP-2); the initial sample brought into contact with atmospheric oxygen for several seconds (PPP-3); the initial dedoped sample (PPP-4); the sample redoped with BF_4^- anions (PPP-5).²⁵

In measurements at the 3 cm EPR band, the PPP-1, PPP-2, and PPP-3 samples give rise to a single asymmetric line with a distinct Dyson form and $g = 2.0029$ (Fig. 1a). The line asymmetry factor A/B (the ratio of the amplitudes of the positive and negative peaks) varies as a function of the conductivity of the sample. When the Cl_3^- dopant is removed, i.e. on passing from the PPP-1 to the PPP-4 sample, the above spectrum is transformed into an axially symmetrical spectrum with $g_{\perp} = 2.0034$ and $g_{\parallel} = 2.0020$ (Fig. 1b). This is accompanied by the broadening of the spectral lines and also by a sharp decrease in the concentrations of spins and charge carriers (Table 2). It is noteworthy that neither in the case of PPP nor in the case of other π -conjugated polymers, investigated previously at the 3 cm EPR band, were axially symmetrical spectra recorded.¹⁵ The above form of the spectrum remains unchanged on further doping of the neutral PP with BF_4^- anions (PPP-5), but in this case some decrease in the spin concentration and a change in the sign of its temperature dependence are observed (Table 2). The minimum excitation energy of the unpaired electron $\Delta E_{\sigma\pi^*} = 5.2$ eV, close to the energy of the first ionisation potential of polycyclic aromatic hydrocarbons,¹³

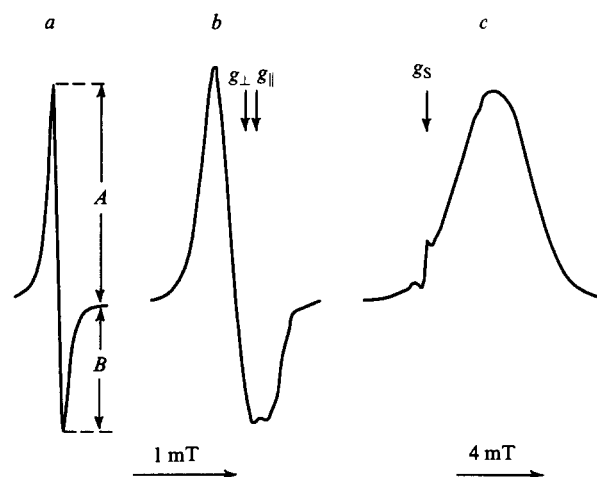


Figure 1. Typical 3 cm EPR absorption spectra of PPP-1–PPP-3 (a) and PPP-4 and PPP-5 (b) samples and the 2 mm in-phase dispersion spectrum of the PPP-4 and PPP-5 samples (c) recorded at room temperature. The narrow line on the right-hand spectrum belongs to the $(\text{DBTTF})_3\text{PtBr}_6$ reference standard with $g_s = 2.00411$. The measured magnetic parameters are presented.

Table 2. The concentration of the paramagnetic centres (N), the d.c. (σ_{dc}) and a.c. (σ_{ac}) conductivities ($\nu_e = 140$ GHz), the line asymmetry parameter (A/B), the line width (ΔB_{PP}), and the spin-lattice relaxation time (τ_1) for polyparaphenylene samples at $T = 300$ K.

Parameters	Sample				
	PPP-1	PPP-2	PPP-3	PPP-4	PPP-5
$10^{-17} N/\text{spin g}^{-1}$	120	320	210	4	0.6
$\sigma_{dc}/\text{S m}^{-1}$	$10^3\text{--}10^4$	—	—	10^{-6}	1
$10^{-5} \sigma_{ac}/\text{S m}^{-1}$	3	4	1.4	—	—
A/B	2.3	2.5	1.4	—	—
$\Delta B_{PP}/\text{mT}$	0.09	0.12	0.22	0.37 ^a	0.47 ^a
$10^6 \tau_1/\text{s}$	0.4	0.5	0.2	~ 100	~ 100

^a The width of the high-field spectral component is presented.

may be calculated, using the difference $\Delta g = g_{\perp} - g_{\parallel} = 1.4 \times 10^{-3}$, from the equation

$$\Delta E_{\sigma\pi'} = \frac{2\lambda_C \rho_C}{\Delta g}, \quad (1)$$

where λ_C is the constant for the spin-orbital interaction of the unpaired electron with a carbon nucleus and ρ_C the electron density on carbon.²⁶ Thus the paramagnetic centres in PPP-4 and PPP-5 can be localised in the vicinity of the polycyclic hydrocarbon cross-links, as predicted previously.¹⁵

At the 2 mm EPR band, the PPP-4 and PPP-5 samples give rise to a bell-shaped signal (Fig. 1c), which arises as a result of the manifestation of the effect due to the rapid adiabatic passage of a nonuniformly broadened line.²⁷ The spin-lattice relaxation time of the paramagnetic centres in these samples, estimated from their spectra, is $\tau_1 \approx 10^{-4}$ s. The rapid passage effects will be examined in greater detail below.

The rate of the spin-spin exchange of the paramagnetic centres in the neutral and redoped PPP has been determined as $\nu_{ex} = 4 \times 10^7 \text{ s}^{-1}$ by analysing the form of the 3 cm and 2 mm EPR spectra.²⁵ For PPP-1, this quantity is $1.8 \times 10^8 \text{ s}^{-1}$ owing to the greater concentration and mobility of the paramagnetic centres. The isotropic g -factor ($\langle g \rangle = \frac{1}{3}(g_{\parallel} + 2g_{\perp})$) for a neutral sample is close to the g -factor for the polymer doped with Cl_3^- anions. This finding indicates the averaging of the components of the g -tensor for the paramagnetic centres as a consequence of the spin 1D-diffusion along the polymer chain of the PPP-1 sample at a minimal rate:

$$\nu_{1D}^0 \geq \frac{(g_{\perp} - g_{\parallel})\mu_B B_0}{h}, \quad (2)$$

where μ_B is the Bohr magneton, B_0 the magnetic field strength, and h the Planck constant. For the PPP sample doped with Cl_3^- anions, this quantity is $\nu_{1D}^0 \geq 6.8 \times 10^6 \text{ s}^{-1}$. Indeed the effective rate of the spin 1D-diffusion, calculated from the equation

$$(\Delta B_{PP}^{\text{mob}})^3 = \frac{\gamma_e (\Delta B_{\perp}^{\text{loc}})^4}{\nu_{1D}}, \quad (3)$$

(here $\Delta B_{PP}^{\text{mob}}$ is the width of the line between the peaks of the PPP-1 samples, $\Delta B_{\perp}^{\text{loc}}$ the width of the perpendicular component of the spectrum of the PPP-4 and PPP-5 samples, and γ_e the gyromagnetic ratio for the electron) proved to be $\nu_{1D} \approx 9 \times 10^{10} \text{ s}^{-1}$ at room temperature. The temperature dependence of the electrical conductivity of the PPP-1 sample, determined using alternating current from the function $A/B(T)$, has the form $\sigma_{ac}(T) \sim T^{-1/3}$. This shows that several conduction mechanisms, including the interchain variable range hopping (VRH) charge transfer and isoenergetic tunnelling of the charge carriers, operate in the doped PPP. The sharp decrease in spin concentration and in the rates of the spin

exchange and relaxation processes on dedoping of the sample (transition from PPP-1 to PPP-4) indicates the annihilation of the majority of the polarons, the 1D-diffusion of which determines the effective electronic relaxation of the entire spin system.

Thus the data obtained make it possible to conclude that, in the highly doped PPP-1 sample, the charge is transferred mainly by the mobile polarons, whereas in PPP-5 charge transfer is effected by diamagnetic bipolarons. On electrochemical substitution of the Cl_3^- anion by the BF_4^- anion, the location of the latter may differ from that of the dopant in the initial sample. The morphology of the PPP redoped with BF_4^- anions may be close to that in the neutral film (PPP-4).

It has been established²⁵ that a film of PPP synthesised from the $\text{C}_3\text{H}_7\text{C}_5\text{H}_4\text{NCl}-\text{AlCl}_3$ melt is characterised by a decrease in the number of benzenoid monomers and an increase in that of the quinonoid ones. This leads to a more ordered structure and to a planar conformation of the polymer, which apparently prevents the collapse of the spin charge carriers to a bipolaron in the highly doped polymer. On dedoping, the anions are 'washed out', which results in an increase in the packing density of the polymer chains. This may prevent the intrafibrillar introduction of BF_4^- anions and may lead to localisation of the dopant molecules in the interfibrillar free volume of the polymer matrix. Such a conformational transition apparently alters the mechanism of charge transfer in the course of the redoping of PPP.

III. Polythiophene

The 3 cm EPR spectrum of neutral PT consists of a single symmetrical line with $g \approx 2.0026$ and a width $\Delta B_{PP} = 0.8 \text{ mT}$ ¹⁵ which indicates the localisation of the spin on the polymer chain and its weak interaction with the sulfur atoms. The low concentration of paramagnetic centres ($N \approx 7 \times 10^{-5}$ of a spin per monomer unit) is associated with the comparatively low degree of defectiveness of this compound. The EPR signal of lightly doped poly(3-methyl)thiophene represents a superposition of a Gaussian line due to the localised paramagnetic centres with $g_1 = 2.0035$ and $\Delta B_{PP} \approx 0.7 \text{ mT}$ and a Lorentzian line with $g_2 = 2.0029$ and $\Delta B_{PP} = 0.15 \text{ mT}$. The latter is characteristic of delocalised paramagnetic centres.²⁸ The overall concentration of paramagnetic centres in this sample is $\sim 3 \times 10^{19} \text{ spins cm}^{-3}$ or about one spin per 300 thiophene rings. After doping, a single Lorentzian component remains. It is symmetrical up to a doping level $z \leq 0.25$ (z is the number of dopant molecules per polymer monomer unit), but becomes asymmetric (Dyson line) for $z > 0.3$. The appearance of the Dyson-like line is accompanied by a significant decrease in the spin-spin and spin-lattice relaxation times,²⁹ which may be a consequence of the increase in the dimensionality of the system. Analysis of the variation of the paramagnetic susceptibility $\chi(z)$ showed that the number of paramagnetic polarons increases during the doping process in the polymer, the polarons recombining to diamagnetic bipolarons for high values of z .

Powder-like PT samples,³⁰ containing different counterions, were investigated at the 2 mm EPR band. The samples were obtained electrochemically from thiophene and bithiophene.

At the 3 cm EPR band, the PT samples synthesised from thiophene and doped with BF_4^- , ClO_4^- , and I_3^- ions give rise to symmetrical lines with $g \approx g_e$ and a width ΔB_{PP} , which varies slightly over a wide temperature range (Table 3), whereas in the spectrum of the PT synthesised from bithiophene and doped with I_3^- anions the lines are appreciably broadened as the temperature increases.

The PT spectra recorded at the 2 mm EPR band are distinguished by a greater variety (Fig. 2). Axially symmetrical spectra, indicating the localisation of the paramagnetic centres on the polymer chains, are characteristic of the polymers PT(BF_4^-) and PT(ClO_4^-). A similar pattern apparently occurs also in the case of PT(I_3^-), the EPR spectrum of which may be broadened owing to the strong spin-orbital interaction of the paramagnetic centres with the counterions.

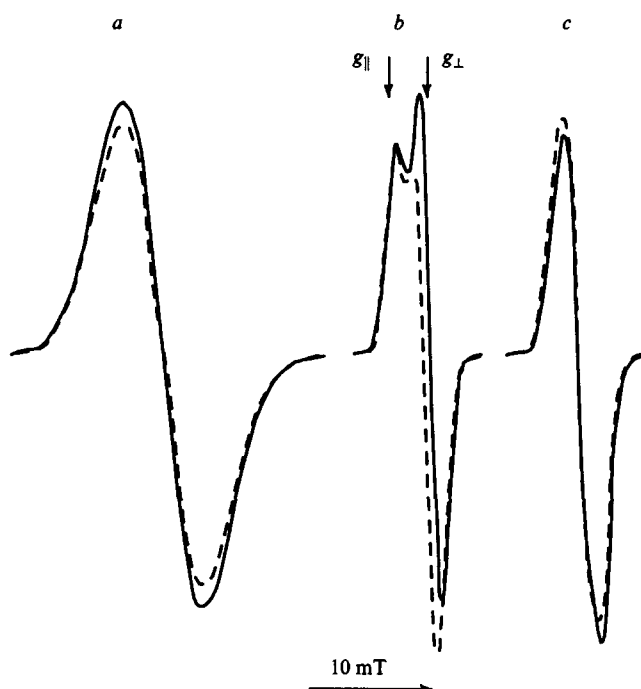


Figure 2. Typical 2mm EPR absorption spectra of polythiophene synthesised electrochemically from thiophene and doped with I_3^- (a), BF_4^- (b), and ClO_4^- (c) anions. The spectra were recorded at $T = 300$ K (continuous line) and 200 K (dashed line).

Table 3 presents the magnetic resonance parameters calculated from the 2 mm EPR spectra, the d.c. and a.c. conductivities of the samples (σ_{dc} and σ_{ac}), and the energies of the excitation of an electron to the nearest level ($\Delta E_{\sigma\pi^*}$). Analysis of the data presented shows that, in the series of anions $I_3^- \rightarrow BF_4^- \rightarrow ClO_4^-$, the quantity $\Delta E_{\sigma\pi^*}$ increases by a factor greater than 4. This transition also leads to an increase in the conductivity of the film and to significant alteration of the concentration of paramagnetic centres. This may indicate charge transfer in PT both by polarons and by bipolarons, the ratio of the concentrations of which depends on the nature and number of the anions introduced into the polymer. The width of the PT spectral lines proved more sensitive to a change in the recording frequency, which indicates a less intense spin exchange in this polymer compared, for example, with PA^{24,31} and PPP.²³

Table 3. The concentration of the paramagnetic centres (N), the electrical conductivity (σ_{dc}), the line width (ΔB_{PP}), the components of the g -tensor, and the energies of the excited electronic state ($\Delta E_{\sigma\pi^*}$) for polythiophene samples at $T = 300$ K.

Parameter	Polythiophene samples doped with the anions			
	I_3^-	BF_4^-	ClO_4^-	$ClO_4^-^a$
$10^{-19} N/\text{spins g}^{-1}$	2	8	5	10
$10^3 \sigma_{dc}/\text{S m}^{-1}$	0.5	1.2	16	11
$\Delta B_{PP}/\text{mT}$				
3 cm band ^b	0.75(0.80)	0.23(0.34)	0.46(0.52)	0.70(0.25)
2 mm band	6.5	1.5	2.6	0.5
g_{\parallel}	2.00679 ^c	2.00412	2.00230	2.00232 ^c
g_{\perp}	2.00232 ^c	2.00266	2.00239	2.00364 ^c
$\Delta E_{\sigma\pi^*}/\text{eV}$	1.6	4.0	7.0	4.5

^a The sample was synthesised from bithiophene. ^b The values of ΔB_{PP} at 77 K are given in brackets. ^c Values calculated from the equation $\langle g \rangle = \frac{1}{3}(g_{\perp} + 2g_{\parallel})$.

On reducing the temperature of the $PT(BF_4^-)$ sample, a Dyson-like line is manifested in the perpendicular component of its EPR spectrum without an appreciable change in the signal intensity. The quantity A/B increases monotonically in the temperature range 100–300 K, which indicates an increase in the electrical conductivity of the sample σ_{ac} , as happens in classical low-dimensional semiconductors. Knowing the characteristic size of the polymer particles δ and using the relation $A/B(\delta)$, it is possible to estimate for amorphous low-dimensional semiconductors³² the electrical conductivity of the sample and also the mobility μ and the rate of the 1D-diffusion of the charge carriers from the formula

$$\sigma_{ac} = N\mu e = \frac{Ne^2 v_{1D} c_{1D}^2}{kT}, \quad (4)$$

where c_{1D} is the lattice constant. The quantities σ_{ac} , μ_{1D} , and v_{1D} calculated for $PT(BF_4^-)$ in this way were found to be respectively $3.6 \times 10^2 \text{ S m}^{-1}$, $1.1 \times 10^{-5} \text{ m}^2 \text{ V}^{-1} \text{ s}^{-1}$, and $3.2 \times 10^{12} \text{ s}^{-1}$ at room temperature.³⁰

Polythiophene, synthesised from bithiophene and doped with ClO_4^- anions, is characterised by a single symmetrical EPR line at the 3 cm band, the width of which decreases monotonically from 0.7 to 0.25 mT on reducing the temperature from 300 to 77 K. In the 2 mm EPR band, this sample also shows a single line over a broad temperature range, which indicates the occurrence of charge transfer in it mainly by delocalised paramagnetic centres. With increase in temperature from 100 to 200 K ($T_c \approx 200$ K), the paramagnetic susceptibility of this sample decreases significantly and, on further rise of temperature, rises sharply (Fig. 3). This is accompanied by a corresponding change in line width, and the inverse relation of the functions $\Delta B_{PP}(T)$ and $\chi(T)$ (Fig. 3). This effect can be accounted for by the annihilation of polaron pairs to bipolarons when the temperature is varied from 100 K to T_c and on subsequent decomposition of the bipolaron into polarons at $T > T_c$, apparently owing to the intensification of the librations of the polymer chains. If one adopts a linear dependence of the rate of decomposition of bipolarons on the frequency of the librations of the polymer chains, then it is possible to estimate the activation energy for the latter process from the $\chi(T)$ behaviour. It proved to be $E_a \approx 0.16 \text{ eV}$ at $T > T_c$. Such polaron–bipolaron transformation is apparently in fact the cause of the unusual broadening, indicated above, of the EPR line of this sample at the 3 cm band, observed on raising the temperature.

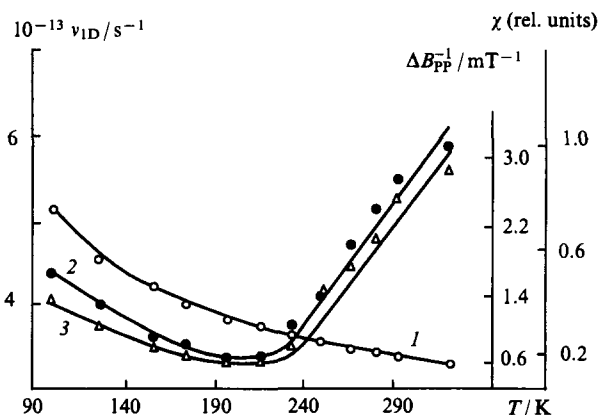


Figure 3. Temperature variations of the rate of diffusion of charge carriers v_{1D} along a polymer chain (1), of the relative paramagnetic susceptibility χ (2), and of the inverse of the line width ΔB_{PP} (3) for polythiophene synthesised electrochemically from bithiophene and doped with ClO_4^- counterions.

As in the spectrum of polythiophene, a Dyson-like line appears in the EPR spectrum of polybithiophene at low temperatures, which reflects the change in the electrical conductivity of the film. Bearing in mind that the concentrations of the polarons and bipolarons are unchanged and using the above procedure, it is possible to determine the rate of 1D-diffusion of the charge carriers in the sample (Fig. 3). At room temperature, this quantity proved to be $v_{1D} = 3 \times 10^{13} \text{ s}^{-1}$, which is similar in order of magnitude to v_{1D} determined for polarons in doped PANI,³³ in which the interchain charge transfer predominates. The weak temperature dependence of the rate of the 1D-diffusion of the charge carriers in bithiophene also indicates the predominance of the interchain charge transfer in this polymer and its increased dimensionality.

IV. Polypyrrole

Neutral PP is characterised by a complex spectrum at the 3 cm EPR band, consisting of a superposition of a narrow (0.04 mT) and a wider (0.28 mT) line with a g -factor ($g = 2.0026$) typical for π -conjugated and aromatic compounds.¹⁵ The concentration of paramagnetic centres in neutral PP corresponds to one spin for several hundreds of monomer rings. The width and intensity of the narrow spectral line are of the activated character, whereas the wider component follows the Curie law. This indicates the existence in neutral PP of two types of paramagnetic centres with different relaxation parameters.

At the same EPR band, doped PP is characterised by an intense single and narrow line ($\sim 0.03 \text{ mT}$) with $g = 2.0028$, which obeys the Curie law in the temperature range 30–300 K.¹⁵ The majority of the results obtained previously indicate that the charge carriers are not responsible for the EPR spectrum of this polymer because there are no correlations between the magnetic susceptibility and the concentration of charge carriers as well as between the line width and the mobility of the carriers. This may be interpreted as a result of the formation of spin-less bipolarons in PP during the doping of the latter. Thus the EPR signal of doped PP cannot yield adequate information about the conduction processes.

The spin probe method, based on the introduction of a stable nitroxyl radical into the test system, may prove more effective in this instance.³⁴ However, hitherto this method has been rarely used in the study of conducting polymers.^{34,35} The reason for this is primarily the fact that the low spectral resolution at $\nu_e \leq 10 \text{ GHz}$ precludes the separate recording of all components of the g - and A -tensors and hence hinders the separate determination of the magnetic parameters of the nitroxyl radicals and the paramagnetic centres localised on the polymer chains, as well as the establishment of the dipole–dipole interaction between different paramagnetic centres. Thus electrochemically synthesised PP, in which the nitroxyl radical was bound covalently to the pyrrole ring, has been investigated.³⁵ However, despite the appreciable concentration of the nitroxyl radicals introduced into the polymer, the 3 cm EPR spectrum of this sample showed no lines corresponding to the spin label.

The spin probe method proved to be more effective in the study of doped PP at the 2 mm EPR band.³⁶

Fig. 4 presents the EPR spectra of 4-carboxy-2,2,6,6-tetramethyl-1-piperidinyloxy (a nitroxyl radical), introduced as the probe and the counterion into a nonpolar model system and PP (electrochemically) simultaneously. The EPR spectrum of the spin-modified PP at the 3 cm band represents a superposition of the lines due to the probe, which is characterised by a rotational correlation time $\tau_c \geq 10^{-7} \text{ s}$, and a superimposed single line due to the paramagnetic centres (R) localised on the chain (Fig. 4a). This superposition of the individual spectra precludes the separate determination of the magnetic resonance parameters of the probe and the radical R in PP and also the analysis of the dipole–dipole broadening of their spectral components.

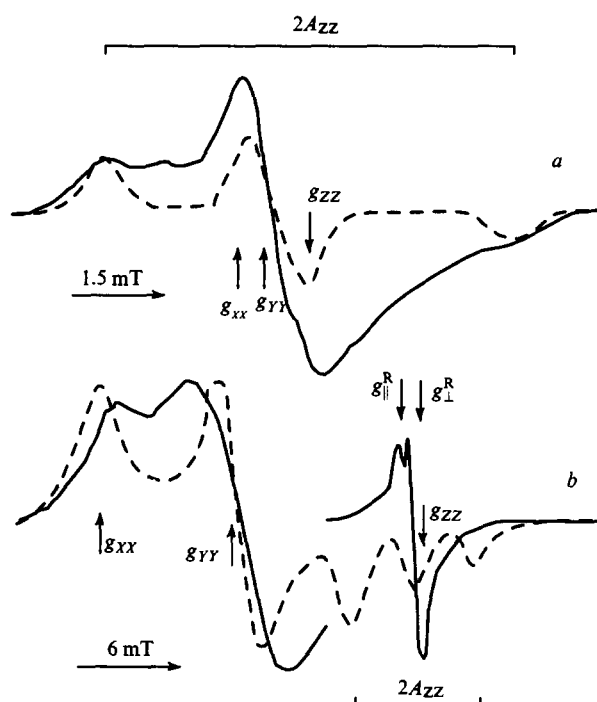


Figure 4. EPR absorption spectra of 4-carboxy-2,2,6,6-tetramethyl-1-piperidinyloxy (a nitroxyl radical) introduced as a spin probe into frozen (120 K) toluene (dashed line) and conducting polypyrrole (continuous line). Recording band: (a) 3 cm; (b) 2 mm. Fig. (a) illustrates the anisotropic spectrum of the localised paramagnetic centres R as well as the measured magnetic parameters of the probe and the radical R.

The EPR spectrum of the spin-modified polymer systems at the 2 mm band has a higher information content (Fig. 4b). All the canonical components of the nitroxyl probe are fully resolved in the spectrum, which permits the direct determination of the principal values of its g - and A -tensors. Furthermore, in the region of the Z -component of the probe spectrum in PP, the axially symmetrical spectrum of the radical R is recorded with the magnetic parameters $g_{\parallel}^R = 2.00380$, $g_{\perp}^R = 2.00235$, and $\Delta B_{PP} = 0.57 \text{ mT}$.

The form of the spectrum of this radical indicates its localisation on the polymer chain, i.e. charge transfer in PP by spin-less bipolarons, as happens in $\text{PPP}(\text{BF}_4^-)$ and $\text{PT}(\text{BF}_4^-)$. The difference $\Delta g = g_{\parallel}^R - g_{\perp}^R = 1.45 \times 10^{-3}$ corresponds to an excited electronic configuration in R with an excitation energy $\Delta E_{\sigma\pi^*} = 5.1 \text{ eV}$, which is close to the excitation energy of the electron in neutral PPP.

The nitroxyl probe in nonpolar toluene is characterised by the following magnetic parameters: $g_{XX} = 2.00987$, $g_{YY} = 2.00637$, $g_{ZZ} = 2.00233$, $A_{XX} = A_{YY} = 0.6$, and $A_{ZZ} = 3.31 \text{ mT}$. In the conducting PP, the quantity g_{XX} diminishes to 2.00906, whereas both the X - and Y -components of the probe spectrum are broadened by 4 mT (Fig. 4b). Analysis of the form of the probe spectrum permits the conclusion that there are no rapid movements of this radical in PP (correlation time $\tau_c \leq 10^{-7} \text{ s}$) even at comparatively high temperatures, which is apparently associated with the small size of the region of localisation of the probe, not exceeding 1 nm.

In neutral PP there are no fragments with an appreciable dipole moment. The dipole–dipole interactions between the radicals may be neglected, because the concentrations of the probe and the paramagnetic centres localised on the chain are small. The changes in the magnetic-resonance parameters of the probe on passing from the model nonpolar system to the conducting polymer matrix, indicated above, may occur as a consequence of the Coulombic interaction of the active fragment

of the probe and the spin-less charge carriers — bipolarons. The effective electric dipole moment of the bipolaron closest to the probe, calculated from the shift of the g_{XX} component, amounted to $\mu_v = 2.3$ D. The shift of the g_{XX} component of the probe g -factor may be calculated within the framework of the electrostatic interaction of the dipoles of the probe and the bipolaron by means of the following procedure. The potential of the electric field induced by the bipolaron at the location of the probe is defined by the expression³⁷

$$E_d = \frac{kT}{\mu_u} (x \coth x - 1), \quad (5)$$

$$x = \frac{2\mu_u \mu_v}{4\pi\epsilon\epsilon_0 kTr^3},$$

where μ_u is the electric dipole moment of the probe, ϵ and ϵ_0 are dielectric constants for the PP and the vacuum respectively, and r is the distance between the active fragment of the nitroxyl radical and the bipolaron. Using the variation of the increment in the isotropic hyperfine interaction constant for the probe due to the electrostatic field of the microenvironment $\Delta a = 7.3er_{NO}I^{-1}E_d$ (here r_{NO} is the distance between the N and O atoms of the active fragment of the probe and I is the resonance overlap integral for the C=C bond) as well as the relation $\partial g_{XX}/\partial A_{ZZ} = 2.3 \times 10^{-3}$ mT for 2,2,6,6-tetramethyl-1-piperidinyloxyl radicals,^{21–23} it is possible to formulate the following equation for Δg_{XX} :

$$\Delta g_{XX} = 6 \times 10^{-3} \frac{er_{NO}kT}{I\mu_u} (x \coth x - 1). \quad (6)$$

Adopting $\mu_u = 2.7$ D,³⁸ $\mu_v = 2.3$ D, and $r_{NO} = 0.13$ nm,²⁶ we obtain $r = 0.92$ nm.

The rate of spin–spin relaxation, which determines the width of the spectral line of the radical, can be formulated as $\tau_2^{-1} = \tau_{2(0)}^{-1} + \tau_{2(D)}^{-1}$ where $\tau_{2(0)}^{-1}$ is the rate of relaxation of a radical which does not interact with the environment and $\tau_{2(D)}^{-1}$ is the increment in the rate of relaxation due to the dipole–dipole interaction. The characteristic time of such interaction τ_c in a polycrystalline sample may be calculated from the broadening of the spectral lines $\delta(\Delta B_{X,Y})$.³⁹

$$\tau_{2(D)}^{-1} = \gamma_e \delta(\Delta B_{X,Y}) \quad (7)$$

$$= \frac{1}{2} \langle \omega^2 \rangle [3J(0) + 5J(\omega_e) + 2J(2\omega_e)],$$

where

$$\langle \omega^2 \rangle = \frac{1}{5} \left(\frac{\mu_0}{4\pi} \right)^2 \gamma_e^4 \hbar^2 S(S+1) N \sum_{r_0}^N \sum_r^N \frac{(3 \cos^2 \vartheta - 1)^2}{r_1^3 r_2^3},$$

$$J(\omega_e) = \frac{2\tau_c}{1 + \omega_e^2 \tau_c^2}.$$

Here μ_0 is the magnetic permeability of a vacuum, $\hbar = h/2\pi$, $\omega_e = 2\pi\nu_e$ is the recording frequency, and ϑ is the angle between the vectors r_1 and r_2 . The inequality $\omega_e \tau_c \gg 1$ holds for the majority of highly viscous condensed systems, so that, by averaging with respect to the angles $\Sigma \Sigma (3 \cos^2 \vartheta - 1)^2 (r_1^{-3} r_2^{-3}) = 6.8 r^{-6}$ and, using the value $\gamma_e \delta(\Delta B_{X,Y}) = 7 \times 10^8$ s⁻¹ and the value $r = 0.92$ calculated above, we obtain $\tau_{2(D)}^{-1} = \gamma_e \delta(\Delta B_{X,Y}) = 3 \langle \omega^2 \rangle \tau_c$ or $\tau_c = 8.1 \times 10^{-11}$ s. Bearing in mind that the average time between translational hops depends on the diffusion coefficient D and the average length of the hop, which is equal to the product of the lattice constant c_{1D} and the half-width of the spin delocalisation on the charge carrier $N_P/2$, i.e. $\tau_c = 1.5 \langle c_{1D}^2 N_P^2 \rangle D^{-1}$, and, taking into account the value $D \approx 5 \times 10^{-7}$ m² s⁻¹ typical for conducting polymers, we obtain $\langle c_{1D} N_P \rangle = 3$ nm, which corresponds approximately to four pyrrole rings. This quantity is close to the width of the bipolaron

in polypyrrole and polyaniline, but is appreciably smaller than N_P obtained for polybithiophene.⁴⁰

Thus the form of the EPR spectrum of the spin-modified PP, recorded at the 2 mm band, indicates extremely slow rotational motions of the probe, apparently as a consequence of the fairly dense packing of the polymer chains in PP. The interaction of the spin-less charge carriers with the active fragment of the spin probe leads to a redistribution of the spin density between the N and O atoms of the nitroxyl radical and hence to a change in its magnetic-resonance parameters. This makes it possible to determine the distance between the radical and the chain, along which the charge carrier moves, and also the effective length of the bipolaron in a randomly oriented polymeric semiconductor.

V. Polyaniline

A characteristic behaviour of polyaniline (PANI) is known⁴¹ to be the insulator/conductor transition, occurring on protonation or oxidation of the polymer, i.e. on transition from its emeraldine base form (EB form) to the emeraldine salt form (ES form). This compound differs from other conjugated polymers in a number of features. Thus, in contrast to PPP, PT, and PP, both the benzene rings and the nitrogen atoms are involved in conjugation in PANI. On protonation or oxidation, the conductivity of the polymer increases by more than 10 orders of magnitude, whilst the number of electrons on the polymer chain remains unchanged.⁴² Polyaniline in the EB form is an insulator. This form is amorphous and contains traces of the ES form, whereas the ES form of PANI contains highly conducting crystalline domains with a characteristic size of 5 nm¹¹ distributed in the amorphous EB phase.

The oxidation or protonation of the EB form of PANI is accompanied by a monotonic increase in the concentration of paramagnetic centres and a narrowing of the line from 0.2 to 0.05 mT in the 3 cm EPR spectrum.^{28,43} The paramagnetic susceptibility of the weakly conducting PANI follows the Curie law, which indicates the formation of single polarons in the polymer chain, whereas Pauli spins, characteristic of the polaron lattice of a highly conducting polymer, have been detected in the ES form of PANI.^{43,44}

The spin dynamics in PANI has been investigated by the complementary EPR and NMR spectroscopic methods.⁴⁵ The frequency dependences $\tau_{1p} \sim \omega_p^{1/2}$ (for nuclear spins) and $\Delta B_{pp}^{-1} \sim \omega_e^{-1/2}$ (for electron spins), obtained for isolated chains of the ES form of PANI, have been interpreted within the framework of the 1D-diffusion of polarons at a rate $\nu_{1D} > 10^{13}$ s⁻¹. The anisotropy of the spin diffusion ν_{1D}/ν_{3D} varies from 10⁴ in the EB form to 10 in the ES form of PANI at room temperature. The correlation found between the spin dynamics and the charge transfer process has been interpreted as evidence in support of the predominantly interchain electron transport. However, this conclusion conflicts with another concept,^{11,46} which predicts the 3D-transport of electrons in massive metal-like domains with a characteristic size 5 nm and 1D-transport of electrons between these domains. Investigations have shown that the charge transfer process in PANI is determined to a significant extent by structural parameters such as the crystallinity of the sample, the size of the crystalline domains, the conformation and degree of orientation of the chains, etc., which depend on the history of the sample and also on the amount of modifying agent introduced into it.

The results of studies on the magnetic and electrodynamic properties of PANI samples with different conductivities by 2 mm EPR spectroscopy are presented below.^{18,47}

Fig. 5 presents the 2 mm EPR spectra of the initial and oxidised PANI samples. Analysis of these spectra showed that at least two types of paramagnetic centres were stabilised in the initial sample, namely an immobilised paramagnetic centre (R¹) (Fig. 5a) with the anisotropic magnetic-resonance parameters $g_{XX} = 2.00535$, $g_{YY} = 2.00415$, $g_{ZZ} = 2.00238$, $A_{XX} = A_{YY} = 0.33$, and $A_{ZZ} = 2.3$ mT, and a more mobile paramagnetic centre (R²) with $g_{\perp} = 2.00351$ and $g_{\parallel} = 2.00212$. The relative

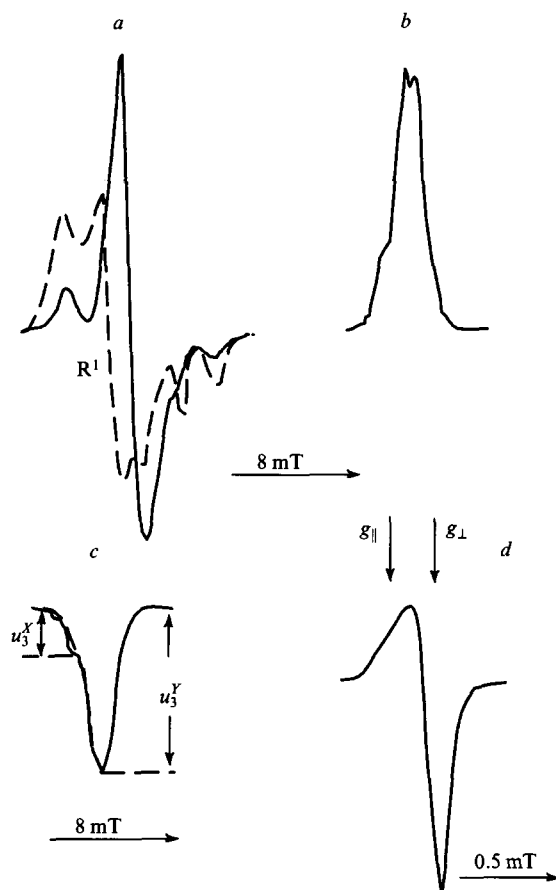


Figure 5. Typical 2 mm EPR absorption spectra (a, d) and the in-phase (b) and $\pi/2$ out-of-phase (c) components of the dispersion signal of neutral (a–c) and oxidised ($z = 0.53$) (d) polyaniline recorded at $T = 300$ K. The dashed lines represent the absorption spectrum of the radical R^1 (a) localised on the chain and the $\pi/2$ out-of-phase component of the dispersion signal of the neutral sample at $T = 200$ K (c).

concentrations of these radicals N_i depend both on the degree of oxidation and on the temperature of the sample (Fig. 6a). The concentrations of paramagnetic centres of both types increase with increasing z (Table 4), which can be accounted for by an increase in the number of spin charge carriers and by the formation of a polaron lattice in PANI for $z \geq 0.3$.

The paramagnetic centre R^1 with an anisotropic EPR spectrum can be attributed to the radical species $(-C_6H_4-NH-C_6H_4-)^{\cdot}$ localised on the polymer chain. Its magnetic parameters differ somewhat from those of the structurally similar radical $-C_6H_4-\dot{N}-C_6H_4-$.²⁶ This is apparently associated with a lower degree of localisation of the unpaired electron on the nitrogen atom ($\rho_N^{\pi} = 0.39$) and with a more planar conformation of the latter radical. The contribution of the CH groups of the radical to g_{XX} is small ($g_{XX} \approx 1.7 \times 10^{-5}$, see Buchachenko and Vasserman²⁶), so that it can be neglected. The energies of the excited electronic configurations of the radical R^1 are $\Delta E_{n\pi^*} = 3.8$ eV and $\Delta E_{\sigma\pi^*} = 6.5$ eV for $\rho_N^{\pi} = 0.61$.⁴⁸

The averaged g -factor of the radicals R^1 ($\langle g \rangle = \frac{1}{3}(g_{XX} + g_{YY} + g_{ZZ})$) is close to the isotropic g -factor R^2 ($\langle g \rangle = \frac{1}{3}(2g_{\perp} + g_{\parallel})$) for the paramagnetic centres R^2 . The polaron diffusing along the polymer chain at an effective rate $v_{1D}^0 \geq 10^9$ s⁻¹ [see Eqn (2)] may therefore be responsible for the EPR spectrum of the radical R^2 .

During the oxidation of the initial PANI sample, the perpendicular component of the EPR spectrum becomes monotonically narrower and the paramagnetic susceptibility increases (Table 4) before the attainment of the degree of oxidation $z = 0.53$, which constitutes additional evidence for the formation in the highly conducting PANI of regions with a high spin density and rapid spin–spin exchange. This fact as well as the decrease in the g -factor for the radical R^2 with increase in z may be associated with the decrease in the spin density on the nucleus of the nitrogen atom and the change in the conformation of the polymer chains. The C–N–C bond angle in PANI is known¹¹ to increase by 22° on passing from the EB to the ES form. Calculation shows that this may alter g_{\perp} only by several per cent. A more significant change in this magnetic parameter is induced by a change in the dihedral angle θ , i.e. the angle between the planes of neighbouring benzene rings. Taking into account the dependence of the overlap integral of the p_z orbitals of the nitrogen atoms and the carbon atom of the PANI benzene ring in the *para*-position relative to the

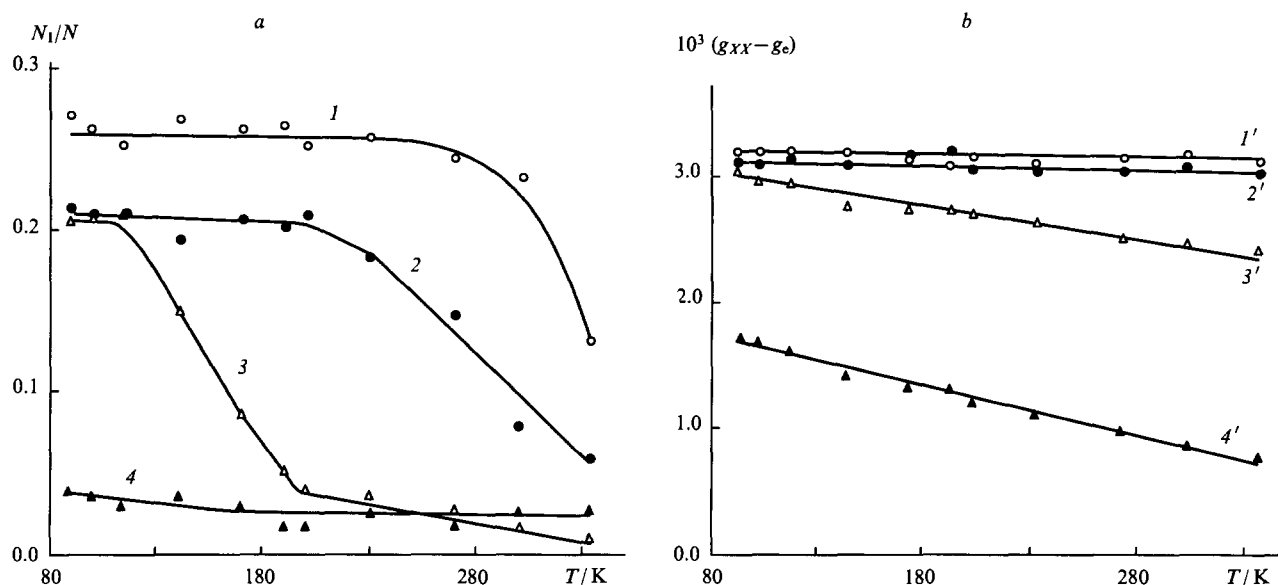


Figure 6. Temperature variations of the relative concentration N_1/N (a) and the g_{XX} -factor (b) of the paramagnetic centres R^1 localised in polyaniline with different degrees of oxidation z : (1) and (1') 0; (2) and (2') < 0.01 ; (3) and (3') 0.02; (4) and (4') 0.2.

Table 4. Dependence of the electrical conductivity (σ_{dc}), the critical temperature (T_0), the Pauli susceptibility (χ_p), the density of states at the Fermi level [$n(\epsilon_F)$], the distance between the polaron level and the Fermi level (A_3), the polaron localisation length (L), the concentration of

paramagnetic centres (N), the line width (ΔB_{PP}), and the spin-spin relaxation time (τ_2) for polyaniline samples at $T = 300$ K on their degree of oxidation z .

Parameter	Degree of oxidation z							
	0.00	0.01	0.02	0.06	0.20	0.30	0.39	0.53
$\sigma_{dc}/S\ m^{-1}$	$5 \cdot 10^{-6}$	$6 \cdot 10^{-6}$	$1 \cdot 10^{-4}$	$2 \cdot 10^{-2}$	100	270	560	1780
$10^{-4} T_0/K$	—	14	—	—	1.2	—	0.97	0.18
$10^6 \chi_p$	~ 0.8	3	—	—	51	—	86	101
$n(\epsilon_F)/eV^{-1}\ mol^{-1}$	0.04	0.09	—	—	1.6	—	2.7	3.2
A_3/eV^a	—	0.04	—	—	0.33	—	0.52	0.61
L/nm	—	0.2	—	—	1.1	—	1.2	6.8
$10^{-19} N/spins\ g^{-1}$	1.0	1.2	3.2	4.7	22	55	91	195
$10^8 \tau_2/s^b$	0.62	0.64	0.82	2.3	5.2	4.5	5.0	15.0
$\Delta B_{PP}/mT$								
3 cm band	1.06	1.02	0.80	0.28	0.125	0.145	0.125	0.035
2 mm band	1.50	1.45	1.31	—	0.60	—	0.29	0.162

^a The values of A_3 were calculated by the formula $A_3 = 0.5 \hbar^2 (3\pi^2 N)^{2/3} m_e^{-1}$. ^b The times τ_2 were calculated by the formula $\tau_2^{-1} = 0.866 \gamma_e \Delta B_{PP}$.

nitrogen atom on the dihedral angle ($I \sim \cos \theta$)¹³ and assuming that $\theta = 56^\circ$ for the initial EB,⁴⁹ it is possible to calculate the effective dihedral angle and the spin density on the nitrogen atom in the ES form of PANI with $z = 0.2$, which are respectively $\theta = 33^\circ$ and $\rho_N^* = 0.42$. The decrease in the angle θ leads to an increase in the transfer integral and hence to a greater delocalisation of the unpaired electron over the benzene rings. Thus the change in the magnetic parameters on oxidation of PANI reflects the transition to a more planar chain conformation.

It is important to note that the shape of the EPR spectrum of the radical R^2 in the ES form of PANI with $z = 0.2$ undergoes major change at 300 K. Whereas the inequality $g_\perp > g_\parallel$ is valid for this sample when $z < 0.2$ and $T \leq 300$ K, the inequality $g_\parallel > g_\perp$ actually holds when $z = 0.2$ and $T \geq 300$ K (Fig. 5). The latter inequality remains unaltered for $z \geq 0.2$ in the temperature range $90 \leq T \leq 330$ K. We recorded a similar transformation of the spectrum previously⁵⁰ on saturation of a PANI sample with water vapour and explained it by a significant change in the conformation of the radical R^2 as a consequence of the formation of H_2O bridges between the polymer chains. On the other hand, in the case described the change in line shape can be accounted for by the transformation of the polymer chains.

The components of the hyperfine structure, arising as a consequence of the interaction of the unpaired electron with the protons of the neighbouring benzene rings, have also been recorded in the EPR spectra of PANI samples with $z \geq 0.3$. The isotropic hyperfine interaction constant a_H is correlated with z and varies in the range 5.0–9.6 μT for different samples, which corresponds to a spin density $\rho_H^* = (2.2-4.3) \times 10^{-3}$. The density of the unpaired electron delocalised over two benzene rings in a solution of the EB form of PANI in dioxane is $\rho_H^* = 1.5 \times 10^{-2}$.⁴⁸ The data obtained therefore indicate the delocalisation of the unpaired electron over a larger number of benzene rings owing to the more planar conformation of the ES samples investigated.

Bell-like components with a Gaussian distribution of the spin packets (Figs 5b and 5c), the intensity and shape of which depend on the amplitude B_m and the frequency ω_m of the high-frequency modulation, the amplitude of the magnetic component of the radiofrequency field B_1 , and also on the spin-spin (τ_1) and spin-lattice (τ_2) relaxation times of the paramagnetic centres, have been recorded in the 2 mm EPR spectra of PANI samples. The appearance of such signals is induced by the effect associated with the rapid adiabatic passage of an inhomogeneously broadened line,²⁷ which may be accounted for as follows.

The shape of an individual spin packet in PANI is determined by the time parameters τ_1 , τ_2 , $(\gamma_e \Delta B_{PP})^{-1}$, ω_m^{-1} , $(\gamma_e B_m)^{-1}$, $(\gamma_e B_1)^{-1}$, and $B_1(dB_0/dt)^{-1}$. The distance between the spin packets which have moved apart is $\Delta\omega_{ij}$ and varies linearly with the recording frequency. On transition to stronger magnetic fields, the frequency ν_{ex} of the spin exchange between the paramagnetic centres with $S = -\frac{1}{2}$ and $g \approx 2$, separated by a distance r , decreases in accordance with the law⁵¹

$$\nu_{ex} \sim \frac{4\mu_B^2}{r^3} \exp\left[\frac{-0.25B_0^2 r^6}{\mu_B^2}\right],$$

as a consequence of which the interaction between the spin packets diminishes and their width begins to depend on the recording frequency.⁵²

$$\Delta B_{PP} = \Delta B_{PP}^0 + \frac{\Delta\omega_{ij}^2}{8\nu_{ex}}. \quad (8)$$

In the adiabatic passage of a saturated signal [i.e. when $\gamma_e \omega_m B_m \ll \gamma_e^2 B_1^2$ and $s = \gamma_e B_1 (\tau_1 \tau_2)^{1/2} \geq 1$, where s is the EPR signal saturation factor], a stationary trajectory of the paramagnetic centre magnetisation vector is established and the succeeding signal projections, for example the dispersion U ,⁵³ with the shape function $g(\nu_e)$ are recorded on the Z , $-Z$, and $-X$ axes.

$$U = u_1 g'(\nu_e) \sin(\omega_m t) + u_2 g(\nu_e) \sin(\omega_m t - \pi) + u_3 g(\nu_e) \sin(\omega_m t \pm \frac{1}{2}\pi). \quad (9)$$

The inequality $\omega_m \tau_1 > 1$ is obtained for the EB form of PANI, so that the dispersion signal is determined mainly by the last two terms of Eqn (9). In this case the relaxation times may be determined from the central amplitude of these components by means of the following formulae:⁵⁴

$$\tau_1 = \frac{3\omega_m(1 + 6\Omega)}{\gamma_e^2 B_{10}^2 \Omega(1 + \Omega)}, \quad (10a)$$

$$\tau_2 = \frac{\Omega}{\omega_m}, \quad (10b)$$

where $\Omega = u_3 u_2^{-1}$ and B_{10} is the value of B_1 for $u_1 = -u_2$.

In the EPR spectra of the ES form of PANI, the passage effects are less appreciable and the relaxation times can therefore be calculated from the formulae⁵⁴

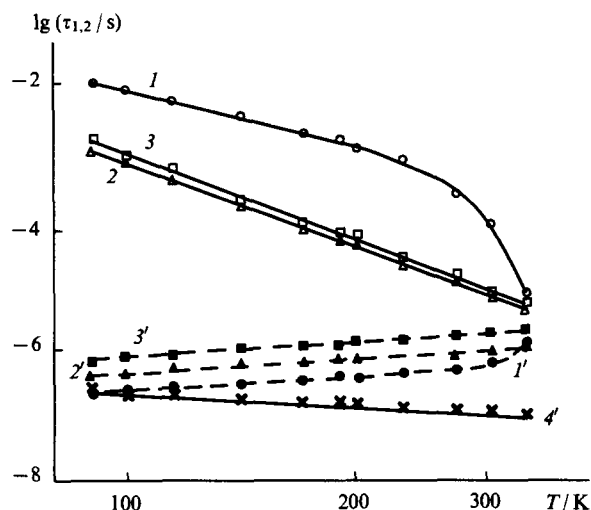


Figure 7. Temperature variations of the effective spin–lattice (τ_1) (curves 1–3) and spin–spin (τ_2) (curves 1'–4') relaxation times of the paramagnetic centres in polyaniline with different degrees of oxidation z : (1) 0; (2) < 0.01; (3) 0.02; (4) 0.2.

$$\tau_1 = \frac{\pi u_3}{2\omega_m u_1}, \quad (11a)$$

$$\tau_2 = \frac{\pi u_3}{2\omega_m(u_1 + 11u_2)}. \quad (11b)$$

Fig. 7 presents the temperature variations of the effective relaxation times of the paramagnetic centres in different PANI samples. Evidently the spin–lattice relaxation time diminishes with increase in z , which indicates an increase in the number and size of the quasi-metallic domains in the ES form of PANI. It also follows from the figure that a temperature dependence of the type $\tau_1^{-1} \sim NT^l$, where $l=3-4$ for $z \leq 0.02$ and $l=0.3$ for $0.02 < z \leq 0.20$, is characteristic of PANI, which is a consequence of the sharp change in the rate of energy transfer from the spin ensemble to the polymer lattice and a change in the mechanism of charge transport during the oxidation of PANI.

The times τ_1 and τ_2 are effective and are determined by the relaxation times of the localised and mobile paramagnetic centres — the radicals R^1 and R^2 at the concentrations N_1 and N_2 respectively — so that for the general case one can write

$$N\tau_{1,2}^{-1} = N_1(\tau_{1,2}^{-1})_{\text{loc}} + N_2(\tau_{1,2}^{-1})_{\text{mob}}, \quad (12)$$

where $N = N_1 + N_2$. This equation permits the separate determination of the relaxation parameters of the trapped and mobile paramagnetic centres in the polymer.

We shall now consider the possibility of using the 2 mm EPR spectroscopic method for the investigation of the dynamics of the polymer chains in PANI and other conducting polymers in which the paramagnetic centres exhibit an appreciable anisotropy of the magnetic parameters. It is seen from Fig. 6b that the quantity g_{XX} for the radical R^1 depends in a complex manner on the degree of oxidation z and the temperature of PANI. The decrease in this parameter with increase in z and/or temperature may be explained both by the increase in the polarity of the microenvironment of the radical R^1 and by the acceleration of the small-scale vibrations of the polymer chain and hence of the radical localised on the latter. The motions of the macromolecules in this and other similar polymers are anisotropic and are characterised by a correlation time $\tau_c \geq 10^{-7}$ s.^{34,55} The 'linear' EPR absorption spectra are usually insensitive to superslow motions and such molecular processes are therefore better investigated by the RF-saturation transfer method (ST-EPR).⁵⁶

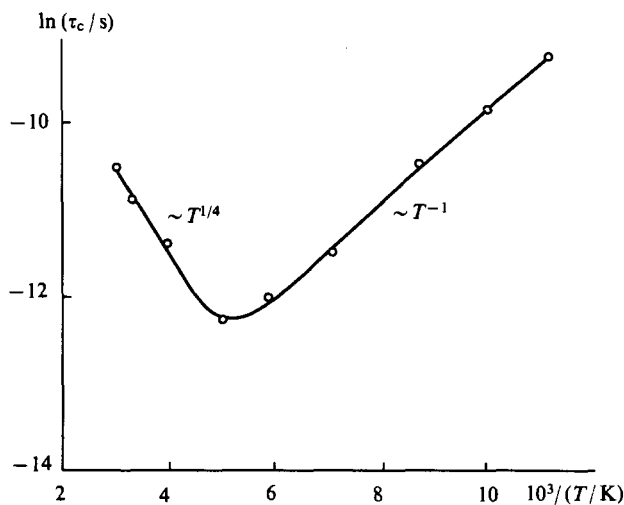


Figure 8. Arrhenius plot for the correlation times τ_c of the anisotropic librations of the polymer chains in the EB form of polyaniline with the degree of oxidation $z = 0$.

The ST-EPR method is based on the introduction into the test system of a nitroxyl label or probe and the recording of the spectrum of this radical under the conditions of the rapid passage of the saturated signal. On rotation of the paramagnetic centres, the above conditions may not be fulfilled for spin packets oriented in a particular way relative to the direction of the external magnetic field, as a result of which the form of the overall spectrum changes. It had been shown earlier²³ that the parameter most sensitive to the anisotropy of the molecular dynamics is the ratio of the components of the derivative of the dispersion signal, $K_{\text{mov}} = u_3^X/u_3^Y$, $\frac{1}{2}\pi$ out-of-phase. The sensitivity of the ST-EPR method also depends on the anisotropy of the magnetic parameters of the paramagnetic centres and on the recording frequency.⁵⁶ Bearing in mind that the paramagnetic centres localised on the polymer chain are themselves paramagnetic labels and are characterised by an appreciable anisotropy of the magnetic parameters, one may expect an increase in the effectiveness of this method in the study of conducting compounds at the 2 mm EPR band.

As can be seen from Fig. 5c, the parameter K_{mov} increases with increase in the temperature of the sample. This is a result of the anisotropic librational reorientations of the pinned polarons around the specified X axis of the polymer chains. The correlation time for the librations of the chains, calculated from the ST-EPR spectra by the method described by the present author,²¹⁻²³ was found to be given by the following expression for the initial PANI sample:

$$\tau_c = 2.4 \times 10^{-7} \exp\left(\frac{0.046}{kT}\right) \text{ s},$$

in the temperature range $200 \leq T \leq 90$ K (Fig. 8). At higher temperatures, the correlation time varies in accordance with the law

$$\tau_c(T) = 61.1 \exp\left[-\left(\frac{T_0}{T}\right)^{1/4}\right] \text{ s},$$

where

$$T_0 = \frac{18.1}{kn(\epsilon_F)L^3} = 1.5 \times 10^7 \text{ K}.$$

Here T_0 is the percolation constant, which depends on the density of states $n(\epsilon_F)$ on the Fermi level ϵ_F and L is the charge carrier localisation length. Using $n(\epsilon_F) = 4.5 \times 10^{-2} \text{ eV}^{-1} \text{ mol}^{-1}$, it is possible to obtain the polaron localisation length in neutral PANI, which is 0.53 nm, and the most probable length of the 3D-hop of the polaron between the chains $R = 0.39L(T_0/T)^{1/4} = 3.1 \text{ nm}$ at

$T = 300$ K. The data obtained indicate a close relation between the molecular spin dynamics in the EB form of PANI. With increase in τ_c or with significant decrease in B_1 , the ST-EPR spectrum becomes insensitive to the molecular dynamics and in this case $K_{\text{mov}} \approx 0.07$. The maximum value of τ_c recorded at the 2 mm EPR band can be estimated from these data as $\sim 10^{-4}$ s at 90 K.

We shall now consider the dynamic parameters of the polaron in PANI. As in the case of a mobile soliton in *trans*-polyacetylene,²⁴ the diffusion of the polaron along the polymer chain is characterised by a translational propagator of motion $P_{\text{tr}}(r, r_0, \tau)$. This quantity determines the probability at a time $t = \tau$ that the i th spin is located in the region $r + dr$ relative to the new position of the j th spin, which was located in the initial instant at the point r_0 relative to the i th spin.

On solving the equation for Brownian diffusion

$$\frac{\partial P_{\text{tr}}(r, r_0, \tau)}{\partial \tau} = \mathbf{D}_{\text{tr}} \Delta P(r, r_0, \tau), \quad (13)$$

we find the propagator for a diffusing polaron subject to the initial condition $P_{\text{tr}}(r, r_0, \tau) = \delta(r_0 - r)$, where $\mathbf{D}_{\text{tr}} = [D_i]$ and i is the unit vector for the molecular coordinate system. For a 1D-system, the above propagator is defined explicitly by the relation³⁹

$$P(r, r_0, \tau)_{1D} = (4\pi v_{1D}\tau)^{1/2} \exp\left[-\frac{(r-r_0)^2}{4v_{1D}\tau}\right] \exp(-v_{3D}\tau). \quad (14)$$

The mobile polaron induces a local magnetic field $B_{\text{loc}}(t)$ at the location of other electron or nuclear spins, influencing thereby the relaxation times of the latter. The relaxation time can therefore be expressed in terms of the frequency function $\tau_{1,2} = f[J(\omega)]$, where

$$J(\omega) = \int_{-\infty}^{+\infty} G(\tau) \exp(-i\omega\tau) d\tau.$$

Here $J(\omega)$ is the spectral density function. The autocorrelation function of a local field $B_{\text{loc}}(t)$ fluctuating in a discrete system is

$$G(\tau) = c_{1D} \sum_{r_0} \sum_r A(r_0, t) P(r, r_0, \tau) F(r_0) F^*(r) dr_0 dr, \quad (15)$$

where $A(r, t)$ is the probability that the spin is at a distance r at time t and is equal to the spin concentration N , while $F(r)$ is the probability that two spins are at a distance r at time t . For frequencies $\omega \ll v_{1D} c_{1D}^2 (r - r_0)^{-2}$ the spectral density function assumes the form:⁵⁷

$$J(\omega) = N J_{1D}(\omega) \sum \sum F(r_0) F^*(r) f_{1D}(|r - r_0|), \quad (16)$$

where $N = N_1 + (1/\sqrt{2})N_2$ is the probability that in the initial instant the spin is in the position r_1 , $J_{1D}(\omega) = (2\pi v_{1D} v_e)^{-1/2}$ for $v_{3D} \ll v_e \ll v_{1D}$ and $J_{1D}(\omega) = (2\pi v_{1D} v_{3D})^{-1/2}$ for $v_{3D} \gg v_e$, $F(r_0) F^*(r) f_{1D}(|r - r_0|) = (3\cos^2 \vartheta - 1)^2 r_1^{-3} r_2^{-3}$, and ϑ is the angle between the vectors r_1 and r_2 .

The relaxation times of the paramagnetic centres in PANI are characterised by the relation $\tau_{1,2} \sim N\omega_e^{1/2}$,^{45,48} so that the experimental results presented in Fig. 7 may be interpreted within the framework of the modulation of the spin relaxation of the 1D-diffusion of a polaron and its interchain hopping 3D-transfer at rates v_{1D} and v_{3D} respectively. Since the electron relaxation is determined mainly by the dipole-dipole interaction between equivalent electron and nuclear spins, it follows subject to the condition $S = I = \frac{1}{2}$, that the equations for the rate of relaxation³⁹ in the polycrystalline sample can be more simply formulated:

$$\begin{aligned} \tau_1^{-1} &= \langle \Delta\omega^2 \rangle [J(\omega_e) + 4J(2\omega_e)] \\ &= 1.16 \times 10^{-43} N (v_{1D})^{-1/2} \sum \sum_i, \end{aligned} \quad (17a)$$

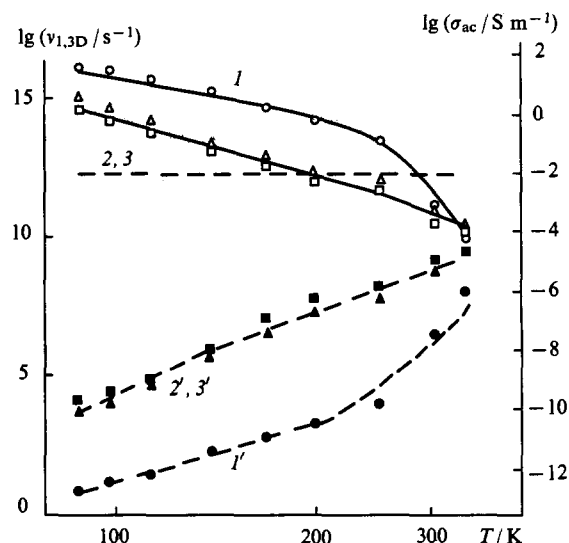


Figure 9. Temperature variations of the rates of diffusion of the polarons along the chain (v_{1D}) and between the chains (v_{3D}) in polyaniline with the degrees of oxidation $z = 0$ (1), < 0.01 (2), and 0.02 (3) and also of the electrical conductivity σ_{ac} calculated within the framework of the isoenergetic (continuous lines) and activated (dashed lines) interchain charge transfer. The horizontal line corresponds to the effective value v_{3D} calculated by Eqns (16) and (17) subject to the condition $\tau_1 \approx \tau_2$ for polyaniline with $z \geq 0.3$.

$$\tau_2^{-1} = \frac{1}{2} \langle \Delta\omega^2 \rangle [3J(0) + 5J(\omega_e) + 2J(2\omega_e)] \quad (17b)$$

$$= 4.13 \times 10^{-38} (v_{1D})^{-1/2} [(v_{3D})^{-1/2} + 2.28 \times 10^{-6}] \sum \sum_i,$$

where $\sum \sum_i$ is the lattice sum equal to $1.21 \times 10^{57} \text{ m}^{-6}$ for PANI.

Fig. 9 presents the temperature variations of the rates of diffusion v_{1D} and v_{3D} of the paramagnetic centres in certain PANI samples under the conditions of spin delocalisation over five monomer units. Evidently the anisotropy of the spin dynamics is a maximum in the initial sample (EB form) and diminishes with increase in the degree of oxidation z . For comparatively high degrees of oxidation ($z \geq 0.2$), the times τ_1 and τ_2 are approximately equal and depend only slightly on temperature in view of the intense spin-spin exchange in the metal-like domains and the increased dimensionality of the system. Bearing in mind that $\tau_2^{-1} \approx \tau_1^{-1}$ it is possible to calculate v_{3D} . It proved to be $1.6 \times 10^{12} \text{ s}^{-1}$ for PANI samples with $z \geq 0.2$ (Fig. 9). The calculated values of v_{1D} are significantly smaller than the rate of 1D-diffusion of the polaron, obtained for PANI by magnetic-resonance methods in weak recording fields.⁴⁵

It had been shown earlier⁴⁵ that the anisotropy of the spin diffusion in PANI at room temperature remains fairly high up to $z = 0.6$, but it follows from Fig. 9 that the ratio v_{1D}/v_{3D} remains fairly high only in neutral and weakly oxidised samples. The dimensionality of PANI increases on oxidation as a result of the intensification of the interaction between the polymer chains, so that the spin diffusion in this polymer becomes almost isotropic for $z \geq 0.2$, which is characteristic of classical 3D-semiconductors. This finding constitutes unambiguous evidence for the formation of massive quasi-metallic domains in the oxidised polymer and for the increase in its dimensionality and crystallinity, which we confirmed in an X-ray diffraction study of PANI.⁴⁷ During the oxidation of the polymer, the concentration of electron traps diminishes, which decreases the probability of the scattering of electrons by lattice phonons and hence leads to a weaker temperature dependence of the relaxation and dynamic parameters of the charge carriers in PANI, as happens in classical inorganic amorphous semiconductors.⁵⁹

If one assumes that the diffusion coefficients D of the spin and diamagnetic charge carriers are identical, it is possible to obtain from Eqn (4) the quantity σ_{1D} , which is 10 S m^{-1} for the sample with $0 \leq z \leq 0.02$ at room temperature whereas σ_{3D} increases in this range of z from 1.0×10^{-3} to 0.5 S m^{-1} . Subject to the condition $v_{1D} \approx v_{3D}$, these quantities are $\sigma_{1D} = (5-18) \times 10^3$ and $\sigma_{3D} = (3-10) \times 10^3 \text{ S m}^{-1}$. Thus the rate of the interchain charge transfer increases with increase in z , which constitutes additional confirmation of the increase in the number and size of the quasi-metallic 3D-domains in PANI.

As in other quasi-one-dimensional polymeric semiconductors, different charge transfer processes may occur in PANI, such as charge transfer along a π -conjugated chain as well as the inter-chain and interfibrillar charge transfer. Evidently the contribution of each of these processes to the bulk conductivity depends on the method of synthesis, structure, and degree of oxidation of the polymer and also on the dynamics of the nonlinear excitations.

The data obtained at the 2 mm EPR band permit a more correct and fuller determination of the mechanism of the charge transfer in PANI. As shown above, the EB form of PANI exhibits a strong temperature dependence of the spin-lattice relaxation time. This means that the hops of the unpaired electron in PANI are accompanied by the absorption or emission of a minimal number of polymer lattice phonons. Since the linkage between the spin and the lattice in the EB form of PANI is fairly strong, multiphonon charge transfer processes predominate in this system. The approach proposed for the description of the motion of solitons in lightly doped *trans*-PA may therefore be used in the study of the spin dynamics in the amorphous regions of PANI.⁶⁰

The essential feature of this approach consists in the phonon-linked interchain tunnelling of the charge between isoenergetic levels of the carriers under the conditions of Coulombic interaction of a soliton with a charge q_1 and an ion with the opposite charge q_2 . The excess charge $\Delta q = q_1 - q_2$ may undergo a phonon-linked transfer, with a finite probability, to a neutral carrier moving along a neighbouring polymer chain. If in the instant of such transfer the charge carrier is also in the vicinity of the ion, then its energy before and after charge transfer remains unchanged. In this case, the components of the electrical conductivity of the polymer, in which the charge is transferred between soliton levels, are determined by the probability that the soliton is located near a charged ion and also by the probability that the energies of the charge carriers are within the limits of kT ,

$$\sigma_{dc} = \frac{k_1 e^2 \dot{\gamma}(T) \xi N_0}{k T R_0} \exp\left(-\frac{2k_2 R_0}{\xi}\right) = \sigma_0 T^n, \quad (18a)$$

$$\begin{aligned} \sigma_{ac} &= \frac{e^2 N_i^2 N_0 \xi_{\parallel}^2 \xi_{\perp}^2 v_e}{384 k T} \left[\ln \frac{2v_e}{N_0 \gamma(T)} \right]^4 \\ &= \sigma_0 v_e T^{-1} \left[\ln \frac{k_3 v_e}{T^{n+1}} \right]^4, \end{aligned} \quad (18b)$$

where $k_1 = 0.45$, $k_2 = 1.39$, and k_3 are constants, $\gamma(T) = \gamma_0 (T/300)^{n+1}$ is the hopping frequency of the charge carrier, $\xi = (\xi_{\parallel} \xi_{\perp}^2)^{1/3}$, ξ_{\parallel} and ξ_{\perp} are the averaged parallel and perpendicular lengths of the charge carrier respectively, $N_0 = N_n N_{ch} (N_n + N_{ch})^{-2}$ (N_n and N_{ch} are the numbers of the neutral and charged carriers per monomer unit respectively), and $R_0 = [(4/3) \pi N_i]^{-1/3}$ is the typical distance between ions at a concentration N_i . The above temperature variations have been obtained experimentally for lightly doped *trans*-PA^{61,62} and other conducting polymers.^{63,64} It can be shown that, within the framework of the approach considered, the following relation is valid:

$$\frac{\sigma(v_e \rightarrow \infty)}{\sigma(v_e \rightarrow 0)} = \frac{\exp(1.9k_1)}{k_1^4}, \quad (19)$$

where $k_1 = (0.4\pi N_i \xi_{\parallel} \xi_{\perp}^2)^{-1/3}$ is a constant. Calculation showed that $\sigma_{ac}/\sigma_{dc} \approx 130$ for PANI at $v_e = 140 \text{ GHz}$.

It is essential to note that the approach described is valid in the case of charge transfers by carriers with a small radius such as solitons. This approach may also be used for the interpretation of the spin dynamics in other conjugated polymers,⁶⁴ for example in tetrathiafulvalene (see below), where charge transfer is effected by nonlinear excitations with a small radius.⁶⁵ Apparently it can also be used for the interpretation of the spin dynamics in PANI when there are N_n polarons with a charge q and N_{ch} bipolarons with a charge $2q$ in this polymer.

Fig. 9 presents the temperature dependence of the electrical conductivity σ_{ac} calculated from Eqn (18b) by using $n = 12.9$ and $\sigma_0 = 2.8 \times 10^{-12} \text{ S m}^{-1} \text{ s K}$ for the initial sample in the EB form and $n = 12.6$ and $\sigma_0 = 8.8 \times 10^{-14} \text{ S m}^{-1} \text{ s K}$ for the sample with $0.02 \geq z \geq 0$, as well as $k_3 = 1 \times 10^{24} \text{ s K}^{n+1}$. A satisfactory agreement of the experimental $v_{1D}(T)$ and theoretical $\sigma_{ac}(T)$ relations obtained for these samples follows from the figure. Bearing in mind that the conductivity of PANI obeys the law $\sigma_{dc}(T) \sim T^a$ ($a = 12-20$) for a low oxidation level,⁴⁷ one may conclude that the charge transfer mechanism considered operates in PANI with $z \leq 0.02$.

An appreciable temperature dependence of σ_{ac} may also be observed on thermal activation of the charge carriers with an energy E_a for activation from their energy level located in the gap to the conductivity band. In this case the conductivities σ_{dc} and σ_{ac} can be determined from the equations⁶¹

$$\sigma_{dc} = \sigma_0 \exp\left(-\frac{E_a}{kT}\right), \quad (20a)$$

$$\sigma_{ac} = \sigma_0 v_e^\gamma T \exp\left(-\frac{E_a}{kT}\right), \quad (20b)$$

where γ is a constant which varies in the range $0.3 < \gamma < 0.8$ depending on the dimensionality of the system. Indeed the $v_{3D}(T)$ relations can be fitted by the function $\sigma_{ac}(T)$ calculated from Eqn (20b) with $\gamma = 0.8$ and $\sigma_{ac}^0 = 3.2 \times 10^{-18} \text{ S m}^{-1} \text{ s}^{0.8} \text{ K}^{-1}$ and $E_a = 0.06 \text{ eV}$ at $T \leq 240 \text{ K}$ or $\sigma_{ac}^0 = 9.1 \text{ S m}^{-1} \text{ s}^{0.8} \text{ K}^{-1}$ and $E_a = 0.9 \text{ eV}$ at $T \geq 240 \text{ K}$ for the sample in which $z = 0$ and with $\sigma_{ac}^0 = 1.4 \times 10^{-11} \text{ S m}^{-1} \text{ s}^{0.8} \text{ K}^{-1}$ and $E_a = 0.13 \text{ eV}$ for samples in which $0.02 \geq z > 0$ (Fig. 9). However, the function $\sigma_{dc}(T)$ for the initial sample has a higher slope than should follow from Eqn (20b). Therefore the activation mechanism of charge transfer can apparently be realised in a polymer with an intermediate degree of oxidation.

The temperature dependence of the electrical conductivity of PANI with $z \geq 0.2$ obeys the law $\sigma_{dc} = \sigma_0 \exp[-(T_0/T)^{1/2}]$.⁴⁷ This is evidence for charge transfer in the oxidised PANI within the framework of the variable range hopping model.⁶⁶ In this case, one can write for the components of the electrical conductivity of a system with a dimensionality d

$$\sigma_{dc} = 0.39 v_0 e^2 \left[\frac{n(\epsilon_F) L}{k T} \right]^{1/2} \exp\left[-\left(\frac{T_0}{T}\right)^{1/(d+1)}\right], \quad (21a)$$

$$\sigma_{ac} = \frac{2}{3} \pi^2 e^2 k T n^2(\epsilon_F) L^5 v_e \left[\ln \frac{v_0}{v_e} \right]^4, \quad (21b)$$

where v_0 is the limiting hopping frequency approximately equal to the frequency of the optical lattice phonon ($v_{ph} \sim 10^{13} \text{ s}^{-1}$).

Using the experimental values of $n(\epsilon_F)$ and the $\sigma_{dc}(T)$ relations, it is possible to determine $v_0 = 3.2 \times 10^{13} \text{ s}^{-1}$. Table 4 presents the constants L , T_0 , and Δ_3 for different PANI samples. It follows from the data presented that the polaron localisation length is approximately equal to the coherence length for the crystalline domains in the ES form of PANI,¹¹ which indicates the 3D-delocalisation of electrons in these regions.

In PANI with $z = 0.53$, charge is transferred between crystalline quasi-metallic domains with a characteristic size 6.8 nm (Table 4), located at a distance $R = 0.25L(T_0/T)^{1/2} = 4.2 \text{ nm}$

($T = 300$ K). The domain consists of polymer chains rolled as a bundle in which the 3D-electron transfer predominates and intense spin-spin exchange takes place. The appearance of a Dyson-like line was recorded in the EPR spectrum of the sample as a consequence of the increase in its conductivity (Fig. 5). Assuming that the characteristic size of the particles is $r_0 \approx 2 \times 10^{-6}$ m, it is possible to calculate the alternating current electrical conductivity of the polymer at room temperature: $\sigma_{ac} = 2.5 \times 10^5 r_0^{-2} v_e^{-1} = 4.5 \times 10^5$ S m $^{-1}$. Next, the constants T_0 and L for an individual domain ($T_0 = 2100$ K and $L = 2.5$ nm) may be determined from Eqn (21b). 3D-Hopping of the polarons takes place within the limits of the domain at a rate $v_{3D} = 1.6 \times 10^{12}$ s $^{-1}$ over a distance $R = 0.39L(T_0/T)^{1/4} = 1.6$ nm at $T = 300$ K. The latter value exceeds significantly the interchain distance as a consequence of the structural disorder in the crystalline domains. The rate of the 1D-diffusion of the polaron at room temperature, determined from the line width of the 3 cm EPR spectrum, is $v_{1D} = 2.0 \times 10^{12}$ s $^{-1}$. The similarity of the rates of diffusion of the polaron along polymer chains and between the chains confirms the quasi-three-dimensional isotropic diffusion of the spin charge carrier in the oxidised polymer. The rate of charge transfer in the vicinity of the Fermi level proved to be $v_F = (2A_2 m_e^{-1})^{1/2} = 4.6 \times 10^5$ m s $^{-1}$.

Thus the 2 mm EPR spectroscopic data obtained confirm the existence in PANI of highly conducting domains dispersed in the amorphous EB phase. On oxidation of the polymer, the number and size of such domains increase and there is also an increase in the dimensionality of the system. This process is accompanied by an increase in the number of Pauli charge carriers and also by an increase in the concentration of polarons. The transition from the EB to the ES form of PANI leads to an increase in the rates of relaxation and electrodynamic processes and to a change in the mechanism of charge transport in the polymer. In the oxidised sample with $z \geq 0.3$, the concentration of paramagnetic centres is approximately equal to the concentration of charge carriers. This permits the conclusion that there is 1D-charge transfer between the quasi-metal domains and 3D-charge transfer in the polaron lattice of these domains by polarons with a small radius in the ES form of PANI.

VI. Polytetrathiafulvalene

The 3 cm EPR spectra of powder-like polytetrathiafulvalene samples, in which the monomer TTF units are linked by phenyl (PTTF-1) or tetrahydroanthracene (PTTF-2) bridges, represents a superposition of the strongly anisotropic spectrum of immobilised paramagnetic centres with $g_{xx} = 2.0147$, $g_{yy} = 2.0067$, and $g_{zz} = 2.0028$ and the almost symmetrical spectrum of mobile polarons with $g = 2.0071$.^{18, 67, 68} The relatively high value of the g -tensor of the radicals indicates an appreciable interaction of the unpaired electron with the sulfur atom nucleus. The spin-lattice relaxation time of the neutral PTTF-1 sample exhibits a temperature dependence of the type $\tau_1 \sim T^{-\alpha}$, where $\alpha \approx 2$ at $100 < T < 150$ K and $\alpha = 1$ at $150 < T < 300$ K.^{67, 68} Doping or heating of the matrix leads to the appearance of a large number of mobile paramagnetic centres and a change in their magnetic and relaxation parameters as a consequence of the conversion of the bipolarons into paramagnetic polarons. However, owing to the low spectral resolution, it proved impossible to analyse using the 3 cm EPR spectra the influence of the relaxation and dynamic parameters of the initial paramagnetic centres on the conducting properties of PTTF in greater detail.

The nature, composition, and dynamics of various paramagnetic centres in the initial and iodine-doped PTTF samples were investigated in greater detail at the 2 mm EPR band.^{18, 23, 69}

Figs 10a and 10c present the EPR absorption spectra of PTTF, from which it is possible to determine more accurately all the components of the g -tensor and also to identify the lines attributed to different paramagnetic centres. Computer simulation demonstrated the presence in PTTF of two types of

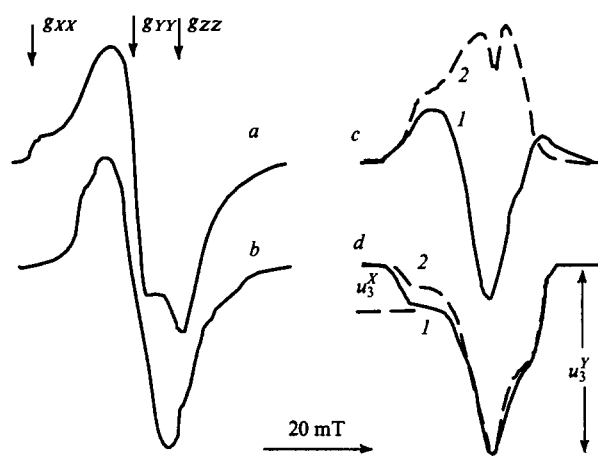


Figure 10. Typical 2 mm EPR absorption spectra (a, c) and also the spectra of the in-phase (b) and $\pi/2$ out-of-phase (d) components of the dispersion signals of the initial (a) and doped (c) polytetrathiafulvalene samples recorded at $T = 300$ K (1) and $T \leq 150$ K (2). The measured magnetic parameters are indicated.

paramagnetic centres with temperature-independent components of the g -tensors. The anisotropic spectrum of PTTF-1 is characterised by the magnetic parameters $g_{xx} = 2.01424$, $g_{yy} = 2.00651$, and $g_{zz} = 2.00235$, whereas the paramagnetic centres with an almost symmetrical spectrum are recorded with $g^p = 2.00706$. The principal values of the g -tensor of the paramagnetic centres localised in PTTF-2 are $g_{xx} = 2.01292$, $g_{yy} = 2.00620$, and $g_{zz} = 2.00251$, while the paramagnetic centres with a weakly asymmetric spectrum are characterised by the parameters $g_{||}^p = 2.00961$ and $g_{\perp}^p = 2.00585$. The ratio of the paramagnetic centres with different forms of the spectrum is 1 : 1.8 for PTTF-1 and 3 : 1 for the neutral PTTF-2.

Since the average g -factors (g) for both types of paramagnetic centres are approximately equal, one may conclude that, as in other conducting polymers, there are in PTTF paramagnetic centres with different mobilities, namely polarons diffusing along polymer chains at a rate $v_{1D}^0 \geq 5 \times 10^9$ s $^{-1}$ and polarons pinned on traps and/or on short polymer chains.

On doping, the comparatively large iodine ions are incorporated into the polymer matrix, increasing the mobility of its polymer chains. This is apparently the cause of the increase in the number of delocalised polarons (Fig. 10c). The components of the g -tensor of the mobile paramagnetic centres in PTTF-1 are fully averaged, whereas in the case of PTTF-2 such averaging takes place only partially. This finding can be accounted for by the different nature and conformations of the monomer units of the polymers.

The width of the spectral components ΔB_{pp}^{loc} of the paramagnetic centres trapped in PTTF-1 depends only slightly on temperature. However, ΔB_{pp}^{loc} for these paramagnetic centres depends on the recording frequency, increasing from 0.28 to 0.38 and then to 3.9 mT ($T = 270$ K) with increase in the recording frequency from 9.5 to 37 and then to 140 GHz respectively. The value ΔB_{pp}^{mob} for mobile polarons changes under these conditions from 1.0 to 1.12 and then to 17.5 mT. The fact that the mobile paramagnetic centres have a wider line than the pinned centres can be accounted for by their stronger interaction with the dopant molecules. This is typical for conducting polymers,^{23, 30} but conflicts with the 3 cm EPR data obtained previously for PTTF-1.^{67, 68}

Following a decrease in temperature by a factor of 2, the components of the spectrum of the mobile polaron in PTTF-1 are narrowed by 2.2 mT, which indicates an increase in the mobility of the polaron. Such a change in ΔB_{pp}^{mob} is analogous to the narrowing of the lines of the spin charge carriers in classical metals.

In the range of resonance frequencies $37 \leq \nu_e \leq 140$ GHz, the line width for the paramagnetic centres varies in accordance with Eqn (8), which indicates a weak interaction between the spin packets in this polymer. As a result of this, at the 2 mm EPR band the paramagnetic centres in PTF are saturated for relatively low values of B_1 , so that rapid passage effects are manifested in the in-phase and $\pi/2$ out-of-phase components of the dispersion signal (Figs 10b and 10d). Since the inequality $\omega_m \tau_1 \geq 1$ is valid for the neutral PTF-2 sample, its dispersion signal U is determined mainly by the last two terms of Eqn (9). Since the condition $\omega_m \tau_1 \leq 1$ holds for the doped samples, their dispersion signal is determined by the u_1 and u_3 terms of this equation.

Modelling of the dispersion spectra showed that they are a superposition of the dominant asymmetric spectrum of the localised polarons with $g_{XX} = 2.01356$, $g_{YY} = 2.00603$, and $g_{ZZ} = 2.00215$ for PTF-1 and $g_{XX} = 2.01188$, $g_{YY} = 2.00571$, and $g_{ZZ} = 2.00231$ for the neutral PTF-2 and of the spectrum of mobile polarons (Fig. 10b).

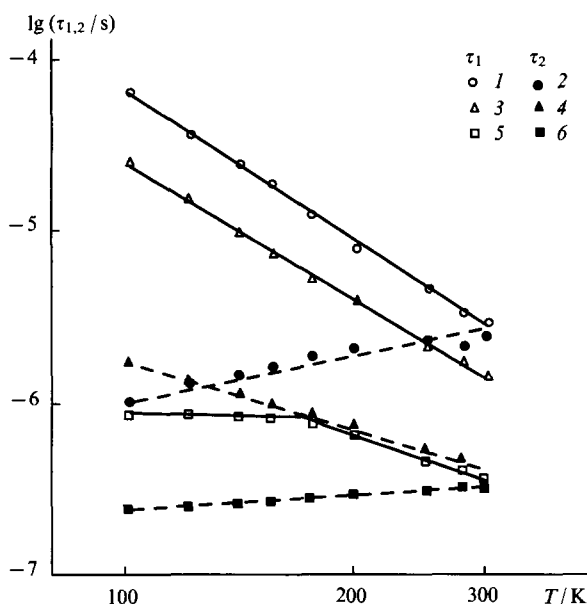


Figure 11. Temperature variations of the effective spin-lattice (τ_1) and spin-spin (τ_2) relaxation times of the paramagnetic centres in polytetrathiafulvalene-1 samples with the doping level $z = 0.4$ (2) and also of polytetrathiafulvalene-2 with the doping levels $z = 0$ (1) and 0.1 (3).

Fig. 11 presents the temperature variations of the effective relaxation times of the paramagnetic centres in both PTF samples calculated from the 2 mm EPR spectra by the equations presented above. The time τ_1 varies with temperature in accordance with the $T^{-\alpha}$ law, where $\alpha \geq 3$ for the trapped and mobile polarons. The exponent α exceeds the corresponding value obtained previously by the spin echo method in the 3 cm EPR band.⁶⁷ The slight difference between the time τ_1^{mob} and τ_1^{loc} may be induced, for example, by the strong interaction between the different paramagnetic centres.

It is seen from Fig. 10d that an increase in temperature leads to an increase in the parameter $K_{\text{mov}} = u_3^X / u_3^Y$. As in the case of PANI, this is a result of the anisotropic librational reorientations of the pinned polarons about a specified X axis of the polymer chains. The correlation time of such molecular motions, calculated by the method described by the present author,²³ was

$$\tau_c = 9.8 \times 10^{-6} \exp\left(\frac{0.02}{kT}\right) \text{ s}$$

for the PTF-1 sample with the maximum value $\tau_c \approx 10^{-4}$ s ($T = 75$ K). The activation energies for the librations and the interchain charge transfer in the doped PTF-1 are

comparable,^{67,69} which indicates interaction of the pinned and mobile polarons in this polymer matrix.

The degree of saturation transfer depends not only on the dynamics and anisotropy of the magnetic parameters of the paramagnetic centres but also on the level of doping of the polymer. Thus the correlation time for the chain librations of the PTF-2 samples, determined by the ST-EPR method, was

$$\tau_c = 5.2 \times 10^{-6} \exp\left(\frac{0.02}{kT}\right) \text{ s.}$$

On doping, the chains of this polymer become more rigid, which leads to a higher slope of the Arrhenius relation for this sample.²³

$$\tau_c = 2.4 \times 10^{-6} \exp\left(\frac{0.04}{kT}\right) \text{ s.}$$

As in the case of PANI, both 1D-diffusion and 3D-hopping of the polaron at rates ν_{1D} and ν_{3D} respectively take place in PTF. Figs 12 and 13 present the temperature variations of these rates for PTF-1 and PTF-2 respectively calculated by Eqns (16) and (17) using the data presented in Fig. 11. If one assumes a spin delocalisation on the polaron equal to five monomer units, then

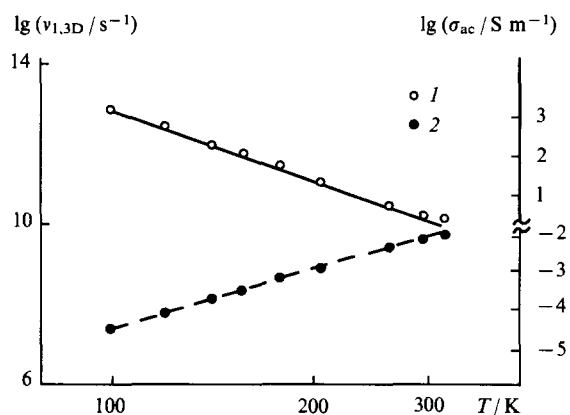


Figure 12. Temperature variations of the rates of diffusion of the polarons along the chain (ν_{1D}) and between the chains (ν_{3D}) and of the electrical conductivity σ_{ac} calculated within the framework of the isoenergetic (continuous line) and activated (dashed line) interchain charge transfer in polytetrathiafulvalene-1 with the doping level $z = 0.4$.

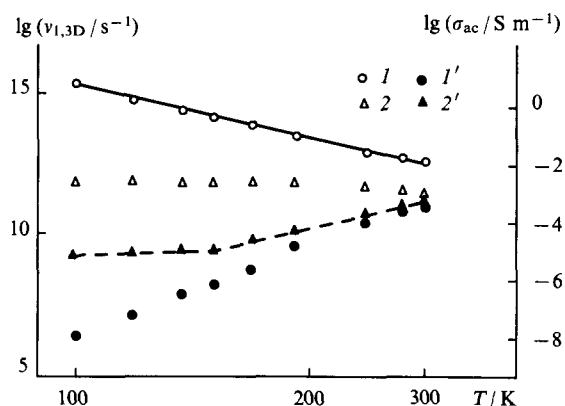


Figure 13. Temperature variations of the rates of diffusion of the polarons along the chain (ν_{1D}) and between the chains (ν_{3D}) in polytetrathiafulvalene-2 samples with the doping levels $z = 0$ (1, 1') and 0.1 (2, 2') and also of the electrical conductivity σ_{ac} calculated within the framework of the isoenergetic (continuous line) and isoenergetic-activated (dashed line) interchain charge transfer.

ν_{1D} is $2 \times 10^{10} \text{ s}^{-1}$ for PTTF-1 and $2 \times 10^{12} \text{ s}^{-1}$ for the neutral PTTF-2 sample at room temperature. This quantity is smaller by at least two orders of magnitude than the frequency of the spin 1D-diffusion in PP⁷⁰ and PANI³³ obtained previously by magnetic-resonance methods at low recording frequencies, but exceeds the frequency ν_{1D}^0 calculated earlier. The anisotropy of the spin dynamics ν_{1D}/ν_{3D} in PTTF at room temperature exceeds 10 and increases as the temperature is reduced.

Evidently the spin dynamics play a significant role in the charge transfer process. When the diffusion coefficients of the spins and charge carriers are equal and for $N_2 = 6.9 \times 10^{-5}$ of an electron per monomer unit, the components of the conductivity of PTTF-1, calculated by Eqn (4), are $\sigma_{1D} \approx 0.1$ and $\sigma_{3D} \approx 4 \times 10^{-3} \text{ S m}^{-1}$ at room temperature. The value σ_{1D} obtained exceeds significantly the electrical conductivity of the sample measured using a direct current ($\sigma_{dc} \approx 10^{-3} \text{ S m}^{-1}$).⁶⁷ Indeed, the macroscopic parameter σ_{dc} which reflects the hopping charge transfer between polymer chains, should not exceed the microconductivity, because $\nu_{1D} \gg \nu_{3D}$. Taking into account the different temperature variations of the conductivities σ_{1D} and σ_{3D} and also the charge transfer in PTTF by polarons with a small radius,⁶⁵ one may postulate that isoenergetic charge transfer takes place in this sample.⁶⁰

As can be seen from Fig. 12, the function $\nu_{1D}(T)$ correlates satisfactorily with the function $\sigma_{1D}(T) = 2.4T^{-1}(81 - 13.6 \ln T)^4$ calculated from Eqn (18b) within the framework of the approach considered. According to Eqn (18a), the isoenergetic charge transport should also lead to the temperature dependence $\sigma_{dc}(T) \approx T^{12.6}$, but the experimental σ_{3D} has a temperature variation of the type⁶⁷

$$\sigma_{3D}(T) \sim \exp\left(-\frac{E_a}{kT}\right).$$

Thus the dynamic process considered must be analysed within the framework of thermally activated polaron hops to the edges of the conductivity band.

Indeed, the temperature variation of the rate of diffusion ν_{1D} for the PTTF-1 sample can be fitted satisfactorily by the function (20b) with $\sigma_0 = 8.3 \times 10^{-14} \text{ S s m}^{-1} \text{ K}^{-1}$, $\nu_e = 1.4 \times 10^{11} \text{ s}^{-1}$, $\gamma = 0.8$, and $E_a = 0.04 \text{ eV}$ (Fig. 13). The value of E_a obtained is close to the activation energy for the interchain charge transfer ($E_a = 0.03 \text{ eV}$) at low temperatures.^{67,68} Furthermore, this quantity corresponds to the activation energy for the librations of the chains in PTTF calculated above. This fact permits the conclusion that the conductivity of PTTF is determined predominantly by the interchain phonon-assisted polaron hopping.

The probability of charge transfer is determined by the strength of the interaction of the electron with the lattice, the interchain transfer of which is accompanied by the absorption of a minimal number m of lattice phonons. It follows from Fig. 12 that the rate of the interchain spin transfer in PTTF-1 varies with temperature in accordance with the law $\nu_{3D} \approx T^{4.7}$. On the other hand, the spin-lattice relaxation time of the paramagnetic centres has a temperature dependence of the type $\tau_1(T) \approx T^{3.6}$ (Fig. 11), which is a consequence of a multiphonon process. Adopting $E'_a = m\hbar\nu_{ph}$ and assuming that the averaged value $\langle m \rangle = 4.2$, one may calculate ν_{ph} for phonons in this sample as $\nu_{ph} = 2.5 \times 10^{13} \text{ s}^{-1}$, which is typical for conducting polymers. Thus, as a consequence of the strong electron-phonon interaction, the conductivity of the polymer is initiated by the librations of the polymer chains and is determined by multiphonon processes.

On passing from PTTF-1 to PTTF-2, the frequency ν_{1D} increases approximately by two orders of magnitude at room temperature (Figs 12 and 13), which is apparently associated with the more planar conformation of the monomer units in PTTF-2. Indeed, the g_{xx} parameter of the g -tensor changes by $\Delta g_{xx} = 1.32 \times 10^{-3}$ in this transition. Bearing in mind the dependence of the overlap integral I and the spin density on the

sulfur nucleus ρ_S on the dihedral angle θ in the form $I \sim \cos \theta$ and $\rho_S \sim \sin \theta$,¹³ it is possible to calculate by Eqn (1) the change $\Delta\theta$ in such a transition, which amounts to 22° . We may note that a similar conformational change occurs on passing from the benzenoid to the quinonoid form of PPP¹² and also on transition from the EB to the ES form of PANI.⁴⁹

If it is postulated that a certain number of bipolarons (concentration N_{BP}) with a charge $2e$ are present in PTTF, an attempt may be made to interpret the spin dynamics in PTTF-2 within the framework of isoenergetic electron transport.⁶⁰ The quantities n and N_{ch} may be determined from the $\nu_{1D}(T)$ relation presented in Fig. 13: $n = 12.2$ and $N_{ch} = N_{BP} = 7.5 \times 10^{-5}$. Using the values $N = 2 \times 10^{23} \text{ m}^{-3}$ and $c_{1D} = 1.2 \text{ nm}$, as well as the data presented in Fig. 13, it is possible to calculate by Eqn (4) the conductivity σ_{1D} , which amounts to 1.8 S m^{-1} at room temperature. Adopting $\xi_{\parallel} = 6 \text{ nm}$, $\xi_{\perp} = 0.6 \text{ nm}$, $N_n = N_p = 6.7 \times 10^{-4}$, $N_0 = 0.11$, and $\sigma_{dc} = 2 \times 10^{-6} \text{ S m}^{-1}$,⁶⁷ we obtain from Eqns (18) $R_0 = 4.1 \text{ nm}$, $\gamma(T) = 4.0 \times 10^{-23} T^{13.2} \text{ s}^{-1}$, and $N_i = 3.3 \times 10^{24} \text{ m}^{-3}$. Fig. 13 shows that the $\sigma_{1D}(T)$ relation, derived from Eqn (18a) for a neutral PTTF-2 sample, fits the function $\nu_{1D}(T)$ fairly satisfactorily.

The rate of diffusion of the polaron in doped PTTF-2 samples varies approximately linearly in the region of low temperatures and is characterised by a high slope at higher temperatures (Fig. 13). This justifies the assumption that the charge transfer in the PTTF polymers is effected within the framework of the variable range hopping model at low temperatures with a contribution by the activated charge transfer at higher temperatures. Putting $L = \xi$, $d = 3$, and $\nu_0 = \nu_{ph} = 3.6 \times 10^{13} \text{ s}^{-1}$, it is possible to determine by Eqn (21) $T_0 = 7.8 \times 10^7 \text{ K}$ and $n(\epsilon_F) = 7.9 \times 10^{-4} \text{ eV}^{-1} \text{ monomer}^{-1}$ for these polymers.

The high-temperature part of the $\nu_{3D}(T)$ relation is described satisfactorily by Eqn (20b) for $\gamma = 0.8$ and $E_a = 0.035 \text{ eV}$ (Fig. 13). The latter quantity is close to the activation energies for the superslow librations of the PTTF polymer chains and also for the interchain charge transfer in PTTF-1. This finding indicates a close relation between the molecular dynamics and the charge transfer process in PTTF and confirms the earlier hypothesis⁷¹ that the fluctuations of the lattice vibrations, including librations, may modulate the interchain electron transfer integral for conducting compounds. The polymer chains in PTTF-1 are less rigid than in PTTF-2, so that the above modulation in this polymer occurs at lower temperatures (Figs 12 and 13).

The intensification of the libron-exciton interactions at high temperatures indicates the formation in doped PTTF of complex quasi-particles — a molecular-lattice polaron.⁷² Within the framework of this phenomenological model, it is postulated that the molecular polaron, the mobility of which is characterised by the temperature variation $\mu_m \sim T$, is additionally coated by a lattice polarisation shell. Since the mobility of the lattice polaron μ_1 is expressed by an activation function, the resultant mobility of the molecular-lattice polaron is expressed by the sum

$$\mu(T) = \mu_m(T) + \mu_1(T) = aT + b \exp\left(-\frac{E_a}{kT}\right), \quad (22)$$

where a and b are constants. Since the formation energies of the molecular polaron in PTTF and polyacetylene crystals are similar, $E_{pm} = 0.15 \text{ eV}$,⁷³ it is possible to determine the formation energy of the molecular-lattice polaron in PTTF as $E_{pml} = E_{pm} + E_{pl} = 0.19 \text{ eV}$. The time necessary for the polarisation of the atomic and molecular orbitals of the polymer is then $\tau_e \approx \hbar E_{pml}^{-1} = 2.2 \times 10^{-14} \text{ s}$ at room temperature. This time is significantly shorter than the characteristic polaron diffusion time in PTTF, i.e. the minimum time of the 1D- and 3D-hops of the charge carriers exceeds significantly the polarisation time of the microenvironment of these carriers in the polymer: $\tau_h \gg \tau_e$. Consequently this inequality is a necessary and sufficient condition for the electronic polarisation of the polymer chains by the charge carriers.

The Fermi velocity v_F of the polarons in PTF is $1.9 \times 10^5 \text{ m s}^{-1}$ (see Ref. 23) and is close to the corresponding value for PANI. The length of the free path l^* of the charge carrier in different PTF specimen is $l^* = v_{1D} c_{1D}^2 v_F^{-1} = 10^{-2} - 10^{-4} \text{ nm}$. The latter quantity is too small to regard the PTF polymer as a quasi-one-dimensional metal.

Thus both 1D- and 3D-spin dynamics occur in PTF, influencing significantly the charge transfer processes. The conductivity of the polymer is determined mainly by the interchain transfer of the positive charge, but, in the analysis of the transport properties of PTF, account must also be taken of the 1D-diffusion of the spin and spin-free charge carriers.

VII. Conclusion

The data obtained demonstrate clearly the advantages of the EPR method in the study of conducting polymers at the 2 mm band. The high spectral resolution with respect to the g -factor achieved in this range makes it possible to record more accurately and separately the components of the g -tensor of organic radicals and hence makes it possible to analyse more fully and correctly the magnetic parameters of paramagnetic centres with different mobilities. The combination of a high resolving power with a low spin-spin cross-interaction permits a more effective employment of the paramagnetic centre steady-state saturation and saturation transfer methods as well as the spin label and probe method for the investigation in this frequency band of the detailed characteristics of the anisotropic molecular and spin dynamics in organic polymeric semiconductors.

The data presented demonstrate the great variety of the electronic processes occurring in organic conducting polymers. The fundamental properties of polymeric semiconductors are determined by the structure and conformation of the polymer chains, the nature and amount of the dopant introduced, and, in the first place, by the dynamics of the nonlinear excitations of the polarons and bipolarons participating in the charge transfer.

The polarons are formed on the chains of the polymer in the initial stage of its doping. With increase in the doping level, they may recombine into bipolarons. Incidentally, this process may be hindered by the structural or conformational characteristics of the polymer. The charge transfer mechanism changes on doping. Thus the conductivity of a neutral and lightly doped polymer are determined largely by the isoenergetic tunnelling of the charge between polymer chains, which is characterised by a fairly strong interaction of the spins with the lattice phonons. At an intermediate doping level, the charge is as a rule transferred by an activated mechanism and this process is initiated by the superslow anisotropic librations of the polymer chains. Finally, the variable range hopping interchain charge transfer, accompanied by comparatively weak scattering of electrons by the lattice phonons, predominates in the relatively highly conducting polymers.

References

1. H Meier *Top. Curr. Chem.* **61** 85 (1976)
2. J M Williams, J R Ferraro, R J Thorn, K D Carlson, U Geiser, H H Wang, A M Kini, M-H Whangbo *Organic Superconductors (Including Fullerenes): Synthesis, Structure, Properties, and Theory* (Englewood Cliffs, NJ: Prentice-Hall, 1992)
3. P Day, in *Handbook of Conducting Polymers* Vol. 1 (Ed. T E Scotheim) (New York: Marcel Dekker, 1986) p. 117
4. G E Wnek, in *Handbook of Conducting Polymers* Vol. 1 (Ed. T E Scotheim) (New York: Marcel Dekker, 1986) p. 205
5. T E Scotheim (Ed.) *Handbook of Conducting Polymers* Vols 1, 2 (New York: Marcel Dekker, 1986)
6. H Kuzmany, M Mehring, S Roth (Eds) *Electronic Properties of Polymers* (Berlin: Springer, 1992)
7. G Zerbi (Ed.) *Polyconjugated Materials* (Amsterdam: North-Holland, 1992)
8. R L Elsenbaumer, L W Shacklette, in *Handbook of Conducting Polymers* Vol. 1 (Ed. T E Scotheim) (New York: Marcel Dekker, 1986) p. 213
9. G Tourillon, in *Handbook of Conducting Polymers* Vol. 1 (Ed. T E Scotheim) (New York: Marcel Dekker, 1986) p. 293
10. G B Street, in *Handbook of Conducting Polymers* Vol. 1 (Ed. T E Scotheim) (New York: Marcel Dekker, 1986) p. 265
11. M E Jozefowicz, R Laversanne, H H S Javadi, A J Epstein, J P Pouget, X Tang, A G MacDiarmid *Phys. Rev. B, Condens. Matter.* **39** 12958 (1989)
12. J L Brédas, in *Handbook of Conducting Polymers* Vol. 2 (Ed. T E Scotheim) (New York: Marcel Dekker, 1986) p. 859
13. V F Traven' *Elektronnaya Struktura i Svoistva Organicheskikh Molekul* (The Electronic Structure and Properties of Organic Molecules) (Moscow: Khimiya, 1989)
14. R R Chance, D S Boudreaux, J L Brédas, R Silbey, in *Handbook of Conducting Polymers* Vol. 2 (Ed. T E Scotheim) (New York: Marcel Dekker, 1986) p. 825
15. P Bernier, in *Handbook of Conducting Polymers* Vol. 2 (Ed. T E Scotheim) (New York: Marcel Dekker, 1986) p. 1099
16. T S Zhuravleva *Usp. Khim.* **56** 128 (1987) [*Russ. Chem. Rev.* **56** 69 (1987)]
17. L D Kispert, L A Files, J E Frommer, L W Shacklette, R R Chance *J. Chem. Phys.* **78** 4858 (1983)
18. H-K Roth, V I Krinichnyi *Makromol. Chem., Makromol. Symp.* **72** 143 (1993)
19. R L Elsenbaumer, P Delannoy, G G Muller, C E Forbes, N S Murthy, H Eskhardt, R H Baughman *Synth. Met.* **11** 251 (1985)
20. O Ya Grinberg, A A Dubinskii, Ya S Lebedev *Usp. Khim.* **52** 1490 (1983) [*Russ. Chem. Rev.* **52** 850 (1983)]
21. V I Krinichnyi *Zh. Prikl. Spektrosk.* **52** 887 (1990) [*Appl. Magn. Reson.* **2** 29 (1991)]
22. V I Krinichnyi *J. Biochem. Biophys. Methods* **23** 1 (1991)
23. V I Krinichnyi *2-mm Wave Band EPR Spectroscopy of Condensed Systems* (Boca Raton, FL: CRC Press, 1995)
24. V I Krinichnyi *Usp. Khim.* **65** 84 (1996) [*Russ. Chem. Rev.* **65** 81 (1996)]
25. L M Goldenberg, A E Pelek, V I Krinichnyi, O S Roshchupkina, A F Zueva, R P Lyubovskaya, O N Efimov *Synth. Met.* **36** 217 (1990)
26. A L Buchachenko, A M Vasserman, in *Stabil'nye Radikaly* (Stable Radicals) (Moscow: Khimiya, 1973) p. 408
27. A A Bugai *Fiz. Tverd. Tela* **4** 3027 (1962)
28. C Menardo, F Genoud, M Nechtschein, J-P Travers, P Hani, in *Electronic Properties of Conjugated Polymers* (Eds H Kuzmany, M Mehring, S Roth) (Berlin: Springer, 1987) p. 244
29. M Schärli, H Kiess, G Harbeck, W Berlinger, K W Blazey, K A Müller, in *Electronic Properties of Conjugated Polymers* (Eds H Kuzmany, M Mehring, S Roth) (Berlin: Springer, 1987) p. 277
30. V I Krinichnyi, O Ya Grinberg, I B Nazarova, L I Tkachenko, G I Kozub, M L Khidekel' *Izv. Akad. Nauk SSSR, Ser. Khim.* **467** (1985)
31. V I Krinichnyi, A E Pelek, Ya S Lebedev, L I Tkachenko, G I Kozub, A L Barra, L C Brunel, J B Robert *Appl. Magn. Reson.* **7** 459 (1994)
32. Z Wilamowski, B Oczkiewicz, P Kacmar, J Blinowski *Phys. Status Solidi B* **134** 303 (1986)
33. M Nechtschein, F Devreux, F Genoud, M Guglielmi, K Holczer *Phys. Rev. B, Condens. Matter.* **27** 61 (1983)
34. A M Vasserman, A L Kovarskii *Spinovye Metki i Zondy v Khimii i Fizike Polimerov* (Spin Labels and Probes in the Chemistry and Physics of Polymers) (Moscow: Nauka, 1986)
35. H Winter, G Sachs, E Dormann, R Cosmo, H Naarmann *Synth. Met.* **36** 353 (1990)
36. A E Pelek, L M Goldenberg, V I Krinichnyi *Synth. Met.* **44** 205 (1991)
37. A L Buchachenko, in *Kompleksy Radikalov i Molekulyarnogo Kisloroda s Organicheskimi Molekulami* (Complexes of Radicals and Molecular Oxygen with Organic Molecules) (Moscow: Nauka, 1984) p. 158
38. A Reddoch, S Konishi *J. Chem. Phys.* **70** 2121 (1979)
39. A Abragam *Principles of Nuclear Magnetism* (London: Oxford University Press, 1961)

40. F Devreux, F Genoud, M Nechtschein, B Villeret, in *Electronic Properties of Conjugated Polymers* (Eds H Kuzmany, M Mehring, S Roth) (Berlin: Springer, 1987) p. 270
41. A A Syed, M K Dinesan *Talanta* **38** 815 (1991)
42. A J Epstein, A G MacDiarmid *J. Mol. Electron.* **4** 161 (1988)
43. M Lapkowski, E M Genies *J. Electroanal. Chem.* **279** 157 (1990)
44. A G MacDiarmid, A J Epstein, in *Science and Application of Conducting Polymers* (Eds W R Salaneck, D T Clark, E J Samuelson) (Bristol: Adam Hilger, 1991) p. 86
45. K Mizoguchi, M Nechtschein, J-P Travers, C Menardo *Phys. Rev. Lett.* **63** 66 (1989)
46. Z H Wang, E M Scherr, A G MacDiarmid, A J Epstein *Phys. Rev. B, Condens. Matter.* **45** 4190 (1992)
47. F Lux, G Hinrichsen, C Christen, V I Krinichnyi, I B Nazarova, S D Cheremisow, M-M Pohl *Synth. Met.* **53** 347 (1993)
48. S M Long, K R Cromack, A J Epstein, Y Sun, A G MacDiarmid *Synth. Met.* **55** 648 (1993)
49. J G Masters, J M Ginder, A G MacDiarmid, A J Epstein *J. Chem. Phys.* **96** 4768 (1992)
50. B Z Lubentsov, O N Timofeeva, S V Saratovskikh, V I Krinichnyi, A E Pelekh, V I Dmitrenko, M L Khidekel *Synth. Met.* **47** 187 (1992)
51. A A Al'tshuller, B M Kozyrev *Elektronnyi Paramagnitnyi Rezonans Soedinenii Elementov Promezhutochnykh Grupp* (Electron Paramagnetic Resonance of Compounds of Intermediate Group Elements) (Moscow: Nauka, 1972) p. 571
52. A Carrington, A D MacLachlan *Introduction to Magnetic Resonance* (New York: Harper and Row, 1967)
53. P R Gullis *J. Magn. Reson.* **21** 397 (1976)
54. A E Pelekh, V I Krinichnyi, A Yu Brezgunov, L I Tkachenko, G I Kozub *Vysokomol. Soedin.* **33** 1731 (1991)
55. G M Bartenev, S Ya Frenkel', in *Fizika Polimerov* (The Physics of Polymers) (Leningrad: Khimiya, 1990) p. 430
56. J S Hyde, L R Dalton, in *Spin Labeling. Theory and Application* Vol. 2 (Ed. L Berliner) (New York: Academic Press, 1979) p. 1
57. M A Butler, L R Walker, Z G Soos *J. Chem. Phys.* **64** 3592 (1976)
58. K Mizoguchi, M Nechtschein, J-P Travers *Synth. Met.* **41** 113 (1991)
59. J S Blakemore *Solid State Physics* (Cambridge: Cambridge University Press, 1985)
60. S Kivelson *Phys. Rev. B, Condens. Matter.* **25** 3798 (1982)
61. A J Epstein, in *Handbook of Conducting Polymers* Vol. 2 (Ed. T E Scotheim) (New York: Marcel Dekker, 1986) p. 1041
62. G Paasch *Synth. Met.* **51** 7 (1992)
63. M El Kadiri, J P Parneix, in *Electronic Properties of Polymers and Related Compounds* (Eds H Kuzmany, M Mehring, S Roth) (Berlin: Springer, 1985) p. 183
64. P Kuivalainen, H Stubb, H Isotalo, P Yli-Lahti, C Holmström *Phys. Rev. B, Condens. Matter.* **31** 7900 (1985)
65. J Patzsch, H Gruber, in *Electronic Properties of Polymers and Related Compounds* (Eds H Kuzmany, M Mehring, S Roth) (Berlin: Springer, 1985) p. 121
66. N F Mott, E A Davis *Electronic Processes in Non-Crystalline Materials* (Oxford: Clarendon Press, 1979)
67. H-K Roth, H Gruber, E Fanghänel, Trinh vu Quang *Prog. Colloid Polym. Sci.* **78** 75 (1988)
68. H-K Roth, W Brunner, G Volkel, M Schrödner, H Gruber *Makromol. Chem., Makromol. Symp.* **34** 293 (1990)
69. V I Krinichnyi, A E Pelekh, H-K Roth, K Lüders *Appl. Magn. Reson.* **4** 345 (1993)
70. F Devreux, H Lecavelier *Phys. Rev. Lett.* **59** 2585 (1987)
71. A Madhukar, W Post *Phys. Rev. Lett.* **39** 1424 (1977)
72. E A Silin'sh, M V Kurik, V Chapek, in *Elektronnye Protssessy v Organicheskikh Molekulyarnykh Kristallakh: Yavleniya Lokalizatsii i Polyarizatsii* (Electronic Processes in Organic Molecular Crystals: Localisation and Polarisation Phenomena) (Riga: Zinatne, 1988) p. 177
73. E A Silin'sh, in *Proceedings of the XIth Symposium on Molecular Crystals, Lugano, Switzerland, 1985*, p. 277

Positively charged lipids: structure, methods of synthesis, and applications

I D Konstantinova, G A Serebrennikova

Contents

I. Introduction	537
II. The structure and synthesis of positively charged lipids	537
III. Applications of positively charged lipids	543

Abstract. Data on the structure, methods of synthesis, and applications of positively charged lipids are presented. Their likely usefulness as antitumour and antiviral agents and also as antagonists of the platelet activating factor and transfection mediators is demonstrated. The bibliography includes 80 references.

I. Introduction

There has been a considerable growth of interest in recent years in a new type of modified glycerolipids containing a positively charged group (cationic lipids). Such interest in compounds of this class is due to the possibility of their wide scale employment in the transportation of genetic material and other macromolecules into cells of animal origin and plant protoplasts and also in the creation of artificial membranes with an affinity for negatively charged cell surfaces. Their antitumour activity, partly associated with the inhibition of protein kinase C and diacylglycerol kinase, is also known. Many representatives of cationic lipids inhibit effectively the replication of the HIV-1 virus. In addition, promising antagonists of the lipid bioregulator — the platelet activating factor (PAF) have been discovered among them. All these features lead to the possibility of devising chemotherapeutic preparations of a new type on the basis of positively charged lipids.

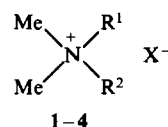
II. The structure and synthesis of positively charged lipids

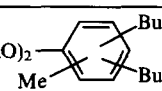
Among positively charged lipids, particular attention has been devoted to glycerol derivatives. Cationic glycerolipids have a wide variety of structures, but their common feature is the presence of a positively charged head, an intramolecularly uncompensated negatively charged group, and one or several long-chain substituents in the hydrophobic part of the molecule. It has been established that the length of the chains of the substituents at the C(1) and C(2) atoms of glycerol, the type of cationic head, and also

the presence of a spacer group, separating it from the glycerol fragment, exert a significant influence on the biological activity exhibited by a particular compound.

1. Tetraalkylammonium derivatives

The quaternary ammonium detergents 1–4 in liposomes have found applications in the transfection of genetic material into cells of animal origin.^{1–3}



Com- pound	Name ^a	R ¹	R ²	X
1	DEBDA	CH ₂ C ₆ H ₅	(C ₂ H ₄ O) ₂ 	OH
2	DTAB	Me	(CH ₂) ₁₁ Me	Br
3	TTAB	Me	(CH ₂) ₁₃ Me	Br
4	CTAB	Me	(CH ₂) ₁₅ Me	Br

^a DEBDA = diisobutylcresoxyethoxyethyltrimethylbenzylammonium hydroxide, DTAB = dodecyltrimethylammonium bromide, TTAB = tetradecyltrimethylammonium bromide, CTAB = cetyltrimethylammonium bromide.

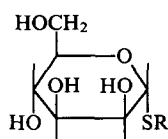
These cationic lipids are fairly widely distributed and are cheap. They can be synthesised by simple chemical reactions and can be incorporated in liposomes having different compositions in order to stabilise the bilayer. The tetraalkylammonium derivatives 5 and 6, incorporating carbohydrates as the structural fragments (the so-called bolaamphiphiles) are regarded as promising amphiphiles for negatively charged polyelectrolytes such as nucleic acids. The presence of the electrically neutral carbohydrate fragment at one end of the long-chain residue and of an electro-positive group at the other ensures their amphiphilic properties.⁴

The mannose bolaamphiphiles 5 have been synthesised by alkylating thio- α -D-mannopyranose with the corresponding ω -iodo(or bromo)- α -trimethylalkylammonio-derivatives.

I D Konstantinova, G A Serebrennikova Department of Chemistry and Technology of Fine Organic Compounds, M V Lomonosov Moscow State Academy of Fine Chemical Technology, 86 prosp. Vernadskogo, 117571 Moscow, Russian Federation. Fax (7-095) 430 79 83. Tel. (7-095) 437 19 25 (I D Konstantinova)

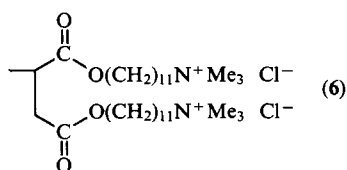
Received 12 July 1995

Uspekhi Khimii 65 (6) 581–598 (1996); translated by A K Grzybowski



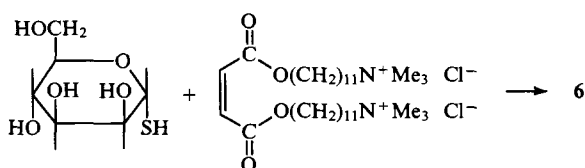
5a-d, 6

R = (CH₂)₁₁C(O)O(CH₂)₂N⁺Me₃ Cl⁻ (5a),
 (CH₂)₁₁C(O)NH(CH₂)₂N⁺Me₃ Cl⁻ (5b),
 (CH₂)₁₁C(O)O(CH₂)₁₁N⁺Me₃ Cl⁻ (5c),
 (CH₂)₉C(O)O(CH₂)₁₁C(O)NH(CH₂)₂N⁺Me₃ I⁻ (5d),

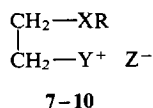


(6)

The bolaamphiphile 6, containing two hydrocarbon chains, has been obtained by adding thiomannose to the corresponding maleic acid diester.



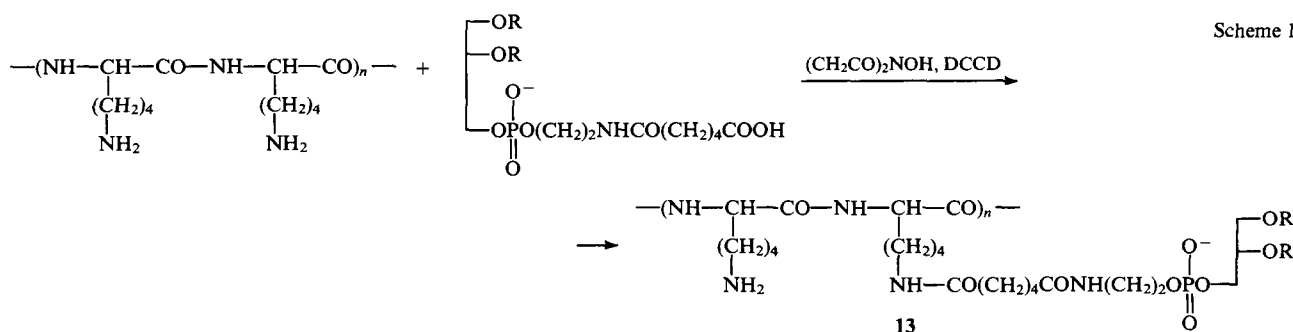
In order to investigate the influence of a series of quaternary ammonium derivatives of types 7–10 on normal and neoplastic cells, a series of such derivatives have been synthesised.^{5–7}



7–10

Compound	R	X	Y	Z
7	(CH ₂) _n Me, n = 14, 16	OC(O)	N(Me) ₂ (CH ₂) ₂ OH	Br
8	H, Ph, (CH ₂) _n Me, n = 11, 13, 15, 17	O	N(Me) ₂ (CH ₂) _n OH, n = 2–4	I
9	(CH ₂) ₁₅ Me	S	N(Me) ₂ (CH ₂) ₂ OH, NC ₅ H ₅	Br
10	(CH ₂) ₆ Me	OC(O)	NMe ₃	I

The synthesis of these compounds is based on the quaternisation of tertiary amines or aromatic heterocyclic bases by β-haloethanolamine with subsequent alkylation or acylation of the free hydroxy-group.

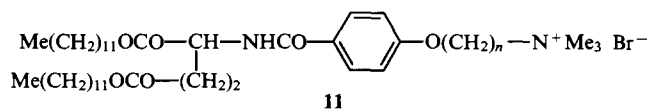


Scheme 1

2. Synthetic amphiphiles — aminoacid derivatives

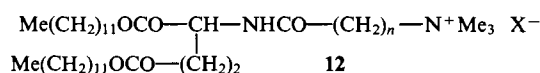
Lipophilic derivatives of aminoacids, peptides, and polyamines have proved fairly effective in the transfection of DNA into eukaryotic cells.

The new cationic amphiphiles 11 and 12 have been recently synthesised from glutamic acid.⁸



11

n = 2, 4, 6, 8



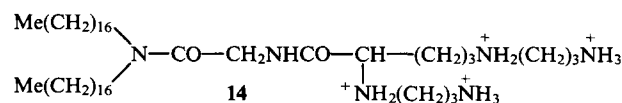
12

n = 1, X = Cl; n = 5, X = Br

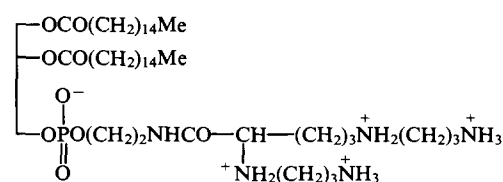
Lipopoly-L-lysine 13 (LPLL) has been attained in accordance with Scheme 1 by the reaction of poly-L-lysine and N-glutarylphosphatidylethanolamine in the presence of N-hydroxysuccinimide and dicyclohexylcarbodiimide (DCCD).⁹

Compound 13 usually includes two molecules of the phospholipid per poly-L-lysine molecule.

Lipophilic polyamines — the lipospermines 14 and 15 — have proved to be effective mediators of the transfection of DNA.¹⁰

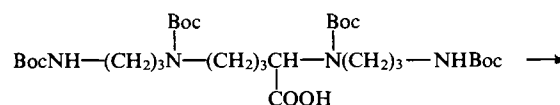


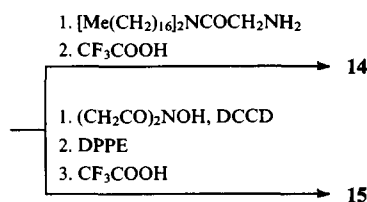
14



15

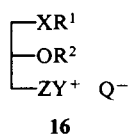
The lipospermines 14 and 15 have been synthesised by the reaction of protected L-5-carboxyspermine with the lipophilic glycine N,N-diheptadecylamide and dipalmitoylphosphatidylethanolamine (DPPE) respectively.





3. Cationic lipids — glycerol derivatives

The commonest type of cationic lipids may be represented by the general formula 16.^{11–15}



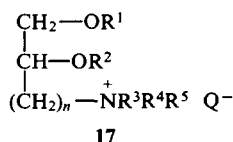
X = O, S, or OCONH; R¹ = alkyl, alkenyl, and acyl (C₁₀–C₂₀), alkyls with aromatic and heterocyclic residues, etc.; R² = long-chain (C₁₀–C₂₀) or short-chain (C₁–C₈) alkyl and acyl substituents; Z = spacer groups of different types (their absence is also possible); Y⁺ = ammonium and sulfonium groups or heterocyclic heads in which positively charged nitrogen or sulfur atoms are incorporated; Q = Hal, AcO, TsO, etc. counterions.

Depending on the nature of the substituents R¹ and R² in the hydrophobic part of the molecule, the cationic lipids of a given type can be subdivided into several varieties, which determine the methods of their synthesis and their applications:

- (a) positively charged lipids with long-chain alkyl substituents [R¹ = R² = Alkyl(C₁₀–C₂₀)];
- (b) lipids with long-chain and short-chain alkyl substituents [R¹ = Alkyl(C₁₀–C₂₀), R² = Alkyl(C₁–C₈)];
- (c) cationic glycerolipids with long-chain acyl substituents;
- (d) mixed type lipids containing alkyl, acyl, acylcarbamoyl, and other types of long-chain and short-chain substituents in various combinations.

a. Cationic lipids with long-chain alkyl substituents

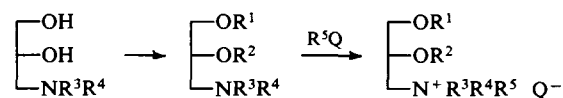
The compounds having the general formula 17 are used for the transfection of various biologically active substances (nucleosides, polynucleotides, peptides, hormones, etc.), containing a negatively charged section, into cells of animal origin and plant protoplasts.^{11–15}



R¹ = R² = alkenyl or alkyl (C₁₀–C₂₀); R³ = R⁴ = R⁵ = Me or Et; n = 1–4 (predominantly n = 1); Q = Hal

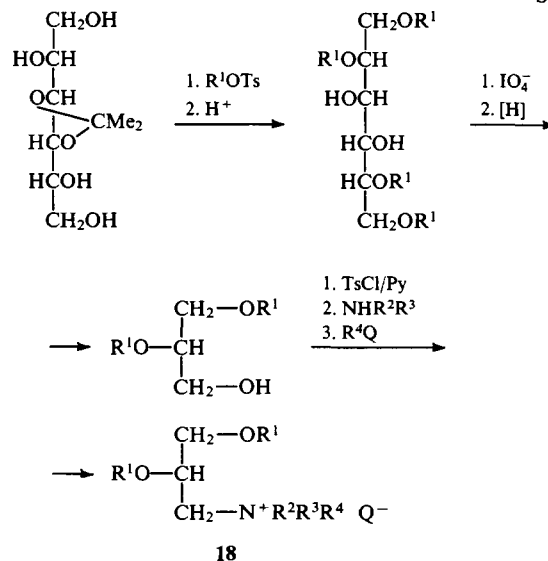
These lipids are usually incorporated in liposomes produced from phosphatidylcholine (PC) or phosphatidylethanolamine (PE) in the molar proportions cationic lipid : phospholipid = 1 : 1. This ratio may vary depending on the type of the transfected substance and the target cells.^{11, 12, 14}

The scheme used in the synthesis of the lipids 17 is fairly simple and includes stages involving the alkylation of the aminodiols system with subsequent quaternisation of the amino-group.^{11, 12}

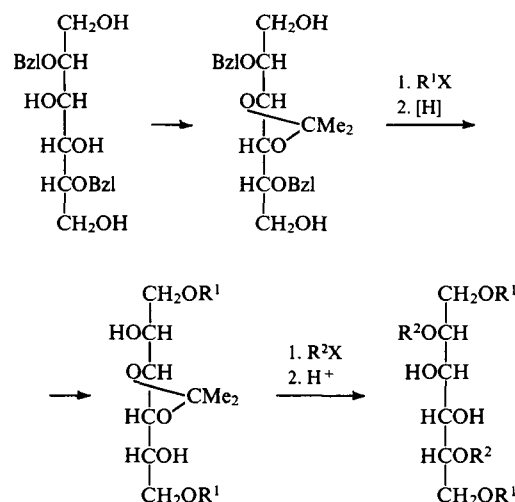


Racemic mixtures are usually obtained via this scheme with R¹ = R², while R³, R⁴, and R⁵ are different or the same but are not incorporated into aromatic systems. Optically active compounds of this type [(S)-isomers] are synthesised via Scheme 2 from 3,4-isopropylidene-D-mannitol.¹⁴

Scheme 2



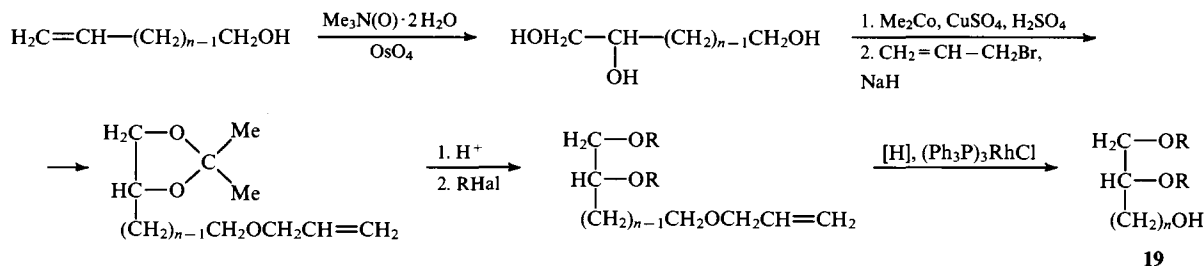
Optically active compounds with various alkyl residues R¹ and R² are synthesised from 2,5-dibenzyl-D-mannitol.



Positively charged glycerolipids of the alkyl type with various substituents in the hydrophobic part of the molecule are then synthesised similarly to Scheme 2.

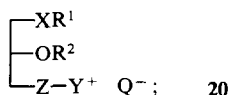
In order to obtain compounds containing a spacer group comprising 2–8 methylene groups, the derivative 19 is synthesised initially (Scheme 3) and is then converted into cationic lipids by the method described above.

Scheme 3



b. Positively charged lipids with long-chain and short-chain substituents of the alkyl type

This group of lipids has been investigated most vigorously because its representatives exhibit an inhibiting activity on the growth of neoplastic cells and are also effective antagonists of the lipid bioregulator of the platelet activating factor. Certain compounds are capable of suppressing the development of the HIV-1 virus. In a general form, the structure of such glycerolipids can be represented as follows:



X = O or S;

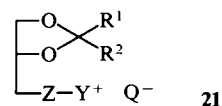
R¹ = alkenyl or alkyl (C₁₀–C₂₀), a branched alkyl, an alkyl with aromatic substituents, naphthylaryl, or aryl;

R² = alkyl (C₁–C₄), a cyclic alkyl, heterocycles (pyridine, triazoline, pyrazine, etc.), H, or CH₂CF₃;

Z = bond, O(CH₂)_n (n = 1–7), (OCH₂CH₂)_n (n = 1–3), S(CH₂)_n (n = 1, 2), a spacer group of the alkyl or arylalkyl type, etc.;

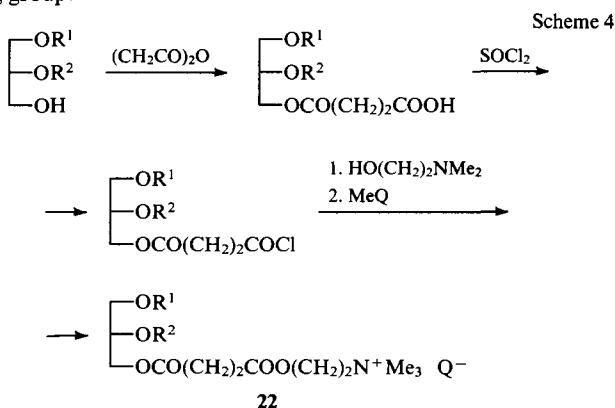
Y = NR¹R²R³, where R¹ = R² = R³ = Me or Et, R¹ = R² = Me and R³ = (CH₂)₂OH or (CH₂)₃OH, or R¹, R², and R³ may be combined into heterocycles; Q = Hal, MsO, TsO, etc.

The groups R¹ and R² may be combined into an acetal ring with a long-chain alkyl group (for example, R¹ = C₁₇H₃₅ and R² = H).^{16, 17}

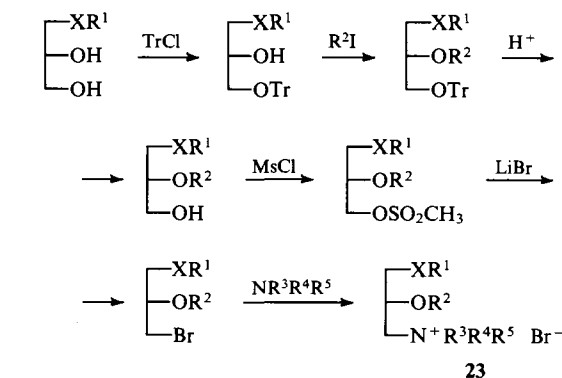


The cationic glycerolipids **22**, containing a spacer group of the succinyl type, are synthesised in accordance with Scheme 4.^{18, 19}

The synthesis of compound **23**, containing a cationic group attached directly to the glycerol fragment, involves the preliminary preparation of disubstituted glycerols using a trityl protecting group.¹⁶

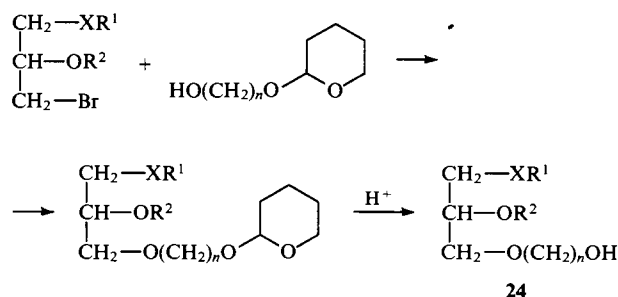


Scheme 4



Various approaches are used in the preparation of compounds containing a spacer group depending on the structure of the latter.

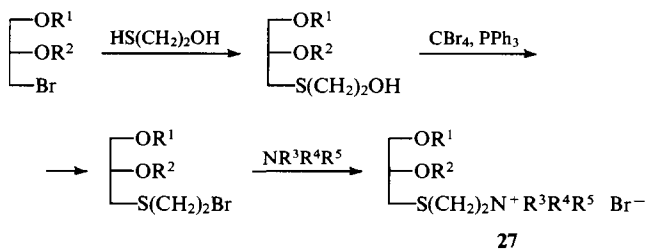
If the quaternary ammonium group is separated from the glycerol fragment by several methylene groups, compound **24** is synthesised and then converted into cationic lipids by traditional methods.¹⁶



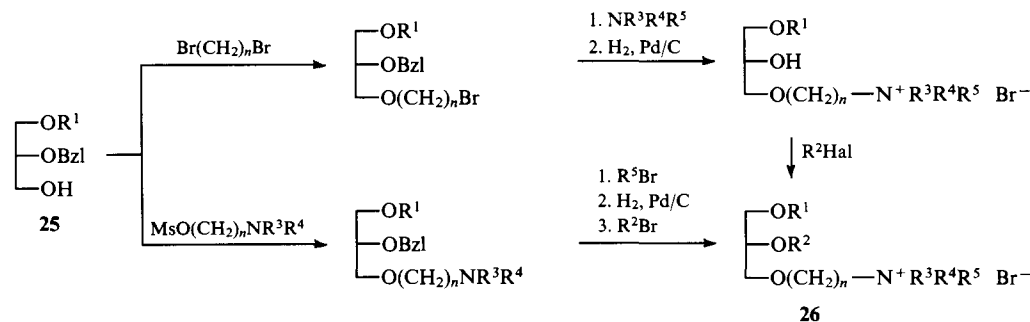
The 3-(2-hydroxyethoxy)- and 3-[2-(2-hydroxyethoxy)-ethoxy]-residues are also used as spacer groups. They are introduced into the molecule by treating the corresponding tosyl derivatives of mono- or di-alkylglycerols with ethylene glycol or diethylene glycol.²⁰

A series of cationic lipids **26** with a spacer group have been obtained from 1-O-alkyl-2-O-benzyl-*rac*-glycerols **25** (Scheme 5).^{21, 22}

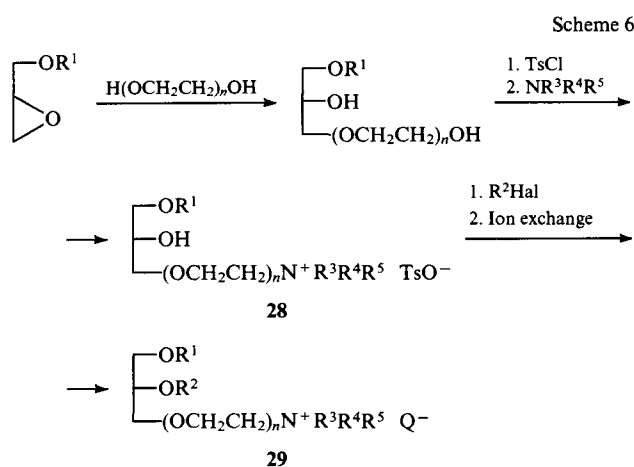
The synthesis of positively charged lipids **27**, having an ethylthio spacer group, has been reported.^{6, 23}



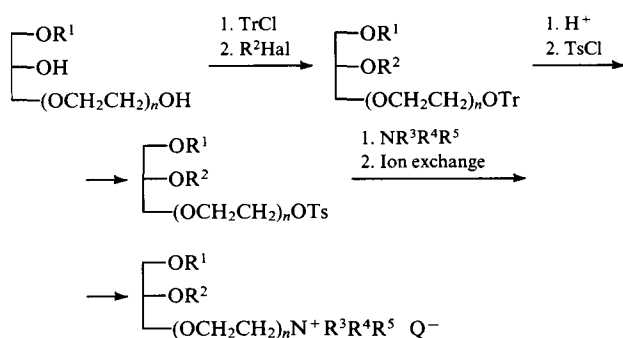
Scheme 5



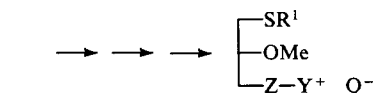
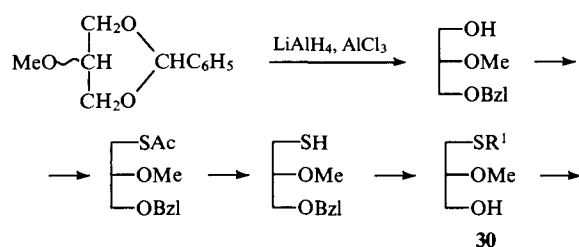
Compounds of types **28** and **29**, containing heterocycles as the substituent R^2 and the $(OCH_2CH_2)_n$ group as the spacer, are synthesised in accordance with Scheme 6.²⁴



The scheme may be modified by employing the trityl protecting group.



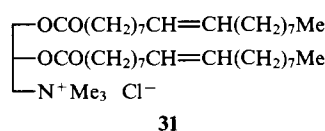
The method involving the reductive cleavage of cyclic acetals has been used in the synthesis of the disubstituted thioglycerol derivative **30**, which is converted into cationic lipids by traditional methods.²⁵



Together with lipids containing alkylammonium groups as the polar head, compounds incorporating various heterocycles have been obtained.^{22, 26, 27}

c. Cationic lipids with long-chain acyl substituents

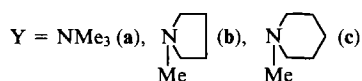
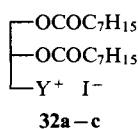
2,3-Dioleoyloxypropyltrimethylammonium chloride **31** (DOTAP) is one of the commonest glycerolipids of this series.



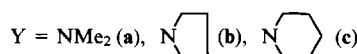
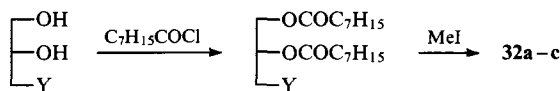
This lipid is used to investigate the processes involving the fusion of liposomes carrying opposite charges, the mixing of the biologically active substances incorporated in them, and their possible transport through a liposomal bilayer.

DOTAP is synthesised by acylating 3-bromopropane-1,2-diol with subsequent quaternisation of the resulting compound with trimethylamine.²⁸

The synthesis of the positively charged lipids **32a–c** containing various cationic groups and higher aliphatic acid residues has been described.⁷



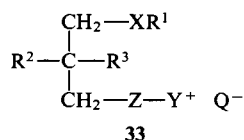
The general scheme for the synthesis of compounds **32** can be represented as follows:



Compounds **32a–c** are inhibitors of the membrane-bound protein kinase C to the same extent as cationic lipids of the alkyl ether type having a short-chain substituent at the C(2) atom of the glycerol fragment.⁷

g. Cationic lipids of the mixed type

Among positively charged glycerolipids of the mixed acylalkyl ether, alkyl ether, or acylcarbamoyl types, a series of effective antagonists of the platelet activating factor as well as compounds with antitumour activity have been discovered. This stimulated the study of the structure–function relations in this class of lipids and led to the synthesis of a large group of compounds having the general formula 33.



X = O, S, OCONH or SCONH;

R¹ = alkyl(C₈–C₂₀), (CH₂)₃OC₁₈H₃₇, (CH₂)₁₀NHCONHMe, CH₂–C₆P₄–Ph, etc.;

R² = OMe, OEt, OCOMe, OCOC₇H₁₅, OCH₂COMe, CH₂CN, NHCOOMe, OCOOMe, NHCONHMe, or heterocycles of the pyrrole, triazole, etc. type;

R³ = H or Me;

Z = O(CH₂)_n, (OCH₂CH₂)_n, OCO(CH₂)_n, (CH₂)_n, CH₂SO₂(CH₂)_n, NHCO(CH₂)_n, NHSO₂(CH₂)_n, N(COMe)SO₂(CH₂)_n, or OCONR(CH₂)_n

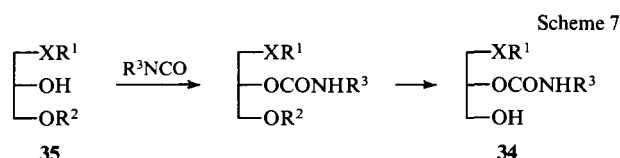
(R = H, Me, COMe, COEt, or COOMe; n = 1–6);

Y = NMe₃, NMe₂CH₂CH₂OH, various heterocycles in which a quaternary nitrogen atom is incorporated, etc.;

Q = Hal, MsO, TsO, etc.

Compounds of the alkylacyl type are synthesised in accordance with the general strategy developed for the preparation of dialkyl lipids with various substituents in the glycerol skeleton using the same selective protecting groups (Bzl, Tr, Ts, benzylidene) and alkylation, acylation, and thioalkylation methods.

The syntheses of compounds containing alkylcarbamoyl and alkoxy-carbonylamino-groups have specific features. They usually involve the preparation of the corresponding disubstituted glycerol derivatives with subsequent introduction of the cationic head by traditional methods.

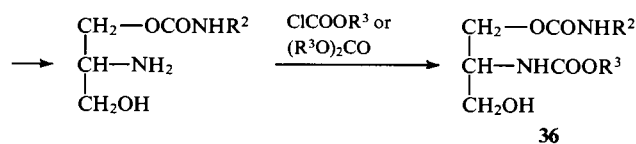
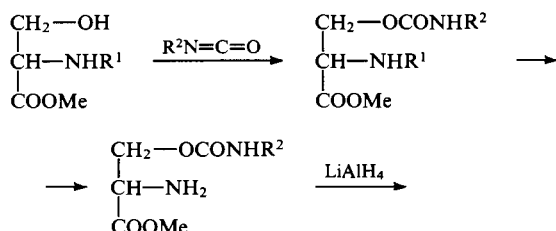


R² = protecting group; R³ = alkyl(C₁–C₃).

The overall strategy for the synthesis of the initial compounds 34 in the preparation of cationic lipids with an alkylcarbamoyl residue at the C(2) atom may be represented by Scheme 7.²⁵

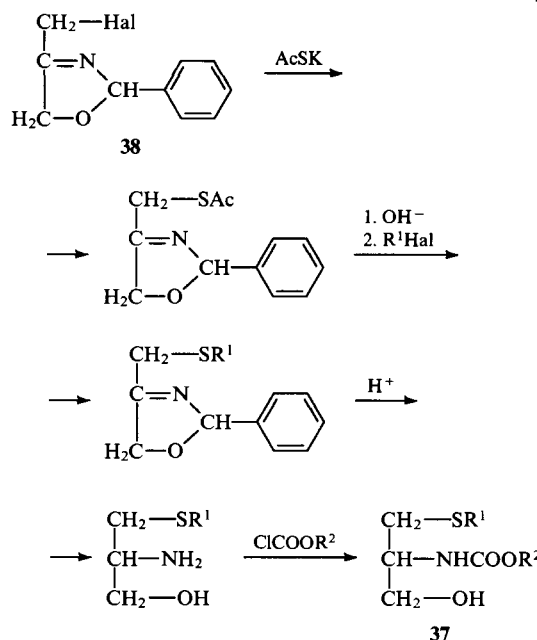
The alkylcarbamoyl group was introduced by the interaction of compound 35 with alkyl isocyanate in the presence of an acid catalyst (AlCl₃) and a base (pyridine, triethylamine).

Compounds 36, containing alkylcarbamoyloxy- and alkoxy-carbonylamino-groups at the C(1) and C(2) atoms respectively, are synthesised in the following manner:²⁵



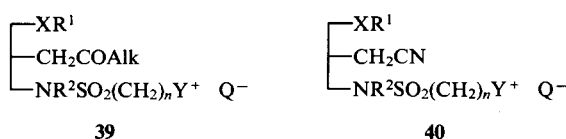
R¹ = protecting group; R² = alkyl(C₁₂–C₂₀); R³ = alkyl(C₁–C₄).

Compound 37, incorporating an alkylthio- and an alkoxy-carbonylamino-group at the C(1) and C(2) atoms respectively, was synthesised from the phenyloxazoline derivative 38 in accordance with Scheme 8.²⁵



R² = Alk(C₁–C₄).

The synthesis of the cationic lipids 39 and 40 with alkanoyl-methyl and cyanomethyl substituents at the C(2) atom of the glycerol fragment has been described in detail.^{20–22, 29}

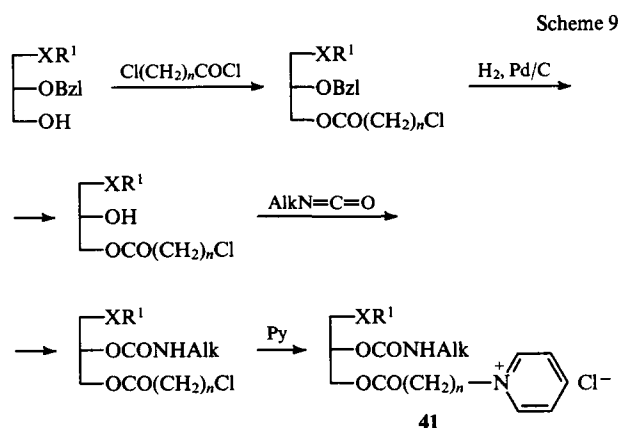


R² = H, Me, COMe, COEt, or COOMe; n = 1–6;

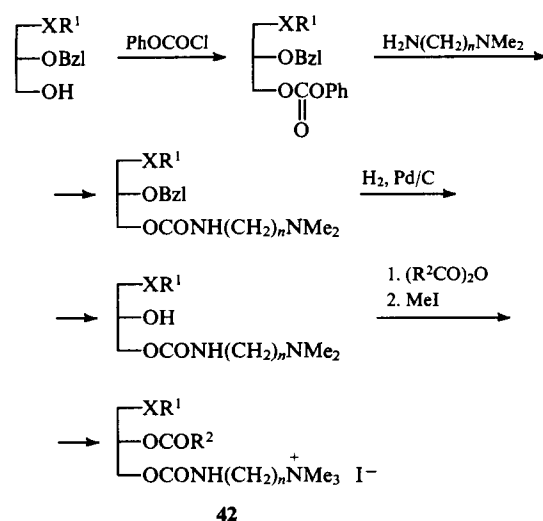
Y = NMe₃, NMe₂CH₂CH₂OH, various heterocycles in which a quaternary nitrogen atom is incorporated, etc.;

Q = Hal, MsO, TsO, etc.

The general approach to the synthesis of lipids 41 having the 1-alkyl-2-carbamoyl structure and containing a cationic head attached via a spacer group of the acyl type is presented in Scheme 9.^{22, 30} The cationic head with a spacer of the acyl type may be obtained via the acylation of the dialkylglyceride of a dimethylaminoalkanoic acid of a suitable type followed by the quaternisation of the dimethylamino-group with methyl iodide.^{31, 32}

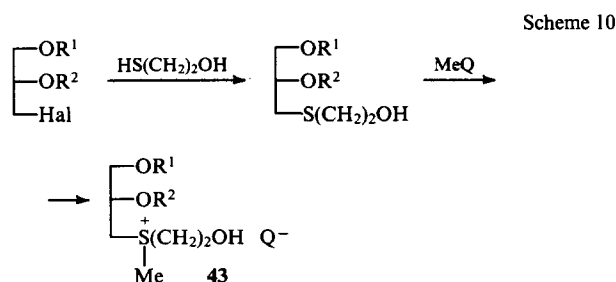


The positively charged lipids **42** — PAF antagonists with a carbamoyl structure — have been obtained by the following method.²⁹



f. Positively charged alkyl ether lipids with a sulfonium cationic head

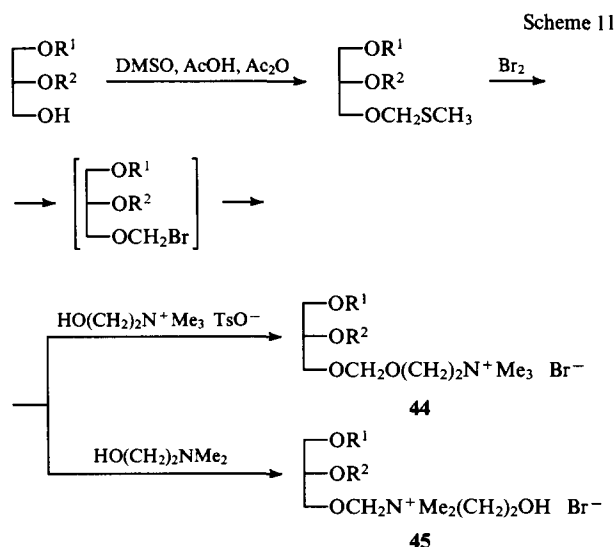
The type **43** lipids are of interest for the study of the mechanism of the inhibition of the membrane-bound protein kinase C (PKC), the growth of neoplastic cells, and the replication of the HIV-1 virus.^{6, 23} They are synthesised in accordance with Scheme 10.



$R^1 = C_{16}H_{33}, C_{18}H_{37}; R^2 = Me, Et; Q = I, TsO.$

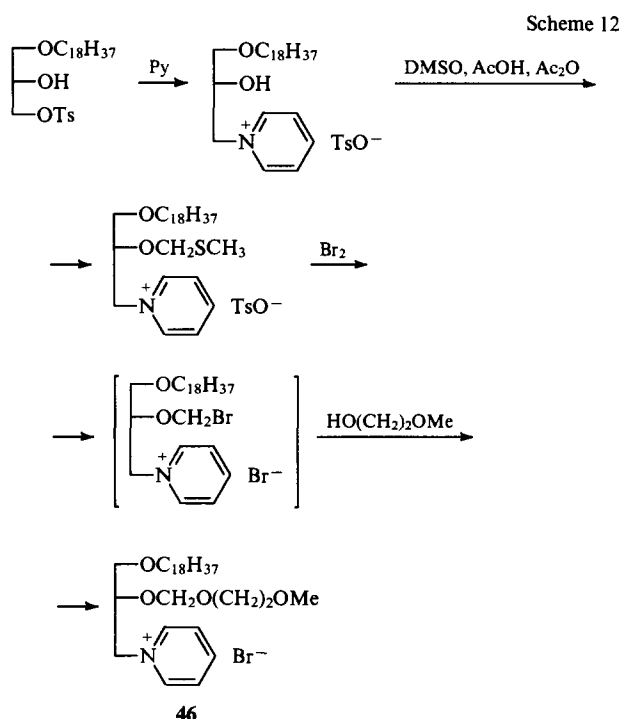
g. Positively charged lipids synthesised by the alkylthioalkylation reaction

Konstantinova et al.³³ were the first to demonstrate in lipid chemistry the possibility of using a modified Pummerer's rearrangement (the alkylthioalkylation reaction)³⁴ in the chemistry of lipids by introducing the $MeSCH_2$ group at a primary



$R^1 = C_{18}H_{37}; R^2 = Me, Et; R^1 = R^2 = C_{16}H_{33}.$

(Scheme 11) or secondary hydroxy-group (Scheme 12) of disubstituted glycerols **44–46**. Subsequent conversion of these highly reactive groups (asymmetric *O,S*-acetals) into α -bromoethers, capable of interacting readily with nucleophiles, leads to prospects for the synthesis of various modified lipids, including positively charged ones.



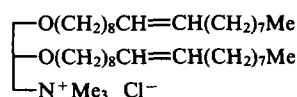
III. Applications of positively charged lipids

1. Cationic lipids in liposomology

Positively charged lipids form liposomes in an aqueous medium or in a buffer solution either individually or in a mixture with other natural phospholipids. For example, an active preparation, known as lipofectin, includes the cationic lipid DOTMA[†] **47** and

[†] *N*-[1-(2,3-dioleoyloxy)propyl]-*N,N,N*-triethylammonium salt.

PE; in molar proportions ranging from 1 : 1 to 3 : 7 depending on the type of cultures of the cells used in transfection.^{11, 12, 14, 35}



47

Cationic liposomes are obtained similarly from the quaternary ammonium derivatives 1–4 (DEBDA, DTAB, TTAB, and CTAB), which exert a stabilising effect on the bilayers formed by PE.^{1, 36, 37} DTAB stabilises the bilayers more effectively than the TTAB and CTAB analogues, the amount of which required to achieve a similar effect is twice as great.

The mechanism of the interaction of cationic liposomes with liposomes incorporating negatively charged or zwitterionic phospholipids has been widely investigated in recent years.^{36–39} The elucidation of the details of this process may explain the interaction of the positively charged liposomes with the cell membrane during the transfection process. It has been shown that the populations of such liposomes may interact with one another in various ways which depend on the lipid composition of the membrane surface and on the ionic strength of the medium.

It has been established that liposomes containing DOTMA and PE interact with the negatively charged membrane lipids and fuse with the cell surface. Different anions can also induce the fusion of cationic liposomes. Thus, for the DOTMA/PE (1 : 1) liposomes, the influence of the anions on the degree of fusion decreases in the sequence citrate > ethylenediaminetetraacetate > phosphate. It is of interest that these liposomes were entirely resistant to fusion in the presence of polyanions. Liposomes of the DOTMA/PE and DOTMA/PC types may fuse at a high citrate concentration. The negatively charged phosphatidylserine (PS) exerts a similar effect even in the absence of polyanions. The interaction of the negatively charged groups in PS with the quaternary ammonium group of DOTMA or DOTAP 31 is apparently sufficient for the fusion of the membranes containing these lipids, while the zwitterionic phospholipid component of these membranes is an additional and decisive factor for membrane conductivity.¹⁵

It is essential to note that the fusion of liposomes in the presence of anions is influenced significantly by the size of the liposomes. For example, liposomes 300 nm in diameter, the composition of which includes didodecylammonium bromide, fuse in the presence of dipicolinic or toluene-*p*-sulfonic acid. On the other hand, if the diameter of the liposomes is < 200 nm, no fusion occurs and only aggregation is observed.¹⁵

Fusion results in the formation of a complex between the liposomes and the anion, which is preceded by the dehydration of the surface of the liposome. Studies are planned in the future on the quantitative determination of the binding capacities of a wide variety of anions in relation to cationic lipids in liposomes and on the determination of the possible dehydration of liposomes in the presence of anions.²⁸

It has been shown that the DOTMA/PC/PE mixed liposomes are entirely resistant to fusion in the presence of polyanions. However, when they were mixed with liposomes containing negative charges on the surface, aggregates were formed readily at the physiological or lower ionic strength. The PC/PE ratio in liposomes has a considerable influence on the degree of aggregation even under the conditions where it is not followed by coalescence (i.e. the mixing of the lipids of the bilayer and/or aqueous compositions). The degree of aggregation is higher the greater the PC/PE ratio. These observations may be useful for the study of the interaction between liposomes having different lipid compositions and also for providing investigators with systems in which the interaction between liposomes is independent of the bond between ions and the lipid surface. The tendency of liposomes to become associated with one another can be readily controlled by varying the ionic composition of the medium.^{15, 28}

The mechanism of the interaction of the DOTMA/PE vesicles with the plasma membranes of cultured cells has not been elucidated. It may be that the binding of DOTMA to the negatively charged sialic acid in gangliosides leads to the destabilisation of the plasma membrane and the coalescence of the liposomes with cells. It is essential to note that cationic liposomes containing cationic amphiphiles with ether and ester bonds interact equally readily with the cell membrane. Furthermore, liposomes containing fluorescent labels are readily disrupted after being incorporated in CV-1 cells.^{28, 40} One of the most interesting properties of positively charged liposomes with a high PE content is their ability to interact with membranes containing surface proteins. Liposomes formed from DOTMA/PE are readily adsorbed on erythrocytes in a medium with the physiological ionic strength.²⁸

A fairly important property of the lipofectin preparation is its toxicity for cells *in vitro* following an increase in the concentration of the cationic lipid above a certain level. The toxicity of the preparations is different for different types of cells and depends on the duration of exposure and the density of the cell culture. It is therefore necessary to optimise the transfection parameters for each cell line.

The quaternary ammonium derivatives 1–4 are even more toxic to the transfected cells. Therefore, out of all the above compounds, the least toxic CTAB is most often employed. It is a cheaper and readily available substitute for DOTMA and DOTAP. Similar observations have been made also for another cationic lipid, namely DEBDA, which is used in studies on plant protoplasts.¹

2. Positively charged lipids as transfection mediators

One of the most interesting fields of medicine — genetic therapy — has been rapidly developing recently. It is essential for the correction of genetic cell defects and for the treatment of genetic diseases. In order to correct genetic defects, normal exogenous genes are introduced into the target cell, where they or the products of their vital activity act together with the defective molecules or replace the latter and hence assist the cell in its normal functioning.

One of the main tasks in genetic therapy is the search for methods which are suitable for the specific and effective introduction of genetic material. It has been shown that under exceptional conditions eukaryotic cells may receive DNA molecules, a proportion of which are localised in the nucleus. However, owing to its large size and charge, the spontaneous permeation of DNA into the cell and its subsequent expression into the nucleus (transfection) are difficult. For this reason, various methods facilitating this process, i.e. inducing cell fusion under specially selected conditions, or mediators of DNA gene transfection have been used. Employment of calcium phosphate, liposomes, retrovirus vectors, electroporation, and microinjection may be included among the effective methods for the transfection of genetic material. In certain cases, the application of polycations such as polylysine, DEAE-dextran, and polyornithine yields satisfactory results. However, all these methods are characterised by a low effectiveness, an unstable introduction of genes, and a poor reproducibility. Furthermore, the compounds employed in this procedure are frequently toxic to the target cells.^{11, 12}

The most modern DNA-transfection methods employ positively charged liposomes as mediators. The use of liposomes capable of transferring genetic material into cells via fusion with the cell membrane is of special interest. Cationic lipids with various structures (compounds 1–4, 11–17, and 47) form together with PE and PC positively charged liposomes which spontaneously produce complexes with polynucleotides. These complexes are adsorbed by the cell surface, fuse with the plasma membrane, and transfer the genetic material to the cytoplasm. Further study of the positively charged liposomes can therefore lead to the creation of convenient and effective systems for the introduction of various biologically active substances into the cell:

nucleosides oligo- and poly-nucleotides, hormones, proteins, and other natural and synthetic macromolecules with a negatively charged section.¹⁴

The current break-through in transfection arose from the preparation lipofectin. It is convenient to use and is effective.^{11–14, 41, 42} The DNA — lipofectin (DOTMA/PE) complex has a network of positive charges, which facilitate its interaction with the negative charges of glycolipids and glycoproteins on the surface of the cell membrane.¹¹

The quaternary ammonium derivatives 1–4 are also sometimes used for DNA transfection. Although the transfecting activity of liposomes containing these compounds is somewhat lower than the activity of lipofectin, nevertheless they can be used as cheap readily available substitutes.^{1, 13, 15, 40, 43}

Apart from DNA transfection, lipofectin is used for the effective introduction of RNA into cells of animal origin and also into the protoplasts of a number of plants. By employing this method, it is possible to introduce up to 70% of RNA.² The RNA — lipofectin complexes are used to investigate the stability of mRNA when they are introduced into cell tissues and embryos. This may lead to the development of a technology in which RNA is used as a medicinal preparation.¹³

Lipofectin is a simple and convenient preparation whereby one can obtain various specific tissue cells or cell lines infected by whole viruses or only by virus vectors in the absence of homologous virus receptors.⁴²

Communications concerning the possibility of the transfection of the vector for the expression of cDNA luciferase into the brain cells of the *Xenopus* and mouse embryos, which permits the lipofection (transfection with the aid of lipofectin) of various functional genes into the cells of the central nervous systems of embryos, have appeared recently.^{42, 44}

The bolaamphiphiles 5 and 6 are also used as ideal amphiphiles for polyanions. The positively charged end of the bolaamphiphile molecule may bind a negatively charged polyanion in aqueous solutions even if it is only sparingly soluble in the latter. However, since these compounds do not possess aliphatic chains arranged in parallel, they are unable to form a stable bilayer. They are therefore more frequently used as models for the investigation of the interaction of liposomes and cell membranes with polyelectrolytes.⁴

Cationic liposomes, prepared by the sonication of aqueous dispersions of lipids or by employing solubilising detergents, are used to incorporate horseradish peroxidase into human erythrocytes *in vitro*. The stability of the modified erythrocytes has been investigated from the standpoint of photohemolysis.³⁵

Behr *et al.*¹⁰ developed a highly effective transfection method based on the ionic binding of plasmids to the lipopolyamines 14 and 15. This procedure has been used for the transfection of lipopolyamines into the endocrine cells of the intermediate lobe of the pituitary gland. Such transfection did not entail changes in the membrane-dependent receptors and did not affect the physiological regulation of the biosynthesis of hormones. The cationic lipopolyamines 14 and 15 do not exert a toxic activity on cells and may be used for the transfection of chromaffine cells and the neurones of the central nervous system. It is of interest that the method does not affect the normal cell growth or the electrochemical characteristics of the peripheral neurones. The introduction of DNA into the epidermal human keratinocytes has also been achieved with the aid of lipopolyamines.⁴⁵

The so called lipopolylysines 13 are some of the most effective mediators of DNA transfection.⁹ Poly-L-lysine is used as the starting material for the synthesis of this preparation because of its biodegradability on entering the cell, in contrast to poly-D-lysine. This preparation is used in the individual state, since its liposomal form (with PC or PE) exhibits only 50% of the activity of the individual form in DNA transfection. Lipopolylysine preparations are at present some of the most active and relatively cheap mediators of the DNA transfection of type L929 mouse cells and human HeLa cells as well as the monkey Vero cells.

The data presented indicate the possibility of using lipofection under *in vivo* conditions. The method using DOTMA, or its analogues belonging to the series of diolealkyl derivatives containing a hydroxyalkyl chain in the quaternary ammonium head, as the cationic lipid has been recognised nowadays as optimal. These compounds enter into the composition of liposomes in a mixture with dioleoylphosphatidylethanolamine (50 mol %).^{46–48}

An aerosol method for the introduction of plasmids for the expression of chloroamphenicol acetyltransferase, which makes it possible to achieve a high lung-specific level of its production in the mouse organism *in vivo*, has been developed recently.⁴⁹

Promising results have been obtained in the lipofection of plasmids, coding the synthesis of the human growth hormone, via the introduction of the preparation intravenously into the mouse organism.⁵⁰

It has been shown that the direct intravenous introduction of DNA — cationic liposome complexes into the organisms of adult animals transfects effectively all types of tissues (the endothelial tissues of blood vessels and the parenchymal cells of the lungs, spleen, lymph nodes, and bone marrow). The expression of the genes introduced remained at a stable level for 9 weeks after transfection. At the present time, these results are being considered from the standpoint of the study of ageing processes at a molecular level.⁵¹

Furthermore, the study of organ tissues and analysis of the cardiac functions of mice and pigs after lipofection *in vivo* has not revealed any pathologies following the employment of deliberately excess doses of the DNA — liposome complex.⁵²

It is essential to note that the transfection method, employing cationic liposomes as mediators, may prove promising in the enzyme- and hormone-substitution therapy of a wide variety of diseases such as sugar diabetes, growth defects, and various blood affections (β -thalassemia, adenosine deaminase deficiency, sickle cell anaemia, etc.).^{14, 49, 50, 53}

3. The use of cationic lipids as inhibitors of the membrane-bound protein kinase C and diacylglycerol kinase

In connection with the study of the influence of lipids of the type of 1-*O*-octadecyl-2-*O*-methyl-*rac*-glycero-3-phosphocholine (ET-18-OMe) on metastases and the growth of a wide variety of neoplastic cell lines, the new quaternary ammonium derivatives of glycerolipids 20 are of great interest. These compounds proved to be effective inhibitors of the membrane-bound protein kinase C (PKC), which regulates the content of phospholipids and Ca^{2+} ions in the cell. The study of the mechanism of the action of this kinase, activated by phosphatidylserine, phorbol esters, and diacylglycerols, has shown that exogenic alkylacylglycerols and dialkyl derivatives are capable of inhibiting this kinase, which is present in HL-60 cells. A similar activity of compounds of types 23 and 32 has been observed in relation to diacylglycerol kinase (DAG).⁷ In order to investigate the molecular interaction of these enzymes with their natural activators, inhibitors, and substrates, a series of dialkyl and diacyl quaternary ammonium derivatives with various structures have been synthesised (compounds 10, 21, 23, 32, etc.)

The study of the activity of PKC in the presence of the above compounds using *rac*-1,2-dioleoylglycerol — $\text{PS} - \text{Ca}^{2+}$ mixtures as activators showed that the manifestation of inhibiting activities requires the presence in its composition of a relatively long-chain alkyl or acyl substituent at the C(1) atom of the glycerol fragment, a short-chain alkyl or acyl substituent at the C(2) atom, and also a functional group capable of forming hydrogen bonds at the C(3) atom. A similar conclusion was reached in relation to DAG when *rac*-1,2-dioleoylglycerol was used as the substrate in the investigations.

Compounds 32a,b proved to be the most active under the experimental conditions, whereas the diol type lipid 10 proved to be inactive in this instance.

During tests of 2-*O*-acetyl-1-*O*-oleoylglycerol as one of the activators, a study was made of the ability of compounds of types **21**, **23**, and **26** to inhibit PKC (obtained from the bovine brain), which made it possible to discover the influence of the structure of these compounds on the inhibition process. Table 1 presents the concentrations corresponding to 50% inhibition of PKC by compounds having different structures.^{16, 54}

The data presented permit the following conclusions:

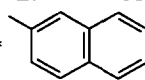
- the replacement of an oxygen atom by a sulfur atom does not alter significantly the activity (cf. compounds **23a** and **23f**);
- the long alkyl chain at the C(1) atom of glycerol plays a decisive role in the manifestation of activity (compound **23e** is inactive);
- significant differences between the activities of compounds containing methoxy- and ethoxy-groups at the C(2) atom of the glycerol fragment have not been observed (compounds **23a** and **23b**);
- the activities are influenced by a change in the length of the chain of the *N,N*-dimethylalkylammonium alcohol; thus the propanol derivative **23g** exhibits a higher activity than compound **23a**;
- the replacement of the 'inverse' choline group by a trialkylammonium group improves the inhibition of the enzyme (a free hydroxy-group alters the activity insignificantly);
- the replacement of the quaternary ammonium group by a hydroxy-group does not influence the inhibition of PKC but fully abolishes the cytotoxicity of these analogues in relation to tumour cells;
- the migration of the quaternary nitrogen atom from the glycerol skeleton to the end of the alkyl chain made up of several methylene groups has only a slight influence on the PKC activity (compounds **26a–c** and **23h**).

In conclusion, one must note that the restriction of the mobility of the glycerol on incorporation of R¹ and R² into a structure of the acetal type does not diminish the activity. Furthermore, the stereospecificity of the compounds synthesised is not a decisive factor in the inhibition of PKC.¹⁶ Preliminary experiments designed to elucidate the mechanism of the inhibition of PKC showed that the compounds quoted block its activation by phosphatidylserine.

Studies which will help to discover for these compounds a correlation between the antineoplastic activity and the ability to inhibit PKC are being prosecuted at the present time.

Table 1. The concentrations corresponding to 50% inhibition (IC₅₀/μmol litre⁻¹) of PKC.^{16, 54}

		$\begin{array}{c} \text{O} \\ \diagup \quad \diagdown \\ \text{O} \quad \text{R}^1 \\ \quad \quad \text{R}^2 \\ \text{N}^+ \text{Me}_2 \text{R}^3 \quad \text{Q}^- \end{array}$		$\begin{array}{c} \text{XR}^1 \\ \text{OR}^2 \\ \text{Z-N}^+ \text{Me}_2 \text{R}^3 \quad \text{Q}^- \end{array}$			
		21		23, 26			
Compound	X	R ¹	R ²	R ³	Q	IC ₅₀	
ET-18-OMe ^a	O	C ₁₈ H ₃₇	Me	Me	—	12	
21	—	C ₁₇ H ₃₅	H	(CH ₂) ₃ OH	Br	13	
23a	S	C ₁₆ H ₃₃	Me	(CH ₂) ₂ OH	Br	27	
23b	S	C ₁₆ H ₃₃	Et	(CH ₂) ₂ OH	Br	37	
23c	S	C ₁₆ H ₃₃	Et	(CH ₂) ₃ OH	Br	26	
23d	S	C ₁₆ H ₃₃	Me	Me	Me	25	
23e	O	Naphth ^b	Me	(CH ₂) ₂ OH	Br	>>40	
23f	O	C ₁₆ H ₃₃	Me	(CH ₂) ₂ OH	I	17	
23g	S	C ₁₈ H ₃₇	Me	(CH ₂) ₃ OH	I	5	
23h	O	C ₁₆ H ₃₃	Me	Me	Br	>40	
23i	O	C ₁₆ H ₃₃	H (instead of OR ²)	Me	Br	>>40	
26a^c	O	C ₁₆ H ₃₃	Me	Me	Br	31	
26b^d	O	C ₁₆ H ₃₃	Me	Me	Br	>40	
26c^e	O	C ₁₆ H ₃₃	Me	Me	Br	>>0	
26d^d	O	C ₁₆ H ₃₃	Et	Me	Br	>>40	

^a Z = OPO₃⁻(CH₂)₂, ^b Naphth = , ^c Z = O(CH₂)₂,
^d Z = O(CH₂)₄, ^e Z = O(CH₂)₆.

4. The antitumour activity of positively charged lipids

It is widely known that positively charged alkyl ether lipids influence the metabolism and growth of neoplastic cell lines. The compound ET-18-OMe and its phosphorus-free analogues

Table 2. Concentrations of lipids with a cationic head in the form of 'reversed' choline corresponding to 50% inhibition of the growth of neoplastic cells.

		$\begin{array}{c} \text{XR}^1 \\ \text{OR}^2 \\ \text{N}^+ \text{Me}_2 (\text{CH}_2)_n \text{OH} \quad \text{Q}^- \end{array}$							
		23, 48							
Compound	X	R ¹	R ²	n	Q	IC ₅₀ /μmol litre ⁻¹	Type of cell	Ref.	
ET-18-OMe	O	C ₁₈ H ₃₇	Me	—	—	2.50 ± 0.31	HL-60	6	
23a	S	C ₁₆ H ₃₃	Me	2	Br	4.66 ± 0.27	HL-60	54	
23b	S	C ₁₆ H ₃₃	Et	2	Br	3.72 ± 0.05	HL-60	54	
23c	S	C ₁₆ H ₃₃	Et	3	Br	2.95 ± 0.36	HL-60	54	
23g	S	C ₁₈ H ₃₇	Me	3	Br	3.55 ± 0.22	HL-60	54	
23e	S	Naphth	Me	2	Br	>10	HL-60	54	
23j	S	C ₁₈ H ₃₇	H	2	I	0.35 ± 0.05	KB	5	
23k	S	C ₁₆ H ₃₃	C ₆ H ₁₁	2	Br	7.15	HL-60	6	
48	S	C ₁₆ H ₃₃	CH ₂ OMe (instead of OR ²)	3	Br	3.46	HL-60	6	

accumulate on the surface of the plasma membrane, inhibiting PKC and certain other kinases, which may be associated with the antineoplastic activity which they exhibit in vitro (HL-60 and KB cells) and in vivo (S-180 and MM46 cells).²⁰ In addition, alkyl ether lipids may accumulate selectively in tumour cells by virtue of the low activity in the latter of the enzymes which cleave ether bonds.^{28, 55} This disturbs the normal biosynthesis of the lipids of the cell membrane and the functions and integrity of the latter.

A series of cationic lipids with an antineoplastic activity have been synthesised. They can be subdivided arbitrarily into five main series:

(1) Lipids with a cationic head in the form of 'inverse' choline (Table 2).

(2) Cationic lipids of the acetal type (Table 3).

(3) Lipids with an ammonium group attached directly to the glycerol fragment (Table 4).

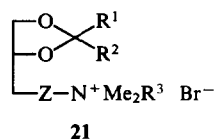
(4) Lipids with a cationic head attached to the glycerol skeleton via a spacer group (Table 5).

(5) Derivatives of cationic lipids of the diol type (Table 6).

All the compounds were investigated from the standpoint of their antineoplastic activity in relation to cells of different types (Tables 2–6). Comparison of the results of experiments performed under similar conditions permits a series of conclusions.

The 'inverse' cholines of the first series have largely proved less active than the compounds of the third and fourth series, the activities of which are comparable with that of the ET-18-OMe reference standard. The presence of the hydroxy-group in the

Table 3. Concentrations of cationic lipids of the acetal type corresponding to 50% inhibition of the growth of neoplastic cells.⁵⁴



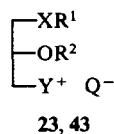
Compound	R ¹	R ²	R ³	IC ₅₀ / μmol litre ⁻¹	Type of cells
21a	C ₁₇ H ₃₅	H	(CH ₂) ₃ OH	6.47 ± 0.24	HL-60
21b	Me	Me	(CH ₂) ₂ OH	> 10	HL-60
21c^a	C ₁₇ H ₃₅	Me	Me	2.82 ± 0.42	HL-60

^a Z = O(CH₂)₄.

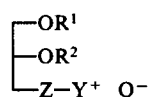
cationic head reduces the activity somewhat. The influence of the heteroatom (S or O) at the C(1) atom of glycerol has not been accurately elucidated.⁵⁴

A decrease in the length of the alkyl substituent at the C(1) atom of glycerol or its replacement by an aromatic system lowers the activity of the compound in relation to the HL-60 cells. Thus compound **23e** (Table 2) shows no activity within the limits of the measured concentrations.

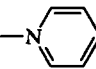
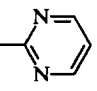
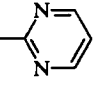
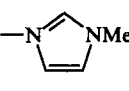
Table 4. Concentrations of lipids with an ammonium group attached directly to the glycerol fragment corresponding to 50% inhibition of the growth of neoplastic HL-60 cells.



Compound	X	R ¹	R ²	Y	Q	IC ₅₀ / μmol litre ⁻¹	Ref.
23h	O	C ₁₆ H ₃₃	Me	NMe ₃	Br	1.59 ± 0.17	54
23i	O	C ₁₆ H ₃₃	H (instead of OR ²)	NMe ₃	Br	1.61 ± 0.10	54
23l	O	C ₁₆ H ₃₃	Et	NEt ₃	Br	0.68 ± 0.11	54
23m	O	C ₁₆ H ₃₃	Et		Br	1.01 ± 0.06	54
23n	O	C ₁₆ H ₃₃	H (instead of OR ²)		Br	0.82 ± 0.24	54
23o	O	C ₈ H ₁₇	Me	NMe ₃	Br	21.15 ± 5.40	6
23p	O	C ₁₆ H ₃₃	Me		Br	1.07 ± 0.30	6
23q	O	C ₁₈ H ₃₇	Et		Br	2.92	6
23d	S	C ₁₆ H ₃₃	Me	NMe ₃	Br	2.20 ± 0.30	43
23r	S	C ₁₆ H ₃₃	Me	NMe ₂ CH ₂ CH(OH)CH ₂ OH	Br	3.62 ± 0.04	6
23s	S	C ₁₆ H ₃₃	Me		Br	8.75	6
23t	S	C ₁₆ H ₃₃	C ₅ H ₁₁	NMe ₃	Br	6.14	6
43	O	C ₁₆ H ₃₃	Me	SMc(CH ₂) ₂ OH	TsO	2.49 ± 0.29	6

Table 5. Concentrations of lipids with a cationic head attached to glycerol via a spacer group corresponding to 50% inhibition of the growth of neoplastic cells.

26, 27, 29, 49

Compound	R ¹	R ²	Z	Y	Q	IC ₅₀ / μg ml ⁻¹	Type of cell	Ref.
ET-18-OMe	C ₁₆ H ₃₃	Me	O(CH ₂) ₂	NMe ₃	Br	2.5 ± 0.31 ^a 0.63	HL-60 KB	6, 54 20
26a	C ₁₆ H ₃₃	Me	O(CH ₂) ₂	NMe ₃	Br	1.85 ± 0.15 ^a	HL-60	54
26b	C ₁₆ H ₃₃	Me	O(CH ₂) ₂	NMe ₃	Br	2.30 ± 0.37	HL-60	54
26c	C ₁₆ H ₃₃	Me	O(CH ₂) ₂	NMe ₃	Br	3.79 ± 0.13 ^a	HL-60	54
26d	C ₁₆ H ₃₃	Et	O(CH ₂) ₄	NMe ₃	Br	1.86 ± 0.04	HL-60	54
26f	C ₁₆ H ₃₃	Et	O(CH ₂) ₄		Br	0.78 ± 0.02	HL-60	54
26g	C ₁₆ H ₃₃	H (instead of OR ²)	O(CH ₂) ₄	NMe ₃	Br	1.56 ± 0.10 ^a	HL-60	54
26h	C ₁₈ H ₃₇	Me	O(CH ₂) ₂	NMe ₃	Cl	1.25 0.16	HL-60 KB	20 20
29a	C ₁₈ H ₃₇	Me	(OCH ₂ CH ₂) ₂	NMe ₃	Cl	1.25 0.32	HL-60 KB	20 20
29b	C ₁₈ H ₃₇	Me	(OCH ₂ CH ₂) ₅	NMe ₃	Cl	1.25 0.16	HL-60 KB	20 20
29c	C ₁₈ H ₃₇	C ₄ H ₉	(OCH ₂ CH ₂) ₂	NMe ₃	Cl	2.5	HL-60	20, 24
29d	C ₁₈ H ₃₇		(OCH ₂ CH ₂) ₂	NMe ₃	Cl	0.31 0.32	HL-60 KB	20, 24, 58 20, 24, 58
29e	C ₁₈ H ₃₇	COCH ₂ Ac	(OCH ₂ CH ₂) ₂	NMe ₃	Cl	20.0	HL-60	20, 24
29f	C ₁₈ H ₃₇	CH ₂ CF ₃	(OCH ₂ CH ₂) ₂	NMe ₃	Cl	2.5	HL-60	20, 24
29g	C ₁₈ H ₃₇		(OCH ₂ CH ₂) ₂		Cl	0.63	HL-60	24, 58
27	C ₁₆ H ₃₃	Me	S(CH ₂) ₂	NMe ₃	Br	2.4	HL-60	6
49a	C ₁₆ H ₃₃	Me	SO ₂ (CH ₂) ₃	NMe ₃	MsO	1.25	HL-60	56
49b	C ₁₆ H ₃₃	Me	SO ₂ (CH ₂) ₆	NMe ₃	MsO	5.0	HL-60	56

^a Expressed in μmol litre⁻¹.

The restriction of rotational mobility in the presence of the acetal system at the C(1) and C(2) atoms of the glycerol fragment diminishes the antineoplastic activity of the compounds. The presence of methoxy- or ethoxy-groups at the C(2) atom does not affect the activity. However, the presence of an alkyl substituent with a long chain containing more than five carbon atoms reduces the activity of the compound sharply. The replacement of the methoxy- and ethoxy-groups by heterocyclic bases of the pyrimidine or pyridazine type induces a slight decrease in the antineoplastic activity.²⁴

Among the compounds of the fourth group, the inhibition of the growth of neoplastic cells diminishes slightly with increase in the length of the spacer group but remains similar to the inhibiting activity of ET-18-OMe.

The presence of a quaternary ammonium or a tertiary sulfonium group is essential for the manifestation of activity, the sulfonium and pyridinium derivatives being the most active.⁶

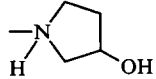
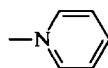
The degree of oligomerisation of the ethyleneoxy-group in compounds with the structure **29** does not play a decisive role for the activation in vitro (Table 5).²⁰ A similar conclusion can be reached also as regards compounds **49a** and **49b** with different numbers of methylene groups separating the sulfo-group from the cationic head.⁵⁶

It is of interest that compound **29**, containing the acetoacetyl group at the C(2) atom of the glycerol fragment, proved to be fairly active against the S-180 and MM46 cells in studies carried out in vivo in contrast to in vitro investigations.²⁰

Table 6. Concentrations of a series of derivatives of cationic lipids of the diol type corresponding to 50% inhibition of the growth of neoplastic cells.

$$\begin{array}{c} \text{—XR} \\ | \\ \text{—Y}^+ \text{—Q}^- \end{array}$$

7, 8, 19

Compound	X	R	Y	Q	IC ₅₀ / μmol litre ⁻¹	Type of cell	Ref.
7	OCO	C ₁₅ H ₃₁	NMe ₂ (CH ₂) ₂ OH	Br	50 ^a	KB	5
8a	O	C ₁₂ H ₂₅	NMe ₂ (CH ₂) ₂ OH	I	0.78 ± 0.03	KB	5
8b	O	C ₁₆ H ₃₃	NMe ₂ (CH ₂) ₂ OH	Br	0.33 ± 0.12	KB	5
8c	O	Ph	NMe ₂ (CH ₂) ₂ OH	Br	> 100	HL-60	5
8d	O	H	NMe ₂ (CH ₂) ₂ OH	Br	> 100	HL-60	5
8e	O	C ₁₆ H ₃₃		Br	1.26 ± 0.36	HL-60	5
19a	S	C ₁₆ H ₃₃		Br	2.28	HL-60	6
19b	S	C ₁₆ H ₃₃	NMe ₂ (CH ₂) ₂ OH	Br	3.95	HL-60	6

^a Expressed in mmol litre⁻¹.

numbers of methylene groups separating the sulfo-group from the cationic head.⁵⁶

It is of interest that compound **29**, containing the acetoacetyl group at the C(2) atom of the glycerol fragment, proved to be fairly active against the S-180 and MM46 cells in studies carried out in vivo in contrast to in vitro investigations.²⁰

Some of the analogues synthesised have been tested in other systems. Thus for cells of the ChaGo and K562-4 lines, the inhibition was similar to that of the cell line 77. The inhibition of the P388 cells in mouse leukemia is comparable to the activity against the KB cells. The cells of the MHC rat hepatoma, obtained from the Morris 7795 hepatoma, were inhibited 2–3 times less effectively than the cells of the 77 line.⁵

There are data⁵⁷ demonstrating that increased concentration of cholesterol in the cell membrane plays a fairly important role in reducing the toxicity of the alkyl ether lipids (AL) to the HL-60 cells.

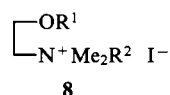
5. The antiviral activity of positively charged lipids

Synthetic lipids of the alkyl type exhibit a broad spectrum of biological activity, including the inhibition of replication of the HIV-1 virus. The exact mechanism of their action is not entirely clear. The HIV infection is a multistage process, which begins with the binding of the HIV to the CD4 receptors of the lymphocytes. After binding, the HIV permeates into the cell either via the direct fusion of the viral coating with the plasma membrane or by virtue of the receptor-dependent endocytosis of the CD4–HIV complex.^{6,59} There are data demonstrating that the blocking of the HIV-dependent phosphorylation of the CD4 receptors by the introduction of a selective PKC inhibitor inhibits effectively the infection of the cell by the virus.

A new class of alkyl ether lipids — potential PKC inhibitors — has been investigated recently as regards their anti-HIV-1 activity. Monolayers or suspension cultures of human T-cells (CEM-ss) were used in these investigations to determine the activity of the structurally modified, phosphorus-free analogues of lipids of the alkyl ether type. The concentration corresponding to 50% inhibition of the growth of the CEM-ss cells and the formation of HIV-1 plaques as well as the decrease in viral budding (the capture by the virus of a portion of the cell membrane on permeation into the cell) were investigated.^{17,60}

The experiments established that treatment of the cells infected by HIV-1 with compounds of this type is not accompanied by an increase in the activity of the reverse transcriptase, which implies different mechanisms of the action of 3'-azido-3'-deoxythymidine (AZT) and cationic lipids.

Electron microscope studies have shown⁶⁰ that there is no viral budding on the surface of a cell membrane in cells infected by HIV-1 and treated with positively charged lipids, but intracellular vacuolar viral particles are present. These data suggests that alkyl ether lipid analogues disturb the process involving the formation of cytoplasmic vacuolar forms of HIV in T-cells. The binding of HIV-1 to CD4 receptors of the T-lymphocytes induces their phosphorylation by means of the phospholipid-Ca²⁺-dependent

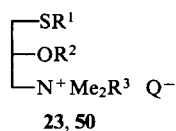


R¹ = C₁₈H₃₇; R² = (CH₂)₂CH(OH)CH₂OH (**8f**);

R¹ = C₁₆H₃₃; R² = (CH₂)₂OH (**8g**), (CH₂)₃OH (**8h**);

PKC, whereupon cationic lipids, inhibiting the kinase, block the intracellular processes involving the development and multiplication of viral particles. The formation of HIV-1 plaques is inhibited via a concentration-dependent mechanism until the virus ceases to act on the growth of human T-cells.

The activities of the following compounds against HIV-1 have been investigated:



Compound	R ¹	R ²	R ³	Q
23a	C ₁₆ H ₃₃	Me	(CH ₂) ₂ OH	Br
23b	C ₁₆ H ₃₃	Et	(CH ₂) ₂ OH	Br
23d	C ₁₆ H ₃₃	Me	Me	Br
23g	C ₁₈ H ₃₇	Me	(CH ₂) ₃ OH	I
23r	C ₁₆ H ₃₃	Me	CH ₂ CH(OH)CH ₂ OH	Br
23u	C ₁₆ H ₃₃	Et	C ₅ H ₅ N ⁺ (instead of N ⁺ Me ₂ R ³)	Br
50	C ₁₆ H ₃₃	Et	OH (instead of N ⁺ Me ₂ R ³)	—

Analysis of the results (Table 7) shows that the formation of HIV-1 plaques in the CEM-ss cells is inhibited within the limits of

Table 7. Concentrations corresponding to 50% inhibition of the formation of HIV-1 plaques and the growth of CEM-ss cells.^{17,60}

Compound	IC ₅₀ for the formation of HIV plaques / μmol litre ⁻¹	IC ₅₀ for the growth of CEM-ss cells / μmol litre ⁻¹	D ^a
AZT	0.004 ± 0.001	5.6 ± 0.8	1400
ET-18-OMe	0.92 ± 0.39	4.0 ± 0.7	4.3
23a	0.37 ± 0.02	2.1 ± 1.0	5.7
23b	0.63 ± 0.18	5.1 ± 0.4	8.1
23d	0.39 ± 0.24	5.3 ± 0.1	13.4
23g	0.41 ± 0.29	4.0 ± 2.7	9.8
23i	0.49 ± 0.23	2.0 ± 0.1	4.1
23k	0.21 ± 0.01	1.1	5.2
8f	0.20 ± 0.05	2.0 ± 0.5	14.5
8g	0.38 ± 0.29	6.0 ± 0.2	15.6
8h	0.24 ± 0.06	1.5 ± 0.1	6.1
50	> 5.0	> 20.0	—

^a D is the differential selectivity defined as the ratio of the concentration corresponding to the inhibition of the growth of the CEM-ss cells to the concentration corresponding to the inhibition of the formation of HIV-1 plaques.

concentrations which are not toxic to the host cells. In order to exhibit anti-HIV-1 activity, compounds of this type must possess long-chain alkyl substituents at the C(1) atom, a short-chain substituent at the C(2) atom, and a quaternary ammonium group at the C(3) atom of glycerol.

The changes in the type of cationic head and in the size of the substituents at the quaternary nitrogen atom do not influence significantly the activity of the compounds.^{17,60} However, in its absence the compound becomes inactive (for example, compound 50).

Unfortunately no data have been obtained which would make it possible to infer the inhibition of the formation of plaques of the type 2 herpes simplest virus (HSV-2) or the inactivation of the intracellular virus, which evidently indicates the selectivity of compounds of this type in their action against HIV-1. This apparently occurs because they interact with the cytoplasmic

membrane (the HIV-1 budding site) and not with the nuclear membrane (the herpes simplest budding site). In addition, the herpes virus does not require PKC for infection and its multiplication is different from that of HIV-1 (Table 7).¹⁷

Studies designed to elucidate the mechanism of the action of alkyl ether lipid analogues, inhibiting infection by HIV-1 and inducing the formation of a defective form of the virus, are being carried out at the present time. It has been shown that lipid antagonists are not inhibitors of reverse transcriptase but disturb the replication of the virus in the last stage. The choice of optimum analogues may provide specialists with effective chemotherapeutic preparations which can be used in the treatment of AIDS either individually or in combination with DNA-interactive anti-HIV-nucleosidic analogues.⁶⁰

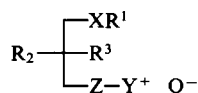
6. Cationic lipids — analogues and antagonists of the platelet activating factor

Numerous specific and nonspecific analogues and antagonists of the platelet activating factor (PAF) have been synthesised and investigated during the last decade. Synthetic derivatives permitting the solution of the problem of the relation between structure and biological activity and the possible therapeutic activity are of special interest.

The numerous PAF antagonists with a lipid structure can be subdivided into the following types: natural phospholipid PAF antagonists, their derivatives, and synthetic compounds. These antagonists are in the main active inhibitors of the binding of PAF to its receptors. Many of them are highly specific in their biological activity with the exception of certain phospholipid analogues, which do not exhibit any appreciable antagonistic activity at high concentrations.^{26,61}

Two methods for the investigation of PAF antagonists under in vitro conditions are most widely used nowadays: inhibition of the PAF-induced aggregation of rabbit, human, and guinea pig platelets, as well as the inhibition of the specific binding of [³H] PAF to cells or isolated membranes.⁶¹ In the in vivo experiments, usually carried out on mice or rabbits, the effect of antagonists on the decrease in pressure, induced by PAF, and also the prevention of the lethal effect of high PAF doses are considered.^{47,62–67}

One of the first phospholipid PAF antagonists, namely CV-3988 (Table 8), was synthesised initially as a powerful antifungal and cytotoxic agent.⁶⁸ The next structural phosphorus-free analogue, CV-6209, proved to be approximately 80 times more active in experiments in vitro.^{26,61,63,69,70} A series of antagonists were synthesised in this connection by substituting the phosphocholine groups of PAF by quaternary ammonium groups of different types, attached to the glycerol fragment via spacer groups. In a general form, the structure of the PAF antagonists can be represented as follows:



The strength of the antagonists in relation to the PAF-induced state depends on their structure and the experimental conditions. For each series of cationic lipids, representatives of which are listed in Table 8, the concentrations corresponding to the inhibition of the PAF-induced aggregation of platelets were obtained. For the majority of them, experiments designed to investigate the influence of the antagonists on the pathological states induced by the introduction of PAF under in vivo conditions were formulated.^{25,35,61–64,71}

The principal requirements which must be met by the structure of the PAF antagonists are listed below:

(a) the long-chain substituent at the C(1) atom attached to glycerol via oxy-, thio-, carbamoyloxy-, and carbamoylthio-groups should have an optimum content of 16–18 carbon atoms;

Table 8. Concentrations corresponding to the 50% inhibition of the aggregation of blood platelets by PAF antagonists (for the experimental conditions and the type of platelets, see the literature sources).

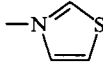
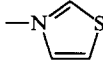
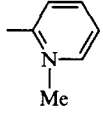
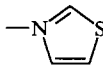
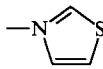
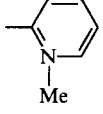
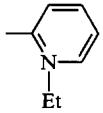
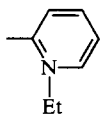
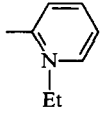
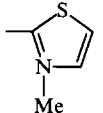
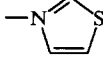
$\begin{array}{l} \text{XR}^1 \\ \\ \text{R}^2 \\ \\ \text{Z}-\text{Y}^+ \quad \text{Q}^- \end{array}$								
Compound	X	R ¹	R ²	Z	Y	Q	IC ₅₀ / μmol litre ⁻¹	Ref.
CV-3988	OCONH	C ₁₈ H ₃₇	OMe	OPO ₃ ⁻ (CH ₂) ₂		—	1.6	26
ONO-6240	O	C ₁₆ H ₃₃	OEt	O(CH ₂) ₇		OMs	0.1	61, 72, 73
CV-6209	OCONH	C ₁₈ H ₃₇	OMe	OCONAcCH ₂		OMs	0.2	35
Ro-18-8736	OCONH	C ₁₈ H ₃₇	NHCOOMe	OCO(CH ₂) ₃		I	0.63	74
Ro-19-3704	OCONH	C ₁₈ H ₃₇	OCOOMe	O(CH ₂) ₄		I	0.1 + 1	74, 75
Ru-45703	O	C ₁₈ H ₃₇	OEt	COO(CH ₂) ₄	NMe ₃	I	8.0	22, 76
33a	O	C ₁₈ H ₃₇	OCOMe	O(CH ₂) ₄	NMe ₃	I	> 100	77
42a	O	C ₁₈ H ₃₇	OCOMe	OCONAcCH ₂ CH ₂	NMe ₃	I	0.88	35
42b	O	C ₁₈ H ₃₇	OCOMe	OCONH(CH ₂) ₂	NMe ₃	Br	8.4	35
42c	OCONH	C ₁₈ H ₃₇	OMe	OCONAc(CH ₂) ₃	NMe ₃	I	8.5	35
42d	OCONH	C ₁₈ H ₃₇	OMe	OCONH(CH ₂) ₂ Me	—	—	> 30	35
51a	OCONH	C ₁₈ H ₃₇	OMe	OCONAc(CH ₂) ₂		Cl	0.2	35
51b	OCONH	C ₁₈ H ₃₇	OMe	OCONAcCH ₂		Cl	0.075	61
51c	OCONH	C ₁₈ H ₃₇	OMe	OCONAcCH ₂		Cl	0.084	61
51d	OCONH	C ₁₈ H ₃₇	OMe	OCONAcCH ₂		Cl	0.091	61
51e	OCONH	C ₁₈ H ₃₇	OMe	OCONAcCH ₂		I	0.41	61
52a	OCONH	C ₁₈ H ₃₇	OMe	NHSO ₂ (CH ₂) ₃	NMe ₃	Cl	48.1	25
52b	OCONH	C ₁₈ H ₃₇	OMe	NHSO ₂ (CH ₂) ₃		I	1.89	25

Table 8 (continued).

Compound	X	R ¹	R ²	Z	Y	Q	IC ₅₀ / μmol litre ⁻¹	Ref.
52c	CONH	C ₁₈ H ₃₇	OMe	NHSO ₂ (CH ₂) ₃		I	5.20	25
52d	S	C ₁₆ H ₃₃	OMe	NHSO ₂ (CH ₂) ₃		I	3.64	25
53a	O	C ₁₆ H ₃₃	H			Br	3.6	78
53b	O	C ₁₈ H ₃₇	H		NMe ₃	Br	31	78
54a	O		—	CONAcCH ₂	—	I	0.38	62, 70
54b	O		—		—	I	0.025	62, 70
54c	CONH	(CH ₂) ₃ CONHC ₁₈ H ₃₇	—		—	Cl	0.044	62, 70
54d	CONH		—		—	I	2.6	62, 70

(b) the configuration of the chiral centre must be analogous to that of PAF (*R*);

(c) the character and bulk of the substituent at the C(2) atom of glycerol must be analogous to those of acetyl;

(d) the replacement of the phosphate group at the C(3) atom by a spacer group of any kind is essential;

(e) the cationic head must have an acceptable structure.

It follows from the data presented in Table 8 that the replacement of the alkyl chain at the C(1) atom of glycerol by aromatic or heterocyclic groups with substituents of different lengths and structure did not lead to a sharp alteration of the antagonistic activity (cf. CV-6209 and **54a**).^{35, 61, 62}

No appreciable differences between the *in vitro* activities of the (*RS*)- and (*R*)(-)- and (*S*)(+)-analogues have been observed (cf. **51b**–**d**). A similar situation has been noted for the compounds SRI 63-072 and SRI 63-119.^{35, 79}

In the case where the spacer group Z is a carbamoyl derivative, the introduction of an acyl substituent into this group increases the blocking of the aggregation of platelets *in vitro* (cf. compounds **42a** and **42b**).^{62, 64, 70} However, when amide bridges, linear imide bonds, and alkyl and certain carbamoyl substituents are used in the spacer group instead of the acyl substituent, the activity decreases fairly appreciably. An increase in the size of the spacer group as a whole induces a similar effect.^{62, 70}

It is preferable to use thiazolinium and pyridinium groups as the cationic head. The presence of the ethyl substituent at the quaternary nitrogen atom in the heterocycle has then the most

favourable effect on the antagonistic activity (compound **51b**).^{35, 61, 70}

PAF antagonists help nowadays to elucidate the possible role of this natural bioregulator in various pathological changes in the organism and also its interaction with other causative agents and immunological mediators of these processes.⁸⁰ Many investigators are actively engaged in the assessment of their clinical activity. The data obtained suggest that it is possible to exert a definite therapeutic effect on asthma, allergic diseases, shock syndromes, the endointoxication of the organism, premature births, psoriasis, and many allergic diseases of the eyes.

In conclusion, it is essential to note that the creation and comprehensive investigation of new positively charged glycerolipids with the aim of discovering among them biologically active substances with an extended spectrum of therapeutic activity is an aspect of bioorganic chemistry and biotechnology of current interest.

References

1. P Pinnoduwage, L Schmitt, L Huang *Biochim. Biophys. Acta* **985** 33 (1989)
2. N Ballas, N Zakai, I Sela, A Loyter *Biochim. Biophys. Acta* **939** 8 (1988)
3. US P. 4 661 663 (1987)
4. J H Fuhrhop, H Tank *Chem. Phys. Lipids* **43** 193 (1987)
5. S C Crumpton, B Goz, K S Ishaq *Anticancer Res.* **8** 1361 (1988)

6. S L Morris-Natschke, F Gumus, C J Marasco, K L Meyer, M Marx, C Piantadosi, M D Layne, E J Modest *J. Med. Chem.* **36** 2018 (1993)
7. J Goddat, H Coste, I Vilgrain, E Chambaz, H Driguez *Lipids* **27** 331 (1992)
8. A Ito, R Miyazoe, J-Y Mitoma, T Akao, T Osaki, T Kunitake *Biochem. Int.* **22** 235 (1990)
9. X Zhou, A L Klibanov, L Huang *Biochim. Biophys. Acta* **1065** 8 (1991)
10. J P Behr, B Demeneix, J P Loeffler, J Perez-Mutul *Proc. Natl. Acad. Sci. USA* **86** 6982 (1989)
11. P L Felgner, G M Ringold *Nature (London)* **337** 387 (1989)
12. P L Felgner, T R Gadek, M Holm, R S Roman, H W Chan, M Wenz, J P Northrop, G M Ringold, M Danielsen *Proc. Natl. Acad. Sci. USA* **84** 7413 (1989)
13. R W Malone, P L Felgner, I M Verma *Proc. Natl. Acad. Sci. USA* **86** 6077 (1989)
14. US P. 4 897 355 (1990)
15. N Duzgunes, J A Goldstein, D S Friend, P L Felgner *Biochemistry* **28** 9179 (1989)
16. C J Marasco, C Piantadosi, K L Meyer, S L Morris-Natschke, K S Ishaq, G W Small, L W Daniel *J. Med. Chem.* **33** 985 (1990)
17. L S Kucera, N Iyer, E Leake, A Raben, E J Modest, L W Daniel, C Piantadosi *AIDS Res. Hum. Retrovir.* **6** 491 (1990)
18. I D Konstantinova, N I Zaitseva, I P Ushakova, G A Serebrennikova *Izv. Akad. Nauk, Ser. Khim.* 1826 (1994)
19. I D Konstantinova, I P Ushakova, G A Serebrennikova *Bioorg. Khim.* **19** 844 (1993)
20. K Ukawa, E Imamiya, H Yamamoto, T Aono *Chem. Pharm. Bull.* **37** 3277 (1989)
21. F Heymans, M C Borrel, C Broquet, J Lefort, J J Godfroid *J. Med. Chem.* **28** 1094 (1985)
22. J J Godfroid, F Heymans, in *Progress in Biochemical Pharmacology* Vol. 22 (Ed. P Braquet) (Basel: Karger, 1988) p. 25
23. P A Tremblay, M Kates *Can. J. Biochem.* **57** 595 (1979)
24. Eur. P. 0 302 744 (1989)
25. Eur. P. 0 321 296 (1988)
26. P Braquet, J J Godfroid, in *Platelet Activating Factor and Related Lipid Mediators* (Ed. F Snyder) (New York: Plenum Press, 1987) p. 191
27. P Braquet, J J Godfroid *Trends Pharmacol. Sci.* **7** 397 (1986)
28. L Stamatatos, R Leventis, M J Zuckermann, J R Silvious *Biochemistry* **27** 3917 (1988)
29. M Takatani, Y Yoshioka, A Tasaka, Z Terashita, Y Imura *J. Med. Chem.* **32** 56 (1989)
30. Eur. P. 0 147 768 (1985)
31. B Wichrowski, S Jouquely, C Broquet, F Heymans, J J Godfroid, J Fichelle, M Worcel *J. Med. Chem.* **31** 410 (1988)
32. K Burri, R Barner, J M Cassal, P Hadvary, G Hirt, in *Proceedings of the Symposium 'Is There a Case for PAF-Acether Antagonists?' Paris, 1985*
33. I D Konstantinova, S G Zavgorodnyi, A I Miroshnikov, I P Ushakova, G A Serebrennikova *Bioorg. Khim.* **21** 71 (1995)
34. S Zavgorodnyi, M Polianski, E Besidsky, V Kriukov, A Sanin, M Pokrovskaya, G Gurskaya, H Lonnberg, A Azhayevev *Tetrahedron Lett.* **32** 7593 (1991)
35. A Di Guilio, A Oratore, M G Tozzi-Ciancarelli, C Grifo, A Finazzi-Agro *Biochem. Int.* **16** 999 (1988)
36. R M Epand, R J B Chen, K S Robinson *J. Am. Chem. Soc.* **111** 6833 (1989)
37. J Gallova, F Devinsky, P I Palgavy *Chem. Phys. Lipids* **53** 231 (1990)
38. T Seimiya, H Miyasaka, T Kato, T Shirakawa, K Ohbu, M Iwahashi *Chem. Phys. Lipids* **43** 161 (1987)
39. I Jaaskelainen, J Monkkonen, A Urtti *Biochim. Biophys. Acta. Biomembranes* **1195** 115 (1994)
40. R Leventis, P I Silvious *Biochim. Biophys. Acta* **1023** 124 (1990)
41. C E Holt, N Garlich, E Cornel *Neuron* **4** 203 (1990)
42. C L Innes, P B Smith, R Langenbach, K R Tindall, L R Boone *J. Virol.* **64** 957 (1990)
43. Br. P. 2 188 900 (1987)
44. T Ono, Y Fujino, T Tsuchiya, M Tsuda *Neurosci. Lett.* **117** 259 (1990)
45. C Staedel, J S Remy, Z X Hua, T R Broker, L T Chow, J P Behr *J. Investigat. Dermatol.* **102** 768 (1994)
46. J H Felgner, R Kumar, C N Sridhar, C J Wheeler, Y J Tsai, R Border, P Ramsey, M Martin, P L Felgner *J. Biol. Chem.* **269** 2550 (1994)
47. S Capaccioli, G Dipasquale, E Mini, T Mazzei, A Quattrone *Biochem. Biophys. Res. Commun.* **197** 818 (1993)
48. S Capaccioli, G Dipasquale, E Mini, T Mazzei, A Quattrone *Biochem. Biophys. Res. Commun.* **200** 1769 (1994)
49. R Stribling, E Brunette, D Liggitt, K Gaensler, R Debs *Proc. Natl. Acad. Sci. USA* **89** 11277 (1992)
50. K L Brigham, B Meyrick, B Christman, J T Conary, G King, L C Berry, M A Magnuson *Am. J. Resp. Cell Mol. Biol.* **8** 209 (1993)
51. N Zhu, D Liggitt, Y Liu, R Debs *Science* **261** 209 (1993)
52. H San, Z Y Yang, V J Pompili, M L Jaffe, G E Plautz, L Xu, J H Felgner, C J Wheeler, P L Felgner, X Gao, L Huang, D Gordon, G J Nabel, E G Nabel *Hum. Gene Therapy* **4** 781 (1993)
53. F O Nestle, R S Mitra, C F Bennett, H Chan, B J Nickoloff *J. Investigat. Dermatol.* **103** 569 (1994)
54. S L Morris-Natschke, K L Meyer, C J Marasco, C Piantadosi, F Rossi, P L Godwin, E J Modest *J. Med. Chem.* **33** 1812 (1990)
55. J F Soodma, C Piantadosi, F Snyder *Cancer Res.* **30** 309 (1970)
56. Eur. P. 0 255 306 (1988)
57. L Diomedea, A Bizzi, A Magistrelli, E Modest, A Nosedà *Int. J. Cancer* **46** 341 (1990)
58. US P. 4 920 134 (1991)
59. A P Fields, D P Bednarik, A Hess, W S May *Nature (London)* **333** 278 (1988)
60. K L Meyer, C J Marasco, S L Morris-Natschke, K S Ishaq, C Piantadosi, L S Kucera *J. Med. Chem.* **34** 1377 (1991)
61. T Y Shen, S B Hwang, T W Doeberber, J C Robbins, in *Platelet Activating Factor and Related Lipid Mediators* (Ed. F Snyder) (New York: Plenum, 1987) p. 153
62. Eur. P. 0 353 474 (1990)
63. K S Wang, M Monden, T Kanai, M Gotoh, K Umeshita, T Ueki, T Mori *Surgery* **113** 76 (1993)
64. A Wissner, M L Carroll, B D Johnson, S S Kerwar, W C Pickett, R E Schaub, L W Torley, M P Trova, C A Kohler *J. Med. Chem.* **35** 4779 (1992)
65. S Desquand *Therapie* **48** 585 (1993)
66. WO PCT 89/07 099 (1989)
67. M Koltai, D Hosford, P Braquet *J. Lipid Mediators* **6** 183 (1993)
68. Z Terashita, S Tsushima, Y Yoshioka, H Nomura, Y Inada, K Nishikawa *Life Sci.* **32** 1975 (1983)
69. Z Terashita, Y Imura, M Takatani, S Tsushima, K Nishikawa, in *The Second International Conference on Platelet Activating Factor and Structurally Related Alkyl Ether Lipids, Gateburg, TN, 1986* p. 29
70. M P Trova, A Wissner, M L Carroll, S S Kerwar, W C Pickett, R E Schaub, L W Torley, C A Kohler *J. Med. Chem.* **36** 580 (1993)
71. W A Thompson, S Coyle, K Vanzee, H Oldenburg, R Trousdale, M Rogy, D Felsen, L Moldawer, S F Lowry, R Maier, D Wittmann *Arch. Surgery* **129** 72 (1994)
72. K Helmut, H K Mangold, in *Progress in Biochemical Pharmacology* Vol. 22 (Ed. P Braquet) (Basel: Karger, 1988) p. 1
73. T Yamamoto, H Ohno, T Yano, T Okada, N Hamonaka, A Kawasaki, in *The Third International Congress of Inflammation, Paris, 1984* p. 513
74. T Miyamoto, H Ohno, T Yano, T Okada, N Hamonaka, A Kawasaki in *Advances in Prostaglandin, Thromboxane, and Leukotriene Research* (Eds O Hayaishi, S Yamamoto) (New York: Raven Press, 1985) p. 15
75. C Mounier, M Hatmi, A Faili, C Bon, B B Vargaftig *J. Pharmacol. Experiment. Therapeutics* **264** 1460 (1993)
76. H K Mangold, N Weber *Lipids* **22** 789 (1987)
77. A Wissner, R E Schaub, P E Sum, C A Kohler *J. Med. Chem.* **29** 328 (1986)
78. Eur. P. 0 336 142 (1989)
79. C M Winslow, R C Anderson, F J D'Aries, G E Frisch, in *New Horizons in Platelet Activating Factor Research* (Eds M L Lee, C M Winslow) (New York: Wiley, 1987) p. 153
80. B M Schreiber, M D Layne, E J Modest *Lipids* **29** 237 (1994)

Adamantane derivatives containing heterocyclic substituents in the bridgehead positions. Synthesis and properties

M-G A Shvekhgeimer

Contents

I. Introduction	555
II. Adamantane derivatives containing heterocyclic nuclei with nitrogen atoms	555
III. Adamantane derivatives containing heterocyclic nuclei with oxygen atoms	578
IV. Adamantane derivatives containing heterocyclic nuclei with sulfur atoms	581
V. Adamantane derivatives containing heterocyclic nuclei with nitrogen and oxygen atoms	585
VI. Adamantane derivatives containing heterocyclic nuclei with nitrogen and sulfur atoms	591
VII. Adamantane derivatives containing other heterocyclic nuclei	594

Abstract. Data on the synthesis, transformations, and applications of adamantane derivatives containing heterocyclic substituents in the bridgehead positions are surveyed, described systematically, and analysed. The bibliography includes 202 references.

I. Introduction

Adamantane was discovered in 1933 in a study of petroleum products.^{1,2} The adamantane molecule is a rigid structure consisting of three fused six-membered carbon rings and having the shape of almost an ideal sphere. The arrangement of carbon atoms in the adamantane molecule is similar to that in the unit cell of the crystal lattice of diamond. The spatial structure, hydrophobicity, and lipophilicity of adamantane ensure favourable conditions for its transport through biological membranes. The introduction of an adamantyl radical into organic compounds changes and often enhances their biological activities. The influence of the adamantyl radical on the hypoglycemic, antitumour, immunodepressive, antibacterial, fungistatic, hormonal, analgesic, antipyretic, anti-inflammatory, cholagogic, antiarrhythmic, sedative, neuroplegic, antimalarial, and anticholine-esterase activities as well as on the central nervous system stimulating activity of the corresponding medicinal preparations have been noted.³ Among various compounds of the adamantane series, those containing heterocyclic substituents in their molecules seem to be especially interesting both from the theoretical and practical standpoints.

Despite the great interest of researchers in the chemistry of adamantane derivatives containing heterocyclic substituents and numerous examples of their practical use, no reviews surveying the literature data on the synthesis, transformations, and practical significance of heteryladamantanes have been published; only separate examples of synthesis or biological activity of heteryladamantanes have been reported.^{4–11} Among the monographs devoted to adamantane,^{12–14} only one paper¹³ contains a mention

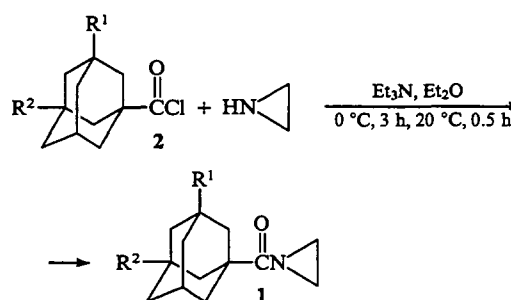
of heteryladamantanes, synthesised before 1975; however, this study also contains virtually no data on the synthesis and properties of adamantane derivatives with heterocyclic substituents.

In our review we survey the published data on the synthesis and properties of adamantane derivatives, the bridgehead positions of which contain heterocyclic radicals either linked directly to the adamantane nucleus or separated from it by a chain of carbon atoms. We consider adamantane derivatives with heterocyclic residues the nucleus of which incorporate nitrogen, oxygen, sulfur, nitrogen and oxygen, or nitrogen and sulfur atoms, as well as residues of other heterocyclic systems.

II. Adamantane derivatives containing heterocyclic nuclei with nitrogen atoms

1. Compounds with three-membered heterocycles

Several methods have been proposed for the synthesis of heteryladamantanes containing residues of three-membered nitrogen-containing heterocycles. A series of *N*-adamantoylaziridines **1** were prepared by the reaction of the acid chlorides **2** with aziridine in the presence of triethylamine.¹⁵



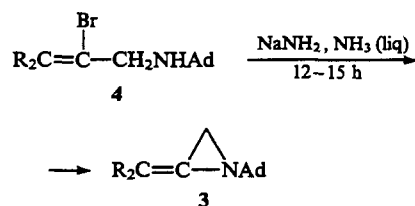
R ¹	R ²	R ¹	R ²	R ¹	R ²
H	H	F	H	Me	Me
Me	H	Cl	H	Me	OH
Ph	H	Br	H	EtO	Et
OH	H	I	H	4-ClC ₆ H ₄	H
MeO	H				

1-(Adamant-1-yl)-2-alkylideneaziridines **3** are formed in a yield of 50% (R = H) or 64% (R = Me) on treatment of the unsaturated bromides **4** with sodium amide in liquid ammonia.¹⁶

M-G A Shvekhgeimer Department of Organic Chemistry and the Chemistry of Dyes, Kosygin Moscow State Textile Academy, ul. Malaya Kaluzhskaya 1, 117918 Moscow, Russian Federation. Fax (7-095) 952 14 40. Tel. (7-095) 955 35 96

Received 2 October 1995

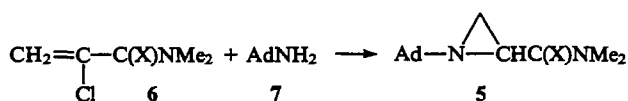
Uspekhi Khimii 65 (7) 603–647 (1996); translated by Z P Bobkova



R = H, Me.

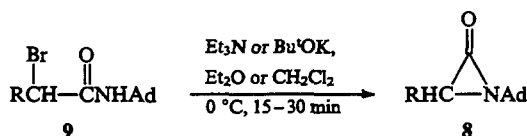
From here on, Ad is adamant-1-yl, C₁₀H₁₅.

Substituted aziridines **5** have been synthesised by the interaction of the vinyl chlorides **6** with 1-aminoadamantane **7**.¹⁷



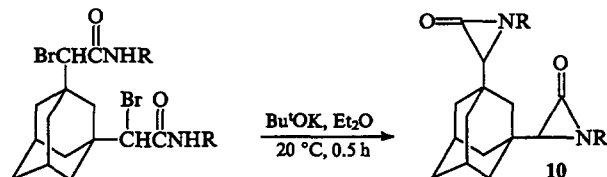
X = H₂, O.

The derivatives of 1-(adamant-1-yl)aziridin-2-one **8** have been obtained by cyclocondensation of *N*-(adamant-1-yl)amides of α-bromocarboxylic acids **9** in 60%–70% yields.^{18–20}



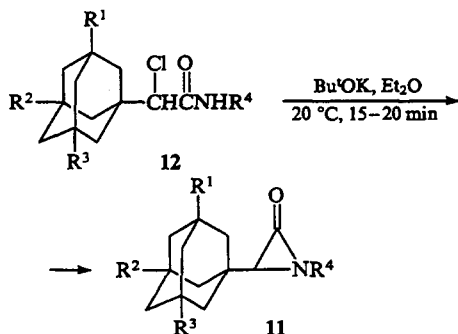
R = Ad (see Ref.18), Bu^t (see Ref.19, 20).

The same method has been used to synthesise compounds **10** containing two aziridinone fragments (yields 60% and 64%).²¹



R = Bu^t, Ad.

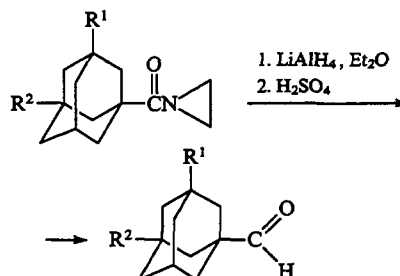
When chloramides **12** are used in this reaction instead of the corresponding bromamides, the aziridinone derivatives **11** are formed equally readily in 60%–70% yields.^{22–24}



R ¹	R ²	R ³	R ⁴	Ref.	R ¹	R ²	R ³	R ⁴	Ref.
H	H	H	Bu ^t	22	H	H	H	Bu ^t	24
Me	Me	Me	Bu ^t	22	Me	Me	Me	Bu ^t	24
H	H	H	Bu ^t	23	Me	H	H	Bu ^t	24
Me	Me	Me	Bu ^t	23	Me	Me	H	Bu ^t	24
Me	Me	Me	cyclo-C ₆ H ₁₁	23	Me	Me	Me	Bu ^t	24
Me	Me	Me	Bu	23	Me	Me	Me	cyclo-C ₆ H ₁₁	24

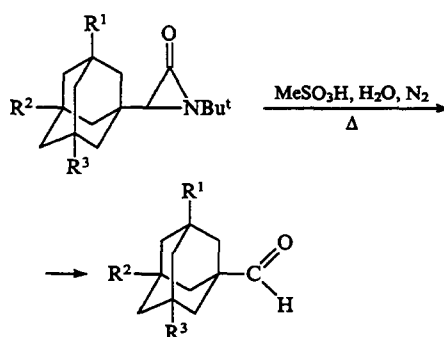
The irradiation of 1-(adamant-1-yl)-4,4-dimethyltriazol-5-one with light from a high-pressure mercury or mercury-xenon lamp in toluene at 15 °C for 4.5 h under a nitrogen atmosphere affords a mixture of products in which 1-(adamant-1-yl)-3,3-dimethylaziridin-2-one was detected by spectral methods.²⁵

Treatment of adamantyl-containing aziridines (reduced preliminarily with lithium tetrahydroaluminate)¹⁵ and adamantyl-containing aziridinones^{23,24,26,27} with strong acids (H₂SO₄ or MeSO₃H) leads to aldehydes of the adamantane series in more than 90% yields.



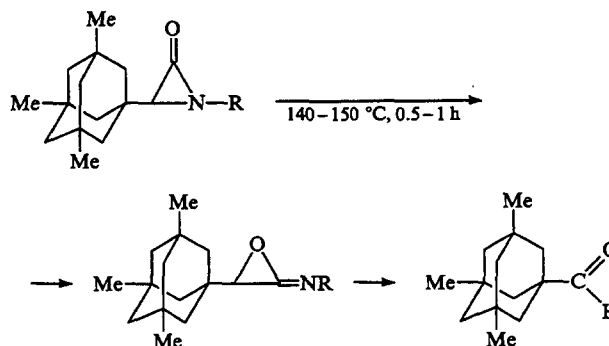
R² = H: R¹ = H, Me, Ph, OH, MeO, F, Cl, Br, I, 4-ClC₆H₄;

R¹ = R² = Me; R¹ = Me, R² = OH; R¹ = EtO, R² = Et.



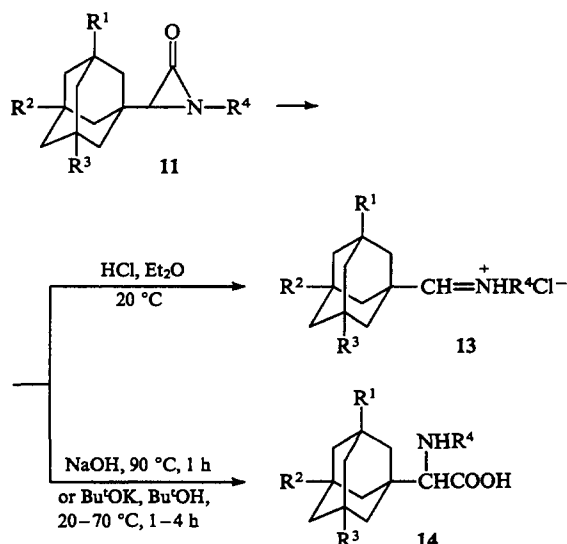
R ¹	R ²	R ³	Ref.
H	H	H	24, 26, 27
Me	H	H	24, 26, 27
Me	Me	Me	24, 26, 27
Me	Me	H	24

The transformation of adamantyl-containing aziridinones into aldehydes can also be carried out in the absence of acids, by heating them at 140–150 °C.²³

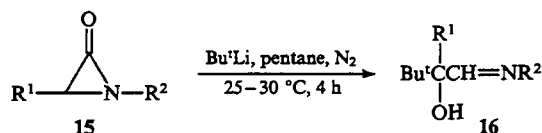


R = Bu, Bu^t, C₅H₁₁.

Treatment of the aziridinone derivatives **11** with HCl in Et₂O gives the salts **13** (yields 95%–96%),^{23,24} whereas the reaction of the compounds **11** with sodium hydroxide or potassium *tert*-butoxide affords the amino acids **14** (yields 63%–94%).



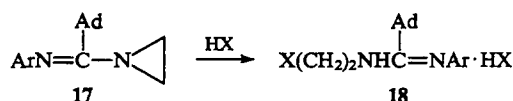
Lithium *tert*-butoxide converts compounds 15 into the alcohols 16 in 75%–85% yields.²⁸



R¹ = Ad, R² = Bu^t, Ad;

R¹ = Bu^t, R² = Ad.

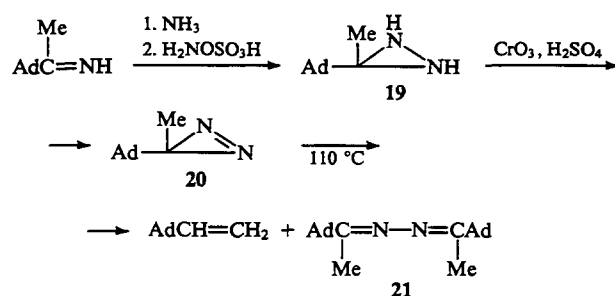
The reaction of azomethines 17 with hydrohalic acids involves the cleavage of the aziridine ring and yields salts 18.²⁹



Ar = Ph, C₆H₄R; X = Cl, Br, I.

1-(Adamant-1-yl)aziridine exhibits antiphlogistic activity and stimulates the central nervous system.³⁰ 1-(Adamant-1-yl)-3-*tert*-butylaziridin-2-one possesses antiviral activity.²¹

The successive treatment of 1-acetyladamantane imine with ammonia and then with hydroxyaminesulfonic acid resulted in the formation of 3-(adamant-1-yl)diaziridine 19, which was converted into 3-(adamant-1-yl)diazirine 20 by the action of chromic anhydride in sulfuric acid. The compound 20 is thermally unstable and is converted on heating into a mixture of vinyladamantane and the azine 21 in a ratio of 5.1 : 1.³¹

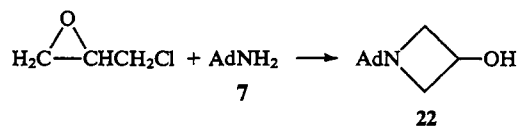


The transformation of the diazirine 20 into vinyladamantane and the azine 21 involves the intermediate formation of the carbene AdC(Me). Diazirines of this type are of interest as

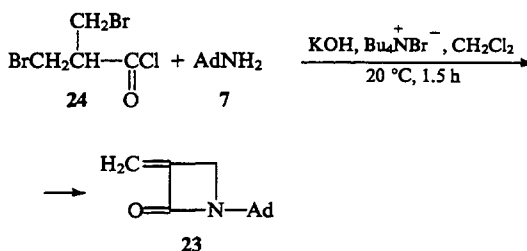
initiators of polymerisation or as reagents for introducing a tracer into cell membrane lipids.³¹

2. Compounds with four-membered heterocycles

In the search for compounds exhibiting an antiarrhythmic activity, the reaction of epichlorohydrin with the amine 7 has been studied. Thus 1-(adamant-1-yl)azetidin-3-ol 22 was obtained in a good yield.³²

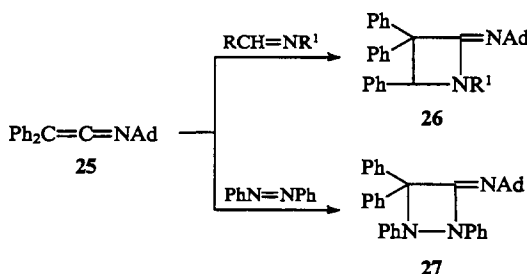


A method for the preparation of 1-(adamant-1-yl)-3-methyleneazetidin-2-one 23 has been developed.³³ The method involves cyclisation of the acid chloride 24 with the amine 7 under the influence of potassium hydroxide under conditions of phase transfer catalysis; the yield of compound 23 is 40%.



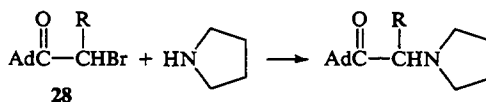
The oxygen atom in the compound 23 can be substituted by sulfur by the action of the Lawesson reagent; this reaction affords 1-(adamant-1-yl)-3-methyleneazetidine-2-thione in 46% yield.³³

Ketenimine 25 enters into cycloaddition reactions with azomethines or with azobenzene; this results in the formation of the azetidine derivatives 26 or diazetidine derivatives 27.³⁴



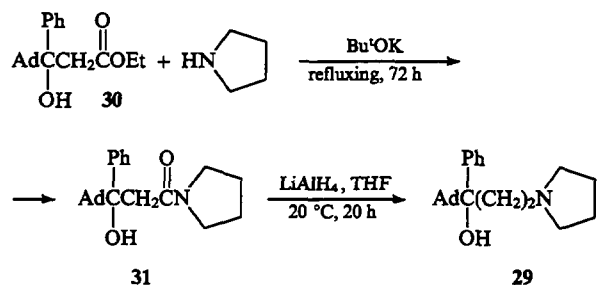
3. Compounds with five-membered heterocycles

A number of methods have been reported for the introduction of a pyrrolidine ring into adamantyl-containing compounds. For example, in the reaction of the bromoketones 28 with pyrrolidine, the bromine atom is substituted by a pyrrolidine residue.³⁵

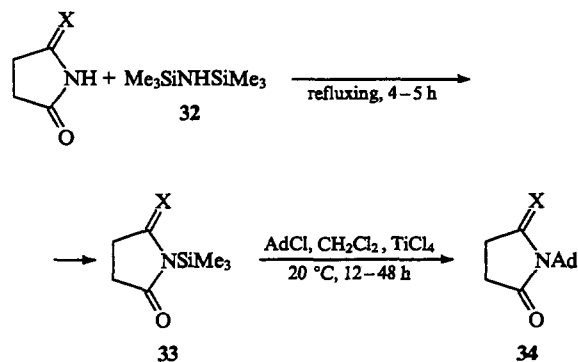


R = H, Me.

The alcohol 29, which causes general depression of the central nervous system, is obtained in 34% yield by refluxing ethyl 3-(adamant-1-yl)-3-hydroxy-3-phenylpropionate 30 in pyrrolidine in the presence of potassium *tert*-butoxide followed by the reduction of the compound 31 thus formed.³⁶

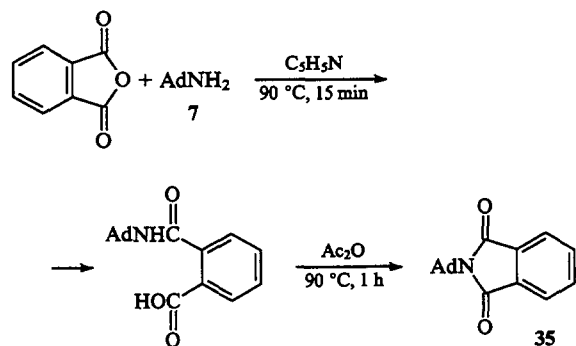


The addition of adamant-1-yl radical to the nitrogen atom of pyrrolidone has been accomplished in two stages: initially, pyrrolidone was refluxed with hexamethyldisilazane 32, and then the resulting *N*-silylated derivative 33 ($X = H_2$) was treated with 1-chloroadamantane in the presence of titanium(IV) chloride and chlorotrimethylsilane. The reaction product 34 ($X = H_2$) and the corresponding adamantylation product 34 ($X = O$) were obtained in a similar way from pyrrolidine-2,5-dione (yield 33%).³⁷



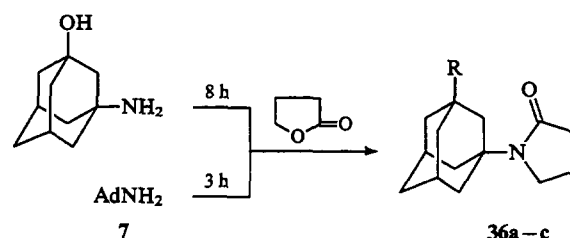
$X = H_2, O$.

N-(Adamant-1-yl)phthalimide 35 has been obtained in 15% yield by the reaction of the amine 7 with phthalic anhydride with subsequent cyclisation of the resulting *o*-(adamant-1-yl)amino-carbonylbenzoic acid with acetic anhydride.³⁸



N-(Adamant-1-yl)maleimide, which possesses antitumour activity and inhibits *Herpes simplex* virus, has been prepared by the reaction of the amine 7 with maleic anhydride followed by cyclisation of the resulting compound $AdNHCOCH=CHCOOH$ with polyphosphoric acid.³⁹

Heating of butyrolactone with the amine 7 and with 1-amino-3-hydroxyadamantane at 200–205 °C leads to *N*-substituted derivatives of pyrrolidone 36a and 36b in 86.5% and 71.5% yields, respectively.



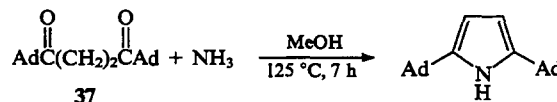
$R = H$ (a), OH (b), $COOH$ (c).

The hydroxy compound 36b can also be obtained from the adamantyl derivative 36a by treating it with a mixture of nitric and sulfuric acids (0–5 °C, 2 h, yield 56.3%). The acid 36c ($R = COOH$), in its turn, can be synthesised in 69.5% yield from the hydroxy derivative and formic acid in the presence of sulfuric acid (20 °C, 5 h).⁴⁰

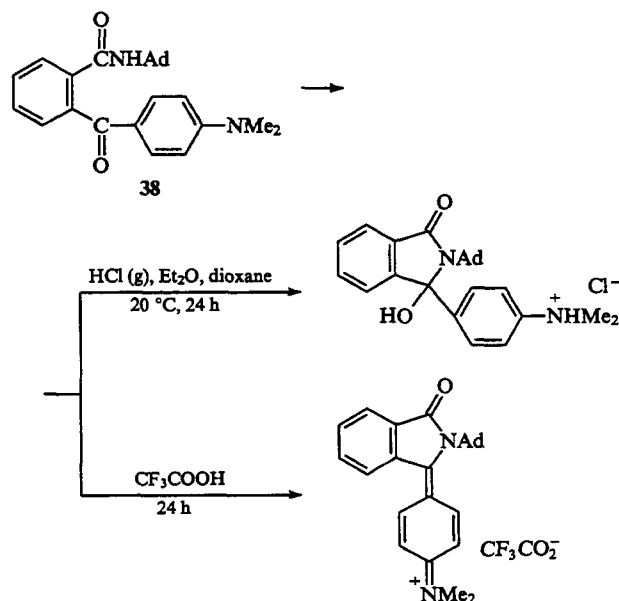
The compounds 36a and 36b exhibit an immunostimulating activity, which is higher for 36a. The introduction of the $COOH$ group exerts no substantial influence on the activity, but decreases markedly the toxicity.⁴⁰

N-(Adamant-1-yl)pyrrolidone and its hydrochloride have been patented as anti-inflammatory agents and also as preparations stimulating the central nervous system and decreasing the cholesterol level.²⁹ *N*-[2-(Adamant-1-yl)ethyl]pyrrolidine and *N*-[3-(adamant-1-yl)propyl]pyrrolidine hydrochlorides have also been recommended as agents influencing the central nervous system.⁴¹

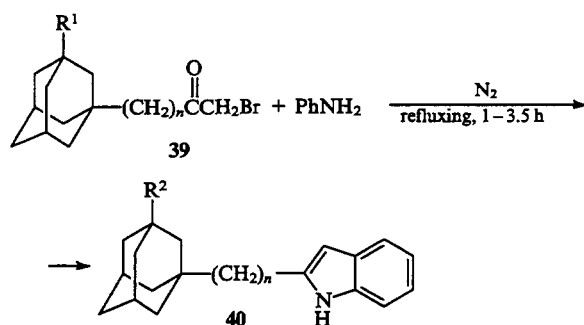
Heating of the diketone 37 with ammonia in a sealed tube affords 2,5-di(adamant-1-yl)pyrrole in a very high yield (95%).⁴²



The cyclisation of compound 38 in the presence of hydrogen chloride or trifluoroacetic acid affords two different salt-type products.⁴³

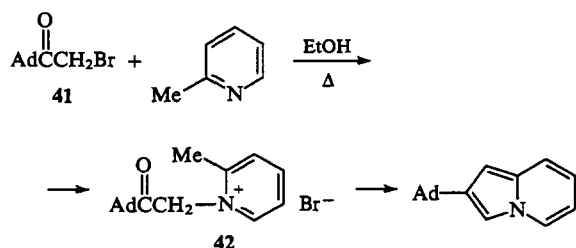


Refluxing of the bromomethyl ketones 39 with aniline leads to their cyclisation into indol derivatives 40 in 48%–94% yields.^{44,45}

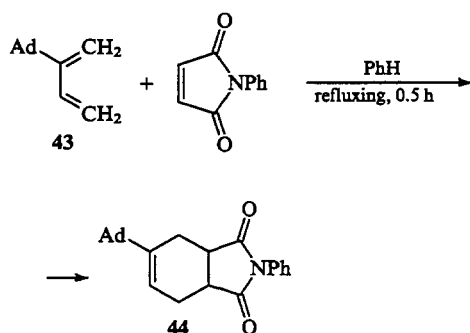


R ¹	R ²	n	Ref.
H	H	0	44, 45
H	H	1	44
CH ₂ Br	CH ₂ Br	0	44
Cl	NHPh	0	44

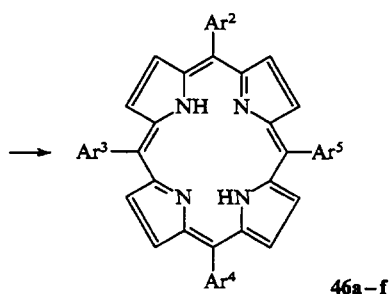
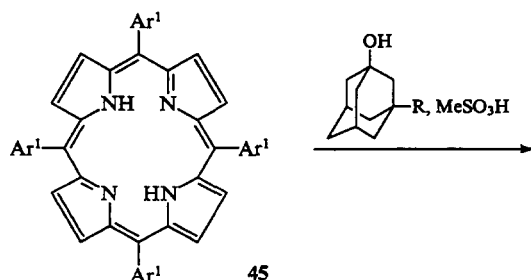
It has been found that the reaction of adamant-1-yl bromomethyl ketone **41** with 2-methylpyridine gives in 50% yield salt **42**, which then cyclises to 2-(adamant-1-yl)indolizine in 58% yield.⁴⁶



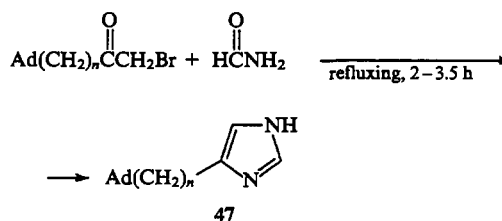
2-(Adamant-1-yl)buta-1,3-diene **43** enters into the Diels-Alder reaction with *N*-phenylmaleimide upon refluxing in benzene to give the corresponding adduct **44** in 63% yield.⁴⁷



The introduction of an adamantane nucleus into the porphyrin derivatives **45** giving rise to compounds **46** has been accomplished by the action of 3-aminomethyl-1-hydroxyadamantane or 3-hydroxyadamantane-1-carboxylic acid in the presence of methanesulfonic acid (see Table 1).⁴⁸

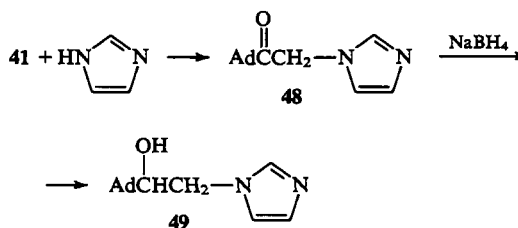


Following refluxing with formamide, the bromoketones $\text{Ad}(\text{CH}_2)_n\text{COCH}_2\text{Br}$ are converted into imidazole derivatives **47** in 43%–51% yields.^{44, 45}

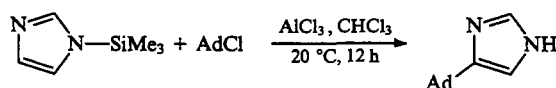


$n = 0, 1.$

The ketone **48**, which is formed in the reaction of the bromomethyl ketone **41** with imidazole, has been reduced to the corresponding alcohol **49**, the derivatives of which have been recommended as bactericides and fungicides.⁴⁹



Japanese investigators^{50, 51} developed a method for the introduction of the adamantyl radical into heterocyclic compounds, which involves the use of organosilicon derivatives of the latter. For example, treatment of *N*-(trimethylsilyl)imidazole with 1-chloroadamantane in the presence of aluminium chloride or titanium(IV) chloride affords 4-(adamant-1-yl)imidazole in 52% yield.⁵¹

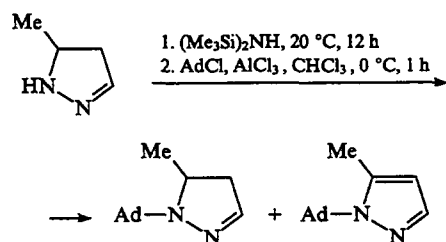
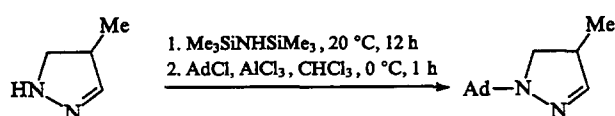


Similarly, in the reaction of 1-(trimethylsilyl)benzimidazole with 1-chloroadamantane, the adamantyl radical adds to the benzene ring rather than to the heterocyclic nucleus; hence, the reaction leads to 5-(adamant-1-yl)benzimidazole (yield 49%).⁵⁰

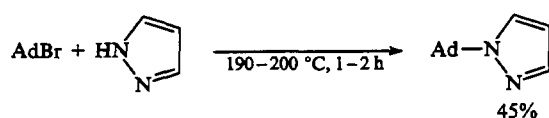
In a more recent study,³⁷ the *N*-adamantylation of nitrogen-containing heterocycles has been carried out by a one-pot procedure: a heterocyclic compound was initially treated with disilazane, and then 1-chloroadamantane and a Lewis acid were added to the reaction mixture; the process was completed, as a rule, at room temperature. 4-Methylpyrazoline was converted in this way into 1-(adamant-1-yl)-4-methylpyrazoline (yield 60%), while the transformation of 5-methylpyrazoline gave 1-(adamant-1-yl)-5-methylpyrazoline (yield 18%) and the product of its dehydrogenation, 1-(adamant-1-yl)-5-methylpyrazole (yield 37%).³⁷

Table 1. Yields of adamantylporphyrins 46.

Compound	R	Ar ¹	Ar ²	Ar ³	Ar ⁴	Ar ⁵	Yield (%)
46a	CH ₂ NH ₂	Ph	Ph	Ph	Ph		42
46b	CH ₂ NH ₂	4-MeOC ₆ H ₄	4-MeOC ₆ H ₄	4-MeOC ₆ H ₄	4-MeOC ₆ H ₄		42
46c	CH ₂ NH ₂	4-MeOC ₆ H ₄	4-MeOC ₆ H ₄		4-MeOC ₆ H ₄		22
46d	CH ₂ NH ₂	4-MeOC ₆ H ₄			4-MeOC ₆ H ₄	4-MeOC ₆ H ₄	22
46e	COOH	Ph	Ph	Ph	Ph		40
46f	COOH	4-MeOC ₆ H ₄	4-MeOC ₆ H ₄	4-MeOC ₆ H ₄	4-MeOC ₆ H ₄		45

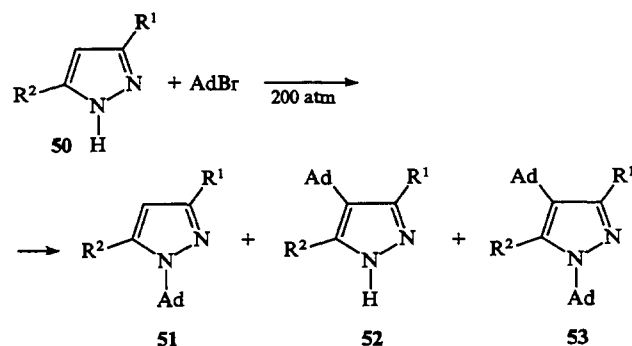


1-(Adamant-1-yl)pyrazole has been obtained by heating pyrazole with 1-bromoadamantane.^{52,53}



1-(Adamant-1-yl)imidazole (yield 74%) and 1-(adamant-1-yl)benzimidazole (yield 69%) were synthesised in a similar way from 1-bromoadamantane and imidazole (or benzimidazole).⁵³

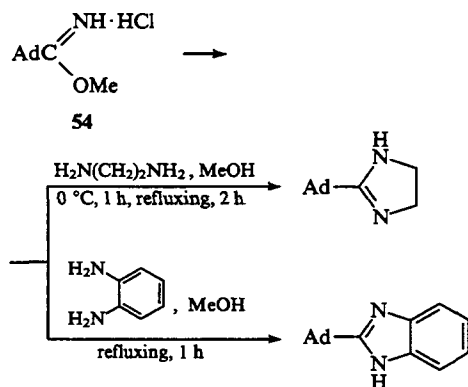
The reactions of 1-bromoadamantane with pyrazole and its alkyl analogues **50** have been studied in detail. It was found that the interaction of AdBr with pyrazole, 3-methylpyrazole, or 3,5-dimethylpyrazole under a pressure of 200 atm may afford one to three reaction products **51–53** depending on the temperature and on the ratio heterocyclic compound : bromide.⁵⁴



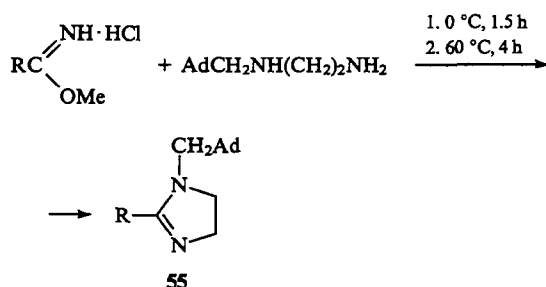
50 : AdBr	T / °C	t / h	Reaction products composition (%)		
			51	52	53
			R ¹ = R ² = H		
2 : 1	120	4	100	0	0
2 : 1	230	4	13	86	1
1 : 2	230	1	14	37	49
			R ¹ = Me, R ² = H		
1 : 1	230	4	78	25	0
2 : 1	230	4	7	90	3
1 : 2	230	4	9	26	65
			R ¹ = R ² = Me		
1 : 1	120	5.5	100	0	0
1 : 1	230	4	0	100	0

In a certain temperature regime, one can obtain only compounds **51**.

The hydrochlorides of iminoesters of carboxylic acids are convenient initial compounds for the synthesis of diverse heterocyclic derivatives. The reaction of methyl adamantane-1-carboximidate hydrochloride **54** with ethylenediamine gives 2-(adamant-1-yl)imidazoline in 92% yield, while the interaction of compound **54** with *o*-phenylenediamine leads to 2-(adamant-1-yl)benzimidazole (yield 71.5%).^{55, 56}

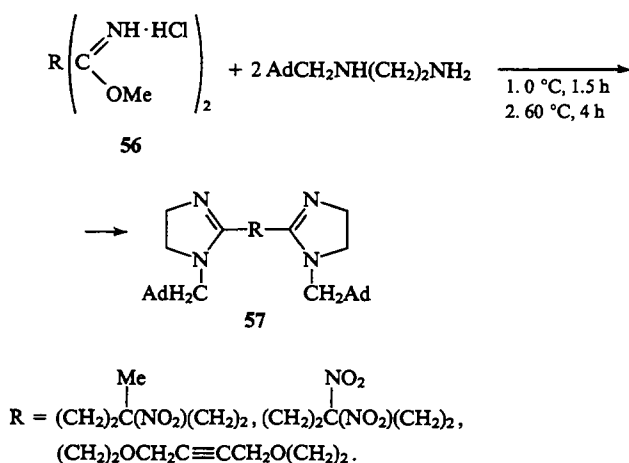


The imidazoline derivatives **55** have been synthesised in 80%–94% yields by cyclocondensation of *N*-(adamant-1-ylmethyl)ethylenediamine with hydrochlorides of various methyl carboximidates.⁵⁶



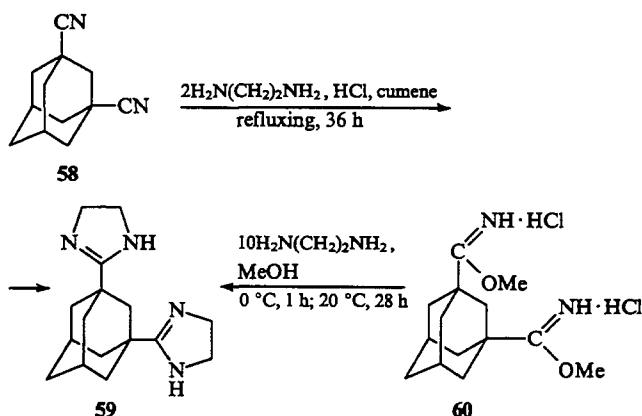
R = Me, Ph, PhCH₂, 5-nitrofuryl-2, 2-(benzimidazol-1-yl)ethyl, 3-nitro-3-methylbutyl.

The reaction of hydrochlorides of methyl iminoesters of dicarboxylic acids **56** with two equivalents of *N*-(adamant-1-ylmethyl)ethylenediamine affords compounds **57** containing two *N*-(adamant-1-ylmethyl)imidazoline fragments in 89%–95% yields.⁵⁶

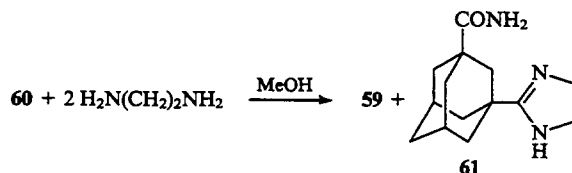


A series of adamantane derivatives containing residues of two identical or different five-membered heterocyclic compounds have been synthesised from 1,3-dicyanoadamantane **58**. Its reaction with ethylenediamine in boiling cumene in the presence of hydrochloric acid gave 1,3-bis(imidazolin-2-yl)adamantane **59** in 86% yield.^{56, 57}

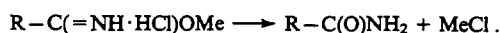
The compound **59** is also formed in 83% yield in the reaction of the diiminoester dihydrochloride **60** with a five-fold excess of ethylenediamine in methanol.^{56, 57}



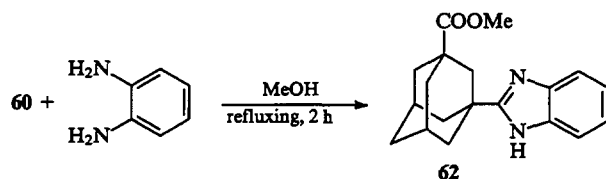
If the reaction of the dihydrochloride **60** involves a stoichiometric amount of ethylenediamine, it leads to the compound **59** and 3-aminocarbonyl-1-(imidazolin-2-yl)adamantane **61**.^{56, 57}



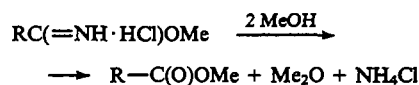
The formation of the amide **61** is accounted for by the fact that one of the iminoester groups undergoes partly the Pinner rearrangement under the reaction conditions



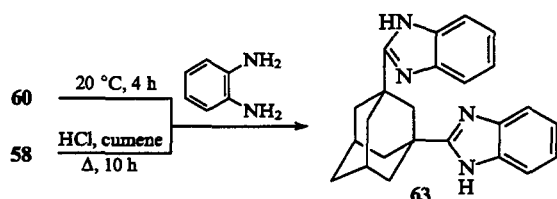
1-(Benzimidazol-2-yl)-3-(methoxycarbonyl)adamantane **62** has been synthesised in 64% yield by the reaction of the dihydrochloride **60** with a stoichiometric amount of *o*-phenylenediamine carried out in boiling methanol.



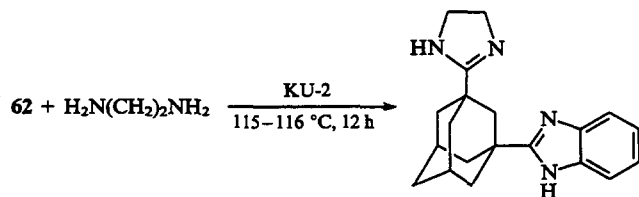
The C(O)OMe group arises via the alcoholysis of the iminoester group.^{56,57}



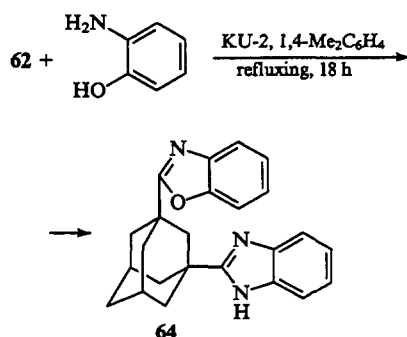
When the dihydrochloride **60** is introduced in the reaction with a fivefold excess of *o*-phenylenediamine at 20 °C, 1,3-bis-(benzimidazol-2-yl)adamantane **63** is obtained in 69% yield. The same compound is formed in 58% yield on refluxing the dinitrile **58** and *o*-phenylenediamine in cumene in the presence of hydrochloric acid.^{56,57}



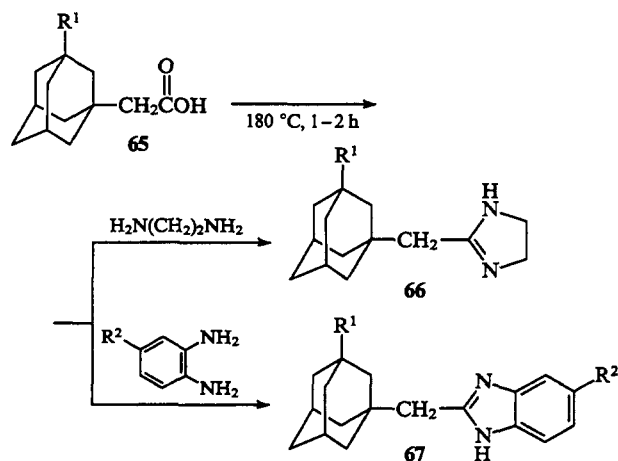
The adamantane derivative containing a benzimidazole residue in the 1-position and an imidazoline fragment in 3-position has been prepared in 71% yield by condensing compound **62** with ethylenediamine in the presence of the KU-2 cation-exchange resin.^{56,57}



Refluxing of the compound **62** with *o*-aminophenol in *p*-xylene in the presence of the KU-2 cation-exchange resin with continuous removal of the water liberated affords 1-(benzimidazol-2-yl)-3-(benzoxazol-2-yl)adamantane **64** in 59% yield.^{56,57}



The carboxylic acids of the adamantane series **65** react with ethylenediamine or with *o*-phenylenediamine at a temperature of 180 °C giving the imidazolines **66** (yields 49% and 56%) or benzimidazoles **67** (yields 32%–42%).⁵⁸

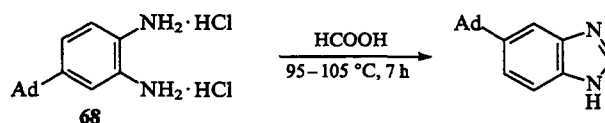


66: R¹ = H, OH;

67: R¹ = H; R² = H, Me, Cl, Br, OH.

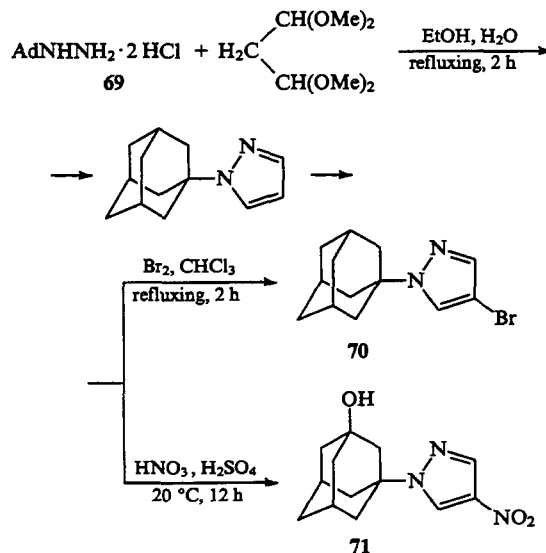
Some of the compounds synthesised were noted to possess antihypertensive and antibacterial activities.⁵⁸

6-(Adamant-1-yl)benzimidazole has been obtained in 98% yield by the cyclocondensation of the bis-hydrochloride **68** with formic acid.⁵⁹

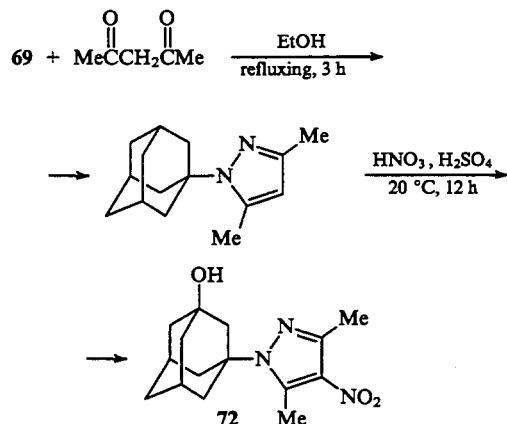


N-(Adamant-1-ylcarbonyl)-*o*-phenylenediamine is converted into 2-(adamant-1-yl)benzimidazole in 96% yield on heating with polyphosphoric acid.⁶⁰

Cyclocondensation of hydrazine or its derivatives with carbonyl compounds is a common method for the synthesis of compounds of the pyrazole series. This method is also used fairly frequently for the synthesis of adamantyl-containing pyrazole derivatives. For example, when *N*-(adamant-1-yl)hydrazine hydrochloride **69** is made to react with the tetramethylacetal of malonaldehyde, 1-(adamant-1-yl)pyrazole is formed in 63% yield; treatment of the latter compound with bromine affords the 4-bromo-derivative **70** (yield 95%). When (adamant-1-yl)pyrazole is treated with a mixture of nitric and sulfuric acids, the nitration of the pyrazole ring and the oxidation of the adamantyl fragment occur simultaneously to give compound **71**, yield 86%.⁶¹

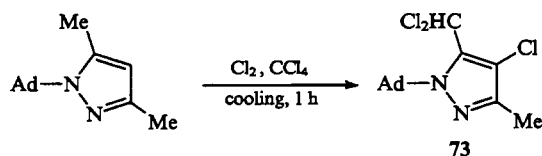


The reaction of pentane-2,4-dione with the dihydrochloride **69** leads to 1-(adamant-1-yl)-3,5-dimethylpyrazole, which is converted into compound **72** in 86% yield on treatment with a mixture of nitric and sulfuric acids.⁶¹

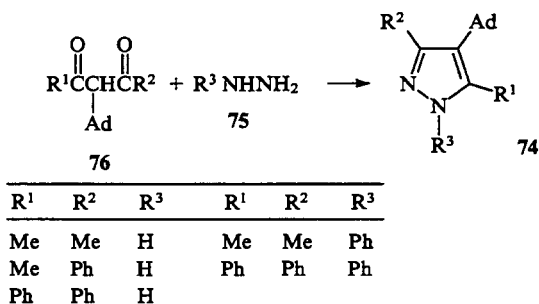


The dihydrochloride **69** reacts with 3-methylpentane-2,4-dione in boiling alcohol (3 h) to give 1-(adamant-1-yl)-3,4,5-trimethylpyrazole (yield 63%).⁶²

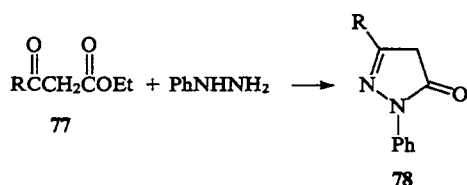
The chlorination of 1-(adamant-1-yl)-3,5-dimethylpyrazole with chlorine carried out with cooling involves both the pyrazole ring and one of the methyl groups and leads to 1-(adamant-1-yl)-4-chloro-5-dichloromethyl-3-methylpyrazole **73** in 43% yield.⁶²



A series of derivatives of 4-(adamant-1-yl)pyrazole **74** have been prepared in 71%–93% yields by the condensation of the hydrazines **75** with the β -diketones **76** carried out in boiling alcohol (1 h), in alcohol at 20 °C (12 h), or without solvent at 130–140 °C (1–1.5 h).⁶³

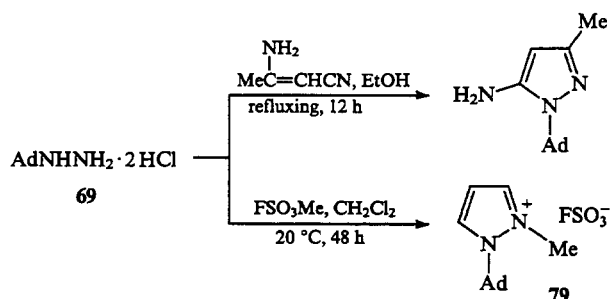


In earlier papers,^{42,64} the products of the interaction of the β -ketoesters **77** with phenylhydrazine have been identified as the pyrazol-5-one derivatives **78** (yields 67%–80%). The reactions were carried out at 20 °C for 3 h in aqueous acetic acid in the case of the ketoester with R = Ad⁴² or without solvent in the case of R = AdCH₂.⁶⁴

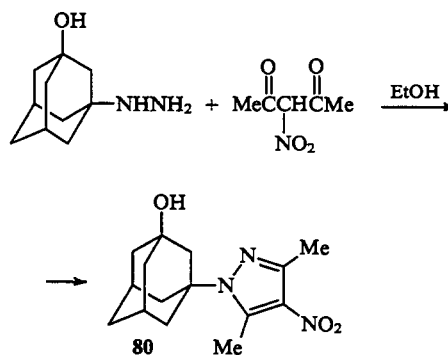


R = Ad, AdCH₂.

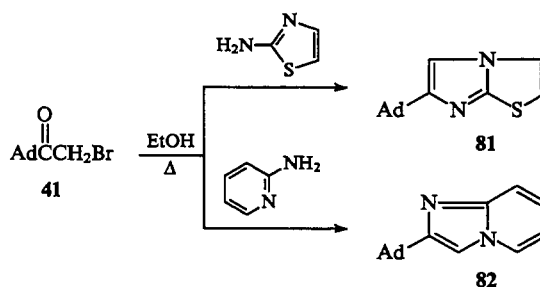
The reaction of the dihydrochloride **69** with β -aminocrotonitrile affords 1-(adamant-1-yl)-5-amino-3-methylpyrazole in 40% yield, whereas the interaction of the compound **69** with methyl fluorosulfonate gives the salt **79** (yield 90%).⁶¹



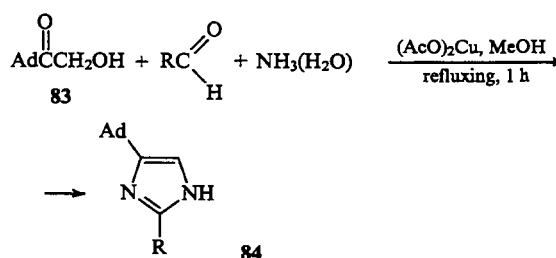
Cyclocondensation of (3-hydroxyadamant-1-yl)hydrazine with 3-nitropentane-2,4-dione leads to compound **80**, which is active against anaerobic bacteria.⁶⁵



The 1-acetyladamantane derivatives, in which one or two hydrogen atoms in the methyl group have been substituted by bromine or by a functional group, have been used as the initial compounds in the syntheses of heteryladamantanes. The bicyclic compounds **81** and **82** were prepared by the condensation of the ketone **41** with 2-aminothiazole and 2-aminopyridine, respectively.⁴⁶

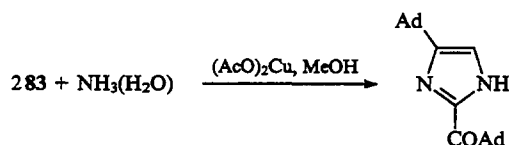


The hydroxy ketone **83** reacts with aldehydes and ammonia in boiling methanol in the presence of copper acetate to give the imidazole derivatives **84**.⁶⁶



R = H (54%), Prⁱ (46%), Ph (54%).

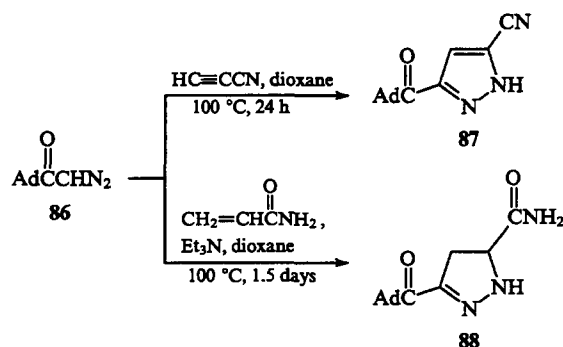
If the hydroxy ketone **83** is made to react with ammonia in the absence of aldehydes, 2-(adamantylcarbonyl)-4-(adamant-1-yl)-imidazole is obtained in 72.5% yield.⁶⁶



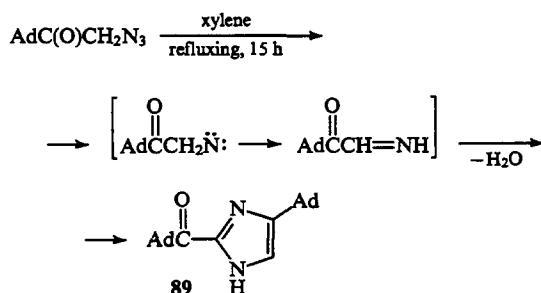
4-(Adamant-1-yl)-2-sulfanylimidazole (**84**, R = SH) has been synthesised in 35% yield by refluxing the hydrobromide **85** with NH_4SCN in water.⁶⁶



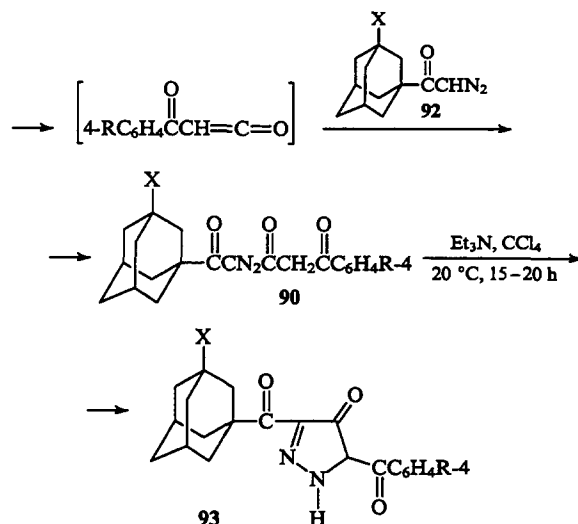
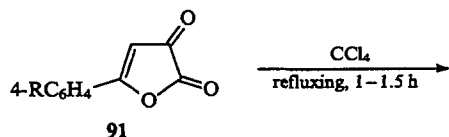
Some investigators have prepared adamantyl-containing pyrazole and pyrazoline derivatives using adamantyl diazomethyl ketones as the initial compounds. The condensation of adamant-1-yl diazomethyl ketone **86** with propionitrile or with acrylamide gives 3-adamantylcarbonyl-5-cyanopyrazole **87** (yield 92%) or 3-adamantylcarbonyl-5-aminocarbonylpyrazoline **88** (yield 14%).⁶⁰



An interesting reaction occurs when adamant-1-yl azidomethyl ketone is heated in xylene; the compound **86** is converted into 2-adamant-1-ylcarbonyl-4-(adamant-1-yl)imidazoline **89** (yield 73%). The authors⁶⁷ believe that the process involves the intermediate formation of nitrene, which is converted into imine, and the latter dimerises with intermolecular abstraction of water.

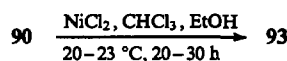


1-(Adamant-1-yl)-5-aryl-2-diazopentane-1,3,5-triones **90**, obtained by heating 5-aryl-2,3-dihydrofuran-2,3-diones **91** with the diazoketones **92** in tetrachloromethane, are converted in the presence of triethylamine into the pyrazolin-4-one derivatives **93** in 63–92% yields.⁶⁸



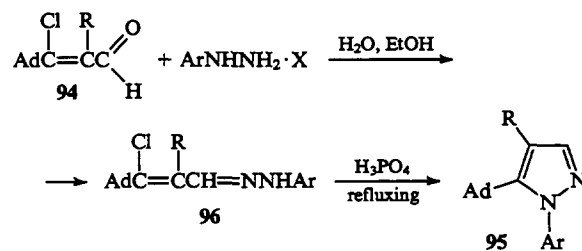
X = H, R = H, Me, OMe, Br, Cl; X = ONO_2 ; R = H, Br.

The transformation of the derivatives **90** into the corresponding pyrazolin-4-ones **93** can also be carried out with nickel chloride as the catalyst.⁶⁹

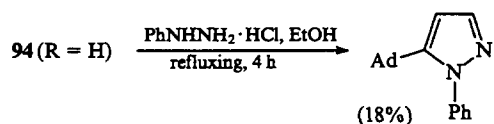


X = H, R = Cl; X = ONO_2 , R = H.

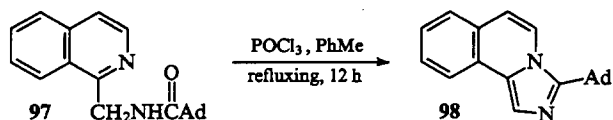
The β -chloroacrolein derivatives $\text{R}^1\text{C}(\text{Cl})=\text{C}(\text{R}^2)\text{CHO}$ offer considerable synthetic opportunities. These compounds are widely used for the synthesis of various heterocyclic derivatives including heteryladamantanes. For example, the aldehydes **94** have been converted into the pyrazole derivatives **95** by two different procedures.^{70,71} One of them⁷⁰ involved the reaction of the aldehydes **94** [Ar = 2,4,6-(NO_2)₃C₆H₂ and C₅H₅] with phenylhydrazine giving the corresponding hydrazones **96**, which were then converted into the target compounds **95**,⁷⁰ whereas according to the other procedure,⁷¹ 5-(adamant-1-yl)-1-phenylpyrazole was obtained without isolation of the intermediate hydrazone **96** (R = H, Ar = Ph).⁷¹



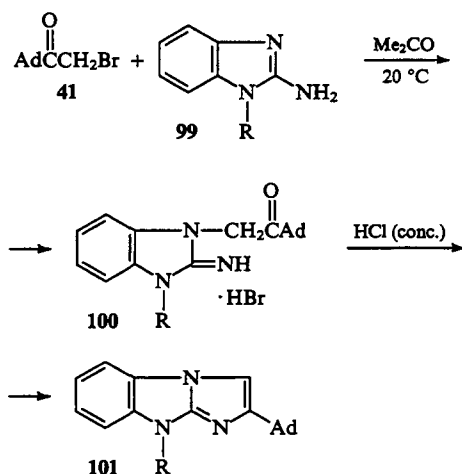
R	Ar	X	t/h		T / °C		Yield (%)	
			95	96	95	96	95	96
H	Ph	HCl	2	24	160	20	48	73
H	2,4,6-(O_2N) ₃ C ₆ H ₂	—	6	0.25	refluxing (AcOH)	100	41	77
Me	2,4,6-(O_2N) ₃ C ₆ H ₂	—	6	0.2	refluxing (AcOH)	100	54	62



Heating of the isoquinoline derivative **97** with an 18% solution of phosphorus oxychloride in toluene affords 3-(adamant-1-yl)imidazo[5,1-*a*]isoquinoline **98** in 90% yield.⁷²

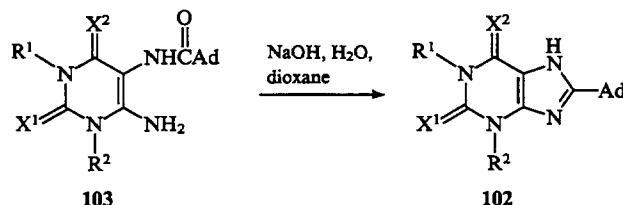


The interaction of the ketone **41** with 2-amino-1-*R*-benzimidazoles **99** leads to the hydrobromides **100** in quantitative yields; on heating with concentrated hydrochloric acid the latter are converted into the tricyclic compounds **101**, which exhibit immunodepressant properties and are psychotropic inhibitors of cytochrome P-450.⁷³



$R = \text{Alk, PhCH}_2, (\text{CH}_2)_2\text{NEt}_2, (\text{CH}_2)_2\text{N}(\text{CH}_2)_2\text{OCH}_2\text{CH}_2$.

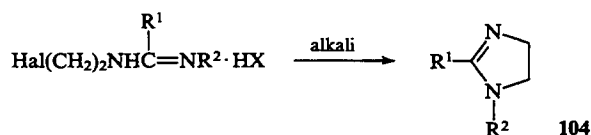
The derivatives of 8-(adamant-1-yl)xanthine or 8-(adamant-1-yl)thioxanthine **102** have been prepared by cyclisation of the amides **103** carried out in dioxane under the action of aqueous sodium hydroxide.⁷⁴



$X^1, X^2 = \text{O, S}; R^1, R^2 = \text{H, Alk, CH}_2\text{CH=CH}_2, \text{CH}_2\text{C}\equiv\text{CH}$.

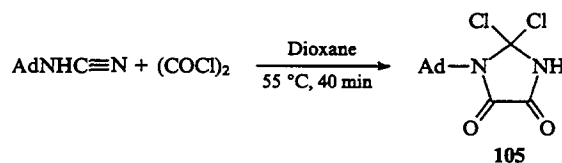
8-(Adamant-1-yl)-1,3-dipropylxanthine, which is an antagonist of adenosine A₁, is formed upon heating 6-amino-5-(nor-adamantanecarbonylamino)-1,3-dipropyluracil with phosphorus oxychloride.⁷⁵

The salts $\text{HalCH}_2\text{CH}_2\text{NHC(R}^1\text{)=NR}^2 \cdot \text{HX}$ cyclise in the presence of alkali to give the imidazoline derivatives **104**.³⁰



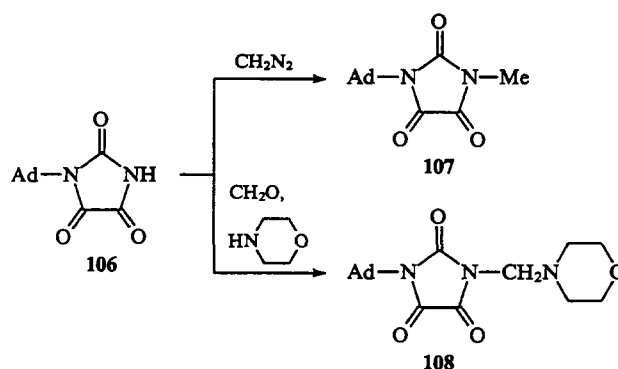
$R^1 = \text{Ad}; R^2 = \text{Ph, C}_6\text{H}_5, \dots, \text{R}_n$.

1-(Adamant-1-yl)-2,2-dichloroimidazolidine-4,5-dione **105**, synthesised from (adamant-1-yl)cyanogen amide and oxalyl chloride, is a promising synthon for the preparation of adamantyl-containing derivatives of imidazolidine-4,5-dione.⁷⁶

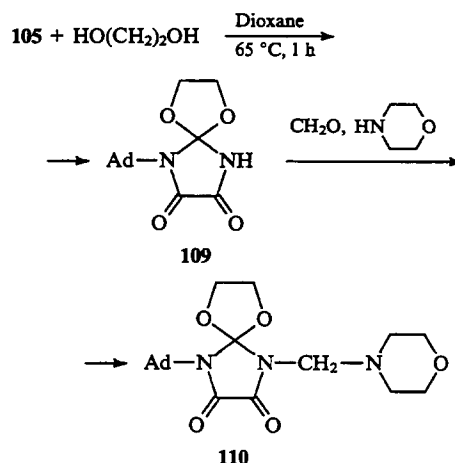


Treatment of the dichloro-derivative **105** with water affords 1-(adamant-1-yl)imidazolidine-2,4,5-trione **106** in 97% yield.⁷⁶

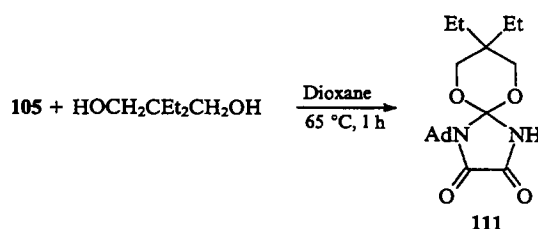
To prepare derivatives of the imidazolidinetriene **106**, namely, compounds **107** and **108** (yields 62% and 92%), the product of the hydrolysis of the dichloride **105** is made to react in situ with diazomethane or with formaldehyde and morpholine.⁷⁶



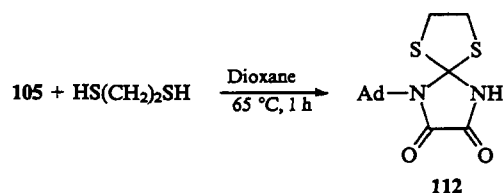
The ketal **109** (yield 48%) is formed in the reaction of adamantylcyanogen amide with oxalyl chloride in the absence of moisture followed by treatment of the resulting dichloride with ethylene glycol; the reaction of the compound **109** with formaldehyde and morpholine leads to the ketal **110** in 77% yield.⁷⁶



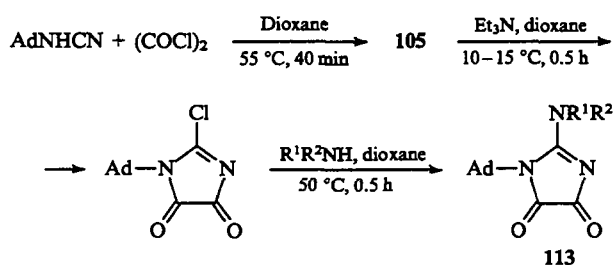
Compound **111** is synthesised from the dichloro-derivative **105** and 2,2-diethylpropane-1,3-diol under similar conditions in 11% yield.⁷⁶



The spiro-compound **112** is prepared in 4% yield by heating the dichloride **105** with ethane-1,2-dithiol in anhydrous dioxane.⁷⁶

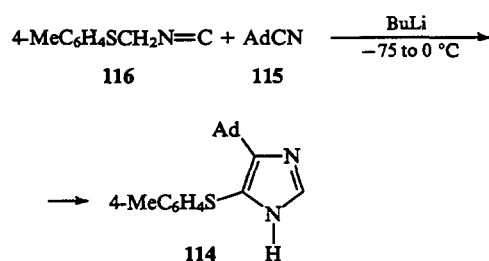


The successive treatment of (adamant-1-yl)cyanogen amide with oxalyl chloride in anhydrous dioxane, with triethylamine, and with secondary amines gives compounds **113** in 65%–90% yields.⁷⁶

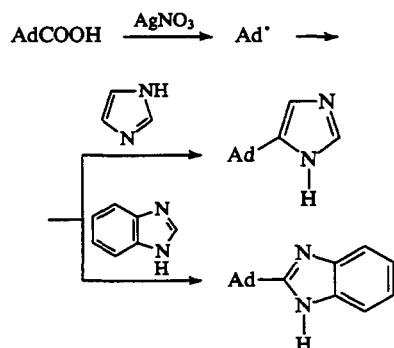


$\text{R}^1 = \text{R}^2 = (\text{PhCH}_2)_2, (\text{Pr}^i\text{CH})_2,$
 $\text{R}^1, \text{R}^2 = -\text{O}(\text{CH}_2\text{CH}_2)_2-, -(\text{CH}_2)_5-.$

The imidazole derivative **114** is formed in 91% yield in the reaction of the nitrile **115** with the isocyanide **116** at low temperature.⁷⁷

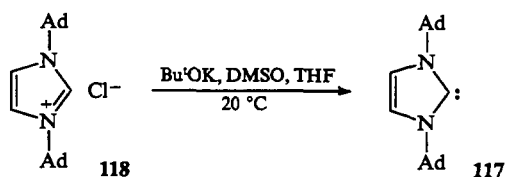


The formation of 2-(adamant-1-yl)imidazole or 2-(adamant-1-yl)benzimidazole from adamantane-1-carboxylic acid and imidazole (or benzimidazole) in the presence of silver nitrate is a homolytic reaction. The Ad^\bullet radical is generated from adamantane-1-carboxylic acid.⁷⁸

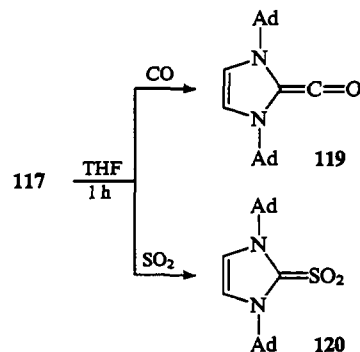


2-(Adamant-1-yl)-1-methylimidazole has been reported⁷⁸ to exhibit antiviral activity.

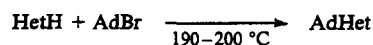
The crystalline carbene **117**, which is stable in the absence of oxygen and moisture, has been synthesised in 96% yield by treating 1,3-di(adamant-1-yl)imidazolium chloride **118** with potassium *tert*-butoxide in dimethyl sulfoxide.⁷⁹



The carbene **117** reacts with carbon monoxide or with sulfur dioxide⁸⁰ in THF giving the ketene **119** (yield 34%) or 1,3-di(adamant-1-yl)imidazole-2-thione *S,S*-dioxide **120**.

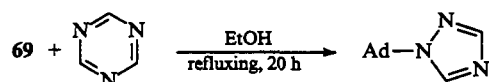


Adamantyl residues have been introduced to the nitrogen atoms in 1,3,4-triazole, 1,2,4-triazole, or benzotriazole by treating these compounds with 1-bromoadamantane with heating.⁵³

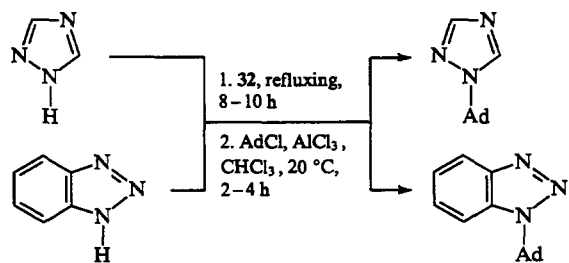


Het = 1,2,4-triazol-1-yl (59%), 1,3,4-triazol-1-yl (3%),
 benzotriazol-1-yl (45%), benzotriazol-2-yl (34%).

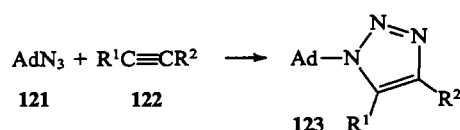
1-(Adamant-1-yl)-1,2,4-triazole is formed in 30% yield on heating *sym*-triazine with the hydrochloride **69** in alcohol.⁵³



1-(Adamant-1-yl)-1,2,4-triazole (yield 70%) and 1-(adamant-1-yl)benzotriazole (yield 60%) have been prepared by a two-stage procedure. The first stage consists in the *N*-silylation of the corresponding heterocyclic compounds by refluxing them with disilazane **32**. In the second stage, the products of the *N*-silylation are treated with 1-chloroadamantane in the presence of aluminium chloride at 20 °C.³⁷



Japanese scientists⁸¹ have studied systematically the 1,3-dipolar cycloaddition of 1-azidoadamantane **121** to alkynes. The reactions of the azide **121** with alkynes **122** are carried out at 110 °C. The yields of the 1,2,3-triazole derivatives **123** vary from 5% to 84%.⁸¹

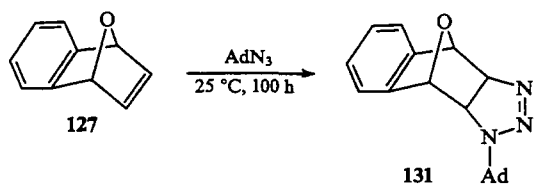
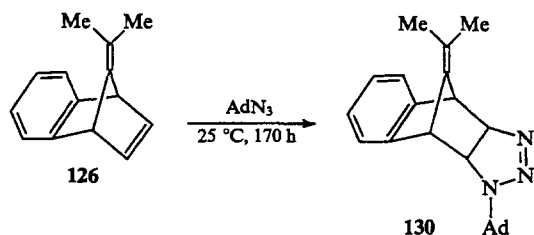
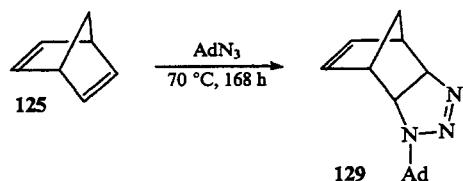
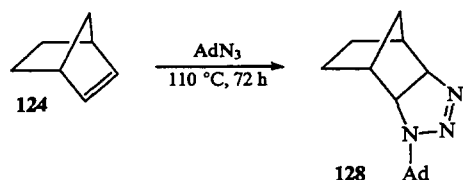


R ¹	R ²	Reaction time / h	Yield of 123 (%)
Ph	H	35	21 ^a
H	Ad	30	67
H	COOMe	11	84
H	CH ₂ OH	5	80 ^b
H	COOEt	50	77
CH ₂ OH	CH ₂ OH	90	32
Ph	Ph	500	17
C(Me)(Et)OH	C(Me)(Et)OH	180	5
COOMe	COOMe	24	77

^a The analogue of 123 with R¹ = H, R² = Ph is formed in 60% yield.

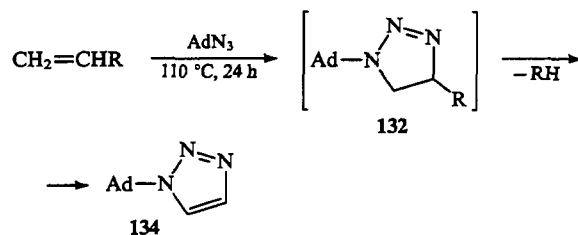
^b The analogue of 123 with R¹ = CH₂OH, R² = H is formed in 11%.

The alicyclic alkenes 124–127 enter into the 1,3-dipolar cycloaddition with adamantyl azide giving the 1,2,3-triazoline derivatives 128–131, their yields ranging from 40% to 70%.⁸¹

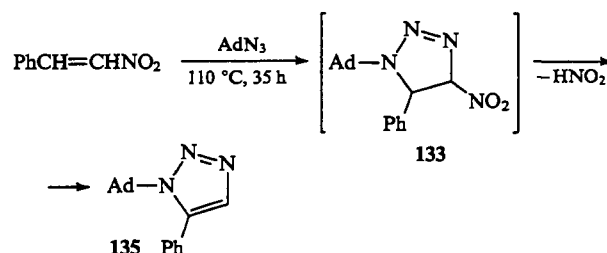


The azide 121 reacts with the ester CH₂ = CHCOOEt at 20 °C and is thus converted into 1-(adamant-1-yl)-4-ethoxycarbonyl-1,2,3-triazoline in 85% yield over a period of 336 h.⁸¹

The reaction of the azide 121 with alkenes CH₂ = CHNO₂, PhCH = CHNO₂, and PhSOCH = CH₂ is more complex. In all these cases, the adducts 132 and 133 formed initially eliminate HNO₂ and PhSOH molecules, and the reaction products are the corresponding 1,2,3-triazole derivatives 134 (yields 73% and 88%) and 135 (yield 66%).⁸¹

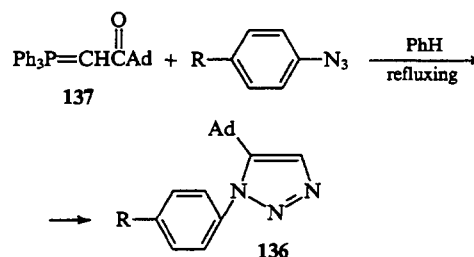


R = NO₂, SOPh.



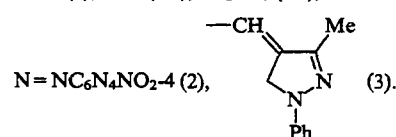
The adduct 131 readily eliminates a C₈H₆O molecule giving rise to 1-(adamant-1-yl)-1,2,3-triazole 134 (yield 71%).⁸¹

To prepare the derivatives of 1,2,3-triazole 136, phosphorus ylide 137 has been used as the second component in the reaction with the azides 4-RC₆H₄N₃. The yields of the adducts 136 vary from 60% to 99%.⁸²

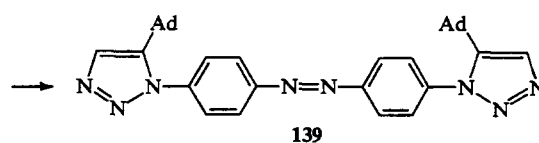
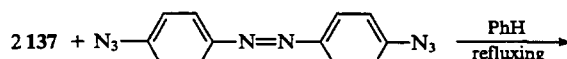
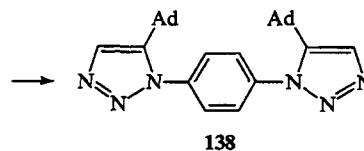
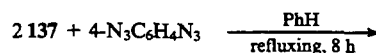


R (reaction time / h) = H (8), F(7), COOMe (3.5), COMe (1.5),

CHO (1), NO₂ (0.5), SO₂CF₃ (0.5), N = NPh (5),

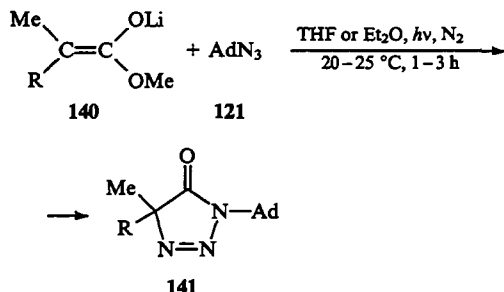


Compounds 138 and 139, which contain two 1,2,3-triazole nuclei each, are obtained in 98% and 93% yields by the interaction of the ylide 137 with 1,4-bis(azido)benzene or with 4,4'-bis(azido)diphenyldiazene.⁸²



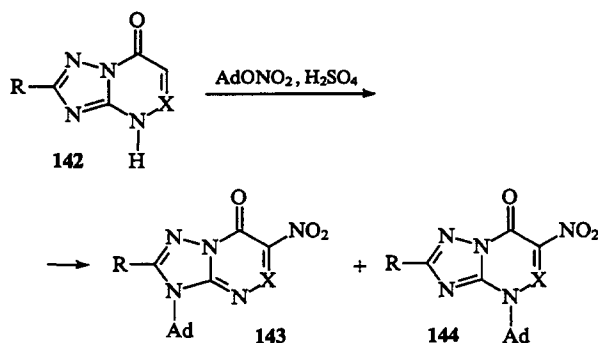
The aryl azides containing electron-donating substituents in the *para*-position with respect to the azido group react with the ylide **137** with difficulty or do not react at all.⁸²

The ester enolates **140** react with the azide **121** on exposure to the radiation from a mercury or mercury-xenon high-pressure lamp to give the 1,2,3-triazol-5-one derivatives **141** in 60%–70% yields.^{25,83}



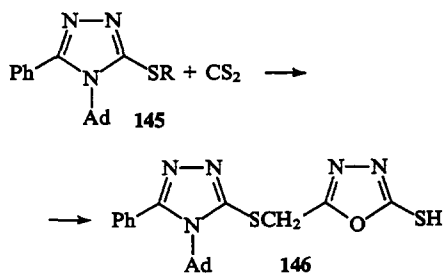
R = Me, Bu^t.

Rusinov et al.⁸⁴ accomplished simultaneous introduction of an adamantyl radical and of a nitro-group by treatment of the bicyclic compound **142** with adamant-1-yl nitrate in the presence of concentrated sulfuric acid. The reaction gave a mixture of two compounds **143** and **144** in an overall yield of >70%.⁸⁴



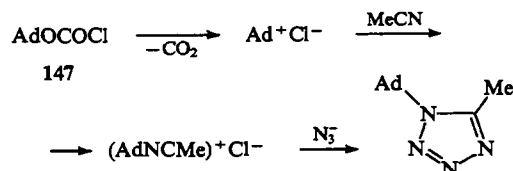
R = H, Me; X = N, CH, CMe, CCF₃.

The 1,3,4-triazole derivatives **145**, which contain in the 2-position the residue of thioglycolic acid hydrazide, react with carbon disulfide to give compounds **146**.⁸⁵

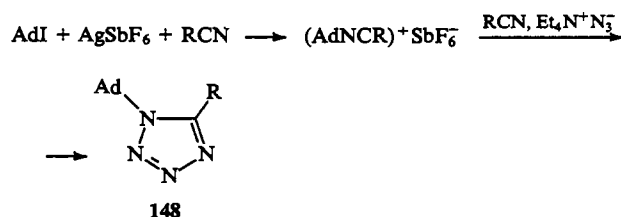


R = CH₂CONHNH₂.

1-(Adamant-1-yl)-5-methyltetrazole has been obtained in 46% yield by the reaction of the chlorocarbonate **147** with acetonitrile and sodium azide at room temperature over a period of 20 h.⁸⁶



The tetrazoles **148** containing alkyl, alkenyl or aryl substituents in the 5-position have been prepared by the interaction of 1-iodoadamantane with silver hexafluoroantimonate and with the corresponding carbonitriles in the presence of the quaternary ammonium salt Et₄N⁺N₃⁻.⁸⁶

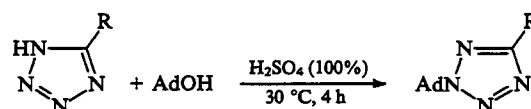


R = Me (71%), Et (29%), Pr (64%), Prⁱ (43%), Ph (21%),

CH₂=CH (20%), CH=CMe₂ (14%), PhCH=CH (49%).

When tetrazole is heated with the bromo-derivative of adamantane at 190–200 °C, two compounds are formed, namely, 1-(adamant-1-yl)tetrazole (yield 24%) and 2-(adamant-1-yl)tetrazole (yield 30%).⁵³

The direct adamantylation of the tetrazole ring has been carried out by treating 5-methyltetrazole and 5-phenyltetrazole with adamantan-1-ol in the presence of sulfuric acid.⁸⁷

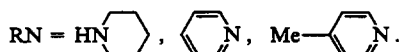
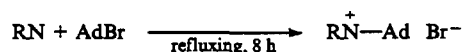


R = Me (57%), Ph (84%).

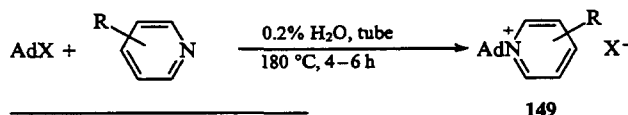
4. Six-membered heterocycles

1-(Adamant-1-yl)-4,4-diarylpiperidines⁸⁸ and *N*-[2-(adamant-1-yl)ethyl]piperidine hydrochloride⁴¹ have been patented as stimulants of the central nervous system.

By refluxing AdBr with piperidine, pyridine, or 4-picoline, the corresponding salts have been synthesised; they have been recommended as antiviral agents.⁸⁹



In a study of reactions of pyridine and its derivatives with 1-bromoadamantane and 1-iodoadamantane, it has been shown that the successful formation of the salts **149** requires that a small amount of water be present in the reaction mixture.⁹⁰

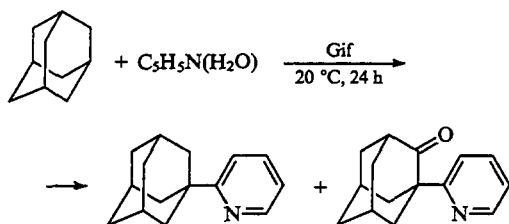


X	R	Yield (%)
Br	H	97
I	H	96
Br	3-Me	62
Br	4-Me	80
Br	3-CONEt ₂	70
Br	4-(pyridyl-4)	98

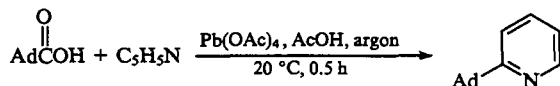
When the reactions are carried out in the absence of water, the salts **149** are formed in low yields. The process should be carried out at 230–250 °C. The corresponding salt with quinoline is not formed.⁹⁰ Steric factors play an important role in this reaction: for

example, the salts **149** cannot be obtained from adamant-1-yl halides with 2-picoline, 2,3-lutidine, or 2,4,6-collidine.

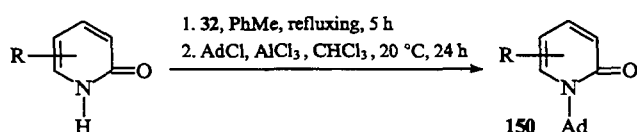
A hydrogen atom in the adamantane molecule can be substituted by a pyridyl radical in the presence of a Gif system ($\text{Fe}-\text{O}_2-\text{Zn}-\text{AcOH}-\text{C}_5\text{H}_5\text{N}$). For example, the reaction of adamantane with pyridine in the presence of this system at 20 °C gives rise to two products: 2-(adamant-1-yl)pyridine and 1-(2-pyridyl)adamant-2-one.⁹¹



The hydrogen atom in the 2-position of pyridine can be substituted by the adamantane residue by a radical mechanism. 2-(Adamant-1-yl)pyridine is formed in 20% yield when a mixture of adamantane-1-carboxylic acid and pyridine is irradiated with a Hanovia lamp (100 W) in the presence of lead(IV) acetate under an argon atmosphere.⁹¹



A method has been developed for the substitution of the hydrogen atom at the nitrogen atom in the 2-pyridone derivatives by the adamantyl fragment.³⁷ For this purpose, this hydrogen atom is substituted by the SiMe_3 group by treating the initial compounds with disilazane **32**, and then the *N*-silylated products are made to react with chloroadamantane in the presence of aluminium chloride. The electronic nature of the substituents in the heterocyclic nucleus of the initial compound exerts the crucial influence on the yields of the reaction products. In the case where electron-withdrawing substituents (Cl or NO_2) are present in the 5-position, the yields of compounds **150** are 53% or 77%. When the initial compound contains an electron-donating methyl group in the 3-, 4-, or 5-position, the yields of the products **150** are much lower (25%, 30%, and 30%, respectively).³⁷

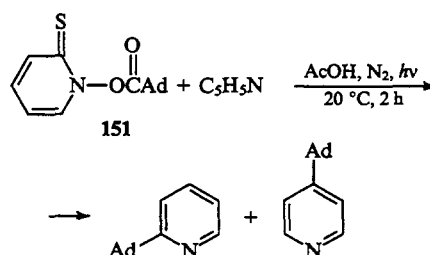


$\text{R} = 5\text{-Cl}, 5\text{-NO}_2, 3\text{-Me}, 4\text{-Me}, 5\text{-Me}$.

The interaction of 2-quinolone with chloroadamantane under similar conditions leads in 72% yield to (adamant-1-yl)-2-quinolone (the position of the adamantyl substituent has not been mentioned in the paper cited).³⁷

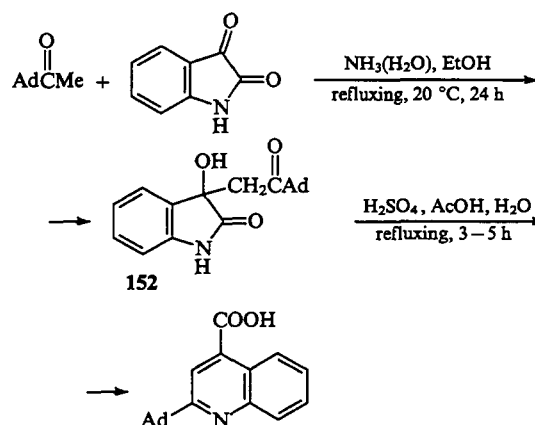
1-(Adamant-1-yl)-2-pyridone has been obtained in 30%–52% yield by the reaction of the chloro-derivative of adamantane with 2-(trimethylsilyloxy)pyridine. The reaction is carried out in the presence of aluminium chloride at 20 °C for 12 h.^{50,51}

The reaction of the compound **151** with pyridine in the presence of acetic acid under irradiation with two tungsten lamps (300 W) leads to a complex mixture of products, among which 2-(adamant-1-yl)pyridine (yield 27.5%) and 4-(adamant-1-yl)pyridine (yield 14%) have been identified.⁹²



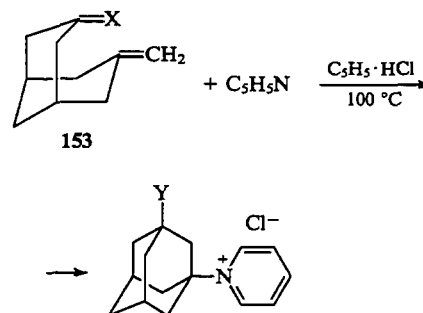
N-(Adamant-1-yl)pyridinium salts are obtained from bromo-adamantane and pyridine. If this reaction is carried out in a sealed tube at 230 °C for 30 h, the yield of adamantylpyridinium bromide is 69%,⁹³ whereas in the reaction carried out at 180 °C for 6 h, the yield reaches 97%.⁹⁴ When bromoadamantane reacts with pyridine in the presence of sodium perchlorate in nitromethane at 0 °C for 4 h and then at 20 °C for 14 h, *N*-(adamant-1-yl)pyridinium perchlorate is formed in 54% yield.⁹⁵

Adamant-1-yl methyl ketone condenses with isatin in the presence of ammonia to give the hydroxy diketone **152**, which is converted into 2-(adamant-1-yl)quinoline-4-carboxylic acid in 94% yield in the presence of sulfuric acid. If the reaction is carried out without isolation of the compound **152**, this acid is formed in a yield of only 5%–10%.⁹⁶



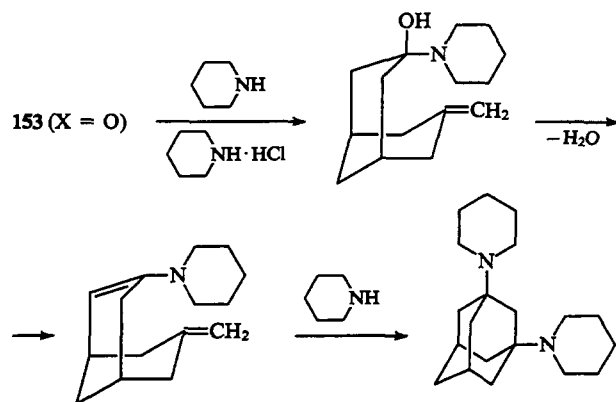
2-(Adamant-1-yl)quinoline has been synthesised in 75% yield by refluxing a mixture of adamant-1-yl methyl ketone with 2-aminobenzaldehyde in an alcoholic solution of potassium hydroxide for 1 h.⁹⁶

In the presence of a weak protic acid, pyridinium chloride, 3,7-dimethylenebicyclo[3.3.1]nonane (**153**, $\text{X} = \text{CH}_2$) and 3-methylenebicyclo[3.3.1]nonan-7-one (**153**, $\text{X} = \text{O}$) react with pyridine yielding the corresponding pyridinium salts.⁹⁷

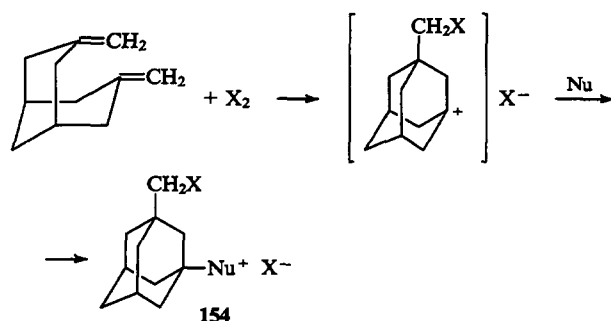


$\text{X} = \text{CH}_2$, $\text{Y} = \text{Me}$; $\text{X} = \text{O}$, $\text{Y} = \text{OH}$.

The reaction of the compound **153** ($\text{X} = \text{O}$) with piperidine in the presence of piperidine hydrochloride follows a different pathway: piperidine adds to the oxo-group, then a molecule of water is eliminated, and finally, the ring closure occurs.⁹⁸



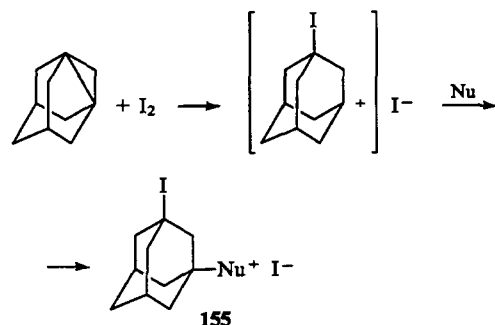
Salts of heteryladamantanes can be obtained from the precursors of adamantane, namely, compounds **153** ($X = \text{CH}_2$) or 1,3-dehydroadamantane, via conjugated intermolecular halamination. A number of salts of 1-heteryl-3-halomethyladamantanes **154** have been synthesised by the reaction of the compound **153** ($X = \text{CH}_2$) with pyridine bases or with quinoline.⁹⁹



$X = \text{I}$: Nu — pyridine, quinoline;
 $X = \text{Br}$: Nu — pyridine, 2-picoline, quinoline.

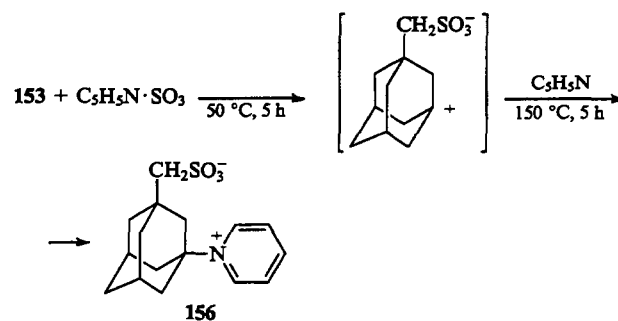
The reactions with bromine were carried out at temperatures from -10 to 0°C over a period of 10 days, whereas the reactions with iodine were conducted at 20°C over 10 days. The yields of the salts **154** varied from 44% to 84%.⁹⁹

The salts **155** have been prepared in 28%–68% yields by the reactions of 1,3-dehydroadamantane with heterocyclic amines and iodine.^{99, 100}

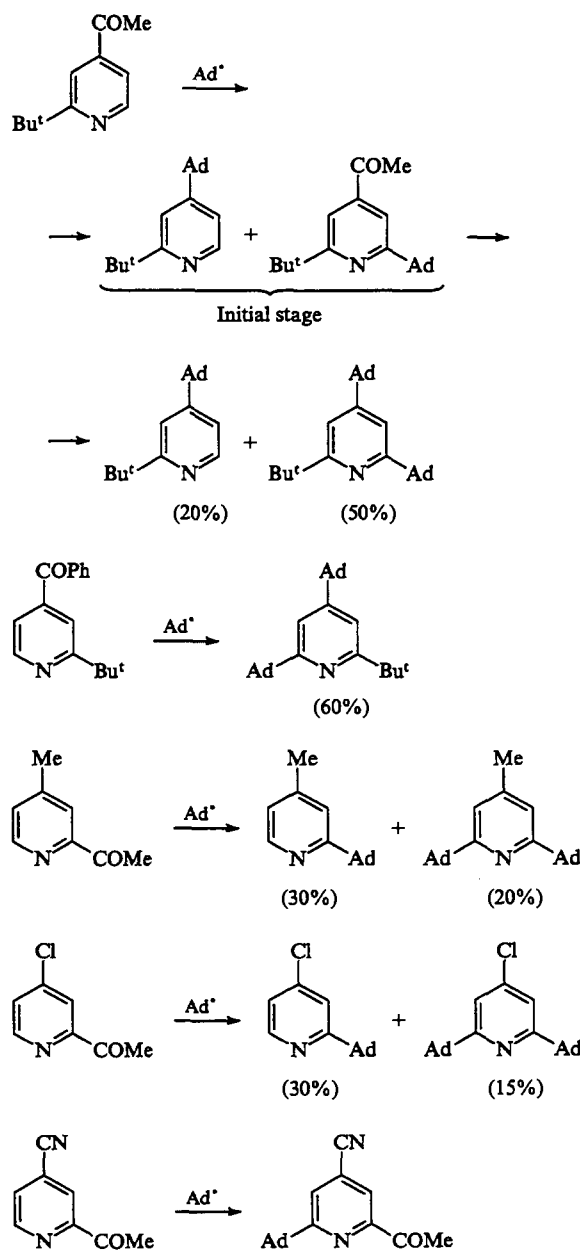


Nu — pyridine, 3-picoline, quinoline, $\text{MeNCH}_2\text{CH}_2\text{OCH}_2\text{CH}_2$.

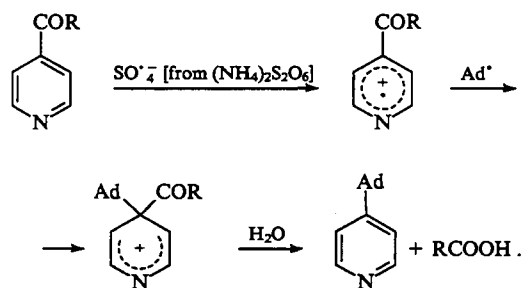
The diene **153** ($X = \text{CH}_2$) reacts with pyridine-sulfotrioxide in pyridine giving the salt **156** in 70% yield.¹⁰¹



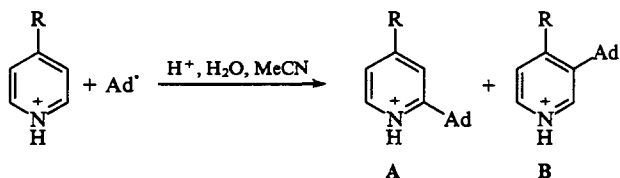
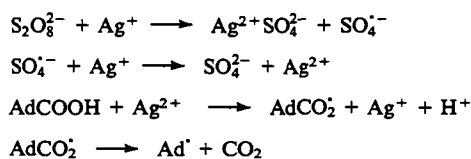
In 1976, a new S_R reaction involving the Ad^\bullet radical was reported.¹⁰² The interaction of adamantane-1-carboxylic acid with ketones of the pyridine series in the presence of ammonium peroxydisulfate and silver nitrate at 80°C in aqueous ammonia and acetonitrile leads to the generation of adamantyl radical, which substitutes the acyl groups, the hydrogen atoms, or both in pyridine bases.



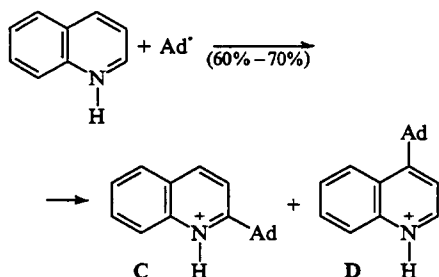
The following scheme of the homolytic *ipso*-substitution has been suggested:¹⁰²



More recently this reaction has been studied¹⁰³ in relation to other compounds and a scheme for the formation of the Ad• radical and of the $\text{SO}_4^{\bullet-}$ radical-anion has been suggested.

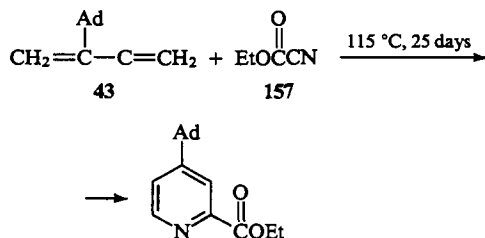


R = CN, COMe; A : B = 92 : 8.

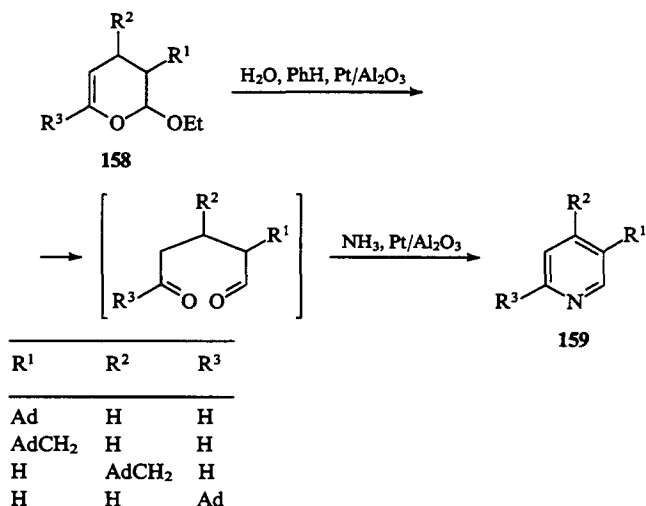


C : D = 97 : 3.

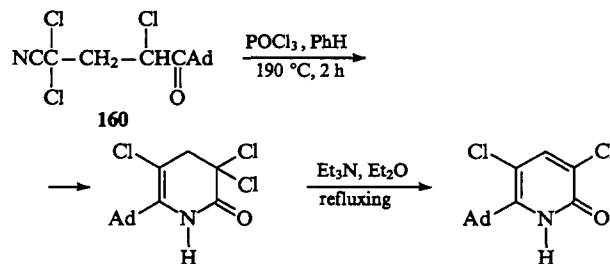
4-(Adamant-1-yl)-2-ethoxycarbonylpyridine has been synthesised in 42% yield by cycloaddition of the diene 43 to the nitrile 157.⁴⁷



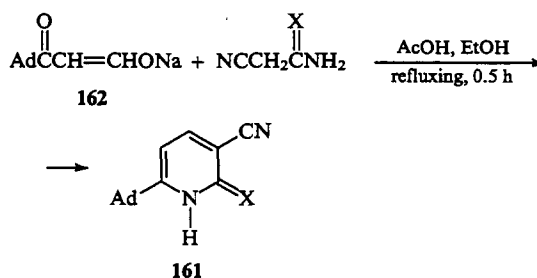
The reaction of the 2,3-dihydropyran derivatives 158 with water in the presence of a platinum catalyst followed by treatment in situ of the resulting 1,5-dicarbonyl compounds with ammonia leads to the pyridine bases 159, their yields being 32%–42%.⁹³



On heating with phosphorus oxychloride in an autoclave the oxonitrile 160 cyclises giving 2-(adamant-1-yl)-3,5,5-trichloro-4,5-dihydro-6-pyridinone in 41% yield; the latter is converted into 6-(adamant-1-yl)-3,5-dichloro-2-pyridone (yield 87%) on treatment with triethylamine.¹⁰⁴

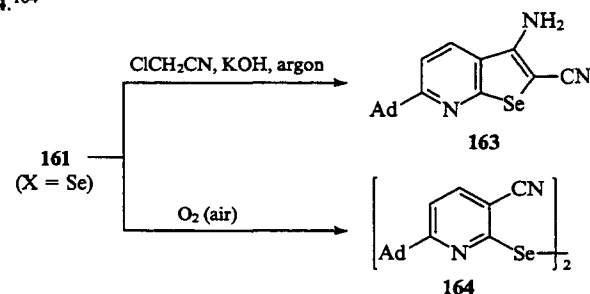


6-(Adamant-1-yl)-3-cyano-2-pyridone (161, X = O) and 6-(adamant-1-yl)-3-cyano-2-pyridoselenone (161, X = Se) have been synthesised in 33% and 52% yields by refluxing the sodium derivative 162 with compounds $\text{NCCH}_2\text{C(X)NH}_2$.¹⁰⁵

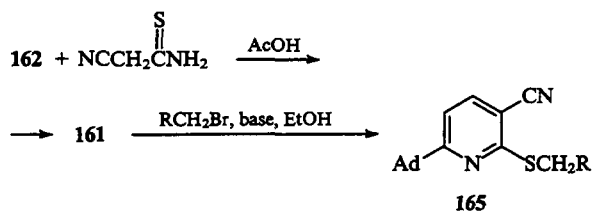


X = O, Se.

The selenone 161 (X = Se) reacts with chloroacetonitrile in the presence of a 10% aqueous solution of potassium hydroxide under an inert atmosphere affording the selenopheno-[2,3-*b*]pyridine derivative 163 (yield 70%), whereas during storage in air the compound 161 is converted into the diselenide 164.¹⁰⁴

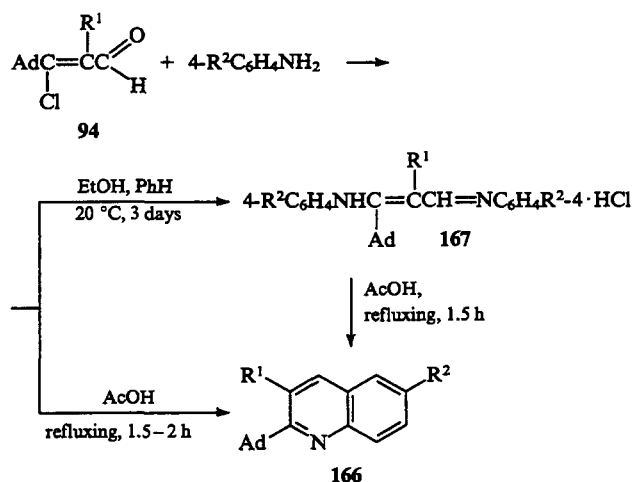


The sulfur-containing analogue **161** ($X = S$) has been synthesised in 62% yield by the cyclocondensation of the sodium derivative **162** with cyanothioacetamide. The pyridine-2-thione **161** ($X = S$) thus obtained reacts with the bromo-derivatives RCH_2Br in the presence of bases to give the sulfides **165** (yields 58%–64%).¹⁰⁶



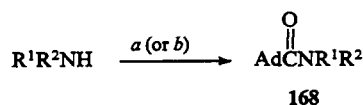
$X = S$; $R = COOMe, COOEt, CN$.

The quinoline derivatives **166** are formed in 43%–63% yields in the reaction of the aldehydes **94** with aniline or 4-bromoaniline^{70, 71} (in some cases, the intermediate salts **167** can be isolated).



$R^1 = H, R^2 = H, Br$; $R^1 = Me, R^2 = H, Br$.

The adamantane-1-carboxamides **168** have been prepared in 72%–92% yields from secondary amines and the acid chloride $AdCOCl$ or the sulfide **169**.^{107, 108}



$R^1 = Et, R^2 = Et$;

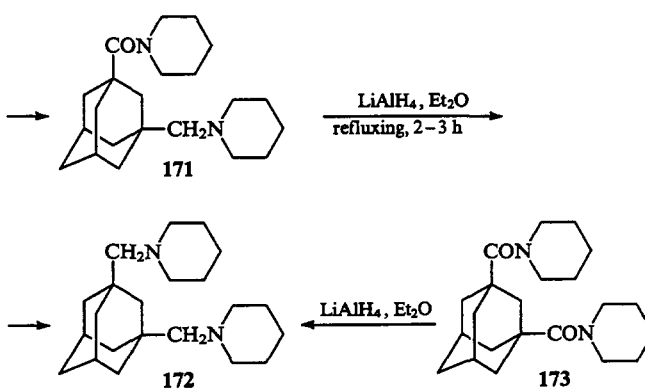
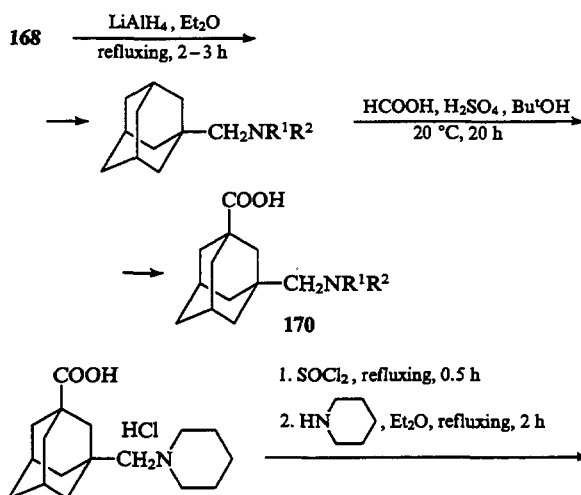
$R^1 + R^2 = -(CH_2)_4-, -(CH_2)_5-, -(CH_2CH_2)_2O-$;

$R^3 = Me, H_2N^+ \text{ (cyclohexyl)}$;

(a) $AdCOCl, Et_2O$ (0–20 °C, 1–12 h);

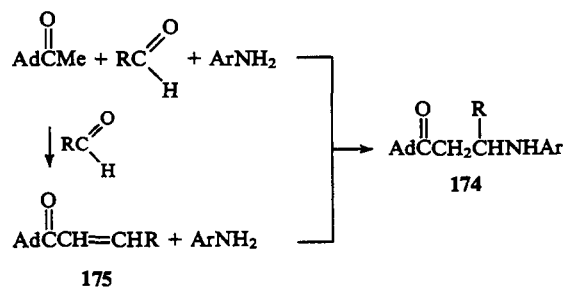
(b) $AdCSR^3$ (**169**) (refluxing, 4–6 h).

The amides **168** have been converted into biologically active compounds **170** via several consecutive stages. First, they were reduced with lithium tetrahydroaluminate to amines (yields 94%–97%) and the latter were converted into the carboxylic acids **170**. The hydrochloride of the amino acid **170** [$R^1 + R^2 = -(CH_2)_5-$] was made to react with thionyl chloride and piperidine to give the corresponding amide **171** (yield 91%), which was then reduced with lithium tetrahydroaluminate to the diamine **172**. The latter can also be obtained by the reduction of the diamide **173** (yield 79%).¹⁰⁷



Hydrochlorides of the acids **170** exhibit analgesic and anti-inflammatory activities.¹⁰⁷

To synthesise the aminoketones **174**, two methods have been suggested, namely, the Mannich reaction of 1-acetyladamantane with aldehydes and arylamines and the addition of arylamines to the α, β -unsaturated ketones **175**, generated from acetyladamantane and aldehydes.¹⁰⁹

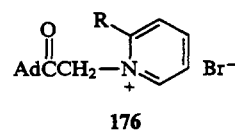


$R = \text{pyridyl-3, pyridyl-4, quinolyl-2, quinolyl-6, quinolyl-7}$;

$Ar = Ph, 2-FC_6H_4, 3-FC_6H_4, 4-FC_6H_4, 4-MeOC_6H_4, \text{naphthyl-2}$.

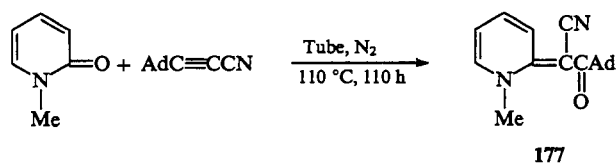
The aminoketones **174** possess a broad spectrum of biological activity: neurotropic, antiviral, antibacterial, fungicidal, psychotropic, and hepatoprotecting activities.¹⁰⁹

Heating of the ketone **41** with 2-aminopyridine or with 2-picoline in alcohol leads to the corresponding salts **176** (yields 96% and 50%).⁴⁶

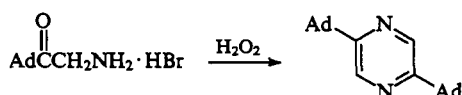


$R = NH_2, Me$.

An unexpected result was obtained when 1-methyl-2-pyridone was heated with 2-(adamant-1-yl)ethyne-1-carbonitrile: compound **177** was found among the reaction products.¹¹⁰



The hydrobromide **85** is converted into 2,5-di(adamant-1-yl)pyrazine in 30.5% yield on treatment with hydrogen peroxide.⁶⁶

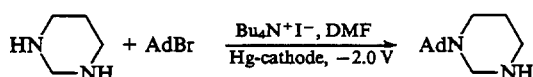


Piperazine derivatives **178** exhibiting an antiviral activity have been prepared by refluxing bromoadamantane with piperazine or with its *N*-monosubstituted derivatives.⁸⁹



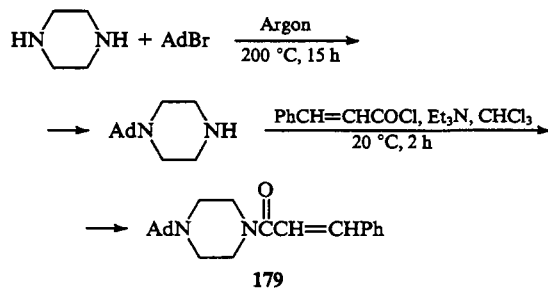
R = H, HOCH₂CH₂, Ad, Ph, 3-Cl, 4-MeC₆H₃.

Hexahydropyrimidine reacts with AdBr under conditions of phase-transfer catalysis at a mercury cathode in a cell with a double G-5 diaphragm giving the corresponding *N*-adamantyl derivative in 70% yield.¹¹¹

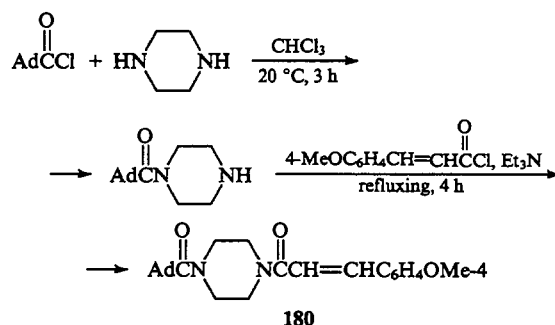


N-(Adamant-1-yl)hexahydropyrimidine and *N*-adamantyl-containing derivatives of other pyrimidines, pyridazines, and pyrazines obtained in a similar way are active against influenza viruses of the H₂N₂A/Singapore type.¹¹¹

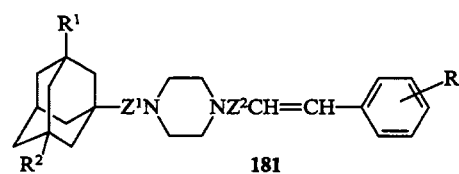
N-(Adamant-1-yl)piperazine, synthesised in 85% yield by heating piperazine with bromoadamantane in an autoclave, has been made to react with cinnamoyl chloride in the presence of triethylamine. The compound **179** formed in this reaction (yield 85%) enhances the cerebral circulation.¹¹²



It has been reported in a patent¹¹³ that *N*-(adamant-1-ylcarbonyl)piperazine has been synthesised in 40% yield by the acylation of piperazine with the acid chloride AdCOCl. The product of acylation was converted into the *N,N'*-diacylpiperazine **180** in 90% yield.¹¹³

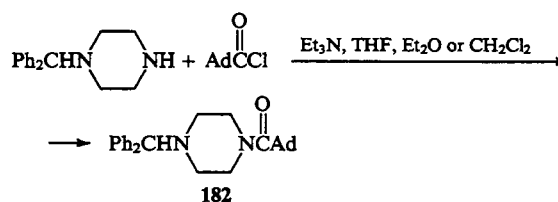


Compounds of the general formula **181** have been patented as substances active with respect to the central nervous system.¹¹³

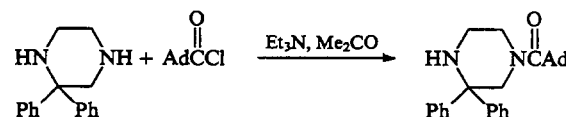


R¹ = H, Me, MeO; R² = H, Me; R³ = H, Me, MeO, Cl, F;
Z¹, Z² = CO, CH₂.

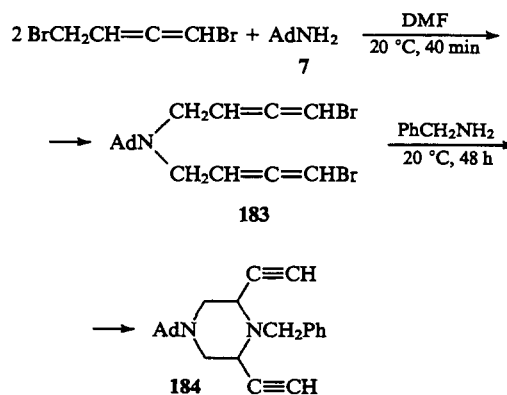
The acylation of *N*-(diphenylmethyl)piperazine with the chloride AdCOCl leads to compound **182** exhibiting high anti-histamine and antiallergic activities.¹¹⁴



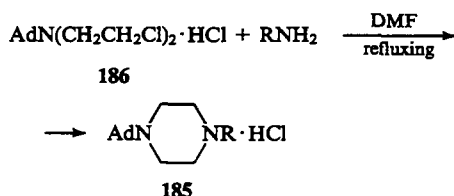
1-(Adamant-1-ylcarbonyl)-3,3-diphenylpiperazine has been synthesised from 3,3-diphenylpiperazine and adamantane-1-carboxylic acid chloride in the presence of triethylamine.¹¹⁵



1,4-Dibromobuta-1,2-diene reacts readily with the amine **7** giving the dibromo-derivative **183**, which is converted into the 1,4-disubstituted piperazine **184** on treatment with benzylamine.¹¹⁶



In 1972, a new method was patented for the synthesis of the *N*-adamantylpiperazines **185**. The method involves cyclisation of the hydrochloride of (adamant-1-yl)bis(2-chloroethyl)amine **186** under the action of primary amines (the yield of compounds **185** ranges from 53% to 70%).¹¹⁷



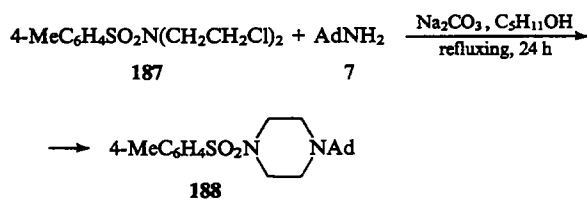
R = cyclo-C₆H₁₁, Pr, Prⁱ, Bu, Bu^t, Ph, PhCH₂, H.

Later, this method was used to prepare a wider set of 1-(adamant-1-yl)-4-R-piperazines with R = H, Me, Et, Pr, Prⁱ, Bu^t, C₅H₁₁, cyclo-C₅H₉, cyclo-C₆H₁₁, cyclo-C₈H₁₅, Ad, Ph, PhCH₂ and CH₂CH₂OH.

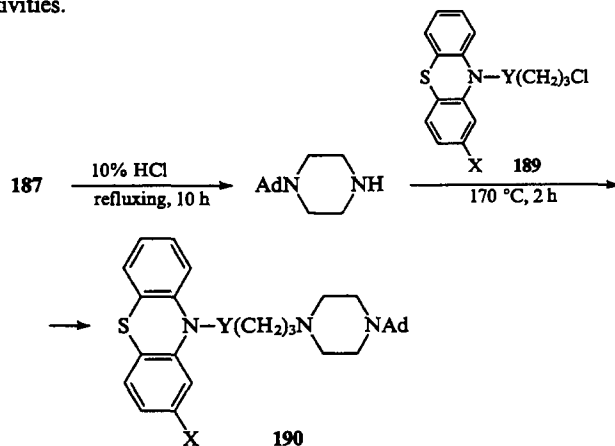
The majority of the hydrochlorides **185** increase the blood pressure. The compounds with R = Et or CH₂CH₂OH have a hypotensive effect, those with R = cyclo-C₆H₁₁ slow down cardiac activity, and the compound with R = Bu^t exhibits a vasodilatory activity and an adrenaline-blocking effect.¹¹⁸

Compounds like **185** are active with respect to the central nervous system, exhibit analgesic and hypothermal activities, and modify the soporific effects of Hexanal, Medinal and chloral hydrate.¹¹⁹

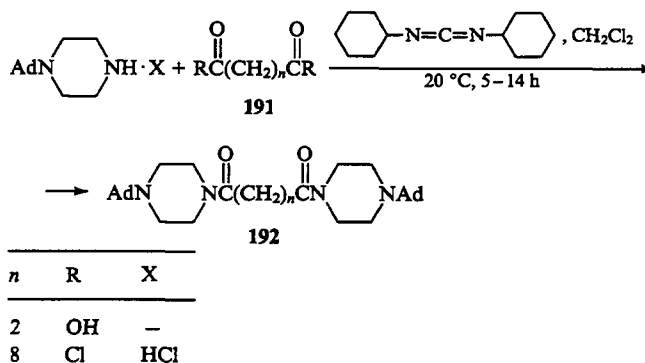
1-(Adamant-1-yl)-4-(tolyl-*p*-sulfonyl)piperazine **188** has been synthesised in 87.5% yield by the condensation of the dichloro-derivative **187** with the amine **7**.¹²⁰



On refluxing in hydrochloric acid compound **188**, is converted into 1-(adamant-1-yl)piperazine (yield 84%), which reacts with the chloro-derivatives **189** to give phenothiazines **190** (yields 49%–50%),¹²⁰ the latter exhibit vasodilatory and psychotropic activities.

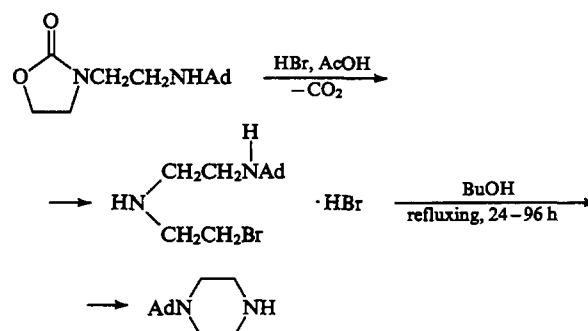


1-(Adamant-1-yl)piperazine and its hydrochloride react with the dicarboxylic acids **191** (in the presence of cyclohexylcarbodiimide) or with the corresponding acyl chlorides giving the diamides **192** (yields 58% and 60%).¹²¹

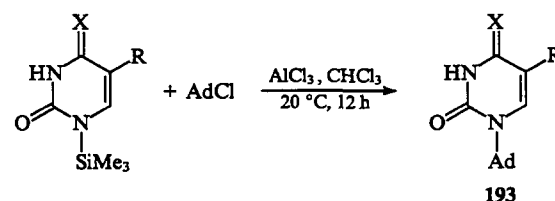


The diamide **192** (n = 8) possesses an immunodepressive activity.¹²¹

Treatment of 3-[2-(adamant-1-ylamino)ethyl]oxazolidin-2-one with hydrobromic acid in glacial acetic acid affords a salt, which cyclises to 1-(adamant-1-yl)piperazine on heating in butyl alcohol.¹²²

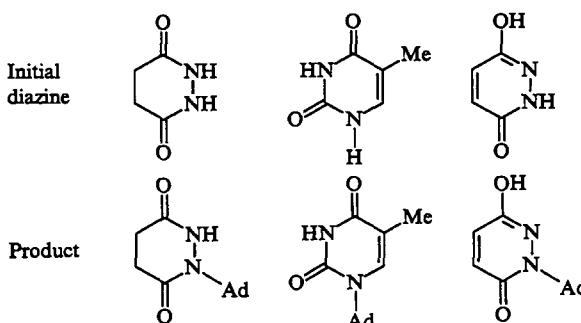


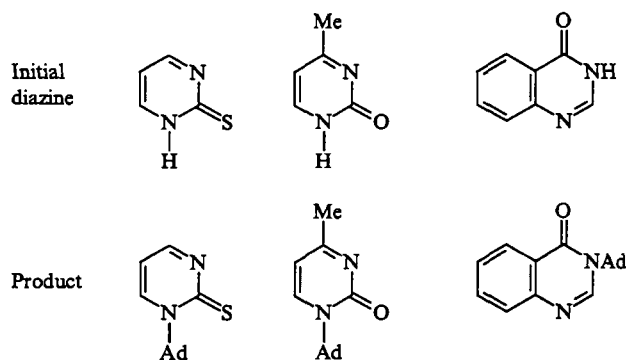
To introduce an adamantyl radical to the nitrogen atom of the cyclic diazines, two procedures have been developed. One of them involves the initial preparation of trimethylsilyl derivatives of diazines, which are then treated with 1-chloroadamantane in the presence of aluminium chloride. Compounds **193** have been synthesised in this way in 38%–53% yields.⁵⁰



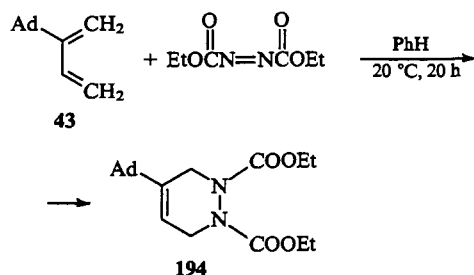
X = O, R = H, F; X = S, R = H.

The second one-pot procedure is used for the synthesis of *N*-adamantyl-diazines more frequently. The *N*-trimethylsilyl derivative of diazine is prepared by refluxing the diazine with the disilazane **32**; the obtained compound is introduced directly into the reaction with 1-chloroadamantane in the presence of aluminium chloride (in CHCl₃, 20 °C).³⁷ We present below the examples of *N*-(adamant-1-yl)azines prepared in this way (yields 38%–61%).³⁷

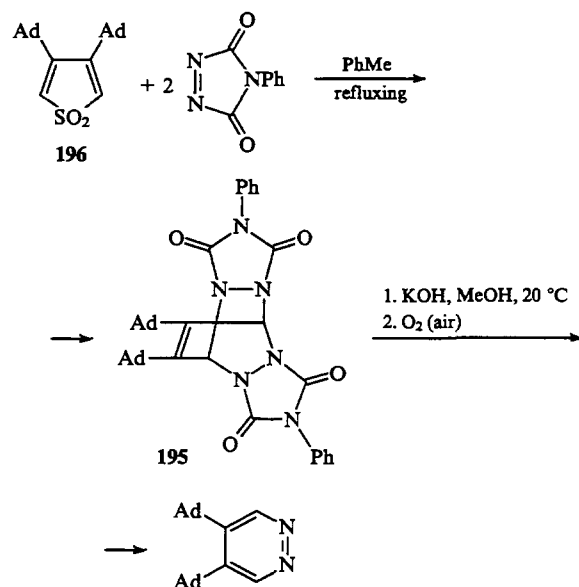




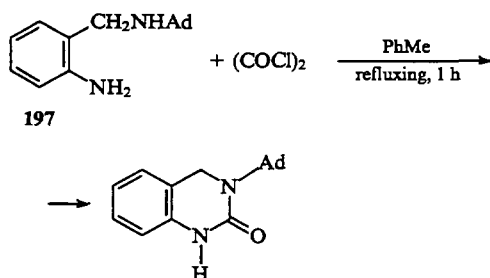
The pyridazine derivative **194** has been obtained in 87% yield by the diene condensation of compound **43** with ethyl diazenedicarboxylate at room temperature.⁴⁷



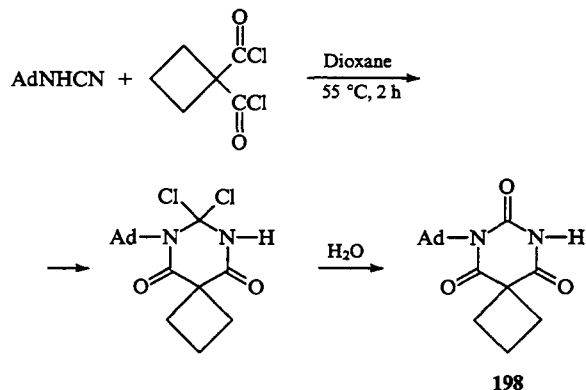
The bis-adduct **195** formed from the cyclic sulfone **196** and an excess of 4-phenyl-1,2,4-triazoline-3,5-dione, is converted into 4,5-di(adamant-1-yl)pyridazine in 56% yield on treatment with potassium hydroxide followed by oxidation in air.¹²³



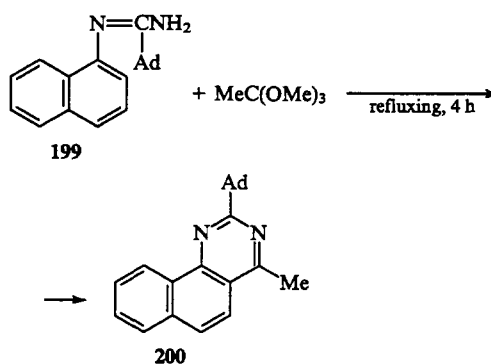
When the diamine **197** is refluxed with oxalyl chloride in toluene, 3-(adamant-1-yl)-1,4-dihydro-2-quinazolinone is formed, which exhibits anti-inflammatory activity.¹²⁴



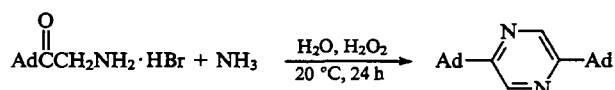
The derivative of barbituric acid **198** has been synthesised in 7% yield by the condensation of (adamant-1-yl)cyanogen amide with cyclobutane-1,1-dicarbonyl dichloride in anhydrous dioxane followed by treatment with water.⁷⁶



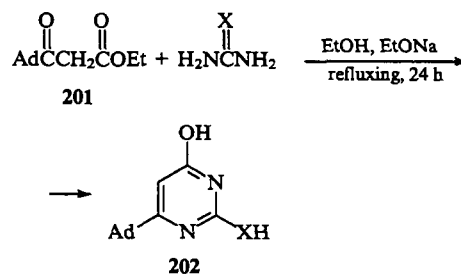
The amidine **199** reacts with the ortho ester MeC(OMe)_3 to give the tricyclic compound **200** (yield 60%).¹²⁵



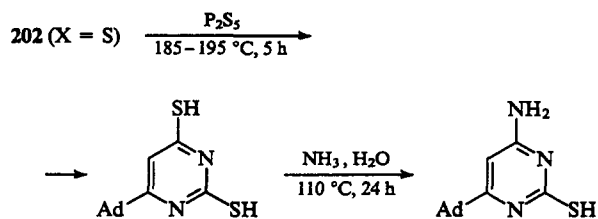
Treatment of adamant-1-yl aminomethyl ketone hydrobromide with aqueous ammonia in the presence of hydrogen peroxide leads to 2,5-di(adamant-1-yl)pyrimidine in 30.5% yield.⁶⁶



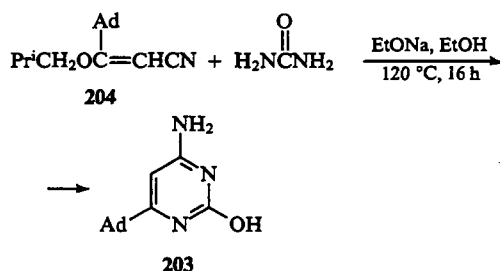
Several other approaches to the synthesis of pyrimidine derivatives containing an adamantane nucleus have been developed. Cyclocondensation of the ester **201** with urea or thiourea in the presence of sodium ethoxide gives rise to 6-(adamant-1-yl)uracil (**202**, X = O) (yield 21.5%) or 6-(adamant-1-yl)thiouracil (**202**, X = S) (yield 60.3%). The latter compound is converted into 6-(adamant-1-yl)-2,4-disulfanylpurimidine by the action of phosphorus pentasulfide and also into 4-amino-6-(adamant-1-yl)-2-sulfanylpurimidine (yield 60.5%) by heating with aqueous ammonia.¹²⁶



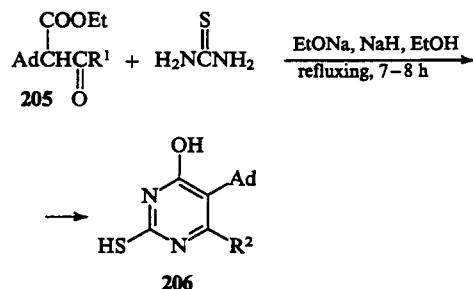
X = O, S.



6-(Adamant-1-yl)cytosine **203** was obtained in 33% yield by the condensation of the nitrile **204** with urea in the presence of sodium ethoxide.¹²⁶

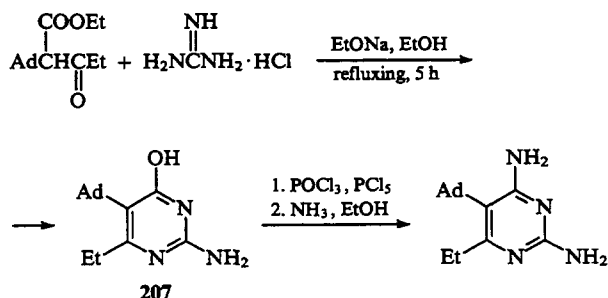


Czech researchers¹²⁷ studied the condensation of compounds of the general formula $\text{R}^1\text{OCC}(\text{R}^2)(\text{Ad})\text{COR}^3$ with urea, thiourea, and guanidine. The interaction of compounds **205** with thiourea in the presence of sodium ethoxide and sodium hydride gives the thioracil derivatives **206** in 27%–68% yield.



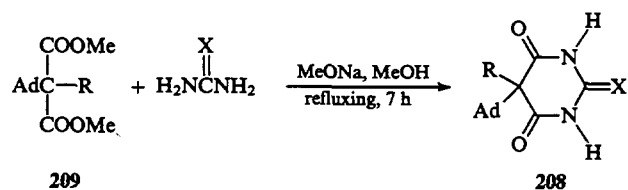
$\text{R}^1 = \text{H}, \text{R}^2 = \text{H}; \text{R}^1 = \text{OEt}, \text{R}^2 = \text{OH}; \text{R}^1 = \text{Me}, \text{R}^2 = \text{Me}.$

The reaction of the oxoester **205** ($\text{R}^1 = \text{Et}$) with guanidine hydrochloride in the presence of sodium ethoxide affords the cytosine derivative **207** (yield 41%), which is converted into 5-(adamant-1-yl)-2,4-diamino-6-ethylpyrimidine by successive treatment with phosphorus oxychloride and phosphorus pentachloride and then with an alcoholic solution of ammonia.



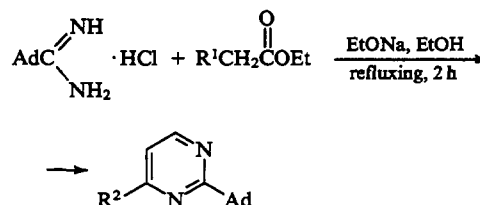
The resulting compound is a 30-fold more effective inhibitor of the growth of mammary carcinoma cells than the compound **206**.¹²⁸

The low-toxicity biologically active compounds **208** have been synthesised in yields of more than 80% by the cyclocondensation of bis-esters **209** with urea or with thiourea in the presence of sodium methoxide.¹²⁹



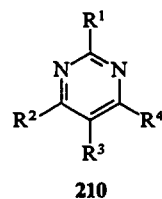
$\text{X} = \text{O}, \text{S}; \text{R} = \text{H}, \text{Me}, \text{Et}, \text{CH}_2\text{CH}=\text{CH}_2.$

Adamantane-1-carboximidamide hydrochloride reacts with ethyl malonate or with ethyl cyanoacetate in the presence of sodium ethoxide to give 2-(adamant-1-yl)-6-hydroxypyrimidine and 2-(adamant-1-yl)-6-aminopyrimidine, respectively.¹³⁰



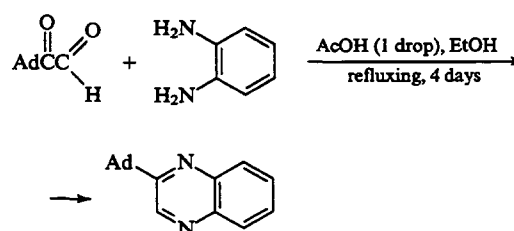
$\text{R}^1 = \text{COOEt}, \text{R}^2 = \text{OH}; \text{R}^1 = \text{CN}, \text{R}^2 = \text{NH}_2.$

The pyrimidine derivatives **210** ($\text{R}^1 = \text{OH}, \text{NH}_2, \text{R}^2 = \text{OH}, \text{R}^3 = \text{H}, \text{R}^4 = \text{Ad}$) inhibit liver folate-reductase and exert a cytostatic effect on tumour cells,¹³¹ whereas the compound **210** ($\text{R}^1 = \text{R}^2 = \text{NH}_2, \text{R}^3 = \text{Ad}, \text{R}^4 = \text{Me}$) has been recommended as an antitumour preparation.¹³²

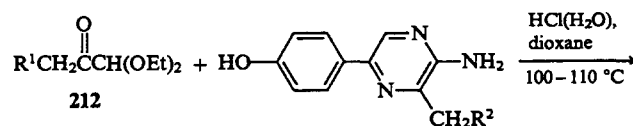


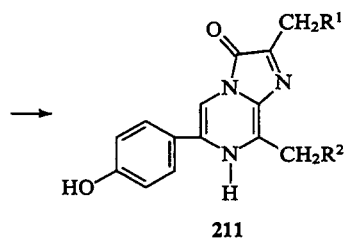
The oxidation of adamant-1-yl aminomethyl ketone hydrobromide with hydrogen peroxide gives 2,5-di(adamant-1-yl)pyrazine in 30.5% yield.⁶⁶

1,2-Diaminobenzene reacts with (adamant-1-yl)glyoxal on heating in alcohol in the presence of acetic acid affording 2-(adamant-1-yl)quinoxaline in 35% yield.⁶⁰



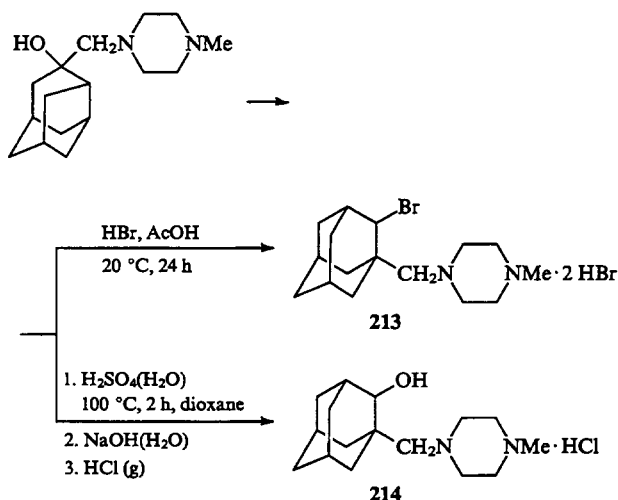
The imidazopyrazine derivatives **211** have been obtained by the condensation of diethyl acetals **212** with 2-amino-3-benzyl-5-(4-hydroxyphenyl)pyrazine or with 3-(adamant-1-ylmethyl)-2-amino-5-(4-hydroxyphenyl)pyrazine in the presence of dilute hydrochloric acid.¹³³



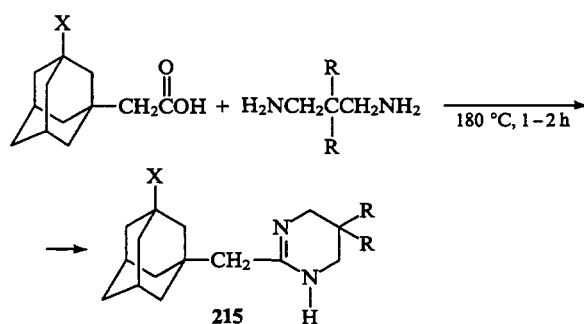


R ¹	R ²	Yield of 211 (%)
Ad	Ph	44
4-HOC ₆ H ₄	Ad	63

4-(4-Methylpiperazin-1-yl)methylprotoadamantan-4-ol is converted into the salt **213** (yield 40%) on treatment with hydrogen bromide, whereas its reaction with sulfuric acid and hydrogen chloride affords the salt **214** (yield 80%).¹³⁴

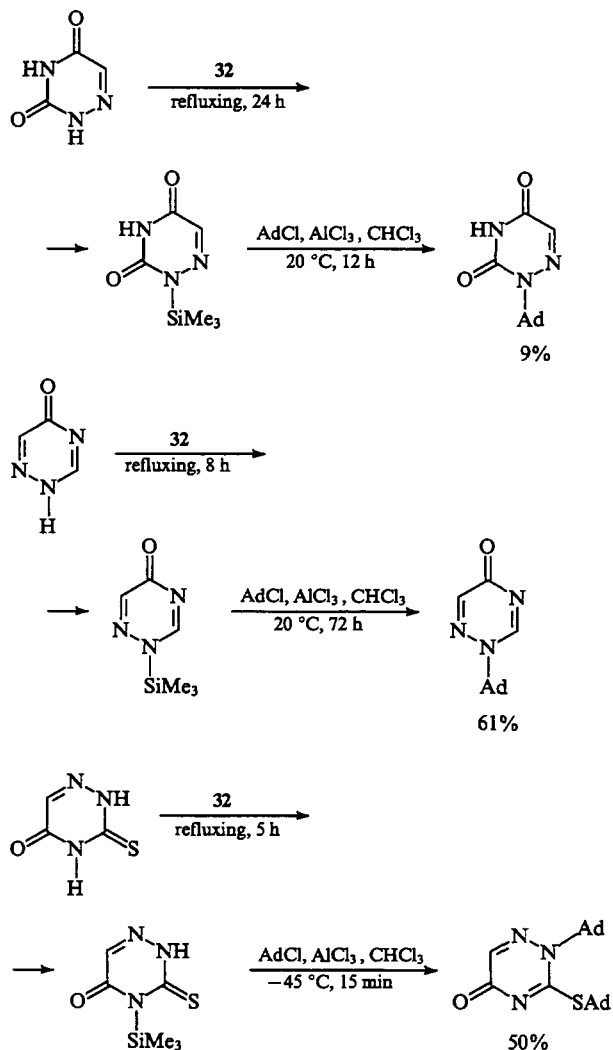


Heating of (adamant-1-yl)acetic acid and (3-hydroxyadamant-1-yl)acetic acid with diamines H₂NCH₂CR₂CH₂NH₂ leads to tetrahydropyrimidine derivatives **215** (yields 30%–59%).⁵⁸

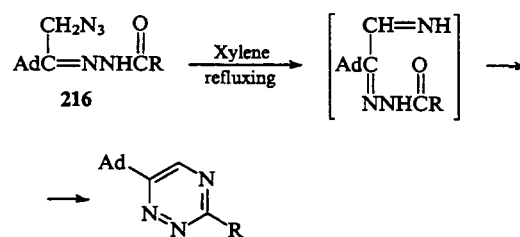


X = H, OH; R = H, Me.

Several methods have been developed for the preparation of 1,2,4-triazine derivatives containing the adamantyl nucleus. Japanese researchers³⁷ have synthesised these compounds in two stages. The first stage involves the reaction of triazine with disilazane **32** giving the trimethylsilyl derivative, which is then made to react with chloroadamantane in the presence of aluminium chloride.

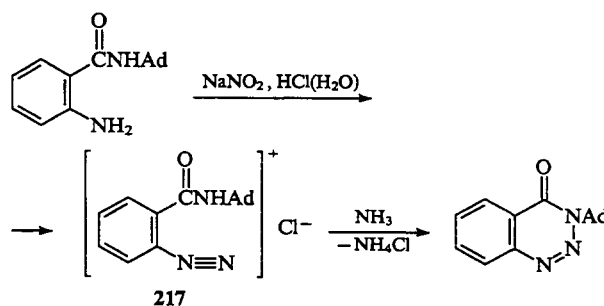


On heating in xylene, the azides **216** cyclise with the elimination of nitrogen giving 3-R-6-(adamant-1-yl)-1,2,4-triazines in 58%–73% yields.¹³⁵

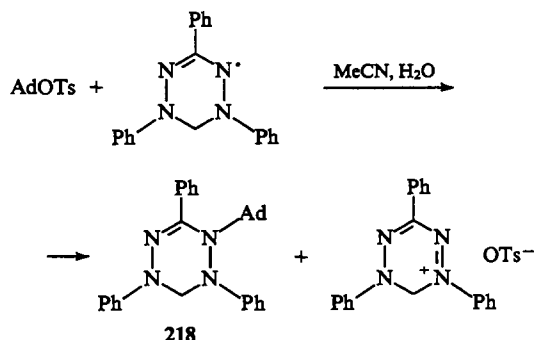


R = Me, Ph, Ad.

The reaction of ammonia with the diazonium salt **217** formed upon diazotisation of the (adamant-1-yl)amide of anthranilic acid gave 3-(adamant-1-yl)-3,4-dihydro-1,2,3-benzotriazin-4-one.^{136, 137}



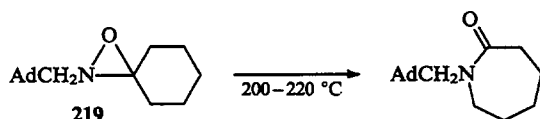
Only one example¹³⁸ of the synthesis of a 1,2,4,5-tetrazine derivative has been reported. 2-(Adamant-1-yl)-1,3,5-triphenyl-1,2,5,6-tetrahydro-1,2,4,5-tetrazine **218** was obtained by the reaction of adamant-1-yl tosylate with 1,3,5-triphenylverdazyl.¹³⁸



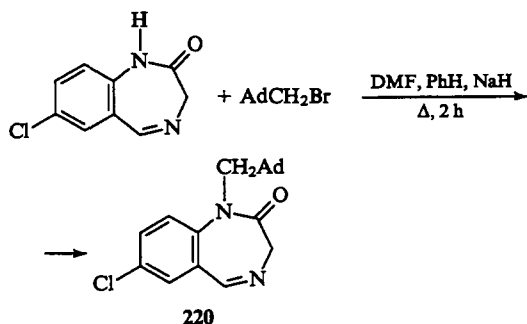
5. Compounds with seven-membered heterocycles

The preparation of *N*-(adamant-1-yl)caprolactam hydrochloride has been described in a patent.²⁹ The authors noted that this compound exhibits an anti-inflammatory activity, stimulates the central nervous system, reduces the cholesterol level, and decreases appetite.

The oxaziridine derivative **219** isomerises on heating above 200 °C into *N*-(adamant-1-ylmethyl)caprolactam in 70% yield.¹³⁹



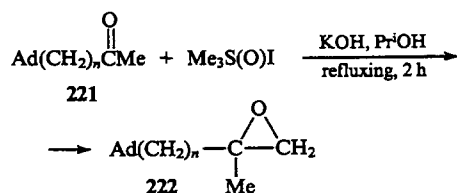
The reaction of 1-bromomethyladamantane with 7-chloro-1,4-benzodiazepin-2-one in the presence of sodium hydride leads to the *N*-alkylation product **220** in 30% yield.¹⁴⁰



III. Adamantane derivatives containing heterocyclic nuclei with oxygen atoms

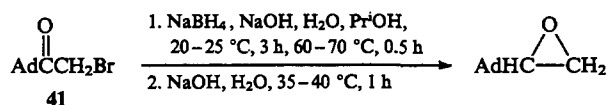
1. Compounds with three-membered and four-membered heterocycles

The ketones **221** of the adamantane series enter into the reaction with oxodimethylsulfonium methylide (which is obtained by treating trimethyloxosulfonium iodide with potassium hydroxide), which affords the oxirane derivatives **222** in 88% and 83% yields.¹⁴¹

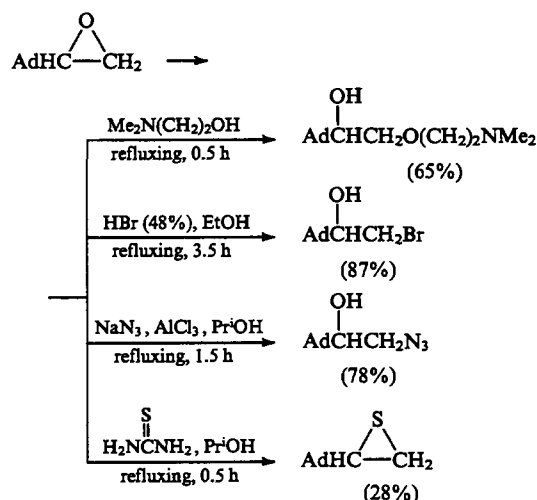


$n = 0, 1.$

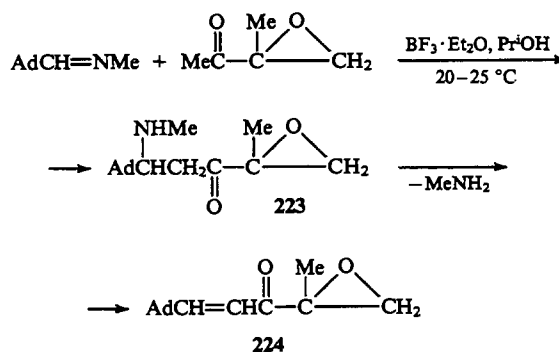
2-(Adamant-1-yl)oxirane has been synthesised in 86% yield in two stages, namely, by the reaction of the ketone **41** with sodium tetrahydroborate in an alkaline medium and the subsequent treatment with aqueous sodium hydroxide.¹⁴²



The same workers¹⁴² studied the transformations of the obtained oxirane in reactions with nucleophilic and electrophilic reagents.

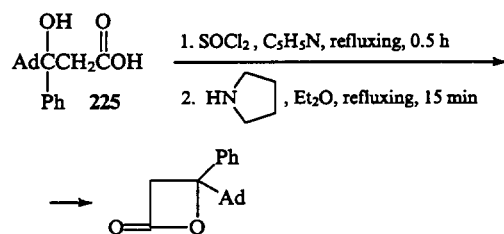


1-Acetyl-1-methyloxirane adds to the imine $\text{AdCH}=\text{NMe}$ in the presence of boron trifluoride etherate to give unstable aminoketone **223**; the latter eliminates methylamine under the reaction conditions and is thus converted into the unsaturated compound **224**.¹⁴³



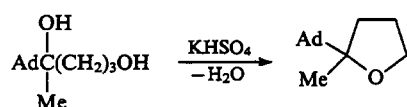
The methods for the synthesis of oxiranes containing an adamantane nucleus have been analysed.¹⁴⁴ These methods include the epoxidation of unsaturated compounds of the adamantane series and transformation of adamantyl-containing ketones. The introduction of an adamantyl fragment into epoxy-polymers was shown to increase their thermal stability and to improve technological characteristics of compositions based on them.

To the best of our knowledge, only one study devoted to the synthesis of adamantane derivatives containing four-membered heterocycles with oxygen atoms has been published.³⁶ It presents the preparation of 2-(adamant-1-yl)-2-phenyloxetan-4-one from the hydroxy acid **225** under the action of thionyl chloride and pyrrolidine (yield 95%).

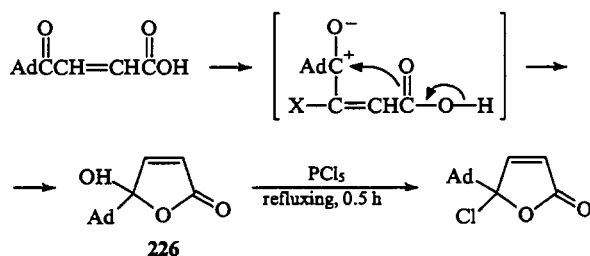


2. Compounds with five-membered heterocycles

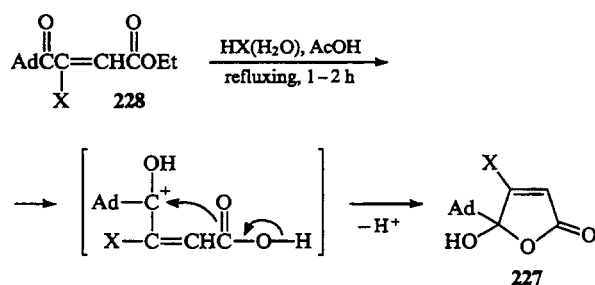
4-(Adamant-1-yl)pentane-1,4-diol undergoes intramolecular dehydration in the presence of potassium hydrogen sulfate, which affords 2-(adamant-1-yl)-2-methyltetrahydrofuran.¹⁴⁵



When 3-(adamantoyl)acrylic acid is exposed to sunlight, it cyclises giving compound **226** in 85.5% yield; the hydroxy-group in the latter is substituted by a chlorine atom under the action of phosphorus pentachloride (yield 39.5%).¹⁴⁶

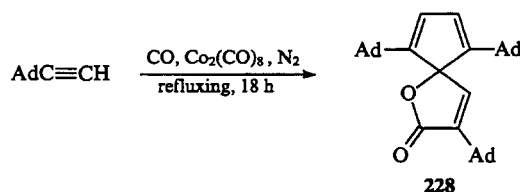


The derivatives of furanone **227** have been synthesised by heating ethyl 2-adamantoyl-2-haloacrylates with hydrohalic acids (yields 84% and 98%).¹⁴⁷

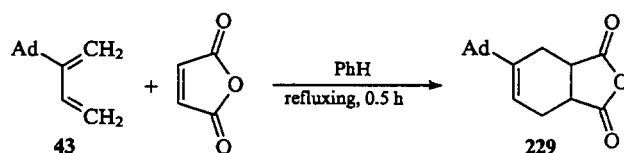


X = Cl, Br.

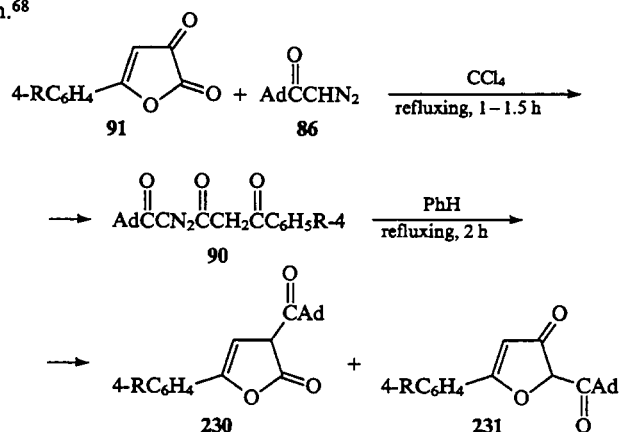
3,6,9-Tri(adamant-1-yl)-1-oxaspiro[4.4]nona-3,6,8-trien-2-one **228** is formed when 1-ethynyladamantane is heated with cobalt carbonyl in light petroleum in a flow of carbon monoxide.¹⁴⁸



The diene **43**, on heating in benzene, enters into diene condensation with maleic anhydride, which leads to the adduct **229** in 70% yield.⁴⁷

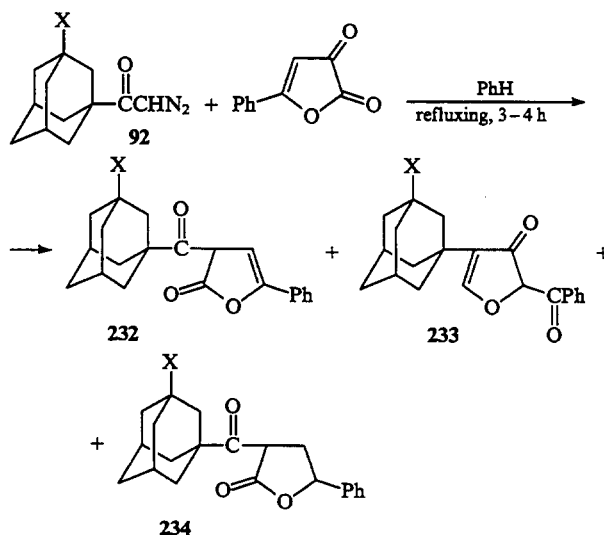


A mixture of adamant-1-ylcarbonyl derivatives of 2,3-dihydrofuran-2-one **230** and 2,3-dihydrofuran-3-one **231** has been synthesised by heating in benzene for 2 h the triketones **90**, which are formed from the diazoketone **86** and dihydrofuran-diones **91**. The compounds **230** and **231** can also be obtained without isolation of the triketones **90**, by refluxing a mixture of dihydrofuran-diones **91** and the diazoketone **86** in benzene for 3 h.⁶⁸



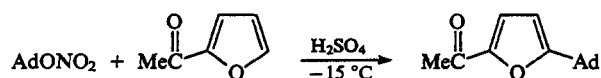
R	Yields (%)	
	230	231
H	38	7
Me	71	10
OMe	47	6
Br	14	9

The reaction of 5-phenyl-2,3-dihydrofuran-2,3-dione with the diazoketones **92** has been described in a patent.¹⁴⁹ This reaction yields one, two or three compounds depending on the nature of the substituent X in the diazoketone: for X = Br, three compounds **232**–**234** are formed, whereas for X = H, two compounds **233** and **234** have been isolated. When X = ONO₂, the reaction yields only compound **232**.

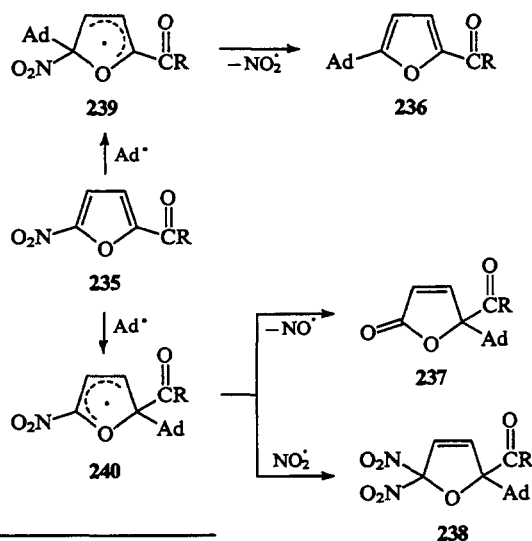


X = H, Br, ONO₂.

The hydrogen atom in the 5-position of 2-acetylfuran is substituted by an adamantyl radical in the reaction with adamant-1-yl nitrate in the presence of sulfuric acid even at -15°C ; the yield of 5-(adamant-1-yl)-2-acetylfuran is 32%.¹⁵⁰

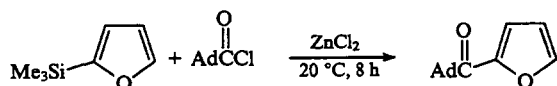


Homolytic *ipso*-substitution in 2-acyl-5-nitrofurans **235** has been studied.¹⁵¹ The reaction of furan derivatives **235** with the Ad \cdot radical [generated from AdCOOH in the presence of $(\text{NH}_4)_2\text{S}_2\text{O}_8$ and AgNO_3 ¹⁰³] results in a mixture of three compounds: 2-acyl-5-(adamant-1-yl)furans **236**, 2-acyl-2-(adamant-1-yl)-2,5-dihydrofuran-5-ones **237**, and 2-acyl-2-(adamant-1-yl)-5,5-dinitro-2,5-dihydrofurans **238**. The authors¹⁵¹ presented the following scheme for these transformations: the reaction of the compounds **235** with the Ad \cdot radical affords pairs of more complex radicals **239** and **240**. The radicals **239** eliminate $\text{NO}_2\cdot$ to give compounds **236**. The transformation of the radicals **240** can follow two pathways: it involves either the loss of $\text{NO}_2\cdot$ resulting in the formation of the compound **237** or, conversely, the addition of $\text{NO}_2\cdot$ leading to the compound **238**.

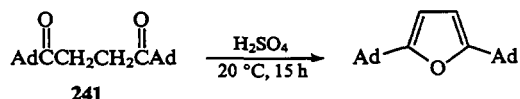


R	Yields (%)		
	236	237	238
H	35	25	15
OMe	31.5	32	10

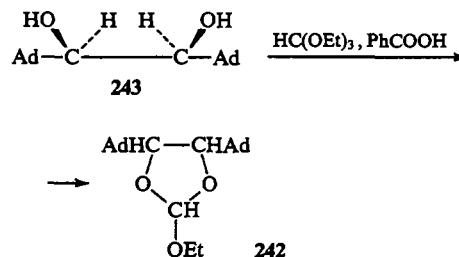
When 2-(trimethylsilyl)furan reacts with the chloride AdCOCl in the presence of zinc chloride, the trimethylsilyl group is substituted by the adamant-1-ylcarbonyl group giving adamant-1-yl 2-furyl ketone in 61% yield.¹⁵²



The cyclocondensation of the diketone **241** in the presence of concentrated sulfuric acid affords 2,5-di(adamant-1-yl)furan in 84% yield.⁴²



A mixture of diastereomers of 4,5-di(adamant-1-yl)-2-ethoxy-1,3-dioxolane **242** has been obtained by heating the *meso*-diol **243** with the ortho ester HC(OEt)_3 in the presence of benzoic acid.¹⁵³

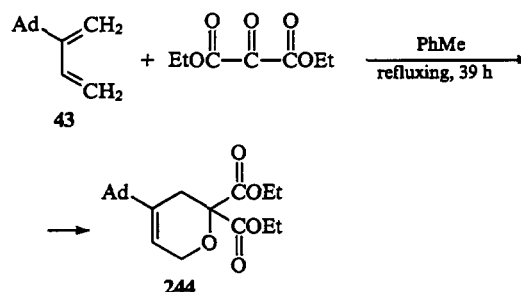


When the dioxolane **242** is heated in benzoic acid at 200°C , stereoselective *cis*-elimination occurs to give *cis*-1,2-di(adamant-1-yl)ethene in 90% yield.¹⁵³

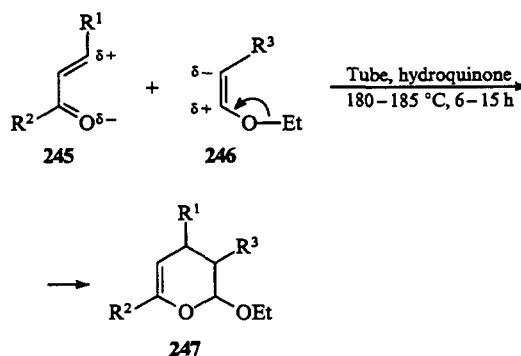


3. Compounds with six-membered heterocycles

The diene **43** in boiling toluene undergoes [4+2]-cycloaddition with the oxo-group of the diethyl ester of mesoxalic acid; the reaction affords the adduct **244** in an almost quantitative yield.⁴⁷

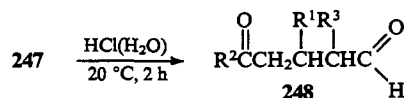


The electron density distribution in the α,β -unsaturated ketones **245** and in the vinyl ethers **246** is favourable for them to enter into [4+2]-cycloaddition. By heating these compounds at $180\text{--}185^{\circ}\text{C}$ in sealed tubes, the dihydropyran derivatives **247** were synthesised in 50%–88% yields.¹⁵⁴

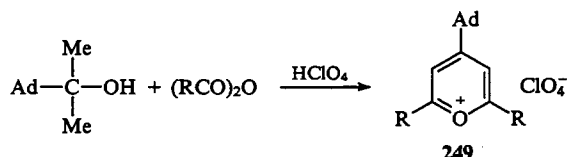


R ¹	R ²	R ³
H	H	Ad
H	H	AdCH ₂
AdCH ₂	H	H
H	Ad	H

When the dihydropyrans **247** are treated with dilute hydrochloric acid at 20 °C, the heterocyclic ring is cleaved and the 1,5-dicarbonyl compounds **248** are obtained in 84%–92% yields.¹⁵⁴

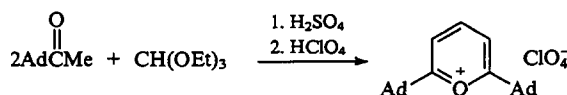


The tertiary alcohol, 2-(adamant-1-yl)propan-2-ol, reacts with perchloric acid and carboxyanhydrides to give 2,6-dialkyl-4-(adamant-1-yl)pyrilium perchlorates **249**.¹⁵⁵

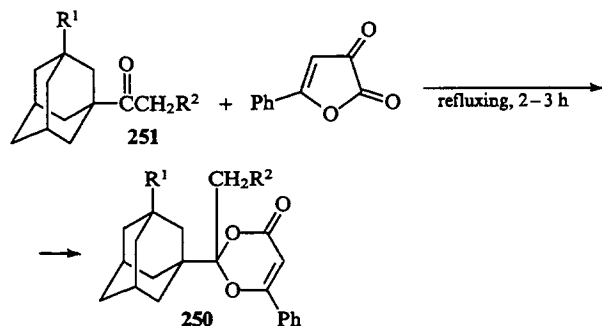


R = Me, Et, Pr.

2,6-Di(adamant-1-yl)pyrilium perchlorate is formed in 22% yield in the condensation of 1-acetyladamantane with ethyl orthoformate in the presence of sulfuric acid followed by the treatment of the reaction product with perchloric acid.¹⁵⁵



A series of adamantyl-containing heterocyclic compounds **250** with two oxygen atoms in the heterocyclic ring have been synthesised by the condensation of the ketones **251** with 5-phenyl-2,3-dihydrofuran-2,3-dione, their yields ranging from 29% to 78%.¹⁵⁶



R¹ = Br: R² = Br, NO₂; R¹ = NO₂: R² = ONO₂;

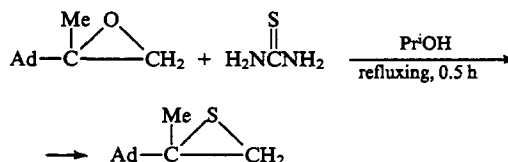
R¹ = Ph: R² = ONO₂; R¹ = ONO₂: R² = Br;

R¹ = H: R² = H, Cl, Br, ONO₂, OSO₂CH₂Ad.

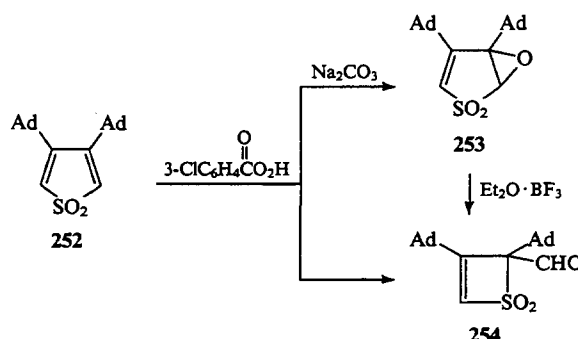
IV. Adamantane derivatives containing heterocyclic nuclei with sulfur atoms

1. Compounds with three-membered and four-membered heterocycles

2-(Adamant-1-yl)-2-methylthiirane is formed in 28% yield on refluxing a mixture of 2-(adamant-1-yl)-2-methyloxirane and thiourea in isopropyl alcohol.¹⁴²

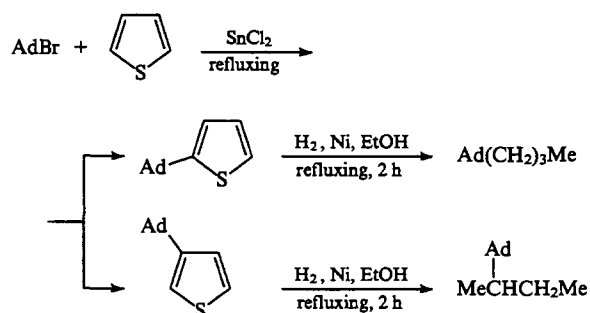


In the only study,¹⁵⁷ which reports synthesis of a compound of the adamantane series containing a four-membered heterocycle with a sulfur atom in the heterocyclic ring, two procedures have been proposed for the transformation of a five-membered ring into a four-membered ring. The cyclic sulfone **252** is converted into the epoxide **253** by reaction with 3-chloroperbenzoic acid in the presence of sodium carbonate; on treatment with boron trifluoride etherate the compound **253** isomerises into the thiete dioxide derivative **254**. Interestingly, the compound **254** is also formed in 78% yield in the reaction of the initial sulfone **252** with 3-chloroperbenzoic acid in the absence of water. This result was explained¹⁵⁷ by the fact that the peracid catalyses the isomerisation of the epoxide **253** formed into the thiete dioxide **254**.

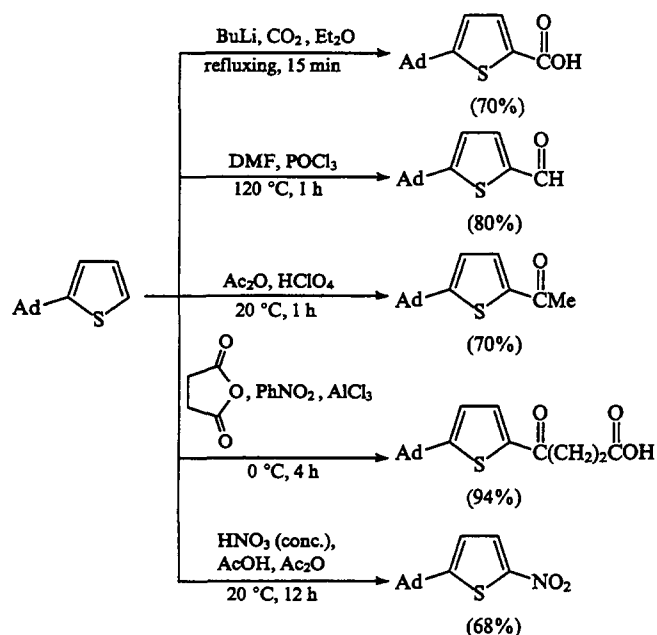


2. Compounds with five-membered heterocycles

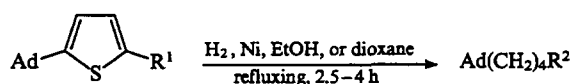
In the presence of tin(II) chloride, thiophene reacts with 1-bromoadamantane to give two adamantylation products, namely, 2-(adamant-1-yl)thiophene (yield 52%) and 3-(adamant-1-yl)thiophene (yield 7%). On treatment with hydrogen over W-7 Raney nickel, the resulting adamantylthiophenes are desulfurised and converted into 1-(adamant-1-yl)butane (yield 80%) and 2-(adamant-1-yl)butane (yield 85%).¹⁵⁸



Substitution reactions in 2-(adamant-1-yl)thiophene have been studied. A series of thiophene derivatives containing an adamantyl radical in the 2-position and various substituents in the 5-position were thus obtained.¹⁵⁹

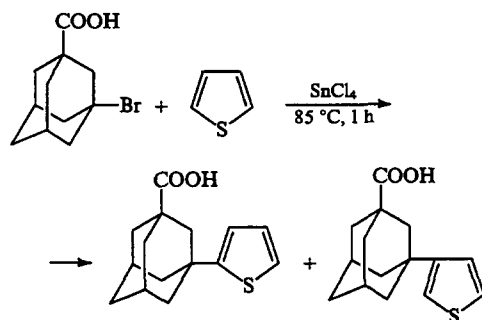


All the above compounds are desulfurised in the presence of the W-7 catalyst in alcohol or in dioxane giving the corresponding adamantane derivatives containing no heterocyclic rings.¹⁵⁹

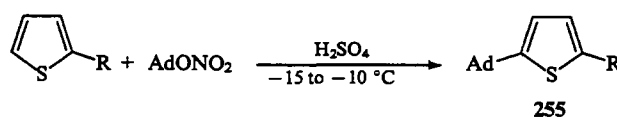


R ¹	R ²	Yield (%)
COOH	COOH	66
CHO	CH ₂ OH	60
COMe	CH(OH)Me	75
CO(CH ₂) ₂ COOH	CH(CH ₂) ₂ CO + CO(CH ₂) ₂ COOH	75 (total)
NO ₂	NH ₂	70

Two compounds, 3-(2-thienyl)adamantane-1-carboxylic acid and 3-(3-thienyl)adamantane-1-carboxylic acid have been obtained in a ratio of 2:1 in 47% overall yield by the reaction of 3-bromoadamantane-1-carboxylic acid with thiophene in the presence of tin(IV) chloride.¹⁶⁰

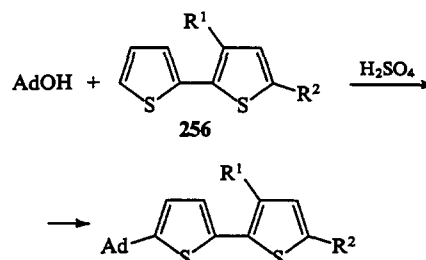


In the presence of concentrated sulfuric acid, adamant-1-yl nitrate reacts with thiophene derivatives containing electron-withdrawing substituents in the 2-position to give compounds **255** (yields 41% and 44%).¹⁵⁰



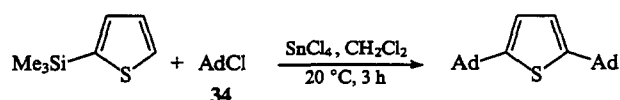
R = NO₂, COOH.

By means of adamant-1-ol, the adamantyl radical has been introduced into the 2,2'-dithienyl derivatives **256**.¹⁶¹

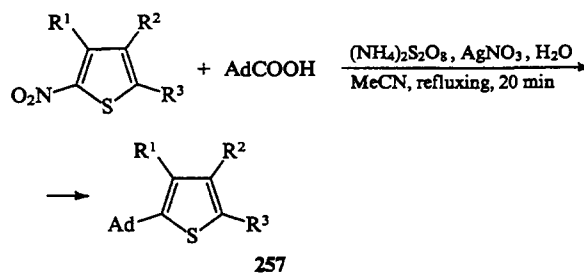


R¹ = H, R² = COMe, CHO, COOH; R¹ = NO₂, R² = H.

It is of interest that even at 20 °C, 2-(trimethylsilyl)thiophene reacts with chloroadamantane **34** to give 2,5-di(adamant-1-yl)-thiophene (yield 65%).³⁷

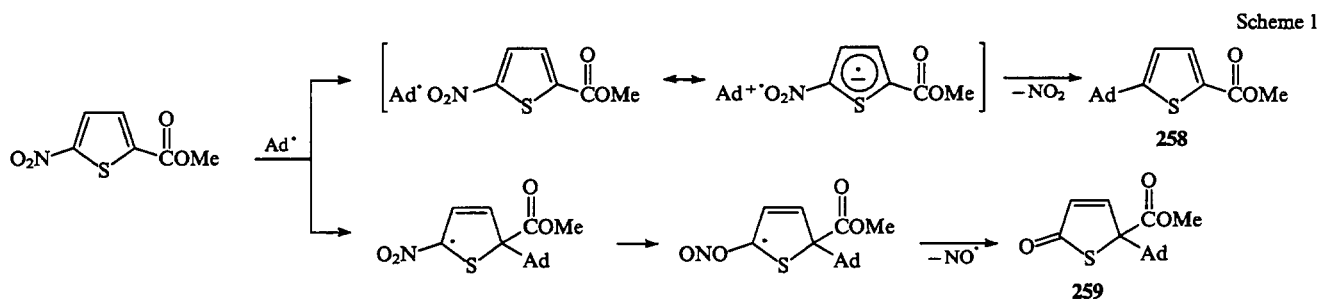


Cogolli et al.^{162, 163} have studied homolytic *ipso*-substitution in the series of thiophene nitro-derivatives under the action of the Ad[•] radical (generated from AdCOOH¹⁰³). The workers¹⁶² described the interaction of the Ad[•] radical with derivatives of 2-nitrothiophene, containing electron-withdrawing substituents in various positions of the thiophene ring; compounds **257** were thus prepared (yields 43%–55%).

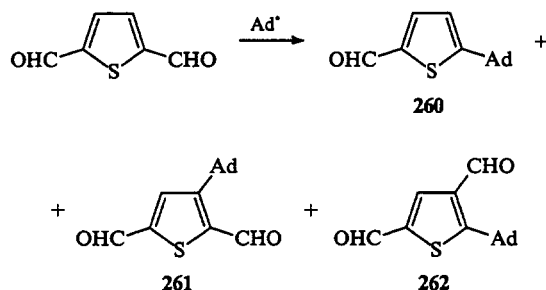


R ¹	R ²	R ³
H	H	SO ₂ Ph
H	H	CHO
H	NO ₂	COOMe
NO ₂	H	COOMe

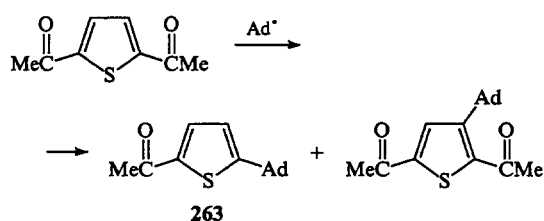
The reaction of Ad[•] with 5-methoxycarbonyl-3-nitrothiophene afforded 2-(adamant-1-yl)-5-methoxycarbonyl-3-nitrothiophene in 50% yield,¹⁶² whereas the interaction of this radical with 5-(methoxycarbonyl)-2-nitrothiophene gave two compounds: the normal product of *ipso*-substitution **258** (yield 55%) and the 'unusual' product **259** (yield 8%). A scheme was suggested to explain these results (Scheme 1).¹⁶³



A more complex picture has been observed in a study of the reactions of the Ad^\bullet radical with thiophene derivatives containing formyl, acetyl, or methoxycarbonyl group in various positions of the thiophene ring.¹⁶³ For example, three compounds were detected among the products of the reaction of the Ad^\bullet radical with 2,5-diformylthiophene, namely, compound **260** (yield 19%), **261** (yield 10%), and **262** (yield 56%), whereas the reaction of 2,4-diformylthiophene with the Ad^\bullet radical gave only compound **262** (yield 60%).¹⁶³

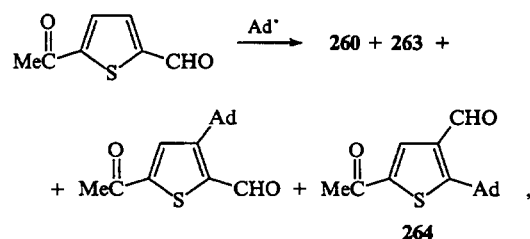


The reaction of 2,5-diacetylthiophene with the Ad^\bullet radical leads to two compounds, 2-acetyl-5-(adamant-1-yl)thiophene **263** (yield 33%) and 2,5-diacetyl-3-(adamant-1-yl)thiophene (yield 16%).¹⁶³



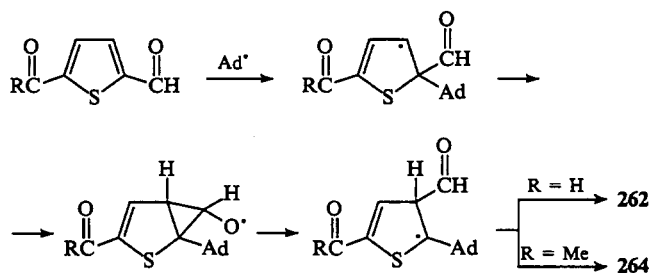
2,5-Di(methoxycarbonyl)thiophene reacts with the Ad^\bullet radical to give 3-(adamant-1-yl)-2,5-di(methoxycarbonyl)thiophene (yield 25%).¹⁶³

The interaction of the Ad^\bullet radical with 2-acetyl-5-formylthiophene is the most complex: four compounds have been isolated and identified among the reaction products, namely, compound **260** (yield 10%), **263** (yield 17%), 2-acetyl-4-(adamant-1-yl)-5-formylthiophene (yield 11%), and 2-acetyl-5-(adamant-1-yl)-4-formylthiophene **264** (yield 13%).¹⁶³

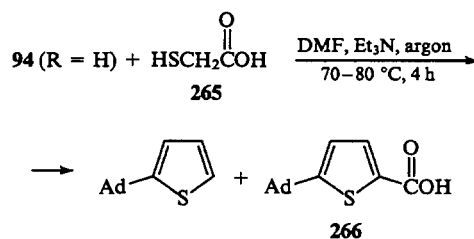


whereas the reaction of 2-acetyl-4-formylthiophene with the Ad^\bullet radical gave the compound **264** as the only product (yield 56%).¹⁶³

The formation of the 'unusual' products **262** and **264** in the reactions of the Ad^\bullet radical with the derivatives of 2-formylthiophene was explained¹⁶³ by assuming a scheme that includes the 1,2-shift of the formyl group.

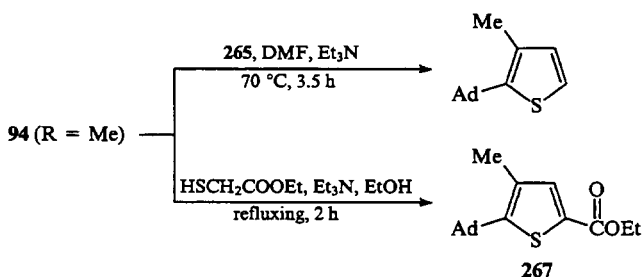


The cyclocondensation of the aldehyde **94** ($\text{R} = \text{H}$) with thioglycolic acid **265** carried out in boiling alcohol in the presence of triethylamine over a period of 5 h gives 5-(adamant-1-yl)thiophene-2-carboxylic acid **266** (yield 4.5%) and 2-(adamant-1-yl)thiophene (yield 34%). The latter is obviously formed via decarboxylation of the acid **266** under the reaction conditions.¹⁶⁴ By conducting this reaction in DMF in an argon flow, the yields of the products can be substantially increased: the acid **266** is formed in 24.6% yield and adamantylthiophene is obtained in 53.4% yield.¹⁶⁵

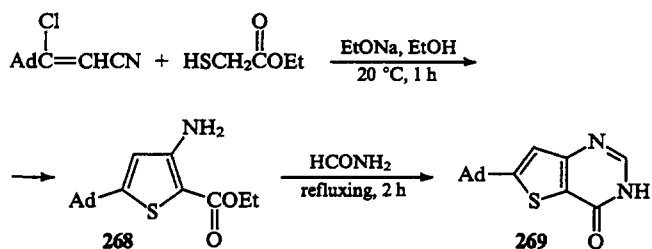


The condensation of the aldehyde **94** ($\text{R} = \text{H}$) with thioglycolic acid anilide in DMF in the presence of triethylamine at 60 °C for 3.5 h led to the anilide of the acid **266** (yield 45.5%).¹⁶⁵

When the aldehyde **94** ($\text{R} = \text{Me}$) has been made to react with the acid **265**, only the decarboxylation product, 2-(adamant-1-yl)-3-methylthiophene, has been isolated in 43% yield. Ethyl 5-(adamant-1-yl)-4-methylthiophene-2-carboxylate **267** was synthesised in 71% yield from the aldehyde **94** ($\text{R} = \text{Me}$) and ethyl thioglycolate.⁷¹

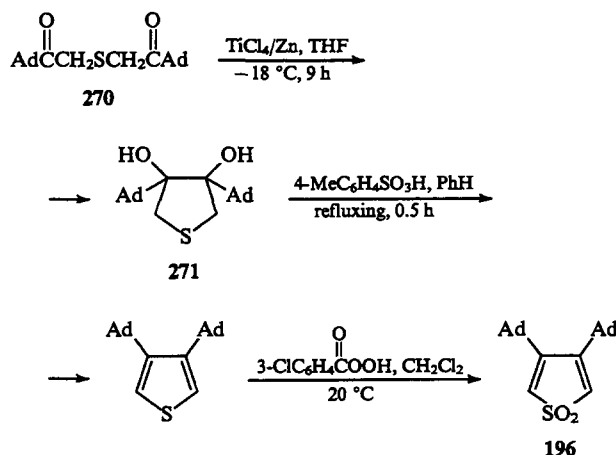


The reaction of 3-(adamant-1-yl)-3-chloroacrylonitrile with ethyl thioglycolate gives the aminoester **268** (yield 40%); heating of the latter with formamide in the presence of sodium ethoxide leads to 6-(adamant-1-yl)thieno[2.3-*e*]pyrimidin-4-one **269** (yield 86.5%).⁷⁰

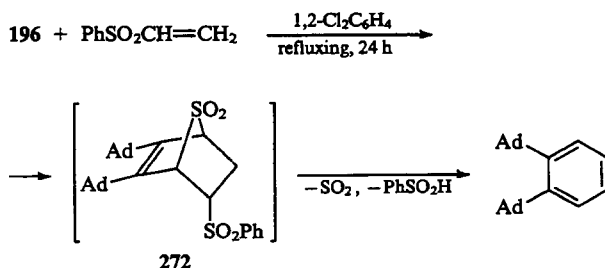


Treatment of 2-(trimethylsilyl)thiophene with AdCOCl in the presence of zinc chloride leads to the substitution of the Me₃Si group by the AdCO group; the reaction affords 2-(adamant-1-ylcarbonyl)thiophene in 82% yield.¹⁵²

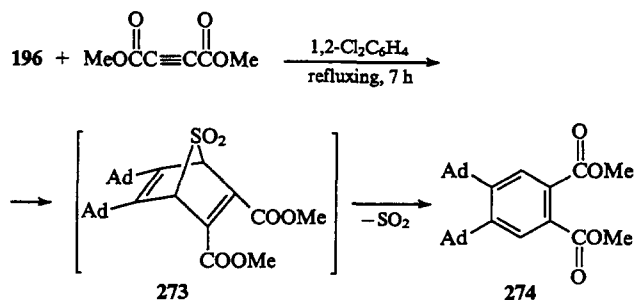
In 1990, an interesting study was published,¹²³ which was devoted to the synthesis and some transformations of 3,4-di(adamant-1-yl)thiophene 1,1-dioxide **196**. The dioxo sulfide **270** was reduced to the diol **271** (yield 34%), which on heating with toluene-*p*-sulfonic acid is converted to 3,4-di(adamant-1-yl)thiophene (yield 60%). The latter is oxidised with 3-chloroperbenzoic acid to the cyclic sulfone **196** in 75% yield.¹²³



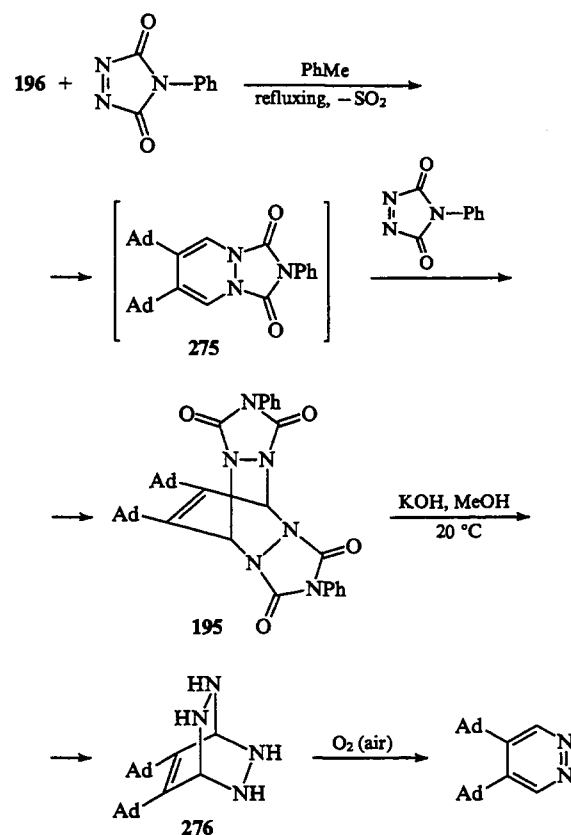
The diene condensation of the sulfone **196** with phenyl vinyl sulfone gives adduct **272**, which decomposes under the reaction conditions into sulfur dioxide, phenylsulfonic acid, and 1,2-di(adamant-1-yl)benzene (yield 92%).¹²³



The cycloaddition of the sulfone **196** to the dimethyl ethylenedicarboxylate also affords an unstable adduct, compound **273**, which loses sulfur dioxide under the reaction conditions and is converted into dimethyl 4,5-di(adamant-1-yl)phthalate **274** in 90% yield.¹²³



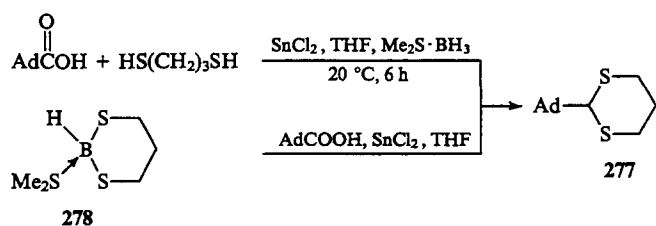
A more complex situation is observed when the sulfone **196** reacts with an excess of 4-phenyl-1,2,4-triazoline-3,5-dione. The adduct **275** of the composition 1:1 is formed initially; it reacts further with one more triazolinedione molecule giving the adduct **195** of the composition 1:2 (yield 71%). Treatment of the latter with potassium hydroxide in methanol gives the bicyclic compound **276** (yield 82%), which is transformed during storage in air into 4,5-di(adamant-1-yl)pyridazine in 82% yield.¹²³



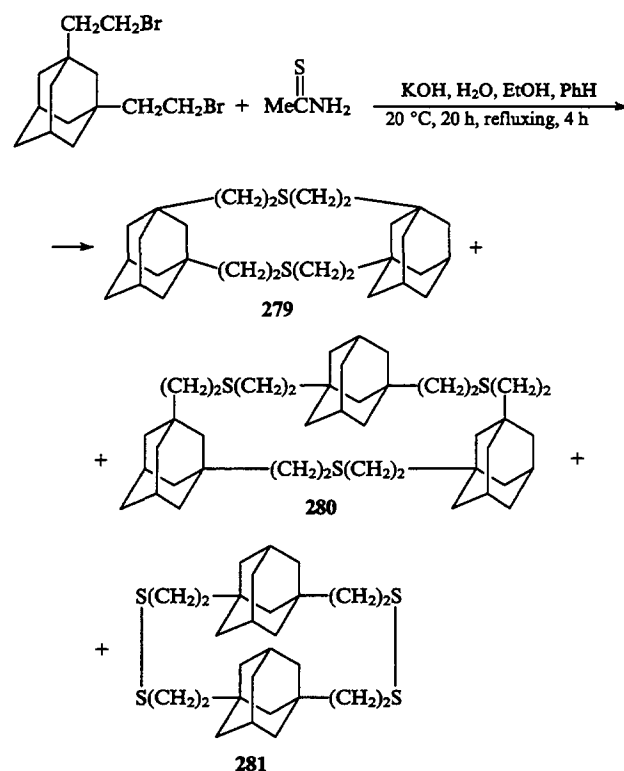
3,4-Di(adamant-1-yl)thiophene in a solution in carbon disulfide in the presence of aluminium chloride is converted into 2,4-di(adamant-1-yl)thiophene in quantitative yield over a period of 6 days at 20 °C.¹²³

3. Compounds with six-membered and larger heterocycles

Two methods for the synthesis of 2-(adamant-1-yl)hexahydro-1,3-dithiane **277** have been reported. One of these methods involves cyclocondensation of adamantane-1-carboxylic acid with 1,3-disulfanypropane in the presence of tin(II) chloride and the complex Me₂S·BH₃, and the other method involves the reaction of the same acid with the complex **278** [obtained preliminarily from HS(CH₂)₃SH and Me₂S·BH₃] in the presence of tin(II) chloride (yield 80%).¹⁶⁶



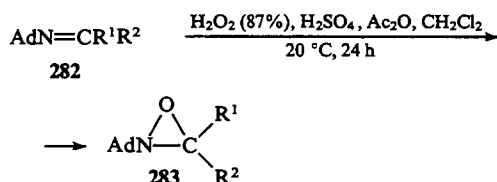
The heterocyclic compounds **279** (yield 34%), **280** (yield 17%), and **281** (yield 3%) containing several adamantane fragments and several sulfur atoms have been synthesised by heating 1,3-bis(2-bromoethyl)adamantane with thioacetamide in the presence of potassium hydroxide.¹⁶⁷



V. Adamantane derivatives containing heterocyclic nuclei with nitrogen and oxygen atoms

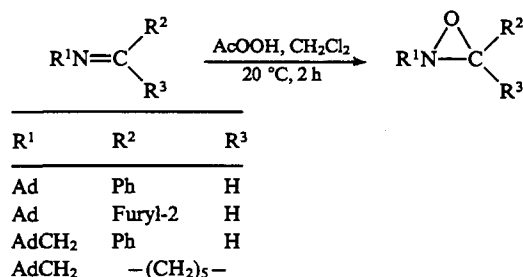
1. Compounds with three-membered heterocycles

Epoxydation of Schiff's bases is a general method for the preparation of oxaziridine derivatives. The Schiff's bases **282** have been converted into the oxaziridines **283** (yield 44%–75%) by treating them with hydrogen peroxide in acetic anhydride in the presence of sulfuric acid.¹⁶⁸

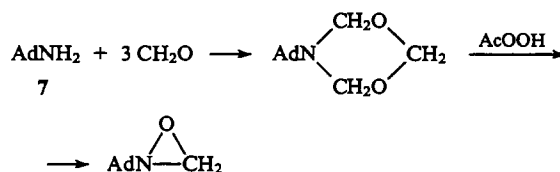


$\text{R}^1 = \text{H}; \text{R}^2 = \text{H, Ph}; \text{R}^1 = \text{cyclo-C}_6\text{H}_{11}, \text{R}^2 = \text{Me};$
 $\text{R}^1 + \text{R}^2 = -(\text{CH}_2)_5-$

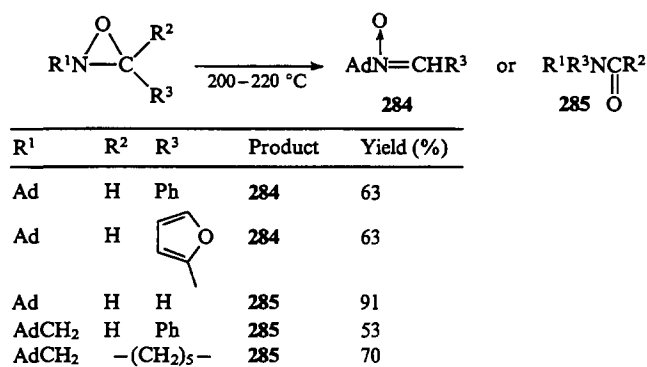
Oxaziridine derivatives have been synthesised by the oxidation of Schiff's bases with peracetic acid; the yields of the oxidation products varied from 47% to 56%.^{31, 139}



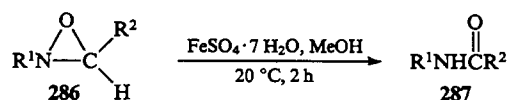
The oxaziridine containing no substituents at the carbon atom was obtained in 29% yield by the oxidation of the product of condensation of the amine **7** with formaldehyde.¹³⁹



The adamantyloxaziridines **283** are fairly thermally stable compounds. However, at temperatures above 200 °C they isomerise to give the nitrones **284** or amides **285**.¹³⁹



The oxaziridines **286** isomerise in the presence of iron(II) sulfate at room temperature to the amides **287** in 70%–76% yields.¹³⁹

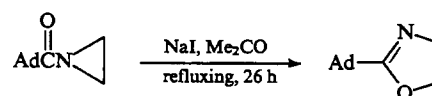


$\text{R}^1 = \text{Ad}, \text{R}^2 = \text{Ph, furyl-2}; \text{R}^1 = \text{AdCH}_2, \text{R}^2 = \text{Ph}; \text{R}^3 = \text{Alk.}$

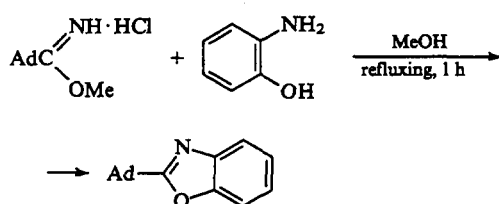
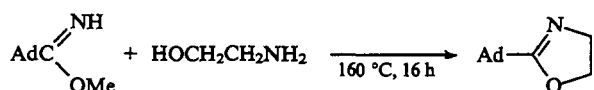
No compounds containing the adamantyl radical linked directly to the oxazetidine ring have been reported in the literature.

2. Compounds with five-membered heterocycles

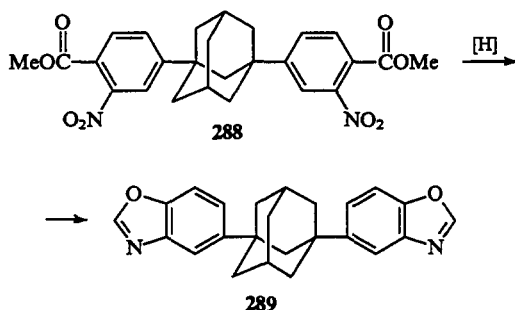
When 1-adamant-1-ylcarbonylaziridine is heated with sodium iodide in acetone, it isomerises to 2-(adamant-1-yl)oxazoline (yield 43%).⁶⁰



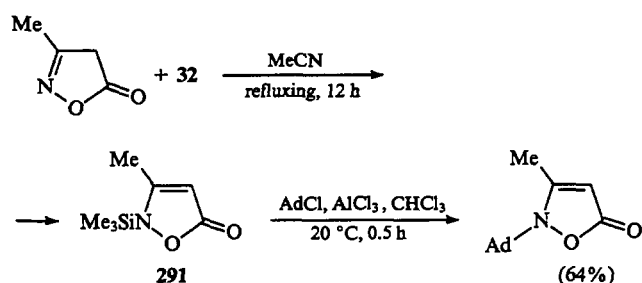
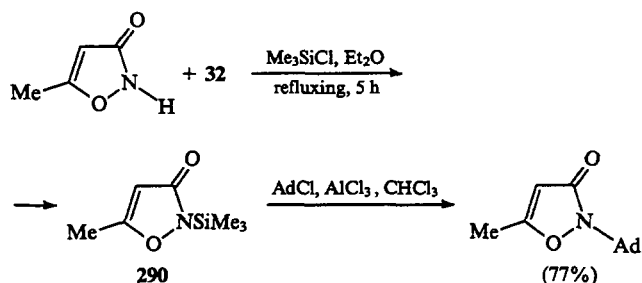
2-(Adamant-1-yl)oxazoline has been synthesised by the condensation of the methyl iminoester of adamantane-1-carboxylic acid with ethanolamine (yield 93%), whereas the reaction of the hydrochloride of the same iminoester with 2-aminophenol gives 2-(adamant-1-yl)benzoxazole (yield 76%).⁵⁵



1,3-Di(benzoxazol-5-yl)adamantane **289** has been obtained by the reduction of the adamantane derivative **288** containing the methyl 2-nitrobenzoate residues in the 1- and 3-positions.¹⁶⁹

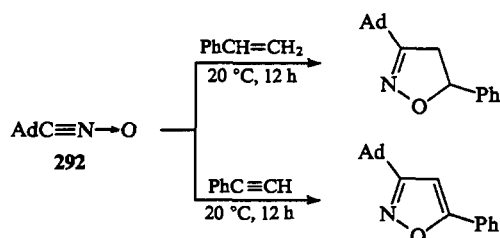


A two-stage procedure proposed for the introduction of adamantyl radical to the nitrogen atoms of 5-methylisoxazolin-3-one or 3-methylisoxazolin-5-one involves *N*-silylation of heterocyclic compounds with disilazane **32** and the subsequent treatment of the resulting silylated products **290** or **291** in situ with 1-chloroadamantane in the presence of aluminium chloride.³⁷



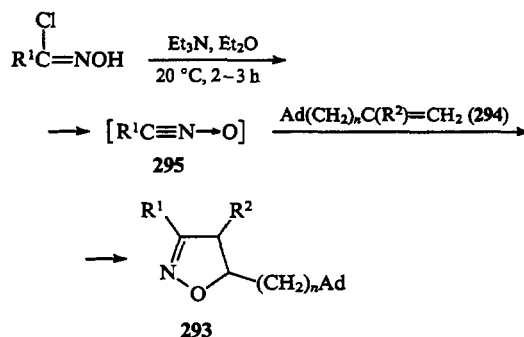
One of the most general methods for the synthesis of isoxazoline and isoxazole derivatives involves the 1,3-dipolar cycloaddition of carbonitrile *N*-oxides to alkenes and alkynes. In 1972, Italian investigators¹⁷⁰ described for the first time the preparation of the *N*-oxide of adamantane-1-carbonitrile **292** and carried out the 1,3-dipolar cycloaddition of the nitrile **292** to styrene and

phenylethyne. The corresponding adducts were obtained in 89% and 69% yields.



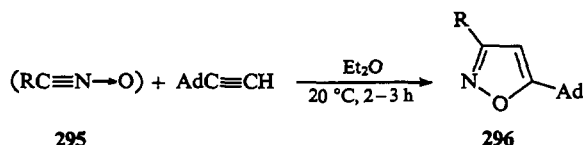
An alternative approach to the synthesis of isoxazolines and isoxazoles containing an adamantyl substituent involves 1,3-dipolar cycloaddition of *N*-oxides of nitriles of aliphatic or aromatic carboxylic acids to unsaturated adamantane derivatives. Carbonitrile *N*-oxides used in situ in these reactions are obtained either by treating hydroxamoyl chlorides with bases or by thermolysis.

The isoxazoline derivatives **293** have been obtained in 63%–98% yields from alkenes **294** of the adamantane series and the aromatic and heterocyclic carboxylic acid nitrile *N*-oxides **295** prepared from the corresponding hydroxamoyl chlorides by treating them with triethylamine.^{171, 172}



$n = 0, 1$; $\text{R}^1 = \text{Ph, 4-MeOC}_6\text{H}_4, 3\text{-O}_2\text{NC}_6\text{H}_4, 4\text{-O}_2\text{NC}_6\text{H}_4, 5\text{-nitrofuryl-2}$; $\text{R}^2 = \text{H, Me}$.

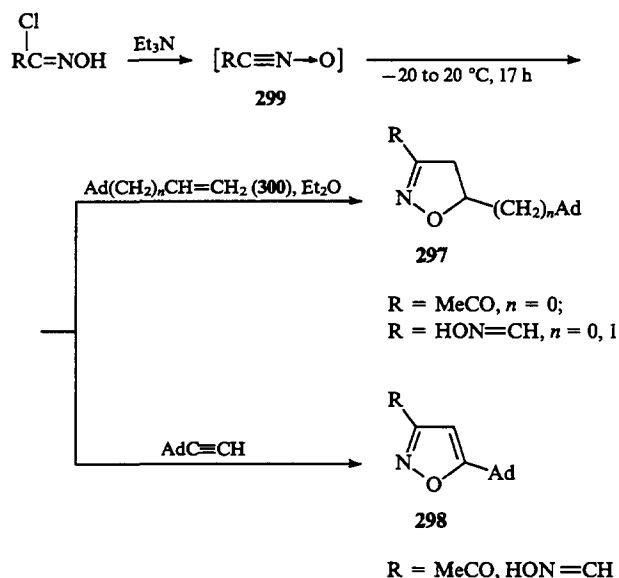
The reaction of 1-ethynyladamantane with nitrile *N*-oxides **295** under similar conditions gives isoxazole derivatives **296** in 68%–95% yields.^{171, 172}



$\text{R} = \text{Ph, 4-MeOC}_6\text{H}_4, 3\text{-NO}_2\text{C}_6\text{H}_4, 4\text{-NO}_2\text{C}_6\text{H}_4, 5\text{-nitrofuryl-2}$.

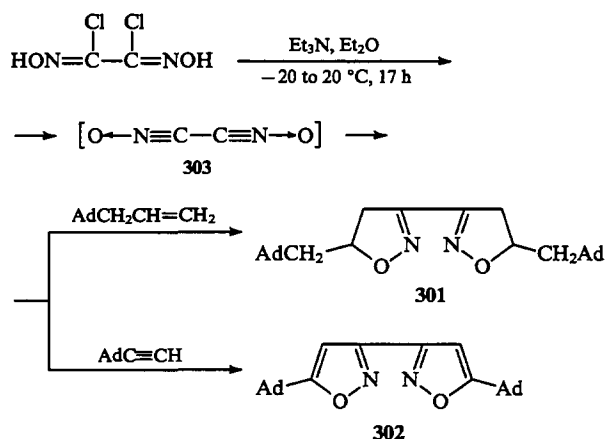
The use of the above procedure permits the preparation of isoxazoline and isoxazole derivatives from unsaturated adamantane derivatives and aliphatic carbonitrile *N*-oxides, their yields ranging from 20 to 40%. The researchers found conditions under which the yields of isoxazolines and isoxazoles increased to 65%.¹⁷²

The isoxazolines **297** and isoxazoles **298** were synthesised in 50–65% yields by the reaction of pyruvonnitrile *N*-oxide (**299**, $\text{R} = \text{MeCO}$) or hydroxyiminoacetonitrile *N*-oxide (**299**, $\text{R} = \text{HON}=\text{CH}$) with alkenes **300** or with 1-ethynyladamantane, respectively.¹⁷¹

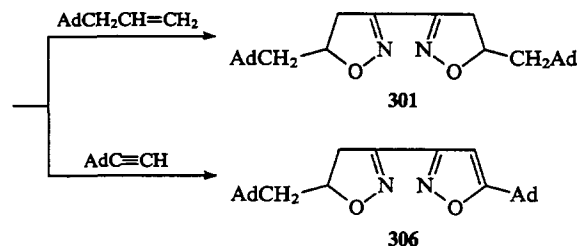
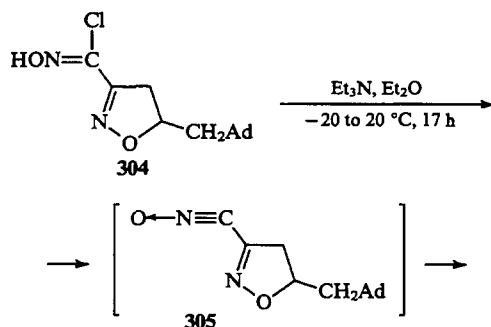


By using aqueous sodium bicarbonate instead of triethylamine in the synthesis of isoxazoline **297** ($\text{R} = \text{HON}=\text{CH}$, $n = 0$), the yield of the latter can be increased to 92%.¹⁷¹

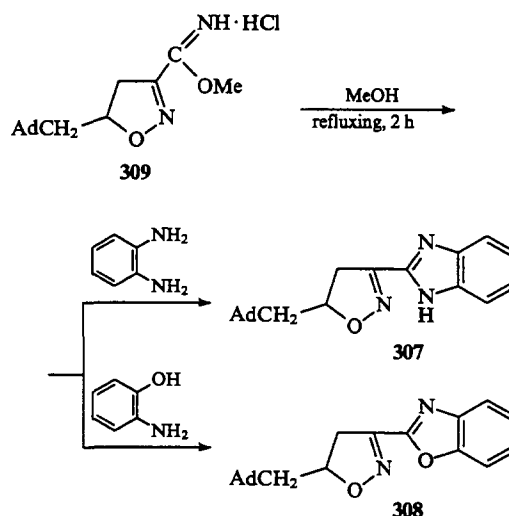
Compounds containing two isoxazoline nuclei **301** or two isoxazole nuclei **302** are formed in the cycloaddition of the bis(*N*-oxide) of oxalic acid dinitrile **303** to 1-allyladamantane or to 1-ethynyladamantane (yields 50 and 42%, respectively).¹⁷²



The hydroxamoyl chloride **304** on treatment with triethylamine is converted into the nitrile *N*-oxide **305**, which reacts with 1-allyl and 1-ethynyladamantane to give compounds **301** and **306** (yields 65% and 35%).¹⁷²

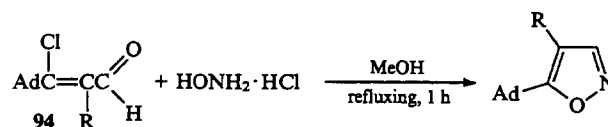


Compound **307** containing isoxazoline and benzimidazole nuclei and compound **308** with imidazoline and benzoxazole nuclei are obtained in 75% and 72% yields by the condensation of the iminoester hydrochloride **309** with *o*-diaminobenzene or *o*-aminophenol.¹⁷²



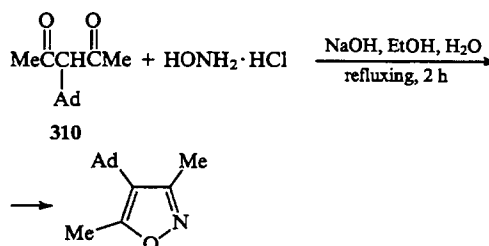
Most of the compounds synthesised from nitrile *N*-oxides and unsaturated adamantane derivatives exhibit a bacteriostatic activity. For example, the adamantyl derivative of isoxazoline **293** with $\text{R}^1 = 5\text{-nitro-2-furyl}$, $\text{R}^2 = \text{Me}$, and $n = 0$ is active against diphtheria and tuberculosis pathogens, the derivative with $\text{R}^1 = \text{Ph}$, $\text{R}^2 = \text{Me}$, and $n = 0$ exhibits a high tuberculostatic activity, and the compound with $\text{R}^1 = 3\text{-O}_2\text{NC}_6\text{H}_4$, $\text{R}^2 = \text{H}$, and $n = 0$ possesses a high antiviral activity.¹⁷²

5-(Adamant-1-yl)- and 5-(adamant-1-yl)-4-methylisoxazoles have been synthesised by the reaction of the aldehydes **94** with hydroxylamine hydrochloride in boiling methanol (yield 90%).¹⁶⁵

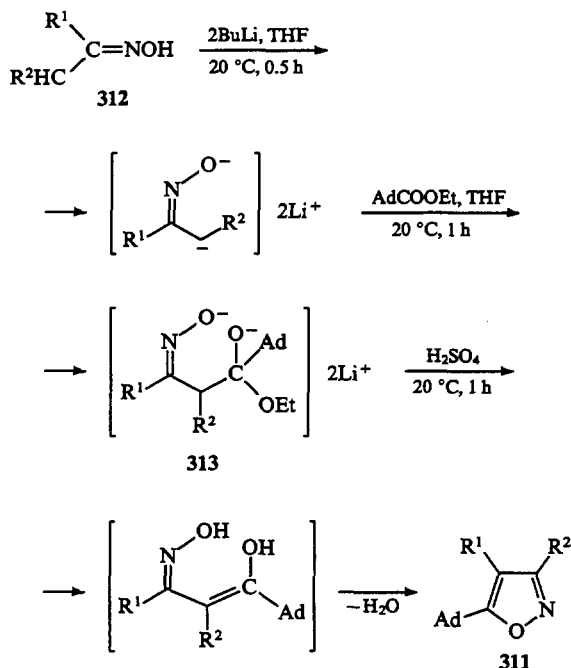


$\text{R} = \text{H}, \text{Me}$.

Refluxing of 3-(adamant-1-yl)pentane-2,4-dione **310** with hydroxylamine hydrochloride in aqueous alcohol gives rise to 4-(adamant-1-yl)-3,5-dimethylisoxazole (yield 70%).⁶⁰

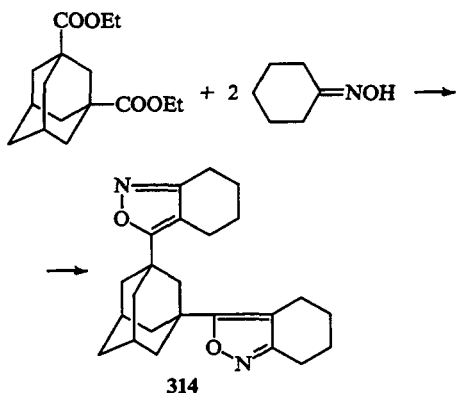


He and Lin proposed¹⁷³ an original method for the synthesis of the oxazole derivatives **311**. The oximes of ketones **312** are converted into the corresponding dianions on treatment with butyllithium. The dianions are introduced into the reaction with ethyl adamantane-1-carboxylate. The resulting salts **313** cyclise to the isoxazoles **311** on treatment with sulfuric acid.¹⁷³

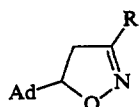


$\text{R}^1 = \text{Me}; \text{R}^2 = \text{H}; \text{R}^1 + \text{R}^2 = -(\text{CH}_2)_3-, -(\text{CH}_2)_4-.$

Compound **314** can be obtained in 64% yield in a similar way from diethyl adamantane-1,3-dicarboxylate and cyclohexanone oxime.¹⁷³

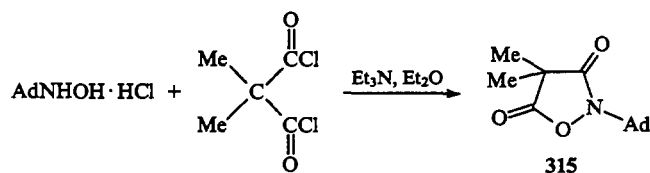


Biological activity of the isoxazoline derivatives has been studied.

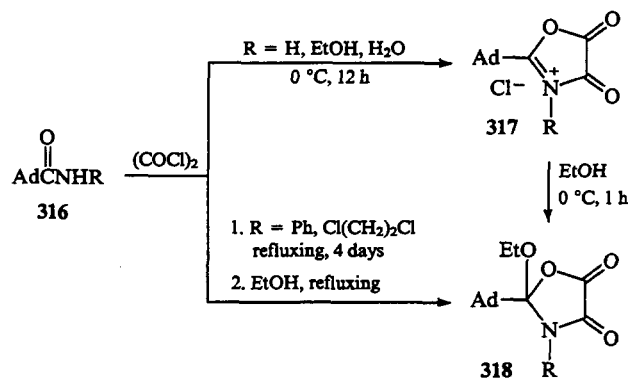


This compound with $\text{R} = \text{Ph}$ was found to exhibit a tuberculo-static activity, and the compounds with $\text{R} = 5\text{-nitro-2-furyl}$ and 5-nitro-2-thienyl exhibit an antibacterial activity.¹⁷⁴

2-(Adamant-1-yl)-4,4-dimethylisoxazolidine-3,5-dione **315** has been obtained in 94% yield by the condensation of *N*-(adamant-1-yl)hydroxylamine hydrochloride with dimethylmalonic acid dichloride.¹⁷⁵

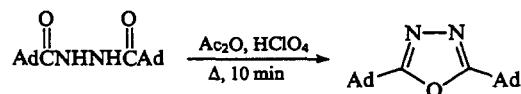


The amide AdC(O)NH_2 is converted initially into the salt **317** (yield 72.5%) by treating it with oxalyl chloride; the interaction of this salt with ethanol results in the formation of the ethoxy-derivative **318** ($\text{R} = \text{H}$, yield 91%). The anilide AdC(O)NHPh is converted into compound **318** ($\text{R} = \text{Ph}$, yield 56%) without isolation of the corresponding salt.^{176, 177}

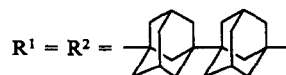
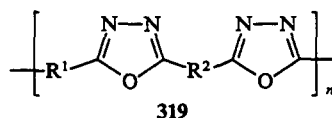


On treatment with ammonia, the compound **318** with $\text{R} = \text{H}$ is converted into the diamide AdCONHCOCONH_2 , whereas refluxing of this compound in dichloromethane for 28 h leads to the acyl isocyanate AdCONCO .¹⁷⁶

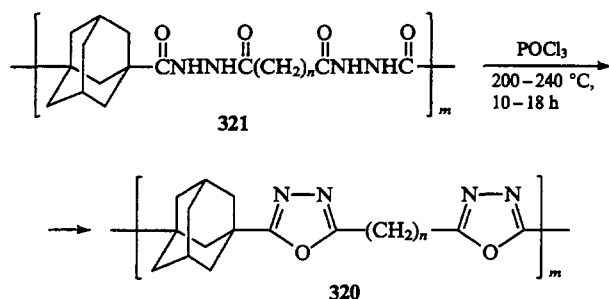
Heating of *N,N'*-di(adamant-1-ylcarbonyl)hydrazine in acetic anhydride in the presence of perchloric acid affords 2,5-di(adamant-1-yl)-1,3,4-oxadiazole in 50% yield.⁶⁰



High-molecular-weight thermostable compounds **319** containing adamantyl and 1,3,4-oxadiazole fragments, which are readily moulded at temperatures above the softening point, have been prepared by heating adamantane-1,3-dicarboxylic acid, diadamant-1,1'-yl-3,3'-dicarboxylic acid, or their chlorides with the dihydrazides of the same acids in polyphosphoric acid (with a content of P_2O_5 of 85%–86%) at 140–160 °C for 6 h.¹⁷⁸

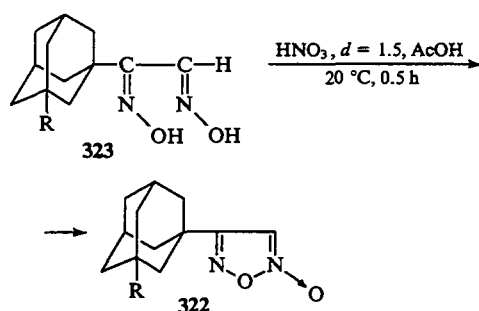


Thermostable polymers are formed in 73–89% yields when *N,N'*-diacylpolyhydrazides **321** are heated with phosphorus oxychloride in vacuo.¹⁷⁹



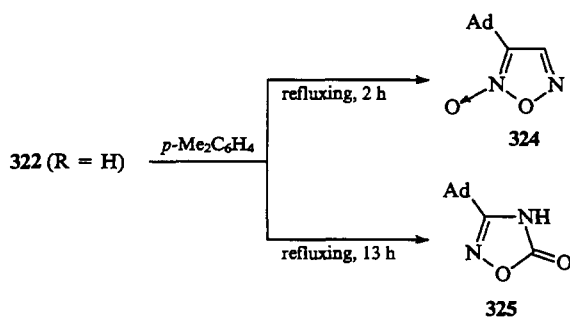
$n = 1-4, 7, 8.$

The furoxans **322** containing an adamantyl radical in the 4-position have been prepared by a known method involving the reaction of the *anti*-glyoximes **323** with a fuming nitric acid in glacial acetic acid. The yields of the furoxans **322** in this reaction are 60%–70%.¹⁸⁰



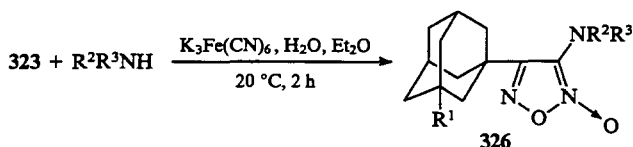
$R = \text{H, Me, Cl, 4-MeOC}_6\text{H}_4.$

On refluxing in *p*-xylene for 2 h the furoxan **322** ($R = \text{H}$) isomerises to the furoxan **324** (yield 22%), whereas on prolonged refluxing (13 h) the isomerisation leads to 3-(adamant-1-yl)-1,2,4-oxadiazol-5-one **325** (yield 50%).¹⁸⁰



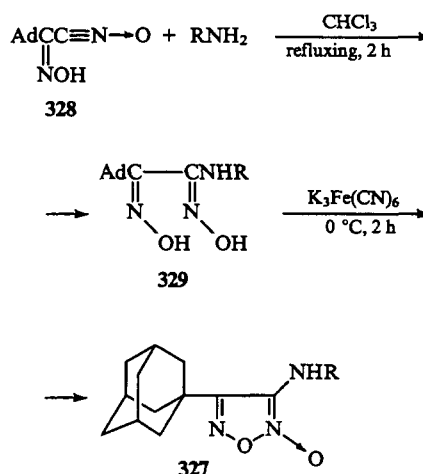
Treatment of the furoxan **322** ($R = \text{H}$) with nitric acid ($d = 1.5$) at 20 °C for 2 h gives rise to the furoxan **322** ($R = \text{ONO}_2$) in 78% yield.¹⁸⁰

In the presence of $\text{K}_3\text{Fe}(\text{CN})_6$, the glyoximes **323** react with secondary amines giving the furoxans **326** containing residues of the secondary amines in the 5-position (yields 33%–64%).¹⁸¹



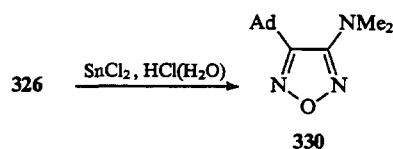
R^1	R^2	R^3	R^1	R^2	R^3
H	Me	Me	OH	Me	Me
Me	Me	Me	H	Et	Et
4-MeC ₆ H ₄	Me	Me	H	-(CH ₂) ₅ -	
Cl	Me	Me	H	(CH ₂ CH ₂) ₂ O	

The furoxans **327** have been obtained by the reaction of the nitrile *N*-oxide **328** with ammonia or methylamine followed by treatment of the resulting glyoximes **329** with potassium hexacyanoferrate(III). The yields of furoxans **327** are 37% ($R = \text{H}$) and 30% ($R = \text{Me}$).¹⁸¹



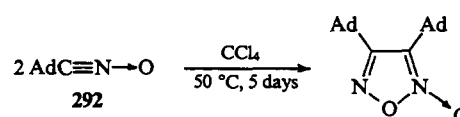
$R = \text{H, Me.}$

The furoxan **326** ($R^1 = \text{H}, R^2 = R^3 = \text{Me}$) is reduced by tin(II) chloride in hydrochloric acid to a furazan derivative, 3-(adamant-1-yl)-4-dimethylamino-1,2,5-oxadiazole **330**.¹⁸¹ The yield of the furazan **330** is 66%.

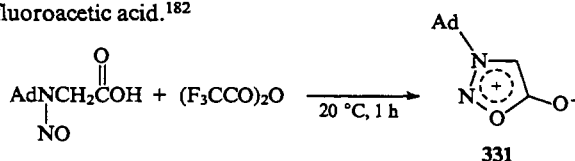


$R^1 = \text{H}, R^2 = R^3 = \text{Me.}$

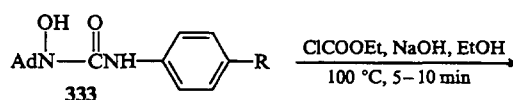
The nitrile *N*-oxide **292** dimerises under mild conditions to give 4,5-di(adamant-1-yl)furoxan (yield 78%).¹⁷⁰

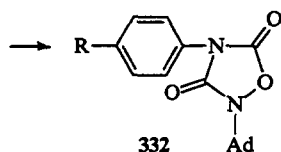


There is only one example of synthesis of a derivative of 1,2,3-oxadiazolidine, namely, 3-(adamant-1-yl)-1,2,3-oxadiazol-5-one **331**. This compound is formed in 80% yield in the reaction in *N*-nitroso-*N*-(adamant-1-yl)glycine with the anhydride of trifluoroacetic acid.¹⁸²



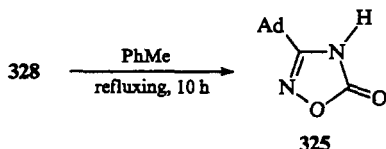
The 1,2,4-oxadiazolidine-3,5-dione derivatives **332** containing an adamantyl radical have been obtained by the condensation of the amides **333** with ethyl chloroformate in the presence of an alcoholic solution of potassium hydroxide (yields 75% and 58%).¹⁸³





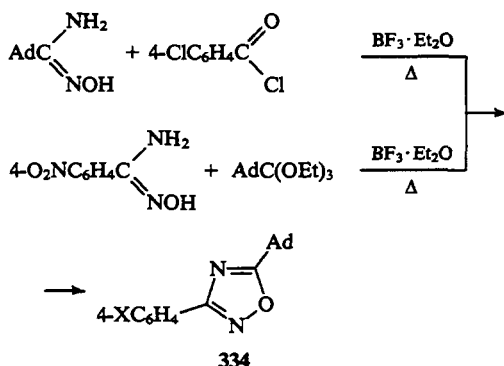
R = H, Cl.

Heating of the nitrile *N*-oxide **328** in toluene affords 3-(adamant-1-yl)-1,2,4-oxadiazol-5-one **325** in 63% yield.¹⁸⁰



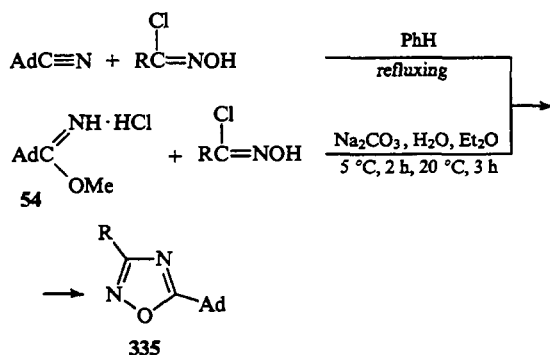
It has been found that the formation of the compound **325** involves cleavage of the furoxan ring, the isocyanate rearrangement of the intermediate nitrile *N*-oxide **328**, and its subsequent cyclisation.¹⁸⁰

The 1,2,4-oxadiazole derivatives **334** have been synthesised from amidoximes and *p*-chlorobenzoyl chloride¹⁸⁴ or from the orthoester $\text{AdC}(\text{OEt})_3$ ¹⁸⁵ in the presence of boron trifluoride etherate with heating (yield 40%).



X = Cl, NO₂.

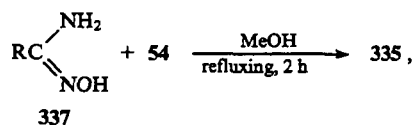
Several procedures have been proposed for the synthesis of adamantyl-containing oxadiazoles. 3-R-5-(Adamant-1-yl)-1,2,4-oxadiazoles **335** have been obtained in 56%–98% yields from the hydroxamoyl chlorides $\text{RC}(\text{Cl})=\text{NOH}$ by two procedures: their thermal condensation with 1-cyanoadamantane or their interaction with the methyl iminoester hydrochloride **54** in the presence of sodium carbonate.^{56, 186}



R (time of refluxing/h) = Ph (40), 3-O₂NC₆H₄ (80),

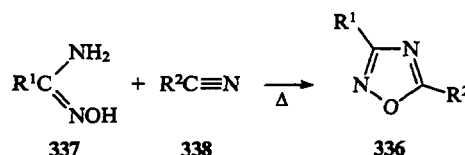
4-O₂NC₆H₄ (110), (110).

Two alternative methods for the synthesis of the 1,2,4-oxadiazole derivatives **335** and **336** are based on the reaction of the amidoximes **337** with the iminoester hydrochloride **54** (the yields of the target compounds varied from 40% to 88%)^{56, 186, 187}



R = Me, PhCH₂, Ad,

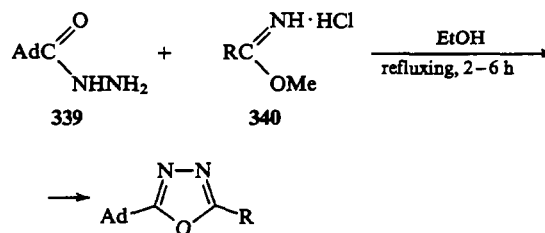
or on the cyclocondensation of amidoximes **337** with carbonitriles **338**.



R¹ = Ad; R² = CCl₃, 2-ClC₆H₄, Ad;

R² = Ad; R¹ = Me, ClCH₂, CCl₃, 2-ClC₆H₄.

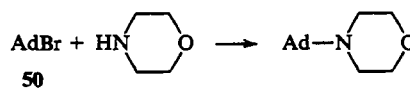
To prepare 2,5-disubstituted derivatives of 1,3,4-oxadiazole, cyclocondensation of the carboxylic acid hydrazides **339** with iminoester hydrochlorides **340** has been used. The yields of the oxadiazole derivatives were 50%–70%.⁵⁶



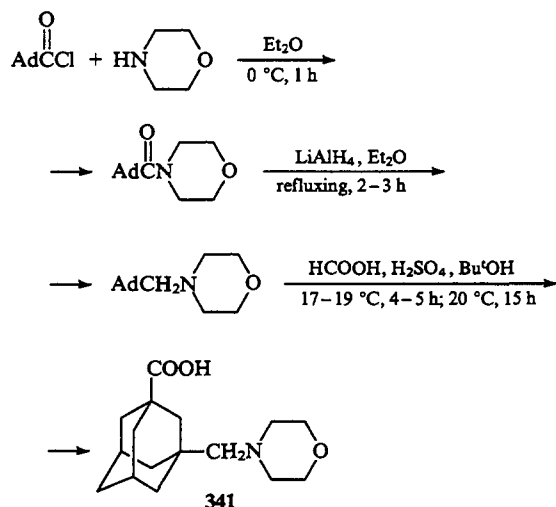
R = Me, Ph, , Ad.

3. Compounds with six-membered heterocycles

Refluxing of a mixture of morpholine and the 1-bromoadamantane for 8 h gives rise to 4-(adamant-1-yl)morpholine, which has been claimed as a compound possessing an antiviral activity.⁸⁹

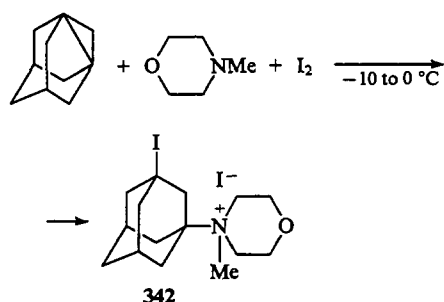


A method for preparing 3-(morpholinomethyl)adamantane-1-carboxylic acid **341** has been proposed. The method includes three stages. The reaction of the chloride AdCOCl with morpholine affords the morpholide of this acid (yield 72%), which is then reduced with lithium tetrahydroaluminate to 1-(morpholinomethyl)adamantane (yield 97%). The latter reacts with formic acid in the presence of sulfuric acid to give the compound **341** in 11% yield.¹⁰⁷

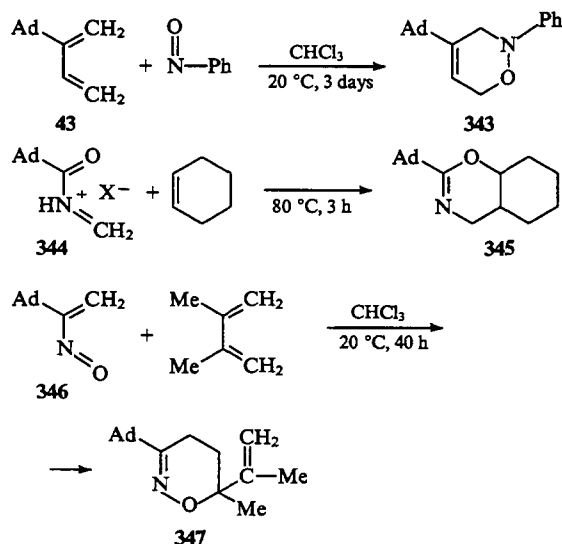


The hydrochloride of the compound **341** exhibits analgesic, anti-inflammatory, antipyretic, and antifibrillar activities.¹⁰⁷

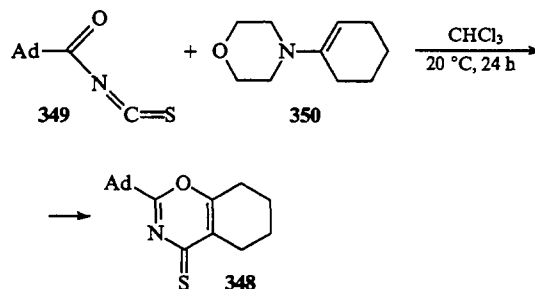
The salt **342** has been obtained in 42% yield from 1,3-dehydroadamantane, 4-methylmorpholine, and iodine by conjugated haloamination.¹⁰⁰



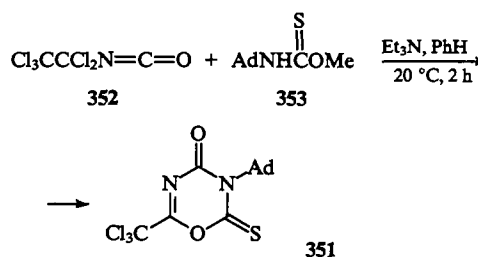
Derivatives of dihydro-1,2- and dihydro-1,3-oxazine have been prepared by diene condensation. 4-(Adamant-1-yl)-2-phenyl-3,6-dihydro-1,2-oxazine **343** has been synthesised in this way from the diene **43** and nitrosobenzene in 51% yield; the adduct **345** was obtained from the diene **344** and cyclohexene in 33% yield; and the interaction of the diene **346** and 2,3-dimethylbuta-1,3-diene gave rise to the adduct **347** (yield 59%).⁴⁷



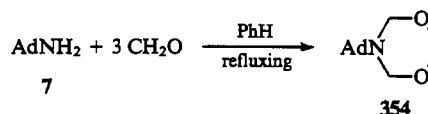
Compound **348** has been synthesised in 50% yield by the diene condensation of adamant-1-ylcarbonyl isothiocyanate **349** with the enamine **350**.⁴⁷



A heteryladamantane, 2-(trichloromethyl)-6-thioxo-5*H*-1,3,5-oxadiazin-4-one **351**, has been obtained in 53% yield by the reaction of perchloroethyl isocyanate **352** with *N*-(adamant-1-yl)-*O*-methylthiourethane **353** in the presence of triethylamine.¹⁸⁸



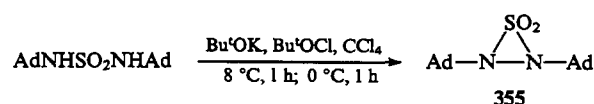
On heating in benzene, AdNH_2 condenses with three formaldehyde molecules affording the derivative of 1,3,5-dioxazine **354** (yield 49%).¹³⁹



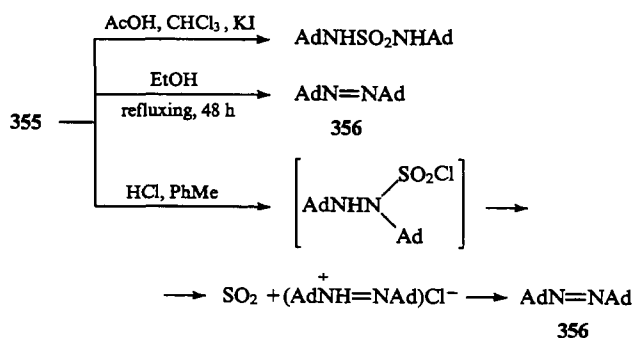
VI. Adamantane derivatives containing heterocyclic nuclei with nitrogen and sulfur atoms

1. Compounds with three-membered and four-membered heterocycles

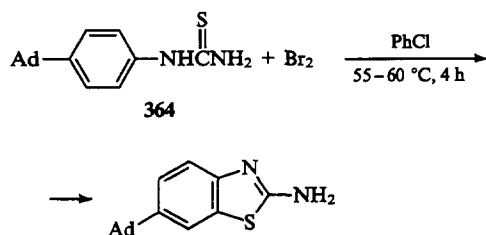
N,N'-Bis(adamant-1-yl)sulfonamide is converted into 2,3-di(adamant-1-yl)thiadiaziridine-1,1-dioxide **355** in 92% yield by treating it with potassium *tert*-butoxide and *tert*-butyl hypochlorite in tetrachloromethane.¹⁸⁹



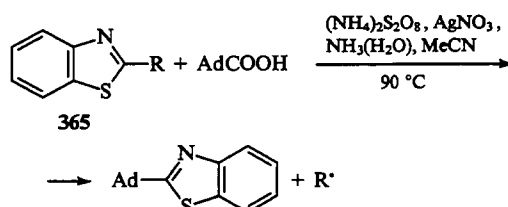
Diadamantylidiazene **356** is formed from the dioxide **355** when it is treated with hydrogen chloride in toluene (yield 100%) or refluxed in ethanol (yield 84%). Treatment of the dioxide **355** with potassium iodide in acetic acid leads to the initial *N,N'*-bis(adamant-1-yl)sulfonamide in 72% yield.¹⁸⁹



6-(Adamant-1-yl)-2-aminobenzothiazole is formed in the reaction of the thiourea derivative **364** with bromine (yield 40%).⁴⁵

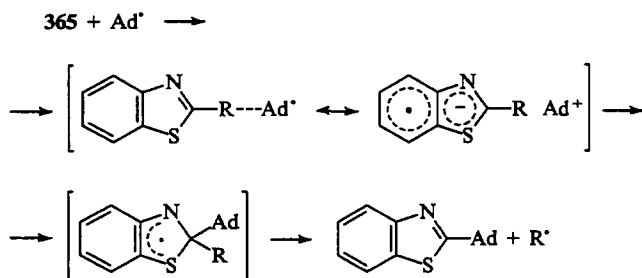


The homolytic *ipso*-substitution in the series of benzothiazole derivatives has been studied fairly comprehensively.¹⁹²⁻¹⁹⁴ The benzothiazole derivatives **365** and the acid AdCOOH were treated with ammonium peroxydisulfate and silver nitrate in acetonitrile in the presence of aqueous ammonia at 90 °C for 20 min. The last stage of this reaction is the displacement of the substituent in the 2-position of the benzothiazole nucleus and its substitution by the adamantyl radical.¹⁹²⁻¹⁹⁴

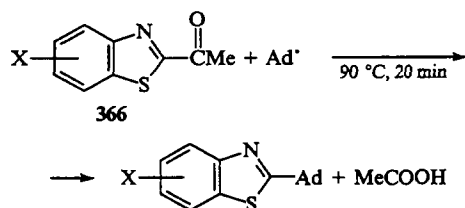


R (yield, %) = PhSO₂ (80), PhSO (80), PhCO (55), MeCO (60), CHO (40), MeS (60), MeO (40), Br (70), Cl (50), F (50),¹⁹² CHO (40), MeCO (60), COEt (60), PhCO (55), 4-ClC₆H₄ (56), 4-MeC₆H₄CO (52), 4-MeOC₆H₄ (50),¹⁹³ NO₂ (100).¹⁹⁴

A possible scheme for this reaction has been suggested.^{192, 193}

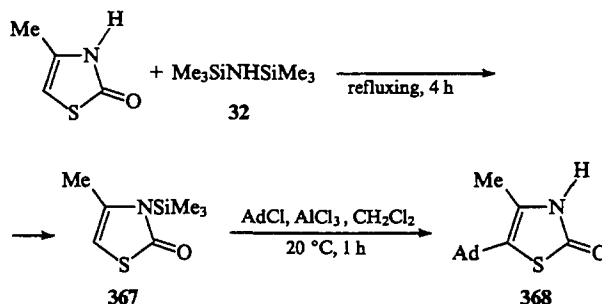


The presence of electron-withdrawing substituents in the 5- or 6-position facilitates this reaction. The relative rates (*v*) of the substitution of the acetyl radical by the adamantyl radical in the 2-acetylbenzothiazole derivatives **366** have been measured.¹⁹³

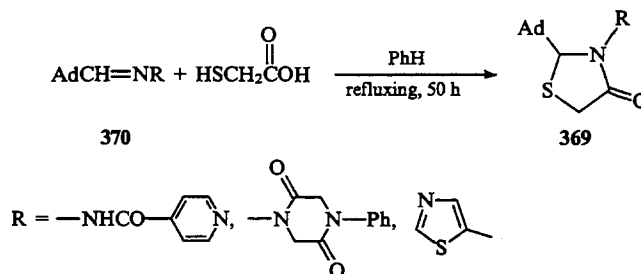


X (*v*) = 6-CN (10.92), 6-Cl (2.30), 5-Cl (2.18), 5-MeO (1.26), H (1.0), 5-Me (0.86), 6-Me (0.6), 6-MeO (0.46).

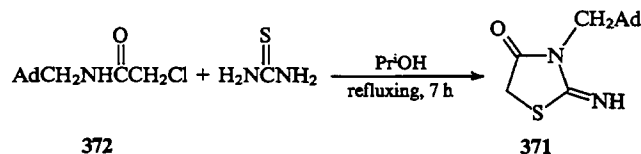
Treatment of compound **367**, obtained by silylation of 4-methyl-3*H*-thiazolin-2-one with disilazane **32**, with 1-chloro-adamantane in the presence of AlCl₃ has led to 5-(adamant-1-yl)-4-methyl-3*H*-thiazolin-2-one **368**.³⁷



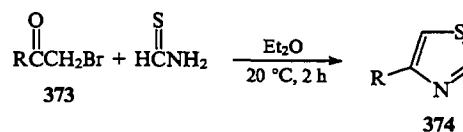
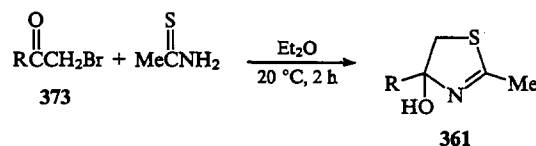
The derivatives of thiazolidin-4-one **369** inhibiting the growth of Gram-positive and Gram-negative bacteria and acting as fungicides have been synthesised by cyclocondensation of the Schiff's bases **370** with thioglycolic acid.¹⁹⁵

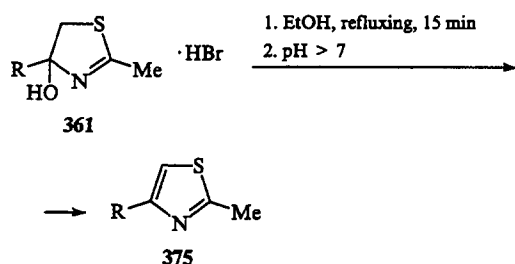


3-(Adamant-1-ylmethyl)-2-iminothiazolidin-4-one **371** is formed on refluxing the chloroacetamide **372** and thiourea in isopropyl alcohol (yield 58%).¹⁹⁶



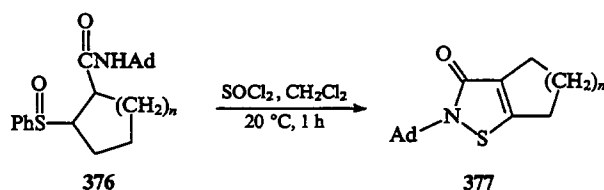
The nature of the radical R in the thioamides RC(S)NH₂ plays the crucial role in their interaction with the ketones **373**. For example, the reaction of MeC(S)NH₂ with the ketones **373** affords the 4-hydroxythiazolines **361**, whereas the interaction of HC(S)NH₂ with these ketones leads to the thiazole derivatives **374**. The yields of all the compounds obtained vary from 70% to 97%. Hydroxythiazoline hydrobromides on refluxing in alcohol are converted into the thiazole derivatives **375**.¹⁹¹





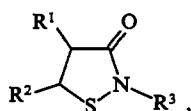
R = Ad, AdCH₂, 3-ClAd, 3-BrCH₂Ad.

Compounds 376 cyclise on treatment with thionyl chloride giving the isothiazolin-3-one derivatives 377, which have been recommended as bactericides and fungicides.¹⁹⁷



n = 1, 2.

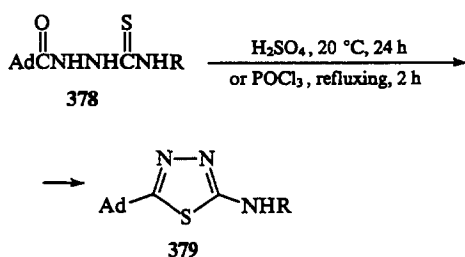
Compounds of the general formula



R¹, R² = H, Hal; R³ = Ad, AdCH₂,

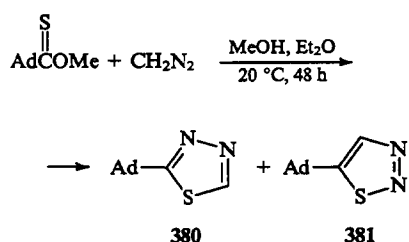
were claimed as bactericides and fungicides in the same patent.¹⁹⁷

The transformation of adamant-1-ylcarbonylthiosemicarbazide 378 into the 2,5-disubstituted 1,3,4-thiadiazoles 379 has been achieved by means of cyclisation agents such as concentrated sulfuric acid or phosphorus oxychloride.¹⁹⁸ When concentrated sulfuric acid was used for R = Me and Et, the yields of the products 379 were 51% and 55%, whereas with phosphorus oxychloride in the case where R = Me, Et, 4-XC₆H₄ (X = F, Cl, Br), and PhCH₂, the yields were 61%–68%.

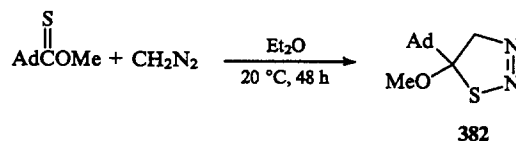


R = H, Me, Et, 4-FC₆H₄, 4-ClC₆H₄, 4-BrC₆H₄, PhCH₂.

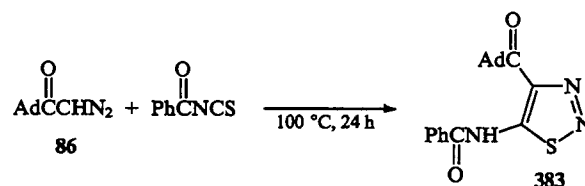
The interaction of the *O*-methyl adamantane-1-carbothioate with diazomethane in a mixture of ether and methanol in the dark gives rise to two compounds: 1,3,4-thiadiazole 380 and 1,2,3-thiadiazole 381 derivatives (yields 7% and 32%).¹⁰⁸



If this reaction is carried out in the absence of methanol only one compound, 5-(adamant-1-yl)-5-methoxy-1,2,3-thiadiazole 382 is formed in 22% yield.¹⁰⁸



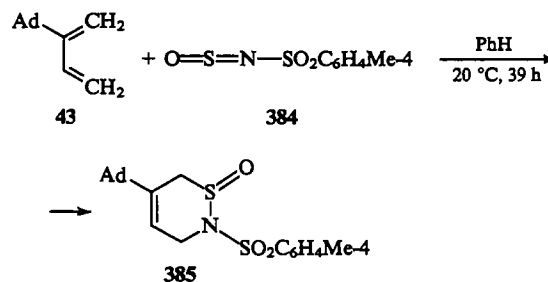
4-Adamant-1-ylcarbonyl-5-benzoylamino-1,2,3-thiadiazole 383 has been synthesised from the ketone 86 and benzoyl thioisocyanate with heating (yield 50%).^{60, 199}



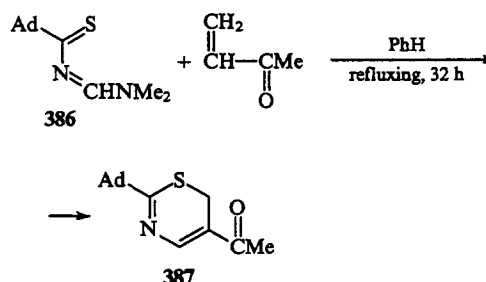
Compound 383 and its 5-arylamino-analogues possess bactericidal and antiviral activities.¹⁹⁹

3. Compounds with six-membered heterocycles

The adamantane derivatives containing six-membered heterocyclic nuclei incorporating nitrogen and sulfur atoms can be obtained by diene condensation. Cyclocondensation of *N*-sulfenyltoluene-*p*-sulfonamide 384 with the diene 43 at ambient temperature affords the 1,2-thiazine derivative 385 (yield 89%).⁴⁷

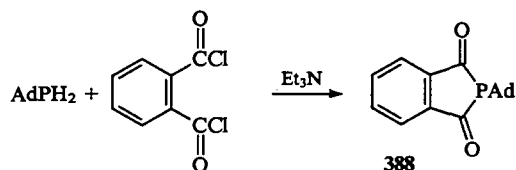


N-(Adamant-1-ylthiocarbonyl)-*N*',*N*'-dimethylformamidine 386 reacts with methyl vinyl ketone on refluxing in benzene giving rise to the 1,3-thiazine derivative 387 (yield 36%).⁴⁷

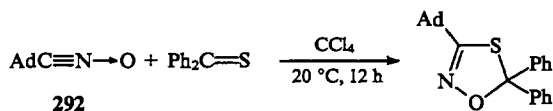


VII. Adamantane derivatives containing other heterocyclic nuclei

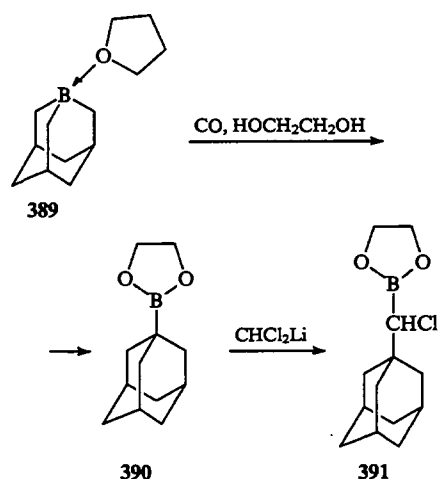
The heterocyclic compound 388 containing a five-membered ring with a phosphorus atom has been synthesised by cyclocondensation of (adamant-1-yl)phosphane with phthalic acid chloride in the presence of triethylamine.²⁰⁰



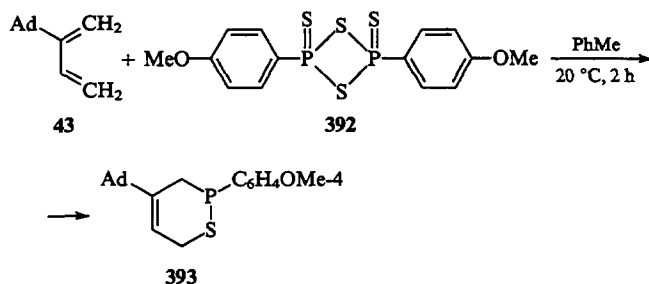
At 20 °C, the nitrile *N*-oxide **292** enters into 1,3-dipolar cycloaddition with thiobenzophenone, which affords 3-(adamant-1-yl)-5,5-diphenyl-1,4,2-oxathiazole in 75% yield.¹⁶⁹



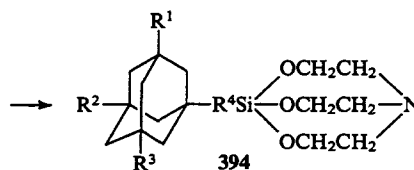
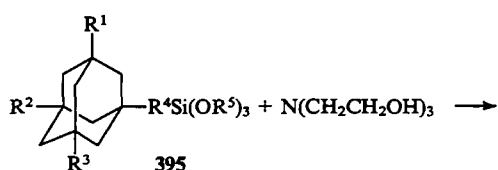
The complex of boraadamantane with tetrahydrofuran **389** reacts with carbon monoxide giving (adamant-1-yl)borodioxolane **390**, interaction of which with lithiodichloromethane gives rise to compound **391**.²⁰¹



The Lawesson reagent **392** can act as the dienophile in diene condensation. For example, the reaction of the diene **43** with this reagent at 20 °C affords the adduct **393** (yield 85%) with sulfur and phosphorus atoms in the heterocyclic moiety.⁴⁷



Compounds **394** have been synthesised in 50%–80% yields by the condensation of adamantane derivatives **395** with triethanolamine.²⁰²



$R^1 = H$; $R^2 = H, Me$; $R^3 = H, Me, Et$;

$R^1 = R^2 = R^3 = Me$; $R^4 = \text{alkylene, arylene, thienylene}$;

$R^5 = \text{alkyl}$.

References

1. S Landa *Chem. Listy* **27** 415 (1933)
2. S Landa, V Michacek *Coll. Trav. Chim. Czechosl.* **28** 4873 (1933)
3. I E Kovalev *Khim.-Farm. Zh.* **11** (3) 19 (1977)
4. H Stetter *Angew. Chem.* **66** 217 (1954)
5. H Stetter *Angew. Chem.* **74** 361 (1962)
6. S N Pandeya *Indian J. Pharm.* **33** 1 (1971)
7. V V Sevost'yanova, M M Krayushkin, A G Yurchenko *Usp. Khim.* **39** 1721 (1970) [*Russ. Chem. Rev.* **39** 817 (1970)]
8. S Hala *Chem. Listy* **71** 18 (1977)
9. A P Khardin, S S Radchenko *Usp. Khim.* **51** 480 (1982) [*Russ. Chem. Rev.* **51** 272 (1982)]
10. E N Bagrii, A T Saginaev *Usp. Khim.* **52** 1538 (1983) [*Russ. Chem. Rev.* **52** 881 (1983)]
11. S D Isaev, A G Yurchenko, S S Isaeva *Fiziologicheski Aktivnye Veshchestva* (15) 3 (1983)
12. R C Bingham, P R Schleyer *Fortschr. Chem. Forsch.* **18** 1 (1971)
13. R C Fort *Adamantan. The Chemistry of Diamond Molecules* (New York: Marcel Dekker, 1976)
14. E N Bagrii *Adamantan: Poluchenie, Svoistva, Primenenie* (Adamantanes: Synthesis, Properties, and Applications) (Moscow: Nauka, 1989)
15. US P. 3 300 480; *Chem. Abstr.* **66** 35 697t (1967)
16. H Quast, R Jakob, K Peters, E-M Peters, H G Schnering *Chem. Ber.* **117** 840 (1984)
17. C Lambert, R Merenyi, B Caillaux, H G Viehe *Bull. Soc. Chim. Belg.* **94** 457 (1985)
18. E R Talaty, A E Dupuy, A E Cancienne *J. Heterocycl. Chem.* **5** 657 (1967)
19. I Lengyel, B D Uliss *J. Chem. Soc., Chem. Commun.* 1621 (1968)
20. E R Talaty, A E Dupuy *J. Med. Chem.* **12** 195 (1969)
21. F D Popp, E B Moynaham *J. Med. Chem.* **13** 1020 (1970)
22. K Bott *Angew. Chem.* **79** 943 (1967)
23. K Bott *Tetrahedron Lett.* 3323 (1968)
24. K Bott *Liebigs Ann. Chem.* **755** 58 (1972)
25. H Quast, B Seiferling *Tetrahedron Lett.* **23** 4681 (1982)
26. K Bott *Angew. Chem.* **80** 970 (1968)
27. K Bott *Angew. Chem., Int. Ed. Engl.* **7** 894 (1968)
28. E R Talaty, C M Untermoeblen *J. Chem. Soc., Chem. Commun.* 204 (1974)
29. DDR P. 200 619; *Chem. Abstr.* **99** 175 767b (1983)
30. Belg. P. 646 581; *Ref. Zh. Khim.* **1** N 299P (1969)
31. E F Novoselov, S D Isaev, A G Yurchenko *Vestn. Kievsk. Politekh. Inst., Ser. Khim. Mashinost. Tekhnol.* **20** 17 (1983)
32. M Laguevre, C Boyer, J Leger, A Carpy *Can. J. Chem.* **67** 1514 (1989)
33. A Commercon, G Ponsinet *Tetrahedron Lett.* **24** 3725 (1983)
34. G A Shvekhgeimer, K I Kobakov, in *Nauchnaya Konferentsiya po Khimii Organicheskikh Poliedranov* (Tez. Dokl.) [Scientific Conference on the Chemistry of Organic Polyhedranes (Abstracts of Reports)] (Volgograd: Volgograd Polytechnic Institute, 1981) p. 105
35. S D Isaev, M I Novikova, A G Yurchenko, L V Korobchenko, G V Vladko, E I Boreko, U Tomsons, I Penke, in *Perspektivy Razvitiya Khimii i Prakticheskogo Primeneniya Karkasnykh Soedinenii* (Tez. Dokl.) [Prospects for the Development of the Chemistry and Practical Applications of Skeletal Compounds (Abstracts of Reports)] (Volgograd: Volgograd Polytechnic Institute, 1992) p. 160
36. C H Cashin, T M Hotten, S S Szinai *J. Med. Chem.* **15** 853 (1972)
37. T Sasaki, A Hakamishi, M Ohno *Chem. Pharm. Bull.* **30** 2051 (1982)

38. M E Herr, R A Johnson, H C Murray, L M Reineke, G S Fonken *J. Org. Chem.* 33 3201 (1968)
39. Jpn. Appl. 60-28 961; *Chem. Abstr.* 103 6 216s (1985)
40. L N Lavrova, Yu A Shalyminova, N V Klimova, N A Artsimovich *Khim.-Farm. Zh.* 16 1197 (1982)
41. Aust. P. 305 973; *Ref. Zh. Khim.* 7 N 280P (1974)
42. H Stetter, E Rauscher *Chem. Ber.* 93 2054 (1960)
43. G A Karlivan, R E Val'ter, R B Kampare, V P Tsiekure *Khim. Geterotsikl. Soedin.* 780 (1979)
44. F N Stepanov, S D Isaev *Zh. Org. Khim.* 6 1195 (1970)
45. E I Dikolenko, S D Isaev *Vestn. Kievsk. Politekh. Inst., Ser. Khim. Mashinost. Tekhnol.* 5 166 (1968)
46. N V Makarova, M N Zemtsova, I K Moiseev *Khim. Geterotsikl. Soedin.* 1580 (1993)
47. T Sasaki, K Shimizu, M Ohno *Chem. Pharm. Bull.* 32 1433 (1984)
48. G V Ponomarev, L N Lavrova, A M Shchul'ga, A S Moskovkin, I M Karnaukh *Khim. Geterotsikl. Soedin.* 1428 (1991)
49. US P. 4 036 975; *Chem. Abstr.* 87 168 032g (1977)
50. T Sasaki, A Usuki, M Ohno *J. Org. Chem.* 45 3559 (1980)
51. T Sasaki, A Usuki, M Ohno *Tetrahedron Lett.* 4925 (1978)
52. P Cabildo, R M Claramunt, I Forfar, C Foces-Foces, A L Llamas-Saiz, J Elquero *Heterocycles* 37 1623 (1994); *Chem. Abstr.* 121 205 265d (1994)
53. M E Gonzalez, B Alarcon, P Cabildo, R M Claramunt, D Saz, J Elquero *Eur. J. Med., Chim. Ther.* 20 359 (1985)
54. P Cabildo, R M Claramunt, I Forfar, J Elquero *Tetrahedron Lett.* 35 183 (1994)
55. G A Shvakhgimer, L K Kuz'micheva, S S Novikov *Izv. Akad. Nauk SSSR, Ser. Khim.* 144 (1974)
56. L K Kuz'micheva, Candidate Thesis in Chemical Sciences, Gubkin Moscow Institute of Petrochemical and Gas Industry, Moscow, 1975
57. G A Shvakhgimer, L K Kuz'micheva *Khim. Geterotsikl. Soedin.* 1654 (1976)
58. W Kuzmickiewicz, F Saczewski, H Foks, R Kaliszan, B Damasiewicz, A Nasal, A Radwanska *Arch. Pharm. (Weinheim, Ger.)* 319 830 (1986)
59. I O Lomidze, D S Zurabishvili, Sh A Samsoniya *Khim. Geterotsikl. Soedin.* 843 (1994)
60. T Sasaki, Sh Eguchi, T Toru *Bull. Chem., Soc. Jpn.* 42 1617 (1969)
61. P Cabildo, R M Claramunt, J Elquero *J. Heterocycl. Chem.* 21 249 (1984)
62. M C Foces-Foces, F H Cano, J P Fayet, M C Vertut, J Elquero *J. Heterocycl. Chem.* 23 1045 (1986)
63. A Gonzalez, J Marquet, M Moreno-Mañas *Tetrahedron* 42 4253 (1986)
64. F N Stepanov, L I Sidorova, N L Dovgan' *Zh. Org. Khim.* 8 1834 (1972)
65. Span. P. 2 008 341; *Chem. Abstr.* 114 164 218a (1991)
66. H Schubert, H-J Born *Z. Chem.* 11 257 (1971)
67. R Y Ning, L H Sternbach *J. Med. Chem.* 13 1251 (1970)
68. Yu S Andreichikov, M P Kolobova *Zh. Org. Khim.* 28 1692 (1992)
69. USSR P. 1 004 373; *Chem. Abstr.* 99 105 243d (1983)
70. V P Litvinov, V S Dermugin, V I Shvedov, V E Shklover, Yu T Struchkov *Izv. Akad. Nauk SSSR, Ser. Khim.* 1858 (1985)
71. V S Dermugin, V I Shvedov, V P Litvinov *Izv. Akad. Nauk SSSR, Ser. Khim.* 2549 (1985)
72. H Zimmer, D G Glasgow, M McClanahan, T Novinson *Tetrahedron Lett.* 9 2805 (1968)
73. N I Avdyunina, I M Zinov'eva, V A Annsimova, B M Petin, N V Klimova, R F Bol'shakova, I S Morozov, in *Perspektivy Razvitiya Khimii i Prakticheskogo Primeneniya Karkasnykh Soedinenii (Tez. Dokl.)* [Prospects for the Development of the Chemistry and Practical Applications of Skeletal Compounds (Abstracts of Reports)] (Volgograd: Volgograd Polytechnic Institute, 1992) p. 155
74. US P. 5 290 782; *Chem. Abstr.* 121 300 909a (1994)
75. Eur. P. 415 456; *Chem. Abstr.* 115 158 836e (1991)
76. G Zinner, H Gross *Chem. Ber.* 105 1714 (1972)
77. A M Leusen, J Schut *Tetrahedron Lett.* 17 285 (1976)
78. R Pellicciari, M C Fioretti, P Cogolli, M Tiecco *Arzneim.-Forsch.* 30 2103 (1980); *Chem. Abstr.* 94 156 821v (1981)
79. A J Arduengo, R L Harlow, M Kleine *J. Am. Chem. Soc.* 113 361 (1991)
80. S N Lyashchuk, Yu G Skrypnik *Tetrahedron Lett.* 35 5271 (1994); Yu G Skrypnik, S N Lyashchuk *Sulfur Lett.* 17 287 (1994); *Chem. Abstr.* 122 81 218q (1995)
81. T Sasaki, Sh Egushi, M Yamayoshi, T Esaki *J. Org. Chem.* 46 1800 (1981)
82. R I Yurchenko, S D Isaev, A G Yurchenko *Khim.-Farm. Zh.* 42 1060 (1976)
83. H Quast, G Meichner, B Seiferling *Liebigs Ann. Chem.* 1891 (1986)
84. V L Rusinov, E N Ulomskii, M N Kushnir, I K Moiseev, A V Yudashkin, in *Perspektivy Razvitiya Khimii i Prakticheskogo Primeneniya Karkasnykh Soedinenii (Tez. Dokl.)* [Prospects for the Development of the Chemistry and Practical Applications of Skeletal Compounds (Abstracts of Reports)] (Volgograd: Volgograd Polytechnic Institute, 1992) p. 41
85. A Tantawy, A E M Barghash *Alexandria J. Pharm. Sci.* 2 50 (1988); *Chem. Abstr.* 111 7302u (1989)
86. D N Kevill, F L Weitl *J. Org. Chem.* 35 2526 (1970)
87. A L Kovalenko, I V Bryukhankov *Zh. Org. Khim.* 30 1698 (1994)
88. BRD P. 2 822 360; *Chem. Abstr.* 90 121 436r (1979)
89. US P. 3 391 142; *Chem. Abstr.* 69 59 281v (1968)
90. V A Sokolenko, N M Svirskaya *Khim. Geterotsikl. Soedin.* 817 (1987)
91. D H R Barton, J Boivin, W B Motherwell, N Ozbalik, K M Schwartzentruber, K Jankowski *Nouv. J. Chem.* 387 (1986)
92. D H R Barton, F Halley, N Ozbalik, M Schmidt, E Young, G Balavoine *J. Am. Chem. Soc.* 111 7144 (1989)
93. F N Stepanov, N L Dovgan', A G Yurchenko *Zh. Org. Khim.* 6 1823 (1970)
94. V A Sokolenko, N M Svirskaya *Izv. Akad. Nauk SSSR, Ser. Khim.* 1677 (1984)
95. A R Katritzky, O Rubio, M Szajba, B Nowak-Wydra *J. Chem. Res. (S)* 234 (1984)
96. I K Moiseev, M N Zemtsova, P L Trakhtenberg, D A Kulikova, I P Skobkina, G N Neshchadin, N V Ostapchuk *Khim.-Farm. Zh.* 22 1448 (1988)
97. V K Gubernatorov, B E Kogai, V A Sokolenko *Izv. Akad. Nauk SSSR, Ser. Khim.* 1203 (1983)
98. V A Sokolenko, V V Rivanenkov, in *Perspektivy Razvitiya Khimii Karkasnykh Soedinenii i Ikh Primenenie v Otrasyakh Promyshlennosti (Tez. Dokl.)* [Prospects for the Development of the Chemistry of Skeletal Compounds and Their Industrial Applications (Abstracts of Reports)] (Kiev: Kiev Polytechnic Institute, 1986) p. 60
99. B E Kogai, V K Gubernatorov, V A Sokolenko *Zh. Org. Khim.* 20 2554 (1984)
100. V A Sokolenko, B E Kogai *Zh. Org. Khim.* 12 1370 (1976)
101. V A Sokolenko, V K Gubernatorov *Izv. Akad. Nauk SSSR, Ser. Khim.* 220 (1990)
102. M Fiorentino, L Testaferri, M Tiecco, L Troisi *J. Chem. Soc., Chem. Commun.* 329 (1976)
103. M Fiorentino, L Testaferri, M Tiecco, L Troisi *J. Chem. Soc., Perkin Trans.* 2 87 (1977)
104. M-G A Shvakhgimer, K I Kobrakov, S S Sychev, V K Promanenko *Dokl. Akad. Nauk SSSR* 294 893 (1987)
105. V P Litvinov, E E Apenova, Yu A Sharanin, A M Shestopalov *Zh. Org. Khim.* 21 669 (1985)
106. V P Litvinov, E E Apenova, Yu A Sharanin, A M Shestopalov *Izv. Akad. Nauk SSSR, Ser. Khim.* 2408 (1984)
107. D Kontonassios, C Sandris, G Tsatsas, S Casadio, B Lumachi, C Turba *J. Med. Chem.* 12 170 (1969)
108. Yu E Klimko, S D Isaev, A G Yurchenko *Zh. Org. Khim.* 30 1688 (1994)
109. N S Kozlov, G P Korotysheva, in *Perspektivy Razvitiya Khimii i Prakticheskogo Primeneniya Karkasnykh Soedinenii (Tez. Dokl.)* [Prospects for the Development of the Chemistry and Practical Applications of Skeletal Compounds (Abstracts of Reports)] (Volgograd: Volgograd Polytechnic Institute, 1992) p. 158
110. R Yalda, H Rehman, Ja M Rao *Tetrahedron* 45 7093 (1989)
111. Eur. P. 358 152; *Chem. Abstr.* 113 78 421j (1990)
112. Jpn. Appl. 77-144 682; *Chem. Abstr.* 88 136 675y (1978)
113. Jpn. Appl. 77-144 680; *Chem. Abstr.* 88 136 676z (1978)
114. Span. P. 2 046 107; *Chem. Abstr.* 121 9423q (1994)
115. US P. 3 869 460; *Chem. Abstr.* 83 28 282f (1975)
116. USSR P. 492 518; *Byull. Izobret.* 43 63 (1975)

117. USSR P. 301 066; *Ref. Zh. Khim.* 2 N 296P (1973)
118. S K Germane, Ya Yu Polis, L Ya Karinya *Khim.-Farm. Zh.* 11 (3) 66 (1977)
119. N V Klimova, L N Lavrova, G V Pushkar', M I Shmar'yan, A P Arendaruk, A P Skoldinov *Khim.-Farm. Zh.* 9 (11) 8 (1975)
120. L I Durakova, N V Klimova, I E Kovalev, L N Lavrova, A P Skoldinov, D A Kharkevich, M I Shmar'yan *Khim.-Farm. Zh.* 14 (5) 26 (1980)
121. R O Vittolin', A A Kimenis *Khim.-Farm. Zh.* 12 (9) 20 (1978)
122. G S Poindexter, M A Bruce, K L LeBoulluec, I Monkovic *Tetrahedron Lett.* 35 7331 (1994)
123. J Nakayama, R Hasemi *J. Am. Chem. Soc.* 112 5654 (1990)
124. W E Coyne, J W Cusic *J. Med. Chem.* 11 1208 (1968)
125. S Robev *Dokl. Bolg. Acad. Nauk* 36 1551 (1983)
126. M Kuchar, J Strof, J Vachek *Collect. Czech. Chem. Commun.* 34 2278 (1969)
127. J P Jonak, S F Zakarzewski, L H Mead *J. Med. Chem.* 14 408 (1971)
128. J P Jonak, S F Zakarzewski, L H Mead *J. Med. Chem.* 15 662 (1972)
129. Czech. P. 145 615; *Chem. Abstr.* 78 58 456e (1973)
130. Jpn. Appl. 75-148 366; *Chem. Abstr.* 85 94 396r (1976)
131. J Soucek, V Slavikova, M Kucher, in *The Seventh Proceedings of the International Congress on Chemotherapy, 1971* Vol. 2, p. 71; *Chem. Abstr.* 79 100 460z (1973)
132. S F Zakarzewski, Z Pavelic, W R Greco, G Bollard, P J Creaven, E Mihich *Cancer Res.* 42 2177 (1982); *Chem. Abstr.* 97 16 786z (1982)
133. T Hirano, R Negishi, M Yamaguchi, F Qichen, Yo Ohmiya, F Tsuchi, M Ohashi *J. Chem. Soc., Chem. Commun.* 1335 (1995)
134. J K Chakrabarti, T M Hotten, S Sutton, D E Tupper *J. Med. Chem.* 19 967 (1976)
135. A I Matveev, I K Moiseev *Khim. Geterotsikl. Soedin.* 275 (1989)
136. A Kreutzberger, H-H Schroder *Tetrahedron Lett.* 11 4523 (1970)
137. A Kreutzberger, H-H Schroder *Arch. Pharm.* 308 161 (1975)
138. A G Yurchenko, E A Ponomareva, P V Tarasenko, V G Gerasimenko, in *Nauchnaya Konferentsiya po Khimii Organicheskikh Poliedranov (Tez. Dokl.)* [Scientific Conference on the Chemistry of Organic Polyhedranes (Abstracts of Reports)] (Volgograd: Volgograd Polytechnic Institute, 1981) p. 45
139. S D Isaev, E F Novoselov, A G Yurchenko *Zh. Org. Khim.* 21 114 (1985)
140. A V Bogatskii, Z I Zhilina, S A Andronati, S D Isaev, A G Yurchenko, Yu I Vikhlyaev, T A Klygul', N Ya Golovenko, S S Isaeva *Fiziologich. Aktivnye Veshchestva* (11) 55 (1979)
141. A K Shiryayev, I K Moiseev *Zh. Obshch. Khim.* 58 1680 (1988)
142. A K Shiryayev, I K Moiseev, E I Boreko, E I Korobchenko, G V Vladko *Khim.-Farm. Zh.* 24(5) 23 (1990)
143. V N Sytin, I G Tishchenko, in *Perspektivy Razvitiya Khimii Karkasnykh Soedinenii i Ikh Primenenie v Otrasyakh Promyshlennosti (Tez. Dokl.)* [Prospects for the Development of the Chemistry of Skeletal Compounds and Their Industrial Applications (Abstracts of Reports)] (Kiev: Kiev Polytechnic Institute, 1986) p. 48
144. A K Shiryayev, I K Moiseev, V F Stroganov *Plast. Massy* (12) 35 (1987)
145. D S Zurabishvili, M O Lomidze, A M Sladkov, in *Nauchnaya Konferentsiya po Khimii Organicheskikh Poliedranov (Tez. Dokl.)* [Scientific Conference on the Chemistry of Organic Polyhedranes (Abstracts of Reports)] (Volgograd: Volgograd Polytechnic Institute, 1981) p. 147
146. M Kuchar *Collect. Czech. Chem. Commun.* 33 880 (1968)
147. M Kuchar, B Kakas *Collect. Czech. Chem. Commun.* 36 2298 (1971)
148. E V Dehmlow, A Winterfeldt *J. Organomet. Chem.* 363 223 (1989)
149. USSR 909 934; *Byull. Izobret.* (15) 280 (1990)
150. USSR P. 1 122 658; *Byull. Izobret.* (11) 86 (1984)
151. P Cogolli, L Testaferri, M Tiecco, M Tingoli *J. Chem. Soc., Chem. Commun.* 800 (1979)
152. T Sasaki, A Nakanishi, M Ohno *J. Org. Chem.* 47 3219 (1982)
153. A P Marchand, D King, S G Bott *Tetrahedron Lett.* 35 8935 (1994)
154. F N Stepanov, N L Dovgan' *Zh. Org. Khim.* 6 1821 (1970)
155. V N Voshula, V I Dulenko, in *Perspektivy Razvitiya Khimii Karkasnykh Soedinenii i Ikh Primenenie v Otrasyakh Promyshlennosti (Tez. Dokl.)* [Prospects for the Development of the Chemistry of Skeletal Compounds and Their Industrial Applications (Abstracts of Reports)] (Kiev: Kiev Polytechnic Institute, 1986) p. 40
156. Yu S Andreichikov, M P Sivkova, N N Shapit'ko *Khim. Geterotsikl. Soedin.* 1312 (1982)
157. H Kamiyama, H Ryuji *Heteroat. Chem.* 4 445 (1993); *Chem. Abstr.* 121 9063x (1994)
158. W Hoek, H Wynberg, J Strating *Recl. Trav. Chim. Pays-Bas* 85 1045 (1966)
159. W Hoek, J Strating, H Wynberg *Recl. Trav. Chim. Pays-Bas* 85 1054 (1966)
160. I Handa, L Bauer *J. Chem. Eng. Data* 29 223 (1984)
161. A V Yudashkin, I K Moiseev, V P Zvolinskii, O A Katkova, in *Perspektivy Razvitiya Khimii Karkasnykh Soedinenii i Ikh Primenenie v Otrasyakh Promyshlennosti (Tez. Dokl.)* [Prospects for the Development of the Chemistry of Skeletal Compounds and Their Industrial Applications (Abstracts of Reports)] (Kiev: Kiev Polytechnic Institute, 1986) p. 135
162. P Cogolli, F Maiolo, L Testaferri, M Tiecco, M Tingoli *J. Chem. Soc., Perkin Trans. 2* 1331 (1980)
163. P Cogolli, L Testaferri, M Tiecco, M Tingoli *J. Chem. Soc., Perkin Trans. 2* 1336 (1980)
164. V P Litvinov, V I Shvedov, V S Dermugin *Khim. Geterotsikl. Soedin.* 1128 (1982)
165. V P Litvinov, V S Dermugin, V I Shvedov, V S Bogdanov *Izv. Akad. Nauk SSSR, Ser. Khim.* 1581 (1984)
166. S Kim, S S Kim, S T Lim, C Ch Shim *J. Org. Chem.* 52 2114 (1987)
167. K Mlinarić-Majerski, D Pavlović, M Juić, B Kojic-Prodić *Chem. Ber.* 127 1327 (1994)
168. S D Isaev, E F Novoselov, A G Yurchenko *Vestn. Kievsk. Politekh. Inst., Ser. Khim. Mashinostr. Tekhnol.* 17 10 (1980)
169. D S Zurabishvili, Z Sh Dzheparidze, I N Gogolashvili, in *Nauchnaya Konferentsiya po Khimii Organicheskikh Poliedranov (Tez. Dokl.)* [Scientific Conference on the Chemistry of Organic Polyhedranes (Abstracts of Reports)] (Volgograd: Volgograd Polytechnic Institute, 1981) p. 146
170. A Dondoni, G Barbaro, A Battaglia, P Giorgianni *J. Org. Chem.* 37 3196 (1972)
171. G A Shvekhgeimer, O A Vol'skaya *Khim. Geterotsikl. Soedin.* 180 (1975)
172. O A Safonova, Candidate Thesis in Chemical Sciences, Gubkin Moscow Institute of Petrochemical and Gas Industry, Moscow, 1975
173. Yu He, N-H Lin *Synthesis* 989 (1994)
174. G N Neshchadin, V S Klimova, T A Zinchenko, A D Koveshnikov, G A Shvekhgeimer, E A Rudzit, in *Khimiya Poliedranov (Tez. Dokl.)* [The Chemistry of Polyhedranes (Abstracts of Reports)] (Volgograd: Volgograd Polytechnic Institute, 1976) p. 123
175. G Zinner, H Ruthe, D Boese *Pharmazie* 29 16 (1974)
176. T Sasaki, Sh Eguchi, T Toru *Tetrahedron Lett.* 9 4135 (1968)
177. T Sasaki, Sh Eguchi, T Toru *Tetrahedron* 25 2909 (1969)
178. A P Khardin, V E Derbisher *Vysokomol. Soedin., Ser. B* 14B 565 (1972)
179. A P Khardin, V E Derbisher *Izv. Vyssh. Uchebn. Zaved., Khim. Khim. Tekhnol.* 15 1238 (1972)
180. M I Kalinina, I K Moiseev *Khim. Geterotsikl. Soedin.* 258 (1988)
181. M I Kalinina, I K Moiseev, V M Pavskii *Khim. Geterotsikl. Soedin.* 1124 (1988)
182. H V Daeniker *Helv. Chim. Acta* 50 2008 (1967)
183. G Zinner, U D Dybowski *Arch. Pharm.* 303 488 (1970)
184. BRD P. 2 415 978; *Chem. Abstr.* 82 16 848m (1975)
185. US P. 3 910 942; *Ref. Zh. Khim.* 11 O 79 (1976)
186. G A Shvekhgeimer, L K Kuz'micheva *Khim. Geterotsikl. Soedin.* 32 (1975)
187. G A Shvekhgeimer, V Yu Rumyantsev, K I Kobakov, in *Perspektivy Razvitiya Khimii i Prakticheskogo Primeneniya Karkasnykh Soedinenii (Tez. Dokl.)* [Prospects for the Development of the Chemistry and Practical Applications of Skeletal Compounds (Abstracts of Reports)] (Volgograd: Volgograd Polytechnic Institute, 1992) p. 55
188. M V Vovk *Zh. Org. Khim.* 30 1700 (1994)
189. H Quast, F Kees *Chem. Ber.* 110 1780 (1977)
190. Jpn. Appl. 71-04 370; *Chem. Abstr.* 75 5888d (1971)
191. F N Stepanov, S D Isaev *Zh. Org. Khim.* 6 1189 (1970)
192. M Fiorentino, L Testaferri, M Tiecco, L Troisi *J. Chem. Soc., Chem. Commun.* 316 (1977)

193. M Fiorentino, L Testaferri, M Tiecco, L Troisi *J. Chem. Soc., Perkin Trans. 2* 1679 (1977)
194. L Testaferri, M Tiecco, M Tingoli *J. Chem. Soc., Chem. Commun.* 93 (1978)
195. G Fenech, P Manforte, A Chimirri, S Grasso *J. Heterocycl. Chem.* 16 347 (1979)
196. V M Plakhotnik, V G Yashunskii *Khim.-Farm. Zh.* 16 1060 (1982)
197. Eur. P. 342 105; *Chem. Abstr.* 112 178 954h (1990)
198. A-A El-Emam, J Lehmann *Monatsh.* 125 587 (1994)
199. Jpn. Appl. 70-27 573; *Chem. Abstr.* 74 3629a (1971)
200. J R Goerlich, C Mueller, R Schmuter *Phosphorus Sulfur Silicon Relat. Elem.* 85 193 (1993); *Chem. Abstr.* 121 108 955w (1994)
201. M E Gurskii, T V Potapova, Yu N Bubnov, in *Perspektivy Razvitiya Khimii i Prakticheskogo Primeneniya Karkasnykh Soedinenii (Tez. Dokl.)* [Prospects for the Development of the Chemistry and Practical Applications of Skeletal Compounds (Abstracts of Reports)] (Volgograd: Volgograd Polytechnic Institute, 1992) p. 3
202. N S Fedotov, E V Boloeva, G E Evert, V D Sheludyakov, V N Solov'ev, E I Bagrii, in *Nauchnaya Konferentsiya po Khimii Organicheskikh Poliedranov (Tez. Dokl.)* [Scientific Conference on the Chemistry of Organic Polyhedranes (Abstracts of Reports)] (Volgograd: Volgograd Polytechnic Institute, 1981) p. 107

Aromatic polyimides with flexible and rigid chains

Z B Shifrina, A L Rusanov

Contents

I. Introduction	599
II. Flexible-chain aromatic polyimides	599
III. Rigid-chain aromatic polyimides	604
IV. Conclusion	607

Abstract. The results of studies in recent years on the synthesis of polyimides with chains which are both flexible and rigid to the maximum extent are surveyed. The characteristic features of the formation of these polymers, their properties, and certain aspects of their practical applications are considered. It is shown that the thermodynamic rigidity of the macromolecules is one of the principal factors which determines the most important properties of polyimides and the materials based on them. The bibliography includes 85 references.

I. Introduction

The development of the chemistry of aromatic polyimides (API) ^{1–5} led to the formation of a large number of polyheteroarylenes exhibiting significantly different properties. One of the most important factors influencing the properties of API is the rigidity of their macromolecules. In terms of this feature, the API may be divided into two principal groups — flexible-chain and rigid-chain polyimides.

The development of the flexible-chain polyimides was stimulated by the need to obtain easily processed polyimides soluble in the usual organic solvents and having wide gaps between the glass transition and decomposition temperatures. ^{6–8} The development of the chemistry of the rigid-chain polymers was in its turn determined by the need to create very strong and high-modulus materials. ^{9, 10}

The molecular designs of the flexible-chain and rigid-chain polyimides are different. The flexible-chain API contain in the main chain asymmetric phenylene (*m*-phenylene) rings and groups which increase the flexibility of the chain (ether, thioether, isopropylidene, hexafluoroisopropylidene, etc.), ^{6–8} whereas in the rigid-chain API the macromolecular chains are extended to the maximum extent and contain predominantly symmetrical *p*-phenylene fragments and heterocycles without any groups increasing the flexibility of the chains. ¹¹

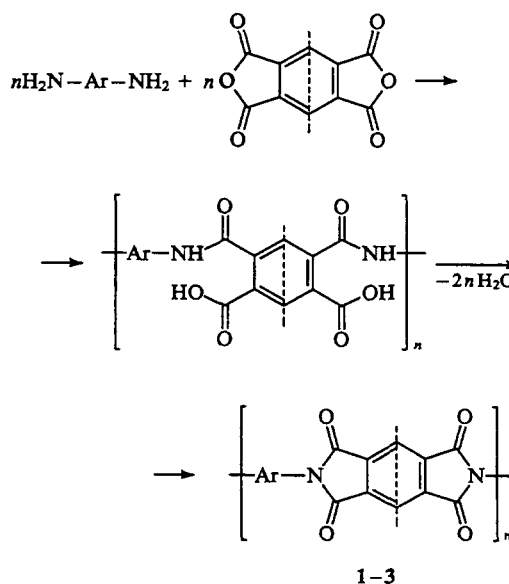
II. Flexible-chain aromatic polyimides

The most important flexible-chain API are polyimides with ether groups in the main chain, the so called polyetherimides (PEI). A wide range of PEI have been obtained as a result of the interaction of various aromatic diamines containing ether groups and the dianhydrides of aromatic tetracarboxylic acids without the same groups ^{1, 12, 13} in accordance with Scheme 1.

The values of the Kuhn segment ($A_f/\text{\AA}$), calculated and determined experimentally ^{14, 15} for certain PEI based on the dianhydride of oxybis(benzene-3,3',4,4'-dicarboxylic) acid (OBBDCA) as well as the properties of these PEI are presented in Table 1.

The use of diamines with *p*-phenylene fragments and of dianhydrides containing only one ether group led to PEI with a 30–37 Å Kuhn segment and a glass transition temperature of 255–290 °C. When the 'dianhydride R' was used instead of OBBDCA, the PEI 3a–e with a 26–32 Å Kuhn segment and a glass transition temperature of 175–215 °C were synthesised (Table 2).

Scheme 1



Z B Shifrina, A L Rusanov Nesmeyanov Institute of Organoelement Compounds, Russian Academy of Sciences, ul. Vavilova 28, 117813 Moscow, Russian Federation.
Fax (7-095) 135 50 85. Tel. (7-095) 135 93 17 (Z B Shifrina)

Received 28 June 1995

Uspekhi Khimii 65 (7) 648–658 (1996); translated by A K Grzybowski

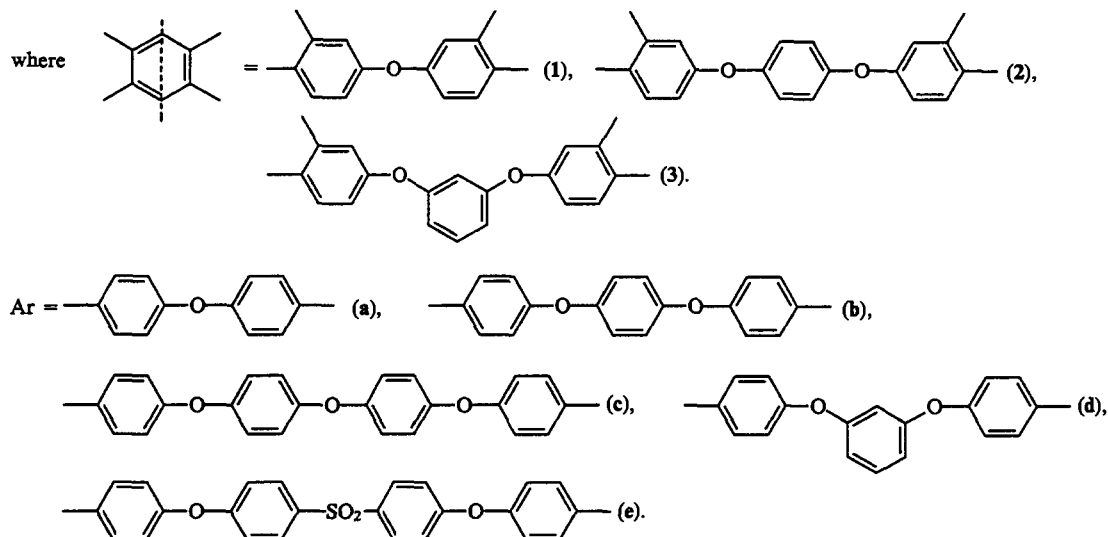


Table 1. The properties of polyimides based on the dianhydride of oxybis(benzene-3,3',4,4'-dicarboxylic) acid.^{14,15}

-Ar-	$T_g/^\circ\text{C}$	$T_{10\%}/^\circ\text{C}$ (TGA)	Properties of films			$A_f/\text{\AA}$
			σ/MPa	$\varepsilon(\%)$	E/GPa	
	270	450–500	160–200	50–100	3.2	36.4
	290	445	141	16	3.1	36.3
	255	460	140–170	50–75	2.7–3.2	29.9

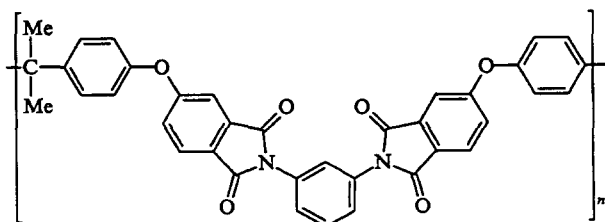
Table 2. Some properties of the polyetherimides 3a–e.

Poly-etherimide	$T_g/^\circ\text{C}$	$T_{10\%}/^\circ\text{C}$ (TGA)	Properties of films		
			σ/MPa	$\varepsilon(\%)$	E/GPa
3a	215	540	120	20	2.6
3b	202	560	125	160	—
3c	174	510	120	90	2.3
3d	197	577	120	160	3.4
3e	205	510	100	60	2.4

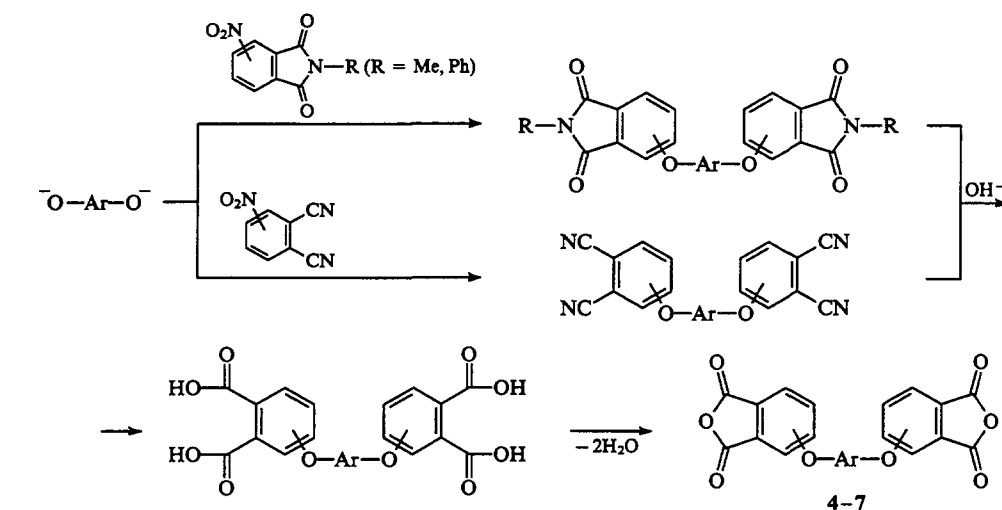
In order to obtain PEI with a smaller Kuhn segment and lower glass transition temperatures it appeared useful to introduce into the macromolecule the largest possible number of ether groups, which increase the flexibility of the chain, as well as *m*-phenylene fragments. A large group of bis(phthalic anhydrides), containing at least two ether groups — bis(etherphthalic anhydrides) (BEPA) — were synthesised. The dianhydrides were obtained by the aromatic nucleophilic nitro-displacement reaction between bisphenoxides and nitrophthalimides or nitrophthalonitriles (Scheme 2).^{6–8,16–21}

The reactions of the BEPA 4–7 with aromatic diamines [*m*-phenylenediamine, bis(4-aminophenyl)ether, bis(4-aminophenyl)methane, etc.] were carried out in accordance with Scheme 3.^{22–34} The PEI were synthesised in the melt,^{22–26} in amide solvents (high-temperature polycondensation),^{27,28} or in nonpolar organic^{22,23,29,30} and phenolic^{31–34} solvents. Particular attention was concentrated on the polymers obtained on the basis of the cheap and readily available *m*-phenylenediamine. Certain properties of these polymers are presented in Table 3.

Among the PEI listed in Table 3, the polymer synthesised from the 'dianhydride A' is the most important and most readily available.

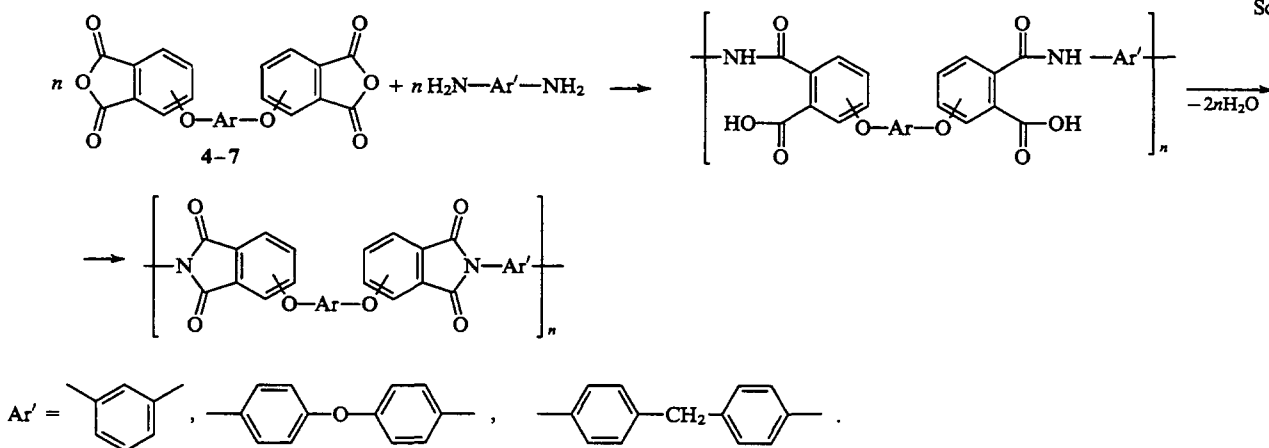


Scheme 2



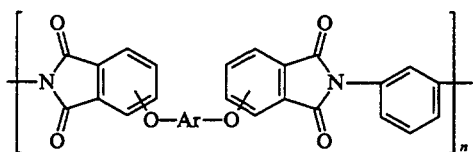
Ar	BEPA	Isomer	Yield (%)	$T_m / ^\circ\text{C}$
	4	3,3'	100.0	228–229.5
		4,4'	89.9	284.5–286
X = O	5	3,3'	98.9	254–255.5
		4,4'	100.0	238–239
X = S	6	3,3'	46.6	257–257.5
		4,4'	97.0	189–190
X = CMe ₂	7	3,3'	97.0	186.5–187.5
		4,4'	85.0	189–190

Scheme 3



This polymer, containing *m*-phenylene ring, ether, and isopropylidene groups in the main chain, is extremely flexible — its Kuhn segment is 19 Å long.³⁵ It was selected as the starting material for the preparation of the ULTEM plastic, which is produced by the General Electric Company.⁶ Certain properties of ULTEM are listed in Table 4. A high transparency and rigidity combined with a high decomposition temperature and fire resistance as well as the absence of smoke formation or combustion are characteristic of this polymer.⁶

Another approach to the synthesis of flexible-chain readily processable PEI is based on the use of aromatic diamines containing several ether groups and *m*-phenylene fragments in the structure of the molecule. A large group of these diamines have been obtained by the interaction of various bisphenoxides with unsubstituted and substituted *m*-dinitrobenzenes^{36–57} by the aromatic nucleophilic nitro-displacement reaction (Scheme 4).

Table 3. The properties of polyetherimides having the general formula ^{6,18}

Initial BEPA	Isomer PEI	[η]/dl g ⁻¹ ^a	T_g /°C (DSC)	$T_{10\%}$ /°C (TGA)		Solubility ^b		
				air	N ₂	<i>N</i> -MP	DMF	CHCl ₃
4	3,3'	0.57	241	460	500	S	S	IS
	4,4'	0.70	224	500	515	S	IS	IS
5	3,3'	0.53	238	480	480	S	S	S
	4,4'	1.04	227	500	490	S	IS	PS
6	3,3'	0.39	236	446	470	S	S	S
	4,4'	0.50	215	460	480	S	S	S
7	3,3'	0.52	231	470	470	S	S	S
	4,4'	0.45	209	480	490	S	IS	S

^a The viscosity η was measured in *m*-cresol at 25 °C. ^b Notation adopted: S = soluble, IS = insoluble, PS = partially.

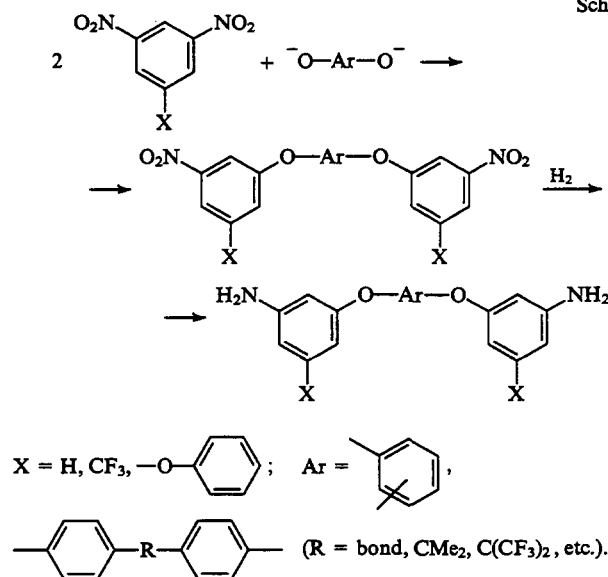
Table 4. The properties of the ULTEM polyimide.⁶

Mechanical properties		Thermal properties	
Tensile strength at yield (yield point)	105 MPa	Glass transition temperature	217 °C
Tensile modulus	3000 MPa	Heat deflection temperature	
Tensile elongation, ultimate	60%–80%	1.85 MPa	200 °C
		0.46 MPa	210 °C
Flexural strength	145 MPa	Limited oxygen index	47
Flexural modulus	3300 MPa	Burn bending UL 94 (vertical)	v-O at 0.64 mm
Compressive strength	140 MPa		
Compressive modulus	2900 MPa	Smoke evolution according to the NBS method	
Gardner impact strength	36 Nm	D_4 after 4 min	0.7
Izod impact strength		D_{max} after 20 min	30
notched	50 J m ⁻¹		
unnotched	1300 J m ⁻¹		

As a rule, the aromatic nucleophilic nitro-displacement reaction takes place readily, provided that the activating groups are located in the *ortho*- and *para*-positions relative to the nitro-group, but in certain cases *meta*-substituted dinitro-compounds can also be involved in the reaction.^{4,6,7}

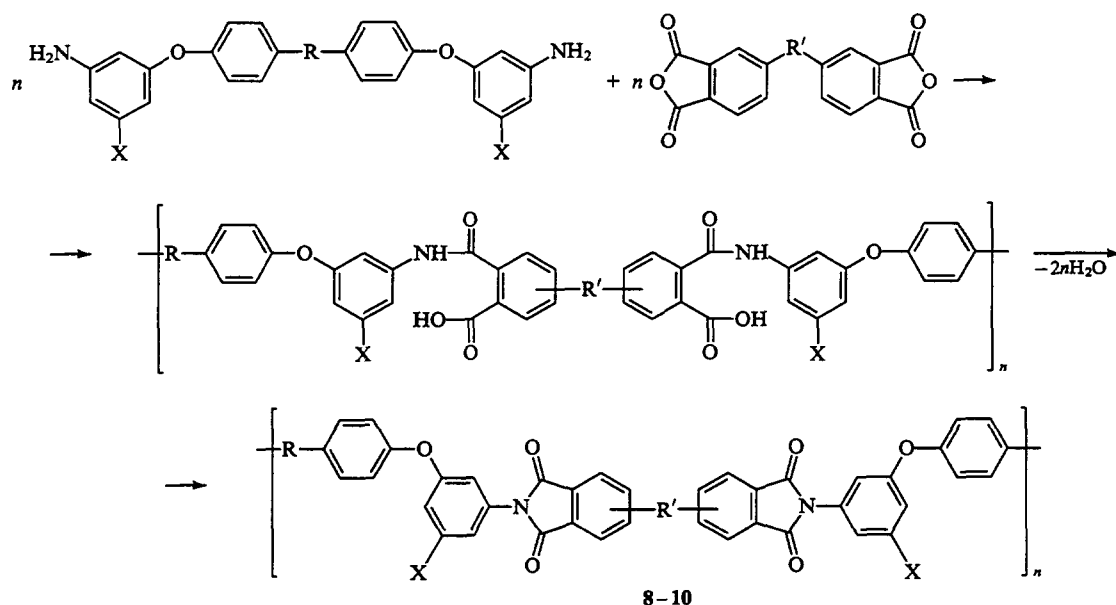
Numerous studies^{36–49} have been devoted to the preparation of diamines from *m*-dinitrobenzene. Among them, products with the isopropylidene and hexafluoroisopropylidene 'bridging' groups are of greatest interest. The PEI involving these diamines have been synthesised in accordance with Scheme 5.

Scheme 4



The reactions were carried out in *N*-methylpyrrolidone (*N*-MP) at room temperature; the intermediate poly(*o*-carboxy)amides were cyclised directly in the reaction solution using as the catalyst either a 1 : 1 pyridine–acetic anhydride mixture or orthophosphoric acid or adding compounds which form azeotropic mixtures with the water evolved during cyclisation. All the reactions took place under homogeneous conditions. Under the conditions of catalysis by orthophosphoric acid or without the use of any catalyst, as a rule high-molecular-mass PEI with a high degree of cyclisation were obtained. Certain properties of the PEI 8 and 9 are presented in Table 5. It follows from the data in Table 5 that the PEI 8 and 9 are characterised by relatively low glass transition temperatures (180–225 °C) and high decomposition temperatures. The melt viscosity of these polymers is fairly low, which makes them suitable for processing by injection moulding.

Scheme 5



X = H: R = CMe₂ (**8**), C(CF₃)₂ (**9**); X = CF₃: R = CMe₂ (**10**)

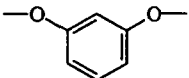
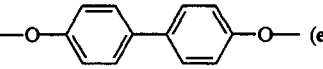
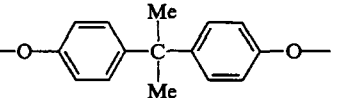
R' = bond (a), C(O) (b), -O- (c),  (d),  (e),  (f).

Table 5. The properties of the polyimides **8** and **9**.^{46, 48}

Polyimide	η_{red}^a /dl g ⁻¹	T_g /°C	$T_{5\%}$ /°C (TGA)	$10^{-3} \eta_{\text{eff}}^b$ /dl g ⁻¹	
				A	B
8a	0.78	210	438	3.9	9.0
8b	0.71	225	443	8.7	28.0
8c	0.69	200	443	5.4	15.0
8d	0.42	180	508	1.8	4.7
8e	0.50	200	484	2.4	5.4
8f	0.59	190	447	2.7	3.5
9a	1.23	220	492	8.6	23.0
9b	0.55	220	492	2.8	4.9
9c	0.55	180	505	0.4	—
9d	0.68	200	517	2.8	7.7
9e	1.07	220	498	5.4	1.5
9f	0.78	200	507	2.9	6.4

^a The viscosity η measured in *m*-cresol at 25 °C. ^b The effective viscosity of the melt (capillary viscosimetry) measured at $\dot{\nu} = 2912 \text{ s}^{-1}$ (A), $\dot{\nu} = 728 \text{ s}^{-1}$ (B) ($\dot{\nu}$ is rate of shearing).

The polyimides obtained are readily soluble in organic solvents — *N*-MP, *m*-cresol, methylene chloride, chloroform, etc. The ready solubility of the polymers is determined by their structure and method of synthesis. The polymers synthesised under mild conditions are known to be more soluble than the polymers obtained at high temperatures.⁵⁸ Thus the polyimides **9a–c**, obtained in accordance with Scheme 5, are readily soluble in *N*-MP and dimethylacetamide (DMA) while the polyimides based on 2,2-[bis(*p*-aminophenoxy)phenylene]propane,⁵⁹ obtained using solid-phase high-temperature cyclisation of polyamidoacids, are insoluble in these solvents. The polyimides based on diamines with trifluoromethyl groups in the benzene ring are even more soluble.^{51, 52} The corresponding diamines were obtained in accordance with Scheme 4; 3,5-dinitro-1-trifluoromethylbenzene

and various bisphenoxides were used as the starting compounds.^{50–52} Attention has been concentrated on the diamine with the isopropylidene bridging group.

The polyimides were synthesised from this diamine and the dianhydrides of the simplest dinuclear tetracarboxylic aromatic acids in *N*-MP without a catalyst in accordance with Scheme 5.⁵² The principal properties of the polyimides **10a–c** are presented in Table 6. As can be seen, the polyimides have low glass transition temperatures (180–210 °C) combined with high decomposition temperatures. The polymers **10a–c** are soluble not only in amide, phenolic, and chlorinated solvents (like the polymers **8** and **9**) but also in cyclohexanone and butyrolactone.

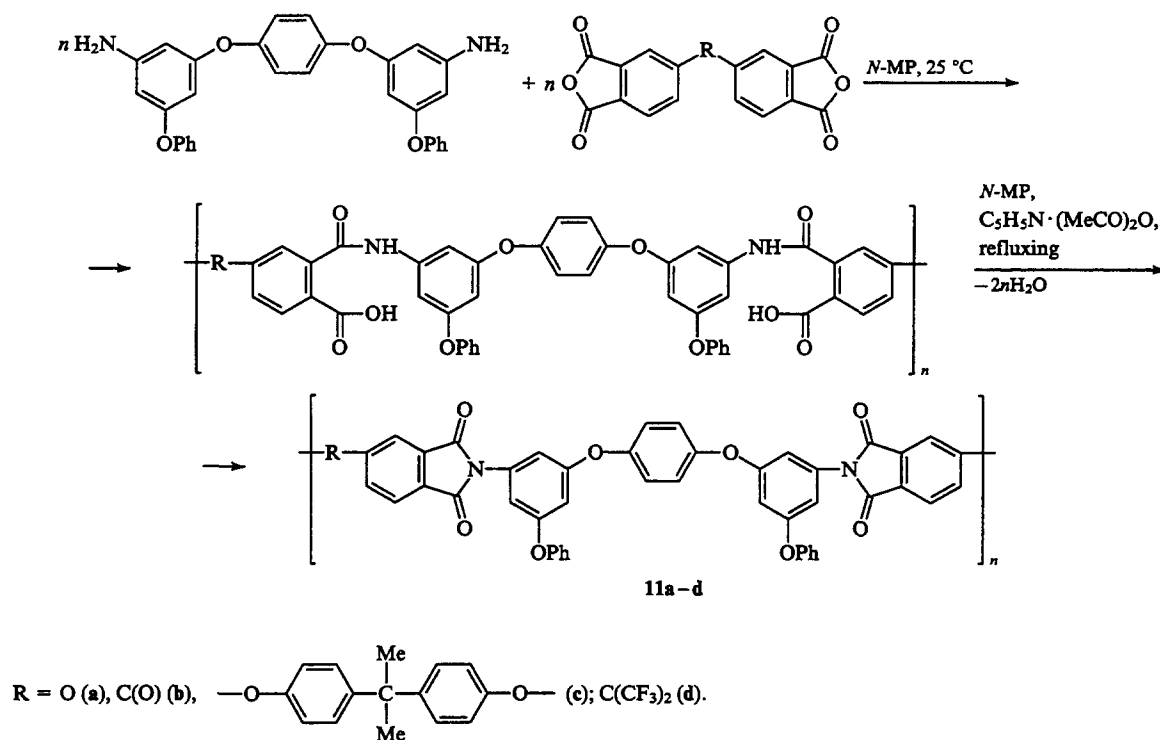
Table 6. The properties of the polyimides **10a–c**.⁵²

Polyimide	η_{red} /dl g ⁻¹ ^a	T_g /°C	$T_{10\%}$ /°C (TGA)
10a	0.46	193	523
10b	0.37	190	502
10c	0.31	180	511

^a The viscosity η measured in *m*-cresol at 25 °C.

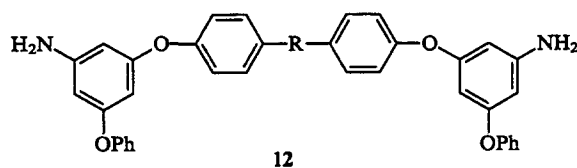
3,5-Dinitrodiphenyl ether can also be used to obtain the diamines. The interaction of the ether with various bisphenoxides leads to nitro-compounds with phenoxide side groups,^{53, 54} the reduction of which results in the formation of the corresponding amines with phenoxide side groups.⁵⁶ The polyimides **11a–d** have been synthesised from a diamine containing a hydroquinone residue.⁵⁷ The synthesis was based on Scheme 6. All the reactions were carried out homogeneously and led to high-molecular-mass polyimides with a high degree of cyclisation. The properties of the polyimides **11a–d** are presented in Table 7. The polyimides obtained were distinguished by relatively low glass transition temperatures combined with high decomposition temperatures and a ready solubility in organic solvents, which led to their being easily processed into articles.

Scheme 6

Table 7. The general properties of the polyimides 11a-d.⁵⁷

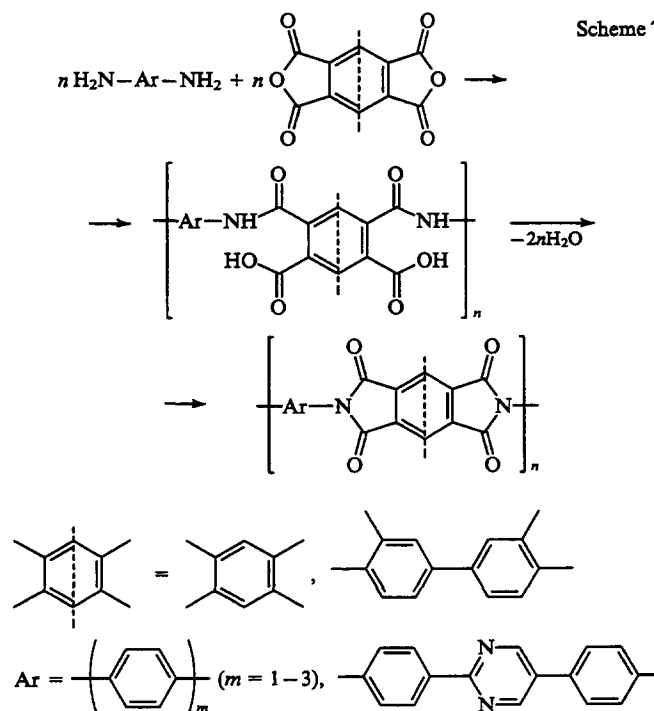
Polyimide	η_{red} / dl g ⁻¹	T_g /°C	$T_{10\%}$ /°C (TGA)	Molecular mass	Properties of films	
					σ /MPa	ϵ (%)
11a	0.67	170	520	47 000	890	4
11b	1.00	190	520	77 000	760	5
11c	0.95	188	500	—	540	5
11d	0.65	205	470	—	530	4

Almost all the polymers are soluble in amide, phenolic and chlorinated solvents, and also in cyclohexanone, acetone, and butyrolactone. The polyimides based on the diamines having the general formula 12 are even more easily processed into articles.



$R = CMe_2, C(CF_3)_2$.

Scheme 7



III. Rigid-chain aromatic polyimides

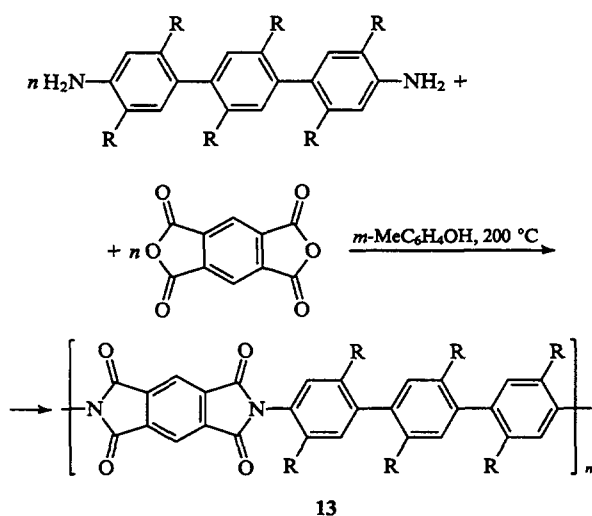
As mentioned above, the macromolecules of rigid-chain aromatic polyimides must be extended to the maximum extent and must contain symmetrical *p*-phenylene fragments and heterocyclic units without 'flexibilising bridges'. The simplest aromatic polyimides with a 'rod' geometry may be obtained from pyromellitic dianhydride or the dianhydride of biphenyl-3,3',4,4'-tetracarboxylic acid and carbocyclic (*p*-phenylenediamine, benzidine, 4',4''-diaminoterphenyl, etc.) or heterocyclic [2,5-bis(*p*-aminophenyl)pyrimidine]diamines⁶⁰⁻⁶⁴ in accordance with Scheme 7.

The high-molecular-mass poly(*o*-carboxy)amides formed in the first stage (in various amide solvents) undergo chemical or thermal cyclodehydration in the second stage, which results in the formation of insoluble polyimides. The value of the Kuhn segment was 625 Å for the polypyromellitimide based on 4',4''-diaminoterphenyl and 1750 Å for the polypyromellitimide based on 2,5-bis(*p*-aminophenyl)pyrimidine, which indicates a high rigidity of the macromolecules.⁶²

It is noteworthy that the evolution of gaseous products during the high-temperature thermal cyclodehydration limits the use of these materials in the industrial manufacture of thick-walled articles.⁶⁰

The studies by various research groups on the problem of the removal of water stimulated investigations of the synthesis of rigid-chain polyimides soluble in organic solvents. Bulky side groups are usually introduced into the macromolecule in order to improve the solubility of polymers. Typical representatives of such groups are long aliphatic segments, for example dodecyl fragments.^{65–68} The reaction of 4,4''-diamino-2,5,2',5'',5''-hexadodecyl-*p*-terphenyl with pyromellitic dianhydride in *m*-cresol at 200 °C using isoquinoline as the catalyst was carried out in accordance with Scheme 8. The polyimide **13** obtained as a result of this reaction was soluble in various organic solvents. However, it is noteworthy that the introduction of aliphatic fragments into the molecules of aromatic polyimides appreciably lowers their thermal stability — the polymers rapidly lose weight starting from 380 °C.

Scheme 8

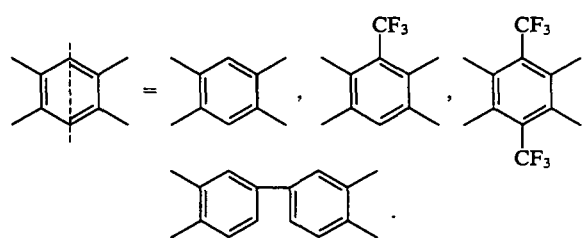
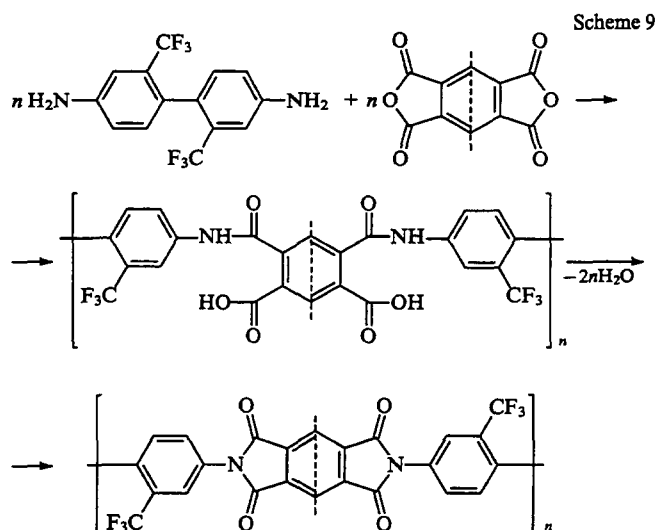


13

R = (CH₂)₁₁CH₃.

Better results were obtained when diamines and/or dianhydrides with trifluoromethyl side groups were used as the starting components.^{69–76} Polyimides based on 2,2'-bis-(trifluoromethyl)-4,4'-diaminobiphenyl and the dianhydrides of pyromellitic, biphenyl-3,3',4,4'-tetracarboxylic, 1-(trifluoromethyl)benzene-2,3,5,6-tetracarboxylic, and 1,4-bis(trifluoromethyl)benzene-2,3,5,6-tetracarboxylic acids have been synthesised by this procedure (Scheme 9).

The synthesis is carried out in two ways — by a two-stage reaction involving the low-temperature synthesis of poly(*o*-carboxy)amides in DMA with subsequent thermal cyclisation in the solid state at 350 °C^{70,71} and by a single-stage polycyclocondensation in boiling *m*-cresol.^{72–76} The polyimide obtained from 2,2'-bis(trifluoromethyl)-4,4'-diaminobiphenyl and the dianhydride of biphenyl-3,3',4,4'-tetracarboxylic acid by polycondensation in *m*-cresol is of greatest interest.^{72–76} This polymer is soluble in hot *m*-cresol. Fibres with a low strength and low elasticity modulus have been obtained by spinning its isotropic solution, but after tenfold drawing at a temperature above 380 °C the strength and the modulus of elasticity improved greatly when a load was applied. The fibres drawn in this way had a tensile strength of 3.2 GPa and an initial modulus of elasticity in excess of 130 GPa. The fibres had excellent thermal stability and retained a high strength and modulus of elasticity at elevated temperatures.



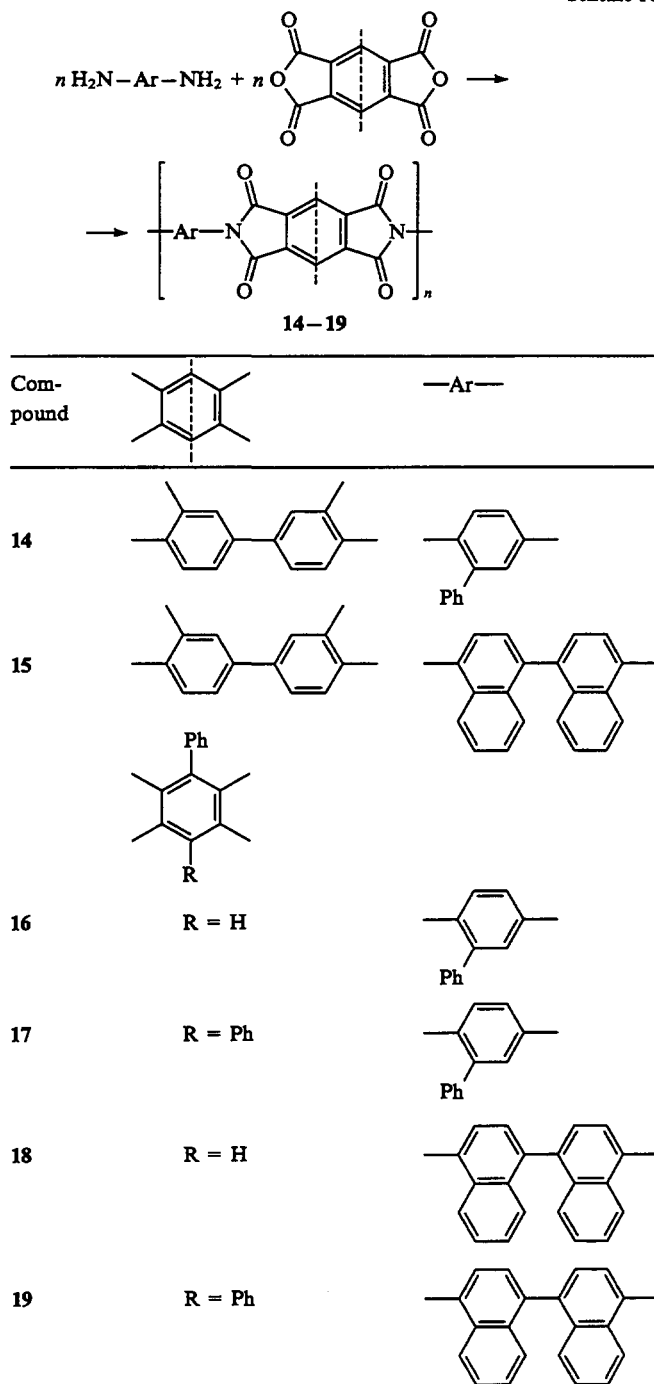
Rigid-chain polyimides soluble in phenolic solvents have been obtained by the interaction of the dianhydride of biphenyl-3,3',4,4'-tetracarboxylic acid with 2-phenyl-*p*-phenylenediamine and 4,4'-diamino-1,1'-binaphthyl⁷⁷ in accordance with Scheme 10. The reaction was carried out in *m*-cresol or *p*-chlorophenol at 200 °C using isoquinoline or tertiary amines as catalysts. The polyimides **14** and **15** are soluble in *m*-cresol and *p*-chlorophenol and have a high viscosity combined with high glass transition temperatures and decomposition temperatures. The same diamines have been used in the reactions with the dianhydrides of 3-phenyl- and 3,6-diphenylpyromellitic acids (Scheme 10).⁷⁸ The properties of the polyimides obtained under the conditions described above are presented in Table 8.

Table 8. The properties of the polyimides 14–19.^{77,78}

Polyimide	η_{\log} / dl g ⁻¹	T_g / °C	$T_{5\%}$ / °C (TGA)	
			N ₂	air
14	0.96	341	565	572
15	4.54	—	585	498
16	0.70	—	560	501
17	2.32	—	557	555
18	1.21	—	578	557
19	3.15	404	546	467

The dianhydride of 3,6-diphenylpyromellitic acid was also made to react with *p*-phenylenediamine, 1,4-diamino-2,3,5,6-tetramethylbenzene, benzidine, 4,4'-diamino-3,3',5,5'-tetramethylbiphenyl, 4,4'-diamino-3,3'-dimethoxybiphenyl, and 4,4'-diamino-2,2'-bis(trifluoromethyl)biphenyl.⁷⁹ The corresponding polyimides were obtained in two ways — by a two-stage synthesis (low-temperature synthesis of poly(*o*-carboxy)amides in *N*-MP with subsequent chemical or thermal imidisation) and a single-stage high-temperature polycyclocondensation in boiling *m*-cresol with isoquinoline as the catalyst. Best results were achieved when the single-stage process was used.

Scheme 10



Among the rigid-chain polyimides synthesised in this way, three polymers (based on dinuclear diamines) proved soluble in *m*-cresol. It is most likely that the improvement of the solubility of these polymers is associated with the nonplanarity of the bisphe-nylene fragments (especially 2,2'-substituted ones).⁸⁰

The intrinsic viscosities of the polymers soluble in *m*-cresol (Table 9) are in the range 0.91–2.63 dl g⁻¹; these are relatively low values for rigid-chain polymers. The mass-average molecular masses of these polymers are 10 000–12 000.

Table 9. Some properties of polyimides having the general formula.⁷⁹

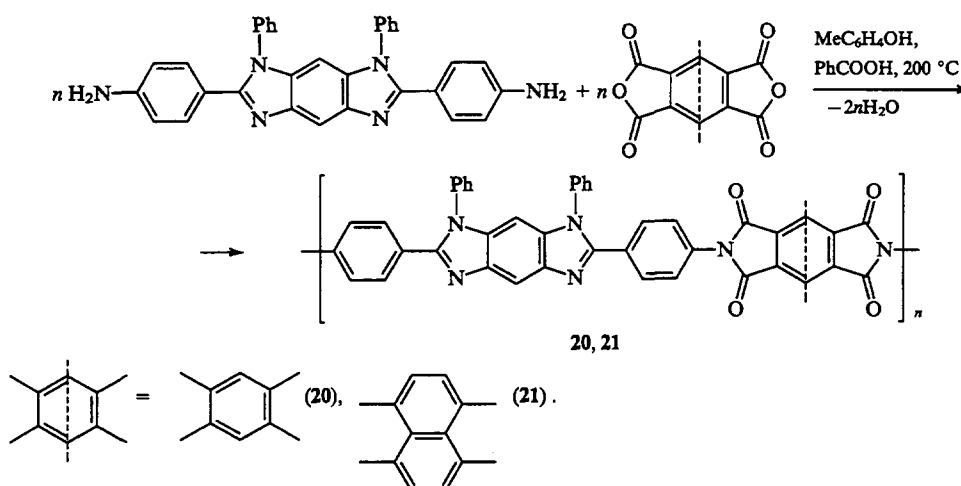
Ar	$[\eta]$ /dl g ⁻¹	$T_{5\%}$ /°C (TGA)	
		N ₂	air
	0.91	520	440
	2.63	475	425
	2.40	585	585

Fibres have been obtained from the polyimide with trifluoromethyl side groups by wet spinning from a hot *m*-cresol solution. The thermooxidative stability of the polyimides synthesised from 4,4'-diamino-3,3',5,5'-tetramethylbiphenyl and 4,4'-diamino-3,3'-dimethoxybiphenyl is relatively low — thermograms indicate 5% weight losses in air at 425 and 440 °C respectively. The low thermal stability of these polymers may be associated with the lack of resistance of the methoxy and methyl groups to oxidation. The thermal stability of the same polymers under nitrogen is much higher (the thermograms indicate 5% weight losses at 475 and 520 °C respectively in this instance). The presence of trifluoromethyl side groups in polyimides increases the thermooxidative and thermal stabilities of the polymers. Thermograms indicate a 5% weight loss at 585 °C in air and under nitrogen.⁷⁹

The rigid-chain polypyromellitimide **20** was obtained from 2,6-di(*p*-aminophenyl)-1,7-diphenylbenzo[1,2,4,5']biimidazole⁸¹ by high-temperature polycondensation in phenolic solvents (Scheme 11). Despite the presence of phenyl substituents, the polyimide **20** hardly dissolves in organic solvents. A polymer with a better solubility was synthesised by the interaction of the same diamine and the dianhydride of naphthalene-1,4,5,8-tetracarboxylic acid.⁸¹ The resulting polynaphthylimide **21** dissolved not only in sulfuric but also in trifluoroacetic acid as well as the tetrachloroethane — phenol mixture. The ready solubility of the polyimide is combined with a high viscosity of the solution and a very high glass transition temperature and decomposition temperature (540 °C).

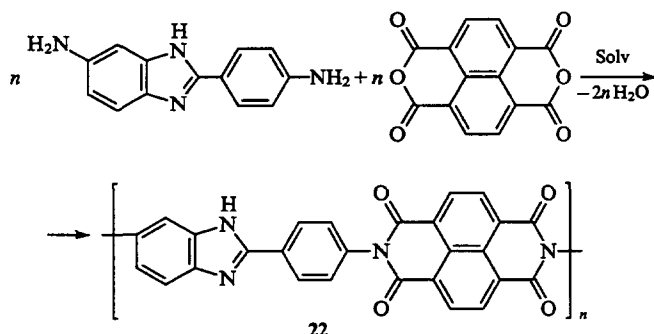
Polynaphthylimides have a series of advantages over polyphthalimides (for example, they are more stable under conditions of hydrolysis and thermolysis),⁸² so that investigators have devoted much attention to the synthesis of soluble polynaphthylimides. The most significant and to some extent unexpected result was obtained in the synthesis of the polyimide from the dianhydride of naphthalene-1,4,5,8-tetracarboxylic acid and an asymmetric diamine — 2-(*p*-aminophenyl)-5(6)-aminobenzimidazole in accordance with Scheme 12.⁸³

Scheme 11



Despite the absence of substituents of any kind in the diamine and the dianhydride, the reaction occurred homogeneously and led to the high-molecular-mass polymer **22** ($M = 120\,000$),⁸⁴ which is soluble (before isolation from the reaction solution) in phenolic solvents. The polymer **22** is moderately rigid — its Kuhn segment is 320 \AA .⁸⁴ Strong and elastic films have been cast from the reaction solutions of the polyimide **22** (Table 10). After heat treatment at 140 °C for 12 h with subsequent maintenance in vacuo at 250 °C for 3 h, the properties of the films improved and after stretching the tensile strength was $930 \pm 10\text{ MPa}$ and the modulus of elasticity was $20 \pm 1\text{ GPa}$.

Scheme 12



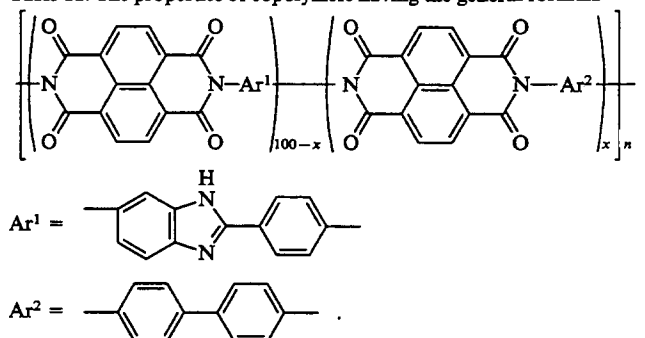
Solv = $\text{MeC}_6\text{H}_4\text{OH}$, PhCOOH (200 °C)

Table 10. The properties of a polynaphthylimidobenzimidazole film (polyimide **22**).⁸³

Test specimen	σ/MPa	$\varepsilon(\%)$	$10^{-3} E/\text{MPa}$
Film after casting	320 ± 10	25 ± 5	4.5 ± 0.5
Film after heating ($140\text{ °C}/12\text{ h}$ and $250\text{ °C}/3\text{ h}$ in vacuo)	470 ± 10	35 ± 5	4.6 ± 0.5
Stretched film	930 ± 10	8 ± 1	20 ± 1

The partial replacement of 2-(*p*-aminophenyl)-5(6)-amino-benzimidazole by benzidine led to a polymer with a larger Kuhn segment and a greater strength and modulus of elasticity (Table 11).⁸⁵

Table 11. The properties of copolymers having the general formula⁸⁵



x (mol %)	$[\eta]/\text{dl g}^{-1}$ (H_2SO_4)	σ/MPa	$\varepsilon(\%)$	$10^{-3} E/\text{MPa}$
0	9.8	320 ± 10	25 ± 5	4.5 ± 0.5
5	11.5	384 ± 21	17 ± 4	10.0 ± 0.5
10	13.0	443 ± 9	17 ± 1	12.9 ± 0.5
15	8.9	417 ± 19	17 ± 2	12.0 ± 0.8
20	11.2	446 ± 19	17 ± 2	15.2 ± 1.6
20	11.2	1174 ^a	4 ^a	29.9 ^a
25	9.4	418 ± 14	20 ± 4	10.7 ± 0.3
30	15.3	418 ± 33	20 ± 4	10.4 ± 0.2
30	15.3	1500 ^a	4 ^a	38.0 ^a

^a Data for oriented (60%) films are presented.

IV. Conclusion

The data considered above indicate considerable advances in the chemistry and technology of the flexible- and rigid-chain polyimides achieved during recent years. Novel methods of synthesis of various bifunctional and tetrafunctional aromatic monomers have been developed and the reactions involving the formation from them of high-molecular-mass polyimides have been investigated. Certain polyimides are of practical as well as academic interest. Further development of this field of polymer chemistry makes it possible to hope that new results will be obtained in the immediate future.

References

1. M I Bessonov, M M Koton, V V Kudryavtsev, L A Laius *Poliimidy — Klass Termostoikikh Polimerov* (Polyimides — Class of Heat-Resistant Polymers) (Leningrad: Nauka, 1983)

2. V V Korshak, A L Rusanov, I Batirov *Novoe v Oblasti Termostoikikh Poliimidov* (New Advances in the Field of Heat-Resistant Polymers) (Dushanbe: Donish, 1986)
3. B Sillion *Compr. Polym. Sci.* **5** 499 (1989)
4. T Takekoshi *Adv. Polym. Sci.* **94** 3 (1990)
5. C E Sroog *Prog. Polym. Sci.* **16** 561 (1991)
6. T Takekoshi *Polym. J.* **19** 191 (1987)
7. A L Rusanov, T Takekoshi *Usp. Khim.* **60** 1449 (1991) [*Russ. Chem. Rev.* **60** 738 (1991)]
8. V V Korshak, A L Rusanov, G V Kazakova, N S Zabel'nikov, G S Matvelashvili *Vysokomol. Soedin., Ser. A* **30** 1795 (1988)
9. F C Frank *Proc. R. Soc. London, A Math. Phys. Sci.* **319** 127 (1970)
10. A J Kinloch, R J Young *Fracture Behaviour of Polymers* (New York; London: Applied Science, 1983)
11. R T Read *Polym. Paint Colour J* **178** 664 (1988)
12. M M Koton *Vysokomol. Soedin., Ser. A* **21** 2496 (1979)
13. Yu N Sazanov, F S Florinsky, M M Koton *Eur. Polym. J.* **15** 781 (1979)
14. S S -A Pavlova, G I Timofeeva, I A Ronova *J. Polym. Sci., Polym. Phys. Ed.* **18** 1175 (1980)
15. T M Birshtein, A N Goryunov *Vysokomol. Soedin., Ser. A* **21** 1990 (1979)
16. US P. 3 838 097 (1974)
17. US P. 3 879 428 (1975)
18. T Takekoshi, J E Kochanowski, J S Manello, M J Webber *J. Polym. Sci., Polym. Chem. Ed.* **23** 1759 (1985)
19. J N Gorvin *Chem. Ind. (London)* **36** 1525 (1969)
20. T J DeBoer, J P Dirkx, in: *The Chemistry of the Nitro- and Nitroso-Groups Part 1* (Ed. H Feuer) (New York: Wiley, 1969) p. 487
21. US P. 3 763 210 (1973)
22. US P. 4 324 882 (1984)
23. US P. 4 293 683 (1983)
24. US P. 3 933 749 (1976)
25. US P. 3 803 085 (1974)
26. US P. 4 281 100 (1983)
27. G S Matvelashvili, G V Kazakova, A L Rusanov, N A Anissimova, A L Narkon *The Second AIM Conference on Advanced Topics in Polymer Science, Gargnano, Italy 1990*, p. 173
28. G S Matvelashvili, A L Rusanov, V M Vlasov, G V Kazakova, O Yu Rogozhnikova *Vysokomol. Soedin.* **37** 1941 (1995)
29. US P. 3 991 004 (1976)
30. US P. 4 634 760 (1986)
31. US P. 3 944 517 (1976)
32. US P. 4 599 396 (1986)
33. US P. 4 612 361 (1986)
34. T Takekoshi, J E Kochanowski, J S Manello, M J Webber *J. Polym. Sci., Polym. Symp.* **74** 93 (1986)
35. A V Pavlov, O M Karanyan, A G Morozov, G S Matvelashvili, G V Kazakova, N A Anissimova, in *Polyimides and other High-Temperature Polymers* (Eds M J M Abadie, B Sillion) (Amsterdam: Elsevier, 1991) p. 173
36. Eur. P. 1 924 80 (1986)
37. Int. P. 8 701 378 (1978)
38. Jpn. P. 62-05 035 (1987)
39. Jpn. P. 62-068 817 (1987)
40. Jpn. P. 62-116 547 (1987)
41. Jpn. P. 62-116 563 (1987)
42. Jpn. P. 62-270 636 (1987)
43. Jpn. P. 04 108 767 (1992)
44. US P. 4 912 197 (1991)
45. US P. 4 914 175 (1991)
46. G S Matvelashvili, A L Rusanov, G V Kazakova, V M Vlasov, N A Anissimova, O Yu Rogozhnikova *Vysokomol. Soedin., Ser. B* **32** 631 (1991)
47. G S Matvelashvili, A L Rusanov, G V Kazakova, V M Vlasov, N A Anissimova, O Yu Rogozhnikova, in *Polyimides and other High-Temperature Polymers* (Eds M J M Abadie, B Sillion) (Amsterdam: Elsevier, 1991) p. 199
48. G S Matvelashvili, V M Vlasov, A L Rusanov, G V Kazakova, N A Anissimova, O Yu Rogozhnikova *Vysokomol. Soedin., Ser. A* **35** 293 (1993)
49. A L Rusanov, E G Bulychева, G S Matvelashvili, G V Kazakova, V M Vlasov, O Yu Rogozhnikova *ACS Polym. Prepr.* **35** 370 (1994)
50. Jpn. P. 1-190 652 (1990)
51. S J Havens, P M Hergenrother *High Perform. Polym.* **518** (1993)
52. A L Rusanov, Z B Shifrina, T N Kolosova, G S Matvelashvili, G V Kazakova, V M Vlasov, O Yu Rogozhnikova *Vysokomol. Soedin.* (1996) (in the press)
53. V A Tartakovsky, S A Shevelev *Commercial Application and Disposal Technologies of Energetic Systems Programme of NATO, Advanced Research Workshop, Moscow, 1994*
54. V A Tartakovsky, S A Shevelev, M Dutov *Proceedings of the 25th International Conference of ICT, Karlsruhe, Germany, 1994* p. 109-1
55. A L Rusanov, L G Komarova, A M Trushkin, S A Shevelev, M D Dutov, O V Serushkina, A M Andrievskii *Vysokomol. Soedin.* **35** 883 (1993)
56. A Shevelev, M Dutov, O Serushkina *Abstracts of the Vth International Conference on Polyimides, Ellenville, USA, 1994* p. 38
57. A L Rusanov *Abstracts of the Vth International Conference on Polyimides, Ellenville, USA, 1994* p. 92
58. F W Harris, W A Feld, in *Structure-Solubility Relationships in Polymers* (New-York: Academic Press, 1977) p. 183
59. Y -S Negi, Y -I Suzuki, I Kawamura, T Nagiwaru, Y Takahashi, M A Kakimoto, Y Imai *J. Polym. Sci., Polym. Chem.* **30** 2281 (1992)
60. J S Wallace, F E Arnold, L S Tan *ACS Polym. Prepr.* **28** 316 (1987)
61. J S Wallace, L-S Tan, F E Arnold *Polymer* **31** 2411 (1990)
62. V N Artem'eva, V V Kudryavtsev, E M Nekrasova, V P Sklizkova, I A Shibaev, N G Stepanov, Yu M Sazanov, T N Fedorova, O P Shkurko, N Borovik *Izv. Akad. Nauk, Ser. Khim.* **2297** (1992)
63. R Yokota, R Horiuchi, H Soma, M Kochi, I Mita *Polym. Prepr. Jpn.* **35** 3304 (1986)
64. M Koshi, T Uruji, T Iizuka, I Mita *J. Polym. Sci.* **C25** 441 (1987)
65. M Wenzel, M Ballauff, G Wegner *Makromol. Chem.* **188** 2865 (1987)
66. F Helmer-Meltzmann, M Ballauff, R C Schulz, G Wegner *Makromol. Chem.* **190** 985 (1989)
67. M Ballauff *Angew. Chem.* **101** 261 (1989)
68. F Helmer-Metzmann, M Rehahn, L Schmitz, M Ballauff, G Wegner *Makromol. Chem.* **193** 1847 (1992)
69. T Matsura, Y Hasuda, S Nishi, N Yamada *Macromolecules* **24** 5001 (1991)
70. T Matsura, M Ishizawa, Y Hasuda, S Nishi *Macromolecules* **25** 3540 (1992)
71. F W Harris, S L-C Hsu, C C Tso *ACS Polym. Prepr.* **31** 342 (1990)
72. S Z D Cheng, Z Wu, M Eashoo, S L-C Hsu, F W Harris *Polymer* **32** 1803 (1991)
73. S Z D Cheng, F E Arnold Jr *ACS Polym. Prepr.* **33** 1 313 (1992)
74. S L-C Hsu, F W Harris, S Z D Cheng, F E Arnold Jr, Anqui Zhang *Macromolecules* **24** 5856 (1991)
75. T Fukai, J C Yang, T Kyu, S Z D Cheng, S K Lee, S L-C Hsu, F W Harris *Polymer* **33** 3621 (1992)
76. T Kyu, J C Yang, S Z D Cheng, S L-C Hsu, F W Harris *Macromolecules* **27** 1861 (1994)
77. R Giesa, U Keller, H-W Schmidt *ACS Polym. Prepr.* **33** 396 (1992)
78. R Giesa, U Keller, P Eiselt, H-W Schmidt *J. Polymer Sci. Polymer Chem.* **31** 141 (1993)
79. F W Harris, S L-C Hsu *High Perform. Polym.* **1** 3 (1989)
80. R A Gaudiana, R A Minns, H G Rogers, R Sinta, L D Taylor *J. Polymer Sci. Polymer Chem. Ed.* **25** 1249 (1987)
81. V V Korshak, A L Rusanov, I Batirov *Dokl. Akad. Nauk SSSR* **240** 88 (1978)
82. A L Rusanov *Adv. Polym. Sci.* **111** 115 (1994)
83. O G Nikol'skii, I I Ponomarev, A L Rusanov, S V Vinogradova, V Yu Levin *Vysokomol. Soedin., Ser. B* **31** 636 (1990)
84. N V Pogodina, N P Evlampieva, V N Tsvetkov, V V Korshak, S V Vinogradova, A L Rusanov, I I Ponomarev *Dokl. Akad. Nauk SSSR* **301** 905 (1988)
85. I I Ponomarev, O G Nikol'skii, Yu A Volkova, A V Zakharov *Vysokomol. Soedin., Ser. A* **36A** 1429 (1994)

Catalytic properties of metal-phthalocyanines in reactions involving hydrogen

E M Sul'man, B V Romanovskii

Contents

I. Introduction	609
II. The structure of phthalocyanines	609
III. The catalytic activity of phthalocyanines and the mechanism of their activation	610
IV. Reactions with participation of hydrogen	610
V. Phthalocyanines on carriers	611

Abstract. The catalytic properties and the mechanism of activation of phthalocyanines in reactions with participation of hydrogen are examined. The mechanism of the catalytic action of phthalocyanines is discussed. Two types of active centres ('metallic' and 'organic') are distinguished in the phthalocyanine molecule. Problems associated with the fixation of phthalocyanine catalysts on carriers are considered. The bibliography includes 120 references.

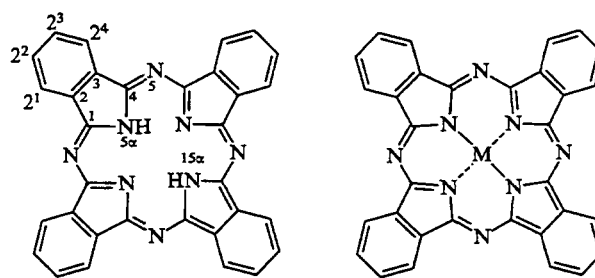
I. Introduction

Phthalocyanines (Pc), which are structural analogues of chlorophyll and haem, were discovered in the 1920s.¹ The complexes of phthalocyanines with alkali and alkaline earth metals contain the metal in an ionic form and may be decomposed by acids and even water, whereas transition metals in complexes with phthalocyanines, which form a covalent bond, are, on the other hand, surprisingly stable.² Phthalocyanines possess a number of unusual properties and have found various applications.^{3–5}

The first information about the catalytic activity of phthalocyanines⁶ appeared in 1938. In the course of the succeeding 55 years, metal-phthalocyanines (PcM) have been used as catalysts of the oxidation of aromatic hydrocarbons^{7–20} propene,^{21–24} aldehydes,²⁵ acids,^{25,26} alkenes^{6,27} alcohols^{8,28} ketones²⁹ sulfur-containing compounds,^{30–34} and nitrogen³⁵ and carbon³⁶ oxides, of the dehydrogenation of alcohols^{37–42} and hydrocarbons,^{43–47} of photodehydrogenation,⁴⁸ of the decarboxylation of carboxylic acids,⁴⁹ of the decomposition of peroxide compounds,^{50–62} hydrazine,^{14,63,64} and formic acid,⁶⁵ of isomerisation,⁷ of polymerisation,⁵⁰ of the ortho–para conversion of hydrogen and deuterium exchange,⁶⁶ of the reduction of nitrogen oxide with hydrogen^{67–69} and with carbon monoxide,^{67,70} of electrochemical processes,⁷¹ and of the reduction of organic compounds.^{37,72–79}

II. The structure of phthalocyanines

The structure of phthalocyanines was first considered by Dent et al.⁸⁰ It was shown by X-ray diffraction^{81,82} that metal-phthalocyanines have planar molecules.



Both crystalline α - and β -modifications of phthalocyanines exist.^{83,84} The mutual phase transitions of the α - and β -forms occur on boiling in acid and organic solvents and also as a result of mechanical and thermal influences. The hypsochromic shift of the IR absorption band of phthalocyanine molecules at 720–730 cm^{-1} is regarded as a sign of the $\alpha \rightarrow \beta$ transition.⁸⁴ In a mixture of the α - and β -forms, this band is split. The distance between the molecules in the crystals of both modifications are the same (Fig. 1), but the orientations of the molecules relative to the

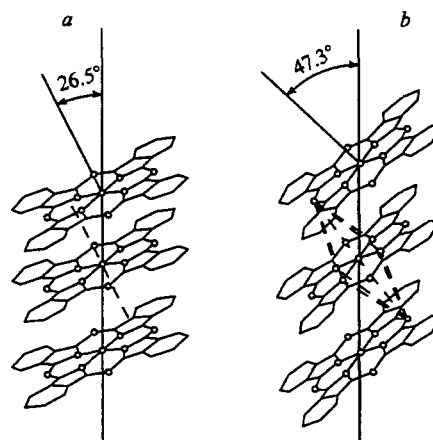


Figure 1. Arrangement of the molecules in the crystals of α -PcM (a) and β -PcM (b).

E M Sul'man Department of Biotechnology and Chemistry, Tver' State Technical University, nab. A. Nikitina 22, 170026 Tver', Russian Federation. Fax (7-082) 231 62 92

B V Romanovskii Laboratory for Kinetics and Catalysis, Department of Physical Chemistry, Chemistry Department, Lomonosov Moscow State University, Vorob'evy Gory, 119899 Moscow, Russian Federation. Fax (7-095) 939 31 85

Received 30 January 1996

Uspekhi Khimii 65 (7) 659–666 (1996); translated by A K Grzybowski

crystallographic axes different.⁸⁵ In the β -form, the metal atom of the chelate unit coordinates the nitrogen atoms of the neighbouring molecules, which serve as extra-ligands relative to the complex forming metal (Fig. 1). The higher stability of the β -form is attributed to the interaction between the metal atom and the nitrogen atoms of the neighbouring PcM molecules.⁸⁶ The different crystalline modifications of PcM can therefore exhibit different catalytic activities.

III. The catalytic activity of phthalocyanines and the mechanism of their activation

By virtue of their high chemical stability,⁶⁶ phthalocyanines can be used as model substances under conditions including catalytic investigations.

The wide variety of the reactions catalysed by metal-phthalocyanines⁸⁷ apparently reflect the characteristic features of their structure. As a consequence of their planar structure and the presence of an extensive electron conjugation system, the phthalocyanine molecules are fairly mobile and are capable of being coordinated to substrate molecules.

In the phthalocyanine molecule, it is possible to distinguish two types of active centres: the 'metallic' centre incorporating the complex forming metal and the 'organic' centre.⁸⁸ The latter includes the nitrogen atoms of the azo-bridges, which have an enhanced electron density. The application of quantum-chemical calculations^{89,90} made it possible to determine the electron populations and the effective charges of the individual atoms in the phthalocyanine molecule and to discover the presence of donor and acceptor centres. The electron populations of the different atoms in the PcCo molecule are characterised by the following values:⁸⁹

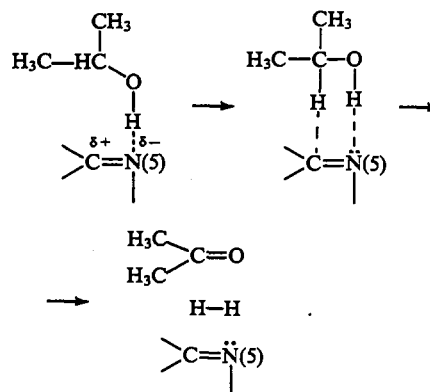
N(5 α)	C(1)	C(2)	C(2')	C(2'')	N(5)
5.148	3.927	3.995	4.031	4.041	5.179

It follows from these data that the nitrogen atoms behave as electron-donating centres. The effective charge on the cobalt atom (+0.359) indicates the interaction of the orbitals of the organic ligand with the atomic orbitals of the metal and electron transfer between the metal and the π -electron system of the ligand. Either the metal or the organic ligand or both centres simultaneously exhibit a catalytic activity in various reactions.⁸ The catalysis by metal-phthalocyanines is influenced by the number of electrons in the $3d^N 4s^2$ atomic orbitals of the metal and in the molecular orbitals of the ligand.⁹¹

Gudkov⁴⁷ put forward the hypothesis that O_2 may be coordinated to PcCo via the central metal atom and the organic ligand. The shielding of the central atom by ligands, for example by pyridine,⁹²⁻⁹⁴ in the axial position hinders the binding of O_2 to the metal of the chelate unit⁹⁵ and hence alters the catalytic activity of PcM in oxidation reactions. The decisive role of the central metal atom in catalysis has been confirmed experimentally.^{6,14} The bond in the $PcM \cdots O_2$ complex is formed as a result of electron transfer both from the π orbital of oxygen to the d_{z^2} orbital of the metal and by the electron transfer in the opposite direction — from the d_{π} orbital of the metal to the antibonding π^* orbitals of oxygen; the first process predominates.³⁷

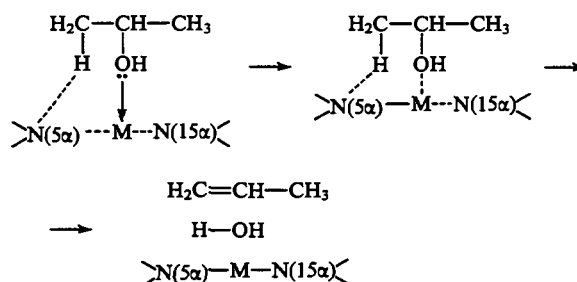
EPR and electronic spectroscopic data have led to the conclusion that O_2 is coordinated to the organic part of the metal complex of phthalocyanine.⁹⁶⁻⁹⁸ Judging from the nature of the spectrum in the visible region,⁹⁷ one may postulate the coordination of O_2 to a ring nitrogen atom. The change in the nature of the EPR spectrum of phthalocyanine in the presence of O_2 ⁹⁹ made it possible also to put forward the hypothesis that oxygen interacts with the central metal atom. However, oxidation of the organic ligand by the metal ion can yield the same results. Thus both the 'organic' and the 'metallic' active centres may be catalytically active.

The studies of the mechanisms of the PcM-catalysed reactions, for example the mechanism of the dehydrogenation of isopropyl alcohol in the presence of complexes of phthalocyanines with transition and nontransition metals, where the metal atom may be shielded, are of undoubted interest.^{40-42,100} It has been suggested that the isopropyl alcohol molecule is activated on the 'organic' active centre. The coordination centre in the organic ligand is the bridging N(5) nitrogen atom, which has a lone pair and forms a bond with the hydrogen atom of the hydroxy group:



The role of the metal of the chelate unit is to ensure electron transfers via the central atom of the PcM molecule.

The dehydration of isopropyl alcohol requires two-centre coordination, where the oxygen atom of the hydroxy group transfers its electron to the metal atom, while the hydrogen atom of the methyl group forms a bond with the nitrogen atom of the chelate unit.

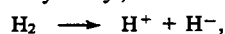


Thus the metal atom may be either an electron acceptor or donor and this determines the specificity of the activity of the PcM.

In the decomposition of formic acid to H_2 and CO_2 on the β -forms of Cu-, Fe-, Co-, Ni-, and Zn-phthalocyanines at 200–300 °C, zero order with respect to the substrate was observed in all cases, while the apparent activation energy was 80–100 kJ mol⁻¹.¹⁰¹ Thus the nature of the central metal atom did not affect the process. Moser and Thomas⁷ believe that the chelate unit, the CH groups of the benzene rings, the nitrogen *meso*-atoms, and the carbon atoms of the pyrrole rings may be reactive. Depending on the type of reaction catalysed, the catalytic activity may be exhibited under certain conditions by either one or several of these centres at once.

IV. Reactions with participation of hydrogen

The available information about the reactions with participation of molecular hydrogen catalysed by metal-phthalocyanines is extremely limited.^{66,102,103} It has been suggested⁶⁶ that in the ortho-para conversion of hydrogen and in deuterium exchange on PcCu and PcH₂, the H-H bond may be dissociated both heterolytically, i.e.



or homolytically, i.e.



The second pathway appears more probable.

Reaction	$E/\text{kJ mol}^{-1}$	
	PcH ₂	PcCu
$\text{p-H}_2 \xrightarrow{150-360^\circ\text{C}} \text{o-H}_2$	24	21
$\text{H}_2 + \text{D}_2 \xrightarrow{<100^\circ\text{C}} 2\text{HD}$	—	42

The apparent activation energies for the ortho-para conversion of H₂ on monomeric and polymeric PcCu are not the same. The polymeric form is capable of desorbing hydrogen in the ratio Cu:H = 1:1, which permits ready diffusion of hydrogen through the polymer.⁶⁶ An increase in the conjugation length on passing from the monomeric to the polymeric phthalocyanine may lead to the equalisation of electron density over the entire PcM molecule, which is accompanied by a decrease in the effective charges on the central metal atom and the organic ligand.

In the related cobalt-tetraphenylporphyrin-TiO₂ (CoTPP/TiO₂) catalytic system,⁶⁷ the porphyrin ring serves as the adsorption centre for hydrogen.

The study of the adsorption of hydrogen on the pre-evacuated CoTPP/TiO₂ and H₂TPP/TiO₂ showed that H₂TPP/TiO₂ and CoTPP/TiO₂ adsorb 13.5 and 19.6 mmol of H₂ per gramme of the catalyst under comparable conditions. This led to the indisputable conclusion that hydrogen is activated by the 'organic' active centre. The study of the kinetics of the reduction of NO on CoTPP/TiO₂ confirmed the dissociative nature of the adsorption of hydrogen.⁶⁷ Fig. 2 shows that nitric oxide is activated by the central metal atom.

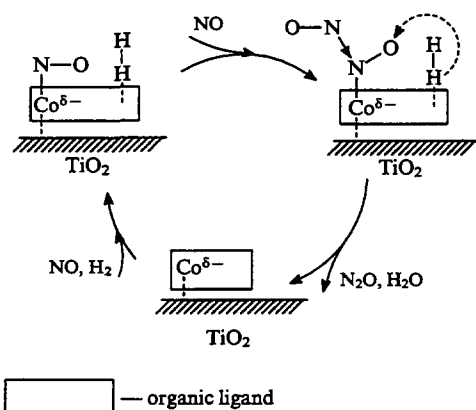
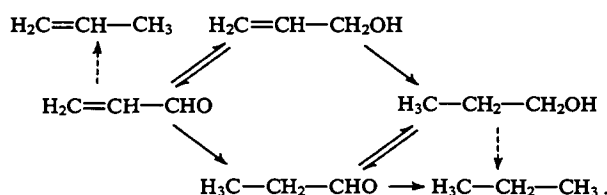


Figure 2. Schematic illustration of the reduction of NO on CoTPP/TiO₂.

The study of the hydrogenation of ethyne by a metal tetrahydroborate in the presence of sulfonated CoTPP led to the conclusion that ethyne is activated on the central metal atom.⁷²

The following scheme has been proposed for the hydrogenation of allyl alcohol on PcNi at 100–300 °C:¹⁰⁴



Other pathways leading to the conversion of allyl alcohol, for example directly into propene, are not taken into account in the above scheme.

In addition, the hypothesis has been put forward that hydrogen is activated on the nitrogen atoms of the PcM molecule.¹⁰⁴ It was later confirmed by other investigators with the aid of adsorption methods.⁶⁷ The independence of the activation of PcM in the isopropyl alcohol dehydrogenation reaction of the nature of the central atom¹⁰⁵ led to the conclusion that the nitrogen atoms of the azo-bridges participate in the activation of isopropyl alcohol.

Thus molecular hydrogen may be activated on both the 'metallic' and 'organic' active centres of metal-phthalocyanines and metal-porphyrins. The results of the study of the hydrogenation of acetylenic alcohols on modified palladium catalysts and carriers led to the hypothesis that the C≡C bond is activated on the 'organic' centre, while hydrogen is activated on the metal.¹⁰⁶

V. Phthalocyanines on carriers

Covalent binding, coordination in the axial position, adsorption methods, and direct synthesis on the carrier surface were used for the fixation of metal-porphyrins, including phthalocyanines, on oxide carriers.⁹⁵ The last two methods are most widely used.

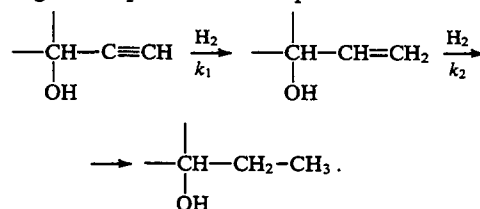
In order to increase the catalytic activity of metal-phthalocyanines and to facilitate the control of the selectivity of the reactions, the fixation of PcM on various carriers is resorted to.^{95, 103, 105–108} This prevents the aggregation of the complexes and makes it possible to achieve molecular dispersion.

A fivefold increase in the catalytic activity of cobalt-phthalocyanine in the oxidation of 2-mercaptoethanol after the fixation of the catalyst on the polymeric carrier was noted.¹⁰⁹ The immobilisation of H₂TPP in a polymer matrix is used for the same purposes.

The catalytic activities of monomeric and polymeric phthalocyanines, deposited on carbon carriers, in the decomposition of H₂O₂ depend on the nature of the complex forming metal and on the characteristic features of the carrier.¹⁰³ The activity of the monomeric phthalocyanines decreases in the sequence Os >> Fe > Ru > Pt > Pd, Ir, whilst that of polymeric ones diminishes in the sequences Fe > Co >> Ni > Cu and Fe > Os, Pt, Ru > Ir, Rh, Pd.

Oxide carriers with a high chemical and thermal stability are widely used for porphyrins.^{95, 107}

The selective hydrogenation of C₅, C₁₅, and C₂₀ acetylenic alcohols in the presence of PcM (M = Pd, Ni, Cu, Co), deposited on oxides (Al₂O₃, SiO₂), has been investigated⁷⁶ varying the nature of the solvent, the PcM deposition method, and the amount of the active component in the carrier. The overall scheme for the hydrogenation process can be represented as follows:



The alcohol dehydrogenation and dehydration reactions take place together with the reactions shown above.

In order to elucidate the influence of the nature of the solvent, a study has been made of the hydrogenation of a C₁₅ acetylenic alcohol in solutions in isopropyl alcohol, methanol, and hexane (0.4 M) in the presence of PcNi/SiO₂ (5% Ni).⁷⁷ The catalyst was prepared by the preliminary impregnation of SiO₂ (specific surface 200 m² g^{−1}) with an aqueous NiCl₂ solution and subsequent treatment with phthalonitrile vapour (250–320 °C), drying, and thermoevacuation. The selectivity and activity of the

catalyst obtained in this way as regards the formation of the C₁₅ ethylenic carbinol were found to be a maximum in hexane and a minimum in methanol.

The influence of the nature of the solvent on the heterogeneous catalytic system is determined by a whole series of factors. The solvent is adsorbed on the catalyst, altering the free energy of the surface and its charge,¹¹⁰ which may affect the mode of the reaction and its selectivity. The solvation constants, the adsorption coefficients, and the rate of conversion of the intermediate surface compound into the reaction products depend on the nature of the solvent.¹¹¹ The adsorption from solutions is competitive in character and the adsorption of substrates can therefore be greatly influenced by the ability of the solvent to form coordinate bonds with the catalyst.⁷⁶

Not only the activity of the catalyst in the reactions involving the hydrogenation of the C≡C bond of acetylenic alcohols but also the mechanism of the catalytic activity depend on the method used to deposit PcM on the oxide (from concentrated H₂SO₄ or benzene). Catalysts obtained by depositing Co-, Cu-, and Ni-phthalocyanines from solutions in H₂SO₄ accelerate the reduction of acetylenic alcohols to the same extent. The catalysts prepared by fixation on a carrier of a PcM from a solution in benzene and those obtained from phthalonitrile can be arranged in the following sequence in terms of their activity in the synthesis of ethylenic alcohols: PcPd > PcNi > PcCo.⁷⁶

The rate of oxidation of propan-2-ol in the presence of PcCo is higher than in the presence of PcNi.⁶⁶ It has been suggested that the catalytically active centre in this reaction is the central metal atom, as in the hydrogenation reaction.⁷⁶

Thus, depending on the method of preparation of the catalyst, different atoms or groups of atoms of the PcM molecule enter into the reaction complex.

When the PcM/oxide heterogeneous systems are used, it is necessary, as in the case of metallic catalysts on carriers, to take into account the interaction between the active component and the carrier, which not only influences the activity of the catalytic system but is also capable of altering the mode of the process.

The higher catalytic activity of PcNi/Al₂O₃ compared with PcNi/SiO₂ can be explained by the influence of the carrier on the active component of the catalyst.⁷⁶ The Ni 2p_{3/2} binding energy (E_b) in the PcNi/Al₂O₃ system proved to be lower by 1 eV than in the initial PcNi (according to a patent,⁶⁹ E_b = 865.0 eV in this case).

The catalytic properties of PcCo deposited on silica gel by direct synthesis on the surface and of PcFe/SiO₂ obtained by the joint grinding of PcFe and SiO₂¹⁰⁵ have been investigated. When the deposited catalyst is used, the reaction of isopropyl alcohol involves predominantly dehydration and not dehydrogenation. This is evidently associated with an increase, as a result of dispersion, in the number of centres responsible for dehydration or with the influence of the carrier on the catalytic activity of PcM. The catalytic activity of PcCo on silochrome, referred to unit mass of the active phase, is higher by 1–2 orders of magnitude than the activity of crystalline PcCo in the reactions of isopropyl alcohol.¹¹²

The highest activity of CoTPP in the reduction of CO is attained when TiO₂ is used as the carrier, whereas in the decomposition of H₂O₂ the best carrier is NiO.^{59, 113} When CoTPP is attached to TiO₂, electron density is transferred from the carrier to the CoTPP molecule, which is accompanied by the formation of a radical-anion and a change in the effective charge on the atoms of the chelate unit. This has been confirmed by XPES data for the binding energies (expressed in eV) in the CoTPP and CoTPP/TiO₂ systems:

	Co 2p _{3/2}	Co 2p _{1/2}	N 1s
CoTPP	781.0	796.4	397.3
CoTPP/TiO ₂	780.2	795.6	398.6

The EPR spectra of benzene solutions of CoTPP and CoTPP/TiO₂ differ appreciably (Fig. 3).¹¹³ Comparison of the electronic absorption spectra of CoTPP in a benzene solution with the spectra of CoTPP deposited on SiO₂ and TiO₂ showed¹⁰⁹ that the use of SiO₂ as the carrier alters the intensity of the absorption bands (AB), whereas new absorption bands appear when the TiO₂ carrier is employed (Fig. 4).

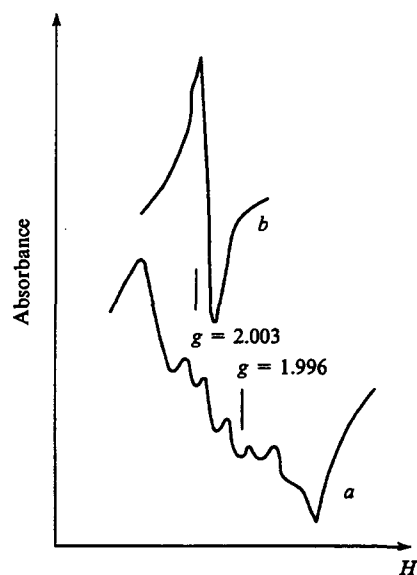


Figure 3. EPR spectra of a benzene solution of CoTPP (a) and of CoTPP deposited on TiO₂ (b). The spectra were obtained at -196 °C after evacuation at 20 °C.

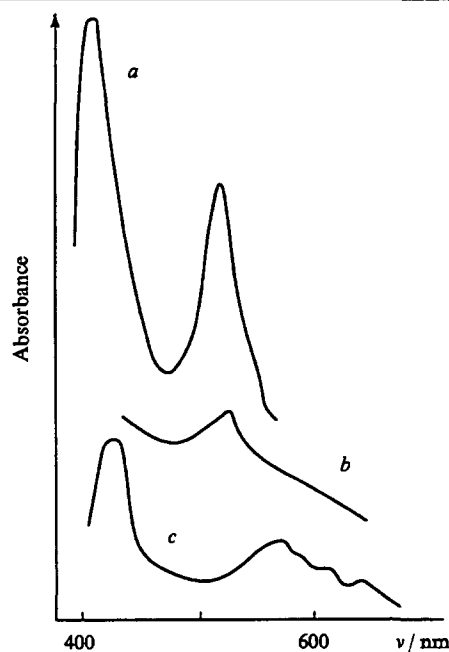
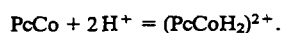


Figure 4. Electronic absorption spectra of CoTPP in benzene solution (a) and of CoTPP deposited on SiO₂ (b) and TiO₂ (c).

An XPES study of cobalt-phthalocyanine deposited on a zeolite led to the conclusion that the carrier influences mainly the nitrogen meso-atoms.⁶⁹ Instead of the narrow N 1s singlet, characteristic of PcCo, a poorly resolved doublet was noted. The Co 2p_{2/3} binding energy hardly changed after the fixation of PcCo on the zeolite. Hence it was concluded that the nitrogen meso-atoms are nonequivalent owing to the protonation of the

immobilised complexes.^{95,114} The acid centres of the carrier are protonated:



In the fixation on oxides chemisorbed water molecules may play the role of the proton-donating species.

Detailed study of the state of the oxygen in the molecular adduct with PcCo immobilised on aluminium oxide¹¹⁵ showed that Al_2O_3 activates specifically the PcCo molecule. The bond between the complex and the surface is then formed via electron transfer from the atomic orbital of the metal in the chelate unit to an unoccupied atomic orbital of a surface aluminium atom.

On passing from the multilayer to the monolayer coverage of the oxide carrier by the phthalocyanine, the catalytic activity of the immobilised PcM increases.⁷⁶ A further tenfold decrease in the PcM concentration on the carrier results in a low catalytic activity. It is noted that the molecules of different gases (CO , O_2 , H_2) are capable of dissolving in the PcM crystal lattice.⁶⁶

One of the authors of the present review investigated the kinetics of the hydrogenation of C_5 and C_{20} acetylenic alcohols on PcCo/SiO_2 (0.2% of PcCo deposited from solution in sulfuric acid) and $\text{PcNi/Al}_2\text{O}_3$ (0.2% of Ni deposited from solution in benzene).⁷⁵ On PcCo/SiO_2 , the dependence of the half-reaction time ($\tau_{0.5}$) for ethynylmethylmethanol (a C_5 acetylenic alcohol) on $q = C_0/C_c$, where C_0 is the initial alcohol concentration and C_c the catalyst concentration, passes through a minimum. The power exponent n is -0.7 and 0.2 respectively for the left- and right-hand branches of the $\tau_{0.5} \sim q^n$ relation. The half-reaction time is directly proportional to the initial concentration of ethynylmethylmethanol.

In order to specify more precisely the site where H_2 is located in the PcM molecule, sorption studies were performed.⁷⁶ The measurements were carried out in solution in hexane at 100°C . After the introduction of the adsorbent into the reaction volume with vigorous stirring sorption of H_2 was observed. The amount of nickel-phthalocyanine corresponding to 1 g of $\text{PcNi/Al}_2\text{O}_3$ is capable of absorbing 0.4×10^{-4} of a mole of H_2 (Table 1). On dividing this figure by the number of moles of nickel in the same gramme of $\text{PcNi/Al}_2\text{O}_3$ (this is equal to 0.35×10^{-4} of a mole), we obtain ~ 1.18 . Thus it is possible to postulate that the H_2 molecule binds preferentially to the central metal atom.

Table 1. The adsorption of hydrogen on Al_2O_3 and $\text{PcNi/Al}_2\text{O}_3$ at 100°C .

Adsorbent	P_{H_2} / MPa	Amount of absorbed hydrogen, $10^4 \text{ V/mol g}^{-1}$
Al_2O_3	0.1	1.07
$\text{PcNi/Al}_2\text{O}_3$ (0.2% Ni)	0.1	1.47
	10.1	2.09
$\text{PcNi/Al}_2\text{O}_3$ (0.2% Ni) in the presence of pyridine ^a	0.1	0.82

^a The amount of pyridine introduced was 8×10^{-5} mol.

In order to test this hypothesis, the Ni atom in PcNi was shielded with pyridine. The pyridine-treated $\text{PcNi/Al}_2\text{O}_3$ sorbed hydrogen less effectively than the carrier. It is known that the pyridine introduced into the system forms an axial coordinate bond with the metal atom in the chelate unit and behaves as an electron donor in relation to the latter.^{92,93} The latter factor suggests that, like the oxygen molecule,⁴¹ the hydrogen molecule can behave as a ligand in relation to the central metal atom.

The interaction of the components of the reaction system with the nitrogen atoms of the pyrrole rings may abolish the influence of the nature of the central metal atom. For example, as a result of the strong effect of the carrier on the metal, the latter may lose the capacity to participate in the activation of hydrogen. Since $\text{PcNi/Al}_2\text{O}_3$ sorbs more hydrogen at an elevated pressure than at

atmospheric pressure (Table 1), one may postulate the coordination of H_2 also to the organic ligand. The retardation of the hydrogenation of the C_5 and C_{20} acetylenic alcohols at $P_{\text{H}_2} > 8.1$ MPa was accounted for by this factor.

The IR spectra of the initial $\text{PcNi/Al}_2\text{O}_3$ (0.2% Ni) catalyst contain absorption bands characteristic of the surface OH groups of aluminium oxide.⁷⁶ After treatment with hexane at 100°C and $P_{\text{H}_2} = 0.1$ MPa, these bands disappeared as a result of the adsorption of hexane on the carrier.¹¹⁶ In the IR spectrum of the hydrogen-treated specimen, absorption bands appeared at 1680 cm^{-1} and those at 1090 and 1165 cm^{-1} intensified (Fig. 5). Using the principle of group frequencies as a guide, the former absorption band was assigned to the vibrations of the $\text{C}=\text{N}$ bond and the last two bands were assigned to $\text{C}-\text{N}$ vibrations, although much caution must be exercised when this is done in relation to a chelate ring. The facts presented indicate that contact between the catalyst and the solvent under hydrogen weakens the interaction of the phthalocyanine ligand with the central metal atom. This may be associated with the transfer of electron density from hydrogen to the metal atom.

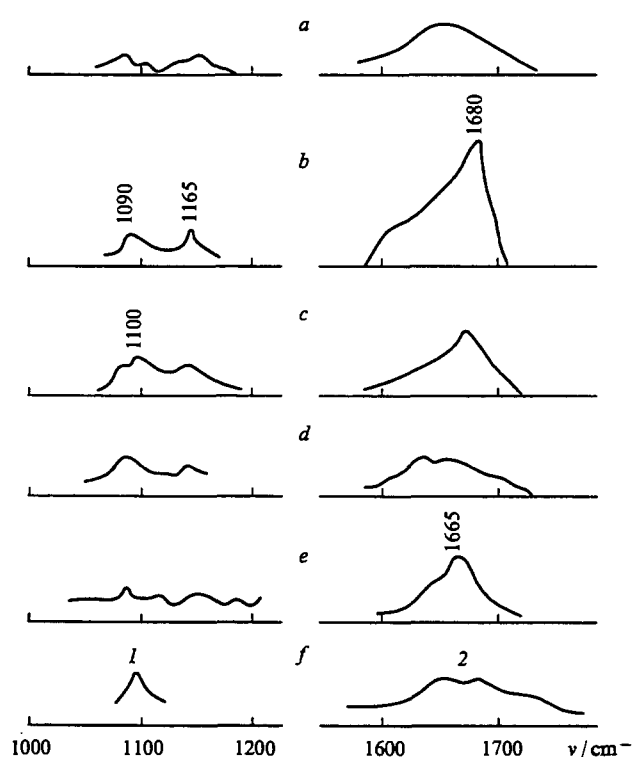


Figure 5. IR spectra of $\text{PcNi/Al}_2\text{O}_3$: (a) initial specimen; (b) specimen obtained after contact with H_2 in hexane; (c) after successive treatment with hydrogen on the C_{20} acetylenic alcohol; (d) after successive treatment with hydrogen and the C_5 acetylenic alcohol; (e) after treatment with pyridine; (f) after treatment with the C_{20} ethylenic alcohol (1) or after successive treatment with pyridine and the C_{20} acetylenic alcohol (2). Only those parts of the spectra are illustrated where a difference was observed between the specimens. The specimens for analysis were prepared as mulls in liquid paraffin.

In order to test this hypothesis, $\text{PcNi/Al}_2\text{O}_3$ was treated with pyridine which is an electron-donating extra-ligand in relation to the metal atom, after which an absorption band appears in the IR spectrum at 1665 cm^{-1} . This band was also assigned to the $\text{C}=\text{N}$ bond vibrations, the intensity of which increases as a result of the coordination. After successive treatment of $\text{PcNi/Al}_2\text{O}_3$ with hydrogen and with a C_{20} acetylenic alcohol, a decrease in the intensity of the 1680 cm^{-1} absorption band was observed, whereas the replacement of the C_{20} by the C_5 alcohol resulted in

the complete disappearance of the absorption. This suggests that acetylenic alcohols with a shorter chain are adsorbed more effectively on phthalocyanine catalysts, i.e. the series based on the adsorption capacity of alcohols, which they exhibit in relation to modified palladium catalysts, is, as it were, reversed.¹¹⁷ In addition, the acetylenic and ethylenic C₂₀ alcohols coordinated to the catalyst absorb at 1100 cm⁻¹. The 1100 cm⁻¹ absorption band is characteristic of the vibrations of the C–O bond in tertiary alcohols.¹¹⁸ Such coordination of alcohols promotes the occurrence of the dehydration reaction together with hydrogenation.

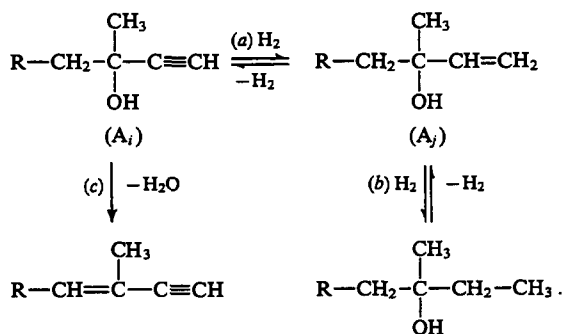
In order to elucidate the centre for the interaction of the acetylenic alcohol with PcNi, the heterogenised catalyst was treated in succession with pyridine and the C₂₀ acetylenic alcohol. This resulted in the disappearance of the absorption at 1665 cm⁻¹. The nickel in the specimen treated in this way was shielded by pyridine and the substrate could be coordinated only to the organic ligand in the PcM, namely to the nitrogen *meso*-atoms. After treatment with pyridine, the catalyst did not exhibit an activity in the hydrogenation of the C₂₀ acetylenic alcohol at 100 °C and P_{H₂} = 0.1 MPa. This can be explained by the impossibility of activating hydrogen on such a catalyst.

No changes are observed after the adsorption of substrates in the IR spectra of the PcCo/SiO₂ catalyst prepared by the adsorption on SiO₂ of cobalt-phthalocyanine from solution in concentrated sulfuric acid. This is caused mainly by the low PcCo concentration (0.2%) on the carrier surface. At this PcCo concentration on the silica gel surface (specific surface 26 m² g⁻¹), the coverage should amount to ~15% of the monolayer coverage and should consist of isolated patches. We may note that even for the 1.5-layer coverage, the molecular PcCo is deposited nonuniformly on silica gel.¹⁰⁵

The apparent activation energy for the hydrogenation of the C₂₀ acetylenic alcohol on PcCo/SiO₂ was approximately 2.3 times smaller than for the hydrogenation of the C₅ acetylenic alcohol, which has been attributed to the different adsorption capacities of these alcohols.

* * *

Thus it has been established by kinetic, adsorption, and IR spectroscopic methods that hydrogen and the acetylenic alcohol are coordinated at different active centres of the immobilised metal-phthalocyanine. The conversion of acetylenic alcohols on phthalocyanine complexes of metals, attached to oxide carriers, can be represented by the following scheme:



If it is supposed that hydrogen and the substrate are activated on different active centres (Z and Z'), then reaction (a) should include the following stages:



where A_i is the substrate and K_i, K_m, and K_n are the equilibrium constants of stages (1), (2), and (3) respectively. The surface reaction must be reversible:



where k₄ and k₋₄ are the forward and reverse rate constants for stage (4) respectively, whilst K_j is the equilibrium constant of stage (5). It is assumed that stages (1), (2), (3), and (5) are fast.

In addition account must be taken of the adsorption of the solvent (hexane) on the carrier and on the PcM.

It is postulated that the substrate and the solvent are adsorbed on the same active centres Z':



where Solv is the solvent and k₆ and k₋₆ are the forward and reverse rate constants for stage (6).

If account is taken only of the adsorption of the solvent and the occurrence of stage (5) in the reverse direction is neglected, then the rate of the reaction under static conditions can be described by the following kinetic equation:

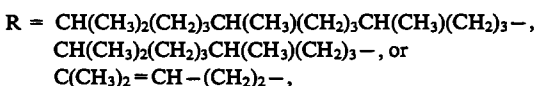
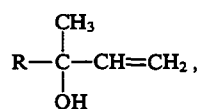
$$W = \frac{k_4 k_{-6} K_i K_m K_n Z'_0 C_a C_H^2}{k_k C_{\text{Solv}}}$$

where C_a, C_H, and C_{Solv} are the concentrations of the acetylenic alcohol, hydrogen, and the solvent respectively and Z'₀ is the total number of active centres for the adsorption of the substrate or the solvent.

If the catalyst concentration C_c is constant and the hydrogenation takes place in concentrated solutions, account must be taken only of the adsorption of the acetylenic alcohol. The rate of reaction can then be represented in the form

$$W = k_4 K_m K_n C_k C_H^2$$

The above investigation led to the development of a procedure for the preparation of ethylenic alcohols having the general formula



by the hydrogenation of the corresponding acetylenic alcohols in the presence of PcM on Al₂O₃ or SiO₂ in an organic solvent.⁷⁶ The yield of the ethylenic alcohols reaches 99.2%–99.8%.

The following general features are characteristic of the selective hydrogenation of acetylenic alcohols on PcM immobilised on inorganic carriers: (a) the process takes place via an intermediate heteroligand complex (solvent–substrate–hydrogen–catalyst–carrier)¹¹⁹ which has a 'multistory' structure; (b) the nature and amount of the components of the complex influence the catalytic activity of the PcM and the process selectivity; (c) the reactants are activated on different active centres ('metallic' and 'organic'). The catalytic system under discussion should be regarded as homogeneous-heterogeneous, which is confirmed by the nonlinear relations between the rates of the reactions and the ratio of the concentrations of the components of these reactions.

By virtue of their unusual properties, metal-phthalocyanines are promising catalysts of many processes.¹⁰³ The immobilisation of the PcM on carriers makes it possible to achieve the maximum catalytic activity per unit mass of the active phase and to regulate the mode of reaction of the substrate. The catalytic activity exhibited by both the central metal atom and the atoms of the organic ligand in the PcM confirms the hypothesis¹²⁰ that 'organometallic' active centres are formed on deposited palladium catalysts and that the substrate and hydrogen are activated separately on centres of different nature.

References

1. P Karrer *Lehrbuch der Organischen Chemie* (Translated into Russian; Leningrad: Goskhimizdat, 1960)
2. D Nenitescu *Chimie Organica de Costin* Vol. 2 (Translated into Russian; Moscow: Izd. Inostr. Lit., 1963)
3. Jpn. Appl. 1 292 066; *Ref. Zh. Khim.* 4 N 252P (1992)
4. Fr. Appl. 2 634 464; *Ref. Zh. Khim.* 4 N 253P (1992)
5. V A Perfil'ev, E A Venediktov, in *5-ya Vsesoyuz. Konferentsiya po Koordinatsionnoi i Fizicheskoi Khimii Porfirinov (Tez. Dokl.)* [The Fifth All-Union Conference on Coordination and Physical Chemistry of the Porphyrins (Abstracts of Reports)] (Ivanovo: Chemical Engineering Institute, 1988) p. 151
6. A H Cook *J. Chem. Soc.* 1761 (1938)
7. P Moser, A L Thomas *J. Chem. Educ.* 41 245 (1964)
8. L M Il'ina, Candidate Thesis in Chemical Sciences, Moscow State University, Moscow, 1974
9. H Kropf *Ann. Chim. (Paris)* 637 73 (1960)
10. H Kropf *Ann. Chim. (Paris)* 637 111 (1960)
11. J M Van Tilborg, A D Vreugdenhi *Tetrahedron* 31 2825 (1975)
12. T I Andrianova, A I Sherle, A A Berlin *Izv. Akad. Nauk SSSR, Ser. Khim.* 531 (1973)
13. S Z Roginskii *Elektronnye Yavleniya v Geterogennom Katalize* (Electronic Phenomena in Heterogeneous Catalysis) (Moscow: Nauka, 1975)
14. S D Levina, T I Andrianova, M M Sakharov *Zh. Fiz. Khim.* 40 1229 (1966)
15. T Hara, V Ohkatsu, T Osa *Chem. Lett.* 103 (1973)
16. T Hara, V Ohkatsu, T Osa *Bull. Chem. Soc. Jpn.* 48 85 (1975)
17. F Shtainbakh *Kinet. Katal.* 16 1094 (1975)
18. V E Errero-Palensuela, S A Borisenkova, V A Seleznev, A V Artemov *Vestn. Mosk. Univ., Ser. 2, Khim.* 19 714 (1978)
19. S A Borisenkova, A V Artemov, V V Kurylev, in *Materialy 4-go Sovetsko-Frantsuzskogo Seminara po Katalizu* (Proceedings of the Fourth Soviet-French Seminar on Catalysis) (Tbilisi: Institute of Physical Chemistry of the Academy of Sciences of the Georgian SSR, 1978) p. 96
20. V E Errero-Palensuela, A V Artemov, S A Borisenkova *Vestn. Mosk. Univ., Ser. 2, Khim.* 20 471 (1979)
21. V Ragaini, P Carniti, C Rainaldi, F Morazzoni *Chim. Ind.* 58 473 (1976)
22. I I Ioffe, G A Zapevalov *Izv. Akad. Nauk Latv. SSR, Ser. Khim.* 430 (1977)
23. S Z Roginskii *Probl. Kinet. Katal.* 15 12 (1973)
24. I I Ioffe, G A Zapevalov, in *Katalizatory, Soderzhashchie Nanesennye Kompleksey (Materialy Vsesoyuz. Soveshchaniya)* [Catalysts Containing Deposited Complexes (Proceedings of All-Union Conference)] (Novosibirsk: Institute of Catalysis, Siberian Branch of the Academy of Sciences of the USSR, 1978) p. 203
25. V Ohkatsu, T Hara, T Osa *Bull. Chem. Soc. Jpn.* 50 696 (1977)
26. S Paquot, F Goursak *Bull. Soc. Chim. Fr.* 17 172 (1950)
27. C Paquot *C. R. Hebd. Seances Acad. Sci.* 209 171 (1939)
28. N I Ionescu, D Popescu *Rev. Roum. Chim.* 27 481 (1982)
29. C Paquot *Bull. Soc. Chim. Fr.* 12 450 (1945)
30. A D Simonov, N N Kundo, E Kh Mamaeva, L A Akimova *Zh. Prikl. Khim.* 50 307 (1977)
31. A D Simonov, I P Keier, N N Kundo *Kinet. Katal.* 14 988 (1973)
32. N N Kundo, I P Keier *Zh. Fiz. Khim.* 42 1352 (1968)
33. S A Borisenkova, E P Denisova, T A Danilova, O I Kozunenkov *Issledovanie Okisleniya Nekotorykh Serosoderzhashchikh Soedinenii v Prisutstvii Ftalotsianinovyykh Kompleksov* Moscow, 1969 (Investigation of the Oxidation of Some Sulfur-Containing Compounds in the Presence of Phthalocyanine Complexes, Moscow, 1969) Article deposited at the All-Union Institute of Scientific and Technical Information (VINITI) No. 1802-74 (1974)
34. V S Pozii, S A Borisenkova, in *6-aya Vsesoyuz. Nauch. Konferentsiya po Okisleniyu Organicheskikh Soedinenii v Zhidkoi Faze "Okislenie-86" T. 2 (Tez. Dokl.)* [The Sixth All-Union Scientific Conference on the Oxidation of Organic Compounds in the Liquid Phase 'Oxidation-86' Vol. 2 (Abstracts of Reports)] (L'vov: L'vov University, 1986) p. 89
35. I Mochida, K Takeyashi, H Fujitsu, K Takashita *Chem. Lett.* 327 (1976)
36. B V Romanovskii, R E Mardaleishvili, V Yu Zakharov *Kinet. Katal.* 18 255 (1977)
37. S Naito, K Tamaru *Z. Phys. Chem.* 94 150 (1975)
38. V Yu Zakharov, O M Zakharova, B V Romanovskii, R E Mardaleishvili *React. Kinet. Catal. Lett.* 6 133 (1977)
39. V Yu Zakharov, O M Zakharova, B V Romanovskii, R E Mardaleishvili *Vestn. Mosk. Univ., Ser. 2, Khim.* 19 137 (1978)
40. S A Borisenkova, L M Il'ina, A P Rudenko *Zh. Fiz. Khim.* 50 1712 (1976)
41. V E Errero-Palensuela, S A Borisenkova, P I Nekrasov *Issledovanie Prevrashchenii Izopropilovogo Spirta v Prisutstvii Katalizatorov Tetraizoporfirinovogo Ryada* Moscow, 1979 (Investigation of the Conversions of Isopropyl Alcohol in the Presence of Catalysts of the Tetraizoporphyrin Series, Moscow, 1979) Article deposited at the All-Union Institute of Scientific and Technical Information (VINITI) No. 1105-79 (1979)
42. F Steinbach, K Hiltner *Z. Phys. Chem.* 83 126 (1973)
43. V Yu Zakharov, Author's Abstract of Candidate Thesis in Chemical Sciences, Moscow State University, Moscow, 1977
44. A Wolberg, J Manassen *J. Am. Chem. Soc.* 92 2982 (1970)
45. J Manassen, A Bar-Ilan *J. Catal.* 17 86 (1970)
46. A Bar-Ilan, J Manassen *J. Catal.* 33 68 (1974)
47. C B Gudkov, Author's Abstract of Candidate Thesis in Chemical Sciences, Moscow State University, Moscow, 1981
48. O L Kaliya, N A Kuznetsova, in *Naukoemkie Khimicheskie Tekhnologii (Materialy II Mezhdunar. Konferentsii) Moscow, 1994* [Chemical Technologies with a High Scientific Content (Proceedings of the Second International Conference) Moscow, 1994] p. 28
49. S A Borisenkova, N E Davidenko, A P Rudenko, in *Katalizatory, Soderzhashchie Nanesennye Kompleksey (Materialy Vsesoyuz. Soveshchaniya)* [Catalysts Containing Deposited Complexes (Proceedings of All-Union Conference)] (Novosibirsk: Institute of Catalysis, Siberian Branch of the Academy of Sciences of the USSR, 1980) p. 129
50. A A Balandin, V I Spitsyn, A P Rudenko, A P Dobrosel'skaya *Kinet. Katal.* 8 808 (1967)
51. J H Kropf *Chem. Eng. Technol.* 36 759 (1964)
52. V A Grin, S N Pobedinskii, in *Voprosy Kinetiki i Kataliza (Mezhvuz. Sb. Nauch. Trudov)* [Problems of Kinetics and Catalysis (Intercollege Collection of Scientific Reports)] (Ivanovo: Ivanovo Chemical Engineering Institute, 1979) p. 66
53. H Kropf, S K Ivanov, R Direks *Ann. Chim. (Paris)* 2046 (1974)
54. H Kropf, S K Ivanov, I Zink *Ann. Chim. (Paris)* 2055 (1974)
55. H Kropf, J Spangenberg, A Hofer, H Wenk *Ann. Chim.* 1242 (1974)
56. P K Tarasenko, S A Borisenkova, V A Novikov *Vestn. Mosk. Univ., Ser. 2, Khim.* 20 380 (1979)
57. H Kropf, J Spangenberg, A Gunst, J Hinrichsen *Ann. Chim. (Paris)* 1242 (1980)
58. S V Vul'fson, O L Kaliya, O L Lebedev, E A Luk'yanets *Zh. Fiz. Khim.* 10 1757 (1974)
59. I Mochida, A Yasutake, H Fujitsu, K Takeshita *J. Phys. Chem.* 86 3468 (1982)
60. S N Pobedinskii, A A Trofimenko, L R Bychkova *Izv. Vyssh. Uchebn. Zaved., Khim. Khim. Tekhnol.* 26 316 (1983)
61. I Okura, N Kim-Thuan, T Keii *J. Mol. Catal.* 5 293 (1979)

62. US P. 4 992 602; *Ref. Zh. Khim.* 4 N 18P (1992)
63. F Steinbach, M Zobel *Z. Phys. Chem.* 111 113 (1978)
64. D M Wagnerova, E Schwertnerova, I Verek-Siska *Collect. Czech. Chem. Commun.* 38 756 (1973)
65. S Tanaka, T Onishi, K Tamaru *Bull. Chem. Soc. Jpn.* 41 2557 (1968)
66. N I Ionescu, P Popescu *Rev. Chim. (Bucharest)* 34 18 (1983)
67. I Mochida, K Setsugu, H Fujitsu, K Takeshita *J. Phys. Chem.* 87 1524 (1983)
68. O M Zakharova, Author's Abstract of Candidate Thesis in Chemical Sciences, Moscow State University, Moscow, 1982
69. Russ. P. 1 703 650; *Byull. Izobret.* (1) 114 (1992)
70. E S Spiro, G V Antoshin, O P Tkachenko, Kh M Minachev, in *Structure and Reactivity of Modified Zeolites* (Amsterdam, 1984) p. 31
71. M R Tarasevich, K A Radyushkina *Kataliz i Elektrokataliz Metalloporfirinami* (Catalysis and Electrocatalysis by Metalloporphyrins) (Moscow: Nauka, 1982)
72. E B Fleischer, M Krishnamurthy *J. Am. Chem. Soc.* 94 1382 (1972)
73. S Naito, M Ichikawa, K Tamaru *J. Chem. Soc., Faraday Trans.* 68 1451 (1972)
74. E M Sul'man, Doctoral Thesis in Chemical Sciences, Institute of Organic Chemistry, Academy of Sciences of the USSR, Moscow, 1989
75. E M Sul'man *Usp. Khim.* 63 981 (1994) [*Russ. Chem. Rev.* 63 923 (1994)]
76. E M Sul'man, Author's Abstract of Doctoral Thesis in Chemical Sciences, Institute of Organic Chemistry, Academy of Sciences of the USSR, Moscow, 1989
77. E M Sul'man, B V Romanovskii, T V Ankudinova, I Yu Tyamina, S P Dorozhko, O S Popov, in *5-ya Vsesoyuz. Konferentsiya po Koordinatsionnoi i Fizicheskoi Khimii Porfirinov (Tez. Dokl.)* [The Fifth All-Union Conference on Coordination and Physical Chemistry of the Porphyrins (Abstracts of Reports)] (Ivanovo: Chemical Engineering Institute, 1988) p. 207
78. USSR P. 1 401 672; *Byull. Izobret.* (21) 270 (1988)
79. S Sakaki, S Mitarai, K Onkubo *Chem. Lett.* 195 (1991)
80. C E Dent, R P Linstead, A R Cove *J. Chem. Soc.* 1039 (1934)
81. J M Robertson, J Woodward *J. Chem. Soc.* 219 (1937)
82. J M Robertson, J Woodward *J. Chem. Soc.* 36 (1940)
83. J H Shap, M Lardon *J. Phys. Chem.* 72 3230 (1968)
84. A I Sidorov, I P Kotlyar *Opt. Spektrosk.* 11 175 (1961)
85. B D Berezin *Koordinatsionnye Soedineniya Porfirinov i Ftalotsionina* (Coordination Compounds of the Porphyrins and Phthalocyanine) (Moscow: Nauka, 1978)
86. T V Silina, B G Aristov *Zh. Vses. Khim. O-va im D I Mendeleeva* 19 77 (1974)
87. A Miyazawa, J Tsutsui, S Yoshitomi, T Sato, Y Yoshimura, H Shimada, N Matsubayashi, A Nishijima *J. Jpn. Petrol. Inst.* 36 291 (1993)
88. S Z Roginskii, M M Sakharov *Zh. Fiz. Khim.* 42 1331 (1968)
89. A M Schaffer, M Gouterman, E R Davidson *Theor. Chim. Acta* 30 9 (1973)
90. V G Maslov *Teor. Eksp. Khim.* 16 93 (1980)
91. K Sakamoto, J Sonobe, F Shibamiya *J. Jpn. Soc. Colour Mater.* 63 385 (1990)
92. F Cariati, D Galizzioli, F Marazzoni, C Busetto *J. Chem. Soc., Dalton Trans.* 556 (1975)
93. F A Walker *J. Am. Chem. Soc.* 95 1154 (1973)
94. N Kawashima, T Suzuki, K Meguro *Bull. Chem. Soc. Jpn.* 49 2029 (1976)
95. B V Romanovskii, in *5-i Mezhdunar. Simpozium po Svyazi Mezdu Gomogennym i Geterogennym Katalizom (Tez. Dokl.)* [The Fifth International Symposium on the Relation between Homogeneous and Heterogeneous Catalysis (Abstracts of Reports)] (Novosibirsk: Institute of Catalysis, Siberian Branch of the Academy of Sciences of the USSR, 1986) Vol. 2, Part 1, p. 40
96. Y Ogata, K Marumo, T Kwan *Chem. Pharm. Bull.* 17 1194 (1969)
97. A E Cahill, H Taube *J. Am. Chem. Soc.* 73 2847 (1951)
98. J M Assour, S E Harrison *J. Phys. Chem.* 68 872 (1964)
99. K Yamamoto, T Kwan *J. Catal.* 18 354 (1970)
100. V A Novikov, Candidate Thesis in Chemical Sciences, Moscow State University, Moscow, 1978
101. T G Borisova, Candidate Thesis in Chemical Sciences, Moscow State University, Moscow, 1982
102. M Hronec, J Ilavsky *Petrochemia* 23 89 (1982)
103. O A Golubchikov, B D Berezin *Usp. Khim.* 55 1361 (1986) [*Russ. Chem. Rev.* 55 768 (1986)]
104. H Kropf, D J Witt *Z. Phys. Chem.* 76 331 (1971)
105. S A Borisenkova, A S Erokhin, V A Novikov *Zh. Fiz. Khim.* 56 2304 (1985)
106. US P. 4 913 802; *Ref. Zh. Khim.* 2 P 186P (1991)
107. T Hara *Chem. Ind. Jpn.* 37 390 (1986)
108. US P. 4 897 180; *Ref. Zh. Khim.* 2 P 187P (1991)
109. T A Maas, M Kuijer, J Zwart *J. Chem. Soc., Chem. Commun.* 86 (1976)
110. A N Frumkin, V E Kazarinov, G Ya Tsyachnaya *Dokl. Akad. Nauk SSSR* 198 145 (1971)
111. D V Sokol'skii *Gidrirovaniye v Rastvorakh* (Hydrogenation in Solutions) (Alma-Ata: Izd. Akad. Nauk Kaz. SSR, 1962)
112. D Gassan, S A Borisenkova, A N Pryakhin *Adsorbtsionnye Ftalotsianinovyie Katalizatory: Metody Polucheniya, Struktura i Kataliticheskaya Aktivnost'. Sistema PcCo-SiO₂* (Adsorption Phthalocyanine Catalysts: Methods of Preparation, Structure, and Catalytic Activity. The PcCo-SiO₂ System, Moscow, 1983) Article deposited at the All-Union Institute of Scientific and Technical Information (VINITI) No. 5343-83 (1983)
113. I Mjchida, K Isuji, K Setsugu *J. Phys. Chem.* 84 3159 (1980)
114. U Ahrens, H Kuhl *Z. Phys. Chem.* 37 1 (1963)
115. M Barzaghi, T Beringhelli, F Morazzoni *J. Mol. Catal.* 14, 357 (1982)
116. A G Kiselev, V I Lygin *Infrakrasnye Spektry Poverkhnostnykh Soedinenii* (Infrared Spectra of Surface Compounds) (Moscow: Nauka, 1972)
117. E M Sulman, O S Popov, A Yermakova, A A Belyaev *React. Kinet. Catal. Lett.* 36 59 (1988)
118. K Nakanishi *Infrared Absorption Spectroscopy* (Translated into Russian; Moscow: Mir, 1965)
119. E I Klabunovskii, A A Vedenyapin *Asimmetricheskii Kataliz. Gidrogenizatsiya na Metallakh* (Asymmetric Catalysis. Hydrogenation on Metals) (Moscow: Nauka, 1980)
120. A I Sidorov, E M Sul'man, L M Bronshtein, T V Ankudinova, Yu E Avtushenko *Kinet. Katal.* 34 87 (1993)

Prospects for the development of methods for the processing of organohalogen waste. Characteristic features of the catalytic hydrogenolysis of halogen-containing compounds

L N Zanaveskin, V A Aver'yanov, Yu A Treger

Contents

I. Introduction	617
II. Comparative characteristics of the methods for the processing and detoxification of organohalogen waste	617
III. Hydrogenolytic methods. Prospects for their development	618
IV. Catalytic systems for hydrogenolysis. The kinetics and mechanisms of the reactions	619

Abstract. Comparative characteristics of methods for the processing and detoxification of organohalogen waste are described. It is shown that the catalytic hydrogenolysis method is the most promising. Numerous catalytic systems used for hydrogenolysis are examined, the influence of the dispersity of the catalysts on their activity is discussed, and data concerning the kinetics and mechanisms of these reactions as well as the possible elementary reactions occurring on the catalyst surface are analysed. Also discussed are the factors determining the reactivity of the C–Hal bonds in the hydrogenolytic reactions. The bibliography includes 159 references.

I. Introduction

One of the most acute problems in the creation and organisation of low-waste ecologically safe industries producing organohalogen compounds involves the processing and detoxification of the waste. An unpleasant feature of this waste is that in almost all cases they are xenobiotics, i.e. products which have no analogues in nature, and there are no natural means of combating them. On the other hand, not all the procedures for the conversion of organohalogen compounds can be used for their utilisation and detoxification. The severe ecological and economic limitations imposed on modern industries producing organohalogen substances give rise to a series of requirements as regards procedures for the treatment of waste from these industries. Such requirements include the renewability of the carbon-containing raw materials or a high commercial value of the products formed, the economic viability of the treatment, a high degree of conversion, the universality of the procedure, and the lack of toxic substances among the products. The prospects for the development of methods for the processing of organohalogen waste should be considered in the light of these requirements.

II. Comparative characteristics of the methods for the processing and detoxification of organohalogen waste

A large proportion of the existing methods for the processing and detoxification of waste from industries producing halogen-containing substances have to some extent exhausted their possibilities. In particular, the disruptive effect of tetrachloromethane on the Earth's ozone layer, discovered in recent years,^{1,2} gives rise to the problem of gradually winding-down the output of industrial chlorolysis, which is a source of this product together with tetrachloroethene. This requirement of the Montreal Protocol^{3,4} is not excessive, since the existing industrial capacity greatly exceeds the need for tetrachloroethene,^{2,5,6} while better technologies have been developed for alternative industrial processes for the production of this substance.^{5,7}

The method for the detoxification of organohalogen waste with the aid of thermal combustion is also unsuitable nowadays, since it leads to the formation of highly toxic products such as chlorine, nitrogen oxides, phosgene, and dioxins.^{1,8–11} Furthermore, thermal combustion requires a large consumption of fuel and gives rise to the irreversible loss of the hydrocarbon raw material, the evolution of carbon dioxide into the environment, and rapid wear of the equipment. The effectiveness of the method for the detoxification of toxic waste in dilute gases is low.^{1,8–12}

The catalytic combustion method is free from the majority of the above deficiencies.^{5,8,12,13} However, despite the notable progress in the development of new catalytic systems for the combustion of organohalogen waste, the range of substances susceptible to detoxification remains comparatively narrow.^{8,14} Evidently this method cannot be regarded as promising, since the irreversible loss of raw material resulting from its application does not conform to the concept of low-waste technologies.

The gas-phase thermal and catalytic dehydrochlorination processes are more attractive^{1,5,8,15–17} because they lead to the possibility of the transformation of organohalogen waste into useful products. However, the range of practical applications of these methods is significantly limited, which is associated either with the lack of demand for the dehydrochlorination products or with the impossibility of achieving the process in principle. In particular, chloromethanes, chlorobenzenes, and chlorobiphenyls cannot serve as the dehydrochlorination objects.

Hydrodehalogenation or hydrogenolysis may be regarded as the most universal and promising method for the treatment and detoxification of organohalogen waste.^{1,2,6,9–12,18–56} Together with ecological safety, it ensures in many instances the regeneration of the initial raw material, which may open a path to the

L N Zanaveskin, Yu A Treger The 'Sintez' Research Institute, Ugreshskaya ul. 2 a/Box 56, 109432 Moscow, Russian Federation. Fax (7-095) 913 92 43. Tel. (7-095) 279 84 09 (L N Zanaveskin), (7-095) 279 85 63 (Yu A Treger)
V A Aver'yanov Department of Chemistry, Tula State Technical University, prosp. Lenina 92, 300600 Tula, Russian Federation. Tel. (7-087) 225 78 09

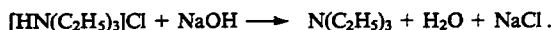
Received 14 September 1995

Uspekhi Khimii 65 (7) 667–675 (1996); translated by A K Grzybowski

creation of low-waste technologies.[†] The regeneration of the raw material from the waste in the industrial production of vinyl chloride and chlorobenzene can serve as an example,^{55, 57, 58} chlorobenzene itself being regenerated in the latter case.^{23, 57-59} In certain cases, hydrogenolysis leads to the formation of useful products which can be used in related industries. Thus the organochlorine waste from the industrial production of *sym*-tetrachloroethane and vinyl chloride based on ethyne may be subjected to thermal hydrogenolysis with formation of gaseous ethyne, ethene, and hydrogen chloride.³⁸ After the absorption of the latter, the hydrogenolysis gases can be combined with the pyrolysis ethyne and directed to the stage in which pure ethyne is isolated. If catalytic hydrogenolysis is used in the treatment designed for the preferential formation of ethane, then the hydrogenolysis gases formed can be directed, after the absorption of hydrogen chloride from them, to the natural gas line, which proceeds to the stage in which pyrolysis ethyne is obtained. Finally, when the hydrocarbons formed as a result of hydrogenolysis cannot be returned to the technological cycle, their employment as a fuel is most rational.¹⁰ The likely usefulness of hydrogenolysis as a detoxification method is emphasised by the recently published data concerning the conversion of polychlorodibenzodioxins, polychlorodibenzofurans, and polychlorobiphenyls into ecologically safe products.⁶⁰

As regards hydrogen chloride, there are two possibilities for its utilisation. The first consists in the preparation of nongaseous hydrochloric acid. This procedure is effective in the exhaustive hydrogenolysis of C₁-C₄ organochlorine compounds, since gaseous organic products sparingly soluble in water are formed, which guarantees a high quality of the acid obtained. The second possibility presupposes the use of hydrogen chloride as the reactant in hydroxychlorination and hydrochlorination processes. This variant is more suitable for hydrogenolytic processes in which liquid organic products are formed: in this case, the hydrochloric acid formed on absorption of gases is contaminated by organic impurities and there is no commercial demand for it. An example of the use of recovered hydrogen chloride as the reactant is provided by the hydroxychlorination of benzene to chlorobenzene.¹⁶

The Exxon Company has proposed a very interesting procedure for the utilisation of the hydrogen chloride obtained in the hydrogenolysis of chlorobenzenes: the hydrogen chloride is extracted from the reaction products treating them with triethylamine⁶¹ and the resulting salt [HN(C₂H₅)₃]Cl is treated with aqueous alkali:



This regenerates triethylamine, which is returned to the technological cycle. Evidently this version of the binding of hydrogen chloride is most effective if the production of organochlorine substances is combined with the production of chlorine and sodium hydroxide in which sodium chloride serves as the raw material.

The principal advantage of the hydrogenolytic processes is the possibility of a flexible selection of the optimum type of treatment of the waste by varying the process parameters, the catalytic or initiating system, the reaction medium, and the hydrogen donors. The practical use of hydrogenolysis for the treatment of waste is not restricted to halogen-containing compounds and this method has been tested successfully on nitrogen-, sulfur-, and oxygen-containing compounds,^{15, 44, 45, 62-74} including the processes for the detoxification of sulfur and nitrogen oxides and CO.^{75, 76} The importance of the hydrogenolytic processes for the detoxification of organoelement compounds, the combustion of which leads to the formation of a series of many highly toxic products, such as

Cl₂, Br₂, sulfur and nitrogen oxides, dioxins, etc., giving rise to new acute ecological problems, must be specially emphasised.

Apart from hydrocarbons, the hydrogenolysis products include hydrogen compounds of the halogens, sulfur, and nitrogen, having distinctly acid or basic properties, which facilitates their extraction by sorption methods. The universality of hydrogenolysis as a method for the detoxification of waste has been confirmed by its effectiveness in the removal of organoelement impurities from waste water and technological gases.^{32, 40, 75, 77-80}

On the other hand, certain hydrogenolytic processes are of independent importance as a method of synthesis of valuable products on an industrial or preparative scale. This applies to the preparation of fluorohydrocarbons by the hydrogenolysis of the corresponding chlorofluorohydrocarbons^{22, 36, 48} and of nitrobenzenes from chloronitrobenzenes,⁸¹ the synthesis of substituted anilines,⁸² the conversion of aliphatic esters into higher alcohols,⁸³⁻⁸⁷ and the synthesis of sterically strained amines,⁸⁸ purine,⁴⁹ and other preparations.^{51, 52, 89, 90}

There has been an extremely interesting communication about the use of hydrogenolysis for the isolation of pure *m*-xylene from a mixture of *m*- and *p*-xylenes.²⁵ The mixture is monochlorinated, which affords a 90% yield of 2-chloro- and 4-chloro-xylenes. The latter are readily separated by distillation and are subjected to further gas-phase hydrogenolysis on a platinum catalyst deposited on activated carbon.

Finally the possibility of converting freons into ecologically safe commercial products^{4, 91-95} is of fundamental importance for the solution of the global problem of the protection of the Earth's ozone layer.

III. Hydrogenolytic methods. Prospects for their development

Hydrogenolysis may be achieved by thermal, catalytic, and reagent procedures. This classification is to some extent arbitrary because it does not reflect the entire wide variety of the reactions underlying these processes. In particular, it is to be expected that the mechanism of the catalytic action of metals differs fundamentally from the mechanism of enzymic hydrogenolysis^{97, 98} and that the metals themselves can perform various catalytic functions depending on the type of the hydrogenolytic agent. Evidently the effect of the majority of metals on gas-phase hydrogenolytic reactions involving molecular hydrogen is determined by homolytic processes on the surface,^{30, 35, 98-105} whereas the liquid-phase catalytic reactions occurring on treatment with alcohols and with formic acid and its salts¹⁰⁶⁻¹⁰⁸ involve the transfer of a hydride anion. Published data concerning the possibility of inducing catalytic reactions involving the hydrogenolysis of organohalogen compounds by microwave radiation¹⁰⁹ constitute yet another piece of evidence for the multiplicity of these processes. In this case, the catalyst (iron oxide) accumulates the radiation energy and transfers it to the chemisorbed molecule of the organohalogen compound. The latter undergoes homolytic decomposition at the C-Cl bond and initiates the radical hydrogenolytic process. The methods involving the electrochemical reduction and reductive coupling of organohalogen compounds¹¹⁰⁻¹¹⁴ may be classified as reagent methods subject only to certain stipulations.

Among the numerous hydrogenolytic methods, the catalytic and thermal methods are of practical interest. The reagent methods, involving the use of expensive hydrogen donors such as Na + ROH, LiAlH₄, Ar₃SnH,^{25, 115-117} NaBH₄,^{63, 118-121} hydrazine,⁸⁰ Zn + protic acid,¹²² and finely dispersed zinc,¹²³ are only of preparative importance.

In the present review, attention is concentrated on the catalytic hydrogenolytic reactions of organohalogen compounds, which are of greatest practical importance and have been comparatively little investigated. The data on the hydrogenolysis of organoelement compounds are used only to reveal the general characteristic features of this group of processes.

[†] In the large-scale industrial production of organochlorine substances, the creation of autonomous treatment plant is economically justified, as has been done by the Union Carbide Company, which has announced the organisation of the treatment of waste from the production of vinyl chloride with a potential output of 10 000 tonnes annually.⁴⁰

IV. Catalytic systems for hydrogenolysis. The kinetics and mechanisms of the reactions

Numerous versions of catalytic hydrogenolysis have been described in the literature. The processes are carried out in both liquid and gas phases. The choice of catalytic systems is fairly wide. The vast majority of the reactions take place on Group IB, VB, VIB, VIIB, and VIII metals, including Pt, Pd, Rh, Ru, Ir, Os, Ni, Co, Fe, Re, Mn, Mo, W, Cr, V, Cu, Ag, and Au.

The properties of metallic catalysts, namely their activity, selective action, useful lifetime, etc. can be modified by fusion with other metals, by the introduction of promoting additives, and by varying the carrier. Catalytic systems based on the Rh-Ir,¹²⁴ Cu-Rh,¹⁸ Co-Mo,⁴⁴ Ni-W,⁴⁵ Ni-Mo,^{45, 125-128} Pd-Pt, Pd-Ga, Pd-Al, Pd-Ru,¹⁰¹ Pd-Sn, Pd-Pb, Pd-Ge, Pd-K, Pd-Fe, Pd-Co, and Pd-Ag^{93, 100, 129} bimetallic alloys have been proposed. Pd, Pt, Ru, Ir, Fe, Co, Ni, Cu, Cd, Ag, Au, V, Cr, Mo, W, Bi, Al, Hg, In, Sn, Te, Si, P, As, and Sb,^{19, 24, 92, 101, 130} aluminium, boron, and titanium salts and oxides,²⁴ phosphines and phosphates,^{5, 130} alkali and alkaline earth metal hydroxides and oxides,^{24, 29, 127} and phosphonium halides³¹ are used as promoting additives to metallic catalysts. The range of carriers for metallic catalysts is fairly wide, including activated carbon,^{80, 93, 130-139} diatomites,¹⁸ aluminium oxide,^{125-129, 135, 136} chromium oxide,¹³⁵ silicon oxide,^{9, 12, 26, 39, 99, 134} iron oxide,¹³⁵ aluminosilicates,²⁴ calcium carbonate,³⁵ zeolites,^{43, 96} and barium sulfate.⁵²

Copper,^{23, 29} palladium,^{137, 138} ruthenium, platinum, and rhodium^{138, 139} salts, chromium, iron, aluminium, nickel, and molybdenum oxides,^{60, 95, 96, 140} silicon oxide,^{9, 12, 26, 39, 99} phosphine complexes of ruthenium rhodium, and iron,^{91, 106, 108} and transition metal coenzymes, namely vitamin B₁₂ (Co), the coenzyme F₄₃₀ (Ni), and hematin (Fe)⁹⁷ merit attention among other occasionally employed catalytic systems. Vitamin B₁₂ is used successfully for the treatment of organochlorine waste (C₂H₃Cl₃, C₆H₆Cl₆, C₆H₃Cl₃, C₆Cl₆, and C₂Cl₄), F₄₃₀ is employed for the hydrodehalogenation of C₆H₅CH₂Cl, *o*-ClC₆H₄CH₂Cl, C₆H₅CH₂CH₂Br, and *p*-BrC₆H₄Br to C₆H₅CH₃, *o*-ClC₆H₄CH₃, C₆H₅CH₃, C₆H₅CH₂CH₃, and C₆H₅Br respectively by formate anions, and hematin is used in the utilisation of organoelement waste such as tetrachloromethane, hexachloromethane, *cis*- and *trans*-dichloroethenes, etc.

The theoretical principles underlying the catalytic hydrogenolysis of organohalogen compounds have been investigated inadequately, while kinetic data are scattered and contradictory. The region in which the reactions occur has been reported only in rare investigations, which to a large extent vitiates the kinetic data obtained and casts doubt on the catalytic activity^{62, 99, 141} and substrate reactivity^{30, 136} series quoted in the literature. We may note that in those studies where the region in which catalytic hydrogenolysis on metals was subjected to a detailed analysis it was not possible to obtain the kinetic region. Thus the radioisotope label method showed that, in the temperature range 193-448 K, the true picture of the chemical interaction on the surface is distorted by adsorption and diffusion factors.¹⁴² Kinetic analysis of the hydrogenolysis of chlorobenzene and 1,2-dichlorobenzene on Ni-Mo/ γ -Al₂O₃ at 275-376 °C indicates that the rate of reaction is limited by adsorption and desorption processes.

Certain investigations were devoted to the solution of practical problems — the search for formal mathematical models of the processes.^{60, 143} However, such models, which are useful for the design of reaction apparatus and the optimisation of process conditions, yield little evidence for the interpretation of the mechanism of the catalytic hydrogenolysis.

Together with the temperature variations of the rates of hydrogenolysis of ethane, methylamine, and chloromethane, the structures and dispersities of the catalyst have been investigated.^{62, 98, 141} This made it possible to give the reaction rates and the pre-exponential factors for a single surface metal atom — the catalyst active centre. The variations in catalytic activity in the Re-Os-Ir-Pt-Au and Ru-Rh-Pd-Ag series are attributed

by the authors to the unequal capacities of ethane, methylamine, and chloromethane for sorption via the C-C, C-N, and C-Cl bonds on the surfaces of these metals.

However, the results obtained are to a large extent vitiated by the arbitrary assumptions adopted by the authors. In particular, one cannot neglect the relation between the activity of a single surface metal atom and the dispersity of the catalyst: it is well known that hydrogenolysis belongs to the class of structure-sensitive reactions, a characteristic feature of which is the dependence of the specific activity on the structure of the reaction centre.¹⁴⁵ The available data indicate a significant influence of the dispersity of the metallic catalysts on their activity in hydrogenolytic reactions.^{65, 102, 129, 145, 146}

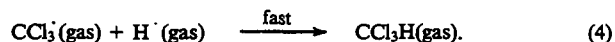
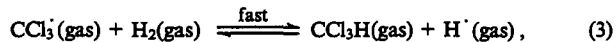
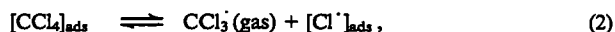
It is hardly correct to determine the activity of the catalysts of the hydrogenolysis of methylamine from the rates of formation of methane and ammonia,⁶² since the authors themselves showed that at least one other side product — (CH₃)₂NH, (CH₃)₃N, (CH₃CH₂)₂NH, or CH₃CN — is formed to an appreciable extent on the majority of the catalysts which they employed (Ru, Pd, Rh, Ag, Re, Os, Pt, Ir, Au). Since the contributions of the main and side reactions depend on temperature, the attempt to determine the activation parameters does not yield reliable results and the observed isokinetic relation between the rates of these reactions cannot serve as an argument in support of a common mechanism of the hydrogenolysis of ethylamine and the side reactions complicating it on different catalytic systems.

Finally, the determination of the activities of the catalysts in the hydrogenolytic reactions of all the compounds investigated, carried out under the conditions of constant partial pressures of the substrate and hydrogen, is based on the doubtful *a priori* hypothesis that the reaction orders with respect to the reactants are equal on each catalyst. Furthermore, the presence of extrema in the catalytic activities presented above may serve as an indication that the rate-limiting stage of the process may also vary as a function of the adsorption capacity of the reactant. For a low adsorption capacity, the rate of reaction may be determined by the adsorption stage, but the greater the strength of the bonds between the chemisorbed species and the surface, the higher the rate of this stage. At the same time, the subsequent interaction of the reacting species on the surface becomes increasingly more difficult and in the limiting case it can become the stage which determines the overall rate of reaction.

The observed dependences of the reactivities of the metals on their positions in the Periodic Table can be explained also by the fact that the most favourable geometrical correspondence between the length of the chemisorption bond and the size of the unit cell of the catalyst crystal lattice is obtained in the region of the extremum.¹⁴⁷ This point of view, based on the multiplet theory of catalysis,¹⁴⁸ is confirmed by the dominant contribution of the entropy factor to the change in the specific activity of single atoms on passing from one metal to another.

The contradictory nature of the data on the kinetics of hydrogenolysis and on the catalytic activity series reflects, in our view, the complexity of the test systems due to the specificity of each catalytic system and the variations in the influence of various factors on the chemical processes occurring. The proposed reaction mechanisms are therefore valid only in specific cases and cannot be extended to other objects of hydrogenolysis. Nevertheless, from a formal point of view, the hydrogenolysis mechanisms discussed in the literature may be divided into two groups. The first group of mechanisms presupposes the adsorption of the components of the reacting systems on the catalytic surface, the interaction of the adsorbed species, and the subsequent desorption of the products from the surface (the Langmuir-Hinshelwood mechanism).^{65, 93, 126} This approach has been used to interpret data on the kinetics of the hydrogenolysis of *p*-chloronitrobenzene to *p*-chloroaniline on ruthenium and platinum catalysts.^{65, 101} A characteristic feature of the proposed mechanism is the continued adsorption of hydrogen on the catalytic surface after it has been saturated by the organic

reactant. According to the authors, the physical preconditions for this to occur are the presence of free sites on the surface owing to the strong dipole-dipole repulsion of the polar nitro-groups of the adsorbed substrate and the small size of the hydrogen molecules. A similar mechanism has been proposed for the hydrogenolysis of tetrachloromethane on the Pt/ η -Al₂O₃ catalyst.³⁵ The observed zero order of the reaction with respect to CCl₄ and the 0.5 order with respect to H₂ was justified by the authors in terms of the following scheme:



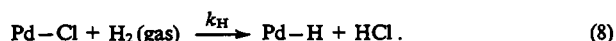
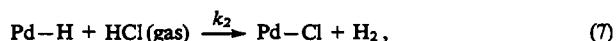
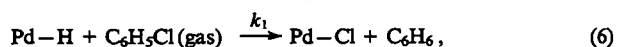
This scheme presupposes the preferential adsorption of CCl₄ on the catalyst surface:



The slight increase in the reaction orders with respect to the reactants as the temperature increases may indicate that the kinetics of the process follow the Langmuir-Hinshelwood mechanism.

Similar kinetic data have been obtained also in a study of the hydrochlorination of *cis*- and *trans*-dichloroethenes on Pt/Al₂O₃.¹³⁶ Although in view of the complexity of the systems investigated the authors themselves refrained from interpreting their data, one may suppose that the observed reaction orders with respect to the dichloroethenes indicate the adsorption saturation of the catalytic surface by the dichloroethenes and that the reaction order of 0.5 with respect to hydrogen corresponds to the dissociative nature of its adsorption.

The second group of mechanisms of catalytic hydrogenolysis is formally based on the analogy of this process with the selective oxidation reactions of hydrocarbons¹⁴⁹ and presupposes the alternate chlorination and reduction of the catalyst, which functions as a hydrogen and chlorine transferring agent between the reactants and the products.^{99, 129} This approach is based on the mechanism, proposed for the hydrogenolytic reactions of chlorobenzene on palladium-rhodium and palladium-tin alloy catalysts, which includes the following stages:



The proposed mechanism is vulnerable to criticism. Firstly, the use in it of the method of stationary concentrations leads to the kinetic equation

$$r = \frac{k_1 k_H P_{C_6H_5Cl} P_{H_2}}{k_H P_{H_2} + k_1 P_{C_6H_5Cl} + k_2 P_{HCl}}, \quad (9)$$

where $P_{C_6H_5Cl}$, P_{H_2} , and P_{HCl} are the current partial pressures of chlorobenzene, hydrogen, and hydrogen chloride respectively. The equation differs from the experimental equation

$$r = \frac{k_1 k_H P_{C_6H_5Cl} P_{H_2}^{0.5}}{k_H P_{H_2}^{0.5} + k_1 P_{C_6H_5Cl} + k_2 P_{HCl}}, \quad (10)$$

indicating a different dependence of the rate of reaction on the partial pressure of hydrogen. Secondly, the observed constants

$$k_2 > k_1 \gg k_H,$$

which follow from the mechanism proposed by the authors, are inconsistent with the available thermochemical data. Thus one should expect that the entropies of activation for reactions (6) and (7) are similar and that the difference between the constants k_1 and k_2 should be determined solely by the difference between the bond dissociation energies $D(C_6H_5-H) - D(C_6H_5-Cl) = 15.3$ kcal mol⁻¹ and $D(H-H) - D(H-Cl) = 1$ kcal mol⁻¹.¹⁵⁰ This difference between the dissociation energies should lead to the inequality $k_1 \gg k_2$, which conflicts with estimates by other workers.^{99, 129}

We believe that the kinetic data on the catalytic hydrogenolysis of chlorobenzenes presented above may be interpreted successfully within the framework of the Langmuir-Hinshelwood model. In this case, the parameters k_H , k_1 , and k_2 of Eqn (10) reflect the adsorption capacity of the components. Indeed, the high value of k_2 is inconsistent with the high polarity of hydrogen chloride and its ability to form hydrogen bonds. On the other hand, the observed dependence of the reaction rate on the partial pressure of hydrogen reflects the dissociative character of its adsorption on platinum group metals, which has been confirmed by numerous experimental data.^{144, 151}

Analysis of the kinetic data shows that they can be usually described within the framework of the Langmuir-Hinshelwood model. The conclusion concerning the dissociative character of the adsorption of hydrogen on the metal surfaces, which follows from the proportionality of the rate of the reaction (or the numerator in the kinetic equation) to $P_H^{0.5}$, is of fundamental importance. The relatively low activation energies for the overall catalytic hydrogenolytic processes (Table 1) is an additional argument in support of the dissociative adsorption of hydrogen.

Table 1. The activation energies (E /kcal mol⁻¹) for the hydrogenolytic reactions.

Reaction	Catalyst	E	Ref.
CH ₃ Cl + H ₂ → CH ₄ + HCl	Ti film	16.1	102
CH ₂ Cl ₂ + H ₂ → CH ₃ Cl + HCl	Ti film	13.4	102
CH ₂ Cl ₂ + 2H ₂ → CH ₄ + 2HCl	Ti film	13.3	102
(CH ₃) ₃ CCl + H ₂ → (CH ₃) ₃ CH + HCl	Pt film	19.0	104
(CH ₃) ₃ CCl + H ₂ → (CH ₃) ₃ CH + HCl	Pd film	18.0	104
C ₆ H ₅ Cl + H ₂ → C ₆ H ₆ + HCl	Pd/Al ₂ O ₃	25.0	129
ClHC=CHCl + H ₂ → → H ₂ C=CHCl + HCl	Pt/Al ₂ O ₃	27.5	136
CH ₃ CH ₂ F + H ₂ → C ₂ H ₆ + HF	Pd/C	12.0	30
CH ₃ CHF ₂ + 2H ₂ → C ₂ H ₆ + 2HF	Pd/C	26.0	30
CH ₃ CF ₃ + 3H ₂ → C ₂ H ₆ + 3HF	Pd/C	26.0	30

The fruitfulness of the Langmuir-Hinshelwood model is confirmed by the fact that it makes it possible to predict the inhibiting effects of the reactants and reaction products on the process and to estimate the adsorption capacities of the components. The lack of sensitivity of the hydrogenolytic reactions to the presence of acid active centres in the catalyst is apparently associated with the high adsorption capacity of hydrogen chloride: the adsorbed hydrogen chloride molecules themselves function as such centres and the contribution of the natural active centres of the catalyst to its catalytic activity becomes negligible. This may account for the failure of our attempts to modify the hydrogenolysis catalysts with alkaline reagents.

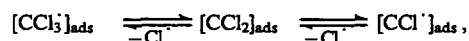
The elucidation of the nature of the elementary stages in the hydrogenolysis of haloalkanes is assisted by analysis of the composition of the products and by special studies of the mechanisms of these reactions. Evidently the substitution of the halogen by hydrogen requires the preliminary dissociation of carbon-halogen bonds. The preferential dissociation of these particular bonds is due to thermodynamic factors, which follow from the comparatively low C-Hal bond energies¹⁵⁰ and high metal-Hal bond energies. This is in fact the driving force of the chemisorption of haloalkanes. The nature of the dissocia-

tion of the C–Cl bonds on the catalytic surface has been investigated in a study¹⁰² devoted to the hydrogenolysis of chloromethane and dichloroethane on titanium, palladium, and other metallic films. The use of the ¹³C and ³⁵Cl isotopes made it possible to establish that the dissociation of the C–Cl bonds is irreversible. It was shown in the same study that the rate of deuterium exchange involving chloroalkanes is negligible compared with the rate of hydrogenolysis. A similar result had been obtained earlier in a study of the hydrogenolysis of chloroethane, bromoethane, and *tert*-butyl chloride on sputtered platinum and palladium films.^{103, 104} The composition of the products formed in the hydrogenolysis of halohydrocarbons shows that the dissociation of the C–Cl bonds is not accompanied by the synchronous attack on the latter by an adsorbed hydrogen atom or another surface intermediate and is an independent elementary stage leading to the formation of surface radicals. The latter, which are kinetically independent species, are involved in further interactions, affording various products depending on the conditions and the type of catalytic system. This is confirmed by the formation of polymerisation products together with the products of the direct substitution of the halogen by hydrogen.

The following types of interactions involving the surface radicals formed as a result of the primary dissociation of the carbon–halogen bonds are possible.

1. Radical recombination reactions. The possibility of these interactions is confirmed by the formation of hexachloroethane as one of the products of the hydrogenolysis of tetrachloromethane on nickel–zeolite catalysts and Pd–Pt, Pd–Ga, Pd–Al, and Pd–Ru metallic alloy membranes.^{43, 101} Tetrafluoroethene is also formed in the hydrogenolysis of difluoromethane on deposited Pd–Fe and Pd–Co catalysts.⁹³ We regard the appearance as a result of the hydrogenolysis of products containing twice the number of carbon atoms compared with the initial organic reactant as a result of the recombination of surface radicals. The observed discrepancy between the degrees of substitution of the carbon atoms in the primary fragments formed and in the recombination products is a consequence of the conversion of the primary fragments into new surface radicals with the same number of carbon atoms. Thus the formation of 1,1,1,2-tetrachloroethane as the product of the hydrogenolysis of tetrachloromethane on Ni–zeolite catalysts⁴³ should be regarded as the result of the recombination of the surface radicals $[\text{CCl}_3]_{\text{ads}}$ and $[\text{CH}_2\text{Cl}]_{\text{ads}}$, the latter being the product of the conversion of the $[\text{CCl}_3]_{\text{ads}}$ radical.

2. Reactions involving the elimination of chlorine radical species. One of the variants of the conversion of the surface radical $[\text{CCl}_3]_{\text{ads}}$ into the radical $[\text{CH}_2\text{Cl}]_{\text{ads}}$ may involve preliminary dechlorination with elimination of a chlorine radical species, i.e.



and the subsequent interaction of the adsorbed fragment with hydrogen. This view, put forward by Mishchenko and Senina,¹⁰⁰ makes it possible to account for the formation of appreciable amounts of methane even at low degrees of conversion under the conditions of the hydrogenolysis of tetrachloromethane. Methane is formed as the dominant substitution product also in the hydrogenolysis of difluoromethane.⁹³ Unique data have been obtained in a study⁴³ where it was shown that the hydrogenolysis of tetrachloromethane on Pt/η-Al₂O₃ leads to the exclusive formation of chloroform and methane with a constant ratio $[\text{CHCl}_3]/[\text{CH}_4]$ over the entire range of degrees of conversion. This result apparently reflects the specificity of the catalytic system employed by the authors as regards the adsorption and reactivity of the intermediate radicals responsible for the formation of CHCl_3 and CH_4 . The hydrogenolytic reactions of polyhalohydrocarbons are evidently consecutive in character.^{19, 30, 41, 136}

3. Radical hydrogenation reactions. The hydrogenation of the surface radicals leads naturally to the formation of hydrogenolysis products. This has been demonstrated kinetically in studies^{93, 102} where an increase in the proportion of the hydrogenolysis

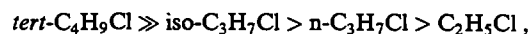
products with increase in the hydrogen concentration was established. The participation of the surface radicals in the hydrogenolytic reaction was confirmed directly by the study of the deuteration of chloroalkanes.^{102–104} On the one hand, the isotopic composition of the alkane formed indicates the structure of the surface radical involved in the hydrogenation and, on the other, it shows that this radical is indeed hydrogenated by hydrogen (deuterium).

4. Reactions involving the elimination of hydrogen atoms. By combining reactions (1)–(3), it is possible to obtain a wide variety of products of the catalytic hydrogenolysis of halogen-containing organic compounds. The contribution of the hydrogen elimination reactions to these processes is in most cases unimportant in view of the high strength of the C–H bonds.¹⁵⁰ Nevertheless, there is direct evidence for the involvement of these reactions in certain hydrogenolytic processes. Thus, in a study of the hydrogenolysis of chloroethane,¹⁰³ the problem arose which of the two intermediates, $[\text{CH}_3\text{CH}_2]_{\text{ads}}$ or $[\text{CH}_3\text{CH}]_{\text{ads}}$, actually participates in the process. It was found that, when the hydrogenation is carried out with deuterium and not hydrogen, the compound CH_3CHD_2 is formed as the product. This made it possible to make a choice in favour of the intermediate $[\text{CH}_3\text{CH}]_{\text{ads}}$. Furthermore, this result confirms the elimination of the hydrogen atom from the intermediate adsorbed species. This possibility has been discussed in connection with a study of the hydrogenolysis of fluorohydrocarbons on a palladium catalyst deposited on activated carbon.³⁰ The probability of the dissociation of the C–H bonds in these compounds are significantly higher than in other halo-derivatives because the C–F bond is characterised by the highest energies.

5. Polymerisation reactions. The occurrence of these reactions has been confirmed by the formation of polymeric products in certain catalytic hydrogenolytic processes. Thus, the formation of a wide range of products from C₁ to C₄ has been noted in a study of the hydrogenolysis of the compounds $\text{CH}_n\text{Cl}_{4-n}$ on Ni, Co, and Fe catalysts.²¹ Polymeric products containing more than two carbon atoms are formed in the hydrogenolysis of chloromethane and dichloromethane on titanium films.¹⁰² The mechanism of the formation of low-molecular-mass polymers has been little studied. One may postulate that this reaction proceeds via the interaction of surface carbene radicals with monoradicals. The acceleration of the formation of C₁–C₄ hydrocarbons from CO and H₂ on Ni, Co, and Fe catalysts following the addition of the compounds $\text{CH}_n\text{Cl}_{4-n}$ to the reaction mixture shows that the mechanism of the formation of the low molecular-mass polymers under the conditions of catalytic hydrogenolysis is similar to the mechanism of the Fischer–Tropsch synthesis.²¹

The data on the reactivities of halohydrocarbons in catalytic hydrogenolytic reactions are fragmentary. Nevertheless, the results of quantitative investigations permit the conclusion that the reactivities of different compounds in these reactions and hence the selectivities of the latter are determined by thermodynamic, polar, steric, and adsorption factors and also by the specificity of the catalytic system.

The antiparallel changes in the rate of hydrogenolysis of different bonds and in the energies of these bonds observed in a number of instances indicate that the thermodynamic factor exerts a decisive influence on the reactivities of the compounds and the selectivities of the reactions. Thus the decrease in the reactivities of chloroalkanes on a palladium catalyst in the sequence



is accompanied by an increase in the C–Cl bond dissociation energies in the same sequence.¹⁰⁴ It has also been shown that the C–Cl bond is more reactive in hydrogenolysis on the Pd/C catalyst than the C–F bond and that at the same time $D(\text{C–Cl}) < D(\text{C–F})$.¹⁵² We may note that the examples quoted are characteristic of platinum group metals, which do not exhibit a high specificity in relation to the adsorption of compounds of different nature.

The operation of the steric factor may be due either to the shielding of the reaction centre by bulky substituents of the substrates or by the dependence of the degree of accessibility of

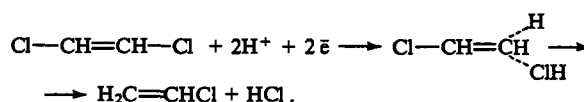
the catalyst active centres on the size of the species being adsorbed. Thus the inhibiting effect of *ortho*-substituents on the rate of hydrogenolysis of the C-Cl bonds of chlorobenzenes and chlorophenols is regarded as a result of the blocking effect of these substituents.^{153, 154} The dependence of the accessibility of the catalyst active centre on the size of the reactant molecules is confirmed by the fact that the adsorption saturation of the catalyst surface by the organic reactant in the hydrogenolysis of *p*-chloronitrobenzene to *p*-chloroaniline is attained sooner than saturation by hydrogen.^{65, 101}

The role of the polar factor is confirmed by the correlation between the rates of hydrogenolysis of the C-Cl bonds in *para*-substituted chlorobenzenes and polychlorobenzenes in the liquid phase on Pd/C and the electron-donating properties of the substituents in the aromatic ring.¹⁵⁵ This dependence has been attributed to the displacement of electron density towards the chlorine atom of the adsorbed substrate, which renders the attack on the latter by the electrophilic adsorbed hydrogen atom more effective. The antiparallel variation of the rate of hydrogenolysis of the C-Cl bonds and of the electron-donating capacities of the substituents in the vapour-phase process¹⁵⁶ indicates a fundamental difference between the mechanisms of the catalytic hydrogenolysis in the vapour and liquid phases. In particular, it has been suggested¹⁵⁶ that the key stage in the vapour-phase hydrogenolysis is nucleophilic attack by a surface hydride anion on the positively charged carbon atom of the C-Cl bond. In all the different mechanisms of the vapour-phase and liquid-phase processes, the polar character of the key stage is postulated in both cases and hence the dependence of the rate of hydrogenolysis on the presence or absence of polar substituents in the substrate.

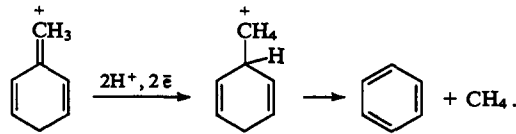
If the rate of catalytic hydrogenolysis is determined by Langmuir-Hinshelwood kinetics, then the composition of the products formed may be controlled by the adsorption capacities of the reactants or their functional groups. The data quoted above, indicating that methane is formed preferentially in the hydrogenolysis of tetrachloromethane, are evidence of the decisive influence of the adsorption factor on the composition of the products.

The inhibiting effect of hydrogen chloride on the hydrogenolytic processes observed in a number of studies has been usually attributed to the adsorption of this component on the surface and the blocking of the catalyst active centres. In order to prevent the blocking of the catalyst active centres by hydrogen chloride, certain processes are carried out in the presence of added alkalis, bases, or buffer mixtures [NaOH, KOH, NH₄OH, NaOOCCH₃-N(C₂H₅)₃, CH₃COONH₄-CH₃COOH, etc.].^{41, 49, 51, 80, 155, 157} The hydrogenation of *o*-chloronitrobenzene is particularly instructive in this respect.¹⁵⁷ The hydrogenolysis of the C-Cl bond predominates in the presence of NaOH, whereas the reduction of the nitro-group predominates in its absence. These and other data suggest that there are active centres of different types on the catalytic surface, each of which is specific to a particular reaction.^{44, 45}

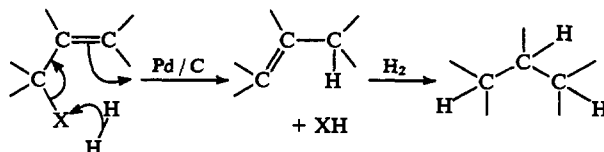
The specificity of the catalysts affects the relative contributions of the different reactions occurring under the conditions of the hydrogenolysis and especially the process selectivity. The role of the adsorption factor noted above is to some extent due to the specificity of the catalyst active centres in relation to the adsorption of the reactants. However, the nature of the specificity of catalytic systems is not restricted solely to adsorption interactions and in the general case one must take into account the structural characteristics of both the catalyst active centre and the reactant. This has been demonstrated in a study¹³⁶ where the hydrogenolysis of dichloroethenes on Pt/Al₂O₃ was investigated. The higher reactivity of the C-Cl bond in these reactants compared with chloroalkanes is due, according to the authors, to the stabilisation by the catalyst active centre of the quasi-tautomeric form of dichloroethene functioning as a surface intermediate in the hydrogenolytic reaction.



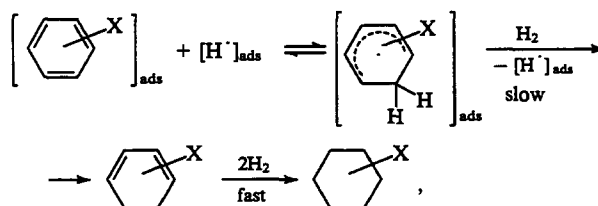
A similar approach has been used to account for the anomalously high reactivities of benzene derivatives.¹³⁶



The increased mobility of the fluorine atom in the hydrogenolysis of allyl, vinyl, benzyl, and aryl fluorides has been attributed to the involvement of the double bond of the adsorbed compound in the substitution of fluorine by hydrogen.¹⁵⁸

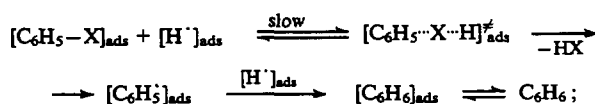


The above examples show that the specific features of the interactions on the surfaces of metallic catalysts are in many respects determined by the structural characteristics of the reactants. The soundest demonstration of this has been achieved in studies^{44, 45} where competing reactions involving the hydrogenolysis of C-X bonds and the hydrogenation of the aromatic rings of the benzene derivatives C₆H₅X (X = OH, OC₂H₅, SC₆H₅, NH₂, NHC₆H₅, F, Cl, Br) were investigated on Ni-Mo, Co-Mo, and W-Mo catalysts deposited on aluminium oxide. The correlation between the rates of ring hydrogenation and the electron-donating properties of the substituents reflects to some extent the electrophilic character of this reaction, i.e.

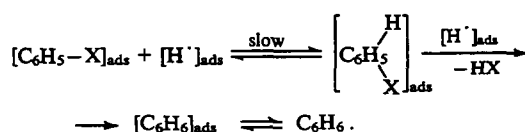


the successful outcome of which is determined by the stabilisation of the intermediate σ -complex. On the other hand, the high reactivity of the compounds C₆H₅X in hydrogenolysis is ensured by the presence of weak electron-donating substituents in the ring. One may postulate two possible pathways leading to hydrogenolysis on the catalytic surface:

(1) the abstraction of the substituent X by an adsorbed hydrogen atom:



(2) the substitution of the group X by a hydrogen atom via *ipso*-attack



Our attempts to observe a correlation between the rates of these reactions, on the one hand, and the heat of the hydrogenolytic reactions and the polarisability of the groups X, on the other, were unsuccessful. This confirms the need to take into

account the energetics of the interactions of the catalyst active centres with the components participating in the rate-limiting stages of the reactions.

Catalytic hydrogenolytic reactions are known to be structure-sensitive, which is manifested by the dependence of the specific activity of the catalyst on the accessibility and structures of the active centres.¹⁴⁴ The structural insensitivity of the hydrogenation reaction presupposes the independence of the activity of the catalytic centres of their structure. On the other hand, in hydrogenolysis the effective interaction between the catalyst active centre and the substrate requires the optimum combination of their structural properties and this is most clearly manifested in the presence of weak electron-donating substituents. The structural sensitivity of the hydrogenolytic reactions is confirmed by the numerous examples of the dependence of the specific activities of the catalysts on their dispersity.^{99, 101, 129, 145, 146} The important role of the modification and of the methods of preparation of the hydrogenolysis catalyst which follows from this has been confirmed by the dependence of their activities and selectivities on the temperatures of their treatment by an inert gas and reductants,^{19, 25, 39, 43, 85} the type of reductant,^{19, 25, 39, 85, 103, 132} the presence of promoting additives,^{19, 21, 24, 28, 29, 31, 132} and also on the treatment of the catalyst by gaseous reagents such HCl, Cl₂, air, H₂O, F₂, H₂S, etc.^{19, 48, 60, 103, 125, 126, 128, 159} The importance of this method of preparation of the catalyst for the specific regulation of its activity has been demonstrated by the results of a study⁴⁷ where the possibility of the 'chemical grafting' of palladium ions on the Al₂O₃ surface with variation of the ionic character of the metal was demonstrated. A vigorous correlation between the ionic character of palladium and its activity was discovered.

The data on catalytic hydrogenolysis considered above indicate the need to formulate systematic studies in which kinetic experiments would be combined with the study of the properties of the catalytic surface, the adsorption equilibria, and the influence of impurities and modification on the activities and selectivities of the catalysts. A special study of the elementary steps on the surface is also required. From the practical point of view, it is important to direct the efforts of investigators to the study of the quantitative aspects of the deactivation and regeneration of the catalysts and to the development of catalytic systems resistant to the action of contact poisons.

References

- Eur. P. 295 454; *Chem. Abstr.* 110 218 521g (1989)
- M Uhliz, I Hrabal, I Beranek *Chem. Prum.* 38/63 77 (1988)
- M Heathcote *Eur. Chem. News* 58 (1530) 21 (1992)
- G M Bickle, T Suzuki, Y Mitarai *Process Safety Environ. Prot.* 70 44 (1992)
- F F Muganlinskii, Yu A Treger, M M Lyushin *Khimiya i Tekhnologiya Galogenorganicheskikh Soedinenii* (The Chemistry and Technology of Organohalogen Compounds) (Moscow: Khimiya, 1991)
- J Zienko, J Myszkowski *Przem. Chem.* 71/6 209 (1992)
- Yu A Treger, L M Kartashov, N F Krishtal' *Osnovnye Khlororganicheskie Rastvoriteli* (Basic Organochlorine Solvents) (Moscow: Khimiya, 1984)
- Eur. Chem. News* 58 (1520) 26 (1992)
- Czech. P. 268 406; *Chem. Abstr.* 114 228 496z (1991)
- R Louw, J A Manion, R Mulder *Resour. Conserv.* 14 365 (1987)
- R Louw, R Mulder *J. Environ. Sci. Health, Part A* 25 555 (1990)
- Czech. P. 268 602; *Chem. Abstr.* 114 228 429e (1991)
- L N Zhanaveskin, Yu A Treger, V A Aver'yanov, in *Tez. Dokl. 2-i Mezhdunar. Nauch. Konferentsii "Naukoemkie Khimicheskie Tekhnologii"*, Moscow - St.-Petersburg, 1994 (Abstracts of Reports at the Second International Scientific Conference 'Chemical Technologies with a High Scientific Content', Moscow - St.-Petersburg, 1994) p. 74
- N M Popova *Katalizatory Ochistki Gazovykh Vybrosov Promyshlennykh Proizvodstv* (Catalysts for the Purification of Gaseous Industrial Waste) (Moscow: Khimiya, 1991)
- B Radomsky, J Szczygial, J Trawczynski *Appl. Catal.* 39 25 (1988)
- Yu A Treger, T D Guzhnovskaya *Intensifikatsiya Khlororganicheskikh Proizvodstv. Vysokoeffektivnye Kataliticheskie Sistemy* (Intensification of Organochlorine Industries. Highly Efficient Catalytic Systems) (Moscow: Khimiya, 1989)
- Jpn. Appl. 03-221 121; *Chem. Abstr.* 116 66 217w (1992)
- Jpn. P. 91-211 735/29 (1991)
- Eur. P. 479 116; *Chem. Abstr.* 115 182 612z (1991)
- Jpn. Appl. 03-133 939; *Chem. Abstr.* 115 182 612z (1991)
- W A A Barneveld, V Ponc J. *Catal.* 88 382 (1984)
- Belg. P. 867 285; *Chem. Abstr.* 90 151 557w (1979)
- US P. 2 886 605 (1959)
- BRD Appl. 2 164 074; *Chem. Abstr.* 79 78 079h (1973)
- O Hinterhofer *Monatsh. Chem.* 105 279 (1974)
- O A Zaidman, E N Verkhutova, E V Sonin, in *Tez. Dokl. 4-i Moskovskoi Konferentsii po Organicheskoi Khimii i Tekhnologii* (Abstracts of Reports at the Fourth Moscow Conference on Organic Chemistry and Technology) (Moscow: Vses. Khim. O-vo im D I Mendeleeva, 1985) p. 209
- BRD Appl. 3 850 807; *Chem. Abstr.* 114 215 119e (1991)
- BRD Appl. 3 804 265; *Chem. Abstr.* 112 7 025b (1990)
- Eur. P. 301 343; *Chem. Abstr.* 111 38 991kh (1989)
- S D Witt, E-C Wu, K-L Loh, Y-N Tang *J. Catal.* 71 270 (1981)
- BRD Appl. 3 941 037; *Chem. Abstr.* 115 182 608s (1991)
- US P. 4 840 722; *Chem. Abstr.* 111 137 373d (1989)
- Czech. P. 268 276; *Chem. Abstr.* 114 246 930r (1991)
- L I Bushneva, S V Levanova, R M Rodova, A M Rozhnov, Yu A Treger, P P Ol'fert *Zh. Prikl. Khim.* 51 200 (1978)
- A H Weiss, B S Gambhir, R B Leon *J. Catal.* 22 245 (1971)
- Eur. P. 379 396; *Chem. Abstr.* 115 182 608s (1991)
- J A Manion, P Mulder, R Louw *Environ. Sci. Technol.* 19 280 (1985)
- J A Manion, R L Louw *Recl. Trav. Chim. Pays-Bas* 108 235 (1989)
- US P. 3 855 347; *Chem. Abstr.* 82 170 003r (1979)
- Eur. Chem. News* 54 (1417) 28 (1990)
- US P. 3 579 596; *Ref. Zh. Khim.* 8 N 14P (1972)
- J A Manion, J H M Dijk, P Mulder, R Louw *Recl. Trav. Chim. Pays-Bas* 107 434 (1988)
- N Naum, Gh Miha'ila, N Billa' *Bull. Inst. Politech. Din IASI, Sec. 2* 31 67 (1985)
- C Moreau, J Jaffre, C Saenz, P Geneste *J. Catal.* 122 448 (1990)
- C Moreau, R Durand, P Geneste, J L Olive, J Bachelier, D Cornet, J C Duchet, J C Lavalley *Prepr. Am. Chem. Soc., Div. Pet. Chem.* 32 298 (1987)
- J A Manion, R Louw *J. Chem. Soc., Perkin Trans. 2* 1547 (1988)
- E Telas, J L Margitfalvi, M Nedelüs, S Göddöls, A Ruckebauer, in *The 6-th International Symposium on Relations between Homogeneous and Heterogeneous Catalysis, Pisa, Italy, 1989* (Lausanne: Elsevier Sequoia, 1989) p. 69
- Jpn. P. 62-252 736; *Chem. Abstr.* 108 111 808n (1988)
- Eur. P. 355 986; *Chem. Abstr.* 113 40 718y (1990)
- S C Chuang, J W Bozzelli *Ind. Eng. Chem., Process Des. Dev.* 25 317 (1986)
- K Isogai, T Kadzama *J. Chem. Soc. Jpn., Pure Chem. Sec.* 88 106 (1967)
- BRD Appl. 2 614 294; *Ref. Zh. Khim.* 14 N 177P (1978)
- Eur. Chem. News* 53 (1383) 12 (1989)
- D H Evans *J. Hazard. Mater.* 27 253 (1991)
- N N Mel'nikov, S R Belan *Khim. Promst* 328 (1989)
- N F Aleshin, in *Issledovanie Plazmennyykh Protssessov i Apparatov* (Investigation of Plasma Processes and Apparatus) (Minsk: Nauka i Tekhnika, 1991) p. 133
- Russ. P. 2 039 731; *Byull. Izobret.* (20) 150 (1995)
- S G Ruban, L N Zhanaveskin, Yu A Treger, V A Aver'yanov, in *Tez. Dokl. XIV Mendelevskogo S'ezda po Obshchei i Prikladnoi Khimii* (Abstracts of Reports at the XIVth Mendeleev Congress on General and Applied Chemistry) (Tashkent: Nauka, 1989) p. 398
- S G Ruban, L N Zhanaveskin, Yu A Treger, V A Aver'yanov, in *Tez. Dokl. Vses. Nauchno-Prakticheskogo Seminara "Opyt Raboty Nauchno-Tekhnicheskoi Obshchestvennosti Vses. Khim. Obshch-va im D I Mendeleeva po Sozdaniyu Ekologicheskii Chistykh Regionov"* (Abstracts of Reports at the All-Union Scientific Practical Seminar 'Experiment at Work by the Scientific and Technical Community of the Mendeleev All-Union Chemical Society on the Creation of Ecologically Clean Regions') (Tula: Tul'sk. Politekh. Inst., 1980) p. 30
- F Murena, V Famiglietti, F Giorgia *Environ. Progr.* 12 231 (1993)

61. *Eur. Chem. News*. **58** (1522) 26 (1992)
62. G Meitzner, W J Mykytka, J H Sinfelt *J. Catal.* **98** 513 (1986)
63. R S Varma, G W Kabalka *Synth. Commun.* **15** 985 (1985)
64. *Eur. P.* 3 325 892; *Chem. Abstr.* **112** 79 939g (1990)
65. A Tijani, B Coq, F Figueras *Appl. Catal.* **76** 255 (1991)
66. M Makabe, H Ito, K Ouchi *Fuel* **69** 575 (1990)
67. R A Cocco, B J Tarachuk *Mater. Res. Soc. Symp. Proc.* **111** 335 (1988)
68. F E Massoth, K Balusanu, J Shabtai *J. Catal.* **122** 256 (1990)
69. V D Statsenko, A Yu D'yakonov, I A Eigenson, E S Apostol *Kinet. Katal.* **29** 616 (1988)
70. V D Statsenko, A Yu D'yakonov, I A Eigenson, A Ya Rozovskii *Kinet. Katal.* **29** 845 (1988)
71. R Louw, J-P Born, O J Harenwinkel, in *Hazardous Waste: Detection, Control, Treatment (Proceedings of the World Conference on Hazardous Waste, Budapest, 1987) Part B* (Amsterdam: Elsevier, 1988) p. 1409
72. B Delmon, J L Dallons *Bull. Soc. Chim. Belg.* **97** 478 (1988)
73. K Shanthi, C N Pillai, J C Kuriacose *Appl. Catal.* **46** 241 (1989)
74. D Melamed *Chem. Eng.* **96** (11) 30 (1989)
75. E Johnson *Chem. Eng.* **96** (11) 39 (1989)
76. Ch Tomas *Catalytic Processes and Proven Catalysts* (New York, London: Academic Press, 1970)
77. F Mureno, V Famiglietti, F Giogia *Environ. Progr.* **12** 23 (1993)
78. S Kovenklioglu, Zh Gao, D Shah, R J Farranto, E M Balko *Aust. Chem. Educ. J.* **38** 1003 (1992)
79. I Ya Mokrousova, Yu A Treger, A A Atasov *Kinet. Katal.* **16** 796 (1975)
80. J B Hoke, G A Gramiccioni, E N Balko *Appl. Catal.* **B 1** 285 (1992)
81. A Kazmierzak, D Gebauer, B Fabak, T Paryczak *Przem. Chem.* **68** 456 (1989)
82. *Jpn. P.* 89-45 345; *Chem. Abstr.* **111** 114 838v (1989)
83. A K Agarwal, M S Wainwright, D L Trimm, N W Cant *J. Mol. Catal.* **45** 247 (1988)
84. A K Agarwal, N W Cant, M S Wainwright, D L Trimm *J. Mol. Catal.* **43** 79 (1987)
85. Ch S Narasimhan, V M Deshpande, K Ramnarayan *Ind. Eng. Chem. Res.* **28** 1110 (1989)
86. V M Deshpande, K Ramnarayan, Ch S Narasimhan *J. Catal.* **121** 174 (1990)
87. J M Tedder, A Nechvatal, A H Jubbs *Basic Organic Chemistry* (New York: Wiley, 1975)
88. G Gondas, L Gera, M Bartok *J. Mol. Catal.* **57** 81 (1989)
89. K Isogai, Ju Sakai *Nippon Kagaku Kaishi* **5** 650 (1986)
90. P Toropainen, J B N Bredenberg *Appl. Catal.* **52** 57 (1989)
91. W Ueda, S Tomioka, Yu Morikawa, M Sudo, Ts Ikawa *Chem. Lett.* **879** (1990)
92. R Ohnishi, W L Wang, M Ichikawa *Appl. Catal. A-Gen.* **113** 29 (1994)
93. B Coq, S Hub, F Figueras, D Tournigant *Appl. Catal. A-Gen* **101** 41 (1993)
94. J Zienko, J Myszkowski *Przem. Chem.* **71** 209 (1992)
95. S Okazaki, H Habutsu *J. Fluorine Chem.* **57** 191 (1992)
96. Ch J Gantzer, L P Wackett *Environ. Sci. Technol.* **25** 715 (1991)
97. L R Wackett, D T Gibson *Appl. Environ. Microbiol.* **54** 1703 (1988)
98. S C Fung, J H Sinfelt *J. Catal.* **103** 220 (1987)
99. P Bodnariuk, B Cog, G Ferrat, F Figueras *J. Catal.* **16** 459 (1989)
100. A P Mishchenko, E V Senina *Izv. Akad. Nauk SSSR, Ser. Khim.* **1664** (1987)
101. B Coq, A Tijani, F Figueras *J. Mol. Catal.* **68** 331 (1991)
102. J R Anderson, B H McConkey *J. Catal.* **11** 54 (1968)
103. J S Campbell, C Kemball *Trans. Faraday Soc.* **57** 809 (1961)
104. J S Campbell, C Kemball *Trans. Faraday Soc.* **59** 2583 (1963)
105. J Sasson, G L Rempel *Tetrahedron Lett.* **3221** (1974)
106. G Viner, I Blum, J Sasson *J. Org. Chem.* **56** 6145 (1991)
107. R Marčec *Croatia Chem. Acta* **63** 203 (1990)
108. T R J Dinesen, M Y Tse, M C Depew, J K S Wan *Res. Chem. Intermediates* **15** 113 (1991)
109. J Chausard, J C Folest, J-Y Nedelec, J Perichon, S Sibille, M Troupel *Synthesis* **369** (1990)
110. T Shono *Electroorganic Chemistry as a New Tool in Organic Synthesis* (Berlin: Springer, 1984)
111. M M Baiser *Tetrahedron* **40** 944 (1984)
112. M Kimura, H Miyahara, N Moritani, Y Sawaki *J. Org. Chem.* **55** 3897 (1990)
113. R Holze, U Fette *J. Electroanal. Chem.* **389** 247 (1984)
114. Th Kauffmann, H Henkler, H Zengel *Angew. Chem.* **74** 248 (1962)
115. G J Karabatsos, R L Skone, S E Sckeppele *Tetrahedron Lett.* **5** 2113 (1964)
116. D H Lorenz, Ph Shapiro, A Stern, E J Becker *J. Org. Chem.* **28** 2332 (1963)
117. R S Varma, G W Kabalka *Synth. Commun.* **15** 151 (1985)
118. K Soai, H Oyamada, M Takase, A Ookawa *Bull. Chem. Soc. Jpn.* **57** 1948 (1984)
119. V F Lavrushin, L M Kutsenko, L M Grin, I Ya Litvin *Ukr. Khim. Zh.* **34** 413 (1968)
120. A Ono *Z. Naturforsch.* **41b** 1568 (1986)
121. Weygand-Hilgetag *Preparative Organic Chemistry* (New York: Wiley, 1972)
122. B Juršiae, A Galošii *Synth. Commun.* **19** 1649 (1989)
123. *US P.* 4 895 995; *Chem. Abstr.* **112** 142 622j (1990)
124. F Gajewski, K German, J Ogonowski, J Rakoczy, K Rutkowski *Politechnika Krakowska. Monogr.* **52** 77 (1987)
125. F Giogia, E J Callagher, V Famiglietti *J. Hazard. Mater.* **38** 277 (1994)
126. B F Hagh, D T Allen *Aust. Chem. Educ. J.* **36** 773 (1990)
127. *US P.* 3 595 931 SShA (1971)
128. M Novak, M Zdrzil *Bull. Soc. Chim. Belg.* **102** 271 (1993)
129. B Coq, F Figueras, in *Proceedings of the Soviet-French Seminar on Catalysis, Novosibirsk, 1990* p. 218
130. *Eur. P.* 290 861; *Chem. Abstr.* **110** 212 330kh (1989)
131. *BRD P.* 2 127 182; *Chem. Abstr.* **76** 126 565 (1972)
132. O Hinterhofer *Ber. Bunsenges. Phys. Chem.* **79** 18 (1975)
133. *US P.* 5 136 113; *Chem. Abstr.* **117** 170 778m (1992)
134. B Rennert, F Turek *Chem.-Ing.-Tech.* **66** 192 (1994)
135. *BRD P.* 3 804 265 (1989)
136. A H Weiss, K A Krieger *J. Catal.* **6** 167 (1966)
137. G S Dasaeva, S M Velichko, Yu A Treger, I I Moiseev *Kinet. Katal.* **31** 858 (1990)
138. *Jpn. Appl.* 03-221 121; *Chem. Abstr.* **116** 66 217w (1992)
139. D T Ferrughelli, I T Horvath *J. Chem. Soc., Chem. Commun.* **806** (1992)
140. *USSR P.* 694 483; *Byull. Izobret.* (40) 85 (1979)
141. J H Sinfelt *Catal. Rev. Sci. Eng.* **9** 107 (1974)
142. S V Narval, S J Thomson *J. Chem. Soc., Faraday Trans. 1* **75** 1798 (1979)
143. L B Fertel, N J Oreilly, K M Callaghan *J. Org. Chem.* **58** 261 (1993)
144. Ch N Satterfield *Heterogeneous Catalysis in Practice* (New York: McGraw-Hill, 1980)
145. H Kubicka, J Okal *React. Kinet. Catal. Lett.* **34** 433 (1987)
146. C Lee, S Gao, L D Schmidt *Stud. Surf. Sci. Catal.* **31** 421 (1987)
147. S L Kiperman *Osnovy Khimicheskoi Kinetiki v Geterogennom Katalize* (Fundamentals of Chemical Kinetics in Heterogeneous Catalysis) (Moscow: Khimiya, 1979)
148. A A Balandin *Sovremennoe Sostoyanie Mul'tipletnoi Teorii Geterogennogo Kataliza* (The Current State of the Multiplet Theory of Heterogeneous Catalysis) (Moscow: Nauka, 1968)
149. P Mars, D M van Krevelen *Chem. Eng. Sci.* **3** 41 (1954)
150. L V Gurvich, G V Karachevtsev, V N Kondrat'ev, Yu A Lebedev, V A Medvedev, V K Potapov, Yu S Khodoev *Energii Razryva Khimicheskikh Svyazei. Potentsialy Ionizatsii i Srodstvo k Elektronu* (Chemical Bond Dissociation Energies, Ionisation Potentials, and Electron Affinities) (Moscow: Nauka, 1974)
151. P G Ashmore *Catalysis and Inhibition of Chemical Reactions* (London: Butterworths, 1963)
152. J R Lacher, A Kianpour, F Oetting *Trans. Faraday Soc.* **52** 1500 (1956)
153. A R Suzdorf, S I Tsyganova, N N Anshits, S V Morozov, A G Anshits *Sib. Khim. Zh.* (6) 131 (1992)
154. A R Suzdorf, S V Morozov, N N Anshits, S I Tsyganova, A G Anshits *Catal. Lett.* **29** 49 (1994)
155. I L Simakova, V A Semikolenov *Kinet. Katal.* **32** 989 (1991)
156. M Kraus, V Bazant, in *Proceedings of the 5th International Congress on Catalysis Vol. 2* (Amsterdam: North-Holland, 1973) p. 1073
157. V Z Sharf, A S Gurovets, I B Slinyakova, L P Finn, L Kh Freidlin, V N Krutii *Izv. Akad. Nauk SSSR, Ser. Khim.* **114** (1980)
158. M Hudlicky *J. Fluorine Chem.* **44** 345 (1989)
159. M K Anwer, A F Spatola *Tetrahedron Lett.* **26** 1381 (1985)

Selective oxidation of gaseous hydrocarbons by bacterial cells

G A Kovalenko

Contents

I. Introduction	625
II. Comparative characteristics of the direct selective oxidation reactions of gaseous hydrocarbons	626
III. Microorganisms as biocatalysts of the direct partial oxidation of gaseous hydrocarbons	626
IV. Microbiological epoxidation of lower alkenes	632
V. Microbiological hydroxylation of gaseous alkanes	635
VI. Conclusion	638

Abstract. Studies on the direct selective oxidation of gaseous C_1 – C_4 alkanes and C_2 – C_4 alkenes to valuable oxygen-containing products (alcohols, methyl ketones, and epoxides) with the aid of the bacterial cells of gas-assimilating microorganisms are surveyed. The resting bacterial cells of the microorganisms grown on gaseous hydrocarbons possess an enzymic monooxygenase activity: they promote the insertion of an oxygen atom into the hydrocarbon molecule with formation of an oxygen-containing product. This process is effected under very mild conditions and is characterised by high selectivity and stereospecificity. It proceeds without the formation of toxic by-products. Certain problems of the practical implementation of biocatalytic oxidation processes, namely the regeneration of the monooxygenase cofactor, the reduction of the toxic effect of the oxygen-containing product formed, as well as the immobilisation of the cells on solid carriers in order to obtain an active and stable heterogeneous biocatalyst for the direct partial oxidation of hydrocarbons are considered. The bibliography includes 111 references.

I. Introduction

There has been a considerable growth of interest in recent years in the preparation of chemical compounds (the products of large scale organic synthesis) by biotechnological and biocatalytic methods. Environmentally pure processes of this kind, entailing a low energy consumption, constitute a real alternative to chemical synthesis and they are therefore being vigorously investigated and developed in all the industrially developed countries. According to certain predictions,¹ 10%–20% of chemical products will be produced by a biotechnological procedure towards the end of the 1990s. The biochemical process involving the direct selective oxidation of saturated and unsaturated hydrocarbons to valuable oxygen-containing products (chiral epoxides, alcohols, methyl ketones, and dicarboxylic acids) is particularly interesting.

The oxidative biotransformation of organic compounds, including hydrocarbon raw materials, occupies one of the leading places among industrial biocatalytic processes. Specific investigations in this field are being undertaken by large chemical companies in Japan (Nippon Mining Co., Nito Chem. Ind.), America (Exxon, Dow Chem., Monsanto, Du Pont), and Western Europe (Hoechst, Bayer, BASF), and also by Western European Universities (Wageningen Agricultural University, the Netherlands). The synthesis of the optical isomers of epoxides derived from unsaturated hydrocarbons (the properties of 31 epoxides have been described), carried out by the Japanese company Nippon Mining Co. on a semi-industrial scale using suspensions of microorganisms of the genus *Nocardia*, is of greatest interest.^{2,3} In the microbiological epoxidation of moderately long chains, the yield of the (*R*)-1,2-epoxides is 80% with an optical purity of 80%–90%.^{2,3} The optically active epoxides obtained are used in fine organic synthesis for the production of medicinal drugs, biologically active substances, and liquid crystals for electronics. Expert estimates have shown that the biotechnological methods of synthesis of the optical isomers of the epoxides may compete with the chemical methods. For example, the annual profit from the sale of the 'biotechnological' epoxypropane may reach 2–3 billion U.S. dollars.¹

The present review considers the biocatalytic approaches to the solution of the problems of the direct partial oxidation of gaseous saturated and unsaturated hydrocarbons (methane, ethane, ethene, propane, propene, butane, butene) to valuable oxygen-containing products (epoxides, alcohols, and methyl ketones). Bacterial cells possessing the required enzymic oxygenase activity are used as biocatalysts of these processes in the immobilised state and also in the form of suspensions of resting (not growing) microorganisms. The characteristic features of the microorganisms employing gaseous hydrocarbons for their growth and the intracellular enzyme systems catalysing the oxidative biotransformation reactions of gaseous hydrocarbons will be briefly described in this review. Particular attention will be devoted to heterogeneous biocatalysts based on immobilised bacterial cells for the oxidative biotransformation of propene into 1,2-epoxypropane.

G A Kovalenko Boreskov Institute of Catalysis, Siberian Branch of the Russian Academy of Sciences,
Prosp. akad. Lavrent'eva 5, 630090 Novosibirsk, Russian Federation.
Fax (7-383) 235 57 66. Tel. (7-383) 235 77 89

Received 15 February 1996

Uspekhi Khimii 65 (7) 676–691 (1996); translated by A K Grzybowski

II. Comparative characteristics of the direct selective oxidation reactions of gaseous hydrocarbons

The processes involving the selective oxidation of light gaseous hydrocarbons to valuable oxygen-containing products constitute the key stages in the chemical processing of gas and petroleum. Some of these processes, in particular the direct selective epoxidation of ethene, have been implemented on an industrial scale, whilst others, for example the direct partial oxidation of gaseous alkanes (methane, ethane, and propane) to valuable oxygen-containing products (alcohols and aldehydes) are at the stage of intense laboratory research. Analysis of the literature data on the selective oxidation of C₁–C₄ hydrocarbons has shown that the heterogeneous oxide catalysts widely used in these processes have fairly limited possibilities: the maximum selectivity in the formation of the target product (80%–95%) is attained only for low degrees of conversion of the initial hydrocarbon (not more than 5%).^{4–6} In order to attain a selectivity up to 70% for a conversion greater than 5%, either nitrous oxide is employed as the oxidant^{5,7} or use is made of catalysts containing precious metals (gold, palladium, and ruthenium).⁸ The literature data on the direct selective oxidation of ethane and propane to alcohols, aldehydes, or methyl ketones are very fragmentary and few in number. The main product of the oxidation of ethane is methanol mixed with ethanol,⁵ while the oxidation of propane gives rise predominantly to acrylic acid.^{9,10}

Biocatalytic processes have attracted the attention of investigators because of their unique features: low energy consumption due to the mild reaction conditions (temperature not exceeding 40 °C), a nearly 100% selectivity regardless of the degree of conversion of the initial substrate, as well as stereospecificity ensuring the formation of chiral compounds. Furthermore, owing to the absence of toxic by-products, biocatalytic processes are environmentally-friendly.

The data presented in Tables 1 and 2 demonstrate the possibilities of biocatalysis in relation to the epoxidation of propene and the hydroxylation of methane by gaseous oxygen as examples. In terms of their principal parameters (activity, yield of products), biocatalysts are at the level of the best heterogeneous chemical catalysts or are superior. The prospects for the oxidative biotransformation of hydrocarbons into valuable oxygen-containing products have been analysed in reviews^{19–21} and the possibility of the practical implementation of such a process under chemical industrial conditions has been considered. The only significant disadvantage of biotechnological processes is the low concentration of the final products in the reaction medium (as a rule an aqueous medium). It does not exceed several tens of millimoles per litre, which gives rise to problems in the isolation of the target substances. Similar problems exist also in heteroge-

Table 2. Comparative characteristics of the processes involving the direct partial oxidation of methane to methanol.

Parameter	Chemical process		Biocatalytic process ^{17,18}
	homogeneous ^a	heterogeneous ^b	
Temperatures / °C	450–550	250–350	20–40
Pressure / atm	25–65	1	1
Conversion of methane per pass (%)	9–13	4–6	27–61
Selectivity with respect to methanol (%)	38–83	83–96	~ 100
Yield with respect to methanol (%)	2–7	3–6	10–60
Productivity with respect to methanol / mmol g ⁻¹ h ⁻¹		0.001–1.7	1–7

^a According to data in Refs 5, 6, and 15. ^b According to data in Refs 5, 6, and 16.

neous catalysts for low degrees of conversion of the initial compound. They can be solved, for example, by selecting a suitable reactor design or by employing a two-phase reaction medium for the extraction and concentration of the final oxygen-containing product.

Thus biocatalytic processes exhibit a high selectivity, ensure the possibility of obtaining the stereoisomers of chemical compounds, require a small energy consumption, and are relatively environmentally clean. They are therefore competitive with the chemical processes in basic organic synthesis.

III. Microorganisms as biocatalysts of the direct partial oxidation of gaseous hydrocarbons

Evidently the first stage in the development of any biotechnological process is screening for microorganisms possessing the necessary enzymic activity. The partial oxidation of saturated and unsaturated gaseous C₁–C₄ hydrocarbons is effected predominantly by gas-assimilating microorganisms. There are only isolated examples where bacterial cells grown on liquid C₅ and higher hydrocarbons oxidise gaseous substrates. For example, suspensions of the bacterial cells of the microorganism *Nocardia*, grown on isoprene, are capable of effectively oxidising propene and butene to the corresponding epoxides.²² Other microorganisms employing C₅–C₁₈ hydrocarbons for their growth do not oxidise gaseous alkanes and alkenes.

The first gas-assimilating bacterium, using methane as the sole source of carbon for its growth, was isolated in its pure form in 1906 and up to 1954 only five species of such bacteria, called methanotrophs, had been described.^{23,24} A profound conviction that microorganisms capable of assimilating chemically inert compounds such as saturated and gaseous hydrocarbons are widely distributed in nature has arisen recently. About 200 strains of methanotrophs have been isolated from their habitats:^{25,26} fresh- and salt-water reservoirs, subterranean and waste waters, muds, soils, coal mines, and even from the rumen of ruminants.²³ Soil microorganisms of the genus *Rhodococcus* utilise propane and butane as a source of carbon.²⁷

Gas-assimilating microorganisms can be divided into the following groups:

(1) methanotrophs (the principal representatives belonging to the genera *Methylococcus*, *Methylosinus*, and *Methylomonas*) which are highly specialised microorganisms using methane as the sole source of carbon and energy; glucose and other organic compounds inhibit completely their growth;

(2) alkane-assimilating microorganisms (the principal representatives belong to the genera *Rhodococcus*, *Mycobacteria*, *Nocardia*, and *Xantobacter*), which utilise ethane, propane, and

Table 1. Comparative characteristics of the processes involving the direct partial oxidation of propene to 1,2-epoxypropane by molecular oxygen.

Characteristic	Chemical heterogeneous process ¹¹	Biocatalytic process ^{12–14}
Temperature / °C	450–550	20–40
Conversion of propene (%)	not above 15	40–80
Selectivity with respect to epoxypropane (%)	25	100
Stereospecificity	Racemic mixture	80%–90% of (<i>R</i>)-1,2-epoxypropane
Toxic side products	aldehydes, carbon monoxide, aromatic compounds	absent

butane are virtually incapable of growing on methane; glucose and certain organic acids support their growth;

(3) alkene-assimilating microorganisms (the principal representatives belong to the genera *Mycobacterium*, *Xantobacter*, and *Nocardia*), which grow on gaseous alkenes (ethene, propene, butene, and butadiene); they are also capable of utilising glucose.

The characteristic differences between the last two groups of microorganisms grown on gaseous hydrocarbons (especially on alkanes) and the same microorganisms grown on glucose or organic acids is the relatively high content of lipids in the cell and the structure of the cell wall, which is a strongly lipophilic formation.²⁸ The cells of *Mycobacterium vaccae* may serve as a typical example: such cells, grown on ethane (propane or n-butane), contain twice as much lipid as the cells grown on acetate (propionate).²⁹ These cells have another interesting feature: when acetate is replaced as the growth substrate by propane, the synthesis of lipids precedes the synthesis of nitrogen-containing compounds (proteins) and cell division, which indicates the important role of lipid materials in the assimilation by the cells of the hydrophobic hydrocarbon substrates necessary for their growth.²⁹ It has now been demonstrated that passive diffusion of the molecules towards the cell and their sorption on the cell wall take place in the initial stage of the assimilation of the hydrocarbon by the microorganisms.^{27, 30} A metabolic process involving active (with an expenditure of energy) transport of the hydrocarbon to the cell, where it is oxidised intracellularly on membrane structures (microsomes), takes place in the next stage.^{27, 28} In *Rhodococcus* sp. grown on propane, an excessive development of the outer membrane of the cell wall is observed and a well developed network of intracellular membrane structures on the periphery of the cells is clearly manifested.²⁷

All the processes involved in the oxidative microbiological transformation of hydrocarbons proceed with participation of molecular oxygen and are effected by enzymic oxygenase complexes (monooxygenases), the structure and functional role of which in the cell metabolism have been widely described in the literature.^{23, 31–33} In the present review, we shall dwell briefly on the structure of the active centre of the key enzyme effecting the primary activation of the gaseous hydrocarbon and the subsequent incorporation into the molecule of one oxygen atom with

formation of an alcohol or epoxide. Such enzyme activity of the microorganisms belonging to the second and third groups is induced by the hydrocarbon in the course of cell growth^{27, 30} (cells then grow relatively slowly and the period for the doubling of the population amounts to tens of hours). The cells grown on glucose or organic acids as a rule do not possess such activity and are incapable of transforming hydrocarbons. The Japanese strain *Nocardia corallina* B-276, the resting cells of which (grown on glucose) are capable of epoxidising alkenes, is an exception.^{34, 35} However, the yield of the epoxide is then almost twice as small as in a medium with cells grown on propene.³⁴

Depending on whether an alkane or an alkene is used as the growth substrate, enzyme complexes having different properties are induced and synthesised in the cell, namely an alkane monooxygenase or an alkene monooxygenase, which are responsible for the primary activation of the gaseous hydrocarbon.^{22, 36} The alkane monooxygenase has a broader substrate specificity than the alkene monooxygenase: it hydroxylates alkanes and epoxidises alkenes, whereas the alkene monooxygenase is only capable of epoxidising alkenes (but is incapable of hydroxylating alkanes). The microorganisms grown on alkenes are as a rule incapable of growing on alkanes. It is of interest that these two enzyme systems (or the cells of microorganisms with an induced enzyme activity) differ from one another also in their stereospecificity: the methane and alkane monooxygenases as a rule form during the epoxidation of C₃–C₄ alkenes a racemic mixture of optical isomers of the epoxides, whereas in the case where alkene monooxygenases are employed an excess (80%–90%) of the enantiomeric forms is observed. In both cases the configuration of the alkene (butene) is retained (Tables 3–7).^{22, 41} The Japanese strain *Nocardia corallina* B-276 has exceptional characteristics: regardless of the growth substrate employed (glucose, alkanes, and alkenes), one of the optical isomers of the epoxide is formed in excess within the cells of this microorganism.^{2, 3}

Two principal types of monooxygenase enzyme systems of microorganisms, capable of assimilating hydrocarbons, including gaseous ones, have now been described and characterised:

(1) monooxygenases containing an oxo- or hydroxo-bridged iron cluster in the active centre are present in the cells of methanotrophs (Fig. 1a);^{32, 33, 62}

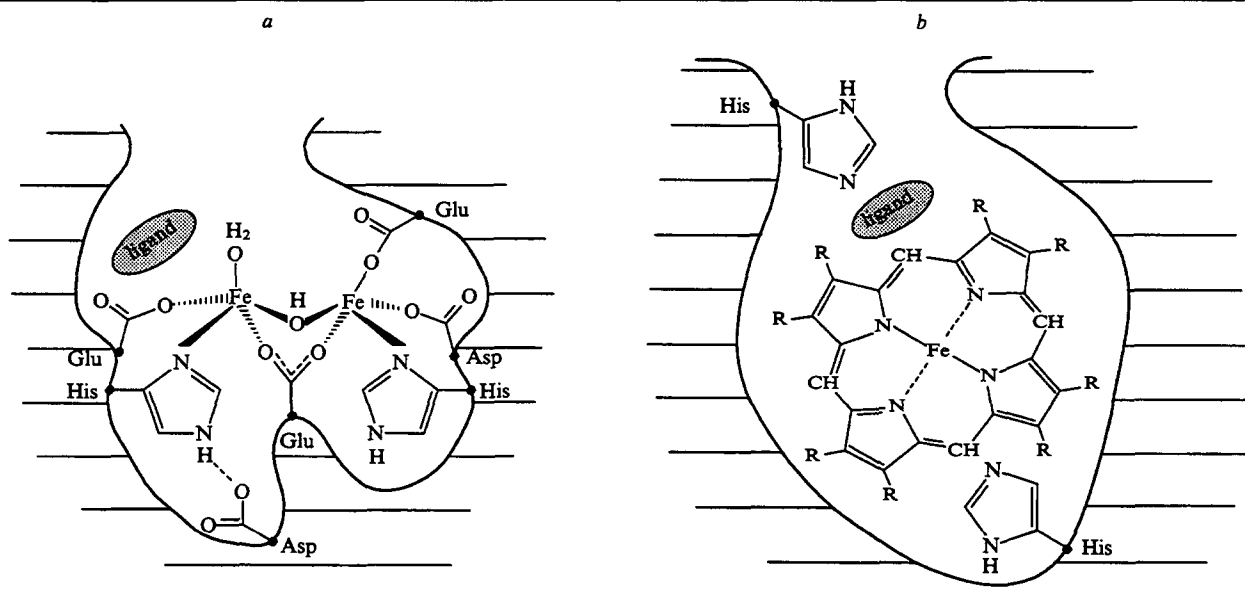


Figure 1. The active centres for the oxidation of hydrocarbon substrates by the monooxygenase of methanotrophs³³ (a) and certain other gas-assimilating microorganisms (b).

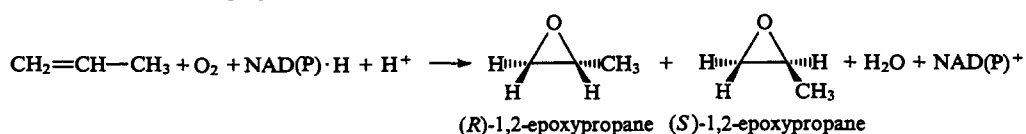
Notation: Asp = aspartic acid residue in the protein component of the monooxygenase; Glu = glutamic acid residue; His = histidine residue; R = hydrocarbon residue in the haem molecule; ligand = low molecular-mass compounds, including substrates (hydrocarbons, oxygen, and inhibitors).

Table 3. Partial oxidation of ethene to epoxyethane by gas-assimilating microorganisms.

Growth substrate	Microorganism (immobilisation method)	<i>a</i> ^a	Ref.	Growth substrate	Microorganism (immobilisation method)	<i>a</i> ^a	Ref.
Methane	Methanotroph H-2	93	37	Ethene	<i>Mycobacterium</i> 2W	4	12
	<i>Methylococcus capsulatus</i> (Bath)	33 [46]	12, 31, 38–40		<i>Mycobacterium</i> E44, 12D, Tu1	3	12
	<i>Methylosinus trichosporium</i> OB3b	16 [16]	12, 31, 39–41		<i>Mycobacterium</i> 32	1	12
	<i>Methylobacterium organophilum</i>	[7.5]	31, 40	Propene	<i>Mycobacterium</i> Py1	50	12, 45–47
					<i>Xantobacter</i> Py2	46	39, 46–48
Ethane	<i>Brevibacterium fuscum</i> ATCC 15993	17.5	42		<i>Mycobacterium</i> Py8	25	12
	<i>Mycobacterium</i> CRL-69	14	42		<i>Mycobacterium</i> Py1 (entrapment in alginate)	6	45
	<i>Arthrobacter</i> CRL-68	8	42		<i>Mycobacterium</i> Py1 (adsorption on sand)	5	45
Propane	<i>Alcaligenes</i> ATCC 15525	43	43	But-1(2)-ene	<i>Mycobacterium</i> By1	19	12
	<i>Pseudomonas fluorescens</i> B-1244	28	43		<i>Xantobacter</i> By2	11	46
	<i>Rhodococcus rhodochrous</i> PNKb1	22	44		<i>Nocardia</i> By1	9	46
	<i>Brevibacterium</i> CRL-56	16	39, 43		<i>Nocardia</i> TB1	2	46
	<i>Rhodococcus erythropolis</i> 3/89	[7]					
n-Butane	<i>Arthrobacter</i> CRL-70	38	42	Buta-1,3-diene	<i>Nocardia</i> TB1	17	46
	<i>Arthrobacter</i> CRL-60	32	42		<i>Mycobacterium</i> B	11	12
	<i>Pseudomonas</i> CRL-71	20	42				
	<i>Mycobacterium</i> E20	15	12	CO ₂ /NH ₄	<i>Nitrosomonas europaea</i>		39

^aThe activity of the cell suspension expressed in nmol min⁻¹ (mg protein)⁻¹ [nmol min⁻¹ (mg dry cells)⁻¹] and determined as the rate of the extracellular accumulation of epoxyethane in the reaction medium. The maximum reaction rates quoted in the literature are presented.

Table 4. Partial oxidation of propene to 1,2-epoxypropane by gas-assimilating microorganisms.



Growth substrate	Microorganisms	<i>a</i> ^a	Enantiomeric composition of product (%)		Ref.
			(R)-isomer	(S)-isomer	
Methane	<i>Methylomonas</i> Z 201	[60]			49
	<i>Methylococcus capsulatus</i>	215 [46]	56	44	31, 39, 40, 41, 50–53
	<i>Methylosinus trichosporium</i> OB3b	175 [30]	57	43	22, 31, 39, 40, 41, 52–54
	Methanotroph H-2	100			37
	<i>Methylosinus</i> CRL	37			40, 55
	<i>Methylobacterium organophilum</i>	22 [21]			31, 40
	<i>Methylomonas albus</i> BG8		53	47	22, 40
	<i>Methanomonas</i> GY-J-3	21 [0.1]			52, 56
Ethane	<i>Mycobacterium</i> E20		47	53	14
	<i>Arthrobacter</i> CRL-60	33			42
	<i>Mycobacterium rhodochrous</i>	27			42
	<i>Brevibacterium fuscum</i>	20			42
Propane	<i>Pseudomonas fluorescens</i> B-1244	102			43
	<i>Nocardia paraffinica</i>	72			43
	<i>Rhodococcus rhodochrous</i> PNKb1	50			44
	<i>Brevibacterium</i> CRL-61	47			43
	<i>Corynebacterium</i> CRL-63	40			43
	<i>Rhodococcus erythropolis</i> 3/89	[9]			57, 58

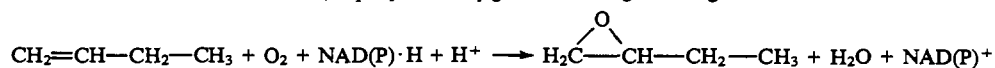
Table 4 (continued).

Growth substrate	Microorganisms	<i>a</i> ^a	Enantiomeric composition of product (%)		Ref.
			(<i>R</i>)-isomer	(<i>S</i>)-isomer	
Propane	<i>Rhodococcus</i> 1r	[1]			50
	<i>Scedosporium</i> A-4	[1]			59
	<i>Nocardia carollina</i> B-276	[0.5]	87	13	22, 34, 39
	<i>Mycobacterium</i> P2y		78	22	22
	<i>Pseudomonas</i> P9y		45	50	22, 39
n-Butane	<i>Arthrobacter</i> CRL-70	58			42
	<i>Pseudomonas fluorescens</i> B-1244	52			42
	<i>Corynebacterium</i> CRL63	40			42
	<i>Mycobacterium</i> E20	17			12
	<i>Mycobacterium vaccae</i>		56	44	22
	<i>Nocardia</i> TB1		68	32	22, 39
	<i>Nocardia</i> IP1		91	9	22, 39
Ethene	<i>Mycobacterium</i> E3	46 [2.5]	93	7	12, 14, 22, 39
					46, 50, 60
	<i>Mycobacterium</i> 2W, Eul	11	93	7	12, 14, 22, 46, 60
	<i>Nocardia carollina</i> B-276	[0.5]	86	14	22, 34, 39
	<i>Mycobacterium</i> E20		88	12	14
	<i>Mycobacterium aurum</i> L1		99	1	22, 39
Propene	<i>Mycobacterium</i> Py1	9.5 ^b			45
	<i>Nocardia corallina</i> B-276	[3.5]			61
	<i>Mycobacterium</i> Py2		97 ^b	3 ^b	14
<i>trans</i> -But-2-ene	<i>Mycobacterium vaccae</i>		61	39	22
	<i>Nocardia</i> TB1	2	60	40	22, 39, 46
Buta-1,3-diene	<i>Mycobacterium</i> B	21	93	7	12, 14
	<i>Nocardia</i> TB1	13	93	7	22, 46
	<i>Nocardia</i> IP1		90	10	22, 39
CO ₂ /NH ₄	<i>Nitrosomonas europaea</i>	—	32	68	22, 39

^a The activity of the resting cells expressed in nmol min⁻¹ (mg protein)⁻¹ [mmol min⁻¹ (mg dry cells)⁻¹] and determined as the rate of the extracellular accumulation of 1,2-epoxypropane in the reaction medium. The maximum reaction rates quoted in the literature are presented.

^b In the presence of 10 mM 1,2-epoxybutane as the inhibitor of the further oxidation of the 1,2-epoxypropane formed.

Table 5. Partial oxidation of butene to 1,2-epoxybutane by gas-assimilating microorganisms.



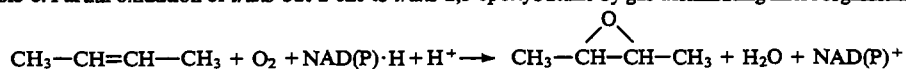
Growth substrate	Microorganisms	<i>a</i> ^a	Enantiomeric composition of product (%)		Ref.
			(<i>R</i>)-isomer	(<i>S</i>)-isomer	
Methane	<i>Methylococcus capsulatus</i>	[11]			31, 40
	<i>Methylobacterium organophilum</i>	[8]			31, 40
	<i>Methylosinus trichosporium</i> OB3b	[4]	39	64	22, 31, 39, 40, 54
	Methanotroph H-2	64.5			37
Ethane	<i>Mycobacterium</i> E20, CRL-69	4	41	59	14, 42
	<i>Brevibacterium fuscum</i>	3			42
	<i>Arthrobacter</i> CRL-68	2			42

Table 5 (continued).

Growth substrate	Microorganisms	a^a	Enantiomeric composition of product (%)		Ref.
			(R)-isomer	(S)-isomer	
Propane	<i>Nocardia paraffinica</i> NNRRL11326	67			43
	<i>Rhodococcus rhodochrous</i> PNKb1	26			44
	<i>Pseudomonas cruceanae</i>	15			43
	<i>Pseudomonas</i> P9y		45	50	22, 39
	<i>Mycobacterium</i> P2y		77	23	22
	<i>Nocardia corallina</i> B-276		84	16	22, 39
n-Butane	<i>Pseudomonas</i> CRL-71	32			42
	<i>Mycobacterium rhodochrous</i>	3			42
	<i>Arthrobacter</i> CRL-60	2			42
	<i>Mycobacterium vaccae</i>		58	42	22
	<i>Nocardia</i> TB1		69	31	22, 39
	<i>Nocardia</i> IP1		87	13	22, 39
Ethene	<i>Mycobacterium</i> E3, E4, Eu, 2D	15	84	16	12, 14, 22, 39, 46
	<i>Mycobacterium</i> E44, 2W	11	83	17	12, 14, 22, 46
	<i>Mycobacterium</i> E20		81	19	14
	<i>Mycobacterium aurum</i> L1		90	10	22, 39
	<i>Nocardia corallina</i> B-276		84	16	22, 39
Propene	<i>Mycobacterium</i> Py10, Py2		95 ^b	5 ^b	14
But-2-ene	<i>Mycobacterium vaccae</i>		64	36	22
	<i>Nocardia</i> TB1	2	63	37	22, 39, 46
Buta-1,3-diene	<i>Mycobacterium</i> B	17	89	11	12, 14
	<i>Nocardia</i> TB1	16	89	11	22, 46
	<i>Nocardia</i> IP1		95	5	22, 39
CO ₂ /NH ₄	<i>Nitrosomonas europaea</i>		29	71	22, 39

^a The activity of the resting cells is expressed in nmol min⁻¹ (mg protein)⁻¹ [nmol min⁻¹ (mg dry cells)⁻¹] and determined as the rate of the extracellular accumulation of 1,2-epoxybutane in the reaction medium. The maximum reaction rates quoted in the literature are presented.

^b In the presence of 10 mM 1,2-epoxypropane as the inhibitor of the further oxidation of the 1,2-epoxybutane formed.

Table 6. Partial oxidation of *trans*-but-2-ene to *trans*-2,3-epoxybutane by gas-assimilating microorganisms.

Growth substrate	Microorganisms	a^a	Enantiomeric composition of product (%)		Ref.
			(R)-isomer	(S)-isomer	
Methane	<i>Methylococcus capsulatus</i>		51	49	22, 39
	<i>Methylomonas albus</i> BG8		50	50	22
	<i>Methylosinus trichosporium</i> OB3b		50	50	22, 39
	<i>Methylocystis parvus</i> OBBP		52	48	22
	<i>Methanotroph</i> H-2	17.5			37
Propane	<i>Nocardia corallina</i> B-276		73	27	22, 39
n-Butane	<i>Nocardia</i> IP1		81	19	22, 39
Ethene	<i>Mycobacterium</i> E3	20	85	15	12, 14, 22, 39, 46
	<i>Mycobacterium</i> 2W	13	78	22	12, 14, 22, 46
	<i>Mycobacterium</i> NCIB 11626		79	21	22
	<i>Mycobacterium aurum</i> L1		87	13	22, 39
	<i>Nocardia corallina</i> B-276		80	20	22, 39

Table 6 (continued).

Growth substrate	Microorganisms	a^a	Enantiomeric composition of product (%)		Ref.
			(R)-isomer	(S)-isomer	
Propene	<i>Mycobacterium</i> Py8	41	93	7	22
	<i>Xantobacter</i> Py2		89	11	22, 39, 46
But-1-ene	<i>Xantobacter</i> By2	22	82	18	22, 46
	<i>Nocardia</i> By1	11	78	22	22, 39, 46
Buta-1,3-diene	<i>Nocardia</i> BT1	19	80	20	22, 46
	<i>Nocardia</i> IP1		81	19	22, 39

^aThe activity of resting cells expressed in $\text{nmol min}^{-1} (\text{mg protein})^{-1}$ and determined as the rate of the extracellular accumulation of *trans*-2,3-epoxybutane in the reaction medium. The maximum reaction rates quoted in the literature are presented.

Table 7. Partial oxidation of buta-1,3-diene to 1,2-epoxybutene by gas-assimilating microorganisms.

$\text{CH}_2=\text{CH}-\text{CH}=\text{CH}_2 + \text{O}_2 + \text{NAD(P)}\cdot\text{H} + \text{H}^+ \rightarrow$ $\rightarrow \begin{array}{c} \text{O} \\ \diagup \quad \diagdown \\ \text{H}_2\text{C}-\text{CH}-\text{CH}=\text{CH}_2 \end{array} + \text{H}_2\text{O} + \text{NAD(P)}^+$				
Growth substrate	Microorganisms	a^a	Ref.	
Methane	<i>Methylococcus capsulatus</i>	[37]	31	
	<i>Methylobacterium organophilum</i>	[23]	31	
	<i>Methylosinus trichosporium</i> OB3b ^b	[21]	31, 40, 54	
	Methanotroph H-2	85.5	37	
Ethane	<i>Brevibacterium fuscum</i> ATCC 159993	1	42	
	<i>Arthrobacter</i> CRL-68	1	42	
	<i>Mycobacterium</i> CRL-69	1	42	
Propane	<i>Nocardia paraffinica</i> ATCC 21198	53	43	
	<i>Nocardia</i> NRRL 11326	16	43	
	<i>Pseudomonas putida</i> ATCC 17453	13	43	
	<i>Brevibacterium fuscum</i> ATCC 159993	6	43	
n-Butane	<i>Brevibacterium fuscum</i> ATCC 159993	3	42	
	<i>Mycobacterium rhodochrous</i>	1	42	
	<i>Pseudomonas</i> CRL-71	0.5	42	
	<i>Arthrobacter</i> CRL-70	0.5	42	

^aThe activity of resting cells expressed in $\text{nmol min}^{-1} (\text{mg protein})^{-1}$ [$\text{nmol min}^{-1} (\text{mg dry cells})^{-1}$] and determined as the rate of the extracellular accumulation of 1,2-epoxybutene in the reaction medium. The maximum reaction rates quoted in the literature are presented.

^bThe ratio (in %) (R)-isomer : (S)-isomer = 36 : 64.

(2) haem-containing monooxygenases of the type of cytochrome P-450 are present in the cells of *Nocardia*,⁶³ *Rhodococcus*,⁶³ *Mycobacterium*,⁶³ *Xantobacter*,⁶⁴ and *Corynebacterium*⁶⁵ (Fig. 1b).

It is noteworthy that the term 'monooxygenase' is applied not to an individual enzyme but to the whole enzyme system, which consists of at least two to three components performing different functions (the electron transport, regulation, and oxidative functions).³² Fig. 1 illustrates the structure of the active centres of the enzyme performing the oxidative function, which consists in the incorporation of an oxygen atom into the hydrocarbon molecule with formation of an alcohol or an epoxide, while the other atom enters into a water molecule (Fig. 2).

The mechanism of the microbiological oxidation of hydrocarbons to alcohols, in particular of methane to methanol, has been thoroughly investigated. There are data showing that the rate-limiting stage of this process is the dissociation of a C-H bond.^{25,32,33} The methane monooxygenase in different strains of methanotrophs has a broad substrate specificity: it hydroxylates C_1 - C_8 alkanes with formation of primary and secondary alcohols,^{32,66} epoxidises C_2 - C_4 alkenes,^{32,54} and oxidises a series of aromatic (benzene, toluene, and styrene) and alicyclic (cyclohexane) hydrocarbons.^{32,67} The ability of methanotrophs to oxidise chloroalkenes (dichloroethene, trichloroethene, and vinyl chloride) with the aid of methane monooxygenase gives rise to prospects for their use in the purification of waste waters: in the first stage, methanotrophs oxidise the chlorinated alkene to the epoxide, which subsequently undergoes degradation with participation of the population of microorganisms, giving rise to nontoxic products — carbon dioxide and chloride ions.⁶⁸⁻⁷⁰

The so called cofactor (or coenzyme), performing the function of an electron donor, is consumed in the course of the biooxidation of hydrocarbons by a monooxygenase (Fig. 2). The natural cofactors for the monooxygenase are the reduced forms of high molecular-mass derivatives of nicotinamide [nicotinamide-adenine dinucleotides NADH or NAD(P)H].

When whole viable cells (and not cell-free enzyme extracts) are used for the oxidative biotransformations, the natural cofactors may be regenerated intracellularly as a result of the occurrence of consecutive enzyme reactions with participation of low molecular-mass substrates. For example, for the methane monooxygenase the effective electron donors are the intermediates products of methane metabolism, namely methanol,⁷¹ formaldehyde,^{41,55} and formate,^{41,55} which are oxidised by intracellular enzymes with formation of the reduced form NAD(P)H. The latter is in its turn consumed by the methane monooxygenase on the oxidation of the hydrocarbon molecule (Fig. 2).^{25,33}

It has been observed that in certain cases the addition of ethanol and ethyl acetate to the reaction medium prolongs the bioepoxidation of propene by mycobacteria. In addition, the rate of formation of epoxypropane increases in their presence.⁶⁰ Apparently these compounds participate in the regeneration of the natural cofactor of the monooxygenase in the above bacteria.

For *Rhodococcus* sp. it has not so far been possible to detect a low molecular-mass electron donor.⁵⁰ Glucose, added to a cell suspension of the Japanese strain *Nocardia corallina* B-276, promotes the regeneration of the monooxygenase cofactor.^{35,72,73} Evidently the solution of the problem of the replacement of the expensive and virtually inaccessible natural cofactors by low molecular-mass substrates may render the oxidative biocatalysis based on resting cells promising from the standpoint of its practical application.

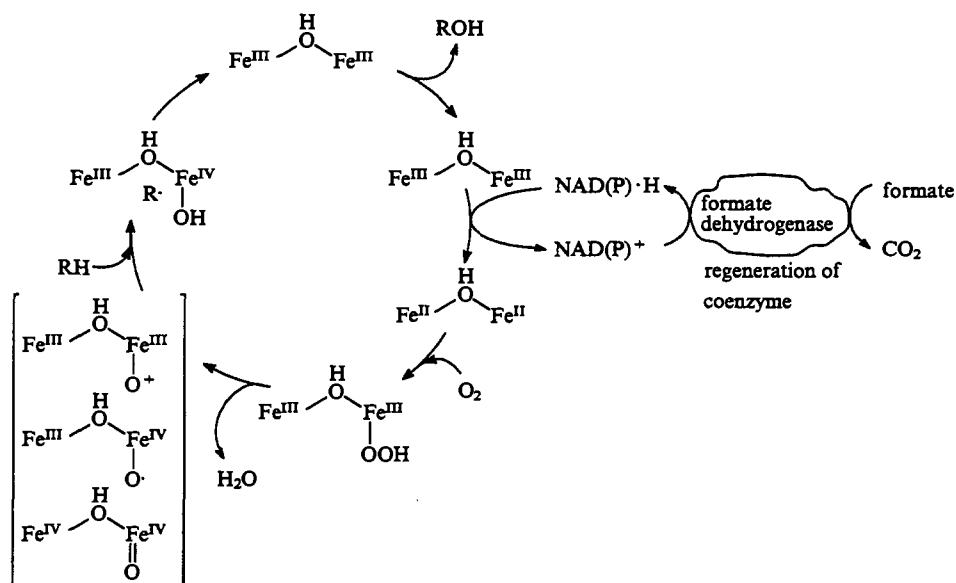


Figure 2. The mechanism of the hydroxylation of the alkanes RH by the monooxygenase of methanotrophs³³ and a possible pathway leading to the regeneration of the coenzyme NAD(P)H as a result of the consecutive enzymic reaction.

Thus the direct selective oxidation of gaseous hydrocarbons can be achieved by biocatalytic methods involving gas-assimilating microorganisms possessing a monooxygenase activity, the process being characterised by a high selectivity and stereospecificity and occurring under mild conditions without the formation of toxic side products (the only possible product of this kind is carbon dioxide).

IV. Microbiological epoxidation of lower alkenes

The microbiological epoxidation of lower alkenes was first achieved in 1963 when it was possible to obtain 1 mg of 1,2-epoxyoctane from oct-1-ene with the aid of *Pseudomonas aeruginosa* cells grown on heptane.⁷⁴ During the last decade, the studies in this field have been carried out by scientific teams from many countries (Table 8). As already noted, certain 'biotechnological' methods of synthesis of epoxides from alkenes have been implemented on a semi-industrial scale.^{2,3} The epoxidation of gaseous alkenes is effected by microorganisms grown both on gaseous alkanes (methane, ethane, and propane) and on gaseous alkenes (ethene, propene, and butene) (Tables 3–7), the monooxygenase of the alkane-assimilating microorganisms having the ability not only to epoxidise alkenes but also to hydroxylate the terminal CH₃ group with formation of unsaturated alcohols.⁷⁸

It is of interest to note that, in the reactions involving the oxidative biotransformation of alkenes effected by *Pseudomonas oleovorans*,⁷⁸ there is no relation whatever between the chemical reactivity of the bonds being oxidised and the oxidative activity of the microorganisms. For example, oct-2-ene is not epoxidised, whereas oct-1-ene is oxidised with formation of 1,2-epoxyoctane; propene is also not epoxidised, but is transformed into allyl alcohol.

The epoxides formed during oxidative biotransformation accumulate extracellularly in the reaction medium, provided that they are not intermediates in the metabolism of the main growth substrate but are formed by virtue of the relatively broad substrate specificity of the monooxygenase. For example, ethene-assimilating mycobacteria, which effectively oxidise propene and butene, effect the extracellular accumulation of their epoxides (Tables 4–6), whereas epoxyethane undergoes further metabolic transformations, which are necessary for cell growth and biosynthesis. In order to prevent the metabolic transformations of the epoxide formed on oxidation of the growth substrate, one may add an inhibitor to the medium. For example, the inhibitor of the

further oxidation of 1,2-epoxypropane, formed by propene-assimilating cells, is the related 1,2-epoxybutane, which undergoes degradation, enabling the epoxypropane to accumulate in the medium.^{45,79}

The epoxides accumulated in the medium have a distinctive toxic activity, since they are capable of alkylating protein molecules and of decomposing membranes (this permits their use as sterilising agents in medical practice, epoxyethane being the most toxic). The inhibition by epoxides is irreversible and specific in relation to monooxygenases, while other vitally important enzymes are only slightly inactivated.⁷⁹ Various microorganisms are unequally susceptible to the action of epoxides: the most stable are the alkene-utilising microorganisms of the genus *Mycobacterium* (they withstand a concentration up to 100 mM), while the

Table 8. Microbiological epoxidation of alkenes.

Alkenes epoxidised	Microorganisms	Research groups
C ₂ –C ₄	Methanotrophs: <i>Methylococcus capsulatus</i> , <i>Methylosinus trichosporium</i>	C T Hou (EXXON Res. & Eng. Co., USA); H Dalton, J C Murrell (University of Warwick, UK)
C ₂ –C ₄	<i>Mycobacterium</i> sp.	J A M de Bont (Agriculture University of Wageningen, The Netherlands)
C ₂ –C ₁₈	<i>Nocardia corallina</i> B-276	K Furuhashi (Nippon Mining Co. Ltd, Japan)
C ₂ –C ₃	<i>Caldariomyces fumago</i> , <i>Flavobacterium Cetus</i> sp.	S L Neidleman (CETUS Corp., USA) ^{75–77}
C ₆ –C ₁₂	<i>Pseudomonas oleovorans</i>	M J de Smet (University of Groningen, The Netherlands)

most sensitive are the methanotrophs (the epoxide exerts a distinct toxic effect on the latter at a concentration less than 10 mM).⁷⁹

The following approaches have been proposed for the practical solution of the problem of reducing the toxic effect of the epoxides and of the concentration and isolation of the valuable oxygen-containing product from the reaction medium: the immobilisation of the cells on/in solid carriers, as a result of which the resistance of the microorganisms to the action of the toxic reagents

as a rule increases; the removal of the epoxide formed from the reaction zone, which is achieved either by its extraction into the solvent phase of a two-phase water-immiscible organic solvent system or by passing a gas stream with subsequent isolation of the target product by absorption in a suitable organic phase.

These approaches may be clearly illustrated in relation to the epoxidation of propene (Table 9). The gas-utilising microorganisms are immobilised mainly via their entrapment into

Table 9. Epoxidation of propene by the immobilised cells of gas-assimilating organisms.

Microorganism	Immobilisation method	Process characteristics		Bioreactor ^b	Ref.
		α^a	other parameters		
<i>Methanomonas</i> GYJ-3	adsorption on sand, zeolite, aluminium oxide, polypropylene paraffin	0.25 (sand) 0.19 (polypropylene)	adsorption: 1.5 (sand), 3.4 mg g ⁻¹ (polypropylene)	G-S, flow type with stationary bed	56
	incorporation in alginate gel	1.2		L-S, periodic with stirring	80
<i>Methylosinus</i> CRL 31, <i>Methylococcus</i> CRLM1, <i>Methylosinus trichosporium</i> OB3b	adhesion in the form of a biofilm on porous glass	8–15	stability: 18 h of continuous operation (regeneration by methanol vapour after each 10 h); conversion of propene: 2.7%	G-S, flow type with stationary bed	31, 55, 71
<i>Methylosinus trichosporium</i> OB3b <i>Methylococcus capsulatus</i> M1	adhesion on glass beads, activated charcoal, silica gel		yield of product: 250–300 nmol min ⁻¹ ; stability: 7 h of continuous operation	G-S	81
<i>Rhodococcus</i> <i>Mycobacterium</i> E3, <i>Methylosinus trichosporium</i>	adsorption on silica gel, carbon, or carbonsaturated aluminium oxide; double immobilisation in the pores of carbonsaturated aluminosilicate	10–20	adsorption, mg g ⁻¹ : 40 (rhodococci), 3 (methanotrophs) stability: after 14 h of continuous operation, 46% of initial activity is retained	L-S, flow type with stationary bed	50
<i>Mycobacterium</i> E3	lyotropic surfactant mesophase in the water-hexane twophase system	26.3			82
	incorporation in alginate gel	0.07	stability: 7 days; productivity: 0.03 g of (<i>R</i>)-epoxypropane per 1 g of cells after 2 days	L-S, flow type with recirculation and stationary bed in a two-phase system water-organic solvent	83, 85, 86, 89
	incorporation in alginate gel	2.3		G-L-S, flow type with fluidised bed	86
<i>Mycobacterium</i> E3, E4, 2W	incorporation in alginate and carrageenan	2.5	stability: 3 h of continuous operation	L-S, periodic with stirring	12, 87, 88
<i>Mycobacterium</i> Py1	on sand		productivity: 0.25 mmol after 4 days	G-S	89
<i>Mycobacterium</i> Eu1	adhesion on lava	2.6 ^c	stability: 20 days of operation (16 cycles 15 h each); conversion of propene: 90%	G-S	60

Table 9 (continued).

Microorganism	Immobilisation method	Process characteristics		Bioreactor ^b	Ref.
		<i>a</i> ^a	other parameters		
<i>Nocardia corallina</i> B-276	emulsion in liquid paraffin	7.1	stability: 9 days of continuous operation, <i>t</i> _{1/2} = 200 h; conversion of propene: 95%–100%; productivity: 2.3 g of epoxyp propane per 1 g of cells	L–L, continuous bubbling of the gas stream	72
<i>Nocardia corallina</i> B-276	adsorption on poly- propylene and polyethylene	5.0–6.8	adsorption: 1.0–2.8 mg g ⁻¹ ; stability: 2–3 days of operation, <i>t</i> _{1/2} = 36 h	G–S, flow type with stationary bed	13
	incorporation in alginate, carrageenan, and urethane matrix	0.9	stability: <i>t</i> _{1/2} = 78 h	G–S, flow type with stationary bed	13
	incorporation in poly- acrylamide gel	1.3–3.7	stability: 7 days without loss of activity	L–S, flow type	90

^a Activity expressed in nmol min⁻¹ (mg dry cells)⁻¹ and determined as the rate of the extracellular accumulation of epoxyp propane in the reaction medium.

^b Notation: G = gas phase; L = liquid phase; S = solid phase.

^c The activity expressed in nmol min⁻¹ (mg protein)⁻¹.

natural organic gels (alginate, carrageenan), in the matrix of which the cells remain virtually intact (integrity, metabolic activity) and retain a fairly high transforming activity and stability.^{12, 13, 60, 80, 83–88, 90} The principal deficiency of organic gels is their swellability, inducing a high hydrodynamic resistance to the flow, and also their decomposition during use by chemical and biological factors.

Another method for the immobilisation of bacterial cells is adsorption (adhesion) on the surfaces of inorganic carriers (silicates, oxides, and carbon materials).^{31, 50, 55, 56, 60, 71, 81, 89} Under these conditions, biofilms are formed as a rule. Covalent immobilisation is used rarely, since the cross-linking agents used for the formation of covalent bonds (dialdehydes and carbodiimides) are usually toxic to cells.

The immobilisation of microorganisms in the mesophases of nonionic surfactants (of the type of polyoxyethylene n-dodecyl ethers with different molecular masses), formed in a water–organic solvent (hexadecane) two-phase system, leads to interesting prospects.⁸² The *Mycobacterium* E3 cells immobilised in this way exhibit the maximum epoxidising activity (Table 9).⁸²

Another nontrivial approach to the immobilisation of enzymes and bacterial cells involves the sealing of the biologically active material with the aid of a gel-forming system within the pores of an inorganic carrier.⁹¹ In essence, this is a double immobilisation method, which combines the advantages of the incorporation of the cells into gels (high biocatalytic activity and stability) and of the use of inorganic carriers (high mechanical strength and resistance to degradation). The heterogeneous biocatalyst obtained in this way exhibits a relatively high enzyme activity and is stable both in storage and under operating conditions (Table 9).⁵⁰

One of the main problems in the immobilisation of enzymes and cells is that of the selection of the optimum carrier and immobilisation procedure. Nowadays the immobilisation of enzymes and cells is approached purely empirically, predominantly on the basis of the tradition which has arisen in a particular research group. However, analysis of a large volume of literature data and our own results enables us to formulate certain general

principles governing the immobilisation and stabilisation of enzymes and microbial cells on/in solid matrices.

The stabilisation of immobilised enzymes and cells is ensured by the mutual correspondence of the characteristics of the biologically active material and the carrier. In the first place, the biomolecule (cell) must correspond exactly to the size of the support pores, as a result of which a multipoint interaction is achieved. For the stabilisation of bacterial cells and the maintenance of their viability in the immobilised state, it is essential that the morphology of the porous space of the carrier should definitely correspond to the biologically active material: the ratio of the pore size to the size (length) of the microorganism should range from 1:5 and the pores of the given size should occupy ~70% of the porous space.⁹² In other words, 1–10 µm macropores should predominate in the support texture.

Another principle is the mutual chemical correspondence of the biomolecule (cell) and the carrier (gel) surface, particularly from the standpoint of their hydrophilic–hydrophobic characteristics.⁹³ For example, microorganisms with a hydrophobic cell wall are sorbed most strongly on a hydrophobic carrier surface (or in a hydrophobic mesophase) and exhibit a relatively high biocatalytic activity and stability.⁸² The practical implementation of the mutual correspondence principles, particularly in the case of the immobilisation of individual enzymes, as a rule promotes the formation of active heterogeneous biocatalysts, which are more stable by a factor of tens and thousands than their homogeneous analogues.

Unfortunately, on immobilisation of whole bacterial cells the stabilisation of the enzyme activity by virtue of the interaction of the microorganisms with the surface of optimum carriers (selected taking into account the mutual correspondence) is not quite so marked and striking as in the case of enzymes. The enzyme activity of whole bacterial cells apparently depends to a large extent on the intracellular microenvironment of the enzymes, which is determined only indirectly by the state of the immobilised bacterial cells.

The mechanisms of the initiation and stabilisation of enzyme activity in immobilised microorganisms may be different in each specific case. For example, an increase in activity may be

promoted by the improvement in gas exchange and in the distribution of nutrient substances,^{94,95} by the structural rearrangement of the membranes leading to an increase in permeability and the acceleration of transport of substrates into the cell,^{96,97} by the change in the physiology of the cells under the influence of the stress accompanying the immobilisation procedure,⁹⁸ etc. Evidently the main advantage of the immobilisation of microbial cells consists in the possibility of obtaining biocatalysts in a heterogeneous form, which makes it possible to carry out biocatalytic processes in a continuous regime in bioreactors of different design and with repeated employment of the biologically active material. The matrix stabilises fairly frequently the enzyme activity of the immobilised bacterial cells and also increases the resistance of the microorganisms immobilised on the carrier surface to the effect of toxic compounds.

Another approach to the solution of the problem of overcoming the inhibiting effect of epoxides on the cells of gas-utilising microorganisms consists in the removal of the epoxide from the reaction zone. Two-phase water-organic solvent (as a rule, n-hexadecane) systems with extraction of the epoxide into the organic phase^{61,83,84,86} and/or the removal of the epoxide, for example epoxyp propane, from the gas stream (where its fraction at 35 °C is ~ 3% of all the molecules⁸⁶) by absorption in di-n-octyl phthalate or by acid hydrolysis in sulfuric acid solution (pH 1, 30 °C) are used for this purpose.⁸⁴ The immobilisation of microorganisms promotes an increase in the resistance of bacterial cells to the action of the organic solvent apparently as a result of the presence of an aqueous microenvironment in the vicinity of the solid carrier surface.

In conclusion, it must be emphasised yet again that certain gas-assimilating microorganisms of the genera *Mycobacteria* and

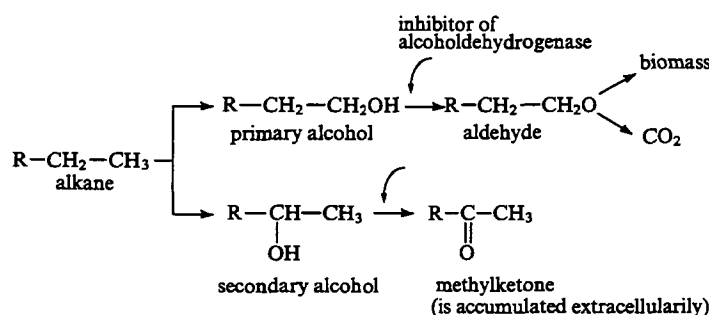
Nocardia are capable of epoxidising unsaturated hydrocarbons stereospecifically, so that only one of the optical isomers is formed in excess, accumulating extracellularly in the reaction medium (Tables 4–7). Another procedure for the preparation of optical isomers of epoxides is based on the fact that certain microorganisms of the genera *Xantobacter*⁹⁹ and *Nocardia* H8¹⁰⁰ are capable of the degradation (utilisation) of only one of the stereoisomers of the racemic mixture, whereas the other isomer of the epoxide accumulates in the medium.

Thus the epoxidation of light alkenes (ethene, propene, and butene) can be achieved by means of the enzymic monooxygenase complexes of alkane- and alkene-utilising microorganisms in free or immobilised forms (Tables 4–7 and 9). One of the main ways of increasing the effectiveness of the alkene bioepoxidation processes is the reduction of the inhibiting effect of the epoxides, which accumulate in the reaction medium and exhibit a very pronounced toxicity. For this purpose, the processes are optimised by employing, for example, immobilised microorganisms in water-organic solvent two-phase systems.

V. Microbiological hydroxylation of gaseous alkanes

As already mentioned, the direct selective oxidation of saturated hydrocarbons to valuable oxygen-containing products (alcohols, aldehydes, ketones, and acids) is the main problem in the chemical processing of natural gas by homogeneous and heterogeneous catalytic methods. The partial oxidation of alkanes is traditionally carried out on oxide catalysts (for example, catalysts based on V₂O₅ or MoO₃), the key parameter of the processes being selectivity. The biotechnological approach to the direct single-

Table 10. Partial single-stage oxidation of gaseous hydrocarbons to alcohols and methyl ketones by atmospheric oxygen with participation of gas-assimilating microorganisms.



Initial hydrocarbon	Product	Microorganisms (growth substrate)	α^a	Inhibitor (concentration)	Ref.
Methane	methanol	<i>Methylococcus capsulatus</i> (methane)	42	none	41
	"	<i>Methylosinus trichosporium</i> (methane) ^b	[149]	phosphate ions (80–100 mM)	18
	"	<i>Methylococcus capsulatus</i> (methane)	[131]	EDTA (10 mM)	52
	"	<i>Methylosinus trichosporium</i> (methane)	[79]	phosphate ions (80–100 mM)	18
	"	"	[50]	EDTA (10 mM)	52
	"	<i>Methylomonas</i> GY-J-3 (methane)	[31]	"	52
	"	<i>Methylosinus trichosporium</i> OB3b (methane)	25 [24]	treatment of cells with cyclopropane; cyclopropanol (0.3 mM)	41, 101, 102
	"	"	[8]	NaCl (0.2 M), EDTA (2 mM), H ₂ (10%)	17

Table 10 (continued).

Initial hydrocarbon	Product	Microorganisms (growth substrate)	α^a	Inhibitor (concentration)	Ref.
Methane	methanol	<i>Methylobacterium organophilum</i> (methane)	7	none	41
	"	<i>Methamonas methanooxidans</i> (methane)	—	iodoacetate (0.003 M)	103
Ethane	ethanol	<i>Methylosinus trichosporium</i> OB3b (methane)	22 [12]	EDTA (2 mM), H ₂ (10%)	17, 41
	"	<i>Methylococcus capsulatus</i> (methane)	33	none	41
	"	<i>Methylobacterium organophilum</i> (methane)	7	"	41
	"	<i>Scedosporium</i> A-4 (propane)	[6]	pyrazole (10 mM)	59
Propane	propan-1-ol	<i>Scedosporium</i> A-4 (propane)	[5]	"	59
	"	<i>Rhodococcus rhodochrous</i> (propane)	—	none	104
	propan-2-ol	Methanotroph H-2 (methane)	25	"	37
	"	<i>Methylosinus trichosporium</i> CRL15 (methane)	18	"	105
	"	<i>Methylococcus capsulatus</i> (methane)	18	"	105, 106
	"	<i>Methylobacterium organophilum</i> (methane)	12.5	"	41, 105–107
	"	<i>Methylosinus trichosporium</i> OB3b (methane)	8 [3]	EDTA (2 mM)	17, 105, 106
	"	<i>Scedosporium</i> A-4 (propane)	[2]	pyrazole (10 mM)	59
	"	<i>Rhodococcus rhodochrous</i> (propane)	—	—	104
	acetone	Methanotroph H-2 (methane)	50	none	37
Propane	"	<i>Methylococcus capsulatus</i> CRL M1 (methane)	42	"	41, 105, 108
	"	<i>Nocardia paraffinica</i> (propane)	33	"	43
	"	<i>Methylobacterium organophilum</i> (methane)	30	"	41, 105, 108
	"	<i>Methylosinus trichosporium</i> OB3b (methane)	25 [3]	"	17, 41, 105, 108
	"	<i>Methylobacter</i> CRL M6 (methane)	17	"	105, 108
	"	<i>Pseudomonas fluorescens</i> (propane)	17	"	43
	"	<i>Methylocystis parvus</i> (methane)	15	"	105, 108
	"	<i>Scedosporium</i> A-4 (propane)	[0.6]	"	109
	"	<i>Mycobacterium smegmatis</i> (propane)	—	—	110
	butan-1-ol	<i>Scedosporium</i> A-4 (propane)	[8]	pyrazole (10 mM)	59
n-Butane	"	<i>Methylosinus trichosporium</i> OB3b (methane)	5	none	41
	"	<i>Methylococcus capsulatus</i> CRL M1 (methane)	2	"	41
	butan-2-ol	Methanotroph H-2 (methane)	33	"	37
	"	<i>Methylococcus capsulatus</i> CRL M1 (methane)	20	"	41, 106
	"	<i>Methylosinus trichosporium</i> OB3b (methane)	10	"	41, 105, 106
	"	<i>Methylomonas</i> CRL (methane)	10	"	105–107
	"	<i>Methylobacterium organophilum</i> (methane)	3	"	41
	"	<i>Scedosporium</i> A-4 (propane)	[2]	pyrazole (10 mM)	59

Table 10 (continued).

Initial hydrocarbon	Product	Microorganisms (growth substrate)	a^a	Inhibitor (concentration)	Ref.
n-Butane	butan-2-one	<i>Nocardia paraffinica</i> (propane)	73	none	43
	"	<i>Brevibacterium</i> CRL 56 (propane)	43	"	43
	"	<i>Methylococcus capsulatus</i> CRL M1 (methane)	33	"	41, 105, 108
	"	<i>Methylobacterium organophilum</i> (methane)	25	"	41, 105, 108
	"	<i>Pseudomonas fluorescens</i> (propane)	20	"	41, 105, 108
	"	<i>Methylosinus trichosporium</i> OB3b (methane)	20	"	41, 105, 108
	"	<i>Methylomonas</i> CRL 8 (methane)	12	"	105
	"	<i>Scydosporium</i> A-4 (n-butane)	[0.3]	"	109
Isobutane	butan-2-one	<i>Mycobacterium smegmatis</i> (propane)	—	—	110
	2-methyl-propan-1-ol	Methanotroph H-2 (methane)	89	none	37
	2-methyl-propan-2-ol	Methanotroph H-2 (methane)	89	"	37
Cyclopropane	cyclo-propanol	<i>Methylosinus trichosporium</i> OB3b (methane)	—	"	102
Propene	allyl alcohol	<i>Pseudomonas oleovorans</i> (n-octane)	—	"	78
	acrylic acid	<i>Mycobacterium convolutum</i> (propane)	—	"	111
But-1-ene	but-3-en-1-ol	<i>Pseudomonas oleovorans</i> (n-octane)	—	"	78

^a The activity is expressed in $\text{nmol min}^{-1} (\text{mg protein})^{-1}$ [$\text{mol min}^{-1} (\text{mg dry cells})^{-1}$] and is determined as the rate of the extracellular accumulation of the oxidation product in the reaction medium. The maximum reaction rates quoted in the literature are presented.

^b Immobilised by covalent binding to DEAE cellulose.

stage oxidation of alkanes by atmospheric oxygen to alcohols and methyl ketones with the aid of the cells of gas-assimilating microorganisms is demonstrated in Table 10.

In the microbiological hydroxylation of alkanes, certain additional problems, which do not exist in the epoxidation of alkenes, arise. One of them involves the search for an effective inhibitor of the further bioconversion of the alcohol formed in the reaction (see the Scheme in Table 10). The point is that, during the growth of microorganisms on saturated hydrocarbons, the primary activation of a C–H bond of the hydrocarbon by the bacterial monooxygenase results in the formation of molecules of a primary or secondary alcohol (Fig. 2), which are converted by alcohol dehydrogenase into an aldehyde or methyl ketone respectively.^{23, 25, 27} The aldehyde molecules then undergo further metabolic transformations, leading to the incorporation of carbon into the biomass, whereas the methyl ketones accumulate in the reaction medium. The problem of the search for an effective universal inhibitor of alcohol dehydrogenase, which would interrupt the cell metabolism at the stage involving the formation of a primary or secondary alcohol, has still not been solved and it apparently should be solved individually in each specific case. Cyclopropanol, pyrazole, and the sodium salt of ethylenediaminetetraacetic acid (EDTA) are the most effective of the inhibitors of bacterial alcohol dehydrogenases investigated (Table 10).

As in the microbiological epoxidation of alkenes, the concentration of the final oxygen-containing product (an alcohol or a methyl ketone) in the reaction mixture does not exceed several tens of millimoles per litre. The hydroxylation process is retarded as a function of time. The causes of this retardation may be as follows: an increase in the rate of bioconversion of the alcohol formed; the consumption of the cofactor (electron donor) required for the oxidative biotransformation of the hydrocarbons; the toxic effect of the alcohol or methyl ketone, accumulated in the reaction medium, on the microbial cell.

Thus the problems of reducing the toxic effect of the oxygen-containing product formed, of the regeneration of the monooxygenase cofactor with the aid of available low molecular-mass substrates of the coupled enzymic reactions, and the isolation of the final oxygen-containing product from dilute buffer solutions arise when the hydroxylation process is carried out. In addition, it is necessary to solve also the problem of inhibiting the further bioconversion of the alcohol formed. The procedures for overcoming some of these difficulties were described above.

There is so far no need for the practical implementation of the biocatalytic alkane hydroxylation processes, since in the basic industrial organic synthesis traditional chemical procedures for the synthesis of alcohols (of methanol from the synthesis gas and of ethanol by the hydration of ethene) are widely employed. In terms of their economic parameters, in particular in terms of the cost of the final oxygen-containing product, they cannot at the moment be competed with.

VI. Conclusion

The alternative biotechnological procedures for the direct selective oxidation of gaseous C_1 – C_4 alkanes and C_2 – C_4 alkenes make it possible to obtain valuable oxygen-containing products — alcohols and epoxides. The single-stage oxidative transformations of hydrocarbons can occur with participation of the bacterial cells of gas-assimilating microorganisms with the necessary monooxygenase enzyme activity. The biocatalytic processes are distinguished by a low energy consumption, because they are carried out under mild conditions and at low temperatures (below 40 °C), by a high selectivity (close to 100%) independent of the degree of conversion of the initial substrate, and, what is most important, by stereospecificity. One optically active stereoisomer may predominate in the oxygen-containing product, which is impossible when the analogous chemical processes are performed. It is at present still too early to consider the replacement of the large scale organic synthesis in industry by oxidative biocatalytic processes, but the scientific investigations performed in this field, which are at the boundary between microbiology and organic chemistry, are quite timely and promising.

References

1. A Sasson *Biotechnology: Advances and Horizons* (Translated into Russian; Moscow: Mir, 1987)
2. K Furuhashi *Biosci. Ind., Jpn.* **45** 468 (1987)
3. K Furuhashi *J. Synth. Org. Chem., Jpn.* **45** 162 (1987)
4. A M Maitra *Appl. Catal.* **104** 11 (1993)
5. R Pitchai, K Kleir *Catal. Rev. Sci. Eng.* **28** 13 (1986)
6. M J Brown, N D Parkyns *Catal. Today* **8** 305 (1991)
7. H-F Liu, R-S Liu, K Y Liew, R E Johnson, J H Lunsford *J. Am. Chem. Soc.* **106** 4117 (1984)
8. Yu S Mardashev, G D Kazakova, L S Ibraeva, in *Tez. Dokl. Vsesoyuz. Konferentsii "Selektivnoe Okislenie Uglevodorodov i Resursosberezhnie Uglevodorodnogo Syr'ya"* (Abstracts of Reports at the All-Union Conference 'Selective Oxidation of Hydrocarbons and Procedures Designed to Economise on Hydrocarbon Resources') (Khar'kov: Khar'kov Polytechnic Institute, 1991) p. 53
9. R K Grasselli, G Centi, F Trifiro *Appl. Catal.* **57** 149 (1990)
10. R Zhao, Z Xu, Z Wang *Petrochem. Technol. (China)* **4** 157 (1995)
11. S V Adel'son, T P Vishnyakova, Ya M Paushkin *Tekhnologiya Neftekhimicheskogo Sintez* (Technology of Petrochemical Synthesis) (Moscow: Khimiya, 1985)
12. A Q H Habets-Crutzen, L E S Brink, C G van Ginkel, J A M de Bont, J Tramper *Appl. Microbiol. Biotechnol.* **20** 245 (1984)
13. L B Wingard Jr, R P Roach, O Miyawaki, K A Egler, G E Klinzing, R S Silver, J S Brackin *Enzyme Microbiol. Technol.* **7** 503 (1985)
14. A Q H Habets-Crutzen, C J M Carlier, J A M de Bont, D Wistuba, V Schurig, S Hartmans, J Tramper *Enzyme Microbiol. Technol.* **7** 17 (1985)
15. P S Yarladda, L F Morton, N R Hunter, H D Gesser *Ind. Eng. Chem. Res.* **27** 252 (1988)
16. H D Gesser, N R Hunter, C B Prakash *Chem. Rev.* **85** 235 (1985)
17. D O Mountford, Y Pybus, R Wilson *Enzyme Microbiol. Technol.* **12** 343 (1990)
18. P K Mehta, S Mishra, T K Ghose *Biotechnol. Bioeng.* **37** 551 (1991)
19. S Vaisman *Biofutur* **52** 53 (1986)
20. V G Debabov *Zh. Vses. Khim. O-va im D I Mendeleeva* **35** 755 (1990)
21. Yosiki Tani *Biosci. Ind., Jpn.* **48** 635 (1990)
22. C A G M Weijers, C G van Ginkel, J A M de Bont *Enzyme Microbiol. Technol.* **10** 214 (1988)
23. E N Kondrat'eva *Khemolitotrofy i Metilotrofy* (Chemolithotrophs and Methylotrophs) (Moscow: Izd. Mosk. Gos. Univ., 1983)
24. E I Kvasnikov, Yu R Malashenko, V A Romanovskaya *Usp. Mikrobiol.* **9** 125 (1974)
25. Yu R Malashenko, V A Romanovskaya, Yu A Trotsenko *Metanokislyayushchie Mikroorganizmy* (Oxidising Methane Microorganisms) (Moscow: Nauka, 1978)
26. I J Higgins, D J Best, R C Hammond *Nature (London)* **286** 561 (1980)
27. I B Ivshina, R A Pshenichnov, A A Oborin *Propanokislyayushchie Rodokokki* (Propane Oxidising Rhodococci) (Sverdlovsk: Ural Scientific Centre of Academy of Sciences of the USSR, 1987)
28. T V Koronelli *Lipidy Mikobakterii i Rodstvennykh Mikroorganizmov* (Lipids of Mycobacteria and Related Microorganisms) (Moscow: Izd. Mosk. Gos. Univ., 1984)
29. J R Vestal, J J Perry *Can. J. Microbiol.* **17** 445 (1971)
30. G K Skryabin, L A Golovleva *Ispolzovanie Mikroorganizmov v Organicheskom Sintez* (The Use of Microorganisms in Organic Synthesis) (Moscow: Nauka, 1976)
31. C-T Hou *Biotechnol. Gen. Eng. Rev.* **4** 145 (1986)
32. R I Gvozdev, N P Akent'eva *Biokhimiya i Fiziologiya Metilotrofov* (The Biochemistry and Physiology of Methylotrophs) (Pushchino: Institute of Biochemistry and Physiology of Microorganisms, 1987)
33. J D Lipscomb *Annu. Rev. Microbiol.* **48** 371 (1994)
34. K Furuhashi, A Taoka, S Uchida, S Suzuki *Eur. J. Appl. Microbiol. Biotechnol.* **12** 39 (1981)
35. K Furuhashi *J. Agr. Chem. Soc., Jpn.* **62** 772 (1988)
36. J A M de Bont, M M Attwood, S B Primrose, W Harder *FEMS Microbiol. Lett.* **6** 183 (1979)
37. T Imai, H Takigawa, S Nakagawa, G-J Shen, T Kodama, Y Minoda *Appl. Environ. Microbiol.* **52** 1403 (1986)
38. D I Stirling, H Dalton *FEMS Microbiol. Lett.* **5** 315 (1979)
39. S Hartmans, J A M de Bont, W Harder *FEMS Microbiol. Rev.* **63** 235 (1989)
40. C-T Hou, R N Patel, A I Laskin, N Barnabe *Appl. Environ. Microbiol.* **38** 127 (1979)
41. C-T Hou, P N Patel, A I Laskin, N Barnabe *FEMS Microbiol. Lett.* **9** 267 (1980)
42. R N Patel, C-T Hou, A I Laskin, A Felix, P Derelanko *J. Appl. Biochem.* **5** 121 (1983)
43. C-T Hou, R N Patel, A I Laskin, N Barnabe, I Barist *Appl. Environ. Microbiol.* **46** 171 (1983)
44. N R Woods, J C Murrell *Biotechnol. Lett.* **12** 409 (1990)
45. J A M de Bont, C G van Ginkel, J Tramper, K Ch A M Luyben *Enzyme Microbiol. Technol.* **5** 55 (1983)
46. C G van Ginkel, H G J Welten, J A M de Bont *Appl. Environ. Microbiol.* **53** 2903 (1987)
47. R S Hamstra, M R Murriss, J Tramper *Biotechnol. Bioeng.* **29** 884 (1987)
48. C G van Ginkel, H G J Welten, J A M de Bont *Appl. Microbiol. Biotechnol.* **24** 334 (1986)
49. Wang Fulai, Zheng Jian, Wang Fang, Chen Jingru, Hu Xiao, Zhao Zhujie *Acta Microbiol. Sin. (China)* **33** 129 (1993)
50. G A Kovalenko, V D Sokolovskii *Biotechnol. Bioeng.* **39** 522 (1992)
51. D J Leak, H Dalton, J Gen *Microbiology* **129** 3487 (1983)
52. G A Kovalenko, V D Sokolovskii *React. Kinet. Catal. Lett.* **48** 447 (1992)
53. C-T Hou, R N Patel, A I Laskin *Adv. Appl. Microbiol.* **26** 41 (1980)
54. A Shigetoshi, O Mitsufumi, O Ichiro *J. Mol. Catal.* **49** L65 (1989)
55. C-T Hou *Ann. N. Y. Acad. Sci.* **434** 541 (1986)
56. Gao Canzhu, Li Zhuben, Ning Zhizhong, Miao Dexun *J. Mol. Catal. (China)* **5** 227 (1991)
57. A K Kulikova, A A Bezzubov, A M Bezborodov *Prikl. Biokhim. Mikrobiol.* **29** 512 (1993)
58. A K Kulikova, E B Letunova, A M Bezborodov *Prikl. Biokhim. Mikrobiol.* **29** 431 (1993)
59. M Onodera, Y Endo, N Ogasawara *Agr. Biol. Chem.* **53** 1947 (1989)
60. A Q H Habets-Crutzen, J A M de Bont *Appl. Microbiol. Biotechnol.* **26** 434 (1987)
61. K Furuhashi, M Shintani, M Takagi *Appl. Microbiol. Biotechnol.* **23** 218 (1986)
62. B G Fox, W A Froland, J E Dege, J D Lipscomb *J. Biol. Chem.* **26** 10 023 (1989)
63. O Asperger, K Wirkner, H-P Kleber *Biocatalysis* **4** 59 (1990)
64. E J Warburton, A M Magor, M K Trower, M Griffin *FEMS Microbiol. Lett.* **66** 5 (1990)
65. J M Wyatt *Trends Biochem. Sci.* **9** 20 (1984)
66. J Colby, D I Stirling, H Dalton *Biochem. J.* **165** 395 (1977)
67. I J Higgins, R C Hammond, F S Sariaslani, D Best, M M Davies, S E Tryhorn, F Taylor *Biochem. Biophys. Res. Commun.* **89** 671 (1979)
68. L Alvarez-Cohen, P L McCarty *Appl. Environ. Microbiol.* **57** 228 (1991)

69. H-C Tsien, G A Brusseau, P S Hanson, L P Wackett *Appl. Environ. Microbiol.* **55** 3155 (1989)
70. P Oldenhius, J Y Oedzes, J J van der Waarde, D B Janssen *Appl. Environ. Microbiol.* **57** 7 (1991)
71. C-T Hou *Appl. Microbiol. Biotechnol.* **19** 1 (1984)
72. O Miyawaki, B Wingard Jr, J S Brackin, R S Silver *Biotechnol. Bioeng.* **28** 343 (1986)
73. K Furuhashi *Chemistry (Jpn.)* **42** 672 (1987)
74. A C van der Linden *Biochim. Biophys. Acta* **77** 157 (1963)
75. Eur. P. 0 082 006 (1983)
76. S L Neileman, J Geigert *Biotechnol. Biochem. Soc. Symp.* **48** 39 (1982)
77. S L Neileman *Hydrocarbon Proces.* **59** 135 (1983)
78. S W May, R D Schwartz, B J Abbott, O R Zaborsky *Biochim. Biophys. Acta* **403** 245 (1975)
79. A Q H Habets-Crutzen, J A M de Bont *Appl. Microbiol. Biotechnol.* **22** 428 (1985)
80. Gao Canzhu, Li Zhuben, Ning Zhizhong, Miao Dexun *J. Mol. Catal. (China)* **4** 291 (1990)
81. US P. 4 348 476 (1982)
82. D Frense, P Miethe, M Langwald, K-H Mohr *Biotechnol. Lett.* **14** 93 (1992)
83. L E S Brink, J Tramper *Biotechnol. Bioeng.* **27** 1258 (1985)
84. L E S Brink, J Tramper *Enzyme Microbiol. Technol.* **9** 612 (1987)
85. L E S Brink, J Tramper *J. Chem. Technol. Biotechnol.* **37** 21 (1987)
86. L E S Brink, J Tramper, K van Triet, K Ch A M Luyben *Anal. Chim. Acta* **163** 207 (1984)
87. A Q H Habets-Crutzen, J A M de Bont *Appl. Microbiol. Biotechnol.* **26** 434 (1987)
88. V D Sokolovskii, G A Kovalenko *Biotechnol. Bioeng.* **32** 916 (1988)
89. J Tramper, L E S Brink, R S Hamstra, J A M de Bont, A Q H Habets-Crutzen, C G van Ginkel, in *Proceedings of the Third European Congress on Biotechnology, Munchen, Weinheim AO, 1984* p. II 269
90. K Furuhashi, S Uchida, I Karube, S Suzuki *Enzyme Eng.* **6** 139 (1982)
91. G A Kovalenko, V D Sokolovskii *Biotechnologia* **3** 612 (1987)
92. R A Messing, R A Opperman *Biotechnol. Bioeng.* **21** 49 (1979)
93. V D Sokolovskii, G A Kovalenko *Biotechnol. Bioeng.* **32** 916 (1988)
94. J Klein, H Ziehr *J. Biotechnol.* **16** 1 (1990)
95. D G Zvyagintsev *Vzaimodeistvie Mikroorganizmov s Tverdyimi Poverkhnostyami* (Interaction of Microorganisms with Solid Surfaces) (Moscow: Izd. Mosk. Gos. Univ., 1979)
96. S V El'chits, V B Pichko, L V Loginenko *Biotechnologia* **4** 89 (1988)
97. J L Galazzo, J E Bailey *Biotechnol. Bioeng.* **34** 1283 (1989)
98. C Fortin, J-Ch Vuilleumard *Biotechnol. Lett.* **12** 913 (1990)
99. C A G M Weijers, A de Haan, J A M de Bont *Appl. Microbiol. Biotechnol.* **27** 337 (1988)
100. C A G M Weijers, J A M de Bont *Enzyme Microbiol. Technol.* **13** 306 (1991)
101. S Masahiro, O Ichido *J. Chem. Soc., Chem. Commun.* 533 (1990)
102. S Masahiro, O Ichido *J. Mol. Catal.* **64** L23 (1991)
103. L R Brown, R J Strawinski, C S McCleskey *Can. J. Microbiol.* **10** 791 (1964)
104. W Ashraf, A Mihdhir, J C Murrell *FEMS Microbiol. Lett.* **122** 1 (1994)
105. C-T Hou, R N Patel, A I Laskin, I Marczak, N Barnabe *Can. J. Microbiol.* **107** (1981)
106. R N Patel, C-T Hou, A I Laskin, A Felix, P Derelanko *Appl. Environ. Microbiol.* **39** 720 (1980)
107. C-T Hou, R N Patel, A I Laskin, I Marczak, N Barnabe *Dev. Ind. Microbiol.* **22** 467 (1981)
108. R N Patel, C-T Hou, A I Laskin, A Felix, P Derelanko *Appl. Environ. Microbiol.* **39** 727 (1980)
109. M Onodera, Y Endo, N Ogasawara *Agr. Biol. Chem.* **52** 1431 (1989)
110. H B Lukins, J W Foster *J. Bacteriol.* **85** 1074 (1963)
111. C E Cerniglia, W T Brevins, J J Perry *Appl. Environ. Microbiol.* **32** 764 (1976)

The problem of the quantitative evaluation of the inductive effect: correlation analysis

A R Cherkasov, V I Galkin, R A Cherkasov

Contents

I. Introduction	641
II. Inductive effect of substituents in the chemistry of organic and organoelement compounds	642
III. The problem of a unified scale of inductive constants	646
IV. An additive model of the inductive effect	647

Abstract. Published data concerning the quantitative estimation of the inductive interaction of functional groups in organic and organoelement compounds are systematically described. Studies carried out by the authors and devoted to the elaboration of a new model of the inductive effect, permitting theoretical calculation of inductive constants of various substituents at any reactive centre, are surveyed. The possibility of using this approach to solve some important theoretical problems associated with the inductive effect such as the inductive influence in organoelement compounds and the inductive effects of alkyl groups is discussed. The bibliography includes 132 references.

I. Introduction

The relationship between the structure and reactivity of organic and organoelement compounds is a fundamental problem in modern chemistry. The overall interaction of a substituent with a reaction centre is usually considered to consist of inductive, resonance, and steric components. The correct separation of these components is one of the main problems hampering further development of quantitative organic chemistry and correlation analysis. The difficulties in solving this problem are associated with the fact that, within the framework of widely used empirical methods in which the influence of substituents is quantitatively evaluated based on standard reaction series, it is extremely difficult (if possible at all) to elaborate any reliable criteria for dividing the overall effect into its elementary constituents. Numerous attempts undertaken along these lines have always been based on certain postulates and assumptions that initially looked quite justified, but sooner or later, following subsequent development of theory and experimental methods, these came into question and were criticised or, in some cases, even totally rejected. A great number of various experimental scales of inductive constants have been developed, the physical meaning of which are quite obscure and the limits of applicability difficult to predict.

This accounts for the interest aroused in recent years in the quantitative evaluation of various effects of substituents by nonempirical methods. Among the latter, nonempirical procedures for the calculation of the total energy of a system and of its constituents, i.e. *ab initio* quantum-chemical calculations, are undoubtedly the most strict. However, the use of these calculations for real reaction series, which are of interest for researchers, is held up for a number of objective reasons. The main reasons are the capacity of computers and of software and the fact that these calculations are very time-consuming and expensive. Therefore, *ab initio* calculations are in fact inexpedient for the vast majority of known reaction series, especially for those involving complex organic and organoelement compounds.

This fact, in its turn, stimulated the development of various non-quantum-chemical calculation methods, the low accuracy of which is largely counter-balanced by their simplicity and intelligible mathematics. Besides, their accuracy is often quite sufficient for the solution of particular problems arising in the studies of reactivities and reaction mechanisms. In our opinion, the most promising approach is the construction of certain models for the manifestation of an effect, these models being usually based on fairly simple physical laws and thus having quite obvious physical meaning. Our experience in the field of the steric effect^{1–3} has demonstrated that modelling is an extremely effective method for the quantitative evaluation of the influence of substituents. For example, the model of the frontal steric effect developed by us makes it possible not only to calculate adequately the steric effect of any substituent at any reaction centre with high accuracy but also to solve many other problems that are difficult to solve or cannot be solved in terms of existing empirical scales.

Thus, it can be said with confidence that modelling is the most promising method for the quantitative analysis of reactivity in physical organic chemistry and in correlation analysis.

In this review we consider the main approaches to the quantitative evaluation of the inductive influence of substituents only within the limits needed to understand the essence of this problem, so as not to duplicate the data covered by reviews and monographs published previously.^{4–11} Attention is focused on the possibility of modelling the inductive effect in order to develop a unified versatile approach to the quantitative theoretical evaluation of the inductive constants of any substituent at any reaction centre. We believe that our model of the inductive effect gives a reliable tool to researchers for the evaluation of the relationship between the structure and the reactivity of organic and organoelement molecules.

A R Cherkasov, V I Galkin, R A Cherkasov Chair of High-Molecular Weight and Organoelement Compounds, Kazan' State University, ul. Lenina 18, 420008 Kazan', Russian Federation.
Fax (7-843) 238 09 94. Tel. (7-843) 231 81 86

Received 30 January 1996

Uspekhi Khimii 65 (8) 695–711 (1996); translated by Z P Bobkova

II. Inductive effect of substituents in the chemistry of organic and organoelement compounds

The idea of the mutual influence of atoms and groups appeared long ago during the development of the theory of chemical structure. Later, investigations of the characteristic features of intramolecular interactions have occupied a prominent place in chemical research. Numerous approaches to the evaluation of the electronic interactions between functional groups in a molecule have been elaborated. Among them, the theory of electron displacements, within the framework of which views on the inductive effect have been developed, is considered the most adequate.⁴

The term 'induction' derives from the Latin word *inductio*. By analogy with the inductive effect in electrostatics, the inductive effect in the theory of reactivity has been historically interpreted as the variation of the electron density on an atom or functional group under the action of certain factors.

The history of the development of opinions on the inductive effect as well as their current application to the theory of reactivity have been surveyed in the monograph by Vereshchagin,⁴ which we repeatedly cite.

In our review, we briefly outline the most significant aspects of the problem in question that relate directly to the quantitative description of the inductive influence of substituents.

1. The nature of inductive effect and the mechanism of its transfer

Although there is no strict mathematical description of the nature of the inductive effect, this is generally clear and reduces to the classical view that electron density flows from the atom with a lower electronegativity to the atom with a higher electronegativity. As early as 1916, Lewis described for the first time the consecutive displacement of the electron pairs forming the bonds along a chain of atoms in relation to chloroacetic acid. Later, this served as the basis for the development of the theory of electron displacements.¹²⁻¹⁴ However, there is still no clear knowledge concerning the mechanism by which the inductive influence is transmitted. Two possible mechanisms for the propagation of this effect are discussed in the literature, both having their pros and cons and their adherents and opponents.

The first mechanism described long ago by Lewis suggests that the influence is transmitted along the bonds by their consecutive polarisation. The electronic asymmetry arising due to the difference between the electron-withdrawing properties of two atoms linked together can propagate along the molecule by a mechanism similar to the electrostatic induction.^{4, 13}

According to this mechanism, each atom or a group of atoms is characterised by the coefficient of conduction of the inductive influence. The conduction coefficient Z does not depend on the position of the unit (atom) between a substituent and a reaction centre. The overall attenuation of the effect in a chain consisting of bridging units $X-A-B-C-Y$ is proportional to the product of the coefficients of attenuation of the inductive influence on each of the intermediate atoms, so

$$\sigma(XABC) = \sigma(X)Z(A)Z(B)Z(C),$$

and for a chain consisting of identical atoms it is written as

$$\sigma(XA_n) = \sigma(X)Z^n(A).$$

The parameters Z are calculated from empirical relations connecting either the σ -constants of the substituents containing and not containing the conducting group (σ - σ method)

$$Z(B) = \frac{\sigma(BX)}{\sigma(X)},$$

or the corresponding reaction parameters ρ (the ρ - ρ method)

$$Z(CH_2) = \frac{\rho(CH_2Y)}{\rho(Y)}.$$

If there exist several paths for the transmission of the inductive influence of a substituent, i.e. the substituent and the reaction centre are separated by several conducting systems, the inductive effect is assumed to propagate along these systems independently and in an additive manner. In the general case, in terms of the 'bond' mechanism, the intensity of an inductive effect should depend on the number of bonds separating the substituent and the reaction centre.

An alternative mechanism of the transfer of inductive effect involves interaction of functional groups through space. This induction mechanism is purely electrostatic in its nature and, like the concept of electron density displacement along bonds, it has been known for a long time. This approach was proposed for the first time by Ingold, who postulated that the intensity of an inductive influence should depend on the presence of an electric field in the space directly adjacent to the molecule.¹⁴ Later, the electrostatic mechanism of the influence of substituents was called the 'field effect'. It has been assumed to occur via electrostatic ion-ion, ion-dipole, and dipole-dipole interactions, the intensity of which is described by various functions of the distance r^{-n} ($n = 2-4$).⁵ In this case, the intensity of the inductive interaction of a substituent with a reaction centre depends directly on intramolecular distances.

In recent years, preference has been given to the field mechanism of the inductive effect; an increasing number of scientists are apt to consider the inductive interaction in terms of the electrostatic concept.^{4, 15} Strictly speaking, the transmission of the influence 'along bonds' and 'through space' should not be regarded as alternative mechanisms. Whereas the field theory accounts well for the very fact of the Coulomb stabilisation of charges arising in a molecule, the nature of their appearance, i.e. the mechanism of the intramolecular redistribution of the electron density, still remains obscure. In any case, electron density redistribution can hardly be conceived without participation of molecular orbitals.

2. Quantitative methods for the evaluation of the inductive effect

The methods that permit the quantitative description of each of the constituents of the overall influence of substituents on the reaction centre (inductive, resonance, and steric) can be divided conventionally into three main groups. Empirical approaches according to which the influence of a substituent is inferred from data on the reactivity or the physical properties of molecules have found the widest application. As a rule, standard procedures of regression analysis are used. The second group of methods is based on quantum-chemical calculations (*ab initio* and semiempirical methods) or on the use of fundamental characteristics of atoms, groups, or molecules that obey particular empirical relations. Methods that involve the construction of formal models of the corresponding interactions based, as a rule, on fairly simple physical laws should also be assigned to this group. Finally, a separate group includes topological approaches, which occupy a certain intermediate position between the methods belonging to the first and second groups.

a. Empirical methods. Inductive interaction constants

Experimental methods for the evaluation of the influence of substituents are based on the possibility of representing the variation of Gibbs free energy in a reaction (ΔG) or the Gibbs energy of activation as a sum of independent constituents^{5, 7, 16}

$$\Delta G = \Delta G_I + \Delta G_R + \Delta G_S.$$

Each term reflects the contribution of a particular substituent effect — inductive (I), resonance (R), or steric (S). The principles of linearity of free energy (LFE) and polylinearity (PL) make it

possible to perform mathematical formalisation of the problem of the relationship between structure and reactivity.

Quantitative evaluation of the inductive influence of substituents became possible for the first time within the framework of the approach developed by Hammett. Based on the LFE principle, he proposed an empirical equation (which has gained wide acceptance) to describe the ionisation of substituted benzoic acids¹⁷

$$\lg(K/K_0) = \rho\sigma,$$

where K and K_0 are the ionisation constants of the corresponding substituted and unsubstituted acids, σ is a universal constant specific for a substituent in the benzene ring, which remains invariable over a reaction series, and ρ is a constant reflecting the sensitivity of the reaction centre to the variation of the influence of a substituent. Since substituents in the benzene ring (especially those occupying the *para*-position) can exert influence by both inductive and resonance mechanisms, the Hammett constants σ are considered to reflect the overall effect, i.e. they incorporate the inductive and resonance constituents.

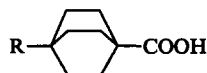
Later, the Hammett method was modified many times, but the vast majority of these modifications referred to the chemistry of aromatic compounds.⁶ For the series of aliphatic compounds, the Hammett relation, as a rule, did not hold. Taft suggested that in the case of aliphatic compounds, steric substituent effects are significant. Hence, for the Hammett relation to be obeyed, steric effects should be separated from electronic effects. Taft accomplished this task based on standard reaction series of the alkaline and acid hydrolysis of alkyl carboxylates.¹⁸

$$\sigma^* = \frac{1}{2.48} \left[\lg \left(\frac{k}{k_0} \right)_B - \lg \left(\frac{k}{k_0} \right)_A \right],$$

$$\lg \left(\frac{k}{k_0} \right)_A = E_s,$$

where σ^* is a substituent constant depending only on its inductive influence, k and k_0 are rate constants for the reactions involving the given compound and the standard compound with the CH_3 substituent, respectively, and E_s is the substituent constant reflecting its steric influence; the indices A and B refer to the otherwise identical reactions of alkaline and acid hydrolysis of fully substituted esters of carboxylic acids. The factor 2.48 was introduced in order to reduce the σ^* scale to the scale of Hammett σ -constants. This procedure was used to determine the purely inductive constants for aliphatic groups.

Another model, which permits direct determination of the inductive influence of substituents, was proposed by Roberts and Moreland in 1953.¹⁹ In this model, dissociation constants for a series of 4-substituted bicyclo[2.2.2]octanecarboxylic acids are used.



In these systems, the resonance mechanism for the transfer of substituent influence to the reaction centre is impossible, and the substituents are reliably removed from the reaction centre owing to the rigid cyclic structure, as in the case of the benzene ring. Thus the steric effect of the substituents is reduced virtually to zero, and the influence of substituents on the reaction centre in the molecules of bicyclooctanecarboxylic acids occurs exclusively by the inductive mechanism. The σ^1 -constants (sometimes, designations σ_1 and σ' are used), which are based on the dissociation of a series of bicyclooctanecarboxylic acids, reflect only the inductive influence of the corresponding substituents.

In place of the bicyclooctanecarboxylic acids, other rigid polycyclic systems can also be used, for example, 3-substituted adamantane-1-carboxylic acids, 3-substituted bicyclo[1.1.1]pen-

tane-1-carboxylic acids, *trans*-4-substituted cyclohexanecarboxylic acids, and quinuclidinium ions.⁴ The inductive constants of substituents determined for these reaction series correlate fairly closely with one another; this confirms the legitimacy of the neglect of all effects except for the inductive effect in this case. However, the specific structure of these model systems does not make it possible to cover the whole set of substituents.

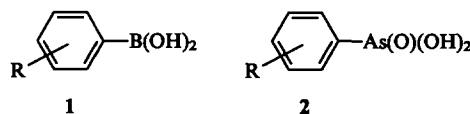
σ -Constants, free from a contribution due to direct polar conjugation, are also used as a measure of the inductive influence of substituents. Substituted benzoic acids are used as the standard reaction series for the determination of these constants. As a rule, only compounds with *meta*-substituents are included in the basic sets; insulation series of compounds, i.e. those in which the reaction centre is separated from the aromatic ring by a saturated group, are used as secondary reaction series. The idea of using insulation reaction series was proposed for the first time by Jaffé,²⁰ who suggested that substituted benzoic acids should be used as a standard reaction series and arylacetic and arylcarboxylic acids should be used as insulation series.

Later this method was widely developed.²¹ A large number of qualitatively similar scales of inductive constants, which have been obtained by the separation of the inductive influence from the conjugation effect in aromatic systems, have been proposed. However, it should be noted that constants 'free from direct polar conjugation' can be regarded as inductive constants only conventionally, because in the standard series of substituted benzoic acids (used in all these approaches), the possibility of conjugation of the aryl and carboxyl groups cannot be ruled out.⁴

At present, a large number of inductive constants for hundreds of diverse substituents have been determined; these constants form more than a dozen of the most extensively used scales. As a rule, they correlate well with one another. Thus, we can say with confidence that the empirical inductive constants, based on standard reaction series, properly reflect the donor-acceptor properties of substituents and can be adequately used in quantitative organic chemistry.

It is also noteworthy that the approach developed by Hammett and Taft for the analysis of organic compounds proved applicable to the reactivity of organoelement compounds.

For example, Jaffé et al.²² noted that the ionisation constants of arylboric 1 and arylarsenous 2 acids obey the Hammett equation, which is also applicable to some other reactions of these compounds.^{20, 23}

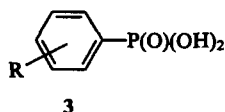


Numerous attempts have been undertaken to use the Hammett-Taft equation for a description of the reactivity of organosilicon compounds. In particular, it was found that the rates of reactions of organosilanes ($\text{R}_n\text{SiH}_{4-n}$) with alcohols, amines, and phenols correlate with the σ - and σ^* -constants of substituents.⁶ However, these attempts can hardly be considered successful, due to the known specific character of organosilicon compounds. For example, it has been proposed²⁴ to introduce new σ_{Si} -constants for organosilicon compounds which reflect, like the Hammett constants, the overall effect of a substituent on a reaction centre.

Relations, similar to the Hammett equation, can also be used to describe the reactivity of organomagnesium and organomercury compounds.⁶ Jaffé^{20, 23} has noted a good correlation of the σ -constants for some organoantimony compounds. In addition, the existence of a correlation between the dissociation constants of various metal complexes and the σ -constants of the substituents in the ligand molecules has been noted in a number of papers. In particular, the Hammett equation appropriately describes the instability constants for Ni- and Ag-pyridinates, Ni- and Fe-1,10-phenanthroline complexes, copper complexes of aromatic carboxylic acids, etc.⁶ In recent years, an ever increasing number

of papers have been published in which correlation equations have been used to describe the reactivity of organometallic compounds, for example, derivatives of zirconium,²⁵ vanadium,²⁶ nickel,²⁷ ruthenium,^{28,29} cobalt,³⁰⁻³² etc.

However, the correlation analysis equations have found the most extensive application in the evaluation of the reactivity of phosphorus compounds. Jaffé²² has shown that the ionisation constants for arylphosphonic acids **3** obey the Hammett equation.



Later, other examples of using correlation equations in the chemistry of trivalent and pentavalent phosphorus derivatives were found. The most general approach to the problem of correlation analysis of the reactivities of organophosphorus compounds (OPC) has been developed by Kabachnik and Mastryukova.^{8,9} They suggested that the dissociation of oxygen-containing acids of tetracoordinated phosphorus should be used as the basic reaction series for OPC and introduced special phosphorus σ^P -constants as a measure of the influence of substituents on the dissociation constant of P(IV) acids in water at 25°C:

$$\lg K = \lg K_0 + \rho \Sigma \sigma^P,$$

where K_0 is the dissociation constant for phosphinic acid $\text{H}_2\text{P}(\text{O})\text{OH}$ [in this case, $\sigma^P(\text{H}) = 0$].

The σ^P -constants have been actively used for many years and are still used to analyse the reactivities of diverse classes of organophosphorus compounds. For example, it has been shown that the $\Sigma \sigma^P$ values correlate linearly with the dissociation constants of various phosphorus-based oxygen- and dithio-acids in aqueous alcohol,³³ with the basicity constants of phosphines,³⁴ with the rate constants for the addition of bromine to esters of vinylphosphonic and phosphonic acids,³⁵ and with benzylolation constants of sodium phosphorus dithioates,³⁶ etc.

These constants have been widely used in our laboratory for the interpretation of the reaction mechanisms and reactivities of thio-derivatives of phosphorus acids; their complex-formation properties,³⁷⁻⁴¹ dissociation constants,⁴²⁻⁴⁴ oxidation potentials,⁴⁵ rate constants for addition reactions,⁴⁶⁻⁵¹ specific solvation energies,^{52,53} and some other properties⁵⁴⁻⁵⁶ have been described in this way. The reactivities of OPC toward reactions involving functional groups attached to the phosphorus atom were described by the σ^P -constants most adequately. However, the use of σ^P for reactions in which the tricoordinated and, especially, tetracoordinated phosphorus atoms themselves act as the reaction centres was not always successful.

Kabachnik and Mastryukova⁹ suggested that the relative contributions of the inductive (σ_I^P) and resonance (σ_R^P) constituents to the σ^P -constants vary on passing from one reaction to another.

$$\lg \frac{k_1}{k_2} = \rho(\sigma_I^P + \alpha \sigma_R^P).$$

It is notable that this equation has been used successfully in a study of the kinetics and mechanism of cyanoethylation of phosphorus dithio-acids.^{49,50}

With the progress of $\sigma\rho$ analysis in organophosphorus chemistry, the opinion has emerged that the σ^P -constants are compound parameters, since they include inductive, resonance, and steric constituents, which can be adequately described by virtue of the classical 'carbon' constants.^{57,58} This is confirmed, for example, by the strictly linear relationship between the steric effects of substituents at phosphorus and carbon atoms.^{59,60}

Consequently, it became widely believed that the nature of substituent effects in the chemistry of organic and organoelement compounds was the same,⁴ and that it was therefore reasonable to use the classical 'carbon' constants in the analysis of reactivities of organoelement compounds.

However, this approach does not necessarily work, and the reactivity of the corresponding classes of compounds is often described much more adequately by the 'special' organoelement constants than by the classical 'carbon' ones.

It should be noted that at present, the question of linearity of the inductive influences of substituents on carbon and heteroatomic (organoelement) reaction centres is not completely clear. This problem is still a sore spot in the quantitative theory of reactivity of organoelement compounds.

At the same time, the data accumulated to date make it possible to conclude that empirical inductive constants are fairly versatile, at least in classical organic chemistry, and that they apparently reflect adequately the inductive influence of substituents.

It should be noted that the methods for the determination of the empirical inductive constants are not at all restricted to the approaches based on consideration of quantitative data on reactivities. It is well known that substituents influence the physical properties of molecules in the ground state. Innumerable examples of correlations of σ constants with diverse physical properties, which are associated in one way or another with the electron density distribution, have been found.^{4,61} Based on these correlations, a large number of extensively used empirical scales of substituent constants have been developed.⁶² Characteristics obtained by NMR,^{4,6,55,63} NQR,^{4,14,64} IR,^{4,6,14,65,66} and photoelectron spectroscopy,⁴ as well as data on dipole moments and polarisability of molecules^{4,6,14,67} are used most frequently for this purpose.

It has been reported that the Hammett equation can be applied to the solution of some mass-spectrometric problems⁶ and to the description of the solvatochromic effect.⁶ Correlation equations have found application in polarography,^{18,25,26,41,68} in the interpretation of fluorescence spectra,⁶⁹ in studies of some gas-phase processes,⁷⁰⁻⁷³ and in the rationalisation of scintillation activity data.⁶ The optical rotation of β -D-galactosides⁶ as well as parameters describing the activity of enzymes,⁷⁴ the electrical conductivity of some crystalline compounds, etc. are correlated with the σ -constants of substituents. The number of known correlations is constantly increasing, since more and more experimental data are quantitatively interpreted in terms of the correlation equations.

Thus, the inductive and other substituent constants can adequately describe both the reactivities and the physical properties of diverse organic and organoelement compounds.

However, the dependences obtained are not necessarily suitable for the determination of new substituent parameters, although they often provide information on the spatial structures of molecules and on the nature and mechanisms of various intramolecular interactions.

In recent years, an increasing number of new complex substituents have appeared in organic and, especially, in organoelement chemistry. These substituents have not been described and some of them cannot in principle be described quantitatively within the framework of empirical methods. Moreover, as noted above, none of the empirical approaches claims or can claim to be a physical model, capable of disclosing the nature and mechanism of the transmission of the inductive influence. In addition, none of the approaches described above possesses a versatile mathematical technique establishing the quantitative relationship between the structure and reactivity of organic and organoelement compounds. Therefore, it is no wonder that interest in the quantitative evaluation of substituent effects based on nonempirical and semiempirical methods has grown so sharply in recent years.

b. Semiempirical methods for the evaluation of inductive effects

Methods based on the formal analysis of a structure with the aim of identifying the correlation between the structure and a property (topological methods) have been used in theoretical organic chemistry for a long time.

The development of the topological approach is largely associated with the application of the methods of graph theory.⁷⁵ An abstract model of the structure, the so-called 'molecular graph', is normally characterised by two matrices, namely, by the adjacency matrix A , in which A_{ij} elements are equivalent to elements A_{ji} and are equal to 1 if the nodes i and j are linked by an edge and to 0 if they are not linked, as well as by the distance matrix D , in which D_{ij} elements are equivalent to D_{ji} and correspond to the number of edges situated on the way from the node i to j . The topological indices are quantitative characteristics of these graphs and are various combinations of elements of both matrices reflecting particular aspects of the molecular structure.

The topological index was used for the first time by Wiener,⁷⁶ who introduced the index W , which denoted the number of edges needed to connect all the pairs of nodes to one another and indicated the degree of branching in the molecule. Later, other indices similar to W were introduced, for example, the index I ,⁷⁷ the Altenburg index,⁷⁸ the Platt index f ,⁷⁹ and the index N_2 derived from it.⁸⁰ The Hosoya index Z ⁸¹ reflects the distance between all the disconnected nodes. The Gutman (M),⁸² Randić (χ),⁸³ and Kier (h_x)⁸⁴ indices show the degree of substitution at each node of the graph.

A new group of information indices I_{pc} and I'_{pc} has been introduced by Bonchev.⁸⁵ These are combinations of W , Z , and χ indices. The group of centric Balaban indices⁸⁶ — the centric index α , the binormal quadratic index α' , and the binormal centric index α'' — reflect the structure of a tree-like graph. These indices are also related to the geometrical structure of the molecule.

All the indices listed above are used in chemistry. Correlations of the topological indices with various parameters have been found, for example, with solubility, boiling point, density, diamagnetic susceptibility, heat of atomisation, formation, and vaporisation, and molar volume. High-quality relationships between the topological indices and steric parameters (molecular volume, molecular refraction, and surface area of the molecules) have been obtained.^{1,57} The correlations of the topological indices with the steric constants from the E_s and V_x empirical scales have been established successfully.

The use of graph theory within the framework of the global 'structure-property' problem frequently leads to adequate results. However, the use of topological indices suffers from obvious drawbacks. Not all the characteristic features of molecular structure are taken into account (for example, the conformation is ignored) and, what is more important, the physical meaning of these indices is obscure. Despite the fact that in some cases the topological indices correlate with electronic parameters (ionisation potential, electron affinity, polarisability, chemical shifts in NMR spectra, optical density, etc.),^{1,57} one cannot speak of serious application of the graph theory to the evaluation of electronic effects of substituents.

Together with the purely topological method for the evaluation of the influence of the structure of molecules on their properties, which does not reflect the distribution and redistribution of the electron density, there exist a number of approaches which take into account to a certain extent the mutual arrangement of atoms and groups.

The modelling of interactions based on the structural characteristics and geometrical parameters in relation to the inductive effect has been accomplished by various procedures. The best known is the Dewar method developed for naphthalene derivatives. Several modifications of this method exist. In terms of one of them, the Hammett constant is described by a two-parameter equation:^{4,74}

$$\sigma = \frac{F_D}{r} + Mq,$$

where F_D is the substituent field (inductive) constant, r is the distance from this substituent to the reaction centre expressed in terms of the aromatic carbon-carbon bond lengths, M is the mesomeric constant, and q is excess charge. The first term describes the field effect and the second term corresponds to conjugation. The F_D and F'_D constants obtained in various modifications of the Dewar method are somewhat different.

Further development of the Dewar approach has been associated with the introduction of other initial scales of substituent constants. For example, the $F_D(S)$ scale, which has been elaborated for the analysis of ^{19}F NMR spectra and which takes into account not only the distance from the substituent to the reaction centre but also the orientation of substituents with respect to the C—F bond,⁴ differs substantially from other scales.

The method of additive determination of inductive constants suggested by Taft,^{4,5} who was the first to introduce the additivity principle for the inductive influence, can be regarded as being 'conventionally topological'. According to this method, the overall inductive influence of a complex substituent is determined by the inductive effects of fragments incorporated in it.

The Dewar approach and the Taft method share the common property that they are based on the analysis of substituent constants themselves, i.e. they can be classified as empirical methods. In addition, both approaches take into account in a certain way the geometry and the electronic structures of molecules: according to Dewar, the influence of substituents on the reaction centre is determined by the distance separating them in space, whereas according to Taft, it is determined by the number and nature of the fragments separating them.

The approach developed in the studies of Tatevskii,^{87,88} which permits quantitative description of intramolecular interactions in saturated hydrocarbons and their derivatives of the same type by virtue of bond increments, is also noteworthy. C—C and C—X bonds are divided into types according to the hybridisation of the carbon atoms and into sub-types according to the number of hydrocarbon substituents at each of them. Both scalar properties — energy characteristics, specific volumes, densities, refractions, etc. — and such properties as bond polarities and dipole moments have been considered within the framework of this approach.

The key feature, which distinguishes semiempirical methods from empirical methods, is that the constants can be calculated theoretically rather than found directly from correlations with the physicochemical properties or reactivity data.

c. Non-empirical methods for the evaluation of the inductive effect

Among non-empirical methods for the evaluation of the inductive influence of substituents, the quantum-chemical approach should undoubtedly be considered the most rigorous. The quantum theory permits the calculation of molecular energies and charges on atoms (the electron density distribution). Thus, consideration of the calculated parameters over a reaction series with variation of a substituent, precluding the conjugation effect, provides a direct path to the description of inductive interactions.

The simplest approach involves the separation of the contributions of the inductive and resonance constituents to the variation of the reaction free energies found by quantum-chemical calculations in a good approximation. Another method involves correlation of the σ_I basic set with the quantum-chemical characteristics of the charge distribution in the molecules incorporating the corresponding substituents.⁴

For various mechanisms of transmission of the inductive influence, different quantum-chemical calculation models are chosen. For example, *ab initio* calculations carried out under the assumption that the inductive influence is transmitted 'along bonds' result in uniform attenuation in *n*-alkyl radicals of the electron density variations caused by the substituent.^{4,62}

In recent years, the method of 'isolated molecules' has been widely used for the modelling of the field effect. In conformity with this method, *ab initio* calculations are carried out in parallel for two systems: for the molecule under study and for a pair of simplest isolated molecules arranged so that the interacting fragments in them are oriented in exactly the same way as in the molecule under study (the X—H H—H system). Thus the value $\Delta q = q_{\text{H(X)}} - q_{\text{H(H)}}$ characterises the inductive effect of the substituent X and proves proportional to the inductive $\sigma_{\text{I(X)}}$ -constant.⁸⁹ This approach served as the basis for the introduction of a new scale of 'theoretical field' constants of substituents T_{F} , determined from the charge variation on the β -hydrogen atom in *para*-substituted styrenes.^{4, 90}

However, the extensive use of quantum-chemical calculations in the analysis of substituent effects is hampered by the insufficient level of their development. In addition to the fact that these methods are time-consuming and require the use of complex software, the level of which does not always correspond to the complexity of the problems solved, quantum-chemical calculations are held up by a number of other objective factors.⁹¹ In particular, the use of various approximations sometimes leads to results that disagree with one another or are even fundamentally contradictory. For example, the charges on the hydrogen atoms in alkanes calculated by various methods can differ not only in magnitude but also in sign.^{4-6, 89}

Thus, it is not surprising that attempts are made now and then to develop formal non-quantum-chemical models for intramolecular electrostatic interactions. The principles of the construction of such models were formulated most clearly by Remick,⁹² Smith and Eyring,⁹³ and Del Re,⁴ who considered dipole moments, and by Pacey et al.,⁹⁴ who analysed the standard enthalpies of formation of substituted alkanes.

Thus, studies on the influence of substituents on the dissociation constants of acids played an important role in the development of the Bjerrum-Kirkwood-Westheimer electrostatic theory. According to this theory, the energy of interaction of the anion resulting from the dissociation of an acid containing a polar substituent, with the substituent dipole⁴ is expressed by the following equation:

$$\lg \frac{K_{\text{X}}}{K_{\text{H}}} = 2.303 \Delta p K = \frac{1}{kT} e \frac{\mu \cos \theta}{\epsilon r^2},$$

where K_{X} and K_{H} are the dissociation constants for the substituted and unsubstituted acids, respectively, μ is the dipole moment in the substituent, ϵ is the dielectric permeability of the medium, r is the distance between the charge and the dipole, and θ is the angle between the vectors r and μ .

Since the parameters for effective dielectric permeabilities were selected empirically, it was necessary to develop a procedure for calculating the ϵ value. This problem was solved by Kirkwood and Westheimer⁹⁵ in terms of a model based on a molecular cavity placed into a continuous dielectric medium. Later this model was repeatedly modified and widely used for the description of the chemical properties of compounds^{4, 95-108} and for the interpretation of some experimental data that cannot be described quantitatively within the framework of the classical correlation analysis involving the Hammett-Taft equation.^{107, 108}

It should be noted that all models based on the electrostatic theory suggest that the charges and dipoles are constant, the electron displacements remaining beyond their consideration. However, it is the laws of electrostatics that ensure the basic similarity between the influence of substituents on the energy characteristics and on the electron density distribution.⁴

* * *

Thus, neither nonempirical approaches nor the construction of electrostatic interaction models currently provides a universal description of the inductive effect; therefore, these approaches

cannot compete with empirical methods for the determination of inductive constants. In turn, experimental approaches based on data on the reactivities and physical properties of compounds do not allow one to reveal comprehensively the physical nature of intramolecular interactions and so do not possess sufficient prognostic potential.

III. The problem of a unified scale of inductive constants

The diversity of approaches to the evaluation of inductive effects in the description of reactivities of organic and organoelement compounds points to a need for the development of a universal scale of inductive constants, which would be suitable for use in any field of organic and organoelement chemistry. Three approaches to the solution of this problem can be suggested:

- (1) the use of several scales in various fields, according to their maximum efficiency;
- (2) the search for a universal scale with several parameters;
- (3) the calculation of the total energy of the system in each particular case.

The first approach reflects the current situation in chemistry: numerous scales of various constants of substituent are currently in use, their success being as a rule difficult to predict, especially in the chemistry of organoelement compounds. Furthermore, a strategy for choosing a particular scale does not exist, and one can hardly be expected in the near future.

The calculation of the total energy of a system is, of course, the most universal method to account for the inductive effect and also of other effects. However, as noted above, a wide use of molecular mechanics and quantum chemistry for the quantitative evaluation of reactivity still seems not to be realisable in the near future.

At present, the second approach, namely, the search for a universal scale having a clear physical meaning, is the optimal method. The interrelations of the existing scales and numerous examples of their use in organic and organoelement chemistry, which indicate the common nature of substituent effects, serve as prerequisites for this approach. The universal scale should be based on structural calculations, since empirical scales depend too much on the particular conditions and on the accuracy of experiments. Finally, the universal character of this scale should be based on extensive experimental verification; in other words, it should describe the maximum possible number of experimental data, a high quality of correlation being maintained.

Obviously, the development of a unified theoretical scale of inductive constants requires the elaboration of a quantitative model of inductive interactions involving intelligible mathematics (as we have done previously for the evaluation of steric constants within the framework of the model of the frontal steric effect.¹⁻³)

The main statement of our steric model is the principle of simple mechanical shielding of the reaction centre by substituents, which hamper the access of the second reagent to it. In conformity with this, the steric constant of a substituent R_{s} is determined in terms of this model from a fairly simple additive equation:^{1-3, 59}

$$R_{\text{s}} = 30 \lg \left(1 - \sum \frac{R_i^2}{4r_i^2} \right), \quad (1)$$

where R_i is the atomic radius of the i -th atom in the substituent and r_i is the distance from this atom to the reaction centre.

The scale of the R_{s} -constants obtained within the framework of the frontal steric effect model is in good agreement with experimental scales and describes adequately the steric influences of diverse substituents. The model possesses a clear physical meaning and permits not only adequate and accurate calculation of the steric effect of any substituent at any reaction centre but also the solution of many other problems that are difficult to solve or cannot be solved in terms of the existing empirical scales. Extensive verification of the applicability of this model to

hundreds of diverse organic and organoelement series revealed no limitations on the use of this approach.¹

It is of interest that an essentially similar approach involving a virtually identical mathematical technique was suggested later by Japanese researchers.^{109, 110} A number of other examples of the successful use of a variety of models for the quantitative analysis of reactivities and substituent effects have been presented in a review.¹

Thus, our experience and analysis of the recent literature data make it possible to state with confidence that modelling as a method for the quantitative evaluation of the influence of substituents represents a clear-cut world trend in the development of quantitative organic chemistry and correlation analysis.

We therefore believed that the use of formal modelling in relation to the problem of the inductive effect could also prove an effective and fruitful approach. In a series of papers we have described a fairly simple model of the inductive effect, which permits the correct theoretical calculation of the inductive constants of diverse substituents at virtually any reaction centre.^{15, 111–119} The essence of the model developed by us, its use in solving practical problems of correlation analysis, and in solving some theoretical problems concerning the inductive effect are presented in the subsequent Section of this review. We believe that this model, owing to its accessibility and relatively simple mathematics, could be quite useful in the everyday practical work of chemists who deal with quantitative organic chemistry and correlation analysis.

IV. An additive model of the inductive effect

1. Basic postulates of the model

Taking into account the fundamental and extensively studied properties of the inductive effect, we developed an approach that makes it possible to model with high accuracy the inductive constants of organic and organoelement substituents and groups in the Taft scale.¹¹¹

According to this approach, the inductive effect of a substituent is determined by the sum of the inductive influences of the atoms contained within it:

$$\sigma^* = \sum_{i=1}^n \frac{(\sigma_A)_i}{r_i^2}, \quad (2)$$

where σ^* is the Taft inductive constant of the substituent; n is the number of atoms in the substituent; and r_i is the distance from a particular atom to the reaction centre; in our model a tetracoordinated carbon atom was chosen as the reaction centre.

The empirical parameter $(\sigma_A)_i$, which we introduce here, determines the capability of an i -th atom of exerting the inductive effect and depends on the chemical nature of the element and on its valence state. We calculated the atomic constants σ_A for a wide range of elements in various valence states by substituting empirical 'tabulated' σ^* -constants in Eqn (2) and solving it for σ_A . The resulting values are presented in Table 1.

This additive approach makes it possible to describe with a relatively high degree of accuracy the inductive constants of diverse substituents, i.e. of virtually all substituents for which the σ^* -constants are available (Table 2).

The σ^* -constants found experimentally (σ_{exp}^*) for most frequently encountered organic substituents form a high-quality correlation with the corresponding constants (σ_{calc}^*) found from Eqn (2). The constant term of this correlation is equal to zero and the slope is equal to unity;¹¹¹ this corresponds entirely to the mean values of these parameters.

$$\sigma_{\text{calc}}^* = (-0.078 \pm 0.022) + (1.029 \pm 0.012) \sigma_{\text{exp}}^* \\ N = 146, R = 0.988, S = 0.148.$$

Table 1. Empirical atomic (σ_A) and group (σ_G) constants, obtained from experimental Taft constants.

Substituent	σ_A	Substituent	σ_G
–F	5.88±0.29	–C=C–	0.94±0.15
–Cl	7.62±0.64	>C=O	3.29±0.24
–Br	8.91±0.73	–COOR	4.48±0.14
–I	9.71±1.24	–NO ₂	10.23±0.29
–O–	3.25±0.06	–CN	7.56±0.45
O=	7.52±0.70	–C≡C–	3.86±0.08
–S–	5.03±0.12	>S=O	8.69±0.55
S=	17.14±1.72	>SO ₂	11.14±0.46
>S=	5.90±0.59	>C=S	8.24±0.19
>S≡	4.20±0.72	–NCS	5.24±0.48
–N<	1.78±0.16	–NCO	4.51±0.42
N≡	11.06±1.54	–NC	6.72 ^a
–N≡	4.89±0.77	–NO	3.55 ^a
>C<	0.00	–N ₃	4.51 ^a
>C=	0.70±0.14	–SCN	10.6 ^a
–C≡	2.90±0.58	≥N→O	7.17 ^a
–P<	1.23±0.32	≥P=O	4.38±0.21
–P≡	1.588±0.24	≥P=S	2.52±0.16

^a Group constants are estimated on the base of unity values of σ^* .

Similar high-quality dependences have been obtained for aromatic,¹¹² organoelement,¹¹³ and charged¹¹⁴ substituents [Eqns (3), (4), and (5), respectively]:

$$\sigma_{\text{calc}}^* = (0.046 \pm 0.025) + (0.944 \pm 0.014) \sigma_{\text{exp}}^* \quad (3)$$

$$N = 127, R = 0.985, S = 0.156,$$

$$\sigma_{\text{calc}}^* = (0.023 \pm 0.015) + (0.994 \pm 0.010) \sigma_{\text{exp}}^* \quad (4)$$

$$N = 124, R = 0.993, S = 0.162,$$

$$\sigma_{\text{calc}}^* = (0.081 \pm 0.093) + (0.999 \pm 0.092) \sigma_{\text{exp}}^* \quad (5)$$

$$N = 29, R = 0.986, S = 0.310.$$

The final dependence, describing more than 400 points, has a correlation coefficient of 0.99,¹¹⁴ i.e. the theoretical inductive constants correspond completely to the experimental data.

$$\sigma_{\text{calc}}^* = (0.031 \pm 0.012) + (0.991 \pm 0.006) \sigma_{\text{exp}}^*$$

$$N = 427, R = 0.991, S = 0.130.$$

The high level of additivity of the model suggested makes it possible to determine the inductive effects of substituents not only using the σ_A -constants of atoms but also (for convenience) using σ_G -constants for groups, which can be obtained similarly to σ_A -constants from an equation resembling Eqn (2).¹¹¹ The σ_G -constants for functional groups most frequently encountered in organic chemistry (C=O, COOR, CN, NO₂, etc.) are also listed in Table 1. The use of the group constants does not diminish the accuracy of the calculations of inductive constants,¹¹¹ which confirms a certain integrity and the high degree of additivity of our approach.

Table 2. Experimental and theoretical [calculated from Eqn (2)] Taft inductive σ^* -constants.

Substituent	σ_{exp}^*	σ_{calc}^*	Substituent	σ_{exp}^*	σ_{calc}^*
-F	3.21±0.17	3.08	-CH ₂ N(CH ₃) ₂	0.09±0.12	0.29
-CH ₂ F	1.10±0.17	1.27	-COCH ₃	1.70±0.05	1.56
-Cl	2.89±0.17	2.43	-COC ₃ H _{7-n}	1.59±0.09	1.56
-CH ₂ Cl	0.96±0.17	1.08	-COC ₄ H _{9-n}	1.45±0.12	1.56
-CHCl ₂	1.95±0.17	2.16	-CH ₂ COCH ₃	0.69±0.17	0.69
-CHClCH ₃	0.83±0.17	1.08	-CH ₂ CHO	0.69±0.17	0.69
-CHClC ₂ H ₅	0.94±0.10	1.08	-CH ₂ CH ₂ CHO	0.15±0.12	0.32
-C ₂ H ₄ Cl	0.30±0.07	0.50	-CH ₂ CH ₂ COCH ₃	0.11±0.12	0.32
-CH ₂ CHClCH ₃	0.24±0.10	0.49	-COOCH ₃	1.94±0.07	2.05
-Br	2.80±0.17	2.36	-COOC ₂ H ₅	1.89±0.07	2.05
-CH ₂ Br	1.15±0.17	1.14	-COOC ₃ H _{7-n}	1.99±0.07	2.05
-CHBrCH ₃	1.09±0.17	1.14	-COOC ₃ H _{7-iso}	1.91±0.07	2.05
-CHBrC ₂ H ₅	0.91±0.10	1.14	-CH ₂ COOH	1.08±0.17	1.23
-CHBr ₂	1.97±0.17	2.28	-CH ₂ COOCH ₃	1.09±0.17	1.23
-CHBrCH ₂ Br	1.33±0.10	1.62	-CH ₂ CH ₂ COOH	0.34±0.17	0.53
-C ₂ H ₄ Br	0.17±0.07	0.48	-CH ₂ CH ₂ COOCH ₃	0.30±0.07	0.53
-CH ₂ CHBrCH ₃	0.25±0.10	0.51	-CH ₂ CH ₂ COOC ₂ H ₅	0.22±0.19	0.53
-I	2.38±0.17	2.00	-NO ₂	4.73±0.17	4.72
-CH ₂ I	0.96±0.17	1.23	-CH ₂ NO ₂	1.37±0.17	1.59
-C ₂ H ₄ I	0.21±0.10	0.39	-CH(CH ₃)NO ₂	1.30±0.17	1.59
-OH	1.60±0.17	1.58	-CH(C ₂ H ₅)NO ₂	1.30±0.17	1.59
-OCH ₃	1.79±0.17	1.63	-CH(NO ₂) ₂	3.03±0.17	3.18
-OC ₂ H ₅	1.68±0.17	1.63	-C(NO ₂) ₃	4.62±0.17	4.77
-OC ₃ H _{7-n}	1.68±0.17	1.63	-CH ₂ CH ₂ NO ₂	0.47±0.17	0.73
-OC ₃ H _{7-iso}	1.61±0.17	1.63	-(CH ₂) ₃ NO ₂	0.48±0.17	0.42
-OC ₄ H _{9-n}	1.68±0.17	1.63	-CN	3.48±0.07	3.37
-OC ₄ H _{9-sec}	1.65±0.17	1.63	-CH ₂ CN	1.15±0.17	1.67
-OC ₅ H _{11-n}	1.55±0.10	1.63	-CH ₂ CH ₂ CN	0.87±0.07	0.78
-OC ₅ H _{10-cyclo}	1.61±0.17	1.63	-(CH ₂) ₃ CN	0.43±0.07	0.50
-OCH ₂ CH ₂ C ₃ H _{7-iso}	1.55±0.17	1.63	-C≡CH	1.75±0.07	1.72
-OCH ₂ C ₄ H _{9-tert}	1.54±0.17	1.63	-C≡C-CH ₃	1.81±0.07	1.79
-OCH(CH ₃)C ₄ H _{9-tert}	1.48±0.17	1.63	-CH ₂ -C≡CH	0.76±0.17	0.82
-OC ₆ H _{11-cyclo}	1.88±0.17	1.63	-CH ₂ CH ₂ -C≡CH	0.19±0.07	0.31
-CH ₂ OH	0.56±0.17	0.54	-(CH ₂) ₃ -C≡CH	0.17±0.07	0.19
-CH ₂ OCH ₃	0.56±0.10	0.54	-SOCH ₃	2.89±0.17	2.87
-CH(OCH ₃) ₂	1.12±0.17	1.08	-CH ₂ SOCH ₃	1.30±0.17	1.18
-CH ₂ OC ₃ H _{7-iso}	0.59±0.11	0.54	-SO ₂ CH ₃	3.72±0.17	3.65
-CH ₂ OC ₃ H _{7-n}	0.61±0.11	0.54	-SO ₂ C ₃ H _{7-iso}	3.59±0.17	3.65
-CH ₂ CH ₂ OH	0.23±0.17	0.54	-CH ₂ SO ₂ CH ₃	1.26±0.17	1.63
-CH ₂ CH ₂ OCH ₃	0.16±0.17	0.22	-NCH ₃ NO ₂	2.40±0.07	2.27
-CH ₂ CH ₂ OC ₂ H ₅	0.23±0.17	0.22	-NHCOCH ₃	1.59±0.07	1.58
-SH	1.61±0.17	1.52	-NHCOC ₂ H ₅	1.59±0.07	1.58
-SCH ₃	1.66±0.17	1.55	-NCS	2.61±0.17	2.67
-SC ₂ H ₅	1.55±0.17	1.55	-CH ₂ NCS	0.94±0.17	0.74
-SC ₃ H _{7-n}	1.48±0.17	1.55	-NCO	2.25±0.17	2.30
-SC ₃ H _{7-iso}	1.55±0.17	1.55	-CH ₂ NCO	0.81±0.17	0.66
-SC ₄ H _{9-n}	1.55±0.17	1.55	-OCH ₂ Cl	2.58±0.17	2.63
-SC ₄ H _{9-sec}	1.48±0.17	1.55	-OCHCl ₂	3.08±0.17	3.28
-CH ₂ SH	0.63±0.17	0.63	-OCH ₂ F	2.33±0.17	2.18
-CH ₂ SCH ₃	0.63±0.10	0.63	-OCHF ₂	2.83±0.17	2.71
-CH ₂ SC ₃ H _{7-n}	0.54±0.10	0.63	-OCHO	3.00±0.17	2.83
-CH ₂ SC ₃ H _{7-iso}	0.57±0.10	0.63	-O-C≡CH	2.67±0.17	2.59
-CH ₂ SC ₄ H _{9-n}	0.57±0.10	0.63	-ONO ₂	3.76±0.07	3.68
-CH ₂ CH ₂ SH	0.19±0.10	0.26	-COBr	2.47±0.17	2.58
-CH=CH ₂	0.40±0.17	0.42	-COF	2.46±0.17	2.56
-CH=CH-CH ₃	0.30±0.17	0.42	-NHCOCH ₃	1.59	1.47
-C(CH ₃)=CH ₂	0.50±0.17	0.42	-OCOCH ₃	2.33±0.20	2.25
-CH=CH-C ₂ H ₅	0.32±0.17	0.42	-CH ₂ OCOCH ₃	0.79±0.07	0.74
-NH ₂	0.72±0.17	0.82	-CONH ₂	1.75±0.17	1.81
-NHCH ₃	0.69±0.12	0.85	-CH ₂ ONO ₂	1.49±0.07	1.62
-NHC ₂ H ₅	0.96±0.12	0.83	-COCN	3.43±0.17	3.23
-N(CH ₃)C ₂ H ₅	0.83±0.12	0.83	-CH=CHCl-trans	0.96±0.07	0.87
-N(C ₂ H ₅) ₂	0.86±0.12	0.83	-CH=CHCl-cis	1.02±0.07	1.20
-CH ₂ NH ₂	0.50±0.12	0.29	-CF=CH ₂	1.57±0.17	1.42
-CH(CH ₃)NHCH ₃	0.01±0.12	0.29	-CH=CHNO ₂ -trans	1.76±0.12	1.55

Table 2 (continued).

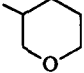
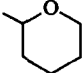
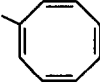
Substituent	σ_{exp}^*	σ_{calc}^*	Substituent	σ_{exp}^*	σ_{calc}^*
$-\text{CH}_2\text{NHCONH}_2$	0.39 ± 0.17	0.64	$-\text{C}_6\text{H}_4\text{NHCHO-}p$	0.81 ± 0.02	0.84
	0.18 ± 0.07	0.22	$-\text{NHCO}_2\text{C}_6\text{H}_5$	1.68 ± 0.17	1.71
	0.27 ± 0.07	0.42	$-\text{C}_6\text{H}_4\text{OCH}_2\text{Cl-}m$	0.88 ± 0.17	1.05
$-\text{CO}-\text{CH}=\text{CH}_2$	1.90 ± 0.17	1.76	$-\text{C}_6\text{H}_4\text{OCH}_2\text{Cl-}p$	0.76 ± 0.17	0.99
$-\text{CO}-\text{C}\equiv\text{CH}$	2.08 ± 0.07	2.28	$-\text{C}_6\text{H}_4\text{OCHCl}_2\text{-}m$	0.90 ± 0.17	1.23
$-\text{CH}=\text{CH}-\text{COOH}$	1.00 ± 0.07	0.99	$-\text{C}_6\text{H}_4\text{OCHCl}_2\text{-}p$	0.96 ± 0.17	1.19
$-\text{CH}_2\text{NHCOCH}_3$	0.45 ± 0.17	0.65	$-\text{C}_6\text{H}_4\text{OCH}_2\text{F-}m$	0.84 ± 0.17	1.00
$-\text{CH}_2\text{CH}_2\text{CONH}_2$	0.18 ± 0.07	0.44	$-\text{C}_6\text{H}_4\text{OCH}_2\text{F-}p$	0.71 ± 0.17	0.96
$-\text{CH}=\text{C}(\text{CN})_2$	2.58 ± 0.07	2.64	$-\text{OC}_6\text{H}_5$	2.47 ± 0.17	2.42
$-\text{CH}=\text{CH}-\text{COOH}$	0.69 ± 0.07	0.65	$-\text{OC}_6\text{H}_4\text{Cl-}m$	2.58 ± 0.17	2.43
$-\text{CH}=\text{CHCOOCH}_3$	1.12 ± 0.07	1.12	$-\text{OC}_6\text{H}_4\text{Cl-}p$	2.63 ± 0.17	2.37
$-\text{CH}_2\text{CH}_2\text{CONHCH}_3$	0.25 ± 0.07	0.44	$-\text{OC}_6\text{H}_4\text{F-}m$	2.52 ± 0.17	2.39
$-\text{SC}(\text{S})\text{CH}_3$	2.80 ± 0.17	2.61	$-\text{OC}_6\text{H}_4\text{F-}p$	2.45 ± 0.17	2.35
$-\text{SC}(\text{S})\text{SC}_2\text{H}_5$	2.86 ± 0.17	2.85	$-\text{OC}_6\text{H}_4\text{I-}m$	2.45 ± 0.17	2.45
$-\text{SC}(\text{S})\text{OC}_2\text{H}_5$	2.60 ± 0.17	2.69	$-\text{OC}_6\text{H}_4\text{I-}p$	2.40 ± 0.17	2.39
	1.00 ± 0.12	0.91	$-\text{OC}_6\text{H}_4\text{NO}_2\text{-}m$	2.77 ± 0.17	2.51
$-\text{C}_6\text{H}_5$	0.75 ± 0.17	0.84	$-\text{OC}_6\text{H}_4\text{CH}_3\text{-}m$	2.34 ± 0.17	2.21
$-\text{C}_6\text{H}_4\text{F-}m$	0.95 ± 0.17	0.87	$-\text{OC}_6\text{H}_4\text{CH}_3\text{-}p$	2.31 ± 0.17	2.21
$-\text{C}_6\text{H}_4\text{F-}p$	0.81 ± 0.17	0.81	$-\text{C}_6\text{H}_4\text{SC}_2\text{H}_5\text{-}p$	0.74 ± 0.17	0.77
$-\text{C}_6\text{H}_4\text{Cl-}m$	0.98 ± 0.17	0.90	$-\text{C}_6\text{H}_4\text{SCH}_3\text{-}m$	0.79 ± 0.02	0.81
$-\text{C}_6\text{H}_4\text{Cl-}p$	0.87 ± 0.17	0.84	$-\text{C}_6\text{H}_4\text{SCH}_3\text{-}p$	0.73 ± 0.02	0.77
$-\text{C}_6\text{H}_4\text{I-}m$	0.90 ± 0.17	0.94	$-\text{SC}_6\text{H}_4\text{Cl-}m$	2.03 ± 0.17	2.18
$-\text{C}_6\text{H}_4\text{I-}p$	0.87 ± 0.17	0.86	$-\text{SC}_6\text{H}_4\text{Cl-}p$	1.98 ± 0.17	2.15
$-\text{C}_6\text{H}_4\text{Br-}p$	0.86 ± 0.17	0.86	$-\text{SOC}_6\text{H}_4\text{Cl-}m$	3.18 ± 0.17	3.24
$-\text{C}_6\text{H}_4\text{CH}_3\text{-}p$	0.59 ± 0.17	0.64	$-\text{SOC}_6\text{H}_4\text{Cl-}p$	3.18 ± 0.17	3.24
$-\text{C}_6\text{H}_4\text{OCH}_3\text{-}m$	0.50 ± 0.17	0.76	$-\text{SO}_2\text{C}_6\text{H}_4\text{Cl-}m$	3.47 ± 0.17	3.83
$-\text{C}_6\text{H}_4\text{OCH}_3\text{-}p$	0.60 ± 0.17	0.74	$-\text{SO}_2\text{C}_6\text{H}_4\text{Cl-}p$	3.51 ± 0.17	3.84
$-\text{C}_6\text{H}_4\text{C}_2\text{H}_5\text{-}p$	0.59 ± 0.17	0.64	$-\text{SC}_6\text{H}_4\text{F-}m$	1.88 ± 0.17	2.14
$-\text{CH}_2\text{C}_6\text{H}_5$	0.26 ± 0.17	0.21	$-\text{SC}_6\text{H}_4\text{F-}p$	1.78 ± 0.17	2.12
$-\text{CH}(\text{CH}_3)\text{C}_6\text{H}_5$	0.36 ± 0.17	0.21	$-\text{SOC}_6\text{H}_4\text{F-}m$	3.17 ± 0.17	3.23
$-\text{CH}_2\text{CH}_2\text{C}_6\text{H}_5$	0.07 ± 0.17	0.09	$-\text{SOC}_6\text{H}_4\text{F-}p$	3.17 ± 0.17	3.22
$-\text{CH}_2\text{C}_6\text{H}_4\text{CN-}p$	0.41 ± 0.17	0.37	$-\text{SO}_2\text{C}_6\text{H}_4\text{F-}m$	3.55 ± 0.17	3.70
$-\text{C}_6\text{H}_4(\text{C}_6\text{H}_9\text{-}tert)\text{-}p$	0.52 ± 0.17	0.64	$-\text{SO}_2\text{C}_6\text{H}_4\text{F-}p$	3.45 ± 0.17	3.70
$-\text{C}_6\text{H}_3(\text{NO}_2)_2\text{-}2,4$	1.89 ± 0.17	2.06	$-\text{SC}_6\text{H}_4\text{NO}_2\text{-}m$	2.04 ± 0.17	2.26
$-\text{C}_6\text{H}_3(\text{NO}_2)_2\text{-}3,5$	1.38 ± 0.17	1.39	$-\text{SC}_6\text{H}_4\text{NO}_2\text{-}p$	2.34 ± 0.17	2.21
$-\text{C}_6\text{H}_4\text{NO}_2\text{-}m$	1.22 ± 0.17	1.02	$-\text{SOC}_6\text{H}_4\text{NO}_2\text{-}m$	3.22 ± 0.17	3.32
$-\text{C}_6\text{H}_4\text{NO}_2\text{-}p$	1.27 ± 0.17	0.92	$-\text{SOC}_6\text{H}_4\text{NO}_2\text{-}p$	3.26 ± 0.17	3.31
$-\text{C}_6\text{H}_4\text{NHCH}_3\text{-}p$	0.55 ± 0.07	0.69	$-\text{SC}_6\text{H}_5$	1.89 ± 0.17	1.99
$-\text{C}_6\text{H}_4\text{NCS-}m$	1.04 ± 0.07	0.83	$-\text{SOC}_6\text{H}_5$	3.24 ± 0.17	3.09
$-\text{C}_6\text{H}_4\text{NCS-}p$	0.95 ± 0.07	0.78	$-\text{SO}_2\text{C}_6\text{H}_5$	3.27 ± 0.17	3.60
$-\text{C}_6\text{H}_4\text{N}(\text{CH}_3)_2\text{-}m$	0.61 ± 0.07	0.71	$-\text{SC}_6\text{H}_4\text{CN-}p$	2.30 ± 0.17	2.17
$-\text{C}_6\text{H}_4\text{N}(\text{CH}_3)_2\text{-}p$	0.43 ± 0.07	0.69	$-\text{SC}_6\text{H}_4\text{CH}_3\text{-}m$	1.90 ± 0.17	1.99
$-\text{C}_6\text{H}_4\text{NH}_2\text{-}m$	0.61 ± 0.07	0.71	$-\text{SC}_6\text{H}_4\text{CH}_3\text{-}p$	1.91 ± 0.17	1.99
$-\text{C}_6\text{H}_4\text{NH}_2\text{-}p$	0.49 ± 0.07	0.67	$-\text{SOC}_6\text{H}_4\text{CH}_3\text{-}m$	3.01 ± 0.17	3.09
$-\text{C}_6\text{H}_4\text{N}_3\text{-}m$	0.88 ± 0.07	0.81	$-\text{SOC}_6\text{H}_4\text{CH}_3\text{-}p$	3.03 ± 0.17	3.09
$-\text{C}_6\text{H}_4\text{ICl}_2\text{-}m$	1.50 ± 0.02	1.25	$-\text{SC}_6\text{H}_4\text{OCH}_3\text{-}m$	1.90 ± 0.17	2.09
$-\text{C}_6\text{H}_4\text{ICl}_2\text{-}p$	1.50 ± 0.02	1.18	$-\text{SC}_6\text{H}_4\text{OCH}_3\text{-}p$	1.67 ± 0.17	2.07
$-\text{C}_6\text{H}_4\text{IF}_2\text{-}m$	1.30 ± 0.02	1.19	$-\text{SOC}_6\text{H}_4\text{OCH}_3\text{-}p$	3.02 ± 0.17	3.15
$-\text{C}_6\text{H}_4\text{IF}_2\text{-}p$	1.31 ± 0.02	1.12	$-\text{SO}_2\text{C}_6\text{H}_4\text{OCH}_3\text{-}m$	3.26 ± 0.17	3.72
$-\text{C}_6\text{H}_4\text{IO}_2\text{-}m$	1.13 ± 0.02	1.19	$-\text{SO}_2\text{C}_6\text{H}_4\text{OCH}_3\text{-}p$	3.25 ± 0.17	3.72
$-\text{C}_6\text{H}_4\text{IO}_2\text{-}p$	1.18 ± 0.02	1.17	$-\text{SC}_6\text{H}_4\text{SCH}_3\text{-}m$	1.94 ± 0.17	2.12
$-\text{C}_6\text{H}_4\text{NHCN-}m$	0.85 ± 0.02	0.87	$-\text{SC}_6\text{H}_4\text{SCH}_3\text{-}p$	1.70 ± 0.17	2.09
$-\text{C}_6\text{H}_4\text{NHCN-}p$	0.74 ± 0.02	0.85	$-\text{C}_6\text{H}_4\text{CN-}m$	1.13 ± 0.03	0.92
$-\text{C}_6\text{H}_4\text{NHCHO-}m$	0.83 ± 0.02	0.87	$-\text{C}_6\text{H}_4\text{CN-}p$	1.21 ± 0.03	0.85
			$-\text{C}_6\text{H}_4\text{CHF}_2\text{-}m$	0.93 ± 0.03	0.96
			$-\text{C}_6\text{H}_4\text{CHF}_2\text{-}p$	0.95 ± 0.03	0.94
			$-\text{C}_6\text{H}_4\text{CHCl}_2\text{-}m$	0.92 ± 0.03	1.02
			$-\text{C}_6\text{H}_4\text{CHCl}_2\text{-}p$	0.93 ± 0.03	0.96
			$-\text{C}_6\text{H}_4\text{CHBr}_2\text{-}m$	0.92 ± 0.03	1.07
			$-\text{C}_6\text{H}_4\text{CHBr}_2\text{-}p$	0.93 ± 0.03	1.00
			$-\text{C}_6\text{H}_4\text{CHI}_2\text{-}m$	0.89 ± 0.03	1.08
			$-\text{C}_6\text{H}_4\text{CHI}_2\text{-}p$	0.89 ± 0.03	1.02
			$-\text{C}_6\text{H}_4\text{CHO-}m$	0.99 ± 0.03	0.89
			$-\text{C}_6\text{H}_4\text{CHO-}p$	1.03 ± 0.03	0.85
			$-\text{C}_6\text{H}_4\text{COOH-}m$	0.95 ± 0.02	0.81

Table 2 (continued).

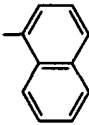
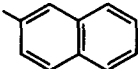
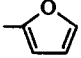

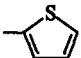
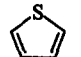
Substituent	σ_{exp}^*	σ_{calc}^*	Substituent	σ_{exp}^*	σ_{calc}^*
$-\text{C}_6\text{H}_4\text{COOH}-p$	1.02 ± 0.02	0.90	$-\text{C}_6\text{H}_4(\text{HgF})-m$	0.94 ± 0.03	0.68
$-\text{C}_6\text{H}_4\text{CH}_2\text{F}-m$	0.78 ± 0.03	0.80	$-\text{Li}$	-2.89 ± 0.50	-2.65
$-\text{C}_6\text{H}_4\text{CH}_2\text{F}-p$	0.77 ± 0.03	0.79	$-\text{OLi}$	0.87 ± 0.50	0.80
$-\text{C}_6\text{H}_4(\text{CH}_2\text{NH}_2)-m$	0.66 ± 0.03	0.68	$-\text{MgBr}$	-3.11 ± 0.5	-3.11
$-\text{C}_6\text{H}_4(\text{CH}_2\text{NH}_2)-p$	0.61 ± 0.03	0.67	$-\text{MgCl}$	-3.16 ± 0.5	-3.16
$-\text{C}_6\text{H}_4(\text{C} \equiv \text{CH})-p$	0.81 ± 0.03	0.75	$-\text{SeCH}_3$	0.94 ± 0.17	1.28
$-\text{C}_6\text{H}_4(\text{CH}_2\text{CN})-m$	0.86 ± 0.03	0.83	$-\text{SeH}$	1.29 ± 0.13	1.28
$-\text{C}_6\text{H}_4(\text{CH}_2\text{CN})-p$	0.83 ± 0.03	0.81	$-\text{SeC}_6\text{H}_5$	1.55 ± 0.07	1.44
$-\text{C}_6\text{H}_4(\text{CH} = \text{CH}_2)-m$	0.71 ± 0.03	0.68	$-\text{SeC}_6\text{H}_4\text{CH}_3-m$	1.66 ± 0.17	1.44
$-\text{C}_6\text{H}_4(\text{CH} = \text{CH}_2)-p$	0.69 ± 0.03	0.66	$-\text{SeC}_6\text{H}_4\text{CH}_3-p$	1.84 ± 0.17	1.44
$-\text{C}_6\text{H}_4(\text{COCH}_3)-m$	0.93 ± 0.03	0.89	$-\text{SeC}_6\text{H}_4\text{Br}-p$	1.42 ± 0.17	1.60
$-\text{C}_6\text{H}_4(\text{COCH}_3)-p$	1.04 ± 0.03	0.83	$-\text{SeC}_6\text{H}_4\text{Cl}-m$	1.52 ± 0.17	1.57
$-\text{C}_6\text{H}_4(\text{COOC}_2\text{H}_5)-p$	1.00 ± 0.03	0.90	$-\text{SeC}_6\text{H}_4\text{Cl}-p$	1.46 ± 0.17	1.54
$-\text{C}_6\text{H}_4(\text{COOCH}_3)-m$	0.95 ± 0.03	0.98	$-\text{SeC}_6\text{H}_4\text{NO}_2-m$	1.66 ± 0.17	1.68
$-\text{C}_6\text{H}_4(\text{COOCH}_3)-p$	1.03 ± 0.03	0.90	$-\text{SeC}_6\text{H}_4\text{NO}_2-p$	1.84 ± 0.17	1.58
$-\text{C}_6\text{H}_4(\text{C} \equiv \text{CCH}_3)-p$	0.74 ± 0.03	0.75	$-\text{SeC}_6\text{H}_4\text{SCH}_3-p$	1.24 ± 0.17	1.52
$-\text{C}_6\text{H}_4[\text{C}(\text{CN})_2\text{CH}_3]-m$	1.13 ± 0.03	1.02	$-\text{SeC}_6\text{H}_4\text{OC}_2\text{H}_5-p$	1.19 ± 0.17	1.50
$-\text{C}_6\text{H}_4[\text{C}(\text{CN})_2\text{CH}_3]-p$	1.11 ± 0.03	0.98	$-\text{SnBr}_3$	2.06 ± 0.08	1.77
	0.77 ± 0.17	0.95	$-\text{SnCl}_2\text{CH}_3$	0.90 ± 0.08	1.08
	0.74 ± 0.17	0.81	$-\text{SnCl}(\text{CH}_3)_2$	0.28 ± 0.08	0.30
	1.02 ± 0.17	1.11	$-\text{Sn}(\text{CH}_3)_3$	-0.04 ± 0.08	-0.30
	0.61 ± 0.17	0.80	$-\text{SnCl}_2\text{C}_6\text{H}_5$	0.98 ± 0.08	1.17
	1.32 ± 0.03	1.28	$-\text{Sn}(\text{CH} = \text{CH}_2)_3$	-0.26 ± 0.08	-0.14
	0.61 ± 0.03	0.76	$-\text{SiBr}_3$	2.39 ± 0.17	2.33
$-\text{As}(\text{CH}_3)_2$	0.78 ± 0.50	0.62	$-\text{SiCl}_2\text{CH}_3$	1.46 ± 0.13	1.40
$-\text{As}(\text{C}_2\text{H}_5)_2$	0.52 ± 0.02	0.62	$-\text{SiCl}(\text{CH}_3)_2$	0.65 ± 0.17	0.64
$-\text{As}(\text{CH} = \text{CH}_2)_2$	0.78 ± 0.50	0.84	$-\text{SiF}(\text{CH}_3)_2$	0.45 ± 0.17	0.55
$-\text{C}_6\text{H}_4[\text{As}(\text{C}_6\text{H}_5)_2]-m$	0.74 ± 0.02	0.76	$-\text{SiH}(\text{CH}_3)_2$	-0.16 ± 0.17	-0.12
$-\text{C}_6\text{H}_4[\text{As}(\text{C}_6\text{H}_5)_2]-p$	0.78 ± 0.02	0.76	$-\text{SiCl}_3$	2.41 ± 0.17	2.16
$-\text{AuP}(\text{OC}_6\text{H}_5)_3$	-4.71 ± 0.02	-4.87	$-\text{C}_6\text{H}_4(\text{SiBr}_3)-m$	1.04 ± 0.03	1.20
$-\text{AuP}(\text{C}_6\text{H}_5)_3$	-5.10 ± 0.02	-5.23	$-\text{C}_6\text{H}_4(\text{SiBr}_3)-p$	1.11 ± 0.03	1.06
$-\text{AuP}(\text{CH}_3)_3$	-5.65 ± 0.02	-5.45	$-\text{C}_6\text{H}_4(\text{SiCl}_3)-m$	1.04 ± 0.03	1.16
$-\text{AuP}(\text{C}_6\text{H}_4\text{CH}_3)_3$	-5.30 ± 0.02	-5.38	$-\text{C}_6\text{H}_4(\text{SiCl}_3)-p$	1.10 ± 0.03	1.12
$-\text{Ga}(\text{CH}_3)_2$	-1.31 ± 0.02	-1.19	$-\text{C}_6\text{H}_4(\text{SiF}_3)-m$	1.09 ± 0.03	1.09
$-\text{Ga}(\text{CH} = \text{CH}_2)_2$	-0.89 ± 0.02	-0.99	$-\text{C}_6\text{H}_4(\text{SiF}_3)-p$	1.17 ± 0.03	1.07
$-\text{Ge}(\text{CH}_3)_3$	-0.04 ± 0.08	-0.14	$-\text{C}_6\text{H}_4(\text{SiH}_3)-m$	0.74 ± 0.03	0.63
$-\text{Ge}(\text{C}_2\text{H}_5)_3$	-0.04 ± 0.08	-0.14	$-\text{C}_6\text{H}_4(\text{SiH}_3)-p$	0.77 ± 0.03	0.63
$-\text{Ge}(\text{C}_6\text{H}_5)_3$	0.28 ± 0.08	0.32	$-\text{C}_6\text{H}_4(\text{SiCl}_2\text{CH}_3)-m$	0.92 ± 0.03	0.98
$-\text{C}_6\text{H}_4(\text{GeBr}_3)-p$	1.22 ± 0.02	1.37	$-\text{C}_6\text{H}_4(\text{SiCl}_2\text{CH}_3)-p$	0.98 ± 0.03	0.94
$-\text{C}_6\text{H}_4(\text{GeCl}_3)-p$	1.27 ± 0.02	1.26	$-\text{C}_6\text{H}_4[\text{SiCl}(\text{CH}_3)_2]-m$	0.82 ± 0.03	0.81
$-\text{C}_6\text{H}_4(\text{GeF}_3)-p$	1.39 ± 0.02	1.11	$-\text{C}_6\text{H}_4[\text{SiCl}(\text{CH}_3)_2]-p$	0.85 ± 0.03	0.79
$-\text{HgBr}$	0.05 ± 0.08	0.06	$-\text{C}_6\text{H}_4[\text{SiF}(\text{CH}_3)_2]-m$	0.79 ± 0.03	0.79
$-\text{HgCH} = \text{CH}_2$	-0.50 ± 0.08	-0.41	$-\text{C}_6\text{H}_4[\text{SiF}(\text{CH}_3)_2]-p$	0.84 ± 0.03	0.77
$-\text{HgOCOCH}_3$	-0.12 ± 0.08	-0.06	$-\text{C}_6\text{H}_4[\text{SiH}(\text{CH}_3)_2]-m$	0.71 ± 0.03	0.63
$-\text{C}_6\text{H}_4(\text{HgCH}_3)-m$	1.00 ± 0.03	0.60	$-\text{C}_6\text{H}_4[\text{SiH}(\text{CH}_3)_2]-p$	0.73 ± 0.03	0.63
$-\text{C}_6\text{H}_4(\text{HgCH}_3)-p$	0.77 ± 0.03	0.60	$-\text{C}_6\text{H}_4[\text{Si}(\text{CH}_3)_3]-m$	0.64 ± 0.03	0.63
$-\text{C}_6\text{H}_4(\text{HgCN})-m$	0.90 ± 0.03	0.72	$-\text{C}_6\text{H}_4[\text{Si}(\text{CH}_3)_3]-p$	0.65 ± 0.03	0.63
$-\text{C}_6\text{H}_4(\text{HgCN})-p$	0.94 ± 0.03	0.70	$-\text{C}_6\text{H}_4[\text{Si}(\text{N}(\text{CH}_3)_2)_3]-m$	0.67 ± 0.03	0.74
$-\text{C}_6\text{H}_4(\text{HgCl})-m$	0.94 ± 0.03	0.70	$-\text{C}_6\text{H}_4[\text{Si}(\text{N}(\text{CH}_3)_2)_3]-p$	0.67 ± 0.03	0.71
$-\text{C}_6\text{H}_4(\text{HgCl})-p$	0.95 ± 0.03	0.69	$-\text{C}_6\text{H}_4[\text{Si}(\text{CH}_3)_2\text{C}_6\text{H}_5]-m$	0.73 ± 0.03	0.67
$-\text{C}_6\text{H}_4(\text{HgF})-p$	0.94 ± 0.03	0.68	$-\text{C}_6\text{H}_4[\text{Si}(\text{CH}_3)_2\text{C}_6\text{H}_5]-p$	0.75 ± 0.03	0.65
			$-\text{C}_6\text{H}_4[\text{SiCH}_3(\text{C}_6\text{H}_5)_2]-m$	0.75 ± 0.03	0.69
			$-\text{C}_6\text{H}_4[\text{SiCH}_3(\text{C}_6\text{H}_5)_2]-p$	0.77 ± 0.03	0.68
			$-\text{C}_6\text{H}_4[\text{Si}(\text{C}_6\text{H}_5)_3]-m$	0.82 ± 0.03	0.74
			$-\text{C}_6\text{H}_4[\text{Si}(\text{C}_6\text{H}_5)_3]-p$	0.83 ± 0.03	0.72
			$-\text{PBr}_2$	1.73 ± 0.17	2.12
			$-\text{P}(\text{CH}_3)_2$	0.55 ± 0.17	0.34
			$-\text{P}(\text{CH} = \text{CH}_2)_2$	0.55 ± 0.17	0.57
			$-\text{PCl}_2$	1.73 ± 0.17	2.05
			$-\text{PF}_2$	2.38 ± 0.17	2.17
			$-\text{PH}_2$	0.17 ± 0.17	0.34
			$-\text{PO}(\text{CH}_3)_2$	1.39 ± 0.07	1.42
			$-\text{PO}(\text{OCH}_3)_2$	2.21 ± 0.07	2.28
			$-\text{PO}(\text{C}_2\text{H}_5)_2$	1.68 ± 0.07	1.42
			$-\text{PO}(\text{CH}_3)\text{OC}_2\text{H}_5$	1.82 ± 0.07	1.85

Table 2 (continued).

Substituent	σ_{exp}^*	σ_{calc}^*	Substituent	σ_{exp}^*	σ_{calc}^*
–PO(C ₃ H ₇ - <i>n</i>) ₂	1.55±0.07	1.42	–C ₆ H ₄ [PO(OH) ₂]- <i>p</i>	1.00±0.03	0.98
–PO(C ₄ H ₉ - <i>n</i>) ₂	1.48±0.07	1.42	–COO [–]	–1.08±0.17	–1.08
–PO(C ₄ H ₉)OC ₄ H ₉	1.62±0.07	1.85	–CH ₂ COO [–]	–0.07±0.17	–0.39
–PO(OC ₄ H ₉ - <i>n</i>) ₂	1.78±0.07	2.28	–CH=CH–COO [–]	–0.03±0.17	0.01
–CH ₂ PO(CH ₃) ₂	0.68±0.07	0.55	– $\bar{\text{C}}\text{H}=\text{CN}$	1.60±0.07	1.70
–CH ₂ PO(OCH ₃) ₂	0.80±0.07	1.21	– $\bar{\text{C}}\text{H}=\text{COOC}_2\text{H}_5$	1.25±0.07	1.15
–CH ₂ PO(CH ₃)OC ₂ H ₅	0.70±0.07	0.88	–SO ₃ [–]	0.89±0.17	0.68
–CH ₂ PO(C ₂ H ₅) ₂	0.62±0.07	0.55	–CH ₂ SO ₃ [–]	–0.09±0.17	0.32
–CH ₂ PO(C ₂ H ₅)OC ₂ H ₅	0.67±0.07	0.88	–S ⁺ (CH ₃) ₂	5.76±0.07	5.85
–CH ₂ PO(C ₃ H ₇ - <i>n</i>) ₂	0.59±0.07	0.55	–CH ₂ CH ₂ S ⁺ (CH ₃) ₂	1.60±0.07	1.12
–C ₆ H ₄ [P(CH ₃) ₂]- <i>m</i>	0.73±0.03	0.67	–(CH ₂) ₃ S ⁺ (CH ₃)C ₂ H ₅	0.73±0.07	0.68
–C ₆ H ₄ [P(CH ₃) ₂]- <i>p</i>	0.72±0.03	0.66	–(CH ₂) ₄ S ⁺ (CH ₃)C ₂ H ₅	0.38±0.07	0.43
–C ₆ H ₄ [PO(CH ₃) ₂]- <i>m</i>	1.01±0.03	0.90	–P ⁺ (CH ₃) ₃	2.51±0.17	2.67
–C ₆ H ₄ [PO(CH ₃) ₂]- <i>p</i>	1.06±0.03	0.84	–P ⁺ (C ₂ H ₅) ₃	1.86±0.17	2.67
–C ₆ H ₄ [P(OCH ₃) ₂]- <i>m</i>	0.79±0.03	0.86	–P ⁺ CH ₃ (C ₂ H ₅) ₂	3.66±0.17	2.67
–C ₆ H ₄ [P(OCH ₃) ₂]- <i>p</i>	0.81±0.03	0.81	–C ₆ H ₄ COO [–] - <i>m</i>	0.60±0.03	0.58
–C ₆ H ₄ [PO(OCH ₃) ₂]- <i>m</i>	0.95±0.03	1.03	–C ₆ H ₄ COO [–] - <i>m</i>	0.55±0.03	0.56
–C ₆ H ₄ [PO(OCH ₃) ₂]- <i>p</i>	1.01±0.03	0.98	–N ⁺ H(CH ₃) ₂ Cl [–]	3.75±0.17	4.01
–C ₆ H ₄ [PO(OC ₂ H ₅) ₂]- <i>m</i>	0.92±0.03	1.03	–N ⁺ H ₂ (CH ₃)Cl [–]	3.69±0.17	4.01
–C ₆ H ₄ [PO(OC ₂ H ₅) ₂]- <i>p</i>	0.97±0.03	0.98	–N ⁺ H ₂ CH ₃	3.76±0.17	4.01
–C ₆ H ₄ [PO(C ₆ H ₅) ₂]- <i>m</i>	1.02±0.03	0.98	–N ⁺ H(CH ₃) ₂	4.38±0.17	4.01
–C ₆ H ₄ [PO(C ₆ H ₅) ₂]- <i>p</i>	1.07±0.03	0.94	–N ⁺ H ₂ C ₂ H ₅	3.75±0.17	4.01
–C ₆ H ₄ PCl ₂ - <i>m</i>	1.08±0.03	1.09	–N ⁺ (CH ₃) ₃ Cl [–]	4.48±0.17	4.01
–C ₆ H ₄ PCl ₂ - <i>p</i>	1.14±0.03	0.98	–N ⁺ H ₂ C ₃ H ₇ - <i>n</i>	3.75±0.17	4.01
–C ₆ H ₄ [P(O)Cl ₂]- <i>m</i>	1.26±0.03	1.32	–N ⁺ (CH ₃) ₃	4.38±0.17	4.01
–C ₆ H ₄ [P(O)Cl ₂]- <i>p</i>	1.34±0.03	1.16	–N ⁺ H ₂ C ₄ H ₉	3.75±0.17	4.01
–C ₆ H ₄ PF ₂ - <i>m</i>	1.05±0.03	1.01	–N ⁺ H ₂ C ₄ H ₉ - <i>iso</i>	3.75±0.17	4.01
–C ₆ H ₄ PF ₂ - <i>p</i>	1.13±0.03	0.95	–N ⁺ H ₃	3.78±0.17	4.01
–C ₆ H ₄ PH ₂ - <i>m</i>	0.74±0.03	0.67	–CH ₂ N ⁺ H(CH ₃) ₂	1.08±0.17	1.48
–C ₆ H ₄ PH ₂ - <i>p</i>	0.73±0.03	0.66	–CH ₂ N ⁺ (CH ₃) ₃	1.02±0.17	1.48
–C ₆ H ₄ [PO(OH) ₂]- <i>m</i>	0.96±0.03	1.03			

2. Inductive effect and the conformation of a substituent

Obviously, within the framework of the model under consideration, the inductive effect of a particular substituent is substantially dependent upon its conformation. In particular, the parameters r_i in Eqn (2), which correspond to the distances from each of the atoms constituting the substituent to the reaction centre, are sensitive to the conformation. On the one hand, this is an argument in favour of the model proposed, because the inductive effects of substituents depend in reality on their conformations.⁴ On the other hand, such a conformational sensitivity may appear at first glance to be an undesirable factor, since the exact conformation of a substituent is not necessarily known and, furthermore, the conformation can change during a reaction or activation.

However, it is easy to see that the number of such substituents in real reaction series is relatively small. For the majority of substituents, the problem of conformational uncertainty either does not exist at all or is easily solved if the occurrence of a particular conformation amongst several possible conformations is obvious. Thus, relying on the above majority of substituents, we can proceed to the reverse procedure, i.e. to determine the conformation in which a substituent exists (for those substituents for which the degree of conformational uncertainty is quite large). In this case, one should merely calculate the inductive effects for each of the possible conformations, compare the values obtained with the experimental inductive constant, and choose the value that is in best agreement with the whole series. An example of such a sort of conformation analysis is presented in Table 3 for the substituents CH₂COR and for *trans*-CH=CHCH₂COOR. We calculated the inductive constants for various possible types of orientation of these substituents with respect to the reaction centre and compared the results with the corresponding experimental values.

It is seen that the acylmethyl substituent has a clear-cut transoid orientation, which is evidently sterically more favourable.

Table 3. Theoretical (σ_{calc}^*) and experimental (σ_{exp}^*) σ^* -constants for the acylmethyl and *trans*-alkoxycarbonylpropenyl substituents.

Substituent	Conformation	σ_{calc}^*	σ_{exp}^*
CH ₂ COR	<i>cis</i>	1.41	
	<i>trans</i>	0.69	0.69
<i>trans</i> -CH=CH–CH ₂ COOR	<i>cis</i>	0.65	0.69
	<i>trans</i>	0.58	

In the case of the *trans*-alkoxycarbonylpropenyl substituent, the difference between the inductive constants of the two conformations considered is relatively small; we present this example in order to demonstrate that conformational transitions do not necessarily exert a substantial influence on the inductive constant.

In any case, the above analysis indicates that the conformational sensitivity of the model under consideration is not a drawback; conversely, this makes the model more flexible and more useful for practical purposes.

3. Critical analysis of the model and its physical meaning

It is clear that our approach to the description of the inductive effect of substituents in terms of the additive Eqn (2) is in essence purely formal. At the same time, the dependence of the σ^* -constants on the reciprocal of the squared distance to the reaction centre confirms in general the electrostatic field nature of the inductive effect, because it reflects the involvement of Coulomb interactions. Besides, good agreement between the

calculated and experimental inductive constants, which is manifested in the high quality of the correlations, indicates that σ_A -constants reflect the actual ability of various elements to exert an inductive influence, depending on their chemical nature and valence state. This raises the question as to what is the physical meaning of the elemental constants σ_A .

To find out what factors largely determine the nature of the σ_A -constants we studied¹¹¹ the quantitative dependences of σ_A -constants on various physical and geometrical parameters used most frequently in the analysis and interpretation of inductive interactions by multifactor regression analysis; a number of interesting regularities were thus identified.

For example, for a broad selection of elements, σ_A -constants follow high-quality correlations with the difference between the electronegativities of a given element and carbon (reaction centre) and with the covalent radius (R) of the element in the corresponding valence state squared:^{111, 115}

$$\sigma_A = 7.840 \Delta\chi R^2. \quad (6)$$

It is obvious that this dependence is in good agreement with both the magnitude and sign of inductive constants.

Eqn (6) indicates that the σ_A -constant, reflecting the ability of an atom to exhibit an inductive effect, depends not only on its electronegativity, which is certainly the motivating force in the displacement of electron density, but is also directly proportional to the surface area of its valence shell (R^2), i.e. to its ability to delocalise the arising charge. Thus, the magnitude of the inductive effect of a particular element (substituent) is determined both by the 'potential difference' ($\Delta\chi$) between this element and the reaction centre and by its 'capacity'.

It should be noted that numerous attempts have been made to find a direct relationship between the inductive constants and some known physical parameters characterising in one way or another the ability of an atom to attract electrons, such as electronegativity,^{120, 121} ionisation potential,¹²⁰ electron affinity,¹²⁰ dipole moment,^{4, 6} degree of ionic character of the bond,^{4, 74} etc., all of which were unsuccessful. However, one would hardly expect that any one parameter alone would be sufficient to describe quantitatively the inductive effect. Even if this were the case, the dependence obtained would be far from simple. This is demonstrated, in particular, by Eqn (6).

It is noteworthy that Eqn (6) almost agrees with the known^{4, 74, 122, 123} dependences of electronegativity on atom size

$$\chi = \frac{aZ}{R^2} + b, \quad (7)$$

which forms the basis for the so-called 'geometrical' systems of electronegativity, for example, the widely used Allred-Rochov scale.^{4, 74, 122, 124} In addition, dependences of the following form are known

$$\chi = \frac{aZ}{R} + b, \quad (8)$$

[Pritchard-Skinner¹²³ and Gordon ($b = 0$)¹²⁴ equations].

From a comparison of relations (6)–(8), it follows unambiguously that the σ_A constants found by us are directly related to the effective nuclear charge Z , or, more precisely, to the difference between the effective nuclear charge of the given atom and that of carbon (ΔZ).

Thus, the σ_A constants have a clear physical meaning, which, in its turn, can throw light on the nature of the inductive effect itself.

Combination of Eqns (2) and (6) gives the following final expression for a Taft inductive constant:

$$\sigma^* = 7.840 \sum_i \Delta\chi_i \frac{R_i^2}{r_i^2}, \quad (9)$$

where $\Delta\chi_i$ is the difference between the electronegativities of the i -th atom in the substituent and the reaction centre, R_i is the covalent radius of the i -th atom, and r_i is the distance from this atom to the reaction centre.

A number of interesting corollaries and relations follow from Eqn (9) (some of them are considered below). In addition, this equation permits the direct calculation of the inductive constant of any substituent at any reaction centre from the fundamental characteristics of atoms and groups.

The relatively complex form of Eqn (9) accounts for the fact that numerous attempts made by various workers to describe quantitatively the inductive effect in an analytical form have so far been unsuccessful, although in some cases and for relatively small selections of substituents, quite satisfactory results have been obtained (see, for example, a number of papers^{4, 6, 120}).

4. Use of the additive model of the inductive effect in the analysis of reactivities of organoelement compounds

The inductive influence of substituents on reaction centres other than carbon is a fundamental problem in the modern theory of reactivity of organoelement compounds.

As noted above, the reactivities of organoelement compounds in correlation analysis are often evaluated using scales of 'special' electronic constants (for example, 'silicon' σ_{Si} or 'phosphorus' σ^P constants).^{4, 74} Like Hammett constants, these values reflect the inductive interaction, conjugation, and steric shielding, i.e. the overall influence of a substituent on a reaction centre. Thus, the special scales are applicable in those cases where the ratios of the constituents forming the overall effect of a substituent and the structure of the reaction centre are similar to those in a standard reaction series for which the constants have been determined.

At the same time, interest in the possibility of using the classical 'carbon' scales of inductive constants to describe the reactivities of organoelement compounds has been frequently shown. Thus, no unified approach to the problem of the linearity of variation of the inductive effects of substituents at various reaction centres has been elaborated so far. Since there is no self-consistency of the operating scales, their use is limited, and their physical meaning is obscure, it is impossible to make a correct comparison of inductive interactions in the chemistry of organic and organoelement compounds.

In our opinion, this problem could be solved fairly legitimately by considering the inductive effects of substituents at carbon and non-carbon reaction centres within the framework of a certain unified approach, which operates with the calculated values of the inductive constants and thus ensures the possibility of their comparative analysis.

We have attempted^{116–119} to solve the problem of linearity of the inductive influences of substituents at carbon and heteroatom reaction centres, which is now of prime importance in the chemistry of organoelement compounds. Solution of this problem would make it possible to identify the limits within which the classical carbon inductive constants are applicable to the evaluation of reactivities of organoelement compounds.

In terms of our approach, the inductive constant of a substituent at a heteroatom reaction centre is either directly calculated from Eqn (9), based on the fundamental characteristics of the reaction centre and of the atoms incorporated in the substituent, or calculated using the basic Eqn (2). In the latter case, an intrinsic ability to exert an inductive influence on the given reaction centre is assigned to each atom and is determined by the magnitude of the corresponding atomic σ_A -constant found from Eqn (6).

It is clear that by analysing the σ_A -constants calculated theoretically for the same atoms at different reaction centres, one can find out whether there is a linear correlation between the inductive influences of atoms and substituents at carbon and non-carbon reaction centres. Using the method of regression analysis, we compared the calculated $\sigma_A(X)$ -constants (reflecting the ability of atoms to exert an inductive influence on heteroatom reaction

centres X) with the $\sigma_A(C)$ -constants, used for the calculation of the inductive effects of substituents at a carbon atom. We obtained correlations of the following form

$$\sigma_A(X) = A_0 + A_1\sigma_A(C). \quad (10)$$

The A_0 and A_1 parameters of the dependences obtained are listed in Table 4. Analysis of these values makes it possible to conclude that the closer the 'inductive' electronegativities of the X and C atoms to each other, the higher the quality of the corresponding correlations and more correct the use of the 'carbon' inductive constants to describe the inductive effect of substituents at the atom X.

Table 4. The parameters of correlations of type (10), which relate the $\sigma_A(X)$ -constants of atoms at various reaction centres (X) to the corresponding values of the $\sigma_A(C)$ -constants.

Reaction centre	A_0	A_1	R	S_0
F	-17.39 ± 1.93	1.69 ± 0.35	0.715	9.051
Cl	-9.07 ± 1.10	1.37 ± 0.20	0.824	5.147
Br	-8.27 ± 0.92	1.32 ± 0.16	0.860	4.309
I	-6.67 ± 0.74	1.26 ± 0.12	0.893	3.475
-O-	-9.03 ± 1.00	1.35 ± 0.18	0.845	4.702
-S-	-5.66 ± 0.62	1.23 ± 0.40	0.916	2.945
-N<	-4.21 ± 0.52	1.17 ± 0.09	0.933	2.475
=C<	-1.44 ± 0.16	1.05 ± 0.02	0.991	0.756
-P<	-1.24 ± 0.14	1.04 ± 0.02	0.993	0.667
Sn	0.73 ± 0.08	0.97 ± 0.01	0.997	0.393
As	-1.96 ± 0.22	1.06 ± 0.04	0.984	1.042
B	0.17 ± 0.02	0.99 ± 0.01	0.999	0.124
Li	6.06 ± 0.67	0.75 ± 0.12	0.795	3.149
Mg	7.69 ± 0.86	0.69 ± 0.15	0.684	4.021
Pb	-1.35 ± 0.15	1.05 ± 0.02	0.992	0.709
Sb	-0.91 ± 0.11	1.02 ± 0.02	0.995	0.527
Ge	0.74 ± 0.08	0.97 ± 0.15	0.997	0.393
Si	0.33 ± 0.05	0.98 ± 0.01	0.998	0.267
Se	-3.34 ± 0.54	0.92 ± 0.09	0.892	2.54
-C≡	-9.82 ± 1.09	1.39 ± 0.19	0.830	5.10
O=	-28.13 ± 3.13	2.18 ± 0.57	0.631	14.65
>P=	-1.94 ± 0.21	1.07 ± 0.03	0.985	1.00

It should be noted that the above correlations cover the whole array of σ_A -constants, including those points corresponding to extremely electron-donating and extremely electron-withdrawing atoms. However, even this broad range of magnitude of σ_A -constants ensures a high quality of correlations of type (10) only if the electronegativity of the reaction centre X deviates from that of carbon by no more than 0.2 unit.

Thus, in the general case, the inductive constants of substituents at different reaction centres are not proportional to one another, i.e. there is no linearity of the inductive effect in the chemistry of organic and organoelement substituents, despite the fact that the nature of inductive interactions certainly remains invariable. Now it is clear that the classical inductive constants of substituents must be used for analysing the reactivities of organoelement compounds with great caution. In addition, it is obvious that the smaller the difference between the electronegativity χ of the reaction centre X and the electronegativity χ_C of carbon and the greater the difference between the electronegativities of the atoms forming the substituent and the electronegativity of carbon, the more correct the use of carbon constants.

It should be noted that since our approach permits fairly easy theoretical calculation of the inductive constant of any substituent at any particular reaction centre, the above problem simply no longer exists within the framework of our model. Thus, in all probability, the use of this model for the quantitative evaluation of the inductive influences of substituents in the reactivities of organoelement compounds will be the most legitimate. This chiefly refers to alkyl substituents, the inductive influence of which is still one of the most acute and disputed problems.

5. The problem of the inductive influence of alkyl substituents

At present, the inductive influence of alkyl substituents is still one of the most uncertain problems in the correlation analysis of the reactivities of organic and organoelement compounds. When the inductive influence of substituents in various reaction series is considered, the points corresponding to alkyl substituents deviate most substantially from the general correlation plots. Hence, it is no wonder that the question of the inductive effects of alkyl substituents has caused the most prolonged discussion in the literature which has not yet been completed.⁴

At present, the overwhelming majority of researchers are inclined to believe that alkyl substituents are incapable of participating in any significant electronic interactions; therefore, their inductive influence is frequently regarded as zero.¹²⁵⁻¹²⁸

However, a number of examples indicate that the inductive effects of alkyl substituents are significant and differ from one another.¹²⁹ Furthermore, correlations have been obtained that relate the inductive constants of alkyl substituents in the Hammett scale to the 'special' constants, reflecting the influence of alkyl groups on non-carbon reaction centres, for example, on the phosphorus atom.⁵⁷ Based on these correlations, the overall influence of alkyl substituents on the phosphorus atom was divided into inductive and resonance constituents. As this was done, the substituents at the phosphorus atom (including alkyl groups) were assumed not to shield sterically the reaction centre due to the large size of the latter.⁹

However, it was later found that, apart from the inductive and resonance constituents, the 'special' constants also incorporate a steric component. Thus, when the overall effect of the substituents on the reaction centre is divided into elementary parts, all three types of interaction should be taken into account.^{57, 130, 131} Moreover, a linear correlation between the inductive and steric influences has been found. This served as additional evidence for the illegitimacy of the inductive constants of alkyl substituents and for the presence of the residual contribution of steric interactions to them. The notion of 'pseudo-inductive' influence of alkyl substituents has even appeared.⁵

Thus, it can be stated that at present, opinions on the inductive effect of alkyl substituents differ widely and are uncertain. Evidently, this is caused by the absence of reliable criteria and of a reliable technique for the division of the overall effect of substituents into inductive, resonance, and steric constituents. In addition, even in those scales in which the inductive constants of alkyl substituents differ from zero, they are still fairly small; in view of the error in the determination of empirical constants, this makes the evaluation of the inductive influence of alkyl groups based on standard reaction series doubtful.

It is also noteworthy that conformations of alkyl substituents are quite diverse, which can make the division of their influence on a reaction centre into elementary contributions even more complicated. At the same time, in view of the fact that almost all real reaction series involve large numbers of alkyl and alkyl-containing substituents, it is clear that a versatile and legitimate approach to the estimation of their inductive influence needs to be developed.

The consideration of inductive effects of alkyl substituents within the framework of the model suggested by us unambiguously implies that it is improper to consider the inductive influence of alkyl groups to be zero. This can be done legitimately only in those cases where a saturated carbon atom acts as the reaction

centre,¹³² whereas in all other situations, as follows from Eqn (9), the inductive effects of alkyl groups can not only be significant but also quite strong (especially in the chemistry of organoelement compounds for which the $\Delta\chi$ value in Eqn (9) is the highest).

Theoretical analysis of the inductive influence of alkyl substituents in terms of our model makes it possible to identify yet another important feature in an analytical form. Since the electronegativities of carbon and hydrogen atoms are close, it is clear that the $\Delta\chi$ values for all the atoms in an alkyl substituent at each particular reaction centre are virtually identical; therefore, in Eqn (9), this value can be factored out from the summation sign. Thus, the inductive influence of alkyl groups is proportional to the sum of the ratios of the squared covalent radii of the atoms incorporated in it to the squared distances from these atoms to the reaction centre:

$$\sigma_{\text{Alk}}(X) = 7.840 \Delta\chi_i \sum_i \frac{(R_i^2)_i}{r_i^2} \quad (11)$$

Within the framework of the frontal steric effect model developed by us previously, a similar ratio was obtained as a measure of the steric shielding of a reaction centre by an atom defining the steric constant R_s of the corresponding substituent. In particular, this follows from Eqn (1), which can be transformed into the simpler expression (12), because, for small values of the argument x , the function $\lg(1-x)$ is known to be linearly related to x :

$$R_s = \text{const} \sum_i \frac{(R_i^2)_i}{r_i^2} \quad (12)$$

Thus, Eqns (11) and (12) indicate that there is a linear relationship and an intrinsic genetic connection between the inductive and steric effects of alkyl substituents. However, this cannot be interpreted as evidence for the illegitimacy of the inductive constants of alkyl groups and for the presence of the residual steric contribution in them, as has usually been done in recent years.⁵

In order to confirm experimentally this statement we calculated the inductive constants for alkyl substituents at various reaction centres in terms of our model and compared the results with the steric constants R_s of the corresponding alkyl groups at the same reaction centres.¹³² The parameters of the resulting correlations are presented in Table 5. It should be noted that the correlation coefficients are about 0.99, i.e. a strictly linear correlation between the inductive and steric influences of alkyl groups really exists.

The results obtained indicate that the sensitivities of reaction centres to the inductive influence of alkyl radicals are dissimilar: the greater the difference between the electronegativities of the reaction centre and carbon, the more significant the inductive effect of alkyl groups on this centre and the more clear-cut its dependence on the number of atoms in the substituent.

Thus, in terms of our inductive model, the problem of the inductive influence of alkyl substituents receives a strict and simple solution which, in our opinion, adequately accounts for the contradictory set of data published on this topic.

Hence, the model of the inductive effect that we have developed permits more than just the legitimate theoretical calculation of the inductive constant of any substituent at any reaction centre for the purposes of the correlation analysis of the reactivities of organic and organoelement substituents. This model also makes it possible to solve many other important problems associated with the inductive effect that cannot be currently solved in terms of other approaches.

Table 5. Parameters of the linear correlations connecting the steric (R_s) and inductive (σ^*) constants of alkyl substituents at various reaction centres ($N = 13$)

$$\sigma_{\text{Alk}}^* = A_1 + A_2 R_s(\text{Alk}).$$

Reaction centre	A_1	A_2	S_0	R
—O—	−0.568 (0.086)	−1.444 (0.031)	0.0751	0.998
—S—	−0.161 (0.030)	−0.929 (0.015)	0.0295	0.999
—N<	−0.250 (0.045)	−0.704 (0.017)	0.0403	0.997
—P<	−0.030 (0.009)	−0.203 (0.005)	0.0094	0.997
—As<	−0.052 (0.009)	−0.337 (0.005)	0.0092	0.999
—B<	0.011 (0.001)	0.032 (0.007)	0.0017	0.997
—Ga<	0.086 (0.015)	0.554 (0.008)	0.0150	0.999
—Hg—	0.024 (0.005)	0.194 (0.003)	0.0048	0.999
>Pb<	−0.038 (0.006)	−0.241 (0.004)	0.0060	0.999
—Sb<	−0.025 (0.004)	−0.144 (0.003)	0.0041	0.998
>Si<	0.017 (0.002)	0.067 (0.001)	0.0026	0.998

References

- V I Galkin, R D Sayakhov, R A Cherkasov *Usp. Khim.* **60** 1617 (1991) [*Russ. Chem. Rev.* **50** 815 (1991)]
- V I Galkin, R A Cherkasov *Reaktsion. Sposob. Org. Soedin. (Tartu)* **18** 111 (1981)
- V I Galkin, R D Sayakhov, R A Cherkasov *Metalloorg. Khim.* **3** 986 (1990)
- A N Vereshchagin *Induktivnyi Effekt* (Inductive Effect) (Moscow: Nauka, 1987)
- V A Pal'm *Osnovy Kolichestvennoi Teorii Organicheskikh Reaktsii* (Fundamentals of the Quantitative Theory of Organic Reactions) (Leningrad: Khimiya, 1977)
- Yu A Zhdanov, V I Minkin *Korrelyatsionnyi Analiz v Organicheskoi Khimii* (Correlation Analysis in Organic Chemistry) (Rostov: Izd. Rostovsk. Univ., 1966)
- C D Johnson *The Hammett Equation* (Cambridge: Cambridge University Press, 1973)
- M I Kabachnik *Dokl. Akad. Nauk SSSR* **110** 393 (1956)
- T A Mastryukova, M I Kabachnik *Usp. Khim.* **38** 1751 (1969) [*Russ. Chem. Rev.* **38** 795 (1969)]
- M Charton *Prog. Phys. Org. Chem.* **13** 119 (1981)
- D D Perrin, B Dempsey, E P Serjeant *pK_a Prediction for Organic Acids and Bases* (London: Chapman and Hall, 1981)
- R A Robinson, in *Elektronnaya Teoriya v Organicheskoi Khimii* (Electronic Theory in Organic Chemistry) (Translated into Russian; Leningrad: ONTI, 1936) p. 115
- C K Ingold, in *Elektronnaya Teoriya v Organicheskoi Khimii* (Electronic Theory in Organic Chemistry) (Translated into Russian; Leningrad: ONTI, 1936) p. 144
- C K Ingold *Structure and Mechanism in Organic Chemistry* (Ithaca, London: Cornell University Press, 1969)
- V I Galkin, A R Cherkasov, R D Sayakhov, R A Cherkasov, in *Tez. Dokl. 1-go Vserossiiskogo Simpoziuma po Organicheskoi Khimii* (Abstracts of Reports of the First All-Russian Symposium on Organic Chemistry) (St.-Petersburg: Nauka, 1995) p. 28
- R W Taft, in *Steric Effects in Organic Chemistry* (Translated into Russian; Moscow: Izd. Inostr. Lit., 1960) p. 562
- L P Hammett *Chem. Rev.* **17** 125 (1935)
- R W Taft *J. Am. Chem. Soc.* **75** 4538 (1953)
- J D Roberts, W T Moreland *J. Am. Chem. Soc.* **75** 2167 (1953)
- H H Jaffé *Chem. Rev.* **53** 191 (1953)
- R W Taft, S Ehrenson, I C Lewis, R E Glick *J. Am. Chem. Soc.* **81** 5352 (1959)
- H H Jaffé, L D Freedman, G O Doak *J. Am. Chem. Soc.* **75** 2209 (1953)
- H H Jaffé *J. Chem. Phys.* **20** 279, 778, 1554 (1952); **21** 415 (1953)

24. A I Shatenshtein *Izotopnyi Obmen i Zameshchenie Vodoroda v Organicheskikh Soedineniyakh* (Isotope Exchange and Substitution of Hydrogen in Organic Compounds, Ch. V) (Moscow: Izd. Akad. Nauk SSSR, 1960)
25. S L Buchwald, R B Nielsen *J. Am. Chem. Soc.* **110** 3171 (1986)
26. D C Crans, S M Schelble, L A Theisen *J. Org. Chem.* **56** 1266 (1991)
27. L A van de Kuil, H Luitjes, D M Grove, J W Zwikker, J W van de Linden *Organometallics* **13** 466 (1994)
28. P Sharpe, N G Aalemeddin, D F Richardson *J. Am. Chem. Soc.* **116** 11098 (1994)
29. F G Bordwell, Jin-Pei Cheng *J. Am. Chem. Soc.* **113** 1736 (1991)
30. A S Dneprovskii, A N Kasatochkin, D Yu Kondakov *Zh. Org. Khim.* **24** 923 (1988)
31. A S Dneprovskii, D Yu Kondakov, A N Kasatochkin *Zh. Org. Khim.* **25** 19 (1989)
32. A S Dneprovskii, A N Kasatochkin, D Yu Kondakov *Zh. Org. Khim.* **25** 1984 (1989)
33. T A Mastryukova, in *Khimiya i Primenenie Fosfororganicheskikh Soedinenii (Tr. II Konf.)* [The Chemistry and Application of Organophosphorus Compounds (Transactions of the Second Conference)] (Moscow: Izd. Akad. Nauk SSSR, 1962) p. 57
34. M I Kabachnik, T A Batsaeva, in *Khimiya i Primenenie Fosfororganicheskikh Soedinenii (Tr. II Konf.)* [The Chemistry and Application of Organophosphorus Compounds (Transactions of the Second Conference)] (Moscow: Izd. Akad. Nauk SSSR, 1962) p. 536
35. A N Pudovik, I V Gur'yanova, R A Cherkasov *Zh. Obshch. Khim.* **37** 2393 (1967)
36. M I Kabachnik, in *Khimiya i Primenenie Fosfororganicheskikh Soedinenii (Tr. II Konf.)* [The Chemistry and Application of Organophosphorus Compounds (Transactions of the Second Conference)] (Moscow: Izd. Akad. Nauk SSSR, 1962) p. 24
37. V F Toropova, M K Saikina, N I Guseva, R A Cherkasov, M G Khakimov *Zh. Obshch. Khim.* **38** 2088 (1968)
38. V F Toropova, R A Cherkasov, N I Savel'eva, A N Pudovik *Zh. Obshch. Khim.* **40** 1043 (1970)
39. V F Toropova, R A Cherkasov, N I Savel'eva, V I Gorshkova, A N Pudovik *Zh. Obshch. Khim.* **41** 1469 (1971)
40. V F Toropova, R A Cherkasov, N I Savel'eva, A A Grigor'eva, I V Shergina, V V Ovchinnikov, A N Pudovik *Zh. Obshch. Khim.* **41** 1673 (1971)
41. V F Toropova, R A Cherkasov, N I Savel'eva, I V Slyusar', A N Pudovik *Zh. Obshch. Khim.* **42** 1485 (1972)
42. R A Cherkasov, V V Ovchinnikov, E N Petrova, V F Toropova, A N Pudovik, in *Khimiya Elementoorganicheskikh Soedinenii III–V Grupp* (The Chemistry of Organoelement Compounds of Groups III–V) (Leningrad: Nauka, 1976) p. 114
43. V V Ovchinnikov, V I Galkin, R A Cherkasov, A N Pudovik *Zh. Obshch. Khim.* **47** 290 (1977)
44. V V Ovchinnikov, V I Galkin, R A Cherkasov, A N Pudovik *Izv. Akad. Nauk SSSR, Ser. Khim.* **2021** (1977)
45. V V Ovchinnikov, A R Garifzyanov, R A Cherkasov, V F Toropova *Zh. Obshch. Khim.* **50** 67 (1980)
46. A N Pudovik, R A Cherkasov, G A Kutyrev, Yu Yu Samitov, A A Musina, E I Gol'dfarb *Zh. Obshch. Khim.* **40** 1987 (1970)
47. R A Cherkasov, G A Kutyrev, V V Ovchinnikov, A N Pudovik *Zh. Obshch. Khim.* **46** 963 (1976)
48. N V Kashina, G A Kutyrev, I P Lipatova, R A Cherkasov, A N Pudovik *Zh. Obshch. Khim.* **44** 504 (1974)
49. R A Cherkasov, V V Ovchinnikov, A N Pudovik *Zh. Obshch. Khim.* **46** 957 (1976)
50. G A Kutyrev, I V Gorokhovskaya, O A Samarina, N V Kashina, R A Cherkasov, E A Ishmaeva, A N Pudovik *Zh. Obshch. Khim.* **47** 348 (1977)
51. N G Khusainova, V I Galkin, R A Cherkasov *Zh. Obshch. Khim.* **60** 995 (1990)
52. V V Ovchinnikov, S V Cherezova, V V Klochkov, A V Aganov, R A Cherkasov, A N Pudovik *Dokl. Akad. Nauk SSSR* **276** 144 (1984)
53. V V Ovchinnikov, G Sh Malkova, A M Polozov, R A Cherkasov, A N Pudovik *Zh. Obshch. Khim.* **56** 20 (1986)
54. V V Ovchinnikov, V I Galkin, E G Yarkova, L E Markova, R A Cherkasov, A N Pudovik *Zh. Obshch. Khim.* **48** 2424 (1978)
55. O E Raevskaya, R A Cherkasov, G A Kutyrev, A N Pudovik *Zh. Obshch. Khim.* **44** 746 (1974)
56. R A Cherkasov, in *Stroenie i Reaktivnaya Sposobnost' Organicheskikh Soedinenii* (The Structure and Reactivity of Organic Compounds) (Moscow: Nauka, 1978) p. 107
57. B I Istomin, V A Baranskii *Usp. Khim.* **51** 394 (1982) [*Russ. Chem. Rev.* **51** 223 (1982)]
58. B I Istomin, V A Baranskii *Reaktivn. Sposob. Org. Soedin. (Tartu)* **12** 963 (1975)
59. V I Galkin, Doctoral Thesis in Chemical Sciences, Kazan' State University, Kazan', 1991
60. V I Galkin, R D Sayakhov, R A Cherkasov *Zh. Org. Khim.* **30** 3 (1994)
61. R Knorr *Tetrahedron* **37** 929 (1981)
62. A N Vereshchagin *Konstanty Zamestitelei dlya Korrelyatsionnogo Analiza* (Substituent Constants for Correlation Analysis) (Moscow: Nauka, 1988)
63. G V Bykov *Istoriya Elektronnykh Teorii Organicheskoi Khimii* (The History of Electron Theories of Organic Chemistry) (Moscow: Izd. Akad. Nauk SSSR, 1963)
64. G K Semin, T A Babushkina, G G Yakobson *Primenenie Yadernogo Kvadrupol'nogo Rezonansa v Khimii* (Applications of Nuclear Quadrupole Resonance in Chemistry) (Leningrad: Khimiya, 1972)
65. N I Sherpina, L V Sherstyannikov, A L Kuznetsov, O G Yarosh, R G Mirakov, M G Voronkov *Izv. Akad. Nauk SSSR, Ser. Khim.* **2716** (1985)
66. M C Pirrung, A T Morehead *J. Am. Chem. Soc.* **116** 8991 (1994)
67. O Exner *Dipole Moments in Organic Chemistry* (Stuttgart: Georg Thieme, 1975)
68. J M Garrison, D Ostavic, T C Buice *J. Am. Chem. Soc.* **111** 4960 (1989)
69. S R Sander, K C Tsou *J. Chem. Phys.* **39** 1062 (1963)
70. R W Taft, J L M Abboud, F Anvia, M Berthelot, M Fujio, I-F Gal, A D Headley, W G Henderson, I Koppel, J H Qian, M Mishima, M Taagepera, S Ueki *J. Am. Chem. Soc.* **110** 1797 (1988)
71. H Takeuchi, M Sugino, T Egana, S Konaka *J. Phys. Chem.* **97** 7511 (1993)
72. G Chuchani, S Pekerar, R M Domingues, A Rotinow, I Martin *J. Phys. Chem.* **93** 201 (1989)
73. I A Koppel, R W Taft, F Anvia, S Z Zhu, L Q Hu, K-S Sung, P D des Marreau, L M Yagupolskii, V L Yagupolskii, N V Ignat'ev, N V Kondratenko, A K Volkonskii, V M Vlasov, R Notario, P C Maria *J. Am. Chem. Soc.* **116** 3047 (1994)
74. L T Kanerva, A M Klibanov *J. Am. Chem. Soc.* **111** 6864 (1989)
75. F Harary *Graph Theory* (Reading, MA: Addison-Wesley Publ., 1969)
76. H Wiener *J. Am. Chem. Soc.* **69** 17 (1947)
77. D H Rouvray, B C Grafford *Afr. J. Sci.* **12** 47 (1976)
78. K Altenburg *Brenn. Chem.* **47** 100 (1966)
79. I R Platt *J. Phys. Chem.* **56** 328 (1952)
80. M Gordon, G R Scartlebury *Trans. Farad. Soc.* **60** 605 (1994)
81. H Hosoye *Bull. Chem. Soc. Jpn.* **44** 2332 (1971)
82. I Gutman, B Ruscic, N Trinagastic, C F Wilcox *J. Chem. Phys.* **62** 3399 (1975)
83. M Randic *J. Am. Chem. Soc.* **97** 6609 (1975)
84. M I Stankevich, I V Stankevich, N S Zefirov *Usp. Khim.* **57** 337 (1988) [*Russ. Chem. Rev.* **57** 191 (1988)]
85. D Bonchev, N Trinastic *J. Am. Chem. Soc.* **67** 4517 (1975)
86. A T Balaban *Theor. Chim. Acta (Berlin)* **53** 355 (1979)
87. V M Tatevskii *Khimicheskoe Stroenie Uglevodorodov i Zakonomernosti v ikh Fizicheskikh Svoistvakh* (The Chemical Structure of Hydrocarbons and Regularities in Their Physical Properties) (Moscow: Izd. Moskovsk. Gos. Univ., 1953)
88. V M Tatevskii, V A Benderskii, S S Yarovoi *Metody Rascheta Fiziko-Khimicheskikh Svoistv Parafinovykh Uglevodorodov* (Methods for the Calculation of the Physicochemical Properties of Paraffin Hydrocarbons) (Moscow: Gostoptekhizdat, 1969)
89. S Marriot, W F Reynolds, R W Taft, R Topsom *J. Org. Chem.* **49** 959 (1984)
90. W F Reynolds, P G Mezey, G K Hamer *Can. J. Chem.* **55** 522 (1977)
91. R D Topsom *Acc. Chem. Res.* **16** 292 (1983)
92. A E Remick *J. Chem. Phys.* **9** 653 (1941)
93. R P Smith, T Ree, J L Magee, H Eyring *J. Am. Chem. Soc.* **73** 2263 (1951)
94. N Lawrencelle, P D Pacey *J. Am. Chem. Soc.* **115** 625 (1993)
95. F H Wesheimer *J. Am. Chem. Soc.* **62** 1892 (1940)
96. F H Wesheimer, M W Shookhoff *J. Am. Chem. Soc.* **61** 555 (1939)
97. C M Judson, M Kilpatrick *J. Am. Chem. Soc.* **71** 3115 (1949)

98. M Kilpatrick, J G Morse *J. Am. Chem. Soc.* **75** 1846 (1953)
99. R C Duty, G Hodel *J. Phys. Chem.* **82** 1016 (1978)
100. M Kilpatrick, C A Arenberg *J. Am. Chem. Soc.* **75** 3812 (1953)
101. H M Peek, T L Hill *J. Am. Chem. Soc.* **73** 5304 (1951)
102. S Ehrenson *J. Phys. Chem.* **81** 1520 (1977)
103. J D S Ritter, S I Miller *J. Am. Chem. Soc.* **86** 1507 (1964)
104. C F Wilcox, J S McIntyre *J. Org. Chem.* **30** 777 (1965)
105. S Siegel, J M Komarmy *J. Am. Chem. Soc.* **82** 2547 (1960)
106. G Ceregolini, N Re *Gazz. Chim. Ital.* **123** 653 (1993)
107. A S Dneprovskii, S A Mil'tsov *Zh. Org. Khim.* **22** 303 (1986)
108. A S Dneprovskii, S A Mil'tsov, P V Arbuzov *Zh. Org. Khim.* **24** 2026 (1988)
109. T Komatsuzaki, K Sakakibara, M Hirota *Tetrahedron Lett.* **39** 3309 (1989)
110. M Hirota, K Sakakibara, J Ishizawa, S Kuroda *Organic Reactivity (Tartu)* **102** 33 (1995)
111. V I Galkin, A R Cherkasov, R D Sayakhov, R A Cherkasov *Zh. Obshch. Khim.* **65** 458 (1995)
112. V I Galkin, A R Cherkasov, R D Sayakhov, R A Cherkasov *Zh. Obshch. Khim.* **65** 469 (1995)
113. V I Galkin, A R Cherkasov, R D Sayakhov, R A Cherkasov *Zh. Obshch. Khim.* **65** 474 (1995)
114. V I Galkin, A R Cherkasov, R D Sayakhov, R A Cherkasov *Zh. Obshch. Khim.* **65** 477 (1995)
115. V I Galkin, A R Cherkasov, R A Cherkasov *Zh. Org. Khim.* **31** 1802 (1995)
116. V I Galkin, A R Cherkasov, I M Sibgatullin, R A Cherkasov *Zh. Org. Khim.* **31** 1352 (1995)
117. V I Galkin, A R Cherkasov, I M Sibgatullin, R A Cherkasov, in *Abstracts of the XIIIth International Conference on Phosphorus Chemistry, Jerusalem, Israel, 1995* p. 143
118. A R Cherkasov, V I Galkin, I M Sibgatullin, R A Cherkasov *Phosphorus Sulfur Silicon Relat. Elem.* **111** 141 (1996)
119. A R Cherkasov, V I Galkin, R A Cherkasov, in *Tez. Dokl. VI Vserossiiskoi Konferentsii po Metalloorganicheskoi Khimii* (Abstracts of Reports of the Sixth All-Union Conference on Organometallic Chemistry) (N.-Novgorod: Izd. N.-Novgorodsk. Gos. Univ., 1995) p. 245
120. N S Imyanitov, G I Shmelev *Zh. Org. Khim.* **25** 900 (1989)
121. W F Reynolds *J. Chem. Soc., Perkin Trans.* **2** 985 (1980)
122. J Huheey *Inorganic Chemistry: Principles of Structure and Reactivity* (New York: Harpercollins College, 1993)
123. S S Batsanov *Izv. Akad. Nauk SSSR, Ser. Khim.* 2701 (1989)
124. J Mullay *J. Am. Chem. Soc.* **106** 5842 (1984)
125. J A MacPhee, J E Dubois *Tetrahedron Lett.* **26** 2471 (1976)
126. M Charton *J. Org. Chem.* **44** 903 (1979)
127. M Charton *J. Am. Chem. Soc.* **99** 5687 (1977)
128. D F De Tar *J. Org. Chem.* **45** 5166 (1980)
129. M I Kabachnik *Usp. Khim.* **48** 1523 (1979) [*Russ. Chem. Rev.* **48** 814 (1979)]
130. B I Istomin, V A Baranskii, E F Grechkin *Reaktsion. Sposob. Org. Soedin. (Tartu)* **12** 69 (1975)
131. V A Baranskii, B I Istomin, A R Kalabina *Reaktsion. Sposob. Org. Soedin. (Tartu)* **13** 263 (1976)
132. V I Galkin, A R Cherkasov, R A Cherkasov *Zh. Org. Khim.* **32** 1362 (1995)

Methods for the measurement of ion mobilities and applications

G V Karachevtsev

Contents

I. Introduction	657
II. Ion mobilities	657
III. Mobility spectrometers and their applications	658
IV. Conclusion	660

Abstract. The results of studies of ion mobilities in gases, yielding information about ion-molecule interaction potentials, are surveyed. The principles of the operation and the characteristics of the ion mobility spectrometers are described. Examples of the applications of plasma chromatography in the study of ions are presented. The bibliography includes 70 references.

I. Introduction

The term mobility of ions is defined as the ratio of the rate of their directed uniform motion through a gas to the strength of the electric field inducing this motion. Ion mobilities in gases are widely used in both fundamental and applied branches of science. For example, the parameters of the interaction potentials have been determined and the bond dissociation energies, equilibrium bond lengths, and vibrational frequencies have been obtained from the mobilities of chromium, cobalt, and nickel ions in helium and neon at different temperatures.^{1,2} Such information is of interest in the study of the physical and chemical characteristics of low-temperature plasma.

Analytical instruments based on measurements of ion mobilities have been developed in recent years. These instruments are known under different names: ion mobility spectrometers,³ drift spectrometers, and plasma chromatographs.^{4,5} The methods for the analysis of ions in these instruments consist in the study of the dependence of the mobilities of ions on their masses and, in a more general case, on the type of ions. Such devices do not require the

creation of a high vacuum, which significantly simplifies their design compared with other analytical apparatus in which ionisation processes are employed (for example, mass spectrometers and electron spectrometers).

A schematic illustration of a drift spectrometer is presented in Fig. 1. A packet of ions with different mobilities is injected into the drift tube with a uniform electric field and an increased gas pressure. The initial packet is then divided into several packets in accordance with the number of different types of ions in the initial packet.

As in mass spectrometers, the ionisation in plasma chromatographs may be achieved by corpuscular radiation and photoradiation and by laser desorption as well as electro- and thermo-sputtering methods.^{6–9}

II. Ion mobilities

Data on ion mobilities in gases have been published in a series of communications.^{10–24} The mobilities of ions depend on their masses, structures, and the effectiveness of energy exchange during their motion in an electric field in gases.

For electric fields usually employed in plasma chromatography at atmospheric pressure, the mobility coefficient K is independent of the electric field strength E . The mobility coefficient is linked by the Einstein relation to the ion diffusion coefficient D

$$K = 1.16 \times 10^4 \frac{D}{T},$$

where the dimensions are $\text{cm}^2 \text{V}^{-1} \text{s}^{-1}$ for K , $\text{cm}^2 \text{s}^{-1}$ for D , and K for T .

The average energy of the ions in the electric field is determined by the parameter E/N (N is the density of the gas) measured in townsend (1 Td = 10^{-17}V cm^2). In plasma chromatography, the typical values of the quantities E/N are 1–2 Td.

Under these conditions, the elastic scattering of ions is determined by the polarisation capture occurring over distances appreciably greater than the geometrical dimensions of the molecule and ion. The mobility coefficient under standard conditions ($N = 2.69 \times 10^{19}$ molecules in 1 cm^3 , $T = 273 \text{ K}$) can be obtained by means of the following expression:

$$K = 13.85 \left(\frac{1}{m} + \frac{1}{M} \right)^{0.5} \alpha^{-0.5},$$

where m is the mass of the ion in a.u., M the mass of the molecule in a.u., and α the polarisability of the molecules in \AA^3 .

The mobility is linked to the reduced mobility K_0 by the relation

$$K_0 = K \frac{273}{T} \frac{P}{760}.$$

Here P is the total pressure in mm Hg.

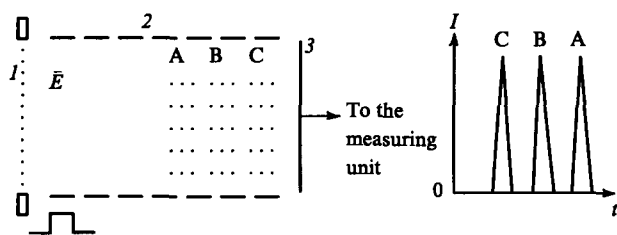


Figure 1. Schematic illustration of a drift spectrometer. (1) Ion shutter ensuring the passage of ions from the ion source to the drift tube (2); (3) ion detector; A, B, C — packets of ions with different mobilities.

G V Karachevtsev Department of Molecular Physics, Moscow Institute of Physics and Technology, Institutskii per. 9, 141700 Dolgoprudnyi, Moscow Region, Russian Federation. Fax (7-095) 408 68 69. Tel. (7-095) 408 55 27

Received 13 May 1995

Uspekhi Khimii 65 (8) 712–717 (1996); translated by A K Grzybowski

With increase in the energy of the relative motion of the ion and the molecule, the radius for the capture of the ion by the molecule diminishes and short-range exchange interactions begin to be manifested between the molecule and the ion. The mobility coefficient begins to depend on the electric field:

$$K = K_{(0)} \left[1 + \alpha_1 \left(\frac{E}{N} \right)^2 \right].$$

Here $K_{(0)}$ is the mobility in a zero electric field and α_1 is a coefficient which takes into account the deviation of the interaction potential from the polarisation potential. Over short distances, this deviation is responsible for the temperature dependence of the mobility coefficients. For example, with increase in temperature during the drift of Li^+ ions in helium, whereupon the short-range exchange forces become repulsive, the mobility coefficient increases, whereas in the drift of H^+ ions, where short-range attractive forces operate, it diminishes.²⁵

We may note that the dependence of the average kinetic energy of the ion w on the temperature of the gas and the rate of drift v is determined by the Vanier formula

$$w = 1.5kT + 0.5mv^2 + 0.5Mv^2,$$

which is frequently employed in kinetic studies.

III. Mobility spectrometers and their applications

The spectrometers, the principle of the operation of which is based on the separation of ions in terms of their mobilities, can be used jointly with the usual high-vacuum mass spectrometers. Such combination requires the overcoming of appreciable technical difficulties, namely the mutual adjustment of the regions of the high and low gas pressures along the ion path,^{26,27} but its advantage is that it ensures the possibility of solving problems inaccessible to each separate method. For example, an apparatus has been described^{28,29} in which a quadrupole mass analyser is placed at the outlet from the plasma chromatograph (Fig. 2) Such devices make it possible to identify accurately the ions constituting a particular chromatographic peak.

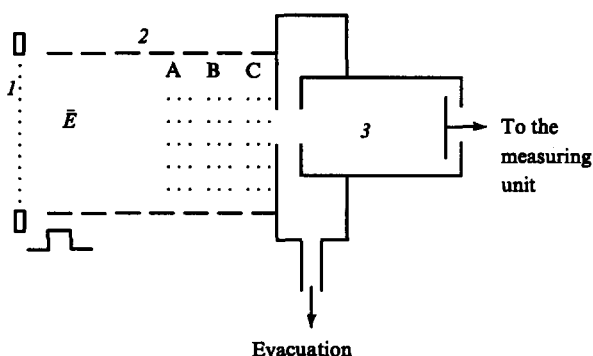


Figure 2. Schematic illustration of tandem drift spectrometer-mass spectrometer apparatus. (1), (2), A, B, C — as in Fig. 1, (3) quadrupole mass analyser.

Another version is possible where the plasma chromatograph is placed after the mass-spectrometric analyser (Fig. 3).³⁰ The carbon clusters C_n^+ , obtained by evaporating graphite on exposure to laser radiation in a helium atmosphere with subsequent hyper-sonic expansion, have been investigated with the aid of such tandem apparatus.^{2,31} The ions of the C_n^+ cluster were accelerated, passed through a mass analyser, retarded, and injected into a drift tube. In this case, it was possible to investigate the structure of ions having the same elemental composition. In particular, the drift times of the $\text{C}_3^+ - \text{C}_6^+$ clusters are the same for each particular C_n^+ ion. For the $\text{C}_7^+ - \text{C}_{10}^+$ ions, there are two resolved mobility

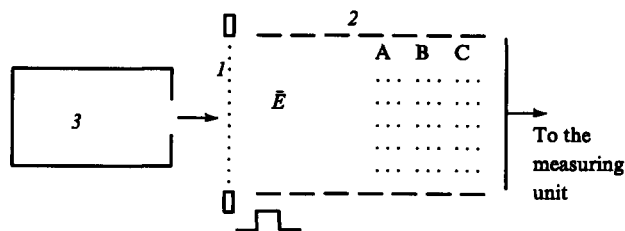


Figure 3. Schematic illustration of a tandem mass spectrometer-drift spectrometer apparatus. (1), (2), A, B, C — as in Fig. 1; (3) mass analyser.

peaks in each case, which corresponds to the presence of two isomeric forms of the clusters — cyclic and linear. The ions having the cyclic clusters have higher mobilities than the linear ones. For the C_{32}^+ cluster, it was found that the composition comprises 23% of monocycles, 71% of bicycles, 2.4% of open fullerenes, and 3.2% of fullerenes. Similar information is available for all the clusters up to C_{61}^+ (Fig. 4).³¹

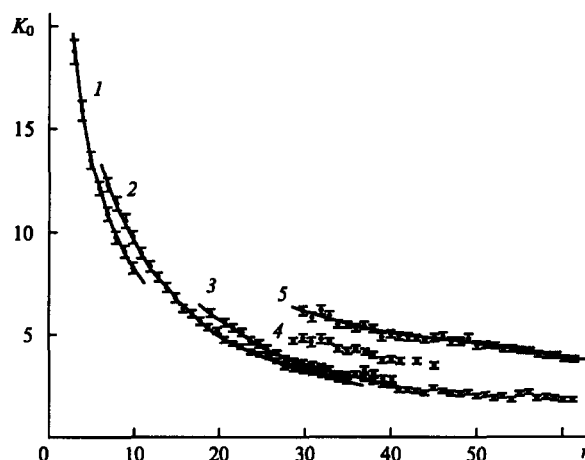


Figure 4. Dependence of the reduced mobility coefficients K_0 for the ions C_n^+ on n for different clusters. (1) Linear clusters; (2) monocyclic clusters; (3) planar polycyclic clusters; (4) open fullerenes; (5) fullerenes.

The theory of the mobility of carbon cluster ions taking into account the geometry and vibrational excitation of the clusters has been examined.³² It was shown, for example, that the mobility increases with increase in the vibrational energy of the cluster. It was observed with the aid of ion mobility spectrometry that the protonation of aniline in the gas phase leads to two isomeric forms.³³ The addition of a proton to the nitrogen atom is most preferred. The addition of a proton to the benzene ring is less probable. Such ions have a higher mobility than the ions protonated at the nitrogen atom.

Other studies of the isomers with the aid of plasma chromatography have also been described.³⁴

The plasma chromatograph can be used effectively as a highly sensitive selective detector in gas chromatography.³⁵ The design of the spectrometers, the method for the introduction of the specimens, and the interpretation of the spectra have been described in detail.³⁶ The plasma chromatograph usually consists of two consecutively arranged drift tubes. The first contains the source of radioactive radiation (a foil containing ^{63}Ni). This tube serves as the reactor for ion-molecule reactions, pure nitrogen, which can usually be obtained from liquid nitrogen, being normally used as the carrier gas. However, the water impurity remains even in highly purified nitrogen, leading, as a result of ion-molecule reactions, to the formation of stable positive ions of the type $\text{H}^+(\text{H}_2\text{O})_n$ and $\text{NO}^+(\text{H}_2\text{O})_n$. When purified air is used as the

carrier gas instead of nitrogen, the composition of the positive ions hardly changes, while the negative ions are of the type $O_2^-(H_2O)_n$.

The addition of trace amounts of organic substances to the carrier gas leads to reactions of the carrier gas ions with the impurity molecules; the products incorporate the impurity molecule. The second tube, fitted with a grid for the injection of ions, serves as an ion-drift spectrometer for the measurement of the spectrum of the ions in terms of their mobilities in the electric field. The spectrum is obtained by employing a weak electric field, which directs the ions formed in the reactor to the drift tube of the spectrometer. The packet of cluster ions moves in the inert pure nitrogen atmosphere, the directions of the streams of ions and nitrogen being opposed (in order to diminish the penetration of the carrier gas, containing the impurity, into the region of the analyser). During the motion of the ions through the drift tube, they are separated into packets with different mobilities. The heavier ions usually have smaller mobilities. The pulses of ions having different masses are recorded with the aid of an electrometer amplifier. The scan of a single spectrum in the mass range up to 400 a.m.u. takes 20 ms. Several hundreds of such spectra are usually summed and averaged in order to increase the accuracy of the experiment. A synchronous detector which integrates the signal during a short time interval moving slowly along the time axis relative to the pulse being injected, is used for this purpose.

The Fourier transformation has been used recently in ion mobility spectrometry.³⁷ The mobility interferogram is obtained with a single transfer of pulses to the modulating grids at the inlet to and outlet from the mobility spectrometer. The pulses are supplied from a rectangular pulse generator with a frequency scan. By applying the Fourier transformation to the interferogram, the usual ion mobility spectrum is obtained. The theory of the method has been described and examples of the measurement of the mobility spectra have been presented (Fig. 5).³⁷ This method may increase the rate of recording of the mobility spectrum and the sensitivity, which is particularly important when the mobility spectrometer is used as the detector for chromatographs.

The detectable amounts of impurities in 100 cm³ of air are 10^{-9} – 10^{-8} g for plasma chromatographs. The use of larger masses of the specimen (10^{-6} g and above) leads to the saturation of the response, the complete consumption of the reactant ions, and the formation of dimeric impurity ions. The interpretation of the mobility spectra then becomes difficult. The ion mobility spectra are also greatly distorted when a drift gas containing impurities which may enter into ion–molecule interactions with the test ions is employed. A discrepancy arises with the mobilities

predicted by the classical theory when fast ion–molecule reactions take place in the system during a period shorter than the drift time. Typical examples of such reactions are the solvation and desolvation of ions by the water molecules present as an impurity in the drift gas.

A useful employment of the ion cluster formation process is also possible, for example, in order to increase the resolving power of plasma chromatographs.³⁸ If the sizes and masses of the ions are similar but the rates of formation of clusters are different, then the addition of cluster-forming gas to the carrier gas leads to an appreciable difference between the masses of the ions analysed and hence between their mobilities. The kinetic characteristics of the ion–molecule processes are similar in plasma chromatography and high pressure mass spectrometry.^{39–42}

Reference data on the kinetic parameters of ion–molecule processes have been published.^{43,44} The rate constants for exothermic bimolecular ion–molecule processes for low ion energies are determined by the long-range charge–induced dipole and charge–permanent dipole forces. These constants are usually of the order of 10^{-9} cm³ s⁻¹ and lower values have been found only in a few instances.⁴⁵

The rate constants for termolecular ion–molecule association reactions are determined by the rate constants for the corresponding bimolecular processes and the lifetimes of the ion–molecule ‘collision’ complexes formed.

The rate constants for termolecular ion–molecule association processes are 10^{-32} – 10^{-21} cm⁶ s⁻¹.^{43,46}

We shall consider the typical conditions in the operation of plasma chromatograms. With the aid of a radioactive radiation source with an activity of ~ 10 μ Ci at atmospheric pressure, it is possible to obtain $\sim 10^{11}$ ions per second. At atmospheric pressure, the carrier gas flow rate is 100 ml min⁻¹, the electric field strength is 250 V cm⁻¹, the duration of the ion-injecting pulse is 0.2 ms, and the recording scanning pulse has the same duration. The spectra are usually obtained with a drift tube temperature of 100–150 °C and for a length of the drift region of 8 cm. For example, the mobility coefficient for the Cl⁻ ion at 150 °C is 4.7 cm² V⁻¹ s⁻¹. This yields a drift time of 8 ms. Watts and Wilders⁴⁷ made a detailed study of the resolving power of a plasma chromatograph. The formula obtained for the determination of the resolving power in the ideal case (when the resolving power is limited by diffusion) is

$$R = 2(EL)^{0.5},$$

where E is the electric field strength in V cm⁻¹ and L the length of the drift tube in cm.

Watts and Wilders⁴⁷ studied the influence of the initial width of the ion packet and of the volume charge of the ions on the resolving power. For example, when account is taken of the finite duration of the ion packet, the formula for the resolving power assumes the following form:

$$R = \frac{L/v + t/2}{(48.4DL/v^3 + t^2)^{0.5}},$$

where t is the duration of the ion packet, v the ion drift velocity, and D the diffusion coefficient.

For small electric field strengths

$$E < 4\pi en,$$

where n is the concentration of ions, a negative influence of the space charge of the ions on the resolving power may be observed. For example, when $E = 2$ V cm⁻¹ and $L = 10$ cm, then appreciable distortion of E due to the space charge will occur for $n = 10^5$ cm⁻³.

Mathematical methods for the reconstruction of poorly resolved peaks are widely used to increase the resolving power. For example, the spectra of chlorine and bromine isotopes have been resolved by this procedure.⁴⁸ Computers are used widely for the recording and treatment of spectra of different types.⁴⁹

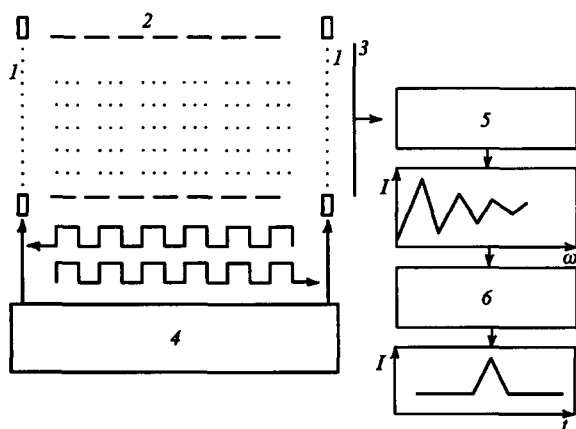


Figure 5. Schematic illustration of a mobility spectrometer with Fourier transformation. (1) and (2) as in Fig. 1; (3) ion collector; (4) generator of rectangular pulses with a variable frequency ω ; (5) electrometer amplifier, analogue–digital transformer, and memory device ensuring the generation of the ion mobility interferogram; (6) Fourier transformation ensuring the generation of the ion mobility spectrum.

One of the principal elements of the design of plasma chromatographs is the grid ion filter. The filters may be of different types. The Tyndall filter consists of two wire grids close to one another and fixed at right angles to the axis of the drift tube. A potential is applied to the grids, i.e. there is a potential difference between them. As a result of this, the ions are not transmitted through the grid for most of the time. However, the potential difference changes sign periodically, which enables the ions to pass through the grid and enter the drift space.

It has been suggested⁵⁰ that the Tyndall filter be modified by employing microchannel plates. Such plates are beginning to be employed widely in various experimental techniques.⁵¹ The design of the modified filter is convenient during assembly, ensures a parallel arrangement of the end faces, is mechanically stable, and is not short-circuited on contamination by conducting particles. The channels in such filters have diameters of 40–80 μm and are perpendicular to the surfaces of the plates (to ensure the effective transmission of ions).

The Bradbury–Nielson filter consists of a single grid made of wires arranged at short distances from one another. A sinusoidal potential is applied between the alternating wires of the grid, the average potential on each wire being equal to the potential of the uniform drift field in the plane of the grid. The ions which reach the grids at the moments when the instantaneous alternating potential is close to zero pass through the filter. A modification has been proposed also for this filter, in which foil strips are employed instead of wires.⁵²

Ion mobility spectrometers in which the electric field vectors and the gas flow rates are directed to one side were examined above. Ion separators with the gas stream directed at right angles to the electric field in which the ions drift have been proposed (Fig. 6).⁵³ Such geometry leads to an increase in the resolving power. However, this requires a much greater stability of the gas flow rate compared with the usual geometry.

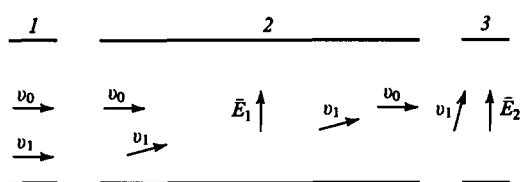


Figure 6. Schematic illustration of an ion mobility spectrometer with a perpendicular arrangement of the electric field and gas flow direction. (1) Ion source; (2) ion selector; (3) ion recorder; v_0 = gas flow rate; v_1 = velocity of ions; E_1 , E_2 = electric field strengths.

Another probable advantage of this scheme is the measurement of the ion spectrum without employing a pulse technique — by recording constant ionic currents at different points in the plane of the collector. The ions are carried away by the gas stream at a steady rate and drift in the electric field at right angles to the stream at rates which depend on the mass of the ions. Heavy ions reach the plane of the collector at a long distance from the inlet, whilst light ions reach it at a short distance, since the drift velocity of light ions is usually greater than the drift velocity of heavy ones.

A procedure has been proposed^{54–56} for the modification of the ion separation method with the gas flow rate and electric field strength vectors arranged at right angles, to one another. The method is based on subjecting the ions to constant and variable electric fields. When the ions are subjected to such an influence, there is an appreciable increase in the effectiveness of the separation, which is determined not only by the difference between the mobilities but also by the difference between the first derivatives of the mobilities with respect to the electric field. Spectrometers in which this modification procedure of the ion separation method is employed have been constructed by the

Ekotek Company (Novosibirsk). The present author and Chentsov have estimated the resolving power of a spectrometer of this type.⁵⁷

IV. Conclusion

The studies on ion mobilities in gases, initiated at the end of the last century by Thomson, Rutherford, Townsend, and Langevin, are still of interest both for fundamental science and for analytical techniques. In fundamental science, such studies make it possible to obtain data on the compositions, structures, and reactivities of ions, which permits a deeper understanding of the general problems of molecular structure and chemical reactivity. Data on gas-phase reactions are also of interest for high-energy chemistry, including radiation chemistry and the chemistry of low-temperature plasma. For example, the rate of recombination of positive and negative ions in plasma is determined directly by the mobilities of these ions.⁵⁸

Definite progress has been noted recently in the improvement of the experimental methods for the study of ion mobilities. Experiments carried out at low temperatures^{59–61} showed that at $T < 10$ K ion mobilities in helium diminish sharply and become lower than the polarisation limit, which may be a consequence of the manifestation of quantum effects. Further theoretical experimental studies are needed to elucidate the nature of the observed low-temperature effects. They may yield information about the mechanisms of low-temperature chemical processes.

The laser technique is being applied to an increasing extent in studies of ion mobilities and not only for the generation of the ions but also for the measurement of the velocity distribution of the drifting ions.⁶² Systems in which the drift tube–laser combination is used may compete with the drift tube–mass spectrometer systems. One may probably expect an expansion of studies in this promising direction. Mobility spectrometers are being increasingly used for analytical purposes. Apart from the studies indicated above concerning their application in the investigation of carbon cluster isomers, there have been studies of the isomers of metallocarbon clusters.^{63–65}

It has been shown that the metal atom may be both incorporated in the carbon network and accommodated in the cavity of fullerene. A further increase in the complexity of the objects investigated is also possible. Studies concerning the application of plasma chromatography for the identification of traces of vapours of drugs and explosives have been continued over many years. In the latest study on the detection of vapours of explosives by plasma chromatography, multiphoton laser ionisation was employed to generate the ions.⁶⁶ Studies on the drift of ions in gases in an electric field continue to develop vigorously.^{67–70}

References

1. G Von Helden, P R Kemper, M T Hsu, M T Bowers *J. Chem. Phys.* **96** 6591 (1992)
2. M T Bowers, P R Kemper, G Von Helden, P A M van Koppen *Science* **260** 1446 (1993)
3. G A Eiceman, Z Karpas *Ion Mobility Spectrometry* (Boca Raton, FL: CRC Press, 1994)
4. T W Carr *Plasma Chromatography* (New York: Plenum, 1984)
5. R H St Louis, H H Hill, Jr *Crit. Rev. Anal. Chem.* **21** 321 (1990)
6. V E Skurat *Poluchenie i Issledovanie Ionov Neletuchikh Soedinenii v Gazovoi Faze [Radiatsionnaya Khimiya (Ser. Itogi Nauki i Tekhniki) {The Generation and Study of the Ions of Non-volatile Compounds in the Gas Phase [Radiation Chemistry (Ser. Advances in Science and Engineering)]}* (Moscow: Izd. VINITI, 1988)
7. *Proceedings of the NATO Advanced Research Workshop on Methods and Mechanisms for Producing Ions from Large Molecules* (Minaki, Canada: Plenum, 1990)
8. C Shumate *Trends Anal. Chem.* **13** 104 (1994)
9. G Von Helden, T Wytenbach, M T Bowers *Science* **267** 1483 (1995)

10. E A Mason, E W McDaniel *The Mobility and Diffusion of Ions in Gases* (New York: Wiley, 1984)
11. E A Mason, E W McDaniel *Transport Properties of Ions in Gases* (New York: Wiley, 1984)
12. W Lindinger, T D Mark, F Howorka (Eds) *Swarms of Ions and Electrons in Gases* (Wien: Springer, 1984)
13. H W Ellis, R Y Pai, E W McDaniel, E A Mason, L A Viehland *At. Data Nucl. Data Tables* **17** 177 (1976)
14. H W Ellis, E W McDaniel, D L Albritton, L A Viehland, S L Lin, E A Mason *At. Data Nucl. Data Tables* **22** 179 (1978)
15. H W Ellis, E W McDaniel, M G Thackston, E A Mason *At. Data Nucl. Data Tables* **31** 113 (1984)
16. L A Viehland, E A Mason *At. Data Nucl. Data Tables* **41** 37 (1995)
17. F Celli, G Waddle, D P Ridge *J. Chem. Phys.* **73** 801 (1980)
18. J W Gallagher, D F Hadson, E E Kunhard, R J van Brunt (Eds) *Nonequilibrium Effects in Ion and Electron Transport* (New York: Plenum, 1990)
19. J Lin, T Su *J. Chem. Phys.* **95** 6471 (1991)
20. W A Wakeham, A S Dickinson, F R W McCourt, V Versovic (Eds) *Status and Future Developments in the Study of Transport Properties. NATO ASI Ser. C, Vol. 361* (Dordrecht, Netherlands: Kluwer Academic, 1992)
21. Z Berant, Z Karpas *J. Am. Chem. Soc.* **111** 3819 (1989)
22. K Giles, E P Crimrud *J. Phys. Chem.* **96** 6680 (1992)
23. E A Mason *Science* **260** 43 (1993)
24. N Ikuta, E Nishi, S Nakajima *J. Phys. Soc. Jpn.* **61** 4425 (1992)
25. F Howorka, F C Fehsenfeld, D L Albritton *J. Phys. B, At. Mol. Phys.* **12** 4189 (1992)
26. D Smith, N D Adams, in *Gas Phase Ion Chemistry* Vol. 1 (Ed. M T Bowers) (New York: Academic Press, 1979) p. 2
27. S L Pozharov *Zh. Tekh. Fiz.* **21** 56 (1982)
28. Z Berant, O Shahal, Z Karpas *J. Phys. Chem.* **95** 7534 (1991)
29. US P. 36 211 240 (1971)
30. S H Kim, K R Betty, F W Karasek *Anal. Chem.* **50** 1784 (1978)
31. G Von Helden, M T Hsu, P R Kemper, M T Bowers *J. Chem. Phys.* **95** 3835 (1991)
32. L D Book, C Xu, G E Scuseria *Chem. Phys. Lett.* **222** 281 (1994)
33. Z Karpas, Z Berant, R M Stimac *Struct. Chem.* **1** 201 (1990)
34. D F Hagen *Science* **260** 115 (1993)
35. H H Hill, Jr, M A Baim *Science* **260** 143 (1993)
36. G E Spangler, M J Cohen *Science* **260** 1 (1993)
37. F J Knorr, R L Eaterton, W F Siems, H H Hill, Jr *Anal. Chem.* **57** 402 (1985)
38. USSR P. 1 627 984; *Byull. Izobret.* (6) 139 (1991)
39. A F Harrison *Chemical Ionization Mass Spectrometry* (Boca Raton, FL: CRC Press, 1983)
40. A A Polyakova, I A Revel'skii, M I Tokarev, L O Kogan, V L Tal'roze *Mass-Spektrol'nyi Analiz Smesei s Primeneniem Ionno-Molekulyarnykh Reaktsii* (Mass-Spectrometric Analysis of Mixtures Using Ion-Molecule Reactions) (Ed. A A Polyakova) (Moscow: Khimiya, 1989)
41. M Sigel', V Fait, in *Kineticheskaya Mass-Spektrometriya i Ee Analiticheskie Primeneniya* (Kinetic Mass Spectrometry and Its Analytical Applications) (Moscow: Institute of Chemical Physics, 1979) p. 132
42. M W Siegel *Science* **260** 95 (1993)
43. L I Virin, R V Dzhagatspanyan, G V Karachevtsev, V K Potapov, V L Tal'roze *Ionno-Molekulyarnye Reaktsii v Gazakh* (Gas Phase Ion-Molecule Reactions) (Moscow: Nauka, 1979)
44. J Ikezoe, S Takebe, A Viggiano *Gas Phase Ion-Molecule Reactions Rate Constants Through 1986. Ion Reaction Research Group of the Mass Spectroscopy Society of Japan, Tokyo, 1987*
45. G V Karachevtsev, A Z Marutkin, V V Savkin *Usp. Khim.* **51** 1849 (1982) [*Russ. Chem. Rev.* **51** 1060 (1982)]
46. V M Smirnov *Iony i Vozbuzhdennyye Atomy v Plazme* (Ions and Excited Atoms in Plasma) (Moscow: Atomizdat, 1974)
47. P Watts, A Wilders *Int. J. Mass Spectrom. Ion Process.* **112** 179 (1992)
48. F W Karasek, R J Laub, E de Decker *J. Chromatogr.* **93** 123 (1974)
49. V V Reznikov, M O Reznikova *Informatsionno-Analiticheskaya Mass-Spektrometriya* (Information Analytic Mass Spectrometry) (Moscow: Nauka, 1992)
50. USSR P. 1 737 770; *Byull. Izobret.* (20) 239 (1992)
51. B N Bragin, M M Butelov, A N Ivanova, V S Malysheva *Prib. Tekh. Eksp.* **1** 192 (1975)
52. K Iinuma, M Takebe *Aust. J. Phys.* **48** 491 (1995)
53. US P. 3 668 388 (1972)
54. USSR P. 966 583; *Byull. Izobret.* (38) 208 (1982)
55. USSR P. 1 337 934; *Byull. Izobret.* (34) 210 (1987)
56. A S Avakumov, I A Buryakov, E V Krylov, in *Fizika Nizkoterturnoi Plazmy. Materialy 7-i Vsesoyuz. Konferentsii* (Physics of Low Temperature Plasma. Proceedings of the Seventh All-Union Conference) (Tashkent: Fan, 1987) Part 1, p. 21
57. G V Karachevtsev, A A Chentsov *Tr. MFTI. Ser. Fiz. Kvantovoi Elektron. (Moscow)* 1996 (in the press)
58. N L Aleksandrov, D A Novitskii *Pis'ma Zh. Tekh. Fiz.* **19** (13) 9 (1993)
59. J Sanderson, H Tanuma, N Kobayashi, Y Kaneko *J. Phys. B, At. Mol. Opt. Phys.* **26** L465 (1993)
60. J Sanderson, H Tanuma, N Kobayashi, Y Kaneko *J. Phys. B, At. Mol. Opt. Phys.* **27** L433 (1994)
61. N Saito, T M Kojima, N Kobayashi, Y Kaneko *J. Chem. Phys.* **100** 5726 (1994)
62. V M Bierbaum, in *SASP-94. Symposium on Atomic, Cluster and Surface Physics. Contributions*. (Eds T D Mark, R Schaittwieser, D Smith) (Maria Alm, Austria: Hintermoos, 1994) p. 29
63. G von Helden, N G Gotts, P Maitre, M T Bowers *Chem. Phys. Lett.* **227** 601 (1994)
64. K B Shelimov, M F Jarrold *J. Am. Chem. Soc.* **117** 6404 (1995)
65. K B Shelimov, D E Clemmer, M F Jarrold *J. Phys. Chem.* **99** 11376 (1995)
66. A Clark, R M Deas, C Kosmidis, K W D Ledingham, A Marshall, R P Singhal, in *Proceedings of the 6th International Symposium on Advance Nucleus Energy Research 'Innovative Laser Technology in Nuclear Energy'* 1994 Vol. 2, p. 521
67. K R Jennings (Ed.) *Fundamentals of Gas Phase Ion Chemistry. NATO ASI Ser.* (New York: Kluwer, 1991)
68. *Proceedings of the 1992 Workshop on Ion Mobility Spectrometry, Mescalero, NM, 1992*
69. *Proceedings of the 8th International Seminar on Electron and Ion Swarms, Trendheim, Norway, 1993*
70. G E Strangler *Anal. Chem.* **65** 3010 (1993)

Physicochemical aspects of the adsorption of sulfur dioxide by carbon adsorbents

S A Anurov

Contents

I. Introduction	663
II. General characteristics of the adsorption of SO ₂ by carbon adsorbents	664
III. The nature of the active centres for the adsorption of SO ₂ on carbon adsorbents	672
IV. Conclusion	674

Abstract. Literature data on the chemistry of the adsorption of sulfur dioxide on carbon adsorbents are surveyed and described systematically. The influence of various factors (the nature of the carbon matrix, the activation method, the chemistry of the adsorbent surfaces, temperature, the composition of the gas stream, etc.) on the sorption of SO₂ by activated carbons and semicokes is examined. The possible ways in which sulfur dioxide interacts with the carbon surface are discussed. The bibliography includes 128 references.

I. Introduction

The protection of the environment from pollution is one of the most important and complex socioecological problems. Nowadays approximately 2.5 billion tonnes of pollutants are discharged into the atmosphere annually.¹ The oxides of carbon, nitrogen, and sulfur, dust, ammonia, and various hydrocarbons are massive pollutants of air. Among them, sulfur dioxide, which on entering the atmosphere is capable of forming sulfuric acid, constitutes the greatest hazard. The acid residues in the form of rain or smoke have a negative effect on human health and the flora and fauna and cause the disintegration of constructional materials. Sulfur dioxide is formed mainly by the combustion of fuel in thermal electric power stations. Nonferrous metallurgy and to a lesser extent the sulfuric acid industry and the regeneration of sulfur by the Klaus method are sources from which large amounts of SO₂ are emitted.

In 1980, major plants, involving solely the combustion of fuel, discharged about 145 million tonnes of SO₂ into the atmosphere in countries of the European Economic Community. In most of the industrially developed countries, governments have adopted measures designed to achieve a sharp reduction of the discharge of sulfur dioxide. The 1989 EEC directive prescribes a reduction in the evolution of SO₂ in three stages and specifies the control periods during which these stages must be completed:² 1993, 1998, and 2003 (Table 1). This will make it possible not only to solve the most important ecological problem but also to economise on

Table 1. The volumes of SO₂ discharged into the atmosphere in EEC countries.

Country	SO ₂ discharged in 1980/10 ³ t	SO ₂ discharged (in 10 ³ t) and the change in the latter relative to 1980 (%)		
		1993	1998	2003
Belgium	530	318/–40	212/–60	159/–70
Denmark	323	213/–34	141/–56	106/–67
Germany	2225	1335/–40	890/–60	668/–70
Greece	303	320/+6	320/+6	320/+6
Spain	2290	2290/0	1730/–24	1440/–37
France	1910	1146/–40	764/–60	573/–70
Ireland	99	124/+25	124/+25	124/+25
Italy	2450	1800/–27	1500/–39	900/–63
Luxembourg	3	1.8/–40	1.5/–50	1.5/–50
The Netherlands	299	180/–40	120/–60	90/–70
Portugal	115	232/+102	270/+135	206/+79
Great Britain	3883	3106/–20	2330/–40	1553/–60

valuable sulfur-containing raw material for the production of sulfuric acid and other chemical products.

Depending on the conditions under which sulfur dioxide is evolved, different methods are applied to remove it from gas streams. One of the most rational and promising procedures involves processes whereby SO₂ is extracted by carbon adsorbents (activated carbons and semicokes), which make it possible to obtain sulfur dioxide in a form suitable for its subsequent use — as a gas enriched in SO₂, liquid sulfur dioxide, elemental sulfur, as well as sulfuric acid. A number of processes for the removal of SO₂ from effluent gases have been devised on the basis of carbon adsorbents.^{3–8} Almost all of them have passed successfully through pilot and experimental-industrial tests and some have been introduced into industry.

Although the carbon adsorption method is already used in industry, the question of the chemistry of the interaction of sulfur dioxide with a carbon surface still remains open. The growing interest in this problem can be accounted for not only by its scientific importance² but also by the necessity to formulate the principal requirements which must be met by carbon adsorbents capable of extracting effectively sulfur dioxide from gas streams.

There are fairly numerous literature data on the adsorption of sulfur dioxide by carbon materials, but there are virtually no surveys devoted to a critical analysis of the experimental data. The review which we published earlier⁹ as well as the attempt by

S A Anurov Mendelev Russian Chemical Engineering University, Miusskaya pl. 9, 125190 Moscow, Russian Federation.
Fax (7-095) 200 42 04. Tel. (7-095) 978 94 51

Received 10 January 1996

Uspekhi Khimii 65 (8) 718–732 (1996); translated by A K Grzybowski

Loskutov and Khlopotov¹⁰ to survey the available data are incomplete and morally obsolete and do not reflect the entire depth of the problem. In the present review, we have attempted to fill the existing gap.

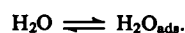
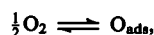
II. General characteristics of the adsorption of SO₂ by carbon adsorbents

1. The forms of the bond between SO₂ and the carbon surface

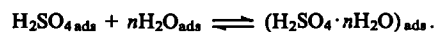
The study of the chemistry of the sorption of SO₂ by carbon adsorbents presupposes the elucidation of the nature of the stages involving the adsorption of sulfur dioxide from a complex gas mixture containing SO₂, O₂, N₂, CO₂, H₂O and other components with subsequent conversion of SO₂ into the final product as well as the establishment of the role played in these stages by individual components of the surfaces of the carbons and semicokes.

The transition of sulfur dioxide to the adsorbed state cannot occur immediately as a result of a single elementary step. The process involving the adsorption of a SO₂ molecule consists of a series of consecutive stages. The characteristics of the sorption process depend on the nature of the sorbent, the technological conditions of the sorption, and the chemical composition of the gas being purified. However, it is always possible to differentiate typical primary or secondary reactions occurring when the gas mixture passes through a layer of the carbon adsorbent.

The primary adsorption processes, occurring when SO₂, O₂, and water vapour are present simultaneously in the gas, can be described by the following equations:¹¹⁻²¹



Next there is a possibility of secondary transformations of the adsorbed components:



On real surfaces, particularly when activated carbons and semicokes are employed, a large set of sorbed forms usually arises. By no means all of them participate directly in the sorption of SO₂. Their influence on the adsorption of sulfur dioxide is manifested, in particular, by the fact that they alter in some way the properties of the carbon surface or simply block individual sections which constitute active centres for the adsorption of SO₂.

The hypothesis of the existence of two forms of bond between carbon dioxide and the carbon surface, each of which is characterised by a definite heat of adsorption and desorption temperature, has been put forward.²²⁻³¹ Analysis of the isobars for the desorption of SO₂ from carbon adsorbents leads to this conclusion. In virtually all cases, there are horizontal sections in the temperature range 100–150 °C (Fig. 1). At low temperatures (< 150 °C), the weakly bound sulfur dioxide, retained on the surface by van der Waals forces, is desorbed. The removal of this portion of SO₂ is achieved rapidly, in 10–20 min, which indicates a low energy of the bond between this form of sulfur dioxide and the surface (Fig. 2, curve 1). If the temperature is raised to 200 °C, the amount of desorbed SO₂ hardly increases.

Above 200 °C, the strongly bound form of SO₂, retained by chemical forces, is desorbed. The chemical nature of the interaction of this portion of SO₂ with the surface is also indicated by the rate of desorption: the process takes place slowly and is completed in 50–90 min (Fig. 2, curve 2).

This view on the forms of the bonds between sulfur dioxide and the carbon surface has been confirmed, on the one hand, by the heats of adsorption and, on the other, by the results of spectroscopic analysis. Thus the heat of adsorption of the part of sulfur dioxide weakly bound to activated carbons and semicokes is

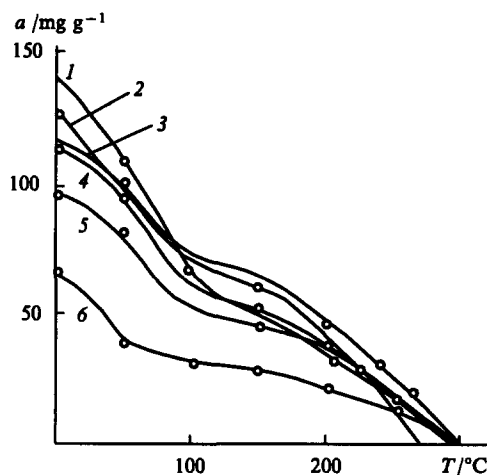


Figure 1. Isobars for the desorption of sulfur dioxide from carbon adsorbents: (1) SKT; (2) AR-3; (3) AG-5; (4) IGI; (5) KAD; (6) BAU.

in all cases less than 50 kJ mol⁻¹.³²⁻³⁹ This makes it possible to claim that this component of the SO₂ is a physically adsorbed form, which is retained on the surface by dispersion forces. The presence of molecularly sorbed SO₂ on the surfaces of carbon adsorbents is indicated also by the existence of the 1350 cm⁻¹ absorption band in the IR spectra of virtually all the Russian and foreign carbon materials saturated by sulfur dioxide.^{40,41}

The strongly bound form of sulfur dioxide has a higher heat of adsorption (> 80 kJ mol⁻¹). In the IR spectra of activated carbons and semicokes, intense absorption bands in the region of 950, 1050, 1170, and 1250 cm⁻¹, associated with sulfur compounds having different degrees of oxidation,^{40,41} correspond to this form. This makes it possible to postulate the occurrence of chemisorption processes.

The ratio of these two forms is determined, on the one hand, by the nature of the adsorbents and, on the other, by the adsorption conditions. The maximum degree of adsorption of sulfur dioxide in the physical form, not exceeding 50% of the overall degree of adsorption, is attained when SO₂ is sorbed from a dry oxygen-free gas. In all cases, the physical adsorption of SO₂ takes place and then, as a result of the chemical reaction with the surface compounds, a particular form of chemisorbed sulfur dioxide arises.

As will be shown below, chemisorption represents the interaction of the adsorbed molecules of sulfur dioxide with basic

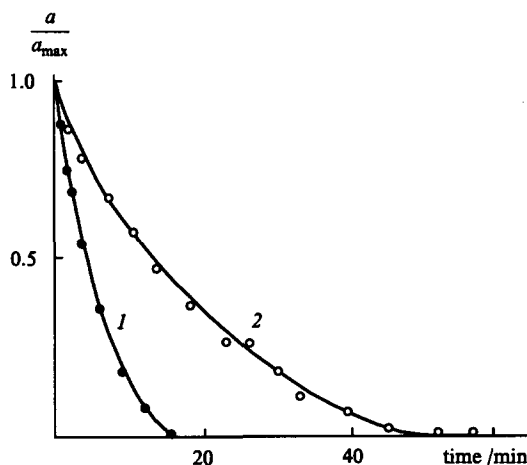


Figure 2. Kinetics of the desorption of sulfur dioxide from the activated carbon AR-3 at different temperatures (°C): (1) 150; (2) 350

oxygen-containing functional groups on the surfaces of carbon adsorbents, which results in the formation of an active complex of the type $C-SO_2$ with a definite chemical reactivity. If it is assumed that each chemisorbed SO_2 molecule occupies only one active centre, it is possible to estimate approximately the total number of primary active centres on the surfaces of adsorbents and the area occupied by the sulfur dioxide molecules. For example, the AR-3 activated carbon with a specific surface $S_{BET} = 730 \text{ m}^2 \text{ g}^{-1}$ can sorb sulfur dioxide from a dry oxygen-containing gas in the maximum amount $a = 125 \text{ mg g}^{-1}$, i.e. 2 mmol g^{-1} . The cross-sectional area of the SO_2 molecule (average diameter $3.38 \times 10^{-10} \text{ m}$) is $S = 8.967 \times 10^{-20} \text{ m}^2$. The overall area occupied by the chemisorbed SO_2 molecules is then

$$S_{\Sigma} = SaN_A = 8.967 \times 10^{-20} \times 2 \times 10^{-3} \times 6.02 \times 10^{23} = 108 \text{ m}^2,$$

which corresponds to 1/7 of the surface of the charcoal (N_A is the Avogadro number). The number of active centres per m^2 of the surface of the charcoal is

$$\frac{aN_A}{S_{BET}} = \frac{2 \times 10^{-3} \times 6.02 \times 10^{23}}{730} = 1.65 \times 10^{18}.$$

The factors which determine both the adsorption capacity of the adsorbents with respect to SO_2 as well as the process chemistry itself are of special interest from the technological point of view. Such factors may be the pore structure of the adsorbent, the quantitative and qualitative composition of the ash, and also the chemical nature of the surface. Furthermore, the process conditions may be of great importance: temperature, composition of the gas mixture, etc.

2. The influence of the pore structure of the adsorbents

One of the most important factors influencing the adsorption capacity of sorbents is known to be their pore structure.^{42,43} It is to be expected that, in the case of purely physical adsorption and when all the micropores of the adsorbent are accessible to the given adsorbate, the adsorption capacity of carbon materials is greater the greater their porosity. This hypothesis has been tested experimentally⁴⁴⁻⁴⁷ using as adsorbents both Russian and foreign industrial activated carbons of different origin and subjected to activation by different methods: SKT, AR-3, AG-3, AG-5, KAD-iodine, and BAU (Russia), Norit-2RL-Extra (the Netherlands), A-G (Poland), and experimental specimens of activated carbons IGI (Russia) and WJ-4 (Poland), the active coke K-14 (Poland), the semicokes PK-1 and PK-2 obtained by pyrolysis from brown coal from the Irsha-Borodinsk deposit, as

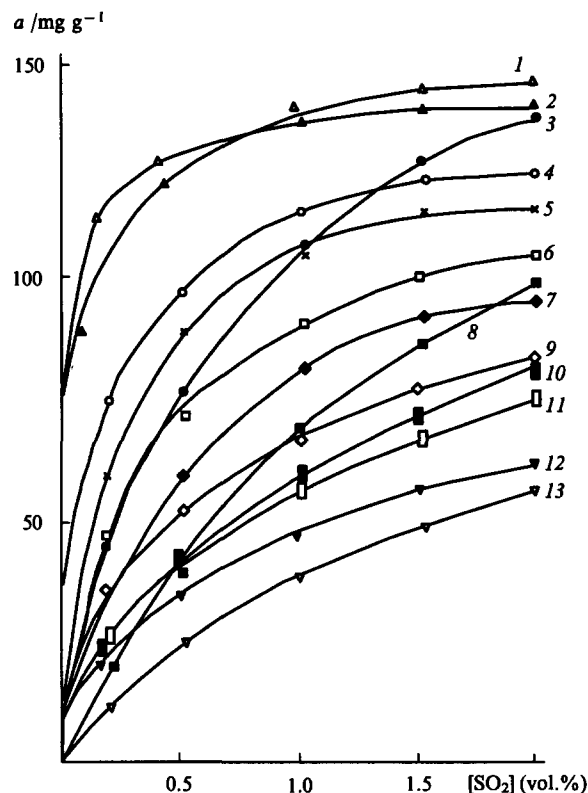


Figure 3. Sulfur dioxide adsorption isotherms on different carbon adsorbents at 25 °C; (1) PK-1; (2) PK-2; (3) SKT; (4) AR-3; (5) KAD; (6) IGI; (7) AG-5; (8) Norit; (9) K-14; (10) A-G; (11) AG-3; (12) BAU; (13) WJ-4.

well as the German carbon black of the Corax LHS type. The parameters of the porous structures of some of the adsorbents investigated are presented in Table 2.

Fig. 3 presents experimental data on the static adsorption of sulfur dioxide from a dry oxygen-free mixture at 25 °C. Among the Russian adsorbents, the highest capacity with respect to SO_2 over the entire range of concentrations investigated is shown by the brown coal semicokes PK-1 and PK-2 (curves 1 and 2). The static adsorption capacities of these adsorbents at a sulfur dioxide concentration in the gas undergoing purification of 0.1 vol.%

Table 2. Characteristics of the porous structures of certain carbon adsorbents.

Parameter	Brand of adsorbent											
	SKT	AR-3	AG-3	AG-5	KAD	BAU	IGI	Norit	WJ-4	AG	K-14	Corax
Total pore volume/ $\text{cm}^3 \text{ g}^{-1}$	0.98	0.70	0.74	0.56	0.70	1.5	0.81	1.09	1.81	0.92	0.43	0.14
Micropore volume/ $\text{cm}^3 \text{ g}^{-1}$	0.51	0.33	0.30	0.27	0.29	0.23	0.40	0.60	0.46	0.28	0.16	0.04
Mesopore volume/ $\text{cm}^3 \text{ g}^{-1}$	0.20	0.07	0.19	0.10	0.15	0.08	0.11	0.09	0.41	0.16	0.03	0.10
Macropore volume/ $\text{cm}^3 \text{ g}^{-1}$	0.27	0.30	0.25	0.19	0.51	1.10	0.30	0.40	0.94	0.48	0.24	—
Specific surface area of mesopore/ $\text{m}^2 \text{ g}^{-1}$	105	48	33	35	110	57	35	72	245	107	16	42
Total specific surface area/ $\text{m}^2 \text{ g}^{-1}$	970	731	427	410	620	584	850	1550	1350	790	790	84
Limiting volume of adsorption space/ $\text{cm}^3 \text{ g}^{-1}$	0.55	0.35	0.3	0.25	0.30	0.20	0.39	—	—	—	—	—
Characteristic energy of the adsorption of standard vapour/ kJ mol^{-1}	21.7	20.1	21.3	20.4	19.7	25.5	19.6	—	—	—	—	—
Characteristic size of micropores/ \AA	5.6	5.9	5.6	5.9	6.1	4.8	6.1	—	—	—	—	—

are respectively 100 and 110 mg g⁻¹.³¹ Among the activated carbons, the highest adsorption capacities are shown by SKT and AR-3 specimens (45.4 and 67.2 mg g⁻¹ respectively),³¹ whilst among the foreign carbon materials the Polish activated coke K-14 has the highest adsorption capacity (50.3 mg g⁻¹).

However, in all cases the adsorption capacities of the carbon sorbents investigated with respect to sulfur dioxide were not correlated with the parameters of their porous structure (the total pore volume, the volumes of the mesopores and micropores, and the limiting volume of the adsorption space W_0) and also with the specific surface. Nevertheless, Grzybek et al.⁴⁷ attributed the increased adsorption capacity of the K-14 coke to the presence in the latter of a definite number of supermicropores. This variety of pores has not been observed in the remaining adsorbents.

Thus the impression is created that the porous structures of carbon adsorbents of different origin and subjected to activation by different methods do not by themselves exert a decisive influence on their adsorption capacities with respect to sulfur dioxide.

However, this conclusion cannot be extended to carbon adsorbents obtained from a single initial material and using a single activation method. Semicoke formation has been achieved^{48,49} by the thermal pyrolysis of brown coal from the Irsha-Borodinsk deposit at 500–800 °C without access of air. The adsorbents synthesised had specific surfaces ranging from 250 to 500 m² g⁻¹. Sulfur dioxide was adsorbed on the specimens obtained at 25 °C from a stream of nitrogen containing 1 vol.% of SO₂. The results are presented in Fig. 4, from which it follows that the adsorption capacity of the semicokes with respect to SO₂ is directly proportional to the specific surface area.

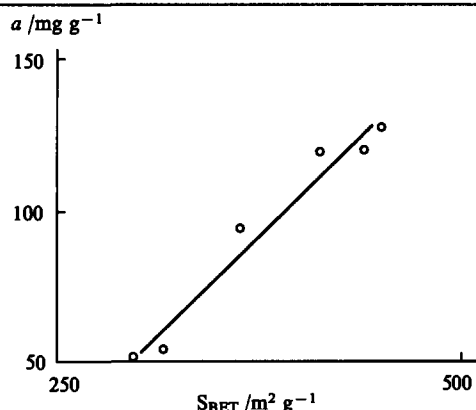


Figure 4. Dependence of the adsorption capacity of the semicoke PK-2 with respect to SO₂ on its specific surface area.

Thus the specific surface of the carbon adsorbents affects their adsorption capacity with respect to SO₂, but only when the same

initial material and the same chemical activation methods are used. An indirect confirmation of this conclusion has been obtained in a study of the influence of the chemistry of the surfaces of carbon materials on the adsorption of sulfur dioxide.^{50,51}

3. The influence of the qualitative and quantitative composition of the ash

The qualitative and quantitative compositions of the ash in activated carbons may be extremely varied and depend as a rule on the nature of the raw materials used to prepare the adsorbents and on the method for their activation. The ash content in the industrial adsorbents ranges from 1 mass % to 17 mass % and the principal components of the ash are compounds of alkali and alkaline earth metals, nickel, iron, manganese, copper, etc. (Table 3).^{52–55} Taking into account the high reactivity of sulfur dioxide, it was natural to expect that the presence of ash in carbon adsorbents exerts a definite influence on its adsorption. This was first noted in studies^{44,46,55–57} in which only the qualitative conclusion was reached that the adsorption capacities of carbons with respect to sulfur dioxide increase with decrease in the ash content. This question has been investigated in greatest detail in a recent study employing Merck and C.Erba activated carbons subjected to complete or partial deashing.⁵⁵ The ash content in the charcoals varied from 0.12 mass % to 3.28 mass %. Sulfur dioxide was adsorbed in the temperature range 130–170 °C from a gas mixture with a composition similar to flue gas containing 0.2 vol.% of SO₂. The thermal desorption of SO₂ from the saturated adsorbent was achieved at 360 °C in a stream of nitrogen.

Figure 5 shows how the ash content in the carbons investigated, the adsorption temperature, and the number of 'adsorption-desorption' cycles influence the adsorption capacities of the specimens with respect to sulfur dioxide. With increase in the duration of the operation (the number of cycles), the adsorption capacities fell in almost all the specimens. However, the capacities of the high-ash adsorbents fell, other conditions being equal, much faster than those of the low-ash specimens. Furthermore, the process was significantly influenced also by temperature: at 170 °C, a more marked decrease in adsorption capacity was observed than at 130 °C.

With increase in the duration of use, the parameters of the porous structures of the high-ash components were greatly impaired — in the first place, the number of micropores and mesopores diminished with a consequent decrease in the specific surface. For example, the specific surface of the C.Erba activated carbon containing 3.28 mass % of ash fell after 10 cycles by approximately 10% (from 835 to 750 m² g⁻¹). Similar but much less marked changes occurred in the low-ash specimens: during this period, S_{BET} for the C.Erba carbon subjected to preliminary deashing (down to 0.12 mass % of ash) diminished only from 850 to 835 m² g⁻¹, i.e. by 1.6%.

Activated carbons with an increased ash content are oxidised more readily than the low-ash carbon materials. Thus, in the

Table 3. Chemical composition of the ash in carbon adsorbents (mass %).

Brand of adsorbent	Na	K	Mg	Ca	Co	Ni	Fe	Mn	Cu	Zn	Cr	Al	Ash
SKT	0.09	0.22	0.06	0.51	0.0008	0.005	0.10	0.002	0.008	0.005	0.009	—	13.9
AR-3	0.15	0.20	0.10	0.55	0.001	0.003	0.58	0.01	0.01	0.003	0.005	—	12.0
AG-3	0.45	0.17	0.42	0.79	0.002	0.006	2.31	0.002	0.02	0.004	—	—	13.0
AG-5	0.39	0.15	0.25	0.60	0.001	0.003	1.72	0.008	0.02	0.004	—	—	10.5
KAD	0.08	0.03	0.05	0.40	0.001	0.002	0.26	0.001	0.004	0.002	—	—	12.6
BAU	0.21	0.35	0.53	3.16	0.001	0.001	0.05	0.004	0.025	0.002	—	—	4.5
IGI	0.28	0.16	0.12	0.83	0.001	0.004	1.23	0.007	0.003	0.003	—	—	17.8
Merc	0.074	0.54	0.031	0.027	—	0.003	0.006	0.002	0.003	—	—	0.089	1.8
C. Erba	0.12	0.64	0.057	0.033	—	0.005	0.02	0.004	0.004	—	—	0.051	3.2

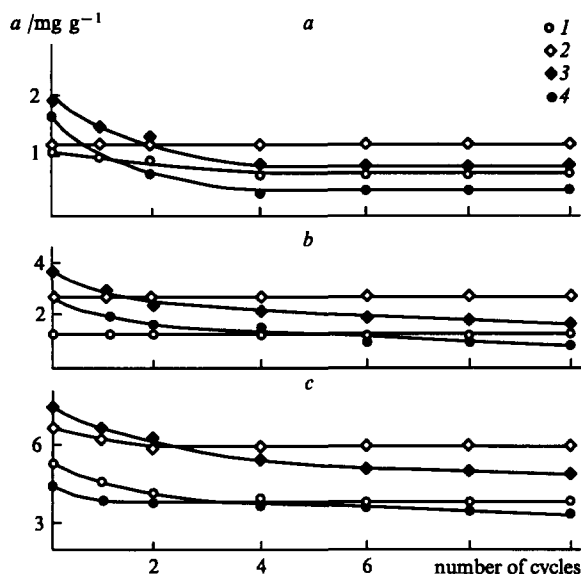


Figure 5. Dependence of the adsorption of sulfur dioxide ($\{\text{SO}_2\}_0 = 0.2 \text{ vol.}\%$) on the Merck and C.Erba activated carbons on the number of 'adsorption-desorption' cycles at 170 °C (a), 150 °C (b), and 130 °C (c) and for different ash contents (mass %): (1) 0.12; (2) 0.13; (3) 1.92; (4) 3.28.

thermal desorption stage at 360 °C, specimens containing more than 3 mass % of ash underwent appreciable oxidation accompanied by the partial surface combustion of the adsorbents and the evolution of CO_2 into the gas phase. The concentration of the bound oxygen in the high-ash carbons then increased by more than 20%, which naturally led to a sharp increase in the number of acid functional groups on their surface. A similar phenomenon is characteristic also of specimens containing 0.12 mass % to 0.13 mass % of ash, but, after similar 10 'adsorption-desorption' cycles, the concentration of oxygen on the surface increased by less than 2%. As will be shown below, the oxidised carbon should have *a priori* a lower adsorption capacity with respect to sulfur dioxide than the initial activated carbon.

Finally, the ash content itself in the low-ash adsorbents remains stable, like the sulfur content in the ash, during the above cycles, whereas in the high-ash specimens the above parameters increase from cycle to cycle. In all probability, this can be explained by the interaction of the adsorbed sulfur dioxide with individual components of the ash, which leads ultimately to the formation of stable compounds of the type of metal sulfates, which do not dissociate at the given temperatures and accumulate in the carbons.

Thus the presence of ash in the carbon adsorbents reduces the adsorption capacity with respect to SO_2 owing to the impairment of the parameters of the porous structure, a decrease in the specific surface, an increase in the degree of oxidation of the surface, and the conversion of the ash components to sulfates, which do not decompose in the course of regeneration and remain on the surface of the adsorbents, blocking the SO_2 specific adsorption centres.

4. The influence of the chemical nature of the adsorbent surfaces

The adsorption and catalytic properties of activated carbons and semicokes are to a large extent determined by the nature of their surfaces. Two types of surface functional groups of carbon materials are distinguished — acidic and basic.^{58–62} Four groups of oxides with different acidities have been identified in oxidised carbons — carboxylic, lactone, phenolic, and carbonyl groups.⁶³ It has been suggested that these groups do not constitute a separate phase but are fragments of a single complex group of

the type of phenolphthalein.⁶⁴ The question of the nature of the basic oxides on the carbon surface still remains open, although the hypotheses of the existence of chromene, quinonoid, benzo-pyrene, and pyrone structures have been put forward.^{65–68}

Numerous investigations have been directed recently to the elucidation of the problem of the influence of the chemistry of the surfaces of carbon adsorbents on the adsorption of sulfur dioxide.^{30, 31, 50, 51, 69–71} It was natural to suppose that basic surface groups are centres for the adsorption of SO_2 molecules. Treatment of the usual carbon adsorbents with air at high temperatures or with nitric acid is known to lead to the appearance of acid oxides on their surfaces and to a gradual disappearance of basic oxygen-containing groups.^{72, 73} The surfaces of the Merck⁵⁰ and AR-3 activated carbons and of the PK-2 semicokes⁵¹ have been modified in this particular way, which made it possible to synthesise adsorbents with different contents of basic functional groups. These specimens were in fact used to identify the centres for the specific adsorption of SO_2 .

A sample of the adsorbent (2–4 g) was saturated at 20 °C with sulfur dioxide in its mixture with nitrogen containing 0.3 vol.% of SO_2 until the attainment of a state of equilibrium. After equilibration, two-step thermal desorption of SO_2 from the carbon sorbents was carried out: initially the process was performed in a stream of nitrogen in the course of 3 h at 150 °C, after which the temperature was raised to 350 °C and the specimen

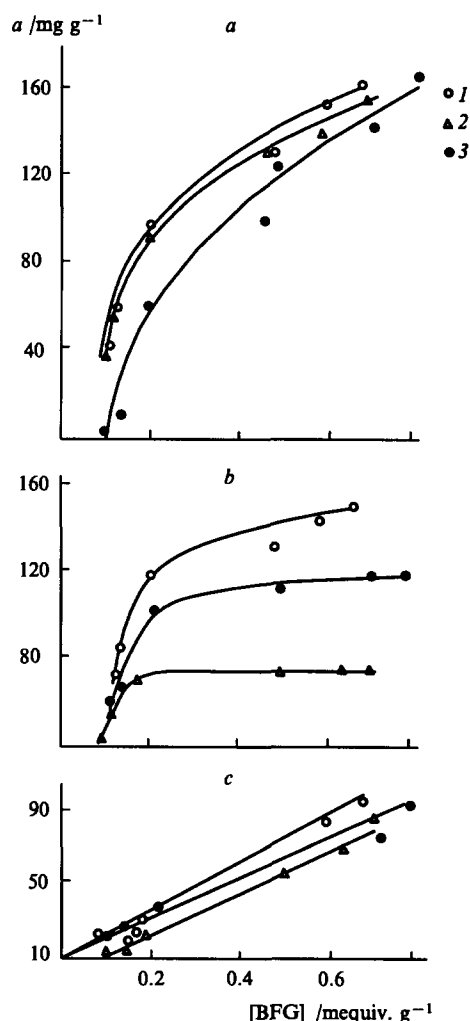


Figure 6. The influence of the concentration of basic functional groups (BFG) on the overall adsorption of sulfur dioxide on carbon adsorbents (a) and on the adsorption of SO_2 in the weakly bound (b) and strongly bound (c) forms at 25 °C ($\{\text{SO}_2\}_0 = 1 \text{ vol.}\%$): (1) SKT; (2) Merck; (3) semicoke PK-2.

was subjected to a stream of nitrogen for 2 h. The SO_2 evolved was trapped in a Drechsel bottle filled with a 5% H_2O_2 solution. The sulfuric acid formed was titrated with 0.05 M NaOH solution in the presence of blue bromophenol.

The influence of the concentration of basic functional groups on the adsorption of sulfur dioxide by various adsorbents can be seen from Fig. 6. The presence of basic oxygen-containing groups on the surfaces of carbon adsorbents has a significant effect on their overall adsorption capacity with respect to SO_2 : the amount of adsorbed SO_2 is proportional to their content (Fig. 6a). Thus the AR-3 activated carbon, which has a low adsorption capacity (about 40 mg g^{-1}), has at the same time few basic oxygen-containing groups ($0.090\text{--}0.127 \text{ mequiv. g}^{-1}$), while carbons with a high adsorption capacity ($140\text{--}160 \text{ mg g}^{-1}$) are also characterised by a high content of basic surface oxides ($0.500\text{--}0.660 \text{ mequiv. g}^{-1}$).

Figures 6b and 6c illustrate the influence the content of basic functional groups in the specimens on the adsorption of SO_2 in the weakly bound (a_1) and strongly bound (a_2) forms. The degree of adsorption of SO_2 in both forms increases in all cases with increase in the content of basic oxides. However, comparison of the relations in Figs 6b and 6c permits the conclusion that the adsorption of SO_2 in the strongly bound form is more sensitive to the presence of basic surface groups and hence to their acid-base characteristics than the adsorption in the weakly bound form.

Figure 7 shows how the concentration of basic oxides on the surface of Merck carbon affects the rate of sorption of SO_2 . It is seen from the figure that the adsorption capacities of specimens containing few basic surface groups are low and are determined mainly by physical adsorption — equilibration occurs rapidly (after 20–30 min). At a high concentration of basic functional groups, the sorption of SO_2 is slow and equilibrium is attained only after 60–90 min. This demonstrates yet again that in this

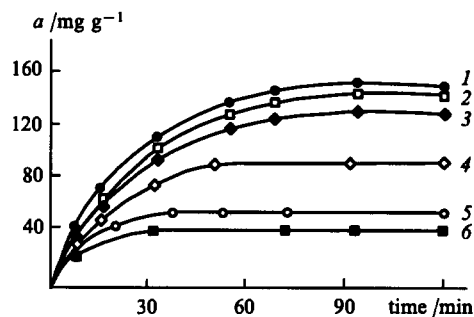


Figure 7. Kinetics of the adsorption of sulfur dioxide ($[\text{SO}_2]_0 = 0.3 \text{ vol. \%}$) on the activated Merck charcoal at 25°C and at the following concentrations of the basic functional groups (mequiv. g^{-1}): (1) 0.685; (2) 0.610; (3) 0.493; (4) 0.190; (5) 0.116; (6) 0.112.

case adsorption includes also chemisorption: almost half of the adsorbed dioxide corresponds to the strongly bound SO_2 .

Thus the concentration of basic functional groups on the surface of carbon materials determines their adsorption capacities with respect to SO_2 . It has a stronger influence on the adsorption of sulfur dioxide in the strongly bound form (heat of adsorption $> 80 \text{ kJ mol}^{-1}$). The amount of weakly bound sulfur dioxide (heat of adsorption $< 50 \text{ kJ mol}^{-1}$) is influenced mainly by the structural characteristics of the adsorbents and in particular by their specific surface areas.

5. The influence of temperature

The question of the influence of temperature on the equilibrium adsorption capacities of carbon adsorbents has been thoroughly investigated.^{20, 21, 39, 74–87} The isotherms illustrated in Fig. 8 correspond to the first type in Brunauer's classification.⁸⁸ A steep

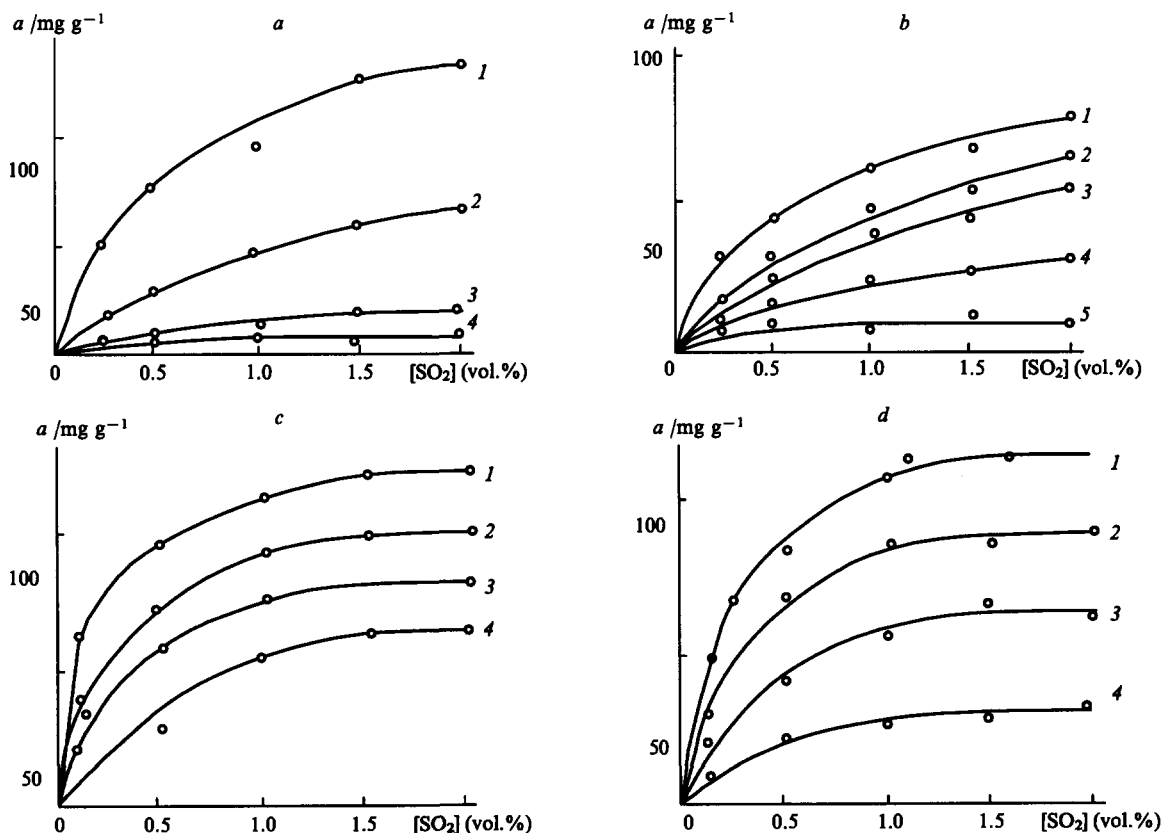


Figure 8. Isotherms for the adsorption of sulfur dioxide on the activated carbons SKT (a), BAU (b), AR-3 (c), and KAD (d) at different temperatures ($^\circ\text{C}$): (1) 25; (2) 50; (3) 100; (4) 150.

rise in the isotherms in the region of relatively low SO_2 concentrations is characteristic of almost all the specimens. This means that carbon adsorbents can serve as an effective means for the extensive removal of sulfur dioxide from gases and can be used to treat gases with a low SO_2 content. With increase in temperature from 20 to 150 °C, the capacities of the adsorbents considered fall by 50%–90% when the SO_2 content in the initial gas mixture is about 1 vol.%. However, at low concentrations of sulfur dioxide (up to 0.5%) the adsorption capacity depends little on temperature, which shows that they would not be useful for the purification of gases with low concentrations and at an elevated temperature.

An increase in temperature has a negative effect on the overall amount of adsorbed sulfur dioxide.^{22, 24} However, the fraction of SO_2 retained on the carbon surface by chemical forces, i.e. as a result of the interaction with basic sulfurous groups, increases approximately by 10% as the temperature rises from 20 to 100 °C, after which it remains constant (Fig. 9). At temperatures above 50 °C, the fraction of chemisorbed SO_2 is in all cases greater than the fraction of the sulfur dioxide bound to the carbon adsorbents by dispersion forces and reaches 55%–70%. Almost all the SO_2 adsorption isotherms on carbon adsorbents can be satisfactorily fitted by the Langmuir monomolecular adsorption equation⁸⁹ or by the Freundlich equation.⁹⁰

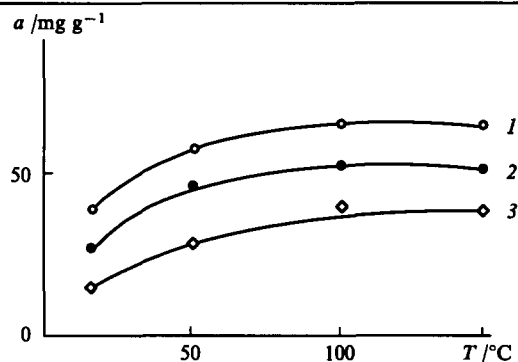


Figure 9. The influence of temperature on the ratio of the weakly and strongly bound forms of SO_2 on the surfaces of carbon adsorbents ($[\text{SO}_2]_0 = 1 \text{ vol.}\%$): (1) SKT; (2) AR-3; (3) PK-2.

6. The influence of oxygen

The influence of oxygen on the adsorption of sulfur dioxide was already noted in the very first studies devoted to the interaction of SO_2 with a carbon surface.^{11, 14, 25, 91–93} However, systematic investigations began only recently and this was associated with the appearance of the hypothesis that the chemical nature of the surfaces of the adsorbents affects SO_2 sorption process.

It was shown above that the sorption of SO_2 from an oxygen-free gas mixture includes chemisorption with formation of a stable chemical compound on the surface. The contribution of chemisorption, which does not exceed 45%–70% of the total amount of the sorbed sulfur dioxide, is determined by the acid–base properties of the adsorbent and the adsorption temperature. Evidently the presence of oxygen in the gas phase should promote chemisorption and in all probability the degree of conversion of SO_2 should increase in parallel with increasing O_2 concentration in the gas.

The adsorption of sulfur dioxide on activated carbons in the presence of oxygen has been investigated in detail in a number of studies.^{26, 29, 51, 84, 94–97, 126} Fig. 10 illustrates the influence of the concentration of the oxygen in the gas stream on the adsorption capacities of the SKT and AR-3 carbons with respect to SO_2 .^{57, 91} In all cases, sulfur dioxide is sorbed in the form of weakly bound (physically bound) and strongly bound (chemically bound) forms,

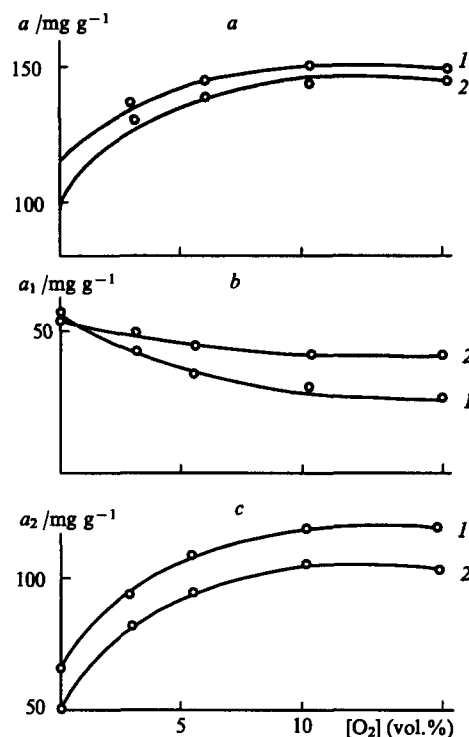


Figure 10. The influence of oxygen concentration in the gas mixture on the overall adsorption of sulfur dioxide by activated carbons (a) and on its physical (b) and chemical (c) adsorption at 25 °C ($[\text{SO}_2]_0 = 1 \text{ vol.}\%$) (1) AR-3; (2) SKT.

the fraction of the chemisorbed SO_2 depending to a large extent on the O_2 concentration in the gas and on the process temperature.

The adsorption capacities of sorbents increase with increasing O_2 content in the gas mixture. The degree of adsorption of SO_2 from a gas containing 10 vol.% of O_2 at 20 °C is approximately 30% greater than the degree of its adsorption from an oxygen-free gas mixture. A further increase in the O_2 content in the gas stream (above 10%) does not lead to an increase in the equilibrium adsorption capacity — virtually all the curves reach a plateau. In all cases, the increase in the adsorption capacities of carbons is caused exclusively by chemisorption processes. As can be seen from Fig. 10b, the amount of physically sorbed sulfur dioxide tends to decrease with increase in the O_2 concentration. As the adsorption temperature rises, this trend weakens and at 100–150 °C the quantity a_1 is almost independent of the O_2 concentration.

On the other hand, the amount of chemisorbed SO_2 increases with increase in the oxygen concentration in the gas mixture (Fig. 10c). At high temperatures, the $a_2 = f[\text{O}_2]$ relation is linear. At low temperatures, an increase in the oxygen content in the gas undergoing purification to above 10 vol.% hardly affects the adsorption of SO_2 in the strongly bound form.

According to a number of investigators,^{51, 96, 97, 126} such influence of the oxygen concentration on the adsorption of sulfur dioxide can be explained by the active sorption of oxygen by carbon adsorbents in the temperature range 0–150 °C. Physical adsorption of oxygen takes place initially, after which it is bound by chemical forces to the most active sections of the carbon's surface, i.e. it passes to the chemisorbed state. Basic oxides, which, as shown above, are centres for the specific adsorption of sulfur dioxide molecules, are formed as a result on the surfaces of activated carbons.^{67, 68, 98, 99} Thus the presence of oxygen in the gas mixture promotes an increase in the total number of SO_2 adsorption active sites, which naturally increases the adsorption capacities of activated carbons with respect to sulfur dioxide.

Table 4. Characteristics of the oxidised adsorbents.

Oxidation conditions		Content of oxygen-containing groups / mequiv. g ⁻¹				
temperature / °C	O ₂ concentration (vol. %)	carboxylic	lactone	phenolic	carbonyl	basic
SKT carbon sorbent						
Initial specimen		0.558	0.594	0.095	0.161	0.653
20	3.0	0.551	0.564	—	0.050	0.927
20	5.0	0.525	0.541	—	0.045	1.253
100	3.0	0.531	0.572	—	0.100	0.896
100	5.0	0.513	0.501	—	0.090	1.269
AR-3 carbon sorbent						
Initial specimen		—	—	0.125	0.100	0.744
20	3.0	—	—	0.104	—	0.986
20	5.0	—	—	0.080	0.020	1.334
100	3.0	—	—	0.100	0.025	0.951
100	5.0	—	—	0.075	0.030	1.395

In order to test this hypothesis, a series of experiments were performed in which the influence of the treatment of carbon adsorbents with oxygen on the chemical state of their surfaces was investigated.⁵¹ The initial adsorbents were maintained for 2 h in a stream of nitrogen at 350 °C, after which they were cooled to the required temperature, continuing the passage of dried N₂ through them. After this, a measured amount of oxygen such that its content was 3 vol.% or 5 vol.% was introduced into the gas stream. The subsequent treatment of the adsorbents by the oxygen-containing mixture was carried out for 2 h at 20 or 100 °C. The conditions of the preceding experiments, in which there was no sulfur dioxide in the gas, were thus virtually reproduced.

After the adsorption of oxygen, the chemical state of the adsorbent surface was studied by the neutralisation method.⁶³ The results presented in Table 4 show that the initial AR-3 carbon possesses predominantly basic groups. The SKT activated carbon contains in addition an appreciable number of acid groups, mainly lactone and carboxy-groups.

Treatment of the adsorbents with nitrogen at 350 °C with subsequent adsorption of oxygen altered in all cases the chemical nature of the carbon surface: the surface acidic groups of virtually all types vanished and the number of basic groups, which constitute some of the sulfur dioxide adsorption centres, increased. The increase in the concentration of basic groups naturally increases the adsorption capacities of the carbons with respect to SO₂.

7. The influence of water vapour

The influence of water vapour on the sorption of SO₂ by carbon adsorbents has been the subject of numerous investigations.^{13, 20, 22, 23, 26, 100} An appreciable increase in the adsorption capacities of activated carbons in the adsorption of SO₂ from moist gas streams has been noted. The views of many investigators on this phenomenon reduce to the postulate that water, which has a considerable chemical affinity for the chemisorbed SO₂, abstracts it from the carbon surface and transfers it to the liquid phase. Thus the blocked SO₂ sorption active centres are liberated and can again participate in the process.

In all probability, a weak point in the above hypothesis is that water is regarded merely as an 'abstracting agent'. Furthermore, studies of the influence of water on the sorption of SO₂ have almost always been performed in the presence of O₂, which naturally has a definite effect on the course of the process itself. A study was therefore made¹⁰¹ of the joint adsorption of sulfur dioxide and H₂O both in the absence of oxygen from the gas mixture and in its presence. The studies were performed by the thermal desorption method on SKT and AR-3 activated carbons and on the PK-2 semicoke. In another series of experiments, the

saturated adsorbents were washed with distilled water and the content of H₂SO₃ and H₂SO₄ was then determined by titration.

a. The influence of water vapour on the adsorption of SO₂ from an oxygen-free mixture

Fig. 11 shows how water vapour influences the adsorption capacity of the SKT activated carbons.¹⁰¹ The ratio of the contributions of physical adsorption and chemisorption in the sorption of SO₂ from a moist oxygen-free gas is determined not only by the nature of the adsorbent and the process temperature⁹⁵ but also by the water vapour content of the gas being purified. The appreciable increase in the adsorption capacity with increase in the H₂O content is due to the increase in the amount of chemisorbed sulfur dioxide (Fig. 11, curve 3), since the physical adsorption of SO₂ (*a*₁) tends to diminish over the entire range of water vapour concentrations (curve 2). This means that the presence of water on the surfaces of carbon adsorbents promotes the appearance of new centres for the chemical adsorption of SO₂.

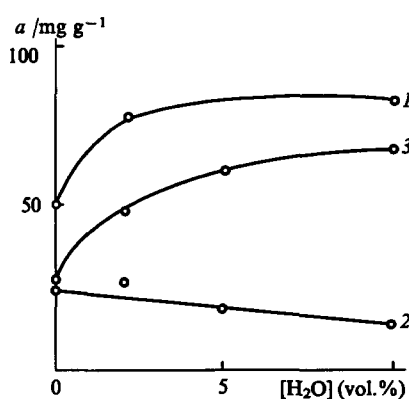


Figure 11. Dependence of the adsorption of sulfur dioxide from an oxygen-free mixture on the activated carbon SKT on the concentration of water vapour adsorption in the gas at 50 °C: (1) overall adsorption; (2) physical adsorption; (3) chemisorption.

The results of the chemical analysis of aqueous extracts, obtained as a result of the washing of saturated adsorbents with water, indicate the presence of sulfuric and sulfurous acids (Fig. 12). The amount of sulfur dioxide washed off the adsorbent in the form of sulfuric acid increases slightly with increase in the concentration of water vapour in the gas. On the other hand, the content of sulfurous acid increases to a much greater extent. This permits the conclusion that in the presence of water vapour the

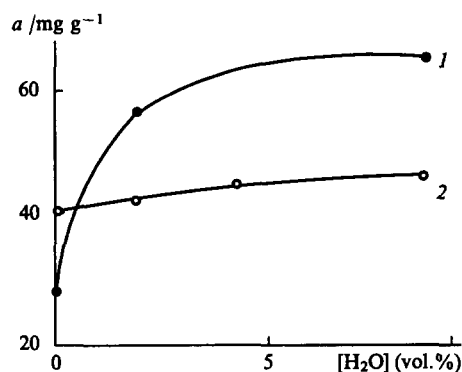


Figure 12. The influence of the concentration of water vapour on the composition of the aqueous extract from the carbon SKT saturated with sulfur dioxide at 50 °C: (1) sulfurous acid; (2) sulfuric acid.

degree of oxidation of sulfur dioxide to the trioxide does not increase. In all probability, the increase in the amount of chemisorbed SO_2 and hence the overall increase in the adsorption capacity of the carbons are induced by other chemical causes, which have a bearing on the presence of water on the surfaces of the adsorbents.

The mechanism of the adsorption of water vapour on activated carbons has been examined in detail.^{58, 102, 103} It has been established that the adsorption capacity of a carbon in relation to water vapour depends greatly on the number of chemically bound oxygen atoms present on the surface as part of the composition of acidic surface oxides, which play the role of primary adsorption centres for water molecules. At low equilibrium pressures, adsorption is ensured mainly by the formation of hydrogen bonds between the water molecules and the primary adsorption centres. The adsorbed water molecules are secondary adsorption centres, which may include other molecules as a result of the formation of hydrogen bonds. With increase in pressure, the probability of adsorption increases as a consequence of the increase in the number of secondary adsorption centres, i.e. the adsorbed molecules themselves.

Bearing in mind the ability of sulfur atoms to form hydrogen bonds,¹²⁷ one may postulate that in the case under consideration the preliminary adsorption of water on the carbon surface results in the appearance of a second variety of adsorption centre, namely adsorbed H_2O molecules, which may retain sulfur dioxide with the aid of hydrogen bonds. Thus, in the presence of water vapour in the gas phase, there are two types of active centres for SO_2 molecules on the carbon adsorbents: basic surface groups^{30, 50, 51} and the protons of the sorbed water molecules, capable of forming hydrogen bonds with sulfur dioxide.^{23, 26} It is natural to postulate that an increase in the concentration of adsorbed water entails also an increase in the number of centres of the second type, which means an increase also in the total number of SO_2 adsorption centres. As a result, the adsorption capacities of the carbon adsorbents with respect to sulfur dioxide increase when the latter is sorbed from a moist gas.

However, one must not forget the possibility of the interaction of some of the sorbed H_2O molecules with the sulfur dioxide chemisorbed on the basic surface centres, resulting in the formation of sulfuric acid.¹¹ The molecules of the latter do not in all probability form strong bonds with the active centres and may be displaced to other sections of the adsorbent surface by virtue of diffusion, liberating the active centres for further oxidation of SO_2 . A slight increase in the amount of sulfuric acid formed in the adsorption process with increase in the H_2O concentration (Fig. 12, curve 1) can be explained by the fact that each active centre of the first type participates repeatedly in the oxidation process.

The sulfur dioxide bound by hydrogen bonds to the adsorbed water is not in the oxidised state and may be washed off the

surfaces of the adsorbents with water in the form of sulfurous acid. This accounts for the marked increase in the H_2SO_3 concentration with increase in the concentration of H_2O (Fig. 12, curve 2). On the other hand, under thermal desorption conditions, SO_2 may be removed from the surface only at temperatures in excess of 200 °C. This is in fact the reason why the quantity a_2 increases with increase in the concentration of H_2O (Fig. 11, curve 3).

In conclusion, we may note that the influence of temperature on the adsorption capacities of carbon adsorbents is less marked than the influence of the concentration of water vapour. This can be explained by the partial compensation for the decrease in adsorption capacity with increase in temperature by the increase in the content of water vapour in the gas stream.

b. The influence of water vapour on the adsorption of SO_2 from a mixture containing oxygen

Analysis of literature data shows that the adsorption capacities of carbon adsorbents in the sorption of SO_2 from a gas containing simultaneously oxygen and water vapour are higher than in all the preceding cases. Fig. 13 shows how the concentration of water vapour influences the adsorption capacity of the AR-3 activated carbon and its components (a_1 and a_2) at 50 °C and a constant oxygen concentration of 5 vol.%.¹⁰¹ With increase in the water vapour content in the gas being purified, the capacity of the adsorbent with respect to SO_2 also increases over the entire range of H_2O concentrations solely as a result of the chemisorption of sulfur dioxide (a_2). The fraction of SO_2 bound to the carbon surface by physical forces diminishes steadily.

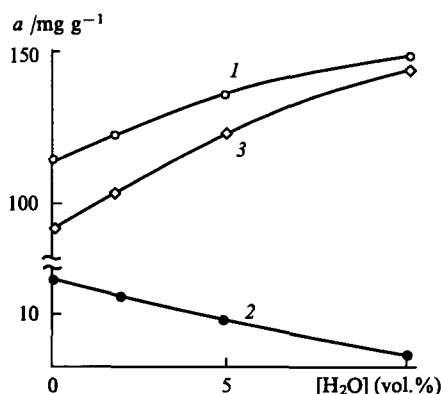


Figure 13. Dependence of the adsorption of sulfur dioxide from a gas containing 5 vol.% O_2 on the carbon AR-3 on the concentration of water vapour at 50 °C: (1) overall adsorption; (2) physical adsorption; (3) chemisorption.

According to the results of the chemical analysis of the solutions formed when the saturated adsorbents are washed with water, the liquid phase contains sulfurous and sulfuric acids (Fig. 14). The fraction of sulfurous acid in the wash waters ranges from 15% to 45% depending on the system parameters and increases with increasing concentration of water vapour.¹²⁸ On the other hand, the concentration of H_2O in the gas being purified hardly affects the content of sulfuric acid. In all probability, the high H_2SO_3 content in the wash waters can be accounted for by a deficiency of oxygen in the system, which prevents more complete oxidation of sulfur dioxide.

The results of the study of the influence of the oxygen concentration on the sorption of sulfur dioxide from a moist gas are presented in Fig. 15. They show that the amount of the oxidised product, washed off the adsorbents in the form of H_2SO_4 , increases with increase in the O_2 content. At an oxygen concentration of 10 vol.% in the gas being purified, virtually complete oxidation of SO_2 is already attained: only sulfuric acid is present in the solution formed.

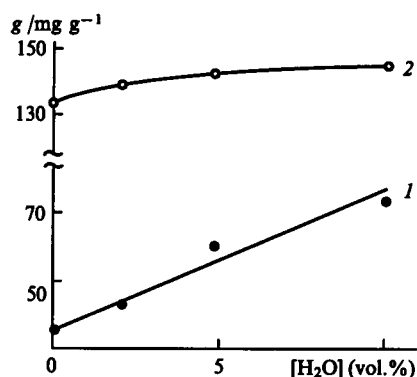


Figure 14. The influence of the concentration of water vapour on the composition of the aqueous extract from the carbon AR-3 saturated with sulfur dioxide at 50 °C in a gas containing 5 vol. % of O₂ (1) sulfurous acid; (2) sulfuric acid.

As in all the previous cases, an increase in temperature has a negative effect on the adsorption capacity, although this is manifested to a much smaller extent because the chemical component of the adsorption process is less subject to the influence of temperature.

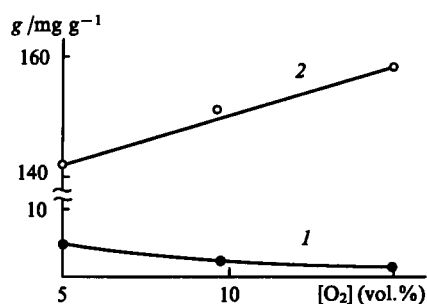


Figure 15. The influence of the concentration of oxygen on the composition of the aqueous extract from the carbon SKT saturated with sulfur dioxide at 50 °C in a gas containing 10 vol. % of H₂O: (1) sulfurous acid; (2) sulfuric acid.

III. The nature of the active centres for the adsorption of SO₂ on carbon adsorbents

1. Infrared spectroscopic study of the interaction of SO₂ with carbon adsorbents

IR spectroscopy is one of the few methods of physicochemical analysis which make it possible to assess quantitatively the nature of the processes occurring in the sorption of sulfur dioxide by optically opaque bodies such as carbon adsorbents, to discover the possible reactions between the components of the gas mixture, and also to identify the final products and the sites of the specific adsorption of SO₂ molecules.

Fig. 16 presents typical IR spectra of the Russian industrial activated carbons SKT, AR-3, and BAU, as well as a cellulose-based carbon adsorbent after their evacuation to a residual pressure of 10⁻⁴ mm Hg at 350 °C for 2 h.^{40,41,104-107} In virtually all cases, weak absorption bands at 1750 and 1710 cm⁻¹ and also moderately intense bands at 900 and 725 cm⁻¹ are observed in the spectra of the activated carbons. Evidently the 1750 and 1710 cm⁻¹ bands may be assigned to the stretching vibrations of the carbonyl groups.¹⁰⁸

The 1600 cm⁻¹ band is attributed to the C=O structures, in which the bond length is greater and the bond multiplicity is smaller than in the carbonyl groups absorbing at higher frequencies.¹⁰⁹ Similar structures are formed with participation of the π

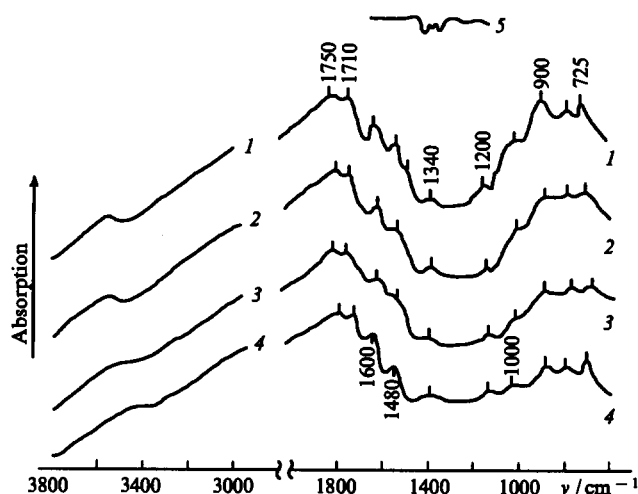
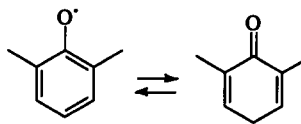


Figure 16. IR spectra of activated carbon evacuated to a residual pressure of 10⁻⁴ mm Hg at 350 °C: (1) AR-3; (2) SKT; (3) BAU; (4) KAD-iodine; (5) gaseous SO₂.

electrons of condensed aromatic systems. In all probability, they can be assigned to the radical-ion structures C=O[•], which are intermediate forms on the way to the formation of carbonyl groups strongly bound to the carbon surface.^{104,106,107,110}



The absorption bands in the range 1340–1480 cm⁻¹ are characteristic of the deformation vibrations of the COOH groups.¹¹¹ The assignment of the bands in the range 1110–1130 cm⁻¹ gives rise to difficulties. The band with a frequency of about 1120 cm⁻¹, observed in the spectrum of oxidised carbon black and graphite oxide, has been assigned¹¹²⁻¹¹⁴ to the stretching vibrations of the C–OH bond, while the similar band (1065 cm⁻¹) in the spectrum of graphite oxide has been assigned¹¹⁵ to the stretching vibrations of the C–OH enolic group. Finally, the absorption in the range 1000–1180 cm⁻¹ is characteristic of the stretching vibrations of the C–O bond.¹⁰⁸

Cooling of the adsorbents in a stream of air after preliminary evacuation at 350 °C leads to the appearance of intense absorption bands at 1800–1830, 1750–1770, 900, 725, and 1230–1250 cm⁻¹ in the IR spectra of the specimens (Fig. 17, curve 2). The presence of doubled bands (at 1830 and 1770 cm⁻¹) in the region of the deformation vibrations of the carbonyl groups C=O and also of intense bands at 900 and 725 cm⁻¹ indicates the

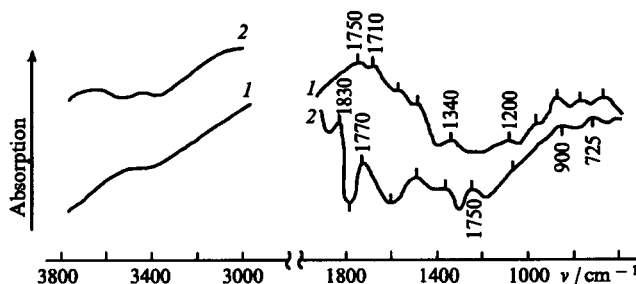
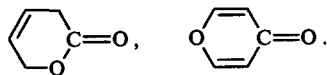


Figure 17. IR spectra of the activated carbon BAU evacuated to a residual pressure of 10⁻⁴ mm Hg at 350 °C (1) and subjected after this procedure to cooling in air to 20 °C (2).

dehydration of the carboxy-groups and the formation of cyclic aromatic systems with participation of π electrons.¹⁰⁶

The intense 1250 cm^{-1} absorption band is characteristic of the vibrations of the C—O—C groups. This means that the most probable form of the basic surface oxides, formed on oxidation of the carbon in a stream of air, comprises unsaturated lactones, in particular α - and γ -pyrones or their derivatives:



Thus IR spectroscopic analysis confirms indirectly the existence on the surface of carbon adsorbents, in an anion-exchange form, of the pyrone structures predicted by Voll and Boehm.^{67,68}

Analysis of the IR spectra of activated charcoals and semicokes saturated by sulfur dioxide from complex gas mixtures permits the conclusion that the adsorption of SO_2 on various carbon adsorbents proceeds via a single mechanism. The physical adsorption of sulfur dioxide, which does not require the presence on the surface of any kind of active centre, is accompanied by the appearance of absorption bands within the comparatively narrow range $1330\text{--}1360\text{ cm}^{-1}$ and at 1150 cm^{-1} (Fig. 18).

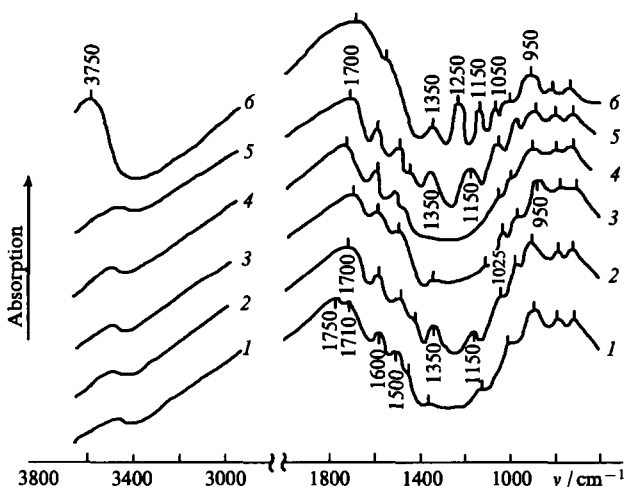


Figure 18. IR spectra of the activated carbon AR-3: (1) after evacuation to 10^{-4} mm Hg at 350°C ; (2) after saturation with sulfur dioxide at 50°C ; (3) after evacuation at 20°C ; (4) after saturation with sulfur dioxide at 100°C ; (5) after preliminary adsorption of SO_2 at 20°C and subsequent saturation with oxygen; (6) after preliminary adsorption SO_2 and O_2 at 20°C and subsequent saturation with water vapour.

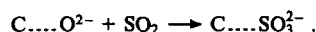
Another portion of the sulfur dioxide is chemisorbed on particular active centres. The bathochromic shift of the 1740 cm^{-1} band, which is characteristic of the stretching vibrations of the carbonyl group, after the adsorption of SO_2 (to 1700 cm^{-1}) and also the fact that the C=O bond remains perturbed also after the removal of the physically sorbed SO_2 indicate that the surface carbonyl groups, playing the role of an electron donor, actually participate in the chemisorption of sulfur dioxide.

One cannot rule out also the interaction of SO_2 with the surface OH groups. Since the change in the stretching vibration frequency of the OH groups of the adsorbents persists also after the removal from the surface of weakly bound sulfur dioxide, one may postulate that SO_2 does not form hydrogen bonds with these groups. At the same time, the positions of the absorption bands of the OH groups and their appreciable half-width indicate the existence of a hydrogen bond. The only explanation of this may be the interaction of the adsorbed SO_2 with the surface hydroxy-groups involving the formation of bisulfites. However, judging

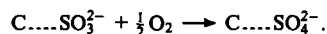
from the intensity of the 1075 cm^{-1} band in the spectrum, the contribution of such interaction is low.

After the adsorption of sulfur dioxide in the presence of water vapour, a broad intense band at 3600 cm^{-1} as well as a moderately intense band in the range $1045\text{--}1073\text{ cm}^{-1}$ appear in the IR spectra of virtually all the adsorbents. These refer respectively to the vibrations of the OH groups of the adsorbed water and of the S—O bisulfites. It is natural to postulate that sulfurous acid is formed on the surfaces of the adsorbents as a result of the interaction of sulfur dioxide with the adsorbed water molecules.

The adsorption of the molecular form of SO_2 may not involve solely the formation of a physical bond with the surface. There is also a possibility of strong adsorption, observed for example, on the SKT and BAU activated carbons. It has been noted¹¹⁶ that SO_2 is capable of forming molecular complexes with pyridine, triethanolamine, and triethylamine, in which sulfur dioxide exhibits the properties of an electron pair acceptor. The absorption bands corresponding to the S—O vibrations, undergo a bathochromic shift in the spectra of such complexes compared with the absorption bands of the free molecule. The surface O^{2-} ions may serve as electron donors in the formation of a complex with the adsorbed SO_2 .^{117,118}



The presence of oxygen in the gas leads to the oxidation of the chemisorbed SO_2 with formation of sulfate ions:



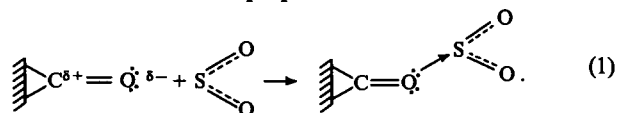
The spectrum of the SO_4^{2-} ions depends to a large extent on the presence of water vapour in the system.

Thus the study of the IR spectra has shown that the strength and nature of the interaction of sulfur dioxide with the surfaces of carbon adsorbents are determined both by the chemical nature of the latter and the composition of the gas mixture. Part of the SO_2 is then sorbed as a result of dispersion (physical) forces in the form of molecularly adsorbed sulfur dioxide. This process, which is not related to the presence on the surface of particular active centres, is accompanied by the appearance of absorption bands in the comparatively narrow range $1330\text{--}1360$ and at 1150 cm^{-1} .

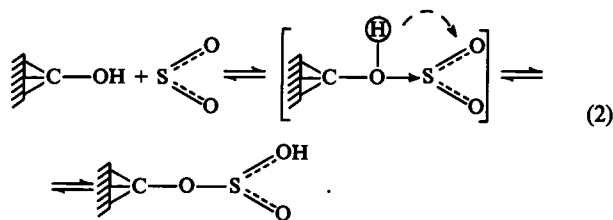
Another portion of sulfur dioxide is bound to the surface by stronger (chemical) forces. This chemisorbed SO_2 is converted on the surfaces of activated carbons and semicokes into sulfur compounds with different degrees of oxidation.

2. The chemistry of the adsorption of SO_2 from a dry oxygen-free mixture

It was shown above that the amount of sulfur dioxide chemisorbed from a dry gas is directly proportional to the concentration of basic functional groups on the carbon surface. At the same time, spectroscopic data indicate unambiguously the existence of pyrone structures on carbons having basic properties. One can therefore postulate that the centres for the specific sorption of SO_2 molecules from a dry oxygen-free mixture are basic oxygen complexes or more precisely, the carbonyl groups of pyrone derivatives. By virtue of the presence of the electron lone pair on the oxygen atom, the carbonyl group possesses weakly basic properties and interacts chemically with sulfur dioxide, which exhibits in this instance the properties of a Lewis acid:

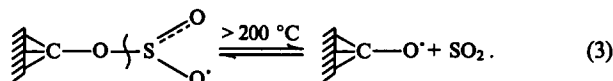


The slight change in the vibration frequency of the OH groups on virtually all activated carbons and semicokes after the removal of the physically adsorbed SO_2 indicates the involvement in the process of surface hydroxy-groups:

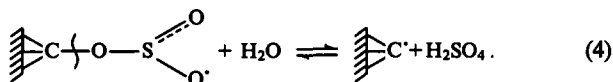


The formation of sulfite compounds on the surfaces of carbon adsorbents has been confirmed also by the existence of absorption bands at 1070, 1025, and 950 cm^{-1} in the IR spectra of all the adsorbents.

Thus the strongly bound form of SO_2 may be regarded as the intermediate sulfite compound $\text{C}-\text{OSO}_2$, in which the sulfur retains the +4 oxidation state. The amount of heat evolved in this process should not be large. Indeed, the isosteric heats of adsorption are 25–63 kJ mol^{-1} depending on the type of adsorbent. At low temperatures, the final product of the adsorption-catalytic process remains on the adsorbent surface and blocks the active sites. At fairly high temperatures, the chemisorbed SO_2 passes to the gas phase in the form of sulfur dioxide.



When the carbon adsorbent saturated with sulfur dioxide comes into contact with water, the chemisorbed SO_2 is abstracted from the surface in the form of sulfuric acid:



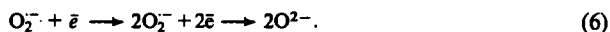
The process proceeds at room temperature and is accompanied by the transfer of electrons from the sulfur atom to the oxygen atoms and the reduction of the surfaces of the adsorbents with formation of electronic defects of the type of oxygen vacancies.

3. The chemistry of the adsorption of SO_2 from a dry oxygen-containing mixture

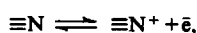
If O_2 is present in the gas phase during the adsorption of sulfur dioxide by carbon adsorbents, then not only chemically but also physically adsorbed oxygen participates in the oxidation of SO_2 . Detailed study of the catalytic properties of carbon in the oxidation reactions of various substances led to the conclusion that the process proceeds via a radical-chain mechanism.^{119–123} In conformity with this hypothesis, oxygen radical-ions are formed in the first stage of the process as a result of the transfer of electrons from heteroatoms via conjugated bonds to physically sorbed O_2 :



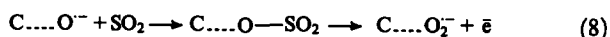
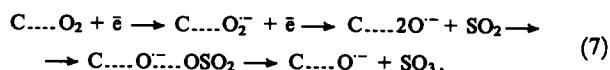
The next oxidation stage determines the order of the reaction with respect to oxygen (0.5) and the overall rate of the process:



The sources of electrons for the formation of superoxides are structural nitrogen atoms and the CN groups, which enter the lattice of the carbon adsorbents, as well as variable-valence metals (M) introduced into the adsorbents to activate and modify them:^{121, 124, 125}



The oxygen radical-ion structures ($\text{O}^{\cdot-}$ and $\text{O}_2^{\cdot-}$) the existence of which on the surfaces of activated carbons and semicokes is confirmed by the presence of an intense 1600 cm^{-1} absorption band in the IR spectra, actually initiate the conversion of SO_2 into SO_3 :



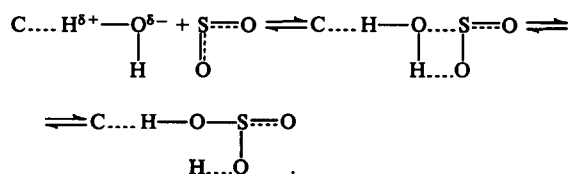
etc.

Another part of SO_2 enters into reactions (1) and (2) with the basic surface oxides of the carbon adsorbents, namely with the carbonyl groups of the pyrone structures and also with the surface hydroxyls, which is indicated by the presence of the 1075 and 1025 cm^{-1} absorption bands characteristic of sulfides in the IR spectra of virtually all activated carbons saturated with sulfur dioxide in the presence of O_2 . Furthermore, after the desorption of the weakly bound SO_2 , a change in the OH group vibration frequencies is observed in the adsorbents.

Thus the centres for the adsorption of sulfur dioxide from dry oxygen-containing mixtures are the oxygen radical-ions $\text{O}^{\cdot-}$ and $\text{O}_2^{\cdot-}$ as well as the carboxy- and hydroxy-groups of the pyrone structures.

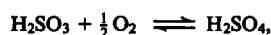
4. The chemistry of the adsorption of SO_2 from a moist oxygen-containing mixture

If the gas streams contain water vapour and oxygen, then, apart from the centres in which reactions (1) and (2) as well as (7) and (8) occur, additional centres for the adsorption of sulfur dioxide appear on the surfaces of carbon adsorbents. The latter are the protons of the preadsorbed H_2O molecules.^{23, 26} The appreciable increase in the adsorption capacities of carbons and semicokes under these conditions is due to the formation of hydrogen bonds between SO_2 and the water molecules sorbed beforehand. Sulfurous acid appears on the surfaces of the adsorbents as a result:



However, the role of water vapour does not reduce solely to the formation of new active centres for the adsorption of sulfur dioxide. In all probability, some of the H_2O molecules react during adsorption on the carbon surface with the chemisorbed sulfur dioxide (in the form of either SO_3 or $\text{SO}_3^{\cdot-}$), forming sulfurous and sulfuric acids. The acids do not form a strong bond with the active centres and are displaced by diffusion to other sections of the surfaces of the adsorbents, liberating the active centres for further chemisorption of new SO_2 molecules. Thus each active centre can participate repeatedly in the adsorption process.

In the presence of oxygen, sulfurous acid is oxidised to sulfuric acid, i.e.



which is in fact the final product of the adsorption of sulfur dioxide on carbon adsorbents. The presence of H_2SO_4 on the surface has also been confirmed by IR spectroscopic analysis (there are absorption bands at 1160 and 1240 cm^{-1} in the IR spectrum).

IV. Conclusion

Summarising, one may say that the adsorption of sulfur dioxide on carbon adsorbents from gas mixtures of different composition is an adsorption-catalytic process, which consists of several stages and leads to the formation of compounds of sulfur in different oxidation states. The adsorption of sulfur dioxide occurs only on adsorbents in an anion-exchange form; oxidised carbon hardly adsorbs SO_2 .

Two types of bonds between sulfur dioxide and the carbon surface are distinguished — a weak bond which is characterised by a heat of absorption $< 50 \text{ kJ mol}^{-1}$ and may be ruptured at a temperature $< 150^\circ\text{C}$, and a strong bond (heat of adsorption $> 80 \text{ kJ mol}^{-1}$) ruptured at temperatures above 200°C . The weak bond is due to van der Waals forces and corresponds to the physical adsorption of SO_2 . The strong bond is formed as a result of chemical interaction between sulfur dioxide and the surface compounds and corresponds to the chemisorption of SO_2 . In the latter case, the most likely centres for the specific adsorption of sulfur dioxide are surface carbonyl and hydroxy-groups of the pyrone structures and their derivatives, which have basic properties, the oxygen radical-ions (O^- and O_2^-), as well as the protons of the adsorbed water molecules.

The degree of oxidation of the adsorbed SO_2 depends on the nature of the adsorbent, the process temperature, and also the presence of O_2 in the gas mixture. Sulfur dioxide is partly oxidised to SO_3 also when SO_2 is sorbed from a dry oxygen-free gas. This is ensured by the oxygen weakly bound the carbon surface and forming part of the composition of the basic surface functional groups. The presence of water vapour in the gas phase promotes an increase in the adsorption capacity as a result of the formation of a strong hydrogen bond between the molecules of the pre-adsorbed water and SO_2 , but the amount of oxidised sulfur dioxide does not increase under these conditions.

The removal of the reaction products from the adsorbent surfaces can be achieved by heating the adsorbents in a stream of an inert gas or by washing with water. The liberated active centres can again participate in the process.

The carbon adsorbents employed in the processes involving the removal of sulfur dioxide from industrial and ventilation gases must satisfy the following principal requirements:

- they must have an extensive pore structure;
- they must exist in the anion-exchange form, i.e. they must possess basic properties;
- they must contain an appreciable amount of structural nitrogen;
- as far as possible, they must include in their composition catalysts for the oxidation of sulfur dioxide to the trioxide.

References

1. A I Rodionov, V N Klushin, N S Torocheshnikov *Tekhnika Zashchity Okruzhayushchei Sredy* (Technology of Environmental Protection) (Moscow: Khimiya, 1989)
2. S H Bruce, in *University of Southampton Colloquium on Environmental and Pollution Sensing*, Southampton, 1990 p. 75
3. H Furkert *Chem. Ind.* **22** 291 (1970)
4. M H Kocker *VGB Kraftwerkstech.* **53** 516 (1973)
5. T Ono *Sangyo Kagai* **5** 326 (1969)
6. F Johswich *Brennst-Warme-Kraft* **14** 105 (1962)
7. F J Ball, S L Torrence, F J Repik *J. Air Pollut. Control Assoc.* **22** 20 (1972)
8. P Steiner, H Juntgen, K Knoblauch *Adv. Chem. Ser.* **139** 180 (1975)
9. S A Anurov, N V Kel'tsev, V I Smola, N S Torocheshnikov *Usp. Khim.* **46** 32 (1977) [*Russ. Chem. Rev.* **46** 16 (1977)]
10. L I Loskutov, M N Khlopotov *Adsorbtsiya Adsorbenty* **28** (1982)
11. O K Davtyan, E N Ovchinnikova *Dokl. Akad. Nauk SSSR* **104** 857 (1955)
12. E N Ovchinnikova, O K Davtyan *Zh. Fiz. Khim.* **30** 1735 (1956)
13. O K Davtyan, E N Ovchinnikova *Zh. Fiz. Khim.* **35** 713 (1961)
14. O K Davtyan, Yu A Tkach *Zh. Fiz. Khim.* **35** 992 (1961)
15. O K Davtyan, B A Manakin, E G Misyuk, Yu N Polishchuk *Zh. Fiz. Khim.* **35** 1186 (1961)
16. O K Davtyan *Zh. Fiz. Khim.* **35** 2582 (1961)
17. Yu A Tkach, O K Davtyan *Zh. Fiz. Khim.* **35** 2727 (1961)
18. H Dratwa, H Juntgen *Staub-Reinhalt. Luft* **27** 30 (1967)
19. H Dratwa, H Juntgen, W Peters *Chem.-Ing.-Tech.* **39** 949 (1967)
20. G N Buzanova, Candidate Thesis in Technical Sciences, Lensovet Leningrad Technological Institute, Leningrad, 1973
21. N N Dobrovol'skii, S I Surinova *Khim. Tv. Topliva* **130** (1977)
22. G N Buzanova, I G Lesokhin, I P Mukhlenov, L I Vinnikov *Khim. Promst (Moscow)* **205** (1972)
23. L I Vinnikov, I P Mukhlenov, I G Lesokhin, G N Buzanova *Khim. Promst (Moscow)* **125** (1973)
24. S A Anurov, N V Kel'tsev, V I Smola, I S Torocheshnikov *Promysh. Sanitarn. Ochistka Gazov* (4) **11** (1974)
25. S A Anurov, Candidate Thesis in Technical Sciences, Mendelev Moscow Chemical Technological Institute, Moscow, 1974
26. I P Mukhlenov, G N Buzanova, L I Vinnikov, I S Safonov *Khim. Promst (Moscow)* **39** (1976)
27. P Davini, F Morelli, R Tartarelli *Chim. Ind.* **59** 11 (1977)
28. P Davini, F Morelli, R Tartarelli *Chim. Ind.* **59** 235 (1977)
29. P Corsi, P Davini, F Morelli, R Tartarelli *Chim. Ind.* **59** 768 (1977)
30. S A Anurov, T V Kutlaeva, V I Smola, in *Problemy Proizvodstva Alyuminiya i Elektroodnykh Materialov (Sb. Nauch. Tr.)* [Problems of the Production of Aluminium and Electrode Materials (Collection of Scientific Reports)] (St.-Petersburg: VAMI, 1992) p. 86
31. S A Anurov, T V Kutlaeva, in *Khimiya i Khimicheskaya Tekhnologiya Neorganicheskikh Veshchestv (Sb. Nauch. Tr.)* [The Chemistry and Chemical Technology of Inorganic Substances (Collection of Scientific Reports)] (Moscow: Mendelev Russian Chemical Technological University, 1996) p. 126
32. M Polanyi, K Welke *Z. Phys. Chem.* **132** 371 (1928)
33. A Magnus, H Giebenhein *Z. Phys. Chem.* **164** 209 (1933)
34. R A Bude, R M Dele *Z. Phys. Chem.* **59** 745 (1955)
35. H L McDermont, B E Lawton *Can. J. Chem.* **37** 637 (1959)
36. I F Berman, V I Smola, in *Pyleulavlvanie i Ochistka Gazov v Tsvetnoi Metallurgii (Sb. Nauch. Tr. Gintsvetmeta)* [Dust Trapping and Purification of Gases in Nonferrous Metallurgy (Collection of Scientific Reports from Gintsvetmet)] (Moscow: Metallurgiya, 1975) p. 147
37. T Allen, D Burevski *Powder Technol.* **28** 139 (1977)
38. W J Murphy, R F Ross, R W Glass *Ind. Eng. Chem., Prod. Res. Dev.* **16** 69 (1977)
39. N N Dobrovol'skii, Z V Lyubimova, S I Surinova, O V Fomkina *Tr. Inst. Goryuchikh Iskopaemykh* **32** 18 (1977)
40. J Zawadzki *Carbon* **25** 431 (1987)
41. S A Anurov *Zh. Fiz. Khim.* **69** 1065 (1995)
42. M M Dubinin *Poristaya Struktura i Adsorbtsionnye Svoistva Aktivnykh Ugley* (Porous Structure and Adsorption Properties of Active Charcoals) (Moscow: Izd. VAKhZ, 1965)
43. M M Dubinin *Adsorbtsiya i Poristost'* (Adsorption and Porosity) (Moscow: Izd. VAKhZ, 1972)
44. K Yamamoto, K Kaneko, L Sekim *Kogyo Kagaku Zasshi* **74** 1582 (1971)
45. M A Kostomarov, S I Surinova *Khim. Tv. Topliva* **3** (1976)
46. I P Mukhlenov, G N Buzanova, E A Kulish, in *Geterogenyye Kataliticheskie Protsessy vo Vzveshennom i Fil'truyushchem Sloe (Sb. Nauch. Tr.)* [Heterogeneous Catalytic Processes in Suspended and Filtering Beds (Collection of Scientific Transactions)] (Leningrad: Lensovet Leningrad Technological Institute, 1977) p. 17
47. T Grzybek, J Jagiello, E Polito, E Wisla *Arch. Gornistwa* **26** 43 (1981)
48. V I Smola, Candidate Thesis in Technical Sciences, Gintsvetmet, Moscow, 1972
49. V I Smola, S A Anurov *Promysh. Sanitarn. Ochistka Gazov* (5) **21** (1976)
50. P Davini *Carbon* **28** 565 (1990)
51. S A Anurov *Zh. Fiz. Khim.* **70** 132 (1996)
52. D A Kolyshkin, K K Mikhailova *Aktivnye Ugli* (Active Charcoals) (Leningrad: Khimiya, 1972)
53. *Aktivnye Ugli (Katalog)* [Active Charcoals (Catalog)] (Cherkassy: NIITEKHIM, 1989)
54. V M Bogdanov, Candidate Thesis in Technical Sciences, Mendelev Moscow Chemical Technological Institute, Moscow, 1989
55. P Davini *Carbon* **31** 47 (1993)
56. E K Rideal, W M Wright *J. Chem. Soc.* **1813** (1926)
57. S Zylbertal *Biochem. Z.* **236** 131 (1931)
58. M M Dubinin *Usp. Khim.* **24** 513 (1955)
59. M M Dubinin, in *Poverkhnostnye Khimicheskie Soedineniya i Ikh Rol' v Yavleniyakh Adsorbtsii* (Surface Chemical Compounds and Their Role in Adsorption Phenomena) (Moscow: Izd. VAKhZ, 1957) p. 9
60. P L Walker (Ed.) *Chemistry and Physics of Carbon* (New York: M Dekker, 1965)
61. C Ischizaki, I Marti *Carbon* **19** 409 (1981)

62. E Papirer, S Li, J-B Donnet *Carbon* **25** 243 (1987)
63. H P Boehm, E Diehl, W Heck, R Sappok *Angew. Chem.* **76** 742 (1964)
64. G P Fedorov, Yu F Zarifyants, V F Kiselev *Zh. Fiz. Khim.* **37** 2344 (1963)
65. V A Garten, D E Weiss, J B Willis *Aust. J. Chem.* **10** 295 (1957)
66. V A Garten, D E Weiss, J B Willis *Aust. J. Chem.* **8** 68 (1955)
67. M Voll, H P Boehm *Carbon* **8** 741 (1970)
68. H P Boehm, M Voll *Carbon* **8** 227 (1970)
69. S Ogawa, S Yamada, T Ochi Kogai to *Taisaku* **21** 475 (1985)
70. H Kitagawa *Kogai* **20** 85 (1985)
71. P Davini *Fuel* **68** 145 (1989)
72. I P Mukhlenov, G N Buzanova, in *Ekologicheskaya Tekhnologiya i Ochistka Promyshlennyykh Vybrosov (Sb. Nauchn. Tr.)* [Ecological Technology and Purification of Industrial Waste (Collection of Scientific Reports)] (Leningrad: Lensovet Leningrad Technological Institute, 1977) p. 17
73. A King *J. Chem. Soc.* 1489 (1937)
74. J Siedlewski, J Zawadzki *Chem. Stosow.* **XVII** 11 (1973)
75. K Arti *Bull. Inst. Phys. Chem. Res.* **13** 135 (1934)
76. K Arti *Bull. Inst. Phys. Chem. Res.* **13** 853 (1934)
77. K Arti *Bull. Inst. Phys. Chem. Res.* **13** 1428 (1934)
78. K Arti *Bull. Inst. Phys. Chem. Res.* **14** 99 (1935)
79. K Arti *Bull. Inst. Phys. Chem. Res.* **14** 1210 (1935)
80. K Arti *Bull. Inst. Phys. Chem. Res.* **15** 254 (1936)
81. S Kasaoka, E Sasaoka *J. Chem. Soc., Jpn. Ind. Chem. Sect.* **74** 2213 (1971)
82. V I Smola, N V Kel'tsev, E S Rakhlin, S A Anurov, in *Pyleulavli-vanie i Ochistka Gazov v Tsvetnoi Metallurgii (Sb. Nauch. Tr. Gintsvetmeta)* [Dust Trapping and Purification of Gases in Nonferrous Metallurgy (Collection of Scientific Reports from Gintsvetmet)] (Moscow: Metallurgiya, 1970) p. 152
83. S A Anurov, N V Kel'tsev, V I Smola, N S Torocheshnikov *Khim. Promst (Moscow)* **113** (1974)
84. V I Smola, S A Anurov, V A Zinkovskii, L G Guseletov *Tsv. Metall.* **30** (1974)
85. N N Dobrovol'skii, Z V Lyubimova, S I Surinova, O V Fomkina *Tr. Inst. Goryuchikh Iskopaemykh* **32** 18 (1977)
86. T Allen, D Burevski *Powder Technol.* **18** 139 (1977)
87. S Anourov, V Smola, N Torotchechnikov, in *Revue Scientifique Sur la Chimie Industrielle (Algerie: l'Universite d' Annaba, 1979)* p. 26
88. S Brunauer *The Adsorption of Gases and Vapors* Vol. 1 (Princeton: Princeton University Press, 1945)
89. I Langmuir *J. Am. Chem. Soc.* **38** 2221 (1916)
90. H Freundlich *Kapillarchemie* (Berlin: VDJ Verlag, 1930)
91. J Siedlewski *Int. Chem. Eng.* **5** 608 (1965)
92. J Siedlewski *Int. Chem. Eng.* **7** 35 (1967)
93. H Dratwa ThD, Tech. Hochschule, Aachen, Germany, 1966
94. W O Stacy, F J Vastola, P L Walker *Carbon* **6** 917 (1969)
95. V I Smola, S A Anurov, N V Kel'tsev *Promysh. Sanitarn. Ochistka Gazov* (1) **15** (1975)
96. P Davini *Carbon* **29** 321 (1991)
97. S A Anurov, T V Kutlaeva, V I Smola, in *Problemy Proizvodstva Alyuminiya i Elektroodnykh Materialov (Sb. Nauch. Tr.)* [Problems of the Production of Aluminium and Electrode Materials (Collection of Scientific Reports)] (St.-Petersburg: VAMI, 1992) p. 91
98. B G Linsen (Ed.) *Physical and Chemical Aspects of Adsorbents and Catalysts* (New York: Academic Press, 1970)
99. B R Puri, B C Kaistha, O P Mahajan *J. Indian Chem. Soc.* **50** 473 (1973)
100. F Johswich *Brennst.-Warme-Kraft* **17** 238 (1965)
101. S A Anurov *Zh. Fiz. Khim.* **69** 1262 (1995)
102. M M Dubinin, E D Zaverina *Dokl. Akad. Nauk SSSR* **92** 111 (1953)
103. M M Dubinin, V V Serpinskiy *Dokl. Akad. Nauk SSSR* **99** 1033 (1954)
104. J Zawadzki *Carbon* **18** 281 (1980)
105. J Zawadzki *Pol. J. Chem.* **52** 2157 (1978)
106. J Zawadzki *Carbon* **16** 491 (1978)
107. J Zawadzki *Carbon* **19** 19 (1981)
108. L J Bellamy *The Infra-Red Spectra of Complex Molecules* (New York: Wiley, 1960)
109. F J Long, K W Sykes *J. Chim. Phys.* **47** 361 (1950)
110. C Ishizaki, I Marti *Carbon* **19** 409 (1981)
111. J B Donnet, F Hueber, N Perol, J Jaeger *J. Chim. Phys.* **60** 426 (1963)
112. A V Kiselev, G A Kozlov, V I Lygin *Zh. Fiz. Khim.* **39** 2733 (1965)
113. V I Lygin, N V Kovaleva, N N Kavtaradze, A V Kiselev *Kolloid. Zh.* **22** 334 (1960)
114. D Hadzi, A Novak *Trans. Faraday Soc.* **51** 1614 (1955)
115. A Van Doorn ThD, Technischa Hogeschool de Delft, Delft, Netherlands, 1957
116. E N Gur'yanova, E S Isaeva, R R Shifrina, S V Moshchenok, V A Chernoplekova, V A Terent'ev *Zh. Obshch. Khim.* **51** 1639 (1981)
117. V I Lygin, R E Tugushev, I K Kuchkaeva *Zh. Fiz. Khim.* **53** 2923 (1979)
118. M A Babaeva, A A Tsyganenko, V N Filimonov *Kinet. Katal.* **25** 921 (1984)
119. B Tereczki, R Kurth, H P Boehm, in *The Preprints Carbon '80 (International Carbon Conference) Baden-Baden, 1980* p. 218
120. H P Boehm, G Mair, T Stohr, A R de Rincon, B Tereczki *Fuel* **63** 1061 (1984)
121. T Stohr, H P Boehm, in *The Preprints Carbon '86 (International Carbon Conference) Baden-Baden, 1986* p. 354
122. T Stohr, H P Boehm, R Schlögl *Carbon* **29** 707 (1991)
123. H Juntgen *Erdoel Kohle, Ergars, Petrochem.* **39** 546 (1986)
124. A I Loskutov, Candidate Thesis in Chemical Sciences, Lensovet Leningrad Technological Institute, Leningrad, 1968
125. I A Kuzin, A I Loskutov *Zh. Prikl. Khim.* **39** 100 (1966)
126. S A Anurov, T V Kutlaeva, in *Khimiya i Khimicheskaya Tekhnologiya Neorganicheskikh Veshchestv (Sb. Nauch. Tr.)* [The Chemistry and Chemical Technology of Inorganic Substances (Collection of Scientific Reports)] (Moscow: Mendelev Russian Chemical Technological University, 1996) p. 131
127. M A Men'kovskii, V T Yavorskii *Tekhnologiya Sery* (Sulfur Technology) (Moscow: Khimiya, 1985)
128. S A Anurov, T V Kutlaeva, in *Khimiya i Khimicheskaya Tekhnologiya Neorganicheskikh Veshchestv (Sb. Nauch. Tr.)* [The Chemistry and Chemical Technology of Inorganic Substances (Collection of Scientific Reports)] (Moscow: Mendelev Russian Chemical Technological University, 1996) p. 135

The influence of chemical structure on the relaxation properties of heat-resistant aromatic polymers

A A Askadskii

Contents

I. Introduction	677
II. The influence of the chemical structure of heat-resistant polymers on their mechanical workability estimated from relaxation measurements	678
III. Stress relaxation and creep curves	689
IV. Low-temperature relaxation processes and transitions in heat-resistant polymers	695
V. The mechanism of the relaxation processes in heat-resistant polymers	699
VI. Networks, blends, and composites based on heat-resistant polymers	702
VII. Conclusion	705

Abstracts. Data concerning the experimental method for the estimation of the mechanical workability of heat-resistant polymers, based on relaxation measurements, as well as concerning procedures for the fitting of stress relaxation and creep curves with the aid of new memory functions are surveyed. The influence of the chemical structures of various heat-resistant polymers (aromatic polyethers and polyamides, polyimides, polybenzoxazoles, polyoxadiazoles, etc.) on their relaxation behaviour is analysed in detail. Attention is concentrated on the relaxation transitions manifested in the glassy state. The mechanism of the deformation and relaxation in heat-resistant polymers, investigated with the aid of the positron annihilation method, is described. The relaxation behaviour of heat-resistant aromatic polymers down to the temperature of liquid helium is considered. Attention is drawn to the relaxation behaviour. The bibliography includes 167 references.

I. Introduction

Studies on the synthesis and properties of heat-resistant polymers began about 40 years ago and have continued fairly vigorously to the present day. Naturally, in the first investigations attention was concentrated on the limiting strength and deformation properties. However, it soon became evident that, in terms of the strength and deformation on rupture, it is impossible to infer objectively the mechanical workability of the materials. Indeed, a polymeric material is never used when subjected to near breaking loads; even under extreme conditions, the polymers can always realistically operate provided that they are subjected to loads and deformations significantly below the limiting values. Naturally, whatever the load and deformation, relaxation processes develop,

the essential feature of which is that at a constant deformation the stress is not constant, as for ideally elastic materials, but relaxes, i.e. diminishes with time. Accordingly, a creep process develops — an increase in deformation with time. The kinetic data for the relaxation processes depend on temperature, i.e. both are manifested whatever the type of load and not only for a constant deformation and load. These processes in fact determine the true mechanical workability of the polymers. The study of relaxation transitions by the dynamic mechanical analysis is particularly important. Such transitions are associated with the freeing of the molecular mobility of different kinetic units, which play an enormous role in the establishment of the properties of the polymer. The study of the mechanism of these transitions and of the influence on the latter by the chemical structure of the heat-resistant polymer has attracted the attention of investigators.

Evidently the above relaxation processes and transitions are important also for composite materials and blends. Significant attention has been devoted in recent years to the mechanism of the relaxation and deformation processes in heat-resistant polymers subjected to a large deformation. The application of positron diagnostic methods (positron annihilation) directly in the relaxation and deformation process made it possible to obtain new data on the changes in the microporous structure of the material. Many questions are associated with the analysis of the nonlinear mechanical behaviour of heat-resistant polymers when the parameters of the relaxation process depend on time and are not constant. Finally, one of the most interesting phenomena, observed in the study of heat-resistant aromatic polymers, consists in the manifestation by the latter of appreciable deformations at low temperatures, down to the temperature of liquid helium, relaxation processes also developing at these temperatures.

All the above questions are dealt with in the present review.

It is noteworthy that the available data on this field were reviewed in 1975 and 1981.^{1,2} New heat-resistant aromatic polymers as well as new methods for the investigation of their relaxation properties have now appeared. The results of the study of the relaxation properties of these polymers using new methods constitute the main content of the review.

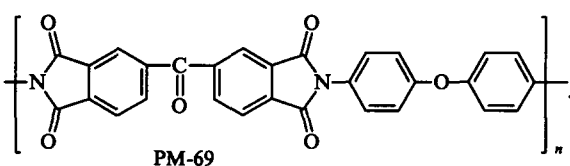
A A Askadskii Laboratory for Polymeric Materials, Nesmeyanov Institute of Organoelement Compounds, Russian Academy of Sciences, ul. Vavilova 28, 117813 Moscow, Russian Federation.
Fax (7-095)135 50 85. Tel. (7-095) 135 93 98
E-mail address: andrey@ineos.ac.ru

Received 10 October 1995

Uspekhi Khimii 65 (8) 733–764 (1996); translated by A K Grzybowski

II. The influence of the chemical structure of heat-resistant polymers on their mechanical workability estimated from relaxation measurements

There are several approaches to the estimation of the mechanical workability of polymeric materials. According to one of them,³ a generalised characteristic which makes it possible to take into account the relaxation processes and the viscoelastic behaviour of polymers, is the temperature dependence of the critical stresses, which limits the region of the mechanical workability of the material. A method has been proposed for the estimation of the critical stresses in solid materials^{3,4} the essential feature is as follows. A series of relaxation curves for different deformations ϵ_0 are plotted at a constant temperature. Fig. 1 presents as an example curves of this kind for the polyimide PM-69



With increase in the deformation ϵ_0 , the stress relaxation curves shift upwards to the region of higher stresses.⁴ However, on further increase in ϵ_0 , the stress relaxation is appreciably accelerated and the relaxation curves begin to shift towards lower stresses (Fig. 1, curve 7). Under these conditions, an appreciable decrease in stress is observed over the entire temperature range for the polyimide only in the initial period of the relaxation process and the decrease in stress intensifies only as ϵ_0 approaches a value close to the yield strength.

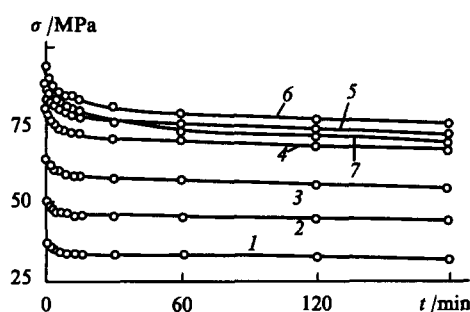


Figure 1. Stress relaxation for polyimide at 220 °C and different initial deformations (%): (1) 2; (2) 3; (3) 4; (4) 6; (5) 8; (6) 10; (7) 12.

After this isochronous dependences of the relaxing stress σ on ϵ_0 are plotted, each of which corresponds to a definite duration of the relaxation process. The isochronous relations as a rule have a maximum, the stress corresponding to the latter being referred to as critical and being designated by σ_c . By carrying out experiments at different temperatures T , one obtains isochronous relations between σ_c and T characterising the possibility of the retention in the material of the maximum stresses σ_c at a specified time t_r .

The isochronous relations for the relaxing stresses in the polyimide PM-69 at different temperatures and for a duration of the stress relaxation of 180 min are presented in Fig. 2. The maximum corresponding to σ_c arises for deformations ϵ_c ranging from 11.2% at 20 °C to 3.3% at 320 °C. This shows that the polyimide is capable of being used over a wide range of deformations without attaining mechanical softening. The isochronous relations for the polyimide have virtually no linear sections, which indicates the nonlinearity of the mechanical properties of the polyimide.

In order to estimate the mechanical workability of the polymeric material from the σ - ϵ_0 isochronous relations obtained

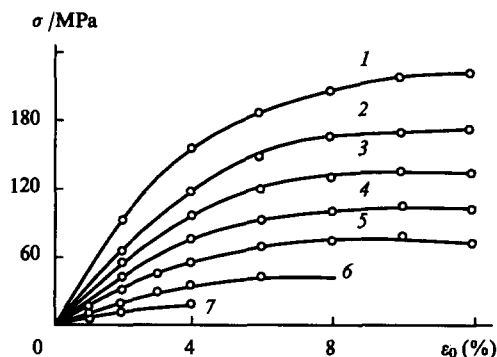
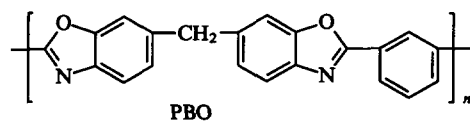


Figure 2. Isochronous variations of the relaxing stress for a process duration of 180 min at different temperatures (°C): (1) 20; (2) 70; (3) 120; (4) 170; (5) 220; (6) 270; (7) 320.

at different temperatures, the temperature dependences of the critical stresses are plotted.

The temperature dependences of the critical stresses for the polyimide PM-69 and polybenzoxazole (PBO) are presented in Fig. 3.



are presented in Fig. 3. The region bounded by these curves and the coordinate axes defines the conditions under which the polymer may be used without softening and without being disrupted (the region of mechanical workability). Having compared the curves in Fig. 3, we may note that the critical stresses and temperatures for the polyimide are higher over the entire temperature range than for PBO.

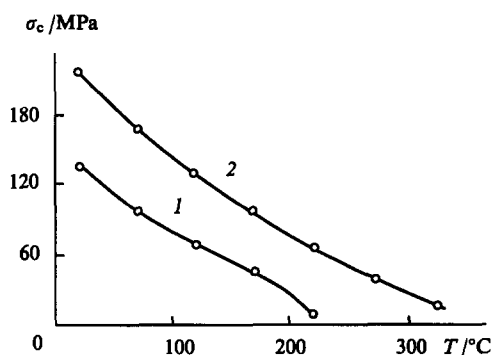


Figure 3. Temperature variations of the critical stresses in PBO (curve 1) and polyimide (curve 2) for a relaxation process duration of 180 min.

In the method for the estimation of mechanical workability,³ the temperature dependences of the critical stresses, obtained for different durations of the relaxation process, are replotted as dependences of the critical stress on the duration of relaxation t_r . The duration of the retention of the critical stress under stress relaxation conditions is a kinetic characteristic of the mechanical workability of the polymer.

The dependences of $\lg t_r$ on $\lg \sigma_c$ for PBO at different temperatures are presented in Fig. 4. Similar dependences have been obtained for the polyimide⁴ and other heat-resistant polymers. In terms of logarithmic coordinates, the $\lg t_r$ - $\lg \sigma_c$ relations for PBO are linear up to 170 °C, whereas at 220 °C a linear section is hardly observed. A linear $\lg t_r$ - $\lg \sigma_c$ relation is as a rule characteristic of other heat-resistant polymers over a very wide temperature range.

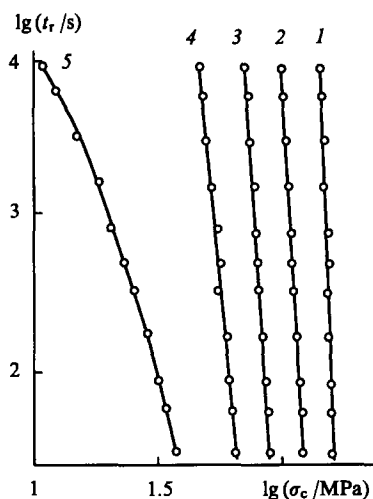


Figure 4. Dependence of the duration of the relaxation process t_r for PBO on the critical stresses at different temperatures (°C): (1) 20; (2) 70; (3) 120; (4) 170; (5) 220.

The slope of this relation, $\tan \alpha$, is a kinetic characteristic of the rate of the relaxation process along the linear sections of the $\lg t_r - \lg \sigma_c$ relations. The temperature dependences of $\tan \alpha$ for PBO and PM-69, obtained from experiments⁴ on the stress relaxation under compression conditions, are presented in Fig. 5. Evidently, the temperature dependences of $\tan \alpha$ are not identical for all the polymers.

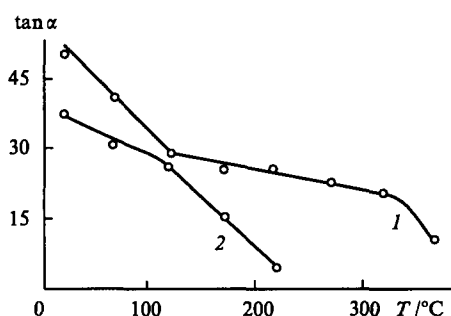


Figure 5. Temperature variation of $\tan \alpha$ for the polyimide PM-69 (curve 1) and PBO (curve 2).

For PBO in the range of comparatively low temperatures, $\tan \alpha$ diminishes somewhat, whilst above 120 °C it increases sharply. In the case of the polyimide, the temperature dependence of $\tan \alpha$ is more pronounced below 120 °C, the rate of relaxation diminishing on further increase in temperature. This shows that in the middle of the temperature range of the glassy state at ~ 120 °C, a transition occurs in both polymers as a result of which the rate of the relaxation processes begins to change. It must be emphasised that the higher the absolute value of $\tan \alpha$ the lower the extent to which the relaxation of critical stresses is manifested. For materials used in rigid constructions, the relaxation of critical stresses must be as small as possible. In terms of this feature, the polyimide is somewhat superior to PBO over the entire temperature range. It is noteworthy that the temperature variation of $\tan \alpha$ for the polyimide consists not of two sections, as has been observed for other heat-resistant polymers, but of three. Along the first section in the region of comparatively low temperatures, $\tan \alpha$ decreases fairly rapidly with increase in temperature; this is followed by a low-slope section, after which $\tan \alpha$ diminishes, which indicates a sharp acceleration of the relaxation near the

softening temperature. Such a dependence is apparently common to heat-resistant polymers; the middle section, where the relaxation of critical stresses is relatively insensitive to temperature, may be of greatest practical importance.

The equation

$$t_r = B\sigma_c^{-\tan \alpha}, \quad (1)$$

where B is a constant for the material, is used to describe the relations between t_r and σ_c .³

The nature of the relations between $\tan \alpha$ and T changes at the temperature of the relaxation transition in the solid glassy state $T_{ss} \approx 120$ °C (Fig. 5) and may be described by the following equation:

$$\tan \alpha = \begin{cases} a + kT & \text{as } T \leq T_{ss} \\ a' + k'T & \text{as } T > T_{ss} \end{cases}, \quad (2)$$

where a , k , a' , and k' are constants.

The nature of the temperature dependences of the parameter B for PBO and the polyimide also changes near 120 °C. This is reflected by the different values of the coefficients in the relations describing the temperature dependence of the parameter B .

$$B = \begin{cases} A_0 \exp \frac{U}{TR} & \text{as } T \leq T_{ss} \\ A'_0 \exp \frac{U'}{TR} & \text{as } T > T_{ss} \end{cases}, \quad (3)$$

where A_0 and A'_0 are pre-exponential factors and U and U' are the activation energies for the relaxation process.

The coefficients in Eqns (2) and (3) are listed in Table 1. Knowing these parameters, it is possible to predict the mechanical behaviour of the polymers over a wide range of temperatures and stresses.

Table 1. The coefficients in Eqns (2) and (3).

Polymer	a	k	a'	k'	$\lg A_0$	$\lg A'_0$	U	U'
PBO	69	-0.109	112	-0.216	-33.9	-163.4	649	1619
PM-69	118	-0.226	45	-0.04	-100.4	-11.4	1264	565

Note. For all the values of the coefficients presented here, σ_c is expressed in MPa, the time t_r in s, and U in kJ mol⁻¹ in calculations by Eqns (2) and (3).

It is noteworthy that the data presented above for PBO and the polyimide have been obtained⁴ from measurements of the relaxation processes under the conditions of uniaxial compression. In another study,⁵ such measurements were carried out under the conditions of uniaxial elongation. One of the differences in the mechanical behaviour of PBO under the conditions of uniaxial compression and elongation is that in the latter case the maxima in the isochronous relations are absent in the temperature range 22–100 °C. The stresses arising in the polymer with the maximum possible deformation are therefore adopted as the critical stresses σ_c (Fig. 6). The acceleration of the relaxation processes at higher temperatures (210–250 °C) for PBO induced the appearance on the isochronous curves of distinct maxima corresponding to the critical stresses.

We may note that it is possible to discover, from the isochronous relations on the one hand, the specified deformation ε_0 capable of maintaining the maximum possible stresses and, on the other, the duration of the retention of the stress of this magnitude in the polymer.

In order to determine the region of the mechanical workability of PBO under extension conditions, we shall consider the temperature dependence of the critical stresses for constant

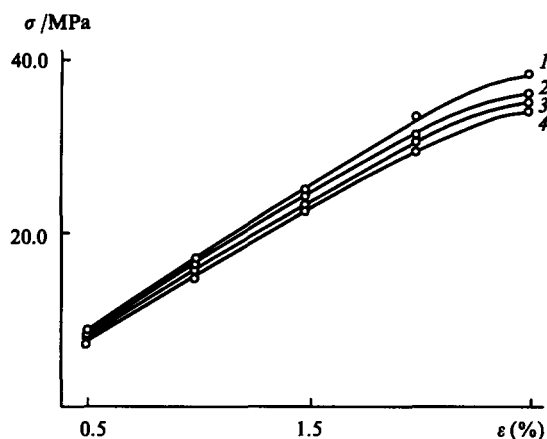


Figure 6. Isochronous dependence of the stress on deformation for PBO at 150 °C and different durations of the relaxation process (min): (1) 1.5; (2) 30; (3) 60; (4) 360.

durations of the relaxation process. If a straight line corresponding to the isothermal state is drawn in Fig. 7, it is possible to determine the function $t_r = f(\sigma_c)$. This relation makes it possible to establish the maximum temperature at which the polymer can withstand a stress of a particular magnitude over a specified time t_r .

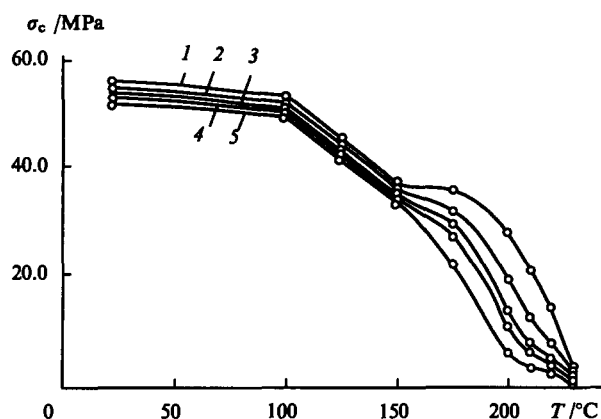


Figure 7. Temperature dependence of the critical stresses for PBO corresponding to different durations of the relaxation process (min): (1) 1.5; (2) 9; (3) 30; (4) 60; (5) 360.

An analytical relation between σ_c and t_r has been obtained⁵ in the form

$$\lg t_r = A[1 - \exp(-B\sigma_c^{-C})], \quad (4)$$

where the parameters A , B , and C depend on temperature. These parameters are listed in Table 2.

Table 2. The parameters A , B , and C in Eqn (4) for PBO.

$T/^\circ\text{C}$	A	B	C
150	4.39	24.1	9.65
175	4.47	5.91	2.63
200	4.56	4.25	2.08
220	5.03	3.24	1.83
230	4.51	1.77	1.41

Note. For all the coefficients quoted, the time t_r is expressed in s and σ in kg cm^{-2} in calculations by Eqn (4).

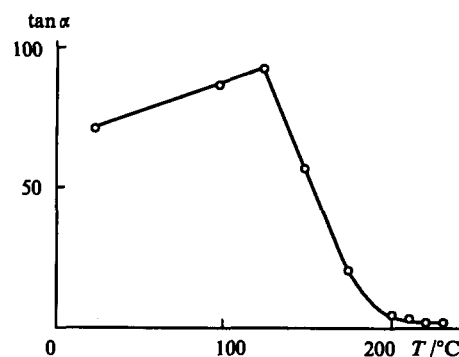
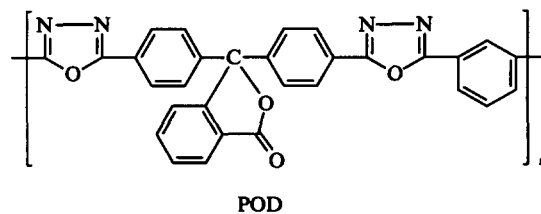


Figure 8. Temperature dependence of $\tan \alpha$ for PBO.

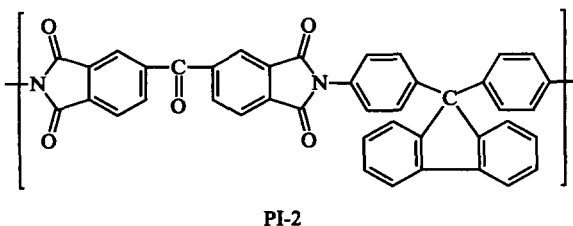
The most important parameter, characterising the kinetics of the relaxation process, is the slope of the linear section of the $\lg t_r - \lg \sigma_c$ relation. For polybenzoxazole, the temperature dependence of the slope $\tan \alpha$ has a characteristic form (Fig. 8); in the range 20–130 °C, $\tan \alpha$ depends only slightly on temperature. Above 130 °C, it diminishes sharply, which indicates the acceleration of the relaxation processes. Such a dependence makes it possible to divide arbitrarily the temperature range of the glassy state into sections, along which the rates of the relaxation processes are different, a sharp acceleration of the relaxation processes being observed in the middle of the temperature range of the glassy state. In this respect, the given polymer behaves similarly to other heat-resistant polymers.

Such substates cannot be observed by the dynamic mechanical analysis, with the aid of which the temperature dependences of the components of the complex modulus of elasticity E^* and of the loss factor $\tan \delta$ are determined at a particular frequency. The relaxation transitions, observed by the dynamic mechanical method, are manifested at temperatures other than those of the transitions observed from the temperature dependence of the parameters of the static stress relaxation. This is evidently associated with the nonlinearity of the mechanical behaviour, which is manifested for the deformations (several %) specified during tests on polymers under static stress relaxation conditions. We shall deal below with this important question whilst analysing the mechanical behaviour of other heat-resistant polymers.

The relaxation properties of two polymers have been studied in detail:⁶ polyoxadiazole (POD)



and the polyimide PI-2



The temperature dependences of the critical stresses σ_c for these polymers are presented in Fig. 9. The difference in the viscoelastic behaviour of polyoxadiazole and the polyimide may be noted.

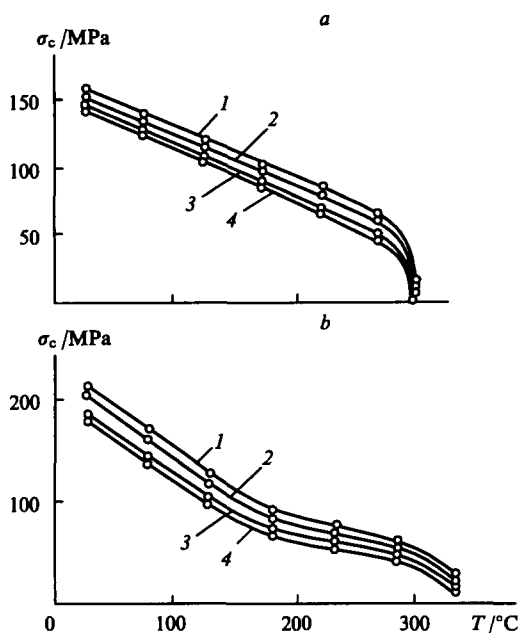


Figure 9. Temperature dependence of σ_c for PBO (a) and the polyimide PI-2 (b) corresponding to different durations of the relaxation process (min): (1) 0.5; (2) 1.5; (3) 15; (4) 60.

At high temperatures, the polyimide PI-2 is superior to POD as regards mechanical stresses which the polymer can withstand without softening for the same temperature and duration of the relaxation process. This is quite natural since PI-2 has a higher glass transition temperature (380 °C compared with 335 °C for POD). However, in the temperature range from 270 to 70 °C, polyoxadiazole is superior as regards critical stresses to PI-2 in the region of comparatively low temperatures.

The temperature dependences of $\tan \alpha$ for the above polymers have been analysed by comparison with other polymers.⁶ These relations are presented in Fig. 10. The temperature dependences of $\tan \alpha$ for polymers of different classes are not the same. The following feature is characteristic of PDO, polyarylate, and a number of other polymers: within a certain range of comparatively low temperatures, $\tan \alpha$ remains almost constant or actually increases, while in the centre of the temperature range, corresponding to the glassy state, it begins to decrease sharply. On further increase in temperature, the sharp decrease in $\tan \alpha$ slows down and a smooth decrease is observed down to the glass transition temperature. This shows that, long before the glass

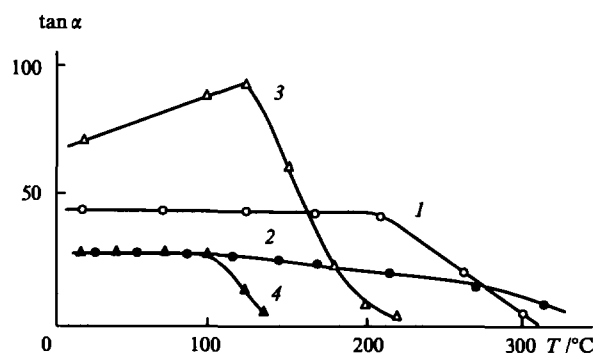


Figure 10. Temperature dependence of $\tan \alpha$ for polyoxadiazole (1), polyimide (2), PBO (3), and the polycarbonate based on bisphenol A (4).

transition temperature is attained, a relaxation transition takes place as a result of which the relaxation processes in the solid glassy state are rapidly accelerated. In essence we are dealing with a solid-solid transition, the latter differing from the γ - and β -transitions, determined by the dynamic mechanical analysis from the temperature variation of the mechanical loss factor. We shall refer to the transition in the solid glassy state described above as the T_{ss} transition. We shall trace the manifestation of the T_{ss} transition for polymers of different structure (Fig. 10).

A weak temperature dependence of $\tan \alpha$ over a wide temperature range is characteristic of polyoxadiazole and the polyimide PI-2. Thus $\tan \alpha$ for polyoxadiazole hardly depends on temperature up to 220 °C and only then begins to decrease appreciably, particularly at 300 °C, i.e. near the glass transition temperature. This trend is even more marked for the polyimide; a sharp decrease in $\tan \alpha$ is observed only at 320 °C, $\tan \alpha$ retaining a virtually constant value over a wide temperature range. In terms of this feature, the above polymers have a significant advantage compared with PBO and polyarylate, because their relaxation properties hardly depend on temperature up to the glass transition temperature.

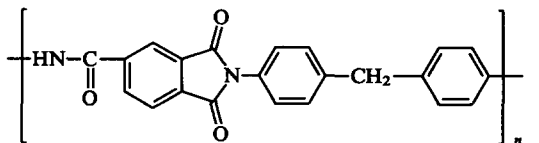
It was noted above that the absolute value of $\tan \alpha$ characterises the rate of relaxation of the critical stresses, i.e. the workability of the polymer under extreme conditions. The higher the value of $\tan \alpha$, the less the extent to which the critical stresses relax. In this respect, PBO is significantly superior to POD and PI-2 in the temperature range 20–120 °C, but the disadvantage is lost as the temperature rises.

Thus heat-resistant aromatic polymers can be divided into two classes taking into account their relaxation properties. The first class includes polymers in which the stress relaxation within a certain range of comparatively low temperatures is manifested to only a slight extent even under extreme conditions (on exposure to critical stresses). However, in the middle of the temperature range of the glassy state observed, the relaxation stress increases sharply, which may lead to the loss of mechanical workability long before the attainment of the glass transition temperature. The second class includes polymers in which the stress relaxation is much more marked (this is indicated by the low values of $\tan \alpha$), but the parameters of the relaxation processes are stable up to the glass transition temperature even under extreme conditions. Such polymers are POD and PI-2.

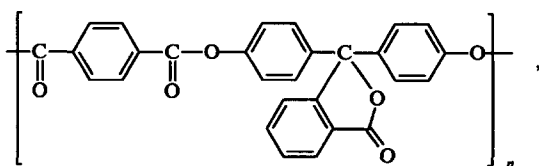
Consequently, if the conditions of use of the polymeric material requires it to retain the stresses established in it, then polymers of the first class must be chosen as such materials. However, these may be usable over a comparatively narrow temperature range. On the other hand, if the polymeric materials must exhibit distinct viscoelastic properties, polymers of the second class must be chosen.

The mechanical behaviour of the following polymers has been investigated:⁷

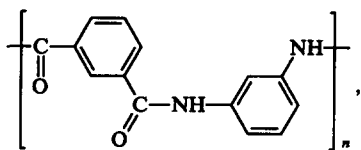
the polyamidoimide



the polyarylate



the aromatic polyamide (Phenylon S-4)



and POD.

In the investigation mentioned above, film specimens were studied under the conditions of uniaxial elongation. For all the heat-resistant systems investigated, a series of relaxation curves were obtained at a constant deformation ϵ_0 over a wide range of variation of the latter in the region of linear and nonlinear viscoelasticity (up to disruptive deformation at different temperatures over a wide range of temperatures of the glassy state of the polymers).

The critical stresses σ_c and their temperature variations were determined from these curves. Such a variation for the polyarylate is presented in Fig. 11, while the temperature variations of $\tan \alpha$

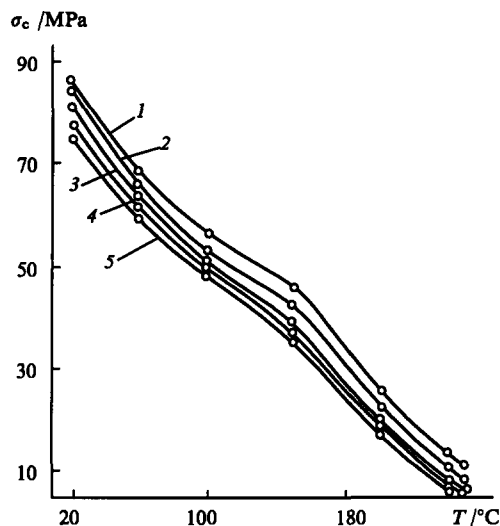


Figure 11. Temperature dependence of the critical stresses in polyarylate for different durations of the relaxation process (min): (1) 1; (2) 3; (3) 10; (4) 30; (5) 60.

for all four polymers are shown in Fig. 12. When account is taken of the temperature variations of $\tan \alpha$, it is possible to divide the temperature range of the glassy state for the systems investigated into sections where the rates of the relaxation processes are

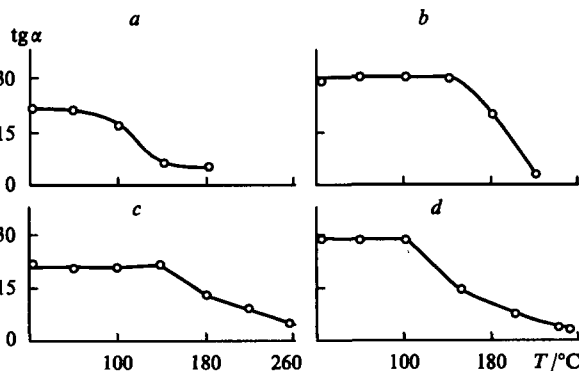


Figure 12. Temperature dependence of $\tan \alpha$ for polyamidoimide (a), POD (b), Phenylon S-4 (c), and polyarylate (d).

different. For all the systems, a sharp acceleration of the relaxation processes is then observed in the middle of the temperature range of the glassy state.

An appreciable expansion of the temperature range in which the parameters of the relaxation behaviour are found to be independent of temperature is characteristic of polyoxadiazole and phenylon S-4 films: compared with polyarylate and polyamidoimide films, the temperature range in which $\tan \alpha$ is constant increases up to 140 °C.

As mentioned above, the critical stress σ_c depends on the time t_r and relaxes in exactly the same way as the usual stresses σ . With increase in process time, the relaxation σ_c slows down and as $t_r \rightarrow \infty$ the relaxation becomes negligible. The corresponding values of σ_c will be referred to (conventionally) as equilibrium critical stresses and will be designated by $\sigma_{c\infty}$.

The temperature dependence of $\sigma_{c\infty}$ confines the region of stresses and temperatures in which there are no rapid relaxation processes, i.e. limits the region of the mechanical workability of the polymers under the conditions of stress relaxation. Fig. 13 presents the temperature variations of $\sigma_{c\infty}$ for four polymers. The influence of the structure of the polymers on their relaxation behaviour may be analysed on the basis of these relations. The first factor to which attention must be drawn is the marked difference between the critical stresses for all the systems in the range of low temperatures. Naturally, the higher the glass transition temperature of the polymer the higher are the temperatures at which finite equilibrium stresses are retained. However, an increase in the heat resistance of the polymer (in particular in the glass transition temperature) promotes a significant increase in the mechanical stresses capable of being retained in the polymeric material under the conditions of stress relaxation and at low temperatures (Fig. 13). At 22 °C the critical equilibrium stress is 53 MPa for the polyamidoimide, 70 MPa for POD, 75 MPa for the polyarylate, and 103 MPa for phenylon S-4.

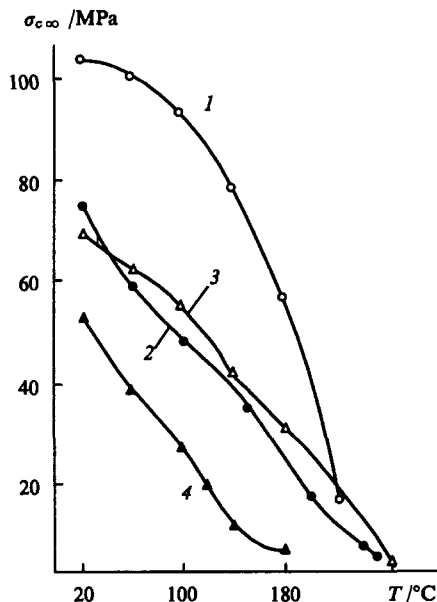


Figure 13. Temperature dependence of the equilibrium critical stresses in Phenylon S-4 (1), polyarylate (2), POD (3) and polyamidoimide (4).

Thus, if the polymeric material is required to retain its workability at high mechanical stresses, then preference must be given to heat-resistant aromatic polymers even in the region of low temperatures.

Extrapolation of the temperature variations of the equilibrium critical stresses to their zero value makes it possible to determine the glass transition temperature of an amorphous

polymer, which is smallest among all the glass transition temperatures determined at finite rates of application of mechanical and thermal influences. This temperature apparently constrains the actual temperature range in which the solid polymer may be used as a constructional material without breaking under the influence of stresses (up to critical stresses).

The crystallisation of polymers is known to increase significantly their strength and resistance to mechanical disruption. For example, phenylon, a crystalline aromatic polyamide, withstands much greater stresses in the temperature range 22–220 °C, without breaking or softening, compared with other heat-resistant systems, although their glass transition temperatures are higher than that of phenylon (Fig. 13). A sharp decrease in the equilibrium critical stresses has been observed for phenylon, although at comparatively low temperatures its mechanical workability is significantly greater. Thus, provided that it is possible, the crystallisation of heat-resistant systems is an effective means of expanding the region of workability towards higher stresses.

It was noted above that the plotting of the temperature variations of the critical stresses is one of the procedures for generalising the results of relaxation measurements. Another method for such generalisation involves the application of the principle of the temperature–time analogy (TTA). According to this principle, one plots master $\lg E_r - \lg(t/a_T)$ relaxation curves, where a_T is the shift factor. Curves are plotted by displacing the $\lg E_r - \lg t$ relaxation curves at different temperatures along the $\lg t$ axis. Fig. 14 presents the initial relaxation curves and the master curve for PBO,⁵ as well as the temperature variation of the shift factor. The latter is a complex function which does not obey the Williams–Landell–Perry equation over the entire temperature range of the glassy state. Each substate has its own $\lg a_T = f(T - T_0)$ relation.

The occurrence of transitions from one substate to another must be taken into account for objective estimation of the mechanical workability of the polymer under the conditions of

stress relaxation. If the polymer is used as a constructional material at temperatures close to the glass transition temperature, it can be subjected to very small loads for a short time. However, when polymeric materials are used under the conditions of variable temperatures, where a transition from one substate to another, involving a sharp acceleration of relaxation processes, is observed, the mechanical workability may be lost at a temperature much lower than the glass transition temperature. Thus the region of stable mechanical workability of PBO is in the temperature range 22–125 °C, which corresponds to a substate in which the rate of relaxation processes is relatively insensitive to temperature.

Fig. 15 presents the initial relaxation curves and the master relaxation curve for PI-2.⁶ The generalised curve for PI-2 is smooth and only a slight decrease in E_r with increase in $\lg t$ is observed.

The temperature variations of the shift factor $\lg a_T$ are well described by the power function

$$\lg a_T = C(T - T_0)^n, \quad (5)$$

where C is a constant for the material, T_0 the reduction temperature, and n the power exponent.

The possibility of describing the dependence of $\lg a_T$ on $T - T_0$ by a power function has been demonstrated also for other heat-resistant polymers.⁸ The quantities C and n depend on the deformation ε . This indicates the nonlinearity of the mechanical behaviour of the polymers. The dependences of C and n on ε are as follows:

$$C = C_0 e^{\gamma \varepsilon}, \quad (6)$$

$$n = a\varepsilon + b, \quad (7)$$

where C_0 , γ , a , and b are constants for the material.

The viscoelastic behaviour of a series of heat-resistant polymers under isothermal stress relaxation conditions was characterised above. The study of the behaviour of heat-resistant

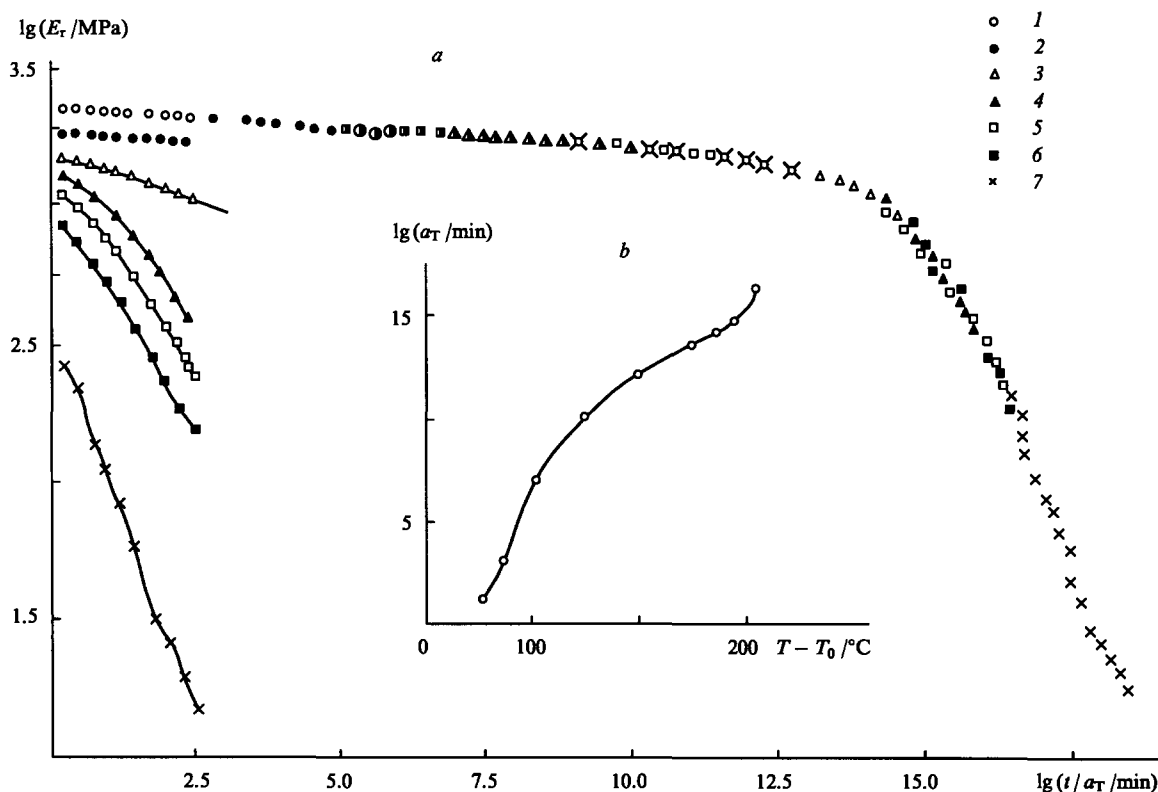


Figure 14. Master curve $\lg E_r - \lg(t/a_T)$ for PBO (a) at $\varepsilon_0 = 1.5\%$ [test temperature (°C): (1) 22; (2) 125; (3) 175; (4) 200; (5) 210; (6) 220; (7) 230; adjusted to a temperature of 22 °C] and temperature dependence of the shift factor a_T (b).

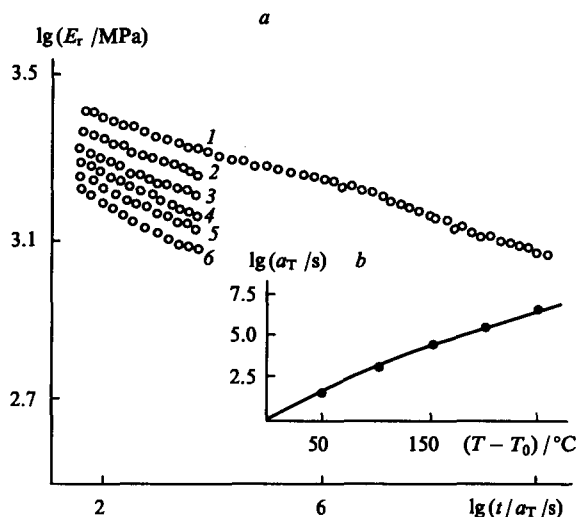


Figure 15. Initial and master relaxation curves (a) and temperature dependence of the shift factor (b) for the polyimide PI-2 at $\varepsilon_0 = 2.8\%$ and different temperatures ($^\circ\text{C}$): (1) 20; (2) 70; (3) 120; (4) 170; (5) 220; (6) 270. Adjusted to a temperature of 20°C .

polymers under creep conditions is also of fundamental interest, because in many cases such polymers are used under precisely such conditions. However, one should note that few investigations of this kind have been made.⁹⁻¹²

The characteristics of the viscoelastic behaviour of heat-resistant bulky polymers under isothermal creep conditions have been investigated in relation to PBO.¹¹ The experiments on creep over the entire range of temperatures and stresses possible for the given polymer made it possible to characterise fully the region of its mechanical workability and to compare it with the similar region under stress relaxation conditions.

Fig. 16 presents, as an example, creep curves obtained at a constant temperature and for different stresses. Evidently the consecutive increase in stress at a constant experimental temperature leads to a steady displacement of the creep curves into the region of greater deformations. The nonmonotonic (accelerated) increase in deformations and in the rate of creep with increase in stress has been observed in the region of high temperatures and stresses.

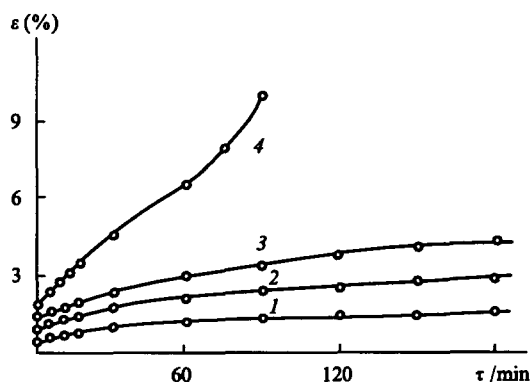


Figure 16. Creep curve at 210°C for different stresses (MPa): (1) 10; (2) 15; (3) 20; (4) 25.

In order to generalise the experimental data on creep, two procedures are used. The first involves the plotting of isothermal dependences of the creep deformation on stress; the critical stresses σ_c , above which the acceleration of the creep process

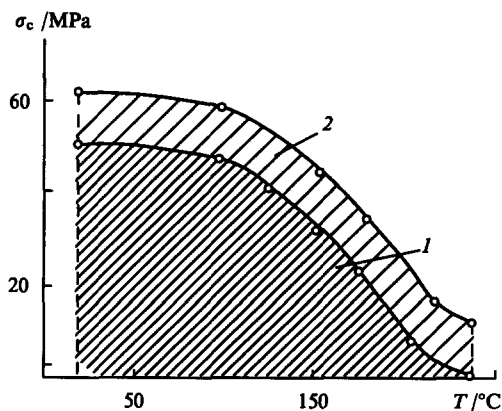
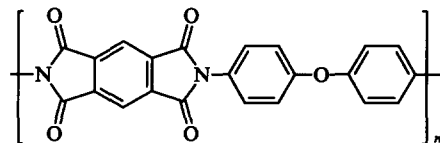


Figure 17. Regions of mechanical workability for PBO under isothermal stress relaxation (region 1) and creep (region 2) conditions.

begins, are determined from the bend in these relations. The $\sigma_c - T$ temperature relation yields a characteristic of the mechanical workability of a heat-resistant material under creep conditions. The regions of workability of PBO under creep and stress relaxation conditions may be compared in Fig. 17. Evidently, the curves confining the region of the workability of PBO are similar, which indicates that the processes underlying the viscoelastic behaviour are common to such cases.

The relaxation properties of a polyimide film based on pyromellitic dianhydride and bis(4-aminophenyl) ether have been investigated in just as much detail under creep conditions.¹²



Apart from the procedure described above, another method has also been used to generalise data on creep, which involves the plotting of master $I = \varepsilon/\sigma$ compliance curves using the principle of the temperature-time analogy. For this purpose, the $\lg I - \lg t$ relations at different temperatures but for constant stresses are shifted along the $\lg t$ axis by an amount $\lg a_T$ until they coincide with the master curve.

The master compliance curves for the polyimide film for different levels of stress are presented in Fig. 18. Evidently, the master compliance curves diverge appreciably, which indicates a nonlinear mechanism of their behaviour. A similar analysis has

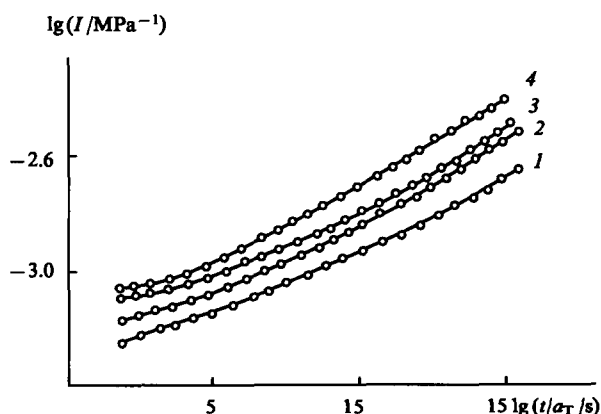
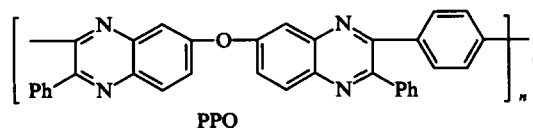


Figure 18. Master compliance curves for a polyimide film corresponding to different stresses (MPa): (1) 50; (2) 70; (3) 90; (4) 110.¹²

been carried out for PBO.¹¹ The relaxation properties of polyphenylquinoxaline (PPQ)

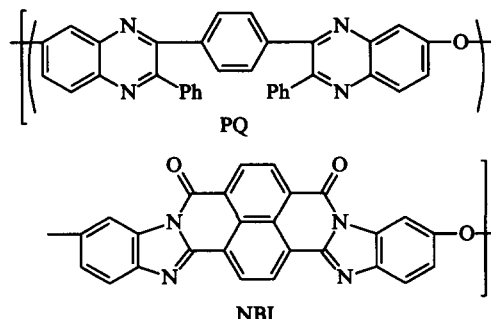


and PI-2 (the chemical structure of the polyimide is shown above) have been investigated as a function of the prehistory of their preparation from solutions.¹³ Pure solvents and their mixtures with a small amount of precipitants were used as solvent media. The addition of precipitants (~2%–5% relative to the solvent) leads to the formation of films with an enhanced strength and a significantly greater deformability. When films are prepared from solution, it is possible to regulate the rate of stress relaxation and creep (Fig. 19). Master compliance curves have been constructed by the horizontal shift along the $\lg t$ axis of compliance curves obtained at a single temperature but for different stresses (Fig. 19a) and for a single stress but at different temperatures (Fig. 19b). In all cases, the compliance of the films obtained from a mixture of the solvent and a precipitant is greater than that of the films obtained from the solvent alone.

Having analysed the relation between three parameters — the intrinsic viscosity $[\eta]$, the Huggins constant K_H , and the second virial coefficient A_2 — Matevosyan et al.¹³ concluded that, judging from the values of A_2 and K_H , the thermodynamic quality of the solvents is impaired after the addition of a small amount of the precipitant. This is quite reasonable. However, judging from the values of $[\eta]$, this property improves. Apparently, the addition of small amounts of the precipitant gives rise to a specific interaction between the polar groups of the polymer and the solvent molecules, which leads to a considerable anisometry of the molecules and to an increase in swelling. As a consequence of this, $[\eta]$ increases, while the mechanical properties of the film obtained from complex solvent media are appreciably superior to those of films obtained from the pure solvent. When large amounts of the precipitant are added, $[\eta]$ diminishes and the properties of the films are markedly impaired. This in fact accounts for the anomalous increase in $[\eta]$.

Thus, by changing the composition of the solvent medium in the preparation of heat-resistant aromatic polymer films from solutions involving the addition to the latter of a small amount of a precipitant, it is possible to regulate within wide limits the relaxation as well as the strength and deformation properties of

the films. This is also indicated by the data obtained in a study¹⁴ of the strength and relaxation properties of films based on the copolymer of phenylquinoxaline (PQ) and naphthoylenebenzimidazole (NBI) having a regular structure.



These systems are characterised by a regular alternation of various heterocyclic fragments, which is in fact responsible for their improved solubility in organic solvents compared with copolymers having an irregular structure and obtained by the interaction of various bis(*o*-phenylenediamines) with 1,4-bis-(phenylglyoxalyl)benzene and the dianhydride of naphthalene-1,4,5,8-tetracarboxylic acid.¹⁵

The high viscous characteristics of the copolymers based on PQ-containing bis(*o*-phenylenediamines) made it possible to obtain films from them. These films have been prepared¹⁴ from two solvent media: *m*-cresol and a 3:1 tetrachloroethane (TCE)–phenol mixture.

The initial and final relaxing stresses[†] for films obtained from the TCE phenol mixture are lower at all temperatures than for films obtained from *m*-cresol (Fig. 20). A significant difference is observed at ~150 °C, where the relaxation processes occur most vigorously. On the one hand, this confirms the existence of a pronounced relaxation transition in the range of temperatures far from the glass transition temperature. On the other hand, this indicates a significant influence of the prehistory of the specimens prepared from the same polymer on their relaxation behaviour.

A similar result has been observed in the analysis of creep data. The specimen prepared from the tetrachloroethane-phenol

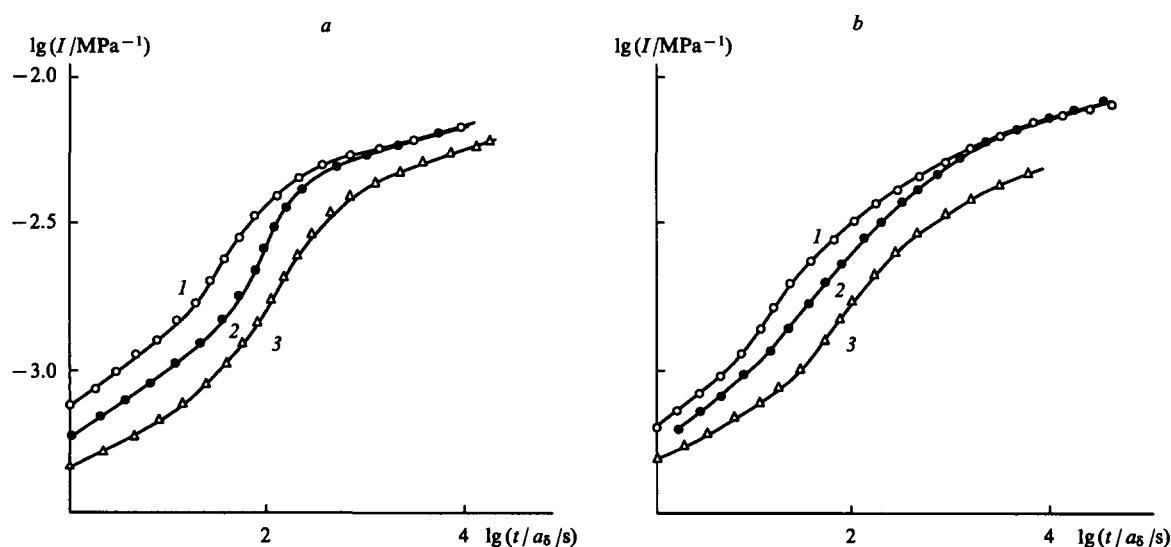


Figure 19. Master compliance curves for polyphenylquinoxaline corresponding to different stresses (*a*) and temperatures (*b*). The films were obtained from chloroform with added 5% of ethanol (1), 2% of toluene (2), and pure chloroform (3).

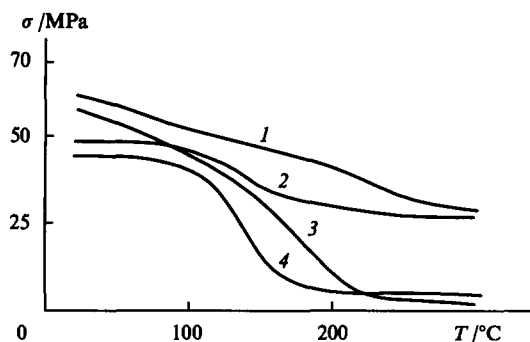


Figure 20. Temperature dependences of the initial (curves 1 and 2) and final (curves 3 and 4) relaxing stresses for copolymer films obtained from *m*-cresol (curves 1 and 3) and from the TCE:phenol = 1:3 mixture (curves 2 and 4). Initial deformation 3%.

mixture has a significantly greater creep deformation at various stresses than the specimen obtained from *m*-cresol. In order to account for these data, the quality of the solvent medium was examined in relation to the polymer. The quality of the solvent may be estimated with the aid of a new solubility criterion introduced by the present author and his coworkers.^{16,17} It has the form

$$\mu \leq 1.374\Phi(\Phi - \sqrt{\Phi^2 - 1 + a}) = \beta, \quad (8)$$

where $\mu = \delta_p^2/\delta_s^2$ (δ_p and δ_s are the solubility parameters of the polymer and the solvent),

$$\Phi = \frac{4(V_p V_s)^{1/3}}{(V_p^{1/3} + V_s^{1/3})^2}, \quad (9)$$

(V_p and V_s are the molar volumes of the repeat unit of the polymer and the solvent respectively), and $a = \gamma_{ps}/\gamma_s$ (γ_{ps} is the interfacial tension at the polymer-solvent boundary and γ_s is the surface tension of the solvent).

The results obtained¹⁴ are presented in Table 3, from which it is seen that in the case of PPQ the quantity μ is much smaller than β for both solvents. Consequently PPQ should dissolve readily in both solvents (which has in fact been observed experimentally), while the presence of PQ units in the copolymer should lead to the appearance or a significant improvement of the solubility when PQ rings are combined with other heterocycles.

Table 3. Solubility criteria for different polymer: solvent pairs.

Solvent	μ	β
PPQ polymer unit		
<i>m</i> -Cresol	0.851	1.100
TCE: phenol	0.897	1.082
PNBI polymer unit		
<i>m</i> -Cresol	0.980	1.080
TCE: phenol	1.080	1.070

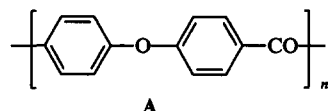
On the other hand, μ for polynaphthoylenebenzimidazole (PNBI) either differs very little from β being smaller, or is greater than the latter; this means that the polymer dissolves very sparingly or is insoluble, which has also been observed experimentally. In the case of a heterounit polymer containing PQ and NBI units, solubility should be observed for different ratios of the PQ and NBI units.

As regards the influence of the quality of the solvent medium, it can be seen from Table 3 that the inequality of the criteria (8) is

enhanced on passing from the TCE-phenol mixture to *m*-cresol. Consequently, on passing from *m*-cresol to the TCE-phenol mixture, the quality of the solvent is somewhat impaired. According to the results of Matevosyan et al.¹³, this should lead to an increase in deformability both under the conditions of continuous uniaxial extension and under creep conditions. In the measurement of the stress relaxation for films obtained from solvents of a poorer thermodynamic quality, the relaxation processes should be more far-reaching, and, other conditions being equal, the decrease in the relaxing stresses should be more pronounced, which has been confirmed experimentally.¹⁴

The results of relaxation measurements carried out under isothermal conditions were examined above. Such experiments require a very long time. However, the method for the determination of the regions of mechanical workability described by the present author³ may prove useful in characterising the mechanical behaviour of polymers over a wide range of temperature and stresses.

The essential feature of the method consists in the measurement of the stresses which arise in the specimen during its thermal expansion whilst retaining a constant deformation imposed initially under the conditions of uniaxial compression. With increase in temperature, the stresses in the specimen increase as a consequence of thermal expansion, and then, as a result of its softening under load, they begin to diminish and become zero on complete softening of the specimen. The temperature dependences of the stress for polyketone A are presented in Fig. 21.¹⁸



The geometrical locus of the maxima on these curves together with the coordinate axes confine the region of stresses and temperatures in which the solid polymeric material is not disrupted and does not soften under the specified conditions of the tests.

Apart from polyketone A, polyketones B and C having the following structure have also been investigated:¹⁸

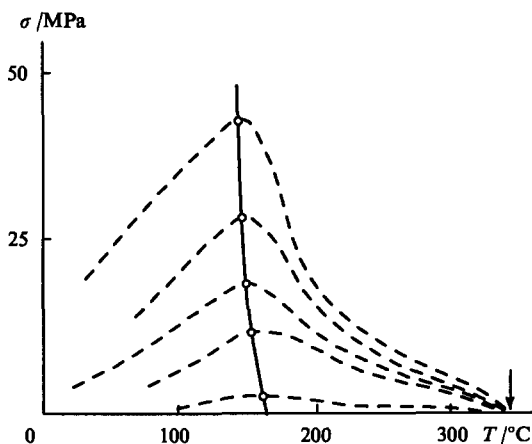
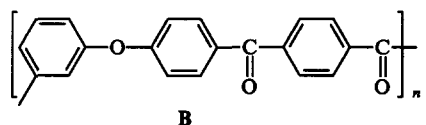
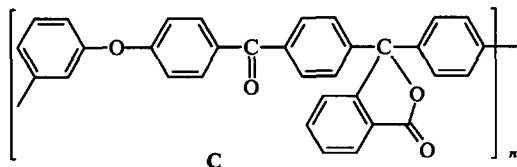


Figure 21. Region of the workability of polyketone A, the arrow indicates the softening temperature, which is close to the melting point.



We shall compare the heat resistances of all three polyketone specimens. For this purpose, we shall combine on one figure the curves confining the regions of the workability of these polymers (Fig. 22). It is seen from the figure that specimens A and B have virtually identical heat resistances and are significantly inferior to specimen C in this respect. All this is valid for the region of comparatively large mechanical stresses. As regards the region of small stresses at high temperatures, preference must be given to the partly crystalline specimens A and B. This is confirmed by the data presented in Fig. 21. For polyketone A, the mechanical stresses appreciably diminish after passing through a maximum, but, with increase in temperature, this decrease slows down and the curves form a 'loop'. The stresses relax very slowly and become zero at a high temperature, close to the melting point. Such relaxation behaviour is characteristic of semi-crystalline polymers.

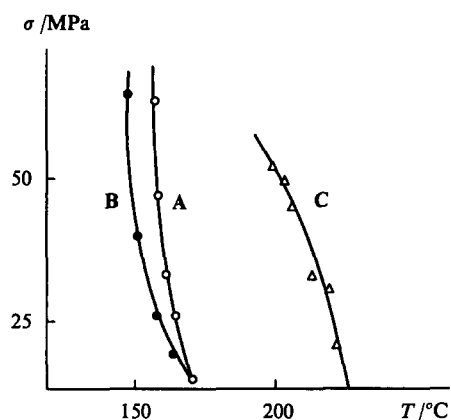
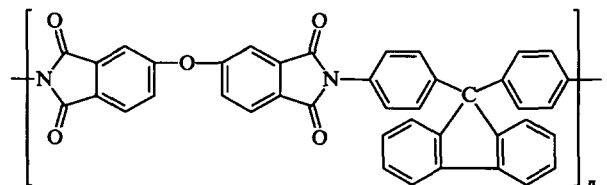


Figure 22. Curves confining the region of the mechanical workability of polyketones A, B, and C.

Thus the crystallisation of aromatic polyketones does not lead to an increase in heat resistance in the region of large mechanical stresses, where the softening of the specimen is associated with the properties of the amorphous component. However, crystallisation increases significantly the temperature at which the specimen softens fully (in the region of low mechanical stresses or in their complete absence).

The influence of the degree of conversion into a monolithic form on the relaxation properties of an aromatic polyimide having the following chemical structure has been studied:¹⁹



The need for such investigations arises because the processing of aromatic heat-resistant polymers by traditional methods (for example by hot pressing) does not always lead to the formation of monolithic specimens, although it is known that even in the nonmonolithic form heat-resistant polymers are capable of withstanding large mechanical loads at elevated temperatures. The following question arises in this connection: to what extent do the

mechanical properties of truly monolithic specimens differ from those of nonmonolithic specimens comprising materials pressed at high temperatures and pressures and consisting of individual grains of the initial powder?

Analysis of the relaxation behaviour of the polyimide¹⁹ showed that the master relaxation curves for specimens with different degrees of conversion into a monolithic form are disposed fairly close to one another. Consequently nonmonolithic specimens of this heat-resistant specimen have good mechanical characteristics close to those for the truly monolithic material.

The mechanical behaviour of heat-resistant aromatic polymers at low temperatures is of special interest. In the early studies,²⁰⁻²⁴ it was already noted that the stability of the heat-resistant polymers is fairly high at low temperatures. A high deformability even at -270°C is characteristic of these polymers.²² Heat-resistant polymers are therefore of significant interest as cold-resistant materials for use in structures associated with cryogenic techniques. However, the characteristic features of the relaxation mechanical behaviour of such polymers at low temperatures have been investigated only recently (one should note that Perepechko and Voloshilov^{23,24} carried out a dynamic mechanical analysis of the polymers).

The stress relaxation and creep processes have been studied in detail for PBO and POD.²⁵ In the study of the stress relaxation and creep in PBO and POD, it was established that the relaxation processes in such polymers are pronounced in the region of low temperatures. Analysis of experimental data on the stress relaxation showed that, over the entire temperature range employed (from 20 to -145°C), a shift of the relaxation curves into the region of higher stresses is observed during the growth of deformation. Under these conditions, the increase in deformation is accompanied by an appreciable acceleration of the relaxation in the initial period. Fig. 23 presents as an example the relaxation curves for PBO at -75°C and for different initial deformations. A decrease in temperature to -145°C leads to a significant retardation of the relaxation processes.

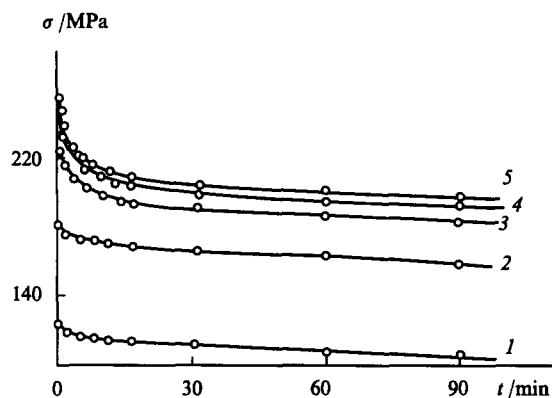


Figure 23. Stress relaxation curves for PBO at -75°C and different initial deformations (%): (1) 4; (2) 6; (3) 8; (4) 9; (5) 10.

A similar pattern in the variation of the relaxation processes is observed in the study of the behaviour of the above polymers under creep conditions. As an example, Fig. 24 presents creep curves for POD at -120°C and for different initial stresses. Evidently, an increase in the applied stress at a constant experimental temperature leads to a steady displacement of the creep curves towards greater deformations. Under these conditions, more marked relaxation processes are observed following an increase in stress. With decrease in temperature, the creep weakens appreciably, although at -50 and -75°C it is manifested quite strikingly.

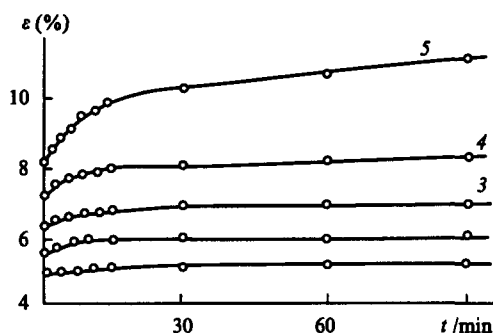


Figure 24. Creep curves for POD at -120°C and different initial stresses (MPa): (1) 120; (2) 180; (3) 220; (4) 260; (5) 290.

It was noted above that, when the temperature is varied in the region of the glassy state, a change in the rate of relaxation processes and the appearance of relaxation transitions are characteristic of heat-resistant polymers. Such transitions have been discovered for heat-resistant polymers in the study of their relaxation properties in the region of raised temperatures. We shall now consider the relaxation transitions at low temperatures.

The temperature dependence of the parameter $\tan \alpha$ for PBO is presented in Fig. 25. Evidently, this relation consists of two sections. In the range from 293 to 203 K, the quantity $\tan \alpha$ changes only slightly. With decrease in temperature in the range from 203 to 128 K, it begins to increase sharply. The greater the value of $\tan \alpha$, the smaller the extent to which the relaxation of stress is manifested. A decrease in temperature leads to a significant alteration of the segmental and group mobilities of macromolecules, which is ultimately reflected in the rate of relaxation.

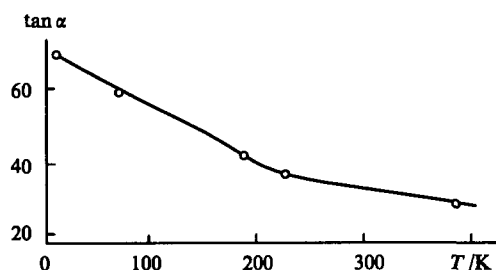


Figure 25. Temperature dependence of $\tan \alpha$ for PBO; deformation 8%.

Thus the temperature dependence of $\tan \alpha$ for PBO makes it possible to observe a relaxation transition at 203 K in the low-temperature region and to identify subregions with different rates of the relaxation processes.

In the range of positive temperatures, a distinct T_{ss} transition is observed for PBO within the glassy state, so that one may conclude that the appearance of several T_{ss} transitions is characteristic of heat-resistant polymers. It must be emphasised yet again that one is dealing with transitions discovered under the conditions of static relaxation measurements, where the degree of deformation is greater by many orders of magnitude than under the conditions of dynamic mechanical analysis, i.e. when the nonlinearity of the mechanical behaviour plays a significant role.

The experiments described above, involving the study of the mechanical behaviour of heat-resistant polymers, were carried out in the range of temperatures from room temperature to the temperature of liquid nitrogen. Subsequently, the temperature range was extended²⁶ down to the temperature of liquid helium. PBO and PI-2 were studied.

The stress-strain curves for PBO and the polyimide PI-2 at different temperatures are presented in Fig. 26. The results showed that the above heat-resistant polymers do not undergo brittle rupture down to 77.3 K. The stress-strain curves have fluidity plateaus, which indicates mechanical softening. The strength properties increase linearly by a factor of ~ 2 – 2.5 on cooling from 300 to 77.3 K.

A quasi-brittle rupture accompanied by a sharp sound, takes place at 4.2 K. In this case, the specimens are deformed up to $\varepsilon = 8\% - 10\%$ for PBO and $\varepsilon = 6\%$ for the polyimide PI-2.

Above 77.3 K, the polymeric specimens did not lose their integrity on deformation up to 25%. At 77.3 K (in liquid nitrogen), the specimens are deformed further up to $\varepsilon \approx 20\%$ beyond the fluidity plateau and then disintegrate, the rupture being accompanied by a sharp sound.

In order to obtain a more objective deformation and rupture picture for heat-resistant polymers at low temperatures, tests have been carried out at different rates of deformation.²⁶ The rate of deformation has little effect on the strength properties of PBO and the polyimide at low temperatures (the changes amount to 10%–20%). The results indicate an anomalous influence of the rate of compression on the strength characteristics of PBO. Thus, on raising the rate of compression from 0.1 to 1 mm min⁻¹, the strength does not increase, as is usually observed, but actually decreases. This is characteristic of all test temperatures. Such an effect can be accounted for only by the different nature of the structural transformations occurring as the rate of compression is changed.

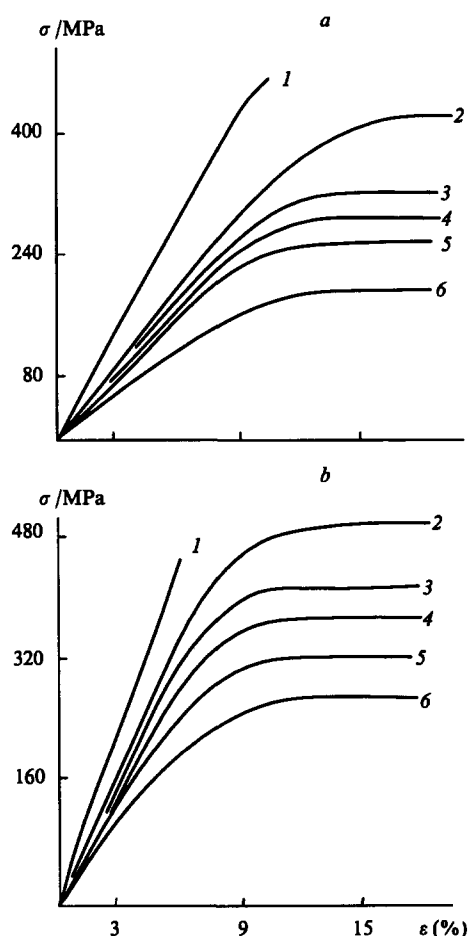
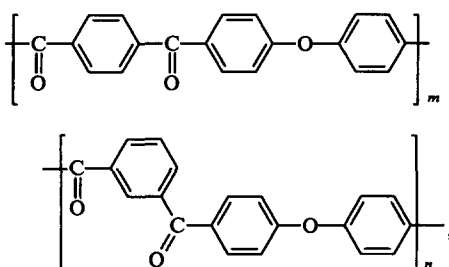


Figure 26. Uniaxial compression curves for PBO (a) and the polyimide PI-2 (b) at different temperatures (K): (1) 4.2; (2) 77.3; (3) 103; (4) 150; (5) 200; (6) 300.

Table 4. The yield stresses for a series of polymers during thermocycling.

Polymer	Temperature range of thermocycling /K	σ_y (MPa) for different numbers of thermocycles												
		0	10	50	100	200	300	400	500	600	700	800	900	1000
MK-M-3	(77–398)±5	88	85	85	85	86	88	87	87	—	—	—	—	—
PBO	(77–473)±5	199	204	200	200	201	200	192	188	—	—	—	—	—
PI-2	(77–473)±5	270	272	271	272	274	273	267	268	263	280	270	268	269
F-4	(77–473)±5	17	15.5	15	16.5	15.4	12.9	—	—	—	—	—	—	—
PKIT	(77–423)±5	191	210	174	189	181	181	192	199	—	—	—	—	—

Another procedure used in the tests for cold resistance consists in the thermocycling of the polymer materials and the study of the influence of such thermocycling on their mechanical properties. This procedure has been used²⁷ for a number of polymers: the polycarbonate MK-M-3,²⁸ the fluoroplastic F-4,[†] the polyimide PI-2, PBO, and the polyketone PKIT having the following chemical structure:



$m:n = 0.7:0.3$.

The resistance of the test polymers to the effects of repeated thermocycles was determined by analysing the state of the PI-2, PBO, and F-4 specimens after heating to 473 ± 5 K, the PK-M-3 specimen after heating to 398 ± 5 K, and the PKIT specimen after heating to 423 K and subsequent rapid cooling with liquid nitrogen.

After a definite number of thermocycles, some of the specimens were used to obtain stress-strain curves at room temperature. The average values of the yield stress σ_y determined from them as a function of the number of thermocycles are presented in Table 4. After 500 thermocycles, the mechanical properties of PK-M-3 hardly changed.

For PBO, the influence of thermocycling up to 300 cycles is also insignificant. On further use, a slight impairment of its properties begins and after the attainment of 500 cycles σ_y diminishes by 5%.

The mechanical properties of the polyimide PI-2 did not change on thermocycling and the polyketone PKIT also showed a high resistance to thermocycling.

In contrast to heat-resistant aromatic polymers, the fluoroplastic (fluoroplast) F-4 exhibited an extremely low resistance to thermocycling. Its yield stress diminishes after only 10 cycles. After 100 cycles, the cracking and disintegration of the specimens begin. It may be that this is associated with the transformation of the crystal structure of the fluoroplastic as a result of cyclic temperature changes.

III. Stress relaxation and creep curves

In the early studies of the stress relaxation and creep processes for heat-resistant aromatic polymers, the Kohlrausch equation

$$\sigma(t) = \sigma_0 \exp\left(-\frac{t}{\tau_r}\right)^k + \sigma_\infty, \quad (10)$$

† Equivalent to Teflon (Translator).

was widely used. Here $\sigma(t)$ is the current (relaxing) stress, σ_0 the initial stress which develops at the moment of the completion of the 'instantaneous' creation of the deformation, τ_r the relaxation time, and σ_∞ the 'equilibrium' stress.

The memory function, leading to this equation, has the form²⁹

$$f(t-\tau) = \frac{E_1}{\tau_r} k \left(\frac{t-\tau}{\tau_r}\right)^{k-1} \exp\left[-\left(\frac{t-\tau}{\tau_r}\right)^k\right], \quad (11)$$

where E_1 is the modulus of elasticity, t the finite duration of relaxation time, τ the current relaxation time, and k a constant for the material.

A similar memory function for the description of the creep process has been used by Bronskii:³⁰

$$\varphi(t-\tau) = I_1 \frac{m}{\theta} \left(\frac{t-\tau}{\theta}\right)^{m-1} \exp\left[-\left(\frac{t-\tau}{\theta}\right)^m\right], \quad (12)$$

where I_1 and m are constants for the material and θ is the retardation time. When this memory function is substituted in the Boltzmann equation, we obtain the following relation for the description of creep under the conditions $\sigma = \sigma_0 = \text{const}$:

$$\varepsilon(t) = \sigma_0 I_\infty \left\{ 1 - \exp\left[-\left(\frac{t}{\theta}\right)^m\right] \right\}. \quad (13)$$

Here $I_\infty = I + I_1$ is the equilibrium compliance, I the 'instantaneous' compliance, and σ_0 the constant stress for which creep is measured.

Eqn (13) describes satisfactorily the creep of polymeric materials. The creep hardly changes after the specimen has been exposed for some time to a constant stress. However, in many instances the so called steady creep section is observed on the creep curves, but the deformation increases with time approximately in accordance with a linear law. To a first approximation, this can be taken into account by formulating the creep memory function in the form

$$\varphi(t-\tau) = I_1 \frac{m}{\theta} \left(\frac{t-\tau}{\theta}\right)^{m-1} \exp\left[-\left(\frac{t-\tau}{\theta}\right)^m\right] + \frac{1}{\eta}, \quad (14)$$

where η is the viscosity of the system.

Having substituted Eqn (14) in the Boltzmann equation, we obtain

$$\varepsilon(t) = \sigma_0 I_\infty \left\{ 1 - \exp\left[-\left(\frac{t}{\theta}\right)^m\right] \right\} + \frac{\sigma_0}{\eta} t, \quad (15)$$

where $\sigma_0 I_\infty = \varepsilon_0$ is the equilibrium deformation.

The most complex question in fitting the Kohlrausch equation to the stress relaxation and creep curves concerns the reliability of the estimation of the parameters of this equation. A detailed description of the procedure for the determination of the parameters of Eqn (15) may be found in the communication of Askadskii et al.³¹

Creep curves for a series of linear and network solid polymer systems based on heat-resistant polymers have been calculated. The parameters of Eqn (15) for such systems are listed in Table 5.

Table 5. Parameters of Eqn (15) for a series of linear and network solid polymer systems.

No.	System	ε_0 (%)	θ /min	m	$10^{-14} \eta$ /P	ξ^a
1	Polyarylate F-2	15.42	1.89	0.37	8.94	0.85
2	Polyphenyl- quinoxaline	13.03	16.81	0.59	6.89	0.62
3	Composition based on 100 parts of F-2 and 50 parts of the epoxy polymer UP-612	8.59	0.097	0.096	6.14	0.16
4	Polyarylate F-2 preheated at 200 °C for 20 h	6.34	3.89	0.093	1.97	0.046
5	Composition based on 100 parts of F-2 and 10 parts of the epoxy polymer UP-612	4.98	0.0084	0.0036	3.77	0.063

^aThe sum of squares of the differences between the calculated and experimental quantities.

The calculated points, obtained with the aid of Eqn (15) and the data in Table 5, fit satisfactorily on the experimental creep curves for different polymers (Fig. 27). The sum of squares of the differences between the calculated and experimental values is in the range from 0.046 to 0.85 (Table 5).

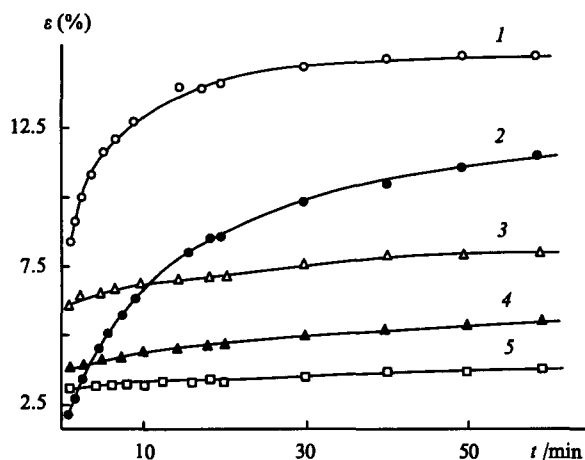


Figure 27. Creep curves for linear and network systems determined for stresses of 400 MPa (curves 1 and 4) 200 MPa (curve 2), 1200 MPa (curve 3), and 600 MPa (curve 5) at 150 °C (curves 1 and 4), 240 °C (curve 2), 20 °C (curve 3), and 90 °C (curve 5).

In further studies of the relaxation properties of heat-resistant polymers, the stress relaxation and creep curves were fitted using new memory functions, proposed by the present author.³² These memory functions are based on the consideration of the change in the entropy of the specimen during stress relaxation. The first memory function was obtained by analysing the kinetics of the interaction of the relaxators and the transition of the 'product' of this interaction to a nonrelaxing material. The term 'relaxator' is applied to various kinetic units, including individual groups of atoms (links, segments), which interact with one another within the limits of their kinetic volumes; undergoing a change in structure during the processes, they are converted into nonrelaxing materials. Here we are dealing not with a chemical interaction but with an interaction of a physical kind. For example, the

formation of microblocks — regions with the densest packing playing the role of physical network nodes — may be assigned to such interactions. During stress relaxation, the microblocks may break down and appear at other sites, which leads ultimately to a decrease in the relaxing stresses. One can consider also other instances of interactions of this kind. For example, the interaction of microdefects within the limits of individual microcavities may lead to their fusion in the course of stress relaxation and to the removal of the stress concentration. Thus, the kinetic units may be of different nature. This leads to the appearance of subsystems which may interact weakly with one another. However, one can apparently identify isotypical units which determine the course of the relaxation process.

If the relaxators considered are isotypical, the memory function assumes the form³²

$$T_1(\tau) = -\frac{S_0}{k_B m_1} \{ [(\alpha - \alpha_0) \ln(\alpha - \alpha_0) + (1 - \alpha + \alpha_0) \ln(1 - \alpha + \alpha_0)]^{-1} - 0.5 \}, \quad (16)$$

where S_0 is the initial entropy of the system (specimen), k_B the Boltzmann constant, $m_1 = m_1^* \int_0^\infty T_1^*(\tau) d\tau$ [here m_1^* is the total number of microheterogeneities in the specimen and $T_1^*(\tau)$ is the time-dependent factor of the memory function, enclosed in braces, in Eqn (19) (see below)], α is the fraction of relaxators relative to the total number of kinetic units in the system, and α_0 the fraction of relaxators which have reacted by the time when the creation of a constant deformation has been completed (the quantity α_0 was assumed³² to be constant for all the materials and equal to 10^{-10}).

The quantity α depends on time and hence the entropy production takes place during the relaxation process i.e. the entropy increases as a consequence of the mixing of the relaxators and nonrelaxators.

Two types of memory functions have been considered.³² As noted above, the first is based on the allowance for the kinetics of the interaction of the relaxators, which is described by an irreversible n th order reaction. In this case, the time variation of α assumes the form

$$\alpha(\tau) = \frac{1}{(1 + k^* \tau / \beta)^\beta}, \quad (17)$$

where $k^* = k c_0^{n-1}$, k is the rate constant for the interaction of the relaxators, c_0 their initial concentration, n the reaction order, and $\beta = (n-1)^{-1}$.

The memory function (16) has a physical significance only when $\alpha(\tau) \geq 0.5$. Here one may note that, if we have a system comprising heterotypical kinetic units where each type introduces a perceptible contribution to the relaxation process, then we have not one but several interaction constants. In this case, the function (16) becomes complicated and this leads formally to the appearance of a spectrum of relaxation times. However, experiments and calculations have shown (see above) that a satisfactory description of the stress relaxation is attained in the presence of only one interaction rate constant.

The second memory function, based on the consideration of the diffusion in the material of the specimen of the nonrelaxators formed, has the form

$$T_2(\tau) = -\frac{S_0}{k_B m_2} \left[\frac{1}{a\tau^\gamma \ln(a\tau^\gamma) + (1 - a\tau^\gamma) \ln(1 - a\tau^\gamma)} + \frac{1}{\ln 2} \right], \quad (18)$$

where $m_2 = m_2^* \int_0^\infty T_2^*(\tau) d\tau$ [here m_2^* is the total number of diffusing microheterogeneities in the specimen and $T_2^*(\tau)$ is the time-dependent factor of the function $T_2(\tau)$ enclosed in square brackets in the equation] and $a\tau^\gamma$ is the fraction of sites occupied at time τ by kinetic units during their random wandering in the lattice³³ (here a is the velocity of an elementary migration step, while γ characterises the influence of constraints).

We shall consider in greater detail the memory functions based on the analysis of the kinetics of the interaction of relaxators and their conversion into a nonrelaxing material.

If this process is considered as an irreversible n th order reaction, then substitution of Eqn (17) in Eqn (16) leads to the following expression:

$$T_1(\tau) = -\frac{S_0}{k_B m_1} \left\{ \left[\frac{1}{(1 + k^* \tau / \beta)^\beta} - \alpha_0 \right] \ln \left[\frac{1}{(1 + k^* \tau / \beta)^\beta} - \alpha_0 \right] + \left[1 - \frac{1}{(1 + k^* \tau / \beta)^\beta} + \alpha_0 \right] \ln \left[1 - \frac{1}{(1 + k^* \tau / \beta)^\beta} + \alpha_0 \right] \right\}^{-1} - 0.5 \quad (19)$$

In a simplified version, when $k^* \tau \ll 1$, the function (19) simplifies to³²

$$T_1(\tau) = -\frac{S_0}{k_B m_1} \{ (k^* \tau + \alpha_0) [\ln(k^* \tau + \alpha_0) - 1] \}^{-1} \quad (20)$$

In order to employ these memory functions in fitting the strain relaxation or creep curves, it is essential to find their integrals for different durations of the relaxation process. Such a procedure has been carried out³⁴ with the aid of a computer for different pairs of the parameters k^* and β and for different process times ranging from 0.5 to 10^5 arbitrary units. The tabulated integrals of the time-dependent factor of the memory function (19) have been published.³⁴

The interaction of the relaxators has been considered^{32, 34} as a unilateral irreversible n th order reaction, i.e. it was assumed that the interacting relaxators are converted into a nonrelaxing material and that this process is irreversible. This factor in fact required the introduction of the condition $\alpha(\tau) \geq 0.5$. In another study,³⁵ the interaction of the relaxators was considered as a reversible bilateral n th order reaction, the kinetic equation for which assumes the form

$$-\frac{d\alpha}{d\tau} = k\alpha^n - k(1 - \alpha)^n \quad (21)$$

Eqn (21) has been formulated subject to the condition that the rate constants for the direct and reverse reactions are the same and equal to k . As a result of this, at the time when the system reaches equilibrium the fractions of the relaxators and nonrelaxators become identical and equal to 0.5.

In order to find the dependence of the degree of conversion α on the time t , the Runge-Kutta numerical method for the automatic selection of the integration step was used.³⁵ The integrals of the time-dependent factor of the function $T_3(\tau)$ were found by computer. This integral has the form $\int_0^t T_3^*(\tau) d\tau$, where

$$T_3^*(\tau) = \{ [(\alpha - \alpha_0) \ln(\alpha - \alpha_0) + (1 - \alpha + \alpha_0) \ln(1 - \alpha + \alpha_0)]^{-1} - 0.5 \} \quad (22)$$

The values of $T_3^*(\tau)$ for different parameters k and β have been published.³⁵

In order to be able to use the functions $T_1(\tau)$, $T_2(\tau)$, and $T_3(\tau)$ to fit the stress relaxation curves, it is essential to substitute them in the Boltzmann equation

$$\sigma(t) = \sigma_0 \left[1 - \int_0^t T_i(\tau) d\tau \right] \quad (23)$$

where σ_0 is the initial stress.

On substituting the functions $T_1(\tau)$, $T_2(\tau)$, and $T_3(\tau)$ in the above equation and going over to the relaxing modulus, we obtain

$$E_r = E_0 \left[1 + \frac{S_0}{k_B m_1} \int_0^t T_1^*(\tau) d\tau \right] \quad (24)$$

$$E_r = E_0 \left[1 + \frac{S_0}{k_B m_2} \int_0^t T_2^*(\tau) d\tau \right] \quad (25)$$

$$E_r = E_0 \left[1 + \frac{S_0}{k_B m_3} \int_0^t T_3^*(\tau) d\tau \right] \quad (26)$$

The time-dependent factors of the functions $T_1^*(\tau)$, $T_2^*(\tau)$, and $T_3^*(\tau)$ are described by Eqns (18) and (19) (the expressions in braces) and Eqn (22) jointly with Eqn (21) respectively.

If Eqns (24)–(26) reproduce satisfactorily the experimental relaxing modulus curves, then the $E_r - \int_0^t T_1^*(\tau) d\tau$, $E_r - \int_0^t T_2^*(\tau) d\tau$, and $E_r - \int_0^t T_3^*(\tau) d\tau$ plots should be linear and their slopes should be respectively $E_0 S_0 / k_B m_1$, $E_0 S_0 / k_B m_2$, and $E_0 S_0 / k_B m_3$; the intercepts on the ordinate axis should be equal to E_0 .

In order to implement the above procedure, it is necessary to have the tabulated integrals $\int_0^t T_1^*(\tau) d\tau$, $\int_0^t T_2^*(\tau) d\tau$, and $\int_0^t T_3^*(\tau) d\tau$. Such data are available.^{34, 35} A computer program, with the aid of which the curves may be fitted has also described in the above communications. Its essential feature is that the values of the above integrals in the form of three sets for different pairs of parameters k^* and β and also α and γ are first introduced into the computer memory. Next each experimental $E_r(t)$ relation is fitted by the linear equation (24), (25), or (26) and the pairs of parameters k^* and β and also α and γ , for which the sum of squares of the deviations of the experimental values of $E_r(t)$ from the calculated ones is a minimum and the correlation coefficient r is a maximum, are chosen automatically.

The stress relaxation curve fitting procedures described above are suitable only in the region of linear mechanical behaviour, where the parameters of the relaxation process are independent of the deformation level. We shall consider briefly the methods for the fitting of relaxation curves also in the nonlinear region of the mechanical behaviour, which is more characteristic of polymers.

At the present time, the commonest method for the fitting of stress relaxation curves in the nonlinear region of mechanical behaviour is one based on Il'yushin's principal cubic theory.³⁶ According to this theory, the relaxation modulus is fitted initially in the linear region of viscoelasticity and then fitting involves the introduction of yet another parameter and the employment of the same memory function but with different parameters—the parameters of the relaxation curves in the nonlinear region. Another procedure involves the employment of equations containing a fractional power exponent of the time, the exponent being assumed to depend on the degree of deformation³⁷ kept constant during the relaxation process. A satisfactory agreement between the experimental and calculated curves is achieved in both cases, but the physical significance of the new parameters introduced is not elucidated.

An approach to the description of the stress relaxation curves in the nonlinear region with the aid of physically well-founded parameters, entering into the memory functions presented above, has been proposed.³⁸ The essential feature of this fitting procedure is as follows: we formulate an expression for the temperature dependence of the rate constant

$$k^* = k_0^* \exp \left(-\frac{\Delta U}{RT} \right),$$

where k_0^* is the pre-exponential factor and ΔU the activation energy for the interaction of the relaxators.

During the deformation of polymers, their free volume is known to increase (in this case, the free volume is understood as the 'empty volume', which represents the difference between the true volume of the polymeric body and the van der Waals volume of the atoms which they occupy in the polymeric body.³⁹ On pronounced deformation of solid (glassy and crystalline) poly-

mers and on transition to the yield stress, the free volume increases to a fairly large value, which facilitates significantly the jumps of kinetic units from one position to another. This actually leads to enforced elasticity, i.e. to enforced softening of the material. It has been postulated³⁸ that the activation energy for the interaction of relaxators decreases with increase in the mechanical stress σ and the rate constant for the interaction of the relaxators was formulated as follows:

$$k^* = k_0^* \exp\left(-\frac{\Delta U_0 - \delta E_r \varepsilon_0}{RT}\right), \quad (27)$$

where E_r is the relaxation modulus, ΔU_0 the initial activation energy for the interaction of the relaxators, $\sigma_r = E_r \varepsilon_0$ the relaxing stress, and δ the fluctuation volume in which the elementary step in the interaction of the relaxators takes place. Then

$$\alpha(\tau) = \left[1 + \frac{\tau k_1^* \exp(\delta E_r \varepsilon_0 / RT)}{\beta}\right]^{-\beta}, \quad (28)$$

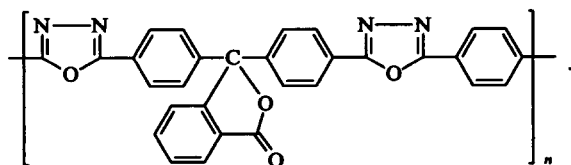
where $k_1^* = k_0^* \exp(-\Delta U / RT)$.

The fitting procedure consists in the determination of the value of δ for which the function $\varphi(\delta)$, representing the sum of squares of the deviations of the experimental values from the calculated ones, is a minimum:

$$\varphi(\delta) = \sum_{i=1}^n (E_{i2} - E_{i1})^2,$$

where n is the number of experimental points and E_{i2} and E_{i1} are the values of the relaxation modulus calculated by Eqn (24) and determined experimentally respectively. The calculations are performed on a computer. The algorithm for the calculations consists in the following steps: the relaxation moduli for the experimental relaxation curves are introduced successively into the computer in order of increasing deformations ε_0 . Each curve introduced, except the first, is compared with the curve which is the average of the relaxation moduli derived from the curves introduced previously. If each modulus for the same relaxation time is smaller for the curve introduced than for the average curve and the arithmetical mean of the relative deviations exceeds 10%, it is assumed that such a curve refers to the nonlinear region of mechanical behaviour. The parameters of the memory function corresponding to the linear region are then calculated for the average curve and the curve referring to the nonlinear region is fitted on their basis.

The relaxation curves for polyoxadiazole have been fitted³⁸ at different temperatures and for different deformations. The results of the calculations are presented in Table 6. In addition to the data in Table 6, we may note that the rate constant k^* for the interaction of the relaxators at both temperatures is 0.1 min^{-1} ; the values of β , $(S_0/k_B m_1) \times 10^4$, and r_1/r_2 [the ratio of the correlation coefficients for the memory functions $T_1(\tau)$ and $T_2(\tau)$ in the nonlinear region of mechanical behaviour] at 21 and 170 °C are respectively 7.2 and 5.2, 0.3 and 0.2, and 0.9991/0.9952 and 0.9981/0.9639. In curve fitting by the method of Askadskii and Valetskii,³⁸ the correlation coefficients at the temperatures indicated are 0.9999 and 0.9997 respectively. Polyoxadiazole having the following structure was investigated:



In terms of absolute magnitude, the correlation coefficients in curve fitting by the above method³⁸ are appreciably greater and much more stable than in fitting by the method of Il'yushin.³⁶

Table 6. The results of the fitting of the parameters of the memory functions for POD in the linear and nonlinear regions of mechanical behaviour.

$\varepsilon(\%)$	$\delta / \text{kJ mol}^{-1} \text{ MPa}^{-1}$	r^a
Temperature 21 °C		
5	0.937	0.9782
5.56	0.840	0.6274
6.12	0.755	0.9915
6.67	0.724	0.9864
Temperature 170 °C		
5.68	0.477	0.9991

^aThe correlation coefficient obtained in fitting by the method of Il'yushin.³⁶

Furthermore, it was noted that the memory function $T_1(\tau)$ fits the relaxation curves for solid polymers in the linear region more satisfactorily than the function $T_2(\tau)$.

We shall consider the results of the study of the relaxation properties of a series of heat-resistant polymers using the memory functions described above. The stress relaxation has been studied in detail⁴⁰ for two polymers—polyoxadiazole and polyimide.

Fig. 28 presents the time variations of the relaxation modulus for POD and polyimide at 20 °C. The data corresponding to the

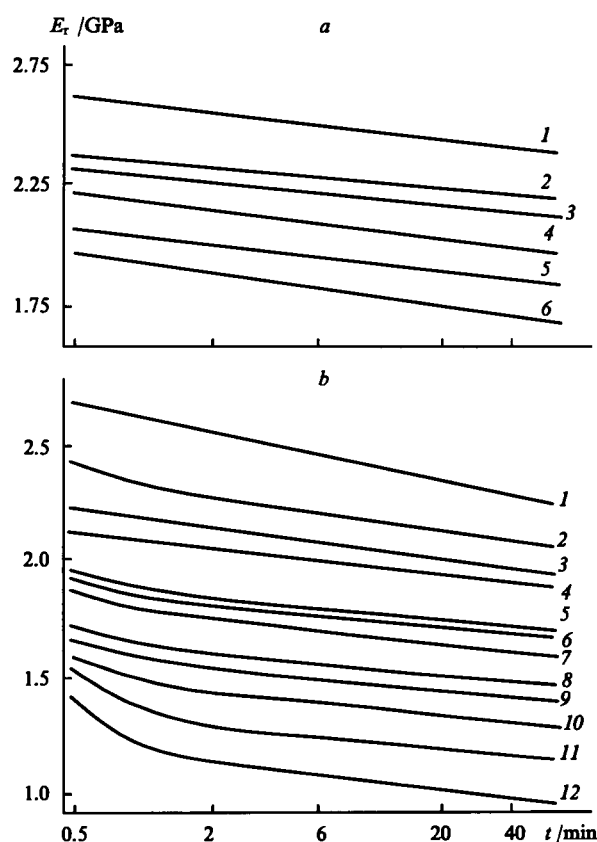


Figure 28. Time variation of the relaxation modulus E_r at 20 °C for polyoxadiazole (a) and polyimide (b) in the linear (curve 1) and nonlinear (curves 2–12) regions.

a: (1) single averaged relation; $\varepsilon(\%)$: (2) 5.56; (3) 6.67; (4) 7.23; (5) 7.78; (6) 8.33;
b: (1) single averaged relation; $\varepsilon(\%)$: (2) 4.46; (3) 5.02; (4) 5.56; (5) 6.82; (6) 8.33; (7) 8.99; (8) 10.23; (9) 11.57; (10) 12.36; (11) 13.95; (12) 15.34.

linear region of mechanical behaviour were averaged and a single relaxation relation was obtained. A deviation from the average relation towards a decrease in E_r is observed at $\varepsilon_0 = 5.56\%$ for polyoxadiazole (Fig. 28a). In the range of ε_0 from 1.7% to 5.0%, linear mechanical behaviour is observed. In terms of this feature, polyoxadiazole is superior to other known polymers, for which the region of nonlinear behaviour begins at significantly smaller deformations.

For polyimide, the deviations from linear mechanical behaviour are observed already at $\varepsilon_0 = 4\%$ (Fig. 28b), while the region of linear mechanical behaviour covers the range of ε_0 from 1.7% to 3.4%, i.e. significantly shorter than the analogous range for polyoxadiazole.

At higher temperatures, the range of deformations in the region of linear behaviour becomes narrower but not uniformly. Fig. 29 presents the temperature variation of the limiting deformation ε_{lim} , for which a linear viscoelastic behaviour is still observed. For polyoxadiazole, ε_{lim} is significantly greater than for polyimide. A common feature of these polymers is a small decrease in ε_{lim} with increase in temperature and also the existence of a region in which ε_{lim} is independent of temperature after which, as the glass transition temperature is approached, ε_{lim} decreases.

The results of the fitting of stress relaxation curves in the linear region of viscoelastic behaviour are presented in Tables 7 and 8.

For the above polymers, the memory function $T_1(\tau)$ 'works' best, its employment leading to a correlation coefficient close to unity, i.e. the experimental and calculated values of E_r are the same. Curve fitting with the aid of the memory function $T_2(\tau)$ leads to a significantly smaller correlation coefficient. Since the memory function $T_1(\tau)$ describes the kinetics of the relaxation of relaxators and their conversion into a nonrelaxing material while the memory function $T_2(\tau)$ describes the kinetics of the diffusion of these kinetic elements in the material, in the given instance the

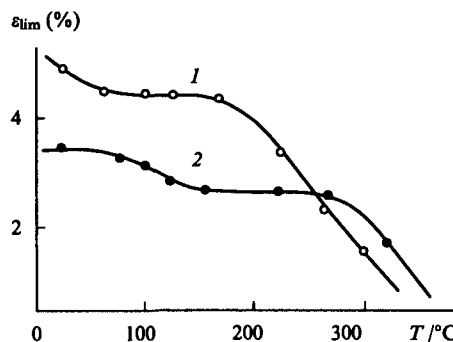


Figure 29. Temperature dependence of the limiting deformation ε_{lim} up to which linear viscoelastic behaviour is retained for PBO (curve 1) and polyimide (curve 2).

rate of the relaxation process is limited by the rate of reaction of the relaxators. The same conclusion has been reached⁴¹ in the analysis of the relaxation behaviour of polybenzoxazole.

The results of the analysis in the form of parameters of the relaxation process and the correlation coefficient r are presented in Tables 9–11.

These data make it possible not only to follow the temperature variation of the parameters of the relaxation processes but also to reach definite conclusions about the changes in the process mechanisms and about the relaxation transitions within the temperature range of the glassy state. We shall therefore consider them in greater detail.

We shall compare the values of all the parameters and the correlation coefficients r when the memory functions $T_1(\tau)$ and $T_3(\tau)$ are used. It can be readily shown (Tables 9 and 10) that all

Table 7. Kinetic parameters of the stress relaxation process for POD determined using the memory functions $T_1(\tau)$ and $T_2(\tau)$.

$T/^{\circ}\text{C}$	Function $T_1(\tau)$						Function $T_2(\tau)$ ^a		
	E_0 /GPa	$\frac{m_1 k_B}{S_0}$	r	β	$10^2 k^*$ /min ⁻¹	n	E_0 /GPa	$\frac{m_2 k_B}{S_0}$	r
20	2.9144	1265	0.9976	0.4	1	3.50	2.6158	428	0.9843
70	2.7504	1660	0.9931	0.8	1	2.25	2.5313	631	0.9627
120	2.6444	1670	0.9996	0.4	1	3.50	2.4394	579	0.9888
170	2.6049	1617	0.9966	0.6	1	2.67	2.3929	601	0.9753
220	2.5228	10945	0.9960	0.2	0.1	6.00	2.2933	613	0.9946
270	2.7575	299728	0.9986	0.2	0.001	6.00	2.2376	175	0.9903
300	1.8074	272	0.9934	0.3	1	4.33	0.9532	52	0.9762

^a At 220 °C, the parameter a was 40.3, whilst at the remaining temperatures it was 0.05; the parameter $\gamma = 0.5$ at all temperatures.

Table 8. Kinetic parameters of the stress relaxation process for polyimide determined using the memory functions $T_1(\tau)$ and $T_2(\tau)$.

$T/^{\circ}\text{C}$	Function $T_1(\tau)$						Function $T_2(\tau)$ ^a		
	E_0 /GPa	$\frac{m_1 k_B}{S_0}$	r	β	$10^2 k^*$ /min ⁻¹	n	E_0 /GPa	$\frac{m_2 k_B}{S_0}$	r
20	3.3259	694	0.9999	0.6	1	2.70	2.6984	223	0.9846
70	3.1109	608	0.9998	0.3	1	4.30	2.4561	172	0.9928
120	3.2992	83	0.9856	0.2	10	6.00	2.5816	249	0.9473
170	2.9620	10375	0.9974	0.2	0.1	6.00	2.6770	583	0.9925
220	3.0221	727	0.9934	0.5	1	3.00	2.4791	233	0.9720
270	2.9483	493	0.9973	0.8	1	2.25	2.1603	149	0.9724
320	4.6264	33	0.9988	0.2	10	6.00	2.1391	60	0.9575

^a At 220 °C, the parameter a was 40.3, whilst at the remaining temperatures it was 0.05; the parameter $\gamma = 0.5$ at all temperatures.

Table 9. Parameters of the memory function $T_1(\tau)$ for PBO.

$T/^\circ\text{C}$	E_0/MPa	$10^2 k^*/\text{min}^{-1}$	n	$\frac{m_1 k_B}{S_0}$	r
22	2574	1	4.33	1533	0.999
100	2336	1	6.00	1975	0.999
125	1986	1	6.00	2118	0.998
150	1829	1	6.00	1517	0.995
175	2007	0.1	6.00	4520	0.998
200	2476	0.1	2.25	2462	0.999
210	2361	1	6.00	286	0.999
220	2522	1	2.25	230	0.996
230	834	1	2.25	222	0.998

Table 10. Parameters of the memory function $T_3(\tau)$ for PBO.

$T/^\circ\text{C}$	E_0/MPa	$10^2 k^*/\text{min}^{-1}$	n	$\frac{m_3 k_B}{S_0}$	r
22	2562	1	4.33	1605	0.999
100	2330	1	6.00	2047	0.999
125	1981	1	6.00	2194	0.998
150	1838	1	6.00	1524	0.995
175	1999	0.1	6.00	3508	0.998
200	2440	0.1	2.25	2513	0.999
210	2361	1	6.00	292	0.999
220	2412	1	2.25	236	0.996
230	796	1	2.25	224	0.998

Table 11. Parameters of the memory function $T_2(\tau)$ for PBO.

$T/^\circ\text{C}$	E_0/MPa	a	$\frac{m_2 k_B}{S_0}$	r
22	2348	0.0403	770	0.989
100	2184	0.0403	826	0.987
125	1857	0.0306	1565	0.997
150	1673	0.0306	1049	0.999
175	1520	0.0209	616	0.997
200	1438	0.0306	137	0.997
210	1304	0.0403	71	0.990
220	1060	0.050	42	0.974
230	332	0.050	38	0.978

Note. The parameter γ was 0.05 at all temperatures.

the parameters and the values of r determined with the aid of the memory functions $T_1(\tau)$ and $T_3(\tau)$ are virtually the same. We may recall that the memory function $T_1(\tau)$ was obtained in the analysis of a unilateral n th order reaction of the relaxators, while the memory function $T_3(\tau)$ was found taking into account the reversible interaction. Consequently, when account is taken of the impossibility of the interconversion of relaxators and non-relaxators, there is no appreciable change in the process kinetics at least for the times t during which the experiment was performed (up to 6 h). This conclusion is in full agreement with the analogous conclusion in another study.³⁵

It is seen from the tables that the correlation coefficients r are very large and approach unity when the memory function $T_1(\tau)$ or $T_3(\tau)$ is employed. When the memory function $T_2(\tau)$ is used (Table 11), the correlation coefficients are significantly lower in the range of comparatively low and high temperatures than the values of r obtained with the aid of the functions $T_1(\tau)$ and $T_3(\tau)$. In the range of moderate temperatures (from 125 to 200 $^\circ\text{C}$), the correlation coefficients are very high when the function $T_2(\tau)$ is

employed [approximately the same as those obtained with the aid of the functions $T_1(\tau)$ and $T_3(\tau)$]. Hence one may conclude (from the standpoints considered) that in the temperature ranges 22–100 $^\circ\text{C}$ and 210–230 $^\circ\text{C}$ the rate-limiting stage of the stress relaxation process is the interaction of the relaxators and their conversion into a nonrelaxing material.

In the temperature range 125–200 $^\circ\text{C}$, the rates of interaction and diffusion of the kinetic units become comparable, as a result of which the relaxation process is described with approximately the same accuracy by all the memory functions. One may note that the correlation coefficients r obtained when the memory function $T_2(\tau)$ is used becomes actually higher than the value of r obtained with the aid of the $T_1(\tau)$ and $T_3(\tau)$ memory functions. This temperature range, in which both mechanisms operate at equal rates, is transitional. The occurrence of a distinct relaxation transition in this temperature range for PBO has been described;⁴ for example, the temperature variation of σ_c for PBO has a characteristic form (Fig. 7): along the first section in the range 22–100 $^\circ\text{C}$, the critical stress depends only slightly on temperature, in the range 100–200 $^\circ\text{C}$, a sharp decrease in σ_c is observed, while in the range 200–230 $^\circ\text{C}$ the decrease becomes less marked.

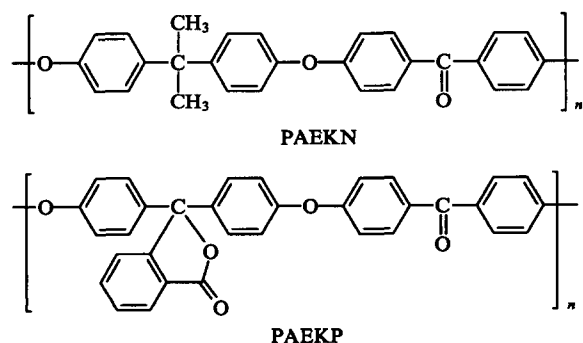
In the region of the T_{gs} transition, the mechanism of the relaxation process changes (Tables 9–11). The rate constant for the interaction of relaxators increases in this range, but the number of relaxators m_1 increases and there is also a sharp increase in the number of kinetic units m_2 participating in the diffusion process. As a result of all these factors, the rates of interaction of the relaxators and of the diffusion of kinetic elements become comparable. With increase in temperature, the rate of interaction of the relaxators increases while the number of relaxators becomes small and changes only slightly with increase in temperature. The same may be said also about the diffusion process.

Another example of the application of the above approach to the analysis of the relaxation behaviour of polymers is the study of the relaxation processes of polyketones subjected to hydrostatic extrusion.⁴²

Numerous aromatic polyketones, including cardo-polyketones, have now been described. These polymers are amorphous or partly crystalline and they are preformed by injection moulding or by pressing. The principal physicomechanical parameters of the polymers are regulated by varying the parameters of the synthesis.⁴³

The possibilities for regulating the structures and properties of these polymers by mechanical treatment have been investigated.^{42,44} One of the promising methods for such treatment is hydrostatic extrusion, which makes it possible to achieve large plastic deformations of the polymers without disruption.

The results of studies of the hydroextrusion process and the structures and physicomechanical properties of the extruded materials — poly(aryl ether ketone) (PAEKN) and poly(aryl ether ketone) based on phenolphthalein (PAEKP) — have been published.⁴²



The polymers were synthesised by nucleophilic substitution of an activated aromatic halogen.

Table 12. Parameters of the memory functions $T_1(\tau)$ and $T_2(\tau)$ obtained in fitting the experimental $\sigma(t)$ relations for PAEKN and PAEKP.

λ	$T/^{\circ}\text{C}$	Function $T_1(\tau)$						Function $T_2(\tau)$					
		r	$10^{-2} \sigma_0$ /MPa	$10^{-2} \sigma_{\infty}$ /MPa	$10^2 k^*$ /min $^{-1}$	n	$\frac{m_1^* k_B}{S_0}$	r	$10^{-2} \sigma_0$ /MPa	$10^{-2} \sigma_{\infty}$ /MPa	$10^2 a$	$10^2 \gamma$	$\frac{m_2^* k_B}{S_0}$
PAEKN													
1.0	—	—	—	—	—	—	—	—	—	—	—	—	—
2.2	20	0.993	2	0.7	0.1	6.0	1.59	0.992	1.5	1.1	6	4	3.50
2.4	20	0.999	2.8	1.3	1.0	6.6	1.888	0.994	2.1	1.4	4	5	3.17
2.8	20	0.991	3.3	1.8	1.0	4.3	2.27	0.981	2.5	1.9	5	5	4.03
2.5	215	0.990	3.4	2.3	0.001	2.25	3.17	0.974	3.1	2.8	4	5	10.25
PAEKP													
1.0	—	0.950	0.70	1.29	1.0	6.0	0.35	0.945	0.62	0.54	5	4	8.19
1.8	170	0.993	1.38	0.79	1.0	4.3	2.34	0.991	1.13	0.90	4	5	5.00
2.6	170	0.965	1.35	0.72	1.0	6.0	2.13	0.981	1.09	0.87	10	3	5.00
1.8	180	0.982	0.78	0.44	10.0	6.0	2.27	0.967	0.66	0.56	4	5	6.55
2.6	180	0.982	1.00	0.66	10.0	3.5	2.28	0.962	0.80	0.66	5	5	5.58
4.0	180	0.997	1.66	0.67	0.01	3.0	1.68	0.988	1.35	1.07	4	5	4.88
6.0	180	0.993	2.14	1.33	10.0	4.3	2.64	0.978	1.69	1.35	5	5	4.95
1.8	190	0.994	1.17	0.57	0.01	1.0	1.93	0.978	0.98	0.81	4	5	5.81
2.6	190	0.929	0.87	0.55	10.0	6.0	2.67	0.933	0.71	0.57	4	5	4.98
6.0	190	0.947	1.64	0.93	100	6.0	2.33	0.907	1.14	0.91	5	5	4.96

Note. For the memory function $T_1(\tau)$, the quantity k^* is proportional to the rate constant for the interaction of the relaxators; the time-dependent factor of the memory functions, $m_1^* k_B / S_0$ and $m_2^* k_B / S_0$, are proportional to the number of microheterogeneities in the specimen.

The stress relaxation curves were determined for the initial and hydroextruded specimens, hydroextrusion being performed up to different degrees of extension λ and at different temperatures T_e (however, always below the glass transition temperature T_g).

For a detailed description of the kinetics of the relaxation processes, the $\sigma(t)$ relations were fitted with the aid of the memory functions $T_1(\tau)$ and $T_2(\tau)$. These memory functions were also used to characterise the relaxation properties of an aromatic polyketone based on isophthalic and terephthalic acids.¹¹ The results of the calculations are presented in Table 12.

Analysis of the parameters of the above memory functions shows that the Boltzmann equation with the memory function $T_1(\tau)$ reproduces best the course of the stress relaxation, although in a number of instances the correlation coefficient r is also fairly close to unity when the memory function $T_2(\tau)$ is used. With increase in λ the quantities σ_0 and σ_∞ as a rule increase. The most significant increase in σ_0 and σ_∞ is characteristic of extruded PAEKN specimens, which have a semi-crystalline structure. The increase in $m_1^* k_B / S_0$, observed for the deformed polymer, indicates an increase in the number of relaxators in the material, the rate of interaction of which in the extruded specimens is on the whole higher than in the cast materials. This is entirely reasonable provided that the relaxators are understood as different kinds of microheterogeneities, which are converted into nonrelaxing structures faster the higher the level of the internal stresses (the latter naturally increases on deformation).

Thus hydroextrusion improves the elastic and relaxation characteristics of aromatic polyketones. In this sense, the most promising material is PAEKN, which is capable of undergoing a structural transition from the amorphous to a partially semi-crystalline modification during the deformation process.

IV. Low-temperature relaxation processes and transitions in heat-resistant polymers

Much attention is devoted nowadays to the analysis of the mechanisms of the relaxation transitions in aromatic polymers, because these transitions influence significantly the macroscopic properties, which depend on the mobility of the structural

elements. Questions of both methodological (methods used for the measurements, the presence of impurities in the monomers analysed) and structural (deliberate alteration of the chemical structure of the repeat unit in the macromolecule for a more clear-cut identification of the mechanisms of the transitions) natures arise in such an analysis. In the dynamic mechanical analysis of heat-resistant aromatic polymers, it is necessary to take into account the fact that many of them contain highly polar groups capable of retaining firmly the solvent with which they are in contact either during synthesis or during the preparation of film materials from solution. The presence of residual solvent promotes the appearance of additional losses and failure to take this into account may lead to erroneous interpretations of the transition mechanism.

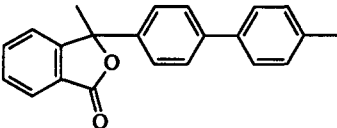
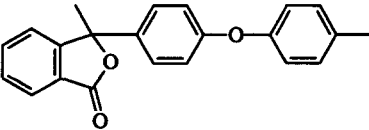
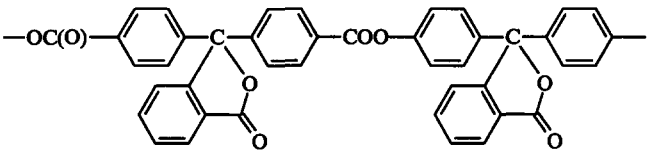
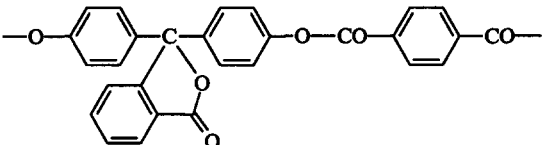
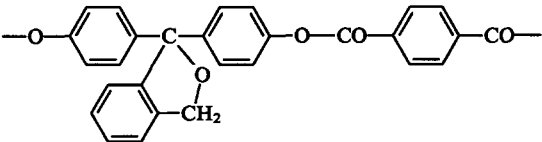
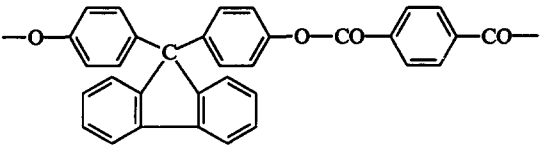
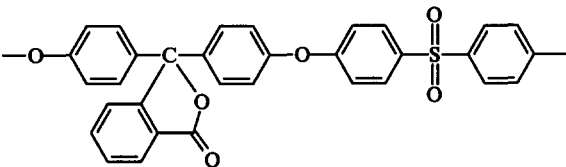
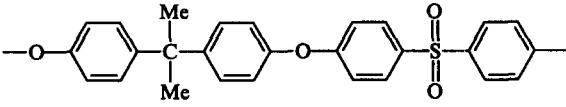
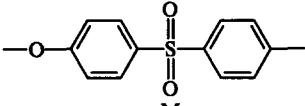
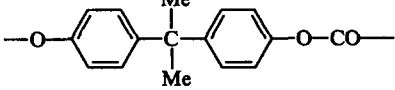
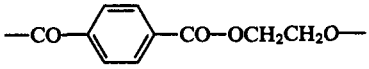
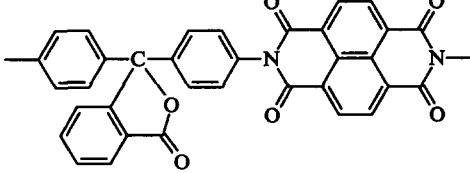
The low-temperature relaxation transitions in heat-resistant polymers have been investigated by numerous workers.^{45–61} Attention was especially concentrated on the temperatures and mechanism of the β -transition. The mechanism of the β -transition has been associated with loss of water in the case of polyimides⁴⁶ and, in another study,⁴⁷ with the interplanar slip in the crystalline regions.

The influence of residual solvents and moisture on the nature of the relaxation transitions has been studied in detail^{51,52} in relation to the polyimide obtained from naphthalene-1,4,5,8-tetracarboxylic acid and anilinephthalein. The diffuse maxima of the loss factor $\tan \delta$, which appear on the plot of temperature variation of $\tan \delta$ for this polyimide, are smoothed out on heat treatment, which eliminates moisture and residual solvents.

It is sometimes assumed that hinge atoms or groups, positioned between aromatic rings, are responsible for the relaxation transitions in aromatic polymers. In order to answer more exactly the questions of the influence of such groups, a specially synthesised series of polyarylenephthalides have been investigated.⁵¹ In this series, polyesters are replaced by polyethers and further by polyphenylenes (Table 13). In other words, particular hinge groups are 'taken away' in succession from the polymers as far as the complete elimination of all types of such groups.

Fig. 30 presents the temperature variations of E' and $\tan \delta$ for a series of such polyheteroarylenes (polymers 1–3 in Table 13).

Table 13. The chemical structures and β -relaxation and glass transition temperatures for a series of heat-treated heat-resistant polymer films.

Compound	Formula of polymer unit	T_{β} /°C ^a	Frequency at T_{β} /Hz	T_g /°C	Frequency at T_g /Hz
1		-96	107	420	79
2		-93	104	270	85
3		-75	104	340	74
4		-67	111	305	75
5		-70	92	255	64
6		-70	88	330	64
7		-88	99	254	76
8		-76	115	177	99
9		-82	87	227	74
10		-70	133	145	103
11		-46	88	90	76
12		-120	119	—	—

^a Temperature at the β -peak maximum.

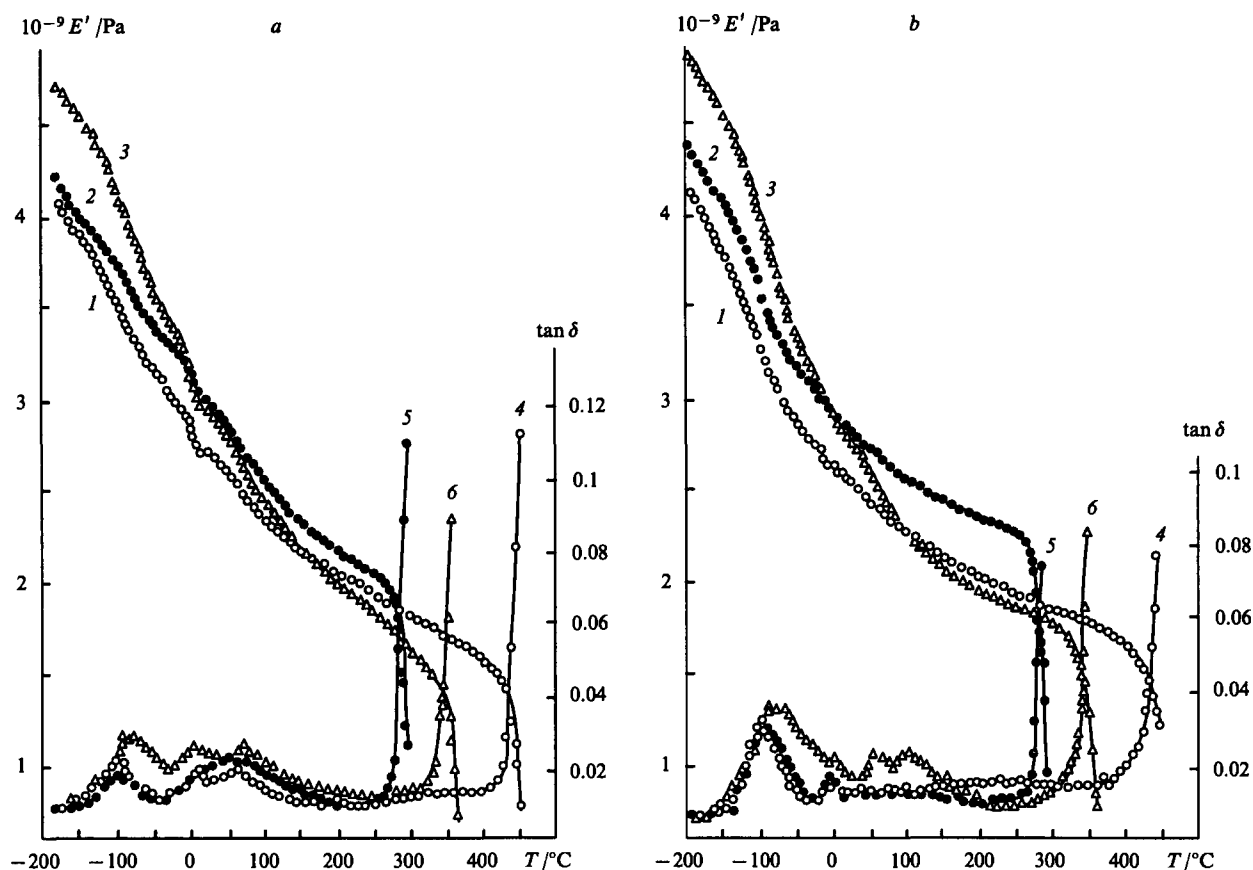


Figure 30. Temperature dependences of E' (curves 1–3) and $\tan \delta$ (curves 4–6) for the initial (a) and heated (b) films of a series of polyheteroarylenes. Number of compounds in Table 13; (1) and (4), 1; (2) and (5) 2; (3) and (6) 3.

Two principal sections may be seen on the temperature variation of the storage modulus E' . The loss factor maxima at -96 , -93 , and -75 °C for the heated polymer 1, 2, and 3 films and at -100 , -95 , and -80 °C for the initial films correspond respectively to a sharp decrease in the storage modulus. Thus, both in the presence and absence of hinge atoms and groups in the main chain, the β -transition is manifested for all the polymers in approximately the same range of temperatures. Consequently, these hinge groups are not responsible for the β -transition.

For all the polymers 1–3, intense loss factor peaks are observed in the intermediate range -30 to 200 °C. Heat treatment at T_g for each polymer smoothes out these peaks to a large extent for polymers 1 and 2, but does not affect appreciably their intensity for polymer 3, containing a highly polar ester group in the main chain. The increase in the polarity of the polymer for the series of bridges between aromatic rings $-$, $-O-$, $-COO-$ leads to an increase in the intensity of the intermediate peaks and influences significantly the relative height of the β -peak. Whereas for the heat-treated polymer 1 and 2 films the increase in the intensity of the β -process is caused mainly by the removal of the residual water and the solvent, for polymer 3, with an ester group in the backbone, this is apparently associated with the redistribution of the intermolecular interactions, limiting the movement of the segments of the chain responsible for the low-temperature transition. Furthermore, the presence of a highly polar ester group in the main chain of polymer 3 intensifies the intermolecular interaction, expanding greatly the region of β -relaxation towards higher temperatures. For polymer 2, containing an ether group in the main chain, this effect is much weaker. The introduction of the polar groups $-O-$ and $-COO-$ into the main chain lowers the glass transition temperature from 420 to 270 and 340 °C for polymers 2 and 3 respectively.

Thus the introduction of ether and ester groups into the main chain of the polymer expands and displaces the maximum of the β -peak towards higher temperatures, on the one hand, but reduces the glass transition temperature, on the other. The contributions of the $-O-$ and $-COO-$ groups to the shift are then directly opposed in relation to the β - and α -transitions.

It may be postulated that the limited rotation of the phenylene groups relative to collinear bonds is responsible for the β -relaxation. However, the observed behaviour cannot be accounted for by this simple mechanism. Indeed, since the hinge atoms and groups facilitate the movement of the phenylene rings (this leads to an increase in the flexibility of the chain and a decrease in T_g), the temperature of the β -transition should be lowered on introduction of the hinge groups. In fact, it increases (Fig. 30 and Table 13).

In the analysis of the mechanism of the β -transition, it is essential to take into account the fact that the polymer in the glassy state consists of a complex system of interacting macromolecules responsible for the existence of regions with different degrees of order and for the relaxation transitions in the main chain of the polymer. From this standpoint, the β -relaxation transition may be accounted for by the freeing of the mobility of large chain segments in the least ordered regions. With increase in temperature, the movement in the more ordered (or more cross-linked as a result of the impurities present in the polymers) regions is freed, such movement being characterised by a higher activation energy necessary to overcome the intermolecular interaction forces. On vitrification, the most ordered and cross-linked segments of the chain are freed. The relative contribution of the polymer chain segments ordered in different ways, taking into account intermolecular interaction, to the overall process involving the freeing of mobility may be determined, for example, in terms of the dynamic loss modulus. The presence of the crystalline

phase in the polymer expands the number of regions with different types of order in chain segments on the assumption that additional energy scattering mechanisms arise. The distribution spectrum of regions with differently ordered chain segments is determined primarily by the specific chemical structure of the chain, the molecular mass distribution, the presence of branches, the impurities present in the polymer, the method of preparation of the test specimen, and also the test conditions.

Even if the hinge atoms and groups are absent from the aromatic polymer, β -relaxation is nevertheless manifested. Hence follows the unambiguous conclusion that these are not the groups responsible for the β -transition.

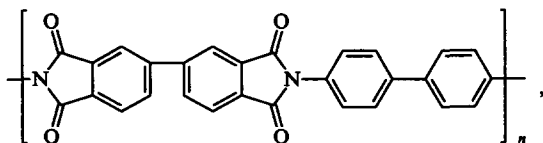
Most investigators associate the mechanism of β -relaxation with the freeing of the molecular mobility of the aromatic rings.⁴⁸⁻⁵⁹ Approximately the same conclusion was reached by Eisenberg and Cavrol.⁶² The results obtained in their study by means of dynamic mechanical analysis indicate that the β -transition in polyimides is associated with the rotation of rigid *p*-phenylene segments and the imide groups around the hinges. However, the authors⁶² believe that the β -transition is manifested by a broad maximum at a positive temperature lower than the glass transition temperature.

The acoustic properties of poly(phenylene sulfide) have been investigated.⁶³ The β -relaxation in this polymer was observed in the temperature range from 193 to 223 K for an amorphous specimen (judging from the temperature variations of the mechanical loss factor). According to the ideas of Lukashov et al.,⁶³ the β -relaxation is associated with the vibrational motion of the phenylene groups in the main chain of the polymer. In the region of α -relaxation, poly(phenylene sulfide) exhibits two transitions due to the freeing of the segmental mobility at two levels of the supermolecular organisation of the polymer. Annealing of the polymer leads to an increase in the transition temperatures in the β -relaxation region.

The influence of flexible alkoxy-groups of different length, located in repeat units of rigid-chain polyesters, on the viscoelastic behaviour of these systems has been investigated.⁶⁴ The results of dynamic mechanical analysis have shown that these polymers have a complex relaxation spectrum. In order to explain the observed spectrum, the authors resort to the concept of different kinds of molecular motion in combination with structural rearrangements on heating. In certain cases, properties typical of liquid-crystal systems were observed.

The relation between the structure and relaxation properties of copolymeric poly(arylene ether ketones) has been investigated.⁶⁵ Different copolymers were synthesised by the partial substitution of hydroquinone in the polyetherketone by resorcinol or hexafluorobisphenol A. In the former case, the dynamic viscosity and the storage modulus for copolymers with a low resorcinol content increased with increase in temperature. The copolymers with a high content of resorcinol residues did not exhibit such unusual behaviour.

The thermal and thermooxidative stabilities, the coefficient of thermal expansion, the glass transition temperature, and the dielectric properties have been investigated in detail for the polyimide having the following structure:⁶⁶

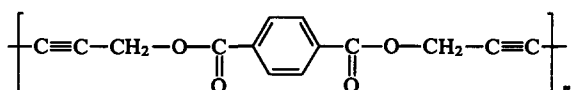
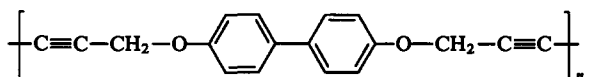
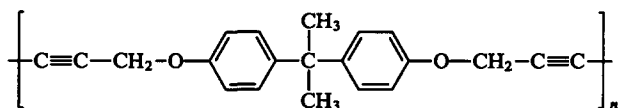


the glass transition temperature of this polymer is $\sim 287^\circ\text{C}$, its coefficient of thermal expansion is $6.98 \times 10^{-6} \text{ K}^{-1}$, and the dielectric constant of films, measured after ageing at 50% humidity, amounts to 2.8–2.9 in the frequency range from 0.1 kHz to 1 MHz.

Relaxation properties have also been investigated for oriented systems (fibres and films) obtained from heat-resistant polymers.

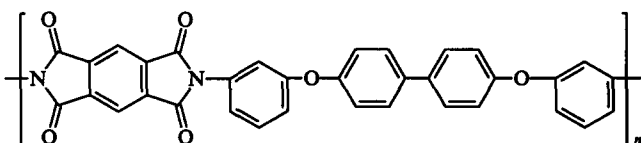
The relation between structure and mechanical properties for highly modular fibres of poly[2,5(6)benzoxazole] has been investigated.⁶⁷ It was found that the modulus of elasticity of the fibres increases from 91 to 133 GPa as a result of treatment of the fibre at 525°C , while the deformation at break falls from 4.3% to 2.0%; the strength of the fibre remains unchanged under these conditions and is above 2.1 GPa. The increase in the modulus is attributed to the development of three-dimensional crystalline order in the fibre.

About all the technologically important fibres are manufactured from linear heat-resistant polymers, such as polyimides, polyoxadiazoles, aromatic polyamides, etc. The modulus and strength of such fibres, measured along the fibre axis, are determined by the strength of the covalent bonds in the chains of these polymers. It has been suggested⁶⁸ that the reduced strength and modulus at right angles to the fibre axis are associated with the weak (compared with chemical bonding) intermolecular interaction involving the formation of hydrogen bonds and dipole–dipole and dispersion interactions arising between the polymer chains in the fibre. An increase in compressive strength in the fibres may be achieved by cross-linking the macromolecules. The authors^{68,69} therefore prepared and characterised three linear polymers with two conjugated triple bonds in each repeat unit:



The third polymer — poly(dipropargyl terephthalate) — crystallises in the solid state on precipitation with water. The crystallisation is in this case the initial stage of the cross-linking process. Thus self-cross-linking fibres may be obtained by a wet method.

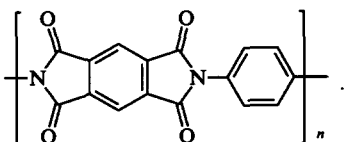
The dynamic mechanical properties and relaxation transitions of the new thermoplastic polyimide



have been studied.⁷⁰ The polyimide films were investigated directly after casting and after zone stretching in order to increase the degree of orientation.⁷¹⁻⁷³ The zone stretching of the polyimide leads to an increase in the modulus of elasticity over the entire temperature range investigated and is accompanied by an increase in the glass transition temperature and a decrease in the mechanical loss factor.⁷⁰

The birefringence of fibres based on heat-resistant polymers has been studied.⁷⁴⁻⁷⁹ A critical analysis of the results has been published.⁸⁰

The influence of the thickness of the coating on the orientation of the chains and the order in polyimides has been investigated.⁸¹ It was found by X-ray diffraction that substrate prepared polyimide films are oriented in such a way that the polyimide chains are preferentially arranged within the plane of the film. The degree of orientation then increases with increase in the content of the rigid polyimide, for example of the kind:



With increase in the thickness of the film, the average degree of orientation falls and the coefficient of volume expansion increases.

The strength and relaxation properties under stretching and compression conditions have been investigated for fibres based on poly-*p*-phenylenebenzobisoxazole and poly-*p*-phenyleneterephthalamide.⁸²

V. The mechanism of the relaxation processes in heat-resistant polymers

The question of the mechanism of the relaxation processes arising on deformation of glassy polymers has attracted constant attention of investigators. The question of the possibility of comparatively large deformations in heat-resistant aromatic polymers has acquired particular interest, such a possibility of existing down to the temperature of liquid helium.

The mechanism of the relaxation process involving the viscoelastic strain recovery of a polyimide film after its preliminary deformation up to a specified elongation has been studied.⁸³ The viscoelastic strain recovery curves (the time variations of the deformation after the specimen has been freed) were fitted with the aid of the memory functions $T_1(\tau)$ and $T_2(\tau)$.

The Boltzmann equation for the viscoelastic strain recovery curves assumes the following form:

$$\varepsilon(t) = \varepsilon_0 \left[1 - \int_0^t T_1(\tau) d\tau \right] \quad (29)$$

or

$$\varepsilon(t) = \varepsilon_0 \left[1 - \int_0^t T_2(\tau) d\tau \right], \quad (30)$$

where ε_0 is the initial deformation at which the load is removed and the shrinking process begins at a constant temperature.

The experiments were performed⁸³ for a commercial PM polyimide film, which was stretched under creep conditions up to the deformation $\varepsilon_0 = 10\%$. The load was then removed and the contraction of the specimen was measured.

The fitting of the strain recovery curves by Eqns (29) and (30) demonstrated⁸³ that these curves are best fitted with the aid of the memory function $T_1(\tau)$ (Table 14). Consequently, from the standpoints considered, the relaxation process in the shrinkage of the specimen after loading is limited by the stage involving the interaction of the relaxators. The rate constant is then small (Table 14). When a load is applied at an elevated temperature, the quantity $k_B m^*/S_0$ is significantly greater than at room temperature.

If the mechanism of the relaxation processes described above is indeed associated with the formation and redistribution of microheterogeneities in the polymeric material, then analysis of positron annihilation in the relaxing specimen may provide an experimental confirmation of this mechanism, because it is precisely with the aid of this method that one can estimate the volumes and nature of the microcavities having dimensions comparable to or somewhat exceeding those of the repeat units of the heat-resistant polymers. The authors⁸³ therefore measured the annihilation spectra in both the initial polyimide specimen and in the prestretched specimen and also during its contraction after the removal of the load.

The measurements showed that the positron annihilation process in the polyimide differs significantly from that usually observed in the majority of polymers. The annihilation spectrum in the polymers is characterised by the presence, as a rule, of three or four components with average lifetimes from 10 ps to 4 ns.⁸⁴⁻⁸⁶ However, a different structure of the spectrum was observed for the polyimide, which was found to have only one, and short-lived, component with $\tau_0 = 0.388$ ns (Fig. 31). The time distribution can be fitted satisfactorily by a single decay line, the slope of which defines the average lifetime.

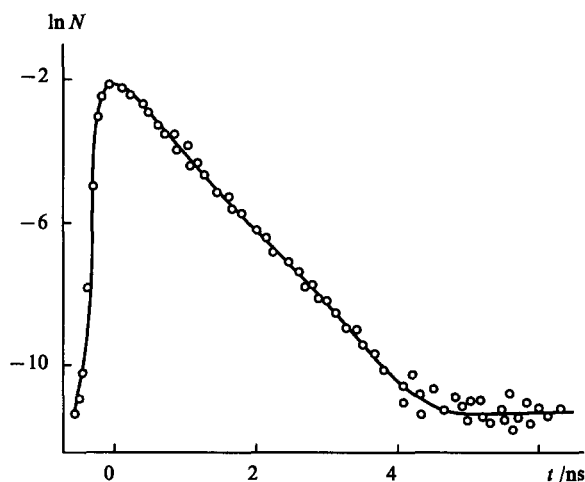


Figure 31. Spectrum of positron lifetimes in the initial polyimide film; N = number of counts in the channel.

The lifetime and the structure of the spectrum suggest that the annihilation in the polyimide occur in the positron state without the formation of a positronium atom of the kind characteristic of metals and semiconductors with a high mobility of electrons and an ordered crystal structure.

In this sense, the polyimide has an electronic structure unique for polymers, characterised by a high degree of uniformity of the electron density function.

In relation to interaction with positrons, the microstructure of the initial (undeformed) polyimide film is defect-free. However,

Table 14. Parameters of the memory functions $T_1(\tau)$ and $T_2(\tau)$ for the polyimide PM film at preliminary load application temperatures of 20 and 200 °C.

$T/^\circ\text{C}$	Function $T_1(\tau)^a$					Function $T_2(\tau)^b$				
	r	$\varepsilon(\%)$	$\frac{m_1 k_B}{S_0} / \text{s}$	$\frac{m_1^* k_B}{S_0}$	β	r	$\varepsilon(\%)$	$\frac{m_2 k_B}{S_0} / \text{s}$	$\frac{m_2^* k_B}{S_0}$	a
20	0.984	26.648	22.440	1.045	0.7	0.848	6.771	118.045	1.266	0.0306
200	0.980	20.559	31.197	1.388	0.3	0.887	8.027	92.598	2.652	0.05

^a k^* was 0.1 s at both temperatures. ^b $\gamma = 0.5$ at both temperatures.

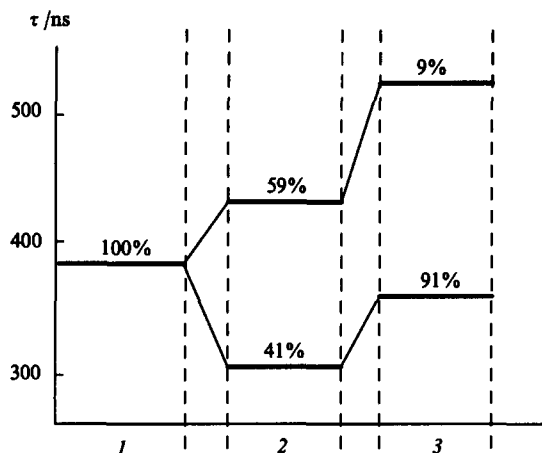


Figure 32. The lifetimes and intensities of the components in the spectra with polyimide the initial polyimide specimen (1) and polyimide specimens subjected to preliminary extension, measured for strain recovery durations of 1 h (2) and 24 h (3).

after deformation, the time aspects change (Fig. 32 and Table 15). Instead of the one component in the deformed specimen, two components are observed: with shorter (τ_1) and longer (τ_2) lifetimes. After strain recovery for 24 h at room temperature, an increase in the lifetimes of both components and a decrease in the intensity of the longer-lived one are observed. The nature of the changes occurring suggest that a rearrangement of the supermolecular structure of the polyimide occurs on deformation: the intermolecular bonds are broken and microdefects — free volumes sufficient to accommodate a positron — are formed. For the long-lived component, the time τ_2 should reflect in this case the changes in the average size, whilst the annihilation intensity I_2 should reflect the concentration of such defects. Similar changes in the spectra have been observed on formation and annealing of defects in metals and semiconductors. These changes are usually analysed with the aid of the positron capture model.⁸⁷ The model reflects qualitatively well changes in the time spectra of the polyimide during its deformation. The decrease in the lifetime of the 'short' component, associated with the annihilation in the defect-free part of the polymer, is due to the high rate of capture in the deformed specimen. After the partial contraction during the strain recovery process, the concentration of the defects falls and the lifetime τ_1 approaches that characteristic of the initial polymer. The intensity I_2 for the long-lived component, formed as a consequence of the annihilation of positrons on defects, also decreases under these conditions. The quantities calculated from the rate of capture spectra for the deformed and partially relaxed specimens are presented in Table 15. The increase in the lifetime τ_2 can be accounted for by the coagulation (the combination of small defects into larger ones) during strain recovery or by the rapid

relaxation of the small pores and hence by the increase in the average capture radius.

The concentration of microdefects after partial relaxation falls by a factor greater than 7, whereupon the free volume induced by deformation diminishes, by a factor of 4.⁸³ The values obtained show that both processes take place — the fusion of the microdefects and the relaxation of the smallest defects — although the intensity of the latter is apparently greater.

Thus a one component spectrum is characteristic of the initial polyimide film. In the deformed specimen, at least two components are observed in the time spectra and are associated with the annihilation of positrons in the free state and the state corresponding to trapping in micropores, which arise on extension. During the relaxation of the structure, the lifetime increases and the intensity of the annihilation of the defective component diminishes. The results obtained with the aid of the positron capture model describe satisfactorily the observed changes in the time distribution and suggest that the structure of the free volume changes on relaxation not only as a result of the rapid recombination of the smallest pores but also as a consequence of the recombination of small pores with formation of long-lived large microcavities.

On the basis of the analysis, the following model of the annihilation of positrons and the mechanism of the relaxation process associated with the latter have been proposed:⁸³ before deformation, all the positrons are annihilated in the state corresponding to their enclosure in small traps with a binding energy slightly exceeding the thermal energy, while after deformation fairly extended regions appear (compared with the positron diffusion length) in which the concentration of small traps (~ 10 nm in size) appreciably diminishes with the simultaneous appearance of loosened regions with deep positron capture centres, in which the positron lifetimes are longer; relaxation takes place in such a way that the pores formed on deformation recombine and in addition increase in size as a result of fusion.

Consequently, having measured the lifetime of the positrons, it is possible to obtain data on the changes in the structure of the unoccupied volume occurring after the deformation of the polyimide film. However, in order to interpret the information obtained, it is necessary to study in detail the nature of the components of the complex annihilation time spectrum characteristic of the nonequilibrium state of the polymer. The problem formulated could not be solved with the aid of one of the positron methods^{84,85} and for this reason a combined study has been carried out⁸⁸ of the annihilation of positrons in the deformed polyimide by measuring the lifetime of the positrons and the angular correlation of the annihilation emission.

Two series of experiments have been described.⁸⁸ In the first series, the polyimide film was subjected to uniaxial extension deformation by 20%. The film was then freed from the clamps and was allowed to relax freely. The lifetime spectra were recorded on a freely relaxing film at 1.5 h intervals. The parameters of the angular correlations were determined at 1 h intervals for 24 h.

In the second series of experiments, the stress relaxation process was investigated for the deformation $\varepsilon_0 = 20\%$. The characteristics of the angular correlations were determined for a film with fixed ends. The measurements were performed with the aid of a device which made it possible to deform specimens directly in the measuring chamber. At the same time the stress relaxation curves themselves (time variation of the stress) were recorded together with the strain recovery curves (time variation of the deformation).

The positron lifetimes obtained from the spectra are presented in Table 16 and in Fig. 33. In the structure of the time spectrum, fitted by three components, changes were observed, after deformation, in the annihilation characteristics, which then gradually relaxed to those characteristic of the initial polyimide specimen.

Three components were differentiated: the lifetime of the first short-lived (170–220 ps) component depended greatly on the relaxation time; the lifetime of the second component

Table 15. Characteristics of the positron annihilation spectra for polyimide film specimens.

Duration of strain recovery at 20 °C/h	τ_0 /ps	τ_1 /ps	τ_2 /ps	I_2 (%)	Rate of capture $10^{-9}k/s^{-1}$
Initial specimen					
—	385±5	—	—	—	—
Deformed specimen					
1	—	294±30	440±17	59±5	0.60±0.15
24	—	361±10	531±30	9±2	0.12±0.05

Table 16. Variation of the annihilation characteristics of a polyimide film as a function of the duration of relaxation after 20% deformation.

Duration of relaxation /s	Lifetime			Angular correlation			
	τ_p /ps	τ_1 /ps	I_2 (%)	FWHM /mrad	Γ_1 /mrad	θ_p /mrad	I_p (%)
Unannealed specimen							
0	365	201	74.3	10.44	10.49	7.14	28.2
1	360	176	73.6	10.77	—	—	—
5	368	208	77.2	10.60	—	—	—
24	362	205	73.0	10.48	10.64	7.14	34.7
240	364	200	74.1	10.43	10.72	6.95	32.3
Annealed specimen							
0	368	220	76.3	—	—	—	—

Note. τ_p , τ_1 , and I_2 are characteristics of the positron lifetime spectra quoted subject to errors of ± 1 , ± 10 , and ± 1.5 respectively; FWHM is the full width at half maximum of the overall spectrum quoted subject to an error of ± 0.05 ; Γ_1 is the FWHM for the first Gaussian quoted subject to an error of ± 0.07 ; θ_p and I_p are the characteristics of the parabolic component of the angular correlation spectrum quoted subject to errors of 0.07 and 1.5 respectively.

(388 ± 10 ps) was independent or depended only slightly on the state of the specimen, but appreciable changes in the intensity of this component were observed; the characteristics of the third component did not change during the experiment.

Experiments involving the measurement of the angular correlation (together with the measurement of the lifetime of the positrons) have also been performed.⁸⁸ Being unable to analyse in detail the results of these measurements we shall only note that, in the experiments with fixed ends (under the conditions of stress relaxation), an increase in the unoccupied volume after deformation

and its subsequent slow relaxation, occurring as a result of the decrease in the concentration of micropores, are well manifested.

Overall, the changes in the macroparameters and microparameters of the polyimide films during the stress relaxation and strain recovery processes after deformation have been revealed by the positron diagnostic method. Nonmonotonic changes in the characteristics of the positron lifetime spectra and the angular correlations of the annihilation photons were observed during the strain recovery period. Two regions corresponding to changes in the positron-sensitive properties of the polyimide, associated with rapid and slow relaxation processes, were differentiated and differences were observed in the nature of the relaxation of the microporous structure of the polymer as a function of the deformation and strain recovery conditions. The observed effects are due to the formation of regions with local freeing of the molecular mobility.

All these experimental facts show that, during the stress relaxation process, the microporous structure of the polymer is rearranged, which is expressed by redistribution of the dimensions of the micropores and their fusion with one another. In this connection, it is of interest to compare the data obtained by the positron diagnostic method with the results of curve fitting with the aid of memory functions (Table 17). In the case of stress relaxation in the linear region of the mechanical behaviour, the correlation coefficient r , obtained using the memory function (19) is close to the value found with the aid of the memory function (18) and amounts to approximately unity. Consequently, the interactions of the relaxators and the diffusion of the microheterogeneities in the specimen take place at approximately the same rate. The fluctuation volume δ is 25.6 \AA^3 per repeat unit of the polymer on $\sim 20\%$ deformation.

Under the conditions of stress relaxation and the recovery of the dimensions of the specimen, the quantities $m_1^*k_B/S_0$ and $m_2^*k_B/S_0$, proportional to the number of microheterogeneities in the specimen, are approximately the same after the removal of the load; on the other hand, $m_2^*k_B/S_0 > m_1^*k_B/S_0$ which indicates a greater number of active microheterogeneities participating in their diffusion in the material. The rate constant for the interaction of the relaxators in the case of stress relaxation is significantly lower (in the linear region of mechanical behaviour) than in the strain recovery relaxation process.

Since the concepts 'relaxator' and 'micropore' are comparable, one may conclude that the relaxation parameters obtained are in good agreement with the microstructural characteristics determined by the positron annihilation technique. During the relaxation of a free film, more favourable conditions are created for the diffusion of micropores and the formation of large and stable packing defects.

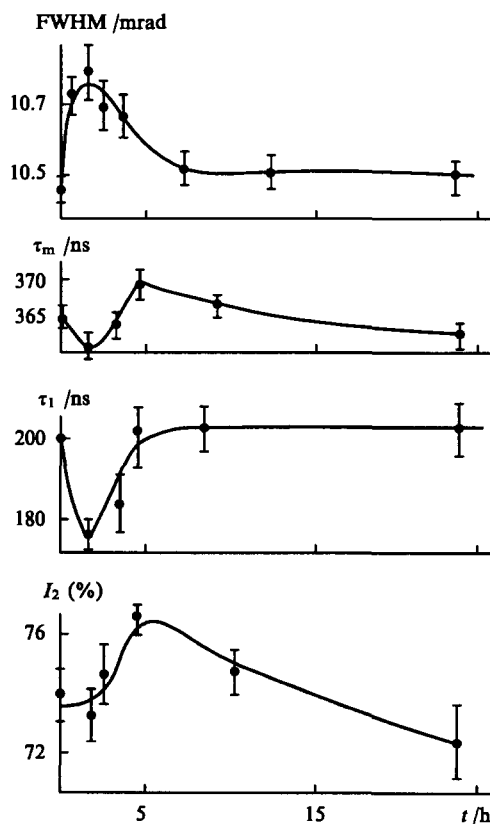


Figure 33. Dependence of the characteristics of the positron lifetime spectra on the relaxation time of a free polyimide film. For legend, see Table 16.

Table 17. Results of the fitting of the stress relaxation and strain recovery curves for polyimide film specimens using the memory functions $T_1(\tau)$ and $T_2(\tau)$.

Function $T_1(\tau)$							Function $T_2(\tau)$					
E_0 /MPa	k^* /min ⁻¹	β	n	$\frac{S_0}{m_1 k_B}$ /min ⁻¹	$\frac{m_1^* k_B}{S_0}$	r	E_0 /MPa	a	γ	$\frac{S_0}{m_2 k_B}$ /min ⁻¹	$\frac{m_2^* k_B}{S_0}$	r
Stress relaxation												
2600.7	10 ⁻⁴	0.2	6	1.84 · 10 ⁻⁵	2.26	0.987	2177	0.0113	0.5	3.88 · 10 ⁻⁴	3.79	0.993
Strain recovery												
—	10 ⁻²	0.7	2.3	1.84 · 10 ⁻³	2.55	0.998	—	0.05	0.5	6.0 · 10 ⁻³	4.77	0.978

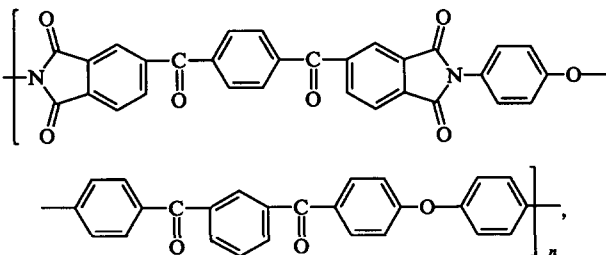
We shall now consider the results of a study designed to analyse the mechanisms of the deformation and relaxation in heat-resistant polymers capable of crystallising and of giving rise to a liquid crystal state.

Wierschke et al.⁸⁹ carried out a theoretical study of the moduli for single poly-*p*-phenylenebenzobisthiazole chains. The study was carried out by the molecular orbital method within the framework of the AMI semiempirical approximation. As a result of the investigation of rigid-chain polymers containing different heteroatoms in the repeat unit, it was found that the charge distribution and the nature of the bonds change on deformation. The moduli of elasticity of the chains obtained in this way were found to be greater than the quantities measured for the real materials. This is attributed both to the presence of heterogeneities in them and to the inadequacies of the computational method itself, which systematically predicts unduly high moduli. These have been mentioned by Shoemaker et al.⁹⁰ The results of the study by Wierschke et al.⁸⁹ permit a comparative analysis of the influence of the chemical structure of heat-resistant polymers on the rigidity of their chains and their mechanical properties.

The moduli of elasticity of the crystalline regions were measured by X-ray diffraction for poly(ether ketone), poly(ether ketone), and poly(*p*-phenylene sulfide).⁹¹ This permitted a further study of the way in which the mechanical properties are related to the conformation of molecular chains and also to the intermolecular interaction in these polymers.

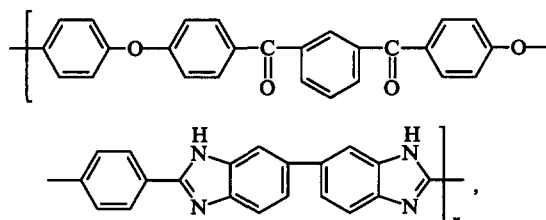
The crystallisation and morphology (which depends on the content of the *meta*- and *para*-isomers) of poly(aryl ketone ketones) have been investigated.⁹² The poly(aryl ketone ketones) were synthesised from diphenyl ether and terephthalic and isophthalic acids. The polymers of this type have two different crystal structures. The addition of the *meta*-isomer diminishes the equilibrium melting point and the rate of crystallisation but increases the flexibility of the chains and the capacity for recrystallisation.

The transition in the crystal phase of the thermoplastic polymer with $T_g = 216^\circ\text{C}$ ⁹³



has been investigated.⁹⁴ It was shown that this polyimide is semi-crystalline and may contain one or two crystalline phases. The mechanical properties of the polyimide films depend significantly on the type and level of crystallinity. Crystallinity promotes a significant increase in the modulus compared with the amorphous polymer, but reduces the capacity for deformation. Its extensive strength depends on the crystal form.

The mechanical properties of different heat-resistant polymers have been studied.^{95–100} Among many heterocyclic polyethers, poly(arylene ether benzimidazole) exhibits the greatest strength. This was demonstrated by tests on nonoriented films of this material.¹⁰¹ The influence of molecular mass on the mechanical properties of heat-resistant polymers



synthesised from 1,3-bis(4-fluorobenzoyl)benzene and 5,5'-bis-[2(4-hydroxyphenyl)-benzimidazole], has been investigated.¹⁰² With decrease in molecular mass, the glass transition temperature and the temperature corresponding to 5% weight loss also diminish. However, the molecular mass does not influence (in the range investigated) the strength of these films and their moduli of elasticity.

Information about the structures and properties of rigid-chain aromatic polymers in the liquid-crystalline state may be found in a review.¹⁰³ Among other investigations in this field, we may mention the study¹⁰⁴ in which the mechanism of the plastic deformation in thermoplastic and thermosetting polyimides and their interpenetrating networks was studied.

VI. Networks, blends, and composites based on heat-resistant polymers

Prepregs based on epoxy-resins have been investigated with the aim of reducing brittleness.¹⁰⁵ The prepregs were modified with aromatic and heat-resistant thermoplastics. The epoxy-resins include systems based on the diglycidyl ethers of bisphenol A and bisphenol F, triglycidyl-*p*-aminophenol, and tetraglycidyl-di-aminophenylmethane. A poly(ether sulfone), polysulfone, and polyimide were chosen as the modifying thermoplastics. It was shown that the brittleness of the epoxy-resins and their relaxation behaviour depend significantly on the type and amount of the modifying agent. The results of dynamic mechanical analysis showed that the modification has only an insignificant influence on the shear modulus and the glass transition temperature. It is noteworthy that, in explaining the results obtained for the initial resins and the composites based on them, the authors¹⁰⁵ did not take into account the chemical interaction between the epoxy-resin and the heat-resistant aromatic polymers.

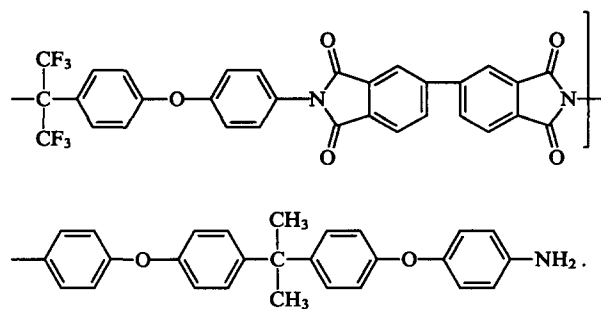
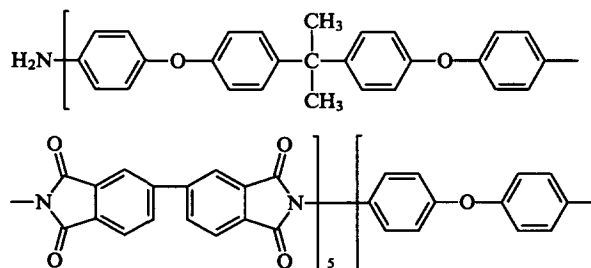
Materials based on epoxy-resins, modified with different amounts of a polyetherimide, have been obtained.^{106,107} The mechanical properties of these materials have been studied in detail.¹⁰⁸ Attention was concentrated on the breakdown rigidity and the rate of liberation of energy. These characteristics increased with increasing content of the polyetherimide as the modifying agent. The authors were able to attain a decrease in the

brittleness of the materials by introducing the poly(ether imide). Under these conditions, the mechanical behaviour is influenced significantly by, for example, parameters such as the initial length of the crack and phase separation processes. Different methods for the reduction of the brittleness of epoxy-resins by the introduction of a second component, which forms an independent phase during the curing process, were proposed in this connection.^{109–114}

Mention may be made of yet another study¹¹⁵ in which the relaxation behaviour of epoxy-resins with added polyetherimide was investigated in detail by means of dynamic mechanical analysis. It was found that the curing temperature and the composition of the blend influence significantly the storage modulus E' , the loss modulus E'' and the mechanical loss factor $\tan \delta = E''/E'$. The quantity E' depends only slightly under these conditions on the content of the polyetherimide in the region of the glassy state. The opposite behaviour occurs in the region of transition from the glassy to the rubbery state: E' increases with increasing content of the poly(ether imide) and the glass temperature shifts under these conditions to the high temperature region. In the rubbery state, E' diminishes with increasing content of the poly(ether imide), which indicates a decrease in the degree of crosslinking. The loss factor $\tan \delta$ decreases with increasing content of the polyetherimide and the $\tan \delta$ maximum shifts at the same time towards higher temperatures with increasing curing temperature. The presence of only one maximum indicates the compatibility of the components.

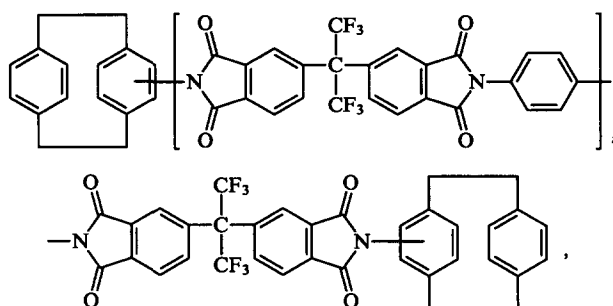
In order to improve the compatibility of the components, one may use a chemical reaction between them.¹¹⁶ This possibility has been implemented in relation to poly(ether ketones). Poly(ether ketones) reacted with polycarbonate, affording the corresponding block copolymers. Despite the fact that the initial components [the poly(ether ketone) and the polycarbonate] were incompatible, the block copolymers based on them were found to be homogeneous and exhibited one α -transition. The moduli of elasticity of the block copolymers were greater than those calculated assuming additivity.

The preparation of blends of heat-resistant polymers with thermoset resins is an effective procedure for improving the mechanical properties of composites. Two approaches to the improvement of the mechanical properties of composites have been described.^{117–119} The first provides for the preparation of 'thermoplastic polymer – thermoset polymer alloys'. The second is associated with the preparation of a system in which thin sheets of heat-resistant thermoplastic polymers serve as spacers in the initial composition with the thermoset polymer. The results of the application of both approaches to the improvement of the mechanical properties of composites have been published.^{120–122} The diglycidyl ether of resorcinol and polyimide oligomers with the following terminal amino-groups were employed in the above studies:



The application of these approaches made it possible not only to improve the mechanical properties of composites but also to facilitate the performance of thermosetting systems.

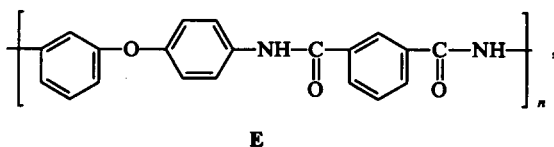
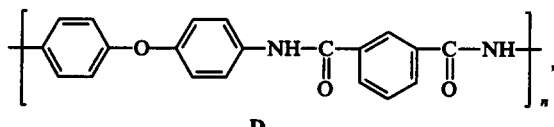
Graphite-reinforced plastics based on the cyclophane resins



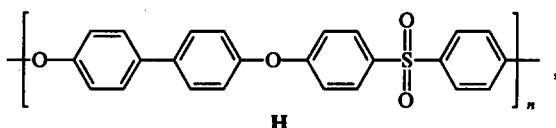
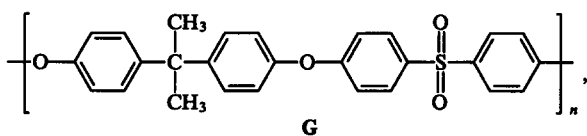
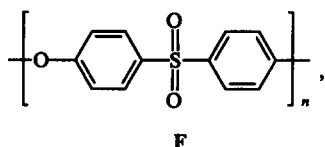
have been investigated.¹²³ The structure of these resins gives rise to a high thermal stability and glass transition temperature and promotes effective cross-linking via their end groups. An effective procedure for the improvement of the mechanical relaxation properties involves also the preparation of semi-interpenetrating polymer networks, in which the linear component is a copolymer based on polyimide.¹²⁴

Analysis of the results of the above studies shows that the most promising ways of improving the mechanical properties of heat-resistant polymers and of developing new types of the latter consists in the synthesis of network systems comprising aromatic oligomers, using, for example, the polycyclotrimerisation reaction, and the preparation of networks with the aid of chemical reactions between oligomers (for example, epoxy oligomers) and heat-resistant aromatic polymers containing in the main chain reactive groups, which can interact chemically with the reactive groups of the oligomer. In certain cases, it is possible to obtain satisfactory mechanical properties without the employment of chemical reactions between the components of the blend. The results of a series of studies, with which we shall deal briefly below, confirm this conclusion. The mechanical behaviour of binary blends of poly(ether sulfone) and poly(phenylene sulfide),¹²⁵ poly(ether sulfone) and poly(ether ketones),^{126–130} poly(ether ketone) and poly(ether imide),^{131, 132} polyamidoimide and an aromatic polyamide,¹³³ polyimides with different types of chemical structure,^{134, 135} polybenzimidazole and polyimides,^{136–142} polybenzimidazole and polyarylate,¹⁴³ and poly(ether ketones) and poly(ether sulfone)¹⁴⁴ has been investigated.

We shall consider in greater detail the results of a study¹⁴⁵ in which binary blends based on two aromatic polyamides



and three poly(ether sulfones)



were investigated.

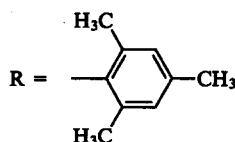
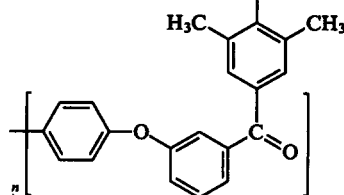
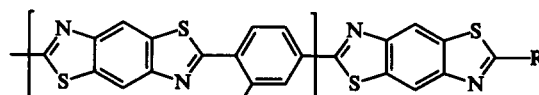
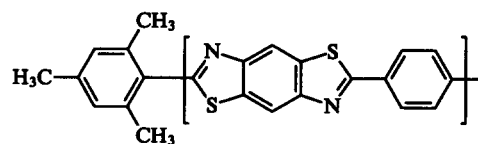
Films made of blends of these polymers were obtained by casting from solutions in *N,N*-dimethylacetamide and *N*-methyl-2-pyrrolidone. These films were investigated by dynamic mechanical analysis, differential scanning calorimetry, and IR spectroscopy; the ultimate mechanical characteristics were also measured. The principal result of this study was the observation of crystallisation induced by the presence of the second component, which entails an increase in the heat resistance of the systems, particularly after their annealing. Test results were achieved for blends based on compounds **D** and **F**. The initial films, for example those prepared from polymers **D** and **F**–**H**, were transparent, but after heat treatment they became opaque and their quality improved.

Thermotropic liquid-crystalline polymers are used nowadays to improve the mechanical properties of heat-resistant polymers. One of the methods of preparation of composites with a high strength and rigidity involves the blending of liquid-crystalline polymers with thermoplastics. There have been fairly numerous studies (see, for example, Refs 146–157) in which the improvement of the mechanical properties of heat-resistant polymer matrices was achieved by adding thermotropic liquid-crystalline polymers to them. Among the heat-resistant polymers, such studies have been performed for poly(ether ketone), poly(ether imide), poly(phenylene sulfide), and polycarbonate. The phenomenon of synergism is characteristic of certain blends of the above polymers and liquid-crystalline polymers.

A series of publications^{156–158} have been devoted to the problem of mechanical anisotropy, which has been observed in blends of liquid-crystalline polymers with heat-resistant aromatic systems.

The studies^{159–162} in which an approach to the preparation of molecular composites was proposed are of significant interest. A molecular composite consists of rigid-chain rod-like polymers, introduced into a polymer matrix, which is made up of a flexible-chain polymer with coiled macromolecules. The rigid-chain macromolecules then serve as strengthening elements of the composite. For example, a graft copolymer based on a rigid-

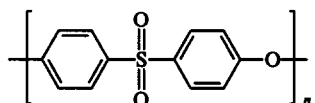
chain polybenzobisthiazole (main chain) and a polyetherketone (side chain) has been synthesised.¹⁶³



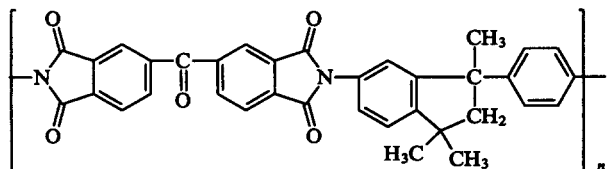
A detailed study of the relaxation properties of this system by dynamic mechanical analysis has been described.¹⁶⁴

In estimating the relaxation properties, it is important to take into account the microphase separation process, which may occur when thermoplastics are blended with thermosetting systems and may also arise on hardening of the composite. The results of studies^{109, 165, 166} in which composites based on blends of a polyethersulfone with an epoxy resin are instructive in this respect. Hardening results in the formation of a two-phase system, which promotes an improvement in the mechanical properties (a decrease in brittleness). Detailed measurements of the enthalpy relaxation have been made for such systems. Subject to a satisfactory fitting of the relaxation curves (for example, with the aid of the Kohlrausch–Williams–Watts function), such measurements can be used to predict the long-term behaviour of polymeric materials under ageing conditions.

Another example of a combined investigation of the relaxation properties may be found in a study¹⁶⁷ in which the behaviour of a blend of the poly(ether sulfone)



and the polyimide



was investigated. These polymers are compatible and their behaviour was investigated by differential scanning calorimetry, dynamic mechanical analysis, and rheological methods. For a polyimide content > 10% microphase layer separation occurred and was manifested by a sharp alteration of the rheological properties. The author also did not rule out the occurrence of a cross-linking process, which may be superimposed on the microphase layer-separation process.

VII. Conclusion

Analysis of the results of relaxation measurements for heat-resistant aromatic polymers permits a series of conclusions about the characteristic features of their mechanical behaviour. One of these conclusions, which at first sight may appear trivial, is that heat-resistant aromatic polymers are capable of withstanding for a long time much greater mechanical loads than traditional plastics in the region of not only high but also moderate and low temperatures. This conclusion is based on the results of measurements of stress relaxation and creep, which show that both processes are less marked than for the usual plastics. Therefore, in creating constructional materials which can be used not only at high but also at low temperatures and for large loads, preference must be given to heat-resistant aromatic polymers. At the same time, it has become evident that, in order to discover the advantages of one set of polymers over others, relaxation measurements are not only desirable but also essential.

One should bear in mind that, even within the class of heat-resistant polymers itself, the structure of the latter has an appreciable influence on their mechanical relaxation properties. For example, in terms of critical stresses, polyimide is superior to PBO; the rate of stress relaxation in polyimide is lower than in PBO. On the other hand, in the range of comparatively low temperatures, polyimide is inferior to PBO in terms of these features.

In dynamic mechanical analysis, heat-resistant aromatic polymers exhibit a series of relaxation transitions associated with the freeing of the molecular mobility of individual groups and segments. A study of the mechanism of these processes by synthesising and investigating a series of polymers in which different hinge atoms and groups are deliberately 'taken away' demonstrated unambiguously that the β -transition in these polymers is associated with the freeing of the molecular mobility of phenylene groups.

However, attention should be concentrated on the characteristics of the mechanical behaviour of heat-resistant polymers, which are manifested in the analysis of relaxation transitions under the conditions of static measurements of stress relaxation and creep. The essential feature of the transitions is that, within the range of the glassy state at temperatures greatly below the glass transition temperature, the relaxation processes are accelerated sharply and the critical stresses are reduced. These transitions play a significant role in an objective assessment of the mechanical workability of polymers. If the polymer is designed for use at variable temperatures and is to be subjected to appreciable mechanical loads, then, on heating to the transition temperature, the mechanical workability may be lost long before the glass transition temperature. The occurrence of these transitions is undoubtedly associated with the linearity of the mechanical behaviour, whereupon appreciable deformations result in a change of the relaxation parameters of the polymer.

Another characteristic feature of the relaxation behaviour of aromatic heat-resistant polymers is that, over a fairly wide temperature range within the region of the glassy state, the parameters of the relaxation processes are relatively insensitive to temperature. This temperature range confines the region of the stable workability of the polymers and it is desirable to take it into account when selecting a polymeric material for each specific task.

One of the significant features of the mechanical behaviour of aromatic polymers is their ability to develop large deformations (i.e. to undergo nonbrittle disruption) in the region of low and ultra-low temperatures. Even at the temperature of liquid helium, the deformation of aromatic polymers attains a large percentage value and relaxation processes are also manifested at these temperatures. Analysis of the mechanisms of deformation and relaxation with the aid of the positron annihilation method has shown (in relation to polyimide) that these polymers have a unique electronic structure and a very narrow size distribution of their pores. It may be that this is the cause of the surprising behaviour at

low temperatures. Aromatic polymers also have another significant advantage over the usual ones (for example, Teflon) — they are capable of withstanding an enormous number of thermocycles over a temperature range from 200 °C to the temperature of liquid nitrogen without loss of mechanical strength.

Finally, many aromatic polymers contain in their chains functional groups (ester, amide, imide, etc. groups) capable of interacting with the functional groups of thermoset oligomers and of curing them. This property is used in creating composite materials based on traditional polymers (for example, epoxy resins), which are strengthened when heat-resistant polymers are introduced into them and lose their brittleness.

References

1. A A Askadskii, G L Slonimskii *Usp. Khim.* **43** 1688 (1975) [*Russ. Chem. Rev.* **43** 767 (1975)]
2. A A Askadskii *Struktura i Svoistva Teplostoikikh Polimerov* (Structure and Properties of Heat-Resistant Polymers) (Moscow: Khimiya, 1981)
3. A A Askadskii *Deformatsiya Polimerov* (Deformation of Polymers) (Moscow: Khimiya, 1973)
4. R B Banyavichyus, A V Ambrazyavichyus, A A Askadskii *Vysokomol. Soedin., Ser. A* **26** 2307 (1984)
5. R B Banyavichyus, A I Marma, A A Askadskii *Vysokomol. Soedin., Ser. A* **21** 1383 (1979)
6. A A Askadskii, Z S Vikhauskas, R B Banyavichyus, A I Marma *Vysokomol. Soedin., Ser. A* **25** 203 (1983)
7. A A Mavricheva, A A Askadskii, V E Gul' *Vysokomol. Soedin., Ser. A* **19** 2379 (1977)
8. A A Askadskii, T V Todadze *Mekh. Kompoz. Mater.* **7** 13 (1980)
9. Yu S Kochergin, A A Askadskii, G L Slonimskii, A P Travnikova, E S Krongauz, V V Korshak *Vysokomol. Soedin., Ser. A* **19** 2543 (1977)
10. Yu S Kochergin, A A Askadskii, S N Salazkin, I A Bulgakova, V F Alekseev, S V Vinogradova, G L Slonimskii, V V Korshak *Vysokomol. Soedin., Ser. A* **20** 880 (1978)
11. R B Banyavichyus, A I Barauskas, A V Ambrazyavichyus, A A Askadskii *Vysokomol. Soedin., Ser. A* **25** 1436 (1983)
12. Z S Vikhauskas, R B Banyavichyus, A A Askadskii, A I Marma *Vysokomol. Soedin., Ser. A* **25** 2351 (1983)
13. M S Matevosyan, A A Askadskii, G L Slonimskii *Vysokomol. Soedin., Ser. A* **29** 761 (1987)
14. V V Korshak, G L Slonimskii, A A Askadskii, A L Rusanov, T V Lekae, M S Matevosyan *Vysokomol. Soedin., Ser. A* **31** 34 (1989)
15. V V Korshak, A L Rusanov, T V Lekae, K A Bychko *Vysokomol. Soedin., Ser. A* **29** 761 (1987)
16. A A Askadskii, Yu I Matveev, M S Matevosyan *Vysokomol. Soedin., Ser. A* **32** 2157 (1990)
17. Yu I Matveev, A A Askadskii *Vysokomol. Soedin., Ser. A* **36** 436 (1994)
18. A A Askadskii, S N Salazkin, K A Bychko, N G Gileva, M G Zolotukhin, G L Slonimskii, S R Rafikov *Vysokomol. Soedin., Ser. A* **31** 2667 (1989)
19. G L Slonimskii, E V Todadze, A A Askadskii *Vysokomol. Soedin., Ser. A* **31** 1305 (1981)
20. E B Trostyanskaya (Ed.) *Termoustoichivost' Plastikov Konstruktsionnogo Naznacheniya* (Heat Resistance of Construction Plastics) (Moscow: Khimiya, 1980)
21. D A Wigley *Mechanical Properties of Materials at Low Temperatures* (New York: Plenum, 1971)
22. T I Sogolova, M I Demina *Mekh. Kompoz. Mater.* **387** (1977)
23. I I Perepechko *Svoistva Polimerov pri Nizkikh Temperaturakh* (Properties of Polymers at Low Temperatures) (Moscow: Khimiya, 1977)
24. I I Perepechko, E B Voloshilov *Vysokomol. Soedin., Ser. A* **19** 1620 (1977)
25. R B Banyavichyus, Z B Migonene, A A Askadskii *Vysokomol. Soedin., Ser. A* **26** 2604 (1984)
26. V V Pustovalov, V S Fomenko, Z B Migonene, A A Askadskii *Vysokomol. Soedin., Ser. B* **32** 363 (1991)

27. A A Askadskii, Z B Migonene, P Yu Zhilyukas, S N Salazkin, A V Samoryadov, V A Sergeev *Vysokomol. Soedin., Ser. B* 32 188 (1991)
28. M Yu Kantsel'son, G A Balaev, in *Polimernye Materialy. Spravochnik* (Polymer Materials. Handbook) (Leningrad: Khimiya, 1982) p. 317
29. G L Slonimskii *Zh. Tekh. Fiz.* 1979 (1939)
30. A P Bronskii *Prikl. Matem. Mekh.* (5) 5 (1941)
31. A A Askadskii, V G Dashevskii, Yu S Kochergin *Vysokomol. Soedin., Ser. B* 19 500 (1977)
32. A A Askadskii *Mekh. Kompoz. Mater.* 403 (1987)
33. R J Gaylord, B Joss, J T Bendler, E A Di Marzio *Br. Polym. J.* 17 126 (1985)
34. A A Askadskii, A L Blyumenfel'd, E G Gal'pern, A L Chistyakov *Vysokomol. Soedin., Ser. A* 30 886 (1988)
35. A A Askadskii, G V Surov, V V Nemchinov, A L Blyumenfel'd, Z S Vikhauskas *Vysokomol. Soedin., Ser. A* 31 1320 (1989)
36. A A Il'yushin, B E Pobedrya *Osnovy Matematicheskoi Teorii Termoviskozoprugosti* (Fundamentals of a Mathematical Theory of Thermoviscoelasticity) (Moscow: Nauka, 1970)
37. A E Yee, R G Bankert, K L Ngai, R W Rendell *J. Polym. Sci., Part B, Polym. Phys.* 26 2463 (1988)
38. A A Askadskii, M P Valetskii *Mekh. Kompoz. Mater.* 441 (1990)
39. A A Askadskii, Yu I Matveev *Khimicheskoe Stroenie i Fizicheskie Svoystva Polimerov* (Chemical Structure and Physical Properties of Polymers) (Moscow: Khimiya, 1983)
40. A A Askadskii, R B Banyavichyus, Z S Vikhauskas, A I Marma, A L Blyumenfel'd *Vysokomol. Soedin., Ser. A* 30 1684 (1988)
41. A A Askadskii, A I Marma, R B Banyavichyus, Z S Vikhauskas *Vysokomol. Soedin., Ser. A* 31 2271 (1989)
42. A A Askadskii, V A Beloshenko, K A Bychko, V V Shaposhnikova, A V Samoryadov, O V Kovriga, S N Salazkin, V A Sergeev, V G Slobodina, Ya V Genin *Vysokomol. Soedin., Ser. A* 36 1143 (1994)
43. B J Jensen, P M Hergenrother *High Perform. Polym.* 1 31 (1989)
44. A A Askadskii, T R Razmadze, S N Salazkin, V A Sergeev, A V Samoryadov, K A Bychko, O V Kovriga, T M Babchinitser, A Varada Radzhulu *Vysokomol. Soedin., Ser. A* 33 1239 (1991)
45. M I Bessonov, M M Koton, V V Kudryavtsev, L A Laius *Polyimides: Thermal Stable Polymers* (New York: Consultants Bureau, 1987)
46. W J Wrasidlo *J. Macromol. Sci., Phys. B* 6 559 (1972)
47. R M Ikeda *J. Polym. Sci., Polym. Lett. Ed.* 4 353 (1966)
48. G M Bartenev, M M Koton *Dokl. Akad. Nauk SSSR* 305 112 (1989)
49. G M Bartenev *Plaste Kautsch.* 36 151 (1989)
50. G A Bernier, D E Kline *J. Appl. Polym. Sci.* 12 493 (1968)
51. O G Nikol'skii, A A Askadskii, S N Salazkin, G L Slonimskii *Mekh. Kompoz. Mater.* 963 (1983)
52. O G Nikol'skii, A A Askadskii, G L Slonimskii *Mekh. Kompoz. Mater.* 901 (1980)
53. E Butta, S D Petris, M Pasquini *J. Appl. Polym. Sci.* 13 1073 (1969)
54. T Lim, V Frosini, V Zaleckas, D Morrow, J A Sauer *Polym. Eng. Sci.* 13 51 (1973)
55. J K Gillham, H C Gillham *Polym. Eng. Sci.* 13 447 (1973)
56. M Kochi, H Shimada, H Kambe *J. Polym. Sci., Polym. Phys. Ed.* 22 1979 (1984)
57. M Kochi, S Isoda, R Yokota, H Kambe *J. Polym. Sci., Polym. Phys. Ed.* 24 1621 (1986)
58. J E Harris, L M Robeson *J. Appl. Polym. Sci.* 35 1877 (1988)
59. R H Pater *Polym. Eng. Sci.* 12 13 (1991)
60. R P Chartoff, T W Chin *Polym. Eng. Sci.* 2 244 (1980)
61. Z Sun, L Dong, Y Zhuang, L Cao, M Ding, Z Feng *Polymer* 33 4728 (1992)
62. M Eisenberg, B Cavrol *J. Polym. Sci., Part C* 35 129 (1971)
63. A Lukashov, V Feofanov, J D Schultze, M Boehning, J Springer *Polymer* 33 2227 (1992)
64. C Schrauwen, T Pakula, G Vegner *Makromol. Chem.* 193 11 (1992)
65. Chul Joo Lee, Tae Won Sohn, Byoung Chul Lim, Van Sik Ha, in *The 34th IUPAC International Symposium on Macromolecules (Book of Abstracts)* Prague, 1992 Sec. 1, p. 286
66. F E Arnold, S Z Cheng, S L-C Hsu, C J Lee, F W Harris *Polymer* 33 5179 (1992)
67. R J Young, P P Ang *Polymer* 33 975 (1992)
68. S Dirikov, Z Chen, D Wang *Polym. Prepr. Am. Chem. Soc.* 33 483 (1992)
69. X Wu, Y Feng, S Dirikov, in *Radiation Curing of Polymeric Materials. ACS Symposium Series 417* (Eds C Hoyle, J Kinstl) (Washington, DC: American Chemical Society, 1990) p. 194
70. Y Aihara, P Gebe *Polym. Prepr. Am. Chem. Soc.* 33 471 (1992)
71. T Kunugi, C Ichinose, A Suzuki *J. Appl. Polym. Sci.* 31 429 (1986)
72. D Grubb, F Keamey *J. Polym. Sci., Part B, Polym.-Phys.* 28 2021 (1990)
73. T Kunugi, A Suzuki, M Hashimoto *J. Appl. Polym. Sci.* 26 1951 (1981)
74. E J Roche, R F Van Kavelaar, G Pausson *Polym. Commun.* 30 151 (1989)
75. A A Hamza, J J Sikorskii *Microscopy* 113 15 (1978)
76. M J Pluta *Microscopy* 149 97 (1988)
77. H H Yang, M P Chouinard, W J Ling *J. Polym. Sci., Polym. Phys. Ed.* 20 281 (1982)
78. A W Harsthorne, D K Laing *Microscopy* 32 11 (1984)
79. N Barakat, A A Hamza *Interferometry of Fibrous Materials* (Bristol: Adam Hilger, 1990)
80. M Pluta *Polymer* 33 1553 (1992)
81. J-H Jou, P-T Huang, H-C Chen, C-N Liao *Polymer* 33 967 (1992)
82. S A Fawas, A N Palazotto, C S Wang *Polymer* 33 100 (1992)
83. A A Askadskii, S A Tishin, V V Kazantseva, O V Kovriga *Vysokomol. Soedin., Ser. A* 32 2437 (1990)
84. A Z Varisov, Yu N Kuznetsov, E P Prokop'ev, A I Filip'ev *Usp. Khim.* 50 1892 (1981) [*Russ. Chem. Rev.* 50 991 (1981)]
85. P Kindl, G Retter *Phys. Status Solidi A* 104 707 (1987)
86. B D Malhotra, R A Petrick *Eur. Polym. J.* 19 457 (1983)
87. C K Hu, G R Gruzalski *Phys. Rev. B* 27 1 (1983)
88. A A Askadskii, S A Tishin, M I Tsapovetskii, V V Kazantseva, O V Kovriga, V A Tishin *Vysokomol. Soedin., Ser. A* 34 (12) 62 (1992)
89. S G Wierschke, J R Shoemaker, P D Haaland, R Pachter, W W Adams *Polymer* 33 3357 (1992)
90. J R Shoemaker, T Horn, P D Haaland, R Pachter, W W Adams *Polymer* 33 3351 (1992)
91. T Nishino, K Nakamae *Polymer* 33 736 (1992)
92. K H Gardner, B S Hsiao, R R Matheson, B A Wood *Polymer* 33 2483 (1992)
93. J R Pratt, T L St Clair, M K Gerber, C R Gautreaux, in *Polyimides: Materials, Chemistry and Characterisation* (Eds C Feger, M M Khojastch, J E McGrath) (Amsterdam: Elsevier, 1989) p. 193
94. C R Cautreaux, J R Pratt, T L St Clair *J. Polym. Sci., Part B, Polym.-Phys.* 30 71; 162 (1992)
95. D M White, T Takekoshi, F J Williams, H M Relles, P E Donahue, H J Klopfer, G R Toncks, J S Manello, T O Matthews, R W Shlueny *J. Polym. Sci., Polym. Chem. Ed.* 19 1635 (1981)
96. J L Hedrick, J W Labadie *Macromolecules* 21 1883 (1988)
97. J W Connell, P M Hergenrother *Polym. Prepr. Am. Chem. Soc.* 29 172 (1988)
98. F W Harris, J E Korieski *Polym. Mater. Sci. Eng.* 61 370 (1989)
99. J W Connell, P M Hergenrother *Polym. Mater. Sci. Eng.* 60 527 (1988); *J. Polym. Sci., Part A, Polym. Chem.* 29 1667 (1991)
100. J W Connell, P M Hergenrother *High Perform. Polym.* 2 211 (1990)
101. J D Smith, J W Connell, P M Hergenrother *Polym. Prepr. Am. Chem. Soc.* 32 193 (1991)
102. P M Hergenrother, J D Smith, J W Connell *Polym. Prepr. Am. Chem. Soc.* 33 411 (1992)
103. M Ballauff *GII* 36 (11) 1095 (1992)
104. B Z Jang, R H Pater, M D Soucek, J A Hinkley *J. Polym. Sci., Part B, Polym.-Phys.* 30 643 (1992)
105. M Stangle, V Alstaat, H Tesh, Th Weber *Adv. Mater. Proceedings of the 12th International European Conference, Maastricht, 1991* p. 33
106. H H Chen, N R Schott *Polym. Prepr. Am. Chem. Soc.* 30 457 (1990)
107. H H Chen, ThD, University of Massachusetts at Lowell, 1991
108. H H Chen, N R Schott *Polym. Prepr. Am. Chem. Soc.* 33 498 (1992)
109. C B Bucknall, I K Partridge *Polymer* 24 639 (1983)
110. R S Raghava *J. Polym. Sci., Part B, Polym.-Phys.* 25 1017 (1987)
111. G R Almen, R K Maskell, V Molhorta, M S Sefton, P T McGrail, S P Wilkinson *SAMPE Symp.* 33 979 (1989)

112. J A Cecere, J L Hedrick, J E McGrath *SAMPE Symp.* 31 580 (1986)
113. J A Cecere, J E McGrath *Polym. Prepr. Am. Chem. Soc.* 27 299 (1986)
114. C B Bucknall, A H Gilbert *Polymer* 30 213 (1989)
115. H H Chen, N R Schott *Polym. Prepr. Am. Chem. Soc.* 33 495 (1992)
116. R J Kumpf, D Nerger, C Lautman, H Pielartzik, R Wehrmann *Polym. Prepr. Am. Chem. Soc.* 32 280 (1991)
117. C B Bucknall, A H Gilbert *Polymer* 30 213 (1989)
118. Eur. P. 0 311 349 (1989)
119. J E Masters, J L Courter, R E Evans *SAMPE Symp.* 31 844 (1986)
120. H Kishi, N Odagiri, K Tobukuro, in *Proceedings of the 3rd European Symposium on Polymer Blends, Cambridge, 1990* A8
121. N Odagiri, H Kishi, T Nakae, in *Proceedings of the American Society for Composites, the 6th Technical Conference, 1991* p. 43
122. N Odagiri, H Kishi *Polym. Prepr. Am. Chem. Soc.* 33 384 (1992)
123. J K Sutter, J Waters, M Schuerman *Polym. Prepr. Am. Chem. Soc.* 33 366 (1992)
124. C L Leung, S Y L Kreisler, A L Landis *Polym. Prepr. Am. Chem. Soc.* 33 508 (1992)
125. H Zeng, K Mai *Makromol. Chem.* 187 1787 (1986)
126. C K Sham, C H Lae, D J Williams, F E Karasz, W J McKnight *Br. Polym. J.* 20 149 (1988)
127. Q Guo, J Huang, T Chen *Polym. Bull.* 20 517 (1988)
128. Q Guo, J Huang, T Chen, H Zhang, Y Yang, C Hou, Z Feng *Polym. Eng. Sci.* 30 44 (1990)
129. Z Wu, Y Zheng, X Yu, T Nakamura, R Yosomiya *Angew. Makromol. Chem.* 171 119 (1989)
130. Z Wu, Y Zheng, H Yan, T Nakamura, T Nozawa, R Yosomiya *Angew. Makromol. Chem.* 173 163 (1989)
131. J E Harris, L M Robeson *J. Appl. Polym. Sci.* 35 1877 (1988)
132. G Crevecoeur, G Groeninckx *Macromolecules* 24 1190 (1991)
133. K Yamada, T Mitsutake, M Takayanagi, T Kajiyama *J. Macromol. Sci., Chem.* A26 891 (1989)
134. R Yokota, R Horiuchi, M Kochi, H Soma, I Mita *J. Polym. Sci., Polym. Lett. Ed.* 26 215 (1988)
135. I Mita, M Kochi, M Hasegawa, T Iizuka, H Soma, R Yokota, R Horiuchi, in *Polyimides: Materials, Chemistry and Characterisation* (Eds C Feger, M M Khojastch, J E McGrath) (Amsterdam: Elsevier, 1989) p. 1
136. L Leung, D J Williams, F E Karasz, W J McKnight *Polym. Bull.* 16 457 (1986)
137. G Guerra, D J Williams, F E Karasz, W J McKnight *J. Polym. Sci., Polym. Phys. Ed.* 26 301 (1988)
138. S Stankovic, G Guerra, D J Williams, F E Karasz, W J McKnight *Polym. Commun.* 29 14 (1988)
139. G Guerra, S Choe, D J Williams, F E Karasz, W J McKnight *Macromolecules* 21 231 (1988)
140. P Musto, F E Karasz, W J McKnight *Polymer* 30 1012 (1989)
141. J Grobelny, D Rice, F E Karasz, W J McKnight *Macromolecules* 23 2139 (1990)
142. D S Lee, G Quin *Polym. J.* 21 751 (1989)
143. T Chung, P N Chen *Polym. Eng. Sci.* 30 1 (1990)
144. R E Rigby *Polym. News* 9 325 (1984)
145. S Nakata, M Kakimoto, Y Imai *Polymer* 33 3873 (1992)
146. G Crevecoeur, G Groeninckx *Polym. Eng. Sci.* 30 532 (1990)
147. G Kiss *Polym. Eng. Sci.* 27 410 (1987)
148. K G Blizard, D G Baird *SPE 44th ANTEC (Proceedings of the Conference) Boston, 1985* Vol. 311, p. 301
149. A I Isaev, M Modic *Polym. Compos.* 8 158 (1987)
150. K G Blizard, D G Baird *Polym. Eng. Sci.* 27 563 (1987)
151. P Zhuang, J L White, T Kyu *Polym. Eng. Sci.* 28 1095 (1988)
152. A Kohli, N Chung, R A Weiss *Polym. Eng. Sci.* 29 573 (1989)
153. US P. 4 835 047 (1989)
154. A Mehta, A I Isaev *Polym. Eng. Sci.* 31 971 (1991)
155. P R Subramanian, A I Isaev *Polymer* 32 1961 (1991)
156. K G Blizard, T S Wilson, D G Baird *Int. Polym. Process.* V 58 (1990)
157. K G Blizard, D G Baird *Int. Polym. Process.* IV 172 (1989)
158. J P de Souza, H H Chen, D G Baird *Polym. Prepr. Am. Chem. Soc.* 33 392 (1992)
159. US P. 4 207 407 (1980)
160. W F Hwang, D R Wiff, G I Benner, T E Helminiak *J. Macromol. Sci. Phys.* B22 231 (1983)
161. T Kyu, T E Helminiak *Polymer* 28 2130 (1987)
162. C S Wang, I J Goldfarb, T E Helminiak *Polymer* 29 825 (1988)
163. M Dotrong, M H Dotrong, R C Evers *Polym. Prepr. Am. Chem. Soc.* 33 477 (1992)
164. U M Vakil, C S Wang, C Y-C Lee, M H Dotrong, M Dotrong, R C Evers *Polym. Prepr. Am. Chem. Soc.* 33 479 (1992)
165. C D Breach, M J Folkes, J M Barton *Polymer* 33 3080 (1992)
166. R S Raghava *J. Polym. Sci., Polym. Chem. Ed.* 25 1017 (1987)
167. K Liang, J Grebowicz, E Valles, F E Karasz, W J McKnight *J. Polym. Sci., Part B, Polym. Phys.* 30 465 (1992)

Methods for the covalent attachment of nucleic acids and their derivatives to proteins

G Ya Sheflyan, E A Kubareva, E S Gromova

Contents

I. Introduction	709
II. Covalent attachment of proteins to nucleic acids by exposure to different types of radiation	709
III. Chemical methods for the covalent attachment of proteins to nucleic acids	714
IV. Covalent attachment of nucleic acids to enzymes based on the mode of enzyme action	716
V. Methods for the identification and isolation of covalent protein–DNA complexes	718
VI. Determination of peptides in a protein bound covalently to nucleic acid	720
VII. Probing the DNA recognising proteins mode of action via cross-linking assay	722
VIII. Conclusion	722

Abstract. The methods for the affinity modification of proteins, specific to nucleic acids, by activated nucleic acid analogues and their components, are considered. The active groups introduced into proteins or nucleic acids and the symmetrical cross-linking agents used to obtain covalent protein–nucleic acid complexes are listed. The methods for the analysis of covalently linked protein–nucleic acid adducts as well as procedures for the identification of the aminoacids in the protein participating in the formation of bonds with nucleic acids are surveyed. The bibliography includes 112 references.

I. Introduction

There are comparatively few methods which make it possible to determine the groups in the protein participating in protein–nucleic acid recognition. The most accurate of these is X-ray diffraction (XRD). However, owing to the poor resolution of X-ray diffraction patterns, the difficulty of isolating sufficient amounts of the protein, and also the differences between the conformations of the macromolecules in solution and in the crystal, this method has not found extensive application. Furthermore, it is not always possible to obtain and isolate specific complexes between proteins and DNA. There are also problems associated with their crystallisation.

Site-specific mutagenesis and chemical modification of the proteins also yield valuable information about the interaction of proteins with nucleic acids, but such experiments require, at least to a first approximation, the knowledge of location of the protein region responsible for this process. A method which makes it possible to identify this region is covalent attachment of proteins to nucleic acids (NA).

Numerous methods for the attachment of proteins to nucleic acids are known at the present time. We have attempted to arrange systematically the available literature data on this question. In our view, the existing methods for the affinity modification of proteins by nucleic acids can be divided into three groups:

- the attachment of proteins to nucleic acids by exposure to different types of radiation;
- chemical methods for the covalent attachment of proteins to nucleic acids;
- covalent attachment of nucleic acids to enzymes based on the mechanisms of the functioning of the latter.

Nucleic acid analogues containing different active groups are usually employed for the affinity modification of the protein. Such groups may be introduced into heterocyclic bases and carbohydrate residues via the terminal or internucleotide phosphate group of the nucleic acid. So, to our mind it is necessary to concentrate attention also on the approaches for the activation of nucleic acids used in each of these methods for the covalent attachment of proteins to nucleic acids.

In the concluding section of the review, the approaches to the identification and isolation of covalent protein–nucleic acid complexes and for the determination of the peptides in the protein bound covalently to the nucleic acid are surveyed. The possibilities for the application of the method involving the covalent attachment of nucleic acid–specific proteins to nucleic acids for the probing of the mechanisms of their interaction are considered.

II. Covalent attachment of proteins to nucleic acids by exposure to different types of radiation

1. Irradiation with UV light

When complexes between proteins and nucleic acids or their analogues are irradiated with UV light, the side chains of the protein become covalently attached to the heterocyclic base residues closest to them (the so-called ‘zero length cross-linking’).

a. Irradiation of complexes between proteins and unmodified nucleic acids with UV light

This method for covalent attachment is used in relation to a wide range of biological systems: from cell nuclei up to isolated and purified proteins in complexes with synthetic oligonucleotides. The conditions for the irradiation of various systems in order to obtain protein–nucleic acid complexes in the appropriate buffer

G Ya Sheflyan, E A Kubareva, E S Gromova Belozerskii Institute of Physical and Chemical Biology at the Lomonosov Moscow State University, Lomonosov Moscow State University, Chemistry Department, Vorob'evy gory, 119899 Moscow, Russian Federation. Fax (7-095) 939 31 81. Tel. (7-095) 939 54 20 (G Ya Sheflyan), 939 31 48 (E A Kubareva), and 939 31 44 (E S Gromova)

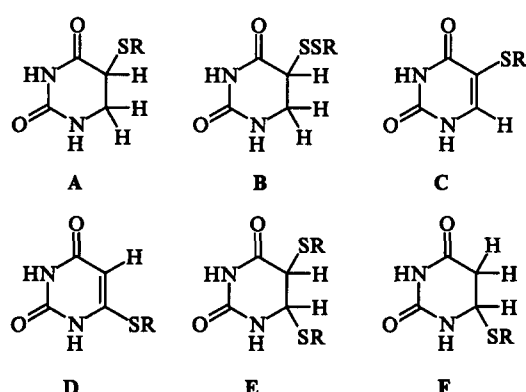
Received 13 December 1995

Uspekhi Khimii 65 (8) 765–781 (1996); translated by A K Grzybowski

solutions are surveyed in Table 1. It is seen from the data presented that the irradiation time varies from 1 min to 4 h and the wavelength is as a rule 254 nm. Under these conditions, the yield of the conjugate varies from 0.1% to 70%. Owing to the complexity of the system, in certain cases it was not possible to determine the yield of the final conjugate, so that the stoichiometry of the complexes is presented instead. It reflects the number of protein molecules per DNA molecule or the number of base pairs of the DNA bound covalently to one protein molecule.

On irradiation with UV light of a protein–nucleic acid complex, the 5,6-double bond of the pyrimidines is excited, which leads to its rupture; a biradical is formed at the 5,6-positions in the pyrimidine ring and reacts with the side chains of the protein.²¹ This reaction mechanism has been established in a detailed study of the products of the irradiation of uracil in the presence of cysteine (Scheme 1).

Scheme 1



R = CH₂CH(NH₂)COOH.

Compounds A, B, E, and F are formed on irradiation with light at a wavelength > 290 nm in the presence of acetophenone, which is a 'trap' for the radicals. It has been suggested that the reaction is reversible. The product C is formed in solutions containing free radical generators, for example oxygen or riboflavin. The irradiation conditions depend on the energy required for the formation of the radical: when the solution contains oxygen, a wavelength of 254 nm is employed, while in the presence of riboflavin the wavelength is 290 nm. Compound C is probably obtained from E as the primary product. Compound D is apparently formed similarly to C, via a free radical in the 5-position in uracil.²²

At the present time, there is no unanimous view in the literature concerning the mechanism of the covalent cross-linking of unmodified nucleic acids with proteins on exposure to UV light. In a number of studies, for example in that of Welsh and Cantor,²¹ it has been suggested that such cross-linking is nonspecific and depends not on the nature of the side chain of the amino acid residue but on the distance between it and the heterocycle. On the other hand, other workers (see Refs 3, 22, and 23) noted the specificity of the formation of the covalent cross-link in relation to definite amino acid residues, for example Ser, Ile, Thr, Arg, and Lys.

Saito et al.³ believe that, when complexes between proteins and nucleic acids are irradiated with UV light, a cross-link is formed between the thymine residue and the ε-amino-group of lysine. The deoxythymidine–L-Lys model system was used to investigate this reaction (Scheme 2).

It was established that, on irradiation with light at a wavelength > 280 nm, the adduct L-Lys–thymidine is not formed. On exposure to UV light, thymidine also interacts with Arg. The reaction involves the α-amino-group of Arg and not the guanidine residue, i.e. Arg in the protein may react with thymidine on irradiation only when it is N-terminal.

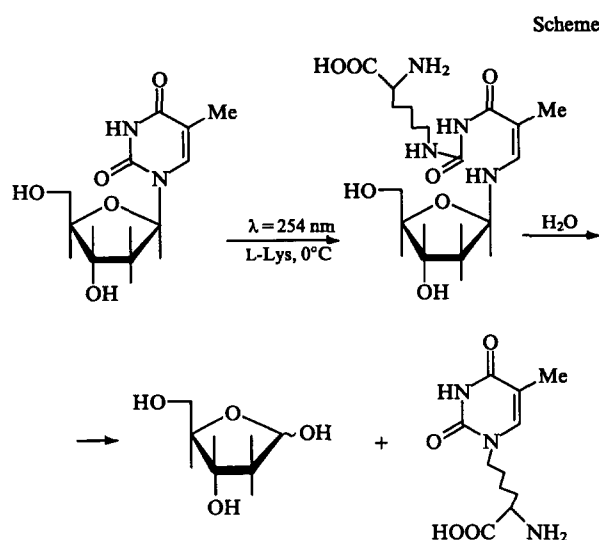
The method for the UV irradiation of proteins and nucleic acids considered in this Section has its advantages and disadvantages.

Table 1. Conditions for the irradiation of complexes between proteins and unmodified nucleic acids and the yields of the reaction products.

Object	Wavelength /nm	Time /min	Yield (%) or stoichiometry of the complex	Ref.
Chick erythrocyte nucleus	254	240	58 ^a , 70 ^c	1
Nucleohistone	230–290	30	see ^b	2
Calf thymus nucleosome	> 250	40	see ^b	3
Cells from a <i>D. melanogaster</i> tissue culture	not indicated	12	see ^b	4
<i>Trypanosoma brucei</i> cells	254	10	see ^b	5
<i>E. coli</i> RNA polymerase and DNA	254	1–4	0.1	6
<i>E. coli</i> RNA polymerase and phage T7 DNA	254	20–240	see ^b	7
<i>E. coli</i> RNA polymerase and poly-d(AT)	254	not indicated	50 (protein : NA = 3 : 1, 6 : 1 and 12 : 1)	8
σ-Factor of <i>E. coli</i> RNA polymerase and phage M13 single-stranded DNA with an oligonucleotide primer	254	20	25 ^c	9
The protein snRNP and RNA	254	30	see ^b	10
DNA polymerase and fragments of the phage T7	254	not indicated	protein : NA from 3 : 1 to 10 : 1	11
Ile-tRNA-synthetase and ATP	253.7	30–40	protein : ATP = 6.7 : 1	12
Replication protein A and single-stranded DNA	UV region	10	see ^b	13
DNA-binding adenovirus protein and p(dT) ₁₄	UV region	20	20 ^a	14
Human protein recognising d(GA) _n and d(GT) _n repeats in DNA and d(GA) _n	254	100	see ^b	15
Guanidine-acetate methyltransferase and SAM ^d	254	240	17–20 ^a	16
DNA methyltransferase CheR from <i>Salmonella</i> <i>typhimurium</i> and SAM	254	40	60–70 ^c	17
DNA methyltransferase Dam from <i>E. coli</i> and SAM	254	5–90	3–4 ^a	18, 19
DNA methyltransferase <i>McpI</i> and SAM	254	60	see ^b	20

^a The yield calculated relative to the protein is indicated. ^b The yield is not indicated. ^c The yield calculated relative to DNA is indicated.

^d S-Adenosyl-L-methionine. ^e The yield calculated relative to SAM is indicated.



The former include the possibility of identifying the amino acid residue closest to the nucleic acid. However, the absence of a covalent adduct after irradiation does not imply the absence of contact between the nucleic acid and protein, since it may be that the activation of the components of the complex by UV irradiation

is insufficient for the reaction to occur. A disadvantage of the method is also the damage to the structure of the nucleic acid and the protein for a high intensity and long duration of the irradiation. Under these conditions, the mutations occurring in nucleic acids interfere with the study of the conjugate (for example, owing to a change in mobility in the gel). The inactivation of the protein, which may occur either as a result of its breakdown on irradiation or owing to covalent cross-linking, cannot serve as a test for the formation of a protein–nucleic acid complex.

b. Irradiation with UV light of complexes of proteins with modified nucleic acid analogues

The cross-linking of proteins to photosensitive nucleic acid analogues is used for the determination of the topology of nucleic acid–protein complexes. Nucleic acids where a bromine atom or the azido-group has been introduced in the 5-position in pyrimidine bases and in the 8-position in the purine bases are used as analogues of this kind.²⁴ The above chemical groups are exposed in the major groove of the double helix. They do not induce a significant change in its structure and do not prevent protein–nucleic acid recognition.

The conditions governing the cross-linking of the bromo- and azido-substituted nucleic acid analogues to proteins are summarised in Table 2. The table shows that the irradiation conditions for the modified nucleic acid analogues are milder than for the unmodified nucleic acids. The yields of the covalently bound

Table 2. Conditions for the irradiation of complexes between proteins and modified nucleic acid analogues and the yields of the reaction products.

Object	Wave-length /nm	Time /min	Yield of complex (%)	Ref.
Restriction endonucleases <i>EcoRI</i> and <i>EcoRV</i> and DNA duplex containing br^5dU	> 300	1	0.05 ^a	25
<i>lac</i> repressor and oligonucleotide with <i>lac</i> -operator sequence containing br^5dU	300–400	20	60 ^b	26, 27
Matrix-binding polypeptide in the transcription complex of pea chloroplasts and DNA containing br^5dU	300–315	20	not indicated	28
Protein of the bacteriophage R17 coat and RNA containing br^5dU	312	3	20 ^a	29
Transcription activator GCN4 from yeast and DNA containing br^5dU	254	1.5	2	30
Cyclic 3',5'-phosphate receptor protein and <i>E. coli</i> DNA containing br^5dU	300–400	not indicated	70 ^b	31
Chromosomal protein of the archaeobacteria MC1 and <i>E. coli</i> DNA containing br^5dU	300–400	not indicated	20 ^b	32
DNA methyltransferase <i>EcoRV</i> and DNA containing 4-thiothymidine	> 310	10–12	18–35 ^a	33
DNA methyltransferase <i>EcoRV</i> and DNA containing 6-thiodeoxyguanosine	> 310	10–12	5–8 ^a	33
Restriction endonuclease <i>EcoRV</i> and DNA containing 4-thiothymidine	> 310	10–12	6 ^a	33
Restriction endonuclease <i>EcoRV</i> and DNA containing 6-thiodeoxyguanosine	> 310	10–12	6 ^a	33
Terminal deoxynucleotidyltransferase and 40-membered DNA containing N_3^5dU	302	1	40–50 ^a	34
DNA polymerase I and oligonucleotide duplex containing N_3^5dU	302	2	40 ^b	35
Carboxy- <i>O</i> -methyltransferase and 8-azido-SAM	254	15	42 ^b	36
<i>E. coli</i> RNA polymerase and N_3^8dA	254	8	not indicated	37
70S Ribosomes and tRNA ^{Phe} of <i>E. coli</i> containing 3- $\{N-[N-(p\text{-azidobenzoyl})\text{glycyl}]\text{-(3-amino-3-carboxypropyl)}\}$ uridine	UV region	2–3	25	38
Endonuclease V of phage T4 and 14-membered DNA duplex containing 3-trifluoromethyl-3-(<i>p</i> -carboxybenzoyl)diazirine	365	30	15 ^a	39

^a The yield calculated relative to the nucleic acid is indicated. ^b The yield calculated relative to the protein is indicated.

protein–nucleic acid conjugates are fairly large and in certain systems amount to 60%.

The introduction of photosensitive groups into a heterocyclic base alters the reaction mechanism. Irradiation of the complexes of bromo-substituted nucleic acid analogues with a protein is accompanied by the loss of the bromine atom and the formation of an unpaired electron in the 5-position of the uracil residue, which may react in different ways with the protein side chains, giving rise to a covalent cross-link.²¹ The only condition for the occurrence of such cross-linking is the proximity of the side chain of the aminoacid residue and of the free radical. Wolfes et al.²⁵ believe that the interaction of the bromine-containing substrates with the Gly, Ser, Phe, Tyr, Trp, Cys, and Met residues, having aliphatic chains or aromatic rings, as possible free radical acceptors is most likely. The mechanism and specificity of this reaction were not investigated in greater detail. Among the advantages of the method considered one should mention the high sensitivity of the modified nucleic acids to UV irradiation, as a result of which the probability of mutations in the nucleic acids and in the protein diminishes owing to the smaller intensity and duration of the irradiation.

The azido-substituted nucleic acid analogues are even more effective in the covalent binding reaction.⁴⁰ In the case of nucleoside residues containing the azido-group in the 8-position in the purine bases or in the 5-position in the pyrimidine bases, the mechanism of the formation of the covalently bound protein–nucleic acid complex is much more complicated. On irradiation with UV light, the photochemical elimination of a nitrogen atom results in the formation not of a radical but of a nitrene, which may react nonselectively with the closest groups regardless of their electrophilicity or nucleophilicity.³⁷ An indirect demonstration of this mechanism has been achieved in a spectrophotometric study of the consequences of the UV irradiation of N₃-dUTP.⁴⁰ After only 20 s, the maximum at 288 nm, corresponding to the azido-derivative of dUTP, vanishes completely. The decrease in absorption after photolysis indicates the rupture of the conjugated ring system of the heterocyclic base (possibly as a result of an intramolecular rearrangement initiated by the formation of the nitrene).

The particular value of the azido-derivatives of nucleic acids consists in the fact that the azido-group is fairly small and does not prevent the formation of hydrogen bonds between the protein and the nucleic acid. Furthermore, the introduction of the azido-group in the 5-position in the pyrimidine residues does not alter the *anti*-conformation of the heterocyclic base of the nucleoside and only induces a slight distortion of the nucleic acid structure.^{40, 41} Reich and Everett⁴¹ compared the kinetic parameters of the interaction of the methyltransferase *EcoRI* with the cofactor SAM (*S*-adenosyl-L-methionine) and also its analogues containing the azido-group in the 8-position of the heterocyclic base. It was found that the constants for binding to the enzyme in the absence of DNA are of the same order of magnitude for the native cofactor and its azido-analogues, amounting to 4.8 and 12.9 μM respectively. The catalytic constant (k_{cat}) and the Michaelis–Menten constant (K_{M}) for SAM and 8-azido-SAM in ternary complexes with the enzyme and with the 12-membered DNA duplex hardly differ, amounting to 4.3 s⁻¹ and 0.335 μM for the native cofactor and to 5.0 s⁻¹ and 0.710 μM respectively for the modified compound. These results indicate the insignificant nature of the changes in the structure of the nucleoside following the introduction of the azido-group. When acted upon by UV light, 8-azido-SAM becomes covalently attached to the enzyme. The specificity of the covalent attachment has been demonstrated by its inhibition on addition of the unmodified cofactor.⁴¹

Another advantage of the azido-derivatives is the fact that the conversion of the azido-group into the nitrene occurs at a much lower intensity of the UV light, which makes it possible to avoid

damage to DNA on irradiation. The initial rates of disruption of the heterocycle on irradiation with UV light at a wavelength of 254 nm have been compared.⁴⁰ It was established that a decrease in maximum absorption for N₃-dUMP was 7000 times faster than for dTTP and 1150 times faster than for br⁵dUMP. Thus the azido-analogues are much more reactive in relation to proteins. There are no data on the specificity of their action.

Thymidine and deoxyguanosine in which the keto-group has been replaced by the thio-group have been tried as photosensitive analogues of nucleosides.³³ It was established that the DNA duplexes modified in this way become covalently attached to restriction–modification enzymes *EcoRI* and *EcoRV* (the conditions for their irradiation are presented in Table 2). It was shown in control experiments that the enzymes themselves retain fully their activity after irradiation; the irradiation of enzymes with unmodified DNA does not lead to the formation of covalently bound adducts; incubation of the components of the complex without irradiation also does not induce the formation of conjugates.

By introducing 4-thiothymidine residues into genes coding for 5S rRNA and tRNA^{Tyr} of the yeast *Saccharomyces cerevisiae*, the interaction of such DNA with transcription factors — TFIIC and TFIIB — was investigated. It was shown that the modification does not prevent the formation of noncovalent specific complexes with the proteins considered. Photoattachment occurred after the preincubation of the complexes on irradiation with UV light at a wavelength of 300 nm for 15 min. The method made it possible to identify the subunits of the transcription factors in contact with particular regions of the transcribed DNA.⁴²

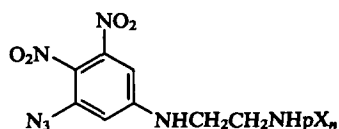
The modification of mRNA and certain ribosomal RNA with the 4-thiouridine residue has been used in the study of the topography of ribosomes in early stages of the transcription.^{43–48} It was shown that, in the transcription involving T7-polymerase, 4-thiouridine triphosphate is incorporated in the synthesised RNA strand in the same way as the unmodified nucleoside triphosphates.^{43–48} When ribosomes containing the modified components were irradiated with UV light at a wavelength > 300 nm for 10 min, cross-links were formed between mRNA and the ribosomal RNA^{43–47} as well as RNA–protein cross-links. The ribosomal proteins bound covalently to a synthetic analogue of mRNA containing the 4-thiouridine residue have been identified.⁴⁸ The method has been used to determine the proteins spatially in close proximity to mRNA at different transcription stages.

We shall consider two possible mechanisms of the reaction of proteins with nucleic acids containing a 4-thiopyrimidine base: in the presence of oxygen and in its absence.³³ In the latter case, the protein is attached to the C(6) atom of the pyrimidine ring with the simultaneous reduction of the 5,6-double bond. The reaction proceeds via a radical mechanism, which involves the elimination of a hydrogen atom from 4-thiopyrimidine in the excited state.

In the presence of oxygen, the 4-thiopyrimidines in the nucleic acid are oxidised to the corresponding 4-sulfonates, which are highly reactive and are subjected to nucleophilic attack by the aminoacid residues of the protein with substitution of the sulfonate group.

There are data concerning the mechanism of the photoattachment of nucleic acids containing 6-thiodeoxyguanosine to proteins. It is believed that they form sulfonate derivatives as a result of irradiation.³³

Another type of activation of nucleic acids involves the formation of oligoribonucleotides or oligodeoxyribonucleotides in which the photoactivated group is not attached directly to the heterocyclic base. Thus oligoribonucleotides containing a dinitrobenzene ring with the azido-group and linked to the 5'-phosphate group via ethylenediamine have been used for the affinity modification of ribosomal proteins.⁴⁹



X = ribonucleoside residue

Mitchell et al.³⁸ modified tRNA with *N*-(*p*-azidobenzoyl)glycine by attaching it to the 3-(3-amino-3-carboxypropyl)uridine residue (the irradiation conditions are presented in Table 2). The mechanism of the reaction involving the attachment of nucleic acids modified in this way to proteins does not differ from that considered above, since in this case too the main photoactivated reactive group is the azido-group.

Apart from the nitrene, a carbene may be used for the covalent attachment to proteins. The formation of a carbene from the diazine-derivative of the nucleic acid is induced by irradiation with UV light.³⁹ The active group — 3-trifluoromethyl-3-(*p*-carboxybenzoyl)diazine — was attached to the internucleotide phosphate in the DNA duplex. As a result of irradiation with UV light at a longer wavelength (Table 2), this group decomposes, affording a carbene. It is postulated that the carbenes are more reactive than the nitrenes and, furthermore, that irradiation with UV light at a longer wavelength is preferable, since it prevents the degradation of the protein.

c. The use of laser radiation

Not only a mercury or mineral lamp but also a laser may be used as a source of UV light. The difference between laser irradiation and the usual irradiation consists in the extremely high power and brief duration of the light pulse. Laser radiation was first used for the covalent attachment of proteins to nucleic acids in relation to the complex between the *E. coli* RNA polymerase and the phage T7 DNA. The reaction mixture was irradiated with a single pulse having an energy of 120 mJ (irradiation time 20 ns, wavelength 248 nm). Depending on the concentration of mercaptoethanol, the yield of the complex varied from 5% to 20%.

The mechanism of the covalent attachment of proteins to nucleic acids on exposure to laser irradiation does not differ from that of the attachment on irradiation by light from a mercury or mineral lamp. However, the use of a brief pulse and the presence of mercaptoethanol as the 'trap' for the long-lived radicals formed on irradiation made it possible to characterise in greater detail the intermediate compounds formed on irradiation by a laser. The lifetime of the radicals formed on irradiation is calculated from the formula

$$\frac{f_0}{f_q} = 1 + K_q t,$$

where f_0 and f_q are the yields of the product of the covalent attachment in the absence and in the presence of mercaptoethanol respectively, K_q is the rate constant for the trapping of radicals, and t the lifetime of the radical.⁵⁰ It was established that $t = 25\text{--}4000$ ns and that approximately half of the radicals are long-lived. Since the lifetime of a particular conformation of the DNA-protein complex proved to be much greater than the duration of the laser pulse, it became possible to 'freeze' a particular structure of the test object, but this is interfered with by the long-living radicals because the latter may react with the protein already after the transition of the system to another state (the so-called diffusion of radicals). In order to avoid such artefacts, it has been suggested that mercaptoethanol be used as a 'trap' for the long-lived radicals.

The yield of the product of the covalent attachment of a protein to the nucleic acid under the influence of laser radiation depends linearly on the irradiation dose, which indicates that only one photon participates in each cross-linking step and that the excitation of only one of the components of the complex is sufficient for the reaction. An advantage of the method is smaller

damage to DNA compared with other methods, the protein fully retaining its native state under these conditions.⁵⁰

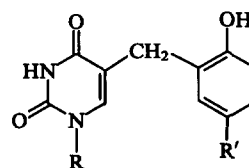
On exposure to laser irradiation, the DNA modified with the psoralen furanoside residue can also be attached to proteins, which has been demonstrated in relation to their attachment to the RNA polymerase of the bacteriophage T7.⁵¹ The irradiation was carried out with the aid of an argon laser having a broad radiation spectrum and a maximum at 366 nm. For an equimolar ratio of DNA and the protein in the reaction mixture, approximately 80% of the DNA is attached covalently to the RNA polymerase. It has been observed by electrophoresis that several isomeric covalent protein-nucleic acid complexes are formed. Degradation of the RNA polymerase under these conditions was not observed. An increase in the irradiation intensity led to a linear growth of the yield of the covalent adducts. The advantages of this method are the short irradiation time and the possibility of 'freezing' the equilibrium states of the DNA-protein complex, which makes it possible to investigate the kinetic constants for this process. Two mechanisms of the attachment of DNA, modified by psoralen furanoside, to a protein have been proposed: (1) via the formation of a singlet oxygen atom, radicals, or radical-ions; (2) by direct photoattachment. It is noteworthy that evidence in support of one of these photoactivation pathways has not been found, but the covalent attachment yield is directly related to the influence of external conditions on the stability of the protein-nucleic acid complex.⁵¹

2. Irradiation from γ -sources

Irradiation from γ -sources has also been used to obtain DNA-protein conjugates. For this purpose, the corresponding complexes were placed in a saturated solution of nitrous oxide.^{52,53} A nucleosome became the object of such studies. A nucleosome consists of a repeating chromatin unit and incorporates DNA consisting of 200 nucleotide pairs and the histones H2A, H2B, H3, and H4.⁵⁴ The study of this system is important for the understanding of the mechanisms of the storage of genetic information.

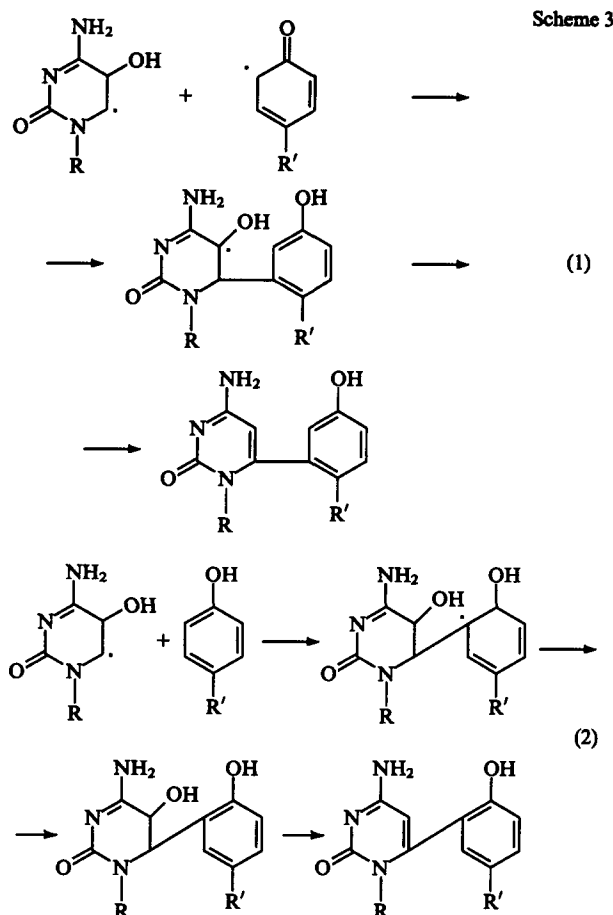
The covalent attachment of histones to DNA occurs on exposure to γ -irradiation. The formation of a covalent bond between the pyrimidine residues of DNA and the tyrosine residues of the protein has been postulated.⁵³ The tyrosine-cytidine system in an aqueous solution of nitrous oxide has been used to model the formation of the DNA-histone conjugate.⁵² The reaction mechanism is as follows. Irradiation of the solution induces the formation of several types of radicals. Hydroxyl radicals react with cytosine and tyrosine, becoming attached to the C(5) carbon atom in the first case and to the aromatic ring with formation of dihydrocyclohexadienyl radicals in the second. Two possible reaction propagation pathways are presented in Scheme 3.

Dizdaroglu et al.⁵³ considered the possibility of the interaction of tyrosine with thymidine on γ -irradiation. Overall, the mechanism of this reaction is similar to that considered above for cytidine, but the radicals are formed as a result of the abstraction of a hydrogen atom from the methyl group of thymidine and not via the 6-position of the heterocycle (as in the case of cytidine).



R = ribose residue, R' = $\text{CH}_2\text{CH}(\text{NH}_2)\text{COOH}$.

The presence of oxygen molecules diminishes the probability of the formation of a covalent protein-nucleic acid complex, since oxygen forms peroxy radicals on interaction with the pyrimidine residues.



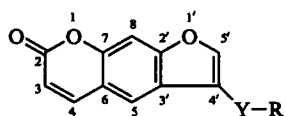
R = ribose residue, R' = CH₂CH(NH₂)COOH.

Arundel et al.⁵⁵ suggest that the covalent attachment of DNA to proteins from HCA-1 cells after their treatment with *N*-methylformamide and γ -irradiation takes place via this mechanism. *N*-Methylformamide does not apparently participate directly in the formation of a cross-link and acts only as a radical trap in order to increase the radiosensitivity of the cells.

Irradiation from γ -sources ensures a specific interaction of DNA with aromatic aminoacid residues in close proximity. However, a serious obstacle to its wide scale employment is the need to use a saturated solution of nitrous oxide, which does not promote the formation of protein-nucleic acid complexes. Furthermore, hard γ -radiation induces mutations.

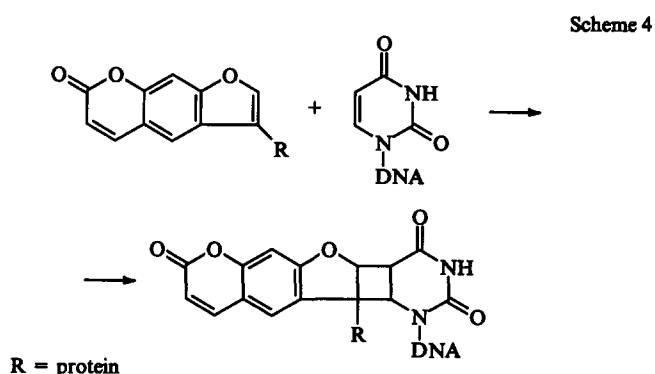
3. Modification of the protein

Modification of the protein side chains with psoralen via the corresponding 'stem' (Y) is most frequently employed.



Y = -NH(CH₂)₂S-, -NMe(CH₂)₂NMe-,
 -NMe(CH₂)₂O(CH₂)₂NMeC(O)(CH₂)₂S-;
 R = protein

In the formation of the protein-nucleic acid complex, psoralen is intercalated in the double helix. When such a complex is irradiated with UV light, monoadducts with an internal cross-link between the furocoumarin and pyrimidine residues are formed. The 3,4- or 4',5'-double bonds of furocoumarin and the 5,6-double bond of the pyrimidine residue participate in the



attachment. This results in the formation of four-membered rings (Scheme 4).^{21, 56}

By altering the length of the stem connecting psoralen to the protein, it is possible to attach it at both short and long distances from the sites of the interaction of the protein and the nucleic acid. A disadvantage of the method is that it is necessary to know beforehand which site in the protein has to be modified.

III. Chemical methods for the covalent attachment of proteins to nucleic acids

For the covalent attachment of proteins to nucleic acids by means of a chemical reaction not involving the generation of radicals with the aid of irradiation, it is necessary either to increase the activity of one of the components of the protein-nucleic acid complex or to introduce into the system a symmetrical cross-linking agent, capable of forming a covalent bond with both components of the complex. Aldehydes are usually employed as agents of this kind.

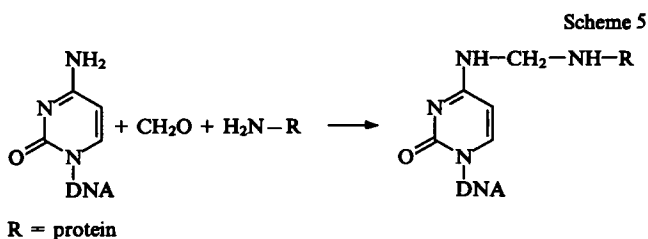
1. The use of symmetrical cross-linking agents

Formaldehyde is used more often than other chemical agents for the covalent attachment of DNA to a protein. The cross-linking of DNA and histones in the nucleosome of the calf thymus nucleus has been achieved in this way. The aim of the study was to identify the sites of contact between DNA and the proteins or to achieve the fixation of protein-nucleic acid complexes in order to prevent their separation during further study on centrifugation and on exposure to other severe treatments.^{57, 58}

Another example of the application of this method is the probing of the structure of the *E. coli* RNA polymerase and its complex with the lac UV5 promoter.⁵⁹

Formaldehyde has also been used to determine the contacts between mRNA or pBR322 DNA with proteins. In this case, covalent attachment was achieved in 3 h at 37 °C on treatment of exponentially growing *E. coli* cells with a 0.75% solution of formaldehyde.⁶⁰

Formaldehyde reacts with the ϵ -amino-group of Lys, affording a hydroxy-methyl derivative, which reacts in its turn with the amino- and imino-groups of DNA.^{21, 57} Formaldehyde also interacts with the DNA adenine and cytosine residues via the exocyclic amino-groups, the protons participating in the formation of Watson-Crick pairs not being involved (Scheme 5).⁶¹



Scheme 6

The endocyclic imino-group of cytosine also reacts with formaldehyde. Furthermore, formaldehyde is attached to the endocyclic imino-groups of the thymine and uracil residues.⁶² Thus the reaction involving the covalent attachment of proteins to nucleic acids on treatment with formaldehyde is specific to lysine residues in the protein but is nonspecific in relation to the heterocyclic bases in the nucleic acid. An advantage of the method is the possibility of the covalent attachment of the protein to DNA without rupturing the structure of the double helix of the latter. Under these conditions, the groups of atoms located in both the major and minor grooves of DNA enter into the reaction. However, the method considered leads to a large number of protein-protein cross-links, which complicates the analysis of the results of the covalent attachment in complex systems, for example in *E. coli* cells.⁶⁰ Apart from formaldehyde, ketones, for example acetophenone and benzophenone, may be used as the cross-linking agents.

Glutaraldehyde and 1-(3-dimethylaminopropyl)-3-ethylcarbodiimide have also been used as symmetrical cross-linking agents. The former reacts with the primary amino-groups of both the protein and the nucleic acid to form Schiff bases. The carbodiimide interacts with the primary amino-groups only of single-stranded DNA.²¹

Cohen et al.⁶³ and Hearst⁶⁴ indicate the possibility of the formation of a bond between DNA and the protein by coordination via the Cr^{6+} ion in the form of a symmetrical covalent or coordination complex between DNA and the enzyme polyadenosyldiphosphoribosylsynthetase. This type of binding has not been investigated, although the conjugates have already been isolated.

2. Activation of nucleic acids

One of the methods for the activation of nucleic acids is acid treatment, which leads to the elimination of purines from DNA. The aldehyde formed as a result of the opening of the furanose ring may react with the amino-groups of the protein to form a Schiff base.⁶⁵ However, this reaction cannot be used directly for the preparation of covalent protein-nucleic acid complexes, since the low pH values and the high ionic strength during the acid treatment interfere with the formation of specific protein-nucleic acid complexes. Levina et al.⁶⁶ therefore proposed that DNA be subjected to preliminary alkylation at the guanine and adenine residues with the aid of dimethyl sulfate and subsequent heating in a neutral medium. The aldehyde groups formed in the DNA interact with the amino-groups of the protein. Next, β -elimination results in the rupture of one of the DNA strands at the site of attachment to the protein. This approach made it possible to determine the sites of contact between DNA and the protein in nucleosomes⁶⁷ and in the complexes between RNA polymerase and the lac UV5 promoter.⁶⁸

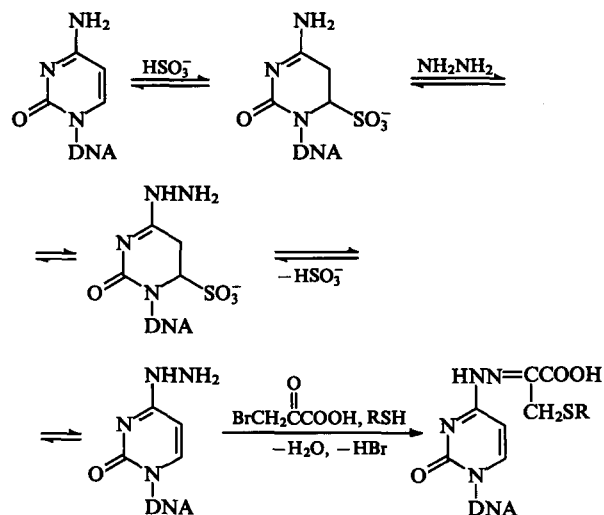
A similar method has been used for the probing of the structure of the hyperacetylated region in nucleosomes. The cell nuclei were treated with dimethyl sulfate for 12 h, after which DNA was depurinated with piperidine with subsequent reduction by sodium tetrahydroborate. This resulted in the formation of covalently bound nuclear particles, in which DNA was attached to the H1/H5 histones.⁶⁹

This method has been used in combination with two-dimensional diagonal electrophoresis for the identification of the proteins forming discrimination contacts with the DNA of the cowpox virus.⁷⁰

A disadvantage of the DNA depurination method, used for the covalent attachment of DNA to DNA-specific proteins, is the distortion of the steric structure of the DNA double helix arising from the multiple methylation of the heterocyclic bases.

Another method for the preparation of protein-nucleic acid conjugates is the modification of the nucleic acid fragments at the heterocyclic bases and the phosphate groups by active alkylating agents.

A procedure for the introduction of a bromoacyl residue into cytidine has been proposed (Scheme 6).⁷¹ The hydrazino-group,

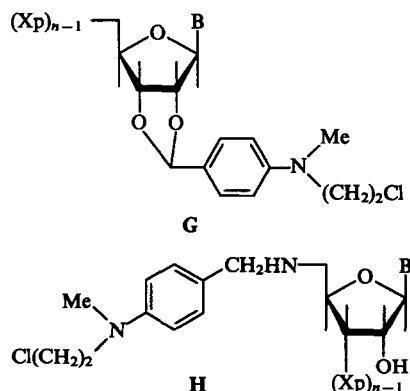


R = protein

introduced into the 4-position of the cytosine ring, interacts with bromopyruvate, which combines with an SH group of the protein. Glutathione has been used as the donor of the SH group in a model system. The optimum conditions for this reaction have been selected. The covalently bound complex of RNA with the protein in the 30S ribosomal subparticle of *E. coli* has been obtained in this way.⁷¹

In another study⁷², the bromoacetyl residue was attached to the 5'-phosphate group of an oligodeoxyribonucleotide. The active derivative of the oligonucleotide obtained — $\text{BrCH}_2\text{CONH}(\text{CH}_2)_2\text{NH-d(pTCTAG)}$ — was used for the affinity modification of the protein of gene 5 of the bacteriophage $\phi 1$. The conditions in the cross-linking reaction were optimal for the formation of a specific protein-nucleic acid complex. The maximum yield of the covalent complex was 20% for a reaction time of 24 h. The decrease in the yield of the protein-nucleic acid complex in the presence of sodium chloride (to 1.3%) and in the presence of competing attachment inhibitors — oligonucleotides not containing an alkyl group (to 9.4%) — demonstrates the specificity of the cross-linking. Since bromoacetate interacts with the nucleophilic centres of the protein, it has been suggested⁷² that the SH group of the cysteine residue of the protein of gene 5 of the bacteriophage $\phi 1$ is alkylated.

Derivatives of oligoribonucleotides containing alkylating groups at the 2',3'-end (G) or the 5'-end (H) have been proposed for the study of the topography of ribosomes.



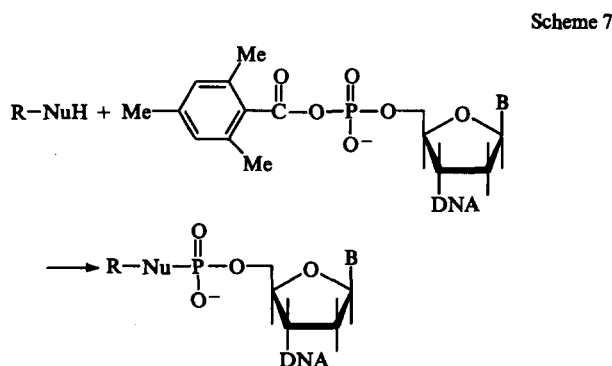
X = ribonucleoside residue,
B = heterocyclic base residue.

Compounds G and H are active alkylating agents and react with ribosomal proteins. The optimum reaction time is believed to be the time required for the half-conversion of the *N*-chloroethyl-*N*-methylamino-group into the ethyleneimmonium cation as a result of the elimination of the chloride ion. The reaction mixtures are incubated at 25 and 37 °C. The yield of the covalent protein–nucleic acid complex is between 10% and 30%.⁴⁹

This method for the introduction of an active group suffers from a disadvantage associated with the modification of only the terminal residues of the oligoribonucleotides, but it has many advantages because of the reactivity of the alkylating groups.

Nucleic acid analogues containing activated terminal phosphate groups are also used for the affinity modification of proteins. The cyclic substituted trimetaphosphate and *N*-cyclohexyl-*N'*-(4-methylmorpholino)ethylcarbodiimide are used as activators. The reaction time is 10 min and the yields of the product of cross-linking to ribosomal proteins are between 1% and 7.5%.⁴⁹

The mixed anhydrides of phosphoric and mesitylenecarboxylic acids in an aqueous medium can phosphorylate different compounds containing nucleophilic groups, for example primary and secondary amines and mercapto-compounds.⁷³ This permits their application in the reaction with a protein. Nucleic acid analogues mesitylated at the terminal phosphate have been used for the covalent attachment to RNase A,⁷⁴ mitochondrial ATPase, myosin,^{73, 75, 76} and other proteins (Scheme 7).

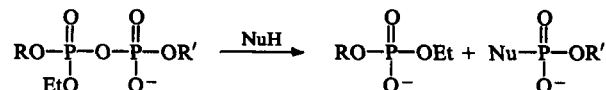


R = protein, Nu = nucleophilic group of the protein,
B = heterocyclic base residue.

The advantages of the mesityl derivatives of oligonucleotides are their stability in aqueous media and low reactivity, which reduces the probability of a nonspecific modification of the protein. According to the results of Sokolova and Tretyakova,⁷⁷ the reactions of the mixed anhydrides of mesitylenecarboxylic and phosphoric acids with strong nucleophiles proceed in several hours, whilst those with weak nucleophiles take several days. The results of the covalent attachment of the mixed anhydride of mesitylenecarboxylic acid and ATP or AMP to myosin were followed from the irreversible inhibition of the enzyme. The reaction time was 1–2 h. In order to obtain the conjugate of RNase A with an oligodeoxyribonucleotide, use was made of reagents such as d[MsC(O)pApApA], d(ApApApMsCO), and d(MsC(O)pTpApGpT), where Ms is the 2,4,6-trimethylbenzoic acid residue. For complexes with a high association constant, the yield of the conjugate was 2%–4% relative to the protein for a reaction time of 7 days. The decrease in the yield of the covalent protein–nucleic acid complex to 0%, which has been noted following a gradual increase in the ionic strength of the solution and when complexes with a low association constant were employed, demonstrates the specificity of the cross-linking.⁷⁴

Shabarova and coworkers⁷⁸ proposed DNA duplexes, containing, in a specified position in the sugar-phosphate backbone, a substituted pyrophosphate group instead of the natural phosphodiester linkage, as affinity reagents for covalent attachment to nucleic acid-recognising proteins. It was established that, in

single-stranded oligodeoxyribonucleotides in an aqueous medium, the anhydride component of the substituted pyrophosphate group is readily and quantitatively cleaved at the phosphorus atom on treatment with nucleophiles via a nucleophilic substitution mechanism. The substitution is accompanied by the formation of a covalent bond between the fragment of the oligodeoxyribonucleotide, bound to the disubstituted phosphate group, and the nucleophile.



NuH = nucleophile,

RO and R'O = fragments of oligodeoxyribonucleotides.

It was shown that the functional groups of the side chains of glutamic acid and arginine may also serve as nucleophiles.⁷⁹

The DNA duplexes containing a substituted pyrophosphate group have been used successfully for the affinity modification of the restriction–modification fragments of *Rsa*I and *Eco*RI⁸⁰ and of the restriction endonuclease *Eco*RII.⁷⁹ These enzymes 'recognise' definite sites in DNA and hydrolyse (restriction endonucleases) or methylate (DNA methyltransferases) them in strictly defined positions. The specificity of their covalent attachment to DNA duplexes with a monosubstituted pyrophosphate internucleotide bond has been demonstrated.^{79, 80}

The advantages of reagents of this type consist in the fact that the substituted pyrophosphate group does not introduce serious changes into the structure of the DNA duplexes; the chemical reaction between the nucleophilic group of the protein and the reactive group of the substrate proceeds at a 'zero distance' between them and, in contrast to photoactive reagents, does not require external activation (for example UV or γ -irradiation). This precludes the possibility of the distortion of the real pattern of the protein–nucleic acid contacts in the interpretation of the results. The disadvantages of the use of DNA duplexes containing a substituted pyrophosphate internucleotide group for the affinity modification of proteins include the need for a close proximity of the nucleophilic group of the protein and the activated group of the nucleic acid and also the lability of the bond formed between the 5'-phosphate group of the oligodeoxyribonucleotide and certain aminoacid residues.

IV. Covalent attachment of nucleic acids to enzymes based on the mode of enzyme action

In the course of the interaction of an enzyme with a nucleic acid, there is a possibility of the formation of a covalently linked protein–nucleic acid intermediate, which then decomposes with formation of the reaction products. In order to achieve the covalent attachment of the protein to the nucleic acid for the study of the structure of the complex by X-ray diffraction or for the determination of the aminoacid interacting with the substrate, it is sufficient to fix this complex at the stage involving the formation of a covalent compound between the enzyme and the nucleic acid.

One of the examples of the use of an enzymic reaction for the preparation of covalent adducts between enzymes and nucleic acid substrate analogues (substrates) is the study of thymidylate synthetase in the interaction with 5-fluoro-2'-deoxyuridine monophosphate (π^5 dUMP). Thymidylate synthetase is an enzyme which transfers a methyl group from 5,10-methylenetetrahydrofolate to uridine with formation of thymidine. The formation of a noncovalent ternary complex, which is converted into a covalent adduct between the protein and the uridine, has been postulated in the interaction of the protein with two substrates. The thiol group of the enzyme attacks the 6-position of the uracil residue in such a way that the C(5) atom can react as a carbanion with methylenetetrahydrofolate.⁸¹ After the transfer of the methyl group from

methylenehydrofolate to the 5-position of uridine, the protein group is eliminated from the 6-position simultaneously with a proton from the 5-position. If a fluorine atom is introduced in place of the hydrogen atom removed, the reaction is blocked at the protein elimination stage.⁸²

The decrease in the growth of lymphocyte cells in a medium containing fl⁵dUMP is also evidence in support of the formation of a covalent adduct, the quantitative characteristics of the process being the same as those of the inactivation of thymidylate synthetase, i.e. the inhibition of cell growth can be accounted for by the interaction of the modified nucleotide with this enzyme.⁸²

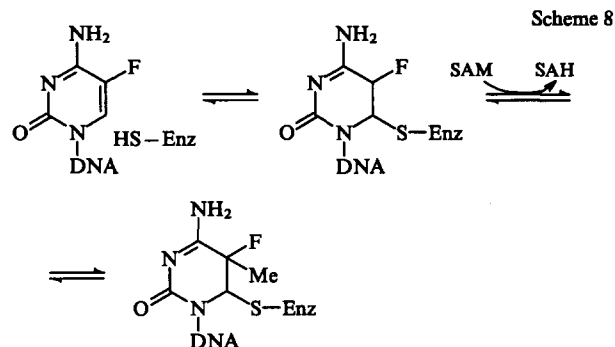
The use of the covalent attachment method is of interest because it makes it possible to determine exactly the stage in which the complex is fixed and to discover the role of the covalently bound aminoacid residue. Under these conditions, the modified nucleotide undergoes the same conformational changes as the substrate. Hence the application of reagents of this kind opens a path to hitherto uninvestigated stages of the catalysis.⁸³ Thus studies have been made^{84,85} of the stereochemical mechanism of the methylation of deoxyuridylylate in relation to the covalent ternary complex of thymidylate synthetase with fl⁵dUMP and 5,10-methylenetetrahydrofolate or 10-propargyl-5,8-dideazafofolate. The high stability of the complexes made it possible to obtain crystals and to investigate their structures by X-ray diffraction. It was shown that, in the formation of the ternary complex, thymidylate synthetase undergoes conformational rearrangements involving four aminoacid residues at the C-end of the protein, which are in immediate proximity to the aromatic ring of the fl⁵dUMP inhibitor.⁸⁵ It has been suggested that before elimination the reaction product undergoes a conformational isomerisation and the pathways leading to its occurrence have been discussed.⁸⁴

The enzymes forming covalent conjugates with the substrate include also DNA [C(5)-cytosine]methyltransferases. It has been virtually demonstrated that they all function via a universal mechanism, according to which in the first stage the nucleophilic aminoacid is attached to the 6-position in the cytosine being modified. In the second stage, the methyl group is transferred from the cofactor SAM to the C(5) carbon atom of cytosine. The introduction of a substituent, which is bound to the carbon atom via a stronger bond than hydrogen, in the 5-position of the base being modified fixes the protein–nucleic acid complex at the covalent adduct stage. It has been suggested that a fluorine atom be used as a substituent of this kind.⁸⁸

The interaction of the modification enzyme *Eco*RII with a DNA duplex containing an azacytidine residue has been investigated.⁸⁶ The formation of the adduct was detected electrophoretically. It was shown that the introduction of azacytidine into the cell system leads to a sharp increase in the expression of the given gene. Bearing in mind the inhibiting effect of this reagent on the methylase *Eco*RII, this fact can be regarded as evidence for the negative regulation by this enzyme of the expression of its gene.⁸⁷

DNA duplexes containing the 5-fluoro-2'-deoxycytidine (fl⁵dC) residue are used for the determination of the aminoacid residues participating in the catalytic step in the methylation of DNA by DNA [C(5)-cytosine]methyltransferases. The conjugate of the methylase *Hae*III with a DNA duplex containing fl⁵dC has been isolated. The substrate in the conjugate was methylated at the C(5) atom of the heterocyclic base. Owing to the presence of fluorine in the 5-position of cytosine, the protein was not split off from the C(6) atom.⁸⁸ Analogous conjugates of DNA duplexes containing fl⁵dC with the enzymes *Eco*RII^{89,90}, *Hha*I,⁹¹ and *dcm*-methyltransferase of *E. coli* K-12⁹² have been isolated. The presence of a covalent complex was demonstrated electrophoretically and detected by autoradiography. The stability of the adduct in denaturing solutions — 6 M urea and 1% solution of sodium dodecyl sulfate (SDS) — was tested. After the denaturation of the protein, the bond between the modified DNA and the methylase in the presence of the cofactor was retained. Kinetic study of the reaction showed that both the enzymic methylation

process and the reaction involving the covalent attachment of the protein to DNA are first-order processes. The results confirm the reaction mechanism proposed previously (Scheme 8).



SAM = S-adenosyl-L-methionine,
SAH = S-adenosyl-L-homocysteine,
Enz = enzyme.

Analysis of the adducts obtained showed that in all cases the Cys residue forms a covalent bond with the carbon atom in the 6-position in cytosine.^{89,90,92} Further studies on these lines lead to the possibility of a detailed description of the stereochemical pathway of the methyl group transfer reaction.⁹¹

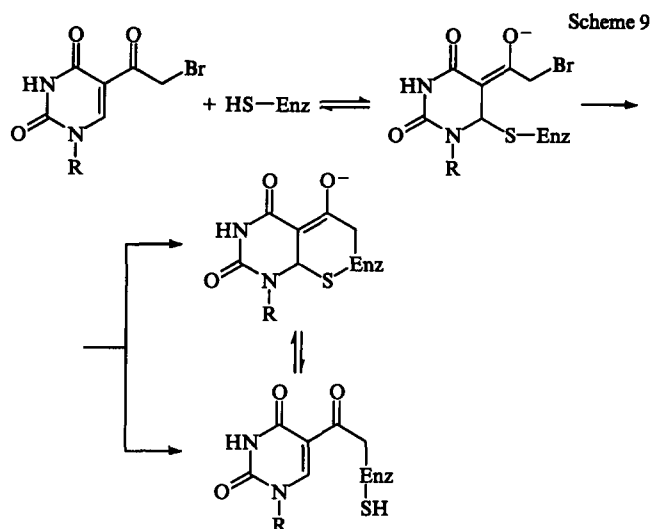
The universality, postulated for DNA [C(5)-cytosine]methyltransferases, extends also to the methyltransferases which interact with RNA. tRNA (m⁵U54)methyltransferase was investigated by Gu and Santi.⁹³ A covalent adduct of this enzyme with tRNA, containing the fl⁵dU residue, was obtained. It proved possible to detect a covalent complex between tRNA (m⁵U54)methyltransferase and RNA, which was stable when treated on a nitrocellulose filter and in electrophoresis under denaturing conditions. It was shown that such adducts are capable of participating in a further methylation reaction and that their formation reaction is reversible.⁹⁴

The preparation of intermediate covalent complexes between topoisomerases and DNA has been described. Topoisomerases are enzymes which alter the number of superturns in cyclic covalently closed DNA, initiating single-stand breaks in DNA.⁹⁵ The topoisomerase of the type I cowpox virus binds specifically to DNA and forms covalent adducts by cleaving the phosphodiester linkage and forming a new bond with the terminal phosphate group produced at the break point. The enzyme recognises in DNA the conservative sequence 5'-(C/T)CCTT-3'. After the uncoiling of the DNA strand, the enzyme transfers the end of the DNA linked to it to the 5'-terminal region of the same strand with regeneration of the covalently closed plasmid ring. The presence of covalent conjugates at an intermediate stage has been demonstrated by transferring the oligonucleotide residue from the complex to the 5'-end of the oligonucleotide and also by blocking the enzymic reaction by an antibiotic inhibiting the activity of topoisomerases, as a result of which the DNA strand remains broken.⁹⁶

It has been suggested⁹⁷ that irreversible inhibitors of the enzymic reaction be employed. Thymidylate synthetase was inhibited by an analogue of uridine triphosphate containing in the 5-position one of the reactive groups: COCH₂Br, CH₂NHCOCH₂I, or NO₂. Such compounds convert reversible enzyme–inhibitor complexes into irreversibly covalently bound complexes. The mechanism of their activity has not been determined accurately, but a possible pathway has been proposed for this process (Scheme 9).

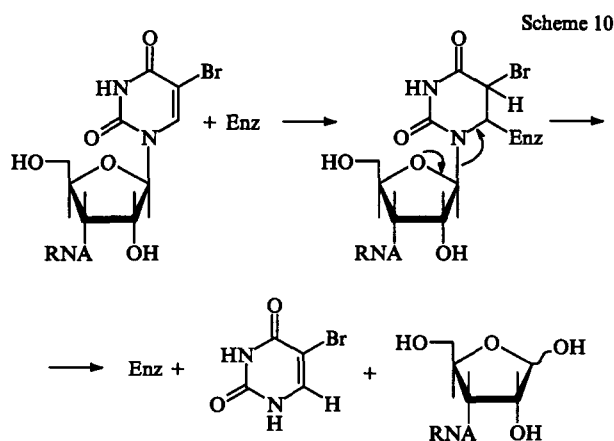
By employing the reagents considered, it is also possible to probe the groups of atoms in the protein which participate in the methylation of the heterocyclic base.

An interesting method involving the employment of tRNA, containing the br⁵U residue, for covalent attachment to amino-



R = ribose triphosphate residue

acyl-tRNA synthetase without activation by UV light has been described.⁹⁸ Although numerous pieces of evidence for the formation of an intermediate covalent adduct between aminoacyl-tRNA synthetase and the uracil ring exist, such compounds had not been obtained earlier. The introduction of a halogen atom, which is highly electronegative, into the heterocyclic base increases the sensitivity of the carbon atom in the 6-position to nucleophiles. The adducts with halogenated uracil derivatives are therefore capable of further rearrangements, leading to the formation of a covalent enzyme-substrate complex. The development of this process leads to the formation of bromouracil and the appearance of a ribose residue at the site occupied previously by 5-bromouracil and of the free enzyme in accordance with Scheme 10.



Optimum conditions for the prevention of the decomposition of the covalent complex were selected: the use of a sulfhydryl reducing agent and of a tenfold excess of 5-bromouridine. The success of the new method was demonstrated in relation to alanine aminoacyl-tRNA synthetase. The inactivation of the enzyme by br⁵U containing tRNA was investigated. It was shown that the elimination of uracil leads to the regeneration of the activity of the protein. The results obtained demonstrate the existence of an intermediate covalent adduct in the functioning of aminoacyl-tRNA synthetases.

V. Methods for the identification and isolation of covalent protein-DNA complexes

For the identification and isolation of covalent protein-nucleic acid adducts, use is made, for example, of the ability of one of the components of the complex to be adsorbed on a carrier and also of the difference between the chemical or physicochemical properties of nucleic acid component of the covalent adduct and of its protein component. Thus, in contrast to the protein, DNA binds to a nitrocellulose filter only under certain conditions. On the other hand, DNA, attached covalently to the protein molecule having an affinity for some kind of polymeric carrier (for example, nitrocellulose), acquires the ability to be precipitated on such filters. The new property can be used to separate the reacted DNA from the free DNA and also to demonstrate that covalent attachment has taken place.

A property of the protein which may be used to identify the covalent adduct is the immune response, i.e. the formation of a specific complex of the given protein with an antibody. In this case, the immunochemical approach may be used to isolate protein-DNA conjugates and for their purification.

The protein bound to the nucleic acid also acquires new features, in its turn, characteristic of the nucleic acid component. One of the applications of this phenomenon is the sedimentation method for the isolation of the attached protein in the case where it is fairly small and does not alter the sedimentation constant of the free nucleic acid in a density gradient. When cells or cell nuclei are irradiated in vivo, this property proves very useful for the isolation of conjugates from complex cell systems. For example, the first stage in the purification of covalent adducts of chromosomal proteins with DNA from a cell culture of *D. melanogaster* tissues has been centrifugation in a CsCl gradient in order to isolate DNA-containing cell fractions.⁴ Gel filtration can also be used for such purposes.

Extraction methods for the isolation of conjugates are associated with the solubility of one of the components in an organic substance, for example of the protein in phenol. The solubility of the protein component in an organic medium promotes the transfer of the covalently bound nucleic acid into the organic phase, whereas the unreacted nucleic acid remains in the aqueous solution.²¹

Examples of the application of methods most frequently used in practical investigations are presented below.

1. Binding to a polymeric carrier

In order to isolate covalent complexes of the DNA adenine methyltransferase (Dam methylase) from *E. coli* with SAM, the protein component of the conjugate was precipitated on a glass filter with 10% trifluoroacetic acid. The presence of a covalent bond between the methyltransferase and the cofactor was demonstrated with the aid of a radioactive label (³H or ¹⁴C) in SAM. As a control, a similar procedure was carried out with a non-covalent complex between the methyltransferase and SAM.¹⁸

The covalent adducts of a DNA-recognising protein from the type 2 adenovirus with ³²P-p(dT)₁₄ were filtered through nitrocellulose filters and washed with solutions containing NaCl or SDS in order to decompose noncovalent specific complexes. The yield of the covalent protein-nucleic acid complex was determined from the radioactivity of the residue on the filter. The same approach (binding on a nitrocellulose filter) was used to purify the covalent adducts of tRNA (m⁵U54)methyltransferase and RNA.⁹³ Toyo Roshi 51 paper filters were used in another study¹⁶ instead of the nitrocellulose filters.

In order to isolate the proteins from the nuclear extract of mouse hybridoma B-cells, participating in the specific recognition of definite DNA sequences, their complexes with oligonucleotides, incorporating not only the binding site but also a 10-membered dA sequence at the 3'-end, were irradiated with UV light. The covalent adducts obtained were isolated on oligo-dT-cellulose. In this case, the elimination of 'unattached' proteins

from the complex was achieved by the formation of an oligo-dA · oligo-dT duplex on a polymer matrix.⁹⁹

Yet another example of the use of a polymeric carrier for the isolation of protein–nucleic acid conjugates is the hybridisation of the products of the treatment with formaldehyde of *E. coli* cells with single-stranded DNA immobilised on cellulose and complementary to the pBR322 plasmid. The conjugates of mRNA and pBR322 DNA with proteins are then separated from the remaining cell material. After being split off from the covalent RNA complex, the protein components were analysed by electrophoretic methods (Laemmli's methods).⁹⁹

2. Electrophoretic isolation methods

Electrophoresis is the most effective method for the isolation of covalently bound protein–nucleic acid conjugates. In the electrophoretic methods of analysis, there is a possibility of the simultaneous determination of both the protein component (by staining with an appropriate dye) and of the nucleic acid (from the ³²P radioactivity). There are two versions of this method differing in the presence or absence of a denaturing agent in the supporting medium.

Thus the isolation of covalent protein–nucleic acid complexes by the 'retardation' method in 1% agarose gel not containing denaturing agents has been described.¹⁰⁰ Covalent adducts of *E. coli* topoisomerase with an oligonucleotide were also identified in a nondenaturing 4.5% polyacrylamide gel.⁹⁶

Two-dimensional electrophoresis in a nondenaturing medium has a greater resolving power. In this case, the reaction mixture is separated initially in one direction, after which one of the components of the protein–nucleic acid complex is subjected to degradation by a chemical or enzymic method and electrophoresis is carried out in the perpendicular direction.²¹ DNA-binding proteins of the cowpox virus, attached covalently to the viral DNA, were identified in this way. The electrophoretic separation in the first direction was carried out in a polyacrylamide gel (the linear acrylamide concentration gradient was from 5% to 15%). In the second direction, the concentration of acrylamide was constant at 12.5%. The proteins were detected from the radioactivity of the ¹²⁵I introduced with the aid of the Bolton–Hunter reagent. The set of marker proteins, used in the electrophoresis in the second direction, made it possible to determine the molecular masses of the attached proteins.

However, the use of nondenaturing gels does not usually afford the complete certainty that the protein–nucleic acid complex is indeed covalent. Denaturing agents, for example SDS or urea, are therefore introduced into the gel. Gel electrophoresis in Laemmli's version with SDS as the denaturing agent is usually employed. The gel concentration varied in different investigations from 10% to 15%.^{10, 17, 19, 25, 29, 33, 34, 87, 101, 102} Preliminary treatment of samples from the SDS procedure with 2-mercaptoethanol, including maintenance for several minutes at 95 °C, guaranteed the complete decomposition of the noncovalent protein–nucleic acid complexes and also the denaturation of the protein. The attachment of nucleic acid fragments to the protein has only a slight influence on the electrophoretic mobility of the latter, because it is abolished by the large negative charge on SDS, while the increase in the mass of the protein after the attachment of the nucleotide or oligonucleotide to the latter is negligible compared with its intrinsic mass. After the electrophoretic separation, the gels are usually stained with a Coomassie dye in order to determine the protein bands and are then dried and autoradiography is carried out in order to visualise the nucleic acid fragments. In the study of Pelle and Murphy,⁵ before determining the positions of the complexes in the gel the latter were transferred by electroblotting on to a nitrocellulose membrane.

After the irradiation of the complexes of a polypeptide present in the transcription complex of the pea and DNA containing br⁵dU the samples were treated with DNase I (in certain experiments an additional treatment with snake venom phosphodiester-

ase was performed).²⁸ After this, they were analysed by electrophoresis in a dilute (5%) polyacrylamide gel.

Nucleic acid was decomposed similarly by micrococcal nuclease and bacterial alkaline phosphatase after the covalent attachment of DNA to histones. A ³²P label was then introduced into the residual oligonucleotide with the aid of polynucleotide kinase (before deposition on a 15% polyacrylamide denaturing gel).⁶⁹ The need for the degradation of DNA is due to its large size and hence low electrophoretic mobility.

The protein component of the complex with nucleic acid can also be subjected to partial cleavage. *N*-Chlorosuccinimide is used for this purpose. After the treatment of the complexes with *N*-chlorosuccinimide, the reaction mixture is deposited on a 10% SDS-containing polyacrylamide gel. The positions of the bands of the partly degraded protein–nucleic acid complex are determined autoradiographically. The set of products of the partial decomposition of such compounds by *N*-chlorosuccinimide is specific to each protein and may be used for the rapid determination of the macromolecules recognising a definite sequence in DNA or RNA.¹⁰³

After covalent attachment to DNA, GCN4 activator of the transcription from yeast was analysed electrophoretically in a gel with another type of denaturing agent—urea. For the denaturation of the 'unattached' complexes, the reaction mixtures were treated with alkali and deposited on a 10% polyacrylamide gel containing 8 M urea. The covalent protein–nucleic acid complex was detected autoradiographically.³⁰

3. Chromatographic isolation methods

Chromatographic methods are more rarely used for the analysis of covalently bound protein–DNA complexes because large amounts of substances are required for the spectrophotometric detection of the reaction products. Nevertheless, for example, in the study of Barbier et al.,²⁶ a mixture of the *lac* repressor with br⁵dU-containing DNA was separated chromatographically on a Sephadex column after irradiation with UV light. When a 200 mM potassium phosphate buffer containing 500 mM KCl was used, the unbound repressor separated from the covalent complex, which was indicated by a well resolved peak. The separation process was followed spectrophotometrically from the absorption at 260 and 280 nm.

The covalent complex of the T4 endonuclease V with an oligonucleotide containing a phenyldiazirine derivative has been isolated on a phosphocellulose column.³⁹

The method for the isolation of the covalent complexes of the methyltransferase *Hae*I with an oligonucleotide containing the fl⁵dC residue by fast protein liquid chromatography (FPLC) on a MonoQ column in a linear NaCl concentration gradient from 0 to 1 M proved effective.⁸⁸

4. Immunochemical methods for the isolation of protein–nucleic acid covalent complexes

Several examples of the use of immunochemical methods for the isolation of protein–nucleic acid covalent complexes have been described in the literature.

The replication protein A was irradiated together with oligonucleotides. After the reaction, the protein and the covalent protein–nucleic acid complex were separated from the unreacted oligonucleotides with the aid of monoclonal antibodies. The reaction mixture was then analysed by the retardation method in a gel.¹³

The proteins from the extract of cell cytoplasm, attached covalently in vitro to nucleic acids, were isolated with the aid of antibodies obtained by the vaccination of mice.⁵

After the covalent attachment of histones to DNA, high-molecular-mass complexes were isolated with the aid of antibodies specific to the acetylated histones.⁶⁹

The protein component of the covalent adduct was determined by the immune precipitation of one of the proteins of the transcription factor II (TBP subunit) after its covalent attachment to DNA as a result of irradiation with UV light.⁴²

VI. Determination of peptides in a protein bound covalently to nucleic acid

The final aim of the covalent attachment of a protein to nucleic acid is the determination of the aminoacids or domains of the protein coming into contact with nucleic acids. To do this, the protein is fragmented after its covalent attachment and its component forming a covalent adduct with the nucleic acid is determined. Numerous methods, both chemical and enzymic, are employed for this purpose.¹⁰⁴ Depending on the conditions, mild acid hydrolysis leads to the formation of large or small protein fragments, but its effect is as a rule nonspecific in relation to particular aminoacid residues and the set of peptides obtained is not reproduced when the hydrolysis of the same protein is repeated. The secondary and tertiary structures of the protein exert some influence on this process. There are also reagents which cleave the peptide bond at a particular aminoacid when the latter is C- or N-terminal. For example, BrCN hydrolyses a specific bond in proteins when methionine is NH₂-terminal.^{105, 106} Bromocyanogen has also been used to determine the DNA-binding domains of the restriction enzymes *EcoRI* and *EcoRV* after their irradiation with UV light in a complex with DNA duplexes containing br³dU residues. Since methionine is rarely encountered in proteins, this made it possible to locate only those regions in the enzymes to which DNA is bound.²⁵ A disadvantage of the method is the severe conditions in the treatment (80% formic acid), under which only the C—C bonds formed on irradiation of protein—nucleic acid complexes with UV light are stable.

The enzymic fragmentation of the protein component of the covalent adduct with the nucleic acid proceeds under milder conditions and is fairly specific when particular proteinases are employed. Rarely and frequently cleaving proteinases are distinguished, which is determined primarily by their specificity and also by the frequency with which certain aminoacids are encountered in proteins. For example, the endopeptidase Lys-C cleaves

proteins into fairly large fragments, which are easier to analyse. However, when this enzyme is employed, it is not possible to locate accurately the active region of the protein. Trypsin is the most frequently employed enzyme. It cleaves the protein specifically at the peptide bonds formed by the carboxy-groups of lysine or arginine.¹⁰⁴ Since the range of aminoacids recognised by them is greater than for the endopeptidase Lys-C, the size of the peptides formed on cleavage is smaller and their number is greater. This complicates the isolation of the peptide bound covalently to the nucleic acid, on the one hand, but it permits a more accurate location of the attached aminoacid, on the other.

When covalent protein—nucleic acid adducts are cleaved by proteolytic enzymes, a large set of peptides is formed, including the protein fragments unattached to the nucleic acid, one or several peptides bound covalently to the nucleic acid, and the products of the hydrolysis of the proteinase itself, because it too may hydrolyse its own peptide bonds (autoproteolysis). In order to avoid autoproteolysis, specially modified trypsin, which hardly undergoes any self-decomposition, is used. For a more complete and exhaustive hydrolysis, the protein is also denatured by 8 M urea, but, since this may prove insufficient, it is treated further with iodoacetamide.¹⁰⁷ After treatment with iodoacetamide, the concentration of urea may be reduced to 2 M, whereupon the effectiveness of the cleavage by trypsin increases sharply, which makes it possible to reduce the trypsin : protein mass ratio to 1 : 25. For this ratio, the autoproteolysis of trypsin is no longer a problem.¹⁰⁸ Table 3 presents the most frequently used methods for the fragmentation of proteins in covalent protein—nucleic acid complexes. In each specific case, the choice of the proteolysis conditions is determined by the effectiveness of the operation of the proteinase (or the chemical reagent) and by the stability of the protein—nucleic acid conjugates. Since the nucleic acid may protect the protein against proteolysis, an individual selection of the protein : proteinase (or reagent) ratio and of the method for

Table 3. Methods for the cleavage of the protein component of the protein—nucleic acid conjugates.

Enzyme or reagent	Enzyme (reagent) concentration or enzyme : substrate mass ratio	Buffer solution for proteolysis	Time /h	Incubation temperature /°C	Ref.
Trypsin	1 : 3.7	83.3 mM tris-HCl, pH 8.0, 16 mM CaCl ₂ , 2 M urea	72	37	51
	1 : 10	2 M urea	4	37	34
	1 : 5000,	25 mM tris-HCl, pH 8.0,	0.3	20	29
	1 : 500,	1 mM EDTA, 0.1 M NaCl			
	1 : 100				
	1 : 25	10 mM tris-HCl, pH 7.5, 4.8 M urea, 0.1 M NaCl	18	25	31
TPCK-trypsin	1 : 20	50 mM NH ₄ HCO ₃ , pH 8.0, 2 M urea	12 (or 48)	37 (or 20)	17
Chymotrypsin	1 : 50,	25 mM tris-HCl, pH 8.0,	0.3	20	14
	1 : 100,	1 mM EDTA, 0.1 M NaCl			
	1 : 200				
	1 : 100 ^a	100 mM NH ₄ HCO ₃	16	37	16
Staphylococcal proteinase V8	1 : 1,	25 mM tris-HCl, pH 8.0,	1	20	14
	1 : 25	1 mM EDTA, 0.1 M NaCl			
	100 µg ml ⁻¹ ^a	50 mM NH ₄ HCO ₃	16	37	89
	36 µg ml ⁻¹	50 mM NH ₄ HCO ₃ , pH 8.0, 0.1 % SDS	12	37	17
Lysine endopeptidase	5 pmol	10 mM K ₃ PO ₄ , pH 6.5, 10% ethylene glycol, 10 mM mercaptoethanol, 2 mM EDTA	4	30	39
<i>o</i> -Iodobenzoic acid	15 mg ml ⁻¹ ^b	80 % AcOH, 4 M guanidine, 1% cresol	24	20	17

^a Preliminary treatment with iodoacetamide. ^b Preliminary treatment with 4-vinylpyridine.

the denaturation of the protein–nucleic acid complex (urea or SDS) is necessary.

After the successful fragmentation of the proteins in their covalent complexes with nucleic acids a new problem arises — the isolation of one or several peptides which were involved in the formation of the covalent adduct with the nucleic acid. Several approaches to the solution of this problem have been described in the literature: the use of electrophoretic methods, extraction into organic solvents, and a different kind of chromatographic purification. Conditions for electrophoresis designed to separate peptides with molecular masses ranging from 1 to 5 kDa have been selected.¹⁰⁹ Phenol extraction of peptides is also used. One purification stage is usually insufficient for the separation of the target compound from other substances, so that column chromatography is almost always used at one of the purification stages.^{108, 109}

Table 4 presents the chromatographic conditions used for the isolation and purification of peptides bound covalently to nucleic acids. For the selection of the column, sorbent, eluent, and other

chromatographic separation conditions, the investigator may use the literature data (Table 4) taking into account the individual features of the conjugate investigated.

After isolation and purification, the amino acid sequence of the peptide is determined.^{108, 110}

Cases are possible where the aim — the determination of the peptide bound covalently to DNA — proves to be unattainable because of the instability of the adduct, insufficient amounts of the protein, and the lack of the necessary equipment. Indirect data are then employed to find the amino acid cross-linked to the nucleic acid. These include the determination of the nature of the bond between the nucleic acid and the protein. Such determination is based on the difference between the reactivities of the functional groups and their hydrolytic stabilities.

If the nucleic acid is attached to the protein via the terminal phosphate group, then, owing to the instability of the covalent complex, problems involving the determination of the peptide usually arise. The phosphodiester or phosphotriester bond formed as a result of the attachment of the protein to hydroxyaminoacids

Table 4. Conditions for the isolation by chromatographic methods of peptides (products of the proteolysis of protein–nucleic acid conjugates) attached covalently to nucleic acids (the separation temperature is not indicated).

Column	Initial eluent	Gradient ^b	Separation time /min	Consumption of eluent /ml min ⁻¹	Detection method ^c	Ref.
Delta-Pak C ₁₈ ; 7.8×300 mm ^a	10 mM CH ₃ COONH ₄ , pH 6.5	70% CH ₃ CN	60	1	SP (214)	18
Delta-Pak C ₁₈ ; 2×150 mm ^a	1.16% CF ₃ COOH	50% CH ₃ CN	60	0.2	SP (214)	18
NAP-10	50 mM NH ₄ HCO ₃	50mM NH ₄ HCO ₃	not indicated	not indicated	SP	34
TSK ODS 120T; 4.6×250 mm	0.05% CF ₃ COOH	48% CH ₃ CN	50	0.8	SP (220)	16
	5 mM NH ₄ HCO ₃	80% CH ₃ CN	50	not indicated	SP (220), RA	16
SynChropak AX300 4.1×250 mm	20 mM K ₃ PO ₄ , pH 6.8, 5% C ₂ H ₅ OH, 50 mM KCl	1 M KCl	90	not indicated	SP (254), RA	14
Waters C ₁₈	100 mM (C ₂ H ₅) ₃ N·CH ₃ COOH, pH 6.8	60% CH ₃ CN	50	not indicated	SP (254), RA	14
Aquapore RP-300; 4.6×250 mm	0.1% CF ₃ COOH	50% Pr ⁱ OH	20	1	SP (220)	39
Beckmann ODS; 4.3×250 mm	50 mM (C ₂ H ₅) ₃ N·CH ₃ COOH	70% CH ₃ CN	45	0.5	SP (222), RA	89
Hydropore-SAX; 4.6×100 mm	50 mM tris-HCl, pH 7.5, 0.5 mM EDTA, 10 mM mercaptoethanol	1 M NaCl	60	1	RA (³ H and ³² P)	51
μBondapak C ₁₈	10 mM CH ₃ COONH ₄ , pH 6.0	80% CH ₃ CN	60	1	SP (214), RA	17
	10 mM CH ₃ COONH ₄ , pH 6.0, 15% CH ₃ CN	45% CH ₃ CN	60	not indicated	SP (214), RA	17

^a Separation temperature 40 °C. ^b Only the gradient-forming component, the concentration of which in the initial eluent increases to the value indicated, is quoted. ^c SP = spectrophotometric method (the wavelength in nm is indicated in brackets); RA = detection based on radioactivity.

is labile under alkaline conditions, the stability of the bond being influenced by the nature of the aminoacid. Thus the adducts with hydroxyaminoacids are more sensitive to alkaline hydrolysis than the adducts with tyrosine. By measuring the dependence of the stability of the covalent protein–nucleic acid complex on the pH, it is possible to reach a conclusion about the nature of the aminoacid bound to the nucleic acid. The phosphodiester nature of the bond may be demonstrated with the aid of snake venom and calf spleen phosphodiesterases, which are able to hydrolyse such bonds.¹¹¹

The nature of the bond between the modification enzyme *EcoRI* and an oligonucleotide has been determined.⁸⁰ The conjugate proved stable in 0.1 M sodium hydroxide solution, but was hydrolysed in 0.1 M hydrochloric acid or in 4 M solution of hydroxylamine at pH 5. This suggested the formation of a covalent bond between the phosphate group of the oligonucleotide and the amino-group of Arg or Lys or the imino-group of His.

VII. Probing the DNA recognising proteins mode of action via cross-linking assay

The covalent attachment method makes it possible to investigate indirectly the protein–nucleic acid interaction because a specific complex is fixed at the binding stage. By varying the parameters of the cross-linking, it is possible to fix different recognition stages.

The complex of the restriction endonuclease *NaeI* and an oligodeoxyribonucleotide duplex containing the *br*³²dU residue has been irradiated with UV light in order to determine the number of enzyme subunits and substrate molecules in the catalytically active enzyme–substrate complex.¹¹² On photoactivation of the substrate in the complex with the protein, a covalent complex was produced. An increase in the reaction time led to the appearance of yet another conjugate. The mobility of the new covalent complex in the polyacrylamide gel corresponds to a macromolecule with a molecular mass approximately twice as great as that of a single *NaeI* subunit. The covalent attachment after additional irradiation time probably resulted in the attachment of a second enzyme molecule to the substrate. This finding constitutes yet another confirmation of the fact that the restriction endonuclease *NaeI* binds to two substrate molecules in the form of a dimer.

The covalent attachment of nucleic acids to proteins on exposure to laser radiation provides even greater possibilities for the indirect study of the mechanism of the protein–nucleic acid interaction. Because of the very short duration of the pulse, it is possible to determine the physicochemical parameters of the protein–nucleic acid recognition — the binding constant.¹⁰¹ The method based on the 'freezing' of the equilibrium states has been used¹⁰¹ for the protein coded for by the 32 gene of the bacteriophage T4 (gp32). This protein binds preferentially to single-stranded DNA. Since during the duration of the pulse there is insufficient time for the protein to pass from one conformational state to another, the yield of the covalent attachment is proportional to the amount of the protein–nucleic acid complexes existing at the given instant, which is determined by the complex formation constant. The dependence of the yield of the product of the covalent attachment on the formation constant of a complex between gp32 and oligo(dT) (known from the literature) was found and the equilibrium constants for other analogous systems were calculated (for example, for the equilibria between gp32 and shorter oligonucleotides, for the same complexes in other buffer solutions, and for the analogous proteins of the same system of the bacteriophage T4). Since the yield of the product of the covalent attachment of gp32 to (dT)_n increases in jumps as a function of the length of the oligomer (up to *n* = 7, there is virtually no covalent attachment of gp32 to the oligodeoxyribonucleotide, while at *n* = 7 the yield of the adduct increases sharply), it has been suggested that the minimum area for the deposition of the protein gp32 on DNA corresponds to seven nucleotide residues. The repeated increase in the yield of the covalent adducts for *n* which is

a multiple of seven confirms this hypothesis, since the deposition of two gp32 molecules on the oligodeoxyribonucleotide now becomes possible.¹⁰¹

Hockensmith et al.¹⁰² chose as the objects of study the proteins coded for by the genes 44 (gp44), 45 (gp45), and 62 (gp62) of the bacteriophage T4, which require nucleotide cofactors as well as Mg²⁺ ions. In the absence of gp45 and also at its low concentrations, DNA forms preferentially covalent adducts with gp44, but, starting from the equimolecular ratio of gp45 and the complex gp44/gp62, the effectiveness of the affinity modification of gp62 increases. Since the protein gp45 has a DNA-dependent ATPase activity, the influence of gp62 on the kinetic parameters of the functioning of gp45 was demonstrated. The nature of the dependence of the covalent attachment of gp44 and gp62 on the gp45 concentration indicates a conformational rearrangement of the DNA-recognising system of the bacteriophage T4 for the equimolecular ratios of all the components. Knowing the yields of the products of the covalent attachment of the proteins considered to (dT)₁₆, (dT)₂₀, (dT)₁₆·(dA)₂₀, (dA)₁₆·(dT)₂₀, and (dT)₂₀·(dA)₂₀, simulating single-stranded DNA, the complexes of the primer and the template, and DNA duplexes with 'blunt' ends, it is possible to determine the disposition of gp32, gp45, and gp62 on the primer, on the template, or on the primer–template complex.

Summarising the foregoing, one should note that a change in the effectiveness of the affinity modification of nucleic acids by proteins reflects conformational transitions and also more complex multisubunit interactions of the latter.¹⁰¹

VIII. Conclusion

Thus the application of the affinity modification method leads to extensive possibilities for the analysis of the structures and mechanisms of the functioning of the proteins interacting with nucleic acids. The principal requirements which must be met by the procedure involving the covalent attachment of a protein to nucleic acids is the creation of optimum conditions for the protein–nucleic acid recognition. The modifications carried out must not distort seriously the structures of the components of the complexes and hence affect the process involving the recognition of nucleic acid analogues by nucleic acid-specific proteins. In our view, the most promising in this sense are the bromo- and azido-substituted nucleic acid analogues as well as nucleic acids containing an activated internucleotide phosphate group. The moderate reactivity of such compounds ensures the specificity of the covalent attachment, since the reaction with the protein becomes possible by virtue of the mutual approach of the reacting centres of both components of the complex.

References

1. T M Cao, M T Sung *Biochemistry* 21 3419 (1982)
2. G R Kunkel, U G Martinson *Nucl. Acids Res.* 5 4263 (1978)
3. I Saito, H Sugiyama, T Matsuura *J. Am. Chem. Soc.* 105 6989 (1983)
4. S V Belikov, A I Belgovsky, O V Preobrazhenskaya, V L Karpov, A D Mirzabekov *Nucl. Acids Res.* 21 1031 (1993)
5. R Pelle, N B Murphy *Nucl. Acids Res.* 21 2453 (1993)
6. D S Gilmour, J T Lis *Proc. Natl. Acad. Sci. USA* 81 4275 (1984)
7. Z Hillel, C-W Wu *Biochemistry* 17 2954 (1978)
8. G F Strniste, D A Smith *Biochemistry* 13 485 (1974)
9. M Buck, W Cannon *Nucl. Acids Res.* 22 1119 (1994)
10. R Mital, Y Albrecht, D Schumperli *Nucl. Acids Res.* 21 1049 (1993)
11. C S Park, Z Hillel, C-W Wu *Nucl. Acids Res.* 8 5895 (1980)
12. V T Yue, P R Schimmel *Biochemistry* 16 4678 (1977)
13. E Seroussi, S Lavi *J. Biol. Chem.* 268 7147 (1993)
14. V Cleghon, D F Klessig *J. Biol. Chem.* 267 17872 (1992)
15. A Aharoni, N Baran, H Manor *Nucl. Acids Res.* 21 5221 (1993)
16. Y Takata, M Fujioka *Biochemistry* 31 4369 (1992)
17. K Subbaramaiah, S A Simms *J. Biol. Chem.* 267 8636 (1992)
18. C Wenzel, W Guschlbauer *Nucl. Acids Res.* 21 4604 (1993)

19. C Wenzel, M Moulard, A Løner-Olesen, W Guschlbauer *FEBS Lett.* **280** 147 (1994)
20. C Taylor, K Ford, B A Conolly, D P Hornby *Biochem. J.* **291** 493 (1993)
21. J Welsh, C R Cantor *Trends. Biochem. Sci.* **9** 505 (1984)
22. A J Varghese *Aging Carcinogenesis Radiat. Biol.* **207** (1976)
23. A Havron, J Sperling *Biochemistry* **16** 5651 (1977)
24. S Maruta, M Burke, M Ikebe *Biochemistry* **29** 9910 (1990)
25. H Wolfes, B A Fleiss, F Winkler, A Pingoud *Eur. J. Biochem.* **159** 267 (1986)
26. B Barbier, M Charlier, J-C Maurizot *Biochemistry* **23** 2933 (1984)
27. R Ogata, W Gilbert *Proc. Natl. Acad. Sci. USA* **74** 4973 (1977)
28. N C Khanna, S Lakhani, K K Tewari *Nucl. Acids Res.* **20** 69 (1992)
29. J M Gott, M C Willis, T H Koch, O C Uhlenbeck *Biochemistry* **30** 6290 (1991)
30. E E Blatter, Y W Ebright, R E Ebright *Nature (London)* **359** 650 (1992)
31. M Katouzian-Safadi, B Blazy, J-I Cremet, J-P Le Caer, J Rossier, M Charlier *Biochemistry* **32** 1770 (1993)
32. M Katouzian-Safadi, B Laine, F Chartier, J-I Cremet, D Belaiche, P Sautiere, M Charlier *Nucl. Acids Res.* **19** 4937 (1991)
33. T T Nikiforov, B A Conolly *Nucl. Acids Res.* **20** 1209 (1992)
34. Y J K Farrar, R K Evans, C M Beach, M S Coleman *Biochemistry* **30** 3075 (1991)
35. C E Catalano, D J Allen, S J Benkovic *Biochemistry* **29** 3612 (1990)
36. S K Syed, S Kim, W K Paik *Biochemistry* **32** 2242 (1993)
37. G A Young, M Woody, C R Vader, R W Woody, B E Haley *Biochemistry* **23** 2843 (1984)
38. P Mitchell, K Stade, M Osswald, R Brimacombe *Nucl. Acids Res.* **21** 887 (1993)
39. N Hori, S Iwai, H Inone, E Ohtsuka *J. Biol. Chem.* **267** 15591 (1992)
40. R K Evans, J D Johnson, B E Haley *Proc. Natl. Acad. Sci. USA* **83** 5382 (1986)
41. N O Reich, E A Everett *J. Biol. Chem.* **265** 8929 (1990)
42. M A Sypes, D S Gilmour *Nucl. Acids Res.* **22** 807 (1994)
43. J Rinke-Appel, N Jünke, R Brimacombe, S Dokudovskaya, O Dontsova, A Bogdanov *Nucl. Acids Res.* **21** 2853 (1993)
44. O Dontsova, V Tishkov, S Dokudovskaya, A Bogdanov, T Döring, J Rinke-Appel, B Greuer, R Brimacombe *Proc. Natl. Acad. Sci. USA* **91** 4125 (1994)
45. O Dontsova, A Kopylov, R Brimacombe *EMBO J.* **10** 2613 (1991)
46. J Rinke-Appel, N Jünke, R Brimacombe, I Lavric, S Dokudovskaya, O Dontsova, A Bogdanov *Nucl. Acids Res.* **22** 3018 (1994)
47. O Dontsova, S Dokudovskaya, A Kopylov, A Bogdanov, J Rinke-Appel, N Jünke, R Brimacombe *EMBO J.* **11** 3105 (1992)
48. S S Dokudovskaya, O A Dontsova, S L Bogdanova, A A Bogdanov, R Brimacombe *Biotechnol. Appl. Biochem.* **18** 149 (1993)
49. G G Karpova, Doctoral Thesis in Chemical Sciences, Moscow State University, Moscow, 1990
50. C A Harrison, D H Turner, D C Hinkle *Nucl. Acids Res.* **10** 2399 (1982)
51. S S Sastry, H P Spielmann, Q S Hoang, A M Phillips, A Sancar, J E Hearst *Biochemistry* **32** 5526 (1993)
52. E Gajewski, M Dizdaroglu *Biochemistry* **29** 977 (1990)
53. M Dizdaroglu, E Gajewski, P Reddy, S A Margolis *Biochemistry* **28** 3625 (1989)
54. L Stryer, in *Biochemistry* Vol. 3 (Translated into Russian; Moscow: Mir, 1985) p. 129
55. C M Arundel, C M Vines, P J Tofilon *Cancer Res.* **48** 5669 (1988)
56. V Jackson *Cell* **15** 945 (1978)
57. G Christiansen, J Griffith *Nucl. Acids Res.* **4** 1837 (1977)
58. K L Brodolin, V M Studitsky, A D Mirzabekov *Nucl. Acids Res.* **21** 5748 (1993)
59. J P Shouten *J. Biol. Chem.* **260** 9929 (1985)
60. J D McGhee, P H von Hippel *Biochemistry* **14** 1281 (1975)
61. J D McGhee, P H von Hippel *Biochemistry* **14** 1297 (1975)
62. M Sugiyama, M Costa, T Nakagawa, T Hidaka, R Ogura *Cells Cancer Res.* **48** 1100 (1988)
63. M D Cohen, C A Miller, L S Xu, E T Snow, M Costa *Anal. Biochem.* **186** 1 (1990)
64. J E Hearst *Annu. Rev. Biophys. Bioeng.* **10** 69 (1981)
65. J W Levinson, L F Leibes, J J McCormic *Biochim. Biophys. Acta*, **447** 260 (1976)
66. E S Levina, S G Bavykin, V V Shick, A D Mirzabekov *Anal. Biochem.* **110** 93 (1981)
67. A D Mirzabekov, S G Bavykin, V L Karpov, O V Preobrazhenskaya, K K Evralidze, V M Tuneev, A F Melinkova, K G Gogvadze, A A Chenchick, R S Beabealashvili *Cold Spring Harbor Symp. Quant. Biol.* **47** 503 (1982)
68. A A Chenchick, R S Beabealashvili, A D Mirzabekov *FEBS Lett.* **128** 46 (1981)
69. K K Ebraldise, T R Hebbes, A L Clayton, A W Thorne, C Crane-Robinson *Nucl. Acids Res.* **21** 4734 (1993)
70. A N Chkheidze, G G Prikhod'ko, V L Karpov, S K Vassilenko, A D Mirzabekov *FEBS Lett* **336** 340 (1993)
71. N Nitta, O Kuge, S Yui, A Tsugawa, H Negishi, H Hayatsu *FEBS Lett.* **166** 194 (1984)
72. M N Vinogradova, V L Drutsa, M G Ivanovskaya, E S Gromova, Z A Shabarova *Biokhimiya* **48** 286 (1983)
73. E V Petushkova, V M Risnik, N I Sokolova, S S Tret'yakova, Z A Shabarova *Biokhimiya* **45** 726 (1980)
74. V L Drutsa, Candidate Thesis in Chemical Sciences, Moscow State University, Moscow, 1978
75. V M Kodentsova, E V Petushkova, S S Tret'yakova, N I Sokolova, Z A Shabarova *Biochem. Int.* **10** 195 (1985)
76. V M Kodentsova, Candidate Thesis in Biological Sciences, Moscow State University, Moscow, 1982
77. N I Sokolova, S S Tret'yakova *Bioorg. Khim.* **9** 1157 (1983)
78. S A Kuznetsova, M G Ivanovskaya, Z A Shabarova *Bioorg. Khim.* **16** 219 (1990)
79. Z A Shabarova, G Ya Sheflyan, S A Kuznetsova, E A Kubareva, O N Sysoev, M G Ivanovskaya, E S Gromova *Bioorg. Khim.* **20** 413 (1994)
80. A A Purmal, Z A Shabarova, R I Gumpert *Nucl. Acids Res.* **20** 3713 (1992)
81. R H Abeles, T A Alston *J. Biol. Chem.* **265** 16705 (1990)
82. S Cox, J Harmenberg *J. Biochem. Biophys. Methods* **25** 17 (1992)
83. K M Ibanetich, D V Santi, in *The Expanding Role of Folates and Fluoropyrimidines in Cancer Chemotherapy* (Eds Y Rustum, J J McGuire) (New York: Plenum, 1988) p. 113
84. D A Matthews, J E Villafranca, C A Janson, W W Smith, K Welsh, S Freer *J. Mol. Biol.* **214** 937 (1990)
85. D A Matthews, K Appelt, S J Oatley, N H Xuong *J. Mol. Biol.* **214** 923 (1990)
86. S Friedman *Nucl. Acids Res.* **14** 4543 (1986)
87. S Som, S Friedman *EMBO J.* **12** 4297 (1993)
88. L Chen, A M McMillan, W Chang, K Ezaz-Nikpay, W S Lane, G L Verdine *Biochemistry* **30** 11018 (1991)
89. S Friedman, N Ansari *Nucl. Acids Res.* **20** 3241 (1992)
90. M W Wyszynski, S Gabbara, E A Kubareva, E A Romanova, T S Oretskaya, E S Gromova, Z A Shabarova, A S Bhagwat *Nucl. Acids Res.* **21** 295 (1993)
91. D S Osterman, G D DePillis, J C Wu, A Matsuda, D V Santi *Biochemistry* **27** 5204 (1988)
92. T Hanck, S Schimdt, H-J Fritz *Nucl. Acids Res.* **21** 303 (1993)
93. X Gu, D V Santi *Biochemistry* **31** 10295 (1992)
94. D V Santi, L W Hardy *Biochemistry* **26** 8599 (1987)
95. F S Spirin (Ed.) *Molekulyarnaya Biologiya. Struktura i Biosintez Nukleinovyykh Kislot* (Molecular Biology. Structure and Biosynthesis of Nucleic Acids) (Moscow: Vysshaya Shkola, 1990)
96. S G Morham, S Shuman *J. Biol. Chem.* **267** 15984 (1992)
97. C B Brouillette, C T-C Chang, M P Mertes *Biochem. Biophys. Res. Commun.* **87** 613 (1979)
98. R M Starzyk, S W Koontz, P Schimmel *Nature (London)* **298** 136 (1982)
99. U Wichser, C Brack *Nucl. Acids Res.* **20** 4103 (1992)
100. J Czichos, M Koehler, B Reckmann, M Renz *Nucl. Acids Res.* **17** 1563 (1989)
101. J W Hockensmith, W L Kubasek, W R Vorachek, P H von Hippel *J. Biol. Chem.* **268** 15712 (1993)
102. J W Hockensmith, W L Kubasek, E M Evertsz, L D Mesner, P H von Hippel *J. Biol. Chem.* **268** 15721 (1993)
103. M Mirfakhraei, A M Weiner *Nucl. Acids Res.* **21** 3591 (1993)

104. S M Avaeva *Khimiya Belka* (Protein Chemistry) Part 1 (Moscow: Replication Laboratory, Faculty of Chemistry, Moscow State University, 1983)
105. E Cross *Methods Enzymol.* 11 238 (1967)
106. W A Schroeder, J B Shelton, J R Shelton *Arch. Biochem. Biophys.* 130 551 (1969)
107. A M Crestfield, S Moore, W H Stein *J. Biol. Chem.* 238 622 (1963)
108. P T Matsudaira (Ed.) *A Practical Guide to Protein and Peptide Purification for Microsequencing* (New York: Academic Press, 1989)
109. R J Simpson, R L Moritz, G S Begg, M R Rubira, E C Nice *Anal. Biochem.* 177 221 (1989)
110. M W Hunkapiler, K Granlund-Moyer, N W Whiteley, in *Methods in Protein Sequence Analysis* (Ed. J E Shively) (Clifton, NJ: Humana Press, 1986)
111. B Juodka, M Pfuetz, D Werner *Nucl. Acids Res.* 19 6391 (1991)
112. B B Baxter, M D Topal *Biochemistry* 32 8291 (1993)

Bacterial polyesters. Synthesis, properties, and applications

B E Geller

Contents

I. Introduction	725
II. Microbiological synthesis of poly(hydroxyalkanoates)	725
III. Structure and properties of poly(hydroxyalkanoates)	729
IV. Biodegradation of poly(hydroxyalkanoates)	731

Abstract. The mechanism of bacterial synthesis of polymers and copolymers of hydroxyalkanoic acids is described. The structural and physicochemical properties of polymers obtained by biosynthesis are identical to those of the polymers obtained by polymerisation of lactones. Polymers and copolymers of hydroxyalkanoic acids are readily crystallisable flexible-chain polymers, capable of forming films and fibres when the degree of polymerisation is higher than 500–600. These compounds are biodegradable. The rate of biodestruction, which leads mainly to oligomeric products, depends on the chemical nature of the compound, on the degree of tacticity in the polymeric chain, and on the degree of ordering in the polymeric substrate. The bibliography includes 105 references.

I. Introduction

The increase in the production and consumption of various polymeric materials has led to increased environmental hazard, including the greenhouse effect. There are some other reasons for this phenomenon, for example:

- the increase in the amount of organic fuel being combusted;
- the increase in the amount of organic raw materials being processed to target products including processing of waste materials;
- the decrease in forest area due to the increase in tree-felling and in the processing of wood;
- the accumulation of waste polymeric materials incapable of biodegradation.

Therefore, the challenge arises to develop new energy-saving methods for the synthesis and processing of polymers accompanied by minimal amounts of CO₂ discharged to the atmosphere. This problem can be solved, for example, by developing biotechnological processes for the synthesis of film-forming and fibre-forming polymers.

Conventional technological schemes for the production of basic polymers [for instance, cellulose, poly(ethylene terephthalate), polypropylene, polyhexanamide, and copolymers of acrylonitrile] require 18–55 GJ of energy per ton of the product. Similar energy expenditure is needed to isolate the target products of microbiological synthesis; however, in this case, the amount of

CO₂ liberated decreases sharply, and the biomass obtained can be included in the hydrocarb energy-chemical cycle.¹

Among the film-forming and fibre-forming polymers that can be synthesised using the microbiological approach, polyesters based on hydroxyalkanoic acids are of considerable interest. Recently, it has been found that some microorganisms are capable of synthesising thermoplastic regular homopolymers and copolymers of β -hydroxyalkanoic acids containing C₁–C₁₁ side groups. Such polymers can undergo biodegradation at a controlled rate.

Comparison of the physicochemical properties of poly(hydroxyalkanoates) (PHA) synthesised by the microbiological method with those of the PHA obtained by polymerisation of the corresponding lactones demonstrated that they are identical, although the primary structures of the polymers are somewhat different. The characteristic features of the polymerisation of lactones were analysed for the first time by Sazonov;² later, studies along these lines were continued.^{3–6} It should be noted that many of the PHA synthesised proved to be biodegradable,⁷ which is very important from the ecological standpoint. PHA are of considerable interest as film-forming and fibre-forming polymers and also as molecular plasticisers compatible with many synthetic and natural polymers.

II. Microbiological synthesis of poly(hydroxyalkanoates)

The target-directed synthesis of polymers based on hydroxyalkanoic acids and their lactones was undertaken for the first time by Van Natta et al.⁸ At present, PHA can be obtained by ionic, hydrolytic, radiation-induced, and UV-induced polymerisation or copolymerisation of β -lactones, δ -lactones, and some other lactones.² Some PHA, for example, poly(ϵ -hydroxyhexanoate) [P(6HH)], are industrial products.

The possibility of using bacterial methods to synthesise PHA was recognised more than 20 years ago, when the accumulation of poly(3-hydroxybutanoate) [P(3HB)] granules in the cytoplasm of the *Alcaligenes eutrophus* bacterium was observed. It was shown that this polymer acts as a reserve compound, i.e. as a source of carbon and energy, for this bacterial culture.^{9–11}

The bacterial P(3HB) is a high-molecular-weight ($\bar{M}_w > 10^5$), readily crystallisable, thermoplastic, biocompatible, and biodegradable polymer.¹² The industrial production of this polymer based on biotechnological processes using *A. eutrophus*¹³ and *A. latus*¹⁴ bacteria was established by the ICI company (UK). By now, procedures for the preparation and properties have been reported for many other polymers built of units of the general formula $\sim[\text{O}-\text{CH}(\text{R})-\text{CH}_2-\text{C}(\text{O})]_n\sim$, where R is a (C₁–C₁₁) saturated,^{15–17} linear unsaturated,^{18–19} or branched unsaturated

B E Geller Department of Chemical Technology of Polymeric Compounds, Mogilev Technological Institute, Prosp. Schmidta 3, 212027 Mogilev, Belarus. Fax (7-022) 244 32 29. Tel (7-022) 244 59 10

Received 13 December 1995

Uspekhi Khimii 65 (8) 782–793 (1996); translated by Z P Bobkova

alkyl,¹⁹ haloalkyl,²⁰⁻²² or aryl²³ radical. It has been shown that microbiological synthesis can be used for the preparation of thermoplastic aliphatic polyesters not only from β -hydroxycarboxylic acids, but also from α -,²⁴ γ -,^{25,26} and δ -hydroxycarboxylic acids.

1. Synthesis of poly(hydroxyalkanoates)

Biosynthesis of homopolymeric and copolymeric PHA by various bacterial strains has been studied in detail by many researchers (Table 1).

Table 1. Bacterial synthesis of various homopolymeric and copolymeric PHA.

Strain	Polymer	Ref.
<i>Alcaligenes eutrophus</i>	(3HB)	27
	(3HB-co-3HP)	24
	(3HB-co-4HB)	26, 28-30, 35
	(3HB-co-3HV)	14, 17, 31, 32
	(3HB-co-5HV)	33
<i>Alcaligenes latus</i>	(3HB-co-3HP)	34
<i>Pseudomonas oleovorans</i>	(3HO)	18
	(3HH-co-3HO)	22

Note. 3HP is 3-hydroxypropionate, 4HB is 4-hydroxybutyrate, 3HV is 3-hydroxyvalerate, 5HV is 5-hydroxyvalerate, 3HH is 3-hydroxyhexanoate, and 3HO is 3-hydroxyoctanoate.

The physicochemical and structural characteristics of PHA obtained using different bacterial strains are very similar.

The biosynthesis pathway of PHA has been considered in detail in relation to the generation of P(3HB) by the *A. eutrophus* culture.^{17,28,31} The block diagram of this process is shown in Fig. 1. The formation of aliphatic acids and their derivatives in organisms is known³⁶ to result from the metabolism of carbohydrates, and the first stage of their formation is one of the last stages of the biodegradation of monosaccharides. The hydroxy-acids thus obtained are subsequently biopolymerised.

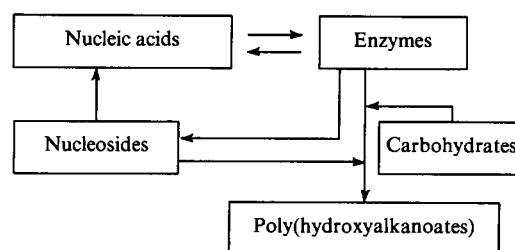
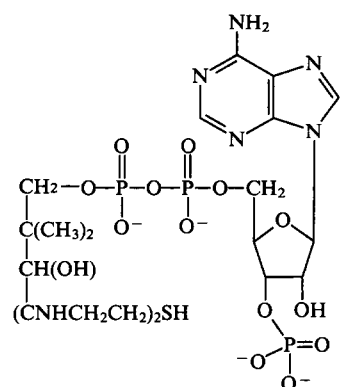


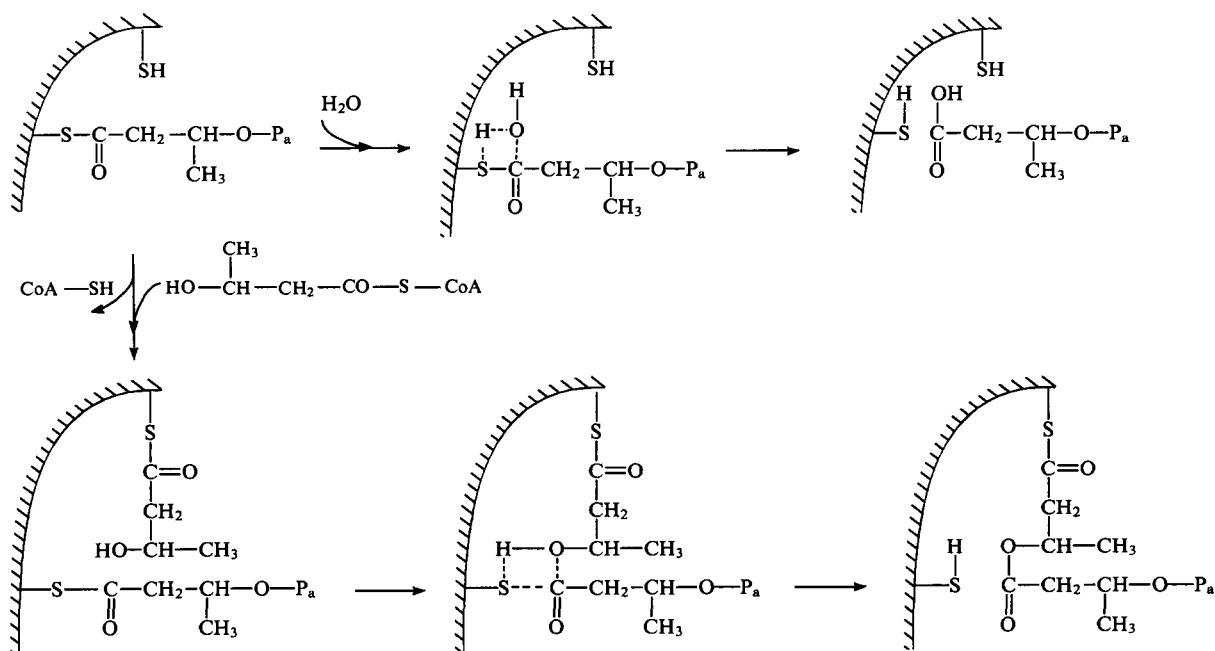
Figure 1. Block diagram of the biosynthesis of poly(hydroxyalkanoates).

The metabolism of carbohydrates occurring with the active participation of the nucleotide adenosinetriphosphate leads to the formation of the compound



coenzyme A (CoA-SH). The acetate of this coenzyme [CoA-SC(O)CH₃] plays an important role in the synthesis of poly-(3-hydroxybutanoate).

P(3HB) and other bacterial PHA are synthesised at 30–35 °C via a series of heterogeneous reactions occurring on the surface of enzymes (Fig. 2).²⁷ Recently, blocks of DNA codons responsible for the synthesis of these enzymes have been determined.^{29, 30, 33} The mechanism of the action of the corresponding enzymes on the



P_a is poly(oligo)hydroxyalkanoates.

Figure 2. Scheme for the enzymic synthesis of P(3HB) with participation of D-(-)-3-hydroxybutyryl-CoA.

dynamics of the synthesis and depolymerisation of P(3HB) has also been considered.³⁷ The polymerase generated by *A. eutrophus* was found to be a polypeptide with $\bar{M}_w = 63\,940$ containing five cystine units, three of which ensure the conformational stability of the enzyme and the other two provide the binding of a hydroxyalkanoic acid molecule on the enzyme surface through the HS groups (Fig. 2). The scheme for this process in relation to the synthesis of P(3HB) is presented in Fig. 3. In the first stage, the enzyme 3-ketothiolase catalyses the reversible condensation of two CoA-SC(O)CH₃ molecules to give the acetoacetyl derivative CoA-SC(O)CH₂C(O)CH₃.

In the second stage, the NADPH-dependent enzyme, acetoacetyl-CoA-reductase (hydrogenase), catalyses the reversible reduction of the acetoacetyl derivative of coenzyme A to D-(-)-3-hydroxybutanoyl-CoA.

The third stage involves a reversible redox reaction catalysed by the NAD-specific dehydrogenase, in which the L-form of 3-hydroxybutanoic acid arising via an independent pathway is converted into the acetoacetyl derivative. The reaction mixture is thus 'fed' with the monomer.

In the fourth stage, the enzyme P(3HB)-polymerase (synthase) catalyses the heterogeneous stereospecific synthesis of P(3HB). The activity of the P(3HB)-polymerase remains virtually invariable during the synthesis of the polyester.

In the fifth stage, depolymerisation of P(3HB) to D-(-)-3-hydroxybutyric acid can occur under the action of the enzyme P(3HB)-depolymerase.

The sixth stage involves the oxidation of the hydroxy-acid with NAD-specific-dehydrogenase to acetoacetic acid, which reacts in the seventh stage with CoA-SH to give CoA-SC(O)CH₂C(O)CH₃.

Evidently, the acetoacetyl derivative of coenzyme A arises as an intermediate both in the synthesis and in the biodegradation of

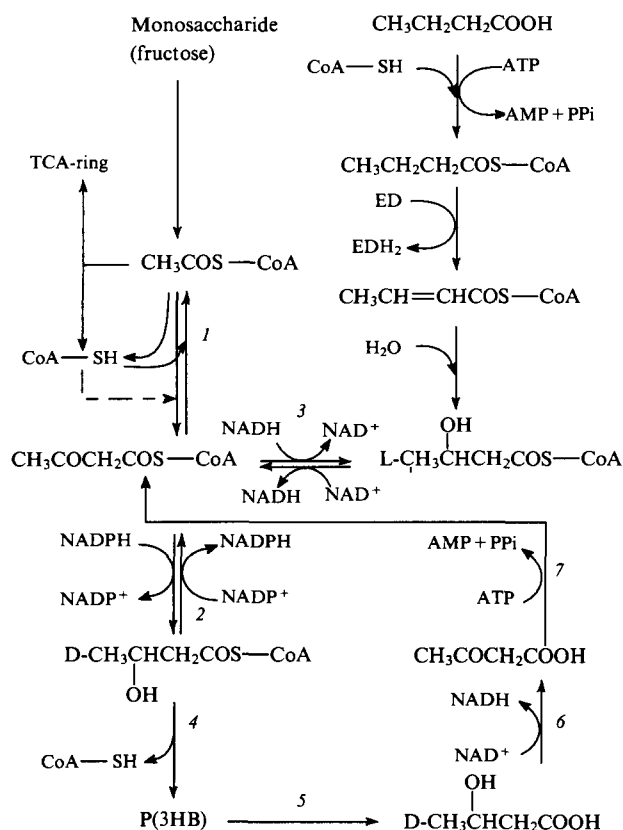


Figure 3. Scheme for the biosynthesis and biodestruction of P(3HB)²⁷ (fructose and butyric acid as the medium); PPi is the amide of nicotinic acid; 'TCA-ring' is the ring of tricarboxylic acids; and ED is the dehydrogenase.

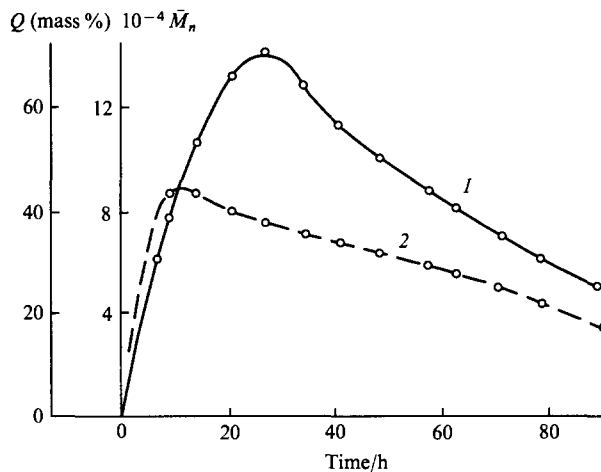
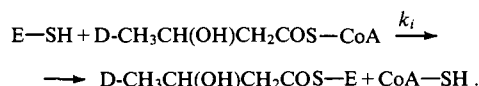


Figure 4. Dynamics of the synthesis of P(3HB) (Q is the polymer yield) with the *Alcaligenes eutrophus* bacteria (1), and of the variation of the molecular weight (\bar{M}_n) of the polymer (2).²⁷

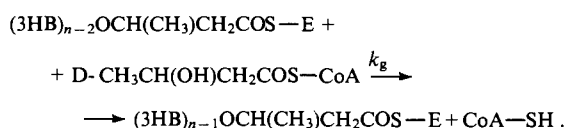
P(3HB). The dynamics of the synthesis of P(3HB) and of the change in the molecular-mass characteristics of the resulting polyester are illustrated in Fig. 4.

The sequence of chemical transformations occurring during the biosynthesis of P(3HB) includes three stages:

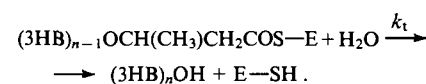
The generation of the polymeric chain:



The growth of the macromolecule:



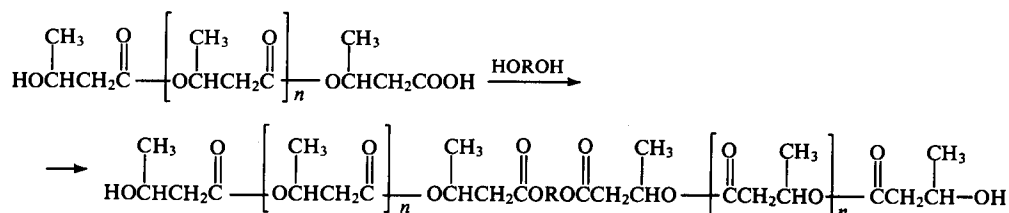
The termination of the polymeric chain:



Here, E is the enzyme and k_i , k_g , and k_t are the rate constants for the chain generation, chain growth, and chain termination, respectively. All three stages are considered as pseudo-first-order reactions.

Under the isothermal conditions of the synthesis, the rate constants k_g and k_t depend on the presence of monomeric carbon sources in the culture medium in which the bacterial strains are grown. As applied to the biosynthesis of P(3HB), this is illustrated by the following data:²⁷

Content/ g dm ⁻³	Rate constants/ h ⁻¹	
	10 ³ k_g	10 ² k_t
Fructose		
5	5.8	28
10	6.6	28
20	6.0	72
Butyric acid		
5	11.2	116
10	8.0	58
20	4.4	150



HOROH = HOCH₂C≡CCH₂OH, HO(CH₂)₄OH, HOCH₂C(CH₃)₂CH₂OH, *cis*-HOCH₂CH=CHCH₂OH.

With the assumptions that the duration of the chain generation stage is much shorter than those of the other stages of the synthesis and that the number of enzyme molecules remains constant during the synthesis, the overall kinetics of the synthesis can be described by the following equation:

$$\bar{P}_n = \frac{\int_0^t R_g dt}{[E] + \int_0^t R_t dt} = \frac{k_g[E]t}{[E] + k_t[E]t}, \quad (1)$$

where \bar{P}_n is the number-average degree of polymerisation, R_g is the rate of the polymeric chain growth, $R_g = k_g[E]$; R_t is the rate of the polymeric chain termination, $R_t = k_t[E]$; and $[E]$ is the concentration of the polymerase. All the kinetic parameters of the process are assumed to be constant during the synthesis. It is clear that the number of P(3HB) molecules produced over the period of time t is

$$N_t = k_g[E]t\bar{P}_{n,t}^{-1} = [E] + k_t[E]t. \quad (2)$$

It follows from equation (2) that $[E]$ can be evaluated from the plot of N_t against t by extrapolating the N_t value to the region $t \rightarrow 0$. It was found that the concentration of the polymerase $[E]$ does not depend on the nature and on the initial concentration of monomeric carbon sources present in the culture medium. Calculations showed that the number of P(3HB)-polymerase molecules is 18 000 per cell.

The accumulation of the polymer in the biomass reaches 75 mass %. Initially, products with $\bar{M}_w = 2 \times 10^6$ are formed; however, during the polymerisation, the \bar{M}_w value decreases to 6×10^5 , whereas the polydispersity of the polymer remains virtually invariable during the whole enzymic cycle: $\bar{M}_w/\bar{M}_n = 2.0 \pm 0.2$. When carbohydrates, hydrocarbons, and acids are no longer present in the culture medium, biodegradation of the polyester begins.

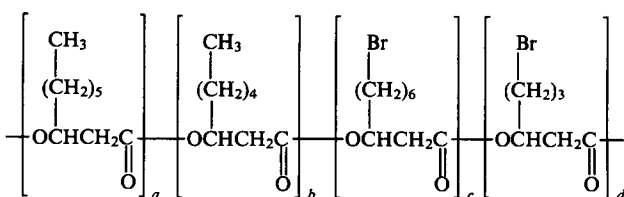
2. Biosynthesis of copolymers of poly(hydroxyalkanoates)

The composition and properties of copolymers obtained by copolymerisation of various hydroxyalkanoates depend only slightly on the bacterial strain chosen. However, the introduction of various monosaccharides as well as alkanes,¹⁸ alkenes,^{18,33} alkanolic acids,^{16,40,41} or alkenolic acids^{19,42} into the culture medium makes it possible to achieve the reproducible synthesis of various PHA copolymers (Table 1). The biosynthesis of poly-(3-hydroxybutyrate-co-3-hydroxypropionate) [P(3HB-co-3HP)], containing 0% to 80% of 3HP units, has been reported.²⁶ The structure and physical properties of the P(3HB-co-3HP) copolymers were studied by ¹H and ¹³C NMR spectroscopy, X-ray analysis, gel-permeation chromatography, differential scanning calorimetry (DSC), and dielectric and dynamic mechanical spectroscopy.

In the primary structure of the copolymers obtained, the 3HB and 3HP units were distributed randomly along the polymeric chain; the molecular weight of these copolymers lies in the range $(1.1 - 3.5) \times 10^5$.

Statistical P(3HB-co-4HB) copolymers with compositions varying over the whole range have been obtained by adding 4-hydroxybutyric acid, butane-1,4-diol, and γ -butyrolactone to the culture medium.^{25,26} The biosynthesis of P(3HB-co-3HV) has been carried out, and characteristic features of its primary structure have been studied.^{9,43-48}

Copolymers of PHA containing brominated repeating units (up to 2–3 mass %) have been prepared²² by cultivation of *Pseudomonas oleovorans* in culture media containing ω -bromoalkanoic acids and octanoic and nonanoic acids. It was noted that in the presence of a bromoalkanoic acid alone, the synthesis of PHA does not occur.



The proportion of bromine-containing units in the PHA remains virtually constant during the synthesis, whereas the yield of PHA initially increases and then decreases asymptotically as the content of carboxylic acids in the culture medium decreases.

The distribution of different units along the chain in all the copolymers of PHA studied is described adequately in terms of Bernoulli probability statistics, and the mole fractions of the copolymers in the polymeric product are described by the Leibnitz formula. For example, the following polynomial is valid for the estimation of the distribution of units in P(3HV-co-3HH-co-3HU), where 3HU is the residue of 3-hydroxyundecanoic acid:^{49,50}

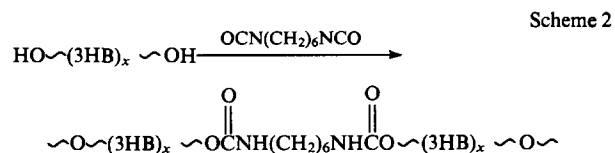
$$P_i = \frac{x+y+\dots+z}{x! \cdot y! \cdot \dots \cdot z!} P_{HV}^x P_{HH}^y \dots P_{HU}^z, \quad (3)$$

P_i is the mole fraction of a comonomer; P_{HV} , P_{HH} , and P_{HU} are the mole fractions of the corresponding comonomers in the PHA.

The polynomial coefficients x , y , \dots , z in the formula (3) characterise the number of probable combinations of the units in the copolymer. The legitimacy of this approach to the description of the primary structure of the macromolecules of PHA copolymers has been confirmed by computer analysis.

Block copolymerisation opens up additional opportunities for varying the primary structure of the PHA. A variant of such synthesis has been described.^{51,52}

The synthesis of a (3HB)_x block copolymer is shown in Scheme 1, and the synthesis of a polyurethane is presented in Scheme 2.



The resulting PHA derivatives exhibit elastomer properties over a fairly broad temperature range and are biodegradable.

The possibility of the enzymic synthesis of high-molecular-weight block copolymers of aliphatic polyesters has recently been considered.⁵³

III. Structure and properties of poly(hydroxyalkanoates)

The possibilities for technical application of PHA depend on the sum of their physicochemical characteristics and on the physico-mechanical properties of the polymeric materials based on them (films, fibres). The presence of the ester bond in the polymeric chain and weak interchain interaction account for a series of specific properties of these polymers. Some physicochemical properties of fibre-forming polymers with $\bar{M}_n = 2 \times 10^4$ based on poly(ϵ -hexanamide) [P(6HA)] and poly(ϵ -hydroxyhexanoate) [P(6HH)] are presented in Table 2.

Table 2. Glass transition temperature (T_g), melting point (T_m), density, and heat capacity at 25 °C of P(6HA) and P(6HH).⁵⁴

Polymer	T_g /°C	T_m /°C	ρ_{25} /kg m ⁻³		C_p /kJ kg ⁻¹ K ⁻¹
			amorphous state	crystalline state	
P(6HA)	52	220	1090	1230	1.512
P(6HH)	-70	69	1081	1200	1.343

The polymeric chains of poly(hydroxyalkanoates) are markedly more flexible than those of the analogous polyamides. PHA obtained by both chemical and microbiological methods are readily crystallisable thermoplastic materials.⁴⁸ Some physicochemical characteristics of various homopolymeric PHA are given in Table 3. These polymers are readily soluble in dichloromethane, dimethylformamide, and some other solvents. The specific features of the supermolecular organisation of a polymeric substrate, including its self-ordering (crystallisation), depend on the special conditions of its synthesis⁵ or biosynthesis,^{7,55,59} on the tacticity of the primary structure of the macromolecules,⁷ and on the conditions of annealing.^{60,61}

For example, rapid cooling of P(3HB) melts leads to its transition to the amorphous state.⁶² However, this polymer readily crystallises, the rate of the accumulation of the crystalline phase being substantially dependent on the temperature of crystallisation (Fig. 5); more precisely, the rate at which spherulites grow increases with temperature and passes through a maximum at $T_c = 80-90$ °C. Crystallographic characteristics of P(3HB), P(3HV), and of P(3HB-co-3HV) copolymers of various compositions have been reported.³² The influence of the degree of crystallinity of PHA on the structural and mechanical properties of these thermoplastic elastomers has been considered.⁶³ These polymers exhibit highly elastic properties both above and below the temperature range of transition to the plastic state (T_p).⁶⁴ When the polymeric substrate is heated above T_p , the proportion

Table 3. Physicochemical properties of poly(hydroxyalkanoates).

Polymer	T_g /°C	T_m /°C	T_{mc}^a /°C	ρ_{25} /kg m ⁻³	$\delta/10^3$ ^b (J m ⁻³) ^{1/2}
P(3HB)	15-16	184	62	1193.4	19.57
P(3HB)	4.0 to -4.5	176	57	1171.2	19.12
P(3HV)	-19 to -20	107	50	1159.7	19.45
P(3HO)	-35 to -37	55	30	1098.1	19.29
P(4HB)	-50 to -51	54	20	1184.2	20.01
P(6HH) ^c	-69 to -70	63	25	1149.3	20.15
P(10HD) ^d	-77 to -78	68	27	1063.2	19.32
P(3H3MB) ^e	76 to 77	245	120	1221.5	22.28

^a T_{mc} is the temperature at which the rate of crystallisation is a maximum;

^b δ is a solubility parameter; ^c P(6HH) is poly(6-hydroxyhexanoate);

^d P(10HD) is poly(10-hydroxydecanoate); ^e P(3H3MB) is poly(3-hydroxy-3-methylbutyrate).

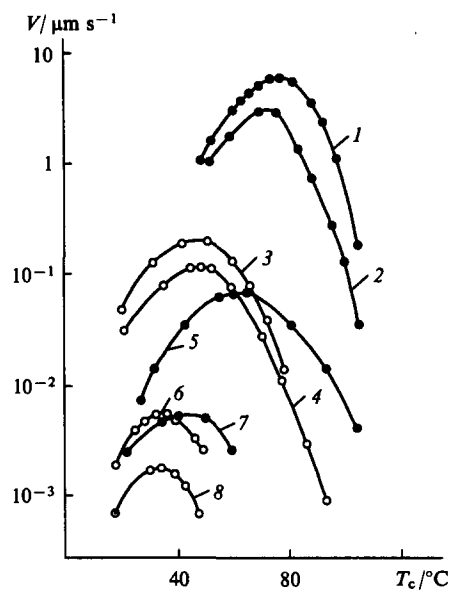


Figure 5. Influence of the temperature of crystallisation (T_c) on the rate of growth of spherulites (V) for P(3HB-co-3HV) copolymers; proportion of the 3HV units, mass %: (1) 0; (2) 8; (3) 95; (4) 82; (5) 19; (6) 71; (7) 34; (8) 55.

of the highly elastic component in the total deformation decreases. On cooling below T_p , the segments of the PHA macromolecules are capable of self-ordering due to the formation of crystalline domains. The appearance of the crystalline domains in the amorphous PHA determines the effect of 'physical links' between the chains in amorphous regions.

It has been suggested⁶⁵ that the hardening of thermoplastic elastomers occurring below T_p can be represented as a 'physical' gel formation. In conformity with this approach, as the degree of crystallinity (α_c) of the polymeric substrate increases, the crystalline domains are converted into crystalline 'clusters'. The size distribution of these 'clusters' is fairly broad. When the critical level of self-ordering ($\bar{\alpha}_c$) is reached, the polymer transforms from the liquid state into the solid state, and the highly elastic component of deformation somewhat decreases. This effect of hardening of the PHA polymeric substrate is referred to as 'the gel formation point' (GP), and its structure is defined as the 'critical gel'. The above description of the hardening of readily crystallisable elastomers (PHA) is similar to that of 'chemical' gel formation studied in detail previously.^{66,67} It is clear that the GP characterises the stage of molecular structuring, during which $\bar{M}_n \rightarrow \infty$, i.e. the kinetic individuality of the chains is lost.

The crystallisation of PHA on cooling has been studied.⁶⁵ The dynamics of the variation of the modulus of elasticity $G(t)$ (defined as the ratio of the stress to the deformation at constant deformation), of the modulus $G''(\omega)$ (defined as the ratio of the stress component that is in phase with the sinusoidally varying deformation component to the magnitude of this deformation), and of the modulus of loss $G''(\omega)$ (defined as the ratio of the stress component phase shifted by 90° with respect to deformation to the magnitude of this deformation) were studied. At constant deformation amplitudes, the $G''(\omega)$ value is a measure of energy dissipation. Since $G(t)$ and $G'(\omega)$ correspond to the stored elastic energy and since the dynamic change at frequency ω is qualitatively equivalent to the change in the nonequilibrium properties at $t = \omega^{-1}$, the $G(t)-t$ and $G'(\omega)-\omega$ dependences plotted in logarithmic coordinates are, to a first approximation, mirror images with respect to the modulus axis of the corresponding plots describing stress relaxation.⁶⁸

According to Winter and Chambon,⁶⁹ in the GP region for $t_0 < t < \infty$, one can write

$$G(t) = St^{-n}. \quad (4)$$

Here, S is the strength of the 'gel' and n is the 'relaxation exponent'. These parameters are the characteristics of a critical 'gel'. At the point of gel formation, the relation $G'(\omega) \sim G''(\omega) \sim \omega^n$ holds at $0 < \omega < \omega_0^{-1}$. In other words, the above dependences plotted in logarithmic coordinates are similar. The loss angle (δ_k) in the GP is independent of ω . Since

$$\delta_k = \frac{\pi}{2} n,$$

then

$$\tan \left[\frac{G''(\omega)}{G'(\omega)} \right] = \tan \left(\frac{\pi}{2} n \right). \quad (5)$$

The latter dependence permits evaluation of the GP of 'physical' gels from $\tan \delta_k$, which has been demonstrated in relation to various crystallisable polymeric systems.⁷⁰ A study of these dependences for P(3HO) showed that the dynamics of crystallisation of PHA depend substantially on the initial temperature of the melt (T_i) and on the temperature of crystallisation of the amorphous polymer obtained by fast cooling (Fig. 6). For example, at 15 °C and 20 °C, the crystallisation of a thermoplastic P(3HO) elastomer occurs by the 'physical' gel formation mechanism with the manifestation of the GP. However, crystallisation of this polymer at 30 °C occurs by a different mechanism. When a P(3HO) melt heated to 90 °C or above is abruptly cooled, the GP is clearly manifested. At lower temperatures of the melt, no GP is observed. Recently,⁷¹ kinetic and thermodynamic aspects of the flexibility and self-ordering of P(3HO) macromolecules in a block have been studied by means of ¹³C NMR spectroscopy. It should be noted that the kinetic features of crystallisation of PHA of identical compositions are somewhat different depending on whether the polymer has been obtained by chemical synthesis or by biosynthesis: in the latter case, the rate of self-ordering is somewhat higher. This is believed⁷² to be due to the plasticising effect of the residual lipids and proteins present in PHA preparations isolated from the biomass.

The crystallographic lattice parameters of P(3HB-co-3HP) specimens with compositions varying over the whole range have been reported.³⁴ It was shown that the rate of radial growth of the copolymer spherulites, containing 11 mol % of 3HP units, under isothermal conditions is approximately 100 times lower than that for homo-P(3HB). Under the conditions of isothermal crystallisation, the degree of crystallinity of the polymeric substrate decreases as the content of the 3HP units in the polymer increases. The crystallographic lattice parameters remain almost constant as the content of 3HB units increases up to 37 mol %. Crystallisation and structural features of the crystalline phase of P(3HB-co-3HV) copolymers have been studied.^{32, 43, 44, 72, 73} Crystallisation of these copolymers has been investigated using films obtained from both melts^{73–75} and solutions.⁴³

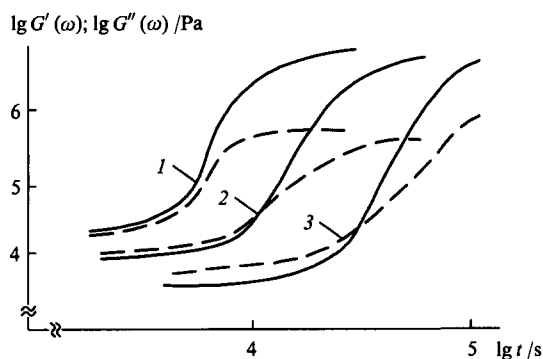


Figure 6. Variation of the $G'(\omega)$ (continuous line) and $G''(\omega)$ (dashed line) moduli as functions of the temperature of crystallisation of P(3HO); $T_i = 90$ °C; $\omega = 1$ rad s⁻¹; T_c /°C: (1) 15; (2) 20; (3) 30.

Crystallographic characteristics of the P(3HB-co-3HV) copolymers of various compositions are listed in Table 4.

Table 4. Structural characteristics of bacterial copolymers P(3HB-co-3HV).³²

Specimen	Type of the lattice	Parameters of the lattice/ nm			α_c (%)	ΔH_0^a /J g ⁻¹
		<i>a</i>	<i>b</i>	<i>c</i>		
P(3HB)	P(3HB)	0.573	1.315	0.596	73	130
P(3HB-co-19% 3HV)	P(3HB)	0.580	1.330	0.599	54	115
P(3HB-co-34% 3HV)	P(3HB)	0.604	1.353	0.600	52	92
P(3HB-co-55% 3HV)	P(3HV)	0.953	0.995	0.559	60	95
P(3HB-co-71% 3HV)	P(3HV)	0.960	1.004	0.558	64	111
P(3HB-co-82% 3HV)	P(3HV)	0.959	1.008	0.560	65	128
P(3HB-co-95% 3HV)	P(3HV)	0.958	1.017	0.558	68	128
P(3HV)	P(3HV)	0.952	1.008	0.556	—	—

^a ΔH_0 is the enthalpy of melting.

When the content of a comonomer is low, the dynamics of crystallisation of PHA copolymers and the structure of the crystalline phase hardly differ from the corresponding characteristics of the homopolymers. In this case, the units of the comonomer act as 'defects' in the crystallographic lattice of the polymeric substrate. However, in some cases, when the distinctions between the sizes and structures of different units are small, the effect of isomorphism is observed.⁷⁶ The ability of the P(3HB-co-3HV) copolymers to form common crystallographic lattices over a wide range of comonomer ratios has led Bluhm et al.⁴⁴ to the hypothesis of diisomorphism, i.e. of the possibility for 3HV units to be incorporated in the crystallographic lattice of P(3HB) and for 3HB units to be incorporated in the lattice of P(3HV). This conclusion was made in a study of the isothermal crystallisation of PHA copolymers in the temperature range from 0 °C to 80 °C by high-resolution ¹³C NMR spectroscopy. It was found that an increase in the temperature of crystallisation results either in a decrease in the degree of crystallinity of the polymeric substrate, when the content of the 3HV units is low, or in its increase, when the content of these units is high (> 50%), which is in agreement with the Bluhm hypothesis.⁷⁷ The rate of radial growth of spherulites of P(3HB-co-3HV) of various compositions in the temperature range from 0 °C to 120 °C is shown in Fig. 5. The maximum rate of growth of the copolymer spherulites is lower than that for P(3HB) and is observed at lower T_c values. It is noteworthy that the physical characteristics of these copolymers depend on the stress of the polymeric material (Table 5).

Table 5. Crystallinity and melting points of P(3HB-co-3HV).

Specimen	Deformation, ϵ_0 (%)	T_m /°C		α_c (%) (25 °C)		
		DSC	IGC	DSC, $\Delta H/\Delta H_0$	X-ray analysis	IGC
P(3HB)	0	179	—	59	64	—
P(3HB-co-7% 3HV)	0	155	—	53	64	68
	4	154	159	49	—	—
	9	154	156	51	—	—
P(3HB-co-21% 3HV)	0	121	—	32	62	65
	4	123	—	35	—	—
	9	121	125	31	—	—
P(3HB-co-27% 3HV)	0	—	—	28	63	60
	4	114	117	23	—	—
	9	112	113	24	—	—

A study of the mechanism of crystallisation of P(3HB-co-3HV) carried out by DSC and by inverse gas chromatography (IGC) has shown⁷⁴ that the melting point of the copolymers decreases with an increase in the content of 3HV units even in the case where the degree of crystallinity remains the same. Apparently, the differences between the melting points (T_m) determined by DSC and IGC are due to the differences in the morphology of PHA specimens. The authors cited⁷⁴ believe that the evaluation of the crystallinity of PHA specimens from their density, which has been proposed in another study,⁷⁸ does not permit one to obtain correct characteristics of the self-ordering of these polyesters.

The physicochemical and mechanical properties of P(3HB-co-4HB) copolymers have been studied over the whole range of comonomer ratios.²⁶ Some physicochemical characteristics of these copolymers are given in Table 6.

Table 6. Physicochemical properties of copolymers P(3HB-co-4HB).²⁶

Proportions of comonomers (mol %)		$10^{-3}\bar{M}_n$	\bar{M}_w/\bar{M}_n	T_c /°C	T_m /°C	ΔH_0 /J g ⁻¹	α_c (%)
(3HB)	(4HB)						
100	0	768	1.9	4	177	130.0	59 ± 5
94	6	494	2.1	-1	162	96.2	56 ± 5
90	10	395	3.0	-3	159	80.1	46 ± 5
72	28	252	2.6	-12	—	—	23 ± 5
15	85	168	3.7	-34	46	62.3	29 ± 5
10	90	327	2.1	-44	48	70.2	—
6	94	315	3.0	-46	48	86.2	42 ± 5
0	100	93	2.4	-50	54	89.7	—

Copolymerisation may lead to a sharp decrease in T_m , in the enthalpy of self-ordering ΔH_0 , and in the degree of crystallinity of PHA (α_c). The mixed amorphous and crystalline nature of the polymeric substrate (for both homopolymeric and copolymeric PHA) has been illustrated by the results of studies of the temperature dependences of relaxation spectra.^{34, 39, 62, 79} The apparent activation energy of the relaxation processes (ΔE_a) is ~ 180 kJ mol⁻¹ (see a published study³⁴). The thermal stability of PHA depends largely on the primary structure of the polymeric substrate. The dynamics of thermal decomposition of linear polyesters of various structures have been analysed.⁸⁰ A kinetic model for the thermodestruction of PHA has been suggested.⁸¹ At 200–300°C this process can formally be described by the following first-order equation:

$$\bar{P}_{n,t}^{-1} = \bar{P}_{n,0}^{-1} + k_d t, \quad (6)$$

where $\bar{P}_{n,0}$ and $\bar{P}_{n,t}$ are the number-average degrees of polymerisation of PHA at the beginning of the isothermal heating and after a period of time t , respectively. The polydispersity of the polymer hardly changes during the process: the ratio \bar{M}_w/\bar{M}_n remains constant.

It has been shown that the thermodestruction decelerates as $\bar{P}_{n,0}$ decreases and that the mechanism of the process depends on the presence of free terminal COOH groups; in the presence of terminal COOH groups, the thermodestruction proceeds by a thermal depolymerisation mechanism, the yield of the corresponding lactone reaching 99% and that of oligomers being only 1%.⁸²

Melts of poly(3-hydroxy-3-methylbutyrate) P(3H3MB), which is a polyester with $T_g = 76$ –77 °C and $T_m = 245$ °C (see Table 3), are fairly stable under a nitrogen atmosphere up to 260–270 °C. As for poly(3-hydroxy-2,2-dimethylpropionate P(3H2MB)), it is thermostable under these conditions up to 300 °C. The maximum rate of thermal depolymerisation (T_{md}) of this polymer has been observed at 450 °C.⁸² When the methyl group is substituted by an alkyl group, the T_{md} value decreases. The larger the alkyl side chain in PHA, the

lower the T_{md} value. The following results were obtained for $\sim[\text{OCH}_2-\text{C}(\text{CH}_3)_2-\text{C}(\text{O})]_n$ polymers:

R	$T_{md}/^\circ\text{C}$
CH ₃	~ 450
CH ₂ CH ₃	415
CH ₂ CH ₂ CH ₃	405
CH ₂ C(CH ₃) ₃	445
CH(CH ₃)CH ₂ CH ₃	390

It has been found²⁶ that when the P(3HB-co-94%4HB) copolymer is kept under nitrogen at 100 °C, its $\bar{P}_{n,0}$ value remains constant. At higher temperatures, thermodestruction becomes more intense, but the \bar{M}_w/\bar{M}_n ratio still remains virtually invariant. The rate of the destruction (k_d) [Eqn (6)] of P(3HB-co-94%4HB) increases from 1.1×10^{-5} to 4.5×10^{-5} min⁻¹ as the temperature is raised from 150 °C to 180 °C. The thermodestruction of this copolymer in this temperature range is also described as statistical depolymerisation. The temperature range in which the thermal depolymerisation occurs shifts depending on the primary structure of the PHA.

The physicochemical properties of films and fibres based on PHA depend essentially on the primary structure of these polyesters and on their molecular-weight characteristics. By analysing the 'load-elongation' curves recorded at 23 °C, Nakamura et al.²⁶ have found the following parameters for P(3HB-co-94%4HB) films: modulus of elasticity 5 MPa, rupture stress (G_r) 39 MPa, ultimate elongation (ϵ_u) 500%. In relation to poly(11-hydroxyundecanoate), it has been shown⁸³ that at $\bar{P}_n \approx 100$, the formation of films and fibres proceeds unsatisfactorily, whereas at $\bar{P}_n \geq 600$, high-strength fibrous and film materials can be obtained.

A systematic study of the sorption activity of films based on bacterial P(3HB) toward vapours of various liquids has been carried out.⁸⁴ It has been found⁸⁵ that the presence of impurities in a polymer has an influence on the supermolecular structure of the polymeric substrate and thus leads to changes in moisture absorption properties and in the thermal stability of the polymer. It was shown⁸⁵ that diffusion coefficients depend on the vapour concentration and on the thermodynamic parameters of the solvents. For example, the empirical dependence of the diffusion coefficient of acetone on the concentration of its vapour in the sorption of acetone by a P(3HB) film is described by the formula $-\ln D = 9.97 - 0.0975$.

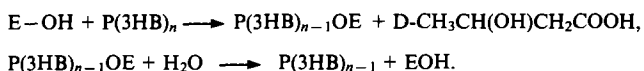
It has been shown in numerous studies that PHA possess a remarkable compatibility (in solutions, melts, and in the solid state) with various natural and synthetic polymers as well as biocompatibility. However, since this property of PHA is largely specific, it will be considered elsewhere.

IV. Biodegradation of poly(hydroxyalkanoates)

Studies performed at ICI⁸⁶ have demonstrated the possibility of effective biodegradation of high-molecular-weight P(3HB) in soil, sea water, bottom-dwelling sediments, and aerobic and anaerobic waste water. Sixteen strains of soil microorganisms were isolated, which are capable of using PHA as an exogenous carbon source and of producing extracellular depolymerases for this purpose. Strains of *Pseudomonas lemoigenes*^{87–90} and *Alcaligenes faecalis*^{91, 92} bacteria can degrade P(3HB) to give trimers and tetramers in the former case or dimers of 3-hydroxyalkanoic acids in the latter case. Recently, PHA depolymerase has been isolated in a pure state from the *Penicillium funiculosum* fungus,⁹³ and the degradation activity of this enzyme toward polymeric and copolymeric PHA has been demonstrated.^{94, 95} As noted above, biodegradation of PHA begins when monomeric carbon sources (monosaccharides, carboxylic acids and their derivatives) are no longer present in the culture medium. During the biodegradation of PHA, \bar{P}_n and the content of PHA in the biomass decrease. At the same time, the number of polymeric chains N_r remains virtually constant. This is due to the fact that the extracellular

PHA-depolymerase is an exo-hydrolase, which destroys the polymeric chain by cleaving the terminal units of 3-hydroxyalkanoic acids.²⁷ Moreover, the polydispersity of the PHA polymeric substrate remains virtually constant and lies in the range $\bar{M}_w/\bar{M}_n = 2.0 \pm 0.3$ even at fairly high degrees of conversion.

It has been found^{7,96} that soluble extracellular P(3HB)-depolymerase produced by *A. eutrophus* can degrade native P(3HB) granules to give monomeric D-(-)-3-hydroxybutyric acid (see Fig. 2). However, information on the structure and properties of this enzyme is quite scarce. It is believed that P(3HB)-depolymerase is a serine esterase having active HO groups.^{92,97} The following sequence of processes has been proposed to describe the destruction of P(3HB) catalysed by this enzyme:²⁷



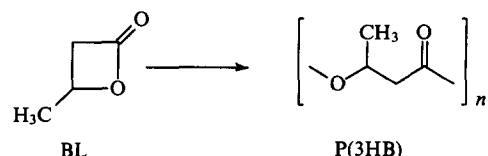
Here, E-OH is P(3HB)-depolymerase. A scheme for this heterogeneous process is shown in Fig. 7. According to a hypothesis,²⁷ the terminal carboxyl groups in P(3HB) react with the positively charged sites on the enzyme 'surface' to yield an active complex. In the case where fructose and butyric acid are used as initial carbon sources in the culture medium, the rate of anaerobic biodegradation of P(3HB) is illustrated by the following data:

Concentration /g dm ⁻³	Biodegradation rate /g h ⁻¹ dm ⁻³
Fructose	
5	0.013
10	0.027
20	0.025
Butyric acid	
5	0.023
10	0.023
20	0.034

The rate of biodegradation of P(3HB) depends substantially on the primary structure of PHA: structural regularity of the chain, and the nature and the sequence of the units in the chain.

The influence of stereoregularity of P(3HB) macromolecules on the dynamics of biodegradation of this polymer has been studied.⁷ For this purpose, electrophoretically homogeneous P(3HB)-depolymerase was isolated from the *Penicillium funiculosum* fungus. The molecular weight of this protein was 38 000. The protein had an isoelectric point at pH 5.8, and its maximum hydrolytic activity was observed at pH 5.5–6.2 and at 30 to 35 °C.⁹⁸ The rate of the biodestruction of PHA is substantially higher than the rate of typical chemical hydrolysis of a polymeric substrate under the same conditions.^{99–103}

Stereoregular PHA were obtained by polymerisation of stereoisomers of β -butyrolactone (BL) in the presence of ionic catalysts according to the following scheme:



The polydispersity of the resulting samples of P(3HB) was low ($\bar{M}_w/\bar{M}_n \approx 1.1–1.5$), the proportion of isomeric units in the copolymers ranging from 50% to 100%. The P(3HB)-depolymerase isolated can catalyse hydrolysis of (R)-P(3HB) but proves inactive with respect to (S)-P(3HB).⁷ As the proportion of (R)-3HB units in the (S,R)-P(3HB) copolymer increases, the rate of biodestruction increases and reaches a maximum when the content of the (R)-3HB units is 75 mol % (Fig. 8). Further increase in the content of the (R)-3HB units (to more than 90 mol %) results in a decrease in the rate of biodestruction. Biodegradation of a P(3HB) copolymer containing (S)- and (R)-units in a 1:1 ratio leads to oligomers with $\bar{P}_n = 3 \pm 1$. The biodegradation of PHA copolymers has also been studied by other workers.^{95, 104}

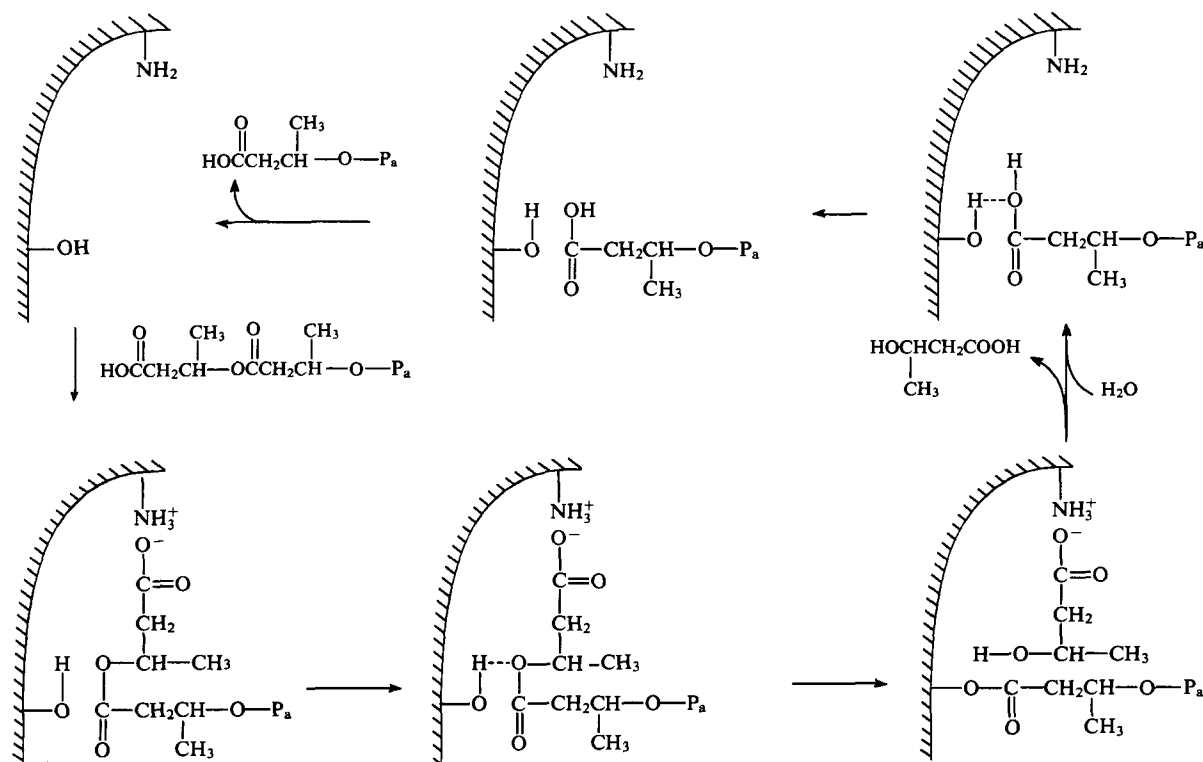


Figure 7. Scheme for the hydrolytic biodestruction of P(3HB) under the action of P(3HB)-depolymerase.²⁷

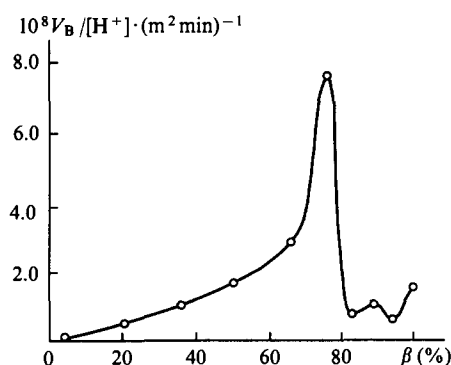


Figure 8. Influence of stereoregularity on the rate of biodegradation of P(3HB); β is the content of the (*R*)-isomer in the stereocopolymer P(3HB), and V_B is the biodestruction rate.

The ability of the extracellular P(3HB)-depolymerase isolated from *Alcaligenes faecalis* to catalyse the hydrolysis of P(3HB-co-4HB) copolymers at 37 °C in a 0.1 M phosphate buffer (pH 7.5) has been studied.²⁶ Data on the dynamics of the variation in the mass of PHA films are shown in Fig. 9. As the content of the 4HB units in the P(3HB-co-4HB) copolymer increases up to 28 mol %, the rate of film destruction increases; however, when the content of the 4HB units exceeds 85 mol %, the rate of destruction diminishes and becomes lower than that in the case of homo-P(3HB).

The dependence of the rate of biodestruction on the composition of P(3HB-co-3HP) is presented in Table 7.

Biodestruction of the P(3HB-co-3HP) at 37 °C in a 0.1 M phosphate buffer (pH 7.5) in the presence of electrophoretically homogeneous P(3HB)-depolymerase isolated from *Alcaligenes faecalis* has been studied.³⁴ As the content of the 3HP units in the copolymer increases up to 20 mol %, the rate of the surface bioerosion of P(3HB-co-3HP) films increases. For higher contents of these units, the rate of destruction of copolymers decreases somewhat. The investigators believe³⁴ that this is due to the specificity of P(3HB) depolymerase.

The rate of the enzymic destruction of PHA has been studied in relation to the P(3HB-co-3HH) copolymer.¹⁰⁵ The influence of the primary structure of the macromolecules of PHA copolymers on the dynamics of biodestruction has been illustrated by Hori et al.⁵¹ The films of polyurethanes synthesised from PHA blocks, various diols, and hexamethylene diisocyanate and having

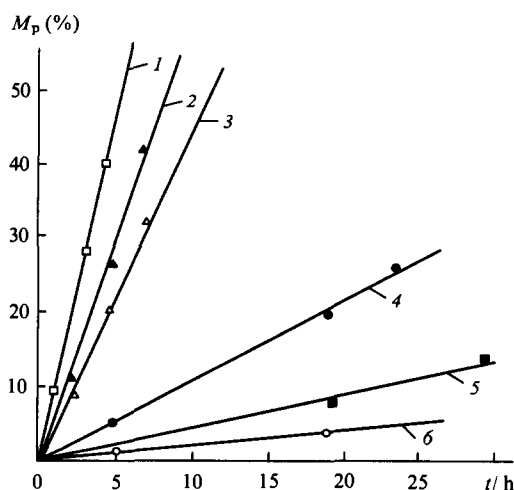


Figure 9. Dynamics of biodestruction of P(3HB)-co-4HB films in aqueous dispersions of P(3HB)-depolymerase at 37 °C and pH 7.5; proportion of (4HB)-units in the copolymer, mol %: (1) 28; (2) 10; (3) 6; (4) 0; (5) 85; (6) 94; M_p is the mass loss.

Table 7. Influence of the composition of P(3HB-co-3HP) on the crystallinity of the polymeric substrate (α_c) and on the loss of mass (M_p) of films during biodestruction.³⁴

PHA	α_c (%)	M_p (%)
P(3HB)	60 ± 5	5.1 ± 1.7
P(3HB-co-7% 3HP)	43 ± 5	17.2 ± 3.4
P(3HB-co-11% 3HP)	41 ± 5	21.7 ± 3.4
P(3HB-co-20% 3HP)	28 ± 5	31.7 ± 5.1
P(3HB-co-37% 3HP)	19 ± 5	26.6 ± 3.4
P(3HB-co-43% 3HP)	16 ± 5	26.3 ± 3.4

$\bar{M}_n = 1.98 \times 10^5$ and $\bar{M}_w/\bar{M}_n = 2.0$ lost about 70% of their mass following the biodegradation at 30 °C for four weeks, whereas the PHA polymer itself was depolymerised by 93%. The variation of the rate of biodegradation of PHA copolymers as a function of the copolymer composition is due to the difference in the degree of structural ordering of the polymeric substrates: as the degree of crystallinity decreases, the rate of destruction increases (see Table 7). Analysis of the biodegradation dynamics makes it possible to conclude that this process is governed by both the specificity of PHA depolymerase and the ordering of the structural elements of the polymeric substrate.

* * *

Film-forming and fibre-forming PHA can be obtained by biosynthesis in fairly high yields and with relatively low power consumption. By varying conditions of the biosynthesis, one can alter the composition and properties of the resulting compounds over a wide range. Polymers and copolymers of hydroxyalkanoic acids are readily crystallisable thermoplastic polymers with flexible chains. They are capable of forming homogeneous mixtures with various natural and synthetic film-forming and fibre-forming polymers, which permits them to be used as high-molecular-weight plasticisers and as diverse additives that change the relaxation spectra of polymeric materials. The biocompatibility of various PHA is also of considerable interest. Many homopolymeric and copolymeric PHA are biodegradable, which accounts for the efficiency of their practical application for the development of polymeric materials that are biodegraded at a controlled rate.

This work was supported by a grant of the International Soros Science Education Program (ISSEP).

References

1. M Steinberg *An Option for the Coal Industry in Utilizing Fossil Fuel Resources with Reduced CO₂-Emissions* (New York: Brookhaven National Laboratory, Upjon, 1989)
2. Yu N Sazonov *Usp. Khim.* **37** 1084 (1968) [*Russ. Chem. Rev.* **37** 463 (1968)]
3. K Teraniashi, M Iida, T Araki, S Jamashita, H Tani *Macromolecules* **7** 421 (1974)
4. M Iida, T Araki, K Teraniashi, H Tani *Macromolecules* **10** 275 (1975)
5. J Zhang, R A Gross, R W Lenz *Macromolecules* **23** 3206 (1990)
6. N Tanahashi, Y Doi *Macromolecules* **24** 5732 (1991)
7. J E Kemmter, S P McCarthy, R A Gross *Macromolecules* **25** 5927 (1992)
8. F I Van Natta, J W Hill, W H Carothers *J. Am. Chem. Soc.* **54** 761 (1932)
9. E A Dawes, P J Senior *Adv. Microbiol. Physiol.* **10** 135 (1973)
10. A J Anderson, E A Dawes *Microbiol. Rev.* **54** 450 (1990)
11. L F Savenkova, E D Zagreba, Z F Gertsberg, R K Ozolin' *Mikrobnaya Konversiya: Fundamental'nye i Prikladnye Aspekty* (Microbial Conversion: Fundamental and Applied Aspects) (Riga: Zinatne, 1990)
12. Y Doi *Microbial Polyesters* (New York: VCH, 1990)
13. H G Segel, G Gottschlak, R V Bartha *Nature (London)* **191** 463 (1966)
14. Eur. P. 0 052 459 (1981); Eur. P. 0 069 467 (1983)
15. M J De Smet, G Eggink, B Witholt, J Kingma, S Wynberg *J. Bacteriol.* **154** 870 (1983)

16. H Brandl, R A Gross, R W Lenz, R C Fuller *J. Appl. Environ. Microbiol.* **54** 1977 (1988)
17. Y Doi, A Tamali, N Kunioka, K Soga *J. Appl. Microbiol. Biotechnol.* **28** 330 (1988)
18. R G Lageveen, G W Huisman, H Presuting, P Katelaar, G Eggink, B Witholt *J. Appl. Environ. Microbiol.* **54** 2924 (1988)
19. K Fritzsche, R W Lenz, R C Fuller *Int. J. Biol. Macromol.* **12** 85 (1990)
20. Y Doi, C Abe *Macromolecules* **23** 3705 (1990)
21. C Abe, J Taima, J Nakamura, Y Doi *Polym. Commun.* **31** 404 (1990)
22. J D Kim, R W Lenz, R C Fuller *Macromolecules* **25** 1852 (1992)
23. J D Kim, R W Lenz, R C Fuller *Macromolecules* **24** 5256 (1991)
24. S Nakamura, M Kunioka, Y Doi *Macromol. Rep.* **28A** 15 (1991)
25. Y Doi, M Kunioka, Y Nakamura, K Soga *Macromolecules* **21** 2722 (1988)
26. Y Nakamura, Y Doi, M Scandola *Macromolecules* **25** 4237 (1992)
27. Y Kawaguchi, Y Doi *Macromolecules* **25** 2324 (1992)
28. M Kunioka, Y Nakamura, Y Doi *Polym. Commun.* **29** 174 (1988)
29. Y Doi, A Segawa, M Kunioka *Int. J. Biol. Macromol.* **12** 108 (1990)
30. Y Doi, A Segawa, S Nakamura, M Kunioka, in *Novel Biodegradable Microbial Polymers* (Ed. E A Dawes) (Dordrecht, Netherlands: Kluwer Academic Press, 1990) p. 37
31. Y Doi, M Kunioka, Y Nakamura, K Soga *Macromolecules* **20** 2988 (1987)
32. M Scandola, G Ceccorulli, M Pizzoli, M Gazzano *Macromolecules* **25** 1405 (1992)
33. Y Doi, A Tamaki, M Soga *Macromol. Chem., Rapid Commun.* **8** 631 (1987)
34. E Shimamura, M Scandola, Y Doi *Macromolecules* **27** 4429 (1994)
35. M Kunioka, Y Kawaguchi, Y Doi *J. Appl. Microbiol. Biotechnol.* **30** 569 (1989)
36. A L Ternay *Contemporary Organic Chemistry* (Philadelphia: Saunders, 1968)
37. D G H Ballard, P A Holmes, P J Senior, in *Recent Advances in Mechanistic and Synthesis Aspects of Polymerisation* (Eds M Fontanill, A Guyot) (Zancaster: Reidel, 1987) p. 219
38. T Nakada, T Fukui, T Saito, K Miki, C Oji, S Matsuda, A Ushijima, K Tomita *J. Biol. Chem.* **256** 625 (1981)
39. T Fukui, M Ito, K Tomita *Eur. J. Biochem.* **127** 423 (1982)
40. H Preusting, A Nijonhuis, B Witholt *Macromolecules* **23** 4220 (1990)
41. R A Gross, C De Mello, R W Lenz, H Brandl, R C Fuller *Macromolecules* **22** 1106 (1989)
42. A Ballistreri, G Montando, G Impallomeni, R W Lenz, J B Kim, R C Fuller *Macromolecules* **23** 1231 (1990)
43. S Bloembergen, D A Holden, G K Hamer, T J Bluhm, R H Marchessault *Macromolecules* **19** 2865 (1986); **22** 1663 (1989)
44. T L Bluhm, G K Hamer, R H Marchessault, C A Fyfe, R P Veregin *Macromolecules* **19** 2871 (1986)
45. Y Doi, M Kunioka, Y Nakamura, K Soga *Macromolecules* **19** 2860 (1986)
46. N Kamiya, Y Jamamoto, Y Inoue, R Chujo, Y Doi *Macromolecules* **22** 1672, 3800 (1989)
47. P P King *J. Chem. Technol. Biotechnol.* **32** 2 (1982)
48. P A Holmes *Phys. Technol.* **16** 32 (1985)
49. A Ballistreri, G Montando, M Giuffrida, R W Lenz, J B Kim, R C Fuller *Macromolecules* **25** 1846 (1992)
50. M S Montando, A Ballistreri, G Montando *Macromolecules* **24** 5051 (1991)
51. Y Hori, M Suzuki, Y Okeda, T Imai, M Sakaguchi, Y Takahashi, A Jamaguchi, S Akatagawa *Macromolecules* **25** 5117 (1992)
52. L P Razumovskii, L L Razumov, A L Iordanskii, G E Zaikov *Kauch. Rezina* **6** 2 (1994)
53. E M Brazwell, D J Filos, C I Morrow *J. Polym. Sci. Part A, Polym. Chem.* **32** 3 (1995)
54. V P Privalko *Spravochnik po Fizicheskoi Khimii Polimerov* (Handbook of the Physical Chemistry of Polymers) Vol. 2 (Kiev: Naukova Dumka, 1984)
55. E A Dawes *Microbial Energetics* (New York: Chapman and Hall, 1986)
56. H Brandl, R A Gross, R W Lenz, R C Fuller *Adv. Biochem. Eng. Biotechnol.* **41** 78 (1990)
57. R N Findlay, D C White *Appl. Environ. Microbiol.* **45** 71 (1973)
58. R J Capon, R W Dunlop, E Z Chisalberti, P R Jeffries *Phytochemistry* **22** 1181 (1983)
59. L L Wallen, W K Rohwedder *Environ. Sci. Technol.* **8** 576 (1974)
60. P J Barham, H H Keller, E L Otun, P A Holmes *J. Mater. Sci.* **19** 2781 (1984)
61. P J Barham, H H Keller *J. Polym. Sci., Polym. Phys. Ed.* **24** 69 (1986)
62. M Scandola, M Pizzoli, G Ceccorulli, A Cesaro, S Paoletti, L Navarini *Int. J. Biol. Macromol.* **10** 373 (1988)
63. R H Marchessault, C J Monasterios, F G Morin, P R Sundararajan *Int. J. Biol. Macromol.* **12** 158 (1990)
64. A A Geller, B E Geller *Prakticheskoe Rukovodstvo po Fizikokhimii Voloknobrazuyushchikh Polimerov* (Practical Manual on the Physical Chemistry of Fiber-Forming Polymers) (Moscow, Leningrad: Khimiya, 1972)
65. H W Richtering, K D Gagnon, R W Lenz, R C Fuller, H H Winter *Macromolecules* **25** 2429 (1992)
66. S P Papkov *Studneobraznoe Sostoyanie Polimerov* (The Gel-Like State of Polymers) (Moscow: Khimiya, 1974)
67. V V Kuleznev, V A Shershnev *Khimiya i Fizika Polimerov* (The Chemistry and Physics of Polymers) (Moscow: Vysshaya Shkola, 1988)
68. J D Ferry *Viscoelastic Properties of Polymers* (New York, London, 1961)
69. H H Winter, F Chambon *J. Rheol.* **30** 367 (1986); **31** 683 (1987)
70. J G Lin, D T Mallin, J C W Chien, H H Winter *Macromolecules* **24** 850 (1991)
71. S Spyros, Ph Dais, R H Marchessanet *J. Polym. Sci., Polym. Phys. Ed.* **33** 367 (1995)
72. G N Barnard, J K M Sanders *J. Biol. Chem.* **264** 32 (1986)
73. M Kunioka, A Tamaki, Y Doi *Macromolecules* **22** 694 (1989)
74. W J Orts, M Romansky, J E Guillet *Macromolecules* **25** 949 (1992)
75. S J Organ, P J Barham *J. Mater. Sci.* **26** 1368 (1991)
76. G Allerga, J W Bassi *J. Adv. Polym. Sci.* **6** 549 (1969)
77. N Kamija, M Bakurai, Y Inoue, R Chujo *Macromolecules* **24** 3888 (1991)
78. H Mitomo, P J Barham, A Keller *Polym. Commun.* **29** 112 (1988)
79. M Scandola, G Ceccorulli, Y Doi *Int. J. Biol. Macromol.* **12** 112 (1990)
80. N Grassie *The Chemistry of High Polymer Degradation Processes* (London: Butterworth, 1956)
81. M Kunioka, Y Doi *Macromolecules* **23** 1933 (1990)
82. L E Manring, R C Bluhm, W J Simonsick, D J Ademan *Macromolecules* **25** 4863 (1992)
83. H Batzer *Macromol. Chem.* **10** 13 (1953)
84. T L Lebedeva, A L Iordanskii, A V Krivandin *Vysokomol. Soedin., Ser. A* **36** 1113 (1994)
85. D R Razumovskii, A L Iordanskii, G E Zaikov *Vysokomol. Soedin., Ser. A* **37** 113 (1995)
86. P A Holmes *Conference on Biological Engineering Polymers* (Cambridge: Churchill College, 1986)
87. P Delagield, M Dondoroff, N J Palleroni, C J Zusty, R Contopoulos *J. Bacteriol.* **90** 1455 (1965)
88. C J Zusty, M Doudoroff *Proc. Nat. Acad. Sci., USA* **56** 960 (1966)
89. M W Stinson, J M Merrick *J. Bacteriol.* **119** 152 (1974)
90. K Nakayama, T Saito, T Fukui, Y Shirakura, K Tomita *Biochim. Biophys. Acta* **827** 63 (1985)
91. T Tanio, T Fukui, Y Shirakura, T Saito, K Tomita, T Kaiho, S Masamune *Eur. J. Biochem.* **124** 71 (1982)
92. J Shirakura, T Fukui, T Saito, Y Okamoto, T Narikawa, K Koide, K Tomita, T Takemasa, S Masamune *Biochim. Biophys. Acta* **880** 46 (1986)
93. C L Brucato, S S Wong *Arch. Biochem. Biophys.* **290** 491 (1991)
94. G P Smith, B Press, D Eberiel, R A Gross, S P McCarthy, D L Kaplan *Polym. Mater. Sci. Eng.* **63** 867 (1990)
95. J M Mayer, M Greenberger, D L Kaplan, R A Gross, S P McCarthy *Polym. Prepr. Am. Chem. Soc., Div. Polym. Chem.* **31** 439 (1990)
96. H Hippe, H G Schlegel *Arch. Microbiol.* **56** 278 (1967)
97. G W Huisman, R Wonink, R Meima, B Kazemier, P Terpstra, B Witholt *J. Biol. Chem.* **266** 2197 (1991)
98. C L Brucato, S S Wong *Arch. Biochem. Biophys.* **290** 497 (1991)
99. C J Holland, A M Jolly, M Jasin, B J Tighe *Biomaterials* **8** 289 (1987)
100. N D Miller, D E Williams *Biomaterials* **8** 129 (1987)
101. Y Doi, Y Kanesawa, Y Kawaguchi, M Kunioka *Macromol. Chem. Rapid Commun.* **10** 227 (1989)
102. J C Knowles, G W Hastings *Biomaterials* **12** 210 (1990)
103. Y Doi, Y Kanesawa, M Kunioka, T Saito *Macromolecules* **23** 26 (1990)
104. G P Smith, B Press, D Eberiel, R A Gross, S P McCarthy, D L Kaplan *Polym. Mater. Sci. Eng.* **63** 867 (1990)
105. E Shimamura, K Kasura, G Kobayashi, T Shiotani, S Ju, Y Doi *Macromolecules* **27** 878 (1994)

Unusual monosaccharides: components of O-antigenic polysaccharides of microorganisms

N K Kochetkov

Contents

I. Introduction	735
II. General observations concerning isolation, determination of structure and identification of monosaccharides and their derivatives present in O-antigenic PS	736
III. Unusual monosaccharides forming a part of O-antigenic PS	738
IV. Non-carbohydrate substituents in monosaccharide units	755
V. Conclusions	765

Abstract. The data on new monosaccharides detected in O-antigenic polysaccharides of Gram-negative bacteria have been surveyed. The results of isolation and structure determination of these unusual monosaccharides have been arranged and described systematically. The NMR spectroscopy techniques are shown to be promising for the O-antigenic polysaccharides structure determination. The information about fine structure of monosaccharides which constitute the base of important class of microbial polysaccharides, is of great significance for applied studies, first of all, the design and synthesis of biologically active substances. The bibliography includes 216 references.

I. Introduction

Carbohydrate-containing biopolymers are among the major components of the living cell where they play a role of building blocks and energy donors and provide for the normal course of some highly specific biological processes coupled with the specific properties of the cell surface. Of those, the most abundant ones are polysaccharides (PS) made up of monomeric units, i.e., monosaccharides. The biological functions of PS specifically correlate with their structure. This structure–function relationship is especially well-defined in PS localised on the cell surface of Gram-negative bacteria. These PS determine the specificity of cell interactions with the environment which reflects on the fine immunochemical characteristics of the bacterium (serological reactions), on the specificity of cell interaction with bacteriophages (phage transformation of the microbial cell) and host tissues as well as on other highly specific biological processes.

The biological specificity of PS is determined by the peculiarities of the molecular structure of these biopolymers which, in turn, depends on the structure of the monomers (monosaccharides) in the biopolymer, their sequence in the polymeric chain and the mode of binding of the monomeric units. Whereas the first two factors, the monomeric composition and the sequence of the monomeric units, are not specific for the PS structure only but also for the structure of proteins and nucleic acids, the last factor determines the type of intermonomer binding and is unique to PS.

This is due to the multifunctionality of monosaccharide residues containing several hydroxy groups at chiral carbon atoms. The existence of several hydroxy groups provides for the formation of several sterically unique intermonomer glycosidic bonds, thus giving rise to a complex (often branched) polymeric chain and increases manifold the possibility of variations in the structure of PS built up from these monomers.

Another circumstance which greatly favours the existence in Nature of a broad spectrum of polysaccharide structures is the diversity of the monomeric units which may serve as building blocks for the polymeric carbohydrate chain. Whereas the diversity of nucleic acids is provided by only four nucleotides, and the number of amino acids in most proteins does not exceed 12–15, the diversity of PS is provided by more than a hundred monosaccharides and their derivatives.

Among the immense variety of PS isolated from natural sources, the most diversified (as regards their structure and monosaccharide composition) and most thoroughly studied are the PS of the outer cell membrane of Gram-negative bacteria. The primary structure of many of those has been established. These PS are important constituents of complex biopolymers, the so-called lipopolysaccharides (LPS)¹ localised on the cell surface of Gram-negative bacteria. Lipopolysaccharides consist of the lipid component (lipid A) incorporated into the microbial cell outer membrane, and the polysaccharide chain which, via a short oligosaccharide (so-called 'core') is attached to the lipid. The polysaccharide chain is exposed on the cell surface and is in direct contact with the environment, thereby providing, together with proteins, a unique pattern ('membrane mosaic') which determines the ultimate specific characteristics of the bacterial surface.

These PS are somatic bacterial antigens generally termed O-antigenic polysaccharides. They represent regularly arranged block polymers which only in rare instances occur as homopolymers but are usually composed of repeating oligosaccharide units, each of which contains 2 to 8 monosaccharide residues.² It may appear that such block organisation of the biopolymer restricts the number of plausible structures of O-antigenic PS. However, actually, because of the above peculiarities (great diversity of intermonomer glycosidic bonds, possibility to form branched chains and a great number of structurally distinct monosaccharides or their derivatives), the number of plausible structures of oligosaccharide units (and, consequently, of corresponding PS) is enormous amounting to tens of thousands (even when the polymer units are built up of only 3–4 monosaccharides).

It should be stressed that in contrast to PS of plant and animal cells, which are as a rule built up of a limited number of the most

N K Kochetkov Zelinskii Institute of Organic Chemistry, Russian Academy of Sciences, Leninskii prosp. 47, 117913 Moscow, Russian Federation. Fax (7-095) 135 53 28. Tel. (7-095) 137 61 48

Received 14 February 1996

Uspekhi Khimii 65 (9) 799–835 (1996); translated by R L Birnova

commonly occurring monosaccharides, PS of microbial origin contain a large number of less abundant monosaccharides often detected exclusively in these biopolymers. Very likely, only antibiotics, many of which also contain unusual monosaccharides, may effectively compete with their great diversity.

So far, the biosynthesis of monosaccharides present in PS, including some structurally unusual ones, has been studied in considerable detail. The pathways of formation of various monosaccharide structures from primary photosynthetic products have been elucidated: these shed more light on the diversity of the monomers utilised by microorganisms for the synthesis of the O-antigenic PS chain. These data have been considered in the review of Shibaev.³

In many cases structurally unusual monosaccharides or their derivatives play the role of the immunochemical dominant group, i.e., of the component that contributes most to the biological specificity of PS. This becomes especially apparent when an unusual component occupies the position of a side-chain substituent of the main linear chain of the biopolymer.

An example of a rare or even unique monomer of microbial PS may be a monosaccharide containing unusual structural groups. Their representatives in O-antigenic polysaccharides are deoxyhexoses, deoxyheptoses, aminodeoxy sugars, aminouronic acids and nonulosonic acids carrying amino groups. In addition to well-known *O*- and *N*-acetyl monosaccharide derivatives and their *O*-methyl ethers, O-antigenic PS have been found to contain, highly specific for this class of biopolymers, *O*- or *N*-acyl derivatives formed by acylation of monosaccharides by hydroxy or dihydroxy acids and amino acids. Another example of unusual derivatives are amides of uronic acids, including those formed by amino groups of amino acid residue. In current literature such fragments are generally termed 'non-carbohydrate substituents'. The monomers containing such unusual *O*- and *N*-substituents were mostly discovered during the last 10–15 years, and their number is rapidly increasing. Their identification and localisation in the polymeric chain is an indispensable part of the modern-day structural chemistry of polysaccharides.

It is especially worth noting that the vast body of experimental material obtained by analysis of the structure, chemical properties and pathways of synthesis of novel monosaccharides (and their non-carbohydrate substituents) present in O-antigenic PS has been found to be extremely important not only for understanding the nature of the biological specificity of carbohydrate polymers but also for further progress in carbohydrate chemistry in general. The data for novel, unusual combinations of functional groups in the monosaccharide molecules have considerably expanded our concepts of the reactivity and stereochemistry of monosaccharides and culminated in the discovery of some novel reactions, giving a new impetus to the elaboration of new methods of organic synthesis. The availability of a great number of carbohydrates differing in their structure has considerably enriched the methodological arsenal of NMR spectroscopy, for which these derivatives served as perfect model compounds.

The present review is dedicated to the consideration of mostly chemical aspects of the problem: it deals with isolation, determination of structure, identification and chemical properties of novel unusual monosaccharides or their unusual derivatives present in O-antigenic PS as monomeric units. In some instances data are given about the same or structurally related monosaccharides found in microbial PS unrelated to O-antigenic PS of Gram-negative bacteria. Some of the data concern the synthesis of certain monosaccharides. Such syntheses were undertaken with the purpose of confirming their structure or obtaining a corresponding, not easily available monosaccharide or its derivative in larger amounts needed for further analysis and application to the solution of research problems or practical tasks. Of the extensive body of synthetic material, we have focussed our attention only on those syntheses that either have a fundamental importance or are novel, effective and practical.

The data on the structure of PS themselves comprising these monosaccharides have been reviewed in one of the recent reports² which also concerns the localisation and type of binding of the monomers in the polysaccharide chain.

Earlier published reviews^{4–6} dedicated to O-antigenic PS covered mainly biological and, particularly, microbiological aspects.

II. General observations concerning isolation, determination of structure and identification of monosaccharides and their derivatives present in O-antigenic PS

In order to determine the structure or to identify an unusual component of the polysaccharide chain by comparison with an authentic sample, the component is sometimes isolated in the individual state as such, as one of its standard derivatives (e.g., acetate) or in a modified form (e.g., as a corresponding alditol). However, the use of contemporary physico-chemical methods, and in the first place, NMR spectroscopy, often permits a conclusion about the structure of the unusual monomer directly in the process of establishment of the structure of the PS itself by using a non-destructive method. In recent studies identification of an already known component of a PS is often performed during the spectral analysis of PS by characteristic signals in the NMR spectrum.

1. Isolation of unusual monosaccharides or their derivatives

The initial O-antigenic polysaccharide is obtained by selective degradation of LPS routinely isolated by extraction of the microbial mass with aqueous phenol.⁷ This is followed by mild acid hydrolysis of LPS with dilute acetic acid, after which the polysaccharide is isolated by a standard, specific for the given PS procedure (for example, ion-exchange chromatography is effectively used for PS containing acidic groups).[†]

After establishment of the presence of an unusual component by conventional monosaccharide analysis of PS or by preliminary analysis of its NMR spectrum, the isolation of the monosaccharide in the pure state is achieved by acid hydrolysis of the PS followed by chromatographic separation of the resulting mixture. For a successful solution of this problem, two mutually exclusive conditions often have to be met: (i) cleavage of the glycosidic bond of the monomer to be isolated during its splitting off from the polysaccharide chain, and (ii) avoidance of partial or even complete degradation of the monomer upon hydrolysis. For example, it is well known that monosaccharides containing one or several deoxy units are unstable in acid media and, although the glycosidic bonds of these monosaccharides are readily cleaved, isolation of the corresponding monomers may pose serious problems. At the same time, the glycosidic bonds of uronic acids or amino sugars having a nonacylated amino group are distinguished by increased resistance to hydrolysis which largely prevents the isolation of the corresponding native monomer in the individual state.

This task is further complicated by the situation when a complex monomer, a monosaccharide derivative containing a non-carbohydrate substituent, is to be isolated. Clearly, in this case the hydrolysis must not be accompanied by cleavage, modification, destruction or rearrangement of the substituting group. If after hydrolysis the unchanged non-carbohydrate substituent can be successfully isolated and identified, a new problem arises as to which monosaccharide of the polymeric chain is concerned and how the substituent is bound.

[†] Examples of standard procedures for isolation and purification of various types of PS can be found in the many-volume monograph *Methods in Carbohydrate Chemistry* Vols I–IX (New York: Academic Press, 1965–1993).

The hydrolytic conditions used to isolate novel components of PS may vary widely depending on the experimental goal. This is pertinent to the choice of the acid (hydrochloric, sulfuric, trifluoroacetic) and its concentration as well as the temperature and duration of hydrolysis. Most commonly, the hydrolytic conditions are selected experimentally, taking into account preliminary data on the monosaccharide composition of the biopolymer. Sometimes, for the isolation of an unusual component, special conditions are applied which may not be suited for achieving complete hydrolytic cleavage of the polysaccharide. In other cases, acetolysis (treatment of PS with an acetic anhydride-acetic acid mixture in the presence of sulfuric or another strong acid, e.g., hydrochloric acid) is used instead of acid hydrolysis; in this case monosaccharides are isolated in the form of full acetates.

Currently, solvolysis with anhydrous HF at reduced or room temperatures is used for depolymerisation of polysaccharides.⁸ The distinctive feature of this method is that it cleaves the glycosidic bonds without any effect on bonds cleaved by hydrolysis, e.g., amide bonds. In particular, the method is used effectively to isolate complex derivatives of monosaccharides with their non-carbohydrate substituents attached.

When an unusual monomeric component fails to be isolated, a short oligosaccharide fragment (usually a disaccharide or a trisaccharide) containing this monosaccharide is obtained. For this purpose, in addition to selective acid hydrolysis, other conventional procedures for partial cleavage of the polysaccharide chain are used, such as oxidation with periodic acid (periodate oxidation) with subsequent Smith degradation,⁹ and in some cases deamination of an amino sugar present in the PS chain is carried out.¹⁰ This simplifies considerably the determination of the structure of the unusual component of a short oligosaccharide in comparison with its identification within PS, mass spectrometry and NMR spectroscopy being helpful tools in the process.

Chromatographic techniques are now being used almost exclusively to isolate monosaccharides, their derivatives and short oligosaccharide fragments from hydrolysates. Preliminary qualitative estimation of the composition of the hydrolysate and identification of an unusual component are carried out using paper chromatography (PC) or thin-layer chromatography (TLC) and by various modifications of liquid or gas-liquid chromatography. On the basis of the preliminary data, the most appropriate method is selected for preparative isolation of the desired component (a monomer or an oligosaccharide).

2. Chemical methods used to establish the structure

With the development of physico-chemical techniques, classical chemical methods used for establishing the structure of monosaccharides and their derivatives gradually lose their significance, although some of them still remain practicable. If a previously unknown monosaccharide was isolated in the pure state, its structure can be determined by routine approaches commonly employed in monosaccharide chemistry, such as methylation and periodate oxidation, which had especially wide application at early stages of microbial PS analysis. The first of these methods (see Practical Guide¹¹) is based on the conversion of free hydroxy groups of a mono-, oligo- or poly-saccharide into *O*-methyl groups. Their localisation in the resulting derivative by using mass spectrometry makes it possible to establish the position of other substituents, deoxy units, and details of the monosaccharide structure.

Oxidation of a monosaccharide with periodate⁹ results in the cleavage of the carbon-carbon bonds between adjacent atoms carrying hydroxy groups which prompts a conclusion about their location and the presence of deoxy units in the monosaccharide. Currently, this method is used widely for selective cleavage of the PS chain with the ultimate goal of obtaining short fragments and is followed by mild acid hydrolysis and reduction (Smith degradation) of the oxidised PS.⁹

Other chemical conversions used to establish the monosaccharide structure involve deamination of amino sugars, as a result

of which the amino group is first deacetylated and the amino sugar derived is treated with nitrous acid (see review¹⁰). This reaction is also employed for selective degradation of the PS chain.^{12,13} In some cases other reactions of monosaccharides, e.g., conversion of monosaccharides into anhydro sugars, lactonisation of uronic acids, etc., may become helpful.

Sometimes, in order to identify a monosaccharide by comparison with the authentic sample, the former is converted into its derivative, e.g., *O*-acetate or *O*-trimethylsilyl ether. Reduction of a monosaccharide with NaBH₄ to the corresponding alditol is especially useful. The latter is converted into the acetate and identified either by direct comparison with an authentic sample or using mass spectrometric analysis.

To establish the absolute configuration of a monosaccharide, this is converted into a glycoside by interaction with an optically active alcohol (most commonly with butan-2-ol or octan-2-ol). The absolute configuration of the initial monosaccharide is inferred from the chromatographic mobility of the glycoside.

Chemical methods used to establish the structure of unusual derivatives of monosaccharides are mostly confined to their degradation into the constituent fragments: a monosaccharide and a non-carbohydrate substituent. To this end, hydrolytic cleavage of a hydroxy group or an amino acid group that is acylating one of the hydroxy groups in the monosaccharide is performed, after which the acid is isolated for further identification. The substitution site in the monosaccharide is determined by one of routine chemical or physicochemical methods.

It should be noted that at the present time such tasks, as well as establishment of the structure of novel monosaccharides, are more easily and effectively accomplished by application of physico-chemical methods alone, while chemical methods are used in counterflow syntheses of new monosaccharides or their unusual derivatives for unambiguous and final identification. Synthesis of novel monosaccharides is usually achieved by regio- and stereo-selective transformation of one of the available monosaccharides by methods routinely used in carbohydrate chemistry. Examples of different syntheses of this sort will be given below.

3. Mass spectrometric analysis

One of the physicochemical methods used to study the structure of sugars is mass spectrometry. The stipulation of the principles for fragmentation of monosaccharide molecules^{14,15} and of alditols derived by their reduction^{16,17} using electron impact has made it possible to use mass spectrometry for effective establishment of their structure. Currently, the most commonly used is mass spectrometry of alditols characterised by more simple and unambiguous fragmentation of the molecule.

For this purpose, a monosaccharide or its derivative is reduced with borohydride or, in special cases, with sodium borodeuteride. This results in the formation of an alditol, in which the primary alcohol group (which often comprises deuterium, CHD-OH, providing the 'labelling' of the group essential for further elucidation of the structure on the basis of the mass spectrum) corresponds to the aldehyde group of the original molecule. The alditol thus obtained is converted into the full acetate which is further subjected to mass spectrometry. It should be emphasised that in the majority of cases this method permits the preservation of the non-carbohydrate substituents present in the monosaccharide and makes mass spectrometry a helpful tool for the analysis of complex derivatives of monosaccharides.

Fragmentation of alditols by electron impact has been studied thoroughly.¹⁸ In particular, a correlation has been established between the relative ease of cleavage of the carbon-carbon bonds in alditols and the nature of the substituent at the carbon atom. On the basis of these data, standard procedures have been developed for establishment of the structure of monosaccharide components of PS (see reviews^{19,20}).

The mode of degradation of carbon-carbon bonds in alditols by electron impact appears to be especially informative in the analysis of the structure of deoxy and aminodeoxy sugars as well

as of monosaccharides containing non-carbohydrate substituents. Such substituents (e.g., a residue of a hydroxy or an amino acid) are also subject to fragmentation by well-known pathways and easily identified, the fragmentation of the alditol skeleton indicating the position of the non-carbohydrate substituent.

Regrettably, mass spectrometric analysis does not allow a conclusion about the stereochemistry of the monosaccharide, since the spatial arrangement of the substituents at the chiral carbon atoms of the monosaccharide skeleton does not appreciably influence the cleavage of the carbon-carbon bonds. Numerous attempts to use mass spectrometry for determination of the configuration of monosaccharides failed and, therefore, NMR spectroscopy is now being used more frequently to establish the polysaccharide structure.

4. NMR spectroscopy

NMR spectroscopy is the major procedure designed to establish the structure of carbohydrates and structurally unusual monomeric components of PS. Sometimes, this method allows a solution of this problem without isolation of monosaccharides in the pure state, directly on the basis of the NMR spectrum of the polysaccharide, and the establishment of the complete structure of PS on the basis of the spectral data alone, i.e., by a non-destructive approach.

Almost all presently known versions of ^1H and ^{13}C NMR spectroscopy are used in polysaccharide chemistry; the use of each of those modifications is defined by the specific goal to be sought (see reviews ²¹⁻²⁶). The techniques based on the measurement of nuclear Overhauser effects (NOE) in the ^1H NMR spectra, which allows a direct determination of the relative spatial position of protons in the monosaccharide molecule, has acquired special importance in recent years.

Among new approaches expressly designed to solve structural problems of polysaccharide chemistry, special mention should be made of computer analysis of ^{13}C NMR spectra.^{24,27} This approach is meant, primarily, for determining the type of binding and the sequence of monosaccharide units in the polysaccharide chain. However, it often appears to be a helpful tool for elucidation of the structure of monosaccharides in PS, particularly, for the determination of their configuration. Thus, this method is now being widely employed for establishment of the absolute configuration of the monosaccharide without its isolation, i.e., directly within the polysaccharide chain.²⁴ The method is based on the determination of the magnitude of the so-called glycosylation effects, i.e., changes in the chemical shifts of the given carbon atoms in the ^{13}C NMR spectrum depending on the stereochemical features (including the absolute configuration) of the neighbouring monosaccharide unit in the polymeric chain.

5. Other physicochemical methods

An important physicochemical constant used in the structural analysis of sugar derivatives is the specific optical rotation. This value is readily determined with a high degree of accuracy and reproducibility and not only serves as an important criterion of the purity of the preparation obtained but is also routinely used for identification of the compound studied by comparison with an authentic sample. The absolute configuration of the monosaccharide under study as well as of oligosaccharides and other derivatives containing this monosaccharide unit can also be determined from the specific optical rotation; for this purpose, the experimentally determined specific optical rotation is compared with the theoretically calculated value for the given monosaccharide or its derivative using Klein's rule.²⁸

In what follows, the description of individual representatives of monosaccharides and their derivatives present in O-antigenic PS will include concrete data on the use of the physicochemical methods mentioned above; this is confined to a brief consideration of only the most important spectral characteristics of the monosaccharide that are critical and sufficient for the elucidation of its structure.

III. Unusual monosaccharides forming a part of O-antigenic PS

1. Pentoses and hexoses

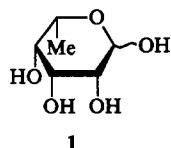
The majority of aldopentoses and aldohexoses widely distributed in Nature are common components of microbial PS. D-Glucose, D-galactose and D-mannose have a peak incidence among hexoses, while D-ribose among pentoses. D-Xylose and D-arabinose are far less abundant.²

Aldoses of the L-series are not common in microbial PS. Thus, only PS of two *Pseudomonas* species contain L-xylose.^{29,30} This sugar was identified by conventional methods of carbohydrate analysis as the acetate of the corresponding alditol.²⁹ The absolute configuration of the (–)-2-octyl glycoside derivative of L-xylose was determined by GLC.³⁰

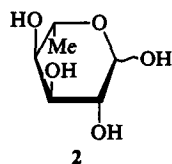
2. Deoxyhexoses

Unlike hexoses which enter into polysaccharides predominantly as D-isomers, deoxyhexoses occur more frequently as L-isomers. Thus, 6-deoxyhexoses, L-rhamnose and L-fucose are common constituents of O-antigenic PS,² whereas D-isomers of these monosaccharides are rare. The D-isomers were isolated in the individual state after acid hydrolysis of PS of *Pseudomonas cepacia* or as O-methyl ethers after hydrolysis of methylated PS and identified by conventional methods. Their absolute configuration was established either by calculation according to Klein (e.g., see Ref. 31) or by GLC of alkyl glycoside derivatives with optically active alcohols (e.g., see Ref. 32). Sometimes, the absolute configuration was determined by a computer analysis of the structure of PS based on their ^{13}C NMR spectra (e.g., see Ref. 27).

Some PS were found to contain even more rare 6-deoxyaldoses. Thus, 6-deoxy-L-talose (1) was detected in PS of several *Pseudomonas* species (*P. fluorescens*,³³ *P. maltophilia*,³⁴ *P. pseudomallei*³⁵) as well as in PS of a strain of *Escherichia coli*.³⁶ This sugar was isolated in the pure state from acid hydrolysates of PS and identified using PC and TLC by comparison with an authentic sample obtained from glycosides of the terpene series.³⁷ Its structure was confirmed by mass, ^1H and ^{13}C NMR spectra, whereas the L-configuration was evident from the specific optical rotation.

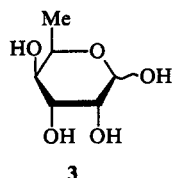


6-Deoxy-L-altrose (2) was detected in *Yersinia enterocolitica*^{38,39} as a component of a homopolysaccharide composed of the pyranose units of this sugar as well as in PS of *Y. pseudotuberculosis* serovar VB, where its furanose form is present in the side chain.⁴⁰ The monosaccharide was identified by direct comparison with the sample isolated earlier from terpene glycosides.³⁷ Its structure as 6-deoxyaldose was corroborated by mass spectrometry and NMR spectroscopy,³⁸ whereas its L-configuration was determined from the specific optical rotation.



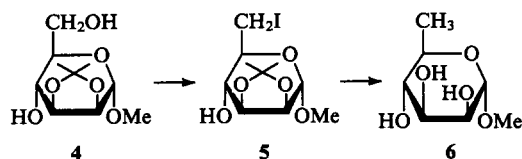
There is evidence⁴¹ that a PS of *Y. enterocolitica* contains 6-deoxy-D-gulose (3) which failed to be isolated in a sufficiently pure state. Its structure was established by comparison with an authentic sample³⁷ using electrophoresis in borate buffer. The stereochemistry of 6-deoxy-D-gulose was determined by analysis of the ^1H NMR spectrum of a partially purified sample. This spectrum contained signals corresponding to the CH_3 group of

6-deoxyhexose and the coupling constant values ($J_{2,3} = 3.5$, $J_{3,4} = 1.5$, $J_{4,5} = 2.25$ Hz) were consistent with the *gulo*-configuration. The absolute configuration was established from the ^{13}C NMR spectrum of the polysaccharide.



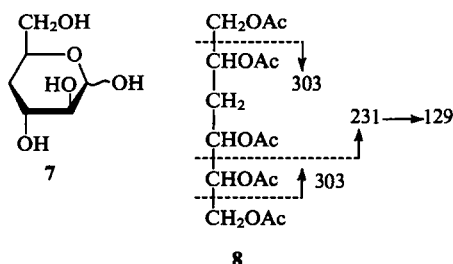
6-Deoxyaldoses can be easily synthesised by routine methods, i.e., by introducing a 6-deoxy unit into the corresponding aldoses. An example is provided by the synthesis of rarely occurring D-rhamnose from D-mannose⁴² (Scheme 1).

Scheme 1



Methyl 2,3-*O*-isopropylidene- α -D-mannopyranoside (4) was converted into the 6-iodo derivative 5 by selective tosylation of the primary hydroxy group and subsequent treatment with NaI. Hydrogenation of the latter over Raney nickel followed by elimination of the isopropylidene group gave the methyl glycoside of D-rhamnose 6.

Other monodeoxyhexoses have not yet been found in O-antigenic PS. Of particular interest is the fact that 2-deoxyhexoses, widespread in many natural glycosides, are absent from bacterial PS at all. There is also no evidence for the presence of 3-deoxyhexoses in PS. The only representative of 4-deoxyhexoses in O-antigenic PS is 4-deoxy-D-*arabino*-hexose (7) detected in some strains of *Citrobacter* (e.g., in *Citrobacter* O36 its pyranose units form a homopolysaccharide,⁴³ whereas in *Citrobacter* PCM 1487 it is present in the side chain of O-antigenic PS⁴⁴). The monosaccharide 7 is distinguished by very high lability and could not be purified after acid hydrolysis of PS, although the reduction of the hydrolysate gave the alditol 8. The mass spectrum of the acetate of 8 contained peaks of the fragments with m/z 303 and 231 and the corresponding secondary fragments which clearly indicates the presence of a C(4)-deoxy unit. The stereochemistry of 7 was determined on the basis of the ^1H NMR spectrum of the polysaccharide itself; the presence of two signals of H(4) at 1.751 (a) and 1.528 (e) ppm also corroborates its structure. The D-configuration was assigned to the monosaccharide 7 on the basis of the specific optical rotation.

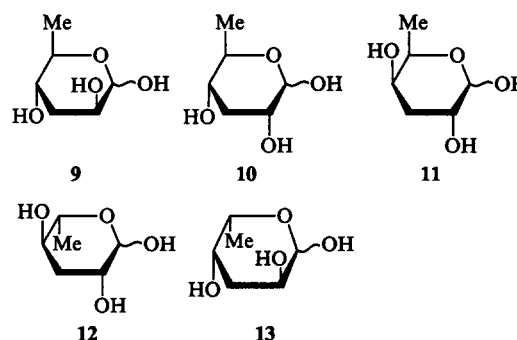


3. 3,6-Dideoxyhexoses

This type of deoxy sugars is widely spread in PS of Gram-negative bacteria and is typical of PS of the genus *Salmonella*.² 3,6-Dideoxyhexoses were detected as components of PS even in pioneer studies of O-antigenic PS of microorganisms. Identification and determination of the structure of 3,6-dideoxyhexoses isolated from various *Salmonella* species demonstrated a direct

correlation between the structure of O-antigenic PS of a certain bacterium and its immunochemical properties. These studies, which dated back to the 1950's, had a great historical impact, for they actually opened up a way for extensive systematic chemical investigations into microbial O-antigenic PS.

Up to the present, five representatives of 3,6-dideoxyhexoses of various configurations are known that are present in PS of a rather large number of Gram-negative bacteria. They are: D-*arabino*-hexose (tyvelose 9), D-*ribo*-hexose (paratose 10), D-*xylo*-hexose (abequose 11), L-*arabino*-hexose (ascarylose 12) and L-*xylo*-hexose (colitose 13). Among these, the first three monosaccharides, which were first discovered by Westphal and Lüderitz during their study of PS of *Salmonella*, are the most widespread.⁴⁵ These compounds are attached as side chains to the main chain of the biopolymer and represent the immunodominant groups, i.e., they determine the immunochemical characteristics of the given microorganism (see review⁴⁶). Thus, PS of *S. paratyphi* contains paratose, PS of *S. typhimurium* abequose, *S. typhi* PS tyvelose.^{2,47} The *Salmonella* of serogroups A–D contain as an indispensable component one of these three 3,6-dideoxyhexoses.



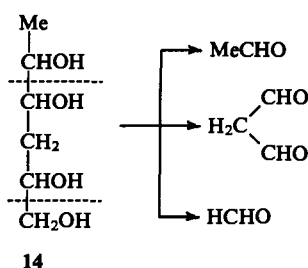
Two species of *Salmonella* were also found to contain colitose⁴⁸ first discovered in PS of *Escherichia coli* O111.⁴⁹ Later, 3,6-dideoxyhexoses were found in PS of other Gram-negative bacteria. Thus, all the five representatives mentioned above were identified in PS of various strains of *Yersinia pseudotuberculosis*;^{50–57} ascarylose was found in PS of *Vibrio cholerae* O3,⁵⁸ abequose in PS of *Citrobacter freundii*,^{59,60} tyvelose in PS of *Eubacterium saburreum*,⁶¹ while colitose occurred in PS of one of *Escherichia coli* strains.⁶²

All the 3,6-dideoxyhexoses mentioned above can be isolated in the individual state after acid hydrolysis of the corresponding PS. Their glycosidic bond which, as with other deoxy sugars, is hydrolysed much more easily than typical glycosidic bonds makes possible their selective cleavage. At the same time, they have increased lability towards acids and their isolation presents some difficulties.

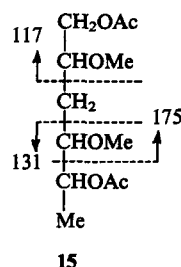
Originally, the structure of 3,6-dideoxyhexoses was established by classical methods. An example is abequose (Scheme 2). The positions of its deoxy units were determined by periodate oxidation of the alditol 14 obtained by the reduction of abequose 11 with LiAlH_4 . Oxidation of the alditol 14 gave formaldehyde, acetaldehyde and malonic aldehyde proving the position of deoxy units at C(6) and C(3) of the hexose skeleton.⁴⁶ The establishment of the absolute and relative configurations of abequose, as with other 3,6-dideoxyhexoses, was possible at that time only by comparison with authentic samples. For this purpose, the synthesis of some representatives of 3,6-dideoxyhexoses was carried out.

More recently, mass spectrometry of alditol acetates obtained by reduction of 3,6-dideoxyhexoses came into routine practice as a means for the establishment of the structure of their skeleton. These derivatives exhibit a peculiar fragmentation which indicates

‡ *Eubacterium saburreum* is not a Gram-negative bacterium.



the position of deoxy units. By way of illustration, the mass spectrum of the alditol acetate **15** obtained by reduction of the *O*-methyl ether of abequose isolated from the hydrolysate of methylated PS of *S. typhimurium* contains fragments with *m/z* 175, 131 and 117 indicating the presence of deoxy units at C(6) and C(3).⁶³



However, the positions of deoxy units in the monosaccharide can be more easily detected by ¹³C NMR spectroscopy. All the spectroscopic characteristics of 3,6-dideoxyhexoses are now well known and readily detectable directly in the NMR spectra of the corresponding PS: a signal in the region 16.0–18.0 ppm shows the presence of a methyl group at C(6), whereas a signal in the region 33–40 ppm the presence of a deoxy unit at C(3).⁶⁴

The configuration of 3,6-dideoxyhexoses, namely, the stereochemistry of C(2) and C(4) can well be defined by the ¹H NMR spectra, the coupling constant values between the C(3)H₂ group and protons at C(2) and C(4) being the most characteristic ones. According to the general regularities, these constants have higher values (11–12 Hz) for *a,a*-protons and lower values (3–5 Hz) for *a,e*- and *e,e*-protons. Thus, the corresponding values for paratose¹⁰ are $J_{3a,4} \approx J_{2,3a} \approx 11$ Hz and $J_{3e,4} \approx J_{2,3e} \approx 4$ Hz, respectively; those for abequose are $J_{2,3e} \approx 4.5$, $J_{2,3a} \approx 12$, $J_{3a,4} \approx 3$ Hz. Identification of 3,6-dideoxyhexoses is now carried out directly from the NMR spectra of the PS itself.

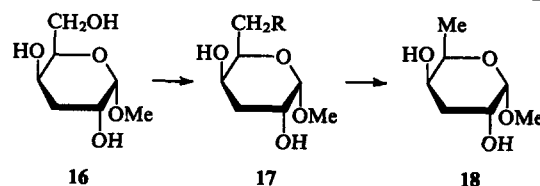
The above data are pertinent to the pyranose form of 3,6-dideoxyhexoses, in which these deoxy sugars are present in almost all bacterial PS. The only exception is PS of *Yersinia pseudotuberculosis* IB, where a 3,6-dideoxyhexose is present in the furanose form.⁵²

Several methods of 3,6-dideoxyhexose synthesis have been described; all are based on the introduction of deoxy units into hexoses having a regular structure by classical methods. This synthesis was originally undertaken to establish the structure of dideoxyhexoses isolated from natural PS.

Of considerable historical importance is the synthesis of the abequose derivative **11** from methyl 3-deoxygalactoside **16** (Scheme 3).⁶⁵ The latter was selectively tosylated at the primary hydroxy group; the tosylate **17** (R = OTs) was converted into the iodide **17** (R = I), reduction of which gave the methyl abequoside **18**. The same methyl abequoside can also be obtained by direct reduction of the tosylate **17** with LiAlH₄. In a similar way, the derivatives of tyvelose (**9**) and paratose (**10**) were synthesised from 3-deoxymannoside and 3-deoxyglucoside,⁶⁶ respectively. Later, paratose was synthesised by direct introduction of a halogen atom at C(6) of a 3-deoxyglycoside.⁶⁷

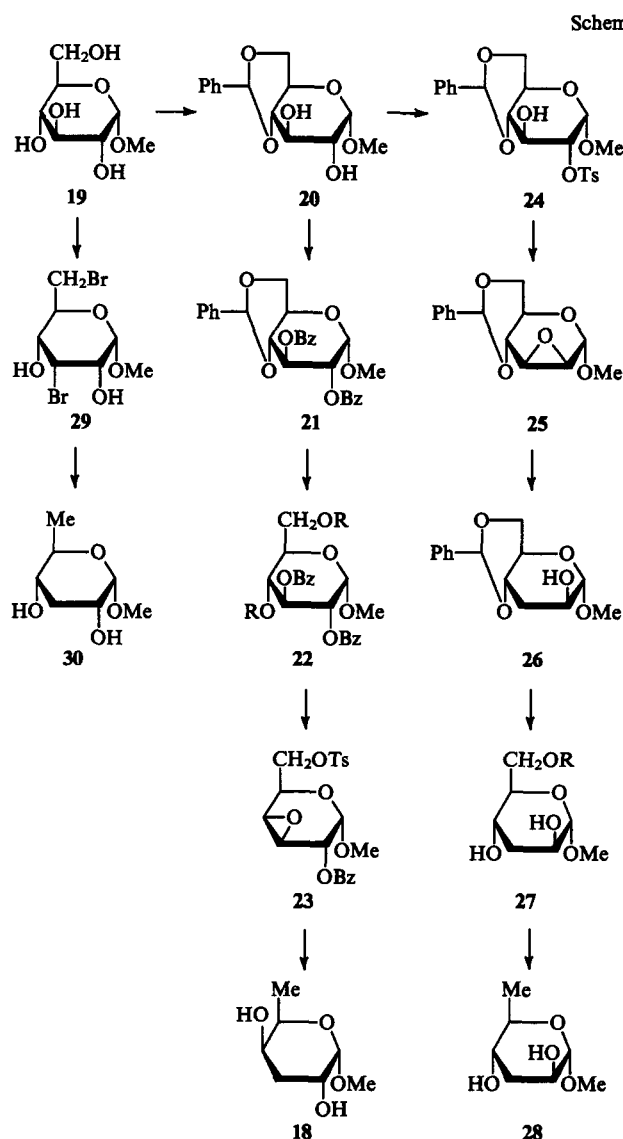
Currently, it has become necessary to develop preparative methods for the synthesis of considerable amounts of 3,6-dideoxyhexoses for the purpose of creating artificial antigens

Scheme 2



Scheme 3

and diagnostic tools. The synthesis of three most important 3,6-dideoxyhexoses⁶⁸ (tyvelose, paratose, abequose) from the most readily available material, the methyl glycoside **19**, is depicted below (Scheme 4).



Scheme 4

To synthesise abequose, methyl α -D-glucopyranoside **19** was converted into the 4,6-*O*-benzylidene derivative **20** and further into its dibenzoate **21**. After elimination of the benzylidene group, the diol **22** (R = H) was converted into the 4,6-di-*O*-tosylate **22** (R = Ts); its treatment with a base gave 6-*O*-tosylate of the 3,4-anhydro sugar **23**. Reduction of the anhydro sugar with LiAlH₄ was accompanied by regio- and stereo-specific opening of the epoxide ring and hydrogenolysis of the *O*-tosyl group resulting in the formation of the abequose derivative **18**.

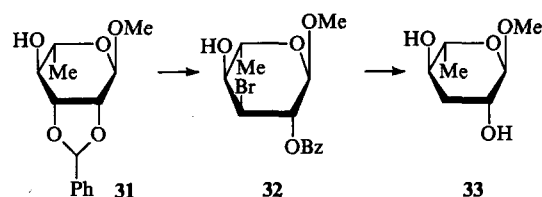
During the synthesis of tyvelose, the benzylidene derivative **20** was subjected to selective tosylation to give the 2-*O*-tosylate **24**. The latter was converted into the 2,3-anhydro derivative **25** which

was converted into the 3-deoxy derivative **26** by the action of LiAlH_4 . After elimination of the benzylidene group and selective tosylation of the hydroxy group at C(6) of the triol **27** ($\text{R} = \text{H}$), the corresponding tosylate **27** ($\text{R} = \text{Ts}$) was reduced and the tyvelose derivative **28** was isolated.

Finally, the paratose derivative **30** was obtained by treatment of the glucopyranoside **19** with tribromoimidazole in the presence of triphenylphosphine (cf. published data⁶⁹) followed by reduction of the dibromide **29** by hydrogenolysis over Raney nickel or with Bu_3SnH in the presence of azo- N,N' -bis-isobutyronitrile.

A rather simple synthesis⁷⁰ of the ascarylose derivative **33** from L-rhamnose is also known (Scheme 5). Methyl 2,3-O-benzylidene- α -L-rhamnopyranoside **31** (readily produced by treatment of methyl rhamnoside with benzaldehyde dimethylacetal in the presence of toluenesulfonic acid) interacts with N -bromosuccinimide with a regiospecific opening of the benzylidene ring to give the 3-bromo derivative **32**, which is reduced with LiAlH_4 into the methyl glycoside of 3,6-dideoxy-L-arabino-hexose (ascarylose) **33**. Colitose⁷¹ was synthesised from the 3,4-O-benzylidene derivative of α -L-fucose by a similar scheme.

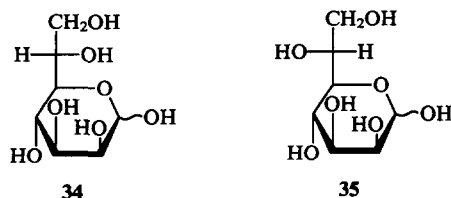
Scheme 5



4. Heptoses

Up to the present, only three heptoses, L-glycero-D-manno-heptose, D-glycero-D-manno-heptose and D-glycero-D-altro-heptose, have been identified as components of O-antigenic PS. The first of these is also a common component of the LPS core of Gram-negative bacteria (see review⁷²).

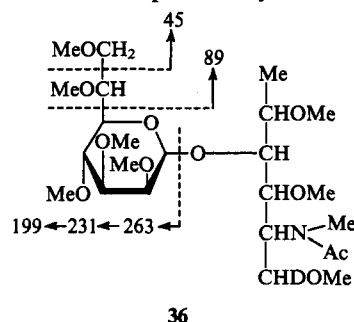
L-Glycero-D-manno-heptose **34** was isolated⁷³ after acid hydrolysis of PS of *Pseudomonas cepacia* IMV 673/2 using ion-exchange chromatography in borate buffer. Its structure was established in the following way. The PS was oxidised with a calculated amount of sodium periodate and then reduced with NaBH_4 . Products of the hydrolysis of the PS thus modified contained mannose resulting from the cleavage of the C(7)–C(6) bond of the heptopyranoside unit. This finding provided evidence for the manno-configuration of the C(2)–C(5) fragment of the monosaccharide and was confirmed by ^{13}C NMR spectroscopic data from the original PS. The retention time of the heptose fraction in a sugar analyser and its ^{13}C NMR spectrum were fully consistent with the corresponding parameters for the enantiomeric D-glycero-L-manno-heptose but differed from that for D-glycero-D-manno-heptose, thus confirming the relative configuration of the monosaccharide as a whole. Its absolute configuration was evident from the specific optical rotation ($[\alpha]_D = +4.8^\circ$) and confirmed by analysis of the glycosylation effects in the ^{13}C NMR spectrum of the polysaccharide.



D-Glycero-D-manno-heptose **35** was found in PS of *Vibrio cholerae* O21 where it is present in the main chain.⁷⁴ The monosaccharide **35** was isolated in the pure state from the acid hydrolysate of PS. In the ^1H NMR spectrum of the methyl

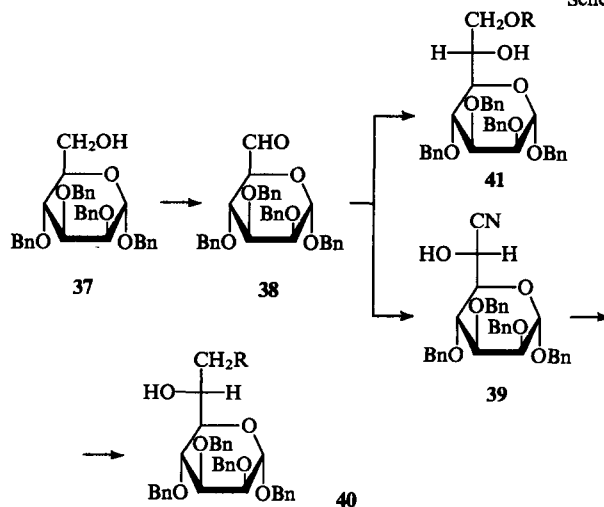
heptoside pentaacetate, the chemical shifts of the signals and the coupling constants for the protons at C(2)–C(5) practically coincided with those for methyl α -D-mannoside tetraacetate, thus corroborating the configuration of the heptose fragment C(2)–C(5). In GLC analysis the mobility of the heptitol acetate derived from the heptose differed from that of the heptitol obtained from L-glycero-D-manno-heptose, and the specific optical rotation ($[\alpha]_D = +74^\circ$) was indicative of the D-configuration.

More recently, D-glycero-D-manno-heptose was also isolated from PS of *Vibrio cholerae* O3.⁵⁸ Its presence was demonstrated by conventional monosaccharide analysis of PS, and its structure confirmed by ^1H NMR spectroscopy of the polysaccharide itself as well as by mass spectrometric analysis of the disaccharide fragment **36** (isolated by acid hydrolysis of the methylated PS followed by reduction with NaBD_4) which contained a heptose residue and an aminodeoxyalditol residue bound to it. The presence in the mass spectrum of a fragment with m/z 263 and the corresponding secondary ions with m/z 231 and 199 as well as of fragments with m/z 45 and 89 indicated the O-methyl ether of a heptose. The final confirmation of the D-glycero-D-manno-heptose structure was provided by counterflow synthesis.

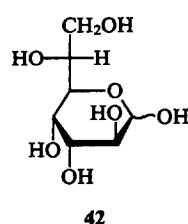


Several procedures for the synthesis of glycero-manno-heptose are known which employ conventional methods of synthesis of higher sugars. The most practicable is shown in Scheme 6.⁷⁵ Thus, benzyl 2,3,4-tri-O-benzyl- α -D-mannopyranoside **37** was subjected to Swern oxidation resulting in the aldehyde **38** whose interaction with HCN gave a mixture of isomers. The cyanohydrin **39** having the D-glycero-D-manno-configuration was isolated by chromatography and reduced to the amino sugar **40** ($\text{R} = \text{NH}_2$) which was further converted into the D-glycero-D-manno-heptose derivative **40** ($\text{R} = \text{OH}$) by treatment with nitrous acid. To obtain the L-glycero-isomer, the aldehyde **38** was condensed with allyloxy-methylmagnesium bromide and the main isomeric alcohol **41** ($\text{R} = \text{allyl}$) having the L-glycero-configuration was chromatographically isolated from the resulting mixture; its deallylation gave a derivative of L-glycero-D-manno-heptose **41** ($\text{R} = \text{H}$).

Scheme 6

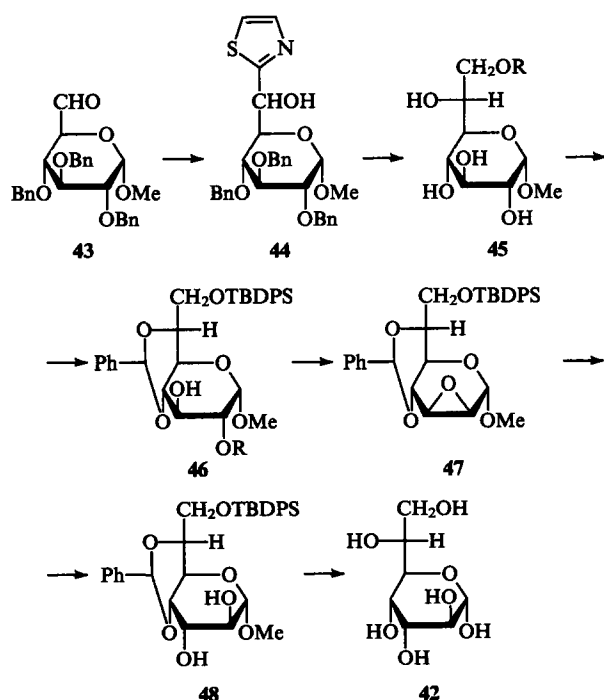


D-Glycero-D-*altro*-heptose **42** was found in PS of *Campylobacter jejuni* O23, together with 6-deoxy-D-*altro*-heptose and their 3-O-methyl ethers, the relative amount of these components of antigenic PS being dependent on both the bacterial strain and, seemingly, on cultivation conditions.⁷⁶ The heptose **42** present in the main chain of PS was isolated after acid hydrolysis of PS in a mixture with its 1,6- and 1,7-anhydro derivatives. The presence in the monosaccharide of the heptose skeleton was confirmed by the mass spectrum of the alditol obtained by reduction. To establish the configuration of the heptose, the polysaccharide was subjected successively to oxidation with a calculated amount of periodate, the glycol system of the C(6)–C(7) fragment is oxidised first, reduction with NaBH₄ and methanolysis. As a result, methyl D-altroside was isolated and identified corroborating the configuration of the heptose fragment C(2)–C(5). The configuration of C(6) was established by direct comparison of the corresponding alditol acetate with an authentic sample obtained from synthetic D-glycero-D-*altro*-heptose. A similar procedure was used to determine the structure of the 3-O-methyl ether of the heptose **42** present in the same PS.⁷⁶



The synthesis of D-glycero-D-*altro*-heptose was carried out⁷⁷ by stereospecific elongation of the carbon chain at C(6) of the glucose derivative **43** by the method of Donadoni⁷⁸ with subsequent inversion of configuration at C(2) and C(3) (Scheme 7). The aldehyde **43** obtained by Swern oxidation of methyl 2,3,4-tri-O-benzyl- α -D-glucopyranoside was converted into the thiazole derivative **44** by reaction with 2-trimethylsilylthiazole. Treatment of the derivative **44** with formic acid and subsequent debenzyla-tion resulted in a mixture of heptoses epimeric at C(6), from which the isomer having the D-glycero-configuration **45** (R = H) was isolated. This was converted into the 7-O-*tert*-butyldiphenylsilyl ether **45** (R = TBDPS) and then into the 4,6-O-benzylidene

Scheme 7

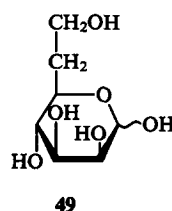


derivative **46** (R = H) which was further converted into the corresponding 2-O-tosylate **46** (R = Ts). The tosylate **46** was routinely converted into the 2,3-epoxy derivative **47** which after treatment with NaOH and *trans*-diaxial opening of the oxide ring gave the monosaccharide derivative **48** having the *altro*-configuration. Elimination of the protective groups resulted in D-glycero-D-*altro*-heptose **42** whose configuration was confirmed by NMR spectroscopic data. The synthetic monosaccharide and that isolated from natural PS were identical.⁷⁶

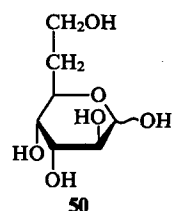
5. Deoxyheptoses

Only two representatives of this class have thus far been detected among monosaccharide components of O-antigenic PS. Both of them are 6-deoxyheptoses.

6-Deoxy-D-*manno*-heptose **49** was detected in PS of *Yersinia pseudotuberculosis* where it is attached as a side chain to the main chain.⁵⁴ The presence of a 6-deoxyheptose in PS was first proved by analysis of the ¹³C NMR spectrum which contains signals characteristic for deoxyaldoses at 34.1 ppm (a methylene group of deoxyaldoses) and 59.0 ppm (a CH₂OH group of deoxyaldoses). The presence in PS of the 6-deoxyheptose **49** was also confirmed by mass spectrometric data of the O-methyl ether of the deoxyheptose glycoside obtained in the pure state after methanolysis of methylated PS.⁵⁴ This heptose was also found in *Pseudomonas pseudomallei* where it forms a homopolysaccharide.³⁵ Its structure and stereochemistry were confirmed by ¹H NMR spectroscopic data: in particular, the coupling constant values were consistent with the *manno*-configuration ($J_{2,3} = 3.5$, $J_{3,4} = 9.1$, $J_{4,5} = 9.5$ Hz). The absolute configuration of **49** was established from the specific optical rotation. The structure of the monosaccharide **49** was also corroborated by counterflow synthesis.

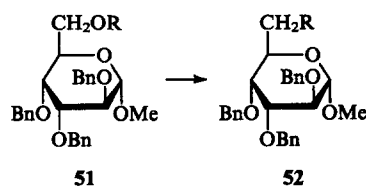


6-Deoxy-D-*altro*-heptose **50** was found in PS of *Campylobacter jejuni* O23A and O23B.⁷⁶ It was isolated in a mixture with its anhydro derivative after acid hydrolysis of PS. The structure of the monosaccharide **50** was confirmed by direct comparison with a synthetic sample of the corresponding alditol hexaacetate, and its D-configuration was established by GLC analysis of glycosides with (*R*)- and (*S*)-butan-2-ols.



The synthesis of 6-deoxy-D-*altro*-heptose⁷⁹ was performed as depicted in Scheme 8.

Scheme 8

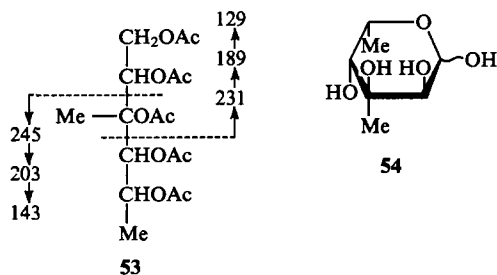


Methyl 2,3,4-tri-*O*-benzyl- α -D-altropyranoside **51** ($R = H$) was converted via 6-*O*-triflate **51** ($R = CF_3SO_2$) into the nitrile **52** ($R = CN$) which, in turn, was converted into a derivative of 6-deoxy-D-altro-heptose **52** ($R = CH_2OH$) by successive reduction with DIBAH, hydrolysis of the resulting imine and reduction of the corresponding aldehyde with $NaBH_4$. The corresponding derivative of 6-deoxy-D-manno-heptose was similarly obtained from the mannose derivative.⁷⁹

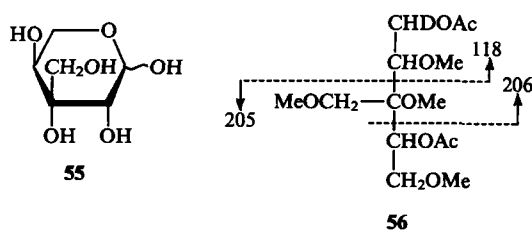
6. Branched monosaccharides

Monosaccharides having a branched carbon chain are a rare class of sugars. These monosaccharides are sometimes found in antibiotics, although some of their representatives were recently detected in O-antigenic PS where they can be localised both in the main chain of the biopolymer and in side chains.

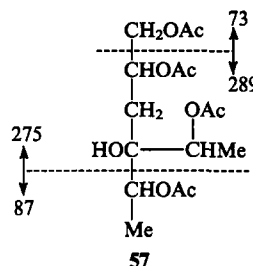
Two representatives of this monosaccharide class were isolated in the pure state after acid hydrolysis of PS of the Gram-negative bacterium *Coxiella brunetti* phase I.⁸⁰ One of those appeared to be identical by its chromatographic characteristics to 6-deoxy-3-*C*-methylgulose (virenose) earlier detected in the antibiotic virenomicin.⁸¹ The structure of the monosaccharide isolated from the O-antigenic PS was also confirmed by the mass spectrum of the fully acetylated alditol **53**. Fragmentation of this compound corresponded to the structure of the parent monosaccharide; in particular, the presence of fragments with m/z 231 and 245 and the corresponding secondary fragments indicated the type and the site of the chain branching. Direct comparison of the natural monosaccharide with the samples of the corresponding monosaccharides of the *manno*-, *talo*- and *gulo*-series isolated from other natural products demonstrated its *gulo*-configuration. However, the specific optical rotation of this monosaccharide differed from that of virenose, for which the D-configuration had been established.⁸¹ Based on these data, the monosaccharide from PS of *Coxiella brunetti* was ascribed the structure of 6-deoxy-3-*C*-methyl-L-gulose **54**.



The second monosaccharide isolated from O-antigenic PS of *Coxiella brunetti* was assigned the structure of 3-*C*-hydroxymethyl-L-lyxose **55**. Successive methylation of PS, acid hydrolysis of methylated PS, reduction of the resulting mixture of methylated monosaccharides with $NaBD_4$ and their acetylation resulted in a mixture of alditol acetates, from which the acetate of the partially methylated alditol **56** corresponding to the branched monosaccharide was isolated. Its fragmentation in mass spectrometric analysis fully confirmed the structure of the skeleton and the positions of the hydroxy groups in the monosaccharide as can be evidenced, in particular, from the presence of fragments with m/z 205, 206 and 118. Determination of configuration of the monosaccharide **55** and its assignment to the L-lyxose series was made by the authors on the basis of synthetic data.

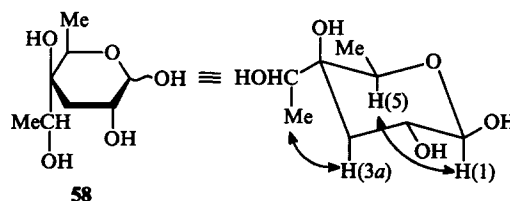


Two other structurally complex monosaccharides belonging to branched octoses were found in O-antigenic PS of several serotypes of *Yersinia*. They were isolated in the individual state after acid hydrolysis of PS and found to be similar in structure with the only difference the configuration of one of the chiral centres. One of those, yersiniose A, was isolated from *Y. pseudotuberculosis* serovar VI,⁸² while the second one, yersiniose B from *Y. enterocolitica* serovar O4,32.⁸³ Reduction of yersinioses A and B with $NaBH_4$ and subsequent acylation resulted in tetraacetates of the corresponding alditols **57**. In this case, one of the hydroxy groups failed to be acetylated under standard conditions that showed its localisation at the tertiary carbon atom. The mass spectra of both alditol tetraacetates appeared to be identical; their fragmentation demonstrated that both yersinioses are 3,6-dideoxy-4-*C*-(1'-hydroxyethyl)hexoses with the identical structure of the carbon skeleton and positions of the hydroxy groups. The same result was obtained by mass spectrometry of methyl glycosides of both monosaccharides.



The NMR spectra of yersinioses A and B also appeared to be almost identical. Thus, the ^{13}C NMR spectrum of yersiniose A contained signals at 13.4 and 16.4 (two CH_3 groups), 35.9 (CH_2 group) and 75.8 ppm (tertiary carbon atom). The signal of C(1) with a low-field chemical shift indicated the D-configuration of the monosaccharide. The 1H NMR spectrum of yersiniose A contained signals at 4.71 [$J_{1,2} = 8.25$ Hz, H(1)], 3.80 [$J_{2,3e} = 5.22$ and $J_{2,3a} = 11.82$ Hz, H(2)], 1.85 [$J_{3a,3e} = 13.86$ Hz, H(3)], 4.18 [$J_{5,6} = 6.63$ Hz, H(5)] and 1.30 ppm [H(6)].

Higher values of the coupling constants ($J_{1,2}$ and $J_{2,3a}$) for yersiniose B present in the β -form show the axial orientation of H(2), whereas NOE data revealed interaction between H(1) and H(5) [i.e., the axial position of H(5)] and the proximity of H(3a) and the CH_3 group of the side chain, thus indicating the equatorial position of the side chain at C(4). These data suggest that yersiniose B has the *xylo*-configuration. Comparison of the ^{13}C NMR spectra for yersinioses A and B revealed that both of them are 3,6-dideoxy-4-*C*-(1'-hydroxyethyl)-D-*xylo*-hexopyranoses **58**. The only distinction between them is in the stereochemistry of the asymmetric centre C(7) in the side chain. This problem was solved by counterflow synthesis of the yersinioses.



To this end, a general procedure for the synthesis of 3,6-dideoxy-4-*C*-(1'-hydroxyethyl)hexoses was elaborated which, in principle, permits the synthesis of any kind of branched octoses of this type. Leaving aside the consideration of relationships between different configurations of the chiral centres in isomeric octoses of this series (see Ref. 84), it is worth noting that the solution of the particular problem of determination of the absolute configuration of the chiral centre C(7) of the isomeric yersinioses, required a stereospecific synthesis of compounds having the D-*xylo*-configuration and distinguished by only the geometry of the chiral centre present in the side chain.

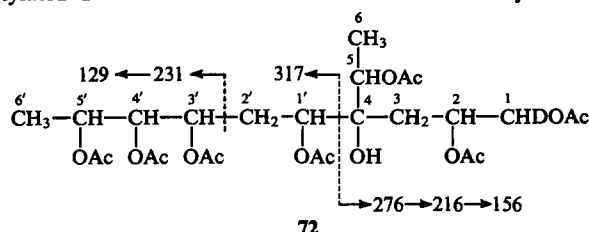
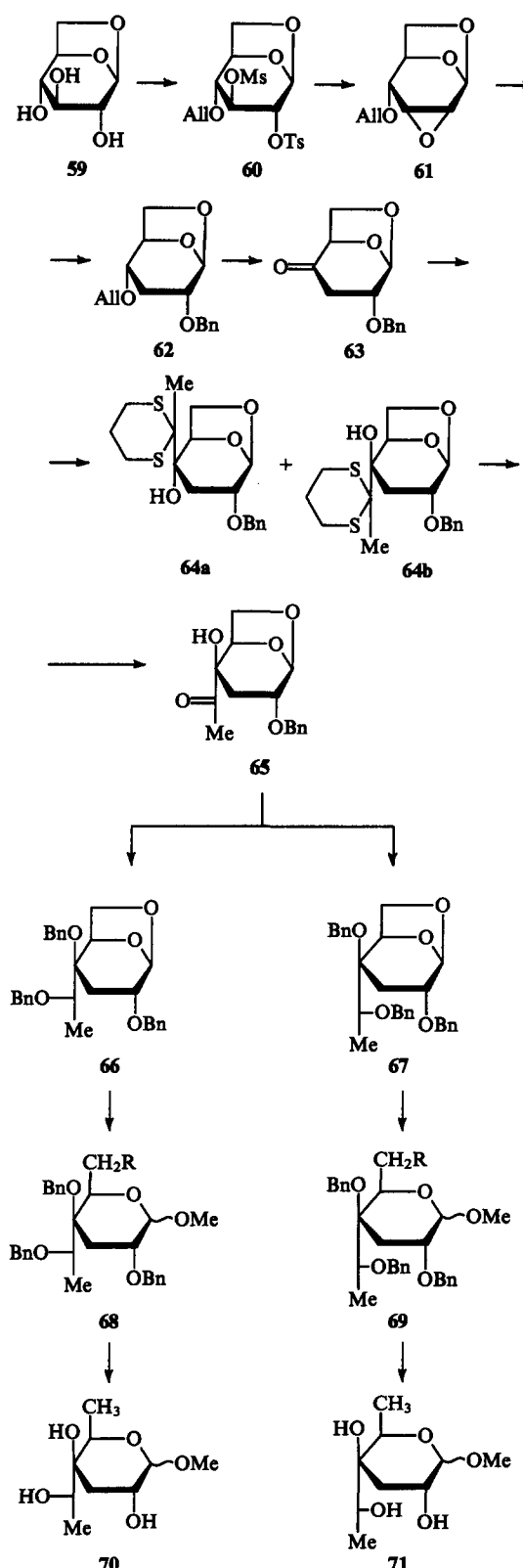
Scheme 9

This rather complex synthesis^{84,85} is depicted in Scheme 9. As the initial compound, 1,6-anhydro- β -D-glucopyranose (levoglucosan **59**) was used, which via a standard set of reactions was converted into 4-*O*-allyl-3-*O*-mesyl-2-*O*-tosyllevoglucosan **60** and then into 1,6:2,3-dianhydro-4-*O*-allyl- β -D-allopyranose **61**. Reduction of the epoxide **61** and subsequent *O*-benzylation gave 1,6-anhydro-4-*O*-allyl-2-*O*-benzyl-3-deoxy- β -D-ribo-hexose **62**. Elimination of the allyl protective group and Swern oxidation of the liberated hydroxy group gave the key intermediate of the synthesis, a derivative of the keto sugar **63**. Its reaction with 2-lithium-2-methyl-1,3-dithiane resulted in a mixture of two alcohols **64a** and **64b** epimeric at C(4) which were separated chromatographically. The structure of the isomers differing in only the configuration at C(4) was established by NMR spectroscopy (including NOE measurements). It appeared that the alcohol **64** has the D-xylo-configuration of the pyranose ring; namely, this compound was selected for further synthesis.

Treatment of the alcohol **64a** with a mixture of HgCl_2 and CdCO_3 gave the ketone **65** which after reduction with NaBH_4 and subsequent benzylation produced two epimeric (with regard to the chiral centre of the side chain) alcohols **66** and **67** in a 2:1 ratio. The absolute configuration of the new chiral centre C(7) in the alcohols **66** and **67** was established by spectroscopic analysis and NOE measurements of isopropylidene derivatives obtained by debenzilation of the initial alcohols **66** and **67**. The side chain of the monosaccharide derivative **67** appeared to have the D-glycero-configuration, and that of **66** the L-glycero-configuration.

To convert the alcohols **66** and **67** into the corresponding yersinioses, the former were exposed to very mild acetolysis and subsequent methanolysis which opened the 1,6-anhydro ring without any accompanying elimination of the *O*-benzyl groups (which might result in a complex mixture of pyranose and furanose forms of yersinioses). The resulting glycosides **68** and **69** ($\text{R} = \text{OH}$) with a free hydroxy group at C(6) were thus obtained. This group was substituted with bromine by treatment with $\text{Ph}_3\text{P}-\text{CBr}_4$ in pyridine. After separation and catalytic hydrogenolysis with simultaneous removal of the benzyl groups, the resulting bromides **68** and **69** ($\text{R} = \text{Br}$) were converted into glycosides of the synthetic yersinioses **70** and **71**. Their comparison with the corresponding derivatives of natural yersinioses isolated from PS using various versions of NMR spectroscopy (of which NOE analysis was the most important one) allowed establishment of the configuration of the chiral centre of C(7) in both monosaccharides. It was found that yersiniose A is 3,6-dideoxy-4-*C*-(L-glycero-1'-hydroxyethyl)-D-xylo-hexopyranose, while yersiniose B 3,6-dideoxy-4-*C*-(D-glycero-1'-hydroxyethyl)-D-xylo-hexopyranose.

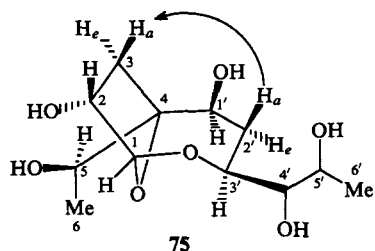
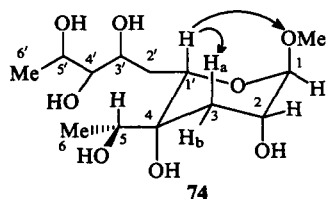
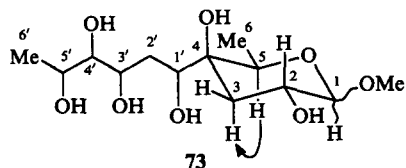
A structurally unique higher monosaccharide with a branched chain has recently been detected in PS of *Pseudomonas caryophylli*.^{86,87} This monosaccharide was isolated in the pure state after acid hydrolysis of PS and called caryophillose. Its ^{13}C NMR spectrum suggested the presence of six CHOH groups (signals around 68–78 ppm), two CH_3 groups (signals in the region 16–17 ppm), two methylene groups (signals in the region 29–32 ppm) and one tertiary carbon atom carrying a hydroxy group (signal at 74 ppm). Reduction of caryophillose with NaBD_4 resulted in a branched alditol which upon acetylation gave the heptaacetate **72**. The fact that one of the hydroxy groups was not acetylated demonstrated its attachment to the tertiary carbon



atom. The type of fragmentation in the mass spectrum of the acetate **72** as well as ^{13}C NMR spectroscopic data indicated that caryophillose comprises 12 carbon atoms, two methyl groups and two methylene units, has a branched chain and is a 3,6-dideoxy-4-*C*-(1',3',4',5'-tetrahydroxyhexyl)hexose.

Determination of the stereochemistry of caryophillose was a challenge. This problem was solved using NMR spectroscopy (including NOE measurements).

Briefly, the essence of this complex study is as follows. Acid methanolysis of the monosaccharide gave two isomeric methyl glycosides of caryophillose **73** and **74**, and one internal glycoside **75**.

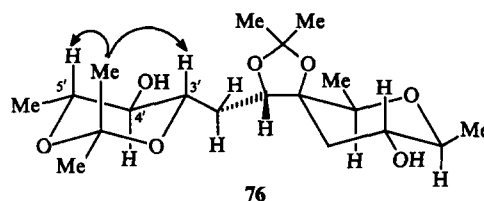


The glycoside **73** formed by closing of the pyranose ring via the hydroxy group at C(5) was isolated as a mixture of α - and β -anomers and had the 4C_1 conformation of the pyranose cycle (as could be evidenced from NMR spectroscopic data). Its 1H NMR spectrum suggested the lack of protons at C(4), thus confirming the site of branching of the carbon chain determined from the mass spectrum of the alditol **72**. An NOE study revealed interaction between H(5) and H(3a) in the glycoside **73** which proved the axial position of H(5). The equatorial position of the aliphatic chain C(1')-C(6') was evident from the spatial proximity of H(5) and H(1') of the side chain. Based on these data, the pyranose ring and, correspondingly, the C(1')-C(6') fragment of caryophillose were assigned the *xylo*-configuration. To establish the spatial structure of this aliphatic fragment of caryophillose was a more complicated task which was solved by complex analysis of the NMR spectra of the glycosides **74** and **75** and of some other derivatives.

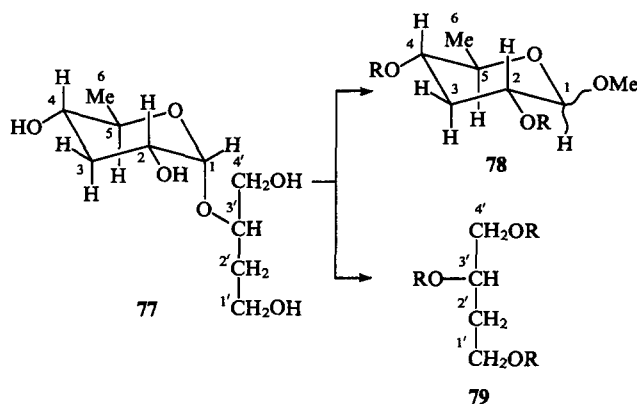
The glycoside **74** isomeric with the glycoside **73** was formed by closing of the pyranose ring via the hydroxy group at C(1') of caryophillose (this was accompanied by stereospecific formation of the β -glycoside alone). The data of the 1H NMR spectrum suggest the glycoside **74** to be in the 1C_4 conformation. NOE measurements with the glycoside **74** and its *O*-acetate reveal that H(1') is closed to the axial methoxy group and, consequently, occupies the axial position as well. Hence, C(1') in the C(1')-C(6') chain has the (*S*)-configuration.

The glycoside **75**, isolated by acid methanolysis of caryophillose, is formed as a result of intramolecular glycosylation involving the hydroxy group at C(3'). Glycosylation gives a bicyclic system containing a furanose ring. The structure of the glycoside **75** was reliably established: the compound has the composition $C_{12}H_{22}O_7$ (as can be evidenced from the FAB mass spectrum); its ^{13}C NMR spectrum is completely consistent with the structure **75**. In the ^{13}C NMR spectrum of the acetate of **75**, the signal of the proton at C(3') (3.88 ppm) lacked the characteristic shift which might result from the presence of a heminal acetoxy group; consequently, C(3') is linked by an acetal (i.e., glycosidic) bond corroborating the accepted structure of the glycoside **75**. The conformation of the glycoside **75** was established by NOE measurements for the protons at C(2) and C(3) as well as at C(1'), C(2') and C(3') in the glycoside **75** itself and its *O*-acetate,

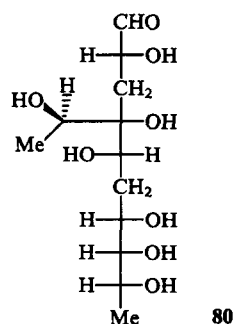
which suggest, in particular, that C(3') has the (*S*)-configuration. To establish the relative configuration at C(4') and C(5') of caryophillose, the 4,1':3',5'-di-*O*-isopropylidene derivative **76** was prepared from the glycoside **73**. NOE measurements for H(3') and H(5') in the 3',5'-*O*-isopropylidene group, forming 1,3-dioxane ring with the chair conformation, show their *cis*-diaxial orientation and *trans*-diaxial position relative to H(4'). Therefore, it was concluded that C(4') and C(5') have the (*R*)-configuration.



The absolute configuration of the C(1)-C(6) and C(1')-C(6') fragments of caryophillose was established mainly on the basis of circular dichroism measurements for each of these fragments.⁸⁸ Methylation analysis revealed that in the PS chain the neighbouring residues of caryophillose are linked by the glycosidic bonds at the hydroxy group localised at C(3'). Therefore, periodate oxidation of the original PS results in the cleavage of the bonds between C(4') and C(5') as well as between C(1') and C(4). As a result, reduction of the oxidation product gives rise to compound **77**, which is a glycoside of 3,6-dideoxy- α -ribo-hexose (paratose), and 1,4-dihydroxybutan-3-ol. The structure of this compound was confirmed by NMR spectroscopy. Methanolysis of the glycoside **77** gives α - and β -glycosides of paratose **78** (R = H) and 1,3,4-trihydroxybutane **79** (R = H). Analysis of the circular dichroism spectra by the method of Nakanishi⁸⁸ was carried out for the *p*-bromobenzoates **78** and **79** (R = *p*-BrC₆H₄CO). A change in the Cotton effect as a function of wavelength indicates that C(2) in the glycoside **78** has the (*R*)-configuration, and C(3') in **79** the (*S*)-configuration.



These data suggested that the caryophillose present in PS is 3,6-dideoxy-4-*C*-(*D*-*altro*-tetrahydroxyhexyl)-*D*-*xylo*-hexopyranose **73**, which is a cyclic form of the higher branched sugar, 3,6,10-trideoxy-4-*C*-[(*R*)-1'-hydroxyethyl]-*D*-*erythro*-*D*-*gulo*-decaose **80**.



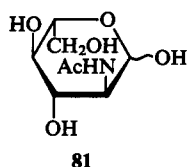
7. Amino sugars

Monosaccharides containing amino groups (amino sugars) of various structure are widespread in bacterial PS. Many of them contain several deoxy units and amino groups in various combinations which contributes largely to the great diversity of known natural amino sugars.

a. Aminodeoxyhexoses

Derivatives of 2-amino-2-deoxyhexoses having the D-gluc-, D-galacto- or D-manno-configuration (glucosamine, galactosamine and mannosamine) are among the most common components of PS of microorganisms. Most often, they are present in the polysaccharide chain as N-acetyl derivatives, although N-acyl derivatives comprising residues of other organic acids are also known (see Section 4).

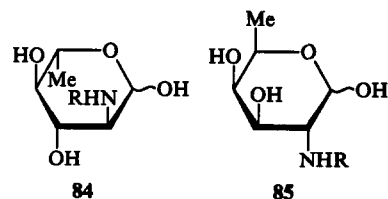
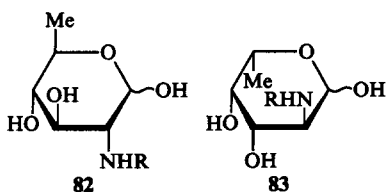
At the same time, O-antigenic PS have been found to contain only one representative of 2-amino-2-deoxyhexoses with the L-configuration, namely, 2-acetyl-amino-2-deoxy-L-glucose **81** detected in PS of *Pseudomonas cepacia* O1.⁸⁹



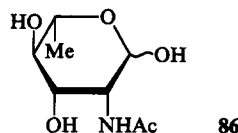
The monosaccharide **81** gave qualitative reactions for amino sugars; the mass spectrum of the aminodeoxyalditol acetate derived was identical to that of the well-known derivative obtained from the D-isomer. The fragmentation observed demonstrated the presence of an acetyl-amino group at C(2). This finding was also confirmed by ¹³C NMR spectroscopic data: the spectrum of PS contained a signal of C(2) at 54.23 ppm. Finally, the structure of this amino sugar was also corroborated by analysis of a disaccharide fragment obtained after Smith degradation of PS. The unusual L-configuration of the monosaccharide was established on the basis of GLC of its glycosides with optically active butan-2-ol and octan-2-ol, by its specific optical rotation⁸⁰ and by comparison of the circular dichroism spectrum of the derived aminodeoxyalditol with that of the corresponding D-isomer.

b. Aminodideoxyhexoses

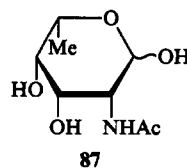
Derivatives of 2-amino-2,6-dideoxyhexoses are widespread in O-antigenic PS. Two of these, 2-amino-2,6-dideoxy-D-glucose (D-quinovosamine) **82** and 2-amino-2,6-dideoxy-L-galactose (L-fucosamine) **83** are common components of O-antigenic PS.² Their enantiomers, L-quinovosamine **84** and D-fucosamine **85** occur less frequently. L-Quinovosamine was found in PS of *Shigella boydii*, *Proteus vulgaris*, *Pseudomonas fluorescens*, etc.,² while D-fucosamine in *Pseudomonas fluorescens* and some species of *Pseudomonas aeruginosa*.² These 2-amino-2,6-dideoxyhexoses are present in the polysaccharide chains as various N-acyl (most frequently N-acetyl) derivatives. They can be isolated in the pure state from acid hydrolysates of PS or after solvolysis of PS with liquid HF. Currently, these monosaccharides are identified directly by the NMR spectra of PS themselves.



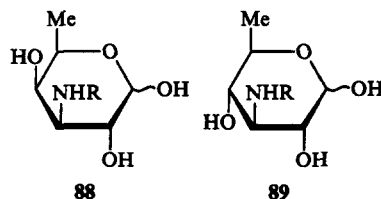
An example of more rare amino sugars of this type present in microbial PS is 2-acetyl-amino-2,6-dideoxy-L-mannose **86** (L-rhamnosamine) detected in *Escherichia coli* O3.⁹⁰ The monosaccharide was isolated in the pure state after acid hydrolysis. Its structure was established by classical methods: periodate oxidation yielded acetaldehyde, thus suggesting the presence of a methyl group (the 6-deoxy fragment); based on different ion-chromatographic behaviour of the monosaccharide and the derivatives of other 2-amino-2,6-dideoxy sugars, the monosaccharide was assigned the structure of an L-rhamnose derivative.



It is interesting to note that another very rare monosaccharide of this class, 2-acetyl-amino-2,6-dideoxy-L-talose **87** (pneumosamine), was identified long ago in a capsular polysaccharide of *Streptococcus pneumoniae* type 5; however, its structure was not strictly confirmed.⁹¹

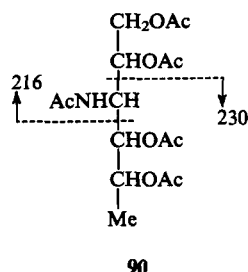


Among other monoaminodideoxyhexoses, O-antigenic PS contain derivatives of 3-amino-3,6-dideoxyhexoses present in the PS chain as N-acyl derivatives (most frequently, as acetyl but sometimes also as derivatives of hydroxy and amino acids; see Section 4). Among monosaccharides of this type, derivatives of 3-amino-3,6-dideoxy-D-galactose **88** (3-amino-3-deoxy-D-fucose) are rather common components of many PS.² An analogue of 3-amino-3,6-dideoxy-D-galactose, 3-amino-3,6-dideoxy-D-glucose **89** (3-amino-3-deoxyquinovose), was found in O-antigenic PS of several species of Gram-negative bacteria: in *Escherichia coli*,⁹² *Hafnia alvei*,⁹³ *Proteus penneri*,⁹⁴ *Pseudomonas fluorescens*,⁹³ *Vibrio mimicus*.⁹⁵ The L-isomer, 3-amino-3,6-dideoxy-L-glucose, was isolated from O-antigenic PS of *Vibrio anguillarum*.⁹⁶ This is the only example of 3-amino-3,6-dideoxyhexoses with the L-configuration detected in O-antigenic PS. This sugar was earlier detected in the LPS core⁹⁷ of *Aeromonas hydrophila* III.



Derivatives of these aminodideoxyhexoses including those of glucose with the L-configuration were isolated from PS in the individual state after acid hydrolysis or solvolysis with liquid HF and, to simplify analysis, converted into N-acetates. To this end, they were deacylated (the N-acyl substituent was eliminated) and then N-acetylated by a routine procedure. The structure of the 3-acetyl-amino-3,6-dideoxyhexoses thus obtained was established by physicochemical methods and confirmed by counterflow synthesis.

An example is the establishment of the structure of 3-acetyl-amino-3,6-dideoxy-D-glucose.^{95,98} The mass spectrum of the full acetate of the aminodeoxyalditol **90** derived from the amino sugar by reduction and subsequent acetylation contained fragments with m/z 230 and 216 which unambiguously indicated the position of the acetyl-amino group at C(3) and of the deoxy unit (CH_3 group) at C(6). This finding demonstrated that the parent sugar has the 3-acetyl-amino-3,6-dideoxyhexose structure.



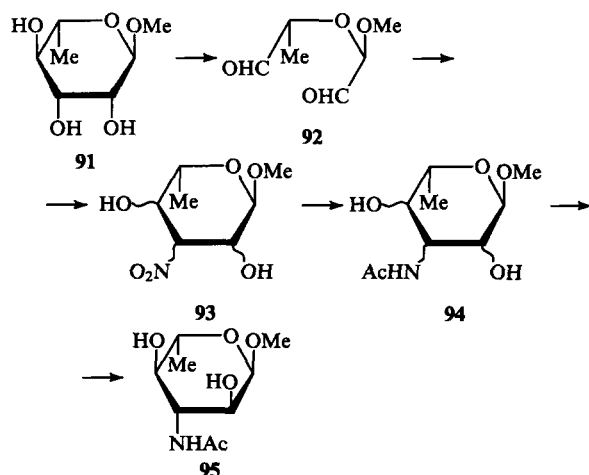
This conclusion was also confirmed by the ^{13}C NMR spectrum containing signals at 18 ppm (CH_3 group) and 55–58 ppm [NHAc -substituent at C(3)]. The ^1H NMR spectrum of the full acetate of the amino sugar glycoside was characterised by the coupling constant values of $J_{2,3}$, $J_{3,4}$ and $J_{4,5}$ exceeding 10 Hz, thus suggesting the *gluco*-configuration of the monosaccharide. Finally, the specific optical rotation ($[\alpha]_D = +26^\circ$) showed that it belongs to the D-series.

The structure of 3-acetyl-amino-3,6-dideoxy-D-galactose⁹⁹ was also confirmed by analysis of the mass spectrum of the corresponding aminodeoxyalditol acetate which exhibited characteristic fragmentation. The ^{13}C NMR spectrum of this compound contained signals at 17 and 52 ppm, and the ^1H NMR spectrum demonstrated the *galacto*-configuration (the coupling constant values were: $J_{2,3} = 10$, $J_{3,4} = 4$, $J_{4,5} = 1$ Hz). The D-configuration was established by comparison with a synthetic authentic sample and confirmed by the specific optical rotation. It is interesting to note that initially this monosaccharide was erroneously assigned the D-*gluco*-configuration,¹⁰⁰ and this error was corrected later.⁹⁸

The structure of 3-acetyl-amino-3,6-dideoxy-L-glucose, the only monosaccharide in this group having the L-configuration,^{96,97} was established by the same methods, and its absolute configuration determined by circular dichroism.

Several methods for the synthesis of 3-amino-3,6-dideoxy-aldoses are known. These compounds were obtained by the classical Fischer–Bayer method (condensation of dialdehydes prepared by oxidation of 6-deoxyhexose glycosides with nitromethane followed by reduction of the nitro group). As an example, we refer to the synthesis of a derivative of 3-acetyl-amino-3,6-dideoxy-L-glucose (Scheme 10).¹⁰¹

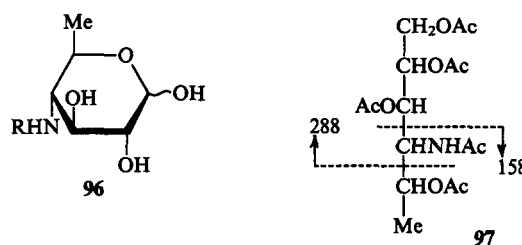
Scheme 10



Methyl- α -L-rhamnopyranoside **91** was oxidised by periodate, and the dialdehyde **92** derived was condensed with nitromethane in the presence of sodium methoxide. The resulting isomeric 3-nitrohexoses **93** were reduced over Raney nickel; the corresponding amino sugars were *N*-acetylated, and then methyl 3-acetyl-amino-3,6-dideoxy- α -L-glucopyranoside **95** was isolated from the resulting mixture of the amino acetates **94** by chromatography in a 26% yield. Other aminodeoxyhexoses can be synthesised by conventional methods based on inversion of the configuration at certain carbon atoms (e.g., see Ref. 102).

The third group of amino sugars present in O-antigenic PS are derivatives of 4-amino-4,6-dideoxyhexoses, although they seem to be less common than their 3-amino analogues. By now, three hexoses of this type having the D-*gluco*-, D-*manno*- or D-*galacto*-configuration have been identified. The amino groups in these monosaccharides are acylated (usually, acetylated).

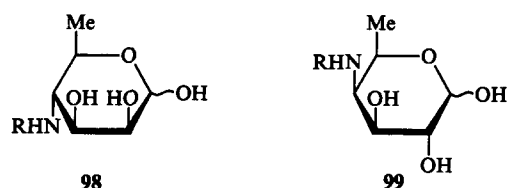
4-Amino-4,6-dideoxy-D-glucose **96** (4-amino-4-deoxy-D-quinovose, viosamine) was first identified as the *N*-acetyl derivative in PS of *Escherichia coli* O7 where it is present in the main chain.¹⁰³ As an *N*-acyl derivative carrying the *N*-acetylglycine residue, it was also found in PS of *Shigella dysenteriae* 7,^{104,105} and as the *N*-formyl derivative in PS of *Francisella tularensis* 15 (tularemia pathogen).¹⁰⁶ Recently this sugar was also detected in PS of *Vibrio anguillarum*¹⁰⁷ and in O-antigenic PS of *Hafnia alvei* 1205 having an unusual polysaccharide chain similar to that of teichoic acids.¹⁰⁸



The monosaccharide **96** was isolated as a structurally complex *N*-acylated derivative after treatment of PS with liquid HF and, to simplify analysis, further converted into the *N*-acetyl derivative. Its structure was studied by physicochemical methods. The mass spectrum of the fully acetylated aminodeoxyalditol **97** derived contained fragments with m/z 288 and 158 as well as the corresponding series of secondary ions indicating the presence of a deoxy unit at C(6) and of an acetyl-amino group at C(4). Such a structure was confirmed by ^{13}C NMR spectroscopic data [signals at 18.0 ppm for a CH_3 group and at 58.2 ppm for C(4)]. The *gluco*-configuration of the monosaccharide was established by ^1H NMR spectroscopic data, and the absolute configuration was confirmed by the specific optical rotation ($[\alpha]_D = +17^\circ$) which almost coincided with the corresponding value for the synthetic sample (see below).

At present, identification of this aminodeoxy sugar (as well as of its isomers) is performed almost exclusively on the basis of NMR spectral data of the initial PS themselves.

4-Amino-4,6-dideoxy-D-mannose **98** (4-amino-4-deoxy-D-rhamnose, perosamine) was first detected as an *N*-acyl derivative with 2-deoxy-L-*glycero*-tetronic acid in O-antigenic PS of *Vibrio cholera* Inaba (Asian cholera pathogen) where it forms a homopolysaccharide.¹⁰⁹ Later, it was found as the *N*-formyl derivative in a homopolysaccharide in O-antigenic PS of *Brucella melitensis* (brucellosis pathogen).¹¹⁰ As some other *N*-acyl derivatives, it is present in PS of several species of *Salmonella*,^{111,112} *Escherichia coli*,^{113,114} *Yersinia*¹¹⁵ and *Xanthomonas*.¹¹⁶ Since 4-amino-4,6-dideoxyhexoses are very unstable in acid media, they were isolated as *N*-acyl derivatives exclusively by solvolysis of PS with liquid HF.

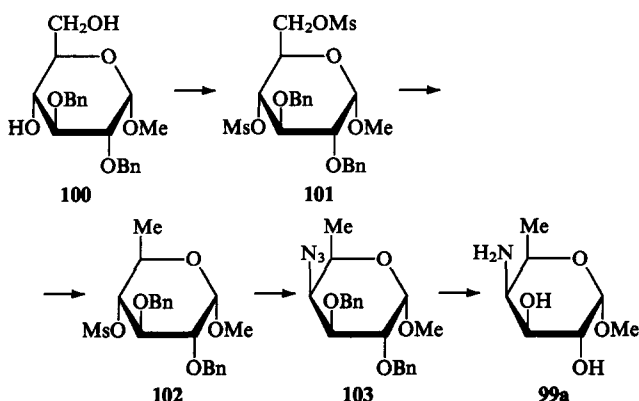


The monosaccharide **98** was identified by the mass spectrum of the corresponding aminoalditol acetate which appeared to be identical with that of the alditol derived from the *gluco*-analogue. That this monosaccharide belongs to the *manno*-series was first demonstrated by deamination with nitrous acid of deacetylated PS: hydrolysis of deaminated PS revealed the presence of D-rhamnose and 6-deoxy-D-allose which could be formed only when the original monosaccharide contained the NH_2 group at C(4) and had the *manno*-configuration.¹⁰⁹ Later, it was confirmed by ^1H NMR spectroscopic analysis of the PS itself that this monosaccharide belongs to the *manno*-series (the coupling constant values were: $J_{2,3} = 4.5$, $J_{3,4} = 10$, $J_{4,5} = 10$ Hz). The absolute configuration of the monosaccharide was established by its conversion into a glucoside with (–)-butan-2-ol.

4-Amino-4,6-dideoxy-D-galactose **99** (4-amino-4-deoxy-D-fucose, tomosamine) occurs less frequently and has thus far been found only in O-antigenic PS of *Escherichia coli* O10¹¹⁷ and *Pseudomonas fluorescens*.¹¹⁸ In the former PS the amino sugar is *N*-acylated by the residue of 3-hydroxybutyric acid and localised in the side chain attached to the main chain of the PS; in the latter case the PS is *N*-acetylated. The amino sugar was isolated after solvolysis of PS with liquid HF ; its structure was established by ^1H NMR spectroscopic data: the position of the *N*-acyl group was proved by a low-field shift of H(4), and the *galacto*-configuration was concluded from the coupling constant values: $J_{2,3} > 10$, $J_{3,4} \sim 4.5$, $J_{4,5} \sim 1.8$ Hz.¹¹⁸

Synthesis of several 4-amino-4,6-dideoxyhexoses was carried out by using a general approach well-known in sugar chemistry: introduction of an amino function into a neutral monosaccharide via the corresponding azide. By illustration, let us consider the synthesis of tomosamine and viosamine¹¹⁹ derivatives from glucose (Scheme 11).

Scheme 11



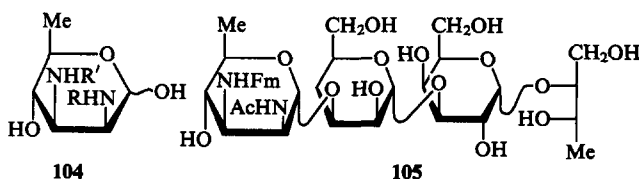
Methyl-2,3-di-*O*-benzyl- α -D-glucopyranoside **100** was converted into the dimesylate **101**, which after interaction with KI, hydration of the corresponding monoiodide and repeated mesylation gave the 4-*O*-mesylate of 6-deoxyglucose **102**. The reaction of the compound **102** with sodium azide accompanied by inversion of the configuration gave the azide **103** hydration of which was accompanied by removal of the benzyl groups to yield the glycoside of tomosamine **99a**. To obtain the *gluco*-analogue, double inversion at C(4) was used: the mesylate **102** was converted into a galactose derivative by reaction with sodium benzoate. The derivative of 4-amino-4,6-dideoxyglucose **96**

($\text{R} = \text{H}$) (viosamine) was obtained via the corresponding azide after debenzoylation and mesylation of the galactose derivative.

c. Diaminotrideoxyhexoses

PS of some Gram-negative bacteria were found to contain amino sugars of unusual structure, which belong to 6-deoxyhexoses containing two amino groups at C(2) and C(3) or at C(2) and C(4) and only one hydroxy group. Diaminotrideoxyhexoses are distinguished by high lability to acids and usually cannot be isolated in the pure state. Their structure was mostly established by NMR spectroscopic and mass spectrometric data for oligosaccharide fragments isolated by partial cleavage of the corresponding PS.

The only representative of 2,3-diamino-2,3,6-trideoxyhexoses in O-antigenic PS is a derivative of 2,3-diamino-2,3,6-trideoxy-D-mannose **104** (2,3-diamino-2,3-dideoxy-D-rhamnose) containing *N*-formyl and *N*-acetyl substituents at the amino groups at C(3) and C(2), respectively.



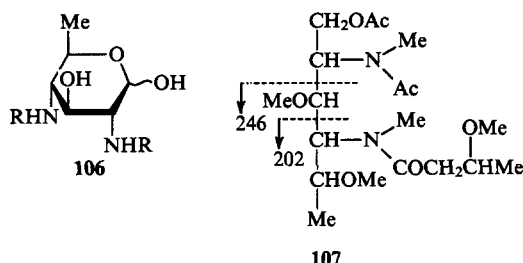
This monosaccharide is a component of PS of *Escherichia coli* O119, where it occupies the position of a lateral substituent of the polysaccharide chain and is an immunochemical determinant.¹²⁰ Its structure was established on the basis of the following data. The PS was oxidised two times with periodate, and the subsequent Smith degradation resulted in the oligosaccharide **105** containing a diaminotrideoxyhexose residue. This finding was confirmed by mass spectrometric data: the FAB mass spectrum of the PS contained a fragment with m/z 215 suggesting the presence of a diaminotrideoxyhexose residue carrying *N*-formyl and *N*-acetyl substituents as well as the corresponding secondary fragments, thus indicating the localisation of the formyl residue at the amino group at C(3). The complex NMR spectra of the tetrasaccharide **105** contained signals of the diaminotrideoxyhexose residue. In the ^{13}C NMR spectra the signals of C(2) and C(3) (52.11 and 53.03 ppm) demonstrated the presence of the acylamino groups at these atoms. The signals at 165 and 168 ppm indicated the presence of a formylamino group, and the signal at 176.36 ppm indicated the presence of an acetylamino group. The signal at 17.86 ppm corroborated the presence of the CH_3 group at C(6). Application of the INEPT technique to NMR spectroscopic analysis revealed localisation of the *N*-acetyl group at C(2) and the *N*-formyl group at C(3).

In the ^1H NMR spectra the coupling constant values ($J_{2,3} = 4.0$, $J_{3,4} = 10.3$, $J_{4,5} = 9.5$ and $J_{5,6} = 6.1$ Hz) suggested the *manno*-configuration for the monosaccharide.

The absolute configuration of the monosaccharide **104** was evident from the NOE data: irradiation of H(1) of this sugar caused a strong effect on the adjacent H(2) in the chain of the oligosaccharide **105** mannose residue. This finding suggested that both monosaccharides have the same absolute configuration. Since mannose had the D-configuration, the novel monosaccharide was also assigned the D-configuration. Therefore, the novel sugar was identified as a derivative of 2,3-diamino-2,3,6-trideoxy-D-mannose.

2,4-Diamino-2,4,6-trideoxyhexoses are more common in PS. Thus, derivatives of 2,4-diamino-2,4,6-trideoxy-D-glucose **106** (bacillosamine) were first detected in PS of the cell wall of *Bacillus licheniformis*¹²¹ and, later, in O-antigenic PS of several species of *Pseudomonas aeruginosa*,¹²² *Pseudomonas aurantiaca*,¹²³ *Vibrio cholerae* O3^{58,124} and *Fusobacterium necroforum*.¹²⁵ A derivative of this amino sugar with the acetylated amino group at C(2) and the amino group at C(4) acylated with 3-hydroxybutyric acid was isolated in the pure state from PS of *P. aeruginosa* O3 only after

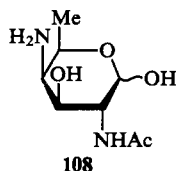
solvolysis with liquid HF.¹²² The ¹³C NMR spectrum of the monosaccharide indicated the presence of a CH₃ group (18.3 ppm) at C(6) and of amino groups at C(2) and C(4) (57.6 and 56.8 ppm). High coupling constant values for the ring protons ($J_{2,3}$, $J_{3,4}$ and $J_{4,5} \approx 10$ Hz) demonstrated unambiguously the *gluco*-configuration of this monosaccharide. The absolute D-configuration was evident from the specific optical rotation ($[\alpha]_D = +36^\circ$). All the characteristic signals of the NMR spectra of the monosaccharide **106** mentioned above were also found in the spectra of the PS itself and of its fragments.



For final establishment of the position of the amino groups and localisation of the acyl substituents by routine degradation of PS, the alditol **107** was obtained by solvolysis with anhydrous HF followed by reduction with NaBH₄ and methylation involving the NH groups. The mass spectrum of the alditol **107** contained fragments with m/z 202 and 246 which confirmed the presence of an *N*-acetyl group at C(2) and of a *N*-hydroxybutyryl group at C(4).¹²²

In subsequent studies, this diamino sugar was not isolated and its identification was carried out by NMR spectroscopy of the initial PS. Mass spectrometry of PS fragments obtained by their cleavage made it possible to establish the structure and localisation of *N*-acyl groups. For instance, it was found that bacillosamine in PS of *Vibrio cholerae* O3 is acetylated at the amino group at C(2) and acylated by the residue of 3,5-dihydroxyhexanoic acid at the amino group at C(4) (see Section 4).⁵⁸

2,4-Diamino-2,4,6-trideoxy-D-galactose (**108**), a monosaccharide isomeric with bacillosamine and having an acetylated amino group at C(2), was found in O-antigenic PS of *Shigella sonnei*.¹²⁶ The monosaccharide **108** failed to be isolated in the pure state even by solvolysis with HF, and its structure was determined on the basis of the ¹³C NMR spectrum of PS which contained signals similar to those observed for its *gluco*-isomer: 17.3 (CH₃ group), 56.6 and 53.0 ppm [C(2) and C(4) substituted by the amino groups]. The D-configuration was assigned to the monosaccharide based on the results of deamination and subsequent hydrolysis of PS. The formation as the main product of 2-acetylamino-2,6-dideoxy-D-glucose and (after reduction) of small amounts of a mixture of 2-acetylamino-2,4,6-trideoxyhexoses allowed a conclusion that the monosaccharide has the *galacto*-configuration.



No more unambiguous proof of the amino sugar configuration is given. The presence in the ¹H NMR spectrum of PS (at pH 10) of a signal at 3.15 ppm with small coupling constant values also confirmed the axial position of the free amino group at C(4) and, correspondingly, the *galacto*-configuration of the monosaccharide.

8. Hexuronic acids

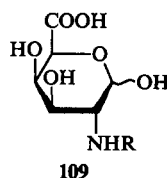
Many O-antigenic PS contain acidic monosaccharides. The presence of such components in PS localised on the surface of the microbial cell confers specific properties on the bacterial envelope. In some cases it protects the cell from external aggressive factors and offers an alternative to the microbial capsule which fulfils a similar protective function in encapsulated bacteria. At the same time, the presence of acidic components in O-antigenic polysaccharides strongly influences the character of the somatic antigen, since it is precisely the acidic monosaccharide that often plays the role of the immunodominant group.

The most common acidic monosaccharides present in the polysaccharide chain of O-antigenic PS are hexuronic acids. Two of those, D-glucuronic and D-galacturonic acids are widespread in nature and are common components of microbial PS of a number of Gram-negative bacteria belonging to different species. Procedures for their identification have been well developed and standardised and their chemistry has been studied in a sufficiently great detail. Uronic acids bearing one or two amino groups occur as well.

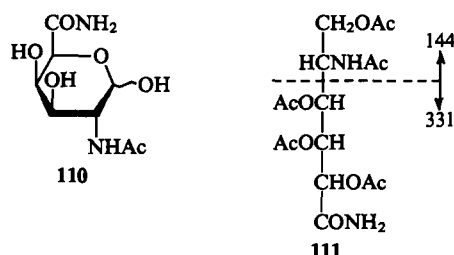
a. 2-Amino-2-deoxyhexuronic acids

O-Antigenic PS have been found to contain some representatives of 2-amino-2-deoxyhexuronic acids with the *D-galacto*-, *D-manno*-, *L-galacto*-, *L-gulo*- and *L-altro*-configuration. In an effort to isolate and to establish the structure of aminuronic acids at various stages of analysis of microbial PS, different approaches were employed depending upon the degree of sophistication of the physicochemical approaches developed at the time when the particular study was carried out. Recent trends are towards the use of NMR spectroscopy of PS for establishment of the structure of aminuronic acids and their fragments and of mass spectrometry of alditols derived by their reduction. Of chemical methods, the most often used is the reduction of the carboxy group of a uronic acid resulting in formation of the corresponding easily identified 2-acylamino-2-deoxyhexose. This allows a direct conclusion about the structure of the initial aminuronic acid including its absolute configuration.

2-Amino-2-deoxy-D-galacturonic acid **109** in the form of its derivatives is found in O-antigenic PS more frequently than other sugars of this class. It is detected in PS of *Shigella dysenteriae* 7,¹⁰⁵ some serotypes of *Pseudomonas aeruginosa*,¹²⁸⁻¹³⁰ *Salmonella arizonae*¹²⁷ and *Vibrio anguillarum*¹⁰⁷ as well as in some capsular PS. A homopolysaccharide built up of residues of this aminuronic acid has long been known as the Vi-antigen of Gram-negative bacteria.¹³¹ The amino group of this and other aminuronic acids is usually acylated (most commonly acetylated), while the carboxy group is free. In PS of some bacteria the carboxy group is present as an amide; sometimes the same PS contains various proportions of both free acid and its amide. 2-Acetylamino-2-deoxy-D-galacturonic acid and its amide as well as other aminuronic acids can be isolated in the pure state using various procedures for PS cleavage: solvolysis with liquid HF, acid hydrolysis, methanolysis, etc.^{127, 128} To separate the amide of *N*-acetylaminogalacturonic acid from the free acid and to isolate it in the pure state, the following approach was used: the PS was first reduced with NaBH₄ in the presence of a water-soluble carbodiimide (the uronic acid residue was thereby converted into 2-acetylamino-2-deoxygalactose, while the amide residue was not reduced) and subjected to solvolysis with liquid HF.

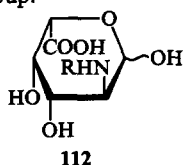


To determine the structure of aminogalacturonic acid derivatives, they were converted into the acetates of the corresponding alditols, and the amides of galacturonic acid into the acetates of the aldonic acid amides. Then, their structure was established by mass spectrometry. Significantly, this approach made it possible to keep the *N*-acyl group residues unchanged and to determine their structure. For example, the presence in the mass spectrum of the acetate of the amide of 5-acetyl-amino-5-deoxygalactonic acid **111** (obtained by reduction and acetylation of the amide of 2-acetyl-amino-2-deoxygalacturonic acid **110**) of fragments with *m/z* 331 and 144 suggests the presence of an *N*-acetyl-amino group in the amide **110** and reveals its position.



The structure of 2-amino-2-deoxygalacturonic acid can be established on the basis of NMR spectroscopic data. Thus, the ^{13}C NMR spectrum contains a signal due to the carboxy group at 173–176 ppm and a signal of C(2) substituted by the amino group at 49–51 ppm. The assignment of the acid to the *galacto*-series was done on the basis of the ^1H NMR spectrum: the coupling constant values for the ring protons were: $J_{2,3} = 11$, $J_{3,4} = 3$ and $J_{4,5} = 1.5$ Hz. The specific optical rotation ($[\alpha]_D = +17.9^\circ$) corroborated the absolute configuration of the monosaccharide.

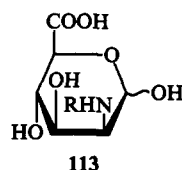
Polysaccharides of some other serotypes of *Pseudomonas aeruginosa* were found to contain the L-isomer of the acid **109**, 2-acetyl-amino-2-deoxy-L-galacturonic acid **112**,^{122,132} which, like its D-isomer, is a component of the main chain of PS. The presence in PS of the uronic acid was also evident from spectral data: the IR spectrum contained an absorption band at 1740 cm^{-1} and the ^{13}C NMR spectrum a signal at 175 ppm belonging to the carboxy group.



Reduction of PS with NaBH_4 and subsequent hydrolysis resulted in isolation and identification of 2-acetyl-amino-2-deoxy-L-galactose (*N*-acetyl-L-galactosamine), thus confirming finally the structure of the monosaccharide **112** including its absolute configuration.

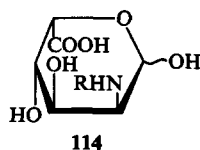
A derivative of 2-amino-2-deoxy-D-mannuronic acid **113** was found in O-antigenic PS of *Vibrio cholerae* O5.¹²⁴ The acid **113** was not isolated in the pure state, and its structure was established by a non-destructive method based on a detailed analysis of NMR spectra of the PS itself. Thus, the ^{13}C NMR spectrum of the aminomannuronic acid residue contained a carboxy group signal at 160–170 ppm; in addition, the presence of the carboxy group of the uronic acid was evident from the absence of H(6) signals in the ^1H NMR spectrum in combination with a characteristic pH dependence of the H(5) proton shift. For confirmation of the acid **113** structure, the polysaccharide was reduced with NaBD_4 and hydrolysed. As a hydrolytic product, a derivative of 6-[$^2\text{H}_2$]-mannosamine was isolated and identified by mass spectrometry as the acetate of the corresponding alditol. The *manno*-configuration of the acid was corroborated by NMR spectroscopic data of the initial PS. The absolute configuration was suggested on the basis of the glycosylation effects determined from the ^{13}C NMR

spectrum taking into account the type of substitution of the adjacent unit in the polysaccharide chain.

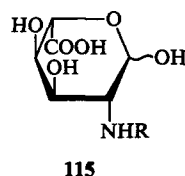


The derivatives of the two other 2-amino-2-deoxyuronic acids, 2-acetyl-amino-2-deoxy-L-guluronic acid and 2-acetyl-amino-2-deoxy-L-alturonic acid, are very rare in occurrence and have thus far been found only in O-antigenic PS.

2-Acetyl-amino-2-deoxy-L-guluronic acid **114** was found in PS of *Alteromonas macleodi* 2MM.¹³³ Its structure was established by a non-destructive method. The presence of the uronic acid residue was confirmed by the signals corresponding to the carboxy group (177.7 ppm) and C(2) substituted by an amino group (52.4 ppm) in the ^{13}C NMR spectrum of the polysaccharide and was also corroborated by a low-field shift of the H(2) signal in the ^1H NMR spectrum (4.38 ppm). The *gulo*-configuration of the acid is evident from the ^1H NMR spectrum of the polysaccharide, in which the coupling constant values for the ring protons are characteristic of the *gulo*-series ($J_{2,3} = 9$, $J_{3,4} = 4.0$, $J_{4,5} = 2$ Hz). The absolute L-configuration of the acid was suggested on the basis of NOE measurements for PS and construction of molecular models.



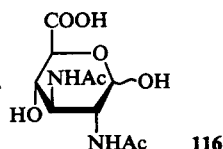
2-Acetyl-amino-2-deoxy-L-alturonic acid **115** was found in PS of *Shigella sonnei*, phase I.^{126,134} It was isolated in the pure state by acid methanolysis of PS followed by *N*-acetylation. Its reduction with NaBH_4 gave 2-acetyl-amino-2-deoxy-L-altrose identified by comparison with an authentic sample using the specific optical rotation.¹³⁴ More recently,¹²⁶ the ^{13}C NMR spectrum of the acid **115** containing, in particular, signals at 175.6 (COOH) and 56.8 ppm [C(2)] was recorded. The L-configuration of the acid was confirmed by the fact that ninhydrin oxidation of 2-acetyl-amino-2-deoxyaltrose derived by its reduction gives L-ribose.¹²⁶



b. 2,3-Diamino-2,3-dideoxyhexuronic acids

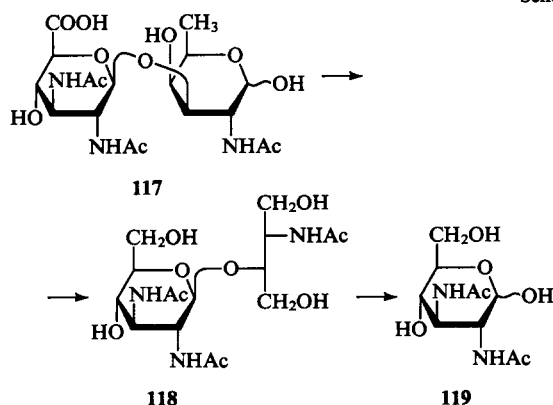
These structurally unique acidic monosaccharides are rare in occurrence and have thus far been detected only in O-antigenic PS of several strains of *Pseudomonas aeruginosa* and one of their representative has been found in PS of *Bordetella*. These monosaccharides are unstable in acid media and not all of them could be isolated in the pure state; determination of their structure posed considerable difficulties which could be obviated by structural analysis of oligosaccharide fragments obtained by partial degradation of PS in combination with a thorough analysis of the NMR spectra of the PS themselves.

Currently, derivatives of 2,3-diamino-2,3-dideoxyuronic acids having the D-*gluco*-, D-*manno*-, D-*galacto*- and L-*gulo*-configurations are known.

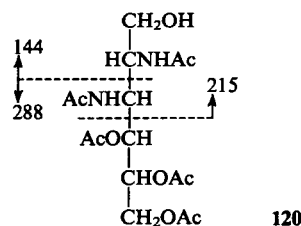


2,3-Acetyl-amino-2,3-dideoxy-D-glucuronic acid **116** was found in PS of *P. aeruginosa* O6.^{135,136} Using this acid as an example, a scheme for structural analysis of these unusual monosaccharides has been elaborated (Scheme 12). The presence in PS of a free carboxy group was confirmed by the presence in the IR spectrum of a band at 1740 cm^{-1} . Solvolysis of PS with liquid HF performed at room temperature gave the disaccharide **117** containing a uronic acid. Successive reduction of the disaccharide with NaBH_4 followed by oxidation with HIO_4 , repeated reduction with NaBH_4 and carboxyl reduction resulted in the compound **118**. Strong acid hydrolysis of **118** and its subsequent *N*-acetylation gave 2,3-diacetyl-amino-2,3-dideoxyhexose **119**. The structure of the acid **119** was established by mass spectrometric analysis of the alditol acetate **120** derived from **119**.

Scheme 12



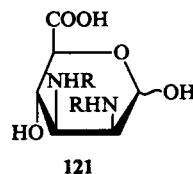
The mass spectrum of the compound **120** contained fragments with m/z 288, 215 and 144; such fragmentation, which is characteristic of 2,3-diacetyl-amino-2,3-dideoxyhexitol acetates, was previously observed for synthetic samples.¹³⁷



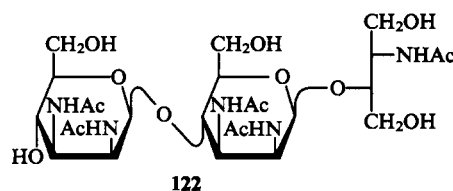
The ^{13}C NMR spectrum of the disaccharide **117** contained signals belonging to the carboxy group (176 ppm) and C(2) and C(3) substituted by the amino group (54.9 and 56 ppm). High coupling constant values of the ring protons in the ^1H NMR spectrum of the monosaccharide **116** ($J_{2,3} = 11.5$, $J_{3,4} = J_{4,5} = 10.0$ Hz) indicated its *gluco*-configuration. The acid **116** was assigned to the D-series on the basis of direct comparison of the diacetyldiaminohexose **119** derived by reduction of **116** with a synthetic sample of 2,3-diacetyl-amino-2,3-dideoxy-D-glucose.¹³⁸

Derivatives of 2,3-diamino-2,3-dideoxy-D-mannuronic acid **121** were found in PS of several serotypes of *Pseudomonas aeruginosa* where they are present in the main chain as one or two residues.^{139,140} The amino groups of the acid appeared to be substituted by acetyl and acetimidoyl (acetamidino) groups. It should be noted that the latter is unique for carbohydrate derivatives and was first detected in O-antigenic PS. The presence of an acetimidoyl group offered some difficulties in elucidation of

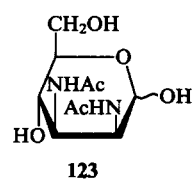
the structure of diaminomannuronic acid derivatives and originally prompted an erroneous conclusion about the presence in PS of a monosaccharide containing a condensed pyrano-imidazoline system.^{139,140} Subsequently this error was corrected.¹⁴¹ Therefore, to simplify the structural analysis, the polysaccharide or its fragments were treated with triethylamine to convert the acetimidoyl group into a more common acetyl group.



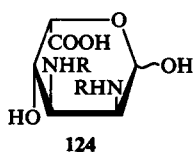
The structure of the acid **121** was established by the scheme described above for the *gluco*-analogue. Evidence for the presence of a carboxy group was derived from the band at 1725 cm^{-1} in the IR spectrum of PS. Successive solvolysis of PS with liquid HF, reduction with NaBH_4 , oxidation with HIO_4 , repeated reduction with NaBH_4 , treatment with triethylamine (conversion of the *N*-acetimidoyl into the *N*-acetyl group) and carboxyl reduction gave the trisaccharide derivative **122**.



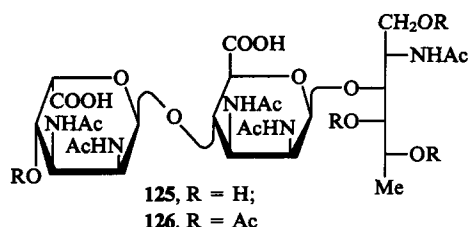
Drastic hydrolysis of **122** afforded 2,3-diacetyl-amino-2,3-dideoxy-D-mannose **123** whose structure was corroborated by mass spectrometry of the corresponding diacetylaminodialditol acetate. Fragmentation of this derivative proceeds by the same pathway as that of the alditol obtained from the *gluco*-analogue. The parameters of the NMR spectra of the diaminuronic acid residue present in the acetate of the trisaccharide **122** confirmed its structure: the ^{13}C NMR spectrum contained signals of C(2) and C(3) carrying NH groups at 52.3 and 52.5 ppm, and the coupling constant values of the ring protons in the ^1H NMR spectrum were consistent with the *manno*-series ($J_{2,3} = 3.9$, $J_{3,4} \approx J_{4,5} = 9.8$ Hz). Finally, the absolute configuration of the diacetylaminodideoxyhexose obtained from PS was confirmed by direct comparison with a synthetic sample of 2,3-diacetyl-amino-2,3-dideoxy-D-mannose.¹⁴³



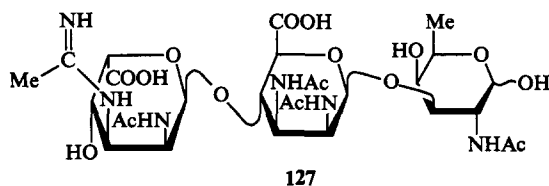
The third isomer of diaminuronic acids of this series, a derivative of 2,3-diacetyl-amino-2,3-dideoxy-L-guluronic acid **124** containing an *N*-acetimidoyl group, was found in PS of several subtypes of *Pseudomonas aeruginosa* O3^{140,143} and *Pseudomonas aeruginosa* immunotype 7.^{143,144} Some of these PS also contained a residue of 2,3-diamino-2,3-dideoxy-mannuronic acid that posed some problems while establishing the structure of the *gulo*-isomer, since interpretation of the NMR spectra of fragments containing both isomeric diaminuronic acids was quite complicated.



The structure of 2,3-diacetyl-amino-2,3-dideoxy-L-guluronic acid in PS of *Pseudomonas aeruginosa* O3 was established using the same scheme as for its *gluco*- and *manno*-analogues. After detection in the IR and NMR spectra of PS of signals for carboxy groups, the polysaccharide was subjected to solvolysis with liquid HF and subsequent treatment as described above. This resulted in a derivative of the trisaccharide **125** containing residues of diaminouronic acids with the *manno*- and *gulo*-configurations that was corroborated by NMR spectroscopy.



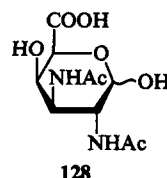
Regretfully, not only the derivative of the diaminoguluronic acid itself but also the product of its reduction, 2,3-diacetyl-amino-2,3-dideoxy-L-gulose, appeared to be rather unstable in acid media. The latter also failed to be isolated and identified. For this reason the structure and the configuration of the diaminoguluronic acid was established by analysis of the complex NMR spectra of the trisaccharide derivative **125** and its acetate **126** (their composition was confirmed by mass spectrometry) using special versions of NMR spectroscopy. It was found that, in addition to the carboxy group, the novel monosaccharide contains two acetamino groups at C(2) and C(3) and has the *gulo*-configuration as evidenced by the coupling constant values for the ring protons in the ^1H NMR spectrum ($J_{2,3} = 4.5$, $J_{3,4} = 3.0$ and $J_{4,5} = 3.0$ Hz). This configuration was finally corroborated by comparison of signals of the carbon atoms belonging to the residue of the acid **124** in the ^{13}C NMR spectrum of the derivative **125** with the spectral characteristics of synthetic samples of all isomeric 2,3-diacetyl-amino-2,3-dideoxyhexoses.¹⁴⁵ This configuration was also established for the oligosaccharide **127**, one of the intermediate products of selective cleavage of PS from *Pseudomonas aeruginosa* immunotype 7, during the analysis of the NMR spectra.¹⁴⁴



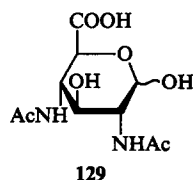
The absolute L-configuration of diaminoguluronic acid was evident from the specific optical rotation of the oligosaccharide **125**. It was finally confirmed by analysis of the ^{13}C NMR spectrum of the trisaccharide **127** using the dependence of the glycosylation effects on the absolute configuration of the neighbouring monosaccharide units. A negative β -effect of glycosylation (0.9 ppm) on C(3) of the diaminomannuronic acid (for which the D-configuration had been established previously) attached to the diaminoguluronic acid residue in **127** by the α -glycosidic bond at position C(4) demonstrated, unambiguously, the L-configuration of 2,3-diacetyl-amino-2,3-dideoxyguluronic acid.

Recently, the fourth isomer of diaminodideoxyhexuronic acids, 2,3-diacetyl-amino-2,3-dideoxy-D-galacturonic acid (**128**), was identified. This acid is a component of O-antigenic PS of the Gram-negative bacteria *Bordetella bronchiseptica* and *Bordetella parapertussis*.¹⁴⁶ Both PS are homopolysaccharides built up of diaminogalacturonic acid residues, the immunochemical difference between the antigens being exclusively due to variations in the structure of the core of the corresponding LPS. The structure of the novel monosaccharide was established without any difficulty by a non-destructive method using NMR spectroscopy. The

presence of signals of the carboxy group (175 ppm) and of C(2) and C(3) bearing amino groups (46.6 and 49.1 ppm) in the ^{13}C NMR spectra and the coupling constant values for the ring protons in the ^1H NMR spectrum characteristic of the *galacto*-series ($J_{2,3} = 10.8$, $J_{3,4} = 3.0$ and $J_{4,5} = 3.0$ Hz), fully confirmed the structure of 2,3-diacetyl-amino-2,3-dideoxygalacturonic acid. The absolute D-configuration was evident from the specific optical rotation of the PS.



Recently, the first representative of 2,4-diamino-2,4-dideoxyuronic acids has been identified. 2,4-Diacetyl-amino-2,4-dideoxy-D-glucuronic acid **129** was found in O-specific PS of *Thiobacillus* IFO 14570.¹⁴⁷ The structure of this PS was established by a non-destructive method using a complex analysis of PS with the help of several versions of NMR spectroscopy, including NOE measurements. This study is an excellent demonstration of contemporary structural analysis of a structurally complex PS using NMR spectroscopy alone. Signals of the diaminoglucuronic acid residue identified in the two-dimensional heteronuclear ^1H - ^{13}C NMR spectrum corroborated the structure of the molecular skeleton: the ^{13}C NMR spectrum contained a signal at 173.0 ppm [COOH group at C(6)] and signals at 55.3 and 56.5 ppm [the carbon atoms at C(2) and C(4) containing NHAc substituents]. Large coupling constant values for the ring protons in the ^1H NMR spectrum (9–10 Hz) showed the *gluco*-configuration of the acid **129**, and the data obtained during NOE measurements proved the D-configuration.



To the above statements concerning hexuronic acids it must be added that sometimes these monosaccharides are present in PS as amides. This fact may have a considerable influence on the immunochemical specificity of the whole biopolymer, since amides, in contrast to the parent acids, are neutral and their presence alters the distribution of charged groups along the polysaccharide chain. In this context, identification of a uronic acid amide and its localisation in the chain are integral parts of structural analysis of O-antigenic PS.

Up to the present, both unsubstituted glycuronamides and more complex compounds of this series with the carboxy group amidated, e.g., by an amino acid, have been found in PS (see Section 5).

Unsubstituted amides of uronic acids were detected in polysaccharides of various classes. For the first time, they were found in PS of several serotypes of *Pseudomonas aeruginosa*,¹²⁸ which contain 2-acetyl-amino-2-deoxy-D-galacturonamide. More recently, this same hexuronamide was detected in PS of *Shigella dysenteriae* 7¹⁰⁵ and *Vibrio anguillarum*.¹⁰⁷

Since identification of unsubstituted hexuronic acids is now being carried out by a non-destructive method on the basis of NMR spectra, and the spectra of the acid and its amide differ insignificantly, the presence of an amide group is usually established by the pH dependence of the position of the H(5) signal in the ^1H NMR spectrum: for an amide the chemical shift of this signal does not depend on pH, while in case of an acid the signal is shifted down-field with a decrease in pH (due to the effect of the adjacent carboxy group).¹⁴⁸ Thus, it was shown that the PS chain

of *Shigella dysenteriae* 7 contains two adjacent units, 2-acetylamino-2-deoxy-D-galacturonic acid and its amide: with a drop in pH from 9 to 1 the signal of H(5) of the acid residue is shifted from 4.40 to 4.63 ppm, whereas the chemical shift of the amide signal remains unchanged.

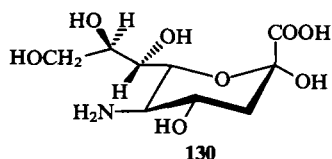
In conclusion, it should be noted that amidation of hexuronic acid residues in the PS chain may also be non-stoichiometric. In this case the same PS may comprise both a free acid and its amide, their quantitative ratio being different for PS of related serotypes or subtypes. This phenomenon was studied for several subtypes of PS of *Pseudomonas aeruginosa* O4 containing residues of both 2-deoxy-2-formylamino-D-galacturonic acid and its amide. By using anion-exchange and reversed-phase chromatography for separation of the trisaccharide fragments obtained from PS after solvolysis with liquid HF and study of the pH dependence of their ^1H NMR spectra, it was found that the degree of amidation of this uronic acid in subgroups O4a,4b, O4a,4d and O4a,4c is 10%, 20% and 0%, respectively.¹⁴⁸ Derivatives of more complex amides of uronic acids containing 'non-carbohydrate substituents' will be considered in Section 5.

9. Glycosonic acids

Glycosonic acids are α -keto acids of the carbohydrate series. These acidic monosaccharides which have a peculiar structure are found in various PS of microbial origin; however, the main source of glycosonic acids is extracellular and capsular PS. The chain of natural glycosonic acids may comprise 5 to 9 carbon atoms; some of those acids contain deoxy units and amino groups.

Most widespread representative of glycosonic acids in the microbial world is 3-deoxy-D-manno-octulosonic acid (KDO), an indispensable component of the inner core of all Gram-negative bacteria.¹⁴⁹ This acid, like some hexulosonic acids as well, was found in capsular PS of *Klebsiella* and some other bacteria (see review⁶).

In the present review we shall restrict our consideration to only some representatives of this class of acidic monosaccharides detected in O-antigenic PS of Gram-negative bacteria. Of those, most widespread is 5-amino-3,5-dideoxy-D-glycero-D-galactononulosonic acid **130** more commonly known as neuraminic acid. Derivatives of this acid having the common name of sialic acids are especially widely distributed in carbohydrate-containing biopolymers of animal tissues where they enter into the carbohydrate chains of glycoproteins and glycolipids and play a crucial role in the determination of specific biological properties and conversions of these biopolymers.¹⁵⁰



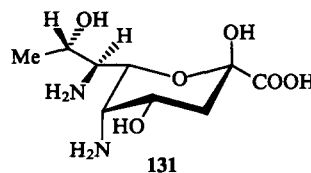
Residues of neuraminic acid and other glycosonic acids are present in the PS chain in the pyranose form **130** and have a deoxy unit adjacent to the anomeric centre. Derivatives of neuraminic acid are distinguished by high acid lability and are destroyed during hydrolysis of the carbohydrate-containing biopolymer. Perhaps, for this particular reason, derivatives of neuraminic acid were first identified in O-antigenic PS not long ago.

So far, *N*-acetyl derivatives of neuraminic acid have been found in O-antigenic PS of several bacteria: *Salmonella arizonae*,^{151, 152} *Citrobacter freundii*,¹⁵² *Escherichia coli*,¹⁵²⁻¹⁵⁶ *Hafnia alvei*^{152, 157} and *Vibrio cholerae*.¹⁵⁸ They are also present in some extracellular PS. One of such polysaccharides, the long known colaminic acid, is a homopolysaccharide composed of residues of *N*-acetylneuraminic acid.¹⁵⁹

Because of the wide occurrence of neuraminic acid derivatives in glycoproteins and glycolipids, their chemical properties and spectroscopic characteristics have been studied in great detail and are comprehensively discussed in reviews.^{150, 160} In this connec-

tion, identification of a neuraminic acid residue (or its derivatives) in O-antigenic PS is now being achieved by a non-destructive method based on the NMR spectroscopic analysis of the PS itself or of its oligosaccharide fragments.

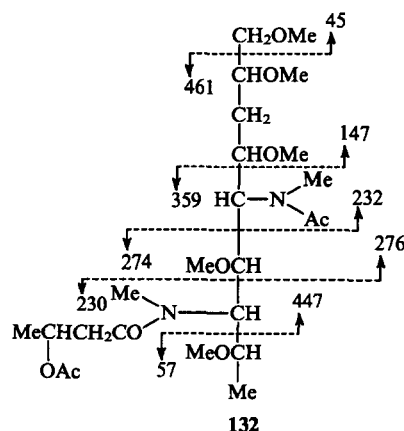
Recently, another two structurally unique representatives of aminodeoxynonulosonic acids have been identified in O-antigenic PS. Derivatives of one of them, 5,7-diamino-3,5,7,9-tetradeoxy-L-glycero-L-manno-nonulosonic acid **131** (pseudaminic acid), were detected in PS of several serotypes of *Pseudomonas aeruginosa*,¹⁶¹⁻¹⁶³ *Shigella boydii* 7^{161, 162, 164} and *Vibrio cholerae* O2.¹⁶⁵



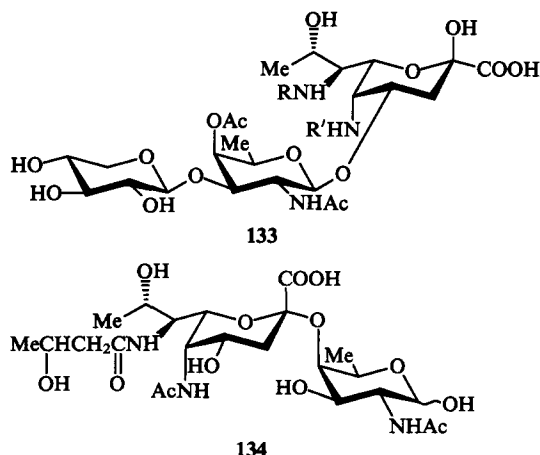
In the monosaccharides of these PS (with the exception of *V. cholerae* PS) the amino group at C(5) is acetylated, while the amino group at C(7) carries a formyl group or a residue of 3-hydroxybutyric acid. In the case of *V. cholerae* PS, the monosaccharide contains an acetylated amino group at C(7) and an acetimidoyl group at the amino group at C(5).

Originally, the presence in these PS of a pseudaminic acid residue was established by a qualitative reaction for *N*-acetylneuraminic acid with the resorcinol reagent.¹⁶⁶ Furthermore, the ^{13}C NMR spectra of the fragments obtained by acid hydrolysis of PS contained signals characteristic of a 3-deoxyaldulosonic acid.

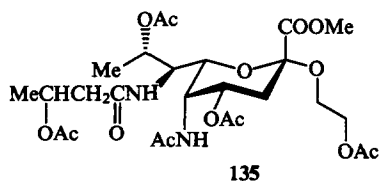
In view of the high lability of pseudaminic acid derivatives towards acids, the establishment of their structure met considerable difficulties. The main approaches^{161, 162, 164} used for determination of their complete structure can briefly be summarised as follows. Carboxy groups of PS isolated from *S. boydii* 7 and *P. aeruginosa* O10 were first reduced, and then the PS were subjected to hydrolysis. This was accompanied by cleavage of the glycosidic bonds of the reduced pseudaminic acid residues; however, the monosaccharide residues themselves that are deprived of their carboxy groups were not destroyed. The products of the hydrolysis were then treated with NaBH_4 . After methylation of the hydroxy groups, the oligosaccharide was solvolysed with liquid HF. The resulting mixture of partially methylated monosaccharides (in which the *N*-acylated amino groups were also *N*-methylated) was reduced with NaBH_4 and acetylated. Chromato-mass spectrometry of the mixture of partially methylated alditol acetates obtained after degradation of PS of *P. aeruginosa* O10 revealed the presence of the alditol **132** containing nine carbon atoms and corresponding to the residue of pseudaminic acid. Its fragmentation allowed establishment of the structure of the skeleton and localisation of deoxy units [at C(3) and C(9)] and aminoacyl substituents [at C(5) and C(7)].



These data were confirmed by NMR spectroscopy of several oligosaccharides containing residues of pseudaminic acid, which were obtained by degradation of PS. For example, the ^{13}C NMR spectrum of the oligosaccharide 133 obtained by very mild acid hydrolysis of PS from *P. aeruginosa* O5 contained signals belonging to the residue of pseudaminic acid: at 99.7 ppm [C(2)] and 34.8 ppm [a deoxy unit at C(3)]. The ^{13}C NMR spectrum of the oligosaccharide 134 obtained by solvolysis of PS from *P. aeruginosa* O10a with liquid HF contained signals at 37.1 ppm [a deoxy unit at C(3)], 49.1 ppm [C(5) carrying an aminoacyl substituent], 54.7 ppm [C(7) carrying an aminoacyl substituent] and 17.7 ppm [a CH_3 group at C(9)]. A slight difference between the chemical shifts in the ^{13}C NMR spectra of the compounds 133 and 134 is attributed to the difference in the substituents of the amino groups of pseudaminic acid in the fragments obtained from different bacteria. The ^1H NMR spectra of the oligosaccharides 133 and 134 fully corroborate the structure described above.



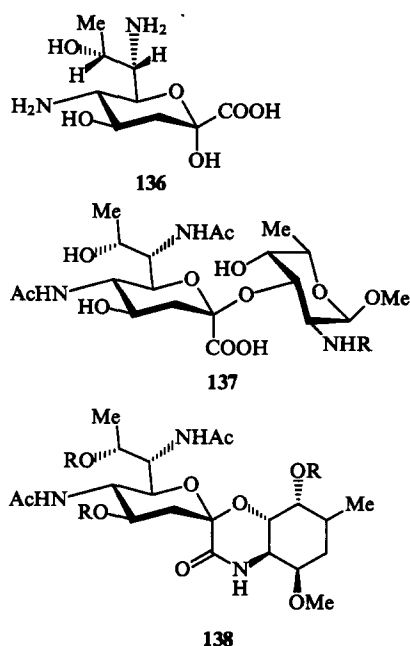
The configuration of pseudaminic acid was established by analysis of the ^1H NMR spectra of the fragment 135 obtained from PS of *S. boydii* 7 by three successive Smith degradations followed by its conversion into the methyl ester and acetylation. The spectrum of the compound 135 is characterised by the following coupling constant values for the ring protons: $J_{3,4} = 13$, $J_{4,5} = 3.5$, $J_{5,6} = 1.6$ Hz, that indicate the axial orientation of H(4) and the equatorial orientation of H(5). The equatorial orientation of the substituent at C(6) was confirmed by NOE measurements which indicated the proximity of H(7) and of the NH proton at C(5).



These data suggest that the C(4)–C(5)–C(6) fragment of pseudaminic acid has the *lyxo*-configuration. A large coupling constant value ($J_{6,7} = 10$ Hz) and a strong NOE on H(5) and H(6) caused by preirradiation of the NH proton at C(7) proved the *erythro*-configuration of the C(6)–C(7) fragment. Finally, the *L-erythro*-configuration of the C(7)–C(8) fragment of pseudaminic acid was established by comparison of the glycosylation effects on C(9) of pseudaminic acid and on C(1) of the glucosamine residue (linked by the glycosidic bond to C(8) of pseudaminic acid in the polysaccharide chain) as well as by analysis of the ^{13}C NMR spectra of model compounds, glycosylated derivatives of D- and L-threonine and of D- and L-*allo*-threonine. These data suggested that the C(7)–C(8)–C(9) fragment of pseudaminic acid is homomorphous with the fragment of L-*allo*-threonine, i.e., that the C(7)–C(8) fragment has the *L-erythro*-configuration. Therefore, pseudaminic acid has the *L-glycero-L-manno*-configuration 131.¹⁶¹

Later, identification of pseudaminic acid derivatives in PS was performed using ^1H and ^{13}C NMR spectroscopy (including NOE measurements) taking into account the above data.^{163,165}

Derivatives of a pseudaminic acid isomer, 5,7-diacylamino-3,5,7,9-tetra-deoxy-D-*glycero*-L-*galacto*-nonulosonic acid 136, were found in O-antigenic PS of *Salmonella arizonae* O61,¹⁶⁷ *Pseudomonas aeruginosa* O13,^{168,169} *Vibrio alginolyticus*¹⁷⁰ and *Legionella pneumophila* 1.¹⁷¹ The amino groups of this nonulosonic acid were acylated by various acids. A derivative was also found which contained an *N*-acetamidino group.¹⁷¹ The complete structure of this acid was established by the same methods as described for pseudaminic acid.^{168,169} Solvolysis of PS of *P. aeruginosa* O13 with an HF solution in methanol resulted in the disaccharide 137 containing residues of the nonulosonic acid 136 and fucosamine. After treatment with acetic anhydride in pyridine, the disaccharide 137 underwent intramolecular cyclisation to give the lactam 138.



The composition of the compounds 137 and 138 was confirmed by determination of their molecular weights using FAB mass spectrometry. The ^{13}C NMR spectra of the compounds 137 and 138 contained signals at 19.7 ppm [a CH_3 group at C(9)], at 54.4 and 53.8 ppm [C(7) and C(5) carrying acylamino groups] and 42–41 ppm [a deoxy unit at C(3)]. The data obtained by ^1H NMR spectroscopy were fully consistent with this structure of the nonulosonic acid skeleton. The presence in the ^1H NMR spectra of characteristic coupling constant values for the ring protons ($J_{3a,3e} = J_{3a,4} = 12$, $J_{3e,4} = 4.2$, $J_{4,5} = J_{5,6} = 10$ Hz) demonstrated the axial orientation of the protons in the C(4)–C(5)–C(6) fragment of the nonulosonic acid and, consequently, its *arabino*-configuration. A small coupling constant value ($J_{6,7} = 2.5$ Hz), which is close to the corresponding value for *N*-acetylneuraminic acid (1.5 Hz) but different from that for pseudaminic acid (10 Hz), indicates the *threo*-configuration of the C(6)–C(7) fragment. Finally, the C(7)–C(8) fragment was also assigned the *D-threo*-configuration which, as in the previous case, was established on the basis of glycosylation data for the nonulosonic acid 136 and model glycosides of *N*-acetylgalactosamine, D- and L-threonine, D- and L-*allo*-threonine.

Therefore, the nonulosonic acid 136 was ascribed the D-*glycero*-L-*galacto*-configuration. Later, this monosaccharide containing various *N*-substituents was detected in PS of other bacteria.^{167,170,171} Its identification was carried out mainly by non-destructive methods on the basis of NMR spectral data, some of which were partly listed above. Analysis of oligosaccharide

fragments obtained by partial cleavage of PS was performed only in a few particular cases.

Among biopolymers containing the nonulosonic acid **136**, PS of *Legionella pneumophila* (the pathogen of a severe lung disease, so-called 'Legionnaires disease') is of special interest.¹⁷¹ This PS is a homopolysaccharide built up of residues of a derivative of 5,7-diamino-3,5,7,9-tetradeoxy-D-glycero-L-galacto-nonulosonic acid with acetamido and N-acetylamino groups at C(5) and C(7), respectively, and is the first example of a polysaccharide of this type. It should be stressed that identification of this nonulosonic acid and establishment of the structure of the whole PS was carried out by a non-destructive method on the basis of NMR spectral data alone.

In conclusion, it should be noted that to finally solve the question concerning the structure and, especially, the configuration of the representatives of this novel class of monosaccharides, it is most desirable to carry out counterflow syntheses of both 5,7-diamino-3,5,7,9-tetradeoxynonulosonic acids **131** and **136**.

IV. Non-carbohydrate substituents in monosaccharide units

As indicated in the Introduction, the second factor determining the differentiation of monomeric components in O-antigenic PS and the diversity of their structures is the presence in PS of so-called 'non-carbohydrate' substituents. The presence of such substituents markedly and, sometimes, dramatically alters the spatial structure of the polysaccharide chain and the general 'topography' of the polysaccharide molecule by exposing on its surface additional polar and hydrophobic groups which eventually determine the specificity of its interaction with the protein (antibody) surface, i.e., its immunologic specificity.

It should be noted that, although the presence of some non-carbohydrate substituents in polysaccharides of various origin, e.g., in plant PS, is well known, these are microbial PS and, particularly, O-antigenic PS of Gram-negative bacteria that contain an especially great variety of such substituents. These substituents can modify hydroxy groups of monosaccharides, amino groups of amino sugars and carboxy groups of acids of the carbohydrate series.

O-Substituted monosaccharides may include ethers or esters, the latter being far more widely spread. Also known are monosaccharides carrying an acetal group linked to two hydroxy groups of a monosaccharide unit.

Exclusively N-acylated derivatives are characteristic for amino sugars, whereas N-alkylated monosaccharides are practically unknown in O-antigenic PS. The carboxy groups of uronic acids appear to be most frequently substituted to give an amide group, both unsubstituted amides and more complex derivatives, including, in particular, an amino acid residue being known. Finally, residues of phosphoric acid and some of its derivatives have also been detected in O-antigenic PS as non-carbohydrate substituents.

Establishment of the structure and localisation of a non-carbohydrate substituent in a carbohydrate unit of PS presents a separate and often complicated problem. Since in recent years the number and diversity of non-carbohydrate substituents detected in O-antigenic PS is growing fast, the search for the most effective ways to solve these problems is becoming more and more important in the chemistry of O-antigenic PS. One of these consists in selective cleavage of the non-carbohydrate substituent with subsequent determination of its structure by conventional methods; however, the problem of its localisation in the polysaccharide chain cannot be solved by this approach. Another approach is confined to isolation of the corresponding substituted monosaccharide followed by its structural analysis. Regrettably, both pathways are not always practicable, since attempts to cleave the non-carbohydrate substituent or to isolate the substituted monosaccharide often result in irreversible changes or even complete destruction of the compounds being isolated. For this

reason, the problem of elucidation of the structure is now being solved using physicochemical methods. This approach permits determination of the nature and localisation of the non-carbohydrate substituent directly by analysis of PS or oligosaccharide fragments obtained by its specific degradation.

1. O-Alkyl substituents

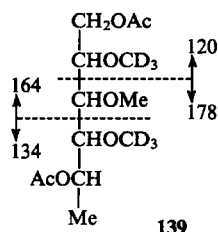
Substitution of hydroxy groups in monosaccharide units of O-antigenic PS with formation of the ether bond occurs rarely. Only O-methyl and 1-carboxyethyl ethers are now known.

a. O-Methyl ethers

Partially methylated monosaccharides are rather widely distributed in plant PS. Among microbial PS, they are mostly found in extracellular and capsular PS as well as in PS of photosynthetic bacteria (see review⁶); in O-antigenic PS they were detected only in a few cases. It is believed that methylation of a monosaccharide hydroxy group takes place during one of the stages of PS biosynthesis, the SMe group of methionine being the donor of the methyl group.

3-O-Methyl-L-xylose was found in PS of *Pseudomonas maltophilia* NCTC 10257,¹⁷² where it occupies the terminal position in the side chains of the branched PS. This sugar was isolated after acid hydrolysis of PS and identified by routine methods (comparison with an authentic sample).

3-O-Methyl-L-rhamnose was isolated from O-antigenic PS of *Klebsiella* O10¹⁷³ by acid hydrolysis. This monosaccharide occupies the terminal position at the non-reducing end of the polysaccharide chain. To establish its structure, the PS was first deuteromethylated with CD₃I and then hydrolysed. The resulting monosaccharide was converted into the alditol acetate **139** and analysed by mass spectrometry. Its mass spectrum contained peaks corresponding to the fragments with *m/z* 164, 134, 178 and 120 which corroborated unambiguously the structure of 3-O-methylrhamnose.



It is likely that the presence of both methylated monosaccharides at the ends of the polysaccharide chains serves as a signal for termination of further elongation of this chain during biosynthesis.

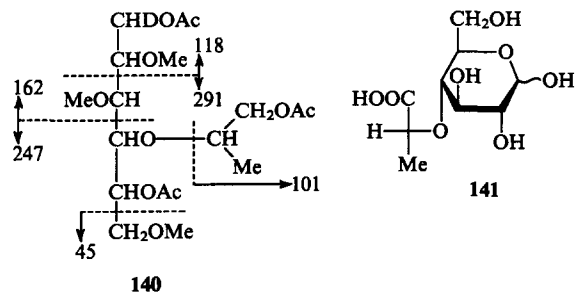
3-O-Methyl-D-glycero-D-altro-heptose and 3-O-methyl-6-deoxy-D-altro-heptose were found in some PS of *Campylobacter jejuni* where they partially substitute hydroxy groups.⁷⁶ Interestingly, the ratio of methylated to non-methylated monosaccharides in PS is determined by the cultivation conditions of these bacteria, although the actual reason for this phenomenon still remains to be elucidated. The structure of both methylated heptoses was established by mass spectrometry of partially methylated alditol acetates derived from PS after deuteromethylation, hydrolysis and reduction (see above).

b. 1-Carboxyethyl ethers (glycolactylic acids)

Glycolactylic acids present in O-antigenic PS contain a residue of lactic acid linked by the ether bond to the sugar molecule. Compounds of this type were first detected in peptidoglycan of the bacterial cell wall (muramic acid and its *manno*-isomer^{174,175}). Later, they were also found in O-antigenic and some other microbial PS (exocellular PS, capsular PS and PS of photosynthetic bacteria). Thus, glycolactylic acids are a rather large group of acidic monosaccharides.

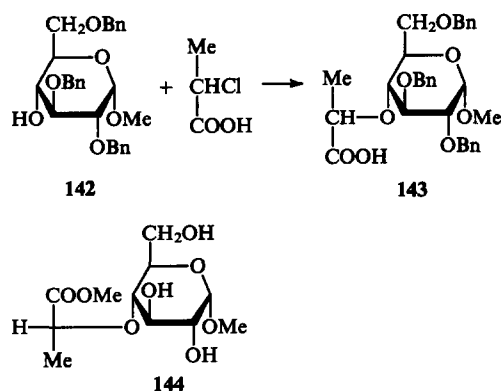
The ether bond in these acids is rather stable; therefore, they can be isolated in the pure state after acid hydrolysis of PS using ion-exchange chromatography. Representatives of this class differ from one another by the nature of the parent monosaccharide, the absolute configuration of the lactic acid residue and its localisation. So far, the following representatives of glycolactic acids have been isolated from O-antigenic PS of Gram-negative bacteria: derivatives of D-glucose, L-rhamnose and 2-acetyl-amino-2-deoxy-D-glucose usually containing a residue of (*R*)-lactic acid, although the derivatives of the (*S*)-isomer are also known. In addition, PS of other microorganisms contain derivatives of D-mannose¹⁷⁶ and D-glucuronic acid.¹⁷⁷

Initially, the structure of glycolactic acid was established by classical chemical methods and mass spectrometry. However, more recent studies employed NMR spectroscopy for this purpose. An illustrative example of the classical approach is the establishment of the structure of glucolactic acid isolated from PS of *Shigella dysenteriae* 3.^{178,179} The substituted monosaccharide was isolated in the pure state from the acid hydrolysate of PS; its ¹H NMR spectrum contained a characteristic signal of a methyl group CH₃—CH at 1.4 ppm (d, *J* = 6.0 Hz). Its treatment with BCl₃ resulted in cleavage of the ether bond to form D-glucose. To establish the site of attachment of the lactic acid residue to the glucose residue, the polysaccharide was methylated, reduced with LiAlH₄ and hydrolysed. The resulting mixture of monosaccharides was converted into alditol acetates by reduction with NaBD₄ and subsequent acetylation. Chromato-mass spectrometry of the alditol acetate mixture revealed the tetraacetate **140** whose fragmentation provided evidence for its structure: a fragment with *m/z* 101 showed the presence of a propanediol residue (formed by reduction of the lactic acid carboxy group), and fragments with *m/z* 118, 291 and 162 indicated the site of its binding to C(4) of glucose. Based on these data, the original monosaccharide was ascribed the structure of 4-*O*-(1'-carboxyethyl)-D-glucose **141**.



The absolute configuration of the lactic acid residue was established by counterflow synthesis of glucolactic acid¹⁷⁹ using condensation of methyl 2,3,6-tri-*O*-benzyl- α -D-glycopyranoside **142** with (*S*)-2-chloropropionic acid (obtained from L-alanine) in the presence of sodium hydride (Scheme 13). Treat-

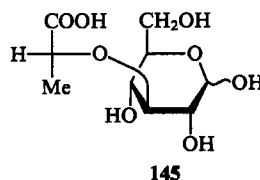
Scheme 13



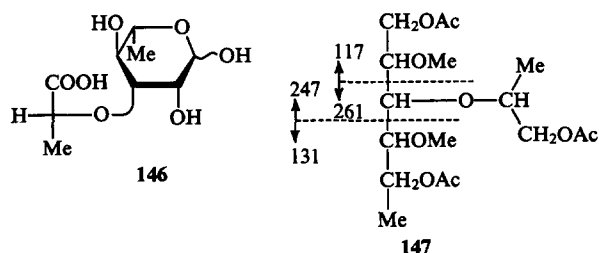
ment of the condensation product **143** with diazomethane and elimination of the benzyl groups gave the methyl glycoside of the methyl ester of the glucolactic acid **144** whose physicochemical characteristics (including the specific optical rotation) were identical to those of the natural product. Thus, in the natural compound the residue of lactic acid has the (*R*)-configuration, and this glycolactic acid is 4-*O*-[(*R*)-1'-carboxyethyl]-D-glucose **141**.

The glycolactic acid **141** was also found in PS of an immunochemically related to *Shigella dysenteriae* 3 bacterium *Escherichia coli* O124 and identified in the same way. Moreover, the PS structures in both bacteria, *S. dysenteriae* 7 and *E. coli* O124, appeared to be identical. This fact provided the first experimental proof that bacteria with identical immunochemical specificity, even those belonging in biological classification to different species, contain the structurally identical PS.¹⁸⁰ Notice that another glycolactic acid, 4-*O*-[(*S*)-1'-carboxyethyl]-D-glucose, isomeric by the lactic acid residue to the glycolactic acid **141**, was isolated from an extracellular PS of the bacterium *Aerococcus viridans*.⁶

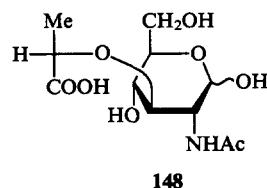
An isomeric glucolactic acid, 3-*O*-[(*R*)-1'-carboxyethyl]-D-glucose **145**, has recently been isolated in the pure state from PS of *Aeromonas haloplanktis*¹⁸¹ after acid hydrolysis of PS with trifluoroacetic acid. Its structure was established by NMR spectroscopy. The ¹H NMR spectrum contained signals characteristic of a lactic acid residue: at 1.45 (d, 7.0 Hz, a CH₃ group) and 4.41 ppm (q, a CH group) as well as signals characteristic of the glucose residue. The ¹³C NMR spectrum also contained signals characteristic of the lactic acid residue: at 19.6 (CH₃ group) and 79.5 ppm (CH group). The signal of C(3) of the glucose residue was shifted down-field to 83 ppm in comparison with the signal of unsubstituted glucose, indicating the binding of lactic acid residue to this atom. This structure was also confirmed by full coincidence of the NMR spectra for the acid **145** and the glucolactic acid isolated from a capsular polysaccharide of *Pseudomonas fragi*, for which the same structure had been established.¹⁸² The D-configuration of the glucose residue was evident from the regularities in the glycosylation effects determined from the ¹³C NMR spectrum of the original PS; the (*R*)-configuration of the lactic acid residue was suggested on the basis of the specific optical rotation of the acid **145**.



The structure of other glycolactic acids was established in a similar way (using the methods available at the time of the investigation). Thus, the 3-*O*-[(*R*)-1'-carboxyethyl]-L-rhamnose **146** (rhamnolactic acid) isolated from *Shigella dysenteriae* 5,¹⁸³ after treatment with BCl₃ gave L-rhamnose, and the mass spectrum of the partially methylated alditol **147** derived from PS revealed the presence of a lactic acid residue bound to C(3) of rhamnose. The (*R*)-configuration of the lactic acid residue was established by counterflow synthesis. More recently, this acid was isolated from PS of *Vibrio fluvialis*¹⁸⁴ and its structure was confirmed by NMR spectroscopy. The ¹H NMR spectrum contained signals at 1.42 and 4.33 ppm (a lactic acid residue) and a set of characteristic signals of the rhamnose residue. The conclusion about the (*R*)-configuration of the lactic acid residue was made on the basis of comparison of the chromatographic behaviour and optical rotation of the sample tested with synthetic samples of the (*R*)- and (*S*)-isomers of this rhamnolactic acid.¹⁷⁰



A glycolactylic acid derived from glucosamine, 2-acetyl-amino-3-*O*-[(*S*)-1'-carboxyethyl]-2-deoxy-D-glucose **148**, was found in O-antigenic PS of *Proteus penneri* 62.¹⁸⁵ Its structure was established by spectral data. The ¹H and ¹³C NMR spectra of the polysaccharide contained signals characteristic of the lactic acid residue [1.31, (d, *J* = 7 Hz) and 4.05 ppm (q) (¹H NMR) and, correspondingly, 20.3, 80.6 and 182.9 ppm (¹³C NMR)] and of the glucosamine residue. The ¹³C NMR spectrum revealed a characteristic down-field shift of the C(3) signal, indicating substitution of the corresponding hydroxy group. The monosaccharide was isolated in the pure state after solvolysis of PS with liquid HF. Its spectrum coincided with that of 2-acetyl-amino-3-*O*-[(*S*)-1'-carboxyethyl]-2-deoxy-D-glucose but differed from that of the well-known muramic acid¹⁷⁴ with the (*R*)-configuration of the lactic acid residue. On the basis of these data and using the specific optical rotation differing markedly from the corresponding value for muramic acid, the novel glycolactylic acid was ascribed the (*S*)-configuration. This compound is known as isomuramic acid.



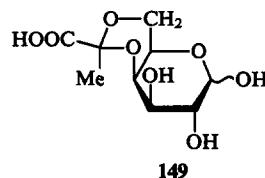
Recently, PS of another serotype of the same species of *Proteus penneri* 35 was found to contain an isomer of isomuramic acid, 2-acetyl-amino-4-*O*-[(*S*)-1'-carboxyethyl]-2-deoxy-D-glucose, whose structure was established by similar methods.¹⁸⁶

Apart from the compounds described above, some other glycolactylic acids were identified. Thus, a capsular PS of *Klebsiella* K37 was found to contain 4-*O*-[(*S*)-1'-carboxyethyl]-D-glucuronic acid,¹⁷⁷ whereas an extracellular PS of *Mycobacterium lacticum* 121 4-*O*-[(*S*)-1'-carboxyethyl]-D-mannose;¹⁷⁶ their structures were established by the approaches described above.¹⁸⁷

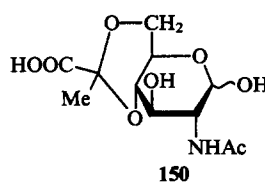
2. Acetal (carboxyethylidene) groups

Monosaccharides carrying acetal groups with two hydroxy groups of the monosaccharide simultaneously substituted by a pyruvic acid residue (carboxyethylidene groups) are rather widely spread in exocellular and capsular PS. Methods have been developed for determination of the structure of their derivatives present in PS. In O-antigenic PS of Gram-negative bacteria, monosaccharides carrying carboxyethylidene groups have thus far been detected only in PS of *Shigella dysenteriae* 9¹⁸⁸ and *Escherichia coli* O149.¹⁸⁹ NMR spectroscopy in combination with chemical methods is used to identify this group. Thus, the ¹H NMR spectrum of PS of *S. dysenteriae* 9 contains a signal at 1.60 ppm that is characteristic of the methyl group of the pyruvic acid residue. This group is not affected by basic treatment of PS but gradually disappears during treatment of PS with dilute acetic acid, thus suggesting the binding of the pyruvic acid residue as an acetal. The nature of the monosaccharide unit carrying this substituent and the substitution site were established by comparing the results of PS methylation before and after its deacetalation with acetic acid: in the former case hydrolysis of methylated PS resulted in 2-*O*-methylgalactose, while in the latter case, in 2,4,6-tri-*O*-methyl-D-galactopyranose. It was thus demonstrated that

the carboxyethylidene group modified the hydroxy groups at C(4) and C(6) of galactose, and the monomeric unit of PS is 4,6-*O*-(1'-carboxyethylidene)-D-galactose **149**.



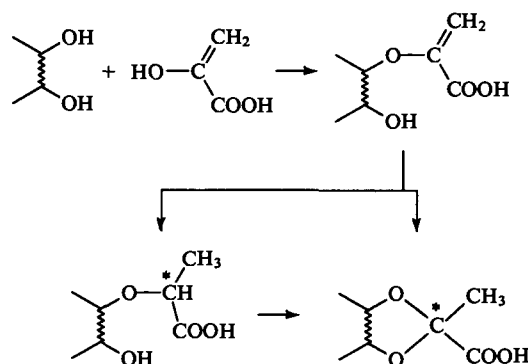
The ¹H NMR spectrum of *E. coli* PS also contains a signal at 1.50 ppm, and the ¹³C NMR spectrum has signals at 25.4 and 101.3 ppm characteristic of the pyruvic acid residue. As in the previous case, the position of this residue was established by comparison of the products of methylation of the native and deacetalised PS which revealed that the carboxyethylidene group binds to C(4) and C(6) of *N*-acetylglucosamine. Therefore, the substituted monosaccharide has the structure of 2-acetyl-amino-4,6-*O*-(1'-carboxyethylidene)-2-deoxy-D-glucose **150**.



Introduction of the carboxyethylidene group into the monosaccharide results in the formation of a new chiral centre whose configuration can be easily established by ¹³C NMR.¹⁹⁰ Depending on the conformation of the dioxane ring of the 4,6-di-*O*-substituted monosaccharide, the methyl and carboxy groups can have either axial or equatorial orientation that can be readily determined by the values of the chemical shifts of the corresponding signals. With the known conformation of the dioxane ring (defined by the structure of the parent monosaccharide), the relative position of the CH₃ and COOH groups determined from the NMR spectra provides direct evidence for the (*R*)- or (*S*)-configuration of the central carbon atom of the acetal group.¹⁹⁰ This approach was used to establish the (*S*)-configuration of the pyruvic acid residue in PS of *E. coli* O149.

The acetal group, like the lactic acid residue in glycolactylic acids, is introduced into PS in the course of PS biosynthesis in the cell by reaction of the corresponding monosaccharide with the enol form of pyruvic acid catalysed by a specific enzyme. The ester formed is probably reduced to give the (*R*)- or (*S*)-isomer of a glycolactylic acid, which, in the case of a suitable spatial arrangement of the adjacent hydroxy group, can further be converted into the corresponding acetal. An alternative pathway, namely, direct binding of the hydroxy group to the double bond of the intermediate enol (Scheme 14), is also not excluded.

Scheme 14



It was thus demonstrated that

3. O-Acyl substituents

Substitution of hydroxy groups in monosaccharide residues of PS by residues of aliphatic acids is common for plant and microbial polysaccharides. Usually, *O*-acetylation takes place but acylation with other aliphatic (including higher fatty acids) and hydroxy acids is also known. Thus, the aliphatic acids C_{12} – C_{16} and hydroxycarboxylic acids of this series are indispensable components of the lipid part of LPS (the so-called lipid A) where they acylate glucosamine residues, thereby providing the high lipophilic character of LPS needed for its fixation in the outer cellular membrane of Gram-negative bacteria.¹

O-Acetylation of particular hydroxy groups in certain monosaccharide units of the *O*-antigenic polysaccharide chain is essential for the determination of immunochemical specificity of PS. To fully characterise this epitope of the *O*-antigen, it is necessary to establish the precise localisation of the *O*-acetyl group. The assignment of the *O*-acetyl group to a certain monosaccharide unit in the PS chain is a routine task which can readily be solved using 1H and ^{13}C NMR spectroscopy.

Evidence for the presence of other *O*-acyl groups in *O*-antigenic PS is almost absent. The only experimental proof seems to be the presence of the *O*-propionyl group in PS of *Vibrio anguillarum*.⁹⁶

The paucity of variation of *O*-acyl groups seems to be remarkable, especially in comparison with the great diversity of aliphatic acids acylating amino groups of monosaccharides in *O*-antigenic PS.

4. N-Acyl substituents

The occurrence of monosaccharides with acylated amino groups in various natural compounds is a common but not compulsory phenomenon, whereas polysaccharides almost always contain residues of amino sugars with acylated amino groups. Most frequently, PS comprise *N*-acetyl derivatives, while derivatives of other organic acids are far less common. The exception is *O*-antigenic PS of Gram-negative bacteria, where the diversity of acids acylating amino groups is rather high and includes simplest aliphatic acids, hydroxy and polyhydroxy acids, and amino acids. Monosaccharides containing two amino groups can be acylated by the same or by two different acids (this is also true of the amino groups in different monosaccharide units of PS).

The great diversity of acids acylating amino groups in *O*-antigenic PS has become especially apparent recently, mainly due to the rapid progress in NMR spectroscopy. At present, the nature of *N*-acyl substituents and their position in PS is almost exclusively established by NMR spectroscopy of the PS themselves or of their fragments obtained by their specific degradation. Mass spectrometry is also used for this purpose.

a. *N*-Acylation by aliphatic acids

The most common substituents in *O*-antigenic PS are *N*-acetyl groups. Their identification is a routine task which is most often solved during interpretation of the NMR spectra of PS (by the presence of characteristic signals of the $NHCOCH_3$ group). For example, in the ^{13}C NMR spectrum the signals at 22.0–24.0 (CH_3 group) and 174–177 ppm (CO group) correspond to this group.

Localisation of the *N*-acetyl group is evident from the characteristic shift caused by this substituent in the neighbouring carbon atom and proton: in the ^{13}C NMR spectrum, it is a signal in the region 45–58 ppm; in the 1H NMR spectrum, the signal of a ring proton in the region 3.8–4.3 ppm. These data, after reliable assignment of the signal, allow both simultaneous identification of the monosaccharide unit carrying this substituent and localisation of the substituent in this unit.

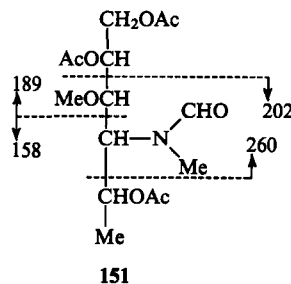
Substitution of the amino group by a residue of formic acid occurs less frequently. *N*-Formyl groups were found in PS of *Escherichia coli* O119,¹²⁰ *Yersinia enterocolitica* O9,¹¹⁵ *Pseudomonas aeruginosa* O4¹²⁸ and related serotypes as well as in PS of *Vibrio anguillarum*,¹⁰⁷ *Brucella*^{110, 191} and *Francisella tularensis*¹⁰⁶ where they are localised in residues of 2,3-diamino-2,3,6-trideoxy-

D-mannose,¹²⁰ 4-amino-4,6-dideoxy-D-mannose,^{110, 115} 2-amino-2-deoxy-D-galacturonic acid^{107, 128} and 4-amino-4,6-dideoxy-D-glucose.¹⁰⁶

The presence of an *N*-formyl group can be readily established by the presence in the ^{13}C NMR spectrum of a signal in the 166–169 ppm region.

Since rotation around the CO–NH bond is restricted, and the NHCHO group may exist in stable *cis*- or *trans*-conformations, a splitting of the proton signals is characteristic of this group. By comparing the intensities of these signals, one can draw a conclusion about the ratio of both conformers.¹⁹² Localisation of the *N*-formyl group in PS is also evident from the NMR spectral data. Thus, a characteristic shift of the signal of the C atom carrying the NHCHO group (45–55 ppm) is observed in the ^{13}C NMR spectrum.

Sometimes, the presence and localisation of the *N*-formyl group is determined by mass spectroscopic analysis. Thus, the aminoalditol 151, whose mass spectrum clearly indicated the presence of an *N*-formyl group and its localisation at C(4) of 4,6-dideoxy-4-(*N*-formylamino)-D-mannose,¹¹⁰ was isolated from PS of the bacterium *Brucella melitensis* after methylation (involving the NH group of the formamide residue), solvolysis with liquid HF and subsequent conversion of the degradation products into acetates of partially methylated alditols.



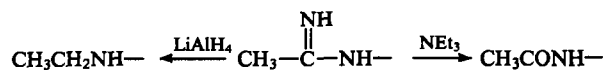
The *N*-formyl group is fully cleaved by mild acid treatment of PS to give a PS with free amino groups. At the same time, this group is stable towards solvolysis with liquid HF and retained in fragments formed by degradation of PS that is employed in their structural analysis.

One of unusual *N*-acylating groups thus far found only in *O*-antigenic PS is the *N*-acetimidoyl (amidino) group, $CH_3C(=NH)-$. It was first detected in PS of several species of *Pseudomonas*,^{143, 144, 193} and, later, in PS of *Vibrio cholerae*,¹⁶⁵ *Salmonella arizonae*^{151, 167} and *Legionella pneumophila*¹⁷¹ where it acylates the amino groups of aminuronic and aminononulosonic acids to form the corresponding amidines.

The *N*-acetimidoyl group has a basic nature and it confers it on the whole PS. Its presence is readily detectable spectroscopically. Thus, the ^{13}C NMR spectrum contains signals at 19.5–21 ppm (CH_3 group) and 167–169 ppm ($N=C-N$ group), whereas the signal of the carbon atom carrying the *N*-acetimidoyl group has a chemical shift of 45–57 ppm; the 1H NMR spectrum contains a singlet at 2.2–2.4 ppm.

The amidino group is not cleaved by treatment with liquid HF; however, upon basic treatment (e.g., with triethylamine) or reduction with $LiAlH_4$, it is converted into the *N*-acetyl amino group or the *N*-ethyl amino group, respectively (Scheme 15). This property is often used in structural analyses of PS or their fragments, since these conversions of the amidino group are readily controlled by NMR spectroscopy. Thus, transformation of the amidino group to the *N*-acetyl amino group is accompanied by the appearance of a signal near 2 ppm in the 1H NMR

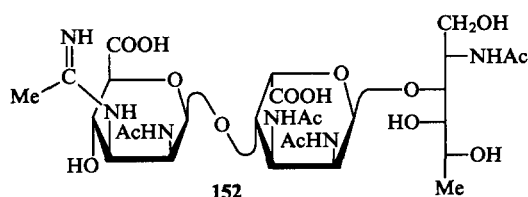
Scheme 15



spectrum and signals near 23 and 176 ppm in the ^{13}C NMR spectrum. When the amidino group is reduced to the *N*-ethylamino group, the changes are even more apparent: the ^1H NMR spectrum becomes a triplet at 1.35 ppm ($J = 7.5$ Hz, CH_3 group) and a quadruplet at 3.2–3.4 ppm (CH_2 group), and the ^{13}C NMR spectrum signals at 11–13 (CH_3 group) and 42–45 ppm (CH_2 group). In the process, the signal of the corresponding C atom of the pyranose ring is shifted to 62 ppm, and that of the attached proton from 3.86 to 3.62 ppm. In the spectra of a specially synthesised model compound, methyl 3-acetimido-1,3,6-dideoxy- α -L-glucopyranose, the changes were essentially the same.¹⁹⁴

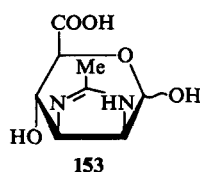
As an example of identification and localisation of the acetimidoyl group, we may refer to the analysis of PS isolated from *Pseudomonas aeruginosa* O2.¹⁴³

The ^{13}C NMR spectrum of this PS contained signals at 19.9 and 167.3 ppm indicating the presence of an acetimidoyl group. Solvolysis of PS with liquid HF and subsequent reduction of degradation products with NaBH_4 gave a derivative of the trisaccharide **152** containing an acetimidoyl group. The composition of the trisaccharide **152** was corroborated by an analysis of the FAB mass spectrum. The ^{13}C NMR spectrum of the compound **152** contained signals characteristic of an acetimidoyl group localised in a residue of 2,3-diamino-2,3-dideoxy-D-mannuronic acid. The signals of the ring carbons, C(2) and C(3), at 50.9 and 55.7 ppm showed the presence of two *N*-containing substituents, one of which was an amidino group. Upon reduction of the trisaccharide **152** with LiAlH_4 , the amidino substituent was converted into the *N*-ethylamino group, corroborated by the corresponding changes in the NMR spectra (see above). Thus, the signal of the ring carbon C(3) was shifted from 57.7 to 61.4 ppm, while after treatment of **152** with triethylamine the amidino group was converted into the *N*-acetyl amino group, and the signal of C(3) shifted to 54.4 ppm. In both cases, the position of the C(2) signal did not change. These data suggest unambiguously that in the PS studied the amidino group is located at C(3) of the diaminomannuronic acid residue.



Similar methods were used to reveal the presence of the *N*-acetimidoyl substituent at the amino group of 2-amino-2,6-dideoxy-D-galactose in PS of *S. arizonae* O21,¹⁵¹ *S. arizonae* O61,¹⁶⁷ *P. aeruginosa* O12 and at the C(5) amino groups of 5,7-diamino-3,5,7,9-tetra-deoxy-L-glycero-L-manno-nonulosonic acid in PS of *Vibrio cholerae*¹⁶⁵ and its D-glycero-L-galactoisomer in PS of *Legionella pneumophila*.¹⁷¹

It is interesting to note that originally the monosaccharide forming a part of PS of several serotypes of *P. aeruginosa* and simultaneously containing an *N*-acetimidoyl and an *N*-acetyl group, was erroneously ascribed, on the basis of spectral data, the structure **153** containing a bicyclic pyrano-imidazoline system (which is quite admissible because the substituents at the C(2) and C(3) atoms were in the equatorial-axial position).^{139,140} This conclusion was revised¹⁴¹ on the grounds that the FAB-mass spectra of fragments obtained by degradation of PS lacked molecular ions corresponding to the imidazoline group but



contained ions corresponding to the acetimidoyl and acetyl amino groups which were localised by the methods indicated above.

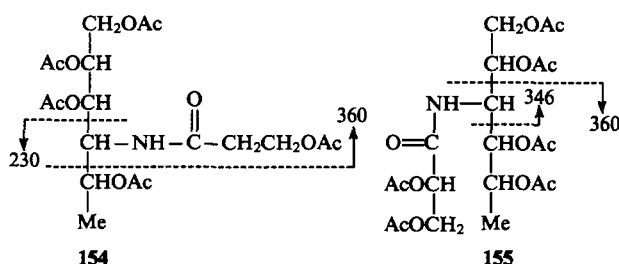
b. *N*-Acylation by hydroxy- and polyhydroxy-acids

Apart from amino sugars *N*-acylated by unsubstituted aliphatic acids, O-antigenic PS often contain derivatives of hydroxy and polyhydroxy acids of the aliphatic series; most commonly, these are C_2 – C_6 acids having one or two hydroxy groups (3-hydroxypropionic, L-glyceric, 3- and 4-hydroxybutyric, 2,4-dihydroxybutyric and 3,5-dihydroxyhexanoic acids). The presence of hydroxy acid residues in the polysaccharide chain confers peculiar characteristics on its peripheral surface by simultaneously exposing both hydrophobic and hydrophilic regions that markedly increases the selectivity of its contacts (e.g., with the surface of an immunoglobulin during antigen-antibody interaction).

Establishment of the structure of hydroxy acids acylating amino groups of monosaccharides and determination of the site of their attachment to the monosaccharide is usually performed simultaneously with establishment of the structure of the monosaccharide itself (most often, using physicochemical methods).

Thus, PS of *Vibrio cholerae* 1875 was found to contain 3-hydroxypropionic acid¹⁹⁵ which acylates the amino group of 4-amino-4-deoxy-D-rhamnose (perosamine). The *N*-acylated monosaccharide was isolated after solvolysis of the polysaccharide with HF. Its structure, including the presence of a residue of 3-hydroxypropionic acid was established by NMR spectroscopy and confirmed by mass spectrometry. In particular, the ^1H NMR spectrum of its acetate contained signals at 4.58 (NH proton), 4.23 and 1.98 ppm (CH_2O and CH_2 groups of the hydroxyacyl residue). The presence and localisation of the 3-hydroxypropionyl residue was corroborated by mass spectrometry of alditol acetate **154**.

L-Glyceric acid was found in PS of *Citrobacter freundii* O32. This biopolymer can only conventionally be regarded as a polysaccharide, because its main chain contains alternating glycosidic and amidic bonds.¹⁹⁶ Glyceric acid acylates the amino group of 3-amino-3,6-dideoxy-D-fucose whose C(2')-hydroxy group is linked by the glycosidic bond to the adjacent residue of the same monosaccharide; as a result, a polymeric chain with alternating bond types is formed. Hydrolysis of the biopolymer with trifluoroacetic acid and subsequent reduction and acetylation of the resulting mixture of fragments gave a derivative of the corresponding alditol **155** whose mass spectrum revealed the presence of a monosaccharide *N*-acetylated by glyceric acid. The presence of the glyceric acid residue in the biopolymer was fully confirmed by characteristic signals in the ^{13}C NMR spectrum: at 173 [C(1)], 80.2 [C(2)] and 62.8 ppm [C(3)]. Glyceric acid was isolated from the acid hydrolysate of the polymer using paper electrophoresis; its specific optical rotation ($[\alpha]_D = -5.5^\circ$) proved the L-configuration.



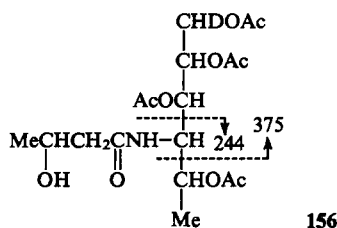
(R)-3-Hydroxybutanoic (β -hydroxybutyric) acid was detected in a number of O-antigenic PS: *Escherichia coli* O10 (where it acylates the amino group of 4-amino-4-dideoxy-D-fucose),¹¹⁷ *Yersinia aldovae*¹⁹⁷ and *Proteus penneri* 16 (where it acylates the amino group of 3-amino-3-deoxy-D-fucose),¹⁹⁸ as well as in PS of several serotypes of *Hafnia alvei* (where it acylates the amino group of glucosamine or of 3-amino-3-deoxy-D-fucose),^{199,200} *Pseudomonas aeruginosa* O5 and O10, *Shigella boydii* O7 [where it acylates the amino group at C(5) or C(7) of 5,7-diamino-3,5,7,9-

tetradecoxy-L-glycero-L-manno-nonulosonic acid],^{162,163} and *Vibrio mimicus* 26768 (where it acylates the amino group of 3-amino-3-deoxy-D-quinovose).⁹⁵

The (S)-isomer of 3-hydroxybutanoic acid occurs less frequently: it was found in PS of *P. aeruginosa* O1 [where it acylates the amino group at C(4) of 2,4-diamino-2,4,6-trideoxy-D-glucose].¹²²

Identification of a 3-hydroxybutanoic acid residue and determination of the site of its attachment to the corresponding monosaccharide in the polysaccharide chain are usually performed by isolation of the N-substituted monosaccharide and its analysis by physicochemical methods. In some cases the PS is methylated, and an O-methyl derivative of the corresponding N-substituted monosaccharide is isolated and analysed. As a typical example, we may refer to identification of the residue of (R)-3-hydroxybutanoic acid in PS of *Escherichia coli* O10.¹¹⁷

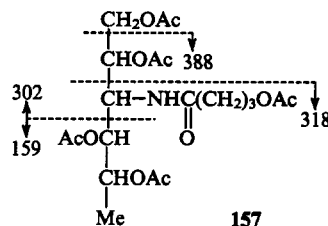
Solvolysis of PS with liquid HF and subsequent mild acid hydrolysis gave, among other fragments, an N-acyl derivative of 4-amino-4-deoxy-D-fucose. This derivative was reduced with NaBD₄ and then acetylated. The mass spectrum of the acetate of the corresponding alditol **156** revealed unambiguously the presence and localisation of the residue of 3-hydroxybutanoic acid in the derivative of 4-amino-4,6-dideoxyhexose. Similar results were obtained in analysis of an O-methylated derivative of this alditol obtained after degradation of the methylated PS. The absolute (R)-configuration of this residue was established by its oxidation with specific D-3-hydroxybutyrate dehydrogenase in the presence of nicotinamide adenosine diphosphate.



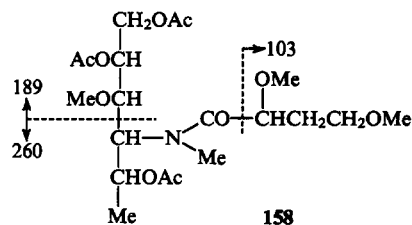
In other cases, e.g., in studies of PS from *P. aeruginosa* and *S. boydii* 7,¹⁶² 3-hydroxybutanoic acid was isolated in the individual state and its structure was confirmed by spectroscopic data. The ¹H NMR spectrum of 3-hydroxybutanoic acid contained signals at 4.25 [H(3'), sextet; $J_{2,3} = J_{3,4} = 6$ Hz], 2.50 [H(2'), doublet] and 1.27 ppm [H(4'), doublet, $J = 6$ Hz]; the ¹³C NMR spectrum contained signals at 180.0 [C(1')], 44.8 [C(2')], 66.2 [C(3')] and 23.5 ppm [C(4')]. These characteristic signals were also detected in the NMR spectra of PS themselves containing residues of 3-hydroxybutanoic acid and are therefore employed for direct spectroscopic identification of this residue. If this acid is isolated in the pure state, its (R)- or (S)-character can be readily established from the specific optical rotation.

Usually, a repeating unit of O-antigenic PS contains not more than one residue of 3-hydroxybutanoic acid; other amino groups are acylated by other acids, most commonly, by acetic acid.¹⁶² Also, PS are known where the same amino group is partially substituted by an acetic acid residue and partially by a 3-hydroxybutanoic acid residue, as in PS of *E. coli* O10 where 60% of the amino groups in the 4-amino-4-deoxy-D-fucose residue are acylated by acetic acid and 40% by 3-hydroxybutanoic acid.¹¹⁷ This makes the polysaccharide chain irregular as could be evident from the NMR spectrum. The question still remains open as to whether such substitution has a heterogeneous character, that is, the same polysaccharide chain contains both substituents, or, in contrast, there exist two different polysaccharide chains, each of which is substituted only by the same residue. Because of the structural similarity of both chains and their rather high molecular mass, they cannot be separated by the currently available methods.

4-Hydroxybutanoic (γ-hydroxybutyric) acid has thus far been found only in O-antigenic PS of *Alteromonas macleodii* 2MM6, where it acylates the amino group of 3-amino-3-deoxy-D-fucose.¹³³ Hydrolysis of PS resulted in an N-acyl derivative of this monosaccharide. The ¹H NMR spectrum of this derivative contains, in addition to signals of the monosaccharide unit, characteristic signals of a residue of 4-hydroxybutanoic acid: at 2.37 [H(2'), triplet, $J_{2,3} = 8.0$ Hz], 1.85 [H(3'), multiplet, $J_{3,4} = 7.0$ Hz] and 3.62 ppm [H(4'), triplet]. The ¹³C NMR spectrum contained signals at 33.3 [C(2')], 28.7 [C(3')] and 61.8 ppm [C(4')]. The mass spectrum of the alditol acetate **157** derived from this monosaccharide confirmed the presence of a 4-hydroxybutanoic acid residue and its localisation at the amino group at C(3) of the monosaccharide.

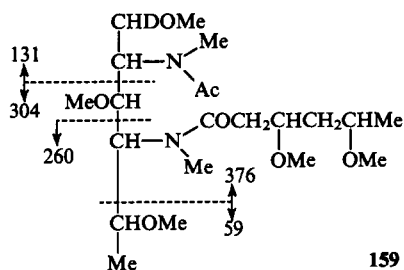


(S)-2,4-Dihydroxybutanoic (3-deoxytetronic) acid was found in O-antigenic PS of *Vibrio cholerae* O1 where it acylates the amino group of 4-amino-4,6-dideoxy-D-mannose (perosamine).¹⁰⁹ This acid was isolated in the pure state after hydrolysis of PS with dilute trifluoroacetic acid and identified by NMR spectroscopy. The ¹³C NMR spectrum of this acid contained signals at 182.8 (CO group), 71.0 (CHOH group), 37.7 (CH₂ group) and 59.8 ppm (CH₂OH group). The ¹H NMR spectrum also fits this structure. The structure and localisation of the residue of (S)-2,4-dihydroxybutanoic acid was established using the mass spectrum of the acetate of the partially methylated alditol **158** obtained by solvolysis of methylated PS with liquid HF and subsequent reduction and acetylation of the corresponding N-acyl derivative of perosamine.



The (S)-configuration (L-glycero-configuration) of the acid residue was evident from the specific optical rotation ($[\alpha]_D = -8^\circ$) and confirmed by the identity of its ester with (R)-octan-2-ol to the corresponding synthetic sample.

3,5-Dihydroxyhexanoic acid was detected in PS of *Vibrio cholerae* O3 where it acylates the amino group at C(4) of 2,4-diamino-2,4,6-trideoxy-D-glucose (bacillosamine).⁵⁸ The other amino group of this monosaccharide is N-acetylated. The presence of 3,5-dihydroxyhexanoic acid in PS was corroborated by the presence in the ¹H NMR spectrum of signals characteristic of the fragment CH₃-CHOH-CH₂-CHOH-CH₂CO. The structure of the acid residue was also confirmed by the ¹³C NMR spectrum which contained signals at 45.0 [C(2')], 66.7 [C(3')], 46.1 [C(4')], 65.3 [C(5')] and 23.7 ppm [C(6')]. The mass spectrum of the methylated alditol **159** derived from PS by a conventional method also confirmed the presence and localisation of this acid residue at the corresponding amino group of bacillosamine. These conclusions are consistent with the results of mass spectrometric analysis of disaccharide fragments obtained by partial degradation of PS.

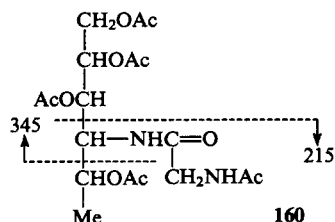


c. N-Acylation by amino acids

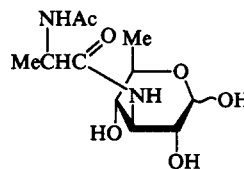
Among amino acids acylating an amino group of an amino sugar, mainly α -amino acids and some other more complex proline derivatives are known. Most commonly, PS contain only one amino acid residue per one repeating unit.

The finding of α -amino acids in PS of microbial origin presents substantial interest since it demonstrates the relationship between the two most important classes of carbohydrate-containing biopolymers: glycoproteins as typical representatives of the animal world and polysaccharides as classical biopolymers of microorganisms. Further expansion of our knowledge in this area may disclose interesting regularities in variations in biosynthetic pathways in the course of evolution.

An example of N-acylation of the chain of O-antigenic PS by an amino acid is acylation of the amino group of 4-amino-4,6-dideoxy-D-glucose (4-amino-4-deoxy-D-quinovose) by glycine, the amino group of the glycine itself being acetylated. This derivative was detected in PS of *Shigella dysenteriae* 7.¹⁰⁵ The residue of N-acetylglycine was first identified in PS using spectroscopic analysis: the ¹³C NMR spectrum contained a characteristic signal of C(2) of glycine at 44.1 ppm. Hydrolysis of PS with dilute HCl resulted in a derivative of 4-amino-4-dihydroxyquinovose; conventional analysis of the hydrolysate using an amino acid analyser revealed glycine. The mass spectrum of the corresponding alditol acetate **160**, derived by a routine procedure, indicated unambiguously the position of the glycine residue.



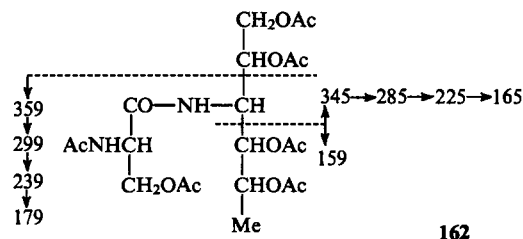
PS of *Proteus penneri* 14 was found to contain residues of D- and L-alanine. The former acylated the amino group of 3-amino-3,6-dideoxy-D-glucose (3-amino-3-deoxy-D-quinovose), while the L-isomer amidated the carboxy group of D-galacturonic acid.⁹⁴ This was the first example of a PS containing two different amino acid residues linked by different bonds to different monosaccharide residues. Solvolysis of PS with liquid HF resulted in the derivative **161** which contained a residue of N-acetyl-D-alanine linked to 3-amino-3-deoxyquinovose. The structure of this compound was confirmed by the mass spectrum of the derived alditol acetate as well as by NMR spectroscopy of the PS itself. The ¹³C NMR spectrum contained signals characteristic of D-alanine at 18.4 [C(2')], 51.8 [C(3')], and 178.3 ppm (CO), and the position of the C(3) signal of the monosaccharide residue (58.4 ppm) proved unambiguously the presence of an acylamino group at this atom.



161

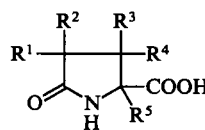
A residue of N-acetyl-L-serine was found in PS of *Escherichia coli* O114^{92,98} where it acylated the amino group of 3-amino-3-deoxyquinovose. The corresponding N-acylated monosaccharide was obtained after solvolysis of PS with liquid HF, from which L-serine was isolated after acid hydrolysis and identified by conventional amino acid analysis. Its L-configuration was established by GLC using an optically active stationary phase.

A routine procedure was used to convert the monosaccharide derivative into the alditol acetate **162** whose mass spectrum revealed fragmentation indicating the presence of a serine residue and its localisation in the monosaccharide (secondary fragments were especially characteristic). The structure of this monosaccharide was also confirmed by ¹³C NMR spectral data.



162

Several O-antigenic PS were found to contain structurally more complex N-acyl substituents related to 5-oxoproline derivatives of the type **163**. They can be regarded as lactams of substituted glutamic acids. Elucidation of their structure required a great deal of effort and was performed with the help of mass spectrometric analysis and NMR spectroscopy. The first substituent of the oxoproline type was detected in PS of *Pseudomonas fluorescens*²⁰¹ where it acylates the amino group of 3-amino-3-deoxyquinovose. The derivative of the N-acylated amino sugar was isolated from the acid hydrolysate of PS and was neutral. Its IR spectrum contained bands at 1660 and 1730 cm⁻¹ which demonstrated the presence of amide and lactam groups in this compound. The molecular weight of the N-acyl substituent, as determined from the FAB mass spectrum, was 156 Da corresponding to the compound of the type **163** containing two methyl groups and one hydroxy group.



163

The ¹³C NMR spectrum of this derivative contained signals confirming the presence of two methyl groups (18.9 and 23.5 ppm), one methylene group (45.8 ppm), two tertiary carbon atoms (71.6 and 78.2 ppm) and two carbonyl groups (175.7 and 179.7 ppm). The ¹H NMR spectrum revealed signals of two isolated methyl groups (1.37 and 1.49 ppm) and a methylene group with nonequivalent protons localised near the carbonyl group [2.45 and 2.65 ppm (AB-system, J_{AB} = 15 Hz)] as well as two NH groups (7.26 and 7.57 ppm), one of which was linked to

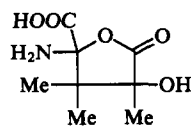
the carbon atom carrying no protons. NOE measurements indicated the *trans*-orientation of the methyl groups. The whole body of experimental evidence suggested that the acylating amino acid can be assigned the structure of 3-hydroxy-2,3-methyl-5-oxoproline **163** ($R^1 = R^2 = H$, $R^3 = R^5 = CH_3$, $R^4 = OH$).

A structurally related substituent (also a derivative of 5-oxoproline) was identified in PS of *Vibrio cholerae* O5,¹²⁴ where it acylates the amino group of 3-amino-3-deoxyfucose. The structure of this amino acid was established exclusively on the basis of the NMR spectra of the PS itself. The ^{13}C NMR spectrum of the polysaccharide (and of the disaccharide fragment derived) contained signals of the methyl (23.4 ppm), methine (69.6 ppm), methylene (45.4 ppm) and CO groups (180.2 ppm). This corresponded to the following signals in the 1H NMR spectrum: 1.37 (methyl), 2.38 and 2.64 (methylene, $J_{H,H} = 17.4$ Hz) and 4.19 ppm (methine) as well as a singlet at 8.62 ppm (NH group). These data which were fully confirmed by several correlations and NOE measurements suggested that the amino acid has the structure of 3-hydroxy-3-methyl-5-oxoproline **163** ($R^1 = R^2 = R^5 = H$, $R^3 = CH_3$, $R^4 = OH$).

This structure of the *N*-acyl substituent was fully confirmed by FAB mass spectrometry of some oligosaccharide fragments obtained by PS degradation. The configuration of the substituent was established by NOE measurements: a strong interaction between the NH proton and H(6) in the monosaccharide residue showed the (*R*)-configuration of C(2') of the proline ring, and an interaction between the CH_3 group of the amino acid and H(4) of the adjacent monosaccharide (2,4-diamino-2,4-dideoxyquinovose), indicated the (*R*)-configuration of C(3') of the proline ring.

The third representative of *N*-acyl substituents of this type, 2,4-dihydroxy-3,3,4-trimethyl-5-oxoproline, was detected in PS of *Vibrio anguillarum*,¹⁰⁷ where it acylates the amino group of 4-amino-4-deoxyquinovose (viosamine). Selective cleavage of PS by solvolysis with liquid HF and by two successive Smith degradations gave several oligosaccharide fragments. Their 1H and ^{13}C spectra contained signals corresponding to a substituted 5-oxoproline residue which was attached to the amino group of 4-amino-4-deoxyquinovose as shown by the position of the signal for C(4) of this monosaccharide (57.4 ppm).

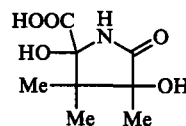
A special study was undertaken to establish the structure of this complex *N*-acyl substituent.²⁰² A derivative of this amino acid was isolated from a complex mixture of fragments obtained by solvolysis of PS with liquid HF and subsequent acid hydrolysis. This derivative displayed an IR spectrum with a band at 1792 cm^{-1} and gave a positive reaction with ninhydrin corresponding to the structure of a lactone carrying a free amino group. This compound was assigned the structure **164**. Its ^{13}C NMR spectrum revealed the presence of eight carbon atoms, two of which belonged to carbonyl groups (171.5 and 172.0 ppm), three other, to methyl groups (15.2, 18.0 and 19.7 ppm) and three more carbon atoms were localised in the ring. Analysis of the 1H NMR spectrum (signals at 1.62, 1.68 and 1.69 ppm) confirmed the presence of three methyl groups. Esterification and subsequent *N*-acylation of the lactone **164** gave a methyl ester whose 1H NMR spectrum contained signals of NH proton (6.14 ppm), OH proton (3.97 ppm) and a methyl group of the ester (3.82 ppm) as well as signals of three methyl groups (1.18, 1.59 and 1.75 ppm). Thus, the lactone **164** appeared to be a butyrolactone containing one amino, one hydroxy, one carboxy and three methyl groups.



164

Mild basic treatment of the butyrolactone **164** resulted in its conversion into a lactam, which, on the basis of the NMR and mass spectra of its *O*-methyl derivative, was assigned the structure

165 correlating with the structure of the lactone **164**. Thus, the *N*-acyl substituent present in the PS chain is 2,4-dihydroxy-3,3,4-trimethyl-5-oxoproline **163** ($R^2 = R^3 = R^4 = CH_3$; $R^1 = R^5 = OH$) (2,4-dihydroxy-3,3,4-trimethylpyrrolutamic acid).²⁰² The stereochemistry of this compound still remains unknown.

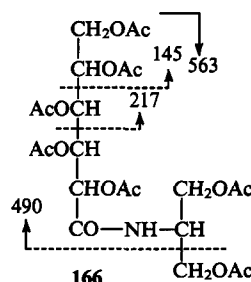


165

5. *N*-Substituents of hexuronic acid amides

As mentioned above, uronic acids occur occasionally in the polysaccharide chain as amides. Only one example of a glycuronic acid amide is known that is formed by an amino alcohol, 2-amino-1,3-dihydroxypropane. This compound was found in PS of *Shigella boydii* 8²⁰³ and *Vibrio cholerae*.¹⁵⁸ The amino alcohol was isolated by paper electrophoresis after strong acid hydrolysis of the PS and identified mass spectrometrically as the *N*-acetate. Its structure was confirmed by counterflow synthesis.

To determine the position of the *N*-substituent, the PS was subjected to solvolysis with liquid HF resulting in isolation of a small amount of an *N*-substituted amide of galacturonic acid. Its structure was established by mass spectrometry of the corresponding alditol acetate **166** derived by a routine procedure. A peak of the molecular ion with m/z 563 confirmed its molecular weight, and a fragment with m/z 490 the presence of a CH_2OH group.



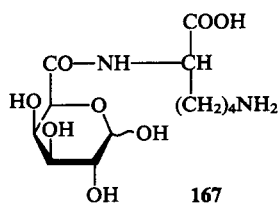
166

α -Amino acids linked by the amide bond to hexuronic acids (*N*-glycuronoyl amino acids) are more widespread. They were found in bacteria of the genus *Proteus*.²⁰⁴

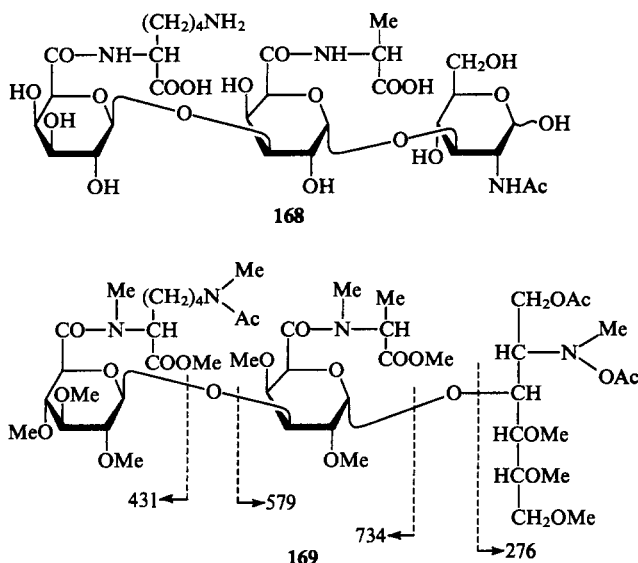
So far, the bacteria *Proteus* have been shown to contain L-alanine (PS of *P. mirabilis* O27 and *P. penneri* 14), L-serine (PS of *P. mirabilis* O28), L-threonine (PS of *P. penneri* O12)²⁰⁵ and L-lysine (PS of *P. mirabilis* O28 and *P. mirabilis* 1959) acylated by D-galacturonic acid, L-lysine being acylated at the α -amino group. In the PS of *P. mirabilis* O27, an L-lysine residue is acylated by D-glucuronic acid.

The presence of a uronic acid amide is revealed by the primary analysis of the ^{13}C NMR spectrum which showed a characteristic signal at 170–172 ppm corresponding to C(6) of uronic acid and signals of an amino acid residue. The presence of an amino acid is confirmed by its isolation using strong acid hydrolysis of PS and conventional analysis on an amino acid analyser. Its configuration was routinely established by the specific optical rotation or by esterification with (*R*)- or (*S*)-butan-2-ol.

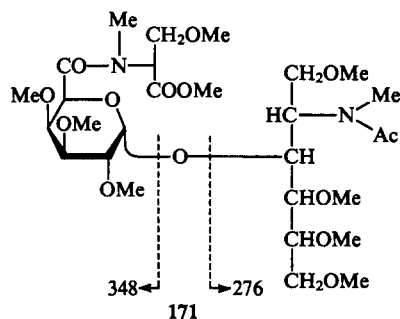
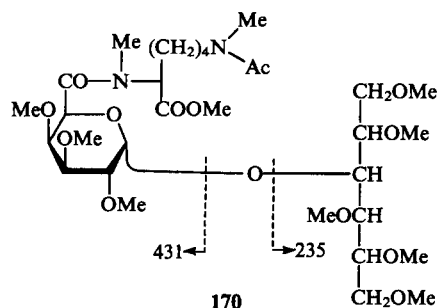
To obtain final evidence for the amide structure, it was isolated in the pure state or within a short oligosaccharide after solvolysis with liquid HF and subjected to mass spectrometric and NMR analyses. Thus, the glycuronamide **167** whose 1H NMR spectrum contained characteristic signals of galacturonic acid and lysine residues was isolated by ion-exchange chromatography from the PS of *P. mirabilis* 1959.²⁰⁶ Notably, the signal of the C(2) proton of lysine appeared to be shifted compared to that of unsubstituted lysine (from 3.20 to 4.35 ppm) suggesting the acylation of the α -amino group of the amino acid.



A similar approach was used to solve a more complex problem, namely, to determine the structure of two different amino acids and the site of their attachment to the corresponding monosaccharide units of the chain. Thus, after solvolysis with liquid HF, the trisaccharide **168** was isolated from the PS of *P. mirabilis* O27²⁰⁷ containing L-alanine and L-lysine residues attached to residues of D-galacturonic and D-glucuronic acids; reduction with NaBH₄ and subsequent methylation of this trisaccharide gave the oligosaccharide **169**. The presence in its FAB mass spectrum of fragments with *m/z* 431, 579, 734 and 276 demonstrated unambiguously that the residue of glucuronic acid at the non-reducing end of the oligosaccharide **169** was amidated by the lysine residue, and the penultimate unit of galacturonic acid by the alanine residue.

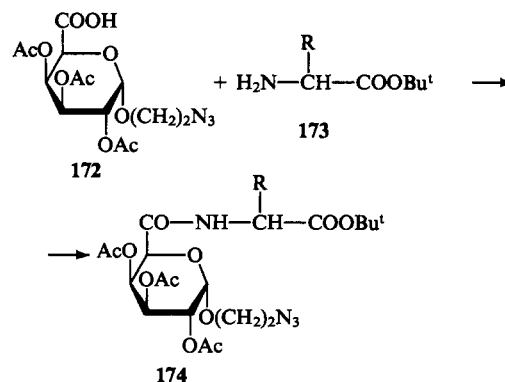


Similarly, localisation of L-lysine and L-serine residues in the PS of *P. mirabilis* O28 was established.²⁰⁸ After mild acid hydrolysis of the PS two disaccharides, one of which contained lysine and the other a serine residue, were isolated from a complex mixture. The acetates of the glycosyl alditols **170** and **171** derived by reduction and methylation were analysed by mass spectrometry. Fragmentation of both compounds clearly demonstrated that the lysine residue was attached to the galacturonic acid bound to the galactose residue and the alanine residue to the galacturonic acid adjacent to the *N*-acetylglucosamine residue in the polysaccharide chain.

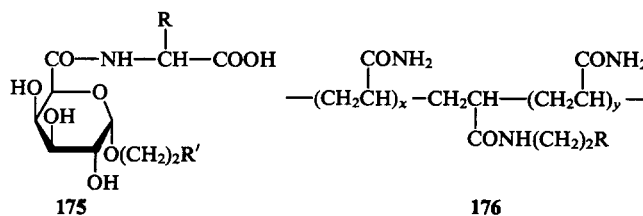


Amino acid residues in PS localised in side chains often represent immunodominant groups, i.e., they define the immunological specificity of the biopolymer. If the same PS contains residues of two different amino acids, an interesting question may arise: which particular amino acid residue plays the role of the determinant? To answer this question is essential from the viewpoint of creating diagnostic tools based on synthetic antigens. To this end, a synthesis of galacturonic acid amides with different amino acids was undertaken with their subsequent conversion to synthetic antigens by immobilisation on a polyacrylamide matrix using copolymerisation.^{209, 210} The synthesis of these amides was carried out in accordance with Scheme 16.²¹¹

Scheme 16



A uronic acid was first converted into the glycoside of 2-azidoethanol the residue of which was further converted into a synthetic antigen. 2'-Azidoethyl-2,3,4-tri-*O*-acetyl- α -galactopyranosiduronate **172** was condensed with the *tert*-butyl ester of the amino acid (in which the functional groups were protected) **173** [R = Me, R = (CH₂)₄NHCOOBu^t, R = CH₂OBu^t, R = CH(Me)OBu^t] in the presence of ethyl 2-ethoxy-1,2-dihydroxyquinoline-1-carboxylate. Deprotection of the condensation products **174** gave the corresponding derivatives of galacturonoyl-D- and -L-alanines, -L-serine, -L-threonine, -D- and -L-lysine **175** (R' = N₃).



The azides **175** (R' = N₃) were hydrogenated to give the amines **175** (R' = NH₂) which were further *N*-acylated by acryloyl chloride. The resulting derivatives of the acrylic acid **175** (R' = NHCOCH=CH₂) were copolymerised with acrylamide (R is a residue of a galacturonoyl amino acid) to give the synthetic antigens **176**.²¹¹

Comparison of the immunological specificity of the artificial antigens thus obtained with that of natural LPS isolated from bacteria allowed identification of the immunodominant group.²¹² Thus, in the PS of *P. penneri* 12 this group is the L-threonine residue, since of all synthetic antigens studied, only the antigen containing this particular amino acid appeared to be active.

6. Phosphate groups

A unique position among substituents affecting the general characteristics of the polysaccharide chain is held by groups containing residues of inorganic acids, such as sulfate and phosphate groups. These groups create fragments with localised charges along the whole length of the biopolymer chain which influence not only the general properties of the polymeric chain but also its determinant sites. There is still no compelling evidence for the presence of sulfate groups in O-antigenic PS, although these groups are widely distributed in other PS, especially in PS of marine organisms, such as algae; evidently this is related to the peculiarities of the mineral composition of their environment.

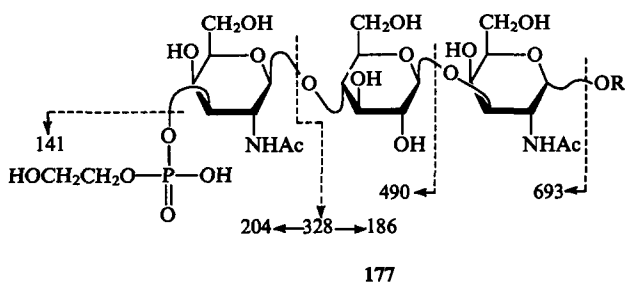
Phosphate groups were detected in many natural PS, including O-antigenic PS; the number of known phosphorylated O-antigenic PS is rapidly increasing. A distinction needs to be drawn between the two modes of incorporation of phosphorus-containing groups into PS. They can be present as substituents attached to one of the hydroxy groups of monosaccharide units in the polysaccharide chain or incorporated into the main skeleton of the polysaccharide linking together, in place of the glycosidic bond, monosaccharide or oligosaccharide fragments of the main chain of the biopolymer. The latter case may be considered as a new type of biopolymers which is not actually a polysaccharide, because its main chain consists of both glycosidic and phosphodiester bonds. Thus, this biopolymer occupies an intermediate position between PS and teichoic acids.

Biopolymers of this type, as well as lipid A, where the phosphate groups are present as components of a disaccharide,¹ are not discussed in the present review.

The presence of O-phosphate substituents in the chains of O-antigenic PS is rather well known. Usually they form phosphodiester groups esterifying a monosaccharide unit and a residue of an alcohol or an amino alcohol.

The presence of the phosphodiester group in PS was confirmed (apart from analysis of PS for phosphorus) by ³¹P NMR spectroscopic data. The nature of the second non-carbohydrate substituent in the phosphodiester group can also be found from NMR spectroscopic data and is finally established during localisation of the phosphodiester group in the PS chain using various approaches as required by the particular experimental goal.

A polysaccharide of the bacterium *Citrobacter* O16²¹³ was found to contain a glycerol phosphate group substituting a hydroxy group of an N-acetylgalactosamine residue. This polysaccharide contained 3% of phosphorus, and its ³¹P NMR spectrum revealed a signal of a phosphodiester group at 0.48 ppm. The presence of glycerol was established by GLC of the acid hydrolysate of the PS. To localise the glycerophosphate group, the PS was subjected to Smith degradation followed by mild acid hydrolysis to afford the oligosaccharide 177 containing the phosphate group.



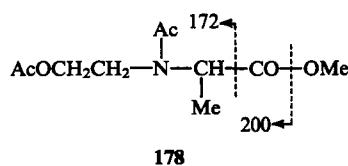
The FAB mass spectrum of the oligosaccharide 177 contained a characteristic fragment with m/z 328 which indicated the presence of a phosphodiester group at the N-acetylgalactosamine residue. This finding was also confirmed by the presence of a fragment with m/z 141 corresponding to the residue of the phosphodiester group modified by oxidation with HIO₄ (the glycerol residue was converted into the ethyleneglycol residue). The presence of fragments with m/z 490 and 693 demonstrated localisation of the phosphorylated monosaccharide at the reducing end of the oligosaccharide 177; this determined its position in the PS chain established by the structural analysis of PS. These data were corroborated by ¹³C NMR spectroscopic data which suggested also that the glycerol phosphate group substitutes the hydroxy group at C(3) of galactosamine since the signal of C(3) is shifted down-field in comparison with the signal of the unsubstituted monosaccharide (72.4 → 76.4 ppm).

The glycerol phosphate group was also found in the PS of *E. coli* O100. This PS has previously been studied by classical methods.²¹⁴ Substitution of one of the hydroxy groups of the monosaccharide chain was demonstrated by cleavage of glycerol phosphate by alkaline hydrolysis of the PS without cleavage of the polymeric chain of PS. The binding of the substituent to one of the hydroxy groups of the rhamnose residue was evident from the stability of the residue of this monosaccharide in the native PS towards periodate oxidation, whereas in the dephosphorylated PS it was destroyed.

In some PS the phosphodiester group contained an ethanolamine residue, as in the PS of *Proteus mirabilis* O27.²⁰⁷ The ³¹P NMR spectrum of the polysaccharide containing 2.5% phosphorus includes a signal at 1.33 ppm which indicates the presence of a phosphodiester group. Ethanolamine was identified after acid hydrolysis of PS by routine methods; its presence was confirmed by the presence in the ¹³C NMR spectrum of signals at 63.2 (CH₂OH) and 41.5 ppm (CH₂NH₂). Both signals, as well as the signals of C(5) and C(6) of N-acetylglucosamine present in the PS, were split due to coupling to the neighbouring phosphorus atom, thus suggesting that the phosphodiester group is linked to C(6) of N-acetylglucosamine. Elimination of the ethanolamine residue upon dephosphorylation of the PS confirmed its attachment to the phosphate group. The phosphodiester group appeared to substitute in the PS only 80% of the monosaccharide residues as determined by analysis of the ¹³C NMR spectrum: it contained two sets of signals for C(4), C(5) and C(6) of glucosamine, of which 80% belonged to the phosphorylated monosaccharide and 20% to the unsubstituted one.

A 2-aminoethyl phosphate group was found in the PS of *P. penneri* 8 where its localisation at C(6) of N-acetylglucosamine was demonstrated using similar approaches.²⁰⁵

A more complex phosphodiester substituent containing a residue of N-(2-hydroxyethyl)-D-alanine was found in PS of *P. mirabilis* O3.²¹⁵ The polysaccharide containing 2.5% of phosphorus was dephosphorylated with concentrated aqueous HF. The resulting amino acid was isolated from the hydrolysate by chromatography and converted into the methyl ester of the N,O-diacetate 178 whose mass spectrum contained ions with m/z 200 (M - OCH₃)⁺ and m/z 172 (M - CH₃COO)⁺ characteristic of fragmentation of the molecular ion of this kind.



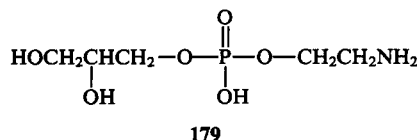
The presence in the ¹³C NMR spectrum of the amino acid of signals at 15.4 (CH₃), 48.8 (CH₂N), 58.2 (CHN), 56.9 (CH₂O) and 172.5 ppm (COOH) correlated with the structure ascribed to this amino acid. Its binding to the phosphate group was confirmed by the fact that signals of CH₂N and CH₂O groups are shifted from 48.3 and 54.7 ppm in the free amino acid to 47.5 and 62.3 ppm in

the PS and were split due to C—P coupling. The binding of this complex phosphodiester substituent to the hydroxy group at C(6) of a galactose unit in the PS chain is evident from the fact that in the ^{13}C NMR spectrum of the native PS the C(5) signal of this monosaccharide is split and shifted up-field as compared with the signal in the dephosphorylated PS (71.8 \rightarrow 70.6 ppm), whereas the C(6) signal is shifted down-field (62.2 \rightarrow 66.0 ppm).

Sometimes, the same PS contains two distinct phosphodiester groups linked to different monosaccharide units. An example is a PS of *P. mirabilis* D52 containing residues of 2-aminoethyl phosphate and ribitol phosphate.²¹⁶

This PS was investigated using classical methods. Apart from phosphorus, it contained 14.5% ribitol and 2.6% ethanolamine which, after strong acid hydrolysis, were isolated and identified by routine methods. Both residues could also be cleaved by alkaline hydrolysis without any cleavage of the polysaccharide chain, thus suggesting their localisation in the side chain but not in the main skeleton of the biopolymer. Reaction of the amino group of ethanolamine with 2,4-dinitrofluorobenzene showed that this group is unsubstituted and that the amino alcohol is phosphorylated at the hydroxy group. The ribitol residue was fully oxidised with HIO_4 to give formaldehyde and formic acid, thus providing a proof for ribitol phosphorylation at one of the primary hydroxy groups.

Localisation of the phosphodiester substituents in the PS chain was determined during establishment of the PS structure, for which purpose the PS was cleaved by acid hydrolysis or several repeated Smith degradations. The resulting oligosaccharides were analysed by classical methods. Thus, analysis of one of the fragments obtained by several repeated Smith degradations of the PS revealed the 2-aminoethyl phosphate group to be localised at C(6) of one of the two galactose residues. This is evident from the structure of the fragment 179 containing the 2-aminoethyl phosphate substituent at the glycerol residue, which is the end product of Smith degradation of the galactose unit.



Localisation of the ribitol phosphate group in the second galactose unit followed from the fact that in the native PS this unit is not oxidised with HIO_4 , whereas in the dephosphorylated PS it undergoes oxidation. The reason is that dephosphorylation results in formation of a vicinal glycol group, and, consequently, the ribitol phosphate group is localised at C(3) of galactose. Since localisation of these galactose units was determined in the course of structural analysis of the PS chain, the distribution of both phosphodiester groups in the chain is also established.

While considering this relatively complex example of structural analysis of a PS, it should be noted that the use of NMR spectroscopy offers a rapid, simple and reliable tool to solve similar problems.

V. Conclusions

In this review data are given on novel, scantily known monosaccharides present in O-antigenic polysaccharides of Gram-negative bacteria, many of which have thus far been detected only in this particular class of natural compounds. These data which were mainly obtained at the Laboratory of Carbohydrate Chemistry, Institute of Organic Chemistry (Russian Academy of Sciences), demonstrated that the old classical concepts of monosaccharides as a small group of structurally related organic substances are contrary to fact.

Monosaccharides represent a wide class of organic compounds integrated by one common property, namely, the ability to form cyclic oxygen-containing systems existing in a tautomeric

equilibrium with the corresponding polysubstituted hydroxy aldehydes or ketones. By appending to these data an ample body of experimental evidence on numerous monosaccharides found in antibiotics and some other natural substances, it may be well to notice that we deal with a large class of compounds whose carbon skeleton comprises very diverse functional groups and substituents, the number of individual representatives increasing largely due to their stereochemical differences determined by the presence of a large number of chiral centres. It should also be remembered that the number of novel monosaccharides carrying more than six carbon atoms (including those with a branched carbon chain) is rapidly increasing.

Such a dramatic widening of the class of monosaccharides calls for new methods and techniques for determination of their structure, conducting stereospecific syntheses and elaboration of new concepts of the spatial structure of their molecules.

The present review shows how important is the application of new methods for establishment of the structure and identification of hitherto unknown monosaccharides and their derivatives. The prominent role of physicochemical studies, without which further progress in this complex branch of organic chemistry would be impossible, becomes especially apparent.

It is quite impossible (and not necessary) to give all the details of structural analysis in a short review like this. An effort has just been made to outline the basic route and general logic which are significantly different in studies of structurally distinct monosaccharides. The syntheses of some representatives of monosaccharides described above illustrate the peculiarities of the stereospecific arrangement of rather complex compounds which may be useful in consideration of pathways of synthesis of other polychiral systems.

It should again be noted in conclusion that the data cited here are essential for development of molecular concepts in related biological sciences: biochemistry, immunochemistry, immunology and molecular biology.

A knowledge of the fine structure of monosaccharides making up the bulk of the important class of microbial polysaccharides, aside from its fundamental natural-scientific significance, is of prime importance for solution of applied tasks, firstly, in the design and synthesis of a new generation of biologically active compounds, especially of medicinal drugs used in chemotherapy and reliable diagnostics of infectious diseases.

References

1. Yu A Knirel', N K Kochetkov *Biokhimiya* **58** 166 (1993)
2. Yu A Knirel', N K Kochetkov *Biokhimiya* **59** 1784 (1994)
3. V N Shibaev *Adv. Carbohydr. Chem. Biochem.* **44** 277 (1986)
4. K Jann, O Westphal, in *The Antigens* Vol. 3 (Ed. M Sela) (New York: Academic Press, 1975) p. 1
5. S G Wilkinson *Surface Carbohydrates of the Prokaryotic Cell* (Ed. I M Sutherland) (London: Academic Press, 1977)
6. B Lindberg *Adv. Carbohydr. Chem. Biochem.* **48** 279 (1990)
7. O Westphal, K Jann, in *Methods in Carbohydrate Chemistry* (Eds R L Whistler, M L Wolfrom) (New York: Academic Press, 1962–1965) p. 325
8. Yu A Knirel, E V Vinogradov, A J Mort *Adv. Carbohydr. Chem. Biochem.* **47** 167 (1989)
9. R L Whistler, M L Wolfrom (Eds) *Methods in Carbohydrate Chemistry* (New York: Academic Press, 1962–1965) p. 58, 467
10. M Williams *Adv. Carbohydr. Chem. Biochem.* **31** 9 (1975)
11. P Jansson, L Kenne, H Liedgren, B Lindberg, G Lönngren *Chem. Commun. Univ. Stockholm* **8** (1976)
12. B A Dmitriev, Yu A Knirel, N K Kochetkov *Carbohydr. Res.* **40** 365 (1975)
13. B A Dmitriev, Yu A Knirel, N K Kochetkov *Carbohydr. Res.* **44** 77 (1975)
14. N K Kochetkov, O S Chizhov *Adv. Carbohydr. Chem.* **21** 39 (1966)
15. N K Kochetkov, O S Chizhov, N V Molodtsov *Tetrahedron* **24** 5587 (1968)

16. L S Golovkina, O S Chizhov, N S Vul'fon *Izv. Akad. Nauk SSSR, Ser. Khim.* 1915 (1966)
17. L S Golovkina, N S Vul'fon, O S Chizhov *Zh. Org. Khim.* 14 737 (1968)
18. H Bjorndal, B Lindberg, S Svensson *Carbohydr. Res.* 5 433 (1967)
19. H Bjorndal, C Hellerquist, B Lindberg, S Svensson *Angew. Chem., Int. Ed. Engl.* 9 610 (1970)
20. G Lönngrén, S Svensson *Adv. Carbohydr. Chem. Biochem.* 29 433 (1974)
21. K Bock, H Thorgersen *Annu. Rep. N.M.R. Spectrosc.* 13 1 (1982)
22. J Dabrowsky, in *Two Dimensional NMR Spectroscopy: Application for Chemists and Biochemists* (New York: VCH, 1987) p. 349
23. J Dabrowsky *Methods Enzymol.* 179 122 (1989)
24. N K Kochetkov, A S Shashkov, G M Lipkind, Yu A Knirel *Sov. Sci. Rev., Sect. B, Part. 2*, 13 1 (1989)
25. K Bock, C Pedersen *Adv. Carbohydr. Chem. Biochem.* 41 27 (1983)
26. K Bock, C Pedersen *Adv. Carbohydr. Chem. Biochem.* 42 193 (1984)
27. G M Lipkind, A S Shashkov, Yu A Knirel, E V Vinogradov, N K Kochetkov *Carbohydr. Res.* 175 75 (1988)
28. W Klyne *Biochem. J.* 47 Xiii (1950)
29. D I Neal, S G Wilkinson *Carbohydr. Res.* 69 191 (1979)
30. N A Kocharova, Yu A Knirel, A S Shashkov, N E Nifantiev, N K Kochetkov, L D Varbanetz, N V Moskalenko, O S Brovanskaya, V A Muras *Carbohydr. Res.* 250 278 (1993)
31. Yu A Knirel', A S Shashkov, M A Soldatkina, N A Paramonov, I Ya Zakharova *Bioorg. Khim.* 14 1208 (1988)
32. E V Vinogradov, A S Shashkov, Yu A Knirel, G M Zdorovenko, L P Solyanik, R I Gvosdyak *Carbohydr. Res.* 212 295 (1991)
33. V A Khomenko, G A Naberezhnykh, V V Isakov, T F Solov'eva, Yu S Ovodov, Yu A Knirel', E V Vinogradov *Bioorg. Khim.* 12 1641 (1986)
34. S G Wilkinson, L Galbraith, W I Anderton *Carbohydr. Res.* 112 241 (1983)
35. Yu A Knirel, N A Paramonov, A S Shashkov, N K Kochetkov, R G Jarullin, S Farber, V I Efremenko *Carbohydr. Res.* 233 185 (1992)
36. F Oerskov, J Oerskov, B Jann *Acta Pathol. Microbiol. Scand.* 71 339 (1967)
37. H Kaufman, P Muhlratt, T Reichstein *Helv. Chim. Acta* 50 2287 (1967)
38. J Hofman, B Lindberg, R Brubaker *Carbohydr. Res.* 78 212 (1980)
39. R P Gorshkova, E N Kalmykova, V V Isakov, Yu S Ovodov *Eur. J. Biochem.* 150 527 (1985)
40. N I Korchagina, R P Gorshkova, Yu S Ovodov *Bioorg. Khim.* 8 1666 (1982)
41. E N Kalmykova, R P Gorshkova, V V Isakov, Yu S Ovodov *Bioorg. Khim.* 14 652 (1988)
42. Yu E Tsvetkov, L V Backinowsky, N K Kochetkov *Carbohydr. Res.* 193 75 (1989)
43. E Romanowska, A Romanowska, C Lugowski, E Katzenellenbogen *Eur. J. Biochem.* 121 119 (1981)
44. A Gamian, E Romanowska, A Romanowska, C Lugowski, J Dabrowsky, K Trauner *Eur. J. Biochem.* 146 641 (1985)
45. O Westphal, O Lüderitz, I Fromme, N Joseph *Angew. Chem.* 65 555 (1953)
46. O Westphal, O Lüderitz *Angew. Chem.* 72 35 (1960)
47. K Jann, B Jann *Handbook of Endotoxin* Vol. 1 (Amsterdam: Elsevier, 1984) p. 138
48. L Kenne, B Lindberg, E Söderholm, D Bundle, D Griffith *Carbohydr. Res.* 111 289 (1983)
49. O Lüderitz *Biochem. Z.* 330 193 (1958)
50. R P Gorshkova, V A Zubkov, V V Isakov, Yu S Ovodov *Bioorg. Khim.* 9 1401 (1983)
51. R P Gorshkova, N I Korchagina, Yu S Ovodov *Eur. J. Biochem.* 131 345 (1983)
52. V V Isakov, R P Gorshkova, S V Tomich, Yu S Ovodov *Bioorg. Khim.* 7 559 (1981)
53. V V Isakov, N A Komandrova, R P Gorshkova, Yu S Ovodov *Bioorg. Khim.* 9 1565 (1983)
54. N A Komandrova, R P Gorshkova, V V Isakov, Yu S Ovodov *Bioorg. Khim.* 10 232 (1984)
55. R P Gorshkova, V V Isakov, L S Shevchenko, Yu S Ovodov *Bioorg. Khim.* 17 252 (1991)
56. R P Gorshkova, V A Zubkov, V V Isakov, Yu S Ovodov *Bioorg. Khim.* 9 1068 (1983)
57. N A Komandrova, R P Gorshkova, V A Zubkov, Yu S Ovodov *Bioorg. Khim.* 15 104 (1989)
58. T Chawdhury, P E Jansson, B Lindberg, J Lindberg, B Gustafson, T Holme *Carbohydr. Res.* 215 303 (1991)
59. N A Kocharova, Yu A Knirel, E S Stanislavsky, in *Abstracts of Reports of the 6th European Symposium on Carbohydrates, Edinburgh, 1991* A51
60. B Jann, K Prehm, K Jann *J. Bacteriol.* 134 462 (1978)
61. J Hofman, B Lindberg, T Hofstad, N Skand *Carbohydr. Res.* 66 67 (1978)
62. B Lindberg, F Lindh, J Lönngrén, A Lindberg, S Svensson *Carbohydr. Res.* 97 105 (1981)
63. G Hellerquist, B Lindberg, S Svensson, T Holme, A Lindberg *Carbohydr. Res.* 8 43 (1968)
64. K Bock, C Pedersen *Adv. Carbohydr. Chem. Biochem.* 41 56 (1983)
65. O Westphal, S Stirn *Liebigs Ann. Chem.* 620 8 (1959)
66. J Fourquey *Bull. Soc. Chim. Fr.* 803 (1959)
67. G Ekborg, P Garregg, B Gothammer *Acta Chem. Scand., Ser. B* 29 765 (1975)
68. A B Levinskii, Candidate Thesis in Chemical Sciences, Institute of Organic Chemistry, Russian Academy of Sciences, Moscow, 1993
69. B Classon, P Garregg, B Samuelson *Can. J. Chem.* 59 339 (1981)
70. I-C Florent, C Monnerat, Q Kuang-Huu *Carbohydr. Res.* 56 301 (1977)
71. D Bundle, S Josephson *Can. J. Chem.* 56 2686 (1978)
72. Yu A Knirel', N K Kochetkov *Biokhimiya* 58 182 (1993)
73. Yu A Knirel', N V Tanatar, M A Soldatkina, A S Shashkov, I Ya Zakharova *Bioorg. Khim.* 14 77 (1988)
74. A A Ansari, L Kenne, B Lindberg, B Gustafson, T Holme *Carbohydr. Res.* 150 213 (1986)
75. K Dzrewiszek, A Zamoiski *Carbohydr. Res.* 150 163 (1986)
76. G O Aspinall, A G McDonald, H Pang *Carbohydr. Res.* 231 13 (1992)
77. N K Khare, R K Sood, G O Aspinall *Can. J. Chem.* 72 237 (1994)
78. A Donadoni, G Fantin, M Fagnolo, A Medici *Tetrahedron* 43 3533 (1987)
79. G O Aspinall, M G McDonald, R S Sood *Can. J. Chem.* 72 247 (1994)
80. S Schramek, I Radzewska-Lebrecht, H Mayer *Eur. J. Biochem.* 148 455 (1985)
81. V V Kulaeva, M K Kudinova, N P Potapova, L M Rubashova, M G Brazhnikova, B V Rozynov, A R Bekker *Bioorg. Khim.* 4 1087 (1978)
82. R P Gorshkova, V A Zubkov, V V Isakov, Yu S Ovodov *Carbohydr. Res.* 126 308 (1984)
83. R P Gorshkova, V A Zubkov, V V Isakov, Yu S Ovodov *Bioorg. Khim.* 13 1146 (1987)
84. V A Zubkov, A F Sviridov, R P Gorshkova, A S Shashkov, Yu S Ovodov *Bioorg. Khim.* 15 192; 538 (1989)
85. V A Zubkov, R P Gorshkova, Yu S Ovodov, A F Sviridov, A S Shashkov *Carbohydr. Res.* 225 189 (1992)
86. M Adinolfi, M Corsaro, C DeCastro, L Lanzetta, M Parilli, A Evidente, P Lavermicoca *Carbohydr. Res.* 267 307 (1995)
87. M Adinolfi, M Corsaro, C DeCastro, L Lanzetta, A Evidente, L Mangoni, M Parilli *Carbohydr. Res.* 274 223 (1995)
88. N Harada, K Nakanishi *Circular Dichroic Spectroscopy-Exiton Coupling in Organic Chemistry* (London: Oxford University Press, 1983)
89. A Cox, S Wilkinson *Carbohydr. Res.* 195 295 (1990)
90. B Jann, K Jann *Eur. J. Biochem.* 5 173 (1968)
91. S A Barker, I S Brimacombe, M I How, M Stacey, J M Williams *Nature (London)* 303 (1961)
92. B A Dmitriev, V L Lvov, N V Tochamysheva, A S Shashkov, N K Kochetkov, B Jann, K Jann *Eur. J. Biochem.* 134 517 (1983)
93. E Katzenellenbogen, E Romanowska, A S Shashkov, N A Kocharova, Yu A Knirel, N K Kochetkov *Carbohydr. Res.* 259 67 (1994)
94. E V Vinogradov, A S Shashkov, Yu A Knirel, N K Kochetkov, Z Sidorczyk, A Swierzko *Carbohydr. Res.* 219 C1 (1991)
95. L Kenne, B Lindberg, M Rahman, M Mosihuzzman *Carbohydr. Res.* 243 131 (1993)
96. I Banoub, F Mishon, H I Holder *Biochem. Cell. Biol.* 65 19 (1987)

97. I Banoub, D Shaw *Carbohydr. Res.* **98** 93 (1981)
98. V L Lvov, N V Tochamysheva, A S Shashkov, B A Dmitriev, K Capek *Carbohydr. Res.* **112** 233 (1983)
99. P-E Jansson, B Lindberg, M Spellman, T Hofstad, N Skaug *Carbohydr. Res.* **137** 197 (1985)
100. W Kondo, F Nakazawa, T Ito *Carbohydr. Res.* **83** 129 (1980)
101. H Baer, K Capek *Can. J. Chem.* **47** 99 (1969)
102. K Capek, J Steffkova, J Jary *Collect. Czech. Chem. Commun.* **31** 1854 (1966)
103. V L Lvov, A S Shashkov, B A Dmitriev, N K Kochetkov *Carbohydr. Res.* **126** 249 (1984)
104. Yu A Knirel', V M Dashunin, A S Shashkov, B A Dmitriev, N K Kochetkov, I L Gofman *Bioorg. Khim.* **13** 1002 (1987)
105. Yu A Knirel, V M Dashunin, A S Shashkov, N K Kochetkov, B A Dmitriev, I L Hofman *Carbohydr. Res.* **179** 51 (1988)
106. E V Vinogradov, A S Shashkov, Yu A Knirel, N K Kochetkov, N V Tochamysheva, S F Averin, O V Goncharova, V S Khlebnikov *Carbohydr. Res.* **214** 289 (1991)
107. H Eguichi, Sh Kaya, Y Araki, N Kojima, Sh Yokata *Carbohydr. Res.* **231** 159 (1992)
108. E Katzenellenbogen, E Romanowska, N A Kocharova, Yu A Knirel, A S Shashkov, N K Kochetkov *Carbohydr. Res.* **231** 249 (1992)
109. L Kenne, B Lindberg, P Unger, B Gustafson, T Holme *Carbohydr. Res.* **100** 341 (1982)
110. V L L'vov, V E Malikov, A S Shashkov, E A Dranovskaya, B A Dmitriev *Bioorg. Khim.* **11** 963 (1985)
111. D Bundle, M Gereken, M Perry *Can. J. Chem.* **64** 255 (1986)
112. M Perry, D Bundle, L MacLean, J Perry, D Griffith *Carbohydr. Res.* **156** 107 (1986)
113. M Perry, D Bundle *Infect. Immunol.* **58** 1391 (1990)
114. M Perry, L MacLean, D Griffith *Biochem. Cell. Biol.* **64** 21 (1986)
115. M Carrof, D Bundle, M Perry *Eur. J. Biochem.* **139** 195 (1984)
116. L DiFabio, M Perry, D Bundle *Biochem. Cell. Biol.* **65** 968 (1987)
117. L Kenne, B Lindberg, C Lugowski, S Svensson *Carbohydr. Res.* **151** 349 (1986)
118. Yu A Knirel, N A Paramonov, A S Shashkov, N K Kochetkov, G M Zdorovenko, S N Veremeychenko, I Ya Zakharova *Carbohydr. Res.* **243** 205 (1993)
119. C I Stevens, P Blumbers, F Daniher, D Henbach, K Taylor *J. Org. Chem.* **31** 2822 (1966)
120. A Anderson, J Richards, M Perry *Carbohydr. Res.* **237** 249 (1992)
121. U Zehavi, N Sharon *J. Biol. Chem.* **248** 433 (1973)
122. Yu A Knirel, E V Vinogradov, A S Shashkov, E Wilkinson, Y Tahara, B A Dmitriev, N K Kochetkov, E S Stanislavsky, G M Mashilova *Eur. J. Biochem.* **155** 659 (1986)
123. Yu A Knirel', G M Zdorovenko, S N Veremeichenko, G M Lipkind, A S Shashkov, I Ya Zakharova, N K Kochetkov *Bioorg. Khim.* **14** 352 (1988)
124. K Hermanson, P-E Janson, T Holme, B Gustafson *Carbohydr. Res.* **248** 199 (1993)
125. K Hermanson, M B Perry, E Altman, J R Brisson, M M Garcia *Eur. J. Biochem.* **212** 801 (1993)
126. L Kenne, B Lindberg, K Petersen, E Katzenellenbogen, E Romanowska *Carbohydr. Res.* **78** 119 (1980)
127. E V Vinogradov, Yu A Knirel, N K Kochetkov, S Schlecht, H Mayer *Carbohydr. Res.* **253** 101 (1994)
128. Yu A Knirel, E V Vinogradov, A S Shashkov, B A Dmitriev, N K Kochetkov, E S Stanislavsky, G M Mashilova *Eur. J. Biochem.* **150** 541 (1985)
129. Yu A Knirel, N A Kocharova, A S Shashkov, N K Kochetkov, E V Kholodkova, E S Stanislavsky *Eur. J. Biochem.* **166** 189 (1987)
130. Yu A Knirel, A S Shashkov, B A Dmitriev, N K Kochetkov *Carbohydr. Res.* **133** C12 (1984)
131. K Heyns, G Kiessling *Carbohydr. Res.* **3** 340 (1967)
132. Yu A Knirel, E V Vinogradov, A S Shashkov, B A Dmitriev, N K Kochetkov, E S Stanislavsky, G M Mashilova *Eur. J. Biochem.* **125** 221 (1982)
133. E L Nazarenko, V A Zubkov, A S Shashkov, Yu A Knirel', R P Gorshkova, E P Ivanova, Yu S Ovodov *Bioorg. Khim.* **19** 740 (1993)
134. T Kontrohr *Carbohydr. Res.* **58** 498 (1977)
135. Yu A Knirel, N A Kocharova, A S Shashkov, B A Dmitriev, N K Kochetkov *Carbohydr. Res.* **93** C12 (1981)
136. B A Dmitriev, N A Kocharova, Yu A Knirel, A S Shashkov, N K Kochetkov, E S Stanislavsky, G M Mashilova *Eur. J. Biochem.* **125** 229 (1982)
137. I Roppel, H Mayer, I Weckesser *Carbohydr. Res.* **40** 31 (1975)
138. H Baer, T Nelson *J. Org. Chem.* **32** 1068 (1967)
139. Yu A Knirel, E V Vinogradov, A S Shashkov, B A Dmitriev, N K Kochetkov, E S Stanislavsky, G M Mashilova *Eur. J. Biochem.* **128** 81 (1982)
140. Yu A Knirel, E V Vinogradov, A S Shashkov, B A Dmitriev, N K Kochetkov, E S Stanislavsky, G M Mashilova *Eur. J. Biochem.* **134** 289 (1983)
141. Yu A Knirel', N A Paramonov, E V Vinogradov, A S Shashkov, B A Dmitriev, N K Kochetkov *Bioorg. Khim.* **12** 995 (1986)
142. R D Guthrie, D Murray *J. Chem. Soc.* 6956 (1965)
143. Yu A Knirel, N A Paramonov, E V Vinogradov, A S Shashkov, B A Dmitriev, N K Kochetkov, E V Kholodkova, E S Stanislavsky *Eur. J. Biochem.* **167** 549 (1987)
144. Yu A Knirel', N A Paramonov, E V Vinogradov, A S Shashkov, N K Kochetkov *Bioorg. Khim.* **12** 992 (1986)
145. Yu A Knirel, E V Vinogradov, N A Kocharova, A S Shashkov, B A Dmitriev, N K Kochetkov *Carbohydr. Res.* **122** 181 (1983)
146. I L DiFabio, M Caroff, D Karabian, J Richards, M Perry *FEMS Microbiol. Lett.* **97** 275 (1992)
147. A S Shashkov, S Campos-Portuguez, H Kochanowski, A Yokota, H Mayer *Carbohydr. Res.* **269** 157 (1995)
148. E V Vinogradov, Yu A Knirel, A S Shashkov, N K Kochetkov *Carbohydr. Res.* **170** C1 (1987)
149. F M Unger *Adv. Carbohydr. Chem. Biochem.* **38** 323 (1981)
150. R Schauer *Adv. Carbohydr. Chem. Biochem.* **40** 132 (1982)
151. E V Vinogradov, N A Paramonov, Yu A Knirel, A S Shashkov, N K Kochetkov *Carbohydr. Res.* **242** C11 (1993)
152. A Gamian, L Kenne *J. Bacteriol.* **175** 1508 (1993)
153. G Kogan, B Jann, K Jann *Carbohydr. Res.* **238** 335 (1993)
154. G Kogan, B Jann, K Jann *FEMS Microbiol. Lett.* **91** 135 (1992)
155. G Kogan, A S Shashkov, B Jann, K Jann *Carbohydr. Res.* **238** 261 (1993)
156. V I Torgov, A S Shashkov, B Jann, K Jann *Carbohydr. Res.* **272** 73 (1995)
157. A Gamian, E Romanowska, U Dabrowski, J Dabrowski *Biochemistry* **30** 5032 (1991)
158. E V Vinogradov, O Holst, J Thomas-Oates *Eur. J. Biochem.* **210** 491 (1992)
159. E I McGuire, S B Binkley *Biochemistry* **3** 247 (1964)
160. I Vliegenhardt, L Dorland, J van Halbeek, J Haverkamp, in *Sialic Acids* (Ed. R Shauer) (Wien: Springer, 1982)
161. Yu A Knirel, E V Vinogradov, V L Lvov, N A Kocharova, A S Shashkov, B A Dmitriev, N K Kochetkov *Carbohydr. Res.* **133** C5 (1984)
162. Yu A Knirel, E V Vinogradov, A S Shashkov, N K Kochetkov, V L Lvov, B A Dmitriev *Carbohydr. Res.* **141** C1 (1985)
163. Yu A Knirel, N A Kocharova, A S Shashkov, B A Dmitriev, N K Kochetkov, E S Stanislavsky, G M Mashilova *Eur. J. Biochem.* **163** 639 (1987)
164. V L L'vov, A S Shashkov, B A Dmitriev *Bioorg. Khim.* **13** 223 (1987)
165. L Kenne, B Lindberg, E Schweda, B Gustafson, T Holme *Carbohydr. Res.* **180** 285 (1988)
166. L Svennerholm *Biochim. Biophys. Acta* **24** 604 (1957)
167. E V Vinogradov, A S Shashkov, Yu A Knirel, N K Kochetkov, J Dabrowsky, H Grosskurth, E S Stanislavsky, E Kholodkova *Carbohydr. Res.* **231** 1 (1992)
168. Yu A Knirel, E V Vinogradov, A S Shashkov, B A Dmitriev, N K Kochetkov, E S Stanislavsky, G M Mashilova *Eur. J. Biochem.* **163** 627 (1987)
169. Yu A Knirel', E V Vinogradov, A S Shashkov, B A Dmitriev, N K Kochetkov *Bioorg. Khim.* **12** 848 (1986)
170. E L Nazarenko, A S Shashkov, Yu A Knirel', E P Ivanova, Yu S Ovodov *Bioorg. Khim.* **16** 1426 (1990)
171. Yu A Knirel, E T Rietschel, R Marre, U Zähringer *Eur. J. Biochem.* **221** 239 (1994)
172. J Brom, K Neel, G Williamson *Biochem. J.* **163** 173 (1977)
173. H Björndal, B Lindberg, W Nimnich *Acta Chem. Scand.* **24** 3414 (1970)
174. R Stange, L Kent *Biochem. J.* **71** 333 (1959)

175. O Hoshino, U Zehavi, P Sinay, R Jeanloz *J. Biol. Chem.* **247** 381 (1972)
176. N K Kochetkov, A F Sviridov, Kh Arifkhodzhaev, O Chizhov, A S Shashkov *Carbohydr. Res.* **71** 193 (1979)
177. B Lindberg, B Lindquist, J Löngren, W Nimmich *Carbohydr. Res.* **49** 411 (1976)
178. N K Kochetkov, B A Dmitriev, L V Bakinovskii, V L L'vov *Bioorg. Khim.* **1** 1238 (1975)
179. N K Kochetkov, B A Dmitriev, V L L'vov *Carbohydr. Res.* **54** 253 (1977)
180. B A Dmitriev, V L L'vov, N K Kochetkov, B Jann, K Jann *Eur. J. Biochem.* **64** 491 (1976)
181. R P Gorshkova, E L Nazarenko, V A Zubkov, E P Ivanova, Yu S Ovodov, A S Shashkov, Yu A Knirel' *Bioorg. Khim.* **19** 327 (1993)
182. L Parolis, H Parolis, G Dutton, P Wing, B Skura *Carbohydr. Res.* **216** 495 (1991)
183. N K Kochetkov, B A Dmitriev, L V Backinowsky *Carbohydr. Res.* **51** 229 (1976)
184. E L Nazarenko, V A Zubkov, A S Shashkov, Yu A Knirel', N A Komandrova, R P Gorshkova, Yu S Ovodov *Bioorg. Khim.* **19** 989 (1993)
185. Yu A Knirel, N A Paramonov, E V Vinogradov, A S Shashkov, N K Kochetkov, Z Sidorczyk, A Swierzko *Carbohydr. Res.* **235** C19 (1992)
186. Yu A Knirel, N A Paramonov, E V Vinogradov, N K Kochetkov, Z Sidorczyk, K Zych *Carbohydr. Res.* **259** C1 (1994)
187. L Kenne, B Lindberg, B Lindquist, J Lönngrén, R Arie, R Brown, I Stewart *Carbohydr. Res.* **51** 287 (1976)
188. B A Dmitriev, Yu A Knirel', E V Vinogradov, N K Kochetkov, I L Gofman *Bioorg. Khim.* **4** 40 (1978)
189. A Adeyeye, P-E Jansson, B Lindberg, S Abbas, S Svensson *Carbohydr. Res.* **176** 231 (1988)
190. P Garegg, P-E Janson, B Lindberg, F Lindh, J Lönngrén, I Kvärnström, W Nimmich *Carbohydr. Res.* **78** 127 (1980)
191. M Caroff, D Bundle, M Perry, I Cherwonogrodzky, I Duncan *Infect. Immun.* **46** 384 (1984)
192. L Kenne, P Unger, T Wehler *J. Chem. Soc., Perkin Trans. 1* 1183 (1988)
193. Yu A Knirel', E V Vinogradov, N A Paramonov, A S Shashkov, N K Kochetkov, E S Stanislavskii, G M Mashilova *Bioorg. Khim.* **12** 1263 (1986)
194. N A Paramonov, Yu A Knirel', N K Kochetkov *Bioorg. Khim.* **17** 1111 (1991)
195. S Kondo, K Ishida, Y Isshiki, Y Haishima, T Iguchi, K Hisatsune *Biochem. J.* **292** 531 (1993)
196. N A Kocharova, Yu A Knirel, A S Shashkov, N K Kochetkov, E V Kholodkova, E S Stanislavsky *Carbohydr. Res.* **264** 123 (1994)
197. V A Zubkov, R P Gorshkova, E L Nazarenko, A S Shashkov, Yu S Ovodov *Bioorg. Khim.* **17** 831 (1991)
198. E V Vinogradov, Z Sidorczyk, A Swierzko, A Rosalski, E Daeva, A S Shashkov, Yu A Knirel, N K Kochetkov *Eur. J. Biochem.* **197** 93 (1991)
199. A Gamian, R Romanowska, H Offenkuch *Eur. J. Biochem.* **186** 611 (1989)
200. E Katrenellenbogen, E Romanowska, U Dabrowska, J Dabrowsky *Eur. J. Biochem.* **200** 410 (1992)
201. G A Naberezhnykh, V A Khomenko, V V Isakov, Yu N Elkin, T F Solov'eva, Yu S Ovodov *Bioorg. Khim.* **13** 1428 (1987)
202. H Eguchi, Sh Kaya, Y Araki *Carbohydr. Res.* **231** 147 (1992)
203. V L L'vov, I V Tokhtamysheva, A S Shashkov, B A Dmitriev, N K Kochetkov *Bioorg. Khim.* **9** 60 (1983)
204. Yu A Knirel, Z Sidorczyk, A Rosalski, I Radziewska-Lebrecht, W Kaca *J. Carbohydr. Chem.* **12** 379 (1993)
205. Z Sidorczyk, A Swierzko, Yu A Knirel, E V Vinogradov, A Chernyak, L Kononov, M Cedzynski, A Rozalski, W Kaca, A S Shashkov, N K Kochetkov *Eur. J. Biochem.* **230** 713 (1995)
206. E V Vinogradov, A S Shashkov, Yu A Knirel', N K Kochetkov, E V Kholodkova, E S Stanislavskii *Bioorg. Khim.* **13** 660 (1987)
207. E V Vinogradov, D Krajewska-Pietrasik, W Kaca, A S Shashkov, Yu A Knirel, N K Kochetkov *Eur. J. Biochem.* **185** 645 (1989)
208. E V Vinogradov, Yu A Knirel', N K Kochetkov, I Radziewska-Lebrecht, V Katsa *Bioorg. Khim.* **19** 1132 (1993)
209. N K Kochetkov, B A Dmitriev, A Ya Chernyak, V I Pokrovskii, Yu Ya Tendetnik *Dokl. Akad. Nauk SSSR* **263** 1277 (1982)
210. N K Kochetkov, B A Dmitriev, A Ya Chernyak, A B Levinsky *Carbohydr. Res.* **110** C16 (1982)
211. A Ya Chernyak, L O Kononov, N K Kochetkov *J. Carbohydr. Chem.* **13** 383 (1994)
212. Z Sidorczyk, A Swierzko, Yu A Knirel, E V Vinogradov, A Ya Chernyak, L O Kononov, M Cedzynski, A Rozalski, N K Kochetkov *Eur. J. Biochem.* **230** 713 (1995)
213. N A Kocharova, J Thomas-Oates, Yu A Knirel, A S Shashkov, U Dabrowska, N K Kochetkov, E S Stanislavsky, E V Kholodkova *Eur. J. Biochem.* **219** 653 (1994)
214. B Jann, K Jann, G Schmidt *Eur. J. Biochem.* **15** 29 (1970)
215. E V Vinogradov, W Kaca, A S Shashkov, D Krajewska-Pietrasik, A Rosalski, Yu A Knirel, N K Kochetkov *Eur. J. Biochem.* **188** 645 (1990)
216. J Gmeiner *Eur. J. Biochem.* **74** 171 (1977)

Natural peroxides. Chemistry and biological activity

G A Tolstikov, A G Tolstikov, O V Tolstikova

Contents

I. Introduction	769
II. Naturally occurring peroxides and their biological activity	770
III. Synthesis of artemisinin, its derivatives and structural analogues	778

Abstract. This review is devoted to the chemistry of natural peroxides and their biologically active analogues. Data are presented on the natural sources of peroxy compounds and pathways of their formation. The structure, stereochemistry and chemical transformations of natural peroxides are considered; the problems of total synthesis of natural peroxy compounds and their structural analogues are also discussed. Data for the biological activity of peroxides are presented. The bibliography includes 134 references.

I. Introduction

The chemistry of peroxy compounds is a vast field which encompasses problems of organic synthesis, macromolecular chemistry, and free-radical processes. These problems have received much attention in the current literature. Lively discussions concern the involvement of peroxy intermediates in biochemical processes; much attention is given, in particular, to the role of peroxy compounds as biologically active metabolites in the synthesis of prostaglandins, thromboxanes, prostacyclins, leukotrienes, hepoxylins, and lipoxins as well as of a wide variety of unsaturated acids with oxygen-containing functions.^{1–6}

Despite the apparently convincing evidence for a relatively high stability of ascaridol, which can be isolated by steam distillation of plant material,^{7,8} further replenishment of the family of natural peroxides has long been considered problematic because of their high lability and short metabolic life.

In this regard, the history of isolation of prostaglandin endoperoxide, one of the key intermediates of prostanoid biosynthesis, commonly known as prostaglandin H₂ (PGH₂) appears to be very typical. This labile compound could be isolated only after isomerase has been blocked with mercury salts by rapid extraction of the culture medium.⁶ However, among the wide variety of natural peroxides stable compounds have been found, which do not require any special precautions connected with their isolation. The formation of stable peroxides by photosensitised oxidation of

terpenes and steroids stimulated the search for the peroxy compounds synthesised by animal and plant organisms.^{9–11}

Beginning in 1970s, the opinion was repeatedly stated that peroxy metabolites can be present in marine organisms. Later, this assumption has often received experimental support. Thus, extracts of sea sponges were found to contain, in addition to the expected 6,9-endoperoxides of sterols, relatively stable 1,2-dioxane and 1,2-dioxolane derivatives and macrocyclic peroxides.

Studies of chemical transformations of natural peroxides revealed that the suggestions of their extreme lability are in many cases unwarranted. For example, some 1,2-dioxane derivatives retain the peroxy group even in the presence of such reagents as complex aluminium hydrides and OsO₄.

Biological assays of peroxides from marine organisms revealed highly active antibacterial, fungicidal, cytostatic, and anticarcinogenic agents.

An event, which changed dramatically many current notions of the natural peroxides, was the discovery by Chinese investigators¹² of a high antimalarial activity of a sesquiterpene peroxylactone artemisinin (qinghaosu) isolated from the wild plant *Artemisia annua* L (sweet wormwood). It is of note in this connection that in traditional Chinese medicine this plant had long been considered to be a highly effective antimalarial agent. The communication by Chinese authors¹² aroused considerable interest among chemists, pharmacologists, and practitioners. The studies performed in a number of laboratories have culminated in the preparation of a drug, which has a number of salient advantages over all currently known antimalarial agents, including the possibility of its application in pregnancy.¹³ It is noteworthy that the discovery of therapeutic properties of artemisinin gave an impetus to the total synthesis of this sesquiterpene and its analogues. Data on the chemistry of artemisinin and other terpenoids isolated from *A. annua* have been reported.^{12, 14}

It is not inconceivable that medicinal drugs of peroxide nature will play a conspicuous role in the therapy of malaria, a disease which presently affects hundreds of millions of people all over the world.¹⁵ It is not therefore surprising that the interest in elaborating the methods of synthesis and bioassay of peroxides has increased considerably during the past decade. Special mention should be made of the prime importance of the general approaches to the synthesis of cyclic peroxides.^{10, 11, 16}

Nowadays, the chemistry of peroxides may be regarded as a new perspective in research in bioorganic chemistry and medicine.

G A Tolstikov Novosibirsk Institute of Organic Chemistry, Siberian Branch of the Russian Academy of Sciences, prosp. akad. Lavrent'eva 9, 630090 Novosibirsk, Russian Federation. Fax (7-383) 235 47 52. Tel. (7-383) 235 16 46

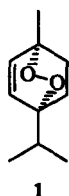
A G Tolstikov, O V Tolstikova Boreskov Institute of Catalysis, Siberian Branch of the Russian Academy of Sciences, prosp. akad. Lavrent'eva 5, 630090 Novosibirsk, Russian Federation. Fax (7-383) 235 57 66. Tel. (7-383) 239 73 50

Received 4 April 1996

Uspekhi Khimii 65 (9) 836–851 (1996); translated by R L Birnova

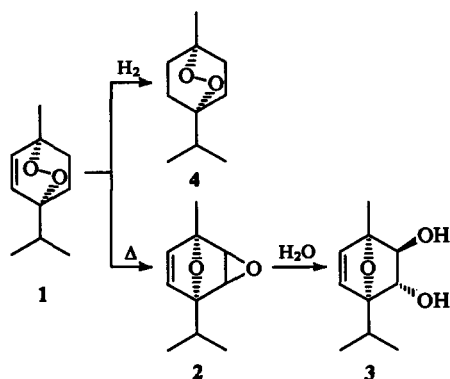
II. Naturally occurring peroxides and their biological activity

The first natural peroxy compound that has been isolated in an individual state is ascaridol **1**, which is present in the so-called chenopodium essential oil obtained by steam distillation of the plant *Chenopodium ambrosioides* L. This plant was cultivated in the USA and other countries specially for the purpose of obtaining an oil known as a potent anthelmintic agent. The peak of chenopodium oil production (up to 50 tons per year) was in 1930–1940.¹⁷ The ascaridol content in this essential oil amounts to 60%. The essential oil of the plant *Chenopodium hircinum* contains 40% of ascaridol. The essential oils of the yarrow *Achillea micrantha* M.B. and *Ajania fastigiata* contain 26%–51% of ascaridol.⁸



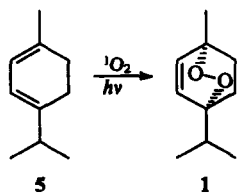
Apart from its potent anthelmintic action, ascaridol **1** is also active with respect to the central nervous system (CNS). It has been shown, in particular, that ascaridol displays a pronounced analgesic activity in the 'acetic convulsions' test and prolongs threefold the pentobarbital-induced anaesthesia. The ability of ascaridol at a dose of 100 mg kg⁻¹ to reduce body temperature in experimental animals by 1.5 °C has been reported.

When heated above 150 °C, ascaridol explodes, which explains the cases of explosive decomposition of the chenopodium oil as a result of careless distillation. Boiling of ascaridol in a solution of *p*-cymene is accompanied by the rearrangement of the peroxy group, eventually resulting in the dioxide **2** being further hydrated into the glycol **3** (Scheme 1). At the same time, the peroxy group of ascaridol appeared to be resistant to catalytic hydrogenolysis. Thus, hydrogenation of ascaridol gives the dihydro derivative **4**.

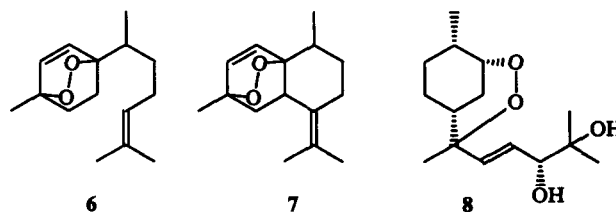


Scheme 1

Synthesis of ascaridol by photosensitised photooxidation of α -terpinene **5** occurs practically quantitatively.¹⁸



Many plants of the *Compositae* family produce sesquiterpene peroxides. For example, the sesquiterpene analogues of ascaridol **6** and **7** were detected in extracts of the plants *Rudbeckia laciniata* and *Senecio paludatus*,¹⁹ while the sesquiterpene peroxydiol qinghaosu-A **8** was isolated from the plant *Artemisia annua* used in Chinese folk medicine as an antimalarial.²⁰ An opinion was expressed that qinghaosu is an artefact, since it had been isolated from the plant that underwent storage.



The wild plant *A. annua* widely distributed throughout the Asian continent contains, apart from the steam-distilled essential oil, terpene extractives including 12 compounds of the cadinane series.

Unquestionably, the most remarkable of these compounds is lactone **9**, artemisinin, isolated and identified by Chinese investigators.^{12, 13} The artemisinin content in *A. annua* does not exceed 0.1%, reaching a maximum two weeks before the flowering of the plant.²¹ A search for other natural sources of artemisinin led to its discovery in the extract of the wormwood *Artemisia apiacea*.²¹ The sweet wormwood growing in Middle Asian countries and Kazakhstan contains up to 0.05% artemisinin.²² The artemisinin content in *A. annua* cultivated in Central Europe does not exceed 0.001%.²³ The interest in artemisinin can be inferred from the communication describing the introduction of the sweet wormwood in the USA.²⁴

Artemisinin possesses rather high antimalarial activity; its use as a medicinal agent is due to its ability to suppress the proliferation of the plasmodium clones resistant to many modern antimalarial drugs.

It is reported that the antimalarial activity of the qinghaosu peroxydiol **8** is of the same order of magnitude as that of artemisinin.²⁵ The assay of all the sesquiterpene peroxydiones described above revealed their significantly lower antimalarial activity than that of artemisinin.²⁶

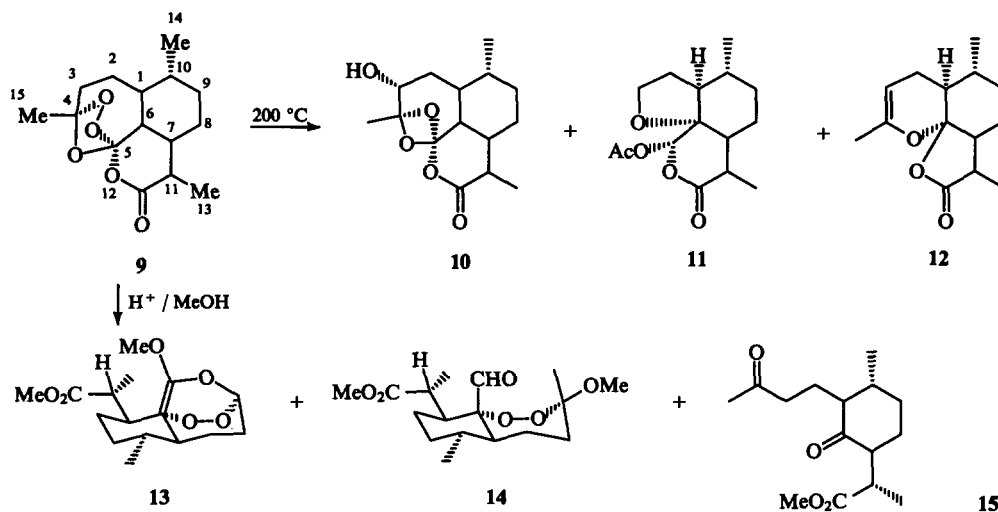
Artemisinin can regulate the plant growth. It has been shown that at a concentration of 5×10^{-6} M artemisinin inhibits the growth of the duckweed *Lemna minor*. Noteworthy, deoxyartemisinin devoid of the peroxy function does not display any inhibitory activity.²⁷

Artemisinin is a sufficiently stable compound, which not only permits its isolation in a pure state, but also makes it possible to obtain a wide range of derivatives retaining the peroxide bridge.

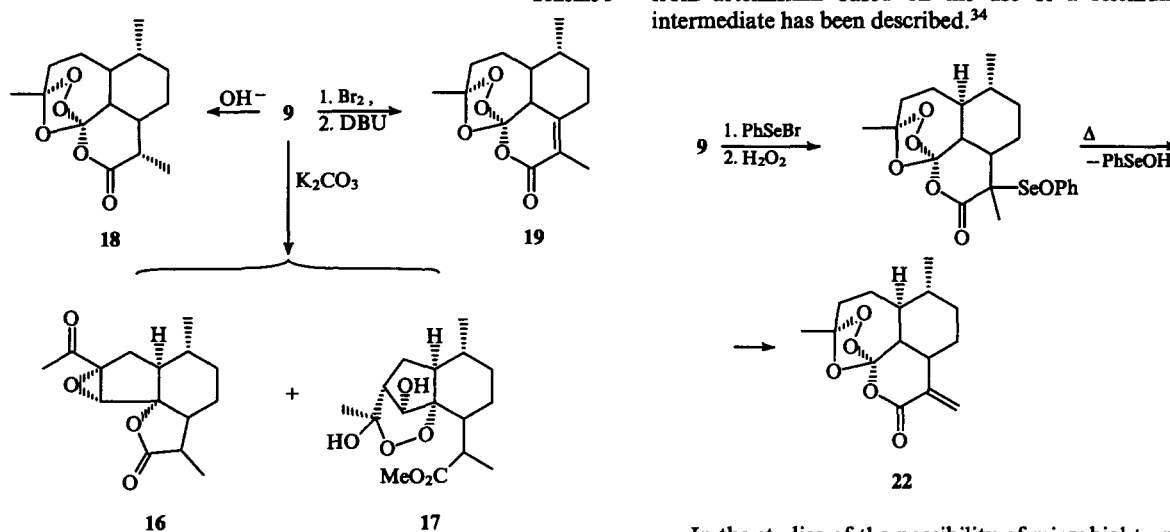
Thermal decomposition of artemisinin results in artemisinin D **10** and the products of more profound rearrangements of the molecule **11**, **12** (Scheme 2).²⁸ Upon treatment with a methanolic acid, artemisinin is converted into peroxy compounds **13** and **14** and the dioxo ester **15**.²⁹

It should be noted that artemisinin, like compounds **13** and **14**, possess high antimalarial activity. Treatment of artemisinin with K₂CO₃ in methanol yields products of intramolecular rearrangement **16**, **17**.³⁰ The preparation of 11-epiartemisinin **18** under alkaline conditions and a two-step conversion of artemisinin into isoartemisitene **19** have been described (Scheme 3).³¹

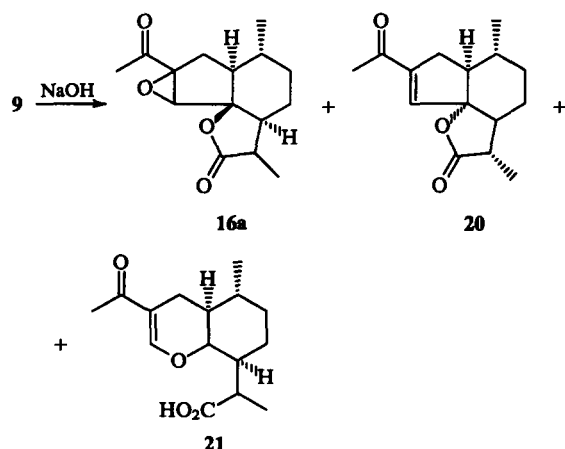
Scheme 2



Scheme 3



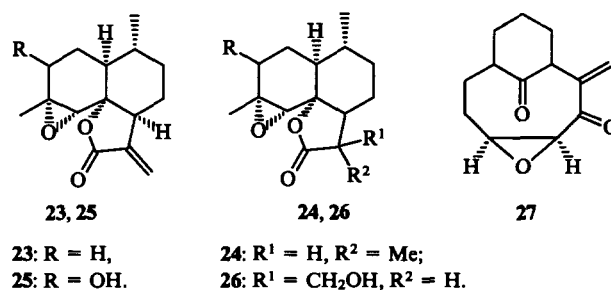
Treatment of artemisinin with alkali gives the epoxy ketone epimer 16a and oxo compounds 20, 21.³²



The peroxy lactone 22, artemisitene, has been found among the minor components of the extract of *A. annua*.^{12, 33} Its synthesis

from artemisinin based on the use of a selenium-containing intermediate has been described.³⁴

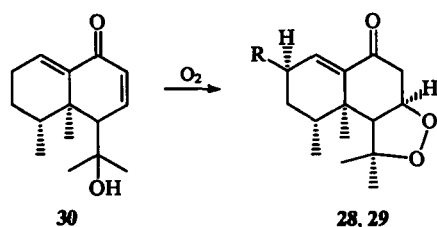
In the studies of the possibility of microbial transformations of artemisinin in the plant, it has been shown³⁵ that *Aspergillus flavipes* converts one of the components of *A. annua*, artemisinin B 23, into the dihydro derivative 24, while *Beauveria bassiana* transforms the compound 23 into the hydroxy lactones 25 and 26.



UV irradiation of artemisinin B gives the product of profound skeletal rearrangement, lumiartemisinin B 27.³⁶

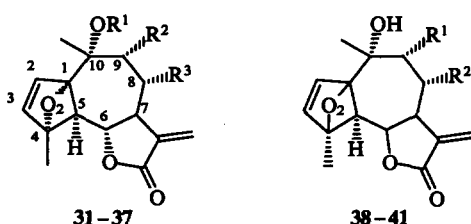
The plant *Nardostachys chinensis* Batalin of the Valerianaceae family is also extensively used in Oriental medicine. To the active extracts of this plant one can refer the oxo peroxides nardosinone 28 and canchone 29.^{37, 38} Nardosinone is a cycloperoxy

derivative of the hydroxyketone **30** (canthone A) and is present in the above plant together with the peroxides **28** and **29**.³⁹



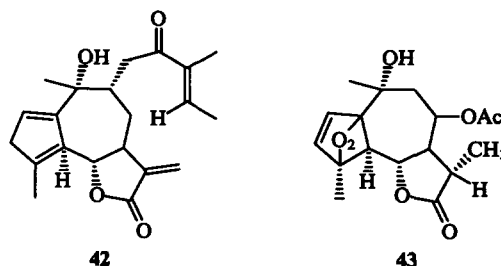
28: R = H, **29**: R = OH.

The isolation of a series of 1,4-peroxy lactones **31–41** of the guaiane type differing in not only substituents, but also in the configuration of the peroxide cycle (Tables 1, 2)^{40–45} has been described. Some of these compounds (e.g., the peroxy lactones **31–33** and **38–41**) manifest weak antimalarial activity.

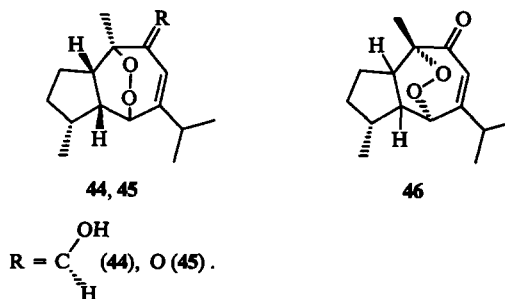


It should be noted that isoachillofolidiene **42**,⁴⁶ the precursor of the peroxides **38–41**, was isolated from the leaves of the yarrow *Achillea millefolium*, while its dihydro derivative **43** was isolated, along with the esomontanine **41**, from the leaves of the yarrow *Artemisia montana* (Scheme 4).⁴⁵

Some sesquiterpenes of the guaiane type contain a peroxide bridge in a 7-membered cycle. For example, the 6 β ,10 β -peroxides,



chanalpinol **44**, chanalpinone **45**, and isochanalpinone **46** were isolated from the plant *Alpinia japonica*.^{47, 48}



One of the constituents of this plant is the peroxide alpinolide **47**. Its structure sheds more light on the biosynthetic pathways of the furoperargones A and B **48**, **49**, which are also present in this plant.

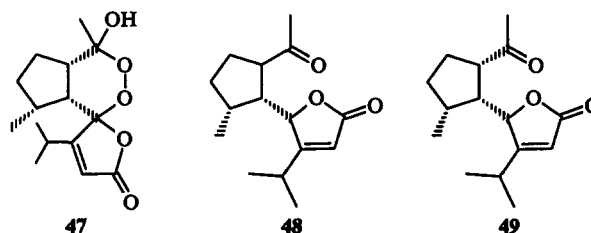
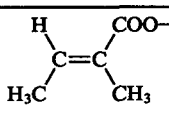
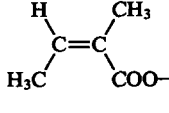
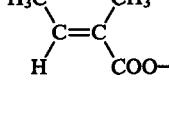


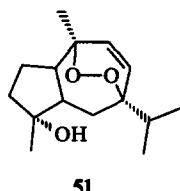
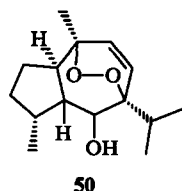
Table 1. Some representatives of 1 α ,4 α -peroxylactones of the guaiane type.

Compound	Name of the peroxide and its source	R ¹	R ²	R ³	Ref.
31	Apressin, <i>Achillea depressa</i>	H	OAc	H	40, 41
32	Isoapressin, <i>Achillea ligustica</i> , <i>A. depressa</i>	Ac	H	H	40
33	Peroxyachifolide, <i>A. millefolium</i>		OH	H	42–44
34	<i>A. millefolium</i>	Ac	OH	H	44
35	<i>A. millefolium</i>		OH	H	44
36	<i>A. millefolium</i>		OH	H	44
37	<i>A. millefolium</i>	H	H		44

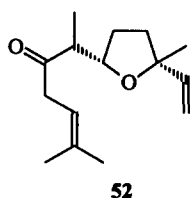
Table 2. Some representatives of 1 β ,4 β -peroxylactones of the guaiane type.

Compound	Name of the peroxide and its source	R ¹	R ²	Ref.
38	β -Peroxyisoachiofolide, <i>Achillea millefolium</i>		H	42-44
39	<i>Athunasia</i>		H	41
40	<i>Athunasia</i>		OH	41
41	Exomontanine, <i>Artemisia montana</i>	H	OAc	45

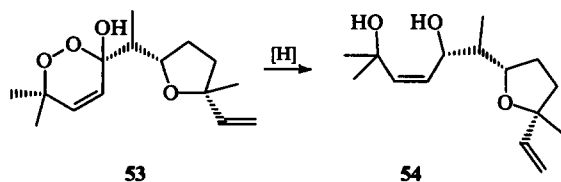
The Peruvian plant *Lialum floribundum* contains 7 β ,10 β - and 1 β ,10 β -peroxides, compounds **50** and **51**.⁴⁹



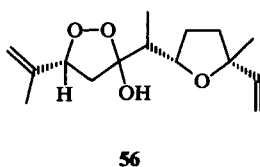
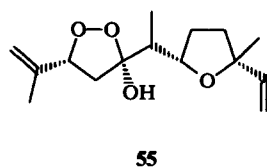
A group of peroxides structurally related to the sesquiterpene alcohol nerolidol has been described. Their precursor is davanone **52** isolated from the leaves of the tansy *Tanacetum vulgare*.⁵⁰



This plant also contains the peroxyketal **53**, whose structure was confirmed by its reduction into the diol **54**.

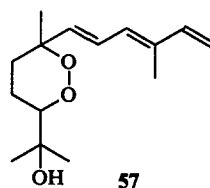


Peroxyketones of the davanone type **55** and **56** were isolated from the extracts of the yarrows *Artemisia maritima* and *A. abrotanum*.^{51, 52}

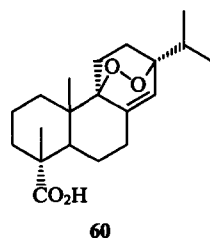
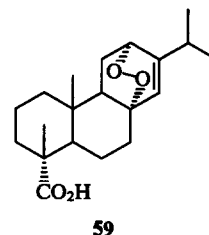
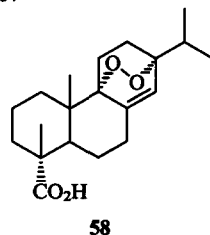


It is to be noted that compounds **53**–**56** possess a weak anti-malarial activity.

The dark blotches formed on the apple peel on storage contain the triene peroxide **57**.⁵³

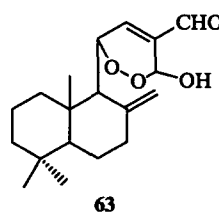
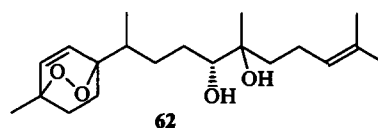
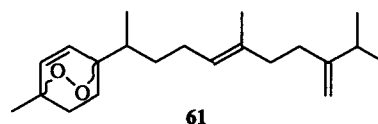


Peroxides of the diterpene type occur less frequently. Endoperoxides formed from resin acids are the most common representatives of this group. The endoperoxides of palustic **58** and levopimaric **59** acids were isolated from the needles of the Siberian fir.⁵⁴

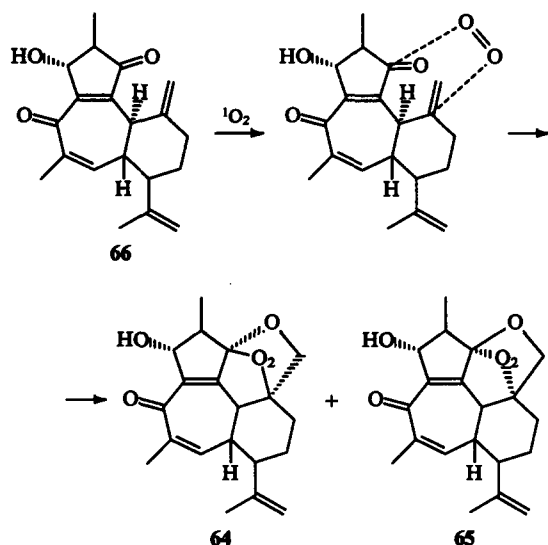


The peroxide **58** and its enantiomer **60** are the components of the plant *Elodea canadensis*.⁵⁵

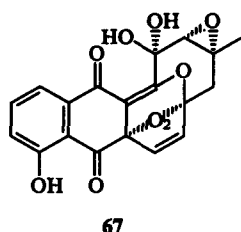
The diterpene analogues of ascaridol differing in the configuration of the peroxide cycle (**61**, **62**) are present in the wormwood *A. absintium*.⁵⁶ The monocyclic peroxydiol **62** was found in the plant *Helichrysum acutatum*.⁵⁷ The plant *Hedichium coronarium* used in Brazilian folk medicine as an antirheumatic agent contains, along with other terpenoids, coronarin B **63**, a peroxide of the labdane type.⁵⁸



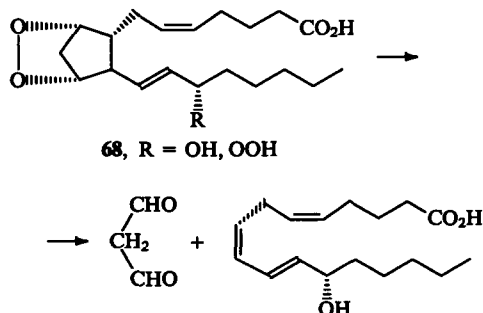
The bark of the tree *Jatropha grossidentata* is used by the Indian population of Paraguay as an antiparasitic means. The active principle of the bark extract are canioyan **64** and bisepicanioyan **65**. It has been suggested that both peroxides are formed as a result of an unusual attack of singlet oxygen at the diketone yatrogrossidione **66**, which has also been isolated from the extract of this plant.⁵⁹



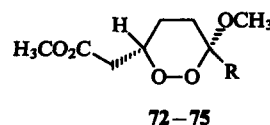
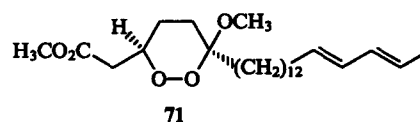
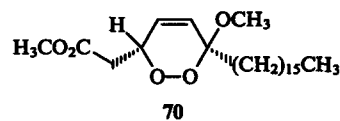
The peroxide **67** is of microbial origin; it is produced by *Streptomyces phaeochomogenes*.⁶⁰



As already mentioned in the Introduction, prostaglandin endoperoxides **68** are formed from arachidonic acid under the action of prostaglandin cyclooxygenase.¹⁻⁶ The main pathways of their metabolism are as follows: synthesis of prostaglandins D₂, E₂, and F_{2α} by isomerases, synthesis of thromboxanes A₂ and B₂ by thromboxane synthetase and prostacyclin synthesis by prostacyclin synthetase; they also undergo degradation resulting in the formation of malonaldehyde and (12*R*)-hydroxyheptadeca-(5*Z*,8*Z*,10*E*)-trienoic acid.⁵

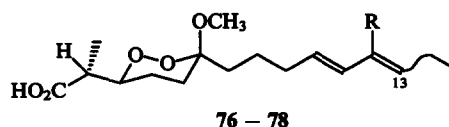


Peroxides isolated from marine organisms constitute a rather large group. Among them, the peroxides MeCH(O_nH)OOEt **69** produced by the Ascidia, *Phallusia mamillata*, *Ascidia ahodori*, *Styela plicata*, and *Halocynthia roretzi* have the most simple structure.⁶¹ Of special interest are the 1,2-dioxane derivatives formed from linear unsaturated acids. For example, chondrillin **70** and xestins A and B **71**, **72** were isolated from the sponges *Xestospongia*⁶² and *Chondriella*,⁶³ while peroxy esters **73**–**75** were isolated from the sponge *Plakortis lita*.⁶⁴ The compounds **69**–**74** possess a cytostatic activity.

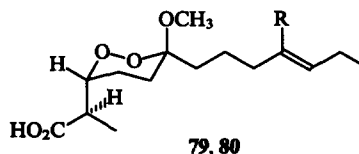


R = (CH₂)_n (n = 12 (**72**), 9 (**73**), 7 (**74**)), (CH₂)₁₁CH₃ (**75**).

The sponges of the *Plakortis* genus produce a wide variety of peroxy acids, five of which [the peroxyplakoric acids A₁, A₂, A₃ (**76**–**78**), B₁ and B₃ (**79**, **80**)] have been isolated and identified.⁶⁵

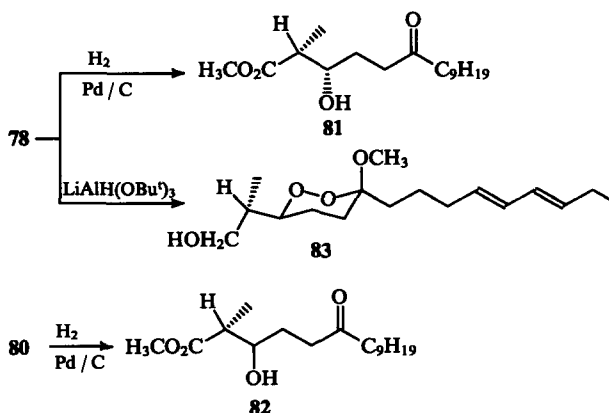


76: R = CH₃, 13*E*,
77: R = CH₃, 13*Z*,
78: R = H, 13*E*.

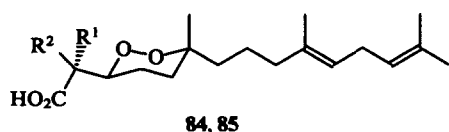


R = CH₃ (**79**), H (**80**).

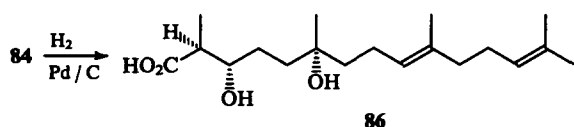
The configuration of the peroxy acids **78** and **80** has been confirmed by their hydrogenation into the diastereoisomeric hydroxy oxo esters **81** and **82**, while the stability of the peroxide cycle is corroborated by the isolation of the compound **83** upon the reduction of the methyl ester of the acid **78** with LiAlH(OBu^t)₃.



The diastereoisomeric isoprenoid peroxy acids **84** and **85** were isolated from the sponges *Latruncularia*.

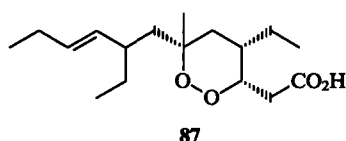


84: $R^1 = \text{CH}_3$, $R^2 = \text{H}$;
85: $R^1 = \text{H}$, $R^2 = \text{CH}_3$.

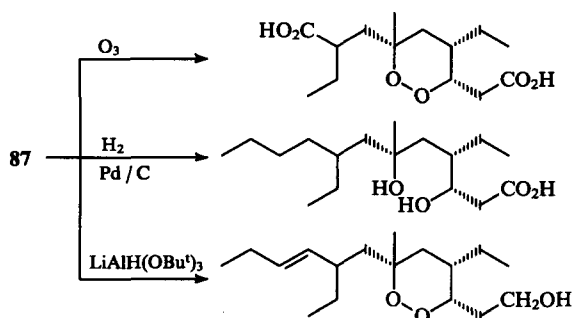


The configuration of the former peroxy acid has been confirmed by hydrogenation into the dihydroxy acid **86**.⁶⁶

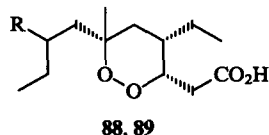
Branched-chain peroxides are produced by some species of marine sponges and, what is remarkable, at surprisingly high concentrations. For example, plakortin **87** was isolated from the reef sponges *Plakortis halihondrioides* with a 5.7% yield of the dry weight.⁶⁷



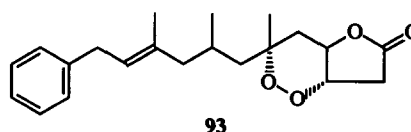
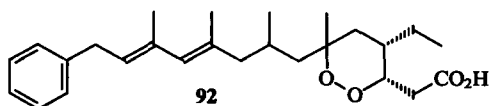
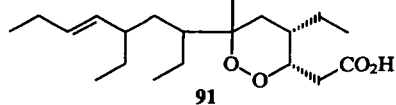
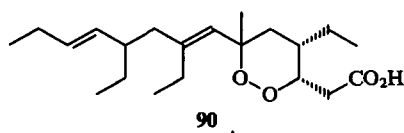
The transformations of this compound carried out in the course of structural analysis, testify to a high resistance of the peroxy group to reducing and oxidising reagents.



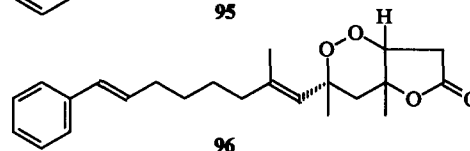
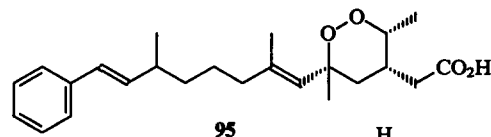
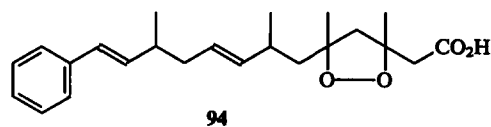
The sponges *Plakortis halihondrioides* contain a wide range of peroxides: 3-epiplakortin **88**, its dihydro derivative **89**, the unstable peroxides **90** and **91**, as well as the aryl-substituted peroxy acid **92**, its methyl ester, and lactone **93**.⁶⁸



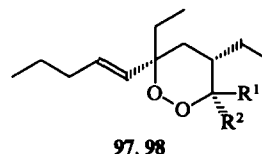
$R = (\text{CH}_2)_2\text{CH}=\text{CHCH}_3$ (**88**), C_4H_9 (**89**)



The sponges of the *Plakortis* genus contain plakininic acids **A** and **B** **94, 95** and plakortolide **96**.^{69, 70}



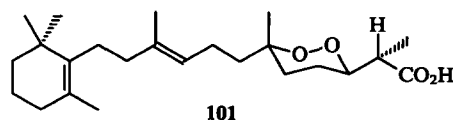
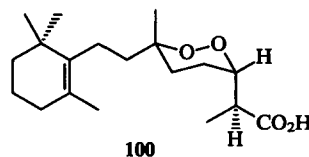
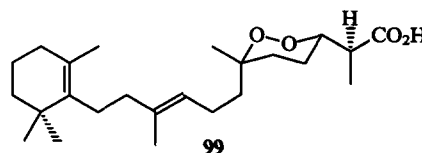
The Caribbean sponge *Chondrosia colletrix* produces the epimeric acids **97** and **98** and their methyl esters, whose content amounts to 6% of the dry weight.⁷¹



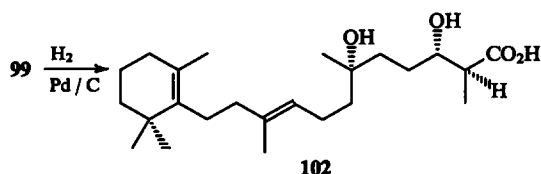
97: $R^1 = \text{CO}_2\text{H}$, $R^2 = \text{H}$;
98: $R^1 = \text{H}$, $R^2 = \text{CO}_2\text{H}$.

It is worth noting that the compounds **95–98** possess antimicrobial and antifungal activities.

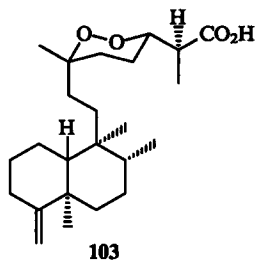
Mono- and bi-cyclic isoprenoid peroxy acids were first described in 1979. It was reported that the sponges *Prianos* dwelling in the Red Sea contain up to 1.5% of the peroxide **99**,⁷² which was also found in the coral reef sponges together with the peroxy acid **100**.⁷³ The sponges of the *Latrunculata* genus contain the peroxide **100** and the peroxy acid mugubilin **101**.⁶⁶



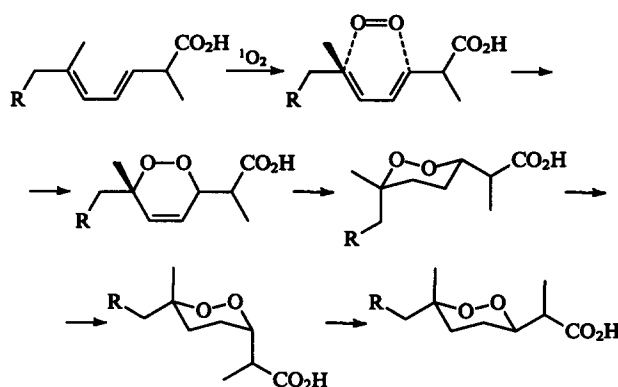
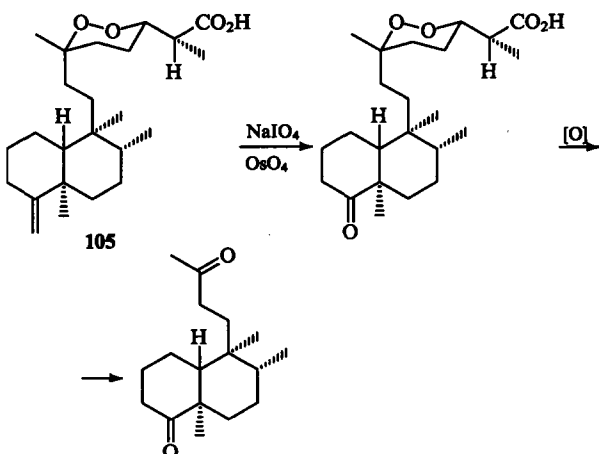
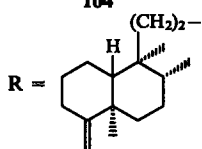
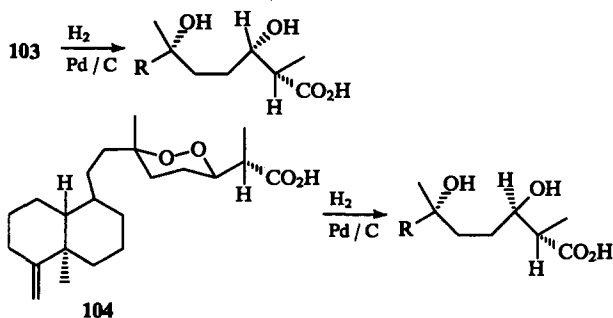
To confirm the configuration of the peroxy group in the compound **99**, the former was hydrogenated resulting in the dihydroxy acid **102**.



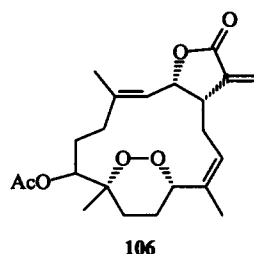
Sigmosceptrellin A 103, whose structure was established by the X-ray analysis, was isolated from the extract of the sponges *Sigmosceptrella laevis*.⁷⁴



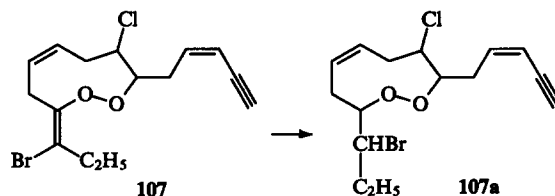
Later, the isolation of sigmosceptrellins B and C 104, 105 and a series of transformations confirming their structure was reported.⁷⁵



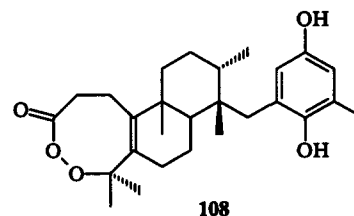
Among metabolites of marine organisms, compounds of a cembrane series were found, which possessed high cancerostatic, antimicrobial, and fungicidal activity.⁷⁶⁻⁸³ For example, the ichthyotoxic coral *Lobophytum denticulatum* contains the cembranoid peroxide denticulatolide 106, whose structure was established by X-ray analysis, while the correct conformations were calculated by using the molecular mechanics method.⁸⁴⁻⁸⁷ The denticulatolide displays an antitumour activity.



The halogen-containing peroxide rhodophytin 107 has been isolated from the algae of the *Laurencia* genus; it isomerises on storage in solution into the compound 107a.^{64, 88}



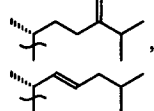
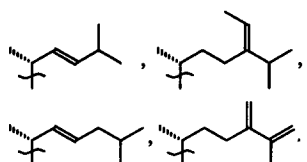
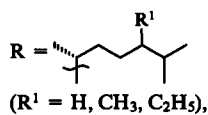
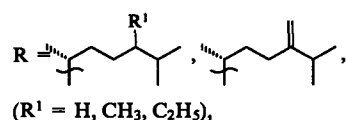
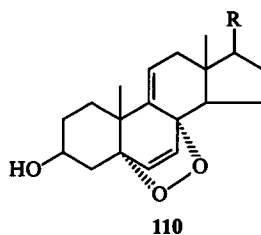
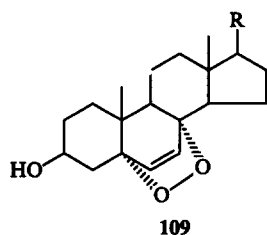
The terpenoid peroxy ester 108 is produced by the brown algae *Taonia atomaria*.⁸⁷



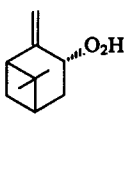
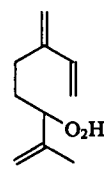
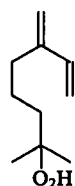
Steroid endoperoxides are distributed in marine organisms fairly widely. For example, the sponge *Tethya aurantia* contains four 6,9-endoperoxides of the type 109;⁸⁷ 16 peroxides, whose structures resembled those of 109 and 110, have been isolated from the extracts of the sponges *Ascidia nigru*, *Dendrogyra cylindrus*, *Thalysias juniperiana*, and *Aplysia dactiolumea*.⁸⁹

The compounds 99–101 have a cytostatic activity, whereas the compounds 102–105 manifest an ichthiostatic action.

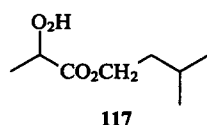
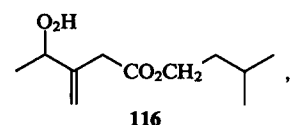
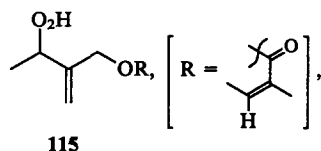
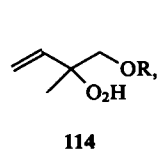
The formation of peroxy acids occurs, most probably, with the participation of enzymes producing singlet oxygen as well as hydrogenases and isomerases.⁶⁶



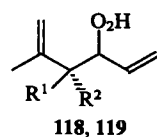
Hydroperoxides of terpene and steroid structures are produced by higher plants and marine organisms. For example, myrcene hydroperoxides 111, 112 have been isolated from the extracts of the leaves of the wormwood *A. annua*,⁹⁰ while the trans-pinocarveyl hydroperoxide 113, from the leaves of the plants *Anthemis nobilis*,⁹¹ *Chenopodium ambrosioides*,⁹² and *Achillea filipendulina*.⁹³



The plant *Anthemis nobilis* contains hydroperoxides, the derivatives of the esters of prenolic and aliphatic alcohols and the acids 114–117.⁹¹

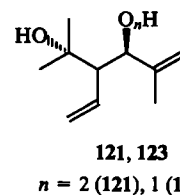
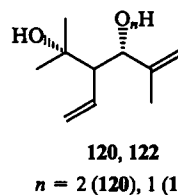


The medicinal plant *Achillea filipendulina* was used as a source of monoterpenes of a new structural type.⁹⁴ The extraction of the aerial parts of this plant results in four hydroperoxides of the achillene series.⁸⁸ Two of them, 118 and 119, have also been found in the extract of the wormwood *A. lamcea*.⁹⁵

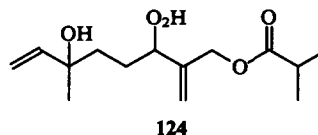


118: R¹ = H, R² = CH=CH₂;
119: R¹ = CH=CH₂, R² = H.

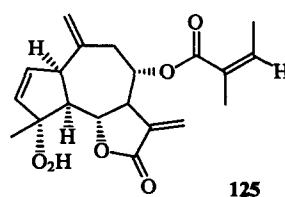
The structure of the hydroperoxides 120 and 121 was corroborated by X-ray analysis and by their reduction into the stereoisomeric diols 122 and 123.⁹⁵



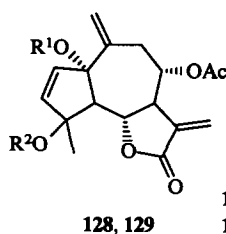
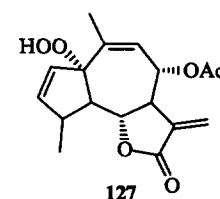
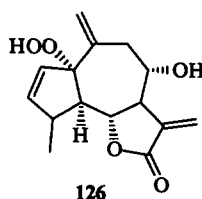
The monoterpene hydroperoxide 124 structurally related to linalool has been isolated from the plant *Ferrea fruticosa*.⁹⁶



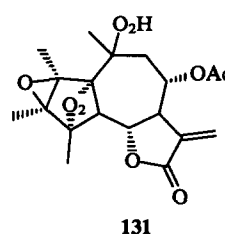
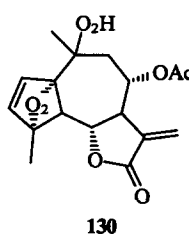
The isolation of several hydroperoxides of the guaiane type has been described. For example, the above-mentioned plant *Anthemis nobilis* contains the hydroxyperoxy lactone 125.⁹¹



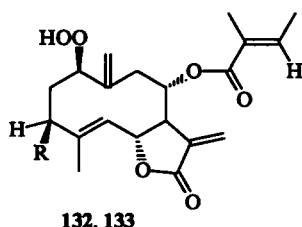
The plant *Cacosmia rugosa* produces the hydroperoxides 126 and 127,⁹⁷ while the peroxy lactone hydroperoxides 130, 131⁹⁸ could be isolated from the plant *Bishopanthus solicens* together with the hydroperoxides 128 and 129.



128: R¹ = OH, R² = H;
129: R¹ = H, R² = OH.

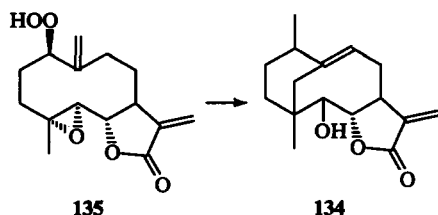


The hydroxyperoxy lactone of the germacrane series 132 has been isolated from the leaves of the plant *Anthemis nobilis*,^{91,99} while its dihydroxy derivative 133 is present in the plant *Ferrea fruticosa*.⁹³

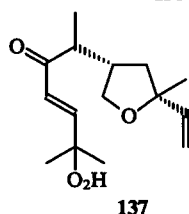
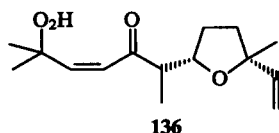


R = H (132), OH (133).

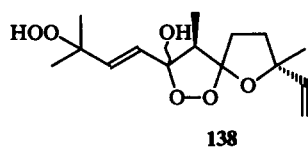
The tansy *Tanacetum vulgare* produces the cryspolide 134. It has been postulated that the latter is formed in the plant from the peroxyartenolide 135.¹⁰⁰



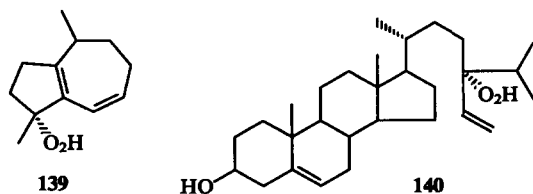
The hydroxyperoxide derivatives of davanone 50 have been isolated from the extracts of the tansy and some wormwood species. For example, flowers of the plant *Tanacetum vulgare* contain the *Z*-hydroperoxide 136, while its leaves contain the *E*-isomer 137.⁵⁰



The latter has been isolated from the southernwood *Artemisia abrotanum*⁵² as well as from the aerial parts of the wormwood *A. maritima*⁵¹ and *A. inculta*.¹⁰¹ The peroxyhydroperoxide 138 is produced by the plant *A. abrotanum*.⁵²



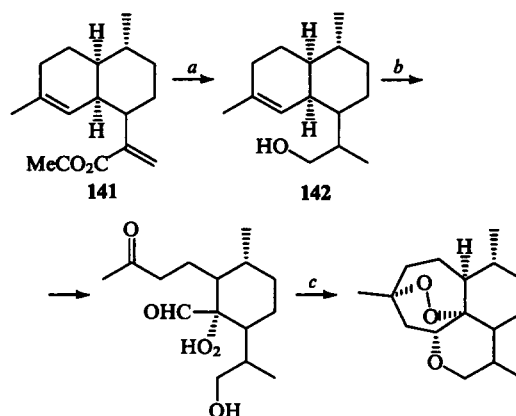
The hydroperoxide clavukerin C 139 has been isolated from the coral *Clavularia koellikeri*,¹⁰² and the steroid 140 is present in the plankton *Phallusia mamillata*.¹⁰³



III. Synthesis of artemisinin, its derivatives and structural analogues

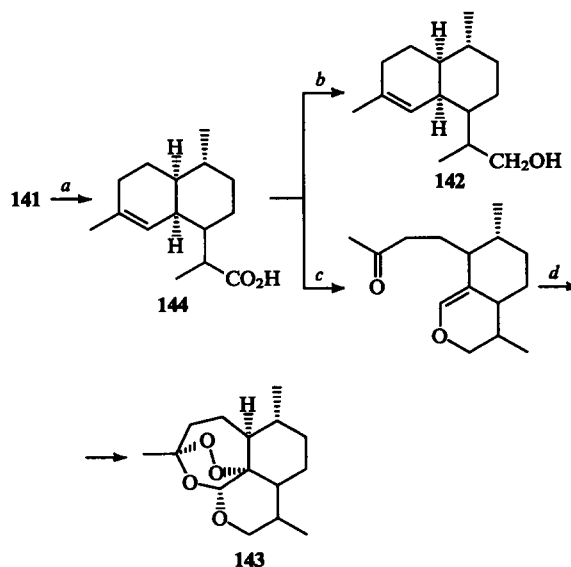
In the discussion of the pathways of synthesis of artemisinin and its structural analogues, we have deliberately excluded from the synthetic schemes those stages which have no principal significance, by omitting certain experimental details. The main attention was then focussed on the methods used in the synthesis of the peroxy fragments of the molecules. They involve the oxidation by singlet (photoexcited) oxygen, ozonisation, and the use of unique reagents, such as $\text{Et}_3\text{SiO}_3\text{H}$.

One of the most promising approaches to the synthesis of artemisinin is based on the use of artemisinic acid 141 as the starting compound. Its content in *Artemisia annua* exceeds by one order of magnitude that of artemisinin, and its isolation is much easier. The synthesis of (+)-deoxyartemisinin 143 can be carried out in only three stages via the hydroxy compound 142.¹⁰⁴



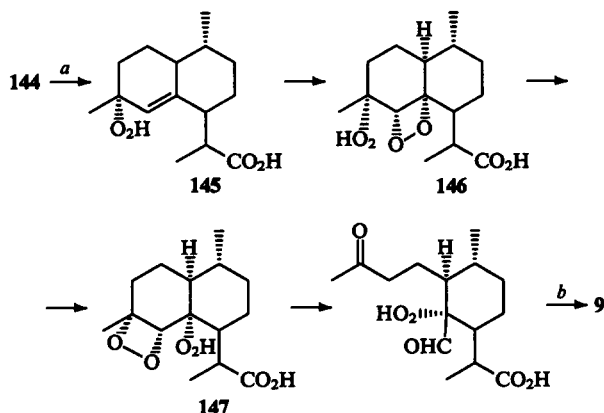
(a) LiAlH_4 , $\text{NiCl}_2 \cdot 6\text{H}_2\text{O}$; (b) O_2 , $h\nu$, Methylene Blue; (c) Dowex H^+ .

An alternative synthesis of the compound 143 has been described, which requires more steps and includes the formation of dihydroxyartemisinic acid 144 at the first stage by reduction of the acid 141 with nickel boride.¹⁰⁵



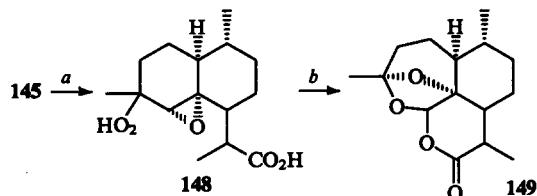
(a) NaBH_4 , $\text{NiCl}_2 \cdot 6\text{H}_2\text{O}$; (b) LiAlH_4 , Et_2O ; (c) O_3 , MeOH , Me_2S , $p\text{-TsOH}$, xylene; (d) O_2 , $h\nu$, Methylene Blue, $\text{CF}_3\text{SO}_2\text{OSiMe}_3$.

The synthesis of artemisinin based on sensitised photooxidation of the dihydroxy acid **144** is initiated by the formation of the hydroperoxide **145** and further proceeds via the dioxetans **146** and **147**.¹⁰⁶



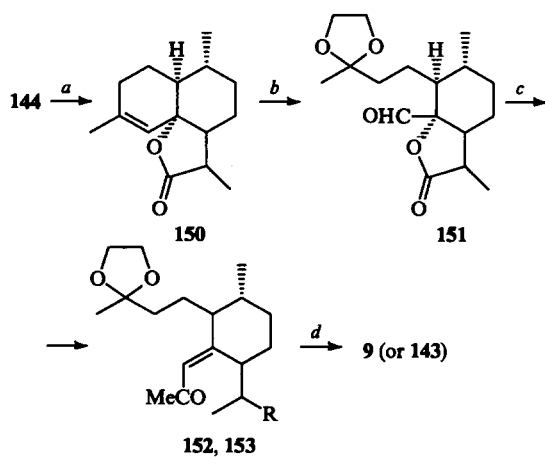
(a) O_2 , $h\nu$, Methylene Blue; (b) Dowex H^+ .

It has to be noted that the unstable epoxide **148** formed from the hydroxyperoxide **145** is converted into the deoxyartemisinin **149**.¹⁰⁷

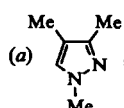


(a) $m\text{-ClC}_6\text{H}_4\text{CO}_3\text{H}$, CHCl_3 ; (b) $p\text{-TsOH}$.

An interesting conversion of dihydroxyartemisinic acid **144** into artemisinin **9** has been described.¹⁰⁸ Its key stage is the allylic oxidation of the acid **144** by the CrO_3 -3,5-dimethylpyrazole complex into the lactone **150**, which after ozonolysis and ketalisation gives the aldehydo lactone **151**. This is followed by the synthesis of the enol ester **152** and the photooxidation sensitised with Bengal rose. This method can also be used to obtain deoxyartemisinin **143** by the reduction of the methoxycarbonyl group in the compound **152** and photooxidation of the compound **153**.



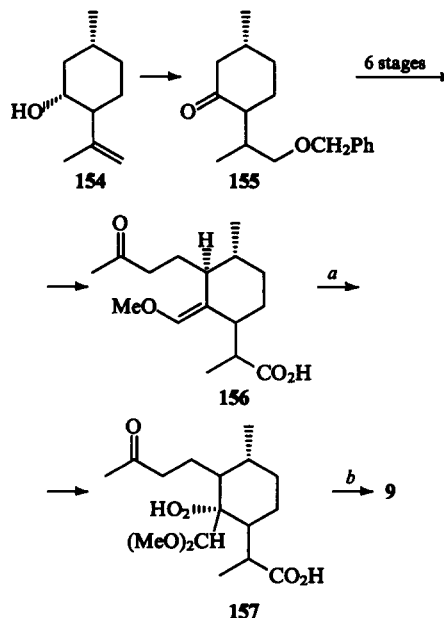
$R = \text{CO}_2\text{Me}$ (**152**), CH_2OH (**153**)



(a) CrO_3 ; (b) O_3 , $[\text{Me}_3\text{SiOCH}_2]_2$, $\text{CF}_3\text{SO}_2\text{OSiMe}_3$;

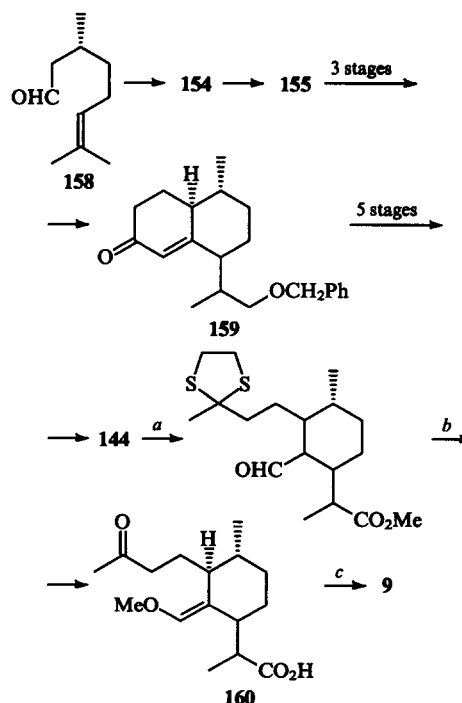
(c) Na -naphthalene, CH_3I ; (d) O_2 , $h\nu$, Bengal Rose, HClO_4 .

The synthesis of artemisinin from more simple optically active precursors are multistep. For example, the use of isopulegol **154** entails its functionalisation to form 8-benzyloxymenthone **155** and the subsequent six-step conversion of the compound **155** into the oxo acid **156**. Photooxidation of the acid **156** in the presence of Methylene Blue gives the hydroperoxide **157**, which further cyclises into artemisinin.¹⁰⁹



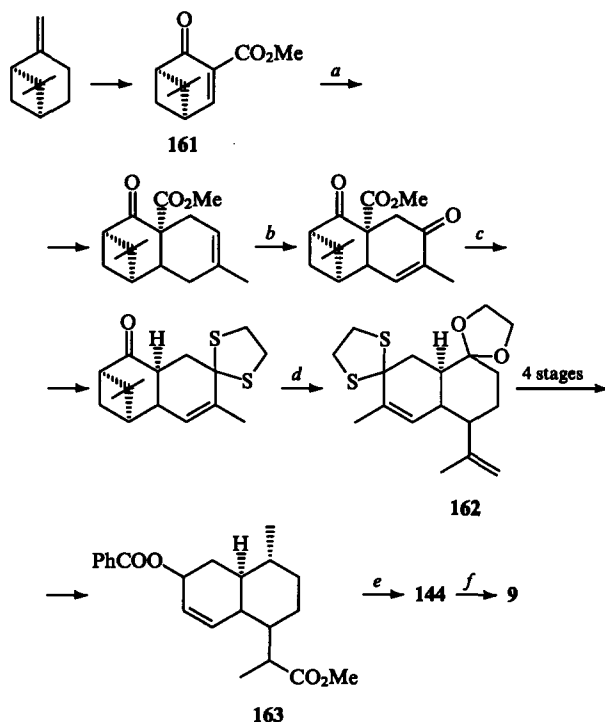
(a) O_2 , $h\nu$, Methylene Blue; (b) HCO_2H , CH_2Cl_2 .

The synthesis of artemisinin based on citronellal **158**, which is readily converted into isopulegol **154** and, further, into the ketone **155**, entails the annelation according to Robinson. The ketone **159** formed thereby is converted into dihydroartemisinic acid **144**, from which artemisinin is then obtained in three steps. Photooxidation of the artemisinin precursor, the compound **160**, was sensitised with Bengal Rose.¹¹⁰



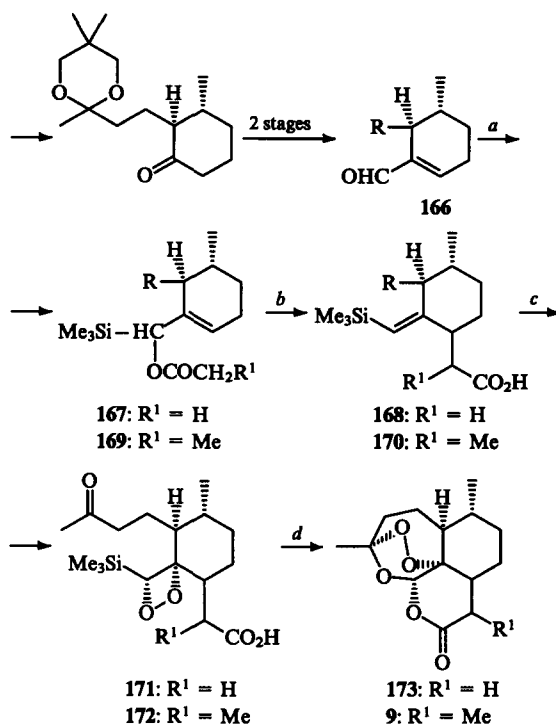
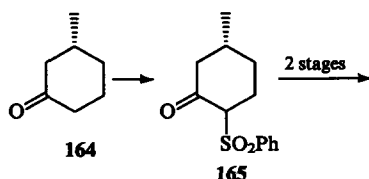
(a) O_3 , Me_2S , $\text{HS}(\text{CH}_2)_2\text{SH}$, $\text{BF}_3 \cdot \text{OEt}_2$; (b) $\text{HC}(\text{OMe})_3$, $p\text{-TsOH}$, HgCl_2 ; (c) O_2 , $h\nu$, Bengal Rose, HClO_4 .

The synthesis of artemisinin based on the use of β -pinene is remarkable in that the specific rotation of the synthetic, optically active (+)-artemisinin did not practically differ from that of the natural sample.¹¹¹ The ZnCl_2 -controlled interaction of dienophile **161** with isoprene, the scission of the picean bond resulting in the ketal **162**, and hydrogenolysis of the benzoyloxy group in the compound **163** by nickel boride giving the dihydroartemisinic acid **144**, are worth noting.



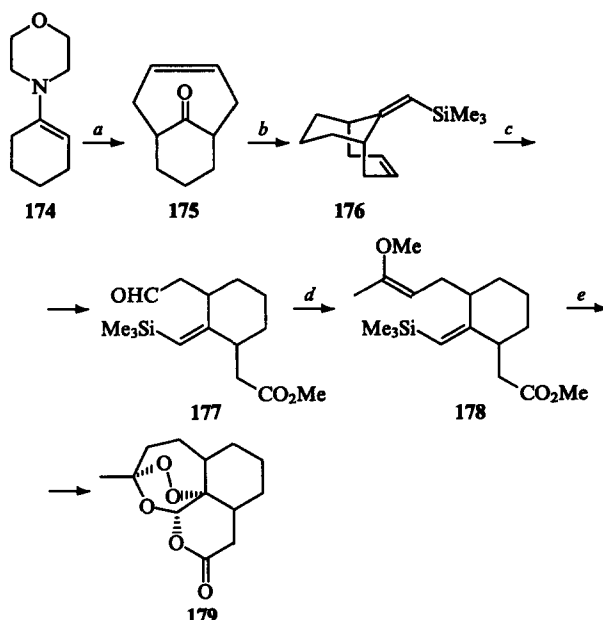
(a) $\text{CH}_2=\text{CH}-\text{CMe}=\text{CH}_2$, ZnCl_2 ; (b) O_2 , $h\nu$, 5,10,15,20-tetraphenyl-21*H*,23*H*-porphyrin, Ac_2O , $\text{C}_5\text{H}_5\text{N}$, 4-dimethylaminopyridine; (c) $(\text{CH}_2\text{SH})_2$, LiI , DMF ; (d) $(\text{CH}_2\text{OH})_2$, $p\text{-TsOH}$; (e) NaBH_4 , $\text{NiCl}_2 \cdot 6\text{H}_2\text{O}$; (f) O_2 , $h\nu$, Methylene Blue, $\text{CF}_3\text{CO}_2\text{H}$, O_2 .

An approach based on the use of the optically active 3-methylcyclohexanone **164** is interesting in that the natural configuration on the C(10) atom in the artemisinin molecule is created initially.¹¹² The synthesis involves via the formation of the oxosulfoxide **165**, which is converted in several steps into the aldehyde **166**. This is followed by a remarkable transformation of the formyl group under the action of the organoaluminium reagent, $(\text{Me}_3\text{Si})_3\text{Al} \cdot \text{OEt}_2$, with subsequent acetylation, resulting in the silyl acetate **167**. The Ireland rearrangement using lithium cyclohexylisopropylamide gives the unsaturated silane **168**. If the propionate **169** is employed instead of the acetate **167**, the rearrangement results in the silane **170**. Ozonisation of the compounds **168** and **170** occurs through the formation of the 1,2-dioxetanes **171** and **172**, which are further converted in the presence of $\text{CF}_3\text{CO}_2\text{H}$ into demethylartemisinin **173** or artemisinin **9**.



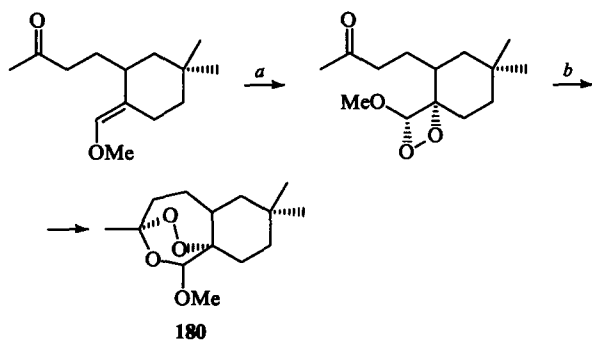
(a) $(\text{Me}_3\text{Si})_3\text{Al} \cdot \text{OEt}_2$; (b) $\text{C}_6\text{H}_{11}\text{Pr}^i\text{NLi}$; (c) O_3 , MeOH ; (d) $\text{CF}_3\text{CO}_2\text{H}$, H_2O .

The total synthesis of 13,14-bisnorartemisinin **179** from non-chiral precursors begins with alkylation of the enamine **174** with (*Z*)-1,4-dichlorobutene.¹¹³ This is followed by olefination of the ketone **175** to give silane **176** and ozonolysis of **176** to form the aldehyde **177**. This elegant synthesis is completed by olefination of the compound **177** and ozonolysis of the enolsilane **178**.



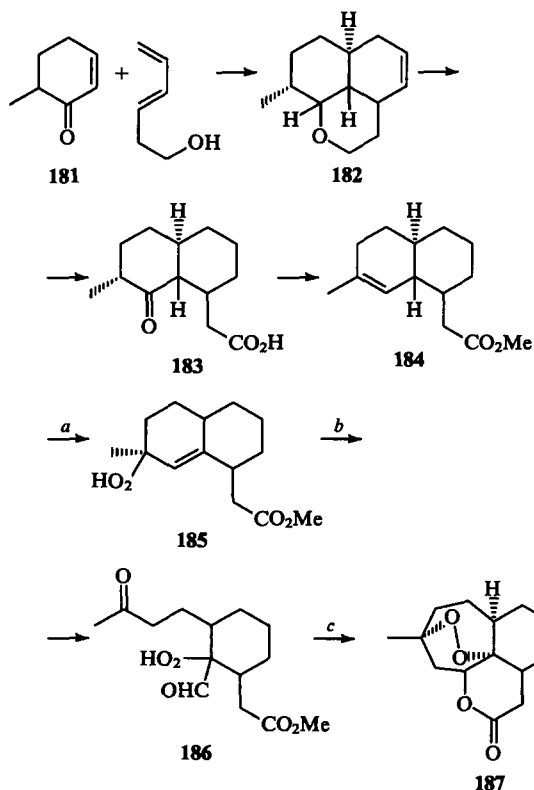
(a) $Z\text{-ClCH}_2\text{CH}=\text{CHCH}_2\text{Cl}$, H_2O ; (b) $\text{LiCH}(\text{SiMe}_3)_2$; (c) O_3 , Ac_2O , CH_2N_2 ; (d) $\text{Ph}_2\text{P}(\text{O})=\text{C}(\text{OMe})\text{Me}$; (e) O_3 , $\text{CF}_3\text{CO}_2\text{H}$.

Singlet oxygen needed for the synthesis of dioxetans can be obtained from the hydrotrioxide, $\text{Et}_3\text{SiO}_3\text{H}$.¹¹⁴ Thus, the synthesis of the model compound **180** exhibiting a high antimalarial activity is realised according to the following scheme:



(a) $\text{Et}_3\text{SiO}_3\text{H}$; (b) $\text{CF}_3\text{SO}_2\text{SiMe}_3$.

A structural analogue of artemisinin was synthesised on the basis of 6-methylcyclohex-2-en-1-ol **181**. The Diels–Alder synthesis of hexa-3,5-dien-1-ol with 6-methylcyclohex-2-en-1-ol gives the hemiketal **182**, whose oxidation and subsequent hydrogenation results in the oxo acid **183**. This is followed by the conversion of the acid **183** into the ester **184** and its photooxidation into the hydroperoxy ester **185** in the presence of Bengal Rose. The resulting ester **185** is subjected to oxidation in the presence of an iron–phenanthroline complex, $\text{Fe}(\text{Phen})_3(\text{PF}_6)_3$, and copper triflate, resulting in the hydroperoxide **186** further cyclised in acid medium into the peroxy lactone **187**.¹¹⁵

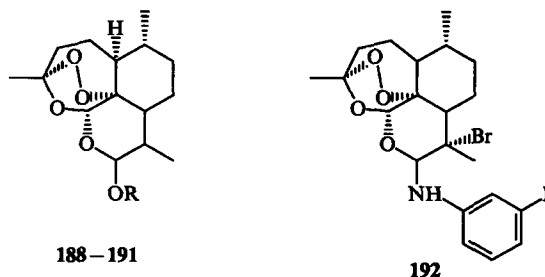


(a) O_2 , $h\nu$, Bengal Rose; (b) O_2 , $\text{Fe}(\text{Phen})_3(\text{PF}_6)_3$, $(\text{CF}_3\text{SO}_2)_2\text{Cu}$; (c) p -TsOH.

The uniqueness of artemisinin as an antimalarial drug¹¹⁶ posed the question as to the synthesis of artemisinin derivatives more active and convenient in application, of which dihydro esters and aminoacetals are becoming increasingly important. For example, the hydrogen succinate **188** in the form of sodium salt

can be used for intravenous administration instead of the poorly water-soluble artemisinin.¹¹⁷

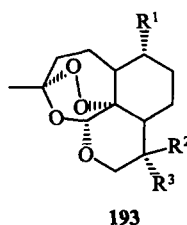
Prolonged activity was found in the glycoside **190**.¹¹⁸ The esters **191**¹¹⁹ and **192**¹²⁰ displayed a high activity against the plasmodia D-6 and W-2.



188: $\text{R} = \text{CO}(\text{CH}_2)_2\text{CO}_2\text{Na}$;
189: $\text{R} = \beta\text{-D-Glu}(1\rightarrow4)\text{-}\beta\text{-D-Glu}$;
190: $\text{R} = \text{CH}_2\text{CO}_2\text{Me}$;
191: $\text{R} = \text{CH}_2\text{C}_6\text{H}_4\text{CO}_2\text{Na}$.

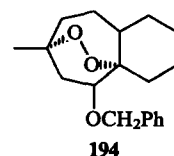
Among aminoacetals, the compound **192**¹²¹ stands out as possessing a remarkably high activity.

More than 70 artemisinin derivatives and analogues of the type **193** have been described;^{122,123} 12-deoxoartemisinin ($\text{R}^1 = \text{Me}$, $\text{R}^2 = \text{R}^3 = \text{H}$) is very promising.

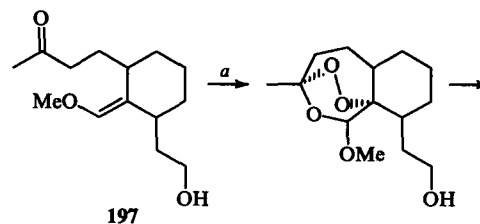


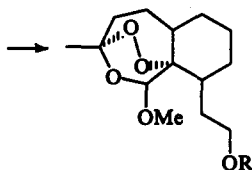
$\text{R}^1 = \text{H}, \text{Me}$;
 $\text{R}^2, \text{R}^3 = \text{H}, \text{OMe}, \text{OCH}_2\text{Ph}$.

Extremely valuable artemisinin analogues have been synthesised. For example, the peroxyacetal **194** is not inferior to artemisinin as regards its activity towards *Plasmodium falciparum* (the Indo-Chinese clone W-2).¹¹⁴



The ester **195** and the carbamate **196** obtained by photooxidation of the enol ester **197** or by its treatment with $\text{Et}_3\text{SiO}_3\text{H}$ displayed, besides a high antiplasmodium activity, also a unique stability. These crystalline peroxides are now undergoing clinical trials.¹²⁴ It should be emphasised that the majority of artemisinin derivatives and analogues are active against those plasmodium clones that are resistant to potent antimalarial agents, such as plasmoquine.





195: R = COC₆H₄CO₂Me

196: R = CONEt₂.

(a) O₂, hv, Bengal Rose or Et₃SiO₃H.

The question of the activity of peroxy compounds against malarial pathogens is worth special discussion, since the search for antimalarial agents that can be obtained economically is a very urgent task. Structurally simple synthetic peroxides, which are promising as antiparasitic agents, have been described.¹²⁵⁻¹³¹

Recent publications deal with the synthesis of stable peroxides as promising drugs.¹³²⁻¹³⁴ Terpene ozonides are the components of medicinal drugs endowed with antimicrobial and antiparasitic activities.¹³³

* * *

The data presented herein attest to the fact that peroxy compounds are widely distributed in natural objects. Contrary to the earlier, common opinion about the lability of most natural peroxides, investigators encounter sufficiently stable substances more and more frequently. The literature data available on the biological activity of natural peroxides may be regarded as a pledge of future progress in the design of medicinal drugs and antiparasitic agents in agroindustrial production. The example of artemisinin, where the investigations in the area of the chemistry of natural peroxides have acquired medical orientation, is very explicit. It is probable that in the near future the list of antiparasitic agents designed for clinical application will be supplemented with not only natural derivatives of artemisinin but also with synthetic peroxy compounds.

Attention should also be paid to such important properties of natural peroxides as their cytostatic, antitumour, and antimicrobial activity as well as the recently detected CNS activity.

Thus, the comprehensive bioassay of both natural and synthetic peroxy compounds is becoming a current problem.

This review has been prepared with the financial support of the Russian Fundamental Research Fund (Grant No. 95-03-08517).

References

1. B Samuelsson, M Goldyne, E Grandström, M Hamberg, S Hammarström, C Malmsten *Ann. Rev. Biochem.* **47** 997 (1978)
2. *The Leucotrienes, Chemistry and Biology* (Eds L Chakrin, D Bailey) (New York: Academic Press, 1984)
3. R P Evstigneeva, G I Myagkova *Usp. Khim.* **55** 843 (1986) [*Russ. Chem. Rev.* **55** 455 (1986)]
4. D A Zabolotskii, G I Myagkova, R P Evstigneeva *Usp. Khim.* **59** 827 (1990) [*Russ. Chem. Rev.* **59** 482 (1990)]
5. K Nicolaou, G Gasic, W Barnette *Angew. Chem.* **90** 360 (1978)
6. M Hamberg, J Svensson, T Wakabayashi, B Samuelsson *Proc. Nat. Acad. Sci. USA* **71** 345 (1974)
7. M I Goryaev, I Pliva, in *Metody Issledovaniya Efirnykh Masel* (Methods of Investigation of Essential Oils) (Alma-Ata: Izd. Akad. Nauk Kaz. SSR, 1962) p. 658
8. A D Dembitskii, Doctoral Thesis in Chemical Sciences, Institute of Bioorganic Chemistry, Academy of Sciences, Uzb. SSR, Tashkent, 1984
9. E G E Hawkins *Organic Peroxides* (London: F F Spon Ltd, 1961)
10. T Wilson *Singlet O₂ Vol. 2* (Ed. A Frimer) (Boca Raton, FL: CRC Press, 1985)
11. E Clennan *Tetrahedron* **47** 1343 (1991)
12. L Jing-Ming, N Mu-Jang, F Ju-Fen, T You-You, W Zhao-Huo, W Yu-Lin, C Wei-Shan *Acta Chim. Sinica* **37** 129 (1979)
13. D Klayman *Science* **228** 1049 (1985)
14. S S Zaman, R P Sharma *Heterocycles* **32** 1593 (1991)
15. J L Vannerstrom, J W Eaton *J. Med. Chem.* **31** 1269 (1988)
16. G L Sharipov, V P Kazakov, G A Tolstikov *Khimiya i Khimiluminesentsiya 1,2-Dioksetanov* (The Chemistry and Chemiluminescence of 1,2-Dioxetanes) (Moscow: Nauka, 1990) p. 287
17. E Gildmeister, F Hoffmann *Die Aetherischen Ole* Vol. IV (Berlin: Akademie-Verlag, 1956) p. 592
18. H Schenk *Angew. Chem.* **61** 434 (1949)
19. F Bohlmann, J Jakupovic, C Zdero *Phytochemistry* **17** 2034 (1978)
20. X-T Liang, D-Q Ju, L Wu, H-C Deng *Acta Chim. Sinica* **37** 231 (1979)
21. R Leirsh, H Soicke, C Stehr, H Tullner *Planta Medica* **387** (1986)
22. Sh Z Kasymov, A Ovezdurdyev, M I Yusupov, I D Sham'yanov, V I Malikov *Khim. Prir. Soedin.* **636** (1986)
23. G Ruecker, R Mayer, D Manns *Planta Medica* **3** 245 (1986)
24. P Huang *Chem. Gud* **8** 290 (1992)
25. W S Zhou, X-X Xu *Acc. Chem. Res.* **27** 211 (1994)
26. G Ruecker, R Walter, D Manns *Planta Medica* **57** 295 (1991)
27. P Chen, G Leather *J. Chem. Ecol.* **16** 1867 (1990)
28. A J Lin, D L Klayman, J H Hochi, J V Silverton, C George *J. Org. Chem.* **50** 4504 (1985)
29. Y Imakura, K Hachiya, T Ikemoto, S Yamashita, M Kihara, S Kobayashi, T Shingu, W K Milhous, K H Lee *Heterocycles* **31** 1011 (1990)
30. W-S Zhon, L Zhang, Z-C Fan, X-X Xu *Tetrahedron* **42** 4437 (1986)
31. N Acton, D Klayman *Planta Medica* **226** (1987)
32. X Shang, C-H He, Q-T Zheng, J-J Yang, X-T Liang *Heterocycles* **28** 421 (1989)
33. N Acton, D L Klayman *Planta Medica* **411** (1985)
34. F S El-Feraly, A Ayalp, M A Al-Jahaya, D R McPhail, A T McPhail *J. Nat. Prod.* **53** 66 (1990)
35. S El-Marakby, F S El-Feraly, H El-Sohly, E Croom, C Hufford *J. Nat. Prod.* **50** 903 (1987)
36. J Flippen-Anderson, R Gilard, C George *Acta Crystallogr., Sect. C, Cryst. Struct. Commun.* **44** 388 (1988); *Chem. Abstr.* **110** 57 862b (1989)
37. G Rücker, A Olbrich *Tetrahedron Lett.* **29** 4703 (1988)
38. G Rücker, Luo Shide, A Olbrich *Arch. Pharm.* **323** 171 (1990)
39. A Bagchi, J Oshima, H Hikino *Phytochemistry* **27** 1199 (1988)
40. M Bruno, W Herz *Phytochemistry* **27** 1871 (1988)
41. E Tsankova, U Kempe, T Norin, I Ognyanov *Phytochemistry* **20** 1436 (1981)
42. G Rücker, D Manns, J Breuer *Arch. Pharm.* **323** 678 (1990)
43. G Rücker, D Manns, J Breuer *Arch. Pharm.* **324** 979 (1991)
44. G Rücker, D Manns, J Breuer *Arch. Pharm.* **326** 901 (1993)
45. M Koreeda, M Nagaki, K Hayami, S Matsueda *Yakugaku Zasshi* **108** 434 (1988); *Chem. Abstr.* **109** 115 918s (1988)
46. G Rücker, A Kielfer, J Breuer *Planta Medica* **58** 293 (1992)
47. H Itokawa, K Watanabe, H Morita, S Mihashi, Y Titaka *Chem. Pharm. Bull.* **33** 2023 (1985)
48. H Itokawa, H Morita, K Osawa, K Watanabe, Y Titaka *Chem. Pharm. Bull.* **35** 2849 (1987)
49. J Jakupovic, A Schuster, F Bohlmann, M Dillon *Phytochemistry* **27** 1771 (1988)
50. G Appendino, P Gariboldi, G Nano, P Tetenyi *Phytochemistry* **23** 2545 (1984)
51. G Rücker, R Breitmeier, R Mayer, D Manns *Arch. Pharm.* **320** 437 (1987)
52. G Rücker, D Manns, S Wilbert *Arch. Pharm.* **326** 457 (1993)
53. M Brimble, P Reay, D Rowan, J Spicer *Chem. N. Z.* **58** 29 (1994); *Ref. Zh. Khim.* **2** E 22 (1995)
54. T V Leibyuk, S A Shevtsov, V A Ralugin *Khim. Prir. Soedin.* **556** (1990)
55. P Monaco, M Parrilli, L Previtera *Tetrahedron Lett.* **28** 4609 (1987)
56. G Rücker, D Manns, S Wilbert *Phytochemistry* **31** 340 (1992)
57. F Bohlmann, W Abraham *Phytochemistry* **18** 1754 (1979)
58. H Itokawa, K Takega *Heterocycles* **35** 1467 (1993)
59. J Jakupovic, M Grenz, G Schmeda-Hirschmann *Phytochemistry* **27** 2997 (1988)
60. S J Gould, X C Cheng, *J. Org. Chem.* **59** 400 (1994)

61. A Nakamura, T Ashino, M Yamamoto *Tetrahedron Lett.* **32** 4355 (1991)
62. E Quinoa, E Kho, L Manes, P Crews, G Bakus *J. Org. Chem.* **51** 4260 (1986)
63. R Wells *Tetrahedron Lett.* 2637 (1976)
64. Sh Sakemi, T Higa, U Anthoni, C Christophersen *Tetrahedron* **43** 263 (1987)
65. M Kobayashi, K Kondo, J Kitagawa *Chem. Pharm. Bull.* **41** 1324 (1993)
66. R Capon, J MacLeod *Tetrahedron* **41** 3391 (1985)
67. M D Higgs, D J Faulkner *J. Org. Chem.* **43** 3454 (1978)
68. D B Stierle, D J Faulkner *J. Org. Chem.* **45** 3396 (1980)
69. B Davidson *Tetrahedron Lett.* **32** 7167 (1991)
70. D W Philipson, K L Rinehart Jr *J. Am. Chem. Soc.* **105** 7735 (1983)
71. D B Stierle, D J Faulkner *J. Org. Chem.* **44** 964 (1979)
72. J Kashman, M Rotem *Tetrahedron Lett.* 1707 (1979)
73. L Manes, G Bakus, Ph Crews *Tetrahedron Lett.* **25** 931 (1984)
74. M Albericci, M Collart-Lempereur, J C Braekman, D Daloze, B Tursch, J P Declercq, G Germain, M van Meerseche *Tetrahedron Lett.* 2687 (1979)
75. M Albericci, J Braekman, D Daloze, B Tursch *Tetrahedron* **38** 1881 (1982)
76. D Faulkner *Nat. Prod. Rep.* **1** 250 (1984)
77. D Faulkner *Nat. Prod. Rep.* **1** 551 (1984)
78. D Faulkner *Nat. Prod. Rep.* **4** 539 (1987)
79. D Faulkner *Nat. Prod. Rep.* **3** 1 (1986)
80. D Faulkner *Nat. Prod. Rep.* **5** 613 (1988)
81. D Faulkner *Nat. Prod. Rep.* **7** 268 (1990)
82. D Faulkner *Nat. Prod. Rep.* **8** 97 (1991)
83. D Faulkner *Nat. Prod. Rep.* **9** 323 (1992)
84. Y Fukazawa, Sh Usui, Y Uchio, Y Shiobara, M Kodama *Tetrahedron Lett.* **27** 1825 (1986)
85. Y Uchio, S Eguchi, J Kuramoto, M Nakayama, T Hase *Tetrahedron Lett.* 26 4487 (1985)
86. A G Gonzalez, J D Martin, C Perez, J Roviroso, B Tagle, J Clardy *Chem. Lett.* 1649 (1984)
87. Y Sheikh, C Djerassi *Tetrahedron* **30** 4095 (1974)
88. W Fenical *J. Am. Chem. Soc.* **96** 5580 (1974)
89. A Gunatilaka, Y Gopichand, F Schmitz, C Djerassi *J. Org. Chem.* **46** 3860 (1981)
90. G Ruecker, R Mayer, D Manns, *J. Nat. Prod.* **50** 287 (1987)
91. G Rücker, R Mayer, K R Lee *Arch. Pharm.* **322** 821 (1989)
92. E Okuyama, K Umeyama, Y Saito, M Satake *Chem. Pharm. Bull.* **41** 1309 (1993)
93. G Rücker, D Manns, N Korber, J Breuer *Arch. Pharm.* **327** 277 (1994)
94. A D Dembitskii, M I Goryaev, R A Yurina, A E Lyutz, S M Vasilyuk *Izv. Akad. Nauk Kaz. SSR, Ser. Khim.* **45** (1978)
95. L Shide, N Bingmei, H Wangyu *J. Nat. Prod.* **54** 573 (1991)
96. F Bohlmann, K Umemoto, J Jakupovic, R King, H Robinson *Phytochemistry* **23** 1669 (1984)
97. F Bohlmann, K Knoll, H Robinson, R King *Phytochemistry* **19** 599 (1980)
98. P Singh, J Jakupovic, F Bohlmann, R King, H Robinson *Phytochemistry* **24** 2110 (1983)
99. R Mayer, G Rücker *Arch. Pharm.* **320** 318 (1987)
100. G Appendino, P Gariboldi, G Nano *Phytochemistry* **21** 1099 (1982)
101. S Khafagy, M Al-Yahya, J Zische, F Bohlmann *Phytochemistry* **23** 1821 (1983)
102. M Kobayashi, Bueng Whu Son, Y Kyogoku, I Kitagawa *Chem. Pharm. Bull.* **32** 1667 (1984)
103. M Guyot, D Davoust, Ch Belaud *Tetrahedron Lett.* **23** 1905 (1982)
104. M Jung, X Li, D Bustos, H El-Sohly, J McChesney *Tetrahedron Lett.* **30** 5973 (1989)
105. B Je, Y-L Wu *J. Chem. Soc., Chem. Commun.* 726 (1990)
106. R J Roth, N Acton *J. Nat. Prod.* **52** 1183 (1989)
107. M Jung, H N ElSohly, E M Croom, A T McPhail, D R McPhail *J. Org. Chem.* **51** 5417 (1986)
108. P Lansbury, D Nowak *Tetrahedron Lett.* **33** 1029 (1992)
109. G Schmid, W Hofheinz *J. Am. Chem. Soc.* **105** 624 (1983)
110. X-X Xu, J Zhu, D Z Huang, W S Zhou *Tetrahedron* **42** 819 (1986)
111. X-Y Liu, W L Yeh, S Y Chew, W S Zhou *Tetrahedron Lett.* **34** 4435 (1993)
112. M A Avery, C Jennings-White, W K M Chong *Tetrahedron Lett.* **28** 4629 (1987)
113. M A Avery, C Jennings-White, W K M Chong *J. Org. Chem.* **54** 1792 (1989)
114. G Posner, C H Oh, W Milhous *Tetrahedron Lett.* **32** 4235 (1991)
115. R K Haynes, G R King, S C Vonwiller *J. Org. Chem.* **59** 4743 (1994)
116. *Annual Reports in Medicinal Chemistry* Vol. 23 (Ed. R Allen) (New York: Academic Press, 1988) p. 327
117. A J Lin, M Lee, D L Klayman *J. Med. Chem.* **32** 1249 (1989)
118. A J Lin, L-Q Li, S L Andersen, D L Klayman *J. Med. Chem.* **35** 1639 (1992)
119. US P. 87 365; *Chem. Abstr.* **110** 193 144w (1989)
120. A J Lin, D L Klayman, W K Milhous *J. Med. Chem.* **30** 2147 (1987)
121. A J Lin, L-Q Li, D L Klayman, C F George, J L Flippen-Anderson *J. Med. Chem.* **33** 2610 (1990)
122. M A Avery, F Gao, W K Chong, S Mehrotra, W K Milhous *J. Med. Chem.* **36** 4264 (1993)
123. M Jung, X Li, D A Bustos, W K Milhous, H N ElSohly, J D McChesney *J. Med. Chem.* **33** 1516 (1990)
124. G H Posner, Ch H Oh, L Gerena, W K Milhous *J. Med. Chem.* **35** 2459 (1992)
125. J L Vennerstrom, J W Eaton *J. Med. Chem.* **31** 1269 (1988)
126. Sh Tani, N Fukamiya, H Kiyogawa, H A Musallam, R O Pick, K H Lee *J. Med. Chem.* **28** 1743 (1985)
127. C Jefford, J Wang, G Bernardinelli *Helv. Chim. Acta* **71** 2042 (1988)
128. J A Kepler, A Philip, Y W Lee, M C Morey, F I Carroll *J. Med. Chem.* **31** 713 (1988)
129. J A Kepler, A Philip, Y W Lee, H A Musallam, F I Carroll *J. Med. Chem.* **30** 1505 (1987)
130. J Vennerstrom, Hong-Ning Fu, W Ellis, A Ager, J Wood, S Andersen, L Gerena, W Milhous *J. Med. Chem.* **35** 3023 (1992)
131. M Avery, F Gao, W Chong, T Hendrickson, W Inman, Ph Crews *Tetrahedron* **50** 957 (1994)
132. K McCullough *Contemp. Org. Synth.* **2** 225 (1995)
133. US P. 5 190 979; *Ref. Zh. Khim.* **90** 85P (1994)
134. Y-S Hon, J-L Yan *Tetrahedron Lett.* **34** 6591 (1993)

Polycondensation reactions catalysed by Ni and Pd complexes as the method for the synthesis of carbo- and hetero-cyclic polyarylenes

A L Rusanov, I A Khotina

Contents

I. Introduction	785
II. Synthesis of polyarylenes by cross-coupling catalysed by palladium complexes	785
III. Synthesis of polyarylenes by cross-coupling catalysed by nickel complexes	790
IV. Synthesis of heterocyclic polyarylenes	792

Abstract. Data on the application of the method of polycondensation cross-coupling catalysed by Pd and Ni complexes for the synthesis of carbo- and hetero-cyclic polyarylenes are systematised and generalised. The bibliography includes 126 references.

I. Introduction

Until recently, the chemistry of carbo- and hetero-cyclic polyarylenes has been among the less studied fields of science on high-molecular compounds.¹ Despite the numerous attempts of investigators to develop new approaches to the synthesis of carbocyclic^{2–11} and heterocyclic^{12,13} polyarylenes, the synthesis of high-molecular polymers having a clearly defined structure seemed to be highly problematic.

The methods of polyarylene synthesis are classified as direct and indirect ones. Direct syntheses employ the monomers already containing the aromatic units, which then become repeating units of the polymers. Characteristic examples of direct polyarylene synthesis are the synthesis of poly-*p*-phenylene according to Kovacic⁹ or using electrochemical methods.^{14,15}

In the case of indirect syntheses, a prepolymer is first prepared, which is converted into polyarylene under the action of definite factors (e.g., thermal treatment). This can be exemplified by the synthesis of insoluble poly-*p*-phenylene starting from a soluble prepolymer, a derivative of poly(5,6-dihydroxy-cyclohex-2-en-1,4-ylene); its pyrolysis gives insoluble poly-*p*-phenylene.^{8,12} The transformation of high-molecular, stereoregular poly(5,6-dicarboxycyclohex-2-en-1,4-ylene) into poly-*p*-phenylene in the presence of H₃PO₄ at 100–250 °C has been described.¹⁶

Unfortunately, both the direct and indirect methods have serious disadvantages. The conditions required for the direct polyarylene synthesis are too drastic for the regiospecific reactions. Therefore, in the case of polyphenylene not only 1,2-, 1,3- and 1,4-disubstituted phenylene fragments of the chain but also trisubstituted units can be formed. Moreover, the molecular weight of the polyarylenes obtained by direct methods are usually low due to the insolubility of polyarylenes.

The indirect method can be used to obtain polyarylenes with high molecular weight; however, the units in the polymers thus formed are not uniform¹⁷ due to the incompleteness of the prepolymer conversions.

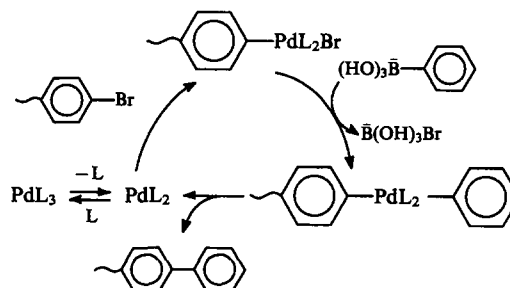
The analysis of literature data revealed that the development of direct methods that would not require drastic conditions for their realisation is the most promising approach to progress in polyarylene chemistry. The problem of polymer solubility must be solved in parallel. The most suitable to this end are polycondensation reactions based on haloaromatic compounds catalysed by transition metal complexes.

II. Synthesis of polyarylenes by cross-coupling catalysed by palladium complexes

1. Synthesis of carbo- and hetero-cyclic polyarylenes by interaction of arene dihalides with aromatic diboronic acids or their derivatives

The first application of cross-coupling reactions catalysed by palladium complexes to the synthesis of polyarylenes was described by Suzuki¹⁸ and Muller.¹⁹ These authors demonstrated that different monobromoaromatic compounds react with benzenboronic acid or its cyclic esters to give high (up to 99%) yields of products.

The same reactions have been described in more recent works.^{20–22} The following scheme for this process has been proposed by Suzuki:²³



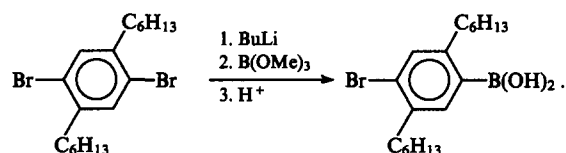
Later, cross-coupling reactions were used for the synthesis of polyarylenes. A great advantage of the polycondensation cross-coupling method is the possibility of introducing various side groups (aliphatic, aromatic, ester, etc.) into the monomers. On the one hand, by introducing side groups one may improve the solubility of the polymers (which is important for their processing) and, to some extent, increase their molecular weight. On the other hand, the use of these groups may confer specific (liquid crystalline, conducting, nonlinear optical) properties on the

A L Rusanov, I A Khotina Nesmeyanov Institute of Organoelement Compounds, Russian Academy of Sciences, ul. Vavilova 28, 117813 Moscow, Russian Federation. Fax (7-095)135 50 85. Tel. (7-095) 135 63 72 (A L Rusanov)

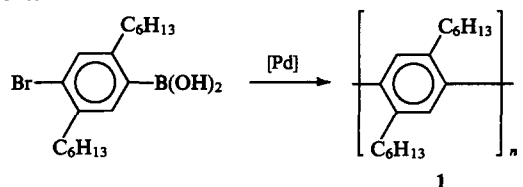
Received 13 July 1995

Uspekhi Khimii 65 (9) 852–864 (1996); translated by R L Birnova

polymer. Cross-coupling reactions have been used, in particular, in the synthesis of alkyl-substituted poly-*p*-phenylenes. The starting monomers were obtained by the treatment of 2,5-di-alkyl-1,4-dibromobenzenes with 1 equiv. of *n*-butyllithium followed by addition of trimethylborate and acid hydrolysis:²⁴



Homopolycondensation of this monomer in the presence of $\text{Pd}(\text{Ph}_3\text{P})_4$ in benzene and subsequent addition of concentrated Na_2CO_3 solution give a colourless polymer soluble in organic solvents:²⁴

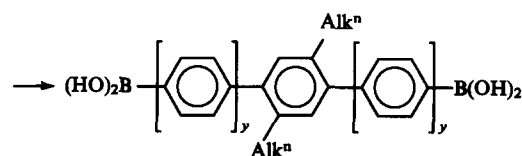
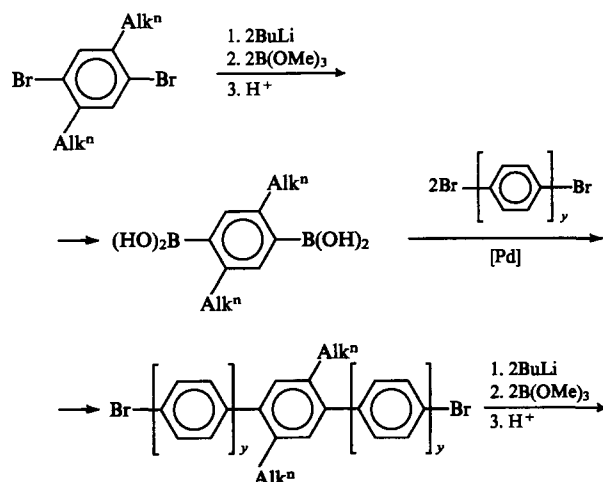


The degree of polymerisation (DP) of the polymer 1 reached 30. The analysis of ^1H and ^{13}C NMR spectra revealed that this reaction is highly regiospecific. The yield of the polymer in this reaction was 100%.

It is noteworthy that in the majority of polycondensation cross-coupling reactions the yields of the polymers vary from 80% to 100% depending on the solubility of the synthetic polymer and its molecular weight.

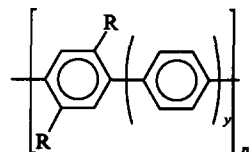
Clearly, if bulky alkyl groups were not introduced into the original monomers, no poly-*p*-phenylenes with DP 30 could be obtained. However, the introduction of these groups plays not only a positive role. In some instances, the introduction of bulky substituents results in conformational changes in the polymer chain, e.g., in disturbance of the coplanarity of the adjacent phenyl groups.^{25–28} Minor departures from coplanarity have no appreciable influence on the electrical and optical characteristics of the polymers; however, if these deviations exceed a certain level, the properties of the polymers change drastically.²⁹

Similar approaches were used to obtain polyphenylenes,²⁴ in which the blocks of unsubstituted *p*-phenylene fragments of varying length were connected via phenylene cycles containing side alkyl groups.³⁰ The synthesis of the original monomers was carried out in accordance with the following scheme:



$y = 1-6$.

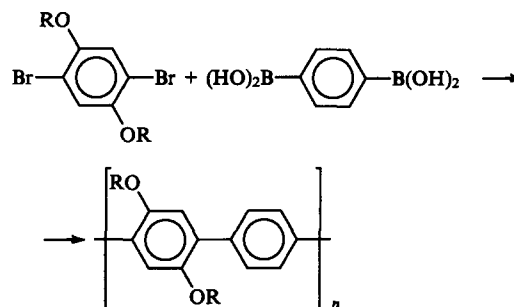
Thus, by combining various diboronic acids with dibromo compounds one can obtain polymers with the general formula:³⁰



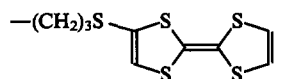
In some cases ($y = 2$), the target products with the molecular weight M_n of 21 000 were synthesised, which corresponds to a degree of polymerisation of 37. In this case, the total number of phenylene groups may amount to 100. To date, this polymer has the highest degree of polymerisation among those obtained by Pd-catalysed polycondensation cross-coupling.

The synthesis of polymers with side alkoxy groups based on dibromides and diboronic acids has been described.¹ A significant advantage of the polycondensation cross-coupling method is the high activity of diboronic acids and their insensitivity with respect to water (e.g., in some of these reactions, an aqueous solution of Na_2CO_3 was used). In some instances, water-soluble palladium complexes, sodium tris[(trisulfonatophenyl)phosphine]palladium(0) (2) and sodium (or potassium) tris[(diphenyl-*m*-sulfonatophenyl)phosphine]palladium(0) (3), were used as catalysts.^{31,32}

The synthesis of water-soluble polymers containing sulfonatealkoxy groups has been described.^{33,34}

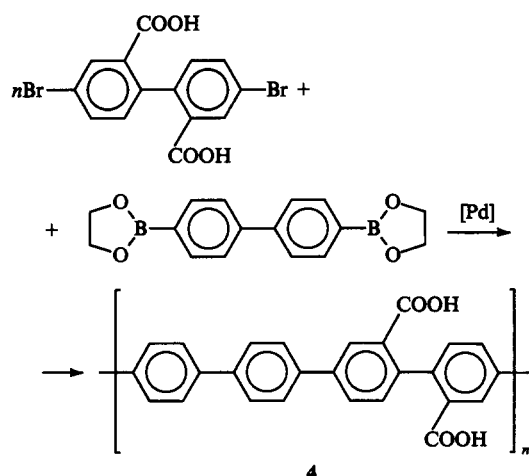


$\text{R} = -(\text{CH}_2)_3\text{SO}_3\text{Na}$,



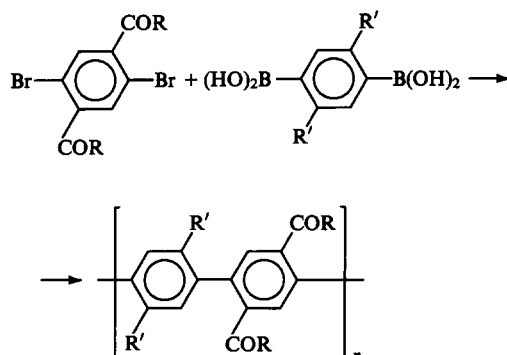
The reactions were carried out in an aqueous medium, to which DMF and K_2CO_3 were added. Palladium complexes 2 or 3 were used as catalysts. The molecular weight was not determined, but, as could be judged from the low bromine content in the polymer based on sodium of 1,4-dibromo-2,5-bis(3-sulfonatopropoxy)benzene and benzene-1,4-diboronic acid (0.5%), it was of about 15 000.

Other water-soluble poly-*p*-phenylenes^{23,32} carrying carboxyl and carboxymethyl groups have also been described. Thus, the polymer 4 with a molecular weight of about 10 000 (DP ~ 25) was synthesised based on 4,4'-dibromo-2,2'-dicarboxybiphenyl and a cyclic ester of 4,4'-biphenyldiboronic acid. The polycondensation reaction was carried out in a weakly alkaline solution (H_2O –DMF, 3 : 1) in the presence of a water-soluble Pd-catalyst.³¹



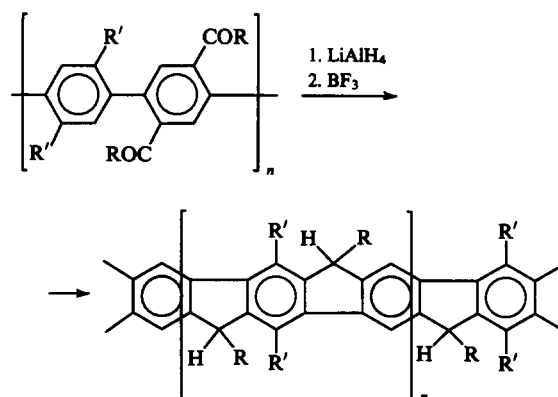
It is noteworthy that cyclic diboronates are more preferable than diboric acids because of their better solubility and ease of purification.

Also, polycondensation was successfully employed in the synthesis of prepolymers of ladder systems.^{35–38} Mullen et al.^{35,38} performed the synthesis of soluble prepolymers based on dialkyl-substituted benzenediboronic acids and dibromobenzenes containing keto, aldehyde, and other groups:



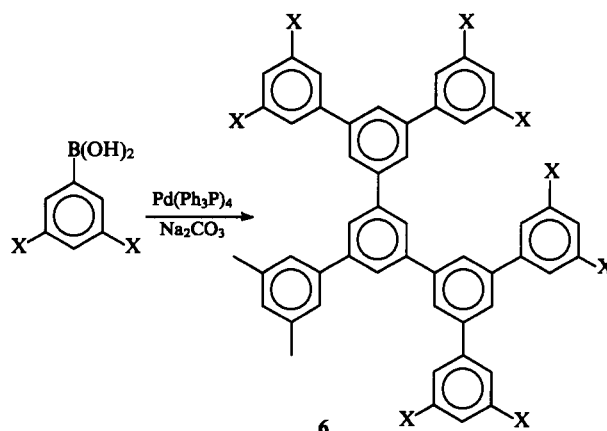
$R = H, C_{10}H_{21}$; $R' = C_6H_{13}$.

Subsequent intramolecular cyclisation converted them into ladder structures devoid of non-cyclised fragments.



The ladder polymers **5** have been synthesised from the prepolymer ($\bar{M}_n = 7800$) based on substituted dibromobenzene carrying acetylene groups and cyclic benzenediboronate (Scheme 1).³⁹

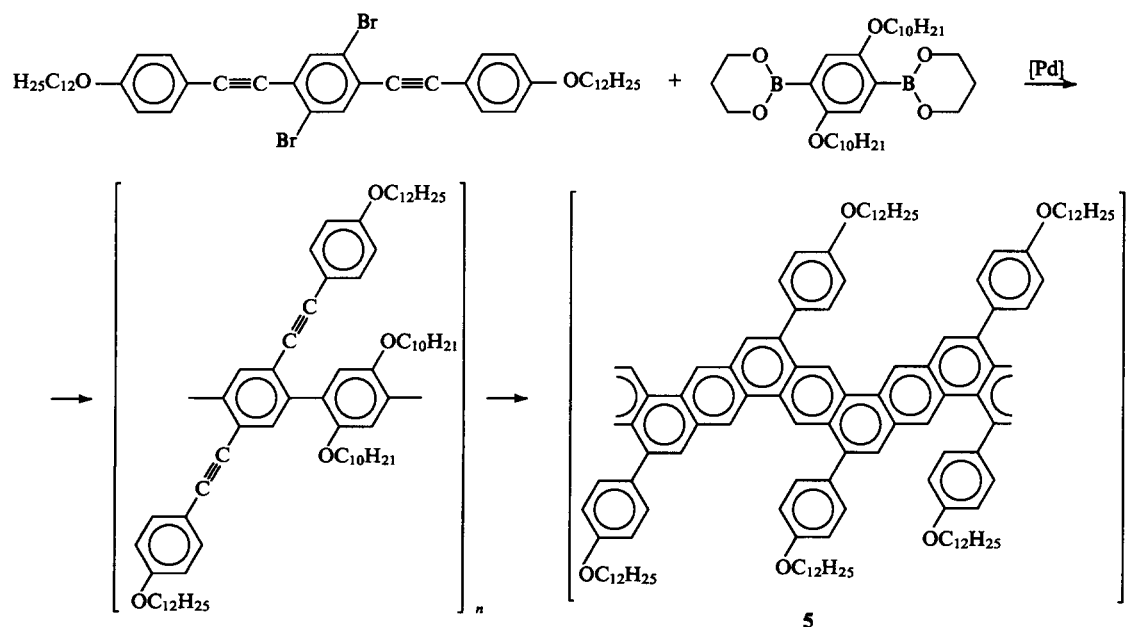
Besides difunctional monomers or monomers of the AB-type, the Pd-catalysed cross-coupling reactions also involve trifunctional benzene compounds of the ABB type. The latter were used to obtain the polymeric dendrites (**6**):^{40,41}



$X = Br$.

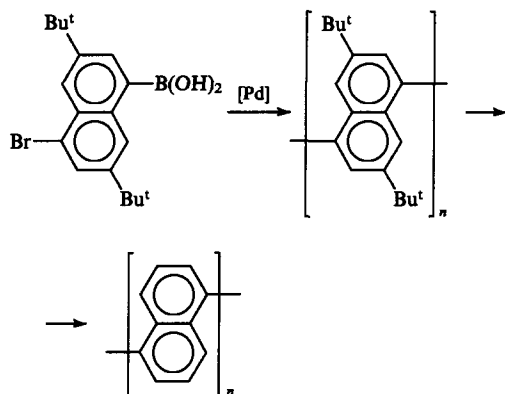
The yield of the product was 80%–95%, $\bar{M}_n = 3820$ and $\bar{M}_w = 5750$. It was readily soluble in THF and *o*-dichlorobenzene.

Scheme 1



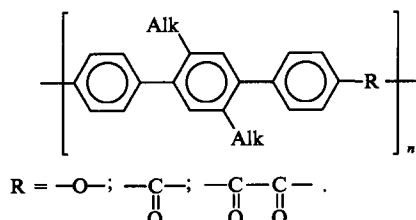
Its viscosity (0.031 dl g^{-1} in THF) was very low which is characteristic of highly branched oligomers. The oligomer **6** had a $T_g = 280^\circ\text{C}$ and did not melt.

Polycondensation cross-coupling is also used in the synthesis of naphthalene compounds. Using this route, a soluble poly(1,5-naphthalene) with a low degree of polymerisation has been synthesised.^{42, 43}



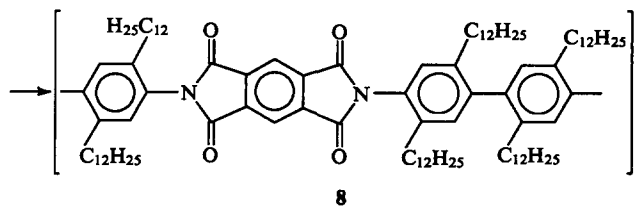
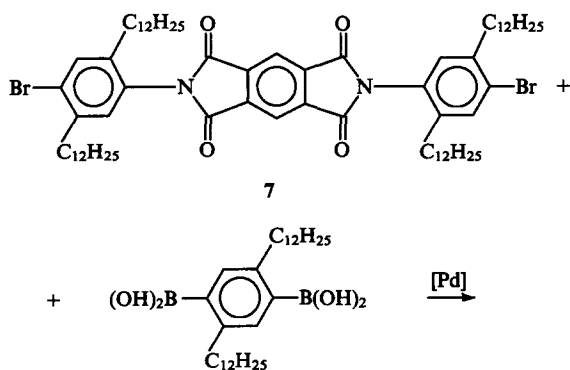
To obtain thermostable polymers, the *tert*-butyl groups are removed from the polymer in alkaline media or by thermal treatment. In this context, the *tert*-butyl groups have a clear advantage over linear alkyl substituents.

A great number of investigations in the area of polycondensation cross-coupling were concerned with the synthesis of polyarylenes and related aromatic polymers containing $-\text{O}-$ and $-\text{CO}-$ groups in their main chains. Thus, the interaction of the 4,4'-dibromodiphenyl ether, 4,4'-dibromobenzophenone or 4,4'-dibromobenzyl with dialkyl-*p*-phenylenediboronic acid gave the corresponding alkyl-containing aromatic polyether, polyketone, and poly- α -diketone.



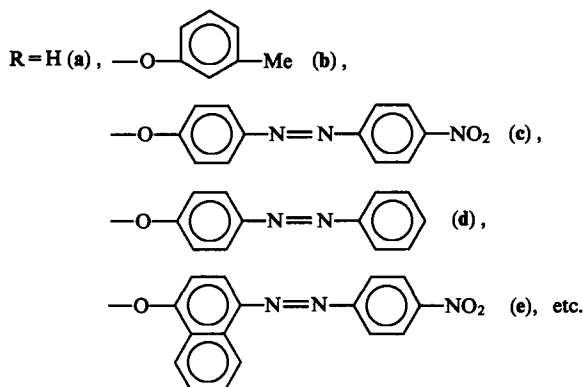
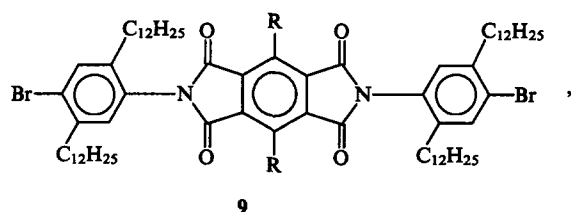
The presence in the side chains of alkyl substituents renders these polymers soluble in ordinary organic solvents.

The cross-coupling reaction opens up new opportunities for the synthesis of such polymers as substituted polyimides.⁴⁴⁻⁴⁶ Recently,⁴⁴ defect-free polyimides **8** based on didodecylphenyldiboronic acid and the dibromide **7** containing imide rings have been synthesised in a heterogeneous medium (aqueous solution of $\text{Na}_2\text{CO}_3/\text{toluene}$) in the presence of the Pd^0 catalyst, $\text{Pd}(\text{Ph}_3\text{P})_4$.



The molecular weight of the polymer **8**, \bar{M}_n , equalled 20 000, which corresponded to a DP of 14. Such polymers can be obtained by conventional polycondensation of dianhydrides and diamines;⁴⁷ however, in some cases (see, for example, Ref. 46) direct synthesis of the polymers seems to be problematic.

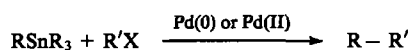
Other imide-containing dibromides, such as the compounds cited in Ref. 46 can also be introduced into the reaction (1):



Here, the radicals R are the residues of dyes which are nonlinear, optically active chromophores. The dibromides **9b-e** enter into the polycondensation reaction with difficulty due to steric hindrances. In this case, up to 50% of the dibromide **9a** was introduced into the reaction simultaneously with the dibromides **9b-e**. The molecular weights of the copolymers so obtained were not very high, they amounted to 17 000 (50% **9a** + 50% **9b** copolymers), whereas the molecular weight of the polymer obtained from dibromide **9a** alone was 41 000 (DP = 11 and 26, respectively).⁴⁶

2. Synthesis of polyarylenes with participation of aromatic organometallic compounds

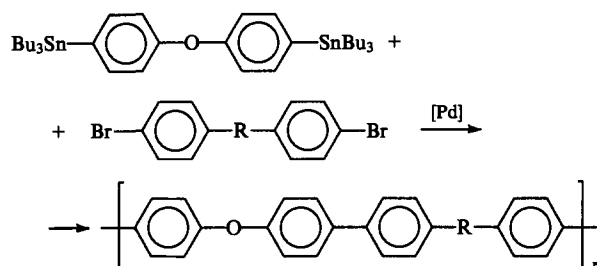
Considerable attention has been recently given to Pd-catalysed reactions between aromatic dihalides and bis(trialkylstannyl) compounds. The chemical stability and ease of purification of organotin compounds have motivated their wide-scale application in organic chemistry.⁴⁸⁻⁵¹



R, R' = aryl, alkyl, alkenyl and alkynyl.

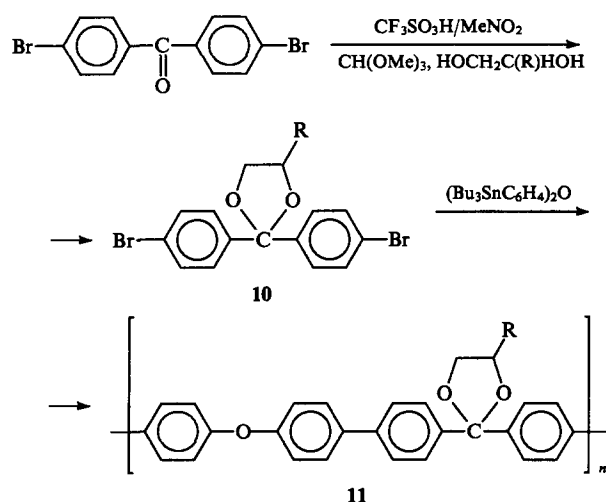
This reaction was first described for aromatic tin derivatives and aromatic halides in Ref. 51. The interaction of bisstannyl compounds and aromatic dihalides was employed in the synthesis of polyarylenes. Thus, the interaction of 4,4'-bis(tributylstannyl)diphenyl ether with various aromatic dihalides^{52, 53} [e.g., with 4,4'-dibromodiphenyl ether (**a**), 4,4'-dibromobenzophenone (**b**), and 4,4'-dibromodiphenyl sulphone (**c**)], in the presence of

$\text{PdCl}_2(\text{Ph}_3\text{P})_2$ in dipolar aprotic solvents gives the polymers whose molecular weights [as can be judged from their residual bromine content 5.2 (a), 1.69 (b), and 0.9% (c)] are 1500, 4800, and 8000, respectively. All the synthetic polymers are poorly soluble in organic solvents; their molecular weights increase with an increase in the polymer solubility. It has been possible to measure the inherent viscosity for the latter polymer, which was equal to 0.22 dl g^{-1} .



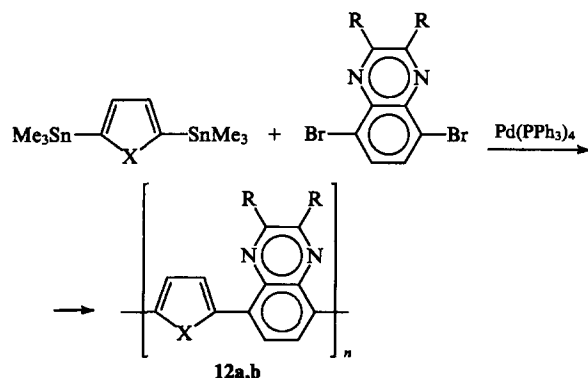
$\text{R} = -\text{O}-(\text{a}), -\text{C}(\text{O})-(\text{b}), -\text{SO}_2-(\text{c})$.

4,4'-Bis(tributylstannyl)diphenyl ether was also used in the synthesis of soluble polyarylenes based on 4,4'-dibromobenzophenone.⁵⁴ Insoluble 4,4'-dibromobenzophenone was converted into the soluble acetal. The reaction was carried out according to the following scheme:



After polycondensation, the acetal groups can be transformed into the ketone groups. The molecular weight of the polymer 11 obtained from the acetal 10 exceeds 25 000 ($\text{DP} > 74$).

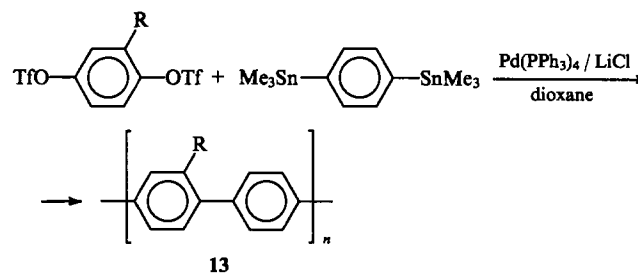
Recently, the synthesis of polymers with alternating electron-deficient quinoxaline cycles and electron-donor thiophene or furan groups, has been carried out.⁵⁵



$\text{R} = \text{C}_7\text{H}_{15}, \text{Ph}; \text{X} = \text{S} (\text{a}); \text{O} (\text{b})$.

The yield of the polymers was 96% and the reduced viscosities varied from 0.37 to 0.47 dl g^{-1} . The polymers 12a,b represent structures with charge transfer between the electron-donor and electron-acceptor groups, which eventually determines their intriguing physical properties.

Another synthetic procedure that makes use of the Pd-catalysts involves the interaction of bistrifluoromethanesulfonates (bistriflates) with bisstannin compounds (in some cases, with aromatic dihalides). Triflates are readily formed from the accessible hydroquinones by their interaction with triflic (trifluoromethanesulfonic) anhydride, $(\text{CF}_3\text{SO}_2)_2\text{O}$ (Trf_2O). This approach applied to alkyl-containing bistriflate and bis(tri-methylstannyl)benzene with catalysis by $\text{Pd}(\text{PPh}_3)_4$ and LiCl resulted in alkyl-containing polyphenylenes 13.^{56, 57}



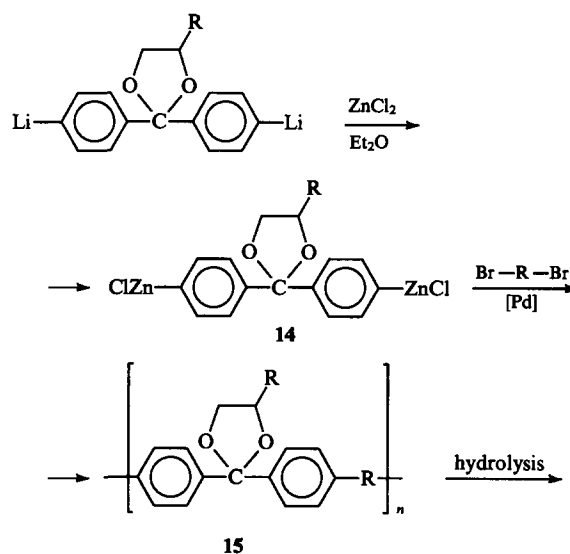
$\text{Trf} = \text{CF}_3\text{CO}_2$;

$\text{R} = (\text{CH}_2)_{10}\text{COOC}_2\text{H}_5, (\text{CH}_2)_x\text{CH}_3 (x = 5, 7, 11)$.

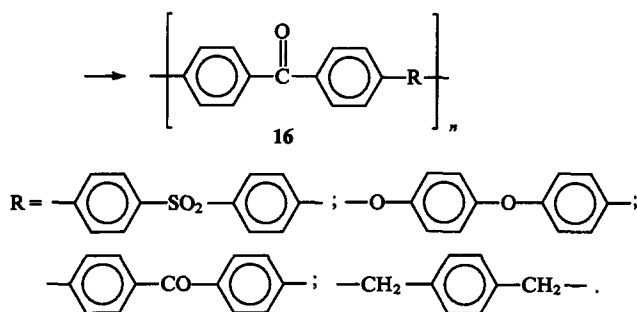
The maximum molecular weight of the resulting oligomer, \bar{M}_n , was 6400.

The palladium-catalysed cross-coupling also makes use of the reactions with other organometallic compounds.⁵⁸ Thus, polycondensation of aromatic dihalides with organotin compounds as well as their interactions with Grignard (see below) and Zn-reagents have been described.⁵³ One of Zn-reagents was synthesised from the corresponding diphenyl ether by transmetalation. Its interaction with 4,4'-dibromodiphenyl ether, 4,4'-dibromop-xylene, and 4,4'-di(bromomethyl)benzene in the presence of $\text{PdCl}_2(\text{Ph}_3\text{P})_2$ in THF was used to synthesise the corresponding oligomers. Of them, the oligomer based on 4,4'-di(bromomethyl)benzene had the highest molecular weight (3100).

Polycondensation of the Zn-reagent 14 obtained from the acetal of 4,4'-dilithiobenzophenone with dibromoderivatives of some aromatic compounds has been carried out.⁵⁴



15



The maximum molecular weight of the acetal polymer 15c, $R = (\text{C}_6\text{H}_4)_2\text{SO}_2$, is not high being up to 6730 ($\text{DP} = 19$).

The crystalline polymer 16 obtained by hydrolysis of the prepolymer 15 has $T_g = 208^\circ\text{C}$ and m.p. 380°C . As regards its crystallinity and other properties, the polymer 16 is closely related to polybiphenylene ether sulfones obtained by other methods.

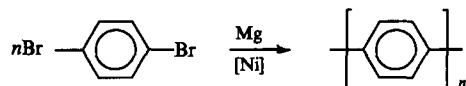
In general, the molecular weights of the polymers based on Zn-reagents are lower than those based on Sn-compounds, apparently due to the better solubility of the latter.

Thus, the use of the polycondensation cross-coupling method in the presence of Pd^0 and Pd^{II} complexes makes it possible to obtain polymers whose molecular weights do not exceed 20 000–25 000. These reactions can be carried out in aqueous media.

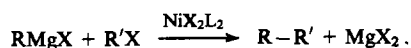
III. Synthesis of polyarylenes by cross-coupling catalysed by nickel complexes

1. Synthesis of polyphenylenes and polyarylenes using Grignard reagents

The cross-coupling reaction of dihalogenoaromatic compounds with Grignard reagents in the presence of various catalysts including predominantly bivalent Ni was first described by Yamamoto^{59, 60} in 1977–78. Thus, the interaction of 1,4-dibromobenzene with 1 equiv. of Mg and a catalytic amount of $\text{NiCl}_2(\text{bipy})$ ($\text{bipy} = 2,2'$ -bipyridyl) or other Ni^{II} compounds in boiling THF resulted in a polymer, which contained exclusively *p*-phenylene groups, with DP of up to 24.



This polycondensation reaction was based on the synthesis described by Tomao and Kumada in 1972.⁶¹

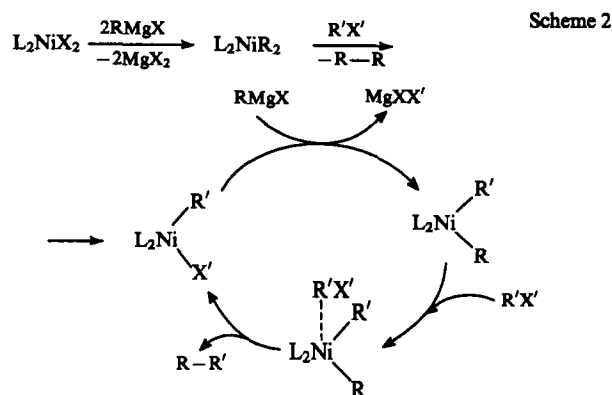


This reaction proceeds selectively and quantitatively under mild conditions.

Later, studies of cross-coupling of aromatic halides and Grignard reagents were further continued in the works,^{22, 62–65} in which not only Ni^{II} but, for the most part, Ni^0 complexes have been used as catalysts. The most probable mechanism for this reaction can be schematised as depicted in Scheme 2.⁶³

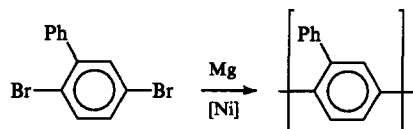
An attempt has been made⁵⁷ to obtain polymers from 4,4'-dibromodiphenyl ether and the Grignard reagent prepared from it. Polycondensation was performed in the presence of $\text{NiCl}_2(\text{dppp})$ [$\text{dppp} = 1,3$ -bis(diphenylphosphino) propane]. However, the final products appeared to be insoluble in the majority of organic solvents and had a low molecular weight (up to 600).

Two most likely reasons for the termination of growth of the poly-*p*-phenylene chain are: (i) the decrease of the product solubility in the course of polycondensation and its precipitation; (ii) chemical factors preventing the growth of the macromolecular chain, such as hydrolysis of its active end.



The fact that phenylene and, particularly, flexible side alkyl groups improve the solubility of low-molecular compounds^{66–69} and polymers^{70–72} predetermined future lines for development of investigations in the field of synthesis of polyphenylenes and polyarylenes based on Grignard reagents, viz., the use of monomers carrying side groups.

Poly(phenyl-1,4-phenylene)⁷³ was synthesised by using the Yamamoto reaction.⁵⁹ 2,5-Dibromobiphenyl was treated with an equimolar amount of Mg in THF and then 1.13 mol % of a nickel catalyst, $\text{NiCl}_2(\text{Ph}_3\text{P})_2$, was added:



The final product was soluble in chloroform; its molecular mass, \bar{M}_w , was 1100–2200 (in some cases, the proportion of an insoluble fraction constituted 13%).

The use of 1,4-dibromobenzene containing side alkyl groups [$R = \text{Alk} (\text{C}_6\text{—C}_{12})$] as monomer resulted in the polymer $[\text{—C}_6\text{H}_2\text{R}_2\text{—}]_n$.⁷⁴

The synthesis of *n*-alkyl-substituted poly-*p*-phenylenes was carried out under conditions described above. The reaction mixture was homogeneous; however, in this case, too, the degree of polymerisation did not exceed 13. The following Ni^{II} compounds were used as catalysts: $\text{Ni}(\text{bipy})\text{Cl}_2$, $\text{Ni}(\text{Ph}_3\text{P})_2\text{Cl}_2$, $\text{Ni}(\text{acac})_2$, and $\text{Ni}(\text{dppp})\text{Cl}_2$ (acac is acetylacetonate). Among those, $\text{Ni}(\text{Ph}_3\text{P})_2\text{Cl}_2$ turned out to be the best catalyst, for it gave the polymer of the highest molecular weight.

Conducting polyarylenes, polytriphenylamines⁷⁵ soluble in benzene and chloroform were synthesised based on 4,4'-dichlorotriphenylamine (a) and 4,4'-dibromo-(4''-methyl)triphenylamine (b) by Ni-catalysed polycondensation using Grignard reagents. $\text{Ni}(\text{bipy})\text{Cl}_2$ was used as the catalyst; it was added only after the formation of the Grignard reagent. This procedure made use of metallic Mg obtained *in situ* by reduction of anhydrous MgCl_2 with metallic potassium. The yield of the oligomers was 63% and 71%, respectively; the degree of polymerisation did not exceed 12.

From the above examples it can be seen that if the polycondensation is performed with the Grignard reagents, the solubility is not crucial in the preparation of high-molecular-weight polymers. The most probable reason for the termination of the chain growth in these reactions is purely chemical, i.e., hydrolysis of Mg-containing terminal fragments by trace amounts of moisture. Moreover, all the polycondensation reactions based on the use of Grignard reagents were carried out in THF, which could also restrict the growth of the polymeric chain.

Hence, the application of Grignard reagents in the cross-coupling reaction is limited due to the fact that they can give rise only to oligomeric products.

2. Synthesis of polymers using Ni⁰ complexes

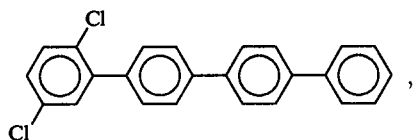
a. Homocondensation of dihaloaromatic compounds

For the first time, the condensation of aryl bromides or iodides in the presence of Ni⁰ complexes in dipolar aprotic solvents has been described in Refs 76–78.

These reactions proceeded under mild conditions but had a number of limitations: (i) their realisation required large amounts of the catalyst, the catalyst to monomer ratio being 1:1; (ii) the reaction conditions must be such that traces of air and moisture must be avoided.

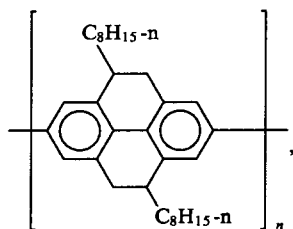
Using this method, Yamamoto et al.^{79,80} succeeded in obtaining poly-*p*-phenylenes and other polyarylenes. As a catalyst, Ni(COD)₂ (COD = cycloocta-1,5-diene) was used. Neutral ligands (Ph₃P or bipy) were also added to the reaction medium. Thus, oligomers with molecular weights of up to 6000 were synthesised based on *p*-dihalobenzenes.⁷⁹ The use of 9,10-dibromoanthracene as monomer gave a stable complex, L_mNiX(C₆H₄X), in high yield; in this case, the oligomer was not formed. Hence, it follows that chain growth also depends on the monomer structure.

Poly-*p*-phenylenes carrying pendant *ter*-phenyl groups have been synthesised⁸¹ from 2,5-dichloroquaterphenyl



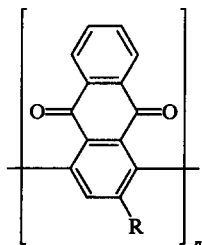
in the presence of the same catalyst, [Ni(COD)₂ + bipy] in DMF; they possess intriguing properties (as regards their conductivity); however, the degree of polymerisation did not exceed 10.

In more recent syntheses employing this catalyst, polymers of higher molecular weights could be obtained, apparently due to perfection of the synthetic procedure, i.e., more extensive purification of monomers and better removal of traces of moisture and oxygen from the reaction medium. Thus, Mullen et al.⁸² succeeded in obtaining soluble poly-*p*-phenylene:



based on the dibromide of substituted tetrahydropyrene; its molecular weight was 35 000 (\bar{M}_w) or 17 400 (\bar{M}_n) (DP = 40).

Later, Yamamoto⁸³ synthesised polyanthraquinone and polymethylantraquinone of high molecular weights (~190 000) from dichlorides:

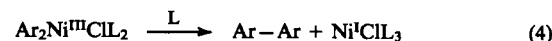
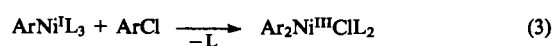


R = H, Me.

An alternative pathway was also proposed.^{84–86} A reactive Ni⁰ catalyst was prepared from catalytic amounts of NiCl₂(Ph₃P)₂ (or NiCl₂) in the presence of excess Ph₃P and a large excess of Zn powder (or some other reducing metal) at 60–80 °C in dipolar aprotic solvents. The reaction was completed within several minutes.

The positive factor in the use of these Ni⁰ catalysts is that aryl chlorides are most active in this process, as distinct from processes described earlier, in which aryl bromides and aryl iodides possess the highest activity.

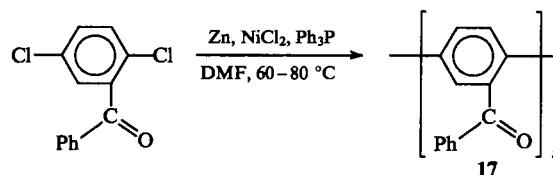
The putative mechanism of this reaction can be illustrated by the following scheme with the synthesis of a bisarene as an example:⁸⁴



L = PPh₃.

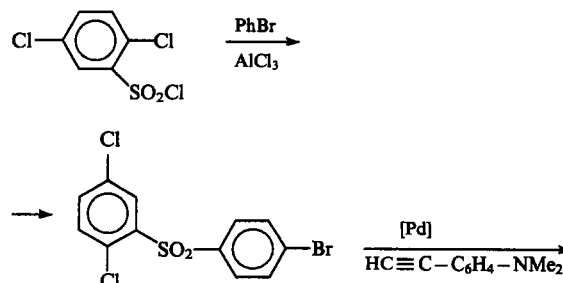
It has been shown that the first step (oxidative attachment of ArCl to Ni⁰ to form a bivalent nickel complex) occurs at rather a high rate. The next step, i.e., the reduction of Ni^{II} to Ni^I, is slow and rate-limiting at the beginning of the reaction when the ArCl concentration is still high. At the end of the reaction, it is the third step that determines the reaction rate. It has been found that the second and third rate-limiting steps are accelerated by the introduction of electron-acceptor substituents into the benzene rings and, *vice versa*, are decelerated with the introduction of electron-donor substituents. In addition, in the presence of electron-donor substituents side reactions can take place, viz., the formation of ArH. This is due to the fact that electron-donor groups stabilise the coordinatively unsaturated Ni^I complex, and the transfer of the phenyl group from the phosphorus to the nickel atom is possible. As the reaction proceeds further, this reaction course can result in the termination of the polymer chain and, consequently, in the synthesis of a low-molecular weight polymer.

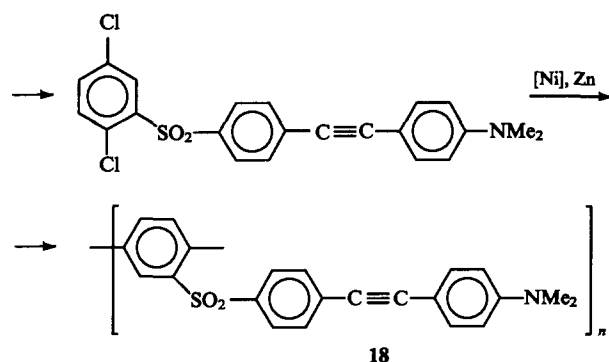
This method was used to obtain soluble poly-*p*-phenylene **17** based on 2,5-dichlorobenzophenone.^{87,88}



The polymer **17** possessed a high inherent viscosity: 1.05 dl g^{−1} when the reaction was carried out for 7 h, and 1.3 dl g^{−1} when the reaction was carried out for 50 h (\bar{M}_w = 60 000, DP = 330, T_g > 205 °C). The polymer was soluble in CHCl₃, in PhOH–CH₂Cl₂ and PhOH–C₂Cl₄ mixtures, formed films, and retained stability in air at temperatures below 500 °C (TGA).

Poly-*p*-phenylenes with side acetylene fragments **18** possessing nonlinear optical properties have been synthesised by Wright.⁸⁹



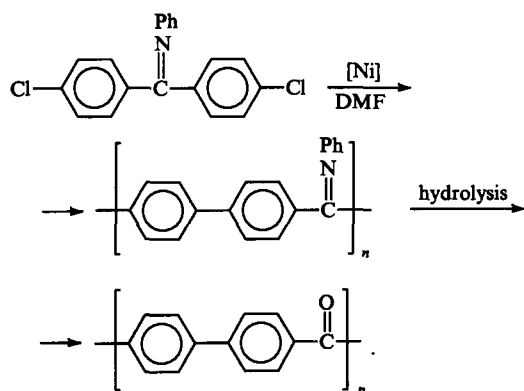


The polymer **18** had a low molecular weight ($\bar{M}_n = 8000$) and was readily soluble in ordinary organic solvents. Its glass transition temperature, T_g , is 220 °C, and its thermal stability is 300 °C (according to TGA).

The synthesis of polyether sulfones $[-C_6H_4-SO_2-C_6H_4-O-C_6H_4-C_6H_4-O-]_n$ and polyether ketones with the following formulae: $[-C_6H_4-C(O)-C_6H_4-X-C_6H_4-C(O)-C_6H_4-]_n$ where $X = O, OC_6H_4O$, has been described.⁹⁰⁻⁹² 4,4'-Bis(*p*-chlorophenoxy)diphenyl sulfone was used as the main monomer during the synthesis of polyether sulfones. Copolymers of 4,4'-bis(*p*-chlorophenoxy)diphenyl sulfone with 4,4'-dichlorodiphenyl sulfone, *p*-dichlorobenzene, etc, were also obtained. Of all polymers, the homopolymer possessed the largest reduced viscosity (0.81 dl g⁻¹); the viscosities of copolymers (in *N*-methylpyrrolidone at 25 °C) were in the range 0.4–0.69 dl g⁻¹.

The efficiency of homopolycondensation and, correspondingly, the molecular weight of the polymers obtained in the presence of Ni⁰ complexes depends on three factors. The most important is the absence of moisture, since in the presence of water aryl halide is reduced to arene,⁹³ eventually resulting in the termination of the chain. The second factor is the inert atmosphere, since even very small amounts of oxygen deactivate the catalyst (nickel oxide formed upon oxidation is not a catalyst under these conditions). The third factor is the purity of Zn (this must possess a well-developed surface and be free of oxygen).

The synthesis of polyarylenes involving Ni⁰ catalysts has also been described in many other papers. Thus, 1,2-bis(4-chlorophenyl)- and 1,2-bis(3-chlorophenyl)-1,1,2,2-tetramethyldisilane were used as monomers;⁸⁸ however, the polymers based on them had low molecular weights, 2400 and 10 000, as could be deduced from GPC data. The polyarylketone obtained from 4,4'-dichlorobenzophenone rapidly formed a precipitate (its molecular weight was as low as 1700). An alternative pathway for the synthesis of polyarylketone from polyketimine with subsequent hydrolysis of the ketimine groups has been proposed:⁸⁸



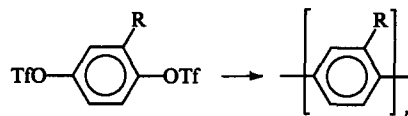
The polymer carrying ketimine groups is more readily soluble than its benzophenone analogue and has an inherent viscosity of

0.25 dl g⁻¹ (when the synthesis is performed in *N*-methylpyrrolidone, the viscosity can amount to 0.36 dl g⁻¹).

Thus, the use of Ni⁰ complexes has made it possible to obtain in some cases high-molecular-weight polymers from monomers carrying electron-acceptor substituents provided stringent conditions of the synthesis are observed.

b. Homopolycondensation of bistriflates

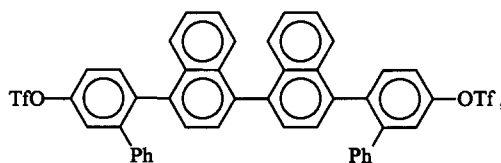
Ni⁰ complexes are ideal catalysts for the homopolycondensation of aromatic substituted bistriflates.^{94,95}



R = Ph, COOMe, Bu^t.

The reaction was carried out with Ni⁰ prepared *in situ* in the presence of excess Zn. It should be noted that the degree of polymerisation of polyphenylenes with phenyl, carboxymethyl, and *tert*-butyl substituents is different,⁹⁰ reaching 15, 30–47 and < 14, respectively. It may be inferred from these data that with triflates the molecular weight was the highest when monomers carrying electron-acceptor substituents were used.

One serious pitfall of this method is that the coupling of monomers can proceed in a 'head-to-tail' and 'head-to-head' manner, resulting in polymers with irregular structures. In this respect, the application of symmetrical monomers seems to be more expedient. Thus, the synthesis of the following monomer:



has been described.⁹¹

Homopolycondensation of this monomer resulted in an oligomer with DP = 7–8 (GPC) with a 33%–35% yield. The oligomer appeared to be nonconjugated due to the non-coplanarity of the benzene nuclei; however, it can be transformed into a conjugated form by intramolecular cyclisation resulting in the formation of triphenylene or perylene structural fragments.

IV. Synthesis of heterocyclic polyarylenes

There is an ample body of evidence concerning the synthesis of low-molecular organic compounds by cross-coupling of halogen derivatives of thiophenes, pyridines, *N*-substituted pyrroles, quinolines, benzotriazoles, ferrocene,⁹⁶ and even halonucleosides with the use of Ni and Pd catalysts.⁹⁷ Attempts have been made to apply this methodology to the synthesis of heteroaromatic polyarylenes (especially, of conducting systems of the polythiophene type).^{79,98-107}

Electrochemical methods or oxidation are used for obtaining heteroaromatic polymers; however, these techniques do not give, with a few exceptions,¹⁰⁸ regular structures.

By contrast, the cross-coupling reaction catalysed by transition-metal complexes allows for regio-specific interactions between the monomers, and correspondingly, the synthesis of polyheteroarylenes of a strictly defined structure. This approach was very extensively used in the synthesis of poly-2,5-thiophenes (to a lesser degree, poly-2,5-selenophene,¹⁰⁹ poly-2,5-pyrroles and related model oligomers).

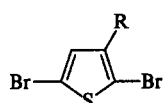
Cross-coupling reactions proved to be very effective in the synthesis of polythiophenes. In addition to the reproducible method for the synthesis of high-molecular-weight poly-2,5-thiophene, other procedures were elaborated for the synthesis of substituted poly-2,5-thiophenes and individual oligomers containing up to 7 cycles. As early as 1980, Lin⁹⁸ and Yamamoto⁹⁹

described the polycondensation of 2,5-dibromothiophene and demonstrated the advantages of nickel catalysts over palladium ones in the synthesis of polythiophene.

Polycondensation cross-coupling aimed at the synthesis of heterocyclic polyarylenes developed along the three main lines: (i) the use of Grignard reagents and their further interaction with heterocyclic halides in the presence of Ni^{II} complexes; (ii) the use of stoichiometric quantities of Ni⁰ complexes; (iii) the use of Ni⁰ complexes synthesised *in situ* in the presence of reducing agents.

Poly-2,5-(thiophene) and its methyl derivatives have been obtained^{98,99,102,103} in the following way: first, Grignard reagents were synthesised from the dibromides in the presence of a stoichiometric amount of Mg. They were subjected to polycondensation in the presence of catalytic amounts of a NiCl₂(bipy) complex in THF (first approach). The resulting product was poorly soluble in organic solvents (22%). The soluble fraction had a molecular weight, $M_n = 1370$.

In more recent studies,^{106,107} the following substituted dibromothiophenes were used:



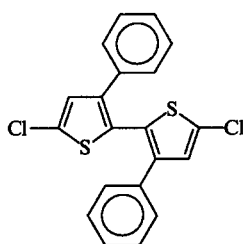
$R = C_{12}H_{25}$, Bu^p , $n-C_6H_{13}$, $(OCH_2CH_2)_nOCH_3$ ($n = 1, 2$) etc.

In both of the studies cited the monomer of the AB type was first obtained: to this end, one bromine atom was substituted by the MgBr group in the presence of the catalyst, Ni(dppp)Cl₂. The experimental conditions were such that the maximum molecular weight, M_w , reached 71 000 (DP = 160). In this case, the yield of the 'head-to-tail' polymer amounted to 99%.

Yamamoto⁷⁹ suggested to use the Ni⁰–Ni(COD)₂ complex in the presence of Ph₃P or bipy for the preparation of substituted ($R = C_6H_{13}$, C_8H_{17} , $C_{12}H_{25}$, CN) and non-substituted polythiophenes (second approach). The molecular weight of polythiophene with $R = C_6H_{13}$ was 52 000 (M_w , light scattering) and 190 000 for the samples obtained after 16 and 48 h, respectively.

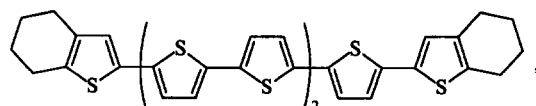
Ueda et al.¹⁰⁰ described the synthesis of poly-3-phenyl-2,5-thiophene based on a chloro-substituted monomer using catalytic amounts of Ni⁰ complexes in the presence of reducing agents (third approach).

A symmetrical monomer with two thiophene groups has been recommended¹¹¹ for the synthesis of polythiophene.



This route precludes the formation of a polymer having an irregular structure. The inherent viscosity of the polymer was rather high rising to 0.23–0.25 dl g⁻¹.

Recently Bauerle^{112,113} has described the synthesis of several intriguing oligothiophenes, such as the heptamer:



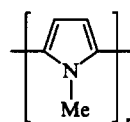
which is a compound of choice for electrochemical studies. It is noteworthy that analogous oligothiophenes were earlier obtained by other methods.^{114–116}

As far as oligo- and poly-pyrroles are concerned, despite the considerable interest of investigators in these compounds (in the

context of materials technology), only a small number of them have been synthesised with the use of the polycondensation cross-coupling method.

Thus, Kovacic^{117,118} reports on the synthesis of phenyl- and benzyl-substituted poly-*N*-methyl-2,5-pyrroles from the corresponding 2,5-dibromopyrroles. After conversion into the corresponding bifunctional Grignard reagents, these pyrroles entered into the polycondensation reaction catalysed by Ni^{II}(acac) in the quantities exceeding the stoichiometric ones. The resulting oligomers were partly soluble in organic solvents but had rather low molecular weights (according to the residual bromine content).

A wide variety of oligomeric unsubstituted poly-*N*-methyl-2,5-pyrroles have been synthesised and fully characterised in the course of detailed studies carried out by Kaufman.¹¹⁹

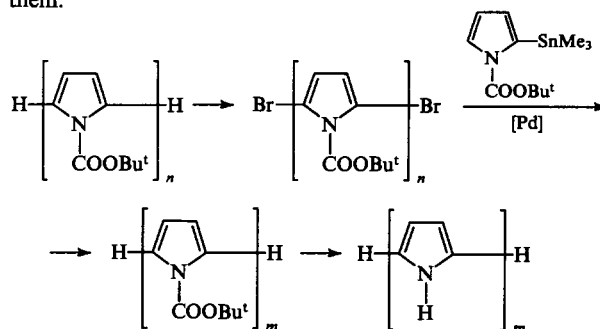


$n = 2, 6, 8, 16$.

It is to be mentioned, however, that the presence of methyl groups at the nitrogen atoms in the pyrrole rings decreases sharply the conductivity of polypyrroles. However, in the above syntheses only *N*-substituted pyrroles could be used, since the unprotected pyrrole is unstable (its sensitivity to even trace amounts of oxidants is well known). Therefore, the progress in the synthesis of conducting polypyrroles could be achieved if the problem of the monomer stability is solved.

The best solution of this problem is the use of *N*-substituted pyrroles provided the protecting group can be removed if required.^{118,119} In this case, polycondensation of monomers results in protected oligomers and polymers, which can be converted into poly-2,5-pyrroles at the final stage of the reaction. *tert*-Butoxycarbonyl was used as the protecting group, since it decomposes completely to form CO₂ and isobutene,¹²⁰ favours an increase in the solubility of intermediate oligomers and polymers and thus facilitates their processing and analysis; it is also an electron acceptor, and, as a consequence, demonstrates a stabilising effect.

Below is given a scheme of the synthesis of the corresponding substituted oligopyrroles and of oligopyrroles prepared from them:



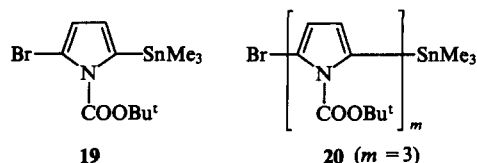
$n = 1, 3, 5, 7; m = n + 2$.

Bromination of *N-tert*-butoxycarbonylpyrrole ($n = 1$) has been carried out according to Gilow.¹²¹ The dibromide thus obtained¹²² reacted with two equivalents of a monotin derivative of *N-tert*-butoxycarbonylpyrrole⁵¹ to give a trimer. Bromination of the trimer at the both terminal α -positions and its repeated reaction with the organotin derivative resulted in further elongation of the chain to yield a pentamer. This pentamer was then repeatedly introduced into the chain growth cycle and so on. The resulting oligomers were fully characterised by spectroscopic methods.¹²³ The crystal structure of some of these compounds was established by X-ray analysis.¹

Heating of each of these polymers at 160–180 °C led to the elimination of the protecting COOBu^t-groups resulting in a series of unprotected oligopyrroles with $m = 3, 5, 7, 9$. According to ¹H and ¹³C NMR data, the deprotection was almost complete: the content of residual COOBu^t-groups did not exceed 4%. The longest pyrrole oligomer known thus far was terpyrrole. It is of note, however, that unprotected oligopyrroles are very unstable compounds, which form gels even at low temperatures; their treatment must be carried out in the absence of air.

The application of Pd-catalysed polycondensation to polypyrrole synthesis is coupled with certain difficulties, which are not still resolved. The attempts to synthesise polypyrroles under conditions of the Suzuki reaction (Pd-catalysed interaction of dihalides with diboronic acids) were unsuccessful, because in the case of pyrrole the electron-rich heteroatom easily loses its functional groups. For example, heating of *N*-tert-butoxycarbonylpyrrole-2-boronic acid in the biphasic toluene/Na₂CO₃ system for 24 h at 50 °C (in the absence of other components of the cross-coupling reaction and catalysts) resulted in a 50% loss of the B(OH)₂ groups, which thus determines the inapplicability of these compounds in the polycondensation reaction.^{124, 125}

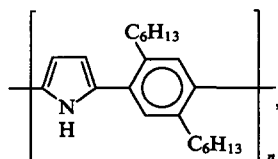
Therefore, an attempt has been made to prepare oligomers based on other monomers. To this end, monomers of the AB-type containing the trimethylstannyl group instead of B(OH)₂ have been synthesised:



Studies of cross-coupling of compounds of this type have shown that monomers **19** and **20** are quite stable.⁵⁰

According to liquid chromatography data, polycondensation of the monomer **19** yields only the oligomers with $n = 3-4$. To elucidate the reason for the low DP of these products, the lowest oligomers were isolated from the mixture and their structure was elucidated. It was found that they contain Me- and SnMe₃-groups as terminal groups rather than Br- and SnMe₃-groups as could be expected for the systems obtained by the interaction of the above monomers. The attempts to prevent the undesirable termination of the chain by varying the reaction conditions have failed. In further studies, an approach well-known in polycondensation has been applied, namely, the use of monomers containing more than one repeating unit. To this end, the terpyrrole monomer **20** was used. The polycondensation again proceeded with difficulty, but since the original monomer contained three structural units, it yielded an oligomer with $n = 10$. Fractionation of a mixture gave an oligomer with 20 *N*-substituted pyrrole rings in the chain ($M_w = 3400$, $M_n = 2800$). After deprotection, this oligomer was further used in electrochemical and optical-spectroscopic studies.

Pyrrole can also be introduced into the reaction of copolymerisation with arylidiboronic acid. The copolymer



was obtained by the interaction of the substituted aromatic diboronic acid with dibrominated protected pyrrole followed by thermal deprotection.¹²⁶ The resulting product had a rather high molecular weight, $M_w = 17\,000-20\,000$.

* * *

It may be inferred from the above that the polycondensation cross-coupling employing transition-metal complexes as catalysts allows one to synthesise soluble carbo- and hetero-chain polyarylenes of a strictly defined structure.

References

1. A-D Schlüter, G Wegner *Acta Polym.* **44** 59 (1993)
2. J K Stille, Y Gillioma *Macromolecules* **4** 515 (1971)
3. J K Stille *Makromol. Chem.* **154** 49 (1972)
4. J M Dineen, A A Volpe *ACS Polym. Prepr.* **19** (2) 34 (1978)
5. W R Krigbaum, K J Krause *J. Polym. Sci., Polym. Chem. Ed.* **16** 3151 (1978)
6. J M Dineen, E E Howell, A A Volpe *J. Polym. Sci., Polym. Chem. Ed.* **23** 282 (1982)
7. D G H Ballard, A Courtis, I M Shirley, S C Taylor *J. Chem. Soc., Chem. Commun.* 954 (1983)
8. K Mukai, T Teshirogi, N Kuramoto, T Kitamura *J. Polym. Sci., Polym. Chem. Ed.* **23** 1259 (1985)
9. P Kovacic, M B Jones *Chem. Rev.* **87** 357 (1987)
10. D R McKean, J K Stille *Macromolecules* **20** 1787 (1987)
11. D G H Ballard, A Courtis, I M Shirley, S C Taylor *Macromolecules* **21** 294 (1988)
12. C B Gortman, R H Grubbs *Conjugated Polymers* (Eds S L Bredas, R Silbey) (Dordrecht: Kluwer, 1991)
13. A F Diaz, J Bargon, in *Handbook of Conducting Polymers* Vol. 1 (Ed. T A Scotchell) (New York: Marcel Dekker, 1986) p. 81
14. T V Vernitskaya, O N Efimov, A B Gavrilov *Elektrokhimiya* **29** 1237 (1993)
15. J-W Lee, D-S Park, Y-B Shim, S-M Park *J. Electrochem. Soc.* **139** 3507 (1992)
16. D L Gin, J K Avlyanov, Y Min, A G MacGiarmind *ACS Polym. Prepr.* **35** (1) 287 (1994)
17. V V Korshak *Raznozhennost' Polimerov* (Different Chains of Polymers) (Moscow: Nauka, 1977)
18. N Miyaura, T Yanagi, A Suzuki *Synth. Commun.* **11** 513 (1981)
19. R B Muller, S Dudar *Organometallics* **3** 1261 (1984)
20. V Snieckas *Chem. Rev.* **90** 925 (1990)
21. J P Callman, L S Hegedus, J R Norton, R G Finke *Principles and Application of Organotransition Metal Chemistry* (Mill Valley: University Science Books, 1987)
22. K Tamao, M Kumada, in *The Chemistry of the Metal-Carbon Bond* Vol. 4 (Ed. F Hartley) (Chichester: Wiley, 1987) p. 819
23. T I Wallow, B M Novak *ACS Polym. Prepr.* **33** (1) 908 (1992)
24. M Rehahn, A-D Schlüter, G Wegner, W J Feast *Polymer* **30** 1060 (1989)
25. A Almennigen, O Bastiansen, L Fernhold, B N Cyvin, S Samdal *J. Mol. Struct.* **128** 59 (1985)
26. G-P Carbonneau, Y Delugeard *Acta Crystallogr., Sect. B, Struct. Crystallogr.* **33** 1586 (1977)
27. C P Brock, R P Minton *J. Am. Chem. Soc.* **111** 4586 (1989)
28. K N Baker, A V Fratine, W W Adams *Polymer* **31** 1623 (1990)
29. J L Bredas, R R Chance, R H Baughman, S Silbey *J. Chem. Phys.* **76** 3673 (1982)
30. M Rehahn, A-D Schlüter, G Wegner *Makromol. Chem.* **191** 1991 (1990)
31. T I Wallow, B M Novak *J. Am. Chem. Soc.* **113** 7411 (1991)
32. A L Casalnuova, J C Calabrese *J. Am. Chem. Soc.* **112** 4324 (1990)
33. P B Baland, A D Child, J R Reynolds *ACS Polym. Prepr.* **35** (1) 257 (1994)
34. A D Child, J R Reynolds *Macromolecules* **27** 1975 (1994)
35. U Scherf, K Müllen *Macromol. Chem., Rapid Commun.* **12** 489 (1991)
36. V Chaturvedi, S Tanaka, K Kaeriyama *Macromolecules* **26** 2607 (1993)
37. K Chmil, U Scherf *Macromol. Chem., Rapid Commun.* **14** 217 (1993)
38. U Scherf, K Müllen *Macromolecules* **25** 3546 (1992)
39. M B Goldfinger, T M Swager *ACS Polym. Prepr.* **35** (1) 273 (1994)
40. Y H Kim, O W Webster *J. Am. Chem. Soc.* **112** 4592 (1990)
41. O W Webster, Y H Kim, F P Gentry, R D Farlee, B E Smart *ACS Polym. Prepr.* **33** (1) 186 (1992)
42. U Fahrenstich, K-H Koch, K Müllen *Macromol. Chem., Rapid Commun.* **10** 563 (1989)
43. U Anton, K Müllen *Macromolecules* **26** 1248 (1993)

44. F Helmer-Metzmann, M Rehahn, L Schmitz, M Ballauff, G Wegner *Makromol. Chem.* **193** 1847 (1992)
45. L Schmitz, M Rehahn, M Ballauff *Polymer* **34** 646 (1993)
46. L Schmitz, M Rehahn *Macromolecules* **26** 4413 (1993)
47. B Sillion *Polyimides and Other Heteroaromatic Polymers (Comprehensive Polymer Science)* Vol. 5. (Eds G Allen, J C Bevington) (Oxford: Pergamon Press, 1989)
48. I P Beletskaya *J. Organomet. Chem.* **250** 551 (1983)
49. T R Bailey *Tetrahedron Lett.* **27** 4407 (1986)
50. J K Stille *Angew. Chem., Int. Ed. Engl.* **25** 508 (1986)
51. A N Kashin, I G Bumagina, N A Bumagin, I P Beletskaya, O A Reutov *Izv. Akad. Nauk SSSR. Ser. Khim.* 479 (1980)
52. M Bochmann, K Kelly *J. Chem. Soc., Chem. Commun.* 532 (1989)
53. M Bochmann, K Kelly, J Lu *J. Polym. Sci., Polym. Chem. Ed.* **30** 2511 (1992)
54. M Bochmann, J Lu *J. Polym. Sci., Polym. Chem. Ed.* **32** 2493 (1994)
55. T Kanbara, Y Miyazaki, T Yamamoto *J. Polym. Sci., Polym. Chem. Ed.* **33** 999 (1995)
56. X Qian, M R Pena *ACS Polym. Prepr.* **35** (2) 860 (1994)
57. X Qian, M R Pena *Macromolecules* **28** 4415 (1995)
58. E Negishi, A O King, N Okakado *J. Org. Chem.* **42** 1821 (1977)
59. T Yamamoto, A Yamamoto *Chem. Lett.* 353 (1977)
60. T Yamamoto, Y Hayashi, A Yamamoto *Bull. Chem. Soc. Jpn.* **51** 2091 (1978)
61. K Tamao, K Sumitani, M Kumada *J. Am. Chem. Soc.* **94** 4374 (1972)
62. K Tamao, K Sumitani, Y Kiso, M Zembayashi, A Fijioaka, S Kodama, J Nakajima, A Minato, M Kumada *Bull. Chem. Soc. Jpn.* **49** 1958 (1976)
63. M Kumada *Pure Appl. Chem.* **52** 669 (1980)
64. Z-J Ni, T-Y Luh *J. Chem. Soc., Chem. Commun.* 115 (1987)
65. M Bochmann, C S Creaser, L Wallace *J. Mol. Catal.* **60** 343 (1990)
66. W Kern, H O Wirth *Kunststoffe* **6** 12 (1959)
67. W Kern, M Seibel, H O Wirth *Makromol. Chem.* **29** 164 (1959)
68. W Kern, H W Ebersbach, I Zieger *Makromol. Chem.* **31** 154 (1959)
69. H Longhals, S Demig, T Potawa *J. Prakt. Chem.* **333** 733 (1991)
70. W Heitz *Chem.-Ztg.* **110** 385 (1986)
71. H Ringsdorf, P Tschirmer, O Hermann-Schönherr, J H Wendorf *Makromol. Chem.* **188** 1431 (1987)
72. M Ballauff *Angew. Chem., Int. Ed. Engl.* **28** 253 (1989)
73. A Noll, N Siegfried, W Heitz *Macromol. Chem., Rapid Commun.* **11** 485 (1990)
74. M Rehahn, A-D Schlüter, G Wegner, W J Feast *Polymer* **30** 1054 (1989)
75. M Ishikawa, M Kawai, Y Ohsawa *Synth. Met.* **40** 231 (1991)
76. M F Semmelhack, L S Ryono *J. Am. Chem. Soc.* **97** 2873 (1975)
77. M F Semmelhack, P M Helquist, L D Jones *J. Am. Chem. Soc.* **93** 5908 (1971)
78. M F Semmelhack, P M Helquist, L D Jones, L Keller, L Mendelson, L Ryono, J Gorzynski, R D Stauffer *J. Am. Chem. Soc.* **103** 6460 (1981)
79. T Yamamoto, A Morita, Y Miyazaki, T Maruyama, H Wakayama, Z Zhou, Y Nakamura, T Kanbara, S Sasaki, K Kubata *Macromolecules* **25** 1214 (1992)
80. T Yamamoto, T Maruyama, Z Zhou, Y Miyazaki, T Kanbara, K Sanechika *Synth. Met.* **41** 345 (1991)
81. M Pomerantz, J P Wong *ACS Polym. Prepr.* **35** (1) 210 (1994)
82. M Kreyenschmidt, F Uckert, K Müllen *Macromolecules* **28** 4577 (1995)
83. T Yamamoto, H Etori *Macromolecules* **28** 3371 (1995)
84. J Colon, D R Kelsey *J. Org. Chem.* **51** 2627 (1986)
85. A S Kende, L S Liebeskind, D M Braitsch *Tetrahedron Lett.* 3375 (1975)
86. T Lembayashi, M Kumada *Tetrahedron Lett.* 4089 (1977)
87. C Y Wang, R P Quirk *ACS Polym. Prepr.* **35** (1) 712 (1994)
88. R W Phillips, V V Sheares, E T Samulski, J M DeSimone *ACS Polym. Prepr.* **35** (1) 367 (1994)
89. M E Wright, E G Toplikar *ACS Polym. Prepr.* **35** (1) 369 (1994)
90. I Colon, G T Kwiatkowski *J. Polym. Sci., Polym. Chem. Ed.* **28** 367 (1990)
91. M Ueda, F Ichikawa *Macromolecules* **23** 926 (1990)
92. G T Kwiatkowski, I Colon, M J El-Hibri, M Matzner *Makromol. Chem., Makromol. Symp.* **54/55** 199 (1992)
93. I Colon *J. Org. Chem.* **47** 2622 (1982)
94. V Percec, S Okita, R Weiss *Macromolecules* **25** 1816 (1992)
95. V Percec, S Okita, J Bae *Polym. Bull.* **29** 271 (1992)
96. R Knapp, M Rehahn *J. Organomet. Chem.* **452** 235 (1993)
97. V N Kalinin *Synthesis* 413 (1992)
98. J W-P Lin, L P Dodek *J. Polym. Sci., Polym. Chem. Ed.* **18** 2869 (1980)
99. T Yamamoto, K Osakada, T Wakabayashi, A Yamamoto *Macromol. Chem., Rapid Commun.* **6** 671 (1985)
100. M Ueda, Y Miyaji, T Ito, Y Oba, T Sone *Macromolecules* **24** 2694 (1991)
101. H Mao, S Holdcroft *Macromolecules* **25** 554 (1992)
102. K Sanechika, A Yamamoto *J. Polym. Sci., Polym. Lett. Ed.* **20** 365 (1980)
103. T Yamamoto, K Sanechika, A Yamamoto *Bull. Chem. Soc. Jpn.* **56** 1497 (1983)
104. C E Brown, P Kovacic, R B Cody Jr, R E Hein, J A Kinsinger *J. Polym. Sci., Polym. Lett. Ed.* **24** 519 (1986)
105. V N Kalinin *Usp. Khim.* **60** 339 (1991) [*Russ. Chem. Rev.* **60** 173 (1991)]
106. R D McCullough, S P Williams, M Jayaraman *ACS Polym. Prepr.* **35** (1) 190 (1994)
107. M Jayaraman, R D McCullough *ACS Polym. Prepr.* **35** (1) 229 (1994)
108. R M Souto Maior, K Hinkelmann, H Eckert, F Wudl *Macromolecules* **23** 1268 (1990)
109. M D Bezoari, P Kovacic, S Gronowitz, A B Hornfeldt *J. Polym. Sci., Polym. Lett. Ed.* **19** 347 (1981)
110. J K Kallitsis, H Naarman *Synth. Met.* **44** 247 (1991)
111. M Ueda, T Ito, Y Seino, Y Ohba, T Sone *Polym. J.* **24** 693 (1992)
112. P Biuerle *Adv. Mater.* **4** 102 (1992)
113. P Biuerle, U Segelbacher, K-U Gardl, D Huttenlocher, A Mehring *Angew. Chem., Int. Ed. Engl.* **32** 76 (1993)
114. W ten Holve, H Wynberg, E E Havinga, E W Meijer *J. Am. Chem. Soc.* **113** 5887 (1991)
115. D Delabougliuse, M Hmyene, G Horowith, A Yassar, F Garnier *Adv. Mater.* **4** 107 (1992)
116. A Yassar, D Delabougliuse, M Hmyene, B Nessak, G Horowitz, F Garnier *Adv. Mater.* **4** 490 (1992)
117. I Khouri, P Kovacic, H M Gillow *J. Polym. Sci., Polym. Lett. Ed.* **19** 395 (1981)
118. P Kovacic, I Khouri, R L Eisenbaumer *Synth. Met.* **6** 31 (1983)
119. T Kaufman, H Lexy *Chem. Ber.* **114** 3674 (1981)
120. W Raval, M P Cava *Tetrahedron Lett.* **26** 6141 (1985)
121. H M Gillow, D E Burton *J. Org. Chem.* **46** 2221 (1981)
122. S Martina, V Enkelmann, G Wegner, A D Schlüter *Synthesis* 613 (1991)
123. S Martina, V Enkelmann, G Wegner, A D Schlüter *Synth. Met.* **51** 299 (1992)
124. S Gronowitz, A-B Hornfeldt, Y Yang *Organic Synthesis: Modern Trends. The 6th IUPAC Symposium* (Ed. O Chizhov) (Oxford: Blackwell, 1987)
125. S Gronowitz, D Peters *Heterocycles* **30** 645 (1990)
126. S Martina, A D Schlüter *Macromolecules* **25** 3607 (1992)

Prospects in the application of alkoxo-technology in heterogeneous catalysis

Yu M Rodionov, E M Slyusarenko, V V Lunin

Contents

I. Introduction	797
II. The mechanisms of the conversion of alkoxides into oxides	797
III. Principal aspects, advantages, and disadvantages of the application of alkoxo-technology in heterogeneous catalysis	799
IV. Regulation of the chemical and phase compositions of oxide systems	800
V. Preparation of coatings and thin films	802
VI. The use of alkoxides for the preparation of carriers and catalysts	803
VII. Achievements of alkoxo-technology in the manufacture of materials structurally similar to carriers and catalysts	807
VIII. Conclusion	808

Abstract. The main principles, characteristic features, advantages, and disadvantages, of the application of alkoxo-technology[†] for the preparation of heterogeneous oxide catalysts and carriers are examined. The bibliography includes 293 references.

I. Introduction

The traditional technologies for the preparation of inorganic oxide materials, including carriers and heterogeneous catalysts, which are based on the use of inorganic acid salts, oxides, and hydroxides as precursors, have to a large extent exhausted their possibilities. The probability that a qualitative jump in the development of this field can be achieved and that the characteristics of materials, can be appreciably improved on their basis is extremely small. One of the promising approaches to the overcoming of many disadvantages of the traditional technology and to the creation of new materials and the improvement of the quality of those already known involves the application as starting materials (precursors) of the alkoxides of various chemical elements (metal alkoxides and alkyl esters of ortho-acids). This method has been called alkoxo-technology. Abroad, alkoxo-technology, which is one of the variants of sol-gel technology, made it possible to initiate the manufacture of a series of advanced materials for microelectronic, optic fibre, aerospace, and other branches of engineering.^{1–3} The number of publications on this topic throughout the world runs into thousands, but in the Russian scientific and patent literature they are represented by few examples and are either of a purely academic character or are concerned with simple variants of alkoxo-technology associated

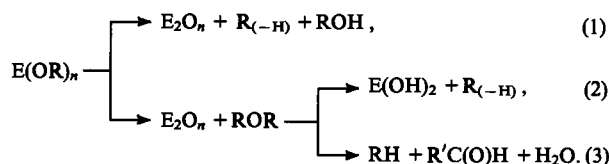
with the employment of only silicon alkoxides or their mixtures with inorganic salts. This situation has led to an underestimate of the possibilities of the use of alkoxo-technology in heterogeneous catalysis. Furthermore, it was evident from the very beginning that the most promising aspect of its practical application involves the preparation of catalysts and carriers for the latter.⁴

The reviews^{5–11} concerning the application of alkoxo-technology in heterogeneous catalysis are relatively inaccessible and are limited to the consideration of a narrow range of problems. The aim of the present review is to survey the most important advances in the field of alkoxo-technology (mainly during the last decade) and also to assess the potential possibilities of its use for the preparation of oxide catalysts and carriers.

II. The mechanisms of the conversion of alkoxides into oxides

Alkoxides are converted into oxides in thermal and thermooxidative degradation and hydrolytic processes and in the interaction with the surface OH groups and hydroxides.

In the synthesis of oxide powders by spray pyrolysis in an inert medium, in the chemical vapour-phase deposition of coatings, and in the preparation of coatings and bulky materials from solutions of alkoxides or the products of their partial hydrolysis, the alkoxides undergo thermal decomposition. A schematic illustration of this process, proposed by Tishchenko as early as the past century,¹² can be represented as follows:



Here the symbol E designates the fundamental element. The composition of the organic product of the thermal degradation (ethers ROR, alkenes $\text{R}_{(-\text{H})}$, alkanes RH, aldehydes $\text{R}'\text{CHO}$, and alcohols ROH) is determined mainly by the nature of the alkyl group and of the chemical element and also by the process temperature. For example, alkaline earth metal oxides are capable of dehydrating ethers and the decomposition of their alkoxides proceeds predominantly via path (2). Alkoxides with

[†] Alkoxide sol-gel methods (Translator).

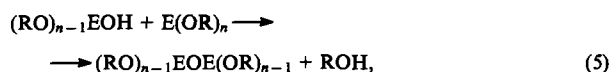
Yu M Rodionov State Institute of the Chemistry and Technology of Organoelement Compounds, shosse Entuziastov 38, 111123 Moscow, Russian Federation. Fax (7-095) 273 13 23. Tel. (7-095) 273 63 69
E M Slyusarenko, V V Lunin Faculty of Chemistry, Lomonosov Moscow State University, Vorob'evy gory, 119899 Moscow, Russian Federation. Fax (7-095) 939 01 71

secondary and tertiary alkyl groups decompose most readily via path (1) (since the heterolytic dissociation of the R—O bond and the abstraction of a proton from the carbonium ion are facilitated under these conditions).¹³ For catalytic purposes, it is desirable to employ the alkoxides derived from higher alcohols, since in this case the oxides formed have the most extensive porous structure. Products of the thermal decomposition of alkoxides are usually nonstoichiometric oxides E_2O_{n-x} and this factor may be used deliberately for the preparation of a series of catalysts. The thermal decomposition conditions are chosen in such a way that certain catalytically active substances are segregated not in the oxide but in the metallic form (the reduction is effected by the organic thermal degradation products). This mechanism can be achieved also in a mixture of an alkoxide (precursor of the porous carrier) and of the salt undergoing thermal decomposition (precursor of the metal catalyst).

The thermal decomposition of alkoxides for the preparation of catalysts and adsorbents is usually carried out under thermooxidative conditions in the presence of O_2 . Together with reaction (1)–(3), the alkyl groups of the alkoxide and of the organic degradation products are oxidised. The compounds formed may interact with the alkoxide: the water evolved in the thermal oxidation hydrolyses the alkoxide, as a result of which the decomposition is sharply accelerated and assumes a chain character.

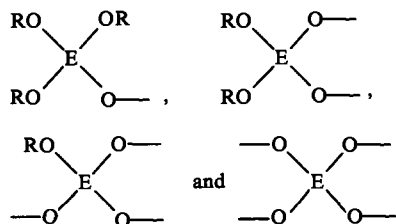
Not only the final process temperature but also the rate of its increase exert a definite influence on the course of the thermooxidative degradation, which is associated with the sintering of the elementoxane skeleton at high temperatures, decrease in the oxidation surface, and hindrance to the diffusion of oxygen and volatile products. Although all this leads to a sharp fall in the rate of decomposition of alkoxides, nevertheless it is not always taken into account in practice.

Alkoxides are usually converted into oxides by hydrolysis in which the following reactions take place:^{14,15}



The hydrolysis [reaction (4)] of the majority of alkoxides proceeds at a high rate and the overall rate of hydrolysis is determined by diffusional and not kinetic factors. In order to complete the condensation with formation of ROH or H_2O [reactions (5) and (6)], an increased temperature and/or the presence of acidic or basic catalysts is usually required. The dimers formed on condensation enter into further reactions with H_2O and alkoxide hydroxides. The composition and structure of the final hydrolysis (hydropolycondensation) product depend mainly on the nature of the chemical element and the alkyl group, the pH of the reaction medium, and the ratio of the alkoxide and water.

If water has been added in an amount theoretically insufficient for the complete elimination of the RO groups via reactions (4)–(6), for example less than 2 moles of H_2O per mole of the alkoxide of a tetravalent element, then alkoxyelementoxane polymers (oligomers) of different structure are formed. The chain of such a polymer includes the following units:



By selecting the reaction conditions, it is possible to regulate the ratio of such units and the ways in which they are joined together and to synthesise polyalkoxyelementoxanes having a predominantly linear or branched structure, which makes it possible to control the porous structure of the oxides formed on their decomposition.

If the hydrolysis of the alkoxides proceeds in an excess of H_2O , then, depending on the nature of the element, the oxides E_2O_n , the hydroxides $E(OH)_n$, or the oxide hydroxides $EO_x(OH)_{n-2x}$, containing residual RO groups, are formed. This is associated with the reversibility of the reactions and the formation of three-dimensional elementoxane skeletons with sterically 'frozen' RO groups incapable of further hydrolysis or condensation with OH groups.

Complete hydrolysis is usually carried out in aqueous alcoholic media with a 10–20-fold excess of H_2O (relative to the theoretical amount). The hydrolysis products are isolated in the first stage in the form of nanometer-sized particles, so that the reaction medium remains optically transparent. Such a solution, called a sol, may be stabilised by special additives and may be used in the deposition of catalytic coatings and as a binder for carriers. Partly chelated alkoxides, for example $Ti(OR)_2(acac)_2$, are often used for the preparation of sols from the readily hydrolysable aluminium, titanium, or zirconium alkoxides, since this ensures a quieter course of hydrolysis (without the formation of powders or gels) and the stabilisation of the sol formed.

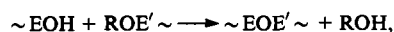
If the sol is not stabilised, the shape and size of the primary particles change during its ageing and gradually combine into various associated species. The sol loses its fluidity and is converted into a gel. The sol–gel transition may be regulated by selecting the solvent and the catalysis and by altering the temperature. An important factor is that this process is fairly controllable and that it does not entail, in contrast to the preparation of a sol from inorganic salts, the laborious washing away of extraneous ions and an increased purity of the product is attained. Although the SiO_2 carriers obtained, for example, from sodium silicates, are cheaper than those obtained from ethyl silicates, they retain 1% of Na_2O even after prolonged washing,¹⁶ which lowers their thermal stability and interferes with a series of catalytic processes.

Water and organic solvents are removed from gels by drying in air at different temperatures or by treatment in an autoclave at temperatures and pressures above the critical values for the solvent being removed (super-critical or hypercritical conditions). Xerogels and aerogels are then obtained respectively. The specific surface (S_{sp}) and the pore volume of the aerogels are somewhat greater than those of the xerogels, but the latter are cheaper and therefore have found more extensive application. Owing to the difference between the capillary tensions in pores with different diameters, large specimens crack and disintegrate during the drying of the xerogels, which, however, does not preclude their application, since the xerogels are usually employed only at starting materials for the preparation of various forms of catalysts and carriers (with the aid of comminution, moulding with a binder, and sintering). In recent years, methods have been developed for the drying of the gels under the usual conditions without cracking.¹⁷ For this purpose, chemical additives, for example formamide, which control the drying process, are introduced into the solutions being hydrolysed.

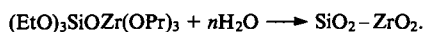
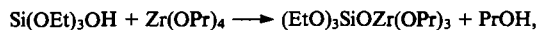
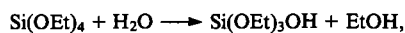
In most cases only one oxide is insufficient for the preparation of a carrier or catalyst with the optimum combination of properties. Mixed oxides are frequently used in heterogeneous catalysis. When alkoxy-technology is employed, they are obtained by the joint hydrolysis of two and more alkoxides or by the hydrolysis of an alkoxide in the presence of inorganic compounds with subsequent drying and partial sintering. The main problem in the hydrolysis of a mixture of alkoxides is that of the generation of mixed elementoxane fragments $E-O-E'$, which ensures the homogeneity of the system at the atomic (molecular) level and ultimately makes it possible to reduce sharply the crystallisation

and sintering temperatures or, conversely, to increase the temperatures of undesirable phase transitions.

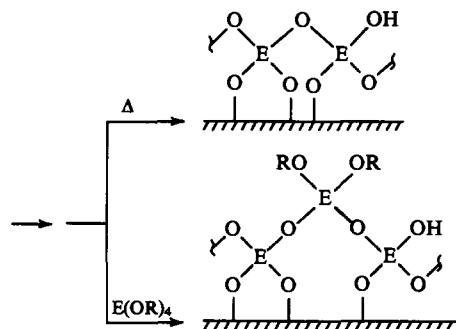
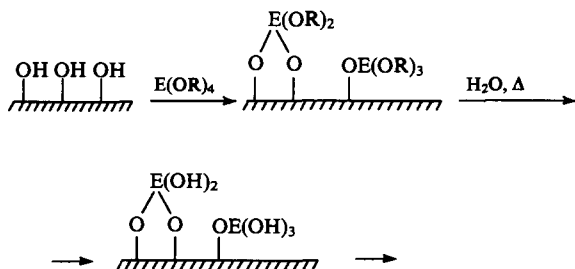
The homogeneity of the distribution of the components, including small amounts of modifying additives, is the principal advantage of alkoxo-technology. Thus a microheterogeneous mixture of SiO_2 and TiO_2 is formed in the SiCl_4 – TiCl_4 system on deposition,¹⁸ whereas the joint hydrolysis of Si(OR)_4 and Ti(OR)_4 leads to the formation of a homogeneous titanosilica gel.¹⁹ When aqueous solutions of aluminium and magnesium salts are made alkaline, mixed hydroxide and oxide hydroxides with a homogeneous distribution of the metals are not formed owing to the difference between their precipitation pH values.²⁰ In contrast, on dissolution of alkoxides in organic solvents, complex formation takes place and the alkoxo-salt $\text{Mg[Al(OR)}_4\text{]}_2$ is formed, partial hydrolysis generating the Al–O–Mg fragment. Homogeneity is also retained on subsequent conversion into oxide hydroxides and oxides.²¹ Mixed E–O–E' fragments are formed mainly on condensation of the RO and OH groups attached to different elements:



It is noteworthy that the rates of hydrolysis and condensation of alkoxides differ significantly. This complicates the task of achieving atomic homogeneity (simple addition of water to a solution of a mixture of alkoxides usually results in the formation of a heterogeneous mixture of oxide and/or oxide hydroxide particles of nanometer size). A series of methods for the solution of the problem have been developed: slow hydrolysis by atmospheric moisture, selection of RO groups, the use of presynthesised mixed alkoxides, the introduction of organometallic catalysts, and preliminary partial hydrolysis of one of the alkoxides. The last method has received the greatest attention.^{22–24} Thus in the manufacture of highly porous ' SiO_2 – ZrO_2 ' carriers, Si(OEt)_4 is initially partially hydrolysed, after which Zr(OPr)_4 is added, and then the final hydrolysis is carried out:²⁵

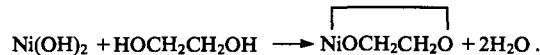


The high chemical reactivity of the RO groups of alkoxides is manifested also when alkoxides come into contact with the OH groups of surfaces and hydroxides. This feature has been used successfully in the modification of the surfaces of catalysts and carriers. The sequence of reactions occurring under these conditions and the structure of the films (monolayer or bilayer in the initial stage of their formation), which are produced when a hydroxylated surface is treated with an alkoxide of a tetravalent element, can be represented as follows:



A similar modification of the surface may be achieved with the aid of anhydrous halides, which are virtually the only alternative to alkoxides. However, this does not afford any significant advantages, whereas the disadvantages of this procedure (among which difficulties in the storage and use of the product and the evolution of hydrogen halides during hydrolysis may be included) are fairly considerable.

The processes in which the precursors of oxide carriers and catalysts are inorganic compounds is of great interest. Alkoxides are then formed or R–O–E fragments are generated. Such processes are based on familiar reactions involving the formation of alkoxides from hydroxy-compounds, on the one hand, and oxides, hydroxides, and the salts of volatile acids (acetic, carbonic, and nitric), on the other.^{26–27} For example, the alkoxide (glycolate) was obtained directly in the reaction mixture in the synthesis of the Ni–SiO_2 catalyst:²⁸



Until recently, attention has been devoted to the specific synthesis of alkoxides from cheap inorganic compounds directly during the preparation of carriers and catalysts, i.e. to the attainment of the chain of reactions inorganic compound \rightarrow alkoxide \rightarrow oxide within the framework of alkoxo-technology.

III. Principal aspects, advantages, and disadvantages of the application of alkoxo-technology in heterogeneous catalysis

The chemical properties of alkoxide and the products of their hydrolysis described above as well as the mechanism of their conversion into oxides provide alkoxo-technology with the following important advantages:

- high purity of the final products (other elements can be fairly readily eliminated from alkoxides even at the synthesis stage or on distillation, and the preparation of powders does not require a milling stage in which the product might be contaminated);
- structural and chemical homogeneity of multicomponent mixtures;
- an appreciable decrease in the phase formation and sintering temperatures;
- simplicity of deposition of coatings with a controllable porosity and thickness on carriers of any shape;
- the possibility of synthesising new crystalline and amorphous compounds, the preparation of which by traditional methods is difficult or impossible;
- high quality of the intermediate products obtained when hydrolysed alkoxides are used as binders for large articles;
- the possibility of obtaining products in the form of fibres and microspheres;
- ecological cleanliness of the processes.

In modern chemical engineering, ecological advantages have assumed particular importance. Firstly, when alkoxides are employed, problems of the purification of waste waters do not arise. Secondly, the alcohols and organic compounds formed when alkoxides are converted into oxides may be fairly readily trapped, reused, or combusted further to CO_2 . This is significantly simpler than neutralisation of nitrogen and sulfur oxides as well as hydrogen halides, which are frequently present in the effluent gases in the synthesis of catalysts from inorganic precursors.

The main disadvantages of alkoxo-technology are as follows:

- the use of organic compounds as solvents;
- the considerable shrinkage in the preparation of dense materials;
- the higher cost of alkoxides compared with inorganic compounds.

The handling of organic compounds (solvents, alcohols, and decomposition products) requires the use of explosion-proof apparatus. However, this is not a significant obstacle to the employment of alkoxo-technology in catalysis, because the manufacture of catalysts is in general distinguished by a high degree of technological sophistication. Similar problems arise (are solved) also in the handling of ammonia, ammonium salts, and acetates.

The appreciable shrinkage during sintering is known to have a negative effect on the preparation of dense, and bulky ceramic materials.²⁹ In heterogeneous catalysis, alkoxides and their hydrolysis products are usually employed for the deposition of thin coatings or as binders in the preparation of bulky carriers and catalysts. In such cases, the problem of shrinkage is not so significant, particularly since the heat treatment is carried out at temperatures such that only partial sintering of the oxide skeleton generated from the alkoxide takes place and the optimum ratio of porosity to strength is ensured (porosity reduces sharply the strength of oxide materials).

The higher cost of alkoxides compared with inorganic compounds is undoubtedly the most important disadvantage of alkoxo-technology. Nevertheless, both in Russia and abroad silicon alkoxides are widely used in the casting of metals in accordance with smeltable models. The world prices of silicon, titanium, and aluminium alkoxides are comparable and are respectively about 3.5, and 3 U.S. dollars per kilogram.³⁰ The reasons why foreign investigators and practitioners in the field of the sol-gel process have turned to its alkoxide version are not discussed in the Russian literature,³¹ so that the hypotheses concerning the use of cheaper inorganic precursors are insufficiently convincing. It is striking that abroad it is regarded economically justified to employ for the preparation of a series of oxide materials not only alkoxides but also even acetylacetonates,^{32,33} the cost of which is higher by a factor of tens.

The application of the mixed alkoxoacetylacetonates $\text{E(OR)}_x(\text{acac})_{n-x}$, also of the acetylacetonates E(acac)_n , is considered in this review, since the latter represent a special kind of alkoxide with an intramolecular coordinate bond and a conjugation system, which are formed with participation of acetylacetone in the enolic form.

Not so much the high cost as the lack of a wide-scale industrial manufacture of aluminium and zirconium alkoxides, which together with silicon and titanium alkoxides are the principal reagents in alkoxo-technology, is a more realistic obstacle to the introduction of the latter in Russia. Their manufacture is now being initiated, but an electrochemical procedure is used for this purpose,³⁴ which differs from the industrial methods of alkoxide synthesis generally adopted in world practice.³⁵

Figure 1 presents schematically the principal aspects of alkoxide use in the technology of heterogeneous catalyst synthesis. This scheme embraces silicon, aluminium, and titanium alkoxides. Sometimes the oxide formed from one alkoxide is catalytically inactive or is insufficiently active. Such an oxide may function as a cocatalyst, a carrier, or an inorganic carrier,

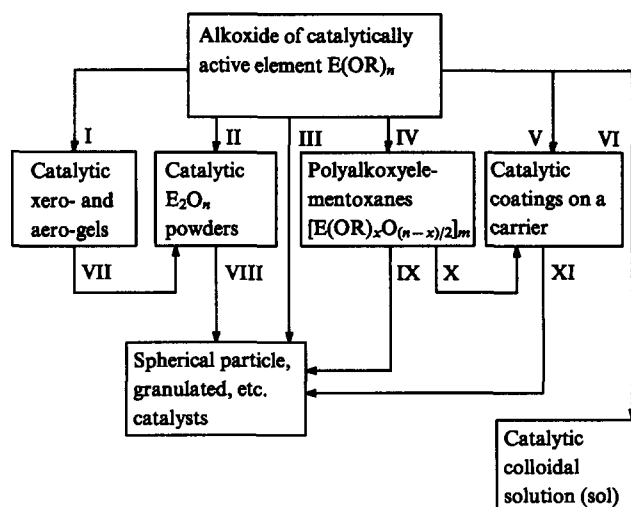


Figure 1. Principal operations in the preparation of intermediate products and catalytic materials from the alkoxides of catalytically active elements.

while the active component may be added to it, for example, in the course of, or after, joint hydrolysis.

There are several ways of synthesising heterogeneous catalysts, including the following operations (Fig. 1): I and II — total hydrolysis and drying, III — hydrolysis accompanied by the introduction of a filler and moulding, IV — partial hydrolysis; V — treatment of the carrier with a liquid or gaseous alkoxide; VI — total hydrolysis with stabilisation of the sol; VII — dispersion; VIII — introduction of inorganic binders (including their introduction via alkoxides) and moulding; IX — preparation of the solution, introduction of the filler, and moulding; X — treatment of the carrier with a polymer solution; XI — introduction of binders and moulding (preparation of fibrous and powdered carriers). The concluding operation in procedures I, III, V and VIII — XI is heat treatment. Specific ways of implementing individual variants of this general scheme will be examined below.

IV. Regulation of the chemical and phase compositions of oxide systems

The purity of the alkoxides, the uniformity of the distribution of the components in their joint hydrolysis mixtures, and the increased reactivity of the oxides formed after the removal of the organic component favour the specific regulation of the chemical and phase compositions of catalyst materials and hence exert a definite influence on their characteristics.³⁶

One of the commonest carriers and also catalysts or cocatalysts in many reactions is porous $\gamma\text{-Al}_2\text{O}_3$. In its preparation, it is necessary to solve a whole series of problems: the formation and stabilisation of a large surface area, the attainment of definite acid — base characteristics, and the retardation (shifts towards higher temperatures) of the $\gamma \rightarrow \alpha$ transition. The last problem is especially important in high-temperature catalysis, since the $\gamma \rightarrow \alpha$ transition is accompanied by an increase in grain size and in the density of the carriers and catalysts, which leads to a sharp decrease in their specific surfaces (S_{sp}) and strength up to disintegration. The use of alkoxo-technology made it possible to achieve significant advances in all these aspects. Thus $\gamma\text{-Al}_2\text{O}_3$ obtained from an alkoxide is distinguished by an increased thermal stability:^{37,38} after heat treatment at 800 °C, the specific surfaces of the alkoxide and nitrate $\gamma\text{-Al}_2\text{O}_3$ are respectively 150 and 50 $\text{m}^2 \text{g}^{-1}$.

The thermal stability of γ - Al_2O_3 increases significantly after the introduction of certain elements in the $\text{Al}(\text{OR})_3$ hydrolysis stage:³⁹ the specific surfaces of γ - Al_2O_3 without additives and following the addition of 4% of ThO_2 , ZrO_2 , and SiO_2 were 80, 99, 88, and $150 \text{ m}^2 \text{ g}^{-1}$ respectively after they had been maintained at 1000°C for 24 h, while the specimens containing 7% of SiO_2 had $S_{\text{sp}} = 116, 98.4$, and $84.9 \text{ m}^2 \text{ g}^{-1}$ after heat treatment at 1100°C for 30, 100, and 400 h respectively. The increase in thermal stability is due to the uniform distribution of the additives in the alumina matrix, which hinders the conversion of the low-temperature modifications of alumina into the thermostable α -form and shifts it into the region of higher temperatures.

Alkali and alkaline earth metal hexa-, undeca-, and dodeca-aluminates have a greater ability than γ - Al_2O_3 to retain an extensive specific surface at temperatures above 900°C . They can be most conveniently synthesised by employing alkoxides or mixtures of alkoxides with acetylacetonates and hydroxides.^{40–44} Thus barium hexaaluminate, obtained by the traditional solid-phase synthesis from BaCO_3 and Al_2O_3 , had $S_{\text{sp}} = 6.3 \text{ m}^2 \text{ g}^{-1}$ after heat treatment at 1300°C , while the specimen obtained by the alkoxide method had $S_{\text{sp}} = 20.2 \text{ m}^2 \text{ g}^{-1}$.⁴²

It is of interest to compare the alkoxide method with other procedures for the preparation of aluminates. For example, the traditional method of preparation of hexaaluminates as carriers for final-combustion catalysts includes the following principal technological operations: fusion of Al_2O_3 , B_2O_3 , and alkaline earth metal oxides at temperatures exceeding 1500°C , maintenance at 750 – 850°C , comminution, leaching with acids (for example, with acetic acid), washing, and drying.⁴⁵ This process is distinguished by high energy consumption, is laborious, and generates a series of ecological problems. When alkoxo-technology is employed, water is simply added to alkoxides and the powders are separated and heat-treated (up to 900°C). Such simplification of the technology combined with an increased heat resistance of the products justifies the view that the alkoxide method is an economically more acceptable procedure for the preparation of aluminate carriers for high-temperature catalysts.⁴³ All these advantages outweigh the disadvantages associated with the increased cost of the alkoxide precursors.

The use of alkoxo-technology makes it possible to regulate the degree of homogeneity in the distribution of the components in multicomponent systems.

Thus, depending on the conditions in the joint hydrolysis of $\text{Al}(\text{OR})_3$ and $\text{Si}(\text{OR})_4$, powders having the mullite composition ($3\text{Al}_2\text{O}_3 \cdot 2\text{SiO}_2$) could have a specific surface of either 6.8 or $38 \text{ m}^2 \text{ g}^{-1}$ after heating at 1500°C .⁴⁶ The degree of homogeneity of the former did not then attain the atomic level (nanocomposite) and that of the latter corresponded to the atomic or nearly atomic level of distribution of the components. In the latter case, the mullite microcrystals were formed at 900 – 1000°C and the vitreous aluminosilicate phase, through which recrystallisation accompanied by a decrease in S_{sp} in fact largely occurs, was then absent from the system.

The aluminomagnesium alkoxide spinel — a promising chemically inert carrier — also has an enhanced thermal stability.⁴⁷ Its specific surface at 1100°C is $30 \text{ m}^2 \text{ g}^{-1}$.⁴⁷

Depending on the alkoxide decomposition conditions (the effect of water or atmospheric moisture, thermal decomposition), γ - Al_2O_3 powders with different acidities, which affect their catalytic properties, are formed.⁴⁸ Thus, in the dehydration of ethanol on one of such powders, the yields of C_2H_4 and Et_2O were 73% and 8% respectively for a conversion of 82%, whereas on γ - Al_2O_3 obtained from inorganic precursors the yields were 2.6% and 10% respectively.

Modification of the chemical composition of the γ - Al_2O_3 surface by treating the latter with $\text{Si}(\text{OR})_4$ and subsequent deposition of palladium or platinum made it possible to obtain a thermostable catalyst capable of ensuring the flame-free combustion of hydrocarbons, diminishing thereby the evolution of CO and NO_x during catalytic combustion.⁴⁹

A special program for the preparation of artificial clays is being developed in Japan. Its aim is to improve the quality and to attain the stability and reproducibility of the properties of promising ceramic materials.⁵⁰ Such clays are used, for example, in the manufacture of ceramic cellular carriers for catalytic converters in internal combustion engines. The possibility of using alkoxides as oxide precursors is being investigated, which is not surprising since Japan is the leader in the introduction of alkoxo-technology. Treatment of natural clays with alkoxides makes it possible to obtain secondary clays with increased inter-layer distances and greater specific surfaces,⁵¹ which ensures the creation of a comparatively cheap heat-resistant and strong ceramics.

Studies carried out by the Nissan Motor Company and the National Chemical Laboratory of Japan have shown that, depending on the structure of the added low-molecular-mass polyether, anatase or rutile may be obtained from $\text{Ti}(\text{OPr})_4$ after hydrolysis and heat treatment.⁵² This is important, since different modifications of TiO_2 have significantly different catalytic properties. For example, anatase is preferable in the selective catalytic reduction of NO_x . The thermal decomposition of $\text{Fe}(\text{NO}_3)_3$ on surfaces modified with organic compounds, for example with ethylene glycol, has also been investigated.⁵³ As noted above, ROE fragments are generated in such systems on heating. Depending on the structure of the modifying agent, coatings having the Fe_2O_3 composition with a spinel or corundum structure are obtained.

The influence of the reaction conditions on the structure and properties of TiO_2 powders, obtained by the thermal decomposition of $\text{Ti}(\text{OPr})_4$ and $\text{TiO}(\text{acac})_2$ at 200 – 300°C , has been studied.⁵⁴ Rutile was obtained from the latter in the presence of ethylene glycol, whereas anatase with $S_{\text{sp}} = 200 \text{ m}^2 \text{ g}^{-1}$ was produced in the presence of toluene, the specific surface not diminishing on heating to 550°C .

Mixed crystalline oxides with the perovskite structure are active catalysts and promising carriers.^{55,56} The catalytic activities of a series of perovskites are comparable with those of noble metals. The inclusion of noble metals in the perovskite lattice increases the chemical and thermal stabilities of mixed catalysts and prevents the volatilisation of the noble metals in the form of oxides, for example, Ru_2O_3 or RuO_3 . The principal obstacle to the wide-scale introduction of catalysts with the perovskite structure is the high temperature of their synthesis ($\sim 900^\circ\text{C}$). This greatly hinders their preparation by the impregnation method. At the same time, the solid-phase synthesis with subsequent dispersion does not ensure the formation of a sufficiently large surface. Even on an inert carrier such as MgAl_2O_4 , only insignificant amounts of a mixed perovskite are formed from a mixture of copper, cobalt, and lanthanum nitrates. Their reaction with the support generates mainly spinels.⁵⁷ The optimum support for the synthesis of a perovskite might be ZrO_2 , but, since this carrier is expensive and has a low S_{sp} , it has not found a wide-scale application.

Low temperature methods of synthesis of perovskites at reduced temperatures (400 – 700°C) employing alkoxo-technology have been developed in recent years.^{58–59} It is to be expected that this will provide a fresh stimulus to the employment of perovskites in heterogeneous catalysis. This is of particularly great current interest for Russia, where chromium-containing catalysts or catalysts based on noble metals are mainly used for the purification of effluent gases.^{56,60} It is noteworthy that abroad the manufacture of the former has been curtailed owing to the high biological activity of chromium(VI) compounds⁶¹ and that of the latter has been reduced because of their high cost.

One of the most important advantages of alkoxo-technology is the possibility of obtaining new crystalline and amorphous phases, the synthesis of which by the traditional methods is difficult or impossible. This is caused mainly by the need to carry out the solid-phase synthesis at high temperatures,⁶² the formation of phases stable in the low-temperature region being impossible under such conditions. Furthermore, in solid-phase synthesis

it is extremely difficult to ensure the homogeneity of multicomponent systems, particularly when small amounts of additives are introduced. On the other hand, when alkoxo-technology is employed, atomic (molecular) homogeneity is already attained at the hydrolysis stage and heat treatment leads mainly to the densification of the oxide skeleton. This results in a decrease in the formation temperature of the crystalline phases and eliminates the liquation phenomenon — heterogeneous separation in glass melts (when amorphous oxides are obtained). Naturally, the transition from the theoretical consideration of the possibility of using alkoxo-technology to its practical implementation requires much effort. Nevertheless, considerable advances have already been achieved on these lines: barium titanates with the ratio $\text{BaO}:\text{TiO}_2 = 1:2$ and $1:5$,⁶³ previously regarded as metastable, the previously unknown compound $5\text{La}_2\text{O}_3 \cdot 2\text{Al}_2\text{O}_3$,⁶⁴ LiNbO_3 films,⁶⁵ and other materials have been obtained. Even though there is as yet no information about the use in heterogeneous catalysis of new crystalline compounds obtained with the aid of alkoxo-technology, data concerning the application of new amorphous materials (for example, in the manufacture of $\text{SiO}_2\text{-ZrO}_2$ porous glasses with an increased ZrO_2 content)²⁵ are already available.

V. Preparation of coatings and thin films

Catalysts obtained by deposition from solutions of catalytically active compounds onto a highly porous carrier with subsequent heat treatment are usually employed in many catalytic reactions, particularly in the external diffusion region. A carrier with a high surface area (primary carrier), treated with solution or suspensions, from which highly porous coatings (secondary carrier) are obtained on heat treatment, is also used as a support. In such cases, aqueous solutions of inorganic salts which can be decomposed by heat treatment (the cheapest and most readily available compounds) are traditionally employed for the introduction of catalytically active elements. However, the thermal decomposition of inorganic salts is usually accompanied by the evolution of corrosive and toxic gases and in addition the nitrates most frequently used are explosive. However, the main disadvantage of this technology is the crystallisation of inorganic salts on evaporation of water, which ultimately rules out the possibility of obtaining a uniform coating (a 'patchy' oxide coating is formed), reduced S_{sp} , and increases the consumption of catalytically active elements.

In multicomponent systems, the situation is aggravated by the occurrence of separate (fractional) crystallisation, since the probability of isomorphism or of the formation of complex salts is low. As a result, heat treatment gives rise to the formation of a microheterogeneous mixture of oxides, the homogenisation of which with formation of a mixed crystalline oxide having the specified structure requires an increased temperature and this leads to sintering accompanied by a decrease in S_{sp} , the formation of relatively inactive phases with participation of the carrier, and the alteration of the component ratio.

The application of alkoxo-technology makes it possible to overcome fairly readily these disadvantages of the traditional technology. The principal advantages of alkoxo-technology are ability of the products of the hydrolysis of alkoxides to form films and the establishment of homogeneity in the hydrolysis stage. The hydrolysis of alkoxides results in the formation of predominantly linear or branched polymers as well as oxide or oxide hydroxide particles of controllable size. The latter are produced either immediately in the form of a sol or (after peptisation) in the form of gels and powders.

Solutions of the hydrolysis products, deposited on supports by immersion, impregnation, or sputtering methods, give rise to uniform organic-inorganic coatings. After drying and moderate heat treatment at temperatures of 400–800 °C, ensuring the elimination of the organic component and the partial sintering of the coatings with retention of their high porosity, such coatings

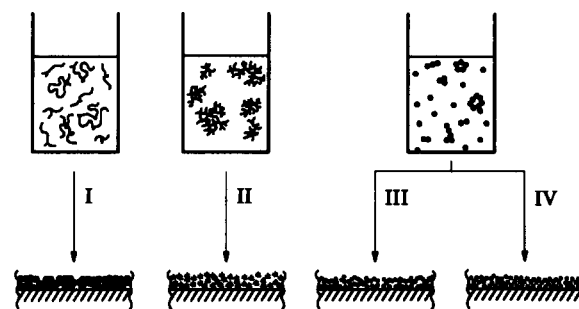


Figure 2. The structure of oxide coatings formed from different hydrolysed alkoxides.

are converted into oxide ones. Their structure is illustrated conventionally in Fig. 2.

Type I coatings are characterised by a low open porosity and have no special importance in catalysis, but they can be used as an oxide binder, which sinters at a low temperature, for example in the preparation of ceramic honeycomb carriers. Type II–IV oxide coatings (films), which have a high open porosity and a large contact surface, are used as carriers and catalysts. The structure of the oxides formed from the alkoxide hydrolysis products obtained under various conditions has been examined in detail.^{66, 67}

For the deposition of coatings, one may use either liquid alkoxides directly or solutions of liquid and solid alkoxides in organic solvents with subsequent hydrolysis by atmospheric moisture and/or heat treatment. However, this method has not found extensive application, because it is fairly difficult to regulate the structure of an oxide coating having an appreciable thickness ($>0.1 \mu\text{m}$). It is more convenient to deposit monolayer and multilayer coatings from dilute solutions of alkoxides. The properties of such coatings, especially monolayer ones, differ significantly from those of bulk-phase materials owing to their anomalous structure (distortion of bond angles and changes in bond lengths and in the electronic state of their atoms), which is particularly important for catalysis. For example, Fe_2O_3 in a surface layer deposited from $\text{Fe}(\text{acac})_3$ on TiO_2 has a lower activity in the oxidation of CO than bulk-phase Fe_2O_3 .⁶⁸ This can be explained by the fact that a monolayer coating of this kind (obtained as a result of interaction with the support) is chemically closer to iron silicate rather than to Fe_2O_3 .

However, monolayer coatings exhibit much more frequently a higher catalytic activity than multilayer ones. Thus the dehydration of ethanol to C_2H_4 on the $\text{Nb}_2\text{O}_5/\text{SiO}_2$ monolayer catalyst obtained from $\text{Nb}(\text{OEt})_5$ proceeds to an extent of 99%–100%, whereas on the analogous impregnation catalyst considerable amounts of Et_2O are formed together with C_2H_4 .⁶⁹ The rate of the esterification reaction between AcOH and EtOH on a monolayer catalyst of this kind is 20 times greater than on massive Nb_2O_5 .⁷⁰ When platinum or nickel is deposited on it, the effect of the strong metal–carrier interaction is not manifested, in contrast to the deposition of the same metals on 'pure' Nb_2O_5 . The dispersity of copper in the Cu/SiO_2 monolayer catalyst obtained by deposition from $\text{Cu}(\text{acac})_2$ solution does not change even after 10 oxidation-reduction cycles, whereas in a multilayer catalyst it is lower immediately after preparation and falls to a particularly large extent after five such cycles have been performed.⁷¹

The surface monolayers obtained by depositing $\text{Nb}(\text{OR})_5$ or its mixture with $\text{Al}(\text{OR})_3$ do not crystallise with formation of Nb_2O_5 or aluminium niobates even after heating at 900 °C.⁷²

V_2O_5 coatings, for the deposition of which one may employ vanadium and vanadyl alkoxides^{73–80} or acetylacetonates,^{81–87} have acquired practical importance. They are used for the selective catalytic reduction of NO_x in effluent gases. Monolayer catalysts containing 2%–4% of V_2O_5 have activities in this reaction comparable to those of catalysts obtained by impregnating the

carrier with NH_4VO_3 solutions or deposited from $\text{V}_2(\text{SO}_4)_3$ solutions containing 20%–24% of V_2O_5 .⁸⁶ Thus the activity of the alkoxide catalyst referred to unit mass of V_2O_5 is almost ten times greater than that of a traditional catalyst obtained from inorganic precursors.

For low surface coverages of the SiO_2 , TiO_2 , Nb_2O_5 , Al_2O_3 , or ZrO_2 carriers by V_2O_5 films obtained from $\text{VO}(\text{OR})_3$, vanadate forms containing one terminal V–O bond and three VO–carrier bridge bonds are formed on the surface.⁷⁵ It has been suggested that vanadium oxide catalysts for the reduction of NO_x be obtained by impregnating cellular carriers with solutions of partly hydrolysed alkoxide-based mixtures, for example, a mixture of $\text{Ti}(\text{O}i\text{Bu})_4$, $\text{VO}(\text{O}i\text{Bu})_3$, and WCl_6 .⁸⁰

The method involving the chemical vapour-phase deposition (CVPD) of the $\text{B}(\text{O}Et)_3$, $\text{Si}(\text{O}Et)_4$, $\text{P}(\text{O}Me)_3$, and $\text{Ti}(\text{OPr}^i)_4$ alkoxides has been used to obtain the $\text{B}_2\text{O}_3/\text{SiO}_2$,^{88–90} $\text{B}_2\text{O}_3/\text{Al}_2\text{O}_3$,⁹¹ $\text{SiO}_2/\text{Al}_2\text{O}_3$,^{92–95} $\text{TiO}_2/\text{carrier}$,⁹⁶ $\text{SiO}_2/\text{aluminosilicate}$,⁹⁷ and $\text{BPO}_4/\text{SiO}_2$ ⁹⁸ catalysts. The supported catalysts obtained from alkoxides by the CVPD method have a higher activity: thus boron oxide is uniformly distributed on the carrier surface even when its content is more than 30% (in the usual impregnation deposition, large B_2O_3 crystals are formed in this case).^{89–90} This promotes a high activity and selectivity (95%–96%) of the catalyst in the rearrangement of cyclohexanone oxime to caprolactam. The $\text{SiO}_2/\text{Al}_2\text{O}_3$ alkoxide catalyst, which has a lower S_{sp} than the industrial catalyst having a similar composition (177 and 360 $\text{m}^2 \text{g}^{-1}$ respectively) has a catalytic activity in the cracking of cresol comparable to that of the latter. This is apparently associated with the fact that it contains a larger number of acid centres.⁹² The fixation of the first layer on deposition of SiO_2 formed from $\text{Si}(\text{O}Et)_4$ on Al_2O_3 takes place as a result of the interaction between the HOAl and EtOSi groups with formation of Al–O–Si fragments. In a nitrogen atmosphere, the residual EtO groups do not decompose, whilst in the presence of oxygen they are oxidised with formation of acetaldehyde and the regeneration of OH groups.⁹³

The formation of catalytic oxide coatings from alkoxides by the CVPD method has also been investigated in other studies.^{99–108} Silicon dioxide, obtained from $\text{Si}(\text{O}Et)_4$, covers only the outer surface of zeolites. This alters the dimensions of the inlet pores with retention of the inner structure of the zeolites and increases sharply the selectivity of the latter in relation to the volume of the reacting molecules, which is indicated, for example, by the results of a study of the cracking of octane isomers.¹⁰¹ Coatings in the form of SiO_2 , deposited from the vapour phase, exhibit a higher chemical reactivity even on an inert carrier such as ZrO_2 . At 550 °C, they partially coalesce with formation of clusters and partly dissolve in the carrier.¹⁰⁷

The method involving the deposition of coatings by treating the carrier with an alkoxide under thermal decomposition conditions is close to CVPD. The $\text{SiO}_2/\text{Al}_2\text{O}_3$ catalyst has been obtained by this procedure.¹⁰⁹ It is assumed that the deposition takes place via the interaction of the EtO groups in $\text{Si}(\text{O}Et)_4$ with Lewis acid centres on the Al_2O_3 surface. However, this explanation cannot be extended to the formation of the second and subsequent layers (the overall increment in the mass of SiO_2 reaches 20%).

A comparative study of several $\text{Pd}/\text{Al}_2\text{O}_3$ impregnation catalysts showed¹¹⁰ that highly disperse palladium particles are formed from PdCl_2 and $\text{Pd}(\text{acac})_2$. On reduction, they are converted into a finely disperse metallic phase, whereas the decomposition of $\text{Pd}(\text{NO}_3)_2$ leads to the formation of large particles.

Aluminium, tantalum, and titanium alkoxides have been used for the modification of the surfaces of porous carriers before deposition of catalytically active metals on the latter.^{111–113} For a comparatively slight increase in the specific surface of the specimens (for example, from 100 $\text{m}^2 \text{g}^{-1}$ for the initial $\gamma\text{-Al}_2\text{O}_3$ to 120 $\text{m}^2 \text{g}^{-1}$ for the modified oxide), this made it possible to increase sharply their activity and to obtain effective catalysts for a series of reactions. Thus the degree of conversion of carbon

monoxide into methane on a modified $\text{Ru}/\text{Al}_2\text{O}_3/\gamma\text{-Al}_2\text{O}_3$ catalyst was 99% for selectivity of 100%, whereas on the usual $\text{Ru}/\gamma\text{-Al}_2\text{O}_3$ catalyst it was 62% with a selectivity of 99%. A similar approach has been used to obtain active $\text{Pd}/\text{TiO}_2/\text{spherical glass bead hydrogenation catalysts}$ ^{114,115} and for the deposition of Al_2O_3 coatings on highly porous SiO_2 carriers.¹¹⁶ It is important to note that this procedure makes it possible to attain a significant catalytic effect for a low consumption of alkoxides.

A modified copper/zeolite catalyst, obtained by ion exchange followed by treatment in a $\text{Ti}(\text{OMe})_4$ solution, has been developed for the catalytic conversion of moist exhaust gases.¹¹⁷ Different additives have different effects on the modification of $\gamma\text{-Al}_2\text{O}_3$ ($S_{sp} = 13.7 \text{ m}^2 \text{g}^{-1}$) with $\text{Ti}(\text{OPr}^i)_4$ or $\text{Si}(\text{O}Et)_4$ solutions in hexane.¹¹⁸ Best coatings with S_{sp} up to 29.4 $\text{m}^2 \text{g}^{-1}$ are formed in the presence of EtOH, PrOH, and PrⁱOH, whereas added surfactants exhibit a negative effect.

A process involving the fixation on honeycomb ceramic carriers of secondary $\gamma\text{-Al}_2\text{O}_3$ carriers, formed from sols obtained by the hydrolysis of $\text{Al}(\text{OR})_3$ and the peptisation of the gels produced, has been patented.¹¹⁹ A disadvantage of the traditional technology for the fixation of secondary carriers from suspension is the accumulation of $\gamma\text{-Al}_2\text{O}_3$ particles in corners of the channels within the honeycomb carrier, which reduces the effectiveness of the catalyst and increases its aerodynamic resistance. The proposed method is free from this disadvantage. In addition, 14.7% of Al_2O_3 , and not 33% as in the formation of a suspension coating, is sufficient for the attainment of $S_{sp} = 25\text{--}30 \text{ m}^2 \text{g}^{-1}$.

A process has been developed for the deposition of alumina coatings on barium aluminate.¹²⁰ A catalyst obtained from platinum salts and a mixture of $\text{Ti}(\text{O}Et)_4$ and $\text{Al}(\text{OPr}^i)_3$ has been designed for use in automobile converters. The mixture of alkoxides is subjected to joint hydrolysis, deposited on a honeycomb carrier, dried, and maintained at 500 °C. The degree of conversion of CO on this catalyst reaches 94% at 250 °C and falls to 81 % after being used for 1000 h at 800 °C (for the usual catalyst, the corresponding conversions are 88% and 75%).¹²¹

VI. The use of alkoxides for the preparation of carriers and catalysts

In studies^{6,41,122–144} on the use of alkoxides for the preparation of carriers and catalysts and of their physicochemical and catalytic properties, attention was concentrated on the chemical mixing method. It has been shown for mixtures of silicon and aluminium alkoxides with aluminium, ruthenium, and copper chlorides that the process should consist of four stages:

- (1) the formation of complexes of the alkoxides and chlorides with organic polydentate ligands;
- (2) hydrolysis with formation of a sol and gel;
- (3) drying and dispersion;
- (4) sintering and reduction in a stream of hydrogen (when copper and ruthenium salts are used).

The introduction of polydentate ligands such as aliphatic diols and low-molecular-mass polyethers makes it possible to monitor the course of the hydrolysis and polycondensation (by virtue of their coordination to the RO groups of the alkoxides or their substitution, the ligands lowering the rates of these reactions), ensures the binding of the metal ions to the elementoxane chains, and regulates the shape and size of the pores as well as S_{sp} . Thus, in the hydrolysis of $\text{Al}(\text{OR})_3$ in the presence of the polyether $\text{Me}(\text{OCH}_2\text{CH}_2)_n\text{OMe}$, micropores with an average diameter of 10 nm predominated in the $\gamma\text{-Al}_2\text{O}_3$ obtained for $n = 2$, whereas for $n = 3$ or 4 a wide size distribution of the pores was observed (from 10 to more than 100 nm).¹³² In the joint hydrolysis of $\text{Si}(\text{OR})_4$ and $\text{Al}(\text{OR})_3$ in the presence of ethylene glycol, 2-methylpentane-1,2-diol, or hexane-1,6-diol, aluminosilicates (3.3% of Al_2O_3) with an average pore diameter of 0.55–0.65 nm were obtained.¹⁴⁰ The structure of the diol introduced has a decisive influence on the specific surfaces of such aluminosilicates (Table 1).

Table 1. The influence of the nature of the ligand on the specific surfaces of the 3.3% Al₂O₃-SiO₂ carriers obtained from alkoxides by the chemical mixing method.¹⁴¹

Ligand	$S_{sp}/m^2 g^{-1}$
Ethane-1,2-diol	399
Propane-1,2-diol	170
Butane-2,3-diol	179
2-Methylpropane-1,2-diol	308
Butane-1,2-diol	315
Pinacol	319
Pentane-1,2-diol	483
Propane-1,3-diol	210
Butane-1,3-diol	222
2-Methylbutane-1,3-diol	545
2-Methylpentane-2,4-diol	486
Butane-1,4-diol	5
Pentane-1,5-diol	365
Hexane-1,6-diol	595
Decane-1,10-diol	734
Dodecane-1,12-diol	637

The homogeneities in the distribution of the components were compared on TiO₂-Al₂O₃ specimens synthesised in different ways: by sintering TiO₂ and Al₂O₃ powders, by precipitating mixtures of oxide hydroxides from aqueous solutions of salts with ammonia or urea, and by chemical mixing.¹⁴⁰

In the last case, the crystallisation of TiO₂ was not noted after heating for 5 h at 550 °C. The specimen remained X-ray-amorphous, which confirmed the high degree of homogeneity attainable when the chemical mixing method is employed. In a number of instances, this is of practical importance.

The catalysts synthesised were tested in reactions involving the partial hydrogenation of benzene, the alkylation of naphthalene, and the conversion of methanol. Data on the partial hydrogenation of benzene to cyclohexene on the Ru-SiO₂ and Ru-Al₂O₃ catalyst obtained by the chemical mixing method and on impregnation catalysts employed for comparison are presented in Table 2.

Chemical mixing was used also in the study of the influence of added metal oxides (10%) on the S_{sp} of alumina.⁴¹ The introduction of SrO, BaO, La₂O₃, and ZrO₂ suppressed the sintering of Al₂O₃ in the range 1000–1200 °C. After heating the BaO-Al₂O₃ mixture for 100 h at 1000 °C, a high specific surface of alumina

Table 2. Partial hydrogenation of benzene to cyclohexene on different ruthenium catalysts.¹³⁴

Method of preparation	Ligand	Catalyst composition	Conversion of benzene (%)	Yield of cyclohexene (mol %)
Chemical mixing (TEOS-AlCl ₃)	ethylene glycol	2% Ru-SiO ₂	86.8	27.0
	ethylene glycol	(2% Ru + 0.2% Cu) SiO ₂	83.3	31.4
	pinacol	(2% Ru + 0.2% Cu) SiO ₂	42.7	14.2
	hexylene glycol	(2% Ru + 0.2% Cu) Al ₂ O ₃	53.1	24.5
		2% Ru-SiO ₂	64.3	8.6
Impregnation		2% Ru-Al ₂ O ₃	54.5	5.3

Note. Reaction temperature 453 K, H₂ pressure 7 MPa, benzene: water = 1.6:1.

(139 m² g⁻¹) was retained, whilst after heating for 3 h at 1200 °C S_{sp} diminished to 96 m² g⁻¹. The addition of CaO, MgO, and CeO₂ accelerated the sintering and reduced the S_{sp} of alumina.

The chemical mixing method was also applied in other studies.^{145–151} It was shown in relation to the selective reduction of NO_x that mixed V₂O₅-TiO₂ catalysts exhibit an enhanced catalytic activity compared with impregnation catalysts.¹⁴⁹

The average rhodium particle size in the Rh/SiO₂ catalyst synthesised using the Rh(NO₃)₃-Si(OEt)₄-HOC₂H₄OH systems increased from 1 to 5.6 nm with increase in the rhodium content from 0.34% to 6.89%. The activity of this catalyst in the PROH decomposition reaction increased sharply for particle sizes of 1–2 nm, when the fraction of metal atoms at the corners and on the edges of microcrystallites was a maximum.¹⁵¹ A similar dependence of the selectivity in the hydrogenation of propionaldehyde on the nickel particle size has been observed on the Ni/SiO₂ catalyst, in which the metal particle size increased from 4 to 12 nm with increase in the nickel content from 2% to 26%.¹⁵⁰ It was shown by IR spectroscopy that the metal particles are retained on the support as a result of the formation of the Ni-O-Si linkage. The cobalt particle size in the Co/TiO₂ catalyst increased from 10 to 40 nm with increase in the reduction temperature to 600 °C, but at ~700 °C, where the anatase-rutile transition takes place, it again decreased to 10–15 nm.¹⁴⁷ The redispersion effect, characteristic solely of catalysts obtained by chemical mixing but not of impregnation catalysts, is apparently due to a strong metal-carrier interaction.

Catalyst powders obtained as a result of the operation of the reaction chain alkoxide → xerogel → powder (Fig. 1, operations I and VII modified by the introduction of inorganic salts and ligands) were considered above. In industry, powders are rarely employed as the finished form of the catalysts, serving mainly as the starting material for the preparation of various bulk-phase catalysts.

Boehmite (AlOOH) powders synthesised via alkoxides have found the greatest practical application.¹¹⁶ Previously they were obtained as side products in the synthesis of higher alcohols by the Ziegler method, but subsequently a number of companies, for example Conoco and Vista,¹⁵² set up a special industrial process. The alkoxide obtained by the reaction of metallic aluminium with an alcohol was hydrolysed, after which boehmite was separated and dried, while the alcohol was regenerated. The process has satisfactory ecological characteristics and the powders synthesised have a high purity and dispersity. They can be readily made to undergo a transition to the sol state by adding water and small amount of acid (in certain cases the addition of acid is not required). The employment of such powders for the deposition of secondary γ -Al₂O₃ coatings on honeycomb carriers made it possible to create Pt/ γ -Al₂O₃/honeycomb carrier catalysts, which, whilst having the same activity as the industrial analogues, contain 10 times less platinum.¹⁵³

The Al₂O₃,^{154–158} SiO₂-TiO₂,^{159–161} TiO₂,^{162–166} SiO₂-Al₂O₃,^{167,168} TiO₂-ZrO₂,¹⁶⁹ SiO₂,²⁸ V₂O₅-Al₂O₃,¹⁷⁰ etc. catalytic powders have been obtained with the aid of alkoxotechnology. By selecting the method of synthesis and the reaction conditions, it is possible to regulate S_{sp} and the size and volume of the pores. For example, in the thermolysis of Al(OR)₃ solutions in secondary and tertiary alcohols, where water is generated *in situ* as a result of the thermal degradation of the alcohols, γ -Al₂O₃ powders with $S_{sp} \approx 500$ m² g⁻¹ are produced.¹⁵⁸ Gels were obtained by preliminary partial hydrolysis of Si(OR)₄ in the Si(OR)₄-Ti(OR)₄ system and were then dried, comminuted, impregnated with chromium salts, and sintered.¹⁵⁹ The uniform distribution of the components promoted an increase in the thermal stability of the resulting 1% Cr/SiO₂-TiO₂ catalytic powders; after heat treatment for 3 h at 850 °C, their specific surface was 404 m² g⁻¹ with a porosity of 2.19 cm³ g⁻¹.

By virtue of the high specific surface of alkoxide powders, they may be pelleted without a binder.¹⁷¹ A powder catalyst of the Fischer–Tropsch process has been obtained by the joint hydrolysis of $\text{Ti}(\text{OPr})_4$ and $\text{Zr}(\text{OPr})_4$ in the presence of $\text{Fe}(\text{OAc})_3$.¹⁶⁹

A spherical shape of the catalytic powder particles is preferred, since this diminishes wear due to abrasion. Porous microspheres 1–100 μm in diameter and with pore dimensions of 10–40 nm were obtained by heating the products of the hydrolysis of $\text{Si}(\text{OR})_4$ at $\text{Ti}(\text{OR})_4$ at 400–900 °C.¹⁷² Microspheres having the composition 3% Y_2O_3 – ZrO_2 with an average diameter of 40–50 μm are formed when products of the joint hydrolysis of the corresponding alkoxides are mixed with alkyl phthalates, the mixture being subsequently forced through a draw plate into high-boiling organic liquids.¹⁷³ The formation of an emulsion in the region of immiscibility of the alkoxide–ethanol–water ternary system was used to obtain SiO_2 – TiO_2 powders having spherical particles with $S_{\text{sp}} \leq 375 \text{ m}^2 \text{ g}^{-1}$ and a controllable diameter from 0.05 μm to 1 mm.¹⁶¹ Alkoxide TiO_2 and Al_2O_3 – TiO_2 microsphere powders, activated by the addition of V_2O_5 and CuO , have found a practical application in the purification of the effluent gases from various industries, while TiO_2 microsphere powders are used in the photochemical decomposition of organic compounds in waste waters.^{174, 175}

Stable TiO_2 or ZrO_2 spherical particle powders, designed for use as carriers and catalysts, with an average diameter of 1–100 μm , pore dimensions of 1–500 nm, and a porosity of 0.1–1 $\text{cm}^3 \text{ g}^{-1}$ have been obtained by the hydrolysis of alkoxides, spray drying of the resulting sols, and heat treatment at 500 °C.¹⁷⁶ The TiO_2 spherical particle powder for the promotion of photochemical reactions has been synthesised by the hydrolysis of $\text{Ti}(\text{OR})_4$ in the presence of HCl .¹⁷⁷ SiO_2 – Al_2O_3 microspheres have been obtained similarly.¹⁶⁷

Porous spherical particle powders may be obtained also without the use of alkoxides, but in most cases the alkoxide procedure is preferred. For example, a high quality SiO_2 microsphere powder with S_{sp} up to 300 $\text{m}^2 \text{ g}^{-1}$ and a porosity of 1.3 $\text{cm}^3 \text{ g}^{-1}$ is obtained by the Vycor process.¹⁷⁸ In terms of resistance to wear, this powder is superior to alkoxide powders. However, the Vycor process consumes a large amount of energy, takes a long time, and, what is most important, is designed mainly for the preparation of high-silica microspheres, whereas alkoxo-technology has virtually unlimited possibilities for the selection of components.

SiO_2 – Al_2O_3 ,^{179, 180} SiO_2 – ZrO_2 ,^{181–183} SiO_2 – TiO_2 ,¹⁸⁴ SiO_2 ,¹⁸⁵ ZrO_2 ,¹⁸⁶ and SiO_2 – B_2O_3 ¹⁸⁷ xerogels have been obtained for use in heterogeneous catalysis. Studies^{187–192} on the joint hydrolysis of $\text{Si}(\text{OR})_4$ and $\text{Zr}(\text{OR})_4$ are of great interest. These investigations have served as a basis for the establishment of the industrial manufacture of highly porous glasses with an increased thermal stability and resistance to alkalis.²⁵ Thus 30% ZrO_2 – SiO_2 glasses have specific surfaces of 392, 350, 250, and 119 $\text{m}^2 \text{ g}^{-1}$ at 300, 500, 800 and 900 °C respectively and lose their porosity completely as a result of sintering only on attainment of 950 °C. After heat treatment at 800 °C, $\text{Ti}(\text{O}i\text{Bu})_4$ xerogels contained 30% of anatase and 70% of rutile; when 5% of Cr_2O_3 was introduced with the aid of $\text{Cr}(\text{acac})_3$, the anatase content increased to 90%.¹⁹³ The addition of different amounts of $\text{R}_4\text{N}^+ \cdot \text{OH}^-$ to a mixture of silicon and aluminium alkoxides made it possible to obtain porous aluminosilicates with a molar ratio SiO_2 : Al_2O_3 from 30:1 to 500:1, $S_{\text{sp}} = 50$ –1000 $\text{m}^2 \text{ g}^{-1}$, a porosity of 0.3–0.6 $\text{cm}^3 \text{ g}^{-1}$, and a pore diameter of 1 nm. They contained no pores with diameters > 3 nm.¹⁶⁸ In order to regulate porosity, it has been suggested that a proportion of 0.03–0.4 of an organic polymer relative to the alkoxide be introduced: on formation of a gel, the latter is segregated as a separate phase, which ensures, after burning it off and sintering, the creation of a highly porous oxide structure.¹⁷⁹

The anomalously high porosities and specific surfaces of alkoxide aerogels are especially valuable in heterogeneous catalysis.^{194–207} Thus the Fe_2O_3 – SiO_2 (Al_2O_3) aerogel catalysts

obtained from $\text{Si}(\text{OMe})_4$ or $\text{Al}(\text{O}i\text{Bu})_3$ and $\text{Fe}(\text{acac})_3$ are more active in the Fischer–Tropsch reaction by 2–3 orders of magnitude than the usual iron-containing catalysts and, what is no less important, do not become saturated with coke, in contrast to the latter.¹⁹⁶ Catalysts with $S_{\text{sp}} = 20$ –700 $\text{m}^2 \text{ g}^{-1}$, a porosity of 1.5–12 $\text{cm}^3 \text{ g}^{-1}$, and an apparent density of 0.003–0.5 g cm^{-3} have been obtained by the joint hydrolysis of $\text{Al}(\text{O}i\text{Bu})_3$ and $\text{Pd}(\text{OAc})_2$ [or $\text{Ni}(\text{OAc})_2$]. They are distinguished by a uniform distribution of the components and the absence of clusters. They are designed for the reduction of nitro-compounds and hydrodesulfurisation.¹⁹⁵ The traditional catalysts based on tin and antimony or molybdenum and bismuth oxides are incapable of accelerating the synthesis of nitriles from unsaturated hydrocarbons and NO, whereas the Ni – Al_2O_3 (SiO_2) aerogel catalyst is highly active and selective in this reaction.^{201, 202}

The γ - Al_2O_3 -based porous ceramic obtained via an aerogel is used as a carrier, retaining $S_{\text{sp}} = 72 \text{ m}^2 \text{ g}^{-1}$ after heating for 5 h at 1200 °C.²⁰⁸ Alkoxo-technology is formally not used in the synthesis of aerogel from Cr_2O_3 ,²⁰⁵ but since CrO_3 and MeOH are used as the starting compounds, it follows that in this process too there is a possibility of the generation and subsequent decomposition of chromium(III) and chromium(IV) methoxides because instances of the formation of alkoxides from CrO_3 and alcohols are known.²⁰⁹ Products analogous to aerogels are formed in the glycothermal synthesis, which involves the treatment of a mixture of $\text{Al}(\text{OPr})_3$ with glycols in an autoclave at 300 °C for 2 h and subsequent heat treatment at ~ 600 °C.¹⁵⁷ The dominant pore diameters in the γ - Al_2O_3 obtained using ethylene glycol, propane-1,3-diol and butane-1,4-diol were respectively 7, 16, and 70 nm, while S_{sp} varied from 184 to 354 $\text{m}^2 \text{ g}^{-1}$. γ - Al_2O_3 modified by the addition of SiO_2 in order to increase its thermal stability has been synthesised by a similar method.²¹⁰

Catalysts with a honeycomb structure, which exhibit low aerodynamic and hydrodynamic resistances and make it possible to perform catalytic processes in liquids and gaseous media in the presence of heterogeneous admixtures, have come to be widely used abroad during recent years. A porous ceramic with a cordierite ($2\text{MgO} \cdot 2\text{Al}_2\text{O}_3 \cdot 5\text{SiO}_2$) composition, a low coefficient of thermal expansion, and a resistance to temperature gradients is most often employed as a carrier for honeycomb catalysts. The Corning Company, which has devoted a considerable amount of attention to alkoxo-technology,^{37, 39, 213–218} is the pioneer and recognised leader in the development and introduction of ceramic honeycomb carriers.^{211, 212} For example, it developed a new type of monolithic honeycomb catalysts with porous catalytic coatings, which are not on the walls (washcoat), as in the traditional catalyst, but within them (washcoat-in-the-wall), which reduces the consumption of expensive metals per unit volume of the catalyst and improves its operating characteristics.²¹⁷ It may be postulated that alkoxo-technology has found an application in the manufacture of a new honeycomb catalyst with an increased operating lifetime.²¹⁹

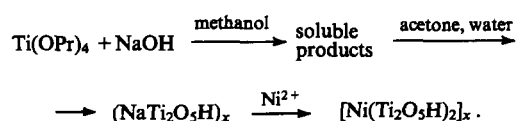
A cordierite ceramic has been obtained in Japan with the aid of alkoxo-technology.^{220–222} For this purpose, a mixture of ethyl silicates with magnesium and aluminium salts was spray pyrolysed, which resulted in the formation of porous cordierite microsphere powders, which were heat-treated in the temperature range 950–1450 °C. The resulting ceramic has a high porosity (48%–92%) and is promising material for honeycomb carriers. The purity of the alkoxide cordierite powders is important, since impurities significantly increase the coefficient of thermal expansion of cordierite²¹² and reduce the heat resistance of the finished product.

In Russia, the large-scale industrial manufacture of ceramic cordierite carriers has not been initiated (mainly owing to the difficulties arising during heat treatment, associated with achieving a compatible combination of the stages involving the synthesis of cordierite and sintering within a narrow process temperature range). Carriers based on glass or polycrystalline fibres (paper, cardboard, fabric, etc.) may serve as an alternative.

The deposition of porous coatings on these materials from aqueous solutions of inorganic salts is difficult because such solutions have no film-forming properties and when they are dried crystallisation takes place. The employment of alkoxides and the products of their hydrolysis makes it possible to overcome these difficulties easily. For example, the carrier and the catalyst may be obtained by impregnating various fabrics having specified mesh dimensions with suspensions based on aqueous alcoholic solutions and silicon, aluminium, and/or titanium alkoxides and oxide powders of the same elements.²²³

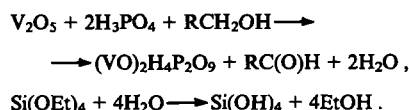
A convenient procedure for the creation of a heat-resistant fibrous oxide structure is the method involving the burning away of a matrix. A fibrous organic material is impregnated with a hydrolysed solution of an alkoxide (in one step or with periodic intermediate drying) and is heat-treated under conditions ensuring the burning away of the organic matrix and the sintering of the oxide coating generated.^{224–226} It has been suggested that heat-resistant highly porous carriers be obtained by the cyclic impregnation of foam-carbon articles with a chelated alkoxide and intervening heat treatment.²²⁷

Elements of alkoxo-technology and ion exchange have been used in a novel method of preparation of catalysts.^{228, 229} According to this method, soluble substitution products are obtained initially by the interaction of titanium, zirconium, or tantalum alkoxides with a methanol solution of NaOH, this being followed by hydrolysis and ion exchange with nickel, palladium, or molybdenum salts.



The catalysts synthesised have a high specific surface ($150\text{--}300\text{ m}^2\text{ g}^{-1}$) and an increased catalytic activity: for a 1% content of the catalytically active metal, they are just as effective in the liquefaction of coal as industrial catalysts with a 15% content of this metal.

Interesting procedures for the employment of alkoxo-technology in the preparation of phosphorus vanadium oxide catalysts for the synthesis of maleic anhydride by the selective oxidation of C_4 hydrocarbons have been proposed. Here the alkoxide VO(OR)_3 may be used as one of the starting compounds in the synthesis of the catalyst,²³⁰ vanadium(IV) and vanadium(III) alkoxides may be formed and segregated in one of the technological stages,²³¹ and, finally, the alkoxides may be formed *in situ* from V_2O_5 and ROH and react with H_3PO_4 .^{232–234} The use of alkoxides has a dual purpose. Firstly, they are the most convenient vanadium compounds suitable for interaction with H_3PO_4 (vanadates or vanadium chlorides are unsuitable for this purpose and the synthesis of vanadium catalysts from a mixture of V_2O_5 powders with P_2O_5 or H_3PO_4 is also impossible). Secondly, alcohols reduce vanadium(V) to vanadium(III) and vanadium(IV), which promotes the attainment of a high activity and selectivity. Another alkoxide, Si(OEt)_4 , is also used in these synthesis, its role consisting mainly in the binding of the water evolved, which facilitates the formation of a cryptocrystalline catalytic powder.



Large foreign companies, for example Union Carbide, Mobil Oil, Chevron, etc., have devoted much attention during the last decade to the use of alkoxides for the preparation of synthetic molecular sieves having the compositions $(\text{Si}_x\text{Al}_y\text{P}_z)\text{O}_2$,^{235, 236} $(\text{M}_x\text{Si}_y\text{Al}_z\text{P}_w)\text{O}_2$ ($\text{M} = \text{Mg, Fe, or Ti}$),^{237–240} $(\text{Ti}_x\text{Al}_y\text{Si}_z)\text{O}_2$,^{241–243} $\text{Al}_2\text{O}_3\text{--P}_2\text{O}_5$,²⁴⁴ etc.,^{245–248} which is associated with increased

reactivity of the oxides and oxide hydroxides formed on hydrolysis of alkoxides. The use of Ti(OR)_4 and of its modified analogues, formed when a proportion of the RO groups are replaced by chelating groups, made it possible to achieve the homogeneous insertion of TiO_2 into the aluminosilicate framework, which could not be achieved when other titanium compounds were employed.²⁴³ The molecular sieves were synthesised by the hydrothermal treatment of a mixture of compounds of the corresponding elements, at least one of which is an alkoxide or a product of its hydrolysis, in the presence of an organic structure-forming agent (alkylamine, pyridine, tetraalkylammonium hydroxide) with subsequent heat treatment in air at $200\text{--}700^\circ\text{C}$ for the complete or partial removal of the structure-forming agent. For example, SAPO-11 aluminosilicon phosphate molecular sieves have been obtained in this way and the 0.5% Pd/SAPO-11 catalyst was prepared from them. The yield of neutral distillates in hydrocracking on this catalyst reaches 75.4%, whereas in the presence of the traditional catalyst having a similar composition it is 64.7%.²³⁵ Evidently in the presence of this effect the question of the increased cost of the precursor alkoxide does not arise. An unusual method of synthesis of molecular sieves has been proposed²⁴⁹ in which Si(OR)_4 serves as the cross-linking agent for alkali metal silicates, titanates, and mixed titanates swollen in the reaction medium.

Many specialists in the field of catalysts manufacture believe (see, for example, Ref. 250) that the main problem nowadays is the creation of carriers with a definite set of characteristics ensuring their functioning under specified conditions rather than the choice of catalytically active elements and their introduction into the catalyst. For example, the widely used $\gamma\text{-Al}_2\text{O}_3$ carriers disintegrate when acted upon by the acid reagents (HCl , SO_3) present in contaminated air or formed during its purification. The replacement of $\gamma\text{-Al}_2\text{O}_3$ by SiO_2 , TiO_2 , ZrO_2 , and their mixtures is the most promising procedure. The choice of inorganic precursors for such carriers is limited and their application does not ensure the attainment of a high porosity and S_{sp} and gives rise to significant ecological problems.

These deficiencies are overcome when alkoxides are employed. Thus, among the available TiO_2 precursors, Ti(OR)_4 is most preferred. It is employed for the preparation of an aqueous TiO_2 sol (a catalyst of photochemical reactions),²⁵¹ microspheres or fibres,²⁵² powders,²⁵³ extruded materials,²⁵⁴ carriers with effective ion-exchange properties [for this purpose, Ti(OR)_4 is hydrolysed in the presence of NaOH or KOH],¹⁶⁶ and also as an organic binder with catalytic properties.²⁵⁵ In most cases, such materials possess a high catalytic activity. For example, the catalysts obtained by depositing the active component on alkoxide-derived TiO_2 powder are more effective in the reduction of NO_x than those obtained by deposition on powdered aerosil, rutile, anatase, or rutile-anatase mixtures.²⁵³

The authors of the present review initiated comprehensive studies on the chemical foundations of alkoxo-technology and its application in heterogeneous catalysis.^{256–259} A method for the joint hydrolysis of two and more alkoxides, ensuring the formation of a large number of mixed elementoxane bonds and affording significant practical advantages (the consumption of organic solvents is reduced, the effectiveness of the process is increased, and the use of inorganic acids and expensive chelating agents is eliminated) has been developed. A method of synthesis of vanadium-containing alkoxide joint hydrolysis products, envisaging the replacement of the usually employed scarce and expensive vanadium alkoxides as precursors by V_2O_5 powder, which is heated jointly with E(OR)_n ($\text{E} = \text{Si, Ti, Zr, P, Al}$) and ROH, has been proposed. The synthesis of oligomeric products by heating one or several metal acetates with high-boiling di- and tri-hydroxy organic compounds has been achieved. This procedure is free from the disadvantages associated with the use of mixtures of acetates (fractional crystallisation, low solubility in water, lack of film-forming properties). Furthermore, the application of the self-

propagating high temperature synthesis weakens significantly the interaction of the deposited catalytic coating with the carrier.

It has been suggested that the heat resistance of the aluminosilicate carrier obtained from Al(OR)_3 and Si(OH)_4 be increased by introducing 0.5% of La_2O_3 .²⁶⁰ For the ratio $\text{Al}_2\text{O}_3:\text{SiO}_2 = 99.5:0.5$, the specific surfaces after heat treatment at 550 °C (3 h) and 1100 °C (24 h) are 242 and 42 $\text{m}^2 \text{g}^{-1}$ in the absence of La_2O_3 and 245 and 72 $\text{m}^2 \text{g}^{-1}$ respectively in its presence. This process has been patented by the Conoco Company on Russian territory.

In recent years, comprehensive studies on the use of alkoxo-technology in heterogeneous catalysis have been initiated in Mexico. Carriers and catalysts with the composition $\text{Pt-Sn/Al}_2\text{O}_3$ [produced by the joint hydrolysis of Al(OBu)_3 and SnBu_4],²⁶¹ $\text{Ru-SiO}_2(\text{Al}_2\text{O}_3)$,²⁶² $\text{SiO}_2\text{-Al}_2\text{O}_3$,²⁶³ Al_2O_3 ,^{180,264} and Pt(Pd)/SiO_2 ²⁶⁵ have been obtained.

VII. Achievements of alkoxo-technology in the manufacture of materials structurally similar to carriers and catalysts

The oxide materials obtained with the aid of alkoxo-technology may be employed in a wide variety of fields. For example, $\text{SiO}_2\text{-TiO}_2$ coatings possess simultaneously catalytic, light reflecting, abrasion-resistant, and electrically insulating properties. The procedures for the preparation of alkoxide materials, developed for use in a specific field, may be employed also in other fields, naturally taking into account the specific requirements as regards some of their properties. It is therefore of interest to examine also the advances of alkoxo-technology in the manufacture of oxide materials structurally similar to carriers and catalysts but having a different functional purpose.

High-temperature superconducting ceramics occupy a special place among such 'related' materials. The main task of alkoxo-technology in this field is the low-temperature synthesis of thin layer multicomponent oxide coatings with a perovskite structure on different supports. The same problem is also faced by heterogeneous catalysis. The fact that many perovskites used nowadays as high-temperature superconductors possess also catalytic properties brings these two aspects even closer together. For example, the high temperature superconducting $\text{YBa}_2\text{Cu}_3\text{O}_7$ perovskite actively catalyses the oxidation of CO and hydrocarbons.²⁶⁶

The low-temperature synthesis of perovskites with the aim of obtaining coatings makes it possible to diminish their chemical interaction with the support and helps to overcome the negative phenomena associated with this factor. During several years of studies (the high-temperature superconductivity of oxide ceramics was not discovered until 1986),²⁶⁷ it has been possible to develop with the aid of alkoxo-technology procedures for the synthesis of superconducting perovskites at temperatures of about 400 °C²⁶⁸ or 650–700 °C,²⁶⁹ whereas the traditional synthesis requires heating above 950 °C. Evidently further advances of alkoxo-technology in the preparation of high-temperature superconducting ceramics still remain in the future. The task of specialists in catalysis is a critical analysis and purposeful employment of these developments.

The principal difference in the requirements which must be met by the oxide materials used as superconductors and catalysts (carriers) concerns the size and distribution of pores. Superconductors and catalysts must have respectively minimum and maximum porosities. In this respect, specialists in catalysis are in the best position, since, owing to the high content of the organic component in the initial mixture and the sharp increase in density on passing from organometallic to inorganic oxide materials, it is much simpler to obtain porous coatings from alkoxides than dense nonporous ones.

Another field close to heterogeneous catalysis is the electronics industry, where the employment of alkoxo-technology for the synthesis of powders with the aim of depositing coatings has been vigorously investigated and introduced.²⁷⁰ For example, NiFe_2O_4 powders with $S_{\text{sp}} = 221 \text{ m}^2 \text{g}^{-1}$ have been obtained from alkoxides.²⁷¹ Evidently these and similar powders can be used also as catalysts for a series of reactions. A review on the preparation of powders for electronics, including their preparation with the aid of alkoxo-technology, has been published.²⁷²

There are no fundamental differences in the structures of the porous oxide coatings used in ultrafiltration or membrane separation and in catalysis. The principal difference concerns the form of the primary carrier and the operating conditions. The employment of alkoxides in the technology for the manufacture of inorganic (ceramic) membranes is the most promising method, since it ensures the possibility of a fine regulation of the pore dimensions within wide limits.^{273,274} Like high-temperature catalysis, the filtration of hot gases or the purification of liquids with subsequent burning away of organic impurities gives rise to the problem of increasing the heat resistance, which is solved, for example, by synthesising aluminate-based membranes by means of alkoxo-technology.⁴⁴ Filtering coatings based on $\gamma\text{-Al}_2\text{O}_3$ and the products of its hydrolysis are most often employed.^{275–278} $\text{TiO}_2\text{-SiO}_2$ membranes with an average pore size of 4 nm and $S_{\text{sp}} = 324 \text{ m}^2 \text{g}^{-1}$ have been obtained from the products of the joint hydrolysis of alkoxides.²⁷⁹ Aluminosilicate membranes, the specific surfaces of which were 217, 384, 456, and 472 $\text{m}^2 \text{g}^{-1}$ with pore radii of 2.21, 2.15, 2.15, and 1.72 nm for the ratios $\text{Al}_2\text{O}_3:\text{SiO}_2 = 5.6:1, 4.4:1, 4.2:1, \text{ and } 1.5:1$ respectively have been obtained by the separate hydrolysis of Si(OMe)_4 and Al(OBu)_3 with formation of sols and subsequent mixing and heat treatment.²⁸⁰ It has been recommended that these membranes be used also in heterogeneous catalysis.

Separating ZrO_2 layers are used in catalysts with metallic carriers, which are employed in the high-temperature purification of gases, for improving the resistance of the metal to oxidation and for increasing the adhesion of the metal to the porous $\gamma\text{-Al}_2\text{O}_3$ carrier.²⁸¹ Such layers, 0.1 μm thick and obtained from Zr(acac)_4 , retained their continuity and did not peel off on heating to 1000 °C.²⁸²

Oxide coatings synthesised from various alkoxides and their mixtures prevent the high-temperature oxidation of metals.^{283–286} They also prevent chemical corrosion and increase the resistance of materials to abrasion. The chemical compositions of the coatings (SiO_2 , TiO_2 , Al_2O_3 , ZrO_2) suggest their possible use in catalysis not only for the creation of separating layers but also directly as acid–base catalysts or carriers. Here one must take into account the difference between the requirements as regards the porosities of protective and catalytic coatings. Special procedures and methods are used to increase the porosity, for example, additives which are burnt off with formation of pores are introduced.

In systems for the catalytic purification of exhaust gases in automobile transport, oxygen sensors prepared from Zr(OR)_4 and ZrO_2 powder are employed.²⁸⁷ After their deposition on a suitable support and the introduction of catalytically active metals, such materials may also function as high-temperature catalysts, for example, in the same systems for the purification of exhaust gases.

It is believed²⁸⁸ that alkoxo-technology will play an important role in the creation of sensors in the future.

One of the most significant advances in modern ceramic technology is the use of the products of the hydrolysis of alkoxides as binders in the preparation of bulky ceramic materials.²⁸⁹ Such binders make it possible to reduce or to eliminate completely the cracking occurring during moulding, drying, and heat treatment (sintering) of the ceramic, improving its strength. This approach has a great future in the manufacture of porous ceramic glass and composite materials,^{290,291} which may be employed also as carriers for heterogeneous catalysts.

VIII. Conclusion

The alkoxides of various chemical elements (as precursors of oxides) have come to be widely used nowadays for the preparation of heterogeneous catalysts and carriers. Large chemical companies of the USA and Japan have shown special interest in alkoxo-technology. Although a considerable proportion of the publications in this field are in the nature of advertisements and many details of the process are not specified, nevertheless there have evidently been significant advances associated principally with the creation of catalytic materials having a high specific surface and porosity and a controllable pore size. The use of alkoxo-technology also makes it possible to obtain heat-resistant carriers and catalysts with a high activity and selectivity combined with a reduced (by an order of magnitude and more) consumption of catalytically active elements. A series of alkoxide catalysts possess unique properties which traditional catalysts lack. The ecological cleanliness of the process involving the preparation of catalysts and carriers by the alkoxo-technological method is very important.

At the same time, the use of alkoxo-technology in heterogeneous catalysis is still at the development stage. Among the numerous possibilities provided by alkoxo-technology, only a small proportion have been realised. For example, possibilities for the low-temperature synthesis of known and especially new crystalline and amorphous compounds are only beginning to be realised. Alkoxo-technology is also used in the preparation of a series of oxide materials structurally similar to catalytic substances but having a different functional purpose. The approaches to the appropriate modifications developed in this connection may be used also in the technology for the manufacture of heterogeneous catalysts and carriers.

In Russia and the Commonwealth of Independent States, adequate attention has not so far been devoted to the application of alkoxo-technology in heterogeneous catalysis. At the same time, some investigations have led to the development of a series of approaches (for example, the synthesis of catalysts via metal resins),^{292,293} which, although they have no direct bearing on alkoxo-technology, can nevertheless find partial applications in the preparation of heterogeneous catalysts by this method.

Studies on alkoxo-technology have been initiated in recent years at the Faculty of Chemistry of the Moscow State University, at the State Institute of the Chemistry and Technology of Organoelement Compounds, at the Institute of Petrochemical Synthesis of the Russian Academy of Sciences, and in certain other scientific establishments. The practical introduction of alkoxo-technology has also begun. Thus the synthesis of boehmite has been implemented in the undertakings of Yaroslavl' and Ufa (the Condea chemie Company).

References

1. B J J Zelinski, D R Uhlman *J. Phys. Chem. Solids* **45** 1069 (1984)
2. D R Ulrich *J. Non-Cryst. Solids* **100** 174 (1988)
3. D R Ulrich *J. Non-Cryst. Solids* **121** 436 (1990)
4. H Dislich *J. Non-Cryst. Solids* **57** 371 (1983)
5. H Yutaka *Catalyst* **28** 250 (1986)
6. F Mizukami *Tech. Jpn.* **22** 8 (1989)
7. Y Imizu *Catalyst* **30** 525 (1988)
8. Y Guan *Tianrangi Huangong* **18** 39 (1993)
9. L G Hubert-Pfalzgraf *New J. Chem.* **11** 663 (1987)
10. M A Cauqui, J M Rodriguez-Izquierdo *J. Non-Cryst. Solids* **147** - 148 724 (1992)
11. A Miyamoto, Y Murakami *Catalyst* **26** 177 (1984)
12. V E Tishchenko *Zh. Rus. Fiz.-Khim. O-va* **31** 394 (1889)
13. K S Mazdiyasi *Ceram. Int.* **8** 42 (1982)
14. G W Scherer *J. Ceram. Soc. Jpn.* **95** 81 (1987)
15. D R Uhlman, B J J Zelinski, G E Wherk, in *Better Ceramics through Chemistry* Vol. I (Eds C J Brinker, D R Ulrich, D E Clark) (New York: North-Holland, 1984) p. 59
16. A B Stiles *Catalyst Supports and Supported Catalysts* (Boston: Butterworths, 1987)
17. L L Hench, in *Science of Ceramic Chemical Processing* (Eds L L Hench, D R Ulrich) (New York: Wiley, 1986) p. 52
18. V E Sokol'skii, V V Sidorchuk, V P Kazimirov, V A Shovskii, G I Batalin, V M Chertov, E K Luchuk *Izv. Akad. Nauk SSSR, Neorg. Mater.* **25** 1178 (1989)
19. B E Yoldas *J. Mater. Sci.* **14** 1843 (1979)
20. V P Chalyi *Gidrokisi Metalov* (Metal Hydroxides) (Kiev: Naukova Dumka, 1972)
21. K Jones, J Davis, G Emblem, P Parkes, in *Better Ceramics through Chemistry* Vol. II (Eds C J Brinker, D R Ulrich, D E Clark) (New York: North-Holland, 1986) p. 111
22. US P. 3 640 093; *Chem. Abstr.* **77** 167 990z (1972)
23. US P. 4 687 652; *Chem. Abstr.* **106** 89 198y (1987)
24. B E Yoldas, D P Partlow *J. Mater. Sci.* **23** 1895 (1988)
25. In *New Materials Developed in Japan* (Tokyo: Toray Research Center, 1987) p. 148
26. R C Mehrotra, R Bohra, D R Gaur *Metal β -Diketonates and Allied Derivatives* (London: Academic Press, 1978)
27. J H Harwood *Industrial Applications of Organometallic Compounds* (London: Chapman and Hall, 1970)
28. A Ueno, H Suzuki, Y Kotero *J. Chem. Soc., Faraday Trans. 1* **79**; 127 (1983)
29. V P Balkevich *Tekhnicheskaya Keramika* (Technical Ceramics) (Moscow: Stroiizdat, 1984)
30. M Guglielmi, G Carturan *J. Non-Cryst. Solids* **100** 16 (1988)
31. M M Sychev *Zh. Prikl. Khim.* **63** 489 (1990)
32. *Jpn. Appl.* 64-9851; *Ref. Zh. Khim.* **24** M 43P (1989)
33. *Jpn. Appl.* 1-23 0425; *Chem. Abstr.* **112** 201 633p (1990)
34. R C Mehrotra *J. Non-Cryst. Solids* **121** 1 (1990)
35. H Okamura, H K Bowen *Ceram. Int.* **12** 161 (1986)
36. V A Dzis'ko *Osnovy Metodov Prigotovleniya Katalizatorov* (Fundamentals of Methods of Preparation of Catalysts) (Novosibirsk: Nauka, 1983)
37. BRD P. 2 317 536; *Chem. Abstr.* **80** 124 226z (1974)
38. BRD P. 2 317 560; *Chem. Abstr.* **80** 52 770z (1974)
39. B E Yoldas *J. Mater. Sci.* **11** 465 (1976)
40. Eur. P. 22 2471; *Chem. Abstr.* **107** 65 510p (1987)
41. F Mizukami, M Wada, S Niwa, M Toba, K Shimizu *J. Chem. Soc. Jpn., Chem. Ind. Chem.* 1542 (1988)
42. M Machida, K Eguchi *J. Am. Ceram. Soc.* **71** 1142 (1988)
43. *Jpn. Appl.* 1-230 425; *Chem. Abstr.* **112** 201 633p (1990)
44. M Chai, K Sekizawa, M Machida, K Eguchi, H Arai *J. Ceram. Soc. Jpn.* **99** 530 (1991)
45. *Jpn. Appl.* 2-217 314; *Ref. Zh. Khim.* **13** L 232P (1991)
46. H Suzuki, Y Tomokiyo, Y Suyama, H Saito *J. Ceram. Soc. Jpn.* **96** 67 (1988)
47. BRD P. 3 319 346; *Chem. Abstr.* **102** 96 926e (1985)
48. E Matijevic *J. Catal.* **89** 560 (1984)
49. Fr. Appl. 2 767 182; *Ref. Zh. Khim.* **17** L 163P (1994)
50. Y Sibasaki *Jpn. Energy Technol. Intell.* **36** 113 (1988)
51. BRD P. 3 619 390; *Chem. Abstr.* **106** 87 156j (1987)
52. *Tech. Jpn.* **24** (4) 80 (1991)
53. F Mizukami, Y Kobayashi, S Niwa, M Toba, K Shimizu *J. Chem. Soc., Chem. Commun.* 1540 (1988)
54. M Inove, H Kominami, H Otsu, T Inui *J. Chem. Soc. Jpn., Chem. Ind. Chem.* 1364 (1991)
55. R J H Voorhoeve, in *Advanced Materials in Catalysis* (Eds J J Barton, R L Garten) (New York: Academic Press, 1977) p. 129
56. N M Popova *Katalizatory Ochistki Gazovykh Vybrosov Promyshlennyykh Proizvodstv* (Catalysts for the Purification of Industrial Waste Gases) (Moscow: Khimiya, 1991)
57. V I Varlamov, V S Komarov, A A Klimenkova *Zh. Prikl. Khim.* **56** 177 (1983)
58. Yu M Rodionov, B V Molchanov, E M Balashova, N I Anikeeva *Metalloorganicheskie Soedineniya pri Poluchenii Vysokotemperaturnykh Sverkhprovodnikov* (Organometallic Compounds in the Preparation of High-Temperature Superconductors) (Moscow: NIITEKhim, 1989)
59. C D Chandler, C Roger, M J Hampden-Smith *Chem. Rev.* **93** 1205 (1993)

60. Yu Sh Matros, A S Noskov, V A Chumachenko *Kataliticheskoe Obezvrezhivanie Otkhodyashchikh Gazov Promyshlennykh Proizvodstv* (Catalytic Detoxification of Industrial Waste Gases) (Novosibirsk: Nauka, 1991)
61. *Chem. Week* **146** 50 (1990)
62. P P Budnikov, A M Gistling *Reaktsii v Smesnykh Tverdykh Veshchestv* (Reactions in Mixtures of Solid Substances) (Moscow: Stroiizdat, 1965)
63. J J Ritter, R S Roth, J E Blendell *J. Am. Ceram. Soc.* **69** 155 (1986)
64. O Yamaguchi, K Sugiura, A Mitsui, K Shimizu *J. Am. Ceram. Soc.* **68** 44 (1985)
65. *Tech. Jpn.* **24** (2) 80 (1991)
66. G W Scherer *J. Non-Cryst. Solids* **100** 77 (1988)
67. M F Gruninger *Ceram. Ind. Int.* **98** 22 (1989)
68. J G Van Ommen, H Bosch, P J Gellings, J R H Ross, in *Studies in Surface Science and Catalysis* Vol. 31 (Amsterdam: Elsevier, 1987) p. 151
69. K Asakura, Y Iwasawa *Chem. Lett.* 859 (1986)
70. M Shirai, K Asakura, Y Iwasawa *J. Phys. Chem.* **95** 9999 (1991)
71. J C Kevlin, M G White *J. Catal.* **135** 81 (1992)
72. S M Maurer, E I Ko *Cuihua Xuebao* **13** 143 (1992)
73. J Nicki, D Dutoit, A Baiker, U Scharf, A Wokaun *Ber. Bunsenges. Phys. Chem.* **97** 217 (1993)
74. E H Brent, B Alfons, S-M Mattias, A Wokaun *J. Catal.* **133** 1 (1992)
75. D Goutman, F W Israel *J. Catal.* **129** 307 (1991)
76. M Glinski, J Kijenski *React. Kinet. Catal. Lett.* **42** 387 (1992)
77. T Okuhara, M Misono *Repis Asahi Glass Found.* **56** 211 (1990)
78. J Kijenski, A Baiker, M Glinski, P Dollenmeier, A Wokaun *J. Catal.* **101** 1 (1986)
79. M Glinski, J Kijenski, in *Studies in Surface Science and Catalysis* Vol. 16 (Amsterdam: Elsevier, 1983) p. 553
80. *Eur. P.* 271 919; *Chem. Abstr.* **109** 78 986q (1988)
81. B N Reddy, M Subrahmanyam *Langmuir* **8** 2072 (1992)
82. B N Reddy, M Subrahmanyam *J. Chem. Soc., Faraday Trans.* 1649 (1991)
83. E T C Vogt, A J Van Dillen, J W Gens, J Biermann, F J J Janssen, in *Proceedings of the 9th International Congress on Catalysis* Vol. 4 (Ottawa: Chemical Institute of Canada, 1988) p. 1976
84. A J Van Hengstum, J G Van Ommen, H Bosch, P J Gellings, in *Proceedings of the 8th International Congress on Catalysis, Weinheim, 1984* p. 287
85. A J Van Hengstum, J G Van Ommen, H Bosch, P J Gellings *Appl. Catal.* **5** 207 (1983)
86. H Barten, F Janssen, F V D Kerkhof, K R Leferink, E T C Vogt, A J Van Dillen, J W Geus, in *Studies in Surface Science and Catalysis* Vol. 31 (Amsterdam: Elsevier, 1987) p. 103
87. E T C Vogt, A J Van Dillen, J W Geus, F J J Janssen *Catal. Today* **2** 569 (1988)
88. S Sato, H Sakurai, K Urabe, Y Izumi *Chem. Lett.* 277 (1985)
89. S Sato, K Urabe, Y Izumi *J. Catal.* **102** 99 (1986)
90. S Sato, S Hasebe, H Sakurai, K Urabe, Y Izumi *Appl. Catal.* **29** 107 (1987)
91. H Sakurai, S Sato, K Urabe, Y Izumi *Chem. Lett.* 1783 (1985)
92. S Sato, M Toita, Y Q Yu, T Sodesawa, F Nosaki *Chem. Lett.* 1535 (1987)
93. S Sato, M Toita, T Sodesawa, F Nosaki *Catalyst* **31** 124 (1989)
94. S Sato, T Sodesawa, F Nosaki, H Shoji *J. Mol. Catal.* **66** 343 (1991)
95. S Sato, M Toita, T Sodesawa, F Nosaki *Appl. Catal.* **62** 73 (1990)
96. S Sato, A Sobczynski, J M White *J. Photochem. Photobiol. A: Chem.* **50** 283 (1989)
97. S Sato, M Hiratsuka, T Sodesawa, F Nosaki *Bull. Chem. Soc. Jpn.* **64** 2214 (1991)
98. S Sato, M Hasegawa, T Sodesawa, F Nosaki *Bull. Chem. Soc. Jpn.* **64** 516 (1991)
99. H Nakajima, M Koya, H Ishida, M Kohno *J. Jpn. Petrol. Inst.* **35** 185 (1992)
100. T Jin, T Okuhara, J M White *J. Chem. Soc., Chem. Commun.* 1246 (1987)
101. Y Murakami, in *Studies in Surface Science and Catalysis* Vol. 44 (Amsterdam: Elsevier, 1989) p. 177
102. M Niwa, T Hattori, Y Murakami *Kagaku Kogaku* **49** 550 (1985)
103. M Niwa, S Kato, T Hattori, Y Murakami *J. Chem. Soc., Faraday Trans. 1* 3135 (1984)
104. M Niwa, Y Kawashima, Y Murakami *J. Chem. Soc., Faraday Trans. 1* 2757 (1985)
105. M Niwa, S Kato, T Hattori, Y Murakami *J. Phys. Chem.* **90** 6233 (1986)
106. Y Teraoka, K Kunitake, S Kagawa, M Iwamoto *J. Chem. Soc. Jpn., Chem. Ind. Chem.* 424 (1983)
107. T Okuhara, J M White *Appl. Surface Sci.* **29** 223 (1987)
108. K Asakura, Y Iwasawa *Catalyst* **32** 55 (1990)
109. V A Smirnov, V V Aleksandrov, V V Khryapchina, S I Kryukov *Zh. Prikl. Khim.* **62** 1141 (1989)
110. A Rakai, D Tessier, F Bozon-Verduraz *New J. Chem.* **16** 869 (1992)
111. US P. 46 86314; *Chem. Abstr.* **108** 114 683d (1988)
112. *Eur. P.* 225 953; *Chem. Abstr.* **107** 156 979q (1987)
113. US P. 4 559 364; *Chem. Abstr.* **104** 209 948a (1986)
114. G Carturan, G Facchin, V Gottardi, G Navazio *J. Non-Cryst. Solids* **63** 273 (1984)
115. G Carturan, G Facchin, G Navazio, V Gottardi, G Cocco, in *Ultrastructure Processing of Ceramics, Glasses and Composites* (New York: Wiley, 1984) p. 197
116. *Eur. P.* 68 603; *Chem. Abstr.* **98** 114 512x (1983)
117. US P. 4 962 075; *Ref. Zh. Khim.* 19 L 190P (1991)
118. A Towato, M Awano, M Sando, A Tsuge *Kagaku Kogaku Ronbunshu* **18** 315 (1993)
119. WO PCT 93-3840; *Chem. Abstr.* **118** 239 916v (1993)
120. *Jpn. Appl.* 5-168 925; *Chem. Abstr.* **119** 166 873n (1993)
121. *Jpn. Appl.* 62-149 338; *Chem. Abstr.* **108** 137143s (1988)
122. F Mizukami *Chem. Chem. Ind.* **42** 875 (1989)
123. M Toba, S Niwa, K Shimizu *J. Chem. Soc. Jpn., Chem. Ind. Chem.* 1523 (1989)
124. F Mizukami *Inst. Electrostat. Jpn.* **14** 376 (1990)
125. F Mizukami *Petrotechnology* **12** 728 (1989)
126. M Toba, S Niwa, K Shimizu, Y Kiyozumi, P Sales, F Mizukami *Catalyst* **29** 394 (1987)
127. F Mizukami *Metals* **59** 73 (1989)
128. F Mizukami, S Matsuzaki, F Furokoki, S Niwa, M Toba, J Imamura *J. Chem. Soc. Jpn. Chem. Commun.* 678 (1986)
129. F Mizukami, S Niwa, M Toba, T Tsuchiya, K Shimizu, S Imai, J Imamura, in *Studies in Surface Science and Catalysis* Vol. 31 (Amsterdam: Elsevier, 1987) p. 45
130. K Mazada, S Miyazaki, T Sano, F Mizukami, K Kuno *J. Chem. Soc. Jpn., Chem. Ind. Chem.* 910 (1992)
131. K Maeda, F Mizukami, S Niwa, M Toba, M Watanabe, K Masuda *J. Chem. Soc., Faraday Trans.* 92 (1992)
132. K Maeda, F Mizukami, M Watanabe, S Niwa, M Toba, S Shimizu *Chem. Ind.* **42** 807 (1989)
133. K Maeda, F Mizukami, M Watanabe, N Avai, S Niwa, M Toba, K Shimizu *J. Mater. Sci. Lett.* **9** 522 (1990)
134. S Niwa, F Mizukami, M Kuno, K Takeshita, H Nakamura, T Tsuchiya, K Shimizu, J Imamura *J. Mol. Catal.* **34** 247 (1986)
135. S Niwa, F Mizukami, J Imamura, K Itabashi *J. Jpn. Petrol. Inst.* **32** 145 (1989)
136. S Niwa, F Mizukami *Yukagaku* **39** 105 (1990)
137. K Maeda, F Mizukami, M Watanabe, N Arai, S Niwa, M Toba, K Shimizu *Catalyst* **31** 132 (1989)
138. M Toba, F Mizukami, A Katayama, S Niwa, K Maeda *Catalyst* **32** 85 (1990)
139. US P. 5 077 032; *Ref. Zh. Khim.* 10 M 70P (1993)
140. F Mizukami, S Niwa, K Furukori, M Toba, T Tsuchiya, K Shimizu, S Imai, J Imamura *Catalyst* **28** 89 (1986)
141. M Toba, S Niwa, K Shimizu, Y Kiyozumi, P Sales, F Mizukami *Catalyst* **9** 394 (1987)
142. S Niwa, F Mizukami, S Isoyama, T Tsuchiya, K Shimizu, S Imai, J Imamura *J. Chem. Tech. Biotechnol.* **36** 491 (1986)
143. S Imai, S Niwa, F Mizukami, M Toba, J Imamura *J. Nat. Chem. Lab. Ind.* **81** 683 (1986)
144. S Niwa, F Mizukami, M Toba, T Tsuchiya, K Shimizu, J Imamura *Catalyst* **31** 421 (1989)
145. K Junya, S Takashy, I Kazuhiro *Chem. Lett.* 211 (1992)
146. T Sodesawa *Petrotechnology* **15** 934 (1992)
147. S Takasaki, H Suzuki, K Takahashi, S Tanabe, A Ueno, Y Kotera *J. Chem. Soc., Faraday Trans. 1* 803 (1984)
148. J M Pearson, H Ryu, W C Wong, K Nobe *Ind. Eng. Chem., Prod. Res. Dev.* **22** 381 (1983)
149. W C Wong, K Nobe *Ind. Eng. Chem., Prod. Res. Dev.* **23** 564 (1984)

150. H Suzuki, S Takasaki, F Koga, K Takahashi, A Ueno, Y Kotera *Catalyst* **24** 58 (1982)
151. S Takasaki, F Koga, S Tanabe, A Ueno, Y Kotera *J. Chem. Soc. Jpn., Chem. Ind.* **998** (1984)
152. *Ceram. Ind.* **134** 21 (1990)
153. L B Larsson, L O Lowendahl, J-E Offerstedt, in *Catalysis and Automotive Pollution Control* (Amsterdam: Elsevier, 1987) p. 333
154. A J Fanelli, J V Burlew *J. Am. Ceram. Soc.* **69** 174 (1986)
155. K Ishiguro, T Tshikawa, N Kakuto, A Ueno, Y Mitarai, T Kamo *J. Catal.* **123** 523 (1990)
156. Eur. P. 199 930; *Chem. Abstr.* **106** 35 522f (1987)
157. J Masashi, H Kominami, M Inoue, T Kominami, T Inue *J. Am. Ceram. Soc.* **73** 1100 (1990)
158. US P. 4 387 085; *Chem. Abstr.* **99** 55 805r (1983)
159. US P. 4 547 557; *Chem. Abstr.* **104** 51 258q (1986)
160. B Karmakar, D Ganguli *Indian J. Technol.* **25** 282 (1987)
161. W T Minehan, G L Messing *J. Non-Cryst. Solids* **121** 375 (1990)
162. J Kiwi, E Borgarello, D Duonghong, M Gratzel, in *Studies in Surface Science and Catalysis* Vol. 16 (Amsterdam: Elsevier, 1983) p. 135
163. T Takahashi, K Abe, T Kai *Kagaku Kogaku Rombunshu* **16** 584 (1990)
164. S Matsuda, A Kato *Appl. Catal.* **8** 149 (1983)
165. J Haber, A Kozlowski, R Kozlowski *J. Catal.* **102** 52 (1986)
166. US P. 5 177 045; *Chem. Abstr.* **118** 155 479s (1993)
167. Jpn. Appl. 1-197 311; *Chem. Abstr.* **112** 11 077n (1990)
168. Eur. P. 340 868; *Chem. Abstr.* **112** 141 758w (1990)
169. US P. 4 624 942; *Chem. Abstr.* **106** 53 062k (1987)
170. US P. 4 560 797; *Chem. Abstr.* **105** 42 377v (1986)
171. Eur. P. 331 396; *Chem. Abstr.* **112** 78 183n (1990)
172. Jpn. Appl. 2-102 138; *Chem. Abstr.* **113** 64 120y (1990)
173. BRD P. 3 616 503; *Chem. Abstr.* **106** 37 502y (1987)
174. G Brambilla, F Frenquellucci *Ceram. Acta* **4** 79 (1992)
175. S Sakka, T Yoko *Ceramurgia* **21** 24 (1991)
176. US P. 5 128 291; *Chem. Abstr.* **117** 156 270h (1992)
177. Jpn. Appl. 5-17 153; *Chem. Abstr.* **118** 257 643h (1993)
178. G Greiner-Baer, M Schaefer *Silikattechnik* **40** 184 (1989)
179. Eur. P. 363 697; *Chem. Abstr.* **113** 28 190n (1990)
180. T Lopez, M Asomoza, L Raso, R Gomez *J. Non-Cryst. Solids* **108** 45 (1989)
181. Jpn. Appl. 1-164 742; *Ref. Zh. Khim.* **12** M 376P (1990)
182. Jpn. Appl. 61-17 443; *Chem. Abstr.* **104** 211 888z (1986)
183. Jpn. Appl. 2-102 131; *Chem. Abstr.* **113** 641 192 (1990)
184. US P. 5 162 283; *Ref. Zh. Khim.* **7** L 217P (1992)
185. Jpn. Appl. 5-58 617; *Chem. Abstr.* **119** 13 920a (1993)
186. Jpn. Appl. 2-111 669; *Ref. Zh. Khim.* **3** M 67P (1992)
187. H Asaoka *J. Mol. Catal.* **68** 301 (1991)
188. Jpn. Appl. 61-83 648; *Chem. Abstr.* **105** 119 530z (1986)
189. M Nogami *J. Am. Ceram. Soc.* **69** 99 (1986)
190. M Nogami *J. Non-Cryst. Solids* **69** 415 (1985)
191. M Nogami *Yogyo Kyokaishi* **93** 195 (1985)
192. M Nogami *Chem. Ind.* **39** 345 (1986)
193. S Doeuff, M Heury, C Sanchez, in *Better Ceramics through Chemistry* Vol. II (Eds C J Brinker, D E Clark, D R Ulrich) (Amsterdam: North-Holland, 1986) p. 653
194. J N Armor, E J Carlson *J. Mater. Sci.* **22** 2549 (1987)
195. US P. 4 469 816; *Chem. Abstr.* **101** 178 415f (1984)
196. F Blanchard, B Pommier, J P Raymond, S J Teicher, in *Studies in Surface Science and Catalysis* Vol. 16 (Amsterdam: Elsevier, 1983) p. 395
197. Eur. P. 186 149; *Chem. Abstr.* **105** 81 719c (1986)
198. S Abouarnadasse, G P Pajonk, S J Teichner, in *Heterogeneous Catalysis and Fine Chemicals* (Amsterdam: Elsevier, 1988) p. 371
199. US P. 4 478 987; *Chem. Abstr.* **102** 25 239x (1985)
200. S J Teichner, in *Aerogels* (Ed. J Fricke) (Berlin: Springer, 1986) p. 22
201. G M Pajonk, S J Teichner, in *Aerogels* (Ed. J Fricke) (Berlin: Springer, 1986) p. 193
202. S Abouarnadasse, G M Pajonk, J E Germain, S J Teichner *Appl. Catal.* **9** 119 (1984)
203. J Chaouki, C Chavarie, D Klevana, G M Pajonk *Can. J. Chem. Eng.* **64** 440 (1986)
204. J N Armor, E J Carlson, P M Zambri *Appl. Catal.* **19** 339 (1985)
205. J N Armor, E J Carlson *Appl. Catal.* **19** 327 (1985)
206. H D Gesser, P C Goswami *Chem. Rev.* **89** 765 (1989)
207. H D Gesser, L Kruczynski *J. Phys. Chem.* **88** 2751 (1984)
208. Jpn. Appl. 4-104 972; *Chem. Abstr.* **117** 218 532f (1992)
209. N Hagihara, H Yamazaki *J. Am. Chem. Soc.* **81** 3160 (1959)
210. M Inoue, H Otzu, H Kominami, T Inue *J. Mater. Sci. Lett.* **11** 269 (1992)
211. I M Lachman *Chem. Eng. Progr.* **81** 29 (1985)
212. I M Lachman *Sprechsaal* **119** 1116 (1986)
213. BRD P. 2 317 516; *Chem. Abstr.* **80** 52 770 (1974)
214. US P. 5 212 130; *Chem. Abstr.* **119** 102 397c (1993)
215. Eur. P. 535 897; *Chem. Abstr.* **119** 11 549n (1993)
216. Eur. P. 197 681; *Chem. Abstr.* **106** 9782w (1987)
217. J L Williams, I M Lachman, in *Proceedings of the 8th World Clean Air Congress* Vol. 4 (Amsterdam: Elsevier, 1989) p. 351
218. Eur. P. 197 645; *Chem. Abstr.* **106** 9783x (1987)
219. *Ind. Ceram.* **93** (1991)
220. Eur. P. 160 267; *Chem. Abstr.* **104** 94 109h (1986)
221. US P. 4 871 693; *Ref. Zh. Khim.* **15** M 177P (1991)
222. Jpn. Appl. 4-338 164; *Chem. Abstr.* **118** 259 875j (1993)
223. BRD P. 3 128 603; *Chem. Abstr.* **98** 56 111c (1983)
224. US P. 4 931 316; *Chem. Abstr.* **113** 102 389c (1990)
225. Jpn. Appl. 2-19 569; *Chem. Abstr.* **113** 137 381w (1990)
226. Jpn. Appl. 2-26 878; *Chem. Abstr.* **113** 157 503r (1990)
227. E Pope, A Almazan, K Kratsch *J. Am. Ceram. Soc.* **74** 1722 (1991)
228. H P Stephens, R D Dosch, F V Stohl *Ind. Eng. Chem., Prod. Res. Dev.* **24** 15 (1985)
229. US P. 4 511 455; *Chem. Abstr.* **102** 28 232a (1985)
230. US P. 4 400 306; *Chem. Abstr.* **99** 146 942z (1983)
231. US P. 4 315 864; *Chem. Abstr.* **96** 143 529x (1982)
232. US P. 5 108 974; *Ref. Zh. Khim.* **19** L 79P (1993)
233. Eur. P. 225 062; *Chem. Abstr.* **107** 178 622v (1987)
234. H S Horowitz, C M Blackstone, A W Sleight, G Teufer *Appl. Catal.* **38** 193 (1988)
235. WO PCT 88-5070; *Chem. Abstr.* **109** 173 377a (1988)
236. Jpn. Appl. 59-35 018; *Chem. Abstr.* **101** 9574b (1984)
237. Eur. P. 158 348; *Chem. Abstr.* **104** 7806 (1986)
238. Eur. P. 121 232; *Chem. Abstr.* **101** 232 979 (1985)
239. Eur. P. 161 488; *Chem. Abstr.* **104** 151 797g (1986)
240. Eur. P. 161 491; *Chem. Abstr.* **104** 36 298h (1986)
241. WO PCT Appl. 85-4855; *Chem. Abstr.* **104** 152 266v (1986)
242. Jpn. Appl. 2-302 314; *Ref. Zh. Khim.* **11** L 261P (1992)
243. US P. 5 160 717; *Ref. Zh. Khim.* **8** L 187P (1994)
244. DDR P. 286 564; *Ref. Zh. Khim.* **6** L 252P (1992)
245. Eur. P. 530 104; *Chem. Abstr.* **118** 194 635j (1993)
246. Eur. P. 530 103; *Chem. Abstr.* **118** 194 634h (1993)
247. Jpn. Appl. 1-257 123; *Chem. Abstr.* **113** 214 793m (1990)
248. US P. 5 094 828; *Chem. Abstr.* **117** 174 514v (1992)
249. B A Aufdembrink, M E Landis, P Chu, I D Johnson, G W Kirker, M K Rubin, in *International Symposium 'Zeolite Chemistry and Catalysis', Praha, 1991* p. 1
250. *Chem. Eng.* **98** 37 (1991)
251. A Leautic, F Babonneau, J Livage *Chem. Mater.* **1** 248 (1989)
252. Jpn. Appl. 5-17 153; *Chem. Abstr.* **118** 257 643h (1993)
253. V M Belousov, V A Zazhygalov, Yu P Saitsev, G A Komashko, A I Pyatnitskaya, in *Soviet-French Seminar on Catalysis* (Novosibirsk: Institute of Catalysis, 1990) p. 21
254. US P. 4 992 406; *Ref. Zh. Khim.* **5** L 218P (1992)
255. Eur. P. 219 284; *Chem. Abstr.* **107** 98 588 (1987)
256. Yu M Rodionov, E M Slyusarenko *Neorg. Mater.* **31** 1499 (1995)
257. Yu M Rodionov, E M Slyusarenko, E A Chernyshev, V V Lunin *Mendeleev Commun.* (1996) (in the press)
258. Yu M Rodionov, E M Slyusarenko, V V Lunin *Dokl. Akad. Nauk* **345** 209 (1995)
259. Yu M Rodionov, E M Slyusarenko, I I Novoshinskii, I V Zhitkov, V F Tret'yakov, E A Chernyshev, V V Lunin, in *Blochnye Nositeli i Katalizatory Sotovoi Struktury (Tez. Dokl. Mezhdunar. Seminara)* [Block Carriers and Catalysts of Honeycomb Structure (Abstracts of Reports at the International Seminar)] (Novosibirsk: Institute of Catalysis, 1995) p. 111, 113
260. USSR P. 1 771 427; *Byull. Izobret* (39) **198** (1992)
261. R Gomez, V Bertiv, M A Ramirez, J Zamudio, P Bosch, I Schifter, T Lopez *J. Non-Cryst. Solids* **147-148** 748 (1992)
262. T Lopez, L Herrera, J Mendez-Vivar, P Bosch, R Gomez, R D Gonzalez *J. Non-Cryst. Solids* **147-148** 773 (1992)
263. T Lopez *React. Kinet. Catal. Lett.* **47** 21 (1992)

264. T Lopez, A Romero, A Chavela, L Razo, R Gomez *React. Kinet. Catal. Lett.* **43** 307 (1991)
265. T Lopez, M Moran, J Navarrete, L Herreva, R Gomez *J. Non-Cryst. Solids* **147–148** 753 (1992)
266. A Jiang, Y Peng, Q-W Zhou, P-Y Gao, H-Q Yuan *Catal. Lett.* **3** 235 (1989)
267. J Bednorz, K Muller *Z. Phys. B* **64** 189 (1986)
268. Jpn. Appl. 1-126 208; *Chem. Abstr.* **111** 246 245j (1989)
269. H S Horowitz, S J McLain, A W Sleight, J D Druliner, P L Gai, M J Van Kavelaar, J L Wagner *Science* **243** 66 (1989)
270. S L Swartz *IEEE Trans. Elec. Insul.* **25** 935 (1990)
271. A Clearfield, A M Cadalla, W H Marlow, T W Livingston *J. Am. Ceram. Soc.* **72** 1789 (1989)
272. T F Limar', A N Borshch, I G Slatinskaya, L P Mudrolyubova, E A Nenasheva *Khimicheskie Metody Polucheniya Sovremennykh Keramicheskikh Kondensatornykh Materialov* (Chemical Methods of Preparation of Current Condenser Materials) (Moscow: NIITEKhim, 1988)
273. K Keizer, A J Burggraaf, in *Scientific Ceramic 14: Proceeding of the 14th International Conference* (Cantenburg: Stoke-on-Trent, 1988) p. 83
274. K K Chan, M Bravstein *Am. Ceram. Soc. Bull.* **70** 703 (1991)
275. T Okubo, M Watanabe, K Kusakabe, S Morooka *J. Mater. Sci.* **25** 4822 (1990)
276. US P. 5 160 352; *Chem. Abstr.* **118** 257 088f (1993)
277. A B Larbot, J A Alary, C G Guizard, L Cot, in *High Technology Ceramics* (Ed. P Vincenzini) (Amsterdam: Elsevier, 1987) p. 2259
278. T Okubo, M Watanabe, K Kusakabe, S Morooka *Kagaku Kogaku* **53** 755 (1989)
279. T Yazawa, H Tanaka, H Nakamichi, K Eguchi, O Yamaguchi *J. Ceram. Soc. Jpn.* **99** 1271 (1993)
280. Eur. P. 536 995; *Chem. Abstr.* **118** 259 871e (1993)
281. BRD P. 3 823 239; *Chem. Abstr.* **110** 236 536v (1989)
282. Jpn. Appl. 63-76 881; *Chem. Abstr.* **109** 161 133e (1988)
283. Fr. P. 2 586 037; *Chem. Abstr.* **107** 60 763p (1987)
284. M Guglielmi, D Festa, P Innocenzi, M Mallawaski *Ceram. Acta* **4** 140 (1992)
285. O De Sanctis, L Gomes, N Pellegri, C Parody, M Marajofsky, A Duran *J. Non-Cryst. Solids* **121** 338 (1990)
286. K Izumi, H Tanaka, M Murakami, T Deduchi, A Morita, N Tohge, T Minami *J. Non-Cryst. Solids* **121** 344 (1990)
287. Jpn. Appl. 63-151 669; *Chem. Abstr.* **109** 195 959n (1988)
288. M Naito *Ceram. Eng. Sci. Proc.* **8** 1106 (1987)
289. *Design News(USA)* 93 (1990); *Byull. Inostr. Nauch.-Tekhn. Inform.* **28** 39 (1990)
290. Jpn. Appl. 1-183 445; *Chem. Abstr.* **112** 83 072e (1990)
291. Jpn. Appl. 2-221 184; *Chem. Abstr.* **113** 117 892k (1990)
292. E V Sidash, V N Belyatskii, S N Mal'chenko, G A Branitskii, S V Baran, V V Ponaryadov *Vestsi Akad. Navuk BSSR, Ser. Khim. Navuk* (6) 31 (1988)
293. M I Ivanovskaya, V V Romanovskaya, G A Branitskii, L S Ivashkevich *Zh. Fiz. Khim.* **68** 232 (1994)

The influence of the medium on the mechanical properties of catalysts

E D Shchukin, L Ya Margolis, S I Kontorovich, Z M Polukarova

Contents

I. Introduction	813
II. The influence of adsorption on the mechanical strength of catalysts	815
III. The effect of the catalytic reaction on the mechanical strength of catalysts	817
IV. Contacts between the particles and internal stresses	818
V. The sintering and strengthening of catalysts	820
VI. Conclusion	820

Abstract. The phenomena involving a decrease in the mechanical strength and durability of catalysts during their use, which can be explained in the light of ideas concerning the mutual influence of the solid phase and the medium during catalysis, are examined. Analysis of the mechanism and the set of conditions inducing these phenomena makes it possible to develop methods for a significant improvement of the quality of a catalyst. It is shown that the appearance on the catalyst surface of a multiplicity of mobile adsorbed atoms on dissociation of chemical bonds during the catalytic reaction can give rise to the acceleration of the surface self-diffusion by a large factor, which promotes a significant decrease in the temperature of the sintering of powdered materials. The bibliography includes 105 references.

I. Introduction

In the study of the mechanisms of catalytic reactions, allowance for the interaction of catalysts with the reaction medium and also for the nature of the surface and the bulk phase of the solid catalyst is extremely important.

In order to ensure a prolonged operation of the catalyst, it is essential to create conditions preventing its disintegration and to increase its mechanical strength. The porous solids of different chemical nature employed in catalysis usually disintegrate under the influence of the reaction medium, the chemical processes occurring on their surfaces, and thermal and internal stresses.^{1–5}

Many examples of the effect of the catalytic process on the mechanical and structural characteristics of catalysts are known: the disruption of contacts between corundum grains,⁶ the detachment and removal of quartz glass macroparticles in the pyrolysis of benzene,⁷ the sputtering of an aluminosilicate catalyst,⁷ and the

disintegration of the nickel catalyst in the decomposition of n-hexyl alcohol.⁸ The disintegration of catalysts (the detachment of solid macroparticles and other types of dispersion of the porous structure) may be associated with the adsorption-induced decrease in mechanical strength (ADS). This question was first formulated as early as the 1960s.^{9,10} It was postulated that there is an analogy between the ADS of catalyst under the real conditions of their operation and the phenomenon which is observed when metals and other solids (ionic and covalent compounds, molecular crystals, amorphous materials, etc.) come into contact with surfactants.¹¹ This phenomenon is due to the decrease in the free surface energy of the grains of the solid material under the influence of the surrounding medium, which must contain adsorption-active components (such are the catalytic conditions).

Such phenomena may (or may not) be accompanied by corrosion, dissolution, the condensation of a new phase, and the formation of films or other phase and chemical transformations (including the reconstruction of the surface, the rearrangement of the lattice, and the formation of a wide variety of structural defects), which influence the mechanical strength of the catalyst. Thus there is the phenomenon of 'catalytic corrosion'¹² expressed by a change in the topography of the surface of platinum, palladium, or nickel under the influence of catalytic hydrogen and ammonia oxidation reactions at comparatively low temperatures. The dynamics of catalytic corrosion and the intensity and mechanism of the rearrangement of the surface of the platinum catalyst have been investigated.¹³ Various aspects of the mutual influence of the reaction medium and the chemical (phase) composition, the structure of the surface, and the activity and selectivity of catalysts have been examined.^{14–16} Numerous data concerning the migration atoms and ions on the surfaces of heterogeneous catalysts during catalysis and the formation and growth of interacting clusters which represent the nuclei of phase formations and structural reconstruction, have been published.^{17–32}

Catalysis and the decrease in the mechanical strength of a solid represent different aspects of the same phenomenon, namely the interaction of the solid with the reaction medium, which induces a change in the bonds within both the solid and the reactant. The catalytic reactions of the initial materials and the changes in the structure of the catalyst, occurring simultaneously, may lead to disintegration of the latter.

E D Shchukin, S I Kontorovich, Z M Polukarova Physicochemical Mechanics Laboratory, Institute of Physical Chemistry, Russian Academy of Sciences, Leninskii prosp. 31, 117915 Moscow, Russian Federation.

Fax (7-095) 952 53 08. Tel. (7-095) 955 44 15 (Z M Polukarova)

L Ya Margolis Heterogeneous Catalysis Laboratory, Semenov Institute of Chemical Physics, Russian Academy of Sciences, ul. Kosygina 4, 117977 Moscow, Russian Federation. Fax (7-095) 938 21 56

Received 27 February 1996

Uspekhi Khimii 65 (9) 881–891 (1996); translated by A K Grzybowski

Shchukin and coworkers^{9,10} showed for the first time that the mechanical strength and durability of catalysts[†] depend to a large extent on the number, distribution, and strength of individual contacts between the catalyst particles and on the magnitude of the residual internal stresses arising under the conditions in the formation of structures. The kinetics of the ADS in disperse porous structures with an open porosity have their specific features: the pores are readily accessible to the reactive medium and the rate of permeation of the latter into the bond rupture zone is not the limiting factor, as in the propagation of a macrocrack in a continuous material. Therefore the influence of the medium on the parameters of a porous catalyst should be manifested relatively rapidly and should be determined by thermodynamic factors.

The studies of Shchukin and coworkers^{9,10} and subsequent systematic theoretical and experimental investigations³³⁻⁸⁸ served as a basis for the creation of a physicochemical theory of the mechanical strength of disperse porous structures. The thermodynamic nature of the ADS (partial compensation of the energy of the ruptured bonds by the interaction with the corresponding 'related' medium) at a macroscopic level is manifested by a decrease in the work of formation of new surfaces, i.e. the work of fracture, and hence by a decrease in mechanical strength. Under conditions close to equilibrium, the effect of the ADS may be expressed quantitatively by the decrease in the free surface energy. It has been observed experimentally that the relation between the decrease in surface energy (σ) and in the mechanical strength (P) of any solids in the corresponding medium is described by the well known Griffith relation

$$\frac{P_0}{P_c} = \sqrt{\frac{\sigma_0}{\sigma}},$$

where the quantities P_0 and σ_0 refer to an inert medium, whilst P_c and σ refer to an adsorption-active medium.

At the same time a definite micromechanism of the facilitation of the rearrangement and rupture of the bonds in the solid corresponds to each specific case of a real decrease in mechanical strength. Either the van der Waals pair potential for spherically symmetrical molecules (noble gas atoms) or the ideas concerning donor-acceptor interactions and the changes in the structure of near-surface zones are used for its description.⁷⁸⁻⁸⁰ The outcome of all these investigations has been the establishment of the characteristics and the mechanism of the disintegration of catalysts' structures in adsorption and catalytic processes and the creation of the scientific foundations for the regulation of the mechanical strength of disperse porous bodies and for the control of cohesion and structure-formation processes.^{1-5,64,66} A set of methods and several series of instruments for a comprehensive estimation of the mechanical properties of materials in different stressed states (under static and dynamic conditions) and also in the processes associated with wear (in various media) have been developed.^{34,35} There have also been other approaches. For example, it has been suggested that the deformation and level of disintegrating stresses can be estimated with the aid of acoustic emission.[‡] The choice of the method for estimating the mechanical strength under the conditions of a catalytic reaction is determined by the type of reactor in which the process takes place (reactors with stationary, fluidised or moving catalyst beds).³⁶ Novel methods for the determination of the mechanical strength of the

catalyst directly under the conditions of catalysis³⁷ and also for the determination of the internal microstresses in porous structures before and after catalysis have been devised.^{38,39} A series of publications have been devoted to the mechanical strength and durability of catalysts. For example, Fenelonov⁸¹ proposed a texture-geometrical model of the mechanical strength of porous bodies, which differs from the model of Rebinder, Shchukin, and Margolis⁹ (RSM) by the allowance for the real statistical packing of the particles. He also obtained an equation for the calculation of the specific strength of a single contact when different methods are employed in tests of mechanical strength, which was checked by employing the results of different investigations.⁸²

The applicability of the postulates of the statistical theory to data on the mechanical strength of catalysts and sorbents [the 'weak link' and 'fibre bunch' (rope) models] has been examined.⁸⁷ The results of tests on porous materials in different stressed states are presented in the same communication and the validity of the equation $PV = \text{const}$ (P = stress, V = deformation) was checked and confirmed.

The influence of the porosity (including the porosity in the 'critical' cross-section) of the catalyst grains and of the conditions in their preparation (temperature and duration of heat treatment) on their mechanical strength have been studied.^{88,89} The dependence of the mechanical properties of catalysts (and the possibility of using these properties for a form of monitoring of the mechanical strength testing methods arising from it) on a series of technological factors (for example on the duration of drying, hydrothermal synthesis in hot water, and drying) has been investigated.⁹⁰ The change in phase composition (during heat treatment) and the rearrangement of the structures of catalysts under the influence of the reaction medium increase the mechanical strength of the grains of cement-containing systems used in organochlorine synthesis,⁹¹ which indicates the occurrence of crystallisation contacts at the interface. The reason for fracture during the employment of copper-containing catalytic systems designed for the oxidation of hydrocarbons and CO to CO₂ is believed to be the extensive reduction of CuO to zerovalent copper accompanied by the formation of highly crystalline phases which leads to the breakdown of interparticle contacts (point and phase contacts).⁹²

The need for the creation of a theoretical basis for the development of a technology for the preparation of industrial catalysts and its implementation has now appeared.^{93,94} The problem of the mechanical strength of the catalyst again arises in this connection. The strength properties of specific catalysts may be determined by extremely diverse factors.

The mechanical properties of solids and materials have been the subject of numerous fundamental and applied sciences. The concept of the thermofluctuation nature of fracture has arisen from solid state physics. In this case, the dependence of durability under load (t) on the applied stress and temperature is described by the familiar Zhurkov equation

$$t = t_0 \exp \frac{U_0 - \gamma P}{kT},$$

where γ is a constant of the material, t_0 the period of the vibrations, and U_0 the dissociation energy of the interatomic bonds.

In the mechanics of granular media, elastic behaviour is considered from the standpoint of the packing of the particles in monodisperse and polydisperse systems and the nature of the contacts. In the statistical theory of mechanical strength, schematised ideas concerning the parameters of the statistical distribution of defects in the bulk of the material are employed for the description of the macroscopic behaviour of bodies under load. Rheology which studies the viscoelastic, viscoplastic, etc. mechanical behaviour of bodies (usually without taking into account their internal structure) describes the changes occurring during their deformations.

[†] Mechanical strength is a characteristic of the resistance of solids to disintegration at a constant rate of deformation. It depends on the type and method of application of an external mechanical load. Durability or long-term mechanical strength is characterised by the time required for the disintegration of the material subjected to a constant load.

[‡] B I Malyshev, O V Dmitrik, R V Fishkin, in *Nauchnye Osnovy Prigotovleniya Katalizatorov* (Scientific Foundations of the Preparation of Catalysts) (Novosibirsk: Nauka, 1984) p. 249.

In the physicochemical mechanics of solids and disperse materials,^{5,11} the strength and mechanical fracture of the material are considered from the standpoint of surface physicochemical interactions, because the rupture of interatomic (chemical) bonds actually leads to the formation of new surfaces and at the instant of their appearance (*in statu nascendi*) they are accessible to the physicochemical influence of the medium, which affects the nature of the deformation and rupture. The rupture of interatomic bonds can be achieved in three ways (in various proportions):

(1) as a result of the work performed by mechanical forces (external and internal stresses) given by

$$Pb^2b\sqrt{\frac{L}{b}} = P\gamma,$$

where b is the lattice period (b is the path traversed and b^2 the area of application of the force), L the characteristic linear parameter describing the defective structure of the body, and $\sqrt{L/b}$ the stress concentration factor;

(2) as a result of the thermal fluctuations

$$kT \ln \frac{t}{t_0},$$

where t is the residence time under load and t_0 the period of the vibrations, whilst the quantity $\ln(t/t_0)$ characterises the increase in the probability of the manifestation of fairly large fluctuations in the course of time;

(3) as a result of the work of adsorption ΔU (which includes the work of reversible physical adsorption, chemisorption, and the chemical reaction),¹¹ which reduces U_0 to $U = U_0 - \Delta U$ and increases the activation volume (i.e. the path leading to the overcoming of the bonding force) to $\gamma' = \gamma + \Delta\gamma$; in this case

$$P\gamma' + kT \ln \frac{t}{t_0} = U.$$

The universal Zhurkov equation, mentioned above, follows from the last equation.

Studies by the method of molecular dynamics, i.e. numerical experiment of a dynamic type (NEDT) of the long-term strength of an individual bond subjected to a constant load have shown⁶⁷ that the logarithm of the average lifetime of an atomic (molecular) bond diminishes linearly with increase in the applied load strictly in accordance with the Zhurkov equation.

The deformation and fracture of a two-dimensional crystal with a concentrator-cavity, the adsorption of a surface-active component on the walls of this cavity, the initiation and growth of a crack when a crystal is subjected to a load in the presence of a second component, and the permeation into the growing crack of foreign atoms which promote its development have been investigated by the NEDT method.⁶⁸ The results agree with the ideas concerning the molecular nature of the Rebinder effect.

II. The influence of adsorption on the mechanical strength of catalysts

One of the first pieces of direct evidence concerning the influence of adsorption on the mechanical strength of porous structures has been the results of a study of porous magnesium hydroxide specimens in the presence of the vapours of various liquids: water, sulfuric acid solutions at different concentrations (the presence of H_2SO_4 ensured a change in the partial pressure of water vapour), ethyl alcohol, benzene, cyclohexane, etc.^{40,41} It was established that the coverage of the surface by 1–4 adsorbate monolayers induces an appreciable decrease in the strength of the magnesium hydroxide specimens (Fig. 1). The principal contribution to the decrease in mechanical strength (by a factor of 1.5–2) corresponds to the range with increasing moisture content up to 1%–1.5%, which corresponds to the formation of a saturated monolayer of the molecules of the medium on the external and internal surfaces of the porous specimen. The decrease in the

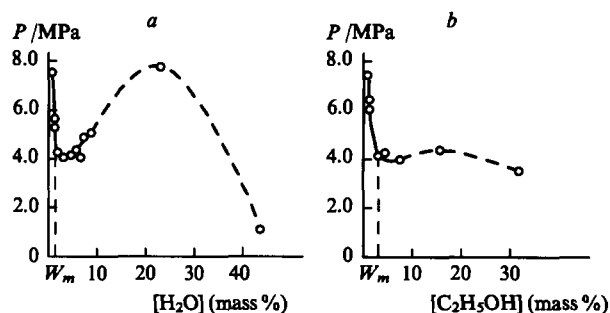


Figure 1. Variation of the compressive strength of magnesium hydroxide specimens during the adsorption of water (a) and ethyl alcohol (b).^{40,41}

mechanical strength of the specimens is not a consequence of the condensation of the adsorbent molecules in contacts between the particles of the solid. The absence of water as an individual phase in magnesium hydroxide (within the limits of monolayer adsorption) has been demonstrated by the NMR method. The true cause is the decrease in the surface energy of the solid on adsorption, i.e. the weakening of the bonds between the atoms (ions) at the surface. The maximum decrease in mechanical strength, attained for a 3%–4% moisture content, is associated with a further decrease in the free surface energy on multilayer adsorption. The subsequent increase in mechanical strength and then its resumed decrease in the presence of high contents of the adsorbate has been explained by the fact that in contrast to continuous media, in disperse porous media the decrease in mechanical strength may be reduced by capillary contracting forces which arise on condensation of the vapour of a liquid in pores.

In the presence of ethyl alcohol, the rise in the curve is not quite so pronounced as in the presence of water owing to the weakening of the capillary contraction forces as a consequence of the smaller surface tension of the boundary with air than for water. The adsorption nature of the decrease in the mechanical strength of magnesium hydroxide specimens in the presence of water is also indicated by the correlation between the relative decrease in the strength of the porous structure and the decrease in the free surface energy of this material ($\Delta\sigma$), which were measured in the presence of water by independent methods (Fig. 2).^{42,43} The quantity $\Delta\sigma$ by which the surface energy decreases, i.e.

$$\Delta\sigma = \sigma_0 - \sigma = RT \int_0^p \Gamma \ln p,$$

(p is the water vapour pressure at which the specimens were moistened) was found from the adsorption (Γ) isotherm for water vapour.

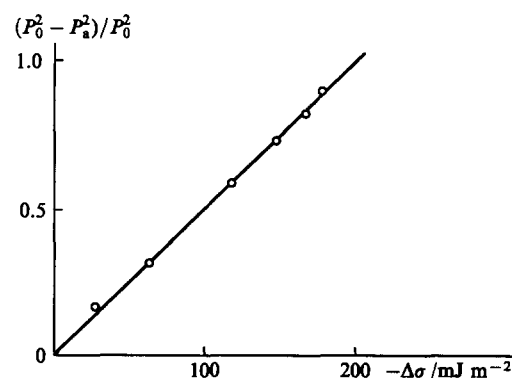


Figure 2. Relation between the decrease in mechanical strength and the decrease in the surface energy of highly disperse porous magnesium hydroxide specimens⁴² in terms of the variables of the Griffith equation.

The relation obtained confirms the validity of the Griffith relation, i.e. a proportionality between the relative decrease in mechanical strength ($(P_0^2 - P_a^2)/P_0^2$ (P_0 and P_a are the mechanical strengths of the dry specimen and the specimen moistened under equilibrium conditions respectively)) and the decrease in surface energy holds for these structures. Hence it follows that $P \sim \sigma^{1/2}$. The quantity $\sigma_0 = 300 \text{ mJ m}^{-2}$, found from the slope of the straight line, has an acceptable value. The same correlation has been observed in the adsorption of water vapour on silica gel.⁹⁵ A relation between the decrease in surface energy and the decrease in the mechanical strength of porous bodies has been indicated.⁴⁴ The values of σ for cement were found from the Griffith equation; for a water : solid (WS) ratio of 0.45, we have $\sigma = 1370 \text{ erg cm}^{-2}$, whilst for WS = 0.60 we have $\sigma = 657 \text{ erg cm}^{-2}$.

The ADS effect for the monomolecular surface coverage by the adsorbate has been observed in experiments with ionic polycrystalline KCl and NaCl immersed in water–dioxane mixtures of different composition.⁴⁵ The decrease in mechanical strength under these conditions was not associated with the impregnation of the grains between the crystals by the liquid.

In the study of the influence of the polarity of the adsorbate on the mechanical strength of porous structures in relation to magnesium hydroxide as an example, it was shown that, in contrast to the polar water and ethanol molecules, the nonpolar benzene and cyclohexane molecules hardly influence the mechanical strength of the hydroxide.⁴¹ Similar features were observed in the study of the decrease in the mechanical strength of pressed calcium carbonate, zinc oxide, sodium chloride, charcoal and silica gel specimens in the presence of water, benzene, and carbon tetrachloride vapours, carbon dioxide, and nitrogen.^{95–97} The specimens on the surfaces of which a saturated monolayer of the molecules of the medium had been adsorbed were found to be the least strong. The effect involving a decrease in mechanical strength was greater the closer were the polarities of the adsorbent and the medium (water on silica gel, benzene on charcoal). This indicates a decrease in mechanical strength with decrease in the free surface energy on adsorption. In all the systems indicated, the decrease in mechanical strength was not accompanied by the occurrence of dissolution and chemical interaction processes. The mechanical strength of ionic polycrystalline sodium and potassium halides in heptane, water, and dioxane decreased to a greater extent the greater was the polarity of the medium.⁴⁵ Thus in water it amounted to 0.2 of the initial value.

The dispersity of the structure-forming particles, the degree of porosity of the medium, and the nature of the individual contacts did not affect the decrease in mechanical strength in adsorption on magnesium hydroxide specimens.⁴¹ It was observed by X-ray diffraction that, in physical and chemical adsorption (for example, of isopropyl alcohol on magnesium oxide⁴⁶ and of water and ethyl alcohol on magnesium hydroxide,⁴⁷) the microdeformations (internal stresses) increase with the consequent adsorption-induced decrease in the strength of the structure. The appearance of internal stresses has been explained by the change in the relation between the resistance of the rigid framework comprising interlinked particles and the Laplace pressure compressing the particles (as a consequence of the decrease in free surface energy on adsorption).

The transition of silica gel to a complex stressed state occurred when it was moistened and dried.⁹⁸ When silica gel was fully immersed in water, air was trapped in the structure and was compressed by the capillary pressure due to the gradually permeating water. As a result, high counterpressures arose in the structure, reaching limiting disruptive values.

The ADS phenomenon was observed also on chemically more complex porous structures: specimens of clays of different mineralogical composition (kaolinite, bentonite), NaA and NaX zeolites,^{48,49} and an aluminosilicate zeolite-containing cracking catalyst.⁵⁰ The mechanical strength of these materials diminished sharply following the adsorption of various substances. The adsorption and especially chemisorption of isopropyl alcohol

induces an appreciable comminution of the block structure of magnesium oxide crystals (an increase in the density of dislocations).⁴⁶ The possible cause of this is the nonuniformity of the adsorption combined with the mechanical anisotropy of the crystals. The relaxation processes occurring after the catalytic reaction again lead to an increase in the size of the blocks and a decrease in the density of dislocations.

Among the multiplicity of the elementary mechanisms for the formation of the texture of catalysts under various conditions, two most common mechanisms of the increase in surface are distinguished. The characteristics of the thermodynamics of highly disperse systems, which determine the direction and driving force of the process, are manifested in these mechanisms.⁹¹ One of the mechanisms involves the growth of the surface in phase transformations, where the decrease in the phase potential compensates for the increase in the surface potential, which is appropriately reflected in the radius of the critical nucleus of the new phase.^{3,91} The second mechanism is associated with the change in entropy. If the interfacial energy is small, the increase in entropy may compensate for the increase in surface energy.³ On the basis of these mechanisms, it is possible to estimate the minimum size of the nucleus or the 'maximum area which can then only decrease in the absence of phase transformations or a sharp decrease in the interfacial energy'.⁸¹

The driving forces and the principal mechanisms of the decrease in the surface (for example, as a result of coagulation) can also be related to the local (in the contact zones) decrease in the interfacial energy.⁴ On the other hand, the specific mechanisms of the processes, including the mechanisms of the change in porosity, may be extremely varied.⁸¹

Examination of the ADS phenomena helps us to understand the mechanisms of certain intermediate stages in the new processes involving the formation of a wide variety of aluminium oxide carriers and catalysts using thermochemical (TCA) and mechanochemical (MCA) methods for the activation of solids (see, for example, Refs 84 and 99–101). Thus it has been shown that, in the transformation of the products of the MCA and TCA of technical hydrated alumina, as a result of hydration, from the amorphous to the pseudoboehmite state (which can be readily converted into various aluminium oxide carriers or binders for catalysts), bonds between the elements of the layered structure (plates) are disturbed by the ADS and by the presence of the disjoining pressure of the liquid phase on the surfaces bounding it.⁸⁴ This results in the cleavage of the highly disperse particles of the products of the TCA into finely disperse (2–5 nm thick) plates and their subsequent hydration. This phenomenon as well as others have been used in creating a low-waste technology for the manufacture of aluminium oxides used as carriers, adsorbents and catalysts.⁸⁴ The formation of surface compounds, which occurs, for example, in the interaction of methanol with magnesium oxide,⁸⁵ is accompanied by the dissociation of the bonds in the alcohol molecule and the liberation of energy. In the chemisorption of ethanol on Al_2O_3 ,⁸⁶ the bonds between the aluminium and oxygen ions are 75%–90% weakened according to quantum-chemical calculations and IR spectroscopic data. The clusters formed and their varieties, participating in the formation of surface compounds, also play a definite role in this process.

Comparison of the behaviour of adsorbates having molecules of different size (water, benzene) made it possible to observe that the filling of the inner cavities of the zeolite crystals (within the limits of sorption capacity) with adsorbate molecules prevents a decrease in mechanical strength of granules.^{48,49} If there is steric hindrance to the permeation of the adsorbate molecules into the cavities, the mechanical strength of the zeolite grains diminishes already for low degrees of adsorption (of the order of monolayer coverage of the surface of the clay binder). A similar 'protective' effect has been observed in the dispersion of brown coal in the presence of water and heptane.⁵¹

The data presented referred to physical adsorption, but in catalytic processes the chemical adsorption of the reactants and reaction products plays the main role.

The influence of chemisorption on the short-term and long-term mechanical strength of disperse porous structures has been investigated in detail in relation to the behaviour of the cobalt-molybdenum catalyst under conditions involving a change in the temperature and pressure of the vapours of the products of the incomplete oxidation of propene (carbon dioxide, acetaldehyde, and especially acrolein).^{52-54, 102, 103} It was established that the degree of disintegration of the catalyst depends on the degree of surface coverage by chemisorbed molecules and on the strength of the chemisorption bond, i.e. on the decrease in free surface energy on chemisorption (Fig. 3).

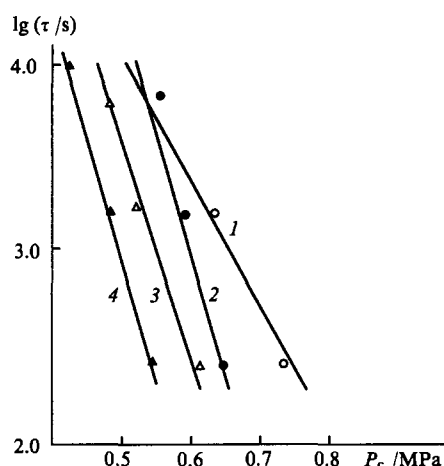


Figure 3. Dependence of the time to fracture of a cobalt-molybdenum catalyst on the applied load in various media at 483 K: (1) nitrogen; (2) carbon dioxide (partial pressure 350 mm Hg); (3) acetaldehyde (60 mm Hg); (4) acrolein (60 mm Hg).⁴⁹

The disintegration of a catalyst as a consequence of chemisorption has been observed also under the conditions where the grains of an alumina-chromium oxide-potassium oxide catalyst were ground up in a stream of n-butane and butenes at elevated temperatures.⁵⁵

III. The effect of the catalytic reaction on the mechanical strength of catalysts

The phenomenon of the accelerated disintegration of the structures of catalysts under the reaction conditions has long been known. Shchukin and coworkers^{9, 10} showed for the first time that the surface phenomena at the interfaces in the porous structures should be regarded as the main causes of the decrease in the mechanical strength and durability of catalysts. A similar view has been expressed in a study of the surface phenomena accompanying a heterogeneous chemical reaction using methods based on the thermodynamics of irreversible processes.¹⁰⁴ If intermediate compounds or a series of states which possess a higher surface activity than the initial and final compounds are formed in a chemical reaction,[§] then their adsorption at the interface reduces the interfacial energy and increases the area of the interface. Consequently, the surface energy of the catalyst should diminish during the catalytic process. A decrease in the hardness of

amalgamated zinc and brass catalysts in the decomposition of aqueous solutions of hydrogen peroxide has been observed experimentally and explained by a decrease in the surface tension of mercury during catalysis.¹⁰⁵ According to the data of Shchukin and Margolis,⁶⁴ the active intermediate complex interacts more strongly with the catalyst surface than the initial reactants and chemisorption appreciably weakens the metal-metal bond. As a result, surface metal atoms are frequently detached on formation of a bond with active adsorbates.

The mechanical strength of sulfur dioxide oxidation catalysts under the reaction conditions differs appreciably from their strength outside the reactor.⁷⁷

The influence of catalysis on the mechanical strength and durability of porous magnesium oxide catalysts in the endothermic isopropyl alcohol dehydrogenation reaction has been studied systematically.^{37, 40, 46, 52, 56, 66, 67} Already 20-30 s after the start of the reactions, even before the establishment of stationary conditions, the compressive strength of the catalyst diminished by a factor of 1.5-2 (the tests were carried out after the cessation of the catalytic reaction and the drying of the grains).^{46, 56} A further increase in the duration of the use of the catalyst induced only a slight decrease in its mechanical strength. It was demonstrated by X-ray diffraction that the internal stresses in the catalyst diminish during the reaction owing to the irreversible rupture of the bonds (contacts between the particles).

Numerous experiments have shown that the mechanical strength of the catalyst decreases with increase in the internal stresses associated both with the genesis of the structure (for example, on pressing a magnesium oxide powder or on dehydration of magnesium hydroxide) and with the catalytic reaction conditions (thermoelastic stresses due to the cyclic changes in temperature during catalysis). The mechanical strength of the catalyst, measured directly during catalysis with the aid of a dynamometric device mounted in a specially constructed reactor,⁵⁷ proved to be lower than after the cessation of the reaction for the same exposure time. It may be that the decrease in the interfacial energy is influenced by the nonequilibrium adsorption of intermediate compounds during catalysis. If the conditions of the catalysis promote the appearance of internal stresses (for example, as a consequence of cyclic changes in temperature), then the mechanical strength decreases significantly not only at the beginning of the process but also throughout it. The decrease in mechanical strength may be accompanied by a change in the specific surfaces of the specimens, but a direct relation between the decrease in mechanical strength and dispersity was not observed.

The decrease in mechanical strength was independent of the change in the specific surface of the porous structure as was confirmed in experiments on the dehydrogenation of isopropyl alcohol on aluminium oxide specimens.⁵⁸

During the catalytic reaction, not only the mechanical strength but also the durability of the catalyst under load decrease. Thus the disintegration time of a magnesium oxide catalyst subjected to a 0.8 MPa load decreases dramatically in the reaction medium (the disintegration time was determined from the projections of the corresponding points on the relations illustrated in Fig. 4 onto the ordinate axis). A decrease in durability under the conditions of catalysis has been observed also for the cobalt-molybdenum catalyst of the incomplete oxidation of propene.⁵²

There are data on the disintegration of sulfate catalysts in stationary and fluidised beds used in the synthesis of sulfuric acid.^{59, 60}

In order to test the hypothesis that the bonds are weakened in the solid under the reaction conditions, CO was oxidised on disperse porous iron and nickel specimens.⁶¹ An increase in the area of contact between the metal particles was observed with an electron microscope.

The migration of crystallites as well as the disappearance of small particles and the appearance of large ones with formation of irregular shapes have been observed also in a study of the

§ The possibility of the appearance of intermediate forms of the interaction in catalytic processes was already noted by D I Mendeleev [see D I Mendeleev *Osnovy Khimii* (Fundamentals of Chemistry) Vol. I (Moscow, Leningrad: Goskhimizdat, 1947) pp. 523, 524].

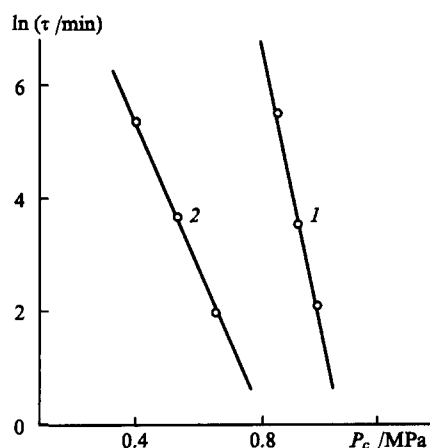


Figure 4. Dependence of the time to fracture of a magnesium oxide catalyst on the applied load at 668 K in nitrogen (line 1) and in the reaction medium during the dehydrogenation of isopropyl alcohol (line 2).

behaviour of the $\text{Ag}/\text{Al}_2\text{O}_3$ catalyst in the ethene oxidation reaction.¹⁰³

These results as well as the data mentioned above concerning the decrease in the durability of the cobalt–molybdenum catalyst in the chemisorption of the reaction products^{52,53} confirm the hypothesis of Shchukin and coworkers,^{9,10} according to which the decrease in the mechanical strength of the specimens under the conditions of catalysis is caused by the simultaneous effect of the internal stresses in the catalyst and of the weakening of the bonds between the atoms (ions) on the surface of the solid as a result of the adsorption of the reacting components, including the effect resulting from the nonequilibrium adsorption of intermediate compounds.

The rate of the surface diffusion (self-diffusion) in iron under the conditions of catalysis and in the absence of the reaction medium has been investigated.⁶² The method involving the 'healing' of a scratched groove was employed: for a specified observation time, the decrease in the depth of the groove δ is proportional to the surface diffusion coefficient D raised to the power $1/4$. It was established that, under the conditions of the synthesis of ammonia at 800 K, the diffusion coefficient of iron atoms on the surface of the catalyst increases by a factor of 10^5 compared with the value of D at the same temperature in the absence of catalysis. This effect is due to the sharp increase in the number of mobile adsorbed atoms as a result of the implementation of the reaction steps (in this case, an exothermic reaction). Similar phenomena have been observed in the hydrogenation of benzene on nickel.⁵⁴ The similarity in the behaviour of these metals in the reaction described above is due to the fact that molecular hydrogen dissociates on these catalysts and atomic hydrogen induces their embrittlement.

It is noteworthy that, under the conditions of experiments⁵⁴ involving the 'healing' of a scratch, the migration mechanism is known to be determined by the surface mass transfer on nickel, since the mechanism involving transfer through the gas phase is impossible owing to the low vapour pressure of nickel, while the bulk diffusion mechanism cannot be achieved because of the considerable predominance of surface self-diffusion over the bulk-phase diffusion at the experimental temperature. The exothermic reaction in which benzene is hydrogenated to cyclohexane at 100 °C and the endothermic cyclohexane dehydrogenation reaction at 350 °C have been investigated.⁵⁴ In control experiments, nickel specimens with scratches were annealed in a stream of hydrogen at 100 °C and in a stream of helium at 350 °C. The smoothing of the scratch was estimated from the decrease in its initial depth. This occurred only under the conditions of the exothermic reaction involving the hydrogenation of benzene to cyclohexane. As in the synthesis of ammonia on iron, the nickel

diffusion coefficient was greater by a factor of 10^4 – 10^5 than the value of D in the absence of catalysis. Since the coefficient D increased only in the presence of an exothermic reaction, it is evident that the energy of the chemical reaction is necessary for the acceleration of the mass transfer.

It has been suggested that this effect is possible also in an endothermic reaction, provided that an intermediate stage proceeds with evolution of energy. The role of catalysis in the rearrangement of the surface consists precisely in facilitating a single nickel adatom formation due to an elementary catalytic step and not in facilitating the subsequent migration of the adsorbed atom over thousands of interatomic distances. In other words, since the scratch is not 'healed' in an endothermic reaction, the increase in D during catalysis may be attributed to the heat of reaction: the energy evolved in each catalytic step is consumed predominantly (or completely) not on heating the catalyst but on the local rupture of the bonds of individual atoms (ions) in the surface layer of the solid (on which or in the vicinity of which the catalytic step occurs), on the 'abstraction' of atoms from the defective region of the crystal lattice (for example, from kinks in the steps on the surface), and on their transition to the state of adsorbed atoms. Since the absolute heat of the reactions investigated calculated per mole exceeds by a factor of 2–3 the energy required for the formation of 1 mole of adsorbed atoms, it was postulated⁵⁴ that 2–3 additional adsorbed atoms, which participate in the diffusional surface mass transfer, arise in each step.

IV. Contacts between the particles and internal stresses

According to the ideas of physicochemical mechanics, the mechanical strength of a solid depends on the nature of the contacts between the particles. The strength of the crystallisation contacts is relatively high, amounting to 10^{-6} N and more. Depending on the conditions in the preparation of the catalysts and on their chemical properties, the number and strength of the individual contacts may vary and hence the mechanical strength also varies. The characteristics of the structure of the solid (defects, dislocations, etc.) are superimposed on the properties of the porous structures of the catalyst.

It has been shown^{37,63} that, in contrast to the decrease in mechanical strength during adsorption, in many cases the adsorption-induced decrease in mechanical strength during catalysis may be sharply weakened with increase in the strength of the contacts in the porous structure. These results have been obtained on specimens of a magnesium oxide catalyst with the same fine and overall porosities, on which the catalytic reaction proceeds at the same rate. Specimens with 'low strength' contacts were formed from a magnesium oxide powder obtained by heating magnesium hydroxide at 1173 K. After moulding, they were annealed at 723 K. Specimens with 'strong' contacts were obtained from hydrated magnesium oxide, by dehydration of magnesium hydroxide specimens at 723 K and following calcination at 1173 K. In both cases the heat treatment conditions were the same and only the sequence of the operations was altered.

Figure 5 presents data on the relative decrease in the compressive strength (along the axis of a cylinder) of magnesium oxide specimens, obtained under the conditions of the dehydrogenation of isopropyl alcohol at 653 K, as function of their porosity (Π). These relations have been attributed^{37,63} to the lower mobility of the chemisorbed molecules ('kinetic difficulties') compared with the mobility of the molecules in the state of physical adsorption. In the latter case, the molecules have sufficient time to migrate, following the tip of the crack opening as a result of the applied stress.

The increase in the durability of the magnesium oxide catalyst containing 15 mass % of added silica, known as white soot, has also been explained by the kinetic difficulties arising following an increase in the strength (area) of the contacts.^{56,62} In the presence of white soot, the longterm strength of this catalyst falls to an

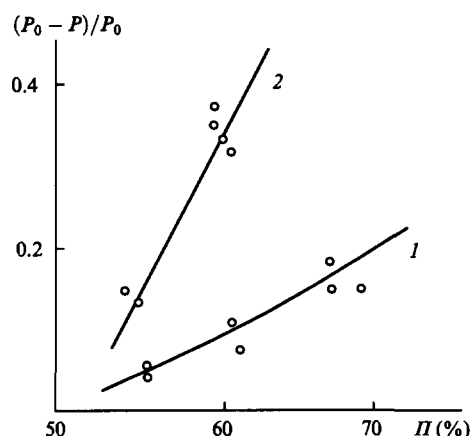


Figure 5. Dependence of the relative decrease in the strength of the samples with 'weak' (line 1) and 'strong' (line 2) contacts on the porosity of a magnesium oxide catalyst under the conditions of the dehydrogenation of isopropyl alcohol at 653 K. P = mechanical strength of the specimen 1 h after the start of the reaction; P_0 = mechanical strength of the initial specimen kept in the reactor at the temperature of the catalytic reaction in a stream of dry nitrogen.

appreciably lesser extent 50 min after the start of the catalytic reaction than in its absence. The specimen with the additive possesses the same and in certain cases a higher catalytic activity. The strengthening of the contacts has been attributed to the improvement in the sintering of the magnesium oxide particles as a result of the chemical interaction with silicon oxide.

The possibility of the reconstruction of the catalyst surface under the conditions of adsorption and the catalytic reaction has been demonstrated.^{7,8} The driving force for the reconstruction of the lattice of the solid is the decrease in the free surface energy. The kinetics of the mass transfer accompanying this phenomenon indicate^{54,62} that, in the course of exothermic catalytic reactions, there is a sharp (by 4–5 orders of magnitude) increase in the coefficient of the surface self-diffusion of the metal atoms on the catalyst surface (the heat of chemisorption, which is always positive, is insufficient for an appreciable acceleration of the surface diffusion). Experiments with porous nickel and iron catalysts have shown that this increases by a factor of 4–6 the strength of the porous structures under the conditions of catalysis by virtue of the increase in the number of adsorbed atoms and their directed diffusion to sites with a changed chemical potential, including contact regions. The same mechanical strength under an inert gas atmosphere as in catalysis may be attained only at an appreciably higher (by 300 °C) temperature. Under the conditions of catalysis, where the self-diffusion coefficient increases by a factor of 10^5 , the calculated sintering temperatures of a series of substances (iron, nickel, magnesium oxide, iron oxide) decrease by several hundreds of degrees; a decrease in the sintering temperature is promoted by a decrease in the activation energy for self-diffusion.⁶²

The relation between the elementary catalytic events and the adsorption mechanisms of the decrease in mechanical strength was established by comparing the processes involving the synthesis of ammonia on an iron catalyst, one of the stages of which is the dissociative chemisorption of hydrogen, and the hydrogen-induced embrittlement of iron.^{64–66} The weakening of the interatomic bonds in molecular hydrogen and in iron are two aspects of a single process: the iron catalyst promotes the dissociation of the bond in the H_2 molecule, while atomic hydrogen facilitates in its turn the rupture of the Fe–Fe bonds in the iron lattice. Nickel, which is a catalyst for exothermic hydrogenation reactions and is also susceptible to hydrogen-induced embrittlement, behaves similarly.

In other words, together with the 'direct' effect of the surface of the solid phase on the reaction kinetics, there is a 'reverse' effect of the medium on the structure of the solid — the catalyst.

The appearance and decomposition of contacts as a result of fluctuating oscillations, the mechanisms of the elementary steps in the deformation and disintegration, and the influence of the medium on these processes have been examined at the atomic-molecular level with the aid of the method of molecular dynamics (numerical experiment of a dynamic type).^{67,68} Analysis of the long-term strength of an individual bond subjected to a constant load showed that the logarithm of the average lifetime of the bond decreases linearly with increase in the applied load, which is strictly consistent with the universal Zhurkov equation.

This approach made it possible to confirm also the idea of the molecular nature of the Rebinder effect. The deformation and fracture of a two-dimensional crystal having a concentrator-cavity during the adsorption of a surface-active component on the walls of the cavity have been explained by the fact that when a crystal is subjected to a load, a crack is initiated, which is followed by its growth and the permeation into the growing crack of surface-active atoms, which promote its propagation.

The principle of the interrelation between the elementary catalytic steps and the adsorption-induced decrease in mechanical strength,^{64–66} i.e. the analogy between the rupture of the interatomic bonds induced by mechanical disintegration and the chemical reaction, has been confirmed in a theoretical analysis of the catalytic cracking of hydrocarbons.⁶⁹ Acid catalysts are used in cracking processes and the reaction proceeds via a stage involving the formation of a carbonium ion. In this connection, it was postulated that the acid agents must facilitate also the mechanical disintegration of the hydrocarbon chain. In order to establish the mechanism of the Rebinder effect and to determine the quantitative characteristics of the adsorption-dependent influence of the medium, a direct quantum-mechanical calculation of the force and energy parameters of single and double C–C bonds during their mechanical rupture was carried out and the influence of the hydrogen cation — the active principle in acid catalysts of the cracking of hydrocarbons — on this process was estimated. The calculation showed that the addition of a proton diminishes the strength of the C–C bond and that the magnitude of the effect depends significantly on the nature of the carbonium ion formed. The interrelation principle has been confirmed also in numerous experimental observations of the rearrangement of the surfaces of catalysts under the conditions of a catalytic reaction.

It was established that the stresses in solids arising during the formation of the structure can both decrease and increase their mechanical strength.² The increase in the mechanical strength of solids has been observed on pressing powders, whereupon phase contacts were produced as a result of the plastic deformation in the contact zone. On the other hand, the presence of residual internal stresses in the solid always induces a decrease in mechanical strength, especially in the study of catalytically active media which accelerate the relaxation of stresses due to the weakening, as a result, of chemisorption of the bonds between the atoms (ions) of the surface.^{2,3} One of the most important conditions governing the increase in the durability of heterogeneous catalysts, sorbents, and carriers is therefore a decrease in the residual internal stresses by the optimisation of structure formation.

Among the procedures for decreasing the residual internal stresses one may name, for example, the regulation of the dispersity of the initial binding substance in the structures arising as a result of the hydration-induced hardening of calcium and magnesium oxides, the introduction of seeds in crystallisation processes, and the addition of some electrolytes (i.e. the creation of conditions promoting a decrease in the supersaturation of suspensions in the aqueous phase during the preparation of the catalyst).^{2,70} An increase in porosity and a decrease in the rigidity of the crystallisation structures are also used to eliminate internal stresses, for example by introducing small amounts of a highly

disperse inert filler, which hinders the formation of phase contacts in the bulk of the material in the initial stages.

Catalysts based on silica and alumina gels having an amorphous matrix constitute a separate group. They acquire special functional (catalytic, adsorption, etc.) properties following the introduction of a crystalline filler, for example, a zeolite. As in crystallisation structures, in these composite structures the internal stresses reach magnitudes close to the mechanical strength of the material itself ($\sim 10^7$ N m⁻²).^{4,71} An increase in the dispersity of the filler crystals and the introduction of anisometric particles are procedures for reducing the residual stresses in such materials.² Thus the introduction into an amorphous aluminosilicate xerogel (a cracking catalyst) of fluorite crystals with a lower dispersity as a filler reduces the internal stresses by a factor greater than two, while small amounts of added ($\sim 2\%$) asbestos fibres diminish microdistortions by a factor of two.²

The internal stresses in catalysts and sorbents become smaller when vibration-induced compaction is used instead of static pressing.^{72,73} In this case, the decrease in the internal stress is accompanied by the simultaneous increase in the density of the structure, increasing its strength,^{1,10} which depends on the number of particles per unit cross-section (the granulometric composition is the same under the conditions of static and vibration-induced compaction). A decrease in the fraction of large pores, which under the conditions of catalysis in the presence of residual stress may play the role of the nuclei of cracks, has an extremely positive effect on the increase in density. It has been shown for the bismuth-molybdenum catalyst of the oxidative ammonolysis of propene that a denser structure with smaller internal stresses obtained by vibrocompaction is also more durable.⁷³ Its catalytic properties remain unchanged under these conditions.

V. The sintering and strengthening of catalysts

Since the coefficient D increases during the catalytic reaction,⁶² a decrease in the sintering (presintering) temperature and hence an increase in the strength of the porous structure of the powdered pressed catalysts compared with similar specimens heat-treated at the temperature of the catalytic reaction but in an inert medium might have been expected. A heterogeneous catalytic reaction proceeds only on the outer or inner surface of the solid catalyst and therefore one should expect that the cause of such strengthening is an increase in the area of the true contact between the particles for an unchanged porosity of the specimens.

Naturally the postulated effect involving the strengthening of catalysts in exothermic reactions may be observed only if it surpasses the effect involving the adsorption-induced decrease in the strength of the porous structure.

The oxidation of CO has been investigated in through-put apparatus at atmospheric pressure under isothermal conditions, where the temperature of the catalyst (carbonyl iron) increase during the reaction by not more than 0.2 °C.^{61,75,76} The reacting gases — oxygen and carbon monoxide in stoichiometric proportions — were supplied to the reactor in a mixture with helium. The influence of the reaction mixture and of its individual components — CO (in a mixture with helium) and O₂ (in a stream of air) as well as H₂ — on the mechanical strength of the catalyst was elucidated. 'Mild' conditions in the preparation of the specimens promoted a decrease in the residual internal stresses and the adsorption-induced decrease in mechanical strength.

Table 1 presents the results of the measurement of the mechanical strengths of carbonyl iron specimens after their annealing in various media. During the reaction at 573 and 623 K, there is a sharp (by a factor of 4–5) increase in the mechanical strength of the catalyst compared with the initial specimen and the specimens annealed in the presence of one of the reaction components. It was demonstrated by means of an electron microscope that the catalyst particles form contact chords, produced during the annealing of the specimen under the reaction

Table 1. The influence of the carbon monoxide oxidation reaction and of the components of the reaction medium on the mechanical strength of the porous structure of the catalyst — carbonyl iron.⁵⁴

Composition of medium (vol. %)	Strength (in MPa) at	
	573 K	623 K
8% CO + 4% O ₂ + 88% He	6.4	7.46
21% O ₂ + 78% N ₂ (air)	2.40	2.88
100% Ar	1.37	1.46
8% CO + 92% He	0.31	0.36

Note. The porosity of the specimens was $57.5 \pm 0.2\%$ before and after catalysis and the mechanical strength was 1.27 MPa.⁵⁴

conditions. In the absence of the reaction medium at the same temperature, the effect is much weaker.

The increase in mechanical strength is due to the increase in the area of contact between the particles as a result of the surface self-diffusion. A sharp increase in the strength of the catalyst for a constant porosity was achieved in this reaction also on specimens of electrolytic nickel.

A decrease in the sintering temperatures of iron and nickel during the catalytic reaction was established experimentally. The strength of the porous structures of iron and nickel in an inert medium increased only at higher temperatures (by 300–350 °C).

Thus the sintering temperatures of metallic powders decrease appreciably under the conditions of an exothermic catalytic reaction. A significant strengthening of the porous structures is then attained as a result of the development of contacts between the particles with retention of the initial porosity, which is important for both catalysts and adsorbents and for membranes. Qualitatively similar results have been obtained on the MgO and V₂O₅ oxide catalysts in exothermic oxidation reactions,^{74,75} but the strengthening effect proved to be smaller in this case than on porous metallic catalysts. This is apparently due to the greater defectiveness (metastability) of the oxides obtained by the decomposition of hydroxides and salts at relatively low temperatures, appreciably those lower than the melting points of the corresponding oxides.

VI. Conclusion

The interaction between the catalyst surface and the molecules of the medium induces certain changes both in the adsorbed molecules and in the catalyst itself. For example, the mechanical strength and durability of the MgO, Co-Mo, Al-Cr-K, etc. catalysts may decrease significantly in the course of the catalytic reaction. Iron may serve as yet another striking example: as a catalyst of the synthesis of ammonia, iron participates in the cleavage (dissociative adsorption) of the hydrogen molecule and is in its turn subjected to hydrogen-induced embrittlement.

The influence of the catalytic reaction on the mechanical properties of the catalyst must be regarded as one of the manifestations of the Rebinder effect — a decrease in the mechanical strength of a solid under the influence of the adsorption active components of the medium, which reduce the surface energy (and the work of disintegration), and of the mechanical stresses induced by the weight of the catalyst layer, collisions, and thermal gradients. The residual internal stresses, arising at different stages in the preparation of the grains, also make their own contribution. The catalyst is therefore, as it were, doomed to accelerated wear precisely by virtue of its purpose.

However, comprehensive analysis made it possible to also discover ways whereby these undesirable effects can be significantly weakened. The strengthening and increase in the stability of granules in an active medium are achieved by the optimisation of the entire technological chain in the preparation of the catalyst by selecting pressing and hydration conditions, by the use of inert carriers, by employing modifying agents during sintering, by

introducing mineral binders, by modifying the contacts themselves, which promotes a decrease in their sensitivity to the medium, by combining finely disperse and coarsely disperse fractions, by adding anisometric (fibrous), including inert, fillers, etc. All this makes it possible to increase drastically the useful life of the catalyst.

At the same time, the weakening of the bonds between the atoms on the surface of the catalyst leads to a sharp increase in the number of mobile atoms and intensification of the surface self-diffusion. Direct observations by the method involving the 'healing' of a scratch indicate an enormous (by 4–5 orders of magnitude) increase in the coefficient of surface self-diffusion. This effect has been observed on iron during the synthesis of ammonia and on nickel during the hydrogenation of benzene.

The intensification of self-diffusion may in its turn intensify the sintering process, making it possible to carry it out at reduced temperatures. The sintering temperatures of iron and nickel powders under the conditions of the oxidation of CO may be reduced by 300 °C without affecting the mechanical strength of the specimens, i.e. it ensures the development of strong contacts between the particles. Similar effects have been observed on the MgO, V₂O₅, and Al₂O₃ catalysts under the conditions of the corresponding reactions.

The approach described leads to new possibilities for the selection of catalysts and the optimisation of the technology of their preparation, the improvement of the processes involving the sintering of high-temperature components, and in general the development of new principles of the treatment of materials.

This review has been written with partial financial support by the International Scientific Fund (grant MLE 300) and the Russian Fundamental Research Fund (grant 95-03-08072).

References

1. E D Shchukin, in *Fiziko-khimicheskaya Teoriya Prochnosti Dispersnykh Struktur i Materialov. Fiziko-khimicheskaya Mekhanika Prirodnykh Dispersnykh Sistem* (Physicochemical Theory of the Strength of Disperse Structures and Materials. Physicochemical Mechanics of Natural Disperse Systems) (Ed. E D Shchukin) (Moscow: Izd. Moskovsk. Gos. Univ., 1985) p. 72
2. E D Shchukin, S I Kontorovich, E A Amelina *Zh. Vses. Khim. O-va im D I Mendeleeva* **34** (2) 23 (1989)
3. E D Shchukin (Ed.) *Uspekhi Kolloidnoi Khimii i Fiziko-khimicheskoi Mekhaniki* (Advances in Colloid Chemistry and Physicochemical Mechanics) (Moscow: Nauka, 1992)
4. E D Shchukin, A V Pertsov, E A Amelina *Kolloidnaya Khimiya* (Colloid Chemistry) (Moscow: Vysshaya Shkola, 1992)
5. E D Shchukin, in *Fiziko-khimicheskaya Mekhanika i Liofil'nost' Dispersnykh Sistem* (Physicochemical Mechanics and Lyophilicity of Disperse Systems) (Kiev: Naukova Dumka, 1981) Vol. 13, p. 46
6. A G Leibush, in *Khimicheskaya Pererabotka Neftnykh Uglevodorodov* (Chemical Processing of Petroleum Hydrocarbons) (Moscow: Izd. Akad. Nauk SSSR, 1956) p. 121
7. A P Rudenko, in *Sovremennye Problemy Fizicheskoi Khimii. Voprosy Kataliza, Adsorbtsii i Fiziko-khimicheskoi Mekhaniki* (Current Problems in Physical Chemistry. Problems of Catalysis, Adsorption, and Physicochemical Mechanics) (Eds Ya I Gerasimov, P A Akishin) (Moscow: Izd. Moskovsk. Gos. Univ., 1968) Vol. 3, p. 263
8. A A Balandin, A P Rudenko, G Stegner *Izv. Akad. Nauk SSSR, Ser. Khim.* **762** (1961)
9. P A Rebinder, E D Shchukin, L Ya Margolis *Dokl. Akad. Nauk SSSR* **154** 695 (1964)
10. E D Shchukin *Kinet. Katal.* **6** 641 (1965)
11. V I Likhtman, E D Shchukin, P A Rebinder *Fiziko-khimicheskaya Mekhanika Metallov* (Physicochemical Mechanics of Metals) (Moscow: Izd. Akad. Nauk SSSR, 1962)
12. S Z Roginskii, I I Tret'yakov, A B Shekhter *Dokl. Akad. Nauk SSSR* **91** 881 (1953)
13. M R Lyubovskii, V V Barelo *Kinet. Katal.* **35** 412 (1994)
14. G K Borekov *Kataliz. Voprosy Teorii i Praktiki* (Catalysis. Problems of Theory and Practice) (Eds K I Zamaraev, G I Panov) (Novosibirsk: Nauka, 1987)
15. G K Borekov *Kinet. Katal.* **21** 5 (1980)
16. A Ya Rozovskii *Katalizator i Reaktsionnaya Sreda* (The Catalyst and the Reaction Medium) (Moscow: Nauka, 1988)
17. K N Spiridonov, O V Krylov, in *Problemy Kinetiki i Kataliza* (Problems of Kinetics and Catalysis) (Moscow: Nauka, 1975) Vol. 16, p. 7
18. V A Khalif, B V Rozentuller, A M Frolov, E L Aptekar', K N Spiridonov, O V Krylov *Kinet. Katal.* **19** 1231 (1978)
19. V P Zhdanov *Elementarnye Fiziko-khimicheskie Protssy na Poverkhnosti* (Elementary Physicochemical Surface Processes) (Ed. K I Zamaraev) (Novosibirsk: Nauka, 1988)
20. L Ya Margolis *Okslenie Uglevodorodov na Geterogennykh Katalizatorakh* (Oxidation of Hydrocarbons on Heterogeneous Catalysts) (Moscow: Khimiya, 1977) p. 327
21. I V Berestetskaya, P Yu Butyagin *Dokl. Akad. Nauk SSSR* **260** 361 (1981)
22. A D Berman, O V Krylov, in *Problemy Kinetiki i Kataliza* (Problems of Kinetics and Catalysis) (Moscow: Nauka, 1978) Vol. 17, p. 112
23. P A Rebinder, E D Shchukin, L Ya Margolis *Dokl. Akad. Nauk SSSR* **154** 695 (1964)
24. F E Massoth *J. Catal.* **30** 204 (1973)
25. J Iwasawa *Adv. Catal.* **35** 187 (1987)
26. G A Somarjai, M A Vantive *Surf. Sci.* **299/300** 487 (1994)
27. C N R Rao, S R S Gopalakrishnan *New Directions in Solid State Chemistry* (London: Cambridge University Press, 1986)
28. J Johansen, A G Andersen (Eds) *Selected Topics in High Temperature Chemistry (Chemical Defects in Solids)* (Amsterdam: Elsevier, 1989)
29. C K D Tomlinson, J H Catlow *J. Phys. Chem. Solids* **51** 477 (1990)
30. R A Buyanov *Kinet. Katal.* **28** 157 (1987)
31. O V Krylov *Kinet. Katal.* **22** 1391 (1982)
32. Sh K Shaikhudinov, V I Kochubei *Usp. Khim.* **62** 443 (1993) [Russ. Chem. Rev. **62** 409 (1993)]
33. E D Shchukin *Izv. Akad. Nauk SSSR, Ser. Khim.* **2424** (1990)
34. E D Shchukin, A I Bessonov, S A Paranskii *Mekhanicheskie Ispytaniya Katalizatorov i Sorbentov* (Mechanical Tests on Catalysts and Sorbents) (Moscow: Nauka, 1971)
35. E D Shchukin, A I Bessonov, in *Standartizatsiya Metodov, Priborov i Ustanovok Kontrolya Kachestva Promyshlennykh Katalizatorov* (Standardisation of the Methods, Instruments, and Equipment for the Quality Control of Industrial Catalysts) (Eds R A Buyanov, N N Bobrov) (Novosibirsk: Institute of Catalysis, Siberian Division of Academy of Sciences of the USSR, 1991) p. 12
36. L F Mel'gunova, A A Samakhov, in *Standartizatsiya Metodov, Priborov i Ustanovok Kontrolya Kachestva Promyshlennykh Katalizatorov* (Standardisation of the Methods, Instruments, and Equipment for the Quality Control of Industrial Catalysts) (Eds R A Buyanov, N N Bobrov) (Novosibirsk: Institute of Catalysis, Siberian Division of Academy of Sciences of the USSR, 1991) p. 36
37. S F Suzdal'tseva, S I Kontorovich, E D Shchukin *Kolloid. Zh.* **39** 814 (1967)
38. E D Shchukin *Dokl. Akad. Nauk SSSR* **173** 139 (1967)
39. S I Kontorovich, E D Shchukin, in *Nauchnye Osnovy Tekhnologii Katalizatorov* (Scientific Foundations of the Technology of Catalysts) (Ed. G K Borekov) (Novosibirsk: Nauka, 1976) p. 131
40. E D Shchukin, M V Dukarevich, S I Kontorovich, P A Rebinder *Dokl. Akad. Nauk SSSR* **167** 1109 (1966)
41. M V Dukarevich, S I Kontorovich, E D Shchukin, in *Tr. Vsesoyuz. Nauchnogo Seminara po Vzaimodeistviyu Materialov Vysokotemperaturnogo Naznacheniya so Sredoi*, Kiev, 1968 (Proceedings of the All-Union Scientific Seminar on Interaction of High-Temperature Materials with the Environment, Kiev, 1968) p. 201
42. V S Yushchenko, M V Dukarevich, V F Chuvaev, E D Shchukin *Zh. Fiz. Khim.* **53** 1556 (1969)
43. E D Shchukin, S I Kontorovich, in *Razrushenie Katalizatorov — Sledstvie Vzaimnogo Vliyaniya Tverdoi Fazy i Reaktsionnoi Sredy. Problemy Dezaktivatsii Katalizatorov* (Disintegration of Catalysts — A Result of the Mutual Influence of the Solid Phase and the Reaction Medium. Problems of the Deactivation of Catalysts) (Novosibirsk: Nauka, 1985) Part 1, p. 3

44. F Wittman Z. *Angew. Phys.* **25** 160 (1968)
45. V Yu Traskin, N V Pertsov, Z N Skvortsova, E D Shchukin, P A Rebinder *Dokl. Akad. Nauk SSSR* **191** 147 (1970)
46. L M Shishlyannikova, S F Suzdal'tseva, S I Kontorovich, E D Shchukin *Kolloid. Zh.* **36** 612 (1974)
47. S F Suzdal'tseva, L M Shishlyannikova, E D Shchukin *Kolloid. Zh.* **48** 1031 (1986)
48. A T Slepneva, B A Lipkind, M V Dukarevich, S I Kontorovich, E D Shchukin *Kolloid. Zh.* **32** 251 (1970)
49. A T Slepneva, S I Kontorovich, B A Lipkind, E A Amelina, E D Shchukin *Kolloid. Zh.* **31** 281 (1969)
50. L V Koval'skaya, Ya V Mirskii, in *Tseolitnye Katalizatory i Adsorbenty* (Zeolite Catalysts and Adsorbents) (Ed. A Z Dorogochinskii) (Moscow: TsNIITE Neftekhim, 1978) p. 78
51. S I Kontorovich, L I Bogomolova, L N Sokolova, E D Shchukin *Khim. Tv. Topliva* **97** (1985)
52. S F Suzdal'tseva, E I Skvortsova, L Ya Margolis, E D Shchukin *Dokl. Akad. Nauk SSSR* **201** 415 (1971)
53. S I Kontorovich, M V Dukarevich, S F Suzdal'tseva, E D Shchukin, in *Materialy V Vsesoyuz. Konf. po Fiziko-khimicheskoi Mekhanike, Ufa, 1971* (Proceedings of the Fifth All-Union Conference on Physicochemical Mechanics, Ufa, 1971) p. 144
54. S I Kontorovich, T P Ponomareva, Ya E Geguzin, Yu S Kaganovskii, E D Shchukin *Poverkhnost'* (1) 111 (1983)
55. S A Paranskii, V N Medvedev, A I Veden'eva, A I Bessonov, O D Sterligov, E D Shchukin *Kinet. Katal.* **12** 473 (1971)
56. E D Shchukin, S I Kontorovich, M V Dukarevich *Dokl. Akad. Nauk SSSR* **175** 882 (1967)
57. S F Suzdal'tseva, S I Kontorovich, E D Shchukin *Kolloid. Zh.* **39** 814 (1977)
58. M V Dukarevich, Candidate Thesis in Chemical Sciences, Institute of Physical Chemistry, Academy of Sciences of the USSR, Moscow, 1968
59. L N Mamaeva, E I Dobkina, I P Mukhlenov, V I Malkiman *Kinet. Katal.* **21** 805 (1980)
60. G R Kotel'nikov, V A Potanov, E D Shchukin, L N Kozina *Kolloid. Zh.* **37** N5 875 (1975)
61. E D Shchukin, S I Kontorovich, N I Girenkova, V K Yatsimirskii, Yu S Kaganovskii, L N Sokolova *Dokl. Akad. Nauk SSSR* **318** 1417 (1991)
62. Ya E Geguzin, N I Girenkova, Yu S Kaganovskii, S I Kontorovich, T P Ponomareva, M V Tovbin, E D Shchukin, in *Nestatsionarnye Protssy v Katalize* (Nonstationary Processes in Catalysis) (Novosibirsk: Institute of Catalysis, Siberian Division of the Academy of Sciences of the USSR, 1979) Part 1, p. 138
63. USSR P. 554 883; *Byul. Izobret.* (15) 57 (1977)
64. E D Shchukin, L Ya Margolis *Poverkhnost'* (8) 1 (1982)
65. E D Shchukin, in *Atomistics of Fracture* (Eds R M Latanision, J R Pickens) (New York: Plenum, 1983) p. 421
66. E D Shchukin, in *Metody Issledovaniya Kataliticheskikh Reaktsii* (Methods for the Investigation of Catalytic Reactions) (Eds G K Boreskov, T V Andrushkevich) (Novosibirsk: Nauka, 1984) p. 142
67. V S Yushchenko, E D Shchukin *Dokl. Akad. Nauk SSSR* **242** 653 (1978)
68. V S Yushchenko, A G Grivtsov, E D Shchukin *Dokl. Akad. Nauk SSSR* **219** 162 (1974)
69. E D Shchukin, V S Yushchenko, T P Ponomareva *Kolloid. Zh.* **53** 319 (1991)
70. S I Kontorovich, Zh G Malikova, E D Shchukin *Kolloid. Zh.* **32** 224 (1970)
71. S I Kontorovich, K A Lavrova, E D Shchukin *Kolloid. Zh.* **37** 57 (1975)
72. I G Shatalova, N S Gorbunov, V I Likhtman *Fiziko-khimicheskie Osnovy Vibratsionnogo Uplotneniya Poroshkovykh Materialov* (Physicochemical Foundations of the Vibration-Induced Compaction of Powdered Materials) (Moscow: Nauka, 1965)
73. Z M Polukarova, I G Shatalova, R K Yusupov, I K Kolchin, L Ya Margolis, E D Shchukin *Neftekhimiya* **8** 899 (1968)
74. E D Shchukin, S I Kontorovich, B V Romanovsky *Abstracts of Reports of the 13th European Conference on Chemistry of Interference*, Kiev, 1994 p. 46
75. E D Shchukin, S I Kontorovich, B V Romanovsky *J. Mater. Sci.* **28** 1937 (1993)
76. E D Shchukin, S I Kontorovich, N I Girenkova, V K Yatsimirskii, Yu S Kaganovskii, L N Sokolova *Mendelev Commun.* 136 (1991)
77. I P Mukhlenov, E I Dobkina, V I Deryuzhkina, V E Soroko *Tekhnologiya Katalizatorov* (Technology of Catalysts) (Khimiya: Leningrad, 1989) p. 114
78. E D Shchukin *Fiz-Khim. Mekh. Mater.* **12** (1) 3 (1976)
79. V S Yushchenko, E D Shchukin *Fiz-Khim. Mekh. Mater.* **4** (10) 46 (1981)
80. ARC Westwood, J S Ahearn, J J Mills *Colloid Surf.* **2** 1 (1971)
81. V B Fenelonov, in *Nauchnye Osnovy Prigotovleniya Katalizatorov* (Scientific Foundations of the Preparation of Catalysts) (Novosibirsk Institute of Catalysis, Siberian Division of Academy of Sciences of the USSR, 1984) p. 130
82. L V Koval'skaya, Author's Abstract of Candidate Thesis in Chemical Sciences, Lensovet Leningrad Technological Institute, Leningrad, 1983
83. V A Dzis'ko *Osnovy Metodov Prigotovleniya Katalizatorov* (Foundations of the Methods of Preparation of Catalysts) (Novosibirsk: Nauka, 1983) p. 264
84. B P Zolotovskii, R A Buyanov, V A Balashov, O P Krivoruchko, A Ya Bakaev, V E Loiko, A A Samakhov, V I Bashin, in *Nauchnye Osnovy Prigotovleniya i Tekhnologii Katalizatorov* (Sbornik Nauchnykh Trudov) [Scientific Foundations of the Preparation and Technology of Catalysts (Collection of Scientific Reports)] (Novosibirsk: Institute of Catalysis, Siberian Division of Academy of Sciences of the USSR, 1990) p. 108
85. R O Kagel, R G Greenlar *J. Chem. Phys.* **49** 1648 (1968)
86. V A Korsunov, I Ya Chuvylkin, G M Zhidomirov, V V Kazanskii *Kinet. Katal.* **22** 938 (1981)
87. L I Titel'man *Obzorn. Informatsiya, Ser. Azotnaya Promyshlennost'* (Review Information, Nitrogen Industry Ser.) (Moscow: NIITEKhim, 1986) p. 30
88. L I Titel'man, in *Nauchnye Osnovy Prigotovleniya i Tekhnologii Katalizatorov* (Sbornik Nauchnykh Trudov) [Scientific Foundations of the Preparation and Technology of Catalysts (Collection of Scientific Reports)] (Novosibirsk: Institute of Catalysis, Siberian Division of Academy of Sciences of the USSR, 1990) p. 61
89. M A Kipnis, in *Tezisy Dokladov III Konferentsii po Nauchnym Osnovam Prigotovleniya i Tekhnologii Katalizatorov, Yaroslavl'*, (Abstracts of Reports at the Third Conference on the Scientific Foundations of the Preparation and Technology of Catalysts, Yaroslavl') (Novosibirsk: Institute of Catalysis, Siberian Division of Russian Academy of Sciences, 1996) p. 123
90. N A Levitskaya, L I Titel'man, G V Makrushina, A I Nechugovskii, E Z Golosman, in *Tezisy Dokladov III Konferentsii po Nauchnym Osnovam Prigotovleniya i Tekhnologii Katalizatorov, Yaroslavl'*, (Abstracts of Reports at the Third Conference on the Scientific Foundations of the Preparation and Technology of Catalysts, Yaroslavl') (Novosibirsk: Institute of Catalysis, Siberian Division of Russian Academy of Sciences, 1996) p. 142
91. I I Kurlyandskaya, I G Solomonik, E D Glazunova, Yu A Treger, E A Boevskaya, E Z Golosman, V I Yakerson, in *Tezisy Dokladov III Konferentsii po Nauchnym Osnovam Prigotovleniya i Tekhnologii Katalizatorov, Yaroslavl'*, (Abstracts of Reports at the Third Conference on the Scientific Foundations of the Preparation and Technology of Catalysts, Yaroslavl') (Novosibirsk: Institute of Catalysis, Siberian Division of Russian Academy of Sciences, 1996) p. 139
92. E Z Golosman, L L Klinova, G I Solomatin, A I Nechugovskii, E A Boevskaya, I A Mamaeva, G V Kozyreva, in *Tezisy Dokladov III Konferentsii po Nauchnym Osnovam Prigotovleniya i Tekhnologii Katalizatorov, Yaroslavl'*, (Abstracts of Reports at the Third Conference on the Scientific Foundations of the Preparation and Technology of Catalysts, Yaroslavl') (Novosibirsk: Institute of Catalysis, Siberian Division of Russian Academy of Sciences, 1996) p. 99
93. R A Buyanov, in *Nauchnye Osnovy Prigotovleniya i Tekhnologii Katalizatorov* (Sbornik Nauchnykh Trudov) [Scientific Foundations of the Preparation and Technology of Catalysts (Collection of Scientific Reports)] (Novosibirsk: Institute of Catalysis, Siberian Division of Russian Academy of Sciences, 1996) p. 3

94. V K Duplyakin, in *Tezisy Dokladov III Konferentsii po Nauchnym Osnovam Prigotovleniya i Tekhnologii Katalizatorov, Yaroslavl'*, (Abstracts of Reports at the Third Conference on the Scientific Foundations of the Preparation and Technology of Catalysts, Yaroslavl') (Novosibirsk: Institute of Catalysis, Siberian Division of Russian Academy of Sciences, 1996) p. 5
95. D Dollimore, G R Heal *J. App. Chem.* **11** 459 (1961)
96. D Dollimore, S Y Gregg *Trans. Br. Ceram. Soc.* **54** 261 (1955)
97. P S Bonsall, D Dollimore, Y Dollimore *Proc. Br. Ceram. Soc.* **6** 61 (1966)
98. G D Dibrov, in *Fiziko-Khimich. Mekhanika Dispersnykh Struktur* (Physicochemical Mechanics of Disperse Structures) (Moscow: Nauka, 1966) p. 32
99. M I Volkov, N V Dvoretiskii, M I Ogil'ko, E G Stepanov, G R Kotel'nikov, in *Tezisy Dokladov III Konferentsii po Nauchnym Osnovam Prigotovleniya i Tekhnologii Katalizatorov, Yaroslavl'*, (Abstracts of Reports at the Third Conference on the Scientific Foundations of the Preparation and Technology of Catalysts, Yaroslavl') (Novosibirsk: Institute of Catalysis, Siberian Division of Russian Academy of Sciences, 1996) p. 89; P Yu Butyagin *Usp. Khim.* **53** 1769 (1984) [*Russ. Chem. Rev.* **53** 1025 (1984)]
100. V V Boldyrev *Izv. Akad. Nauk SSSR, Ser. Khim.* **2228** (1990)
101. A Kapoor, R T Yang, C Wong *Catal. Rev. Sci. Eng.* **31** 43 (1989)
102. E Ruckenstein, S H Lee *J. Catal.* **109** 100 (1988)
103. A A Zhukhovitskii, V A Grigoryan, E Mikhailik *Poverkhnostnye Yavleniya v Rasplavakh i Voznikayushchikh iz Nikh Tverdykh Fazakh* (Surface Effects in Melts and in the Solid Phases Originating from Them) (Nal'chik: Kab.-Balkarsk. Kn. Izd., 1965)
104. V A Grigoryan, A A Zhukhovitskii, L S Shvindlerman, M I Chikonosova *Zh. Fiz. Khim.* **40** 1144 (1966)
105. F C Tompkins, in *Surface Science. Recent Progress and Perspectives* (Eds T S Jayadevian, R Vandselow (Boca Raton. FL: CRC Press, 1974) p. 235

Inner valence molecular orbitals and the structure of X-ray photoelectron spectra

Yu A Teterin, S G Gagarin

Contents

I. Introduction	825
II. General notions	826
III. Theoretical consideration	827
IV. The structure of X-ray photoelectron spectra	830
V. Contribution of inner valence molecular orbitals to chemical bonding	839
VI. Conclusion	845

Abstract. X-Ray photoelectron spectroscopy (XPS) and theoretical calculations show that under certain conditions inner valence molecular orbitals (IVMOs) can form within a rather broad binding energy range (15 eV to 50 eV) in compounds of many elements of the Periodic Table. This results in the appearance of a fine structure in their X-ray photoelectron spectra. The structure of X-ray photoelectron spectra associated with electrons of IVMOs correlates with contributions of the filled atomic orbitals (AOs) to the IVMO formation and the structure of compounds. In certain cases, the total contribution of electrons of the inner valence molecular orbitals to the bond energy in molecules and compounds is comparable to that of electrons of the outer valence molecular orbitals. This phenomenon is extremely important and new in principle for chemistry. The bibliography includes 128 references.

I. Introduction

X-Ray photoelectron spectra of compounds of various elements of the Periodic Table often exhibit, instead of the expected atomic singlets and doublets associated with spin-orbital interaction, a more complicated structure. This spectral fine structure can appear due to the formation of molecular orbitals (MOs),^{1–8} multiplet splitting, dynamic effect, multielectron excitation, etc.^{7–10} Recently, much attention has been paid to the analysis of the reasons for the appearance of fine structure in X-ray photoelectron spectra of various compounds since it gives information on the physical and chemical properties and the structure of compounds, the nature of chemical bonds in them, oxidation states of constituent atoms, etc.^{10–20} Although this problem is far from being completely solved, it becomes possible in certain cases to obtain unique information on compounds using the characteristics of the fine structure of X-ray photoelectron spectra.

Basically, the electrons of non-filled low-energy shells of neighbouring atoms (with energies ranging from 0 eV to ~15 eV) have been traditionally taken into account in spectral studies of the nature of chemical bonds. To some extent, it was facilitated by the widespread use of excitation sources of visible and UV-radiation in atomic and molecular spectroscopy. In most cases, X-ray emission spectroscopy studies of a wide range of compounds utilised the same interval of energies. Although, from the standpoint of quantum chemistry, the contribution of deep-lying filled atomic shells to the formation of MOs is well established,^{21,22} it has been believed that the effect of these electrons on chemical bonding could be neglected compared to that of weakly-bound (from 0 eV to ~15 eV) electrons.

Progress in precision XPS, with soft X-ray radiation ($h\nu < 1.5$ keV) as a source of excitation, allowed the study of fine structure in the spectra of both weakly-bound and inner electrons. In X-ray photoelectron spectra of compounds taken in the interval from ~15 eV to ~50 eV, instead of separate lines associated with electrons of filled atomic subshells, a more complex structure attributed to electrons of MOs is observed.

Studies of the fine structure in X-ray photoelectron spectra of compounds of various elements of the Periodic Table have shown that, in many cases, rather strong interaction between the electrons of low-energy AOs, closed in the ground state, results in the formation of MOs lying in the energy range from 0 eV to ~50 eV.^{1–8, 11–16, 23–28} This fact agrees with predictions of theoretical calculations.^{29–33} Thus, clear experimental evidence of arrangement of filled AOs into MOs has been attained. However, the significant binding energy difference between certain pairs (bonding and antibonding) of low-lying MOs (from ~15 eV to ~50 eV) in some compounds allowed one to suggest that the perturbation induced by electrons of these MOs substantially affect bond strengths in these compounds.^{1–6}

To this end, from the practical viewpoint, it is expedient to divide the X-ray photoelectron spectra into three regions depending on the electron binding energy. The first region (from 0 eV to ~15 eV) typically involves a poorly-resolved structure corresponding to the outer valence molecular orbitals (OVMOs), which are mainly built up of partially filled valence atomic orbitals. The second region (~15 eV ... 50 eV) exhibits a well-resolved structure associated with electrons of the inner valence molecular orbitals (IVMOs) which are mainly composed of closed atomic shells. Peaks that belong to the third region (more than 50 eV) reflect inner(core) MOs (CMOs) primarily consisting of deep-lying inner (core) AOs. However, due to the limited resolution of X-ray photoelectron spectrometers, separate peaks of electrons of

Yu A Teterin Russian Research Centre 'Kurchatov Institute', Kurchatov sq., 1, 123182 Moscow, Russian Federation, Fax (7-095) 882 58 04.

S G Gagarin Fossil Fuel Institute, Ministry of Fuel and Energetics of the Russian Federation, Leninskii prosp., 29, 117910 Moscow, Russian Federation, Fax (7-095) 952 55 21

Received 18 December 1995

Uspekhi Khimii 65 (10) 895–919 (1996); translated by E F Valeev

these CMOs cannot be observed even in the spectra of homonuclear gaseous molecules.¹ When we proceed to correlation of the structure of a compound with the structure of its IVMOs, the expedience of this division is most evident.

It should be noted that one cannot strictly divide MOs into categories of CMOs, IVMOs, and OVMOs, when considering the IVMO problem in general terms of the formation of MOs in various compounds. The character of the IVMOs in light-element compounds discussed in this review is closer to that of conventional OVMOs. Some of IVMOs of compounds containing heavy atoms are like CMOs. In other words, we should carefully consider this question for each particular compound. Moreover, although *de facto* the term 'IVMO' for light-element compounds has been used earlier, scientists started using this term for heavy-atom compounds only recently, since the existence of fine structure that could be interpreted in terms of the formation of IVMOs had been discovered in X-ray photoelectron spectra in the energy range of ~ 15 eV... ~ 50 eV.²⁻⁶

As has been mentioned in previous studies,^{17,20} one of the reasons that a group of MOs referred to as IVMOs should be considered separately from the rest of MOs is that the peaks corresponding to IVMOs are well resolved, unlike those corresponding to OVMOs, and the fine structure associated with them depends on the nearest environment of the absorbing atom in the molecule or cluster. We should mention that, simultaneously with the appearance of a fine structure, multielectron effects can manifest themselves in the low-energy region of X-ray photoelectron spectra. It has been shown^{1,17-20} that multielectron effects give rise to additional bands, as a rule, of much lower intensity than that of the major peaks, and a certain smearing of the spectrum. However, the spectral structure determined by the ground and final electronic states of the system with a vacancy after photoemission almost always remains firmly pronounced.

Fine structure observed in X-ray photoelectron spectra of shells of various compounds are evidence that multielectron effects play a noticeable role in their formation. However, one should keep in mind that XPS is of greatest practical use for a wide range of researchers when the spectra can be interpreted in terms of the one-electron approximation.

In the present review we discuss the IVMO problem from the general viewpoint. An attempt has been made to answer the following questions:

1. How common is IVMO formation for compounds of various elements of the Periodic Table?
2. What qualitative and quantitative information on physico-chemical properties can be obtained from the spectral parameters of the IVMO-assigned fine structure?
3. How significant is the role of IVMOs in chemical bonding and what is the overall contribution of electrons of these orbitals to the covalent component of the bond energy?

For the sake of simplicity, we interpret the spectra containing fine structure using atomic notation as well as molecular ones.

II. General notions

In terms of the MO LCAO model, chemical bonding in diatomic molecules occurs by filling MOs with the common electrons. The positive, negative, or zero contribution of an electron to the bond energy depends upon the character of the corresponding MO (bonding, antibonding, or non-bonding). This concept was developed to the largest extent in the consideration of the nature of the chemical bond in diatomics, viz., homonuclear molecules of $D_{\infty h}$ symmetry and heteronuclear ones of $C_{\infty v}$ symmetry. The main qualitative postulate, which defines the relative bond energy in a diatomic molecule, is that the bond energy contributions of the electrons to the bonding and the corresponding antibonding MOs are approximately equal. The bond order, determining the bond strength, equals half the difference in populations of the bonding and antibonding MOs.^{21,22,34-37} Therefore, the number of excessive 'bonding' electrons is considered to be the measure of

the bond strength.^{35,38-41} However, this rule is approximate,^{21,35} since a molecule is destabilised by the electrons of antibonding MOs to a somewhat greater extent than stabilised by electrons of the corresponding bonding MOs.

The bonding or antibonding character of individual MOs can be established experimentally from the deviation, ΔR_e , of the internuclear distance from its equilibrium value in the ground state,^{41,42} variations in dissociation energy ΔD_e ,^{37,41,43} and vibrational frequencies occurring due to the ionisation.⁴⁴ The MO character can be estimated roughly by consideration of the specific distribution of electron density in internuclear space²¹ and on the basis of difference electron density maps $\Delta\rho$,³⁹ i.e. a difference between the molecular electron density and initial atomic electron densities.

As mentioned earlier,^{21,22,34-41} the contributions of the electrons of the bonding and antibonding IVMOs to the covalent component of the bond energy compensate each other. Thus, the overall chemical bonding in a molecule is solely attributed to the electrons of OVMOs. Thus, it is believed that in a diatomic molecule AB of $C_{\infty v}$ symmetry, where A and B are second Period elements, as a first approximation, the bonding (3σ) and antibonding (4σ) IVMOs, which are composed of the $2s$ AOs of neighbouring atoms, in the first approximation do not affect the A-B bonding. Populations of the 1π , 5σ , and $2\pi^*$ OVMOs formed by the $2p$ AOs determine the total bond order. In homonuclear molecules A_2 , such orbitals are classified as $2\sigma_g$ and $2\sigma_u^*$ IVMOs. The corresponding OVMOs within the framework of the D_{2h} symmetry point group are classified as the $1\pi_u$, $3\sigma_g$, and $1\pi_g$ outer valence molecular orbitals. This concept of the negligibly small influence of the electrons of MOs formed by doubly-occupied AOs on chemical bonding had been so widely used that it almost became an axiom. It is represented in a number of monographs^{21,34,38,39,43,44} and textbooks for college students^{35,37,40,41} and school teachers.^{45,46} Until recently, attempts to revise this established model have hardly been undertaken.

However, the first *ab initio* calculations on the CO molecule (e.g., see review⁴⁷) indicate either a weakly-bonding or antibonding character of the 5σ OVMO. The latter is usually used to explain the increased vibrational frequency of the CO^+ as well as $CO\delta^+$ ions, where δ^+ is a small charge induced upon the adsorption of the CO molecule on electron-deficient centres of a solid surface, compared to that of the neutral molecule. In an attempt to tailor this fact to a simple scheme of MO formation, the authors⁴⁴ assigned the bond order of the carbon-oxygen bond as 2 instead of 3, that is determined by four electrons in the 1π OVMO. It was considered that the electrons of the 3σ and 4σ IVMOs do not contribute to the chemical bonding owing to the mutual compensation of bonding and antibonding effects.

Another approach (see Refs 41, 44) implies a non-bonding character of the 3σ IVMO of the CO molecule (it is occupied by a lone electron pair of the O atom). The triple bond in the molecule is attributed to two electrons of the 4σ IVMO and four electrons of the 1π OVMO. In contrast, the authors of another study²¹ assumed that the 4σ IVMO and 5σ OVMO are non-bonding, while the electrons in the 3σ IVMO and 1π OVMO account for the bond order 3.

Traditionally, triple bond formation in the CO molecule is attributed to the electrons of the $5\sigma^2$ and $1\pi^4$ OVMOs.^{34,43} We should note that, according to the valence bond approach,⁴⁸ the bond order in the CO molecule is intermediate between 2 and 3 due to the contribution of resonance structures, namely, $:C \equiv O:$ and $:C \equiv \dot{O}$.

Recently, attempts to quantify the bonding character of MOs in the CO molecule have been undertaken based on division of the total Hartree-Fock energy⁴⁹ and the values of Mulliken MO populations.⁵⁰ In these studies, the 3σ electrons were found to contribute significantly to the binding of C and O atoms in the CO molecule. Qualitative arguments in favour of the participation of the inner valence electrons in chemical bonding can be obtained by linear transformation of the 4σ IVMO and 5σ OVMO.⁴² It has

been found that electrons occupying these MOs are essentially the lone pairs, and the $3\sigma(2\sigma_g)$ IVMO and $1\pi(1\pi_u)$ OVMO are involved in the triple bond formation in CO (or N_2).

Studies of the electronic structure of compounds by XPS^{1-9, 17-20, 26-28} and theoretical calculations conducted at different levels of theory^{3, 4, 29-32, 49-57} have demonstrated that the conventional concept of the dominant participation of electrons of the OVMOs in chemical bonding is too rough an approximation.

III. Theoretical consideration

At present, there is no unified qualitative measure that allows the contribution of electrons of individual MOs to the bond strength, even for diatomic molecules, to be estimated. This quantity must be additive, i.e. the total bond energy must be equal to the sum of the individual MO contributions with respect to their populations. This condition is satisfied in the Mulliken bond population theory and in various quantum-chemical bond strength characteristics based on division of the total molecular energy into orbital and other components. Criteria concerned with an internuclear force, which arise due to changes in MO populations, are also of interest. This section discusses possible approaches to the solution of this problem.

1. Contribution of electrons to bond populations

In this approach, the contributions of electrons to the bond strength are estimated from Mulliken populations of MOs and AOs.⁴⁷ Within the MO LCAO approximation for a heteronuclear molecule AB, every pair of interacting orbitals satisfies the following equation:

$$\psi^\pm = \frac{1}{(2 \pm 2S)^{1/2}} (\chi^A \pm \chi^B), \quad (1)$$

where ψ^+ and ψ^- are the bonding and antibonding MOs respectively, χ^A (χ^B) an atomic orbital or, more generally, a linear combination of atomic orbitals of the atom A (B), and S is an absolute value of the overlap integral between χ^A and χ^B . The one-electron density in these MOs is defined as follows:

$$|\psi^\pm|^2 = \frac{1}{2(1 \pm S)} [|\chi^A|^2 + |\chi^B|^2] \pm \frac{1}{1 \pm S} \chi^A \chi^B. \quad (2)$$

The bonding space is an area between two planes passing through nuclei A and B perpendicularly to the bond axis. If χ is a non-hybrid AO, then the electron densities $|\chi^A|^2$ and $|\chi^B|^2$ contribute equally to the total electron density, not only in the bonding space, but also in the rest of space. The second term in Eqn (2) is the charge density localised essentially in the internuclear area. Therefore, one may consider this term as a qualitative measure of the bonding (antibonding) character of the MO. If ψ is the sp hybrid AO, then the first term in Eqn (2) also contributes to the bond order. The second term integrates to the following expression:

$$n(j_\pm, AB) = \pm \int \frac{1}{1 \pm S} \chi^A \chi^B d\tau = \pm \frac{S}{1 \pm S}, \quad (3)$$

which is the contribution of an electron in the j th MO to Mulliken's bond population. It follows from Eqn (3) that the contribution of an electron in the bonding MO ψ_i^+ is positive while the contribution of an electron in the antibonding MO ψ_i^- is negative and is larger in magnitude.

For diatomic heteronuclear molecules, the j th MO is expressed as:

$$\psi_j = c_j^A \chi^A + c_j^B \chi^B, \quad (4)$$

and the contribution of the electron in this MO to the bond population is:

$$n(j, AB) = 2c_j^A c_j^B \int \chi^A \chi^B d\tau. \quad (5)$$

Since the contributions are additive, the total population of the A–B bond is:

$$n(AB) = \sum_j N_j n(j, AB), \quad (6)$$

where N_j is the population of the j th MO.

In multiatomic molecules, $n(j, AB)$ refers to pairs of adjacent atoms. The partial contribution of an electron on the j th MO is defined as follows:

$$n(j) = \sum n(j, AB), \quad (7)$$

where the sum is taken over all the bonds.

2. Estimation of orbital character by separation of the total energy

Different kinds of interactions within the quantum-chemical approach are widely treated by separation of the total energy of a multiatomic molecule into one-, two-, three-, and four-centre components. The method of the complete neglect of differential overlap (CNDO/2)⁵⁵ serves as an example. The total energy E_{tot} within this method assumes the form:

$$E_{tot} = \sum_A E_A + \sum_{B,A} E_{AB}, \quad (8)$$

where E_A and E_{AB} are corresponding one- and two-centre components. The latter has the form:

$$E_{AB} = 2 \sum_\mu^A \sum_\nu^B p_{\mu\nu} H_{\mu\nu} - \frac{1}{2} \sum_\mu^A \sum_\nu^B p_{\mu\nu}^2 \gamma_{AB} + Z_A Z_B R_{AB}^{-1} - p_{AA} Z_B \gamma_{AB} - p_{BB} Z_A \gamma_{AB} + p_{AA} p_{BB} \gamma_{AB}, \quad (9)$$

where $p_{\mu\nu}$ is referred to as the bond order, the result of interaction of the μ -AO of atom A with the ν -AO of atom B; $H_{\mu\nu}$ are elements of the core Hamiltonian, γ_{AB} are repulsion integrals of the electrons of the s -type functions, Z_A (Z_B) is the charge of the nucleus (the effective value is used for the valence shell), p_{AA} (p_{BB}) is the electron density of the atoms.

The first term in Eqn (9) is referred to as the resonance energy.⁵⁶ Its magnitude characterises the covalent component of the A–B bond. The other terms denote the exchange component of the energy, core–core repulsion energy, potential energy of electrons of the atom A in the field of the core B, potential energy of electrons of the atom B in the field of the core A, and energy of electron–electron repulsion for atoms A and B respectively.

Despite the variational nature of the CNDO/2 approach, its semiempirical character does not yield total energy values that correspond to the results obtained with more rigorous approaches or from experiment. However, atomisation energies and bond energies of molecules can be estimated from components of the total energy in Eqn. (8).⁵⁷ It will be shown (see Section V.1) that the results of CNDO/2 calculations can provide an estimate of the bonding character of MOs. To this end, the resonance energy E_{AB}^R is separated into contributions E_α^R of individual MOs:

$$E_{AB}^R = \sum_\alpha E_\alpha^R, \quad (10)$$

$$E_\alpha^R = 2n_\alpha \sum_i^A \sum_j^B c_{i\alpha} c_{j\alpha} H_{ij},$$

where n_α is the population of the α MO, H_{ij} the core Hamiltonian, $c_{i\alpha}$ and $c_{j\alpha}$ are the coefficients of the i th and j th AOs in an expansion of the α MO by atomic orbitals found from self-consistent field (SCF) calculation, CNDO/2. The positive (negative) sign of the contribution E_α^R to the resonance energy corresponds to the antibonding (bonding) character of the α MO.

3. Estimation of the orbital character within the orbital force approach

According to the Hellmann–Feynman theorem, the internuclear force is equal to the expectation value of $\partial\hat{H}/\partial R$, where \hat{H} is the Hamiltonian and R is the internuclear distance.

Forces acting on nuclei in a molecule are determined as derivatives of the potential energy with respect to internal bond lengths and bond angles or cartesian coordinates. These forces can also be calculated from the known wave functions. Regarding a diatomic molecule AB, the total force acting on the nucleus A is:

$$F_A(R) = \frac{Z_A}{R^2} \left(Z_B - n_e R^2 \int \psi_{AB}^* \frac{\cos\theta_{\mu A}}{r_{\mu A}^2} \psi_{AB} d\tau \right), \quad (11)$$

where n_e is the total number of electrons, R is the internuclear distance, μ is the electron index, A is the atom index, $r_{\mu A}$ is the distance from the μ th electron to the nucleus A, $\theta_{\mu A}$ is the angle between the bond direction and radius-vector of the μ th electron of the atom A, $d\tau$ is the space unit. At $R = R_e$, $F_A = -F_B = 0$, therefore the second term in Eqn (11) must be equal to Z_B , i.e.

$$n_e R_e^2 \int \psi_{AB}^* \frac{\cos\theta_{\mu A}}{r_{\mu A}^2} \psi_{AB} d\tau = Z_B. \quad (12)$$

This term reflects the contribution of electrons to the total force acting on the nucleus. Within the MO LCAO approach, the following expression is valid for each MO:

$$\eta_i = R^2 N_i \int \phi_i^* \frac{\cos\theta_{\mu A}}{r_{\mu A}^2} \phi_i d\tau, \quad (13)$$

where ϕ_i is the MO, N_i is the number of electrons in the i th MO. Subject to Eqns (12) and (13), it follows that:

$$\sum_i \eta_i = Z_B, \quad (14)$$

where the integration is performed over the occupied MOs.

A modified orbital force f_i , which determines a one-electron contribution to the total force,¹⁷ can be introduced

$$f_i = \frac{Z_B}{N_i R^2} \eta_i, \quad (15)$$

This force is also additive, i.e.

$$\sum_i N_i f_i = \frac{Z_B^2}{R^2}. \quad (16)$$

The force f_i can be calculated from the derivative of the orbital energy vs. the internuclear distance. Indeed, according to the Fock equation for the MO

$$\hat{F}\phi_i = E_i\phi_i, \quad (17)$$

it follows that:

$$E_i' = \frac{dE_i}{dR} = \int \phi_i^* \left| \frac{d\hat{F}}{dR} \right| \phi_i d\tau. \quad (18)$$

Since

$$\hat{F} = \hat{h} + \hat{G},$$

where \hat{h} is the one-electron Hamiltonian, \hat{G} is the operator of the electron–electron electrostatic interaction, then

$$E_i' = f_i + \int \phi_i^* \left| \frac{d\hat{G}}{dR} \right| \phi_i d\tau. \quad (19)$$

According to Eqn (19), f_i differs from E_i' only by electron–electron repulsion terms. These terms can be estimated using the values of E_i' and f_i listed in Table 1.

Presumably, the second term in Eqn (19) equals f_i times a constant factor. Then Eqn (19) takes the form:

$$E_i' \simeq f_i + cf_i = (1+c)f_i. \quad (20)$$

A correlation plot of E_i' versus f_i using the data in Table 1 proves this assumption (Fig. 1). According to this plot, the coefficient c equals approximately 0.23. Therefore, Eqn (20) may be rewritten:¹⁷

$$E_i' \simeq 1.23f_i. \quad (21)$$

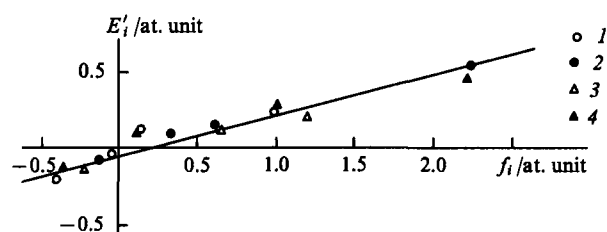


Figure 1. Dependence of the derivatives of the orbital energies E_i' on the orbital forces f_i for: (1) O_2 ; (2) B_2 ; (3) C_2 ; (4) N_2 (1 at. unit = 8.24×10^{-8} N).¹⁷

The orbital forces can be substituted by E_i' values in a semiquantitative estimation of the relative contributions of electrons of individual MOs to the covalent bonding, since the total covalent component of the bond energy of the molecule can be represented as the sum of the orbital energies with respect to their populations.⁵⁹ Ruedenberg⁶⁰ has suggested an empirical correlation between the total covalent component of the Hartree–Fock energy E of a molecule and the sum of the orbital energies of the occupied MOs:

$$E \simeq k \sum_i N_i E_i, \quad (22)$$

where k is a constant.

Table 1. The orbital forces f_i and derivatives of the MO energies ($E_i'/10^{-8}$ N).¹⁷

Molecule	$2\sigma_g$ IVMO		$2\sigma_u$ IVMO		$1\pi_u$ OVMO		$3\pi_g$ OVMO		$1\pi_u$ OVMO	
	E_i'	f_i	E_i'	f_i	E_i'	f_i	E_i'	f_i	E_i'	f_i
B_2	0.824	5.257	-0.585	-1.121	0.634	2.711	—	—	—	—
C_2	1.524	10.086	-1.162	-1.953	1.038	5.043	—	—	—	—
N_2	3.486	18.087	-1.195	-3.123	2.175	8.199	0.709	1.014	—	—
O_2	4.227	18.573	-1.640	-3.280	1.838	8.240	1.129	1.104	-1.607	2.694

From Eqn (22),

$$F = -\frac{\partial E}{\partial R} \cong -k \sum_i N_i E_i' \quad (23)$$

Roedenberg's value $^{60} 3/2$ for k in Eqn (22) differs somewhat from 1.23 in Eqn (21). Apparently, the coefficient in Eqn (21) varies for series of diatomic molecules made up of elements of different Periods. The same is valid for the constant k in Eqn (22). Goscinsky⁶¹ also noted the approximate character of the estimation of the orbital forces from E_i' . He suggested a technique for calculation of the derivatives, which takes into consideration the MO relaxation occurring during the ionisation of a molecule. According to this approach, a force arising on nuclei due to the removal of an electron from the i th MO equals the derivative of the energy of the ion (i) with respect to the internuclear distance at the equilibrium point of the initial molecule:

$$\tilde{f}_i = -\left. \frac{dE_i^i(R)}{dR} \right|_{R_e} \quad (24)$$

Koopmans's theorem states that

$$E_i^i(R) = E(R) - E_i(R), \quad (25)$$

where $E(R)$ is the total energy of the ground state of the molecule. Then within this approach,

$$\tilde{f}_i = E_i' \quad (26)$$

Taking into account MO reorganisation caused by a change in the populations, we obtain:

$$\tilde{f}_i = E_i' + \left. \frac{dE_i^{\text{rel}}(R)}{dR} \right|_{R_e} \quad (27)$$

where $E_i^{\text{rel}}(R)$ is the relaxation energy of the system upon removal of an electron from the i th MO. A method for the determination of the contribution of MO relaxation within the transition operator approach has been suggested.⁶¹

The effect of relaxation is automatically taken into account if orbital forces are determined from experimental rather than the calculated spectral data.⁶² In this case, the orbital forces are referred to as the orbital vibronic constants.^{63,64,65} A deformation force, which arises on nuclei upon vertical electron excitation or ionisation of a diatomic molecule, is determined as a derivative of the potential energy of the final state versus the interatomic distance at the transition point. For a Morse potential we may write²¹

$$U(x) = D_e[\exp(-2\beta x) - 2\exp(-\beta x)], \quad (28)$$

where D_e is the depth of the well, β is a variable parameter, and x is the deviation of the interatomic distance R from its equilibrium value R_e . Then the classical force \tilde{f} is determined as follows:

$$\tilde{f} = -\left. \frac{dU(x)}{dx} \right|_{x^*} = -2D_e\beta[\exp(-\beta x^*) - 2\exp(-2\beta x^*)], \quad (29)$$

where x^* is the difference between the equilibrium distances in the initial and final states.

4. Relationship between various characteristics of the orbital contributions

Most simply, the estimation of the MO contribution to the bonding is determined as a part of the Mulliken bond population associated with this MO. The values of the bond populations for a series of diatomic molecules and the values of the orbital forces for some of them⁴⁷ are listed in Table 1. Correlation plots of the bond population vs. the orbital force f_i for the valence MOs of C_2 , N_2 , and O_2 shown in Fig. 2 yield straight lines. This reflects the approximate character of the bond order as an index of the bond

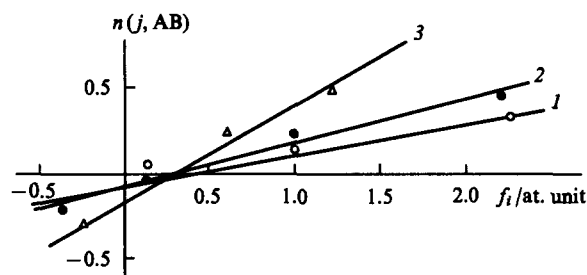


Figure 2. Dependence of the bond populations $n(j, AB)$ on the orbital forces f_i for valence MOs of (1) O_2 , (2) N_2 , and (3) C_2 .⁶⁵

strength. We have to note that only the MO contributions to the bond order $n(j, AB)$ calculated within the extended Hückel approach correlate satisfactorily with other characteristics, such as the orbital forces f_i , and the orbital vibronic constants for MOs of the same molecule.¹⁷ The CNDO/2 calculations for N_2 , CO, NO, O_2 , C_2 , and CN have been carried out in order to test whether the bonding character of MOs can be estimated from values of the orbital resonance energy.⁶⁵ For the first four molecules, the orbital vibronic constants, which had been calculated earlier from spectral data,⁶² were used as the bonding indices. The values of the orbital vibronic constants for the last two molecules were calculated from the corresponding wave functions of OVMOs.⁶² The total number of data points reached 20. The correlation between the CNDO/2 resonance orbital energies and the orbital vibronic constants has been established (Fig. 3). Characteristically, the plot yields a straight line through the origin of coordinates, and the correlation has the form:

$$a_\alpha = -7.1 E_\alpha^R, \quad (30)$$

where a_α is the orbital vibronic constant (in 10^{-8} N) and E_α^R is the resonance orbital energy in atomic units. The orbital vibronic constants of arbitrary MOs can be calculated from the orbital contribution to the resonance energy using this dependence. In particular, it makes possible the determination of the orbital vibronic constants of IVMOs for which spectral data are currently unavailable.

Ab initio calculations of the electronic structure of molecules N_2 ,^{66,67} CO,^{67,68} and a radical CH⁶⁹ have provided the values of derivatives (E_α') at the equilibrium interatomic distances. Graphical analysis reveals a correlation between E_α' and a_α of the form:

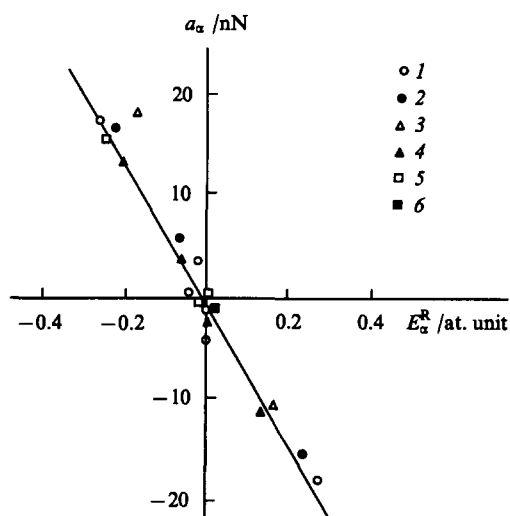


Figure 3. Dependence of the orbital vibronic constants a_α on the orbital resonance energies E_α^R for: (1) N_2 ; (2) CO; (3) O_2 ; (4) NO; (5) CN; (6) C_2 .⁶⁵

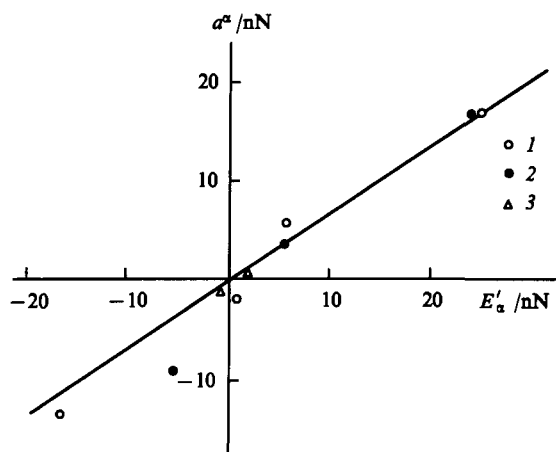


Figure 4. Correlation of the orbital vibronic constants a_α with the derivatives of the MO energies E'_α for: (1) CO; (2) N₂; (3) CH.⁶⁵

$$a_\alpha = 0.71E'_\alpha, \quad (31)$$

where both E'_α and a_α are expressed in nN (Fig. 4). Obviously, Eqn (31) can also be applied to calculations of the missing orbital vibronic constants. We should keep in mind that formula (31) was derived with a limited number of data points due to incomplete sets of experimental a_α values rather than due to the absence of *ab initio* studies with varied R .⁶² Consequently, an examination of the correlation between E'_α and E_α^R would be helpful for verification of Eqn (31). This challenge is feasible since non-empirical $E_\alpha(R)$ dependences have been published for a number of diatomic molecules and the corresponding CNDO/2 values of E_α^R can be readily calculated. With this in mind, we appended the values of the orbital energy derivatives from *ab initio* calculations for molecular hydrides LiH, BeH, BH, NH, and HF^{69,70} to the list of those for N₂, CO₂, and CH, so that the total number of data points reached 32. From least-squares analysis of the data collected

$$E'_\alpha = b_0 + b_1E_\alpha^R$$

the coefficients b_0 and b_1 were found to be equal to 0 and -10 respectively. Thus the correlation between the non-empirical derivatives of the orbital energies and the semiempirical values of the orbital resonance energies has the form:

$$E'_\alpha = -10E_\alpha^R. \quad (32)$$

Composition of Eqns (32) and (30) corroborates Eqn (31). Also, it can be demonstrated that the CNDO/2 derivatives of the orbital energies are of certain interest for the estimation of orbital vibronic constants. Indeed, reasoning by analogy with Eqn (32), we have

$$E'_\alpha(\text{CNDO/2}) = -10.9E_\alpha^R. \quad (33)$$

On other hand,

$$a_\alpha = 0.65E'_\alpha(\text{CNDO/2}). \quad (34)$$

The last two dependencies corroborate additionally the validity of Eqn (30). It can be deduced from Eqns (33) and (34) that the non-empirical and CNDO/2 values of E'_α correlate. The dependence presented in Fig. 5 confirms this expectation.

According to the data mentioned above, derivatives of the orbital energy versus the internuclear distance can serve as an estimate of orbital vibronic constants in diatomic molecules.¹⁷ It is not surprising that CNDO/2 values are successfully used on even terms with non-empirical data since the initial parametrisation of the semiempirical method employed *ab initio* data for small molecules. At the same time, the derivatives E'_α obtained in terms of the extended Hückel method correlate with the orbital vibronic

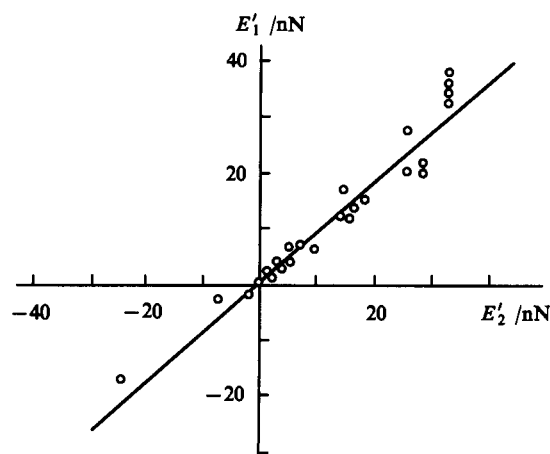


Figure 5. Correlation of the derivatives of the orbital energies E'_1 obtained from *ab initio* calculations with those, E'_2 , obtained from SCF CNDO/2 calculations for N₂, CO, CH, LiH, BeH, BH, NH, and HF.⁷⁰

constant to a lesser extent although satisfactory results can still be obtained in certain cases. The same holds for the correlation between the orbital vibronic constants and the Mulliken orbital populations (Fig. 6).

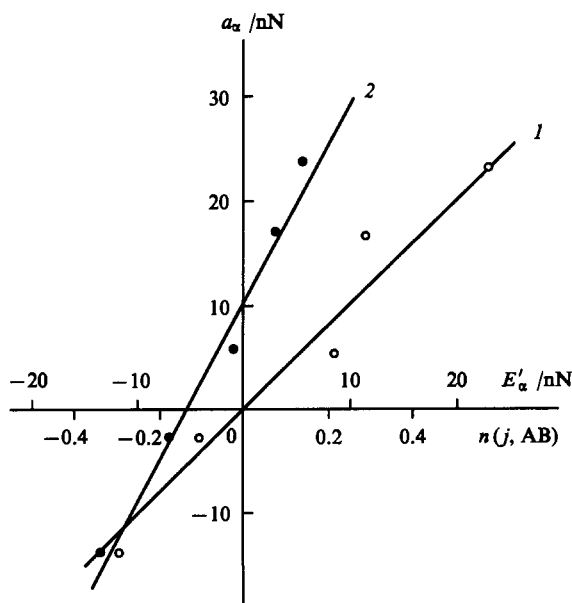


Figure 6. The orbital vibronic constants a_α for the CO molecule as functions of the bond strength indexes calculated within the extended Hückel approach: (1) $n(j;AB)$; (2) E'_α .¹⁷

IV. The structure of X-ray photoelectron spectra

X-Ray photoelectron spectroscopy is based on the photoeffect.¹ Under exposure to exciting X-ray radiation, e.g., $\text{MgK}_{\alpha 1,2}$, photoelectrons with kinetic energy of up to ~ 1.2 keV are emitted. The electron energy is measured to an accuracy of 0.1 eV. As a result, the binding energies (electronic work functions) of inner and outer levels of the compound under examination can be determined up to a constant factor from the Einstein equation.

An X-ray photoelectron spectrum represents the number of photoelectrons (peak intensity I expressed in relative units) plotted against the binding energy E_b (in eV). To enable compar-

ison of X-ray photoelectron spectra, they are calibrated against a known value of the binding energy E_b of electrons of a certain shell of a standard substance, e.g., gold (Au 4f_{7/2}).

The X-ray photoelectron spectra of the compounds to be discussed in this review were obtained in the gas phase¹ and solid state.^{17–20} High-resolution spectra of solid compounds are usually obtained with the monochromatic AlK_{α1,2} (1486.6 eV) characteristic X-ray radiation and a low-energy electron gun. Samples are usually prepared as dense layers precipitated from inert solvents or depressed on an indium support. Experiments are carried out either at ambient or liquid-nitrogen temperatures. All the spectra discussed are reduced to the same scale in which the binding energy E_b of the C 1s electrons in hydrocarbons was set equal to 285.0 eV (except for gas-phase spectra).

Fine structures in X-ray photoelectron spectra are often interpreted using calculations of the electronic structure of molecules and clusters performed mainly by non-relativistic SCF methods, namely, the SCF CNDO/2, SCF X α -SW,^{29, 55, 71–75} and SCF X α -DV.^{31, 32, 76–80}

The formation of IVMOs between neighbouring atoms requires that:

(a) the energies of the corresponding filled AOs are comparable;

(b) these AOs possess the same symmetry type with respect to the interatomic axis;

(c) the interatomic distance is sufficient for effective overlap of these AOs.^{17, 21, 81–85}

According to (a) and (b), it is anticipated that IVMOs effectively form in homonuclear molecules, and, with (c) satisfied, IVMOs can form in heteronuclear compounds too.

Such difficulties as fast oxidation and decomposition of highly-reactive compounds as well as the influence of aggressive species, e.g. F₂, Cl₂, etc., on units of the spectrometer often arise in XPS studies of these compounds, for which the formation of IVMO is expected. Generally, these difficulties are not fundamental since the current level of the experimental technique is sufficient to overcome such problems. However, XPS studies are preferably performed with stable inert compounds to obtain the most reliable results. It is the main factor that defines up to now the set of available spectra of homo- and heteronuclear compounds.

We should also mention that solid compounds form a lattice where electronic states are described in terms of the band structure. In a certain approximation, the bands represent MOs, thus they reflect the electronic structure of clusters typical of a given compound in the solid phase. This seems to be quite admissible for the less-delocalised core electrons, and the corresponding peaks in X-ray photoelectron spectra are broadened. Such broadening due to effects of the solid lattice gives maxima, attributable to the band structure, which are referred to as peaks for the sake of simplicity and attributed to electrons of individual clusters.

In this review we discussed X-ray photoelectron spectra of compounds of group IVA–VIIA elements, lanthanide oxides and fluorides (except for Pm compounds), and a wide range of actinide series compounds.

1. Manifestation of inner valence molecular orbitals in X-ray photoelectron spectra

a. Homonuclear molecules and clusters of group IVA–VIIA elements

X-Ray photoelectron spectra of solid compounds under consideration reveal a fine structure occurring in the low-energy region. Since the electronic configuration of these elements is ns^2np^m , where $2 \leq m \leq 5$, this fine structure can be concerned considerably with the interaction of ns electrons. A simpler fine structure appears in the spectra of gaseous diatomic molecules of these elements (Fig. 7). In this case, on the one hand, homonuclear molecules provide the most favourable conditions for IVMO

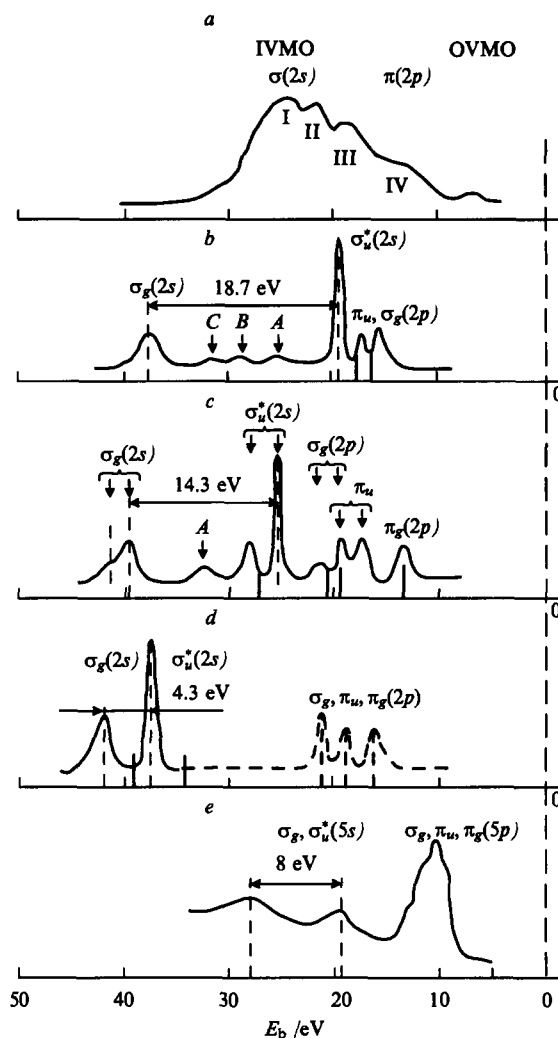


Figure 7. The X-ray photoelectron spectra of pyrographite ($E_b(\text{C}1s) = 290$ eV) (a)²⁵ and gaseous N₂ (b),¹ O₂ (c),¹ F₂ (d),²³ and I₂ (e).²⁴ The bond lengths (in Å) are 1.42 (C–C), 1.098 (N≡N), 1.207 (O=O), 1.417 (F–F) and 2.666 (I–I).

formation; on the other hand, rigorous theoretical studies of the electronic structure of these compounds can be performed and interpreted relatively easily.

The results of the CNDO/2 and X α -DV theoretical calculations^{1, 32, 51, 56, 86, 87} for the N₂ molecule, establish that the two most intense low-energy peaks in the X-ray photoelectron spectra of this molecule, separated by 18.7 eV, are associated essentially with the electrons of the antibonding $2\sigma_u^*$ and bonding $2\sigma_g$ IVMOs. The calculated gap (ΔE_{theor}) between the binding energies of electrons of the $2\sigma_g$ and $2\sigma_u^*$ IVMOs in the N₂ molecule equals 16.9 eV (X α -DVM) and 18.1 eV (CNDO/2) at the equilibrium distance $R_e = 0.109$ nm.^{51, 56} The fine structure of the X-ray photoelectron spectrum of N₂ theoretically modelled at the SCF X α -DVM level (bond length $R = 0.106$ nm, $\Delta E_{\text{theor}} = 18.59$ nm) is shown in vertical lines below the experimental spectrum (Fig. 7 b). The scales of the experimental and theoretical spectra do not match; the binding energy differences of the N 1s electrons are not equal ($|E_{\text{exp}}(\text{N } 1s) - E_{\text{theor}}(\text{N } 1s)| = 7.5$ eV). Additional peaks (A, B, and C) attributable to multielectron effects, characteristic losses, and MgK $\alpha_{3,4}$ excitation appear in the X-ray photoelectron spectrum of N₂.¹ The spectrum of the weakly-bound electrons of the nitrogen molecule is an exemplary demonstration of IVMO formation in molecules.

The spectrum of the O_2 molecule provides yet another example.¹ In the low-energy region of its spectrum, as in the spectrum of N_2 , two peaks associated with electrons of the $2\sigma_g$ and $2\sigma_u^*$ IVMOs appear; the binding energy gap ΔE_{exp} between them equals 14.3 eV (Fig. 7 c). These IVMOs to a great extent consist of the $O\ 2s$ AOs. Since O_2 is paramagnetic, multiplet splitting of the electronic states appears in the spectrum. Thus, every peak except for one of the π_g^* electrons is split into two components corresponding to the $^2\Sigma^-(^2\Pi)$ and $^4\Sigma^-(^4\Pi)$ possible electronic states of the system after electron photoemission. Additional peaks (A, B,...) associated with multielectron effects, characteristic losses, and the $MgK_{\alpha,3,4}$ excitation are present in the O_2 spectrum as well as in the spectrum of N_2 .¹ The theoretically predicted spectrum obtained within the framework of the SCF X α -DVM approach³² is represented by vertical lines in Fig. 7 under the experimental one.

Theoretical predictions of X-ray photoelectron spectra of diatomic molecules, namely N_2 , CO, O_2 , NO, etc., taking into account multielectron effects demonstrate that configuration interaction somewhat complicates the spectra calculated within the one-electron approximation.¹ However, one-electron spectra can be used in considering the IVMO formation since they are much like the experimental spectra.

The binding energy difference between electrons of the $2\sigma_g$ and $2\sigma_u^*$ IVMOs in the F_2 molecule is essentially smaller than those in N_2 and O_2 and equals $\Delta E_{exp} = 4.28$ eV.²³ The results of the SCF X α -DV calculation³² of the electronic structure for the F_2 molecule ($\Delta E_{theor} = 5.6$ eV) are shown in Fig. 7 d and compared with the experimental spectrum. Another detailed study on the IVMO formation in the F_2 molecule, in which the contribution of the IVMO electrons to the bond energy was estimated, was accomplished at the SCF X α -SW level of theory.⁷³

There is a slight difference between the low-energy part of the spectrum of molecular iodine in gaseous and condensed states.²⁴ In the region of the $I\ 5s$ electrons (~ 15 eV–35 eV), two broadened peaks are present in both spectra.²⁴ These peaks are attributed to the σ_g and σ_u^* IVMOs that refer to the $I\ 5s-5s$ interaction. The energy difference between these IVMOs is of about 8 eV (see Fig. 7), although the bond in the I_2 molecule is relatively long ($R_e = 0.2666$ nm) to result in such a considerable difference in energy. Therefore, it was hypothesised¹⁷ that the energies of these IVMOs differ much less and the peaks associated with them appear at around $E_b = 19$ eV. However, this assumption still has to be confirmed by theoretical calculations.

The calculated electronic structure of the C_2 molecule⁸⁸ implies also an essential feature of the $C\ 2s-C\ 2s$ overlap resulting in the formation of the $2\sigma_g$ and $2\sigma_u^*$ IVMOs. At the interatomic distance $R_e = 0.1242$ nm, the binding energy difference between electrons of the $2\sigma_g$ and $2\sigma_u^*$ IVMOs is 18.2 eV, which substantially extends the energy range of the X-ray photoelectron spectrum of C_2 compared to the atomic spectrum of carbon. This accounts for a larger width (~ 25 eV)^{17,25} of the low-energy band in highly-oriented pyrolytic graphite (Fig. 7 a) and diamond compared to the width of the valence band in solid Si and Ge, which possess the diamond-type structure.¹⁷ Since the X-ray photoelectron spectra of graphite and diamond recorded in this region are essentially associated with the $C\ 2s$ electrons,^{17,25} it was postulated⁸⁸ that the base of the valence band is strongly lowered due to the IVMO formation by the $C\ 2s$ AOs.

Peaks attributed to electrons of the IVMOs arising mainly from the $ns-ns$ interaction are also present in X-ray photoelectron spectra of other homonuclear compounds of Group IVA–VIIA elements (see Refs 17, 52, 72 and Figs 8 and 9). The binding energy difference between the electrons of the IVMOs decreases as the atomic number Z increases.^{17,20} In other words, the character of the IVMOs is getting closer to that of the inner (core) MOs, i.e. the overlap between occupied and vacant valence AOs decreases. A similar tendency in the formation of IVMOs is observed when the atomic number increases in a Period.

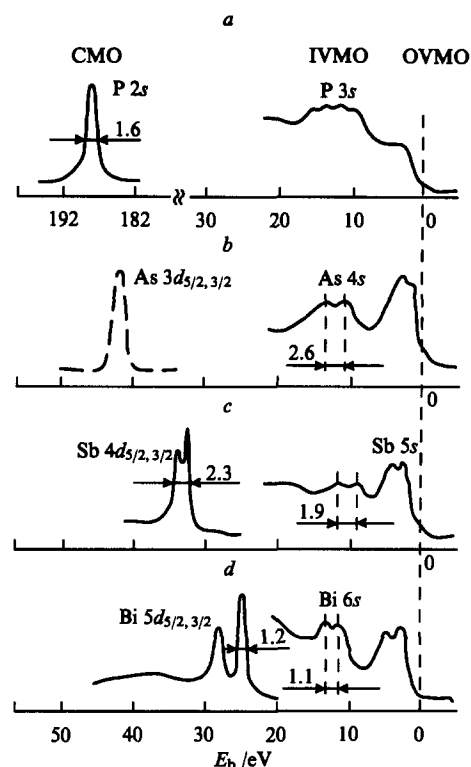


Figure 8. The X-ray photoelectron spectra of red phosphorus (a), As (b),¹¹ Sb (c), and Bi (d) in the solid state.⁷² Here and elsewhere the CMO and IVMO spectra are not calibrated in terms of intensity. In this case, for phosphorus, the intensity of the CMO spectrum is 15 times that of the IVMO one; the intensity of the CMO spectra of As, Sb and Bi is 20 times that of the IVMO one.

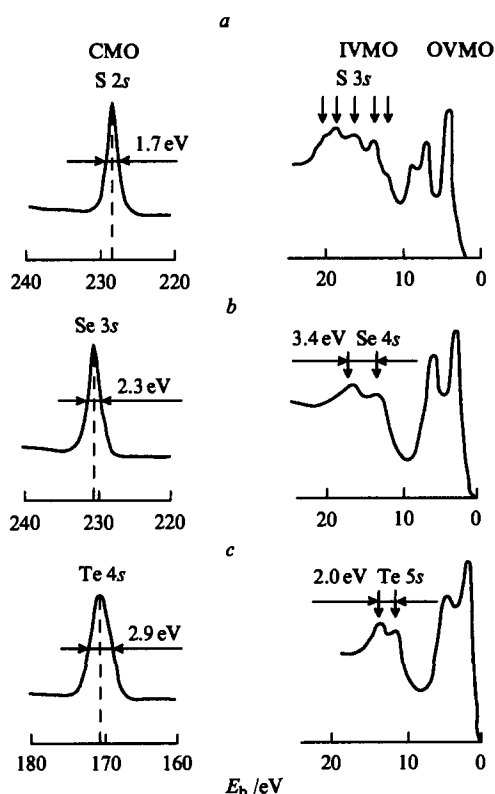


Figure 9. The X-ray photoelectron spectra of solid S (a), Se (b), and Te (c).⁵²

b. Heteronuclear compounds of group IVA – VIIA elements

In some cases, the very fact of the formation of IVMOs in heteronuclear compounds as well as in homonuclear ones can be established definitely on the basis of characteristics of the fine structure in their X-ray photoelectron spectra. It becomes feasible since IVMO formation does not lead to an appearance of separate peaks, but to a complex fine structure in the energy range of ~ 15 eV to ~ 50 eV of the X-ray photoelectron spectra of a heteronuclear compound. Separate peaks can often be classified as being associated with the electrons of IVMOs based on the cooperative analysis of characteristics of the fine structure in spectra of inner and outer electrons. The X-ray photoelectron spectra can then be interpreted qualitatively in terms of group theory. However, in certain cases, especially if electrons of AOs contributing to the IVMOs have significantly different photoionisation cross-sections, a rigorous assignment of the peaks attributed to these MOs can be performed with the aid of theoretical calculation. Thus, the O 2s peak in the X-ray photoelectron spectrum of SiO₂ has a shoulder on its high-energy slope and it is significantly broadened (Fig. 10). This structure of the spectrum of O 2s cannot be attributed to the participation of the oxygen atoms in different types of chemical bonding since the spectrum of O 1s electrons consist of one, relatively narrow peak. The electronic structure of the Si₂O₇⁴⁻ cluster calculated at the SCF X α -DV level¹⁷ points to a noticeable interaction between the electrons of the Si 3s and O 2s AOs resulting in IVMO formation (Fig. 10). This result agrees with published data.³³

A complex structure is observed in the F 2s region of the X-ray photoelectron spectra of compounds [CpMn(CO)₂NO]⁺PF₆⁻, [CpMn(CO)(NO)PPh₃]⁺PF₆⁻, and [CpMn(NO)(PPh₃)₂]⁺PF₆⁻, where Cp is cyclopentadienyl (Fig. 10).¹⁷ This structure cannot be attributed to the fluorine atoms with different effective charges since the F 1s electrons are represented with one symmetrical, relatively narrow peak. Thus, it was suggested¹⁷ that the structure of the F 2s peak of the PF₆⁻ cluster can be partially assigned to the interaction between the F 2s and P 3s AOs resulting in IVMO formation.

An analogous peak profile is observed in the F 2s region of the X-ray photoelectron spectrum of SF₆. Its three components are identified as the 1a_{1g}, 1t_{1u}, and 1e_g MOs (in descending order of the absolute energy values).¹ These orbitals comprise the F 2s and S 3s, F 2s and S 3p, and F 2s and F 2p AOs to an extent of 64 and 33, 77 and 20, and 98 and 2 percent respectively. Since the electron configurations of sulfur {3s²3p⁴} and phosphorus {3s²3p³} atoms are similar, the X-ray photoelectron spectrum of the PF₆⁻ cluster has been interpreted by analogy with the SF₆ spectrum.

Instead of an expected single peak, two peaks of electrons of the 1a₁ and 1t₂ IVMOs are observed in the X-ray photoelectron spectrum of gaseous CF₄. These MOs consist of the F 2s and C 2s AOs to an extent of 69 and 27, and 82 and 15 percent respectively. A fine structure associated with electrons of the filled AOs, which take part in the IVMO formation, also appear in the X-ray photoelectron spectra of NO, CO, CH₃OH, H₂O, and H₂S.¹ It has been noted^{74,89} that the structure of the O 2s region of the X-ray photoelectron spectra of the MO oxides, where M denotes Ca, Sr, and Ba, is associated with the IVMOs made up partially of the M *np* and O 2s AOs of neighbouring atoms. This is consistent with the results of an electronic structure calculation for the CaO₆¹⁰⁻ of O_h symmetry (the SCF X α -SW method was used).⁷⁴

The interpretation of fine structure in the low-energy region of the X-ray photoelectron spectra of La-, Y-, Bi-, and Tl-based high-temperature superconductors^{90–92} has revealed that IVMOs form in these due to interaction between the O 2s AOs and the closest-in-energy-shell of metal atoms in these compounds. Previously,^{93,94} the fine structure in the X-ray photoelectron spectra of these compounds led to the hypothesis that all the elements in high-temperature superconductors possess shells with energies close to that of the O 2s AO. Then, by correlation of the oxidation state of metal ions with their radii, the range of elements that can form HTSC has been defined.⁹³

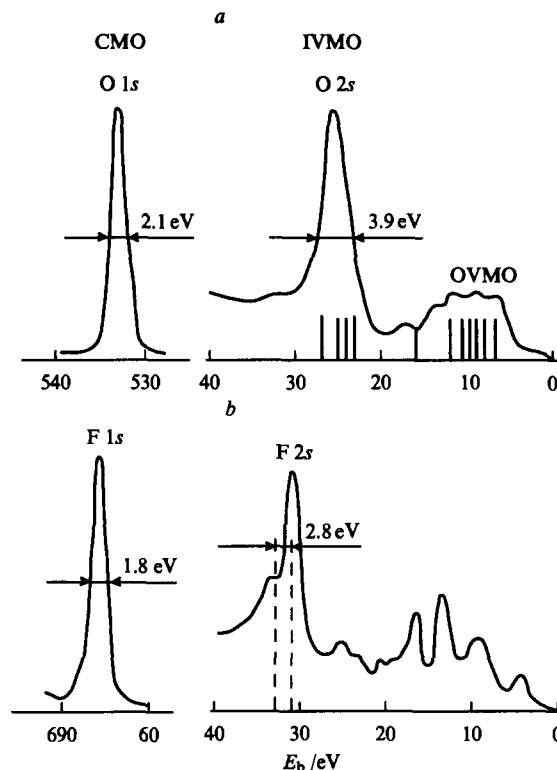


Figure 10. The X-ray photoelectron spectra of SiO₂ (a) and the manganese organometallic compound [CpMn(CO)₂NO]⁺PF₆⁻ (b). Vertical lines show the theoretically predicted spectra of the outer electrons.¹⁷

c. Lanthanide compounds

With all other conditions satisfied IVMO formation also requires that the energies of the corresponding occupied AOs of neighbouring atoms are comparable.²¹ In this connection, lanthanide compounds are of great interest since the energies of Ln 5p (where Ln designates a lanthanide element) and O (F) 2s orbitals are close in magnitude. As the atomic number increases from 57 (La) to 71 (Lu), the binding energy of the Ln 5p_{3/2} electrons in lanthanide oxides ranges within the limits from 17.7 to 27.5 eV.¹⁹ The binding energies of the O 2s electrons (~ 21 eV) fall approximately in the middle of this interval. All lanthanide oxides from La to Lu (except for Pm) have been studied by XPS.^{19, 78–80}

The structures of the oxides vary in a series, and, in certain cases, the oxidation states of metal atoms vary too. Therefore, two sets of isostructural lanthanide compounds, viz. *o*-methoxybenzoates and diphenylacetates, have been studied (for all but promethium compounds) to solve the problem of IVMO formation (Fig. 11).¹⁹ These compounds are non-hygroscopic, stable in high vacuum, and insensitive to exciting X-ray radiation. Therefore one could expect that the compounds considered do not undergo structural changes and decomposition during the spectra collection.

Together with the expected separate peaks of Ln 5p_{3/2,1/2} and O 2s electrons, a fine structure is observed in the region of the binding energies of Ln 5p and O 2s electrons in the X-ray photoelectron spectra of all the compounds studied (Fig. 11). The most complex fine structures are observed in the mid-row lanthanide oxides since in this case the Ln 5p and O 2s AOs are closest in energy.^{4,5} Theoretical calculations for various Ln–O bond lengths have been performed for clusters LnO₇¹¹⁻ and LnO₆²⁻ of C_{3v} and D_{3d} symmetry types respectively at the SCF X α -DV level and for a cluster LnO₃³⁻ of D_{3h} symmetry type at the SCF X α -SW level of theory. The results obtained support the assumption that the fine structure in the spectra of lanthanide compounds is partly associated with interaction of the Ln 5p and O 2s shells resulting in

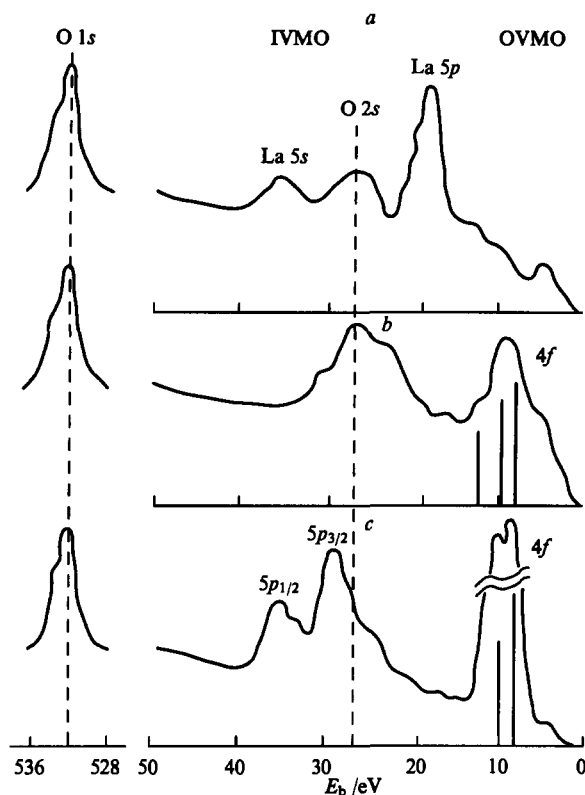


Figure 11. The X-ray photoelectron spectra of La (a), Eu (b), and Lu (c) (LnL_3 *o*-methylbenzoates). Vertical lines represent the theoretical metal 4f spectra.⁴

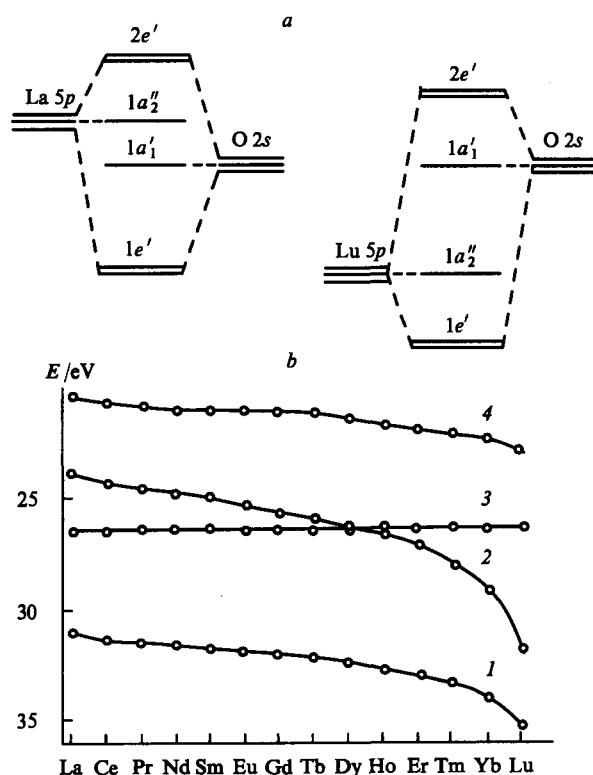


Figure 12. The IVMO diagram (a), dependence of the energies of the IVMOs, which consist of the Ln 5p and O 2s AOs, on the atomic number of the lanthanide element (b) for the cluster LnO_3^{3-} (symmetry group D_{3h}).⁴ (1) $1e'$, (2) $1a_2'$, (3) $1a_1'$, (4) $2e'$.

IVMO formation (Fig. 12). However, the calculations⁴ performed do not take into account the relativistic effects, and the cluster LnO_3^{3-} does not exactly represent the structure of the oxygen-containing compounds under consideration. Therefore, a direct, quantitative comparison of the theoretical and experimental results is not possible. However, the very fact of IVMO formation can be proved by the calculation results.

Spectra of lanthanide fluorides also exhibit fine structure in the region of F 2s electrons.^{19,82} These structures cannot be attributed to the presence of fluorine atoms in different oxidation states since only one relatively narrow peak corresponds to the F 1s electrons in the X-ray photoelectron spectrum. It was therefore assumed that the structure observed is concerned with the IVMO electrons.^{19,82} The results of the SCF X α -DV calculation⁹⁵ of the electronic structure for cluster LaF_{11}^{8-} of D_{3h} symmetry group agree qualitatively with these experimental data.

d. Actinide compounds

In XPS studies of actinide compounds, much attention has been paid to uranium compounds. It is on the basis of their X-ray photoelectron spectra that the most interesting conclusions on the role of the An 5f electrons (where An is an actinide element) in chemical bonding in actinide compounds⁹⁶ and on the contribution of the low-energy filled subshells to the bonding have been derived.^{2, 3, 6, 18, 78}

It is most convenient to consider the participation of the U 5f electrons in chemical bonding with stable uranium oxides as an example. Uranium dioxide UO_2 has a fluorite-type (CaF_2) structure, while the trioxide UO_3 is built up of planar networks of tetragons centered with nearly linear uranyl UO_2^{2+} fragments.¹⁸ This fragment serves as a basis for many oxygen-containing uranium compounds with various ligands in its equatorial plane. Special attention is drawn to the low-energy part of the X-ray photoelectron spectra of these compounds.

A high extent of localisation of the non-bonding U 5f electrons on the uranium atoms in UO_2 has been suggested from a neutron diffraction study.⁹⁷ The electronic configuration of the U atom in UO_2 is $\{\text{Rn}\} 5f^2$, where $\{\text{Rn}\}$ is that of the Rn atom in the ground state. This conclusion has been corroborated with XPS^{18,96} and theoretical studies.^{3,31,54}

A rather narrow peak corresponding to the U 5f electrons is found near the Fermi level in the X-ray photoelectron spectrum of UO_2 (Fig. 13 a). This peak is absent in the spectrum of $\gamma\text{-UO}_3$, but, instead of separate peaks of the U $6p_{3/2,1/2}$ and O 2s electrons, a fine structure is observed in the region of the U 6p and O 2s electrons. Binding energies of the electrons that account for different components of the spectrum change with variation in the U–O bond length in the UO_2^{2+} fragment of various compounds. In particular, the difference in energies between the components in the U $6p_{3/2}$ region of the spectra is the most convenient for measurements. This difference may serve as a measure of the bond length $R_{\text{U}-\text{O}}$ in the UO_2^{2+} fragment of various compounds.^{2, 3, 6, 14, 18, 76, 85}

The X-ray photoelectron spectra of UO_2 , UF_4 , and other non-uranyl compounds do not exhibit such a complex structure in the region of the U $6p_{3/2}$ electrons. Therefore, the fine structure observed in this spectral interval cannot be attributed to the dynamic effect.¹⁸ Also, the most intense peak of this structure cannot be explained by multielectron excitation. The latter give rise to so-called 'shake-up' satellites of relative intensity of $\sim 20\%$ with respect to that of the major peaks in the spectra of inner electrons. The structures of the low-energy part of X-ray photoelectron spectra of uranyl-containing compounds differ essentially in relative intensities of the constituent peaks, their energy distribution, and relative distances from the structure associated with multielectron excitation and observed in the inner electron spectra of these compounds.⁷⁸ The presence of two components in the U $6p_{1/2}$ and O 2s region of the spectrum of $\gamma\text{-UO}_3$ (see Fig. 13) is not consistent with the splitting of the U $6p_{3/2}$ component in the crystal field.¹⁴

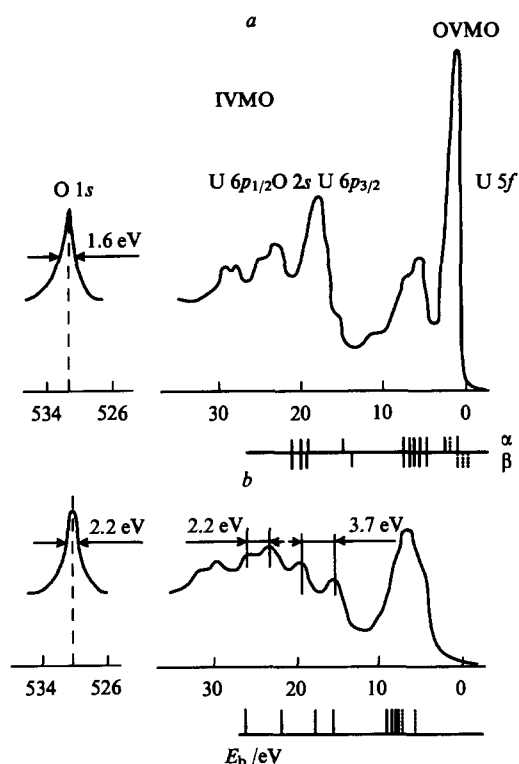


Figure 13. The X-ray photoelectron spectra of uranium oxides UO_2 (a) and $\gamma\text{-UO}_3$ (b) and the corresponding energy levels calculated at the SCF $\text{X}\alpha\text{-SW}$ level of theory.³

Experimental data^{2, 3, 6, 78, 83} and the results of theoretical studies performed within the framework of the SCF $\text{X}\alpha\text{-SW}$ ^{3, 29} and SCF $\text{X}\alpha\text{-DV}$ ³⁰ approaches demonstrate that the complex structure in the U 6p and O 2s region of the spectra is concerned with the IVMOs that comprise U 6s, U 6p, and O 2s AOs.

The spin-orbit splitting energies of the U 6p and Th 6p levels differ for the corresponding fluorides, oxides and pure metals (Table 2).^{98–101} The variation in the splitting of the level under discussion for Th and its compounds is not attributed to a

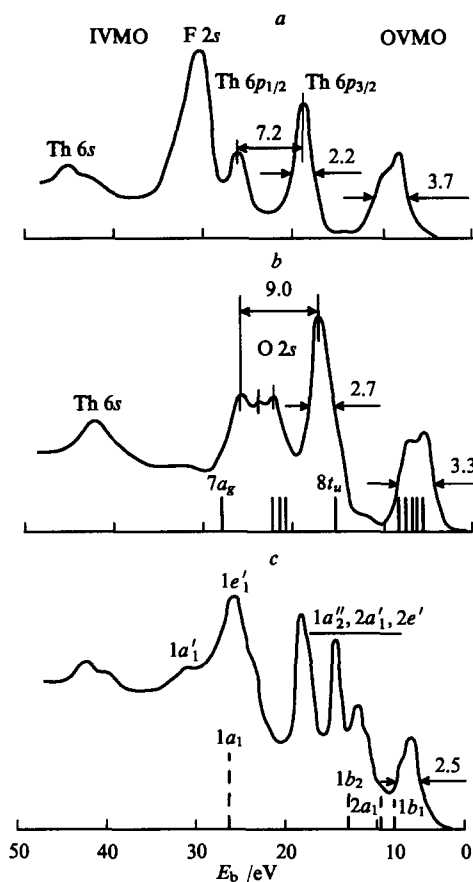


Figure 14. The X-ray photoelectron spectra of weakly-bound Th electrons in ThF_4 (a), ThO_2 (b)⁸¹ (solid vertical lines represent the electron energies for the cluster ThO_8^{2-} of the O_h symmetry),⁵⁴ thorium nitrate (c) (dashed lines represent the experimental spectrum of H_2O).¹ The designation of the molecular orbitals of NO_3^- (D_{3h} symmetry group) are shown at the top).

coincidence of the Th 6p peaks and neighbouring ligand peaks since the effect should be reversed in that case (Fig. 14). The

Table 2. The binding energy difference ΔE_b between subshells in Th, U, and their compounds.⁷⁶

Metal or compound	ΔE_b /eV ^a						Ref.
	$6p_{3/2} - 6p_{1/2}$	$6p_{3/2} - 6s_{1/2}$	$6p_{3/2} - 4f_{1/2}$	$6s_{1/2} - 4f_{7/2}$	$5d_{5/2} - 4f_{7/2}$	$X 2s_{1/2} - X 1s_{1/2}$	
ThO_2	9.0	25.4	317.8	292.4	248.0	508.2	17
	8.5	—	317.6	—	247.9	508.0	98
ThF_4	7.2	26.1	318.2	291.1	248.1	655.7	17
$\text{Th}(\text{NO}_3)_4 \cdot 4\text{H}_2\text{O}$	—	25.3	317.4	292.1	248.0	506.6	17
Th	7.5	—	316.6	—	247.6	—	17
	7.9	24.8	316.5	291.7	247.7	—	98
Th_{theor}	9.2	28.7	318.8	290.1	248.0	—	99
UO_2	10.5	27.6,	362.5	335.3,	283.6	507.2	17
		29.4		333.5	—	—	
	10.6	27.8	362.5	334.7	283.8	507.9	98
UF_4	—	28.2	362.6	334.4	283.6	655.7	17
	11.7	—	362.8	—	—	655.4	100
U	10.0	—	360.6	—	283.0	—	17
	10.0	27.1	360.6	333.5	283.2	—	78
U_{theor}	10.4	31.0	360.9	329.9	283.0	—	79
$\gamma\text{-UO}_3$	—	—	363.0,	—	284.0	505.9,	17
			366.7			508.1	

^a $\Delta E_b = E_b M n l_i j_i - E_b M n l_k j_k$.

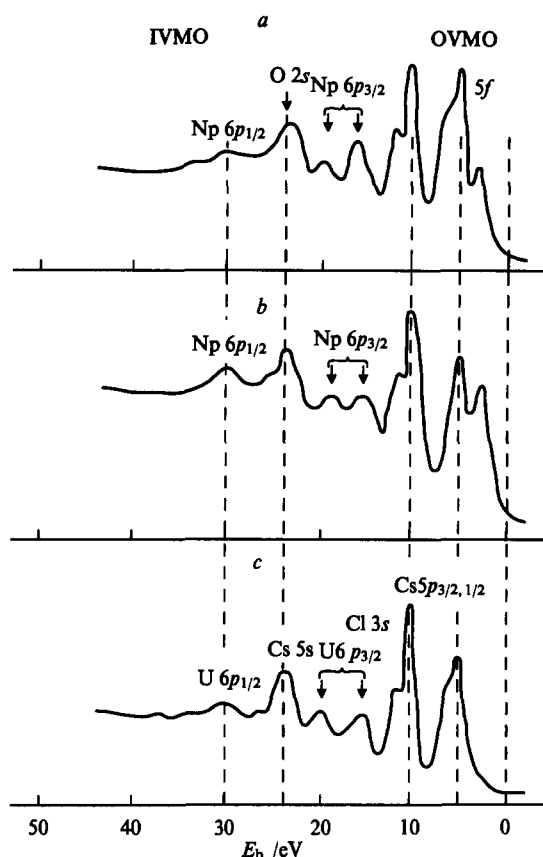


Figure 15. The X-ray photoelectron spectra of weakly-bound electrons of $\text{Cs}_2\text{NpO}_2\text{Cl}_4$ (a), $\text{Cs}_3\text{NpO}_2\text{Cl}_4$ (b), and $\text{Cs}_2\text{UO}_2\text{Cl}_4$ (c) single crystals.¹⁰³

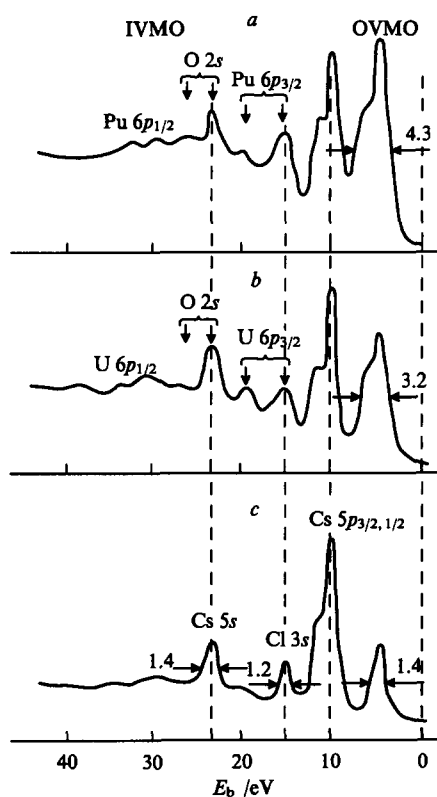


Figure 16. The X-ray photoelectron spectra of weakly-bound electrons of $\text{Cs}_2\text{PuO}_2\text{Cl}_4$ (a), $\text{Cs}_2\text{UO}_2\text{Cl}_4$ (b), and CsCl (c) single crystals.¹⁰³

multiplet splitting effect also does not account for this splitting as long as these compounds are diamagnetic. Extensive experimental data¹⁻⁸ show that spin-orbit splitting of inner levels of metal ions depends slightly on the properties of their ligand environment. With this in mind, it was suggested that electrons of the low-energy subshells of Th and U are affected by the chemical bonding in these compounds and take part in IVMO formation.

It is evident from general considerations that, for example, IVMO formation by the Th(U) 6p and O 2s AOs lowers the binding energy of the Th(U) 6p_{3/2} state, etc. It has been mentioned¹⁸ that other effects that shift the energy of low-energy AOs can affect MO formation. Such shifts can be most rigorously detected if the difference in binding energy between the inner valence electrons and deep-lying electrons of core atomic shells in Th and U and their compounds is considered (Table 2). These data accord with the participation of at least Th(U) 6p_{3/2} electrons in chemical bonding in the compounds under discussion.

The binding energy difference between the Th 5d_{5/2} and 4f_{7/2} inner atomic levels is the same for thorium and its compounds within the standard error of measurement. Thus, the essentially increased energy difference between the Th(U) 6p_{3/2} and Th(U) 4f_{7/2} electrons in Th compounds compared to that in Th metal is a fairly reliable criterion of the contribution of the Th(U) 6p_{3/2} and F(O) 2s electrons to the chemical bonding in thorium (uranium) oxides and fluorides.^{81, 101} It has been noted¹⁸ that this difference can be measured most accurately since the corresponding peaks are relatively narrow and hardly overlap with other peaks. Calculations have confirmed a significant participation of the fully occupied Th(U) 6p and O 2s AOs in the formation of IVMOs in uranium and thorium dioxides.^{31, 54}

To establish experimentally the formation of IVMOs by An 6p and O 2s AOs in compounds containing AnO_2^{2+} groups, a series of isostructural single crystals of U, Np, and Pu compounds ($\text{Cs}_2\text{UO}_2\text{Cl}_4$, $\text{Cs}_3\text{NpO}_2\text{Cl}_4$, $\text{Cs}_2\text{NpO}_2\text{Cl}_4$, $\text{Cs}_2\text{PuO}_2\text{Cl}_4$) and polycrystalline samples of Np compounds ($\text{Cs}_2\text{NpO}_2(\text{CH}_3\text{COO})_3$, $\text{RbNpO}_2(\text{NO}_3)_2 \cdot 2\text{H}_2\text{O}$, $\text{NaNpO}_2(\text{CH}_3\text{COO})_3$)¹⁰²⁻¹⁰⁴ have been studied by XPS. From analysis of the spectra of the low-energy and inner electrons of these compounds in the X-ray photoelectron spectra of the corresponding oxides and cesium chloride as well as the photoionisation cross-section,¹⁰⁵ it has been concluded¹⁰²⁻¹⁰⁴ that IVMOs form in the compounds of Np and Pu considered as well as in uranyl compounds. The inner valence electrons account for the fine structure in the low-energy region of the X-ray photoelectron spectra of these species (Figs 15 and 16). These results are in satisfactory agreement with the results of electronic structure calculations for clusters AnO_2^{2+} (An = U, Np, Pu) of $D_{\infty h}$ symmetry within the framework of non-relativistic SCF $X\alpha$ -SW^{104, 106} and relativistic^{107, 108} approaches as well as clusters $\text{AnO}_2\text{Cl}_4^{2-}$ (An = U, Np, Pu) at the relativistic $X\alpha$ -DV level of theory.¹¹¹ The structure of the X-ray photoelectron spectra of the 'new product' from the Chernobyl nuclear plant¹⁰⁹ and americium nitrate¹¹⁰ are also consistent with these results.

It follows from the examples considered in this Section that IVMOs form effectively in compounds of any elements of the Periodic Table if certain conditions are satisfied.

2. Relationship between the structures of compounds and the structures of their X-ray photoelectron spectra

The interpretation of fine structure in an X-ray photoelectron spectrum concerned with IVMOs often utilises not only experimental data, but also results of rather tedious and complicated calculations of the electronic structure of the compound within the framework of the $X\alpha$ - and other methods that require powerful hardware.^{32, 106-108} However, the correct model cluster cannot be always chosen at once. In some cases, only approximate data on the structure of the compound are available (especially for amorphous ones). All these factors increase the CPU time required to execute the calculations of the electronic structure. Therefore, qualitative information on the structure of the com-

pound under study obtained from its spectrum is rather helpful, e.g. see Ref. 109.

Several reasons account for the importance of this information. First, reliable information defines a range of species where the formation of IVMOs is expected, thus more precise laborious calculations can be accomplished for them in order to examine the contribution of the IVMO electrons to the chemical bonding. Second, this is useful when relativistic effects are to be taken into account in the interpretation of the spectrum. Third, a possible qualitative interpretation of fine structure in X-ray photoelectron spectra extends the scope of X-ray photoelectron spectroscopy for applied studies of the physicochemical properties of matter.^{6, 78, 109}

From the standpoint of group theory, it is expected that fine structure in an X-ray photoelectron spectrum attributed to the IVMO electrons reflects the local environment of the specified atom. The structure of the X-ray photoelectron spectrum is determined by the symmetry point group of the cluster comprising the central atom and the ligands from the closest coordination shells. It is also obvious that the distance between the peaks corresponding to the electrons of different IVMOs must depend on the bond lengths in the cluster. If the IVMO-associated structure in the spectrum is pronounced, then the relative positions of the ligands with respect to the central atom can be easily determined.^{17, 20, 78} Estimation of the contribution of the electrons of the inner closed shells to chemical bonding can also be performed. With an experimental or theoretically predicted correlation of the binding energy of the IVMO electrons with the bond lengths in the specified cluster, e.g., UO_2^{2+} , available, the bond lengths in the UO_2^{2+} fragment in any compound or on a solid surface can be determined.¹⁸ It has been mentioned^{20, 85} that information of this kind for amorphous compounds cannot be obtained with the same ease since X-ray diffraction cannot be applied for bond length determination in them. Thus, if bond lengths in a cluster have not been determined, then the calculation should be carried out for a certain range of expected distances. We shall consider these points with examples.^{1, 17–20, 78}

As has been mentioned above (see Section IV.1), the simplest fine structure is observed in the spectra of diatomic molecules N_2 , O_2 , F_2 , and I_2 (Fig. 7). Two filled ns AOs form two IVMOs, one of them, in accordance with conventional quantum-chemical notation for the two-level system, is formally referred to as the bonding $\pi\sigma_g$ MO, and the other as the antibonding $\pi\sigma_u^*$ MO.²¹ A considerable energy difference between these two IVMOs (18.7 eV in N_2) points to a significant interaction of electrons of doubly-occupied levels. We should note that, up to the present, the maximum reported to date energy difference is that between $\pi\sigma_u^*$ and $\pi\sigma_g$ IVMOs observed in the X-ray photoelectron spectrum of N_2 .^{1, 51, 56} Despite configuration interaction complicating the fine structure in this region of the spectrum,^{86, 87} the peaks corresponding to the electrons of these orbitals are easily distinguished from others (Fig. 7).

The interaction between the electrons of subshells of carbon atoms in the planar layers of pyrographite is of more complex character, therefore, the spectrum of C 2s electrons does not exhibit a sharp fine structure associated with a system of IVMOs (Fig. 7a).²⁵ Nevertheless, the spectrum shows interaction between the C 2s electrons of neighbouring atoms. This interaction manifests itself in the appreciable broadening of the valence band⁸⁸ compared with that in the spectra of weakly-bound electrons in solid Si, Ge, and Sn possessing analogous structures.¹⁷

Fine structures are observed in the ns region of the spectra of solid P, As, Sb, and Bi (the electronic configuration of atoms is $\{\text{ns}^2\text{np}^3\}$)⁷² as well as in solid S, Se, and Te (the atomic electronic configuration is $\{\text{ns}^2\text{np}^4\}$) (Figs 8 and 9).⁵² It is known that, in solid sulfur, atoms are arranged in 8-membered twisted rings, and, in solid Se and Te, atoms form linear zigzag chains.^{52, 72} A diagram of the energies of IVMOs consisting of the occupied ns AOs versus the number of atoms in a planar closed ring or linear chain has been constructed (Fig. 17).⁵² These models are closely related to

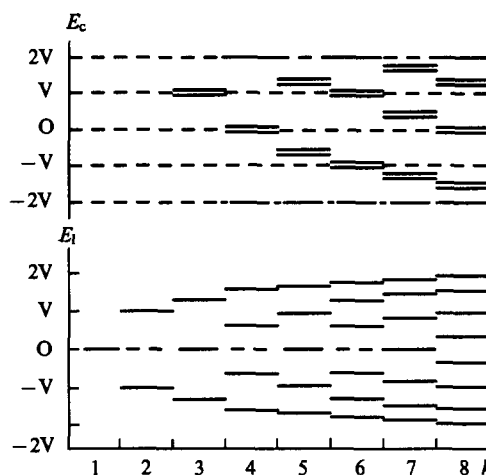


Figure 17. Dependence of the IVMO diagram on the number of atoms in a molecular system (E_c denotes the energy of the ring system, E_l the energy of the linear system, V a relative (Hückel) energy unit).⁵²

the real picture. The number of fully-occupied IVMOs increases with the number of atoms k in the ring. The closest agreement between the theoretical and experimental spectra of S 3s electrons is reached at $k = 8$. The spectrum considered comprises five peaks in a 1:2:2:2:1 ratio which agrees satisfactorily with the experimental data (see Fig. 9). The linear-chain model does not explain the structure of the spectrum of S 3s electrons in solid sulfur. At the same time the predicted and experimental spectra of Se 4s and Te 5s electrons best fit a linear model with small even k (see Figs. 9 and 17).⁵² The Se 4s and Te 5s spectra of ion-bombarded surfaces of solid Se and Te reveal a single relatively narrow peak^{17, 52} with the concurrent disappearance of two peaks, which indicates atomisation of Se and Te on the samples' surface, i.e. the weakening of chemical bonding between neighbouring atoms. This phenomenon may be useful for practical study of radiation-induced damage and defects.

A dependence between the difference ΔE_b in binding energies of the IVMO electrons and the bond length R_{X-X} in solid Se, Te, As, Bi, etc. has been revealed (Fig. 18). A linear correlation of ΔE_b with R_{X-X} suggested previously¹¹ has a purely illustrative significance.

In transition 3d metal disulfides and diselenides, the sulfur and selenium atoms form clusters X_2^{2-} with a marked interaction between the X ns electrons of neighbouring atoms.¹⁶ Two peaks associated with electrons of IVMOs are therefore present in the S 3s and Se 4s X-ray photoelectron spectra.¹⁶ An analogous phenomenon is observed in the X-ray photoelectron spectrum of CuP_2 , where, instead of a single peak, two peaks separated by ~4.5 eV are present in the P 3s region of the spectrum. It has been noted¹⁶ that these two peaks are concerned with the interaction of P 3s orbitals. For the S_2^{2-} cluster, a qualitative agreement between the theoretical and experimental dependences between the binding energy difference ΔE_b of inner valence electrons and the bond length R_{S-S} has been found (Fig. 19). The theoretical dependence obtained within the framework of the CNDO/2 method¹⁷ differs by about 3 eV from the experimental one.

Cluster models can be used to illustrate the correlation of the energy and structure of IVMOs in lanthanide compounds with the structure of the local environment of the metal atom and the distances R_{Ln-X} to the nearest atoms. Within the non-relativistic approximation for the cluster LnO_3^{3-} of D_{3h} symmetry, the IVMO spectrum associated with the Ln 5p and O 2s AOs corresponds to four energy levels. The highest and lowest ones are the two-fold degenerate $1e'$ and $2e'$ IVMOs, and the two others are the quasi-atomic $1a_1'$ and $1a_2'$ IVMOs (Fig. 12a).⁴ The energies of the $1e'$ and $2e'$ MOs must depend on the bond length R_{Ln-O} to a greater extent than those of the $1a_1'$ and $1a_2'$ MOs. The dependence of the

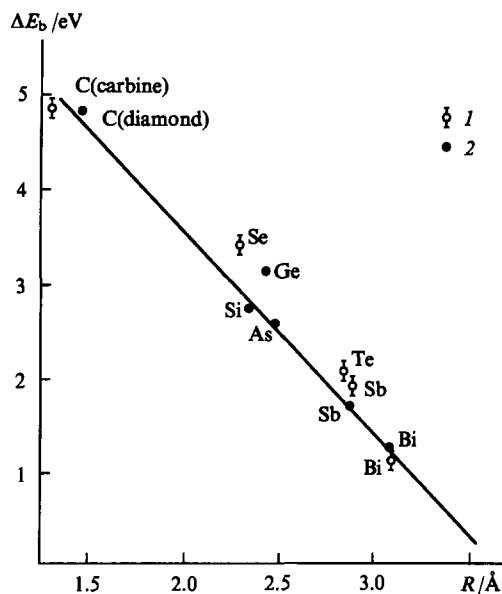


Figure 18. Dependence of the energy gap ΔE_b between the IVMOs, which consist of the ns AOs, in solids on the bond lengths R . An equation $\Delta E_b = 8.0 - 2.2R$ is in qualitative agreement with results of studies described in Refs 52, 72 (1) and Ref. 11 (2).

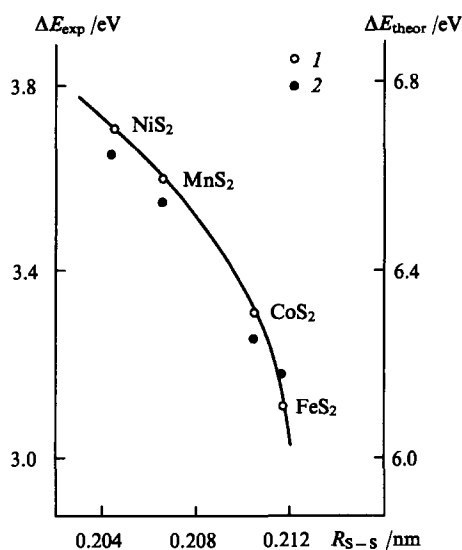


Figure 19. Dependence of the binding energy difference between the $3\sigma_u^*$ and $3\sigma_g$ IVMOs associated with the $S\ 3s$ AOs on the bond length R_{S-S} in the S_2^{2-} cluster of the $3d$ transition metal disulfides: (1) experiment; (2) theoretical results.⁵²

energies of these MOs on the atomic number Z of the central $4f$ element has been calculated for various R_{Ln-O} values at the SCF $X\alpha$ -SW level of theory (Fig. 12 b).⁴ The energy was calibrated with respect to the energy of the quasiatomic $1a_1'$ IVMO associated mainly with the $O\ 2s$ AO.

The structure of IVMOs for cluster LnO_3^{3-} obtained in terms of group theory is in qualitative agreement with computational results.⁴ The IVMO structure for clusters LnO_7^{11-} (symmetry group C_{3v}) and LnO_6^{9-} (symmetry group D_{3d}) is different.⁷⁸⁻⁸⁰ Electronic structure calculations for lanthanide compounds within the relativistic approach would enable more precise quantitative comparison of theoretical and experimental data.

Oxygen-containing actinide series compounds are the species structural information on which, namely the structure of the local environment of the metal atom and its oxidation state, can be determined from the fine structure corresponding to electrons of IVMOs in their X-ray photoelectron spectra.^{3, 6, 17, 18, 85, 106, 107, 111} Most clearly this can be illustrated with the spectra of uranium compounds. The results of calculations demonstrate that taking into account the relativistic effects leads essentially to the strong splitting of the $U\ 6p_{1/2}$ component of the doublet and hardly affects the energy of the $U\ 6p_{3/2}$ electrons.³¹ Thus, the interpretation of the spectrum in the region of the $U\ 6p_{3/2}$ and $O\ 2s$ electrons can be carried out within the non-relativistic approach.³

Substantially different structures of uranium dioxide and trioxide give rise to a fundamental distinction in the spectra of weakly-bound electrons (Fig. 13). Since the $U-O$ bond in the UO_2^{2+} fragment of UO_3 is much shorter than the equatorial $U-O$ bonds, in the first approximation, the structure of the valence region of the spectra is determined by this fragment. It has been mentioned^{6, 85} that, within the non-relativistic approximation, the correlation diagram of IVMOs consisting of the $U\ 6s$, $U\ 6p$, and $O\ 2s$ AOs makes it possible not only to rationalise the structure of the spectra of the uranium oxides under discussion, it can also be helpful in the investigation of the structures of these compounds (Fig. 20).^{6, 85} According to this scheme, variations in the $U-O$ bond lengths in clusters UO_8^{12-} and UO_2^{2+} slightly influence the energies of the quasi-atomic t_{2g} , t_{2e} (in UO_8^{12-}), and π_u (in UO_2^{2+}) MOs, but can have a substantial effect on the t_{1u} , t_{1u}^* (in UO_8^{12-}), σ_u , σ_u^* , σ_g , and σ_g^* (in UO_2^{2+}) IVMOs. In practice, this phenomenon permits the determination of the structures of oxides and the bond lengths in them.

However, this diagram does not describe completely the structure observed in the spectrum of γ - UO_3 .^{2, 3, 6} It is concerned with the fact that it does not take into account the influence of the ligands in the equatorial plane of the UO_2^{2+} fragment on the spectra of the valence electrons of oxygen. Apparently, this

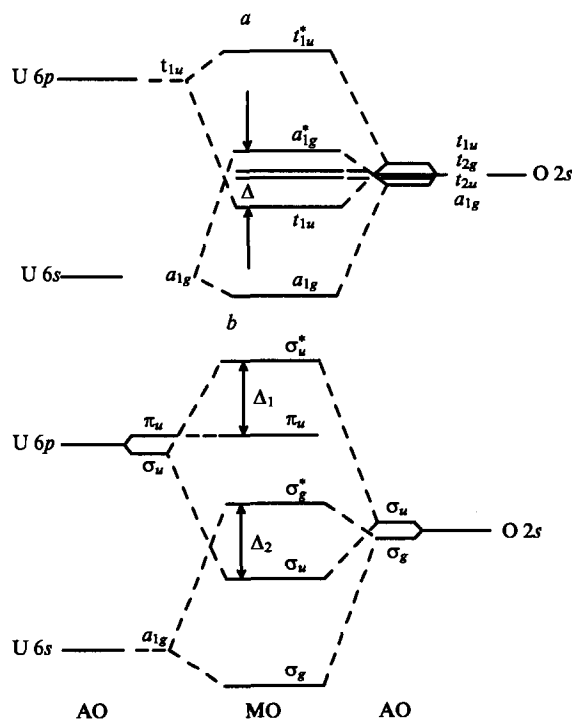


Figure 20. The diagram of IVMOs attributed to the interaction of the $U\ 6p$ and $O\ 2s$ AOs for clusters UO_8^{12-} (a) (O_h symmetry group) and UO_2^{2+} (b) (D_{oh} symmetry group).^{6, 85}

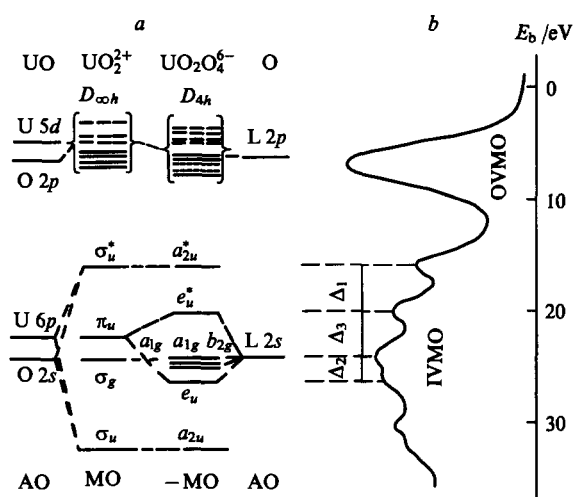


Figure 21. The principal scheme for MO formation in clusters UO_2^{2+} ($D_{\infty h}$ symmetry group) and $UO_2O_4^{6-}$ (D_{4h} symmetry group) (a) and the X-ray photoelectron spectrum of γ - UO_3 (b).¹⁰⁶

influence gives rise to additional IVMOs consisting of the U 6p and O 2s AOs. In the scheme, which accounts for the effect of the equatorial ligands on the structure of IVMOs of the UO_2^{2+} ion, these MOs correspond to the e_u and e_u^* orbitals (Fig. 21).¹⁰⁶ The latter scheme almost completely describes qualitatively the structure of the valence electron region of uranyl compounds. The results of theoretical calculations for clusters of uranyl compounds,^{3, 106} which take into account the effect of the equatorial ligands are consistent with the results obtained from this scheme.

Thus, the experimental correlation of the energy gap between the two components in the U 6p_{3/2} region of the spectrum (in Fig. 20, they are related to the a_{2u}^* and e_u^* IVMOs) with the U—O bond length in the UO_2^{2+} fragment in a series of uranyl compounds becomes comprehensible.^{17, 85} The results of semiempirical calculations¹⁰⁶ of structural characteristics of clusters $UO_2L_n^{m-}$ are consistent with this dependence. In certain cases, the phase content of natural uranium oxides and some bond lengths in them have been determined from these data.^{2, 6, 17, 85} The correlation of the structure of a compound with the fine structure in the X-ray photoelectron spectra of the valence region has also been studied in a series of Np, Pu (Figs 15 and 16),^{102–104} and Am¹¹⁰ compounds.

Since ThO_2 and UO_2 have similar structures,¹⁷ their spectra (Figs 13 and 14) have much in common (see Fig. 20). Thus, in the O 2s region, the structure associated with the t_{1u} IVMO is observed. In the Th 6p_{1/2} region of the X-ray photoelectron spectrum of $Th(NO_3)_4 \cdot 4H_2O$, peaks corresponding to the $1a'_1$ and $1e'_1$ IVMOs of the NO_3^- cluster are present.⁸¹

In many cases, the fact of the formation of IVMOs in various compounds can be authenticated by the presence of fine structure in the region of weakly-bound electrons in their X-ray photoelectron spectra. This structure can often be interpreted without recourse to rigorous theoretical calculations by a simple approach based on group theory.^{17, 20, 78} A correlation of the structure of a compound, i.e., bond lengths, with the structure of their spectra associated with the inner valence electrons has been established. It allows in some cases the retrieval of qualitative and quantitative information on the structure of compounds, which is exceptionally important for amorphous materials.

V. Contribution of inner valence molecular orbitals to chemical bonding

From the viewpoint of quantum-chemical theory, provided certain conditions are satisfied, MOs can be formed from arbitrary low-lying filled AOs.^{21, 22} The contribution of electrons to the chemical bonding is defined with a specific model describing the bond formation. The chemical bonding in homonuclear molecules is assumed to occur essentially due to the electrons of valence atomic shells,^{21, 22} and the electrons of inner closed shells contribute to the chemical bonding to a lesser extent and destabilise the bonds. Thus, in a molecule A_2 , two occupied 1s AOs can form a bonding $1\sigma_g$ and antibonding $1\sigma_u^*$ MOs. The bonding MO stabilises the bond to a lesser degree than the antibonding one destabilises it.²¹ Therefore, the total contribution of the CMO electrons to the covalent component of the bond energy is negative. In particular, this explains the instability of the helium molecule He_2 .²¹

However, as follows from experimental data on light-element compounds, both filled and valence shells with the same principal quantum number contribute to the chemical bonding.¹ Calculations of the electronic structure of light-element diatomic molecules within the MO LCAO approach have indicated that the occupied low-energy AOs do not form 'pure' CMOs but mix with valence AOs.^{1, 51, 52, 56, 73, 88} These CMOs lose their 'inner' character and have to be considered collectively with the OVMOs. They are referred to as IVMOs since they have not fully become the valence ones.^{51, 56}

The question of the participation of the electrons of filled low-energy shells in chemical bonding for light-element compounds has been considered to some extent. However, it had barely been raised for heavy-element compounds until recently.^{17, 85} Consider, for example, an established fact of the formation of IVMOs in uranyl compounds by the U 6p and O 2s AOs.^{2, 3, 6} If these MOs consisted solely of the U 6p and O 2s AOs, they would not be referred to as valence MOs. However, they were given the name 'IVMO' since they also consist of the valence U 7s, 6d, 4f, and O 2p AOs.

The question of the role of the low-energy closed shells of heavy elements (lanthanide compounds, actinide compounds, etc.) in chemical bonding raised on the basis of XPS studies^{2–6, 26, 27, 78} is very important. Its examination will help in understanding the nature of chemical bonding in these compounds, furnish an explanation of the existence of unique nearly linear stable fragments, AnO_2^{2+} , in certain actinide compounds, etc. However, difficulty in rigorous theoretical calculations for actinide series compounds is now evident. Therefore, as has been mentioned,^{17, 20} the first step is to consider the participation of inner electrons in chemical bonding for the most simple molecules,^{51–53, 56, 71, 73–75, 88} and then to proceed to heavy-element compounds.

1. Simple models

Examination of correlations of MO energies with interatomic distances can help understanding of the formation of these MOs.^{3, 4, 51–53, 56, 72, 73, 85, 112} The N_2 molecule is the most convenient subject for examination of this kind. Calculations of the MO energies for N_2 at different interatomic distances were carried out at the SCF CNDO/2 and SCF X α -DV levels (Fig. 22).^{51, 56} The results obtained by these two approaches are in good conformity with each other. They display the same trend of changes in the orbital energies with decrease in the bond length and the same order of MO energies at the equilibrium interatomic distance $R_e = 0.109$ nm. They also give comparable values of the binding energy gap between electrons of the bonding $2\sigma_g$ and antibonding $2\sigma_u^*$ IVMOs.

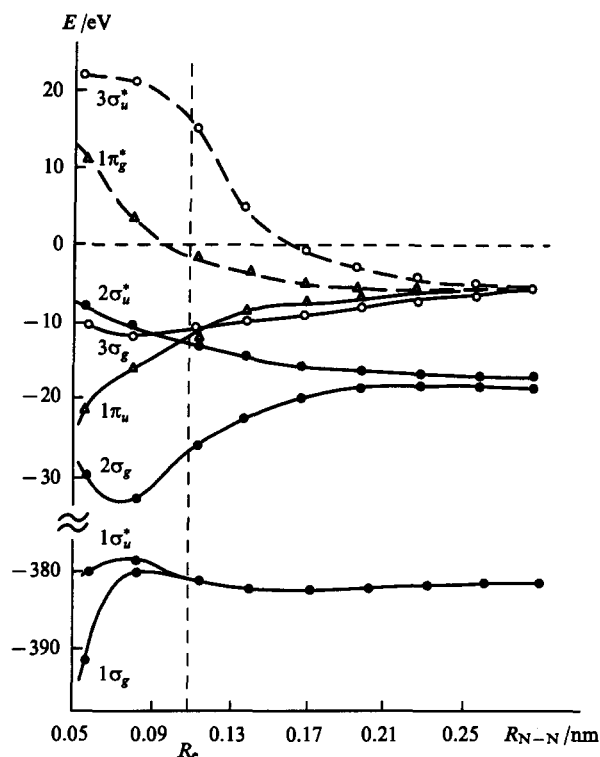


Figure 22. The SCF X α -DV orbital energies of N₂ as functions of the bond length R_{N-N} (R_e is the equilibrium distance).^{51, 56}

As nitrogen atoms are brought together to the equilibrium distance, not only the orbital energies, but also the order of MO as regards their energies change. This results in the formation of the $1\sigma_g$ and $1\sigma_u^*$ CMOs and $2\sigma_g$ and $2\sigma_u^*$ IVMOs, which, to a substantial degree, are contributed by the N 1s and N 2s AOs respectively. An increase in the energy of the doubly-degenerate $1\pi_u$ VMO made up of the $2p_x$ and $2p_y$ AOs is greater in magnitude than that of the $3\pi_g$ VMO that is primarily composed of the $2p_z$ AO. It points to a greater contribution of the $1\pi_u$ VMO to the covalent component of the N–N bond compared with that of the $3\sigma_g$ VMO. Weak dependence of the energies of the $2\sigma_u^*$ and $3\sigma_g$ MOs on the interatomic distance ranging from R_e to $R = 0.35$ nm indicates insignificant values of the corresponding orbital force f_i and thus essentially non-bonding character of the N 1s AOs.

In a certain approximation, the contribution of the N 1s electrons to the chemical bonding in N₂ can be neglected since the energies of the $1\sigma_g$ and $1\sigma_u^*$ CMOs hardly depend on the interatomic distance within the same interval. As the atoms continue to close with each other, the energy of the $1\pi_u$ VMO increases and that of the $3\sigma_g$ VMO decreases. Such behaviour could be attributed to an increase in the overlap integral of $2p_x$ and $2p_y$ AOs and a decrease in that of $2p_z$ AOs of neighbouring atoms at small R . At $R \leq R_e$, the energies of the $1\sigma_g$ and $1\sigma_u^*$ CMOs behave like those of the $2\sigma_g$ and $2\sigma_u^*$ IVMOs at $R > R_e$. The energies of the antibonding $1\sigma_u^*$ and $2\sigma_u^*$ MOs depend on the interatomic distance to a lesser extent than the energies of the corresponding bonding $1\sigma_g$ and $2\sigma_g$ MOs.

Changes in orbital energies of N₂ with decreasing bond length can be easily followed in a simple scheme (Fig. 23).^{51, 56} This scheme may be used for consideration of any homonuclear diatomic molecule formed from p -block elements $\{ns^2np^m\}$. An example of a molecule where MOs are formed by individual AOs (the $1\sigma_g$ and $1\sigma_u^*$ CMOs, $2\sigma_g$ and $2\sigma_u^*$ IVMOs, and $3\sigma_g$, $1\pi_u$, $1\pi_g^*$ and $3\sigma_u^*$ VMOs are represented) is shown in Fig. 23 a. The value of the splitting $\Delta'_i > \Delta_i$ ($i = 1, 2, 3$), and $\Delta_+ = \Delta_i + \Delta'_i$ depends on the bond length. Totally occupied CMOs destabilize the bond. Since the difference $\Delta_- = |\Delta'_i - \Delta_i|$ is not too great, decrease of the bond

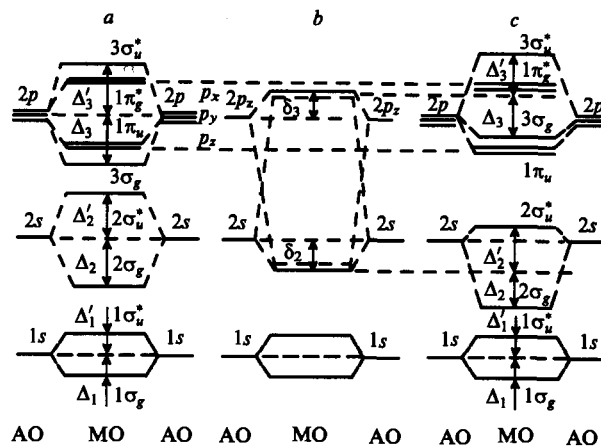


Figure 23. Scheme of formation of OVMOs, IVMOs, and CMOs in a nitrogen molecule: (a) — overlap of 2s and $2p_z$ AOs is neglected; (b) — the 's-p' interaction; (c) — with 2s-2p overlap taken into account.^{51, 56}

length causes comparable changes in energies of the bonding and antibonding MOs. It is observed for $1\pi_u$ and $1\pi_g^*$ VMOs (Fig. 22). Unlike the π -type MOs, the σ -type MOs are formed by the 2s AOs as well as the $2p_z$ AOs. At $R_e = 0.109$ nm, the 2σ and $2\sigma_u^*$ IVMOs and $3\sigma_g$ VMO consist of the 2s and $2p_z$ AOs in 84 : 16, 69 : 31, and 84 : 16 ratios respectively. In Fig. 23 b, the formation of the σ -type MO by the $2p_z$ and 2s AOs is schematically shown. The magnitude of this 's-p' interaction also depends on the bond length. Bonding and antibonding MOs shift in opposite directions to the same extent if the 's-p' interaction affects them equally (Fig. 23 b). In reality, this interaction does not affect each type of MO equally, thus it gives rise to an even more asymmetrical shift of the MO energies from their initial values. With regard to this, with decrease in the bond length in the N₂ molecule, the 'centre of mass' of the σ -type VMOs shifts to a greater extent than that of the IVMOs, i.e., formally, $\delta_3 > \delta_2$ (see Figs 22 and 23). Thus the order of MOs may change, as is observed in the $1\pi_u$ – $3\sigma_g$ pair of VMOs. Also, the overlap between the $2p_z$ AOs decreases at shorter R compared with that of the $2p_x$ and $2p_y$ AOs, and it affects the energies of the $1\pi_u$ and $3\sigma_g$ VMOs.

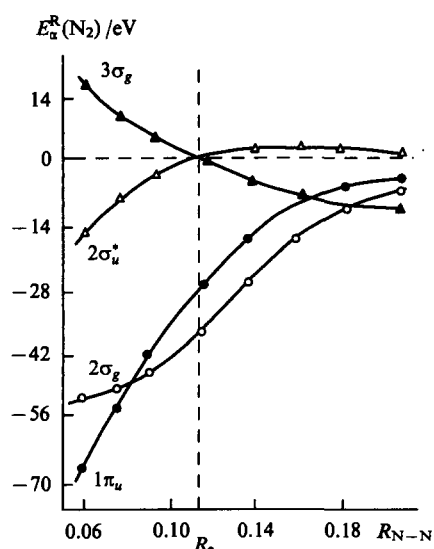
Despite the formalism of the separation of the total interaction between the electrons of neighbouring atoms, this simple approach, not taking into account atomic s-p hybridisation, furnishes an explanation of the observed changes in the orbital energies with decrease of the N–N bond length and inversion of the $3\sigma_g$ and $1\pi_u$ MOs. Also, it explains the non-bonding character of the $2\sigma_u^*$ and $3\sigma_g$ MOs and the positive contribution of the $2\sigma_g$ and $2\sigma_u^*$ IVMOs to the bond energy in N₂. Estimation of contributions of individual MOs to the chemical bonding in N₂ within the CNDO/2 approach has been based on analysis of the resonance energy E_{AB}^R (see Eqn 10) that represents the degree of covalence of the bond A–B (Fig. 24).^{51, 52, 56} The contributions of electrons of the $1\sigma_g$ and $1\sigma_u^*$ CMOs to the bond energy were not estimated.

We should mention that the results obtained do not conform to the conventional viewpoint on the character of the chemical bond in N₂.^{21, 22} To a certain approximation, as before, this bond may be treated as a triple bond, which is not attributed to electrons of the $3\sigma_g$ and $1\pi_u$ OVMOs,^{21, 22} but to electrons of the $1\pi_u$ OVMO and $2\pi_g$ IVMO. The contribution to the N≡N bonding of electrons of the $2\sigma_g$ IVMO, which primarily consists of N 2s AOs, is comparable with that of electrons of the twofold-degenerate $1\pi_u$ OVMO.^{51, 56}

The F₂ molecule, in which both the antibonding $1\pi_g^*$ and bonding $1\pi_u$ OVMOs are totally-occupied is yet another example of the contribution of the inner valence electrons to the chemical bonding. According to the traditional model of the formation of a

Table 3. Energies of MOs (eV) and their content (%) for different bond lengths R_{F-F} (nm) in F_2 calculated at the CNDO/2 level.⁷³

Molecular orbital	$R_1 = 0.05$				$R_e = 0.1417$				$R_2 = 0.20$			
	E_1	2s AO	2p _z AO	2p _x (2p _y) AO	E_e	2s AO	2p _z AO	2p _x (2p _y) AO	E_2	2s AO	2p _z AO	2p _x (2p _y) AO
3σ _g OVMO	22.83	79	21	—	2.05	5	95	—	−5.91	—	100	—
1π _g OVMO	−1.00	—	—	100	−22.09	—	—	100	−23.69	—	—	100
3σ _g OVMO	−16.13	21	79	—	−22.73	2	98	—	−16.20	—	100	—
1π _u OVMO	−46.86	—	—	100	−25.77	—	—	100	−24.17	—	—	100
2σ _u IVMO	−40.60	39	61	—	−41.99	5	95	—	−44.41	100	—	—
2σ _g IVMO	−78.51	90	10	—	−49.74	98	2	—	−45.89	100	—	—

**Figure 24.** Dependence of E'_α quantities, which characterise the MO contribution to the covalent bonding, on the bond length R_{N-N} for N_2 .^{51,56}

chemical bond,^{21,22} the contributions of electrons of these OVMOs and of electrons of the bonding $2\pi_g$ and antibonding $2\pi_u^*$ IVMOs are assumed to mutually neutralise. However, this assumption is not valid since the dependence of the MO energies in F_2 on the bond length R_{F-F} (see Ref. 73) points to different orbital forces f_i for the $2\sigma_g$ and $2\sigma_u^*$ IVMOs.

The estimation of the contributions of the electrons of various MOs to the chemical bonding in F_2 within the approach of separation of total energy demonstrates that, at an equilibrium distance R_e , the influence of electrons of the $1\pi_u$ and $1\pi_g^*$ OVMOs compensate each other, and the contribution of electrons of the $2\sigma_g$ IVMO is somewhat greater than that of electrons of the $2\sigma_u^*$ IVMO.⁷³ As a result, the covalent component of the $F-F$ bond is mainly associated with the electrons of the $3\sigma_g$ OVMO and, partly, $2\sigma_g$ IVMO. The latter accounts for 44% of the total covalent component of the bond energy. Thus, the substantial contribution of the IVMOs to the chemical bonding in F_2 is attributed to mixing of fully-occupied and valence AOs (Table 3).

The quantum-chemical estimation of bonding (antibonding) character of MOs for F_2 was also accomplished with the aid of the orbital force f_α approach. The calculation utilised the SCF X α -SW method with respect to the orbital relaxation within the framework of the transition state principle.⁷³ The X-ray photoelectron spectrum of the weakly-bound electrons of F_2 has been used for the data interpretation (see Fig. 7).²³ Unlike the X α -calculation, *ab initio*¹¹³ and semiempirical CNDO/2⁷³ calculations give the wrong order of the MO energies within the Koopmans's approximation (Table 4): the $3\sigma_g$ OVMO is between two π -type MOs, which does not agree with the order determined experimentally (see Fig. 7). The results obtained at these levels of theory are less precise than those obtained by X α -methods of calculation. The

Table 4. Vertical ionisation potentials for valence electrons of F_2 at the equilibrium bond length $R_e = 0.1417$ nm.

Calculation method	IP /eV					Ref.
	1π _g [*] OVMO	1π _u OVMO	3σ _g OVMO	2σ _u [*] IVMO	2σ _g IVMO	
Experiment	15.9	18.8	21.1	37.5	41.8	23
<i>Ab initio</i>	18.0	21.9	20.3	40.7	47.8	113
X α -DBM	16.0	18.6	20.8	33.7	39.3	32
CNDO/2	22.1	25.8	22.7	42.0	49.7	73
X α -SW	16.8	19.5	20.7	34.7	39.5	73

X α -SW modification is preferable for the interpretation of the binding energies of electrons of IVMOs.

The values of the derivatives E'_b (of the orbital forces f_i) at the equilibrium interatomic distance $R_e = 0.1417$ nm in the F_2 molecule show that the electrons of the $2\sigma_g$ IVMO make the largest contribution to the bonding in the system. The $2\sigma_u^*$ IVMO destabilises the $F-F$ bond, but does not entirely compensate the stabilisation from the $2\sigma_g$ IVMO (Table 5).

Table 5. Orbital forces E'_b for valence orbitals of F_2 at the equilibrium distance $R_e = 0.1417$ nm.¹⁷

Molecular orbital	$E'_b / 10^{-8}$ N per electron,		
	<i>ab initio</i> ^a	CNDO/2	X α -SW
1π _g [*] OVMO	−0.93	−0.89	−0.71
1π _u OVMO	0.98	0.89	1.79
3σ _g OVMO	1.69	1.08	1.43
2σ _u [*] IVMO	−1.24	−0.96	−1.78
2σ _g IVMO	2.42	2.05	2.85

^a Calculated from cited in Ref. 113 MO energies at two distances R_{F-F} equal to 0.1336 and 0.1417 nm.

In the X-ray photoelectron spectrum of F_2 , the peak corresponding to the $2\sigma_g$ electrons is broader than that corresponding to the $2\sigma_u^*$ electrons (their half-widths are 2.7 and 1.6 eV respectively).²³ Several final states of the system after photoemission could account for this distinction. Theoretical calculation in terms of the configuration interaction can corroborate this assumption. A dependence of the gradient of the ionisation potential of these orbitals on the bond length R_{F-F} could be another reason; this is in full agreement with results of the X α -SW calculation. Actually, the ratio of $2\sigma_u^*$ and $2\sigma_g$ peaks' half-widths is 0.59, while the ratio of the absolute values of the orbital forces f_α is 0.62 (Table 5).

Despite the different profiles assigned to the different contributions of electrons of the $2\sigma_u^*$ and $2\sigma_g$ IVMOs to the chemical bonding in F_2 , the integral intensities of these peaks are almost equal,²³ which points to their essentially identical photoionisation cross-sections, and thus to equal 2s character of these IVMOs. The results of the X α -SW calculation⁷³ are also consistent with this

Table 6. Energies E_b and distribution of electronic charge Q (%) for valence orbitals of F_2 at the equilibrium distance $R_e = 0.1417$ nm for ground and transition states.⁷³

Molecular orbital	E_b /eV	Charge Q in areas			
		atomic		interatomic	outer
		F 2s	F 2p		
Ground state					
$1\pi_g^*$ -OVMO	10.50	0	79.2	15.0	5.8
$1\pi_u$ -OVMO	13.50	0	70.7	23.1	6.2
$3\sigma_g$ -OVMO	14.56	2.2	77.3	11.7	8.8
$2\sigma_u^*$ -IVMO	28.31	81.8	2.0	11.1	5.1
$2\sigma_g$ -IVMO	33.18	78.3	2.0	17.1	2.6
Transition state					
$1\pi_g^*$ -OVMO	16.80	0	80.8	14.4	4.8
$1\pi_u$ -OVMO	19.50	0	72.8	22.0	5.2
$3\sigma_g$ -OVMO	20.70	2.4	78.5	11.3	7.8
$2\sigma_u^*$ -IVMO	34.70	82.7	1.9	10.8	4.6
$2\sigma_g$ -IVMO	39.50	79.0	2.0	16.7	2.3

premise (Table 6). Different contributions of the $2\sigma_u^*$ and $2\sigma_g$ IVMOs would imply a significant dependence of the photoionisation cross-sections on the energy of the levels in question, a dependence that is unlikely due to the close binding energies of electrons of the $2\sigma_u^*$ and $2\sigma_g$ IVMOs (see Table 5). It follows from Table 6 that the IVMOs are built up mainly of the F 2s AOs, the contributions of which are nearly the same and change little during the relaxation of the ionised system. An essential contribution of the F 2s AO to the $2\sigma_u^*$ IVMO accounts for the significant stabilisation of this MO, unlike that in N_2 molecule, which is characterised by a greater percentage of the N_2 2p AO.^{51,56} The energy gap between the IVMOs in F_2 (4.3 eV, Table 4) is much smaller than the corresponding value (18.7 eV) in N_2 .^{51,56} Specific characteristics of the IVMO in F_2 also account for a clearly bonding character of the $3\sigma_g$ OVMO (Table 5), as soon as this OVMO consists mainly of the F 2p_σ AOs (see Table 6).

Analogous results have also been obtained for other diatomic Group IV–VIIA second and third Period molecules and clusters.^{17, 52, 71, 72, 88}

The same reasoning can be applied to the dependence of the orbital energies of the uranyl fragment UO_2^{2+} on the bond length R_{U-O} obtained within the framework of the SCF X α -SW approach (Fig. 25).^{3, 106} The dependence obtained is in a good qualitative agreement with the corresponding data for N_2 . As atoms are brought together, the energies of the antibonding $8\sigma_u^*$ (UO_2^{2+}) and $2\sigma_u^*$ (N_2) IVMOs change to a lesser extent than the energies of the corresponding bonding $7\sigma_u$ and $2\sigma_g$ IVMOs, thus a considerable contribution of the $8\sigma_u^*$ and $7\sigma_g$ electrons to the bonding in UO_2^{2+} is suggested. As has already been mentioned for N_2 , this effect arises due to the mixing of the valence and doubly-occupied low-energy AOs of adjacent atoms leading to the formation of IVMOs. Apparently, this mixing also accounts for the inversion of the $7\pi_u$, $9\sigma_u$, $4\sigma_g$, and $12\sigma_g$ OVMOs of the uranyl fragment caused by a change in the U–O bond length (Fig. 25). The MO contributions to the chemical bonding were estimated from the values of orbital forces f_i calculated from the E_i vs. R_{U-O} dependences.¹¹³ It has been found that, at $R_{U-O} = 0.173$ nm, electrons on IVMOs account for 29% of the total electron contribution in the uranyl cluster.

The calculation of the electronic structure of the uranyl cluster by the SCF X α -DV method yields similar results (Figs 26 and 27).⁷⁷ In Fig. 27, vacant MOs are shown as dashed lines, and occupied MOs as solid lines. Presented in the Figure are the atom content, energies (to the left), and the E_α^R values (to the right), which characterise the contribution of IVMOs to the

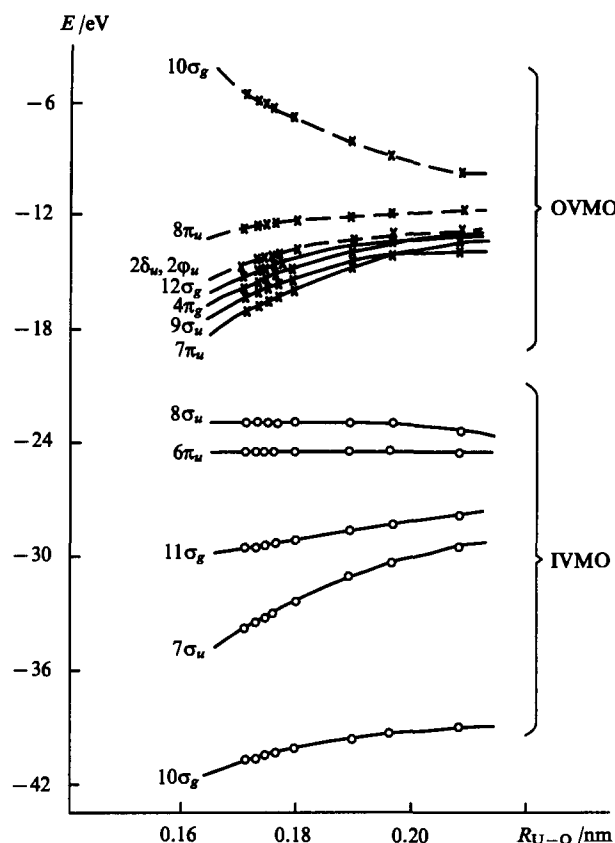


Figure 25. Dependence of the MO energies for the cluster UO_2^{2+} (symmetry group $D_{\infty h}$) on the bond length R_{U-O} calculated in the SCF X α -SW approach.¹⁰⁶

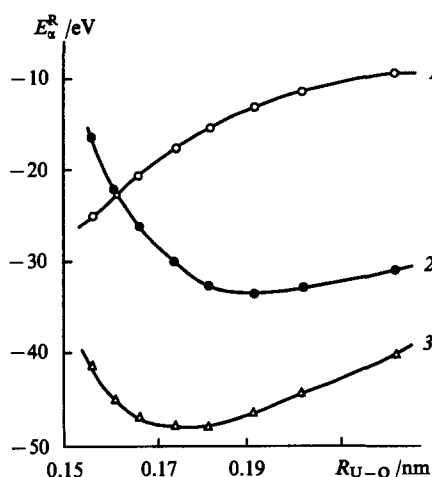


Figure 26. Dependence of the energy contribution of electrons of the IVMOs (1), OVMOs (2), and of the total electron contribution (3) to the covalent bonding E_α^R on the bond length R_{U-O} for UO_2^{2+} .⁷⁷

covalent bonding of the cluster UO_2^{2+} . At $R_{U-O} = 0.173$ nm, the electrons of IVMOs account for 37% of the total electronic contribution in UO_2^{2+} . Similar calculations have also been performed for the cluster $UO_2Cl_2^{2-}$ of D_{4h} symmetry.¹⁷ The contributions of the electrons of OVMOs and IVMOs to the chemical bonding in UO_2^{2+} somewhat depend on the bond lengths R_{U-O} (Fig. 26).

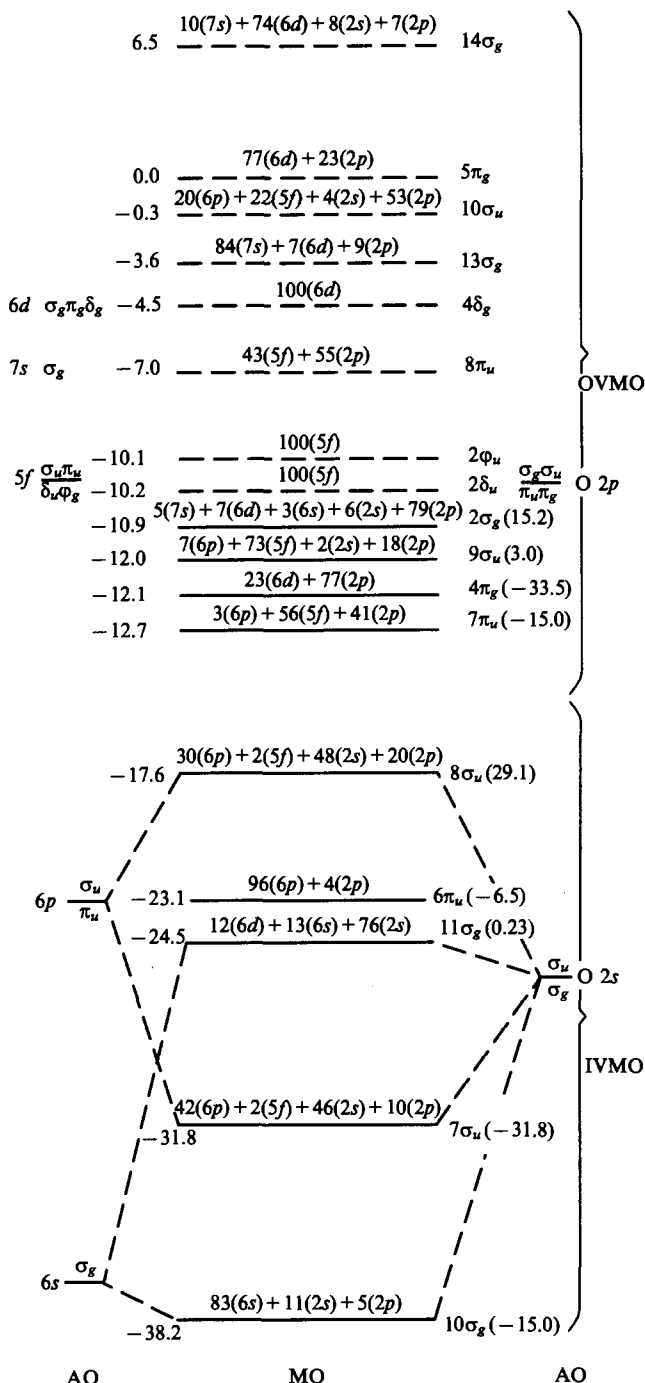


Figure 27. The MO diagram for UO_2^{2+} (symmetry group $D_{\infty h}$) at $R_{\text{U-O}} = 0.173$ nm (the SCF X α -DV method). Energies of MOs (in eV), their content (%), and the values of E_{α}^R (in eV) characterising the MO contribution to the covalent bonding are displayed in parentheses.⁷⁷

2. Crystal framework

From the data presented above we may assume that the inner valence electrons contribute to the chemical bonding not only in molecules, but also in crystals. In essence, this applies to covalent crystals. To this end, quantum-chemical calculations of the band structure of black phosphorus have been made.⁷⁵ The choice of the subject of study is concerned with the monoatomic character of the crystal lattice, which excludes the ionic component of the bonding, the availability of reliable crystallographic data¹¹⁴ and of X-ray photoelectron spectra obtained with a synchrotron radiation source.¹¹⁵ The calculations of the band structure of black phosphorus have been carried out by the crystal orbital

method within the framework of the extended Hückel method (EHM) by a program described in a previous study.¹¹⁶

The crystal lattice of black phosphorus is built up of crimped layers.¹¹⁴ The unit-cell dimensions a , b , and c are 0.33136, 1.0478, and 0.43763 nm respectively. Each phosphorus atom has three closest neighbours within the layer at a distance of 0.2244, 0.2224, and 0.2224 nm. The layers are separated from each other so that the minimum distance between two phosphorus atoms belonging to adjacent layers is 0.3592 nm. At this distance, the overlap integral between the two atomic Slater 3s and 3p orbitals, the exponential factors of which have been defined according to Clementi¹¹⁷ is close to zero. Therefore, the basic aspects of the band structure of black phosphorus can be described satisfactorily within a two-dimensional representation with four atoms per unit cell.

The unit cell of the layer consists of two pairs of phosphorus atoms. The bond axes make an angle of 44.17° with the crystallographic a axis.¹¹⁴ The distance $R_{\text{P-P}}$ within pairs is 0.2224 nm, the distance between the axes of pairs along the c axis is 0.2130 nm. Translational constants along two perpendicular directions are equal to the values of constants a and c , respectively.

The two-dimensional Brillouin zone for the layer under consideration is rectangular, its centre is designated as Γ ; points J and K refer to the middle of the longest side and the vertex of the Brillouin zone, respectively. Direction $\Gamma \rightarrow J$ is denoted as Σ_1 , $J \rightarrow K$ as Σ_2 , and $K \rightarrow \Gamma$ as Σ_3 .

The energies of the crystal valence orbitals $E_i(k)$ are determined along these directions and in points Γ , J , and K from the secular equation:

$$\sum_{\nu} [F_{\mu\nu}(k) - S_{\mu\nu}(k)E_i(k)]c_{i\nu}(k) = 0, \quad (35)$$

where $F_{\mu\nu}(k)$ and $S_{\mu\nu}(k)$ are matrix elements of the one-electron operator and the overlap integral between the Bloch basis functions, respectively.

For the P 3s and 3p AOs, the orbital ionisation potentials have been taken as recommended by Charkin.¹¹⁸ Eqn (35) as applied to the band structure calculations was examined first by Messmer¹¹⁹ and then was successfully employed by Nishida¹²⁰ and Hoffmann et al.¹²¹ The crucial point of this approach is a proper choice of parameters.¹²² As shown below, data on the orbital exponent factors¹¹⁷ and ionisation potentials¹¹⁸ lead to a satisfactory description of the valence band structure of black phosphorus.

With a basis set incorporating the P s and p orbitals for four atoms in a unit cell (each atom has five valence electrons), the LCAO equation (35) yields 16 crystal orbitals; the lowest 10 of them are doubly occupied. Dispersion curves calculated for 10 occupied and two vacant crystal orbitals are shown in Fig. 28. The energy zero corresponds to the top of the valence band reached

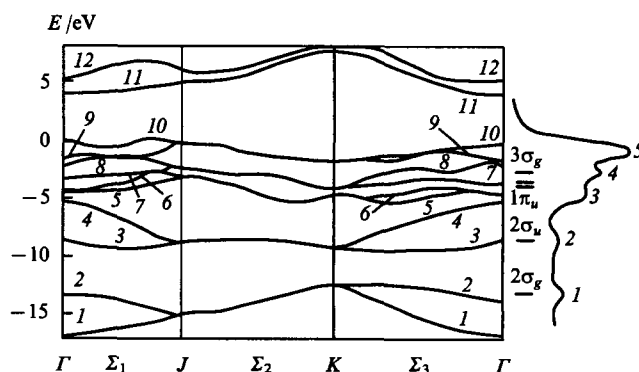


Figure 28. The dispersion curves of the energy bands in black phosphorus calculated by the extended Hückel method,⁷⁵ and from its photoelectron spectrum.¹¹⁵ Horizontal lines represent levels of a cluster P_2 .

near the point J along the direction Σ_1 . According to the calculation, black phosphorus possesses the semiconducting properties.

The two lowest valence crystal orbitals are genetically linked with the $2\sigma_g$ IVMO of the diatomic cluster P_2 , the next two, with the $2\sigma_u$ IVMO. Three pairs of the upper filled crystal orbitals originate from the $1\pi_u$ and $3\sigma_g$ OVMOs. The corresponding crystal orbitals are degenerate along the direction Σ_2 . The photoelectron spectrum of a single crystal of black phosphorus obtained at a photon energy of 110 eV¹¹⁵ is shown on the right side of Fig. 28.¹¹⁵ Five distinct peaks sequentially spaced by 2.0, 1.9, 4.2, and 4.6 eV appear in the spectrum. All features of the photoelectron spectrum including the energies and relative heights of the peaks are represented satisfactorily by the calculated dispersion curves. The positions of MOs of the P_2 cluster at $R_{P-P} = 0.2224$ nm are displayed also in Fig. 28. As is seen, the splitting of the $2\sigma_g$ and $2\sigma_u$ IVMOs composed of the P $3s$ AOs with addition of P $3p_z$ AOs describes well the relative positions of peaks 2 and 1, while the $1\pi_u$ and $3\sigma_g$ MOs fall near the centroid of peaks 3–5. Thus, the qualitative features of the chemical bonding in black phosphorus crystals can be understood even in terms of diatomic interactions, i.e. in a close-order approximation, while the details of the electronic structure are determined by the band character of the wave functions.

In diatomic molecules, the orbital vibronic constants determined from spectral data can serve as a quantitative measure of the contributions of electrons to the chemical bonding. It has been shown that orbital vibronic constants correlate intimately with the orbital forces f_i [see Eqn (24)] defined as derivatives of the orbital energies $E_i(R)$ versus the interatomic distance R at the equilibrium point R_e , where i is an orbital index. Provided the orbital energies are obtained from *ab initio* calculations, the plot of orbital vibronic constant versus f_i yields a line through the coordinate origin.⁵³ To verify the legitimacy of this approach within the adopted semi-empirical Hoffmann method, the dependences $E_i(R)$ have been calculated⁷⁵ and the orbital forces f_i determined for N_2 (an analogue of P_2),⁷⁵ so far as the orbital vibronic constants for N_2 are available.^{53, 65}

The correlation plot of the orbital vibronic constants of N_2 versus the orbital forces f_i calculated according to Eqn (24) at the experimental equilibrium distance R_e (see Refs 17, 75) is presented in Fig. 29. It may be concluded that the extended Hückel method is quite suitable for estimating the orbital vibronic constants. It has also been found that orbital vibronic constants correlate with the contributions $n(j, NN)$ of individual MOs to the total bond order.⁵³ Therefore, Mulliken orbital bond populations are also applicable to the calculation of the orbital vibronic constants. The

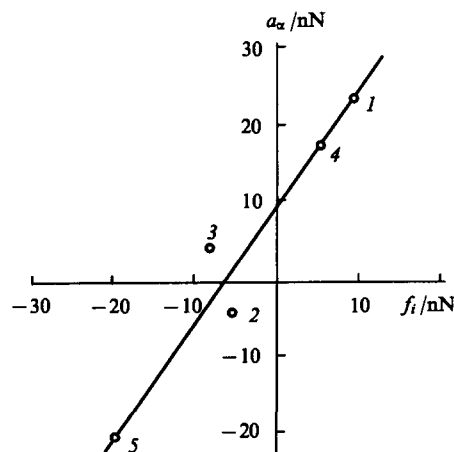


Figure 29. Dependence of the orbital vibronic constants a_α on the orbital forces f_i for N_2 (the extended Hückel calculation): (1) $2\sigma_g$; (2) $2\sigma_u$; (3) $2\sigma_g$; (4) $1\pi_u$; (5) $1\pi_g$.⁷⁵

$n(j, NN) - f_i$ correlation for N_2 , a correlation which is also confirmed by calculation for P_2 ,⁷⁵ is evident from comparison of Fig. 29 and data from Ref. 53.

We should mention that the $2\sigma_g$ IVMO plays a particular role in the chemical bonding in P_2 as well as in N_2 . Thus, orbital forces according to the EHM can be regarded as quantum-chemical indexes in the qualitative analysis of electronic contributions to chemical bonding.

As has been mentioned,^{17, 75} it seems natural to extend this approach to band structure calculations for solids. To this end, a solution of the secular equation (35) is differentiated with respect to R . For the sake of convenience, two additional calculations should be carried out at $R = R_e - \Delta R$ and $R = R_e + \Delta R$, where ΔR is a small variation of the interatomic distance. The value of 0.001 nm for variations of all distances in a unit cell has been adopted in calculations of the band structure of black phosphorus. The dispersion curves obtained have been numerically differentiated with respect to R , and the orbital forces have been determined at various points of the two-dimensional Brillouin zone for the dispersion curves presented in Fig. 28. The results obtained are listed in Table 7; the average directions of Σ_1 , Σ_2 , and Σ_3 in the Brillouin zone are referred to these points. As follows from Table 7, the inner valence crystal orbitals 1 and 2 display slightly bonding character (the positive sign of the corresponding orbital forces). The higher crystal orbitals exhibit either a weakly-bonding (non-bonding) or antibonding (the negative sign of the orbital forces) character. The lower vacant crystal orbitals 11 and 12 possess highly antibonding character, as expected. However, the values of the orbital forces f_i depend on the coordinates of the point in the Brillouin zone. For example, at the point K , all crystal orbitals are less bonding, the inner valence crystal orbitals included. The angular dependence of the indexes of interatomic bonding f_i of crystal orbitals, e.g. 1 and 2, can be used in studies of the anisotropy of properties of black phosphorus and other compounds.

Table 7. Orbital forces ($f_i / 10^{-8}$ N) for the energy bands of the black phosphorus.⁷⁵

Dispersion curve number	Points of the two-dimensional Brillouin zone					
	Γ	Σ_1	J	Σ_2	K	Σ_3
12	-2.9	-3.9	-8.4	-8.3	-8.0	-7.2
11	-4.5	-6.0	-6.4	-7.3	-6.4	-4.5
10	-2.4	-2.6	-3.2	-1.7	-1.0	-2.0
9	-2.1	-1.1	-3.1	-1.7	-0.9	-1.1
8	-0.1	-1.7	-1.9	-0.6	-0.2	-1.4
7	-1.2	-1.5	-1.6	-0.6	-0.2	0.3
6	-2.1	-1.3	0.4	0.1	0.5	-0.3
5	0.7	0.6	0.4	0.1	0.5	0.6
4	0.9	0.0	0.5	-0.3	-0.1	-1.0
3	-2.1	-0.3	0.5	-0.3	-0.1	-0.9
2	2.2	1.8	1.8	1.1	-0.3	1.1
1	2.5	2.3	1.8	1.1	-0.2	1.7

The results of the study imply a prevailing contribution of the electrons of inner valence bands of atomic crystal to the covalent bonding. When considering the electronic structure of solids within the framework of the band theory, the IVMOs of the diatomic cluster, which is a building block of the crystal lattice, possess a bonding character as well.

Thus the contribution of the electrons of the inner valence MOs to the chemical bonding cannot be neglected. In certain cases, it is comparable with that of the electrons of the valence MOs.

VI. Conclusion

Widespread use of XPS in the studies of the electronic structure of molecules and solids consisting of diverse elements of the Periodic Table have provided unique results on the interaction between the electrons of the closed low-energy subshells of neighbouring atoms. In many cases, this interaction is strong enough so that one cannot neglect it in the analysis of the electronic structure of compounds. The X-ray photoelectron spectra of such compounds usually reveal a fine structure in the region of weakly-bound electrons (~ 15 – 50 eV). The parameters of this fine structure, attributed to the inner valence electrons, reflect structural characteristics of the compounds. Experimental XPS data on the formation of IVMOs, the interrelation of the fine structure of X-ray photoelectron spectra with the structure of compounds, and the data on the participation of the inner valence electrons in chemical bonding are in good agreement with results of theoretical calculations. Qualitative interpretation of the structure of X-ray photoelectron spectra in the region of the inner valence electrons by means of group theory allows a wide range of researchers to apply XPS in various structural studies, for instance on radiation-induced damage and defects in solids.

We should note that the role of IVMOs in the formation of compounds and in the determination of their physico-chemical and structural features, has not been firmly established yet. In particular, this topic has been little covered for lanthanide and actinide series compounds. However, currently, there are several examples of the practical application of the concept of effective (experimentally observed) formation of IVMO in the explanation of experimental data. These are an inversion of the $3\sigma_g$ and $1\pi_u$ IVMOs and the exceptionally high bond strength of N_2 ;^{51, 56} the relatively broad valence band (25.2 eV) in graphite and diamond, and energies of the C—C bonds within graphite layers;^{25, 88} the appearance of a fine structure in the ~ 15 – 50 eV range of the X-ray photoelectron spectra of lanthanide^{4, 5} and actinide series^{2, 3, 102, 103} compounds; the relation of the characteristics of fine structure in X-ray photoelectron spectra of compounds containing actinide series^{18, 109, 123} and other¹⁷ elements with the structure of the local environment and the bond lengths to the closest ligand atoms; the appearance of a fine structure in the emission spectra of lanthanide¹⁹ and uranium¹²⁴ compounds and in the electron conversion spectra of uranium compounds^{125, 126} if electrons with bonding energy within the ~ 15 – 50 eV range contribute to these spectra.

One cannot rule out [the possibility] that the formation of IVMOs in actinide series compounds explains the formation of stable groups AnO_2^{2+} . We should also note that a new method has been proposed to determine U—O distances, which can help in the identification of the products of reactions of uranium compounds with solid surfaces.^{109, 123, 127, 128}

Thus, taking into account the results considered hitherto, the following conclusions, which answer the questions listed in the 'Introduction', can be derived:

1. Under certain necessary conditions, IVMOs can form in compounds containing virtually any element of the Periodic Table.
2. The fine structure in X-ray photoelectron spectra associated with the inner valence electrons allows one to assess the contribution of electrons of the occupied AOs to the chemical bonding, the local environment of atoms under consideration, and the bond lengths in compounds.
3. In certain instances, the overall contribution of the inner valence electrons to the bond energy is comparable to that of the valence electrons. This phenomenon is novel and important for chemistry.

References

1. K. Siegbahn, C. Nordling, G. Johansson, J. Hedman, P. F. Heden, K. Hamrin, U. Gelius, T. Bergmark, L. O. Werme, R. Manne, Y. Baer *ESCA Applied to Free Molecules* (Amsterdam: North-Holland, 1969)
2. Yu. A. Teterin, V. M. Kulakov, A. S. Baev, A. G. Zelenkov, I. V. Mel'nikov, N. B. Nevzorov, V. A. Strel'tsov, in *Tez. Dokl. Soveshchaniya "Rentgenovskie i Rentgenoelektronnye Spektry i Elektronaya Struktura Metallov, Splavov i Khimicheskikh Soedinenii"* (Abstracts of Reports of the Meeting 'X-Ray and X-Ray Electron Spectra and Electronic Structure of Metals, Alloys, and Chemical Compounds' (Izhevsk: Physicotechnical Institute, 1979) p. 25
3. Yu. A. Teterin, A. S. Baev, R. V. Vedrinskii, A. L. Gubskii, A. G. Zelenkov, A. P. Kovtun, V. M. Kulakov, V. P. Sachenko *Dokl. Akad. Nauk SSSR* **256** 381 (1981)
4. Yu. A. Teterin, A. S. Baev, V. M. Kulakov, A. L. Gubskii, A. P. Kovtun, S. B. Pirkes, G. N. Makushova *Dokl. Akad. Nauk SSSR* **259** 416 (1981)
5. Yu. A. Teterin, A. S. Baev, V. M. Kulakov, N. B. Nevzorov, S. B. Pirkes, T. A. Krasovskaya, in *Fizicheskie i Matematicheskie Metody v Koordinatsionnoi Khimii* (Physical and Mathematical Methods in Coordination Chemistry) (Kishinev: Shtiintsa, 1980) p. 75
6. Yu. A. Teterin, V. M. Kulakov, A. S. Baev, N. B. Nevzorov, I. V. Melnikov, V. A. Strel'tsov, L. G. Mashirov, D. N. Suglobov, A. G. Zelenkov *Phys. Chem. Miner.* **7** 151 (1981)
7. V. I. Nefedov, V. I. Vovna *Elektronnaya Struktura Khimicheskikh Soedinenii* (Electronic Structure of Chemical Compounds) (Moscow: Nauka, 1987)
8. V. I. Nefedov, V. I. Vovna *Elektronnaya Struktura Organicheskikh i Elementoorganicheskikh Soedinenii* (Electronic Structure of Organic and Organoelement Compounds) (Moscow: Nauka, 1989)
9. D. V. Korol'kov *Elektronnoe Stroenie i Svoistva Soedinenii Neperekhodnykh Elementov* (Electronic Structure and Properties of Compounds of Non-transition Elements) (St-Petersburg: Khimiya, 1992)
10. V. M. Kulakov, Yu. A. Teterin *Priroda (Moscow)* (2) 78 (1978)
11. L. Ley, R. A. Pollak, S. P. Kowalczyk, R. McFeely, D. A. Shirley *Phys. Rev. B, Solid State, Ser. 3* **8** 641 (1973)
12. V. I. Nefedov *Zh. Strukt. Khim.* **15** 1093 (1974)
13. F. Jelinek, R. A. Pollak, M. W. Shafer *Matter. Res. Bull.* **9** 845 (1974)
14. B. W. Veal, D. J. Lam, W. T. Carnall, H. R. Hoekstra *Phys. Rev. B, Solid State, Ser. 3* **12** 5651 (1975)
15. E. P. Domashevskaya, V. I. Nefedov, in *Rentgenovskaya Fotoelektronnaya Spektroskopiya* (X-Ray Photoelectron Spectroscopy) (Kiev: Naukova Dumka, 1977) p. 86
16. H. Heid, R. Hemmel, C. F. Bruggen, C. Haas *J. Solid State Chem.* **33** 17 (1980)
17. Yu. A. Teterin, S. G. Gagarin *Vnutrennie Valentnye Molekulyarnye Orbitali i Vliyaniye ikh Elektronov na Kharakter Khimicheskoi Svyazi Soedinenii* (Inner Valence Molecular Orbitals and the Influence of Their Electrons on the Character of the Chemical Bonds in Compounds) (Moscow: TsNIIatominform, 1985)
18. Yu. A. Teterin, A. S. Baev *Rentgenovskaya Fotoelektronnaya Spektroskopiya Soedinenii Legkikh Aktinoidov* (X-Ray Photoelectron Spectroscopy of Light Actinide Compounds) (Moscow: TsNIIatominform, 1986)
19. Yu. A. Teterin, A. S. Baev *Rentgenovskaya Fotoelektronnaya Spektroskopiya Soedinenii Lantanoidov* (X-Ray Photoelectron Spectroscopy of Lanthanide Compounds) (Moscow: TsNIIatominform, 1987)
20. Yu. A. Teterin, in *Rentgenovskie Elektronnye Spektry i Khimicheskaya Svyaz'* (X-Ray Electron Spectra and the Chemical Bond) (Eds V. V. Gorchakov, V. I. Vovna, V. I. Nefedov) (Vladivostok: The Far East State University, 1986) p. 165
21. C. A. Coulson *Valence* (Oxford: Oxford University Press, 1961)
22. M. Orchin, H. H. Jaffé *The Importance of Antibonding Orbitals* (Geneva: Palo Alto, 1967)
23. P. Weightman, T. D. Thomas, D. R. Jennison *J. Chem. Phys.* **78** 1652 (1983)
24. W. R. Salaneck, R. W. Bigelow, H. J. Freund, E. W. Plummer *Phys. Rev. B, Condens. Matter.* **24** 2403 (1981)

25. A S Baev, A G Zelenkov, V M Kulakov, B V Odinov, V P Smilga, Yu A Teterin, Yu P Tumanov, O K Chugunov *Zh. Strukt. Khim.* **21** 29 (1980)
26. Yu A Teterin, A P Kovtun, S G Gagarin, N B Nevzorov, A S Baev, Yu P Dikov, in *Tez. dokl. XII Mendelevskii S'ezd po Obshchei i Prikladnoi Khimii* (Abstracts of Reports of the XII Mendeleev Congress on General and Applied Chemistry) (Moscow: Nauka, 1981) No 3, p. 131
27. A S Baev, V M Kulakov, Yu A Teterin, N G Gorshkov, L G Mashirov, D N Suglobov, in *Tez. dokl. XII Mendelevskii S'ezd po Obshchei i Prikladnoi Khimii* (Abstracts of Reports of the XII Mendeleev Congress on General and Applied Chemistry) (Moscow: Nauka, 1981) No 1, p. 154; *Radiokhimiya* **24** 576 (1982)
28. V A Terekhov, L N Marshakova, N P Sergushin, E M Smolyarenko, Yu A Teterin, E P Domachevskaya *Fiz. Tverd. Tela* **24** 283 (1982)
29. M Boring, J H Wood *J. Chem. Phys.* **63** 638 (1975)
30. P F Walch, D E Ellis *J. Chem. Phys.* **65** 2387 (1976)
31. V A Gubanov, A Rosen, D E Ellis *Solid State Commun.* **22** 219 (1977)
32. G L Gutsev, F F Levin *Zh. Strukt. Khim.* **20** 771 (1979)
33. T Sasaki, H Adachi *Int. J. Quantum Chem.* **18** 227 (1980)
34. W Haberditzl *Basteine der Materie und Chemische Binding* (Berlin: VEB Deutscher Verlag der Wissenschaften, 1972)
35. K B Yatsimirskii, V K Yatsimirskii *Khimicheskaya Svyaz'* (The Chemical Bond) (Kiev: Vishcha Shkola, 1975)
36. L A Blyumenfel'd, A K Kukushkina *Kurs Kvantovoi Khimii i Stroenie Molekul* (Textbook of Quantum Chemistry and Molecular Structure) (Moscow: Izd. Moskovsk. Gos. Univ., 1980)
37. Yu N Kukushkin, E I Maslov *Stroenie Atomov i Khimicheskaya Svyaz'* (The Structure of Atoms and the Chemical Bond) (Leningrad: Izd. Leningradsk. Gos. Univ., 1973)
38. J N Murrell, S F A Kettle, J M Tedder *Valence Theory* (New York: Wiley, 1965)
39. M J S Dewar, R C Dougherty *The PMO Theory of Organic Chemistry* (New York: Plenum, 1975)
40. V I Minkin, B Ya Simkin, R M Minyaev *Teoriya Stroeniya Molekul (Elektronnye Obolochki)* [The Molecular Structure Theory (Electron Shells)] (Moscow: Vysshaya Shkola, 1979)
41. K S Krasnov *Molekuly i Khimicheskaya Svyaz'* (Molecules and the Chemical Bond) (Moscow: Vysshaya Shkola, 1977)
42. G Henrici-Olive, S Olive *Coordination and Catalysis* (Wainheim: Verlag Chemie, 1977)
43. F A Cotton, G Wilkinson *Advanced Inorganic Chemistry* (New York: Interscience, 1966)
44. E Cartmell, G W A Fowles *Valence and Molecular Structure* (London: Butterworth, 1978)
45. T I Krasovitskaya *Elektronnye Struktury Atomov i Khimicheskaya Svyaz'* (The Electronic Structures of Atoms and the Chemical Bond) (Moscow: Prosveshchenie, 1980)
46. V I Kornev, M N Konyukhov *Stroenie Atoma i Priroda Khimicheskoi Svyazi* (The Structure of the Atom and the Nature of the Chemical Bond) (Izhevsk: Physicotechnical Institute, 1972)
47. M Kotani, K Ohno, K Kayama, in *Handbuch der Physik* Vol. 37/2 (Berlin: Springer, 1961) p. 173
48. R D Harcourt *Qualitative Valence-Bond Descriptions of Electron-Rich Molecules: Pauling '3-Electron Bonds' and 'Increased-Valence' Theory* (Berlin: Springer, 1982)
49. M S Gopinathan, C Ravimohan *Chem. Phys. Lett.* **85** 307 (1982)
50. K Hermann, P S Bagus, C R Brundle, D Menzel *Phys. Rev. B, Condens. Matter* **24** 7025 (1981)
51. Yu A Teterin, S G Gagarin, Yu P Dikov, G L Gutsev *Dokl. Akad. Nauk SSSR* **268** 921 (1983)
52. Yu A Teterin, A S Baev, S G Gagarin, A P Kovtun *Dokl. Akad. Nauk SSSR* **273** 156 (1983)
53. S G Gagarin, Yu A Teterin, Yu P Dikov *Zh. Fiz. Khim.* **57** 2624 (1983)
54. V A Gubanov, A Rosen, D E Ellis *J. Inorg. Nucl. Chem.* **41** 975 (1979)
55. G M Zhidomirov, A A Bagatur'yants, I A Abronin *Prikladnaya Kvantovaya Khimiya* (Applied Quantum Chemistry) (Moscow: Khimiya, 1979)
56. Yu A Teterin, S G Gagarin, Yu P Dikov, G L Gutsev, V V Nemoshkalenko *Teor. Eksp. Khim.* **19** 259 (1983)
57. S G Gagarin, I A Lygina, in *Kvantovaya Khimiya* (Quantum Chemistry) (Kishenev: Shtiintsa, 1975) p. 50
58. R F W Bader, W H Henneker, P E Cade *J. Chem. Phys.* **46** 3341 (1967)
59. A M Gul'maliev, I V Stankevich *Zh. Fiz. Khim.* **46** 2711 (1972)
60. K Ruedenberg *J. Chem. Phys.* **66** 375 (1977)
61. O Goscinski, in *Quantum Science. Methods and Structure* (Eds J-L Calais, O Goscinski, J Linderberg, Y Ohrn) (New York: Plenum, 1976) p. 427
62. S G Gagarin *Koord. Khim.* **6** 215 (1980)
63. I B Bersuker *Kinet. Katal.* **18** 1268 (1977)
64. S G Gagarin, Yu A Teterin *Zh. Strukt. Khim.* **25** (4) 125 (1984)
65. S G Gagarin, Yu A Teterin *Zh. Strukt. Khim.* **25** (6) 18 (1984)
66. P E Cade, K D Sales, A C Wahl *J. Chem. Phys.* **44** 1973 (1966)
67. R K Nesbet *J. Chem. Phys.* **40** 3619 (1964)
68. H Lefebvre-Brion, C M Moser, R K Nesbet *Chem. Phys.* **34** 1950 (1961)
69. P E Cade, W M Huo *J. Chem. Phys.* **47** 614 (1967)
70. S G Gagarin, Yu A Teterin *Zh. Fiz. Khim.* **58** 3015 (1984)
71. S G Gagarin, Yu A Teterin *Zh. Neorg. Khim.* **29** 1915 (1984)
72. Yu A Teterin, A D Sidorenko, S G Gagarin, in *Kvantovaya Khimiya Tverdogo Tela. Preprint UNTs AN SSSR* (Quantum Chemistry of Solids. Preprint of the Ural Scientific Centre of the Academy of Sciences of the USSR) (Sverdlovsk, 1984) p. 55
73. S G Gagarin, Yu A Teterin, in *Kvantovaya Khimiya Tverdogo Tela. Preprint UNTs AN SSSR* (Quantum Chemistry of Solids. Preprint of the Ural Scientific Centre of the Academy of Sciences of the USSR) (Sverdlovsk, 1984) p. 58; *Teor. Eksp. Khim.* **21** 211 (1985)
74. S G Gagarin, Yu A Teterin *Zh. Fiz. Khim.* **59** 920 (1985)
75. S G Gagarin, Yu A Teterin, in *Kvantovaya Khimiya Tverdogo Tela. Preprint UNTs AN SSSR* (Quantum Chemistry of Solids. Preprint of the Ural Scientific Centre of the Academy of Sciences of the USSR) (Sverdlovsk, 1984) p. 68; *Zh. Strukt. Khim.* **26** (4) 54 (1985)
76. Yu A Teterin, M V Ryzhkov, V A Gubanov, S G Gagarin, in *Kvantovaya Khimiya Tverdogo Tela. Preprint UNTs AN SSSR* (Quantum Chemistry of Solids. Preprint of the Ural Scientific Centre of the Academy of Sciences of the USSR) (Sverdlovsk, 1984) p. 62
77. Yu A Teterin, M V Ryzhkov, V A Gubanov, S G Gagarin, in *Voprosy Atomnoi Nauki i Tekhniki (Ser. Obshchaya i Yadernaya Fizika)* [Problems in Atomic Science and Engineering (General and Nuclear Physics Ser.)] (Moscow: TsNIIatominform, 1984) Vol. 4, No 29, p. 91; *Dokl. Akad. Nauk SSSR* **284** 915 (1985)
78. Yu A Teterin, Doctoral Thesis in Physicomathematical Sciences, Institute of Chemical Physics of the Academy of Sciences of the USSR, Moscow, 1989
79. M V Ryzhkov, V A Gubanov, Yu A Teterin, A S Baev *Phys. Rev. B, Condens. Matter.* **59** 1; 7 (1985)
80. M V Ryzhkov, V A Gubanov, Yu A Teterin, A S Baev *Zh. Neorg. Khim.* **30** 2475 (1985)
81. Yu A Teterin, A S Baev, S G Gagarin, V D Klimov *Radiokhimiya* **27** 3 (1985)
82. Yu A Teterin, A S Baev, S G Gagarin *Radiokhimiya* **28** 318 (1986)
83. Yu A Teterin, A S Baev, L G Mashirov, D N Suglobov *Radiokhimiya* **28** 460 (1986)
84. Yu A Teterin, A S Baev, L G Mashirov, D N Suglobov, in *Voprosy Atomnoi Nauki i Tekhniki (Ser. Obshchaya i Yadernaya Fizika)* [Problems in Atomic Science and Engineering (General and Nuclear Physics Ser.)] (Moscow: TsNIIatominform, 1986) Vol. 36, No 3, p. 60
85. A S Baev, Yu A Teterin, in *Voprosy Atomnoi Nauki i Tekhniki (Ser. Obshchaya i Yadernaya Fizika)* [Problems in Atomic Science and Engineering (General and Nuclear Physics Ser.)] (Moscow: TsNIIatominform, 1986) Vol. 36, No 3, p. 60
86. J Schirmer, L S Cederbaum, W Domcke, W Von Niessen *Chem. Phys.* **26** 149 (1977)
87. N Honjou, T Sasajima, F Sasaki *Chem. Phys.* **57** 475 (1981)
88. Yu A Teterin, S G Gagarin, A S Baev, in *Poverkhnostnye i Teplofizicheskie Svoistva Abrazov. Preprint ISM AN USSR* (Surface and Thermal Properties of Diamonds. Preprint of the Institute of Structural Materials of the Academy of Sciences of Ukr. SSR) (Kiev, 1985) p. 17
89. M I Sosulnikov, Yu A Teterin *J. Electron. Spectrosc. Relat. Phenom.* **59** 111 (1992)
90. Yu A Teterin, M I Sosulnikov *Appl. Supercond.* **3-6** 457 (1993)

91. Yu A Teterin, M I Sosulnikov, Yu A Petrov *J. Electron. Spectrosc. Relat. Phenom.* **68** 469 (1994)
92. Yu A Teterin, M I Sosulnikov, L D Shustov *J. Electr. Spectr. Relat. Phenom.* **68** 453 (1994)
93. Yu A Teterin, V M Kulakov, V V Lomonosov, A S Baev, M I Sosul'nikov, in *Voprosy Atomnoi Nauki i Tekhniki*. (Ser. *Yaderno-Fizicheskie Issledovaniya*) [Problems in Atomic Science and Engineering (Nuclear-Physical Investigations Ser.)] (Moscow: TsNIIatominform, 1990) Vol. 5, No 13, p. 71
94. Yu A Teterin, A S Baev, M I Sosul'nikov, Yu N Simirskii *Sverkhprovodimost: Fiz., Khim., Tekhnika* (3) 25 (1988)
95. V M Ryzhkov, N I Medvedeva, A F Golota, M Ya Khodos, V A Gubanov *Zh. Strukt. Khim.* **26** (6) 76 (1985)
96. Yu A Teterin, V M Kulakov, A S Baev, A G Zelenkov, N B Nevzorov, I V Mel'nikov, V A Strel'tsov, L G Mashirov, D N Suglobov *Dokl. Akad. Nauk SSSR* **255** 434 (1980)
97. B C Frazer, G Shirane, D E Cox, C E Olsen *Phys. Rev. A* **140** 1448 (1965)
98. J C Fuggle, A F Burr, L M Watson, D J Fabian, W Lang *J. Phys. F* **4** 335 (1974)
99. K N Huang, M Aojagi, M N Chen, B Crasemann, H Mark *At. Data Nucl. Data Tabl.* **18** 243 (1976)
100. J J Pireaux, N Martensson, R Didriksson, K Siegbahn, J Riga, J Verbist *Chem. Phys. Lett.* **46** 215 (1977)
101. Yu A Teterin, A S Baev, in *Voprosy Atomnoi Nauki i Tekhniki* (Ser. *Obshchaya i Yadernaya Fizika*) [Problems in Atomic Science and Engineering (General and Nuclear Physics Ser.)] (Moscow: TsNIIatominform, 1985) Vol. 4, No 33, p. 53
102. Yu A Teterin, A S Baev, L G Mashirov, D N Suglobov *Dokl. Akad. Nauk SSSR* **276** 154 (1984)
103. Yu A Teterin, A S Baev, L G Mashirov, D N Suglobov *Dokl. Akad. Nauk SSSR* **277** 131 (1984)
104. Yu A Teterin, A S Baev, A D Sidorenko, S G Gagarin, in *Rentgenovskaya Spektroskopiya Tverdogo Tela. Preprint UNTs AN SSSR* (X-Ray Spectroscopy of Solids. Preprint of the Ural Scientific Centre of the Academy of Sciences of the USSR) (Sverdlovsk, 1984) p. 23
105. J H Scofield *J. Electron. Spectrosc. Relat. Phenom.* **8** 129 (1976)
106. A L Gubskii, A P Kovtun, Yu A Teterin, A S Baev *Elektronnoe Stroenie i Struktura RES Uranilovykh Soedinenii. Preprint IAE* (Electronic Structure of X-Ray Electron Spectra of Uranyl Compounds. Preprint of the Institute of Atomic Energy) (Moscow, 1984) No 4053/12
107. V A Glebov *Elektronnoe Stroenie i Svoistva Uranilovykh Soedinenii* (Electronic Structure and Properties of Uranyl Compounds) (Moscow: Energoatomizdat, 1983)
108. G V Ionova, V G Pershina, V I Spitsin *Elektronnoe Stroenie Aktinoidov* (Electronic Structure of the Actinides) (Moscow: Nauka, 1986)
109. Yu A Teterin, A S Baev, S A Bogatov *J. Electron. Spectrosc. Relat. Phenom.* **68** 685 (1994)
110. Yu A Teterin, A S Baev, N G Yakovlev, in *Voprosy Atomnoi Nauki i Tekhniki* (Ser. *Obshchaya i Yadernaya Fizika*) [Problems in Atomic Science and Engineering (General and Nuclear Physics Ser.)] (Moscow: TsNIIatominform, 1992) Vol. 3, p. 58
111. M V Ryzhkov, V A Gubanov, Yu A Teterin, A S Baev *Radiokhimiya* **33** (1) 22 (1991); **34** (1) 85 (1992)
112. Yu A Teterin, S G Gagarin, in *Voprosy Atomnoi Nauki i Tekhniki* (Ser. *Obshchaya i Yadernaya Fizika*) [Problems in Atomic Science and Engineering (General and Nuclear Physics Ser.)] (Moscow: TsNIIatominform, 1984) Vol. 4, No 29, p. 89
113. P E Cade, A C Wahi *At. Data Nucl. Data Tables* **13** 339 (1974)
114. A Brown, S Rundqvist *Acta Crystallogr.* **19** 684 (1965)
115. M Taniguchi, S Suga, M Seki, H Sakamoto, H Kanzaki, Y Alkahama, S Terada, S Endo, S Narita *Solid State Commun.* **45** 59 (1983)
116. S G Gagarin *Zh. Fiz. Khim.* **57** 1212 (1983)
117. E Clementi, D L Raimondi *J. Chem. Phys.* **38** 2686 (1963)
118. O P Charkin *Stabil'nost' i Struktura Gazoobraznykh Neorganicheskikh Molekul, Radikalov i Ionov* (Stability and Structure of Inorganic Gaseous Molecules, Radicals, and Ions) (Moscow: Nauka, 1980)
119. R P Messmer *Chem. Phys. Lett.* **11** 589 (1971)
120. M Nishida *Phys. Rev. B, Solid State, Ser. 3* **95** 263 (1979)
121. L A Grunes, R D Leapman, C N Hoffmann, A B Kunz *Phys. Rev. B, Condens. Matter* **5** 7157 (1982)
122. S G Gagarin, Yu A Kolbanovskii *Kinet. Katal.* **23** 1454 (1982)
123. Yu A Teterin, A S Baev, K E Ivanov, L G Mashirov, D N Suglobov *Radiokhimiya* **38** (4) 365 (1996)
124. Yu A Teterin, V A Terekhov, K E Ivanov *Dokl. Akad. Nauk* **345** 365 (1995)
125. V I Zhudov, A G Zelenkov, V M Kulakov, B V Odinov, Yu A Teterin, in *Tez. Dokl. XXX Vsesoyuz. Soveshchaniya po Yadernoi Spektroskopii i Struktura Atomnogo Yadra* (Abstracts of Reports of the XXX All-Union Conference on Nuclear Spectroscopy and the Structure of the Atomic Nucleus) (Leningrad: Nauka, 1980) p. 614
126. D P Grechukhin, V I Zhudov, A G Zelenkov, V M Kulakov, B V Odinov, A A Soldatov, Yu A Teterin *Pis'ma Zh. Eksp. Teor. Fiz.* **31** 627 (1980)
127. Yu A Teterin, V I Nefedov, K E Ivanov, A S Baev, G Gaipel', T Raikh, Ch Niche *Dokl. Akad. Nauk* **344** 206 (1995)
128. V I Nefedov, Yu A Teterin, T Raikh, Kh Niche *Dokl. Akad. Nauk* **348** 634 (1996)

Low-temperature functionalisation of alkanes and cycloalkanes by 'classical' and 'non-classical' (superacidic) Friedel–Crafts complexes

I S Akhrem, A V Orlinkov, M E Vol'pin (deceased)

Contents

I. Introduction	849
II. Functionalisation of isoalkanes and activated cycloalkanes by equimolar complexes $\text{RCOX} \cdot \text{AlCl}_3$ and related systems	850
III. Functionalisation of alkanes and cycloalkanes with aprotic organic superacidic complexes $\text{RCOX} \cdot 2\text{AlCl}_3$	853
IV. Reactions of acylium salts with saturated hydrocarbons in protic superacids	857
V. The nature of the active complexes in acyl halide–aluminium halide systems	858
VI. Conclusion	862

Abstract. The results of studies on direct functionalisation of activated alkanes and cycloalkanes under the action of 'classical' Friedel–Crafts complexes (*viz.* equimolar complexes of acyl halides with aluminium halides) and related systems containing smaller or somewhat larger amounts of aluminium halide are surveyed. The studies carried out during the last decade on functionalisation of saturated hydrocarbons devoid of tertiary carbon atoms, by aprotic organic superacids $\text{RCOX} \cdot 2\text{AlCl}_3$ are summarised. Reactions of alkanes with acylium cations in superacidic media are considered. The published data on the structure of complexes $\text{RCOX} \cdot \text{AlCl}_3$ and $\text{RCOX} \cdot 2\text{AlCl}_3$ and on the nature of the active complexes in the reactions of arenes with acylium cations and with complexes $\text{RCOX} \cdot \text{AlCl}_3$ in both acidic and organic media as well as in the reactions of alkanes with acylium salts in protic superacids and with superacidic complexes $\text{RCOX} \cdot 2\text{AlCl}_3$ in aprotic solvents are analysed. The prospects for the synthesis of organic compounds from alkanes and cycloalkanes under the action of complexes of acyl halides with aluminium halides are outlined. The bibliography includes 128 references.

I. Introduction

Alkanes and cycloalkanes, which are the major components of oil and natural gas, still remain the most promising raw material for the synthesis of organic compounds. Although there is a possibility, in principle, to carry out direct functionalisation of alkanes and cycloalkanes and although some selective reactions of this type have been reported, only few saturated hydrocarbons are used currently in organic synthesis. Therefore, Mendeleev's words that to use petroleum as a fuel is like firing a furnace with banknotes are still timely.

The main difficulties that hamper selective one-stage functionalisation of alkanes (or cycloalkanes) arise because compounds

of this class are inert and, hence, the products of their transformations are more reactive than the initial hydrocarbons.

In the early 1970s, a new stage in the chemistry of alkanes began. Since then, two non-traditional approaches are being developed successfully, which have given an impetus to the new 'low-temperature' chemistry of alkanes. (Low-temperature catalysts for transformations of alkanes have indubitable advantages over catalysts that are active at elevated temperatures, since the former make it possible to perform more selective processes and to work under thermodynamically more favourable conditions.¹). The activation of the C–H bonds in alkanes, including methane, by transition metal complexes in solution has been discovered.^{2–4} Over the past two and half decades, a wide range of transition metal complexes and lanthanide and actinide derivatives that are capable of activating alkanes have been described, the scientific fundamentals for the metallocomplex activation of C–H σ -bonds have been created, and processes for the transformation of alkanes and cycloalkanes into their derivatives (alkenes, oxidation products, carbonyl compounds, *etc.*) have been developed. The 'biomimetic' approach based on the development of activating systems, similar to metalloenzymes acting in living nature, proved quite promising.

At about the same time as the first transition metal complexes activating alkanes were described, the activation of saturated hydrocarbons by protic superacids was discovered.^{5–7} The use of these systems made it possible to accomplish for the first time cracking, isomerisation, alkylation, and some other reactions of alkanes under mild conditions, at high rates, and with good yields of products. It has been shown that direct functionalisation of nonactivated cycloalkanes and alkanes including methane in protic acid media is, in principle, possible, and some examples of selective reactions of this type have been reported.

A great achievement in the chemistry of alkanes has been the elucidation of the mechanism of σ -bond activation by protic superacids and evidence for the existence of hypervalent carbon and for the formation of a two-electron three-centre ($2e-3c$) transition state. The intermediates in these reactions, namely, derivatives of pentacoordinated and hexacoordinated carbon, carbonium ions, and carbenium ions, the existence of which had been postulated previously, were generated and studied experimentally.⁵ As a result of these studies, the views on the mechanism of the electrophilic activation of alkanes, which had previously been speculative, became substantially more profound and acquired a reliable theoretical base. The Nobel prize in chemistry awarded to Olah in 1994 for his pioneering studies on the activation of alkanes by protic superacids reflected the recogni-

I S Akhrem, A V Orlinkov Laboratory of complex organometallic catalysts, Nesmeyanov Institute of Organoelement Compounds, Russian Academy of Sciences, ul. Vavilova 28, 117813 Moscow, Russian Federation. Fax (7-095) 135 50 85
Vol'pin M E Director of the same Institute

Received 15 April 1995

Uspekhi Khimii 65 (10) 920–935 (1996); translated by Z P Bobkova

tion of his fundamental contribution to the chemistry of alkanes⁷ and, simultaneously, the recognition of the current interest in this subject.

Among the new approaches to the chemistry of alkanes, which have been successfully developed during the past two decades, gas-phase reactions of alkanes with metal ions⁸⁻¹⁷ and with metal atoms or small clusters¹⁷⁻²⁸ are noteworthy. The former have provided valuable information concerning the mechanisms of the activation of C-H and C-C bonds and on the energies of M-H and M-C bonds. The studies on the reactions of alkanes with metal atoms and small clusters have led to the development of new active heterogeneous catalysts^{17,18} and to the direct synthesis of organometallic compounds from alkanes.^{26,27}

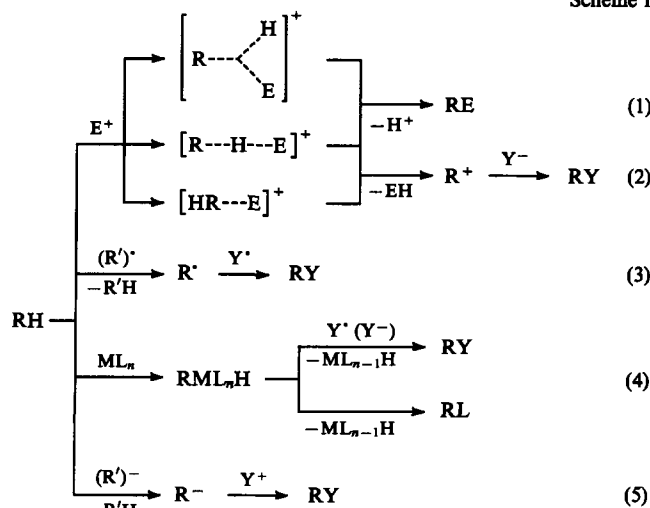
The traditional field involving gas-phase reactions of alkanes in the presence of heterogeneous catalysts, which still occupy a prominent position among industrial processes, has also been substantially revolutionised. Great progress has been achieved in studies on the structures of heterogeneous catalysts and mechanisms of reactions involving them (including industrial processes) as well as in the development of a new generation of catalysts.²⁰⁻³⁴ The elaboration of novel catalysts for the oxidation of alkanes based on polyoxometallates ('inorganic porphyrin'), which combine the advantages of homogeneous systems (selectivity and controllability of processes; see Chapter VIII in the published book²) with stability, which is the basic advantage of heterogeneous catalysts, especially significant for industry, demonstrates the fruitfulness of using different approaches for solving a common problem.

In recent years, some selective radical processes of functionalisation of alkanes have been reported. The photoinduced single electron transfer (SET), which has been achieved using photochemical oxidising agents (for example, tetracyanobenzene) generating radical cations from saturated hydrocarbons, can serve as an example. The subsequent exothermal transformation of the alkyl radical cation into the alkyl cation, which then adds to the radical derived from the oxidising agent, affords a functional derivative of the alkane.³⁵ Somewhat earlier, Crabtree (see for example, Chapter III in the published book²) has proposed another method for the generation of alkyl radicals from alkanes; this involved the use of photoexcited mercury atoms. The alkyl radicals thus formed can undergo cross-coupling with other radicals generated in the system. For example, the interaction of cyclohexane and methanol yields the cross-coupling product, cyclo-C₆H₁₁CH₂OH, in addition to the products of dimerisation of the radicals — (cyclo-C₆H₁₁)₂ and (CH₂OH)₂. Crabtree believes that this approach is quite promising for practical purposes, because it permits a large number of catalytic cycles. In this respect, the 'mercury' method compares favourably with the dehydrogenation of alkanes under the action of phosphine complexes of transition metals, which are readily deactivated during the reactions. Unfortunately, the Hg/hv and Hg/hv/H₂ systems are relatively ineffective for the transformation of methane or other alkanes with strong C-H bonds.

The simplest pathways to the functionalisation of alkanes are shown in Scheme 1. Obviously, compounds of the same type can react by different mechanisms. For example, metal complexes can act either as electrophiles or as radicals or react by the oxidative addition mechanism.

The electrophilic functionalisation (1), electrophile-promoted nucleophilic functionalisation (2),^{5,6} the radical mechanism (3), and the metalcomplex mechanism (4) of hydrogen substitution in a saturated hydrocarbon²⁻⁴ shown in the Scheme have been proved, while reaction (5) has not been performed so far. However, since the H/D isotope exchange in saturated hydrocarbons including methane under the action of strong nucleophiles is well known,³⁶⁻³⁹ this functionalisation pathway seems possible, although it is unlikely to play a noticeable role in the chemistry of alkanes, because the reagents needed for the irreversible functionalisation are difficult to select.

Scheme 1



It can be concluded from the foregoing that the chemistry of alkanes has developed vigorously over the last 20–25 years. It has been reported² that the number of publications devoted to the activation of alkanes and their catalytic reactions increases exponentially and doubles every 3–4 years. The advances made in this field bring closer the solution of the problem of the direct synthesis of organic compounds from alkanes and cycloalkanes.

The present review is devoted to the functionalisation of alkanes and cycloalkanes by complexes of acyl halides with aluminium halides.

Studies on the transformations of saturated hydrocarbons under the action of equimolar Friedel–Crafts complexes have been carried out desultorily for 65 years. The reported examples of functionalisation of activated saturated hydrocarbons seemed to be of purely abstract interest. However, recently it has been shown that, in some cases, the acylation of activated cycloalkanes with these systems can be applied to organic synthesis.

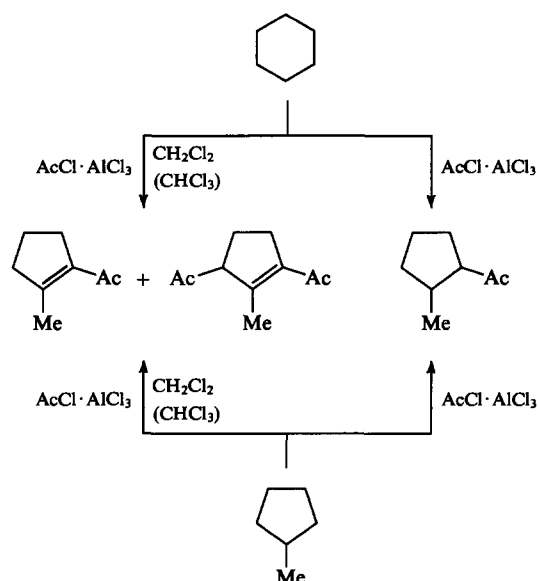
The discovery of the 'superacidic' properties of the RCOX·2AlX₃ complexes has opened new prospects in the chemistry of alkanes.⁴⁰ The RCOX·2AlX₃ complexes, which were called by us aprotic organic superacids (AOS) proved extremely reactive toward *n*-alkanes and non-activated cycloalkanes under mild conditions,⁴¹ which markedly distinguishes them from the equimolar complexes RCOX·AlX₃, which are inert with respect to these substrates. Regarding their activity in the initiation of transformations of alkanes, AOS surpass not only the known systems based on aluminium halides but also the strongest protic superacids. In the presence of AOS, functionalisation of linear alkanes and nonactivated cycloalkanes has been accomplished; among these processes, novel reactions of alkanes were found. It is also essential that, although AOS readily initiate transformations of alkanes and cycloalkanes accompanied by the rupture of C–C bonds, the fragmentation processes can be suppressed under certain conditions and a one-stage selective functionalisation of saturated hydrocarbons can be performed.

II. Functionalisation of isoalkanes and activated cycloalkanes by equimolar complexes RCOX·AlCl₃ and related systems

The discovery of the activating influence of aluminium chloride on acyl halides made by Friedel and Crafts in the late XIX century marked the beginning of the fruitful use of the complexes RCOX·AlX₃ in organic chemistry and, actually, the beginning of the use of catalysis in organic synthesis. However, the use of RCOX·AlX₃ complexes has long been confined only to reactions of unsaturated or aromatic compounds.⁴²⁻⁴⁵ The use of these

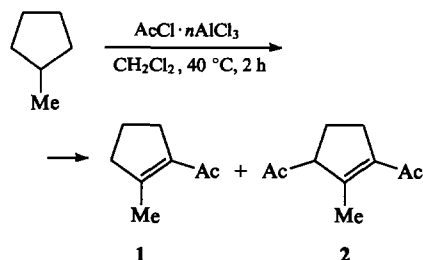
complexes for transformations of alkanes and cycloalkanes was far from being equally successful. The first studies in this field were carried out by Nenitzescu, Zelinsky, Hopff, and other researchers^{46–53} as early as the 1930s. The results of these studies have been discussed in monographs^{42,43} and in a review.⁵⁴

In early papers, only qualitative experiments were carried out. For example, it was found that stirring cyclopentane, acetyl chloride, and aluminium chloride in a molar ratio of 3 : 1 : 1.1 for two days affords acetylcyclopentane.⁴⁷ If methylcyclopentane is used instead of cyclopentane and the ratio of the reagents is 5 : 1 : 1.2, 2-acetyl-1-methylcyclopentane is formed in three days.⁴⁶ Later, reactions of cyclohexane, methylcyclopentane, methylcyclohexane, and decalin in the presence of $\text{AcCl} \cdot n\text{AlCl}_3$ ($n = 0.8–1.5$) were studied in detail by various researchers. It was found that the transformations of cyclohexane and methylcyclopentane carried out in the medium of the hydrocarbon itself lead to the corresponding saturated ketones, while in a solvent (CH_2Cl_2 or CHCl_3), α,β -unsaturated ketones or diketones of the cyclopentane series are formed.^{55–64}



Acetylation of methylcyclopentane, cyclohexane, methylcyclohexane, and decalin with the reaction conditions are shown in Scheme 2.^{55–58}

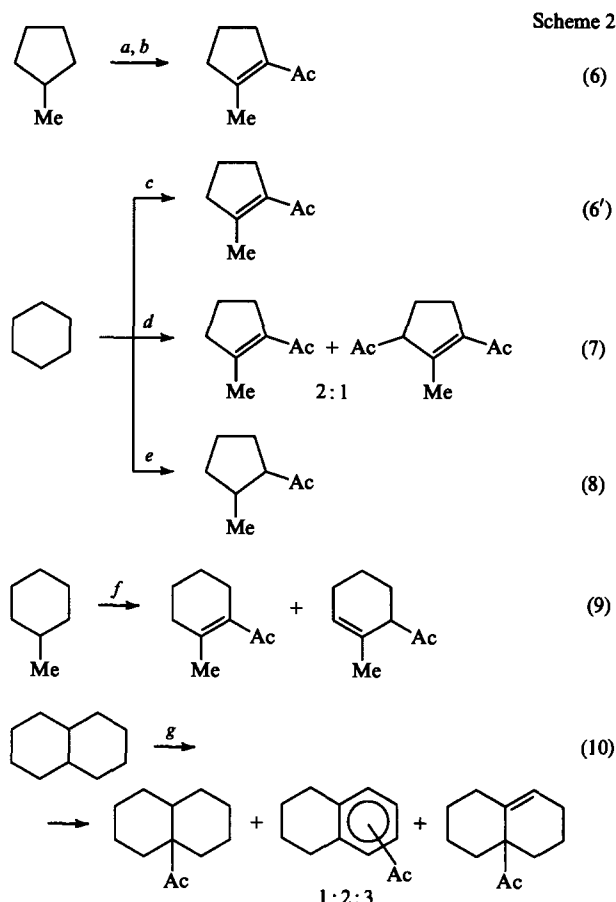
Thorough investigation of the acetylation of methylcyclopentane carried out recently has made it possible to increase the overall yield of the monoacetylated product 1 and diacetylated product 2 to 65%–70%.⁶⁴



The ratio of 1 and 2 depends on the $[\text{AcCl}]:[\text{AlCl}_3]$ ratio. When this is 2 : 1.5, the yield of the compound 2 is 50%.

Although the exact mechanism of the formation of the diketone 2 is unknown, the researchers cited presented some facts indicating that it is formed *via* enol derivative 3 rather than by the direct acylation of the unsaturated ketone 1 (Scheme 3).

In keeping with this scheme is the fact that treatment of the enol derivative 3 with AlCl_3 or TiCl_4 gives the diketone 2 in a quantitative yield. Conversely, acylation of 1 leads mostly to

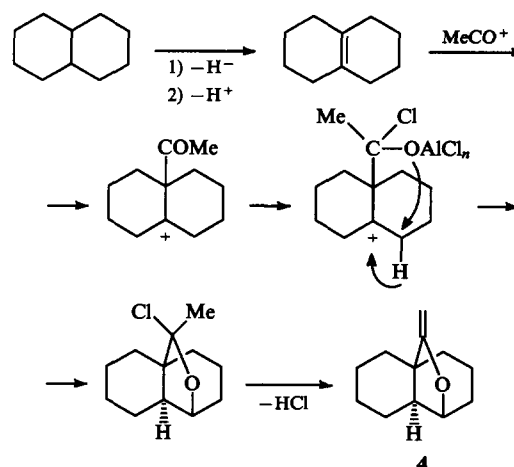


- (a) $\text{AcCl} \cdot \text{AlCl}_3$, 20 °C, 5 h (yield 27%);⁵⁵
 (b) $\text{AcCl} \cdot \text{AlCl}_3$, 40 °C, 2 h (yield 50%);⁵⁶
 (c) $\text{AcCl} \cdot \text{AlCl}_3$, 60 °C, 5 h, 20 °C, 12 h (yield 36%);⁵⁷
 (d) $\text{AcCl} \cdot \text{AlCl}_3$, 40 °C, 24 h + 20 °C, 18 h (yield 58%);⁵⁶
 (e) $\text{AcCl} \cdot \text{AlCl}_3$, 20 °C, 17 h (yield 30%);⁵⁸
 (f) $\text{AcCl} \cdot 0.8\text{AlCl}_3$, 60 °C, 70 h (total yield 13%);⁵⁸
 (g) $\text{AcCl} \cdot 1.5\text{AlCl}_3$, 20 °C, 48 h (total yield 71%).⁵⁹

heavy products in which the proportion of the diketone 2 is very low.⁶⁴

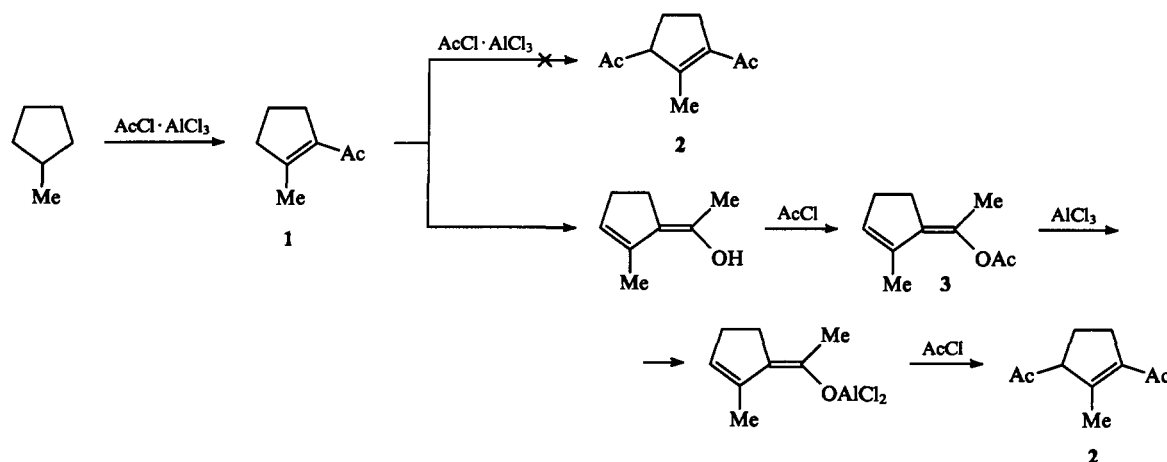
The acetylation of methylcyclohexane and decalin occurs with the retention of the structures of the initial cycloalkanes.

Unlike reactions (6)–(9) (Scheme 2), acetylation of decalin [reaction (10)] is conducted with a substantial excess of aluminium



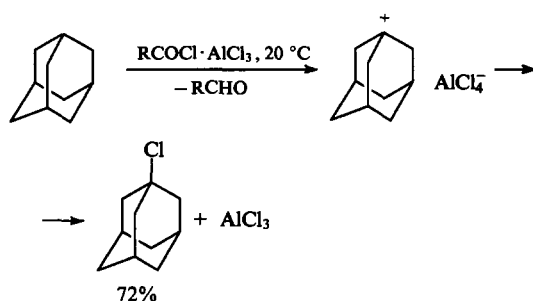
$[\text{RH}]:[\text{AcCl}]:[\text{AlCl}_3] = 1:2.4:1.5$; CH_2Cl_2 , 10 °C, 10 h (yield 46%).

Scheme 3



chloride. Although this reaction is not selective, the overall yield of acylated products is quite high. A decrease in the amount of aluminium chloride in the $\text{AcCl} \cdot n\text{AlCl}_3$ system to $n < 1$ and a decrease in the temperature change sharply the direction of the reaction. Instead of the decalin acylation products, vinyl ether 4 is formed.⁶³ It was shown that only *cis*-decalin enters into this process, while *trans*-decalin is inactive. The scheme proposed for the transformation of *cis*-decalin into the vinyl ether 4 involves the formation of 9,10-decalene, which is then acylated giving a tertiary carbocation. The latter undergoes an axial shift and cyclisation and, after elimination of HCl , it is finally converted into the vinyl ether 4.^{63, 64}

When cyclic hydrocarbons that are not prone to form alkenes are made to react with $\text{RCOCl} \cdot \text{AlCl}_3$ systems, halogenation products rather than acylation products are formed.⁶⁵ For example, treatment of adamantane with $\text{RCOCl} \cdot \text{AlCl}_3$ leads to 1-chloroadamantane.



$[\text{AdH}]:[\text{RCOCl} \cdot \text{AlCl}_3] = 1:1$; $\text{R} = \text{Me}, \text{Pr}^n, \text{Pr}^i, \text{cyclo-C}_6\text{H}_{11}$ ($\text{R} \neq \text{Ph}$).

At 50°C and at the molar ratio $[\text{RCOCl} \cdot \text{AlCl}_3]:[\text{AdH}] = 6:1$, dichloroadamantane is formed in a good yield, instead of 1-chloroadamantane.⁶⁵

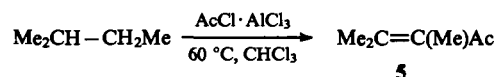
The only transformation observed for linear and branched alkanes in earlier studies, was their acylation, which led predominantly to the formation of saturated ketones and, to a lesser degree, of unsaturated ketones.^{47, 55, 66–69} The yields of the acylation products were extremely low even after prolonged heating of the reactants.



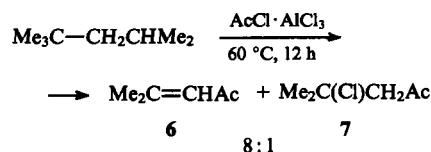
$n = 4–6$.

n-Butane does not react with $\text{AcCl} \cdot \text{AlCl}_3$ at room temperature. However, if a mixture of *n*-butane with $\text{AcCl} \cdot \text{AlCl}_3$ (molar ratio 3:1) is stirred for 15 h at 60°C without a solvent, $\text{Me}_2\text{CHCH}_2\text{Ac}$, formed in a very low yield can be detected. The same product is also obtained from isobutane.⁶⁶

Pentane and hexane can be acylated by prolonged stirring with $\text{AcCl} \cdot \text{AlCl}_3$ at room temperature without a solvent. For example, when *n*-pentane reacted with $\text{AcCl} \cdot \text{AlCl}_3$ for 8 h, the formation of a mixture of $\text{Me}_2\text{CHCH}(\text{Me})\text{Ac}$ and $\text{Me}_2\text{C}=\text{C}(\text{Me})\text{Ac}$ was qualitatively detected.⁶⁷ Under similar conditions, *n*-hexane is converted into $\text{Me}_2\text{CHCH}(\text{Et})\text{Ac}$ and $\text{Me}_2\text{C}=\text{C}(\text{Et})\text{Ac}$. The indirect data reported by Nenitzescu et al.⁴⁷ suggest that the yield of $\text{Me}_2\text{CHCH}(\text{Et})\text{Ac}$ relative to AcCl does not exceed 5%. Japanese workers⁵⁵ have studied the interaction of isopentane with $\text{AcCl} \cdot \text{AlCl}_3$ by heating the reactants ($[\text{RH}]:[\text{AcCl} \cdot \text{AlCl}_3] = 1:1$) in a solvent. Under these conditions, only the unsaturated ketone 5 was obtained in a yield of no more than 6%.⁵⁵



Prolonged heating of isooctane, which readily undergoes cracking, with the $\text{AcCl} \cdot \text{AlCl}_3$ complex gives rise to the unsaturated ketone 6 and compound 7, resulting from its further chlorination, the degree of conversion of the initial hydrocarbon not exceeding 37%.



Yet another interesting route for the transformation of alkanes containing a tertiary carbon atom in the presence of $\text{AcCl} \cdot \text{AlCl}_3$ systems (excess AcCl is normally used) has been reported by French researchers.^{70, 71} They found that, apart from the products resulting from monoacylation of isoalkanes (2-methylbutane, 2-methylpentane, 3-methylpentane, and 2,3-dimethylbutane), diacylated and triacylated compounds are formed intermediately; under the reaction conditions, they are converted into a mixture of pyrylium salts and, after treatment of the reaction mixture with NH_4OH , they are transformed into a mixture of pyridinium salts. The transformation of isopentane into a mixture of four pyrylium salts is illustrated in Scheme 4.⁷⁰

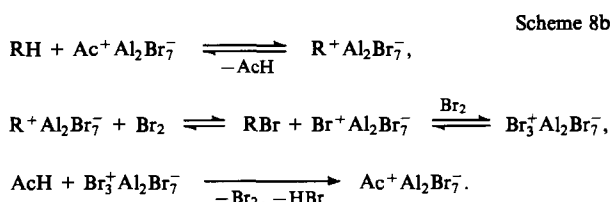
Pyrylium salts are synthesised at $25–53^\circ\text{C}$ over a period of 5–23 h without a solvent or in CHCl_3 . The yields of the products depend strongly on the reaction conditions and do not exceed 20%–25%.⁷⁰ The reactions of 2,2,4-trimethylpentane, which readily undergoes cracking, with $\text{RCOCl} \cdot \text{AlCl}_3$ systems ($\text{R} = \text{Me}, \text{Et}, \text{Pr}^i$) afford isobutane, saturated and unsaturated

Table 2. Ionic bromination of *n*-alkanes and cycloalkanes catalysed by the AcBr·2AlCl₃ complex and AlCl₃ in CH₂Cl₂ at 0 ° (according to a published study⁷⁸).

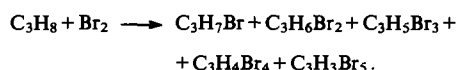
RH	Catalyst (Ct)	<i>t</i> /h	[RH] : [Br ₂] : [Ct]	Overall yield of mono-bromides (% relative to Ct)	Proportion of mono-bromides in the bromide mixture (%)
n-C ₄ H ₁₀	AcBr·2AlCl ₃	2.7	10 : 4 : 1	54 ^a	91
	AcBr·2AlCl ₃	2.7	10 : 4 : 1	142 ^b	—
n-C ₅ H ₁₂	AcBr·2AlCl ₃	1.5	10 : 4 : 1	203	91
	AcBr·2AlCl ₃	2.0	20 : 10 : 1	369	—
n-C ₆ H ₁₄	AlCl ₃	2.0	20 : 10 : 1	7	—
	AcBr·2AlCl ₃	0.5	10 : 4 : 1	66	95
n-C ₇ H ₁₆	AlCl ₃	0.5	10 : 4 : 2	0	—
	AcBr·2AlCl ₃	1.0	10 : 4 : 1	90	78
cyclo-C ₅ H ₁₀	AcBr·2AlCl ₃	2.0	10 : 4 : 1	55	100
	AlCl ₃	2.0	10 : 4 : 2	4	100
cyclo-C ₆ H ₁₂	AcBr·2AlCl ₃	2.0	10 : 4 : 1	133	100
	AcBr·AlCl ₃	2.0	10 : 4 : 1	0	—

^a At 10 °C. ^b At 20 °C.

Another possibility is that a carbocation (R⁺) is generated from RH by the action of the superacid RCO⁺Al₂Br₇[−]; this carbocation withdraws Br[−] from Br₂ thus forming a bromide.



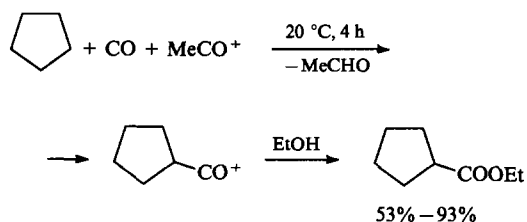
Both schemes include stages in which the catalyst is regenerated. The Ac⁺Al₂Br₇[−] complex is the catalyst of the bromination shown in Scheme 8b, whereas in the process shown in Scheme 8a, this complex initiates the reaction catalysed by the Br₃⁺Al₂Br₇[−] complex. By increasing the amount of Br₂ in the initial mixture and the reaction period, one can accomplish polybromination of alkanes, for example, of propane.



The overall yield of polybromopropanes is quantitative relative to Br₂.

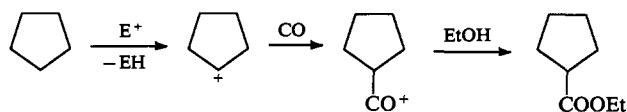
b. Carbonylation of cyclopentane

Acetyl bromide initiates carbonylation of cyclopentane with CO in the presence of excess AlBr₃ (AlBr₃ : MeCOBr > 1.8).⁷⁹ This reaction occurs at room temperature and under atmospheric pressure and, after treatment of the reaction mixture with ethanol, it leads to the corresponding ester.

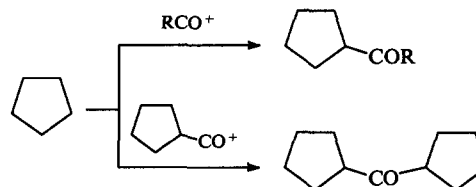


The selectivity of this reaction is 90%–99% and the yield of the ester varies from 53% to 93% depending on the proportion of AlBr₃. Dicyclopentyl ketone and acetylcyclopentane are formed as side products. The equimolar AcBr·AlBr₃ complex is inert under these conditions.

The mechanism suggested for this reaction is similar to that of the known Haaf–Koch reaction,⁸⁰ which includes generation of a carbocation from a cycloalkane through the action of an electrophile and subsequent addition of a CO molecule leading to the formation of an acylium-cation.



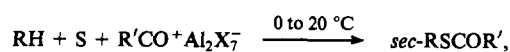
Side reactions:



It is significant that in the presence of AOS, alkanes and cycloalkanes have been introduced into reactions of new types (see Sections c and d).

c. The synthesis of RSCOR'

Compounds RSCOR' have been synthesised from alkanes (or cycloalkanes) RH, elementary sulfur, and the R'COX·2AlX₃ complexes in 25%–60% yields relative to the initial sulfur (Table 3).⁸¹



RH = C₃H₈, n-C₄H₁₀, n-C₅H₁₂, cyclo-C₅H₁₀, cyclo-C₆H₁₂;
R'CO⁺ = MeCO⁺, PrCO⁺, PhCO⁺.

With cycloalkanes, the corresponding dicycloalkyl sulfides R₂S (R = cyclo-C₅H₉, cyclo-C₆H₁₁) are formed in small yields. The mechanisms possible for this reaction are shown in Scheme 9.

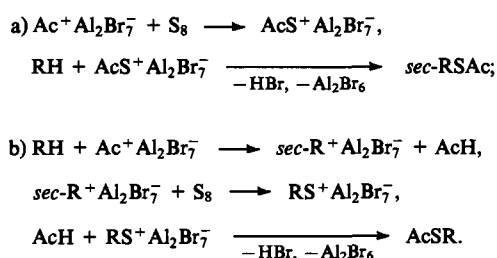
In the case of hydrocarbons containing tertiary carbon atoms (isobutane, methylcyclohexane, adamantane), which are usually more reactive than *n*-alkanes and than unsubstituted cycloalkanes, organosulfur compounds either are not formed at all under the conditions studied or are formed in low yields.

In the presence of Al₂Br₆ or the equimolar MeCOBr·AlBr₃ complex, no organosulfur compounds are formed from alkanes and sulfur, which is in agreement with published data indicating that alkanes are inert with respect to sulfur at low temperatures.

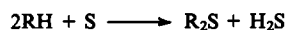
Table 3. One-stage synthesis of organosulfur compounds RSCOR' from alkanes (cycloalkanes), elemental sulfur, and R'COCl·2AlBr₃ complexes (according to a published study⁸¹).

RH	R'	T/°C	t/h	RSCOR'	Yield relative to S (%)
C ₃ H ₈	Me	20	2	Pr ⁱ SCOMe	47
n-C ₄ H ₁₀	Me	0	2.5	Bu ⁱ SCOMe	29
cyclo-C ₅ H ₁₀	Me	0	2	cyclo-C ₅ H ₉ SCOMe	45
cyclo-C ₆ H ₁₂	Me	0	4	cyclo-C ₆ H ₁₁ SCOMe	60
	Pr	0	4	cyclo-C ₆ H ₁₁ SCOPr	52
	Ph	0	4	cyclo-C ₆ H ₁₁ SCOPh	34

At elevated temperatures, the reactions of alkanes with sulfur are non-selective and ineffective.^{82, 83}



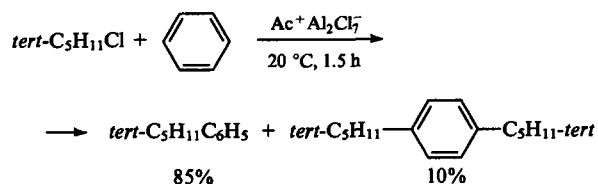
Note for comparison that sulfurisation of alkanes (or cycloalkanes) with elementary sulfur in CF₃SO₃H giving rise to the corresponding (or isomeric) disulfides proceeds only upon prolonged reaction at a high temperature.⁸⁴



RH	T/°C	t/h	Reaction product	Yield relative to the reacted sulfur (%)
cyclo-C ₅ H ₁₀	150	12	(cyclo-C ₅ H ₉) ₂ S	46
C ₃ H ₈	150	62	Pr ₂ S	47
			(mixture of isomers)	
iso-C ₄ H ₁₀	125	10	Bu ₂ S	33

d. Alkylacylation of aromatic hydrocarbons with alkanes (or cycloalkanes) in the presence of RCO⁺Al₂X₇⁻ complexes

The ability of superacidic RCO⁺Al₂X₇⁻ complexes to acylate under mild conditions not only unsaturated compounds⁸⁵ but also alkanes^{40, 41, 72} seemingly precludes the possibility of alkylation of aromatic compounds in the presence of these complexes. However, it has been found that the acylating ability of these complexes is suppressed in the presence of alkyl halides, and they act as catalysts for alkylation, for instance, of benzene.⁸⁶

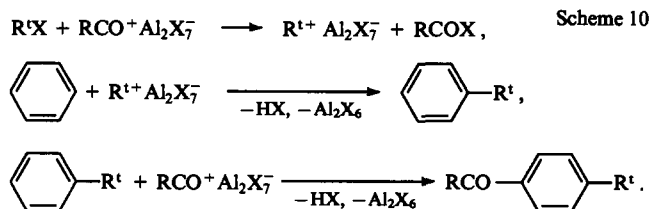


$$[\text{C}_6\text{H}_6]:[\text{tert-C}_5\text{H}_{11}\text{Cl}]:[\text{Ac}^+ \text{Al}_2\text{Cl}_7^-] = 180:36:1.$$

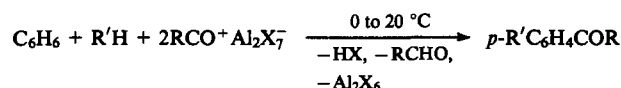
Alkylated aromatic ketones *tert*-C₅H₁₁C₆H₄COMe are formed as side products in these reactions. The yield of the alkylated aromatic ketones can be increased to 57% (relative to

Ac⁺Al₂Cl₇⁻) when the molar ratio of the reactants is 5:15:1. The reaction is completed over a period of 5 min at 20 °C.

Apparently, the alkylacylation of benzene with alkyl halides involves generation of a carbenium ion, which alkylates benzene. Subsequently acylation of the alkylated benzene occurs (Scheme 10).



Since alkanes can give rise to carbenium ions in the presence of RCO⁺Al₂X₇⁻ complexes, they can be successfully used, instead of alkyl halides, as alkylating agents for aromatic hydrocarbons.^{86, 87} These reactions result in the formation of alkylated aromatic ketones (Scheme 10). The one-stage alkylacylation of benzene with isoalkanes or *n*-alkanes in the presence of the RCO⁺Al₂X₇⁻ complexes occurs at 0–20 °C. The yields of alkylacylation products reach 65%–87% (Table 4). The yields of non-alkylated aromatic ketones, the products of a competing reaction, are relatively low (3%–20%). Isobutane and *n*-butane can be used as alkylating agents. Butylated ketones are normally obtained in somewhat lower yields (up to 68%) but they are also the major reaction products.

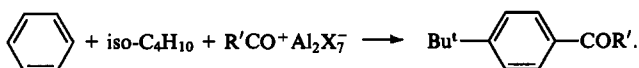


R' = Buⁱ, Buⁿ, *n*-C₅H₁₁, 2,3-Me₂C₄H₇, cyclo-C₅H₈Me;

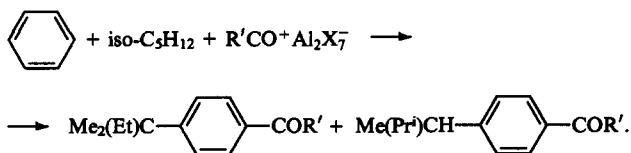
R = Me, Pr, Ph; X = Cl, Br.

Alkylacylation reactions result in good yields of products only when an excess of the 'alkylating system' (R'H + RCO⁺Al₂X₇⁻) is used, the molar ratio [R'H]:[RCO⁺Al₂X₇⁻]:[C₆H₆] is (10 to 15):(3 to 12):1, and the experimental procedure is thoroughly followed.^{86, 87}

Alkylacylation of benzene with isobutane occurs regioselectively and leads to the *para*-isomers of the corresponding ketones.



The reaction of benzene with isopentane gives equal amounts of *para*-substituted ketones differing in the structure of the pentyl group.



Alkylacylation of bromobenzene is more selective than that of benzene, the yield of the corresponding ketone reaching 74%–82% (see Table 4). The reaction with isobutane affords only one isomer, 2-bromo-4-*tert*-butylacetophenone.⁸⁶

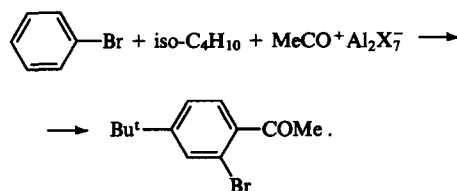


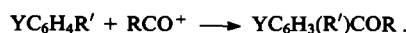
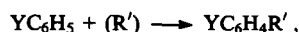
Table 4. One-stage alkylation of benzene and bromobenzene with alkanes (cycloalkanes) and $\text{RCO}^+ \text{Al}_2\text{X}_7^-$ complexes.

Run	R'H	RCO ⁺ Al ₂ X ₇ ⁻		[RCO ⁺ Al ₂ X ₇ ⁻]: :[PhY]	T/°C	t/min	Yield of products relative to ArH (%)	
		R	X				R'C ₆ H ₃ (Y)COR	YC ₆ H ₄ COR
Benzene								
1	iso-C ₄ H ₁₀	Me	Cl	12:1	0	30	62	35
2	iso-C ₄ H ₁₀	Me	Cl	12:1	20	40	68	32
3	iso-C ₄ H ₁₀	Me	Br	6:1	0	30	48	41
4	iso-C ₄ H ₁₀	Pr	Br	6:1	0	30	54	23
5	iso-C ₄ H ₁₀	Ph	Cl	6:1	0	30	35	18
6	iso-C ₅ H ₁₂	Me	Br	6:1	20	5	87	3
7	iso-C ₅ H ₁₂	Me	Br	3:1	20	5	65	12
8	iso-C ₅ H ₁₂	Me	Cl	6:1	20	5	81	20
9	iso-C ₅ H ₁₂	Me	Br	6:1	20	5	73	3
10	iso-C ₆ H ₁₄	Me	Cl	6:1	20	5	82	18
11	cyclo-C ₅ H ₉ Me	Me	Cl	6:1	20	5	58	11
Bromobenzene								
12	iso-C ₄ H ₁₀	Me	Br	6:1	0	60	82	4
13	iso-C ₄ H ₁₀	Me	Cl	6:1	0	60	79	22
14	iso-C ₅ H ₁₂	Me	Cl	6:1	0	20	74	Traces
15	n-C ₄ H ₁₀ ^a	Me	Cl	6:1	0	30	40	5

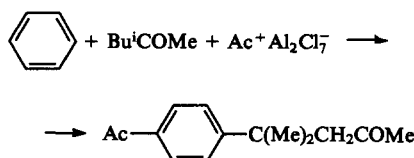
^a Before the reaction, the initial alkane was held for 3 h with a catalytic amount of $\text{RCO}^+ \text{Al}_2\text{X}_7^-$.

Apparently, the *para*-bromo-*tert*-butylbenzene formed initially isomerises into the more stable *meta*-isomer in the presence of a strong aprotic superacid. The acylation of the *meta*-isomer into the *para*-position with respect to the *tert*-butyl group gives rise to the reaction product observed. Activated arenes (toluene, naphthalene, and *meta*-xylene) also form alkylation products, but their yields do not exceed 10% of the yields of products obtained by the direct acylation of arenes. At the same time, arenes that contain strong electron-withdrawing groups (nitrobenzene and acetophenone) remain unchanged under the reaction conditions. This fact suggests that the reactions under consideration occur as the initial alkylation of arenes followed by acylation of the alkylated arenes. Apparently, in the case where the aromatic compound is activated toward an electrophilic attack, the acylation and alkylation reactions proceed at comparable rates. Therefore, in the presence of excess acylating agent, the acylation occurs as the prevailing process. The difference between the acylation and alkylation rates increases on passing from activated aromatic compounds to benzene and, especially, to bromobenzene, which is inert toward electrophiles. Therefore, in these cases, the initial alkylation is the predominant or even the only reaction pathway.

Apparently, the scheme of the alkylation with alkanes (or cycloalkanes) is similar to Scheme 10 and differs from it only by the absence of the stage for the regeneration of the acylium cation.⁸⁶



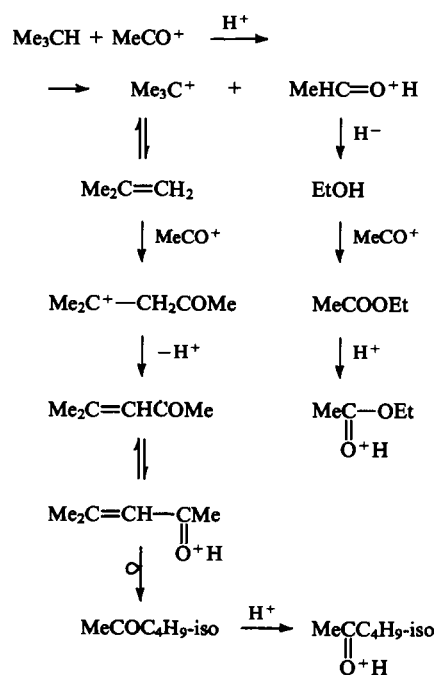
We have also detected the 'alkane-type' reactivity of Bu^t-COMe in its interaction with benzene, which resulted in the formation of the corresponding product of the alkylation of benzene in 40% yield.⁸⁶

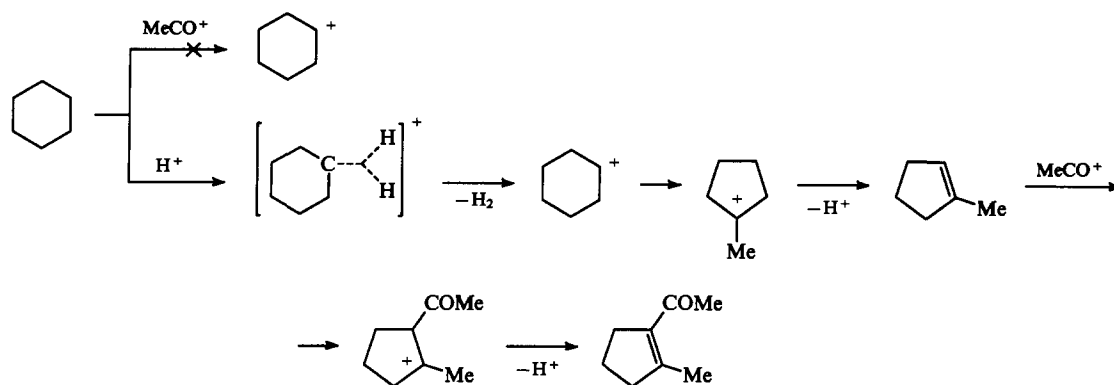


IV. Reactions of acylium salts with saturated hydrocarbons in protic superacids

Reactions of saturated hydrocarbons with acylium salts in a medium of a protic superacid were described for the first time by Brouwer and Kiffen.⁸⁸ They showed that in the HF–BF₃ and HF–SbF₅ systems at 25 °C, acylium ion detaches a hydride ion from the tertiary carbon atom in isobutane, isopentane, or methylcyclopentane. In the case of isobutane, the degree of conversion of an acylium salt amounts to 90% over a period of 12 h. The acylium salt is transformed into protonated ethyl acetate, which arises, in the authors' opinion,⁸⁸ via the interaction of MeCO⁺ with the ethanol resulting from the reduction of MeCO⁺ by the isoalkane. The conversion of isobutane leads initially to protonated mesityl oxide (Scheme 11). The second-order rate constant for this reaction is $3 \times 10^{-5} \text{ l mol}^{-1} \text{ s}^{-1}$.

Scheme 11

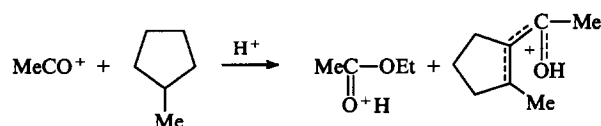




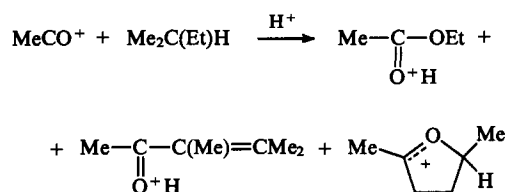
Scheme 12

When the duration of the process is more than 12 h, the mesityl oxide formed is reduced by isobutane to give protonated isobutyl methyl ketone.

Methylcyclopentane reacts with MeCO^+ in a protic acid in a similar way and gives rise to protonated 1-acetyl-2-methylcyclopentene and ethyl acetate.



The reaction involving isopentane yields a more complex mixture of products.



When cyclohexane is treated with MeCO^+ in excess $\text{HSO}_3\text{F}-\text{SbF}_5$, an α,β -unsaturated ketone — 1-acetyl-2-methylcyclopentene — is formed in 44% yield.⁸⁹ It was suggested that the dehydrogenation of cyclohexane is due to the generation of a carbocation upon the action of the superacid $\text{HSO}_3\text{F}-\text{SbF}_5$ on the cycloalkane rather than to the hydride transfer to the MeCO^+ cation.^{90,91} Thus, the role of MeCO^+ reduces only to acylation of the alkene existing in an equilibrium with the carbenium ion (Scheme 12).

It should be noted that with *n*-alkanes, hydride transfer barely takes place under the same conditions. For example, when butane has been in contact with a solution of $\text{MeCO}^+\text{BF}_4^-$ in $\text{HF}-\text{BF}_3$ for 72 h, the transformation occurred by no more than 1%, and the rate constant for this reaction, as estimated by Brouwer and Kiffen,⁸⁸ did not exceed $2 \cdot 10^{-8} \text{ l mol}^{-1} \text{ s}^{-1}$. No transformations of *n*-alkanes have been observed when they were treated with MeCO^+ in excess $\text{HSO}_3\text{F}-\text{SbF}_5$.⁸⁹

V. The nature of the active complexes in acyl halide – aluminium halide systems

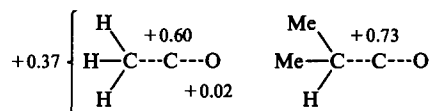
Evidently, the abstraction of a hydride ion from a saturated hydrocarbon by a superelectrophile leading to a carbocation is the key stage of the functionalisation of alkanes and cycloalkanes. This process includes one or several stages and occurs either by the classical Olah scheme [Eqns (1) and (2) in Scheme 1]⁹² or by a different mechanism.

From studies of equimolar $\text{RCOX}-\text{MX}_n$ systems, which were started as early as the beginning of this century and developed most significantly in the 1960–1970s, the structures of these

systems in the solid state and in solution are well known (see, for example, reviews^{44,93,94} and monographs^{43–45,93–96}).

The solid $\text{RCOX} \cdot \text{AlX}_3$ complexes ($\text{R} = \text{Alk}$, $\text{X} = \text{Cl}, \text{Br}$) exist as ionic acylium salts or donor-acceptor complexes.⁹⁴ The structures of $\text{MeCO}^+\text{AlCl}_4^-$,⁹⁷ and $\text{RC}(\text{Cl})=\text{O} \rightarrow \text{AlCl}_3$ [$\text{R} = \text{Et}$,⁹⁸ C_6H_5 ,⁹⁹ and *o*- and *p*- MeC_6H_4]¹⁰⁰] were determined by X-ray diffraction analysis. The cationic fragment MeCO^+ in the ionic complex $\text{MeCO}^+\text{AlCl}_4^-$ is linear, which corresponds to *sp*-hybridisation of the carbonyl carbon atom. The C–C–O angle is close to 180° , and the C–O bond is markedly shorter than the $\text{C}_{\text{sp}^2}=\text{O}$ bonds in ketones and acyl halides and even than that in CO. The structure of the AlCl_4^- moiety is close to tetrahedral.

X-Ray diffraction data provide valuable information also on the electron density distribution in acylium cations. The positive charge in the acylium cation $\text{C}(2)\text{H}_3\text{C}(1)\text{O}^+$ has been shown to be mostly localised on the C(1) atom and on the hydrogen atoms attached to C(2) but not on the oxygen atom. In fact, the $\text{C}(1) \cdots \text{Cl}$ and $\text{C}(2)\text{H}_3 \cdots \text{Cl}$ intramolecular distances between the nonbonded atoms are almost always smaller than the sums of the van der Waals radii of the corresponding atoms, whereas the $\text{Cl} \cdots \text{O}$ distances are greater than the sum of the covalent radii of Cl and O. This conclusion was totally confirmed by the data of an *ab initio* LCAO MO SCF calculation.¹⁰¹ The results of this quantum-chemical calculation are in good agreement with the experimental values of bond lengths and bond angles shown in Scheme 13.



Scheme 13

The electron density distribution in the MeCO^+ ion inferred from an X-ray diffraction structural study of $\text{MeCO}^+\text{SbF}_6^-$ (see Ref. 102) is, in our opinion, less probable,⁹⁴ because, according to these data, the charge on the hydrogen atom (+0.07) in CH_3CO^+ is close to that in ethane, which is at variance with a number of other studies indicating that the hydrogen atoms in the acylium cation carry a substantial positive charge.

According to X-ray diffraction studies, the Lewis acid in nonionic $\text{RCOX} \cdot \text{AlX}_3$ complexes is coordinated to the electron pair of the oxygen atom of the acyl halide. This follows from the presence of Al–O bonds in these compounds. The Al–O bond lengths vary in the range 1.820–1.847 Å, and they are only slightly larger than the Al–O bond lengths in such stable compounds as aluminosilicates (1.79 Å). The complex formation involving oxygen results in the elongation of the C–O bond (1.21–1.24 Å) compared to this bond in noncoordinated RCOX (1.17 Å).¹⁰³ It is significant that the C–O and C–Cl bond lengths are much the same in various donor-acceptor complexes, which apparently indicates that their strengths are similar. Conversely, the C–C bond lengths in donor-acceptor complexes of the aliphatic and aromatic series are markedly different. For example, the C(1)–C(2) bond length in the complex $\text{EtC}(\text{Cl})=\text{O} \rightarrow \text{AlCl}_3$ is close to the length of the classical $\text{C}_{\text{sp}^3}-\text{C}_{\text{sp}^2}$ bond, while the Ar–C bond

in complexes like $\text{ArC(X)=O} \rightarrow \text{AlX}_3$ is shorter than the Ar-C bond in a non-coordinated ArC(X)=O molecule.⁹⁴ A specific feature of the geometry of the donor-acceptor complexes $\text{ArC(X)=O} \rightarrow \text{AlX}_3$ is a substantial increase in the bond angles with respect to 120° typical of an sp^2 -hybridised carbon atom. This distortion of the angles has been attributed¹⁰⁴ to steric effects occurring upon packing of the molecules in a crystal. The geometry of the O-AlCl_3 fragment is that of a somewhat distorted tetrahedron.⁹⁴

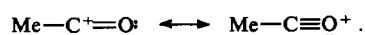
According to ^{81}Br NQR data,¹⁰⁵ the $\text{AcBr} \cdot \text{AlBr}_3$ complex at 77 K is an ionic acetylum salt. The same complex obtained in a solution in CH_2Br_2 at 77 K exists as the ionic salt $\text{MeCO}^+[\text{AlBr}_4 \rightarrow \text{CH}_2\text{Br}_2]^-$.

The $\text{RCOX} \cdot \text{AlX}_3$ systems have been studied in a broad range of solvents (CH_2Cl_2 , CH_2Br_2 , CHCl_3 , $\text{C}_2\text{H}_4\text{Cl}_2$, $\text{C}_6\text{H}_5\text{NO}_2$, MeNO_2 , SO_2 , HF , $\text{CF}_3\text{SO}_3\text{H}$, etc.) by IR, Raman, and ^1H , ^{13}C , and ^{27}Al NMR spectroscopy.^{41, 94, 106–109} The whole set of the results obtained indicate that in the solvents listed above, except for strong protic acids, the systems under study exist exclusively as donor-acceptor complexes (the state of these systems in SO_2 is less definite⁹⁴).

1. Acylation of arenes

Since 1877, when the AlCl_3 -catalysed acylation of aromatic hydrocarbons was discovered by Friedel and Crafts,¹¹⁰ the mechanism of this reaction has been intensely studied both by the same researchers and by many others. The current views on the nature of the active species involved in this process and the arguments in favour of the concept outlined are the following.¹¹¹

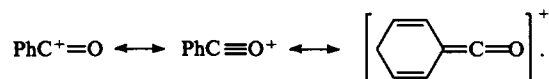
The acetylum cation is a relatively weak electrophile due to the resonance stabilisation of the carbocation centre by the electron pairs of the oxygen atom.



Therefore, it seems unlikely that benzene or other non-activated arenes would react with the acetylum cation or with the donor-acceptor complex, which is even less reactive. In fact, a study of the influence of the acidity of the medium on the rate of acetylation and benzoylation of benzene, toluene, and chlorobenzene with $\text{MeCO}^+ \text{SbF}_6^-$ and $\text{PhCO}^+ \text{SbF}_6^-$ has led to the conclusion that in an acidic medium, the protonated acetylum $\text{MeC}^+ = \text{O}^+ \text{H}$ or $\text{PhC}^+ = \text{O}^+ \text{H}$ is the main reacting species.¹¹¹ For example, the reaction of benzene with $\text{MeCO}^+ \text{SbF}_6^-$ carried out in CF_3COOH ($H_0 = -2.7$) at 5°C for 12 h, yields less than 10% of acetophenone, while chlorobenzene remains unchanged over a period of 24 h under the same conditions. The rate of acetylation increases by a factor of 10 and more on passing from a solvent with $H_0 = -12$ (a mixture of CF_3COOH with $\text{CF}_3\text{SO}_3\text{H}$) to a solvent with $H_0 = -14$ ($\text{CF}_3\text{SO}_3\text{H}$).¹¹¹ The NMR data indicate that for $H_0 = -12$, the proportion of the MeCO^+ ion in the complex is 60%, whereas for $H_0 = -14$, it reaches 75%. Calculations show that if it were the acetylum cation that acted as the reactive species, the acylation rate would increase by a factor of less than 2 following the change in the acidity from $H_0 = -12$ to $H_0 = -14$.

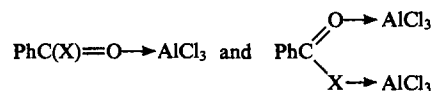
Unlike benzene and chlorobenzene, toluene, which is more reactive, gives acetylation products in 55% yield over a period of 12 h at 0°C in CF_3COOH . However, the ratios of the isomers resulting from the acetylation of toluene in CF_3COOH and $\text{CF}_3\text{SO}_3\text{H}$ are markedly dissimilar, which indicates that the process occurs by different mechanisms in the media with different acidities. Conversely, the isomeric compositions of the acylation products obtained in media with $H_0 = -10$ and -18 are identical. It has been assumed that toluene, which is an activated arene, is capable of being acetylated with the MeCO^+ ion in low-acidity media. The strong acid HSbF_5X formed in this reaction also can catalyse subsequent reactions. In a medium with higher acidity, the reaction involving the protonated acetylum cation is the main route for the acylation of toluene.

The benzoylation of arenes with $\text{PhCO}^+ \text{SbF}_6^-$ follows the same regularities. It is noteworthy that an increase in the benzoylation rate is observed at a higher acidity than $H_0 = -14$, although spectral studies indicate that at $H_0 = -14$, the system exists exclusively as the ionic salt $\text{PhCO}^+ \text{SbF}_6^-$.¹¹¹ The fact that benzoylation requires more acidic media than acetylation has been explained¹¹¹ by the lower reactivity of aryl cations ArCO^+ compared to that of the acylium cations AlkCO^+ , which is due to the contribution of ketene-like structures.



It has also been suggested that the species formed from two acceptor molecules play an important role in the acylation of arenes in organic media. This hypothesis was stated for the first time by Gillet to account for the activating influence of AlCl_3 on the synthesis of ketones from arenes and $\text{RCOX} \cdot \text{AlCl}_3$ complexes.¹¹² The hypothesis of Gillet was soon confirmed experimentally.

A kinetic study of the AlCl_3 -catalysed benzoylation of aromatic hydrocarbons¹¹³ has led to a complex equation for the rate constant, most closely consistent with the concept of participation of complexes of two types



Based on a kinetic study of the acylation of arenes with acetyl chloride in the presence of AlCl_3 in dichloroethane, *ortho*-dichlorobenzene, or in excess acetyl chloride, the workers cited¹¹³ concluded that complexes of three types participate in the reaction, namely, $\text{MeCO}^+ \text{AlCl}_4^-$, $\text{MeC(Cl)=O} \rightarrow \text{AlCl}_3$, and $\text{Cl}_3\text{Al} \leftarrow \text{ClC(Me)=O} \rightarrow \text{AlCl}_3$.

Other investigators,¹¹⁴ who have also studied the acylation of benzene with $\text{RCOCl} \cdot \text{AlCl}_3$ complexes in dichloroethane, have shown that this reaction can be described by a simpler equation

$$v = k[\text{ArH}][\text{RCOCl} \cdot \text{AlCl}_3]$$

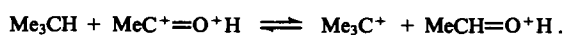
The benzoylation of arenes with acyl halides in the presence of AlBr_3 , at $[\text{AlBr}_3]:[\text{PhCOBr}]$ molar ratios of 1 and 1.5 has been shown¹¹⁵ to obey second-order kinetics. Further increase in the amount of AlBr_3 results in a change in the reaction mechanism. In this case, the reaction rate is described by a third-order equation. The rate constants (k) for the benzoylation in a trichlorobenzene solution are given below.

$[\text{AlBr}_3]:[\text{PhCOBr}]$	1	1.5	2	2.5	3
k	0.4	6.0	128	225	327

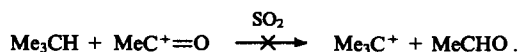
It is seen from the above data that on passing from the $\text{PhCOBr} \cdot \text{AlBr}_3$ system to the $\text{PhCOBr} \cdot 2\text{AlBr}_3$ system, the rate constant for benzoylation increases by a factor of 320. When the quantity of AlBr_3 is further increased, the rate constant smoothly and slightly increases. The researchers¹¹⁵ could not explain this phenomenon, and they stated only that the electrophilicity of $\text{PhCOBr} \cdot n\text{AlBr}_3$ systems at $n = 2$ is markedly higher than that at $n = 1$.

2. The nature of active species in reactions of activated alkanes with acylium salts in media of protic superacids

The results obtained for reactions of isobutane with the acetylum cation are in full agreement with the above data on the protonated acylium cations as the species responsible for the acylation of arenes in acidic media. Brouwer and Kiffen⁸⁸ have reported on the hydride transfer from isobutane to the acetylum cation generated from acetic acid in an $\text{HF}-\text{BF}_3$ medium.



At the same time, Olah and coworkers¹¹⁶ have shown that in aprotic solvents such as SO_2 , SO_2ClF , AsF_3 , and CH_2Cl_2 this reaction with the acetylium cation does not occur.

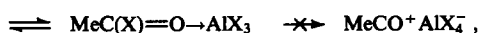
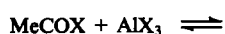


The views about a crucial role for protonated acetylium are in agreement with the results of calculations, which indicate that the abstraction of a hydride ion from isobutane by the acetylium cation in the gas phase requires $8.5 \text{ kcal mol}^{-1}$. The protonated acylium dication has not been detected by ^1H NMR; however, in the IR spectrum of the acetylium cation in a protic superacid, a shift of the frequency corresponding to the carbonyl group has been observed. Calculations have shown that a global minimum on the potential energy surface corresponds to the $[\text{MeC}-\text{OH}]^{2+}$ structure.¹¹⁷ It should be noted that the $\text{C}_2\text{H}_4\text{O}^{2+}$ dication has also been observed in the gas phase by mass spectrometry.¹¹⁸

3. The nature of active species generated in aprotic superacids $\text{RCOX} \cdot 2\text{AlX}_3$ and responsible for their reactivity toward alkanes

In order to understand the reason for the high reactivity of the $\text{RCOX} \cdot 2\text{AlX}_3$ complexes, which differs so markedly from the reactivity of the corresponding equimolar $\text{RCOX} \cdot \text{AlX}_3$ complexes, we have studied the structures of both types of complexes in the solid state and in solutions in CH_2X_2 using ^{81}Br NQR, ^1H , ^{13}C , ^{27}Al , and ^{17}O NMR (in the solid state and in solutions), IR, and Raman spectroscopy.^{41, 105, 109} It was found that in the solid state complexes of both types are ionic acylium salts differing only in the structure of the anions: $\text{MeCO}^+ \text{Al}_2\text{X}_7^-$ for $\text{MeCOX} \cdot 2\text{AlX}_3$ or $\text{MeCO}^+ \text{AlX}_4^-$ for $\text{MeCOX} \cdot \text{AlX}_3$. This conclusion is at variance with the suggestion of Bertoluzza, who has attributed the structure $(\text{Ac}^+ \cdot \text{AlCl}_3)^+ \text{AlCl}_4^-$ to the isolated complex $\text{AcCl} \cdot 2\text{AlCl}_3$.¹¹⁹

In CH_2X_2 solutions, the former complexes exist as equilibrium mixtures of acylium salts $\text{MeCO}^+ \text{Al}_2\text{X}_7^-$ and donor-acceptor complexes $\text{MeC}(\text{X})=\text{O} \rightarrow \text{Al}_2\text{X}_6$, whereas the latter exist exclusively as coordination complexes $\text{MeCO}(\text{X})=\text{O} \rightarrow \text{AlX}_3$.

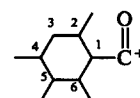


Thus, only $\text{RCOX} \cdot 2\text{AlX}_3$ ($\text{R} = \text{Alk}$), which are active in the reactions with alkanes, are able to generate effectively acylium cations in low-polarity solutions, and this is their basic difference from the corresponding equimolar complexes. A comparison of two pairs of complexes: $\text{MesCO}^+ \text{Al}_2\text{Br}_7^-$ and $\text{MesCO}^+ \text{AlBr}_4^-$ ($\text{Mes} = 2,4,6\text{-Me}_3\text{C}_6\text{H}_2$), on the one hand, and $\text{Ac}^+ \text{Sb}_2\text{F}_{11}^-$ and $\text{Ac}^+ \text{SbF}_6^-$ in SO_2 , on the other hand, has shown that only acylium salts with dimeric anions are active in the reactions with alkanes under mild conditions (Table 5).¹²⁰

The very close similarity of the ^1H and ^{13}C NMR spectra of active and inactive complexes of the composition $\text{RCOX} \cdot n\text{AlX}_3$ ($n = 1, 2$) differing only in the structure of the anion (Table 6) gave grounds to suggest that it is not the acylium salts themselves that

Table 6. ^{13}C NMR spectra of $\text{MesCO}^+ \text{X}^-$ salts with anions $\text{X}^- = \text{AlBr}_4^-$ and $\text{X}^- = \text{Al}_2\text{Br}_7^-$ (δ , ppm).¹²⁰

δ , ppm		Assignment
$\text{X}^- = \text{AlBr}_4^-$	$\text{X}^- = \text{Al}_2\text{Br}_7^-$	
21.4	21.7	C(2)-CH ₃
23.7	24.2	C(4)-CH ₃
85.3	84.6	C(1)
153.7	153.9	C(2)
130.9	131.5	C(3)
162.1	163.1	C(4)
159.2	159.7	CO



Note. In the ^{27}Al NMR spectra of the $\text{MesCO}^+ \text{AlBr}_4^-$ and $\text{MesCO}^+ \text{Al}_2\text{Br}_7^-$ complexes, the corresponding shifts of the ^{27}Al nuclei are 79.4 ($\Delta = 12 \text{ Hz}$) and 93.0 ppm ($\Delta = 930 \text{ Hz}$).

are responsible for the superacidic properties of the $\text{RCOX} \cdot 2\text{AlX}_3$ systems. It was suggested that in solutions, the acylium salts with the dimeric anions Al_2X_7^- occur in an equilibrium with more electrophilic ionic complexes, namely, cationic acylium complexes of the type **10a** or **10b** in which the cation is additionally coordinated to the Lewis acid.^{41, 94, 120}

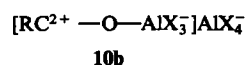
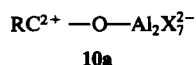
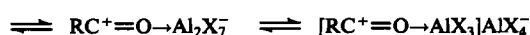


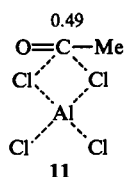
Table 5. Comparison of the activities of acylium salts with monomeric and dimeric anions in the cracking of *n*-alkanes and in the isomerisation of trimethylenenorbornane **9** (according to a published study¹²⁰).

Hydrocarbon (RH)	Acylium salt (A)	[RH]:[A]	t/h	Conversion of RH (%)	Products (yields relative to RH, mass %)
<i>n</i> -C ₈ H ₁₈	$\text{Ac}^+ \text{SbF}_6^-$	1:1	3.0	0	—
<i>n</i> -C ₈ H ₁₈	$\text{Ac}^+ \text{Sb}_2\text{F}_{11}^-$	1:1	3.0	100	iso-C ₄ H ₁₀ (31) + oligomer (59)
<i>n</i> -C ₈ H ₁₈	$\text{Ac}^+ \text{Sb}_2\text{F}_{11}^-$	1:1	1.0	100	iso-C ₄ H ₁₀ (36) + oligomer (56)
<i>n</i> -C ₁₂ H ₂₆ ^a	$\text{Ac}^+ \text{Sb}_2\text{F}_{11}^-$	1:1	2.0	85	see ^b
<i>n</i> -C ₈ H ₁₈ ^c	$\text{MesCO}^+ \text{AlBr}_4^-$	1:4	0.5	0	—
<i>n</i> -C ₈ H ₁₈ ^c	$\text{MesCO}^+ \text{Al}_2\text{Br}_7^-$	1:4	0.5	100	see ^b
<i>n</i> -C ₁₂ H ₂₆ ^c	$\text{MesCO}^+ \text{AlBr}_4^-$	1:2	0.5	0	—
<i>n</i> -C ₁₂ H ₂₆ ^c	$\text{MesCO}^+ \text{Al}_2\text{Br}_7^-$	1:2	0.5	100	see ^b
9	$\text{MesCO}^+ \text{AlBr}_4^-$	1:10	5.0	0	—
9	$\text{MesCO}^+ \text{Al}_2\text{Br}_7^-$	1:10	5.0	37	adamantane (37)
9	$\text{MesCO}^+ \text{Al}_2\text{Br}_7^-$	1:10	8.0	86	adamantane (54)

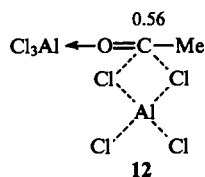
^a In SO_2 . ^b Not determined. ^c In CH_2Br_2 .

It is clear that the additional coordination should lead to a more electrophilic cation, which in its extreme form, can be represented as the acylium dication. The fact that these species are difficult to detect experimentally must be due to their very low concentration.

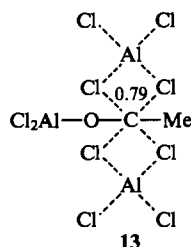
Data about the complexes that can be generated in the $\text{MeCOCl} \cdot n\text{AlCl}_3$ systems ($n = 1-3$) have also been obtained by semiempirical CNDO quantum-chemical calculations. The most significant conclusion which can be drawn from these calculations is that in the systems containing an excess of aluminium chloride ($n = 2$ and 3), the formation of complexes **12** and **13**, in which the carbonyl carbon atoms carry larger positive charges than this carbon atom in the acetylium cation **11**, is in principle possible.¹²¹



$$H_0 = -185 \text{ kcal mol}^{-1}$$



$$H_0 = -322 \text{ kcal mol}^{-1}$$



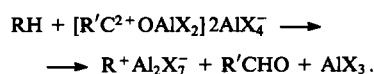
$$H_0 = -423 \text{ kcal mol}^{-1}$$

In the complex **12**, which can be regarded as the acetylium cation with a donor–acceptor bond $=\text{O} \rightarrow \text{AlCl}_3$ (**10b**) postulated previously as a key intermediate, the electron density on all the atoms in the $\text{MeC}=\text{O}$ fragment is substantially lower than that in the non-coordinated cation **11**: the positive charge on the carbonyl carbon atom is $+0.56$. The structure of **13**, which also corre-

sponds to a local minimum on the potential energy surface, is of special interest. The complex **13** can be regarded as a system incorporating a $\text{Cl}_2\text{Al}-\text{OC}^2+\text{Me}$ dication and two AlCl_4^- anions. The charge on the carbon atom in this complex reaches a record value of $+0.79$.

Table 7 presents the enthalpies of the reactions, which characterise the relative stabilities of the $\text{MeCOCl} \cdot n\text{AlCl}_3$ complexes. From the data given in the Table, it follows that the reactions (1) and (2) leading to charged species are strongly endothermic. The formation of the polar complex **11** requires less energy than the formation of separated ions. It should be taken into account that these data refer to the gas phase, whereas the energies of formation of the ions in solution can be much lower due to solvation and agglomeration. In fact, the existence of acetylium salts in solution has been proved, although calculations for the reactions (1) and (2) indicate that their formation requires a lot of energy ($110.5 \text{ kcal mol}^{-1}$). The formation of donor–acceptor complexes of the composition 1 : 1 and 1 : 2 involves either release of energy or absorption of a small quantity of energy. It is significant that the formation of the complex **12** and even of the dicationic complex **13** in the reaction of acetyl chloride with AlCl_3 (but not with Al_2Cl_6) is energetically favourable, unlike the formation of the acetylium complex **11**.

Thus, the complexes **12** and **13** can be regarded as the most likely key superelectrophiles, which are responsible for the high activity of acyl halides (in the presence of excess aluminium halides) with respect to alkanes. Apparently, the role of the complex **13** is manifested only when the reaction mixture contains a substantial excess of aluminium halide. The generation of the carbenium ions from alkanes under the action of $\text{RCOX} \cdot 2\text{AlX}_3$ can be represented as follows:



At present, the idea concerning the participation of dications or even of multicharged positive ions in organic reactions is becoming more and more popular.^{117, 121}

Table 7. Enthalpies (ΔH) of reactions, characterising the stability of the $\text{MeCOCl} \cdot n\text{AlCl}_3$ complexes (according to a published study¹²¹).

Number of the reaction	Reaction	$\Delta H/\text{kcal mol}^{-1}$
(1)	$\text{MeCOCl} + \frac{1}{2} \text{Al}_2\text{Cl}_6 \longrightarrow \text{O}=\text{C}^+\text{Me} + \text{AlCl}_4^-$	110.5
(2)	$\text{MeC}(\text{Cl})=\text{O} \rightarrow \text{AlCl}_3 + \frac{1}{2} \text{Al}_2\text{Cl}_6 \longrightarrow \text{MeC}(\text{Cl})=\text{O} \rightarrow \text{AlCl}_2^+ + \text{AlCl}_4^-$	98.3
(3)	$\text{MeCOCl} + \frac{1}{2} \text{Al}_2\text{Cl}_6 \longrightarrow (\text{MeC}^+\text{O})\text{AlCl}_4^-$ 11	35.7
(4)	$\text{MeC}(\text{Cl})=\text{O} \rightarrow \text{AlCl}_3 \longrightarrow \text{MeC}(\text{Cl})_2\text{OAlCl}_2$	24.9
(5)	$\text{MeCOCl} + \frac{1}{2} \text{Al}_2\text{Cl}_6 \longrightarrow \text{MeC}(\text{Cl})=\text{O} \rightarrow \text{AlCl}_3$	-7.5
(6)	$\text{MeCOCl} + \frac{1}{2} \text{Al}_2\text{Cl}_6 \longrightarrow \text{MeC}(\text{O})\text{Cl} \rightarrow \text{AlCl}_3$	5.4
(7)	$\text{MeCOCl} + \text{Al}_2\text{Cl}_6 \longrightarrow \text{MeC}(\text{Cl})=\text{O} \rightarrow \text{Al}_2\text{Cl}_6$	-2.9
(8)	$\text{MeCOCl} + \text{Al}_2\text{Cl}_6 \longrightarrow [\text{MeC}=\text{O} \rightarrow \text{AlCl}_3]^+ \text{AlCl}_4^-$ 12	-4.4
(9)	$\text{MeCOCl} + \frac{3}{2} \text{Al}_2\text{Cl}_6 \longrightarrow [\text{MeC}^{2+} \text{OAlCl}_2] 2\text{AlCl}_4^-$ 13	75.4
(10)	$\text{MeCOCl} + 3\text{AlCl}_3 \longrightarrow [\text{MeC}^{2+} \text{OAlCl}_2] 2\text{AlCl}_4^-$ 13	-2.3

VI. Conclusion

The high selectivity and the ease of one-stage functionalisation reactions, the high yields of products, and the accessibility of both initial compounds and $\text{RCOX} \cdot n\text{AlX}_3$ complexes (which are obtained by mere mixing of acyl halides with aluminium halides) suggest that the reactions considered above can be of interest as methods for the laboratory syntheses of organic compounds from alkanes and cycloalkanes.

The 'classical' Friedel–Crafts complexes can find application in the functionalisation of activated saturated hydrocarbons. The superacidic $\text{RCOX} \cdot 2\text{AlX}_3$ complexes substantially extend the possibilities for the direct functionalisation of alkanes and make it possible to perform selective and effective transformations of linear alkanes and simple cycloalkanes into functional derivatives.

The conclusion that dication-type species play a key role in the reactions of alkanes with $\text{RCOX} \cdot 2\text{AlX}_3$ complexes has stimulated the search for new superelectrophilic complexes, which would be more accessible and more convenient to work with than the complexes based on acyl halides and would open the way to new types of functionalisation. Testing of a number of systems in which the generation of dications is, in principle, possible has led in recent years to new aprotic superacids, which are quite promising regarding the functionalisation of alkanes.^{123–128} The direct one-stage synthesis of organic compounds from saturated hydrocarbons may be accomplished in the near future, at least, for lower alkanes and cycloalkanes, which are relatively resistant to cracking. The subsequent important and complicated task is to develop new superacids containing no aluminium halides. The advantages of such systems are obvious. In this case, the problem of catalyst regeneration as well as ecological problems would be solved more easily.

Advances in the development of homogeneous aprotic superacids also seem very important for the elaboration of solid superacids of a new generation, which play a crucial role in the chemistry of alkanes.

This work was partially supported by the Russian Foundation for Basic Research (Grant 96-03-33255) and by the International Science Foundation (Grant MRA 000). During the preparation of this review, we were encouraged and given practical support by Professor Yu. T. Struchkov. To our great sorrow, we could not express our gratitude to him fully — it remains in our hearts.

References

1. *Heterogeneous Catalysis in Practice* (Ed. C N Satterfield) (New York: McGraw-Hill, 1984)
2. C L Hill (Ed.) *Activation and Functionalization of Alkanes* (New York: Wiley-Interscience, 1989)
3. *New J. Chem.* **10/11** 13 (1989)
4. *Activation of Saturated Hydrocarbons by Transition Metal Complexes* (Ed. A E Shilov) (Dordrecht: Reidel, 1985)
5. G A Olah, G K S Prakash, J Sommer *Superacids* (New York: Wiley-Interscience, 1985)
6. G A Olah, G K S Prakash, in *The Chemistry of Alkanes and Cycloalkanes* Part 13 (Eds S Patai, Z Rapport) (Chichester: Wiley-Interscience, 1992) p. 609
7. G A Olah *Nobel Lecture. Angew. Chem., Int. Ed. Engl.*, **13/14** 1393 (1995)
8. J Allison, R B Freas, D P Ridge *J. Am. Chem. Soc.* **101** 1332 (1979)
9. R B Freas, D P Ridge *J. Am. Chem. Soc.* **102** 7129 (1980)
10. B S Larsen, D P Ridge *J. Am. Chem. Soc.* **106** 1912 (1984)
11. P B Armentrout, J L Beauchamp *J. Am. Chem. Soc.* **102** 1736 (1980); **103** 784 6628 (1981)
12. R D Radecki, J Allison *Organometallics* **5** 4110 (1986)
13. R Georgiadis, E R Fisher, P B Armentrout *J. Am. Chem. Soc.* **111** 4251 (1989)
14. S W Buchner, B S Freiser *Polyhedron* **7** 1583 (1988)
15. K Eller, H Schwarz *Chem. Rev.* **91** 1121 (1991)
16. K Eller *Coord. Chem. Rev.* **126** 93 (1993)
17. I S Akhrem, M E Vol'pin *Usp. Khim.* **59** 1906 (1990) [*Russ. Chem. Rev.* **59** 1118 (1990)]
18. S C Davis, K J Klabunde *J. Am. Chem. Soc.* **100** 5973 (1978)
19. R J Remick, T A Asunta, P S Skell *J. Am. Chem. Soc.* **101** 1320 (1979)
20. S C Davis, S J Severson, K J Klabunde *J. Am. Chem. Soc.* **103** 3024 (1981)
21. G Vitulli *J. Organomet. Chem.* **239** 23 (1982)
22. K Matsuo, K Klabunde *J. Catal.* **73** 216 (1982)
23. K J Klabunde, Y Imizu *J. Am. Chem. Soc.* **106** 2721 (1984)
24. I S Akhrem, S V Reznichenko, N M Chistovalova, V V Grushin, M E Vol'pin *Catal. Lett.* **20** 275 (1993)
25. P Gallezo, in *Tez. Dokl. V Mezhdunar. Simpoziuma po Svyazi Mezhd. Homogennym i Geterogennym Katalizom* (Abstracts of Reports of the Fifth International Symposium on the Correlation between Homogeneous and Heterogeneous Catalysis) (Novosibirsk: Institute of Catalysis, Siberian Branch of Academy of Sciences of the USSR, 1986) Vol. 3, Part 2
26. J A Bandy, G M Cloke, M L H Green *J. Chem. Soc., Chem. Commun.* **240** (1984); **355** (1985)
27. M L H Green, G Parker *J. Chem. Soc., Chem. Commun.* **1467** (1984)
28. S Davis, K J Klabunde *Chem. Rev.* **82** 153 (1982)
29. *Characterisation of Catalysts*. (Eds J M Thomas, R M Lambert) (Chichester: Wiley-Interscience, 1980)
30. G A Somorjai *Science* **201** 489 (1978)
31. S C Davis, F Zaera, G A Somorjai *J. Catal.* **77** 439 (1982)
32. J M Thomas *Pure Appl. Chem.* **60** 1517 (1988)
33. J R Engstrom, D W Goodman, W H Weinberg *J. Am. Chem. Soc.* **110** 8305 (1988)
34. G A Somorjai *Pure Appl. Chem.* **60** 1499 (1988)
35. M Mella, M Freccero, A Albini *J. Chem. Soc., Chem. Commun.* **41** (1995)
36. A I Shatenshtein *Usp. Fiz. Nauk* **1** 153 (1963)
37. M Ichikawa, K Kawase, K Tamaru *J. Chem. Soc., Chem. Commun.* **177** (1972)
38. S M Yunusov, M A Ilatovskaya, S Rumel', M German, E I Mysov *Izv. Akad. Nauk SSSR, Ser. Khim.* **1214** (1989)
39. M A Ilatovskaya, S Rumel', Yu V Isaev, S M Yunusov, V D Lenenko, M German, M Varen, Yu N Novikov, V B Shur *Izv. Akad. Nauk SSSR, Ser. Khim.* **1935** (1991)
40. I S Akhrem, A V Orlinkov, E I Mysov, M E Vol'pin *Tetrahedron Lett.* **22** 3891 (1981)
41. M Vol'pin, I Akhrem, A Orlinkov *New J. Chem.* **13** 771 (1989)
42. *Friedel-Crafts and Related Reactions* Vol. 1 (Ed. G A Olah) (New York: Wiley-Interscience, 1963)
43. *Friedel-Crafts and Related Reactions* Vol. 3 (Ed. G A Olah) (New York: Wiley-Interscience, 1964)
44. P H Gore *Chem. Rev.* **55** 229 (1955)
45. S Patai, in *The Chemistry of Acyl Halides* Parts 4 and 8 (London: Wiley-Interscience, 1972) p. 547
46. C D Nenitzescu, C N Ionescu *Ann. Chim.* **491** 189 (1931)
47. C D Nenitzescu, I P Cantuniary *Chem. Ber.* **65** 807 1449 (1932)
48. C D Nenitzescu, I P Cantuniary *Ann. Chim.* **510** 269 (1934)
49. F Unger *Chem. Ber.* **65** 467 (1932)
50. N D Zelinsky, E M Tarasova *Ann. Chim.* **508** 113 (1934)
51. N D Zelinsky, E M Tarasova *Chem. Ber.* **65** 1249 (1932)
52. C D Nenitzescu, E Cioranescu, I P Cantuniary *Chem. Ber.* **70** 277 (1937)
53. H Hoppff *Chem. Ber.* **65** 482 (1932)
54. S D Nenitzescu *Usp. Khim.* **27** 399 (1957)
55. I Tabushi, K Fujita, R Oda *Tetrahedron Lett.* **5455** (1968)
56. R Pardo, M Santelli *Tetrahedron Lett.* **3843** (1981)
57. I Tabushi, K Fujita, R Oda *Tetrahedron Lett.* **4247** (1968)
58. L Otows, H Tudos, L Radics *Chem. Ind.* **18** 597 (1970)
59. G Baddeley, F Wrench *J. Chem. Soc.* **1324** (1959)
60. G Baddeley, B G Heaton, J W Rurburn *J. Chem. Soc.* **4713** (1960)
61. K E Hardling, K S Clement, J C Gilbert, R Wiechman *J. Org. Chem.* **49** 2049 (1984)
62. H-Y Ha, K-P Park *Bull. Korean Chem. Soc.* **9** 411; 2049 (1988)
63. M S Ahmad, G Baddeley, B G Heaton, J M Rasburn *Proc. Chem. Soc.* **395** (1959)
64. C Morel-Fourrier, J -P Dulcere, M Santelli *J. Am. Chem. Soc.* **113** 8062 (1991)
65. I Tabushi, J Hamuro, R Oda *Nippon Kagaku Zasshi* **89** 794 (1968)

66. H Hopff, C D Nenitzescu, D A Isacescu, I P Cantuniary *Chem. Ber.* **69** 2244 (1936)
67. C D Nenitzescu, I Chicos *Chem. Ber.* **68** 1584 (1935)
68. H Pines, N E Hoffman *J. Am. Chem. Soc.* **76** 4417 (1954)
69. I Tabushi, K Fujita, R Oda, M Tsuboi *Tetrahedron Lett.* 2581 (1969)
70. M Arnaud, A Pedra, C Roussel, J Metzger *J. Org. Chem.* **44** 2972 (1979)
71. M Arnaud, A Pedra, C Roussel *Heterocycles* **20** 761 (1983)
72. I S Akhrem, A V Orlinkov, L V Afanas'eva, M E Vol'pin *Dokl. Akad. Nauk SSSR* **298** 107 (1988)
73. H Stetter, G Wulff *Chem. Ber.* **93** 1366 (1966)
74. N C Deno, D N Lincoln *J. Am. Chem. Soc.* **88** 5357 (1966)
75. A V Orlinkov, I S Akhrem, L V Afanas'eva, M E Vol'pin *Izv. Akad. Nauk SSSR, Ser. Khim.* 2185 (1988)
76. G A Olah, P Schilling *J. Am. Chem. Soc.* **95** 7680 (1973)
77. Y Halpern *Isr. J. Chem.* **13** 99 (1975)
78. I S Akhrem, A V Orlinkov, S V Vitt, L V Afanas'eva, M E Vol'pin *Izv. Akad. Nauk SSSR, Ser. Khim.* 2028 (1989)
79. I S Akhrem, S Z Bernadyuk, M E Vol'pin *Mendeleev Commun.* 188 (1993)
80. H Koch, W Haaf *Angew. Chem.* **72** 628 (1960)
81. A V Orlinkov, I S Akhrem, L V Afanas'eva, S V Vitt, M E Vol'pin *Izv. Akad. Nauk SSSR, Ser. Khim.* 105 (1991)
82. H Hopff, R Roggero, G Valkanas *Rev. Chim. (Bucharest)* **7** 921 (1962); *Chem. Abstr.* **61** 4201 (1964)
83. Br. P. 783 037 (1957)
84. G A Olah, Q Wang, G K S Prakash *J. Am. Chem. Soc.* **112** 3697 (1990)
85. A I Nesmelov, A V Orlinkov, V B Murachev, I S Akhrem, V S Byrikhin, M E Vol'pin *Izv. Akad. Nauk SSSR, Ser. Khim.* 2233 (1988)
86. I S Akhrem, A V Orlinkov, S V Vitt, L A Afanas'eva, M E Vol'pin *Izv. Akad. Nauk SSSR, Ser. Khim.* 1253 (1993)
87. I Akhrem, A Orlinkov, M Vol'pin *J. Chem. Soc., Chem. Commun.* 257 (1993)
88. D N Brouwer, A A Kiffen *Recl. Trav. Chem., Pays-Bas* **92** 689 (1973)
89. J Bertram, J -P Coleman, M Fleischmann, D Pletcher *J. Chem. Soc., Perkin Trans. 2* 374 (1973)
90. G A Olah, Y Halpern, J Shen, Y K Mo *J. Am. Chem. Soc.* **95** 4960 (1973)
91. G A Olah, J A Olah *J. Am. Chem. Soc.* **93** 1251 (1971)
92. P R Schreiner, P v R Schleyer, H F Schaefer, III *J. Am. Chem. Soc.* **115** 9659 (1993)
93. B Chevrier, R Weiss *Angew. Chem., Int. Ed. Engl.* **13** 1 (1974)
94. A V Orlinkov, I S Akhrem, M E Vol'pin *Usp. Khim.* **60** 1049 (1991) [*Russ. Chem. Rev.* **60** 524 (1991)]
95. B Chevrier, A M White *Carbonium Ions* Vol. 5 (New York: Wiley-Interscience, 1976) p. 2049
96. D Seyferth *Organometallic Chemical Reviews. Library 9* (Amsterdam: Elsevier, 1980) p. 19
97. J M Carpentier, R Weiss *Acta Crystallogr., Sect. B* **28** 1421 (1972)
98. J M Carpentier, R Weiss *Acta Crystallogr., Sect. B* **28** 1437 (1972)
99. S E Rasmussem, N C Broth *Acta Chem. Scand.* **20** 1351 (1966)
100. B Chevrier, J M Carpentier, R Weiss *Acta Crystallogr., Sect. B* **28** 2659 (1972)
101. D R Yarkony, H F Schaefer *J. Chem. Phys.* **63** 4317 (1975)
102. F P Boer *J. Am. Chem. Soc.* **90** 6706 (1968)
103. A J Gordon, R A Ford *The Chemists Companion. A Handbook of Practical Data, Techniques, and References* (New York: Wiley Interscience, 1972)
104. B Chevrier, J M Carpentier, R Weiss *J. Am. Chem. Soc.* **94** 5718 (1972)
105. I Yu Amiantov, T L Khotsyanova, I S Akhrem, A V Orlinkov, M E Vol'pin *Zh. Strukt. Khim.* **25** 46 (1984)
106. G A Olah, M E Moffatt, S J Kuhn *J. Am. Chem. Soc.* **86** 2198 (1964)
107. J Wilinsky, R Kurland *J. Am. Chem. Soc.* **100** 2233 (1978)
108. S Brownstein, B Glavincevsky *J. Org. Chem.* **47** 1005 (1982)
109. I S Akhrem, A V Orlinkov, V I Bakhmutov, P V Petrovskii, P I Pekhk, E G Lipmaa, M E Vol'pin *Dokl. Akad. Nauk SSSR* **284** 627 (1985)
110. C Friedel, J M Crafts *C. R. Hebd. Seances Acad. Sci.* **84** 1392 (1877)
111. Y Sato, M Yato, P Ohwada, S Saito, K Shudo *J. Am. Chem. Soc.* **117** 3037 (1995)
112. G Gillet *Ind. Chem. Belg.* **3** 235 (1962)
113. R Corriu, M Dore, R Thomassin *Tetrahedron* **28** 5819 (1971)
114. A Kawasaki, G Ogata *Tetrahedron* **28** 217 (1972)
115. H C Brown, G Marino *J. Am. Chem. Soc.* **81** 3303 (1959)
116. G A Olah, A Germain, H C Lin, D A Forsyth *J. Am. Chem. Soc.* **97** 2928 (1975)
117. G A Olah *Angew. Chem.* **32** 775 (1993)
118. W Koch, G Frenking, H Schwarz, F Maquin, D Stahl *Int. J. Mass. Spectrom. Ion. Process.* **63** 59 (1985)
119. A Bertoluzza *Estrada dai Rend. Accad. Naz. dei XI, Ser. IV* Rome, 1969, Vol. XX; quoted by *J. Chem. Soc. A* 366 (1969)
120. I S Akhrem, A V Orlinkov, V I Bakhmutov, L V Afanas'eva, M E Vol'pin *Izv. Akad. Nauk SSSR, Ser. Khim.* 2490 (1990)
121. I V Stankevich, A L Chistyakov, I S Akhrem, A V Orlinkov, M E Vol'pin *Izv. Akad. Nauk SSSR, Ser. Khim.* 854 (1993)
122. T Ohwada, N Yamagata, K Shudo *J. Am. Chem. Soc.* **113** 1364 (1991)
123. I Akhrem, A Orlinkov, M Vol'pin *J. Chem. Soc., Chem. Commun.* 671 (1993)
124. S Z Bernadyuk, M E Vol'pin *Mendeleev Commun.* 183 (1994)
125. I Akhrem, L Afanas'eva, A Orlinkov, M Vol'pin *Mendeleev Commun.* 131 (1994)
126. I S Akhrem, A V Orlinkov, L V Afanas'eva, E T Mysov, M E Vol'pin *Tetrahedron Lett.* **36** 9365 (1995)
127. A Orlinkov, I Akhrem, S Vitt, M Vol'pin *Tetrahedron Lett.* **37** 3363 (1996)
128. I Akhrem, S Gudima, M Vol'pin *Chem. Eur. J.* **2** 812 (1996)

The structure and properties of block poly(vinylidene fluoride) and systems based on it

V V Kochervinskii

Contents

I. Introduction	865
II. The specific effect of solvents on the conformational characteristics of the chains of poly(vinylidene fluoride) obtained by polymerisation or crystallisation from solution	868
III. The influence of various factors on the polymorphism of poly(vinylidene fluoride) in the isotropic state	871
IV. Characteristics of the solid-state transformations under the conditions of tensile deformations	877
V. Characteristics of the crystallisation of poly(vinylidene fluoride) under the conditions of uniaxial compression and high pressures	882
VI. The polymorphism of the poly(vinylidene fluoride) induced by strong electric fields	884
VII. The influence of irradiation on the structure of poly(vinylidene fluoride) and its copolymers	892
VIII. Characteristics of the dynamics of the chains in the block state of isotropic and anisotropic poly(vinylidene fluoride) specimens	895
IX. Structural characteristics in the crystallisation of poly(vinylidene fluoride) in blends with other polymers	901
X. Conclusion	909

Abstract. The influence of external factors on the formation of various polymorphic modifications of poly(vinylidene fluoride) (PVDF) and the copolymers and blends based on it is examined. It is shown that the formation of a particular conformational structure of the PVDF chains may be controlled by regulating, for example, the fraction of irregular 'head to head' ('tail to tail') attachments and by selecting a suitable comonomer or component of the blend. It is shown that polar modifications of PVDF may be obtained by its crystallisation from solutions in specific solvents. The important role of high pressures was noted in block crystallisation. Solid-phase transformations may be initiated with the aid of tensile and compressive deformations (within certain temperature ranges), high electric fields, and exposure to radiation. It is shown that both the type of the lattice and the variety of the morphology of the PVDF change on crystallisation in a blend with amorphous poly(methyl methacrylate). The characteristics of the dynamics of the block PVDF chains, obtained predominantly with the aid of dielectric spectroscopy, have proved sensitive to the polymorphism and the kind of morphology and may yield additional information about the structure of the noncrystallising regions of the polymer under consideration. The bibliography includes 383 references.

I. Introduction

A systematic treatment of the structure and properties of poly(vinylidene fluoride) (PVDF) is of interest because it has effective piezoelectric and pyroelectric properties.^{1,2} It is one of the most promising polymeric ferroelectrics. It is used for practical purposes in the polarised state (for example, in various kinds of

transducers³), so that knowledge of the mechanism of the structural changes in strong electric fields is obligatory. Analysis of published studies has shown that polarisation processes depend on the characteristics of the structure and the nature of the molecular mobility in crystalline and amorphous regions.

One of the most informative methods for the study of the microstructure of PVDF chains is high-resolution nuclear magnetic resonance, NMR spectra of polymer solutions being recorded. A series of peaks, associated with defects in the 'head to head' or 'tail to tail' attachment, may be distinguished for ¹⁹F nuclei.⁴ As the apparatus improved, it became possible to obtain spectra at higher frequencies,^{5–8} which yield detailed information about the microstructure of the PVDF chain. In particular, the influence of the suspension (or emulsion) polymerisation method on the microstructure of the PVDF chain has been discussed.⁷ In order to obtain additional information, data on the ¹³C resonance^{9–10} or the resonances involving all three nuclei entering into the composition of the chain (¹H, ¹³C, and ¹⁹F) at once¹¹ are resorted to. The application of two-dimensional NMR spectroscopy^{12,13} has also expanded the existing ideas about the microstructure of the PVDF chain. This method is used in the study of the microstructure of the chains in vinylidene fluoride (VDF) copolymers with perfluoroalkyl trifluorovinyl ethers,¹⁴ trifluoroethene (TrFE),¹⁵ tetrafluoroethene (TFE), or hexafluoropropene.^{16,17} Having estimated the spin-spin coupling constants for neighbouring sections of PVDF in the *trans*-(*T*) or *gauche*-conformations (*G*), it is possible to estimate their proportions. For example, the fraction of the *TT* conformations for the monochlorobenzene–dimethyl sulfoxide solvent mixture increases significantly when the fraction of monochlorobenzene is reduced.¹⁸ It is assumed that there must exist a correlation between the conformations of the VPVF chains in solution and in the block state.

The crystalline phases of PVDF and of its copolymers are characterised by the presence of at least four polymorphic modifications [α (II), β (I), γ (III), and α (IV)]. These modifications are distinguished by the conformational structure of the chain and by the nature of the packing of the macromolecules in the unit cell of the crystallites. The characteristic conformational

V V Kochervinskii Troitsk Institute for Innovation and Fusion Research
142092 Troitsk, Moscow Region, Russian Federation.
Fax (7-095) 334 57 76. Tel. (7-095) 334 04 44

Received 23 October 1995

Uspekhi Khimii 65 (10) 936–987 (1996); translated by A K Grzybowski

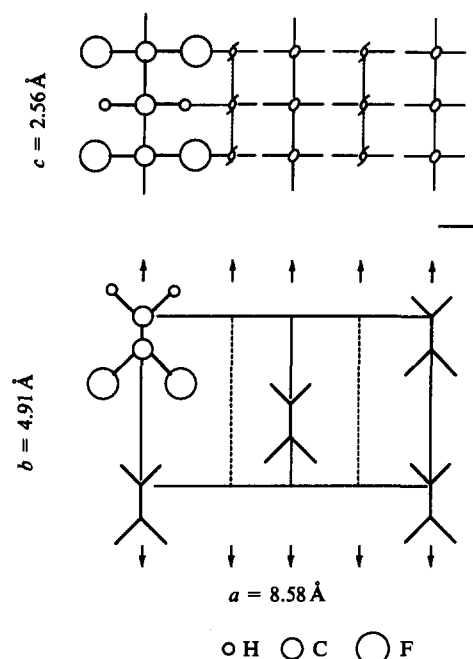


Figure 1. The structure of the crystal lattice of the β modification of PVDF.^{19, 36}

chain structures for three of the modifications listed above are presented in Figs 1–3. Evidently conformations of the $TGT\bar{G}$, $T_3GT_3\bar{G}$, and ‘planar zigzag’ types are characteristic of the α phases, γ phases, and β phases respectively.¹⁹ One may note that, owing to the phenomenon of rotational isomerism involving the hydrocarbon skeleton of the chain, the transition from the ‘planar

zigzag’ conformation to the $TGT\bar{G}$ conformation is accompanied by an almost twofold increase in the identity period along the chain (c axis of the cell).

The Raman and IR spectroscopic methods are known to be ‘sensitive’ to the short-range order, i.e. they should be more informative as regards the chain conformation. Numerous literature data on the vibrational spectra of PVDF have confirmed this.^{19–35} Table 1 presents the results of the study of PVDF crystallised in three different modifications — their symmetries and characteristic vibrational frequencies. It follows from the tabulated data that there exist a series of characteristic absorption bands for each conformation and that this can be used to identify a particular PVDF conformation.

Since Table 1 presents mainly the characteristics of localised vibrations, it should be supplemented by data on the low-frequency vibrations characterising as a rule the lattice modes of motion. Thus, according to Latour et al.,²⁰ these modes for PVDF crystallised as the α , β , and γ phases are characterised by absorption bands at 100, 70, and 90 cm^{-1} respectively.

The need to characterise PVDF and its copolymers by the degree of crystallinity α frequently arises. The so called ‘crystalline’ or ‘amorphous’ bands are usually found for this purpose in spectroscopic practice for crystallisable polymers. Such bands have been found also for PVDF. The bands at 600, 740, and 905 cm^{-1} have been classified as amorphous and those at 1180 and 1235 cm^{-1} have been classified as crystalline.^{34, 35} According to Kobayashi et al.,²⁵ the 489 cm^{-1} band for PVDF crystallised in the β and γ modification should also characterise the nonordered phase. The 442 cm^{-1} band characterises the chain vibrations in the ‘planar zigzag’ conformation present in the crystal whereas the 510 cm^{-1} band is characteristic of such conformers in the crystalline and amorphous phases.¹⁵ The conclusion that bands sensitive to the presence of fragments with long *trans*-sequences is useful for practical purposes: these are vibrations with frequencies of 840 and 1275 cm^{-1} .²⁷ Regions which may yield information

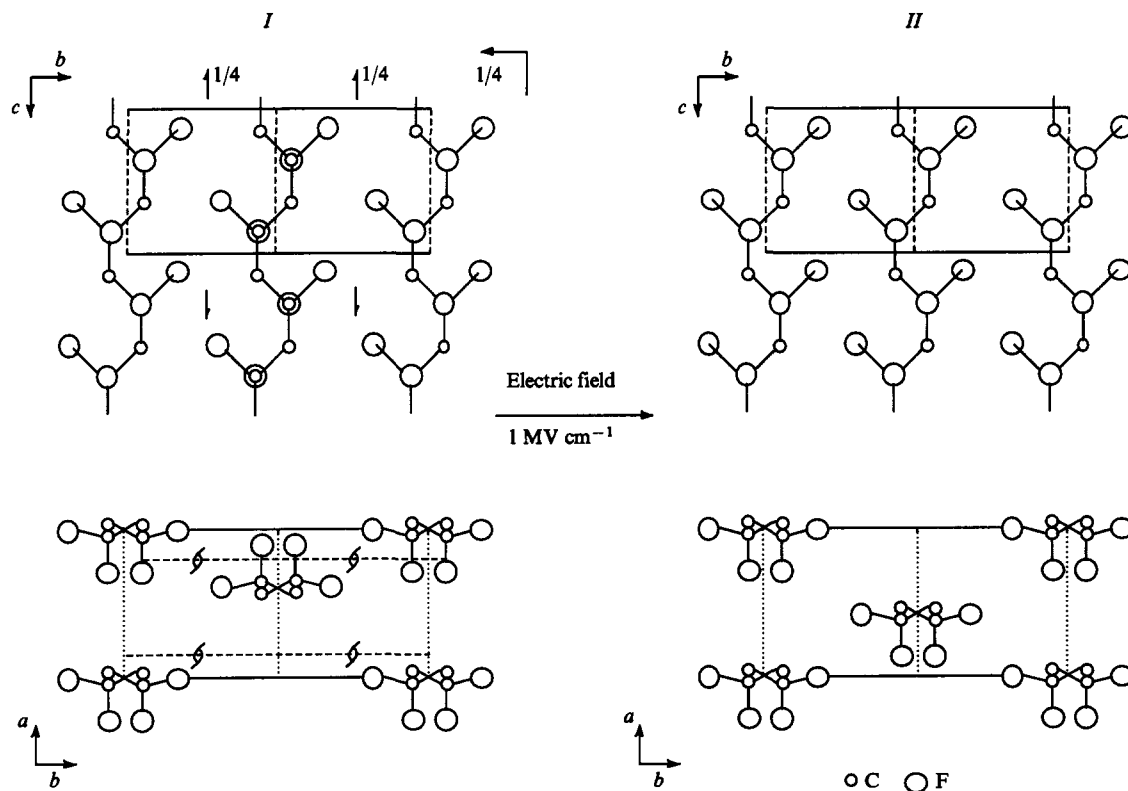


Figure 2. The structure of the crystal lattice of the α modification of PVDF with parallel chains (I) and the phase transition to the α_p phase on 180° rotation and translation by $c/2$ of the central chain (II).¹⁹

Table 1. The assignments of the IR absorption bands for the α , β , and γ phases.¹⁹

α Phase ($TGT\bar{G}$)			γ Phase ($T_3GT_3\bar{G}$)			β Phase (TT)		
I	II	III	I	II	III	I	II	III
3026	A'	$\nu_a \text{CH}_2$	3023	A'	$\nu_a \text{CH}_2$	3020	B_1	$\nu_a \text{CH}_2$
	A''			A''				
2986	A''	$\nu_a \text{CH}_2$	2981	A''	$\nu_s \text{CH}_2$	2978	A_1	$\nu_s \text{CH}_2$
	A'			A'				
1425	A	$\delta \text{CH}_2 - \omega \text{CH}_2$	1431	A'	$\delta \text{CH}_2 - \omega \text{CH}_2$	1430	A_1	δCH_2
1404	A'	$\delta \text{CH}_2 + \omega \text{CH}_2$	1406	A'	$\delta \text{CH}_2 + \omega \text{CH}_2$	1400	B_1	$\omega \text{CH}_2 - \nu_a \text{CC}$
1385	A''	$\delta \text{CH}_2 + \omega \text{CH}_2$						
1294	A'	$\nu_a \text{CF}_2 - r \text{CF}_2$						
1213	A''	$\nu_a \text{CF}_2 + \omega \text{CH}_2$	1234	A''	$\nu_a \text{CF}_2 + \omega \text{CH}_2$			
1185	A''	$\nu_a \text{CF}_2 + l \text{CH}_2$	1176	A''	$\nu_a \text{CF}_2 + l \text{CH}_2$	1180	B_2	$\nu \text{CF}_2 - r \text{CF}_2 + r \text{CH}_2$
1150	A''	$\nu_a \text{CC} - \nu_a \text{CF}_2$	1140	A''	$\nu_a \text{CC} - \nu_s \text{CF}_2$			
976	A'	$l \text{CH}_2$						
874	A'	$\nu_a \text{CC} + \nu_a \text{CF}_2$	880	A''	$\nu_a \text{CC} + \nu_s \text{CF}_2$	880	A_1	$\nu_s \text{CF}_2 + \nu_a \text{CC}$
855	A'	$r \text{CH}_2$	838	A'	$r \text{CH}_2$	840	B_2	$r \text{CH}_2 - \nu_a \text{CF}_2$
			813	A'	$r \text{CH}_2$			
796	A'	$r \text{CH}_2$	792	A''	$r \text{CH}_2$			
765	A''	$\delta \text{CF}_2 + \delta \text{CCC}$	776	A'	δCF_2			
			723	A''	δCF_2			
			688	A''	δCF_2			
			656	A''	δCF_2			
615	A'	$\delta \text{CF}_2 - \delta' \text{CCC}$	552	A'	δCF_2			
			511	A''	δCF_2	508	A'_1	δCF_2
532	A''	δCF_2	482	A'	$\delta \text{CF}_2 + \omega \text{CF}_2$	490		
490	A'	$\delta \text{CF}_2 + \omega \text{CF}_2$	430	A'	$r \text{CF}_2$	470	B_1	ωCF_2
410	A'	$r \text{CF}_2$	400	A''	$r \text{CF}_2$	445	B_2	$r \text{CF}_2 + r \text{CH}_2$
			348	A''	$l \text{CF}_2 + r \text{CF}_2$			
355	A'	$l \text{CF}_2 + r \text{CF}_2$	300	A'	$l \text{CF}_2 + \omega \text{CF}_2$			
287	A'	$l \text{CF}_2 + \omega \text{CF}_2$						

Note. Designations adopted: I—band (cm^{-1}); II—symmetry; III—type of vibration.

about the defects of 'head to head' attachment have been differentiated by calculating the densities of vibrational states in PVDF chains.³¹

We shall consider certain crystallographic aspects of the packing of the chains in the unit cell. Fig. 1 presents the unit cell parameters for β -phase crystals. According to Servet et al.¹⁹ and Lando and Doll³⁶, this is an orthorhombic cell belonging to the $Cm2m$ space group and the density of the crystal is 1.97 g cm^{-3} . Fig. 2 presents a schematic illustration of the unit cell of the α

phase with a parallel arrangement of the chains in the lattice. In this case, the cell is monoclinic with the Cc space group, whereas for antiparallel chains it is orthorhombic with the space group $P2_1cn$. In both cases, the cell is found to be nonpolar, since the two chains in the repeat unit have opposite dipole moments. The α_p phase[†] differs from the α phase only by the fact that the overall dipole moment per cell is not zero. The appearance of additional extinctions of the reflections in the case of the α_p phase indicates its greater symmetry compared with the α phase.

The nature of the packing of the chains in the PVDF γ phase is illustrated in Fig. 3. The workers who have studied systematically

† The mechanisms of the formation of this form will be discussed below.

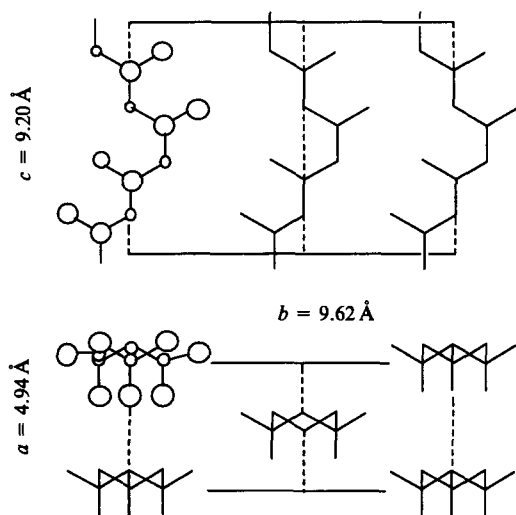


Figure 3. The structure of the crystal lattice of the γ modification of PVDF.¹⁹

Table 2. X-Ray reflections and structure factors F_{hkl} for the PVDF β phase.³⁸

hkl	$d' / \text{\AA}$	θ / deg	F_{hkl}
200	4.29	10.35	9.31
110	4.26	10.42	16.6
001	2.56	17.53	7.2
310	2.47	18.18	5.15
020	2.46	18.3	5.4
201	2.20	20.53	1.1
411	2.19	20.57	5.7
400	2.15	21.06	1.5
220	2.13	21.21	0.24
311	1.78	25.69	
021	1.77	25.79	
401	1.64	27.96	

Table 3. X-Ray reflections and structure factors F_{hkl} for the α and α_p phases of PVDF.³⁸

hkl	$d/\text{\AA}$	θ/deg	F_{hkl}	
			α	α_p
100	4.96	8.94	36	0
020	4.82	9.20	52	52
110	4.41	10.07	83	100
011	4.17	10.66		
120	3.46	12.89	56	0
021	3.34	13.36	72	72
111	3.19	13.98	48	52
121	2.77	16.17	39	0
130	2.7	16.61	45	56
031	2.64	16.99		
200	2.48	18.11	42	64
040	2.41	18.66	9	9
210	2.4	18.72	49	0
131	2.33	19.33		
002	2.31	19.49	47	47
012	2.25	20.07		
220	2.21	20.46		
140	2.17	20.83		
041	2.14	21.15		
211	2.13	21.21		
102	2.09	21.6		
022	2.08	21.72		
112	2.05	22.13		
221	1.99	22.79		
230	1.96	23.12		
141	1.96	23.13		
122	1.92	23.66		
032	1.88	24.27		

Table 4. The calculated and experimental interplanar spacings and the indexing of reflections for γ phase crystals.¹⁹

hkl	$d/\text{\AA}$		hkl	$d/\text{\AA}$	
	experiment	calculation		experiment	calculation
020	4.81	4.81	024	2.07	2.07
110	4.38	4.39	114		2.04
			133		2.04
021		4.26	150	1.76	1.79
022	3.34	3.32	223		1.79
			151		1.76
130	2.69	2.69	134		1.75
			240		1.72
023	2.58	2.59			
131		2.58	241	1.63	1.69
			204		1.68
200	2.46	2.47	152		1.67
			044		1.66
041	2.30	2.32	310		1.62
132		2.32	241		1.61
004		2.30	060		1.60
221	2.14	2.14	311		1.60
042		2.13	224		1.59
			061		1.58

the PVDF structure hold different views concerning the crystallographic identification of the γ phase. One of the reasons for this is the difficulty of obtaining the γ phase in the oriented state. Another one is the possibility of the formation of two modifications of the γ phase. According to Weinhold et al.³⁷ this may be the cause of the assignment of the γ phase to the orthorhombic system with the $C2cm$ space group, on the one hand, and to the

monoclinic system with the Cc space group, on the other. Tables 2–4 present the angular positions of the principal reflections with their identifications and their structure factors (F_{hkl}) for all four polymorphic modifications of PVDF considered.

II. The specific effect of solvents on the conformational characteristics of the chains of poly(vinylidene fluoride) obtained by polymerisation or crystallisation from solution

An attempt has been made³⁹ to obtain PVDF single crystals by crystallisation from solution. A 90:10 mixture of monochlorobenzene and dimethylformamide was used as the solvent. At a solution concentration of 0.01%–0.1% and with the solutions cooled slowly, crystals of the α phase were obtained with a thickness of the lamellae of 90 \AA , the chain axis being arranged at right angles to the surface of the crystal. According to the assignment, crystals with a monoclinic lattice in the β modification were obtained as a result of precipitation from dimethyl sulfoxide. This can hardly be regarded as reliable, since later this conclusion was not confirmed by any investigator using the same solvent. Crystallisation from a good solvent such as dimethyl sulfoxide is most likely to result in the γ phase. For example, Makarevich and Sushko³⁵ and Gal'perin et al.⁴⁰ arrived independently at this conclusion. The crystallisation conditions apparently play a by no means secondary role. Thus, according to the results of Gal'perin et al.,⁴⁰ crystallisation from solution in a good solvent (dimethyl sulfoxide or dimethyl formamide) affords the γ modification of PVDF only at a temperature of the support below 140–150 $^{\circ}\text{C}$. Analysis of the formation of films from solutions in variable solvents showed that the crystals of the γ phase are obtained from solutions in acetone, dimethyl sulfoxide, and ethyl methyl ketone, whilst those of the α phase are obtained from solutions in methyl propyl ketone, dipropyl ketone, butyl methyl ketone, acetophenone, cyclohexanone, or their mixtures.³⁵ The presence of the α phase on crystallisation from solution in cyclohexanone (on the surface of water) has been confirmed indirectly by the presence of spherulites in the crystallised films⁴¹ which are usually produced by crystals of this modification.

The conclusion that the γ phase is formed on crystallisation from a mixture of good and poor solvents for PVDF³⁹ has been confirmed by the results of a study⁴² where monochlorobenzene was again used as the poor solvent, whilst the good solvent was dimethylacetamide. According to this study,³⁹ the γ phase crystallises at a concentration of 0.1%, whereas at a concentration of $\sim 0.5\%$ the α modification is actually produced. It has been noted that the crystals of the γ phase are very resistant to an electron beam, i.e. they are not converted into an amorphous form in the course of 10 min and longer (for comparison, we may note that the crystals of the α phase are preserved for 0.5 min and those of polyethylene for 1.5 min).

The influence of ionogenic impurities (in the polymer and in the solvent) on the characteristic features of the crystallisation process may be traced in relation to solutions of PVDF in cyclohexanone. Thus crystallisation from a 0.02% solution of PVDF in cyclohexanone is accompanied by the formation of a pseudohexagonal structure.⁴³ This was inferred from the ratio of the unit cell parameters: $a/b = 1.73$ (for the pseudohexagonal structure, $a/b = \sqrt{3}$). Taking into account literature data, Miller and Raison⁴³ concluded (in contrast to Makarevich and Sushko³⁵) that PVDF crystallises as a mixture of β and γ phases. However, it was established with the aid of a series of methods for monitoring the crystal structure that crystallisation from this solvent is accompanied by the formation of the α phase or its mixture with the γ phase.⁴⁴ In the latter case, the X-ray method did not permit the estimation of the contributions of each phase and their fractions were therefore calculated from IR spectroscopic data: the γ phase was assumed to be associated

with the presence of absorption bands at 430 and 776 cm^{-1} in addition to others.

Comparison of the published data permits the conclusion that the polymorphic modifications deduced by different investigators for solutions of PVDF in the same solvents are poorly reproducible. This forced Grubb and Choi⁴⁴ to postulate the important role of ionogenic impurities in crystallisation processes. The same workers confirmed this hypothesis later⁴⁵ in relation to dilute (0.01%) and concentrated (5%–9%) solutions of PVDF in dimethylacetamide (or in its mixture with monochlorobenzene). It was observed that an increase in the concentration of ionogenic impurities leads to an increase in the fraction of the γ phase if the polymer crystallises as a mixture of the α and γ phases. This is explained by the fact that, under the conditions governing the formation of crystals with intrinsic polarisation, the latter possess an appreciable electrostatic energy. For example, on the assumption that the perpendicular and parallel components of the dipole moment for the orthorhombic lattice of the γ phase crystal are 4×10^{-30} and 3.4×10^{-30} C m respectively, the surface charge densities on the 100 and 001 planes were found to be $P_a = 0.073$ and $P_c = 0.062$ C m⁻². As a result of an increase in the concentration of ionogenic impurities, the latter are deposited on a plane having the opposite charge and give rise to a depolarising field. An appreciable decrease in electrostatic energy thus has a favourable effect on the crystallisation of the polymer in a polar phase.

The high energy of the electrostatic interaction between the PVDF chains is apparently one of the causes of an unusual phenomenon — the displacement of the solvent from the bulk phase in experiments on the swelling of PVDF in various solvents, including those having a high affinity for the polymer (for example, in dimethylformamide).⁴⁶ Experiments on the swelling of biaxially oriented PVDF film in various solvents (or their mixtures) have shown that the equilibrium swelling tends to decrease with increase in the amount of precipitant in dimethylformamide — water and acetonitrile–water mixtures. It was noted that even the best solvents have a low affinity for the polymer, which is approximately the same for the α and β modifications. The remark by Chapiro et al.⁴⁶ that all solvents are spontaneously desorbed from the film after its removal from the medium (liquid or gaseous) owing to the higher energy of the polymer–polymer interaction is significant.

Yet another contradiction, noted when data on the crystallisation of PVDF from acetone were compared, can probably also be accounted for by the influence of ionogenic impurities on the nature of the polymorphic modification formed when PVDF crystallises from solutions. According to the data of Makarevich and Sushko,³⁵ this process results in the formation of the γ phase, whilst according to those of Kochervinskii et al.⁴⁷ this should be the α phase, since bands typical of the $TGT\bar{G}$ conformers were observed in the IR spectrum: 100, 214, 287, 411, and 530 cm^{-1} , etc. It is noteworthy that the crystallisation from acetone in the latter study⁴⁷ was accompanied also by a significant change in the nature of the morphology. If the polymer crystallises from the melt, spherulites with a high birefringence coefficient are formed. In contrast to this, spherulites were hardly noted in the film crystallised from acetone.

Yet another cause of the contradictions noted in different investigations may be failure to take into account other factors, for example, the molecular mass, the characteristics of the molecular mass distribution (MMD), the number of 'head to head' defects, the form of the end groups, etc., data on which are not always reported. One should apparently consider separately the characteristics of crystallisation from solutions not of the homopolymer but of the VDF–TFE 94/6 copolymer, which, in contrast to the homopolymer, crystallises from the melt at once mainly as the β phase.^{32,48} It has been observed that the crystallisation of this copolymer from an 8% solution in pure dimethylformamide leads to the formation of the β phase with a morphology comprising spherulites with an average size of 2–3 μm .⁴⁸ The crystallisation of the same copolymer from

solution in a 76:24 dimethylformamide–ethyl acetate mixture leads to an appreciable alteration of the morphology of the β phase formed. In this case, the spherulites are no longer formed and the film (in contrast to the film obtained from pure dimethylformamide) is characterised by an optical transparency which is several times greater. Analysis of the results of X-ray analysis has shown³² that the size of the crystallites for the coexisting ferroelectric and paraelectric phases is smaller in the case of crystallisation from the solvent mixture and the fraction of the paraelectric phase is also reduced.

It appears attractive to use the phenomenon of epitaxy for the formation of the required polymorphic PVDF modification. In this case, one should consider the results of several studies in which the crystallisation of PVDF from solution onto a support of a particular crystal was investigated. Thus the crystallisation of the homopolymer of the Kynar 460 type ($M_w = 451\,000$, $M_n = 160\,000$) from 6.3 vol.% solution in dimethylacetamide on the surface of a KBr crystal at 60 °C leads to the formation of a nonoriented γ phase,²⁶ while crystallisation of the same crystal (on the 001 plane) from a dilute solution (0.1%) of PVDF in dimethylformamide at a temperature of the support of 165 °C leads to the formation of lamellar crystals of the β phase oriented along two directions in the 110 plane of the support.⁴⁹ An exact correspondence of the lattices in epitaxial crystallisation is not obligatory, since the difference between the identity periods of the substrate and support ranges from 4.3% to 5.6%. Analysis of electron diffraction patterns has shown that the bc plane of the unit cell of the PVDF β phase grows parallel to the plane of the support, the growth being directed predominantly along the b axis. Crystallisation from a dilute solution of PVDF in dimethylformamide onto the 001 plane on the surface of muscovite or NaCl at 180 °C has been investigated.⁵⁰ The γ phase formed is characterised by a monoclinic cell with a 93 °C angle and the $T_3GT_3\bar{G}$ conformation of the chain. The possibility of the formation on NaCl of two lattices with mirror symmetry relative to the 001 plane of the substrate has been demonstrated. According to the ideas developed, the possibility of the formation of a modification of the γ phase with antiparallel packing of the dipoles in the cell is not ruled out. Epitaxial crystallisation of a copolymer of vinylidene fluoride and vinyl fluoride (molar ratio 95/5) has been investigated.⁵¹ The crystallisation was carried out from a 0.1% solution in nitrobenzene at 90–105 °C onto the 001 planes of NaCl and KCl crystals. Lamellar crystals with a rod-like morphology are formed in both cases (according to electron microscope data). Electron diffraction patterns have shown that more perfect crystals are formed on the KCl support than on the NaCl support, although their size is greater in the latter case.

The differences are explained by the unequal concentrations of specific defects on the surface of the support, which are the nucleation sites. The above copolymer crystallises as the orthorhombic β phase, which has been confirmed by electron diffraction data. The reflections have been indexed as $0kl$, which implies that the bc plane of the cell grows parallel to the plane of the support.

The studies of the influence of the conditions of the synthesis of PVDF on its crystallographic and conformational characteristics must be analysed in the light of the data considered. In one of the early studies,⁵² the characteristics of the polymer obtained for different methods of initiating the polymerisation of VDF were compared. It was shown that the change from chemical to radiation-induced initiation is accompanied by a transition from the β phase crystals to those of the weakly ordered α phase. It was observed later that the decisive factor in the formation of a particular polymorphic modification is nevertheless the medium and not the initiation method.⁵³ Indeed, whereas the radiation-induced initiation in the gas phase is characterised by the formation of the relatively imperfect α phase, the transition in an aqueous medium is accompanied by the appearance of β crystals, i.e. the 'planar zigzag' conformation of the chain proves to be more favourable for the chain in a polar condensed medium in which the polymerisation takes place.

The study of the influence of the initiation method on the nature of the morphology of the films obtained on crystallisation from solution of the polymerisation products has shown that, regardless of the molecular mass of the polymer, chemical initiation always results in the formation of spherulites with an average size of 1–12 μm .⁵³ On radiation-induced initiation, the spherulites are formed in the film only for molecular masses below 2×10^5 . With increase in molecular mass, dendritic crystals appear initially and then structures of the 'shish-kebab' type. PVDF obtained by the radiation-induced cross-linking has been characterised in greater detail by Doll and Lando.⁵⁴ Analysis showed that the polymerisation conditions do not affect significantly the number of 'head to head' defects, which varied in the range from 6.8% to 9.7%, but may be reflected appreciably in the molecular mass of the chain formed. For example, the radiation polymerisation of VDF in acetone is accompanied by an appreciable decrease in the intrinsic viscosity of the product compared with that of the commercial polymer obtained by suspension polymerisation. At the same time, this leads to an increase in the melting point of the former by 15–17°.

Polymerisation in dimethylacetamide, dimethylformamide, and dimethyl sulfoxide is accompanied by the crystallisation of the polymer with the 'planar zigzag' conformation (β phase), but the polymers are distinguished by instability and are degraded on heat treatment. Polymerisation in fluorine-containing solvents (trifluoroacetic acid, etc.) leads to a high-molecular-mass product, which may ensure the formation of a well oriented state under the conditions of uniaxial stretching. Fairly unusual properties have been reported for PVDF obtained by a special type of polymerisation ensuring single additions of the repeat units to the chain.⁵⁵ The polymer obtained exhibits a weak absorption of water and has enhanced electrical parameters (specific volume resistance, breakdown potential, etc.) The effective electret characteristics of the films obtained from the above polymer are also included among its quite unusual properties (admittedly these were not subsequently confirmed by any investigator). Thus it has been noted that the electret charge (with a surface density of 10–20 CGSE charge units per cm^2) may be retained for ten years and does not require preliminary protection by 'short circuiting' the charged surfaces. The electret charge is also more resistant to the effect of temperature and various media (air, oil, solvents).

Certain properties of polymer with a reduced number of 'head to head' defects in the chains (2.7%–3.2%) have been reported.⁵⁶ New types of initiators and catalysts (for example, Ziegler–Natta catalysts) were employed in this investigation. Comparison of the characteristics of this polymer and those of commercial PVDF (having 6% of irregular attachments) showed that the extinction of the absorption bands characteristic of the different polymorphic modifications of the polymer varies in the sequence $\alpha > \beta > \gamma$, whereas for the commercial product it varies in the sequence $\alpha < \beta < \gamma$. According to the results of Liepins et al.,⁵⁶ the crystallisation of the new polymer from hot dimethylformamide results in the formation of crystals of the α phase[†] whilst the crystallisation of the commercial PVDF affords crystals of the β phase. Thus, when the concentration of the chemical irregularities along the PVDF chain is reduced, the $TGT\bar{G}$ conformation becomes energetically more favourable than the $T_3GT_3\bar{G}$ or 'planar zigzag' conformation.

In a number of studies,^{57–61} attention was concentrated on the investigation of the influence of the end groups in the PVDF chains on the properties of the polymer, including its properties in the block state. It was noted that the radical polymerisation of VDF in an aqueous medium under the influence of two different initiators — potassium persulfate (PPS) and β -hydroxyethyl *tert*-

butyl peroxide (HETBP) — is accompanied by a significant change in the properties of the polymer obtained. When PPS was used, the number of volatile substances in the latter proved to be higher by an order of magnitude,⁵⁸ which was manifested by a reduced thermal stability of the polymer.⁵⁹ The results obtained by analytical methods, including isotope analysis,⁶¹ showed that CH_3 end groups predominate in polymerisation with participation of HETBP, whereas in polymerisation involving PPS there is a possibility of the formation of hydroxy-groups at the ends. In the version involving the addition of $\sim\text{CH}_2\text{--CF}_2\text{--OH}$ groups, the latter prove to be unstable and there is a possibility of dehydrofluorination reactions with elimination of HF in accordance with the mechanism $\sim\text{CF}_2\text{--OH} \rightarrow \text{HF} + \sim\text{CF}=\text{O}$.⁵⁹ The thermal stability and the electrophysical characteristics of the polymer are impaired under these conditions. According to the ideas developed,⁵⁹ this difference in the macroproperties can be explained precisely by the type of end groups, since other characteristics of the microstructure hardly differed in the two polymers (the number of irregular attachments, the molecular mass of the chain).

The difference between the end groups in PVDF noted above can be manifested also in finer details on the formation of the polymer by crystallisation from the melt. It has been shown⁶² that, in the isothermal crystallisation of polymers under identical conditions, the spherulites formed for PVDF with PPS proved more perfect and were larger than for PVDF with HETBP. Under the conditions of nonisothermal crystallisation in PVDF with PPS, only 'normal' spherulites were formed, whereas for the other initiator it was possible to find also 'anomalous' spherulites, differing from the former in the way in which the lamellae were packed along the spherulite radius. Films based on PVDE with HETBP, obtained on rapid nonisothermal crystallisation, may involve the formation of spherulites with a bimodal size distribution, in contrast to the films based on PVDE with PPS. The difference between the end groups and hence between the morphologies of the films affected indirectly also the characteristics of the molecular mobility in the nonordered phase in the vitrification region.⁶² Whereas the average relaxation times differed only slightly in the two polymers, this could not be said of either the form of the relaxation time distribution curve or of the magnitude of the total dielectric absorption.

Several investigations touched upon the question of the influence of the polymerisation temperature on the properties of the polymer obtained. Thus, according to the data of Madorskaya et al.,⁶³ for the copolymerisation of VDF with TEF, an increase in the synthesis temperature from 303 to 373 K gives rise to a tendency towards an increase in the number of 'head to head' defects (from 3.5% to 4.7%)[§] for an approximately similar molecular mass of the chain. This leads to a small decrease in the equilibrium melting point and the enthalpy of fusion and to an almost two fold increase in the half-crystallisation time. An increase in polymerisation temperature leads to an increase not only in the number of chemical irregularities in the chain but also in the number of branches in them. For another VDF copolymer (with fluorovinyl ether), an increase in emulsion polymerisation temperature leads to even more striking changes: whereas at low synthesis temperatures the copolymer is characterised by a unimodal molecular mass distribution, at high temperatures it has a bimodal distribution. It is concluded that an increase in the synthesis temperature increases the low-molecular-mass fraction. The study of various factors influencing the microstructure of the VDF homopolymer with the aid of gel-permeation chromatography, electron microscopy, and sedimentation analysis showed that the kinetic parameters of the polymerisation process, the molecular mass distribution, and the dimensions of the latex particles depend primarily on the presence of the emulsifying

† In this and all other casts where one is dealing with crystallisation from a solution in hot dimethylformamide of a VDF/TFE copolymer, one should note that the process is accompanied by dehydrofluorination reactions with formation in the chain of new functional group of the type $-\text{CH}=\text{CF}-$, $\text{CH}=\text{CF}_2$, $\text{C}=\text{O}$.

§ Cais and Soane⁶⁴ also arrived at the same conclusion in the analysis of the NMR spectra of two types of PVDF with different numbers of chemical irregularities in the chain.

agent in the reaction medium. The polymer synthesised in the presence of the latter is linear, in contrast to the randomly branched polymer formed in a system without an emulsifying agent.⁶⁵

III. The influence of various factors on the polymorphism of poly(vinylidene fluoride) in the isotropic state

For the practical use of PVDF, for example in sensors of different kinds,³ the choice of crystallisation conditions which would ensure the formation of the required polymorphic modification is important. It was shown above that this can be achieved by selecting a suitable solvent in crystallisation from solution. In the present section, attention is concentrated on the analysis of the characteristics of crystallisation from the melt (at not very high pressures) with emphasis on the discovery of the role of defects in the chemical attachment of units to the chain and on the previous thermal history of the specimen being crystallised.

Doll and Lando devoted several of their studies of the polymorphism in PVDF^{36, 37, 66–70} to the discovery of the influence of 'head to head' type defects (HHTT) on the characteristic features of its crystallisation. The fraction of the above defects was varied by copolymerisation with TFE or TrFE. It was shown that the VDF/TFE 93/7 copolymer is in the polymorphic β modification even in the isotropic state on crystallisation from the melt, whereas the homopolymer always constitutes the α phase under the same crystallisation conditions. Here it is evidently necessary to emphasise the special role of the TFE comonomer, since the VDF/TrFE 91/9 copolymer still crystallises, like the homopolymer, in the form of the α phase. Different workers attribute this to the easier cocrystallisation of the CF_2CF_2 groups with similar groups in PVDF, where the latter also enter into the composition of the usual chemical irregularities of the homopolymer chains. Tables 5 and 6 present the interplanar spacings d and the indexing of the reflections for the β phases of the homopolymer and the VDF/TFE 93/7 copolymer. The tables show that the spacings d , in particular for the intermolecular reflection 200, differ appreciably in these phases.

Table 7 presents the unit cell parameters for PVDF and three of its copolymers. Evidently the introduction of the TFE comonomer into the chain leads to an appreciable loosening of the lattice in the basal plane precisely for the β phase.

The equilibrium packing density in the crystal depends on the number of the defects noted above, so that one may expect also their influence on the kinetic parameters of the crystallisation. This influence has been studied in detail in the crystallisation of the α phase.^{71–73} The kinetics of the crystallisation of a large

Table 6. Indexing of the reflections for the isotropic specimens of the β phase of the VDF/TFE 93/7 copolymer.³⁶

hkl	$d/\text{\AA}$ (experiment)	hkl	$d/\text{\AA}$ (experiment)
200	4.42	021	1.78
001	2.55	221	1.67
310	2.50	401	1.67
020	2.20	420	1.67
111	2.20	510	1.49
201	2.20	600	1.21
400	2.20	112	1.21
311	1.81	240	1.21
		520	1.21

Table 7. The lattice constants for PVDF and its copolymers.³⁶

Composition	Phase	Unit cell parameter / \AA		
		a	b	c
PVDF	α	9.63	5.02	4.62
PVDF/PTFE 91/9	α	9.59	4.98	4.66
PVDF	β	8.47	4.90	2.56
PVDF/PTFE 93/7	β	8.85	5.00	2.55
PVDF/PTFE 83/17	β	8.84	5.03	2.54

number of PVDF specimens differing both in the number of 'head to head' defects and in the molecular mass have been investigated.⁷⁴ The fraction of the former was varied in the range 3.3%–6.1%, while the molecular mass was varied by more than an order of magnitude from 52 000 to 703 000. Differential scanning calorimetric (DSC) data were interpreted in terms of the Hoffman–Weeks relation in the model with nucleation on folded chains. The following relation is valid for this model:

$$T = T_0 \left(1 - \frac{2\sigma_e}{\Delta H_f l} \right), \quad (1)$$

where T is the experimentally measured melting point, T_0 the equilibrium melting point for a perfect crystal with an infinite thickness, σ_e the free energy of the 'fold surface' of the nucleus, ΔH_f the heat of fusion per unit volume of the crystal, and l the thickness of the lamella.

One of the tasks in the study by Chen and Frank⁷⁴ was to elucidate the question of the location of the 'head to head' defects, namely whether they enter into the composition of the lamella or are displaced on crystallisation into the interlamellar region. Evidently, the former is valid, since the thermodynamic stability of the crystallites decreases with increase in the fraction of the above defects. For a hypothetical defect-free specimen, $T_0 = 481.3$ K is obtained. It has been noted that the linearity of the T –fraction of HHTT relation agrees with the prediction based on Flory's theory⁷⁵ and on the Sanchez model⁷⁶ if it is assumed that the 'head to head' defect can be regarded as a comonomer unit. The degrees of crystallinity calculated from the heats of fusion on the assumption that $\Delta H_f = 1570$ cal mol^{−1} also decrease linearly with increase in the fraction of the defects. The degrees of crystallinity based on DSC data, corrected by the linear dependence of ΔH_f on the fraction of defects, agree very well with the degrees of crystallinity obtained from density data. The degree of crystallinity of a specimen free of the above defects, found by extrapolation, is 82.5%. The study of PVDF specimens with approximately the same number of irregular junctions but differing in molecular mass has led to the conclusion that the degree of crystallinity may depend also on the molecular mass, other conditions being equal.

The above experimental facts, indicating the influence of the HHTT type defects on the nature of the packing of the chains in

Table 5. Indexing of the reflections and the corresponding interplanar spacings for the PVDF β phase in the form of oriented fibres.³⁶

hkl	$d/\text{\AA}$ (experiment)	hkl	$d/\text{\AA}$ (experiment)
110	4.24	600	1.41
200	4.24	121	1.36
001	2.56	511	1.36
020	2.45	530	1.36
310	2.45	002	1.28
111	2.19	040	1.24
201	2.19	112	1.24
220	2.13	202	1.24
400	2.13	331	1.24
021	1.77	601	1.24
221	1.64	240	1.18
401	1.64	530	1.18
330	1.41		

the lattice, initiated the development of studies on the theoretical justification of the above phenomenon. For this purpose, the nature of the variation of the potential energy of both isolated PVDF chains and of block PVDF as the number of defects in the HHTT form or in the form of the TFE comonomer is varied was analysed in detail.⁷⁷ For an isolated chain having the *TGTG* conformation, an increase in the number of defects of both types leads to a linear increase in the potential energy. For an isolated chain in the 'planar zigzag' conformation, the potential energy also increases linearly with increase in the number of defects in the form of the TFE comonomer, whereas for the HHTT defects it diminishes. Therefore the potential energy of an isolated PVDF chain with the 'planar zigzag' conformation and a content of HHTT defects in excess of 10% also proves to be lower than for a chain with the *TGTG* conformation (in contrast to defect-free chains). However, the use only of data on intramolecular interactions (isolated chain) can give rise to serious errors in the conclusions concerning the influence of the number of defects on the properties of a real block polymer, since it is obligatory to take into account also the change in the nature of the packing (intermolecular interactions). For PVDF with 5% of type HHTT defects, it has been shown that some increase in the potential energy minimum is observed for both forms of the polymer. More complete data are presented in Table 8.

Evidently the introduction of 5% of HHTT defects into the chain has a more significant influence on the intermolecular component of the energy. Comparison of the nature of the change in the total energy for the β and α phases in the monoclinic system (usually adopted by the majority of investigators) has shown that the changes are greater in the former case. This agrees qualitatively with the conclusion that the loosening of the α phase lattice is less marked compared with the β phase when comonomers are introduced into the PVDF chain (Table 7).

In order to develop their concept, Chen and Frank⁷⁴ investigated the influence of the concentration of the HHTT defects on the characteristics of the solid-phase $\alpha \rightarrow \gamma$ transformation. We shall consider the principal features (based on the data of different investigators) of this transformation. Ishida and coworkers and Prest and Luca⁷⁸⁻⁸⁰ should apparently be regarded as the first to report the possibility of this process, their papers being published at approximately the same time. In the study of the annealing defects in PVDF, it was shown⁷⁸ that the γ phase, or more precisely its further two modifications, appear during high-temperature annealing in the α phase of PVDF specimens crystallised from the melt.⁷⁹ The above phases were identified from specific absorption bands: these are the 530, 767, 796, and 855 cm^{-1} bands for the α phase and the 510, 779, 809, and 833 cm^{-1} bands for the γ phase (Table 1). In the general case, three melting endotherms were observed on the DSC curves, one of which is presented in Fig. 4. It was shown by spectroscopic methods that the lowest-temperature fusion peak (P_3) is associated with the α phase, and that the two peaks at higher temperatures (P_2 and P_1) are associated with the γ phase. It has been suggested that the fraction of the latter be estimated from the ratio of the optical densities of the 510 and 530 cm^{-1} absorption bands:

$$F(\gamma) = \frac{D_{510}}{0.81D_{530} + D_{510}} \quad (2)$$

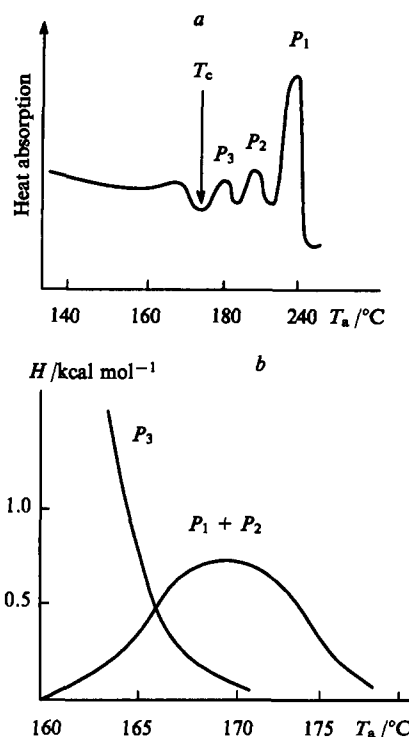


Figure 4. The melting endotherm for PVDF crystallised as the α phase after high-temperature annealing (a) and the variation of the ratio of the peaks on the melting endotherm as a function of the annealing temperature (b).⁷⁹

Eqn (2) was obtained by interpreting the results of experiments with different film thicknesses. Such experiments made it possible to determine the molar absorption coefficients of the above bands: $K_\alpha = 10 \times 10^3$ and $K_\gamma = 8.1 \times 10^3 \text{ cm}^2 \text{ mol}^{-1}$. The variation of the fractions of the α and γ phases as a function of the annealing temperature T_a is illustrated in Fig. 4b. Evidently in the range $T_a = 160-170^\circ\text{C}$ the fraction of the former phase decreases sharply, whilst that of the second increases appreciably. This has been attributed to the occurrence of the high-temperature solid-state transformation $\alpha \rightarrow \gamma$. The equilibrium melting points of the α and γ phases, found with the aid of the Hoffman-Weeks relations, are 188 and 218°C respectively. Prest and Luca⁸⁰ investigated the high-temperature crystallisation of PVDF, the morphology of the PVDF being studied together with the phase analysis. According to their data,⁸⁰ the melting endotherm is also characterised by three fusion peaks, but (in contrast to the paper by Osaki and Ishida⁷⁹) the peak with the intermediate temperature is assigned to the fusion of the β phase. The morphology of the specimen is characterised by the presence of spherulites with negative birefringence (Δn) and a bimodal size distribution. The largest spherulites (with a high Δn) are attributed to the α phase, whilst the small ones (with a low Δn) are attributed to the β phase. The γ phase crystals produce structures which give rise to a specific pattern in crossed polarisers, called by Prest and Luca⁸⁰ a 'wagon wheel', and not a Maltese cross.

Table 8. The energies of two polymorphic modifications of PVDF with and without allowance for type HHTT defects.⁷⁷

Modification of PVDF	β Phase			Monoclinic α phase			Triclinic α phase		
	I	II	III	I	II	III	I	II	III
Without HHTT	-16.4	-64.5	-80.9	-21.6	-57.7	-79.3	-21.6	-63.9	-85.5
With 5% of HHTT	-16.6	-58.6	-75.2	-19.5	-56.5	-76	-19.5	-56.3	-76.4

Note. The following designations have been adopted for the energy (kcal mol^{-1}): I — intramolecular; II — intermolecular; III — total.

Somewhat later, the same investigators concluded⁸¹ that the acceleration of the crystallisation process in the $\alpha \rightarrow \gamma$ transformation may be ensured by introducing surface-active additives. The tentative mechanism of their action is believed to be associated with the fact that, on fusion of the α phase, the molecules of the additives retard the diffusion of the chains in the melt and hence increase the probability of the stabilisation of the fluctuation nuclei of the γ phase. These questions were investigated in greatest detail in a series of studies.^{82–85} Their authors observed three types of spherulites depending on the crystallisation temperature T_c . For low T_c ($< 150^\circ\text{C}$), spherulites with the α phase are produced, whilst at higher T_c the so called mixed spherulites are formed where large spherulites of the α phase and small spherulites of the γ phase coexist. The latter have a low Δn owing to the poor regularity of the arrangement of the lamella along the spherulite radius. For still higher T_c , spherulites of the pure phase are formed. As in the study of Prest and Luca,⁸⁰ they are characterised by the 'wagon wheel' scattering figure. A general feature has been noted for the two types of PVDF: for low T_c , the α spherulites grow faster than the mixed ones, whereas for higher T_c the mixed spherulites actually increase faster than the α spherulites. It is concluded that the solid-state transformation $\alpha \rightarrow \gamma$ begins in mixed spherulites at the boundaries of coexistence of the α and γ phases. The latter grows in the direction opposite to that of the growth of the α phase spherulite. It was shown that the rate of the transition $\alpha \rightarrow \gamma$ along the spherulite radius is much higher than in the tangential direction.

The questions concerning the possible degradation of the polymer and the high crystallisation temperatures necessary for the $\alpha \rightarrow \gamma$ transition have been examined.⁸⁵ Attention was drawn to the fact that the specimens crystallised under the conditions mentioned above (high temperatures and long times) have a yellowish colour. It is believed that thermal degradation reactions may occur under these conditions together with the transformations $\alpha \rightarrow \gamma$. The colouring of the specimens is heterogeneous in character, since the colour centres are mainly located in the regions of the γ phase formed. It has been suggested that the chains in this phase have an increased intramolecular energy. In stressed chains of this kind, the occurrence of dehydrofluorination reactions with formation of $\text{CH}=\text{C}-\text{CH}=\text{CF}$ groups, responsible for the appearance of the colour, is more likely at high temperatures.⁸⁵ The mechanism of the parallel occurrence of the thermal degradation reactions can apparently be also more complex if account is taken of data on the characteristics of the dynamics in PVDF.

As in the above studies,^{80–85} Kochervinskii et al.⁶² observed two types of spherulites, which differed in the magnitude of the Δn and in the average size, on high-temperature nonisothermal crystallisation of two types of the homopolymer (with different end groups). On the basis of the results of the analysis of the form of the absorption bands for the symmetrical and antisymmetrical stretching vibrations of the methylene groups, the small spherulites were attributed to the γ phase.⁶² Attention was drawn to the fact that the PVDF obtained by suspension polymerisation (PVDF-S) exhibits, under identical crystallisation conditions, a higher degree of the $\alpha \rightarrow \gamma$ transformation and a more intense colour than the PVDF obtained by emulsion polymerisation (PVDF-E). This means that the thermal degradation reactions should occur more vigorously for PVDF-S. The relaxation times of the cooperative forms of motion in the noncrystalline regions, extrapolated to the region of the crystallisation temperatures for PVDF-S, proved to be several orders of magnitude shorter than in PVDF-E. Since the amorphous sections in the crystallising polymers may be 'weak' sites in the thermal degradation reactions, the probability of such processes should be higher precisely in PVDF-S, where the average relaxation time is shorter (the frequency of the reorientations of the segments of the amorphous phase is higher). One may postulate that the higher degree of the $\alpha \rightarrow \gamma$ transformation noted in PVDF-S can be explained precisely by the characteristic features of its dynamics in the nonordered

regions of the polymer. Indeed, the packing density of the γ phase lattice is higher than that of the α phase lattice. The polymorphic transformations $\alpha \rightarrow \gamma$ should therefore be accompanied by an increase in the free volume, which is naturally located in the interlamellar regions. Since the relaxation times of the chains of the amorphous phase are inversely proportional to the fraction of the free volume, there should in fact be shorter relaxation times in PVDF-S, which has been confirmed experimentally.⁶²

Conclusions similar to those examined above have been obtained also in a study⁸⁶ where the crystallisation in the temperature range $151\text{--}161^\circ\text{C}$ was also accompanied by the formation of spherulites of two types. The DSC curves reached in this study are qualitatively similar to those presented by Osaki and Ishida⁷⁹ (Fig. 4). Morra and Stein⁸⁶ also observed three fusion peaks but only the P_2 and P_1 peaks were attributed to the fusion of the γ and γ' phases respectively. It was postulated that the first phase is formed on crystallisation, whilst the second is produced as a result of the transformation $\alpha \rightarrow \gamma$. It is assumed that the formation of the α phase is kinetically favourable, whilst that of the γ phase is favoured by thermodynamic factors. On the one hand, it is concluded that the γ and γ' modifications are crystallographically identical but differ markedly morphologically. On the other hand, the α and γ' modifications have identical morphologies but are crystallographically completely different.

In experiments with wide variation of the molecular masses of PVDF and the type HHTT defects, an attempt was made⁸⁷ to discover the characteristic features of the influence of the latter on the polymorphic transformations $\alpha \rightarrow \gamma$. The dependence of the degree of transformations $\alpha \rightarrow \gamma$ on the content γ of phase spherulites was found from DSC data. According to the authors,⁸⁷ the observed linear relation confirms the conclusion that the polymorphic transition $\alpha \rightarrow \gamma$ occurs mainly along the boundaries of the coexisting phases. The influence of the concentration of the HHTT defects both on the fraction of the interlamellar amorphous phase and on the content of γ spherulites was considered for PVDF specimens crystallised at 433 K in the course of 24 h. In the first case, the increase in irregularities increases sharply the fraction of amorphous regions. In the second case, it was concluded that an increase in the fraction of chemical irregularities in the PVDF chain should be reflected in a complex manner in the degree of polymorphic transformations $\alpha \rightarrow \gamma$. This conclusion is due to the fact that the fractions of the amorphous interlamellar phase and of γ spherulites have opposite effects on the degree of the $\alpha \rightarrow \gamma$ transformation.

Thus the experimental data indicate the possibility of the high-temperature polymorphic transformation $\alpha \rightarrow \gamma$. In a series of studies,^{88–90} this transition was predicted theoretically — by calculating the free energy of the PVDF chain in various conformations.

A number of studies^{91–97} have dealt with questions concerning the detailed specification of the conformational rearrangements in PVDF chains in the transition mentioned above. The authors began with the concept that regions of conformational disorder arise (the presence of kink bonds), a confirmation of which was found in the consistent blurring of the 02 ξ reflections.⁹² Fig. 5 presents the detailed pattern of the changes in the chain conformation for α phase crystals in the region of the formation of 'kink' defects, where sections of the chain in the $TGT\bar{G}$ conformation alternate with bonds in the 'planar zigzag' conformation, the number of which may be even or odd. Model studies on different versions of the formation of kink bonds led to the conclusion that the formation of kinks with an odd number of monomer units is more probable. The best agreement with experiment occurs if it is assumed that the kink contains one monomer unit (two neighbouring bonds in the TT position). For its formation, it is necessary to postulate the transition $TGT\bar{G} \rightarrow T\bar{G}TG$, which takes place as a result of a 'flip-flop' type of movement with subsequent transition from G or \bar{G} to T . It is emphasised that the first stage of this transition is decisive.

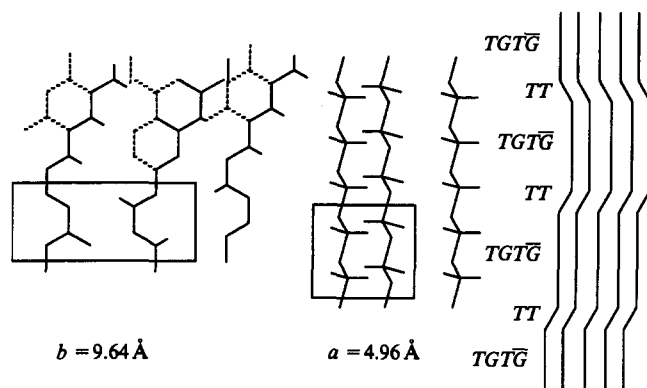


Figure 5. Schematic illustration of the formation of kink bonds in the α modification of PVDF.⁹⁷

Overall, the nature of the transition should be distinguished by its cooperativeness.

According to Lovinger's conclusions,⁹⁸ 'flip-flop' movements with participation of three bonds are more favourable than movements involving five–seven bonds. This means that the conformational rearrangement in the transition must proceed via a two-stage mechanism. An intermediate state (with a low potential energy) is formed in the first stage in accordance with the scheme



The second stage involves the formation of the polar lattice of the γ phase, which should be accompanied by the reorientation of each second chain of the cell, which may occur as a result of the inverse movements of the chain with the altered conformation (Fig. 6b).⁹⁷

We shall now deal with the analysis of a series of results obtained in the study of the formation of the isotropic ferroelectric β phase of the pure VDF homopolymer on crystallisation from the melt in accordance with a definite regime.

The appearance of β crystals on quenching thin (~ 100 nm) films of the PVDF melt in a medium with liquid nitrogen, melting ice, or even in water at room temperature was reported by Hsu and Geil.⁹⁹ It is emphasised that a significant factor in this process is the film thickness. For example, for a film μm thick, β crystals are formed only in the surface, whereas α crystallites are produced in the bulk phase. Later the same workers investigated this phenomenon in greater detail.¹⁰⁰ They varied the temperature of the quenching agent more widely and the results of electron diffraction were supplemented by the results of the study of the

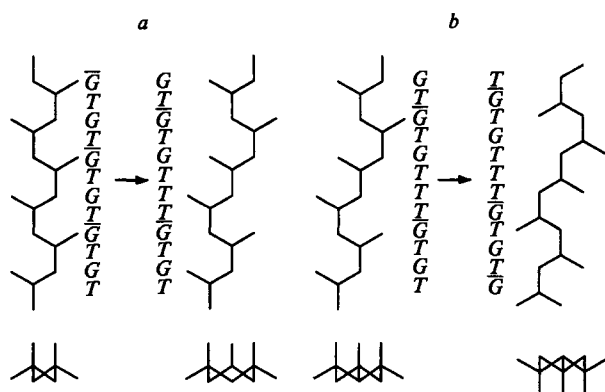


Figure 6. Two modes of molecular motion associated with the solid-state transformation $\alpha \rightarrow \gamma$. (a) Segmental 'flip-flop' motion; (b) inverse motion.⁹⁷

morphology of the films formed on quenching. According to data obtained by transmission electron microscopy, the most homogeneous structure is obtained in films quenched in liquid isopentane. At quenching temperatures of 136 and 273 K, inhomogeneous 20–30 nm sections are seen. At a quenching temperature of 288 K, it is possible to see the appearance of individual fibrils with a transverse dimension of 25 nm and a length up to several hundreds of nanometers. An increase in the quenching temperature to 313 K complicated the morphology somewhat, but crystals of the β phase are formed in all cases. The possibility of obtaining the latter at fairly high quenching temperatures has been confirmed also by other workers.^{101, 102} In these studies the 'planar zigzag' conformations, detected from the 470, 510, 840, and 1280 cm^{-1} absorption bands, were noted for films at a quenching temperature of 303 K. An increase in temperature to 358 K leads to the formation of the α and γ phases together with the β crystals, the size and perfection of the α and γ crystals increasing with increase in the quenching temperature.¹⁰⁰ The morphology of the films becomes more complicated: together with fibrils, structures of incomplete spherulites appear.

Similar results were obtained also in another study, where type KF200 PVDF films 10–15 μm thick were quenched from the melt in melting ice. The appearance of absorption bands at 442, 470, and 510 cm^{-1} , characteristic of the 'planar zigzag', was also noted in the IR spectra of the quenched films. However, it is significant that the conformers obtained apparently serve as nuclei in the subsequent annealing, since the intensity of the above band increases. The results of X-ray studies have shown that the annealing is accompanied by the improvement of the β phase crystals, since the narrowing of the main intermolecular 100, 200 reflection is observed.

Figures 7 and 8 illustrate the scheme which explains the appearance of β crystals on crystallisation under the conditions of rapid quenching. It is postulated that the rate of nucleation is characterised by a distribution curve, the rate maximum for the α phase being displaced towards higher temperatures compared with that for the β phase (Fig. 7). The time taken to traverse the $T_3 - T_4$ (t_α) temperature range depends on the rate of cooling of the melt (Fig. 8). Then the rate of cooling is high, t_α proves to be low and there is insufficient time for the formation of the nuclei of the α phase. Since the maximum in the rate of nucleation for the β phase is displaced towards lower temperatures, the time taken to traverse the temperature range $T_1 - T_2$ is longer and may be sufficient for the formation of β crystals. Estimates¹⁰³ have shown that such crystals may be formed at rates $> 800 \text{ K s}^{-1}$. The above hypothesis has been confirmed also by the results of thermal analysis.^{104, 105} An increase in the rate of cooling of the melt of the VDF homopolymer creates a tendency towards a displacement of the main crystallisation peak towards lower temperatures, whilst quenching in liquid nitrogen leads to its shift into the region of temperatures actually below 300 K.

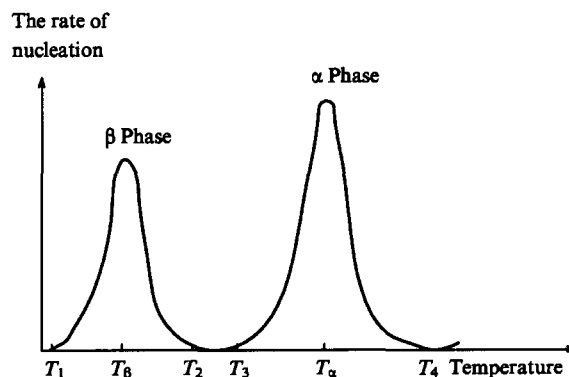


Figure 7. Temperature variation of the rate of nucleation for the α and β phases.¹⁰³

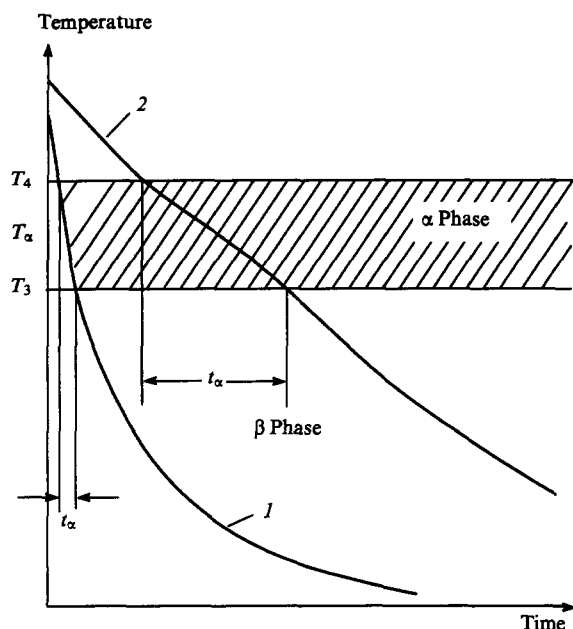


Figure 8. Diagram illustrating the formation of α and β crystallites on rapid (1) and slow (2) quenching.¹⁰³

Under real experimental conditions (fairly thick specimens and not unduly high rates of cooling), nuclei of both phases are apparently formed, although their fraction in the α modification may in fact be low. This is confirmed by the fact that, together with the bands due to the β phase, there are a further two bands (612 and 765 cm^{-1}) characteristic of the $TGT\bar{G}$ conformations.¹⁰³ Analysis of the X-ray diffraction profile indicates that there are few nuclei of the α phase and they do not attain large sizes, since reflections characteristic of the α phase have not been noted. Annealing of the quenched specimens leads to an increase in the number of $TGT\bar{G}$ conformers, since the intensity of the above bands increases. The possible structure of such defective regions of the α phase has been examined on the basis of the results of thermal analysis.^{104, 105} It was noted that, on rapid cooling of the melt ($\geq 10 \text{ K min}^{-1}$) of the VDF homopolymer, an additional endotherm appears on the DSC curves in the range 320–350 K of the kind not observed for specimens obtained at low rates of cooling.¹⁰⁵ The appearance of this endotherm had been attributed to the existence of conformational disorder in the imperfect crystals of the α phase (condis-crystal). In terms of Takahashi's concept,¹⁰⁶ when the PVDF chains have the same $TGT\bar{G}$ conformation, they may assume four possible orientations under the conditions of nonequilibrium crystallisation temperatures (Fig. 9) — AC , $\bar{A}C$, $A\bar{C}$, and $\bar{A}\bar{C}$. Evidently the fluorine atoms may be located above (\bar{C}) or below (C) and to the left (\bar{A}) or to the right (A) relative to the molecular axis. Since the CF bonds have a high dipole moment, such orientations are characterised by different directions (upwards or downwards) of the axial component of the dipole moment. The transition from the A to the \bar{A} orientation is possible as a result of rotation about the c axis, while the C and \bar{C} states are obtained by the mirror reflection relative to this axis. The transitions between the above orientations, occurring as a result of the movement of the entire chain are impossible because of the very high activation barrier, but they can be achieved as a result of local conformational rearrangements.

The studies, mentioned above, of the influence of the copolymerisation of VDF with TFE and TrFE⁶⁷ on the change in the equilibrium polymorphic modification of the homopolymer have greatly developed recently. This was caused by two facts. On the one hand, it was the discovery of ferroelectric properties in PVDF: it was found, in the presence of fairly high contents of the second component, that the ferroelectric–paraelectric transitions in the

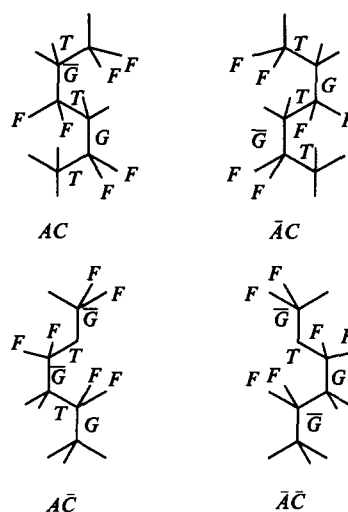


Figure 9. The possible orientations of the chains of the PVDF α phase in the $TGT\bar{G}$ conformation.¹⁰⁵

VDF/TrFE copolymers and fusion proper differ appreciably as regards temperature, which makes it possible to employ this copolymer as a model compound for the study of the mechanism of the appearance of ferroelectric properties in organic polymers. On the other hand, modifications of the materials employed, particularly those with increased piezoelectric constants, were needed for practical purposes. Therefore, when it was shown for a series of VDF/TrFE copolymers¹⁰⁷ that an approximately equimolar component ratio in the copolymer leads to a significant increase in both the electromechanical coupling factor and in the piezoelectric constant d , the interest in the study of the structures of the above copolymers increased.

Initially Lovinger et al.¹⁰⁸ demonstrated in relation to the VDF/TrFE 52/48 copolymer that the specimen crystallised from the melt consists of a mixture of two disordered crystalline phases, one of which is characterised by the 'planar zigzag' conformation, whereas the other has the 3/1 helical conformation. The wide variation of the composition of the copolymer made it possible to obtain later more detailed information about its crystal structure.¹⁰⁹ On the basis of the analysis of the results of detailed X-ray diffraction patterns and spectra over a range of temperatures, the authors concluded that the low-temperature phase (LTP), a cooled phase (CP), and a high-temperature phase (HTP) exist in the isotropic state. Comparison of model calculations with experiment showed that the 'planar zigzag' conformation in the LTP should be characterised by a deviation from the plane by an angle 2σ . As for the β phase of the VDF homopolymer,^{110, 111} this conclusion follows from the passage of the relative difference between the calculated and observed structure factors (the R factor) through a minimum as the angle σ is varied. When such chains are packed in the cell, the following parameters of the low-temperature phase are obtained: monoclinic system, $a = 9.12 \text{ \AA}$, $b = 5.25 \text{ \AA}$, c (chain axis) $= 2.55 \text{ \AA}$, $\beta = 93^\circ$, tilt angle (in the 130 plane) $= 3^\circ$. The scheme of the transitions in the above copolymers¹⁰⁹ shows that the transition from the ordered LTP to the fully disordered HTP proceeds via the formation of the intermediate (cooled) phase CP. The model of the conformational rearrangements in an isolated chain in this transition is illustrated in Fig. 10. An increase in temperature is accompanied by the appearance of 'skew' bonds (S and \bar{S} in Fig. 10) for the chain in the 'planar (distorted) zigzag' conformation. A further increase in temperature leads to the appearance of single bonds in the G or \bar{G} conformation, which corresponds to the chain conformation in the cooled phase.

The transition from LTP to CP is accompanied by a change in the unit cell parameters ($a = 9.16 \text{ \AA}$, $b = 5.43 \text{ \AA}$, $c = 2.53 \text{ \AA}$, and

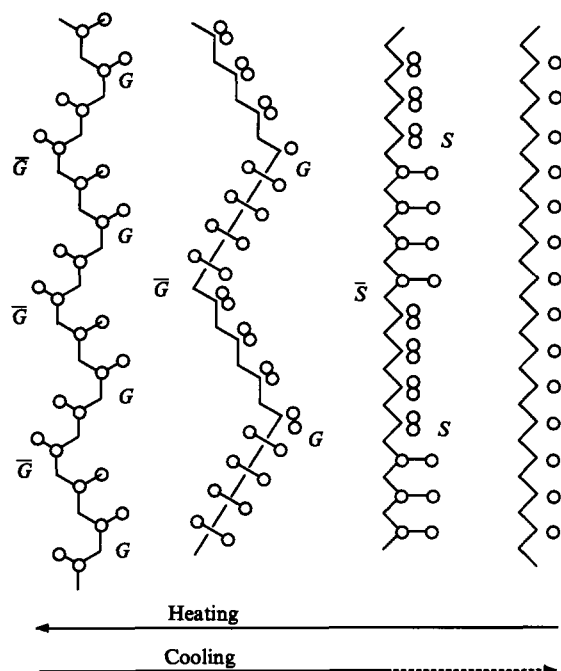


Figure 10. A model of the conformational changes in the single chain of the VDF/TrFE 55/45 copolymer during heating-cooling cycles.¹⁰⁹

$\beta = 93^\circ$) and an appreciable increase in the tilt angle (in the 130 plane) to 18° . The packing of such chains in the cell of the cooled phase is presented in Fig. 11. This lattice may be considered also in the light of the concept of a crystal with kink bonds. The transition from the cooled phase to the high-temperature phase on further increase in temperature is accompanied by the accumulation of conformational irregularities, which, according to IR spectroscopic data, represent a set of sequences of the type $TGT\bar{G}$ and $T_3GT_3\bar{G}$. To a first approximation, the lattice is characterised by hexagonal packing with the parameters $d' = 9.75 \text{ \AA}$ and $b' = 5.63 \text{ \AA}$ ($d'/b' = \sqrt{3}$). Taking into account these values, the calculated and experimentally observed interplanar spacings d and the structure factors \sqrt{I} for a series of reflections are presented in Table 9.

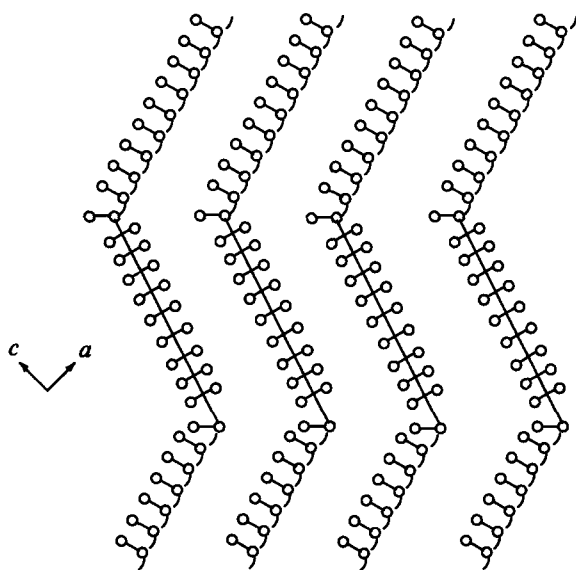


Figure 11. A model of the structure of the crystal of the cooled phase for the VDF/TrFE 55/45 copolymer.¹⁰⁹

Table 9. Interplanar spacings and structure factors for the reflections due to the high-temperature phase of the VDF/TrFE 55/45 copolymer.¹⁰⁹

hkl	Calculation		Experiment	
	$d/\text{\AA}$	\sqrt{I}	$d/\text{\AA}$	\sqrt{I}
200	4.87	35.4	4.88	38.4
110	4.87			
310	2.81	5.1	2.83	3.2
020	2.81			
400	2.44	3.7	2.44	3.0
220	2.44			
510	1.84	2.2	1.85	1.8
420	1.84			
130	1.84			
600	1.62	(2.2)		
330	1.62			
620	1.41	(0.9)		
040	1.41			

Evidently, there is a satisfactory agreement between the measured and calculated parameters, which confirms the correctness of the chosen lattice. Overall, the lattice is found to be nonpolar and the chains may execute rotational motions with large amplitudes. According to Tashiro et al.,¹⁰⁹ the crystal in this state may resemble one of the varieties of a rotator phase. When the HTP is cooled, the reverse transition of the type HTP \rightarrow CP takes place and is accompanied by the conformational rearrangements noted above (Fig. 10). The cooling of the CP is not accompanied by the reverse transition to the LTP. In this case, chains with conformations of the type

...TTTTTTTTTSTTTTTTTTTT \bar{S} TTTTTTTTTT...

are found to be frozen.

For the occurrence of the transition from the CP to the LTP, one may deform the specimen or subject it to a strong field.

The attempt to find definite analogies between the formation of the structure on quenching of the above 65/35 copolymer and of the homopolymer yielded a somewhat unusual result.¹¹² It was found that the ferroelectric-paraelectric transition (according to DSC data) in the quenched copolymer is observed at a higher temperature than in the specimen with slow rate crystallisation. Annealing of the quenched specimen (at 120 and 140 $^\circ\text{C}$) leads to a decrease in the temperature of this transition, although the fraction of the long sequences with the 'planar zigzag' conformation, entering into the composition of the ferroelectric phase, increases under these conditions.

In order to investigate the influence of the polarity of the comonomer in the VDF copolymers on the nature of the crystal structure formed, a study was made of a wide range of VDF copolymers with nonpolar tetrafluoroethene, the fraction of the latter being varied within wide limits (19%–100%).¹¹³ Comparison of the structural data with those for the copolymer of VDF with the polar TrFE comonomer shows that the nature of the phases formed and their interconversions are similar. Admittedly certain nuances were also observed for the 81% VDF content in the VDF/TFE copolymers. Thus the temperature of the LTP \rightarrow HTP transition (with a conformational change from *trans*- to *gauche*-) proved to be close to the melting point. In the case of high VDF contents, such transitions become more diffuse and the hysteresis phenomena are weaker than in the VDF/TrFE copolymers.

The crystallisation of the VDF/TFE 94/6 copolymers from the melt (or from solution) always leads to the coexistence of the ferroelectric and paraelectric phases at room temperature. The presence of the former was inferred from the 100, 200 reflection, whilst the presence of the latter was associated with the broadened reflection in the range $2\theta \approx 18^\circ$ ($\text{CuK}\alpha$ radiation).³² The morphology of the films obtained is characterised by the presence of

spherulites which become small and defective on quenching from the melt¹¹⁴ or a morphology in the form of aggregates of optically anisotropic rods is established.⁴⁸ For crystallisation conditions involving quenching, an unusual phenomenon has been observed — the formation of sections of the α phase, the presence of which was inferred from the appearance of either the weak 021 reflection¹¹⁴ or of strong intermolecular 020, 110 reflections.^{115,116} The latter phase proved to be metastable, since even on heating to 70 °C the above reflections are markedly weakened.^{117,118} The crystallisation of the copolymers (predominantly as the polar β phase) is accompanied, according to spectroscopic data,^{48,114} by the formation of irregular sequences in the $TGT\bar{G}$ and $T_3GT_3\bar{G}$ conformations, the ratio of which depends on the previous thermal history of the specimen.

The study of Roussel et al.¹¹⁹ was devoted to the influence of the molecular mass on the kinetics of the crystallisation of PVDF. When the DSC method was employed, the crystallisation kinetics were described in terms of the constants of the Avrami equation. It was noted that the rate of crystallisation was lowest in the case of the PVDF with an intermediate molecular mass. According to the authors, this unusual phenomenon could not be associated with different crystallographic forms, since the specimens were selected taking into account IR spectroscopic data. However, the exponent in the Avrami equation could reach 11. The reason for this is believed to be the fact that the additional type HHTT irregularities in certain specimens may serve as additional nucleation centres. It is believed that the above crystallisation anomalies are bounded on the side of high degrees of supercooling.

The influence of the crystallisation temperature on the possibility of polymorphic transformations in PVDF has been investigated¹²⁰ mainly with the aid of a spectroscopic technique. The PVDF produced by the Atochem Company (France) in the form of thin (6 μm) films was crystallised from a concentrated solution in dimethylacetamide. On varying the crystallisation temperature, appreciable changes were observed in the IR spectra, which is explained by crystallisation in the form of different modifications. The presence of the α , β , and γ phases was inferred from the presence in the IR spectrum of the 766, 840, and 510 cm^{-1} bands respectively. The fraction of a particular modification was estimated from their intensities. In particular, it was shown that, on prolonged high-temperature (160–185 °C) crystallisation, predominantly the γ phase is formed. This result agrees qualitatively with earlier data.^{78–85} A new feature in the above study¹²⁰ is the observation of the influence of the crystallisation temperature on the ratio of the α and β phases in isotropic films. It was shown that a decrease in temperature (from 160 to 50 °C) leads to a significant increase in the fraction of the β phase in its mixture with the α phase for the same (20 min) crystallisation time. This feature is not fortuitous, since a similar relation has been observed also for a solution of PVDF in dimethylformamide. At a fundamental level the observed phenomenon may have a common basis with the $\alpha \rightarrow \beta$ transformation in the low-temperature deformation of PVDF.

IV. Characteristics of the solid-state transformations under the conditions of tensile deformations

More than twenty years ago, the ferroelectric properties of PVDF and of its copolymers were unknown, but in the studies of Lando¹²¹ and Gal'perin¹²² attention was already drawn to the possibility of the polymorphic transformations $\alpha \rightarrow \beta$ on uniaxial stretching of PVDF films. It was shown that a decrease in the temperature of the uniaxial stretching and an increase in the draw ratio promote an increase in the latter. It was noted, in particular, that orientation at low temperatures (< 60 °C) leads to an abrupt $\alpha \rightarrow \beta$ transition, which is also accompanied by the formation of microcracks in the matrix. At higher temperatures the transition becomes smoother, i.e. the crystals of the α phase are initially

oriented along the draw direction, after which the polymorphic transformation takes place in them. Small angle diffraction has shown that an increase in the draw temperature (T_d) is accompanied, on the one hand, by an increase in the long period, and, on the other, by an increase in the intensity of the small angle reflection. Furthermore, a change has also been noted in the nature of the diffraction patterns: whereas at low T_d the reflection has the form of a vertical line or four points, at high T_d it has the form of two points. Annealing of the oriented PVDF films in the isometric or free state has shown¹²³ that in the latter case a transition from the fibrillar structure to the lamellar structure, accompanied by a change from the c -texture to the a -texture, is observed.

For PVDF films with an oriented β phase, the nature of the structural transformations on annealing may depend significantly on the previous history of the specimens. Thus, when an unannealed specimen is heated, shrinkage stresses σ arise in it already at 40 °C, reaching a maximum ($\sim 1.5 \text{ kg mm}^{-2}$) at 120 °C.¹²⁴

In the specimen (with fixed ends) annealed up to 140 °C, these stresses are insignificant, after which they also increase, although their maximum values are appreciably lower ($\sim 0.5 \text{ kg mm}^{-2}$), while the maximum is displaced towards higher temperatures — to ~ 180 °C. In both cases, the decrease in σ is attributed to the fusion of the β phase crystals, since the intensity of the principal 110, 200 reflections due to the β phase decreases under these conditions (to zero at 189 °C). However, when a specimen with free ends was heated, a sharp fall in the intensity of the above reflection occurred at 166 °C, i.e. for the free state the melting point of the β crystallites is lower by more than 20 °.

An analytical description of the $\alpha \rightarrow \beta$ interconversion in PVDF on uniaxial stretching has been formulated in a study¹²⁵ the authors of which used the method developed¹²⁶ for the estimation of the fraction of the α phase N_2 under the conditions of its coexistence with the β phase. The experimental dependences of N_2 on the draw ratio λ , expressed in semilogarithmic coordinates, are linear, i.e. the following relation holds:

$$N_2 = 1 - \frac{\ln \lambda}{10.8 - 29/RT}, \quad (3)$$

where 29 kJ mol^{-1} is the potential barrier to the $\alpha \rightarrow \beta$ transformation.

Temperature has a significant influence on the effective tensile stress, so that the $N_2 - \sigma$ relation is linear (Fig. 12). Extrapolation of this relation showed that the complete disappearance of the α

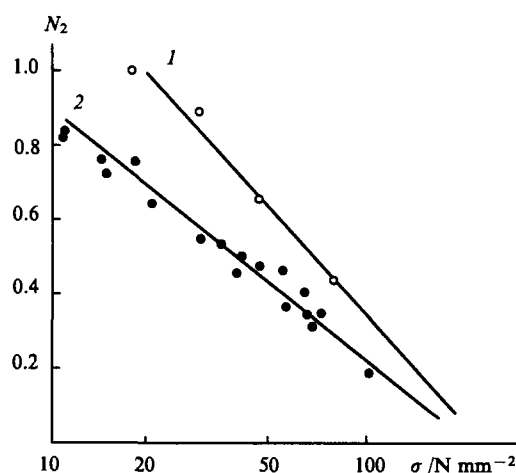


Figure 12. Dependence of the fraction of the α phase (N_2) on the tensile stress in the uniaxial drawing of PVDF before (1) and after (2) the formation of a neck.¹²⁵

phase requires a stress of 180 N mm^{-1} . Evidently, other conditions being equal, the $\alpha \rightarrow \beta$ transformation takes place more effectively in the region where the material assumes the form of a neck. This conclusion has been confirmed by the data of Matsushige and Takemura,¹²⁷ which also showed that the main $\alpha \rightarrow \beta$ transformation on uniaxial stretching begins in the region of deformations where the material assumes the form of a neck. Under the conditions of uniaxial stretching of PVDF, the existence of a critical deformation where intense rotation of the crystals of both modifications begins has been established. For example, the effective rotation in the direction of stretching, for both the newly formed β crystals and for the remaining α crystals, takes place in the range $\lambda = 2-2.5$.¹²⁵

The importance of the role of the tensile stresses in the polymorphic $\alpha \rightarrow \beta$ transformation has been emphasised also in another study.¹²⁸ Taking into account the role of temperature as regards the values of σ , the author also showed that the values of σ may be raised by increasing the rate of deformation. For large draw ratios ($\lambda = 7$), the final values of Young's modulus (E) in the PVDF specimens may depend significantly on the previous thermal history of the isotropic specimens crystallised from the melt. Thus it was found that Young's modulus for films with the same value of λ is higher in the case of slow crystallisation of the initial films obtained by quenching. The maximum values of E in the direction of the draw axis are $\sim 4 \text{ GPa}$, whereas along the c axis they are 177 GPa (according to X-ray diffraction data), which is comparable to the theoretical value of 237 GPa for β phase crystals.

It was found with the aid of the dependence of E on λ for films of one kind, obtained at different draw temperatures, that, other conditions being equal, the decrease in T_d leads to an increase in E . This can be explained [in conformity with Eqn (3)] by an increase in the fraction of the β phase, for which E in the direction of the c axis is found to be greater than E for the α phase. However it appears that this is not the only reason. Such doubts arise from the results of studies^{129,130} in which uniaxial stretching processes were investigated in specimens of the VDF/TFE 94/6 copolymer. Here it was also found that a decrease in T_d leads to an increase in E (according to the results of acoustic measurements). However, since this copolymer crystallised in isotropic films in the form of the β modification, the polymorphic $\alpha \rightarrow \beta$ transition noted above was absent, as in the homopolymer. For this reason, the increase in E for films with different T_d was attributed to the different microstructures of the noncrystallising regions. In particular, it was shown that in films with a lower T_d the latter are characterised by an increased concentration of chain sections in the 'planar zigzag' conformation, while the packing density in them should be greater, since there is a steady decrease in the intensity of the maximum of the small angle meridional X-ray scattering.

The results of the analysis of the acoustic characteristics indicate that one may expect a high content of stressed chains passing through films with a lower T_d . NMR data for PVDF specimens with different draw ratios agree qualitatively with this conclusion. This can also be inferred from the decrease in the mobility of the 'fast' protons associated with the noncrystallisable chain sections in specimens with larger draw ratios.¹³¹

The nature of the polymorphic transformation $\alpha \rightarrow \beta$ occurring on uniaxial stretching affects also the morphology being established. Thus the diffraction pattern produced by a laser beam which has passed through a deformed PVDF film, crystallised in the isotropic state with formation of α phase spherulites, has been investigated.^{132,133} It was observed that at high T_d there is intense equatorial scattering, which indicates the existence of spherulites deformed in the direction of the draw axis. At low T_d , there exist, together with the latter spherulites also undeformed spherulites with the initial phase, which was inferred from the 'anomalous' eight-lobe dispersion pattern. It is assumed that the mechanism involving the 'retwisting' of the lamellae on deformation plays an important role in spherulites disposed favourably in relation to the direction of action of the external force and that the transition

from the α to the β modification may proceed as a result of local fusion and subsequent recrystallisation.¹³² As the draw temperature is reduced due to the higher viscosity of the noncrystallising sections, the external stress may be effectively transmitted to the crystallites of the α phase, reaching critical values for the $\alpha \rightarrow \beta$ transition noted above.¹³³

For intermediate draw ratios, the 'anomalous' eight-lobe H , scattering pattern (in crossed polarisers) has been observed also in the polymorphic $\gamma \rightarrow \beta$ transition.¹³⁴ An analogy between the $\alpha \rightarrow \beta$ and $\gamma \rightarrow \beta$ transitions was noted, although the required deformation energy for the former is found to be greater than for the latter. Indeed, the complete transformation can be achieved at $T_d = 80^\circ \text{C}$ and $\lambda = 4$. On the other hand, in the case of the $\gamma \rightarrow \beta$ polymorphic transition with the same λ , it takes place fully at a draw temperature as high as $T_d = 150^\circ \text{C}$. An unusual feature of the latter transformation is the fact that the appearance of the β phase is noted not immediately after the start of the orientation of the initial crystallite but in the deformation process, where the orientation function reaches 0.25.

In the light of the foregoing, one may conclude that the preparation of PVDF with highly oriented γ phase crystals is by no means a simple task. Indeed, the procedure usually employed, involving the uniaxial stretching of an isotropic film with γ phase crystallites, fails because of the $\gamma \rightarrow \beta$ transformation noted above. In this connection, the results of a study¹³⁵ in which a novel method of preparation of such PVDF was proposed are of interest. The scheme reduces to the following features. In the first stage, an isotropic film with α phase crystallites was oriented at 150°C up to $\lambda = 4-5$ without the polymorphic $\alpha \rightarrow \beta$ transition. In the second stage, the film obtained was polarised in a field with $E = 1 \text{ MV cm}^{-1}$, after which the crystals of the α phase were converted into the polar α_p form. In the third stage, the film obtained was annealed isometrically at temperatures above 120°C (it is even better when $T > 170^\circ \text{C}$), after which the formation of the γ phase was observed. The presence of the latter was inferred from the presence of specific absorption bands in the vibrational spectra — at $300, 430, 656, 776$, and 813 cm^{-1} .

A method was proposed in the same study for the quantitative estimation of the fraction of the γ phase $\rho(\gamma)$ from the optical densities D of the 410 and 430 cm^{-1} bands. It was found that

$$\rho(\gamma) = \frac{D_{430}}{rD_{410} + D_{430}}, \quad (4)$$

where $r = K_{430}/K_{410}$, while K_{430} and K_{410} are the molar absorption coefficients for the 430 and 410 cm^{-1} bands respectively, the values of which proved to be similar. The kinetics of the increase in the fraction of the γ phase, calculated by Eqn (4) for different annealing temperatures in the $\alpha_p \rightarrow \gamma$ transition stage, have shown that an increase in the annealing temperature leads not only to an increase in the rate of transformation on the initial section but also increases the equilibrium value of $\rho(\gamma)$.

According to Brillouin scattering data, under the conditions of the uniaxial stretching of PVDF it is possible to estimate the changes in its nonordered regions.¹³⁶ Thus a significant increase in the velocity of ultrasound V_s in the direction of the draw axis with increase in λ has been observed. The ultrasonic wavelength is $\sim 10^3 \text{ \AA}$, while the side of the crystallite is $\sim 10 \text{ \AA}$, so that the orientation function determined should characterise the rotations of the chains both in the crystal and the amorphous phase. The velocity of ultrasound can be estimated from the following relation:

$$V_s \approx \left(\frac{E}{\rho} \right)^{1/2},$$

where ρ is the density. The increase in V_s with increase in ρ during the drawing process was attributed by the authors to a more significant increase in Young's modulus. Comparison of the values of E for the crystals of the α and β phases shows that an increase in Young's modulus during drawing cannot be attributed

solely to the polymorphic transition $\alpha \rightarrow \beta$ and account must be taken of the possibility of the partial additional crystallisation of the chains in the amorphous phase.

In order to investigate in greater detail the mechanism of the polymorphic transformation $\alpha \rightarrow \beta$ on uniaxial stretching, the changes in a series of physical characteristics were followed in oriented PVDF films where the initial polymers differed both in the number-average molecular mass M_n and by in polydispersity factor M_w/M_n . In particular, it was shown that higher values of Young's modulus (~ 6 GPa) are more likely to be obtained on uniaxial stretching on a polymer the M_n value for which is lower and that the isotropic specimen should be prepared by slow crystallisation.¹³⁷

The PVDF films used for practical purposes were treated in a high electric field, so that the orientation of the 'polar' b axis of the lattice in relation to the plane of the film is very important. The data of Mizuno et al.¹³⁸, who carried out structural studies on PVDF films obtained by the double orientation method, merit attention in this connection. It was shown that, for a film subjected to repeated uniaxial restretching in a direction perpendicular to that of the initial stretching ($T_d \leq 100^\circ\text{C}$, the initial specimen was quenched), the b axis of the cell is in the plane of the film. It was noted that the rolling of a PVDF film subjected to uniaxial stretching and different heat treatment conditions make it possible to obtain textures in which the b axis may form angles of 0° , 30° , and 60° with the plane of the film.

Detailed studies of the morphology in thin and thick PVDF films by electron microscopy, electron diffraction, and X-ray diffraction (large or small angle diffraction) indicate significant differences between the structures of thick films oriented at low ($80\text{--}90^\circ\text{C}$) and high ($130\text{--}140^\circ\text{C}$) temperatures.¹³⁹ Approximately 85% of well oriented but highly defective β phase crystals and $\sim 15\%$ of residual virtually unoriented α crystals were observed for the former films in the region of the macroscopic neck (with 280% deformation). The residues of the unoriented α phase are visible even for deformations of $\sim 350\%$, whereupon the growing neck can reach the ends of the specimen. The long period (in the direction of stretching) is ~ 10.5 nm, which is less than for the initial specimen (13.0 nm). The ellipsoidal microcracks arising under these conditions are located between the microfibrils. In hot drawing, the $\alpha \rightarrow \beta$ transition proceeds somewhat differently: initially the α phase is transformed into microfibrils and then, after the attainment of critical stresses, the polymorphic transition begins. At both high and low temperatures, the deformation occurred heterogeneously, since the regions of the initial α phase remain even for an elongation of 500%.

For polar polymers with fairly high dielectric losses, it is of interest to employ nontraditional heating sources for the specimen during the drawing process. For example, microwave heating may be employed for this purpose. Drawing with this method of heating in polyoxymethylene specimens leads to appreciable improvements in the elastic characteristics.^{140–142} or PVDF, this heating method is of interest for a number of reasons. On the one hand, the increased dielectric losses at high frequencies (at room temperature) provide a basis for effective uniform heating throughout the bulk of the specimen by the energy of the UHF field. On the other hand, the similarity of the frequencies of the electromagnetic field to the average reorientation frequencies of the polar segments in the nonordered phase makes it possible to 'pump' the internal energy precisely into the amorphous regions of the PVDF, which play an important role in the processes involving the deformation of a partly crystalline polymer. The data of a study¹⁴³ where a magnetron with a power of 1.2 kW and a working frequency of 2.45 GHz was used for heating of the kind described above merit attention in this connection.

Comparison of the limiting PVDF draw ratios and of the acoustic modulus for traditional and UHF heating of the specimen showed that the use of the latter method does not afford a significant increase in the elastic characteristics compared with the

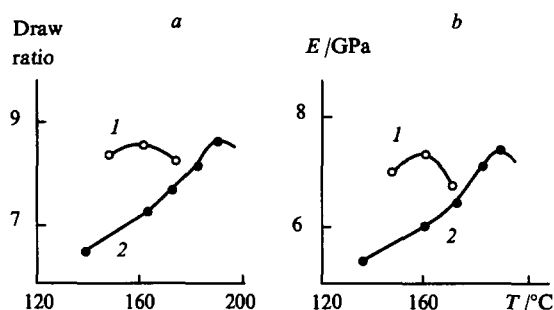


Figure 13. Dependence of the maximum draw ratio (a) and the acoustic modulus (b) in PVDF specimens on the drawing temperature for HF (1) and traditional (2) heating.¹⁴³

traditional heating of the specimen from an external source. According to the authors, the reason for this is that, in contrast to polyoxymethylene, in PVDF the range of temperatures most favourable for maximum stretching is close to the melting point (Fig. 13). In the range of stretch temperatures $150\text{--}160^\circ\text{C}$ (appreciably below the melting point), UHF heating yields a higher maximum draw ratio and hence the highest acoustic modulus. This feature may be a consequence of the local heating of the amorphous regions of PVDF noted above. We may note that Nakagawa and Amano¹⁴³ obtained PVDF specimens with the highest draw ratio (8.6) and acoustic modulus (7.5 GPa).

The influence of the state of the melt on the characteristics of the orientation crystallisation of PVDF has been studied.¹⁴⁴ The initial specimen was subjected to preliminary radiation-induced cross-linking, after which it was melted. Next the specimen was stretched to different values of λ and recrystallised isothermally. The task formulated was to trace the influence of the initial function of the orientation of the chains in the melt and of the density of the cross links in it on the values of the orientation function for the crystallites and the amorphous phase after recrystallisation. On the basis of data obtained by X-ray diffraction and birefringence, it was concluded that in this type of process the c axis in the crystal of the α phase formed is disposed along the direction of stretching of the melt, while the chains of the amorphous phase are perpendicular to this direction. It was found that the orientation state of both phases after recrystallisation depends both on the density of the cross links and on the chain orientation function in the amorphous melt, the role of the latter factor being decisive. Here it is also useful to quote the values of the intrinsic birefringence obtained from optical measurements. Thus the intrinsic birefringence is $\Delta_{c,\alpha}^0 = 0.145 \pm 0.002$ for the crystal of the α modification, whereas for the amorphous phase we have $\Delta_a^0 = 0.098 \pm 0.017$.

The method involving the solid-phase extrusion of polymers, which in many instances yields high orientation characteristics, occupies a definite place in film technology. In this connection, one should mention a series of studies^{145–147} in which this technique was used to obtain oriented PVDF films. The extrusion conditions selected by Mead et al.¹⁴⁶ corresponded to a pressure of 0.23 GPa in the extruder and a temperature of 160°C . The change in melting point corresponding to a pressure change of 1 Pa is 3.3 degree. The pressures employed yield an increase in melting point by 76°C . For this reason, deformations under conditions such that the temperature was much lower than the melting point of PVDF at the normal pressure corresponded to the chosen deformation regimes. It was shown that an increase in draw ratio is accompanied by an increase in the degree of crystallinity and in the magnitude of the birefringence. The phase composition in the film is characterised by a mixture of the α and β crystals, while the morphology is represented predominantly by the folded-chain form of the crystals with a large period of 20 nm. Contradictory results were obtained, according to X-ray data, the fraction of the

crystals of the α phase is greater than that of the β phase, while IR spectroscopy shows that the crystals of the β phase predominate. The discrepancies may be avoided by postulating that the chosen extrusion regime ensures more intense conformational transformations of the type $TGT\bar{G} \rightarrow (TT)_n$ in the nonordered regions than in the crystal. By selecting the extrusion regimes it is possible to achieve the optimum conditions for the $\alpha \rightarrow \beta$ transformation. Indeed, it has been reported¹⁴⁷ that extruded films predominantly in the β modification have been obtained by this method; at the same time, one should expect a high correlation with the arrangement of the chains of the amorphous phase, since the measured birefringence indicated for the extruded films is $\Delta n = 67 \times 10^{-3}$, which had never been noted previously in the literature.

The mechanical characteristics of the PVDF films are improved also when nontraditional orientation methods are used for polymers, for example, rolltruding.¹⁴⁸ At rolling temperatures of 140–160 °C, there is a twofold increase (for the main rolling direction) in Young's modulus and a 12-fold increase in the ultimate strength.

In uniaxial or biaxial mechanical stretching of PVDF films, there is a possibility of the appearance of all kinds of long defects (of the type of voids). It therefore seems promising to develop methods effecting orientation crystallisation without mechanical influences. Lovinger and Wang¹⁴⁹ carried out the zone crystallisation of PVDF at zone migration velocities of 0.6–20 $\mu\text{m min}^{-1}$ and a zone temperature of 153 °C. Analysis of the results obtained by polarisation microscopy, X-ray diffraction, and IR spectroscopy demonstrated that crystallisation in the form of the α phase predominates. Weakly developed β phase spherulites serve mainly as nuclei of α spherulites deformed in the direction of migration of the zone. Analysis of the nature of the diffractometer traces and of the dichroism of a series of IR absorption bands with a known value of the transition moment vector permitted the conclusion that the b axis of the lattice is oriented along the direction of migration of the zone. We may note that, in the textured specimens obtained by mechanical stretching, the cell c axis is aligned along this direction. A version of the zone stretching of PVDF films at high rates or zone migration has been described.¹⁵⁰ Having selected the stretching conditions, specimens with well oriented crystals and preferential crystallisation in the form of both α and β phases were obtained.

The problem of the formation of voids in PVDF films on uniaxial stretching may be of applied importance since, the formation of microcracks in the bulk of the film is accompanied by a decrease in its relative permittivity. Under certain conditions, this may lead to an increase in the piezoelectric constant g for the polarised films, which affects the output characteristics of the energy converters based on these materials. Specialists of the Thorn-EMI Company (England) and of Leeds University have been most actively concerned with this problem. In particular, they developed a method for the preparation of PVDF films with voids resulting from cold drawing ($T_d = 80$ °C) at high rates.¹⁵¹ The nature of the morphology arising under these conditions has been studied in detail by electron microscopy.^{152, 153} It was shown that the voids have the form of an ellipsoid with transverse spans, i.e. they may be regarded as a form of crazing. The voids were disposed between fibrils and were characterised by a fairly wide size distribution. In one case, the average size of the voids in the longitudinal direction was 1.5 μm ,¹⁵² whilst in another it was ~ 5 μm ,¹⁵³ although in both cases their volume fraction was estimated as 17%.

In a study of the mechanical shear anisotropy in oriented PVDF films, it was shown that the presence of voids in the bulk phase promotes an increase in virtually all the components of the elastic pliability tensor.¹⁵⁴

Certain details of the formation of the voids in the cold drawing ($T_d = 80$ °C) of PVDF have been investigated by Kochervinskii et al.⁴⁷ Attention was drawn to the fact that the probability of the formation of voids under identical cold drawing conditions may depend significantly on the nature of the initial

supermolecular structure. Two PVDF films, obtained by quenching from the melt and by slow crystallisation, were investigated. Spherulites differing significantly in size and degree of defectiveness were detected in them by the method involving small angle scattering of polarised light. The spherulites in the quenched films were an order of magnitude smaller, while the internal arrangement of some of them was characterised by the disposition of the lamella at an angle of 45° relative to the radius of the spherulite (the so called 'anomalous' spherulites). The morphology of the two films was different after cold drawing. For the quenched film, the H_v -diffractometer trace had the form of an eight-lobe figure, arising, as noted above,^{132, 133} from the presence of deformed and undeformed spherulites. A stronger equatorial scattering in crossed polarisers and a decrease in density and transparency caused by the formation of ellipsoidal voids are characteristic of the stretched film with large spherulites.

A similar result was also obtained on cold drawing ($T_d = 20$ °C) of films of the VDF/TFE 94/6 copolymer.⁴⁸ The formation of voids in the bulk phase (according to small-angle X-ray scattering data) is also observed in the film where the presence of β phase spherulites was noted in the initial state. The formation of voids is apparently accompanied by local releases of the stress, which should affect the conformational characteristics of the crazed films. In the case of the homopolymer, this is accompanied by a decrease in the fraction of the β phase in the oriented state,³³ while for the VDF/TFE 94/6 copolymer crystallised as the β phase this is accompanied by the appearance in the oriented state of sections of the chains in the $TGT\bar{G}$ conformation, which is not characteristic of the given polymorphic modification.^{155, 156} The fraction and nature of the microstructure of the voids formed may be regulated by isometric annealing processes and under certain conditions it is possible to achieve a decrease in, on the one hand, the concentration of the voids and, on the other, in the concentration of 'defective' conformations of the $TGT\bar{G}$ and $T_3GT_3\bar{G}$ types.^{155–157}

The detection by the spectroscopic method of these conformations in the VDF/TFE copolymer,^{114, 129, 130} which crystallises as the polar β phase with the 'planar zigzag' conformation, most probably confirms the concept that conformational defects of the kink bonds are present in the PVDF crystals.^{91–97} The above defects may play a significant role in polymorphic transformations during uniaxial drawing. This has been confirmed, for example, by data¹⁵⁸ according to which the high-temperature drawing of PVDF is accompanied by the formation of an oriented α phase. Electron diffraction patterns reveal certain 'anomalies'. Thus the 110 reflection due to the α phase has the form not of a point but of a strip which coincides with the direction of the c axis. Diffuse halo blurring (from the $hk0$ direction) is characteristic of the 002 reflection. The authors also attributed the observed 'anomalies' to the appearance of kink bonds. Instead of the $TGT\bar{G}TGT\bar{G}TGT\bar{G}$ sequence, one should expect in this case the $TGT\bar{G}TTTGT\bar{G}$ combination, where the conformational defects arise due to cooperative segmental 'flip-flop' motions between the $T\bar{G}TG$ and $TGT\bar{G}$ conformations. Defects of this kind for the oriented α form of PVDF arise also during prolonged isometric annealing.⁹²

It follows from the overall analysis of the data that the kink bonds noted above tend to aggregate into chains, which are disposed in the 001 plane.¹⁵⁸ The observed diffuse halo near the 200, 110 reflection, due to the oriented polar β phase,¹⁵⁹ is also caused by the appearance of bent kink bonds. In this case, this is attributed to the insertion of type GT_nG or $TGT\bar{G}$ sections of the chain into the chain with the 'planar zigzag' conformation. The authors of the concept developed believe that the solid-state transformation $\alpha \rightarrow \beta$ has a two-step mechanism: the $\gamma \rightarrow \beta$ transition takes place initially and is followed by the $\gamma \rightarrow \beta$ stage.⁹⁴ It is postulated that the kink bonds in the initial α phase constitute an intermediate phase between the α and γ modifications and can therefore facilitate significantly the occurrence of the first stage of the transformation.

The presence of chain sections in the $TGT\bar{G}$ and $T_3GT_3\bar{G}$ conformations in the VDF/TFE 94/6 copolymer, which crystallises from the melt or from solution immediately as the polar β phase,¹³⁰ can be regarded as evidence for the presence of kink bonds. Their role in the uniaxial stretching processes involving isotropic films of the above copolymer, unaccompanied by a polymorphic transformation, is also extremely significant. Thus it has been shown that identical stretching conditions for the two films are characterised by a greater deformation energy density in the case of the specimen with a lower content of conformational defects in the initial state.¹³⁰ The structure of the oriented film arising under these conditions is characterised by a higher Young's modulus and a higher deformation-induced acoustic response.¹²⁹ The higher residual polarisations¹⁶⁰ and piezoelectric responses¹²⁹ in such films after treatment in an electric field show that the role of the kink bonds must be taken into account also in the technological development of methods for the preparation of films designed for practical purposes.

The stabilities of various polymorphic modifications of PVDF under the conditions of the operation of uniaxially stretching stresses σ have been justified theoretically and predicted.⁸⁸ Calculation of the free energy taking into account the interchain and intrachain interactions leads to the conclusion that at least five different phases may exist in PVDF: α , β , γ , σ , (α_p) and m (melt). Analysis of the phase diagram for PVDF in a state of mechanical stress has demonstrated the possibility of the existence of a large number of metastable states.⁸⁸ At room temperatures under the conditions of the operation of uniaxially stretching stresses, the α phase may exist only in a metastable state owing to the increased free energy, which agrees well with the characteristics of the $\alpha \rightarrow \beta$ transformation described above.

It has been shown^{161,162} that the above transition under the conditions of uniaxial stretching proceeds in the neck formation stage in the specimen so that the structural studies devoted to the

necking phenomenon in PVDF may extend the ideas concerning the mechanism of the polymorphic transformations $\alpha \rightarrow \beta$. The conclusions of certain investigators on this question are of interest in this connection. Thus according to Kochervinskii,¹⁶³ the variation of the short- and long-range order parameters as a function of T_d led the authors to the conclusion that crystallisation processes should occur in the region of the formation of a neck in PVDF and should be preceded by the passage of the system through a strongly disordered or even fused state. However, in the study of the Raman spectra in the course of the deformation of PVDF it was observed¹⁶² that not only does the $\alpha \rightarrow \beta$ transformation occur in the region of the neck but there a marked increase in the degree of crystallinity (Fig. 14a). At the same time, as can be seen from the figure, the medium is heated intensely in the region of the neck, such heating depending on the rate of deformation. This factor is apparently decisive for the 'anomalous' decrease in the velocity of ultrasound on formation of a neck in the VDF/TFE 94/6 copolymers.^{114,163} The decrease in the velocity of sound under these conditions may reach 15% and the intensity of the transition of the material to the disordered state may depend significantly on its previous thermal history.

Specimen 2, for which the isothermal crystallisation time was five times longer than for specimen 1, has a lower concentration of defective conformers ($TGT\bar{G}$ and $T_3GT_3\bar{G}$), a larger size of the spherulite R_c , a higher density ρ , and an increased fraction of the basic 'planar zigzag' conformations (Table 10).

Table 10. Spectroscopic and morphological characteristics of isotropic films of the VDF/TFE 94/6 copolymer obtained by crystallisation from the melt.¹¹⁴

Frequency /cm ⁻¹	D/d for specimen 1 ^a	D/d for specimen 2 ^b
$(TT)_n$ conformation		
442	60	122
70	54	86
$T_3GT_3\bar{G}$ conformation		
431	47	106
300	9	15
90	34	163
$TGT\bar{G}$ conformation		
411	48	45
287	16	4
214	18	6

^a For specimen 1, $\rho = 1.8031 \text{ g cm}^{-3}$ and $R_c = 3.4 \text{ }\mu\text{m}$.
^b For specimen 2, $\rho = 1.807 \text{ g cm}^{-3}$ and $R_c = 4.6 \text{ }\mu\text{m}$.

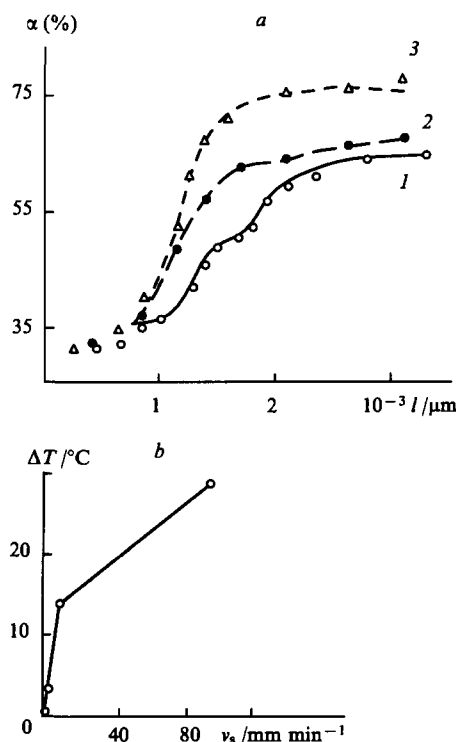


Figure 14. Dependence of the degree of crystallinity (α) on the distance (l) to the neck formation boundary at different rates of deformation (v_s) (a) and variation of the temperature in the region of the formation of a neck on uniaxial drawing of PVDF (b).¹⁶²
 v_s (mm min⁻¹): (1) 0.1; (2) 10; (3) 100.

It may be inferred from the values of $\rho(\gamma)$ calculated by Eqn (4) that an increase in the crystallisation time is accompanied by a redistribution of the relative amounts of the conformational defects, i.e. chain sections are enriched in the isomers with the $T_3GT_3\bar{G}$ conformation as a result of their transition from the $TGT\bar{G}$ conformation.

Specimen	$\rho(\gamma)$	$\frac{D_{287}}{D_{300}}$	$\frac{D_{411}}{D_{442}}$	$\frac{D_{214}}{D_{442}}$	$\frac{D_{100}}{D_{70}}$
1	0.49	1.8	0.8	0.29	0.67
2	0.70	0.88	0.37	0.04	0.46

An increase in the number of chains in the 'planar zigzag' and $T_3GT_3\bar{G}$ (which are closer to a planar zigzag than $TGT\bar{G}$) conformations is in fact apparently the cause of the weaker disordering in the transitional region involving the formation of the oriented β phase (Fig. 15).

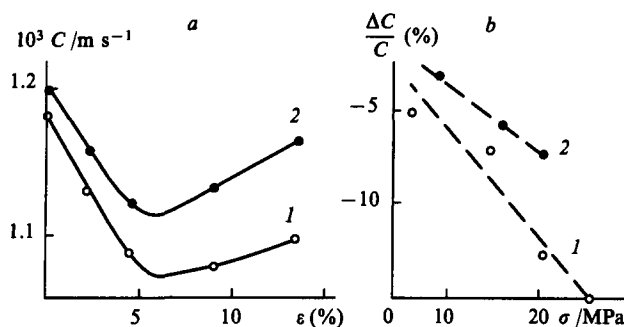


Figure 15. Dependence of the longitudinal velocity of sound on the deformation (a) and the relative change in the velocity of sound as a function of the stress in the region of the formation of a neck in two specimens of the VDF/TFE 94/6 copolymer (b).¹¹⁴ Specimen: (1) 1; (2) 2.

The structure and morphology of the latter for films obtained at different T_d may differ significantly.¹²⁹ This follows also from the consistent changes in the long period L and in the intensity of the small angle meridional maximum on the X-ray diffraction curves (Fig. 16). An increase in T_d is accompanied by an increase in L and in the intensity, as mentioned above, the latter being probably due to the increase in the difference between the densities of the crystalline and amorphous regions along the direction of stretching. As can be seen from the same figure, this is accompanied by consistent changes in the response recorded by acoustic (from the velocity of sound) or optical (from the magnitude of the birefringence) methods. In particular, for the specimen with the highest draw temperature, the optical anisotropy in the film for small deformations hardly changes, while the velocity of sound actually diminishes somewhat. The increased concentration of 'defective' isomers noted for oriented films with a high T_d ¹²⁹ shows that the microstructure of the noncrystallising sections in such systems may determine also the response to external influences (mechanical¹²⁹ or electrical¹⁶⁰). This may prove useful in its turn for the understanding of the mechanism of the piezoelectric response in such systems.

V. Characteristics of the crystallisation of poly(vinylidene fluoride) under the conditions of uniaxial compression and high pressures

The uniaxial stretching effects influence significantly the phase equilibrium in the crystalline PVDF phase and one may therefore expect that the conditions in the uniaxial or all-sided compression also lead to an alteration in the nature of the polymorphic transformations. This hypothesis was confirmed more than 25 years ago in the pioneer studies by Doll and Lando.¹⁶⁴⁻¹⁶⁶ It was shown that isothermal crystallisation from the PVDF melt, which is usually accompanied by the formation of the α modification, leads to the crystallisation of the γ phase (or its mixture with the α phase) on raising the pressure to 2000–5000 atm, the probability of this increasing with decrease in the degree of supercooling.¹⁶⁵ For the VDF/TFE 93/7 copolymer, which usually crystallises as the low-melting β phase (melting point 139 °C), an increase in pressure to 5000 atm leads to the formation of the same modification but with a melting point higher by 20 °C.¹⁶⁶ The same rule holds also for isotropic specimens textured as a result of uniaxial stretching and crystallised at normal and elevated pressures.¹⁶⁶ The results of differential thermal analysis have shown that an increase in pressure at the crystallisation of isotropic specimens is only one of the conditions for the formation of the β phase, the other condition being the maintenance of a low degree of supercooling. It has been shown by electron microscopy that crystallisation under pressure is accompanied by a significant increase in the long period (to 68 nm compared with the usual values of 10–15 nm).¹⁶⁷ An increase in pressure to 3000 atm increases linearly the melting point both of the VDF homopolymer and of its copolymer with TFE, the entropy of fusion diminishing under these conditions.

Similar results have been obtained also in a study whose authors observed the polymorphic transition $\alpha \rightarrow \beta$ in the high-temperature annealing of specimens with the α phase under a pressure of 4000 atm. It was noted (as in the above studies¹⁶⁵⁻¹⁶⁷) that a decrease in the annealing temperature lowers the effectiveness of this transition. It was demonstrated later¹¹⁰ that, by making the conditions for the annealing of the isotropic PVDF specimens more severe (a pressure of 4500 atm and a temperature of 292 °C), it is possible to ensure also the $\alpha \rightarrow \beta$ transformation. The extent of such transformations can be increased by optimising the PVDF crystallisation conditions under high pressure.¹⁶⁹ For this purpose, changes were made both in the temperature (from

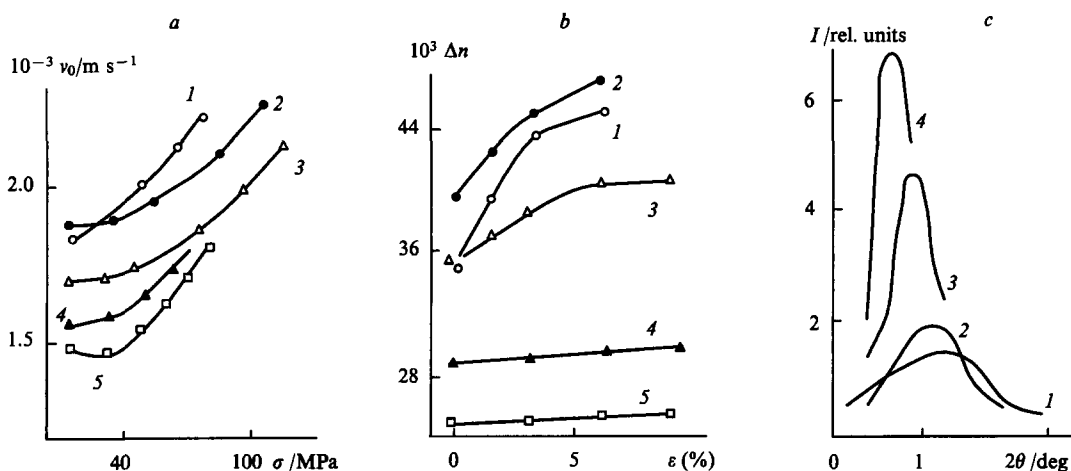


Figure 16. Variation of the longitudinal velocity of sound (a) and birefringence (b) as well as small angle X-ray diffraction curves (c) for oriented films of the VDF/TFE copolymer obtained at different temperatures (°C): (1) 60; (2) 80; (3) 100; (4) 120; (5) 140.¹²⁹

Table 11. Characteristics of the crystallisation conditions and the parameters of the PVDF structure during formation under increased pressure.¹⁶⁹

P_i /kbar	P_f /kbar	T_i /°C	T_f /°C	Fraction of β phase (%)	α (%)	$\Delta T/\Delta P$ /K kbar ⁻¹
0.93	6.25	213.1	254.4	4	51	7.76
1.15	6.38	217.3	255.6	12	50	7.32
1.45	6.21	225.8	257.3	19	52	6.62
1.80	6.4	231.9	261.0	95	60	6.33

the initial T_i to the final T_f and in the temperature (from the initial T_i to the final T_f) and in the pressure (from the initial P_i to the final P_f) of this process as a result of which it is possible to vary appreciably both the fraction of the β phase and the degree of its crystallinity. This is illustrated by the data in Table 11.

The nature of the changes in the parameters of the unit cells in the PVDF crystals formed under pressure has been investigated.¹⁷⁰ For this purpose, the changes in the interplanar spacings were followed in specimens of the α and β phases under pressure. In the α modification of PVDF, they proved lower in the 110 plane than in polyethylene (PE), whereas along the axis of the macromolecule the opposite was true. The variation of the unit cell parameter of the α phase along the b axis was found to be greater than along the a axis, whereas for the β modification the changes in the interplanar spacings along the normals to the 110, 200, 020, and 310 planes are similar. It has also been shown that the compressibility of the lattice decreases in the direction $PE \rightarrow PVDF_\alpha \rightarrow PVDF_\beta$. The study of the volume compressibility β_v with the aid of physicochemical characteristics in block PVDF specimens crystallised as the β modification evidently makes it possible to obtain definite information about the structure of the nonordered regions.¹⁷¹ Thus, it has been shown that, under the conditions of the crystallisation of PVDF in the form of one modification, β_v for the oriented specimens proved to be always lower than for the isotropic ones. On the assumption that the degree of crystallinity is constant, this can be accounted for solely by the denser packing of the chains of the amorphous phase in the former. The large fraction of the latter phase in PVDF (> 50%) is believed to be the main cause of the abrupt change in Young's modulus with increase in pressure, where the vitrification of the nonordered regions is postulated.¹⁷¹ The role of the latter is manifested also by the dependence of the linear expansion coefficient L of the specimens with a nonoriented phase on the pressure P described by the polynomial

$$L = A + BP + CP^2 + DP^3, \quad (5)$$

where $A = 2.540$, $B = -1.733 \times 10^{-2}$, $C = -1.605 \times 10^{-3}$, and $D = -1.386 \times 10^{-4}$.

The two bends in the temperature variations of the linear expansion coefficient (at -50 and 22 °C) are attributed to transitions in the amorphous phase and the crystal respectively.

In a series of studies Matsushige and coworkers^{127, 171–175} also indicated the possibility of the $\alpha \rightarrow \beta$ transformation on crystallisation (or annealing) under high pressure. The presence of three endothermic fusion peaks for the PVDF specimens crystallised in this way is attributed to the fusion of the residues of the α phase and of the regions of the β phase, which results in the formation of folded-chain crystals and extended chain crystals (ECC).^{171–175} It was noted that such crystals have significantly different morphologies: a spherulite structure was observed for the folded-chain crystals, whereas for the ECC lens-like formations with dimensions of ~ 10 μm were noted. The corresponding melting points (at the normal pressure) are respectively 190 and 207 °C, both increasing linearly with pressure. As the PVDF specimens with the β phase crystallised under a high pressure are heated under normal conditions, the reflections characteristic of the β phase remain unchanged up to 189 °C (which is not the case in the oriented specimens with the β phase). This indicates the high stability of the above modification and the absence of the reverse transition $\beta \rightarrow \alpha$ up to the temperature indicated.¹⁷⁴ The results of

the study of the high-temperature annealing of specimens of the PVDF phase under a pressure of 4000 kg cm⁻² have shown that the virtually complete transition $\alpha \rightarrow \beta$ takes place over a period of 165 min at 278 °C (the melting point of the α phase is 286 °C). A decrease in the annealing temperature lowers the rate of the transformation. The activation energy for the above transition (calculated from kinetic data for the initial stage of the process) has been estimated as 30 kcal mol⁻¹.¹⁷³

When pressure was applied to an oriented PVDF specimen containing a small amount of the residual α phase, a uniaxial deformation arose, which led to the complete disappearance of the α phase.¹⁷⁶ In addition, X-ray photographs at different angles relative to the initial c texture have shown that the $h00$ planes of the β phase crystal lattice are located in the plane of the film, the 001 direction again coinciding with the direction of the initial extension, so that the $h00$ planar texture is produced. It is believed that the 100 and 110 planes in PVDF (as in polyethylene) are the closest packing planes with the maximum interplanar spacing. Slip should occur along the above planes in most cases. The formation of fault bands and twinning are characteristic of the structure formed under these conditions.

In the case of the uniaxial compression of isotropic films with the α phase, it was found that the shape of the pistons may play a significant role in the $\alpha \rightarrow \beta$ transformation.^{175, 177} The rectangular shape is preferable for the chosen conditions (5000 kgf cm⁻² and 125 °C). In this case, the X-ray diffraction pattern proved to be similar to those for the extended specimens, the degree of orientation of the β crystallites reaching 95%.¹⁷⁵ The results of the study of the compression process at variable temperatures have shown that the most complete $\alpha \rightarrow \beta$ transformation takes place at 125 °C. On the other hand, on extension an increase in temperature (under the conditions of constant deformation) leads to a decrease in the extent of the above transformation. It is therefore concluded that the mechanisms of the $\alpha \rightarrow \beta$ transitions on compression and extension are different. With increase in pressure, there is also a change in the mechanism of the transformation on extension. At a temperature above 130 °C, uniaxial stretching proves ineffective for the $\alpha \rightarrow \beta$ transition. However, if it is carried out under a pressure of 4000 kgf cm⁻², then the transition occurs up to draw temperatures in the range 250–265 °C.¹²⁷ The changes in the nonordered phase in high-temperature annealing processes under a high pressure have been investigated in a study¹²⁷ of the $\alpha \rightarrow \beta$ transitions in relation to single crystals of the α phase. In particular, the above transformation goes to completion in such crystals over a period of 15 min at 533 K and a pressure of 400 MPa. Presumably the nonordered phase gives rise to definite hindrance to the $\alpha \rightarrow \beta$ transition, since the annealing at the same pressure of a PVDF specimen with a lower degree of crystallinity requires 165 min and a temperature of 551 K for the 100% yield of the β phase.¹⁷³

The structural transformations for different versions of the uniaxial and all-sided compression should be reflected also in the electromechanical characteristics of the polarised PVDF films.

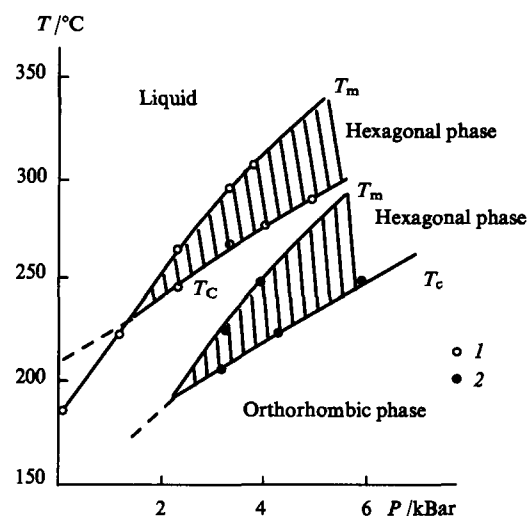
Table 12 shows that, during annealing at a high pressure, the piezoelectric constants of uniaxially extended films increase by a factor of 3.5–4. Drawing under a high pressure requires the optimisation of the process with respect to temperature. For the variant involving uniaxial compression, the piezoelectric moduli may be increased appreciably by combining the film deformation and polarisation processes.

Table 12. Piezoelectric properties of PVDF specimens obtained by different methods.¹²⁷

Preparation conditions	Piezoelectric stress constant $10^2 d_{31}/\text{C m}^{-2}$	Elastic modulus /GPa	Piezoelectric strain constant $d_{31}/\text{pC N}^{-1}$
1 kgf cm ⁻² drawing and 75 °C	1.0	1.5	6.7
Drawing (annealing) under 4000 kgf cm ⁻² pressure and 278 °C for 30 min	3.5	1.3	27
Drawing under 4000 kgf cm ⁻² pressure at different temperatures /°C			
165	2.7	1.4	20
200	3.0	1.4	21
250	4.1	1.6	26
265	1.7	1.3	13
Uniaxial compression at 5000 kgf cm ⁻² and 125 °C			
Poling after compression	1.5	1.5	8.0
Poling during compression	2.8	1.5	19

For the VDF homopolymer with crystals of the β phase, an increase in pressure to 4.5 kbar increases its melting point by more than 100 °C.¹⁷⁰ For the VDF/TrFE 70/30 copolymer, in which the melting point and the temperature of the ferroelectric–paraelectric transition are different, an increase in pressure is accompanied by an increase (albeit in accordance with different laws) in the regions of both transitions. The nature of the above phenomenon has been investigated in detail in studies^{179–181} of the structural changes under the influence of high pressure in ferroelectric VDF/TrFE copolymers having different compositions. In particular, it has been shown for PVDF/TrFE 54/46 that under normal conditions (room temperature, normal pressure) the crystal structure is characterised by the coexistence of the paraelectric and ferroelectric phases, to which correspond different angular positions of the main intermolecular reflection.¹⁷⁹ An increase in pressure to 450 GPa is accompanied, together with the general shift of the reflections towards larger angles, also by a significant weakening of the paraelectric component, the above changes being reversible.¹⁷⁹ An increase in pressure in the copolymers indicated is accompanied, according to X-ray and electrophysical measurements, by an appreciable shift of the region of the ferroelectric–paraelectric transition towards higher temperatures.¹⁸⁰

A combined study of the structural and electrophysical properties of films of the VDF/TrFE 94/6 copolymer resorting to X-ray diffraction, scanning electron microscopy, and thermal analysis data has shown that crystallisation at high pressures is accompanied by the formation of lamellar crystals of the β phase with hexagonal packing and a thickness of 100–200 nm, which retain their stability at very high temperatures. By generalising these data, the authors¹⁸¹ were able to put forward a phase diagram for the VDF/TrFE 94/6 copolymer (Fig. 17). It follows from the latter, in particular, that the melting point and the Curie point (T_c) increase with pressure according to different laws and that the hexagonal phase may be present only at high pressures. As a result of the analysis of the morphology of the supermolecular structures formed, it was later concluded that the ECC regions are formed when crystallisation from the melt gives rise to a metastable hexagonal phase, which may be subsequently converted into a stable orthorhombic phase.^{182, 183}

**Figure 17.** The P – T phase diagram for the PVDF/TrFE 94/6 copolymer.¹⁸¹

(1) curves obtained in the heating regime; (2) curves for the cooling regime; hexagonal phase — paraelectric; orthorhombic phase — ferroelectric.

VI. The polymorphism of the poly(vinylidene fluoride) induced by strong electric fields

The dipole moment of the monomer unit of the PVDF chain in the 'planar zigzag' conformation is 7×10^{-30} C m,¹⁸⁴ so that it is natural to expect a high sensitivity of this polymer to strong fields. Indeed, numerous experimental data have confirmed this. High fields may affect the crystal lattice, altering the nature of the supermolecular formations in the PVDF and the isomeric composition of its chain. The above changes are usually observed by large- and small-angle X-ray diffraction methods, the method based on the small angle scattering of polarised light, and IR and Raman spectroscopy. Examination of the polymorphic transformations in PVDF under the influence of high fields can be usefully begun with a simpler case where a PVDF specimen crystallised as the β phase, in which a polymorphic should not be expected, is subjected to the action of the field. Such a case has been described in a study¹⁸⁴ where the β phase was obtained as a result of low-temperature drawing and subsequent annealing. The nature of the change in the profile of the principal β phase reflection 200, 110 after poling (in a 60 MV m⁻¹ field) showed that the polar cell uncoils under the influence of the field.

Another variant of the behaviour of PVDF in a high field has been examined in studies,^{185, 186} where crystallisation led to the formation of a mixture of the α and β modifications. Fig. 18 presents X-ray diffraction curves for the initial (biaxially oriented) film and the film treated in a corona discharge. Evidently, poling in the corona discharge even at a potential of 5 kV leads to the disappearance of the 100 and 020 reflections of the α phase and to an increase in the principal 200, 110 reflection of the β phase. The intensity of the latter increases significantly with the simultaneous decrease in yet another reflection (110) of the α phase with increase in the potential to 10 kV, which has been attributed to the polymorphic $\alpha \rightarrow \beta$ transition. Certain details of the structural changes occurring under these conditions may be noted by analysing the data in Table 13. In particular, it is seen that, after the treatment of the film in the field, the principal reflections of both the α and β phases shift towards small angles and are broadened at the same time. The former fact, indicating some 'loosening' of the transverse dimensions of the crystallites, has been attributed to the deformation of the bond angles in the main chain as a result of the interaction of the field with the polar CF₂ bonds. On the other hand, the broadening of the β reflection after

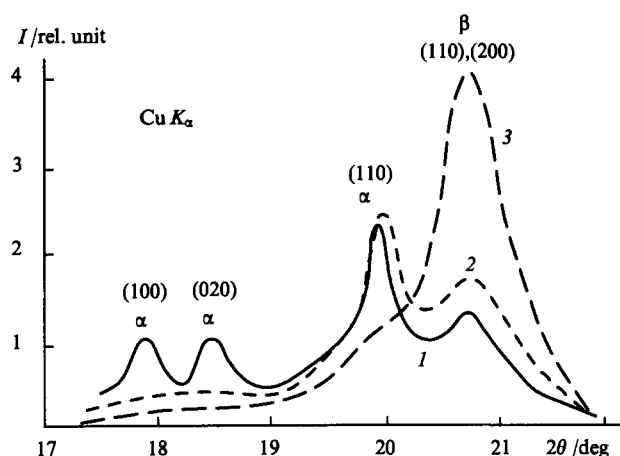


Figure 18. Diffraction curves for the initial PVDF film (1) and the film charged in a corona discharge (2, 3).¹⁸⁵ Potential in the corona discharge (kV): (2) 5; (3) 10.

charging the film is due to the decrease in the size of the crystallites or an increase in their defectiveness.

For oriented PVDF films containing only 5% of the β phase, the effect of the 1.5 MV cm^{-1} field did not lead to the appearance of any new reflections, but a number of those arising from the initial film changed significantly.¹⁸⁷ A similar phenomenon in low fields was noted also in other investigations.^{188, 189} A significant change in the concentration of the groups in the $TGT\bar{G}$ conformation was not then found¹⁸⁷ and it was therefore postulated that a new crystallographic modification α_p (δ -) is formed under these conditions.

The $\alpha \rightarrow \alpha_p$ transition leads to the formation of a new cell in which the dipole moments of two chains are parallel (Fig. 2). This transition requires the rotation of one chain by 180° (as a result of the energy of the external field and temperature) with a translational displacement along the axis of the macromolecule over a distance $c/2$. The identity periods of the new lattice are then found to be the same as in the α phase, but the structure factors for a series of the reflections may differ appreciably (Table 14).

The appearance of the new 110, 200 reflection of the β phase in higher fields^{188, 189} indicates that two stages in the structural rearrangement should be expected for the α phase: in accordance with the scheme $\alpha \rightarrow \alpha_p \rightarrow \beta$. In low fields, the $\alpha \rightarrow \alpha_p$ transition takes place without changes in the chain conformation and in the geometry of the lattice, the unit cell becoming polar under these conditions. The last factor is apparently the reason why certain reflections from the α_p phase undergo a change in intensity or are altogether extinguished (Table 14). However, this transition is not

Table 14. The structure factors for the reflections due to the α and α_p modifications of PVDF.¹⁸⁸

hkl	2θ /deg	Structure factor /rel. units	
		α phase	α_p phase
100	17.88	60	0
020	18.41	86	86
110	20.13	137	165
120	25.77	92	0
021	26.73	119	119
111	27.97	79	85
121	32.35	65	0
130	33.20	75	93
200	36.2	69	106
210	37.44	81	0
040	37.41	14	14
002	38.99	78	78

accompanied by any significant changes in the initial morphology.¹⁹⁰ In higher fields, conformational rearrangements of the type $TGT\bar{G} \rightarrow (TT)_n$ begin, which entail a change in the type of the unit cell. The structural rearrangements noted above are accompanied by the rotation of the dipoles relative to the direction of the field and by a change in the relative intensities of a series of characteristic bands in the IR spectrum.¹⁹¹ It is postulated that the rotations of the dipoles for the chain sections in the $(TT)_n$ conformation proceed with greater difficulty than for the chain sections in the $TGT\bar{G}$ conformation.¹⁹² Analysis of the kinetics of the variation of the intensity of the 512 cm^{-1} band (characteristic of segments with the 'planar zigzag' conformation) after the application of a rectangular electric field pulse permitted the conclusion that there are fast and slow stages in the orientation of the dipoles.¹⁹³ The former is attributed to the rotation of small crystals and the latter to the slow rotation of the chains in the crystal. It is postulated that the slow stage of the orientation process should not reduce solely to 'flip-flop' motions with 180° rotation of the chain, which are inactive in the IR region.¹⁹³

For the cyclic variation of the strength of the field and of its polarity, the orientation processes are in the nature of hysteresis. This can be inferred from Fig. 19, in which the intensity curves for two absorption bands sensitive to the 'planar zigzag' conformation are presented. If A and B are initial points, then the antiparallel nature of the curves is due to the difference between the directions of the transition moment vector for the two bands: for the 512 cm^{-1} band, it is parallel to the dipole moment of the CF_2 group, while for the 446 cm^{-1} band it is perpendicular.¹⁹³ The retention of a definite orientation of the dipoles after the removal of the high field is apparently one of the factors needed for the establishment of a residual poling in PVDF films.

Table 13. X-Ray diffraction data for the initial (biaxially oriented) PVDF film and PVDF film treated in a corona discharge.

Thickness of specimen / μm	Data from Refs 110 and 111			Data from Ref. 186					
				before treatment in discharge			after treatment in discharge		
	2θ /deg	phase	plane	I	II	III	I	II	III
16	17.9	α	100	17.7	11.2	—	17.7	1	—
	18.4	α	020	18.4	3.4	—	18.4	1	—
	20.1	α	110	20.0	54.52	0.00614	19.4	3.3	—
	20.85	β	110	20.7	45.16	0.00636	20.16	63.25	0.00883
25			200						
	20.1	α	110	20.15	76.5	0.00448	19.9	11.2	—
	20.85	β	110	20.9	93.5	0.00537	20.6	109.6	0.00846
			200						

Note. The following designations have been adopted: I — Bragg angle 2θ /deg; II — area /arbitrary units; III — integral width /rad.

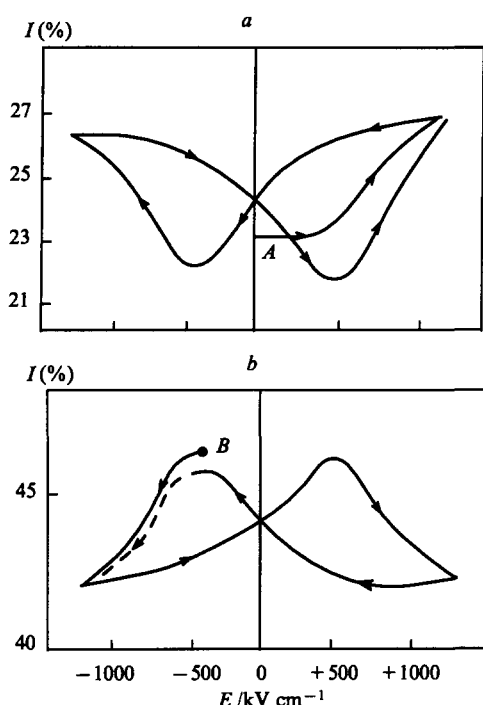


Figure 19. The hysteresis character of the 512 cm^{-1} (a) and 446 cm^{-1} (b) band intensity curves for a variable field in a PVDF film. A and B — initial points.¹⁹²

The above hypothesis that the $\alpha \rightarrow \alpha_p$ transition is not accompanied by a change in the nature of the H_V dispersion pattern¹⁹⁰ was refined to some extent data by the data of Broussoux et al.¹⁹⁴ They observed an increase in the intensity at the centre of the pattern when a PVDF film in the α_p modification was placed in a high field. Since the crystals of the α_p phase are polar, the forces acting on them alter the form of the orientation function $N(\alpha)$ for the crystallites in the spherulite. This should disturb the order in which the crystallites are arranged along the spherulite radius and should increase the scattering intensities at the centre of the pattern. During the repolarisation of the PVDF films in an 800 kV cm^{-1} field, the above changes in intensity occur over several minutes.¹⁹⁴ In high fields, this can be explained only by the influence of the space charge.

In a later study¹⁹⁵ by the same workers, the role of plastic deformation in the $\alpha \rightarrow \alpha_p \rightarrow \beta$ polymorphic transformations on poling of PVDF films was investigated. The change in the nature of the orientation of the β phase crystals under the influence of a high field was estimated (from the 201, 111 reflection) for this purpose. In one case, the poling was carried out after rolling the film and in another both processes were combined. Furthermore, by employing together with the X-ray method yet another variant of the IR spectroscopic distorted total internal reflection method, they estimated the nature of the orientation both in bulk and on the surface. The results demonstrate appreciable differences for the two poling methods. When the rolling and poling are carried out separately, the orientation in bulk proved to be less marked than on the surface and for the latter it is significantly more pronounced on the side of the positive electrode. This difference is attributed to the change in the local field as a result of the injection of carriers from the electrode. On the other hand, when the rolling and poling processes are combined, the difference between the orientations on the surface and in bulk are insignificant, as for different signs of the potential on the surface of the poling film. Owing to the high mobility of the chains, the plastic deformation processes promote an effective 'dissipation' of the space charge of the injected carriers and thereby smoothe out the inhomogeneity of the poling along the film cross-section.

The experimental critical fields for the $\alpha \rightarrow \alpha_p$ ($100\text{--}150\text{ MV m}^{-1}$) and $\alpha \rightarrow \beta$ (500 MV m^{-1}) transitions¹⁸⁸ have been confirmed, as regards order of magnitude, by calculations of the local free energy in terms of the average field approximation.¹⁹⁶ A decrease in the fields with increase in the poling temperature has also been predicted, in agreement with experimental data.¹⁹⁷ On raising the temperature from 20 to 65°C , coercive fields decrease by a factor of 2 as a consequence of the initiation of thermal defects, which should facilitate the above transitions. It is significant that this concerns only conformational defects, since irregularities in the 'head to head' attachment of groups actually increase the intramolecular potential barrier to the transition under consideration.¹⁹⁸ If it is postulated that the conformational defect is produced in the form of a kink of the kind mentioned above, the $\alpha \rightarrow \alpha_p$ transition can be modelled by the motion of a defect along a chain.¹⁹⁹ According to this model, the rate of migration of the kink depends on the field strength. At 373 K and for a field strength of 100 MV m^{-1} , the rate is $\sim 10\text{ m s}^{-1}$. This means that the kink migrates over a lamella 10 nm thick over a period of $\sim 1\text{ ns}$.

Estimates have shown that the proposed mechanism of the $\alpha \rightarrow \alpha_p$ transition requires $\sim 1\text{ ms}$ for the 180° rotation of the chain. For a quantitative justification of the proposed model, it was postulated²⁰⁰ that the motion of the kink along the chain in the form of soliton waves is the basis of the mechanism for the polarisation of the longitudinal component of the dipole moment, observed in PVDF films. Calculations based on the proposed hypothesis yield an activation energy for the migration process of $\sim 10\text{ kcal mol}^{-1}$ in the case of an ideal chain. This is an order of magnitude higher than the value obtained in dielectric relaxation experiments. It is assumed that the difference may be smaller if account is taken of the 'head to head' defects which actually exist in the chains and of the stressed bonds which may arise in the crystal or at its boundary with the nonordered phase. Another mechanism of the growth of the domain disposed most favourably relative to the polarising field has been proposed.²⁰¹ The mechanism is based on the idea of the twisting of the boundaries.²⁰² It has been shown that the additional energy per chain for 180° rotation in the conformation with minimum energy is 42 kJ mol^{-1} . The energy barrier which is overcome during the migration of the boundary along the chain is not less than 7.5 kJ mol^{-1} per repeat unit. This is comparable with the energy gain of 1.45 kJ mol^{-1} on transpolarisation of PVDF in a 2 MV cm^{-1} field.

The above structural transformation occurs only for high field strengths. Indeed, in the crystallisation of PVDF from solution in dimethylformamide in a 100 kV cm^{-1} field, neither the formation of a new phase nor a change in the form of the spherulite were observed.²⁰³ However, even at 115°C appreciable changes in the intensity of the 616 cm^{-1} band are observed only for field strengths in excess of 100 MV m^{-1} .^{204, 205} In the temperature range $50\text{--}70^\circ\text{C}$, the increase in the intensity of the conformational rearrangements occurring in the field (350 MV m^{-1}) agrees qualitatively with the data of Lu et al.¹⁹⁷ The regions of mobility in the PVDF crystal phase observed in this range by the dielectric method necessitate the assumption that above motions should play an important role in structural rearrangement processes under the influence of a field. This has been confirmed by data²⁰⁵ showing that, under the conditions of an identical field, an increase in the poling temperature from 20 to 100°C leads to an increase in the fraction of the β phase formed from 60% to 95%. Data obtained in studies on depolarisation processes in such specimens indicate that the temperature range $50\text{--}70^\circ\text{C}$ is important also for the deorientation processes involving some of the dipoles in polarised PVDF specimens and the β phase formed under these conditions remains stable up to high temperatures.²⁰⁵ The deorientation processes affect also the relaxation of the modulus in PVDF films in the early stages of stress relaxation.²⁰⁶ It must be noted that the mobility in these experiments (mentioned above) may also have a positive effect on the elastic properties,

since after longer times the inverse increase in the modulus is observed, which is most probably attributable to additional crystallisation.

Kepler et al.²⁰⁷ investigated the possibility of the theoretical estimation of the changes in the degree of crystallinity α in PVDF films with the β phase under the influence of an electric field. Estimates have shown that an increase in α with increase in field strength should be linear with a coefficient of $2.8 \times 10^{-11} \text{ V m}^{-1}$. The experimental coefficient was found to be somewhat higher, namely $(1.8 \pm 0.2) \times 10^{-11} \text{ V m}^{-1}$. One of the causes of the difference between the coefficients is, according to the authors, the difference between the relative permittivities of the amorphous and crystalline phases, giving rise to an inhomogeneity in the effect of the field on them. Yet another cause of the above difference may be the irreversible changes in the intermolecular packing of the PVDF chains under the influence of high fields. This can be inferred from the appreciable frequency shift of the characteristic bands in the IR spectra of PVDF on exposure to a strong electric field, which is reflected in Table 15.

Table 15. Variation of the band frequencies in the IR spectrum of PVDF during poling and after poling.²⁰⁸

Bond / cm^{-1}	Type of vibration	Frequency / cm^{-1}		
		before poling	during poling	after poling
976	$\nu(\text{CH}_2)$	975.9	974.8	975.8
796	$\gamma(\text{CH}_2)$	796.4	796.3	796.3
765	$\sigma(\text{CF}_2) + \sigma(\text{CCC})$	765.1	764.3	764.0
614	$\sigma(\text{CF}_2) + \sigma'(\text{CCC})$	614.7	614.0	614.3
530	$\sigma(\text{CF}_2)$	532.3	533.5	532.7
845	$\gamma(\text{CH}_2) + \nu_a(\text{CF}_2)$	843.5	846.0	844
510	$\sigma(\text{CF}_2)$	510.1	510.9	510.4

The same tendency towards a displacement of a series of β phase bands after the poling process towards higher frequencies has been noted also for the VDF/TFE 75/25 copolymer.²⁰⁹ The state of the more ideal packing of the chains after polarisation can be judged from the narrowing of the above bands and from the simultaneous increase in the density from 1.875 to 1.895 g cm^{-3} .²⁰⁹ As in the study of Kepler et al.,²⁰⁷ the polarisation of the VDF homopolymer is accompanied by an increase in α , but this occurs without change in the size of the crystallites. This finding indicates the formation of additional ordered regions from the amorphous phase.²¹⁰

The changes in the intensity of the 510 cm^{-1} band during the cyclic variation of the field applied to a biaxially oriented PVDF

film²¹¹ agree qualitatively with the changes in the intensity of this band found by Naegle and Yoon.¹⁹³ Comparison of the coercive fields obtained from spectroscopic data and from the field dependences of the electric shift showed that in the latter case they are appreciably greater. The 510 cm^{-1} band is characteristic of both the β and γ phases (Table 1). For this reason, Guy and Unsworth²¹¹ believe that one of the causes of the difference between the coercive fields is the presence together with the β phase of small amounts of the γ phase, which may have high coercive fields. Another cause is most probably the fact that the 510 cm^{-1} band is sensitive to the presence of 'planar zigzag' conformations not only in the crystal but also in the amorphous phase. The hysteresis phenomena for the latter should undoubtedly be characterised by lower coercive fields than the domain switching processes in the crystal, which are in fact responsible for the characteristics of the hysteresis in electrophysical experiments.

The influence of the poling temperature on the nature and kinetics of the structural transformations in PVDF in the range $20\text{--}100^\circ\text{C}$ has been investigated.²¹² For films with three different thicknesses, the changes in the intensities of the 510 and 530 cm^{-1} bands, which characterise the 'planar zigzag' and $TGTG$ conformations respectively, were analysed mainly. Fig. 20a presents the dependence of the relative change in the intensity of the 530 cm^{-1} band as a function of the polarising field strength. Evidently an increase in the poling temperature leads to an approximately linear displacement of the structural rearrangement region towards lower fields (Fig. 20b). The kinetics of the variation of the intensity of the 530 cm^{-1} band when a high field (2.1 MV cm^{-1}) acts on a PVDF film shows that the equilibrium value of ΔI_{530} is attained after $40\text{--}60$ min. The domain switching times in such fields should be less than 10^{-3} s.¹²⁷ The considerable differences between the domain switching and structural rearrangement times make it possible to put forward certain considerations about the details of the latter. When a field is applied to a specimen, the reorientation of crystallites takes place initially in the first stage. In the new position, the latter generate an internal field, which promotes the occurrence of orientation processes in the amorphous phase itself and at its boundaries with crystallites. The slowest stage in this process is the diffusion-controlled generation of a space charge both from the free carriers present in the initial state (before the application of the field) and as a consequence of the injection of charges from the electrodes.

A confirmation of the hypothesis of the occurrence of structural rearrangement processes in the amorphous phase may be found in the results of the study of Hsu et al.,²¹² although the authors did not draw attention to this fact. Indeed, during the poling process the 490 and 470 cm^{-1} absorption band intensities are redistributed, a decrease in that of the former and an increase in that of the latter being noted. These bands are attributed to the amorphous regions and their changes imply that poling leads to a

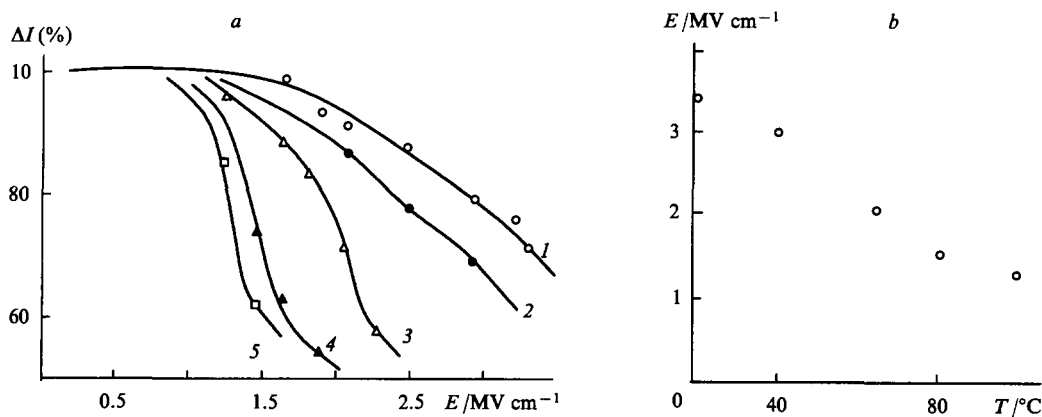


Figure 20. Field dependences of the relative change in the intensity of the 530 cm^{-1} absorption band at different poling temperatures (a) and temperature dependence of the critical fields in the structural rearrangement (b).²¹² T ($^\circ\text{C}$): (1) 20; (2) 40; (3) 65; (4) 80; (5) 100.

decrease in the fraction of the *gauche*-conformation as a result to the transition to the *trans*-conformation.

Yet another rather unpredicted phenomenon was later observed.²¹³ In previous sections, it was shown that the $\alpha \rightarrow \gamma$ transition initiated by prolonged high-temperature annealing of films with crystals of the α phase or by the crystallisation of PVDF from the melt with slight supercooling. The crystallisation of PVDF from the melt with high degrees of supercooling has been investigated in a 0.07 MV cm^{-1} electric field.²¹³ An experiment involving crystallisation with the same degree of supercooling but in the absence of an electric field was carried out as a control. It was observed that in the latter case PVDF always crystallised as the α phase. On the other hand, IR spectroscopic data showed that crystallisation in a weak field is accompanied by the appearance of an appreciable amount of the γ phase. This was inferred from the appearance of the 815, 776, 510, and 430 cm^{-1} bands characteristic of the T_3GT_3G conformation. It is significant that the fraction of the γ phase increases with decrease in the degree of supercooling and reaches 70% in the best cases. This phenomenon may be not only of academic interest but may also find a practical application.

The characteristics of the structural transformations under the influence of strong electric fields have been observed also for the VGF/TrFE 75/25 copolymer, which crystallises immediately as the ferroelectric β phase in the absence of the field.²¹⁴ It was observed by IR spectroscopy that the number of long sections of the chains in the 'planar zigzag' conformation (the 850 and 1290 cm^{-1} bands) changes in different ways following the application of a strong field depending on the temperature. Thus the application of a field at room temperature, which differs markedly from the Curie temperature, leads to a decrease in the concentration of the above sections (this is not observed for the VDF homopolymer), whereas at temperatures close to the Curie point the opposite behaviour is noted. It is believed that the improvement of order occurs only if it has been disturbed in the initial state (in the absence of a field) owing to large thermal fluctuations.

Transitions under the influence of a field on PVDF films obtained by different methods have been observed by X-ray diffraction, IR spectroscopy, and DSC.²¹⁵ Variation of the method of preparation showed that the threshold fields for the structural transformations of the α phase may be 0.6 and 1.6 MV cm^{-1} .

In a series of studies designed to estimate the possible structural changes in PVDF after and during the treatment by operation of strong electric fields, NMR spectroscopy was employed.^{216–210} Significant changes were noted in the direction of the b axis of the lattice in a field of 1 MV cm^{-1} even at room temperature.²¹⁶ Variation of the field strength demonstrated an appreciable decrease in the fraction of mobile protons in fields of $1.5–1.6 \text{ MV cm}^{-1}$,²¹⁷ whilst analysis of the second moment of the absorption line indicates the presence, together with the crystalline phase, of highly oriented chains of the nonordered phase, the fraction of which may reach 0.14.²¹⁸

The distribution function for the b and c axes of the lattice in PVDF films after their poling has been analysed.²¹⁹ Comparison of the intensities of the 111 and 001 reflections for the PVDF β phase before and after poling shows that a high field affects not only the distribution functions for the polar axes of the lattice (b) but also the distribution functions for the axes of the macromolecules (c). At the same time, it was noted that, despite the high fields the distribution of the b axes relatively to the normal to the film surface remains fairly wide. According to the authors²¹⁹, this creates potential possibilities for increasing the residual poling P_r in the ferroelectric PVDF by a factor of at least 2.²¹⁹ In the case of uniaxially extended PVDF films, P_r can be partly increased by selecting the conditions for preliminary isometric annealing. Thus it has been shown that such annealing at high temperatures ($160–180^\circ \text{C}$) is accompanied by an appreciable increase in P_r (from 51.4 to 65.2 mC m^{-2}).²²⁰ This is attributed to a considerable increase (from 45% to 68%) in the degree of crystallinity

under such annealing conditions. Somewhat later, Takase et al.²²¹ showed that such annealing is accompanied by an increase in the chain packing density in the lattice of the β crystallites and by an increase in their perfection. At the same time, these structural changes decrease appreciably (from 67.0 to $41.3 \mu\text{s}$) the domain switching times for a 2 MV cm^{-1} field in the ferroelectric phase.²²¹

The structural transformations in oriented PVDF films, crystallised as a mixture of the α and β phases, have also been investigated by the method of X-ray pole figures.²²² Analysis of the data shows that the distribution of the orientations of the dipoles along the direction of polarisation begins to change appreciably already in fields of 80 MV m^{-1} , although the nature of the distribution is restored after the removal of the field. Such low threshold fields may be associated with the high draw ratio ($\lambda = 6$) of the initial film. A field-induced increase in crystallinity has been observed,²²² which corresponds qualitatively to the data of Kepler and Anderson.¹⁸⁴ The dependence of the additional increment in the degree of crystallinity in PVDF films on the polarising field strength (Fig. 21) indicates nevertheless also certain differences with the above study. Whereas in the latter a monotonic linear dependence was noted in the entire range of fields, it can be seen from the figure that in the range $160–100 \text{ MV m}^{-1}$ an 'anomalous' decrease in the degree of crystallinity takes place. The cause of such decrease is probably the competitive effect of two processes. In low fields, the structures of the crystallites, the polar axis of which assumes a favourable disposition relative to the external field, are built up (using the chains of the amorphous phase). In a higher field, the energy of the latter is sufficient to initiate the rotation of single chains in crystals with an unfavourable disposition. Such rotations may disrupt the crystals, which in fact leads to a decrease in the degree of crystallinity. One should also note that, after the field has been switched off, the degree of crystallinity falls significantly. This finding most probably indicates that the reversible component or the increase in the degree of crystallinity is effected via a transition to an ordered state of some of the chains of the amorphous phase (or of its boundaries with the crystal). After the removal of the electric field, these regions again pass to the disordered state.

The contributions of the dipoles of the crystalline and amorphous phases to the field-induced orientation processes have been divided on the basis of a modified scheme for IR spectroscopic analysis, which provides for the possibility of altering the angle at which the beam enters the textured PVDF films.²²³ Use was made of a uniaxially extended film in which the fraction of the residual α phase was less than 5%, i.e. the polymorphic transformation under the influence of the field could be neglected

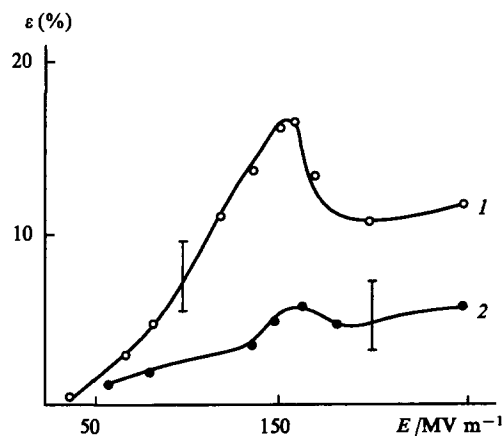


Figure 21. Dependence of the additional increment in the degree of crystallinity in PVDF films on the poling field strength.²²² (1) With the field applied; (2) after the removal of the field.

and the changes in the IR spectra could be unambiguously attributed solely to the change in the orientation of the dipoles. Two vibrational bands (at 510 and 445 cm^{-1}), characterising the 'planar zigzag' conformations were selected. The former corresponds to the CF_2 groups in both phases, while the latter corresponds only to the dipoles in the crystallites. Analysis of these data showed that, whereas in the initial state the dipoles form an angle of $42\text{--}44^\circ$ relative to the normal to the film, after the application of a 2.4 MV cm^{-1} field the angle is 27° for the 510 cm^{-1} band and 18° for the 44 cm^{-1} band. The significant difference between these values demonstrates unambiguously that, for the same field, the dipoles are better oriented in the crystal than in the amorphous phase.

A general thermodynamic approach to the quantitative description of the influence of the field on the crystallisation of PVDF (in the α or γ phases) has been developed.²²⁴ The authors of this study began with the concept of homogeneous primary nucleation. The free energy of formation (in the absence of a field) of N cylindrical particles with a length L and an area A may be found from the relation

$$\Delta F_0 = -NLA\Delta f + 2NA\sigma_e + 2L\sqrt{NA\pi}\sigma, \quad (6)$$

where Δf is the free energy of fusion of a crystal with a unit volume and σ_e and σ are the end-face and lateral surface free energies of the nucleus respectively. In order to take into account the contribution of an electric field with a strength E_0 , a modified Guggenheim approximation was used. The free energy function $F(T, V, E_0)$ assumes the following form for the formation of a crystalline nucleus with a volume V_c and a permanent polarisation P_0 :

$$F(T, V, E_0) = F_0(T, V) - V_c P_0 E_0 - \frac{V_c \epsilon_0 \epsilon E_0^2}{2}. \quad (7)$$

where ϵ is the relative permittivity of the system. Experiments designed to investigate the Kerr effect in PVDF demonstrated a weak orientation of the chains in an electric field. On this basis, it was assumed that the induced polarisation is much smaller than the permanent polarisation. Taking this into account, the authors²²⁴ concluded that there is a large difference between the nucleation processes in an electric field for particles with polar and nonpolar phases. The overall free energy equation for crystallisation in nonpolar (α) and polar (γ) phases subjected to a field is

$$\Delta F = -NAL(\Delta f + PE_0) + 2NA\sigma_e + 2L\sqrt{NA\pi}\sigma. \quad (8)$$

For the α phase, in which the permanent polarisation is zero, P has the significance of the induced polarisation P_i :

$$P = P_i = \epsilon_0 \epsilon_a \frac{(\epsilon_c - \epsilon_a)}{(\epsilon_a + \epsilon_c)} E_0. \quad (9)$$

For the polar γ phase, one should consider, for the reason stated above, only the permanent polarisation P_p , which is linked to the polarisation of the crystal P_c and the relative permittivities of the crystal (ϵ_c) and the melt (ϵ_a) by the relation

$$P = P_p = \frac{2\epsilon_a}{\epsilon_a + \epsilon_c} P_c. \quad (10)$$

By differentiating Eqn (10), it is possible to find the values of the critical parameters: the concentration N_c^* , the size L_c^* and the free energy of formation ΔF_c^* of a nucleus with the critical size in an electric field. For temperatures which are not far below the equilibrium melting point T_m^0 the expression for ΔF_c^* is

$$\Delta F_c^* = \frac{\Delta h \Delta T}{T_m^0},$$

where Δh is the enthalpy of fusion and $\Delta T = T_m^0 - T$ is the degree of supercooling.

Taking into account all the above considerations, the rate of nucleation J_e may be found from the equation

$$J_e = K' \exp \frac{-U_0}{k(T - T_\infty)} \exp \frac{-\Delta F_c^*}{kT}, \quad (11)$$

where K' is a constant, U_0 is the activation energy for the transfer of the species comprising the nucleus ($1.5 \text{ kcal mol}^{-1}$), and $T_\infty = T_g - 30 \text{ K}$.

For analysis, it is more convenient to use the relative change in the rate of nucleation in a field (J_e) and in its absence (J_0) rather than Eqn (11). Such relations (in terms of semilogarithmic coordinates) as a function of field strength for different degrees of supercooling ΔT are presented in Fig. 22. In particular, it is seen that the effects of the field on the crystallisation of the polar and nonpolar modifications of PVDF are different. Whereas the field intensifies nucleation in the γ phase, and to a more significant extent for lower degrees of supercooling, the opposite effect is observed for the α phase (with a nonpolar cell). The theory developed has been confirmed qualitatively by the results of experiments^{203,212} and investigation²²⁵. According to the data obtained in the last study, the application of a 0.1 MV cm^{-1} field during crystallisation does indeed accelerate significantly (for the same crystallisation temperatures) the rate of formation of the γ phase, 100% conversion being achieved already at temperatures of $\sim 165^\circ \text{C}$. The field alters significantly also the form of the dependence of the total degree of crystallinity (taking into account the α and γ phases) on the crystallisation temperature.

However, the theoretical ideas which have been developed do not account for a series of new experimental relations. Thus it has been observed²²⁵ that the morphology arising in PVDF specimens crystallised in high fields and at high temperatures is not homogeneous along the film area. Indeed, the spherulites which have appeared during crystallisation at different depths differed both in size and birefringence, on the one hand, and in concentration, on the other. We may note that the sign of the potential on the electrode is an important factor for the formation of crystallites. For example, near the positive electrode the nucleation density is always greater than in the vicinity of the negative electrode. In the light of the theory developed, the latter factor should be most probably attributed to the fact that the permanent polarisation in the vicinity of the positive electrode is always greater than near the negative one.²²⁶ Direct observations of the crystallisation process have shown²²⁵ that the role of the field does not reduce to the direct inhibition of the rate of formation of the α phase, as predicted by the theory.²²⁴ The decrease in the number and

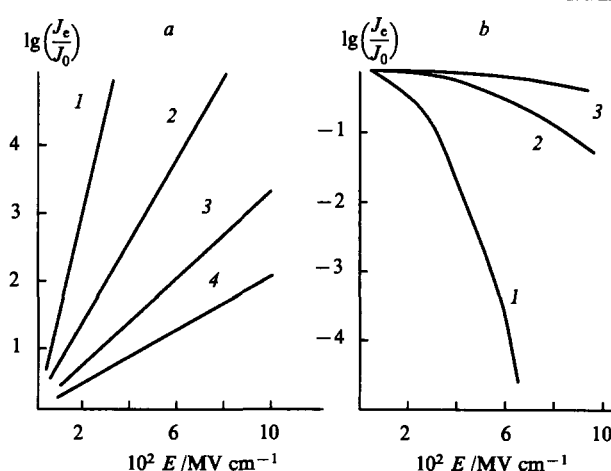


Figure 22. Dependence of the relative change in the rate of nucleation with and without the application of the field with different degrees of supercooling for the γ phase (a) and the α phase (b).²²⁴ ΔT ($^\circ \text{C}$): a: (1) 30; (2) 40; (3) 50; (4) 60; b: (1) 5; (2) 10; (3) 15.

average size of the α spherulites occur as a result of the acceleration of the processes involving the crystallisation of the γ phase spherulites. It has also been noted that, whereas in the absence of the field γ spherulites of approximately equal size are obtained, crystallisation in a field lowers the above homogeneity. The intensity of the depolarisation in the scattered light pattern is also reduced, which has been attributed to the disturbance of the radial disorder of the b axes of the γ phase crystallites in the spherulite under the influence of the field. The fact that disc-shaped spherulites in which the radial direction is in the plane of the film arise near the negative electrode indicates that the field affects not only the processes involving the formation and growth of the nuclei but also the secondary crystallisation processes accompanied by the formation of a supermolecular structure.

This conclusion agrees with the results of a study²²⁷ which confirms, in particular, the theoretical conclusion²²⁴ that the field has an inhibiting effect on the crystallisation of the α phase. However, results which cannot be predicted by the theory have been obtained for γ phase crystals. For example, it has been observed that the nature of the morphology generated may depend significantly on the configuration of the electrodes. An increase in the rate of growth of γ spherulites under the influence of the field has been observed only for direct contact between the specimen and both electrodes. In contrast to the results of Marand et al.,²²⁴ disc-shaped γ spherulites were formed near the positive electrode. Experiments on crystallisation, where one or both electrodes were blocked, showed that such conditions affect appreciably the nature of the morphology produced. Apparently, this can be most reasonably explained by the appearance of local electric fields, arising due to the injection of carriers from the metal into the polymer and captured by traps in the latter.

The VDF/TrFE copolymer exhibits ferroelectric properties most distinctly. The structural transformations in an electric field as a function of the number of triangular pulses applied to the specimen have been investigated for this polymer.²²⁸ The amplitude value of the field strength was 160 MV m^{-1} and the pulse frequency was 0.001 Hz . For an isotropic specimen crystallised as a mixture of the α , β , and possibly γ phases, a virtually complete $\alpha \rightarrow \beta$ transition was observed after only 6–8 pulses and the residual polarisation and the coercive field also attained the equilibrium values. Comparison of the temperature variations of the principal reflections from two polarised specimens in the same investigation made it possible to reach an important conclusion concerning the role of the morphology in the stability of the structure formed under the influence of the field. Isotropic and uniaxially extended specimens were compared, the nature of the X-ray diffraction by both being identical. The former crystallised with formation of thick lamellar crystals with a thickness of $\sim 0.1 \mu\text{m}$, while in the latter a typical fibrillar morphology with the usual ($\sim 100\text{\AA}$) longitudinal dimensions of the crystals was observed. For isotropic specimens, the principal 200, 110 reflection of the β phase remains constant up to $\sim 150^\circ\text{C}$, while for the oriented specimen its intensity begins to change appreciably above $70\text{--}80^\circ\text{C}$. The above differences have also been confirmed indirectly: the higher piezoelectric constant d of the oriented specimen shows that the nature of the structural changes following the application of mechanical loads differs significantly for the isotropic and textured polarised films.

The nature and dynamics of the domain structure were elucidated for the same copolymer (with the composition 65/35) by determining on the real time scale the changes in the structural characteristics during the ferroelectric switching of the specimen.²²⁹ The influence of the poling field strength, primarily on the size of the β phase crystallites and on their perfection, has been tested in relation to the oriented specimen. For this purpose, the integral widths (B) of the 110, 220 and 330 reflections, i.e.

$$B = \frac{1}{L_{110}} + \frac{(my)^2 m^2}{d_{110}}, \quad (12)$$

were estimated for three specimens obtained by polarisation in 60, 90, and 200 MV m^{-1} fields. Here L_{110} is the transverse dimension of the crystallite in the direction of the normal to the 110 plane, m is the diffraction order, $y = \langle d_{110} \rangle / d_{110}$ the degree of defectiveness of the second kind in the crystal, and d_{110} the interplanar spacing.

The analysis showed primarily that the main contribution to B comes from the size of the crystallite, which increases from 19 to 39 nm in the field change indicated above. The defectiveness of the crystal was within the limits of 3% and tended to decrease somewhat on poling. Data on the dynamics of the structural changes in the transposing of a nonoriented specimen, obtained on the real time scale, are valuable and unique. The increase in the electric displacement on switching the poling is accompanied by characteristic changes in the parameters of the 110 reflection of the polar β phase (Fig. 23). The intensity of the reflection at the maximum as well as its integral intensity at the characteristic time pass through a minimum, while the integral width passes through a maximum. Evidently, the parameters of the above reflection vary within the limits of several per cent and in a number of

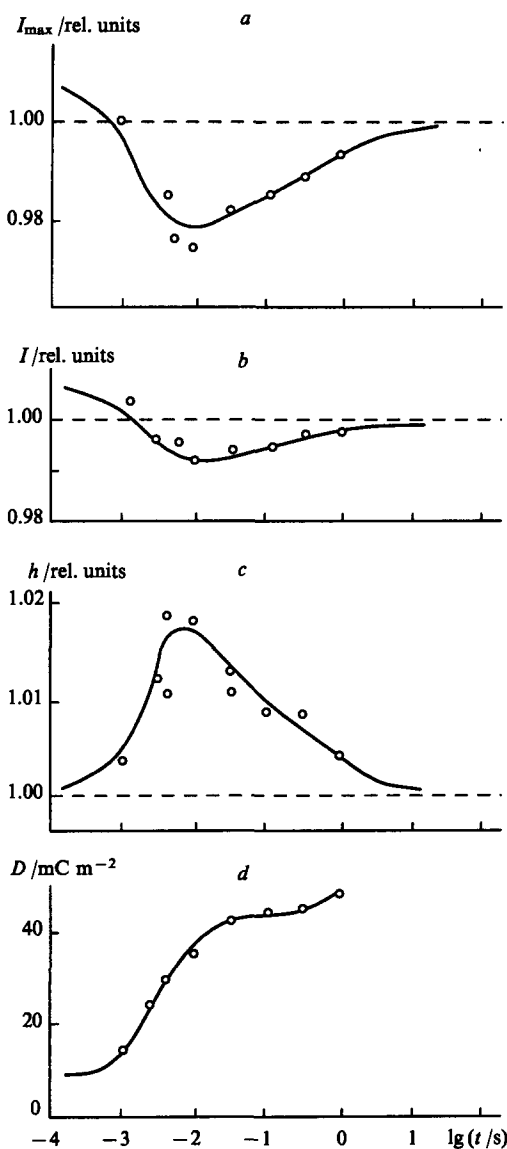


Figure 23. Time variations of the intensity of the maximum (a), the integral intensity (b), the width (c), and the electric displacement (d) of the 110 reflection during the switching of the poling of the VDF/TrFE copolymer.²²⁹

instances their monotonic variation may be observed. The latter presupposes a large contribution to processes responsible for the characteristic features of the supermolecular structure. The nature of the change of the integral intensity indicates the 180° rotation of the chains on transposing of the specimen, in contrast to the 60° model which is frequently employed.

The new reflections observed by Servet and Rault²³⁰ and later also by Newman and Scheinbeim²³¹ and Weinhold et al.²³², which could not be indexed in terms of the lattices of any of the known polymorphic transformations, are important for the understanding of the details of the mechanism of the structural transformations in PVDF under the influence of strong electric fields. More detailed study showed²³³ that the reflections of the new superlattice in a specimen with the polar α phase are located in the vicinity of the reflections characteristic of the β form: 110, 200, 001, and 111, 201.

We discussed above a series of results indicating the existence in the α phase of kink bonds, which are detected from the characteristic features of the scattering in the vicinity of the reflections mentioned above. Taking this into account, the hypothesis was put forward that the reflections from the superlattice are reflections from ordered regions formed by aggregates of the kink bonds. Thus the new form is intermediate between the polar modification of the α phase and the β phase in the course of the field-induced type $\alpha \rightarrow \alpha_p \rightarrow \beta$ transformation. Calculations showed that the probability of intramolecular rearrangements on formation of the new form may depend significantly on the parity of the number of bonds n passing to the 'planar zigzag' conformation when the conformational defects noted above are formed. As an example, one may consider two schemes of transformations for even and odd values of n :²³³

...TGTGTGTGTGTGTGTG...

...TTTGTGTGTGTGTGTG...

1

...TGTGTGTGTGTGTGTGTG...

...TTTTGTGTGTGTGTGTG...

2

It may be said that the transformation in accordance with Scheme 2 should take place preferentially compared with Scheme 1. Indeed, whereas the rearrangements in the second scheme are effected as a result of transitions of G or \bar{G} bonds to T bonds, in Scheme 1 there are in addition the transitions $G \rightarrow \bar{G}$ and $\bar{G} \rightarrow G$, which require the cooperative motion of the entire chain. Fig. 24 presents two variants of the chain conformations (with an odd number of bonds in the repeat unit) for the new form. The presence of chain sections with the $G\bar{T}\bar{G}$ conformation between the bonds in the 'planar zigzag' conformation makes it possible to regard the polar β phase and the new modification as conformationally incommensurable. Fig. 24 shows that two features are characteristic of the above superlattice. Firstly, the identity period along the axis of the macromolecule is found to be greater than for the β phase with the 'planar zigzag' conformation. Furthermore, the appearance of a definite tilt angle for the axes of the macromolecules forming the triclinic lattice is characteristic of this superlattice.

Partly crystalline polymers, including PVDF, are known to have a heterogeneous structure. The presence of a large volume fraction of a nonordered phase complicates the molecular mechanism of the structural rearrangements in PVDF under the influence of strong electric fields. The elucidation of the role of the amorphous phase and of its microstructure in the above phenomena should be the subject of separate investigations. A series of experimental results indicating the nontrivial role of the microstructure in the changes occurring under the influence of a field are presented below. The paper of Sen et al.²³⁴, who described a study of the influence of added plasticiser (tricresyl phosphate) on the nature of the field-induced structural transformations, should probably be regarded as the first communication of this kind. Despite the fact that the plasticiser molecules should be

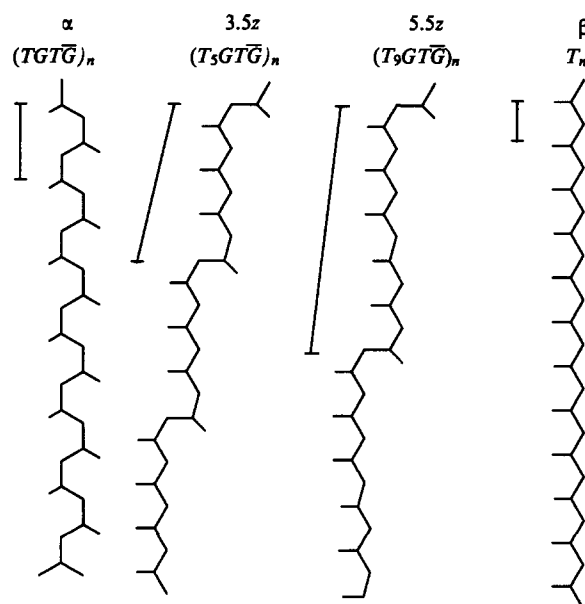


Figure 24. Molecular models for the conformations of the chains in the PVDF superlattice.²³³

located predominantly in regions with an increased free volume, i.e. in the amorphous phase, it was found that the plasticiser influences significantly the characteristics of the polymorphic transition which occurs particularly in the crystalline regions. In plasticised PVDF, the $\alpha \rightarrow \alpha_p \rightarrow \beta$ transitions occur in the presence of appreciably lower fields than in the nonplasticised polymer. As a result of this, the fraction of the β phase formed in the plasticised PVDF is found to be higher almost by a factor of 2 under the same polarisation conditions. The accompanying increase in macroscopic characteristics such as the residual polarisation and the relative permittivity leads also to higher values of the piezoelectric constants d_{31} and e_{31} . A qualitatively similar result has been obtained also in a study²³⁵ where the plasticiser for PVDF was poly(ethylene glycol).

Direct evidence for the important role of the nonordered phase in the strong field-induced structural transformations has been obtained in a study¹⁶⁰ where uniaxially extended VDF/TFE 94/6 copolymer films were investigated. It was shown that, in the presence of high fields, hysteresis-type electric displacement and switching current curves arise for the films. These characteristics for two films with draw temperatures of 60 and 140°C (for the same draw ratio $\lambda = 4$) may be compared in Fig. 25. Evidently, the remanent electric displacements (as well as their maximum values) differ appreciably. The current hysteresis curves also differ significantly. Structural studies have shown that the above copolymer forms the β modification with the 'planar zigzag' conformation under the usual crystallisation conditions.^{32, 160} However, taking into account the increased concentration of bonds in the $TGT\bar{G}$ and $T_3GT_3\bar{G}$ conformations of films oriented at high draw temperatures,¹⁶⁰ one may assume that the difference between the current hysteresis curves is caused by the characteristic features of the microstructure of the amorphous regions. This confirms the small angle X-ray diffraction curves (in the meridional direction) for the same films (Fig. 16). The higher intensity of the maximum for films with an increased draw temperature is most probably due to the greater difference between the densities in the amorphous and crystalline regions. If the β modification is produced in all the films, then the foregoing finding must be attributed to the less dense packing of the amorphous regions along the direction of stretching. The characteristics of the microstructure of the amorphous region affect the remanent and maximum electrical displacement for field strengths in excess of the critical values, where a remanent poling appears (Fig. 25). The

Table 16. Physical characteristics of the VDF/TFE 94/6 copolymer films uniaxially oriented up to the draw ratio $\lambda = 4$ at different temperatures.¹⁶⁰

$T_d / ^\circ\text{C}$	R at different frequencies $/\text{cm}^{-1}$				$L / \text{\AA}$	$l / \text{\AA}$	n/N
	470	490	508	600			
60	17	1.8	3.4	3.0	88	78	
80	15	1.7	3.3	2.9	120	84	0.102
100	14	1.6	3.1	3.1	189	98	0.082
120	7	1.2	2.3	2.6	221	113	0.049
140	6.7	0.8	2.1	1.4	189	102	0.049

Note. The following notation has been adopted: R — dichroic ratios for a series of specific IR bands; L — long period of the crystal; l — longitudinal dimension of the crystal; n — number of chains per unit area in the amorphous phase; N — ditto in the crystal.

increased response to the external field depends significantly on the degree of orientation of the chain in the amorphous regions (Table 16).

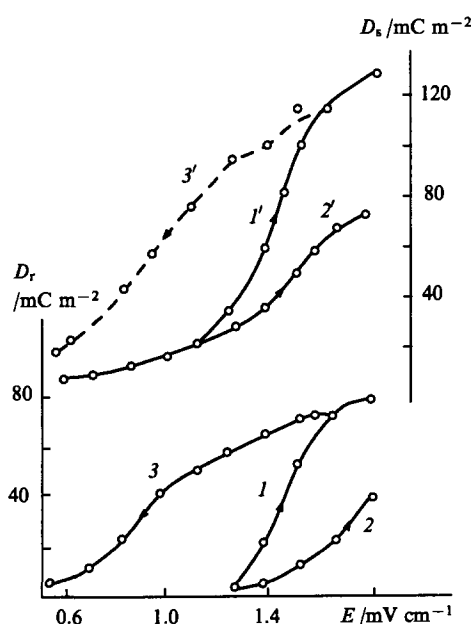


Figure 25. The field dependences of the remanent (1–3) and maximum (1'–3') electric displacements for films of the VDF/TFE 94/6 copolymer uniaxially oriented at 60 °C (1, 3, 1', 3') and 140 °C (2, 2').¹⁶³

The dichroic ratios at frequencies of 470, 490, and 600 cm^{-1} are attributed only to the amorphous phase, whereas at a frequency of 508 cm^{-1} they are believed to be due to the 'planar zigzag' conformers in both phases. Evidently the increase in T_d leads to a decrease in R for all the frequencies specified. At the same time, this is accompanied by an increase in the size of the amorphous gaps obtained in the form of the difference between the long period and the longitudinal size of the crystal.

The decrease in size between neighbouring crystallites is accompanied by an increase in the number of stressed chains passing through them [tie-tough-chains (TTC)], which is indicated by acoustic relaxation data.¹²⁹ At the polarisation temperature (in our case, this is 20 °C), the amorphous regions are in the rubber state, i.e. their compliance is an order of magnitude higher than in the crystalline phase. This means that the polar chains of the amorphous phase should respond in the first place to the increase in the external field strength. The presence of 'planar zigzag' conformers, for which the transverse component of the dipole moment is greater than for the $TGT\bar{G}$ and $T_3GT_3\bar{G}$ conformations because the field strength vector is perpendicular to the surface of the film, is of great importance in this connection. The TTC

regions may play a very important role in these phenomena, since the same chain may enter into both regions mentioned above and into the β phase crystal itself. As a result of this, the rotations in the TTC chains arising under the influence of the field should be transmitted also to the chains of the crystal, leading ultimately to their reorientation as a whole.

Thus the response in textured films of PVDF and its copolymers may be intensified by bringing them closer to the texture of the 'ideal single crystal'. As has been seen, this requires a decrease in the conformational heterogeneity along the chain, an increase in the size of the noncrystalline regions, and an increase in the fraction of the TTC within them.

Special attention must be given to the role of the texture in the materials investigated. The creation of a definite texture in films of the VDF/TFE 94/6²³⁶ and VDF/TFE 71/29²³⁷ copolymers, which can be characterised by the average orientation, promotes a decrease in the coercive fields and an increase in the residual polarisation. The reason is probably that, when a texture is formed, there is a tendency for the arrangement of the axes of the macromolecules in the plane, which facilitates the interaction of the field with the transverse component of the dipole moment, rigidly linked to the main chain.

The role of the amorphous phase in ferroelectric response phenomena can also be seen in relation to isotropic films. A common feature has been observed in the copolymers having the above compositions. For films with a lower degree of crystallinity (this was inferred from the densities and relative permittivities) lower coercive fields and hence greater remanent pollings were noted.^{160, 237} This was attributed to the greater compliance of the amorphous phase chains and to the initiation of the intrinsic ferroelectric polarisation in the neighbouring β phase crystals.

VII. The influence of irradiation on the structure of poly(vinylidene fluoride) and its copolymers

The structural-chemical transformations in PVDF have been investigated by spectroscopic methods.²³⁸ It was shown that an increase in the radiation dose promotes the accumulation of both vinyl $-\text{CH}=\text{CF}_2$ (1715 cm^{-1}) and vinylidene $>\text{C}=\text{CF}_2$ (1750 cm^{-1}) groups. Radiation-chemical processes occur more often on irregularities than on ideal chains. Branches and 'head to head' defects are included among the former. The fraction of irregularities was estimated from high-resolution NMR spectroscopic data. At least two types of radicals, detected in the oriented PVDF specimens, may correspond to the α and β modifications present in such specimens. The appearance of intermediate species (carbonium ions), which are manifested in the form of luminescence peak on the temperature curves of radiothermoluminescence has also been detected.

According to empirical rules, chain rupture reactions should predominate on irradiation in polymers with a structure of the type $(-\text{CH}_2\text{CR}_1\text{R}_2-)$; on the other hand, mainly cross-linking has been noted in PVDF chains. The ratio of the probabilities of scission and cross-linking steps on γ -irradiation has been esti-

mated as 0.35, which leads to an increase in the gel fraction to 0.7 rupture for a dose of 10 Mrad.²³⁹ The hypothesis²³⁸ that the dissociation and cross-linking reactions are linked, which should be associated with the migration of a radical centre (charge) along the chain to the location of the irregularity, has also been confirmed by a study²⁴⁰ of the irradiation of PVDF by accelerated electrons. The sequences of another comonomer can also serve as irregularities of this kind. Therefore, an increase in the gel fraction in the copolymer of VDF and hexafluoropropene compared with the homopolymer confirms qualitatively the above hypothesis. Additives promoting the formation of a three-dimensional network also play a significant role in cross-linking processes on irradiation. This can be inferred from the increase (other conditions being equal) in the gel fraction following the introduction of a sensitizer into the irradiated PVDF.^{240, 241}

The form of the energy-carrying species is important for the processes occurring on irradiation. For example, comparison of data concerning the influence of irradiation by electrons and protons on the strength characteristics of PVDF indicates a significant difference between them. It was observed that, in order to reduce the relative elongation at break by a factor of 2, a proton flux smaller by a factor of ~ 20 than the electron flux is needed.²⁴² These results are related to the data obtained in a study²³⁹ where it was shown that irradiation of PVDF with γ -rays and α -particles leads to a significant difference between the initial free radicals formed. The kinetics of the recombination of such radicals also differ significantly: in the case of γ -rays, the radicals begin to recombine already above 77 K, whereas under the conditions of α -irradiation, the radicals are stable up to 240 K. The dependence of the concentrations of the above radicals on the irradiation dose shows that fast recombinations takes place immediately in the region of the tracks formed along the paths traversed by the particles.

The nature of the radiation damage in the case of helium ions may depend significantly on the energy of the incident particles (for the range 0.4–4.5 MeV).²⁴³ For an energy of 0.4 MeV, the helium ions, which have a path length of only 27 μm , are responsible for an 86% decrease in crystallinity relative to the initial value, while the solubility of the irradiated specimen is reduced by 76%. Such changes in characteristics have been attributed to the probability of the formation of a hydrogen atom, which may rapidly diffuse in space.

By following the dielectric relaxation process associated with micro-Brownian motion in the amorphous regions of PVDF, it is possible to refine the nature of the radiation-chemical transformations and their location. Thus a decrease in the intensity of the above process for irradiation doses of 30–40 Mrad suggests that cross-linking occurs in the amorphous regions, which results in the creation of a definite steric hindrance to the reorientation of a chain segment.^{244, 245} The possible appearance of polyene chains may give rise to an increase in the intensity of the process under consideration for lower irradiation doses.²⁴⁵ It is believed that the cross-links appearing on irradiation may be located not only in particularly nonordered regions but also on the surfaces of lamellae, since an increase in the irradiation dose lowers the intensity of the α -process associated with motion in crystalline regions.²⁴⁵ The observations of irreversible changes in dielectric losses are of interest. After the cessation of irradiation, the latter return to the initial values.²⁴⁴ This phenomenon may be associated with the accumulation of carriers, which may then fall into deep traps.

Studies on the structural changes occurring in PVDF and its copolymers on irradiation began as early as the beginning of the 1980s but developed to a greater extent only in the last 15 years. One may name a large number of studies in which it has been shown that the degrees of crystallinity α of a series of polymers increase for low irradiation doses.^{246–253} This behaviour is common to crystallising polymers, including PVDF.^{254, 255} The nature of the above phenomenon has not been discussed by the authors of the studies mentioned, so that analysis of the con-

formational changes in the chains of PVDF during its irradiation may 'throw light' on this effect.^{256, 257} On γ -irradiation in air of uniaxially and biaxially extended films of the PVDF homopolymer, a weakening of the intensities of the bands associated with the $TGT\bar{G}$ conformations and, conversely, the intensification of a series of bands corresponding to the 'planar zigzag' conformation were observed.^{256, 257} This occurred predominantly in the range of irradiation doses up to 50 Mrad, i.e. in the region where an increase in the degree of crystallinity has also been noted. The radiation-induced conformational rearrangements in PVDF chains were most probably located predominantly in amorphous regions of the polymer, since the intensities of the bands attributed to the nonordered phase changed most significantly. This follows from the fact that, after irradiation at a dose of 30 Mrad, the intensity of the 470 cm^{-1} band increased appreciably at the expense of the weakening of the 490 cm^{-1} band. These bands are attributed to the 'planar zigzag' and $TGT\bar{G}$ conformations of the PVDF chains in the nonordered regions.²⁵⁷ The above finding therefore indicates the possibility of conformational rearrangements on irradiation. For a biaxially oriented film, this effect is due to the most marked.²⁵⁶ The intensity of the 600 and 740 cm^{-1} bands, due to the particular amorphous regions in PVDF, decreased after irradiation, which agrees with DSC data.^{256, 257}

The above results are to some extent correlated with the conclusions reached in studies^{258, 259} in which structural changes in irradiated PVDF specimens were recorded by the X-ray method. The authors of these investigations observed a series of interesting effects due to the influence of large irradiation doses. For example, it was shown that powders are more resistant to irradiation than the film prepared from them, which was accounted for by the role of oxygen. For specimens in various polymorphic forms, an increase in the irradiation dose was accompanied by a decrease in the order characteristics. However the stability of the β modification proved greater than that of the α modification. Whereas the initial specimens crystallised as the α form, at doses of 500–600 Mrad the $\alpha \rightarrow \beta$ polymorphic transition took place.

The significant differences between the irradiation doses inducing structural changes found by Kosmynin and Gal'perin,^{258, 259} on the one hand, and a number of other workers,^{254–257} on the other, can be explained by the fact that in the latter the changes concern predominantly the nonordered regions (or regions adjoining the crystal), whereas in the former the crystals proper were considered.

In the case of VDF copolymers with small amounts of added TFE, the trend in the structural changes on irradiation becomes similar to that for the homopolymer. This is confirmed by the nature of the changes in the diffractometer traces for isotropic specimens of the VDF/TFE 94/6 copolymer after irradiation with doses up to 10 Mrad.^{115, 116} After irradiation, the intensity of the 001 and 210, 111 reflections increases, since the order in the above directions is 'improved'. The broadened reflection at $2\theta = 18^\circ$ is due to the presence of highly disordered paraelectric phase in the initial specimen. Therefore the decrease in the intensity of the above reflection after irradiation can be explained by the partial paraelectric–ferroelectric transition. More significant changes in the structures of the above copolymers have been observed in uniaxially extended specimens for which X-ray photographs were taken in the meridional direction. The intensity of the amorphous halo, adjoining the 001 reflection, decreased significantly after irradiation under these conditions. These results are qualitatively correlated with DSC and IR spectroscopic data.^{254–257}

The initial copolymer specimens may be crystallised in a definite metastable state where the crystalline phase consists mainly of the paraelectric α phase^{117, 118} characterised by the 020, 110, and 021 reflections. The structural changes in the copolymer with increase in the irradiation dose are shown in Fig. 26. For the initial specimen, the intensity of the 110, 200 reflection due to the ferroelectric β phase present was found to be appreciably lower than that of the 110 reflection due to the α

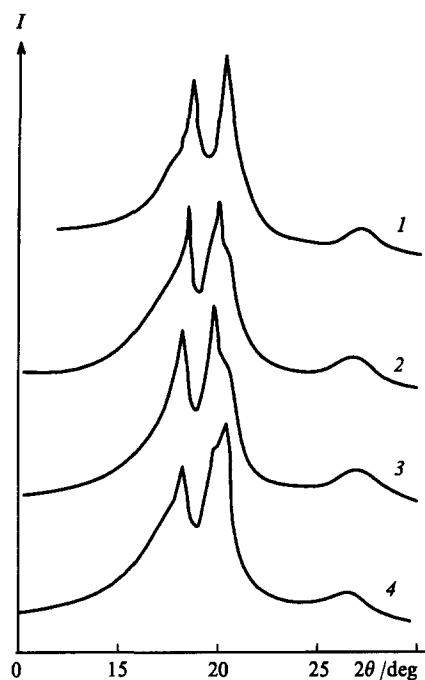


Figure 26. Dynamics of the variation of the diffractometer traces for isotropic metastable films of the VDF/TrFE 94/6 copolymer after γ -irradiation.^{115, 116}
Irradiation dose (Mrad): (1) 0; (2) 1; (3) 10; (4) 48.

phase, where former is manifested by the presence of a shoulder (on the side of larger angles) for the latter reflection. With increase in the irradiation dose, the intensity of the β phase reflection rises and for a dose of 10 Mrad, the reflection is fairly well resolved as a consequence of the decrease in the half-width. On the other hand, the increase in the dose to 40 Mrad leads to the equalisation of the intensities of the above reflections due to the α and β phases, which is manifested by some broadening of the resolved doublet. At high irradiation doses, changes were noted also in the region of the 020 reflection ($2\theta = 18.4^\circ$) due to the α phase, where together with the latter a broadened halo arises, indicating the appearance of perturbations in the paraelectric phase. In conformity with the foregoing and also in view of the increase in the intensity of the intramolecular 201, 111 reflection due to the ferroelectric β phase, one may infer the radiation-induced $\alpha \rightarrow \beta$ transition.^{115, 116}

The mechanism of the above structural transformations in PVDF and its copolymers with TFE is most probably determined by the ferroelectric nature of these polymers. The nature of the changes in the 470 and 490 cm^{-1} absorption bands for the uniaxially extended PVDF after irradiation agrees with those for the film after treatment in a corona discharge.²⁵⁷ In the latter case, the above conformational changes of the type $TGT\bar{G} \rightarrow (TT)_n$ occur under the influence of the field, including the field generated by the surface layer of the injected charges and charges captured by deep traps. The irradiation of PVDF is accompanied by an appreciable increase in the dielectric loss factor, which can be accounted for, with a high degree of probability, by the appearance of additional free carriers.²⁴⁴ Bearing in mind the high penetrating capacity of γ -radiation, their concentration is on average the same throughout the volume, in contrast to the charges in the corona polarisation of PVDF, which are located predominantly on the surface of the film. The decrease in the conductivity of the PVDF films after the cessation of irradiation may be associated with carrier recombination processes. However, bearing in mind their low mobility, capture by deep traps must be regarded as a more likely cause. In the case of the strongly polar ferroelectric β phase crystal, the carriers may be located on charged planes.

Thus local internal fields, sufficiently strong to induce the above conformational transformations, may be generated at these sites. If one begins with this mechanism, then the location planes (in isotropic specimens) are 201, 111, since the intensity of the reflection from them changes most significantly.

The structural transformations under discussion may occur via an epitaxial crystallisation mechanism where sequences of the chain in the $TGT\bar{G}$ conformation, undergoing a transition to the 'planar zigzag' conformation, may undergo additional crystallisation, producing neighbouring regions of the ferroelectric β phase. This mechanism is supported by spectroscopic data, according to which the above conformational transformations are manifested most distinctly in films containing the crystals of the α and β phases.^{256, 257} Naturally, in structural modification processes account must be taken also of the role of the chemical changes in the PVDF chains on irradiation.

As mentioned above, the advantages of the cross-linking processes occurring in the amorphous regions have been confirmed both by the nature of the decrease in the intensity of the dielectric absorption for the micro-Brownian motion in the amorphous regions^{245, 260} and by the decrease in the coefficient of thermal expansion of the lattice in the a and b directions in the cell.²⁶¹ However, the nature of the morphology, which is extremely variable in such systems, may affect the ratio of the yields of the scission and cross-linking reactions. Analysis of the changes in the mechanical characteristics in PVDF and in its copolymers with TFE on irradiation shows that in the oriented state there is an increase in the fraction of tie-tough-chains in the amorphous phase, in which degradation reactions should predominate although the polymer as a whole may remain in the cross-linked state.²⁶² The above significant change in the ratio of the intensities of the amorphous halo and of the 001 reflection after irradiation of a uniaxially extended specimen of the PVDF copolymer also confirms the hypothesis put forward. Indeed, the scission processes on the TTC should facilitate the thermal motion processes in the remaining fragments, as a result of which they may be incorporated in the neighbouring crystals of the β phase, increasing their size and perfection in the direction of the 001 plane.

Copolymers of VDF with TFE in which the fraction of the latter comonomer is low and its chemical structure is similar to that of PVDF were considered in the studies quoted above. This may explain the similarity of the behaviour on irradiation of the above copolymers and PVDF.

Another object for which radiation-induced physicochemical changes have been studied in detail is the copolymer of VDF with trifluoroethene. In contrast to TFE, the latter has a structure differing appreciably from that in the homopolymer. It may be that this factor is one of the reasons why these copolymers behave differently from the homopolymer and the VDF/TFE copolymer.

On γ -irradiation of the VDF/TrFE 65/35 copolymer, it was observed that an increase in the dose is accompanied by the impairment of the structural characteristics.²⁶³ Thus irradiation with a dose of 120 Mrad at room temperature of a specimen consisting of the ferroelectric phase leads to its transition to the paraelectric state, which may be inferred from the shift of the main intermolecular reflection towards lower angles (Fig. 27). If the crystal is in the paraelectric state, irradiation of the specimen is accompanied by significant changes in the initial structure. The ferroelectric-paraelectric transition becomes in this case more diffuse and shifts towards lower temperatures. The latter has been noted also on irradiation of these copolymers by accelerated electrons.²⁶⁴

The results of experiments^{265–268} for the same copolymer but with the composition 70/30 indicate a qualitatively similar conclusion. Irradiation of thin films (7 μm) with a beam of electrons having an energy of 100 keV leads to a smooth displacement of the Curie point with increase in the irradiation dose towards lower temperatures, which, however, are always found to be higher than the glass transition temperature.²⁶⁵ The

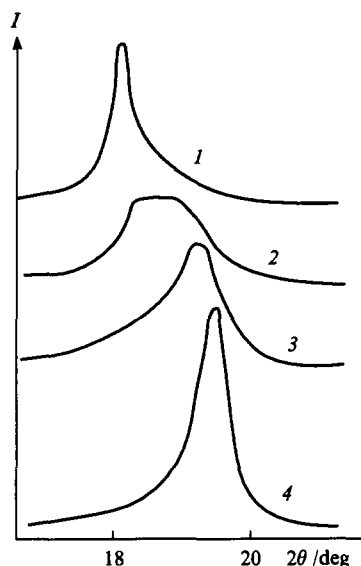


Figure 27. The nature of the variation of the profile of the 200, 110 reflection due to the ferroelectric phase on γ -irradiation of the VDF/TrFE 65/35 copolymer.²⁶³ Irradiation dose (Mrad): (1) 120; (2) and (3) 60; (4) 0; (1), (3) and (4) irradiation at room temperature; (2) irradiation at 120 °C.

experiments failed to confirm the conclusion²⁶³ that more intense processes, leading to the impairment of order, take place when the crystal is in the paraelectric phase. According to the temperature dependence of the internal friction, accelerated electrons convert the copolymer into the amorphous form and lead to the accumulation of defects in the crystallites.²⁶⁷

The last conclusion has been confirmed also by X-ray diffraction data, which showed that an increase in the irradiation dose induces a decrease in the packing density in both the paraelectric and ferroelectric phases of the copolymer.²⁶⁶ At the same time, it was established that, for the same irradiation dose, more significant changes are noted for the paraelectric phase. A new phenomenon has been observed: an increase in the energy of electrons (from 100 keV to 3 MeV) leads, under the conditions of the same irradiation dose, to less significant decrements in the melting and Curie points. It is believed that electrons with a higher energy cause the preferential conversion of the copolymer into an amorphous form, whereas particles with a lower energy are mainly responsible for specific defects within the crystals. The decrease in the average size of the crystallite, noted in such processes, is not the main cause of the decrease in the melting and Curie points.²⁶⁸ The process involving a decrease in the energy of the dipole interactions as a result of the increase in the concentration of the double bonds and carbonyl and other new groups arising on irradiation is believed to be more important. The decrease in the melting and Curie points with increase in the irradiation dose is fairly well described by a model taking into account the decrease in the internal pressure.^{268, 269}

Thus one may see a significant difference between the radiation-induced structural changes in the VDF homopolymer and in the VDF/TrFE copolymer, on the one hand, and in the VDF/TrFE copolymers, on the other. One of the reasons for this may be associated with the chemical structure of the TrFE unit (CH_2CFH), which, in contrast to the TFE unit (CF_2CF_2), is 'chemically incommensurate' with the VDF repeat unit (CF_2CH_2). The fact that the glass transition temperatures in PVDF and TrFE (in contrast to PVDF and TFE) differ markedly may be regarded as confirmation of this postulate.

Other causes of the significant differences in behaviour on irradiation of the VDF/TrFE and VDF/TFE copolymers may be associated with the fact that in the former the fraction of TrFE is

fairly large (30–35 mol %). A decrease in the latter (to 20 mol %) does not alter the situation fundamentally, since radiation-induced conformational rearrangements of the type $(\text{TT})_n \rightarrow \text{TGT}\bar{\text{G}}$ and $(\text{TT})_n \rightarrow \text{T}_3\text{GT}_3\bar{\text{G}}$ have been noted in such copolymers on irradiation with γ -rays at doses as low as 1–10 Mrad. In the homopolymer, the opposite rearrangements take place.^{256, 257} Yet another cause of the differences may be that all the VDF/TrFE copolymers were investigated in the isotropic state, whereas the 'anomalous' behaviour on irradiation of the homopolymer and VDF/TFE copolymer was noted in uniaxially or biaxially oriented states. Copolymers in the latter states are known to be metastable systems in which the role of internal stresses may be manifested to a greater extent. It is noteworthy that a more detailed study of the behaviour of the VDF/TrFE copolymers at low irradiation doses is needed.

VIII. Characteristics of the dynamics of the chains in the block state of isotropic and anisotropic poly(vinylidene fluoride) specimens

For the practical employment of PVDF films as the material of the active element in energy transducers, it is necessary to know their stable electrophysical parameters.³ This requirement cannot be met without the knowledge of the characteristics of the molecular mobility and of the mechanism of the relaxation phenomena in films. Taking into account the high degree of heterogeneity of the test materials, it is possible to obtain from the characteristics of the molecular mobility information about the structural features of the nonordered phase, which frequently cannot be achieved by classical structural methods. In this section, attention is concentrated on the analysis of studies predominantly on the dielectric relaxation of the test materials, since this method has recently undergone a new development and proved very informative in the analysis of the microstructures of PVDF-based blends.

As early as the beginning of the 1970s, when the valuable properties of PVDF for practical purposes were not known, a series of studies of the molecular mobility in PVDF copolymers by the dielectric relaxation method appeared.^{270–272} This polymer has a high dipole moment per monomer unit (7×10^{-30} C m) and is superior to others as regards the glass transition temperature. This in fact explains the great early interest in it and the high information content afforded by the dielectric relaxation method. The ferroelectric properties of these polymers, discovered subsequently, led to additional possibilities for the above method.²⁷⁰ The majority of investigators observed three or four types of molecular motion in these compounds. In the α modification of PVDF crystals, these are always four different forms of motion. The forms of molecular mobility are usually designated as δ , γ , $\beta(\alpha_a)$, and $\alpha(\alpha_c)$.[†]

An example of the temperature variations of the real (ϵ') and imaginary (ϵ'') components of the complex relative permittivity in PVDF for different electric field frequencies is presented in Fig. 28. The two separate dispersion regions in order of increasing temperature are attributed to $\beta(\alpha_a)$ and $\alpha(\alpha_c)$ relaxations. The lower-temperature regions of the δ and γ mobilities are not seen, but the nature of the variation of ϵ' and ϵ'' in them is the same. The generalisation of ideas about the mechanisms of the above types of mobility can be more conveniently begun by the analysis of the mobilities in the low-temperature regions (at temperatures below the glass transition region of PVDF).

According to Sasabe et al.,²⁷⁴ the γ mobility is described by the Arrhenius equation with an activation energy of 2.1 kcal mol⁻¹ and is determined by localised kinetic units. There are two contradictory views concerning the location of such units. Thus, according to Yano,²⁷³ they should be located in the amorphous phase. However, in a later study²⁷⁵ the contrary claim was made

[†] Here and henceforth double designations for relaxation are given, since in the literature these processes are designated in different ways.

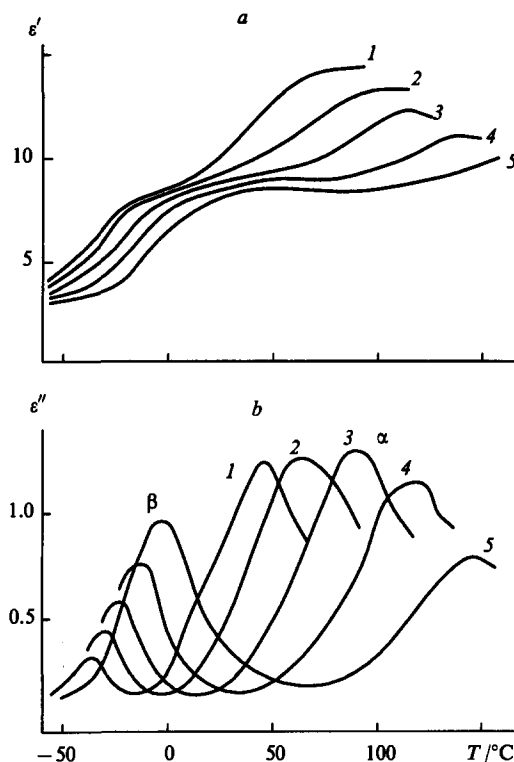


Figure 28. Temperature dependence of the components of the complex relative permittivities ϵ' (a) and ϵ'' (b) in the region of the β and α dispersions of PVDF.²⁷³

Frequency (Hz): (1) 10; (2) 100; (3) 1000; (4) 10 000; (5) 100 000.

that they should constitute crystalline regions. This was based on the observation of a single low-temperature γ -relaxation process on VDF specimens in the α modification. The region of the δ mobility is located near 50 K.²⁷⁶ A detailed study²⁷⁷ has shown that the δ mobility is due to the defects in the α phase lattice. This conclusion was confirmed by the decrease in the intensity of the δ mobility with increase in the degree of crystallinity as the crystallisation conditions were varied. It is significant that this mobility is generated precisely by the defects in the α phase. In specimens of the VDF/TrFE copolymer, which crystallises as the β modification, the above mobility was not observed.²⁷⁷

A similar conclusion was reached in a study²⁷⁶ where there was no δ process in the PVDF specimens with the β phase obtained as a result of uniaxial stretching. At the same time it was noted that a region of ϵ relaxation is present in such specimens, occurring at still lower temperatures (~ 20 K). The activation energy for this process is ~ 1.9 kJ mol⁻¹, whilst that for the δ process is 12.6 kJ mol⁻¹. It has been shown that poling decreases the intensity of the ϵ process severalfold. This finding indicates that the ϵ process is associated with defects in the β phase lattice. The activation parameters for the δ and ϵ relaxation and the temperature ranges where they are manifested differ significantly, so that the defects in the lattices of the α and β modifications responsible for the mobility under discussion are different.²⁷⁶

The curves for the temperature and frequency dependences of ϵ' and ϵ'' for one of the VDF/TFE copolymers have been discussed.²⁷⁸ A characteristic feature of the β relaxation is the increase in the loss factor to a maximum with increase in temperature. The characteristics of this process in the above copolymer are common also to PVDF (Fig. 28) and one may therefore consider them in greater detail.

Analysis of the shape of the above curves shows that they are described satisfactorily by the Williams–Watts equations.²⁷⁹ The

experimental frequency dependences of ϵ'' correspond to those calculated from the relation

$$\epsilon' - \epsilon_\infty - i\epsilon'' = (\epsilon_0 - \epsilon_\infty) \sum_{n=1}^{\infty} (-1)^{n-1} \frac{\Gamma(n\beta + 1)}{\Gamma(n+1)} (i\beta\tau)^{-n\beta}, \quad (13)$$

where i is an imaginary number, ϵ_0 and ϵ_∞ are the limiting relative permittivities at low and high frequencies, β is the parameter of the distribution of the relaxation times ($1 \geq \beta > 0$), $\Gamma(n+1)$ is the gamma function, and τ is the relaxation time. The temperature dependences (in terms of the Arrhenius coordinates) of the frequencies corresponding to the ϵ'' maxima are not linear and it has been shown²⁷⁸ that they can be described by a modified Williams–Lundell–Ferry (WLF) equation in the form proposed by Brereton:²⁸⁰

$$\lg f_{\max} = A + \frac{C_1(T - T_g)}{C_2 + (T - T_g)} + \lg\left(1 - \frac{T_g}{T}\right), \quad (14)$$

where A , C_1 , C_2 , and T_g are numerical constants.

The above form of the curve is characteristic of processes occurring in the glass transition of polymer. The dispersion region under discussion should therefore be associated with the micro-Brownian motion of the chains in the nonordered regions. A series of experimental facts may be regarded as confirmation of this conclusion. For example, the intensity of the above process decreases steadily with increase in the degree of crystallinity of PVDF and its copolymers.^{273, 274, 281} The constant T_g in Eqn (14) agrees with the point corresponding to the characteristic break on the temperature dependences of the coefficient of thermal expansion²⁷⁸ or the specific volume.²⁸¹ The significant decrease in the intensity of the micro-Brownian motion of the chains after irradiation²⁸² may also serve as confirmation of the validity of the assignment of the above process.

Indeed, as shown above, irradiation is accompanied by cross-linking predominantly in the nonordered regions, which should lead to an increase in the steric hindrance to the reorientation of the segments. The enthalpies ΔH and entropies ΔS of relaxation are usually determined from the temperature variations of the relaxation times. For the given process in PVDF with the α phase, ΔH varies from 22 to 41 kcal mol⁻¹ while ΔS varies from 50 to 120 e.u. in the temperature range from 3 to -30 °C.²⁷³ Taking into account these values as well as the enthalpy of vaporisation for a monomer unit, equal to 3.8 kcal mol⁻¹, it has been found²⁷³ that the number of repeat units in the kinetic segment is 23.

The presence of crystalline regions in the bulk of PVDF may give rise to a difference in the relaxation behaviour in the vicinity of T_g compared with that in purely amorphous polymers. The significant difference (by almost 30 °C) between the experimental T_g (-38 °C) and its value calculated by the WLF equation (-67 °C), whilst in the amorphous polymers the difference is 5–6 °C, may be regarded as confirmation of this finding. The reason for the appearance of this difference may be that, as the amorphous polymers approach the equilibrium glass transition temperature, the size of the cooperatively rearranged region should approach a microscopic size, whereas in the crystallising polymers it should be restricted to the size of the nonordered region between crystallites. The same anomalies in the glass transition have been explained²⁸⁰ by the influence of the local field effects (allowance for the correlated motion of dipoles).

In order to discover the reasons for the observed increase in ϵ''_{\max} with temperature in the region of the $\beta(\alpha_a)$ dispersion, Nakagawa and Ishida²⁸³ modelled this type of mobility. It was found that the increase in ϵ''_{\max} mentioned above is associated with the increase in the absorption $\Delta\epsilon = \epsilon_0 - \epsilon_\infty$. It was shown in relation to two specimens (quenched and annealed) that $\Delta\epsilon$ passes through a diffuse maximum in the temperature range 30–80 °C. General relations yield

$$\Delta\epsilon = \frac{4\pi N\bar{\mu}^2\xi}{3kT}, \quad (15)$$

where N is the number of repeat units, $\bar{\mu}^2$ the mean square of the effective dipole moment per monomer unit, ξ the local field factor, k the Boltzmann constant, and T the absolute temperature.

Calculation of $\bar{\mu}^2$ on the assumption of an Onsager internal field showed that all its values are higher than μ_0^2 ($\mu_0 = 1.93$ D is the dipole moment of difluoromethane). The quantity μ^2 was expressed in the form $\bar{\mu}^2 = (\mu_s^2/n_s)g_n$, where μ_s is the dipole moment of the 'segment' containing n_s repeat units and g_n is the correlation factor. For $g_n > 1$, the correlated motion of neighbouring dipoles takes place in the nonordered regions and in fact may be responsible for the characteristics of the relaxation behaviour in the vicinity of the glass transition region.²⁸⁰ The passage of $\Delta\epsilon$ for the β relaxation considered through a maximum is known to be characteristic of order-disorder transitions, in particular of the ferroelectric-paraelectric transformation in the test systems. The latter occurs in the crystalline phase of PVDF and its copolymers. However, the observation of the above dielectric anomalies, for example in highly polar vinylidene cyanide/vinyl acetate copolymers, shows²⁸⁴ that in the amorphous phase of such systems there may be regions with an intermediate form of order analogous to that observed in polymeric liquid crystals. If it is assumed that a definite proportion of the amorphous phase of PVDF is in the nematic phase, the local nematic-isotropic liquid transition will be accompanied by the dielectric anomalies noted above.

A reasonable interpretation of a large number of new experimental data for crystallising polymers nevertheless requires ideas concerning the existence of regions with an intermediate order. It may be that the detection of the isotropic and anisotropic components of the amorphous phase in the VDF/TFE 94/6 copolymers constitutes a confirmation of the above hypothesis.¹¹⁵ The above change in the average interplanar spacing in the sections of the anisotropic phase noted above most probably indicates the occurrence of the postulated nematic-isotropic liquid transition.¹¹⁷ The similar postulated transition in the amorphous component of the PVDF with the α phase is significantly more diffuse and is displaced towards lower temperatures compared with the transition in the VDF/TFE copolymer.²⁸³ This can be explained by the higher fraction in the latter of segments in the 'planar zigzag' conformation than in the VDF homopolymer.

Indeed the modelling of the dynamics of the chains in the amorphous phase of PVDF shows that the best agreement between the calculated and experimental temperature variations of μ^2 is observed only if the neighbouring segments in contact are in the GG or $G\bar{G}$ conformations.²⁸³ If the dipole interactions are decisive in the establishment of the above order, it is possible to find an explanation of the lower transition temperature in the homopolymer²⁸³ compared with the VDF/TFE copolymer.^{117, 118} When neighbouring segments are in contact, the transverse component of the dipole moment relative to the axis of the macromolecule is limiting. The transverse component of the dipole moment of the segments with the GG and $G\bar{G}$ conformations is known to be smaller than that for the segments with the predominant 'planar zigzag' conformation (as in the VDF/TFE copolymer). Accordingly, the lower energy of the interaction in the former does actually lead to a displacement of the transition under consideration in the homopolymer towards lower temperatures.

Since the packing of the chains in the amorphous phase is less dense than in the crystal, the presence of a free volume in this phase is postulated. The role of the latter for β -mobility processes may be traced, for example, from the significant increase in the relaxation times in the VDF/TrFE 73/27 copolymer with increase in pressure.^{285, 286} The free volume causes the displacement of the end groups into the amorphous phase and various kinds of chemical perturbations in the chain (branches, etc.) on crystallisation of PVDF. This can explain the changes in the width of the

relaxation times spectrum and in the effective dipole moment per monomer unit in PVDF obtained by the emulsion and suspension polymerisation methods.⁶²

As the glass transition temperature is approached, the frequency dependences of ϵ'' are greatly broadened. The role of the free volume effects in such broadening has been investigated in a series of studies.²⁸⁷⁻²⁹¹ It was postulated that the relaxation time τ obeys the Doolittle equation:

$$\ln \tau = \ln \tau_0 + \frac{1}{f}. \quad (16)$$

Here f is the fraction of the free volume:

$$f = f_0 + \alpha_f(T - T_0), \quad (17)$$

where α_f is the temperature coefficient of the increase in the free volume. Under these conditions, the frequency dependence of ϵ'' can be described by the function

$$\epsilon''(\omega) = \int_0^1 \epsilon_f''[\omega, \tau(f)] F(f) df, \quad (18)$$

where $\epsilon_f''[\omega, \tau(f)]$ is the loss factor corresponding to the segments with the free volume fraction f and $F(f)$ is the normalised free volume distribution function. The latter was specified in the form

$$F(f) = \frac{(f - f_1) \exp[-(f - f_1)/\lambda]}{\lambda}, \quad (19)$$

where f_1 is the minimum volume and λ the parameter of the width of the distribution.

Comparison of the calculated and experimental relations $\epsilon''(\omega)$ shows that, at temperatures approaching the glass transition temperature, the significant broadening of the curves is determined in the first place by the free volume distribution effects whereas at higher temperatures account must also be taken of the distribution of the relaxation times.

Textured PVDF films are usually employed in practice. From the analysis of the influence of, for example, uniaxial stretching on the nature of the micro-Brownian motion in the nonordered regions, one may formulate general relations.^{272, 281, 292} In all cases the uniaxial stretching process did not lead to an appreciable alteration of the relaxation times, but the total absorption $\Delta\epsilon$ increased steadily. This implies [in conformity with Eqn (15)] an increase in the effective dipole moment per monomer unit. There may be several causes of the increase. In a textured film, the chains in the amorphous phase assume a definite preferred orientation, which can be inferred, for example, from the appearance of the IR dichroism of the 600 cm^{-1} absorption band, which is sensitive to the presence of the amorphous phase.¹²⁹ In this case the quantity $3kT$ in Eqn (15) for the isotropic film should be reduced when account is taken of the anisotropy in the disposition of the chains in the amorphous phase. Another cause, apparently decisive, is that the conformation of the sequences of the chain in the amorphous gaps may change in the oriented state. The probability that chain sections entering into the region of higher local mechanical stresses will pass to the 'planar zigzag' conformation increases. The sequences of the TTC mentioned above apparently constitute the 'limiting case' for the scheme mentioned above, since increased mechanical stresses cause their transition to the 'planar zigzag' conformation.¹⁶⁰

For an anisotropic film, one may speak of three components of the relative permittivity. Under the usual conditions of the measurement (electrodes deposited on the surface of the film), one should be dealing with the component ϵ_{33} if the direction 3 coincides with the normal to the surface. If the chain of a textured amorphous phase is located predominantly in the plane of the film, then the values of ϵ_{33} depends significantly on the transverse component of the dipole moment. As mentioned above, this component for the chain sequences in the 'planar zigzag' conformation is greater than for the sequences with the $TGT\bar{G}$

conformation. For this reason, the increase in $\Delta\epsilon$ in the textured films agrees with the increase within the plane of the films in the number of chain sections of the amorphous phase in the 'planar zigzag' conformation. Evidently data concerning the anisotropy of the dielectric desorption in the regions of the β dispersion for specimens of uniaxially extended PVDF may serve as confirmation of this correspondence.²⁹³ After drawing, the specimens were cut out in a way such that in one case the electrodes were located perpendicular and in another parallel to the draw axis. It was found ϵ''_{\max} in the region of β relaxation is almost three times greater in the second case than in the first.

The high-temperature $\alpha(\alpha_c)$ relaxation process is unambiguously associated with motions in the PVDF crystalline phase. This has been confirmed by the observation of the $\alpha(\alpha_c)$ mobility in crystalline mats²⁷⁵ and also by the increase in the intensity of the above process with increase in the degree of crystallinity.²⁷⁴ The majority of investigators assume that this mobility occurs predominantly in the α modification of PVDF crystals. This is based on numerous data showing that, in specimens where the α and β phases coexist, an appreciable decrease in the intensity of the $\alpha(\alpha_c)$ relaxation is observed.^{273, 281, 292} Furthermore, there is evidence that this process is altogether absent from PVDF specimens obtained in the γ phase,²⁹⁴ while in the PVDF copolymers, where the α phase is usually not formed, it is extremely weak.²⁷⁸ There exists also a communication,²⁹⁵ which unfortunately has been confirmed by only one other investigation,²⁹⁶ stating that in specimens with coexisting α and β phases two $\alpha(\alpha_c)$ relaxation regions are observed. The low-temperature region is attributed to the motion of the chains in the crystals of the α phase, while the high-temperature region is attributed to relaxation in β phase crystals.

Analysis of the above studies shows that in all cases the relaxation times are described by Arrhenius equations and the activation parameters are characterised by the quantities $\Delta H = 24 \text{ kcal mol}^{-1}$ and $\Delta S = 23-26 \text{ e.u.}$ ^{273, 281} Detailed analysis of the characteristics of this process shows that they may reflect fine details of the microstructure. For example, it has been observed that the increase in the fraction of 'head to head' defects in PVDF chains reduces the intensity of the α relaxation.²⁷³ The thickness of the lamellae in the above process affects the mobility parameters: an increase in thickness is accompanied by an increase in mobility.^{273, 283} Annealing, which usually leads to the thickening of the lamellae, is also accompanied by an appreciable increase in the average α relaxation times.²⁸³ One of the characteristic features of the process is that it exhibits anisotropy. The results of three different studies^{293, 297, 298} indicate unambiguously that, when the field vector \vec{E} is arranged perpendicular to the draw axis, the intensity of the process is higher than in the case where these directions coincide.

The mechanism of the processes in the above dispersion region has been discussed in greatest detail by Nakagawa and Ishida²⁸³ and Myjamoto et al.²⁹⁸ In the first study, the discussion began with the postulate that motions of two types are possible in folded-chain crystals: the motion in the surface itself (loops and other defects) and rotation of the chain (or of its section) in the bulk phase with a small longitudinal displacement. The number of monomer units in the fold (n_f) was estimated from the thickness of the lamella using electron microscope data. It was found that, for the range $n_f = 50-130$, the reorientation frequencies of the moving segments varied linearly. It was therefore concluded that the rigid rod approximation used in the study is correct for the kinetic unit. Comparison of the calculated and experimental relations shows that the enthalpy of activation for the above transition is determined mainly by the fold in the chain. Analysis of the experimental $\Delta\epsilon(T)$ relations enabled the authors²⁹⁸ to conclude that the rotations of sections of the lamellae within the crystal make the dominant contribution to α relaxation, but with the stipulation that motion within the folds cannot be fully excluded under these conditions. The chains in the folds are more mobile than within the crystal, but the contribution of the

latter to the process is decisive because of the high resultant dipole moment.

The above studies^{293, 297, 298} confirm the conclusion that the chains in the internal regions of the crystal make the main contribution to the α -relaxation process. Indeed, after orientation, the normal to the surface of the folds coincides with the draw axis. Under these conditions, the inner chains of the lamellae are arranged at right angles to the direction of orientation. Taking into account the fact that the perpendicular component of the dipole moment of the PVDF chain in the $TGT\bar{G}$ conformation is greater than the parallel component, the absorption when the field is applied perpendicular to the draw axis should be more intense, which has in fact been observed.^{293, 297, 298}

The mechanism of the α relaxation has also been considered by Myjamoto et al.²⁹⁸ with the aid of the same two positions model. Using the dependence of $\Delta\epsilon$ on the angle between the field vector and the stretch direction and having assumed that the longitudinal component of the dipole moment μ_{11} varies, the authors obtained a reasonable explanation of the relations noted above. Conformational analysis shows that such a case may occur, for example, in the $TGT\bar{G} \rightarrow GT\bar{G}T$ transition within a section of the lamella. This transition is possible, since even when account is taken of the activated state (in the form of the 'planar zigzag' conformation), which requires a 10% deformation along the axis of the macromolecule, the change in the conformation is then local and significant translational migrations of the chain as a whole are not required. Despite the fact that the fluorine atoms should move in such conformational transition along the c axis, the packing of the chains along the a and b axes changes little. The mechanism of the $TGT\bar{G} \rightarrow GT\bar{G}T$ conformational change presupposes the existence between chain sequences with different conformations of a defect (of the 'head to head' or conformational type), which may migrate along the chain as a result of thermal excitation and may induce a change in the dipole moment component μ_{11} .

According to another model, the position of the defect within the chain is fixed and the initiation of the above conformational transformation begins on the surface of the lamella as a result of a 'wormlike' excitation and is then transferred to another surface. In both models, account is taken of the important role of chemical defects, although the importance of conformational defects is not denied. It is assumed that with the aid of the latter one can explain a series of 'anomalous' effects in the characteristics of the α relaxation. Thus, when the relaxation times of the above process were compared for two specimens (isotropic and oriented), it was observed that, although in the former case the long period (and tentatively also the thickness of the lamella) is greater than in the latter (150 and 135 Å respectively), the relaxation time in it is an order of magnitude shorter than in the latter. It is assumed that, owing to the uniaxially stretching, the concentration of conformational defects changes in the second specimen and these in fact influence the rate of the relaxation processes. The proposed two positions model begins with a single relaxation time, whereas experiments yield a distribution of times. This discrepancy may vanish if account is taken of the distribution of the lamellae with respect to thickness and also of the distortions in the form of the potential energy function as a result of the presence of defects.

When α relaxation was observed in the region of high temperatures, usually at low frequencies of the electric field, anomalously high values of the ϵ' and ϵ'' components were noted. This has been attributed to the influence of impurities causing high losses due to dc conductivity. It was observed that they can be significantly reduced by maintaining the PVDF specimens at elevated temperatures in an electric field, where electrolytic processes take place.²⁹⁹ An increase in the electric field strength accelerates the decrease in the above conductivity during the electrolytic process. The imposition of a $\sim 20-30 \text{ kV cm}^{-1}$ electric field lowers the values of ϵ' at high temperatures, this being manifested to the greatest extent at low frequencies.²⁹⁹ After the field has been switched off, the increased conductivity is partly

restored. Nevertheless, it has been shown that, in cases where the α process was masked by losses due to dc conductivity, annealing of the specimens subjected to the field made it possible to observe the above process distinctly. Experiments with mercury electrodes showed that calcium ions make a large contribution to the ionogenic impurity conductivity.²⁹⁹

For theoretical justification of the above experimental facts, it has been suggested³⁰⁰ that the experimental ϵ' and ϵ'' each have two components:

$$\epsilon' = \epsilon'_i + \epsilon'_p, \quad (20)$$

$$\epsilon'' = \epsilon''_i + \epsilon''_p, \quad (21)$$

where the components with subscripts i and p denote the contributions of the ionic impurities and the polymer itself respectively. Taking into account the fact that only some of the impurities dissociate, their contributions to the components of the complex relative permittivity are defined by the relations³⁰⁰

$$\epsilon'_i = \frac{2v_0q^2}{lkT\pi^{0.5}} \left(\frac{D_0}{f}\right)^{3/2} \exp\left[-\left(\frac{3E_d}{2} + \frac{W}{2\epsilon_0}\right)/kT\right], \quad (22)$$

$$\epsilon''_i = \frac{2v_0q^2}{kT} \left(\frac{D_0}{f}\right)^{3/2} \exp\left[-\left(E_d + \frac{W}{2\epsilon_0}\right)/kT\right], \quad (23)$$

where v_0 is the concentration of mobile ions, l the thickness of the specimen, q the ionic charge, D_0 the diffusion coefficient of the ion, f the field frequency, E_d the activation energy for the diffusion of the ion, and W the ion dissociation energy.

Taking into account the relations obtained, a series of quantitative characteristics were found for the ionogenic impurities in PVDF. Thus at 160 °C the diffusion coefficient proved to be $D_0 = 4.36 \times 10^{-7} \text{ cm}^2 \text{ s}^{-1}$, which (on the assumption that the ions are univalent) corresponds to their mobility $\mu = 1.2 \times 10^{-5} \text{ cm}^2 \text{ V}^{-1} \text{ s}^{-1}$ ($\mu = qD_0/kT$) and the concentration $v_0 = 6.8 \times 10^{14} \text{ cm}^{-3}$ (at a concentration of monomer units of $1.7 \times 10^{22} \text{ cm}^{-3}$). The activation energies for the dissociation of ions and their diffusion have been estimated as 342 and 34 kcal mol⁻¹ respectively. An interesting fact was noted: prolonged (10 days) annealing at 160 °C of PVDF specimens leads to an appreciable decrease in the contribution of the ionic impurities to the low-frequency dielectric characteristics.

The anomalously high values of ϵ' and ϵ'' at low frequencies in the region of fusion of the PVDF α phase crystals have also been noted by Yano et al.³⁰¹ It was shown that there is a sharp fall of ϵ' and an increase in ϵ'' in the range 153–155 °C (according to DSC data the melting point is 157 °C). Analysis of the conductivity in this system before and after fusion indicates significant differences. In particular, the independence of the conductivity of the electric field frequency was noted for the melt. It was proposed that the melt be regarded as a homogeneous medium and that the nature of the conductivity in it is similar to that in an electrolyte solution. In this case, the dielectric parameters depend on the characteristics of the electrical double layer at the electrolyte–electrode boundary and Eqns (22) and (23) should be valid. According to the equations, the conductivity should be frequency-independent and the relations between ϵ'_i and $\lg f$ should be characterised by a coefficient of 3/2. Interpretation of the experimental data confirmed the validity of the chosen model: the conductivity indeed proved to be frequency-independent and the above coefficient was close to the predicted value, namely 1.67–1.79. At temperatures below the melting point, the homogeneous medium model was not confirmed. This may be inferred if only from the fact that the conductivity proved to be a function of the field frequency. The correct interpretation of experimental data can be achieved if account is taken of the differences between the values of ϵ' and of the conductivities of the crystalline and amorphous regions.

Similar anomalies in the behaviour of ϵ' and ϵ'' in the fusion region have been observed also on VDF/TFE copolymers.²⁷⁸ The loss factors in this region vary in accordance with the law

$$\epsilon'' = A\omega^{-m}, \quad (24)$$

where A is an empirical constant and m is a constant which varied in the range 0.3–0.5 as a function of temperature and the conductivity of the specimen. Eqn (24) is characteristic of the polarisation of the space charge of ionogenic impurities³⁰² and it too confirms the necessity to take into account the heterogeneity (in terms of the electrical characteristics) in systems based on PVDF at elevated temperatures.

The Maxwell–Wagner polarisation process under discussion has also been detected in uniaxially extended PVDF films³⁰³ and its characteristics (mainly the loss factor at the maximum) proved to be extremely sensitive both to the phase ratio in PVDF and to the state of orientation of the chains in its nonordered regions. It is noteworthy that the characteristics of the electrical heterogeneity for the ordered and nonordered regions have been found to be sensitive to the polarisation process in the corona discharge, since under these conditions the intensity of the interlayer polarisation process diminishes significantly.³⁰³

This process has been investigated in greater detail in a study³⁰⁴ where the high-temperature transition $\alpha \rightarrow \gamma$ was considered. If the crystals are obtained in the γ modification, the low-frequency dependences of ϵ' are found to differ significantly from those for the case where PVDF crystallises as the α phase (Fig. 29). Indeed, in the former case the values of ϵ' at low

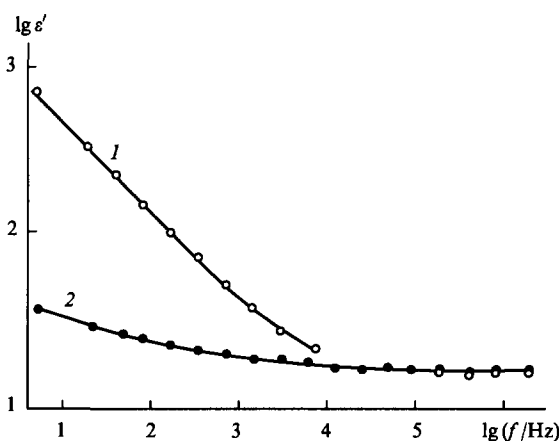


Figure 29. Frequency dependences of the high-temperature relative permittivity for PVDF films crystallised as the γ modification (1) and the α modification (2) at 160 °C.³⁰⁴

frequencies are significantly higher and do not obey the law $\epsilon' (f^{-3/2})$, as happens in the case of α PVDF. As already mentioned above, this law is characteristic of electrode polarisation and this mechanism is therefore inapplicable to crystals of the PVDF γ phase. This conclusion is confirmed also by the dependence of ϵ' for PVDF films in both modifications on the thickness of the specimen (Fig. 30). Evidently, in the case of crystals of the α modification an explicit dependence of ϵ' on thickness is observed (which is characteristic of electrode polarisation, whereas for films with the γ modification ϵ' remains approximately constant. The interlayer (Maxwell–Wagner) polarisation mentioned above may serve as another possible explanation of the observed relaxation process with an activation energy of 627 kJ mol⁻¹. For spherical crystals with a conductivity σ_2 and a relative permittivity ϵ_2 , immersed in an amorphous matrix with the corresponding values of σ_1 and ϵ_1 , the frequency f of the loss maximum can be found from the equation³⁰⁵

$$f = \frac{2(\sigma_1 + \sigma_2)}{2\epsilon_1 + \epsilon_2}. \quad (25)$$

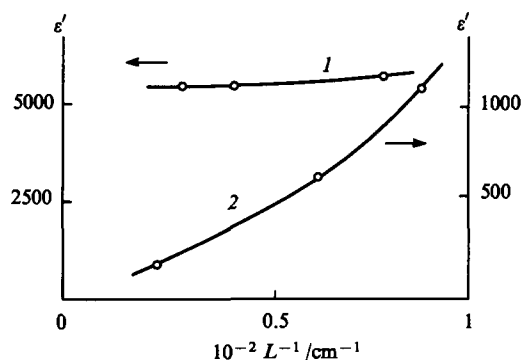


Figure 30. Dependence of the high-temperature relative permittivity on the thickness of PVDF films crystallised as the γ modification (1) and the α modification (2) at 165 °C.³⁰⁴ Frequency (Hz): (1) 0.2; (2) 0.1.

Since the γ phase crystals have an uncompensated dipole moment per unit cell, $\sigma_1 \gg \sigma_2$ and $\epsilon_2 \gg \epsilon_1$ and Eqn (25) may be replaced by

$$f = \frac{4\sigma_1}{\epsilon_2} \quad (26)$$

The equilibrium value $1.5 \times 10^{-10} \Omega^{-1} \text{ cm}^{-1}$, obtained after 15-h maintenance of the specimen at 185 °C in a 400 V cm^{-1} field, was used as σ_1 . The frequency f calculated by Eqn (26) is 0.6 Hz, which differs by more than two orders of magnitude from the experimental value.

The possibility of orientational motions of the γ crystals as a whole was considered as an alternative mechanism of the high-temperature relaxation process mentioned above. This is based on the linear dependence of ϵ''_{max} for the process on the heat of fusion of the γ phase crystals (DSC data), which indicates that the magnitude of the absorption is determined mainly by the volume fraction of the γ phase crystals. The possibility of the motion of the crystals as a whole in this process does not lack justification. Indeed, with increase in the long period (linked directly to the size of the crystalline lamella), the maximum of the mechanical loss modulus shifts towards higher temperatures. Finally, yet another argument in support of the hypothesis that the crystal moves as a whole follows from estimates $\Delta\epsilon$ by Eqn (15) using the experimental numbers of monomer units per kinetic unit. It proved to be 6×10^3 repeat units. This number exceeds by more than an order of magnitude the number of monomer units in a lamella of the usual size ($\sim 10^2$ units). Osaki et al.³⁰⁴ does not discuss the reason for this discrepancy but the latter may indicate the involvement in the given transition of motions accompanying a ferroelectric–paraelectric transition in which cooperative effects should prevail.

Indeed the above relaxation region is in the vicinity of the melting point, where a ferroelectric–paraelectric transition has been postulated for the VDF homopolymer in a polar form (as in the given instance). The relation between the mobility in the crystalline phase and the motions in a ferroelectric transition may be inferred from the nature of the temperature variation of the dielectric parameters in the VDF/TrFE copolymer, which is known to be ferroelectric³⁰⁶ and for which the temperature of the above transition differs from the melting point. Here too one observes a high-temperature mobility in the crystalline phase, which is characterised by high values of $\Delta\epsilon$. Analysis of the temperature variation of the latter shows that its increase with increasing temperature represents the onset of the anomalous rise in $\Delta\epsilon$ in the region of the ferroelectric transition.³⁰⁶

Mention should be made of the results of a study³⁰⁷ of the mechanism of the high-temperature relaxation in PVDF. The low-frequency dielectric characteristics of PVDF films with α -phase crystals were investigated. Here attention was concentrated on the role of the material of the electrodes. Aluminium and gold, for

which different temperature variations of the components of the complex conductivity had been found, were employed. The authors explained the highly intense $\tan \delta$ maximum (amounting to 12–25!) at low frequencies by the manifestation of the space charge at the material–electrode interface. However, in contrast to other investigators, they believe that the majority carriers are the F^- and H^+ ions. This presupposes the presence in the bulk of the film of a finite number of HF molecules which should be partly dissociated. This hypothesis is confirmed by a whole series of facts. For example, one of them is that the presence of excess fluorine has been observed in the bulk of PVDF by the method of reverse Rutherford scattering.³⁰⁷ A finite number of the $(-\text{CH}=\text{CF}-)$ groups have been found in the initial state of different PVDF films from the characteristic IR absorption bands. Such groups may be formed by the reaction



initiated by thermal energy or irradiation.³⁰⁰ A sufficient amount of HF may be formed by this reaction already at ~ 60 °C.³⁰⁹ Thus taking into account the presence of the H^+ and F^- ions in the bulk phase, the low-frequency $\tan \delta$ maximum should be attributed to the behaviour of these ions in a variable electric field.³⁰⁷ It is believed that the mobility of the hydrogen cations is significantly greater than that of the fluoride ions, so that the former accumulate near the negative electrode at ultralow frequencies, creating a space charge, which is in fact responsible for the relaxation process under discussion.

The less mobile fluoride ions are captured by traps, but their role may vary significantly for different electrode materials. If the electrode material is aluminium, then, under the influence of the combined action of a high temperature and a weak variable field, the fluoride ions, having reached the electrode, may diffuse into the latter. This is confirmed by the detection of fluoride ions in the surface of the electrode after the application of the combined influence mentioned above.³⁰⁷ X-Ray photoelectron spectroscopic data demonstrate that the fluoride ions which have migrated into the electrode can react with the aluminium atoms to form new compounds.^{310,311}

Thus analysis of data on the high-temperature relaxation shows that the mechanism of the above processes may be fairly complex. A number of workers have noted the dependence of its characteristics on experimental parameters such as the magnitude and duration of the effect of the field.³¹²

Information about the relaxation process can be obtained by the method of thermostimulated depolarisation currents, with the aid of which processes involving local and segmental mobility at low temperatures can also be detected.³¹³ Above room temperature, it is possible to detect even two interlayer polarisation processes. One of them (the low-temperature process) is attributed to the formation of a space charge at the boundaries between the amorphous phase and the nonpolar crystals of the α modification, whilst the other 'senses' these boundaries with the polar (β , α_p) modifications.^{314,315} In a later study³¹⁶ on specimens with crystals of both the polar and nonpolar phases, only one relaxation process, associated with the space charge, was detected. However, at high temperatures three additional current maxima, the temperatures of which are correlated with the melting points of the α , β , and γ modifications of the PVDF crystals, were noted.

Despite the high information content of the electrical methods for the assessment of relaxation process, there have been a number of studies where it was shown that certain forms of mobility in PVDF are inactive. For example, according to the results of McBrierty et al.,³¹⁷ the relaxation process, associated with the motion of the folds on the surface of the lamellae and noted in experiments on dynamic mechanical relaxation by the dielectric method, was not observed. A similar conclusion was reached in a study³¹⁸ where two mechanical relaxation regions (α_1 and α_2) were found in all the PVDF specimens (isotropic and oriented with the crystals of the α and β modifications) at high temperatures, the higher-temperature region (α_2) being assigned to the

motions preceding the fusion of the crystal. It follows from the results of the study that the mechanisms of the relaxation in mechanical and electric fields in the region of the glass transition of the oriented specimens may differ. This is indicated, in particular, by the finding that, in a mechanical field, the β process is more intense in the case of a parallel disposition of the force vector and the orientation axis,³¹⁸ whereas in an electric field the opposite behaviour obtains.^{293, 297}

An attempt has been made at a detailed comparison of the relaxation processes in PVDF and polyethylene on the basis of the results obtained by mechanical spectroscopy.³¹⁹ In the region lying below the glass transition temperature, two relaxation processes (γ_1 and γ_2) were observed in polyethylene, their parameters being close to those of the γ and δ relaxation processes (discussed above) obtained by dielectric measurements. A reasonable agreement between the activation energies and the normalised relaxation time spectra for the processes in both polymers made it possible to postulate that the mechanisms of the γ and δ processes in PVDF are similar to those of the γ_1 and γ_2 processes in polyethylene. According to the results of Yamada et al.,³²⁰ the γ_1 relaxation should be attributed to the local modes of motion of the nonordered chains in the interlamellar regions, whilst the lower-temperature relaxation region (γ_2) should be assigned to the motion in the surfaces of the lamellae.

The same situation occurs also for the region of the high-temperature α relaxation of PVDF, for which the normalised relaxation time spectra agree well with those for the α_2 relaxation in polyethylene. The similarity in the relaxation behaviour of PVDF and polyethylene is also supplemented by the fact that two transitions (α_1 and α_2) can be noted in the high-temperature region for both polymers.³¹⁹

IX. Structural characteristics in the crystallisation of poly(vinylidene fluoride) in blends with other polymers

Examination of the questions associated with the structural characteristics in the crystallisation of PVDF in blends with other polymers will be useful for a number of reasons. One of them is related to the possibility of supplementing and expanding the ideas concerning the characteristic features of the modification of the structure and properties of polymer blends in which one or both components are crystallisable. By crystallising PVDF in blends with other polymers, it is possible to regulate specifically the conformational structure of its chains, which is important in the practical employment of PVDF-based materials for piezoelectric and pyroelectric sensors. The possibility of the modification in such blends of the morphology and optical properties of PVDF is regarded as their additional advantage when they are used as materials with nonlinear optical properties.

Since the blends of PVDF with polymethacrylates have been studied in greatest detail, it is more convenient to begin the analysis of the results precisely with studies in which these blends were investigated. The orientation process in polymeric materials is frequently used to impart improved mechanical properties to the latter. For PVDF, this process is frequently used also for the formation of the ferroelectric β phase, which determines practically important phenomena such as the piezoelectric effect and the second-order optical nonlinearity. However, the orientation of a polymeric material is accompanied by the appearance of birefringence Δn , the magnitude of which is determined by the difference between the refractive indices along (n_1) and across (n_2) the direction of stretching. When a textured material is used for optical elements (windows, discs, lenses, etc.), the birefringence effect is undesirable. One of the possible ways of suppressing this effect has been noted in relation to blends of atactic poly(methyl methacrylate) (PMMA) with PVDF. Such blends are known to be compatible in the melt and cooling of the latter affords a homogeneous optically transparent material.³²⁰ When the com-

position of the blend was varied, it was shown that the refractive index of the isotropic phase varies linearly with increase in the fraction of PVDF.³²¹ This follows from the Lorentz–Lorenz relation for multiphase mixtures, in which the characteristic dimensions of the regions corresponding to different components are smaller than the light wavelength. PVDF is present in a partly crystalline state and is characterised by the densities $\rho_c = 2.0 \text{ g cm}^{-3}$ and $\rho_a = 1.6 \text{ g cm}^{-3}$ in the crystalline and amorphous states; the refractive indices of these phases have been estimated as $n_c = 1.48$ and $n_a = 1.37$. The value of n_c for PVDF is close to that for the amorphous PMMA (1.49). Therefore a decrease in the light scattering effects and an improvement of transparency compared with pure PVDF are to be expected for crystallisable PVDF/PMMA blends with a high content of the first component.

The effect of the deformation-induced birefringence has been observed on noncrystallisable blends with a PVDF content not exceeding 60 mass %. In this case Δn proved to be a linear function of the draw ratio λ , the slope of which depended significantly on the composition of the blend. In the PVDF/PMMA 40/60 and 20/80 blends, Δn was surprisingly low even for high draw ratios. The reason for this may be found by analysing the dependence of Δn on the composition of the blend for $\lambda = 2$ (Fig. 31). For a certain composition of the blend (for $\lambda = 2$, this is a blend having the composition 17/83), Δn proves to be zero. A further decrease in the PVDF concentration leads to negative values of Δn . The components of the above blend have different signs of the double refraction, so that, by varying their ratio, it is possible to select a composition such that the birefringence is compensated for a certain value of λ .

The foregoing is valid for amorphous blends with a particular previous thermal history. These questions have been investigated in detail in a study,³²² where the composition of the components blended in the melt was varied within wider limits. When the components are fully compatible in given proportions in the melt, the cooling of the latter may lead to the crystallisation of PVDF,^{323–336} the characteristic features of which may depend also on the annealing temperature.³²² In particular, if the annealing is carried out at temperatures in the range between the glass transition temperatures of PMMA and PVDF crystallisation may be observed in blends containing more than 10% of PVDF.³²² The amorphous phases of both components are apparently fairly compatible since a single glass transition temperature has been noted in the blends. It decreases monotonically with increase in the fraction of PVDF in conformity with the mixing rule for a two-component mixture^{337, 338}

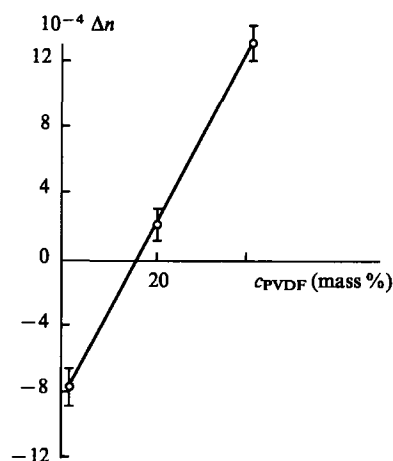


Figure 31. Dependence of the birefringence on the blend composition in amorphous oriented ($\lambda = 2$) specimens.³²¹

$$\lg T_g = \frac{M\Delta C_p \ln T_g + M'\Delta C_p' \ln T_g'}{M\Delta C_p + M'\Delta C_p'} \quad (27)$$

where T_g , M , and ΔC_p are respectively the glass transition temperature, the mass fraction, and the difference between the heat capacities of VDF in the region of the glass transition of the components; the primed quantities refer to PMMA.

A decrease in the fraction of PVDF in the blend hardly affects the thickness of the lamellae formed (Fig. 32). Under the conditions of reduced crystallinity, this implies that the introduction of PMMA promotes mainly a decrease in the rate of nucleation. It follows from the relations presented in Fig. 32 that, for blends enriched in PMMA, the morphology of the structural elements formed is characterised by an increase in the intercrystallite spacings.

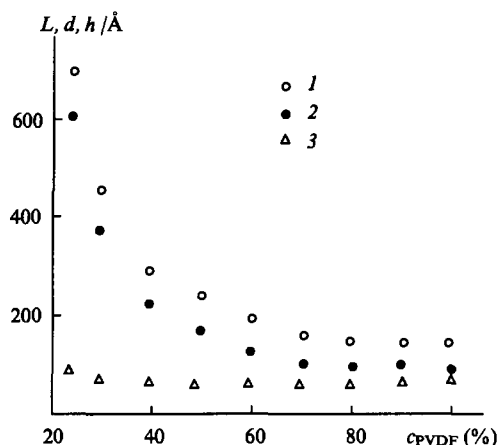


Figure 32. Dependence of the large period (1), the size of the amorphous layers (2), and the thickness of the lamellae (3) on the fraction of PVDF in PVDF/PMMA blends annealed at 140 °C.³²²

The satisfactory compatibility of PVDF with PMMA is confirmed by the negative value of the Flory-Huggins parameter (B). According to numerous data,^{330,339-341} blends of PVDF with poly(ethyl methacrylate) (PEMA) are also compatible. The polymers PMMA and PEMA are incompatible and it is therefore difficult to predict the nature of the compatibility of PVDF with PMMA/PEMA copolymers. This problem has been solved in experiments involving the study of the fusion of PVDF in blends with PMMA/poly(ethyl methacrylate) (PEMA) copolymers over a wide range of compositions.³⁴² The parameter B was estimated from the equation^{324,339}

$$T = T_0 + B \frac{V}{\Delta H} T^0 \Phi^2 \quad (28)$$

where T_0 and T are respectively the melting points of pure PVDF and in the blend, $\Delta H/V$ is the heat of fusion of PVDF per unit volume (44.0 cal cm⁻³), and Φ is the volume fraction of the noncrystallisable polymer in the blend.

According to the pair interaction model,³⁴³ the parameter B for such blends may be estimated with the aid of the relation

$$B = B(\text{MMA/VDF})\Phi(\text{MMA}) + B(\text{EMA/VDF})\Phi(\text{EMA}) + B(\text{MMA/EMA})\Phi(\text{MMA})\Phi(\text{EMA}). \quad (29)$$

The experimental values of B for blends of PVDF with the copolymers PMEMA of different composition are presented in Fig. 33. Evidently, with increase in the amount of MMA in the copolymer, B diminishes. Positive values of $B(\text{MMA/EMA})$ in Eqn (29), indicating the repulsive nature of the intramolecular interactions between neighbouring units in the copolymer, yield

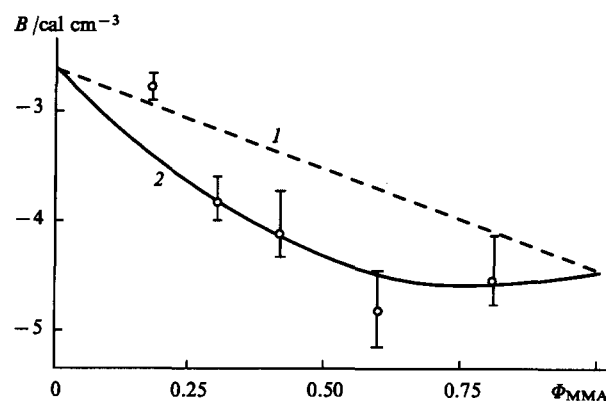


Figure 33. Dependence of the Flory-Huggins parameter for the PVDF/PMEMA blend on the composition of the copolymer. (1) $B(\text{MMA/EMA}) = 0$ (2) $B(\text{MMA/EMA}) = 3.25 \text{ cal cm}^{-3}$.

the best agreement between the calculated curve and the experimental points.

The compatibility of PVDF with low homologues of the methacrylate series (PMMA and PEMA) breaks down for higher homologues of this series.³⁴⁴ Since the concentration of carbonyl groups in the latter diminishes, it has been suggested that these groups in the methacrylates actually play a significant role in the compatibility processes. In this connection, a study has been made³⁴⁵ of the influence on the compatibility processes of both these and other functional groups and elements, for example oxygen or sulfur in ether groups. For this purpose, questions concerning the compatibility of PVDF with poly(methoxymethyl methacrylate) (PMOMMA) and poly(methylthiomethyl methacrylate) (PMTOMA) were examined. For the former, the existence of a single glass transition temperature indicates the compatibility of the components. The parameter B found from Eqn (28) is -14.5 J cm^{-3} . This is an intermediate value for blends of PVDF with PMMA and PEMA. It was shown that the upper critical miscibility temperature (determined from the turbidity temperature) diminishes almost by 100 °C with increase in the fraction of PMOMMA to 0.5. The PVDF/PMTOMA blends are turbid at all temperatures and two glass transition temperatures are observed for them regardless of composition. This means that these blends are incompatible. The melting point of the PVDF crystals in the blends diminishes slightly with increase in the fraction of PMOMMA, which indicates some change in the dimensions and perfection of the crystals. One may assume that the role of PMTOMA in these blends reduces mainly to the effective suppression of nucleation, since the degree of crystallinity (for a PMTOMA fraction of 0.5) decreases almost by a factor of 2 according to measurements of the heat of fusion. The reasons for such a striking difference in the behaviour of the blends of PVDF with methacrylates, is seen by the authors of the study in the increased volume of the side group in PMTOMA compared with PMOMMA. Yet another cause of the above difference is attributed to the lower electronegativity of the sulfur atom compared with the oxygen atom.

The amorphous phase in a blend with a crystallisable polymer is known to decrease the rate of crystallisation of the latter in all cases.^{346,347} This law is valid also for the PVDF/PMMA³²⁸ and PVDF/poly(ethyl acrylate)³⁴⁰ blends. The details of this phenomenon have been investigated in a study³⁴⁹ where the rate of growth of the spherulites was investigated with variation of both the crystallisation temperature of the PVDF/PMMA blend and of the molecular mass of the second component. It was found that, depending on the temperature, the crystallisation can occur in three regimes, which differ in the rates of secondary nucleation and surface growth. At the same crystallisation temperature, an increase in the molecular mass of PMMA in a blend of one composition leads to a decrease in the rate of growth of the

spherulite. The experimental data are best described within the framework of the modified Hoffman–Lauritzen theory, which takes into account the two-step diffusion-controlled mechanism.

The high-resolution nuclear magnetic resonance (NMR) technique with spinning of the specimen at the magic angle is nowadays frequently employed to analyse the microstructures of polymers in the block state. Potentially this method can be used also for the analysis of the details of the interaction in blends if blending at the molecular level is accompanied by a change in the electronic states for the resonating nuclei. The approximate similarity of the magnetisation parameters for these nuclei in the PMMA and PVDF chains has been demonstrated³⁵⁰ on the basis of the characteristics of the resonance of the ^{13}C nuclei. When this was taken into account, the experiments involving the ^{13}C and ^{19}F nuclei with cross-polarisation showed that PMMA and PVDF are at least partly blended at the molecular level. This method has been developed (in relation to the blends under consideration) in a study³⁵¹ where data involving the resonance of not only the ^{19}F and ^{13}C nuclei but also ^1H nuclei were employed.

For PVDF/PMMA blends with a wide range of compositions, the experimental data are best described in terms of the model which takes into account the presence of four different phases. The presence of pure PVDF is postulated in the first phase. On the experimental time scale, the presence of protons arising from PMMA is not detected. The second phase includes the regions in which the chains of both components are mixed at the 'truly molecular' level and the main transfer of magnetisation from protons to fluorine is ensured directly by the ^1H – ^{19}F -depolarisation processes. The third phase is close to the previous one but, in contrast to the latter, it should be controlled to a greater extent by spin diffusion processes. Finally, the fourth phase includes regions of pure PMMA, manifesting depolarisation and spin diffusion processes. On the basis of their experiments, the authors³⁵¹ were able to calculate the fractions of the first and fourth phases and also to estimate the dimensions and ratios of the components in the domains comprising the second and third phases for blends with a wide range of ratios of the initial components.

Table 17 shows that in the blend with 20% of PMMA the latter is wholly in the blended state. In virtually all the blends, the mixed second and third phases have virtually the same composition as regards the monomer ratio. The 80/20 blend is an exception, which is due to the dilution effect. The dimensions of the domains comprising the above phases also vary only slightly with composition and are respectively 7 and 6 Å.³⁵¹

Later Papavoine et al.³⁵² demonstrated in relation to the PMMA/PVDF 60/40 blend that the method being developed has a high information content also for the assessment of the kinetics of phase separation. In the experiments, the initial blends were heated under pressure at 200 °C (i.e. above the melting point of the PVDF crystals where the components are fully compatible) and were then rapidly cooled to 77 K. The kinetics of the phase separation were then followed in the isothermal annealing regime (at 120 and 140 °C) by the method described above (the increase in the fractions of the first and fourth phases was estimated). It was found that at both annealing temperatures the attainment of the equilibrium value occurs at approximately the same time in terms

of the fractions of both the first and fourth phases. The accumulation of the first phase, i.e. of the regions of pure PVDF, should be accompanied by the crystallisation of the latter. This has been confirmed qualitatively by DSC data (the appearance of the fusion endotherm for annealed specimens). Comparison of the increase in the degree of crystallinity during annealing at 140 °C on the basis of the results obtained by both methods shows that, according to DSC, these values are systematically lower by approximately the same amount. The authors believe that this is not fortuitous and attribute it to the fact that in the NMR method the first phase must include also the interfacial regions at the crystal–amorphous phase boundaries, the presence of which has been demonstrated by numerous dielectric relaxation experiments.

Shilov et al.³⁵³ investigated the differences between the phase ratios in bulk and on the surfaces of PVDF/PMMA blends. The X-ray photoelectron spectroscopic method, yielding information about the microstructure at depths of 4–5 nm, was employed. Specimens of two types were investigated, one of which consisted of a thin (0.2 µm) film of the 50/50 blend. Heating of the specimen in 40 °C steps directly in the spectrometer chamber demonstrated that up to 373 K the form of the XPES spectra does not change. Annealing at a temperature $T \geq 413$ K leads to an increase in the intensities of the lines corresponding to the carbon in the CF_2 bond and, conversely, to a decrease in the intensities of the lines due to the carbon in the $\text{C}=\text{O}$ group. On fusion of the blend, this process intensifies to an even greater extent as a result of the weakening of the specific interactions between the blend components. All the foregoing considerations can be accounted for solely by a redistribution of the blend components in the above annealing regimes, as a result of which the surface is enriched in PVDF at depths of 5 nm.

This conclusion is confirmed by the results of the study of specimens of the second kind which were of the 'sandwich' type: a thin layer of PMMA was deposited on top of a layer of PVDF. In the initial state, the lower PVDF layer in the specimen was almost fully covered by PMMA, but thermostatic treatment of the specimen at 413 K leads to the redistribution of the intensities of the components of the lines due to carbon in the CF_2 and $\text{C}=\text{O}$ groups mentioned above. The kinetics of this process are described by a power relation with the exponent $n \approx 0.5$, which is characteristic of diffusion-controlled processes. Since the density of PVDF is higher than that of PMMA the direction of the processes involving the inversion of the distribution of the components in the surface must be opposed to the direction of the force of gravity gradient. According to the authors,³⁵³ a surface energy minimum should correspond to the state of equilibrium, since one is dealing with the structure of the surface. The surface tensions of PMMA and PVDF are respectively 40.2 and 32.7 mN m⁻¹.³⁵⁴ The surface energy minimum therefore requires the emergence of PVDF onto the surface, which has been noted experimentally.³⁵³

In connection with the possible formation of polymorphic modifications in PVDF crystals, a test of the influence of the amorphous phase of the blend on the crystallisation of PVDF in a particular modification is of current interest. If PVDF crystallises with formation of α and γ spherulites for low degrees of supercooling, the addition of PMMA leads to a decrease in the concentration of the large (α) spherulites, which in addition become loosely packed.⁸⁶ Thus isotropic films become enriched in spherulites formed by the γ phase. According to other data,³⁴⁵ PMMA can influence also the form of the polymorphic modification of the PVDF crystals produced in the isothermal annealing regime at temperatures above the glass transition temperature of the blend after its quenching from the melt.

DSC, IR spectroscopic, and X-ray diffraction data have shown that the crystallisation of PVDF/PMMA blends leads mainly to the formation of the α phase, but, if the component ratio is 70/30, the ferroelectric β phase is produced. These questions have been investigated in detail for textured films. In

Table 17. The fractions of the first and fourth phases and the monomer ratio in the second and third phases for PVDF/PMMA blends of different composition.³⁵¹

PMMA/PVDF	Fraction of first phase	Fraction of fourth phase	Monomer ratio	Monomer ratio in second and third phases
20/80	0.75	0	0.16	0.65
40/60	0.35	0.10	0.43	0.59
60/40	0.15	0.30	0.96	0.75
80/20	0.10	0.30	2.56	1.99

particular the role of PMMA in polymorphic changes has been investigated in the formation of PVDF films under the conditions of a high longitudinal gradient in the flow of the melt.³⁵⁶ It was shown that, under the above conditions, pure PVDF crystallises as a mixture of the α and β modifications, the fraction data of the former amounting to 62%. Scanning electron microscopic data indicate that this entails the formation of lamellar crystals. When 20 mass% of PMMA is introduced into PVDF, the fraction of the β phase increases by 20% under the same crystallisation conditions, while the morphology becomes mixed, i.e. acicular crystals appear together with lamellar ones. A similar conclusion was reached also in a later study¹⁰² where it was shown that the addition of PMMA also increases the fraction of the β phase formed, while the morphology changes from lamellar to fibrillar. A new feature is the finding that the number of fibrillar β phase crystals increases with increase in the molecular mass of the polymethacrylates.

The influence of the form and concentration of the amorphous component in the blend with PVDF on the nature of the morphology generated on crystallisation of the latter has been investigated in detail.³⁵⁷ Blends of PVDF with PMMA, the styrene/MMA copolymer (S-MMA), and poly(methyl acrylate) (PMA) were studied. It was noted that, whereas the lower critical miscibility temperature (LCT) in PVDF/PMMA blends is $\sim 350^\circ\text{C}$, it is significantly reduced for the PVDF/S-MMA system with increase in the amount of styrene in the copolymer. When the styrene content reaches ≥ 0.15 , the blend becomes incompatible, since the LCT becomes comparable to the equilibrium melting point of the α modification of PVDF. As in an earlier study,⁸⁶ pure PVDF crystallised at low degrees of supercooling with formation of the α and γ spherulites, but, in contrast to the study quoted, when polymethacrylates were added, fine differences were noted in the supermolecular structures produced. The α spherulites of pure PVDF have a fine fibrillar structure, which the γ spherulites lack.

For the PVDF/S-MMA blends, the α phase spherulites are converted into dendrites, the size of which diminishes, other conditions being equal, with increase in the fraction of the amorphous component. An even higher content of the latter leads to the crystallisation of PVDF in the form of small circular spherulites. The formation of dendrites is explained by the appearance in the growing front of fluctuations in the concentration of PVDF chains and by the transition of the crystallisation process to the diffusion-controlled region. Only circular spherulites are usually observed for PVDF/PMA blends. This is attributed to the lower glass transition temperature of PMA (and hence also of the blend) compared with PMMA, which should lead, other conditions being equal, to the acceleration of the stages involving diffusional control during crystallisation. The last blend is interesting also because it is possible to observe in it the crystallisation of PVDF under the conditions of very high 'dilution', i.e. when its volume fraction is only 0.3.

The above changes in the properties of blends of PVDF with polymethacrylates suggest the occurrence of specific interactions in these components. Their nature has been investigated by IR spectroscopy.³⁵⁹ Attention was concentrated in the above study³⁵⁹ on the analysis of the form and frequencies of the stretching vibrations of the carbonyl (C=O) group of PMMA. Preliminary studies on solutions of low-molecular-mass homologues of PMMA in the form of methyl acetate (MAC) and methyl pivalate (MPA) have shown that the solvent polarity may alter significantly the characteristics of the above band up to its splitting. The occurrence of significant interactions may be deduced by analysing the form of the absorption band due to the vibrations of the carbonyl group in MAC and MPA, which were introduced into the matrices of different polymers (Fig. 34). Evidently in the case of inert matrices (PE, PTFE) the absorption bands remain narrow and are displaced towards higher frequencies. In contrast to this, bands due to the PVDF matrix are significantly broadened and are displaced appreciably towards

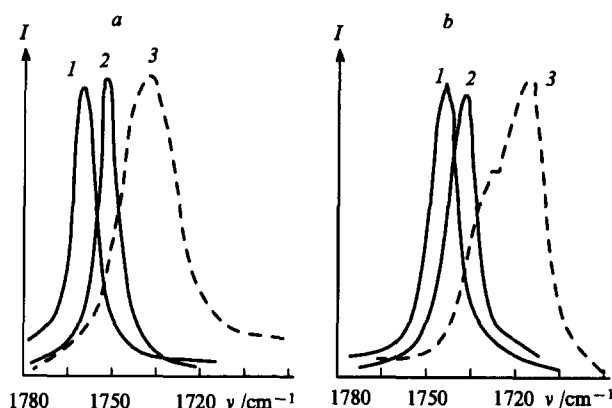


Figure 34. The form and position of the band due to the stretching vibrations of the C=O group of methyl acetate (a) and methyl pivalate (b) in various matrices.³⁵⁹ (1) PTFE; (2) PE; (3) PVDF.³⁵⁹

low frequencies. The authors formulated in greater detail the mechanism of the specific interactions in blends, having considered the system comprising the VDF/chlorotrifluoroethene copolymer swollen in deuterated MAC.

By following the doublet absorption in the region of symmetrical and antisymmetrical stretching vibrations of the methylene groups in PVDF in the copolymer, it was shown that the swelling of the copolymer in MAC leads to a significant bathochromic shift of the bands. It was therefore concluded that the C=O groups may form hydrogen bonds with VDF units. When account is taken of similar data for low-molecular-mass compounds, the enthalpy of such bonds, calculated from the frequency shift of the absorption bands, is found to be $\sim 1 \text{ kcal mol}^{-1}$. This conclusion has been confirmed also on passing from model systems to polymer blends. The changes in the region of the absorption bands due to the carbonyl group for pure PMMA and PMMA in the PVDF/PMMA 50/50 blend show that in the latter case the band shifts somewhat towards lower frequencies, which can be seen distinctly from the difference spectra for specimens of the annealed and quenched blends, having the same composition. The excess absorption on the high-frequency side and the negative absorption on the lower-frequency side imply in this case that this annealing, leading to the crystallisation of PVDF, diminishes the number of specific contacts between PMMA and PVDF.

It was possible to demonstrate the occurrence of specific interactions also in relation to other functional groups, in particular for the methyl ether group $\text{O}-\text{CH}_3$ and the α -methyl group of PMMA. An increase in temperature leads to a decrease in the intensities of the above absorption bands for pure PMMA. The addition of 15 mass % of PVDF leads to exactly the same change. As a result of specific interactions, the latter effectively weakens the intermolecular interactions in PMMA chains. This is reflected also by the decrease in the glass transition temperature of the blends with increase in the fraction of PVDF noted above [see Eqn (27)]. Shilov et al.³⁵³ also concluded that specific interactions occur in PVDF/PMMA blends, where the carbonyl group of PMMA should be involved. This conclusion is based on the analysis of the X-ray photoelectron spectral lines.

The specific interactions between PMMA and PVDF may be the cause of an unusual phenomenon noted for the PVDF/PMMA 80/20 blend. The study by Tsutsumi et al.³⁶⁰ was devoted to the estimation of the internal field E_i in the polarised specimen. The method involving the introduction of small amounts of a dye (dimethylaminonitrostilbene) was used and measurements were made of the differences between the absorption spectra in the visible region before and after poling in a field with a strength E . For sufficiently high poling fields, the internal field proved to be higher than the poling field (Fig. 35 a). In the highest poling fields,

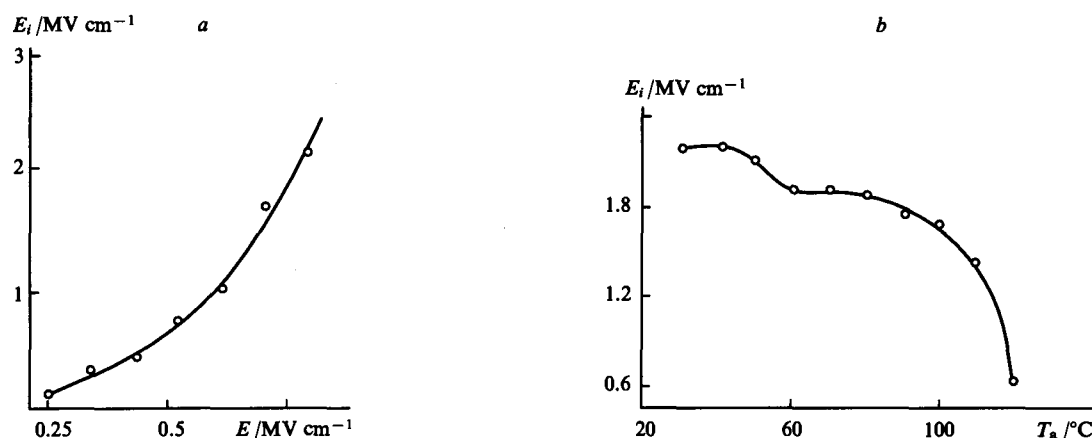


Figure 35. Dependence of the internal field E_i on the strength of the poling field (a) and the annealing temperature (b) in PVDF/PMMA 80/20 blends.³⁶⁰

the field ratio may be more than two, this conclusion being confirmed also for another type of dye.³⁶¹

As a result of the specific interactions between the PVDF and PMMA chains in the amorphous phase, the glass transition temperature in the blend of the above composition becomes 60 $^{\circ}\text{C}$.³⁶⁰ At a poling temperature of 80 $^{\circ}\text{C}$, these interactions are weakened and the poling field causes the preferential orientation of not only the ferroelectric crystals but also of the polar segments in the amorphous phase. Cooling of the specimen after poling in the presence of a field to room temperature creates a new situation for the blend compared with the VDF homopolymer. Indeed, since $T_g = -40$ $^{\circ}\text{C}$ for the latter, it follows that at room temperature the ordered dipoles in the amorphous phase should undergo depolarisation after the removal of the field and the internal field is then generated only by crystallites. In contrast to this, for the above blend at room temperature the ordered dipoles of the amorphous phase should be frozen, since its glass transition temperature is 60 $^{\circ}\text{C}$. For this reason, the resultant internal field at room temperature is generated in this case, in contrast to PVDF, both by the polar crystals and by the ordered domains in the amorphous region. This hypothesis is confirmed by the data presented in Fig. 35b. Evidently heating of the specimen of the poling blend lowers E_i precisely in the region of the glass transition temperature, where the specific interactions between the PVDF and PMMA chains are effectively weakened. It can also be seen from the same figure that the main contribution to the depolarisation process comes nevertheless from crystals in which the appearance of mobility at temperatures above 100 $^{\circ}\text{C}$ leads to a more significant decrease in E_i .

The study of Tsutsumi et al.³⁶⁰ was also concerned with the problem of the influence of PMMA on the polymorphism of PVDF. X-Ray diffraction data have shown that, whereas the homopolymer crystallises as the α phase, its blends with PMMA having the composition specified above are characterised by the presence of the β phase after quenching from the melt. This has also been noted in other studies.^{345,357} However, it would be premature to reach an unambiguous conclusion concerning the role of PMMA as regards polymorphism, since many results indicate some uncertainty. For example, when the blend is prepared by deposition from a compatible polar solvent (dimethylacetamide), then, as for the pure homopolymer, it crystallises as the γ modification.³⁶² In the absence of α phase crystals, it is impossible to observe the high-temperature $\alpha(\alpha_c)$ relaxation. However, later data³⁶³ showed that the form of the crystallographic modification may depend also on the type of the support on which the film is deposited. In particular, the case of the PVDF/PMMA 60/40 blend from solution onto an aluminium support promotes crystallisation as the α modification.

Together with indirect data on the polymorphism in PVDF, the dielectric relaxation method applied to blends can also yield

new information about the details of the morphology produced. This is illustrated by the results of a series of studies where the relaxation processes in compatible PVDF blends were investigated by the dielectric method. The temperature dependences of the loss factor at a frequency of 100 kHz were analysed for pure PVDF and its blends with PMMA having different compositions.^{365–367} Two relaxation regions can be clearly distinguished for the homopolymer. They are attributed, in order of increasing temperatures, to the $\beta(\alpha_a)$ and α_c processes. For blends, the kinetics of both processes are the same as the fraction of PMMA increases to 60% their intensity diminishes steadily without a change in the temperature of the ϵ'' maximum. The latter factor for the high-temperature process can be readily accounted for from the standpoint of the mechanisms of the α_c relaxation in PVDF. Indeed, as already mentioned, it can be attributed to motions of the chains in the crystals of the α modification of PVDF. A decrease in the fraction of the latter is therefore equivalent to a decrease in the number of crystals, which should lead to the observed decrease in the intensity of the peak without its displacement as regards temperature. The $\beta(\alpha_a)$ process is unusual. As mentioned above, according to the unanimous view of all investigators this process is attributed to the micro-Brownian motion of the chains in the amorphous region during glass transition. If the low-temperature peak for blends is also related to the glass transition, then it is impossible to account for the independence of the temperature of the above process as the fraction of PMMA in the blend increases. If the amorphous phase of PVDF is compatible with that in PMMA (this is indicated by the presence of a single glass transition temperature), then, as the fraction of the latter increases, the glass transition region should shift towards higher temperatures, as indicated by Eqn (27). The observed constancy of the low-temperature relaxation peak clearly conflicts with these conclusions.

This factor as well as the fact that the $\beta(\alpha_a)$ relaxation is observed distinctly only when the α_c process is detected made it necessary to postulate that the observed low-temperature process has to be related not to glass transition but to the motion in the interfacial region along the crystal–amorphous PVDF phase boundaries. The same idea has been developed in a study³⁶⁸ in which compatible PVDF blends were investigated, but this time with PEMA. Fig. 36 presents the temperature variations of the loss factor ϵ'' for this blend at a frequency of 200 kHz.

In contrast to PMMA, poly(ethyl methacrylate) has a lower glass transition temperature (60 $^{\circ}\text{C}$), so that yet another relaxation region (β_1) is observed together with the $\beta(\alpha_a)$ and α_c dispersions for blends with a high PVDF content. Comparison of DSC data shows that this relaxation region has to be attributed to the glass transition process in the mixed regions of the amorphous phase of PVDF and PEMA. It was found that the temperature variations of the relaxation frequencies for the

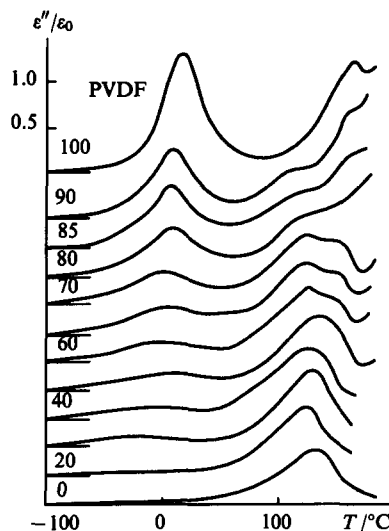


Figure 36. Temperature dependence of the loss factor at a frequency of 200 kHz in PVDF/PEMA blends.³⁶⁸ The numerals on the curves represent the fraction of PVDF in the blend.

homopolymer and the slowly cooled blends enriched in PVDF fit satisfactorily on a single relation. This made it possible to claim that the low-temperature relaxation region in PVDF and in its crystallisable blends with PEMA is associated with the mobility in the interfacial regions of the crystal. Furthermore, the fraction of such regions W_i may be estimated from the relation³⁶⁸

$$W_i = W - (W_c - W_m), \quad (30)$$

where W is the overall fraction of PVDF in the blend, W_c the fraction of the crystalline phase, and W_m the fraction of PVDF in the blended state. The last was estimated from T_g for the blend, while W_c was calculated from the enthalpy of fusion. The values of W_i were compared with the relaxation force $\Delta\epsilon$. It was shown that there is a linear relation between them. The maximum value of $\Delta\epsilon$ (5.5) corresponds to the relaxation in the homopolymer, for which the fraction of interfacial regions reaches 0.35. As can be seen, this value may constitute more than half the degrees of crystallinity in PVDF usually reported.

However, the view of Yoon et al.³⁶⁷ and Ando et al.³⁶⁸ concerning the nature of the low-temperature relaxation region in PVDF blends is not shared by everyone. Thus Saito and Stuhn³⁶⁹ questioned the validity of the conclusions reached. This is based on, for example, the temperature variations of the loss factor ϵ'' at two frequencies for pure PVDF and in blends with PMMA having the 60/40 composition (Fig. 37). Evidently the regions of the ϵ'' maximum for low-temperature relaxation at a high frequency are approximately the same for the homopolymer and the blend, as mentioned in the earlier studies.^{367, 368} However, at a frequency of 100 Hz the differences between the temperatures of the maxima are very striking. This served as a basis for the conclusion that it is not the α_a process but some other process which contributes to the low-temperature relaxation.

Fig. 38 presents comparative frequency dependences of ϵ'' in the glass transition region for pure PVDF and its blend with PMMA. Evidently, the peak for the homopolymer exhibits a high-frequency asymmetry, which was attributed to the contribution by the local mobility in the region of $\beta(\gamma)$ relaxation. The overall curve was subdivided into two components (α_a and β) by adjusting the experimental points to agree with the calculated ones with the aid of the empirical Havriliak–Negami relation:

$$\epsilon^*(\omega) = \epsilon_\infty + \frac{\epsilon_0 - \epsilon_\infty}{[1 + (i\omega\tau)^2]^\gamma}, \quad (31)$$

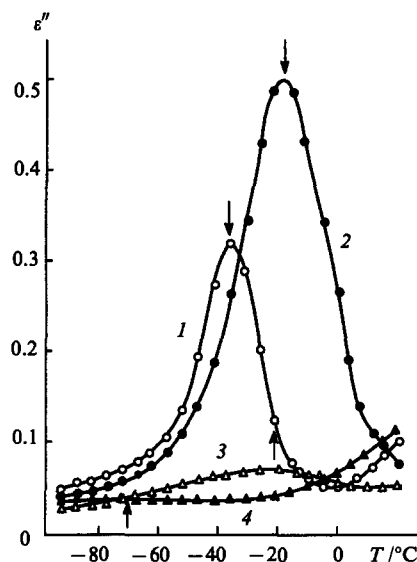


Figure 37. Temperature dependence of the loss factor in PVDF (1, 2) and in the PVDF/PMMA 60/40 blend (3, 4) at frequencies of 100 Hz (1, 4) and 10 kHz (3, 2).³⁶⁹

where the parameters $0 \leq \alpha$ and $\gamma \leq 1$ describe respectively the broadening and asymmetry of the relaxation time distribution function, while ϵ_0 and ϵ_∞ are the extrapolated static and high-frequency relative permittivities. At the temperature indicated in Fig. 38, the curve for the β process in PVDF is described satisfactorily by the parameters $\Delta\epsilon = 0.69$, $\lg v_m = 4.0$, $\alpha = 0.32$, and $\gamma = 1$.

The same frequency dependences of ϵ'' for the blend at the same temperature are presented in Fig. 38b, where the high-frequency maximum is described (after separation from the postulated low-frequency maximum) by the parameters $\Delta\epsilon = 0.43$, $\lg v_m = 4.3$, $\alpha = 0.34$, and $\gamma = 1$. As can be seen, the parameters of the β process for the homopolymer and the blend are virtually identical. This justifies the assumption that the low-temperature relaxation in PVDF/PMMA blends is determined by the contribution not of the α_a process but of the local mode of motion (β process). The temperature dependence of the relaxation frequencies in the blend and in the homopolymer are presented in Fig. 39. They confirm the above conclusion, since in both cases the relaxation frequencies and the activation energies (determined from the slopes of the relations presented) for the β and α_c process are virtually identical.

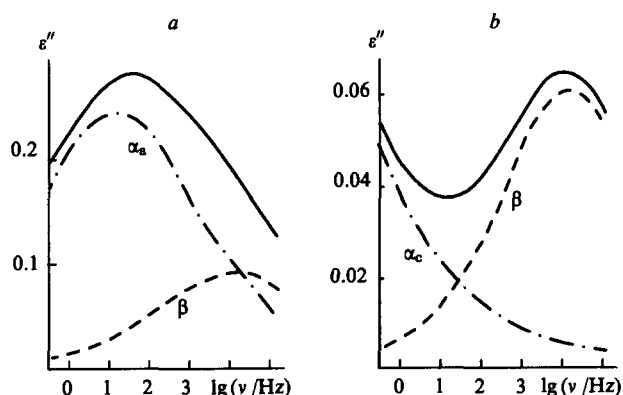


Figure 38. Frequency dependences of the loss factor at -40°C for pure PVDF (a) and for the PVDF/PMMA 60/40 blend (b).³⁶⁹ α_a , α_c , β — contributions of the corresponding relaxation regions.

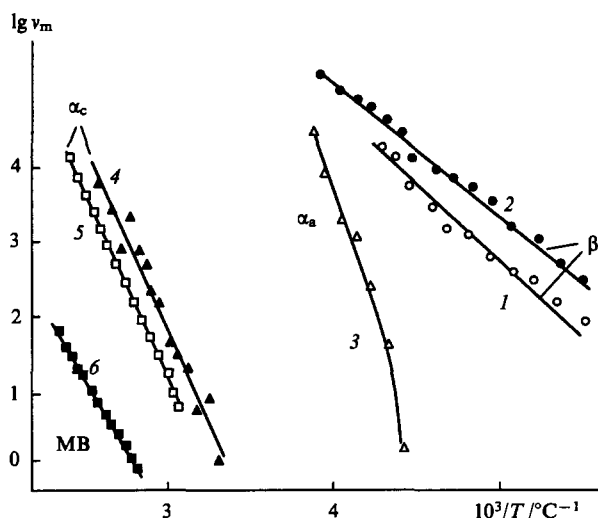


Figure 39. Temperature dependences of the relaxation frequencies in pure PVDF (1, 3, 4) and in the PVDF/PMMA 60/40 blend (2, 5, 6).³⁶⁹ α_a , α_c , β , MW — contributions of the corresponding relaxation regions.

The α_a process in the homopolymer cannot be described by the Arrhenius relation, as noted also by Ando et al.³⁶⁸ Ando et al.³⁶⁸ thought that one of the main arguments in support of their hypothesis is the agreement between the correlation frequencies for the homopolymer and the blend, which cannot be observed in the case of PVDF/PMMA according to the data of Saito and Stuhn.³⁶⁹ However, one can assume that there are no special contradictions in the experimental data of the two studies.^{368, 369} Indeed, the sections of the curve corresponding to the relaxation frequencies in the ranges $\nu > 10^4$ Hz and $\nu < 10^4$ Hz were discussed in the first and second studies respectively (Fig. 39). Evidently, with increase in frequency, the α_a and β relaxation processes approach one another and one may expect that they would coincide. Despite the rigorous quantitative analysis of the results for the low-temperature relaxation in PVDF/PMMA blends, the conclusions reached by Saito and Stuhn³⁶⁹ are nevertheless regarded as controversial. Indeed, if the low-temperature relaxation in the PVDF/PMMA blend is induced mainly by the contribution of the local β process in PVDF, then, under the conditions of the compatibility of the amorphous phases of both components, one has to postulate that the $\beta(\gamma)$ process in PVDF is associated with the local mobility precisely in the amorphous regions. However, this conclusion is not always confirmed experimentally, since there are data (see, for example, Osaki and Ishida²⁷⁵) showing that this process has to be related to the crystalline phase.

The demonstration by Saito and Stuhn³⁶⁹ that the characteristics of the interfacial regions at the amorphous phase–crystal boundary in the homopolymer and in the PVDF/PMMA blend differ significantly is more valuable. This is confirmed by the frequency dependences of ε'' at 90 °C for the PVDF/PMMA blend and the homopolymer (Fig. 40). Evidently they differ significantly: a maximum associated with the α_c relaxation, on which an intense rise in ε'' due to the occurrence of a vigorous low-frequency relaxation process via the Maxwell–Wagner (MW) interlayer polarisation mechanism is superimposed, has been observed for PVDF. As can be seen from Fig. 40a, the above relaxation process can be distinguished in the case of a blend, since the experimental ε'' points in the low-frequency region are satisfactorily fitted for the superposition of the MW process and when account is taken of the dc-conductivity. Compared with the homopolymer, the MW polarisation process in the blend is displaced towards higher frequencies. This made it possible to describe the given relaxation process in terms of the parameters of Eqn (31): $\Delta\varepsilon = 22.5$, $\lg\nu_m \approx 0.3$, $\alpha = 0.72$, and $\gamma = 1$.

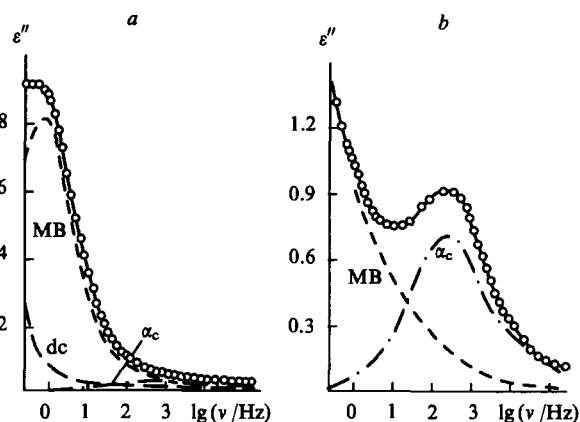


Figure 40. Frequency dependences of the loss factor at 90 °C in the PVDF/PMMA 60/40 blend (a) and in pure PVDF (b).³⁶⁹ Components: dc — dc conductivity; M = Maxwell–Wagner relaxation; α_c — α_c relaxation.

Thus the difference noted between the parameters of the MW polarisation in the homopolymer and in its blend with PMMA makes it possible to assume that, owing to the increased affinity of the chains of both components, PMMA fragments are inserted not only in the PVDF amorphous phase proper but also into the regions of the interfaces noted above. Only this hypothesis can explain (at least qualitatively) the observed differences, since the ratio of the relative permittivities and the mobility of the carriers in the region of the interfaces, which in fact control the MW polarisation processes, should change under these conditions.

It is of interest to examine the characteristics of the blending of PMMA not only with PVDF but also with its copolymers. In the first place, attention was turned to the VDF/TrFE copolymer, which gives rise to a ferroelectric phase immediately on crystallisation from the melt.³⁷⁰ The VDF/TrFE 78.5/21.5 copolymer was used and the blends were prepared by precipitation from solution in dimethylacetamide. As for the PVDF/PMMA blend, in the case of the copolymer an increase in the fraction of the amorphous component lowers the melting point of the PVDF crystals formed. Taking this into account, the Flory–Huggins parameter was estimated from Eqn (29) as -0.329 , which is less than in the case of the homopolymer. This means that the introduction of TrFE into the VDF chain of the monomer promotes an intensification of the interaction between these blend components. It may be that this accounts for a series of the features noted below.

X-Ray diffraction data have shown that an increase in the fraction of PMMA in the blend with the copolymer hardly affects the unit cell parameters of the ferroelectric phase and leads merely to a decrease in its volume fraction. Crystallisation persists even in 65/35 blends and both the Curie and melting points change little under these conditions. The degree of crystallinity diminishes linearly with increase in the fraction of PMMA to 40% and for its higher values the blend is obtained in the amorphous state. Comparison of IR spectroscopic data and the concentrations of the groups of the copolymer in the 'planar zigzag' and $TGT\bar{G}$ conformations showed that the introduction of PMMA into the copolymer promotes an increase in the concentration of the former.

The copolymer considered comprises two polar comonomers. It is of interest to proceed to the consideration of a VDF copolymer in which the second comonomer is nonpolar. A fairly high fraction of this comonomer may affect the mechanism of the interaction of the blend components, since specific interactions between the PMMA chains and a nonpolar comonomer may be disturbed. The most suitable compound for this purpose is the copolymer of VDF with tetrafluoroethylene, which, like the

previous copolymer, can give rise to a ferroelectric phase in the isotropic state.³⁷¹

The use of the VDF/TFE 80/20 copolymer, the properties of which are similar to those of the VDF/TrFE copolymer, made it possible to test the role of the polarity of the second monomer. The monotonic variation of the refractive index and the single glass transition temperature obtained on varying the composition ratio indicate that the above blends are compatible. Analysis of X-ray data has shown that crystallisation ceases when the fraction of the copolymer is less than 70%. Evidently this corresponds approximately to the critical value for VDF/TrFE copolymer in a blend with PMMA (~65%). This similarity is most probably associated with the fact that in both copolymers crystallisation proceeds with formation of the polar ferroelectric β phase. For higher contents of PMMA in the blend with the VDF/TFE copolymer, the latter no longer crystallises. The nature of the amorphous halo indicates the compatibility of the components in the nonordered state: with increase in the fraction of PMMA, the angular position of the halo shifts monotonically towards lower angles as a consequence of the increase in the average distances between the molecules.

The different chemical composition of the second comonomer is, however, manifested in a different way. Yet another endotherm, associated with the phase separation process, which is recorded also from the appearance of the turbidity point, has been noted on the DSC curves in the range of temperatures above the melting point. Both methods yielded approximately similar characteristic temperatures, but, what is most interesting, the turbidity point varied very significantly. The variation may be described by a curve with a minimum as a function of the increase in the fraction of the copolymer in the blend. It has been shown that a maximum variation of the enthalpy of phase separation corresponds to the region of the minimum in the phase separation point. The Flory-Huggins parameter is then found to depend on the composition, but remains negative over the entire concentration range. The increase in this parameter as the concentration of the copolymer is reduced shows that PMMA-enriched blends are characterised by a weaker interaction of the components. This has also been noted for the PVDF/PMMA blend³³² on the basis of small angle X-ray scattering data. The specific role of the nonpolar comonomer TFE in PVDF chains most probably attributes to the fact that the lowest values of B are found to be higher than for the blend of pure PVDF and PMMA.

From the practical point of view, it is important to have compatible PVDF blends with a high glass transition temperature. For this purpose, it is of interest to consider as the blend component the noncrystallising highly polar polyvinylpyrrolidone (PVP), the glass transition temperature of which is ~200 °C. The above components are satisfactorily compatible in the melt.^{372,374} It was observed that the introduction of PVP greatly reduces the melting point of the PVDF crystals, the formation of which is fully inhibited for a PVP content of ~40 mass %. The melting point depends on the molecular mass of PVP and decreases with increase in the fraction of the latter. Analysis of the details of the dynamic relaxation in the above systems shows that a decrease in the fraction of PVP in noncrystallising heterogeneous blends with PVDF leads to a significant decrease also in the glass transition temperature: for a PVP fraction of 0.4, it diminishes to ~120 °C.³⁷⁴

If the PVDF/PVP blends crystallise, then the presence of three-phases is noted: the crystals of PVDF, homogeneously blended domains with a quasi-constant composition, and the purely amorphous PVDF phase. In view of the very low Flory-Huggins parameter, very strong interactions are postulated between the components of the blend in the second phase.

The possibility of regulating the energy of the specific interactions of the components can be ensured by introducing ions into the polymer chain. In this connection, it is of interest to examine the questions concerning structure formation in a blend of PVDF with the tetrafluoroethene-perfluorovinyl ether copolymer with a sulfonic acid group at the end [Nafion (NAF)].³⁷⁵ In the study of

the morphology on crystallisation of PVDF in such a blend, obtained by precipitation from dimethylacetamide and dimethylformamide, it was shown that the average size of the spherulite is always greater when the component ratio is approximately equal. Mixed spherulites of the α and γ modifications have been observed for the PVDF/NAF 40/60 and 60/40 blends, as in pure PVDF under certain crystallisation conditions. The size and shape of the spherulites formed depend not only on the blend composition but also on the film deposition temperature. α Spherulites grow predominantly at 150 °C, whereas the small spherulites of the γ phase grow mainly at 70 and 90 °C. The latter property is new compared with pure PVDF and is apparently due to the presence of the ionomer.

An increase in temperature in a film of a blend with a spherulitic morphology to 185 °C is accompanied by the disappearance of spherulites when the system melts. However, a further increase in temperature leads to a catastrophic growth of scattering intensity (for parallel polarisers) and a displacement of the scattering region towards small angles. This is attributed to the thermoinduced phase separation of the spinodal type. By resorting to dielectric relaxation data in the region of the α_c transition, it was possible to establish that the temperature of the maximum increases linearly with increase in the fraction of NAF. On this basis, it is concluded that this pair of components is partly compatible as a result of the specific interactions between the PVDF groups and NAF ions. A detailed study of the kinetics of the phase separation (above the melting point of PVDF) showed that the characteristic point may depend significantly on the heating rate. At a constant heating rate (0.2 K min⁻¹), the turbidity point varies as a function of blend composition along a curve with a minimum for a blend with 60 mass% of NAF. Treatment of the experimental data from the standpoint of the scaling theory has shown that, for a small thickness of the blend films (10 μ m), the growth of domains with concentration fluctuations in the region of the phase separation is more likely to be two-dimensional in character.

One may deal separately with the results of several studies in which problems of compatibility in blends of PVDF with an other crystallisable polymer were considered. The blends of PVDF with poly(vinyl fluoride) (PVF) have been investigated in greatest detail in this connection.^{376,377} The results of X-ray analysis have shown that the phenomenon of isomorphism (crystallisation of both components with the same lattice) is characteristic of them for virtually any component ratio.³⁷⁶ The reason for this is apparently the identity of the chemical bonds in the repeat units of the monomers and hence the similarity of the lattices of each polymer. Thus the most intense intermolecular reflection due to the β phase is characterised by the interplanar spacings $d = 4.31$ Å in PVF and 4.39 Å in PVDF. It is significant that even small amounts of PVF added to PVDF stabilise the 'planar zigzag' conformation in the latter.³⁷⁶

The same feature has been noted also for the blend of PVDF with another crystallisable polymer — poly(ethylene glycol).³⁷⁸ The manifestation of cocrystallisation effects has also been observed for the blend of PVDF with the chlorotrifluoroethylene/VDF 77/23 copolymer. Under the conditions of the preparation of blend films from a common solvent, a single melting endotherm due to the fusion of the PVDF crystals is manifested, the melting point shifting insignificantly towards lower temperatures as the PVDF fraction is diminished. At the same time, this leads to an appreciable decrease in the degree of crystallinity and in the size of the spherulites. The authors tend to see the significant difference between the degrees of crystallinity α in the blend with 10% of PVDF compared with the pure homopolymer, taking into account its fraction in the blend, as the manifestation of the cocrystallisation effects in the above blends: whereas $\alpha = 53\%$ for PVDF, for the blend with 10% of the homopolymer (in the case of a noncrystallisable copolymer) α should be 5.3%, but the actually observed value is 9.9%.

The practical tasks in the search for new materials with high piezoelectric characteristics suggest the creation of composite systems with classical inorganic ferroelectric fillers (of the type of BaTiO_3), which are introduced into the organic polymer matrix. In this connection, the specific interactions between PVDF and PMMA, in particular, may be reflected also in the final piezoelectric properties. Indeed, the three-layer dielectric in the form of PVDF combined with PMMA (filled with BaTiO_3) has a high piezoelectric constant d_{33} , which, however, is insufficiently stable. An increase in d_{33} may be attained in another system, where the buffer layer consists of a polyetherurethane elastomer,³⁸⁰ the highly polar groups of which may stabilise the structure and hence the piezoelectric properties as a result of the interaction with the corresponding fragments of the PVDF chains.

The filling of PVDF simply with BaTiO_3 particles is also of practical interest, since the latter have a higher Curie temperature, which makes it possible, in principle, to obtain a combined material not only with high piezoelectric characteristics but also with a wider range of temperatures at which it can be employed. Possible structural modifications both in PVDF and in the particles of the added filler have been suggested for this purpose.^{381,382} The X-ray diffraction method, employed for the same purpose, has been applied over a wide range of scattering angles in order to isolate nonoverlapping reflections from individual blend components. Pure PVDF crystallised as the α modification while the introduction of even 10% of BaTiO_3 greatly reduced the intensity of the corresponding reflections, which can be explained by a decrease in the degree of crystallinity. The observation of the characteristic reflections for BaTiO_3 with increase in its content in the blend indicates that they are somewhat displaced into the region of smaller angles. This is treated as evidence for the appearance of internal stresses in such composites.

Finally, one should deal with yet another study on PVDF blends with inorganic fillers. This concerns PVDF composites with $\gamma\text{-Fe}_2\text{O}_3$ particles.³⁸³ The author's aim was to test the occurrence of the thermal decomposition of $\text{Fe}(\text{CO})_5$ in a chemically inert matrix. However, this study may be regarded as a contribution to the development of a new method for the preparation of materials with an interesting combination of electrical and magnetic properties.

The formation of fine $\gamma\text{-Fe}_2\text{O}_3$ particles as a result of the decomposition reactions of the initial compounds is accompanied primarily by the formation of an insoluble polymer. These processes are most probably actually responsible for the fact that, on crystallisation of PVDF, the large spherulites (which arise in the homopolymer) are no longer observed in the blend, while the mechanical characteristics of the latter change significantly in the region of the high elasticity plateau. Optical microscope and small angle X-ray scattering data indicate that the degree of crystallinity in blends diminishes significantly. Analysis of the morphology of the blends produced clearly indicates the occurrence of processes involving the phase separation of the components. The cluster structure was typically analysed by the method of X-ray probes and it was found that the concentration of iron within the particles is higher than in the surrounding polymer matrix. Analysis of X-ray and electron diffraction indicates the possibility of the occurrence of reactions between the magnetic particles and PVDF with formation of FeF_2 compounds. It is believed that the latter are produced in the course of the formation of a three-dimensional network in the polymer matrix. On the other hand, most of the disperse phase has the $\gamma\text{-Fe}_2\text{O}_3$ structure. The proposed method is promising for the preparation of organic materials containing small magnetic particles (the size of the latter is 50–100 Å).

X. Conclusion

The possibilities of the polymorphic transformations in PVDF and in its copolymers under the influence of various external factors have been analysed in the present review. It has been

shown that a particular crystallographic modification may be obtained not only as a result of the operation of various physical factors but also as a result of the introduction into the PVDF chain of, for example, 'head to head' defects or certain comonomers. It is significant that the specific effects of the solvent can also be used as an effective factor in the formation of particular structure of PVDF films from appropriate solutions. It is emphasised that the concentration and type of ionogenic impurities in solution can then affect the type of the polymorphic modification formed.

The operation of factors such as high pressure and tensile deformation are used for practical applications, where one needs to obtain polar modifications of PVDF, for example for pyro- and piezo-electric transducers. Examination of the polymorphism in PVDF induced by high electric fields may be used, on the one hand, to discover the fundamental characteristics of the behaviour of polymeric dielectrics in electric fields and, on the other, for recommendations concerning the practical preparation of the active elements used in the energy converters mentioned above. It has been shown in relation to a series of recent studies that yet another (nontraditioned) method for the modification of the structure of PVDF and crystallising polymers in general is irradiation.

The characteristics of the dynamics of polymer chains in PVDF and its copolymers may serve as a basis for the prediction of the occurrence of relaxation processes in the systems considered, which is important for the creation of materials with stable and specified properties.

It is shown that specific modification of the structures of the polymer systems considered may be achieved also with the aid of blends with polymers and nonpolymeric components. In a number of cases, it is possible to improve by this procedure certain optical characteristics of the materials formed, which makes them competitive in relation to other materials used in elements with nonlinear optical properties.

References

1. H Kawai *Jpn. J. Appl. Phys.* **8** 975 (1969)
2. G M Sessler *J. Acoust. Soc. Am.* **70** 1596 (1981)
3. V V Kochervinskii *Usp. Khim.* **63** 383 (1994) [*Russ. Chem. Rev.* **63**]
4. C W Wilson *J. Polym. Sci. Part A, Polym. Chem.* **1** 1305 (1963)
5. R C Ferguson, E G Brame *J. Phys. Chem.* **83** 1397 (1979)
6. V A Lovchikov, A M Shlyakov, I M Dolgopolskii *Issledovanie Stroeniya Makromolekul Metodom YaMR Vysokogo Razresheniya* (Investigation of the Structure of Macromolecules by the High-Resolution NMR Method) (Moscow: TsNIIITEI Nefteperer. Neftekhim. Prom., 1983)
7. R C Ferguson, D W Ovenall *Am. Chem. Soc. Polym. Prepr.* **25** 340 (1984)
8. A E Tonelli, F C Schilling, R E Cais *Macromolecules* **15** 849 (1982)
9. F A Bovey, F C Schilling, T K Kwey, H L Frish *Macromolecules* **10** 559 (1977)
10. A E Tonelli, F C Schilling, R E Cais *Macromolecules* **14** 560 (1981)
11. F C Schilling *Am. Chem. Soc. Polym. Prepr.* **22** 407 (1981)
12. M Bruch, F A Bovey, R E Cais *Macromolecules* **17** 2547 (1984)
13. R E Cais, J M Kometani *Macromolecules* **18** 1334 (1985)
14. V P Sass, A S Shashkov, A I Konkin, R I Rabinovich, I M Dolgopolskii, V S Sokolov *Vysokomol. Soedin., Ser. A* **17** 1086 (1975)
15. T Yagi, M Tatemoto *Polym. J.* **11** 429 (1979)
16. E M Murasheva, A S Shashkov, A A Dontsov *Vysokomol. Soedin., Ser. A* **23** 632 (1981)
17. R E Cais, J M Kometani *Anal. Chim. Acta.* **189** 101 (1986)
18. J Ando, H Kobayashi, R Chuio, in *Proceedings of the US-Japanese Polymer Symposium* (New York: Springer, 1984) p. 173
19. B Servet, D Bruussoux, F Micheron, R Bisaro, S Res, P Merenda *Rev. Techn. Thomson-CSF* **12** 761 (1980)
20. E L Gal'perin, Yu V Strogalin, M P Mlenik *Vysokomol. Soedin.* **7** 933 (1965)
21. G Cortili, G Zerbi *Spectrochim. Acta* **23A** 285 (1967)

22. G Cortili, G Zerbi *Spectrochim. Acta* **23A** 2216 (1967)
23. F J Boerio, J G Koenig *J. Polymer Sci., Part A, Polym. Chem.* **9** 1517 (1971)
24. G Cessae, J G Curro *J. Polym. Sci., Polym. Phys. Ed.* **12** 695 (1974)
25. M Kobayashi, K Tashiro, H Tadokoro *Macromolecules* **8** 158 (1975)
26. M Bachmann, W J Gordon, J I Koenig, J B Lando *J. Appl. Phys.* **50** 6106 (1979)
27. M Kobayashi, K Tashiro, H Tadokoro *Macromolecules* **14** 1757 (1981)
28. M Latour, A Montaner, M Galtier, G Geneves *J. Polym. Sci., Polym. Phys. Ed.* **19** 1121 (1981)
29. L Lanchlan, J F Rabolt *Macromolecules* **19** 1049 (1986)
30. L N Pirozhnaya, O B Zubkova, L A Gribov *Zh. Prikl. Spektrosk.* **48** 65 (1988)
31. G Borinetti, G Zannoni, G Zerbi *J. Mol. Struct.* **224** 425 (1990)
32. V V Kochervinskii, V A Glukhov, V G Sokolov, V F Romadin, E M Murasheva, Yu K Ovchinnikov, N A Trofimov, B V Lokshin *Vysokomol. Soed., Ser. A* **30** 1969 (1988)
33. V V Kochervinskii *Vysokomol. Soed., Ser. A* **33** 2106 (1991)
34. N N Makarevich *Zh. Prikl. Spektrosk.* **7** 341 (1965)
35. N N Makarevich, N I Sushko *Zh. Prikl. Spektrosk.* **11** 917 (1969)
36. W W Doll, J B Lando *J. Macromol. Sci., Phys.* **B2** 205 1968
37. S Weinhold, M A Bachmann, M H Litt, J B Lando *Macromolecules* **15** 1631 (1982)
38. M Latour, N Abo Dorro, J L Galigne *J. Polym. Sci., Polym. Phys. Ed.* **22** 345 (1984)
39. K Okuda, T Yoshida, M Sugito, M Asahina *J. Polym. Sci., Polym. Phys. Ed.* **5** 465 (1967)
40. E L Gal'perin, B P Kosmynin, R A Bychkov *Vysokomol. Soed., Ser. B* **12** 555 (1970)
41. E L Gal'perin, Doctoral Thesis in Chemical Sciences, Karpov Physicochemical Research Institute, Moscow, 1980
42. E L Gal'perin, V F Mindrul, N I Nikanorova, N I Titanskaya *Vysokomol. Soedin., Ser. B* **14** 37 (1972)
43. R L Miller, J J Raison *J. Polym. Sci., Polym. Phys. Ed.* **14** 2325 (1976)
44. D T Grubb, K W Choi *J. Appl. Phys.* **52** 5908 (1981)
45. D T Grubb, P Cebe, K W Choi *Ferroelectrics* **57** 12 (1984)
46. A Chapiro, Z Mankowski, N Schmitt *J. Polym. Sci., Polym. Chem. Ed.* **20** 1791 (1982)
47. V V Kochervinskii, V A Glukhov, V G Sokolov, L Ya Modorskaya, B V Lokshin *Vysokomol. Soed., Ser. A* **31** 2590 (1989)
48. V V Kochervinskii, V A Glukhov, V G Sokolov, B I Ostrovskii *Vysokomol. Soed., Ser. A* **31** 154 (1989)
49. A J Lovinger *Polymer* **22** 412 (1981)
50. A S Lovinger *Macromolecules* **14** 322 (1981)
51. C M Balik, R Farmer, E Baer *J. Mater. Sci.* **14** 1511 (1979)
52. E L Gal'perin, S S Dubov, E V Volkova, M P Mlenik, L A Bul'ygina *Vysokomol. Soedin.* **8** 2033 (1966)
53. E L Gal'perin, B P Kosmynin, V F Mindrul, V K Smirnov *Vysokomol. Soed., Ser. B* **12** 594 (1970)
54. W W Doll, J B Lando *J. Appl. Polym. Sci.* **14** 1767 (1970)
55. J Hoshi *Mod. Plast.* **48** 110 (1971)
56. R Liepins, J R Surlis, N Morosoff, V J Stannett *J. Polym. Sci., Polym. Chem. Ed.* **16** 3039 (1978)
57. L N Pirozhnaya, V Ya Maksimov, L I Tarutina, L Ya Madorskaya *Zh. Prikl. Khim.* **55** 2758 (1982)
58. L Ya Madorskaya, N I Loginova, N E Shadrina, M S Kleshcheva, Yu A Panshin *Vysokomol. Soed., Ser. B* **22** 904 (1980)
59. L Ya Madorskaya, N N Loginova, A M Lobanov, Yu A Panshin *Vysokomol. Soed., Ser. A* **25** 2144 (1983)
60. E G Erenburg, L V Pavlova, A I Konshin, A M Greis, I P Dolgopol'skii, I T Poddubnyi *Vysokomol. Soed., Ser. A* **25** 365 (1983)
61. L Ya Madorskaya, M V Samoilov, G A Otradina, M P Agapitov, V P Budtov, T G Mksenko, E Yu Kharcheva, N H Loginova *Vysokomol. Soed., Ser. A* **26** 2577 (1984)
62. V V Kochervinskii, T E Danilyuk, L Ya Modorskaya *Vysokomol. Soed., Ser. A* **28** 619 (1986)
63. L Ya Madorskaya, N N Loginova, L P Kastorskii, O V Kuz'michev, V L Maksimov, A M Lobanov *Vysokomol. Soed., Ser. A* **28** 1284 (1986)
64. R E Cais, N J A Sloane *Polymer* **24** 179 (1983)
65. G A Otradnaya, L Ya Madorskaya, V M Belyaev, K A Vylegzhanina, O K Belomutskaya, T V Kornilova *Vysokomol. Soed., Ser. A* **32** 872 (1990)
66. S Weinhold, M A Backmann, M H Litt, J B Lando *Macromolecules* **15** 1631 (1982)
67. W W Doll, J B Lando *J. Macromol. Sci.* **4B** 309 (1970)
68. S Weinhold, M H Litt, J B Lando *J. Appl. Phys.* **51** 5145 (1980)
69. S Weinhold, M H Litt, J B Lando *Macromolecules* **13** 1178 (1980)
70. M A Bachmann, J B Lando *Macromolecules* **14** 40 (1981)
71. G Welch, R L Miller *J. Polym. Sci., Polym. Phys. Ed.* **14** 1683 (1976)
72. C Mancarella, E Martuselli *Polymer* **18** 1240 (1977)
73. Y S Yadav, P C Jain *J. Macromol. Sci., Phys.* **25** 335 (1984)
74. L T Chen, C W Frank *Ferroelectrics* **57** 51 (1984)
75. P J Flory *Trans. Faraday Soc.* **51** 848 (1955)
76. J C Sanchez, R K Eby *J. Res. Natl. Bur. Stand. A, Phys. Chem.* **77** 353 (1973)
77. B L Farmer, A J Hopfinger, J B Lando *J. Appl. Phys.* **43** 4293 (1972)
78. K Nakagawa, Y Ishida *J. Polym. Sci., Polym. Phys. Ed.* **11** 2153 (1973)
79. S Osaki, Y Ishida *J. Polym. Sci., Polym. Phys. Ed.* **13** 1071 (1975)
80. W M Prest, D J Luca *J. Appl. Phys.* **46** 4136 (1975)
81. W M Prest, D J Luca *J. Appl. Phys.* **49** 5042 (1978)
82. A J Lovinger, H D Keith *Macromolecules* **12** 919 (1979)
83. A J Lovinger *J. Polym. Sci., Polym. Phys. Ed.* **18** 793 (1980)
84. A J Lovinger *Polymer* **21** 1317 (1980)
85. A J Lovinger, M Freed *Macromolecules* **13** 989 (1980)
86. B S Morra, R S Stein *J. Polym. Sci., Polym. Phys. Ed.* **20** 2261 (1982)
87. L T Chen, C W Frank *Macromolecules* **18** 2163 (1985)
88. N C Banik, F P Boyle, T J Sluckin, P L Taylor, S K Tripathy, A J Hopfinger *Phys. Rev. Lett.* **43** 456 (1979)
89. N C Banik, P L Taylor, S K Tripathy, A J Hopfinger *Macromolecules* **12** 1015 (1979)
90. N C Banik, F P Boyle, T J Sluckin, P L Taylor, S K Tripathy, A J Hopfinger *J. Chem. Phys.* **72** 3191 (1980)
91. Y Takahashi, M Kohyama, H Tadokoro *Macromolecules* **9** 870 (1976)
92. Y Takahashi, H Tadokoro *Macromolecules* **13** 1316 (1980)
93. Y Takahashi, H Tadokoro, A Odajima *Macromolecules* **13** 1318 (1980)
94. Y Takahashi, Y Matsubara, H Tadokoro *Macromolecules* **13** 334 (1982)
95. Y Takahashi *Kobunshi* **33** 696 (1984)
96. Y Takahashi *Polym. J.* **15** 733 (1983)
97. Y Takahashi, H Tadokoro *Ferroelectrics* **57** 187 (1984)
98. A J Lovinger *J. Appl. Phys.* **52** 5934 (1981)
99. C C Hsu, P H Geil *J. Appl. Phys.* **56** 2404 (1984)
100. C C Hsu, P H Geil *Polym. Commun.* **27** 105 (1986)
101. D-C Yang, Y Chen *J. Mater. Sci. Lett.* **6** 599 (1987)
102. D-C Yang, Y Chen, D-D Song *Chem. J. China. Univ.* **14** 1325 (1993)
103. Y Oka, N Koizumi *Bull. Inst. Chem. Res. Kyoto Univ.* **63** 192 (1985)
104. K Loufakis, B Wunderlich *Polymer* **26** 1875 (1985)
105. R Loufakis, B Wunderlich *Macromolecules* **20** 2471 (1987)
106. Y Takahashi *Polym. J.* **15** 733 (1983)
107. T Yagi *Kindzoku Khemen Gidzyutsu (J. Metal. Finish. Soc. Jpn.)* **37** 640 (1986)
108. A J Lovinger, G T Davis, T Furukawa, M G Broadhurst *Macromolecules* **15** 323 (1982)
109. K Tashiro, K Takano, M Kobayashi, Y Chatani, H Tadokoro *Polymer* **25** 195 (1984)
110. H Yasegawa, M Kobayashi, H Tadokoro *Polym. J.* **3** 591 (1972)
111. R Hasegawa, Y Takanashi, Y Chatani, H Tadokoro *Polym. J.* **3** 600 (1972)
112. Y Oka, Y Murata, N Koizumi *Polym. J.* **18** 417 (1986)
113. K Tashiro, H Kaito, M Kobayashi *Polymer* **33** 2915 (1992)
114. B B Kochervinskii, V A Glukhov, V F Romadin, V G Sokolov, B V Lokshin *Vysokomol. Soed., Ser. A* **30** 1916 (1988)
115. V V Kochervinskii, N N Kuz'min, A N Zadorin *Vysokomol. Soedin.* (1997) (in the press)

116. V V Kochervinskii, N N Kuzmin, in *Proceedings of the Fifth Russian-Japanese Symposium on Ferroelectricity* (Moscow: Moscow State Univ., 1994) p. 132
117. V V Kochervinskii, N N Kuz'min *Neorg. Mater.* **31** 859 (1995)
118. V V Kochervinskii, N N Kuz'min, in *Proceedings of the International Symposium "Ferro-Piezoelectric Materials and their Applications"* (Moscow: Karpov Physicochemical Research Institute, 1994) RO-2-22
119. S Roussel, K L Mgelroy, L N Judovits *Polym. Eng. Sci.*, **32** 1300 (1992)
120. R Gregorio M Cestari *J. Polym. Sci., Part B, Polym. Phys.* **32** 859 (1994)
121. J B Lando, H G Olf, A Peterlin *J. Polym. Sci., Polym. Chem. Ed.* **4** 941 (1966)
122. B P Kosmynin, E L Gal'perin, D Ya Tsvankin *Vysokomol. Soed., Ser. A* **12** 1254 (1970)
123. B P Kosmynin, E L Gal'perin, D Ya Tsvankin *Vysokomol. Soed., Ser. A* **14** 1365 (1972)
124. K Matsushige, T Takemura *J. Polym. Sci., Polym. Phys. Ed.* **18** 1665 (1980)
125. U Kofer, R Hirte *Acta Polym.* **34** 352 (1983)
126. U Kofer, R Hirte *Acta Polym.* **33** 434 (1982)
127. K Matsushige, T Takemura, in *Proceedings of the 55th Meeting of the American Chemical Society, Atlanta, 1983* No 4, p. 1
128. E L Nix, L Holt, J C McGrath *Ferroelectrics* **32** (1-4) 103 (1981)
129. V V Kochervinskii, V F Romadin, V A Glukhov, V G Sokolov, M A Saidakhmetov *Vysokomol. Soed., Ser. A* **31** 1381 (1989)
130. V V Kochervinskii, V A Glukhov, V G Sokolov, V F Romadin, B I Ostrovskii, S Yu Kuznetsova *Vysokomol. Soed., Ser. A* **31** 2311 (1989)
131. J Clements, G R Davies, I M Ward *Polymer* **26** 208 (1985)
132. D K Das-Gupta, D B Shier *J. Appl. Phys.* **49** 5685 (1978)
133. B Servet, D Broussoux, F Micheron *Rev. Tech. Thomson-CSF* **12** 796 (1980)
134. B Servet, D Broussoux, F Micheron *J. Appl. Phys.* **52** 5926 (1981)
135. B Servet, D Broussoux, F Micheron, R Bisaro, S Ries, P Merenda *Rev. Techn. Thomson-CSF* **12** 761 (1980)
136. C H Wang, D B Cavanaugh, Y Hashidaki *J. Polym. Sci., Polym. Phys. Ed.* **19** 941 (1981)
137. J Humpreys, I M Ward, E L Nix, J C McGrath *J. Appl. Polym. Sci.* **30** 4069 (1985)
138. T Mizuno, K Nakamura, N Murayama, K Okuda *Polymer* **26** 853 (1985)
139. T C Hsu, P H Geil *J. Mater. Sci.* **24** 1219 (1989)
140. T Konaka, S Nakagawa, S Yamakawa *Polymer* **26** 462 (1985)
141. Y Takeuchi, K Nakagawa, S Yamikawa *J. Polym. Sci., Polym. Phys. Ed.* **23** 1193 (1985)
142. Y Takeuchi, K Nakagawa, F Yamamoto *Polymer* **26** 1929 (1985)
143. K Nakagawa, M Amano *Polym. Commun.* **27** 310 (1986)
144. K Spector, R S Stein *Macromolecules* **24** 2083 (1991)
145. A G Kolbek, D R Uhlmann *J. Polym. Sci., Polym. Phys. Ed.* **15** 27 (1977)
146. W T Mead, A E Zachariades, T Shimada, R S Porter *Macromolecules* **12** 473 (1979)
147. T Shimada, A E Zachariades, W T Mead, R S Porter *J. Cryst. Growth* **48** 334 (1980)
148. E M Berg, D C Sun, J H Magill *Polym. Eng. Sci.* **29** 715 (1989)
149. A J Lovinger, T T Wang *Polymer* **20** 725 (1979)
150. D T Grubb, F R Kearney *J. Polym. Sci., Part B, Polym. Phys.* **28** 2071 (1990)
151. J C McGrath, L Holt, D M Jones *Ferroelectrics* **50** 339 (1983)
152. G W Andrews, A R Piercy *J. Mater. Sci. Lett.* **5** 969 (1986)
153. P Leaver, M I Cunningham *J. Mater. Sci. Lett.* **6** 705 (1987)
154. E L V Levis, I M Ward *J. Polym. Sci., Part B, Polym. Phys.* **27** 1375 (1989)
155. V V Kochervinskii *Neorgan. Mater.* **31** 851 (1995)
156. V V Kochervinskii, in *Proceedings of the International Symposium "Ferro-Piezoelectric Materials and their Applications"* (Moscow: Karpov Physicochemical Research Institute, 1994) 0-7-6
157. V V Kochervinskii, V A Glukhov, V G Sokolov, B V Lokshin *Vysokomol. Soedin., Ser. A* **31** 282 (1989)
158. R M Cohil, J Petermann *Polymer* **22** 1612 (1981)
159. Y Takahashi, A Odajima *Rep. Progr. Polym. Phys. Jpn.* **23** 161 (1980)
160. V V Kochervinskii, V G Sokolov *Vysokomol. Soedin., Ser. A* **33** 1625 (1991)
161. J Frile *Makromol. Chem., Makromol Symp.* **72** 131 (1993)
162. Y Takahashi, T Zakoh, N Hanatani *Colloid Polym. Sci.* **269** 781 (1991)
163. V V Kochervinskii, V A Glukhov, S Yu Kuznetsova *Vysokomol. Soed., Ser. A* **29** 1530 (1987)
164. W W Doll, J B Lando *J. Macromol. Sci., Phys.* **B2** 219 (1968)
165. W W Doll, J B Lando *J. Macromol. Sci., Phys.* **B4** 889 (1970)
166. W W Doll, J B Lando *J. Macromol. Sci., Phys.* **B4** 897 (1970)
167. R Hasegawa, Y Tanabe, M Kobayashi, H Tadokoro *J. Polym. Sci., Part A, Polym. Chem.* **8** 1079 (1970)
168. J Scheinbien, C Nakafucu, B A Newman, K D Pae *J. Appl. Phys.* **50** 4399 (1979)
169. B A Newman, C H Yoon, K D Pae *J. Mater. Sci.* **14** 2391 (1979)
170. K D Pae, C Vijayan, R Renfree, K T Chung, J I Schenbeim, B A Newman *Ferroelectrics* **57** 245 (1984)
171. K Matsushige, K Nagata, T Takemura *Jpn. J. Appl. Phys.* **17** 467 (1978)
172. K Matsushige, T Takemura *J. Polym. Sci., Polym. Phys. Ed.* **16** 921 (1978)
173. K Matsushige, T Takemura *J. Cryst. Growth* **48** 343 (1980)
174. K Matsushige, T Takemura *J. Polym. Sci., Polym. Phys. Ed.* **18** 1665 (1980)
175. K Matsushige, K Nagata, I Imada, T Takemura *Polymer* **21** 1391 (1980)
176. A I Ozerin, M B Konstantinopol'skaya, Yu A Zubov *Vysokomol. Soed., Ser. A* **16** 2511 (1974)
177. K Sakuoku, T Itoh, S Kunimura *Jpn. J. Appl. Phys. Pt 2* **24** 175 (1985)
178. G A Samara *J. Polym. Sci., Part B, Polym. Phys.* **27** 39 (1989)
179. T Horiashi, K Matsushige, T Takemura *Jpn. J. Appl. Phys.* **25** L 465 (1986)
180. E Akacuge, S Taki, T Horiuchi *Kyusyu Daigaku Kagaku Syukho* **59** 655 (1986)
181. H Ohigashi, T Watanabe, G R Li, T Hattori, S Takanashi *Jpn. J. Appl. Phys.* **1** 30 111 (1991)
182. M Hikosaka, K Sakurai, H Ohigashi, T Koizumi *Jpn. J. Appl. Phys.* **1** 32 2029 (1993)
183. M Hikosaka, K Sakurai, H Ohigashi, A Keller *Jpn. J. Appl. Phys.* **1** 33 214 (1994)
184. R G Kepler, R A Anderson *J. Appl. Phys.* **49** 1232 (1978)
185. D K Das-Gupta, K Doughty *J. Phys. J. Appl. Phys.* **11** 2415 (1978)
186. D K Das-Gupta, K Doughty *IEEE Trans. Ind. Appl.* **1A-14** 448 (1978)
187. D Naeegele, D Y Yoon, M G Broadhurst *Macromolecules* **11** 1297 (1978)
188. G T Davis, J E McKinney, M G Broadhurst, S S Roth *J. Appl. Phys.* **49** 4998 (1978)
189. G T Davis, H Scugh *Polymer* **20** 772 (1979)
190. D K Das-Gupta, K Doughty, D B Shier *J. Electrostat.* **7** 267 (1979)
191. J P Luongo *J. Polym. Sci., Polym. Chem. Ed.* **10** 119 (1972)
192. R D Southgate *J. Appl. Phys. Lett.* **28** 250 (1976)
193. D Naeegele, D Y Yoon *J. Appl. Phys. Lett.* **33** 132 (1978)
194. D Broussoux, B Servet, F Micheron *Rev. Tech. Thompson-CSF* **13** 2 (1981)
195. B Servet, S Ries, D Broussoux, F Micheron *J. Appl. Phys.* **55** 2763 (1984)
196. N C Banik, P L Taylor, A I Hopfinger *J. Appl. Phys. Lett.* **37** 49 (1980)
197. F J Lu, D A Waldman, T Hsu *J. Polym. Sci., Polym. Phys. Ed.* **22** 827 (1984)
198. A J Lovinger *Macromolecules* **14** 225 (1981)
199. H Dvey-Aharon, P L Taylor, A I Hopfinger *J. Appl. Phys.* **51** 5184 (1980)
200. J D Clark, P L Taylor, A I Hopfinger *J. Appl. Phys.* **52** 5903 (1981)
201. D U Reneker, J Mazur *Bull. Am. Phys. Soc.* **29** 324 (1984)
202. D U Reneker, J Mazur *Polymer* **24** 1387 (1983)
203. B Tynenska, A Galeski, M Kryszewski *Polym. Bull.* **4** 171 (1981)
204. R Danz *Acta Polym.* **33** 1 (1982)
205. R Danz *Polym. Bull.* **7** 497 (1982)
206. T T Wang *J. Appl. Phys.* **53** 1828 (1982)
207. R G Kepler, R A Anderson, R R Lagasse *Phys. Rev. Lett.* **48** 1274 (1982)

208. F J Lu, S L Hsu *Polymer* **25** 1247 (1984)
209. M Latour *Polymer* **18** 278 (1977)
210. M Latour, H Abo Dorra, J L Galogne *J. Polym. Sci., Polym. Phys. Ed.* **22** 245 (1984)
211. I J Guy, J Unsworth *J. Appl. Phys.* **61** 5374 (1987)
212. S L Hsu, F J Lu, A Waldman, M Mathukumar *Macromolecules* **18** 2583 (1985)
213. F J Lu, S L Hsu *Macromolecules* **19** 326 (1986)
214. N M Reynolds, K J Kim, C Chang, S L Hsu *Macromolecules* **22** 1092 (1989)
215. M A Marcus *IEEE Trans. Electr. Insul.* **E1-21** 519 (1986)
216. D Geschke, P Holstein, M Mendler *Acta Polym.* **39** 206 (1988)
217. K Frigge, D Geiss, A Janke, W Konstler *Acta Polym.* **39** 169 (1988)
218. F Ishii, T Sawatari, A Odajima *Jpn. J. Appl. Phys.* **27** 1047 (1988)
219. L C Kopferberg *J. Appl. Phys.* **64** 2316 (1988)
220. Y Takase, J I Scheinbeim, B A Newman *J. Polym. Sci., Part B, Polym. Phys.* **27** 2347 (1989)
221. Y Takase, J I Scheinbeim, B A Newman *J. Polym. Sci., Part B, Polym. Phys.* **28** 1593 (1990)
222. D Geiss, C Rusher *Progr. Colloid. Polym. Sci.* **80** 119 (1989)
223. A Biichmann, D Geiss *Polymer* **32** 215 (1991)
224. H L Marand, R S Stein, G M Stack *J. Polym. Sci., Part B, Polym. Phys.* **26** 1361 (1988)
225. H L Marand, R S Stein *J. Polym. Sci., Part B, Polym. Phys.* **27** 1089 (1989)
226. H Sussner, K Dransfeld *J. Polym. Sci., Polym. Phys. Ed.* **16** 529 (1978)
227. P Saikiewicz *J. Polym. Sci., Part B, Polym. Phys.* **32** 313 (1994)
228. K Koga, N Nakano, T Hattori, H Ohigashi *J. Appl. Phys.* **67** 965 (1990)
229. Y Takahashi *Jpn. J. Appl. Phys., Part. 1* **33** 202 (1994)
230. B Servet, J Rault *J. Phys. (Paris)* **40** 1145 (1979)
231. B A Newman, J I Scheinbeim *Macromolecules* **16** 60 (1983)
232. M Weinhold, M Litt, J B Lando *Ferroelectrics* **57** 277 (1984)
233. Y Takahashi *J. Appl. Phys.* **67** 4060 (1990)
234. A Sen, J I Scheinbeim, B A Newman *J. Appl. Phys.* **56** 2433 (1984)
235. A Wedel, R Danz, D Geiss, A Leets *Wiss. Z. Elektrotech.* **26** 222 (1988)
236. V V Kochervinskii, V G Sokolov, V M Zubkov *Vysokomol. Soed., Ser. A* **33** 530 (1991)
237. V V Kochervinskii, E M Murasheva *Vysokomol. Soed., Ser. A* **33** 2096 (1991)
238. Z F Il'icheva, I A Slovokhotova, I G Akhvediani *Vysokomol. Soed., Ser. A* **18** 209 (1976)
239. B K Passal'skii, D A Sachuk, L N Goichenko, Ya I Lavrentovich *Vysokomol. Soed., Ser. B* **22** 107 (1980)
240. I Klier, A Vokal *Radiat. Phys. Chem.* **38** 457. (1991)
241. T B Vinogradova, V K Matveev, A G Sirota, V T Shirinyan *Vysokomol. Soed., Ser. B* **30** 691 (1988)
242. T Sasuga, S Kawanishi, T Seguchi, I Kohno *Polymer* **30** 2054 (1989)
243. M A Said, C M Balik, J D Carlson *J. Polym. Sci., Part B, Polym. Phys.* **26** 1457 (1988)
244. V K Matveev, N A Smirnova, L Ya Madorskaya, N N Loginova, V K Milinchuk *Vysokomol. Soed., Ser. B* **32** 762 (1990)
245. Y Nabata *Jpn. J. Appl. Phys. 1* **29** 2755 (1990)
246. S K Bhabeja, E H Andrews *J. Appl. Polym. Sci.* **34** 2809 (1987)
247. M Norkis, I Raiter, S Sholnik, A Siegmman, P Eyster *J. Macromol. Sci., Phys.* **26** 37 (1987)
248. V M Aslamian, V S Vardanian, M N Avetisyan, S S Filikian, S R Ayvasian *Polymer* **29** 755 (1987)
249. L Minkova *Colloid Polym. Sci.* **266** 6 (1988)
250. S K Bhateja, E N Andrews, S M Yarbough *Polymer* **21** 739 (1989)
251. S K Bhateja, S M Yarbough, E N Andrews *J. Macromol. Sci., Phys.* **29** 1 (1990)
252. A M Hindeleh, R Hosemann, G Hinricsen, H Springer *J. Polym. Sci., Part B, Polym. Phys.* **28** 267 (1990)
253. I Nishimoto, S Haisupakin, T Imui *Radiat. Phys. Chem.* **32** 413 (1992)
254. A D Pae, S K Bhateja, B A Gilbert *J. Polym. Sci., Part B, Polym. Phys.* **25** 717 (1987)
255. Z Zhao, J Chu, X Chen *Radiat. Phys. Chem.* **43** 523 (1994)
256. K A Verkhovskaya, V V Kochervinskii *Vysokomol. Soed., Ser. A* **32** 1669 (1990)
257. V V Kochervinskii *Vysokomol. Soed., Ser. A* **35** 1978 (1993)
258. B P Kosmynin, E L Gal'perin *Vysokomol. Soed., Ser. A* **14** 1603 (1972)
259. E L Gal'perin, B P Kosmynin *Vysokomol. Soed., Ser. A* **15** 2556 (1973)
260. A Collins, R De Batist, R Gevers *Radiat. Phys. Chem.* **16** 225 (1980)
261. Sh T Tuigiev, A N Kuznetsova, A M Mukhamadieva *Vysokomol. Soed., Ser. AB* **27** 375 (1985)
262. P P Khlyabich, A G Sirota, V P Budtov *Vysokomol. Soed., Ser. A* **32** 1444 (1990)
263. A Odajima, Y Takase, T Ishibashi, K Yuasa *Jpn. J. Appl. Phys. 2* **S24** 881 (1985)
264. A J Lovinger *Macromolecules* **18** 910 (1985)
265. B Daudin, M Dubus, J F Legrand *J. Appl. Phys.* **62**. 994 (1987)
266. F Macchi, B Daudin, J F Legrand *Nucl. Instrum. Methods Phys. Res. B* **46** 324 (1990)
267. F Macchi, B Daudin, J Hillairet, J Lanzier, J B Ngoma, J Y Cavaille, J F Legrand *Nucl. Instrum. Methods, Phys. Res. B* **46** 334 (1990)
268. B Daudin, J F Legrand, F Macchi *J. Appl. Phys.* **70** 4037 (1991)
269. Y Tsugita, T Nose, T Hata *Polymer* **3** 580 (1972)
270. S P Kabin, S G Malkevich, G P Mikhailov, B I Sazhin, A L Smolyanskii, L V Chernikov *Vysokomol. Soed.*, **3** 618 (1961)
271. T Wentink *J. Appl. Phys.* **32** 1063 (1961)
272. Y M Ishida, M Watanabe, K Yamafuji *Kolloid-Z.* **200** 48 (1964)
273. S Yano *J. Polym. Sci., Part A, Polym. Chem.* **8** 1057 (1970)
274. H Sasabe, S Saito, M Asahina M Kakutani *J. Polym. Sci., Polym. Chem. Ed.* **7** 1405 (1969)
275. S Osaki, Y Ishida *J. Polym. Sci., Polym. Phys. Ed.* **12** 1727 (1974)
276. H Arisawa, O Yano, Y Wada *Ferroelectrics* **32** 39 (1981)
277. Y Nabata *Jpn. J. Appl. Phys.* **29** 319 (1990)
278. N Koizumi, J Hagino, Y Murata *Ferroelectrics* **32** 141 (1981)
279. G Williams, D C Watts *Trans. Faraday Soc.* **66** 80 (1970)
280. M G Brereton, G R Davies, A Rushworth, J Sprence *J. Polym. Sci., Polym. Phys. Ed.* **15** 583 (1977)
281. N Koizumi, S Yano, K Tsunashima *J. Polym. Sci., Polym. Phys. Ed.* **7** 59 (1969)
282. V K Matveev, S E Vaisberg, V L Karpov *Plast. Massy* (9) 45 (1971)
283. K Nakagawa, Y Ishida *J. Polym. Sci., Polym. Phys. Ed.* **11** 1509 (1973)
284. S Tasaka, K Miyasato, M Yoshikawa, S Miyata, M Ko *Ferroelectrics* **57** 267 (1984)
285. S Tasaka, N Inagaki, T Okutani, S Miyata *Polymer* **30** 1639 (1989)
286. S Utoh *Jpn. J. Appl. Phys.* **30**. L1516 (1991)
287. Y Abe, M Kakizaki, T Hideshima *Jpn. J. Appl. Phys.* **24** 1074 (1985)
288. M Kakizaki, Y Abe, T Hideshima *Jpn. J. Appl. Phys.* **25** 485 (1986)
289. T Anada, M Kakizaki, T Hideshima, in *IUPAC the 32nd International Symposium on Macromolecules, Kyoto 1988*
290. T Anada, M Kakizaki, T Hideshima *Jpn. J. Appl. Phys.* **29** 322 (1990)
291. T Anada, M Kakizaki, T Hideshima *Rep. Progr. Polym. Phys. Jpn.* **33** 361 (1990)
292. A Peterlin, J D Holbrook-Elwell *J. Mater. Sci.* **2** 1 (1967)
293. M E Baird, P Blackburn, B W Delf *J. Mater. Sci.* **10** 1248 (1975)
294. G K Rashmi, P K C Pillai *J. Mater. Sci.* **22** 2006 (1987)
295. H Kukutani *J. Polym. Sci., Polym. Chem. Ed.* **8** 1177 (1970)
296. S Shen, L Wu, B Chen, B Wu *Gaofenzi Tunsun* (4) 241 (1984)
297. B I Sazhin, M P Eidel'nant, V I Shul'gin *Vysokomol. Soed., Ser. B* **11** 384 (1969)
298. Y Myjamoto, H Mijaji, K Asai *J. Polym. Sci., Polym. Phys. Ed.* **18** 597 (1980)
299. S Osaki, S Uemura, Y Ishida *J. Polym. Sci., Polym. Chem. Ed.* **9** 585 (1971)
300. S Uemura *J. Polym. Sci., Polym. Phys. Ed.* **12** 1177 (1974)
301. S Yano, K Tadano, K Adki *J. Polym. Sci., Polym. Phys. Ed.* **12** 1875 (1974)
302. N Koizumi, T Hanai *Bull. Inst. Chem. Res. Kyoto Univ.* **42** 115 (1964)
303. D K Das Gupta, K Douguty *Ferroelectrics* **32** 69 (1981)

304. S Osaki, T Kotaka *Ferroelectrics* **32** 1 (1981)
305. K W Wagner *Arch. F. Electrotech.* **2** 371 373 383 (1914)
306. N Koizumi, N Nakawa, H Habuka *Ferroelectrics* **57** 99 (1984)
307. M-C Felix-Vandorpe, M Maitrot, R Ongaro *Phys. J. Appl. Phys.* **18** 1385 (1985)
308. M Kozaki, H Obeshima, M Ieda *J. Phys. Soc. Jpn.* **29** 1012 (1970)
309. A J Lovinger, D J Freed *Bull. Am. Phys. Soc.* **25** 221 (1980)
310. H P Jillis, K M Boyle, R L Long *Am. Chem. Soc. Polymer. Prepr.* **19** 468 (1978)
311. P K Wu, G -R Yang, X F Ma, T -N Lu *Appl. Phys. Lett.* **65** 508 (1994)
312. M Abkovitz, G Pfister *J. Appl. Phys.* **46** 2559 (1975)
313. T Takamatsu, E Fukada *Rep. Progr. Polym. Phys. Jpn.* **13** 363 (1970)
314. T Mizutani, T Yamada, M Ieda *J. Phys. J. Appl. Phys.* **14** 1139 (1981)
315. T Mizutani, T Yamada, M Ieda *J. Phys. J. Appl. Phys.* **15** 289 (1982)
316. L S Wu, H Shen, in *Proceedings of the International Conference on Properties and Applied Dielectric Materials, Xian 1985*, Vol. 2 (1), p. 437
317. V S Mc Brierty, D C Douglass, T A Weber *J. Polym. Sci., Polym. Phys. Ed.* **14** 1271 (1976)
318. R Sakamoto, Y Abe, S Yano *Rep. Progr. Polym. Phys. Jpn.* **23** 353 (1980)
319. Y Abe, M Kakizaki, T Hedeshima *Ferroelectrics* **57** 9 (1984)
320. Y Yamada, M Kakizaki, T Hideshima *Jpn. J. Appl. Phys.* **21** 352 (1983)
321. B R Hahn, J H Wendorff *Polymer* **26** 1619 (1985)
322. W Ulmann, J H Wendorff *Compos. Sci. Technol.* **23** 97 (1985)
323. J S Noland, N N C Hsu, R Saxon, J M Schmitt *Adv. Chem. Ser.* **99** 15 (1971)
324. T Nishi, T T Wang *Macromolecules* **8** 909 (1975)
325. D R Paul, J O Altamirano *Adv. Chem. Ser.* **142** 371 (1975)
326. M M Coleman, J Zarian, D F Varnell, P S Painter *J. Polym. Sci., Polym. Lett. Ed.* **15** 745 (1977)
327. D J Hourston, J D Hughes *Polymer* **18** 1175 (1977)
328. T T Wang, T Nishi *Macromolecules* **10** 421 (1977)
329. E Roerdink, G Challa *Polymer* **19** 173 (1978)
330. D R Paul, J W Barlow, R E Bernstein, D C Wahrmund *Polym. Eng. Sci.* **18** 1225 (1978)
331. E Roerdink, G Challa *Polymer* **21** 509 (1980)
332. J H Wendorff *J. Polym. Sci., Polym. Phys. Ed.* **18** 439 (1980)
333. T K Kwei, H L Frisch *Macromolecules* **11** 1267 (1978)
334. B S Morra, R S Stein *J. Polym. Sci., Polym. Phys. Ed.* **20** 2243 2261 (1982)
335. B S Morra, R S Stein *Polym. Eng. Sci.* **24** 311 (1984)
336. C Nakafuku, M Yasuniwa *Polym. J.* **19** 845 (1987)
337. P R Couchman *Macromolecules* **11** 1156 (1978)
338. P R Couchman *Macromolecules* **13** 1272 (1980)
339. P L Inken, D R Paul, J W Barlow *Polym. Eng. Sci.* **16** 593 (1976)
340. T K Kwei, G D Patterson, T T Wang *Macromolecules* **9** 780 (1976)
341. M Galin, L Maslanko *Eur. Polym. J.* **23** 923 (1987)
342. S H Goh, K S Slow *Polym. Bull.* **20** 393 (1988)
343. D R Paul, J W Barlow *Polymer* **25** 487 (1984)
344. D C Wahrmund, R E Bernstein, J W Barlow, D R Paul *Polym. Eng. Sci.* **18** 677 (1978)
345. S H Goh, S Y Lee, Y F Chang *Polym. Bull.* **25** 257 (1991)
346. R M Briber, P Knoury *Polymer* **28** 38 (1987)
347. C J Ong, F P Price *J. Polym. Sci., Polym. Symp.* **63** 59 (1978)
348. G C Alfonso, T P Russel *Macromolecules* **19** 1143 (1986)
349. H Saito, T Okada, T Hamam, T Inoue *Macromolecules* **24** 4446 (1991)
350. C N Klein Douwel, W E J R Maas, W S Veeman, G H Werumeus-Buning, J M J Vankan *Macromolecules* **23** 406 (1990)
351. W E J R Maas, W A C Vander Heijden, W S Veeman, J M J Vankan, G H Werumeus-Buning *J. Chem. Phys.* **96** 4698 (1991)
352. C H M Papavoine, W E J R Maas, W S Veeman, G H Werumeus Buning, J M J Vankan *Macromolecules* **26** 6611 (1993)
353. V V Shilov, V N Bliznyuk, S A Tyurin, V I Povstugar, S G Bystrov *Vysokomol. Soedin., Ser. A* **30** 1633 (1988)
354. V P Privalko *Spravochnik po Fizicheskoi Khimii Polimerov. Svoistva Polimerov v Blochnom Sostoyanii* (Handbook on the Physical Chemistry of Polymers. Properties of Polymers in the Block State) (Kiev: Nauk. Dumka, 1984) Vol. 2, p. 273
355. C Leonard, J L Kalary, L Monnerie, D Broussoux, B Servet, F Miciuron *Polym. Commun.* **24** 110 (1983)
356. W Kaufmann, J Petermann, N Reynolds, E L Thomas, S L Hsu *Polymer* **30** 2147 (1989)
357. D Braun, M Jacobs, G P Hellmann *Polymer* **35** 706 (1994)
358. R E Bernstein, C A Cruz, D R Paul, J W Barlow *Macromolecules* **10** 681 (1977)
359. C Leonard, J L Halary, L Monnerie *Polymer* **26** 1507 (1985)
360. N Tsutsumi, Y Ueda, T Kiyatsuki, A S Dereggi, G T Davis *J. Appl. Phys.* **74** 3366 (1993)
361. T Tsutsumi, G T Davis, A S De Reggi *Macromolecules* **24** 6392 (1991)
362. R G K Narula, P K C Pillai *J. Macromol. Sci., Phys.* **B26** 185 (1987)
363. G K Narula, P K C Pillai *J. Mater. Sci. Lett.* **8** 608 (1989)
364. G K Narula, P K C Pillai *J. Mater. Sci. Lett.* **9** 130 (1990)
365. B R Hahn, J H Wendorff, D Y Yoon *Macromolecules* **17** 718 (1985)
366. B R Hahn, O Hermann-Schönherr, J H Wendorff *Polymer* **28** 201 (1987)
367. D Y Yoon, Y Ando, S Rojstaczer, S K Kumar, G C Alfonso *Makromol. Chem., Makromol. Symp.* **50** 183 (1991)
368. Y Ando, T Hanada, K Saiton *J. Polym. Phys.* **B32** 179 (1994)
369. H Saito, B Stuhn *Polymer* **35** 475 (1994)
370. K Saito, S Tasaka, S Miyata *Nippon Kagaku Kaishi* (10) 1909 (1985)
371. N Hamazaki, J W Cho, S Miyata *Polym. J.* **23** 333 (1991)
372. M Galin *Macromol. Chem., Rapid Commun.* **9** 119 (1984)
373. M Galin *Makromol. Chem.* **188** 1391 (1987)
374. G Caccorolli, M Pizzoli, M Scandola, G G Alfonso, A Turturro *Polymer* **30** 1251 (1989)
375. T Kyu, J-C Yang *Macromolecules* **23** 176 182 (1990)
376. G Natta, G Allegra, T W Bassi, D Siamso, G Caporiccio, E Torti *J. Polym. Sci., Polym. Chem. Ed.* **3** 4263 (1965)
377. G Guerra, F Karasz, W J Mecnicht *Macromolecules* **19** 1935 (1986)
378. Yu S Lipatov, G M Semenovich, S S Makovei *Dokl. Akad. Nauk Ukr. SSR* **6** 43 (1986)
379. A Siegmann, G Cohen, Z Baraam *J. Appl. Polym. Sci.* **37** 1481 (1989)
380. K Mazur *IEEE Trans. Electr. Insul.* **27** 782 (1992)
381. G Muralidhar, P K C Pillai *J. Mater. Sci. Lett.* **6** 33 (1987)
382. C Muralidhar, P K C Pillai *J. Mater. Sci.* **23** 410 (1988)
383. S Reich, E P Goldberg *J. Polym. Sci., Polym. Phys. Ed.* **21** 869 (1983)

Capillary gas-solid chromatography

V G Berezkin

Contents

I. Introduction	915
II. The discovery of capillary gas chromatography and its development	916
III. Retention of compounds subjected to capillary gas-solid chromatography	918
IV. Broadening of chromatographic zones in open tubular gas adsorption capillary columns	919
V. Methods for the preparation of open tubular gas adsorption capillary columns	921
VI. The use of open tubular gas-solid capillary columns	925

Abstract. The current state of gas adsorption chromatography on open tubular capillary columns is analysed. The history of the development of this method and its role in gas chromatography are considered. The preparation of open tubular adsorption capillary columns, fundamentals of the theory of retention and of broadening of chromatographic zones, and the use of columns of this type in practical analytical chemistry are discussed. The bibliography includes 148 references.

I. Introduction

Gas chromatography is among the main analytical methods; it is used successfully in various branches of industry such as the petrochemical, chemical, and gas industry, etc., in pharmaceuticals, in the control of environmental pollution, in medicine, in agriculture, and also in scientific research.^{1–6}

Currently, capillary gas chromatography is used most frequently. Indeed, according to a bibliometric study,⁷ 83% of the publications devoted to chromatography refer to the use of capillary columns and, according to McNair's data,⁸ capillary columns account for 80% of all gas-chromatographic columns purchased. In recent years, a new type of capillary column, namely, open tubular gas adsorption (or gas-solid) capillary columns have been used advantageously in analytical practice. This makes it possible to solve numerous practically important analytical problems that cannot be solved with the use of conventional gas-liquid columns.

The aim of the present review is to analyse critically the data on capillary gas adsorption chromatography, in particular, studies by Russian scientists, who have made a substantial contribution to the development of this technique.

The vigorous development of capillary chromatography during the last 10–15 years is due to a number of advantages of capillary columns over the conventional packed columns. Firstly, open tubular capillary columns are 10–1000 times more efficient than the classical packed columns. Secondly, capillary columns

permit separation of a wider range of heavy (high-boiling) compounds, since chromatography on these columns is carried out at lower temperatures than on packed columns. Thirdly, with the open tubular capillary columns, a substantially higher rate of separation can be achieved. Fourthly, the decrease in the size of columns ensures a more reproducible regime of separation. Finally, the procedures for working with capillary columns became much simpler when flexible quartz columns with polymeric coatings^{9,10} or with a more thermostable metallic coating^{11,12} have been introduced into the chromatographic practice. The latter columns were proposed for the first time in Russia.¹¹ The above advantages have stimulated the development of not only gas-liquid but also gas-solid capillary chromatography.

The separating capacity of a chromatographic column (R) is determined by three factors:

$$R = \frac{\alpha - 1}{\alpha} \frac{\sqrt{N}}{4} \frac{k}{1 + k} = SEC, \quad (1)$$

where α is the relative retention of two components that form a pair, critical for separation; N is the number of theoretical plates; k is the capacity factor of the second component being separated; and S is the selectivity index of the column (of the sorbent used)

$$S = \frac{\alpha - 1}{\alpha}; \quad (2)$$

E is the efficiency index of the column

$$E = \frac{\sqrt{N}}{4}; \quad (3)$$

C is the capacity index of the column

$$C = \frac{k}{1 + k}. \quad (4)$$

The capacity index C plays an important role when the capacity factors of the compounds being separated are small; for large k values, the capacity index approaches unity.

When the operation of open tubular capillary columns is analysed, their high efficiency is usually noted; however, the fact that the high selectivity of the sorbent used is also a very important factor having a considerable influence on the chromatographic separation, is often neglected.

V G Berezkin Laboratory of Chromatography, A V Topchiev Institute of Petrochemical Synthesis, Russian Academy of Sciences, Leninskii prosp. 29, 117912 Moscow, Russian Federation.
Fax (7-095) 230 22 24. Tel. (7-095) 955 42 74

Received 19 March 1996

Uspekhi Khimii 65 (11) 991–1012 (1996); translated by Z P Bobkova

The selectivity index [see Eqn (1)] has the greatest influence on the degree of separation. In the case of poorly separable peaks ($\alpha \approx 1.0$), the selectivity index increases proportionally to $(\alpha - 1)$

$$S = \frac{\alpha - 1}{\alpha} \approx \alpha - 1, \quad (5)$$

hence,

$$R = (\alpha - 1)EC. \quad (6)$$

The selectivity of a sorbent is usually the most significant criterion for its possible use. Selective sorbents used in gas chromatography include not only absorbents (stationary liquid phases) but also adsorbents. A special place among the latter belongs to geometrically ordered solids (for example, molecular sieves) or adsorbents with specific properties (for example, organic hydrophobic adsorbents) or adsorbents with extended surface, etc.

In view of this, it is natural to extend the use of solid adsorbents to capillary gas chromatography, i.e. to develop gas adsorption (gas-solid) capillary chromatography.

Gas adsorption chromatography has the following advantages.¹³

1. Enhanced selectivity and sorption capacity of adsorbents, which make it possible to separate organic or inorganic compounds having similar physicochemical properties. Examples are provided by the separation on molecular sieves, graphitised carbon black, or organic polymeric adsorbents.
2. The higher efficiency of separation compared to that in gas-liquid chromatography (GLC), which is due to the fact that mass exchange processes occur more rapidly than those in GLC.
3. The sufficiently high thermal stability of adsorbents.
4. The possibility of separating gases and volatile compounds at 40–50 °C with conventional gas chromatographs.
5. The lower 'noise' of the detector, which is due to the fact that the adsorbents are usually non-volatile.

The unique features of gas adsorption chromatography have also attracted the attention of Giddings,¹⁴ who has written: 'One immediate advantage of gas-solid chromatography resides in the fact that a surface coated with any reasonable degree of uniformity will exhibit a coefficient of the resistance to mass transfer substantially smaller than the corresponding coefficient for a liquid adsorption layer in gas-liquid chromatography. The second immediate advantage of gas-solid chromatography resides in the great potential selectivity of the adsorption process. Surface adsorption is potentially capable of offering the most versatile and selective characteristics of any of the known retentive mechanism. The rigidly fixed forces of a solid surface contrast sharply with the fluid forces of a liquid phase.'

Of course, the gas-solid chromatography is not free from certain drawbacks. These are the following:

1. Some non-reproducibility of sorption and chromatographic characteristics of the adsorbents used (compared to those of stationary liquid phases).
2. Asymmetry of chromatographic zones resulting from some non-linearity of adsorption isotherms.
3. A higher probability (compared to that in GLC) of irreversible adsorption and catalytic transformations of the compounds being analysed on the surface of an adsorbent.
4. The narrow range of commercially available adsorbents for gas-solid chromatography.

Juxtaposition of the advantages and drawbacks of gas adsorption chromatography shows that the advantages of this variant are much more significant than its drawbacks. This is also supported by the fact that columns with such adsorbents as alumina, silica, graphitised carbon black, molecular sieves, organic polymers, etc. are widely used in practice.

The advantages of gas adsorption chromatography can be fully realised by using its capillary variant.

II. The discovery of capillary gas chromatography and its development

The author of capillary chromatography Golay was the first to point out the theoretical possibility of preparing open tubular capillary columns with a sorbent layer arranged on the inner walls. In 1960 he wrote: 'Why not make a semipacked column with a large open passage in the centre, say, nine-tenths as large as the column inside diameter, and with a large thin layer of packing material in the remaining space on the periphery? The answer is why not indeed? I believe that such columns constitute nearly ideal columns for a wider range of analysis than present-day smooth tubular columns.'¹⁵ Note that the researcher did not indicate what particular variant of chromatography, i.e. gas-liquid or gas-solid chromatography, it would be expedient to accomplish on a capillary column with porous walls.

Some years later, open tubular gas adsorption capillary columns with their inner walls coated by an adsorbent layer were produced independently by several researchers in Russia and Germany. For example, in 1961, Kalmanovskii *et al.*,¹⁶ who studied the modification of glasses with chlorotrimethylsilane during the production of various glass capillary columns have noted that: 'the separation on non-modified capillaries proved poor (Fig. 1a), the retention time of acetone being much longer than those for other compounds and its peak being markedly asymmetrical. This indicates that the capillary surfaces contain a large number of polar sites. When the surface of these non-modified capillaries was coated with a silicone oil film, the separation became better (Fig. 1b). The modification of the capillary surface with chlorotrimethylsilane (Fig. 1c) led to clear-cut separation and to a change in the order of elution (acetone emerged first!) with respect to that with the unmodified capillary made of the same glass (*cf.* Fig. 1a). Modified capillaries can be used for analytical purposes directly in the gas adsorption version of the capillary chromatography.'¹⁶

Further, the researchers noted that the application of a silicone oil film to the surface of a modified capillary improved the separation to a greater degree (Fig. 1d) than its application to a non-modified capillary (see Fig. 1b). It is also noteworthy that the modification of the capillary surface with chlorotrimethylsilane was performed by an unusual procedure during the production of the capillary. The initial tube, from which the capillary was to be drawn, was filled with liquid chlorotrimethylsilane. At high temperature (~700 °C), chlorotrimethylsilane apparently decomposed, and interaction of the products thus formed with the glass surface yielded an adsorption layer on the inner walls of the capillary column. The chromatograms shown in Fig. 1 were obtained at 25 °C with glass capillaries with a length of 15–20 m and with an inner diameter of 0.3 mm.

Mohnke and Saffert^{17,18} have prepared a gas adsorption capillary column with a silica layer by prolonged (30 h) etching of the inner surface of a Jena glass capillary by aqueous ammonia at 170–180 °C. This yields a 10–20 µm thick silica layer. Note that Mohnke and Saffert were the first to point to a very important application of capillary gas chromatography, namely, to the separation of isotopes and nuclear-spin isomers of gases. A good degree of separation of nuclear-spin isomers and isotopes of hydrogen was achieved even in the first studies on capillary gas adsorption chromatography (Fig. 2).¹⁸

A fundamentally new suspension method for the preparation of open tubular absorption columns, based on the deposition of an adsorbent layer on the inner walls of a capillary from a suspension, has been proposed by Halasz and Horvath.^{19,20} The preparation of an adsorbent in columns of this type is independent of the material of the inner walls of the column and does not involve any transformations of it. Fig. 3 presents a chromatogram of a fast separation of aromatic hydrocarbons on graphitised carbon black layered onto the inner walls of a copper capillary. Kirkland²¹ manufactured for the first time an open tubular capillary column (75 m × 5 mm) with boehmite (Al₂O₃) and

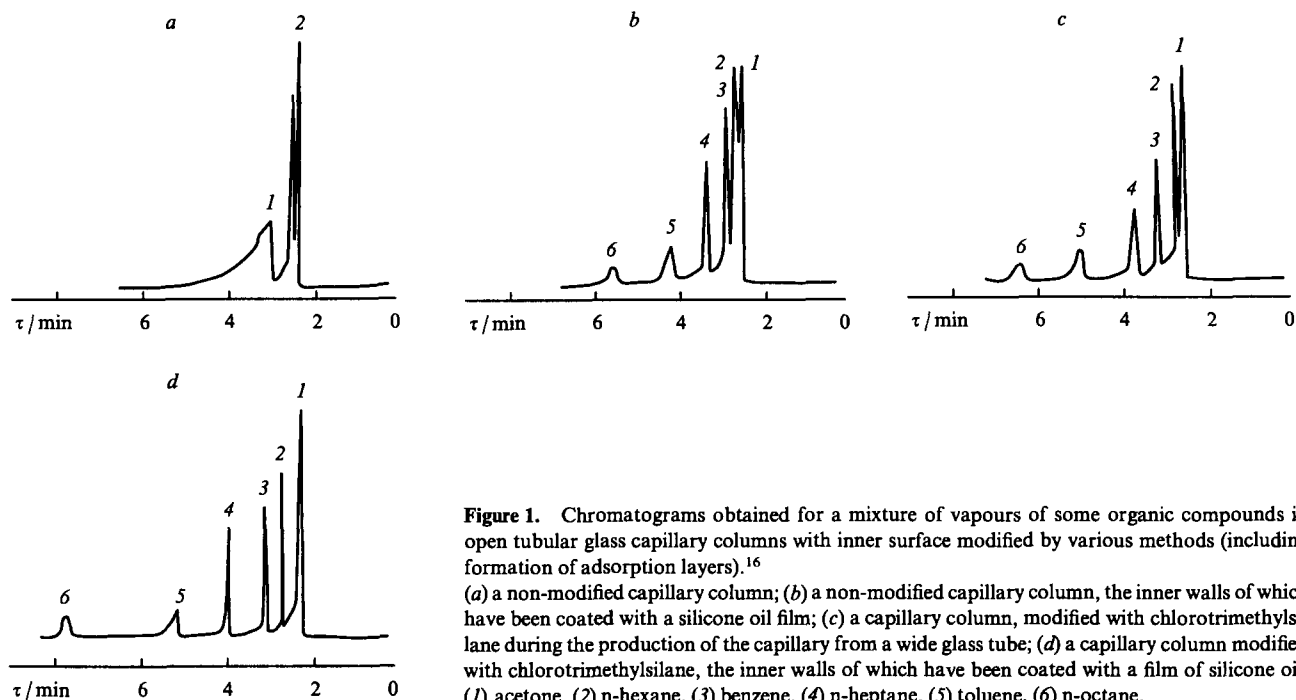


Figure 1. Chromatograms obtained for a mixture of vapours of some organic compounds in open tubular glass capillary columns with inner surface modified by various methods (including formation of adsorption layers).¹⁶

(a) a non-modified capillary column; (b) a non-modified capillary column, the inner walls of which have been coated with a silicone oil film; (c) a capillary column, modified with chlorotrimethylsilane during the production of the capillary from a wide glass tube; (d) a capillary column modified with chlorotrimethylsilane, the inner walls of which have been coated with a film of silicone oil; (1) acetone, (2) n-hexane, (3) benzene, (4) n-heptane, (5) toluene, (6) n-octane.

showed the possibility of using this column for the fast separation of Freons.

Among the pioneering studies dealing with the adsorption capillary chromatography, the works of Weiher,²² Petitjean and Leftault,²³ Schwartz,²⁴ Liberti and coworkers,^{25–29} and of Ilkova and Mistryukov³⁰ should be mentioned.

An important role in the development of the capillary chromatography in columns with a porous layer on the inner walls (capillary columns with adsorbent layers constitute a particular case), has been played by the studies of Ettre and coworkers^{31–33} and, especially, by their review³⁴ devoted to the theory, methods for production, practical application, and prospects of the development of surface-layered open tubular capillary columns for gas-liquid chromatography.

Thus, the results of the very first studies on the adsorption capillary columns demonstrate, firstly, the high resolving power of the method, which is manifested most clearly in the separation of isotopes, and, secondly, the fact that separation takes little time.

During the last 10–15 years, interesting studies and important practical applications of open tubular gas-adsorption columns have been accomplished by de Nijs, de Zeeuw, Mohnke, and coworkers;^{35–40} the 'Chrompack' company (the Netherlands) has

begun the commercial manufacture of some types of these columns based on alumina, molecular sieves, and polymeric adsorbents (see for example Ref. 41).

In our opinion, classification of capillary columns is important in gas chromatography. It has been noted (see for example Ref. 42) that some researchers confuse the term 'open tubular capillary columns with a porous layer on the inner walls' (PLOT) with the term 'open tubular capillary columns with inner walls coated with a layer of a solid material' (WCOT). It is expedient to distinguish various types of columns according to the following features: first, the presence (or absence) of a porous layer on the inner walls of a capillary column and second, the presence (or absence) of a layer of a stationary liquid phase on the inner walls of a column (Fig. 4).

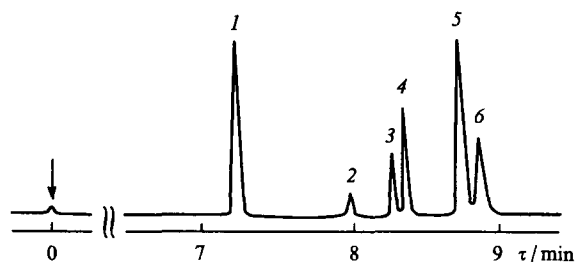


Figure 2. Chromatogram for the separation of nuclear spin isomers and isotopes of hydrogen in an open tubular adsorption glass capillary column.¹⁸

The 80 m long open tubular capillary column contained a 20 μ m thick silica layer as an adsorbent; $T = 77.4$ K; neon was used as the carrier gas; (1) helium, (2) *p*-protium, (3) *o*-protium, (4) DH, (5) *o*-deuterium, (6) *p*-deuterium.

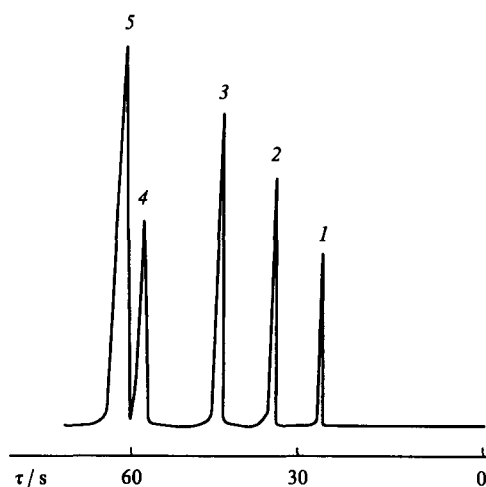


Figure 3. Chromatogram obtained for the separation of aromatic hydrocarbons in an open tubular capillary column containing graphitised carbon black.¹⁹

A 15 m \times 0.25 mm silver-plated copper column was used, the concentration of graphitised carbon black was 5.4 mg m^{-1} ; $T = 245$ °C; hydrogen was used as the carrier gas;

(1) benzene, (2) toluene, (3) ethylbenzene, (4) *m*-xylene, (5) *o*- and *p*-xylenes.

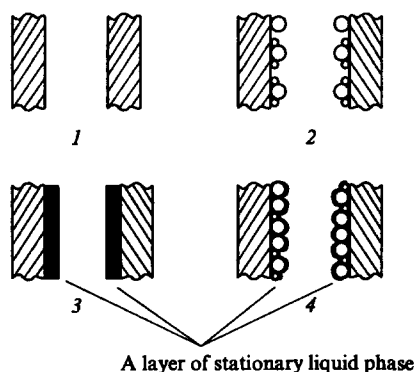


Figure 4. Various types of open tubular capillary columns.

(1) Open gas adsorption (gas-solid) column with smooth walls (an adsorbent); (2) open gas adsorption (gas-solid) column with inner walls coated with an adsorbent layer; (3) open gas-liquid-solid column with smooth walls (a solid support); (4) open gas-liquid-solid column with inner walls coated with an adsorbent layer (a solid support).

In the case of open tubular capillary columns with smooth walls (i.e. containing no porous layer), in which non-porous inner walls of the capillary are used as the adsorbent, an equilibrium in the system 'gas-planar adsorbent' under consideration is established quite rapidly; however, unfortunately, the capacity of these columns is relatively low. The theoretical possibility of using these columns was noted for the first time by Berezkin and Volkov.⁴³

Columns, the inner walls of which are coated with a layer of a solid adsorbent, are most widely used in the analytical practice. Columns containing a solid adsorbent layer modified with small amounts of non-volatile liquid phases should also be classified as adsorption columns. Characteristics of open tubular capillary columns modified with non-volatile liquid phases can be found, for example, in the following studies.⁴⁴⁻⁴⁶

The contribution of an adsorption mechanism to the retention can also be significant in the classical columns with a layer of a stationary liquid phase on smooth walls. For example, this is the case with the chromatography of n-alkanes in open tubular capillary columns with a poly(ethylene glycol) layer.^{47,48}

This review is mostly devoted to open tubular capillary columns, the inner walls of which are coated with a layer of a solid adsorbent (gas-solid chromatography).

III. Retention of compounds subjected to capillary gas-solid chromatography

Retention in gas adsorption chromatography is determined both by the nature of the surface of the adsorbent and by its structure. The mechanism of retention is discussed in detail in a number of monographs.⁴⁹⁻⁵⁴ Kiselev^{13,51} has shown that the retention volume V_N is directly proportional to the surface area (S_{ad}) of the adsorbent in the column (it has been assumed that at relatively low coverages, the accessibility of the adsorbent surface does not change):

$$V_N = K_s S_{ad}, \quad (7)$$

where K_s is the coefficient of distribution of the substance subjected to chromatography between the adsorbent surface and the gas phase.

Note an important specific feature of the gas-solid chromatography, namely, the fact that the retention of compounds depends on the nature of the mobile phase. The replacement of light carrier gases by heavy gases leads to dynamic modification of the adsorbent surface, to a decrease in the coefficients of distribution of compounds being analysed in the 'solid adsorbent-gas' system, and, hence, to a decrease in retention times.

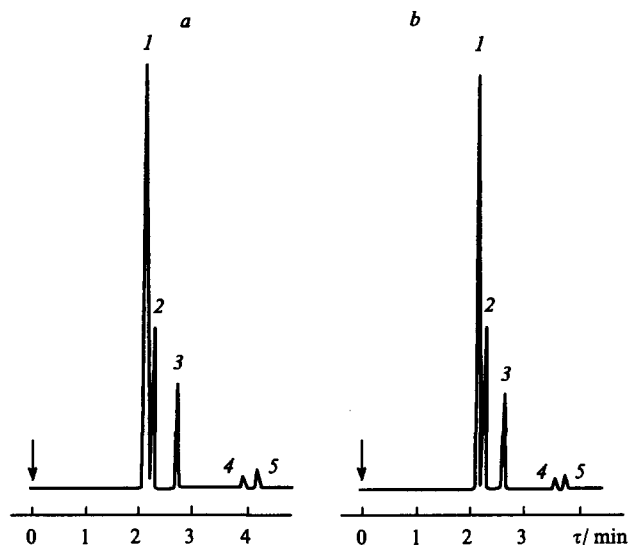


Figure 5. Chromatograms for a mixture of hydrocarbons separated in an open tubular capillary column with alumina using helium (a) and carbon dioxide (b) as carrier gases.

(1) Methane, (2) ethane, (3) propane, (4) isobutane, (5) n-butane. A 50 m × 0.32 mm column with Al_2O_3/KCl was used; $T = 100^\circ C$, flame ionization detector, flow splitting 1/50.

The chromatograms of gaseous hydrocarbons obtained on a column with alumina using two carrier gases (helium and carbon dioxide) are presented in Fig. 5. It is seen that the retention times, especially those of heavy compounds, decrease in the case where the heavy carrier gas (carbon dioxide) is used. An influence of water vapour on the modification of the adsorbent (Al_2O_3) and on the retention in the capillary adsorption chromatography has been noted by de Nijs.³⁵

A further important specific feature of the capillary adsorption chromatography is the dependence of retention on the pressure of the carrier gas. The influence of the average carrier gas pressure in a column on retention values (for example, on the capacity factors) of compounds subjected to high-performance gas-solid capillary chromatography was studied systematically for the first time by Berezkin et al.⁵⁵ for various carrier gases and for the pressure range used in the conventional capillary gas chromatography (1–5 atm at the inlet of the capillary column). It is noteworthy that owing to the high resolving power of open tubular capillary columns, the experimental conditions that can have an influence on the retention are especially significant in capillary chromatography.⁵⁶ For example, in order to decrease the time required for separation by increasing the velocity of the carrier gas in the column, it is necessary to change the pressure at the inlet of the column (and, consequently, the average pressure in the column within the pressure range specified above).

The results of a study of the dependence of the capacity factor on the average pressure of the carrier gas in the column are presented in Table 1. It follows from these data that retention depends both on the nature of the carrier gas and on its pressure in the column.

To explain this, we shall use the known regularities of the adsorption of mixtures. If we assume that the adsorption of molecules of volatile compounds A and C occurs upon their collision with an unoccupied adsorption site on the surface of a solid adsorbent and that the rate of desorption of these molecules is proportional to the surface area occupied by the adsorbed molecules, the adsorption isotherm can be described by the following equations:⁵⁷

$$a_A = \frac{K_{AC} a_C}{1 + K_{CC} c_C + K_{AC} a_C}, \quad (8a)$$

Table 1. Dependence of the capacity factors of gaseous hydrocarbons on the average pressure of the carrier gas in a capillary column.⁵⁵

\bar{P} /atm	Propene	Butane	But-1-ene	\bar{P} /atm	Propene	Butane	But-1-ene
H₂ as the carrier gas				He as the carrier gas			
1.0	0.80	1.51	3.27	1.0	0.88	1.68	3.66
1.6	0.81	1.52	3.29	1.6	0.89	1.71	3.73
2.8	0.80	1.54	3.24	2.8	0.89	1.72	3.75
3.4	0.81	1.53	3.22	3.4	0.89	1.71	3.71
4.1	0.84	1.56	3.24	4.1	0.88	1.69	3.63
N₂ as the carrier gas				CO₂ as the carrier gas			
1.0	0.87	1.65	3.61	1.0	0.64	1.17	2.46
1.6	0.88	1.68	3.64	1.6	0.59	1.08	2.24
2.8	0.87	1.65	3.58	2.8	0.54	0.95	1.91
3.4	0.86	1.62	3.52	3.4	0.49	0.88	0.80
4.1	0.85	1.59	3.45	4.1	0.44	0.80	1.58

$$a_C = \frac{K_C c_C}{1 + K_C c_C + K_A c_A}, \quad (8b)$$

where a_A and a_C are concentrations (g g^{-1}) of the adsorbed compounds A and C, respectively; K_A and K_C are adsorption coefficients of the compounds A and C; and c_A and c_C are the concentrations (g l^{-1}) of A and C in the gas phase. Subsequently, A stands for the compound being chromatographed and C stands for the carrier gas.

From Eqns (8), the following equation has been derived,⁵⁵ which relates the capacity factor (k) to the average pressure of the carrier gas in the column (\bar{P}):

$$\frac{1}{k} = a + b\bar{P}, \quad (9)$$

where

$$a = \frac{\beta}{K_A}, \quad (10a)$$

$$b = aK_C, \quad (10b)$$

β is the ratio (v/v) of the phases occurring in the column, a_p and b_p are coefficients from Eqn (9). By using the above equations, one can determine the parameters of Eqn (8) for adsorption of a gas mixture.

The experimental data obtained are adequately described by Eqn (9) (Fig. 6). Such a processing of experimental results makes it possible to find the parameters of Eqn (9); i.e. in this case, gas chromatography can be used as a physicochemical method for determining parameters of the equation describing the adsorption of mixtures. Note that a variation of the pressure of a carrier gas at the inlet of the column is associated with a variation of its linear velocity; therefore, in this case, a dependence of the capacity factor (i.e. of the retention of a substance) on the linear velocity of the carrier gas can be manifested.

The nature of the carrier gas exerts a substantial influence on the retention of compounds in the capillary gas adsorption chromatography. It is clear that the rules that make it possible to pass from the retention values observed with one carrier gas (G_1) to the values characterising retention of the same compounds when another carrier gas is used (G_2) are of practical interest. Recently[†] the following correlation has been established:

$$k(G_2) = Ak(G_1) + B, \quad (11)$$

where $k(G)$ is the capacity factor of a compound with carrier gas G, and A and B are constants. It was shown in the same study that the efficiency of separation is substantially improved by using carbon dioxide, passed at the optimal velocity, as the carrier gas.

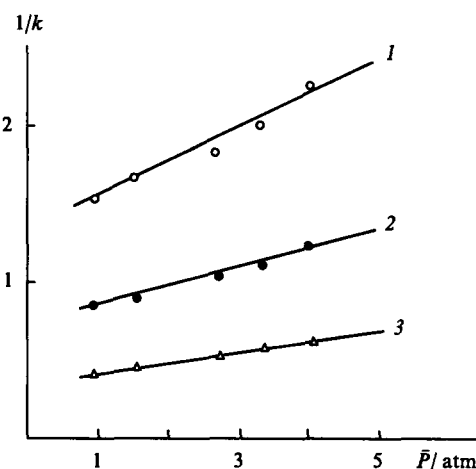


Figure 6. Dependence of $1/k$ on the average pressure of a carrier gas (carbon dioxide) in the column.

(1) Propylene, (2) butane, (3) but-1-ene. Experimental conditions: a $50 \text{ m} \times 0.32 \text{ mm}$ column; $\text{Al}_2\text{O}_3/\text{KCl}$ as the adsorbent; $T = 90^\circ \text{C}$.

The above features characterising the dependence of the retention of compounds being analysed on the properties of the mobile phase should also be taken into account in the practical use of capillary adsorption columns.

IV. Broadening of chromatographic zones in open tubular gas adsorption capillary columns

Broadening of chromatographic zones during their migration along the column is influenced by the character of movement of the carrier gas in the column, by the diffusion of the substances being separated in mobile and stationary phases, by the rate of interfacial mass transfer, and by characteristics of the adsorption layer used.^{13, 34, 51–53, 58–64}

Already in first studies on capillary chromatography, Golay^{58–60} proposed that, in order to increase the capacity index of the column, one should apply a layer of stationary liquid phase onto a porous layer of a solid support located on the inner walls of

[†] See V G Berezkin, I V Malyukova, V R Alishoev, J de Zeeuw *J. High Resol. Chromatogr.* **19** 272 (1996).

a capillary column rather than directly onto the smooth walls of the column. If the thickness of the film formed by the stationary liquid phase on separate particles of the solid support is the same as that formed on the smooth walls of the capillary, then the amount of the stationary liquid phase per unit length of the column becomes much higher, since the interior surface of the solid support is much greater in this case. This results in a decrease in the ratio of the phase volumes

$$\beta = \frac{V_g}{V_l}$$

(where V_g is the volume of the gas phase in the column and V_l is volume of the stationary liquid phase in the column), in an increase in the capacity factor k , and, hence, enhances the separation.

To describe broadening of chromatographic zones in open tubular capillary columns with walls coated by a porous layer, Golay has obtained the following equation:^{14,15}

$$H = \frac{2D_g}{u} + \left[\frac{1+6k+11k^2}{(1+k)^2} + \frac{(8+32k)a_2}{(1+k)^2} + \frac{8k^2}{(1+k)^2} \frac{a_1^2}{a_2} \right] \frac{r^2 u}{24D_g} + \left[\frac{k^3}{6(1+k)^2} \frac{1+2a_2}{F} \right] \frac{r^2 u}{K_D^2 D_l}, \quad (12)$$

where H is the height equivalent to a theoretical plate (HETP); D_g is the coefficient of diffusion of the compound under analysis in the gas phase; u is the linear velocity of the carrier gas; k is the capacity factor of the compound under analysis; $a_1 = d_i/r$ (d_i is the average length of the tortuous channels in the porous layer covering the inner walls of the column); $a_2 = d_g/r$ (d_g is the effective thickness of the gas layer in the porous layer covering the inner walls of the column); r is the internal radius of the column; F is the ratio of the surface area of the liquid phase to the surface area of the capillary walls; K_D is the coefficient of distribution of the substance under analysis between the mobile and stationary phases; and D_l is the diffusion coefficient in the liquid phase.

The last term in Eqn (12) reflects the resistance to the mass transfer in the liquid phase and it is inversely proportional to F . This implies that the efficiency of a capillary column should increase with an increase in the degree of porosity of the near-surface layer (H decreases with an increase in F). Thus, the idea of a capillary column with a porous layer of a solid support has already been included in the derivation of this equation. However, it should be noted that this equation, like other Golay equations, was obtained first of all for gas-liquid-solid (or gas-liquid) chromatography.⁴⁸

An equation relating HETP to the linear velocity of the carrier gas for gas adsorption chromatography has been proposed by Giddings.^{65,66} The first terms in the Giddings equation virtually coincide with those in the Golay equation. These equations differ, firstly, in the term that reflects the resistance to the mass transfer in the adsorption layer located on the inner walls of the capillary column and, secondly, in the allowance for the influence of the carrier gas pressure differential along the column on the broadening of chromatographic zones. The Giddings equation can be represented in the following way:

$$H = \frac{2D_g}{u_0} + \left[\frac{1+6k+11k^2}{24(1+k)^2} \right] \frac{r^2 u}{D_g} f_1 + \frac{8}{a_k u_m} \left(\frac{k}{k+1} \right)^2 \frac{V_g}{S} f_n u_0 f_0, \quad (13)$$

where u_0 is the linear velocity of the carrier gas at the outlet of the column.

$$u_0 = \frac{L}{t_m f_2}, \quad (14)$$

where L is the length of the column; and t_m is the 'dead time' of the column;

$$f_1 = \frac{9}{8} \frac{(P^4 - 1)(P^2 - 1)}{(P^3 - 1)}, \quad (15)$$

$$f_2 = \frac{3}{2} \frac{(P^2 - 1)}{(P^3 - 1)} \quad (16)$$

($P = P_i/P_0$, P_i and P_0 are carrier-gas pressures at the inlet and outlet of the column, respectively), a_k is the accommodation coefficient; u_m is the average velocity of the molecules of the substance under analysis in the gas phase, S is the overall surface area of the adsorbent layer in the column, and f_n is a factor reflecting the heterogeneity of the adsorbent.

If we neglect the influence of the pressure differential on the broadening of chromatographic zones (i.e. $f_2 \approx 1$, $f_1/f_2 \approx 1$), the Giddings equation for an adsorption capillary column assumes the form:

$$H = \frac{2D_g}{u} + \left(\frac{C_{gp}}{D_g} + C_{ad} \right) u \quad (17)$$

or

$$H = \frac{2D_g}{u} + Cu, \quad (18)$$

where

$$C = \frac{C_{gp}}{D_g} + C_{ad} = C_g + C_{ad}, \quad (19)$$

$$C_{gp} = \frac{1+6k+11k^2}{24(1+k)^2} r^2, \quad (20)$$

$$C_{ad} = \frac{8}{a_k u_m} \frac{V_g}{S} f_n \frac{k}{(1+k)^2}, \quad (21)$$

$$C_g = \frac{C_{gp}}{D_g}. \quad (22)$$

To verify whether Eqn (18) is in agreement with experimental results, it is convenient to write it in the following form:

$$Hu = 2D_g + Cu^2. \quad (23)$$

The D_g values can be calculated from the equation proposed by Fuller et al.⁶⁷ or by another theoretical method (see, for example, a published study⁶⁸). If we find the values for the resistance to mass transfer C for compounds subjected to chromatography with two carrier gases in an open tubular adsorption capillary column, then we can determine the real coefficients of resistance to the mass transfer in the gas phase (C_g) and in the adsorption layer (C_{ad}). The theoretical methods have been developed earlier by Perrett and Purnell for gas-liquid chromatography.⁶⁹

The first estimate of the coefficients of resistance to mass transfer from the Golay-Giddings equation was carried out by the Dutch researchers de Nijs and de Zeeuw.³⁶ They considered the chromatography of buta-1,3-diene in an open tubular adsorption capillary column (with alumina as the adsorbent) with helium and nitrogen as carrier gases and obtained the following values for $C \times 10^4$: C_g (butadiene in helium) = 1.3; C_g (butadiene in nitrogen) = 4.6; C_{ad} = 1.8. Thus, C_g and C_{ad} are of the same order of magnitude.

For comparison, we present the coefficients of resistance to mass transfer C_g and C_l reported by Cramers et al.⁷⁰ for the chromatography of tridecane in an open tubular capillary column with the inner walls coated with a stationary liquid phase layer. For a $24.7 \text{ m} \times 0.55 \text{ mm}$ column (with the CP-Sil 5-CB silicone as the stationary liquid phase, $T = 150^\circ \text{C}$), the following values have been reported, $C \times 10^4$: the coefficients of resistance to mass transfer in the gas phase C_g (tridecane in helium) = 2.8; C_g (tridecane in nitrogen) = 10.6; the coefficient of resistance to mass transfer in the liquid phase $C_l = 4.1$. It follows from these data that the coefficients of resistance to mass transfer for the gas-solid and gas-liquid variants of capillary chromatography are of the same order of magnitude.

A similar study has been carried out for a capillary gas adsorption column of the 'Chrompack' company (the Netherlands), the inner walls of which have been coated with a layer of the adsorbent $\text{Al}_2\text{O}_3/\text{KCl}$.⁴³ The results of this study are presented in Table 2. The values listed were determined from the linear Eqn (18). The results obtained are in good agreement with the experimental data.

Table 2. Coefficients of the Golay–Giddings equation for the separation of gaseous hydrocarbons in a capillary column with alumina.

Carrier gas	Calculation		Experiment	
	$D_g^a / \text{cm}^2 \text{ s}^{-1}$	$B^b / \text{cm}^2 \text{ s}^{-1}$	$B / \text{cm}^2 \text{ s}^{-1}$	C / s
For the analysis of ethane				
He	0.68	1.4	1.2	2.4
N ₂	0.22	0.44	0.45	6.8
CO ₂	0.175	0.35	0.36	8.0
For the analysis of propane				
He	0.56	1.11	0.96	3.0
N ₂	0.17	0.34	0.36	8.6
CO ₂	0.14	0.27	0.29	11.0
For the analysis of n-butane				
He	0.43	0.86	0.80	7.2
CO ₂	0.11	0.22	0.22	24.0

^a Calculated by the Fuller–Schettler–Giddings method.⁶⁷ ^b $B = 2D_g$.

The coefficients of diffusion of compounds subjected to chromatography in a carrier gas can be found from the coefficient B and calculated from the Fuller–Schettler–Giddings equation.⁶⁷

Thus, the values found using the Golay–Giddings equation are in satisfactory agreement with the experimental results for open tubular capillary columns both in the type of functional dependence and in the magnitudes of the diffusion coefficients for substances in the gas phase, which are determined from the experimental chromatographic data. For example, the coefficient

of diffusion for butane in helium, found from the Golay equation, is $0.40 \text{ cm}^2 \text{ s}^{-1}$, while the corresponding diffusion coefficient calculated from the Fuller–Schettler–Giddings equation is $0.44 \text{ cm}^2 \text{ s}^{-1}$.

It is noteworthy that the experimental data obtained by Goretti et al.⁷¹ have also been in good agreement with Eqn (18). These investigators used open tubular glass capillary columns, the inner walls of which were coated with a graphitised carbon black layer. The parameters B and C determined from their experimental results are listed in Table 3. It follows from these data that when the velocity of a carrier gas is more than 30 cm s^{-1} , the major contribution to the broadening of the zones corresponding to the compounds under analysis is made by the term reflecting the resistance to mass transfer.

To describe the dependence of HETP on the linear velocity of the carrier gas for open tubular gas adsorption columns, the following equation has been proposed⁷² (which is valid provided that the thickness of the porous adsorbent layer σ is much smaller than the radius of the column r (i.e. $\sigma/r \ll 1$):

$$H = \frac{2D_g}{u} + \frac{11k^2 + 6k + 1}{24(k+1)^2} \frac{r^2}{D_g} u + \frac{1}{3} \left(\frac{k}{k+1} \right)^2 \frac{\sigma r}{D_p \chi} u, \quad (24)$$

where D_p is the diffusion coefficient of the substance being analysed in the porous layer of the adsorbent (note that normally $D_p < D_g$), and $\chi = V_{pg}/V_p$, where V_{pg} is the pore volume in the adsorbent and V_p is the volume of the whole porous layer.

This equation implies that the H value decreases (the efficiency of the column increases), firstly, as the radius of the capillary column decreases and, secondly, as the degree of porosity of the adsorption layer increases. These dependences agree qualitatively with the experimental results.

In conclusion, it should be mentioned that the authors of some recent studies (see for example Ref. 73) have noted that the dependences of HETP on the linear velocity of the carrier gas observed experimentally for adsorption capillary columns do not agree with the Golay–Giddings equation.

V. Methods for the preparation of open tubular gas adsorption capillary columns

Methods for the preparation of open tubular adsorption capillary columns have some specific features which distinguish them from the known techniques used for the production of capillary columns with a stationary liquid layer.

Only methods for the production of adsorption capillary columns with a porous adsorbent layer have been reported. Columns of this type are characterised by high capacities and stable performance.

A method for the preparation of open tubular columns has to meet fairly stringent requirements.

(1) A method should ensure uniform distribution of the layer of an adsorbent over the whole inner surface of a capillary;

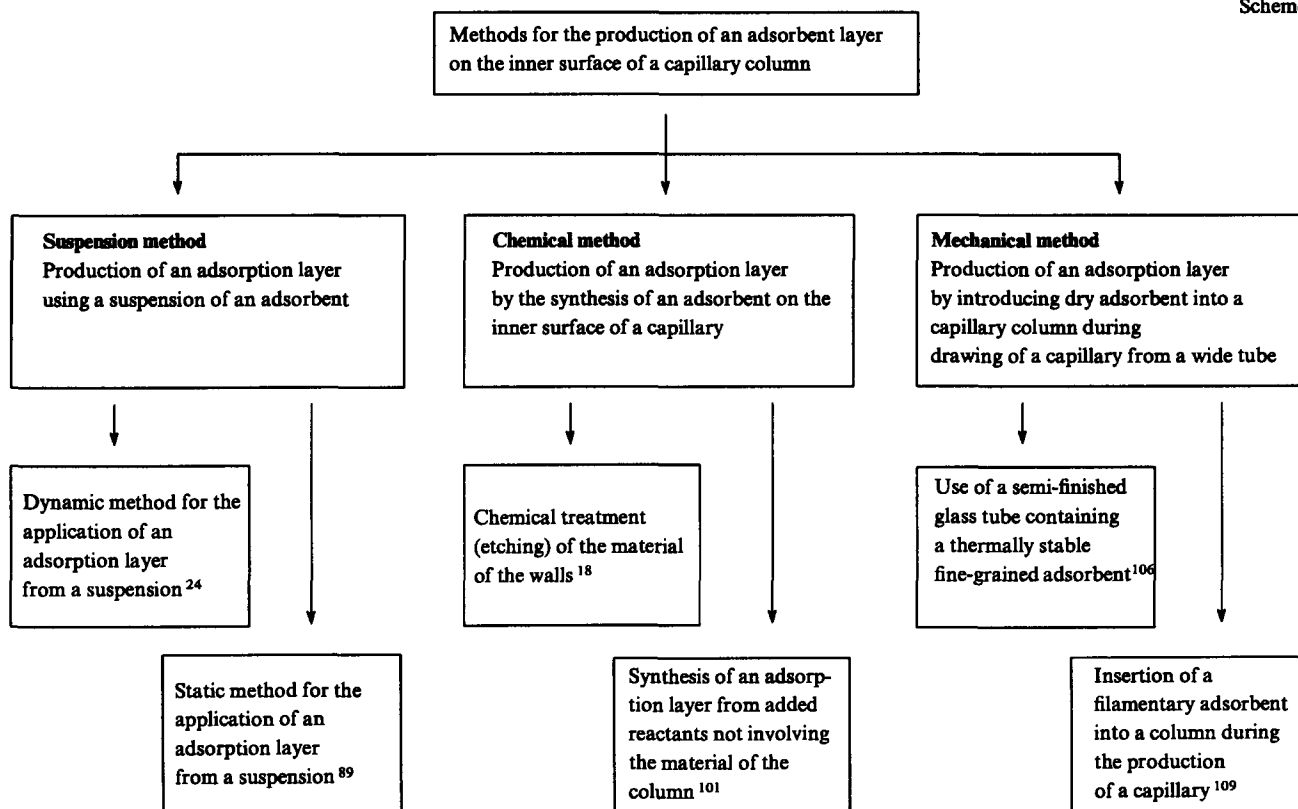
(2) the particles of the adsorption layer should be fixed fairly rigidly on the surface of the capillary;

Table 3. Characteristics of the processes of chromatography of isobutane (I) and n-butane (II) on gas adsorption capillary columns with graphitised carbon black of the MT type ($7 \text{ m}^2 \text{ g}^{-1}$).

Size of the column ^a /m × mm	Thickness of the sorbent layer/μm	K		$B / \text{cm}^2 \text{ s}^{-1}$		$10^3 C / \text{s}$		$H_{\text{min}} / \text{mm}$	
		I	II	I	II	I	II	I	II
9.6 × 0.2	100	1.00	1.54	0.17	0.13	5.7	6.0	—	1.41
11.0 × 0.25	65	1.97	3.02	0.17	0.14	8.3	10.0	—	1.26
11.0 × 0.3	45	1.57	2.42	0.17	0.15	6.4	7.1	—	1.64
11.0 × 0.2 ^b	100	2.05	3.14	0.17	0.13	4.3	4.5	—	0.91

^a The length (m) and the diameter (mm) of columns are given. ^b In this column, graphitised carbon black of the FT type was used ($15 \text{ m}^2 \text{ g}^{-1}$).

Scheme 1



(3) a method should ensure the possibility of preparing capillary columns with reproducible characteristics;

(4) a method should be suitable for producing adsorption layers based on various adsorbents;

(5) the procedure involved should take little time.

Development of a procedure satisfying all these requirements is a fairly complicated task involving various aspects.

The characteristics of the known methods for the preparation of open tubular adsorption capillary columns are shown in Scheme 1. It can be seen that three main techniques have been described to date, namely, suspension, chemical, and mechanical (construction) technique in which dry sorbent is introduced into a glass tube during the production of a capillary.

1. Suspension technique

The suspension method is similar to that used to apply a stationary liquid phase onto the inner walls of a capillary column. An adsorbent is dispersed in an appropriate liquid medium and introduced into a column as a suspension, and the volatile liquid is then removed. As in the 'classical' procedure for the deposition of a stationary liquid phase, dynamic and static versions of the suspension method have been developed. The main specific feature of the latter is heterogeneity (or microheterogeneity) of the system introduced into a capillary in order to prepare an open tubular adsorption column. In this case, the suspension which migrates along the capillary is a non-newtonian liquid, which often exhibits clear-cut thixotropic properties. During the flow of this liquid, the particles are segregated according to their sizes, in conformity with the regularities of flow chromatography in a force field.⁷⁴⁻⁷⁸ As a result, the rheological properties of the suspension vary during the application or during the filling of the column and hence, it is difficult to obtain an adsorbent layer which is uniform over the whole length of the capillary.

Nevertheless, the suspension method has been used even in the earliest works on the capillary adsorption chromatography. For example, silica has been applied onto the inner surface of polymeric, copper, or steel capillaries with lengths ranging from

4 m to 400 m and with an internal diameter of ~ 0.5 mm.^{24,75,79} It was noted that the use of suspensions containing micron-size particles is associated with some difficulties and that colloidal solutions of silica are preferred. Schwartz et al.²⁴ used a 22% sol of silica in a water-isopropyl alcohol system. After removal (evaporation) of the dispersion medium, a thin layer of solid silica remained on the inner walls of the capillary. The workers²⁴ did not mention whether a suspension stabiliser, which is usually present in systems of this sort, has remained on the silica particles after drying. Apparently, surfactants, which are used as stabilisers of suspensions, modify the surface and, consequently, have an influence on the retention.

The particle size in these sols does not exceed $0.02 \mu\text{m}$; therefore, the adsorption layer has a large specific surface area. A column produced by the suspension method was used to separate pentane and hexane isomers. However, the specific efficiency of the column, calculated from the chromatograms, did not exceed 100 theoretical plates per metre. In all probability, this low efficiency is due to the fact that the solid sorbent particles are nonuniformly distributed over the inner surface of the column. This is a result of the disadvantages peculiar to the dynamic method (fluctuations of the velocity at which the suspension meniscus moves and instability of the film formed), as well as of some specific features of the suspension.

Schwarz et al.⁷⁹⁻⁸¹ have prepared adsorption columns using larger silica particles ($\sim 4 \mu\text{m}$) with the surface modified with an organic surfactant, because the use of adsorbent particles with a size not exceeding that of colloidal particles can lead to the formation of a dense adsorption layer, which substantially hampers mass transfer.

The modified silica was applied by the dynamic method as a 7.5% suspension in *n*-hexane. The glass capillary column thus formed with a length of 120 m and with an inner diameter of 0.5 mm permitted separation of 13 isomeric C_5 - C_7 hydrocarbons over a period of 18 min. The specific efficiency of the column determined in relation to 2,4-dimethylpentene was 550 theoretical plates per metre.⁷⁹⁻⁸¹

In the early 60s, the dynamic method for the application of a solid support was used by the Perkin-Elmer company for the commercial production of copper gas-liquid capillary columns with a length of 15–30 m and 0.5 mm in diameter, meant for quick analysis of light gaseous hydrocarbons.⁸²

Capillary adsorption columns with graphite have been obtained by application of graphitised carbon black by the dynamic method.^{19,20} 15 m long copper columns with an internal diameter of 0.25 mm, the inner surface of which was coated with silver, were treated with a suspension of carbon black preliminarily graphitised at 3000 °C. The suspension was prepared by intense stirring (8000 rpm) of a mixture consisting of 15 g of carbon black, 220 ml of trichlorotrifluoroethane, and 30 ml of tetrachloromethane. Thus, the dispersion medium of this suspension had a density of $\sim 1.5 \text{ g cm}^{-3}$. The high density of the dispersion medium made it possible to obtain a fairly stable suspension, which passed through a column without aggregation of particles. The surface area of the capillary column thus obtained was 0.2–0.8 m², which made it possible to separate all the isomers of heptane at 245 °C.¹⁹

Ultrasonic treatment of graphite suspensions has been proposed in order to increase their stability.^{71,83,84} A suspension consisting of 0.25 g of Carboxpack A, 5 ml of dichloromethane, and 20 ml of tetrachloromethane was sonicated (frequency 20 to 24 kHz and amplitude 2 μm). The optimal time of irradiation was 40 min. The suspension thus prepared was passed through a column at a velocity of 0.6 ml min⁻¹ in both directions. The glass capillary column used was 10–15 m long and 0.4–0.5 mm in diameter.

A suspension of graphitised carbon black 'Sterling MT' prepared in a similar way has also been used for the production of an adsorption capillary column. The suspension was passed through a column with a reduced pressure at the outlet. This was possible, because the suspension had a low viscosity, due to the fact that its concentration did not exceed 1%.⁸⁴ However, the amount of the sorbent applied in this way proved insufficient to be used efficiently in the adsorption variant of chromatography. Therefore, the layer thus formed was used as a solid support for a stationary liquid phase, i.e. in the absorption–adsorption variant of chromatography.

Purcell⁸⁵ has used the dynamic method to prepare a column coated from the inside by a layer of 5 Å molecular sieves with a particle size of up to 20 μm . Later, the 'Chrompack' company has started the production of columns with molecular sieves applied by the dynamic method.⁴¹ The most interesting results on the application of an adsorbent layer by the dynamic method have been obtained with alumina suspensions.

The first attempt along this line was undertaken by Kirkland,²¹ who used Al₂O₃ as the fibrous mineral boehmite. Microscopic studies have shown that an elementary fibre of this mineral has a length of $\sim 1000 \text{ Å}$ and a diameter of 50 Å; the fibres are joined in aggregates $\sim 2 \mu\text{m}$ in diameter. The specific surface area of this sorbent is 275 m² g⁻¹. To prepare an adsorption column, a 7% aqueous sol of boehmite was injected into a glass (or stainless-steel) capillary of length 10 m and with an inner diameter of 0.25 mm (or 0.5 mm). When the suspension was passed and the adsorption layer was dried, the capillary column was ready for use. This column made it possible to separate a number of Freons; however, its efficiency was not very high.

The dynamic method for the application of Al₂O₃ has been developed further by Schneider et al.⁸⁶ They noted the following advantages of glass capillary columns, the walls of which are coated by an alumina layer, over metallic capillaries: (1) the adsorption activity of the walls of the columns is low; (2) finely powdered alumina is readily applied onto a glass surface without any fixing agents and forms thin layers, which do not fall off the walls even when the capillary is deformed within its elasticity limits; (3) the process of application and the quality of the column can be monitored visually; (4) glass capillaries of any size can be easily produced in a laboratory.

The following procedure can serve as an example of filling a capillary column. The suspension is prepared by mixing 20 g of alumina (obtained by calcination of aluminium hydroxide with particles no larger than 2 μm) with 70 ml of a 5% colloidal solution of Al₂O₃ and with 0.3 ml of glacial acetic acid. The resulting suspension is exposed to ultrasound, filtered through 300 mesh sieves, and allowed to stand for 24 h for maturing. The suspension thus obtained possessed thixotropic properties.

The use of a colloidal solution of alumina provides a dispersion medium with high density and viscosity, which increases the stability of the suspension. In addition, colloidal particles of alumina cement large particles of the sorbent and thus fix them additionally on the capillary surface.

Prior to the application of Al₂O₃, the capillary column is washed with 1% acetic acid. For the deposition of an alumina layer onto the inner walls of the column, the suspension is pressed through a capillary at a velocity of 4 ml min⁻¹. At this rate, 0.6 ml of the suspension is sufficient to coat 15 m of the column. As the final stage of the process, the column is stored for 10 h and is subsequently dried at room temperature in a flow of nitrogen. A 65 m long column of diameter 0.4 mm is dried for a week at a nitrogen pressure of 0.3 MPa at the inlet.

After drying, the column is activated for 3 h at 300 °C. The column thus obtained has been reported⁸⁷ to contain $\sim 6 \text{ mg}$ of Al₂O₃ per metre. The quantity of the sorbent can be varied over a relatively wide range by varying the viscosity of the suspension, the velocity at which it is pressed through the column, or the volume of the suspension introduced in one portion.

To decrease the adsorption activity, the column is washed twice with a 2% solution of potassium chloride. After repeated drying and heating, the column is ready for use. The columns obtained in this way are sufficiently efficient for the separation of various substances. For example, their efficiency with respect to the peak for 3-methylbut-1-yne (the capacity factor is 7.1) is 700 tp m⁻¹. Altogether more than 50 light hydrocarbons present in a gas mixture in concentrations of about 1 part per billion each, were separated under isothermal conditions at 130 °C. A similar procedure for the application of an adsorbent onto inner walls of the column has been employed by de Nijs³⁵ to prepare quartz capillaries, which have been widely used for capillary columns in recent years. The application by virtue of the dynamic method requires using concentrated suspensions, since the amount of an adsorbent remaining in the column is only that contained in the thin film formed after passing the suspension. It is of interest that when a suspension prepared from spherical silica gel particles with a diameter of $\sim 5 \mu\text{m}$, meant for high performance liquid chromatography (HPLC), is passed through a column, only a loose monolayer of silica gel particles covering only 50% of the whole inner surface of the capillary is formed.

Preparation of capillary columns containing a barium sulfate layer (a solid adsorbent) on the surface has been reported.⁸⁷ Barium sulfate (which is an ionic adsorbent) is known to exhibit high selectivity in the separation of polar organic compounds.⁸⁸

The barium sulfate used as the adsorbent in open tubular capillary columns was prepared separately by the reaction between 1.5 M solutions of barium chloride and sodium sulfate. The precipitate was filtered off and washed, until chloride ions were no longer detected ($S = 10.2 \text{ m}^2 \text{ g}^{-1}$). Barium sulfate was applied onto the inner walls of a capillary column (Pyrex) by the dynamic method. The solvent was removed and then the columns were conditioned at a temperature programmed to increase to 250 °C. Since the asymmetry A_s of the columns obtained amounted to 4.5 with respect to benzene, they were modified by a dynamic method using small amounts of poly(ethylene glycol) (Carbowax 3000) and polydimethylsiloxane (E-301). After modification, the efficiency of the columns sharply increased (from 900 to 2500 tp m⁻¹) and the chromatographic zones became more symmetrical. The retention of compounds in this column is caused by both adsorption and absorption processes.

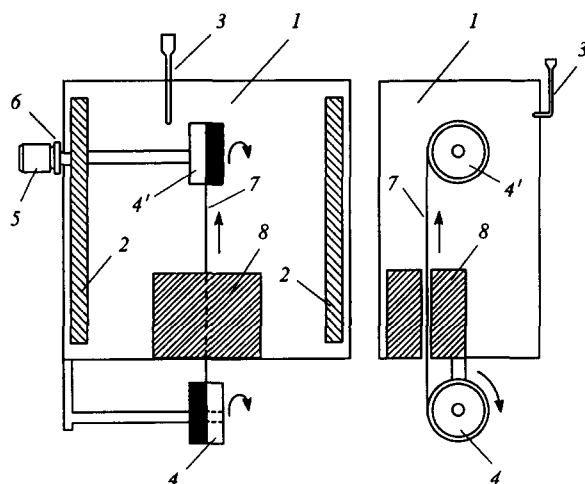


Figure 7. Arrangement for the production of open tubular adsorption capillary columns by applying an adsorbent to their inner walls using a high-pressure static method.⁸⁹

(1) Air thermostat, (2) heater, (3) thermometer, (4, 4') reels, (5) electric motor, (6) connection, (7) capillary tube, (8) heated metallic unit.

To increase the thickness of the layer, attempts have been made to use the static variant of the suspension technique. Horvath⁸⁹ has constructed a special device (Fig. 7) for this purpose. A metallic capillary column was completely filled with a suspension of a sorbent in a volatile solvent; then one of the ends of the column was closed, while the other end was introduced into an air thermostat heated to 90–150 °C (through a metallic unit heated to 200–250 °C). The volatile liquid was evaporated in the metallic unit, and its vapour did not condense owing to the high temperature.

A similar device modified by Mistryukov et al.³⁰ has been used by Guiochon et al.⁹⁰ for the preparation of an open tubular capillary column containing 'Sterling FTG' graphitised carbon black. Initially, a 5% suspension of carbon black in dichloromethane was prepared. When squalane (0.05%) was used as the stabiliser, this suspension was stable over 24 h. This procedure makes it possible to apply 10 mg m⁻¹ of the sorbent. A mixture of *o*-, *m*- and *p*-xylenes was separated at 165 °C in columns (19 m × 0.5 mm). The use of a 20% suspension of carbon black and a high-pressure static method made it possible to increase the thickness of the layer to 20 µm.⁹¹

A simple method for the production of adsorption capillary columns has been proposed.⁹² Silica particles (5 µm) and carbon particles were suspended in a solvent, together with polydimethylsiloxane. The suspension was passed through a column (25 m × 0.32 mm), then the column was dried and heated. This gave a very stable layer.

Using the device proposed by Horvath,⁸⁹ Ettre et al.³¹ have manufactured a capillary column containing a layer of Johns-Manville diatomite with an average thickness of 60 µm. In view of the fact that a sorbent with a particle size of 10 µm was used, it can be inferred that it was possible to deposit ~6 layers of the sorbent in one entry. Apparently, this result could not be achieved by the dynamic method. However, the static procedure also suffers from some drawbacks. First of all, the necessity to fill capillaries with a suspension should be regarded as being a drawback, i.e. this method, too, does not make it possible to avoid movement of a suspension along the tube. Consequently, the structure of the suspension is disturbed, particles are combined into aggregates, which are nonuniformly distributed along the column, and this leads to the formation of an inhomogeneous layer and decreases the efficiency of the separating system. In addition, this method is applicable only to volatile dispersion media, which usually possess low densities.

2. Chemical synthesis of an adsorbent on the inner surface of a capillary column

Conduction of chemical reactions yielding adsorbents directly in a column has been employed already in the early papers dealing with the preparation of open tubular capillary columns. A possible advantage of this method is that the preparation of an adsorption layer does not require using suspensions and involves only homogeneous reagents, which easily fill the whole column and can be easily removed from it. In addition, this technique provides the possibility of repeating the reaction in order to increase the thickness of the adsorption layer.

a. Etching of a capillary

The first attempts to use the technique under consideration involved preparation of a sorbent by a chemical transformation of the material from which the column was produced. This approach has been used most widely in relation to glass columns; in this case, etching or leaching of the walls by various procedures affords layers of adsorption-active silica gel.

The first results obtained by this approach have been published in a number of papers.^{16–18, 93} Kiselev et al.⁹³ have separated gaseous hydrocarbons C₁–C₄ in column (10 m × 0.5 mm), which had been preliminarily treated for a short period with 0.1 M HCl and then washed with distilled water.

Mohnke and Saffert^{17, 18} have filled a capillary of length 80 m with a diameter of 0.27 mm with a 17% solution of ammonia, sealed both ends of the column, and kept it for 70 h at 170 °C. After that, the liquid was removed, and the column was dried at 190 °C in a flow of a carrier gas. This procedure yielded a ~20 µm thick adsorption layer on the inner surface of the capillary. The column thus produced was used for the separation of isotopes and nuclear spin isomers of hydrogen.

Alkaline etching of glass has also been used by other researchers.^{28, 94–96} Their procedure involved treatment of the walls of a column with a 20% solution of NaOH for 6 h followed by activation in a flow of nitrogen at 200 °C. The columns thus produced proved suitable for the separation of oxygen and nitrogen isotopes.

The production of open tubular capillary columns, containing an internal porous layer with a fixed thickness, by etching has been patented.^{97, 98} Initially, a two-layer column was produced from a two-layer half-finished article consisting of two coaxial tubes. The outer tube was made of a chemically stable glass, while the inner tube was made of a chemically less stable sodium borosilicate glass. The resulting two-layer capillary was treated with alkali, which led to almost complete leaching of the inner glass layer. The porous glasses thus obtained were used as adsorbents in a capillary column. Porous glasses are known to be used successfully in gas chromatography (see for example Ref. 99).

Similar procedures have been proposed for covering the inner surface of a column with alumina (keeping aluminium capillaries in a flow of oxygen²³) or with copper(II) oxide (treatment of copper capillaries with 40% HNO₃ followed by oxidation with dry oxygen).¹⁰⁰

The known methods for chemical treatment of capillary walls are facile but not versatile and are limited only to glass (or, more rarely, to metallic) columns. In addition, the composition and properties of the resulting adsorption layer are markedly dependent on the composition of the material of the column, which can vary.

b. Synthesis of an adsorbent inside the column

A variety of adsorbents (and capillary adsorption columns) can be obtained by synthesising them inside the columns. The walls of the column are not involved in these processes. An example is provided by the reported¹⁰¹ synthesis of an inorganic adsorbent, crystalline barium carbonate, on the walls of a capillary, which makes it possible to obtain a markedly more extended surface. This method has been applied successfully to a quartz capillary column.¹⁰²

Apparently, a similar method can also be used for the preparation of capillary columns containing barium sulfate (as an adsorbent). First, barium hydroxide is applied to the inner surface of a column and then gaseous sulfur trioxide is passed through it.

Recently, a method for the production of a capillary column containing an adsorption silica layer has been proposed. The method is based on hydrothermal treatment of a sol of silica directly in a capillary column.¹⁰³ A capillary is filled with a silica sol, then a part of the sol (15%–20% in the case of glass columns) is displaced from the column by a compressed gas, in order to avoid damage of the column during its subsequent heating; then both ends are hermetically closed, and the column is kept in a thermostat at 180–210 °C for several hours. Under these conditions, a silica film forms on the inner surface of the column; this results from two processes occurring in parallel, namely, dissolution of small particles of the sol and polymerisation of silica gel on the surface of the column having a large radius of curvature. Washing and drying afford a stable and relatively uniform coarse-pored layer of silica, which is not washed out from the walls. The thickness of the layer depends on the concentration of the sol and on the duration of treatment. The optimum concentration of the sol is 0.1%–1.5%. At higher concentrations, the thickening of the silica film on the surface ceases, and coagulation of the sol in the bulk occurs instead. When the sol concentration is lower than 0.1%, dissolution predominates, and the silica film does not form at all. Under the conditions specified, the treatment of the column should last for 5–11 h. Heating for a longer period does not lead to any substantial increase in the layer thickness, since the rate of polymerisation markedly decreases at the end of heating. Shorter heating results in the formation of a very thin layer with low adsorption activity. The columns obtained in this way can be used advantageously for quick analysis of light hydrocarbons.¹⁰³

Volkov et al.¹⁰⁴ have proposed a simple method for producing an adsorption layer based on magnesian cement.

It is noteworthy that the technique involving synthesis of an adsorbent inside a capillary has also been used to produce adsorption capillary columns with organic hydrophobic adsorbents.¹⁰⁵

3. Mechanical method (formation of an adsorption layer during production of a glass capillary)

When a glass capillary is manufactured, a ready-for-use sorbent can be introduced into it without being converted into a suspension. Since a capillary is drawn from a relatively wide tube, a sorbent can be easily placed into it before drawing.

Halasz and Heine¹⁰⁶ have produced in this way columns with alumina. In order to preserve an open passage inside the column, they inserted a steel wire 1 mm in diameter into it. As the tube was drawn, alumina particles were captured by the softened glass. The resulting 2 m long column was an intermediate version between a packed column and an open tubular capillary column and exhibited a relatively high efficiency, 3500 tp m^{-1} with respect to ethylene.

In a later modification of this technique, the diameter of the wire was diminished to the size of the inner passage in the column, and the wire itself passed through the area of softening and ended in the capillary (Fig. 8). This design permitted the diameter of the inner tube in the column and, hence, the thickness of the layer to be exactly specified. For example, Grant¹⁰⁷ has manufactured a column with an inner diameter of the capillary of 0.3 mm and with a 100 μm thick alumina layer by using a 0.1 mm thick tungsten wire. In this study, lithium chloride was used as a binding agent in the preparation of the adsorption column. The height equivalent to a theoretical plate for this column was ~ 0.5 mm.

Since this technique involves heating of adsorbents to high temperatures (700–800 °C), the range of adsorbents used is limited to thermally stable substances withstanding temperatures up to the temperature of glass softening. Therefore, apart from alumina, graphitised carbon black has been used. Goretti et al.¹⁰⁸ has produced by this method capillary columns with a length of ~ 10 m containing 50–100 μm thick layers of graphitised carbon

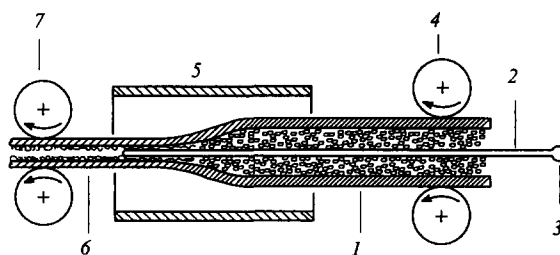


Figure 8. Arrangement for the production of open tubular adsorption columns during drawing of a capillary from a wide tube.¹⁰⁷

(1) Pyrex tube (outer diameter 9 mm, inner diameter 5 mm) filled with particles of a solid packing material (support or adsorbent) and with particles of anhydrous lithium chloride, (2) tungsten wire (diameter 0.3 mm), (3) the point of fastening of the tungsten wire, (4) feeding rollers, (5) electric furnace, (6) the column with a sorbent layer on the inner walls being produced, (7) pulling rollers.

black. The efficiency of the columns obtained was $\sim 1500 \text{ tp m}^{-1}$, their permeability being relatively high.

According to the interesting method proposed by Liberti et al.,¹⁰⁹ a graphitised fibre (7.5–10 μm in diameter) was inserted into the initial tube. When this tube was drawn into a capillary by the usual procedure, the fibre reeled out of the spool and entered the capillary; as this occurred, a gap of 0.2–0.3 mm remained inside the capillary. The length of the column thus obtained varied from 1.5 to 10 m, and the inner diameter varied from 0.4 to 0.5 mm.

In our opinion, application of an adsorption layer during the production of a glass capillary from a wide tube is among the most promising techniques; however, it also suffers from some drawbacks. Firstly, it is applicable only to thermally stable adsorbents (for example, polymeric adsorbents cannot be used in this method). Secondly, to obtain a tightly fixed adsorption layer, a specific binding material should be selected for each type of adsorbent and for each material of the column. Thirdly, in the case of sorbents, which are unstable in air at high temperatures, the process must be conducted under an inert atmosphere, which complicates the apparatus used.

The method for the production of open tubular adsorption capillary columns by synthesising sorbents directly in the capillary permits the simultaneous solution of two problems — preparation of the sorbent and its fixing to the walls. However, it is applicable to a limited range of adsorbents.

In our opinion, the suspension method is most universal as regards the preparation of open tubular capillary columns. However, in this method, too, the problem of fixing an adsorbent on the inner walls of a capillary column has not been solved. The way of fixing and the substance suitable for this purpose should be specially selected. What particular method is optimum in each case depends apparently on the type of sorbent used and on the material of the column.

In conclusion, it should be noted that the problem of the preparation of open tubular capillary columns with walls coated by an adsorption layer cannot be regarded as already solved. This delays somewhat the application of the adsorption capillary chromatography. Elaboration of new methods for the preparation of highly efficient open tubular capillary columns is a basic challenge in the development of capillary gas adsorption chromatography.

VI. The use of open tubular gas-solid capillary columns

At present, gas-solid capillary chromatography is widely used in analytical practice. The area of application of gas adsorption capillary columns is constantly extending. In 1995, columns of this type were presented at the Pittcon-95 workshop by four well-known companies from the USA alone (Table 4). However, the

Table 4. Some characteristics of new capillary gas adsorption columns presented at the Pittcon-95 workshop.¹¹⁰

Sorbent	Thickness of the sorption layer / μm	Dimensions of the column ^a /m \times mm	Notes
Carboxen-1006 column from Supelco			
Carbon molecular sieves, $S = 750 \text{ m}^2 \text{ g}^{-1}$	—	$30 \times 0.32 (0.53)$	Separation of permanent gases and $\text{C}_1 - \text{C}_3$ hydrocarbons, temperatures of up to 250°C
Gas-Pro-GSC column from Astec			
Not indicated	—	$(5-60) \times 0.32$	C_{10} and lighter hydrocarbons; carbon, sulfur, and nitrogen oxides; sulfur and halogen-containing organic compounds, permanent gases
HP PLOT Molsieve column from Hewlett-Packard			
5A Molecular sieves	12.50	Various	Permanent gases, separation of argon and oxygen at ambient temperatures, separation of krypton and nitrogen
RT Molsieve 13X column from Restek			
13 X Molecular sieves	1.2-4.0	$(15; 30) \times (0.32; 0.53)$	Permanent gases, 13X molecular sieves ensure faster and more effective separation than 5A molecular sieves
RtD PLOT column from Restek			
Divinylbenzene	2	30×0.53	Permanent gases and hydrocarbons, separation of air, carbon dioxide, light hydrocarbons, natural gas
Supel Q PLOT column from Supelco			
Divinylbenzene	—	$30 \times (0.32; 0.53)$	$\text{C}_1 - \text{C}_{10}$ hydrocarbons, chlorofluorohydrocarbons, sulfur-containing gases

^a The length (m) and the diameter (mm) of the columns are given.

current level of practical application of open tubular capillary columns is far from their real potential. While developing new analytical procedures, one should take into account the advantages and the limitations of the gas-adsorption chromatography (see above). The adsorption capillary chromatography is a hybrid method combining the advantages of the adsorption and capillary versions of chromatography.

Considering the advantages of capillary columns over packed columns, only the higher efficiency of the former is often mentioned. At the same time, capillary columns are also characterised by higher rates of separation (quicker analysis), by more reproducible temperature regimes, by small sizes of the apparatus

needed, and by lower consumption of carrier gases and sorbents; they also extend the field of application of gas adsorption chromatography, due to lower separation temperatures.

In order to select the optimum conditions while developing a procedure for separation, it is expedient to consider a plot that makes it possible to estimate quickly the number of theoretical plates needed (and, hence, the length of the column), if the selectivity and capacity of the adsorbent used are known.

Figure 9 shows the dependence of the number of theoretical plates needed for separation (N_r) on the selectivity of the sorbent used (α) for compounds characterised by different capacity factors (k):

$$N_r = \varphi[(\alpha-1), f^2]. \quad (25)$$

The influence of the capacity factor is reflected in this plot by the following function

$$f^2 = \left(\frac{k+1}{k} \right)^2 = \left(1 + \frac{\beta}{K_D} \right)^2, \quad (26)$$

each f^2 value being matched by a particular curve:

$$N_r = \varphi[(\alpha-1), f^2] = \text{const}. \quad (27)$$

Let us consider an example of practical application of the plot shown in Fig. 9. Assume that we have to determine the number of theoretical plates needed to separate two components with $\alpha = 1.05$ and $K_D = 100$ in a column with $\beta = 40$. For this pair of compounds, $f^2 = 2$. For the characteristic curve $f^2 = 2$, the point $\alpha-1 = 0.05$ on the abscissa in Fig. 9 corresponds to the point $N_r = 16000$ theoretical plates on the ordinate. Thus, we determined the desired efficiency of the column, which is needed to separate the pair of compounds in question.

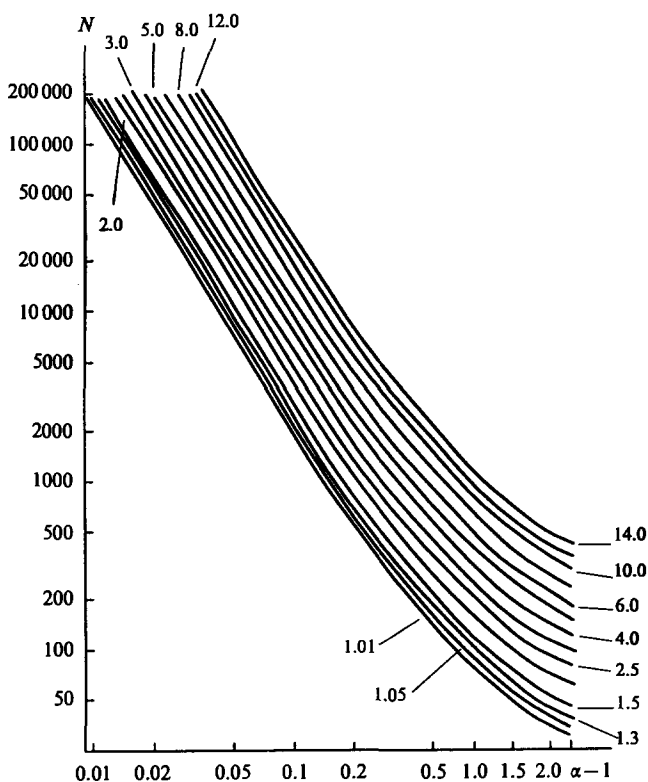


Figure 9. Graphical determination of the number of theoretical plates N_r , needed to separate a pair of compounds, depending on the selectivity of the sorbent α and the parameter f^2 , which is determined by the capacity factor k .¹¹¹

The numbers on the curves give the magnitudes of f^2 .

An important field of practical application of gas chromatographic analysis is the analysis of impurities.^{13,52,61,63,112} Sensitivity (detection limit) is often a crucial characteristic of a method used for this kind of analysis. As samples become larger, the sensitivity of determination increases, but the efficiency of the column simultaneously decreases. Therefore, the dependence of the efficiency (i.e. of the HETP) on the size of the sample being analysed is of practical interest regarding the optimisation of the separation conditions, since to achieve a higher sensitivity, the samples subjected to analysis should be as large as possible.

The dependence of HETP on the size of the sample in the capillary chromatography determines whether a capillary column without a flow splitter can be used, and also whether the use of a particular column in the traditional methods for the determination of impurities would be expedient. The dependence of the chromatographic zone broadening on the size of the sample under analysis has been discussed in a number of studies (see for example Refs 61,63,112).

It would be convenient to evaluate this dependence quantitatively using a linear equation relating HETP to the size of the sample. An equation of this type has been proposed.¹¹³ It is in satisfactory agreement with the experimental results obtained for open tubular capillary columns containing a stationary liquid layer (as an adsorbent) and for packed capillary columns.¹¹⁴

The dependence of the efficiency of a column on the size of the sample under analysis has been studied in relation to an open tubular gas adsorption column with alumina-coated inner walls (produced by 'Chrompack').⁴³ The experimental results were processed in terms of the following equation:¹¹³

$$\sqrt{H} = \sqrt{H_0} + \lambda W, \quad (28)$$

where H_0 is the limiting HETP value corresponding to the sample size approaching zero, λ is a constant determined by characteristics of the system in question; W is the size of the sample injected into the column (or a quantity proportional to it). Eqn (28) makes it possible to determine both the H_0 value and the variation of H as a function of W .

The dependences $\sqrt{H} = \Psi(W)$ corresponding to Eqn (28) and obtained in experiments with the same open tubular capillary column but using different methods for the injection of the sample (with and without a flow splitter), are shown in Fig. 10. The plots of HETP against the size of the sample in these coordinates are linear, which experimentally confirms Eqn (28). When the sample is introduced with a flow splitter, the efficiency of the column increases (the \sqrt{H} value decreases). However, as regards the increase in the sensitivity, the least flow splitting (i.e. the least possible discharge) or even no splitting are desirable.

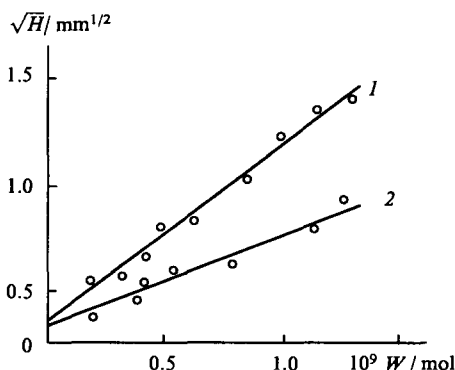


Figure 10. Dependence of \sqrt{H} on the size of the sample under analysis for *n*-butane in an open tubular capillary adsorption column with inner walls coated with alumina, the sample being injected without a flow splitter (1) and with a flow splitter (2).⁴³

A 50 m \times 0.32 mm quartz column from Chrompack (Netherlands) with an alumina layer and a flame ionisation detector were used; $T = 100^\circ\text{C}$.

Note that irrespective of the method used for the injection of samples (with or without a flow splitter), the limiting value of the efficiency of the column H_0 is nearly the same. This specific feature of the dependence observed is additional evidence for the validity of Eqn (28).

The results obtained indicate that an open tubular packed column with inner walls coated with an adsorption layer can also be used in a gas chromatograph without a flow splitter (although in this case, the efficiency markedly decreases). However, the decrease in the efficiency is not very significant for a fairly broad range of analytical procedures.

At present, gas adsorption chromatography is used most frequently for the analysis of volatile compounds with various isotope compositions, of inorganic and organic gases, of volatile organic polar compounds, and of aqueous solutions of organic compounds.

The separation of nuclear spin isomers and isotopes of hydrogen¹⁸ was the first prominent example of the practical application of the adsorption capillary chromatography (see Fig. 2). Later, it has been shown that the time required for the separation of the nuclear isomers of protium and deuterium could be shortened by decreasing the temperature of the column to 47 K.¹¹⁵

Oxygen isotopes ($^{16}\text{O}_2$ and $^{18}\text{O}_2$) have been separated in an adsorption capillary column⁹⁶ (Fig. 11). The adsorption layer on the inner walls of a glass column was produced by etching the walls with 20% NaOH for several hours at 100°C . When this process was prolonged enough (more than 4 h), clear separation of the isotopes was achieved. The efficiency of the capillary columns used was $\sim 350\,000$ theoretical plates. A mixture of nitrogen (65%) and helium (35%) was used as the carrier gas.

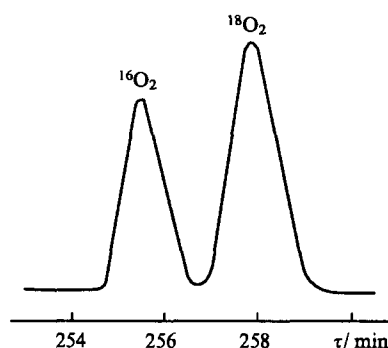


Figure 11. Chromatogram for the separation of a mixture of $^{16}\text{O}_2$ and $^{18}\text{O}_2$ isotopes in an adsorption glass capillary column (175 m \times 0.3 mm) at 77 K, and with the N_2 (65%)–He (35%) binary carrier gas.⁹⁶

Nitrogen isotopes ($^{14}\text{N}_2$ and $^{15}\text{N}_2$) have been separated by Cartoni and Possanzini⁹⁴ in an open tubular gas adsorption glass capillary column, the inner walls of which had been etched in order to produce an adsorption layer. The procedure for the preparation of this column has been reported.⁹⁵

Figure 12 shows the chromatogram for the separation of the nitrogen isotopes. The experiment lasted for ~ 3 h; however, only partial separation was achieved. It is obvious that the separation can be markedly improved, for example, by optimising its conditions.¹¹⁶

It is noteworthy that the nitrogen isotopes have been separated on a sorbent with a very low selectivity ($\alpha = 1.006$). A mixture of helium and carbon dioxide (45%) was used as the carrier gas, the latter also acting as a modifying agent for the adsorption layer of silica coating the walls of the column.

A sharp separation of neon isotopes (^{20}Ne and ^{22}Ne) has been achieved by Purer et al.¹¹⁶ at a low temperature (19 K). The height equivalent to a theoretical plate for the glass column used (82 m \times 0.28 mm) amounted to 0.8 mm at $k = 0.8$ and $\alpha = 1.06$.

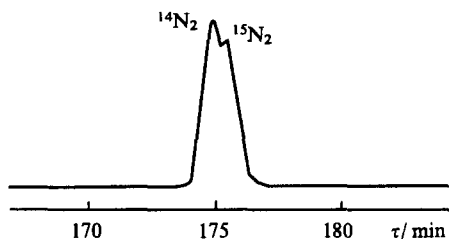


Figure 12. Chromatogram for the separation of nitrogen isotopes.⁹⁴

An open tube glass capillary column (175 m × 0.28 mm) with walls coated by an adsorption layer obtained by etching and a mixture of helium and carbon dioxide (45%) as the carrier gas were used; $T = 77$ K.

Complete separation of neon isotopes can be achieved if a shorter column (45 m) is used.

To obtain the adsorption layer on the walls, the initial capillary was etched with 10% sodium hydroxide for 6 h at 100 °C according to the procedure proposed by Brunner and Cartoni.²⁸ It has been reported¹¹⁶ that mixtures containing ²¹Ne can also be separated by this procedure.

The separation of hydrogen isotopes¹⁸ has certainly stimulated studies aimed at the separation of isotopically substituted molecules of organic compounds.

Figure 13 presents a chromatogram obtained for the separation of methanes with different isotopic compositions.²⁷ It is of interest that not only the methane molecules containing different hydrogen isotopes but also those with different carbon isotopes were separated in this experiment. Thus, we can agree with the opinion stated sometimes that a chromatograph is also a simple and cheap mass spectrometer.

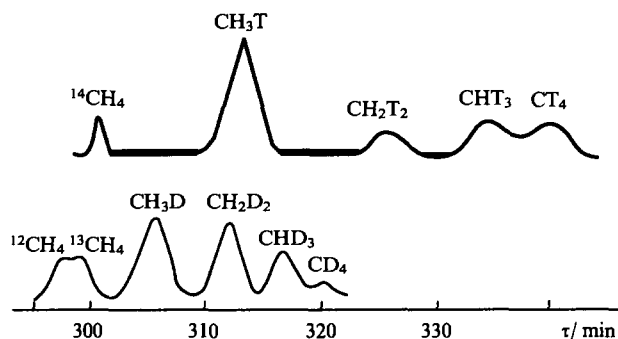


Figure 13. Chromatogram for the separation of deuterated and tritiated methanes.²⁷

The separation of methanes (see Fig. 13) was carried out using an open tubular adsorption capillary column containing a silica layer, which had been etched with a sodium hydroxide solution, according to a previously described procedure.²⁸ The column used was fairly effective (70 000 theoretical plates), and the peaks were symmetrical even at low temperatures. A mixture of helium (30%) and nitrogen (70%) was used as the carrier gas. A clear separation of tritiated methanes in a substantially more prolonged experiment has been also reported.¹¹⁷

In our opinion, the use of adsorption capillary columns with molecular sieves as the adsorbent holds the greatest promise for the separation of isotopically substituted molecules. Separation of molecules of gaseous compounds differing in the isotope composition is a promising branch of capillary gas adsorption chromatography.

Some progress has been achieved in the separation of isotopically substituted liquid organic compounds. For example, separation of benzene and deuteriobenzene and of toluene and

deuteriotoluene has been reported.¹⁰⁸ This was accomplished on a capillary column with a layer of graphitised carbon black.

The above examples indicate that adsorption capillary columns can be successfully used for the separation of isotopically substituted compounds. Further studies along this line will substantially simplify tracer techniques.

The separation of inorganic and organic gases in capillary columns is of great practical significance. In our opinion, capillary columns with molecular sieves are the most promising. Purcell⁸⁵ was the first to use columns of this type for the separation of permanent gases. An interesting example of using 13 Å molecular sieves for separation of hydrocarbons of various types in capillary columns has also been reported.^{118–120}

The procedure used currently for the separation of permanent gases in an open tubular flexible quartz capillary column with molecular sieves was apparently described for the first time by de Zeeuw and de Nijs,¹²¹ Verga,¹²² who has used a similar column, has demonstrated that columns of this type are suitable for solving a number of practically important problems. He used a highly sensitive helium ionisation detector. Fig. 14 shows the results of separation of a standard mixture of permanent gases in helium and of determination of carbon monoxide present in air in a concentration of 2–3 ppm. It is noteworthy that oxygen and argon (3 ppm) are clearly separated under these conditions at 35 °C.

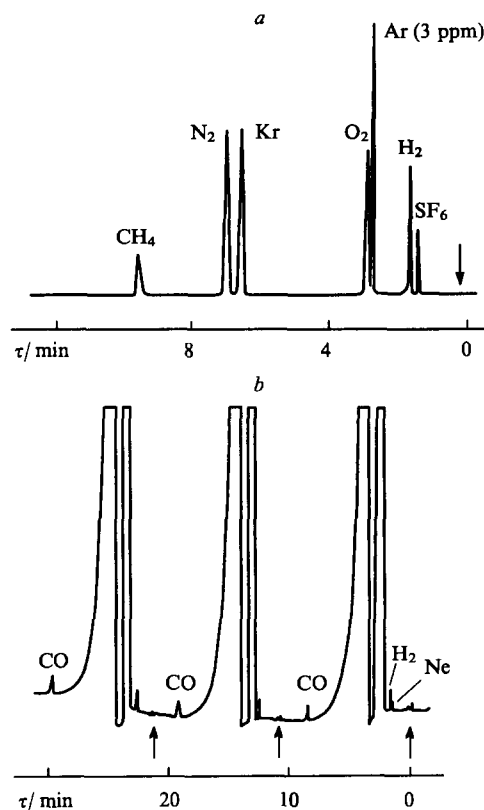


Figure 14. Chromatogram for the separation of a mixture of permanent gases in helium at 35 °C (a) and for determination of carbon dioxide in air at 80 °C (b).¹²²

A 25 m × 0.32 mm column with 5 Å molecular sieves was used.

Oxygen and argon as well as samples of methane differing in the hydrogen isotope composition have been separated¹²³ in a capillary column with 5 Å molecular sieves at room temperature.

Among the numerous fields of application of open tubular adsorption capillary columns, space research should be mentioned. For example, for the studies dealing with the atmosphere of Titan (a satellite of Jupiter), a procedure for the analysis of a gas

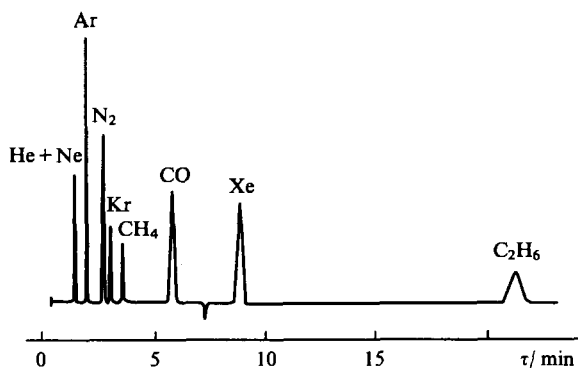


Figure 15. Chromatogram for the separation of a mixture of inorganic and hydrocarbon gases in a quartz adsorption column.⁷³ A 10 m × 0.53 mm column with 5 Å molecular sieves was used (the adsorption layer was 50 μm thick); $T = 90^\circ\text{C}$; hydrogen with a velocity of 2 ml min^{-1} at the outlet of the column was used as the carrier gas, the flow spitting was 1 : 40, and a katharometer was used as the detector.

mixture simulating qualitatively the suggested composition of the atmosphere of this satellite has been developed by Vanssay et al.⁷³ (Fig. 15).

Analysis of mixtures of gaseous hydrocarbons and light hydrocarbons is a practically important problem. Alumina is widely used for the separation of these compounds. The analytical potential of columns containing alumina was demonstrated for the first time by Schneider et al.⁸⁶

A significant contribution to the perfection of columns of this type has been made by researchers of the 'Chrompack' company.^{35-37, 41, 124} In recent years, this company has been manufacturing open tubular capillary columns based on metallic capillaries with an inert inner surface coated with a layer of an inert material (Ultimet column). Two modifications of these columns containing alumina are produced; they differ in the salt used for the modification.¹²⁵ The columns containing $\text{Al}_2\text{O}_3/\text{KCl}$ are less polar than those with $\text{Al}_2\text{O}_3/\text{Na}_2\text{SO}_4$. Chromatograms obtained in the separation of a mixture of C_1 – C_4 hydrocarbons using columns of both types are shown in Fig. 16. It is advisable to use the columns with $\text{Al}_2\text{O}_3/\text{Na}_2\text{SO}_4$ as the adsorbent for the separation of a mixture of butenes.

Capillary columns with alumina are also used for the separation of light halocarbons. The data on retention obtained experimentally for halo-derivatives of hydrocarbons in a capillary adsorption column with Al_2O_3 (60 m × 0.32 mm) have been supplemented by the data on the retention obtained by calculations.¹²⁶ The calculations have been mostly carried out by two methods — correlation equations^{127,128} and additive schemes.¹²⁹ High resolving power of adsorption capillary columns with Al_2O_3 has been noted;¹²⁶ the researchers were able to separate such isomers as $\text{CF}_2\text{ClCF}_2\text{Cl}$ and CF_3CFCl_2 (previous attempts to separate these isomers in gas-liquid capillary columns have failed).

Adsorption capillary columns possess relatively high capacities; therefore, they are suitable for the analysis of impurities.

While considering the range of practical application of capillary columns with alumina, one should mention the possibility of conducting fast analysis of gaseous hydrocarbons (the analysis can take no more than 100 s).¹²⁴ This is of special interest for the purposes of industry.

Adsorption capillary columns are successfully used in complex chromatographic systems for fast separation of mixtures containing components with different boiling points.

The separation of complex multicomponent mixtures can be substantially improved if sorbents, optimum for the selective separation of individual fractions of the mixture (or even of individual groups of compounds) are specially selected for each particular case. Therefore, gas chromatographic systems with adaptable structures have been used for a fairly long period in

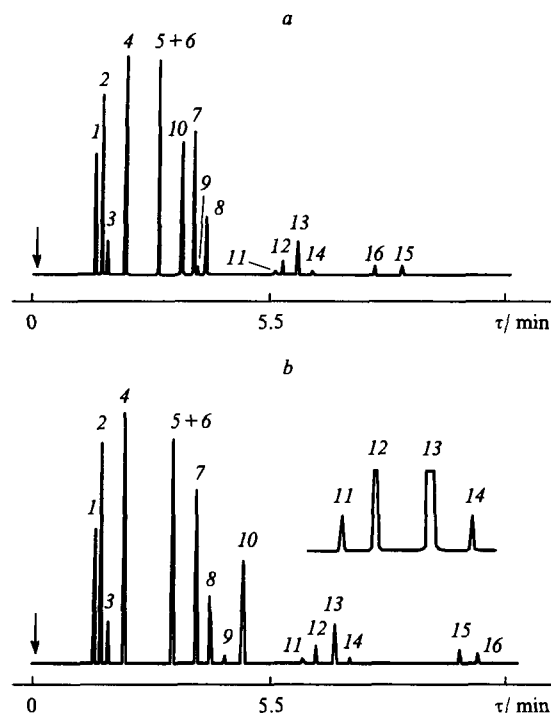


Figure 16. Chromatogram for the separation of C_1 – C_4 hydrocarbons in special metallic capillary columns with $\text{Al}_2\text{O}_3/\text{KCl}$ (a) and $\text{Al}_2\text{O}_3/\text{Na}_2\text{SO}_4$ (b).¹²⁵

Peaks: (1) methane, (2) ethane, (3) ethene, (4) propane, (5) cyclopropane, (6) propene, (7) isobutane, (8) butane, (9) propadiene, (10) acetylene, (11) *trans*-but-2-ene, (12) but-1-ene, (13) isobutene, (14) *cis*-but-2-ene, (15) buta-1,3-diene, (16) methylacetylene. A 50 m × 0.32 mm column and hydrogen as carrier gas were used, the temperature increased from 70 to 130°C at a rate of 5°C/min .

gas chromatography on packed columns, especially for industrial purposes. These schemes make it possible to change automatically, during the analysis, the order in which the columns are connected and the direction of the carrier-gas flow in the individual sections (or in the whole scheme) and also to include individual columns into the scheme or to exclude them from it. Thus, the conditions for the separation of individual groups of compounds can be optimised, the time required for the analysis can be shortened, and the stability of the operation of the columns used can be increased.

The use of such schemes also in the capillary chromatography would certainly be expedient and would markedly improve the separation. The first gas chromatograph 'Siechromat' based on an adaptable multicolumn scheme was developed by Siemens (Germany). Fig. 17 shows two chromatograms obtained in the separation of a mixture of C_1 – C_8 hydrocarbons in *n*-pentane with this instrument. The boiling points and chromatographic characteristics of the components of this mixture were essentially different. Initially, this mixture was separated at 75°C in an open tubular capillary column (24 m × 0.27 mm), the inner walls of which were coated with a modified clay (Bentone-34) impregnated with di-*iso*-decyl phthalate. This main column ensured clear separation of benzene (11), toluene (12), ethylbenzene (13), *p*-xylene (14), *m*-xylene (15), and *o*-xylene (16). The C_1 – C_5 light hydrocarbons were rapidly eluted from the column; therefore, they were responsible for one common peak in the chromatogram.

Fast separation of light hydrocarbons was achieved by injecting them into another open tubular capillary column (80 m × 0.4 mm), the inner walls of which were coated with a layer of alumina modified with potassium chloride. The separation in this column was carried out at 15°C . Light hydrocarbons — methane (1), propane (2), propene (3), isobutane (4),

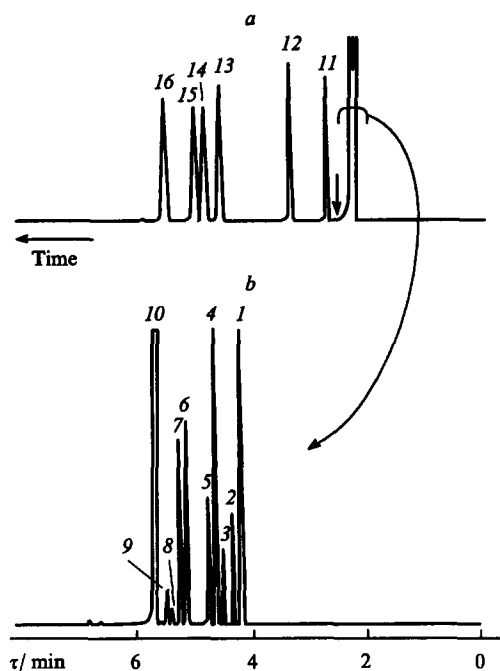


Figure 17. General chromatogram for the separation of C_1 – C_8 hydrocarbons in an open tubular capillary column (a) and the partial chromatogram for the fraction of C_1 – C_5 hydrocarbons (b).¹³⁰ Experimental conditions 24 m \times 0.27 mm columns with Bentone-34 impregnated with diisodecyl phthalate as adsorbent (a) and a 80 m \times 0.4 mm column with alumina (b).

n-butane (5), but-1-ene (6), *trans*-but-2-ene (7), butadiene (8), isobutene (9), and *cis*-but-2-ene (10) — were separated in this column. The separation in the two capillary columns occurred simultaneously, the time required for the process in each column not exceeding 6 min. This example clearly illustrates the advantages of using adaptable multicolumn schemes in gas chromatography and the possibility of increasing markedly the separating capacity of capillary chromatography. These schemes make it possible to gain a larger amount of chromatographic information than a traditional single analysis.

Chromatographic schemes in which adsorption capillary columns are used together with packed columns have also been reported (see for example Ref. 131). Poy and Cobelli¹³¹ have shown experimentally that the use of a gas chromatograph with a flame-ionisation detector ensures fairly high reproducibilities of the retention values and of the proportions of the components determined for a mixture subjected to the analysis (Table 5). The results obtained by these workers can be regarded as experimental justification for using open tubular capillary columns for analytical and physicochemical purposes.

At present, porous organic polymers are used fairly frequently as adsorbents in adsorption chromatography (especially for polar compounds).^{132, 133} Capillary columns with porous organic adsorbents have been used¹²⁵ for the analysis of the following classes of compounds: C_1 – C_5 alcohols, C_2 – C_7 fatty acids, C_1 – C_2 haloalcohols, C_1 – C_5 hydrocarbons, solvents, C_1 – C_5 aldehydes, gases, mixtures of gases with water, C_3 – C_8 ketones, and C_1 – C_9 thiols.

The use of porous organic polymers as adsorbents offers a number of advantages; the main of them are high homogeneity of the surface with controllable (within certain limits) porosity and hydrophobicity of particular types. Therefore, porous polymers can be figuratively regarded as organic polymeric phases that have come to a standstill.

Open tubular capillary columns containing a polymeric layer on the inner walls were produced for the first time by Hollis,¹⁰⁵

Table 5. Reproducibility of retention values and concentrations of components found in a mixture being analysed for an open tubular gas adsorption capillary column from Chrompack.

Compound	Retention time		Concentration	
	τ /min	R (%) ^a	c , %	R (%) ^a
CO ₂	2.11	0.5	5.3	0.8
O ₂	2.58	0.3	1.1	0.7
N ₂	2.58	0.3	4.4	0.6
CH ₄	(3.77) ^b (5.54)	(0.25) ^b (0.15)	5.0	0.8
CO	4.33	0.25	4.9	0.7
C ₂ H ₆	6.91	0.15	2.2	0.6
C ₂ H ₄	8.05	0.12	0.6	0.7
C ₃ H ₈	9.05	0.10	2.1	0.8
C ₃ H ₆	10.28	0.12	1.9	0.6
iso-C ₄ H ₁₀	11.73	0.10	0.4	0.8
n-C ₄ H ₁₀	12.13	0.10	7.4	0.5
iso-C ₄ H ₈	13.05	0.10	6.7	0.5
C ₄ H ₈	13.95	0.10	4.83	0.5
2- <i>trans</i> -C ₄ H ₈	14.27	0.10	10.80	0.4
2- <i>cis</i> -C ₄ H ₈	14.66	0.10	4.7	0.7
Buta-1,3-diene	16.28	0.09	38.8	0.8
n-C ₅ H ₁₂	22.18	0.08	1.0	0.8

^a R — mean square deviation from the average value. ^b The numbers above the bar refer to a packed column, those below the bar refer to a capillary column. The statistical data were obtained from 10 experiments (calculations were carried out by the internal normalisation method).

while the modern variant of these columns based on flexible quartz capillaries has been developed by Dutch researchers of the 'Chrompack' company;^{39, 125, 134} the same researchers have also developed special metallic capillary columns with polymeric adsorbents.³⁸ Fig. 18 presents three chromatograms obtained for the separation of C_1 – C_4 hydrocarbons using three different types of columns. It is seen that the retention of hydrocarbons on the organic adsorbent differs sharply from that on methylsilicone and alumina; in the case of the organic adsorbent, groups of hydrocarbons differing in the number of carbon atoms in their molecules can be clearly distinguished. Examples of successful separation of polar organic compounds in columns of this type have been reported.^{38, 39, 123, 125}

Note that natural organic adsorbents can also be used in capillary columns. Fig. 19 shows the results of the separation of organic acids of natural origin on a natural polymer, *Staphylococcus aureus* cells. A quite satisfactory degree of separation was achieved. The use of natural adsorbents seems promising.

Gas capillary chromatography has been used for the separation of hydrocarbons and nitriles.^{136, 137} Porapak Q and Al₂O₃/KCl were used as adsorbents, a thin layer of which covered the inner walls of a capillary column. Good results were achieved with the PoraPLOT Q column (10 m \times 0.32 mm); in the case of the PLOT Al₂O₃/KCl column, nitriles are held tightly, some of the peaks being asymmetrical.

Determination of buta-1,3-diene in air carried out using a PLOT capillary column containing Al₂O₃/KCl (50 m \times 32 mm) has been described by Finnish researchers.¹³⁸

Columns with traditional adsorbents, for example, with graphitised carbon black, also find practical application. 'Structural sensitivity', which is manifested in the separation of isomers, is a specific feature of graphitised carbon black used as an adsorbent. This feature, which is very attractive for an analyst, can be illustrated by the separation of hydrocarbons, the chromatogram for which is shown in Fig. 20. All the three isomers of xylene were separated in a capillary column with

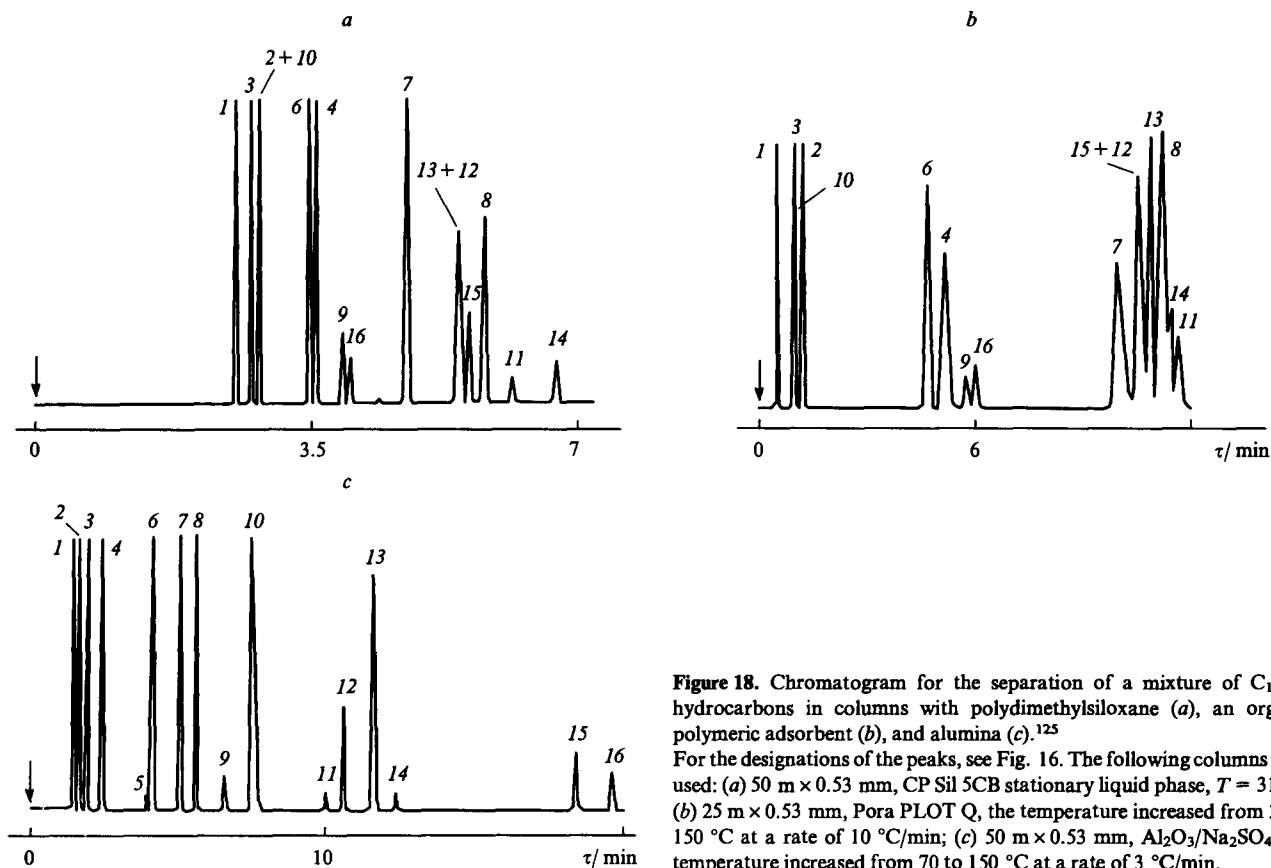


Figure 18. Chromatogram for the separation of a mixture of C_1 – C_4 hydrocarbons in columns with polydimethylsiloxane (a), an organic polymeric adsorbent (b), and alumina (c).¹²⁵ For the designations of the peaks, see Fig. 16. The following columns were used: (a) 50 m \times 0.53 mm, CP Sil 5CB stationary liquid phase, $T = 31^\circ\text{C}$; (b) 25 m \times 0.53 mm, Pora PLOT Q, the temperature increased from 35 to 150 °C at a rate of 10 °C/min; (c) 50 m \times 0.53 mm, $\text{Al}_2\text{O}_3/\text{Na}_2\text{SO}_4$, the temperature increased from 70 to 150 °C at a rate of 3 °C/min.

graphitised carbon black. In another study,¹³⁶ adsorption columns with Carbo-pack B modified with a non-volatile liquid phase have been used; these columns are usually called Carbon Layer Open Tubular (CLOT) columns.

Graphitised carbon black can be used for the analysis of mixtures of halohydrocarbons. The results of separation of some halohydrocarbons in an adsorption capillary column (Carbo-pack B + 1% SP 1000) are shown in Fig. 21.

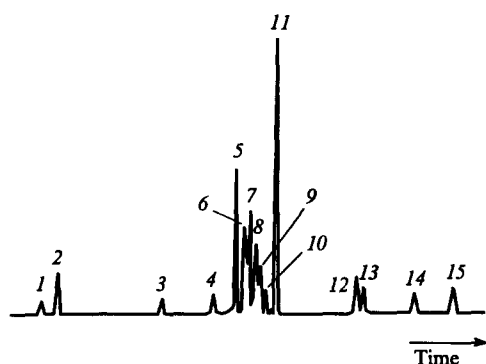


Figure 19. Chromatogram for the separation of unsaturated acids in an open tubular capillary column in which *Staphylococcus aureus* cells were used as the adsorbent.¹³⁵

Acids: (1) 14:1 tetradecenoic; (2) 14:0 myristic; (3) 15:0 pentadecanoic; (4) $c\Delta^8$ 16:1 *cis*-hexadec-8-enoic; (5) $c\Delta^9$ 16:1 *cis*-hexadec-9-enoic (palmitic); (6) $c\Delta^{10}$ 16:1 *cis*-hexadec-10-enoic; (7) $c\Delta^{11}$ 16:1 = $t\Delta^9$ 16:1 *cis*-hexadec-11-enoic and *trans*-hexadec-9-enoic; (8) $t\Delta^{10}$ 16:1 *trans*-hexadec-10-enoic; (9) $t\Delta^{11}$ 16:1 *trans*-hexadec-11-enoic; (10) $t\Delta^{12}$ 16:1 *trans*-hexadec-12-enoic; (11) 16:0 palmitic; (12) $c\Delta$ 17:0 *cis*-methylene-hexadecanoic; (13) $t\Delta$ 17:0 *trans*-methylenehexadecanoic; (14) 18:0 octadecenoic; (15) 18:0 stearic.

Columns with graphitised carbon black are used mostly for the separation of gaseous and relatively light hydrocarbons; however, Brunner et al.¹⁴¹ have shown that they can also be used for the determination of some herbicides in water.

A practically significant separation of halo-derivatives of hydrocarbons in open tubular capillary columns containing a layer of solid adsorbents on the inner surface of the capillary has been studied by de Zeeuw et al.¹⁴² They showed that the PLOT columns with $\text{Al}_2\text{O}_3/\text{KCl}$ are very selective towards the separation of volatile compounds of this type; however, proportions of some of these compounds in the mixture changed during the elution.

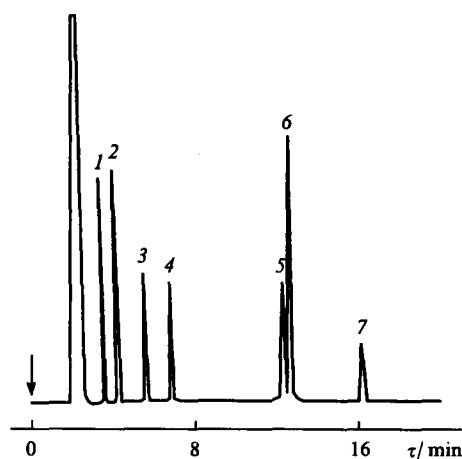


Figure 20. Chromatogram for the separation of a mixture of aromatic hydrocarbons in a capillary column with graphitised carbon black.¹³⁹ (1) n-Octanol; (2) benzene; (3) n-nonane; (4) toluene; (5) *p*-xylene; (6) *m*-xylene; (7) *o*-xylene. A 30 m \times 0.32 mm column with Carbo-pack B was used; $T = 60^\circ\text{C}$; helium was used as the carrier gas.

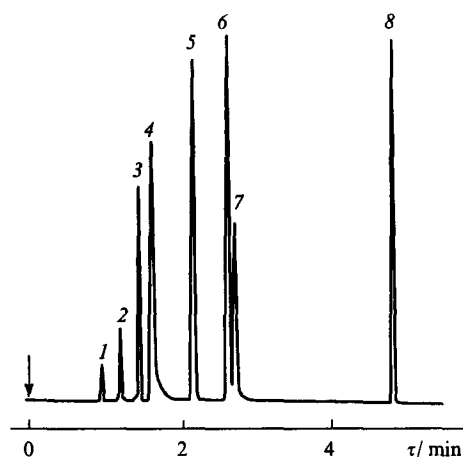


Figure 21. Chromatogram for the separation of a mixture of halohydrocarbons in a capillary column with Carboxpack B modified with 1% of a stationary liquid phase.¹⁴⁰

(1) CFC 12; (2) CFC 114; (3) CFC 11; (4) $C_2H_2Cl_2$; (5) CFC 113; (6) CH_3CCl_3 ; (7) CCl_4 ; (8) C_2Cl_4 . A 32 m \times 0.53 mm column was used; hydrogen was used as the carrier gas, $T = 30^\circ C$ (2 min) followed by heating to $180^\circ C$ at a rate of $20^\circ C/min$.

The use of capillary columns with the PoraPLOT Q adsorbent is promising for the analysis of chlorofluoro-derivatives of hydrocarbons.

Bruner et al.¹⁴³ have developed a procedure for the determination of hydrocarbons and amines in a capillary column with graphitised carbon black modified with various liquid phases.

Stationary liquid phases are widely used for the modification of solid adsorbents in gas adsorption chromatography. The retention in these systems can be described in terms of the additive absorption-adsorption theory.¹⁴⁴ In recent years, colloidal stationary liquid phases have been used in order to increase the capacity of the columns and to change their selectivity.^{145,146}

The field of application of gas adsorption capillary columns is progressively extending, and the number of companies producing these columns is increasing.¹⁴⁷

Unfortunately, the use of open tubular adsorption capillary columns in Russia is still limited, although these columns can be manufactured in almost any chromatographic laboratory.¹⁴⁸

* * *

The use of capillary gas adsorption chromatography makes it possible to improve markedly the main characteristics of chromatographic separation of volatile compounds (selectivity, efficiency, speed, the area of application, etc.). Capillary gas-adsorption chromatography is a modern version of the adsorption chromatography, which makes it possible to take full advantage of this earliest version of gas chromatography.

The wide experience accumulated by researchers from various countries forms a strong basis for the extensive use of adsorption capillary columns for solving numerous important routine problems.

From our viewpoint, in the future, attention should be concentrated on the following branches of gas adsorption capillary chromatography: the theory and optimisation of the separation conditions, reproducible methods for the manufacture of capillary columns, and the extension of the number of various selective adsorbents used in the capillary variant of chromatography.

The author is grateful to Academician I I Moiseev for useful discussion and to the Scientific Council of the subprogramme 'Priority Branches of the Chemical Science' for supporting this work.

References

1. E Hefmann (Ed.) *Chromatography* (Amsterdam: Elsevier, 1983)
2. K A Gol'bert, M S Vigdergauz *Vvedenie v Gazovuyu Khromatografiyu* (Introduction to Gas Chromatography) (Moscow: Khimiya, 1990)
3. C F Poole, S K Poole *Chromatography Today* (Amsterdam: Elsevier, 1991)
4. V G Berezkin, Yu S Drugov *Gas Chromatography in Air Pollution Analysis* (Amsterdam: Elsevier, 1991)
5. V G Berezkin, V S Gavrichev, L N Kolomiets, A A Korolev, V N Lipavskii, N S Nikitina, V S Tatarinskii *Gazovaya Khromatografiya v Neftekhimii* (Gas Chromatography in Petroleum Chemistry) (Moscow: Nauka, 1975)
6. K I Sakodinskii, V V Brazhnikov, S A Volkov, V Yu Zel'venskii, E S Gankina, V D Shatts *Analiiticheskaya Khromatografiya* (Analytical Chromatography) (Moscow: Khimiya, 1993)
7. V G Berezkin, M A Koshevnik *Zh. Analit. Khim.* **47** 80 (1992)
8. H M McNair *LC-GC Int.* **6** 740 (1993)
9. R D Dandeneau, E H Zerenner *J. High Resol. Chromatogr.* **2** 351 (1979)
10. K J Hyver (Ed.) *High Resolution Gas Chromatography* (Hewlett-Packard, 1989)
11. I V Aleksandrov, V R Alishoev, V G Berezkin, M N Budantseva, M E Zhabotinskii, A A Korolev, O E Shushpanova *USSR P. 1 097 060; Byull. Izobret.* (9) (1994)
12. S R Lipsky, M L Duffy *J. High Resol. Chromatogr.* **9** 376 (1986)
13. A V Kiselev, Ya I Yashin *Gas und Flüssigadsorption Chromatographie* (Heidelberg: Huethig Verlag, 1985)
14. J C Giddings *Anal. Chem.* **36** 1173 (1964)
15. M J E Golay, in *Gas Chromatography 1960 (Edinburgh Symposium)* (Ed. R P W Scott) (London: Butterworths, 1960) p. 139
16. V I Kalmanovskii, A V Kiselev, V P Lebedev, I M Savinov, N Ya Smirnov, M M Fiks, K D Shcherbakova *Zh. Fiz. Khim.* **35** 1386 (1961)
17. M Mohnke, W Saffert *Chem. Techn.* **13** 685 (1961)
18. M Mohnke, W Saffert, in *Gas Chromatography 1961* (Ed. M Van Swaay) (London: Butterworths, 1963) p. 216
19. L Halasz, C Horvath *Nature (London)* **197** 71 (1963)
20. L Halasz, C Horvath *Anal. Chem.* **35** 349 (1963)
21. J J Kirkland *Anal. Chem.* **35** 1296 (1963)
22. R Weiher, in *Handbuch der Gas-Chromatographie* (Eds E Von Leibnitz, H G Struppe) (Leipzig: Akademische Verlagsgesellschaft, 1966) p. 329
23. D L Petitjean, C J Leftault *J. Gas Chromatogr.* **1** 18 (1963)
24. R D Schwartz, D L Braseaux, G R Shoemaker *Anal. Chem.* **35** 496 (1963)
25. G Goretti, A Liberti, G Nota, in *Gas Chromatography 1968* (Ed. C L A Harbour) (London: Institute of Petroleum, 1968) p. 22, 30
26. F A Brunner, G P Cartoni, A Liberti, in *Advances in Gas Chromatography 1965 (Houston Symposium)* (Eds A Zlatkis, L S Ettre) (Evanston, IL: Preston Technical Abstracts Co., 1966) p. 106
27. F A Brunner, G P Cartoni, M Possanzini *Anal. Chem.* **41** 1122 (1969)
28. F A Brunner, G P Cartoni *Anal. Chem.* **36** 1522 (1964)
29. A Liberti, in *Gas Chromatography 1966 (Rome Symposium)* (Ed. A B Littlewood) (London: Institute of Petroleum, 1967) p. 95
30. E L Ilkova, E A Mistryukov *J. Chromatogr. Sci.* **9** 569 (1961)
31. L S Ettre, J E Purcell, S D Norem *J. Gas Chromatogr.* **3** 181 (1965)
32. J E Purcell, L S Ettre *J. Gas Chromatogr.* **4** 23 (1966)
33. L S Ettre, J E Purcell, K Billeb *Separation Sci.* **1** 777 (1966)
34. L S Ettre, J E Purcell, in *Advances in Chromatography Vol. 10* (Eds J C Giddings, R A Keller) (New York: Plenum, 1974) p. 1
35. R de Nijs *J. High Resol. Chromatogr.* **4** 612 (1981)
36. R de Nijs, J de Zeeuw *J. Chromatogr.* **279** 41 (1983)
37. J de Zeeuw, R C M de Nijs, L T Henrich *J. Chromatogr. Sci.* **25** 71 (1987)
38. J de Zeeuw, J Buyten, J Peene, M Mohnke *LC-GC Int.* **7** 644 (1994)
39. J de Zeeuw *LC-GC Int.* **4** 36 (1991)
40. L Henrich, J de Zeeuw *J. Chromatogr. Sci.* **26** 198 (1988)
41. *Chrompack General Catalog* (Middelburg: Chrompack Int., 1992)

42. W Jennings *Glass Capillary Columns in Gas Chromatography* (New York: Academic Press, 1980)
43. V G Berezkin, S M Volkov *Chem. Rev.* **89** 287 (1989)
44. F Brenner, G Crescentini, F Mangani *Chromatographia* **30** (9) 565 (1990)
45. G Castello, S Vezzani, P Moretti *J. High Resol. Chromatogr.* **17** 31 (1994)
46. A di Corcia, A Liberti, in *Advances in Chromatography* Vol. 14 (Eds J C Giddings, E Grushka, J Cazes, Ph R Brown) (New York: Marcel Dekker, 1976)
47. V G Berezkin, in *Advances in Chromatography* Vol. 27 (Eds J C Giddings, E Grushka, P R Brown) (New York: Marcel Dekker, 1987) p. 1
48. V G Berezkin *Gas-Liquid-Solid Chromatography* (New York: Marcel Dekker, 1991)
49. N N Avgul', A V Kiselev, D P Poshkus *Adsorbtion Gazov i Parov na Odnorodnykh Poverkhnostyakh* (Adsorption of Gases and Vapours on Homogeneous Surfaces) (Moscow: Khimiya, 1975)
50. A V Kiselev, D P Poshkus, Ya I Yashin *Molekulyarnye Osnovy Adsorbtionnoi Khromatografii* (Molecular Foundations of Adsorption Chromatography) (Moscow: Khimiya, 1986)
51. A V Kiselev *Mezhmolekulyarnye Vzaimodeistviya v Adsorbtii i Khromatografii* (Intermolecular Interactions in Adsorption and Chromatography) (Moscow: Vysshaya Shkola, 1986)
52. G Guiochon, C L Guillemain *Quantitative Gas Chromatography* (Amsterdam: Elsevier, 1988)
53. J C Giddings *Dynamics of Chromatography* (New York: Marcel Dekker, 1965)
54. W Rudzinski, in *Chromatographic Theory and Basic Principles* (Ed. A Jonsson) (New York: Marcel Dekker, 1987) p. 157
55. V G Berezkin, I V Malyukova, V R Alishoev *J. Chromatogr. A* **699** 155 (1995)
56. V G Berezkin *Russ. Khim. Zh.* **38** (1) 21 (1994)
57. G M Panchenkov, V P Lebedev *Khimicheskaya Kinetika i Kataliz* (Chemical Kinetics and Catalysis) (Moscow: Khimiya, 1974)
58. M J E Golay, in *Gas Chromatography 1957 (Lansing Symposium)* (Eds V J Coates, H J Noebels, I S Fagerson) (New York: Academic Press, 1958) p. 1
59. M J S Golay, in *Gas Chromatography 1958 (Amsterdam Symposium)* (Ed. M H Desty) (London: Butterworths, 1958) p. 36
60. M J E Golay *Anal. Chem.* **40** 382 (1968)
61. A V Kiselev, Ya I Yashin *Gazoadsorbtionnaya Khromatografiya* (Gas-Adsorption Chromatography) (Moscow: Nauka, 1967)
62. V Berezkin, G Stoev, O Georgiev *Prilozhna Kapilarna Gazovaya Khromatografiya* (Applied Capillary Gas Chromatography) (Sofia: Nauka i Izkustvo, 1986)
63. M Lee, F Yang, K Bartle *Open Tubular Gas Chromatography* (New York: Wiley-Interscience, 1984)
64. K K Tesarik, K Komarek *Kapilarni Kolony v Plynove Chromatografii* (Capillary Columns in Gas Chromatography) (Prague: SNTL, 1984)
65. J C Giddings *Anal. Chem.* **35** 439 (1963)
66. J C Giddings *Anal. Chem.* **36** 1170 (1964)
67. E N Fuller, P P Schettler, J C Giddings *Ind. Eng. Chem.* **58** (5) 19 (1966)
68. R C Reid, J M Prausnitz, T U Sherwood *The Properties of Gases and Liquids* (New York: McGraw-Hill, 1977)
69. R H Perrett, J H Purnell *Anal. Chem.* **34** 1336 (1962)
70. C A Cramers, C F van Tilburg, C P M Schutjes, J A Rijks, G A Rutten, R de Nijs, in *Proceedings of the Fifth International Symposium on Chromatography* (Ed. J A Rijks) (Amsterdam: Elsevier, 1983) p. 76
71. G Goretti, A Liberti, G Nota *Chromatographia* **8** (9) 486 (1975)
72. V V Ugrozov *Zh. Fiz. Khim.* **61** 1274 (1987)
73. E de Vanssay, P Capilla, D Coscia, L Do, R Sternberg, F Raulin *J. Chromatogr.* **693** 255 (1993)
74. J C Giddings *Separation Sci.* **1** 123 (1966)
75. J C Giddings, M N Myers, J F Moellmer *J. Chromatogr.* **149** 501 (1978)
76. J C Giddings, M N Myers, K D Caldwell, J W Pan *J. Chromatogr.* **195** 261 (1979)
77. V P Andreev, L S Reifman *Nauchnaya Apparatura* **1** (3) 3 (1986)
78. J Janca *Field-Flow Fractionation* (New York: Marcel Dekker, 1988)
79. R D Schwartz, D J Brasseau, R G Mathews *Anal. Chem.* **38** 303 (1966)
80. R G Mathews, J Torres, R D Schwartz *J. Chromatogr.* **186** 183 (1979)
81. R G Mathews, J Torres, R D Schwartz *J. Chromatogr.* **199** 97 (1980)
82. L S Ettre, in *Open Tubular Column in Gas Chromatography* (Norwalk: Perkin Elmer, 1965) p. 107
83. D A Fridrissberg *Kurs Kolloidnoi Khimii* (A Course on Colloid Chemistry) (Leningrad: Khimiya, 1984)
84. G Nota, G Goretti, M Arrenvale, G Marino *J. Chromatogr.* **95** 229 (1974)
85. J E Purcell *Nature (London)* **201** 1321 (1964)
86. W Schneider, J C Frohner, H Bruderrech *J. Chromatogr.* **155** 311 (1978)
87. S A Nenaidenko, L D Belyakova, O G Larionov, V R Alishoev, V G Berezkin *Zh. Fiz. Khim.* **67** 2033 (1993)
88. L D Belyakova, L M Strokina *J. Chromatogr.* **365** 31 (1986)
89. C Horvath D Th, Goethe University Frankfurt am Main, BRD, 1963
90. G Vidal-Madjar, S Behassy, M Gonnord, D Arpino, G Guiochon *Anal. Chem.* **49** 768 (1977)
91. T Welsch, W Engewald, J Poerschmann *J. Chromatogr.* **148** 143 (1978)
92. Yun Hao, K E Markides, M L Lee, in *Book of Abstracts Presented at Pittcon 95* (New Orleans, LA: Ernest N Morial Convention Center, 1995) Paper 1187
93. S P Zhdanov, V I Kalmanovskii, A V Kiselev, M I Fiks, Ya I Yashin *Zh. Fiz. Khim.* **36** 1118 (1962)
94. G P Cartoni, M Possanzini *J. Chromatogr.* **39** 99 (1969)
95. W Bocola, F Brunner, G P Cartoni *Nature (London)* **209** 200 (1966)
96. F Brunner, G P Cartoni, A Liberti *Anal. Chem.* **38** 298 (1966)
97. L M Rappoport, G P Ermakova, V G Berezkin, S K Krashennnikov, A A Konstantinov, V R Alishoev, E N Viktorova, A V Chernobrovov USSR P. 708 220; *Byull. Izobret.* (1) 169 (1980)
98. L M Rappoport, G P Ermakova, V G Berezkin, S K Krashennnikov, A A Konstantinov, V R Alishoev, E N Viktorova, A V Chernobrovov USSR P. 726 035; *Byull. Izobret.* (13) 16 (1980)
99. E Von Leibnitz, H G Struppe (Eds) *Handbuch der Gaschromatographie* (Leipzig: Akademische Verlagsgesellschaft Geest and Portig, 1984)
100. Ch D Lentzi, W Hoevertmann, in *The 14th Pittsburgh Conference on Analytic Chemistry, Pittsburgh, PA, 1963* p. 99
101. K Grob, G Grob, Jr *Chromatographia* **10** 186 (1977)
102. V G Berezkin, T P Popova, A A Korolev, V E Shiryayeva, G F Shalygin *Zavod. Lab.* **56** (3) 15 (1990)
103. S M Volkov, V I Anikeev, V G Berezkin USSR P. 1 318 904; *Byull. Izobret.* (23) 156 (1987)
104. S M Volkov, T F Kuznetsova, E N Barketina, in *Khromatograficheskie Metody v Khimii, Biologii i Meditsine (Materialy Konferentsii)* [Chromatographic Methods in Chemistry, Biology, and Medicine (Conference Proceedings)] (Minsk: Ministry of Public Health of Republic Belorussia, 1995) p. 42
105. O L Hollis *J. Chromatogr. Sci.* **11** 337 (1973)
106. I Halasz, E Heine *Nature (London)* **194** 971 (1962)
107. D W Grant *Presenius Z. Anal. Chem.* **236** 118 (1968)
108. G Goretti, A Liberti, G Nota *J. Chromatogr.* **34** 282 (1968)
109. A Liberti, G Nota, G Goretti *J. Chromatogr.* **38** 96 (1968)
110. R E Majors *LG-GC Int.* **8** 312 (1995)
111. V G Berezkin, G M Bolotov *Neftepererabotka Neftekhimii* **6** 45 (1972)
112. V G Berezkin, V S Tatarinsky *Gas Chromatographic Analysis of Trace Impurities* (New York: Consultants Bureau, 1973)
113. V G Berezkin, O L Gorshunov *Zh. Fiz. Khim.* **42** 2587 (1968)
114. A Malik, A R Jumaev, V C Berezkin *J. High Resol. Chromatogr.* **9** 312 (1986)
115. A Purer, R L Kaplan *J. Chromatogr. Sci.* **9** 59 (1971)
116. A Purer, R L Kaplan, D R Smith *J. Chromatogr. Sci.* **4** 504 (1969)
117. F Cacace, M Schuller *J. Labelled Compd.* **11** 313 (1975)
118. J V Brunnoek, L A Luke *Anal. Chem.* **40** 2158 (1968)
119. J V Brunnoek, L A Luke *Anal. Chem.* **41** 1126 (1969)
120. N L Soulages, A M Brieva *J. Chromatogr.* **101** 365 (1974)
121. J de Zeeuw, R C M de Nijs *Chrompack News* **12** (1) 1 (1985)

122. G R Verga *J. High Resol. Chromatogr.* **8** 456 (1985)
123. M Mohnke, J Heybey *J. Chromatogr.* **471** 31 (1989)
124. R C M de Nijs, J de Zeeuw, in *Capillary Chromatography (Proceedings of the V International Symposium, Riva del Garda, 1983)* (Ed. J Rijks) (Amsterdam: Elsevier, 1983) p. 11
125. J de Zeeuw, J Buyten, J Peene, M Mohnke *Metal Capillary PLOT Columns Coated with Al₂O₃, Molsieve and Porous Polymer Adsorbents (Chrompack Information)* (Middelburg: Chrompack Int., 1994)
126. S V Konyukhova, B N Maksimov, I G Zenkevich *Zh. Prikl. Khim.* **67** 135 (1994)
127. S V Konyukhova, I G Zenkevich, B N Maksimov *Zh. Analit. Khim.* **49** 307 (1994)
128. I G Zenkevich, S V Konyukhova, B N Maksimov *B N Zh. Fiz. Khim.* **67** 1474 (1993)
129. I G Zenkevich *Zh. Org. Khim.* **28** 1827 (1992)
130. G Schomburg, F Weeke, F Muller, M Oreans *Chromatographia* **16** 87 (1982)
131. F Poy, L Cobelli *J. Chromatogr.* **349** 17 (1985)
132. O L Hollis *Anal. Chem.* **38** 309 (1966)
133. K I Sakodinskii, L I Panina *Polimernye Sorbenty dlya Molekulyarnoi Khromatografii* (Polymeric Sorbents for Molecular Chromatography) (Moscow: Nauka, 1977) p. 166
134. L de Zeeuw, R C M de Nijs, J C Buijten, J A Poene, in *Proceedings of the 8th International Symposium on Capillary Chromatography Vol. 1* (Ed. P Sandra) (Heidelberg: Huethig, 1987) p. 171
135. V F Gal'chenko, L V Andreev, Yu A Trotsenko *Taksonomiya i Identifikatsiya Obligatnykh Metanotrofnikh Bakterii* (Taxonomy and Identification of Obligatory Methane-Trophic Bacteria) (Pushchino: Scientific Centre of Biological Investigations, Academy of Sciences of the USSR, 1986)
136. L Do, F Raulin *J. Chromatogr.* **481** 45 (1989)
137. L Do, F Raulin *J. Chromatogr.* **514** 65 (1990)
138. K Peltonen, R Vaaranrinta *J. Chromatogr. A* **710** 237 (1995)
139. L M Sidisky, M V Robillard *J. High Resol. Chromatogr.* **16** 116 (1993)
140. F Brunner, G Crescentini, F Mangani *Chromatographia* **30** 565 (1990)
141. F Brunner, L Lattanzi, F Mangani, M A Rezaii *Chromatographia* **38** 98 (1994)
142. J de Zeeuw, D Zwiep, J W Marinissen, in *Proceedings of the 17th International Symposium on Capillary Chromatography, Wintergreen (USA), 1995* p. 406
143. F Bruner, M A Rezai, L Lattanzi *Chromatographia* **41** 403 (1995)
144. V G Berezkin *Zh. Analit. Khim.* **51** 148 (1996)
145. A A Fedyanin, L G Usova *Zavod. Lab.* **57** (2) 14 (1991)
146. M S Vigdergauz, S I Kirsh, N T Karabanov *Khromatografiya v Sisteme Gaz-Kolloid* (Chromatography in the System Gas-Colloid) (N Novgorod: N Novgorod State University, 1992)
147. R E Majors *LC-GC Int.* **9** 346 (1996)
148. V R Alishoev, V G Berezkin, I V Malyukova *Zavod. Lab.* **60** (12) 6 (1994)

Fluoroalkoxy-derivatives of trivalent phosphorus: synthesis and reactivity

V F Mironov, I V Konovalova, L M Burnaeva, E N Ofitserov

Contents

I. Introduction	935
II. The influence of fluorine-containing substituents on the properties of the P(III) atom. Photoelectron spectroscopic and electrochemical data	935
III. Synthesis of fluoroalkoxy-derivatives of P(III)	938
IV. Reactions of fluoroalkyl phosphites	948
V. Conclusion	966

Abstract. The review surveys and gives a systematic account of the electronic structures, syntheses, and chemical properties of fluoroalkyl derivatives of trivalent phosphorus (phosphites, thiophosphites, and amidophosphites). The methods of preparation and reactivities of fluoroalkyl phosphites are compared with those of unsubstituted phosphites. The bibliography includes 420 references.

I. Introduction

Derivatives of trivalent phosphorus are of key importance in the synthesis of a wide variety of organophosphorus compounds with different coordinations at the phosphorus atom and exhibit in most cases pronounced nucleophilic properties. This is associated with the accessibility of the lone pair (LP) of the phosphorus atom in the above derivatives and with the ease of their conversion into compounds with a phosphoryl group.

Various aspects of the influence of alkyl-, alkoxy-, amido-, etc. substituents on the reactivity of trivalent phosphorus compounds have been described in fair detail in the literature, but there have been no surveys of the influence of fluorine atoms, although a number of questions, concerning, for example, the electronic structures of fluorinated derivatives of P(III), have been discussed in monographs.^{1–3}

A systematic description of the syntheses and chemical properties of fluoroalkoxy-derivatives of trivalent phosphorus and the identification and possible explanation of their characteristic features compared with the unsubstituted analogues are the subject of the present review.

II. The influence of fluorine-containing substituents on the properties of the P(III) atom. Photoelectron spectroscopic and electrochemical data

The introduction of a fluorine atom into trivalent phosphorus compounds almost always alters the properties of the derivatives obtained compared with their nonfluorinated analogues, although as a rule the fluorine atom in such derivatives is not a reaction centre or a leaving group. In order to give a systematic account of data concerning the influence of fluorine on the properties of the P(III) atom, it is useful to examine four conventional groups of compounds containing P and F atoms: (1) compounds with a P–F bond; (2) compounds containing the P–C–F fragment (the F atom occupies the α -position relative to the P atom — these are usually CF_3 derivatives); (3) compounds containing the P–E–C–F fragment, where E = C, O, S, Se, N, etc. (the F atom occupies the β -position relative to the P atom); (4) compounds with the P–E–C–C–F fragment (the F atom occupies the γ position relative to the P atom). The available information about the reactivities of the first two groups of compounds have been surveyed.^{4–9} The chemistry of the compounds belonging to the third group, in which E = S, Se, or Te, has been scarcely investigated. Among the compounds with E = C, the pentafluorophenyl derivatives have been most thoroughly investigated.¹⁰ In compounds with P–E–C–C–F fragments, the fluorine and phosphorus atoms are separated by four bonds and the inductive effect of the fluorine atom on phosphorus in them should be minimal. Nevertheless, experimental data indicate an appreciable influence of the fluorine atoms on the phosphorus centre in such compounds.

According to X-ray photoelectron spectroscopic data, the replacement of a hydrogen atom by fluorine in an organic compound leads to profound perturbations of the electronic core of the molecule as far as the 1s level of carbon. The binding energy of the electrons of the carbon atom $E(\text{C}1s)$ in the $\text{CF}_n\text{H}_{4-n}$ molecule then increases by ~ 2.7 eV for each fluorine atom introduced.¹ On passing from ethane to trifluoroethane ($\text{C}_2\text{H}_6 - \text{CF}_3$), an additive increase in the binding energy for the β -carbon $E(\text{C}\beta 1s)$ is also observed, although to a lesser extent than in methane (from 290.7 to 292.1 eV).

The additivity breaks down when an oxygen atom is introduced at the β -carbon atom. Thus, on passing from ethanol to trifluoroethanol, $E(\text{C}\beta 1s)$ changes by only 0.3 eV (from 292.5 to 292.8 eV), while on replacement of one hydrogen atom in

V F Mironov Laboratory for Renewable Natural Raw Materials, Arbuzov Institute of Organic and Physical Chemistry, Russian Academy of Sciences, ul. akad. Arbuzova 8, 420083 Kazan, Russian Federation. Fax (7-843)275 22 53. Tel. (7-843)276 73 84

I V Konovalova, L M Burnaeva Department of Macromolecular and Organoelement Compounds, Kazan State University, ul. Lenina 18, 420008 Kazan, Russian Federation. Fax (7-843)238 09 94

E N Ofitserov Department of Natural Science, Ul'yanovsk State University, ul. L'va Tolstogo 42, 432700 Ul'yanovsk, Russian Federation

Received 11 September 1995

Uspekhi Khimii 65 (11) 1013–1051 (1996); translated by A K Grzybowski

$C_\alpha F_3 C_\beta H_3$ by OH groups, $E(C_\alpha 1s)$ does not change [$E(C_\alpha 1s) = 297.8$ eV]. It follows from these data that the manifestation of the inductive effect for $C_3 1s$ on passing from ethane to trifluoroethane is almost five times greater ($\Delta = 1.4$ eV) than on passing from ethanol to trifluoroethanol ($\Delta = 0.3$ eV). This phenomenon is classified as the β -effect of the fluorine atom.¹¹

Calculations¹² yield a negative charge on the carbon atom in the β -position relative to fluorine. Thus in ethane the charge on the carbon atom is zero, while in CF_3CH_3 we have $q^{C_\alpha} = 0.60 - 0.72$ e and $q^{C_\beta} = (-0.09) - (-0.11)$ e, i.e. the presence of the fluorine atom increases the electron density on the β -carbon atom and diminishes it on the C_α atom. The consequences of the β -effect of the F atom are particularly strikingly manifested, as will be seen below, in the case of fluorinated alkoxy-derivatives of P(III). In order to explain it, the concepts of hyperconjugation,^{11,13-15} antibonding orbitals,^{16,17} and the perfluoro-effect¹¹ have been resorted to.

According to Davis et al.¹² and Bock et al.,¹⁸ the effect can be accounted for by the fact that the strong acceptance of electronic charge by fluorine via the system of σ -bonds is accompanied by the reverse polarisation of the π -electron system or the σ^* orbitals. Overall, if the charges on the carbon atoms of ethane are zero, the substitution of a hydrogen atom by fluorine leads to the appearance of an effective positive charge of 0.24 e at the α -carbon atom and of a negative charge of -0.03 e at the β -atom; the charge on the fluorine atom is -0.23 e. These features are fully retained for ethene and benzene.¹

By virtue of its small size (the van der Waals radius of fluorine is 0.14 nm), close to that of the hydrogen atom (0.12 nm), the fluorine atom is capable of substituting all the hydrogen atoms in linear molecules. When all the valences of the carbon atom in the carbon chain are saturated by fluorine atoms, the carbon skeleton passes from the zigzag to the helical shape, whereupon the electronegative fluorine atoms fully protect the carbon skeleton against attack by nucleophiles.^{19,20} The helix exhibits a 180° twist for each 13 carbon atoms. In a weakened form, this effect is probably manifested also in fluoroalkyl phosphites, particularly those with long fluorinated carbon chains.

In order to estimate the quantitative influence of fluorine on various properties of the molecule, photoelectron spectroscopy (PES) has been widely used together with X-ray spectroscopy.²¹⁻²³ A characteristic feature of the photoelectron spectra of organofluorine compounds is the absence of narrow (without a vibrational structure) bands, typical for ionisation with participation of nonbonding MOs, although formally the molecules contain a large number of fluorine lone pairs (n_F), whereas such narrow bands are observed for the chloro- and bromo-derivatives. The broad bands present in the spectra of organofluorine compounds, frequently with vibronic structures, indicate that in the organofluorine compounds there are no true n_F orbitals. The photoelectron spectra of fluoroalkanes, fluoroalkenes, and fluoromethyl derivatives of nitrogen subgroup elements, i.e. simple and planar molecules, almost fully reproduce the photoelectron spectra of hydrocarbon analogues, although they are displaced towards higher ionisation potentials (IP). However, the effect of the perfluoroalkyl substituent, postulated²⁴ and defined as a shift towards higher IP (without changes in the sequence, energy differences, and symmetry type of the MO for the n and σ MO of the central atom) when alkyl groups are replaced by perfluoroalkyl groups, is not a general rule for fluorinated molecules, because it requires a correspondence between the nature of the MO and the energies and symmetries of the fluorinated and hydrocarbon analogues. This is possible only subject to the condition of the complete localisation of the orbitals n_F on the fluorine atoms, which in its turn conflicts with the nature of the photoelectron spectra.

The ionisation potential of the molecule is a measure of the difference between the energies of formation of the molecule and the molecular ion (radical-cation). The replacement of a hydrogen atom by an alkyl group with electron-donating properties leads to

the stabilisation of the radical-cation, while the replacement by a fluorine atom or a fluorinated alkyl (σ -acceptors) results in destabilisation. The σ -acceptor effect of the CF_3 group is then intensified by its weak π -acceptor effect, while the effect of the F atom is weakened by the donor influence.³

The complex nature of the effect of the CF_3 group has been demonstrated recently.²⁵ Thus, when a F atom is replaced by the CF_3 group in fluoroalkenes, the π levels of the molecule are strongly stabilised with some destabilisation of the σ levels. For example, on passing from $CF_2=CF_2$ to $(CF_3)_2C=C(CF_3)_2$, the π -type HOMO energy diminishes by 3.8 eV, while the LUMO (π^*) energy decreases by 2.1 eV. Under these conditions, the occupied π - and σ -type MO approach one another. The CF_3 group induces a marked alternation of the charge (the appearance of a negative charge on the β -carbon atom and of a positive charge on the α -carbon atom). Thus the overall effect of the CF_3 group in perfluoroalkene is electron-donating (M-acceptor, σ -donor). Evidently, the electronic effects of the CF_3 group on the F atom can change depending on the nature of the fragment to which they are attached. Thus, using the LCAO-MO SCF methods supplemented by the optimisation of the geometrical parameters, it has been shown that the $C_\alpha - C_\beta$ distance decreases with increase in the number of CF_3 groups at the α -atoms of the carbanions $CF_3CH_2^-$, $(CF_3)_2CF^-$, and $(CF_3)_3C^-$, which indicates the existence of negative hyperconjugation at the fluoroalkyl substituents.²⁶

In simple, planar molecules, the substitution of hydrogen by fluorine leads to a more pronounced stabilisation of the σ MO than the π MO. The preferential σ -stabilisation on fluoro-substitution is called the perfluoro-effect. The ranges of the π -electron IP then overlap markedly and the composition of the fluorinated derivatives changes qualitatively compared with that of the nonfluorinated analogues.²⁷

The photoelectron spectra of fluorinated alcohols have a complex form with broad overlapping bands.²⁸⁻³⁰ Overall, they are subject to the effect of the perfluoroalkyl group, i.e. they have the same band sequence as in the spectra of the usual alcohols which has undergone an almost parallel shift into the region of higher potentials; furthermore, quantum-chemical calculations^{28,29,31} yield the same sequence of the MO. The highest occupied molecular orbital of alkanols and their fluoro-derivatives is not a pure n_O orbital. The contributions of the $2p$ AOP of oxygen to the HOMO in the series CH_3CH_2OH , CH_2FCH_2OH , $(CF_3)_3COH$ are 43%, 41%, and 27% respectively. This suggests that the n_O orbitals, like the n_F orbitals, are not fully localised on oxygen and fluorine.

In trifluoroethanol, the CF_3 group is separated from the oxygen atom by the CH_2 unit, which weakens both the σ_1 -effect and the conjugation effect.

Extremely interesting data have been obtained in the study of fluorinated alcohols by the ^{17}O and ^{13}C NMR methods.³² It was found that the influence of fluorine in the β - and γ -positions ($F_\beta - C - O$, $F_\gamma - C - C - O$) is manifested much more strikingly in the ^{17}O NMR spectra than in the ^{13}C NMR spectra. Bearing in mind that the quantity $\delta_O(\delta_C)$ is linearly related to the charge on the corresponding atom and hence to the electron density,³³ one may reach certain conclusions about its distribution. The fluorine atoms in the β -position relative to the oxygen (and carbon) atom exert a powerful deshielding effect ($\Delta_O = 36 \pm 5$ ppm) on the oxygen atom (the β -effect), whereas the F_γ atoms exert a weak shielding effect ($\Delta_O = 10 \pm 3$ ppm). The above effects may be accounted for by the different manifestations of the effect due to the field of the fluorine atom.³⁴

The vertical IP for fluorine-containing phosphites have been determined.³⁵⁻³⁷ It was shown that the replacement of hydrogen atoms by fluorine increases significantly IP_1 , which largely corresponds to ionisation with participation of the n_P orbital. Thus the IP_1 for the phosphites 2 and 4 exceed the IP_1 for the phosphites 1 and 3 by 1.33–1.37 eV (Table 1). Finally, the IP_1 for tris(hexafluoroisopropyl) phosphite 5 is greater than IP_1 for phosphorus trichloride by 0.29 eV, i.e. the electron-accepting

Table 1. Photoelectron spectroscopic data for certain P(III) derivatives.

Compound	IP ₁ (<i>n</i> _P)/eV	IP ₂ (<i>n</i> _O)/eV	Ref.
(CH ₃ CH ₂ O) ₃ P (1)	9.0	10.3	38, 39
(CF ₃ CH ₂ O) ₃ P (2)	10.37	11.71	35
(CH ₃ CH ₂ CH ₂ O) ₃ P (3)	8.85	10.18	37
(CHF ₂ CF ₂ CH ₂ O) ₃ P (4)	10.18	11.07	36
[(CF ₃) ₂ CHO] ₃ P (5)	10.81	11.94	37
PCl ₃	10.52	—	40
PBr ₃	9.35	—	40

effect of the hexafluoroisopropyl substituent exceeds that of the chlorine atom. Overall, the photoelectron spectra of the fluorinated phosphites resemble those of the usual phosphites, but they are displaced towards higher ionisation potentials, i.e. the perfluoroalkyl effect rule holds in this case, since the sequence and symmetry of the MO (*n*_P, *n*_O, σ_{CC}) are retained.

It has been shown⁴⁰ that the IP₁ in the PX₃ series increase in proportion to the IP₁ of the functional hydrides HX (the fluorinated phosphites 2, 4, and 5 are not an exception). The relation between IP(PX₃) and IP(HX) is linked to the parallel manifestation of the inductive effect of the substituent X and the mixing of the orbitals *l*_P and *n*_X.⁴⁰ Thus the contribution of the 3*p* AO LP of phosphorus to the HOMO increases in the sequence C₆F₅P(NEt₂)₂ < C₆F₅P(NCS)₂ < C₆F₅P(OMe)₂ in conformity with the increase in the IP₁(HX): HNEt₂ (8.15) < HNC (9.94) < HOMe (10.96).⁴¹ The IP(*n*_P) for the phosphites 2, 4, and 5 exceed those for the phosphonites enumerated, like the IP(*n*_O) of fluorinated alcohols, so that the contribution of the phosphorus 3*p* AO to the HOMO increases, with an overall increase in IP(*n*_P), on passing from the phosphites P(OR)₃ and the phosphonites C₆F₅PX₂ to the fluorinated phosphites 2, 4, and 5 and P(OC₆F₅)₃. Under these conditions, the *n*_P orbital to which the 3*p* AO of phosphorus contributes significantly (from 75% to 87% according to different estimates),⁴⁰ is also capable of *n*_P– σ_{C-O}^* conjugation.

The electron-accepting nature of the C–O σ^* -bond increases as a result of the introduction of the fluorinated substituent at the carbon atom. In the usual compounds, the *n*_P– σ_{C-O}^* interaction in the P(III)–O–C fragment is weak, since the excitation is localised mainly on the carbon atom.^{42,43} In fluorinated phosphites, such interaction is apparently more effective; here there is a partial delocalisation of the *n*_P electrons to the C–O σ -bond. An appreciable delocalisation of the *n*_P electrons has been noted for the compound P(OC₆F₅)₃, which has been investigated by X-ray emission spectroscopy (PK _{β}).⁴¹

The enhancement of the electron-accepting properties of the OR_F substituents via the σ_1 mechanism is accompanied by an increase in the electrophilicity of the P–O σ^* -bonds, the electron deficiency occurring predominantly on the phosphorus atom, because it is less electronegative than oxygen. Bearing in mind the electronic interaction occurring in the O–CH₂–CF₃ fragment and enhancing the electron-accepting properties of the orbital σ_{CO}^* , one may postulate that the conjugation of the P–O σ^* -bond and the *n*_O electrons, characteristic of the usual P(III) compounds, is unlikely in compounds with this fragment.

Thus, by virtue of the strong electron-accepting effect of the fluoroalkoxy-groups, a significant electron density deficiency arises on the phosphorus atom, which imparts electrophilic properties to the latter. Hence one should expect a greater reactivity of R_F phosphites in reactions with nucleophiles compared with R_H phosphites.

One of the consequences of the replacement of the H atoms by F atoms in phosphites is the strengthening of the C–O bond, i.e. an increase in its energy. This change in the bond energy may be explained on the basis of the orbital model of *n*_O– σ_{C-C}^* hyperconjugation.^{16,42,43} The introduction of fluorine atoms lowers the energy of the σ_{C-C}^* orbital, which is localised predominantly on

the terminal carbon atom of the C–CF₃ fragment and increases the effectiveness of its interaction with *n*_O.

The transfer of electron density from the oxygen atom to the fluorinated alkyl group is possible both via the σ_1 mechanism and via a mechanism involving *n*_O– σ_{C-C}^* and σ_{C-O} – σ_{C-F}^* conjugation. Furthermore, the substituent CF₃(R_F) exhibits a π -acceptor effect,³ which may occur via the mechanism involving the hyperconjugation of the antibonding MO of the CF₃ group localised on the carbon atom with the π -type MO of the CH₂ fragment. All this strengthens the C–C and C–O bonds, i.e. stabilises the σ levels and enhances the electron-accepting properties of the alkoxy-fragment OR_F.

The photoelectron spectra of cyclic phosphites containing electron-accepting substituents (CF₃)₂CH have been investigated.³⁷ The results are presented in Table 2.

The first two potentials, IP₁ and IP₂, in the photoelectron spectra of benzodioxaphospholanes 6–9 and the salicyl derivatives 13 and 14 correspond to the ionisation of two π orbitals of the benzene ring, *a*₂(π) and *b*₁(π), perturbed by the effective interaction with the antisymmetric (*n*_O[–]) and symmetrical (*n*_O⁺) combinations of the group orbitals of oxygen. Under these conditions, the *a*₂(π)–*n*_O⁺ orbital is the HOMO.

The ionisation potential IP₃ of the benzophospholanes 6–9 corresponds to the ionisation of the *n*_P orbital, exceeding the IP₁(*n*_P) for the analogous phospholanes 10–12 by 0.35–0.6 eV. The reason for the increase in IP₃(*n*_P) in the benzophospholanes 6–9 is the effective interaction. The replacement of one oxygen atom in compounds 6 and 7 by an ester group (compounds 13 and 14) leads to an appreciable increase in the energies of the *a*₂(π) and *b*₁(π) orbitals, but at the same time facilitates the ionisation of the *n*_P orbital. This is consistent with the M effect of the C(O)O group.


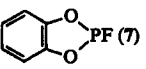
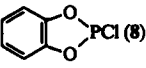
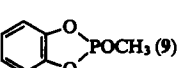
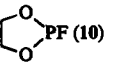
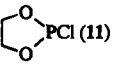

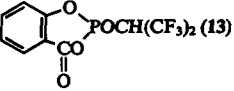
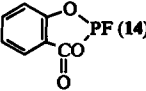
Naturally the *n*_O⁺–*a*₂(π) and *n*_O⁺–*b*₁(π) conjugation is just as effective as the *n*_O⁺– π interaction. The *n*_O– π^* conjugation shifts electron density from the oxygen atom to the ring.

It follows from the foregoing that cyclic benzodioxaphospholanes and unsubstituted dioxaphospholanes contain an extremely electrophilic phosphorus atom, the positive charge on which is comparable to that for acyclic fluorinated phosphites (the ionisation potentials of such compounds are very high). If weak electron-accepting substituents, such as NR₂, OMe, or OSiMe₃, are present at the phosphorus atom in the phospholane, then the σ_{PO}^* orbitals, localised mainly on the phosphorus atom, behave as acceptors in the σ_{PO}^* –*n*_X conjugation,⁴⁴ the electrophilicity of the σ_{PO}^* orbitals of the cyclic fragment increasing after the introduction of the benzene ring owing to *n*_O– π^* conjugation. On the other hand, if there are strong π -acceptor substituents, for example OC₆F₅, OCH(CF₃)₂, or OCH₂CF₃, at the phosphorus atom, then the nature of the electronic interactions of the cyclic fragment with the exocyclic substituent changes. In this case, the electrophilicity of the σ_{PO}^* orbital weakens, and the *n*_O– σ_{PX}^* interactions are intensified, which diminishes somewhat, in its turn, the *n*_O– π^* conjugation. Thus the IP₁(π_1) and IP₂(π_2) for compounds 6 and 7 increase by ~0.45 and ~0.30 eV compared with the corresponding ionisation potentials of compound 9 (Table 2).

The photoelectron spectroscopic data for fluorinated phosphites examined above show that the IP₃(*n*_P) for these compounds are higher by 1.3–2 eV compared with the ionisation potentials of the unsubstituted phosphites, which should undoubtedly be reflected in the electrochemical properties of fluoroalkyl phosphites. The study of the electrochemical behaviour of fluoroalkyl phosphites^{37,45–47} has shown that acyclic derivatives are not oxidised in the accessible range of potentials (for example, compounds 2, 4, and 5), which is fully consistent with photoelectron spectroscopic data. Table 2 presents also the half-wave oxidation potentials (*E*_{1/2}/V) of some of the fluorinated P(III) derivatives investigated. They were obtained by the voltammetric method at a platinum electrode in acetonitrile (25 °C).⁴⁷

The value of *E*_{1/2} quoted^{48,49} for tris(tetrafluoropropyl) phosphite 4 (0.85 eV) is erroneous and has not been reproduced.

Table 2. Photoelectron spectroscopic data for certain cyclic phosphites (IP/eV).³⁷

Compound	IP ₁ (π_1) $a^2(\pi) - n_O^+$	IP ₂ (π_2) $b_1(\pi) - n_O^-$	IP ₃ (n_P)	$E_{1/2}/V$
 (6)	8.89	9.58	10.75	1.59, 2.03
 (7)	8.90	9.53	11.11	1.58, 1.85
 (8)	8.86	9.57	10.55 ($n_P - n_O - n_{Cl}$)	—
 (9)	8.45	9.26	10.33	1.29, 1.99
 (10)	10.74(n_P)	11.19(n_O)	12.51(σ_{CC})	—
 (11)	10.20(n_P) ⁴⁸	—	—	—
 (12)	9.55(n_P) ⁴⁸	—	—	—
 (13)	9.42(π_1)	9.80(π_2)	10.30 ($n_P + n'_O$)	2.34
 (14)	9.54	10.04	10.43	—

This is understandable because the value of $E_{1/2}$ determined by the above workers^{48,49} is actually lower than $E_{1/2} = 1.68$ V for $P(OEt)_3$.⁵⁰ One-electron and (according to cyclic voltammogram data) irreversible waves were observed on the voltammograms for fluoroalkyl phosphites derived from catechol and salicylic acid. The reaction centre in these compounds is the benzene ring and an electron is abstracted from the HOMO which is the $a_2(\pi) - n_O^*$ orbital.

The calculated number of electrons for cyclic fluoroalkyl phosphites is less than integral values, which may be associated with the interaction of the radical-cation formed with the initial phosphite. This leads to the formation of dimeric species, for example in the case of bis(trifluoroethyl) phenylphosphonite.⁵¹

The shift of the potential $E_{1/2}$ to the negative region for compound 13 and its analogues⁴⁷ is associated with the presence of the electron-accepting substituent $C(O)O$ in the ring, which agrees with the higher ionisation potential of the $a_2(\pi)$ orbital.

Thus electrochemical oxidation, photoelectron spectroscopic, NMR spectroscopic, and calculated data clearly indicate that the phosphorus in fluorinated cyclic and acyclic phosphites has a very high $IP(n_P)$, carries an appreciable effective positive charge, and exhibits (together with nucleophilic properties) pronounced electrophilic properties. As a result of the characteristic features of the electronic interactions in the fluoroalkoxy-group, it is difficult to split off R_F from phosphonium centres compared with the splitting off of R_H . For this reason, one should expect the ready elimination of this group in the corresponding nucleophilic reactions, i.e. the easier cleavage of the $P-OR_F$ bond compared with the $P-OR_H$ bond. The easier elimination of the CF_3CH_2O group compared with CH_3CH_2O has been noted⁵² in relation to the aminolysis of the esters $RCOOCH_2CF_3$. In this sense, the chemistry of fluoroalkyl phosphites resembles that of P(III) halides, which is known to reduce largely to nucleophilic substitution reactions at the phosphorus atom. Furthermore, the chem-

istry of fluoroalkyl phosphites is significantly richer and is not restricted solely to the nucleophilic reactions indicated above. The difference in the behaviour of fluoroalkyl phosphites and P(III) halides, having similar $IP(n_P)$, may be due to the difference in the hybridisation of the phosphorus lone pairs, which has predominantly s character in the case of phosphorus halides and is distinguished by a significant contribution of p character in the case of trialkyl phosphites.^{2,40} Finally, the formation of products with a phosphoryl group from fluorinated phosphites should be more convenient than their formation from unsubstituted phosphites.

III. Synthesis of fluoroalkoxy-derivatives of P(III)

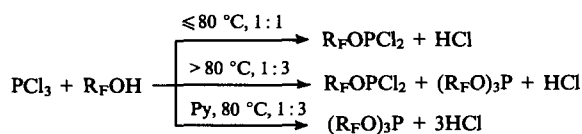
1. Reactions of P(III) halides with fluorine-containing alcohols

Various methods of synthesis of P(III) derivatives containing fluorinated substituents have been developed: reactions involving phosphorylation of fluorinated alcohols by P(III) acid halides and amides, alcoholysis and transamination reactions, interaction of P(III) derivatives with hexafluoroacetone, etc.

The interaction of P(III) halides with fluorinated alcohols is one of the most frequently employed approaches to the synthesis of fluoroalkyl phosphites. As we have already noted, fluorinated alcohols are relatively weak nucleophiles. They are less basic than the usual alcohols.³¹ Being fairly acidic ($pK \approx 4-12$),^{53,54} R_F -alcohols react with difficulty with P(III) chlorides, in contrast to R_H -alcohols. They are unusually inert in reactions proceeding via the intermediate formation of carbonium ions, which indicates a strong interaction of the oxygen lone pair with the fluoroalkyl fragment (the 'mesomeric' nature of the bonds).⁵⁵ Quantum-chemical calculations,³¹ carried out for CF_3CH_2OH , $CF_3CH_2O^-$, $(CF_3)_2CHOH$, and $(CF_3)_2CHO^-$, indicate shortening of the C-O bond in fluoroalcohol anions (compared with

R_F -alcohols) and a corresponding increase in the length of the C–F and C–C bonds and an increase in the effective negative charge on the CF_3 and $(CF_3)_2CH$ fragments, which is interpreted as the manifestation of the field effect.³¹ The nucleophilicity of $P(OR_F)_3$ differs little from that of PX_3 ($X = Cl, Br$). This probably explains the inertness of fluoroalkyl phosphites when acted upon by hydrogen halides so that in the synthesis of R_F phosphites from PX_3 there is no need to employ bases in order to bind the HX.

Phosphites based on fluorinated alcohols — tris(2-fluoroethyl) phosphite and tris(2,2,2-trifluoroethyl) phosphite — were first obtained from PCl_3 .^{56,57} It was noted that, in the interaction of PCl_3 with linear R_F -alcohols, mainly trialkyl phosphites are formed together with a small amount of R_F -dialkyl chlorophosphites.^{57–59} Further studies^{60–62} demonstrated that the result depends on the ratio of the initial compounds, the reaction conditions, and the catalyst. At 80 °C and for the ratio $PCl_3 : R_FOH = 1:1$, it is possible to isolate dichlorophosphites, the yield of trialkyl phosphites increasing with increase in temperature. The latter are formed almost quantitatively if the initial alcohol is employed in (2–3)-fold excess. We have frequently noted that the acid phosphite $(R_FO)_2PHO$ is frequently formed as a side product, i.e. the reaction of fluoroalkyl phosphites with PCl_3 does nevertheless occur to a slight extent (up to 10%–15%). It becomes the main reaction in the case of 2-fluoroethanol, which affords bis(2-fluoroethyl) phosphites in a high yield on treatment with PCl_3 .⁶³ The addition of a catalyst (pyridine) accelerates the reaction significantly and improves the yield of the trialkyl phosphite.^{60,61}

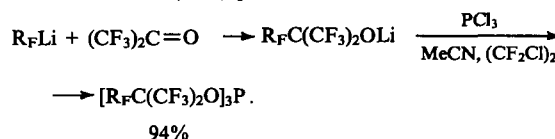


The catalytic role of pyridine is seen in relation to the synthesis of tris(hexafluoroisopropyl) phosphite **5**: at 25 °C, hexafluoroisopropyl alcohol does not react with PCl_3 (1:1), on prolonged heating the phosphite **5** is formed in 70% yield,⁶⁴ while in the presence of pyridine the reaction ends after 2 h and the yield of the phosphite **5** is almost quantitative.⁶⁵ Tertiary alcohols such as $(CF_3)_2MeCOH$, do not react with PCl_3 even at 90 °C,⁶⁴ whereas the alcohols R_FMe_2COH [$R_F = CF_3, CHF_2CF_2, CHF_2(CF_2)_3$], taken in an appropriate amount, interact with PCl_3 in the presence of pyridine as catalyst, affording high yields of the dichloro- and monochloro-phosphites $Cl_{3-n}P(OCMe_2R_F)_n$ ($n = 1, 2$).⁶⁶ Pentafluorophenol reacts with PCl_3 on heating to form (depending on the initial reactant ratio) predominantly $C_6F_5OPCl_2$ or a mixture of $(C_6F_5O)_2PCl$ and $P(OC_6F_5)_3$, all three compounds being separated by distillation.⁶⁷

Numerous studies (see, for example, Refs 57 and 68–73) have been made of the interaction of PBr_3 with fluorinated alcohols, but their results are contradictory. On the whole, PBr_3 reacts more readily with fluoro-alcohols than PCl_3 , but the reaction proceeds via several paths. For the ratio $PBr_3 : R_FOH = 1:3$, fluorine-containing trialkyl phosphites are formed in high yields.^{57,73} Attempts to obtain bromo- and dibromo-phosphites were unsuccessful. The preparation of the dibromophosphite $CHF_2(CF_2)_3CH_2OPBr_2$ has been reported in only one study.⁷² In the case of trifluoroethanol and the fluoroalkanols $CH_2F(CH_2)_nOH$ ($n = 1, 2, 5, 7$), an appreciable amount of the fluoroalkyl bromide is produced.^{68–71} Such results are associated both with the greater tendency of P(III) bromides to disproportionate compared with the chlorides and with the more effective

dealkylation of fluoroalkyl phosphites by HBr. Tris(fluoroalkyl) phosphites, dialkyl chlorophosphites, chlorophosphonites, and chlorophosphinites, their fluorinated analogues, asymmetric fluoroalkyl phosphites, and amidophosphite have been obtained in high yields by Arbuzov's method via alkoxides.^{58,64,74} These reactions proceed smoothly and, depending on the initial reactant ratio, lead to mono-, bis-, or tris-(fluoroalkyl) phosphites. However, here too dismutation occurs in certain cases, particularly in the synthesis of fluoroalkyl phosphites with linear groups.

Lithium alkoxides are usually employed in the synthesis of fluoroalkyl phosphites.^{64,74–88} Sometimes (see, for example, San et al.⁷⁴) lithium alkoxide is obtained beforehand from R_FLi [$R_F = CF_2CF_2OCF(CF_3)_2$] and hexafluoroacetone.

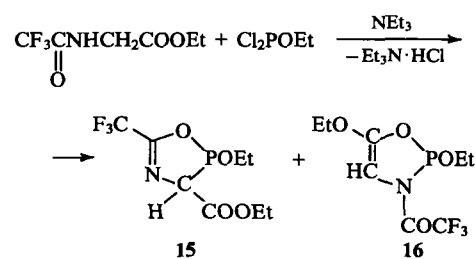


Bis(fluoroalkyl) chlorophosphites show a much greater tendency to disproportionate than dialkyl chlorophosphites. Nevertheless they have been obtained in a number of studies from PCl_3 and the corresponding alcohols both in the presence^{59,89,90} and absence^{58,59,66} of a base. Other approaches to the synthesis of bis(fluoroalkyl) chlorophosphites have also been proposed: the exchange reactions of $P(OCH_2CF_3)_3$ with BCl_3 and PCl_3 ,⁵⁸ as well as the exchange reactions of PX_3 with lithium R_F -alkoxides.^{76,89}

Fluoroalkyl difluorophosphites and bis(fluoroalkyl) fluoro-phosphites are obtained by the reactions of PF_3 with R_F -alcohols or R_FOLi and R_FONa ^{77,78,82,91} by fluorinating bis(fluoroalkyl) chlorophosphites and fluoroalkyl dichlorophosphites with SbF_3 .^{81,92,93} The synthesis of the phosphite containing mobile halogen atoms [$(Pr^iO)_2POCCl(CCl_3)CF(CF_3)(SO_2F)$] described by Eleev et al.,⁹⁴ gives rise to doubts owing to the presence of extremely reactive fragments in this compound.

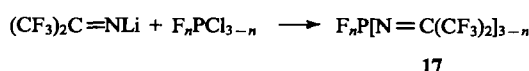
Table 3 presents acyclic P(III) compounds obtained by phosphorylating fluorinated alcohols or their alkoxides by P(III) halides; it also lists cyclic phosphites containing an exocyclic fluoroalkoxy-substituent, as well as compounds obtained from fluorinated diols and their lithium derivatives.^{53,54,56–165}

An extremely interesting example of phosphorylation leading to the isomeric azaphospholines **15** and **16** has been described.¹⁶⁶ On heating, 1,3,5-oxazaphospholine **15** ($\delta_P = 166$ ppm) is converted into 1,3,2-oxazaphospholine **16** ($\delta_P = 112$ ppm)



Phosphorylation of the potassium and silver salts of 2,3,4,5-tetrakis(trifluoromethylthio)pyrrole (HetM) by treatment with PCl_3 , $PhPCl_2$, Ph_2PCl , PI_3 , and PBr_3 afforded fluorinated heterocyclic amidophosphites:¹⁶⁷ Het_2PCl , $PHet_3$, Het_2POEt , Het_nPPh_{3-n} ($n = 1, 2, 3$). The chemistry of these compounds has been surveyed by Weiss.¹⁶⁸

Another interesting type of fluorinated P(III) amides comprises phosphorylated derivatives of hexafluoroacetone imine **17**.¹⁶⁹



$n = 1, 2, 3.$

Table 3. Acyclic and cyclic fluoroalkyl phosphites.

Compound	R _F	R (or NR ₂)	R' (or X)	Ref.
(R _F O) ₃ P	CF ₃ CH ₂	—	—	57, 58, 95
	CHF ₂ (CF ₂) _n CH ₂ (n = 1, 3, 5)	—	—	58–61, 73
	CH ₂ FCH ₂	—	—	56
	CF ₃ CF ₂ CH ₂	—	—	59
	CF ₃ (CF ₂) ₂ CH ₂	—	—	59
	C ₆ F ₁₃ CH ₂ CH ₂	—	—	75
	(CF ₃) ₂ CH	—	—	64, 65, 76, 77, 88, 96
	CF ₃ MeCH	—	—	64
	(CF ₃) ₂ CMe	—	—	64
	CF ₃ CMe ₂	—	—	64
	(CF ₃) ₂ C(CN)	—	—	78, 79
	(CF ₃) ₂ CFO(CF ₂) ₂ C(CF ₃) ₂	—	—	74
	(ClCF ₂) ₂ C(CN)	—	—	80
	C ₆ F ₅ CH ₂	—	—	97
	C ₆ F ₅	—	—	67, 92, 98
(R _F O) ₂ PCl	CF ₃ CH ₂	—	—	58, 99
	CHF ₂ CF ₂ CH ₂	—	—	58, 59, 89, 90
	CF ₃ CF ₂ CH ₂	—	—	59, 100
	CF ₃ (CF ₂) ₂ CH ₂	—	—	59, 100
	(CF ₃) ₂ CH	—	—	64, 76, 81
	CHF ₂ CF ₂ CMe ₂	—	—	66
	(CF ₃) ₂ CMe	—	—	64
	CF ₃ CMe ₂	—	—	64
	C ₆ F ₅	—	—	67
R _F OPCl ₂	CHF ₂ (CF ₂) _n CH ₂ (n = 1, 3, 5)	—	—	58, 60–62
	CF ₃ CH ₂	—	—	64
	(CF ₃) ₂ CH	—	—	64
	(CF ₃) ₂ CMe	—	—	64
	CF ₃ CMe ₂	—	—	64
	CHF ₂ (CF ₂) ₃ CMe ₂	—	—	66
	CF ₃ CEt ₂	—	—	66
	CHF ₂ CF ₂ CMe ₂	—	—	67
	C ₆ F ₅	—	—	67
	MeOCC(CF ₃) ₂	—	—	79
	Cl ₂ POCH ₂ (CF ₂) _n CH ₂ (n = 2, 3)	—	—	101
	(CF ₃) ₂ CHCH ₂	—	—	102
(R _F O) ₂ PF	(CF ₃) ₂ CH	—	—	81
	(CF ₃) ₂ C(CN)	—	—	78
	C ₆ F ₅	—	—	103
R _F OPF ₂	CF ₃ CH ₂	—	—	91
	(CF ₃) ₂ CH	—	—	77, 103, 104
	CHF ₂ (CF ₂) ₃ CH ₂	—	—	92
	CHF ₂ CF ₂ CH ₂	—	—	93
	(CF ₃) ₂ C(CN)	—	—	82
	C ₆ F ₅	—	—	103
	(CF ₃) ₂ CH	—	—	104
	(CF ₃) ₂ Cl	—	—	104
	(CF ₃) ₂ CBr	—	—	104
R _F OPBr ₂ R _F OP(OR) ₂	CH ₂ F(CF ₂) ₃ CH ₂	—	—	73, 92
	CH ₂ FCH ₂	Et	—	63
	CHF ₂ CF ₂ CH ₂	Et	—	105
	FSO ₂ CF(CF ₃)CCl(CCl ₃)	Pr ⁱ	—	94
	C ₄ F ₉ C≡CCH ₂	Et	—	106
	C ₄ F ₉ C≡CCHMe	Et	—	106
	EtOCCCH=CCF ₃	Et	—	107
	MeC(O)CH=CCF ₃	Et	—	108
	Bu ⁱ C(O)CH=CCF ₃	Et	—	108
	PhN=CCF ₃	Et	—	109
	(CF ₃) ₂ CH	Ph	—	110
	CHF ₂ (CF ₂) ₃ CH(NHCOOEt)	Et	—	111

Table 3 (continued).

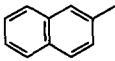
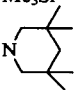
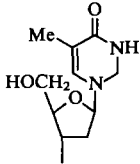
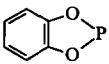
Compound	R _F	R (or NR ₂)	R' (or X)	Ref.
R _F OP(OR)(OR')	CHF ₂ CF ₂ CH ₂	4-(4-PhNHC ₆ H ₄)C ₆ H ₄		112
(R _F O) ₂ POR	CH ₂ FCH ₂	Et	—	63
	CHF ₂ CF ₂ CH ₂	Et	—	113
	EtOOCCH = CCF ₃	Et	—	108
	(CF ₃) ₂ CH	Pr ⁱ	—	88, 114
	(CF ₃) ₂ CH	Ph	—	110
(R _F O) ₂ PNR ₂	C ₂ F ₅ CH ₂	Et	—	100, 115
	C ₂ F ₅ CH ₂	H	—	100
	CF ₃ CH ₂	Me ₃ Si	—	83
	CHF ₂ CF ₂ CH ₂	Me ₃ Si	—	116
	CHF ₂ CF ₂ CH ₂	N = C = O	—	89, 117
	CHF ₂ CF ₂ CH ₂	N = C(Ph)OMe	—	89, 117
	CHF ₂ CF ₂ CH ₂	N = C(Ph)OEt	—	89, 117
	C ₃ F ₇ CH ₂	Et	—	100
	C ₃ F ₇ CH ₂	H	—	100
	(CF ₃) ₂ CH	H	—	84
	(CF ₃) ₂ CH	NHMe	—	84
	(CF ₃) ₂ CH	NHBu ^t	—	84
	(CF ₃) ₂ CH	Me	—	118
	(CF ₃) ₂ CH	Et	—	118
	(CF ₃) ₂ CH	Me ₃ Si	—	118
	(CF ₃) ₂ CH		—	118
(R _F O)(R'O)PNR ₂	(CF ₃) ₂ CHCH ₂	Pr ⁱ		102
	Et ₂ N(EtO)POCH ₂ (CF ₂) ₃ CH ₂	Et	Et	100, 119
(RO) ₂ PN(R _F) ₂	3-CF ₃ C ₆ H ₄	Et	—	120
(RO) ₂ PNR _F R'	3-CF ₃ C ₆ H ₄	Et		120
(R _F O)P(Cl)NR ₂	(CF ₃) ₂ CHCH ₂	Pr ⁱ	—	102
(R _F O)P(NR ₂) ₂	EtOOCCH = C(CF ₃)	Et	—	108
	(CF ₃) ₂ CH	Pr ⁱ	—	121
	CHF ₂ (CF ₂) ₃ CH(NHCOOEt)	Et	—	111
(R _F O)PRX	(CF ₃) ₂ CH	Me	(CF ₃) ₂ CHO	87, 122
	CF ₃ CH ₂	Me	CF ₃ CH ₂ O	105, 123
	CHF ₂ (CF ₂) _n CH ₂	Me	CHF ₂ (CF ₂) _n CH ₂ O	124
	(n = 1, 3)		(n = 1, 3)	
	C ₂ F ₅ CH ₂	CF ₃	NEt ₂	115
	CF ₃ CH ₂	CF ₃	CF ₃ CH ₂ O	125
	CHF ₂ (CF ₂) _n CH ₂	CF ₃	CHF ₂ (CF ₂) _n CH ₂ O	126
	(n = 1, 3)		(n = 1, 3)	
	CHF ₂ (CF ₂) _n CH ₂	C ₂ F ₅	CHF ₂ (CF ₂) _n CH ₂ O	126
	(n = 1, 3)		(n = 1, 3)	
	C ₂ F ₅ CH ₂	CF ₃	NH ₂ , NEt ₂ , Cl	100, 115
	C ₂ F ₅ CH ₂	C ₂ F ₅	NH ₂ , NEt ₂ , Cl	100, 115
	C ₂ F ₅ CH ₂	C ₃ F ₇	NH ₂ , NEt ₂ , Cl	100, 115
	C ₃ F ₇ CH ₂	CF ₃	NH ₂ , NEt ₂ , Cl	100, 115
	C ₃ F ₇ CH ₂	C ₂ F ₅	NH ₂ , NEt ₂ , Cl	100, 115
	C ₃ F ₇ CH ₂	C ₃ F ₇	NH ₂ , NEt ₂ , Cl	100, 115
	CF ₃ CH ₂	Et	CF ₃ CH ₂ O	125
	CF ₃ CH ₂	CCl ₃	CF ₃ CH ₂ O	125
	CHF ₂ CF ₂ CH ₂	Et	CHF ₂ CF ₂ CH ₂ O	105
	CHF ₂ (CF ₂) ₅ CH ₂	Et	CHF ₂ (CF ₂) ₅ CH ₂ O	105
	CHF ₂ (CF ₂) ₃ CH ₂	Et	CHF ₂ (CF ₂) ₃ CH ₂ O	124
	(CF ₃) ₂ CH	Et	(CF ₃) ₂ CHO	86

Table 3 (continued).

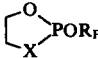
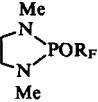
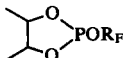
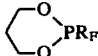
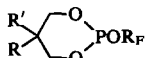
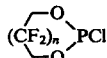
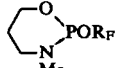
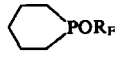
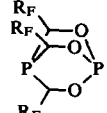
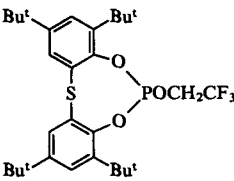
Compound	R _F	R (or NR ₂)	R' (or X)	Ref.
(R _F O)PRX	C ₄ F ₉ CH ₂	CH ₂ =CH	C ₄ F ₉ CH ₂ O	127
	C ₄ F ₉ CH ₂	CH ₂ ClCH ₂	C ₄ F ₉ CH ₂ O	127
	CHF ₂ (CF ₂) ₂ CH ₂	CH ₂ =CH	CHF ₂ (CF ₂) ₂ CH ₂ O	127
	CHF ₂ (CF ₂) ₂ CH ₂	CH ₂ ClCH ₂	CHF ₂ (CF ₂) ₂ CH ₂ O	127
	CHF ₂ CF ₂ CH ₂	EtOCH=CH	CHF ₂ CF ₂ CH ₂ O	128
	CF ₃ CH ₂	Ph	F	129
	(CF ₃) ₂ CH	Ph	F	87, 129, 130
	C ₃ F ₇ CH ₂ CH ₂	Ph	C ₃ F ₇ CH ₂ CH ₂ O	131
	CF ₃ CH ₂	Ph	CF ₃ CH ₂ O	95, 105, 123, 132, 133
	CHF ₂ CF ₂ CH ₂	Ph	CHF ₂ CF ₂ CH ₂ O	105
	(CF ₃) ₂ CH	Ph	(CF ₃) ₂ CHO	81, 87, 96
	(CF ₃) ₂ CH	Bu ^t	F	81, 130
	(CF ₃) ₂ CH	Bu ^t	Cl	81
	(CF ₃) ₂ CH	Bu ^t	Me	130
	(CF ₃) ₂ CH	C ₆ F ₅	(CF ₃) ₂ CHO	81
	(CF ₃) ₂ CH	Me	Me	87, 122
	(CF ₃) ₂ CH	CF ₃	CF ₃	81, 87
	(CF ₃) ₂ CH	Et	Et	86
	(CF ₃) ₂ C(CN)	CF ₃	CF ₃	134
	(CF ₃) ₂ CH	Ph	Ph	96, 135
	CHF ₂ CF ₂ CH ₂	Ph	Ph	136
	CF ₃ CH ₂	—	O	137, 140
	CF ₃ CH ₂	—	S	137, 140
	CF ₃ CH ₂	—	NMe	137, 140
	(CF ₃) ₂ CH	—	O	96, 135
	(CF ₃) ₂ CH	—	S	96, 135
	(CF ₃) ₂ CH	—	NMe	96, 135
	CHF ₂ CF ₂ CH ₂	—	O	138, 139
	EtOOCCH=CCF ₃	—	O	107, 108
	CF ₃ CH ₂	—	—	137, 140
	(CF ₃) ₂ CH	—	—	137, 140
	CHF ₂ CF ₂ CH ₂	—	—	138, 139
	CHF ₂ CF ₂ CH ₂ O	—	—	138
	CF ₃ CH ₂ O	—	—	141
	(CF ₃) ₂ CHO	—	—	141
	C ₃ F ₇	—	—	119
	(CF ₃) ₂ CH	Bu ^t	H	141–143
	(CF ₃) ₂ CH	Ph	H	143
	(CF ₃) ₂ CH	Me	Me	141, 142
 (n = 2, 4)	—	—	—	101
	CF ₃ CH ₂	—	—	144
	CF ₃ CH ₂	—	—	145
	(CF ₃) ₂ CH	—	—	145
	CF ₃	—	—	146
	CHF ₂ CF ₂	—	—	146
	CHF ₂ (CF ₂) ₃	—	—	146

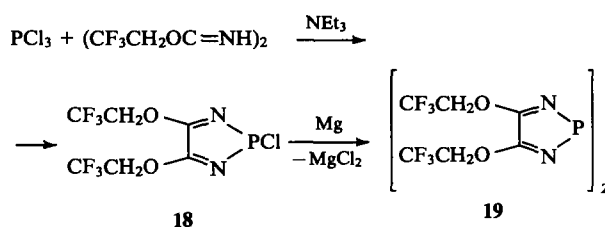
Table 3 (continued).

Compound	R _F	R (or NR ₂)	R' (or X)	Ref.
	(CF ₃) ₂ CH	H	—	143, 147
	(CF ₃) ₂ CH	Thymin-1-yl	—	143, 147
	(CF ₃) ₂ CH	—	—	143
	(CF ₃) ₂ CH	H	—	148
	CF ₃ CH ₂	H	—	37
	CHF ₂ CF ₂ CH ₂	H	—	138
	CHF ₂ (CF ₂) ₃ CH ₂	H	—	148
	CHF ₂ (CF ₂) ₃ CH ₂	H	—	149
	C ₆ F ₅	H	—	148, 149
	CF ₃ CH ₂	Bu ^t	—	150
	CF ₃ CH ₂	Bu ^t	—	151–153
	CF ₃ C(O)	Bu ^t	—	151–153
	(CF ₃) ₂ CH	Bu ^t	—	151–153
	—CH ₂ (CF ₂) _n CH ₂ — (n = 2, 3)	Bu ^t	—	153
	CF ₃	—	NEt ₂	154, 155
	CF ₃	—	OBu ^t	154
	CF ₃	—	NH ₂	155, 156
	CF ₃	—	NMe ₂	155
	CF ₃	—	NHBu ^t	155
	CF ₃	—	NH(SiMe ₃)	155
	CF ₃	—	N(SiMe ₃) ₂	155
	CF ₃	—	F	157–159
	CF ₃	—	Cl	158
	CF ₃	—	Br	158
	CF ₃	—	(CF ₃) ₂ CHO	157, 160
	CF ₃	—	Me ₃ SiO	160
	CF ₃	—	CF ₃ COO	160
	CF ₃	—	I	160
	CF ₃	—	H	160
	CF ₃	—		161
	CF ₃	—		162
	—	—	—	163
	—	—	EtO	164
	—	—	Et ₂ N	164
	(CF ₃) ₂ CH	—	—	37, 103
	CHF ₂ CF ₂ CH ₂	—	—	165
	CHF ₂ (CF ₂) ₃ CH ₂	—	—	103
	C ₆ F ₅	—	—	165

Table 3 (continued).

Compound	R _F	R (or NR ₂)	R' (or X)	Ref.
	—	—	—	150

The 1,3,2-diazaphospholines **18** and **19**, containing trifluoroethyl groups, have been obtained from PCl_3 and $(\text{CF}_3\text{CH}_2\text{OC}=\text{NH})_2$.¹⁷⁰



2. Transesterification, transamination, alcoholysis, and acidolysis

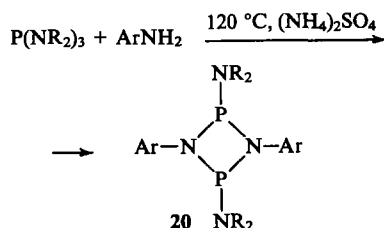
Certain R_F phosphites and amidophosphites have been obtained by the transesterification of phosphites with trifluoroethanol.¹⁷¹ Transesterification proceeds more readily in the case of P(III) derivatives with 'acid' residues, whereas the transesterification of $\text{P}(\text{OMe})_3$ is difficult.¹⁷¹

There are few examples of the alcoholysis of P(III) amides by R_F -alcohols.^{113, 143, 144, 172, 173} Bearing in mind that fluorinated alcohols are extremely acid reagents, one may expect that alcoholysis with their participation would be facilitated by virtue of protophilic cooperation.¹⁷² Indeed, the alcoholysis of amides by R_F -alcohols proceeds under comparatively mild conditions^{113, 173} and, depending on the ratio of the P(III) amide and $\text{R}_F(\text{OH})$, leads to full phosphites and mono- and di-amidophosphites, i.e. $\text{P}(\text{OR}_F)_3$, $\text{Et}_2\text{NP}(\text{OR}_F)_2$, and $(\text{Et}_2\text{N})_2\text{POR}_F$, where $\text{R}_F = \text{CHF}_2(\text{CH}_2)_3\text{CH}_2$ or $\text{CHF}_2(\text{CF}_2)_{11}\text{CH}_2$ and also to cyclic phosphites, for example to 1,3,2-dioxaphosphorinane with the exocyclic substituent $\text{OCH}_2\text{C}_3\text{F}_7$.¹⁷²

The alcoholysis of cyclic amides by hexafluoroisopropyl alcohol also takes place under mild conditions at 20 °C in CH_2Cl_2 .^{143, 147}

The interaction of trifluoropropanol with *o*-phenylene trifluoroacetyl phosphite affords a high yield of the corresponding full phosphite.¹⁷⁴

The transamination reaction has been used¹⁷⁵ to obtain fluorinated diazadiphosphetides **20**.

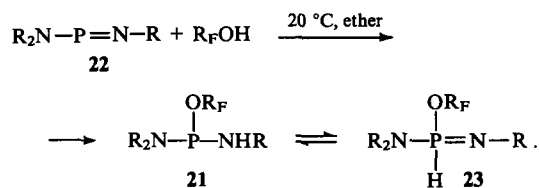


$\text{R} = \text{Et}, \text{Me}$; $\text{Ar} = 2\text{-CF}_3\text{C}_6\text{H}_4, 2,4\text{-F}_2\text{C}_6\text{H}_3, 2\text{-CF}_3\text{-4-ClC}_6\text{H}_3, 2\text{-Me-3-FC}_6\text{H}_3$.

Examples of the acidolysis of the amides $(\text{R}_F\text{O})_2\text{PNEt}_2$ and $(\text{R}_F\text{O})(\text{R}'_F)\text{PNEt}_2$ ($\text{R}_F = \text{C}_2\text{F}_5, \text{C}_3\text{F}_7$; $\text{R}'_F = \text{CF}_3, \text{C}_3\text{F}_7$) by HCl in order to obtain the corresponding R_F chlorophosphites are available in only one communication.¹⁰⁰

3. Reactions involving the addition of dicoordinate phosphorus to alcohols

The R_F phosphites **21** have been synthesised from dicoordinate phosphorus compounds $\text{R}_2\text{N}-\text{P}=\text{NR}$ **22**.¹⁷⁶

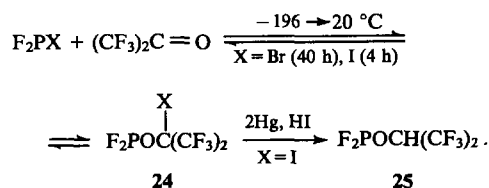


$\text{R} = \text{Me}_3\text{Si}, \text{Bu}^t$.

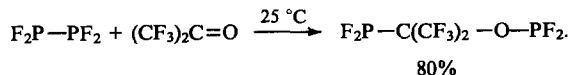
The diamidophosphite **21** is in equilibrium with the amide **23**, the stability of which increases by virtue of the presence of the electron-accepting group R_FO .

4. Reactions of P(III) derivatives with hexafluoroacetone

The reactions of P(III) derivatives with hexafluoroacetone are extremely diverse. The products of these reactions are usually compounds with the phosphorane structure. The reactions of hexafluoroacetone with chloro-, bromo-, and pyro-phosphites, as well as acyl phosphites, in which the final products are P(III) derivatives, are therefore of special interest. The insertion of hexafluoroacetone in a $\text{P}-\text{Hal}$ bond without change in the coordination at the phosphorus atom was first described in 1967.¹⁰⁴ The phosphite **24** ($\text{X} = \text{I}$) formed in this reaction was reduced to compound **25**.



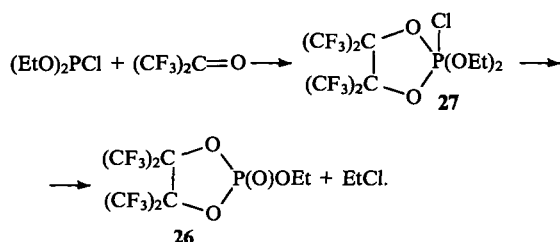
It was later shown that hexafluoroacetone may also be inserted in the $\text{P}-\text{P}$ bond of tetrafluorodiphosphine.¹⁷⁷



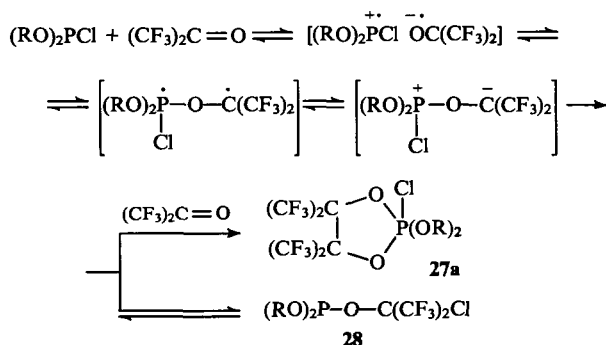
A whole range of compounds are formed in the reactions of the diphosphines Me_2PPMe_2 and $\text{Me}(\text{Bu}^t)\text{PPMe}(\text{Bu}^t)$ with hexafluoroacetone owing to the instability of the phosphinites $\text{R}_2\text{PC}(\text{CF}_3)_2\text{OPR}_2$ formed initially.¹⁷⁸

The reactions of phosphines containing a $\text{P}-\text{H}$ bond with hexafluoroacetone have been examined in reviews.^{179, 180}

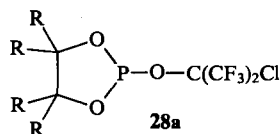
The interaction of chlorophosphites with $(\text{CF}_3)_2\text{CO}$ was first described by Knunyants and coworkers,¹⁸¹ who obtained σ^4 -dioxaphospholane **26**.



Later the reactions of dialkyl chlorophosphites with $(\text{CF}_3)_2\text{C}=\text{O}$ were investigated in greater detail.^{182, 183} It was shown that at -40°C the insertion products **28** are formed almost quantitatively, whereas on raising the temperature to 20°C a mixture of products **26**–**28** is formed.

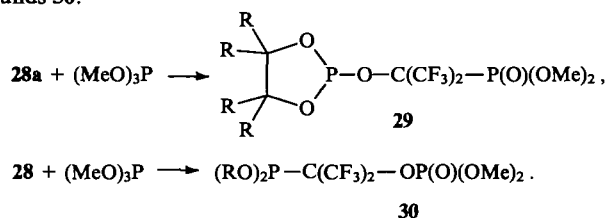


It has been suggested that the first reaction step involves one-electron transfer from the phosphite to the ketone, i.e. a radical mechanism operates.[†] When cyclic chlorophosphites are made to react with hexafluoroacetone, only the insertion products **28a**, which are more stable than the phosphites **28**, are obtained.

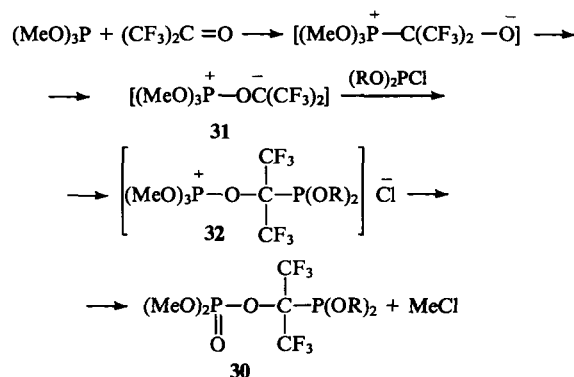


R = H, Me.

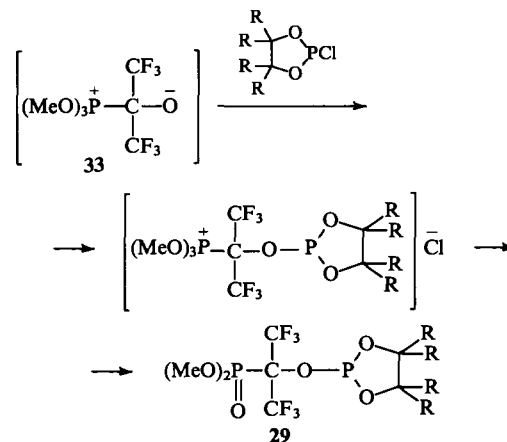
The authors of the studies quoted, suggest that the phosphites **28** enter into the Arbuzov reaction with trimethyl phosphite, forming compound **29**, whereas the phosphites **28** afford compounds **30**.



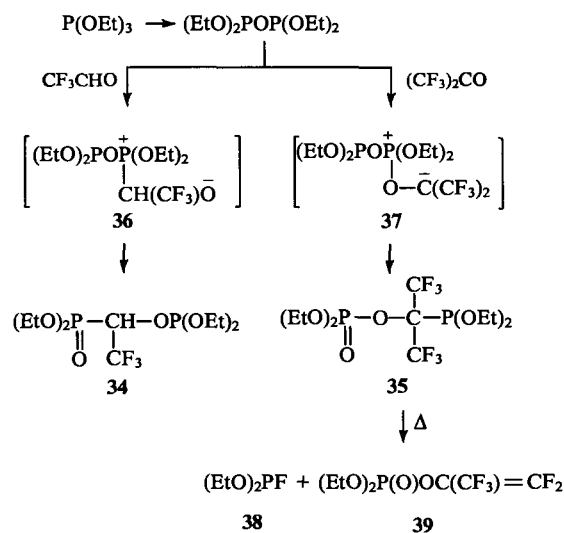
We believe that the product **30** cannot be obtained from the phosphite **28**. Careful analysis of the experimental part of the study of Heine and Rosenthaler¹⁸² confirms our view. Apparently the first reaction stage is the interaction of hexafluoroacetone with the more nucleophilic trimethyl phosphite. The resulting dipolar ion P^+OC^- **31** reacts as a C-nucleophile with $(\text{RO})_2\text{PCl}$, affording the salt **32**. The elimination of MeCl from the latter leads to the phosphonite **30**.



Bearing in mind the greater electrophilicity of cyclic chlorophosphites compared with the acyclic ones, it is logical to assume that they have sufficient time to 'capture' the dipolar ion P^+CO^- :

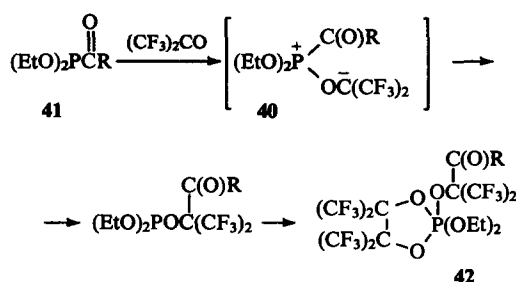


The treatment of the mechanism of the formation of compounds **29** and **30** presented here has been confirmed, from our point of view, by results¹⁸⁴ which show that hexafluoroacetone and fluoral react with triethyl phosphite to form compounds **34** and **35** with different types of substitution at the phosphorus atom, because the $\text{P}(\text{OEt})_2$ group migrates in different dipolar ions **36** and **37**. Thermolysis of compound **35** leads to the fluoro-phosphite **30** and the vinyl phosphate **39**.

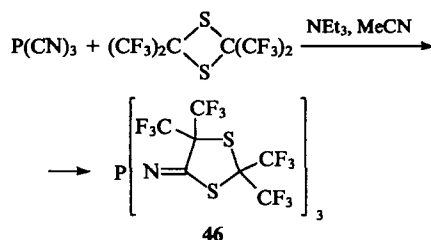
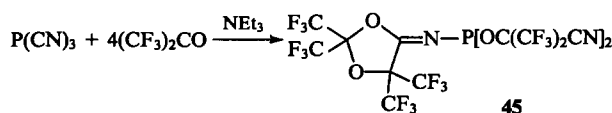
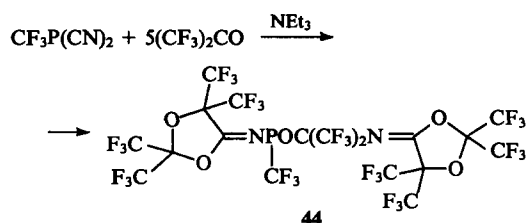
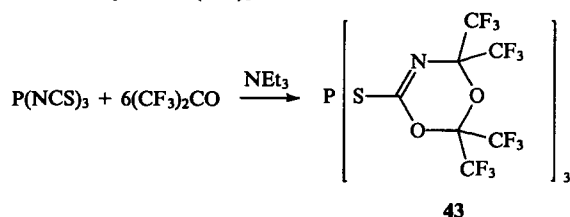


The reaction of the acyl phosphonite $(\text{EtO})_2\text{PC}(\text{O})\text{R}$ (R = Prⁱ, Bu^t, OMe) with hexafluoroacetone apparently proceeds via the same path.¹⁸⁵ If hexafluoroacetone is taken in excess, the σ^5 -1,3,2-dioxaphospholane **42** is formed.

[†] The proposed mechanism was taken from data presented in Professor Rosenthaler's lecture delivered in Tallin in 1989. More detailed data have not been published.

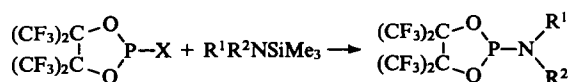
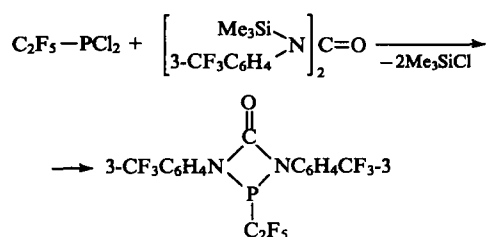


The complex phosphites **43–45**, incorporating heterocyclic fragments, have been obtained from hexafluoroacetone and phosphines containing the $\text{N}=\text{C}=\text{S}$ and $\text{C}\equiv\text{N}$ groups.^{186–188} It was noted that the interaction of the above reactants entails the isomerisation of the isothiocyanate group to the thiocyanate group and of the nitrile group to the isonitrile group. The structure of compound **43** ($\delta_{\text{P}} = 89.3$ ppm) has been demonstrated by X-ray diffraction.¹⁸⁸ The hexafluoroacetone dimer reacts similarly with $\text{P}(\text{CN})_3$.¹⁸⁹

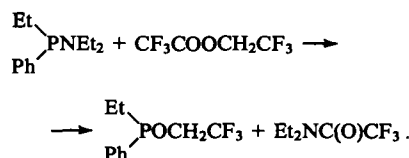


5. Other approaches to the synthesis of fluoroalkoxyfluoroalkylamino-derivatives of P(III)

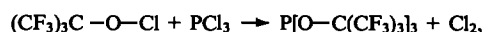
Amido- and amino-phosphites are obtained by the interaction of silylated amides and amines with P(III) chlorides:^{155, 188, 190}



The reactions of aminophosphines with R_F -esters of perfluorocarboxylic acids proceed with retention of configuration at the phosphorus atom.¹⁹¹



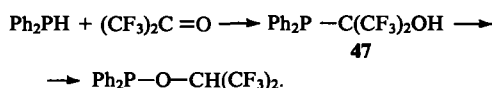
The interaction of phosphorus trichloride with perfluoro-*tert*-butyl hypochlorite is accompanied by the formation of tris(perfluoro-*tert*-butyl) phosphite.¹⁹²



The chlorine liberated does not then react with the phosphine. Attempts to employ this approach in order to obtain $\text{P}(\text{OCF}_3)_3$ from CF_3OCl and PCl_3 proved unsuccessful, since in this case CF_3OCl behaves as a fluorinating agent, being converted into the very stable COF_2 .¹⁹²

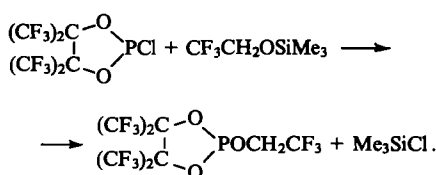
The compounds $(\text{CF}_3\text{O})_3\text{PO}$, $(\text{CF}_3\text{O})\text{P}(\text{O})\text{Cl}$, and $(\text{CF}_3\text{O})\text{P}(\text{O})\text{Cl}_2$ have been detected among the reaction products by mass spectrometry. It was not possible to detect any kind of P(III) derivatives.

Apart from the reactions listed above, the rearrangement $\text{PCO} \rightarrow \text{POC}$ in the series of α -hydroxyphosphines is also used to obtain fluorinated phosphines. This reaction was first described in 1974 for (1-hydroxyperfluoroisopropyl)diphenylphosphine **47** — the product of the reaction of diphenylphosphine with hexafluoroacetone.¹⁷⁷



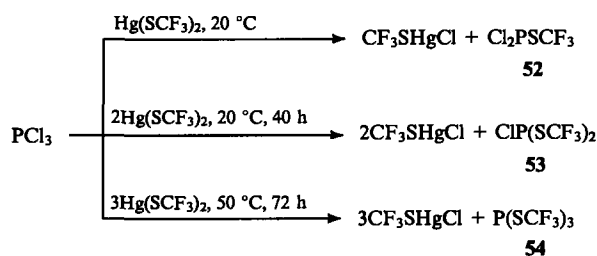
It was found that the rearrangement of the phosphine **47** is effectively catalysed by tertiary phosphines and that the higher the nucleophilicity of the phosphine the faster the rearrangement. The possibility of the occurrence of this reaction for the products of the reaction of bis(*tert*-butyl)phosphine and *tert*-butylmethylphosphine with hexafluoroacetone has been indicated,¹⁹³ but more detailed information has not been published.

It has been suggested¹⁶⁰ that $\text{CF}_3\text{CH}_2\text{OSiMe}_3$ be used for the synthesis of fluoroalkyl phosphites. The corresponding phospholane was obtained in a high yield.



6. Bis(fluoroalkyl) phosphites

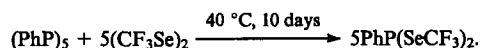
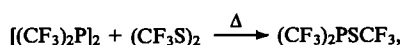
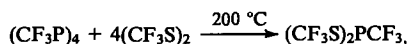
The classical method of synthesis of dialkyl phosphites — the reaction of P(III) chloride with alcohols — cannot be extended to fluorine-containing dialkyl phosphites. The only exception is the reaction of P(III) chlorides with $\text{FCH}_2\text{CH}_2\text{OH}$.⁶³ The synthesis of phosphites containing a large number of fluorine atoms by this method is impossible because of the difficulty of splitting off the fluorinated alkyl group. Indirect approaches to the synthesis of bis(fluoroalkyl) phosphites by the reaction of $\text{R}_\text{F}\text{OH}$ with PCl_3 were therefore developed. Thus bis(fluoroalkyl) phosphites have been obtained by the reaction of PCl_3 with $\text{R}_\text{F}\text{OH}$ in the presence of methanol¹⁹⁴ or *tert*-butyl alcohol.



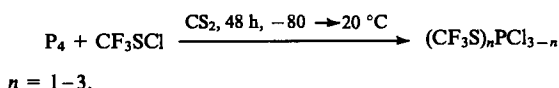
The products **52–54** are liquids, which are separated by distillation at the usual pressure. A quartet ($\delta_P = 194.4$ ppm, $^3J_{\text{PF}} = 24$ Hz), a septet ($\delta_P = 143$ ppm, $^3J_{\text{PF}} = 22$ Hz), and a decet ($\delta_P = 85$ ppm, $^3J_{\text{PF}} = 20$ Hz) correspond to them respectively in the ^{31}P NMR spectra.²¹⁷

$\text{CF}_3\text{SP}(\text{CF}_3)_2$,^{218, 219} $\text{CF}_3\text{SeP}(\text{CF}_3)_2$,²¹⁸ CF_3SPF_2 ,²²⁰ CF_3SePF_2 ,²²¹ $\text{PhP}(\text{SeCF}_3)_2$,²²² $(\text{CF}_3\text{Se})_2\text{P} - \text{P}(\text{SeCF}_3)_2$,²²² $\text{P}(\text{SeCF}_3)_3$,²²² and $\text{PhP}(\text{SCF}_3)_2$ ²²³ were synthesised similarly. The initial compounds employed were the corresponding phosphorus iodides. $\text{Hg}(\text{SeCF}_3)_2$ was used to synthesise the selenides. In the ^{31}P NMR spectrum, a decet with $\delta_P = 65$ ppm ($^3J_{\text{PF}} = 14.9$ Hz) corresponds to the selenophosphite $\text{P}(\text{SeCF}_3)_3$.²²⁰ This compound is unstable, its decomposition resulting in the segregation of $\text{CF}_3\text{SeSeCF}_3$ and the formation of a polymer. The ^{19}F and ^{31}P NMR spectra of the selenophosphinite $(\text{CF}_3)_2\text{PSCF}_3$ have also been described.²²⁴

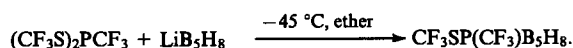
Subsequently several approaches were developed for the synthesis of fluorinated thio- and seleno-phosphites. Thus it has been suggested that the reaction of polyphosphines with CF_3SSCF_3 ^{225, 226} and $\text{CF}_3\text{SeSeCF}_3$ ²²² be used for the synthesis of CF_3E derivatives of $\text{P}(\text{III})$, in which $\text{E} = \text{S}$ or Se .



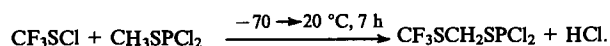
Fluorinated thiophosphines have been obtained by the reaction of R_FSCl with white phosphorus.²¹⁷



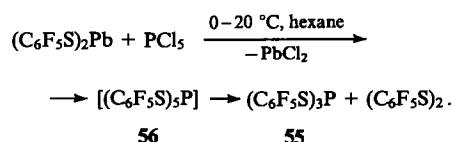
The synthesis of an organoboron derivative of thiophosphine has been described.^{225, 226}



The reaction of trifluoromethanesulfonyl chloride with methyl dichlorothiophosphite involves the substituent CH_3S .²²⁷



The interaction of PCl_5 with $\text{Pb}(\text{SC}_6\text{F}_5)_2$ constitutes yet another unusual approach to the synthesis of thiophosphites. Tris(pentafluorophenyl) thiophosphite **55** has been obtained by this procedure.^{97, 228} The phosphorane **56** formed initially in this reaction is extremely unstable and decomposes to the thiophosphite **55** and a disulfide.

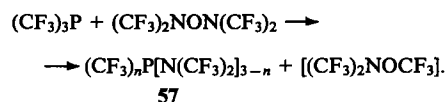


The chemistry of the CF_3E derivatives of $\text{P}(\text{III})$ has been only slightly developed. The reactions with S_8 ,^{219, 223, 229} EtOH ,²¹⁶ and

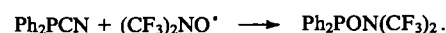
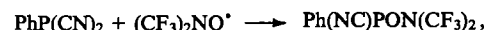
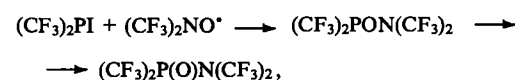
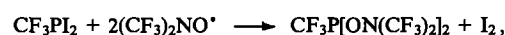
$\text{CF}_n\text{Cl}_{3-n}\text{SCl}$ ($n = 1, 2, 3$)²¹⁷ and the oxidation of the phosphite **54**²²⁹ have been studied. The complexes of perfluoroalkyl-substituted phosphites $(\text{CF}_3)_2\text{PECF}_3$ ($\text{E} = \text{S}, \text{Se}$) with molybdenum and manganese carbonyls have been synthesised.^{230, 231}

c. Perfluoroalkyl amidophosphites

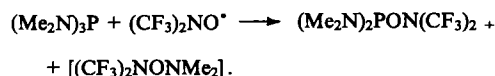
Perfluoroalkylaminophosphines **57** ($n = 1, 2, 3$) have been obtained by the exchange reactions of tris(trifluoromethyl)phosphine with $[(\text{CF}_3)_2\text{N}]_2\text{O}$.²³²⁻²³⁴



The interaction of the stable bis(trifluoromethyl)nitroxyl radical with $\text{E}(\text{III})$ ($\text{E} = \text{P}, \text{As}, \text{Sb}$) derivatives has been investigated.²³⁵⁻²³⁹ $\text{P}(\text{III})$ compounds were obtained only when phosphorus hydrides,²³⁵ iodides,^{236, 237} and cyanides²³⁸ were used as the initial compounds. It is suggested that the reactions proceed via a radical mechanism.



The amidophosphite $(\text{Me}_2\text{N})_2\text{PON}(\text{CF}_3)_2$ can be obtained from hexamethylphosphorous triamide and bis(trifluoromethyl)nitroxyl.²⁴⁰



The analogous arsenic and antimony compounds are more stable than the phosphorus compounds.^{239, 241}

Other perfluoroalkyl and nitrogen derivatives, for example $(\text{CF}_3)_2\text{NONO}$ and CF_3NO , are not only inserted into the $\text{CF}_3 - \text{P}$ bond but also oxidise the compounds formed to $\text{P}(\text{V})$ derivatives.²⁴¹⁻²⁴³ Bis(trifluoromethyl)phosphine adds to CF_3NO with retention of the coordination at the phosphorus atom, forming the amidophosphine $(\text{CF}_3)_2\text{PN}(\text{OH})\text{CF}_3$.²⁴³

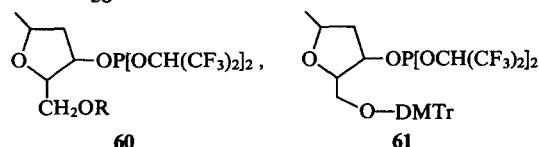
IV. Reactions of fluoroalkyl phosphites

As a result of the presence of the fluorinated substituent R_F , fluoroalkyl phosphites and related compounds (phosphonites, phosphinites, etc.) exhibit a reduced reactivity in nucleophilic reactions and an enhanced reactivity in electrophilic reactions compared with alkyl phosphites. The characteristic features of the chemical behaviour of the R_F -derivatives of $\text{P}(\text{III})$ are caused by the difficulty of cleaving the $\text{O} - \text{R}_F$ bond owing to the strong electron-accepting properties of polyfluorinated groups. The inertness of the polyfluorinated radicals derived from the fluoroalkanol $\text{CHF}_2(\text{CF}_2)_n\text{CH}_2\text{OH}$ ($n = 1, 3$)²⁴⁴ in reactions involving the formation of polyfluoroalkylcarbenium ions^{60, 245} provides grounds for the hope that stable phosphoranes may be obtained from them. The chemistry of the latter has been developed vigorously precisely as a result of the introduction of fluorinated substituents at the phosphorus atom.²⁴⁶⁻²⁴⁸

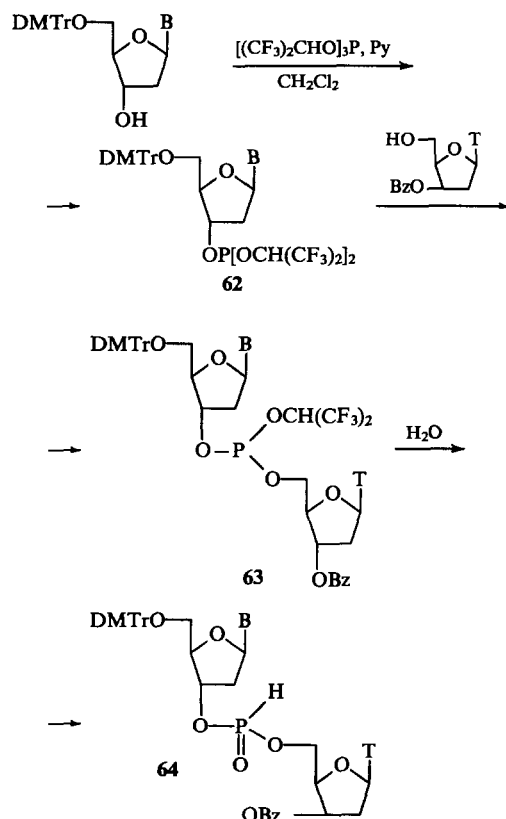
1. Reactions of fluoroalkyl phosphites with retention of the coordination the phosphorus atom

Reactions involving nucleophilic substitution at the phosphorus atom, which behaves as an electrophilic centre, must take first place among the reactions involving retention of the coordination at the phosphorus(III) atom. Such reactions are extremely characteristic of R_F -phosphites. They include alcoholysis, trans-

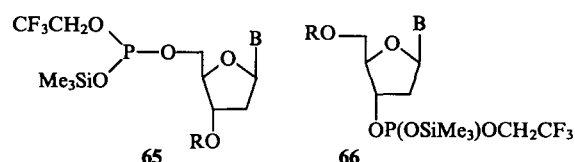
Dimethyl 1-hydroxymethylphosphonate interacts readily with tris(tetrafluoropropyl) phosphite, forming the phosphite $(\text{MeO})_2\text{P}(\text{O})\text{CH}_2\text{OP}(\text{OCH}_2\text{CF}_2\text{CHF}_2)_2$.¹¹³ Tris- and bis-(fluoroalkyl) phosphites proved to be exceptionally mild phosphorylating agents in the synthesis of oligonucleotides.^{88, 114, 249–256} It has been suggested that tris(hexafluoroisopropyl) phosphite be used as the most convenient reagent for the synthesis of DNA oligomers by the phosphite method. Various type **58–61** phosphites are obtained initially from the deoxyribonucleoside phosphite.



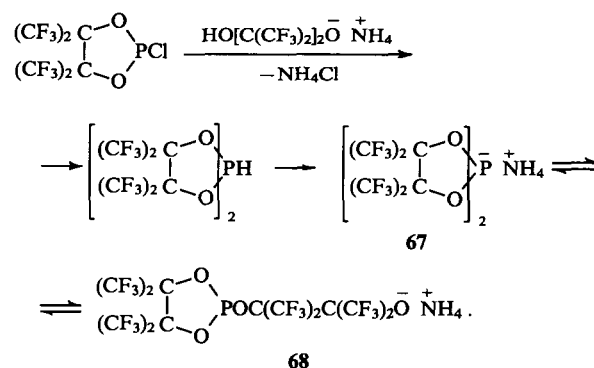
A mild synthesis of oligodeoxyribonucleotides employing the phosphites **62**–**64** as key intermediates has been described.¹¹⁴



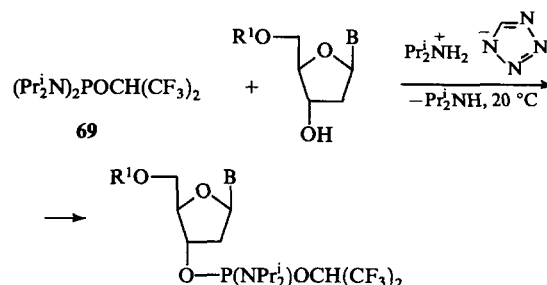
The ready hydrolysis of phosphites or the reactions with nucleosides are used in the synthesis of *H*-phosphonate-nucleotides and oligonucleotides. Data on the phosphorylation of oligonucleotides by certain fluorinated P(III) derivatives can be found in a recently published review.²⁵⁷ It has also been suggested that bis(hexafluoroisopropyl) phosphite,^{199, 201} bis(trifluoroethyl) phosphite,^{195, 196, 198, 258, 259} and bis(trifluoroethyl) trimethylsilyl phosphite²⁶⁰⁻²⁶³ be used for the phosphorylation of oligonucleotides and natural and common alcohols. The P(III) derivatives **65** and **66** are formed initially in the phosphorylation of nucleosides by bis(trifluoroethyl) trimethylsilyl phosphite.²⁶⁰



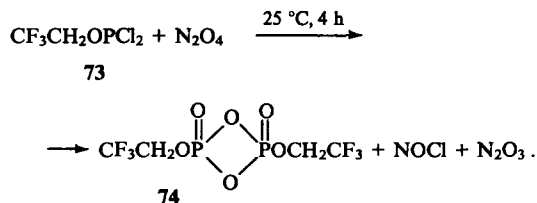
The nucleophilic substitution reactions of a series of phosphites containing the perfluoropinacol fragment have been investigated.^{264, 265} The electrophilicity of the phosphorus atom in these systems is so high that it was possible to obtain the relatively stable bicyclic phosphoranide intermediate **67**.



The reactions involving the phosphorylation of the alcohols by R_F phosphites proceed under very mild conditions (20 °C). Thus the reaction of the amidophosphite $(Pr_2N)_2POCH(CF_3)_2$ **69** with deoxyribonucleosides takes place selectively with formation of diisopropylamine.¹²¹



In certain studies, bases such as pyridine have been used as catalysts of the phosphorylation by R_F phosphites,¹⁹⁹⁻²⁰¹ while triethylamine has been used as the catalyst for reactions involving the addition of bis(fluoroalkyl) phosphites to carbonyl compounds such as CF_3CHO , $CF_2ClCOCFCl_2$, $(ClCF_2)_2C=O$, $(CF_3)_2C=O$,²⁶⁶ and $PhC(O)CHCl_2$ ²⁶⁷ and the alkylation of such phosphites by halogen-containing crown-ethers.^{268,269} In the alkylation of bis(trifluoroethyl) phosphite by functionally substituted alkyl bromides, sodium hydride is added to the reaction mixture.²⁷⁰ In many cases, the reaction is carried out for a long time at a high temperature (80–140 °C).

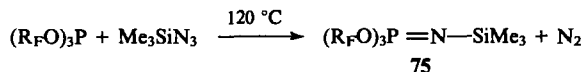


Sulfur adds to tris- and bis-(fluoroalkyl) phosphites with much greater difficulty than to the corresponding alkyl phosphites. The reaction takes place only after prolonged heating in dioxane^{61, 62, 164, 292} or pyridine.²⁹³ Only one reaction involving the addition of selenium to a phosphite, leading to the selenophosphate $\text{CF}_3\text{CH}_2\text{OP}(\text{Se})(\text{OCH}_2)_2$, has been described in the literature.²⁹⁴

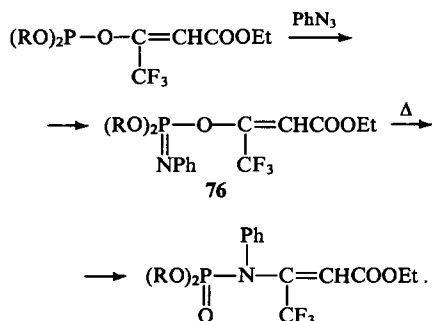
2-Nitro-1,1,3,4,4-pentachlorobuta-1,3-diene, which has electrophilic properties and contains fairly mobile terminal chlorine atoms, reacts fairly readily with fluoroalkyl phosphites, but, in contrast to other types of nucleophiles (for example, amines), only its nitro-group is involved. This results in the oxidation of phosphites to phosphates in high yields.²⁹⁵ The rate of reaction increases with increasing nucleophilicity of the phosphite.

b. The Staudinger reaction

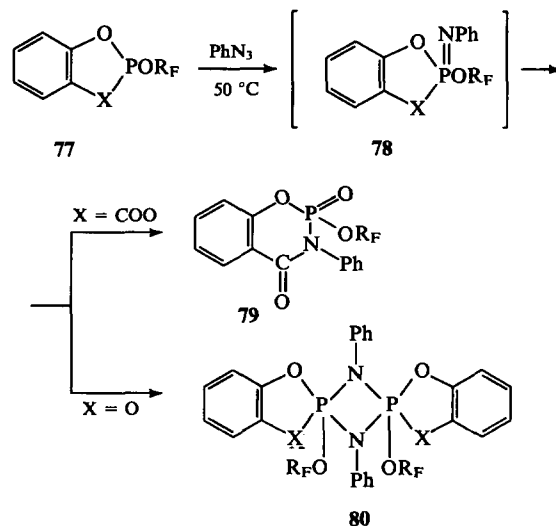
Fluoroalkoxy-derivatives of P(III) enter into the Staudinger reaction with greater difficulty than the R_H analogues, the type 75 iminophosphoranes formed are stable and do not undergo imide-amide rearrangement.²⁹⁶⁻³⁰¹


$$R_F = CF_3CH_2.$$

This course of the reaction becomes understandable in the light of data obtained recently on the imide–amide rearrangement,³⁰² which proceeds via an intermolecular chain mechanism with the intermediate formation of carbonium ions. Thus the rearrangement of the iminophosphorane **76** takes place on heating.^{107, 108}



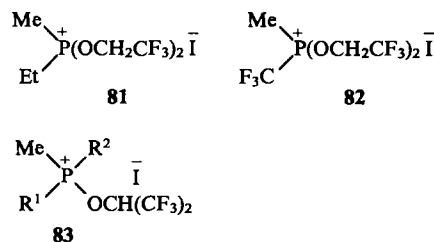
It was found that the result of the Staudinger reaction for the cyclic fluoroalkyl phosphites **77** — derivatives of salicylic acid — depends significantly on the nature of the exocyclic substituent R_F at the phosphorus atom.^{103,303} If $R_F = C_6F_5$, then the intermediate iminophosphorane **78** readily undergoes the imide — amide rearrangement, affording σ^4 -1,3,2-oxazaphosphorinane **79**, but, if $R_F = CF_3CH_2$ or $CHF_2(CF_2)_nCH_2$ ($n = 1, 3$), then the intermediate **78** is almost fully converted into the diazadiphosphetidine **80**. When catechol derivatives are used, only the diazadiphosphetidines **80** are formed.


$$X = O, COO; R_F = CF_3CH_2, CHF_2(CF_2)_nCH_2 (n = 1, 3), C_6F_5.$$

c. The Arbuzov reaction and its nonclassical variants

Tris(perfluoroalkyl) phosphites do not isomerise even at 250 °C.^{60, 62} The Arbuzov reaction of tris(tetrafluoropropyl) phosphite with MeI (1 : 1 ratio) takes place at 220 °C in a stainless steel test tube,^{60, 62, 304} whilst the iodide $\text{CHF}_2\text{CF}_2\text{CH}_2\text{I}$ does not react with the above phosphite.⁶² The kinetics of such reactions have been investigated³⁰⁵ and it has been shown that the rate-determining stage is nucleophilic attack on the P(III) atom. The decrease in the nucleophilicity of the latter is apparently more important for the Arbuzov reaction than the enhancement of the electrophilicity of the C_α atom in the $\text{R}_\text{F}\text{CH}_2\text{O}$ group, which favours elimination via an $\text{S}_{\text{N}}2$ mechanism. It is of interest to note that, in the reaction of the phosphite $(\text{EtO})_2\text{POCH}_2\text{CH}_2\text{F}$ with EtI, a mixture of the phosphonates $(\text{EtO})_2\text{P}(\text{O})\text{Et}$ and $(\text{EtO})(\text{CH}_2\text{FCH}_2\text{O})\text{P}(\text{O})\text{Et}$ is formed, whereas the reaction with MeI affords only the phosphonate $(\text{EtO})(\text{CH}_2\text{FCH}_2\text{O})\text{P}(\text{O})\text{Me}$.⁶³ The reaction temperature decreases after the addition of MeOH,³⁰⁴ which is associated with the fact that, not the initial phosphite, but the transesterification product interacts with RI.

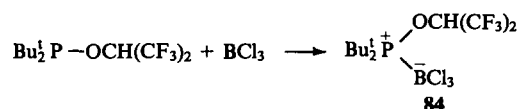
In the presence of two alkyl substituents at the P(III) atom, its fluoro alkoxy-derivatives form the quasi-phosphonium salts **81–83** with MeI.^{122, 125, 177, 178, 306}


$$R^1, R^2 = \text{Me, Et, Ph, Bu}^t.$$

These salts do not decompose up to 100–140 °C, which is due, according to the authors, to the electron-accepting influence of the CF₃ groups on the α -carbon atom.

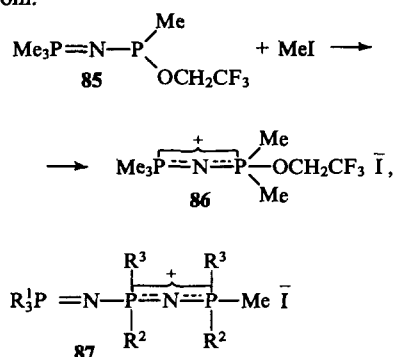
However, it is known that electron-accepting substituents accelerate the substitution reaction via an S_N2 mechanism,³⁰⁷ so that, for example, the stability of compound **83** may be associated either with the effective shielding of the C_α atom in the hexafluoroisopropyl group or with the fact that the elimination stage has significant features of an S_N1 process.³⁰⁸

The preparation of the salt **84**, stable up to 150 °C, has been reported.³⁰⁶



For the salt **84**, the exchange processes do not occur even at 100–150 °C.

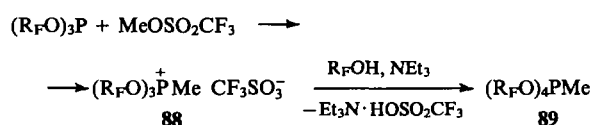
The stable quasi-phosphonium salt **86** has been obtained by the interaction of MeI with the imine **85**.^{125, 306} The authors believe that the stability of the salt **86** and its analogues **87** is due to the delocalisation of the positive charge on the phosphorus atom.



$\text{R}^1 = \text{Me}_2\text{N}$, $\text{R}^2 = \text{CF}_3\text{CH}_2\text{O}$ or Ph , $\text{R}^3 = \text{CF}_3\text{CH}_2\text{O}$.

In the quasi-phosphonium salts examined above, an electron-donating amide or alkyl group was always present together with the fluorinated substituent at the phosphorus atom, stabilising the positive charge on the latter.

It has been shown³⁰⁹ that tris(fluoroalkyl) phosphites are capable of forming the quasi-phosphonium salts **88** with methyl triflate.

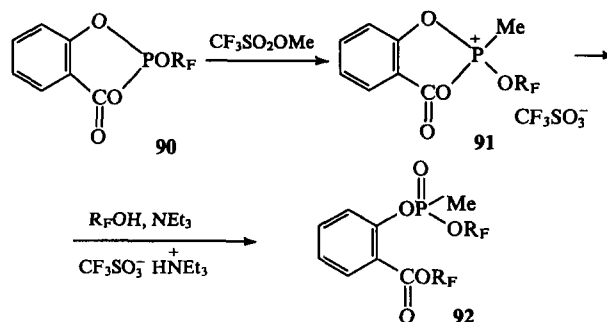


$\text{R}_\text{F} = \text{CF}_3\text{CH}_2$, $\text{CHF}_2\text{CF}_2\text{CH}_2$, $\text{CHF}_2(\text{CF}_2)_3\text{CH}_2$.

The latter are converted into the phosphoranes **89** in a high yield. The interaction of R_F phosphites is much slower than that of R_H -phosphites.^{310–312} The phosphite **5** with $\text{R}_\text{F} = (\text{CF}_3)_2\text{CH}$ reacts at 120–150 °C,¹⁰³ while the phosphites **2** and **4** with $\text{R}_\text{F} = \text{CF}_3\text{CH}_2$ and $\text{CHF}_2(\text{CF}_2)_n\text{CH}_2$ ($n = 1, 3$) react at 20 °C. The salts **88** formed have significantly weaker alkylating properties than R_H -phosphonium triflates. This follows from the inertness of tris(fluoroalkyl) phosphites in relation to fluoroalkylphosphonium triflates. Even in the presence of 50 mass % of the triflates **88** in the reaction mixture, the latter do not react with the initial phosphites, whereas R_H phosphites react via a cationic chain mechanism at an exceptionally high rate.^{310–312} Another significant difference between the R_F -quasi-phosphonium salts and the R_H -salts is the ability to react with R_F -alcohols at the phosphorus atom, i.e. to phosphorylate alcohols, whereas R_H -phosphonium triflates alkylate alcohols.³¹³

In contrast to acyclic fluoroalkyl phosphites, the cyclic phosphites **90** — derivatives of salicylic acid — react more slowly with methyl triflate. This has been established^{37, 103} in a study of

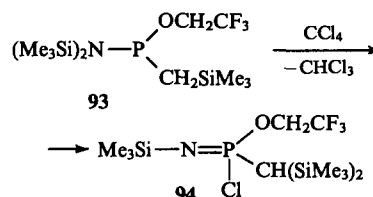
the competing reaction of the phosphites **4** and **90** ($\text{R}_\text{F} = \text{CHF}_2\text{CF}_2\text{CH}_2$) with $\text{MeOSO}_2\text{CF}_3$ by the ^{31}P NMR method. The stability of the cyclic salts **91** was found to be lower than that of the acyclic analogues **88**.



$\text{R}_\text{F} = \text{CF}_3\text{CH}_2$, $\text{CHF}_2\text{CF}_2\text{CH}_2$.

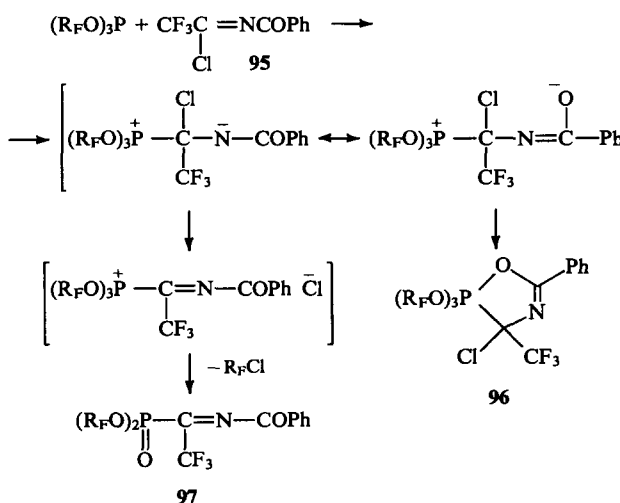
The salts **91** behave in this reaction merely as acylating agents, forming the phosphonate **92** in the reaction with tetrafluoropropanol.

The reactions of carbon tetrachloride with fluoroalkyl phosphonites^{105, 314} take place after prolonged heating in CH_3CN , while those with tris(fluoroalkyl) phosphites do not occur at all. The interaction of the silyl amidophosphonite **93** with CCl_4 leads to the PCl -iminophosphine **94**.³¹⁵



It has been noted that the elimination of CHCl_3 in this reaction is promoted by nonpolar solvents and by the absence of steric shielding of the protons of the CH_2Si fragment in compound **93**.

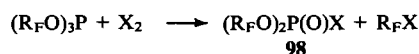
The interaction of N -benzoyltrifluoroacetimidoyl chloride **95** with tris(tetrafluoropropyl) phosphite proceeds with formation of σ^5 -1,4,2-oxazaphospholine **96** ($\delta_\text{P} = -41.7$ ppm) and the phosphonate **97**.³¹⁶



$\text{R}_\text{F} = \text{CHF}_2\text{CF}_2\text{CH}_2$.

Striking differences between cyclic and acyclic fluoroalkyl phosphites, on the one hand, and the corresponding unsubstituted phosphites, on the other, have been observed in the reactions of these compounds with the halogens, which lead, depending on the structure of the $\text{P}(\text{III})$ derivative, to different products —

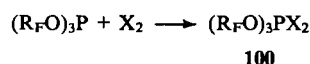
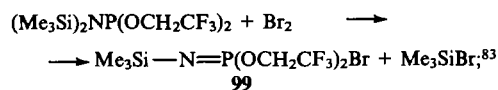
halophosphates **98**, *P*-haloimines **99**, and the phosphoranes **100** and **101**.^{57, 64, 65, 76, 77, 83, 87, 96, 98, 284, 317–319}



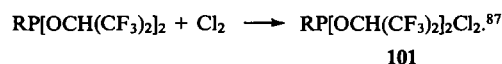
$\text{X} = \text{Cl}, \text{Br}; \text{R}_\text{F} = \text{CF}_3\text{CH}_2, \text{CF}_3\text{CMe}_2, (\text{CF}_3)_2\text{CMe}, \text{CF}_3\text{MeCH},$
 $\text{CHF}_2\text{CF}_2\text{CH}_2, \text{CHF}_2(\text{CF}_2)_3\text{CH}_2$; ^{57, 284, 315}



$\text{R}_\text{F} = \text{CF}_3\text{CMe}_2$,⁶⁴ $\text{CHF}_2\text{CF}_2\text{CH}_2$,²⁸⁴



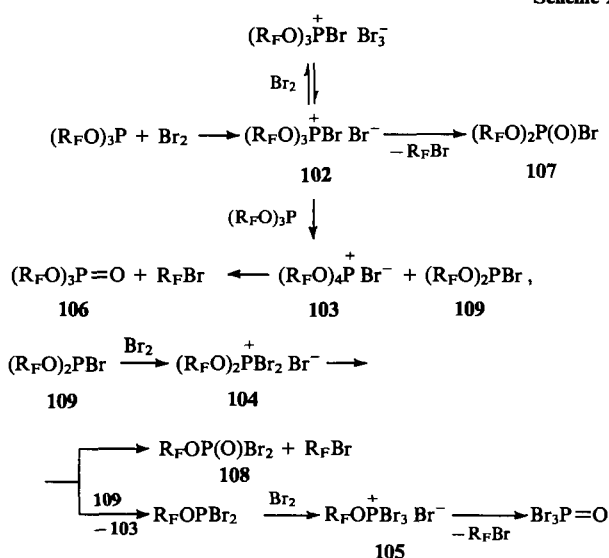
$\text{R}_\text{F} = (\text{CF}_3)_2\text{CH}$ ^{65, 76, 77, 96, 317}; C_6F_5 , ^{98, 316}



It is noteworthy that the compounds containing the $\text{CH}(\text{CF}_3)_2$ substituent react with the halogens to form the stable phosphoranes **100** and **101**.

The interaction of tris(tetrafluoropropyl) phosphite with bromine has been investigated by the dynamic ³¹P NMR method (Scheme 2).²⁸⁴ As in the case of triethyl phosphites,^{320, 321} this results in the formation of the quasi-phosphonium intermediate **102**. A further three quasi-phosphonium salts **103–105** were detected in the reaction mixture, and, depending on the ratios of the reactants and the order in which they were mixed, different phosphates **106–108** and the bromophosphite **109** were obtained.²⁸⁴

Scheme 2



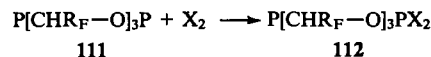
$\text{R}_\text{F} = \text{CHF}_2\text{CF}_2\text{CH}_2$.

Despite the presence of electron-accepting substituents destabilising the phosphonium centre, the stability of the bromide **102** is higher than that of its close analogue $(\text{EtO})_3\text{P}^+\text{Br}^-$ **110**. In this case, it is impossible to explain the greater stability of the fluorinated salt by the increase in the fraction of the phosphorane formed in the possible phosphonium \rightleftharpoons phosphorane equilibrium because, according to ³¹P NMR spectroscopic data, the chemical shifts, which are very sensitive to the position of equilibrium

between phosphonium salts and phosphoranes, are virtually identical for the two salts **102** and **110** ($\delta_\text{P} = 13–15$ ppm).[†] This effect is apparently due to the fact that substitution at the C_α atom has certain features characteristic of an $\text{S}_\text{N}1$ process. Only in this case would fluorinated radicals reduce the rate of cleavage.

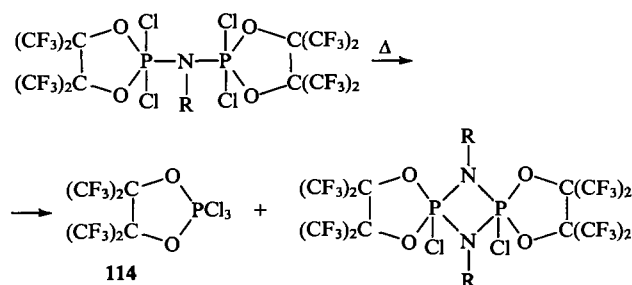
Another specific difference in the behaviour of the salts **102** and **110** is the ability of the former to enter into disproportionation reactions with the initial phosphites.

The tricyclic phosphites **111** also afford the phosphoranes **112**.^{48, 49}

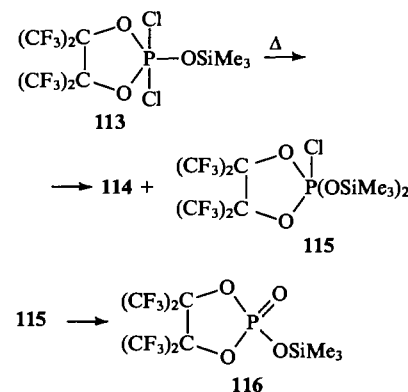


$\text{X} = \text{Cl}, \text{Br}; \text{R}_\text{F} = \text{CF}_3, \text{CHF}_2\text{CF}_2, \text{CHF}_2(\text{CF}_2)_3$.

The stability of the phosphoranes increases significantly if a perfluoropinacol fragment is introduced at the phosphorus atom.^{155, 157, 158, 160, 162} It effectively stabilises the bipyramidal phosphorus structure.^{162, 319, 322} The stabilisation effect is so strong that it is actually possible to obtain halophosphoranes with substituents such as CH_2Ph ,¹⁵⁷ NH_2 , NHBu^t , $\text{N}(\text{SiMe}_3)_2$, NMe_2 , and OSiMe_3 .^{155, 160} The thermolysis of these compounds proceeds in an extremely unusual manner:



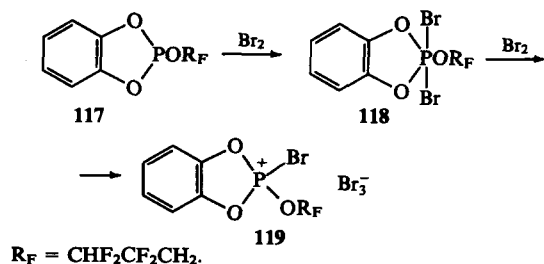
$\text{R} = \text{Me}, \text{Bu}^t$.



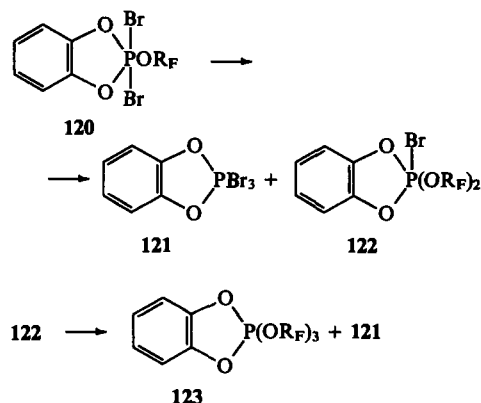
In the case of compound **113**, the latter initially disproportionates to the phosphoranes **114** and **115** after which the phosphorane **115** is converted into the phosphate **116**.¹⁶⁰

The catechol derivative **117** reacts with bromine to form the relatively stable phosphorane **118**, its stability being significantly higher than that of the bis(ethoxy)derivative,³²⁰ which readily decomposes to the phosphate via the Arbuzov reaction. In an excess of bromine, the phosphorane **118** forms the quasi-phosphonium salt **119**. When the phosphorane **118** is allowed to stand (at 20 °C), it disproportionates with formation of P(III) and P(V) derivatives.³²³

[†] The value $\delta_\text{P} = 2$ ppm quoted ⁴⁸ for compound **102** is erroneous.

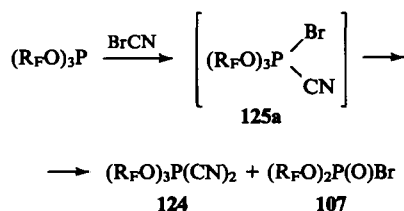


The hexafluoroisopropyl derivative **120** disproportionates to the phosphoranes **121** and **122**, the latter being subsequently converted into a mixture of the phosphoranes **121** and **123**.³²⁴



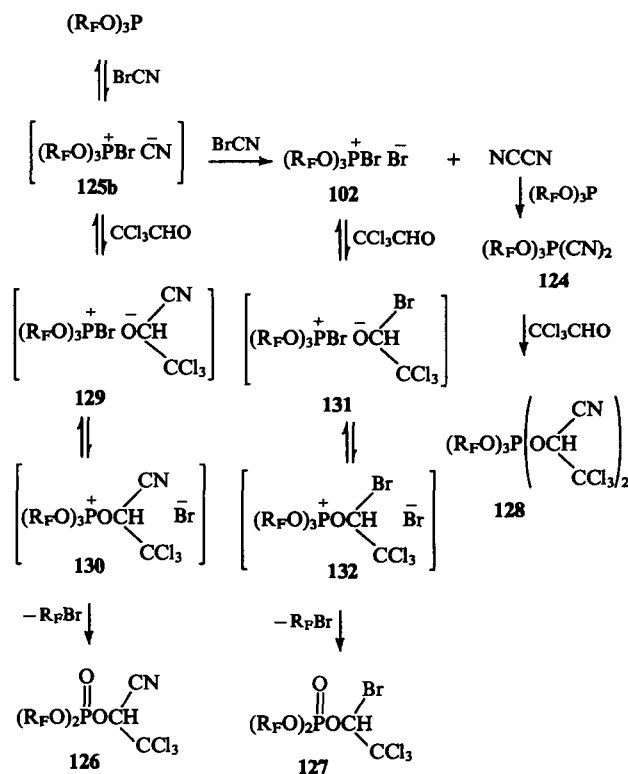
The fluorination of acyclic fluoroalkyl phosphites by fluorine,¹³² the azide $\text{CF}_3\text{CHFCF}_2\text{N}_3$,³²⁵ or perfluoroepoxypropane³²⁶ leads to difluorophosphoranes. The reaction of bis(tetrafluoropropyl) phosphite with the perfluoroepoxypropane dimer and trimer proceeds with the preferential formation of the tetrafluoropropyl ester of monofluorophosphorous acid and bis(tetrafluoropropyl) fluorophosphate.³²⁷

Bromocyanogen reacts slowly with R_F -alkyl phosphites, forming the dicyanophosphoranes **124** and the bromophosphates **107**,^{328, 329} whereas only phosphates are obtained from the R_H phosphites.³³⁰ It has been suggested that the process proceeds via the intermediate **125a**.

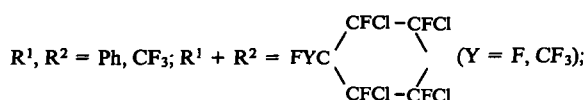
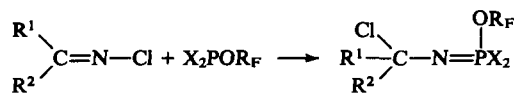
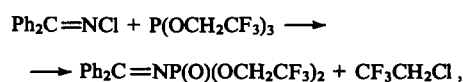


$\text{R}_F = \text{CHF}_2\text{CF}_2\text{CH}_2, \text{CHF}_2(\text{CF}_2)_3\text{CH}_2.$

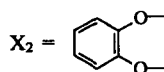
The nature of the intermediate (**125a** or **125b**) was established when the above reaction was carried out in the presence of a third reagent — chloral.³³¹ The phosphates **126** and **127** and the phosphorane **128** were obtained in this case, indicating the initial appearance of the quasi-phosphonium intermediate **125b**, which may react with the initial bromocyanogen. The interaction of the intermediates **124**, **125b**, and **102** with chloral leads to the final compounds **126**–**128**. The formation of the phosphates **126** and **127** includes the initial appearance of the salts **129** and **131** and their subsequent conversion via ligand exchange into the phosphonium salts **130** and **132**.



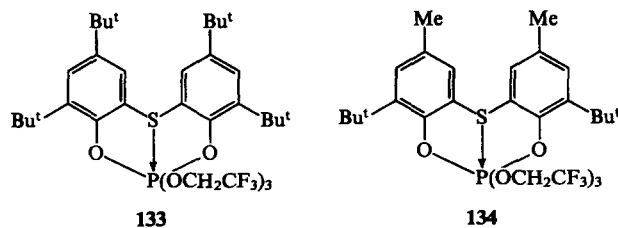
It has been shown^{329, 332, 333} that *N*-chloroamines react with R_F -alkyl phosphites to form iminophosphines, but the intermediate monochlorophosphoranes were not detected.

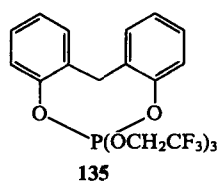


$\text{X} = \text{CF}_3\text{CH}_2\text{O}; \text{CHF}_2\text{CF}_2\text{CH}_2\text{O};$



An interesting approach to the synthesis of fluoroalkoxyphosphoranes has been proposed.^{334–337} It consists in the successive treatment of tris(trifluoroethyl) phosphite with diisopropylchloroamine and bisphenol, the role of a base being assumed by the amine produced during the reaction. The eight-membered heterocyclic compounds **133**–**135** were obtained in this way.

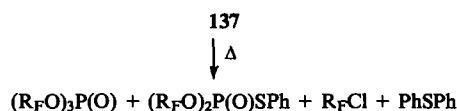
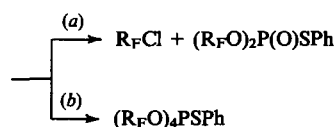
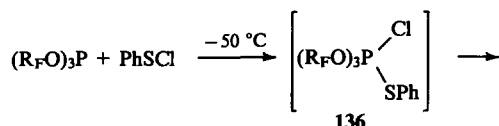




The structure of compound **134** was demonstrated by X-ray diffraction. The determination of the conformations of these phosphoranes was important for the understanding of the interaction of phosphates with the active sites of enzymes in the presence of sulfur-containing aminoacids.³³⁸

The interaction of P(III) derivatives with the halogens and sulfur(II, IV, VI) halides has many features in common and represents a nonclassical variant of the Arbuzov reaction.^{330, 339} In contrast to the halogens, sulfur halides have two different centres (the sulfur and halogen atoms), which are readily polarisable and are accessible to nucleophilic attack by the P(III) atom.³³⁹

Considerable attention has been devoted in the literature (see, for example, Refs 148 and 340–345) to the reactions of sulfur(II, IV, VI) chlorides with R_F -derivatives of P(III). Thus benzenesulfonyl chloride interacts with R_F -phosphites to form mixtures of compounds.³⁴²

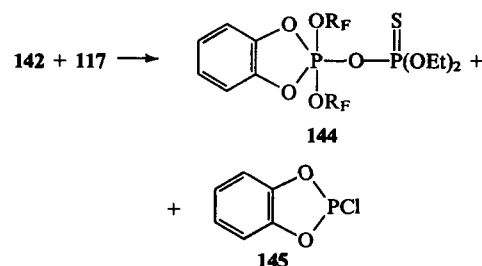
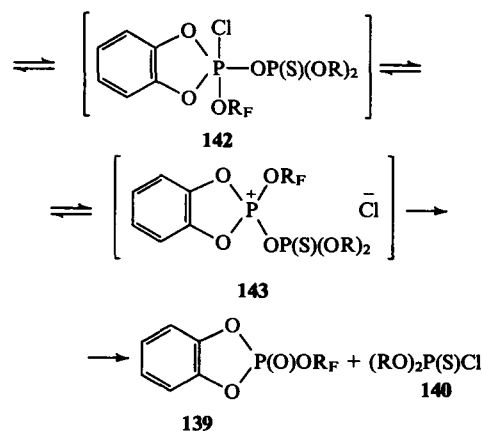
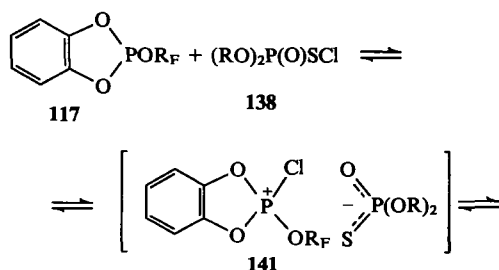


$R_F = CHF_2(CF_2)_nCH_2$, $n = 1, 3$;

(a) 20 °C; (b) –50 °C, R_FOH , NEt_3 .

The intermediate **136** was not detected, but its presence was deduced from the formation of the unstable monothiophosphorane **137** as a result of the treatment of the reaction mass with a mixture of the corresponding alcohol and triethylamine at –50 °C.

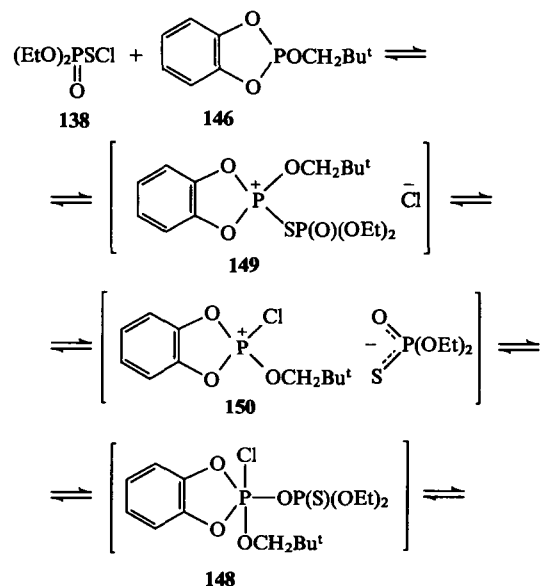
The interaction of acyclic and cyclic fluoroalkyl phosphites with dialkyl phosphonosulfonyl chlorides **138** is accompanied by the deoxygenation of the latter.^{103, 148, 344, 345} The catechol derivatives **117** also react similarly with compounds **138**^{148, 344, 345} with the preferential formation of the phosphate **139** and the chlorothiophosphate **140**.

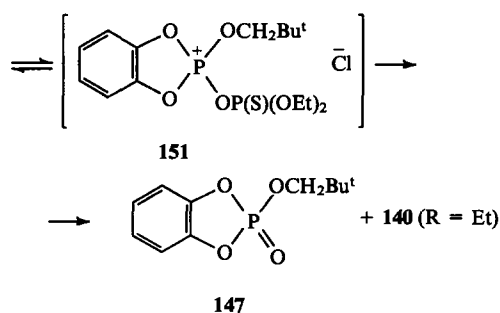


$R = Me, Et, Pr$; $R_F = CHF_2CF_2CH_2, CF_3CH_2, CHF_2(CF_2)_3CH_2$.

The reaction probably begins with halogenophilic attack on the phosphorus atom and the formation of the quasi-phosphonium salt **141**, which is in equilibrium with the phosphorane **142**. The latter is converted via the salt **143** into the main products **139** and **140**. The formation of small amounts of the phosphorylated phosphoranes **144** and of the *o*-phenylene phosphite **145** during the disproportionation process, which has been investigated in detail in relation to the reactions of the phosphites **117** with bromine, also constitutes evidence in support of the formation of the chlorophosphorane **142**.³²³

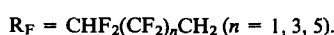
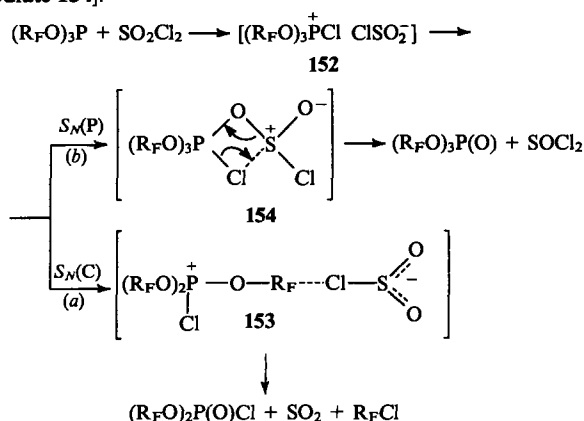
The mechanism of the reaction of the neopentyl *o*-phenylene phosphite **146** with the sulfonyl chloride **138** ($R = Et$), which also leads mainly to the phosphates **140** ($R = Et$) and **147**, has been recently investigated by dynamic ³¹P NMR (from 100 °C).³⁴⁶ The authors were able to detect the intermediate **148**, which is analogous to the phosphorane **142** postulated above. On this basis, it was concluded that the sulfur atom in compound **138** is initially attacked with subsequent two-step ligand exchange.



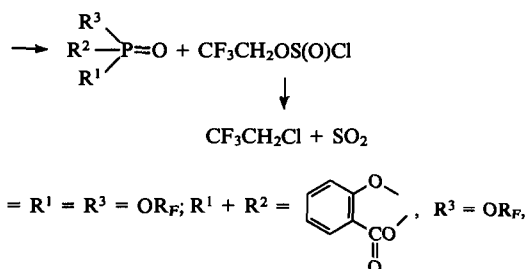
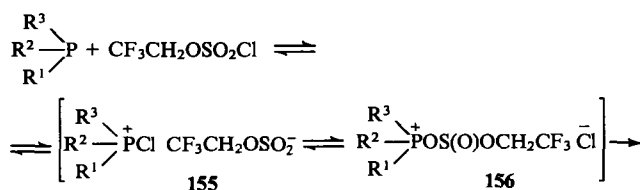


However, despite such a low reaction temperature, the intermediates **149**–**151** were not detected. In our view, the data presented in no way disprove the halogenophilic deoxygenation mechanism and cannot serve as proof that the sulfur atom is attacked. The high rates of the reactions of the sulfonyl chloride **138** with both the usual and fluorinated phosphites may indicate orbital control in these reactions or initial one-electron transfer from the phosphorus atom to the $\sigma_{\text{S-Cl}}^*$.

In the reactions of sulfonyl chloride with fluoroalkyl phosphites, the formation of chlorophosphates is accompanied by oxidation to phosphates.³⁴⁴ It has been suggested that the chlorophosphonium salt **152** formed initially enters into nucleophilic substitution reactions either at a carbon atom [path (a), intermediate **153**] or at the phosphorus atom [path (b), intermediate **154**].



It has been noted³⁴⁴ that the high electronegativity of the $\text{R}_\text{F}\text{O}$ [$\text{R}_\text{F} = \text{CHF}_2(\text{CF}_2)_n\text{CH}_2$] group hinders the elimination of R_F in the reaction with SO_2Cl_2 and promotes the formation of oxidation products. However, if the elimination stage were bimolecular, as described above, then the electron-accepting substituent R_F would be split off easily. It has to be assumed that the formation of the $\text{P}=\text{O}$ bond in the given reaction must take place before the attack by the Cl^- ion on R_F , i.e. the process should possess features of an $\text{S}_\text{N}1$ mechanism of fission of an alkyl group, which is naturally hindered by electron-accepting substituents such as fluorine atoms. It is doubtful if the intermediate **154** has the character of a phosphorane. Monochlorophosphoranes have been obtained only for $\text{R}_\text{F} = \text{CH}(\text{CF}_3)_2$ ³⁴¹ and in all the remaining cases only quasi-phosphonium salts are formed from acyclic fluoroalkyl phosphites. Ligand exchange in the salt **152** and nucleophilic attack on the sulfur atom are therefore more probable, as shown in relation to trifluoroethyl chlorosulfate.

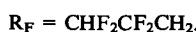
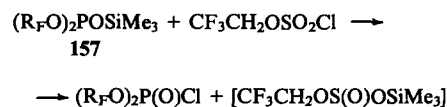


where $\text{R}_\text{F} = \text{CF}_3\text{CH}_2, \text{CHF}_2\text{CF}_2\text{CH}_2, \text{CHF}_2(\text{CF}_2)_3\text{CH}_2, (\text{CF}_3)_2\text{CH}, \text{C}_6\text{F}_5$.

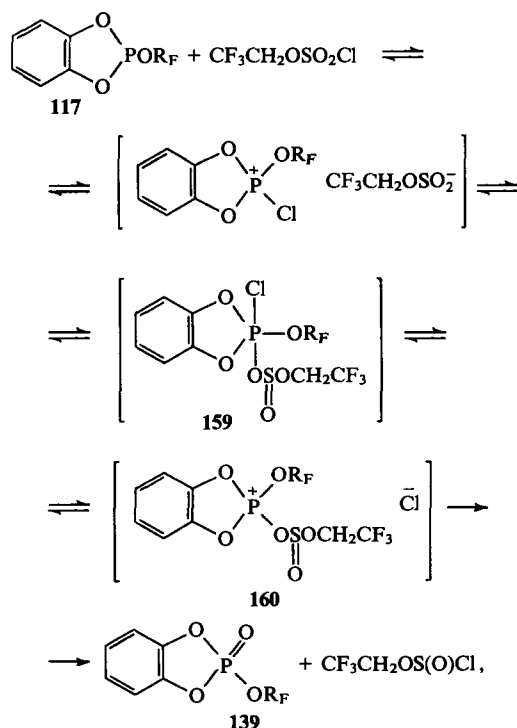
The reactivity of trifluoroethyl chlorosulfate towards fluoroalkyl phosphite is lower than that of sulfonyl chloride.^{103, 344}

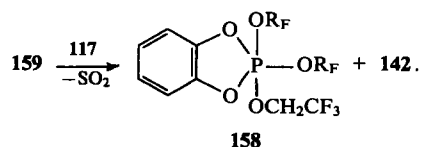
According to the authors, the reactions involve the initial formation of the chlorophosphonium salt **155** and subsequent ligand exchange with formation of the intermediate **156**, the decomposition of which leads exclusively to a phosphate (the yield is quantitative).

The fact that the first stage in the reaction of trifluoroethyl chlorosulfate with R_F -phosphites is nucleophilic attack on the chlorine atom is confirmed by the results of the reaction of trifluoroethyl chlorosulfate with the silyl phosphite **157**, which leads to a bis(fluoroalkyl) chlorophosphate.³⁴⁴

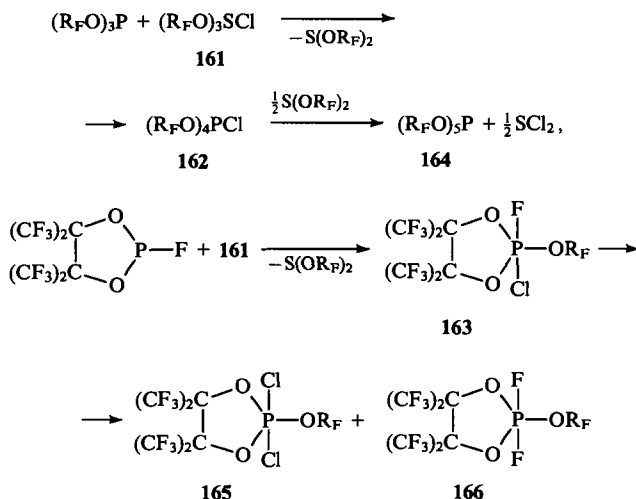


In contrast to the reactions examined above, the interaction of trifluoroethyl chlorosulfate with fluoroalkyl *o*-phenylene phosphites **117** takes place with formation of the phosphoranes **158** and the phosphates **139**. The phosphoranes **158** are obtained as a result of ligand exchange between the initial phosphite and the intermediate chlorophosphorane **159**. However, the main path in the reaction of the latter is transition via the salt **160** to the phosphate **139**.





The chlorosulfurane **161** readily reacts with R_F phosphites to form the phosphoranes **162** and **163**,^{340,344} which are converted into compounds **164**–**166** as a result of exchange reactions with the initial chloride **161** and disproportionation.

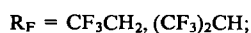
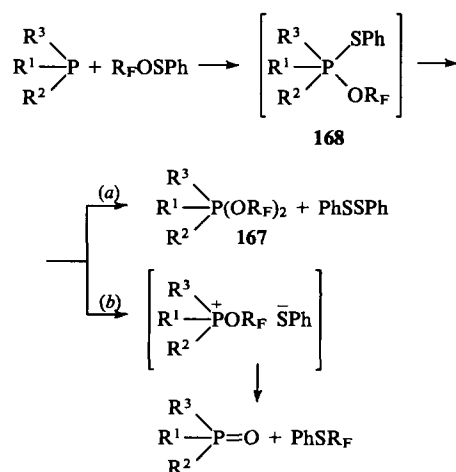


Thus the reactions of fluoroalkyl phosphites with sulfur chlorides and bromine have shown that a whole series of characteristic features, associated primarily with the low nucleophilicity of the P(III) atom and the hindrance to the elimination of the fluoroalkyl group from quasi-phosphonium intermediates, are typical of fluorinated P(III) derivatives. This leads to new reaction paths and unusual ways in which halophosphoranes and quasi-phosphonium salts are stabilised, such as transition to P(V) and P(III) compounds via exchange and disproportionation reactions.

It is known from theoretical studies and data on the stability of phosphorus(V) compounds^{246,248} that electronegative groups stabilise the phosphorane molecule. As we have already noted, fluoroalkoxy-groups have electron-accepting properties and effectively stabilise phosphorane structures and this is the reason why much attention has been devoted in the literature to the synthesis of stable phosphoranes from R_F -phosphites.

The stable phosphoranes **167** have been synthesised^{95–97,135,140,150} via the reaction of R_F -phosphites with sulfenic acid esters (Scheme 3).

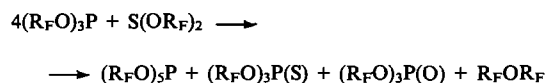
Scheme 3



R^1	R^2	R^3
CF_3CH_2O	CF_3CH_2O	CF_3CH_2O
Ph	CF_3CH_2O	CF_3CH_2O
Ph	Ph	CF_3CH_2O
C_6F_5O	C_6F_5O	C_6F_5O
$(CF_3)_2CHO$	$(CF_3)_2CHO$	$(CF_3)_2CHO$
$(CF_3)_2CHO$	$(CF_3)_2CHO$	Ph
$(CF_3)_2CHO$	Ph	Ph
	$-OCH_2CH_2O-$	$(CF_3)_2CHO$
	$-SCH_2CH_2S-$	$(CF_3)_2CHO$
	$-MeNCH_2CH_2NMe-$	$(CF_3)_2CHO$

It was suggested that, in the interaction of R_F -phosphites with sulfenic acid esters, the P atom is inserted in the S–O bond with formation of the alkoxythiophosphorane **168**. Such mixed phosphoranes have been obtained for $R^1 = R^2 = R^3 = CF_3CH_2O$ and $(CF_3)_2CHO$ ^{95,96} ($\delta_P = 50–54$ ppm). Next, the phosphorane **168** reacts via path (a) with yet another $PhSOR_F$ molecule, forming the pentaalkoxyphosphorane **168**. Path (b) operates for substituents at the phosphorus atom with more pronounced electron-donating properties.

The interaction of the hexafluoroisopropyl ester of sulfoxylic acid with fluoroalkyl phosphites results in the formation of a mixture of products.³⁴¹



3. Reactions of fluoroalkoxy-derivatives of P(III) with carbonyl compounds and their aza-analogues

The reactions of fluoroalkoxy-derivatives of P(III) with carbonyl compounds have been investigated for a comparatively small number of carbonyl compounds, among which most attention has been devoted to hexafluoroacetone. This is not fortuitous, because the latter forms with various P(III) derivatives σ^5 -1,3,2- or σ^5 -1,4,2-dioxaphospholanes, which are of great interest in view of their stability and the possibility of studying the structures of pentacoordinate phosphorus compounds, the role of which in biochemical processes is very important.^{143,347} The importance of fluoroalkoxyphosphoranes in organic synthesis has also been increasing.³⁴⁸

a. Bis(fluoroalkyl) phosphites

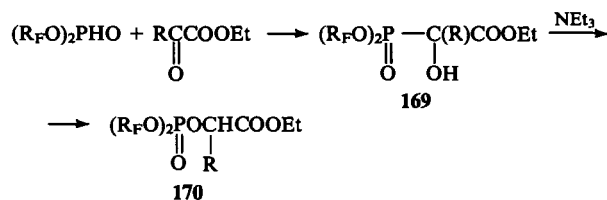
Bis(fluoroalkyl) phosphites are stronger acids than dialkyl phosphites.⁴⁷ The nucleophilicity of phosphorus in the P(III)-tautomeric form of bis(fluoroalkyl) phosphites is lower than in dialkyl phosphites.

The products of the phosphonate–phosphate rearrangement (hexafluoroisopropyl phosphates) have been obtained in the interaction of bis(fluoroalkyl) phosphites with $(CF_3)_2C=O$ in the presence of NEt_3 .^{160,266} Fluorodialkyl phosphites readily add to fluoral and chloral with formation of 1-hydroxyphosphonates,^{62,208} which are converted into phosphates or vinyl phosphates on heating in the presence of NEt_3 . Hexafluoroacetone *N*-benzenesulfonylimine reacts with bis(tetrafluoropropyl) phosphite to form a stable 1-aminoalkylphosphonate.³⁴⁹

The kinetics and mechanism of the addition of bis(fluoroalkyl) phosphites to benzylideneacetone, chalcone, butyl cinnamate and *p*-methoxycinnamate, and also to a phenylglyoxylic acid ester have been investigated.^{350,351} The reduced reactivity of bis(fluoroalkyl) phosphites in the Abramov and Pudovik reactions as well as certain specific features of their behaviour uncharacteristic of the usual dialkyl phosphites have been noted. For example, an excess of bis(fluoroalkyl) phosphite in the reaction of benzylideneacetone in the presence of R_FONa lowers the rate of reaction compared with the rate of reaction of

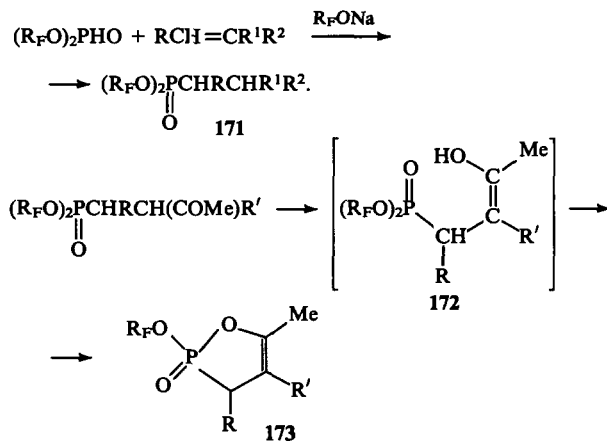
dialkyl phosphites, which the authors attribute to the formation of fairly stable hydrogen-bonded complexes between the free acid and its anion.

The esters of α -ketocarboxylic and mesoxalic acids react with bis(fluoroalkyl) phosphites to form the 1-hydroxyphosphonates **169**. The phosphonate obtained from ethyl pyruvate ($R = Me$) partly undergoes the phosphonate-phosphate rearrangement during distillation, while the analogous phosphonate synthesised from the phenylglyoxylic acid ester ($R = Ph$) is fully converted into the rearrangement product **170**.^{99, 352}


$$R_F = CF_3CH_2, CHF_2CF_2CH_2; R = Me, Ph, COOEt.$$

The fluoroalkyl groups at the phosphorus atom in the 1-hydroxyalkyl phosphonate obtained from bis(tetrafluoropropyl) phosphite and 2-acetoxyethyl methyl ketone promote a more ready occurrence of the phosphonate-phosphate rearrangement compared with the fluoroalkyl groups in the 1-hydroxyalkyl-phosphonate obtained from diethyl phosphite.¹¹⁶

The reactions of bis(fluoroalkyl) phosphites with ethylideneacetylacetone and ethyl acetoacetate and benzylidenemalonate are exothermic. In the presence of a catalyst, they lead to the phosphonates **171**.³⁵³ On heating, compounds **171** cyclize (probably via the enolic form **172**) to the $\sigma^{\alpha-1}$ -2-oxaphospholenes **173**.


$$R = \text{Me, Ph}; R^1, R^2 = \text{MeCO, COOEt}; R_F = \text{CF}_3\text{CH}_2, \text{CHF}_2\text{CF}_2\text{CH}_2.$$

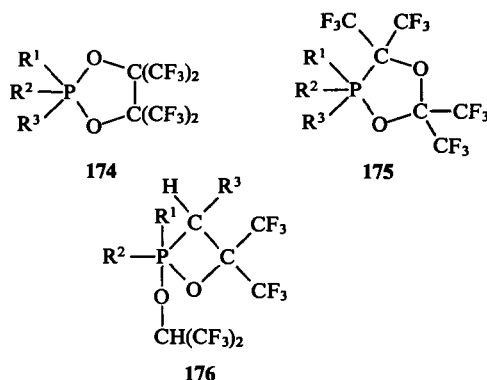
An analogue of the phosphonates **171**, containing OEt substituents instead of OR_F, cyclises under much more severe conditions than compounds **171**, which is associated with the greater leaving capacity of the fluoroalkoxy-group compared with the ethoxy-group. The phosphonate **171**, obtained from benzyldienemalonic ester which is incapable of enolisation, does not give rise to the phospholene **173**.

b. Fluoroalkyl phosphites, phosphonites, phosphinites, and amidophosphites

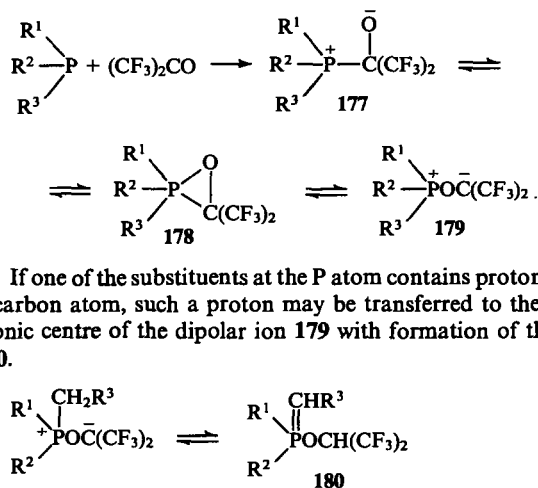
Fluoroalkyl phosphites, amidophosphites, phosphinites, and phosphonites have been allowed to react with hexafluoroacetone,^{84-86, 118, 122, 130, 141, 155, 161, 177, 178, 354, 355} diacetyl,¹⁶¹ perfluorodiacetyl,^{137, 140, 143, 144, 147} carboxylic α -ketoacid esters,³⁵¹ benzoynitrile,⁹⁰ *o*-anthraquinone,¹³³ diethyl mesoxalate,³⁵⁶ *o*-chloranil,^{357, 358} halogen-containing esters of di- and trifluoro-

acetoacetic^{356,359} and pyruvic³⁶⁰ acids, 1,1-dichloroacetophenone,²⁶⁶ pentafluorophenylbromoacetophenone,³⁶¹ dimethyl trichloroacetylphosphonate,⁹⁰ fluorinated aldehydes,^{49,208} and chloral and bromal.^{362,363}

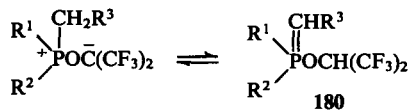
Hexafluoroacetone reacts with fluorinated P(III) derivatives to form phospholanes of three types: σ^5 -1,3,2- and σ -1,4,2-dioxaphospholanes **174**^{85, 86, 118, 122, 130, 141, 142, 161, 177, 178, 355} and **175**^{14, 86} respectively, as well as σ^5 -1,2-oxaphosphetanes **176**^{84, 86, 122, 130, 155, 177, 178, 354}. In the case of fluoroalkyl phosphites, mainly the σ^5 -1,3,2-dioxaphospholanes **174** are formed.


$$R^1, R^2, R^3 = \text{Ph, Et, Me, RO, (CF}_3)_2\text{CHO.}$$

It has been suggested that P(III) initially attacks the carbon atom of the carbonyl group with formation of the dipolar ion 177, which is converted into the zwitterion 179 via the phosphorane 178.



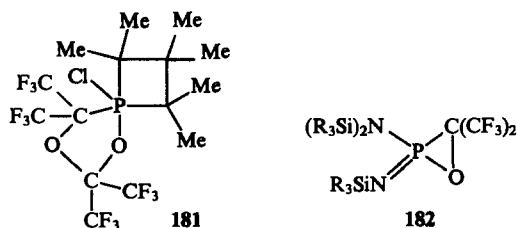
If one of the substituents at the P atom contains protons at the α -carbon atom, such a proton may be transferred to the carbanionic centre of the dipolar ion 179 with formation of the ylide 180.



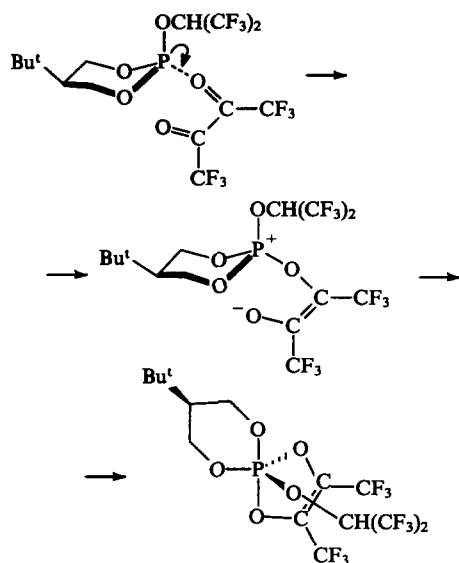
The addition of a second acetone molecule to the intermediates 177, 179, and 180 leads to the final reaction products 174–176. The intermediates 177–179 were not detected by any methods.

It is noteworthy that analysis of the available data on the reactions of P(III) derivatives with hexafluoroacetone, in which σ^5 -1,4,2-dioxaphospholanes are formed,^{86, 122, 181, 364–369} does not reveal the causes of the formation of the latter and the factors promoting the appearance of 1,3,2-dioxaphospholanes. 1,4,2-Dioxaphospholanes have been obtained from cyclic and acyclic P(III) derivatives containing both electron-donating (NR_2) and electron-accepting [F , $\text{OCH}(\text{CF}_3)_2$] substituents, as well as bulky groups. A particularly effective example is quoted in a study³⁶⁶ in which the synthesis of the phosphorane **181** is described.

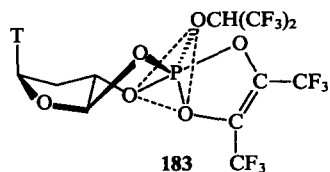
The structure of compound **182** is interesting as a model of the intermediate **178** containing a three-membered ring.³⁷⁰



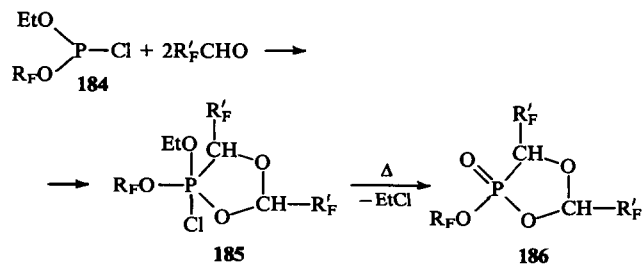
The reactions of cyclic fluoroalkyl phosphites with perfluoro-diacetyl have been investigated^{143, 144, 147} and it has been shown that they proceed stereospecifically — with retention of configuration at the phosphorus atom. The authors believe that this is a consequence of the attack by P(III) on the oxygen atom.



It has been suggested that the phosphorane **183** be used as a phosphorus-containing model of the P(V)-intermediate cyclic nucleotide for enzymic reactions. It has been shown by NMR (500 MHz) that the phosphorinane ring exists predominantly in the twist-conformation.



Fluoral and tetrafluoropropanal react with fluoroalkyl phosphites^{49, 208} and fluoroalkyl chlorophosphites^{49, 136} to form σ^5 -1,4,2-dioxaphospholanes. For example, the chlorophosphite **184** forms an unstable intermediate monochlorophosphorane **185** ($\delta_P = -40$ ppm), which is readily converted into the σ^5 -1,4,2-dioxaphospholane **186**:

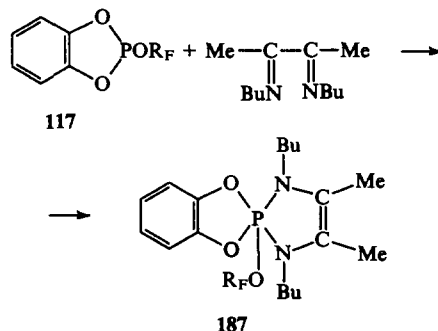


R_F = CF₃CH₂, R'_F = CHF₂CF₂.

Diethyl mesoxalate,³⁵⁶ *o*-chloranil,^{356, 357} and the ethyl ester and nitrile of phenylglyoxylic acid³⁵² react with fluoroalkyl

phosphites to form σ^5 -1,3,2-dioxaphospholanes; the reactions take place under more severe conditions than those with alkyl phosphites.

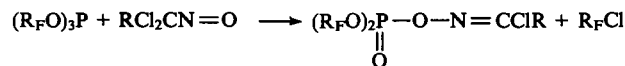
A single example of the interaction of the fluoroalkyl phosphites **117** with α -diimines³⁷¹ to form the σ^5 -1,3,2-diazaphospholine **187** has been described.



R_F = (CF₃)₂CH, CF₃CH₂.

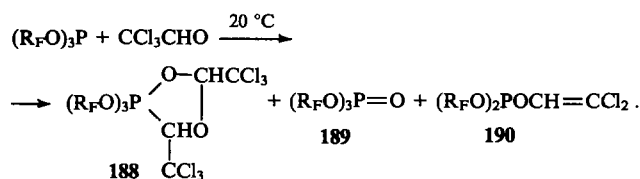
It is noteworthy that alkyl phosphites do not interact with mono- and di-imines.³⁷²

Carbonyl compounds containing a mobile halogen atom have been less studied in reactions with fluoroalkoxy-derivatives of P(III) — there have been only a few communications on this topic. Thus tris(tetrafluoropropyl) phosphite undergoes the Perkow reaction with chloral (in a stainless steel tube at a temperature > 200 °C),^{60, 62} with halogen-containing esters of di- and tri-fluoroacetoacetic³⁵⁸ and pyruvic⁹⁰ acids, with 1,1-dichloroaceto-phenone,²⁶⁷ with pentafluorophenylbromoacetophenone,³⁶¹ and with dimethyl trichloroacetylphosphonate.⁹⁰ Tris(tetrafluoropropyl) phosphite also undergoes the Perkow reaction with polychloronitrosoethanes.³⁷³

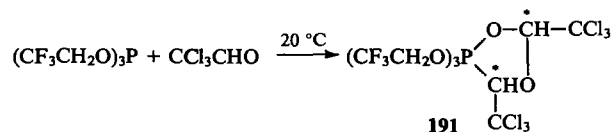


R_F = CHF₂CF₂CH₂, R = ClCH₂, Me.

A detailed reinvestigation of the reaction of tris(fluoroalkyl) phosphites with chloral showed³⁶³ that it begins even at 20 °C and leads mainly to the σ^5 -1,4,2-phosphorane **188**, the phosphate **189**, and small amounts of the vinyl phosphite **190**.

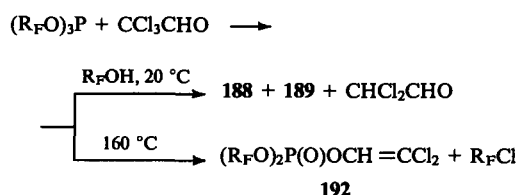


The fundamental results obtained in the study of the reactions of fluoroalkyl phosphites with chloral are briefly surveyed below.^{103, 362, 363, 374, 375} In the first place, it was possible to demonstrate the reversibility of the formation of the phosphorane **188**, which decomposes at 100 °C into the initial compounds and is reformed at 20 °C.³⁶⁰ In the case of tris(trifluoroethyl) phosphite, the corresponding phosphorane **191** was isolated in the form of one diastereoisomer;³⁷⁵ the stereoselectivity of the reaction is > 90%.

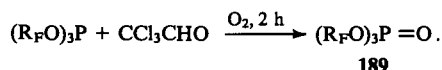


An extremely unusual fact was noted in the reaction of the phosphite P(OR_F)₃ with chloral in the presence of the alcohol R_FOH: together with the phosphate **189**, the fraction of which increases, the phosphorane **188** is also produced.^{103, 363} The

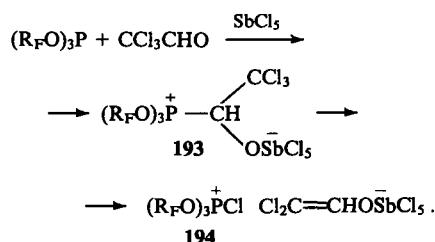
product of the Perkow reaction — the vinyl phosphate **192** — is formed only at 160 °C.^{60, 62, 363} Hence it follows that fluoroalkyl phosphites react with chloral predominantly at the carbonyl group, but the dechlorination of the CCl₃ substituent also takes place to a slight extent.



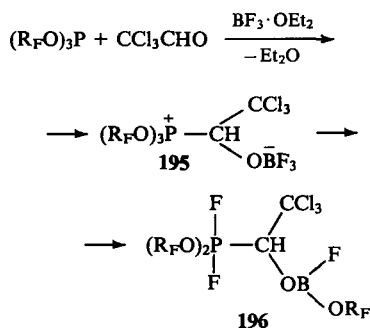
Chloral proved to be an effective catalyst of the oxidation of fluoroalkyl phosphites by oxygen.³⁶²



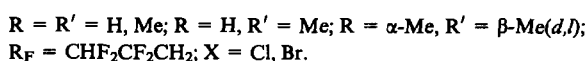
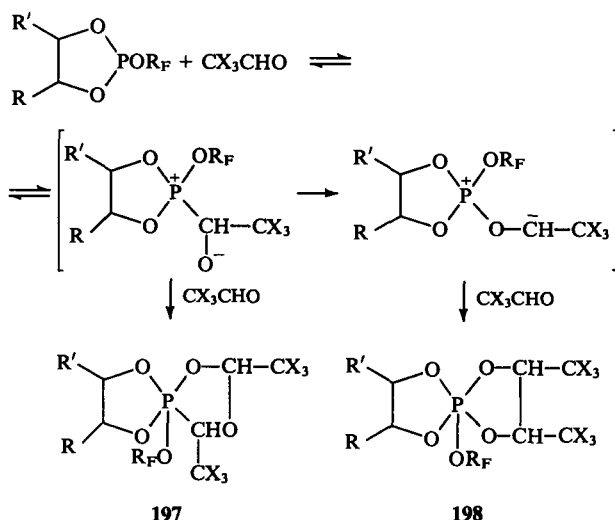
The initial attack on the carbon atom of the carbonyl group has been confirmed also by the results of the reaction of chloroalkyl phosphites with chloral in the presence of Lewis acids.³⁷⁴ When SbCl₅ was used, the betaine **193** with a P—C bond, stabilised by coordination to the Lewis acid at the anionic centre, was obtained. At 20 °C, the betaine **193** is slowly converted into the quasi-phosphonium salt **194** with a P—Cl bond.



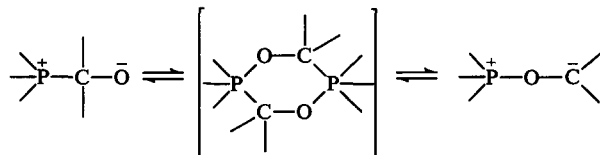
The betaine **195** ($\delta_\text{P} = 26$ ppm), obtained by the interaction of tris(fluoroalkyl) phosphite with chloral in the presence of BF₃·OEt₂, undergoes various reactions on heating, one of which is intramolecular fluorination to the difluorophosphorane **196** ($\delta_\text{P} = -57.9$ ppm, $^1J_\text{PF} = 894$ Hz).³⁶³



The asymmetric fluoroalkyl phosphites (R_FO)₂POR, containing one nonfluorinated substituent, react with chloral to form σ⁵-1,4,2-phospholanes with a P—C bond [R = Et, (EtO)₂P(O)CH₂], which are stable at 20 °C.¹¹³ We obtained the same result for cyclic fluoroalkyl phosphites.^{138, 139} The reaction with chloral led to the isolation for the first time of both σ⁵-1,4,2-dioxaphospholanes **197** and σ⁵-1,3,2-dioxaphospholanes **198**, the structures of which were confirmed by NMR data ($\delta_\text{P} = -20$ to -30 ppm for compound **197** and -42 to -50 ppm for compound **198**). Bromal gives rise to 1,4,2-dioxaphospholanes **197** only.



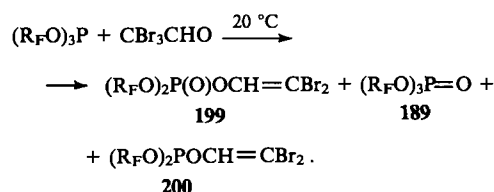
There exist two points of view in the literature concerning the mechanism of the rearrangement $\text{P}^+ - \text{C} - \text{O}^- \rightarrow \text{P}^+ - \text{O} - \text{C}^-$. One of them is that of Ramirez,³⁷⁶ who believes that the rearrangement proceeds via the formation of a six-membered cyclic diphosphorane, i.e. is bimolecular. This cyclic diphosphorane has been recently obtained from PhCHO and ethyl pinacol phosphite,³⁷⁷ which confirmed this mechanism.



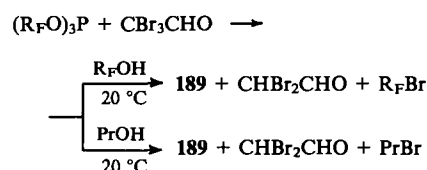
According to the second point of view, the rearrangement involves the formation of a three-membered transition state (or intermediate) on the path to the POC adduct, i.e. follows a unimolecular path.^{378, 379} Theoretically, one cannot rule out also the possibility of a direct electrophilic attack by P on the oxygen atom of the C=O group.³⁷⁹

When σ⁵-1,3,2- and σ⁵-1,4,2-dioxaphospholanes are formed simultaneously, their ratio should be affected by the dilution. When the C=O group is attacked simultaneously at the O and C atoms, the dilution of the reaction mixture should not lead to a significant change in the ratio of the phospholanes **197** and **198**. Where the rearrangement follows a bimolecular mechanism, dilution should diminish the fraction of the phospholane **198**. When the P atom attacks the C=O group at the C atom with an intramolecular rearrangement, the fraction of the phospholane **198** should increase with dilution. The experimental data obtained¹³⁹ for *d*, *l*-2,3-butylene tetrafluoropropyl phosphite and chloral have shown that the fraction of the phospholane **198** increases with dilution, whilst that of the isomer **197** falls, which confirms the intramolecular character of the rearrangement $\text{P}^+ - \text{C} - \text{O}^- \rightarrow \text{P}^+ - \text{O} - \text{C}^-$ in the case of chloral.

The results obtained in the study of the reaction of bromal with fluoroalkyl phosphites differ from those for chloral.^{363, 375} Bromal is much more reactive than chloral. When bromal is employed, the vinyl phosphate **199** and the phosphate **189** are formed as the main products. The dibromovinyl phosphite **200** was also detected in a small amount.

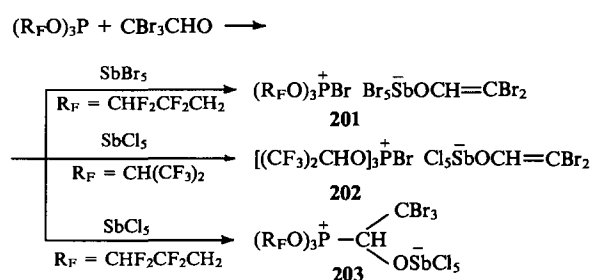


When this reaction is carried out in the presence of an alcohol, the phosphate **189** (yield ~97%) and the aldehyde CHBr_2CHO are formed. This reaction has been proposed in the literature as a test reaction for the halogenophilic mechanism.^{380, 381} Under these conditions, even the use of a much less acid alcohol (propanol) affords more than 90% of the phosphate **189**.^{103, 363}

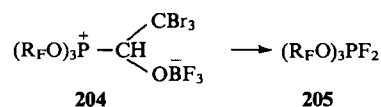


Taking into account the difference between the reactivities of chloral and bromal and also the fact that the rate-determining stage in the Perkow reaction is the nucleophilic attack by the phosphorus atom, a halogenophilic mechanism has been proposed for the reactions of fluoroalkyl phosphites with bromal.^{103, 363}

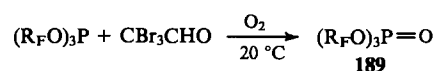
The use of a third reagent (a Lewis acid) in the reaction with bromal on the whole confirms that the bromine atom is attacked, but in this case the shielding of both the carbonyl group and of the phosphorus atom by bulky substituents plays a certain role. Thus, when SbBr_5 is used as the Lewis acid, the quasi-phosphonium salt **201** with a P—Br bond is formed. The salt **202** is obtained similarly from the branched tris(hexafluoroisopropyl) phosphite and SbCl_5 .¹⁰³ On the other hand, the interaction of the complex $\text{CBr}_3\text{CHO} \cdot \text{SbCl}_5$ with tris(tetrafluoropropyl) phosphite leads to the formation of the betaine **203**.³⁷⁴



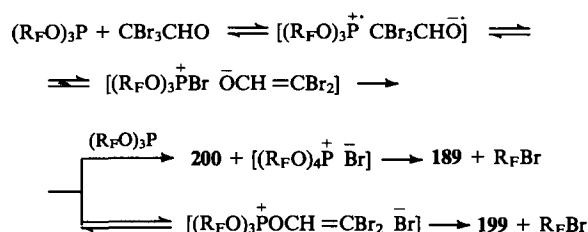
The betaine **204**, stabilised by coordination to BF_3 , is converted into the difluorophosphorane **205** ($\delta_\text{P} = -77.9$ ppm, $^1J_\text{PF} = 729.6$ Hz) after being kept at 20°C .



When oxygen is bubbled through a mixture of a phosphite and bromal, the oxidation product — the phosphate **189** — is formed in 100% yield.³⁶²



This is an extremely important result, indicating the appearance of radical species during the reactions of fluoroalkyl phosphites with bromal, i.e. the occurrence of a one-electron transfer. Only in this case is there a possibility of catalysis of the reactions of phosphites with paramagnetic oxygen. A possible mechanism of the interaction of fluoroalkyl phosphites with bromal is presented below.¹⁰³



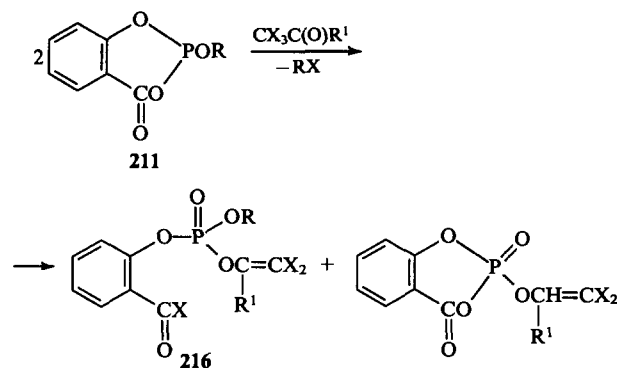
We may note that the appearance of small amounts of vinyl phosphite as well as bromophosphites in reactions with bromine is associated with ligand exchange between the quasi-phosphonium intermediates and the initial fluoroalkyl phosphite.

The interaction of the phosphite **117** with chloral and bromal is complex.^{103, 382, 383} P(III) derivatives, formed on cleavage of the CCl_3 group and representing disproportionation products, were detected together with σ^5 -1,3,2- and σ^5 -1,4,2-dioxaphospholanes in the reaction with chloral.³⁸³

The replacement of chloral by bromal increases the contribution of the processes accompanied by the partial reduction of the CBr_3 group. The reaction products are the monocyclic pentaalkoxyphosphorane **206**, the phosphate **139**, and a small amount of the vinyl phosphite **207** (Scheme 4).³⁸² It was also possible to make the interesting observation that the above reaction is accelerated on UV irradiation.¹⁰³ These data as well as the results of the interaction of oxygen with the phosphite **117** in the presence of bromal, leading to the phosphate **139**, indicate the occurrence of one electron transfer in the reaction with bromal. The interaction of the phosphite **117** with bromal in the presence of $\text{R}_\text{F}\text{OH}$ leads to the phosphate **139**, the phosphorane **208**, and dibromoacetaldehyde, which also confirms that the phosphorus atom attacks the bromine atom of bromal. When the last reaction is carried out in the presence of a base, the phosphorane **208** becomes the only phosphorus-containing reaction product.³⁸²

On heating, the phosphorane **206** decomposes to the vinyl phosphate **210**; when it is kept for a long time at room temperature in an acid medium, symmetrisation results in the formation of various phosphoranes containing both one and two catechol fragments and different acyclic substituents.

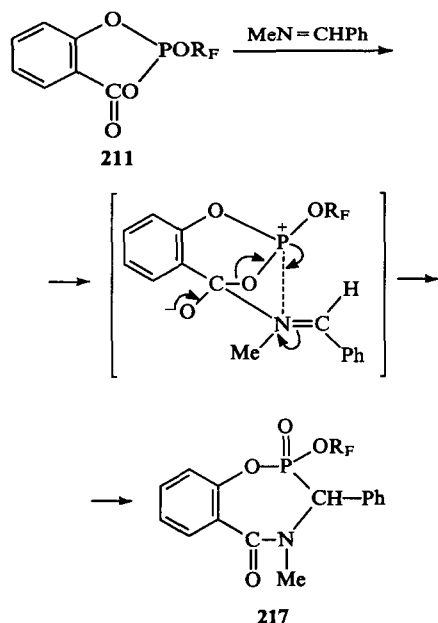
Thus the reaction of the phosphite **117** with bromal proceeds via a halogenophilic mechanism with the intermediate formation of the bromophosphorane **209**, which adds to the $\text{C}=\text{O}$ bond of bromal, affording the phosphorane **206**. The monobromophosphorane **209** is unstable and decomposes to the vinyl phosphate **210** at 20°C .



$R = \text{CF}_3\text{CH}_2, \text{CHF}_2\text{CF}_2\text{CH}_2, \text{Me}, \text{Bu};$

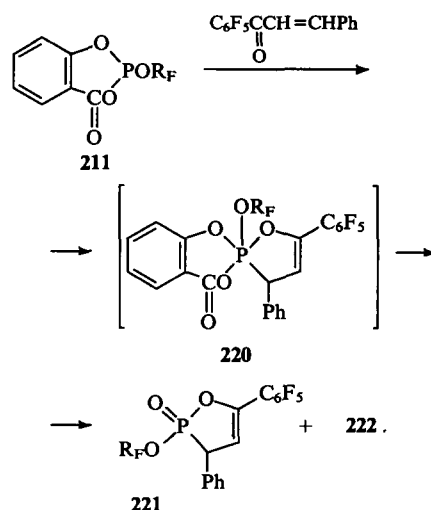
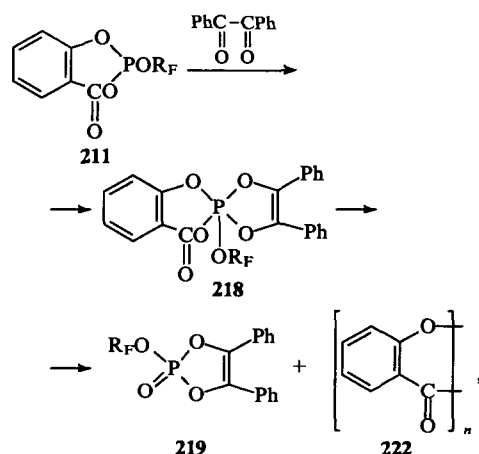
$R^1 = \text{H}, X = \text{Br}; R^1 = (\text{MeO})_2\text{P(O)}, X = \text{Cl}.$

Fluoroalkyl salicyl phosphites **211** interact readily with imines to form 1,4,2-oxazaphosphhepanes **217**.³⁹² It has been suggested that the imine nitrogen atom behaves as a nucleophile.



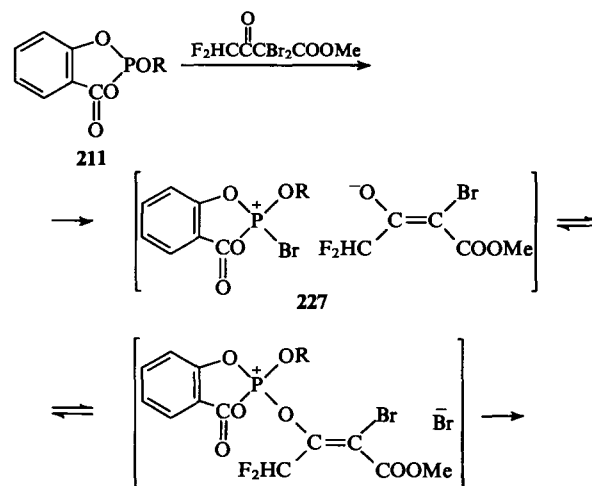
$R_F = (\text{CF}_3)_2\text{CH}_2, \text{CF}_3\text{CH}_2.$

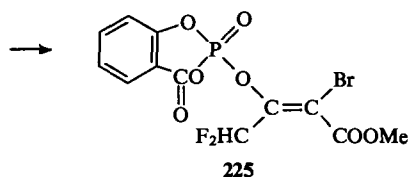
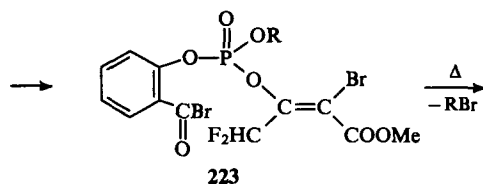
Dibenzoyl reacts with the phosphite **211** ($R_F = \text{CF}_3\text{CH}_2$) to form the unstable σ^5 -1,3,2-dioxaphospholene **218**, which readily eliminates the salicylic acid fragment on heating and is converted into σ^4 -1,3,2-dioxaphospholene **219**.^{390,391}



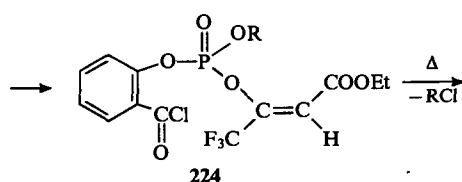
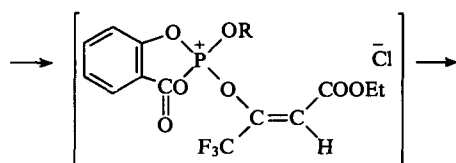
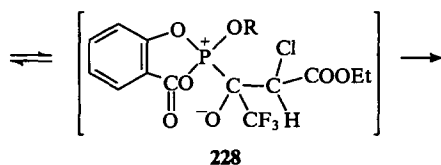
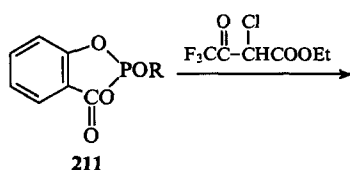
Despite the presence of the electron-accepting pentafluorophenyl substituent, 1-pentafluorophenyl-3-phenylprop-2-en-1-one (the *trans*-isomer) reacts with salicyl trifluoroethyl phosphite only on heating.^{390,391} As in the case of dibenzoyl, the final product is a σ^4 -1,2-oxaphospholene **221**, which does not contain a salicylic acid fragment. The 1,4-adduct (the phosphorane **220**) formed initially is unstable and decomposes to the phospholene **221** under the reaction conditions.

The esters of halogen-substituted acetoacetic acids undergo the Perkow reaction with the salicyl phosphites **211**, the process being accompanied by the regioselective cleavage of the anhydride fragment (in the case of fluoroalkyl salicyl phosphites) or partial elimination of the acyclic group (in the case of alkyl salicyl phosphites).^{358,359} The reactions are highly stereoselective and, when a dibromo-ester is used, lead to the isomers **223** with the *trans*-disposition of the ester group and the phosphorus-containing fragment (yield more than 90%), whereas in the case of the chloro-ester they lead to the thermodynamically more stable *cis*-isomers **224** (yield 60%–80%). The phosphates **223** and **224** cyclise on heating with formation of compounds **225** and **226**. Taking into account the greater reactivity of the dibromo-ester compared with the chloro-ester, one may assume that, when the former is employed, a halogenophilic mechanism operates (the intermediate **227** is formed), whereas in the case of the chloro-ester there is attack on the carbon atom of the carbonyl group (the intermediate **238** is formed).





R = Et, CF₃CH₂, CHF₂CF₂CH₂;



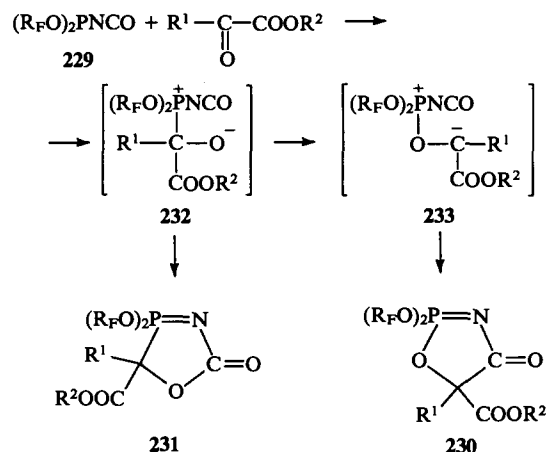
R = Et, CF₃CH₂, CHF₂CF₂CH₂.

d. Bis(fluoroalkyl) isocyanatophosphites

The introduction of fluorinated substituents into the molecules of isocyanatophosphites not only lowers the nucleophilicity of the phosphorus atom in these compounds in reactions with carbonyl compounds and their aza-analogues but also determines a whole series of specific features of the behaviour of these isocyanates: the formation of the products of the dimerisation of σ⁴-1,3,2-oxazaphospholines and the complete absence of the products of the imide-amide rearrangement, cycloaddition to the P=N bond, and the formation of stable phosphoranes.^{89, 90, 117, 233, 352, 393} Certain aspects of the influence of fluoroalkyl groups on the reactivity of isocyanatophosphites in reactions with carbonyl compounds have been demonstrated.³⁴⁵

Thus the formation of stable σ⁴-1,3,2- and σ⁴-1,3,4-oxazaphospholines and **231** is characteristic of the interaction of fluoroalkyl isocyanatophosphite **229** with phenylglyoxylic and

pyruvic acid esters.^{117, 361} The oxazaphospholines obtained from unsubstituted isocyanatophosphites are unstable and undergo rapidly the imide-amide rearrangement.^{394, 395}

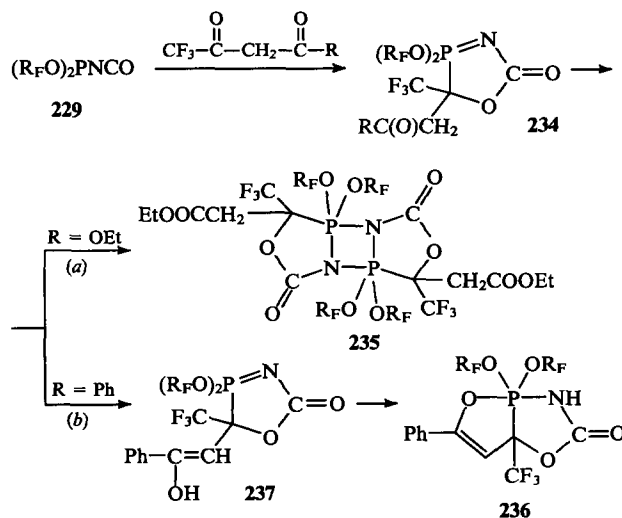


R_F = CHF₂CF₂CH₂; R¹ = Me, Ph; R² = Me, Et.

It has been suggested that in the case of compound **229** the phosphorus atom attacks initially the carbon atom of the carbonyl group with formation of the dipolar ion **232** which subsequently undergoes either intramolecular cyclisation with formation of the product **231** or the phosphonate-phosphate rearrangement to the dipolar ion **233** and subsequent cyclisation to the azaphospholine **230**.

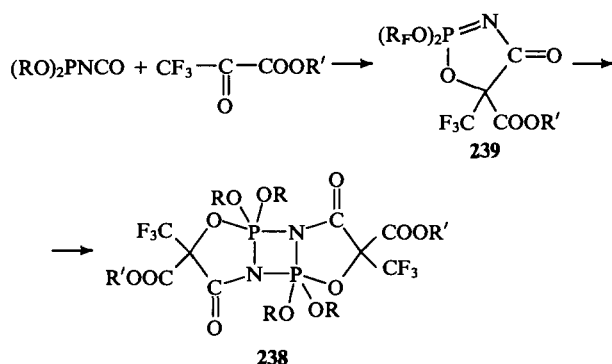
The reduced reactivity of fluoroalkyl isocyanatophosphites compared with the nonfluorinated analogues in the reactions with ethyl phenylglyoxylate and dibenzoyl has been demonstrated by differential thermal analysis.¹¹⁷

In the reactions of the isocyanatophosphite **229** with trifluoroacetoacetic ester^{393, 396} and benzoyltrifluoromethylacetone,³⁹⁷ the corresponding intermediate 1,3,4-oxazaphospholine **234** dimerises in the former case with formation of diphosphatricyclodecane **235** [path (a)], while in the latter it is converted into the bicyclooctene **236** as a result of intramolecular cyclisation via the enolic form **237** [path (b)].



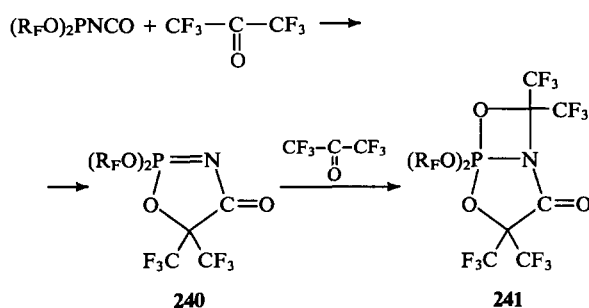
R_F = CHF₂CF₂CH₂.

Bis(tetrafluoropropyl) isocyanatophosphite and diphenyl isocyanatophosphite react with trifluoropyruvic acid esters to form the dimers **238** (σ⁴-1,3,2-oxazaphospholines **239** are intermediates in these reactions, whereas the interaction of dimethyl isocyanatophosphite with the above esters leads to a mixture of σ⁴-1,3,2- and σ⁴-1,4,2-oxazaphospholines.³⁹⁸



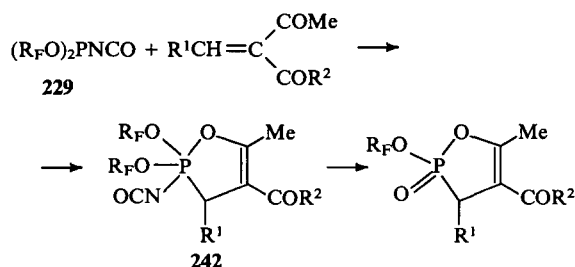
R = CHF₂CF₂CH₂, Ph; R' = Me, Et.

In contrast to trifluoropyruvic acid esters, hexafluoroacetone adds to the intermediate azaphospholine **240** with formation phosphabicycloheptanes **241**.^{361, 398}



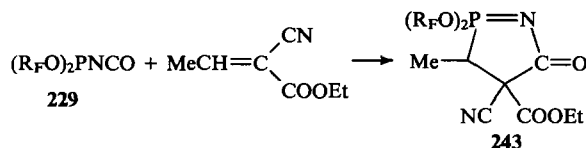
R = CHF₂CF₂CH₂, CF₃CH₂.

The relatively stable intermediate σ⁵-1,2-oxaphospholenes **242** have been detected by ³¹P NMR in reactions of fluoroalkyl isocyanatophosphite **229** (R_F = CHF₂CF₂CH₂) with alkylidene-β-dicarbonyl compounds.³⁹⁹



R¹ = Me, Ph; R² = Me, OEt; R_F = CHF₂CF₂CH₂.

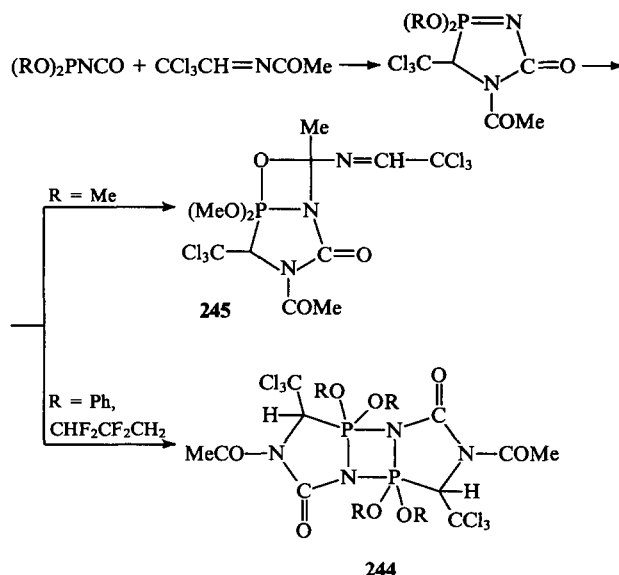
Fluorinated substituents stabilise the structure of σ⁴-1,2-azaphospholine **243**, formed in the reaction of the phosphite **229** with ethylidenecyanoacetic ester.



R_F = CHF₂CF₂CH₂.

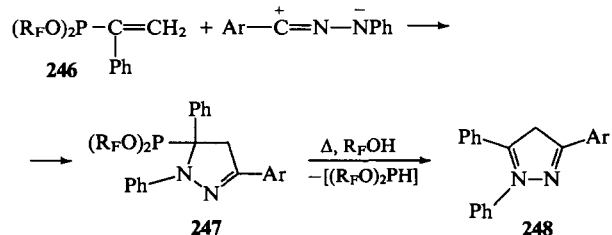
Such stabilisation is due to the high resistance of the R_F-O bond to cleavage, which occurs readily in the imide-amide rearrangement of R_H-isocyanatophosphites.

Bis(tetrafluoropropyl) and diphenyl isocyanatophosphites react with *N*-trichloroethylidenecetamine to form substituted diphosphatricyclodecanes **244**,⁴⁰⁰ whereas dimethyl isocyanatophosphite affords the phosphabicycloheptane **245**.



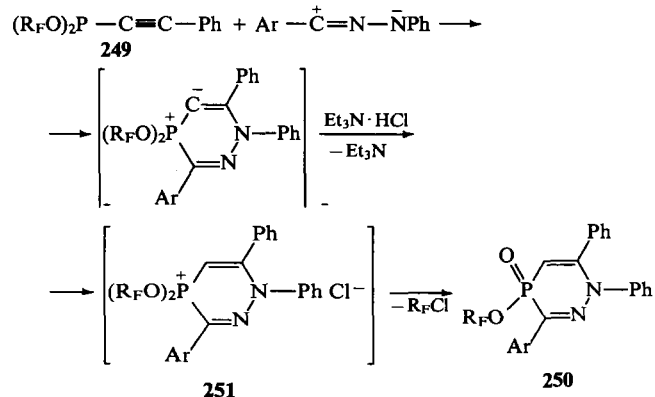
e. Fluoroalkyl-substituted alkenyl and alkynyl phosphonites

Fluoroalkyl-containing alkenyl and alkynyl phosphonites, first obtained by Erofeeva and coworkers,⁴⁰¹⁻⁴⁰³ have been allowed to react with nitrilimines. The reactions of the usual alkenyl phosphonites with nitrilimines proceed with participation of phosphorus as the reaction centre and lead to cyclic [3 + 3]-adducts.⁴⁰⁴ The fluorinated phosphonite **246** undergoes [3 + 2]-cycloaddition without the incorporation of the phosphorus atom in the heterocycle. The pyrazolines **247** formed (δ_P = 187-189 ppm) are unstable and are converted on heating into pyrazole derivatives **248**.



Ar = Ph, 4-O₂NC₆H₄, R_F = CF₃CH₂.

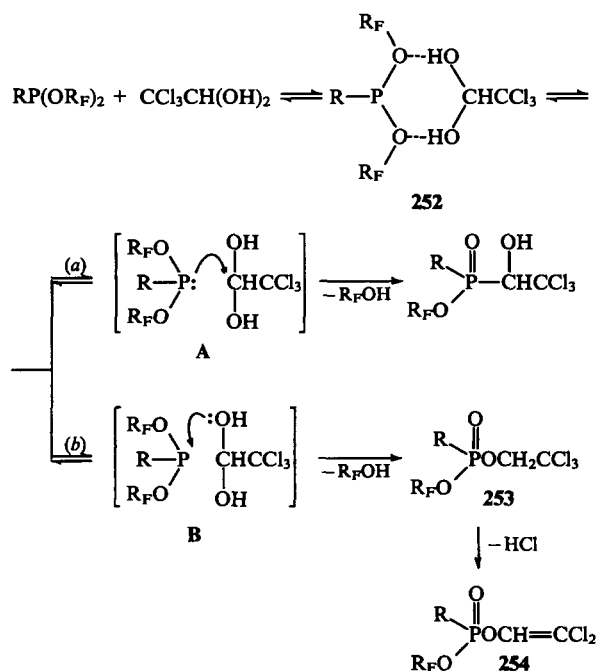
The alkynyl phosphonite **249** as well as its fluorine-free analogue undergo [3 + 3]-cycloaddition to the nitrilimine with formation of σ⁴-1,2,4-diazaphosphorine derivatives **250**. It has been suggested that the reaction proceeds via the intermediate formation of the phosphonium salts **251**.⁴⁰²



R_F = CF₃CH₂.

4. Reactions of fluoroalkyl phosphites with aldehyde hydrates

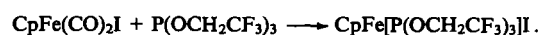
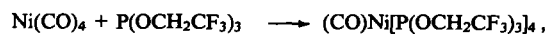
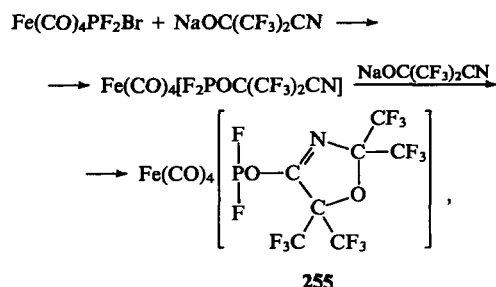
Since the reactions of fluoroalkyl phosphites with aldehyde hydrates have a number of characteristic features, they are considered in a separate section. It has been shown in a series of studies^{124, 405–414} that, when fluoroalkyl phosphites react with aldehyde hydrates, phosphates and α -hydroxyphosphonates are formed. For example, the hydrates $\text{CF}_3\text{CH}(\text{OH})_2$ and $(\text{CF}_3)_2\text{C}(\text{OH})_2$ give rise to phosphates,⁴⁰⁵ while chloral hydrate and $\text{H}(\text{CF}_2\text{CF}_2)_n\text{CH}(\text{OH})_2$ ($n = 1, 2, 3$) afford predominantly α -hydroxyphosphonates.^{408, 410, 411} This reaction has been considered in detail in relation to chloral hydrate.⁴¹² The authors⁴¹² believe that the 'molecular association complex' **252** arises in the first stage, where there is either attack by the phosphorus atom on a carbon atom (A) or by an oxygen atom on the phosphorus atom (B), which lead to an α -hydroxyphosphonate and phosphate respectively.



It is noteworthy that not only the structure of the 'molecular association complex' **252** but also the path leading to the formation of the phosphate **254** [path (b)], presupposing the elimination of HCl from trichloroethyl phosphate **253**, give rise to doubts, since it is known that P(III) and P(V) compounds with the OCH_2CCl_3 substituent are extremely stable (for example the quasi-phosphonium salts,^{46, 211, 415}) while the oxygen atom in the $\text{P}-\text{O}-\text{R}_\text{F}$ group is a very weak electron donor (the electron density on this atom is reduced by the electron-accepting effect of the substituent R_F).

5. Complex formation

There have been several studies^{294, 416–418} in which the use of fluoroalkoxy-derivatives of P(III) in the synthesis of iron and nickel complexes has been described.



The proposed structure of complex **255**⁴¹⁶ was questioned¹⁸⁸ in view of the complexity of the IR spectra (more than seven $\nu_{\text{C}=\text{O}}$ bands), which is associated with the occurrence of side reactions and hydrolysis.

V. Conclusion

The above analysis of the reactivities and the systematic description of the syntheses and properties of fluoroalkyl derivatives of P(III) revealed, on the one hand, a whole series of characteristic features of the syntheses and chemical behaviour of fluoroalkyl phosphites, associated with the influence of fluorinated substituents on the phosphorus atom, and, on the other hand, it made it possible to obtain many new data concerning the mechanisms of known reactions, such as the interactions with the halogens, sulfur halides, halocarbonyl compounds, etc. On the whole, the introduction of fluorine atoms diminishes the nucleophilicity of the P(III) atom and lowers the rate of reaction, because in most of the cases considered nucleophilic attack by the phosphorus atom is probably the rate-determining stage of the reaction. However, the introduction of electron-accepting fluorinated substituents does not affect the rate of interaction with bromine and dialkylphosphonosulfonyl chlorides, which in our view is associated with the ready polarisability of the chlorine and bromine atoms.

The appreciable deficiency of electron density on the phosphorus atom in fluoroalkyl phosphites and the presence of a lone pair with a fairly high ionisation potential impart to these compounds the character of a biphilic reagent, capable of both nucleophilic and electrophilic attack. In certain reactions, it is actually difficult to determine the kind of species that phosphorus represents (electrophilic or nucleophilic), which from our point of view may be associated with orbital control in these reactions, where the initial step is a two-sided exchange interaction of the $n_\text{P}-\pi^*$ and σ^*-n types; here n_P is the lone pair of the phosphorus atom and σ^* is an antibonding orbital of the $\text{R}_\text{F}\text{O}-\text{P}$ bond localised on phosphorus and constituting the LUMO, whereas π^* and n are the LUMO and the HOMO of the organic reactants.⁴¹⁹ The possibility of applying orbital control rules to the reactions of phosphines with alkyl halides and carbonyl compounds is discussed in a recently published communication.⁴²⁰

The study of fluoroalkyl phosphites as potential biphilic reagents in reactions with different nucleophiles and electrophiles is promising not only because there is a possibility of new varieties of the reactions and of new ways of stabilising the intermediates but also in terms of a purely practical aspect — for the very mild phosphorylation of natural alcohols and for the synthesis of new types of phosphorylating agents and phosphorus derivatives with diverse useful properties.⁵⁵

One of the most important and interesting differences between fluoroalkyl phosphites and the R_H derivatives is the reduced rate at which the fluoroalkyl group is split off from the phosphonium centre and the stabilisation of intermediate structures of the phosphorane and phosphonium types. The increase in the stability of quasi-phosphonium compounds is due to the stability of the $\text{O}-\text{R}_\text{F}$ bond. In certain cases, the $\text{R}_\text{F}-\text{O}$ bond is not cleaved at all, although for the R_H derivatives of P(III) the dealkylation stage takes place fairly readily and on the whole obeys the rules governing nucleophilic substitution at a carbon atom via an $\text{S}_\text{N}2$ mechanism (the Perkow and Arbuzov reactions and the nonclassical variants of the latter). In this sense, the weakening of the nucleophilic properties of the P(III) atom is more significant than the increase in the electrophilicity of the CH_2 carbon atom in the $\text{R}_\text{F}\text{CH}_2\text{O}$ fragment.

The appearance of new paths in the interaction of P(III) derivatives with halogen-containing reagents is a consequence of the retardation or complete suppression of the elimination of the

fluoroalkyl group from phosphonium intermediates. These include reactions with retention of the coordination on the phosphorus atom, the disproportionation of haloquasi-phosphonium or phosphorane intermediates in the presence of the initial P(III) derivatives, and the very ready conversion of P(III) compounds into P(V) compounds. In the reactions considered, R_H derivatives of P(III) are as a rule converted into compounds with a phosphoryl group.

References

1. G G Furin, A V Zibarev, L N Mazalov, V D Yumatov *Elektronnaya Struktura Ftororganicheskikh Soedinenii* (Electron Structure of Organofluorine Compounds) (Moscow: Nauka, 1988)
2. V A Naumov, L V Vilkov *Molekulyarnye Struktury Fosfororganicheskikh Soedinenii* (Molecular Structures of Organofluorine Compounds) (Moscow: Nauka, 1986)
3. L M Yagupol'skii *Aromaticheskie i Geterotsiklicheskie Soedineniya s Ftorsoderzhashchimi Zamestitelyami* (Aromatic and Heterocyclic Compounds with Fluorine-Containing Substituents) (Kiev: Naukova Dumka, 1988)
4. A V Fokin, M A Landau *Ftoridy Fosfora i Ftorolefny* (Phosphorus Fluorides and Fluoro-Olefins) (Moscow: Nauka, 1989)
5. A A Krolevets, A G Popov, in *Neorganicheskaya Khimiya, T. 17 (Ser. Itogi Nauki i Tekhniki)* [Inorganic Chemistry (Advances in Science and Engineering Series)] (Moscow: Izd. VINITI, 1989) Vol. 17, p. 1
6. J-L Verlicchie, *ThD, Univ. Paul Sabatier, Toulouse*. 1979; *Ref. Zh. Khim.* 22 Zh 345 (1979)
7. A B Burg *Acc. Chem. Res.* 2 353 (1969)
8. F Kober *Chem.-Ztg.* 111 127 (1987)
9. G G Furin *Usp. Khim.* 62 267 (1993) [*Russ. Chem. Rev.* 62 243 (1993)]
10. M Fild, O Glemser *Fluorine Chem. Rev.* 3 129 (1969)
11. R E Banks, J C Tatlow *J. Fluor. Chem.* 33 227 (1986)
12. D W Davis, M S Banna, D A Shirley *J. Chem. Phys.* 60 237 (1974)
13. A A Korkin *Usp. Khim.* 61 865 (1992) [*Russ. Chem. Rev.* 61 (1992)]
14. B B Zverev *Zh. Org. Khim.* 22 465 (1986)
15. R Deslongchamps *Stereoelectronic Effects in Organic Chemistry* (Oxford: Pergamon Press, 1983)
16. A J Kirby *The Anomeric Effect and Related Stereoelectronic Effects at Oxygen* (Berlin: Springer, 1981)
17. E N Tsvetkov, A A Korkin, in *Khimiya i Primenenie Fosfororganicheskikh Soedinenii (Tr. VIII Vsesoyuz. Konf.)* [The Chemistry and Applications of Organophosphorus Compounds (Proceedings of the VIIIth All-Union Conference)] (Moscow: Nauka, 1987) p. 211
18. H Bock, R Damm, L Lentz *Inorg. Chem.*, 23 1535 (1984)
19. G Zigemund, V Shvertfeger, A Feiring, B Smarsh, G Vogel, B Mak Kusik, in *Organicheskaya Khimiya, T. 30 (Ser. Itogi Nauki i Tekhniki)* [Organic Chemistry (Advances in Science and Engineering Series)] (Moscow: Izd. VINITI, 1993) Vol. 30, p. 29
20. N Ishikawa, Y Kobayashi (Eds) *Fluorine Compounds. Chemistry and Application* (Kodansha Scientific, 1979)
21. V I Nefedov, V I Vovna *Elektronnaya Struktura Organicheskikh i Elementoorganicheskikh Soedinenii* (Electron Structure of Organic and Organoelement Compounds) (Moscow: Nauka, 1989)
22. L Asbrink, W von Niessen, G Bieri *J. Electron Spectrosc., Relat. Phenom.* 24 293 (1981); *Ref. Zh. Khim.* 10 B 109 (1982)
23. L Asbrink, W Von Niessen, G Bieri *J. Electron. Spectrosc., Relat. Phenom.* 26 173 (1982); *Ref. Zh. Khim.* 20 B 126 (1982)
24. S Elbel, H Tom Dieck, R Demuth *J. Fluor. Chem.* 19 349 (1982)
25. I N Rozhkov, Yu A Borisov *Izv. Akad. Nauk, Ser. Khim.* 1334 (1992)
26. D A Dixon, T Fukunada, B E Smart *J. Am. Chem. Soc.* 108 4027 (1986)
27. G H King, J N Murrell, R J Suffolk *J. Chem. Soc., Dalton Trans.* 564 (1972)
28. I A Koppel', U Kh Mel'der, R I Pikver *Reakts. Sposobn. Org. Soedin. (Tartu)* 20 45 (1983)
29. I A Koppel', U Kh Mel'der, R I Pikver *Reakts. Sposobn. Org. Soedin. (Tartu)* 20 204 (1983)
30. A N Hardin, C Sandorfy *J. Fluor. Chem.* 5 435 (1975)
31. I A Koppel', U Kh Mel'der *Reakts. Sposobn. Org. Soedin. (Tartu)* 20 3 (1983)
32. K Werner, B Wrackemeyer *J. Fluor. Chem.* 31 183 (1986)
33. B I Ionin, B A Ershov, A I Kol'tsov *YaMR Spektroskopiya v Organicheskoi Khimii* (Nuclear Magnetic Resonance Spectroscopy in Organic Chemistry) (Leningrad: Khimiya, 1983)
34. W Alcock, T C Khor *J. Am. Chem. Soc.* 100 7799 (1978)
35. A H Cowley, M Lattman, R A Montag, J G Vercade *Inorg. Chim. Acta* 25 L 151 (1977); *Chem. Abstr.* 88 81 540t (1978)
36. V V Zverev, T N Sinyashina, V F Mironov *Zh. Obshch. Khim.* 60 796 (1990)
37. V V Zverev, O Yu Mironova, Z G Bazhanova, V F Mironov *Zh. Obshch. Khim.*, 63 2573 (1993)
38. R P Arshinova, V V Zverev, Ya Ya Villem, N V Villem *Zh. Obshch. Khim.*, 51 1757 (1981)
39. N V Villem, Ya Ya Villem, O V Saks *Uchen. Zapiski Tartussk. Gos. Univ.* 131 (1984)
40. V V Zverev *Zh. Obshch. Khim.* 54 1060 (1984)
41. S A Krupoder, G G Furin, G G Yakobson, G N Dolenko, L L Mazalov, A Sh Sultanov, I I Furler *J. Fluor. Chem.* 22 305 (1983)
42. E N Tsvetkov, A A Korkin *Teor. Eksp. Khim.* 21 39 (1985)
43. N D Epitotis *Theory of Organic Reactions* (Berlin: Springer, 1978)
44. E N Tsvetkov, A A Korkin *Teor. Eksp. Khim.* 21 159 (1985)
45. O Yu Mironova, G K Budnikov, V F Mironov *Zh. Obshch. Khim.* 63 2505 (1993)
46. O Yu Mironova, G K Budnikov, A S Romakhin *Zh. Obshch. Khim.* 64 1396 (1994)
47. O Yu Mironova, Candidate Thesis in Chemical Sciences, Kazan' State University, Kazan', 1995
48. Yu G Shermolovich, E A Danchenko, A V Solov'ev, V V Trachevskii, L N Markovskii *Zh. Obshch. Khim.* 56 560 (1986)
49. L N Markovsky, E S Kozlov, Yu G Shermolovich *Heteroatom. Chem.* 2 87 (1991)
50. A S Romakhin, E V Nikitin, O V Parakin, Yu A Ignat'ev, B S Mironov, Yu M Kargin *Zh. Obshch. Khim.* 56 2597 (1986)
51. W B Gara, B P Roberts *J. Chem. Soc., Chem. Commun.* 949 (1975)
52. J Radell, J W Connolly *J. Chem. Eng. Data* 6 282 (1961)
53. W A Sheppard, C M Sharts *Organic Fluorine Chemistry* (New York, 1969)
54. S Kumar, S R Palit *Adv. Fluorine Chem.* 6 69 (1971)
55. A A Krolevets, in *Organicheskaya Khimiya, T. 6 (Ser. Itogi Nauki i Tekhniki)* [Organic Chemistry (Advances in Science and Engineering Series)] (Moscow: Izd. VINITI, 1986) Vol. 6, p. 1
56. I L Knunyants, O V Kil'disheva, E G Bykhovskaya *Zh. Obshch. Khim.* 19 101 (1949)
57. L C Krogh, T S Reid, H A Brown *J. Org. Chem.* 19 1124 (1954)
58. M V Lenton, B Lewis *Chem. Ind.* 946 (1965)
59. V N Prons, M P Grinblat, A P Klebanskii *Zh. Obshch. Khim.* 41 483 (1971)
60. A V Fokin, A F Kolomiets, V A Komarov, A I Rapkin, K I Pasevina, A A Krolevets *Dokl. Akad. Nauk SSSR* 237 619 (1977)
61. A V Fokin, A F Kolomiets, V A Komarov *Izv. Akad. Nauk SSSR, Ser. Khim.* 159 (1979)
62. A V Fokin, A F Kolomiets, V A Komarov, A I Rapkin, K I Pasevina, O V Verenikin *Izv. Akad. Nauk SSSR, Ser. Khim.* 163 (1979)
63. M I Kabachnik, E I Golubeva, D M Paikin, M P Shabanova, N M Gamper, L F Efimova *Zh. Obshch. Khim.* 29 1671 (1959)
64. M Tariq, J-M Shreeve *Inorg. Chem.* 25 3830 (1986)
65. V F Mironov, I V Konovalova *Zh. Obshch. Khim.* 63 2537 (1993)
66. V M Adamov, V A Babain, B N Belyaev, D A Vasil'ev, D A Mikhalev, A E Ritati *Zh. Obshch. Khim.* 58 2774 (1988)
67. V F Mironov, I V Konovalova, E N Ofitserov, E I Gol'dfarb *Zh. Obshch. Khim.* 62 2231 (1992)
68. R E A Dear, E L M Pattison *J. Am. Chem. Soc.* 85 622 (1963)
69. H Machleidt, W Grell *Liebigs Ann. Chem.* 690 79 (1965)
70. E Elkik, M Le Blanc *C.R. Hebd. Seances Acad. Sci., Ser. C* 269 173 (1969); *Chem. Abstr.* 71 101 615a (1969)
71. V M Dixit, F M Laskovic, W J Noall, C D Poulter *J. Org. Chem.* 46 1967 (1981)
72. A A Krolevets, L I Ragulin *Zh. Obshch. Khim.* 55 461 (1985)
73. A A Krolevets, L I Ragulin, V I Shevchenko, E I Lyubimova *Zh. Obshch. Khim.* 56 584 (1986)
74. K K San, C Tamborski, K C Eapen *J. Fluor. Chem.* 17 457 (1981)
75. M S Benefice, H Blaucou, A Commeyaras *J. Fluor. Chem.* 30 171 (1985)

76. D Dakternieks, G-V Rosenthaler, R Schmutzler, in *The First Acts Congress International Composes Phosphorus*, 1977 (Paris: Inst. Mond. Phosphate, 1978) p. 591; *Chem. Abstr.* **89** 122 281a (1978)
77. D Dakternieks, G-V Rosenthaler, R Schmutzler *J. Fluor. Chem.* **11** 387 (1978)
78. D P Bauer, J K Ruff *Inorg. Chem.* **22** 1686 (1983)
79. F Mares, J Smith *J. Org. Chem.* **41** 1567 (1976)
80. T Mill, J O Rodin, R M Silverstein, C Woolf *J. Org. Chem.* **29** 3715 (1964)
81. D Dakternieks, G-V Rosenthaler, R Schmutzler *Z. Naturforsch., B, Chem. Sci.* **33** 507 (1978)
82. M Lustig *Inorg. Chem.* **7** 2054 (1969)
83. R H Wisian-Neilson, R H Neilson *Inorg. Chem.* **19** 1875 (1980)
84. R Franke, D Dakternieks, R W Gable, B F Hoskins, G-V Rosenthaler *Chem. Ber.* **118** 922 (1985)
85. R Franke, G-V Rosenthaler, R Giacomo, D Dakternieks *Phosphorus Sulfur* **20** 107 (1984)
86. U V Allworden, I Tsegai, G-V Rosenthaler *Phosphorus Sulfur* **21** 177 (1984)
87. D Dakternieks, G-V Rosenthaler, R Schmutzler *J. Fluor. Chem.* **12** 413 (1978)
88. H Hosaka, T Watanabe, Y Suzuki, H Takaku *Heteroatom. Chem.* **2** 197 (1991)
89. I V Konovalova, N V Mikhailova, L A Burnaeva, A N Pudovik *Zh. Obshch. Khim.* **53** 1715 (1983)
90. I V Konovalova, L A Burnaeva, E K Khusnutdinova, G S Khafizova, A N Pudovik *Zh. Obshch. Khim.* **55** 2189 (1985)
91. E L Lines, L F Centofanti *Inorg. Chem.* **12** 2111 (1973)
92. V A Chazov, Yu N Studnev, L I Ragulin, A V Fokin *Zh. Obshch. Khim.* **59** 1294 (1989)
93. V F Mironov, E N Ofitserov, I V Konovalova, P P Chernov, A N Pudovik *Izv. Akad. Nauk SSSR, Ser. Khim.* **2118** (1990)
94. A F Eleev, V K Chekalin, A F Ermolov, A P Kutepov, G A Sokol'skii *Zh. Vses. Khim. O-va im D I Mendeleeva* **26** 103 (1981)
95. D B Denney, D Z Denney, P J Hammond, Wang Yu Pin *J. Am. Chem. Soc.* **103** 1785 (1981)
96. D B Denney, D Z Denney, P J Hammond, Wang Yu Pin *J. Org. Chem.* **48** 2159 (1983)
97. D B Denney, D Z Denney, Lun Tsu Liu *Phosphorus Sulfur* **13** 1 (1982)
98. V F Mironov, I V Konovalova, A N Pudovik *Zh. Obshch. Khim.* **61** 255 (1991)
99. I V Loginova, Candidate Thesis in Chemical Sciences, Kazan' State University, Kazan', 1993
100. V N Prons, M P Grinblat, A L Klebanskii *Zh. Obshch. Khim.* **45** 2423 (1975)
101. M Tariq, J-M Shreeve *Inorg. Chem.* **25** 4081 (1986)
102. Jpn. P. 04-112 894; *Chem. Abstr.* **117** 171 961c (1992)
103. V F Mironov, Doctoral Thesis in Chemical Sciences, Kazan' State University, Kazan', 1995
104. M Lustig, W E Hill *Inorg. Chem.* **6** 1448 (1967)
105. V I Krutikov, E S Semenova, I G Maslennikov, A N Lavrent'ev *Zh. Obshch. Khim.* **53** 1557 (1983)
106. H Collet, P Calas, A Commeyras *J. Chem. Soc., Chem. Commun.* **1152** (1984)
107. T V Kim, E I Kiseleva, A D Sinita *Zh. Obshch. Khim.* **54** 228 (1984)
108. T V Kim, E I Kiseleva, A D Sinita *Zh. Obshch. Khim.* **57** 807 (1987)
109. A D Sinita, D M Malenko, L A Repina, R A Loktionova, A K Shurubura *Zh. Obshch. Khim.* **56** 1262 (1986)
110. Br. P. 1 575 236; *Ref. Zh. Khim.* **8** N 69P (1981)
111. E A Suvalova, T I Chudakova, P P Onys'ko, A D Sinita *Zh. Obshch. Khim.* **65** 1223 (1995)
112. USSR P. 907 002; *Ref. Zh. Khim.* **5** N 183P (1983)
113. I V Konovalova, E N Ofitserov, V F Mironov, A N Pudovik *Izv. Akad. Nauk SSSR, Ser. Khim.* **1432** (1983)
114. H Hosaka, Y Suzuki, Gog-Kim Sang, H Takaku *Tetrahedron Lett.* **32** 785 (1991)
115. USSR P. 255 268; *Ref. Zh. Khim.*, **22** N 123P (1970)
116. I A Alekseichuk, E N Ofitserov, I V Konovalova *Zh. Obshch. Khim.* **62** 786 (1992)
117. I V Konovalova, L A Burnaeva, E K Khusnutdinova, A N Pudovik *Zh. Obshch. Khim.* **56** 1245 (1986)
118. R Francke, R Di Giacomo, D Dakternieks, G-V Rosenthaler *Z. Anorg. Allg. Chem.* **519** 141 (1984)
119. V N Sharov, A L Klebanskii *Vysokomol. Soedin., Ser. A* **15** 2453 (1973)
120. S D Tupchienko, T N Dudchenko, A D Sinita *Zh. Obshch. Khim.* **56** 2519 (1986)
121. H Takaku, T Watanabe, S Hamamoto *Tetrahedron Lett.* **29** 81 (1988)
122. G-V Rosenthaler *Z. Naturforsch., B, Chem. Sci.* **33** 131 (1978)
123. E-P Flindt *Z. Anorg. Allg. Chem.* **479** 57 (1981)
124. T V Palagina, V I Krutikov, A V Naidenov, A N Lavrent'ev *Zh. Obshch. Khim.* **56** 2696 (1986)
125. I G Maslennikov, A N Lavrent'ev, G N Prokof'eva, T B Alekseeva *Zh. Obshch. Khim.* **52** 529 (1982)
126. V V Golovanov, A N Lavrent'ev, I G Maslennikov, M G Golovanova *Zh. Obshch. Khim.* **62** 827 (1992)
127. A I Vali, Z A Rogovin, L S Sletkina, Yu A Cheburkov *Vysokomol. Soedin., Ser. B* **15** 33 (1973)
128. L V Krylov, V V Kormachev, V A Kukhtin *Zh. Obshch. Khim.* **46** 2513 (1976)
129. A F Jansen, L J Kruczynski *Can. J. Chem.* **57** 1903 (1979)
130. D Dakternieks, G-V Rosenthaler, K Sauerbrey, R Schmutzler *Chem. Ber.* **112** 2380 (1979)
131. US P. 3 246 030; *Ref. Zh. Khim.* **15** P 254P (1967)
132. J Ruppert *Z. Anorg. Allg. Chem.* **477** 59 (1981)
133. N Lowther, P D Beer, C D Hall *Phosphorus Sulfur* **35** 133 (1988)
134. D W Mc Kennon, M Lustig *J. Fluor. Chem.* **7** 321 (1976)
135. D B Denney, D Z Denney, Liu Lun Tsu *Huaxue Xuebao* **42** 293 (1984); *Chem. Abstr.* **101** 211 284n (1984)
136. Yu G Shermolovich, A V Solov'ev, E A Danchenko, L M Markovskii *Zh. Obshch. Khim.* **55** 291 (1985)
137. Liu Lun Tsu *Huaxue Xuebao* **42** 1204 (1984); *Chem. Abstr.* **102** 113 612u (1985)
138. I V Konovalova, E N Ofitserov, T N Sinyashina, V F Mironov, A N Pudovik *Izv. Akad. Nauk SSSR, Ser. Khim.* **1164** (1987)
139. E N Ofitserov, V F Mironov, T N Sinyashina, P P Chernov, A V Il'yasov, I V Konovalova, A N Pudovik *Dokl. Akad. Nauk SSSR* **306** 218 (1989)
140. D B Denney, D Z Denney, Liu Lun Tsu *Phosphorus Sulfur* **22** 71 (1985)
141. R Bohlen, H Hacklin, J Heine, W Offerman, G-V Rosenthaler *Phosphorus Sulfur* **27** 321 (1986)
142. Yu Jaehoon, A E Sopchik, A M Arif, W G Bentrude, G-V Rosenthaler *Heteroatom. Chem.* **2** 177 (1991)
143. J H Yu, A M Arif, W G Bentrude *J. Am. Chem. Soc.* **112** 7451 (1990)
144. J H Yu, W G Bentrude *J. Am. Chem. Soc.* **110** 7897 (1988)
145. H Hacklin, G-V Rosenthaler *Phosphorus Sulfur* **36** 165 (1988)
146. Yu G Shermolovich, E A Danchenko, A V Solov'ev, L N Markovskii *Zh. Obshch. Khim.* **55** 2218 (1985)
147. H Yu, W G Bentrude *Tetrahedron Lett.* **30** 2195 (1989)
148. V F Mironov, R A Mavleev, I V Konovalova, R A Cherkasov *Zh. Obshch. Khim.* **62** 701 (1992)
149. V F Mironov, R A Mavleev, E N Ofitserov, I V Konovalova, A N Pudovik *Zh. Obshch. Khim.* **62** 1184 (1992)
150. W M Abdou, M R Mahran *Phosphorus Sulfur* **26** 119 (1986)
151. R Keat, D S Rycroft, D G Thompson *J. Chem. Soc., Dalton Trans.* **1224** (1979)
152. W A Kamil, M R Bond, J-M Shreeve *Inorg. Chem.* **26** 2015 (1987)
153. W A Kamil, M R Bond, R D Willett, J-M Shreeve *Inorg. Chem.* **26** 2829 (1987)
154. V N Volkhovitskii, L I Zinov'eva, E G Bykhovskaya, I L Knunyants *Zh. Vses. Khim. O-va im D I Mendeleeva* **19** 470 (1974)
155. W Storzer, D Schomburg, G-V Rosenthaler *Z. Naturforsch., B, Chem. Sci.* **36** 1071 (1981)
156. W Storzer, G-V Rosenthaler, R Schmutzler *Chem. Ber.* **114** 3609 (1981)
157. G-V Rosenthaler, R Bohlen, W Storzer, A E Sopchik, W G Bentrude *Z. Anorg. Allg. Chem.* **507** 93 (1979)
158. G-V Rosenthaler, K Sauerbrey, J A Gibson, R Schmutzler *Z. Anorg. Allg. Chem.* **450** 79 (1979)

159. G-V Roschenthaler, J A Gibson, R Schmutzler *Chem. Ber.* **110** 611 (1977)
160. R Bohlen, G-V Roschenthaler *Z. Anorg. Allg. Chem.* **513** 199 (1984)
161. W Storz, G-V Roschenthaler *Z. Naturforsch., B, Chem. Sci.* **33** 305 (1978)
162. G-V Roschenthaler *Z. Naturforsch., B, Chem. Sci.* **37** 281 (1982)
163. E E Nifant'ev, T S Kukhareva, V I Dyachenko, A F Kolomiets *Zh. Obshch. Khim.* **63** 706 (1993)
164. E E Nifant'ev, T S Kukhareva, V I D'yachenko, A F Kolomiets, V K Bel'skii, L K Vasyanina *Izv. Akad. Nauk, Ser. Khim.* 1817 (1995)
165. V F Mironov, I V Konovalova, R A Mavleev, A Sh Mukhtarov, E N Ofitserov, A N Pudovik *Zh. Obshch. Khim.* **61** 2150 (1991)
166. D M Malenko, L I Nesterova, S N Luk'yanenko, A D Sinita *Zh. Obshch. Khim.* **59** 2626 (1989)
167. A Haas, F Weiss *Z. Anorg. Allg. Chem.* **518** 234 (1984)
168. F Weiss, *ThD, Chem. Ruhr-Univ. Bochum*, 1983; *Ref. Zh. Khim.* **17** Zh 358D (1985)
169. R F Swindell, D P Babb, T J Ouellette, J-M Shreeve *Inorg. Chem.*, **11** 242 (1972)
170. H Roesky, H Hofmann *Z. Naturforsch., B, Chem. Sci.* **39** 1315 (1984)
171. SAR P. 7 007 990; *Chem. Abstr.* **76** 99 104r (1972)
172. E E Nifant'ev, L N Ivanova *Zh. Obshch. Khim.* **41** 2192 (1971)
173. USSR P. 759 523; *Ref. Zh. Khim.* **15** N 84P (1981)
174. I V Konovalova, E N Ofitserov, V F Mironov, V I Kostyuk, A N Pudovik *Zh. Obshch. Khim.* **53** 1945 (1983)
175. E Fluck, P Wachter *Liebigs Ann. Chem.* **1125** (1979)
176. V D Romanenko, A V Ruban, N N Kalibabchuk, S V Iksanova, L N Markovskii *Zh. Obshch. Khim.* **51** 1726 (1981)
177. G N Bockerman, R W Parry *J. Fluor. Chem.* **7** 1 (1976); *Ref. Zh. Khim.* **12** V38 (1976)
178. G-V Roschenthaler, U V Alloworden, R Schmutzler *Polyhedron* **5** 1387 (1986)
179. E Evangelidou-Tsolis, F Ramirez, J E Pilot, C P Smith *Phosphorus Sulfur* **4** 121 (1974)
180. E Evangelidou-Tsolis, F Ramirez, J F Pilot, C P Smith *Phosphorus Sulfur* **4** 109 (1974)
181. V N Volkhovitskii, I L Knunyants, E G Bykhovskaya *Zh. Vses. Khim. O-va im D I Mendeleeva* **18** 112 (1973)
182. J Heine, G-V Roschenthaler *Chem. Ber.* **121** 379 (1988)
183. R Franke, J Heine, G-V Roschenthaler *Phosphorus Sulfur Silicon Relat. Elem.* **49/50** 377 (1990)
184. V L Foss, N V Lukashev, Yu N Tsvetkov, I F Lutsenko *Zh. Obshch. Khim.* **52** 2183 (1982)
185. M V Prishchenko, M V Livantsov, N V Boganova, I F Lutsenko *Zh. Obshch. Khim.* **59** 2783 (1989)
186. J Lucas, Amirzadeh-asl, H W Roesky *Phosphorus Sulfur* **18** 69 (1983)
187. H W Roesky, N K Homsy, M Noltemeyer, G M Sheldrick *Angew. Chem.* **96** 1002 (1984)
188. H W Roesky, J Lucas, K-L Neber, D Habibollah, E Egert, M Noltemeyer, G M Sheldrick *Chem. Ber.* **118** 2396 (1985)
189. H W Roesky, K S Dhatathreyan *J. Chem. Soc., Chem. Commun.* 1053 (1984)
190. H W Roesky, K Ambrosius, M Banek, W S Sheldrick *Chem. Ber.* **113** 1847 (1980)
191. L Horner, M Jordan *Phosphorus Sulfur* **8** 235 (1980)
192. Qui-Chee Mir, R W Shreeve, J-M Shreeve *Phosphorus Sulfur* **8** 331 (1980)
193. G-V Roschenthaler, D Dakternieks *J. Fluor. Chem.* **16** 563 (1980); *Ref. Zh. Khim.* **13** B 1038 (1981)
194. A N Makarov, E M Khaikis, A S Rodygin *Zh. Obshch. Khim.* **55** 1485 (1985)
195. D E Gibbs, C Larsen *Synthesis* 410 (1984)
196. H Takaku, H Tsuchiya, K Imai, D E Gibbs *Chem. Lett.* 1267 (1984)
197. USSR P. 1 117 302; *Ref. Zh. Khim.* **18** O 362P (1985)
198. Jpn. P. 0-120 890; *Chem. Abstr.* **104** 34 307m (1986)
199. O Sakatsume, H Yamane, H Takaku *Nucleosides, Nucleotides* **8** 1033 (1989); *Chem. Abstr.* **112** 99 112d (1990)
200. H Takaku, S Yamakage, O Sakatsume, M Ohtsuki *Chem. Lett.* 1675 (1988)
201. Jpn. P. 02-32 085; *Chem. Abstr.* **113** 59 539n (1990)
202. V F Mironov, I V Konovalova *Zh. Obshch. Khim.* **63** 2228 (1993)
203. Yu A Mandel'baum, P G Zaks, H H Mel'nikov *Zh. Obshch. Khim.* **36** 44 (1966)
204. US P. 3 293 306; *Chem. Abstr.* **66** 104 686g (1966)
205. USSR P. 390097 SSSR; *Ref. Zh. Khim.* **19** N 115P (1974)
206. A N Lavrent'ev, I G Maslennikov, S V Mayakova *Zh. Obshch. Khim.* **64** 1212 (1994)
207. I G Maslennikov, A N Kirichenko, A N Lavrent'ev *Zh. Obshch. Khim.* **62** 272 (1992)
208. L N Markovskii, N P Kolesnik, Yu L Bakmutov, A A Kudryavtsev, Yu G Shermolovich *Zh. Obshch. Khim.* **53** 1994 (1983)
209. R Bohlen, G-V Roschenthaler *Z. Anorg. Allg. Chem.* **578** 47 (1989)
210. D E Young, L R Anderson, W B Fox *J. Chem. Soc., Chem. Commun.* 736 (1971)
211. G Kloter, K Seppelt *J. Am. Chem. Soc.* **101** 347 (1979)
212. L M Yagupolskii *J. Fluor. Chem.* **1** 1 (1987)
213. F M Mukhametshin, in *Novye Floriguyushchie Reagenty v Organicheskoy Sintezе* (New Fluorinating Agents in Organic Synthesis) (Novosibirsk: Nauka, 1987) p. 140
214. A I Rakhimov *Khimiya i Tekhnologiya Floriganicheskikh Soedinenii* (The Chemistry and Technology of Organofluorine Compounds) (Moscow: Khimiya, 1986)
215. W Mahler *Inorg. Chem.* **18** 352 (1979)
216. H J Emel'us, H Pugh *J. Chem. Soc.* 1108 (1960)
217. A Haas, D Winkler *Z. Anorg. Allg. Chem.* **468** 68 (1980)
218. H J Emel'us, K J Packer, N Welman *J. Chem. Soc.* 2529 (1962)
219. P Dehnert, J Große, W Hildebrandt, D Le Van Z. *Naturforsch., B, Chem. Sci.* **34** 1646 (1979)
220. G H Sprenger, J-M Shreeve *J. Fluor. Chem.* **4** 201 (1974)
221. C J Marsden *J. Fluor. Chem.* **5** 423 (1975)
222. A Darmadi, A Haas, M Kaschani-Motlagh *Z. Anorg. Allg. Chem.* **448** 35 (1979)
223. T Vakratsas *Chem. Chron.* **7** 125 (1978)
224. K J Packer *J. Chem. Soc.* 960 (1963)
225. J B Mishra, A B Burg *Gov. Rep. Ann. (US)* **71** 50 (1971); *Chem. Abstr.* **76** 14 656z (1972)
226. J B Mishra, A B Burg *Inorg. Chem.* **11** 664 (1972)
227. D B Denney, D Z Denney, Liu Lun Tsu *Huaxue Xuebao* **42** 340 (1984); *Ref. Zh. Khim.* **23** Zh 365 (1984)
228. L K Peterson, A B Burg *J. Am. Chem. Soc.* **86** 2587 (1964)
229. A Haas, D Rafiy-Heidarlu, D Winkler *Chem.-Ztg.* **99** 331 (1975)
230. J Große, D Le Van Z. *Naturforsch., B, Chem. Sci.* **35** 694 (1980)
231. J Große, J Vetter, D Rehder *Z. Naturforsch., B, Chem. Sci.* **40** 975 (1985)
232. H G Ang, W S Lien *J. Fluor. Chem.* **4** 447 (1974)
233. L D Freedman, G O Doak *J. Organomet. Chem.* **180** 111 (1979)
234. H G Ang, W S Lien *J. Fluor. Chem.* **11** 419 (1978)
235. H G Ang *J. Chem. Soc., Chem. Commun.* 1320 (1968)
236. H G Ang, K F Ho *J. Fluor. Chem.* **8** 497 (1976)
237. H G Ang, K K So *J. Fluor. Chem.* **21** 221 (1982)
238. H G Ang, F K Lee *J. Fluor. Chem.* **47** 111 (1990)
239. H G Ang, K K So *J. Fluor. Chem.* **27** 433 (1985)
240. Y O El Nigumi, H J Emel'us *J. Inorg. Nucl. Chem.* **32** 3213 (1970)
241. H G Ang, K K So *J. Fluor. Chem.* **22** 95 (1983)
242. H G Ang, K K So *J. Fluor. Chem.* **27** 411 (1985)
243. H G Ang, K K So *J. Fluor. Chem.* **27** 451 (1985)
244. R N Haszeldine *J. Chem. Soc.* 1757 (1953)
245. K N Campbell, J O Knobloch, B K Campbell *J. Am. Chem. Soc.* **72** 4380 (1950)
246. L N Markovskii, N P Kolesnik, Yu G Shermolovich *Usp. Khim.* **56** 1564 (1987) [*Russ. Chem. Rev.* **56** 894 (1987)]
247. L N Markovskii, V Yu Abramov, Yu G Shermolovich *Ukr. Khim. Zh.* **57** 1291 (1991)
248. Yu G Shermolovich, Doctoral Thesis in Chemical Sciences, Institute of Organic Chemistry, Academy of Sciences of Ukr. SSR, Kiev, 1988
249. O Sakatsume, M Ohtsuki, C B Reese *Nucl. Acids Res.* **17** 3689 (1989); *Ref. Zh. Khim.* **13** E176 (1990)
250. O Sakatsume, H Yamone, N Yamamoto *Tetrahedron Lett.* **30** 6375 (1989)
251. Jpn. P. 03-236 396; *Chem. Abstr.* **117** 49 168j (1992)
252. H Komatsu, T Ichikawa, M Nakai, H Takaku *Nucleosides, Nucleotides* **11** 85 (1992)

253. A A Kraevskii, N B Tarusova, Zhu Qing Yu, P Vidal, Chou Ting Chao, P Baron, B Polsky, Jiang Xiang Jun, J Matulic-Adamic *Nucleosides* 11 177 (1992)
254. H Hosaka, Y Suzuki, H Nakamura, H Furakoshi, H Nakashima, N Yamamoto, H Takaku *Nucleosides, Nucleotides* 11 669 (1992)
255. H Hosaka, H Nakamura, H Funakoshi, H Takaku *Chem. Lett.* 935 (1992)
256. T Watanabe, H Sato, H Takaku *J. Am. Chem. Soc.* 111 3437 (1989)
257. A Yu Zamyatina, A S Bushnev, V I Shvets *Bioorg. Khim.* 20 1253 (1994)
258. E Kuyl-Yeheskiely, C M Tromp, G A van der Marel, J H van Boom *Tetrahedron Lett.* 28 4461 (1987)
259. B Lal, A K Gangopadhyay *J. Chem. Soc., Perkin Trans. 1* 1993 (1992)
260. W Dabkowski, F Cramer, J Michalski *J. Chem. Soc., Perkin Trans. 1* 1447 (1992)
261. J Kaziaki, J Tsunehiko, K Susumu, T Hiroshi *Nucleosides, Nucleotides* 4 669 (1985)
262. W Dabkowski, F Kramer, J Michalski *Phosphorus Sulfur Silicon Relat. Elem.* 75 91 (1993)
263. Jpn. P. 60-120 897; *Ref. Zh. Khim.* 15 O141P (1986)
264. G-V Rosenthaler, R Bohlen, W Storzer *J. Fluor. Chem.* 23 470 (1983)
265. D Schomburg, W Storzer, R Bohlen, W Kuhn, G-V Rosenthaler *Chem. Ber.* 116 3301 (1983)
266. A V Fokin, Yu N Studnev, A I Rapkin, K I Pasevina, O V Verenikin, A F Kolomiets *Izv. Akad. Nauk SSSR, Ser. Khim.* 1655 (1981)
267. I G Maslennikov, L I Matus, A N Lavrent'ev *Zh. Obshch. Khim.* 62 1280 (1992)
268. V I Kal'chenko, N A Parkhomenko, L I Atamas', L N Markovskii *Zh. Obshch. Khim.* 59 712 (1989)
269. V I Kal'chenko, L I Atamas', N A Parkhomenko, L N Markovskii *Zh. Obshch. Khim.* 60 2248 (1990)
270. S D Broady, J E Rexhansen, E J Thomas *J. Chem. Soc., Chem. Commun.* 708 (1991)
271. L V Nesterov, N E Krepyseva *Zh. Obshch. Khim.* 53 50 (1983)
272. L G Spears, A Liao, D Minsek, E S Lewis *J. Org. Chem.* 52 61 (1987)
273. F A Bakhtiyarova *Sintez Ammonievnykh Solei Dialkilfosforistyk Khlor* (The Synthesis of Ammonium Salts of Dialkylphosphorous Acids) Article deposited at the ONIITEKhim, Cherkassy, 1982, No 746khp-D82; *Ref. Zh. Khim.* 20 Zh 345 (1982)
274. N Yamazaki, T Iguchi, F Higashi *Chem. Lett.* 185 (1977)
275. Jpn. P. 77-42 858; *Chem. Abstr.* 87 134 558t (1977)
276. M J Gallagher, R Garbutt, Liu Yuan Hua, Gum Hee Lee *Phosphorus Sulfur Silicon Relat. Elem.* 75 201 (1993)
277. T Kh Gazizov, L N Usmanova, A N Pudovik *Zh. Obshch. Khim.* 58 1916 (1988)
278. E E Nifant'ev *Khimiya Gidrofosforil'nykh Soedinenii* (The Chemistry of Hydrophosphoryl Compounds) (Moscow: Nauka, 1983)
279. I G Maslennikov, S V Mayakova, A N Lavrent'ev *Zh. Obshch. Khim.* 63 1432 (1993)
280. D Ludewig, W Eiserbeck, E Feike *Z. Chem.* 24 290 (1984)
281. DDR P. 222 596; *Chem. Abstr.* 104 149 167h (1986)
282. E-P Flindt *Z. Anorg. Allg. Chem.* 447 97 (1978)
283. E-P Flindt *Z. Anorg. Allg. Chem.* 487 119 (1982)
284. E N Ofitserov, V F Mironov, T N Sinyashina, A N Chernov, A V Il'yasov, I V Kononova, A N Pudovik *Zh. Obshch. Khim.* 60 1711 (1990)
285. S F Aleinikov, V I Krutikov, A V Golovanov, I G Maslennikov, A N Lavrent'ev *Zh. Obshch. Khim.* 53 1678 (1983)
286. A V Fokin, Yu N Studnev, A I Rapkin, K I Pasevina, A F Kolomiets *Izv. Akad. Nauk SSSR, Ser. Khim.* 1641 (1981)
287. Yu G Shermolovich, E A Danchenko, A V Solov'ev *Zh. Obshch. Khim.* 56 560 (1986)
288. S M Ramos, J C Owrtusky, P M Keehn *Tetrahedron Lett.* 26 5895 (1985)
289. F El Khatib, A M Caminade, M Koenig *Phosphorus Sulfur* 20 55 (1984)
290. J R Lloyd, N Lowther, C D Hall *J. Chem. Soc., Perkin Trans. 2* 245 (1985)
291. A G Davies, D Griller, B P Roberts *J. Chem. Soc., Perkin Trans. 2* 2224 (1972)
292. USSR P. 755 790; *Ref. Zh. Khim.* 3 T 43P (1981)
293. I G Maslennikov, S V Mayakova, A N Lavrent'ev *Zh. Obshch. Khim.* 63 1540 (1993)
294. S M Socol, J G Verkade *Inorg. Chem.* 25 2658 (1986)
295. V F Mironov, L A Burnaeva, E N Ofitserov, I V Kononova *Zh. Obshch. Khim.* 63 2237 (1993)
296. E P Flindt, H Rose *Z. Anorg. Allg. Chem.* 428 204 (1977)
297. E P Flindt, H Rose, H C Marsmann *Z. Anorg. Allg. Chem.* 430 155 (1977)
298. E P Flindt *Z. Anorg. Allg. Chem.* 461 193 (1980)
299. Jpn. P. 04-178 395; *Chem. Abstr.* 117 234 256z (1992)
300. US P. 533 564; *Chem. Abstr.* 116 129 876h (1992)
301. K Matyjaszewski, R Montague, J Dauth, O Nuyken *J. Polym. Sci. Part A, Polym. Chem.* 30 813 (1992); *Ref. Zh. Khim.* 2 S 495 (1994)
302. T L Shcherbina, A P Laretina, V L Gilyarov, M I Kabachnik *Izv. Akad. Nauk, Ser. Khim.* 690 (1994)
303. V F Mironov, R A Mavleev, E N Ofitserov, I V Kononova, A N Pudovik *Zh. Obshch. Khim.* 62 1184 (1992)
304. I G Maslennikov, L N Kirichenko, A V Garabadzhiu, L S Koshcheeva, A N Lavrent'ev, E G Sochilin *Zh. Obshch. Khim.* 50 1648 (1980)
305. I G Maslennikov, A N Lavrent'ev, I Ya Kuz'mina, L N Kirichenko *Zh. Obshch. Khim.* 51 1567 (1981)
306. D Dakternieks, G-V Rosenthaler *Z. Anorg. Allg. Chem.* 504 153 (1983)
307. C K Ingold *Structure and Mechanism in Organic Chemistry* (Ithaca: Cornell University Press, 1969)
308. D Cooper, S Trippett, C White *J. Chem. Res. (S)* 234 (1983)
309. V F Mironov, R A Mavleev, I V Kononova, E N Ofitserov, A N Pudovik *Izv. Akad. Nauk SSSR, Ser. Khim.* 946 (1991)
310. R H Hudson *Top. Phosphorus Chem.* 11 339 (1983)
311. E S Lewis, D Hamp *J. Org. Chem.* 48 2025 (1983)
312. E S Lewis, K S Colle *J. Org. Chem.* 46 4369 (1981)
313. S E Fry, N J Pienta *J. Org. Chem.* 49 4877 (1984)
314. V I Krutikov, I G Maslennikov, A N Lavrent'ev *Zh. Obshch. Khim.* 53 1982 (1983)
315. R R Ford, M A Goodman, R Neilson, A K Roy, U G Wettermark, P Wisian-Neilson *Inorg. Chem.* 23 2063 (1984)
316. P P Onys'ko, T V Kolodka, A A Kudryavtsev, A D Sinitisa *Zh. Obshch. Khim.* 63 1562 (1993)
317. L N Markovskii, N P Kolesnik, Yu G Shermolovich *Zh. Obshch. Khim.* 49 1764 (1979)
318. V F Mironov, I V Kononova, A N Pudovik *Zh. Obshch. Khim.* 62 2388 (1992)
319. G-V Rosenthaler, W Storzer *J. Fluor. Chem.* 16 533 (1980)
320. J Michalski, M Pakulski, A Skowronska *J. Chem. Soc., Perkin Trans. 1* 833 (1980)
321. J Gloede *Z. Chem.* 28 352 (1988)
322. G-V Rosenthaler, W Storzer *Angew. Chem.* 94 212 (1982)
323. E N Ofitserov, V F Mironov, T N Sinyashina, E I Gol'dfarb, I V Kononova, A N Pudovik *Zh. Obshch. Khim.* 60 768 (1990)
324. I V Kononova, I Glede, V F Mironov *Zh. Obshch. Khim.* 64 1348 (1994)
325. S A Lermontov, A V Popov, I I Sukhozhenov, I V Martynov *Izv. Akad. Nauk SSSR, Ser. Khim.* 215 (1989)
326. S A Lermontov, I M Rakov, I V Martynov *Izv. Akad. Nauk SSSR, Ser. Khim.* 2848 (1990)
327. Ya V Zachinyaev, V F Mironov, A I Ginak, I V Kononova *Zh. Obshch. Khim.* 64 1364 (1994)
328. Yu G Shermolovich, N P Kolesnik, L N Markovskii *Zh. Obshch. Khim.* 56 217 (1986)
329. Yu G Shermolovich, N P Kolesnik, S V Iksanova, V V Trachevskii, L N Markovskii *Zh. Obshch. Khim.* 56 1193 (1986)
330. H Miller *Top. Phosphorus Chem.* 2 133 (1965)
331. V F Mironov, I V Kononova, L M Burnaeva *Zh. Obshch. Khim.* 65 401 (1995)
332. L N Markovskii, Yu G Shermolovich, V I Abramov, V S Talanov, V I Staninets *Zh. Obshch. Khim.* 58 2447 (1988)
333. Yu G Shermolovich, V Yu Abramov, L N Markovskii *Zh. Obshch. Khim.* 61 1725 (1991)
334. T K Prakasha, R O Day, R R Holmes *Inorg. Chem.* 31 1913 (1992)

335. T K Prakasha, S D Burton, R O Day, R R Holmes *Inorg. Chem.* **31** 5494 (1992)
336. T K Prakasha, R O Day, R R Holmes *Inorg. Chem.* **32** 4360 (1993)
337. R R Holmes, T K Prakasha, R O Day *Phosphorus Sulfur Silicon Relat. Elem.* **75** 249 (1993)
338. T K Prakasha, R O Day, R R Holmes *J. Am. Chem. Soc.* **115** 2690 (1993)
339. Yu G Gololobov, N I Gusar' *Sul'fenilkhloridy* (Sulfenyl Chlorides) (Moscow: Nauka, 1989)
340. G-V Rosenthaler *Angew. Chem.* **89** 900 (1977)
341. G-V Rosenthaler *Z. Anorg. Allg. Chem.* **479** 158 (1981)
342. Yu G Shermolovich, N P Kolesnik, V V Vasil'ev, P E Pashinnik, L N Markovskii *Zh. Obshch. Khim.* **51** 542 (1981)
343. V A Chazov, Yu N Studnev, L I Ragulin, A A Ustinov, A V Fokin *Izv. Akad. Nauk SSSR, Ser. Khim.* **146** (1988)
344. V F Mironov, R A Mavleev, I V Konvalova, R A Cherkasov *Zh. Obshch. Khim.* **64** 1358 (1994)
345. I V Konvalova, V F Mironov, L A Burnaeva *Zh. Obshch. Khim.* **63** 2509 (1993)
346. E Krawczyk, A Skowronska, J Michalski, J Mikolajczak *J. Chem. Soc., Perkin Trans. 1* 851 (1993)
347. W H Voncken, H M Buck *Rec. Trav. Chim. Pays-Bas* **93** 210 (1974)
348. T Kubota, S Mayashita, T Kitazume, N Ishikawa *J. Org. Chem.* **45** 5052 (1980)
349. G F Il'in, A F Kolomiets, G A Sokol'skii *Zh. Obshch. Khim.* **51** 2143 (1981)
350. V I Galkin, I V Loginova, I V Konvalova, L A Burnaeva, R A Cherkasov *Zh. Obshch. Khim.* **63** 2467 (1993)
351. V I Galkin, I V Loginova, I V Konvalova, L M Burnaeva, R A Cherkasov *Zh. Obshch. Khim.* **65** 41 (1995)
352. I V Konvalova, L A Burnaeva, I V Loginova, A P Pudovik *Zh. Obshch. Khim.* **61** 2476 (1991)
353. I V Konvalova, V F Mironov, E G Yarkova, I V Loginova, L A Burnaeva, T B Makeeva, A N Pudovik *Zh. Obshch. Khim.* **63** 2000 (1993)
354. H Hacklin, G-V Rosenthaler *Z. Anorg. Allg. Chem.* **561** 49 (1988)
355. G-V Rosenthaler, K Sauerbrey, R Schmutzler *Z. Naturforsch., B, Chem. Sci.* **34** 107 (1979)
356. V F Mironov, L A Burnaeva, I V Konvalova, G A Khlopushina, R A Mavleev, P P Chernov *Zh. Obshch. Khim.* **63** 25 (1993)
357. I V Loginova, L A Burnaeva, A N Pudovik, in *Tez. Dokl. V Mezhd. Konf. "Karbonil'nye Soedineniya v Sintezе Geterotsiklov"* (Abstracts of Reports at the Intercollege Conference 'Carbonyl Compounds in the Syntheses of Heterocycles') (Saratov: Saratov State University, 1992) p. 13
358. V F Mironov, M B Bobrov, R A Mavleev, R M Aminova, I V Konvalova, K I Pashkevich, P P Chernov *Zh. Obshch. Khim.* **63** 797 (1993)
359. V F Mironov, L A Burnaeva, M B Bobrov, K I Pashkevich, I V Konvalova, R M Aminova *Zh. Obshch. Khim.* **64** 1362 (1994)
360. V F Mironov, R A Mavleev, L A Burnaeva, I V Konvalova, A N Pudovik, P P Chernov *Izv. Akad. Nauk SSSR, Ser. Khim.* **565** (1993)
361. I G Maslennikov, L I Matus, L N Kirichenko, I Yu Mansurova, A N Lavrent'ev *Zh. Obshch. Khim.* **61** 1578 (1991)
362. T N Sinyashina, V F Mironov, E N Ofitserov, I V Konvalova, A N Pudovik *Izv. Akad. Nauk SSSR, Ser. Khim.* **1451** (1988)
363. V F Mironov, T N Sinyashina, E N Ofitserov, I V Konvalova *Zh. Obshch. Khim.* **64** 1366 (1994)
364. J A Gibson, G-V Rosenthaler, K Sauerbrey, R Schmutzler *Chem. Ber.* **110** 3214 (1977)
365. R Bohlen, J Heine, W Kuhn, W Offermann, J Stelten, G-V Rosenthaler, W G Bentrude *Phosphorus Sulfur* **27** 313 (1986)
366. R K Oram, S Trippett *J. Chem. Soc., Perkin Trans. 1* 1300 (1973)
367. E Duff, D R Russell, S Trippett *Phosphorus Sulfur* **4** 203 (1974)
368. H Hacklin, G-V Rosenthaler *Chem.-Ztg.* **111** 143 (1987)
369. B M Dahl, O Dahl, S Trippett *J. Chem. Soc., Perkin Trans. 1* 2239 (1981)
370. G-V Rosenthaler, K Sauerbrey, R Schmutzler *Chem. Ber.* **111** 3105 (1978)
371. T V Gryaznova, V F Mironov, M G Khanipova, I V Konvalova, A M Kibardin, A N Pudovik *Zh. Obshch. Khim.* **64** 1738 (1994)
372. A M Kibardin, A N Pudovik *Zh. Obshch. Khim.* **63** 2430 (1993)
373. I V Martynov, A N Ivanov, T A Epishina, V B Sokolov *Izv. Akad. Nauk SSSR, Ser. Khim.* **1086** (1987)
374. V F Mironov, T N Sinyashina, E N Ofitserov, I V Konvalova, A N Pudovik *Zh. Obshch. Khim.* **62** 1288 (1992)
375. I V Konvalova, L M Burnaeva, V F Mironov, I V Loginova, A N Pudovik *Izv. Akad. Nauk SSSR, Ser. Khim.* **2876** (1990)
376. F Ramirez, I Ugi, in *Khimiya i Primenenie Fosfororganicheskikh Soedinenii (Tr. V Konf.)* [The Chemistry and Applications of Organophosphorus Compounds (Proceedings of the Fifth Conference)] (Moscow: Nauka, 1974) p. 138
377. B Tangour, M T Boisdon, G Malavaud, J Barrans *Tetrahedron* **44**, 6087 (1988)
378. I L Vladimirova, A F Grapov, V I Lomakina, in *Reaktsii i Metody Issledovaniya Organicheskikh Soedinenii* (Reactions and Methods of Investigation of Organic Compounds) (Moscow: Khimiya, 1966) Vol. 16, p. 1
379. A J Kirby, S G Warren *The Organic Chemistry of Phosphorus* (Amsterdam: Elsevier, 1967)
380. Yu G Gololobov, T V Kolodka, A S Oganesyan, A N Chernega, M Yu Antipin, Yu T Struchkov, P V Petrovskii *Zh. Obshch. Khim.* **56** 1708 (1986)
381. A S Oganesyan, O A Zagulyaeva, I V Semushkina, V P Mamaev, P V Petrovskii, A N Chernega, M Yu Antipin, Yu T Struchkov, Yu G Gololobov *Zh. Obshch. Khim.* **57** 2234 (1987)
382. E N Ofitserov, V F Mironov, T N Sinyashina, I V Konvalova, A N Pudovik *Zh. Obshch. Khim.* **60** 39 (1990)
383. I V Konvalova, V F Mironov, R A Mavleev, M G Davlieva, E N Ofitserov, in *Sovremennoe Sostoyaniye i Perspektivy Razvitiya Teoreticheskikh Osnov Proizvodstva Khlororganicheskikh Produktov (Tr. V Vsesoyuzn. Nauchn. Konf.)* [Current State and Prospects for the Development of Theoretical Foundations of the Production of Organochlorine Productions (Proceedings of the Fifth All-Union Scientific Conference)] (Baku: Azerbaijan State University, 1991) Part 2, p. 133
384. L V Chvertkina, P S Khokhlov, V F Mironov *Usp. Khim.* **61** 1839 (1992) [*Russ. Chem. Rev.* **61** 1009 (1992)]
385. V F Mironov, E N Ofitserov, A N Pudovik *J. Fluor. Chem.* **54** 299 (1991)
386. V F Mironov, L A Burnaeva, V M Krokhaliev, V I Saloutin, I V Konvalova, R A Mavleev, P P Chernov *Zh. Obshch. Khim.* **62** 1425 (1992)
387. V F Mironov, L A Burnaeva, I V Konvalova, V M Krokhaliev, in *Proceeding of the 10th European Symposium on Fluorine Chemistry, Padua, Italy, 1992* p. 180
388. V F Mironov, I V Konvalova, L A Burnaeva, in *Khimiya. Programma "Universitety Rossii"* (Chemistry. The 'Universities of Russia' Program (Moscow: Izd. Moskovsk. Gos. Univ., 1994) No. 1, p. 121
389. V F Mironov, R A Mavleev, E N Ofitserov, T N Sinyashina, I V Konvalova, A N Pudovik *Izv. Akad. Nauk SSSR, Ser. Khim.* **1676** (1991)
390. V F Mironov, T A Zyblikova, I V Konvalova, R G Gainullin *Novosti YaMR v pis'makh* (1) 134 (1995)
391. V F Mironov, I V Konvalova, T A Zyblikova *Zh. Obshch. Khim.* **64** 1974 (1994)
392. V F Mironov, I V Konvalova, L M Burnaeva, G A Khlopushina, Yu S Shastina *Zh. Obshch. Khim.* **64** 1217 (1994)
393. N M Kashtanova, Author's Abstract of Candidate Thesis in Chemical Sciences, Kazan' State University, Kazan', 1984
394. A N Pudovik, I V Konvalova, L A Burnaeva *Synthesis* **793** (1986)
395. A N Pudovik, I V Konvalova *Sov. Sci. Rev. B., Chem.* **6** 225 (1984)
396. I V Konvalova, L A Burnaeva, E G Yarkova, N M Kashtanova, A N Pudovik *Zh. Obshch. Khim.* **56** 1242 (1986)
397. I V Konvalova, L A Burnaeva, N M Kashtanova, R D Gareev, A N Pudovik *Zh. Obshch. Khim.* **54** 2445 (1984)

398. I V Konovalova, L A Burnaeva, E K Khusnutdinova, R N Kamaletdinova, A N Pudovik *Zh. Obshch. Khim.* **59** 278 (1989)
399. I V Konovalova, E K Khusnutdinova, L A Burnaeva, G Kh Fakhrutdinova, A N Pudovik *Zh. Obshch. Khim.* **58** 2771 (1988)
400. I V Konovalova, Yu G Trishin, L A Burnaeva, E K Khusnutdinova, V N Chistokletov, A N Pudovik *Zh. Obshch. Khim.* **58** 1292 (1988)
401. Yu G Trishin, M R Erofeeva, V N Chistokletov *Zh. Obshch. Khim.* **59** 1196 (1989)
402. M R Erofeeva, Yu G Trishin, V N Chistokletov *Zh. Obshch. Khim.* **59** 2146 (1989)
403. M R Erofeeva, Author's Abstract of Candidate Thesis in Chemical Sciences, Leningrad Technological Institute, Leningrad, 1989
404. V V Kosovtsev, V N Chistokletov, A A Petrov *Zh. Obshch. Khim.* **41** 2649 (1971)
405. S F Aleinikov, I G Maslennikov, A N Lavrent'ev *Zh. Obshch. Khim.* **52** 2134 (1982)
406. S F Aleinikov, V I Krutikov, I G Maslennikov, A V Kashkin, A N Lavrent'ev *Zh. Obshch. Khim.* **53** 1537 (1983)
407. S F Aleinikov, V I Krutikov, A N Lavrent'ev *Zh. Obshch. Khim.* **53** 2438 (1983)
408. S F Aleinikov, V I Krutikov, I N Rogozina, A N Lavrent'ev *Zh. Obshch. Khim.* **55** 576 (1985)
409. S F Aleinikov, V I Krutikov, I N Rogozina, A N Lavrent'ev *Zh. Obshch. Khim.* **55** 2710 (1985)
410. V I Krutikov, A V Naidenov, T V Palagina, V B Lebedev, A N Lavrent'ev *Zh. Obshch. Khim.* **58** 2063 (1988)
411. V I Krutikov, A V Naidenov, T V Palagina, A N Lavrent'ev *Zh. Obshch. Khim.* **89** 98 (1989)
412. V I Krutikov, A V Naidenov, T V Palagina, A N Lavrent'ev *Zh. Obshch. Khim.* **59** 1995 (1989)
413. V I Krutikov, I V Ofrina, E A Kalavardova *Zh. Obshch. Khim.* **61** 840 (1991)
414. L N Markovskii, A V Solov'ev, V E Pashinnik, Yu G Shermolovich *Zh. Obshch. Khim.* **55** 1015 (1985)
415. L N Markovskii, A V Solov'ev, Yu G Shermolovich *Zh. Obshch. Khim.* **50** 2184 (1980)
416. D P Bauer, W M Douglas, J K Ruff *J. Organometal. Chem.* **57** C19 (1973)
417. J-M Shreeve, S M Williamson *J. Organometal. Chem.* **249** C13 (1983)
418. J-M Shreeve, S M Williamson *Organometallics* **2** 1104 (1984)
419. G Klopman (Ed.) *Chemical Reactivity and Reaction Paths* (New York: Wiley, 1974)
420. A Ya Dorfman, L V Levina, T V Petrova, V S Emel'yanova, G S Polimbetova *Zh. Obshch. Khim.* **60** 840 (1990)

Dependence of the extraction ability of organic compounds on their structure

A M Rozen, B V Krupnov

Contents

I. Introduction	973
II. Monodentate neutral organophosphorus compounds	974
III. Organic sulfoxides	976
IV. Variation of extraction ability and the complex formation mechanism as the reaction centre is varied and the basicity of the extractants increases	977
V. Characteristic features of extraction by amine and arsine oxides	979
VI. Salts of amines and quaternary onium bases	979
VII. The influence of the length and degree of branching of substituents on the extraction ability of organic compounds	980
VIII. The use of quantum-chemical calculations for predicting extraction ability	982
IX. Bidentate neutral organophosphorus compounds and the anomalous aryl stabilisation effect	984
X. Polydentate neutral extractants — crown-ethers	989
XI. Organic acids	991
XII. Organic acid salts	994
XIII. The influence of diluents on the extraction ability of organic compounds	995
XIV. Examples of the development of new extractants	996

Abstract. Data on the dependence of the extraction ability of the principal classes of organic compounds on their structure are surveyed. Mono- and bi-dentate neutral organophosphorus compounds (NOPC), sulfoxides, amines, quaternary ammonium, arsonium, and phosphonium bases, amine and arsine oxides, organophosphorus acids and their salts, and crown-ethers are examined. It is shown that the extraction ability of the NOPC in relation to any metal increases with increase in the basicity of the extractant and diminishes when electronegative substituents are introduced into its molecule. With increase in the basicity of neutral extractants, qualitative changes in the complex formation mechanisms are observed. The influence of diluents on the extraction ability of organic compounds is analysed. Methods for predicting extraction ability are considered. Examples of the use of the above rules for the development of new extractants are presented. The bibliography includes 157 references.

I. Introduction

The search for highly effective extractants is an important scientific and practical problem. The understanding of the dependence of the extraction ability (EA) of organic compounds on their structure has played the role of a compass in this search.

Such a dependence is of interest also when the general problem of the reactivity of compounds is considered.

The extraction of metal salts and acids is based on the chemical interaction (complex formation) of these substances with the extractant and may be regarded as a heterogeneous

chemical reaction. The effective extraction constant K_{ex} (the abbreviated term describing the equilibrium constant of the extraction reaction) is a quantitative characteristic of the extraction ability. For example, for the reaction



where TBP = tributyl phosphate, K_{ex} is determined from the Law of Mass Action taking into account the activity coefficients of the extracted compound in the aqueous phase (γ_{\pm}):

$$K_{ex} = \frac{\bar{K}_{ex}}{\gamma_{\pm}^v},$$

$$\bar{K}_{ex} = \frac{[\text{UO}_2(\text{NO}_3)_2(\text{TBP})_2]}{[\text{UO}_2^{2+}][\text{NO}_3^-]^2[\text{TBP}]^2},$$

where \bar{K}_{ex} is the concentration extraction constant and v the number of ions into which the metal salt dissociates in the aqueous phase ($v = 3$). The distribution coefficient (D) can be used as the characteristic of the EA, but only when the compounds present in the aqueous phase at macroconcentrations are not extracted. Otherwise, the changes in D when the structure is varied can reflect not only the changes in the EA of the extractant but also the changes in the concentration of the free extractant.[†] If the salt extracted from the aqueous phase is the same, the changes in the extraction constant when the structure of the extractant is varied reflect the changes in the constant for the complex formation

[†] This happened, for example, in a pioneer study where an apparent linear correlation between the distribution coefficients of uranyl nitrate in extraction from nitric acid solutions by a series of NOPC and the P=O bond vibrational frequency was obtained solely due to experimental errors, which were discovered when the results of the above study¹ were compared with more accurate data.² In addition, the extraction constant is much more informative than the distribution coefficient: knowing \bar{K}_{ex} , it is possible to reproduce the extraction isotherm and to find the dependence of D on the process conditions.

A M Rozen, B V Krupnov State Scientific Centre — Bochvar All-Russian Inorganic Materials Research Institute P. O. Box 369, 123060 Moscow, Russian Federation. Fax (7-095) 196 41 68

Received 8 April 1996

Uspekhi Khimii 65 (11) 1052–1079 (1996); translated by A K Grzybowski

reaction between the salt and the extractant. Admittedly in the traditional approach to the description of extraction (see, for example, Sekine³) this is not quite correct. In this approach, the transfer of the extractant to the aqueous phase is considered as the first stage of the process, the formation of a complex with a metal or an exchange reaction with the latter in the aqueous phase is the second stage (or the third, if the extractant dissociated in the aqueous phase), while the transfer of the compound formed from the aqueous phase to the organic phase is considered to be the last stage. Under these conditions, the extraction constant is related in a complex manner to the complex formation constant in the aqueous phase β_{aq} and also depends on the distribution constants of the extractant and the complex, the last being usually unknown.

This approach arose in the initial period of the use of extraction when water-soluble extractants were employed (especially in analytical chemistry). However, extractants which are sparingly soluble in the aqueous phase are usually employed nowadays. The approach based on the consideration of complex formation in the organic phase⁴ is therefore more useful.

For neutral sparingly soluble extractants, the Gibbs free energy of extraction ΔG_{ex} represents the difference between the Gibbs free energies of the solvation and hydration processes:^{5,6}

$$\Delta G_{ex} = \Delta G_{solv} - \Delta G_{hydr}, \quad (1)$$

and since $\Delta G_{ex} = -RT \ln K_{ex}$ and $\Delta G_{solv} = -RT \ln \beta_{org}$, where β_{org} is the complex formation constant in the organic phase, we find

$$K_{ex} = \beta_{org} \exp \frac{\Delta G_{hydr}}{RT}, \quad (2)$$

i.e. K_{ex} is proportional to the complex formation constant in the organic phase β_{org} and characterises the stability of the complex.

The thermodynamic parameters of the hydration of many metals have been published⁵⁻⁸ and most fully in the last of the studies quoted (examples are presented in Table 1). Evidently the hydration energies increase when the nitrate ion is replaced by the chloride ion, and with increase in the charge and with decrease in the radius of the cation. Extraction becomes correspondingly more difficult. For extraction to be effective (K_{ex} of the order of unity), it is necessary to compensate for the hydration energy, i.e. the complex formation energy in the organic phase must be of the same order as G_{hydr} . In principle, such complex formation energies may be attained if the process proceeds via an electron donor-acceptor (EDA) mechanism. However, for the extraction of alkaline earth elements, a high electron-donating capacity of the extractants is necessary and for $AlCl_3$ it is altogether impossible to select effective extractants. To a certain extent, it is possible to obviate the difficulties associated with hydration by choosing salts with a reduced hydration of the anion; it is also possible to extract the ion with its hydration shell (the hydrate-solvate extraction mechanism⁹).

On the other hand, the most effective procedure involves the transition from the solvate to the cation-exchange mechanism of extraction:

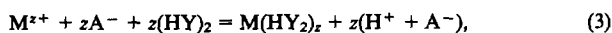


Table 1. The Gibbs free energies and enthalpies of hydration of salts of metals (kcal mol⁻¹).

Compound	$-\Delta G_{hydr}$	$-\Delta H_{hydr}$	Compound	$-\Delta G_{hydr}$	$-\Delta H_{hydr}$
HCl	10.7	14.8	ThCl ₄	—	56.7
NaCl	2.1	-0.9	HNO ₃	7.3	7.95
MgCl ₂	30.3	37.2	NaNO ₃	1.5	-4.9
CaCl ₂	15.5	19.8	Mg(NO ₃) ₂	21.2	21.8
LaCl ₃	21.0	33	Ca(NO ₃) ₂	12.8	4.5
AlCl ₃	61.1	78.1	LiNO ₃	5.6	0.6
UO ₂ Cl ₂	16.4	28.1	UO ₂ (NO ₃) ₂	6.1	20.3

where HY is an organic acid. In the aqueous phase, the salt molecule MA_z is replaced by z molecules of the inorganic acid HA. Depending on the sign of the transhydration energy,

$$\Delta \Delta G_{hydr} = z\Delta G_{hydr}(HA) - \Delta G_{hydr}(MA_z)$$

it is actually possible to achieve a gain in extraction energy, which intensifies extraction.

The most correct method for predicting EA is the quantum-chemical calculation of the complex formation energy with subsequent determination of the partition functions and entropies of the components.[†] Unfortunately, this approach is possible only in a semiempirical approximation for inorganic acids or organic compounds.^{10,11} In most cases, especially for d and f elements, the direct (especially nonempirical) quantum-chemical calculation for extraction complexes is impossible. Therefore, correlations between the extraction constant and various characteristics of the extractant associated with its reactivity are widely used for predicting EA. The following are usually employed: (1) the characteristics of the structural groups, for example the electronegativities of the groups in substituents,¹² the reaction constants of these groups [the Taft (σ^*)¹⁸ and Kabachnik (σ^p)^{13,14} constants] on the assumption that the influence of these groups is additive: (2) the characteristics of an isolated extractant molecule as a whole — the electron density (charge) on the functional atom, the ionisation potential¹⁵, and the energy of the core $1s$ levels;¹⁶ (3) the characteristics of the reactivity of the molecule as a whole — basicity, determined experimentally from the energies of test reactions with simplest electron acceptors¹⁷⁻²¹ or by quantum-chemical calculations of the energies of complex formation with a proton [proton affinities (PA)], Li^+ , LiH , etc.^{16,22}

The dependences of EA on the structure of the extractants and the possibility of predicting it on the basis of various correlations are analysed in the present review. The dependences were established mainly in relation to the extraction of the actinides, but are nevertheless of a general character.[§]

II. Monodentate neutral organophosphorus compounds

At the time of the publication of the first studies on extraction using alcohols, ethers, and ketones, the chemical nature of the process was still obscure. Owing to the low EA of the reagent, the extraction isotherms obtained in these investigations did not in the main have a saturation section characteristic of the formation of compounds (Fig. 1, curves 1 and 2). The relation between extraction ability and structure was not traced and it was only noted that EA diminishes with increase in the C/O ratio, i.e. as the hydrocarbon chain is lengthened.^{23,24} The introduction of tributyl phosphate in the 1950s²⁵⁻³⁰ led to revolutionary changes both in the technology (EA increased by 5-6 orders of magnitude and it became possible to extract uranyl and plutonium nitrates without employing salting-out agents) and in the theory of the processes [a saturation section, frequently indicating the formation of compounds (Fig. 1, curves 3 and 4), appeared on the extraction isotherms].³⁰

† Strictly speaking, a calculation taking into account the influence of the solvent is necessary. However, it has been established in a number of studies that a weakly polar solvent exerts a comparatively weak influence on the complex formation and extraction energies which is due to the compensation of diluent-extractant and diluent-extracted complex interactions (see below).

§ The review is based largely on the results of studies carried out under the supervision of A M Rozen during the last 30 years. Z I Nikolotova, N A Kartasheva, E I Moiseenko, Z I Nagnibeda, Yu I Murinov, B V Martynov, A S Skotnikov, L P Kharkhorina, V G Yurkin, and B V Krupnov participated actively in these investigations. Studies by other workers are naturally also discussed.

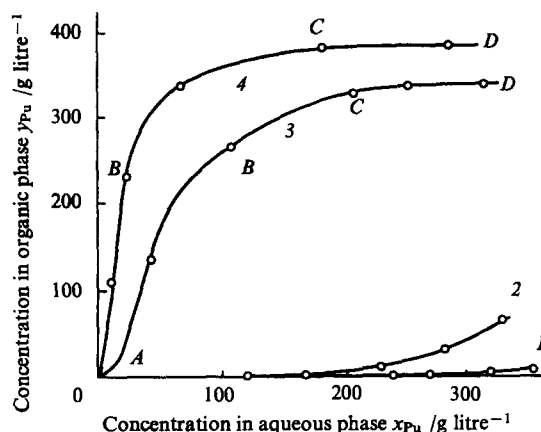


Figure 1. Isotherms for the extraction of Pu(IV) by neutral organic compounds ($x_H = 0.1$ M).

Extractant: (1) dibutyl ether (DBE); (2) diethyl ether (DEE); (3) TBP; (4) diisopentyl methylphosphonate (DPMP); AB — initial section of the isotherm determined by dissociation into ions; BC — section corresponding to moderate nonideality; CD — saturation section.

Neutral organophosphorus compounds are the first class of compounds for which the dependence of EA on the structure has been studied systematically. For phosphates, phosphonates, phosphinates, and phosphine oxides, the reaction centre (RC) is the PO group and the composition of the complexes remains unchanged (for example, the disolvates of tetravalent and hexavalent actinides, the trisolvates of trivalent actinides and lanthanides), while extraction ability increases appreciably. A correlation has been proposed¹² between $\ln K_{ex}$ for uranyl nitrate and nitric acid, on the one hand, and the sums of the electronegativities of the groups of the substituents (X) in the above series:

$$\ln K_{ex} = A - B \sum X - \rho \sum l, \quad (4)$$

where A is a constant which depends on the reaction series (the class of the extractant and the individuality of the compound extracted), B is the coefficient of the sensitivity to electronegativity, ρ the coefficient of the sensitivity to the length of the hydrocarbon chain, l the effective length of the hydrocarbon chain of the substituent (in the case of normal groups, $l = n_C$), and the values of X are determined from the spectral scale (Table 2).

The following considerations also lead to Eqn (4).³¹ On the one hand, since the complexes are formed via an EDA mechanism, one can suppose that EA is greater the greater the electron density on the donor atom. Rozen and Denisov³¹ put forward more logical considerations, which may make it possible to estimate the coefficient B :

Table 2. The electronegativities and Taft constants for certain substituents.^{6, 12}

Substituent	X	σ^*
F	4.0	—
Cl	3.0	—
CCl ₃	2.95	2.65
ClCH ₂	2.60	1.05
Cl(CH ₂) ₂	2.32	—
C ₆ H ₅	2.34	0.6
CH ₃	2.07	0.0
Alk	2.0	-0.13
RO	2.9, 2.4*	1.50, 0.75*
H	2.3	0.49

* Effective values.

$$\ln K_{ex} = a + b|q|,$$

where a and b are constants and q is the charge. On the other hand, according to the results of approximate quantum-chemical calculations,^{32, 33}

$$|q| = a'' - b'' \sum X,$$

where a'' and b'' are constants. When account is taken of these relations, Eqn (4) is obtained. When calculations are made relative to a standard compound, Eqn (4) leads to the Hammett-Taft equation.¹⁴

$$\ln \frac{K_{ex}}{K_0} = -B \sum (X - X_0) - \rho \sum (l - l_0) = r^* \sum \sigma^* + d \sum E_s. \quad (5)$$

Here the subscript 0 refers to the characteristics of the standard state, r^* and d are coefficients, and E_s is the steric hindrance constant.

In fact it has been found¹⁴ that $X = 2.07 + \sigma^*/2$, i.e. the Taft constants represent relative electronegativities.

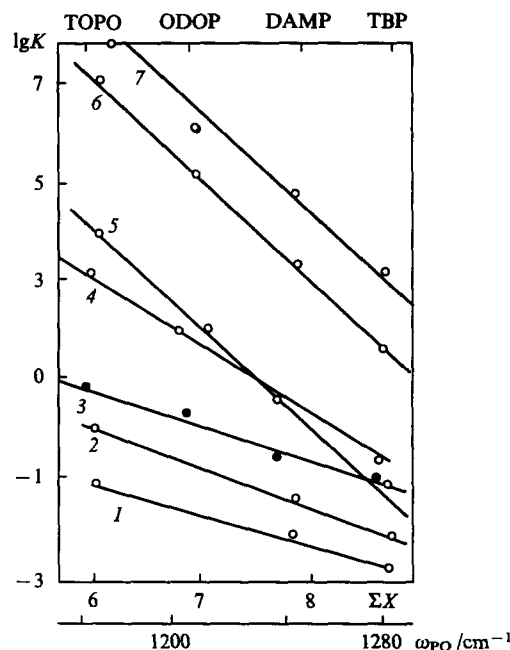


Figure 2. Dependence of EA on the sum of the electronegativities of the substituents (ΣX) and the stretching vibrational frequencies (ω_{PO}) in the extraction of certain compounds by monodentate NOPC.

Compound extracted: (1) manganese nitrate; (2) potassium permanganate; (3) nitric acid; (4) americium nitrate; (5) uranyl chloride; (6) uranyl nitrate; (7) plutonium nitrate. ODOP = octyl dioctylphosphinate; TOPO = trioctylphosphine oxide.

The following conclusion follows from Eqn (4): the EA of monodentate NOPC decrease after the introduction of electronegative substituents. This conclusion is fairly general, being valid for any metals (Fig. 2). However, in order to obtain a general correlation when a wider class of NOPC, including the C_6H_5 , CCl_3 , $ClCH_2$, and $Cl(CH_2)_2$ groups, is considered (Fig. 3), Eqn (4) had to be refined.^{12, 34} Effective (reduced) electronegativities were introduced for the alkoxy-groups ($X_{ef} = 2.4$ and $\sigma_{ef}^* = 0.75$). The possible reason for this is that X and σ^* describe only the inductive effect, whereas for RO the resonance effect is also observed.[†]

† One cannot rule out also the explanation based on the jump in entropy on passing from one subclass to another (for example, from phosphates to phosphonates).¹⁴

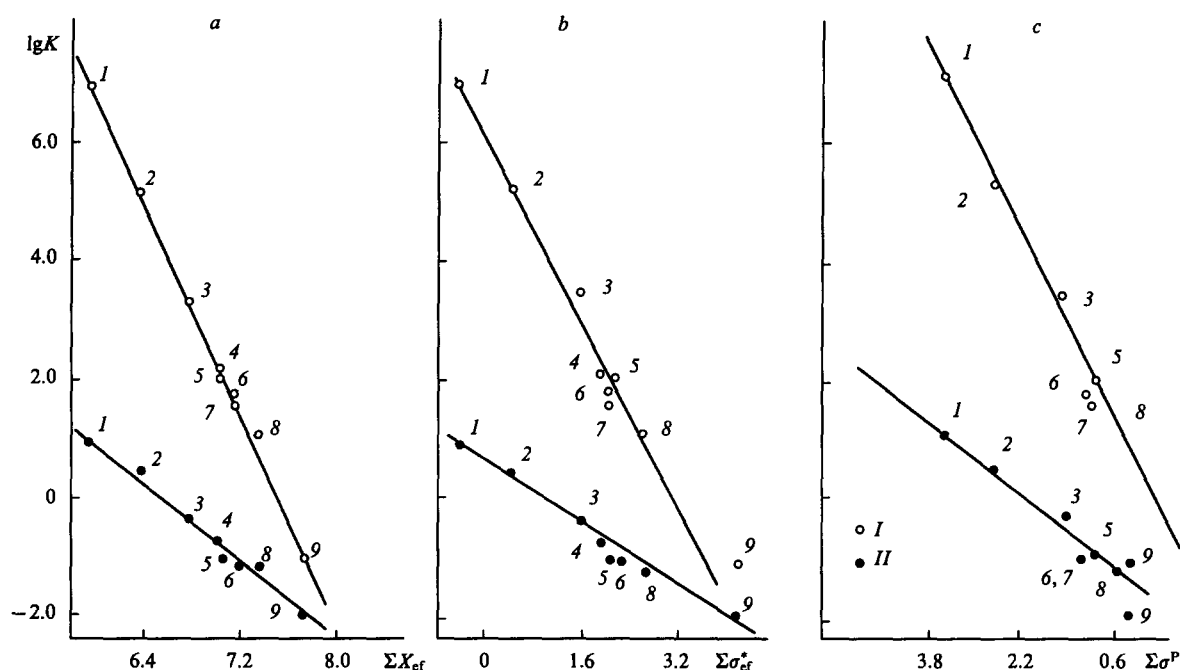


Figure 3. Dependence of the extraction ability of NOPC on the sum of the effective electronegativities (a), the effective Taft constants (b), and the Kabachnik constants (c) of the substituents.

Extractant: (I) TOPO; (2) ODOP; (3) DPMP; (6) TBP; (7) trioctyl phosphate; (4), (5), (8), and (9) (iso-C₅H₁₁O)₂RPO, R = C₆H₅ (4), Cl(CH₂)₂ (5), ClCH₂ (8), or CCl₃ (9); substance extracted: (I) UO₂(NO₃)₂; (II) HNO₃.

Instead of Eqn (4), one can write

$$\begin{aligned} \ln K_{\text{ex}} &= A - B\Sigma X_{\text{ef}} - \rho\Sigma l = \\ &= A - B\Sigma X + B'\Sigma\sigma_{\text{res}} - \rho\Sigma l, \end{aligned} \quad (6)$$

where σ_{res} is the resonance interaction constant and $X_{\text{ef}} = X - \sigma_{\text{res}}B/B'$.

Eqn (6) is equivalent to the use of Kabachnik constants:

$$\lg \frac{K_{\text{ex}}}{K_0} = r^P \Sigma \sigma^P,$$

where $\sigma^P = \sigma_{\text{ind}}^P + \sigma_{\text{res}}^P$ is the Kabachnik constant taking into account the resonance effect, and including also the term $\rho\Sigma l/r^P$. The correlation with σ^P does not therefore require the introduction of effective quantities.

The advantage of electronegativity over the constants σ^* and σ^P is a more clear-cut physical significance. Electronegativities may be determined independently of any reactions. Unfortunately, there are no independent methods for the determination of σ_{res}^P . The energy of the 1s orbitals is an independent quantum-chemical parameter characterising the molecule as a whole and equivalent to ΣX_{ef} . The decrease in EA with increase in the electronegativities of the substituents is characteristic of any class of neutral compounds (the only exception, in the case of bidentate NOPC, is discussed below).

III. Organic sulfoxides

Systematic studies on extraction by sulfoxides (in which the reaction centre is the SO group) began and developed vigorously at the beginning of the 1970s. The research groups led by Rozen, Mikhailov, and Torgov published more than 20 papers. They have been reviewed by Nikitin et al.³⁵

It was established that, in terms of their extraction ability, aliphatic sulfoxides approach phosphonates. Cyclic sulfoxides are obtained by oxidising petroleum sulfides. Their EA is higher by a factor of 2–3 (owing to the contribution by the entropy factor) than that of aliphatic sulfoxides. The dependence of EA on the

structure of the sulfoxide is described by Eqns (4) and (5). The difference from NOPC consists in a higher sensitivity of EA to the influence of substituents (higher values of B in the above equations). Thus the replacement of a single alkyl group by the phenyl group in NOPC lowers the degree of extraction of uranium by a factor of 17, while in the case of sulfoxides the decrease is by a

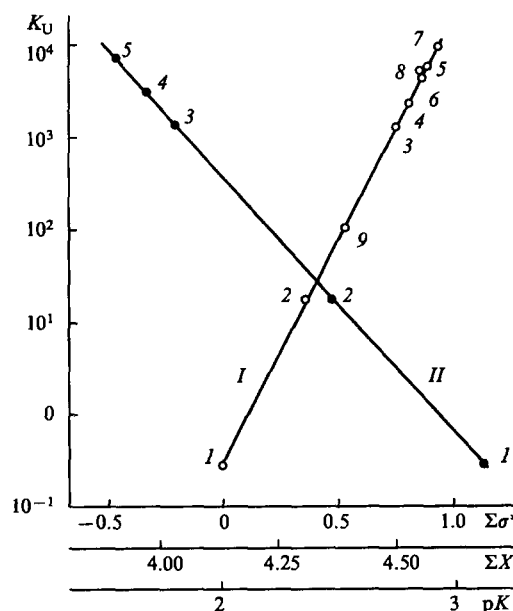


Figure 4. Dependence of the uranyl nitrate extraction constant on the basicity (I) and the sum of the electronegativities of the substituents or the Taft constants (II) of the extractants.

Extractant: (I) diphenyl sulfoxide; (2) hexyl phenyl sulfoxide; (3) dihexyl sulfoxide; (4) cyclohexyl hexyl sulfoxide; (5) hexyl tolyl sulfoxide; (7) 2-amyltetrahydrothiopyran sulfoxide; (8) DPMP; (9) TBP.

factor of 40. Fig. 4 presents the dependences of the extraction constant of uranyl nitrate (K_U) on the basicity and on the sum of the electronegativities or Taft constants of the sulfoxides.

IV. Variation of extraction ability and the complex formation mechanism as the reaction centre is varied and the basicity of the extractants increases

The dependence of extraction ability on the structure of organic compounds has also been investigated for carbonyl compounds and arsine and amine oxides (the reaction centres are the CO, AsO, and NO groups respectively). The extraction by compounds of this type is associated with the formation of electron donor-acceptor complexes, so that the more marked the electron-donating properties of the extractants (characterised by their basicity) the higher the EA. A linear correlation between $\ln K_{ex}$ and the basicity is frequently observed under these conditions [see, for example, Refs 34–37 (Fig. 5)]:

$$\ln K_{ex} = a + bpK \quad (7)$$

We may note that the dependence of EA on the electronegativity of the substituents in the extracting molecule examined above is a special case of the dependence of EA on the basicity. It has been shown in relation to extraction by sulfoxides that the extraction of uranyl nitrate and the basicity of sulfoxides depend on the sum of the electronegativities of the substituents:

$$\ln K_{ex} = 3.04 - 5.23\Sigma(X - 2); \quad (8a)$$

$$pK = 2.67 - 0.94 \Sigma(X - 2), \quad (8b)$$

which is equivalent to the dependence of the EA in relation to uranium on the basicity:

$$\ln K_{ex} = -11.38 + 5.6pK, \quad (8c)$$

i.e. Eqns (4) and (7) are equivalent for a class of extractants with a single reaction centre. Eqn (8b) implies that, when electronegative substituents are introduced into the extractant molecule, the electron-donating capacity of the latter (its basicity) diminishes and there is corresponding decrease also in the EA [Eqns (8a) and (8c)].

There exist several basicity scales which are determined experimentally [for example by titration with perchloric acid in nitromethane (pK),¹⁷ by the reaction with pentachlorophenol,^{8,19} and by the calorimetry of the interaction with antimony pentachloride (Gutmann donor numbers) and other Lewis acids].^{20,21} In connection with the development of quantum chemistry and the ion cyclotron resonance spectroscopic methods, gas-phase basicity and proton affinity scales,^{41,42} which are free from the influence of the solvent, are increasingly used at the present time.[†] Table 3 gives an idea about the above scales.

Table 3. Extractant basicity scales.

Compound	Proton affinity / kcal mol ⁻¹	Donor number ^{43,44}	Energy of H bond with H ₂ O ⁴⁵	Taft–Rozen basicity ¹⁹ (C ₆ Cl ₅ OH)
ROH	189.0±1.5	18.0	—	—
R ₂ O	200.2	—	—	0.98
R ₂ CO	190.5	17.0	2.7	1.18
cyclo-C ₆ H ₁₁	—	—	—	1.30
NR ₂ RCO	214.5	26.6; 27.8	—	—
(NR ₂) ₂ CO	219.5	29.6	—	—
(PhO) ₃ PO	—	—	—	1.73
(RO) ₃ PO	217.0	23.7; 25.2	3.9; 4.0	2.56
(RO) ₂ RPO	—	31.2	4.0	2.74
(RO)R ₂ PO	—	32.0	4.8	—
R ₃ PO	224.5	33.8	5.0; 5.3	3.64
(NR ₂) ₃ PO	229.5	38.6	—	—
R ₂ SO	—	29.8	4.4	2.58
R ₃ NO	238.0	—	6.9	—

† It has been shown^{38,39} that considerable differences are observed between the proton basicities in the gas phase and in solution. At the same time, it has been found⁴⁰ that the differences between the energies of the complex formation reactions with metal salts in the gas phase and in weakly polar solvents are small.

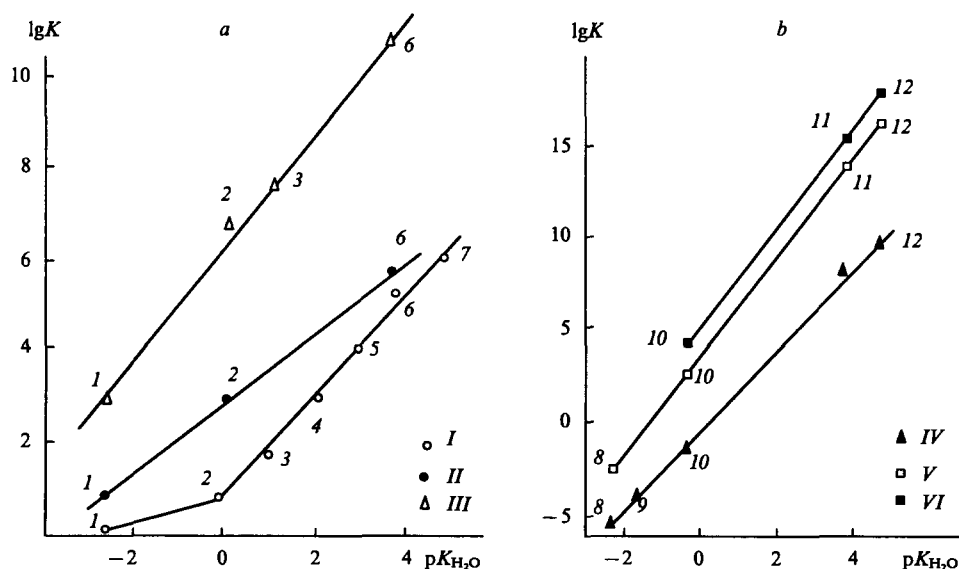


Figure 5. Dependence of the extraction constants of nitric acid (I), americium (II), and uranyl (III) nitrates (a) and of the monosolvates (IV) and disolvates (V) of perchloric and pertechnetic (VI) acids (b) on the basicity of neutral extractants. Extractant: a: (1) Ph₃PO; (2) R₃PO; (3) Ph₃AsO; (4) Ph₂RAsO; (5) PhR₂AsO; (6) R₃AsO; (7) R₃NO; b: (8) TBP; (9) Ph₃PO; (10) TOPO; (11) R₃AsO; (12) R₃NO.

The above scales, based on allowance for the donor–acceptor interactions in solution, have a certain advantage in the prediction of complex formation constants in solutions. Here it is desirable that the nature of the interactions underlying the scale should not vary over the entire basicity range. This condition is not satisfied by the basicity scale based on the titration of the extractant with perchloric acid in nonaqueous media. Only the basicities of strong electron donors (ranging from R_3PO to R_3NO) have been determined by this procedure, while weak bases are not protonated under these conditions. Unfortunately the scales constructed using the interaction energy with weak proton donors (water or phenol) exhibit a low sensitivity to changes in the electron-donating capacities of the extractants. A more sensitive scale is based on the interaction energy with a stronger proton donor — pentachlorophenol. This scale has been used successfully in establishing correlations with EA for a wide range of extractants — from the weakest (alcohols, ethers, and ketones) to fairly strong (sulfoxides and NOPC).[‡] The above condition is most readily fulfilled when the scale is constructed on the basis of the interaction with a metal salt. This is in fact the reason why the Gutmann donor number scale has come to be widely used.

With increase in the basicity of the extractant, not only is there an increase in the stability of the complex observed but the complex formation mechanism also changes. Thus in the extraction of nitric acid, the hydrate solvate mechanism [the coordination of an extractant molecule via a water molecule, for example $HNO_3 \cdot H_2O_2 \cdot (TBP)_2$] is readily replaced by the solvate mechanism (the formation of a molecular hydrogen-bonded complex with a direct bond between the donor atom of the extractant and the proton of the acid extracted, for example $TBP \cdot HNO_3$ and $TOPO \cdot HNO_3$). On further increase in basicity, complexes involving proton transfer are formed ($R_3XOH^+ \cdot NO^-$, where $X = As$ or N).³⁴ A similar complex formation mechanism has been found also in the extraction of strong acids (HCl , H_3ClO_4 , $HReO_4$, $HTcO_4$, etc.) with formation of both monocomplexes $[LH]^+ A^-$ and dicomplexes $[LHL]^+ A^-$.^{46–48} The extraction constants for the latter are especially high (Table 4). The stronger the inorganic acid, the lower the basicity of the extractant for which the transition to the new mechanism takes place.

Table 4. The extraction constants of inorganic acids in the form of the proton-transfer complexes $[LH]^+ A^-$ (K_1) and $[LHL]^+ A^-$ (K_2).

Acid	Extractant			
	R_3AsO		R_3NO	
	K_1	K_2	K_1	K_2
HNO_3	—	—	8.0×10^7	4.0×10^{11}
HCl	—	—	5.0×10^5	3.0×10^7
$HReO_4$	1.0×10^{10}	4.8×10^{15}	3.6×10^{11}	7.2×10^{17}
$HTcO_4$	3.0×10^{10}	2.4×10^{16}	1.0×10^{12}	2.8×10^{18}

A change in the extraction mechanism leads to significant alterations of the extraction ability. The nature of the dependence of the degree of extraction of acids on the basicity of the extractant is then determined to a considerable degree by the strength of the acid being extracted. Torgov and Nikolaeva[§] found that, in the

extraction of weak acids (phenols, phosphoric or acetic acid), the extraction mechanism (the formation of a hydrogen bond) does not change over the entire range of basicities of the extractants and lgK_{ex} varies linearly with the donating capacity of the extractant. Amine oxides possess the highest extraction ability in relation to weak acids. It is of interest that amines are not included in these correlations: having a gas-phase proton affinity similar to that of amine oxides and a higher protonation energy in solution, amines form hydrogen-bonded complexes, the stability of which does not exceed that of complexes formed by phosphine oxides which are less basic in protonation reactions. Furthermore, amines extract weak acids with even lower distribution coefficients than phosphine oxides (for example 3.11 for the extraction of phenol with TOPO and only 1.23 for its extraction with trioctylamine); this may be associated with steric hindrance.

The dependences of lnK_{ex} on the basicity of the extractant for moderately strong acids (for example, nitric acid) have a break on passing from complexes with an intermolecular hydrogen bond to those involving proton transfer (Fig. 5).³⁶ Quantum-chemical calculations have shown⁵¹ that this break is due to the increase in the sensitivity of the energy of the complex to the basicity of the extractant after the change in the complex formation mechanism. We put forward the hypothesis¹¹ that, by altering the 'threshold' of the transition through the selection of the extractant and the diluent, it is possible to obtain a significant increase in the separation coefficients for acids in their mixtures.

The lgK_{ex} of strong acids (for example, perchloric and pertechnetic), which form proton-transfer complexes over the entire range of basicities of the extractant, increases almost linearly (by 15–18 units) with increase in basicity as the substituents and the reaction centre are varied (SO , PO , AsO , NO) (Fig. 5b).^{37, 46, 47}

The formation of proton-transfer complexes in the extraction of metal salts results in the manifestation, together with coordination to the oxide oxygen and the formation of a solvate [for example $UO_2(R_3XO)_2(NO_3)_3$], also of coordination to the cation LH^+ , for example $R_3XOH^+ UO_2(NO_3)_3^-$ (Rozen et al.³⁶ called this the amine mechanism). Attempts to separate the contributions of the oxygen and amine mechanisms have been undertaken.^{36, 47}

The discovery of the amine (anion-exchange) mechanism of the extraction of actinides by the oxides R_3AsO and R_3NO made it possible to explain the similarity of the distribution coefficients of uranium and plutonium in extraction by amines and amine and arsine oxides (Fig. 6).[¶]

For arsine oxides, a transition to the cation-exchange mechanism is observed in the region of low acidity.⁴⁹

In the extraction of metal salts, the changes in the complex formation mechanism are similar to the changes in the mechanism of the formation of complexes by acids over a wide range of basicities of neutral extractants. In extraction by weakly basic extractants (for example, by ethers or ketones), the hydrate-solvate mechanism is favourable. In this case, the extractant is unable to displace a water molecule from the first hydration shell and the metal ion is extracted together with the latter, since the separation of the hydrated ion from the outer hydration shell requires less energy than its separation from the inner shell. Under these conditions, the extractant is in the outer sphere of the complex and is coordinated to the metal ion via a water molecule.[†]

Stronger extractants decompose the first hydration shell and extract the metal without water molecules.

The most basic extractants (arsine and amine oxides) extract the metal via the amine mechanism.

‡ One cannot be certain that the complex formation mechanism does not change for the strongest bases — for example, arsine and amine oxides. A change in this mechanism would lead to considerable errors in prediction.

§ I V Nikolaeva *Vzaimosvyaz' Ekstraktsionnoi Sposobnosti Oksidov 2-Nonilpyridina i Triizooamilfosfina i Sostoyaniya ikh Kompleksov s Kislotami v Nevodnykh Sredakh* (Relation between the Extraction Ability of 2-Nonylpyridine and Triisopentylphosphine Oxides and the State of their Complexes with Acids in Nonaqueous Media). Author's abstract of Candidate Thesis in Chemical Sciences, Institute of Inorganic Chemistry, Siberian Branch of the Russian Academy of Sciences, Novosibirsk, 1996.

¶ For R_3NO , such similarity was observed as early as 1964⁵⁰ but until the publication of the study of Rozen et al.³⁶ was not understood.

† For the characteristic features of the extraction via the hydrate-solvate mechanism, see Yu A Zolotov.⁹

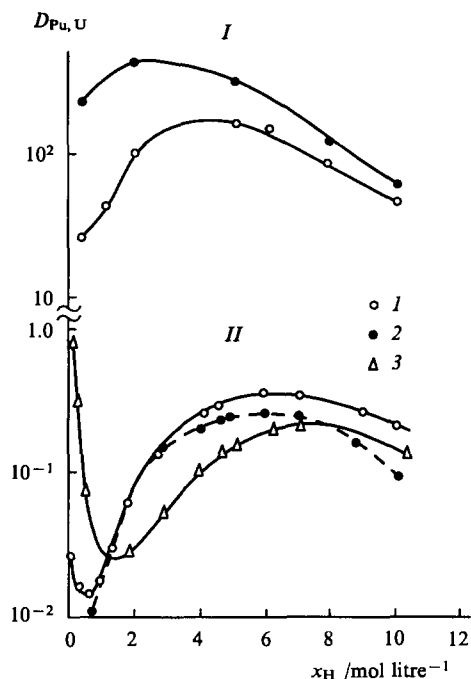


Figure 6. Dependence of the distribution coefficients of Pu^{4+} (I), and UO_2^{2+} (II) on acidity in extraction by trioctylamine oxide (I), trioctylamine (2), and trioctylarsine oxide (3) (extractant concentration in benzene 0.1 M).

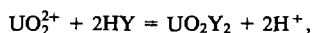
V. Characteristic features of extraction by amine and arsine oxides

In the extraction of metals by arsine and amine oxides, the formation of proton-transfer complexes $(LH^+)A$ between the extractant and the inorganic acid, similar to amine salts, is accompanied also by complex formation via the anion-exchange mechanism. For example, the complexes $LH^+[UO_2(NO_3)_3]^-$ and $(LH^+)_2[Pu(NO_3)_6]^{2-}$ where $L = R_3AsO$ or R_3NO , are formed.³⁴ Thus at high basicities the boundary between neutral extractants and amines is obliterated.

At a low acidity of the aqueous phase, yet another change in the extraction mechanism is observed. It is particularly pronounced in the case of arsine oxides. Fig. 6 shows that, at HNO_3 concentrations less than 1.5 M, the distribution coefficient of uranium increases with decrease in x_H , i.e. R_3AsO begins to extract like an organic acid.³⁶ The dependence of the distribution coefficient on the pH (Fig. 7) characteristic of extraction by organic acids, i.e.

$$\lg D = a + zpH \quad (9)$$

(z is the valence of the cation), is observed. One may conclude³⁶ that the arsine oxide molecule rearranges and tentatively is converted into the acid $R_3As(NO_3)OH$. The reaction proceeds via the cation-exchange mechanism, for example via the reaction



where Y is apparently $R_3As(NO_3)O$. Such rearrangement may account also for the surprising phenomenon observed in a number of studies:^{52–55} in the weakly acid region, the degree of extraction of $Pu(IV)$ and $Pu(VI)$ increased after the replacement of the alkyl groups in the arsine oxide by the more electronegative phenyl groups, which, as we have seen above, leads to a weakening of extraction when NOPC and sulfoxides are employed. However, when account is taken of the 'acid rearrangement', everything becomes clear, since in extraction by organic acids an increase in the electronegativity of the substituents leads to an increase in the

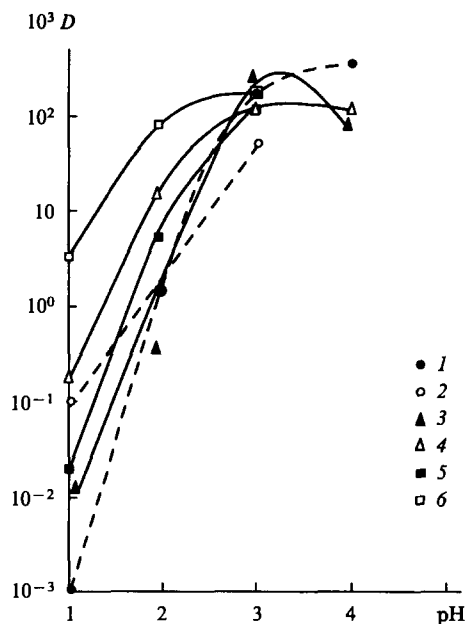


Figure 7. Dependence of the distribution coefficients of U(VI) (1, 2), Pu(VI) (3, 4), and Np(VI) (5, 6) on the pH in extraction by arsine oxides Ph_3AsO (1, 3, 5) and R_3AsO (2, 4, 6).⁵²

strength of the acid and in the degree of extraction by the cation-exchange mechanism.

We may note yet another, albeit less striking, anomaly, which has been observed in the extraction of nitric acid by arsine oxides.⁵⁶ In the weakly acid region, the extraction constant K_{1H} for the first acid molecule depends on the electronegativity of the substituents and on the basicity of the arsine oxides in conformity with Eqns (4) and (7) (for Ph_3AsO , $Ph_2AlkAsO$, $PhAlk_2AsO$, and Alk_3AsO , the constant is 3×10^2 , 3×10^3 , 5×10^4 , and 5×10^5 respectively); in the strongly acid region, the isotherms for the extraction of HNO_3 by all four arsine oxides are virtually identical [see Rozen et al.⁵⁶ (Table 3)].

If inorganic acids are extracted by R_3AsO and R_3NO with extraction constants in the range 10^6 – 10^{10} , they immediately become actual competitors of the metals and are no longer salting-out agents (like HNO_3 in the extraction of metal salts by TBP).

In conclusion we may note that, by varying the substituents and the reaction centre (SO, PO, AsO, NO), it is possible to alter the EA of organic oxides in any required direction by 15–18 orders of magnitude (Fig. 5b).³⁷

VI. Salts of amines and quaternary onium bases

Inorganic acids are extracted by amines via an addition reaction⁵⁵ with extraction constants of 10^5 – 10^7 , characteristic of the formation of proton-transfer complexes, i.e. the amine salts, for example $(R_3NH)^+A^-$. Amine salts are in their turn effective extractants for acids and metal salts. In the latter case, extraction can be described either as anion exchange or as an addition reaction: the two types of reaction are thermodynamically indistinguishable. In the complexes formed [for example, $(R_3NH)^+(UO_2A_3)^-$ or $(R_3NH)_2^+(PuA_6)_2^{2-}$], the metal is present in the anion and the extractant is in the outer sphere of the complex.⁵⁷ However, in the extraction of platinum metals, very stable complexes with a direct metal–amine nitrogen atom coordinate bond, called insertion complexes, were detected together with the anion-exchange complexes.⁵⁸

The electronegativity of hydrogen (2.3) is higher than that of an alkyl group (2.0), so that EA increases in the series primary amine salts < secondary amine salts < tertiary amine salts < quaternary ammonium (QA) salts (Fig. 8). The difference

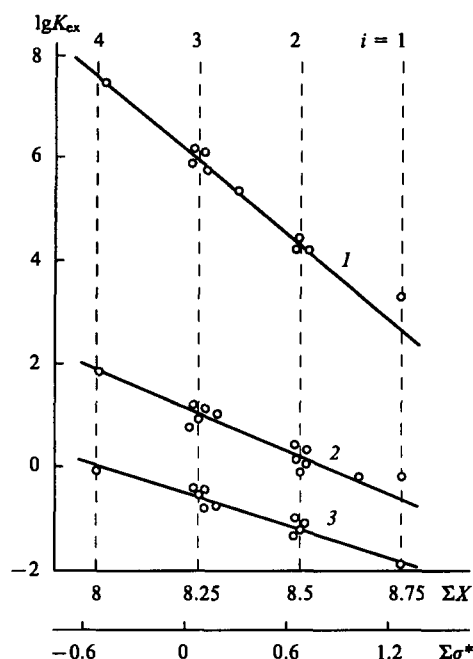


Figure 8. Dependence of EA on the electronegativities sum and the Taft constants of the extractants in the extraction of Pu(VI) (1), U(VI) (2), and HNO₃ (3) by salts of primary amines — quaternary ammonium bases series [R_iNH_{4-i}]⁺NO₃⁻, where *i* = 1, 2, 3, 4.⁶⁰

between amines and NOPC consists in a higher sensitivity to changes in EA ($B_{Pu} = 6.8$ instead of 4.8 for NOPC) and the length of the substituents. The question of the influence of association requires separate discussion. One should only note that, owing to the differences between the degrees of polymerisation, the above series is sometimes found to break down: primary amines extract more effectively than tertiary amines.

The correlation for the EA of amine salts may be represented also in the form of the dependence on the basicity; a linear increase in $\lg K_{ex}$ with increase in pK is observed in the above series. When the nature of the substituents in the amine molecules is varied widely, linear correlations are observed for the EA within the limits of each subclass of amines — primary, secondary, etc. (the corresponding straight lines are parallel). The increase in EA with increasing pK is characteristic of the anion-exchange extraction mechanism while on formation of coordination insertion complexes the opposite relation holds: the stability of the complexes increases in the series tertiary amines < secondary amines <

< primary amines, i.e. as the steric hindrance to coordination is weakened.

The extraction ability of amine salts depends also on the nature of the anions. Shmidt⁵⁹ proposed a two parameter correlation of the extraction constant with the hydration parameter ΔG_{hydr} and the influence of the diluent (ID):

$$\lg K_{ex} = \lg K_{ex 0} + a\Delta G_{hydr} + bBP. \quad (10)$$

The extraction ability of quaternary onium salts $R_4X^+NO_3^-$ (where R = octyl) in the series with X = N, As, or P has been investigated in relation to the extraction of nitric acid and uranyl and plutonium nitrates.³⁶ It was found that EA varies little in the above series. Thus the isotherms for the extraction of nitric acid by the nitrate salts of all three bases virtually coincide (Fig. 9a), while for uranyl and plutonium nitrates (Figs 9b and 9c) a slight decrease in EA is observed [for example, the concentration constants for the extraction of the uranyl monocomplex $R_2X^+(UO_2(NO_3)_3)^-$ are respectively 5.3, 5.0, and 4.7 for the above extractant salts] Fig. 9 shows that significant changes occur only when a second organic phase is formed: in the series N—As—P, the compatibility of the complexes formed with the diluent (CCl₄) increases appreciably. Apparently the polarity and hence the degree of polymerisation of the extractants and complexes decrease somewhat in the above series. The first factor leads to a decrease in EA, whilst the second results in the improvement of the compatibility of the complexes with the solvent. The smallness of the changes in EA in the above series confirms the generally accepted idea that the interaction between the bulky cation in the outer sphere of the complex and the MA_{2-i}^{n-i-} anion is predominantly electrostatic. The important role of the cation-anion hydrogen bond is indicated by the fact that the smallness of the changes in EA in the series N > As > P does not correspond to the change in the size of the central atom (N < P < As), but coincides with the EA series for the oxides R_3XO .

VII. The influence of the length and degree of branching of substituents on the extraction ability of organic compounds

The overall steric effect of the substituents in extraction by neutral and ion-exchange compounds is determined by at least five factors. An increase in the bulk and degree of branching of the substituents leads as a rule to a decrease in the electronegativity of the substituent, a decrease in the solubility of the extractant in the aqueous phase, an increase in the steric hindrance to complex formation, a decrease in the degree of polymerisation of the extractant, and a decrease in the rotational partition function.⁶¹

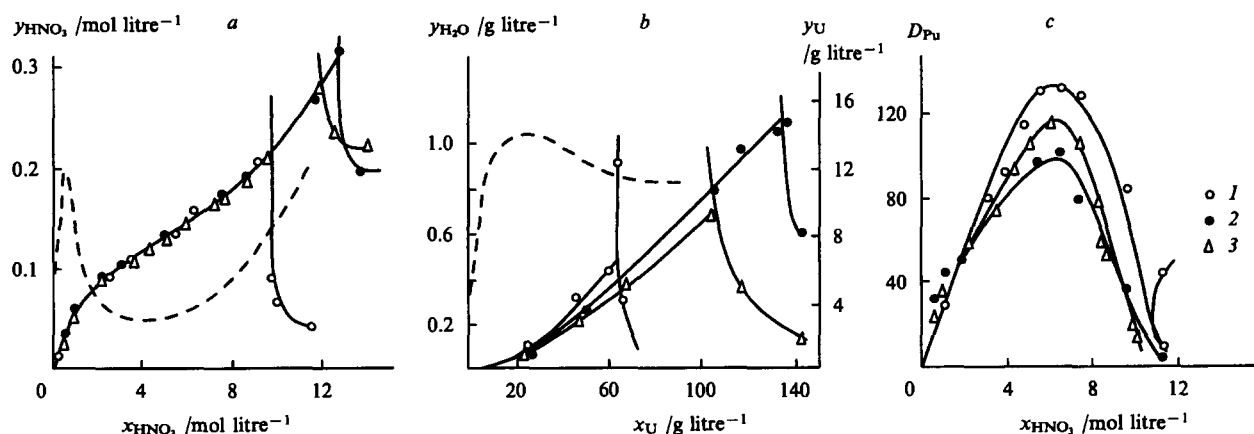


Figure 9. Extraction isotherms of nitric acid (a) and uranyl (b) and plutonium (c) nitrates by onium nitrates $R_4X^+NO_3^-$, where X = N (1), P (2), and As (3) (extractant concentration in CCl₄ 0.1 M); dashed curves — extraction of water.

The first two factors promote an increase in EA, while the others tend to decrease it. Evidently, for a moderate length of the alkyl substituents, the first two factors exert the greatest influence, whilst the importance of the remaining factors increases as a rule for bulky and branched substituents.

The length of the hydrocarbon chain of the substituent n_C particularly for the normal structure, influences comparatively slightly the extraction ability of NOPC and amine salts. Weak maxima have been noted on the $K_{ex} = f(n_C)$ curves for $n_C = 5-8$ (Fig. 10). These can be readily accounted for by the operation of the factors listed above. For NOPC, the coefficient ρ in Eqn (4) is small: $\rho(\text{UO}_2) = \rho(\text{Pu}) = 0.01$; for amine salts, it is appreciably higher: $\rho(\text{Pu}) = 0.12$ (see also Fig. 10 *b*).

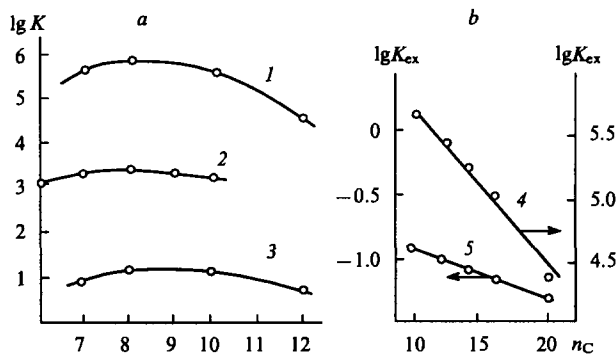


Figure 10. The influence of the length of the hydrocarbon chain in symmetrical trialkylamines on the extraction of uranyl and plutonium nitrates (*a*) and plutonium nitrate and nitric acid (*b*).

Substance extracted: (1) and (4) Pu(VI); (2) and (3) U(VI); (5) HNO₃. Extractant: (1), (3), and (5) amines; (2) and (4) phosphonates.

In the early studies on extraction (see, for example, Glueckauf and coworkers^{23, 24}) a marked decrease in the extraction constant with increase in the length of the hydrocarbon substituent was noted when extraction by undiluted alcohols and ethers was investigated. This relation could not be explained since the chemical nature of extraction was not yet understood. At the present time, the explanation is evident: when account is taken of the formation of complexes, the extraction constant (or more precisely the distribution constant) is proportional to L_0^q , where L_0 is the initial concentration of the extractant (on the molar scale) and q is the solvation number. The initial extractant concentration diminishes with increase in the length of the hydrocarbon chain and in the molecular mass ($L_0^q = 9.8, 7.5$, and $5.9 \text{ mol litre}^{-1}$ for diethyl, dipropyl, and dibutyl ethers respectively). The third factor apparently also plays a role, because hydrocarbon chains are attached directly to the donor centre — the oxygen atom.

The influence of steric hindrance is clearly manifested in the extraction of uranyl and trivalent lanthanide and actinide nitrates by the amides of alkylphosphoric acids. Very high EA of such compounds have been reported, in particular of the hexabutyl phosphorous trisamide (HBTA), which greatly exceeds the EA of trialkylphosphine oxides.[‡] A careful check of the extracting properties of HBTA⁶⁶ led to unexpected results. It was found that, in extraction by nitric acid, where monosolvates are formed both with HBTA and TOPO, the extraction isotherms virtually coincide (Fig. 11); a slight excess (in favour of HBTA) was observed only at a high HNO₃ concentration, i.e. in the region

where semisolvate and one-third solvates are formed. On the other hand, in extraction by hydrochloric, perchloric, and sulfuric acids, where disolvates are formed, HBTA extracts much less effectively than TOPO (Fig. 12, Table 5). A decrease in extraction occurs also in the extraction of uranyl nitrate, where disolvates are also

‡ The greater complex-forming capacity of the amides is indicated also by the higher Gutmann donor number, although the gas-phase basicities of the amides and phosphine oxides are practically identical.⁴¹

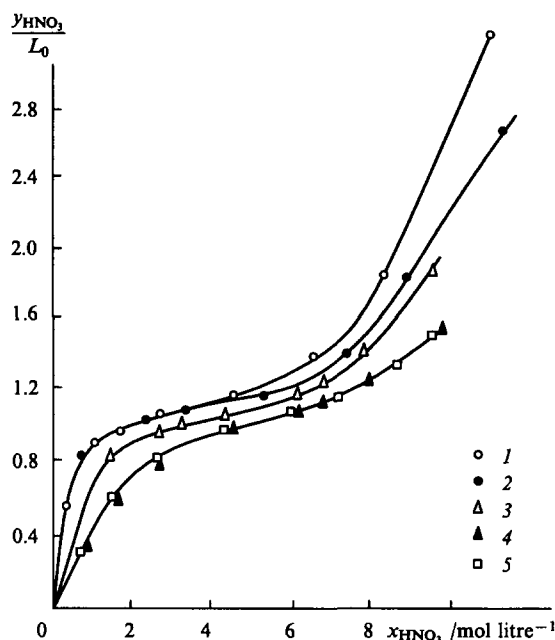


Figure 11. Extraction isotherms of HNO₃ by extractant solutions in benzene.

Extractant: (1) HBTA; (2) TOPO; (3) (NBu₂)₂BuOPO; (4) NBu₂(BuO)₂PO; (5) DPMP; extractant concentration (mol litre⁻¹): (1) and (2) 0.25; (3)–(5) 1.0.

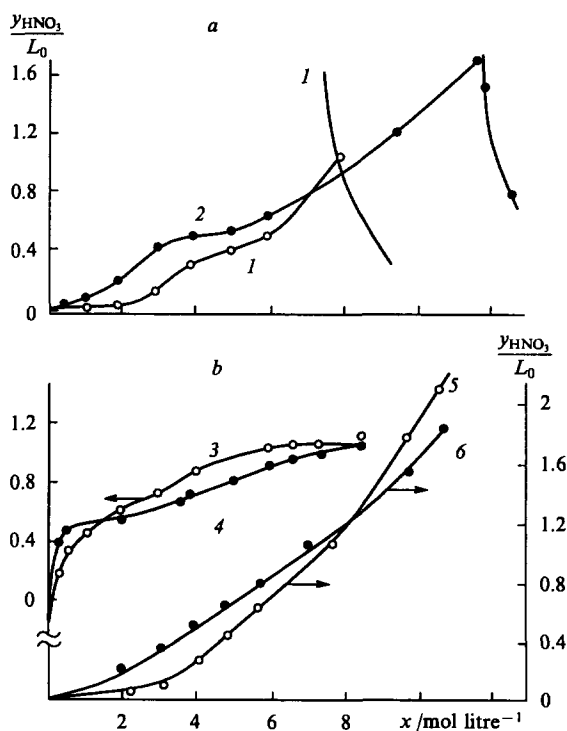


Figure 12. Extraction isotherms of acids by extractant solutions in benzene (0.25 M).

Acid: *a*: (1) and (2) H₂SO₄; *b*: (3) and (4) HClO₄; (5) and (6) HCl; extractant: (1), (3), and (5) HBTA; (2), (4), and (6) TOPO.

Table 5. Constants for the extraction of acids by solutions of TOPO and HBTA in benzene in the form of disolvates (K_2), monosolvates (K_1), hemisolvates ($K_{1/2}$), and one-third solvates ($K_{1/3}$).

Acid	Extractant	K_2	K_1	$10^3 K_{1/2}^a$	$K_{1/3}^a$
HNO ₃	TOPO	0	18.5	1.7	1.4×10^{-5}
	HBTA	0	18.5	2.9	3.3×10^{-5}
HClO ₄	TOPO	1620	0.98	0	0
	HBTA	112	0.91	0.0048	2
HCl	TOPO	0.146	0.02	2.2×10^{-4}	—
	HBTA	0.014	0.0049	—	2.34×10^{-2}
H ₂ SO ₄	TOPO	29.7	0.27	2.8×10^{-4}	—
	HBTA	1.42	0.07	3.5×10^{-4}	—

^a The increased constants $K_{1/2}$ and $K_{1/3}$ for HBTA may be associated with coordination to the nitrogen atom.

formed. The lowest degree of extraction (lower by 3–4 orders of magnitude) is that of the trivalent americium and cerium, which are extracted in the form of disolvates. These results can be explained solely by the influence of the steric hindrance generated by the amide groups, the steric effect increasing non-linearly. For example, for uranyl nitrate, we have

$$\lg K_{\text{ex}}[(\text{NR}_2)_n\text{R}_3\text{—}_n\text{PO}] = \lg K_{\text{ex}}(\text{R}_3\text{PO}) - 0.15n^2.$$

The steric and electronic structures and the electron-donating capacities of a series of carbonyl compounds with amide groups, namely the ketone–carboxylic acid amide–urea series, have also been investigated. It was found that the nonadditivity of the influence of the amide groups in these systems (the strong influence of the first amide group and the weak influence of the second) is due to the geometrical hindrance to the conjugation in substituted amides and ureas. This hindrance increases with increase in the number of amide groups and in the length of the hydrocarbon groups (this system is examined in greater detail below). A characteristic feature of extraction with participation of amides is the strong influence of the length of the amide groups on the compatibility with HNO₃ solutions and even on the stoichiometry of the complex-formation reaction.⁶⁷ Thus, whereas, in the extraction of uranyl nitrate by the amide OctC(O)NR₂, where Oct = C₈H₁₇, the disolvate ($K_2 = 9.6$, $K_3 = 0.7$) is formed preferentially for R = Bu, in the case where R = C₁₂H₂₅ the main product is the trisolvate ($K_3 = 6.3$, $K_2 = 1.2$). Taking into account the increase in steric hindrance, one may postulate that the extractant molecule in the trisolvate is coordinated via a water molecule.

VIII. The use of quantum-chemical calculations for predicting extraction ability

It was shown above that equations similar to Eqns (4) and (5) have been obtained for neutral oxygen-containing compounds, amine salts, and quaternary ammonium salts. At the same time, the electronegativities and constants of the substituents may be used to predict EA only for short series of compounds with one reaction centre. The employment of these parameters is also limited by the assumption that the influence of the substituent is additive. This assumption is in many cases invalid.^{67, 68} Thus in the series of ketone–amide–urea carbonyl compounds, the effects of the first and second amide groups are not equivalent⁵⁴, i.e. there is no additivity. It is therefore useful to employ characteristics calculated by quantum-chemical methods, which are free from the assumption that the influence of the substituents is additive.

Examination of the correlation of EA with quantum-chemical parameters in different series of neutral compounds permits certain conclusions. It is possible to test the hypothesis put forward in early studies that EA is determined by the electron density (charge) on the functional atom. For this purpose, the effective charges on the oxygen atom of the phosphoryl group in a series of NOPC have been calculated. It was found that in the general case the accuracy of the estimates of the effective charges by different molecular orbital methods may be insufficient for a reliable prediction (which is aggravated also by the arbitrary features of the method of analysis of the Mulliken populations itself.)

A more reliable characteristic of the distribution of electron density in the molecule is the energy of the molecular core levels, the values of which not only depend on the effective charge on the atom but also take into account the influence of the field of other atoms.

The correlation between the energy of the 1s core levels of the donor oxygen atom ($E_{1s,O}$) and EA is characteristic for a large series of extractants with different reaction centres (Fig. 13). The nonlinearity of the dependence of $\lg K_{\text{ex}}$ on $E_{1s,O}$ is apparently due to the changes in the complex formation mechanism (noted above) with increase of the extractant basicity. On the other hand, the deviation of the points corresponding to amides and ureas indicates the restricted nature of the correlations deduced from the characteristics of isolated extractant molecules. The point is that in compounds of this kind an appreciable stabilisation of the system occurs directly on complex formation as a result of the conjugation of the bonds. The use of the energies of test reactions for prediction of EA therefore appears more justified. In addition, such energies make it possible to take into account simultaneously components of the energy of the EDA interactions such as the electrostatic, charge-transfer, geometrical ligand rearrangement, and polarisability components. Indeed, the points corresponding to amides and ureas, which deviate in Fig. 13, in Fig. 14 are found to be close to the overall correlation describing the dependence of EA on the energy of the simplest test reaction, namely protonation.

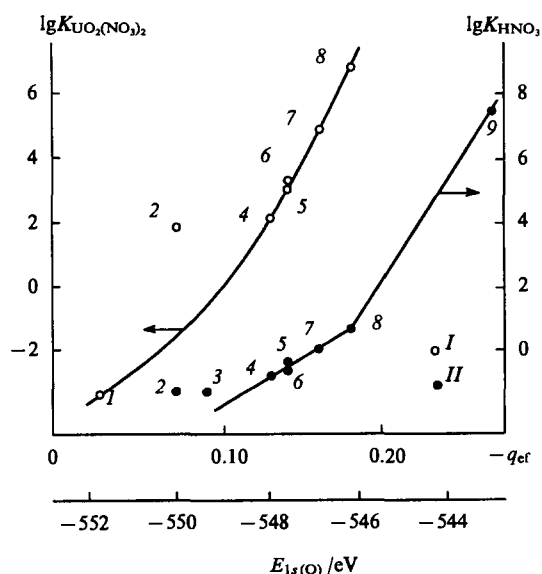


Figure 13. Dependence of the uranyl nitrate (I) and nitric acid (II) extraction constants on the energy of the 1s core levels of the oxygen atom and the effective charge on the oxygen atom. Extractant: (1) R₂CO; (2) (NR₂)₂RCO; (3) (NR₂)₂CO; (4) (RO)₃PO; (5) R₂SO; (6) (RO)₂RPO; (7) (RO)R₂PO; (8) R₃PO; (9) R₃NO.

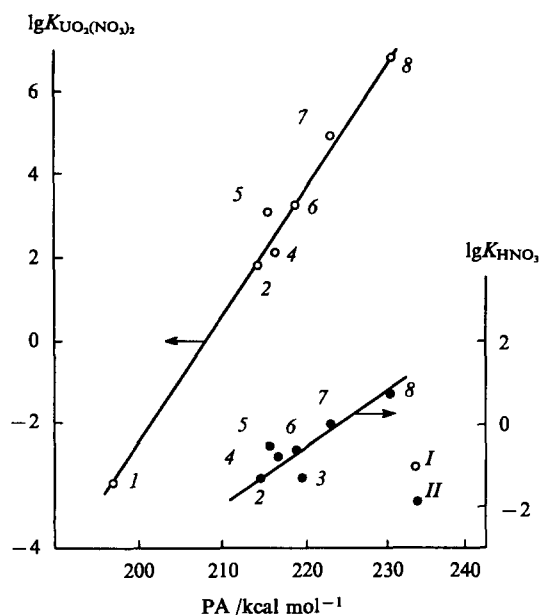


Figure 14. Dependence of the uranyl nitrates (I) and nitric acid (II) extraction constants on the proton affinity calculated by the AM1 method. Extractant: (1) R_2CO ; (2) $(NR_2C)RCO$; (3) $(NR_2)_2CO$; (4) $(RO)_3PO$; (5) R_2SO ; (6) $(RO)_2RPO$; (7) $(RO)R_2PO$; (8) R_3PO .

The ketone-carboxylic acid amide-urea series (three points in Fig. 15) merits a more detailed consideration because this is one of the examples of the nonadditivity of the influence of the substituents. The effects arising from the introduction into the ketone molecule of the first and second amide groups are non-equivalent. The introduction of the first group increases the degree

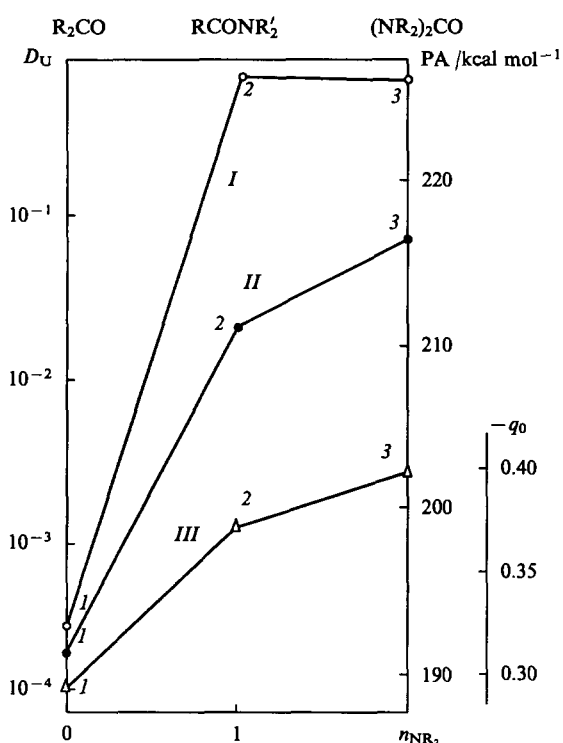


Figure 15. Dependence of the distribution coefficient of uranyl nitrate (I), the proton affinity (II), and the effective charge on the oxygen atom (III) on the structure of the extractants. Extractant: (1) ketone; (2) carboxylic acid amide; (3) urea.

of extraction of uranyl nitrate by three orders of magnitude, whilst the second contributes little.⁶ The frequencies of the carbonyl group vibration (ν_{CO}), the solvate shift of the frequency of the hydroxy-groups of phenol on complex formation ($\Delta\nu_{OH}$), the Gutmann donor number (D_N), and the entropy of formation of a complex with BF_3 (ΔH) also change in steps (Table 6). It is clear that, since the standard correlation approaches presuppose the additivity of the influence of the substituents, they are ineffective in this case. On the other hand, the characteristics calculated by the quantum-chemical method — the charges on the oxygen atom, the energies of the core levels, and the proton affinity (PA) — also vary stepwise in the above series, like the physicochemical properties (Fig. 15), and may be used for correlation with extraction data (PA is employed for correlation within a large series of compounds with different reaction centres). The advantages of the quantum-chemical approach to the interpretation and prediction of EA have been strikingly manifested for the series of compounds considered.^{68, 69}

Table 6. Properties of carbonyl compounds.

Compound	$10^2 D$		ν_{CO} /cm ⁻¹	$\Delta\nu_{OH}$ /cm ⁻¹	D_N	ΔH /kcal mol ⁻¹
	U(VI)	Pu(VI)				
R_2CO	0.037	0.068	1730	74	17.0	18.2
$NR_2C(O)R$	88.5	26.0	1640	200	27.8	26.8
$(NR_2)_2CO$	89.0	56.4	1642	208	29.6	26.0

Together with protonation, reactions with the simplest Lewis acids — H_2O , HNO_3 ,¹⁶ Li^+ , LiH , $LiCl$, $AlBr_3$, AlH_3 , etc. — may also be used as the test reactions.²² The thermodynamic parameters of the complex formation reactions between NOPC and the above acceptors have been calculated quantum-chemically by the modern semiempirical MNDO and AM1 methods.⁶⁹ It was found that the above reaction series is isentropic, which demonstrates the validity of the correlation between EA and the enthalpies of complex formation.

An advantage of the prediction of EA from the values of PA is the relative simplicity of the calculation of EA. At the same time, limitations have also been discovered. Calculations have shown that, in the case of complexes with a weak EDA interaction, alkylphosphine oxides form more stable complexes than their phenyl-substituted analogues, i.e. the phenyl group behaves as an electronegative substituent.²² This is manifested also in all the known cases of the extraction of metals by monodentate NOPC.^{6, 12, 34} For example, in the NOPC series, the introduction of one phenyl group instead of an alkyl group diminishes the extraction constant by a factor of 17 for uranyl nitrate and a factor of 8 for americium nitrate. On the other hand, in the formation of more stable complexes with a proton an inversion is observed: phenyl substituents become electron donors. Therefore in the presence of amphoteric substituents in the reaction series, reactions not with a proton but with a weaker acceptor must be used as the test processes. The test reaction with water, which is ideal from this standpoint, suffers from a significant disadvantage — a small variation of the enthalpy of complex formation within the limits of the reaction series.

§ The main cause of the weak influence of the second amide group is the steric hindrance to the conjugation of the lone pair on the nitrogen atom of the amide group with the π -electron system of the carbonyl bond.

IX. Bidentate neutral organophosphorus compounds and the anomalous aryl stabilisation effect

Bidentate neutral organophosphorus compounds (BDNOPC) are powerful extractants. Analysis of the dependences of the distribution coefficients of americium presented in Figs 16 and 17 shows that in extraction by BDNOPC these coefficients are higher by 3–6 orders of magnitude than in extraction by monodentate NOPC. In particular, they are promising for the extensive extraction of the actinides from waste in radiochemical industries. At the same time, they are of considerable interest because of the unusual dependence of EA on the structure of the extractants. Deviations of relations (4) and (7) have been observed in the study of the extraction ability of alkylendiphosphine dioxides $R'_2P(O)(CH_2)_nP(O)R''_2$,⁷¹ and carbamoylmethylphosphine oxides $R'R''P(O)CH_2C(O)NR'''$ (abbreviated to $R'R''/R'''$). Admittedly, on formation of complexes with monodentate coordination, characteristic of the extraction of inorganic acids (HNO_3 , $HClO_4$),^{70,71} relations (4) and (7) hold qualitatively. The introduction of electronegative substituents at the phosphorus atom in place of alkyl groups lowers the degree of extraction [in particular, in the 4Oct–2Oct2Ph–4Ph series (Fig. 18)].

Eqn (4) then holds quantitatively for HNO_3 : the dependence of the logarithm of the extraction constant on the sum of the electronegativities or the Taft constants of the substituents is linear.⁷⁰ Deviations from linearity have been observed for $HClO_4$ (Fig. 19): the introduction of the first two phenyl groups greatly reduces EA, while the introduction of the next two groups has a smaller effect. In the extraction of trivalent actinides and lanthanides, complexes with bidentate coordination are formed. In this case, the replacement of alkyl groups by more electronegative groups such as $AlkO$ or $Cl(CH_2)_2$ also lowers EA (Table 7). However, when phenyl (or other aryl) group which have the electronegativity like $Cl(CH_2)_2$ are introduced into molecules of

¶ The following abbreviations have been adopted below: if $n = 1$ and $R' = R''$ the extractant is designated by 4R, if $R' \neq R''$ the designation is $2R'2R''$, and if $n > 1$ and $R' = R'' = Ph$ the designation of the extractant is 4Ph(CH_2)_n.

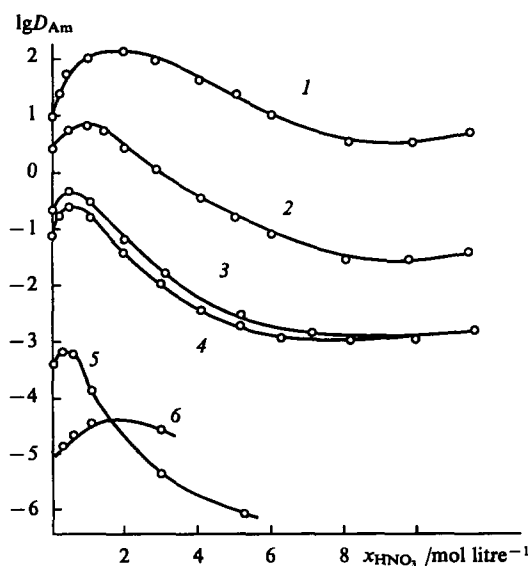


Figure 16. Dependence of the distribution coefficient of americium in extraction by solutions of methylenediphosphine dioxides in dichloroethane (0.01 M) and of triphenylphosphine oxide and TOPO in dichloroethane (0.02 M) on the acidity. Extractant: (1) 4Ph; (2) 2Ph2Oct; (3) 4Oct; (4) 4Bu; (5) TOPO; (6) triphenylphosphine oxide (TPPO).

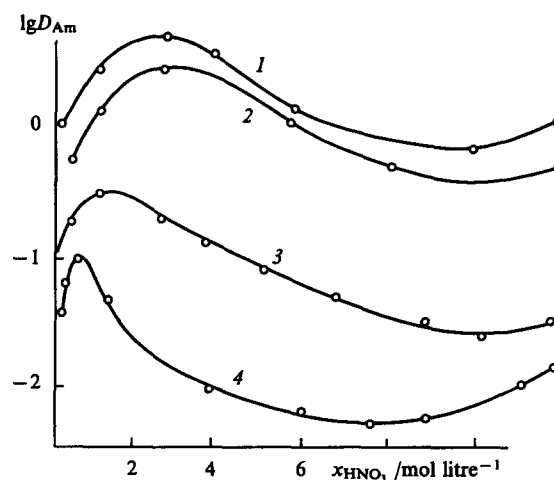


Figure 17. Dependence of the distribution coefficient of americium nitrate in extraction by solutions of carbamoylmethylphosphine oxides in dichloroethane (0.05 M). Extractant: (1) Tol_2/Bu_2 ; (2) Ph_2/Bu_2 ; (3) $OctPh/Bu_2$; (4) Oct_2/Bu_2 .

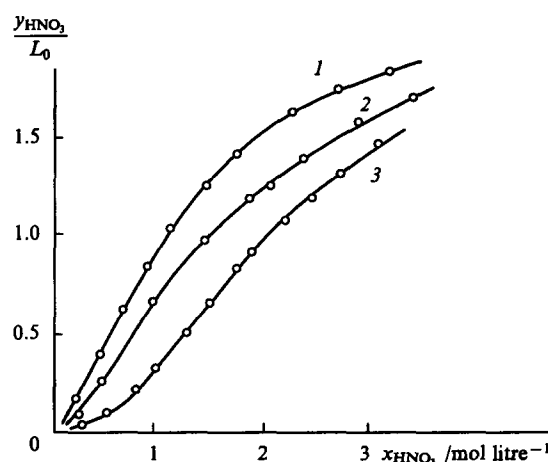


Figure 18. Isotherms for the extraction of nitric acid by solutions of methylenediphosphine dioxides in dichloroethane (0.025 M). Extractant: (1) 4Oct; (2) 2Oct2Ph; (3) 4Ph.

extractants Nos 1 and 4, instead of alkyl groups, relations (4) and (7) are infringed. Despite the increase in the electronegativity of the substituents and the decrease in the basicity of the methylenediphosphine dioxides, the distribution coefficients and extraction constants of trivalent americium and the lanthanides increase almost by two orders of magnitude (Figs 16 and 20). This effect, first observed by Rozen et al.⁷⁴ and discussed in a number of communications,^{22,72–79,81–87} has been called the anomalous aryl stabilisation (AAS). The data presented in Table 7 indicate

Table 7. The effective constants for the extraction of americium(III) from nitric acid solutions of $R'_2P(O)CH_2P(O)R''_2$ in the form of disolvates (determined by a method involving dilution in dichloroethane).^{72–74}

No	Extractant		ΣX	K_{ex}
	R'	R''		
1	Oct	Oct	8.0	1.6×10^7
2	BuO	Bu	9.6	5.0×10^3
3	$Cl(CH_2)_2$	$Cl(CH_2)_2$	9.32	3.5×10^3
4	Oct	Ph	8.66	1.0×10^8
5	Ph	Ph	9.32	6.5×10^8
6	Bz	Bz	—	8.0×10^3
7	EtO	Ph	9.46	2.2×10^3

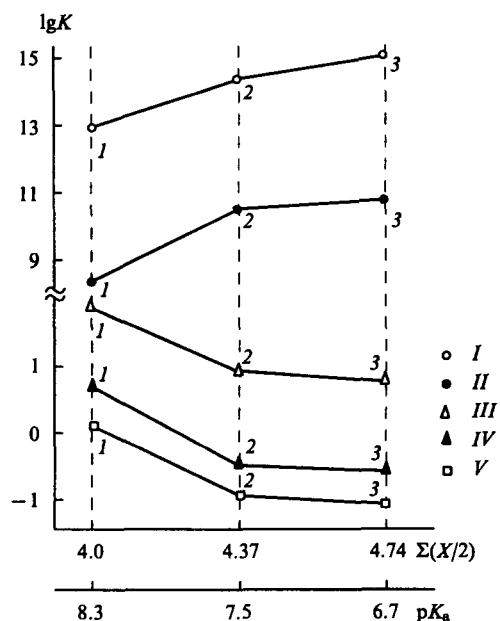


Figure 19. Dependence of the effective perchloric acid and americium extraction constants on the basicity and the sum of the electronegativities of methylenediphosphine dioxides.⁷¹

Substance extracted: (I) americium trisolvate; (II) americium disolvate; (III) molecular form of perchloric acid disolvate; (IV) perchloric acid monosolvate; (V) ionic form of perchloric acid disolvate; extractant: (1) 4Oct; (2) 2Oct2Ph; (3) 4Ph.

that the effect is associated not with the electronegativity but with the chemical nature of the aryl groups.

Yatsimirskii, Kabachnik, and coworkers⁸⁰ found in their conductimetric study of the formation of complexes by methylenediphosphine dioxide with certain metals in acetonitrile that the constant for the formation of a complex between NaI and 4Ph is somewhat higher than for the alkyl-substituted dioxide. However,

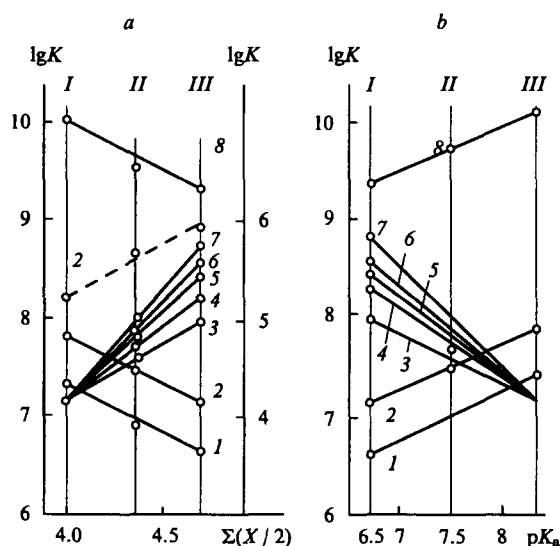


Figure 20. Dependence of the extraction constants for the actinides and lanthanides by extraction with solutions of methylenediphosphine dioxides on the sum of the electronegativities of the substituents (a) and the basicity (b).

Diluent: dichloroethane (continuous lines, left-hand scale), chloroform (dashed line, right-hand scale); extractant: (I) 4Ph; (II) 2Oct2Ph; (III) 4Oct; substance extracted: (1) Pu(VI); (2) U(VI); (3) Pr(III); (4) Pm(III); (5) Eu(III); (6) Cm, Pu(III); (7) Am(III); (8) Pu(IV).

they did not pay attention to this result, did not point it out in their conclusions, and did not note the anomaly. This may have been because the dependence of the complex formation constant on the basicity of the ligand was not investigated (and possibly also because the effect differs little from the experimental error, which in view of the abundance of assumptions made in the method, the authors estimated very optimistically as within the limits of 20%). The authors confined themselves to the hypothesis that an exotic compound is formed: a six-membered ring is not closed via two oxygen atoms through a metal cation but via an anion — through phosphorus. After more than a decade since the anomaly had been discovered by Rozen et al.⁷⁴, Yatsimirskii et al.⁸⁰ carried out a systematic study in which they replaced acetonitrile by tetrahydrofuran and found⁸¹ that the AAS effect is observed on formation of complexes of alkali metal and copper ions with methylenediphosphine dioxides and carbamoylmethylphosphine oxides in ionising solvents (Table 8).

Table 8. The logarithms of the stability constants of the alkali metal complexes ML^+ of $R'R''P(O)CH_2C(O)NEt_2$ and $R_2P(O)CH_2P(O)R_2$ in tetrahydrofuran.⁸¹

M	Ph ₂ /Et ₂	PhBu/Et ₂	Bu ₂ /Et ₂	4Ph	4Bu
Li	3.69	3.38	3.11	4.72	3.92
Na	3.59	3.24	3.08	—	—
K	2.73	2.48	2.35	—	—

The AAS effect is observed in various media [HNO_3 (Fig. 16), HCl , and H_2SO_4 (Fig. 21)] and is particularly large in perchloric acid solution (Fig. 22), which we believe can be accounted for by the increase in the solvation number as a consequence of the decrease in the denticity of the metal-anion bond (the extraction constant for the trisolvate is $\sim 10^{13}$). The increase in lgK_{ex} as phenyl groups are introduced is nonlinear (the first two groups make the main contribution).⁷⁷ The AAS effect depends also on the nature of the trivalent element (Fig. 20).^{74,78} In the case of tetravalent and hexavalent actinides, the distribution coefficients increase following the replacement of alkyl groups by phenyl groups, while the extraction constants diminish slightly [there is 'apparent' stabilisation (Fig. 23)]. This can be explained by the

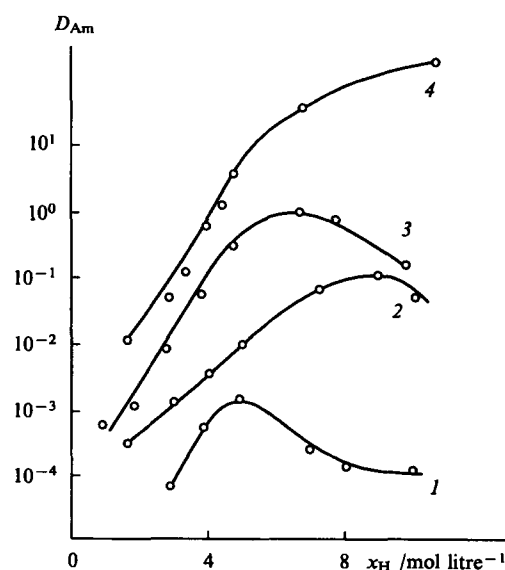


Figure 21. Dependence of the distribution coefficient of americium in extraction by solutions of diphosphine dioxides in dichloroethane (0.01 M) from sulfuric acid (1, 3) and hydrochloric acid (2, 4) solutions on the acidity: (1) and (3) 4Oct; (2) and (4) 4Ph.

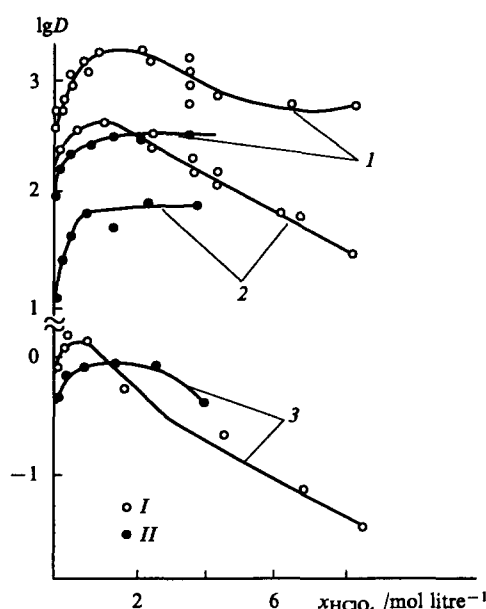


Figure 22. Dependence of the distribution coefficients of americium (I) and europium (II) in extraction by solutions of methylenediphosphine dioxides in dichloroethane (0.001 M) from perchloric acid solutions.⁷⁵ Extractant: (1) 4Ph; (2) 2Oct2Ph; (3) 4Oct.

fact that the increment in ΔG due to the AAS ($\sim 3 \text{ kcal mol}^{-1}$ for two phenyl groups according to the estimate by Rozen et al.⁷⁸) is insufficient for the given elements to overcome the negative inductive effect of the phenyl groups (we may recall that the coefficients of the sensitivity to electronegativity B in extraction by NOPC are 3.1 for americium and 4.6 for tetravalent and hexavalent actinides, i.e. are much greater). On the other hand, the increase in the distribution coefficient is attained as a result of the suppression of the extraction of HNO_3 by electronegative aryl groups and the corresponding increase in the concentration of the free extractant.⁸²

When chloroform is used as the diluent, true AAS is observed for tetravalent and hexavalent actinides (Fig. 20a). This can be explained by the enhancement of the oxygen–chloroform interaction in the 4Ph–2Ph2Oct–4Oct series with a corresponding decrease in the EA for oxygen. When chloroform is employed, the solvation number probably increases from two to three^{5,76} as a consequence of the depolymerisation of the extractant.⁷⁶ Nor can

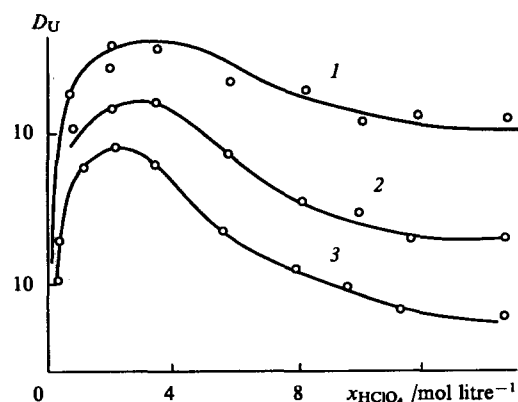


Figure 23. Dependence of the distribution coefficients of uranium in the extraction of uranyl nitrate by methylenediphosphine dioxides (apparent AAS). Extractant: (1) 4Ph; (2) 2Oct2Ph; (3) 4Oct.

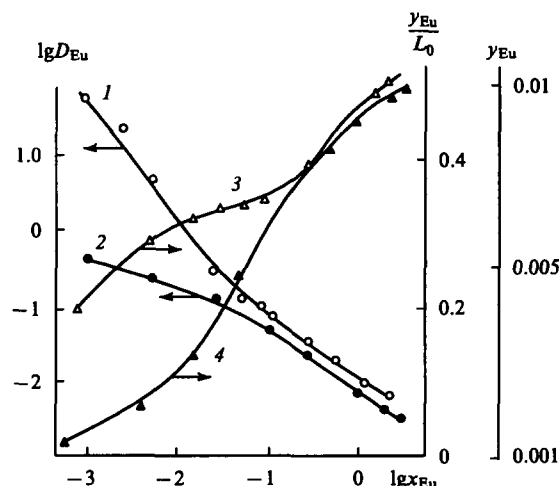


Figure 24. Distribution coefficients (1, 2) and isotherms (3, 4) for the extraction of macroamounts of europium by solutions of methylenediphosphine dioxides in dichloroethane (0.02 M). Extractant: (1) and (3) 4Ph; (2) and (4) 4Oct.

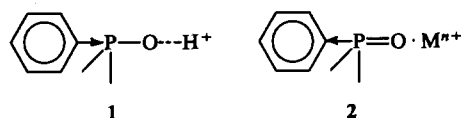
one rule out the interaction of chloroform with the methylene bridge of the dioxide.⁷⁸

An unexpected result was observed in the extraction of macroamounts of europium nitrate by solutions of tetraalkyl- and tetraphenyl-methylenediphosphine dioxides in dichloroethane. Whereas in the extraction of microamounts of americium or europium by the above extractants in dichloroethane the formation of disolvates was observed (according to data concerning the influence of dilution in dichloroethane), in the extraction of europium nitrate the distribution coefficient diminishes rapidly as the extractant is saturated with europium, owing to the formation of a trisolvate [a small plateau is observed on the extraction isotherm (Fig. 24)], after which the distribution coefficients for the extractants are the same.⁷⁶

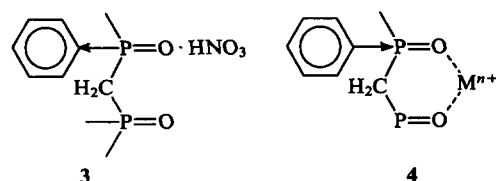
The anomalous aryl stabilisation in the extraction of americium has been noted also for carbamoylmethylphosphine oxides (Fig. 17);^{84–87} as for methylenediphosphine dioxides, the effect is enhanced in perchloric acid solution.^{88–90} However, owing to the lower extraction ability of carbamoylmethylphosphine oxides compared with methylenediphosphine dioxides, extraction from sulfuric acid solutions was not observed. Finally, the AAS has been observed⁸¹ in the formation of complexes of alkali metal ions and CuCl with carbamoylmethylphosphine oxides and methylenediphosphine dioxides (Table 8).

The occurrence of the AAS and the breakdown of relations (4) and (7) in extraction with BDNOPC indicate a significant rearrangement of the extractant molecule on complex formation. Therefore, as in extraction by amides, the prediction of EA on the basis of the characteristics of an isolated extractant molecule becomes incorrect.

The question arises of the nature of the AAS. Calorimetric measurements (unfortunately there has only been one such study⁷⁶) indicate the bonding nature of the effect. A possible explanation, first put forward by ourselves,²² is the amphoteric nature of the aryl groups. Depending on the electron-accepting capacity of the group to which the phenyl group is attached, the latter may function both as an electron donor and acceptor.²² Quantum-chemical calculation has shown²² that in a complex of a monodentate NOPC with a proton (structure 1), the phenyl group is an electron donor. When the proton is replaced by a metal cation (structure 2) or an acid molecule, the phenyl group behaves as an electronegative substituent.



This means that the electron accepting capacity of the group attached to the phenyl substituent in structure 2 is lower than in structure 1 and is insufficient for the conversion of Ph from an electron-accepting into an electron-donating substituent. The same has been observed in the formation of a complex by a BDNOPC with monodentate coordination for example, in the extraction of nitric acid (structure 3).



On the other hand, for the bidentate coordination of the extractant to the metal (structure 4), the six-membered ring formed has a reduced electron-accepting capacity and the phenyl group is converted from an electron acceptor into an electron donor.

The disappearance of the AAS when the phenyl group is separated from the phosphorus atom by a CH_2 group (in the extraction of the tetraenzyl derivative of methylenediphosphine dioxide) indicates the π - π conjugation of the Ph group with the PO group, arising on formation of the complex (a six-membered ring) and also on delocalisation of the electron density from the Ph group to the ring. The decrease in the AAS almost by three orders of magnitude when the methylene bridge between the phosphorus atom is replaced by an ethylene group, its complete disappearance after the introduction of a propylene bridge (Fig. 25), and its restoration when a vinylene bridge is introduced (despite the expansion to a seven-membered ring), as well as the high mobility of the protons of the methylene bridge[†] in the complex also

[†] Shcherbakova has shown⁷⁶ that these protons acquire the capacity for deuterium exchange, which is absent in the isolated extractant molecule.

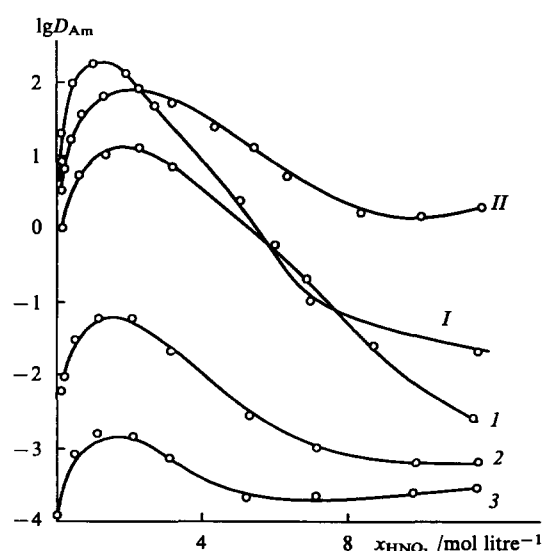


Figure 25. The influence of the length and structure of the bridge on the extraction of americium by $\text{cis-R}_2\text{P}(\text{O})\text{CH}=\text{CHP}(\text{O})\text{R}_2$ and $\text{Ph}_2\text{P}(\text{O})(\text{CH}_2)_n\text{P}(\text{O})\text{Ph}_2$. Extractant: (I) cis-4Tol with a vinylene bridge; (II) cis-4Ph with a vinylene bridge; (1)–(3) $4\text{Ph}(\text{CH}_2)_n$, where $n = 1$ (1), 2 (2), 3 (3).

indicate the chemical nature of the effect. One may postulate that the ring is 'aromatised' — the formation of a single system of conjugated bonds.

Thus there are arguments in support of the chemical (electronic) nature of the AAS effect. On the other hand, some evidence indicates its entropic character. Firstly, this conclusion has been reached⁷⁴ on the basis of the determination of the enthalpy of extraction from the temperature variation of the concentration extraction constant for trivalent americium in the series $4\text{Oct}-2\text{Oct}2\text{Ph}-4\text{Ph}$ (Table 9). Secondly, the changes in the extraction of HNO_3 , in the IR spectra of the PO group, and in X-ray photoelectron spectra indicate a decrease in the electron-donating capacity of the oxygen atom in the phosphoryl group in the above series (which, admittedly, does not rule out stabilisation on complex formation and cyclisation via the metal cation).

Table 9. The americium extraction constants and the enthalpies of extraction calculated from their temperature dependence (0.01 M solutions of the extractants in dichloroethane).⁷⁴

Parameter	4Oct	2Oct2Ph	4Ph	4Ph(CH ₂) ₂
K_{Am}	1.5×10^7	1×10^8	6.3×10^8	5×10^5
$-\Delta H$ (calc) /kcal mol ⁻¹	15.0	14.2	13.0	11.6

In their study of the extraction of Am(III) by carbamoylmethylphosphine oxides, Chiarizia and Horwitz⁹¹ noted that the AAS is observed only for a high polarity of the diluent (when the diluent parameter $\text{ID} > 3$, for example, nitrobenzene, nitromethane, and chloroform). In weakly polar media (tetrachloroethene, carbon tetrachloride, and *o*-xylene) the effect is absent; the solvation number then increases from 2 to 3. Taking into account these data, the authors concluded that the AAS is an effect of the diluent. However, by analysing our results,⁸³ we found that in extraction by methylenediphosphine dioxides the AAS effect is observed also when a weakly polar solvent (benzene) is employed (Fig. 26). It may be that the results of the above study⁹¹ can be accounted for by the loss of bidentate coordination with increase in the solvation number. At the same time Japanese investigators,^{92,93} who studied the NMR spectra, showed that carbamoylmethylphosphine oxides in trisolates are coordinated as bidentate species to cerium and europium atoms. Admittedly, the highly polar deuteriochloroform was used as the diluent, which may be the reason for the retention of the bidentate coordination.

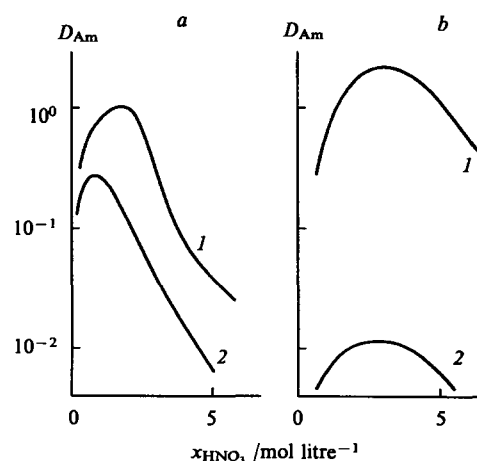


Figure 26. Isotherms for the extraction of americium(III) by 0.01 M solutions of methylenediphosphine dioxides in benzene (a) and chloroform (b). Extractant: (1) 4Ph; (2) 2Ph2Oct.

Thus the causes of the AAS have not been fully established and the contributions of the electronic and entropic effects have not been separated. Despite this, the AAS effect is useful in practice. In contrast to monodentate NOPC, including phosphine oxides which extract effectively tetravalent and hexavalent actinides but are ineffective in the extraction of trivalent actinides and lanthanides, the bidentate NOPC, especially those containing aryl groups, extract trivalent actinides with very high distribution coefficients.

The extraction ability of BDNOPC is influenced by the length and structure of the alkylene bridge. It was found that this influence depends both on the nature of the substituents in the BDNOPC molecule and on the properties of the compound extracted. For example, in the extraction of uranyl nitrate by alkylendiphosphine dioxides with alkyl substituents, the influence of the length of the bridge is small and the highest EA is observed in the case of the ethylene bridge (Fig. 27a).⁹⁴ The chelation effect is then small (<10), but, if uranyl nitrate is replaced by the perchlorate, the chelation effect is 10^5 and is suppressed on lengthening the bridge, i.e. the AAS effect, which is suppressed following an increase in the length of the bridge, is observed. In the case of aryl substituents, the effect of the bridge length is very strong (Figs 25 and 27) probably because the AAS effect is suppressed; in the case of the propylene bridge, the EA is lowest and corresponds to the electronegativity of the aryl

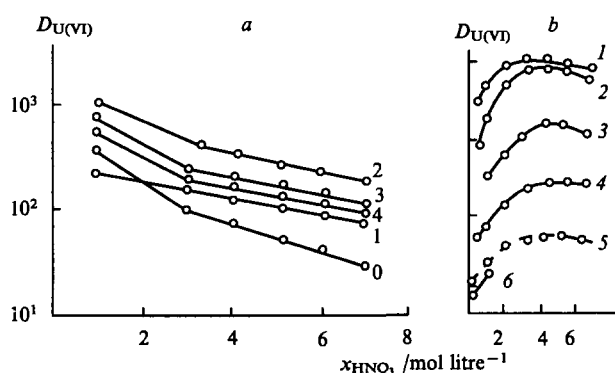


Figure 27. The influence of the length and structure of the bridge on the extraction of U(VI) by diphosphine dioxides.

(a) Extraction by tetrahexylalkylendiphosphine dioxides; the numerals opposite the curves indicate the length of the alkylene bridge; (0) extraction by TOPO; (b) extraction by dioxides with vinylene and alkylene bridges.

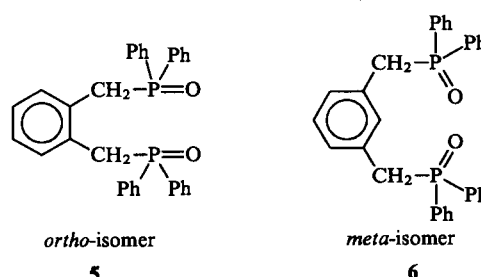
Extractant: (1) *cis*-4Tol; (2) *cis*-4Ph; (3) 4Ph; (4) 4Ph(CH₂)₂; (5) EtPh₂PO; (6) *trans*-4Ph.

substituents. As we have already mentioned, when a vinylene bridge is introduced in the *cis*-position, the conjugation and the AAS are restored but in the case of uranyl nitrate an appreciably higher EA is attained than for the dioxide 4Ph,⁹⁵ while in the extraction of americium the EA is lower⁸⁸ (Figs 27b and 25) by an order of magnitude in nitric acid and by as much as three orders of magnitude in perchloric acid. The dioxide with a vinylene bridge 'catches up' with the dioxide 4Ph only when the phenyl substituents are replaced by tolyl substituents (Fig. 25). Apparently the electronic and steric effects also play a role in this case. We may note that the difference between the shapes of the $D = f([HNO_3])$ curves for UO_2^{2+} and Am^{3+} can be explained by the difference between the stoichiometries: in the reaction with UO_2NO_3 , the monosolvate is formed together with the disolvate,⁹⁵ which lowered the displacing effect of HNO_3 and shifts the maximum in the distribution coefficient towards higher nitric acid concentrations.

The study of the influence of the replacement of hydrogen in the methylene bridge of methylenediphosphine dioxides and carbamoylmethylphosphine oxides by various substituents, for example, in the compounds $Ph_2P(O)CHY(O)PPh_2$ ($Y = C_3H_7$, CH_3 , or Cl) in the extraction of the actinides, showed that in all cases such replacement lowers appreciably the distribution coefficients.^{87,97,98} We found⁹⁷ that the AAS vanishes for $Y = C_6H_5$, i.e. both protons of the methylene bridge are needed for the appearance of the effect. Despite the decrease in EA, which is particularly marked (by four orders of magnitude) in perchloric acid solution, the selectivity diminishes. However, in the case of the methylenediphosphine oxide 4Ph, the introduction of a pyridine group into the methylene bridge increases significantly the distribution coefficient for the transplutonic element/lanthanide element pair.¹⁰⁰ For alkali metals, the introduction of methyl groups into the bridge increases the stability of the complexes.⁸¹ Steric effects apparently play an important role.

The influence of substituents in the benzene ring on the EA of the tetraaryl-methylenediphosphine dioxides 4Ar in chloroform has been investigated¹⁰¹ in relation to the extraction of uranium (trisolvates are extracted; $K_U = 0.7 \times 10^8$ may be found from the data¹⁰¹ for 4Ph). On passing from the unsubstituted phenyl group to *p*-tolyl (i.e. after the introduction of the CH_3 group into the benzene ring), the extraction constant increased by a factor of 1.5; after the introduction of a p - CH_3O group, the increase was by two orders of magnitude; the CH_3O group in the *meta*-position does not increase the degree of extraction. The replacement of CH_3O by C_4H_9O causes an additional increase in the constant by a factor of ~ 2 . The introduction of halogen-containing groups diminishes the solvation number from 3 to 2 and leads to a very marked decrease in the degree of extraction: for $Ar = ClC_6H_4$, BrC_6H_4 , p - $CF_3C_6H_4$, and *m*- $CF_3C_6H_4$, the extraction constants are respectively 130, 110, 70, and 14, i.e. diminish with increase in the electronegativity of the groups introduced. When alkyl groups attached to phosphorus atoms were introduced into the benzene rings of carbamoylmethylenephosphine oxides,¹⁰² an increase in the degree of extraction was observed, as for methylene diphosphine dioxides. The influence of the substituent at the nitrogen atom on the EA of carbamoylmethylphosphine oxides has also been investigated;¹⁰³ it proved to be weak and, when a phenyl group was introduced, there was no AAS effect.

Chmutova, Myasoedov, and coworkers^{104,105} investigated the extraction of nitric acid, americium, uranium, and plutonium by bidentate organophosphorus compounds with a rigid bridge (a benzene ring fragment) — the *ortho*- and *meta*-isomers of xylylenediphosphine dioxides (see also Rozen's review⁷⁹). It was found that the introduction of two $CH_2P(O)Ph_2$ groups in the *ortho*-position increases the selectivity of the separation of the U/Pu and Pu/Am pairs: the separation factor reaches 10^3 – 10^4 . This result has no practical significance (such separation factors are obtained also in extraction by TBP), but it is important because it indicates a possible way of increasing the selectivity by employing steric hindrance or rigid units †.



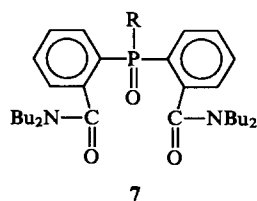
† The idea that rigid units should be used to improve selectivity is due to Kabachnik.¹⁰⁰

It is of interest that the *meta*-isomer of tetraphenylxylylenediphosphine **6** exhibits a much lower selectivity and basicity than the *ortho*-isomer **5**,^{194, 105} but it extracts actinides with appreciably greater distribution coefficients. The degree of extraction of americium by the *meta*-isomer is higher by three orders of magnitude — for example, $K_{ex\ o} = 3.26 \times 10^2$ and $K_{ex\ m} = 4.9 \times 10^5$ for tetra(*p*-tolyl)xylylenediphosphine dioxide. On the other hand, the degree of extraction of uranium and plutonium increases only severalfold on passing from the *ortho*- to the *meta*-isomers. The uranium/americium separation factor therefore diminishes by two orders of magnitude. These surprising results were explained¹⁰⁶ by the fact that, owing to steric hindrance, in the extraction by the *ortho*-isomer only complexes involving monodentate coordination are formed with the actinides. Under these conditions, the trivalent elements are poorly extracted (as in extraction by TBP), so that the An(IV)/An(III) or An(VI)/An(III) separation improves. On the other hand, in extraction by the *meta*-isomer complexes involving bidentate coordination are formed as a consequence of the decrease in steric hindrance, the degree of extraction of americium increases, and the Am/U and Am/Pu separation is less effective.

Judging from data on the extraction of nitric acid by tetraphenylxylylenediphosphine dioxide, the *meta*-isomer should be more basic: $K_{1o} = 0.0336$, $K_{1m} = 0.51$. This has also been confirmed by the AM1 quantum-chemical calculation: the *meta*-isomer forms more stable complexes with nitric acid than the *ortho*-isomer ($\Delta H = -8.6$ and -7.1 kcal mol⁻¹ respectively), which agrees with the observed difference between the extraction constants. It has been suggested¹⁰⁶ that, in the determination of *ortho*-isomer basicity by titrating the reagent with perchloric acid in nitromethane, a complex involving the bidentate coordination of the proton is formed. This in fact leads to an increased formal basicity. Indeed, our calculations by the AM1 method have shown that the *ortho*-isomer effects the bidentate coordination of the proton (the distance between the oxygen atoms of the phosphoryl groups is $R = 2.3$ Å) and with a much higher interaction energy ($PA = 256.2$ kcal mol⁻¹) than the *meta*-isomer, for which the coordination of the proton is monodentate ($R_{O...O} = 6.1$ Å, $PA = 224.1$ kcal mol⁻¹). On the other hand, the *meta*-isomer forms a more stable complex with the lithium cation than the *ortho*-isomer ($R_{O...O} = 2.8$ and 3.9 Å, $\Delta H = -41.8$ and -6.8 kcal mol⁻¹).

A phenomenon resembling the true AAS has been observed in such systems for a ten-membered ring.¹⁰⁵ The americium extraction constants have been determined for tetra(*p*-tolyl)-*m*-xylylenediphosphine and tetrabutyl-*m*-xylylene dioxides as 4.89×10^5 and 2.5×10^5 respectively. However, an americium extraction constant of 1.45×10^4 has been found for tetraphenyl-*m*-xylylenediphosphine dioxide, i.e. there is no true aryl stabilisation. Apparently for this ring size the energy increment corresponding to the AAS (~ 1 kJ per mole of Ph) is small and is insufficient to overcome the negative inductive effects of the phenyl group; the operation of steric factors may also prove to be important.

Carboxylic acid diamides are also effective bidentate extractants, for example, $CH_2[C(O)NOctMe]_2$, which has been proposed as an extractant for the actinides.¹⁰⁷ The tridentate dicarbamoylphosphine oxides **7** are interesting because the AAS effect is observed when the methyl group is replaced by the phenyl group.¹⁰⁸



The study of extraction by polyphosphine oxides containing three and four phosphoryl groups showed that the increase in EA compared with that of the dioxides was insignificant.¹⁰⁹

X. Polydentate neutral extractants — crown-ethers

Polydentate extractants (crown-ethers) are known to be stereospecific. The stereospecificity is manifested predominantly (not always owing to the flexibility of the rings) in the electrostatic interaction occurring in processes involving the extraction of alkali and alkaline earth metals. In the extraction of acids and metal salts (strong electron acceptors), electronic effects, especially EDA interaction play an important role.^{110–113}

In order to obtain quantitative data necessary for the determination of the dependence of the EA of crown-ethers on the structure, a study was made⁹⁸ of the extraction of nitric acid and plutonium, neptunium, uranyl, and thorium nitrates by crown-ethers of the type 18-crown-6 with different substituents. 18-Crown-6, dibenzo-18-crown-6, dicyclohexyl-18-crown-6, as well as dibenzo-ethers with alkyl or alkoxy-groups introduced into the benzene ring were used.⁵

The data obtained permit the conclusion that the rules characteristic of extraction by monodentate compounds hold. Thus, with increase in acidity, curves with a maximum (Pu) are observed. These are due to the combination of the salting-out and displacing effects of the acid.²⁷ The concave initial section of the uranium and thorium extraction isotherms is due to the dissociation of the salts in the aqueous phase. Plutonium and thorium form disolvates with crown-ethers, whilst uranium and HNO₃ form monosolvates. The extraction of actinides by crown-ethers depends greatly on their oxidation state as, in the case where monodentate extractants, for example, TBP, are used. The extraction ability increases in the sequence Th(IV) < Np(IV) < Pu(IV), etc.

At the same time, the equilibria involving crown-ethers are more complex than those involving monodentate extractants. The intense extraction of HNO₃ by crown-ethers is noteworthy: for an acidity > 6 M, it is much more pronounced than the extraction employing the most 'powerful' extractant among the NOPC — the phosphine oxide TOPO (Fig. 28 a). The complexes (HNO₃)_h(H₂O)_h·L, containing from one to twenty or more acid molecules per ligand molecule, are formed. The equilibrium has been described¹¹⁰ as the formation of a polymer chain with attenuation (a decrease in the constant for the addition of the last acid molecule with increase in its number). The usual description with the aid of a single constant¹¹¹ is inappropriate here. The first extraction constants observed for crown-ethers are higher than for ordinary ethers by two–three orders of magnitude, which indicates polydentate coordination. The thorium extraction isotherm was found to be complex. For thorium, dilution yields an apparent solvation number of 1, whereas according to saturation data it is 2. This contradiction has been explained¹¹⁰ by the dissociation of the complex in the organic phase. The constants for extraction by crown-ethers are presented in Table 10.

§ The extraction of HNO₃ and actinide nitrates has been investigated by Yakshin and coworkers.^{111, 112} Unfortunately the complexity of the equilibria in systems with crown-ethers (especially in the extraction of HNO₃, see below) was not taken into account in the above studies, the extraction constant was determined from one point, and a check was not made to make sure that the isotherm as a whole is described for this value of the constant (distribution data are not presented by Yakshin et al.¹¹¹). As a result, the quantitative extraction characteristics found by Yakshin and coworkers^{111, 112} and quoted in a review¹¹⁴ are only qualitative and may differ from the true values severalfold.

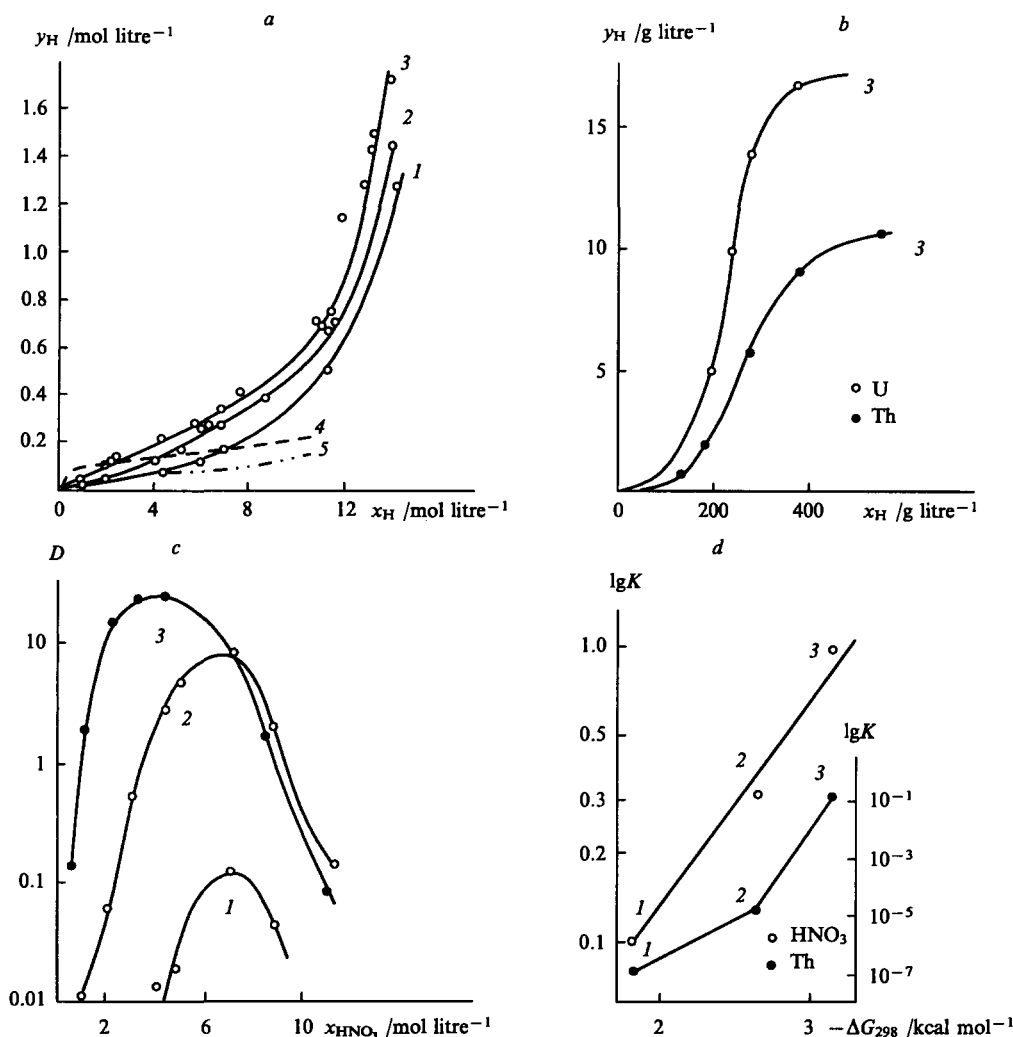


Figure 28. Isotherms for the extraction of HNO₃ (a), uranium and thorium (b), and plutonium (c) by solutions of crown-ethers in dichloroethane (0.1 M) and dependence of the extraction constant on the basicity (the energy of the interaction with phenol) (d). Extractant: (1) dibenzo-18-crown-6; (2) 18-crown-6; (3) cyclohexyl-18-crown-6; (4) TOPO; (5) TBP.

The dependence of the extraction ability of crown-ethers on structure is similar to that for neutral monodentate compounds. In particular, it is possible to control the EA of crown-ethers by varying the substituents. According to Eqns (4) and (7), EA increases with decrease in the electronegativity of the substituents (phenyl < alkyl < cyclohexyl) and the corresponding increase in

the basicity of the crown-ether (for example, the energy of the reactions of the ethers with phenol¹¹³) in the series dibenzo-18-crown-6 < 18-crown-6 < dicyclohexyl-18-crown-6 (Fig. 28 d).

The nonlinearity of the correlation may be associated with an insufficiently correct allowance for the solubility of 18-crown-6 in the aqueous phase. The introduction of alkyl groups into the benzene ring of dibenzo-18-crown-6 has little effect on its EA, while an alkoxy-group increases the EA to the level of the EA of 18-crown-6 (i.e. the same rules are observed as in extraction by BDNOPC, but they are less stringent).

The results constitute fairly convincing proof of the important role of electronic factors. A detailed survey of data on the extraction properties and the complex-forming capacities of crown-ethers may be found in a monograph.¹¹⁴ Different contributions to the complex-formation energy have been analysed.^{115, 116}

Unfortunately crown-ethers extract trivalent actinides and lanthanides very weakly (the basicity of the oxygen in the ether group is low). It would be useful to develop macrocyclic extractants for the extraction and fine separation of trivalent actinides and lanthanides.

Table 10. The concentration (\bar{K}) and effective (K) constants for extraction by crown-ethers (0.1 M in dichloroethane).¹¹⁰

	HNO ₃	UO ₂ (NO ₃) ₂	Th(NO ₃) ₄	Pu(NO ₃) ₄	Np(NO ₃) ₄
Dibenzo-18-crown-6					
\bar{K}	0.1 (0.026)	0.004 (0.062)	6.5×10^{-10}	~5	—
K	—	0.01	1.6×10^{-7}	—	~1.5
18-Crown-6					
\bar{K}	0.3 (0.036)	— (0.036)	3.0×10^{-8}	~40	—
K	0.01	—	1.0×10^{-5}	—	~5
Dicyclohexyl-18-crown-6					
\bar{K}	1.0 (0.50)	0.20 (0.72)	5.0×10^{-4}	~1000	—
K	0.15	0.5	0.1	—	~100

Note. The numbers in brackets represent the data from Refs 111–113.

XI. Organic acids

Organophosphorus acids (R^1R^2POOH) and carboxylic acids ($RCOOH$) are frequently used as extractants. The presence of the functional groups PO and OH in the organophosphorus acids and of CO and OH in carboxylic acids permits the extraction of a metal via both the cation-exchange and solvate or mixed mechanisms. We shall consider these mechanisms in relation to organophosphorus acids (OPA).

1. Extraction via the cation-exchange mechanism

The cation-exchange extraction mechanism predominates in the weakly acid region. When account is taken of the dimerisation of the acid, the process is described by Eqn (3) and the extraction ability is characterised by the equilibrium constant of this reaction. The metal cation extracted replaces the proton of the organic acid and is at the same time coordinated to the oxygen atom of the phosphoryl group.

Thus both functional groups (PO and OH) participate in the coordination. This is the reason for the characteristic feature of the influence of the structure of the OPA on their extraction ability in extraction via the cation-exchange mechanism. The change in the electronegativity of the substituents X has the opposite effect on the reactivity of the groups PO and OH: with increase in the electronegativity, the strength of the acid and the EA of the OH group increase, but the electron-donating capacity and the extraction ability of the oxygen atom of the phosphoryl group diminish.³⁴ As a result, in contrast to NOPC for which the dependence of EA on the structure is universal, in extraction by OPA the nature of the influence of the structure depends on the nature of the element extracted and on the way in which this element reacts with each centre. Thus the acid strength and the degree of extraction of trivalent actinides and lanthanides, which form predominantly an ionic bond and are weakly coordinated to the oxygen atoms of the PO group, increase in the series $R_2POOH - R(RO)POOH - (RO)_2PCOH$ (i.e. with increase in the electronegativity of the substituents). Conversely, the degree of extraction of tetravalent and hexavalent actinides, which are strongly coordinated to the PO group (they form predominantly a covalent bond) weakens in this series (Fig. 29). One may assume that^{6,34,49}

$$\lg \tilde{K}_{ex} = A' + (B_{OH} - B_{PO}) \Sigma X. \quad (11)$$

In the extraction of trivalent actinides and lanthanides, $B_{OH} > B_{PO}$ and the extraction ability of OPA increases with

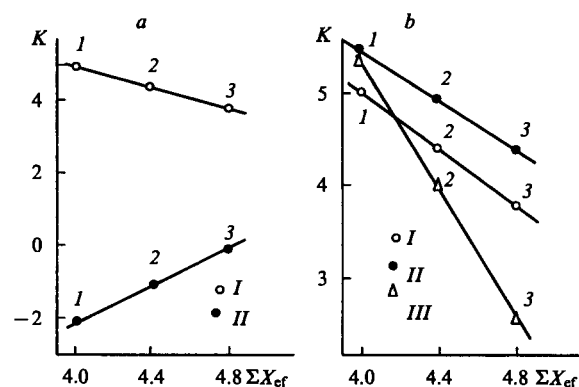
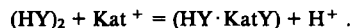


Figure 29. Dependence of the extraction ability of organophosphorus acids [the $(RO)_2POOH$ (1)– $RORPOOH$ (2)– R_2POOH (3) series] on the sum of the effective electronegativities.

(a) Constants for the extraction of UO_2^{2+} (I) and Am^{3+} (II) via the ion-exchange mechanism; (b) constants for the extraction of UO_2 via the ion-exchange (K_1), exchange-solvate (K_{12}), and solvate (K_2) mechanisms.

increase in the electronegativity of the substituents. $B_{OH} < B_{PO}$ in the extraction of uranyl, so that the opposite dependence of EA on the electronegativity holds.

The above explanation was confirmed also by semi-empirical AM1 and PM3 quantum-chemical calculations.¹¹⁷ We used the enthalpy (ΔH_{exch}) of the gas-phase exchange reaction as a characteristic of the EA



In the determination of ΔH_{exch} (in contrast to the determination of the enthalpy of the extraction reaction), no account was taken of the hydration energies of protons and cations (transhydration energies), which remain unchanged if only the extractant is varied. The assumption that the nonspecific solvation has only a slight effect on the process energy relations is therefore fully justified. The overall process may be represented as consisting of two stages: (1) deprotonation of the acid dimer molecule; (2) formation of cyclic complexes. ΔH_{exch} is the sum of the enthalpies of these reactions. The acids R^1R^2POOH , where $R^1, R^2 = R, RO$ ($R = \text{Alk}$), and Cl, were examined and model ions were chosen as the acceptor (Kat^+) — 'hard' $AlBr_2^+$ and 'soft' (HgH^+). According to Pearson's theory, the former ion should form predominantly ionic bonds and the latter predominantly covalent bonds.

As can be seen from Fig. 30, the calculated ΔH_{exch} increases for $AlBr_2^+$ and decreases (slightly) for HgH^+ with increase in acid strength in the series $R_2POOH - RORPOOH - (RO)_2POOH - Cl_2POOH$, which agrees with the experimental extraction data presented above.

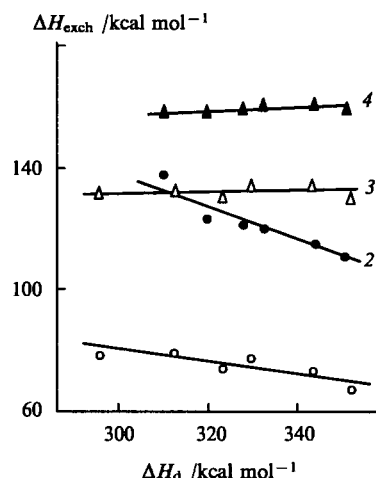


Figure 30. Dependence of the enthalpy (ΔH_{exch}) of the exchange reaction between organophosphorus acids and $AlBr_2^+$ (1, 2) and HgH^+ (3, 4) on the enthalpy of the organophosphorus acid deprotonation reaction (ΔH_d). Calculation by the AM1 (1, 3) and PM3 (2, 4) methods.

Figure 31 presents the variation of constants for the extraction of trivalent americium and promethium by organophosphorus acids over a wide range of variation of ΣX and the acid strength (pK).¹¹⁸ Evidently, by increasing the electronegativity of the substituents and hence the acid strength, it is possible to increase the extraction of trivalent lanthanides and actinides by several orders of magnitude. Alkylphenylphosphoric acid has the highest EA ($pK = 1.4$);[†] a further increase in EA could probably be achieved by the replacement of the alkoxy-group by PhO ($pK = 0.8$) and ClC_6H_4O ($pK = 0.2$).

[†]The quality of the correlation is unsatisfactory possibly because we employed old data; as in the case of NOPC, an effective electronegativity ($X_{ef} = 2.2$) had to be introduced for the RO group.

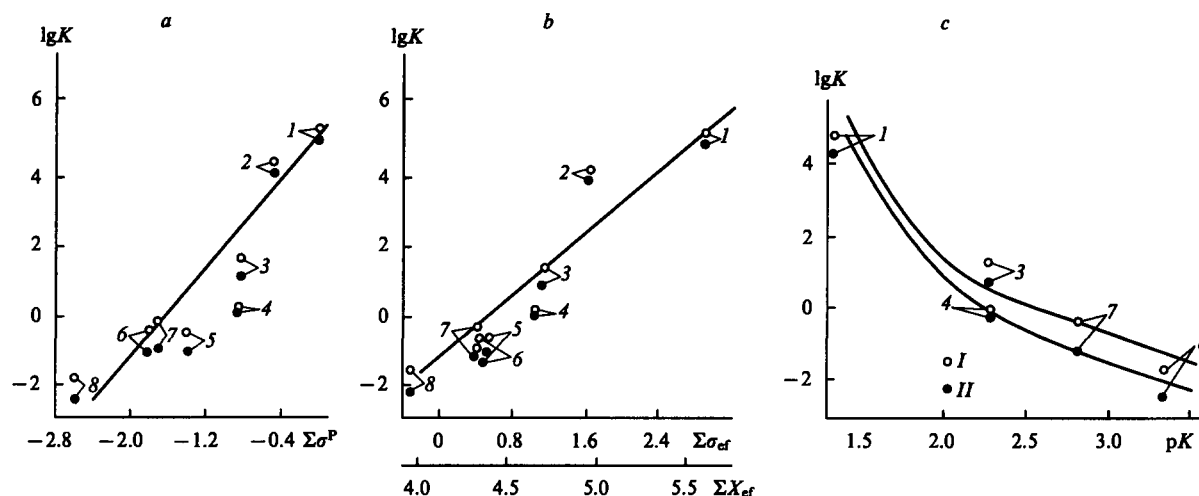
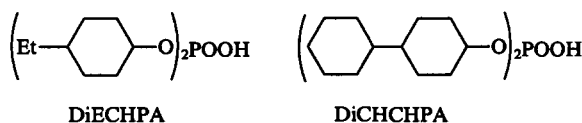


Figure 31. Dependence of the constants for the extraction of promethium (I) and americium (II) by the organophosphorus acids R^1R^2POOH on the Kabachnik (a) and Taft (b) substituent constants and pK (c) over a wide range of basicities.

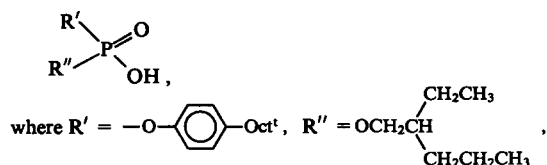
Extractant: (1) ROC_6H_5L ; (2) $ROCICH_2L$; (3) ROC_6H_5L ; (4) $(RO)_2L$; (5) $ROCH_3L$; (6) RC_6H_5L ; (7) $RORL$; (8) R_2L , where R = di-2-ethylhexyl and L = $POOH$.

Together with the increase in EA, an important aspect of the improvement of OPA as extractants is, firstly, an increase in the phase stability of their complexes as a result of the suppression of polymerisation which leads to the formation of gels insoluble in the diluent and reducing the capacity of the extractant; secondly an increase in selectivity, especially in the separation of lanthanides and actinides. Both problems can be solved by optimising the hydrocarbon chain. About 30 years ago, diethylhexylphosphoric acid (D2EHPA) began to be used. It exhibits a higher selectivity and phase stability than di-n-octylphosphoric acid as a result of the branching in the β -position. However, it has been recently observed that free D2EHPA and some of its complexes are polymerised to an extent exceeding dimerisation.^{119,120} A further improvement of the properties of OPA by lengthening the hydrocarbon chain is possible, but a better solution has been proposed¹²¹ — the replacement of alkyl substituents by the bulky ethylcyclohexyl [diethylcyclohexylphosphoric acid (DiECHPA)] or cyclohexylcyclohexyl [dicyclohexylcyclohexylphosphoric acid (DiCHCHPA)] substituents:

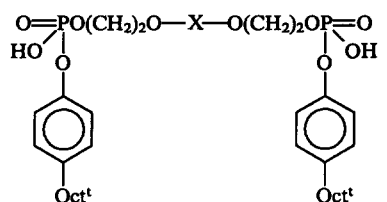


The bulky substituents suppress polymerisation in the extraction of the lanthanides; the formation of gels was not observed and the capacity c_M/c_{HR} increased (for example to 40% and 35% respectively in the case of neodymium instead of 25% for D2EHPA) and the total energy of the complexes $Nd(HR_2)_3$, calculated by the molecular modelling method, increased by a factor of 2 and 3 — from 550 for D2EHPA to 1120 for DiECHPA and 1700 kcal mol⁻¹ for DiCHCHPA. There was also a significant increase, compared with D2EHPA in the extraction ability for DiCHCHPA (by 1–2 orders of magnitude) (Fig. 32) and in the selectivity (especially for the La/Ce and Gd/Ho pairs).

It has been shown¹²² that the monobasic acid (a D2EHPA analogue)



is a more effective extractant than D2EHPA. It was shown in the above study that dibasic acids having the general formula



are effective for the extraction and separation of the lanthanides. Here X may be $-(CH_2)_2-$, $o\text{-C}_6\text{H}_4$, or $p\text{-C}_6\text{H}_4$. The dibasic acid containing a phenyl group in the *para*-position (*p*-DA) in the middle of the bridge proved to be the most effective and selective (predominantly in relation to the heavy lanthanides). The authors explain their results by the steric hindrance generated by the bridge and the advantage of *p*-DA by the rigidity of the bridge with a phenyl group in the *para*-position. It is noted that *p*-DA is

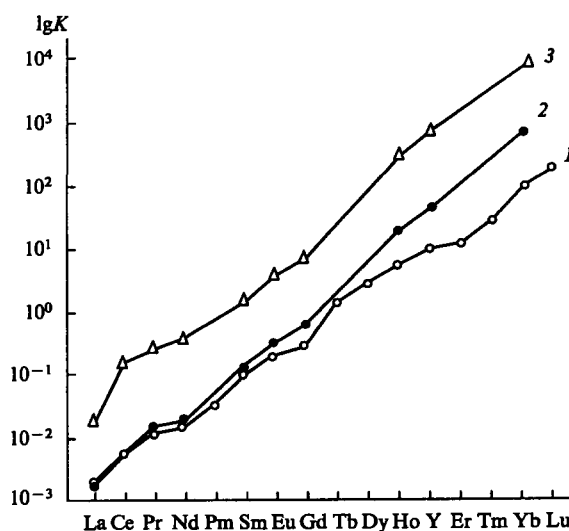


Figure 32. Dependence of the extraction equilibrium constant on the atomic number of the lanthanide.

Extractant: (1) D2EHPA; (2) DiECHPA; (3) DiCHCHPA.

Table 11. Extraction of the lanthanides by the organophosphorus acids R^1R^2POOH .

R^1	R^2	pK_a	$\lg K_{ex}$				$\beta_{Sm/Nd}$	$\beta_{Yb/Y}$
			Nd	Sm	Y	Yb		
PenCHMeCH ₂ CH ₂ O	PenCHMeCH ₂ CH ₂ O	3.25	1.56	2.23	4.36	5.23	4.68	7.41
PenCHMeCH ₂ CH ₂	Me ₃ CCH ₂ O	4.15	-0.55	0.61	2.86	3.75	14.45	7.76
PenCHMeCH ₂ CH ₂	BuCHEtCH ₂ O	4.21	-0.99	0.12	2.55	3.61	12.88	11.48
PenCHMeCH ₂ CH ₂	HexCHMeO	4.37	-1.46	-0.51	1.89	2.94	8.91	11.22
PenCHMeCH ₂ CH ₂	PenCHMeCH ₂ CH ₂ O	4.08	-0.81	0.34	2.75	3.99	14.13	17.38
Pr ⁱ	Me ₃ CCH ₂ O	4.37	-0.80	0.86	2.76	3.24	45.71	3.02
Pr ⁱ	PenCHMeCH ₂ CH ₂ O	4.36	-0.56	0.61	2.59	3.72	4.79	13.49
BuCHEtCH ₂ O	Me ₃ CCH ₂ O	4.39	-1.19	-0.14	2.21	3.14	11.22	8.51
BuCHEtCH ₂ O	PenCHMeCH ₂ CH ₂ O	4.42	-1.45	-0.40	1.88	2.91	11.48	10.72
HexCHMe	Me ₃ CCH ₂ O	4.51	-1.24	0.11	2.22	2.71	22.39	3.09
HexCHMe	PenCHMeCH ₂ CH ₂ O	4.37	-0.92	-0.06	2.30	3.31	7.20	10.23
PenCHMeCH ₂ CH ₂	PenCHMeCH ₂ CH ₂	5.12	-2.20	-1.27	0.93	2.06	8.51	13.49

Note. The following designations have been adopted: Pen = C₅H₁₁; Hex = C₆H₁₃.

present in solution as the trimer (the remaining dibasic acids are dimerised).¹²²

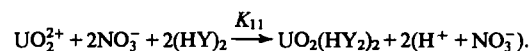
Interesting results have been obtained in the study of Yuan et al.¹²³ The influence of steric factors was investigated in relation to the extraction of the lanthanides by alkylphosphonic acids $R(RO)POOH$ with different structures of the alkyl and alkoxy-chains. It was noted that, for a virtually identical basicity ($pK = 4.1-4.5$), the acids differ by an order of magnitude as regards both their EA and selectivity (Table 11). The branching of the alkyl chain increases the degree of separation predominantly of the heavy lanthanides, while the branching of the alkoxy-chain increases the separation of the light lanthanides. The influence of branching is greater the closer it is to the central phosphorus atom.

In the same study,¹²³ an attempt was made to discover by the molecular mechanics and quantum-chemical methods the optimum conformation of the acids and to investigate the influence of their structure on electronic characteristics.

2. Extraction by the exchange-solvate and solvate mechanisms

We have already mentioned that the extraction by OPA is not confined to the cation-exchange complex-formation mechanism. With increase in the acidity of the aqueous phase, this mechanism is suppressed and new mechanisms arise. We shall examine this problem in relation to the extraction of uranyl as example.

In the weakly acid region, the cation-exchange extraction mechanism predominates; for example, for uranyl we have



Under these conditions, the distribution coefficient of uranium (like those of other metals) rapidly diminishes with increasing acidity ($D_U \sim x_{HNO_3}^{-2}$). However, as can be seen from Fig. 33, this decrease is replaced by an increase — a minimum and then a maximum in the distribution coefficient is observed (at acidities of 3 and 6 M respectively for D2EHPA).^{49,127} This indicates a change in the complex formation mechanism. It has been

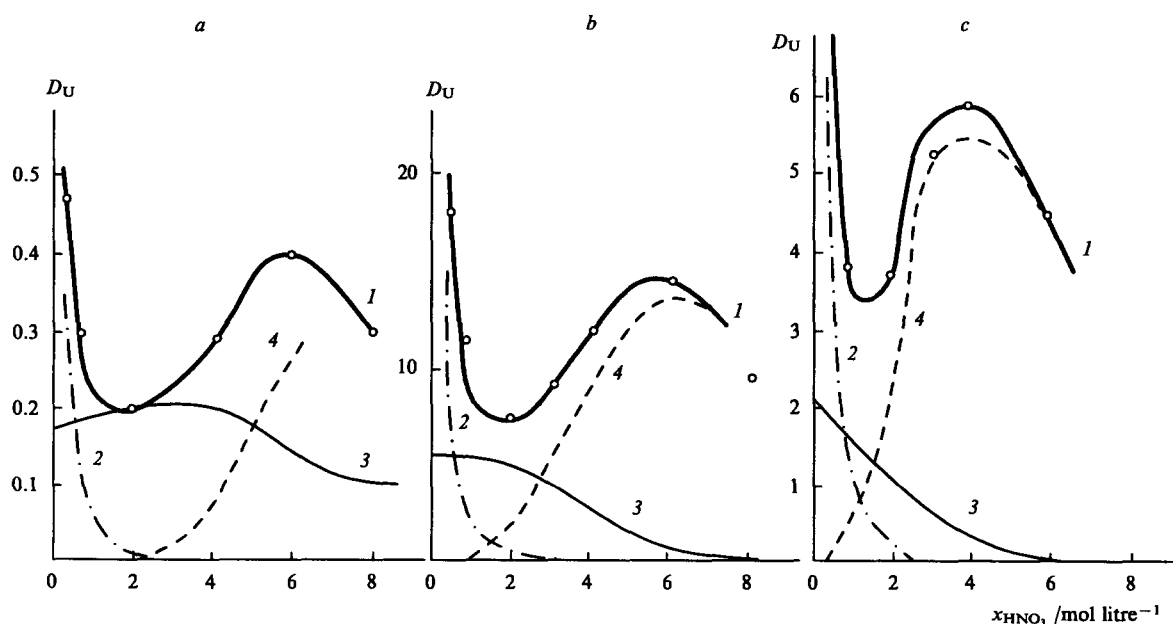
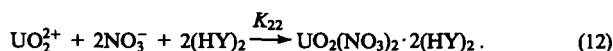


Figure 33. The contributions of different mechanisms to the extraction of U(VI) by diheptylphosphoric (a), phosphonic (b), and phosphinic (c) acids (0.0005 M in *o*-xylene).

(1) Experimental data; (2) ion-exchange mechanism; (3) exchange-solvate mechanism; (4) solvate mechanism.

suggested^{125, 126} that the cation-exchange extraction mechanism is replaced by the solvate mechanism:



However, it has been shown^{124, 127} that the ideas of the above workers^{125, 126} are too simplified and that the description of the result is erroneous. Agreement with experiment was achieved on the assumption that the activity coefficients of uranyl nitrate in the aqueous phase γ_{\pm} are constant, whereas they increase from 0.5 to 2.5, i.e. by a factor of 5, as the ionic strength is raised from 0.5 to 10, while the value of γ_{\pm}^3 in the equation of the Law of Mass Action increases by a factor of 100.

In reality it was found that, as the acidity increases, the second extraction reaction is not reaction (12) but the formation of an exchange-solvate complex containing one inorganic and one organic anion:



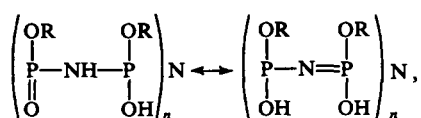
On the other hand, reaction (12) hardly occurs for D2EHPA: $K_{11} = 10^4$, $K_{12} = 3 \times 10^4$, and $K_{22} < 10$, possibly owing to steric hindrance (for di-n-octyl phosphoric and di-n-heptylphosphoric acids, $K_{22} = 5 \times 10^2$, i.e. an appreciable albeit relatively small value).

The role of solvate formation by reactions (12) and (13) increases in the series alkylphosphoric–phosphonic–phosphinic acids, i.e. with increase in the electron-donating capacity of the oxygen atom of the phosphoryl group.^{34, 49} The 'sensitivity' of the extraction constant to changes in the structure of the substituents (their electronegativity) in the course of the transition from the ion-exchange to the exchange-solvate and solvate mechanisms intensifies (Fig. 29).

In the extraction of ions of higher valence, the picture becomes more complicated, since there is a possibility of the appearance of several exchange-solvate complexes, for example, the formation of MY_3NO_3 , $\text{MY}_2(\text{NO}_3)_2$, and $\text{MY}(\text{NO}_3)_3$ for Pu(IV). The hypothesis has been put forward⁴⁹ that the symmetrical exchange-solvate complex $\text{MY}_2(\text{NO}_3)_2$ exists, but no evidence was quoted. We may note that the extraction of Pu(IV), which is effectively coordinated by the oxygen atom in the phosphoryl group,³⁰ weakens, like that of uranyl, in the series phosphinic–phosphonic–phosphoric acids, i.e. with increase in the electronegativity of the substituents and with decrease in the EA of the PO group.⁴⁹

3. Extraction by bidentate phosphonitrilic acids

The extraction ability of OPA is greatly reduced by dimerisation, which results in the binding of both reaction centres — PO and OH. Accordingly there is a possibility of a new way of controlling their EA: the creation of obstacles to dimerisation, for example, the employment of multiunit polyphosphonitrilic acids. These acids have been proposed as extractants by Laskorin et al.¹²⁸ Indeed, it has been found^{129, 130} that the constants for the extraction of americium and europium by polyphosphonitrilic acids are 8 orders of magnitude higher than the constants for the extraction of these elements by D2EHPA. For the tetravalent and hexavalent actinides, the increase in EA was comparatively small. This can be accounted for by the fact that the intensification of the extraction of Am(III) and Eu(III) was assisted by the imide rearrangement



since the number of OH groups, successfully coordinating trivalent elements, increased, but at the same time the PO groups, which coordinate tetravalent and hexavalent actinides most effectively, disappeared.

An advantage of the polydentate phosphonitrilic acids as extractants is a very high EA, whilst their disadvantage is a low selectivity.

XII. Organic acid salts

The acid salts of certain metals (Zr, Hf, Ti, etc.) are known to exhibit higher EA than the corresponding phosphoric acids.^{131–133} This phenomenon is usually explained by the enhancement of the acid properties; the salt [for example, $\text{ZrY}_4(\text{HY})_2$] may be regarded as a strong metalloid acid (for example, H_2ZrY_6), assuming implicitly that the dependences of EA on the structures of the acids and their salts obey common rules. In this case, one may postulate that the possibilities for increasing the EA of the salts (and hence of increasing the concentration of the inorganic acid at which these extractants are capable of extracting radionuclides effectively) are far from exhausted. Stronger organic acids, for example, sulfonic acids, may be used.

At the same time we do not believe that this is the only explanation, since an increase in acidity may be accompanied by the simultaneous decrease in the energy of the complex formation reaction with the metal cations. Quantum-chemical calculation has shown that OPA salts are indeed stronger extractants than the acids themselves,¹¹⁷ but the main reason for the differences between the extraction abilities of the OPA and their acid salts with metals are the differences between the energies of the steric strain in the ligands.¹³⁴

The salts of organic acids with inorganic bases, for example R_4NY (binary extraction proposed by Khol'kin^{135, 136}) are of great interest as extractants. The binary extractant belongs to the neutral group. For example, the extraction reaction of the acid H_mB takes place in accordance with the equation:

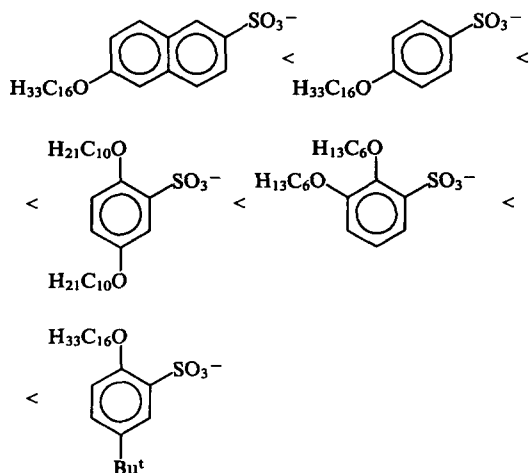


However, the initial section of the extraction isotherm is linear and the distribution coefficient is approximately constant,^{135–137} whereas in the extraction by the usual neutral extractants at $x \rightarrow 0$, $D \rightarrow 0$.²⁷ It can be shown that the binary process is analogous to extraction by neutral extractants with dissociation of the compounds in the organic phase:



In both cases the number of species (ions) does not change in the extraction process, so that we have $D(0) = \text{const}$, when $x \rightarrow 0$.^{137, 140} However, there are incomparably greater possibilities for controlling the binary process. In particular, the EA of the binary extractant may be increased by employing a weaker acid HY; the extraction constant $K(\text{H}_m\text{B}) \approx K_a^{-m}$, where K_a is the dissociation constant of the acid HY. This fact has been confirmed in the extraction of inorganic acids and platinum metals.¹³⁸ In the latter case, the binary extractants have a great advantage over inorganic salts of amines and quaternary ammonium bases because they do not form insertion complexes and make it possible to achieve back-extraction readily.

We may note that the EA of binary extractants may be determined not only by the strength of the acids but also by the operation of steric factors. For example, the degree of extraction of H_2PdCl_4 by tetraoctylammonium alkyl(alkoxy)sulfonates increases in the series of the following anions derived from sulfonic acids of similar strength:



i.e. it increases with increase in the number of substituents and in the length of the chains of the alkyl groups.¹³⁸

Cobalt dicarbollides, which effectively extract caesium (at HNO_3 concentrations up to 4–6 M), strontium, and trivalent actinides and lanthanides, are unusual acid extractants.¹³⁹

XIII. The influence of diluents on the extraction ability of organic compounds

The nature of the diluent has a comparatively weak influence on extraction by monodentate neutral compounds, for example, NOPC, but has a strong influence on extraction by BDNOPC. What is the explanation? We may recall that the effective extraction constant is ^{5, 34, 140}

$$K = \frac{K_T \gamma_L^q}{\gamma_c}, \quad (14a)$$

where K_T is the thermodynamic extraction constant, γ_L and γ_c are the activity coefficients of the extractant and the complex respectively, and q is the solvation number. The thermodynamic constant is independent of the nature of the diluent and its influence is determined by the parameter

$$\text{dil} = \frac{\gamma_L^q}{\gamma_c}. \quad (14b)$$

The activity coefficients of the extractant and the complex in basic diluents (saturated and aromatic hydrocarbons, aprotic chloroderivatives) have been determined experimentally in relation to the extraction of uranyl nitrate by TBP [the complex $\text{UO}_2(\text{NO}_3)_2\text{L}_2$]^{141, 142} and the uranyl salt of D2EHPA [the complex $\text{UO}_2(\text{HY}_2)_2$].¹⁴³ Table 12 presents the values of γ_L and γ_c at zero concentrations of the extractants complexes and also the values of $\text{dil}(0)$ and $\text{dil}/\text{dil}_{\text{CCl}_4} = D/D_{\text{CCl}_4}$. Comparison of the measured values of dil with experimental extraction data indicates satisfactory agreement. The coefficients γ_L for various diluents differ markedly (for example, by an order of magnitude for benzene and hexane). Since in the above systems $q = 2$, one might have expected differences between the parameters dil and D by two orders of magnitude. However, as can be seen from Table 11, the activity coefficients of the complex change 'in the same direction' as γ_L and a compensation takes place — the values of dil and D for various diluents differ little from one another (dilution with chloroform, where dil and D are significantly reduced, is an exception).

In order to understand the results, one has to take into account the fact that the activity coefficients and dil are determined by the operation of three factors:³⁴ (1) the athermal effect (the increase in entropy on mixing molecules differing in size and shape); (2) van der Waals forces; (3) chemical interaction (the last factor dimin-

Table 12. Characteristics of diluents based on measurements of the activity coefficients and extraction data.⁵

Parameter	CCl_4	C_6H_6	C_6H_{14}	CHCl_3
Extraction of uranyl nitrate by TBP [complex extracted $\text{UO}_2(\text{NO}_3)_2(\text{TBP})_2$]				
$\gamma_L(0)$	0.38	0.38	4.36	0.01
$\gamma_c(0)$	0.15	0.06	13.3	0.08
$\text{dil}(0) = \gamma_L^2(0)/\gamma_c(0)$	1.0	2.42	1.55	0.013
$\text{dil}/\text{dil}_{\text{CCl}_4} = (D/D_{\text{CCl}_4})$ (experiment)	1.0	2.35	1.5	0.03
Extraction of uranyl by D2EHTA [complex extracted $\text{UO}_2(\text{HR}_2)_2$]				
$\gamma_L(0)$	0.052	0.040	0.61	0.0039
$\gamma_c(0)$	0.0047	0.0028	0.15	0.00016
$\text{dil}(0) = \gamma_L^2(0)/\gamma_c(0)$	0.58	0.55	2.44	0.097
$\text{dil}/\text{dil}_{\text{CCl}_4}$	1.0	0.95	4.2	0.16
D/D_{CCl_4} (experiment)	1.0	0.97	4.7	0.14

ishes both γ_L and γ_c). It can be shown that the effects of the first two factors on γ_L and γ_c cancel out even for the opposite sign of nonideality (for example, for hexane and benzene). The compensation is most complete on formation of monosolvates (in particular, this is why HNO_3 is most sensitive to the nature of the diluent) and is satisfactory on formation of disolvates, but when trisolvates are formed the athermal effects for benzene and CCl_4 cancel out incompletely; since $\gamma_L^3 \ll 1$, dil and D decrease compared with saturated hydrocarbon diluents. On the other hand chemical reactions do not cancel out at all. They are in fact decisive, the interaction with the extractant diminishing dil and D while that with the complex increasing them. The chemical interactions with the diluents CCl_4 and C_6H_6 are comparatively weak and do not play any role; in the case of C_6H_{14} , they are altogether absent. On the other hand, the interaction with CHCl_3 is significant (a hydrogen bond having an energy of $\sim 5 \text{ kcal mol}^{-1}$ is formed with TBP) and is stronger with the extractant than with the complex because in the latter the oxygen of the PO group is blocked by the metal extracted. There is a corresponding significant decrease in γ_L^2 and in the degree of extraction [by a factor of 30 for TBP (Table 11)].

In the absence of appreciable chemical interactions, the activity coefficients of the extractants and the complex are correlated,³⁴ which makes it possible to describe the influence of the diluent by means of one parameter.¹⁴⁴

Thus in the extraction of metals and acids by monodentate extractants, the inert diluent does not usually affect the dependence of EA on the structure of the extractants. Hence in the vast majority of the systems investigated, the degree of extraction by the organic oxides R_nXO increases in the sequence $\text{TBP} < \text{dioctyl sulfoxide (DOSO)} < 2\text{-nonylpyridine-}N\text{-oxide (2-NPO)} < \text{triisopentylphosphine oxide (TPPO)}$ regardless of the nature of the diluent and the compound extracted. The extraction of acids by solutions of 2-NPO and TPPO in diluents with different solvating capacities constitutes the few existing exceptions.^{145, 146} The relative extraction abilities of these extractants are determined by the form in which the complexes extracted exist, the latter depending on the nature of the acid and the diluent.^{145, 146} For example, in the extraction of moderately strong acids (HNO_3) in weakly solvating diluents (heptane, CCl_4 , benzene), hydrogen-bonded complexes are formed for both extractants, their extraction constants being higher for TPPO than for 2-NPO. In more strongly solvating diluents (chloroform, 1,2-dichloroethane), the state of the complex with TPPO does not change whereas the complex with 2-NPO exists as an ion pair. Owing to

the increased solvation of the ion pair by the diluent, the extraction constants for 2-NPO are higher than those for TPPO.

For bidentate extractants (diphosphine dioxides and carbamoylphosphine oxides), the influence of the diluent proved very strong (see, for example, Fig. 26). When chloroform, which interacts with the reaction centres of BDNOPC is used, the degree of extraction is reduced, as in the case of monodentate extractants. However, when a polar diluent (dichloroethane), which reacts weakly with oxygen, is employed, a marked increase (almost by two orders of magnitude) in the degree of extraction is observed. Apparently dichloroethane reacts with the complex (possibly with the protons of the methylene group⁸³), which, as stated above, leads to an increase in the degree of extraction. When different substituents are introduced into the methylene bridge of methylenediphosphine dioxides and carbamoylmethylphosphine oxides in place of one of the hydrogen atoms, not only does the degree of extraction diminish and the AAS disappear, but the influence of diluents is also significantly weakened.¹⁴⁷ Apparently diluents do indeed interact with the bridge protons⁸³ and their acidity falls sharply on substitution.

We may note that diluents capable, like chloroform, of reacting with the reaction centres and of blocking them may alter qualitatively the dependence of EA on the extractant structure. If this dependence is described by Eqn (4) and the extractant-diluent interaction constant (K_{Ld}) is described by a similar equation but with other values of the coefficients A' and B' , the following equation is valid:

$$\lg K = \lg \frac{K_0}{K_{Ld}} = A - A' + (B - B')\Sigma X, \quad (15)$$

where K_0 is the extraction constant in the absence of interaction of the extractant with the diluent. If $B' > B$, the dependence of $\lg K$ on ΣX may change sign, which is in fact observed in the extraction of tetravalent and hexavalent actinides by methylenediphosphine dioxides when dichloroethane is replaced by chloroform (Fig. 20 a).

XIV. Examples of the development of new extractants

The regularities described above were used to solve two problems of practical importance in the radiochemical technology.

1. Improvement of the first principal extraction cycle in the regeneration of spent fuel from atomic power plants. Development of an extractant as a substitute for tributyl phosphate

Tributyl phosphate, which is widely used in the radiochemical technology, has optimal extraction properties. It extracts uranium and plutonium very effectively and there is no need for salting-out agents. The second essential operation — back-extraction (stripping) of the above elements — is also carried out comparatively readily if TBP is used; here there is no need for the introduction of additional reagents and it is sufficient to alter the acidity and the temperature of the medium. However, TBP suffers from a series of disadvantages. The main one is the comparatively low solubility of plutonium dissolved by TBP in saturated hydrocarbons. For 30% solutions of TBP in alkanes (with a hydrocarbon chain length $n_C = 12-14$) at room temperature, the solubility exceeds only slightly 30 g litre⁻¹ in terms of plutonium. Therefore, in the processing of mixed uranium-plutonium fuel with a high plutonium concentration and also in the refining of plutonium, there is a risk of the formation of a second organic phase and danger of inadmissible process perturbations (in particular, the loss of nuclear safety). Furthermore, TBP is comparatively readily soluble in the aqueous phase, which leads to loss of the extractant, and in refining it can lead to contamination of the product with phosphorus.

In the search for new extractants (taking into account the results described above), it was endeavoured to retain the extraction ability at the level of that of TBP but at the same time to alter the physical properties of the extractant.

It has been shown that EA changes markedly following a change in the chemical nature of the substituents in the extractant molecule and only slightly when the hydrocarbon chain is altered. Consequently, it is necessary to retain the chemical nature of the substituents, i.e. to employ trialkyl phosphates (if phosphonates, even those containing only the electronegative phenyl substituent, are used, difficulties arise with back-extraction). On the other hand, the physical properties may be 'regulated' by optimising the hydrocarbon chain — by increasing its length and by employing branching (this lowers the tendency towards polymerisation, improves compatibility with diluents, and at the same time lowers the solubility in the aqueous phase).

In accordance with these recommendations, the extraction properties of certain trialkyl phosphates, in which the overall length of the hydrocarbon chain varied from 12 (TBP) to 21 (triheptyl phosphate), were investigated. Triisopentyl phosphate (TIPP, $n_C = 15$) and diisobutyl isooctyl phosphate (DIBIOP, $n_C = 16$) proved to be best.¹⁴⁸⁻¹⁵⁰

The use of TIPP solves the problem of the extraction of plutonium from concentrated solutions, because a second organic phase is not formed even after the complete saturation of the extractant by plutonium. On the other hand, if one goes over to DIBIOP, i.e. the hydrocarbon chain is increased by one more atom, then the second organic phase is ruled out also in the presence of thorium nitrate (Fig. 34). The distribution coefficients differ little from one another when TIAP, TIBIOP, and TBP are used (Fig. 35) and the rates of phase separation are comparable. An advantage of both extractants is reduced (by a factor greater than 10) solubility in the aqueous phase, which diminishes the contamination of the products with phosphorus subject to the condition that mechanical losses have also been eliminated.

Triisopentyl phosphate and diisobutyl isooctyl phosphate have undergone successful tests on the highly irradiated fuel (100 GW d t⁻¹) in fast reactors (the activity of the solutions was up to 10³ Ci litre⁻¹ and the concentration of plutonium was up to 30 g litre⁻¹). The risk of radiation damage to the extractant was prevented by employing centrifugal extractors with a short phase contact time.

The parameters of the extraction and purification of valuable components were better than in the case where TBP was employed (including its use on a cascade of mixing-settlers).¹⁵¹ Under the

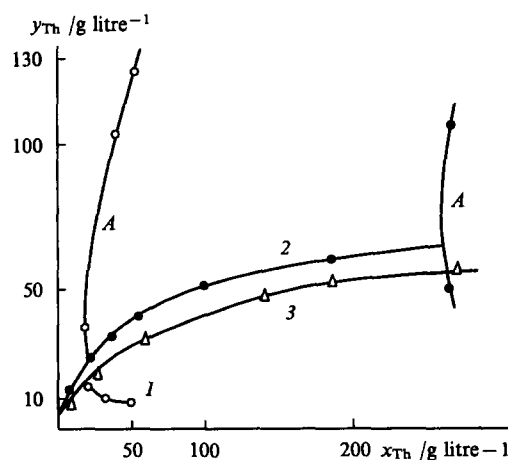


Figure 34. Isotherms for the extraction of thorium by 30% TBP (1), 33% TPAP (2), and 35% diisobutyl isooctyl phosphate (DIBIOP) (3) in *n*-tetradecane. Concentration of extractant in *n*-tetradecane (%): (1) 30, (2) 33, (3) 35; A — region corresponding to separation into two phases.

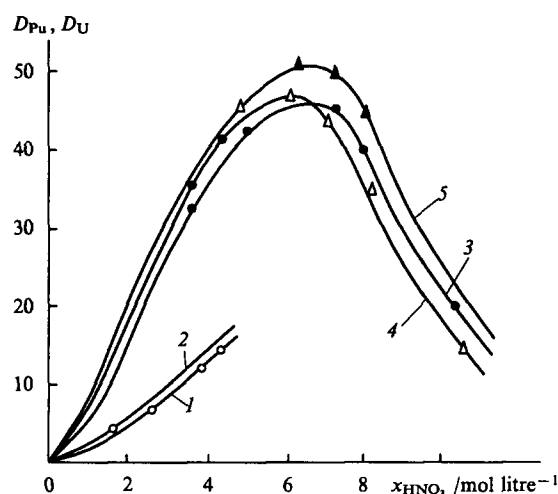


Figure 35. Dependence of the distribution coefficients of Pu(IV) (1, 2) and U(VI) (3–5) on acidity in extraction by solutions of TBP (1, 4), TPAP (2, 5), and DIBIOP (2, 3) in n-tetradecane.

supervision of Nikiforov, Zakharkin, Smelov, and others, triisooamyl phosphate has been used successfully, instead of TBP, on an industrial scale under factory conditions for the regeneration of the spent fuel from water–water power reactors (more than 100 m³ of the 33% extractant in a hydrocarbon diluent was employed).^{152–154} As expected, the new extractant did not introduce negative aspects into the technology: the uranium, plutonium, and neptunium separation factors as well as the decontamination coefficients from radionuclides characteristic of systems with TBP were consistently reproduced. At the same time, it made it possible to reduce appreciably (by a factor of 1.5) the losses of the extractant. This effect is more pronounced if the mechanical loss of the organic phase, which is the same for TIPP and TBP, is eliminated. The employment of TIPP in the refining extraction of plutonium fundamentally expanded the technological possibilities in this stage of the process: the degree of concentration of plutonium was increased and the monitoring of its accumulation in different stages within extractors was simplified.

2. Extractants for the deep extraction of transplutonic elements from radiotechnological waste

Monodentate organophosphorus extractants (even the strongest phosphine oxides, for example, TOPO) are relatively unsuitable for the extraction of transplutonic elements from waste. When TBP is used, it is necessary to introduce a salting-out agent, while phosphine oxides extract americium effectively, but only at a low acidity (up to 0.3 M)¹⁵⁵ and their use requires the neutralisation of the solution. The decrease in the degree of extraction with increase in acidity is associated with the competition by nitric acid for the free extractant: the nitric acid extraction constant is high and the concentration of the free extractant is inversely proportional to it.

Thus an extractant with an increased EA in relation to trivalent actinides and at the same time with a reduced EA in relation to HNO₃ is needed. Surprisingly, these seemingly incompatible requirements can be met by employing the unusual properties of the bidentate organophosphorus compounds — methylenediphosphine dioxides and carbamoylmethylphosphine oxides. Indeed, when electronegative aryl substituents are introduced into the molecules of these compounds, an AAS effect is observed and the extraction of americium and other actinides, involved in bidentate coordination, is enhanced; at the same time, these substituents suppress the extraction of HNO₃, which is involved in monodentate coordination. As a result, a double gain is achieved (Figs 16 and 17): the distribution coefficients of americium increase (compared with the distribution coefficients

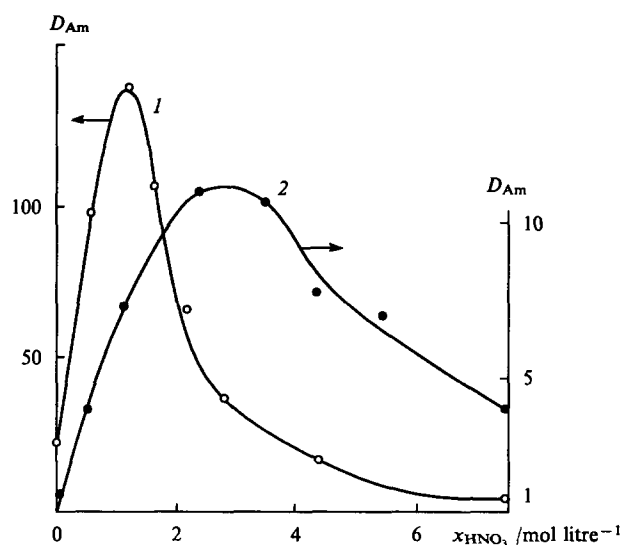


Figure 36. Dependence of the distribution coefficient of Am(III) on acidity in extraction by solutions of 2Tol2Ph (1) and Tol₂/Bu₂ (2) in trichlorobenzene. Concentration of lanthanides in the aqueous phase 10 g litre⁻¹; concentration of the extractant in the organic phase 0.3 M.

when phosphine oxides are used) by 3–5 orders of magnitude and a possibility is created for extensive extraction of the actinides from solutions of any acidity without any kind of preparation of the latter.

The extractants recommended in Refs 156 and 177 — carbamoylphosphine oxide and diphosphine dioxides — have undergone a successful test in the processing of the highly irradiated fuel mentioned above (the activity of the initial aqueous solution was ~ 10³ Ci litre⁻¹).¹⁵¹ The distribution coefficients are presented in Fig. 36. (In order to simulate the conditions in the extraction from the vaporised refined product in the first cycle, 10 g litre⁻¹ of lanthanides was introduced into the aqueous phase.)

The above developments are protected by patents.^{148, 156}

References

1. L L Burger *J. Phys. Chem.* **62** 590 (1958)
2. T V Healy, I Kennedy *J. Inorg. Nucl. Chem.* **10** 128 (1959)
3. T Sekine, in *Proceedings of the International Solvent Extraction Conference, ISEC'88 Vol. 1* (Moscow: Nauka, 1988) p. 15
4. A M Rozen, in *Proceedings of the International Solvent Extraction Conference, ISEC'90, Kyoto, 1990 Vol. A* (Amsterdam: Elsevier, 1992) p. 92
5. A M Rozen, in *Khimiya Ekstraktsii* (Chemistry of Extraction) (Ed. V A Mikhailov) (Novosibirsk: Nauka, 1984) p. 84
6. A M Rozen, in *Proceedings of the International Solvent Extraction Conference, ISEC'88 Vol. 1* (Moscow: Nauka, 1988) p. 62
7. A M Rozen *Dokl. Akad. Nauk SSSR* **249** 134 (1979)
8. A M Rozen *Zh. Fiz. Khim.* **69** 441 (1995)
9. Yu A Zolotov *Usp. Khim.* **32** 220 (1963) [*Russ. Chem. Rev.* **32** 107 (1963)]
10. A M Rozen, B V Krupnov *Zh. Fiz. Khim.* **68** 737 (1994)
11. A M Rozen, B V Krupnov, in *Proceedings of the International Solvent Extraction Conference on Organic Substances, ISECOS'92 Vol. 1* (Voronezh: Nauka, 1992) p. 8
12. A M Rozen, Z I Nikolotova *Zh. Neorg. Khim.* **9** 1725 (1964)
13. T A Mastryukova, M I Kabachnik *Usp. Khim.* **38** 1751 (1969) [*Russ. Chem. Rev.* **38** 795 (1969)]
14. A M Rozen, N A Konstantinova *Dokl. Akad. Nauk SSSR* **161** 132 (1966)
15. A M Rozen, N M Klimenko, B V Krupnov, A S Nikiforov *Dokl. Akad. Nauk SSSR* **287** 915 (1986)

16. A M Rozen, N M Klimenko, B V Krupnov, in *Proceedings of the International Solvent Extraction Conference, ISEC'88 Vol. 1* (Moscow: Nauka, 1988) p. 70
17. V V Yakshin, M I Tymonyuk, L I Sokal'skaya, B N Laskorin *Dokl. Akad. Nauk SSSR* **247** 128 (1979)
18. R S Taft, D Gurka *J. Am. Chem. Soc.* **91** 4801 (1969)
19. A M Rozen, Yu I Murinov, Yu E Nikitin, V S Pilyugin *Radiokhimiya* **16** 118 (1974)
20. B N Laskorin, V V Yakshin, N M Meshchakov, V G Yagodin, in *Proceedings of the International Solvent Extraction Conference, ISEC'88 Vol. 1* (Moscow: Nauka, 1988) p. 99
21. B N Laskorin, V V Yakshin, L I Sokal'skaya *Dokl. Akad. Nauk SSSR* **223** 1405 (1975)
22. A M Rozen, N M Klimenko, B V Krupnov, in *Tez. Dokl. IX Vsesoyuz. Konf. po Ekstraksii, Adler, 1991* (Abstracts of Reports of the IXth All-Union Conference on Extraction, Adler, 1991) (Moscow: Nauka, 1991) p. 16
23. E Glueckauf, H McKay, A Mathieson *Trans. Faraday Soc.* **47** 437 (1951)
24. H McKay, A Mathieson *Trans. Faraday Soc.* **47** 428 (1951)
25. H McKay, in *Khimiya Yadernogo Goryuchego* (The Chemistry of Nuclear Fuel) (Moscow: ONTI, 1954) p. 499
26. S Karpacheva, L Kharkhorina, A M Rozen *Zh. Neorg. Khim.* **2** 6 (1957)
27. A M Rozen *At. Energ. (Russia)* **2** 445 (1957)
28. A M Rozen, L P Kharkhorina *Zh. Neorg. Khim.* **2** 1956 (1957)
29. A M Rozen, E I Moiseenko *Zh. Neorg. Khim.* **4** 1209 (1959)
30. A M Rozen, E I Moiseenko, in *Ekstraksiya* (Extraction) No. 2 (Moscow: Atomizdat, 1962) p. 235
31. A M Rozen, D A Denisov *Radiokhimiya* **18** 921 (1976)
32. E L Wagner *J. Am. Chem. Soc.* **85** 161 (1963)
33. O A Raevskii, V B Bel'skii, V V Zverev *Izv. Akad. Nauk SSSR. Ser. Khim.* 2491 (1973)
34. A M Rozen *Radiokhimiya* **10** 273 (1968)
35. Yu E Nikitin, Yu I Murinov, A M Rozen *Usp. Khim.* **45** 223 (1976) [*Russ. Chem. Rev.* **45** 1155 (1976)]
36. A M Rozen, Z I Nikolotova, N A Kartasheva *Dokl. Akad. Nauk SSSR* **209** 1369 (1973)
37. A M Rozen, Z I Nikolotova, N A Kartasheva, A S Skotnikov *Radiokhimiya* **25** 603 (1983)
38. M I Kabachnik *Usp. Khim.* **48** 1523 (1979) [*Russ. Chem. Rev.* **48** 813 (1979)]
39. L M Epshtein, A V Iogansen *Usp. Khim.* **59** 229 (1990) [*Russ. Chem. Rev.* **59** 134 (1990)]
40. I P Romm, Doctoral Thesis in Chemical Sciences, Karpov Institute of Physical Chemistry, Moscow, 1986
41. J C Bollinger, R J Houriet, C W Kern *J. Am. Chem. Soc.* **107** 5352 (1985)
42. D H Aue, M T Bowers, in *Gas Phase Ion Chemistry* Ch. 9 (Ed. M T Bowers) (New York: Academic Press, 1979)
43. E N Gur'yanova, I P Gol'dshtein, I P Romm *Donorno-Akseptornaya Svyaz'* (The Donor-Acceptor Bond) (Moscow: Khimiya, 1973)
44. V Gutmann *The Donor-Acceptor Approach to Molecular Interaction* (New York: Plenum, 1978)
45. B N Sharapov, Candidate Thesis in Chemical Sciences, All-Union Research Institute of Chemical Technology, Moscow, 1975
46. A M Rozen, A S Skotnikov *Dokl. Akad. Nauk SSSR* **259** 869 (1981)
47. A M Rozen, A S Skotnikov *Zh. Neorg. Khim.* **27** 1272 (1982)
48. A M Rozen, Z I Nikolotova, N A Kartasheva, A V Fokin *Dokl. Akad. Nauk SSSR* **265** 1193 (1982)
49. A M Rozen, Z I Nikolotova, N A Kartasheva, B V Martinov, L A Mamaev, D A Denisov *Radiokhimiya* **16** 682 (1974); *J. Inorg. Nucl. Chem., Suppl.* **229** (1976)
50. I Kennedy, J Perkins *J. Inorg. Nucl. Chem.* **26** 1601 (1964)
51. A M Rozen, N M Klimenko, B V Krupnov *Zh. Fiz. Khim.* **68** 941 (1994)
52. A M Rozen *Zh. Neorg. Khim.* **29** 1886 (1984)
53. B N Laskorin, V V Yakshin, V A Belova, E A Filippov, G G Arkhipova *Radiokhimiya* **20** 702 (1978)
54. B N Laskorin, V V Yakshin, E A Filippov, N A Lyubosvetova *Dokl. Akad. Nauk SSSR* **249** 651 (1979)
55. B N Laskorin, V V Yakshin, N A Lyubosvetova *Usp. Khim.* **50** 860 (1981) [*Russ. Chem. Rev.* **50** 454 (1981)]
56. A M Rozen, Z I Nikolotova, N A Kartasheva, L I Kasumova *Zh. Neorg. Khim.* **23** 113 (1978)
57. V S Shmidt *Ekstraksiya Aminami* (Extraction by Amines) (Moscow: Atomizdat, 1980)
58. L M Gindin *Ekstraktsionnye Protessy i Ikh Primenenie* (Extraction Processes and Their Applications) (Moscow: Nauka, 1984)
59. V S Shmidt, in *Khimiya Ekstraksii* (Chemistry of Extraction) (Ed. V A Mikhailov) (Novosibirsk: Nauka, 1984) p. 96
60. A M Rozen, Z I Nagnibeda *Radiokhimiya* **13** 284 (1971)
61. E G Chudinov *Preprint from Kurchatov Institute of Atomic Energy* No 2125 (1971)
62. C Gonnet, A Lamotte, M Portbault *Anal. Chim. Acta*, **62** 227 (1972)
63. E A Filippov, G G Arkhipova, V A Belov, D I Skorovarov, B N Laskorin, V V Yakshin, in *Primenenie Fosforazotorganicheskikh Kompleksoobrazovatelei v Protessakh Zhidkostnoi Ekstraksii Urana i Transuranovykh Elementov* (Application of Nitrogen-Containing Organophosphorus Complex-forming Agents in Occurring in Liquid Extraction of Uranium and Transuranic Elements) (Moscow: Atomizdat, 1978) p. 2
64. V V Yakshin, M I Tymonyuk, B N Laskorin *Dokl. Akad. Nauk SSSR* **258** 965 (1981)
65. L I Sokal'skaya, Candidate Thesis in Chemical Sciences, All-Union Research Institute of Chemical Technology, Moscow, 1975
66. A M Rozen, A S Nikiforov, Z I Nikolotova, N A Kartasheva, L I Sokal'skaya *Dokl. Akad. Nauk SSSR* **298** 661 (1988)
67. A M Rozen, Z I Nikolotova, N A Kartasheva, L G Andruskii, I V Pastukhova *Radiokhimiya* **34** 49 (1992)
68. A M Rozen, N M Klimenko, B V Krupnov *Zh. Fiz. Khim.* **63** 1239 (1989)
69. A M Rozen, B V Krupnov *Zh. Fiz. Khim.* **69** (1995)
70. A M Rozen, Z A Berkman, Z I Nikolotova *Radiokhimiya* **18** 490 (1976)
71. A M Rozen, Z I Nikolotova, N A Kartasheva *Zh. Neorg. Khim.* **23** 76 (1978)
72. A M Rozen, Z I Nikolotova, N A Kartasheva *Radiokhimiya* **19** 709 (1977)
73. A M Rozen, Z I Nikolotova, N A Kartasheva *Radiokhimiya* **32** 70 (1990)
74. A M Rozen, Z I Nikolotova, N A Kartasheva *Dokl. Akad. Nauk SSSR* **222** 1151 (1975); *Radiokhimiya* **17** 237 (1975)
75. A M Rozen, Z I Nikolotova, N A Kartasheva *Dokl. Akad. Nauk SSSR* **237** 148 (1977); *Radiokhimiya* **20** 725 (1978)
76. A M Rozen, V V Akhachinskii, N A Kartasheva, Z I Nikolotova, N I Chirin, E G Chudinov *Dokl. Akad. Nauk SSSR* **263** 938 (1982)
77. A M Rozen, Z I Nikolotova, N A Kartasheva *Zh. Neorg. Khim.* **24** 1642 (1979)
78. A M Rozen, Z I Nikolotova, N A Kartasheva *Radiokhimiya* **28** 407 (1986)
79. A M Rozen *J. Radioanal. Nucl. Chem., Artic.* **143** 341 (1990)
80. K B Yatsimirskii, M I Kabachnik, Z I Shcheka, T Ya Medved', E I Sinyavskii, Yu M Polikarpov *Teoret. Eksp. Khim.* **4** 446 (1968)
81. K B Yatsimirskii, M I Kabachnik, E I Sinyavskaya *Zh. Neorg. Khim.* **29** 884 (1984)
82. A M Rozen, Z I Nikolotova, N A Kartasheva *Radiokhimiya* **17** 772 (1975)
83. A M Rozen, A S Nikiforov, Z I Nikolotova, N A Kartasheva *Dokl. Akad. Nauk SSSR* **286** 667 (1986)
84. M K Chmutova, N P Nesterova, N E Kochetkova, O E Koiro, B F Myasoedov *Radiokhimiya* **24** 31 (1982)
85. M K Chmutova, N E Kochetkova, O E Koiro, B F Myasoedov, T Ya Medved', N P Nesterova, M I Kabachnik *J. Radioanal. Chem.* **80** 63 (1983)
86. A M Rozen, A S Nikiforov, Z I Nikolotova, N A Kartasheva, A V Fokin *Dokl. Akad. Nauk SSSR* **285** 165 (1985)
87. B F Myasoedov, M K Chmutova, N E Kochetkova, O E Koiro, G A Prilylova, N P Nesterova, T Ya Medved', M I Kabachnik *Solv. Extr. Ion Exch.* **4** 61 (1986)
88. M K Chmutova, M Yussonnua, M N Litvina, N P Nesterova, B F Myasoedov, M I Kabachnik *Radiokhimiya* **32** 56 (1990)
89. M K Chmutova, M N Litvina, N P Nesterova, N E Kochetkova, B F Myasoedov, M I Kabachnik *Radiokhimiya* **32** 88 (1990)

90. M K Chmutova, M N Litvina, N P Nesterova, B F Myasoedov, M I Kabachnik *Solv. Extr. Ion Exch.* **10** 439 (1992)
91. R Chiarizia, E P Horwitz *Solv. Extr. Ion Exch.* **10** 101 (1992)
92. T Nakamura, C Miyake *Solv. Extr. Ion Exch.* **12** 931 (1994)
93. T Nakamura, C Miyake *Solv. Extr. Ion Exch.* **12** 951 (1994)
94. J E Mrochek, J W O'Laughlin, C V Banks *J. Inorg. Nucl. Chem.* **27** 603 (1965)
95. L I Arkhipova, Z A Berkman, L E Bertina, M I Kabachnik, A M Rozen *Dokl. Akad. Nauk SSSR* **209** 1093 (1973)
96. A M Rozen, Z I Nikolotova, N A Kartasheva *Radiokhimiya* **18** 846 (1976)
97. A M Rozen, Z I Nikolotova, N A Kartasheva *Radiokhimiya* **25** 609 (1983)
98. N E Kochetkova, O E Kairo, N P Nesterova, T Ya Medved', M K Chmutova, B F Myasoedov, M I Kabachnik *Radiokhimiya* **28** 338 (1986)
99. A M Rozen *Radiokhimiya* **33** 14 (1991)
100. G V Bodrin, L A Ivanova, E I Matrosov, M K Chmutova, Yu M Polikarpov, B F Myasoedov, M I Kabachnik *Radiokhimiya* **34** 65 (1992)
101. B N Laskorin, M I Kabachnik, L E Bertina, T Ya Medved', V G Kosykh, K F Yudina, A M Nepryakhin, in *Khimiya Protseessov Ekstraktsii* (The Chemistry of Extraction Processes) (Moscow: Nauka, 1972) p. 81
102. M K Chmutova, L A Ivanova, N E Kochetkova, N P Nesterova, B F Myasoedov, A M Rozen *Radiokhimiya* **37** 422 (1995)
103. M K Chmutova, M N Litvina, G A Pribylova, N P Nesterova, V E Klimenko, B F Myasoedov *Radiokhimiya* **37** 430 (1995)
104. B F Myasoedov, G V Bodrin, M K Chmutova, T Ya Medved', Yu M Polikarpov, M I Kabachnik *Solv. Extr. Ion Exch.* **1** 689 (1983)
105. M K Chmutova, G V Bodrin, M N Litvina, A G Matveeva, E I Matrosov, P L Khizhnyak, B F Myasoedov, M I Kabachnik *Radiokhimiya* **31** 83 (1989)
106. A M Rozen *Radiokhimiya* **32** 54 (1990)
107. C Cuillerdier, H Hubert, P Hoel, C Musikas, in *Proceedings of the International Solvent Extraction Conference, ISEC'88* Vol. 1 (Moscow: Nauka, 1988) p. 291
108. A M Rozen, Z I Nikolotova, N A Kartasheva *Radiokhimiya* **32** (3) 70 (1990)
109. B N Laskorin, D I Skorovarov, L A Fedorova, V V Shatalov, E A Filippov *At. Energ. (Russia)* **28** 383 (1970)
110. A M Rozen, Z I Nikolotova, N A Kartasheva *Dokl. Akad. Nauk SSSR* **263** 1165 (1982)
111. V V Yakshin, E V Filippov, V M Abashkiin, B N Laskorin *Dokl. Akad. Nauk SSSR* **241** 159 (1978)
112. V V Yakshin, E V Filippov, V M Abashkiin, B N Laskorin *Dokl. Akad. Nauk SSSR* **247** 1398 (1979)
113. V M Abashkin, V V Yakshin, B N Laskorin *Dokl. Akad. Nauk SSSR* **257** 1374 (1983)
114. Yu A Zolotov, A A Formanovskii, I V Pletnev, S G Dmitrenko, M L Beklemishev, N V Isakova, E N Morosanova, N A Pasekova, L K Shpigun, R D Tsingarelli, I N Torocheshnikova *Makrotsiklicheskie Soedineniya v Analiticheskoi Khimii* (Macrocyclic Mechanisms in Analytical Chemistry) (Moscow: Nauka, 1993)
115. A A Varnek, A S Glebov, O M Petrukhin, R P Ozrov, in *Proceedings of the International Solvent Extraction Conference, ISEC'88* Vol. 1 (Moscow: Nauka, 1988) p. 264
116. A Yu Tsvadze, A A Varnek, V E Khutorskoi *Koordinatsionnye Soedineniya Metallov s Kraun-Ligandami* (Coordination Compounds of Metals with Crown Ligands) (Moscow: Nauka, 1991)
117. A M Rozen, B V Krupnov, in *Tez. Dokl. X Konf. po Ekstraktsii Ufa-94* (Abstracts of Reports at the Xth Conference on the Extraction, Ufa-94) (Moscow: Nauka, 1994) p. 51
118. A M Rozen, in *Proceedings of the International Solvent Extraction Chemistry Conference* (Göteborg: North-Holland, 1967) p. 167
119. A M Rozen, V G Yurkin, Yu V Kononov, M P Shapovalov, B V Krupnov *Zh. Fiz. Khim.* **69** 245 (1995)
120. A M Rozen, V G Yurkin, Yu V Kononov, M P Shapovalov *Zh. Fiz. Khim.* **70** 504 (1996)
121. K Yoshizuka, T Shinohara, K Ohto, K Inoue, in *Proceedings of the International Solvent Extraction Chemistry Conference, ISEC'96* Vol. 1 (Melbourne: University of Melbourne, 1996) p. 317
122. M Goto, S Matsumoto, F Nakashio, K Yoshizuka, K Inoue, in *Proceedings of the International Solvent Extraction Chemistry Conference, ISEC'96* Vol. 1 (Melbourne: University of Melbourne, 1996) p. 281
123. Ch Yuan, S Li, H Feng, in *Proceedings of the International Solvent Extraction Chemistry Conference, ISEC'96* Vol. 1 (Melbourne: University of Melbourne, 1996) p. 329
124. A M Rozen, B V Martynov, V I Anikin *Dokl. Akad. Nauk SSSR* **199** 838 (1971)
125. T Healy, J Kennedy *J. Inorg. Nucl. Chem.* **10** 128 (1959)
126. C Hardy *J. Inorg. Nucl. Chem.* **21** 348 (1961)
127. A M Rozen, B V Martynov, V I Anikin *Radiokhimiya* **15** 24 (1973)
128. B N Laskorin, E A Filippov, D I Skorovarov, V A Kuznetsov *USSR P.* **181** 812; *Byull. Izobret.* (10) 80 (1966)
129. A M Rozen, V I Volk, Z I Nikolotova, N A Kartasheva *Radiokhimiya* **23** 809 (1981)
130. A M Rozen, V I Volk, Z I Nikolotova, N A Kartasheva *Zh. Neorg. Khim.* **27** 131 (1982)
131. B J Weaver *J. Inorg. Nucl. Chem.* **30** 2233 (1968)
132. N A Plesskaya, O A Sinegribova, G A Yagodin *Zh. Neorg. Khim.* **22** 16 (1977)
133. A A Vashman, I V Mukhin, I S Pronin, V S Smelov, V N Shesterikov *Zh. Neorg. Khim.* **32** 1050 (1987)
134. A M Rozen, B V Krupnov *Zh. Fiz. Khim.* **70** (1996) (in the press)
135. A I Khol'kin, V I Kuz'min *Zh. Neorg. Khim.* **27** 2080 (1982)
136. A I Khol'kin, V I Kuz'min, G L Pashkov, G L Pashkov, N V Protasova, O A Logutenko, V V Belova, I N Fleitikh *Izv. Sib. Otd. Akad. Nauk SSSR, Ser. Khim. Nauk* **3** (1990)
137. A M Rozen, A I Khol'kin *Dokl. Akad. Nauk SSSR* **301** 661 (1988)
138. V V Belova, A I Khol'kin, T I Zhidkova *Tsvet. Metal.* **26** (1995)
139. B Ya Galkin, V M Esmantovskii, L N Lazarev, R I Lyubtsev, V N Romanovskii, L Kodlezova, M Kyrsh, I Rais, in *Proceedings of the International Solvent Extraction Conference, ISEC'88* Vol. 4 (Moscow: Nauka, 1988) p. 215
140. A M Rozen, in *Ekstraktsiya* (Extraction) No. 1 (Moscow: Atomizdat, 1962) p. 5
141. A M Rozen, L P Kharkhorina, V G Yurkin *Dokl. Akad. Nauk SSSR* **153** 1387 (1963)
142. A M Rozen, L P Kharkhorina, V G Yurkin *Zh. Neorg. Khim.* **12** 244 (1967)
143. A M Rozen, V G Yurkin *Dokl. Akad. Nauk SSSR* **207** 1165 (1972)
144. V S Shmidt, K D Rybakov *At. Energ. (Russia)* **50** 403 (1981)
145. V G Torgov, M K Drozdova *Izv. Sib. Otd. Akad. Nauk SSSR, Ser. Khim. Nauk* **11** (1985)
146. V G Torgov, I V Nikolayeva, M K Drozdova, in *Proceedings of the International Solvent Extraction Conference, ISEC'88* Vol. 1 (Moscow: Nauka, 1988) p. 91
147. A Yu Shadrin, I V Smirnov, R N Kiseleva, N P Nesterova, Yu M Polikarpov, M I Kabachnik *Radiokhimiya* **35** 70 (1993)
148. *USSR P.* **841** 402; *Byull. Izobret.* (14) 319 (1982)
149. A M Rozen, A S Nikiforov, Z I Nikolotova, V S Shmidt, N A Kartasheva *Dokl. Akad. Nauk SSSR* **274** 1139 (1984)
150. A M Rozen, A S Nikiforov, Z I Nikolotova, N A Kartasheva *At. Energ. (Russia)* **59** 413 (1985)
151. A S Nikiforov, B S Zakharkin, E V Renard, A M Rozen, in *Proceedings of the International Solvent Extraction Conference, ISEC'88* Vol. 4 (Moscow: Nauka, 1988) p. 168
152. A M Rozen, A S Nikiforov, B S Zakharkin *At. Energ. (Russia)* **72** 453 (1992)
153. E G Dzekun, G A Laptev, V D Mel'nikov, V I Osnovin, V M Starikov, V P Ufimtsev, V V Dolgov, A N Levishchev, A M Nudel', V G Shatsillo, A B Yastrebov, V M Dubrovskii, A N Kondrat'ev, V A Kurnosov, A V Serov, B V Nikipelov, B S Zakharkin, E A Nenarokomov, A S Nikiforov, A M Rozen, V S Smelov, A S Solovkin *At. Energ. (Russia)* **72** 432 (1992)
154. A M Rozen, A S Nikiforov, B S Zakharkin, N A Kartasheva, Z I Nikolotova, in *Proceedings of the International Solvent Extraction Chemistry Conference, ISEC'93* Vol. 3 (York: Elsevier, 1993) p. 1615
155. Z I Nikolotova *Spravochnik po Ekstraktsii* (Handbook on Extraction) Vol. 1 (Ed. A M Rozen) (Moscow: Atomizdat, 1976)

156. USSR P. 601 971; *Byull. Izobret.* (35) 2571 (1979)
157. A M Rozen, Z I Nikolotova, N A Kartasheva, in *Proceedings of the International Solvent Extraction Conference, ISEC'88 Vol. 4* (Moscow: Nauka, 1988) p. 133

Electrochemical syntheses based on elemental phosphorus and phosphorous acid esters

A P Tomilov, I M Osadchenko, A V Khudenko

Contents

I. Introduction	1001
II. Syntheses based on the anodic oxidation of phosphorus	1001
III. Cathodic activation of phosphorus	1003
IV. Anodic oxidation of phosphorous acid and electrochemical syntheses based on it	1004

Abstract. The literature data on the electrochemical synthesis of phosphorous acid and phosphoric acid esters from elemental phosphorus are surveyed. The possible mechanisms of the electrode processes are discussed. The procedures for the employment of electrolysis in the preparation of various derivatives of phosphorous acid esters are examined. The bibliography includes 63 references.

I. Introduction

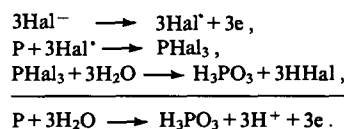
The syntheses of phosphorus-containing compounds based on elemental phosphorus have become important because they make it possible to reduce significantly the amount of industrial waste compared with the classical methods employing phosphorus chlorides. The review of Dorfman et al.¹ published in 1993 contains information about the chemical methods for the syntheses of phosphorus-containing compounds from elemental phosphorus, but electrochemical methods are not considered although numerous studies demonstrating that this aspect is promising have been published during the last decade. It has been established that phosphorus exhibits an electrochemical activity in both anodic and cathodic processes. This makes it possible to obtain various phosphorus-containing compounds in a single stage and under mild conditions. Electrochemical methods have been used successfully also for the syntheses of various phosphorous acid esters. Although in many cases the details of the mechanisms of the electrode processes occurring remain obscure, the synthetic possibilities of the electrochemical methods are evident. The aim of the present review is to survey the experimental data which have accumulated hitherto in this field.

II. Syntheses based on the anodic oxidation of phosphorus

It has been found that in alkaline and acid solutions white phosphorus gives rise to a distinct oxidation wave at a carbon paste anode at a potential of 1.08 V.² According to coulometric

measurements, between 12 and 16 electrons are consumed in the oxidation of a phosphorus molecule in acid solutions. On these grounds, it is concluded that the anodic oxidation of phosphorus results in the formation of a mixture phosphoric and phosphorous acids. In an alkaline medium, the process is complicated by the oxidation of PH_3 — the product of the interaction of phosphorus with water.

The development of a process for the preparation of phosphorous acid by oxidising a suspension of white phosphorus in the presence of hydrogen halide solutions constitutes an interesting attempt at the practical employment of the anodic oxidation of phosphorus.³ The best yield of phosphorous acid is attained in the presence of hydriodic acid. Hydrobromic acid yielded somewhat poorer results. It is postulated that the anodic process includes several stages: the generation of the free halogen, the interaction of the latter with phosphorus, and finally the hydrolysis by water of the phosphorus trihalide formed in the second stage to phosphorous acid.



The hydrogen halide is not consumed in the process but acts as a homogeneous catalyst. It is recommended that a two-phase electrolyte, constituting a mixture of water and benzene, be employed.

This method makes it possible to obtain only relatively dilute solutions of phosphorous acid, since the accumulation of the acid during electrolysis leads to its partial oxidation to phosphoric acid. Furthermore, the phosphorous acid formed contains a small admixture of the hydrogen halide, the complete elimination of which is difficult.

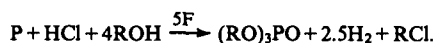
The direct synthesis of phosphoric acid is of much greater interest. The possibility, in principle, of obtaining phosphoric acid esters by electrolysis suspensions of red phosphorus in an aliphatic alcohol was first demonstrated by Varshavskii et al.⁴ The electrolysis was carried out in a diaphragm-free electrolyser with an anode and cathode made of graphite. During electrolysis, the solution containing a suspension of red phosphorus in an aliphatic alcohol was saturated with dry hydrogen chloride. It was noted that the change in current density in the range from 400 to 1000 A m^{-2} and at temperatures from 20 to 50 °C hardly affects the yield of trialkyl phosphates. It is suggested that the overall anodic oxidation process proceeds in accordance with the equation

A P Tomilov, A V Khudenko State Institute of Organic Chemistry and Technology, shosse Entuziastov 23, 111024 Moscow, Russian Federation. Fax (7-095) 273 22 18.

I M Osadchenko Institute of Chemical Problems in Ecology, ul. Mira 19a, 400066 Volgograd, Russian Federaton. Fax (7-844) 236 30 97

Received 19 July 1995

Uspekhi Khimii 65 (11) 1080–1088 (1996); translated by A K Grzybowski



However, the amount of alkyl chloride isolated proved to be much smaller than might have been expected from the above equation. The following phosphoric acid esters have been obtained by this method:

Ester	(MeO) ₃ PO	(EtO) ₃ PO	(BuO) ₃ PO	(C ₅ H ₁₁ O) ₃ PO
Yield (%)	77.5	55.0	88.3	83.1

Subsequently, the direct synthesis of alkyl phosphates was investigated at a greater depth. The reports that other transfer catalysts have been used instead of hydrogen chloride merits attention. Thus the employment of copper(II) chloride as the transfer catalyst has been described.⁵

It was shown that CuCl₂ oxidises white phosphorus:



The anodic process reduces to the regeneration of CuCl₂ by the oxidation of copper(I) chloride. The introduction of HCl lowers the yield of trialkyl phosphate and promotes the formation of a dialkyl phosphite. The electrolysis is carried out in an electrolyser with a diaphragm and, in order to increase the solubility of phosphorus, toluene-alcohol mixtures and not pure alcohol are used. Under optimum conditions [current density $(2-6) \times 10^{-3} \text{ A cm}^{-2}$, $CuCl_2 : P_4 \geq 20$], the yield of alkyl phosphates is nearly quantitative. One cannot rule out the possibility of the formation in this process of copper phosphide as an intermediate, since it has been reported that triethyl phosphate has been obtained in a high yield by the anodic dissolution of copper phosphide in ethyl alcohol.⁶

The anodic oxidation of a suspension of white phosphorus in an acetonitrile-alcohol mixture in the presence of tetrabutylammonium iodide as the supporting electrolyte has been studied in detail.⁷⁻¹⁰

Interesting studies have been carried out by Romakhin et al.,¹⁰ who followed the changes in the outward appearance of the catholyte. It was noted that, soon after the current has been switched on, the state of the white phosphorus changes. It is converted into a dark-yellow deposit with a high phosphorus content, which is insoluble in organic solvents. It is postulated that oligomeric structures are formed in this stage, decomposing in the course of electrolysis (Fig. 1).

This accounts for the low rate of formation of monomeric phosphorus-containing products at the beginning of the electrolysis, the rate increasing significantly towards the end of the process.

It has been found that, under the conditions of diaphragm electrolysis, alkyl phosphates are formed only in an insignificant yield and the presence of trialkyl phosphites was also detected.

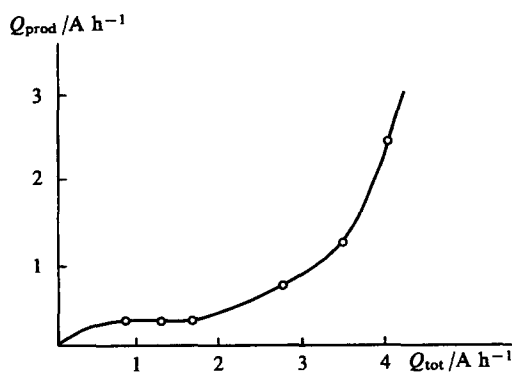


Figure 1. Dependence of the amount of electricity (Q_{prod}) consumed in the formation of triethyl phosphite on the total amount of electricity (Q_{tot}) in the electrolysis of a suspension of phosphorus in acetonitrile in the presence of ethanol.¹⁰

The diaphragm-free electrolysis,⁸ where the trialkyl phosphate is formed with participation of both the cathodic and anodic reactions, proved to be more effective.

After the theoretical amount of electricity has been passed, more than 95% of the phosphorus taken is converted into monomeric products. In the electrolysis of a suspension of white phosphorus in the aliphatic alcohol-acetonitrile-tetrabutylammonium iodide system, dialkyl alkylphosphonates $(RO)_2P(O)R$ and dialkyl phosphites $(RO)_2P(O)H$ are formed in addition to trialkyl phosphates. The yield of the former depends significantly on the electrolysis conditions, particularly on the presence of moisture.¹¹ Unfortunately, the mechanism of this reaction is not discussed in the above study.¹¹ Thus, in the electrolysis of a suspension of white phosphorus in the presence of ethanol at 18–25 °C and a current density of 5 A cm^{-2} , the following dependence of the yield of the electrolysis products on the water content in the reaction mass was obtained:

H ₂ O : P ₄ (in moles)	Yield (%)	
	(EtO) ₃ PO	(EtO) ₂ P(O)H
In the absence of water	81.1	8.9
0.255	73.0	13.8
0.328	70.1	18.8
1.000	72.5	27.0
3.125	50.1	17.4

Thus an increase in the water content lowers appreciably the yield of trialkyl phosphate. In the absence of water, the electrolysis of white phosphorus in the alcohol-acetonitrile-tetrabutylammonium iodide system is accompanied by the formation of a mixture of phosphoric acid esters,⁸ the yield of which varies as a function of the nature of the alcohol.

Alcohol	Yield with respect to phosphorus (%)		
	(RO) ₃ PO	(RO) ₂ P(O)H	(RO) ₂ P(O)R
MeOH	70	11	3
EtOH	69	9	14
BuOH	66	7	15

The yields quoted were not obtained under optimum conditions and can be improved when the process is optimised.

The employment of tetraalkylammonium iodides as the supporting electrolytes has the advantage that the alkyl iodide formed during electrolysis is reduced at the cathode, affording the corresponding hydrocarbon and generating the supporting electrolyte at the same time. Ultimately, the overall process scheme may be formulated as follows:



This method is inapplicable to the synthesis of triaryl phosphates, because phenol and its derivatives interact with phosphorus under these conditions, giving rise to a mixture of triaryl phosphates and triaryl phosphites.¹²

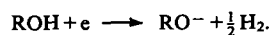
Alcohol	Yield with respect to phosphorus (%)	
	(ArO) ₃ PO	(ArO) ₃ P
PhOH	20	46
<i>o</i> -MeC ₆ H ₄ OH	32	38
<i>p</i> -ClC ₆ H ₄ OH	32	11

The process is accompanied by the passivation of the anode. The addition of pyridine eliminates the passivation, but in this case the main product of the electrolysis becomes the triaryl phosphite. Thus in the presence of pyridine the yield of $P(OPh)_3$ increases to 78%, whilst that of $(PhO)_3PO$ remains 20%.

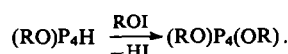
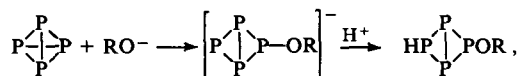
The question of the mechanism of the formation of trialkyl phosphates in the electrolysis of a suspension of phosphorus in the

presence of an aliphatic alcohol and a halide salt merits separate consideration.

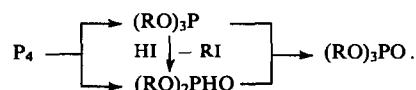
According to Budnikova et al.,¹¹ the first step in the electrochemical process is the reduction of an alcohol molecule at the cathode and the formation of alkoxide ions.⁹



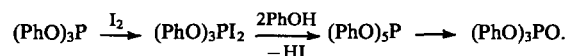
The P–P bond in the phosphorus molecule is ruptured by the alkoxide ions generated at the cathode (in the presence of a large excess of phosphorus, there is a possibility of the formation of polymeric structures) and the resulting ROP_4^- anion is protonated and subsequently interacts with the alkyl hypophosphite generated at the anode:



Subsequent alkoxylation ultimately leads to a full phosphorous acid ester, which is oxidised to an alkyl phosphate at the anode. On the basis of the above considerations, a mechanism has been proposed for the possible processes occurring during electrolysis in a single-solution electrolyser of alcoholic solutions of tetrabutylammonium iodide in the presence of white phosphorus:¹¹



In the case of phenols, a triaryl phosphite is formed in the first stage of the electrolysis. It reacts with the iodide and phenol generated at the anode, affording a pentaphenoxyphosphorane; the latter is partly converted into a triaryl phosphate at the anode:¹²

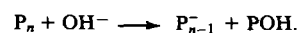


The above data demonstrate that the electrolysis of a suspension of phosphorus in aliphatic alcohols (when halide salts are used as the supporting electrolyte) may be regarded as a way of obtaining phosphoric acid esters, bypassing the stage involving the formation of phosphorus halides. In the study of the formation of alkyl phosphates, the cathodic activation of white phosphorus and the possibility of the anodic oxidation of phosphites to phosphates were observed. These two possibilities merit independent consideration.

III. Cathodic activation of phosphorus

As already mentioned, the electrochemical synthesis of trialkyl phosphates from white phosphorus may be achieved with a satisfactory yield only in an electrolyser without a diaphragm, i.e. the cathodic process plays in this case a significant role, inducing the activation of phosphorus molecules.

The formation of active phosphorus species in chemical processes has been frequently discussed in the literature. For example, in a study of the reactions of elemental phosphorus with electrophiles in a highly basic medium, it was suggested that the P–P bond is ruptured by the base:¹³



Phosphorus is also activated by amines.¹⁴ Thus in the presence of triethylamine, white phosphorus reacts with epoxyethane.

The high reactivity of red phosphorus in the presence of copper halides has also been explained by the dissociation of the P–P bond:¹⁵

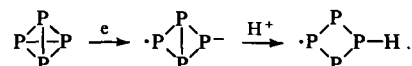


We shall now consider the possible paths leading to the activation of white phosphorus molecules in cathodic processes.

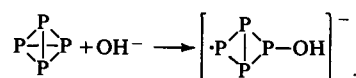
White phosphorus is known to be electrochemically active and gives a wave in the region of -1.90 V.¹⁶ The process involves the transfer of 12 electrons to the P_4 molecule and the final reduction product is phosphine.^{17,18} However, in a study of the electrochemical reduction of a suspension of white phosphorus in 50% acetic acid (with addition of potassium acetate in order to increase the electrical conductivity), it was noted that part of the phosphorus (12.3%) in the cathodic compartment is converted into phosphorus acids. Thus, phosphorous, hypophosphorous, and orthophosphoric acids were detected among the reaction products in proportions of 45:55:5 by weight.¹⁹ Particular experiments demonstrated that white phosphorus does not react with the catholyte.

Another interesting fact was observed in the electrochemical reduction of a suspension of white phosphorus in an acid solution at a lead cathode.²⁰ In the first instants of the electrolysis, gaseous products are hardly evolved at the cathode (Fig. 2), the joint evolution of hydrogen and phosphine being observed only after some time. The yield of phosphine increases sharply, exceeding 100% relative to the amount of electricity passed through the system. As phosphorus is consumed, the yield of hydrogen increases and reaches the theoretical value. This experiment demonstrated that involatile phosphorus compounds are formed initially and are converted during electrolysis into phosphine.

There are different views on the nature of the active phosphorus species formed initially at the cathode. The formation of partly hydrogenated phosphorus molecules, arising in the course of its reduction, appears most probable. For example,



Another path, involving the generation of nucleophilic species in the cathodic compartment, is also possible. For example,



Yield with respect to current (%)

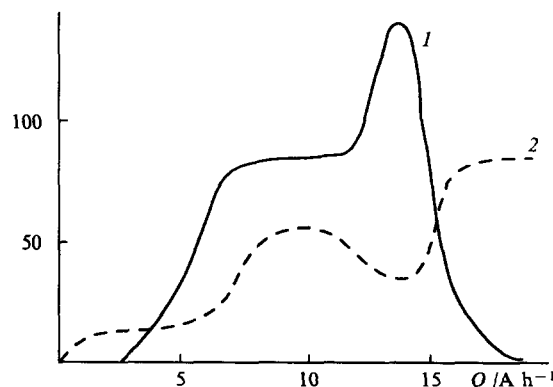
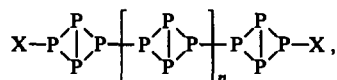


Figure 2. The formation of phosphine (1) and hydrogen (2) in the electrolysis of a suspension of phosphorus in sulfuric acid solution.²⁰

The radical species produced in both cases can give rise, in the presence of an excess of phosphorus, to polymeric structures of the type



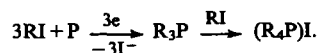
where X = H or OH. Such structures are usually formed in the first stage of the electrolysis.

The example of the reduction of phosphorus at a lead cathode described above agrees well with the first mechanism, according to which higher phosphorus hydrides are formed initially, whereas the formation of phosphorus acids in the cathodic compartment would be more logically explained on the basis of the second mechanism. This mechanism also demonstrates the role of the cathodic process in the synthesis of trialkyl phosphates. One may postulate that the mechanism of the activation of phosphorus depends on the electrolysis conditions and principally on the material on the cathode. On metals with a high hydrogen overpotential, the reduction of P_4 and the formation of lower phosphorus hydrides (the first mechanism) are more likely, whereas on metals with a low hydrogen overpotential the activation of phosphorus by the nucleophile generated at the cathode is more probable. In particular, in the preparation of trialkyl phosphates, phosphorus is activated by the alkoxide ions formed at the cathode.

The electrochemical activation of phosphorus molecules may be used for various synthetic purposes. For example, the possibility of obtaining phosphites by the electrolysis of a suspension of red phosphorus in an aqueous solution of ethylenediamine has been demonstrated.²¹ The phosphite is formed in the cathodic compartment of the electrolyser, the yield with respect to the red phosphorus taken amounting to ~40%. Under the same conditions but in the absence of ethylenediamine, the only product of the reduction of red phosphorus is phosphine.²² Since phosphorus does not react chemically in an aqueous solution of ethylenediamine, it remains to postulate that phosphites are formed as a result of the interaction of electrochemically activated phosphorus molecules with water. When this process is carried out in an electrolyser with a platinum anode but without a diaphragm, the yield of the phosphite increases slightly.²³ This shows that the phosphite is formed exclusively from cathodically activated phosphorus.

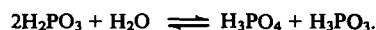
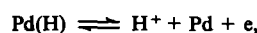
The formation of organophosphorus compounds in the electrolysis of suspensions of white phosphorus in aprotic solvents in the presence of alkyl halides^{24,25} and unsaturated compounds²⁶ can apparently be also accounted for by the cathodic activation of phosphorus. In all cases, the formation of the corresponding phosphines was observed. For example, the electrolysis of a suspension of white phosphorus in acetonitrile in the presence of styrene afforded a series of compounds, the main one being the monosubstituted phosphine $\text{PhCH}_2\text{CH}_2\text{PH}_2$ (26%). The other reaction products were the di- and tri-substituted phosphines $(\text{PhCH}_2\text{CH}_2)_2\text{PH}$ (0.5%) and $\text{P}(\text{PhCH}_2\text{CH}_2)_3$ (2.5%) and also the diphosphine $[(\text{PhCH}_2\text{CH}_2)_2\text{P}]_2$ (1.0%).²⁶

In the presence of alkyl halides, tertiary phosphines are formed preferentially, reacting with the excess alkyl halide to form quaternary phosphonium salts:



IV. Anodic oxidation of phosphorous acid and electrochemical syntheses based on it

Free phosphorous acid in 0.5 N H_2SO_4 gives rise to a distinct oxidation wave at a potential of +0.52 V relative to the saturated calomel electrode (s. c. e.) at a palladium electrode.²⁷ It is suggested that under these conditions phosphorous acid is oxidised via a catalytic dehydrogenation mechanism:²⁸

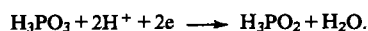


Orthophosphoric acid is the product of the oxidation of phosphorous acid. At a platinum anode in an alkaline medium, the oxidation takes place with a current yield of ~40%.^{29,30} The addition of potassium iodide to the solution increases the yield of orthophosphoric acid to 66%.³¹ At a graphite anode in the presence of 0.5 N HCl, phosphorous acid is oxidised fairly effectively, but this requires the passage of 180% of electricity relative to the theoretical amount, whereupon phosphorous acid is almost fully oxidised (97%).

In an alkaline solution, the oxidation takes place effectively even at a nickel anode, but a fully defined ratio of disodium hydrogen phosphite and sodium hydroxide is then necessary. The optimum ratio disodium hydrogen phosphite:sodium hydroxide = 1.6:1.0 makes it possible to attain a degree of oxidation of 99% with a current yield of 43%. The process can be carried out also in a diaphragm-free electrolyser, since the losses in reduction do not exceed 1%–3%.³²

The sodium salts of phosphorous acid are polarographically active. Thus sodium dihydrogen phosphite has a reduction wave with $E_{1/2} = -0.605$ V ($n = 0.4$), whereas disodium hydrogen phosphite has one with $E_{1/2} = -0.42$ V ($n = 0.7$).³³ Unfortunately the nature of these waves has not been discussed.³³

In an aqueous solution, the product of the electrochemical reduction of phosphorous acid is phosphonous acid:³⁴



The formation of phosphine has also been observed.³²

Electrochemical synthesis based on acid phosphite esters merits separate consideration. The characteristic features of their electrochemical behaviour are determined by the equilibrium

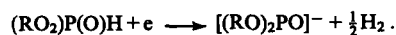


which is almost fully displaced towards four-coordinate phosphorus.

In the accessible range of potentials, dialkylphosphorous acids are not oxidised,³⁵ but in aprotic media they give rise to a reduction wave at transition metal cathodes.³⁶ Thus, in acetonitrile in the presence of quaternary ammonium salts as supporting electrolytes, dimethyl phosphites have the following reduction potentials (in V) at different cathodic materials:

Phosphine	Pt	Ni	Fe	Cu
$(\text{MeO})_2\text{P(O)H}$	1.88	1.88	1.90	2.00
$(\text{EtO})_2\text{P(O)H}$	1.89	—	2.06	2.04

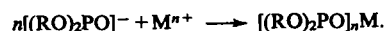
It is suggested that the cathodic process leads to the formation of anions, since the evolution of hydrogen is observed at the cathode:



Four-coordination of the phosphorus atom in the anion is indicated by the finding that diaphragm-free electrolysis with a soluble anode leads to dialkyl phosphite salts with a metal–phosphorus bond.³⁶ In this case, the anodic process consists in the dissolution of the anode material and its transition to an ionic state:



The interaction of the phosphite anions generated at the cathode with the metal cations leads to the formation of salts:^{36,37}



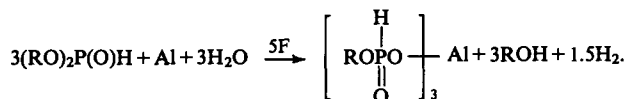
The formation of the corresponding platinum salt has been described in a study³⁷ where a platinum electrode was employed.

In aqueous solutions of alkali metal halides, dialkyl phosphites are oxidised to dialkyl phosphates at a graphite anode:^{38,39}



The oxidation is carried out at a current density not exceeding 0.01 A cm^{-2} and a temperature of $30\text{--}35^\circ\text{C}$. The yield of phosphates is 75%–80%. In the electrolysis of lower dialkyl phosphites ($\text{Alk} = \text{C}_1\text{--C}_3$), the process is accompanied by partial hydrolysis with formation of monoalkylphosphoric acids.

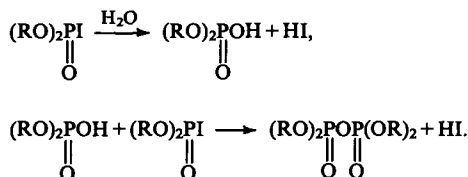
In the electrolysis of an aqueous solution of dialkylphosphorous acid with an aluminium anode, aluminium alkyl phosphate was obtained in a yield of 90%–95%:⁴⁰



This process was used as a basis for the industrial preparation of the Russian-produced systemic fungicide EFAL'-50.⁴¹ The technological scheme is significantly simplified as a result of the employment of a diaphragm-free electrolyser fitted with aluminium electrodes. The electrolysis is carried out with an alternating current at a frequency of 50 Hz.⁴²

The aluminium salt can be obtained similarly from methylphosphonic acid.⁴³

The electrolysis of dialkyl phosphites in a nonaqueous medium using an insoluble graphite anode leads to a complex mixture of products, more than 60% of which comprises tetraalkyl pyrophosphate $(\text{RO})_2\text{P}(\text{O})\text{OP}(\text{O})(\text{OR})_2$.⁴⁴ The mechanism of its formation is not clear. It has been suggested that, since hydriodic acid is used as supporting electrolyte, the acyl iodide formed at the anode reacts with water, giving rise to a dialkyl phosphite; the latter reacts with a second acyl iodide molecule:⁴⁵



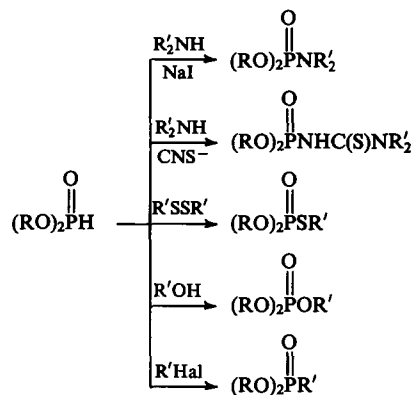
However, from our point of view this mechanism is unlikely, since the use of even thoroughly dried acetonitrile does not lower the yield of pyrophosphate. A similar reaction occurs in the electrolysis of acetonitrile solutions of alkyl alkylphosphonates, leading to the formation of dialkyl dialkylpyrophosphonates $(\text{RO})\text{RP}(\text{O})\text{OP}(\text{O})\text{R}(\text{OR})$.⁴⁴ Data on the electrosynthesis of pyrophosphates and pyrophosphonates from phosphorous acid esters are presented below (the mechanism of this reaction has not been investigated):

$(\text{RO})_2\text{POP}(\text{OR})_2$						
R	Et	Pr ⁿ	Bu ⁿ			
Yield / $10^3 \text{ mol A}^{-1} \text{ h}^{-1}$	12.2	11.1	11.0			
$(\text{RO})\text{MePOPMe}(\text{OR})$						
R	Et	Pr	Pr ⁱ	Bu	Bu ⁱ	n-C ₃ H ₁₁ iso-C ₃ H ₁₁
Yield / $10^3 \text{ mol A}^{-1} \text{ h}^{-1}$	12.3	8.8	11.6	7.9	10.4	6.3 10.1
$(\text{RO})\text{EtPOPEt}(\text{OR})$						
R	iso-C ₃ H ₇	iso-C ₄ H ₉				
Yield / $10^3 \text{ mol A}^{-1} \text{ h}^{-1}$	11.2	10.2				

Although, as already mentioned, the acid phosphite esters themselves do not undergo anodic oxidation, they react readily with the halogens generated at the anode, forming reactive acyl

halides. This reaction has been used successfully for the synthesis of compounds with P–N, P–S, and P–O bonds. The possibility of the electrochemical formation of the P–C bond was later demonstrated.

The overall mechanism of the electrochemical phosphorylation reactions of organic compounds can be represented as follows:

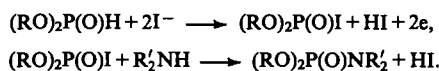


We shall examine these reactions in greater detail.

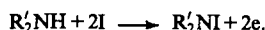
1. Synthesis of amidophosphates

The formation of amidophosphates in a high yield has been noted in the electrolysis of acetonitrile solutions of dialkyl phosphites containing an alkali metal iodide as the supporting electrolyte to which a secondary amine has been added. The process is carried out in a diaphragm-free electrolyser with platinum electrodes. The yields of the amidophosphates as a rule exceed 75%. For example, when dimethyl phosphite was coupled with dipropylamine, the yield of the amidophosphate was 76%, while the yields in the reactions with dibutylamine and morpholine were 83% and 80% respectively.⁴⁶

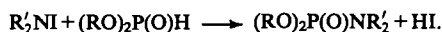
The most probable reaction path involves the anodic iodination of the phosphite:



An alternative path involving the anodic iodination of the amine is also possible:

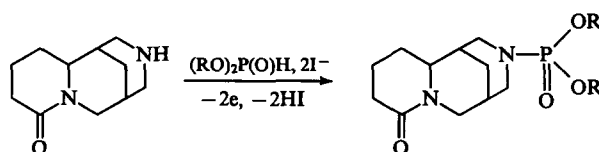


The iodoamine formed as a result of this reaction reacts subsequently with the phosphite:



On the basis of voltammetric measurements and quantum-mechanical calculations, preference is given to the first path.⁴⁷

This reaction has been used successfully for the phosphorylation of various alkaloids. For example, cytosine has been phosphorylated electrochemically:

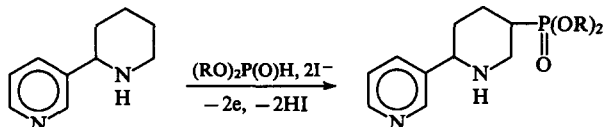


The reaction was carried out in the presence of tetraethylammonium bromide with added free iodine as the supporting electrolyte. The following yields of the phosphorylation products were obtained depending on the nature of R:⁴⁸

R	Me	Et	Pr	Pr ⁱ	Bu ^t
Yield (%)	53	84	78	73	70

L-Ephedrine,⁴⁹ lupinine,⁵⁰ pyrazidol,⁵¹ salsolidine,⁵² and anabasine^{48, 53} have been phosphorylated in 85%–91% yields.

The phosphorylation of anabasine is represented by the following overall equation:



The yield of the phosphorylated product depends on the nature of the group R:

R	Me	Et	Pr ⁿ	Pr ⁱ	Bu ⁿ
Yield (%)	79.0	91.2	86.4	86.0	87.1

In the phosphorylation of quinine, it was established that the hydroxy-group is initially oxidised to the carbonyl group with formation of the corresponding quinone, which is then phosphorylated to the α -hydroxyphosphonate.⁵⁴

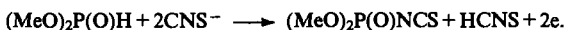
As already mentioned, the phosphorylation of amines takes place with iodine as the transfer catalyst. Other halogens proved to be appreciably less effective. Thus the following dependence of the yield of the target product on the nature of the halogen-containing additive has been obtained in the synthesis of the diethylamide of ethylphosphorous acid:¹⁴

Additive	I ₂	NaI	NaBr	NaCl
Yield (%)	94	92	36	4

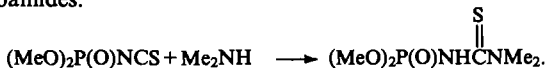
It is of interest to note that lupinine is most effectively phosphorylated in the presence of crown-ethers to which lithium chloride has been added.⁵⁰ The presence of surfactants has apparently a favourable effect on the process.

2. Synthesis of thioamides

If during the electrolysis of acetonitrile solutions of dialkyl phosphites in the presence of secondary amines ammonium thiocyanate is used instead of sodium iodide, the nature of the products changes significantly. The synthesis of *N*-phosphorylated thioamides has been observed. Cyclic voltammetric data and quantum-mechanical calculations have shown that the most probable mechanism for the simplest dimethyl phosphite–dimethylamine system involves the interaction of the phosphite with the iodine thiocyanate formed at the anode:⁵⁵



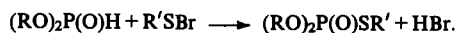
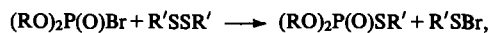
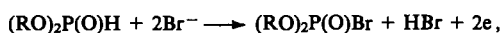
The thiocyanato-derivative obtained as a result of this reaction then reacts with the amine, affording *N*-phosphorylated thioamides:



This reaction has been used successfully for the phosphorylation of ephedrine alkaloids. The corresponding phosphorylated thioamides were obtained in 48%–53% yield. The phosphorylated quinine and lupinine thioamides are formed in approximately the same yield.⁵⁶

3. Synthesis of thiophosphates

The electrochemical generation of the halogens makes it possible to achieve the coupling of dialkylphosphorous acid with disulfides, which results in the formation of compounds with a P–S bond. The following process mechanism has been proposed on the basis of polarisation measurements for the initial components:



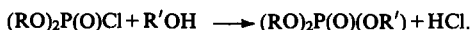
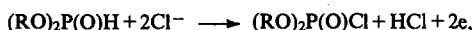
Best results were obtained in the presence of bromide salts; the reactions with other halides are less successful (see, for example, Torii et al.⁴⁵):

Additive	NaI	NaBr	NaCl
Yield of $(\text{EtO})_2\text{P}(\text{O})\text{SPh}$ (%)	73	91	59

The coupling of diethyl phosphite with diphenyl disulfide is carried out in an electrolyser without a diaphragm, which made it possible to obtain coupling products with entirely satisfactory yields. For example, in the coupling of dimethyl phosphite with diphenyl disulfide, dibenzyl disulfide, and bis(ethoxycarbonylmethyl) disulfide, the yields of the coupling products were 61%, 71%, and 75% respectively.

4. Synthesis of trialkyl phosphates

The anodic oxidation of dialkyl phosphites in an alcoholic solution in the presence of chloride ions makes it possible to obtain trialkyl phosphates in high yields.⁵⁷ It has been suggested that in the first stage the phosphite undergoes anodic chlorination to the acyl chloride, which then reacts with the alcohol, affording the corresponding trialkyl phosphate:



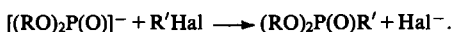
This method made it possible to obtain phosphoric acid esters with various substituents. Although the yield of the esters synthesised in this way is somewhat lower than in the syntheses examined previously, the method is nevertheless preparatively important. Thus, when dimethyl phosphite was coupled with methyl, ethyl, and propyl alcohols, the yields of the corresponding trialkyl phosphates were 46%, 57%, and 63% respectively. The syntheses were carried out using perchloric acid with added lithium chloride as the supporting electrolyte. The anode was made of vitreous carbon and a diaphragm electrolyser was used, although the need for a diaphragm in this process can hardly be justified.

5. Synthesis of phosphonates

The cathodic reduction of dialkyl phosphites in the presence of halogen-containing compounds leads to phosphonates. The mechanism of this process differs significantly from those examined above. The primary process is apparently the cathodic reduction of the dialkyl phosphite with formation of the anion $(\text{RO})_2\text{P}(\text{O})^-$:³⁶



The anion reacts further with the halogen-containing compound:³⁶

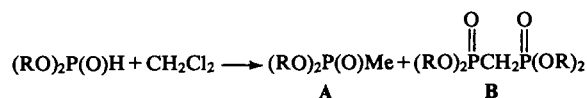


The electrochemical synthesis of phosphonates was first described by Petrosyan and Niyazymbetov.⁵⁸ The process was carried out in a diaphragm electrolyser at a platinum anode in acetonitrile at a current density of 0.003–0.005 A cm⁻² at 20 °C. A 0.3 M solution of tetraethylammonium bromide was used as the supporting electrolyte.

The starting compounds were dimethyl, diethyl, and diphenyl phosphites as well as methyl and benzyl iodides and chlorides. The yields of the corresponding phosphates were in the range 55%–65%.

An interesting modification of this reaction has been proposed.⁵⁸ In it, methylene chloride containing 0.3 M tetraethylammonium bromide and 0.015–0.03 M phosphite (Pt cathode) was used as the catholyte, while the anolyte was a 0.3 M solution of tetraethylammonium bromide in methylene chloride to which

cyclohexene had been added to bind the bromine evolved. The reaction proceeds in accordance with the equation:

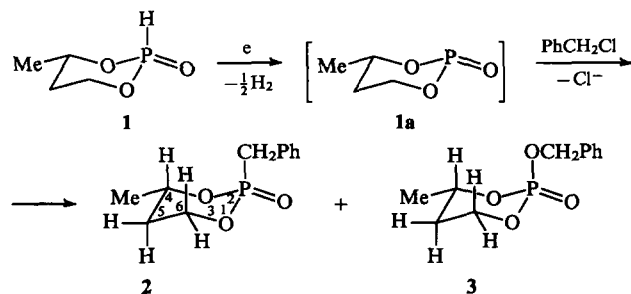


R = Me, Et, Ph.

The yields of the products **A** and **B** depend on the amount of electricity passed through the system. Thus, when three Faradays are passed per mole of the phosphite, mainly product **A** is formed, its yield amounting to 75% for dimethyl phosphite, 72% for diethyl phosphite, and 51% for diphenyl phosphite. It was later shown⁵⁹ that the alkylation of phosphites in the presence of small amounts of water proceeds more successfully than in the anhydrous solvent. The following composition of the catholyte has been recommended for alkylation: solution containing 2 mmol of the phosphite and 3 mmol of the alkyl halide in 25 ml of dimethylformamide containing 4 mmol of tetrabutylammonium as the supporting electrolyte and 4 mmol of water.

For example, the coupling of diethyl phosphite with butyl iodide has been achieved under these conditions in 74% yield, but in the reactions with butyl bromide, benzyl bromide, and benzyl chloride the yields were 49%, 60% and 55% respectively. These data show that compounds containing a sufficiently mobile halogen atom must be used as the coupling component. In other examples, the yields of the phosphonates vary in the range 56%–58%.

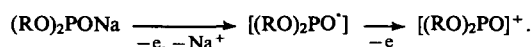
The electrochemical alkylation of *cis*-2-hydro-4-methyl-2-oxo-1,3,2-dioxaphosphorinane **1** with equatorially oriented methyl and oxo-groups proceeds stereoselectively and leads to 2-benzyl-4-methyl-2-oxo-1,3,2-dioxaphosphorinane in 60%–70% yield.⁶⁰ Together with the phosphonate **2**, the phosphate **3** was isolated. The mechanism of the formation of the latter has not yet been investigated.



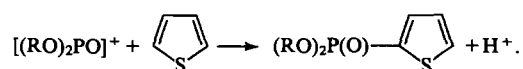
In contrast to dialkyl phosphites, the sodium salts of dialkylphosphorous acids are readily oxidised at a platinum anode in solution in acetonitrile in the presence of sodium perchlorate as the supporting electrolyte.⁶¹

R in (RO) ₂ PONa	Et	Pr ⁱ	Pr ⁿ	Bu ⁿ
<i>E</i> _{1/2} /V	0.45	0.50	0.63	0.63

It is suggested that the oxidation proceeds in accordance with the equation:



The electrolysis of such a system in the presence of aromatic and heterocyclic compounds leads to the corresponding phosphonates, for example,



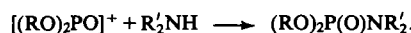
Apart from thiophene, furan, quinoline, and naphthalene have been introduced into this reaction. The yield of the phosphorylation products varied in the range 25%–30%, the reaction

being accompanied by the formation of a number of side products, such as $(\text{RO})_2\text{P}(\text{O})\text{H}$, $(\text{RO})_2\text{P}(\text{O})\text{R}$, and $(\text{RO})_3\text{PO}$.⁶¹

In the presence of secondary amines, amidophosphite diesters were synthesised at the oxidation potential of sodium dialkyl pyrophosphite.⁶² It is suggested that the reaction proceeds via the following path:



In the presence of a large excess of the amine in the solution, the following process may occur:⁶³



The following amidophosphites have been synthesised electrochemically: $(\text{EtO})_2\text{PNet}_2$, $(\text{BuO})_2\text{PNet}_2$, and $(\text{BuO})_2\text{PNBu}_2$ in 30%, 20%, and 32% yields respectively.

* * *

The data presented in this review show that electrolysis can be used successfully for the synthesis of trialkyl phosphates from white and red phosphorus. Data on the catalytic influence of copper halides on the synthesis of alkyl phosphates merit attention. The study of the characteristic features of the formation of trialkyl phosphates demonstrated the possibility, in principle, of the direct synthesis of phosphites from elemental phosphorus and also the possibility of the electrochemical oxidation of phosphites and dialkyl phosphites to the corresponding phosphates and pyrophosphates. It is noted that electrolysis is a promising procedure for the preparation of various derivatives of dialkyl phosphites.

The authors thank the International Scientific-Technical Centre (grant No. 136) for financial support in the writing of this review.

References

1. Ya A Dorfman, M M Aleshkova, G S Polimbetova, L V Levina, T V Petrova, R R Abdreimova, D M Doroshkevich *Usp. Khim.* **62** 928 (1993) [*Russ. Chem. Rev.* **62** 877 (1993)]
2. M Barry, Ch Tobias *Electrochem. Technol.* **4** 502 (1966)
3. D A White, M J Dolan *J. Electrochem. Soc.* **127** 1175 (1977)
4. S L Varshavskii, A P Tomilov, Yu D Smirnov *Zh. Vses. Khim. O-va im D I Mendeleeva* **7** 598 (1962)
5. Ya A Dorfman, R R Abdreimova, V N Statsyuk, G S Polimbetova, D N Akbaeva, S M Aibasova, in *Novosti Elektrokhimii Organicheskikh Soedinenii* (Tez. Dokl. XIII Soveshchaniya po Elektrokhimii Organicheskikh Soedinenii) [New Advances in the Electrochemistry of Organic Compounds (Abstracts of Reports at the XIIIth Meeting on the Electrochemistry of Organic Compounds)] (Tambov: Tambov Institute of Chemical Machine Building, 1994) p. 42
6. USSR P. 1 244 927; *Byull. Izobret.* (26) 256 (1986)
7. A S Romakhin, I M Zaripov, Yu G Budnikova, Yu A Ignat'ev, E V Nikitin, A P Tomilov, Yu M Kargin *Elektrokhiya* **25** 780 (1980)
8. A S Romakhin, Yu G Budnikova, I M Zaripov, Yu M Kargin, E V Nikitin, A P Tomilov, Yu A Ignat'ev, V V Smirnov *Izv. Akad. Nauk, Ser. Khim.* 1322 (1992)
9. A V Bukhtiarov, V N Golyshin, O V Kuz'min *Zh. Obshch. Khim.* **56** 1356 (1986)
10. A S Romakhin, I M Zaripov, Yu G Budnikova, Yu M Kargin, E V Nikitin, A P Tomilov, Yu A Ignat'ev *Izv. Akad. Nauk, Ser. Khim.* 1328 (1992)
11. Yu G Budnikova, Yu M Kargin, I M Zaripov, A S Romakhin, Yu A Ignat'ev, E V Nikitin, A P Tomilov, V V Smirnov *Izv. Akad. Nauk, Ser. Khim.* 2033 (1992)

12. Yu G Budnikova, Yu M Kargin, I M Zaripov, A S Romakhin, Yu A Ignat'ev, E V Nikitin, A P Tomilov *Izv. Akad. Nauk, Ser. Khim.* 2039 (1992)
13. N K Gusarova, B A Trofimov, S F Malysheva, S N Arbuzova, S I Shaikhudinova, V I Dmitriev, A V Polubentsev, A I Albanov *Zh. Obshch. Khim.* 63 53 (1993)
14. B E Ivanov *Izv. Akad. Nauk, Ser. Khim.* 2244 (1989)
15. Ya E Dorfman, R R Abdreimova, L V Levina, T V Petrova *Zh. Obshch. Khim.* 59 481 (1989)
16. A P Tomilov, I M Osadchenko *Zh. Analit. Khim.* 21 1498 (1966)
17. I N Brago, A P Tomilov *Elektrokhimiya* 4 697 (1968)
18. A P Tomilov, I N Brago, I M Osadchenko *Elektrokhimiya* 4 1153 (1968)
19. I M Osadchenko, A P Tomilov *Zh. Obshch. Khim.* 39 469 (1969)
20. N Ya Shandrinov, A P Tomilov *Elektrokhimiya* 4 237 (1968)
21. I M Osadchenko, A P Tomilov *Elektrokhimiya* 29 408 (1993)
22. I M Osadchenko, A P Tomilov *Elektrokhimiya* 29 406 (1993)
23. I M Osadchenko, A P Tomilov *Zh. Prikl. Khim.* 65 1034 (1995)
24. L V Kaabak, M I Kabachnik, A P Tomilov *Zh. Obshch. Khim.* 36 2060 (1966)
25. L F Filimonova, L V Kaabak, A P Tomilov *Zh. Obshch. Khim.* 39 2174 (1969)
26. L V Kaabak, N Ya Shandrinov, A P Tomilov *Zh. Obshch. Khim.* 40 584 (1970)
27. Trasatti, A Alberti *J. Electroanal. Chem.* 12 236 (1966)
28. A M Lunyatskas *Tr. Akad. Nauk Lit. SSR* 3 42 (1965)
29. USSR P. 461 057; *Byull. Izobret.* (7) 47 (1975)
30. A Hickling, D Johnson *J. Electroanal. Chem.* 13 100 (1967)
31. I M Osadchenko, A P Tomilov, V V Rublev *Elektrokhimiya* 9 1492 (1973)
32. M Baudler, D Shellenberg *Z. Anorg. Allg. Chem.* 340 113 (1965)
33. M Baudler, A Bougardt *Z. Anorg. Allg. Chem.* 350 186; 203 (1967)
34. Fr. P. 1130 548 (1957)
35. A P Tomilov, Yu M Kargin, I N Chernykh, in *Elektrokhimiya Elementorganicheskikh Soedinenii. Elementy IV, V, VI Grupp Periodicheskoi Sistemy* (Electrochemistry of Organoelement Compounds. Elements of Groups IV, V, and VI) (Moscow: Nauka, 1986) p. 118
36. A V Bukhtiarov, V V Mikheev, A V Lebedev, Yu G Kudryavtsev *Zh. Obshch. Khim.* 61 889 (1991)
37. V F Pavlichenko, A E Presnov, A P Tomilov *Elektrokhimiya* 31 538 (1995)
38. I M Osadchenko, A P Tomilov, in *Novosti Elektrokhimii Organicheskikh Soedinenii (Tez. Dokl. XII Soveshchaniya po Elektrokhimii Organicheskikh Soedinenii)* [New Advances in the Electrochemistry of Organic Compounds (Abstracts of Reports at the XIIth Meeting on the Electrochemistry of Organic Compounds)] (Karaganda: Institute of Organic Chemistry and Coal Chemistry, 1990) p. 57
39. USSR P. 601 284; *Byull. Izobret.* (13) 79 (1978)
40. I M Osadchenko, A P Tomilov *Elektrokhimiya* 26 596 (1990)
41. I M Osadchenko, A P Tomilov *Khim. Promst* 612 (1995)
42. I M Osadchenko, A P Tomilov, in *Novosti Elektrokhimii Organicheskikh Soedinenii (Tez. Dokl. XIII Soveshchaniya po Elektrokhimii Organicheskikh Soedinenii)* [New Advances in the Electrochemistry of Organic Compounds (Abstracts of Reports at the XIIIth Meeting on the Electrochemistry of Organic Compounds)] (Tambov: Tambov Institute of Chemical Machine Building, 1994) p. 109
43. I N Osadchenko, A P Tomilov *Zh. Prikl. Khim.* 68 1036 (1995)
44. V F Pavlichenko, A E Presnov, A P Tomilov *Zh. Obshch. Khim.* 65 1347 (1995)
45. S Torii, H Tanaka, N Sayo *J. Org. Chem.* 44 2938 (1979)
46. S Torii, N Sayo, H Tanaka *Tetrahedron Lett.* 46 4471 (1979)
47. A M Gazaliev, M Zh Zhurinov, B I Tuleulov, S D Fazylov, in *Novosti Elektrokhimii Organicheskikh Soedinenii (Tez. Dokl. XII Soveshchaniya po Elektrokhimii Organicheskikh Soedinenii)* [New Advances in the Electrochemistry of Organic Compounds (Abstracts of Reports at the XIIth Meeting on the Electrochemistry of Organic Compounds)] (Karaganda: Institute of Organic Chemistry and Coal Chemistry, 1990) p. 63
48. A M Gazaliev, M Zh Zhurinov, S D Fazylov *Novye Bioaktivnye Proizvodnye Alkaloidov* (New Biologically Active Derivatives of Alkaloids) (Alma-Ata: Gilym, 1992)
49. A M Gazaliev, M Zh Zhurinov, S D Fazylov, in *Novosti Elektrokhimii Organicheskikh Soedinenii (Tez. Dokl. XII Soveshchaniya po Elektrokhimii Organicheskikh Soedinenii)* [New Advances in the Electrochemistry of Organic Compounds (Abstracts of Reports at the XIIth Meeting on the Electrochemistry of Organic Compounds)] (Karaganda: Institute of Organic Chemistry and Coal Chemistry, 1990) p. 47
50. A M Gazaliev, S N Beletskii, M Zh Zhurinov, A E Khovanskikh, E B Maizel', K D Mukanova, in *Novosti Elektrokhimii Organicheskikh Soedinenii (Tez. Dokl. XII Soveshchaniya po Elektrokhimii Organicheskikh Soedinenii)* [New Advances in the Electrochemistry of Organic Compounds (Abstracts of Reports at the XIIth Meeting on the Electrochemistry of Organic Compounds)] (Karaganda: Institute of Organic Chemistry and Coal Chemistry, 1990) p. 43
51. A M Gazaliev, M Zh Zhurinov, A N Tabyganova, A S Esaliev, in *Novosti Elektrokhimii Organicheskikh Soedinenii (Tez. Dokl. XII Soveshchaniya po Elektrokhimii Organicheskikh Soedinenii)* [New Advances in the Electrochemistry of Organic Compounds (Abstracts of Reports at the XIIth Meeting on the Electrochemistry of Organic Compounds)] (Karaganda: Institute of Organic Chemistry and Coal Chemistry, 1990) p. 49
52. A M Gazaliev, M Zh Zhurinov, T S Omarov, in *Novosti Elektrokhimii Organicheskikh Soedinenii (Tez. Dokl. XII Soveshchaniya po Elektrokhimii Organicheskikh Soedinenii)* [New Advances in the Electrochemistry of Organic Compounds (Abstracts of Reports at the XIIth Meeting on the Electrochemistry of Organic Compounds)] (Karaganda: Institute of Organic Chemistry and Coal Chemistry, 1990) p. 42
53. A M Gazaliev, M Zh Zhurinov, S A Dyusembaev, A A Abduvakhadov, D N Danilov, Z Tilyabaev, in *Novosti Elektrokhimii Organicheskikh Soedinenii (Tez. Dokl. XII Soveshchaniya po Elektrokhimii Organicheskikh Soedinenii)* [New Advances in the Electrochemistry of Organic Compounds (Abstracts of Reports at the XIIth Meeting on the Electrochemistry of Organic Compounds)] (Karaganda: Institute of Organic Chemistry and Coal Chemistry, 1990) p. 41
54. A.M. Gazaliev M. Zh. Zhurinov S.I. Balitskii, in *Novosti Elektrokhimii Organicheskikh Soedinenii (Tez. Dokl. XII Soveshchaniya po Elektrokhimii Organicheskikh Soedinenii)* [New Advances in the Electrochemistry of Organic Compounds (Abstracts of Reports at the XIIth Meeting on the Electrochemistry of Organic Compounds)] (Karaganda: Institute of Organic Chemistry and Coal Chemistry, 1990) p. 46
55. A M Gazaliev, S D Fazylov, N M Ivanova, R Z Kasenov, in *Novosti Elektrokhimii Organicheskikh Soedinenii (Tez. Dokl. XIII Soveshchaniya po Elektrokhimii Organicheskikh Soedinenii)* [New Advances in the Electrochemistry of Organic Compounds (Abstracts of Reports at the XIIIth Meeting on the Electrochemistry of Organic Compounds)] (Tambov: Tambov Institute of Chemical Machine Building, 1994) p. 34
56. A M Gazaliev, S D Fazylov, R Z Kasenov, A B Tateeva, M Zh Zhurinov, in *Novosti Elektrokhimii Organicheskikh Soedinenii (Tez. Dokl. XIII Soveshchaniya po Elektrokhimii Organicheskikh Soedinenii)* [New Advances in the Electrochemistry of Organic Compounds (Abstracts of Reports at the XIIIth Meeting on the Electrochemistry of Organic Compounds)] (Tambov: Tambov Institute of Chemical Machine Building, 1994) p. 96
57. H Ohmori, S Nakai, V Sekiguchi, M Masui *Chem. Pharm. Bull.* 27 1700 (1979)
58. V A Petrosyan, M E Niyazymbetov *Izv. Akad. Nauk SSSR, Ser. Khim.* 1945 (1988)
59. V A Petrosyan, M E Niyazymbetov, T K Baryshnikova, V A Dorokhov *Dokl. Akad. Nauk SSSR* 302 852 (1988)
60. V A Petrosyan, E N Nifant'ev, M E Niyazymbetov, R K Magdeeva, N S Magometova, V K Bel'skii *Izv. Akad. Nauk, Ser. Khim.* 444 (1996)
61. M Kimura, T Yamashita, T Kurata, Y Sawari *J. Chem. Soc., Chem. Commun.* 259 (1990)
62. E V Nikitin, A S Romakhin, O V Parakin *Dokl. Akad. Nauk SSSR* 258 678 (1981)
63. E V Nikitin, A S Romakhin, O V Parakin *Zh. Obshch. Khim.* 54 1262 (1984)

Spatial and electronic structure of vinyl and allenyl chalcogenides

L M Sinegovskaya, B A Trofimov

Contents

I. Introduction	1009
II. Rotational isomerism in vinyl and allenyl chalcogenides	1010
III. Rotational isomerism in divinyl chalcogenides	1019
IV. Electronic structure of vinyl and allenyl chalcogenides	1022
V. Conclusion	1035

Abstract. Alkyl vinyl chalcogenides show a complex picture of rotational isomerism and are characterised by the presence of several qualitatively different types of stable conformers. The features of conformational structure of these compounds can be understood only by considering the stationary states altogether. Conformational analysis of divinyl chalcogenides indicates that the potential energy surface of internal rotation should be considered not as just a source of information on rotational isomerism; rather, it is a tool in a search for stationary states corresponding to definite intervals of variation of internal molecular coordinates. The principal details of the orbital structure of allenyl ethers and vinyl chalcogenides including a weak dependence of the structure and relative location of higher occupied π -MOs of alkyl vinyl chalcogenides on the nature of the heteroatom and the structure of the alkyl substituent are discussed. The common feature of chalcogenides is the presence of a low energy excited state of σ -symmetry. The excited states of π -symmetry are always located higher on the energy scale than the states of σ -symmetry. The bibliography includes 198 references.

I. Introduction

The interest in electronic and conformational structures of vinyl systems of the type $\text{CH}_2=\text{CHXR}$ ($\text{X} = \text{O}, \text{S}, \text{Se}, \text{Te}$, $\text{R} = \text{Alk}$, and $\text{CH}=\text{CH}_2$) stems from a number of important features specific to rotational isomerism in compounds of this class. First of all, the number of existing rotamers may exceed the number expected on the basis of canonical concepts about the nature of rotational isomers. In the majority of cases, the deviation of atoms from their equilibrium position are small, and the observed properties of the molecular system can be satisfactorily described in terms of the harmonic oscillator approximation. In the case of large deviations from equilibrium in molecules existing in several rotameric forms, quantum mechanical analysis leads to a revision of conclusions on the nature and the number of stable conformers.

According to traditional concepts, hindered internal rotation about $\text{C}_{sp^2}-\text{X}$ ($\text{X} = \text{O}, \text{S}, \text{Se}, \text{Te}$) bonds in molecular systems of alkyl vinyl chalcogenides provides three conformations, namely, *s-cis*-, *s-trans*-, and *gauche*- (non-planar).[†] The reason for hindered rotation about the $\text{C}_{sp^2}-\text{X}$ bonds can be both the interaction of the multiple bond π -electrons with the lone electron pair on the chalcogen atom (p, π -interaction) and purely steric interaction of substituent R with the hydrogen atoms of the vinyl group. For these types of molecules, the most important information on rotational isomerism is the number of stable conformers and their parameters. Mutual counterbalance between the changes in structural parameters in internal rotation and the electron distribution in different conformations opens the way to understanding both the properties of the compounds and the effect on them of external factors, such as electric and magnetic fields, medium, and temperature.

Typical of vinyl chalcogenides are rotameric forms characterised by torsional intramolecular motion of large amplitude. The peculiarities of the conformational structure of these compounds can be understood by considering the whole ensemble of stationary states. The most comprehensive information on rotational isomerism in alkyl vinyl chalcogenides can be gained from the internal rotation potential curve, and in divinyl chalcogenides, from the corresponding potential surface constructed as a function of rotational angles about $\text{C}_{sp^2}-\text{X}$ bonds. Alkyl vinyl chalcogenides are characterized by rotation about the $\text{C}_{sp^3}-\text{X}$ bond, in addition to the rotation about the $\text{C}_{sp^2}-\text{X}$ bond; for R other than Me, internal rotation in the alkyl substituent also takes place. This increases the number of rotational states and hampers the use of many methods of investigation. In this connection, an increased interest in the simplest analogues of compounds under study such as vinyl alcohol and ethenethiol is well understood.

The problem of the relationship between conformational isomerism, electronic structure, physicochemical properties, and reactivity in vinyl heteroatomic systems has first been formulated for vinyl ethers and sulfides in generalising papers.^{1,2} In these studies, the main achievements in this field were summed up, and novel approaches (and solutions) were contemplated. These studies have stimulated systematic investigations in this field carried out in the last two decades^{3–21} including also vinyl compounds of selenium,^{9,11,13} tellurium,^{4,9,11,13} and nitrogen.^{16–20} A significant part of these investigations was performed by the NMR method on various nuclei. Large areas of this

L M Sinegovskaya, B A Trofimov Irkutsk Institute of Organic Chemistry, Russian Academy of Sciences, ul. Favorskogo 1, 664033 Irkutsk, Russian Federation. Fax (7-395) 235 60 46

Received 25 April 1996

Uspekhi Khimii 65 (12) 1091–1123 (1996);
translated by M G Ezernitskaya

[†] Hereinafter, the terms *cis*- and *trans*-conformers refer to *s-cis*- and *s-trans*-conformers of chalcogenides.

research are summarized in theses^{9,13,16,18} and reviews.^{3,4,6-8} However, recent results obtained by other methods have not been considered altogether except for a thesis,²¹ in which the results of the study of the electronic and spatial structures of vinyl and allenyl chalcogenides by IR, Raman, UV, and PE spectroscopy methods, conformational analysis, quantum-chemical calculations, and normal coordinate analysis have been summarized.

The present review gives a systematic account and critical examination of investigations of the electronic and conformational structures of vinyl and allenyl chalcogenides carried out by complementary theoretical and experimental methods (gas electronography, microwave, vibrational, UV and PE spectroscopy, dipole moments).

II. Rotational isomerism in vinyl and allenyl chalcogenides

1. Vinyl alcohol and ethenethiol

For a long time, vinyl alcohol has not been available for experimental studies and has been considered as an unstable tautomeric form of acetaldehyde. Only in 1967 was vinyl alcohol identified by its mass spectrum in the analysis of the products of oxidation of dideuteroacetylene.²² The NMR spectrum of vinyl alcohol (without its isolation from the products of photolysis of acetaldehyde) was reported.²³ The molecular structure of vinyl alcohol was elucidated from the MW spectra.^{24,25} The analysis of the MW spectra favours the preferential planar *cis*-conformation of the molecule having the following geometric parameters: $r(\text{C}=\text{C}) = 1.33 \text{ \AA}$, $r(\text{C}-\text{O}) = 1.37 \text{ \AA}$, CCO bond angle is equal to 120° . Experimental parameters of the less stable *trans*-conformer of vinyl alcohol were obtained later by MW spectroscopy.²⁶ The analysis of rotational constants for the *trans*-rotamer and its deuterioisotopomer ($\text{CH}_2=\text{CHOD}$) gave the following geometry: $r(\text{C}=\text{C}) = 1.32 \text{ \AA}$, $r(\text{C}-\text{O}) = 1.38 \text{ \AA}$, the COD bond angle is 122° . The C=C bond distance in vinyl alcohol is somewhat shorter than the corresponding bond lengths in ethene²⁷ and propene.²⁸ Shortening of the C—O bond length and an increase in the CCO bond angle is observed in vinyl alcohol as compared to saturated alcohols (1.43 \AA and 120° , respectively).²⁹ The energy difference of 4.5 kJ mol^{-1} was calculated for *cis*- and *trans*-conformers of vinyl alcohol from the variation of relative intensities in the MW spectrum.²⁶

The characteristics of vinyl alcohol derived from IR, UV, and NMR spectra³⁰⁻³² are useful for the detection of this alcohol and other simple enol compounds among intermediates of chemical reactions. The absorption bands for the *cis*-rotamer and for all by-products formed in its synthesis were assigned based on the analysis of the IR spectra of vinyl alcohol and nine of its isotopomers and from normal coordinate analysis.³² Five absorption bands are observed in the photoelectron spectrum of vinyl alcohol.^{33,34} The low-energy band has a fine structure with a vibrational interval of 1400 cm^{-1} . The low-frequency component of this band is assigned to the *cis*- and the high-frequency component is assigned to the *trans*-conformer.³³

According to the IR and MW spectra, the sulfur analogue of vinyl alcohol, ethenethiol, is also a mixture of two conformers.³⁵⁻⁴⁰ A detailed analysis of the IR spectra of ethenethiol^{36,37} in the gas phase, crystal state (at 300 K), and in argon and nitrogen matrices has shown that the molecule exists as *cis*- and *trans*-conformers, the *cis*-form being more favourable in energy, as in the case of vinyl alcohol. The normal coordinate analysis for *cis*- and *trans*-conformations indicates that the stretching C—S, bending C=C—H, and torsional S—H vibrations depend most of all on conformations.³⁷

The planar *cis*- and 'quasi'-*trans*-conformers of ethenethiol and its deuterated isotopomers have been studied by MW spectroscopy.^{35,36,38,40} The following geometric parameters were obtained for the most stable *cis*-conformer: $r(\text{C}=\text{C}) = 1.34 \text{ \AA}$, $r(\text{C}-\text{S}) = 1.76 \text{ \AA}$, bond angles CCS and CCH are equal to 126.9 and 95.8° , respectively.⁴⁰ Internal rotation about the

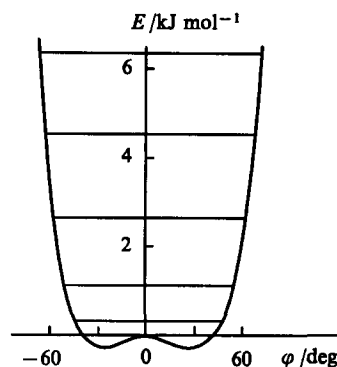


Figure 1. The potential function of internal rotation for the *trans*-conformer of vinylthiol.³⁹

$\text{C}_{sp^2}-\text{S}$ bond results in a decrease in the CCS angle by 5° and in an increase in the C—S bond length by 0.02 \AA . The characteristics of an ethenethiol rotamer and its SD-isotopomer differing from the *cis*-form in the ground and three excited vibrational states were also obtained from the MW spectra.³⁹ The dipole moments and rotational constants corresponding to the CCS and CSH bond angles equal to 122 and 98° , respectively, were determined. The potential curve of internal rotation for *trans*-ethenethiol was obtained in this work (Fig. 1). The ground vibrational state of this 'quasi'-*trans*-conformer (according to the authors' terminology) is above the barrier of 19 cm^{-1} at 26° separating the two minima relative to the zero of the planar conformation.

Considerable progress in studies of the conformational properties of α,β -unsaturated ethers and sulfides has been achieved with the use of *ab initio* calculations, which allow one to estimate the population of one conformation or another and the probability of the interaction of a lone electron pair of a heteroatom with the π -electron system.⁴¹⁻⁴⁶ One of the first theoretical studies of this type was the calculation on vinyl alcohol and ethenethiol,⁴² which confirmed that both compounds have two rotational isomers, the *cis*-conformer being more stable. The maximum in the potential curve of internal rotation for vinyl alcohol corresponds to a dihedral angle (ϕ) of 90° , and for ethenethiol it corresponds to 60° (Fig. 2). The second minimum for ethenethiol corresponds to a torsional angle of 150° .

ab initio Calculations for vinyl alcohol have been performed with full optimization of the geometry of vinyl alcohol using STO-3G and 4-31G basis sets.⁴³⁻⁴⁵ These calculations have also confirmed that the molecule exists in two planar conformations: *cis*- and *trans*-. For a series of substituted vinyl alcohols $\text{XCH}=\text{CHOH}$ ($\text{X} = \text{H}, \text{CN}, \text{F}$),⁴⁶ the potential as a function of the internal rotation about the $\text{C}_{sp^2}-\text{S}$ bond calculated in the 4-21G basis set appeared to depend substantially on the nature of substituent X (Fig. 3) Internal rotation in these molecules is

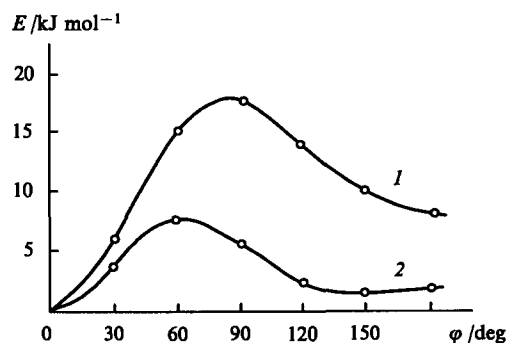


Figure 2. The potential functions of internal rotation for vinyl alcohol (1) and vinylthiol (2).⁴²

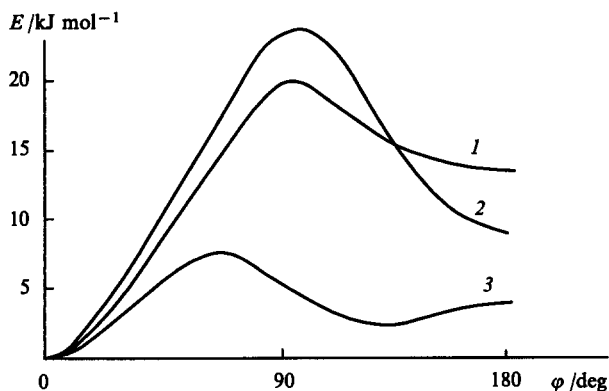


Figure 3. The potential functions of internal rotation for molecules $\text{XHC}=\text{CHOH}$.⁴⁶ X = H (1), CN (2), F (3).

accompanied by changes in the CCO angle and the C–O bond length.^{45, 46}

The energy difference between the conformers of vinyl alcohol is equal to 9.4 (STO-3G),⁴⁴ 9.0 (4-31G),⁴⁴ 7.1–7.9 (3-21G),⁴⁵ and 11.8 (4-21G)⁴⁶ kJ mol^{-1} , which agrees with the value of 7.9 kJ mol^{-1} (*spd*) obtained from the calculation using a partial geometry optimization.⁴² The barrier to internal rotation separating the *cis*- and *trans*-forms of vinyl alcohol is equal to 17.3,⁴⁶ 17.6,⁴² and 17.9 kJ mol^{-1} .⁴⁵

The internal rotation potential curves for ethenethiol obtained by *ab initio* calculations in various basis sets (STO-3G, 3-21G, 44-31G, and *spd*) were compared with those obtained by molecular mechanics (MM) methods (Fig. 4).^{47, 48} The *cis*-conformation is the most stable in all basis sets. The planar *trans*-form is the second stable conformer of ethenethiol in the STO-3G basis while in the 44-31G, 3-21G, and *spd* basis sets, the second stable conformer is a *gauche*-rotamer with a rotational angle about the C_{sp^2} –S bond of 120–135°. The rotational barrier obtained by the MM method (3.8 kJ mol^{-1}) is lower somewhat compared to those determined by other methods (5.9 (44-31G),⁴⁷ and 7.9 kJ mol^{-1} (*spd*).⁴² The value of the barrier calculated using the STO-3G basis appeared to be significantly higher (16.7 kJ mol^{-1})⁴⁶ than those calculated in other basis sets. For this reason the prediction that the *trans*-form is the second stable conformation, most probably, cannot be considered to be correct.

Potential curves for internal rotation about the C_{sp^2} –S bond in ethenethiol obtained from the MW spectroscopy data⁴⁹ are presented in Fig. 5a. In the region corresponding to the *trans*-conformation, there are two minima with torsional angles of about 156° (0.87 π) and 204° (1.13 π) separated by a barrier of about 0.14 kJ mol^{-1} . The ground vibrational state of the *trans*-conformer is above that small barrier. The *cis*-conformer of

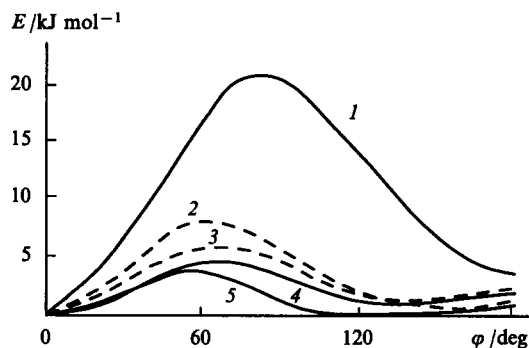


Figure 4. The potential functions of internal rotation for vinylthiol⁴⁷ obtained by different methods: (1) STO-3G, (2) *spd*, (3) MM, (4) 44-31G, (5) 3-21G.

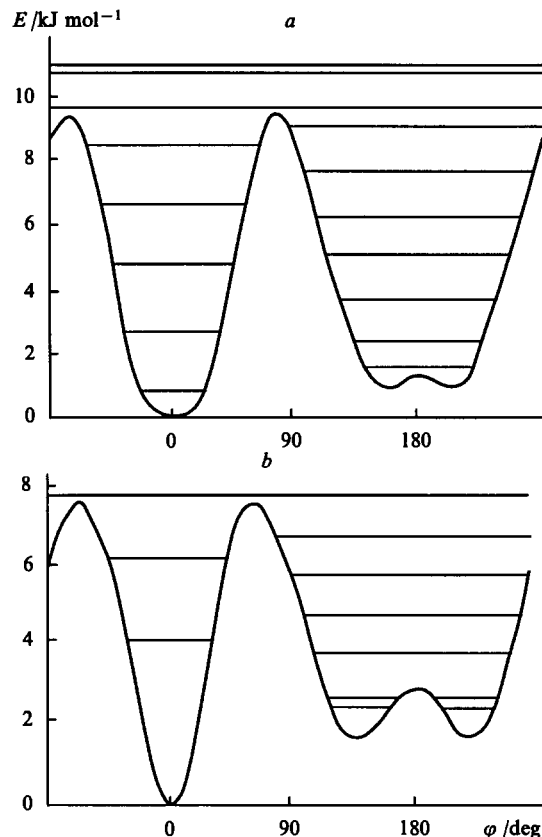


Figure 5. The experimental (a) and theoretical (b) functions of internal rotation for vinylthiol.⁴⁰

vinylthiol is 0.6 kJ mol^{-1} more stable, and the rotational barrier separating the *cis*- and *trans*-conformers is equal to 9.5 kJ mol^{-1} . The *ab initio* calculation in the 4-21G basis gave the internal rotation potential and the positions of stationary energy levels corresponding to the planar *cis*- and 'quasi'-*trans*-states as well as to the non-planar *gauche*-form (Fig. 5b).⁴⁹

The potential function for internal rotation about the C_{sp^2} –S bond in ethenethiols $\text{XCH}=\text{CHSH}$ (X = H, CN, Me, F are *trans* oriented with respect to the sulfur atom) depends substantially on the nature of the substituent (Fig. 6).^{49, 50} The relative stability of the planar *cis*-conformer increases as the electron acceptor

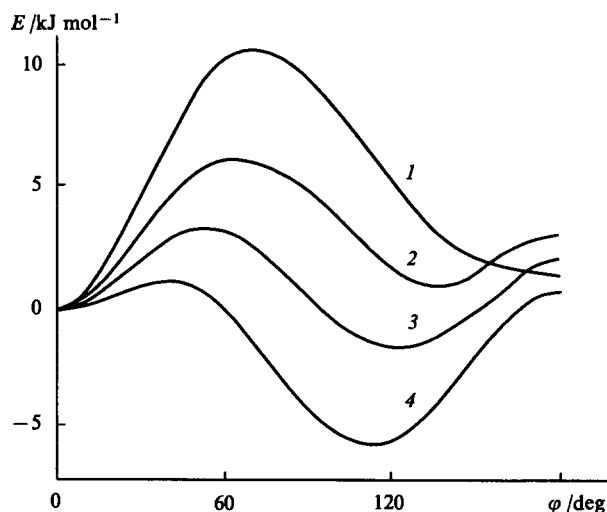


Figure 6. The potential functions of internal rotation for molecules $\text{XHC}=\text{CHSH}$.⁴⁹ X = H (1), CN (2), CH_3 (3), F (4).

properties of the substituent increase; for $X = F$, the acceptor properties of which are lowered due to the competitive p, π -interaction in the $F-C=C$ system, only the *gauche*-rotamer exists in the system.

2. Alkyl vinyl ethers

The existence of rotational isomerism in vinyl ethers was first established from Raman and IR spectroscopy^{1,52-59} and was confirmed later by studies of ultrasonic relaxation⁵¹ and microwave spectroscopy.⁶⁰ From the very beginning, there were different opinions about the number and structure of stable conformers. The study of the temperature dependence of absorbance of triplet components in the range of double bond stretching vibrations allowed one to conclude⁵⁶ that the most stable conformation is characterised by two bands (1613 and 1650 cm^{-1}) whereas the less stable form is characterised by one maximum at 1642 cm^{-1} . The appearance of the third band in the 1600 cm^{-1} region (with the highest frequency) in the vibrational spectra of alkyl vinyl ethers is explained by Fermi resonance between the $\nu(C=C)$ and $\omega(CH_2=)$ vibrations.⁶¹ The temperature dependences of integral intensities of the components of the same triplet in the Raman spectrum of *n*-butyl vinyl ether allowed one to assign each of the three components to a particular rotamer and to calculate the difference between their energies.⁶² Assuming the existence of three possible conformations (two planar, *cis*- and *trans*-, and one non-planar, *gauche*-), one could calculate the frequencies and eigenvectors of the normal modes for methyl vinyl ether, which were in a satisfactory agreement with experimental data.⁵⁸ At the same time, the relaxational behaviour of methyl, ethyl, and 2-chloroethyl vinyl ethers indicates that there is an equilibrium between the planar conformations (*cis*- and *trans*-).⁵¹ Vibrational spectra of methyl vinyl ether and its deuterio-isotopomers have been studied and the band assignment according to symmetry and eigen vectors has been proposed.⁶³ It is noted that this molecule exists at room temperature in the planar *cis*-form, and at lower temperature it exists in the planar *trans*-form (or nearly *trans*-), which follows from the appearance of a number of new bands in the spectra. From the analysis of Raman and IR spectra of methyl vinyl ether it also follows that the *s-trans*-conformation is less stable.⁶⁴⁻⁶⁶ The same conclusions have been derived from the analysis of PE spectra of alkyl vinyl ethers⁶⁷⁻⁶⁹ with normal alkyl substituents.

Analysis of the rotational structure of $CH_2=$ out-of-plane bending modes (820 cm^{-1}) has led to a conclusion^{61,70,71} that the most stable conformation in methyl and ethyl vinyl ethers has a sickle-like (*cis*-) form. It was suggested^{61,70} that the other conformation should have a non-planar structure. These conclusions^{61,70,71} have received additional and independent support from the analysis of MW,⁶⁰ Raman and IR⁷²⁻⁷⁴ spectra of methyl vinyl ether. The study of vibrational spectra of methyl vinyl ether in the gas phase allowed the identification of a less preferred 'skew' rotamer with a torsional angle of 144°.⁷²

The IR spectra of vinyl ethers are very useful in determining the conformer ratio. An analysis of extensive experimental data and literature assignments allowed the major bands of the vinyloxy group to be ascribed to particular conformations. For example, the following maxima correspond to the planar conformer: a low-frequency component of a band in the region of $\sim 820 \text{ cm}^{-1}$ [$\omega(CH_2=)$];^{61,70,75,76} a high-frequency component of a band at $\sim 960 \text{ cm}^{-1}$ [$\omega(CH=)$];^{61,70,76} a very strong broad band around 1200 cm^{-1} [$\nu(C-O)$];^{56,61,70} a narrow band of medium intensity at 1320 cm^{-1} [$\delta(CH=)$];^{61,70} a low-frequency component of a triplet in the 1600 cm^{-1} region (usually, $\sim 1620 \text{ cm}^{-1}$) [$\nu(C=C)$];^{56,61,62,70} The following peaks correspond to the non-planar conformer: a high-frequency shoulder on the band at 820 cm^{-1} ,^{61,70,75,76} a low-frequency component of a doublet in the region of 950 cm^{-1} [$\omega(CH=)$];⁶⁶ weak peaks in the region of 1150–1050 cm^{-1} [$\nu(C-O)$] (for example, 1138 cm^{-1} in methyl vinyl ether⁶⁴ and 1143, 1100, 1081,

1048 cm^{-1} in ethyl vinyl ether⁷⁰); the middle component of a triplet in the range of 1640 cm^{-1} [$\nu(C=C)$].^{56,61,62,70}

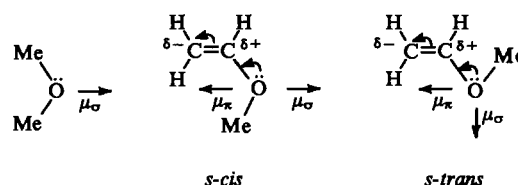
The aim of the studies⁷⁷⁻⁷⁹ was to elucidate, using the IR spectra of alkyl vinyl ethers, the influence of the structure of alkyl substituent on the relative intensities of bands belonging to different conformations without going into details of their spatial structure. A comparative analysis of IR spectra of ethyl vinyl ether indicates that the conformation ratio depends very strongly on the degree of branching of the substituent at the α -carbon atom.⁷⁷ For methyl and alkyl vinyl ethers with normal substituents the planar conformers dominate, whereas the relative intensities of the bands of the planar conformer decrease abruptly with an increase in branching in the substituent up to the disappearance of some of them; simultaneously, the bands of the non-planar conformer appear and their intensities increase. *tert*-Butyl and *tert*-pentyl vinyl ethers exist virtually as one non-planar conformer. Indeed, all the vibrational bands of the planar conformer in the spectra of these ethers decrease in intensity or disappear. This is most clearly illustrated in the 1600 cm^{-1} region, where only one high-frequency component of the very strong multiplet remains, which belongs to the non-planar conformation.

The possibility to apply *ab initio* calculations to analyse the vibrational spectra of methyl vinyl ether has been shown.⁸⁰ A theoretical force field has been composed and corrected by scaling factors, which have been either transferred from simpler molecules $CH_2=CHF$ and Me_2O or selected by calculation of the rotation about the $C_{sp^2}-O$ bond. The method of stepwise determination of scaling factors gave a satisfactory agreement between the calculated and experimental data.

The molecular structure of methyl vinyl ether was also studied by electron diffraction.^{42,81} Along with the problem of the determination of the molecular geometry of the major rotamer, an attempt was made to solve the problem of the existence of a second less-preferable form. In an earlier paper⁸¹, the *gauche*-conformer with an angle between the $C=C-O$ and $C-O-C$ planes between 80–110° has been favoured. Later, the results of *ab initio* calculations referring to the planar *s-trans*-structure of the second stable rotamer have convinced the authors to reconsider their experimental data and to conclude that these data do not contradict the supposition about the planar structure of the second rotamer in methyl vinyl ether.⁴²

Important results concerning the spatial and electronic structure of alkyl vinyl ethers were obtained from the study of their dipole moments.¹ For alkyl vinyl ethers $CH_2=CHOR$, unprecedented dependences of dipole moments on the structure of the alkyl substituent⁸² and temperature⁸³ were established. The reason for these features is a close relationship between p, π -interaction and conformational isomerism. Mere consideration of the dipole moment vectors for dimethyl and methyl vinyl ethers leads to the conclusion that the dipole moment of the latter depends on the torsional angle provided that the p, π -interaction is accompanied by polarisation of the double bond (Scheme 1):

Scheme 1



The existence of this polarisation follows from the consideration of the dipole moment values of alkyl vinyl ethers with normal and branched alkyl substituents (Table 1).⁸⁴⁻⁸⁶

In methyl vinyl ether, which exists preferentially as the *s-cis*-conformer,⁸⁵ the directions of π and σ constituents are opposite. Therefore, in this case, it is worth estimating the π -constituent as the difference (0.36 D) between the moments of dimethyl ether and methyl vinyl ether (as in Ref. 87). Of course, one should bear

Table 1. Dipole moments of vinyl and dialkyl ethers.

Ether	μ /D	Ref.
CH ₂ =CHOMe	1.0	84
	1.1	85
CH ₂ =CHOEt	1.19	84
CH ₂ =CHOPr ⁿ	1.19	84
CH ₂ =CHOPr ⁱ	1.47	84
CH ₂ =CHOBu ⁿ	1.20	84
	1.25	85
CH ₂ =CHOBu ⁱ	1.14	84
	1.20	85
CH ₂ =CHOBu ^t	1.81	84
CH ₂ =CHOPent ⁿ	1.22	84
CH ₂ =CHOPent ^t	1.84	84
(CH ₂ =CH) ₂ O	1.10	84
	1.06	85
Me ₂ O	1.31	85
	1.25	86
Et ₂ O	1.27	85
	1.22	86
(Pr ⁿ) ₂ O	1.13	85
EtOBu ^t	1.29	84

in mind that the π -moment value obtained in this way includes the induced π -moment and the contribution due to the difference in the moments of the C_{sp²}-O and C_{sp²}-O bonds. However, estimations of dipole moments of other conformations by the addition of π and σ vectors⁸⁷ are erroneous in principle, because they do not take into account the changes in the degree of p,π -interaction (and therefore, the π -constituent) due to violation of coplanarity. For a non-planar *gauche*-conformation (where the angle is 90°) the π -constituent should be absent or, at least, should be much less than that for the planar conformation. The consideration of the molecular model shows that for such a conformation, the σ -moment vector forms an angle of ~55° with the double bond plane, and the directions of its projection to this plane and the C_{sp²}-O bond coincide.

A significant difference between the dipole moments of conformers of alkyl vinyl ethers could be rationalised in terms of electronegativity of a substituent R.⁸⁸ The validity of this supposition follows from a close linear dependence of the dipole moment on inductive (σ^*) and steric (E_s) constants of the substituent R. The study of temperature dependence of dipole moments⁸³ allowed one to choose between the inductive and conformational nature of the difference in dipole moments in the series of alkyl vinyl ethers in favour of the latter.

The dielectric behaviour of alkyl vinyl ethers with non-branched substituents was shown to differ substantially from that of vinyl ethers with bulky branched substituents. In the former case, the dipole moment increases markedly with temperature, and in the latter case it decreases. For methyl vinyl ether, the dipole moments measured in a broad temperature interval are in line with the concept about the equilibrium of two rotamers in octane and benzene solutions.^{83,89} It was concluded⁸³ that a decrease in the dipole moments of alkyl vinyl ethers with Prⁱ, Bu^t, Pent^t substituents as temperature increases is caused, not by an increase in the population of the less polar form, but rather by violation of coplanarity of the molecular fragment CH₂=CHO during torsional vibrations. It is evident that an increase in the population of excited torsional vibrational states can affect significantly the experimental dipole moment only if the torsional mode has a sufficiently large amplitude. A W-shaped potential curve of internal rotation has been proposed,⁸³ which can explain qualitatively the dielectric behaviour of all the alkyl vinyl ethers studied.

In addition to the experimental studies of rotational isomerism in vinyl ethers discussed, numerous publications concerning theoretical considerations^{42,45,63,64,80,90-101} indicate that the

planar *cis*-conformation is the most favourable in energy, while the structure of a second less stable conformer is still disputable. The potential curve of internal rotation for methyl vinyl ether was obtained in the CNDO/2 approximation; its shape depends significantly on the COC angle.^{90,91} According to these calculations, the second less stable conformer has a non-planar *gauche*-structure. It is also possible that coplanarity in the *trans*-form is violated.^{42,92}

One of the first *ab initio* calculations⁹⁴ yielded the potential curve of internal rotation for methyl vinyl ether. The minima of the potential function correspond to torsional angles of 0° (*s-cis*-form) and 180° (*s-trans*-form). The conformer energy difference was calculated as 2.2 kJ mol⁻¹.⁹⁴ The potential curve of internal rotation for methyl vinyl ether was calculated using the STO-3G and 4-31G basis sets.^{95,96} The potential curve obtained is shown in Fig. 7.⁹⁶ The geometry optimization was performed in the STO-3G basis. The calculations predict two stable conformations for methyl vinyl ether: planar *cis*- and planar *trans*-. The conformer energy differences of 4.02 kJ mol⁻¹⁹⁵ and 4.2 kJ mol⁻¹⁹⁶ calculated in the STO-3G basis, are in satisfactory agreement with the experimental value (4.8 kJ mol⁻¹) obtained by gas electronography;⁴² the values of 10.3 kJ mol⁻¹⁹⁵ and 9.6 kJ mol⁻¹⁹⁶ calculated in the 4-31G basis appeared to be twice as high.

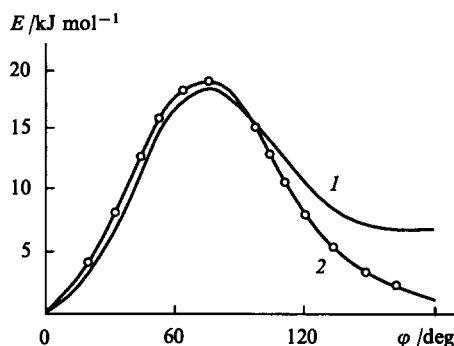


Figure 7. The potential function of internal rotation about the C_{sp²}-O bond in vinyl methyl ether.⁹⁶

The method of calculation: (1) 4-31 G, (2) STO-3G.

The potential as a function of internal rotation for methyl vinyl ether was calculated in the 6-31G and 6-31G* basis sets with full geometry optimization.⁹⁷ A region in the potential curve with two flattened minima (torsional angle CCOC is 156.7–159.4°) and a barrier between them corresponds to a less favourable conformer (Fig. 8). The stationary state energies are located above the barrier; they are associated with the vibration of the Me group with large amplitude relative to the equilibrium position

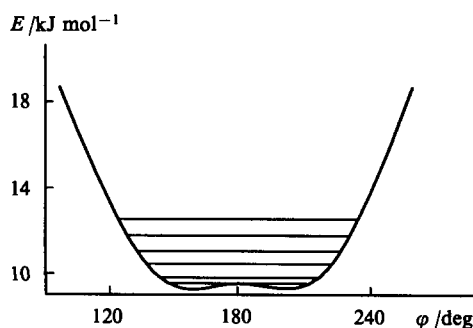


Figure 8. The potential function of internal rotation for vinyl methyl ether in the region of location of the *trans*-conformer and the positions of the steady energy levels (the calculation using the 6-31 G* basis set).⁹⁷

corresponding to the planar *trans*-form. The energy difference between the lowest energy levels of the *cis*- and *trans*-forms, 8.3 kJ mol^{-1} (6-31G) and 9.9 kJ mol^{-1} (6-31G*), is in agreement with the experimental value (7.1 kJ mol^{-1}) obtained for the gas phase by IR spectroscopy.⁷⁴

An *ab initio* calculation in the 4-21G basis with full geometry optimisation gave comprehensive data on the structure of three conformers, *s-cis*- (0°), *s-trans*- (180°), and skew (168°).⁹⁸ The population of the skew conformer is 1–5%, the energy difference between *s-cis*- and *s-trans*-rotamers is equal to 12.4 kJ mol^{-1} . However, according to other *ab initio* calculations for methyl vinyl ether,⁴⁵ torsional angles of 0° (*s-cis*-) and 150° (*gauche*-) correspond to the stable states, the first being more favourable by 7.9 – 8.8 kJ mol^{-1} .

Hence, most of the studies on rotational isomerism in vinyl ethers show that these ethers exist as two stable conformers. One of them is planar (*cis*-), the other is characterised by a relative motion with large amplitude of the molecular fragments and an effective non-coplanarity, which depends on the structure of the vinyl substituent.

3. Allenyl ethers

Allenyl ethers ($\text{CH}_2=\text{C}=\text{CHOR}$) are close analogues of vinyl ethers. Their unsaturated fragment is represented by two orthogonal π -systems. The spatial structure of allenyl methyl ether has been investigated by various physico-chemical methods.^{102–112} The interest in allenyl ethers is easily understandable because they are both valuable initial substances for organic syntheses and convenient models for investigations of the relationship of, and mutual influence between, conformational isomerism and p, π -interaction. Experimental data obtained by gas electronography indicate that at room temperature allenyl methyl ether exists only in the planar *cis*-conformation; the second conformer was not detected.¹⁰² This conclusion was confirmed by an analysis of coupling constants in the ^1H NMR spectrum of allenyl methyl ether.^{103, 104}

According to these data, alkyl allenyl ethers with non-branched substituents possess preferential planar *cis*-conformation, and homologues with branched substituents exist essentially in the planar *trans*-conformation. Conformational analysis of vinyl and phenyl allenyl ethers¹⁰⁴ allowed one to conclude that the planar *trans*-conformation predominated and the content of the *cis*-conformer was $\sim 10\%$.

The molecular structure of allenyl methyl ether was also studied by MW spectroscopy.¹⁰⁵ The overall dipole moment was determined in the ground state ($\mu = 0.96\text{D}$). The barrier to internal rotation of the methyl group was obtained from the splitting of transitions in the excited state ($V_3 = 11.86 \text{ kJ mol}^{-1}$). The values obtained were assigned to the planar *cis*-form. PE spectroscopic data and semiempirical MNDO/3 calculations showed that allenyl methyl ether exists as two conformers *s-cis*- and *s-trans*-, the former dominating.¹⁰⁶ Raman and IR spectra of allenyl methyl ether were studied using *ab initio* calculations within the 3-21G and 6-31G* basis sets. From the data obtained it was concluded that allenyl methyl ether has two conformers, viz, the planar *cis*-form and the non-planar *gauche*-form with a torsional angle of 140° . The energy difference of 11.2 kJ mol^{-1} for conformers was calculated from the temperature dependence of intensities of the bands sensitive to conformations. The potential curve of internal rotation for allenyl methyl ether was obtained¹¹³ (Fig. 9). In the range of the second stable conformer, there are two small minima separated by a barrier of 1.42 kJ mol^{-1} , which correspond to enantiomeric forms. Large amplitude intramolecular motion of fragments of the molecule relative to the planar *trans*-form corresponds to the stationary energy states arranged above the barrier.

Rotational isomerism and the breakdown of local C_3 , symmetry of the methyl group have been studied using vibrational spectra [IR (gas, liquid), Raman (liquid)] of allenyl methyl ether and its deuterio-isotopomer, $\text{CH}_2=\text{C}=\text{CHOCD}_3$.¹¹⁴ Specific

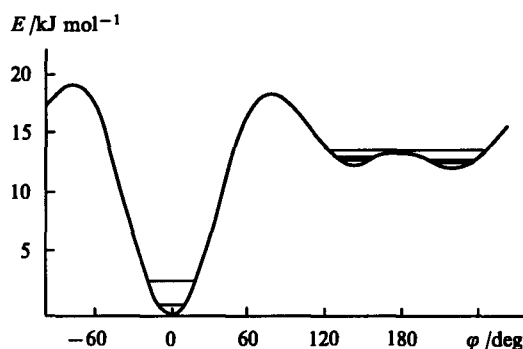


Figure 9. The potential function of internal rotation for allenyl methyl ether.¹¹³

interactions in the fragments $\text{CH}_2=\text{C}=\text{CHO}$ and COC can manifest themselves in vibrational spectra due to the orthogonal arrangement of the π -systems in allenyl methyl ether. It is difficult to estimate the coupling of these vibrations directly from experimental spectra. It became possible only by comparing experimental results and *ab initio* calculations.

The calculation of the equilibrium geometry and the force field was carried out by the gradient method using the 4-21G basis assuming the *cis*-conformer to be the most stable.¹¹⁴ Scaling factors were transferred from simpler dimethyl ether and allene molecules, and for the rotation about the $\text{C}_{sp^2}-\text{O}$ bond these were selected from calculations. The scaling factors were determined by fragments, which gave a satisfactory agreement of calculated and experimental frequencies.¹¹⁴

Similar to Fermi resonance between $\nu_s(\text{CH}_3)$ and $2\delta_s(\text{CH}_3)$, there is a resonance between the $\nu_{as}(\text{CH}_3)$ and $2\delta_{as}(\text{CH}_3)$ modes. Comparative analysis of a splitting value of the degenerate $\nu_{as}(\text{CH}_3)$ mode of C_3 , symmetry and the frequency shift for this mode upon isotopic substitution indicates that asymmetry of the C–H bond lengths in the methyl group of allenyl methyl ether is the same as in methyl vinyl ether.^{115, 116}

The antisymmetric stretching mode of the allenyl fragment $\nu_{as}(\text{C}=\text{C}=\text{C})$ at 1960 cm^{-1} is not coupled and localised in double bonds, while the $\nu_s(\text{C}=\text{C}=\text{C})$ mode at 1054 cm^{-1} is coupled with the vibrations of the COC and CH_3 groups. The frequencies of $\text{C}=\text{C}=\text{C}$ bending modes occur in the low-frequency range at 270 and 170 cm^{-1} ; the bending mode of the COC group contributes largely to the band at 170 cm^{-1} . The band responsible for the torsional motion relative to the CCC axis (612 cm^{-1}) is intense in the Raman spectrum and weak in the IR spectrum. This is explained by substantial changes in the molecular polarisability and a weak dependence of the dipole moment on the torsional motion of the allenyl fragment. Apparently, the perturbation introduced by the orthogonal π -system to the interaction of the lone pair electron with π -electrons of the double bond of the $=\text{C}=\text{C}(\text{H})\text{O}$ fragment does not influence significantly the effects of electron density delocalisation.

Analysis of experimental spectra of allenyl methyl ether and its deuterio-isotopomer allowed one to identify the bands corresponding to the stretching modes of the CH and CH_2 groups. A band of medium intensity in the IR spectrum and a strong line in the Raman spectrum with a frequency of 3046 cm^{-1} were assigned to the stretching mode of the C–H bond.¹¹⁴ It is identical in frequency and eigenvector with that of the analogous group in methyl vinyl ether.

The feature distinguishing allenyl methyl ether from methyl vinyl ether is an anomalous intensity ratio of the vibrational bands $\nu_s(\text{CH}_2)$ and $\nu_{as}(\text{CH}_2)$. The intensity of $\nu_{as}(\text{CH}_2)$ in methyl vinyl ether is significantly higher than that of $\nu_s(\text{CH}_2)$, while, according to the calculation for allenyl methyl ether, confirmed by experimental results, the derivative of the dipole moment with respect to the normal coordinate is by an order of magnitude larger for

$\nu_s(\text{CH}_2)$ than for $\nu_{as}(\text{CH}_2)$. A similar picture is observed in the spectra of other molecules containing the allenyl group,¹¹⁷ which might be rationalised in terms of peculiar features of the electronic structure of the allene framework.

In the IR spectrum of allenyl methyl ether in the gas phase, the A-type band with a frequency of 1430 cm^{-1} belongs to the bending mode $\delta(\text{CH}_2)$.¹¹⁴ This assignment differs from the assignment¹¹³ of this band to $\delta(\text{CH}_3)$, which has been made without analysis of the rotational structure of the deuterio-isotopomer. A low intensity δ_{CH_2} bending mode at 1015 cm^{-1} manifests itself as a C-type band in the IR spectrum. According to calculation, it contains a contribution from a wagging mode, which features a departure of the α -hydrogen atom from the plane of the $\text{C}=\text{C}-\text{O}$ fragment.¹¹⁴

Analysis of rotational contours in the IR spectrum of allenyl methyl ether allowed one to assign the bands in the $850\text{--}920\text{ cm}^{-1}$ range since in this range, the stretching COC mode gives rise to a band of the A type at 918 cm^{-1} , which is coupled with the wagging modes of the CH_2 group (895 cm^{-1}) and the bending mode of the allene framework.

In order to investigate rotational isomerism in allenyl methyl ether and in its deuterio-isotopomer, their IR spectra in various solvents (CCl_4 , C_7H_{16} , $\text{C}_4\text{H}_9\text{Br}$, MeCN) were measured over a wide temperature range.¹¹⁴ A normal coordinate analysis was carried out for various orientations of the COC and CCO fragments specified by the COCC torsional angle. The bands in the vibrational spectrum sensitive to conformations were identified by calculation. For allenyl methyl ether in the condensed state, two weak bands at 572 cm^{-1} (Raman) and 960 cm^{-1} (IR) were revealed, which, probably, belong to the modes of a second conformer differing from the *cis*-conformer in population and geometry. No features of the second conformer were detected in the gas-phase spectra. The splitting of the $\nu_s(\text{C}=\text{C}=\text{C})$ and $\nu_{as}(\text{C}=\text{C}=\text{C})$ bands cannot originate from conformational changes because it remains in the spectra of the gas phase, condensed and solid states. The bands observed on the high-frequency side of $\nu_{as}(\text{C}=\text{C}=\text{C})$ and on the low-frequency side of $\nu_s(\text{C}=\text{C}=\text{C})$ seem to belong to a series of so-called 'hot' transitions.

It follows from the above account that the planar *cis*-conformer with the methyl group of distorted C_{3v} local symmetry is the most preferable in energy for allenyl methyl ether. The splitting value of the degenerate $\nu_{as}\text{CH}_3$ mode of C_{3v} symmetry and the position of the low-frequency component of the Fermi resonance lead to the conclusion that the structures of methyl vinyl and allenyl methyl ethers are similar.

4. Alkyl vinyl sulfides

The molecular structure of the sulfur analogue of methyl vinyl ether, methyl vinyl sulfide, has been studied by both experimental and theoretical methods. The conclusions made from these investigations concerning the nature of possible stable conformers and their energy characteristics do not always coincide.^{42, 118–124} Thus the data of MW¹²⁰ and PE spectroscopy¹²⁵ indicate that methyl vinyl sulfide exists at room temperature only in the *cis*-conformation, whereas electronography shows that methyl vinyl sulfide exists as two conformers, *cis*- and *gauche*-, in the ratio of 33:66¹²¹ and 38:62.⁴² The content of the *gauche*-conformer was estimated as 11%–21%.¹²² The electronographic data reported^{42, 121, 122} and the MW and Raman spectra of methyl vinyl sulfide were analysed¹²³ using a static (considering small amplitude modes) and a dynamic (including large amplitude modes) models. The differences observed were explained by the fact that the use of the static model is incorrect because this model cannot be applied to high-temperature measurements as well as in the cases when the barrier separating the conformers is relatively high as is the case for methyl vinyl sulfide.

Dipole moments of alkyl vinyl sulfides appeared to be very much similar to those of alkyl vinyl ethers. In the series $\text{CH}_2=\text{CHSR}$ ($\text{R} = \text{Me}, \text{Et}, \text{Pr}^i, \text{Bu}^i$) a significant increase in

dipole moments is observed with an increase in branching of alkyl substituent.¹²⁶

R	Me	Et	Pr ⁿ	Pr ⁱ	Bu ⁿ
μ, D	1.35	1.47	1.44	1.58	1.41
R	Bu ⁱ	Bu ^s	Bu ^t	Pent ^t	cyclo-C ₆ H ₁₁
μ, D	1.40	1.59	1.69	1.70	1.60

However, the difference in dipole moments of *tert*-butyl vinyl sulfide and methyl vinyl sulfide at 298 K is only 0.35 D, which is more than twice as low as that of *tert*-butyl vinyl and methyl vinyl ethers (0.74 D). A smaller dipole moment value for methyl vinyl sulfide than that of the saturated analogue, ethyl methyl sulfide (1.60 D), as in methyl vinyl ether, indicates the same direction of polarization due to p, π -conjugation.

The temperature dependence of the dipole moments of alkyl vinyl sulfides is analogous to that observed for alkyl vinyl ethers with the only difference that the variation range is substantially narrower.⁸³ For alkyl vinyl sulfides with normal substituents, the temperature dependence originates from a change in the populations of *s-cis*- and *gauche*-conformations; for branched substituents, it is due to a change in the vibrational level populations of the *gauche*-conformation, i.e. the temperature dependence is determined by a different degree of deviation of the SR group from the equilibrium position as the planar form is approached.

Methyl vinyl sulfide was intensively studied by IR spectroscopy.^{3, 5, 124, 127–131} A detailed investigation of IR-active vibrations of the molecule has been given.^{118, 124, 127} The bands sensitive to conformational changes were revealed. The results of these studies agree except for the assignment of the band at 1430 cm^{-1} , which has earlier been assigned to the bending mode of the vinyl groups ($\text{CH}_2=$).¹¹⁸ In more recent studies,^{124, 127} it was assigned to the out-of-plane bending vibration of the methyl group, and the $\delta(\text{CH}_2=)$ mode was associated with the bands in the range of $1360\text{--}1390\text{ cm}^{-1}$.

Out-of-plane bending ($\text{CH}_2=$) ($860\text{--}880\text{ cm}^{-1}$) and C–S stretching ($600\text{--}750\text{ cm}^{-1}$) modes are sensitive to rotational isomerism and give rise to several bands, the number and intensity of which vary with the change in the structure of the alkyl substituent at the sulfur atom.^{124, 127, 128} The band at 860 cm^{-1} was assigned¹²⁴ to the planar *cis*-conformer, and the higher-frequency band ($\sim 880\text{ cm}^{-1}$), to the *gauche*-rotamer. A trend of increasing frequency of $\omega(\text{CH}_2=)$ (860 cm^{-1}) with increase in the electron-acceptor properties of the substituent was noted¹³¹ in the spectra of substituted vinyl sulfides. Bearing in mind the IR spectra of vinyl ethers,^{77–79} one can relate these changes to the increase in the population of the less conjugated non-planar conformer due to the shift of the lone electron pair of the sulfur atom toward the acceptor.

It is noticed¹²⁸ that the band at 678 cm^{-1} [$\nu_s(\text{C}-\text{S})$], which dominates in the spectra of alkyl vinyl sulfides with non-branched substituents, becomes less intense in the spectra of *sec*-alkyl vinyl sulfides and is absent in the spectra of *tert*-alkyl vinyl sulfides. The latter have the only band at 730 cm^{-1} assigned to *gauche*-rotamer modes.¹²⁸ A comparison of relative intensities of the bands in the ranges mentioned shows that vinyl sulfides are irregular as regards to conformation, and the proportion of the dominating stable *cis*-rotamer decreases with an increase in substituent branching. *tert*-Alkyl vinyl sulfides exist virtually completely in the *gauche*-conformation.

The band due to the double-bond stretching mode exhibits a doublet with absorption maxima in the range of $1575\text{--}1585\text{ cm}^{-1}$ (Fig. 10).¹²⁹ As the alkyl substituent branching increases, the intensity of the low-frequency component decreases and that of the high-frequency component increases. In the spectrum of *tert*-butyl vinyl sulfide, the low-frequency band is absent. A similar picture is observed in the IR spectra of vinyl ethers.^{1, 77} Hence, IR spectra of alkyl vinyl sulfides adequately reflect changes in the conformer ratio depending on the substituent structure.

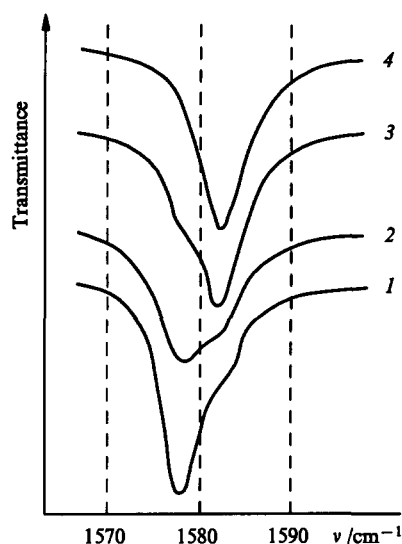


Figure 10. The band contour of the stretching vibration of the double bond in the IR spectra of compounds $\text{CH}_2=\text{CHSAlk}$.¹²⁹ Alk = Me (1), Et (2), Pr^i (3), Bu^i (4).

IR spectroscopic data and quantum mechanical consideration of rotational isomerism gave the potential energy curve for internal rotation in methyl vinyl sulfide.¹²⁹ In the spectrum the doublet band of the double bond stretching mode has maxima at 1577 and 1581 cm^{-1} . The relative intensity of the low-frequency component decreases and that of the high-frequency component increases with temperature. The effect of alkyl substituent branching in a series of alkyl vinyl sulfides as well as the existence of a temperature dependence of relative intensities of the doublet components permitted their assignment to different conformations of the vinylthio group.¹²⁹ Since the intensity of the C=C bond stretching mode due to the substituent resonance effect is independent of the inductive effect influence and since the σ constants are equal in the substituent series AlkS ,¹³⁰ the extinction for methyl vinyl sulfide in the *gauche*-conformation may be assumed to be equal to that for *tert*-butyl vinyl sulfide.

The temperature dependence of the $\nu(\text{C}=\text{C})$ band contour has been analysed. The relationship between $\ln(c_{\text{cis}}/c_{\text{gauche}})$, obtained using the temperature dependence of *tert*-butyl vinyl sulfide, and $1/T$ gives the following enthalpy and entropy difference for the rotamers: $\Delta H = 6.1 \text{ kJ mol}^{-1}$, $\Delta S = -1.74 \text{ J K}^{-1} \text{ mol}^{-1}$. The energy difference obtained for methyl vinyl sulfide conformers is close to those found earlier (kJ mol^{-1}): 9.63,¹³² 5.86,¹²⁴ 7.95,¹²³ 3.3–3.7,¹²² 7.9.¹³³

Based on the quantum model of conformational isomerism, the internal rotation potential curve parameters were selected so as to correlate the number and energies of all the stationary states with the observed temperature behaviour of the conformer ratio (Fig. 11).¹²⁹ The stationary energy spectrum of the molecular rotation is found from the solution of the Schrödinger equation:¹²⁹

$$\left[-\frac{\hbar^2}{2J} \frac{\partial^2}{\partial \varphi^2} + U(\varphi) \right] \phi(\varphi) = \epsilon \phi(\varphi)$$

with the potential $U(\varphi)$ in the form:

$$U(\varphi) = U_n(\varphi) + \frac{1}{2} \sum_{k=1}^3 V_k (1 - \cos k\varphi),$$

where $U_n(\varphi)$ is the energy of steric hindrance, V_k is the characteristic internal rotation barrier about the $\text{C}_{\text{sp}^2}-\text{S}$ bond, J is the reduced moment of inertia of the molecule, and φ is the rotation angle.

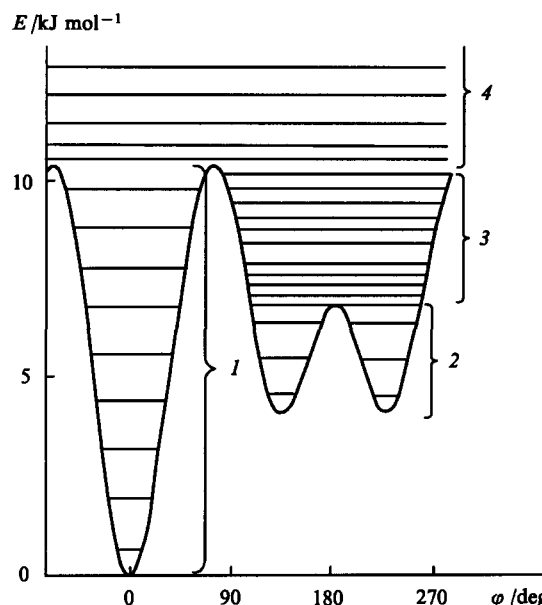


Figure 11. The potential function of internal rotation for vinyl methyl sulfide and the positions of the stationary energy levels. States: *cis* (1), *gauche* (2), 'quasi'-*trans* (3), and free rotation (4).¹²⁹

As is seen from Fig. 11, the methyl vinyl sulfide molecule is an ensemble of four types of rotamers corresponding to four types of stationary states, namely, planar *cis*-states (1), *gauche*-states with rotation angles about the $\text{C}_{\text{sp}^2}-\text{S}$ bond of $132 \pm 3^\circ$ (2), the states above the *trans*-barrier ('quasi'-*trans*-states) associated with a large amplitude intramolecular mode having the equilibrium position in the planar *trans*-form (3), and the states of free rotation (4). The bands of the *gauche*- and 'quasi'-*trans*-states seem to differ somewhat in frequency, therefore, the width of the band at 1581 cm^{-1} is, on the average, 1.35 times larger than that of the band at 1571 cm^{-1} . A maximum in the potential curve corresponding to the planar *s-trans*-conformation is typical of the methyl vinyl sulfide molecule. The barrier separating the *gauche*-forms is equal to 2.5–2.9 kJ mol^{-1} .¹²⁹ There are two or three energy levels in the potential well of the *gauche*-conformer. The energy difference between lower *gauche*- and *cis*-levels (3.8–4.2 kJ mol^{-1}) differ substantially from the formal enthalpy difference of rotamers obtained on the basis of the static model of rotational isomerism (6.1 kJ mol^{-1}). The barrier to *cis-gauche*-transition is equal to 9.8–10.6 kJ mol^{-1} .

Optimal parameters of the potential V_k were obtained,¹²⁹ which correspond to the minimum of the fitness criterion F

$$F = \left\{ \frac{1}{K} \sum_{i=1}^2 \left[\ln \left(\frac{c_{\text{cis}}}{c_{\text{gauche}}} \right)_{\text{calc}} - \ln \left(\frac{c_{\text{cis}}}{c_{\text{gauche}}} \right)_{\text{exp}} \right]^2 \right\}^{1/2}.$$

The value of $V_1 = 2.7 \pm 0.1 \text{ kJ mol}^{-1}$ means that the energy of the interaction between the lone electron pair on the sulfur atom and π -electrons of the double bond differs for planar *cis*- and *trans*-conformations. The interaction is more effective for the *cis*-form than that for the *trans*-rotamer. A value of $V_2 = 7.9 \pm 0.8 \text{ kJ mol}^{-1}$ is an average estimate of the interaction energy. The value of $V_3 = 6.3 \pm 0.4 \text{ kJ mol}^{-1}$ appeared to be unexpectedly high, probably, due to hybridisation intermediate between sp^2 - and sp^3 -hybridisations of the sulfur valence electrons.

The potential function for methyl vinyl sulfide (Fig. 11)¹²⁹ is qualitatively similar to that of ethenethiol (Fig. 5).⁴⁰ The barriers to *cis-gauche*-transitions are practically the same, while the barrier separating two *gauche*-forms is significantly higher for methyl vinyl sulfide (2.9 kJ mol^{-1}) than that for ethenethiol (0.14 kJ mol^{-1}). As a result, there are several (2 or 3) energy

levels in the potential well for the *gauche*-conformer of methyl vinyl sulfide.

The spatial structure of methyl vinyl sulfide was the subject of semiempirical and *ab initio* calculations. Semiempirical calculations were used for the analysis of the correlation between the structure of sulfur compounds and their various experimental characteristics such as electronic and PE spectra, and dipole moments. An analysis of publications⁴¹ of this type leads to the conclusion that the interaction between the lone electron pair on the sulfur atom and the double bond π -electrons should be taken into account to interpret practically all the experimental data. CNDO/2 calculations of methyl vinyl and divinyl ethers and sulfides have been performed in *sp* and *spd* approximations in order to compare the electronic transfer effect through the hetero atom.¹³⁴ It was concluded that the transfer is more effective in the case of the sulfur atom due to $p\pi-d\pi$ interaction. Vacant orbitals were taken into consideration in the calculation though the question of whether it is necessary to include these into the basis set is still being debated.^{135,136} For vinyl sulfides, the passage from the *sp* to the *spd* approximation leads to a basically different conclusion on the nature of the sulfur atom: the sulfur atom is a π -donor within the *sp* basis, while it becomes a π -acceptor within the *spd* basis.¹³⁴ The CNDO/2 calculation in the *sp* approximation yielded the energies of *cis*- and *trans*-conformers for β -substituted methyl vinyl sulfides ($XCH=CHSMe$, $X = Me, OMe, SMe$)¹³⁷ with a fixed geometry.¹²¹ It was shown that the *cis*-rotamer is more favourable in energy. The energy differences between conformers are as follows: 2.8, -3.6, and 2.4 kJ mol⁻¹ for $X = Me, OMe$, and SMe , respectively. The corresponding enthalpy differences obtained from the equilibrium constants are 1.9 kJ mol⁻¹, 9.9 kJ mol⁻¹, and 2.8 kJ mol⁻¹.¹³⁷ An analysis of the interactions in $XCH=CHX$ ($X = OMe, SMe$) has been carried out by the CNDO/2 method.¹³⁸ For these systems the *trans*-conformer appeared to be more favourable than *cis*-conformer. The calculated conformer energy differences are: 20.4 and 1.7 kJ mol⁻¹ for $X = SMe$ and OMe , respectively.

Considerable progress has been made in the analysis of conformational transitions in α,β -unsaturated sulfides using *ab initio* calculations. The efficiency of these calculations depends upon the approximation used, upon the type and set of the basis functions. *ab initio* Calculations are used for the analysis of the role of *nd*-AOs in the formation of chemical bonds by the sulfur atom in different valence states. It was concluded¹³⁵ that a meaningful, in quantitative terms, population of the 3*d*-AO is observed only for compounds with an increased coordination number of sulfur. The authors¹³⁵ believe that the 3*d*-AOs should be always taken into account as polarisation corrections in *ab initio* calculations; for compounds with a higher valence, they might play the role of real orbitals. The solution of a conformational problem requires that sulfur 3*d*-AOs should also be included in the basis for the correct representation of the wave function geometry.

Potential functions for internal rotation about the $C_{sp^2}-S$ bond for vinyl sulfides have been obtained by *ab initio* calculations.^{47,48,92,123,139} The internal rotation potential for methyl vinyl sulfide was shown to depend strongly on the basis set used (Fig. 12).^{47,48} The *cis*-conformation was found to be the more stable regardless of the basis used, whereas the next conformation might be either *trans*- (STO-3G) or *gauche*-form with different values of the CCSC torsional angle (3-21G, 44-31G). The potential obtained by the MM method is analogous to that calculated within the 44-31G basis.⁴⁸ For a long time, the preference of the *cis*-conformer in methyl vinyl sulfide and in methyl vinyl ether was considered as an experimental fact. Later in theoretical studies,^{95,140,141} it was suggested that the preference can result from the interaction between the σ -orbitals of two methyl hydrogen atoms and π -orbitals of the double bond. In the range of *trans*-conformation in the potential curve of methyl vinyl sulfide, there is a small maximum separating two *gauche*-forms (Fig. 12).⁴⁷ The barrier height is equal to 0.84 kJ mol⁻¹, which is

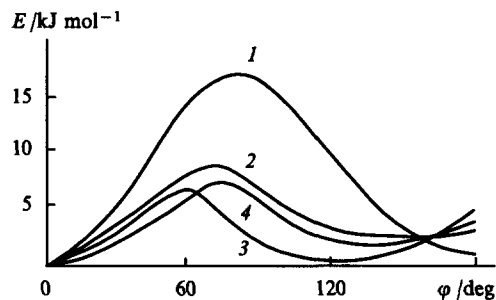


Figure 12. The potential functions of internal rotation about the $C_{sp^2}-S$ bond in vinyl methyl sulfide.⁴⁸

The method of calculation: (1) STO-3G, (2) 44-31 G, (3) 3-21 G, (4) MM.

insufficient for the existence of a stationary state of the *gauche*-type.

The energy differences calculated for methyl vinyl sulfide conformers, 2.9 kJ mol⁻¹ (44-31G),⁴⁷ 0.8 kJ mol⁻¹ (3-21G),⁴⁸ and 0.8 kJ mol⁻¹ (MM),⁴⁸ are markedly lower than the experimental values obtained from the IR spectra (4.9 kJ mol⁻¹ and 6.7 kJ mol⁻¹).^{124,129} A higher value (9.6 kJ mol⁻¹) is obtained from a temperature dependence study of the PE spectra of methyl vinyl sulfide.¹³² Electronography^{42,121} gives the energy difference as close to zero.

5. Allenethiol and allenyl sulfides

ab initio Calculations for allenethiol and allenyl methyl sulfide have been performed.⁴⁷ The calculation for allenethiol within the STO-3G basis⁴⁷ revealed two stable forms, *cis* and *trans*. The potential curves of internal rotation for allenethiol and ethene-thiol are similar. The conformer energy differences for these molecules are practically the same and are equal to ~4.6 kJ mol⁻¹.⁴⁷

The calculations for allenyl methyl sulfide and methyl vinyl sulfide within the STO-3G and 44-31G basis sets give similar results.⁴⁷ Both calculations predict the greater stability of the *cis*-conformation for allenyl methyl sulfide. According to the calculation within the STO-3G basis, the next conformation is *trans*, while the calculation within the 44-31G basis gives a *gauche*-conformation as the next stable one (Fig. 13). The internal rotation potential curve for allenyl methyl sulfide is more flattened (44-31G, Fig. 13) than that for methyl vinyl sulfide (44-31G, Fig. 12), and the energy maximum corresponds to a dihedral angle of 65–70°. The rotational barrier for allenyl methyl sulfide is 5.5 kJ mol⁻¹, which is 3.3 kJ mol⁻¹ lower than that for methyl vinyl sulfide (8.8 kJ mol⁻¹).

The corresponding barriers obtained in the STO-3G basis⁴⁷ are 12.6 kJ mol⁻¹ for allenyl methyl sulfide and 16.4 kJ mol⁻¹ for methyl vinyl sulfide.

The energy minimum in the potential curve for allenyl methyl sulfide corresponds to a torsional angle of ~120°. In the range of

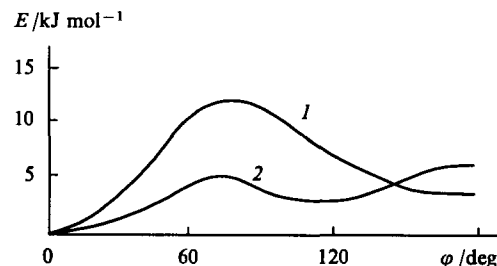


Figure 13. The potential functions of internal rotation for allenyl methyl sulfide.⁴⁷

The method of calculation: (1) STO-3G, (2) 44-31G.

trans-conformation, there is a low barrier of 4.2 kJ mol⁻¹ separating two *gauche*-forms. The energy difference between *cis*- and *trans*-conformers is higher for allenyl methyl sulfide than that for methyl vinyl sulfide (4.6 kJ mol⁻¹ and 1.2 kJ mol⁻¹ in the STO-3G basis and 7.5 kJ mol⁻¹ and 3.8 kJ mol⁻¹ in the 44-31G basis, respectively).⁴⁷ This seems to be due to the difference in spatial interaction between the Me group and the β -hydrogen, which is of a repulsive character in methyl vinyl sulfide and is absent in allenyl methyl sulfide.

ab initio Calculations⁴⁷ predict two stable conformers for allenyl methyl sulfide. PE spectroscopic data and semiempirical quantum calculations of allenyl methyl sulfide suggest two planar conformers, *cis* and *trans*.¹⁰⁶ At the same time, an electronic investigation of allenyl methyl sulfide indicates only one planar *cis*-conformation.¹⁰² The same follows from the ¹H NMR study of alkyl allenyl sulfides.¹⁰³

6. Methyl vinyl selenide and methyl vinyl telluride

Analysis of vibrational spectra of methyl vinyl selenide and methyl vinyl tellurides suggests the presence of rotational isomers: it makes it possible to estimate the torsional angles between the CXC and XCC planes (X = Se, Te) and to assess the degree of interaction of the heteroatom with the double bond. Band assignments in the IR and Raman spectra of methyl vinyl selenide and methyl vinyl telluride were proposed based on a normal coordinate analysis.^{142–144} The starting point for the discussion of the spectra of the molecules under study was a normal coordinate analysis of methyl vinyl sulfide and its deuterio-isotopomers.¹²⁷ The force fields of the vinyl and methyl groups of these molecules are mutually transferable, which indicates that their electronic structures are similar. While the force constant matrices are consistent, the frequencies of C–X modes differ significantly, which might be due to the difference in heteroatom masses, geometry and force constants of the C–S–C, C–Se–C, and C–Te–C groups. The C_{3v} local symmetry of the methyl group breaks down^{127, 142, 143} in the case of methyl vinylchalcogenides. Analysis of the IR spectra of liquids and solutions in a temperature range of 193–353 K allowed one to suppose that methyl vinyl selenide^{142, 145, 146} and methyl vinyl telluride^{143, 147, 148} have rotational isomers.

Normal vibration frequencies calculated for various values of the CXCC torsional angle were correlated with the experimental frequencies.^{142, 143} The bending $\delta(\text{XCC})$ and $\delta(\text{CXC})$ modes are sensitive to changes in the torsional angle. Rotational isomers should manifest themselves most distinctly in the range of the stretching $\nu(\text{CXC})$ modes. Unfortunately, in the case of methyl vinyl selenide, it was impossible to analyse the frequency changes in this region due to the overlap of bands of the stretching (CSeC) and out-of-plane bending (Se–C_{sp²}–H) modes.¹⁴²

According to the calculation for methyl vinyl telluride, the 500–600 cm⁻¹ region should contain the bands due to out-of-plane bending modes of the vinyl group as well as the symmetric and antisymmetric stretching C–Te modes. Only one band is observed in the IR (at 519 cm⁻¹) and Raman spectra (at 530 cm⁻¹) of liquid methyl vinyl telluride at 298 K, whereas in the IR spectrum¹⁴³ of a CS₂ solution of methyl vinyl telluride at 193 K, this band is composed of three components at 512, 521, and 527 cm⁻¹. The band due to double bond stretching vibrations appears as a doublet with absorption maxima at 1582 cm⁻¹ and 1585 cm⁻¹ for methyl vinyl selenide and 1572 cm⁻¹ and 1577 cm⁻¹ for methyl vinyl telluride (in heptane solutions). The temperature dependence of the relative intensities of doublet components is analogous to that for methyl vinyl sulfide.¹²⁹ The intensity of the low-frequency band decreases, and that of the high-frequency band increases with a rise in temperature. Obviously, the doublet nature of the $\nu(\text{C}=\text{C})$ band of methyl vinyl selenide and methyl vinyl telluride is due to the presence of several rotamers in solution.

The enthalpy and entropy differences have been calculated¹⁴⁷ for rotamers of methyl vinyl telluride: $\Delta H = 4.6$ kJ mol⁻¹,

$\Delta S = -11.1$ J K⁻¹ mol⁻¹. The ΔH value reflects the lowering of the rotational barrier from sulfur to tellurium. The high-frequency doublet component in the spectra of methyl vinyl selenide and methyl vinyl telluride corresponds, as for methyl vinyl sulfide, to several rotamers with large amplitude torsional motion or with above-barrier free rotation. A significant ΔS value indicates the presence of a large number of stationary energy levels corresponding to the high-frequency absorption band.

The data presented point to a similarity of the conformational structures of methyl vinylchalcogenides. It is reasonable to suppose that the low-frequency doublet component in the spectra of methyl vinyl selenide and methyl vinyl telluride, as in the case of the corresponding sulfide, belongs to the planar *s-cis*-form. This is confirmed by comparison of half-widths of the high-frequency doublet components.^{129, 142, 147} The half-widths of the low-frequency components are virtually the same for all the chalcogenides considered, whereas the half-widths of the high-frequency doublet components are different: 5.5 cm⁻¹ for methyl vinyl telluride, 8.0 cm⁻¹ for methyl vinyl selenide, and 10.2 cm⁻¹ for methyl vinyl sulfide. Evidently, the high-frequency doublet component of methyl vinyl telluride belongs preferentially to one type of stationary state. Apparently, the contribution of the *p*, π -interaction stabilising planar conformations is less, and the barrier separating two *gauche*-forms seems to be higher for methyl vinyl telluride than those for methyl vinyl sulfide.

In order to solve the problem of possible *p*, π -interaction in methyl vinyl telluride and methyl vinyl sulfide, the conformational energy has been calculated as a sum of energies of interaction between atoms separated by more than two bonds¹⁴⁷ and energies of bond angle strains.^{149–151} The dependence of the conformational energy on the angle of rotation about C_{sp²}–Te and C_{sp²}–S bonds is presented in Fig. 14. It is seen that steric hindrance is practically absent in the *s-cis*-form of methyl vinyl telluride. The difference in the energies of steric hindrance between the planar *cis*- and *trans*-forms is 0.7 kJ mol⁻¹ (for the sulfide it is 4.4 kJ mol⁻¹). The planar *s-cis*-form in methyl vinyl telluride is stabilised by electronic interactions of the same type as in the case of methyl vinyl sulfide, i.e. due to *p*, π -interaction. The energy of this interaction is 5.3 kJ mol⁻¹, which is twice as low as the energy of the same interaction in methyl vinyl sulfide (10.4 kJ mol⁻¹).

Thus, investigations of rotational isomerism in vinyl chalcogenides have revealed unexpected, and remarkable in many respects peculiarities of their molecular and electronic structure. Alkyl vinyl chalcogenides have two qualitatively different types of stable conformers. One of them is characterised by a definite torsional angle and small deviations from the global minimum of potential energy. The other is associated with a large amplitude relative motion of the fragments of the molecule within a flat-bottomed potential well. This motion can include more than one minimum in the internal rotation potential curve.

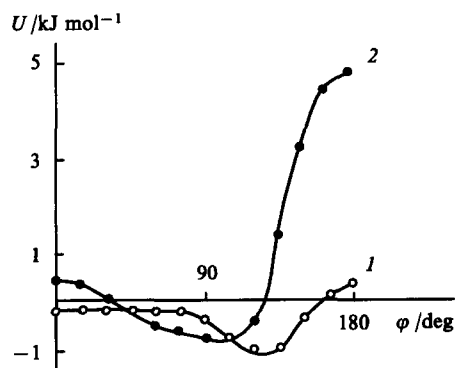


Figure 14. The dependence of the energy of steric strain on the angle of internal rotation for vinyl methyl telluride (1) and vinyl methyl sulfide (2).¹⁴⁷ For the planar *s-trans*-form $\phi = 0$.

III. Rotational isomerism in divinyl chalcogenides

The presence of two unsaturated fragments in the immediate vicinity of the heteroatom in divinyl chalcogenides poses new problems of the competition in the interaction of the double bond π -electrons with the lone electron pair, of the possibility of a 'through' conjugation of the π -systems of the vinyl groups, and of a correlation between the barriers to internal rotation in alkyl vinyl and divinyl compounds. The most comprehensive information about rotational isomerism in divinyl chalcogenides can be gained from the potential surface composed as a function of angles of rotation about $C_{sp^2}-X$ bonds. In the case of divinyl chalcogenides, the internal rotation potential energy surface should be considered not only as source of information on rotational isomerism, but as a tool for a search for the stationary states corresponding to changes in the internal molecular coordinates.

A method of build up and analysis of potential energy maps was used to determine the number and the nature of rotational isomers of divinyl chalcogenides.⁵ The most essential component of the potential energy, the energy of steric hindrance, was calculated by the MM method (Table 2).⁵

Table 2. The energies of steric strain U_n in various conformations for molecules $CH_2=CHXCH=CH_2$ ($X = O, S, Se, Te$).⁵

Conformation	$U_n/\text{kJ mol}^{-1}$			
	O	S	Se	Te
A (<i>trans-trans</i>)	3.8	2.5	2.0	1.8
B (<i>cis-trans</i> , planar)	14.5	12.9	8.4	5.1
C (<i>cis-trans</i> , deviation by 15°)	11.3	9.0	5.5	3.2
D (<i>cis-cis</i> , planar)	52.7	53.5	41.4	31.8
E (<i>cis-cis</i> , deviation by 38°)	9.4	5.3	2.7	1.0
F (<i>cis-cis</i> , deviation by 45°)	7.6	3.2	1.3	0.3

1. Divinyl ether

Electron diffraction study of the molecular structure of divinyl ether has led to the conclusion that the planes of the double bonds are turned by about 20° relative to the plane of the symmetrical *trans-trans*-conformation.¹⁵² However, the analysis of MW spectroscopic data for divinyl ether¹⁵³⁻¹⁵⁵ revealed a non-planar *cis-trans*-conformer. A deviation from the planar structure is supposed to be due to strong repulsion between the hydrogen atoms in the α - and β -positions of the *trans*- and *cis*-vinyl groups, respectively. The special feature of the *cis-trans*-conformation is the existence of a tunnel transition through an insignificant potential barrier, which manifests itself as a splitting of rotational transitions.¹⁵⁴ Taking into account tunnel splitting of rotational transitions made it possible to increase the accuracy of the calculation of frequencies of *cis*- and *trans*-conformers in the MW spectrum of divinyl ether.¹⁵⁵

A study of the vibrational spectra of gaseous and liquid divinyl ether has provided evidence for the preferential planar *cis-trans*-conformation of C_s symmetry, however, the possibility of the existence of a second, less stable conformation having no symmetry elements (C_1) is also not ruled out.¹⁵⁶ Divinyl ether was shown¹⁵⁷ to exist as an equilibrium mixture of two conformers with an energy difference of 2.5 kJ mol⁻¹. Analysis of relative band intensities in the IR and Raman spectra and line polarisability in the Raman spectra leads to the conclusion that the planar *trans-trans*-conformer is the most stable, while the second conformer has no elements of symmetry.¹⁵⁷ An investigation of the band shapes of the COC stretching modes in the IR spectrum of gaseous divinyl ether has been performed¹⁵⁸ based on a theoretical simulation of profiles of these bands in different conformers. At 300 K, divinyl ether was shown to contain 80% of *cis-trans*-conformer with torsional angles of 13° and 145° and 20% of *trans-trans*-conformer.

ab initio Calculations have been carried out in order to investigate rotational isomerism in divinyl ether.¹⁵⁷⁻¹⁶⁰ Two stable conformations have been predicted:¹⁵⁷ the first energy minimum corresponds to the *trans-trans*-form, and the second belongs to a non-planar conformation with torsional angles of 135° and 20°. A potential energy map has been constructed for divinyl ether,¹⁵⁹ and three stable conformations have been predicted corresponding to the potential energy minima of 0, 11.4, and 10.0 kJ mol⁻¹ (Fig. 15). These conformations are non-planar *cis-trans*- (torsional angles 147.4° and -17.4°; C_1), planar *trans-trans*- (torsional angles 180°, 180°; C_{2v}), and near-planar *cis-cis*- (torsional angles 31.5° and 31.5°; C_2). The conformer geometry was optimised¹⁵⁹ within the STO-3G basis, relative energies were optimized within the basis 4-31G. The geometry of *cis-cis*-, *trans-trans*-, and *cis-trans*-conformers of divinyl ether were obtained by a gradient method within the 4-31G basis.¹⁵⁸ The difference in the conformer energy (0; 6.6, and 4.5 kJ mol⁻¹, respectively) differ from those obtained in another study.¹⁵⁹ The calculation of divinyl ether within the 6-31G** basis yielded two stable conformers:¹⁶⁰ a near-planar *cis-trans*-conformer as the most energy-favourable and the planar *trans-trans*-conformer with an energy difference of 1.5 kJ mol⁻¹.

A steric hindrance map for divinyl ether obtained by the MM method is given in Fig. 16.³ The steric hindrance energy was calculated by varying ϕ_1 from 0° to 360° and ϕ_2 from 0° to ϕ_1 with a step of 15° (ϕ_1 and ϕ_2 are the rotation angles of the first and the second vinyl groups relative to the planar *cis-cis*-structure, respectively). A minimum of steric hindrance (-5.65 kJ mol⁻¹) belongs to a non-planar form, which results from the *trans-trans*-conformation by rotating two vinyl groups in opposite directions by an angle of about 75° (Fig. 16). Steric hindrance energies for other conformations are listed in Table 2.

The potential energy for different conformations of divinyl ether was calculated as a sum of energies of steric hindrance and p,π -interaction. The values obtained from the *ab initio* calculation for methyl vinyl ether⁹⁴ were used as p,π -interaction energies for divinyl ether. Analysis of the potential energy map for divinyl ether (Fig. 17) shows that there are three different conformations corresponding to the minima of potential energy. In two non-planar quasi-degenerate *trans-trans*-forms, the vinyl groups deviate from the COC plane by $\phi_1=130^\circ$, $\phi_2=130^\circ$, and $\phi_1=130^\circ$, $\phi_2=-130^\circ$ (energy -26.1 kJ mol⁻¹). In a non-planar *cis-trans*-form, the rotational angle of one vinyl group is

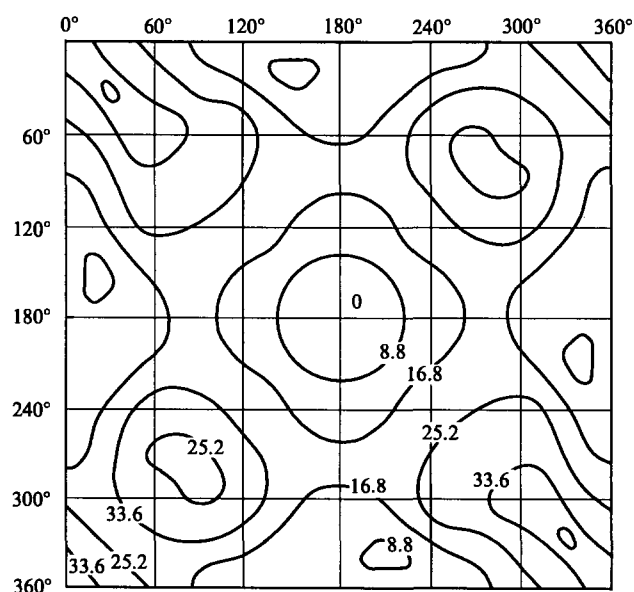


Figure 15. The map of the potential surface for the internal rotation in divinyl ether.¹⁵⁹

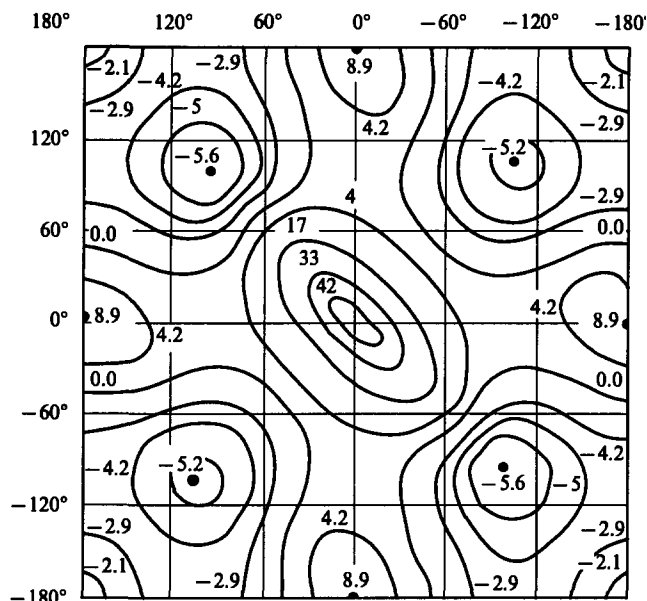


Figure 16. The map of steric hindrance energy for divinyl ether.³

about 10° and that of the other about 50° (energy -28.0 kJ mol⁻¹). These forms are separated by a barrier of -20.9 kJ mol⁻¹. The potential map (Fig. 17) does not take into consideration either effects connected with competition for the interaction of the double bond π -electrons with the lone electron pair of the oxygen atom or 'through' conjugation.

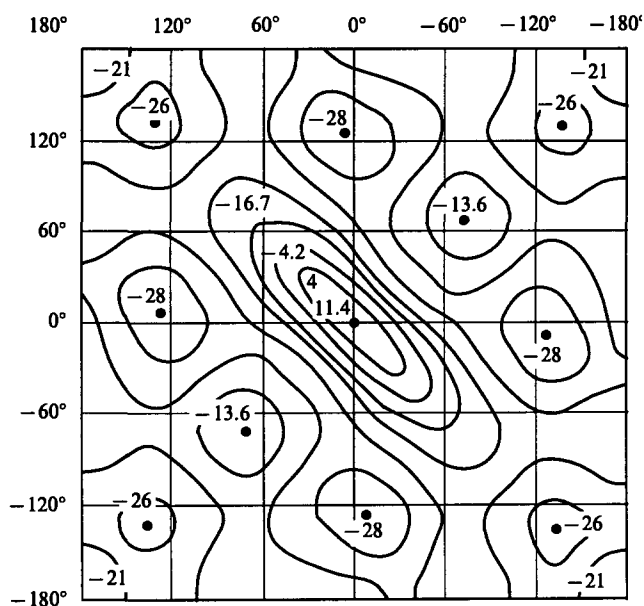


Figure 17. The map of potential energy for divinyl ether.³

2. Divinyl sulfide

The molecular structure of divinyl sulfide was studied by gas electronography.¹⁶¹ Only one *cis-trans*-conformer with CSCC torsional angles of 32° and -148° having no elements of symmetry was detected in gaseous divinyl sulfide at room temperature. The basic structural parameters of the molecule are as follows: $r(\text{C}-\text{S})=1.758 \text{ \AA}$, $r(\text{C}=\text{C})=1.342 \text{ \AA}$; angles CSC 101.8°, SCC 123.7°. Similar torsional angles were obtained by the MM method (38°, 124°)⁴⁸ and by an *ab initio* calculation within the 3-21G basis (18° and 116°).⁴⁸ Low accuracy in the

electronographic determination of some structural parameters for divinyl sulfide is probably due to large-amplitude intramolecular motion. Therefore the presence of a second (minor) conformer cannot be ruled out.

Rotational isomerism in divinyl sulfide was also studied by vibrational spectroscopy.¹⁶²⁻¹⁶⁴ Analysis of the temperature dependence of intensities of the bands sensitive to conformations in the spectra of gaseous, liquid, and solid divinyl sulfide shows the presence of two conformers.¹⁶³ There is a dynamic equilibrium between the *cis-trans*- and *trans-trans*-conformations in liquid and solution, and in the crystal state only the planar *trans-trans*-conformation exists.¹⁶³ The conformer enthalpy difference is close to zero. Theoretical vibrational spectra of stable conformers of divinyl sulfide have been calculated¹⁶⁰ within the 6-31G** basis. The calculations showed that a non-planar *trans-trans*-conformer is the most favourable, a *cis-trans*-conformer is the next, in which the vinyl group deviates from the CSC plane by 20°; the energy difference between these conformers is 0.71 kJ mol⁻¹. The populations of the individual *trans-trans*-conformer at 300 K was calculated to be 57% and that of the *cis-trans*-conformer, 43% (Table 3).

Table 3. Calculated energy differences and populations for conformers of divinyl chalcogenides.¹⁶⁰

Compound	ΔE , /kJ mol ⁻¹	Statistical weight	Population at 300 K	
			calculation	experiment
(CH ₂ CH) ₂ O				
<i>trans-trans</i>	+ 1.46	1	22	20 ^a
<i>cis-trans</i>	0.0	2	78	80
(CH ₂ =CH) ₂ S				
<i>trans-trans</i>	0.0	2	57	50 ^b
<i>cis-trans</i>	+ 0.71	2	43	50
(CH ₂ =CH) ₂ Se				
<i>trans-trans</i>	0.0	2	60	
<i>cis-trans</i>	+ 0.1	2	40	
(CH ₂ =CH) ₂ Te				
<i>trans-trans</i>	0.0	2	71	
<i>cis-trans</i>	+ 2.26	2	29	

^a The data of Ref. 158; ^b the data of Ref. 155.

^a The data of Ref. 158; ^b the data of Ref. 155.

The internal rotation potential curves for divinyl sulfide have been calculated within the STO-3G and 3-21G basis sets and by the MM method with a fixed *trans-trans*-conformation of one vinyl group (Fig. 18).⁴⁸ These potential functions differ significantly from those for ethenethiol (Fig. 4)⁴⁸ and methyl vinyl sulfide (Fig. 12).⁴⁸ The calculation in the STO-3G basis reveals the *trans-trans*-conformation to be the most stable. Two stable conformations, very similar in energy are obtained in the 3-21G basis and by the MM method: *cis-trans*- (0° and 120°, *C_s* symmetry) and *cis-cis*- (120° and 120°, *C₂* symmetry).⁴⁸ ΔE values for the conformers calculated by these methods differ significantly: 5.0 kJ mol⁻¹ (3-21G) and 1.3 kJ mol⁻¹ (MM). The results obtained by the MM method are believed⁴⁸ to be more reliable because the dipole moment (1.48 D) calculated by the MM method fits better the experimental value of 1.07–1.2 D than that calculated within the 3-21G basis (1.9 D).

The conformational energy of divinyl sulfide was calculated^{5,140} as the sum of contributions of the p,π -interaction stabilising the planar arrangement of each of the C–S–C=C fragments and the steric hindrance (Table 2). Minimum steric hindrance is unique to the non-planar *trans-trans*-form with a deviation of the vinyl groups to the both sides of the CSC plane by an angle of ~80°. The planar *cis-cis*-form has a hindrance energy of 53.5 kJ mol⁻¹ (Table 2). Rotation about the C–S bonds in the

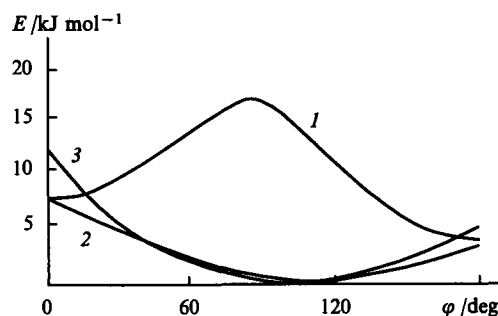


Figure 18. The potential functions of internal rotation for divinyl sulfide ($\varphi_2 = 180^\circ$).⁴⁸ The method of calculation: (1) STO-3G, (2) 3-21G, (3) MM.

opposite direction by less than 30° results in a conformation in which steric hindrance changes into stabilization due to Van der Waals interaction.

Quantitative estimation of the p, π -interaction energy in divinyl sulfide was determined¹⁴⁰ from the known internal rotation potential curve for methyl vinyl sulfide.¹²⁹ A part of the internal rotation potential of methyl vinyl sulfide was used in the calculation of the potential energy map for divinyl sulfide:

$$V(\varphi) = V_1 \frac{1 - \cos \varphi}{2} + V_2 \frac{1 - \cos 2\varphi}{2} + V_3 \frac{1 - \cos 3\varphi}{2},$$

where φ is the torsional angle of the rotation about the $C_{sp^2} - S$ bond for methyl vinyl sulfide; V_1 is the first-order barrier connected with the *cis*-preference; V_2 is the second-order barrier numerically equal to a half of the p, π -interaction energy; V_3 is the third-order barrier due to hybridisation of the lone electron pair of the sulfur atom, which is intermediate between sp^3 - and sp^2 -hybridisations. Since the *cis*-preference in divinyl sulfide molecules cannot take place, the p, π -interaction energy can be described by the equation:

$$V(\varphi_1, \varphi_2) = V_2 \left(\frac{1 - \cos 2\varphi_1}{2} + \frac{1 - \cos 2\varphi_2}{2} \right) + V_3 \left(\frac{1 - \cos 3\varphi_1}{2} + \frac{1 - \cos 3\varphi_2}{2} \right),$$

where $V_2 = 7.9 \pm 0.8 \text{ kJ mol}^{-1}$ and $V_3 = 6.3 \pm 0.4 \text{ kJ mol}^{-1}$.

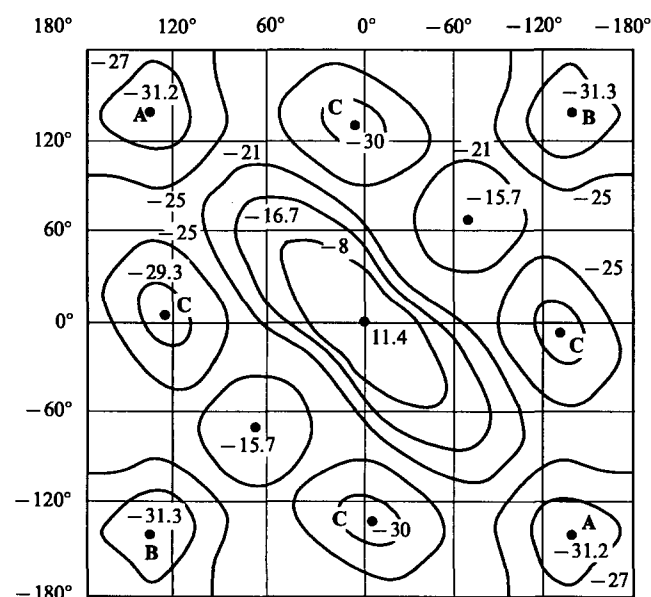


Figure 19. The map of potential energy for divinyl sulfide.¹⁴⁰

The potential energy map for divinyl sulfide is presented in Fig. 19. The planar *trans-trans*-form corresponds to a local maximum rather than to the minimum of potential energy. Two more favourable quasi-degenerate forms have virtually the same energy and correspond to torsional angles $\varphi_1 = 137^\circ$, $\varphi_2 = 137^\circ$ (*trans-trans*-conformer A) and $\varphi_1 = 137^\circ$, $\varphi_2 = -137^\circ$ (*trans-trans*-conformer B). There is also a local minimum at $\varphi_1 = 125^\circ$, $\varphi_2 \sim 0^\circ$ (*cis-trans*-conformer C). The latter conformer is 0.84 kJ mol^{-1} less preferential than the former ones.

Complete understanding of rotational isomerism requires that excited states be taken into account. In the range of excitation energies up to 8 kJ mol^{-1} , there are states in the divinyl sulfide molecule in which torsional angle varies within the limits from -90° to $+90^\circ$ relative to the *trans-trans*-conformation.¹⁴⁰ The stationary state D includes simultaneously potential wells of both *trans-trans*-conformers A and B. Here, large-amplitude intra-molecular motion takes place and the above-barrier states are

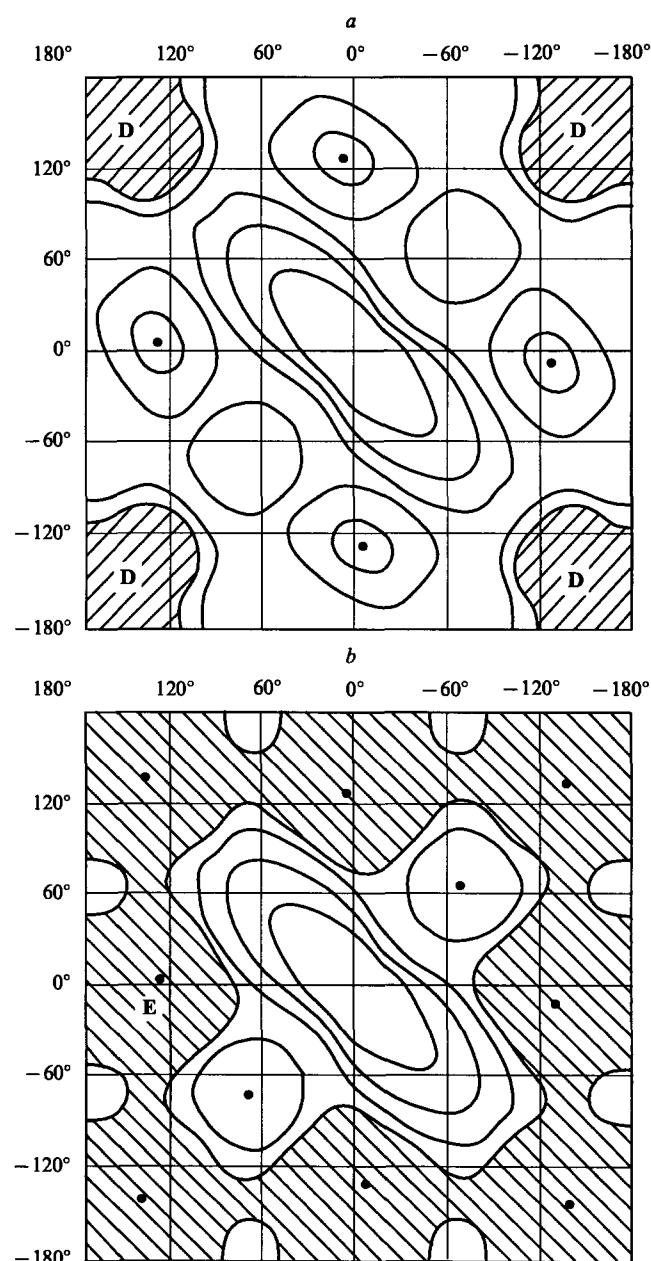


Figure 20. The stationary states of internal rotation¹⁴⁰ for divinyl sulfide: (a) type D with the energy to 8.0 kJ mol^{-1} , (b) type E with the energy above 8.0 kJ mol^{-1} .

becoming occupied. In this range of excitation energies, along with the stationary states of the D type (Fig. 20 a), excited states of the *cis-trans*-conformer C localised near the potential energy minimum are realised.

At excitation energies above 8 kJ mol^{-1} , the stationary state includes conformations that can have, with a few exceptions, practically any values of torsional angles φ_1 and φ_2 (stationary states of the E type, Fig. 20 b).¹⁴⁰ Complete equivalence of the double bonds is characteristic of all the stationary states, except for the *cis-trans*-conformer C in which one of the vinyl groups is practically not involved in the p, π -interaction.

Hence, the potential as a function of the internal rotation about the $C_{sp^2}-S$ bond for methyl vinyl sulfide was transferred (with some corrections) to the rotation about analogous bonds in the divinyl sulfide molecule.¹⁴⁰ Five types of stationary states have been characterised (A-E), two of which have no analogues among stable conformers in a classical sense.

3. Divinyl selenide and divinyl telluride

In this section, the published data on the structure of divinyl selenide and divinyl telluride are presented.^{4, 5, 144, 160, 165} Theoretical vibrational spectra of these molecules have been obtained,¹⁶⁰ the analysis of which revealed two stable non-planar *trans-trans*- and *cis-trans*-conformations. The conformer energy differences and their populations at 300 K are listed in Table 3. A proportion of the more stable *trans-trans*-conformer increases with increase in the mass of chalcogenide. For divinyl sulfide and divinyl telluride, the *trans-trans*-conformer is preferential in energy. Recently the IR spectra of divinyl telluride in the gas, liquid, and solid states and the spectra at low temperatures in various matrices (argon, nitrogen, xenon, and krypton) have been measured and the bands sensitive to conformations have been found.¹⁶⁰

It is interesting to compare the geometrical parameters of conformers for divinyl chalcogenides.¹⁶⁰ With an increase in the chalcogenide mass, the C-X bond length increases and the C-X-C angle decreases, the angle is somewhat less in the *trans-trans*-conformer than that in the *cis-trans*-conformer.

Potential energy maps were obtained for divinyl selenide and divinyl telluride: they were constructed as functions of rotational angles about $C_{sp^2}-X$ (X = Se, Te) bonds.⁵ The steric hindrance energies calculated for different conformations by varying the angles φ_1 from 0° to 360° and φ_2 from 0° to φ_1 with a step of 15° are presented in Table 2.

For all the chalcogenide conformations, steric hindrance energies vary in the series $O > S > Se > Te$. Of the two structural factors, bond lengths and bond angles, exerting opposite influence on steric hindrance, the key role belongs to the increase in the C-X bond lengths. For all vinyl chalcogenides, the planar *cis-cis*-conformation (D) is the most sterically hindered (Table 2), the *trans-trans*-form (A) is the least hindered. The steric hindrance energy of the non-planar *cis-cis*-conformation (F) for divinyl sulfide, divinyl selenide and divinyl telluride is close to, or is lower than that of the *trans-trans*-conformer (A), and only for divinyl ether is it twice higher (Table 3). This conformation results from the planar *cis-cis*-form by rotating the vinyl groups to the opposite directions by an angle of 45° .

Thus, the potential energy maps for divinyl chalcogenides give a comprehensive idea of the steric structure. The potential of internal rotation about the $C_{sp^2}-X$ bonds (X = O and S) in alkyl vinyl chalcogenides can be transferred (with some corrections) to the rotation about analogous bonds in the corresponding divinyl chalcogenides. The latter exist as three non-planar stable conformers: two quasi-degenerate *trans-trans*- and one *cis-trans*-conformer. A complete picture of rotational isomerism in divinyl chalcogenides involves not only the ground, but also excited vibrational states, which are characterised by large-amplitude intramolecular motion encompassing more than one local minima in the potential energy map.

IV. Electronic structure of vinyl and allenyl chalcogenides

1. Photoionisation of vinyl ethers

Interesting and important regularities have been established on the basis of photoelectron investigations of organic compounds.¹⁶⁶ Ionisation potentials of organic molecules depend significantly on the structure of substituents at the atom ionised;^{167, 168} within one class compounds, these are dictated exclusively by the inductive effect.¹⁶⁸⁻¹⁷¹ However, ionisation processes should also be very sensitive to other intramolecular effects of the structure. In particular, considerable contributions to the ionisation energy might be expected from the interaction of a cation radical with neighbouring double bonds and heteroatoms. These contributions can be identified and measured as deviations from a regression line reflecting the relationship between the ionisation potential and inductive effect (for example, by sums of the substituent σ^* constants). Adiabatic ionisation potentials have been obtained for a series of vinyl ethers by the photoionisation method.^{1, 172} By analogy with alcohols and other classes of compounds¹⁶⁸⁻¹⁷¹ in which a linear dependence of the ionisation potential on the σ^* constants is quite unambiguous, a variation of ionisation potentials in the series of vinyl ethers can be supposed to originate primarily from the inductive effect. The correlation between the adiabatic ionisation potentials (I) and substituent inductive constants ($\Sigma\sigma^*$) is presented in Fig. 21; the correlation parameters are somewhat different for saturated (dialkyl and cyclic) (line 1) and divinyl (line 2) ethers.

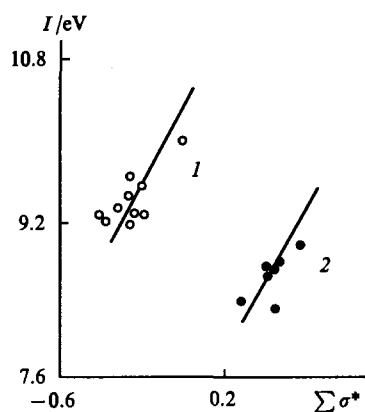


Figure 21. The correlation of ionisation potentials (I) of ethers with inductive constants of substituents ($\Sigma\sigma^*$).¹⁷² (1) aliphatic and cyclic ethers, (2) vinyl ethers.

The independent correlation for alkyl vinyl ethers can be explained¹⁷² by p, π -conjugation in the radical cation. An energy gap separating lines 1 and 2 indicates an inequivalence in the coupling of the oxygen AOs with the orbitals of the sp^2 - or sp^3 -hybridised carbon atoms. Correlation processing points against multiple correlations with three arguments ($\Sigma\sigma^*$, Δn , and E_a) for diorganyl and vinyl ethers.^{1, 172} One of the reasons for the uncertainty of the regressions is a strong dependence between the arguments.

Analysis of the correlation $I = f(\Sigma\sigma^*)$ has shown^{1, 172} that other effects do not manifest themselves as distinctly as the inductive one. The deviation of the points exceeding significantly the accuracy of the ionisation potential measurement indicates a contribution of structural effects.^{1, 172} It cannot be ruled out that steric interactions might contribute. A linear dependence of the second ionisation potential (I_2) for alkyl vinyl ethers on the ionisation potentials of a standard series of alkyl iodides I_{R1} ¹⁷³ and the existence of two different curves for compounds with linear (Me, Et, Buⁿ) and branched (Prⁱ, Bu^s, Bu^t) substituents has been found.⁶⁸ It was explained by a change in the conformational

state of the vinyl ether with the introduction of a bulky substituent.

2. PE spectra of alkyl allenyl ethers

PE spectra of alkyl allenyl ethers^{106, 112, 174–176} have been studied and interpreted on the basis of the orbital energy values calculated by semiempirical and *ab initio* methods. The electronic structure of alkyl allenyl ethers was compared with that of alkyl vinyl ethers.¹⁷⁵ The latter are formal analogues of alkyl allenyl ethers except for the fact that the allenyl fragment comprises two orthogonal π -systems. The electronic structure of alkyl allenyl ethers is fully dictated by the interaction of the lone electron pair on the oxygen atom with the π -electrons of the double bond. The same interaction affects the steric configuration and, to some extent, the relative stability of the conformers.

The sequence of the π -type occupied molecular orbitals in alkyl allenyl ethers is considered¹⁷⁵ to be a result of the interaction between the fragmentary π - and n -MOs. According to the orbital correlation diagram (Fig. 22), four bands are expected to exist and observed in the low-energy range of the PE spectrum^{87, 93, 174, 175} (Table 4). In the spectra of allenyl methyl and allenyl ethyl ethers, bands 1 and 2 have a fine structure, which corresponds to the stretching $C=C=C$ modes of the radical cation and is therefore considered to be the vibrational structure.^{112, 174} At the same time, the structure of band 1 in the PE spectrum of allenyl methyl ether is supposed¹⁰⁶ to be associated with the presence of *cis*- and *trans*-conformers. However, according to the gas electronography data,¹⁰² the *cis*-conformation dominates at room temperature (other conformers were not detected).

The low-energy band (8.77 eV) is assigned to the MO which involves the p, π -interaction of the oxygen atom with the π -system of the $C_\alpha = C_\beta$ bond. The next band (10.33 eV) corresponds to the π -MO of the $C_\beta = C_\gamma$ allenyl fragment. Consecutive replacement of the Me group by Et, Prⁿ, Prⁱ, Buⁿ, and Bu^t groups leads to a low-energy shift of the first and second band maxima by 0.1–0.3 eV (Table 4).

The third band in the spectra of alkyl allenyl ethers (11.25–11.97 eV) belongs to the π_1 -MO, which is a bonding combination of the oxygen lone electron pair and the π -MO of the $C_\alpha = C_\beta$ group.

The fourth band (12.28 eV) in the PE spectrum of allenyl methyl ether results from the ionisation of the π_1 and $n_O(\sigma)$ levels. The MNDO calculation shows¹⁷⁵ that a level deeper than that of the π_1 -MO corresponds to the lone electron pair on the oxygen atom. For methyl vinyl ether, the band at 12.2 eV is assigned⁶⁹ to the $n_O(\sigma)$ level. For alkyl allenyl ether, this level is associated with the band in the range of 11.5–12.3 eV.¹⁷⁵ For allenyl methyl ether, this band (12.28 eV) originates from the ionisation of a nearly pure lone electron pair of the oxygen atom, whereas for compounds with R = Et, Prⁿ, Prⁱ, Buⁿ, and Bu^t, a strong coupling between the $n_O(\sigma)$ -MO and the σ_{CC} -MO is observed. As the

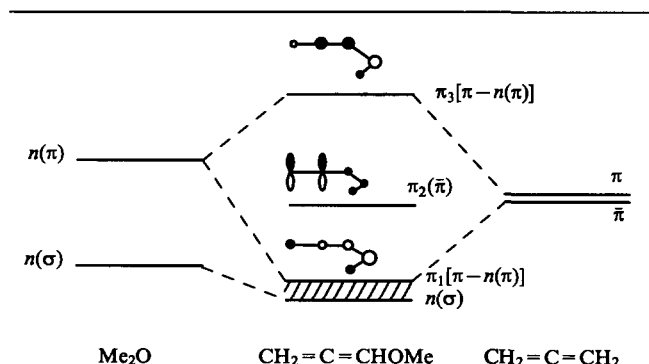


Figure 22. The correlational orbital diagram for the molecule $CH_2=C=CHOMe$.¹⁷⁵

Table 4. Vertical ionisation potentials for compounds $H_2C=C=CHOR$.¹⁷⁵

R	Ionisation energy ^a / eV			
	$I_1(\pi_3)$	$I_2(\pi_2)$	$I_3(\pi_1)$	$I_4[n_O(\sigma)]$
Me	8.8	10.3	11.9	12.3
Et	8.7	10.2	11.7	11.9
Pr ⁿ	8.6	10.2	11.5	see ^b
Bu ⁿ	8.6	10.2	11.4	see ^c
Pr ⁱ	8.6	10.1	11.4	11.6
Bu ^t	8.6	9.9	11.25 ± 0.1	11.5
$CH_2CH=CH_2$	8.8	10.0	11.9	12.4

^a The band assignment is given in parentheses; ^b a system of overlapping bands with an overall maximum at 12.2 eV; ^c the same with a maximum at 12.3 eV.

substituent length and branching increase, the coupling efficiency between the $n_O(\sigma)$ - and σ_{CC} -MOs increases.¹⁷⁵

Since the ionisation potential I_3 for alkyl allenyl ethers is analogous to I_2 for alkyl vinyl ethers,⁶⁹ the relationship between I_3 and the ionisation potentials for a standard series of alkyl iodides (I_{RI}) (I_{RI} values were found by PE spectroscopy¹⁷³) is also true:¹⁷⁵ $I_3 = 1.63$ eV, $I_{RI} = 3.60$ eV. $r = 0.994$, $s_0 = 0.03$ (the standard deviation s_0 does not exceed the experimental error of ~ 0.05 eV). For compounds with R = Prⁱ, and Bu^t, the points deviate from the regression line by a value approximately equal to s_0 , therefore, there is no reason to set apart these compounds from the series of alkyl allenyl ethers (Table 4). The relationship $I_3 = f(I_{RI})$ is entirely determined by the inductive effect of the substituent. In this case, no conformational effects are revealed. Since the ionisation potentials of alkyl iodides are in turn linearly related to the substituent inductive constants (σ^*),^{169–171} which have a more general character, the latter can be used for the correlation of orbital energies.

An MNDO calculation of the angular dependence of orbital energies ($-\epsilon_i$) for allenyl methyl ether has been carried out (Fig. 23).¹⁷⁵ The $\epsilon(\pi_1)$ value is rather sensitive to the departure from planarity and is practically the same for *s-cis*- and *s-trans*-conformations. Therefore, the existence of a common linear dependence $I_3 = f(I_{RI})$ indicates that all the alkyl allenyl ethers studied have a planar conformation. If for allenyl methyl ether it is definitely *s-cis*-, then the *s-trans*-conformation seems to be favoured for $CH_2=C=CHO-Bu^t$.

The comparison of total energies of possible conformers (*cis*-, *trans*-, and *gauche*-) for alkyl allenyl ethers obtained by the

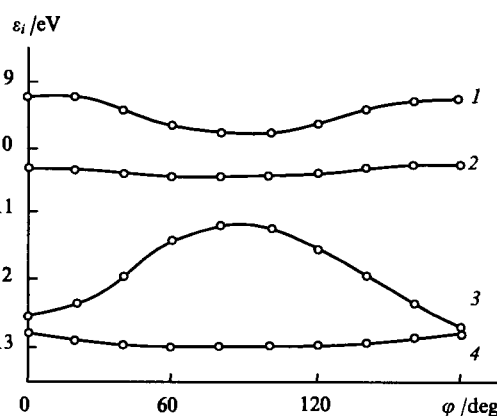


Figure 23. The angular dependence of orbital energies ($-\epsilon_i$) for $CH_2=C=CHOMe$ (the MNDO method):¹⁷⁵ (1) $\epsilon_1(\pi_3)$, (2) $\epsilon_2(\pi_2)$, (3) $\epsilon_3(\pi_1)$, (4) $\epsilon_4(\sigma)$.

MNDO method¹⁷⁵ shows that the *s-cis*-form of the $C=C-C-O-R$ fragment is the most stable in compounds with normal substituents. For compounds with branched substituents, the most stable conformation is the *s-trans*-form.

3. PE spectra of allenyl vinyl ethers

There are no published data on the electronic structure of allenyl vinyl ether $CH_2=C=CHOCH=CH_2$. In this connection, an empirical band assignment in its PE spectrum¹⁷⁷ was based on comparison of the spectrum with those of divinyl ether and allenyl methyl ether.¹⁷⁵ The spectrum of allenyl vinyl ether contains five well-resolved bands in the range of 8.0–16.0 eV (Table 5). The first two bands have fine structure. As in alkyl allenyl ethers,^{112, 174} the fine structure may be ascribed to the vibrational structure of corresponding states of the cation radical. The next band of allenyl vinyl ether has a distinct maximum at ~10.55 eV. The fourth broad band seems to result from the overlapping of several components with maxima at about 12.55 eV. The introduction of a Pr^n substituent into the α -position of the allene group leads to a shift of the band maxima by 0.3–0.4 eV.¹⁷⁷

Table 5. Vertical ionisation potentials for allenyl vinyl ethers.¹⁷⁷

R in compound	Ionisation potential ^a /eV				
$CH_2=C=C(R)OCH=CH_2$	$I_1(\pi_4)$	$I_2(\pi_3)$	$I_3(\pi_2)$	$I_4[n_O(\sigma)]$	$I_5(\pi_1)$
H	8.7	10.2	10.6	12.5	12.5
<i>cis-cis</i>	8.9	10.3	10.3	12.8	14.1
<i>trans-trans</i>	8.9	10.2	10.3	12.9	14.0
Pr^n	8.4	9.9	10.2 (sh)	12.2	11.8 (sh)
$CH_2=CHOCH=CH_2$	9.0	10.5		12.4	12.6

^a Band assignment is given in parentheses.

The orbital correlational diagram based on the interaction of the fragmentary π -orbitals of ethene and the hypothetical allenyl alcohol molecule was used for a quantitative analysis of the PE spectrum of allenyl vinyl ether¹⁷⁷ (Fig. 24). The sequence of one-electron levels for allenyl vinyl ether was determined from the MNDO data.¹⁷⁷ (Fig. 24). The first band (π_4 -MO) corresponds to the HOMO composed of an antibonding combination of the lone electron pair of the oxygen atom, π -orbitals of the vinyl group (π_1 -MO) and the $C_\alpha=C_\beta$ bond of the allene fragment (π -MO). The second band (10.22 eV) is associated with ionisation from the π_3 -MO, which has a node at the oxygen atom and is antibonding. MOs of the vinyl (π_1 -MO) and allenyl $C_\alpha=C_\beta$ (π -MO) groups

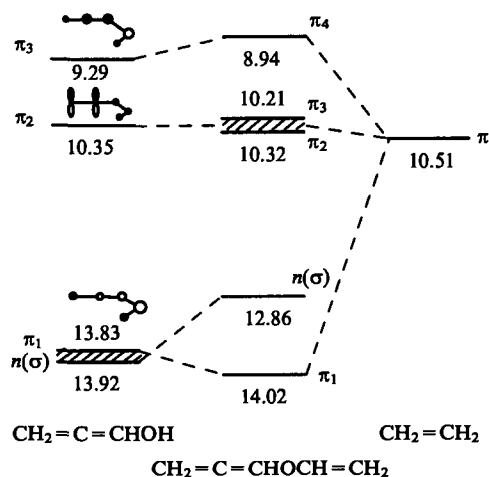


Figure 24. The orbital correlational diagram for hypothetical allenyl alcohol, ethylene, and $CH_2=C=CHOCH-CH_2$.¹⁷⁷

contribute decisively to this orbital. A molecular orbital orthogonal to the rest of the π -system ($\bar{\pi}$ -MO) gives rise to the third band (10.55 eV). The fourth band with a maximum at 12.54 eV results from ionisation from two MOs, a π -MO and an almost pure lone electron pair of the oxygen atom, $n_O(\sigma)$. The π_1 -MO is a bonding combination of the lone electron pair of the oxygen and the fragmentary MOs of the vinyl and allenyl $C_\alpha=C_\beta$ groups. Thus, the structure and sequence of occupied π_4 -, π_3 -, and π_1 -MOs are similar to those for divinyl ether¹⁷⁷ (Table 5).

An MNDO calculation of orbital energies for planar conformations¹⁷⁷ has shown that the bands in the PE spectrum of allenyl vinyl ether can be shifted by ~0.1 eV on transition from the *trans-trans*- to the *cis-cis*-conformation. The difference in the orbital energy values for the *cis-cis*- and *trans-trans*-conformations of allenyl vinyl ether is within the experimental errors of the PE spectroscopy method (0.1 eV for potential difference).

4. PE spectra of vinyl sulfides and selenides

The sequence of three higher occupied MOs of dialkyl sulfides and selenides does not depend on the nature of the chalcogenide:¹⁷⁸ $n_X(b_1) < \sigma_1(a_1) < \sigma_2(b_2)$. The effect of the heteroatom is reduced primarily to an increase in the energy of MOs and the contribution of atomic orbitals of the element (X) to these MOs with an increase in the element atomic number. Structural changes (chain length, branching) of the substituent in each series lead also to the expected effects.

The empirical approach to the low-energy range of PE spectra of vinyl derivatives allowed one to conclude that the relative arrangement of MOs in vinyl sulfides and selenides is practically independent of the nature of the heteroatom and the structure of the hydrocarbon substituent¹⁷⁹ (Table 6, Fig. 25): $\pi_2 < \pi_1 < \sigma_1 < \sigma_2$ ($CH_2=CH-X-Alk$), $\pi_3 < \sigma_1 < \pi_1 < \sigma_2$ ($CH_2=CH-X-CH=CH_2$). On going from dialkyl sulfides

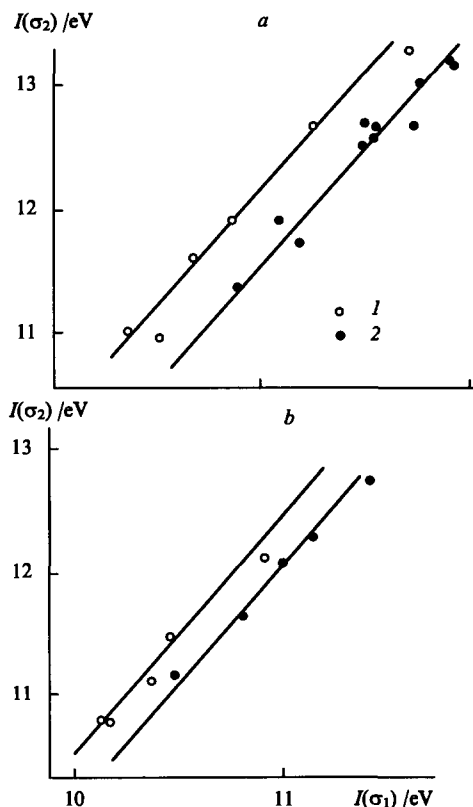
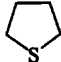
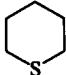
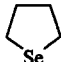

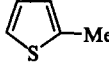
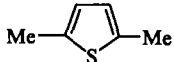
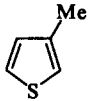
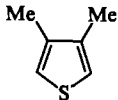
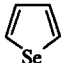
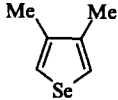
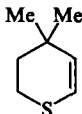


Figure 25. The correlation of σ -MO energies for diorganyl sulfides (a) and diorganyl selenides (b).¹⁷⁹ (1) Saturated, (2) unsaturated.

Table 6. Vertical ionisation potentials for diorganyl sulfides and five-membered heterocyclic compounds.

R	Ionisation energy /eV					ΔI_{σ}	Ref.
	π (or n_X)	π_1	π_2	σ_1	σ_2		
Me ₂ S	8.7			11.3	12.7	1.4	178
	8.4			10.9	11.9	1.0	178
Et ₂ S	8.4			10.7	11.6	0.9	178
	8.4			10.6	11.0	0.4	178
(Pr ⁱ) ₂ S	8.3			10.7	11.0	0.6	178
Me ₂ Se	8.4			11.0	12.0	1.0	178
	8.1			10.5	11.4	0.9	178
Et ₂ Se	8.2			10.4	11.1	0.7	179
(Pr ⁱ) ₂ Se	8.0			10.2	10.8	0.6	179
(Bu ⁿ) ₂ Se	8.0			10.2	10.8	0.6	179
	8.9	9.5	12.3	12.0	13.2	1.2	178
	8.3	9.0	12.4	11.8	13.0	1.2	179
	8.2	9.0	11.9	11.5	12.5	1.0	179
	8.5	9.1	12.5	11.9	13.1	1.2	179
	8.6	8.9	12.1	11.8	12.6	0.9	179
	8.8	8.9	12.1	11.5	12.7	1.2	179
	8.3	8.7	11.4	11.1	11.9	0.8	179
CH ₂ =CHSMe	8.4	11.0		11.6	12.6	1.0	179
(CH ₂ =CH) ₂ S	8.5	10.4	11.9	11.6	12.7	1.1	179
	8.1	10.9		11.2	11.7	0.1	69
CH ₂ =CHSeMe	8.3	10.8		11.2	12.2	1.0	179
CH ₂ =CHSeEt	8.2	10.7		10.9	11.6	0.7	179
CH ₂ =CHSeBu ^t	7.9	9.7		10.5	11.1	0.6	179
(CH ₂ =CH) ₂ Se	8.3	10.3	11.5	11.0	12.0	1.0	179

and selenides to unsaturated derivatives with the same number of atoms, the stabilisation of the σ_1 - and σ_2 -MOs becomes non-equivalent, which indicates a different efficiency of coupling of the element (S, Se) AOs with the orbitals of the sp^2 - and sp^3 -hybridized carbon atoms. These differences lead to a splitting of the dependence $I(\sigma_2) = f[I(\sigma_1)]$ into two parts. One dependence includes saturated and the other includes unsaturated derivatives (Fig. 25). Analysis of the energies of the MOs of saturated and unsaturated diorganyl sulfides and selenides allowed one to state two general

concepts, which facilitate the assignment of the ' σ '-bands in the PE spectra of alkyl vinyl and divinyl derivatives: i) the energy gap ΔI_{σ} separating the σ_1 - and σ_2 -MOs does not exceed a limiting value corresponding to the simplest representatives of the series and decreases with an increase in the substituent size (Table 6); ii) there is a linear correlation between the σ_1 - and σ_2 -MO energies, its parameters being somewhat different for saturated and unsaturated compounds of sulfur and selenium (Fig. 25).¹⁷⁹

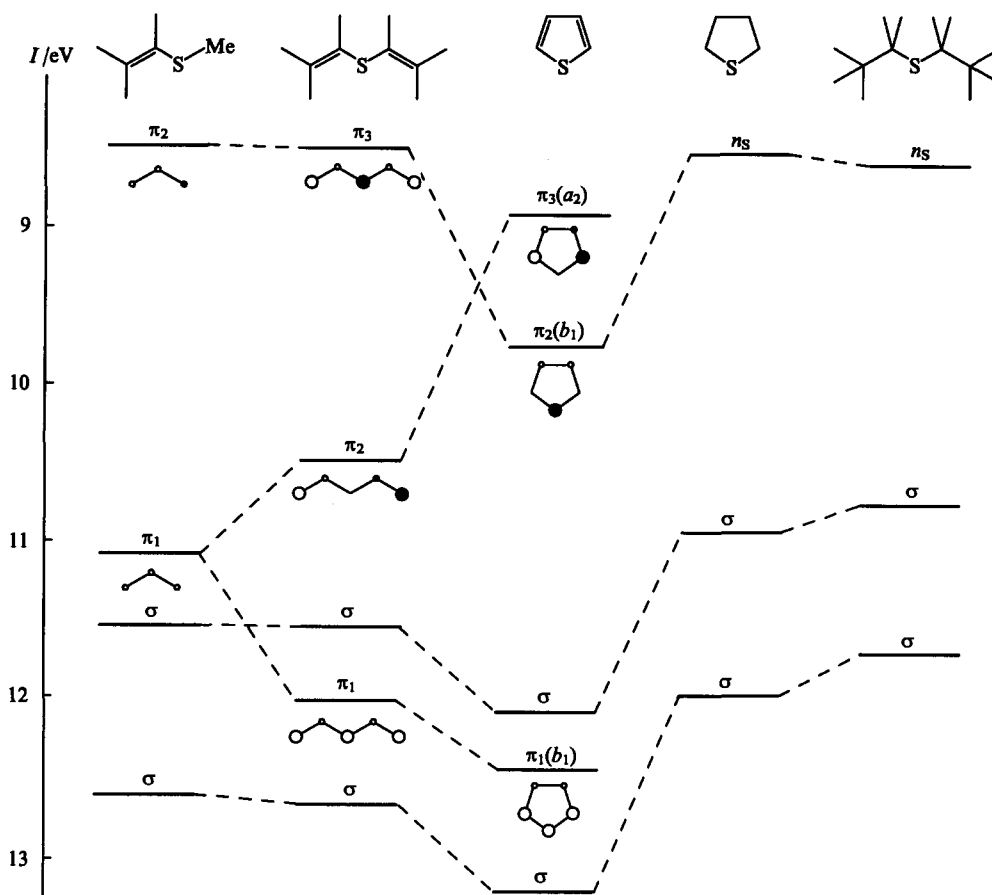


Figure 26. The orbital correlational diagrams for sulfur saturated and unsaturated derivatives.¹⁷⁹

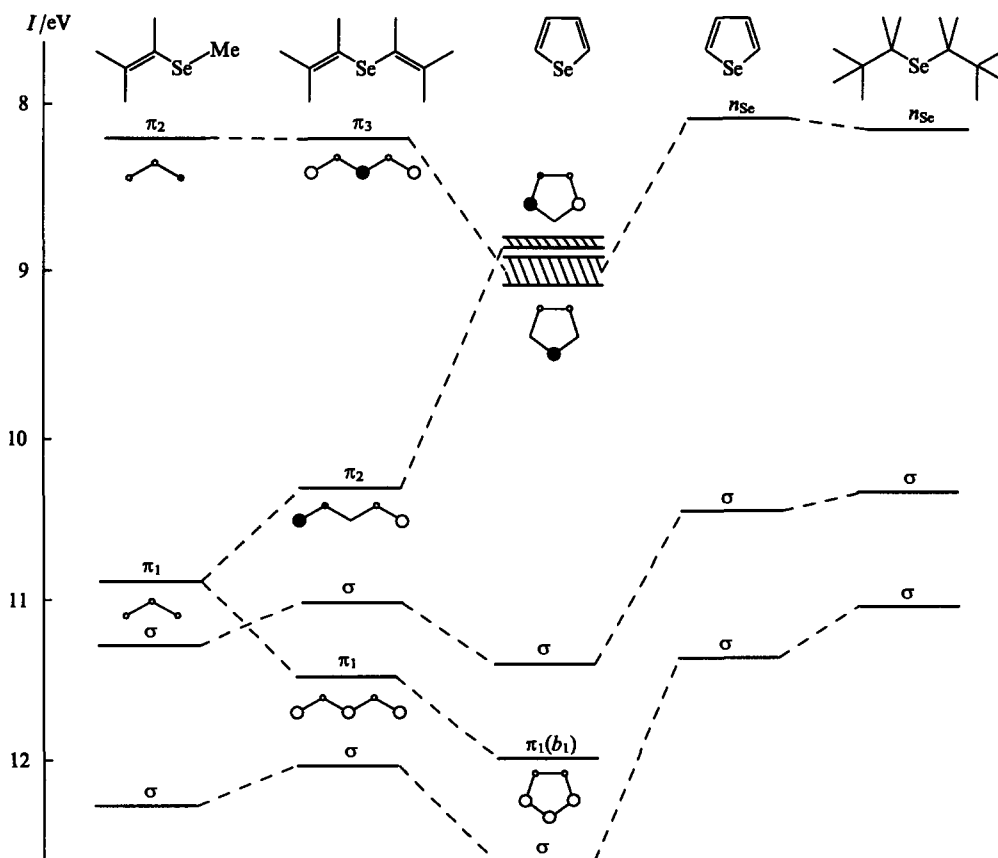



Figure 27. The orbital correlational diagrams for selenium saturated and unsaturated derivatives.¹⁷⁹

The HOMOs also have common features. Comparison of dialkyl, alkyl vinyl, and divinyl sulfides and selenides shows that the first vertical ionisation potential I_1 (Table 6) practically does not change due to a rather weak coupling of p_x -AOs of a heteroatom with fragmentary π -MOs. The localisation of the orbital electron density mostly on the heteroatom and the terminal C_β atom is typical of HOMOs (I_1) of vinyl sulfides and selenides. This order of electron distribution gives reason to suppose that the transition from divinyl chalcogenides to saturated heterocyclic derivatives of sulfur and selenium will be accompanied by a strong stabilisation of the π_3 -MO in the selenium derivatives. This is confirmed by the position of the first band in the PE spectra of divinyl sulfide and thiophene. The stabilisation of the π_3 -MO leads to the inversion of the sequence of the two higher π -MOs. The PE spectra of divinyl selenide and selenophene consisting of a system of overlapping bands, are less indicative. Nevertheless, the mutual position of the first two bands makes it possible to state that the passage from divinyl selenide to selenophene results in, at least, quasi-degeneracy of the boundary π -MOs. The orbital correlational diagrams¹⁷⁹ for saturated and unsaturated sulfur and selenium derivatives indicate that the passage from saturated to unsaturated compounds of sulfur and selenium and to the corresponding cyclic structures leads to the stabilization of σ_1 - and σ_2 -MOs (Figs 26, 27).

For unsaturated sulfur compounds, comparison of results of the empirical approach to the estimation of their orbital structure with the results of the MNDO calculation (Table 7) shows that qualitative and quantitative agreement was obtained for each compound.¹⁷⁹ Calculations have been made for equilibrium planar *s-cis*-, *s-trans*-, *s-trans-s-trans*- (C_{2v}) forms and a non-planar *cis-trans*-form (C_1) of rotamers.¹⁷⁹ π -MO energy differ-

Table 7. Theoretical and experimental assignment of bands in the PE spectra of divinyl sulfide and related compounds.¹⁷⁹

Compound	Assignment		MNDO		
	empirical		MO	$-\epsilon_i/\text{eV}$	
	MO	I_i/eV	MO		
$\text{CH}_2=\text{CHSMe}$	π_2	8.4	π_2^a	9.4 ^b	9.3 ^c
	π_1	11.0	π_1	11.8 ^b	11.7 ^c
	σ_1	11.6	σ_1	12.4 ^b	12.1 ^c
	σ_2	12.6	σ_2	12.9 ^b	13.4 ^c
$\text{CH}_2=\text{C}=\text{CHSMe}$	π_3	8.3	π_3	9.0 ^b	9.0 ^c
	π_2	9.7	π_2	10.2 ^b	9.0 ^c
	π_1	10.9	π_1	11.4 ^b	11.4 ^c
	σ_1	11.8	σ_1	12.0 ^b	11.9 ^c
	σ_2	13.3	σ_2	13.8 ^b	14.0 ^c
$(\text{CH}_2=\text{CH})_2\text{S}$	π_3	8.5	π_3^e	8.8 ^d	8.7 ^e
	π_2	10.4	π_2	10.7 ^d	10.7 ^e
	σ_1	11.6	σ_1	11.7 ^d	11.6 ^e
	π_1	11.9	π_1	12.4 ^d	12.4 ^e
	σ_2	12.7	σ_2	12.8 ^d	13.0 ^e
$\text{CH}_2=\text{C}=\text{CHSCH}=\text{CH}_2$	π_4	8.3	π_4^e	8.7 ^b	8.6 ^e
	π_3	9.9	π_3	10.3 ^d	10.2 ^e
	π_2	10.3	π_2	10.6 ^d	10.6 ^e
	σ_1	12.0	σ_1	12.3 ^d	12.3 ^e
	π_1				
	σ_2	13.2	σ_2	13.8 ^d	13.7 ^e
	—	—	$\pi_3(1a_2)$	9.5	
	—	—	$\pi_2(2b_1)$	10.0	
	—	—	σ_1	12.8	
	—	—	$\pi_1(1b_1)$	13.3	

^a The assignment based on the *ab initio* calculation; ^b *s-cis*-form; ^c *s-trans*-form; ^d *cis-trans*- for $(\text{CH}_2=\text{CH})_2\text{S}$ and $\text{CH}_2=\text{C}=\text{CHSCH}=\text{CH}_2$; ^e *s-trans-s-trans*- (C_{2v}) for $(\text{CH}_2=\text{CH})_2\text{S}$ and $\text{CH}_2=\text{C}=\text{CHSCH}=\text{CH}_2$.

ences for these rotamers are extremely small, that is why the problem of rotational isomerism cannot be solved at the level of the first band in the PE spectrum. In the PE spectrum observed, the shape of the first band rules out the existence of a remarkable concentration of a less favourable rotamer differing from the major rotamer in torsional angles.

Adiabatic potentials for a series of diorganyl sulfides have been measured by the photoionisation method,^{1,180} and conjugation energies in radical cations have been estimated by correlation analysis. Two-parameter approximation¹⁸⁰ yielded the plots (Fig. 28) showing that saturated and unsaturated representatives of the series correlate with the inductive Taft constants to form two independent regressions. The contributions of hyperconjugative and steric effects into the ionisation potential value were found with the requisite statistical accuracy: they make up ~20% of the contribution of the inductive effect.¹⁸⁰ At the same time, conjugation effects contribute significantly to the ionisation potentials, too (Fig. 28). The existence of independent linear dependences for saturated and unsaturated representatives of the series (Fig. 28, lines 1 and 2, respectively) is due to the conjugation between the radical-cation centre and the adjacent double bond. The energy of this conjugation can be estimated^{1,180} by deviations of the points for α,β -unsaturated sulfides from the basic correlational curve. For vinyl sulfides, it is equal to 1.0–1.3 eV.

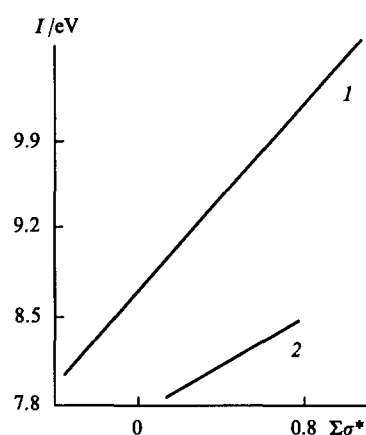


Figure 28. The dependence of ionisation potentials (I) of diorganyl selenides on inductive constants of substituents ($\Sigma\sigma^*$).¹⁸⁰ (1) Unsaturated and cyclic organylthiols and sulfides, (2) vinyl sulfides.

5. Allenyl methyl sulfide and allenyl vinyl sulfide

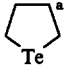

Among unsaturated sulfides, allenyl methyl sulfide and allenyl vinyl sulfide occupy a somewhat unusual position (Table 7).¹⁷⁹ It might be expected that their orbitals, except for an additional π -MO localised at the $C_\beta=C_\gamma$ fragment (9.7 eV for allenyl methyl sulfide and 9.9 eV for allenyl vinyl sulfide) would follow the regularities found for vinyl sulfides. The similarity was, however, found only for allenyl vinyl sulfide (Fig. 25, Table 7). According to the data obtained by the MNDO method, which has shown a good performance in the case of other α,β -unsaturated sulfides, the energies of the σ_1 - and σ_2 -MOs of allenyl methyl sulfide fit the correlational curve of saturated sulfides (Fig. 25). The σ_2 -MO energy for allenyl methyl sulfide is only 0.45 eV higher than the corresponding MO for methanethiol.¹⁷⁸ Unlike other analogous compounds, the σ_2 -MO of allenyl methyl sulfide seems to be localised to a significantly greater extent within the $\text{S}-\text{C}_{sp^3}$ fragment. Other MOs of allenyl sulfides, except for the π -MO localised within the $C_\beta=C_\gamma$ fragment, are qualitatively the same as those for vinyl sulfides. The band assignment in the PE spectra of allenyl sulfides is given in Table 7.

6. PE spectra of vinyl tellurides

PE spectra of dimethyl telluride and some other dialkyl chalcogenides have been described.^{181,182} An analysis of their orbital structure has been performed for model dimethyl derivatives of C_{2v} symmetry.¹⁸² Three lowest-energy bands in the PE spectra of these compounds are associated with electron removal from the antibonding MO of the lone electron pair of the chalcogen atom and from two $\sigma_{1,2}$ bonds.

In the PE spectra of dialkyl tellurides in the range of 7.5–11.4 eV, as well as in the case of analogous sulfides and selenides, there are three bands (Table 8, Fig. 29a). The lowest-energy and the narrowest band is unambiguously assigned to the MO with the major contribution of the tellurium p_z -AO. Two broader bands result from the ionisation of the σ -bonds (Fig. 29a). Successive elongation of the hydrocarbon chain leads to a low-energy shift of all the bands. For saturated tellurides as well as for other dialkyl chalcogenides, there is a linear dependence between the higher σ -MO positions (Fig. 30).¹⁸³ An energy gap value ΔI_σ separating σ_1 - and σ_2 -MOs decreases systematically with an increase in alkyl substituent length and branching (Table 8). In other words, the behaviour of σ -MOs in dialkyl tellurides is completely similar to that of the corresponding sulfides and selenides.

Table 8. Vertical ionisation potentials for diorganyl tellurides.¹⁸³

Compound	Ionisation energy / eV			
	$\pi(\pi_{Te})$	σ_1	$\pi(C=C)$	σ_2
Me_2Te^a	7.9	10.3	—	11.3
$CH_2=CHTeMe$	7.9	10.3	10.6	11.4
Et_2Te	7.7	9.9	—	10.6
$(Pr^i)_2Te$	7.8	9.7	—	10.4
$(Pr^i)_2Te$	7.6	9.5	—	10.0
$CH_2=CHTePr^i$	7.8	9.7	10.5	10.4 (sh)
$(Bu^n)_2Te$	7.6	9.6	—	10.2
$CH_2=CHTeBu^n$	7.7	9.8	10.5	10.5
$(CH_2=CH)_2Te$	7.9	10.4	10.0, 11.0	11.4
	7.7	10.0	—	10.7
	8.4	10.8	8.9, 11.5	11.8

^a The data of Ref. 178.

Analysis of PE spectra of vinyl tellurides has been carried out¹⁸³ using the empirical approach.¹⁷⁹ The PE spectra of vinyl tellurides contain four well-resolved bands (Table 8, Fig. 29b, c). The low-energy band remains narrow. Moreover, for vinyl tellurides its position is practically the same as for dimethyl telluride. The replacement of an alkyl group by the vinyl group in the diorganyl telluride does not lead to a significant interaction of the fragmentary π -orbital with the p_z -AO of the tellurium atom, i.e. the first band relates to the MO localised primarily on the heteroatom. The second and the fourth bands belong to σ -MOs. Unlike saturated and unsaturated sulfur and selenium compounds, in tellurium compounds, the σ -MO energies correlate in the same manner (Fig. 30). The correlation extends also to the σ -MOs of divinyl telluride and tellurophene, thus indicating an equivalent coupling of the tellurium AOs with the orbitals of the sp^2 - and sp^3 -hybridized carbon atoms.¹⁸³ The third MO of vinyl tellurides is responsible for a slightly bonding combination of the π -MO of the vinyl fragment and the tellurium p_z -AO with a lesser contribution of the latter.

More detailed information on the structure of π -MOs in divinyl telluride can be obtained by comparing them with those of tellurophene. The π -MO of tellurophene can easily be com-

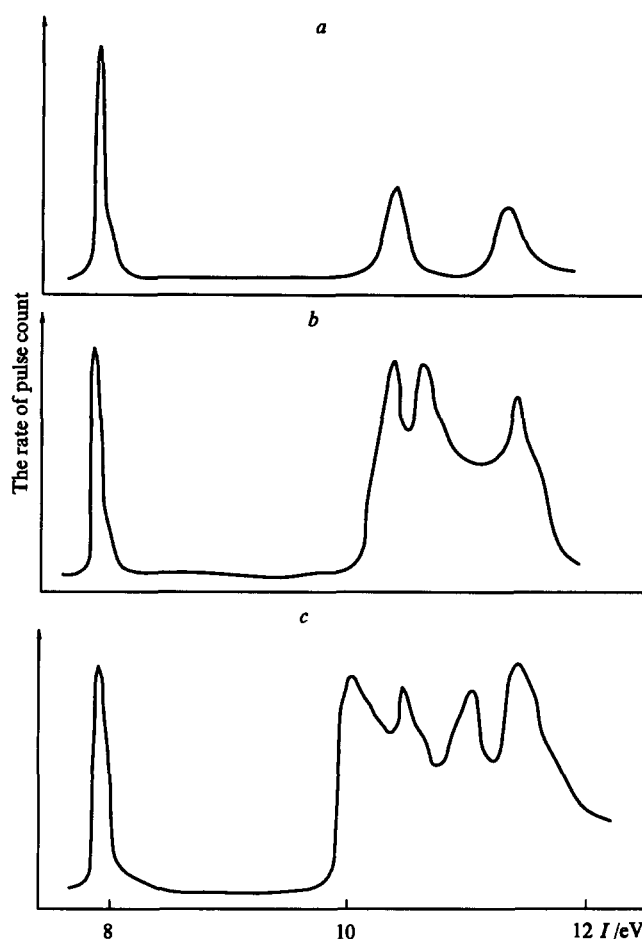


Figure 29. The PE spectra of dimethyl telluride (a),¹⁸² vinyl methyl telluride (b), and divinyl telluride (c).¹⁸³

posed from symmetry considerations.¹⁸³ The PE spectroscopic data (Table 8, Fig. 31) indicate that the passage from divinyl telluride to tellurophene leads to a remarkable increase in the first ionisation potential (0.5 eV). This is not due to the formation of the ordinary bond between the terminal carbon atoms of divinyl telluride, because the analogous structural variation for saturated compounds (tetrahydrotellurophene¹⁸⁴) affects only slightly this

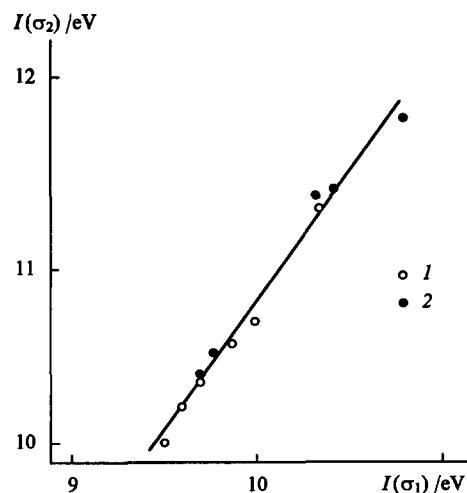


Figure 30. The correlation between the energies of σ -MOs for unsaturated (1) and saturated (2) organyl tellurides.¹⁸³

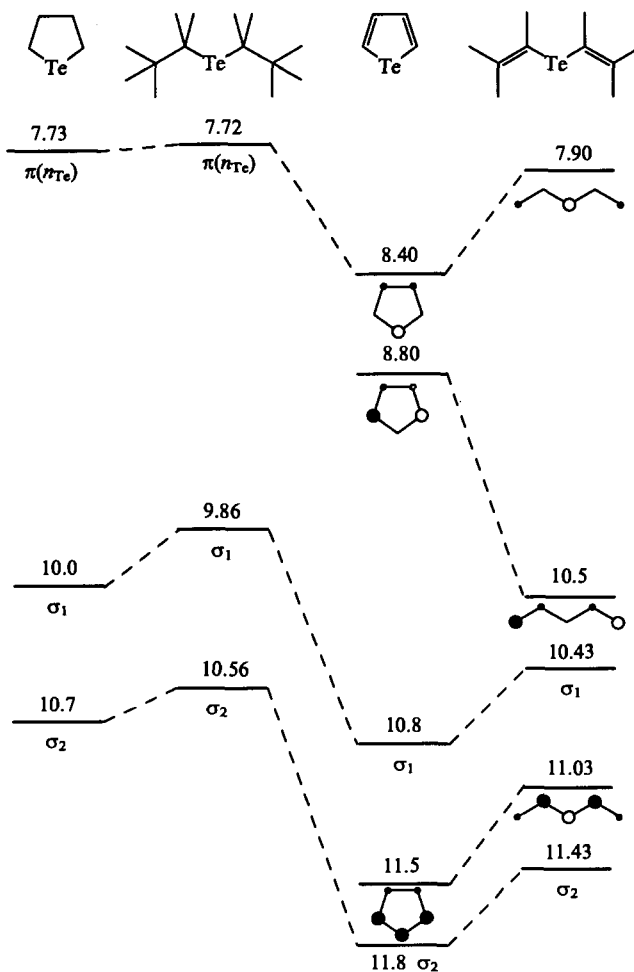


Figure 31. The orbital correlational diagrams for tellurium saturated and unsaturated derivatives.¹⁸³

value. Apparently, stabilising interactions arise upon heterocyclisation. These interactions can be adequately rationalised only assuming that the HOMO structure for tellurophene is of the same type as that for the preferential rotamer of divinyl telluride. The correlation of the other π -MOs (Fig. 31) leads to the conclusion that the second occupied π -MO of divinyl telluride is an antibonding combination of orbitals of the vinyl fragment, and the lowest MO is, naturally, completely bonding.

Thus, the analysis of the PE spectral features of dialkyl, alkyl vinyl, and divinyl tellurides altogether gave the rationale for the nature of their MOs and allowed the empirical assignment to be made: the low-energy band for alkyl vinyl tellurides results from the ionisation of the MO with the dominating contribution of the tellurium p_z -AO, the second and the fourth bands correspond to the σ -MOs, the third band belongs to the π -MO. The orbital structures of divinyl telluride and tellurophene are of the same type.

7. UV absorption spectra of alkyl vinyl sulfides

UV absorption spectra are the subject of a large number of studies.^{69, 132, 185–191} Nevertheless up to now, there is no unequivocal understanding of the nature of electronic transitions observed in liquid and in the gas phase. A discussion^{69, 132, 185–191} about the band assignment in the near UV range for methyl vinyl sulfide is remarkable. The most long-wave transition was assigned to the first transition of the Rydberg series $\pi \rightarrow n_s$, and the next to the $\pi \rightarrow \pi^*$ -type.⁶⁹ However, according to other data¹⁹¹ the first long-wave band originates from the $n \rightarrow \sigma$ or $\sigma \rightarrow \sigma^*$ excitation, and the second band is associated with the $\pi \rightarrow \pi^*$ transition. Both

transitions are considered^{133, 190} to belong formally to the same ($\pi \rightarrow \pi^*$) type, but to correspond to two rotamers. Experimental data accumulated to date allowed one to perform systematic analysis of UV spectra of alkyl vinyl sulfides.¹⁹² An empirical analysis of the full spectrum of gaseous methyl vinyl sulfide has been carried out.⁶⁹ In addition to the $\pi \rightarrow \pi^*$ transition, the spectrum of methyl vinyl sulfide is represented by three Rydberg series: $\pi \rightarrow n_s$, $\pi \rightarrow np$, and $\pi \rightarrow nd$. Rydberg transitions fall primarily in the vacuum ultraviolet range and are inaccessible for comparative investigations in solutions. In the near UV range there are $\pi \rightarrow \pi^*$, $\pi \rightarrow 4p$, and $\pi \rightarrow n_s$ transitions, the latter is believed⁶⁹ to be of the lowest energy in the series. Comparison (cf. with¹⁹³) of the UV spectrum of methyl vinyl sulfide in the gas phase with those of solutions^{189, 191} in hexane, dioxane, and ethanol, in which no narrow peaks of sufficient intensity were found at 204 nm, indicates that the most short-wave transition is largely of the Rydberg character. The quantum defect δ for this transition is relatively low, $\delta \sim \pm 0.59$ where

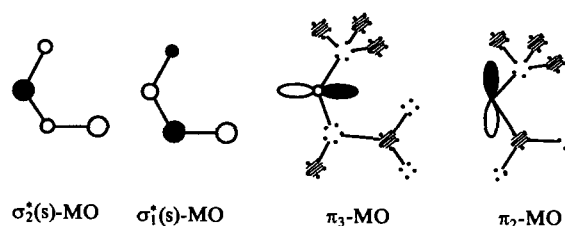
$$\delta = n - \left(\frac{R}{T}\right)^{1/2},$$

here R is the Rydberg constant, $T = I_1 - n$, n is a quantum number. Therefore, indeed, this transition can be assigned to the Rydberg transition of the $\pi \rightarrow 4p$ type.¹⁹² An interesting feature of this transition is a dependence of the relative intensity of the corresponding band on the substituent structure, which decreases as the length of a hydrocarbon substituent and branching increase (Fig. 32); for compounds with $R = \text{tert-butyl}$ and tert-pentyl , Rydberg transitions cannot be reliably assigned.¹⁹⁴

The most long-wave band of methyl vinyl sulfide broadens on passage from the gaseous state to solution. It also broadens upon substitution of the methyl group for another alkyl substituent. Bulky substituents increase its absolute intensity (in solution). Sometimes even a slightly pronounced fine structure appears (Fig. 32, Table 9). For $R = \text{tert-butyl}$ and tert-pentyl the intensity of this band increases, and a separate peak is observed (Fig. 32). An isotope effect was quite unexpected. In the case of methyl vinyl sulfide and its deuterio-isotopomer $\text{CD}_2 = \text{CDSMe}$, the absorbance ratio of the maxima of the long-wave band and the neighbouring ' π ' band (D_{244}/D_{225}) in the gas phase is 0.225, while in the spectrum of $\text{CH}_2 = \text{CHSCD}_3$ this ratio is 1.35 times larger. The band half-width also increases (from 1540 cm^{-1} to 2130 cm^{-1}). Data on the deuteration effect also show that the methyl group orbitals (σ -symmetry) take part in the first excited state of methyl vinyl sulfide. The long-wave band of methyl vinyl sulfide might therefore be supposed to belong to the $\pi \rightarrow \sigma^*$ transition.

CNDO/C calculations indicate that yet another $\pi \rightarrow \sigma^*$ -transition should exist in the UV range separated from the first one by an interval of $\sim 1300 \text{ cm}^{-1}$ (Scheme 2; s -AOs are marked with a dotted line). The band at $\sim 196 \text{ nm}$ in the spectrum of methyl vinyl sulfide in solution corresponds to the second $\pi \rightarrow \sigma^*$ -transition (Fig. 32, Table 10). In the spectrum of gaseous methyl vinyl sulfide, the band corresponding to this transition coincides with the components of a vibrational progression of the Rydberg $\pi \rightarrow 4p$ transition. A complex contour of the short-wave absorption band in gaseous methyl vinyl sulfide does not allow vibrational modes of this transition to be reliably identified.¹⁹²

Scheme 2



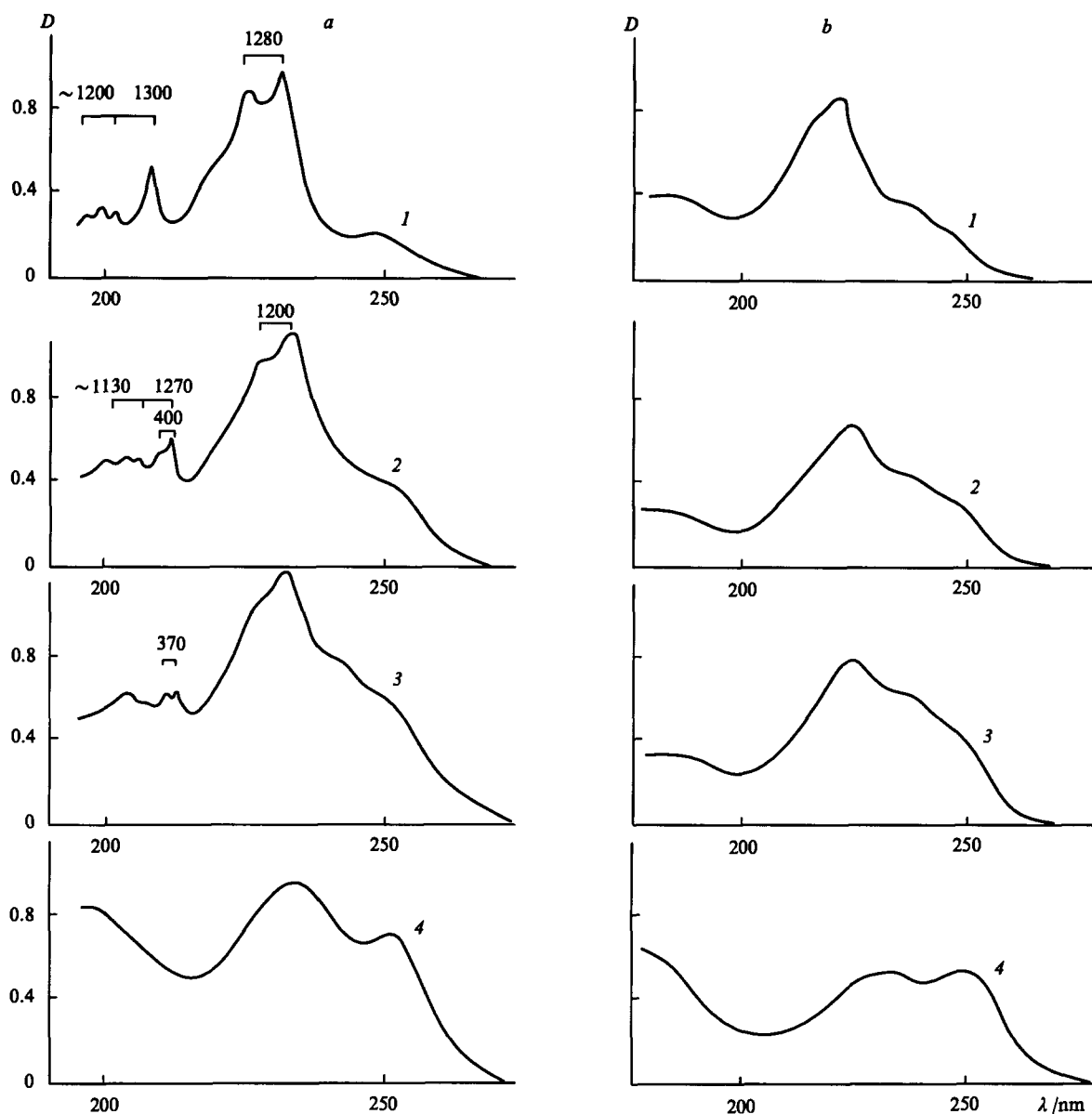


Figure 32. The UV absorption spectra of sulfides $\text{CH}_2=\text{CHSR}$, where $\text{R} = \text{Me}$ (1), Et (2), Bu^i (3), Pent^i (4), in the gaseous state (a) and in a hexane solution (b).¹⁹²

The $\pi \rightarrow \pi^*$ transition band with peaks in the range of 225–236 nm in the spectrum of gaseous methyl vinyl sulfide has a fine structure (the distance between the components is $\sim 1000\text{--}1300\text{ cm}^{-1}$), which disappears in the solution spectra.¹⁹²

Thus, the following energy sequence of transitions is observed in the UV spectra of alkyl vinyl sulfides:¹⁹² $\pi \rightarrow \sigma^* < \pi \rightarrow \pi^* < \pi \rightarrow np < \pi \rightarrow \sigma^*$.

8. UV absorption spectra of alkyl vinyl selenides

UV spectra of vinyl selenides have been studied.^{191,192} The type and the sequence of electronic transitions have been determined (Fig. 33). Comparison of UV spectra of methyl and ethyl vinyl selenides in the gaseous and condensed state identifies the Rydberg transition at $\lambda = 202\text{ nm}$ and 204 nm , respectively. A relatively low magnitude of the quantum defect (0.48) makes it possible to assign these bands to the $\pi \rightarrow 5p$ type (Table 9). $\pi \rightarrow \sigma^*$ transitions in alkyl vinyl selenide are red-shifted as compared to those in the corresponding sulfides, on the average, by 4600 cm^{-1} and occur in the range of 265–270 nm and at 220 nm (Table 10). In the spectrum of methyl vinyl selenide (Fig. 33), the band corresponding to the $\pi \rightarrow \pi^*$ transition has fine structure (1000,

600, $\sim 600\text{ cm}^{-1}$), which differs from that for the analogous sulfur compounds (Fig. 32). Moreover, substitution of the methyl group for the ethyl group leads to a change in the Franck–Condon contour of the absorption band (Fig. 33). This gives grounds to suppose that the ‘ π ’ band of methyl vinyl selenide coincides with the band of the Rydberg transition ($\lambda = 236\text{ nm}$), which distorts the profile of the absorption band in the gas phase. In solution, the Rydberg band disappears or decreases in intensity (Fig. 33, Table 10). The quantum defect of the Rydberg transition (0.88) corresponding to the band at 236 nm allowing one to assign it to the $\pi \rightarrow 5s$ type.

This assignment has further support. The first ionisation potentials for dimethyl and methyl vinyl selenides (to which Rydberg series converge) are close: 8.33 eV and 8.29 eV, respectively.¹⁷⁹ Therefore, their Rydberg $n_{\text{Se}} \rightarrow 5s$ and $\pi \rightarrow 5s$ transitions will also be close. In the spectrum of gaseous Me_2Se there is a narrow peak at $\lambda = 236\text{ nm}$, which is not registered in solution.¹⁹¹ Its quantum defect ($\delta = 0.94$) is in full accord with the Rydberg transition from the series $n_{\text{Se}} \rightarrow n_{\text{S}}$.¹⁹⁶ The following sequence of electronic transitions was found for alkyl vinyl selenides:¹⁹² $\pi \rightarrow \sigma^* < \pi \rightarrow \pi^* \sim \pi \rightarrow ns < \pi \rightarrow \sigma^* < \pi \rightarrow np$ (Tables 9, 10).

Table 9. Rydberg ($np \rightarrow \pi$) transitions for organyl chalcogenides (gaseous phase).¹⁹²

Compound	I_1 ^a /cm ⁻¹	Transition (ν /cm ⁻¹) ^b	λ /nm	δ ^c
H ₂ S	84451	65963 ^d	152	0.56
Me ₂ S	76304	57250 ^d	175	0.60
Et ₂ S	74933	56000 ^e	178	0.59
(Bu ^t) ₂ S	72836	54000 ^e	185	0.585
Me ₂ Se	70013	51165 (287; 698; 1004; 1316) ^d	195	0.59
Et ₂ Se	68077	49000 (~600; 1160)	204	0.60
EtSPri ⁱ	67400	48600 (~550; 1110)	206	0.585
CH ₂ =CHSMe	68077 ^e	49200 (1300; ~1200)	203	0.59
CH ₂ =CHSEt	67840 ^f	48480 (400; 1270; ~1150)	206	0.62
CH ₂ =CHSPri ^a	67430 ^f	48000 (~400; 1280)	208	0.625
CH ₂ =CHSPri ⁱ	67350 ^f	48520 (1240)	206	0.585
CH ₂ =CHSBu ^a		47800	209	
CH ₂ =CHSBu ^a		48160 (~1200)	208	
CH ₂ =CHSBu ⁱ	67350 ^f	48270 (370)	260	0.60
CH ₂ =CHSBu ^t	66710 ^f	—	—	—
CH ₂ =CHSPent ^t		~48000 (very weak)	~206	
CH ₂ =CHSCD ₃		49240 (1210; ~1200)	203	
CD ₂ =CDSMe		49200 (1000; 1200)	203	
H ₂ Se	79692	60600 ^d	165	0.60
Me ₂ Se	67432	49200 (~233; ~595; 981; 129) ^d	203	0.55
CH ₂ =CHSeMe	66867	~49000	~204	0.48
CH ₂ =CHSeEt	66141	48900	205	0.48
H ₂ Te	73723	55000 ^e	182	0.58
Me ₂ Te	63641	46240 (180; ~530; 898; 1252) ^d	216	0.49
CH ₂ =CHTeMe	63398	46700 (~200)	~214	0.44

^a The data of Ref. 178; ^b the vibrational quantum number is given in parentheses; ^c while estimating, the major quantum number was decreased by 1, 2, 3 for S, Se, and Te, respectively; ^d an analysis of the vibrational structure see in Ref. 195; ^e the data of Ref. 195; ^f calculated from the data of Ref. 180: $I_1 = I_1 + 0.2$ /eV.

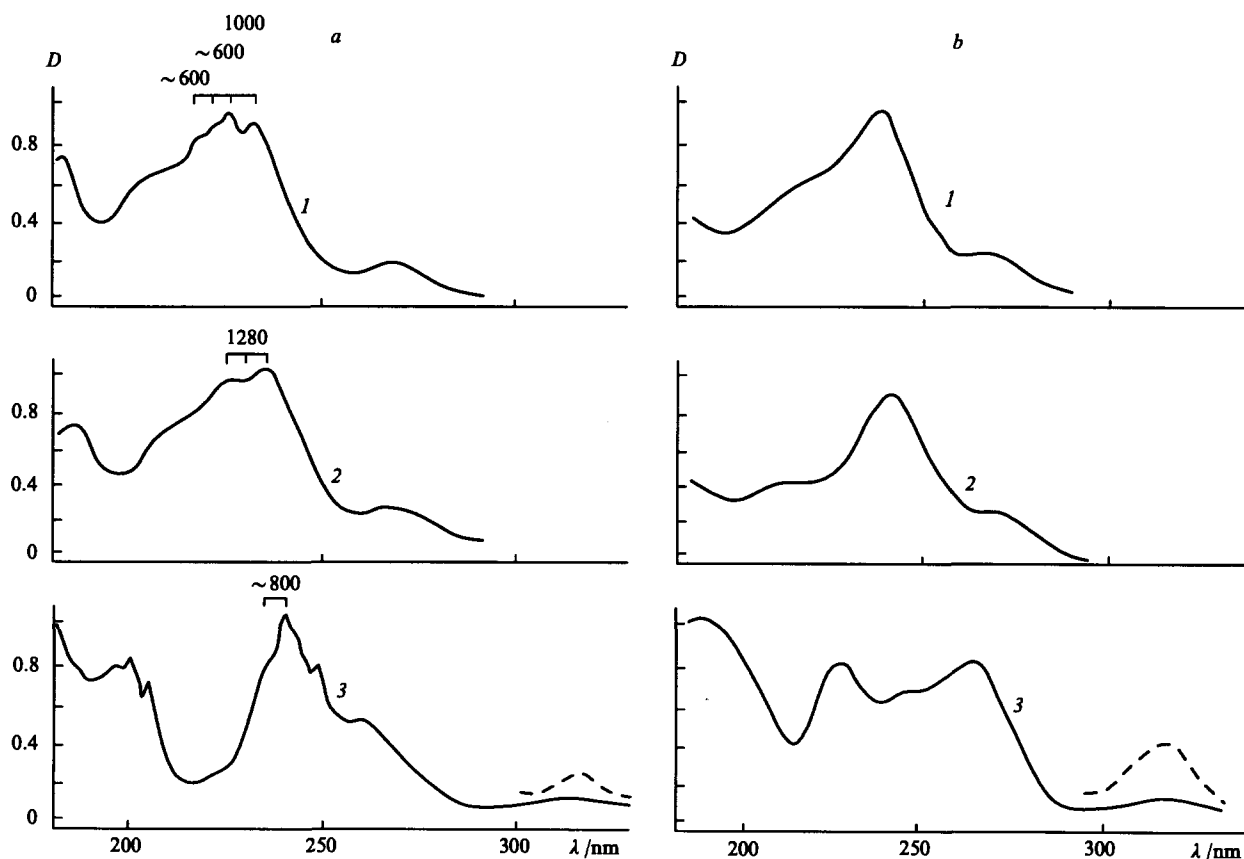
**Figure 33.** The UV absorption spectra of vinyl selenides CH₂=CHSeMe (1), CH₂=CHSeEt (2), and vinyl methyl telluride CH₂=CHTeMe (3) in the gaseous state (a) and in a heptane solution (b).¹⁹²

Table 10. Electronic transitions in the near UV region for vinyl chalcogenides.¹⁹²

Compound	Medium ^a	Transition (λ /nm)		
		$\pi \rightarrow \sigma^*$	$\pi \rightarrow \pi^*$	$\pi \rightarrow \sigma^*$
CH ₂ = CHSMe	GP	243	225 (1280; ~1300) ^b	196
	HX	238–250	227 (~1000)	< 198
CH ₂ = CHSEt	GP	241–246	226 (1200)	199
	HX	247–253	229	< 194
CH ₂ = CHSP ⁿ		238–244		
	GP	240–246	226 (~1150)	200
	HX	244–250	228	< 198
CH ₂ = CHSBu ⁿ		~238		
	GP	238–247	226	< 199
	HX	244–250	230	~198
CH ₂ = CHSBu ⁱ		~238 (sh)		
	GP	~244 (sh)	230 (~1150)	200
		232–238		
	HX	~250 (sh)	228	< 196
CH ₂ = CHSBu ^t		239		
	GP	247	227	199
	HX	~250 (sh)	231	< 194
		235–241		
CH ₂ = CHSP ⁱ	GP	247	227 (~1250)	197
		235–238		
	HX	~252 (sh)	231	
		~240 (sh)		
CH ₂ = CHSBu ^t	GP	249	229	
	HX	251	235	< 199
CH ₂ = CHSPent ^t	GP	249	229	198
	HX	251	235	< 192
CH ₂ = CHSCD ₃	GP	241	225 (1260; 1300)	196
CD ₂ = CDSMe	GP	244	225 (1160; ~1150)	196
CH ₂ = CHSeMe	GP	266	230 (~600; ~600)	~220
	HP	268	240	< 220
CH ₂ = CHSeEt	GP	267	238 (~640)	~221
	HP	271	242	218
CH ₂ = CHSePr ⁱ	HP	272	243	~219
CH ₂ = CHSeBu ^t	HX	273	244	~219
CH ₂ = CHTeMe	GP	330	243	259
	HP	331	232	266
CH ₂ = CHTeEt	HP	332	230	267
CH ₂ = CHTePr ⁿ	HP	329	229	268
CH ₂ = CHTePr ⁱ	HP	333	229	268
CH ₂ = CHTeBu ⁿ	HP	328	228	267

^a Accepted notations: GP — gaseous phase, HX — hexane, HP — heptane; ^b the vibrational quantum number is given in parentheses.

9. UV absorption spectra of alkyl vinyl tellurides

Alkyl vinyl tellurides absorb in the range of 200–330 nm (Table 9, 10, Fig. 34).¹⁹² The $\pi \rightarrow \sigma^*$ transitions in the UV spectrum of methyl vinyl telluride are strongly (by $\sim 7100 \text{ cm}^{-1}$) red-shifted even in comparison with those in methyl vinyl selenide, and are located at 259 and 329 nm in the gas phase. For methyl vinyl sulfide band intensities of $\pi \rightarrow \sigma^*$ transitions are of the same order ($\sim 10^3$), whereas dramatic redistribution takes place on going to vinyl telluride, i.e. with an increase in the mass of the heteroatom (Fig. 33). In the spectrum of a heptane solution of methyl vinyl telluride, the extinction ratio of long-wave and short-wave bands of $\pi \rightarrow \sigma^*$ transitions is $\sim 6 \times 10^{-2}$. This is probably due to localisation of the MOs of methyl vinyl telluride within the CTeC fragment having high symmetry (C_2 or C_{2v}). For the ground state of methyl vinyl telluride such a supposition is confirmed by PE spectroscopic data. In contrast to sulfides, the higher occupied π -MO in unsaturated tellurides contains a dominating contribution from the tellurium p_z -AO (I_1 values are the same for Me_2Te and $\text{CH}_2 = \text{CHTeMe}$).¹⁸³ UV spectra show that it is true of the excited state with an electron in the σ_1^* -MO and the vacant π -MO.

As was already noted, the long-wave σ band profile in the spectra of vinyl sulfides is dictated by the phase state and the structure of the alkyl substituents. In the spectra of alkyl vinyl tellurides, the contours of both σ -bands depend on none of these. Irreducible representations b_1 , a_1 , and b_2 correspond to the HOMO of the π -type and to two low-lying vacant σ^* -orbitals of the ground state of methyl vinyl telluride. Hence, it follows that the transitions will be one-configurational, and one of them [$^1A_1 \rightarrow ^1B_1$ ($^1b_1^1a_1^*$) or $^1A_1 \rightarrow ^1A_2$ ($^1b_1^1b_2^*$)] is symmetry-forbidden (in the absence of electronic-vibrational interactions).

A transition of the $\pi \rightarrow \pi^*$ -type is responsible for the band at $\lambda = 243 \text{ nm}$ (gas) with a vibrational splitting of $\sim 800 \text{ cm}^{-1}$ in the UV spectrum of methyl vinyl telluride. The splitting is significantly higher than the frequency of the CTeC stretching mode in the ground state,¹⁴³ thus indicating that the bond becomes stronger upon excitation. The passage from gas to solution causes a red shift (1000 cm^{-1}) in the respective spectra.

It is known that in the UV spectrum of Me_2Te , the first Rydberg transitions of the series $n\text{Te} \rightarrow 6s$ and $n\text{Te} \rightarrow 6p$ are observed at 250 nm and 216 nm. Comparison of the spectra of methyl vinyl telluride in the gas phase and in solution and the fact that the first

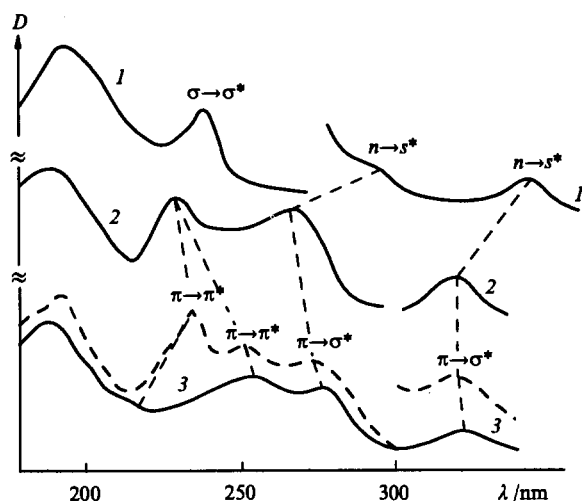


Figure 34. The UV absorption spectra of diorganyltellurides Et_2Te (1), $\text{CH}_2=\text{CHTeEt}$ (2), and $(\text{CH}_2=\text{CH})_2\text{Te}$ (3) in a heptane solution. The spectrum of $(\text{CH}_2=\text{CH})_2\text{Te}$ in the gaseous phase is shown in a dotted line.¹⁹⁷

ionisation potentials of this compound¹⁸³ and Me_2Te are practically the same (7.90 and 7.89 eV) made it possible¹⁹² to assign the bands at 250 nm and 214 nm to the $\pi\rightarrow 6s$ and $\pi\rightarrow 6p$ Rydberg transitions, respectively.

Hence, the following sequence of electronic transitions is observed in the UV spectra of alkyl vinyl tellurides:¹⁹² $\pi\rightarrow\sigma^* < \pi\rightarrow\sigma^* < \pi\rightarrow\pi^* < \pi\rightarrow\pi^* < \pi\rightarrow\pi^*$.

Thus, the common feature of the simplest unsaturated compounds of S, Se, and Te is the presence of a low-energy excited state¹⁹² in which an electron occupies the σ_1^* -MO, and a vacancy arises on the π -MO. From the practical point of view, it is important that in the UV spectra of alkyl vinyl chalcogenides, the energies of $\pi\rightarrow\sigma_1^*$ transitions are approximately constant: for sulfides it is 9970 cm^{-1} in the gas phase, for selenides and tellurides it is $\sim 8000\text{ cm}^{-1}$. Quite different behaviour is typical of two higher occupied σ -MOs of the ground state: an energy gap between the transitions decreases with complication of the structure.^{179,183} With the increase in the atomic number of the chalcogen, the $\pi\rightarrow\sigma^*$ and $\pi\rightarrow\pi^*$ transitions exhibit a systematic red shift, the former being more sensitive to the nature of the element than the latter.¹⁹²

10. UV absorption spectra of divinyl chalcogenides

The following concepts^{179,183} were used in the assignment of electronic transitions in the UV spectra of divinyl chalcogenides (Figs 34, 35):¹⁹⁷ a) the energy gap between the σ band maxima is practically independent of the alkyl substituent length and branching and somewhat decreases with an increase in the heteroatom atomic number; and b) the energies of two higher occupied σ -MOs of organyl chalcogenides are linearly related. These properties of $\pi\rightarrow\sigma^*$ transitions could make the band assignment in the absorption spectra of divinyl chalcogenides substantially easier if data were available on similar transitions in the series $\text{CH}_3-\text{CH}_2\text{XCH}_2-\text{CH}_3$, $\text{CH}_2=\text{CHXCH}_2-\text{CH}_3$, $\text{CH}_2=\text{CHXCH}=\text{CH}_2$ (for saturated compounds, the $\pi\rightarrow\sigma^*$ transitions are actually identical to the $n_x\rightarrow\sigma^*$ ones). Unfortunately, only long-wave $n_x\rightarrow\sigma^*$ transitions are known for saturated cyclic sulfides, which have an extremely low intensity because they are symmetry-forbidden.¹⁹⁴ For dialkyl sulfides, these bands overlap with an intense band associated with the $\sigma\rightarrow\sigma^*$ excitation.¹⁹⁴ For dialkyl sulfides in the gas phase and in solution, both $n_{\text{Te}}\rightarrow\sigma^*$ transitions are shown¹⁹⁷ to have an intensity quite sufficient for reliable detection, and are located in a more long-wave region than the transition of the $\sigma\rightarrow\sigma^*$ type (Table 11,

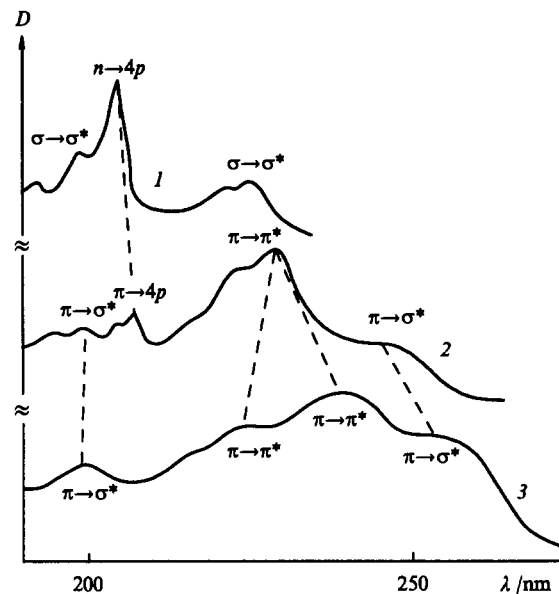


Figure 35. The UV absorption spectra of diorganylsulfides Et_2S (1), $\text{CH}_2=\text{CHSEt}$ (2), and $(\text{CH}_2=\text{CH})_2\text{S}$ (3) in the gaseous phase.¹⁹⁷

Fig. 34). It can be seen from Table 11 that the $\Delta\sigma^*$ values for saturated and unsaturated tellurides differ insignificantly.

The energies of two higher occupied σ -MOs of diorganyl chalcogenides are known^{179,183} to be linearly interrelated. Similar relationship can also be true of two low-lying vacant σ^* -MOs because in the molecules of high symmetry they are rearrange by the same irreducible representations as the higher occupied σ -MOs do. Analysis of UV spectra of diorganyl chalcogenides in which both $\pi\rightarrow\sigma^*$ -transitions are satisfactorily resolved (Table 11), reveals indeed a linear correlation of their energies, which is true for all the compounds considered regardless of the chalcogen type and the number of unsaturated fragments (Fig. 36).¹⁹⁷ Taking this into account, the following energy sequence was obtained for electronic transitions in the UV absorption spectra of divinyl chalcogenides:¹⁹⁷

for Te: $\pi\rightarrow\sigma^* < \pi\rightarrow\sigma^* < \pi\rightarrow\pi^* < \pi\rightarrow\pi^*$;

for S and Se: $\pi\rightarrow\sigma^* < \pi\rightarrow\pi^* < \pi\rightarrow\pi^* < \pi\rightarrow\sigma^*$.

Changes in the Franck-Condon absorption profile for divinyl telluride with regard to the phase state (Fig. 34) indicate

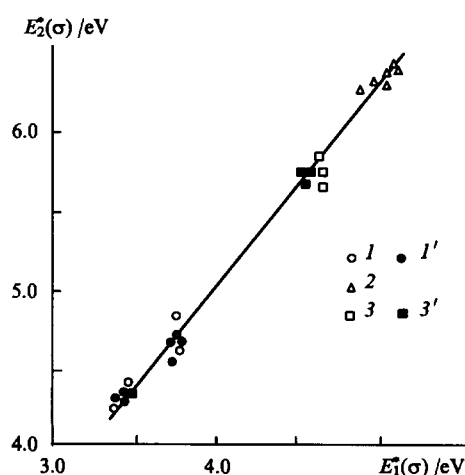


Figure 36. The correlation between the energies of the $\pi(n)\rightarrow\sigma^*$ transitions for tellurides (1, 1'), selenides (2), and sulfides (3, 3') in the gaseous state (1–3) and in a heptane solution (1', 3').¹⁹⁷

Table 11. Characteristics of electronic transitions for diorganyl chalcogenides.¹⁹⁷

Compound	$\pi \rightarrow \sigma^*$ transition ^a			$\sigma \rightarrow \sigma^*$ transition ^a
	E_1^*/eV	E_1^*/eV	$\Delta\sigma^*$	E_1^*/eV
Heptane				
Me ₂ Te	3.38 (1.9)	4.24 (2.2)	0.86	5.18 (3.8)
CH ₂ =CHTeMe	3.75 (2.5)	4.67 (3.7)	0.92	—
EtTeMe	3.42 (1.9)	4.29 (2.6)	0.87	5.24 (3.8)
CH ₂ =CHTeEt	3.72 (2.6)	4.64 (3.6)	0.91	—
(Pr ⁿ) ₂ Te	3.41 (2.1)	4.25 (2.3)	0.84	5.21 (3.8)
CH ₂ =CHTePr ⁱ	3.72 (2.5)	4.63 (3.5)	0.91	—
(Bu ⁿ) ₂ Te	2.46 (1.9)	4.30 (2.6)	0.84	5.27 (3.8)
CH ₂ =CHTeBu ⁿ	3.77 (2.6)	4.64 (3.6)	0.87	—
(CH ₂ =CH) ₂ Te	3.72 (2.6)	4.49 (3.7)	0.77	—
CH ₂ =CHSeEt	4.58 (3.3)	5.70 (3.3)	~1.10	—
CH ₂ =CHSePr ⁱ	4.56 (3.3)	5.66 (3.4)	1.10	—
CH ₂ =CHSeBu ^t	4.54 (3.4)	5.70 (3.5)	~1.20	—
Gaseous phase				
Me ₂ Te	3.36	4.23	0.87	sec ^b
CH ₂ =CHTeMe	3.76	4.79	1.03	—
Et ₂ Te	3.43	4.30	0.87	sec ^b
(CH ₂ =CH) ₂ Te	3.77	4.58	0.81	—
CH ₂ CHSeMe	4.66	5.70	~1.10	—
CH ₂ =CHSeEt	4.65	5.60	~0.90	—
(CH ₂ =CH) ₂ Se	4.64	5.80	~1.20	—
CH ₂ =CHSMe	5.10	6.33	1.23	—
CH ₂ =CHSCD ₃	5.13	6.33	1.20	—
CD ₂ =CDSMe	5.08	6.32	1.24	—
CH ₂ =CHSAm ^t	4.98	6.27	1.29	—
(CH ₂ =CH) ₂ S	4.90	6.22	1.32	—

^a Extinction coefficient (lg ε) is given in parentheses; ^b the bands of the $\sigma \rightarrow \sigma^*$ transition and the Rydberg transition overlap.

that in the gas phase the short-wave $\pi \rightarrow \pi^*$ transition overlaps with the Rydberg $\pi \rightarrow ns$ transition. Among $\pi \rightarrow \pi^*$ transitions in divinyl chalcogenides, the most short-wave transition is the least intense. A great difference in intensities of the σ -bands for divinyl telluride (Fig. 34) can be easily rationalised on the assumption of its planar conformation (C_{2v}). For a non-planar form (C_2) of divinyl chalcogenides, an $^1A < ^1B$ sequence corresponds to π^* excited states. The 1B state is associated with the electronic configuration $a^2b^1b^*a^1$, and the position of the a -symmetry orbitals depends slightly on the central atom, therefore, there is a

near-linear correlation between the energy (E^*) of the $^1A \rightarrow ^1B$ transition in divinyl chalcogenides and their first ionisation potentials (Fig. 37).¹⁹⁷

11. UV absorption spectra of allenyl ethers

Electronic transitions in the UV spectra of alkyl allenyl and allenyl vinyl ethers have been analyzed.^{175,177} Two bands were observed in the spectra of heptane solutions, which had a tendency for a blue shift ($\sim 2-3$ nm) on going to a polar solvent (Table 12). The bands of alkyl allenyl ethers belong to the $\pi \rightarrow \pi^*$ and $\bar{\pi} \rightarrow \pi^*$ transitions partially allowed due to electronic-vibrational interaction in the allene group.¹⁷⁵ In allenyl vinyl ethers, the long-wave band corresponds to the transition localised within the allene fragment, and the short-wave band belongs to the $\pi \rightarrow \pi^*$ transition.¹⁷⁷

In a series of alkyl allenyl ethers, the most significant changes in the UV spectra were observed for $\text{CH}_2=\text{C}=\text{CHOBu}^t$.¹⁷⁵ The electronic transition corresponding to the long-wave band appeared to be the most sensitive. In addition to a blue shift of this band by ~ 16 nm relative to its position in allenyl methyl ether, its half-width nearly doubles.

In order to study the possible influence of stereoisomerism in alkyl allenyl ethers on the nature and position of electronic transitions, CNDO/C calculations for the molecules $\text{CH}_2=\text{C}=\text{CHOMe}$ and $\text{CH}_2=\text{C}=\text{CHOBu}^t$ have been carried out.¹⁷⁵ The one-configurational long-wave transition appeared to be symmetry-forbidden (it belongs to the $\pi \rightarrow \pi^*$ type). The next $\bar{\pi} \rightarrow \pi^*$ transition occurs at 4.83–4.86 eV. The energy gap between the bands observed in the ranges of 255–275 nm and 208–213 nm in the spectra of alkyl allenyl ethers corresponds to the difference in the calculated energies of the $\pi \rightarrow \pi^*$ and $\bar{\pi} \rightarrow \pi^*$ transitions. A blue shift of the long-wave band in $\text{CH}_2=\text{C}=\text{CHOBu}^t$ as compared to that in allenyl methyl ether can be explained by a difference in the conformations of these

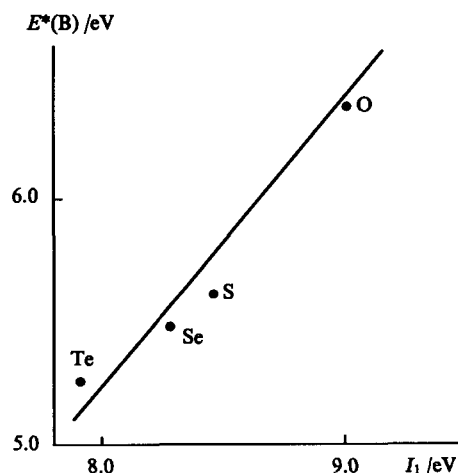


Figure 37. The dependence of the energies of $^1A \rightarrow ^1B$ transitions for divinyl chalcogenides in the gaseous phase on the first ionisation potential (I_1). Points are the experimental values of $E^*(B)$ in the gaseous phase.¹⁹⁷

Table 12. The UV absorption spectra of allenyl ethers.^{175,177}

Compound	Solvent	λ /nm (lg ϵ)	
CH ₂ =C=CHOMe	C ₇ H ₁₆	274 (2.0);	212 sh (3.3)
	EtOH	270 (1.9);	210 sh (3.4)
	MeCN	269 (2.0);	210 sh (2.5)
CH ₂ =C=CHOEt	C ₇ H ₁₆	272 (2.0);	211 sh (3.2)
	EtOH	269 (2.0);	210 sh (3.3)
	MeCN	268 (2.0);	210 sh (3.3)
CH ₂ =C=CHOPr ⁿ	C ₇ H ₁₆	272 (1.9);	211 sh (3.2)
	EtOH	270 (1.9);	211 sh (3.1)
CH ₂ =C=CHOPr ⁱ	C ₇ H ₁₆	271 (2.0);	211 sh (3.3)
	EtOH	268 (1.9);	211 sh (3.2)
CH ₂ =C=CHOBu ⁿ	C ₇ H ₁₆	272 (1.9);	211 sh (3.3)
	EtOH	269 (1.9);	211 sh (3.2)
CH ₂ =C=CHOBu ⁱ	C ₇ H ₁₆	271 (1.9);	211 sh (3.2)
	EtOH	269 (1.9);	211 sh (3.1)
CH ₂ =C=CHOBu ^t	C ₇ H ₁₆	258 (2.0);	208 sh (3.5)
	EtOH	257 (1.9);	208 sh (3.5)
CH ₂ =C=CHOCH ₂ CH=CH ₂	C ₇ H ₁₆	272 (1.9);	213 sh (3.5)
	EtOH	270 (1.8);	213 sh (3.3)
CH ₂ =C=CHOCH=CH ₂	C ₇ H ₁₆	265 (2.4);	213 (4.1)
	EtOH	263 (2.5);	211 (4.3)
	MeCN	261 (2.4);	210 (4.2)
CH ₂ =C=C(Me)OCH=CH ₂	C ₇ H ₁₆	267 (2.4);	216 (4.0)
	EtOH	266 (2.4);	214 (4.0)
CH ₂ =C=C(Pr ⁱ)OCH=CH ₂	C ₇ H ₁₆	269 (2.3);	216 (4.2)
	EtOH	267 (2.4);	215 (4.3)
CH ₂ =C=C(Pr ⁿ)OCH=CH ₂	C ₇ H ₁₆	270 (2.4);	215 (10940)
	EtOH	269 (2.4);	214 (10775)
(CH ₂ =CH) ₂ O	C ₇ H ₁₆	—	210 (14430)
	EtOH	—	209 (19880)

molecules. However, the calculations for *cis*- and *trans*-rotamers in allenyl methyl ether show that the electronic transition energies depend little on the nature of the planar conformation. Violation of the orthogonal character of the π -systems of the allene fragment does not substantially affect spectral characteristics as well.¹⁷⁵ The calculated electronic spectrum of CH₂=C=CHOBu^t, in which

the *tert.* butyl substituent is rotated relative to the C_{sp}²—O bond by 30–60° (from the planar *s-trans*-form), indicates that the long-wave band is 3–9 nm blue-shifted. It should be borne in mind that for this compound C₂ symmetry might break if there is the only minimum in the internal rotation potential curve corresponding to the *s-trans*-rotamer. Presumably, the shape of the internal rotation potential ensures significant population of the excited torsional-vibrational states, for which large-amplitude motion is typical. It explains a larger width of the long-wave band in CH₂=C=CHOBu^t as compared to that in allenyl methyl ether but does not explain a spectral shift because a vibration amplitude of 60° can hardly be supposed.

Another possible reason is the presence of a non-planar *gauche*- or near-*gauche*-form along with the planar *s-trans*-form. In this case, however, the extinction for the *gauche*-conformer should be, at least, two orders of magnitude higher than that for the planar one. This situation does not seem probable since the long-wave transition is symmetry-forbidden for alkylallenes. Thus, the reason for a blue shift of the long-wave band in CH₂=C=CHOBu^t as compared to that in the spectrum of allenyl methyl ether remains obscure.

The most short-wave electronic transition was calculated¹⁷⁵ to have an energy > 6 eV and corresponds to the $\pi \rightarrow \pi^*$ transition observed for alkyl vinyl ethers in the range of 190–200 nm.¹⁹⁸

According to CNDO/C calculations for allenyl vinyl ether,¹⁷⁷ the long-wave transition is located at 308.6 eV ($f=0$) and belongs to the $\pi \rightarrow \pi^*$ type. The next transition belongs to the $\bar{\pi} \rightarrow \pi^*$ type of the allene fragment. Unlike the corresponding transitions in allenyl methyl ether, the long-wave transitions in allenyl vinyl ether are two-configurational (Table 13).¹⁷⁷ The short-wave transition in allenyl vinyl ether is mostly one-configurational. The calculation shows that the corresponding band is located in the range of 210–215 nm and originates from the $\pi \rightarrow \pi^*$ excitation.

V. Conclusion

The investigations of rotational isomerism in vinyl and allenyl chalcogenides summarised in the present review have revealed remarkable peculiarities of the molecular and electronic structure of this group of compounds. Two qualitatively different types of stable conformers exist. One of them is characterised by a definite torsional angle and small deviations from the global minimum of potential energy. The other is associated with large-amplitude relative motion of molecular fragments encompassing not one, but several local minima in the internal rotation potential curve. Methyl vinylchalcogenides represent an ensemble of stationary

Table 13. The UV absorption spectra of allenyl methyl, allenyl vinyl, and divinyl ethers.¹⁷⁷

Molecule (rotamer)	λ_{exp} /nm	lg ϵ	λ_{calc} /nm	f_i	Transition	Dominating conformation (contribution)
CH ₂ =C=CHOMe (<i>s-cis</i>)	274	2.0	316.6	0.0000	$\pi \rightarrow \pi^*$	1–2* (1.00)
			255.3	0.0002	$\bar{\pi} \rightarrow \pi^*$	2–1* (1.00)
	212 (sh)	3.3	204.1	0.9680	$\pi \rightarrow \pi^*$	1–1* (0.83) 2–2* (0.53)
CH ₂ =C=CHOCH=CH ₂ (<i>trans-trans</i>)	265	2.4	308.6	0.0000	$\pi \rightarrow \pi^*$	1–3* (0.89) 3–3* (0.45)
			260.0	0.0001	$\bar{\pi} \rightarrow \pi^*$	2–1* (0.65) 2–2* (0.75)
	213	4.1	212.7	1.0820	$\pi \rightarrow \pi^*$	1–1* (0.88) 2–3* (0.37)
			189.4	0.0800	$\pi \rightarrow \pi^*$	1–2* (0.89) 1–1* (0.36)
(CH ₂ =CH) ₂ O (<i>trans-trans</i>)	210	4.2	196.4	0.6520	$\pi \rightarrow \pi^*$	1–1* (0.99)
			181.5	0.0258	$\pi \rightarrow \pi^*$	1–2* (0.03)

states corresponding to planar *cis*-, *gauche*-, free rotational, and 'quasi'-*trans*-states, in which large-amplitude molecular motion occurs relative to the planar *trans*-form. The existence of three non-planar stable forms, viz, two quasi-degenerate *trans-trans*- and one *cis-trans*-, as well as large amplitude intramolecular motion at high temperatures and, occupancy of above-barrier states under these conditions are typical of internal rotation in divinyl chalcogenides.

The following features are typical of the ground state of alkyl vinyl chalcogenides: a) a weak dependence of the structure and the relative arrangement of higher occupied π -MOs on the nature of the heteroatom and the structure of substituent; b) the existence of a linear correlation between the energies of higher occupied σ -MOs, the parameters of which are dictated by the nature of the heteroatom and the number of unsaturated groups. For alkyl vinyl and divinyl chalcogenides, the lowest energy corresponds to the state, in which an electron migrates to the σ^* -MO and a vacancy arises in the π -MO. Excited states of π -symmetry are located higher on the energy scale as compared to those of σ -symmetry. The latter are more sensitive to the nature of the heteroatom.

References

1. B A Trofimov *Geteroatomnye Proizvodnye Atsetilena. Novye Polifunktsional'nye Monomery, Reagenty i Poluprodukty* (Heteroatomic Derivatives of Acetylene. New Polyfunctional Monomers, Reagents, and Intermediate Products) (Moscow: Nauka, 1981)
2. B A Trofimov, Doctoral Thesis in Chemical Sciences, Leningrad State University, Leningrad, 1970
3. L M Sinegovskaya, V V Keiko, B A Trofimov *Sulfur Rep.* 7 337 (1987)
4. N K Gusarova, A A Tatarinova, L M Sinegovskaya *Sulfur Rep.* 11 1 (1991)
5. B A Trofimov, S V Amosova *Divinilsul'fid i ego Proizvodnye* (Divinyl Sulfide and Its Derivatives) (Novosibirsk: Nauka, 1983)
6. Yu L Frolov, in *Khimiya Organicheskikh Soedinenii Sery* (The Chemistry of Organic Sulfur Compounds) (Ed. L I Belen'kii) (Moscow: Khimiya, 1988) p. 288
7. Yu L Frolov, in *Khimiya Organicheskikh Soedinenii Sery* (The Chemistry of Organic Sulfur Compounds) (Ed. L I Belen'kii) (Moscow: Khimiya, 1988) p. 240
8. V M Bzhezovskii, G A Kalabin, in *Khimiya Organicheskikh Soedinenii Sery* (The Chemistry of Organic Sulfur Compounds) (Ed. L I Belen'kii) (Moscow: Khimiya, 1988) p. 250
9. V M Bzhezovskii, Candidate Thesis in Chemical Sciences, Irkutsk Institute of Organic Chemistry, Siberian Branch of the Academy of Sciences of the USSR, Irkutsk, 1977
10. V B Modonov, Candidate Thesis in Chemical Sciences, Irkutsk Institute of Organic Chemistry, Siberian Branch of the Academy of Sciences of the USSR, Irkutsk, 1978
11. L M Sinegovskaya, Candidate Thesis in Chemical Sciences, Irkutsk Institute of Organic Chemistry, Siberian Branch of the Academy of Sciences of the USSR, Irkutsk, 1979
12. D F Kushnarev, Candidate Thesis in Chemical Sciences, Irkutsk State University, Irkutsk, 1979
13. G A Kalabin, Doctoral Thesis in Chemical Sciences, Irkutsk State University, Irkutsk, 1982
14. R Kh Zacheslavskaya, Candidate Thesis in Chemical Sciences, Leningrad State University, Leningrad, 1984
15. R B Valeev, Candidate Thesis in Chemical Sciences, Irkutsk State University, Irkutsk, 1984
16. M V Sigalov, Candidate Thesis in Chemical Sciences, Irkutsk State University, Irkutsk, 1984
17. E Yu Shmidt, Candidate Thesis in Chemical Sciences, Irkutsk State University, Irkutsk, 1988
18. L B Krivdin, Doctoral Thesis in Chemical Sciences, Irkutsk State University, Irkutsk, 1989
19. M V Sigalov, Doctoral Thesis in Chemical Sciences, Irkutsk State University, Irkutsk, 1995
20. A V Afonin, Doctoral Thesis in Chemical Sciences, Irkutsk State University, Irkutsk, 1982
21. L M Sinegovskaya, Doctoral Thesis in Chemical Sciences, Irkutsk Institute of Organic Chemistry, Siberian Branch of the Russian Academy of Sciences, Irkutsk, 1994
22. J M Hay, D Lyon *Nature (London)* 216 790 (1967)
23. B Blank, H Fischer *Helv. Chim. Acta* 56 506 (1973)
24. S Saito *Chem. Phys. Lett.* 42 399 (1976)
25. M Rodler, A Bauder *J. Am. Chem. Soc.* 106 4025 (1984)
26. M Rodler *J. Mol. Spectrosc.* 114 23 (1985)
27. K Kuchitsu *J. Chem. Phys.* 49 4456 (1968)
28. D R Lide Jr, D Christensen *J. Chem. Phys.* 35 1375 (1961)
29. W Gordy, R L Cook (Eds) *Microwave Molecular Spectra* (New York: Interscience, 1970)
30. J L Rippoll *Nouv. J. Chim.* 3 195 (1979)
31. M Hawkins, L Andrews *J. Am. Chem. Soc.* 105 2523 (1983)
32. M Rodler, C E Blom, A Bauder *J. Am. Chem. Soc.* 106 4029 (1984)
33. B Albrecht, M Allan, E Haselbach, L Neuhaus, P A Carrupt *Helv. Chim. Acta* 67 216 (1984)
34. G Y Matti, O I Osman, J E Upham, R J Suffolk, H W Kroto *J. Electron Spectrosc. Relat. Phenom.* 49 195 (1989)
35. M Tanimoto, S Saito *Chem. Lett.* 637 (1977)
36. V Almond, S W Charles, J N Macdonald, N L Owen *J. Chem. Soc., Chem. Commun.* 483 (1974)
37. V Almond, S W Charles, J N Macdonald, N L Owen *J. Mol. Struct.* 100 223 (1983)
38. M Tanimoto, V Almond, S W Charles, J N Macdonald, N L Owen *J. Mol. Spectrosc.* 78 95 (1979)
39. M Tanimoto, J N Macdonald *J. Mol. Spectrosc.* 78 106 (1979)
40. V Almond, R R Permanand, J N Macdonald *J. Mol. Struct.* 128 337 (1985)
41. A Mangini *Atti Acad. Naz. Lincei CI, Sci. Fis. Mat. Nat., Ser. 2* 14 31 (1977)
42. S Samdal, H M Seip *J. Mol. Struct.* 28 193 (1975)
43. W Bouma, D Poppinger, L Radom *J. Am. Chem. Soc.* 99 6443 (1977)
44. W J Bouma, L Radom *J. Mol. Struct.* 43 267 (1978)
45. R H Nobes, L Radom, N L Allinger *J. Mol. Struct.* 85 185 (1981)
46. C Plant, K Spencer, J N Macdonald *J. Mol. Struct.* 140 317 (1986)
47. J Kao *J. Am. Chem. Soc.* 100 4685 (1978)
48. J Kao, C Eyermann, E Southwick, D Leister *J. Am. Chem. Soc.* 107 5323 (1985)
49. C Plant, J N Macdonald, J E Boggs *J. Mol. Struct.* 128 353 (1985)
50. J N Macdonald, N L Owen, M Rosolini *J. Mol. Struct.* 159 229 (1987)
51. M S Groot, J Lamb *Proc. R. Soc. London, A Math. Phys. Sci.* 242 36 (1957)
52. J Mikawa *Bull. Chem. Soc. Jpn.* 29 110 (1956)
53. W H T Davison, G B Bates *J. Chem. Soc.* 2607 (1953)
54. G D Meakins *J. Chem. Soc.* 4170 (1953)
55. A Kirmman, P Chancel *Bull. Soc. Chim. Fr.* 1338 (1954)
56. M L Brey, B Tarrant *J. Am. Chem. Soc.* 79 6533 (1957)
57. S W Charles, F C Cullen, N L Owen *J. Chem. Soc., Faraday Trans. 2*, 483 (1974)
58. E M Popov, G I Kagan *Opt. Spektrosk. (Russia)* 194 (1962)
59. M Sakakibara, F Inagaki, I Haarada, T Shimanouchi *Bull. Chem. Soc. Jpn.* 49 46 (1976)
60. P Cahill, L P Gold, N L Owen *J. Chem. Phys.* 48 1620 (1968)
61. N L Owen, N Sheppard *Trans. Faraday Soc.* 60 634 (1964)
62. E M Popov, N S Andreev, G I Kagan *Opt. Spektrosk. (Russia)* 37 (1962)
63. I S Ignatyev, A N Lasarev, M L Smirnov, M L Alpert, B A Trofimov *J. Mol. Struct.* 72 25 (1981)
64. B Cadioli, E Gallinella, U Pincelli *J. Mol. Struct.* 78 215 (1982)
65. A R Katritzky, R F Pinzelli, R D Topsom *Tetrahedron* 28 3441 (1972)
66. E Gallinella, B Cadioli *Chem. Phys. Lett.* 77 533 (1981)
67. H Friege, M Klessinger *J. Chem. Res. (S)* 208 (1977)
68. H Friege, M Klessinger *Chem. Ber.* 112 1614 (1979)
69. A A Planckaert, J Doucet, C Sandorfy *J. Chem. Phys.* 60 4846 (1974)
70. N L Owen, N Sheppard *Spectrochim. Acta* 22 1101 (1966)
71. N L Owen, N Sheppard *Proc. Chem. Soc.* 264 (1963)
72. J R Durig, D A C Compton *J. Chem. Phys.* 69 2028 (1978)
73. J R Durig, D J Gerson *J. Mol. Struct.* 71 131 (1981)
74. J F Sullivan, T J Dickson, J R Durig *Spectrochim. Acta, Part A* 42 113 (1986)

75. B A Trofimov, A S Atavin, O N Vylegzhanin, G A Kalabin *Izv. Akad. Nauk SSSR, Ser. Khim.* 1602 (1969)
76. D B Cunliffe-Jones *Spectrochim. Acta* **21** 245 (1965)
77. B A Trofimov, N I Shergina, A S Atavin, E I Kositsyna, A V Gusarov, G M Gavrilova *Izv. Akad. Nauk SSSR, Ser. Khim.* 116 (1972)
78. B A Trofimov, A S Atavin, A V Gusarov *Izv. Akad. Nauk SSSR, Ser. Khim.* 1457 (1971)
79. B A Trofimov, N I Shergina, A S Atavin, E I Kositsyna, A V Gusarov, G M Gavrilova *Zh. Prikl. Spektrosk.* **14** 282 (1971)
80. I S Ignatyev *J. Mol. Struct.* **246** 279 (1991)
81. N L Owen, H M Seip *Chem. Phys. Lett.* **5** 162 (1970)
82. B A Trofimov, I S Emel'yanov, N E Yasel'man, A S Atavin, B V Prokop'ev, A V Gusarov, G N Vanyukhin, M M Ovchinnikova *Reakts. Sposobn. Org. Soedin.* **6** 934 (1969)
83. B A Trofimov, V B Modonov, T N Bazhenova, B I Istomin, N A Nedolya, M L Al'pert, G G Efremova, S P Sitnikova *Izv. Akad. Nauk SSSR, Ser. Khim.* 89 (1979)
84. B A Trofimov, V B Modonov, M G Voronkov *Dokl. Akad. Nauk SSSR* **211** 608 (1973)
85. O A Osipov, V I Minkin, A D Garnovskii *Spravochnik po Dipol'nym Momentam* (Handbook of Dipole Moments) (Moscow: Vysshaya Shkola, 1971)
86. L S Povarov *Usp. Khim.* **36** 1533 (1967) [*Russ. Chem. Rev.* **36** 656 (1967)]
87. M J Aroney, R J W Le Fevre, G L D Ritchie, J D Saxby *Aust. J. Chem.* **22** 1539 (1969)
88. B A Trofimov, V B Modonov, T N Bazhenova, N A Nedolya, V V Keiko *Reakts. Sposobn. Org. Soedin.* **11** 745 (1975)
89. O N Vylegjanin, V B Modonov, B A Trofimov *Tetrahedron Lett.* 2243 (1972)
90. R Kh Zacheslavskaya, L Ya Rappoport, B A Trofimov, G N Petrov *Reakts. Sposobn. Org. Soedin.* **13** 416 (1976)
91. J J Rao *J. Am. Chem. Soc.* **100** 4685 (1978)
92. E Taskinen, H Lahteenmaki *Tetrahedron* **32** 2331 (1976)
93. D G Lister, P Palmieri *J. Mol. Struct.* **32** 355 (1976)
94. B Cadioli, U Pincelli *J. Chem. Soc., Faraday Trans. 2*, **68** 991 (1972)
95. F Bernardi, N D Epiotis, R L Yates, H B Schlegel *J. Am. Chem. Soc.* **98** 2385 (1976)
96. I G John, L Radom *J. Mol. Struct.* **36** 133 (1977)
97. E Gallinella, B Cadioli *J. Mol. Struct.* **249** 343 (1991)
98. W Pyckhout, P van Nuffel, C van Alsenoy, L van Enden, H J Geise *J. Mol. Struct.* **102** 333 (1983)
99. M Leibovitch, A J Kresge, M R Peterson, I G Csizmadia *J. Mol. Struct. Theochem.* **230** 349 (1991)
100. B Cadioli, E Gallinella *J. Mol. Struct.* **216** 261 (1990)
101. S W Charles, F C Cullen, N L Owen *J. Mol. Struct.* **18** 183 (1973)
102. J M J M Bijen, J L Derissen *J. Mol. Struct.* **15** 229 (1972)
103. N J Koole, M J A Bie, P E Hansen *Org. Magn. Reson.* **22** 146 (1984)
104. L B Krivdin, V V Shcherbakov, A G Proidakov, G A Kalabin, B A Trofimov, O A Tarasova, S V Amosova *Zh. Org. Khim.* **24** 1024 (1988)
105. T Ogata, K Sugimoto *J. Mol. Struct.* **190** 61 (1988)
106. P C Burgers, C W Worrell, M P Groenewege *Spectrosc. Lett.* **13** 381 (1980)
107. W Runge, W Kosbahn *Ber. Bunsenges Phys. Chem.* **80** 1330 (1976)
108. W Runge, W Kosbahn, J Kroner *Ber. Bunsenges Phys. Chem.* **81** 841 (1977)
109. W Runge *Z. Naturforsch., B, Chem. Sci.* **32** 1296 (1977)
110. W Runge *Z. Naturforsch., B, Chem. Sci.* **33** 932 (1978)
111. W Runge *Z. Naturforsch., B, Chem. Sci.* **34** 118 (1979)
112. J Kamphuis, H J Bos, C W Worrell, W Runge *J. Chem. Soc., Perkin Trans. 2* 1509 (1986)
113. A Rastelli, E Gallinella, M Burdisso *J. Mol. Struct.* **196** 79 (1989)
114. S V Eroshchenko, L M Sinegovskaya, O A Tarasova, Yu L Frolov, B A Trofimov, I S Ignatyev *Spectrochim. Acta, Part A*, **46** 1509 (1990)
115. N Lazarev, I S Ignat'ev, T F Tenisheva *Kolebaniya Prostykh Molekul so Svyazyami Si—O* (Vibration of Simple Molecules with Si—O Bonds) (Leningrad: Nauka, 1980)
116. I S Ignat'ev, T F Tenisheva *Kolebatel'nye Spektry i Elektronnoe Stroenie Molekul s Uglerod-Kislородnymi i Kremnij-Kislородnymi Svyazyami* (Vibrational Spectra and Electronic Structure of Molecules with Carbon—Oxygen and Silicon—Oxygen Bonds) (Leningrad: Nauka, 1991)
117. J Blanc, Ch Brecher *J. Chem. Phys.* **36** 139 (1988)
118. E M Popov, G I Kagan *Opt. Spektrosk. (Russia)* **730** (1961)
119. B A Trofimov, B A Shainyan, in *The Chemistry of Sulfur-Containing Functional Groups* (Eds S Patai, Z Rappoport) (New York: Wiley, 1993) p. 659
120. R E Penn, R F Curl Jr *J. Mol. Spectrosc.* **24** 235 (1967)
121. S Samdal, H M Seip *Acta Chem. Scand.* **25** 1903 (1975)
122. J L Derissen, J M J M Bijen *J. Mol. Struct.* **16** 289 (1973)
123. S Samdal, H M Seip, T Torggrimsen *J. Mol. Struct.* **57** 105 (1979)
124. J Fabian, H Krober, R Mayer *Spectrochim. Acta, Part A* **24** 727 (1968)
125. H Bock, C Wagner, K Wittel, J Sauer, D Seebach *Chem. Ber.* **107** 1869 (1974)
126. B A Trofimov, V B Modonov, Yu L Frolov, E P Vyalykh, T N Bazhenova, N K Gusarova, G G Efremova, S V Amosova *Reakts. Sposobn. Org. Soedin.* **13** 57 (1976)
127. A N Surushkin, Yu L Frolov, V V Tuturina, L M Sinegovskaya, N K Gusarova, A M Vasil'tsov, E F Kalistratova *Izv. Akad. Nauk SSSR, Ser. Khim.* 1780 (1985)
128. B A Trofimov, Yu L Frolov, L M Sinegovskaya, V B Modonov, E I Kositsyna, S V Amosova, N K Gusarova, G G Efremova *Izv. Akad. Nauk SSSR, Ser. Khim.* 340 (1977)
129. V V Keiko, L M Sinegovskaya, N A Kalinina, N K Gusarova, M L Al'pert, B A Trofimov *Zh. Obshch. Khim.* **4** 875 (1982)
130. A R Katritzky, R F Pinzelli, M V Sinnott, R D Topsom *J. Am. Chem. Soc.* **92** 6861 (1970)
131. M F Shostakovskii, A S Atavin, S V Amosova, B A Trofimov *Izv. Akad. Nauk SSSR, Ser. Khim.* 1852 (1968)
132. C Muller, W Schafer, A Schweig, N Thon, H Vermeer *J. Am. Chem. Soc.* **98** 5440 (1976)
133. A M Panov, G V Ratovskii, V I Rakhlin, R G Mirskov, M G Voronkov *Izv. Akad. Nauk SSSR, Ser. Khim.* 1526 (1982)
134. O Kajimoto, M Kobayashi, T Fueno *Bull. Chem. Soc. Jpn.* **46** 2316 (1973)
135. M E Dyatkina, N M Klimenko *Zh. Strukt. Khim.* **14** 173 (1973)
136. G L Bendazzoli, F Bernardi, P Palmieri *Theor. Chim. Acta* **17** 61 (1970)
137. M Prochazka, T Vondrak, J Polakova *Coll. Czech. Chem. Commun.* **48** 286 (1983)
138. N D Epiotis, S Sarkanen, D Bjorkquist, L Bjorkquist, R Yates *J. Am. Chem. Soc.* **96** 4075 (1977)
139. K M Marstokk, H Mollendal *Acta Chem. Scand.* **44** 692 (1990)
140. V V Keiko, L M Sinegovskaya, B A Trofimov *Izv. Akad. Nauk SSSR, Ser. Khim.* 1531 (1991)
141. D Bond, P R Schleyer *J. Org. Chem.* **55** 1003 (1990)
142. A N Surushkin, L M Sinegovskaya, Yu L Frolov, N K Gusarova, V A Potapov, B A Trofimov *Izv. Akad. Nauk SSSR, Ser. Khim.* 1283 (1987)
143. A N Surushkin, L M Sinegovskaya, Yu L Frolov, N K Gusarova *Izv. Akad. Nauk SSSR, Ser. Khim.* 2783 (1986)
144. A N Surushkin, L M Sinegovskaya, Yu L Frolov, N K Gusarova, V A Potapov, in *Tez. Dokl. Vsesoyuzn. Konf. po Khimii Nepredel'nykh Soedinenii, Kazan', 1986* (Abstracts of Reports at the All-Union Conference on the Chemistry of Unsaturated Compounds, Kazan', 1986) Part 3, p. 17
145. L M Sinegovskaya, V V Keiko, V A Potapov, N K Gusarova, B A Trofimov, in *The XVth European Congress on Molecular Spectroscopy, Sofia, 1983* (Abstracts of Reports) p. 165
146. V V Keiko, L M Sinegovskaya, N A Kalinina, N K Gusarova, V A Potapov, in *Tez. Dokl. Vsesoyuzn. Konf. po Khimii Nepredel'nykh Soedinenii, Kazan', 1986* (Abstracts of Reports of the All-Union Conference on the Chemistry of Unsaturated Compounds, Kazan', 1986) Part 3, p. 16
147. V V Keiko, L M Sinegovskaya, N A Kalinina, N K Gusarova, A A Tatarinova, B A Trofimov *Izv. Akad. Nauk SSSR, Ser. Khim.* 331 (1987)
148. L M Sinegovskaya, V V Keiko, N K Gusarova, B A Trofimov, in *The Second Soviet-Indian Symposium on Organometallic Chemistry, Irkutsk, 1989* (Abstracts of Reports) p. 34
149. V G Dashevskii *Konformatsii Organicheskikh Molekul* (The Conformations of Organic Molecules) (Moscow: Khimiya, 1974)

150. D G Lister, J N Macdonald, N L Owen *Internal Rotation and Inversion. An Introduction to Large Amplitude Motions in Molecules* (New York: Academic Press, 1978)
151. W J Orville-Thomas (Ed.) *Internal Rotation in Molecules* (New York: Wiley, 1974)
152. L L Borricelli, O Bastiansen *Acta Chem. Scand.* **3** 201 (1949)
153. C Hirose, R F Curl Jr *J. Mol. Spectrosc.* **38** 358 (1971)
154. C Hirose, S Maeda *J. Mol. Spectrosc.* **72** 62 (1978)
155. L H Coudert *J. Mol. Spectrosc.* **132** 13 (1988)
156. A D H Claue, A Danti *J. Mol. Spectrosc.* **22** 371 (1967)
157. B Cadioli, B Fortunato, E Gallinella, P Mirone, U Pincelli *Gazz. Chim. Ital.* **104** 369 (1974)
158. W Pyckhout, C van Alsenoy, H J Geise, B van der Veken, G Pieter *J. Mol. Struct.* **130** 335 (1985)
159. I G John, L Radom *J. Mol. Struct.* **39** 281 (1977)
160. K Sohlberg, B L Baker, S P Leary, N W Owen, J C Facelli, B A Trofimov *J. Mol. Struct.* **354** 55 (1995)
161. B Rozsondai, Z E Horvath *J. Chem. Soc., Perkin Trans. 2* 1175 (1993)
162. B Fortunato, M G Giorgini *Gazz. Chim. Ital.* **106** 1005 (1976)
163. A B Remizov, T G Mannafov, F R Tantasheva *Zh. Obshch. Khim.* **45** 1402 (1975)
164. A B Remizov *Zh. Prikl. Spektrosk.* **25** 748 (1976)
165. B A Trofimov, N K Gusarova, A A Tatarinova, V A Potapov, L M Sinegovskaya, S V Amosova, M G Voronkov *Tetrahedron* **44** 6739 (1988)
166. V I Vovna, F I Vilesov *Uspekhi Fotoniki* (Advances in Photonics) (Leningrad: Leningrad State University, 1975)
167. P K Pyldoya, V A Pal'm *Reakts. Sposobn. Org. Soedin.* **4** 786 (1967)
168. F I Vilesov *Uspekhi Fotoniki* (Advances in Photonics) (Leningrad: Leningrad State University, 1969)
169. B W Levitt, L S Levitt *Experientia* **26** 1183 (1970)
170. L S Levitt, B W Levitt *Chem. Ind.* 990 (1970)
171. L S Levitt, B W Levitt, C Parkanyi *Tetrahedron* **28** 3369 (1972)
172. B A Trofimov, U Kh Mel'der, R I Pikver, E P Vyalykh, N A Nedolya *Izv. Akad. Nauk SSSR, Ser. Khim.* 2731 (1974)
173. B J Cocksey, J H D Eland, C J Danby *J. Chem. Soc. (B)* 790 (1971)
174. J Kroner, W Kosbahn, W Runge *Ber. Bunsenges Phys. Chem.* **81** 826 (1977)
175. L M Sinegovskaya, S V Eroshchenko, O A Tarasova, S V Amosova, Yu L Frolov, B A Trofimov *Izv. Akad. Nauk SSSR, Ser. Khim.* 81 (1990)
176. V K Turchaninov, Yu R Mirskova, S V Eroshchenko *Izv. Akad. Nauk, Ser. Khim.* 48 (1995)
177. S V Eroshchenko, L M Sinegovskaya, O A Tarasova, S V Amosova, Yu L Frolov, B A Trofimov *Izv. Akad. Nauk SSSR, Ser. Khim.* 2011 (1989)
178. V I Nefedov, V I Vovna *Elektronnaya Struktura Organicheskikh i Elementoorganicheskikh Soedinenii* (The Electronic Structures of Organic and Organoelement Compounds) (Moscow: Nauka, 1989)
179. V K Turchaninov, L M Sinegovskaya, S V Eroshchenko, A F Ermikov, B A Trofimov *Izv. Akad. Nauk SSSR, Ser. Khim.* 2317 (1991)
180. B A Trofimov, U Kh Mel'der, E P Vyalykh *Teor. Eksp. Khim.* **11** 165 (1975)
181. F S Chang, V Y Yong, J W Prather, K L Cheng *J. Electron Spectr. Relat. Phenom.* **40** 363 (1986)
182. S Craddock, R A Whiteford *J. Chem. Soc., Faraday Trans. 2* **68** 281 (1972)
183. L M Sinegovskaya, A A Tatarinova, N K Gusarova, B A Trofimov *Izv. Akad. Nauk SSSR, Ser. Khim.* 935 (1991)
184. S Pignataro, G Distefano *Chem. Phys. Lett.* **26** 356 (1974)
185. S Sice *J. Phys. Chem.* **64** 1573 (1960)
186. P P Shorygin, M F Shostakovskii, E N Prilezhaeva, L G Shkurina, L G Stolyarova, A P Genich *Izv. Akad. Nauk SSSR, Otd. Khim. Nauk* 1571 (1961)
187. M Prochazka, V Palecek *Coll. Czech. Chem. Commun.* **32** 3149 (1967)
188. Yu L Frolov, L M Sinegovskaya, N K Gusarova, O A Zasyadko, S V Amosova, B A Trofimov *Izv. Akad. Nauk SSSR, Ser. Khim.* 458 (1975)
189. Yu L Frolov, L M Sinegovskaya, N K Gusarova, S V Amosova, B A Trofimov *Zh. Prikl. Spektrosk.* **27** 860 (1977)
190. G V Ratovskii, A M Panov, A N Mirskova, A V Martynov, M G Voronkov *Izv. Akad. Nauk SSSR, Ser. Khim.* 1748 (1979)
191. L M Sinegovskaya, Yu L Frolov, N K Gusarova, V A Potapov, B A Trofimov *Izv. Akad. Nauk SSSR, Ser. Khim.* 115 (1985)
192. L M Sinegovskaya, V K Turchaninov *Izv. Akad. Nauk, Ser. Khim.* 2080 (1992)
193. H Lami *Chem. Phys. Lett.* **48** 447 (1977)
194. L B Clark, W T Simpson *J. Chem. Phys.* **43** 3666 (1965)
195. G Herzberg *Molecular Spectra and Molecular Structure* (Toronto, 1966)
196. J D Scott, G C Causley, B R Russell *J. Chem. Phys.* **59** 6577 (1973)
197. V K Turchaninov, L M Sinegovskaya, B A Trofimov *Izv. Akad. Nauk, Ser. Khim.* 831 (1994)
198. P P Shorygin, T N Shkurina, M F Shostakovskii, E P Gracheva *Izv. Akad. Nauk SSSR, Otd. Khim. Nauk* 1011 (1961)

Thermodynamics of polyolefins

B V Lebedev

Contents

I. Introduction	1039
II. Elements of the thermodynamics of polymerisation and polymers	1040
III. Calorimetric research methods	1041
IV. Heat capacity	1042
V. Thermodynamic parameters of fusion	1046
VI. Parameters of vitrification and of the vitreous state	1048
VII. Thermodynamic functions	1049
VIII. Thermochemical characteristics	1053
IX. Thermodynamic parameters of the formation reactions of polyolefins	1054
X. Principal regularities and characteristics of the thermodynamic properties of polyolefins and of the parameters of their formation reactions	1058

Abstract. The thermodynamic properties of polyethylene, polydeuteroethylene, polypropylene, polybut-1-ene, polyprop-1-ene, poly-3-methylbut-1-ene, polyhex-1-ene, polyisobutylene, poly-4-methylpent-1-ene, and polydec-1-ene as well as the thermodynamic parameters of their formation reaction in the temperature range 0–600 K are considered. The recommended thermodynamic quantities are presented. The characteristic feature of the variation of the thermodynamic properties and parameters of the formation reactions of polyolefins are described in terms of the compositions and structures of the initial monomers and polymers and their physical state and temperature at the standard pressure. The bibliography includes 115 references.

I. Introduction

The use of olefins of various composition and structure in polymerisation and copolymerisation reactions has led to considerable possibilities for the synthesis of polyolefins with new valuable operating properties.¹ Extensive theoretical and applied studies have been carried out in this connection on the synthesis of the initial monomers and on the properties of the polyolefins formed and their applications.^{1–4} One of the dominant aspects of such studies at the present time is the search for appropriate catalytic systems, the study of the kinetics and mechanisms of the polymerisation and copolymerisation reactions, and the determination of the influence of the method of synthesis of polyolefins on their physical properties.^{1–5} The effectiveness of the theoretical and applied developments is significantly improved if use is made of the advances in the thermodynamics of polymers and polymerisation. In the foreword to the American edition of H Sawada's book 'Thermodynamics of Polymerisation', the Editor, Prof. O'Driscoll, noted justifiably that any description of polymer-

isation which does not include thermodynamics is incomplete and the solution of certain problems is altogether impossible without a thermodynamic analysis.⁶ It is noteworthy that the role of thermodynamics in the understanding of polymerisation processes has now been recognised and the thermodynamic aspects of polymerisation have been used systematically for the solution of current problems in polymer chemistry. Unfortunately, suitable data on the thermodynamic properties of polymers and the corresponding monomers are not always available. These data may be obtained mainly as a result of specific and laborious precise calorimetric studies. The majority of such studies have not been systematic. Because of this, the results obtained are scattered through scientific periodicals. The thermodynamic foundations of the technology of the synthesis of polymers may be used in theoretical and applied developments (see, for example, Lebedev and coworkers^{7,8}). The discovery of the dependence of the thermodynamic properties and parameters of reactions on the compositions and structures of the reactants is particularly valuable because they can be used successfully for the estimation of the corresponding quantities for polymers and polymerisation reactions which have not yet been investigated (for example, those described by Vasil'ev⁹ and Lebedev and Yevstropov¹⁰).

The aim of the present review is the analysis, critical selection, and survey of the thermodynamic properties of polyolefins and the parameters of their formation reactions over a wide temperature range and the determination of the dependences of the above properties and reaction parameters on the compositions and structures of the reactants and their physical states and on temperature at the standard pressure.

General information about the polymers considered in this review is presented in Table 1. All polyolefins are high-molecular-mass compounds, which rules out influence of molecular mass on their thermodynamic properties and on the parameters of the polymerisation reactions of the initial monomers. The calculations and estimations of the thermodynamic properties refer to 1 mole of the monomer repeat units of the macromolecules. In the tables of the thermodynamic properties and processes, the values quoted usually refer to the amorphous and crystalline states; if necessary, they can be readily estimated for any degree of crystallinity.

B V Lebedev Institute of Chemistry at the Lobachevskii Nizhnii Novgorod State University, prosp. Gagarina 23/5, 603600 Nizhnii Novgorod, Russian Federation. Fax (7-831) 235 64 80. Tel. (7-831) 265 64 50. E-mail: lebedev@nnov.sovam.com

Received 7 May 1996

Uspekhi Khimii 65 (12) 1124–1148 (1996); translated by A K Grzybowski

Table 1. General information about the polyolefins under consideration.

Name	Monomer repeat unit		Micro-structure (tacticity)
	formula	mass	
Polyethylene	—C ₂ H ₄ —	28.054	—
Polydeutero-ethylene	—C ₂ D ₄ —	32.086	—
Polypropylene	—C ₃ H ₆ —	42.080	Atactic, isotactic, syndiotactic
Polybut-1-ene	—C ₄ H ₈ —	56.104	Isotactic
Polyisobutylene ^a	—C ₄ H ₈ —	56.104	—
Polypent-1-ene	—C ₅ H ₁₀ —	70.134	Isotactic
Poly-3-methyl-but-1-ene	—C ₅ H ₁₀ —	70.134	"
Polyhex-1-ene	—C ₆ H ₁₂ —	84.163	"
Poly-4-methyl-pent-1-ene	—C ₆ H ₁₂ —	84.163	"
Polydec-1-ene	—C ₁₀ H ₂₀ —	140.268	"

^a Amorphous specimen; in all the remaining cases, the specimens were partly crystalline.

II. Elements of the thermodynamics of polymerisation and polymers

In any physical state, real polymers exist in a state of metastable thermodynamic equilibrium,¹¹ so that the methods for the investigation of classical thermodynamics¹² are applicable to them, as well as other metastable systems. In particular, the theory of the occurrence of chemical reactions and their equilibria based on the Second Law of Thermodynamics is fully applicable to polymerisation processes.^{13,14} The following characteristics are the thermodynamic parameters of polymerisation reactions: the thermodynamic constant of the polymerisation-depolymerisation process K_{pol}° and the equilibrium concentration of the monomer $[M]_e^{\circ}$ in the equilibrium reaction mixture; the enthalpy $\Delta_{\text{pol}}H^{\circ}$, the entropy $\Delta_{\text{pol}}S^{\circ}(T)$, and the Gibbs free energy $\Delta_{\text{pol}}G^{\circ}(T)$ of polymerisation; the upper (T_{cel}°) and lower (T_{low}°) limiting polymerisation temperatures.^{6,13-15} The circle in the superscript position indicates that the thermodynamic parameters of the polymerisation process occurring at the standard pressure $p^{\circ} = 101.325$ kPa are considered.

The Law of Mass Action is expressed by the following relation for the polymerisation reaction:

$$K_{\text{pol}}^{\circ} = \frac{1}{[M]_e^{\circ}} \quad (1)$$

In their turn, K_{pol}° and $[M]_e^{\circ}$ are related to the standard Gibbs free energy of polymerisation by the van't Hoff equation.

The equilibrium concentration of the monomer can be expressed in terms of the enthalpy and entropy of polymerisation:

$$\ln [M]_e^{\circ} = \frac{\Delta_{\text{pol}}H^{\circ}(T)}{RT} - \frac{\Delta_{\text{pol}}S^{\circ}(T)}{R},$$

where R is the gas constant.

This equation is frequently used to obtain the values of $\Delta_{\text{pol}}H^{\circ}(T)$ and $\Delta_{\text{pol}}S^{\circ}(T)$, assuming that the enthalpy and entropy are independent of temperature in the experimental range of the latter. Subject to this condition, $\ln [M]_e^{\circ}$ is plotted against $1/T$ on the basis of the values of $[M]_e^{\circ}$ measured at several temperatures. This is usually a straight line, so that

$$\Delta_{\text{pol}}H^{\circ}(\Delta T) = -R \operatorname{tg} \alpha,$$

$$\Delta_{\text{pol}}S^{\circ}(\Delta T) = R \lim_{(1/T) \rightarrow 0} (\ln [M]_e^{\circ}),$$

where α is the slope of the straight line. The enthalpy and entropy of polymerisation are the averages of the quantities in the temperature range of measurement of $[M]_e^{\circ}$.

The temperature variations of K_{pol}° and $[M]_e^{\circ}$ are expressed by the van't Hoff equation of the reaction isobar.

The influence of temperature on $[M]_e^{\circ}$ is determined by the numerical value and sign of the enthalpy of polymerisation. The greater the numerical value of $\Delta_{\text{pol}}H^{\circ}$, the more marked is the variation of $[M]_e^{\circ}$, and, if $\Delta_{\text{pol}}H^{\circ} < 0$, then $[M]_e^{\circ}$ increases with increasing temperature and conversely. All the formation reactions of polyolefins are exothermic, so that the equilibrium yield of the polymer produced by them increases with decrease in temperature.

The influence of pressure on the polymerisation-depolymerisation equilibrium constant K_N , expressed in terms of the mole fraction of the monomer in the reaction mixture, is described by the equation^{11,16}

$$\left(\frac{\partial \ln K_N}{\partial p} \right)_T = - \frac{\Delta_{\text{pol}}V}{RT},$$

where $\Delta_{\text{pol}}V$ is the difference between the molar volumes of the polymer and the monomer at the specified temperature and pressure. For moderate pressure (p), one can use the approximate relation

$$\ln K_N = \ln K_N^{\circ} - \frac{\Delta_{\text{pol}}V^{\circ}p}{RT},$$

where $\Delta_{\text{pol}}V^{\circ}$ is the difference between the molar volumes of the polymer and the monomer at the standard pressure. Since $\Delta_{\text{pol}}V^{\circ} < 0$ in the polymerisation of olefins, an increase in pressure is favourable as regards the yield of the polymers. This equation is applicable to the case where the pressure amounts to tens and even hundreds of atmospheres.

The temperature dependences of the enthalpy, entropy, and Gibbs free energy are expressed by the Kirchhoff and Gibbs-Helmholtz equations.¹⁶

The influence of temperature on $\Delta_{\text{pol}}H^{\circ}(T)$ and $\Delta_{\text{pol}}S^{\circ}(T)$ is determined by the numerical values and signs of $\Delta_{\text{pol}}C_p^{\circ}(T)$ and $\Delta_{\text{pol}}H^{\circ}$, while its influence on $\Delta_{\text{pol}}G^{\circ}(T)$ is determined by the numerical value and sign of $\Delta_{\text{pol}}H^{\circ}(T)$. For the polymerisation reactions of olefins, $\Delta_{\text{pol}}C_p^{\circ}(T)$ and $\Delta_{\text{pol}}H^{\circ}(T)$ are usually negative. As a result of this, the numerical values of $\Delta_{\text{pol}}H^{\circ}(T)$ and $\Delta_{\text{pol}}S^{\circ}(T)$ increase with increasing temperature but remain negative, while $\Delta_{\text{pol}}G^{\circ}(T)$ diminishes with a consequent decrease in the yield of the polymer corresponding to thermodynamic equilibrium; on the other hand, it increases with decrease in temperature.

The dependences of the enthalpy, entropy, and Gibbs free energy on pressure are expressed by the following equations:¹⁷⁻²⁰

$$\Delta_{\text{pol}}H = \Delta_{\text{pol}}H^{\circ} + \int_{p^{\circ}}^p \Delta_{\text{pol}}V(p)dp - T \int_{p^{\circ}}^p \left[\frac{\partial \Delta_{\text{pol}}V(p)}{\partial T} \right]_p dp,$$

$$\Delta_{\text{pol}}S = \Delta_{\text{pol}}S^{\circ} - \int_{p^{\circ}}^p \left[\frac{\partial \Delta_{\text{pol}}V(p)}{\partial T} \right]_p dp,$$

$$\Delta_{\text{pol}}G = \Delta_{\text{pol}}G^{\circ} + \int_{p^{\circ}}^p \Delta_{\text{pol}}V(p)dp,$$

where p° is the standard pressure.

$\Delta_{\text{pol}}H^{\circ}(T)$ and $\Delta_{\text{pol}}S^{\circ}(T)$ for the polymerisation of olefins are negative, whilst the entropy factor $T\Delta_{\text{pol}}S^{\circ}(T)$ increases faster with temperature than $\Delta_{\text{pol}}H^{\circ}(T)$, so that at the upper limiting temperature T_{cel}° the enthalpy and the entropy factor are equalised and $\Delta_{\text{pol}}G^{\circ}(T_{\text{cel}}^{\circ}) = 0$. It can be shown that at moderate pressures

$$\ln T_{\text{cel}} = \ln T_{\text{cel}}^{\circ} + \frac{\Delta_{\text{pol}}V^{\circ}(T_{\text{cel}}^{\circ})p}{\Delta_{\text{pol}}H^{\circ}(T_{\text{cel}}^{\circ})}.$$

Pressure can amount to tens and in certain cases even thousands of atmospheres.¹¹ At $T < T_{\text{ceil}}^{\circ}$, the equilibrium in the polymerisation reaction is displaced towards the formation of the polymer, whereas at $T > T_{\text{ceil}}^{\circ}$ it is actually displaced towards the initial monomer. At temperatures close to T_{ceil}° and higher, the polymer rapidly depolymerises to the initial monomer under kinetic conditions.^{13–15} Since $\Delta_{\text{pol}}V^{\circ}(T_{\text{ceil}}^{\circ})$ and $\Delta_{\text{pol}}V^{\circ}(T_{\text{ceil}}^{\circ})$ for the polymerisation reaction are negative, their ratio is positive and T_{ceil}° accordingly increases with increase in pressure. This leads to the expansion of the range of temperatures favouring polymerisation and to the thermodynamic stability of the polymer.

Heat capacity is one of the most important thermodynamic quantities entering into key thermodynamic relations.^{16, 21, 22}

A series of quantum theories of the heat capacities of chain structures — linear polymers have now been developed: the Stockmayer–Hecht theory²³ based on the analysis of the vibrational spectrum of the lattice formed by the polymer chains; Tarasov's theory of the heat capacities of chain structures²⁴ based on the analysis of the vibrational spectrum of a one-dimensional continuum (rigid string); Lifshits's theory²⁵ also based on the consideration of the vibrational spectrum of a one-dimensional continuum. In contrast to Tarasov, Lifshits chose thin rods (needles) as the one-dimensional continuum. All the above theories of heat capacity have been analysed critically by Godovskii,²⁶ who demonstrated convincingly that Lifshits's theory of heat capacity has the greatest physical justification. However, Tarasov's theory has nevertheless found extensive practical application.²⁴ It is expressed analytically by the following equation:

$$C_{v1,3} = D_1 \left(\frac{\theta_1}{T} \right) - \frac{\theta_3}{\theta_1} \left[D_1 \left(\frac{\theta_3}{T} \right) - D_3 \left(\frac{\theta_3}{T} \right) \right], \quad (2)$$

where D_1 and D_3 are symbols for the Tarasov and Debye heat capacity functions respectively, θ_1 and θ_3 are the characteristic Tarasov and Debye temperatures, and θ_3/θ_1 expresses the degree of interaction of the chains. The generalised expression for the Tarasov and Debye heat capacity functions assumes the form²⁴

$$C_{v,m} = 3mR \left(\frac{T}{\theta_m} \right)^m \int_0^{\theta_m/T} \frac{(\theta_m/T)^{m+1} \exp(\theta_m/T)}{[\exp(\theta_m/T) - 1]^3} d \frac{\theta_m}{T},$$

where $m = 1$ or 3 .

Chernoplekov²⁷ compiled tables of the heat capacities of chain structures, which greatly facilitate practical calculations of the skeletal contribution to the heat capacities of chain polymers. The characteristic temperatures θ_1 and θ_3 are usually determined by an inverse calculation from the experimental measurements of the heat capacities of specific polymers over a temperature range. Eqn (2) has been used particularly fruitfully by Wunderlich and coworkers, for example, in two studies^{28, 29} for the calculation of the heat capacities of linear polymers over a wide temperature range (frequently from 0 to 1000 K). The contribution of atomic vibrations to the heat capacities of polymers has been calculated from vibrational spectroscopic data using the Einstein heat capacity function.

The absolute value of the entropy $S^{\circ}(T)$ of a polymer is expressed by the following equation:

$$S^{\circ}(T) = S^{\circ}(0) + \int_0^T C_p^{\circ}(T) d \ln T + \sum \Delta_{\text{tr}} S^{\circ},$$

where $S^{\circ}(0)$ is the zero-point (residual) entropy of the polymer at $T = 0$ K, $C_p^{\circ}(T)$ is the temperature dependence of the heat capacity, and $\Delta_{\text{tr}} S^{\circ}$ is the entropy of phase transitions.

For vitreous and partially crystalline polymers, $S^{\circ}(0)$ is non-zero owing to the imperfection of the crystals, the thermodynamically nonequilibrium configurations of the macromolecules frozen at the glass transition temperature of the polymer T_g° , and certain other possible factors. The attempts at a theoretical

estimation of $S^{\circ}(0)$, undertaken in a number of studies,^{30–32} usually lead to values ranging from 10 to 20 J mol^{−1} K^{−1}. Strictly speaking, the zero-point entropy of a crystalline polymer is nonzero also owing to the imperfection of the crystals and because the polymer is a mixture of macromolecules having different masses.^{11, 33} However, it has been shown³¹ that the corresponding entropy of mixing of polymers in any physical state is close to zero in cases where the average degree of polymerisation is greater than 100. It has been suggested that the quantity $S^{\circ}(0)$ could be neglected without significant error for polymers with a degree of crystallinity of 100%.

A number of investigators^{34–36} developed a method for the estimation of $S^{\circ}(0)$ for polymers in the amorphous state from calorimetric measurements for partially crystalline polymers. The values of $S^{\circ}(0)$ for more than 100 vitreous polymers of different chemical composition and structure have now been obtained from the results of the corresponding calorimetric measurements. These results have largely confirmed the theoretical estimates. It was found that in most cases $S^{\circ}(0)$ is $\sim 10\%$ of $S^{\circ}(298.15 \text{ K})$ for the corresponding polymers in the amorphous state. It is also of interest that $S^{\circ}(0)$ amounts to between 10% and 80% (in most cases $\sim 50\%$) of the entropies of fusion of the corresponding polymers with $\alpha = 100\%$.^{11, 13} It is not permissible to neglect $S^{\circ}(0)$ in accurate thermodynamic calculations.

It has been established^{37–39} that the configurational entropy S_{conf}° makes the main contribution to $S^{\circ}(0)$ and that frequently we have $S_{\text{conf}}^{\circ} \approx S^{\circ}(0)$. It has also been shown that S_{conf}° can be readily estimated from the formula³⁷

$$S_{\text{conf}}^{\circ} = \int_{T_2^{\circ}}^{T_g^{\circ}} \Delta C_p^{\circ}(T_g^{\circ}) d \ln T, \quad (3)$$

where $\Delta C_p^{\circ}(T_g^{\circ})$ is the increase in heat capacity on devitrification of the polymer at T_g° , while T_2° is the Kauzmann temperature^{37, 40} and $T_g^{\circ}/T_2^{\circ} \approx 1.29$. The quantities in Eqn (3) may be determined experimentally.

Thus the methods developed for the estimation of $S^{\circ}(0)$ made it possible to overcome the significant difficulties in the calculations of $S^{\circ}(T)$ and $\Delta_{\text{pol}} S^{\circ}(0)$, which in its turn opened a way to the full employment of calorimetric data for the calculation of the polymerisation–depolymerisation equilibrium.

III. Calorimetric research methods

1. Combustion calorimetry

The enthalpies of polymerisation of olefins have been calculated mainly from the experimental combustion energies of the monomers and the corresponding polymers. The reactants were combusted in bomb calorimeters.^{41–45} Typical conditions in the measurements of combustion energies have been published.⁴⁶ A calorimeter with an isothermal jacket and a static bomb was used. The design of the calorimeter and the experimental method were similar to those described by Skuratov et al.⁴²

2. Adiabatic vacuum calorimetry

The temperature dependences of the heat capacity and of the temperatures and enthalpies of physical transformations at low and moderate temperatures have been investigated in adiabatic vacuum calorimeters.^{47–51} A number of olefins and polyolefins have been investigated in an adiabatic fully automated vacuum calorimeter, the design and method of employment of which have been described.^{51–53}

3. Dynamic calorimetry

An automated differential calorimeter, working in accordance with the triple thermal bridge principle, is usually employed for measurements by dynamic calorimetry.⁵⁴ The design and method of employment of the calorimeter have been described.^{55, 56} A characteristic feature of the measurements of C_p° in this calorimeter is that it is calibrated for each individual measurement.

The sensitivity of the calorimeter has been raised to $1.3 \times 10^{-2} \text{ J K}^{-1}$ and the error of the heat capacity measurements has been reduced to 1%–4%. However, since in the experiments of Lebedev et al.⁵⁷ the heat capacities of the test substances in the temperature range 250–340 K were measured in an adiabatic vacuum calorimeter subject to an error of 0.2% and the conditions of the measurements in a dynamic calorimeter were chosen so that the values of C_p° obtained in the above temperature range were the same in both calorimeters, it was assumed⁵⁷ that, at $T > 340 \text{ K}$, C_p° measured in the dynamic calorimeter is subject to an error within the range 0.5%–1.5%.

It was shown that the temperature and method of measurement make it possible to obtain C_p° for solid and liquid substances with an error up to 1%, the temperatures of physical transformations can be measured with an error up to 1.0 K, while the enthalpies of the transformations are subject to an error up to 0.8%.³⁰

IV. Heat capacity

The heat capacities C_p° of polyolefins in the range from 5–10 to 350 K have been investigated as a rule in adiabatic vacuum calorimeters, while those at $T > 350 \text{ K}$ have been determined in dynamic calorimeters. In adiabatic vacuum calorimeters, between 90 and 150 experimental C_p° values were obtained in 10–25 series. The calorimeter tube was charged with between 2 and 6 g of the test substance. The heat capacity of the specimens was 50%–70% relative to the overall heat capacity of the calorimeter tube with the test substance. The experimental values of C_p° were averaged by the method of least squares. The scatter of the points around the corresponding averaging curves was 0.7% in the range 5–30 K, 0.07% in the range 30–150 K, and 0.02% in the range 150–340 K. In the study of substances in the dynamic calorimeter, the C_p° measurements were performed under the conditions of continuous heating of the calorimeter with the test substance. The rate of heating was varied from 16.7×10^{-3} to $8.3 \times 10^{-3} \text{ K s}^{-1}$ for the same substance in different series. The duration of a single measurement was ~ 20 –25 s.

All the polyolefins investigated are partly crystalline polymers with the exception of the fully amorphous polyisobutylene and polyhex-1-ene.

Figure 1 presents a typical temperature dependence of the heat capacity of a partly crystalline polymer. Evidently, the heat capacity of a mixture of the vitreous and crystalline polymers increases smoothly in the range from the temperature at the beginning of the measurements from 6 K to the temperature of the onset of devitrification of the amorphous part of the specimen of 260 K (AR). In the range of devitrification temperatures, C_p° increases comparatively sharply with increase in temperature (RN) and then rises smoothly up to the temperature of the onset of the fusion of the crystalline part of the polymer (NQ). The fusion of the crystals is responsible for the anomalous variation of the heat capacity in the fusion range (QSHUE). The heat capacity of the polymer melt increases with increasing temperature (EF). Before proceeding to the analysis of the published data on the heat capacities of polyolefins, we shall make several remarks concerning the methods for the determination of the degree of crystallinity of polymers.

The degree of crystallinity of polyolefins α is determined as a rule from calorimetric data with the aid of the following equations:^{26, 58, 59}

$$\alpha = 100 \left(1 - \frac{\Delta C_p^\circ(\alpha)}{\Delta C_p^\circ(\alpha = 0)} \right), \quad (4)$$

$$\alpha = 100 \frac{\Delta_{\text{fus}} H^\circ(\alpha)}{\Delta_{\text{fus}} H^\circ(\alpha = 100\%)}, \quad (5)$$

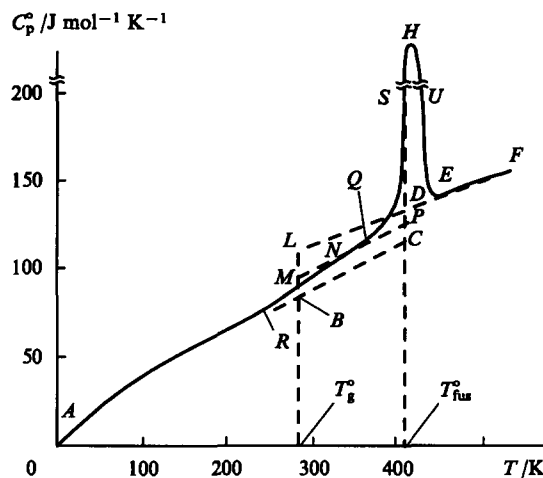


Figure 1. Typical temperature variation of the heat capacity of a partly crystalline polymer for isotactic polybut-1-ene as an example.^{69–71} State of the polymer: ABC — crystalline, $\alpha = 100\%$, AB — vitreous, LD — highly elastic, DEF — liquid, AR — partly crystalline (form I, $\alpha \approx 77\%$; amorphous component in the vitreous state), RNQ — ditto, but with the amorphous component of the polymer in the highly elastic state; QSHUE — apparent heat capacity in the melting range of the crystals of form I.

where $\Delta C_p^\circ(\alpha)$ and $\Delta C_p^\circ(\alpha = 0)$ are respectively the increase in the heat capacity at the glass transition temperature T_g° of the partly crystalline and fully amorphous ($\alpha = 0$) polymer, while $\Delta_{\text{fus}} H^\circ(\alpha)$ and $\Delta_{\text{fus}} H^\circ(\alpha = 100\%)$ are the enthalpies of fusion of the polymer with a degree of crystallinity α and of the fully crystalline polymer.

$\Delta C_p^\circ(\alpha)$ and $\Delta C_p^\circ(\alpha = 0)$ were obtained graphically (sections BM and BL in Fig. 1). Point B was found by the linear extrapolation of the temperature dependence of the heat capacity of the partly crystalline polymer between $T < T_g^\circ$ and T_g° . Point B corresponds to the heat capacity of a mixture of the vitreous and crystalline materials, but C_p° is assumed to be equal at this point to the heat capacity of the polymer in the vitreous state. This is based on the experimentally observed equality of the heat capacities of the same polymer in the vitreous, partly crystalline, and even fully crystalline states at $T < T_g^\circ$ within the limits of the error of the measurements (differences between the values of C_p° less than 0.2%).^{36, 60} Point M corresponds to the heat capacity of the same mixture of crystals with the amorphous component of the polymer in the highly elastic state. It was obtained by extrapolating the $C_p^\circ = f(T)$ relation (section NQ) between the end of the devitrification of the amorphous component and the onset of the prefusion of the crystalline component of the polymer. The increase in C_p° (section B) is associated with the devitrification of the amorphous component of the polymer. Point L was found by the linear extrapolation of the relation $C_p^\circ = f(T)$ for the liquid polymer (EF) into the region of its T_g° . Section BL corresponds to the increase in heat capacity owing to the segmental mobility of the macromolecules, which appeared in the course of the devitrification of the polymer in the amorphous state (the α -transition).⁶¹

On slow stepwise cooling, it is possible to measure the heat capacities of certain polymers in the range from point E to L (for example the heat capacity of the polymer in the highly elastic state in Fig. 1), whereupon the deviations of the C_p° points from the corresponding straight line DL are comparable to the error of the measurements of the heat capacity. Depending on the cooling conditions, the polymers are obtained in both amorphous and partly crystalline states. It is sometimes possible to measure C_p° in both states,^{62, 63} whereupon the $C_p^\circ = f(T)$ relation for the polymer in the highly elastic state is located as a rule on the prolongation of the temperature variation of the heat capacity of the liquid (FE) to point L. Clearly the ratio of the sections BM/BL is equal to the fraction of the amorphous component of the polymer, while the

difference $1 - BM/BL$ represents the fraction of the crystalline component of the polymer. The degrees of crystallinity of the polymers found from calorimetric and X-ray diffraction data agree subject a discrepancy which is usually within the limits of 3%–5%.⁶⁴

In conclusion, we may note that the calorimetric method for the determination of the degree of crystallinity from the increase in the heat capacity at T_g° yields satisfactory results for low and moderate degrees of crystallinity, but may lead to significant errors for higher values of α .²⁶

Polyethylene (PE) is one of the most thoroughly investigated polymers. Approximately 50 studies have been published in which the results of calorimetric investigations on ~100 polyethylene specimens having linear and branched structures, different molecular masses (from 2.5×10^4 to 8×10^6), and different degrees of crystallinity (from 25% to 97%) have been published for temperatures ranging from 0.16 to 570 K. All the published investigations have been thoroughly analysed and surveyed by Wunderlich and coworkers.⁶⁵ They obtained as a result the temperature variations of the heat capacity of PE in the crystalline, vitreous, highly elastic, and liquid states at temperatures in the range 0–600 K. It was shown that C_p° for crystalline PE increases smoothly with increase in temperature in the range from 0 to 360 K, after which there is a sharp rise in heat capacity owing to the onset of fusion, which occurs in the range 360–414 K. An anomalous $C_p^\circ = f(T)$ relation corresponds to the fusion process.

The heat capacity of vitreous PE also increases smoothly with increase in temperature from 0 to 200 K, after which the rise of C_p° becomes appreciably faster owing to devitrification, which is completed at 250 K. In the highly elastic and liquid states, the heat capacity of PE is a linear function of temperature. In the region of very low temperatures, C_p° of crystalline PE obeys the Debye T^3 law (in the range 1–9 K), while C_p° of vitreous PE is described by the equation

$$C_p^\circ = aT^3 + bT,$$

where a and b are constants. A similar relation is characteristic also of other amorphous solids. At temperatures in the ranges from 0 to 60 K and from 150 to 414 K, the heat capacities of amorphous and crystalline PE differ markedly, that of amorphous PE being higher. An additive dependence of the heat capacity on the degree of crystallinity of PE is manifested. In the range 60–150 K, the heat capacities of crystalline and amorphous PE are close: the differences do not exceed $\pm 2\%$. The heat capacity of branched PE is always slightly higher than that of the linear polymer. Differences between the heat capacities were not discovered in a study of PE specimens having different molecular masses (from 6×10^4 to 1×10^6) in the same physical state.

Polydeuteroethylene (PDE). The results of the study of the temperature variation of C_p° of polydeuteroethylene have been published.^{66,67} Rabinovich et al.⁶⁶ investigated in an adiabatic vacuum calorimeter a PDE specimen with a degree of deuteration of 93% and a degree of crystallinity of 72% in the range 80–310 K. The molecular mass of the polymer is not indicated. The results of experimental measurements of C_p° were extrapolated to 100% crystallinity on the basis of the proportionality of the differences between the heat capacities of the polymer in the amorphous and crystalline states. The values of C_p° of the fully crystalline PDE were in their turn extrapolated to 100% degree of deuteration assuming that the difference between the heat capacities of PDE and PE at a specified temperature is proportional to the deuterium content. The heat capacity of PDE has been investigated⁶⁷ in adiabatic vacuum and dynamic calorimeters in the temperature ranges 5–330 and 330–450 K respectively. The degree of deuteration of the test specimen was 98%, its degree of crystallinity was ~92%, and its molecular mass was 2×10^5 . The error of the measurements was ~0.2% in adiabatic vacuum calorimeters^{66,67} and from 0.5 to 1.5% in a dynamic calorimeter.⁶⁷ The results obtained by Lebedev and Smirnova⁶⁷ are presented in Fig. 2. Evidently there are several characteristic

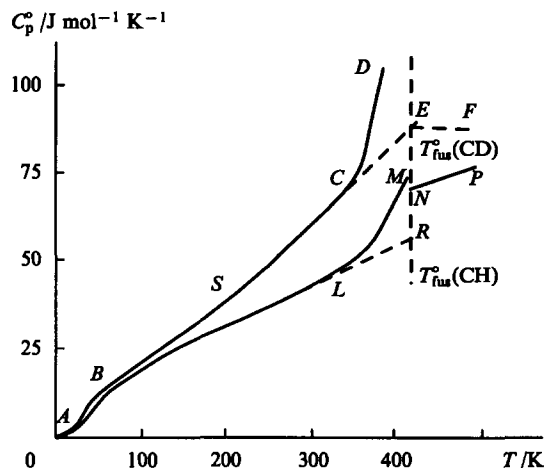


Figure 2. Heat capacities of polydeuteroethylene (ABSCFE)⁶⁷ and polyethylene (ALMNP).⁶⁵

State of the polymer: ABSC — crystalline, $\alpha = 92\%$, EF — liquid, CD — apparent heat capacity in the melting range; AL — crystalline, $\alpha = 100\%$, NP — liquid, LMN — apparent heat capacity in the melting range; T_{fus}^{CD} and T_{fus}^{CH} — melting points of polydeuteroethylene and polyethylene respectively, RN — increase in heat capacity on fusion of polyethylene; for the explanation of the remaining symbols, see text.

sections on the $C_p^\circ = f(T)$ curve corresponding to the variation of the heat capacity with increasing temperature: 0–60 K (AB) — along this section, C_p° increases rapidly; 60–200 K (BS) — the range in which C_p° is a linear function of temperature, which occurs for all chain polymers; 200–350 K (SC) — the section along which the rate of change of C_p° is higher than along the preceding section, which may be associated with the devitrification of the amorphous component of the specimen; $T > 350$ K (CD) — along this section, C_p° increases sharply owing to the fusion of the polymer crystals. The heat capacity of the polymer melt (EF) is a linear function of temperature and a very weak one at that.

Comparison of the heat capacities C_p° found in the above two investigations^{66,67} shows that, according to the data of Lebedev and Smirnova,⁶⁷ the heat capacity in the range 20–220 K is 3%–10% higher than in the study of Rabinovich et al.,⁶⁶ in the temperature range 220–260 K the heat capacities virtually coincide, while in the range 260–310 K the heat capacities are 3%–6% lower according to the data of Rabinovich et al.⁶⁶ The above discrepancies between the values of C_p° are apparently a consequence of the different degrees of deuteration and crystallinity of the test specimens and also of the above assumptions in the extrapolations.

Polypropylene (PP). More than 25 studies have been published in which the results of calorimetric measurements of the heat capacities of 34 specimens of atactic, isotactic, and syndiotactic PP are presented. Specimens with molecular masses from 8.9×10^3 to 6.4×10^5 and degrees of crystallinity from 10% to 65% were investigated. The heat capacity was determined in the temperature range 0.5–600 K. Atactic PP specimens are amorphous, while those of isotactic and syndiotactic PP are partly crystalline. All the published results have been thoroughly analysed and surveyed by Gaur and Wunderlich.⁶⁸

The heat capacity of vitreous atactic PP increases smoothly with increasing temperature in the range from 0 to 230 K; at 230 K, a more rapid rise of the heat capacity is observed, apparently owing to the onset of devitrification. The heat capacity of crystalline PP also increases smoothly with temperature in the range 0–280 K. At $T > 280$ K, the growth of C_p° accelerates, which may be associated with the onset of the fusion of the polymer. In the highly elastic and liquid states, C_p° is a linear function of temperature.

In the crystalline state, the heat capacities C_p° of isotactic and syndiotactic PP are virtually identical; in the liquid state, the heat capacities of atactic, isotactic, and syndiotactic PP are identical in the experimental temperature range.

The heat capacity of vitreous PP is higher throughout than that of crystalline PP. In the range from 20 to 150 K, the difference between the values of C_p° diminishes from 30% to 5%, in the range 150–200 K it is within the limits of 5%, while in the range 260–460 K the difference between the C_p° of highly elastic and crystalline PP is 25%. In the range 20–150 K and also between the glass transition temperature and the melting point, C_p° of partly crystalline PP is linear function of the degree of crystallinity. The heat capacity of a partly crystalline specimen is higher the lower its degree of crystallinity.

Polybut-1-ene. The temperature variation of C_p° of isotactic polybut-1-ene specimens in the partly crystalline and liquid states has been investigated in the range 5–630 K.^{69–71} The degree of isotacticity of the test specimens was ~90% and the degree of crystallinity of the polymer varied from 44% to 83% depending on the crystallisation conditions. The crystalline component of polybut-1-ene formed under these conditions consisted of one crystalline modification or a mixture of two or three possible crystalline modifications: rhombohedral, tetragonal, and hexagonal structures, which are designated as forms I, II, and III respectively.⁷²

Lebedev and coworkers⁶⁹ investigated a specimen of isotactic polybut-1-ene with a degree of crystallinity of 77%. The crystalline component of the specimen consisted of form I. The heat capacities of the specimen were measured in the temperature ranges 6–35 and 200–304 K. Dainton et al.⁴⁷ investigated C_p° of a polybut-1-ene specimen with a degree of crystallinity of 44%, the crystalline component of the polymer consisting of a mixture of two crystalline modifications: 37% of form I and 7% of form II. The heat capacity measurements were performed in the range 22–310 K. Bares and Wunderlich⁷¹ published C_p° data for polybut-1-ene in the vitreous, highly elastic, and liquid states in the temperature range 10–600 K.

Wilski and Grever⁷⁰ investigated C_p° of the polymer in the range 250–430 K, but do not quote numerical values, confining themselves to a plot of the temperature variation of C_p° .

A common feature of all the polybut-1-ene specimens investigated is the equality of the heat capacities virtually within the limits of the errors of measurement at temperatures below T_g° for the polymer. The values of C_p° of the melt, found by Lebedev and coworkers,⁶⁹ also agree with those published by Bares and Wunderlich.⁷¹ In the range 22–33 K, the data of Dainton et al.⁴⁷ and Lebedev et al.⁶⁹ differ only within the limits of 1%, but in the range 0–22 K the heat capacities are significantly higher according to the results of Dainton et al.⁴⁷ However, one should bear in mind that Dainton et al.⁴⁷ obtained then by extrapolating the dependence of the measured values of C_p° on T in accordance with the Debye heat capacity function. In the range 200–220 K, which precedes the devitrification of the amorphous part of the polymer, the heat capacity according to the results of Lebedev et al.⁶⁹ is ~1.5% smaller than that measured by Dainton et al.⁴⁷ This can apparently be accounted for by the influence of the difference between the degrees of crystallinity (44% and 77%) on the heat capacity of polybut-1-ene in the given temperature range and, in particular by the difference between the effects of the reinforcement^{11,73} of the vitreous component of the polymer by the crystals which hinder the excitation of the segmental mobility of the macromolecules. Overall, the temperature dependence of the heat capacity of polybut-1-ene is a typical $C_p^\circ = f(T)$ relation for partly crystalline polymers.

In order to obtain the temperature dependence of the heat capacities of polybut-1-ene in the crystalline and amorphous states from the experimental heat capacities of a partly crystalline polymer, use was made of the method described in detail by Lebedev.^{11,60} This method is based on the fact that the C_p° of partly crystalline polymers at $T < T_g^\circ$ virtually agrees with the

heat capacity of the polymers in the vitreous and crystalline states within the limits of the error of the measurement; the linear relation $C_p^\circ = f(T)$ in the range from 50–60 K up to the glass transition temperature is observed for all the chain polymers investigated hitherto.²⁶ The authors assumed that the extrapolation of C_p° of a partly crystalline polymer from T_g° to T_{fus}° correctly reflects the heat capacity of the polymer in the crystalline state, while the linear extrapolation of the heat capacity of the polymer in the liquid state to T_g° describes correctly, in its turn, the heat capacity of the polymer in the highly elastic state. All the above extrapolations are presented in Fig. 1. In order to obtain the temperature dependence of the heat capacity of the polymer in the highly elastic state (EDL), Bares and Wunderlich⁷¹ extrapolated the temperature dependence of the heat capacity of liquid polybut-1-ene (FE) to T_g° .

Polyisobutylene. The results of calorimetric studies on the temperature dependence of the heat capacity of polyisobutylene in the vitreous and highly elastic states have been published by Ferry and Parks⁷⁴ and Furukawa and Reilly.⁷⁵ The measurements of C_p° were performed in adiabatic vacuum calorimeters. Ferry and Parks⁷⁴ studied the C_p° of a low-molecular-mass ($M_n = 49 \times 10^3$) polymer specimen in the range 118–295 K. Furukawa and Reilly⁷⁵ investigated a high-molecular-mass ($M_n = 1.35 \times 10^6$) polymer with a narrow molecular mass distribution ($M_w/M_n = 1.16$). Comparison shows that the heat capacity of the low-molecular-mass polyisobutylene is always 1%–2% higher than that of the high-molecular-mass polymer, apparently as a consequence of the difference between the molecular masses of the test specimens (by a factor greater than 3000). The nature and characteristics of the variation of the heat capacities of the low- and high-molecular-mass polyisobutylenes do not exhibit any differences: the heat capacities C_p° of the polymer in the vitreous and crystalline states increase smoothly with increase in temperature; in the vitrification ranges, $C_p^\circ = f(T)$ varies in the usual way.¹¹ Wunderlich and Baur²¹ averaged the values of C_p° quoted by Ferry and Parks⁷⁴ and Furukawa and Reilly⁷⁵ and published a table of the heat capacities of polyisobutylene in the range 0–380 K.

Polypent-1-ene. The temperature variation of the heat capacity of isotactic polypent-1-ene has been investigated by Wunderlich and coworkers⁷⁶ in the range 220–430 K and by Lebedev et al.⁷⁷ in the range 9–500 K. The degree of isotacticity of the test polymer specimens was 80%–95% and their degree of crystallinity was 0%⁷⁶ and 60%.⁷⁷ The experimental values of C_p° quoted in the above studies^{76,77} agree to within 1%. The temperature variation of the heat capacity of polypent-1-ene is typical for partly crystalline polymers. In the range 220–260 K, the amorphous component devitrifies, whilst in the range 330–390 K the crystalline component melts. The heat capacities of the polymer in the crystalline and amorphous states were found by extrapolation, as for polybut-1-ene (see above).

Poly-3-methylbut-1-ene. The temperature variation of the heat capacity of isotactic poly-3-methylbut-1-ene has been investigated by Lebedev and coworkers⁷⁸ in the range 8.5–650 K. The degree of isotacticity of the test specimen was ~95% and its degree of crystallinity 70%. On cooling melts of the initial specimen, the degree of crystallinity changed from 50% to 88% during their crystallisation and annealing. The amorphous component of the polymer devitrified in the range 300–370 K and the crystalline component melted in the range 500–610 K. Some irregularity in the temperature variation of C_p° in the range 370–500 K is probably associated with the recrystallisation processes during the heating of the polymer. The temperature variation of the heat capacity in the range 8.5–300 K exhibits no singularities of any kind: C_p° increases smoothly with increasing temperature. Immediately after the end of fusion, small endothermic effects were noted on the temperature variation of the heat capacity. For example, such an effect occurred for the initial poly-3-methylbut-1-ene specimen in the range 605–620 K. The maximum heat capacity $C_{p,max} = 230.0 \text{ J mol}^{-1} \text{ K}^{-1}$ corresponds to 612 K. The

deviation of the heat capacity from its normal value at this temperature is $\sim 8 \text{ J mol}^{-1} \text{ K}^{-1}$.

It is noteworthy that the disposition of the $C_p^\circ = f(T)$ curves for the melt depended on the previous history of the specimens. This can apparently be accounted for by the retention of a certain amount of structure in the polymer after the fusion of its crystalline component and its subsequent decomposition, which requires an energy expenditure. A similar phenomenon has been observed also for poly-4-methylpent-1-ene.

Polyhex-1-ene. Bourderiat et al.⁴⁹ published the results of a study of the temperature variation of the heat capacity of polyhex-1-ene in the range 20–300 K. The measurements were performed in an adiabatic vacuum calorimeter. The test polymer specimen exists in the above temperature range in the vitreous and highly elastic states (Fig. 3). Devitrification occurs in the range 200–225 K. In other respects, the temperature dependence of the heat capacity of polyhex-1-ene exhibits no singularities, increasing smoothly with temperature. The error of the measurements of C_p° was 0.2%–0.4%. We may note that this type of $C_p^\circ = f(T)$ relation is typical for fully amorphous polymers.

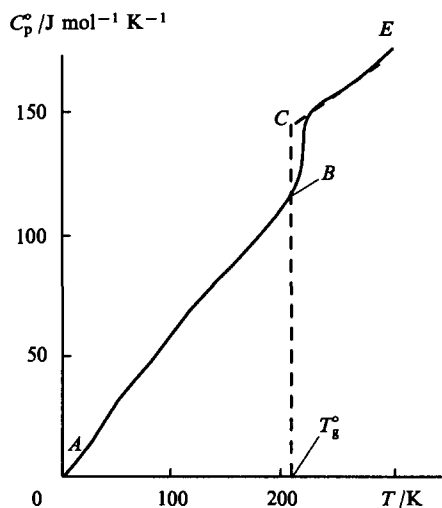


Figure 3. Typical temperature dependence of the heat capacity of an amorphous polymer for isotactic polyhex-1-ene as an example.⁴⁹ State of the polymer: *AB* — vitreous, *CE* — highly elastic; *BC* — increase in heat capacity on devitrification.

Poly-4-methylpent-1-ene. The temperature variation of the heat capacity of isotactic poly-4-methylpent-1-ene was investigated by Karasz et al.⁴⁸ in the range 77–540 K, by Melia and Tyson⁷⁹ in the range 80–320 K, and by Lebedev et al.⁸⁰ in the range 7–670 K. The degree of isotacticity of the test specimens was ~ 95 and the degree of crystallinity was 30%,⁴⁸ 65%,⁷⁹ and between 35% and 40%.⁸⁰ The experimental values obtained by Lebedev et al.⁸⁰ in the range 77–300 K are smaller by $\sim 1\%$ than the data published by Karasz et al.⁴⁸ and higher by 0.5%–1.7% than the results quoted by Melia and Tyson,⁷⁹ the scatter of the experimental points being $\sim 2\%$.

Figure 4 presents the temperature variation of the heat capacity of poly-4-methylpent-1-ene. The amorphous component of the polymer devitrified in the range 270–320 K and the crystalline component melted in the range 470–557 K for the initial specimen and 450–550 K for specimens obtained on cooling and crystallisation of the initial specimen.

Apart from devitrification and fusion, two additional anomalies in the heat capacity were manifested on the $C_p^\circ = f(T)$ curve for the initial polymer specimen: one in the range 360–390 K (between the glass transition temperature and the melting point) and the other in the range 575–600 K (at temperatures above the melting temperature range, i.e. in the polymer melt). In all the

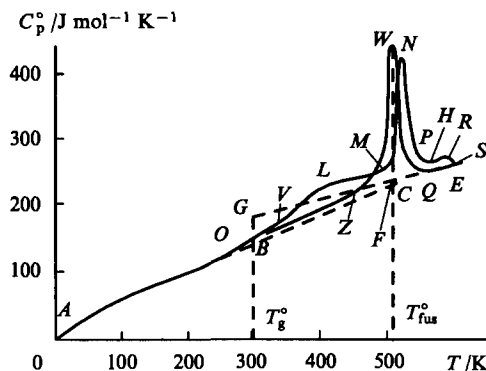


Figure 4. Heat capacity of isotactic poly-4-methylpent-1-ene.^{48, 79, 80} State of the polymer: *ABC* — crystalline, $\alpha = 100\%$, *AB* — vitreous, *GF* — highly elastic, *FQE* — liquid (isotropic melt). *AOVLMNPHRS* — heat capacity of the initial specimen (after synthesis and purification): *AB* — partly crystalline, $\alpha = 35\%$, amorphous component of the polymer in the vitreous state; *OVL* — partly crystalline, $\alpha = 35\%$, amorphous component in the highly elastic state; *MNP* — apparent heat capacity in the melting range; *PHRS* — heat capacity of a melt containing condiscrystals, *HRS* — apparent heat capacity in the melting range of the condiscrystals, *AOZ* — heat capacity of the polymer with $\alpha = 40\%$ (obtained by cooling the melt of the initial specimen), amorphous component of the polymer in the vitreous state from 0 K to T_g° , amorphous component of the polymer in the highly elastic state from T_g° to 440 K (point *Z*); *ZWQ* — apparent heat capacity in the melting range.

subsequent experiments, these anomalies were not reproduced. The dependences of the heat capacity in the temperature range corresponding to the end of devitrification and up to the temperature of the onset of fusion coincided within the limits of 1.5%. The errors of the measurements were approximately the same. In each of the experiments, the heat capacity of the melt increased smoothly with rising temperature from T_{fus}° to 610–670 K, but the positions of the $C_p^\circ = f(T)$ curves relative to one another fell systematically from experiment to experiment becoming stabilised only in the fourth–fifth experiments (*QE*). At 600 K, C_p° decreased by $\sim 5.5\%$ from the first to the fourth and fifth experiments. The anomaly in the heat capacity in the range $T_g^\circ - T_{fus}^\circ$ was discovered by Karasz et al.⁴⁸ Its appearance was attributed to the presence in the poly-4-methylpent-1-ene specimens, together with the main crystalline modification, of a small amount of another crystalline modification formed in the synthesis of the polymer. Hitherto five different crystalline modifications are known for this polymer.^{81, 82} The anomaly in C_p° in the poly-4-methylpent-1-ene melt is apparently caused by the presence in the latter of mesomorphic formations,⁸³ which gradually decompose from experiment to experiment during the measurements of the heat capacities of the melts. In the fourth and fifth experiments,⁸⁰ the melt probably becomes fully isotropic.

Polydec-1-ene. The temperature variation of the heat capacity of isotactic polydec-1-ene has been investigated in adiabatic vacuum and dynamic calorimeters in the range 5–450 K.^{78, 84} The degree of isotacticity of the test polymer was 90% and its degree of crystallinity was 35%. Approximately 200 experimental values of C_p° were obtained in 20 series reflecting the sequence of the measurements. The averaged $C_p^\circ = f(T)$ curves are presented in Fig. 5. The amorphous component of the polymer devitrified in the temperature range 190–230 K (*NP*).

The fusion of the crystalline component of polydec-1-ene was observed in the range 240–315 K; it occurred in two stages, to each of which corresponded an apparent temperature variation of the heat capacity: *RZQM* and *MUSF*. It was found that polyolefins with bulky side substituents form crystals, like other polymers with a similar structure,⁸⁵ as a result of the crystallisation of the main polymer chains and the crystallisation of the side substituents;⁸⁶ for polydec-1-ene, they are designated by crII and

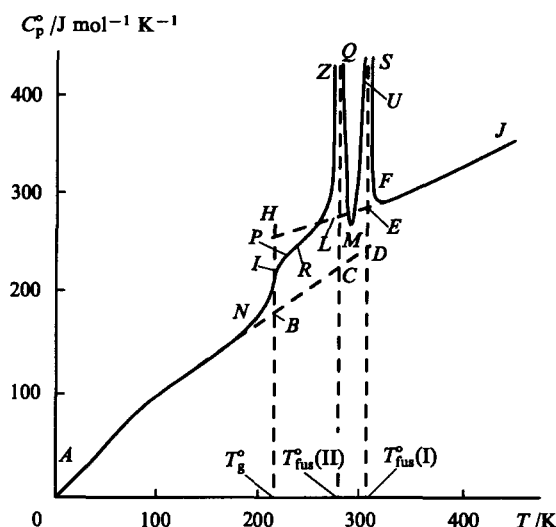


Figure 5. Heat capacity of isotactic polydec-1-ene.⁸⁴

State of the polymer: *ABC* — crII and crI crystals, *CD* — crI crystals; *AB* — vitreous, *HLE* — highly elastic, *EJ* — liquid; *ANPR* — partly crystalline ($\alpha = 35\%$); the amorphous component of the polymer in the vitreous state along section *AN* and in the highly elastic state along section *PR*; *NP* — heat capacity in the vitrification range; *RZQM* — apparent heat capacity in the melting range of crII crystals; *MUSF* — apparent heat capacity in the melting range of crI crystals.

crI respectively. On slow cooling of the polymer melt, it was possible to measure its heat capacity in the supercooled (highly elastic) state between 270 K and a temperature below the melting points of crII and crI crystals. The attempts at a more extensive supercooling terminated in each case by the spontaneous crystallisation of the polymer with the simultaneous formation of crI and crII crystals, after which the heat capacity was described by the *RZQMUSF* curve (Fig. 5). The temperature variation of the heat capacity of the polymer in the partly crystalline (*AN*), supercooled liquid (*LE*), and liquid (*EFJ*) states exhibits no singularities of any kind: it increases smoothly with increasing temperature.

V. Thermodynamic parameters of fusion

The thermodynamic parameters of fusion have been obtained for all the polyolefins investigated (Table 2) with the aid of dynamic calorimeters. The temperature corresponding to the maximum apparent heat capacity in the melting range of the polymer was adopted as the melting point T_{fus}^0 . For example, for polybut-1-ene this is the temperature at point *H* in Fig. 1. The results of

experiments with the lowest rate of heating of the calorimeter with the test substance ($< 2.7 \times 10^{-2} \text{ K s}^{-1}$) were normally employed for this purpose in accordance with the recommendations of Bernshtein and Egorov.⁸⁷ The enthalpies of fusion $\Delta_{fus}H^0(\alpha)$ were measured as a rule in three experiments and the average result with an arithmetical mean deviation was adopted as $\Delta_{fus}H^0(\alpha)$. In a separate experiment, $\Delta_{fus}H^0(\alpha)$ was calculated as the difference between the integrals of the temperature variations of C_p^0 in the melting range, obtained from the apparent (*QSHUT*) and normal (*QPDE*) heat capacity curves (Fig. 1). All the polymers investigated were partly crystalline with the exception of the fully amorphous polyisobutylene and polyhex-1-ene. The enthalpies of fusion $\Delta_{fus}H^0(\alpha)$ were obtained in experiments for a degree of crystallinity α . The molar enthalpies of fusion of the fully crystalline polymers were calculated from the formula⁸⁸

$$\Delta_{fus}H^0(\alpha = 100\%) = 100 \frac{\Delta_{fus}H^0(\alpha)}{\alpha} \quad (6)$$

The entropy of fusion $\Delta_{fus}S^0(\alpha = 100\%)$ was calculated from the values of $\Delta_{fus}H^0(\alpha = 100\%)$ and T_{fus}^0 by the formula

$$\Delta_{fus}S^0(\alpha = 100\%) = \frac{\Delta_{fus}H^0(\alpha = 100\%)}{T_{fus}^0} \quad (7)$$

We shall now consider the characteristic features of the behaviour of certain polyolefins on fusion and crystallisation. Depending on the conditions in the crystallisation of polybut-1-ene (the nature of the solvent, the rate of cooling of the melts, etc.), crystals of forms I, II, and III are produced. On heating, the crystals usually melt without interconversions, but Clampitt and Hughes⁸⁹ observed a spontaneous transition of the crystals of form II into those of form I, which occurred at $\sim 300 \text{ K}$ in the course of seven days. The temperatures and enthalpies of fusion of crystals of forms I–III, measured calorimetrically, have been published by Lebedev et al.⁶⁹ and those of crystals of forms I and II have been published by Wilski and Grever.⁷⁰

As an example, we shall consider the results of an experiment designed to determine the thermodynamic parameters of the fusion of polybut-1-ene published by Lebedev et al.⁶⁹ Fig. 6 presents the temperature variations of the heat capacity of the initial polymer specimen (curve 1) and the specimens obtained by crystallising its melt directly in the calorimeter on cooling from 500 to 200 K at different rates: 5×10^{-2} (curve 2) and $1.5 \times 10^{-2} \text{ K s}$ (curve 3). The initial specimen was crystallised from solution in isooctane during its precipitation with isopropyl alcohol, whereupon the crystalline form III was formed. Crystals of form III melted in the range 280–385 K and their fusion was completed by the onset of the crystallisation of the melt in form II. This is indicated by an exothermic process which completes the

Table 2. Thermodynamic parameters of the fusion of polyolefins.

Polymer	Crystal ^a	T_{fus}^0/K	$\Delta_{fus}H^0/\text{kJ mol}^{-1}$	$\Delta_{fus}S^0/\text{J mol}^{-1} \text{ K}^{-1}$	$\Delta C_p^0(T_{fus}^0)/\text{J mol}^{-1} \text{ K}^{-1}$	Ref.
Polyethylene	cr	414.6	8.8 ± 0.1	21.2 ± 0.2	—	65, 83
Polydeuteroethylene	cr	415	—	—	—	67
Polypropylene	cr	460.7	9.2 ± 0.8	20.0 ± 1.6	—	68, 83
Polybut-1-ene	crI	406.8	7.11	17.5	15.7	69, 70
	crII	393.0	3.68	9.36	—	69, 70
	crIII	374.0	2.67	7.14	—	69
Poly-pent-1-ene	cr	388	5.58	14.4	16.1	77, 83
Poly-3-methylbut-1-ene	cr	584	6.04	10.4	1.5	78
Poly-4-methylpent-1-ene	cr	508	10.2	19.5	11.5	80
Polydec-1-ene	crII	276	6.43	23.3	—	84
	crI	301	7.23	24.0	39.0	78

^a crI — crIII are different crystalline forms.

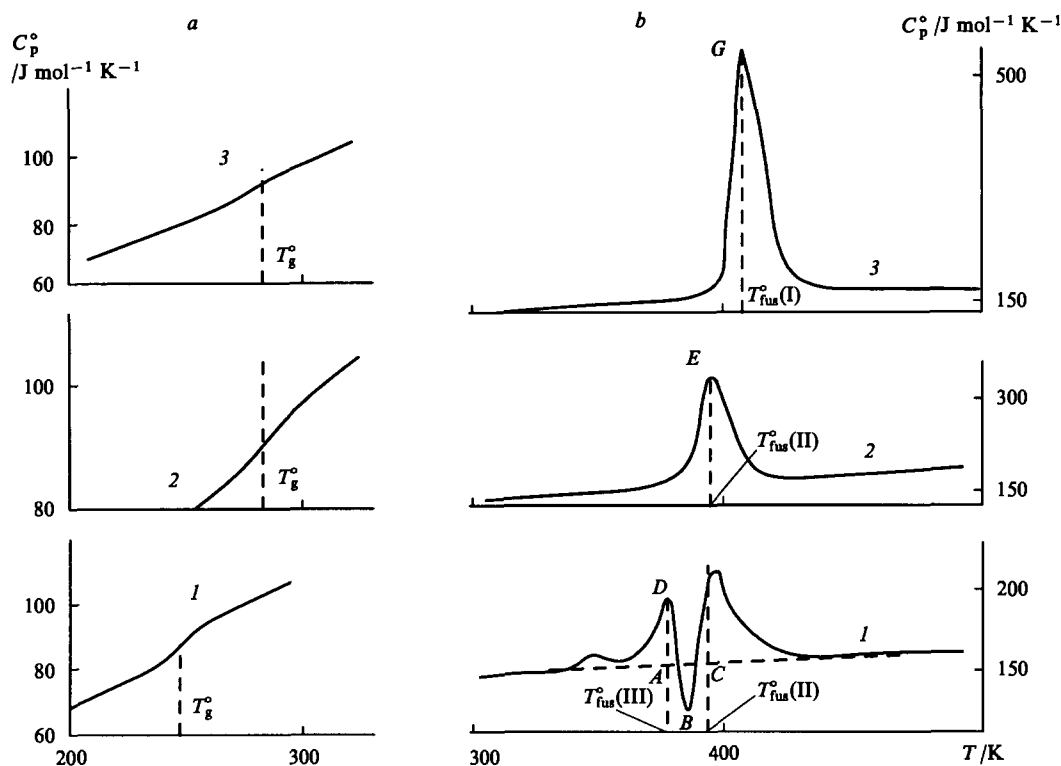


Figure 6. Heat capacity of isotactic polybut-1-ene in the temperature ranges 200–300 K (a) and 300–600 K (b) (according to dynamic calorimetric data, heating rate $1.7 \times 10^{-2} \text{ K s}^{-1}$).

(1) Specimen containing 65% of crystals of form III (with a hexagonal structure) and after their fusion and crystallisation of the amorphous component—crystals of form II (with a tetragonal structure); (2) specimen containing 83% of crystals of form II; (3) specimen containing 77% of crystals of form I (with a rhombohedral structure).

fusion of crystals of form III and precedes the fusion of crystals of form II (the ABC exotherm in Fig. 6b, curve 1). The crystals of form II produced melted in the range 340–420 K (the endotherm in the same figure). We may note that, on crystallisation from solution, the initial specimen had a degree of crystallinity of 65% (crystals of form III).

On cooling of the melt at a rate of $5 \times 10^{-2} \text{ K s}^{-1}$, crystals of form II, constituting 83% of the mass of the specimen, were formed. Crystals of form II melted in the range 340–420 K (Fig. 6b, curve 2), as for the initial polybut-1-ene specimen (curve 1). When the melt was cooled at a rate of $1.5 \times 10^{-2} \text{ K s}^{-1}$ (approximately three times lower than in the previous case), crystals of form I were produced, the degree of crystallinity amounting to 77%. The crystals melted in the range 350–450 K (curve 3). We may note that at this or slightly higher rate of cooling of the melt, a mixture of crystals of forms I and II was formed (10% and 40% respectively). This has also been observed by Dainton et al.⁴⁷ on slow cooling of the melt, a mixture consisting of 7% of crystals of form I and 37% of those of form II was obtained. The degree of crystallinity of the test polymer specimens was determined by Eqn (4) from the values of $\Delta C_p^\circ(\alpha)$ at the glass transition temperature. The values of $\Delta C_p^\circ(\alpha)$ were found graphically from the curves describing the temperature variation of the heat capacity and incorporating devitrification regions (Fig. 6a, curves 1–3). $\Delta C_p^\circ(T_g^\circ)$ is $9.7 \text{ J mol}^{-1} \text{K}^{-1}$ for the specimen containing crystals of form III, $4.3 \text{ J mol}^{-1} \text{K}^{-1}$ for the specimen with crystals of form II, and $58 \text{ J mol}^{-1} \text{K}^{-1}$ for the specimen with crystals of form I. The increase in heat capacity on devitrification of polybut-1-ene in the amorphous state is $\Delta C_p^\circ(\alpha = 0) = 27.5 \text{ J mol}^{-1} \text{K}^{-1}$ (section BL in Fig. 1).

The melting temperature ranges were determined graphically as the temperatures of the onset and end of the anomalous changes in heat capacity caused by fusion (apparent heat capacity endo-

therms in Fig. 6b, curves 1–3). The temperatures corresponding to the maximum heat capacity in the melting range were adopted as the melting points (points D, E, and G on curves 1–3). The enthalpies of fusion $\Delta H^\circ(\alpha)$ were determined by the method involving the continuous injection of energy: for the crystalline forms II and I in three experiments in each case and for form II in one experiment. This yielded $\Delta H^\circ(\alpha = 65\%) = 1.735 \text{ kJ mol}^{-1}$ for form III, $\Delta H^\circ(\alpha = 83\%) = 2.754 \text{ kJ mol}^{-1}$ for form II, and $\Delta H^\circ(\alpha = 77\%) = 5.475 \text{ kJ mol}^{-1}$ for form I. The molar enthalpies of fusion of each form were calculated by Eqn (5) from the corresponding values of $\Delta H^\circ(\alpha)$ and α . The entropies of fusion were calculated by Eqn (6) from the enthalpies of fusion and the melting points. All the thermodynamic parameters of fusion are listed in Table 2. The data of Lebedev et al.⁶⁹ and Wilski and Grever⁷⁰ agree satisfactorily. Judging from the entropy of fusion, the crystalline form I (rhombohedral crystals) is most ordered, while form III is least ordered. Wilski and Grever⁷⁰ established that form III is thermodynamically least stable. We may note that form III cannot be obtained under the conditions of calorimetric experiments on crystallisation of melts of isotactic polybut-1-ene. Furthermore, the determination of the melting temperature range for crystals of form III, crystallised from solution, is complicated by the onset of the crystallisation of the melt in form II, which masks the termination of the fusion of form III. All these factors preclude accurate measurements of the enthalpy of fusion of form III. The enthalpy and entropy of fusion of form III listed in Table 2 must therefore be regarded as only estimates.

According to data quoted by Andrianova⁷² and Raff and Doak,⁹⁰ polybut-1-ene can exist in two crystalline modifications: I (crystals with a monoclinic lattice) and II (crystals with an orthorhombic lattice). It was established that polybut-1-ene usually exists in the crystalline modification I, while modification II is formed extremely rarely. The melting points of modifications I and II are respectively 403 and 348 K. The enthalpies of fusion of

the polymer have been published.^{48,76,77} Their numerical values vary from 3.98 to 6.28 kJ mol⁻¹. The results of calorimetric measurements of the thermodynamic parameters of fusion⁷⁷ are listed in Table 2.

The thermodynamic characteristics of the fusion of poly-3-methylbut-1-ene were determined in four experiments.⁷⁸ In all the experiments, the fusion of the polymer began in the range from 500 to 540 K and ended at 610 K. The melting temperatures corresponding to the maximum apparent heat capacity varied in the melting range from 576.8 to 584.9 K from experiment to experiment. The rates of heating of the calorimeter with the test substance increased under these conditions from 1.7×10^{-2} to 3.3×10^{-2} K s⁻¹. Table 2 lists the value of T_{fus}^0 for the initial specimen (heating rate 1.7×10^{-2} K s⁻¹). For poly-3-methylbut-1-ene specimens with degrees of crystallinity of 50%, 70%, 81%, and 88%, the values of $\Delta_{fus}H^0(\alpha) = 3.04, 4.23, 4.91$, and 5.31 kJ mol⁻¹ respectively were obtained. They were recalculated for the polymer with 100% crystallinity by Eqn (6). The melting range of poly-3-methylbut-1-ene has been published as 513–583 K.⁹¹ Minsker et al.⁹² give $T_{fus}^0 = 545$ K for a specimen of isotactic poly-3-methylbut-1-ene with a degree of crystallinity of 90.5%.

Lebedev et al.⁸⁰ carried out five experiments on the fusion of poly-4-methylpent-1-ene (heating rate $\sim 3 \times 10^{-2}$ K s⁻¹) and obtained a series of melting points ranging from 521.7 K in the first experiment for the initial specimen to 508.5 K in the fifth experiment. A decrease in T_{fus}^0 from experiment to experiment was noted. In the fourth and fifth experiments, the values of T_{fus}^0 virtually coincided. A similar phenomenon has also been observed by Andrianova.⁷² The arithmetical mean of the values of T_{fus}^0 found in the fourth and fifth experiments was adopted as T_{fus}^0 for poly-4-methylpent-1-ene (Table 2). The enthalpy of fusion of the crystalline component of the specimen, obtained in the first experiment, is lower than in the fourth and fifth experiments (in the latter experiments the values of $\Delta_{fus}H^0$ are virtually identical). The value found by Karasz et al.⁴⁸ was adopted as the enthalpy of fusion of the polymer with a crystallinity of 100%.

The apparent heat capacities in the melting range of crystals of forms II and I of isotactic polydec-1-ene were measured with continuous heating of the calorimeter containing the test substance at a rate of 8×10^{-3} K s⁻¹.⁸⁴ The temperature corresponding to the maximum apparent heat capacity $C_{p,max}^0 = 555.3$ J mol⁻¹ K⁻¹ in the melting range was adopted as the melting point $T_{fus}^0(II)$ of the crystals formed by the main chains; the temperature corresponding to $C_{p,max}^0 = 495.3$ J mol⁻¹ K⁻¹ in the melting range of crystals of form I was adopted as the melting point $C_{p,max}^0(I)$ of the crystals formed by the side substituents. The enthalpies of fusion were found to be $\Delta_{fus}H^0(\alpha = 35\%; II) = 2.25$ kJ mol⁻¹ and $\Delta_{fus}H^0(\alpha = 35\%; I) = 2.53$ kJ mol⁻¹. These values were recalculated for 100% crystallinity. The degree of crystallinity was calculated by Eqn (4) from calorimetric data:⁸⁴ $\Delta C_p^0(T_g^0; \alpha = 0) = 60$ and $\Delta C_p^0(T_g^0; \alpha) = 39$ J mol⁻¹ K⁻¹. In the calculations of the degree of crystallinity, it was assumed that the value α found refers to

crystals of both form II and I. This means that, on crystallisation of the main chains of the polymer, the corresponding amount of side substituents crystallises simultaneously. In several consecutive measurements of $\Delta_{fus}H^0(II)$ and $\Delta_{fus}H^0(I)$ for different degrees of crystallinity α , it was found that the ratio

$$\frac{\Delta_{fus}H^0(II)}{\Delta_{fus}H^0(I)} = 0.7 \pm 0.2.$$

is approximately constant.

VI. Parameters of vitrification and of the vitreous state

The parameters of the vitrification and the vitreous state of the polyolefins investigated are listed in Table 3. The glass transition temperature T_g^0 was determined from the point of inflection in the plots of the temperature variation of the entropy $S^0(T) = f(T)$ in the vitrification range. The error of the determination of T_g^0 by this method is usually 0.5–1.0 K.

The availability of the relations $C_p^0 = f(T)$ for the amorphous and crystalline states and also of the temperatures and enthalpies of the physical transformations made it possible to estimate the differences between the enthalpies of the polymers in the vitreous and crystalline states $H_g^0(0) - H_{cr}^0(0)$ at $T = 0$ K and the residual (zero-point) entropy in the vitreous state $S_g^0(0)$. The corresponding calculations were performed by means of published equations,^{11,33,93} which assumed the following form for polyolefins:

$$H_g^0(0) - H_{cr}^0(0) = \int_0^{T_{fus}^0} [C_p^0(cr) - C_p^0(g)] dT + \Delta_{fus}H^0,$$

$$S_g^0(0) = \int_0^{T_{fus}^0} [C_p^0(cr) - C_p^0(g)] d \ln T + \Delta_{fus}S^0,$$

where $C_p^0(cr)$ and $C_p^0(g)$ are the temperature functions of the heat capacities of the polymer in the crystalline and vitreous states respectively.

The configurational entropy S_{conf}^0 of the vitreous polymer was calculated by Eqn (3). The Kauzmann temperature T_2^0 was found graphically from the entropy diagram, as had been done, for example, for polybut-1-ene (Fig. 7). The ratio T_g^0/T_2^0 for the polymeric and monomeric glasses is usually 1.29,^{37,38} so that S_{conf}^0 was estimated from the formula³⁷

$$S_{conf}^0 = \Delta C_p^0(T_g^0) \ln 1.29.$$

It is especially convenient for the estimation of S_{conf}^0 for vitrifying but not crystallising polymers.

According to dynamic calorimetric data,⁶⁹ the devitrification of polybut-1-ene specimens (Fig. 6) with degrees of crystallinity of 65%, 77%, and 83% occurred in the temperature ranges 230–255 K, 265–270 K, and 270–295 K respectively. The glass transition temperatures of these specimens were found to be 249 K for the first and 282 K for the other two. A dependence of

Table 3. Parameters of the vitrification process and of the vitreous state of polyolefins.

Polymer	T_g^0 /K	$\Delta C_p^0(T_g)$ J mol ⁻¹ K ⁻¹	$S_g^0(0)$	S_{conf}^0	$H_g^0(0) - H_{cr}^0(0)$ /kJ mol ⁻¹	Ref.
Polyethylene	237	21.0	5.4	3.2	5.0	65
Polypropylene	260	19.2	1.1	4.4	4.2	68
Polybut-1-ene	249	27.5	6.7	7.0	3.7	69
Polyisobutylene	200	22.6	—	5.7	—	76
Polypent-1-ene	238	21	3.8	2.3	2.4	77
Poly-3-methylbut-1-ene	327	32.1	0	8.2	1.9	78
Polyhex-1-ene	216	29	—	7.4	—	49, 96
Poly-4-methylpent-1-ene	300	33.6	8	8.6	5.6	80
Polydec-1-ene	208	60	26	15.3	8.4	84

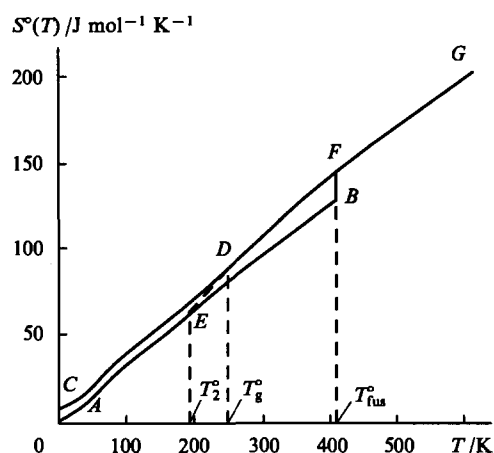


Figure 7. Entropy diagram for polybut-1-ene.

State of the polymer: AEB — crystalline, CD — vitreous, DF — highly elastic, FG — liquid, ED — hypothetical glass; AC — residual (zero-point) entropy of the glass, BF — entropy of fusion.

the vitrification temperature ranges and of the glass transition temperatures on the degree of crystallinity of the test specimens was traced. The higher the values of α , the higher the temperature range to which the temperature range of vitrification and T_g° are displaced. This is apparently caused by the effect due to the reinforcement of the vitreous component of the polymer by crystals,⁷³ as a consequence of which difficulties arise in the excitation of the segmental mobility of the polybut-1-ene macromolecules. The temperature T_g° obtained for poly-3-methylbut-1-ene agrees satisfactorily with $T_g^\circ = 327$ K published by Andrianova.⁷² It is of interest that the zero-point entropy of this polymer in the vitreous state was found to be zero. Strictly speaking, within the limits of experimental error and the errors associated with the assumptions made in calculations, it is equal to the zero-point entropy of the polymer in the crystalline state. It has been shown^{11,93} that $S_{cr}^\circ(0) = 0$ for polymers in the crystalline state. Apparently, the same features are characteristic of poly-3-methylbut-1-ene as for poly-4-methylpent-1-ene.⁸⁰ With decrease in the degree of crystallinity, the density of the amorphous part of the polymer increases, i.e. short-range order becomes more marked with decrease in the long-range order in the disposition of the units of the macromolecules in the crystal lattice.⁸⁰ As a result of the operation of these two effects (the increase in entropy on breakdown of long-range order and its diminution on enhancement of short-range order), the entropy changes are compensated because the above factors act in opposition.

For polyolefins at 0 K, the difference between the enthalpies of the vitreous and crystalline states varies from 1.9 kJ mol⁻¹ (for poly-3-methylbut-1-ene) to 8.4 kJ mol⁻¹ (for polydec-1-ene). The error in the values of $H_g^\circ(0) - H_{cr}^\circ(0)$ is $\sim 10\%$. Vitreous polymers, which are in principle capable of crystallising, exist in a metastable state owing to the high activation energy for the rearrangement and the extremely long relaxation times associated with this fact. Clearly the difference between the Gibbs free energies of the vitreous and crystalline states $\Delta G^\circ(a; cr)$ constitutes an estimate of the metastability of the amorphous polymer under the given conditions. For the temperature range between 0 K and T_{fus}° , the above quantity may be calculated from the difference between the enthalpies $\Delta H^\circ(a; cr)$ and the entropies $\Delta S^\circ(a; cr)$ of the amorphous and crystalline states at any temperature within the above range by the formula¹¹

$$\Delta G^\circ(a; cr) = \Delta H^\circ(a; cr) - T \Delta S^\circ(a; cr),$$

$\Delta H^\circ(a; cr)$ and $\Delta S^\circ(a; cr)$ can be readily calculated in their turn from the values of $H_g^\circ(0) - H_{cr}^\circ(0)$ and ΔS° and the temperature variations of the heat capacities of the polymer in the amorphous (vitreous and highly elastic) and crystalline states in the above

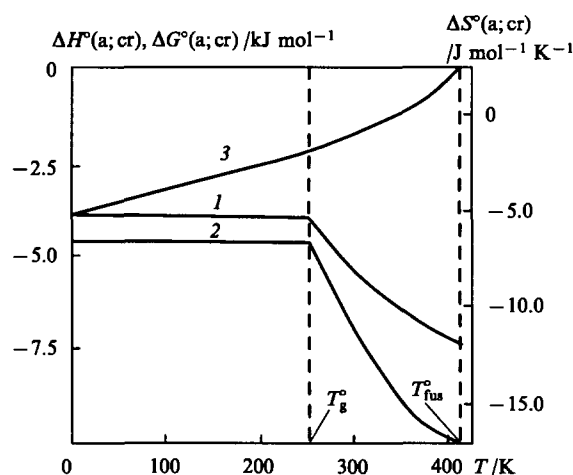


Figure 8. Temperature dependences of the enthalpy (1), entropy (2), and Gibbs free energy (3) of the transition of polybut-1-ene from the amorphous to the crystalline state in the temperature range from 0 K to T_{fus}° .

temperature range, as has been done, for example, in the studies of Lebedev and coworkers.^{7,94} Typical temperature variations of $\Delta G^\circ(a; cr)$, $\Delta H^\circ(a; cr)$, and $\Delta S^\circ(a; cr)$ are presented in Fig. 8 in relation to polybut-1-ene.

VII. Thermodynamic functions

The thermodynamic functions of polyolefins in the range 0–600 K have been calculated with the aid of their experimental heat capacities and the temperatures and enthalpies of the physical transformations. For this purpose, the heat capacity of the polymer was usually extrapolated from 5–10 to 0 K using the Debye function⁵⁹

$$C_p^\circ = nD\left(\frac{\theta_D}{T}\right), \quad (8)$$

where n and θ_D are specially selected parameters. They are usually chosen so that Eqn (8) describes the experimental heat capacities C_p° , or the average heat capacities for the range 5–15 K obtained from them, subject to an error not exceeding 1%–1.5%. In the calculation of the functions, it was assumed that at $T < 5$ –10 K the above equation reproduces the heat capacity of the polymer with the same error. Wunderlich⁹⁵ usually employed the two-parameter Tarasov heat capacity function [see Eqn (2)] to extrapolate the heat capacities of polymers. For example, the corresponding characteristic temperatures for polyethylene in the crystalline state are $\theta_1 = 519$ K and $\theta_3 = 158$ K.

The heat capacity of polyhex-1-ene was extrapolated from 20 to 0 K in terms of the specially selected equation⁹⁶

$$C_p^\circ = 0.0258T + 0.02950T^2 + 0.000417T^3.$$

Since virtually all the polymers investigated are partly crystalline with the exception of polyisobutylene and polyhex-1-ene, their thermodynamic functions were calculated by the method which makes it possible to evaluate the functions of the polymers in the fully amorphous and crystalline states from the experimental data on properties of the partly crystalline polymers.^{11,36}

The functions (Table 4) were calculated on a computer by means of the equations^{11,94}

$$H^\circ(T) - H^\circ(0) = \sum \int_0^T C_p^\circ(T) dT + \sum \Delta_{fus} H^\circ,$$

$$S^\circ(T) = \sum \int_0^T C_p^\circ(T) d \ln T + \sum \Delta_{fus} S^\circ,$$

Table 4. Thermodynamic functions of polyolefins under standard pressure.

T/K	$C_p^\circ(T)$	$H^\circ(T) - H^\circ(0)$	$S^\circ(T)$	$-[G^\circ(T) - H^\circ(0)]$	T/K	$C_p^\circ(T)$	$H^\circ(T) - H^\circ(0)$	$S^\circ(T)$	$-[G^\circ(T) - H^\circ(0)]$
Polyethylene ⁶⁵					Polypropylene ⁶⁸				
<i>Crystalline state</i>					<i>Crystalline state</i>				
5	0.0249	0.000032	0.0084	0.00001	10	0.5538	0.001099	0.1342	0.000242
10	0.1931	0.000488	0.0654	0.000176	20	3.572	0.02043	1.354	0.006638
15	0.6336	0.002416	0.2158	0.000821	30	7.065	0.04381	3.470	0.03028
20	1.459	0.007468	0.5008	0.00255	40	10.20	0.1605	5.942	0.07718
25	2.446	0.01718	0.9306	0.00609	50	13.02	0.2768	8.526	0.1494
30	3.676	0.03242	1.482	0.01205	100	26.25	1.258	21.60	0.9022
40	6.376	0.08226	2.898	0.03366	150	37.57	2.862	34.46	2.306
50	9.046	0.1598	4.618	0.07106	200	47.63	4.994	46.66	4.336
100	18.91	0.8808	14.22	0.5410	298.15	65.17	10.56	69.05	10.03
150	25.74	2.004	23.24	1.481	350	73.94	14.16	80.16	13.90
200	31.14	3.428	31.40	2.850	400	82.42	18.07	90.61	18.17
250	37.10	5.128	38.96	4.610	450	90.90	22.40	100.8	22.96
298.15	43.40	7.070	46.04	6.656	460.7	92.72	23.39	103.0	24.05
350	49.32	9.474	53.46	9.238	<i>Liquid state</i>				
400	54.76	12.08	60.40	12.08	460.7	112.7	32.59	123.0	24.05
414.6	56.32	12.89	62.40	12.98	500	118.6	37.14	132.5	29.10
<i>Liquid state</i>					<i>Vitreous state</i>				
414.6	71.70	21.66	83.58	12.98	0	0	0	1.1	0
450	74.76	24.27	89.56	16.03	10	1.076	0.002311	1.39	0.0116
500	79.08	28.16	97.68	20.72	20	5.077	0.03262	3.33	0.0340
550	83.41	32.17	105.4	25.80	30	8.721	0.1021	6.10	0.0810
600	87.74	36.44	112.9	31.26	40	11.89	0.2054	9.05	0.1571
<i>Vitreous state</i>					50	15.01	0.3398	12.03	0.2617
0	0	0	5.4	0	100	28.51	1.445	26.83	1.238
5	0.1133	0.000139	5.44	0.0270	150	39.48	3.152	40.52	2.926
10	0.7418	0.002046	5.68	0.0547	200	49.63	5.374	53.24	5.274
15	1.756	0.0082	6.26	0.0857	260	64.92	8.792	68.09	8.911
20	2.804	0.01966	6.81	0.1165	<i>Highly elastic state</i>				
25	3.978	0.03574	7.56	0.1525	260	82.29	8.792	68.09	8.911
30	5.210	0.0595	8.396	0.1924	298.15	88.07	12.05	79.76	11.73
40	7.800	0.1245	10.24	0.2854	350	95.91	16.81	94.48	16.26
50	10.29	0.2150	12.26	0.3979	400	103.5	21.80	107.8	21.32
100	19.49	0.9766	22.45	1.269	450	111.0	27.16	120.4	27.02
150	28.12	2.162	31.94	2.629	460.7	112.7	28.36	123.0	28.31
200	37.20	3.796	41.28	4.460	Polybut-1-ene ⁶⁹				
<i>Highly elastic state</i>					<i>Crystalline state (crI)</i>				
250	57.44	6.034	51.18	6.761	5	0.1943	0.00023	0.0585	0.00005
298.15	61.62	8.900	61.66	9.484	10	1.350	0.0037	0.4883	0.0012
350	66.12	12.21	71.88	12.95	15	3.272	0.0150	1.382	0.0057
400	70.44	15.63	81.00	16.77	20	5.480	0.0368	2.620	0.0156
414.6	71.70	16.66	83.58	17.99	25	7.790	0.0699	4.091	0.0323
Polydeuteroethylene ⁶⁷					30	10.11	0.1147	5.714	0.0567
<i>Crystalline state</i>					40	14.86	0.2396	9.272	0.1313
5	0.6056	0.00035	0.0748	0.000023	50	19.26	0.4105	13.07	0.2428
10	0.4884	0.00180	0.2752	0.000949	100	37.78	1.848	32.26	1.378
15	1.293	0.00610	0.6116	0.003080	150	53.37	4.138	50.62	3.455
20	2.392	0.01521	1.128	0.007353	200	67.39	7.167	67.95	6.423
25	3.750	0.03044	1.802	0.01461	250	80.36	10.86	84.39	10.23
30	5.270	0.05301	2.621	0.02561	298.15	92.85	15.03	99.61	14.67
40	8.315	0.1209	4.553	0.06120	300	93.33	15.20	100.2	14.85
50	11.51	0.2198	6.745	0.1144	350	106.3	20.19	115.5	20.25
100	21.33	1.076	18.22	0.7457	400	119.3	25.83	130.6	26.40
150	29.15	2.335	28.32	1.913	406.8	121.0	26.65	132.6	27.29
200	37.89	4.007	37.88	3.569	<i>Liquid state</i>				
250	46.16	6.104	47.20	5.697	406.8	136.7	33.76	150.1	27.29
298.15	54.13	8.518	56.02	8.183	450	144.7	39.83	164.3	34.08
300	54.52	8.619	56.35	8.287	500	153.9	47.29	179.9	42.69
350	62.92	11.55	65.38	11.33	550	163.1	55.22	195.1	52.07
400	71.25	14.91	74.34	14.82	600	172.3	63.61	209.7	62.19
415	74.00	16.04	77.12	16.01					

Table 4 (continued).

T/K	$C_p^\circ(T)$	$H^\circ(T) - H^\circ(0)$	$S^\circ(T)$	$-[G^\circ(T) - H^\circ(0)]$	T/K	$C_p^\circ(T)$	$H^\circ(T) - H^\circ(0)$	$S^\circ(T)$	$-[G^\circ(T) - H^\circ(0)]$
Polybut-1-ene ⁶⁹					<i>Vitreous state</i>				
<i>Vitreous state</i>					0	0	0	3.8	0
0	0	0	6.7	0	5	0.266	0.00033	3.9	0.0192
50	19.26	0.4105	19.7	0.576	10	1.765	0.00488	4.5	0.0401
100	37.78	1.848	38.9	2.04	15	3.815	0.0185	5.5	0.064
150	53.37	4.138	57.3	4.46	20	6.881	0.0447	7.0	0.095
200	67.39	7.167	74.6	7.76	25	10.93	0.0891	9.0	0.1359
249	80.10	10.78	90.7	11.8	30	14.24	0.1524	11.3	0.1866
<i>Highly elastic state</i>					40	20.06	0.3244	16.2	0.3236
249	107.6	10.78	90.7	11.8	50	25.48	0.5524	21.2	0.5076
298.15	116.7	16.29	110.9	16.8	100	49.15	2.447	46.6	2.213
300	117.0	16.51	111.6	17.0	150	67.95	5.392	70.2	5.135
350	126.2	22.59	130.4	23.1	200	85.90	9.248	92.2	9.200
400	135.5	29.13	147.9	30.0	238	105.0	12.78	108.4	13.02
406.8	136.7	30.06	150.1	31.0	<i>Highly elastic state</i>				
Polyisobutylene					238	126.0	12.78	108.4	13.02
<i>Vitreous state</i>					250	129.6	14.32	114.7	14.36
0	0	0	5.70	0	298.15	143.8	20.90	138.8	20.48
5	0.129	0.000084	5.74	0.02861	300	144.4	21.17	139.6	20.71
10	1.010	0.00254	6.04	0.0579	350	159.1	28.75	163.0	28.30
15	3.007	0.01243	6.81	0.0896	388	170.2	35.01	179.9	34.79
20	4.662	0.03167	7.91	0.1264	Poly-3-methylbut-1-ene ⁷⁸				
25	6.300	0.05918	9.12	0.1689	<i>Crystalline state</i>				
30	7.838	0.09448	10.41	0.2177	5	0.564	0.000738	0.190	0.00021
40	10.76	0.1877	13.07	0.3350	10	2.874	0.00902	1.241	0.00339
50	13.68	0.3098	15.78	0.4793	15	4.873	0.02875	2.813	0.01345
100	30.97	1.411	30.36	1.625	20	7.390	0.05992	4.582	0.03172
150	48.59	3.406	46.29	3.538	25	10.35	0.1056	6.608	0.05965
200	64.50	6.234	62.45	6.257	30	13.18	0.1641	8.736	0.09795
<i>Highly elastic state</i>					40	18.84	0.3253	13.33	0.2080
200	87.11	6.234	62.45	6.257	50	23.60	0.5383	18.07	0.3650
250	97.79	10.84	82.97	9.901	60	28.24	0.7966	22.76	0.5691
298.15	109.3	15.82	101.2	14.34	70	32.78	1.102	27.46	0.8203
300	109.7	16.03	101.8	14.53	80	37.45	1.453	32.14	1.118
350	122.4	21.83	119.7	20.07	90	41.92	1.850	36.81	1.463
380	130.2	25.61	130.1	23.82	100	46.08	2.290	41.45	1.854
Polypent-1-ene ⁷⁷					150	64.65	5.068	63.72	4.490
<i>Crystalline state</i>					200	81.70	8.729	84.67	8.204
5	0.266	0.00033	0.081	0.00007	250	99.00	13.26	104.8	12.94
10	1.765	0.00488	0.649	0.0016	298.15	116.2	18.47	123.8	18.44
15	3.815	0.0185	1.722	0.0074	300	117.0	18.69	124.5	18.67
20	6.881	0.0447	3.209	0.0195	350	132.8	24.94	143.8	25.38
25	10.93	0.0891	5.171	0.0402	400	148.5	31.97	162.5	33.04
30	14.24	0.1524	7.473	0.0717	450	163.9	39.78	180.9	41.62
40	20.06	0.3244	12.38	0.1708	500	179.4	48.36	199.0	51.12
50	25.48	0.5524	17.44	0.3198	550	194.5	57.71	216.8	61.52
100	49.15	2.447	42.75	1.828	584	204.7	64.50	228.7	69.09
150	67.95	5.392	66.38	4.565	<i>Liquid state</i>				
200	85.90	9.248	88.44	8.441	584	206.0	70.54	239.1	69.09
250	104.1	14.00	109.6	13.39	600	210.0	73.87	244.7	72.97
298.15	121.5	19.43	129.4	19.15	640	216.2	82.40	258.5	83.03
300	122.2	19.66	130.2	19.39	<i>Vitreous state</i>				
350	140.4	26.22	150.4	26.40	0	0	0	0	0
388	154.1	31.82	165.5	32.39	5	0.564	0.000738	0.190	0.00021
<i>Liquid state</i>					10	2.874	0.00902	1.241	0.00339
388	170.2	37.40	179.9	32.39	15	4.873	0.02875	2.813	0.01345
400	173.8	39.46	185.1	34.60	20	7.890	0.05992	4.582	0.03172
450	188.5	48.52	206.5	44.39	25	10.35	0.1056	6.608	0.05965
500	203.2	58.31	227.1	55.23	30	13.18	0.1641	8.736	0.09795
					40	18.84	0.3253	13.33	0.2080

Table 4 (continued).

T/K	$C_p^\circ(T)$	$H^\circ(T) - H^\circ(0)$	$S^\circ(T)$	$-[G^\circ(T) - H^\circ(0)]$	T/K	$C_p^\circ(T)$	$H^\circ(T) - H^\circ(0)$	$S^\circ(T)$	$-[G^\circ(T) - H^\circ(0)]$
Poly-3-methylbut-1-ene ⁷⁸					<i>Crystalline state</i>				
<i>Vitreous state</i>					298.15	139.2	22.18	150.9	22.80
50	23.60	0.5383	18.07	0.3650	350	161.0	29.98	174.9	31.24
60	28.24	0.7966	22.76	0.5691	400	183.0	38.58	197.8	40.56
70	32.78	1.102	27.46	0.8203	450	204.0	48.24	220.6	51.02
80	37.45	1.453	32.14	1.118	500	225.0	58.97	243.2	62.62
90	41.92	1.850	36.81	1.463	508	228.0	60.78	246.8	64.58
100	46.08	2.290	41.45	1.854	<i>Liquid state</i>				
150	64.65	5.068	63.72	4.490	508	239.5	71.02	267.0	64.58
200	81.70	8.729	84.67	8.204	550	248.9	84.31	292.1	76.36
250	99.00	13.26	104.8	12.94	600	256.5	96.93	314.1	91.52
298.15	116.2	18.47	123.8	18.44	<i>Vitreous state</i>				
300	117.0	18.69	124.5	18.67	0	0	0	8	0
327	125.9	21.97	135.0	22.16	5	0.483	0.0006	8.1	0.0399
<i>Highly elastic state</i>					10	3.250	0.0090	9.2	0.0830
327	158.0	21.97	135.0	22.16	15	6.900	0.0343	11.2	0.1336
350	161.7	25.64	145.8	25.39	20	10.78	0.0784	13.7	0.1957
400	171.2	33.97	168.0	33.25	25	14.60	0.1421	16.5	0.2712
450	180.6	42.76	188.7	42.17	30	18.00	0.2236	19.5	0.3611
500	189.9	52.03	208.3	52.10	40	24.30	0.4364	25.6	0.5864
584	206.0	68.65	239.1	70.90	50	29.85	0.7075	31.6	0.8725
Polyhex-1-ene ^{77,96}					60	35.10	1.032	37.5	1.218
<i>Vitreous state</i>					70	40.35	1.410	43.3	1.622
0	0	0	7.3	0	80	45.70	1.840	49.1	2.084
10	2.803	0.0104	9.0	0.0798	90	50.90	2.323	54.7	2.603
20	9.092	0.0684	12.8	0.188	100	55.90	2.857	60.4	2.797
30	16.42	0.1939	17.8	0.340	150	77.55	6.206	87.2	6.877
40	23.68	0.3954	23.6	0.5467	200	97.25	10.58	112.2	11.86
50	30.17	0.6648	29.6	0.8128	250	118.7	15.98	136.2	18.07
60	36.69	1.000	35.6	1.138	300	140.0	22.44	159.7	25.47
70	42.68	1.398	41.8	1.527	<i>Highly elastic state</i>				
80	48.28	1.853	47.9	1.974	300	173.6	22.44	159.7	25.47
90	53.76	2.364	53.8	2.480	350	189.4	31.52	187.7	34.16
100	59.08	2.929	59.7	3.048	400	205.3	41.38	214.0	44.22
150	84.94	6.513	88.6	6.783	450	221.1	52.04	239.1	55.56
200	111.3	11.44	116.8	11.92	500	237.0	63.50	263.2	68.10
215.5	119.2	13.20	125.2	13.78	508	239.5	65.40	267.0	70.24
<i>Highly elastic state</i>					Polydec-1-ene ⁸⁴				
215.5	147.7	13.20	125.2	13.78	<i>Crystalline state (crII and crI)</i>				
250	159.6	18.46	147.8	18.49	5	0.600	0.000836	0.214	0.000236
298.15	177.5	26.59	177.5	26.33	10	3.810	0.01013	1.392	0.00379
300	178.5	26.92	178.6	26.66	15	8.750	0.04105	3.830	0.01639
Poly-4-methylpent-1-ene ⁸⁰					20	14.67	0.09925	7.136	0.04347
<i>Crystalline state</i>					25	21.24	0.1888	11.11	0.08882
5	0.483	0.0006	0.1458	0.0001	30	27.82	0.3117	15.57	0.1553
10	3.250	0.0090	1.194	0.0030	40	39.64	0.6484	25.17	0.3585
15	6.900	0.0343	3.196	0.0136	50	51.39	1.104	35.28	0.6605
20	10.78	0.0784	5.706	0.0357	60	62.48	1.673	45.64	1.065
25	14.60	0.1421	8.532	0.0712	70	72.25	2.348	56.02	1.573
30	18.00	0.2236	11.49	0.1212	80	80.91	3.115	66.25	2.185
40	24.30	0.4364	17.57	0.2665	90	88.45	3.962	76.22	2.898
50	29.85	0.7075	23.60	0.4725	100	96.09	4.885	85.94	3.709
60	35.10	1.032	29.50	0.7381	150	137.3	10.73	132.8	9.186
70	40.35	1.410	35.31	1.062	200	174.2	18.52	177.3	16.95
80	45.70	1.840	41.05	1.444	250	211.2	28.17	220.2	26.89
90	50.90	2.323	46.73	1.883	276	230.1	33.90	242.0	32.90
100	55.90	2.857	54.36	2.379	<i>Crystalline state (crI)</i>				
150	77.55	6.206	79.22	5.677	276	230.1	40.33	265.3	32.90
200	97.25	10.58	104.2	10.27	298.15	246.1	45.61	283.7	38.97
250	118.7	15.98	128.2	16.08	301	249.0	46.31	286.0	39.79

Table 4 (continued).

<i>T</i> /K	$C_p^\circ(T)$	$H^\circ(T) - H^\circ(0)$	$S^\circ(T)$	$-[G^\circ(T) - H^\circ(0)]$	<i>T</i> /K	$C_p^\circ(T)$	$H^\circ(T) - H^\circ(0)$	$S^\circ(T)$	$-[G^\circ(T) - H^\circ(0)]$
Polydec-1-ene ⁸⁴					<i>Vitreous state</i>				
<i>Liquid state</i>					50	51.39	1.104	61.6	1.966
301	287.8	53.54	310.0	39.79	60	62.48	1.673	71.6	2.611
350	307.3	68.08	354.7	56.07	70	72.25	2.348	82.0	3.378
400	335.2	84.13	397.6	74.89	80	80.91	3.115	92.3	4.253
450	363.7	102.6	438.7	95.80	90	88.45	3.962	102.2	5.220
<i>Vitreous state</i>					100	96.09	4.885	111.9	6.285
0	0	0	26.0	0	150	137.3	10.73	158.8	13.06
5	0.600	0.000836	26.2	0.129	200	174.2	18.52	203.3	22.10
10	3.810	0.01013	27.4	0.2619	208	180.5	20.03	210.5	23.75
15	8.750	0.04105	29.8	0.4030	<i>Highly elastic state</i>				
20	14.67	0.09925	33.1	0.5587	208	260.5	20.03	210.5	23.75
25	21.24	0.1888	37.1	0.7340	250	270.0	31.01	258.5	33.62
30	27.82	0.3117	41.6	0.9302	298.15	286.1	44.36	307.3	47.26
40	39.64	0.6484	51.2	1.392	301	287.8	45.15	310.0	48.16

Note. The thermodynamic functions presented have the following dimensions: $C_p^\circ(T)$ and $S^\circ(T)$ — J mol⁻¹ K⁻¹, $H^\circ(T) - H^\circ(0)$ and $G^\circ(T) - H^\circ(0)$ — kJ mol⁻¹.

$$G^\circ(T) - H^\circ(0) = [H^\circ(T) - H^\circ(0)] - TS^\circ(T),$$

where C_p° is the temperature variation of the heat capacities of the substances in the crystalline, vitreous, highly elastic, and liquid states (see, for example, Fig. 1). In the calculations of the entropy for polyisobutylene and polyhex-1-ene, it was assumed that their zero-point entropy is equal to the configurational entropy. The errors in the calculated functions are on average 1%–1.15% at $T < 20$ K, 0.5% in the range 20–50 K, ~0.2% in the range 50–340 K, and 0.5%–2% in the range 340–600 K.

VIII. Thermochemical characteristics

The thermochemical characteristics of polyolefins are listed in Table 5. The enthalpies of combustion were obtained from the experimental combustion energies $\Delta_c U$ measured calorimetrically. Since all the polymers investigated were partly crystalline, the

$\Delta_c U(\alpha)$ were found in the experiments. The results were recalculated for the standard state and the values of $\Delta_c U^\circ(\alpha)$ were obtained. They were used to calculate the enthalpies of combustion $\Delta_c H^\circ(\alpha)$. The enthalpies of combustion of the polymer in the crystalline and amorphous (vitreous or highly elastic) states were calculated in their turn from the values of $\Delta_c H^\circ(\alpha)$ and the molar enthalpy of fusion of the polymer with $\alpha = 100\%$ (calculated for $T = 298.15$ K) by means of the following relations:

$$\Delta_c H^\circ(\text{cr}) = \Delta_c H^\circ(\alpha) + (1 - \alpha)\Delta_{\text{fus}}H^\circ(298.15 \text{ K}),$$

$$\Delta_c H^\circ(\text{a}) = \Delta_c H^\circ(\alpha) - \alpha\Delta_{\text{fus}}H^\circ(298.15 \text{ K}).$$

Here α is expressed as a fraction. The enthalpy of fusion of the polymer at 298.15 K was calculated by the equation

$$\Delta_{\text{fus}}H^\circ(298.15 \text{ K}) = \Delta_{\text{fus}}H^\circ(T_{\text{fus}}^\circ) + \int_{T_{\text{fus}}}^{298.15 \text{ K}} [C_p^\circ(\text{a}) - C_p^\circ(\text{cr})]dT.$$

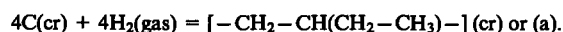
Table 5. Thermochemical characteristics of polyolefins at 298.15 K and the standard pressure.

Polymer	Physical state ^a	$-\Delta_c H^\circ$	$-\Delta_f H^\circ$	$\Delta_f G^\circ$	$\Delta_f S^\circ$	$\ln K_f^\circ$	Ref.
		/kJ mol ⁻¹			/J mol ⁻¹ K ⁻¹		
Polyethylene	cr	1289.8±0.3	58.9±0.3	5.2±0.9	215.0±1.3	0.912	45, 46, 107
	h.e	1306.6±0.3	52.1±0.3	10.8±0.9	210.9±1.3	1.889	
Polydeuteroethylene	cr	1304.9±0.9	74.6±0.9	-1.7±1.3	244.4±1.0	-0.298	46, 67
	h.e	1312.2±0.9	67.1±0.9	1.0±1.3	228.3±1.3	0.170	
Polypropylene	cr	1951.4±0.4	86.2±0.4	10.1±0.9	339.7±1.5	1.775	45, 46
	h.e	1957.1±0.4	80.4±0.4	17.7±0.9	329.0±1.5	3.096	
Polybut-1-ene	cr	2609.8±0.4	107.6±0.4	25.2±1.0	475.4±1.6	4.420	45, 69
	h.e	2614.7±0.4	102.7±0.4	26.8±1.0	434.1±1.6	4.518	
Polypent-1-ene	cr	3250.9±1.9	145.0±1.9	18.7±2.8	551.9±1.8	3.267	46, 77
	h.e	3254.8±1.9	145.0±1.9	19.7±2.8	542.3±1.8	3.449	
Poly-3-methylbut-1-ene	cr	3225.7±2.5	141.0±2.5	25.3±3.0	557.8±2.0	4.432	46, 78
	g	3257.2±2.5	139.5±2.5	26.8±3.0	557.5±2.0	4.695	
Poly-4-methylpent-1-ene	cr	3898.7±1.8	177.4±1.8	21.4±2.4	666.7±1.2	3.749	46, 80
	g	3901.4±1.8	174.7±1.8	24.1±2.4	666.7±1.2	4.222	

^a The following designations of the states of the polymers have been adopted: cr — crystalline, g — vitreous (glassy), h.e. — highly elastic.

We may note that the application of the Kirchhoff equation is possible subject to the condition that the calculation is performed for a constant pressure. In the present instance, it is carried out at the standard pressure (101.325 kPa).

The thermochemical parameters of the formation reaction (the enthalpies $\Delta_f H^\circ$, the entropies $\Delta_f S^\circ$, and the Gibbs free energies $\Delta_f G^\circ$) of the test compounds were calculated from their calorimetric enthalpies of combustion (Table 5) and the absolute entropies (Table 4) and also the enthalpies of formation of liquid water and gaseous carbon dioxide and the entropies of carbon in the form of graphite and gaseous hydrogen, published in handbooks.⁹⁷ The methods used for the corresponding calculations have been described.^{42, 57} For example, $\Delta_f H^\circ$, $\Delta_f S^\circ$, and $\Delta_f G^\circ$ for polybut-1-ene correspond to the following reaction occurring at 298.15 K and the standard pressure:⁶⁹



The Gibbs free energy was calculated from the values of $\Delta_f H^\circ$ and $\Delta_f S^\circ$ by the equation

$$\Delta_f G^\circ = \Delta_f H^\circ - T \Delta_f S^\circ.$$

IX. Thermodynamic parameters of the formation reactions of polyolefins

The methods used to calculate the thermodynamic parameters of the polymerisation reactions from calorimetric data have been described.^{11, 13, 80} The enthalpy of polymerisation $\Delta_{\text{pol}} H^\circ$ was calculated from the enthalpies of combustion of the monomer $\Delta_c H_M^\circ$ and the corresponding polymer $\Delta_c H_P^\circ$ at 298.15 K and 101.325 kPa.

$$\Delta_{\text{pol}} H^\circ = \Delta_c H_M^\circ - \Delta_c H_P^\circ.$$

For other temperatures, the enthalpies of polymerisation were found from the Kirchhoff equation:

$$\Delta_{\text{pol}} H^\circ(T) = \Delta_{\text{pol}} H^\circ(298.15 \text{ K}) + \Delta[H^\circ(T) - H^\circ(298.15 \text{ K})], \quad (9)$$

where $\Delta[H^\circ(T) - H^\circ(298.15 \text{ K})]$ is the difference between the enthalpies of heating of the polymer and monomer in the range 298.15 K–T.

The entropy of polymerisation $\Delta_{\text{pol}} S^\circ(T)$ was calculated from the entropies of the polymer $S_P^\circ(T)$ and the monomer $S_M^\circ(T)$ at the corresponding temperatures:

$$\Delta_{\text{pol}} S^\circ(T) = S_P^\circ(T) - S_M^\circ(T).$$

The Gibbs free energy was calculated from the values of $\Delta_{\text{pol}} H^\circ(T)$ and $\Delta_{\text{pol}} S^\circ(T)$

$$\Delta_{\text{pol}} G^\circ(T) = \Delta_{\text{pol}} H^\circ(T) - T \Delta_{\text{pol}} S^\circ(T).$$

The concentrations of the monomer $[M]_e^\circ$ and the polymer $[P]_e^\circ$ in the equilibrium reaction mixture, corresponding to thermodynamic equilibrium, were estimated from the relations

$$[M]_e^\circ = \exp \frac{\Delta_{\text{pol}} G^\circ(T)}{RT},$$

$$[P]_e^\circ = 1 - \exp \frac{\Delta_{\text{pol}} G^\circ(T)}{RT}.$$

The limiting polymerisation temperatures T_{cel}° of the processes investigated were found from the point of intersection of the relations

$$\Delta_{\text{pol}} H^\circ(T) = f(T) \quad (10a)$$

and

$$T \Delta_{\text{pol}} S^\circ(T) = f(T) \quad (10b)$$

or estimated by Dainton's method.¹³

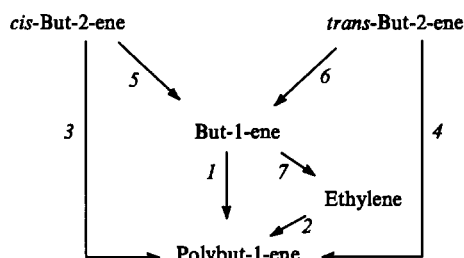
The results of the calculations are presented in Table 6. The standard enthalpy of polymerisation of gaseous ethene to partly crystalline polyethylene at 298.15 K, published by Sawada,⁹⁸ the thermodynamic functions of polyethylene,⁶⁵ the temperature dependence of the heat capacity, and the temperatures and enthalpies of the physical transformations of the monomer^{99, 100} were chosen as the initial data for the calculation of the thermodynamic parameters of the polymerisation of ethene. For propene, use was made of the value of $\Delta_{\text{pol}} H^\circ(\text{gas; cr and gas; a})$ at 298.15 K obtained by Joshi and Zvolinskii⁴⁵ and Richardson and Parks,¹⁰¹ its thermodynamic functions⁶⁸ and $C_p^\circ = f(T)$, and the temperatures and enthalpies of the phase transitions.^{102, 103}

The enthalpies of the polymerisation of isobutene have been published.^{104–107} In order to determine the thermodynamic parameters of the polymerisation, the value of $\Delta_{\text{pol}} H^\circ(\text{gas; a})$ at 298.15 K, given by Parks and Mocher,¹⁰⁷ was selected. All the other data necessary for the calculations were found in publications describing the temperature variations of the heat capacities and the temperatures and enthalpies of the physical transformations for polyisobutylene^{74–76} and isobutene.^{103, 108}

The limiting polymerisation temperatures, estimated from Eqns (10), amounted to 670 K for ethene and 550 K for propene; the estimation of this parameter for isobutene by Dainton's method¹³ yielded 390 K.

The thermodynamic parameters of the processes leading to the formation of isotactic polybut-1-ene (Scheme 1) for the temperature range 0–600 K under standard pressure have been published by Lebedev et al.⁶⁹ The enthalpies of the processes at 298.15 K and 101.325 kPa were calculated from the standard enthalpies of formation of the monomers, taken from Stull et al.,¹⁰³ and the enthalpies of formation of the polymer (Table 5). For other temperatures, the enthalpies of the processes $\Delta_r H^\circ$ were calculated from the temperature variation of the heat capacity and the temperatures and enthalpies of the phase transitions of the reactants quoted in the literature^{69, 109} and in Tables 2 and 5. The entropies of the processes $\Delta_r S^\circ$ were calculated from the absolute entropies of the reactants, while the Gibbs free energies $\Delta_r G^\circ$ were evaluated from the values of $\Delta_r H^\circ$ and $\Delta_r S^\circ$ for the corresponding temperatures.

Scheme 1



The upper limiting temperatures T_{cel}° for the direct conversion of but-1-ene, *cis*- and *trans*-but-2-enes, and ethene into isotactic polybut-1-ene (processes 1, 3, 4, and 2) were estimated by Dainton's method¹³ from the quantities $\Delta_r H^\circ$ and $\Delta_r S^\circ$ for the polymerisation reaction. They are respectively 520, 500, 490, and 640 K.

The following relations hold at different temperatures:

$$\Delta_r G^\circ < 0 \text{ at } T < T_{\text{cel}}^\circ,$$

$$\Delta_r G^\circ = 0 \text{ at } T = T_{\text{cel}}^\circ,$$

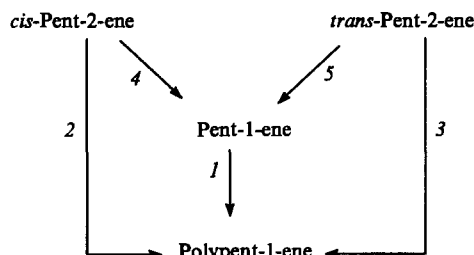
$$\Delta_r G^\circ > 0 \text{ at } T > T_{\text{cel}}^\circ.$$

This means that at $T < T_{\text{cel}}^\circ$ the equilibria in the processes are displaced towards the formation of the polymer and the polymer produced is thermodynamically stable in relation to depolymerisation to the initial monomer; at $T > T_{\text{cel}}^\circ$, the polymer is unstable in relation to the above monomers and rapidly depolymerises under kinetic conditions. In contrast to processes 3 and 4, processes 5 and 6 have lower limiting temperatures — 830 and 910 K respectively. It has been shown^{3, 110} that isotactic polybut-1-ene can be obtained from *cis*- and *trans*-but-2-enes after their

isomerisation to but-1-ene, the yield of the polymer being low. This can be explained by the fact that, since $\Delta_r G^\circ$ for processes 5 and 6 is positive, the equilibrium concentration of but-1-ene in the reaction mixture is low. The reaction equilibrium is displaced towards an increase in the concentrations of but-1-ene with increase in temperature, since $\Delta_r G^\circ$ diminishes. This should increase the yield of polybut-1-ene.

The poly-pent-1-ene formation reactions may be represented by the Scheme 2:

Scheme 2



Chao and Hell¹¹¹ calculated the thermodynamic parameters of processes 1–5 for the temperature range 0–500 K from the results of Lebedev et al.⁷⁷ and the corresponding data on the initial monomers,^{77,111} the enthalpies of the processes at 298.15 K from the enthalpies of formation of the reactants (see Table 5 and Lebedev et al.⁷⁷ and Chao and Hell¹¹¹), and the enthalpies of the processes at other temperatures from the Kirchhoff formula [Eqn (9)]. The temperature variations of the heat capacities and the temperatures and enthalpies of the physical transformations of the reactants were used in the calculations (see Tables 2–4 and Lebedev et al.⁷⁷ and Chao and Hell¹¹¹). The results show that the monomer \rightleftharpoons polymer equilibria in processes 1–3 are displaced towards the formation of poly-pent-1-ene: over the entire temperature range investigated, $\Delta_{\text{pol}} G^\circ < 0$; the absolute values of $\Delta_{\text{pol}} G^\circ$ for the processes decrease with increase in temperature. The enthalpies and entropies of these processes are also negative, which is the reason for the existence of the upper limiting polymerisation temperatures T_{ceil}° . Estimation by Dainton's method¹³ yielded the following values: 590 K for process 1, 560 K for process 2, and 550 K for process 3. Evidently, the thermodynamic characteristics of the polymerisation reactions of the isomeric pentenes diminish in the sequence pent-1-ene > cis-pent-2-ene > trans-pent-2-ene.

One should bear in mind that poly-pent-1-ene is not obtained directly in processes 2 and 3;³ its formation is preceded by the stage involving the conversion of *cis* and *trans*-pent-2-enes into pent-1-ene (processes 4 and 5). The $\Delta_r G^\circ$ for these processes are positive. This means that the reaction equilibrium is displaced to the left. However, since at elevated temperatures the Gibbs free energies $\Delta_r G^\circ$ of the processes are small, the equilibrium reaction mixtures contain a certain amount of pent-1-ene formed from *cis* and *trans*-pent-2-enes. For example, at 500 K the mole fractions of pent-1-ene in the reaction mixture are ~ 0.20 (process 4) and ~ 0.10 (process 5). These concentrations were calculated from the thermodynamic equilibrium constants for these processes K_r° , which were in their turn evaluated from the equation of the van't Hoff isotherm.

As the temperature decreases, the equilibrium concentrations of pent-1-ene in the above processes also decrease. This is the reason for the low rates of conversion of *cis* and *trans*-pent-2-enes into poly-pent-1-ene and the low yield of the polymer during the reaction time. This situation may be altered as a result of the search for more effective isomerisation catalysts, an increase in the concentration of the catalyst in the reaction mixture, or the discovery of physicochemical conditions leading to the displacement of the equilibria 4 and 5 to the right. However, one should bear in mind that the increase of, for example, the pressure does not shift the equilibrium because reactions 4 and 5 proceed without change in the number of moles of the reactants. Varia-

tion of the solvent is also apparently relatively ineffective, since the physicochemical properties of the isomers are similar and the nature of their interaction with the solvent is virtually the same.

An increase in temperature may be comparatively effective. Extrapolation of the $\Delta_r H^\circ = f(T)$ and $T\Delta_r S^\circ = f(T)$ relations for the process under consideration leads to temperatures of 2800 and 1700 K at which the $\Delta_r G^\circ$ for processes 4 and 5 changes sign (from plus to minus). However, the upper limiting temperature of the polymerisation of pent-1-ene is only 590 K, so that the limits within which the temperature can be varied are restricted.

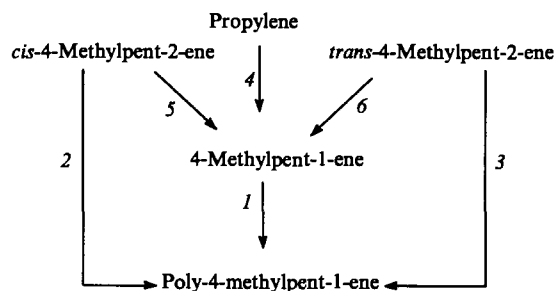
The thermodynamic parameters of the polymerisation of 3-methylbut-1-ene have no singularities of any kind:^{78,111} $\Delta_{\text{pol}} H^\circ$ and $\Delta_{\text{pol}} S^\circ$ are negative throughout and their absolute values increase with increasing temperature; the Gibbs free energy of polymerisation is negative, diminishing with increase in temperature; the upper limiting polymerisation temperature is $T_{\text{ceil}}^\circ = 572$ K.

The enthalpy of the polymerisation of liquid hex-1-ene to highly elastic polyhex-1-ene at 298.15 K and 101.325 kPa is -101 kJ mol⁻¹. This value was obtained by the author of the present review from the enthalpies of formation of the liquid monomer $\Delta_f H^\circ(298.15 \text{ K}) = -72.38$ kJ mol⁻¹ (see Ref. 103) and the highly elastic polymer $\Delta_f H^\circ(298.15 \text{ K}) = 173.6$ kJ mol⁻¹, calculated from the equation quoted by Lebedev and Kiparisova.⁴⁶ The calculated enthalpy of the polymerisation of hex-1-ene, $\Delta_{\text{pol}} H^\circ = -82.8$ kJ mol⁻¹, published by Lebedev and Lebedev,⁹⁶ is significantly too low.

The thermodynamic functions of hex-1-ene in the range 0–300 K have been published by Lebedev and Lebedev.⁹⁶ All these data, together with the results presented in Table 4, have been used to calculate the thermodynamic parameters of the polymerisation of hex-1-ene in bulk in the range 0–300 K (Table 6). Evidently the change in the standard Gibbs free energy $\Delta_{\text{pol}} G^\circ(T)$ is negative throughout, while the numerical values are such that one may conclude that the equilibrium is almost fully displaced to the right. Extrapolation based on the $\Delta_{\text{pol}} H^\circ(T) = f(T)$ and $T(\Delta_{\text{pol}} G^\circ(T)) = f(T)$ relations for the liquid monomer \rightarrow highly elastic polymer process leads to an upper limiting polymerisation temperature of 865 K. The thermodynamic equilibrium concentration of the monomer in the reaction mixture $[M]_e^\circ = 2 \times 10^{-12}$ M was estimated from the equation of the van't Hoff isotherm and the value of $\Delta_{\text{pol}} G^\circ(300 \text{ K})$.

The reactions leading to the formation of isotactic poly-4-methylpent-1-ene may be represented by the Scheme 3:

Scheme 3



The reactions leading to the polymerisation of 4-methylpent-1-ene and *cis* and *trans*-4-methylpent-2-enes to poly-4-methylpent-1-ene in bulk and the reaction in which propene dimerises to 4-methylpent-1-ene have upper limiting polymerisation temperatures which are respectively 590, 540, 530, and 570 K. The numerical values of T_{ceil}° were found graphically from the intersection of the corresponding temperature variations of the enthalpies and the entropy factors: $\Delta_r H^\circ = f(T)$ and $T\Delta_r S^\circ(T) = f(T)$. The enthalpies and entropies were taken from Table 6. At $T < T_{\text{ceil}}^\circ$, the equilibria in processes 1–4 in Scheme 3 are displaced towards the formation of the reaction products ($\Delta_r G^\circ < 0$). The enthalpies and entropies of these processes are

Table 6. The enthalpies (kJ mol^{-1}), entropies ($\text{J mol}^{-1} \text{K}^{-1}$), and Gibbs free energies (kJ mol^{-1}) of the polymerisation of olefins in bulk with formation of polyolefins under standard pressure.

T/K	Physical state of reactants ^a	$-\Delta_{\text{pol}}H^\circ$	$-\Delta_{\text{pol}}S^\circ$	$-\Delta_{\text{pol}}G^\circ$	T/K	Physical state of reactants ^a	$-\Delta_{\text{pol}}H^\circ$	$-\Delta_{\text{pol}}S^\circ$	$-\Delta_{\text{pol}}G^\circ$
Ethene \rightarrow polyethylene ^b					<i>trans</i>-But-2-ene \rightarrow polybut-1-ene ⁶⁹				
0	cr;cr	86.50	0	86.50	200	l;cr	70.9	99.9	50.9
	cr;g	80.95	-5.4	80.95		l;g	67.2	93.2	48.6
100	cr;cr	88.59	34.9	85.10	298.15	gas;cr	96.4	195	38.3
	cr;g	82.92	26.7	80.25		gas;h.e	91.5	184	36.8
200	gas;cr	108.7	171	74.44	400	gas;cr	95.7	193	18.6
	gas;g	102.7	161	70.42		gas;h.e	88.7	175	18.6
298.15	gas;cr	108.8	172	57.52	500	gas;l	83.0	170	-1.9
	gas;h.e	101.4	156	54.80	600	gas;l	80.4	165	-18.6
400	gas;cr	108.8	172	40.04	Isobutene \rightarrow polyisobutylene ^c				
	gas;h.e	99.63	151	39.11	0	cr;g	37	-5.7	37
500	gas;l	98.61	148	24.81	50	cr;g	37	2.6	37
600	gas;l	97.02	145	10.20	100	cr;g	39	20.3	36
Propene \rightarrow polypropylene ^b					150	l;g	47	81.7	34
0	cr;cr	76.65	0	76.65	200	l;h.e	49	97.1	30
	cr;g	72.44	-1.1	72.44	250	l;h.e	51	102.5	25
100	l;cr	82.07	74.8	74.59	298.15	gas;h.e	72	183.5	17
	l;g	77.67	69.6	70.72	300	gas;h.e	72	184.1	17
200	l;cr	87.14	111	64.90	350	gas;h.e	71	180.1	8
	gas;g	82.55	105	61.61	380	gas;h.e	70	178.2	2
298.15	gas;cr	106.5	198	47.59	Pent-1-ene \rightarrow polypent-1-ene ⁷⁷				
	gas;h.e	100.8	187	45.11	0	cr;cr	82	0	82
400	gas;cr	106.3	197	27.50		cr;g	80	-4	80
	gas;h.e	98.37	180	26.45	100	cr;cr	84	24	81
500	gas;l	95.96	175	8.71		cr;g	81	20	80
But-1-ene \rightarrow polybut-1-ene ⁶⁹					200	l;cr	95	117	72
0	cr;cr	71.8	0	71.8		l;g	93	113	70
	cr;g	68.1	6.7	68.1	298.15	l;cr	99	133	60
	gas;cr	78.1	12.8	71.8		l;h.e	95	124	58
	gas;g	68.1	6.1	68.1	300	l;cr	99	133	59
100	l;cr	77.8	75.5	70.2		l;h.e	95	125	58
	l;g	74.1	68.9	67.2	400	gas;l	117	198	38
200	l;cr	83.1	114	57.2	500	gas;l	113	190	18
	l;g	79.5	107	58.0	<i>cis</i>-Pent-2-ene \rightarrow polypent-1-ene ⁷⁷				
298.15	gas;cr	108	207	45.8	0	cr;cr	73	0	73
	gas;h.e	103	196	44.3		cr;g	71	-4	71
400	gas;cr	107	204	25.4	100	cr;cr	75	20	73
	gas;h.e	99.7	187	24.8		cr;g	72	16	71
500	gas;l	94.0	182	3.2	200	l;cr	87	114	64
600	gas;l	91.0	177	-14.7		l;g	85	111	63
<i>cis</i>-But-2-ene \rightarrow polybut-1-ene ⁶⁹					298.15	l;cr	91	129	52
0	cr;cr	61.6	0	61.6		l;h.e	87	120	51
	cr;g	58.0	-6.7	58.0	300	l;cr	90	129	52
100	cr;cr	62.9	20.7	60.8		l;h.e	87	121	51
	cr;g	59.3	14.0	57.9	400	gas;l	109	195	31
200	l;cr	74.8	106	53.6	500	gas;l	105	185	12
	l;g	71.1	99.0	51.3	<i>trans</i>-Pent-2-ene \rightarrow polypent-1-ene ⁷⁷				
298.15	gas;cr	101	201	40.8	0	cr;cr	69	0	69
	gas;h.e	95.7	190	39.2		cr;g	67	-4	67
400	gas;cr	99.0	196	20.5	100	cr;cr	70	18	69
	gas;h.e	92.1	179	20.4		cr;g	68	14	66
500	gas;l	85.7	172	0.3	200	l;cr	83	111	61
600	gas;l	82.6	166	-17.2		l;g	81	102	59
<i>trans</i>-Бутен-2 \rightarrow полибутен-1 ⁶⁹					298.15	l;cr	87	127	49
0	cr;cr	56.3	0	56.3		l;h.e	83	118	48
	cr;g	52.7	-6.7	52.7	300	l;cr	87	127	49
100	cr;cr	57.4	17.0	55.7		l;h.e	83	119	48
	cr;g	53.8	10.3	52.7	400	gas;l	106	194	29
					500	gas;l	103	186	10

Table 6 (continued).

<i>T</i> /K	Physical state of reactants ^a	$-\Delta_{\text{pol}}H^\circ$	$-\Delta_{\text{pol}}S^\circ$	$-\Delta_{\text{pol}}G^\circ$	<i>T</i> /K	Physical state of reactants ^a	$-\Delta_{\text{pol}}H^\circ$	$-\Delta_{\text{pol}}S^\circ$	$-\Delta_{\text{pol}}G^\circ$
3-Methylbut-1-ene → poly-3-methylbut-1-ene⁷⁸					4-Methylpent-1-ene → poly-4-methylpent-1-ene⁸⁰				
0	cr;cr	71	0	71	298.15	l;cr	99	131	60
	cr;g	70	0	70		l;g	94	122	58
100	cr;cr	73	20	71	400	gas;cr	126	214	41
	cr;g	72	20	70		gas;h.e	118	198	39
200	l;cr	84	112	61	500	gas;cr	124	209	19
	l;g	83	112	60		gas;h.e	114	189	20
298.15	gas;cr	112	211	49	600	gas;l	107	175	-2
	gas;g	111	211	48	<i>cis</i>-4-Methylpent-2-ene → poly-4-methylpent-1-ene⁸⁰				
400	gas;cr	112	211	28	298.15	l;cr	93	134	53
	gas;h.e	109	206	27		l;g	87	126	49
500	gas;cr	111	210	6	400	gas;cr	121	220	33
	gas;h.e	107	201	6		gas;h.e	110	197	31
600	gas;l	104	198	-14	500	gas;cr	119	215	12
640	gas;l	104	196	-22		gas;h.e	113	207	9.5
Hex-1-ene → polyhex-1-ene⁹⁶					600	gas;l	103	183	-7
0	cr;g	84	-7.3	84	<i>trans</i>-4-Methylpent-2-ene → poly-4-methylpent-1-ene⁸⁰				
50	cr;g	85	-2.3	85	298.15	l;cr	88	130	49
100	cr;g	86	9.9	84		l;g	82	128	44
150	l;g	97	94.3	83	400	gas;cr	117	216	31
200	l;g	100	111	78		gas;h.e	106	194	28
250	l;h.e	101	116	72	500	gas;cr	115	214	8
298.15	l;h.e	101	118	66		gas;h.e	102	186	9
300	l;h.e	101	118	66	600	gas;l	99	182	-10
4-Methylpent-1-ene → poly-4-methylpent-1-ene⁸⁰					Dec-1-ene → polydec-1-ene⁸⁴				
0	cr;cr	82	0	82	0	crII;crII,crI	97	0	97
	cr;g	77	-8	77		crII;g	89	-26	89
	g;cr	84	15	84	100	crII;crII,crI	98	13	97
	g;g	79	7	79		crII;g	90	-13	91
100	cr;cr	83	28	80	200	crI;crII,crI	108	68	95
	cr;g	78	20	76		crI;g	100	42	92
	ov.l;cr	87	60	81	298.15	l;crI	123	141	81
	ov.l;g	82	52	77		l;h.e	116	118	81
200	l;cr	94	111	72	350	l;l	117	121	75
	l;g	89	103	69	400	l;l	118	123	69
					450	l;l	119	125	62

^a The following designations of the states of the polymers have been adopted: l — liquid, gas — gaseous, ov.l — supercooled liquid.

^b L Ya Tsvetkova's data. ^c N Smirnova's data.

negative throughout and their numerical values depend on the physical state of the reactants and increase with increasing temperature.

The isomerisation reactions of *cis* and *trans*-4-methylpent-2-enes (processes 5 and 6) have neither an upper nor a lower limiting temperature, which is characteristic of processes for which $\Delta_r H^\circ > 0$ and $\Delta_r S^\circ < 0$.¹¹ For this reason, the change in the Gibbs free energy is positive. In processes 5 and 6 under consideration, the free energies $\Delta_r G^\circ$ have small positive values: $\Delta_r G^\circ < 10 \text{ kJ mol}^{-1}$. This means that a small amount of 4-methylpent-1-ene is present in the equilibrium reaction mixture of the isomers. In this case, a shift of the equilibrium is possible provided that 4-methylpent-1-ene is continuously removed from the reaction mixture, for example when it is polymerised to poly-4-methylpent-1-ene, which does in fact occur in the isomeric polymerisation of *cis*- and *trans*-alk-2-enes to polyalk-1-enes.³

Owing to the similarity of the heat capacities of 4-methylpent-1-ene and the *cis*- and *trans*-isomers of 4-methylpent-2-enes, the influence of temperature on $\Delta_r H^\circ(T)$ and $\Delta_r S^\circ(T)$ is small. The enthalpies of the processes were calculated from the enthalpies of formation of 4-methylpent-1-ene,¹¹² *cis*- and *trans*-methylpent-2-enes,¹⁰³ propene,¹⁰³ and poly-4-methylpent-1-ene.⁸⁰ The entropies of the reactants required for the calculation of $\Delta_r S^\circ(T)$ were taken from Lebedev et al.⁸⁰ and Stull et al.¹⁰³

As for other olefins, the enthalpy and entropy of the polymerisation of dec-1-ene are negative throughout.⁸⁴ It follows from this that the polymerisation process has an upper limiting temperature. Indeed, $\Delta_{\text{pol}} G^\circ(T)$ decreases in absolute magnitude with increase in temperature and becomes zero at $T_{\text{ceil}}^\circ = 890 \text{ K}$, while at $T > T_{\text{ceil}}^\circ$ it is positive throughout. T_{ceil}° was estimated by Dainton's method.¹³ The T_{ceil}° obtained is apparently appreciably higher than the temperature of the onset of the thermal degradation of the polymer.

X. Principal regularities and characteristics of the thermodynamic properties of polyolefins and of the parameters of their formation reactions[†]

1. Thermodynamic functions

Since the C₂-C₆ and C₁₀ polyolefins with linear side substituents which have been investigated differ from one another by the number of methylene groups in these substituents, one may expect, for the same physical state of the polymers and under identical temperatures and pressures, a regular change in the thermodynamic properties as a function of the number of carbon atoms *n* in the repeat units of the polymers, as happens, for example, in the paraffins,¹¹³ polyalkenes,⁷ polyaldehydes,¹¹⁴ and polylactones.⁶⁴

The existence of such relations is due to the regular additive contribution of the methylene groups to the corresponding properties of the above polymers. It was found that this is fully valid also for polyolefins. As an example, Figs 9–11 present the isotherms (298.15 K) of the thermodynamic properties of polyolefins. Evidently, the dependences of the heat capacity *C_p*^o, the enthalpy *H*^o(*T*) – *H*^o(0), the entropy *S*^o(*T*), and the Gibbs free energy on *n* are represented by straight lines described satisfactorily by the equations

$$C_p^o(\text{cr}) = -8 + 25.5n, \quad (11)$$

$$C_p^o(\text{h.e.}) = 8 + 27.8n, \quad (12)$$

$$[H^o(T) - H^o(0)](\text{cr}) = -1.1 + 4.0n, \quad (13)$$

$$[H^o(T) - H^o(0)](\text{h.e.}) = -2.42 + 4.68n, \quad (14)$$

$$S^o(\text{cr}) = -21.2 + 30.2n, \quad (15)$$

$$S^o(\text{h.e.}) = -17.8 + 32.2n, \quad (16)$$

$$[G^o(T) - H^o(0)](\text{cr}) = 6.1 - 5.2n, \quad (17)$$

[†]Prepared jointly with the senior scientific member of the Institute of Chemistry at the Nizhni Novgorod State University, Candidate in Chemical Sciences N N Smirnova.

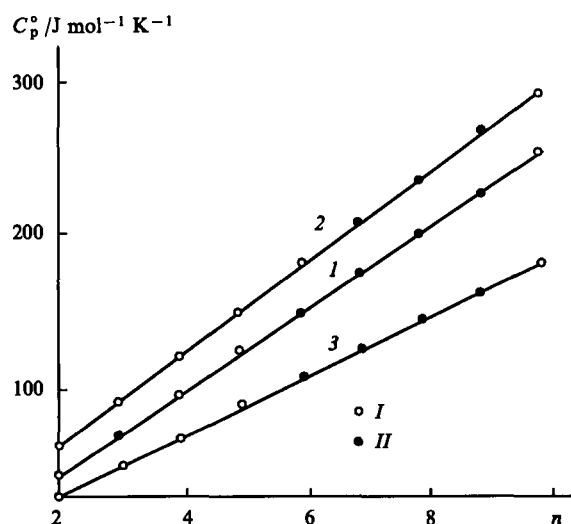


Figure 9. Isothermal dependences of the heat capacities of polyolefins with linear side substituents on the number of carbon atoms *n* in the monomer repeat unit.

State of the polymer: (I) crystalline; (2) highly elastic at *T* = 298.15 K; (3) crystalline and vitreous at *T* = 200 K; (I) experimental values; (II) extrapolated data.

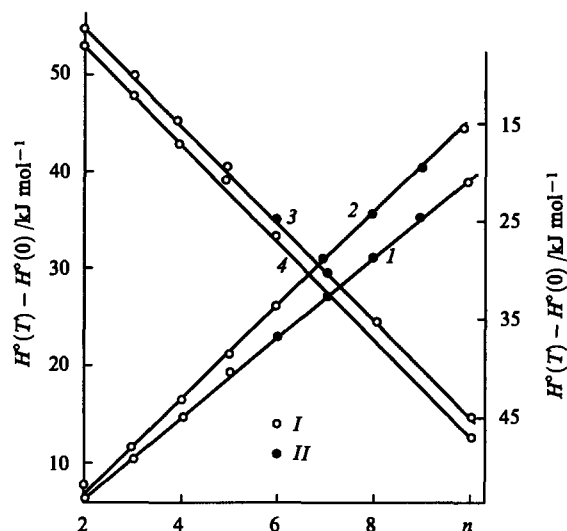


Figure 10. Isothermal dependences of the enthalpies (1, 2) and Gibbs free energies (3, 4) of polyolefins with linear side substituents on the number of carbon atoms *n* in the monomer repeat unit at 298.15 K.

State of the polymer: (I) and (3) highly elastic; (2) and (4) crystalline; (I) experimental values; (II) extrapolated data.

$$[G^o(T) - H^o(0)](\text{h.e.}) = 3.5 - 5.1n. \quad (18)$$

The equations were obtained using experimental *C_p*^o data and data calculated from the temperature variations of the heat capacities, the temperatures and enthalpies of the physical transformations, and the enthalpies, entropies, and Gibbs free energies of the polyolefins investigated. The corresponding experimental values of *C_p*^o agree, subject to an error to within 2.5%, with the heat capacities calculated by Eqns (11) and (12); the enthalpies calculated by Eqns (13) and (14) and the entropies calculated by Eqns (15) and (16) agree with experimental values to within 2% and 3% respectively. This makes it possible in its turn to estimate the numerical values for a series of hitherto uninvestigated polyolefins in the same physical states and for the same physical conditions. The results of these estimates by Eqns (11)–(18) are presented in Table 7 for the closest analogues of the polyolefins investigated. We suggest that the errors of these estimates for *C_p*^o, *H*^o(*T*) – *H*^o(0), *S*^o, and *G*^o(*T*) – *H*^o(0) are within the limits of 3%.

Table 7. Thermodynamic functions of a series of higher polyolefins calculated by Eqns (11)–(18) for *T* = 298.15 K and *p* = 101.325 kPa.

Substance	Physical state	<i>C_p</i> ^o (<i>T</i>)	<i>S</i> ^o (<i>T</i>)	<i>H</i> ^o (<i>T</i>) – <i>H</i> ^o (0)	– [<i>G</i> ^o (<i>T</i>) – <i>H</i> ^o (0)]
		/J mol ^{–1} K ^{–1}		/kJ mol ^{–1}	
Polyhept-1-ene	cr	171	190	26.9	29.7
	h.e	203	208	30.3	31.7
Polyoct-1-ene	cr	196	220	30.9	34.7
	h.e	230	240	35.0	36.6
Polynon-1-ene	cr	222	251	34.9	39.9
	h.e	258	272	39.7	41.4
Polyundec-1-ene	cr	273	311	42.9	49.8
	h.e	314	336	49.1	51.1
Polydodec-1-ene	cr	298	341	46.9	54.8
	h.e	342	369	53.7	56.3

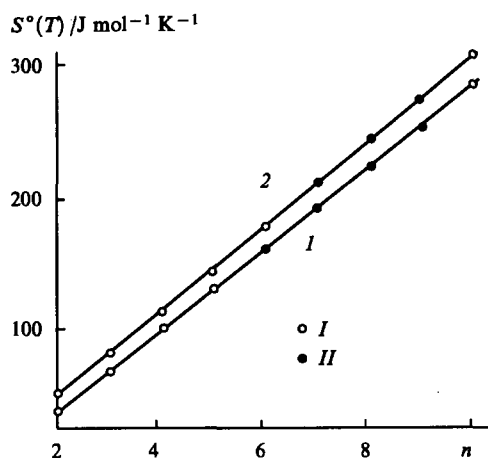


Figure 11. Isothermal dependences of the entropies of polyolefins with linear side substituents on the number of carbon atoms n in the monomer repeat unit.

State of the polymer: (I) crystalline; (2) highly elastic at $T = 298.15$ K; (I) experimental values; (II) extrapolated data.

2. Thermochemical parameters of the formation reactions

The enthalpies of combustion $\Delta_c H^\circ$ and formation $\Delta_f H^\circ$ and the entropies of formation $\Delta_f S^\circ$ of the C_2 – C_6 polyolefins investigated as well as their thermodynamic functions are described satisfactorily by the relations between the thermochemical parameters and the number of carbon atoms in the monomer repeat unit in the macromolecule. At $T = 298.15$ K and the standard pressure, we have

$$\Delta_c H^\circ(\text{cr}) = -4.3 - 648.95 n, \quad (19)$$

$$\Delta_c H^\circ(\text{h.e.}) = -7.97 - 649.5 n, \quad (20)$$

$$\Delta_f H^\circ(\text{cr}) = 4.4 - 30.4 n, \quad (21)$$

$$\Delta_f H^\circ(\text{h.e.}) = 8.35 - 29.9 n. \quad (22)$$

The deviations of the experimental enthalpies of combustion from the corresponding straight lines [Eqns (19) and (20)] are within the limits of 2.3% and the deviations of the enthalpies of formation [Eqns (21) and (22)] are within the limits of 5%.

Under the same physical conditions, the entropies of formation of the polyolefins considered are described by the following equations

$$\Delta_f S^\circ(\text{cr}) = -6.1 - 108 n, \quad (23)$$

$$\Delta_f S^\circ(\text{h.e.}) = -3.8 - 105.4 n. \quad (24)$$

Table 8. The enthalpies of combustion and thermochemical parameters of the formation of a series of higher polyolefins calculated by Eqns (19)–(24) for $T = 298.15$ K and $p = 101.325$ kPa.

Substance	Physical state	$-\Delta_c H^\circ$ /kJ mol ⁻¹	$-\Delta_f H^\circ$	$\Delta_f G^\circ$	$-\Delta_f S^\circ$ /J mol ⁻¹ K ⁻¹
Polyhept-1-ene	cr	4547	208.4	18.8	762
	h.e.	4554	201.0	20.2	742
Polyoct-1-ene	cr	5196	238.8	20.6	870
	h.e.	5204	230.9	21.6	847
Polynon-1-ene	cr	5845	269.2	22.4	978
	h.e.	5853	260.8	23.0	952
Polyundec-1-ene	cr	7143	330.0	26.0	1194
	h.e.	7152	320.6	26.2	1163
Polydodec-1-ene	cr	7792	360.4	27.8	1302
	h.e.	7802	350.5	27.9	1269

The deviations of the experimental values of $\Delta_f S^\circ$ from the calculated entropies are within the limits of 2%.

The relations discovered also made it possible to estimate the corresponding thermodynamic characteristics for the hitherto uninvestigated polyolefins and to calculate $\Delta_f G^\circ$ from the values of $\Delta_f H^\circ$ and $\Delta_f S^\circ$ for these substances (Table 8).

3. Thermodynamic parameters of fusion

Polymorphism is characteristic of higher polyolefins.^{72, 90} Starting with polydecene,⁸⁶ two types of crystals appear on crystallisation: those formed by the main chains of the macromolecules and by the side substituents respectively. The thermodynamic parameters of the fusion of various crystalline modifications of the same polyolefin differ markedly. For example, the crystalline form III of polybut-1-ene melts at 374 K, while form I melts at 407 K; the enthalpies and entropies of the fusion of these forms are respectively 2.67 and 7.11 kJ mol⁻¹ and 7.14 and 17.5 J mol⁻¹ K⁻¹. The melting points of the polydec-1-ene crystals formed by the main chains and side substituents (276 and 301 K) differ by 25 K, whereas their enthalpies and entropies of fusion differ only slightly. For the majority of polyolefins, having several crystalline modifications the thermodynamic parameters of the fusion of one or two have been investigated. For example, poly-4-methylpent-1-ene is known to be capable of forming five different crystalline modifications.⁸⁰

The thermodynamic characteristics of only one of them have been investigated hitherto (Table 2).⁸⁰ Owing to the insufficient amount of experimental data, the search for quantitative regularities in the thermodynamic characteristics of the fusion of polyolefins is so far difficult. One may only note that, among the polyolefins investigated, polydecene has the lowest melting point (276 K). Crystals of form II, formed from the main chain, melt at this temperature. The highest melting point is that of poly-4-methylpent-1-ene (508 K). Polybut-1-ene (crystalline form III) has the lowest enthalpy of fusion (2.67 kJ mol⁻¹), whilst poly-4-methylpent-1-ene has the highest enthalpy of fusion (10.24 kJ mol⁻¹). The entropies of fusion of polyolefins are in the range from 7 to 20 J mol⁻¹ K⁻¹.

4. Parameters of the vitrification process and of the vitreous state

The glass transition temperatures of polyolefins with linear side chains decrease from 249 K for polybut-1-ene to 208 K for polydec-1-ene. For polyolefins with branched side substituents, T_g° is greater than for polyolefins with unbranched substituents. For example, the glass transition temperatures of poly-3-methylbut-1-ene and poly-4-methylpent-1-ene are respectively 327 and 300 K. T_g° for poly-3-methylbut-1-ene is higher by 100 K than for its structural isomer poly-4-methylpent-1-ene, while T_g° for poly-4-methylpent-1-ene is higher than that for polyhex-1-ene. This interesting fact requires additional analysis.

The increase in heat capacity on devitrification $\Delta C_p^\circ(T_g^\circ)$ is in the range from 21 to 34 J mol⁻¹ K⁻¹ for all the polyolefins investigated and corresponds, on according to Wunderlich,⁸³ to between 2.5 and 3 'beads' — kinetically independent atomic groups — in the monomer repeat unit of the polymer. However, $\Delta C_p^\circ(T_g^\circ) = 60$ J mol⁻¹ K⁻¹ for polydec-1-ene, which corresponds to virtually five 'beads'. Clearly this is due to the appearance of additional independently vibrating atomic groups in connection with the increase in the length of the side substituent.

In the vitreous state at $T = 0$ K, the entropies of the polymers $S_g^\circ(0)$ are small for the majority of higher polyolefins, varying from 0 for poly-3-methylbut-1-ene to 8 for poly-4-methylpent-1-ene. The fact that $S_g^\circ(0)$ is zero for poly-3-methylbut-1-ene is associated with the characteristic features of its structure in the crystalline and vitreous states, the same as for poly-4-methylpent-1-ene, which have been examined in detail.⁸⁰ The main reason is that in the crystalline polymer the packing density of the fragments of the macromolecules is smaller than in the vitreous

polymer. In particular, this leads to a decrease in T_g° as well as the density of such polymers with increase in the degree of crystallinity. Conversely, these parameters increase as the polymer passes from the partly crystalline to the amorphous glassy state.

The value $S_g^\circ(0) = 26 \text{ J mol}^{-1} \text{ K}^{-1}$, usual for amorphous polymers, has been observed for polydec-1-ene. For understandable reasons, the polymers in the vitreous state have an excess enthalpy compared with the crystalline state. In polyolefins, this excess $H_g^\circ(T) - H_{cr}^\circ(0)$ varies from 2 J mol^{-1} for poly-3-methylbut-1-ene to 8.4 J mol^{-1} for polydec-1-ene.

5. Thermodynamic characteristics of polymerisation reactions

In the temperature range investigated, the formation reactions of the higher polyolefins by the polymerisation of the corresponding monomers in bulk under standard pressure are thermodynamically allowed. The standard Gibbs free energy $\Delta_{pol}G^\circ$ is negative throughout. At 298.15 K and the standard pressure, $\Delta_{pol}G^\circ$ is in the range from 80 kJ mol^{-1} for the polymerisation reaction of but-1-ene to 116 kJ mol^{-1} for the polymerisation of dec-1-ene (the monomers and the polymers are in the liquid and highly elastic states respectively). Clearly the monomer \rightleftharpoons polymer reaction equilibrium is almost fully displaced towards the formation of the polymer. The enthalpies $\Delta_{pol}H^\circ$ and entropies $\Delta_{pol}S^\circ$ are also negative, so that all the processes considered have the corresponding upper limiting polymerisation temperatures. It is noteworthy that they are all comparatively high and are in the range from 390 K for polyisobutylene to 890 K for polydec-1-ene.

Figure 12 presents the dependences of the enthalpies, entropies, and Gibbs free energies for the polymerisation of olefins in bulk with formation of the corresponding higher polyolefins at 298.15 K and 101.325 kPa on the number of carbon atoms n in the molecules of the initial olefins and the corresponding monomer repeat units in the polymer macromolecules produced (the monomers and polymers were in the liquid and highly elastic states respectively). Evidently, the enthalpies (heats) of the polymerisation reactions increase smoothly from ethene ($n = 2$) to dec-1-ene ($n = 10$), curve 1 tending to a constant value of $\Delta_{pol}H^\circ$ with increase in n .

Lebedev and Rabinovich¹¹⁸ showed that the enthalpy of the polymerisation of a monomer via a C=C bond may be represented by the following sum:

$$\Delta_{pol}H^\circ(T) = \Delta E_{at} + \Delta E_{conj} + \Delta E_{s.s.} + \Delta E_{mol} + \Delta[H^\circ(T) - H^\circ(0)], \quad (25)$$

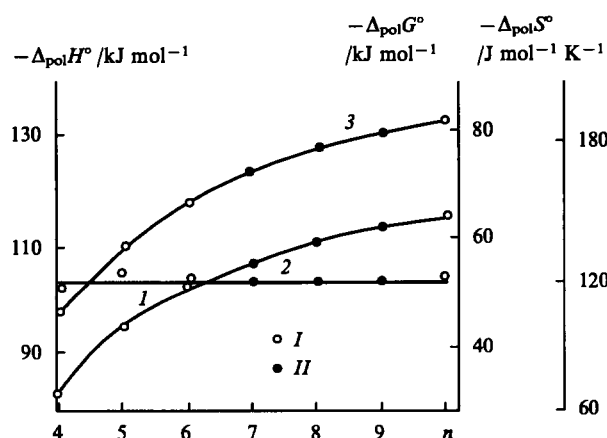


Figure 12. The enthalpies (I), entropies (2), and Gibbs free energies (3) of the polymerisation of olefins in bulk at $T = 298.15 \text{ K}$ and the standard pressure. Monomers and polymers in the liquid and highly elastic states respectively; (I) experimental values; (II) extrapolated data.

where ΔE_{at} is the difference between the average energies of the atomic C=C bond being ruptured and the two atomic C—C bonds being formed, ΔE_{conj} is the difference between the conjugation energies of the atomic bonds in the monomer and the polymer, $\Delta E_{s.s.}$ is the difference between the energies of the steric strain in the polymer and the monomer, ΔE_{mol} the difference between the energies of the intermolecular interaction in the monomer and the polymer at 0 K, and $\Delta[H^\circ(T) - H^\circ(0)]$ the difference between the energies associated with the heating of the polymer and the monomer. It is known that $\Delta E_{at} = 88 \text{ kJ mol}^{-1}$, $\Delta E_{conj} = 9 \text{ kJ mol}^{-1}$ (the hyperconjugation energy in the monomer), $\Delta E_{s.s.} < 4 \text{ kJ mol}^{-1}$ for the polymerisation reactions of monosubstituted vinyl monomers, and $\Delta E_{mol} = 34 \text{ kJ mol}^{-1}$ for the monomers having the same structure. It is found that the change of $\Delta_{pol}H^\circ$ is caused solely by the contribution of $\Delta[H^\circ(T) - H^\circ(0)]$. In fact, the experimental values of $\Delta[H^\circ(T) - H^\circ(0)]$ increase with increase in n and agree, within the limits of the error of the calculations and the assumptions made, with the values obtained by converse calculation from Eqn (25). For example, the experimental and calculated values of $\Delta[H^\circ(T) - H^\circ(0)]$ are 34 and 32 kJ mol^{-1} respectively for the polymerisation of but-1-ene; for polypent-1-ene, the respective values are 40 and 41 kJ mol^{-1} . In both cases, the monomer and the polymer are in the gaseous and highly elastic states respectively at 298.15 K; under these conditions, Eqn (25) yields the best results.

The entropy of polymerisation $\Delta_{pol}S^\circ$ (the monomer and polymer are in the liquid and highly elastic states respectively) at 298.15 K is approximately constant. The decrease in the entropy of the reaction is caused mainly by the formation of chains and corresponds to the rule established by Dainton and Ivin.¹³ According to this rule, the polymerisation of liquid monomers via the C=C bond to amorphous polymers leads to a decrease in entropy by $105\text{--}125 \text{ J mol}^{-1} \text{ K}^{-1}$ (usually by $125 \text{ J mol}^{-1} \text{ K}^{-1}$). In the polymerisation of the above olefins, the entropy diminishes by $120 \text{ J mol}^{-1} \text{ K}^{-1}$.

The Gibbs free energy of polymerisation, like the enthalpy of polymerisation, also gradually increases with increase in n and the form of the dependence of $\Delta_{pol}G^\circ$ on n (Fig. 12, curve 3) resembles the corresponding dependence of $\Delta_{pol}H^\circ$ on n (curve 1). This is of course associated with the fact that $\Delta_{pol}H^\circ$ varies with increase in n , while the entropy factor $T\Delta_{pol}S^\circ$ ($T = 298.15 \text{ K}$) is constant and independent of n . It therefore follows from the equation

$$\Delta_{pol}G^\circ = \Delta_{pol}H^\circ - 298.15 \Delta_{pol}S^\circ$$

that the forms of the curves representing the $\Delta_{pol}H^\circ$ and $\Delta_{pol}G^\circ$ isotherms as a function of n should be identical.

The existence of smooth dependences of the enthalpies, entropies, and Gibbs free energies of the polymerisation of olefins on n made it possible to estimate the thermodynamic characteristics of the polymerisation reactions of olefins (at 298.15 K and 101.325 kPa) for which experimental determinations have not yet been made. The results of the estimates are as follows (kJ mol^{-1}):

	Hept-1-ene	Oct-1-ene	Non-1-ene
$-\Delta_{pol}H^\circ$	107	111	114
$-\Delta_{pol}G^\circ$	72	76	79

In all cases, the monomer and polymer were in the liquid and highly elastic states and the entropy of polymerisation was $120 \text{ J mol}^{-1} \text{ K}^{-1}$.

In conclusion we may note that, in the analysis and generalisation of the thermodynamic characteristics of polyolefins and the parameters of the polymerisation reactions of the corresponding olefins published in the literature, the most reliable values were selected (Tables 2–6). These parameters are recommended for practical use. The quantitative dependences of the thermodynamic properties and parameters of the reactions on the composition and structure of the monomer repeat units in the macromolecules of the polyolefins, on the physical state of the

reactants, and on temperature at the standard pressure have been discovered. They have been used to estimate the numerical values for the corresponding polyolefins in the series polyethylene to polydecene which have not yet been investigated experimentally.

References

1. B A Krentsel, I V Kissin, V J Kleiner, L L Stotskaya *Polymers and Copolymers of Higher α -Olefins* (Germany: Hanser Pallichen) 1996 (in the press)
2. S S Ivanchev, A V Kryzhanovskii, I I Gapon, E L Ponomareva *Vysokomol. Soedin., Ser. A* **32** 66 (1990)
3. K Endo, R Ueda, T Otsu *Polym. J.* **23** 1173 (1991)
4. R B Seymour, T Chang (Eds) *Advances in Polyolefins* (New York: Plenum, 1987)
5. W Kaminsky, H Sinn (Eds) *Transition Metals and Organometallics as Catalysts for Olefin Polymerisation* (Berlin: Springer, 1988)
6. H Sawada *Thermodynamics of Polymerisation* (New York: Marcel Dekker, 1978)
7. B Lebedev, N Smirnova *Makromol. Chem. Phys.* **195** 35 (1994)
8. B V Lebedev, T G Kulagina, N N Smirnova, E G Kiparisova, N V Novoselova *Zh. Fiz. Khim.* **69** 551 (1995)
9. V G Vasil'ev, Author's Abstract of the Candidate Thesis in Chemical Sciences, N Novgorod State University, N Novgorod, 1994
10. B Lebedev, A Yevstropov *Makromol. Chem.* **185** 1235 (1984)
11. B V Lebedev *Termodinamika Polimerov* (Thermodynamics of Polymers) (Gor'kii: Gor'kii State University, 1989)
12. A Munster *Chemische Thermodynamik* (Berlin: Akademie-Verlag, 1969)
13. F S Dainton, K J Ivin *Quart. Rev.* **12** 61 (1958)
14. A V Tobolsky *Properties and Structure of Polymers* (New York: Wiley, 1960)
15. V A Kabanov, V P Zubov *Zh. Vses. Khim. Ova im D I Mendeleeva* **9** 620 (1964)
16. P W Atkins *Physical Chemistry* (Oxford: Oxford University Press, 1977)
17. Ya A Kalashnikov *Fizicheskaya Khimiya Veshchestv pri Vysokikh Davleniyakh* (Physical Chemistry of Substances at the High Pressures) (Moscow: Vysshaya Shkola, 1987)
18. M Ratzsch, Z Wiss Z. *Thechn. Hochsch. Chem. Lenna. Merseburg* **13** 328 (1972)
19. D J Steine, P Witmer *Makromol. Chem.* **8** 61 (1969)
20. J Osuji, M Okamoto, in *Proceeding of the Fourth International Conference of High Pressure*, Kyoto, 1974 p. 689
21. B Wunderlich, H Baur *Heat Capacities of Linear High Polymers* (New York: Springer, 1970)
22. O M Poltorak *Termodinamika v Fizicheskoi Khimii* (Thermodynamics in Physical Chemistry) (Moscow: Vysshaya Shkola, 1991)
23. W H Stockmayer, C E Hecht *J. Phys. Chem.* **21** 1954 (1953)
24. V V Tarasov *Zh. Fiz. Khim.* **24** 111 (1950)
25. I M Lifshits *Zh. Eksp. Teor. Fiz.* **22** 471 (1952)
26. Yu K Godovskii, in *Teplofizika Polimerov* (Thermophysics of Polymers) (Moscow: Khimiya, 1982) p. 14
27. A G Chernoplekov *Zh. Fiz. Khim.* **15** 878 (1951)
28. J Jin, B Wunderlich *J. Phys. Chem.* **95** 9000 (1991)
29. J Jin, A Boller, B Wunderlich, B V Lebedev *Thermochim. Acta* **234** 103 (1994)
30. H N V Temperley *J. Res. Natl. Bur. Stand.* **56** 55 (1956)
31. I Gutzow, Z. *Phys. Chem.* **221** 153 (1962)
32. I Gutzow, in *Stekloobraznoe Sostoyanie* (The Vitreous State) (Moscow: Nauka, 1965) p. 62
33. B V Lebedev, I B Rabinovich *Dokl. Akad. Nauk SSSR* **237** 641 (1977)
34. N Bekkedahl, H Matheson *J. Res. Natl. Bur. Stand.* **15** 503 (1935)
35. E Passaglia, H K Kevorkian *J. Appl. Phys.* **34** 90 (1963)
36. B V Lebedev, I B Rabinovich *Vysokomol. Soedin., Ser. B* **18** 416 (1976)
37. A B Bestull, S S Chang *J. Chem. Phys.* **40** 3781 (1964)
38. G Adam, G H Gibbs *J. Chem. Phys.* **43** 139 (1965)
39. A Milchev, I Gutzow *J. Macromol. Sci. Phys., Ser. B* **21** 583 (1982)
40. V G Rostiashvili, V I Irzhak, B A Rozenberg, in *Steklovanie Polimerov* (Vitrification of Polymers) (Leningrad: Khimiya, 1987) p. 37
41. K V Kir'yanov, V I Tel'noi, in *Tr. po Khimii i Khimicheskoi Tekhnologii (Mezhvuzovskii Sbornik)* [Transactions on Chemistry and Chemical Technology (Intercollegiate Collection)] No. 4 (Gor'kii: Gor'kii State University, 1975) p. 109
42. S M Skuratov, V P Kolesov, A F Vorob'ev *Termokhimiya* (Thermochemistry) Part 2 (Moscow: Moscow State University, 1966) p. 13
43. F D Rossini (Ed.) *Experimental Thermochemistry* (New York: Interscience, 1956)
44. D E Roberts, W W Walton, R B Jessup *J. Polym. Sci.* **2** 420 (1947)
45. R M Joshi, B J Zvolinski *Macromolecules* **1** 25 (1968)
46. B V Lebedev, E G Kiparisova *Zh. Fiz. Khim.* **70** 1351 (1996)
47. F S Dainton, D M Evans, F E Hoare, T P Melia *Polymer, Part II* **3** 263 (1962)
48. F E Karasz, H E Bair, J O'Reily *Polym. J.* **8** 547 (1967)
49. J Bourderiat, A Berton, J Chaussey, R Isnard, J Odin *Polym. Sci.* **14** 167 (1973)
50. B V Lebedev, V Ya Lityagov, in *Termodinamika Organicheskikh Soedinenii (Mezhvuzovskii Sbornik)* [Thermodynamics of Organic Compounds (Intercollegiate Collection)] No. 5 (Gor'kii: Gor'kii State University, 1976) p. 89
51. V M Malyshev, G A Mil'ner, E L Sorkin, V F Shibakin *Priory i Tekhnika Eksperimenta* **6** 195 (1985)
52. B V Lebedev, T A Bykova, V G Vasil'ev, B Wunderlich *Zh. Fiz. Khim.* **68** 15 (1994)
53. E T Westrum, G T Furukawa, J P McCullough *Experimental Thermodynamics* Vol. 1 (Eds J P McCullough, D W Scott) (New York: Plenum)
54. M Sh Yagfarov *Zh. Fiz. Khim.* **43** 1620 (1969)
55. B A Gusev, A A Vechev, I I Kantarovich, S V Dalidovich, in *Termodinamika Organicheskikh Soedinenii (Mezhvuzovskii Sbornik)* [Thermodynamics of Organic Compounds (Intercollegiate Collection)] (Gor'kii: Gor'kii State University, 1988) p. 72
56. E A Gusev, S V Dalidovich, A A Vechev *Thermochim. Acta* **92** 379 (1985)
57. B V Lebedev, N N Smirnova, E G Kiparisova, V G Vasil'ev, N Yu Surkova, V I Kleiner, B A Krentsel' *Vysokomol. Soedin., Ser. A* **35** 767 (1993)
58. M Dole *Fortsch. Hochpolym.-Forsch.* **2** 221 (1960)
59. Yu K Godovskii *Teplofizicheskie Metody Issledovaniya Polimerov* (Thermophysical Methods for the Investigation of Polymers) (Moscow: Khimiya, 1976)
60. B V Lebedev, Doctoral Thesis in Chemical Sciences, Moscow State University, Moscow, 1979
61. G M Bartenev, G M Sinitsina, N V Khikhlovskaya, A V Danilov *Vysokomol. Soedin., Ser. A* **34** 1 (1992)
62. V G Vasil'ev, A G Strikovskii, B V Lebedev, in *Termodinamika Organicheskikh Soedinenii (Mezhvuzovskii Sbornik)* [Thermodynamics of Organic Compounds (Intercollegiate Collection)] (Gor'kii: Gor'kii State University, 1989) p. 13
63. B V Lebedev, N N Mukhina, E G Kiparisova, in *Fiziko-Khimicheskie Osnovy Sintez i Pererabotki Polimerov (Mezhvuzovskii Sbornik)* [Physicochemical Foundations of the Synthesis and Processing of Polymers (Intercollegiate Collection)] No. 4 (Gor'kii: Gor'kii State University, 1979) p. 36
64. A A Evstropov, Candidate Thesis in Chemical Sciences, Gor'kii State University, Gor'kii 1981
65. U Gaur, B Wunderlich *J. Phys. Chem. Ref. Data* **10** 119 (1981)
66. I B Rabinovich, L I Pavlinov, G P Krylova *Zh. Fiz. Khim.* **41** 2044 (1967)
67. B V Lebedev, N N Smirnova, in *Tez. Dokl. Vserossiiskoi Konf. po Termicheskoi Analizu* (Abstracts of Reports at the All-Russian Conference on Thermal Analysis) (Kazan': Kazan' State University, 1996) p. 220
68. U Gaur, B Wunderlich *J. Phys. Chem. Ref. Data* **10** 1051 (1981)
69. B V Lebedev, L Ya Tsvetkova, V G Vasil'ev, V I Kleiner, B A Krentsel' *Vysokomol. Soedin., Ser. A* **35** 1941 (1993)
70. H Wilski, T Grever *J. Polym. Sci., Part C, Polym. Lett.* **6** 33 (1964)
71. V Bares, B Wunderlich *J. Polym. Sci., Polym. Phys. Ed.* **11** 861 (1973)
72. G P Andrianova *Fizikokhimiya Poliolefinov* (The Physical Chemistry of Polyolefins) (Moscow: Khimiya, 1974)
73. I B Rabinovich, A N Mochalov, L Ya Tsvetkova, T B Khlyustova, Ye M Moseyeva, V A Maslova *Acta Polymerica* **34** 482 (1983)

74. J D Ferry, G S Parks *J. Chem. Phys.* **4** 70 (1936)
75. G T Furukawa, M L Reilly *J. Res. Natl. Bur. Stand.* **56** 285 (1956)
76. U Gaur, B B Wunderlich, B Wunderlich *J. Phys. Chem. Ref. Data* **12** 29 (1983)
77. B V Lebedev, N N Smirnova, E G Kiparisova, D G Faminskii, V G Vasil'ev, V F Vasilenko *Vysokomol. Soedin., Ser. A* **35** 1951 (1993)
78. E G Kiparisova, N N Smirnova, B V Lebedev, in *Abstracts of Reports of the First Southeast Asian Symposium on Thermophysical Properties, Kuala Lumpur, Malaysia, 1995*
79. T P Melia, A Tyson *Makromol. Chem., B* **109** 87 (1967)
80. B V Lebedev, N N Smirnova, V G Vasil'ev, E G Kiparisova, V I Kleiner *Vysokomol. Soedin., Ser. A* **36** 1413 (1994)
81. N N Kuz'min, E I Matukhin, V M Polikarpov, E M Antipov *Vysokomol. Soedin., Ser. A* **34** 63 (1992)
82. P Corradini, G Avitabile *Eur. Polym. J.* **4** 2 (1968)
83. B Wunderlich *Macromolecular Physics* (New York: Academic Press, 1976)
84. B V Lebedev, N N Smirnova, E G Kiparisova, V I Kleiner, M I Tokar *Vysokomol. Soedin.* **38** (1996) (in the press)
85. V G Vasil'ev, B V Lebedev, N V Novoselova *Vysokomol. Soedin., Ser. A* **35** 621 (1995)
86. K Soga, D Lee, T Shino *Makromol. Chem.* **190** 2683 (1989)
87. V A Bernshtein, V M Egorov *Differentsial'naya Skaniruyushchaya Kalorimetriya v Fizikokhimii Polimerov* (Differential Scanning Calorimetry in the Physical Chemistry of Polymers) (Leningrad: Khimiya, 1960)
88. J Wiley *J. Polym. Sci., Polym. Chem. Ed.* **9** 1907 (1971)
89. B H Clampitt, R H Hughes *Am. Chem. Soc. Polym. Prepr.* **4** 468 (1963)
90. R A Raff, K W Doak (Eds) *Crystalline Olefins Polymers Part II* (New York: Wiley, 1964)
91. In *Entsiklopediya Polimerov* (Encyclopedia of Polymers) (Moscow: Sovetskaya Entsiklopediya, 1974) Vol. 2, p. 202
92. K S Minsker, A G Liakumovich, Yu A Sangalov, O D Svirskaya, V N Korobeinikova, A Kh Gazizov *Vysokomol. Soedin., Ser. A* **16** 2751 (1974)
93. I B Rabinovich, B V Lebedev *Vysokomol. Soedin., Ser. A* **21** 2025 (1979)
94. B V Lebedev, T G Kulagina, N N Smirnova *J. Chem. Thermodyn.* **26** 941 (1994)
95. B Wunderlich *Thermochim. Acta* **214** 103 (1993)
96. B V Lebedev, N K Lebedev *Termodinamika Poligeksena-1 v Oblasti 0–300 K* (Thermodynamics of Polyhex-1-ene in the Range 0–300 K) Article deposited at the All-Union Institute of Scientific and Technical Information (VINITI), Moscow, 1974, No2118
97. V P Glushko (Ed.) *Termicheskie Konstanty Veshchestv* (Thermal Constants of Substances) Nos 1–5 (Moscow: Izd. VINITI, 1965–1972)
98. H Sawada *J. Macromol. Sci., Part C, Polym. Lett.* **3** 313 (1969)
99. C J Egan, J D Kemp *J. Am. Chem. Soc.* **59** 1264 (1937)
100. F D Rossini, J W Knoviton *J. Res. Natl. Bur. Stand.* **19** 249 (1937)
101. J Richardson, G H Parks *J. Am. Chem. Soc.* **61** 3545 (1939)
102. E D Coon, F Daniels *J. Phys. Chem.* **37** 1 (1933)
103. D R Stull, E F Westrum, G C Sinke *The Chemical Thermodynamics of Organic Compounds* (New York: Wiley, 1969)
104. F S Dainton, K J Ivin *Trans. Faraday. Soc.* **46** 331 (1950)
105. A Evans, M Polanyi *Nature (London)* **152** 738 (1943)
106. R Biddulph, W Longworth, J Renfold *Polymer* **1** 521 (1960)
107. G Parks, H Mocher *J. Polym. Sci., Polym. Chem. Ed.* **A1** 1973 (1963)
108. S S Todd, G S Parks *J. Am. Chem. Soc.* **58** 134 (1936)
109. K Takeda, O Yamomura, H Soga *J. Phys. Chem. Solids* **52** 607 (1991)
110. B A Krentsel', V I Kleiner, L L Stotskaya *Vysshie Poliolefiny* (Higher Polyolefins) (Moscow: Khimiya, 1984)
111. J Chao, K R Hell *Thermochim. Acta* **64** 285 (1983)
112. H F Bartolo, F D Rossini *J. Phys. Chem.* **64** 1685 (1960)
113. D Tox, M M Lates, A Weissberger (Ed.) *Physics and Chemistry of the Organic Solid State Part I* (New York: Interscience, 1965)
114. B V Lebedev, V G Vasil'ev *Vysokomol. Soedin., Ser. A* **39** (1997) (in the press)
115. B V Lebedev, I B Rabinovich, in *Tr. po Khimii i Khimicheskoi Tekhnologii (Mezhvuzovskii Sbornik)* [Transactions on Chemistry and Chemical Technology (Intercollegiate Collection)] No. 2 (Gor'kii: Gor'kii State University, 1972) p. 68

Thermodynamics of polylactones

B V Lebedev

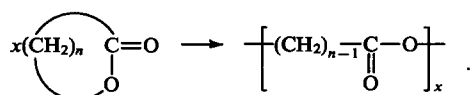
Contents

I. Introduction	1063
II. Calorimetric research methods	1065
III. Heat capacity	1065
IV. Thermodynamics of fusion	1070
V. Parameters of vitrification and the vitreous state	1072
VI. Thermodynamic functions	1073
VII. Thermochemical characteristics	1073
VIII. Thermodynamic parameters of the polymerisation reactions of lactones	1076
IX. The regularities and characteristics of the thermodynamic properties of polylactones and of the parameters of the polymerisation reactions of lactones	1078

Abstract. The thermodynamic properties of polylactones and the thermodynamic parameters of their formation reactions involving the polymerisation of lactones in the range 0–400 K are examined on the basis of the results of calorimetric studies. The selected thermodynamic quantities which have been recommended for use are presented. The regularities and characteristics of the thermodynamic properties and parameters of the lactone polymerisation reaction and their dependence on the composition, structure and physical state of the reactants and on temperature at the standard pressure are described. The bibliography includes 99 references.

I. Introduction

Polylactones are obtained by the polymerisation of the corresponding lactones in accordance with the scheme



The interest in the thermodynamic properties of polylactones and the thermodynamic parameters of the reactions involving their synthesis is due to the wide variety of theoretical and applied studies on reactants and reactions^{1–5} in connection with the good prospects for the practical employment of polylactones as complex aliphatic polyesters with a chain structure.^{6–8} A series of polylactones and their copolymers are being manufactured industrially and are used in practice. As an example, one may point to polyglycolide and its copolymers with lactide, which are used in medicine as biocompatible surgical materials,^{7,9} and to polypivalolactone^{10,11} and poly-β-butyrolactone,^{3,8} which are used as biodegradable materials. The thermodynamic character-

istics of polylactones and their formation reactions are needed in the planning and implementation of theoretical and applied developments designed to obtain and process these materials and in the development of industrial technologies for their manufacture and conversion into articles.¹² The thermodynamic parameters of the polymerisation reactions of lactones are used in the search for the optimum physical conditions in their implementation, ensuring the maximum yield of products, for the determination of the temperature ranges of thermodynamic stability of polylactones relative to their depolymerisation to the initial monomers, and also for the determination of the temperature ranges corresponding to the existence of the polymers in particular physical states, which in many respects determine their specific applications.^{13,14}

Spontaneous polymerisation of the monomers takes place when the Gibbs free energy $\Delta_{\text{pol}}G(T, p)$ decreases.¹⁵ The standard Gibbs free energy $\Delta_{\text{pol}}G^\circ(T)$, characterising the state of thermodynamic equilibrium in the reaction, indicates directly the possibility or impossibility in principle, from the thermodynamic standpoint, of the conversion of the lactone into the corresponding polylactone under specific physicochemical conditions.^{13,15,16} For $\Delta_{\text{pol}}G^\circ(T) < 0$, the process equilibrium is displaced to the right — towards the formation of the polymer, while for $\Delta_{\text{pol}}G^\circ(T) > 0$ it is actually displaced to the left and the monomer predominates in the equilibrium reaction mixture. If the positive standard Gibbs free energy is less than 40 kJ mol^{–1}, then change of the physicochemical conditions in carrying out the reaction may lead to a change in the sign of $\Delta_{\text{pol}}G(T)$ and to a shift of the equilibrium to the right.¹⁶ For $\Delta_{\text{pol}}G^\circ(T) > 40$ kJ mol^{–1}, the spontaneous reaction is thermodynamically prohibited. In this case, the conversion of the monomer into the polymer is possible only with expenditure of energy from outside.

If the positive value of $\Delta_{\text{pol}}G^\circ(T)$ is small, then a low equilibrium polymer concentration corresponds to it in the equilibrium reaction mixture. If it is possible to create conditions such that the polymer formed is removed continuously from the equilibrium reaction mixture, then the conversion of the monomer into the polymer can be continued until the complete exhaustion of the monomer. Realistically this is possible, for example, in cases where the polylactone formed is insoluble in the reaction mixture and precipitates.¹⁷ Calculations have shown that the standard Gibbs free energy for δ-valerolactone and ε-caprolactone are

B V Lebedev Institute of Chemistry at the Lobachevskii Nizhnii Novgorod State University, prosp. Gagarina 23/5, 603600 Nizhnii Novgorod, Russian Federation. Fax (7-831) 235 64 80. Tel. (7-831) 265 64 50. E-mail: lebedev@nnov.sovam.com

Received 8 July 1996

Uspekhi Khimii 65 (12) 1149–1169 (1996); translated by A K Grzybowski

negative, whilst those for γ -butyrolactone are positive.¹³ Accordingly, δ -valerolactone and ϵ -caprolactone are readily converted into the corresponding polymers under the influence of catalysts; γ -butyrolactone cannot be polymerised under the same physico-chemical conditions. However, an increase in pressure from 10^5 to 2×10^9 Pa alters the sign of $\Delta_{\text{pol}}G(T)$ and leads to the virtually complete conversion of the monomer into poly- γ -butyrolactone.

The yield of the polymer corresponding to thermodynamic equilibrium and the content of the residual monomer in the polymer at any temperature for which the standard Gibbs free energy is known may be readily calculated from the values of $\Delta_{\text{pol}}G^\circ(T)$.¹⁴ $\Delta_{\text{pol}}G^\circ(T)$ may be calculated if the enthalpies $\Delta_{\text{pol}}H^\circ(T)$ and entropies $\Delta_{\text{pol}}S^\circ(T)$ of polymerisation are known. The latter are usually found from the results of calorimetric measurements. The calculation of these quantities from the equilibrium concentrations of the monomer $[M]_e$ in the reaction mixture as a function of temperature, as averages for a certain temperature range in which $\Delta_{\text{pol}}H^\circ(T)$ and $\Delta_{\text{pol}}S^\circ(T)$ are independent of temperature or depend little on the latter, is possible in principle.¹⁸ When this method is used, it is necessary to monitor rigorously the onset of the polymerisation-depolymerisation equilibrium in the reaction mixture at a specified temperature and pressure.^{18–20} One must bear in mind that the approach to equilibrium is frequently slow, usually owing to the high viscosity of the reaction mixture.

For several of the lactone polymerisation reactions investigated, the quantities $\Delta_{\text{pol}}H^\circ$ have been obtained from the enthalpies of combustion Δ_cH° of the monomers and the corresponding polymers or from their enthalpies of formation Δ_fH° at 298.15 K and the standard pressure. For other reactions, $\Delta_{\text{pol}}H^\circ$ has been measured directly during polymerisation in calorimeters. We may note that the quantity $\Delta_{\text{pol}}H^\circ(T)$ is independently important as the initial parameter for the calculation of the energy balances in the development of industrial technologies for the synthesis of polymers.

The entropies of polymerisation of lactones $\Delta_{\text{pol}}S^\circ(T)$ are calculated from the absolute entropies of the reactants, which are evaluated in their turn from the experimental temperature variations of the heat capacities and the temperatures, and enthalpies of the physical transformations of the polymers and monomers using the Third Law of Thermodynamics.²¹ For these calculations, it is necessary that the heat capacities of the test substances should be measured from as low temperatures as possible. The absolute entropies of the monomers are calculated in the usual way,²¹ whilst their calculation for the polymers is complicated by the fact that in any physical state the entropies of the polymers at $T = 0$ K are not zero,^{22,23} since polymers have a zero-point (residual) entropy $S^\circ(0)$.^{22–24} This is associated with the fact that polymers, particularly polylactones, are partly crystalline or amorphous and constitute a mixture of macromolecules having different masses.^{23,24} Furthermore, when polymers are cooled the conformations of the macromolecules are frozen at the glass transition temperature T_g° . On further cooling, such macromolecules do not pass to the state corresponding to thermodynamic equilibrium owing to the enormous activation energy for the rearrangement of their constituent segments and give rise to the so called conformational contribution S_{conf}° to the zero-point entropy of the polymer.^{25–27} There are also other causes of the existence of $S^\circ(0)$.²³

The problem of the zero-point entropy remained for a long time a serious obstacle to the calculation of the absolute entropies of polymers and hence to the employment of calorimetric methods for the determination of the thermodynamic parameters of polymerisation reactions.^{24,28} A consequence of the neglect of the values of $S^\circ(0)$ for polymers was serious errors in the calculations of $\Delta_{\text{pol}}G^\circ(T)$, $[M]_e$, and the polymerisation-depolymerisation equilibrium constants, K_{pol}° .

Lebedev and Rabinovich²⁹ found a way of estimating the zero-point entropies of polymers in the amorphous state from experimental temperature variations of the heat capacities and the

temperatures and enthalpies of the physical transformations of partly crystalline polymers. An approximate method for the determination of the configurational entropies S_{conf}° of amorphous polymers from the increments in their heat capacities on devitrification $\Delta C_p^\circ(T_g^\circ)$ at T_g° and from the ratio $T_g^\circ/T_2^\circ \approx 1.29$, where T_2° is the Kauzmann temperature,³⁰ has been proposed.^{25,26} It was shown that the configurational entropy constitutes the main contribution to the zero-point entropies of polymers and in many cases S_{conf}° is close or even equal to $S^\circ(0)$.^{25–27} Thus the problem of the calculation of the absolute entropies of polymers from calorimetric data has been virtually solved. The values of $\Delta_{\text{pol}}S(T)$ for more than 150 polymerisation reactions of monomers, including many lactones, have now been found from the absolute entropies of the reactants.

The physical transformations occurring on heating or cooling the test substances are manifested clearly in the temperature variations of the heat capacity, and the temperatures and enthalpies of these transformations may be measured accurately. By employing the heat capacities and the temperatures and enthalpies of the physical transformations, the enthalpies $H^\circ(T) - H^\circ(0)$, the entropies $S^\circ(T)$, and the Gibbs free energies $G^\circ(T) - H^\circ(0)$ may be found. These thermodynamic functions are used in their turn to calculate the enthalpies, entropies, and Gibbs free energies of the polymerisation processes. The thermochemical parameters Δ_fH° , Δ_fG° , Δ_fH° , and K_f° of the formation of the monomers and polymers are calculated from the standard enthalpies of combustion and $S^\circ(298.15 \text{ K})$. The degrees of crystallinity α of partly crystalline polymers are also estimated from calorimetric data.^{31,32}

$$\alpha = 100 \left[1 - \frac{\Delta C_p^\circ(\alpha)}{\Delta C_p^\circ(\alpha = 0)} \right], \quad (1)$$

$$\alpha = 100 \frac{\Delta_{\text{fus}}H^\circ(\alpha)}{\Delta_{\text{fus}}H^\circ(\alpha = 100\%)}, \quad (2)$$

where $\Delta C_p^\circ(\alpha)$ and $\Delta C_p^\circ(\alpha = 0)$ are respectively the increments in heat capacity on devitrification of the polymers at T_g° for the polymer with a degree of crystallinity α and for the fully amorphous polymer and $\Delta_{\text{fus}}H^\circ(\alpha)$ and $\Delta_{\text{fus}}H^\circ(\alpha = 100\%)$ are the enthalpies of fusion of the polymer with a degree of crystallinity α and the fully crystalline polymer.

The properties of polymers in the amorphous and crystalline states are estimated with the aid of the thermodynamic properties of the partly crystalline polymers. The method used for such estimations has been described.^{29,33} The results permit, apart from the calculation of $S^\circ(0)$ for amorphous polymers, also the calculation of the difference between the zero-point enthalpies of the polymer in the vitreous and crystalline states $H_g^\circ(0) - H_{\text{cr}}^\circ(0)$ at $T = 0 \text{ K}$.^{33,34} Using the values of $S^\circ(0)$ and $H_g^\circ(0) - H_{\text{cr}}^\circ(0)$ as well as the temperature variations of the heat capacities of the monomers in the amorphous and crystalline states, it is possible to find the thermodynamic parameters of the conversion of the amorphous polymer into the crystalline form: $\Delta H^\circ(a;cr)$, $\Delta S^\circ(a;cr)$, and $\Delta G^\circ(a;cr)$ in the range $0 - T_{\text{fus}}^\circ$. The values of $\Delta G^\circ(a;cr)$ represent a kind of estimate of the absolute thermodynamic stability of the amorphous polymer in relation to its crystalline state.^{35,36}

Polylactones are convenient objects for the determination of the dependences of the changes in the properties and thermodynamic parameters of the polymerisation reactions on the compositions and structures of the reactants — the monomer repeat units in the polymer macromolecules. In a series of polylactones, the composition changes by a CH_2 group on passing from one polylactone to another. This gives rise to a regular variation of the melting points and glass transition temperatures, heat capacities, thermodynamic functions, thermochemical parameters of formation, thermodynamic parameters of the polymerisation reactions, and other characteristics. If the above variations can be found, it is possible to estimate the properties of hitherto

uninvestigated polymers, as has been done for the alkanes,³⁵ polyalkenes,³⁶ and polyalkynynes.³⁷

In the present review, partly crystalline high-molecular-mass polylactones are examined (Table 1). For the polymers the degree of crystallinity of which has been determined, the latter proved to be somewhat greater than 60%. The masses of the monomer repeat units in the macromolecules of the polylactones were taken from Domalsky.³⁸

II. Calorimetric research methods

1. Combustion calorimetry

Combustion calorimetry is used in direct measurements of the combustion energies $\Delta_c U$. The enthalpies of combustion $\Delta_c H^\circ$ and formation $\Delta_f H^\circ$ of compounds at 298.15 K and the standard pressure are calculated from the values of $\Delta_c U$. They are in turn necessary for the calculation of the enthalpies of polymerisation $\Delta_{pol} H^\circ$ under the same physical conditions. For this very purpose, Sunner and coworkers,³⁹ Hall,⁴⁰ Andruzzi,⁴¹ and Kiparisova and the author of the present review³⁶ carried out experiments designed to determine $\Delta_c H^\circ$ and $\Delta_f H^\circ$ for lactones and the corresponding polylactones. The calorimetric apparatus and the methods used to measure $\Delta_c U$ by the above investigators did not differ fundamentally and in general were similar to those described by Skuratov et al.⁴² However, Sunner and coworkers³⁹ used a rotating bomb calorimeter[†].

Lebedev and Kiparisova³⁶ used a calorimeter with an isothermal jacket and a static bomb of the inverted type. In the calculation of the combustion energies $\Delta_c U$ under the conditions in the bomb calorimeter, the usual thermochemical corrections were taken into account.⁴² The values of $\Delta_c U$, adjusted to the standard pressure, were then used to calculate $\Delta_c H^\circ$ and $\Delta_f H^\circ$.

The majority of the values of $\Delta_c H^\circ$ were determined with an error of $\sim 0.02\%$.

2. Adiabatic vacuum calorimetry

Adiabatic vacuum calorimetry has been used to measure the temperature variation of the heat capacity C_p° and the temperatures and enthalpies of the physical transformations of polylactones in the range from 13.8 to 320 K. The thermodynamic parameters of fusion T_{fus}° , $\Delta_{fus} H^\circ$, and $\Delta_{fus} S^\circ$, the parameters of vitrification and the vitreous state T_g° , the increase in heat capacity on devitrification of the polymer $\Delta C_p^\circ(T_g^\circ)$, the zero-point $[S^\circ(0)]$ and configurational (S_{conf}°) entropies, the Kauzmann temperature T_2° , and the difference $H_g^\circ(0) - H_{cr}^\circ(0)$ were obtained from the above measurements. Hitherto virtually all the measurements of C_p° for polylactones in the range 13.8–370 K have been carried out on a thermophysical apparatus, the design of which and also the methods of measurement have been published.^{13,43} Overall, the analysis of the calibrations and checks of the calorimeter employed and of the experimental method permitted the conclusion that the error in the measurements of C_p° for the polymer was to within 1% in the range 13.8–20 K, 0.5% in the range 30–90 K, and 0.25% in the range 90–370 K; the error in the measurement of the temperature was 0.01 K in conformity with the International Practical Temperature Scale (IPTS-68) and that in the enthalpies of the transformations was 0.25%.

An adiabatic calorimeter of the Gal'chenko–Popov type was used in the measurements of the heat capacity in the range 300–550 K. The design of the calorimeter and the method of measurement have been described.^{44,45}

3. Differential scanning calorimetry

Differential scanning calorimetry (DSC) has been used in the study of polylactones mainly to obtain the melting points, the crystallisation temperatures, and the enthalpies of fusion.^{46–50}

Wunderlich and coworkers⁵⁰ used this method to investigate the temperature variation of the heat capacity, the glass transition temperature, the crystallisation temperature, and the melting point of polypivalolactone. The principles underlying the design of the differential scanning calorimeters and of the methods for their employment have been examined in a series of studies^{51–55} and on the whole are well known. The results obtained are consistent throughout with the data of the U S National Bureau of Standards⁵⁶ to within approximately $\pm 0.1\%$. The details of the methods of measurement are described by Jin and Wunderlich.⁵⁷

4. Isothermal calorimeter of the Mathews type

An isothermal calorimeter of the Mathews type has been used for the direct measurements of the enthalpies of polymerisation of a series of lactones with formation of the corresponding polylactones. The enthalpy of polymerisation was determined from the mass of carbon tetrachloride vaporised at its normal boiling point (349.66 ± 0.05 K) by the energy evolved on polymerisation of the monomer. The design of the calorimeter and the experimental method have been described.⁵⁸ The reliability of the operation of the calorimeter has been confirmed by the exact reproduction of Joshi's precision experiments⁵⁹ on the polymerisation of methyl methacrylate and styrene.⁶⁰ The values of $\Delta_{pol} H^\circ$ obtained for these monomers did not differ from those quoted by Joshi⁵⁹ by more than 0.3%.

III. Heat capacity

Polyglycolide. The polymerisation of glycolide with ring opening leads to the formation of polyglycolide. According to the formula of its smallest repeat unit (Table 1), it can be formally regarded as a polylactone which might have been obtained from a three-membered lactone, the latter apparently not existing owing to the high ring strain energy. The results of calorimetric measurements of the heat capacity of a partly crystalline ($\alpha = 67\%$) polyglycolide with a molecular mass (found from the viscosity) of 3.8×10^4 have been published by Lebedev et al.⁶¹ The heat capacity was determined in adiabatic calorimeters with an error of $\sim 0.3\%$ in the range 13.8–335 K⁴³ and $\sim 0.7\%$ in the range 335–550 K.⁴⁴ In the ranges 13.8–250, 340–450, and 501–550 K, the heat capacity of the polyglycolide increases smoothly with increasing temperature (Fig. 1). The rapid increase in C_p° in the range 250–345 K is associated with the devitrification of the amorphous component of the specimen, while the sharp increase in heat capacity and the break in the $C_p^\circ - T$ plot in the range 440–501 K are caused by the fusion of the crystalline component of the test specimen. Overall, the temperature variation of the heat capacity of polyglycolide is typical of that for partly crystalline polymers.¹⁴ in the range from 60–80 K up to the temperature of the onset of

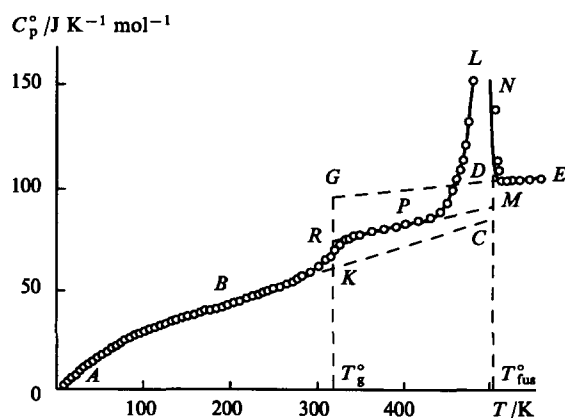


Figure 1. The heat capacity of polyglycolide:⁶¹ ABRPM — with 67% crystallinity, AKC — crystalline, AK — vitreous, GD — highly elastic, DE — liquid; PLND — apparent heat capacity in the melting range.

[†] All the characteristics of the calorimeter employed by the above workers may be found in the paper of Lebedev and Kiparisova.³⁶

Table 1. The polylactones considered in the review.

Polylactones	Monomer repeat unit		Polylactones	Monomer repeat unit	
	formula	mass /g mol ⁻¹ ^a		formula	mass /g mol ⁻¹ ^a
Polyglycolide	$\left[\text{CH}_2 - \underset{\text{O}}{\underset{\parallel}{\text{C}}} - \text{O} \right]$	58.038	Poly- β -ethyl- α,α -dimethyl- β -propiolactone	$\left[\text{CH}(\text{C}_2\text{H}_5) - \text{C}(\text{CH}_3)_2 - \underset{\text{O}}{\underset{\parallel}{\text{C}}} - \text{O} \right]$	128.171
Poly- β -propiolactone	$\left[(\text{CH}_2)_2 - \underset{\text{O}}{\underset{\parallel}{\text{C}}} - \text{O} \right]$	72.063	Poly- β -methyl- β -propiolactone	$\left[\text{CH}(\text{CH}_3) - \text{CH}_2 - \underset{\text{O}}{\underset{\parallel}{\text{C}}} - \text{O} \right]$	86.090
Poly- α,α -dimethyl- β -propiolactone	$\left[\text{CH}_2 - \text{C}(\text{CH}_3)_2 - \underset{\text{O}}{\underset{\parallel}{\text{C}}} - \text{O} \right]$	100.117	Poly- γ -butyrolactone	$\left[(\text{CH}_2)_3 - \underset{\text{O}}{\underset{\parallel}{\text{C}}} - \text{O} \right]$	86.090
Poly- α -ethyl- α -methyl- β -propiolactone	$\left[\text{CH}_2 - \text{C}(\text{CH}_3)(\text{C}_2\text{H}_5) - \underset{\text{O}}{\underset{\parallel}{\text{C}}} - \text{O} \right]$	114.144	Poly- δ -valerolactone	$\left[(\text{CH}_2)_4 - \underset{\text{O}}{\underset{\parallel}{\text{C}}} - \text{O} \right]$	100.117
Poly- α -methyl- α -n-propyl- β -propiolactone	$\left[\text{CH}_2 - \text{C}(\text{CH}_3)(\text{C}_3\text{H}_7) - \underset{\text{O}}{\underset{\parallel}{\text{C}}} - \text{O} \right]$	128.171	Polyoxacarbonyl-1,4-cyclohexylene	$\left[\text{C}_6\text{H}_{10} - \underset{\text{O}}{\underset{\parallel}{\text{C}}} - \text{O} \right]$	126.155
Poly- α -isopropyl- α -methyl- β -propiolactone	$\left[\text{CH}_2 - \text{C}(\text{CH}_3)(\text{CH}(\text{CH}_3)_2) - \underset{\text{O}}{\underset{\parallel}{\text{C}}} - \text{O} \right]$	128.171	Poly- ϵ -caprolactone	$\left[(\text{CH}_2)_5 - \underset{\text{O}}{\underset{\parallel}{\text{C}}} - \text{O} \right]$	114.149
Poly- α -methyl- α -pentyl- β -propiolactone	$\left[\text{CH}_2 - \text{C}(\text{CH}_3)(\text{C}_5\text{H}_{11}) - \underset{\text{O}}{\underset{\parallel}{\text{C}}} - \text{O} \right]$	156.224	Poly- γ -methyl- ϵ -caprolactone	$\left[(\text{CH}_2)_2 - \text{CH}(\text{CH}_3) - (\text{CH}_2)_2 - \underset{\text{O}}{\underset{\parallel}{\text{C}}} - \text{O} \right]$	128.171
Poly- α,α -diethyl- β -propiolactone	$\left[\text{CH}_2 - \text{C}(\text{C}_2\text{H}_5)_2 - \underset{\text{O}}{\underset{\parallel}{\text{C}}} - \text{O} \right]$	128.171	Poly- ϵ -methyl- ϵ -caprolactone	$\left[\text{CH}(\text{CH}_3) - (\text{CH}_2)_4 - \underset{\text{O}}{\underset{\parallel}{\text{C}}} - \text{O} \right]$	128.171
Poly- α -ethyl- α -n-propyl- β -propiolactone	$\left[\text{CH}_2 - \text{C}(\text{C}_2\text{H}_5)_2(\text{C}_3\text{H}_7) - \underset{\text{O}}{\underset{\parallel}{\text{C}}} - \text{O} \right]$	142.197	Poly- α,ϵ -dimethyl- ϵ -caprolactone	$\left[\text{CH}(\text{CH}_3) - (\text{CH}_2)_3 - \text{CH}(\text{CH}_3) - \underset{\text{O}}{\underset{\parallel}{\text{C}}} - \text{O} \right]$	142.197
Poly- α -ethyl- α -n-butyl- β -propiolactone	$\left[\text{CH}_2 - \text{C}(\text{C}_2\text{H}_5)_2(\text{C}_4\text{H}_9) - \underset{\text{O}}{\underset{\parallel}{\text{C}}} - \text{O} \right]$	156.224	Poly- η -caprylolactone	$\left[(\text{CH}_2)_6 - \underset{\text{O}}{\underset{\parallel}{\text{C}}} - \text{O} \right]$	128.171
Poly- α,α -di-n-propyl- β -propiolactone	$\left[\text{CH}_2 - \text{C}(\text{C}_3\text{H}_7)_2 - \underset{\text{O}}{\underset{\parallel}{\text{C}}} - \text{O} \right]$	156.224	Poly- λ -lauro lactone	$\left[(\text{CH}_2)_7 - \underset{\text{O}}{\underset{\parallel}{\text{C}}} - \text{O} \right]$	142.197

Table 1 (continued).

Polylactones	Monomer repeat unit		Polylactones	Monomer repeat unit	
	formula	mass /g mol ⁻¹ ^a		formula	mass /g mol ⁻¹ ^a
Poly- α -n-butyl- α - n-propyl- β -propiolactone	$\left[\text{CH}_2 - \text{C}(\text{C}_3\text{H}_7)(\text{C}_4\text{H}_9) - \underset{\text{O}}{\underset{\parallel}{\text{C}}} - \text{O} \right]$	170.343	Polynonanolactone	$\left[(\text{CH}_2)_8 - \underset{\text{O}}{\underset{\parallel}{\text{C}}} - \text{O} \right]$	156.224
Poly- α,α -dimethyl- β -methyl- β -propiolactone	$\left[\text{C}(\text{CH}_3)_2 - \text{CH}(\text{CH}_3) - \underset{\text{O}}{\underset{\parallel}{\text{C}}} - \text{O} \right]$	114.144	Polydecanolactone	$\left[(\text{CH}_2)_9 - \underset{\text{O}}{\underset{\parallel}{\text{C}}} - \text{O} \right]$	170.343
Polyundecanolactone	$\left[(\text{CH}_2)_{10} - \underset{\text{O}}{\underset{\parallel}{\text{C}}} - \text{O} \right]$	184.278	Polytetradecanolactone	$\left[(\text{CH}_2)_{13} - \underset{\text{O}}{\underset{\parallel}{\text{C}}} - \text{O} \right]$	226.358
Polydodecanolactone	$\left[(\text{CH}_2)_{11} - \underset{\text{O}}{\underset{\parallel}{\text{C}}} - \text{O} \right]$	198.305	Polypentadecanolactone	$\left[(\text{CH}_2)_{14} - \underset{\text{O}}{\underset{\parallel}{\text{C}}} - \text{O} \right]$	240.385
Polytridecanolactone	$\left[(\text{CH}_2)_{12} - \underset{\text{O}}{\underset{\parallel}{\text{C}}} - \text{O} \right]$	212.331	Polyhexadecanolactone	$\left[(\text{CH}_2)_{15} - \underset{\text{O}}{\underset{\parallel}{\text{C}}} - \text{O} \right]$	254.505

^a Values taken from Domalsky.³⁸

the devitrification of the amorphous component of the polymer, the heat capacity is a linear function of temperature; the heat capacity of liquid polyglycolide is also a linear function of temperature, as for many other polymers.^{50,62}

Poly- β -propiolactone. The results of calorimetric measurements of the heat capacity of poly- β -propiolactone have been published.⁶³ The specimen was obtained by the polymerisation of β -propiolactone. The mass-average (\bar{M}_w) and number-average (\bar{M}_n) molecular masses of the polymer were respectively 3×10^4 and 8.3×10^3 , the polydispersity coefficient was $\bar{M}_w/\bar{M}_n = 3.8$, and the degree of crystallinity was $\alpha = 79\%$. The heat capacity of poly- β -propiolactone was measured in an adiabatic vacuum calorimeter⁴³ in the temperature range 13.8–330 K with an error of $\sim 0.3\%$ and in an adiabatic calorimeter⁴⁴ in the range 330–400 K with an error of $\sim 1\%$. The devitrification of the amorphous component of the specimen began at 240 K (Fig. 2), its completion being masked by the onset of the fusion of the crystalline component; the break in the C_p° – T relation in the melting range is also associated with this factor. In the range 100–210 K, the heat capacity is a linear function of temperature and is described by the following equations subject to an error of $\pm 0.3\%$:

$$C_p^\circ = 14.7 + \frac{T}{4},$$

where C_p° is the molar heat capacity of the polymer expressed in $\text{J mol}^{-1} \text{K}^{-1}$. The heat capacity of the poly- β -propiolactone melt is also a linear function of temperature. The temperature variations of the heat capacity of poly- β -propiolactone in the amorphous and crystalline states have been plotted on the basis of the experimental data by the method proposed in the study of Lebedev and Rabinovich²⁹ (Fig. 2).

Poly- β -methyl- β -propiolactone (poly- β -butyrolactone) is obtained by the polymerisation of β -butyrolactone with ring opening^{64,65} or from (*R*)-3-hydroxybutyric acid under the influence of microorganisms in the course of enzymic reactions.^{8,66} Lebedev et al.⁶⁷ investigated the temperature variation of the heat capacity of a poly- β -methyl- β -propiolactone specimen obtained from (*R*)-3-hydroxybutyric acid by a biotechnological method.⁶⁸ The number-average molecular mass of the polymer was 10^5 and its degree of crystallinity was 66%. The specimen was highly isotactic. The heat capacity was measured in the temperature range 10–490 K: in an adiabatic vacuum calorimeter (AVC)⁶⁸ in

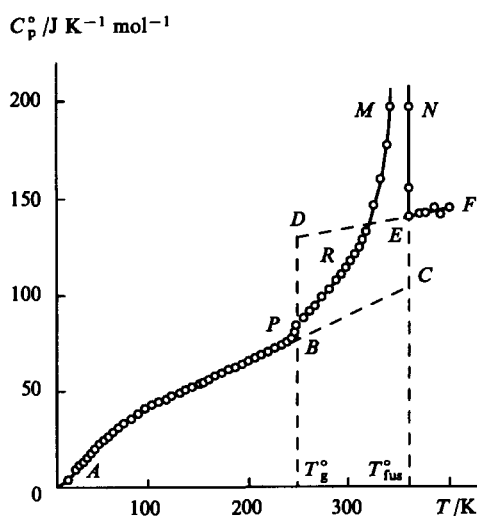


Figure 2. Temperature dependence of the heat capacity of poly- β -propiolactone.⁶³

State of the polymer: *ABC* — crystalline; *AB* — vitreous; *DE* — highly elastic; *EF* — liquid; *APR* — partly crystalline, $\alpha = 79\%$; *RMNE* — apparent heat capacity in the melting range.

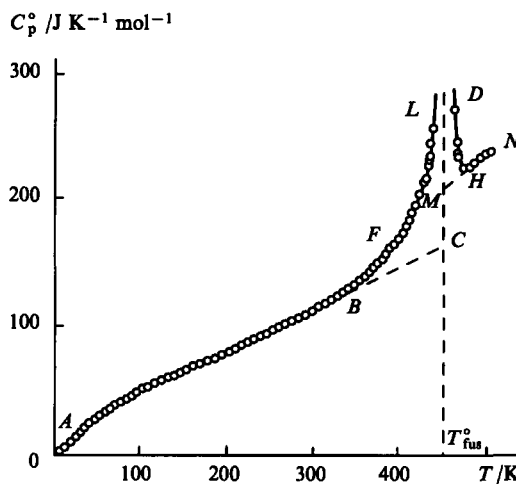


Figure 3. Temperature dependence of the heat capacity of poly- β -methyl- β -propiolactone.⁶⁷

State of the polymer: *ABC* — crystalline; *MHN* — liquid; *ABF* — partly crystalline, $\alpha = 66\%$; *FLDH* — apparent heat capacity in the melting range.

the temperature range 10–340 K with an error of $\sim 0.2\%$ and in a dynamic calorimeter (DC)⁶⁹ in the range 340–490 K with an error of 0.5%–1.5%. The results are presented in Fig. 3.

A characteristic feature of the temperature variation of the heat capacity of poly- β -methyl- β -propiolactone obtained is the absence of the devitrification of the amorphous component of the specimen — only the fusion of the crystalline component is manifested. Such relations are usually characteristic of polymers with a degree of crystallinity close to 100% (more than 90%). In the given instance, it was only 66%. For virtually the same degree of crystallinity, the devitrification of polyglycolide (Fig. 1) is manifested very clearly. The reason for this is probably the degree of interaction of the crystalline and amorphous components in partly crystalline polymer specimens — microheterogeneous systems.⁷⁰ It appears that the greater the uniformity in the distribution of the microheterogeneous crystalline and amorphous components in the bulk of the specimen, the greater the uniformity in their mutual influence and, in particular, in the reinforcement of the amorphous component of the polymer by crystals, which prevents the excitation of segmental motions in the polymer molecules on devitrification.^{71,72}

Poly- α,α -dimethyl- β -propiolactone (polypivalolactone). The heat capacity of poly- α,α -dimethyl- β -propiolactone has been determined by Wunderlich and coworkers⁵⁰ in a DSC-7 differential scanning calorimeter in the range 140–550 K at a rate of heating of the calorimeter with the test substance of $1.7 \times 10^{-1} \text{ K s}^{-1}$. A specimen with a molecular mass of 2.5×10^5 was investigated; the degree of crystallinity of the initial specimen was 51%. The devitrification of the amorphous component of the polymer in the range 260–280 K (section *BC*) and two transitions were manifested on the temperature variation of the heat capacity (Fig. 4, curve *J*): the first transition in the form of a diffuse hump (*DGN*) and the second in the form of the typical temperature variation of the apparent heat capacity of the polymer in the melting range (*NRSU*).

The first transition begins at 380 K, the maximum apparent heat capacity (point *G*) corresponds to 421.5 K, and the end of the transformation is masked by the onset of the fusion process. The nature of the transition is not altogether clear. However, one may postulate that it is due to the transformation of one crystalline modification of poly- α,α -dimethyl- β -propiolactone into another.

Poly- α,α -dimethyl- β -propiolactone is known to be capable of forming three crystalline modifications — α , β , and γ .^{73,74} The crystals melt in the range 497–530 K. The maximum apparent heat capacity corresponds to 511 K. The temperature variation of

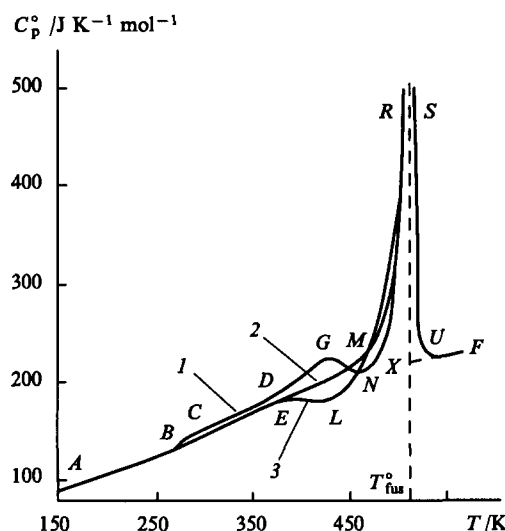


Figure 4. Temperature dependence of the heat capacity of poly- α,α -dimethyl- β -propiolactone.⁵⁰

(1) Initial specimen; (2) specimen obtained by natural cooling of the melt in air; (3) specimen obtained by cooling the melt with liquid nitrogen (cooling rate 5.3 K s⁻¹); for the significance of the letter designations, see text.

C_p° of the polymer melt cooled naturally from 540 K in air is described by curve 2 in Fig. 4. It was found that the degree of crystallinity in the specimen obtained in this way is 68%. Only fusion, which begins at 502 K and ends at 530 K, is manifested on the curves describing the $C_p^\circ = f(T)$ relation; the maximum in the apparent heat capacity corresponds to 513 K.

The third series of measurements was carried out for a specimen of poly- α,α -dimethyl- β -propiolactone obtained by rapid cooling of the polymer melt with liquid nitrogen (rate of cooling ~ 5.3 K s⁻¹). Vitrification was again manifested on the $C_p^\circ = f(T)$ relation (Fig. 4, curve 3) together with an exothermic transformation (ELN section) and fusion. Even on such rapid cooling, the polymer was obtained in a highly crystalline form, its degree of crystallinity being close to that of the initial specimen. Repeated measurements of C_p° in the range 150–260 K and averaging of the latter yielded the following equation which makes it possible to determine the heat capacity of the polymer with an error of $\sim 0.3\%$:

$$C_p^\circ = \exp[-48.06197 + 27.29137 \ln T - 4.791726(\ln T)^2 + 0.28686(\ln T)^3], \quad (3)$$

where C_p° is expressed in J mol⁻¹ K⁻¹.

For the liquid polymer, the following equation was obtained also as a result of several experimental measurements:

$$C_p^\circ = 112.4 + 0.221T,$$

which reproduces satisfactorily (with an error of $\pm 0.13\%$) the heat capacities in the range 510–550 K.

Using the results of experimental determinations of the heat capacity and the vibration frequency of the atoms and atomic groups in poly- α,α -dimethyl- β -propiolactone, Wunderlich and coworkers⁵⁰ calculated the heat capacity of the polymer in the range 0.1–1000 K. The isochoric heat capacity, C_v , as well as the contributions to this quantity by skeletal and atomic vibrations calculated per monomer repeat unit in the polylactone macromolecules were estimated for the same range.

Poly- γ -butyrolactone. The results of the study of the temperature variation of the heat capacity of poly- γ -butyrolactone in an adiabatic vacuum calorimeter⁴³ at temperatures in the range 13.8–340 K have been published by Evstropov et al.⁷⁵ The error of the measurements was 0.3%. The test specimen was obtained

by the bulk polymerisation of γ -butyrolactone under a pressure of 2×10^6 kPa, because at the usual pressure the monomer does not polymerise. The number-average molecular mass of the polymer was $\bar{M}_n = 3 \times 10^3$ and its degree of crystallinity was $\alpha = 67\%$. The amorphous component of the specimen devitrified in the range 200–235 K and the crystalline component melted in the range 245–335 K. In the course of slow stepwise cooling of poly- γ -butyrolactone melt, Evstropov et al.⁷⁵ were able to measure the C_p° of the polymer in the supercooled liquid (highly elastic) state up to a temperature 12 K below its melting point. Overall, the plot of the temperature variation of the heat capacity of poly- γ -butyrolactone has a form similar to that of the plot of the same relation for poly- β -propiolactone (Fig. 2).

Poly- δ -valerolactone. Evstropov et al.⁷⁶ Published the results of a study of the temperature variation of the heat capacity of poly- δ -valerolactone in an adiabatic vacuum calorimeter⁴³ in the range 13.8–340 K. The error of the measurements of C_p° was $\sim 0.3\%$. The test specimen was obtained by the polymerisation of δ -valerolactone. The viscosity-average and number-average molecular masses of poly- δ -valerolactone were respectively 3.6×10^3 and 1.4×10^3 , the polydispersity coefficient was ~ 2.5 , and the degree of crystallinity of the specimen was 70%. The $C_p^\circ - T$ plot was similar to that presented in Fig. 2 for poly- β -propiolactone. The amorphous component of the polymer devitrified in the range 190–215 K and fusion, accompanied by a break in the $C_p^\circ = f(T)$ function, occurred in the range 250–330 K. On slow stepwise cooling of the polymer melt, it was possible to measure its heat capacity in the supercooled liquid state — from the melting point corresponding to thermodynamic equilibrium down to a temperature 10 K below it.

Poly- ϵ -caprolactone. The results of calorimetric studies of the heat capacity of poly- ϵ -caprolactone have been published by Lebedev and coworkers.^{77,78} The measurements in an adiabatic vacuum calorimeter⁴³ in the range 13.8–340 K were carried out with an error of $\sim 0.3\%$,⁷⁷ while those in a differential scanning calorimeter in the range 77–360 K were subject to an error of $\sim 1.5\%$.⁷⁸

Since all the subsequent calculations and conclusions are based on the treatment of the results of Lebedev et al.⁷⁷, we shall note the most important characteristics of the polymer which they investigated. The poly- ϵ -caprolactone specimen was obtained by the polymerisation of ϵ -caprolactone ($\bar{M}_w = 2.9 \times 10^4$, $\alpha = 63\%$). The temperature variation of the heat capacity of the polymer had no singularities: it increased smoothly with increase in temperature, a more rapid rise in C_p° being observed, as for other polylactones, in the devitrification range for the amorphous part of the specimen (200–245 K); the sharp rise in C_p° and the break in the $C_p^\circ - T$ plot in the range 298–336 K are due to the fusion of the crystalline component of the polymer. The differences between the heat capacities quoted in the above two studies^{77,78} do not exceed 1.5% in the range 90–130 K, 0.5% in the range 130–200 K, and 1% in the range 200–250 K.

Polyundecanolactone. The temperature variation of the heat capacity of polyundecanolactone in the temperature range 0–370 K has been published by Evstropov.⁷⁹ The measurements of C_p° were carried out in an adiabatic vacuum calorimeter⁴³ in the range 14–366 K subject to an error of $\sim 0.3\%$. The test specimen was obtained by the polymerisation of undecanolactone. The viscosity-average and number-average molecular masses of the polymer were 3.4×10^4 and 1.0×10^4 respectively. The degree of crystallinity of the specimen was 73%. The $C_p^\circ - T$ plot was similar to that presented in Fig. 2 for poly- β -propiolactone. The amorphous component of the specimen devitrified in the range 190–270 K and fusion, accompanied by a break in the $C_p^\circ = f(T)$ relation, occurred in the range 270–365 K. On slow stepwise cooling of the polyundecanolactone melt, it was possible to measure its heat capacity in the supercooled liquid (highly elastic) state in the temperature range from T_{fus}° to 350 K, which is 15 K below the melting point of polyundecanolactone.

Polytridecanolactone. The results of the study of the temperature variation of the heat capacity of polytridecanolactone in the range 0–370 K have been published by Lebedev et al.⁸⁰ The polymer specimen investigated was obtained by the polymerisation of tridecanolactone. The intrinsic viscosity of polytridecanolactone, measured in chloroform at 298 K, was 0.82 dl g⁻¹ and its degree of crystallinity was 75%. The heat capacity was determined in an adiabatic vacuum calorimeter⁴³ in the range 14–370 K. The error of the values of C_p° obtained was ~0.3%. The devitrification of the amorphous component began at 200 K and its end was masked by the incipient fusion of the crystalline component in the range 280–365 K. The polytridecanolactone melt hardly supercooled. Overall, the $C_p^\circ - T$ plot is similar to that presented in Fig. 2 for poly- β -propiolactone.

Polypentadecanolactone.⁸¹ The heat capacity of polypentadecanolactone was determined in an adiabatic vacuum calorimeter⁴³ in the range 13.8–372 K with an error of ~0.3%. The test specimen was obtained by the polymerisation of pentadecanolactone. The intrinsic viscosity of a solution of the polymer in chloroform at 298 K was 0.93 dl g⁻¹ and the degree of crystallinity of the polymer was 77%. The $C_p^\circ - T$ plot for polypentadecanolactone is similar to the plot presented in Fig. 3 for poly- β -methyl- β -propiolactone. The amorphous component devitrified in the range 200–270 K. In the range 140–200 K, the heat capacity of polypentadecanolactone is described by the equation

$$C_p^\circ = 51.34 + 1.0659T,$$

The deviation of the experimental C_p° points from those calculated by the equation is throughout within the limits of 0.2%. The heat capacity of the fused specimen, like that of other polylactones, is a linear function of temperature. In contrast to some of the preceding polylactones, polypentadecanolactone does not supercool in the liquid state.

IV. Thermodynamics of fusion

The fusion of all partly crystalline polylactones takes place over a wide temperature range. The $C_p^\circ - T$ plots in the melting range have left-hand branches, which ascend comparatively rapidly with increase in temperature, and rapidly descending right-hand branches (Figs. 1–4). Fig. 5 presents typical integral and differential fusion curves for polylactones in relation to poly- ϵ -caprolactone as an example.⁷⁷ They reflect the distribution of the crystals with respect to the melting points. Evidently poly- ϵ -caprolactone melts in the range 210–337 K, approximately 70% of the mass of the crystals melting over a comparatively narrow temperature range (328–337 K), and most of them melt at 336 K.

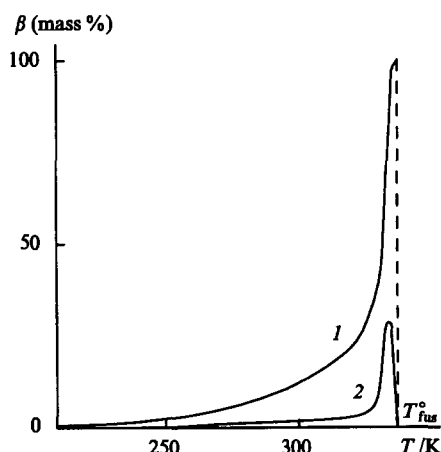


Figure 5. Temperature dependence of the fraction of the melt in the crystalline component of a poly- ϵ -caprolactone specimen ($\alpha = 75\%$).⁷⁷ Integral (1) and differential (2) curves.

The nonisothermal nature of fusion is known to be caused by the polycrystallinity of polymers — the presence of a set of different metastable and crystalline formations with ultramicroscopic and microscopic dimensions and with different chemical potentials. For ultramicroscopic dimensions of the crystals, the Gibbs free energy of the surface constitutes a significant proportion of the total Gibbs free energy G . Below the melting point corresponding to thermodynamic equilibrium, $G(\text{cr}) < G(\text{l})$ and at this temperature $\Delta G = 0$. This condition is attained at different temperatures for small crystals of different size: the smaller the crystal, the lower its melting point. This is in fact the reason for the nonisothermal nature of fusion.¹⁴ The fact that the crystallisation of the polymer does not entail the formation of microscopically ideal crystals of one definite type, the chemical potential of which depends only on the temperature and pressure, can also be accounted for by mainly kinetic causes.

Table 2 presents the thermodynamic parameters of the fusion of polylactones found from the results of calorimetric measurements. The greatest number of data have been obtained by adiabatic vacuum calorimetry. The melting points, corresponding to thermodynamic equilibrium, of defect-free ideal polymer crystals are presented for polylactones investigated by this method. For their calorimetric determination, measurements were made of the melting points T_F° , corresponding to thermodynamic equilibrium, for fractions F of the polymer melt. It was found that, for the polylactones investigated, the $T_F^\circ - F^{-1}$ plots are straight lines described satisfactorily by the equation

$$T_F^\circ = T_0^\circ - F^{-1}(T_0^\circ - T_1^\circ), \quad (4)$$

where T_1° and T_0° are the melting points, corresponding to thermodynamic equilibrium, of the crystals of the polymer specimen employed and a hypothetical defect-free crystal of the same polymer respectively. The above equation is used mainly for low-molecular-mass substances.⁸³ For example, the following results have been obtained for poly- ϵ -caprolactone:⁷⁷

F^{-1}	4.456	2.610	1.305	1.071
T_F° / K	314.584	325.586	334.408	335.420.

$T_1^\circ = 336$ K was obtained from the $T_F^\circ - F^{-1}$ plot for $F^{-1} = 1$ and $T_1^\circ = 342$ K was found by extrapolation for $F^{-1} = 0$.

The enthalpies of fusion of the test specimens of the polymers were measured by the method involving the continuous injection of energy⁸² and were calculated by the equation

$$\Delta_{\text{fus}} H^\circ(\alpha) = \left\{ \Delta H_i^\circ - \int_{T_i^\circ}^{T_{\text{fus}}^\circ} C_p^\circ(\text{s}) dT - \int_{T_{\text{fus}}^\circ}^{T_f^\circ} C_p^\circ(\text{l}) dT - \int_{T_i^\circ}^{T_f^\circ} C_{\text{cal}} dT \right\} \frac{M}{m}, \quad (5)$$

where ΔH_i° is the amount of energy consumed in the heating of the calorimeter with the test substance from the initial experimental temperature T_i° to the final temperature T_f° , $C_p^\circ(\text{s})$ and $C_p^\circ(\text{l})$ are the temperature variations of the heat capacities of a polymer specimen (placed in the calorimeter) with a mass m in the solid (s) and liquid (l) states, C_{cal} is the heat capacity of the empty calorimeter, and M is the molecular mass of the specimen.

The average value of $\Delta_{\text{fus}} H^\circ(\alpha)$ was calculated from the results of 3–4 experiments and was then used to calculate the molar enthalpy of fusion of the crystalline polymer $\Delta_{\text{fus}} H^\circ(\alpha = 100\%)$ from the formula

$$\Delta_{\text{fus}} H^\circ(\alpha = 100\%) = \frac{\Delta_{\text{fus}} H^\circ(\alpha)}{\alpha}, \quad (6)$$

where α is the degree of crystallinity.

In the study of the fusion process by differential scanning and dynamic calorimetry, the temperatures corresponding to the maximum apparent heat capacity in the melting range or the

Table 2. Thermodynamic parameters of the fusion of polylactones.

Poly lactone	$T_{\text{fus}}^{\circ} / \text{K}$	$\Delta_{\text{fus}}H^{\circ}(\alpha = 100\%) / \text{kJ mol}^{-1}$	$\Delta_{\text{fus}}S^{\circ}(\alpha = 100\%) / \text{J mol}^{-1} \text{K}^{-1}$	$\Delta C_p^{\circ}(\alpha = 100\%) / \text{J mol}^{-1} \text{K}^{-1}$	Method of determination	Ref.
Polyglycolide	501 ± 1	11.8 ± 0.5	24 ± 1	20	DSC	61
Poly-β-propiolactone	366 ± 1	10.2 ± 0.5	29.9 ± 1.4	35	AVC	63
Poly-α,α-dimethyl-β-propiolactone	513	14.9	29.0	44	DSC	47, 50
Poly-β-methyl-β-propiolactone	454	12.6	27.7	45	DC	8, 67
Poly-α,α-diethyl-β-propiolactone	531	21.0	40.0	—	DSC	49
Poly-γ-butyrolactone	338 ± 1	13.2 ± 0.3	39.4 ± 0.6	29	AVC	75
Poly-δ-valerolactone	331 ± 2	18.2 ± 0.3	55 ± 1	40	AVC	76
Poly-ε-caprolactone	342 ± 1	19.0 ± 0.3	55.5 ± 1.1	38	AVC	77, 78
Poly-η-caprylactone	354	24.4	70	—	Interpolation	82
Poly-λ-lauro lactone	358	28.2	79	—	"	82
Polynonanolactone	361	31.9	88.5	—	"	82
Polydecanolactone	363	35.6	98	—	"	82
Polyundecanolactone	365 ± 1	38.2 ± 0.8	105.2	64	AVC	79
Polydodecanolactone	366	43	118	—	Interpolation	82
Polytridecanolactone	368 ± 1	46 ± 1.5	125 ± 4	63	AVC	80
Polytetradecanolactone	369	51	137	—	Interpolation	82
Polypentadecanolactone	371 ± 1	56 ± 2	151 ± 6	87	AVC	81

maximum temperature of the melting range were adopted as T_{fus}° .⁶⁹ This is in fact the usual explanation of the discrepancies between the melting points quoted in different publications for the same polylactone. Unfortunately the temperatures T_{fus}° obtained by differential scanning calorimetry at specific rates of heating of the calorimeter with the test substance have not been adjusted to the zero heating rate. The enthalpies of fusion $\Delta_{\text{fus}}H^{\circ}(\alpha)$ were also determined in several experiments. The method has been described, for example, by Lebedev et al.⁸⁴ The average value of $\Delta_{\text{fus}}H^{\circ}(\alpha)$ obtained was then recalculated as $\Delta_{\text{fus}}H^{\circ}(\alpha = 100\%)$ by Eqn (6).

The entropies of fusion $\Delta_{\text{fus}}S^{\circ}(\alpha = 100\%)$ for all the polylactones (Table 2) were found from the enthalpies $\Delta_{\text{fus}}H^{\circ}(\alpha = 100\%)$ and the melting points T_{fus}° by the equation

$$\Delta_{\text{fus}}S^{\circ}(\alpha = 100\%) = \frac{\Delta_{\text{fus}}H^{\circ}(\alpha = 100\%) }{T_{\text{fus}}^{\circ}} \quad (7)$$

The heat capacity change $\Delta C_p^{\circ}(\alpha = 100\%)$ on passing from the crystalline to the liquid polymer at the melting point was found graphically. For example, $\Delta C_p^{\circ}(\alpha = 100\%)$ for polyglycolide is represented by section CD in Fig. 1.

In conclusion we may note that the results of measurements of the melting point and enthalpy of fusion of poly-β-propiolactone by differential scanning calorimetry have been published by Crescenzi et al.⁴⁶ $T_{\text{fus}}^{\circ} = 357 \text{ K}$ and $\Delta_{\text{fus}}H^{\circ}(\alpha = 100\%) = 9.6 \text{ kJ mol}^{-1}$. The enthalpy of fusion agrees satisfactorily with the value published by Lebedev et al.⁶¹ (Table 2), while the melting point is significantly lower, which is natural since Lebedev et al.⁶¹ calculated the melting point for an ideal defect-free poly-β-propiolactone crystal. Kort and Glet⁸⁵ gave the melting point and the specific enthalpy of fusion for poly-α-methyl-α-n-propyl-β-propiolactone as 370 K and 8 J g^{-1} , but there are no data on the degree of crystallinity of the test specimen. For this reason, it is impossible to calculate $\Delta_{\text{fus}}H^{\circ}(\alpha = 100\%)$ for this polymer.

Kort and Glet⁸⁵ found that the melting point of poly-γ-butyrolactone is 334–335 K. This also differs slightly from the temperature quoted in Table 2. The reason for the difference is the same as in the case of poly-β-propiolactone. Tadokoro et al.⁸⁶

determined $T_{\text{fus}}^{\circ} = 326 \text{ K}$ for poly-δ-valerolactone, which is 5 K lower than the corresponding temperature in Table 2. The values $\Delta_{\text{fus}}H^{\circ}(\alpha = 100\%) = 19 \pm 2 \text{ kJ mol}^{-1}$ and $T_{\text{fus}}^{\circ} = 336 \text{ K}$ have been obtained⁷⁸ for poly-ε-caprolactone in adiabatic vacuum calorimetry. The same quantities found by differential scanning calorimetry⁴⁶ proved to be $\Delta_{\text{fus}}H^{\circ}(\alpha = 100\%) = 15.9 \text{ kJ mol}^{-1}$ and $T_{\text{fus}}^{\circ} = 336 \text{ K}$. The enthalpies of fusion found from the results of Lebedev et al.⁷⁷ and Beraty⁷⁸ agree, while the value measured by Crescenzi et al.⁴⁶ is apparently too low.

We may note that, according to our observations,¹⁴ the decrease in the melting points of polymers ($\Delta T_{\text{fus}}^{\circ} = T_0^{\circ} - T_1^{\circ}$) is usually between 4 and 10 K, which is much larger than for the corresponding monomers with approximately the same content of impurities in the usual sense. In the case of polymers, the end groups of the macromolecules and crystal defects are also regarded as impurities.

In conclusion, we shall give a list of the melting points of di- and tri-alkyl-substituted poly-β-propiolactones published by Cornibert et al.⁸⁷ and Thielaut et al.⁸⁸

Poly lactone	$T_{\text{fus}}^{\circ} / \text{K}$
Poly-β-propiolactone	357
Polyα,α-dimethyl-β-propiolactone	513
Poly-α-ethyl-α-methyl-β-propiolactone	398
Poly-α-methyl-α-n-propyl-β-propiolactone	370
Poly-α-isopropyl-α-methyl-β-propiolactone	298
Poly-α-methyl-α-pentyl-β-propiolactone	327
Poly-α,α-diethyl-β-propiolactone	531
Poly-α-ethyl-α-n-propyl-β-propiolactone	478
Poly-α-n-butyl-α-thyl-β-propiolactone	453
Poly-α,α-di-n-propyl-β-propiolactone	530
Poly-α-n-butyl-α-n-propyl-β-propiolactone	500
Poly-α,α-di-n-butyl-β-propiolactone	518
Poly-α,α-dimethyl-β-methyl-β-propiolactone	458
Poly-β-ethyl-α,α-dimethyl-β-propiolactone	423

V. Parameters of vitrification and the vitreous state

Table 3 presents the parameters of the vitrification and the vitreous state of polylactones obtained from the results of calorimetric measurements by adiabatic vacuum and differential scanning calorimetry; the glass transition temperatures of a series of polylactones have been found by the torsional pendulum (TP) method.⁹¹ The temperature of the onset of the devitrification of polylactones in partly crystalline states is distinctly manifested on the temperature variations of C_p° (see, for example, Figs 1 and 2). However, the end of the devitrification process is in most cases masked by the incipient partial fusion of polylactones and it is therefore difficult to determine the temperature at which devitrification comes to an end. Nevertheless, one may conclude that polylactones are devitrified in the range from 20 K (for example, in the case of poly- α,α -dimethyl- β -propiolactone⁵⁰) to 60 K (for polyundecanolactone⁷⁹). The glass transition temperature T_g° is usually close to the average temperature of the vitrification range, but can be determined more accurately from the point of inflection in the $C_p^\circ - T$ and $S^\circ(T) - T$ plots.⁹²

We may note that, since vitrification is a relaxation process,¹⁴ it follows that in the vitrification temperature range the relaxation time of the conformational motions of the segments is of the same order of magnitude as the duration of the experiment (the time required to supply energy to the system). The results of the determination of T_g° therefore depend on the rate at which measurements are made and on the method of the preliminary heat treatment of the polymers (for example, quenching and annealing). The glass transition temperature of poly- β -propiolactone has been found as 245 ± 2 K by the torsional pendulum method,⁹⁰ which is slightly below the value obtained by the AVC method (Table 3). For a rapidly cooled specimen of poly- α,α -dimethyl- β -propiolactone, $T_g^\circ = 259.8$ K,⁵⁰ while for a specimen with a degree of crystallinity of 79% it amounts to 267.8 K. The following values of T_g° have been found for poly- ϵ -caprolactone by different investigators using the torsional pendulum method: 202 K,⁸⁹ 209 K,⁹² and 218 K.⁹³ The lowest value of T_g° corresponds to the fully amorphous polymer specimen and the highest to the specimen with the highest degree of crystallinity.

Thus an increase in the degree of crystallinity leads to an increase in T_g° . This can apparently be explained by the effect of

the reinforcement of the amorphous component of the polymer by crystals, which hinder the excitation of the motion of the segments of the macromolecules on devitrification.⁷¹ As a result of this, the devitrification of partially crystalline polymers occurs at higher temperatures, in contrast to amorphous polymers in which there is no reinforcement effect.

The increase in heat capacity on devitrification of the fully amorphous polymer at the glass transition temperature has been found graphically (Table 3). For example, $C_p^\circ(T_g^\circ)$ for poly- β -propiolactone is represented by section *DB* in Fig. 2. The justification of the validity of the extrapolation of the heat capacity, presented, for example, in Fig. 2, has been described in detail.²⁹ The difference between the enthalpies of the polymer in the vitreous and crystalline states and the zero-point (residual) entropies of the polymers in the vitreous state at 0 K have been calculated by the equations^{24, 29, 34}

$$H_g^\circ - H_{cr}^\circ(0) = \int_0^{T_{fus}} [C_p^\circ(cr) - C_p^\circ(a)]dT + \Delta_{fus}H^\circ(\alpha = 100\%), \quad (8)$$

$$S_g^\circ(0) = \int_0^{T_{fus}} [C_p^\circ(cr) - C_p^\circ(a)]d\ln T + \Delta_{fus}S^\circ(\alpha = 100\%), \quad (9)$$

where $C_p^\circ(a)$ and $C_p^\circ(cr)$ are respectively the temperature functions of the heat capacity of the polymer in the vitreous or highly elastic amorphous ($\alpha = 0$) and crystalline ($\alpha = 100\%$) states (see sections *ABDE* and *ABC* respectively in Fig. 2); $\Delta_{fus}H^\circ(\alpha = 100\%)$ and $\Delta_{fus}S^\circ(\alpha = 100\%)$ are the enthalpy and entropy of fusion of the crystalline polymer.

The enthalpies, entropies, and Gibbs free energies of polyglycolide, poly- β -propiolactone, and poly- ϵ -caprolactone in the amorphous and crystalline states have been calculated for the range $0 - T_{fus}$.^{13, 14, 77} It was postulated that the difference between the Gibbs free energies is an absolute measure of the metastability of the polymer in the amorphous state in relation to its crystalline state. As an example, Fig. 6 presents typical temperature dependences of the above quantities in the range $0 - T_{fus}$ for poly- ϵ -caprolactone.⁷⁷ Evidently the absolute enthalpy and entropy increase with increasing temperature, while the Gibbs free energy diminishes and becomes zero at T_{fus} .

Table 3. Parameters of the vitrification and of the vitreous state of polylactones.

Polylactone	T_g° /K	$\Delta C_p^\circ(T_g^\circ)$ /J K ⁻¹ mol ⁻¹	$H_g^\circ(0) - H_{cr}^\circ(0)$ /kJ mol ⁻¹	$S_g^\circ(0)$ /J K ⁻¹ mol ⁻¹	Method	Ref.
Polyglycolide	318	16	5.9	10	AVC	61
Poly- β -propiolactone	249	53	4.9	10	AVC	63
Poly- α,α -dimethyl- β -propiolactone	260	39	—	16	DSC	50
Poly- γ -butyrolactone	214	58	7.9	19	AVC	75
Poly- δ -valerolactone	207	65	11.7	30	AVC	76
Poly- ϵ -caprolactone	209	60	12.5	31	AVC	77, 78
Poly- γ -methyl- ϵ -caprolactone	220	—	—	—	TP	89
Poly- ϵ -methyl- ϵ -caprolactone	233	—	—	—	TP	89
Poly- α,ϵ -dimethyl- ϵ -caprolactone	240	—	—	—	TP	89
Poly- η -caprolactone	228	—	—	—	TP	90
Poly- λ -laurolactone	235	—	—	—	TP	90
Polyundecanolactone	227	111	27	66	AVC	86
Polydodecanolactone	248	—	—	—	TP	80
Polytridecanolactone	229	146	31	75	AVC	89
Polypentadecanolactone	251	167	41	100	AVC	81

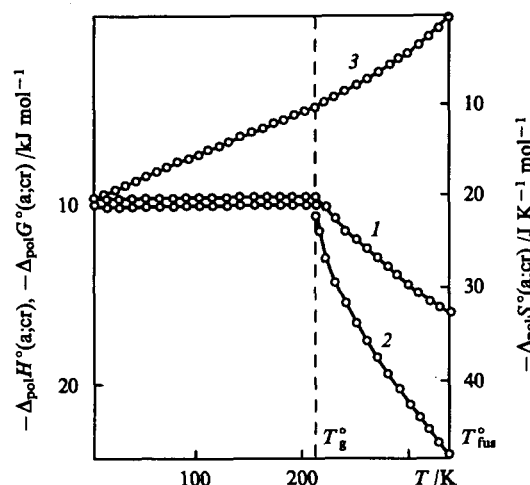


Figure 6. The enthalpies (1), entropies (2), and Gibbs free energies (3) of amorphous and crystalline poly-ε-caprolactone in the range from 0 K to the melting point.⁷⁷

VI. Thermodynamic functions

The thermodynamic functions of polylactones were calculated for the range from 10–14 to 350–550 K (largely with an error of 0.2%–0.3%) from the results of the study of their heat capacities in adiabatic vacuum calorimeters: the enthalpy $H^\circ(T) - H^\circ(0)$, the entropy $S^\circ(T)$, and the Gibbs free energy $G^\circ(T) - H^\circ(0)$; the smoothed heat capacities $C_p^\circ(T)$ were found (Table 4). For the range 0–14 K, the C_p° were obtained by extrapolating the experimental data in terms of the Debye heat capacity formula

$$C_p^\circ(T) = nD\left(\frac{\theta_D}{T}\right), \quad (10)$$

where D is the symbol of the Debye heat capacity and n and θ_D are special parameters chosen so that Eqn (10) describes the values of C_p° in the range from 14 to 20–25 K with an error not exceeding 0.5%–1.0%. It was assumed that at $T < 14$ K it reproduces C_p° with approximately the same error. For example, $n = 3$ and $\theta_D = 93.1$ in Eqn (10) for poly-ε-caprolactone.⁷⁷ For the same parameters, the equation describes the experimental C_p° for the polymer in the range 14–20 K with an error within the limits of 1%.

The thermodynamic functions were calculated from the equations

$$H^\circ(T) - H^\circ(0) = \int_0^T C_p^\circ(T) dT + \Delta_{\text{fus}} H^\circ(\alpha = 100\%), \quad (11)$$

$$S^\circ(T) = S_g^\circ(0) + \int_0^T C_p^\circ(T) d \ln T + \Delta_{\text{fus}} S^\circ(\alpha = 100\%), \quad (12)$$

$$G^\circ(T) - H^\circ(0) = [H^\circ(T) - H^\circ(0)] - TS^\circ(T), \quad (13)$$

where $C_p^\circ(T)$ is the temperature dependence of the heat capacity of polylactones in the given physical state: vitreous, crystalline, highly elastic, and liquid. The values of $C_p^\circ(T)$ were determined from the experimental measurements of the heat capacity of partly crystalline polylactones. The corresponding method has already been published.²⁹ In the calculation of the absolute entropies of the polymers, account was taken of the zero-point entropies $S_g^\circ(0)$ (Table 3).

The heat capacities and thermodynamic functions of polylactones with any degree of crystallinity α can be readily calculated from the numerical values of such functions for the polylactones in the crystalline and amorphous states. This calculation is correct because all the properties listed can be regarded as additive functions of the degree of crystallinity at the specified temperature and pressure. Having designated the property by X , we obtain

$$X(\alpha) = X(\alpha = 1) + [X(\alpha = 0) - X(\alpha = 1)](1 - \alpha), \quad (14)$$

where α is expressed as a fraction.

VII. Thermochemical characteristics

Table 5 presents the enthalpies of combustion ($\Delta_c H^\circ$) and formation ($\Delta_f H^\circ$), the entropies $\Delta_f S^\circ$ and the Gibbs free energies $\Delta_f G^\circ$ of formation of polylactones in the crystalline and amorphous states at 298.15 K and standard pressure, as well as the logarithms of the thermodynamic equilibrium constants of the formation reactions of these compounds from the simple substances in their standard states. For all the compounds listed in Table 5, except poly-β-propiolactone and poly-ε-caprolactone, the combustion energies $\Delta_c U^\circ(\alpha)$ were measured. The values of $\Delta_c U^\circ(\alpha)$, adjusted to the standard pressure [$\Delta_c U^\circ(\alpha)$], were used to calculate the enthalpies of combustion at the standard pressure $\Delta_c H^\circ(\alpha)$. The enthalpies of combustion of the polymers in the crystalline and amorphous (vitreous or highly elastic) states were calculated by the equations

$$\Delta_c H^\circ(\text{cr}) = \Delta_c H^\circ(\alpha) + (1 - \alpha)\Delta_{\text{fus}} H^\circ(298.15 \text{ K}), \quad (15)$$

$$\Delta_c H^\circ(\text{a}) = \Delta_c H^\circ(\alpha) - \alpha\Delta_{\text{fus}} H^\circ(298.15 \text{ K}), \quad (16)$$

where $\Delta_c H^\circ(\alpha)$ is the enthalpy of combustion of the polymer with a degree of crystallinity α and $\Delta_{\text{fus}} H^\circ(298.15 \text{ K})$ is the molar enthalpy of fusion of the fully crystalline polymer at 298.15 K. The latter quantity is hypothetical and it was calculated, using the molar enthalpy of fusion of the crystalline polymer at T_{fus}° and the temperature variations of the heat capacities for the polymer in the crystalline and amorphous states, by the Kirchhoff equation¹⁵

$$\Delta_{\text{fus}} H^\circ(298.15 \text{ K}) = \quad (17)$$

$$= \Delta_{\text{fus}} H^\circ(T_{\text{fus}}^\circ) + \int_{T_{\text{fus}}^\circ}^{298.15 \text{ K}} [C_p^\circ(\text{a}) - C_p^\circ(\text{cr})] dT.$$

This equation may be employed because the calculations relate to a constant (standard) pressure.

The quantities $\Delta_c H^\circ(\text{cr})$ and $\Delta_c H^\circ(\text{a})$ for poly-β-propiolactone and poly-ε-caprolactone were calculated from their enthalpies of formation, which were in their turn evaluated from the enthalpies of the polymerisation of the corresponding monomers to the crystalline and amorphous polymers and the enthalpies of formation of the monomers.

The enthalpies and entropies of formation of the polylactones were calculated from $\Delta_c H^\circ(\text{cr})$, $\Delta_c H^\circ(\text{a})$, the enthalpies of formation of liquid water and gaseous carbon dioxide, the absolute entropies of the polymers in crystalline and amorphous states (Table 4), and the entropies of carbon in the form of graphite and gaseous hydrogen and oxygen at $T = 298.15 \text{ K}$ and $p = 101.325 \text{ kPa}$. The Gibbs free energies of formation of the polymers were found from the formula

$$\Delta_f G^\circ = \Delta_f H^\circ - 298.15 \Delta_f S^\circ. \quad (18)$$

The logarithms of the thermodynamic equilibrium constants of the formation reactions of the polylactones from the simple substances were calculated from the $\Delta_f G^\circ$:

$$\lg K_f^\circ = \frac{-\Delta_f G^\circ}{2.303R \cdot 298.15}. \quad (19)$$

Any thermochemical parameter of a polylactone with any degree of crystallinity may be determined by Eqn (14) using the thermochemical characteristics (Table 5). The additivity of the properties of partly crystalline polymers is a consequence of the fact that they are heterogeneous (microheterogeneous) systems.

We may note in conclusion that Hall⁴⁰ measured in three experiments the energy of combustion of partly crystalline poly-α,α-dimethyl-β-propiolactone (polypivalolactone) and calculated

Table 4. Thermodynamic functions of polylactones.

T/K	$C_p^\circ(T)$	$H^\circ(T) - H^\circ(0)$	$S^\circ(T)$	$G^\circ(T) - H^\circ(0)$	T/K	$C_p^\circ(T)$	$H^\circ(T) - H^\circ(0)$	$S^\circ(T)$	$G^\circ(T) - H^\circ(0)$
Polyglycolide ^{61, 82}					Crystalline state				
<i>Crystalline state</i>					200	77.83	11.67	86.23	8.460
5	0.100	0.00010	0.024	0.000017	298.15	110.8	17.67	123.1	18.73
10	0.7735	0.00195	0.253	0.00058	400	146.9	31.12	160.9	33.23
15	2.184	0.00921	0.824	0.00315	454	166.0	39.57	180.7	42.47
20	3.973	0.02450	1.691	0.00932	<i>Liquid state</i>				
25	5.960	0.04933	2.791	0.02044	454	210.9	52.18	208.4	42.47
50	16.04	0.3324	10.23	0.1790	500	234.2	62.37	229.8	52.53
100	30.47	1.529	26.43	1.094	Poly-γ-butyrolactone ^{75, 82}				
200	48.22	5.495	53.05	5.110	<i>Crystalline state</i>				
298.15	65.15	11.06	75.45	11.43	5	0.19	0.00024	0.062	0.00007
400	82.60	18.59	97.00	20.22	10	1.47	0.00376	0.501	0.00125
501	99.85	27.80	117.5	31.06	15	4.38	0.0181	1.63	0.00629
<i>Liquid state</i>					20	7.87	0.0487	3.37	0.0186
501	120.0	39.10	140.1	31.06	25	11.57	0.0973	5.52	0.0407
550	121.8	45.02	151.3	38.20	30	15.30	0.1645	7.96	0.0743
<i>Vitreous state</i>					50	28.41	0.6062	18.95	0.3416
10	0.7735	0.00195	9	0.0875	100	51.76	2.660	46.50	1.990
15	2.184	0.00921	10	0.134	150	68.48	5.679	70.75	4.934
25	5.960	0.04933	12	0.238	200	84.70	9.505	92.64	9.024
50	16.04	0.3324	19	0.595	250	101.3	14.15	113.3	14.18
100	30.47	1.529	35	1.92	298.15	117.9	19.63	133.4	20.34
200	48.22	5.495	62	6.80	337.5	130.3	24.29	147.8	25.61
298.15	65.15	11.06	84	14.0	<i>Liquid state</i>				
318	68.55	22.36	88	15.6	337.5	159.3	37.56	187.1	25.61
<i>Highly elastic state</i>					345	161.0	38.75	190.7	27.03
350	114.2	16.03	99	18.7	<i>Vitreous state</i>				
400	116.0	21.78	115	24.0	5	0.19	0.00024	18.7	0.094
501	120.0	33.74	140	36.5	10	1.47	0.00376	19.1	0.187
Poly-β-propiolactone ⁶³					15	4.38	0.0181	20.4	0.288
<i>Crystalline state</i>					20	7.87	0.0487	21.7	0.385
10	1.39	0.00352	0.473	0.00121	30	15.30	0.1645	26.8	0.638
20	5.65	0.0375	2.66	0.0157	50	29.41	0.6062	37.8	1.281
30	11.20	0.1212	5.98	0.0581	100	51.76	2.660	65.4	3.871
40	16.56	0.2608	9.96	0.1374	150	68.48	5.679	89.6	7.753
50	21.22	0.4507	14.17	0.2580	214	89.30	10.76	117.6	14.38
100	40.13	2.018	35.15	1.497	<i>Highly elastic state</i>				
150	52.84	4.345	53.85	3.732	250	150.8	16.13	140.6	19.00
200	65.29	7.300	70.77	7.853	298.15	155.5	23.50	167.6	26.47
250	77.15	10.88	86.67	10.79	337.5	159.3	29.70	187.1	33.45
298.15	89.74	14.91	101.4	15.32	Poly-δ-valerolactone ⁷⁶				
366	106.6	21.57	121.5	22.88	<i>Crystalline state</i>				
<i>Liquid state</i>					5	0.19	0.00024	0.060	0.00006
366	142.0	31.77	149.3	22.88	10	1.51	0.00386	0.503	0.00117
400	154.0	36.75	162.3	28.18	15	4.38	0.0182	1.622	0.00613
<i>Vitreous state</i>					20	8.00	0.0489	3.368	0.01846
10	1.39	0.00352	10.5	0.102	25	12.05	0.0989	5.578	0.04060
20	5.65	0.0375	12.7	0.217	30	16.33	0.1698	8.154	0.07479
30	11.20	0.1212	16.0	0.358	50	32.16	0.6598	20.32	0.3564
50	21.22	0.4507	24.2	0.758	100	61.11	3.062	52.47	2.186
100	40.13	2.018	45.2	2.497	150	80.91	6.629	81.13	5.541
150	52.84	4.345	63.9	5.234	200	99.64	11.14	107.0	10.25
200	65.29	7.300	80.8	8.854	250	118.3	16.59	131.2	16.21
245	76.50	10.49	95.1	12.81	298.15	136.3	22.72	153.6	23.08
<i>Highly elastic state</i>					331	148.6	27.40	168.5	28.37
298.15	134.8	17.51	111.0	15.58	<i>Liquid state</i>				
366	142.0	26.90	149.3	27.74	331	188.9	45.60	223.5	28.37
Poly-β-methyl-β-propiolactone ⁶⁷					350	192.2	49.22	234.1	32.72
<i>Crystalline state</i>					<i>Vitreous state</i>				
5	0.2294	0.0003	0.0787	0.0001	5	0.19	0.00024	29.8	0.149
10	1.720	0.00447	0.6010	0.0015	10	1.51	0.00386	30.3	0.299
15	4.487	0.0198	1.805	0.0727	15	4.38	0.0182	31.4	0.453
20	7.937	0.0507	3.560	0.0205	20	8.00	0.0489	33.2	0.615
25	11.45	0.0995	5.720	0.0436	30	16.33	0.1698	38.0	0.970
50	26.24	0.5783	18.41	0.3420	50	32.16	0.6598	50.1	1.845
100	47.23	2.447	43.50	1.901					

Table 4 (continued).

T/K	$C_p(T)$	$H^\circ(T) - H^\circ(0)$	$S^\circ(T)$	$G^\circ(T) - H^\circ(0)$	T/K	$C_p(T)$	$H^\circ(T) - H^\circ(0)$	$S^\circ(T)$	$G^\circ(T) - H^\circ(0)$
Poly-δ-valerolactone ⁷⁶									
<i>Vitreous state</i>					<i>Vitreous state</i>				
100	61.11	3.062	82.3	5.168	200	199.7	21.70	272	32.7
150	80.91	6.629	110.9	10.00	227	221.6	27.39	299	40.5
207	102.3	11.85	140.3	17.19	<i>Highly elastic state</i>				
<i>Highly elastic state</i>					250	341.4	35.14	331	47.6
250	174.8	19.20	172.5	23.93	298.15	360.7	52.04	393	65.1
298.15	183.2	27.82	204.0	33.0	365	387.5	77.05	467	93.4
331	188.9	33.93	223.5	40.02	Polytridecanolactone ⁸⁰				
Poly-ϵ-caprolactone ⁷⁷					<i>Crystalline state</i>				
<i>Crystalline state</i>					5	0.37	0.00032	0.074	0.00005
10	2.42	0.0060	0.79	0.0019	10	3.30	0.0082	1.05	0.0023
20	10.72	0.0690	4.82	0.0274	15	9.62	0.0402	3.55	0.0131
30	20.66	0.2246	10.99	0.1052	20	17.36	0.1073	7.36	0.0399
40	30.17	0.4811	18.31	0.2512	25	25.98	0.2156	12.16	0.0884
50	37.95	0.8216	25.87	0.4721	30	35.26	0.3679	17.68	0.1625
100	71.14	3.611	63.20	2.709	40	53.21	0.8098	30.27	0.4010
150	94.19	7.750	96.45	6.718	50	70.45	1.430	44.05	0.7725
200	116.9	13.03	126.7	12.31	100	137.2	6.781	115.6	4.779
250	139.7	19.44	155.2	19.36	150	185.6	14.87	180.5	12.21
298.15	161.6	26.70	181.7	27.47	200	234.1	25.36	240.6	22.76
342	181.5	34.22	205.2	35.96	250	282.6	38.28	298.0	36.22
<i>Liquid state</i>					298.15	329.3	53.01	351.8	51.88
342	219.3	53.22	260.8	35.96	368	397.1	78.38	428.0	79.11
350	221.6	54.98	265.9	38.09	<i>Liquid state</i>				
<i>Vitreous state</i>					368	459.7	124.4	553.0	79.11
10	2.42	0.0060	31.8	0.312	<i>Vitreous state</i>				
20	10.72	0.0690	35.8	0.647	5	0.37	0.00032	75	0.37
30	20.66	0.2246	42.0	1.04	10	3.30	0.0082	76	0.75
40	30.17	0.4811	49.3	1.49	15	9.62	0.0302	78	1.13
50	37.95	0.8216	56.9	2.02	20	17.36	0.1073	81	1.52
100	71.14	3.611	94.2	5.81	25	25.98	0.2156	86	1.94
150	94.19	7.750	127.5	11.38	30	35.26	0.3679	92	2.38
200	116.9	13.03	157.7	18.51	50	70.45	1.430	118	4.48
209	121.0	14.10	162.9	19.95	100	137.2	6.781	190	12.2
<i>Highly elastic state</i>					150	185.6	14.87	255	23.3
250	192.5	21.74	196.3	27.34	200	234.1	25.36	315	37.6
298.15	206.5	31.35	231.4	37.64	229	262.4	32.56	348	47.1
342	219.3	40.68	260.8	48.45	<i>Highly elastic state</i>				
Polyundecanolactone ^{79, 82}					416.0	41.21	384	54.8	
<i>Crystalline state</i>					298.15	433.9	61.67	459	75.2
5	0.42	0.00053	0.138	0.00016	368	459.7	92.87	553	111
10	3.38	0.0083	1.11	0.0027	Polypentadecanolactone ⁸¹				
15	8.51	0.0374	3.39	0.135	<i>Crystalline state</i>				
20	14.81	0.0950	6.66	0.0382	5	0.46	0.00057	0.148	0.00017
25	22.33	0.1876	10.76	0.0814	10	3.47	0.0091	1.21	0.0030
30	29.93	0.3179	15.49	0.1468	15	10.07	0.0429	3.86	0.0150
40	45.56	0.6953	26.24	0.3543	20	18.48	0.1136	7.86	0.0437
50	60.18	1.225	38.00	0.6749	25	28.29	0.2298	13.01	0.0954
100	117.8	5.803	99.18	4.115	30	38.89	0.3979	19.11	0.1753
150	158.9	12.74	154.9	10.49	40	59.66	0.8925	33.19	0.4352
200	199.7	21.70	206.2	19.53	50	79.33	1.587	48.62	0.8434
250	240.2	32.70	255.1	31.07	100	157.2	7.690	130.1	5.320
298.15	279.7	45.22	300.8	44.46	150	210.8	16.94	204.4	13.72
365	333.8	65.72	362.6	66.64	200	264.5	28.81	272.3	25.65
<i>Liquid state</i>					250	317.8	43.37	337.1	40.96
365	387.5	103.9	467.3	66.64	298.15	369.2	59.91	397.4	58.57
400	401.5	117.7	503.4	83.66	370	446.2	89.36	485.6	90.50
<i>Vitreous state</i>					<i>Liquid state</i>				
10	3.38	0.0083	67	0.66	370	533.1	145.4	637	90.50
20	14.81	0.0950	73	1.37	<i>Vitreous state</i>				
30	29.93	0.3179	81	2.11	5	0.46	0.00057	100	0.50
50	60.18	1.225	104	3.98	10	3.47	0.0091	101	1.00
100	117.8	5.803	165	10.7	15	10.07	0.0429	104	1.52
150	158.9	12.74	221	20.4	20	18.48	0.1136	108	2.05

Table 4 (continued).

T/K	$C_p^\circ(T)$	$H^\circ(T) - H^\circ(0)$	$S^\circ(T)$	$G^\circ(T) - H^\circ(0)$	T/K	$C_p^\circ(T)$	$H^\circ(T) - H^\circ(0)$	$S^\circ(T)$	$G^\circ(T) - H^\circ(0)$
Polyundecanolactone⁸¹									
<i>Vitreous state</i>					<i>Highly elastic state</i>				
30	38.89	0.3979	119	3.17	251	486.9	43.68	438	66.3
50	79.33	1.587	149	5.86	298.15	504.9	67.07	524	89.2
100	157.2	7.690	230	15.3	370	533.1	104.5	637	131.4
150	210.8	16.94	304	28.7					
200	264.5	28.81	372	45.6					
250	317.8	43.37	437	65.9					

Note. The thermodynamic functions quoted have the following dimensions: $C_p^\circ(T)$ and $S^\circ(T)$ — $J \text{ mol}^{-1} \text{ K}^{-1}$; $H^\circ(T) - H^\circ(0)$ and $G^\circ(T) - H^\circ(0)$ — kJ mol^{-1} .

Table 5. The enthalpies of combustion and thermochemical parameters of the formation of polylactones at $T = 298.15 \text{ K}$ and $p = 101.325 \text{ kPa}$ per mole of the repeat unit in the polymers.

Polymer	Physical state ^a	$-\Delta_c H^\circ$ $/\text{kJ mol}^{-1}$	$-\Delta_f H^\circ$ $/\text{kJ mol}^{-1}$	$-\Delta_f S^\circ$ $/\text{J mol}^{-1} \text{ K}^{-1}$	$-\Delta_f G^\circ$ $/\text{kJ mol}^{-1}$	$\lg K_f^\circ$	Ref.
Polyglycolide	cr	705.7 ± 0.8	367.2 ± 0.8	271.6 ± 0.5	286.2 ± 1.0	50.33	
	g	717.5 ± 0.8	355.6 ± 1.3	263.1 ± 1.5	277.1 ± 1.7	48.73	36, 61
Poly- β -propiolactone	cr	1340.2 ± 4.0	412 ± 4.0	382.0 ± 1.0	298.0 ± 4.0	52.20	
	h.e	1347.2 ± 4.0	405 ± 4.0	372.4 ± 1.3	294.0 ± 4.2	51.50	36, 63
Poly- β -methyl- β -propiolactone	cr	2003.2 ± 0.8	428.3 ± 0.8	496.3 ± 1	280.3 ± 1.1	49.16	
	g	2010.6 ± 0.8	421.0 ± 0.8	482.3 ± 1	277.2 ± 1.1	48.62	36, 67
Poly- γ -butyrolactone	cr	2002.4 ± 0.9	429.0 ± 1.2	486.2 ± 0.5	284.0 ± 1.4	49.81	
	h.e	2014.3 ± 0.9	417.1 ± 1.2	452.0 ± 1.2	282.2 ± 1.6	49.50	36, 75
Poly- ϵ -caprolactone	cr	3313.9 ± 2.4	476.3 ± 2.4	710.4 ± 1.3	264.5 ± 2.8	46.39	
	h.e	3328.4 ± 2.2	461.8 ± 2.4	660.7 ± 1.5	264.8 ± 2.6	46.45	36, 76
Polyundecanolactone	cr	6539.4 ± 3.3	648.0 ± 3.3	1117 ± 3	315.0 ± 3.9	55.25	
	h.e	6573.3 ± 3.3	613.8 ± 3.3	1024 ± 4	308.5 ± 4.4	54.11	36, 79
Polytridecanolactone	cr	7857.1 ± 4.0	689.0 ± 4.0	1494 ± 4	243.7 ± 5.2	42.75	
	h.e	7897.2 ± 5.0	649.1 ± 5.0	1387 ± 6	235.7 ± 7.8	41.34	36, 89
Polyundecanolactone	cr	9157.0 ± 6.7	747.3 ± 6.7	1721 ± 3	234.2 ± 3.9	41.08	36, 81
	h.e	9206.1 ± 7.7	698.2 ± 7.7	1590 ± 4	224.1 ± 8.9	39.31	

^a The following designations for the states of the polymers have been adopted: cr — crystalline, g — vitreous (glassy), h.e. — highly elastic.

from the results its enthalpy of combustion as $\Delta_c H^\circ(\alpha) = -2631.7 \text{ kJ mol}^{-1}$. The degree of crystallinity was unknown.

Andruzzi⁴¹ measured the combustion energies of five specimens of polyoxacarbonyl-1,4-cyclohexylene with different molecular masses — from 2.1×10^3 to 1×10^6 . All the specimens investigated were partly crystalline. The number of combustion experiments was 15. Calculation of the enthalpy of combustion showed that $\Delta_c H^\circ(\alpha)$ at $T = 298.15 \text{ K}$ varies from -3686.9 ± 7.6 to $-3700.3 \pm 9.0 \text{ kJ mol}^{-1}$. The authors believe that the reason for the differences is different degrees of crystallinity of the test specimens and also the different contents of the *cis*- and *trans*-units in the polymer. The results of the determination of $\Delta_c H^\circ(\alpha)$ obtained by Hall⁴⁰ and Andruzzi⁴¹ can be regarded only as estimates.

VIII. Thermodynamic parameters of the polymerisation reactions of lactones

The enthalpies of the polymerisation of β -propiolactone,³⁹ δ -valerolactone,⁷⁶ and ϵ -caprolactone⁷⁷ were measured directly in calorimeters;^{58, 94} those of glycolide,^{61, 95} α, α -dimethyl- β -propiolactone,⁴⁰ γ -butyrolactone,⁷⁵ 2-oxabicyclo[2.2.2]octan-3-one,⁴¹ undecanolactone,⁷⁹ tridecanolactone,⁸⁰ and pentadecanolactone⁸¹ were calculated from the experimental enthalpies of combustion of the monomers and polymers. In all cases, the polylactones were partly crystalline, so that the enthalpies of polymerisation were obtained from experimental data for the

processes liquid monomer \rightarrow partly crystalline polymer, i.e. $\Delta_{\text{pol}} H^\circ(l; \text{p.cr})$. The values obtained were used to calculate the enthalpies of polymerisation for the processes liquid monomer \rightarrow crystalline or amorphous (vitreous or highly elastic) polymer. The calculations were performed using the equations¹³

$$\Delta_{\text{pol}} H^\circ(l; \text{cr}) = \Delta_{\text{pol}} H^\circ(l; \text{p.cr}) + \int_T^{T_{\text{fus}}} [C_p^\circ(\text{p.cr}) - C_p^\circ(\text{cr})] dT - (20)$$

$$- (1 - \alpha) \Delta_{\text{fus}} H^\circ(T),$$

$$\Delta_{\text{pol}} H^\circ(l; \text{a}) = \Delta_{\text{pol}} H^\circ(l; \text{p.cr}) + \int_T^{T_{\text{fus}}} [C_p^\circ(\text{p.cr}) - C_p^\circ(\text{a})] dT - (21)$$

$$- \alpha \Delta_{\text{fus}} H^\circ(T),$$

where T is the temperature at which the enthalpy of polymerisation was determined experimentally and the calculation was performed; in those cases where the enthalpies of polymerisation were determined from the enthalpies of combustion the temperature was $T = 298.15 \text{ K}$, whereas in the direct measurements in the calorimeter $T \approx 350 \text{ K}$. The enthalpy of fusion of the polylactone $\Delta_{\text{fus}} H^\circ(T)$ at the temperature of the determination of the enthalpy of polymerisation was calculated by Eqn (17).

For other temperatures, the $\Delta_{\text{pol}} H^\circ$ were calculated from the Kirchhoff formula (Table 6):

Table 6. The enthalpies (kJ mol⁻¹), entropies (J mol⁻¹ K⁻¹), and Gibbs free energies (kJ mol⁻¹), of the polymerisation of lactones in bulk with formation of polylactones ($p = 101.325$ kPa).

T/K	Physical states of monomer and polymer ^a	$-\Delta_{\text{pol}}H^\circ$	$-\Delta_{\text{pol}}S^\circ$	$-\Delta_{\text{pol}}G^\circ$	T, K	Physical states of monomer and polymer ^a	$-\Delta_{\text{pol}}H^\circ$	$-\Delta_{\text{pol}}S^\circ$	$-\Delta_{\text{pol}}G^\circ$
<i>Glycolide</i> → <i>polyglycolide</i> ⁶¹					<i>ε-Caprolactone</i> → <i>poly-ε-caprolactone</i> ⁷⁷				
0	crII;cr	16.7	0	16.7	298.15	l;cr	31	54	15
	crII;g	5.1	-8.4	5.1		l;h.e	17	4	16
200	crII;cr	16.9	2.7	16.4	350	l;l	13.7	8	11
	crII;g	5.3	-5.8	6.5	<i>ξ-Oenantholactone</i> → <i>poly-ξ-oenantholactone</i> ⁹⁶				
298.15	crII;cr	17.0	3.2	16.1	400	l;l	16	1	16
	crII;g	5.4	-5.3	6.9	<i>η-Caprylolactone</i> → <i>poly-η-caprylolactone</i> ⁹⁶				
350	crI;cr	17.7	5.2	15.8	298.15	l;cr	37	60	19
	crI;h.e	4.5	-8.0	7.3		l;h.e	19	-2	20
500	l;cr	27.8	32.5	11.5	400	l;l	16	1	16
	l;h.e	10.3	9.0	5.8	<i>λ-Lauro lactone</i> → <i>poly-λ-lauro lactone</i> ⁹⁶				
550	l;l	15.7	8.8	10.9	298.15	l;cr	43	61	25
<i>β-Propiolactone</i> → <i>poly-β-propiolactone</i> ⁶³						l;h.e	21	-7	23
0	cr;cr	68	0	68	400	l;l	19	-5	21
	cr;g	63	-10	63	<i>Nonanolactone</i> → <i>polynonanolactone</i> ⁹⁶				
100	cr;cr	69	17	67	400	l;l	22	-12	27
	cr;g	64	7	63	<i>Decanolactone</i> → <i>polydecanolactone</i> ⁹⁶				
200	cr;cr	70	24	65	400	l;l	24	-18	31
	cr;g	65	14	62	<i>Undecanolactone</i> → <i>polyundecanolactone</i> ¹³				
298.15	l;cr	82	74	60	0	crII;cr	43	0	43
	l;h.e	75	54	59		crII;g	16	-67	16
400	l;l	74	51	54	100	crII;cr	42	2	42
<i>α,α-Dimethyl-β-propiolactone</i> →						crII;g	16	-64	22
→ <i>poly-α,α-dimethyl-β-propiolactone</i> ^{40,96}					200	crII;cr	42	-5	43
298.15	l;p.cr	84	74	62		crII;g	15	-71	29
<i>γ-Butyrolactone</i> → <i>poly-γ-butyrolactone</i> ⁷⁵					298.15	l;cr	62	69	41
0	cr;cr	-6.5	0	-6.5		l;h.e	28	-24	35
	cr;g	-14	-19	-14	400	l;l	27	-25	37
100	cr;cr	-6	9	-7	<i>Dodecanolactone</i> → <i>polydodecanolactone</i> ⁹⁶				
	cr;g	-14	-10	-13	400	l;l	17	-25	27
200	cr;cr	-5	13	-7.5	<i>Tridecanolactone</i> → <i>polytridecanolactone</i> ⁸⁰				
	cr;g	-13	-6	-12	0	crII;cr	22	0	22
298.15	l;cr	7	65	-13		crII;g	-9	-74	-9
	l;h.e	-5	30	-14	100	crII;cr	22	-1	22
350	l;l	-6	29	-16		crII;g	-9	-75	-2
400	gas;l	28	118	-19	200	crII;cr	20	-9	22
<i>δ-Valerolactone</i> → <i>poly-δ-valerolactone</i> ⁷⁶						crII;g	-10	-83	7
0	crIV;cr	12.5	0	12.5	298.15	crI;cr	38	50	23
	crIV;g	1	-30	1		crI;h.e	-2	-57	15
100	crIV;cr	13	-6	13.5	400	l;l	6	-26	17
	crIV;g	1.5	-24	4	<i>Tetradecanolactone</i> → <i>polytetradecanolactone</i> ⁹⁶				
200	crII;cr	14.5	17	11	400	l;l	2	-26	12
	crII;g	3	-13	5.5	<i>Pentadecanolactone</i> → <i>polypentadecanolactone</i> ⁸¹				
	l;cr	27.5	65	8	0	crI;cr	31	49	31
298.15	l;h.e	10.5	15	6		crII;cr	14	0	14
350	l;l	10	13	5.5		crII;g	-35	-100	-35
<i>2-Oxabicyclo[2.2.2]octan-3-one</i> →					100	crI;cr	31	54	26
→ <i>poly-2-oxabicyclo[2.2.2]octan-3-one</i> ⁴¹						crII;cr	-37	-109	-15
298.15	cr;cr	21				crII;g	36	-99	-30
	l;cr	35	76	12	200	crI;cr	31	55	20
<i>ε-Caprolactone</i> → <i>poly-ε-caprolactone</i> ⁷⁷						crII;cr	12	-10	14
0	cr;cr	17	0	17		crII;g	-37	-109	-15
	cr;g	7	-31	7	298.15	crI;cr	39	86	13
100	cr;cr	17	1	17		crI;h.e	-10	-41	2
	cr;g	7	-30	10	400	l;l	-2	-23	8
200	cr;cr	16	-1	16	<i>Hexadecanolactone</i> → <i>polyhexadecanolactone</i> ⁹⁶				
	cr;g	7	-32	13	400	l;l	0	-21	8

^a The following designations of the states of the reactants have been adopted: cr — crystalline, g — vitreous (glassy), h.e. — highly elastic, l — liquid, gas — gaseous, crI, crII, crIV — different crystalline modifications, p.cr — partly crystalline.

$$\Delta_{\text{pol}}H^\circ(T) = \Delta_{\text{pol}}H^\circ(298.15 \text{ or } 350 \text{ K}) + \Delta[H^\circ(T) - H^\circ(0)], \quad (22)$$

where $\Delta[H^\circ(T) - H^\circ(0)]$ is the difference between the enthalpies of heating the monomer and the polymer, which may be calculated from the data in Table 4.

We may note the characteristic features of the experimental determinations of the enthalpies of the polymerisation of β -propiolactone, α, α -dimethyl- β -propiolactone, and 2-oxabicyclo[2.2.2]octan-3-one. The enthalpy of the bulk polymerisation of β -propiolactone was measured by Sunner and coworkers³⁹ in a Calvet calorimeter⁹⁴ in seven experiments at $T = 298.15 \text{ K}$. $\Delta_{\text{pol}}H^\circ(\alpha) = -80 \pm 3.8 \text{ kJ mol}^{-1}$ was found. The degree of crystallinity was not determined, but it was possible to measure the enthalpy of fusion of the crystalline component of the polymer as $\Delta_{\text{fus}}H^\circ(\alpha) = 7.5 \text{ kJ mol}^{-1}$. Using the value of $\Delta_{\text{fus}}H^\circ$ ($\alpha = 100\%$) (Table 2), Evstropov et al.⁶³ estimated the degree of crystallinity as 75%. This made it possible in its turn to calculate the enthalpy of the polymerisation of β -propiolactone to crystalline and amorphous poly- β -propiolactone⁶³ (Table 6).

The enthalpy of the polymerisation of α, α -dimethyl- β -propiolactone to poly- α, α -dimethyl- β -propiolactone at $T = 298.15 \text{ K}$ was found by Hall:⁴⁰ $\Delta_{\text{pol}}H^\circ(\text{l.p.cr}) = -84 \text{ kJ mol}^{-1}$. It was calculated using the results of the determinations of the enthalpies of combustion of the monomer and the polymer. In order to determine Δ_cH° for the monomer, four experiments were performed, while in the case of the polymer three experiments were carried out. The purity of the monomer specimen was 99%; the polymer was not characterised and it is only known that it was partly crystalline. From this it follows that the value of $\Delta_{\text{pol}}H^\circ$ obtained must be regarded only as an estimate.

Andruzzi⁴¹ gives $\Delta_{\text{pol}}H^\circ(\text{cr;cr}) = -20.9 \pm 2.3 \text{ kJ mol}^{-1}$ for the polymerisation of 2-oxabicyclo[2.2.2]octan-3-one to poly-2-oxabicyclo-1,4-cyclohexylene at $T = 298.15 \text{ K}$. It was obtained from the enthalpies of combustion of the monomer and the polymer. The enthalpy of combustion of the monomer was measured in five experiments and that of the polymer in fifteen experiments. A polymer with \bar{M}_n from 2.1×10^3 to 1×10^6 was used. Analysis of the products of the combustion of the monomer and the polymer showed that the CO_2 content was 99.50 mass%–99.72 mass% relative to the theoretical amount. For the monomer in the crystalline state, $\Delta_cH^\circ = -3717.5 \pm 1.3 \text{ kJ mol}^{-1}$ while for the polymer $\Delta_cH^\circ(\alpha) = -3686.9 \pm 7.6$ to $-3700 \pm 9.8 \text{ kJ mol}^{-1}$. The reasons for the differences between the enthalpies of combustion of the polymer are probably different degrees of crystallinity and also different contents of the *cis*- and *trans*-units in the macromolecules. Andruzzi⁴¹ attempted to measure $\Delta_{\text{pol}}H^\circ$ directly in the calorimeter, but did not succeed because of the unduly low rate of the polymerisation process. Furthermore, he estimated $\Delta_cH^\circ(\text{l;cr})$ as $-76 \pm 10 \text{ kJ mol}^{-1}$. Clearly the value of $\Delta_{\text{pol}}H^\circ$ quoted must be regarded as an approximate estimate.

The entropies of the polymerisation reactions of the lactones (Table 6) were calculated from the entropies of the reactants (Table 4):

$$\Delta_{\text{pol}}S^\circ(T) = S^\circ(\text{M}) - S^\circ(\text{P}), \quad (23)$$

where $S^\circ(\text{M})$ and $S^\circ(\text{P})$ are the absolute entropies of the monomer and the polymer respectively at a temperature T .

The Gibbs free energies of the processes were calculated from a $\Delta_{\text{pol}}H^\circ(T)$ and $\Delta_{\text{pol}}S^\circ(T)$ by the formula

$$\Delta_{\text{pol}}G^\circ(T) = \Delta_{\text{pol}}H^\circ(T) - T\Delta_{\text{pol}}S^\circ(T). \quad (24)$$

The equilibrium concentration of the monomer $[M]_e^\circ$ in the reaction mixture at thermodynamic equilibrium may be determined from the standard Gibbs free energy:

$$[M]_e^\circ = \exp \frac{\Delta G_{\text{pol}}^\circ(T)}{RT}, \quad (25)$$

while the equilibrium concentration of the polymer in the same mixture may be found from the formula

$$[P]_e^\circ = 1 - \exp \frac{\Delta_{\text{pol}}G^\circ(T)}{RT}. \quad (26)$$

Table 7 presents the limiting polymerisation temperatures of lactones, mainly for the liquid monomer \rightarrow liquid polymer processes. They were estimated graphically from the point of intersection of the $\Delta_{\text{pol}}H^\circ = f(T)$ and $T\Delta_{\text{pol}}S^\circ = f(T)$ relations^{14, 18} or by Dainton's method.¹⁸

Table 7. The upper limiting polymerisation temperatures of lactones in bulk under standard pressure.

Lactone	$T_{\text{cel}}^\circ / \text{K}$	Method of determination ^a	Ref.
Glycolide	1800	D	61
β -Propiolactone	1450	D	63
α, α -Dimethyl- β -propiolactone	1135	D	This work
δ -Valerolactone	760	G	76
ϵ -Caprolactone	900	G	77

^a The following designations have been adopted: D — Dainton's method, G — graphical method.

IX. The regularities and characteristics of the thermodynamic properties of polylactones and of the parameters of the polymerisation reactions of lactones

1. Thermodynamic parameters of fusion

Figure 7 presents the dependences of the melting points and the enthalpies and entropies of fusion of polylactones on the composition of the monomer repeat units, each of which has one methylene group more than the preceding one.⁹⁶ Evidently T_{fus}°

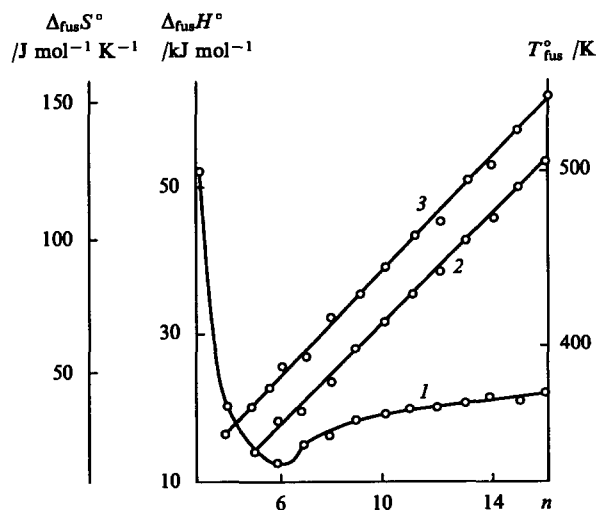


Figure 7. Dependence of the thermodynamic parameters of fusion of polylactones on the number of atoms and atomic groups in the monomer repeat unit of the polymer.⁹⁶

(1) Melting point; (2) enthalpy of fusion; (3) entropy of fusion.

initially decreases rapidly from 501 K for polyglycolide to 331 K for poly- δ -valerolactone and then slowly increases to 371 K for polypentadecanolactone. On further increase in the number of CH₂ groups in the monomer repeat unit in polylactone, T_{fus}° would apparently increase, tending in the limit to T_{fus}° for polyethylene (405 K).⁹⁷

Thielaut et al.⁸⁸ investigated the influence of the composition and structure of the alkyl substituents on the melting points of di- and tri-alkyl-substituted poly- β -propiolactones. Qualitative examination of the results showed that polymers having a more symmetrical structure also have higher melting points; polyesters with the same substituents at the α -carbon atom have the highest T_{fus}° . The dependences of $\Delta_{fus}H^{\circ}$ and $\Delta_{fus}S^{\circ}$ on n are linear and are described by the following equation subject to an error of several percent:

$$\Delta_{fus}H^{\circ} = -5.5 + 3.74n, \quad (27)$$

$$\Delta_{fus}S^{\circ} = -9.0 + 9.75n. \quad (28)$$

The existence of these simple relations made it possible to estimate the corresponding parameters of fusion for polylactones which have not yet been investigated (Table 2).

Comparison of the melting points of polylactones and the corresponding lactones showed¹³ that T_{fus}° for the polymers is higher than for the monomers. The maximum difference between the T_{fus}° is 126 ° for poly- β -propiolactone and β -propiolactone. With increase in the ring size in lactones, ΔT_{fus}° gradually decreases to 62 ° for polypentadecanolactone and pentadecanolactone. The enthalpies of fusion of polylactones are also higher than for the lactones, usually by a factor of 1.2–1.5, while in the case of the polymers obtained from macrocyclic monomers ($n > 10$) the increase is severalfold. It is of interest that the entropies of fusion of (4–6)-membered lactones are equal to or somewhat greater than the $\Delta_{fus}S^{\circ}$ for the corresponding polylactones; $\Delta_{fus}S^{\circ}$ for (7–16)-membered monomers is smaller than for the corresponding polymers — several times smaller for lactones with $n > 12$.

2. Parameters of vitrification and of the vitreous state

The dependence of T_g° for polylactones on the number of atomic groups in the monomer repeat unit⁸² has a form similar to the dependence of T_{fus}° presented in Fig. 7. In the series from four-membered to seven-membered polylactones, T_g° decreases from 318 to 209 K and then increases comparatively slowly to 251 K for polypentadecanolactone. The influence of substitution by methyl groups on T_g° for poly- ϵ -caprolactone has been discovered.⁹³ $T_g^{\circ} = 213$ K for poly- ϵ -caprolactone, 233 K for poly- ϵ -methyl- ϵ -caprolactone, and 220 K for poly- γ -methyl- ϵ -caprolactone and poly- α , ϵ -dimethyl- ϵ -caprolactone. Koleske and Lundberg⁹⁰ compared the glass transition temperatures of polylactones obtained by the polymerisation of (4–16)-membered lactones. It was found that the difference between the glass transition temperatures of the corresponding polymers and monomers is $\Delta T_g^{\circ} = 70 \pm 3$ K. β -Propiolactone and poly- β -propiolactone and also ϵ -caprolactone and poly- ϵ -caprolactone, for which the corresponding differences are 103 and 33 K, are exceptions in the above series.

The $\Delta C_p^{\circ}(T_g^{\circ})$ data obtained for polylactones conform to the familiar Wunderlich rule⁹⁸ that the heat capacity increases on devitrification of amorphous polymers by 11.5 ± 1.7 J K⁻¹ per mole of beads: for polylactones, the increment is 12.5 ± 2.5 J K⁻¹ per mole of beads. The values of $H_g^{\circ}(T) - H_{cr}^{\circ}(0)$ and $S_g^{\circ}(0)$ (Table 3) increase linearly with increase in n , the deviations from the corresponding straight line not exceeding 10%. The accuracy of the calculation of the above quantities is the same.

3. Thermodynamic functions

The dependences of C_p° , $H^{\circ}(T) - H^{\circ}(0)$, $S^{\circ}(T)$, and $G^{\circ}(T) - H^{\circ}(0)$ on n for polylactones at a specified temperature and the standard pressure are straight lines, provided that all the polylactones are in the same physical state.^{13,82} For example, at $T = 298.15$ K and

$p = 101.325$ kPa, the thermodynamic functions for crystalline polylactones are described (subject to an error within the limits of 1%) by the linear equations

$$C_p^{\circ} = -2.2 + 23.42n, \quad (29)$$

$$H^{\circ}(T) - H^{\circ}(0) = 0.46 + 3.732n, \quad (30)$$

$$S^{\circ}(T) = 7.85 + 24.46n, \quad (31)$$

$$-[G^{\circ}(T) - H^{\circ}(0)] = 1.87 + 3.559n. \quad (32)$$

The dependences of the heat capacities of polylactones on n at different temperatures are presented in Fig. 8. The linear relations between the thermodynamic functions and n are undoubtedly associated with the additivity of the corresponding contributions of the methylene groups to particular properties of polylactones. The existence of these relations makes it possible to estimate reliably the thermodynamic functions of polylactones in the series from four-membered to 20-membered polylactones which have not yet been studied experimentally (Table 4).

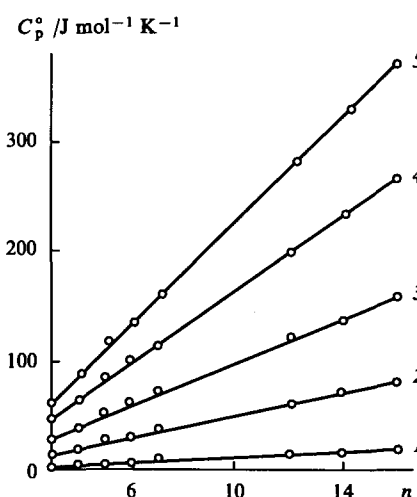


Figure 8. Heat capacity isotherms for polylactones as a function of the number of atoms and atomic groups in the monomer repeat unit of the polymer.⁸² T/K : (1) 20; (2) 50; (3) 100; (4) 200; (5) 300.

4. Thermochemical characteristics

Using the data in Table 5, Kiparisova and Lebedev⁹⁹ fitted by the method of least squares the linear dependences of the thermochemical characteristics of polylactones on the number of carbon atoms ($n' = 3, 4, 6, 11, 13$, and 15) in the monomer repeat units of the macromolecules for $T = 298.15$ K and the standard pressure.

The following relations were found for the enthalpies of combustion and formation of polylactones in the crystalline and vitreous or highly elastic states per mole of the repeat units:

$$\Delta_c H^{\circ}(\text{cr}) = -598.2 + 650.0n', \quad (33)$$

$$\Delta_c H^{\circ}(\text{g}) = -591.8 + 652.8n', \quad (34)$$

$$\Delta_f H^{\circ}(\text{cr}) = -316.8 - 29.0n', \quad (35)$$

$$\Delta_f H^{\circ}(\text{g}) = -318.4 - 25.7n'. \quad (36)$$

The deviations of the experimental values of $\Delta_c H^{\circ}(\text{cr})$ and $\Delta_c H^{\circ}(\text{g})$ from the corresponding straight lines [Eqns (33) and (34)] do not exceed 0.2%, while the deviations of the $\Delta_f H^{\circ}(\text{cr})$ and $\Delta_f H^{\circ}(\text{g})$ do not exceed 2%.

The following relations were established for the entropies of formation:

$$\Delta_f S^{\circ}(\text{cr}) = -4.7 - 111.6n', \quad (37)$$

$$\Delta_f S^\circ(\text{g}) = -5.7 - 103.0n' \quad (38)$$

The deviations of the experimental points from the calculated $\Delta_f S^\circ(\text{cr})$ and $\Delta_f S^\circ(\text{g})$ are within the limits of 10%.

The equations found for the Gibbs free energies are as follows:

$$\Delta_f G^\circ(\text{cr}) = -315.9 + 4.3n', \quad (39)$$

$$\Delta_f G^\circ(\text{g}) = -316.6 + 5.0n'. \quad (40)$$

The deviations of the experimental data from the calculated values of $\Delta_f G^\circ(\text{cr})$ and $\Delta_f G^\circ(\text{g})$ are within the limits of 15%. It has been suggested⁹⁹ that the above equations will prove useful for the estimation of the corresponding thermochemical characteristics of the hitherto uninvestigated polylactones of the series considered. The chemical characteristics found for such polylactones by Eqns (33)–(40) will apparently be subject to approximately the same error as the values found experimentally.

In conclusion, we may note that poly- β -methyl- β -propiolactone and poly- γ -butyrolactone are structural isomers (according to the data of Holmers,⁸ poly- β -methyl- β -propiolactone is an isotactic polymer). Their thermochemical characteristics are fairly close (Table 5) and their enthalpies of combustion and formation in the crystalline state are simply identical. In this connection, the obvious conclusion arises that the $\Delta_c H^\circ$ and $\Delta_f H^\circ$ can also be estimated for other methylsubstituted crystalline polylactones — structural isomers of the polymers investigated.

5. Thermodynamic parameters of polymerisation

Figure 9 presents the Gibbs free energies of polymerisation of lactones in the range from 0 to 400 K at $p = 101.325$ kPa.^{13,96} Evidently the values of $\Delta_{\text{pol}} G^\circ$ for each lactone vary within a fully defined range as a function of temperature (the sections enclosed between curves 1 and 2). This range depends on the compositions, structures, and physical states of the reactants. $\Delta_{\text{pol}} G^\circ < 0$ for four- and (6–13)-membered lactones, while $\Delta_{\text{pol}} G^\circ$ for (14–18)-membered lactones assumes both positive and negative values; for the five-membered lactone, $\Delta_{\text{pol}} G^\circ > 0$. With increase in ring size, the limits of the variation of $\Delta_{\text{pol}} G^\circ$ increase from -54 – -68 kJ mol⁻¹ for β -propiolactone ($n = 4$) to -31 – -29 kJ mol⁻¹ for pentadecanolactone ($n = 16$). All the lactones can be arranged in a series in terms of the values of $\Delta_{\text{pol}} G^\circ$ for liquid monomer \rightarrow liquid polymer processes: β -propiolactone > undecanolactone > decanolactone > dodecanolactone > nonadecanolactone > nonanolactone > η -caprylactone > tridecanolactone > ϵ -caprolactone > ϕ -oenantholactone > pentadecanolactone > δ -valerolactone > lactones with

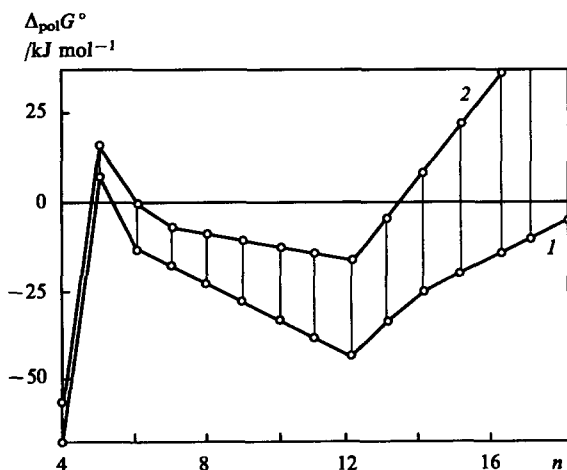


Figure 9. The Gibbs free energies of polymerisation of lactones in the range 0–400 K.^{13,96}
Process: (1) $\text{M}(\text{cr}) \rightarrow \text{P}(\text{cr})$ at 200 K; (2) $\text{M}(\text{cr}) \rightarrow \text{P}(\text{g})$ at 0 K.

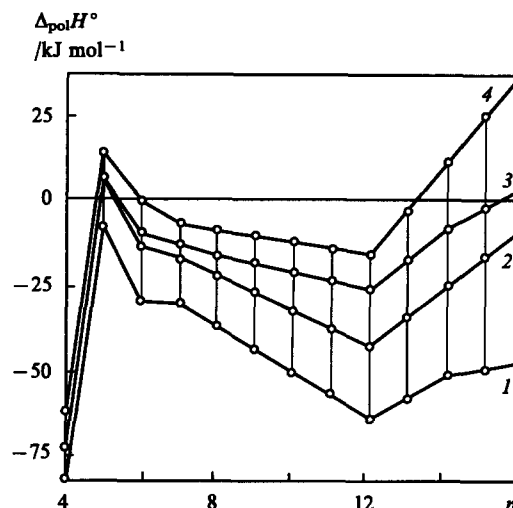


Figure 10. The enthalpies of polymerisation of lactones in the range 0–400 K.^{13,96}
Process: (1) $\text{M}(\text{l}) \rightarrow \text{P}(\text{cr})$ at 300 K; (2) $\text{M}(\text{cr}) \rightarrow \text{P}(\text{cr})$ at 0 K; (3) $\text{M}(\text{l}) \rightarrow \text{P}(\text{l})$ at 370 K; (4) $\text{M}(\text{cr}) \rightarrow \text{P}(\text{g})$ at 0 K.

$n > 20 > \gamma$ -butyrolactone. The sequence thus obtained represents the thermodynamic series for the polymerisabilities of the lactones.

For the same lactone, the $\Delta_{\text{pol}} H^\circ$ for the polymerisation reactions with reactants in different physical states can be arranged in the following sequence: $\text{M}(\text{l}) \rightarrow \text{P}(\text{cr}) > \text{M}(\text{cr}) \rightarrow \text{P}(\text{cr}) > \text{M}(\text{l}) \rightarrow \text{P}(\text{l}) > \text{M}(\text{cr}) \rightarrow \text{P}(\text{g})$, where M is the monomer and P the polymer. The consecutive arrangement of curves 1–4 corresponds to this series in Fig. 10. The $\Delta_{\text{pol}} H^\circ(\text{l}; \text{l})$ increase in the direction from the four-membered to the five-membered lactone, after which they diminish towards the 12-membered lactone, and then again increase. This type of variation of $\Delta_{\text{pol}} H^\circ$ on passing from the four-membered to the 16-membered lactone is caused by the variation of the ring strain energy E . The ring strain energy is evolved on polymerisation of lactones with ring opening, making the main contribution to $\Delta_{\text{pol}} H^\circ(\text{l}; \text{l})$. For example $\Delta_{\text{pol}} H^\circ(\text{l}; \text{l}) = -6$ kJ mol⁻¹ for tridecanolactone, while $E = 8$ kJ mol⁻¹.

As the temperature varies from 0 to 400 K, the entropies of polymerisation of lactones assume both positive and negative values (Fig. 11). As was to be expected, $\Delta_{\text{pol}} S^\circ$ has minimum

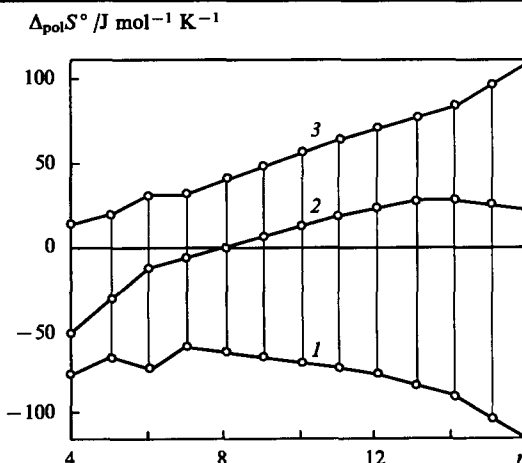


Figure 11. The entropies of polymerisation of lactones in the range 0–400 K.^{13,96}
Process: (1) $\text{M}(\text{l}) \rightarrow \text{P}(\text{cr})$ at 330 K; (2) $\text{M}(\text{l}) \rightarrow \text{P}(\text{l})$ at 370 K; (3) $\text{M}(\text{cr}) \rightarrow \text{P}(\text{g})$ at 200 K.

values for the $M(l) \rightarrow P(cr)$ processes and maximum values for the $M(cr) \rightarrow P(g)$ processes. For the $M(l) \rightarrow P(cr)$ process, the entropy of polymerisation varies from -76 for the four-membered ring to $-116 \text{ J mol}^{-1} \text{ K}^{-1}$ for the 16-membered ring, while for the process $M(cr) \rightarrow P(g)$ the variation is from 14 to $108 \text{ J mol}^{-1} \text{ K}^{-1}$ respectively. The increase in $\Delta_{pol}S^\circ$ for the process $M(cr) \rightarrow P(g)$ is due to the contribution from the zero-point entropy of the polymer $S_g^\circ(0)$, which increases with n . The gradual expansion of the range of variation of $\Delta_{pol}S^\circ$ on passing from the four-membered to the 16-membered ring is associated with the influence of the entropies of the phase transitions of the reactants. The variation of $\Delta_{pol}S^\circ$ for the processes $M(l) \rightarrow P(l)$ is interesting (Fig. 11, curve 2). With increase in n , the quantity $\Delta_{pol}S^\circ(l;l)$ initially increases from $53 \text{ J mol}^{-1} \text{ K}^{-1}$ for β -propiolactone to $26 \text{ J mol}^{-1} \text{ K}^{-1}$ for tridecanolactone and then decreases. If curve 2 is imagined to be prolonged into the range of values $n > 16$, then $\Delta_{pol}S^\circ(l;l) = 0$ at $n \approx 22-25$. This means that rings of this size and larger ones as well as the corresponding repeat units in the polyester macromolecules are entropically indistinguishable. Since rings of this size are of course unstrained, it follows naturally that $\Delta_{pol}G^\circ = 0$ for such structures.

None of the lactones examined in this review has a lower limiting polymerisation temperature. A series of processes have an upper limiting temperature T_{ceil}° . The numerical values of T_{ceil}° are determined by the ratio of a $\Delta_{pol}H^\circ$ and $\Delta_{pol}S^\circ$ at T_{ceil}° . Thus $T_{ceil}^\circ = 1450 \text{ K}$ for β -propiolactone, which is due to the high value of $\Delta_{pol}H^\circ(l;l) = -74 \text{ kJ mol}^{-1}$ and the relatively low value of $\Delta_{pol}S^\circ = -51 \text{ J mol}^{-1} \text{ K}^{-1}$. On passing to δ -valerolactone, $\Delta_{pol}H^\circ$ diminishes sharply and there is only a slight decrease in $\Delta_{pol}S^\circ$. Both these factors lead to $T_{ceil}^\circ = 760 \text{ K}$ for δ -valerolactone. Lactones in which the number of ring members is between 9 and 16 have neither a lower nor an upper limiting temperature because $\Delta_{pol}H^\circ(l;l) < 0$, and $\Delta_{pol}S^\circ > 0$ for these substances.

References

1. Yu N Sazanov *Usp. Khim.* **37** 1084 (1968) [*Russ. Chem. Rev.* **37** 463 (1968)]
2. E B Lyudvig, Doctoral Thesis in Chemical Sciences, L Ya Karpov Physicochemical Research Institute, Moscow, 1981
3. J E Kemnitzer, S P McCarty, R A Grop *Macromolecules* **26** 1221 (1993)
4. D W Grijpma, A J Nijenhuis, A G Penning *Polymer* **31** 2201 (1990)
5. R Deanini *Rolym. Plast. Technol. Eng.* **31** 229 (1992)
6. In *Entsiklopediya Polimerov* (Encyclopedia of Polymers) (Moscow: Sovetskaya Entsiklopediya, 1974) p. 2
7. H Kus, A Kozłowska *Polym. Med.* **2** 375 (1972)
8. P A Holmers, in *Developments in Crystalline Polymers* (Ed. D S Basset) (London: Elsevier, 1988) p. 1
9. Jpn. P. 259 026; *Ref. Zh. Khim.* **18** T 434P (1991)
10. US P. 3 326 938; *Ref. Zh. Khim.* **17** N 87P (1968)
11. US P. 3 291 820; *Ref. Zh. Khim.* **7** N 73P (1968)
12. H Sawada *Thermodynamics of Polymerisation* (New York: Marcel Dekker, 1978)
13. A A Evstropov, Candidate Thesis in Chemical Sciences, Gor'kii State University, Gor'kii 1981
14. B V Lebedev *Termodinamika Polimerov* (Thermodynamics of Polymers) (Gor'kii: Gor'kii State University, 1989)
15. O M Poltorak *Termodinamika v Fizicheskoi Khimii* (Thermodynamics in Physical Chemistry) (Moscow: Vysshaya Shkola, 1991)
16. D R Stull, E F Westrum, G C Sinke *The Chemical Thermodynamics of Organic Compounds* (New York: Wiley, 1969)
17. M Melchior, H Kehl, H Hocker *Macromol. Chem., Rapid Commun.* **15** (1997) (in the press)
18. F S Dainton, K J Ivin *Quart. Rev.* **12** 61 (1958)
19. A V Tobolsky *Properties and Structure of Polymers* (New York: Wiley, 1960)
20. V A Kabanov, V P Zubov *Zh. Vses. Khim. O-va im. D I Mendeleeva* **9** 620 (1964)
21. B P Nikol'skii (Ed.) *Fizicheskaya Khimiya* (Physical Chemistry) (Leningrad: Khimiya, 1987)
22. H N V Temperley *J. Res. Natl. Bur. Stand.* **56** 55 (1956)
23. I Gutzow *Z. Phys. Chem.* **221** 153 (1962)
24. B V Lebedev, I B Rabinovich *Dokl. Akad. Nauk SSSR* **237** 641 (1977)
25. A B Bestul, S S Chang *J. Chem. Phys.* **40** 3781 (1964)
26. G Adam, G H Gibbs *J. Chem. Phys.* **43** 139 (1965)
27. A Milchev, I Gutzow *J. Macromol. Sci.-Phys.* **B21** 583 (1982)
28. T P Melia *J. Appl. Chem.* **11** 461 (1964)
29. B V Lebedev, I B Rabinovich *Vysokomol. Soedin., Ser. B* **18** 416 (1976)
30. W Kauzmann *Chem. Rev.* **43** 218 (1948)
31. Yu K Godovskii, in *Teplofizika Polimerov* (Thermophysics of Polymers) (Moscow: Khimiya, 1982) p. 14
32. B Wunderlich *Macromolecular Physics* (New York: Academic Press, 1976)
33. B V Lebedev, Doctoral Thesis in Chemical Sciences, Moscow State University, Moscow, 1979
34. I B Rabinovich, B V Lebedev *Vysokomolek. Soedin., Ser. A* **21** 2025 (1979)
35. D Tox, M M Lates, A Weissberger (Eds) *Physics and Chemistry of the Organic Solid State* (New York: Interscience, 1965)
36. B V Lebedev, E G Kiparisova *Zh. Fiz. Khim.* **70** 1351 (1996)
37. B Lebedev, N Smirnova *Makromol. Chem. Phys.* **195** 35 (1994)
38. E Domalsky *J. Phys. Chem. Ref. Data* **19** 881 (1990)
39. B Borjesson, J Nakase, S Sunner *Acta Chem. Scand.* **20** 11 (1975)
40. H K Hall *Macromolecules* **1** 488 (1969)
41. F Andruzzi *Makromol. Chem.* **181** 923 (1980)
42. S M Skuratov, V P Kolesov, A F Vorob'ev, in *Termokhimiya* (Thermochemistry) (Moscow: Moscow State University, 1966) Part II, p. 13
43. B V Lebedev, V Ya Lityagov, in *Termodinamika Organicheskikh Soedinenii (Mezhvuzovskii Sbornik)* [Thermodynamics of Organic Compounds (Intercollegiate Collection)] No. 5 (Gor'kii: Gor'kii State University, 1976) p. 89
44. V A Kirillin, A E Sheindlin, in *Issledovanie Termodinamicheskikh Svoistv Veshchestv* (Investigation of the Thermodynamic Properties of Substances) (Moscow: Gosenergoizdat, 1963) p. 335
45. M M Popov, G L Gal'chenko *Zh. Obshch. Khim.* **21** 2220 (1951)
46. V Crescenzi, G Manzini, G Calzolari, C Borri *Eur. Polym. J.* **8** 449 (1972)
47. C Borri, S Bruckner, V Crescenzi, G Fortuna, A Mariano, P Scarazzato *Eur. Polym. J.* **7** 1525 (1971)
48. L A Pilato, J V Koleska, B L Joesten *Am. Chem. Soc. Polym. Prepr.* **17** 824 (1976)
49. J Norman, M Aubin, R E Prud'homme *Makromol. Chem.* **180** 769 (1979)
50. J Grelbowicz, M Varma-Nair, B Wunderlich *Polym. Adv. Technol.* **3** 51 (1992)
51. B Wunderlich *J. Phys. Chem.* **69** 2078 (1965)
52. Yu K Godovskii *Teplofizicheskie Metody Issledovaniya Polimerov* (Thermophysical Methods for the Investigation of Polymers) (Moscow: Khimiya, 1976)
53. M Sh Yagfarov, Doctoral Thesis in Chemical Sciences, Institute of Organic and Physical Chemistry, Kazan', 1986
54. V A Bernshtein, V M Egorov *Differentsial'naya Skaniruyushchaya Kalorimetriya v Fizikokhimii Polimerov* (Differential Scanning Calorimetry in the Physical Chemistry of Polymers) (Leningrad: Khimiya, 1960)
55. W Hemminger, G Hohne *Calorimetry Fundamentals and Practice* (Weinheim: Verlag Chemie, 1983)
56. D C Ginnings, G T Furukawa *J. Am. Chem. Soc.* **75** 522 (1953)
57. J Jin, B Wunderlich *J. Thermal Anal.* **36** 765; 1519 (1990)
58. L Ya Tsvetkova, B V Lebedev, N K Lebedev *Zh. Fiz. Khim.* **50** 798 (1976)
59. R M Joshi *J. Polym. Sci.* **56** 313 (1962)
60. N K Lebedev, Candidate Thesis in Chemical Sciences, Gor'kii State University, Gor'kii, 1980
61. B V Lebedev, A A Evstropov, E G Kiparisova, V I Belov *Vysokomol. Soedin., Ser. A* **20** 29 (1978)
62. K Lofakic, B Wunderlich *J. Phys. Chem.* **92** 4205 (1988)
63. A A Evstropov, B V Lebedev, T G Kulagina, E B Lyudvig, B G Belen'kaya *Vysokomol. Soedin., Ser. A* **21** 2038 (1979)

64. J Chang, R A Gross, R V Lenz *Macromolecules* **23** 3206 (1990)
65. J Hori, M Suzuki, A Yamaguchi, T Nishishita *Macromolecules* **26** 5533 (1993)
66. J Doi *Microbial Polyesters* (Weinheim: VCH, 1990)
67. B V Lebedev, T A Bykova, E G Kiparisova, V G Vasil'ev *Makromol. Chem. Phys.* **197** 1553 (1996)
68. V M Malyshev, G A Mil'ner, E L Sorkin, V F Shibakin *Pribory i Tekhnika Eksperimenta* **6** 195 (1985)
69. E A Gusev, S V Dalidovich, A A Vecher *Thermochim. Acta* **92** 379 (1985)
70. G M Bartenev, S Ya Frenkel' *Fizika Polimerov* (The Physics of Polymers) (Leningrad: Khimiya, 1990) p. 94
71. I B Rabinovich, A N Mochalov, L Ya Tsvetkova, T B Khlyustova, Ye M Moseyeva, V A Maslova *Acta Polym.* **34** 482 (1983)
72. G M Bartenev, G M Sinitsina, N V Khikhlovskaya, A V Danilov *Vysokomol. Soedin., Ser. B* **34** 3 (1992)
73. R E Prud'homme, R H Marchessault *Makromol. Chem.* **175** 2705 (1974)
74. B Wunderlich *Macromolecular Physics* Vol. 3 (New York: Academic Press, 1980)
75. A A Evstropov, B V Lebedev, E G Kiparisova, V A Alekseev, G A Stashina *Vysokomol. Soedin., Ser. A* **22** 2450 (1980)
76. A A Evstropov, B V Lebedev, T G Kulagina, N K Lebedev *Vysokomol. Soedin., Ser. A* **24** 568 (1982)
77. B V Lebedev, A A Evstropov, N K Lebedev, E A Karpova, E B Lyudvig, B G Belen'kaya *Vysokomol. Soedin., Ser. A* **20** 1974 (1978)
78. Ch H Beaty, DTh, University of Massachusetts, 1972
79. A A Evstropov, Author's Abstract of Candidate Thesis in Chemical Sciences, Gor'kii State University, Gor'kii 1981
80. B V Lebedev, A A Evstropov, E G Kiparisova, N P Sheveleva *Vysokomol. Soedin., Ser. B* **23** 551 (1981)
81. A A Evstropov, B V Lebedev, E G Kiparisova *Vysokomol. Soedin., Ser. A* **25** 1679 (1983)
82. B Lebedev, A Yevstropov *Makromol. Chem.* **185** 1235 (1984)
83. Yu I Aleksandrov *Tochnaya Kriometriya Organicheskikh Veshchestv* (Exact Cryoscopy of Organic Substances) (Leningrad: Khimiya, 1975)
84. B V Lebedev, T G Kulagina, V J Telnoy, V G Vasil'ev *Makromol. Chem. Phys.* **196** 3487 (1995)
85. F Kort, W Glet *J. Polym. Sci., Polym. Phys. Ed.* **4** 685 (1966)
86. H Tadokoro, M Kabayashi, H Joshidome, T Kazuo, D Makino *J. Chem. Phys.* **49** 3359 (1968)
87. G Cornibert, R H Marchessault, A E Allegrezza, R W Lenz *Macromolecules* **6** 676 (1973)
88. R Thielaut, N Fischer, J Etienne, J Coste *Ind. Plast. Modern* **14** 13 (1962)
89. C G Seefried, J V Koleske *J. Macromol. Sci.* **10** 579 (1974)
90. J V Koleske, R D Lundberg *J. Polym. Sci., Polym. Chem. Ed.* **10** 323 (1972)
91. L E Nielsen *Rev. Sci. Instr.* **22** 690 (1951)
92. S Alford, M Dole *J. Am. Chem. Soc.* **77** 4774 (1955)
93. C G Seefried, J V Koleske *J. Polym. Sci., Polym. Phys. Ed.* **13** 851 (1975)
94. H A Skinner, in *Experimental Thermochemistry* (New York: Interscience, 1962)
95. B V Lebedev, A A Evstropov, E G Kiparisova, E B Lyudvig, G S Sanina *Dokl. Akad. Nauk SSSR* **236** 668 (1977)
96. B V Lebedev, A A Evstropov *Dokl. Akad. Nauk SSSR* **264** 102 (1982)
97. B Wunderlich, G Czornyj *Macromolecules* **10** 906 (1977)
98. B Wunderlich *Table of Properties of Linear Macromolecules and Small Molecules* (Knoxville: University of Tennessee, 1991)
99. E G Kiparisova, B V Lebedev *Zh. Fiz. Khim.* **70** (1996) (in the press)

Michael synthesis of esters of β -amino acids: Stereochemical aspects

N N Romanova, A G Gravis, Yu. G. Bundel'

Contents

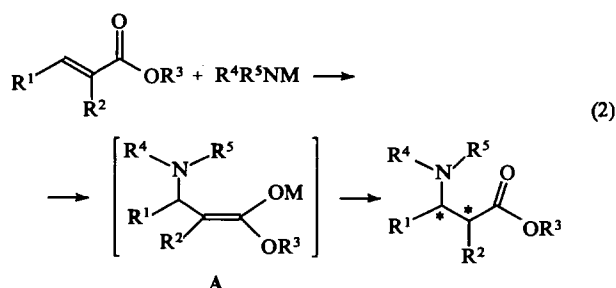
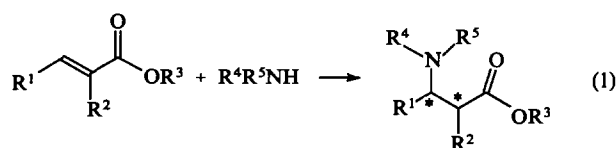
I. Introduction	1083
II. Nucleophilic addition of amines to esters of α,β -unsaturated acids	1083
III. Nucleophilic addition of metal amides to esters of α,β -unsaturated carboxylic acids	1086
IV. Stereochemistry of nucleophilic addition of amines and metal amides to esters of α,β -unsaturated carboxylic acids	1090
V. Mathematical modelling of structures of the transition states in the Michael nucleophilic addition	1091

Abstract. Published data dealing with the synthesis of esters of β -amino acids by nucleophilic addition of amines and metal amides to esters of α,β -unsaturated carboxylic acids are considered. Information on the influence of various factors on the chemical yield and diastereoselectivity of the Michael reaction is discussed systematically. The bibliography includes 70 references.

I. Introduction

During recent years, extensive studies on the synthesis and stereochemistry of β -lactams, which are fragments of numerous natural biomolecules, have been carried out. Since the biological activity of β -lactams is associated with only one of all possible diastereomers,^{1,2} the attention of researchers is focused on the problem of asymmetric synthesis of homochiral β -lactams.^{3–5} Chiral β -amino acids⁶ or their esters, which are difficult to obtain, are precursors of these compounds.

The simplest method for the synthesis of β -amino esters is the conjugate addition of primary or secondary amines (reaction 1) or the corresponding metal amides (reaction 2) to esters of α,β -unsaturated carboxylic acids.



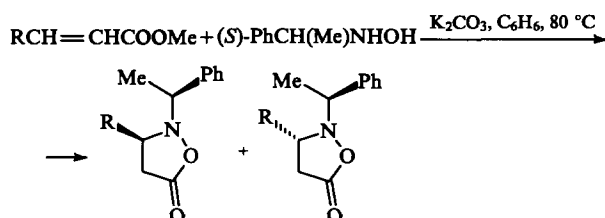
These reactions (if R^1 and/or $\text{R}^2 \neq \text{H}$) result in the formation of a chiral centre at the C_β (and/or C_α) atom and, in some cases, if certain conditions are satisfied, asymmetric synthesis of esters of β -amino acids becomes possible.

II. Nucleophilic addition of amines to esters of α,β -unsaturated acids

The conditions of the syntheses of β -amino esters from primary amines and α,β -unsaturated carboxylates are presented in Table 1. Polar solvents such as alcohols or carboxylic acids are usually employed as the reaction medium. Aprotic solvents, in particular THF, are also used; in some cases, the addition occurs only in a polar medium.⁷

Primary amines do not react with esters of α,β -unsaturated carboxylic acids under ordinary conditions, except for some individual cases (Table 1, entries 1, 2, 6, and 41); therefore, to prepare β -amino esters, the process of addition must be activated.¹⁷

Thermal activation of this reaction leads to satisfactory results; primary amines react most readily with methyl hydroxybenzylacrylate (yields 92%–95%, see entries 3 and 4 in Table 1). With crotonates (entries 12–15, 17, and 18) and cinnamates (entries 38 and 39), the yields of β -amino esters are as low as 14%–47%. It can be seen that an increase in the size of the substituent at the β -carbon atom decreases the chemical yields of the resulting β -amino esters from 26%–47% to 14%–16%. Similar results were also obtained for the addition of (*S*)- α -phenylethylhydroxylamine to methyl esters of α,β -unsaturated carboxylic acids.¹⁸



N N Romanova, A A Gravis, Yu. G. Bundel' Department of Chemistry, Moscow State University, Vorob'evy Gory, 119899 Moscow, Russian Federation. Fax (7-095) 932 88 46. Tel. (7-095) 939 53 76

Received 17 April 1996

Uspekhi Khimii 65 (12) 1170–1180 (1996); translated by Z P Bobkova

The yields of isoxazolidinones, which are formed in this reaction and can be readily reduced to β -amino acids, decrease from 91% (in the case of 4-methylpentenoic acid) to 54% (in the case of cinnamic acid).

The Michael reaction can also be activated by high pressure.¹⁹ This can be illustrated by the addition of benzylamine and α -methylbenzylamine to substituted menthyl crotonates (cf.

Table 1. Conditions of reactions of primary amines with esters of α,β -unsaturated carboxylic acids.



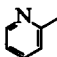
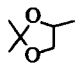
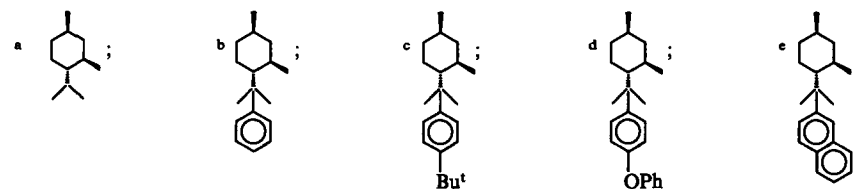
No	R ¹	R ²	R ³	R ⁴	<i>t</i> /h	<i>T</i> /°C	Solvent	<i>P</i> /atm	Catalyst	Yield (%)	d.e. ^a (%)	Ref.
1	H	CH(OH)Me	Me	CH ₂ Ph	48	20	MeOH	1	None	99	64	8
2	H	CH(Me)OSiMe ₂ Bu ^t	Me	CH ₂ Ph	48	25	MeOH	1	"	90	91	8
3	H	CH(OH)Ph	Me	CH ₂ Ph	2	70	MeOH	1	"	95	54	8
4	H	CH(OH)Ph	Me	CH ₂ Ph	40	67	THF	1	"	92	57	8
5	H	CH(OH)Me	Me	CH ₂ Ph	40	67	THF	1	"	77	49	8
6	H	CH(OH)Ph	Me	CH ₂ Ph	46	0	MeOH	1	"	98	61	8
7	H	H	Me		—	118	AcOH	1	"	90	—	9
8	H	Me	Me	Bu ^t	24	30	MeCN	1	"	0	—	10
9	H	Me	Me	Bu ^t	24	30	MeCN	1	Yb(OTf) ₃	4	—	10
10	H	Me	Me	Bu ^t	24	30	MeCN	3000	None	11	—	10
11	H	Me	Me	Bu ^t	24	30	MeCN	3000	Yb(OTf) ₃	47	—	10
12	Me	H	Me	(<i>R</i>)-CH(Me)Ph	12	78	EtOH	1	None	40	7	11
13	Me	H	Me	(<i>S</i>)-CH(Me)Ph	12	78	EtOH	1	"	47	7	11
14	Me	H	Et	(<i>S</i>)-CH(Me)Ph	6	78	EtOH	1	"	28	13	12
15	Me	H	Me	(<i>R</i>)-CH(Me)Ph	4	78	EtOH	1	"	35	<4	13
16	Me	H	Me	CH(Me)Ph	120	20	CH ₂ Cl ₂	13817	"	60	5	14
17	Me	H	<i>l</i> -Menthyl ^b	CH ₂ Ph	12	78	EtOH	1	"	26	2	11
18	Me	H	<i>l</i> -Menthyl ^b	(<i>R</i>)-CH(Me)Ph	12	78	EtOH	1	"	28	5	11
19	Me	H	<i>l</i> -Menthyl ^b	(<i>S</i>)-CH(Me)Ph	12	78	EtOH	1	"	25	15	11
20	Me	H	<i>l</i> -Menthyl ^b	CH ₂ Ph	72	20	MeOH	4935	"	35	10	14
21	Me	H	8-Ph- <i>l</i> -menthyl ^c	(<i>R</i>)-CH(Me)Ph	24	50	CH ₂ Cl ₂	13817	"	60	50	14
22	Me	H	8-Ph- <i>l</i> -menthyl ^c	(<i>S</i>)-CH(Me)Ph	24	50	CH ₂ Cl ₂	13817	"	60	60	14
23	Me	H	8-Ph- <i>l</i> -menthyl ^c	CH ₂ Ph	96	50	MeOH	14804	"	90	60	14
24	Me	H	8- <i>p</i> -Bu ^t C ₆ H ₄ - <i>l</i> -menthyl ^d	CH ₂ Ph	24	25	MeOH	14804	"	65	75	14
25	Me	H	8- <i>p</i> -PhOC ₆ H ₄ - <i>l</i> -menthyl ^e	CH ₂ Ph	24	25	MeOH	14804	"	90	95	14
26	Me	H	8-Naphth- <i>l</i> -menthyl ^f	CH ₂ Ph	24	25	MeOH	14804	"	50	>99	14

Table 1 (continued).

No	R ¹	R ²	R ³	R ⁴	t/ h	T/°C	Solvent	P/ atm	Catalyst	Yield (%)	d.e. ^a (%)	Ref.
27	Me	H	Et	CH ₂ Ph	6	20	CH ₂ Cl ₂	1	La(OTf) ₃	95	—	15
28	Me	H	Et	CH ₂ Ph	6	20	CH ₂ Cl ₂	1	Sm(OTf) ₃	95	—	15
29	Me	H	Et	CH ₂ Ph	25	20	CH ₂ Cl ₂	1	Yb(OTf) ₃	92	—	15
30	Me	H	Et	CH ₂ Ph	6	20	THF	1	Yb(OTf) ₃	97	—	15
31	Me	H	Et	CH ₂ Ph	6	20	EtOH	1	Yb(OTf) ₃	95	—	15
32	Me	H	Et	CH ₂ Ph	6	20	MePh	1	Yb(OTf) ₃	92	—	15
33	Me	H	Et	CH ₂ Ph	4.5	20	CH ₂ Cl ₂	1	TiCl ₄	28	—	15
34	Me	H	Et	CH ₂ Ph	17	20	THF	1	YbCl ₃	28	—	15
35	Me	H	Et	CH(Me)Ph	12	20	THF	1	Yb(OTf) ₃	26	32	15
36	Me	H	Et	CH ₂ Ph	15	20	CH ₂ Cl ₂	1	Yb(OTf) ₃	42	—	10
37	Me	H	Et	CH ₂ Ph	24	30	MeCN	1	Yb(OTf) ₃	100	—	10
38	Ph	H	Et	(<i>R</i>)-CH(Me)Ph	12	78	EtOH	1	None	16	17	11
39	Ph	H	Et	(<i>S</i>)-CH(Me)Ph	12	78	EtOH	1	"	14	19	11
40	CH ₂ CH(OMe) ₂	H	8-Ph- <i>l</i> -Menthyl ^c	CH ₂ Ph	24	20	MeOH	12830	"	85	60	14
41		H	Me	CH ₂ Ph	50	−50	None	1	"	85	100	16

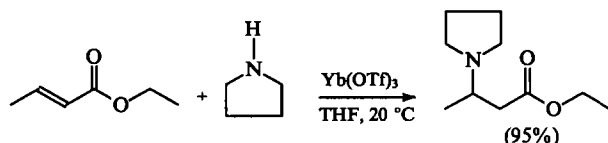
^a In Tables 1–4, d.e. stands for diastereomeric excess;

entries 17–19 and 20–26 in Table 1). The chemical yields vary between 50% and 90% and depend on the nature of the substituent in the substrate.

The use of titanium tetrachloride (Table 1, entry 33) or of ytterbium chloride (entry 34) as catalysts of the conjugate addition does not favour an increase in the yield of β -amino esters (yield ~28%); in addition, the amide of the initial α,β -unsaturated carboxylic acid is formed in these reactions as a side product in approximately the same yield (26%).

When various 2-chloro-2-cyclopropylideneacetates react with (4*S*,5*R*)-4,5-diphenyloxazolidin-2-one in THF in the presence of 10 mol.% of sodium hydride and a small amount of DB-18-C-6 crown ether, the corresponding 1,4-addition products are formed in chemical yields of 57%–88%.²⁰

Recently it has been shown¹⁵ that highly oxophilic lanthanide triflates, which are currently widely used in organic catalysis,²¹ accelerate the Michael reaction, in particular the addition of benzylamine to ethyl crotonate (Table 1, entries 27–32). The yields of the target products in these reactions are 92%–97%, and no side products are formed. In the presence of ytterbium triflate, pyrrolidine easily adds to ethyl crotonate giving the corresponding product in 95% yield; however, α -phenylethylamine, which is sterically more hindered, does not react so readily: the yield of the corresponding product is only 26% (see Table 1, entry 35).

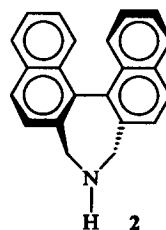


The catalytic addition of amines to esters of α,β -unsaturated acids occurs at room temperature over a period of several hours. Both polar (ethanol) and non-polar (toluene) solvents have been used as the reaction media. The best results were achieved with THF as the solvent and ytterbium triflate as the catalyst. Variation of the polarity of the reaction medium or the use of triflates of other lanthanides do not lead to any substantial changes in the yield of the reaction product (Table 1, entries 30–32, 27–29).

More recent studies^{10, 22, 23} have confirmed that lanthanide triflates are preferred as catalysts in the Michael conjugate addition over other Lewis acids, since the latter are more prone to form complexes with amines thus decreasing their reactivity. The use of acetonitrile as the solvent increases the chemical yield of β -amino esters to 100% (Table 1, entries 36 and 37). In the case of sterically more hindered *tert*-butylamine, a considerable increase in the chemical yield can be achieved by using a combination of activating factors, such as high pressure and a catalyst (ytterbium triflate). Under these conditions, even secondary amines (for example, diisopropylamine and diisobutylamine) enter into the reaction with esters of α,β -unsaturated carboxylic acids. The main contribution to the increase in the chemical yields of the reaction products is made by pressure (Table 1, entries 8–11).

The addition of primary amines and cyclic secondary amines to esters of α,β -unsaturated carboxylic acids also led to satisfactory yields of products (39%–72%), when baker yeast was used as the catalyst.²⁴

Acyclic secondary amines do not usually react with esters of α,β -unsaturated carboxylic acids,^{14, 15} whereas cyclic secondary amines, for example, piperidine:^{15, 22, 23, 25} react to give products in very high chemical yields (up to 100%). For example, 2,7-dihydro-1*H*-dinaphtho[2,1-*c*:1',2'-*e*]azepine **2** adds to methyl crotonate to afford the corresponding product in 68% yield.²⁶



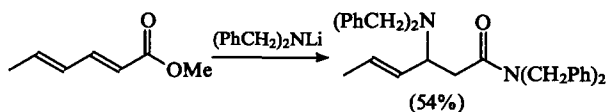
The reaction is carried out with excess methyl crotonate, with boiling, and without a solvent.

Analysis of the data presented in Table 1 indicates that when sterically less hindered reactants are used and when the optimal reaction conditions (solvent, temperature, pressure, and catalyst) are chosen, esters of β -amino acids can be synthesised in high yields.

III. Nucleophilic addition of metal amides to esters of α,β -unsaturated carboxylic acids

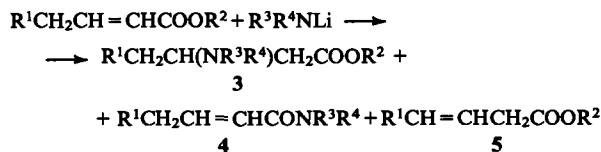
In recent years, metal amides, which have found wide application in asymmetric synthesis, have been used with increasing frequency for the nucleophilic addition to esters of α,β -unsaturated carboxylic acids.²⁷

Primary and some secondary lithium amides react with esters of α,β -unsaturated carboxylic acids as strong bases. Therefore, apart from the target esters of β -amino acids **3**, which are formed in relatively low yields, these reactions afford the corresponding amides **4** or esters of β,γ -unsaturated carboxylic acids **5** (Table 2), these compounds being the main reaction products. In some cases, β -aminoamides have also been detected among the products.³⁴



Side products **5** are also formed when sterically hindered secondary lithium amides react with esters of α,β -unsaturated carboxylic acids (Table 2, entries 9 and 10). For example, the formation of esters **5** in this reaction has been explained³³ by the fact that in the six-membered transition state, the amide attacks

Table 2. Products of the interaction of lithium amides with esters of α,β -unsaturated carboxylic acids.



No	R ¹	R ²	R ³	R ⁴	Yield (%)			Ref.
					3	4	5	
1	H	Me	(<i>R</i>)-CH(Me)Ph	H	28	35	—	13
2	H	Me	CH ₂ Ph	H	20	60	—	28
3	H	Me	Pr ⁱ	Pr ⁱ	44	—	14	28
4	H	Et	Pr ⁱ	Pr ⁱ	—	—	92	29
5	H	Me	SiMe ₃	SiMe ₃	—	—	9	28
6	H	Et	Pr ⁱ	Pr ⁱ	—	—	23	30
7	Br	Me	Pr ⁱ	Pr ⁱ	—	—	<5	31
8	Ph(Z) ^a	Me	CH ₂ Ph	SiMe ₃	—	—	95	32
9	Ph(E) ^a	Bu ^t	(<i>R</i>)-CH(Me)Ph	CH ₂ Ph	69	—	20	33
10	Ph(Z) ^a	Bu ^t	(<i>R</i>)-CH(Me)Ph	CH ₂ Ph	—	—	92	33

^a The configuration of the initial ester is given in parentheses.

the protons of the methylene group, located in the γ -position with respect to the carbonyl group in the substrate, and thus induces the rearrangement of the double bond to the β,γ -position. This process is markedly facilitated if the initial ester has the *cis*-configuration.

The nucleophilic properties of secondary lithium amides, which are more bulky, dominate over their basic properties. Therefore, they preferentially add to the β -position with respect to the carbonyl group, which results in the formation of β -amino esters as the main (and practically the only) reaction products (Table 3). The reaction is usually carried out at a low temperature for 15–30 min. Varying the temperature conditions (from -78 to $+20^\circ\text{C}$) exerts no substantial influence on the chemical yield of β -amino esters.^{13, 29, 45} The best results have been achieved by using a 1.5-fold excess of the amide.⁴⁴ Lithium benzyl(α -phenylethyl)amide **7** is used most often in these conjugate addition reactions.

Good results have also been obtained when the lithium derivative of the above-mentioned dihydro-4*H*-dinaphthoazepine and lithium benzyl(trimethylsilyl)amide have been used as nucleophiles (chemical yields of up to 88% and of 77%–99%, respectively). When symmetrical lithium bis(α -phenylethyl)amide is used, the yield of the corresponding β -amino esters decreases to 23% due to the steric hindrance arising in the amide itself during the nucleophilic attack.⁴⁸ The introduction of substituents in one of the benzene rings in lithium benzyl(α -phenylethyl)amide exerts no influence on the final result of the reaction (Table 3, entries 60–62).

The introduction of a methyl group in the α -position with respect to the carbonyl group of the ester also decreases the yields of the corresponding β -amino esters from 77%–92% to 21%–61% (cf. entries 1, 2 and 7, 8 as well as entries 17, 18 and 21, 22, etc. in Table 3). The nature of the radical located in the β -position with respect to the carboxyl group of the substrate and the nature of the ester group exert as a rule no substantial influence on the chemical yield in the nucleophilic addition of metal amides to the double bond. The yield of β -amino ester increases somewhat if the initial ester contains a silyl group^{46, 49} (Table 3, entries 51–53 and 54).

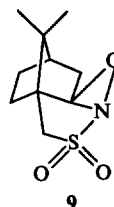
The conjugate addition of lithium amides occurs more successfully with the *trans*-isomers of α,β -unsaturated esters. In those cases where the corresponding *cis*-isomers are used, the chemical yield decreases from 80% to 39% (see Table 3, entries 42 and 43). However the *cis*-configuration of cyclic esters does not influence the yield of the final β -amino ester (Table 3, entries 14, 15, and 26, 30–32).

The solvent exerts substantial influence on the addition. The reaction is usually carried out in polar aprotic solvents such as THF or 1,2-dimethoxyethane (DME). Less polar solvents, for example, toluene or its mixtures with THF, are also used sometimes. The addition of an excess of a crown ether (12-crown-4) increases the chemical yield of β -amino esters by a factor of 1.5–2 (cf. entries 36 and 41 as well as 47 and 48 in Table 3), whereas the addition of polar solvents (in particular, HMPTA) considerably decreases the yield (from 44% to 18%–28%) (Table 3, entries 36, 38, and 39).^{44, 50} Since the basic properties of amides are enhanced in a polar medium, the interaction of ethyl crotonate with lithium diisopropylamide in THF containing some HMPTA affords the isomeric β,γ -unsaturated ester **5** as the only product (see Table 2, entry 4), whereas in the absence of HMPTA, the reaction occurs as a 1,4-addition in nearly quantitative yield (90%).²⁹

Various protonating agents have been used to decompose the β -aminoenolates **A** formed upon 1,4-addition (see reaction 2); a saturated aqueous solution of ammonium chloride, alcohols, or a buffer solution with pH 7 are employed most frequently. The best result has been achieved by using sterically hindered 2,6-di-*tert*-butylphenol. The use of acetic acid as the protonating agent leads to a decrease in the chemical yield of β -amino ester from 40% to 21% (cf. entries 6 and 8 in Table 3), and when aqueous acetic acid is used, the final product may polymerise.⁵¹

If an alkyl halide is added to the reaction mixture instead of a protonating agent, the β -aminoenolate **A** is alkylated at the α -carbon atom (the so-called tandem reaction) resulting in the formation of α -alkyl- β -amino ester **8** (Table 4). An increase in the size of the radical R^5 in the alkylating agent usually deteriorates the chemical yield of the product **8** (see entries 10 and 11; 12 and 13; and 15 and 16 in Table 4). The nature of the substituents in the amide and in the ester is not crucial for the occurrence of the tandem reaction.

When (+)-(camphorsulfonyl)oxaziridine **9**

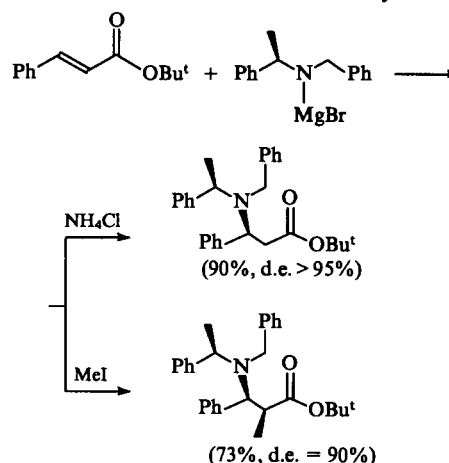


is used as a hydroxylating agent, α -hydroxy- β -amino esters **10** can be prepared (Table 5). If a phenyl substituent occurs in the β -position with respect to the carbonyl group, the yield of the final product is higher than those obtained with compounds containing aliphatic substituents (entries 2, 3, and 5–8 in Table 5). However, replacement of the phenyl group by a benzyl group leads to a sharp decrease in the product yields (entries 2 and 9; 3 and 10). It is of interest that when lithium (*S*)-benzyl(α -phenylethyl)amide is used, the yield of the product **10** is higher than with the (*R*)-isomer (Table 5, entries 7–10). The nature of the alkyl radical in the ester group exerts an ambiguous influence on the yield of the α -hydroxy- β -amino esters.

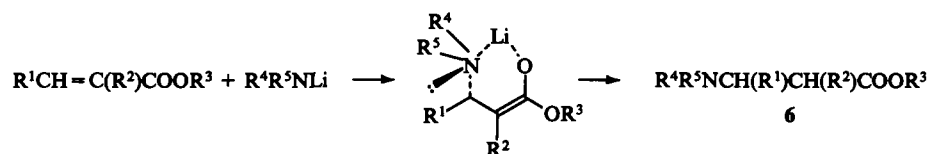
The conjugate addition of amides of other metals to esters of α,β -unsaturated carboxylic acids has not been studied in detail. It has been found that titanium amides like $\text{Ti}(\text{NR}_2)_4$, $\text{ClTi}(\text{NR}_2)_3$, and $\text{Cl}_2\text{Ti}(\text{NR}_2)_2$ ($R = \text{Me}, \text{Et}$) add to acrylates, crotonates, and cinnamates to give the corresponding β -amino esters in good chemical yields (34%–97%); however, amides of β,γ -unsaturated acids (21%–39%) are often formed as side products. The formation of the latter can be completely eliminated by using esters with bulky ester groups.⁵⁹

Lithium amidocuprates $(\text{R}_2\text{N})_2\text{CuLi}$ add to esters of α,β -unsaturated carboxylic acids yielding β -amino esters as the main reaction products,^{33, 60, 61} although in this case, too, small amounts of β,γ -unsaturated carboxamides are formed.³³

Magnesium benzyl(α -phenylethyl)amide has been used successfully in the conjugate addition to *tert*-butyl cinnamate,⁶² as well as in an addition reaction followed by α -alkylation.

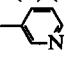


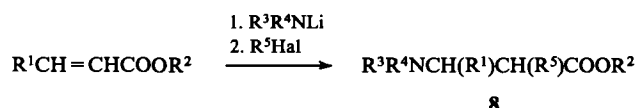
The chemical yields of products in the latter reactions are comparable with the yields of the same products in the similar reactions involving the corresponding lithium amides (Table 3, entry 18; Table 4, entry 15).

Table 3. Conditions of the reactions of secondary lithium amides with esters of α,β -unsaturated carboxylic acids.

No	R ¹ *	R ²	R ³	Solvent	Protonating agent	Yield of 6 (%)	d.e. (%)	Ref.
A. Lithium (<i>R</i>)-benzyl(α -phenylethyl)amide								
1	Me	H	Me	THF	NH ₄ Cl	75	> 95	35
2	Me	H	Me	THF	NH ₄ Cl	85	95	13
3	Me	H	Bu ^t	THF	NH ₄ Cl	75	> 95	35
4	Me	H	Bu ^t	THF	NH ₄ Cl	82	> 99	13
5	Me	H	CH ₂ Ph	THF	NH ₄ Cl	88	95	13, 36
6	Me	Me	Me	THF	AcOH	21	71	37
7	Me	Me	Me	THF	pH 7	23	82	37
8	Me	Me	Me	THF	2,6-(Bu ^t) ₂ C ₆ H ₃ OH	40	82	37
9	Me	Me	CH ₂ Ph	THF	pH 7	11	> 82	37
10	Me	Me	Bu ^t	THF	pH 7	43	88	37
11	Me	Me	Bu ^t	MePh	Bu ^t OH	78	20	37
12	Me	Me	Bu ^t	MePh	pH 7	70	60	37
13	Me	Me	Bu ^t	MePh/THF	pH 7	75	90	37
14	Me	Me	Bu ^t	MePh/THF	2,6-(Bu ^t) ₂ C ₆ H ₃ OH	72	> 99	37
15	Et	Me	Bu ^t	MePh/THF	2,6-(Bu ^t) ₂ C ₆ H ₃ OH	65	> 99	37, 38
16	Ph	H	Me	THF	NH ₄ Cl	77	> 95	35
17	Ph	H	Bu ^t	THF	2,6-(Bu ^t) ₂ C ₆ H ₃ OH	92	95	39
18	Ph	H	Bu ^t	THF	NH ₄ Cl	87	95	35
19	Ph	Me	Me	THF	pH 7	38	87	37
20	Ph	Me	Me	THF	2,6-(Bu ^t) ₂ C ₆ H ₃ OH	37	93	37
21	Ph	Me	Bu ^t	MePh/THF	2,6-(Bu ^t) ₂ C ₆ H ₃ OH	61	> 99	37
22	Ph	Me	Bu ^t	MePh/THF	2,6-(Bu ^t) ₂ C ₆ H ₃ OH	61	99	39
23	Ph	CH ₂ Ph	Bu ^t	MePh/THF	2,6-(Bu ^t) ₂ C ₆ H ₃ OH	45	> 98	39
24	<i>p</i> -C ₆ H ₄ CH ₂ OPh	H	Me	THF	NH ₄ Cl	78	> 99	13
25	C ₇ H ₁₅	H	Bu ^t	THF	NH ₄ Cl	91	> 95	40
26	-(CH ₂) ₄ -		Bu ^t	THF	2,6-(Bu ^t) ₂ C ₆ H ₃ OH	70	> 95	41
B. Lithium (<i>S</i>)-benzyl(α -phenylethyl)amide								
27	CH=CHPh	H	Me	THF	NH ₄ Cl	81	100	42
28	CH=CHPh	H	Pr ⁱ	THF	NH ₄ Cl	83	100	42
29	CH=CHPh	H	Bu ^t	THF	NH ₄ Cl	98	100	42
30	-(CH ₂) ₃ -		Bu ^t	THF	2,6-(Bu ^t) ₂ C ₆ H ₃ OH	85	71	41
31	-(CH ₂) ₃ -		Bu ^t	THF	2,6-(Bu ^t) ₂ C ₆ H ₃ OH	65	> 98	43
32	-(CH ₂) ₄ -		Bu ^t	THF	2,6-(Bu ^t) ₂ C ₆ H ₃ OH	70	> 95	41, 43
C. Lithium derivative of (<i>R,S</i>)-azepine 2								
33	Me (<i>E</i>)	H	Bu ^t	DME	NH ₄ Cl	83	97	44
34	Pr ⁱ (<i>E</i>)	H	Bu ^t	DME	NH ₄ Cl	69	94	44
35	Bu ^t (<i>E</i>)	H	Bu ^t	DME	NH ₄ Cl	74	97	44
36	C ₇ H ₁₅	H	Me	THF	NH ₄ Cl	44	90	44
37	C ₇ H ₁₅	H	Me	DME	NH ₄ Cl	32	91	44
38	C ₇ H ₁₅	H	Me	THF/HMPA = 4:1	NH ₄ Cl	18	50	44
39	C ₇ H ₁₅	H	Me	THF/HMPA (20 eq.)	NH ₄ Cl	28	84	44
40	C ₇ H ₁₅	H	Me	MePh	NH ₄ Cl	6	50	44
41	C ₇ H ₁₅	H	Me	THF/12-C-4 (4 eq.)	NH ₄ Cl	60	95	44
42	C ₇ H ₁₅ (<i>E</i>)	H	Bu ^t	DME	NH ₄ Cl	80	96	44
43	C ₇ H ₁₅ (<i>Z</i>)	H	Bu ^t	DME	NH ₄ Cl	39	78	44
D. Lithium derivative of (<i>S</i>)-azepine 2								
44	Me	Me	Bu ^t	DME	NH ₄ Cl	63	> 95	45
E. Lithium derivative of (<i>R</i>)-azepine 2								
45	C ₇ H ₁₅	H	Pr ⁱ	DME	NH ₄ Cl	63	93	44
46	C ₇ H ₁₅	H	Pr ⁱ	THF/12-C-4 (8 eq.)	NH ₄ Cl	65	89	44
47	C ₇ H ₁₅	H	Bu ^t	THF/12-C-4 (4 eq.)	NH ₄ Cl	88	94	44
48	C ₇ H ₁₅	H	Bu ^t	THF/12-C-4 (1 eq.)	NH ₄ Cl	43	88	44
49	C ₇ H ₁₅	H	Bu ^t	DME	NH ₄ Cl	80	> 97	44

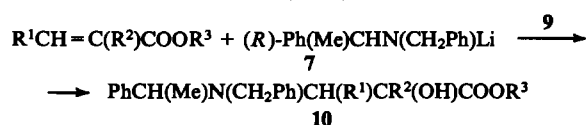
Table 3 (continued).

No	R ¹ ^a	R ²	R ³	Solvent	Protonating agent	Yield of 6 (%)	d.e. (%)	Ref.
F. Lithium benzyl(trimethylsilyl)amide								
50	Me	H	Me	THF	AcOH/THF	88	—	28
51	CH(Me)OSiMe ₂ Bu ^t	H	Bu ^t	THF	MeOH	91	8	46
52	CH(Me)OSiPh ₂ Bu ^t	H	Bu ^t	THF	MeOH	99	78	46
53	CH(Me)OSiPr ₃	H	Bu ^t	THF	MeOH	95	80	46
54	(<i>S</i>)-CH(Me)OCPh ₃	H	Bu ^t	THF	MeOH	77	100	46
55	C ₇ H ₁₅	H	Me	THF	MeOH	86	—	32
G. Lithium (<i>R</i>)-(α-phenylethyl)(trimethylsilyl)amide								
56		H	Et	THF	NH ₄ Cl	64	> 99	47
H. Lithium (<i>R,R</i>)-bis(α-phenylethyl)amide								
57	Me	H	Me	THF	NH ₄ Cl	57	> 99	13
58	Me	H	CH ₂ Ph	THF	NH ₄ Cl	23	98	13
59	Me	H	Bu ^t	THF	NH ₄ Cl	27	> 99	13
I. Lithium (<i>R</i>)-(3,4-dimethoxybenzyl)(α-phenylethyl)amide								
60	Me	H	Me	THF	NH ₄ Cl	68	95	13
61	Me	H	CH ₂ Ph	THF	NH ₄ Cl	74	96	13
62	Me	H	Bu ^t	THF	NH ₄ Cl	83	> 99	13
J. Lithium (<i>S</i>)-allyl(α-phenylethyl)amide								
63	Me	H	Bu ^t	THF	NH ₄ Cl	92	> 99	36
64	Et	H	Bu ^t	THF	NH ₄ Cl	85	> 99	36
65	Pr ⁱ	H	Bu ^t	THF	NH ₄ Cl	88	> 99	36
66	Ph	H	Bu ^t	THF	NH ₄ Cl	97	> 99	36
67	CH=CHMe (<i>E</i>)	H	Bu ^t	THF	NH ₄ Cl	78	> 98	36

^a Configuration of the initial ester is given in parentheses.Table 4. Addition of lithium amides to esters of α,β -unsaturated carboxylic acids with simultaneous α -alkylation.

Number of reaction	R ¹ ^a	R ²	R ³	R ⁴	R ⁵	Yield of 8 (%)	d.e. (%)	Ref.
1	Me	Bu ^t	<i>(S)</i> - 2		Me	71	85	45
2	Me	Me	Pr ⁱ	Pr ⁱ	C ₈ H ₁₇	58	100	52
3	Ph	Bu ^t	CH ₂ Ph	CH ₂ Ph	Me	71	> 90	35
4	Me(<i>Z</i>) ^a	Me	SiMe ₃	CH ₂ Ph	Me	88	6	53
5	Me(<i>E</i>) ^a	Me	SiMe ₃	CH ₂ Ph	Me	68	38	53
6	Me(<i>Z</i>) ^a	Me	SiMe ₃	CH ₂ Ph	C ₈ H ₁₇	81	18	52, 53
7	Me(<i>E</i>) ^a	Me	SiMe ₃	CH ₂ Ph	C ₈ H ₁₇	60	80	53
8	Me	Me	(<i>R</i>)-CH(Me)Ph	CH ₂ Ph	Me	50	9	35
9	Me	Me	(<i>R</i>)-CH(Me)Ph	CH ₂ Ph	CH ₂ Ph	54	50	35
10	Me	Bu ^t	(<i>R</i>)-CH(Me)Ph	CH ₂ Ph	Me	60	15	35
11	Me	Bu ^t	(<i>R</i>)-CH(Me)Ph	CH ₂ Ph	CH ₂ Ph	42	0	35
12	Ph	Me	(<i>R</i>)-CH(Me)Ph	CH ₂ Ph	Me	61	85	35
13	Ph	Me	(<i>R</i>)-CH(Me)Ph	CH ₂ Ph	CH ₂ Ph	55	50	35
14	Ph	Me	(<i>R</i>)-CH(Me)Ph	CH ₂ Ph	CH ₂ CH=CH ₂	79	50	35
15	Ph	Bu ^t	(<i>R</i>)-CH(Me)Ph	CH ₂ Ph	Me	78	15	35
16	Ph	Bu ^t	(<i>R</i>)-CH(Me)Ph	CH ₂ Ph	CH ₂ Ph	46	43	35

^a Configuration of the initial ester is given in parentheses.

Table 5. Addition of lithium amides to esters of α,β -unsaturated carboxylic acids with simultaneous α -hydroxylation.

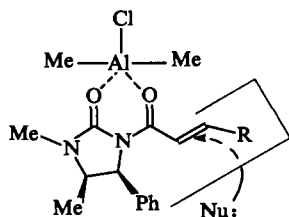
No	R ¹	R ²	R ³	Yield of 10 (%)	d.e. (%)	Ref.
1	Ph	H	Me	43	>90	54
2	Ph	H	Bu ^t	86	92	54, 55
3 ^a	Ph	H	Bu ^t	89	>98	54, 56
4	Me	H	Me	55	75	54
5	Et	H	Bu ^t	53	>90	54
6	Me	H	Bu ^t	36	>90	54
7	C ₇ H ₁₅	H	Bu ^t	63	88	40, 57
8 ^a	C ₇ H ₁₅	H	Bu ^t	85	92	40
9	CH ₂ Ph	H	Bu ^t	41	20	33, 58
10 ^a	CH ₂ Ph	H	Bu ^t	63	91	33
11	Me	Me	Bu ^t	54	83	54

^a The (S)-isomer of the amine was used.

IV. Stereochemistry of nucleophilic addition of amines and metal amides to esters of α,β -unsaturated carboxylic acids

The reactions of chiral amines, in particular, of α -phenylethylamine, with esters of α,β -unsaturated carboxylic acids are characterised by relatively low stereoselectivities (d.e. = 0%–19%, d.e. is diastereomeric excess), irrespective of the type of activation used: high temperature, high pressure, or a catalyst. The interaction of azepine **2** with methyl crotonate without a solvent is an exception; in this case, diastereomeric excess is 61%.²⁶

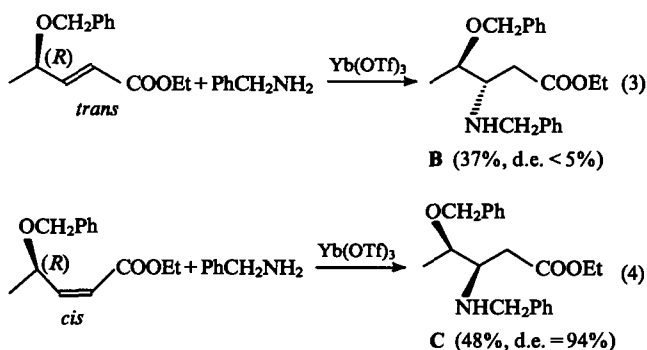
When the conjugate addition of amines to esters of α,β -unsaturated carboxylic acids is carried out with the catalytic activation by lanthanide triflates, the diastereomeric excess is only 12%–31%.^{15, 22, 23} However, in the case where the substrate molecule can be fixed due to the coordination of the catalyst to the oxygen atoms of the carbonyl groups in the substituted amide of α,β -unsaturated acid, presented below, the steric restrictions thus arising cause the nucleophile to attack the substrate from the side that is sterically less hindered. Consequently, 1,4-addition occurs stereoselectively (d.e. up to 80%).^{63, 64}



Reactions of benzylamine with acrylic acid derivatives having a chiral substituent in the α -position with respect to the carbonyl group are fairly stereoselective: d.e. is 49%–91% (Table 1, entries 1–6). The presence of a bulky substituent in the β -position with respect to the carbonyl group of the ester is probably the main factor responsible for the stereospecific character of the addition (Table 1, entry 41), although the fact that this reaction was carried out at a negative temperature and without a solvent should apparently also be taken into account. The presence of a bulky ester group also increases the stereoselectivity of the reaction (entries 21–24) and, in some cases (entries 25 and 26), it even makes the reaction stereospecific.

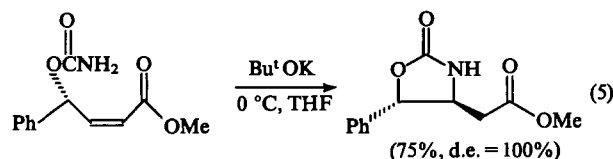
However, the stereoselectivity of the conjugate 1,4-addition of amines to esters of α,β -unsaturated carboxylic acids is influenced

most strongly by the geometric isomerism in the initial esters. It has been shown that, despite the fact that isomeric ethyl esters are characterised by the same (R)-configuration at the C γ atoms, the *trans*-isomer reacts with benzylamine non-stereoselectively (reaction 3), whereas the reaction of the *cis*-isomer is highly stereoselective (reaction 4); the absolute configuration at the β -carbon atom in diastereomer **C**, formed as the major product, is opposite to that in diastereomer **B**.¹⁵



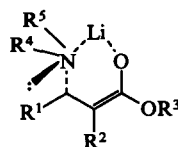
A similar picture has been observed when 1,4-addition has been carried out with lithium amides: the β -amino esters formed are characterised by the opposite configuration at the β -carbon atom.^{44, 52, 53, 65} In this case, the stereoselectivity of the process depends to a lesser degree on the geometry of the initial ester (see Table 3, entries 42 and 43).

It should be specially noted that the intramolecular addition of the ω -amino-group, incorporated in the substituent at the asymmetric C γ atom, to a double bond (reaction 5) is stereospecific.^{66, 67}

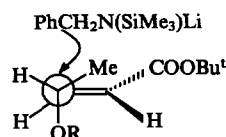


Apparently, the high degree of diastereoselectivity observed in reactions (4) and (5) is due to the appearance of steric restrictions hampering the attack of the nucleophile from one of the sides of the substrate.

Unlike amines, lithium amides react with α,β -unsaturated esters with high degrees of diastereoselectivity (see Table 3); only one of all the possible diastereomers is often formed. The stereoselectivity of these reactions can be accounted for by the fact that, due to the high ability of lithium cation to participate in coordination, the formation of a six-membered transition state is favourable and, consequently, the nucleophile adds predominantly from one side of the substrate.

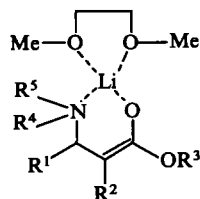


Bulky chiral substituents located in the γ -position with respect to the carbonyl group of the ester also increase the stereoselectivity of the addition. For example, it has been suggested⁴⁶ that the addition of lithium benzyl(trimethylsilyl)amide to butyl esters of silyl-substituted acrylic acids (entries 51–54 in Table 3) from the sterically hindered side is impossible.



However, neither the size of the group located in the β -position, nor the nature of the substituent in the α -position, nor the size of the ester group has a noticeable influence on the stereoselectivity of the addition of lithium amides to esters of α,β -unsaturated carboxylic acids.

In solvents such as THF and DME, which are capable of forming chelates with the β -aminoenolate produced during the reaction, the selectivity of conjugate addition is higher (d.e. = 90%–91%) than that in toluene (d.e. = 50%) (Table 3, entries 36, 37, and 40).⁴⁴

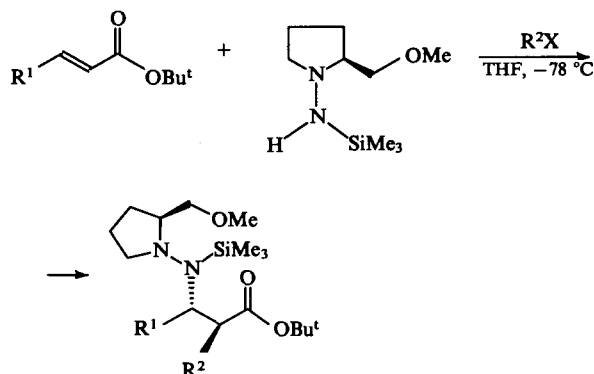


Unlike the products of simple addition of metal amides to a double bond, α -alkyl- β -amino esters resulting from the tandem 1,4-addition and simultaneous α -alkylation contain two asymmetrical centres at the α - and β -carbon atoms of the ester and are formed as mixtures of diastereomers with relatively low d.e. values. Only in some cases has stereospecific reaction been accomplished (Table 4, entries 2 and 3).

The reaction of lithium piperidide with *tert*-butyl α -naphthoate in the presence of methyl iodide as an alkylating agent occurs non-stereoselectively yielding a fairly large amount (32%) of a side product, α -naphthamide, whereas the similar reaction involving α - and β -naphthyloxazolines is stereospecific and affords no side products.⁶⁸ It is noteworthy that lithium benzyl(α -phenylethyl)amide does not react with *tert*-butyl α -naphthoate under these conditions.

High stereoselectivity in the tandem reaction can be achieved by using magnesium benzyl(α -phenylethyl)amide as the nucleophile. This leads not only to an increase in the diastereomeric excess (from 15% to 90%) compared to that attained with the corresponding lithium amide (see Table 4, entry 15), but also to the change in the absolute configuration of the asymmetric centre arising at the α -carbon atom in the ester.⁶²

If the substituent R^1 at the β -carbon atom in the initial *tert*-butyl ester is an aliphatic group, the diastereomeric excesses obtained in the reactions of these esters with (*S*)-(-)-2-methoxymethyl-1-trimethylsilylamino pyrrolidine are 63%–96%. In the case where R^1 is an aromatic substituent, the interaction is stereospecific (d.e. > 96%).⁶⁹



The reactions of tandem addition with simultaneous α -hydroxylation occur with high diastereoselectivity (d.e. = 75%–99%), except for the interaction of (*R*)-benzyl(α -phenylethyl)amine with *tert*-butyl γ -phenylcrotonate (Table 5, entry 9). Apparently, this is due to the presence of steric restrictions hampering the interaction of the (*R*)-isomer with the above substrate.³³

Thus, it follows from the analysis of the published data that the nature of the substituent in the substrate molecule is the main factor influencing the chemical yield in the conjugate addition of amines to esters of α,β -unsaturated carboxylic acids, whereas the geometry of the initial ester is the main factor determining the stereoselectivity of the process. The diastereomeric excess obtained in these reactions does not usually exceed 60% (Table 1). In the case where the reactions involve lithium amides, both the chemical yield and the stereoselectivity depend mostly on the geometry of the ester as well as on the solvent and the character of the protonating agent used.

In conclusion, it should be noted that at present, the addition of metal amides to esters of α,β -unsaturated carboxylic acids is the method of choice for the asymmetric synthesis of esters of β -amino acids. The most significant progress in this field of research has been achieved by a group of English scientists headed by S. Davies (Oxford).^{13, 35–41, 43, 48, 49, 54–58, 62}

V. Mathematical modelling of structures of the transition states in the Michael nucleophilic addition

The stereochemical outcome of the conjugate addition of amines or lithium amides to esters of α,β -unsaturated carboxylic acids can be reliably predicted in some cases by virtue of molecular mechanics modelling of the structure of the transition state of the process.^{48, 70} In the modelling, the tetrahedral angle of the attack and the N–C β bond length in the transition state are taken fixed (it should be noted that variation of the angle of the attack by a nucleophile has no substantial influence on the final stereochemical outcome of the process⁴⁸). It is believed that the H–N...C β –C α torsional angle is the main factor determining the stereochemistry of the reaction (if lithium amide is used, the position of the proton is occupied by the unshared electron pair at the nitrogen atom). The depths of the minima in the plot of the transition state energy versus the magnitude of the torsional angle are mostly determined by the spatial arrangement of the alkyl radicals in the nucleophile and by their structures. The natures of the substituents in the ester group and in the β -position with respect to the carbonyl group in the substrate and their mutual arrangement are also significant. In addition, in the reactions involving lithium amide, the possibility of chelate formation (the lithium atom can fix the structure of the transition state) should also be taken into account. A lower energy of the transition state corresponding to a particular minimum means that the probability of the formation of this transition state is greater.

The use of the energies of the transition states corresponding to minima in the calculation of Boltzmann distribution makes it possible to predict with high accuracy the ratio between the diastereomers of β -amino esters formed in the reaction; however, this is true only for kinetically controlled processes.⁷⁰ An increase in the difference between the energies of the transition states for the minima results in an increase in the stereoselectivity of conjugate addition. The absolute configuration of the reaction product depends on the structure of the most probable transition state.

The efficiency of this method has been demonstrated in relation to the reactions of azepine 2 and its lithium derivative with methyl crotonate⁷⁰ and the reaction of lithium benzyl(α -phenylethyl)amide with *tert*-butyl cinnamate.⁴⁸

Thus, despite the fact that the systems in question are very complex and, therefore, the number of assumptions (based on analysis of empirical features) is large, mathematical modelling of transition states can be used to predict the stereochemical outcome of the conjugate addition of amines or lithium amides to esters of α,β -unsaturated carboxylic acids.

The work was supported by the Russian Foundation for Basic Research (Project No. 96-03-32157) and the State Commission of

the Russian Federation on Higher Education (Science and Engineering Programme 'Fine Organic Synthesis', grant FT-28).

References

1. V S R Rao, T K Vasudevan *CRC Crit. Rev. Biochem.* **14** 173 (1983)
2. N N Romanova *Khim.-Farm. Zh.* **19** (1990)
3. D J Hart, D C Ha *Chem. Rev.* **89** 1447 (1989)
4. M J Brown *Heterocycles* **29** 2225 (1989)
5. F H Van der Steen, G Van Koten *Tetrahedron* **47** 7503 (1991)
6. H Estermann, D Seebach *Helv. Chim. Acta* **71** 1824 (1988)
7. P R Bovy, J G Rico *Tetrahedron Lett.* **34** 8015 (1993)
8. P Perlmutter, H Tabone *Tetrahedron Lett.* **29** 949 (1988)
9. Z-I G Beresnevichyus, V Yu Vilyunas, V I Raudelyunas, R S Baltrushis *Khim. Geterotsikl. Soedin.* **80** (1992)
10. G Jenner *Tetrahedron Lett.* **36** 233 (1995)
11. M Furukawa, T Okawara, Y Terawaki *Chem. Pharm. Bull.* **25** 1319 (1977)
12. R Kinas, K Pankiewicz, W J Stec, P B Farmer, A B Jarman *J. Org. Chem.* **42** 1650 (1977)
13. S G Davies, O Ichihara *Tetrahedron Asymmetry* **2** 183 (1991)
14. J d'Angelo, J Maddaluno *J. Am. Chem. Soc.* **108** 8112 (1986)
15. S Matsubara, M Yoshioka, K Utimoto *Chem. Lett.* 827 (1994)
16. S Matsunaga, T Sakanaki, H Nagaoka, Y Yamada *Tetrahedron Lett.* **24** 3009 (1983)
17. S I Suminov, A N Kost *Usp. Khim.* **38** 1933 (1969) [*Russ. Chem. Rev.* **38** 884 (1969)]
18. S W Baldwin, J Aube *Tetrahedron Lett.* **28** 179 (1987)
19. K Matsumoto, A Sera, T Uchida *Synthesis* **1** (1985)
20. M Es-Sayed, C Gratkowski, N Krass, A I Meyer, A de Meijere *Tetrahedron Lett.* **34** 289 (1993)
21. G A Holander *Chem. Rev.* **92** 29 (1992)
22. N N Romanova, A G Gravis, R A Gracheva, D V Davydov, Yu G Bundel', in *Mezhvuzovskii Kollokvium 'Khimiya Azotistyk Geterotsiklov', Chernogolovka, 1995* (Intercollegiate Colloquium 'The Chemistry of Nitrogen-Containing Heterocycles', Chernogolovka, 1995) p. 62
23. N N Romanova, A G Gravis, I F Leshcheva, L D Ashkinadze, R A Gracheva, M E Akat'eva, Yu G Bundel' *Vestn. Mosk. Univ., Ser. 2, Khim.* **76** (1996)
24. K Rama Rao, Y V D Nageswar, H M Sampath Kumar *Tetrahedron Lett.* **32** 6611 (1991)
25. S G Pyne, R Griffith, M Edwards *Tetrahedron Lett.* **29** 2089 (1988)
26. J H Hawkins, G C Fu *J. Org. Chem.* **51** 2820 (1986)
27. P J Cox N, N S Simpkins *Tetrahedron Asymmetry* **2** 1 (1991)
28. N Asao, T Uyehara, Y Yamamoto *Tetrahedron* **44** 4173 (1988)
29. J L Herrmann, G R Kieczkowski, R H Schlessinger *Tetrahedron Lett.* **24** 33 (1973)
30. M W Rathke, D Sullivan *Tetrahedron Lett.* 4249 (1972)
31. R D Little, J R Dawson *Tetrahedron Lett.* **21** 2609 (1980)
32. T Uyehara, N Shida, Y Yamamoto *J. Org. Chem.* **57** 3139 (1992)
33. M E Bunnage, S G Davies, C J Goodwin, O Ichihara *Tetrahedron* **50** 3975 (1994)
34. Y Yamamoto, N Asao, T Uyehara *J. Am. Chem. Soc.* **114** 5427 (1992)
35. S G Davies, J A S Walters *J. Chem. Soc., Perkin Trans. 1* 1129 (1994)
36. S G Davies, D R Fenwick *J. Chem. Soc., Chem. Commun.* 1109 (1995)
37. S G Davies, O Ichihara, I A S Walters *J. Chem. Soc., Perkin Trans. 1* 1141 (1994)
38. S G Davies, O Ichihara, I A S Walters *Synlett* 117 (1994)
39. S G Davies, N M Garrido, O Ichihara, I A S Walters *J. Chem. Soc., Chem. Commun.* 1153 (1993)
40. M E Bunnage, A J Burke, S G Davies, C J Goodwin *Tetrahedron Asymmetry* **6** 165 (1995)
41. S G Davies, O Ichihara, I Lenoir, I A S Walters *J. Chem. Soc., Perkin Trans. 1* 1411 (1994)
42. N Asao, N Tsukada, Y Yamamoto *J. Chem. Soc., Chem. Commun.* 1660 (1993)
43. S G Davies, O Ichihara, I A S Walters *Synlett* 461 (1993)
44. J M Hawkins, T A Lewis *J. Org. Chem.* **57** 2114 (1992)
45. J M Hawkins, T A Lewis *J. Org. Chem.* **59** 649 (1994)
46. N Asao T. Shimada N. Tsukada Y. Yamamoto. *Tetrahedron Lett.* **35** 8425 (1994)
47. J G Rico, R J Lindmark, T E Rogers, P R Bovy *J. Org. Chem.* **58** 7948 (1993)
48. J F Costello, S G Davies, O Ichihara *Tetrahedron Asymmetry* **5** 1999 (1994)
49. S G Davies, C J R Hedgecock, J M McKenna *Tetrahedron Asymmetry* **6** 827 (1995)
50. I Suzuki, H Kin, Y Yamamoto *J. Am. Chem. Soc.* **115** 10139 (1993)
51. J G Rico *Tetrahedron Lett.* **35** 6599 (1994)
52. T Uyehara, N Asao, Y Yamamoto *J. Chem. Soc., Chem. Commun.* 1410 (1987)
53. N Asao, T Uyehara, Y Yamamoto *Tetrahedron* **46** 4563 (1990)
54. M E Bunnage, A N Chernega, S G Davies, C J Goodwin *J. Chem. Soc., Perkin Trans. 1* 2373 (1994)
55. M E Bunnage, S G Davies, C J Goodwin *J. Chem. Soc., Perkin Trans. 1* 1375 (1993)
56. M E Bunnage, S G Davies, C J Goodwin *J. Chem. Soc., Perkin Trans. 1* 2385 (1994)
57. M E Bunnage, A J Burke, S G Davies, C J Goodwin *Tetrahedron Asymmetry* **5** 203 (1994)
58. M E Bunnage, S G Davies, C J Goodwin *Synlett* 731 (1993)
59. A Hosomi, T Yanagi, M Hojo *Tetrahedron Lett.* **32** 2371 (1991)
60. N Shida, T Uyehara, Y Yamamoto *J. Org. Chem.* **57** 5049 (1992)
61. N Shida, C Kabuto, T Niwa, T Ebata, Y Yamamoto *J. Org. Chem.* **59** 4068 (1994)
62. M E Bunnage, S G Davies, C J Goodwin, I A S Walters *Tetrahedron Asymmetry* **5** 35 (1994)
63. R Amoroso, G Cardillo, P Sabatino, C Tomasini, A Trere *J. Org. Chem.* **58** 5615 (1993)
64. G Cardillo, A de Simone, L Gentilucci, P Sabatino, C Tomasini *Tetrahedron Lett.* **35** 5051 (1994)
65. T Uyehara, N Asao, Y Yamamoto *J. Chem. Soc., Chem. Commun.* 753 (1989)
66. M Hirama, T Shigemoto, Y Yamazaki *J. Am. Chem. Soc.* **107** 1797 (1985)
67. M Hirama, T Shigemoto, S Ito *J. Org. Chem.* **52** 3342 (1987)
68. M Shimano, A I Meyers *J. Org. Chem.* **60** 7445 (1995)
69. D Enders, W Bettray, G Raabe, J Runsink *Synthesis* 1322 (1994)
70. K Rudolf, J Hawkins, R Loncharich, K Houk *J. Org. Chem.* **53** 3879 (1988)